Can. J. Chem. Downloaded from www.nrcresearchpress.com by 190.90.36.8 on 09/04/12
For personal use only.

Canadian Journal of Chemistry

Issued by THE NATIONAL RESEARCH COUNCIL OF CANADA

VOLUME 37 JANUARY 1959 NUMBER 1

ORGANIC DEUTERIUM COMPOUNDS

XXI. SYNTHESIS OF DEUTERATED AZOBISMETHANE[1]

A. T. MORSE,[2] T. F. MASSIAH,[2] AND L. C. LEITCH

ABSTRACT

Deuterated azobismethane was synthesized in the conventional way from dimethyl sulphate and hydrazine.

The principal sources of methyl radicals for photochemical investigations are acetone, dimethyl mercury, and azomethane. Deuteromethyl radicals are similarly obtained from the corresponding deuterated compounds, of which only acetone-d_6 and bistrideuteromethyl-mercury have been reported (2). It seemed of interest to prepare deuteroazobismethane, since it is the only convenient way of obtaining methyl-d_3 radicals for certain work.

With the exception of 2,2′-azobispropane-2,2′-d_2, which was reported by us a few years ago (8), deuterated azoalkanes are unknown. The synthesis of azoalkanes from aldehydes or ketones via the azines and 1,2-dialkylhydrazines described in that paper is not applicable to the preparation of azomethane or deuteroazomethane because condensation of formaldehyde and hydrazine hydrate gives rise to polymers rather than the azine. Furthermore, formaldehyde-d_2, which is required in the present instance, is very difficult to prepare (1). Initially, lithium aluminum hydride reduction of 1,2-diacylhydrazines was found to be unsuccessful. This was also experienced by Hinman (6). However, we were led to reinvestigate this reaction by the appearance of a paper by Stewart (10) on the facile preparation of formic-d acid which readily yields 1,2-diformyl-d_2 hydrazine. Eventually, 1,2-dimethylhydrazine was obtained in 50% yield when 1,2-diformylhydrazine was reduced with a large excess of $LiAlH_4$ in dioxane as a solvent. However, the excessive cost of lithium aluminum deuteride precludes the use of the method for preparing more than very small quantities of azomethane-d_6.

As methyl-d_3 iodide is now readily available (9), methylation of 1,2-dibenzoylhydrazine was attempted with methyl iodide instead of dimethyl sulphate, but no methylation took place under a variety of conditions. Consequently, the method of Folpmers (3) and Hatt (5) remained the only practical route to azomethane-d_6:

$$C_6H_5CONHNHCOC_6H_5 + 2(CD_3)_2SO_4 + 2NaOH \rightarrow C_6H_5CON{=}NCOC_6H_5 + 2CD_3NaSO_4 + 2H_2O$$

$$C_6H_5CON(CD_3)N(CD_3)COC_6H_5 \xrightarrow{HCl} CD_3NH\overset{+}{N}H_2CD_3Cl^-$$

$$CD_3NHNHCD_3 \xrightarrow{HgO} CD_3N{=}NCD_3$$

[1]*Manuscript received September 4, 1958.*
Contribution from the Research Chemical Department of Merck and Company, Limited, Montreal, and the Division of Pure Chemistry, National Research Council, Ottawa, Canada.
Issued as N.R.C. No. 4959.
[2]*Present address: Merck and Company, Limited, Montreal, Que.*

In our first experiments with dimethyl-d_6 sulphate the ester was prepared from methyl-d_3 alcohol and chlorosulphonic acid. This method was somewhat inconvenient because methyl-d_3 alcohol had to be prepared from the bromide. Recent work from this laboratory on the preparation of deuterated esters from methyl-d_3 bromide and silver salts of the acids (7) held out the promise that dimethyl-d_3 sulphate might be prepared from methyl-d_3 bromide and silver sulphate. These reactants did in fact give the inorganic ester in 90% yields. From the investigations of Gragorov (4) on the mobility of radicals it would appear that deuterated dimethyl sulphate could also be prepared by exchanging methyl-d_3 iodide with normal dimethyl sulphate or preferably a homologous sulphate ester. This method is probably less convenient than the one described.

The succeeding steps in the synthesis of azomethane-d_6 paralleled those used to prepare the light compound (8) and call for no special comments.

EXPERIMENTAL

Dimethyl-d_6 Sulphate

(*a*) *By direct esterification of methyl-d_3 alcohol.*—To chlorosulphonic acid (665 g; 6.0 moles), cooled to −15° C in a 1-liter flask fitted with a dropping funnel, a reflux condenser, and a magnetic stirrer, methyl-d_3 alcohol (175 g; 5.0 moles) was added dropwise while maintaining the temperature below 0° C. After the addition of alcohol had been completed the reaction mixture was fractionated under reduced pressure in a Vigreux column. The yield of dimethyl-d_6 sulphate, b.p. 69 to 71° C/11 mm, n_D^{25} 1.3858, was 309 g (90%).

(*b*) *From methyl-d_3 bromide and silver sulphate.*—Methyl-d_3 bromide was prepared as described in a previous paper of this series (9). Silver sulphate (31.0 g; 0.1 mole) was ground to a fine powder in a mortar and placed in a heavy-walled glass tube which was then constricted near the top to facilitate sealing later. Methyl-d_3 bromide (21.0 g; 0.22 mole) was condensed into the tube on a vacuum manifold. The sealed tube was then heated for 4 to 5 hours at 100° C. The contents of the cold tube was washed out with ether into a gravity funnel. The silver iodide on the funnel was washed several times with small portions of ether. The combined ether extracts were freed of solvent and the residue was distilled in a Späth bulb from an air bath at 50° C under 0.1 mm on the vacuum line. The yield of product, n_D^{20} 1.3851, was 10.6 g (85%). The index of refraction of normal dimethyl sulphate is 1.3860.

sym-Dimethyl-d_6 Dibenzoylhydrazine

To a stirred suspension of 40 g (0.165 mole) 1,2-dibenzoylhydrazine in 300 ml of 2% sodium hydroxide solution heated to 80° C were added dropwise and simultaneously from two dropping funnels, 65 ml (0.65 mole) of dimethyl-d_6 sulphate and 125 ml of 50% aqueous sodium hydroxide solution. After it was stirred for an additional hour at 80° C the reaction mixture was set aside to crystallize in the refrigerator. The crystalline solid which had separated was collected on a funnel and dissolved in 50 ml of chloroform. The solution was dried over magnesium sulphate and treated with 100 ml of a 50% mixture of ether and pentane. After the mixture had been allowed to stand at 0° C in the refrigerator for several hours the crystals were filtered off and washed with pentane. Yield: 23 g (24.4%), m.p. 85–86° C.

1,2-Dimethyl-d_6-hydrazine

The dibenzoyldimethyl-d_6-hydrazine obtained above (23.0 g; 0.085 mole) was heated under reflux for 3 hours with 95 ml of 35% concentrated hydrochloric acid. The reaction

Can. J. Chem. Downloaded from www.nrcresearchpress.com by 190.90.36.8 on 09/04/12
For personal use only.

mixture was steam-distilled to remove benzoic acid and then evaporated to dryness in a flash evaporator. The residue of crude 1,2-dimethyl-d_6-hydrazine monohydrochloride was dissolved in 40 ml of water and added slowly with stirring to 100 ml of 50% aqueous sodium hydroxide. The base liberated was purified and freed of water by distillation on the vacuum line through a U-tube filled with potassium hydroxide pellets. Yield: 5.3 g, n_D^{24} 1.4188 (95.5%).

Bisazomethane-d_6

A solution of 1,2-dimethyl-d_6-hydrazine (5.3 g; 0.08 mole) in 50 ml of water was added to a stirred suspension of 22.0 g (0.11 mole) of yellow mercuric oxide in 40 ml of water in a flask with a reflux condenser to which was attached a spiral trap cooled to −78° C in a bath of acetone and solid carbon dioxide. After addition of the base was completed the reaction mixture was slowly heated to reflux. The apparatus was swept with a slow stream of nitrogen. The yield of azomethane-d_6 which analyzed 99.3 atom % deuterium by mass spectrometry was 3.2 g (62.2%).

1,2-Dimethylhydrazine

1,2-Diformylhydrazine (22.0 g; 0.25 mole) was extracted in a Soxhlet by a refluxing solution of 66 g (2.0 mole) of lithium aluminum hydride in 1 liter of dioxane. After 24 hours the hydride was decomposed by careful addition of water. Inorganic hydroxides were removed by centrifugation. The filtrate was acidified and evaporated to dryness in a flash evaporator. The residue was dissolved in the minimum amount of water and the solution added to an excess of 50% alkali. The supernatant layer of insoluble 1,2-dimethylhydrazine was distilled off on a vacuum manifold. Yield: 7.5 g (50%). It was converted into azomethane by oxidation with mercuric oxide as described in ref. (8). The azo compound was identified by mass analysis.

ACKNOWLEDGMENTS

The technical assistance of Mr. D. Kovachic and Mr. W. M. Andrejchyshyn is greatly appreciated.

REFERENCES

1. BANNARD, R. A., MORSE, A. T., and LEITCH, L. C. Can. J. Chem. **31**, 351 (1953).
2. BEVEGE, E. E., RENAUD, R., and LEITCH, L. C. Can. J. Chem. **31**, 1259 (1953).
3. FOLPMERS, M. T. Rec. trav. chim. **34**, 34 (1915).
4. GRAGOROV, I. P. Doklady Akad. Nauk S.S.S.R. **99**, 101 (1954).
5. HATT, H. H. Organic syntheses, coll. vol. II. John Wiley & Sons, Ltd., New York. 1944. p. 208.
6. HINMAN, R. L. J. Am. Chem. Soc. **78**, 1645 (1956).
7. ISABELLE, M. E. and LEITCH, L. C. Can. J. Chem. **36**, 440 (1957).
8. RENAUD, R. and LEITCH, L. C. Can. J. Chem. **32**, 545 (1954).
9. RENAUD, R. and LEITCH, L. C. Can. J. Chem. **34**, 179 (1956).
10. STEWART, R. Can. J. Chem. **35**, 766 (1957).

Can. J. Chem. Downloaded from www.nrcresearchpress.com by 190.90.36.8 on 09/04/12
For personal use only.

Can. J. Chem. Downloaded from www.nrcresearchpress.com by 190.90.36.8 on 09/04/12
For personal use only.

POTATO X VIRUS

PART II. PREPARATION AND PROPERTIES OF PURIFIED, NON-AGGREGATED VIRUS FROM TOBACCO[1]

M. E. REICHMANN

ABSTRACT

When sap from tobacco, infected with potato X virus, was dialyzed against 0.05 *M* and then against 0.005 *M* sodium citrate, no aggregation of the virus was detected after ultracentrifugation. Flow birefringence measurements were made to compare virus preparations obtained by ultracentrifugation of untreated sap and of sap that had been treated with various buffers. Only versene and citrate were found to prevent aggregation. The influence of pH in the range 5.7–7.3 was very slight. Possible explanations of this effect are discussed.

Nitrogen and phosphorus content and the sedimentation constant of the purified, non-aggregated virus are reported.

INTRODUCTION

An investigation of size and size distribution of viruses in solution requires that special precautions be taken, during the process of isolation and purification, not to change these characteristics. Even in the case of the most studied virus, the tobacco mosaic virus, few authors emphasize this point (1) and only recently has the preparation of purified uniform tobacco mosaic virus been described (2).

The irreversible end-to-end aggregation of potato X virus in the process of purification is a well-known phenomenon (3, 4, 5). In a previous publication from this laboratory the size and size distribution of potato X virus in tobacco sap was reported (6). For more accurate studies a purified preparation was needed. This paper describes conditions under which this virus can be isolated without alteration in its state of aggregation. Preliminary conclusions concerning the nature of the aggregation processes are drawn from some of the properties of this preparation.

EXPERIMENTAL

Purification

The potato X virus and the conditions under which it was grown in tobacco have been described previously (6). Freshly frozen tobacco leaves were squeezed with a mortar and pestle. The sap was centrifuged at 4000 r.p.m. for 30 minutes. The brown supernatant was dialyzed overnight against a large volume of 0.05 *M* sodium citrate. The dialysis bags were then transferred to a large volume of 0.005 *M* sodium citrate and the dialysis continued for another 10 hours. The sap was then centrifuged at 4000 r.p.m. for 20 minutes and the supernatant was ultracentrifuged at 75,000$\times g$ for 90 minutes. The pellet was water-clear with a brown core in the center. After decantation the pellet was resuspended in 0.005 *M* sodium citrate. It dissolved readily except for the brown core which was insoluble. The insoluble material was removed by slow centrifugation and the supernatant was submitted to two additional cycles of ultracentrifugation and slow centrifugation in 0.005 *M* sodium citrate. The final pellet obtained was water-clear and dissolved readily with only traces of insoluble material. In contrast, virus material prepared from sap that had not been treated with sodium citrate was slower to dissolve and the amounts of insoluble material in each step were larger.

[1]*Manuscript received July 6, 1958.*
Contribution No. 3, Chemistry Division, Science Service, Canada Department of Agriculture Research Laboratory, Vancouver, B.C.

Flow Birefringence Measurements

The extinction angles χ were measured at different velocity gradients G in a small flow birefringence apparatus manufactured by Rao Instrument Company, Brooklyn, New York (7). Comparisons between different samples were made in a concentration range of 0.08 to 0.02% virus in 0.005 *M* sodium citrate. The extinction angles were found independent of virus concentration in this range. In Fig. 1 typical extinction angles vs. gradient measurements are shown for virus in sap, virus purified as described above, and virus isolated from untreated sap by one ultracentrifugation. The low extinction angles of the latter sample confirm findings reported in the literature that the virus aggregates under these conditions (3, 4, 5). Similar results were obtained whether the virus was resuspended in distilled water or in 0.005 *M* citrate. Moreover, each ultracentrifugation – slow centrifugation cycle increased the amount of aggregated material.

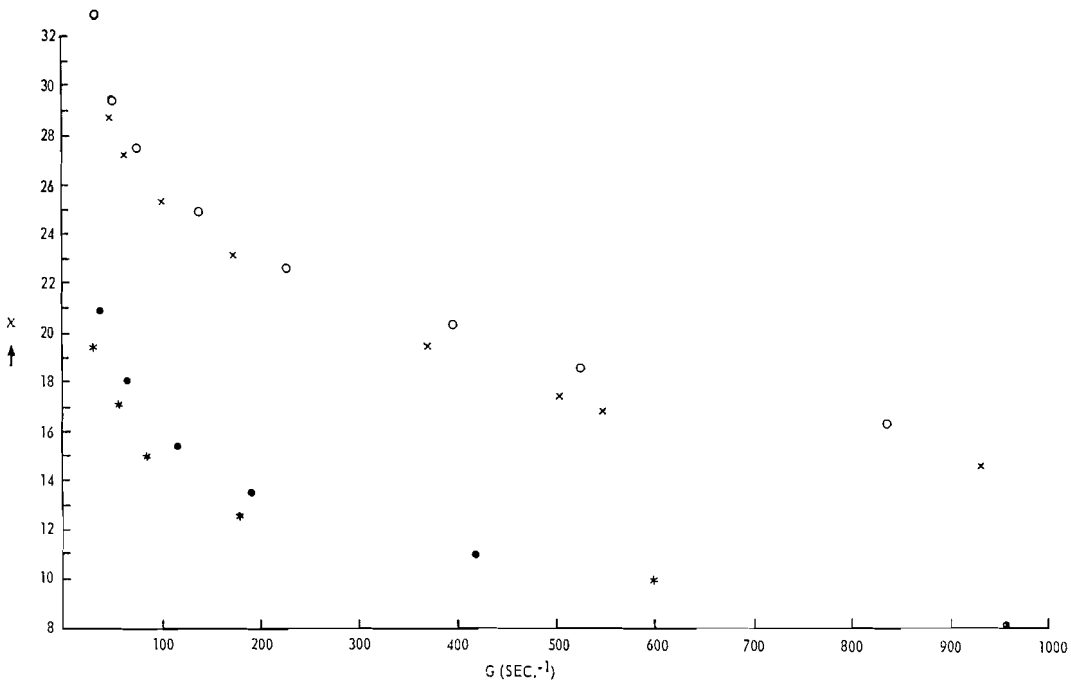

FIG. 1. Extinction angle χ vs. gradient G plot: ×, virus in sap; ●, once ultracentrifuged and dissolved in 0.005 *M* sodium citrate; *, once ultracentrifuged and dissolved in distilled water; ○, ultracentrifuged after citrate treatment.

On the other hand, virus obtained from citrate-treated sap showed virtually no change in the χ vs. G curve. The small shift towards higher extinction angles was probably a result of minor losses of aggregated material in the process of ultracentrifugation.

In Fig. 2, δ, the phase difference in degrees, divided by the concentration c (in per cent virus) is plotted for the purified non-aggregated material. The downward curvature in this plot indicates the rigid nature of the particle. This is in agreement with similar earlier measurements of the virus in tobacco sap (6).

The Effect of pH and Ionic Strength

To speed up the purification procedure several short cuts were attempted. One aliquot of a sap was dialyzed against 0.05 *M* sodium citrate and a second aliquot was dialyzed

Can. J. Chem. Downloaded from www.nrcresearchpress.com by 190.90.36.8 on 09/04/12
For personal use only.

directly against 0.005 *M* sodium citrate. Both samples showed an increase in aggregation after ultracentrifugation. To test the effect of pH, citrate buffer at pH 5.7 was used. Other ions were also tested. The results are summarized in Tables I and II.

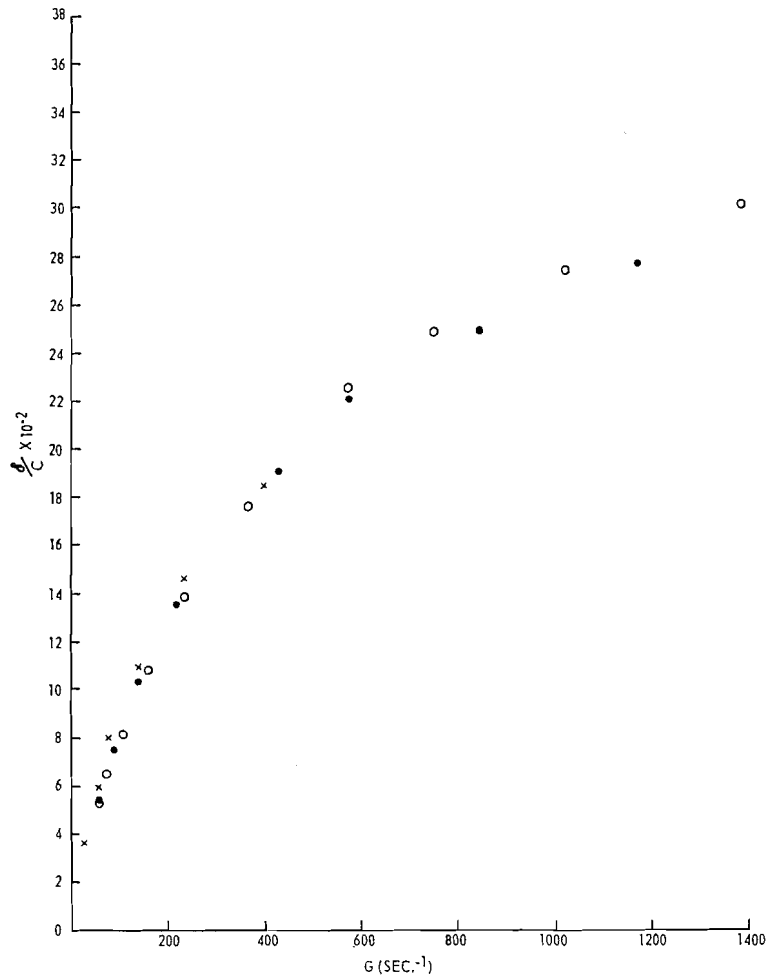

FIG. 2. Amount of birefringence divided by concentration, plotted against velocity gradient. Purified non-aggregated virus in 0.005 *M* sodium citrate.

The purified non-aggregated virus was insoluble in water in the complete absence of electrolytes. When thoroughly dialyzed against distilled water, the virus solution became turbid and upon centrifugation at 4000 r.p.m. for 20 minutes practically all the virus was in the pellet. This pellet could be redissolved in 0.005 *M* sodium citrate. Flow birefringence measurements indicated that no aggregation occurred in this process.

Nitrogen and Phosphorus Content

Kjeldahl nitrogen was determined using essentially the procedure of Miller and Miller (8). The theoretical curves and experimental data were determined on a Beckman DU spectrophotometer at 480 mμ, in a concentration range of 0.06 to 0.12 mg of nitrogen. Phosphorus content was determined by the method of Michelson (9). The virus concentration was obtained from dry weights at 100° C in a vacuum oven by subtracting

Can. J. Chem. Downloaded from www.nrcresearchpress.com by 190.90.36.8 on 09/04/12
For personal use only.

TABLE I

The influence of various ions and of pH on the tendency of potato X virus to aggregate after ultracentrifugation

Dialysis of sap	Solvent after ultracentrifugation	Aggregation
0.05 *M* Na citrate followed by 0.005 *M* Na citrate	0.005 *M* Na citrate	−
0.05 *M* Na citrate	0.05 *M* Na citrate	+
	0.005 *M* Na citrate	++−
0.005 *M* Na citrate	0.005 *M* Na citrate	+
0.05 *M* citrate buffer, pH 5.7, followed by 0.005 *M* of same buffer	0.005 *M* citrate buffer, pH 5.7	+−
0.05 *M* versene, pH 7.2, followed by 0.005 *M* of same buffer	0.005 *M* versene, pH 7.2	−
0.05 *M* K phosphate buffer, pH 7.2, followed by 0.005 *M* of same buffer	0.005 *M* K phosphate buffer, pH 7.2	+
0.005 *M* K phosphate buffer, pH 7.2	0.005 *M* K phosphate buffer, pH 7.2	+
0.05 *M* NaCl, pH 7.2 (adjusted with NaOH), followed by 0.005 *M* of same buffer	0.005 *M* NaCl, pH 7.2 (adjusted with NaOH)	+

NOTE: −, No change.
+, Low extinction angles (approximately like points ● in Fig. 1).
++−, Slight lowering of extinction angles (by 3° at 250 sec^{-1}).
+−, Very slight lowering of extinction angles (by 1° at 250 sec^{-1}).

TABLE II

The influence of various ions on the tendency of purified potato X to aggregate after ultracentrifugation

Dialysis of purified non-aggregated virus	Solvent after ultracentrifugation	Aggregation
0.005 *M* NaCl, pH 7.2 (adjusted with NaOH)	0.005 *M* NaCl, pH 7.2 (adjusted with NaOH)	−
0.005 *M* phosphate, pH 7.2	0.005 *M* phosphate, pH 7.2	−
0.1 *M* phosphate, pH 5.7	0.1 *M* phosphate, pH 5.7	+

NOTE: −, No change.
+, Lower extinction angles (see points ● in Fig. 1).

the dry weight of the citrate solvent. The nitrogen and phosphorus values were 15.7±0.4% and 0.59±0.02% respectively. These data are in good agreement with the values found by Loring (4).

Serology

Antisera were prepared by injecting the citrate-treated, three times ultracentrifuged preparation into rabbits. These sera were compared by means of the complement fixation serological technique (10, 11) with sera prepared from four times ultracentrifuged – slow centrifuged aggregated material. In addition to antibodies against virus, traces of antibodies against normal plant proteins were detected in all sera. However, the virus, given cyclic centrifugation only, produced considerably more of these antibodies than the citrate-treated virus.

Ultraviolet Absorption

An attempt was made to determine the extinction coefficient at 260 mμ. It was found that in 0.005 *M* sodium citrate Beer's law was not followed in a virus concentration range of 0.01 to 0.045% indicating interactions of the chromophoric groups. The same was true when higher sodium citrate concentrations or 0.05–0.1 *M* phosphate buffer at

Can. J. Chem. Downloaded from www.nrcresearchpress.com by 190.90.36.8 on 09/04/12
For personal use only.

pH 7.2 were used. At pH 5.7 in 0.1 *M* phosphate, however, the extinction coefficient was independent of concentration. An average value of 26.8 g virus/100 ml cm was derived.

The ultraviolet absorption spectrum under these conditions showed a minimum at 245 mμ and a broad maximum at 260 mμ. The ratio of the 260/280 mμ absorptions was 1.20. After correction for scattering from measurements at 320 to 410 mμ (12) this ratio became 1.19. On the other hand, virus prepared by four cycles of ultracentrifugation – slow centrifugation from sap untreated with sodium citrate had a 260/280 mμ ratio of 1.30 when corrected for scattering.

Sedimentation

The sedimentation coefficient of the non-aggregated purified preparation was determined in 0.1 *M* phosphate buffer, pH 5.7, in a virus concentration range 0.25–0.02%. Photographs were taken at 4-minute intervals in a Spinco Model E Analytical Ultracentrifuge at 25,980 r.p.m. The sedimentation coefficients were converted to corresponding values at 20° C in water. The least-squares line derived from the data followed the equation $1/S_{20} \times 10^{10} = 8.49 + 4.58\ c$ giving a sedimentation coefficient S_{20} of 117.7 Svedbergs at zero concentration. Similar studies at pH 7.1 reported in the literature gave the value 123.5 Svedbergs (5). As stated in reference (5) the preparation contained a small amount of material that sedimented very rapidly. With the preparations described in this paper, however, there was no indication of the presence of material other than that contained in the major peak. Figure 3 represents the ultracentrifuge patterns of a 0.25% and 0.02% solution respectively.

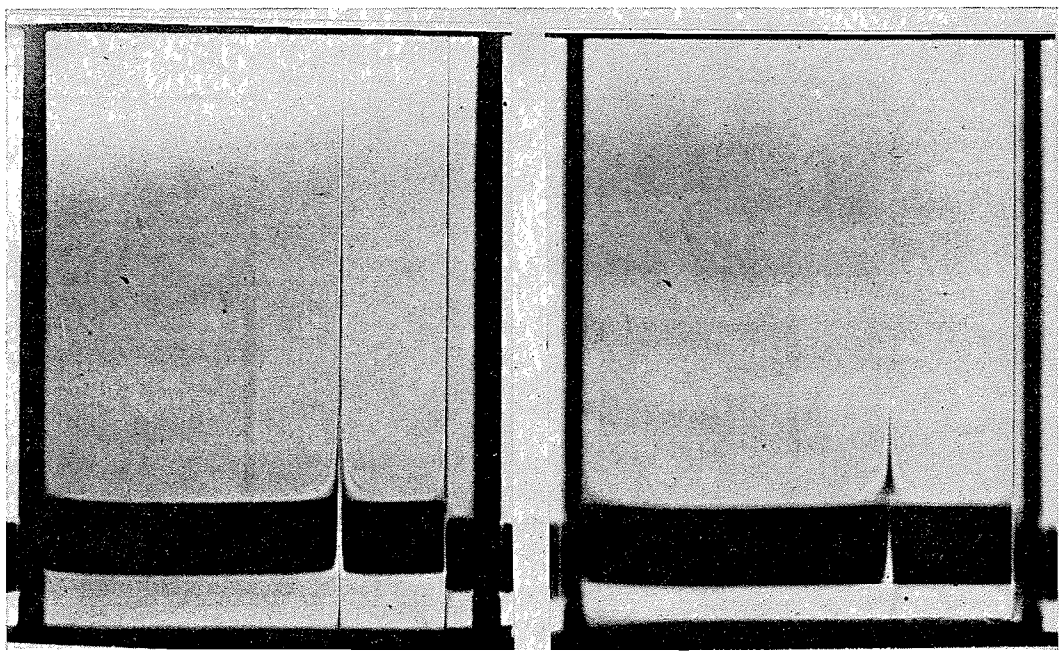

Fig. 3. Sedimentation pattern of purified non-aggregated virus in 0.1 *M* phosphate, pH 5.7. Virus concentrations 0.25% and 0.02% bar angles 70 and 55° respectively. Sedimentation from right to left.

DISCUSSION

The data in Table I indicate that when potato X virus in tobacco sap was exposed to 0.05 *M* sodium citrate, some of its structural features connected with its tendency to aggregate end-to-end irreversibly were altered. Once this change had taken place the

Can. J. Chem. Downloaded from www.nrcresearchpress.com by 190.90.36.8 on 09/04/12
For personal use only.

virus only aggregated when ultracentrifuged at high ionic strength. The influence of pH in the range 5.7–7.4 was very small. Versene buffer at pH 7.2 under the same conditions had a similar effect, while potassium phosphate and sodium chloride were not active. The data in Table II furnished further evidence indicating irreversible changes in the virus structure. In contrast to the untreated virus, the preparation purified with citrate did not aggregate when ultracentrifuged after "exhaustive" dialysis against 0.005 *M* phosphate or sodium chloride at pH 7.2. At higher salt concentrations, however, aggregation occurred.

Recently a more critical attitude to the degree of purity in tobacco mosaic virus preparations has revealed that treatment with citrate and other ions alters the composition of these preparations (13, 14, 15, 16). Thus Ginoza *et al.* (13) were able to prepare colorless pellets of a group of strains of T.M.V. after citrate, versene, and phosphate treatments, while the untreated virus when ultracentrifuged always gave amber-colored pellets. This color was found to be associated with small nucleoprotein molecules that were split off the virus during these procedures. The amount of nucleoprotein removed increased with increasing phosphate concentration and at higher temperatures. Pirie (15) also reported the release of labile phosphorus-containing compounds when T.M.V. was exposed to citrate.

It is possible that the tendency of potato X virus to aggregate is linked with the presence of phosphorus-containing or other compounds that are removed when potato X virus is treated with 0.05 *M* citrate or versene at 5° C. The action of such compounds could be either limited to the facilitation of a close approach of virus particles, similar to the non-specific action of electrolytes, or could be of a more specific nature. The change in the 260/280 mμ absorption ratio cannot be taken as evidence for the splitting of such compounds. It merely indicates that the surrounding of the chromophoric groups has changed under the influence of citrate.

The possibility of heavy metals participating in the aggregation processes cannot be ruled out. The chelating properties of citrate and versene would lead to considerations similar to those made in connection with preparations of colorless T.M.V. pellets (13).*

Finally, the chemical purity of the preparation described in this paper should be considered. The complement fixation experiments indicate that a higher degree of purity has been achieved than in samples prepared by techniques described in the literature. The author is well aware, however, that it may be subject to the same criticism as T.M.V. preparations obtained by ultracentrifugation (15, 17, 18). As stated in the introduction, the main concern of this study was to preserve the size and size distribution intact. Methods offered by critics of the degree of purity of virus preparations unfortunately change these properties in the case of most viruses. Consequently, to the author's knowledge no method is available at the present time which would completely satisfy both the criteria of chemical purity and the requirements for physicochemical studies.

REFERENCES

1. WATANABE, I. and KAWADE, Y. Bull. Chem. Soc. Japan, **26**, 294 (1953).
2. BEODTKER, H. and SIMMONS, N. S. J. Am. Chem. Soc. **80**, 2550 (1958).
3. BAWDEN, F. C. Plant viruses and virus diseases. Chronica Botanica Company, Waltham, Mass. 1950.
4. LORING, H. S. J. Biol. Chem. **126**, 455 (1938).
5. LAUFFER, M. A. and CARTWRIGHT, T. E. Arch. Biochem. Biophys. **38**, 371 (1952).
6. REICHMANN, M. E. Can. J. Chem. **36**, 1603 (1958).

**In one of our preparations the tobacco leaves were squeezed in a stainless steel Carver press basket. The sap in this preparation darkened very rapidly on standing, indicating the presence of traces of metals from the press. The citrate-treated, purified virus when dialyzed against 0.1 M phosphate buffer at pH 5.7 aggregated and most of it came out of solution. This behavior was never observed in preparations squeezed by a mortar and pestle.*

Can. J. Chem. Downloaded from www.nrcresearchpress.com by 190.90.36.8 on 09/04/12
For personal use only.

7. EDSALL, J. T., RICH, A., and GOLDSTEIN, M. Rev. Sci. Instr. **23**, 695 (1952).
8. MILLER, G. L. and MILLER, E. E. Anal. Chem. **20**, 481 (1948).
9. MICHELSON, O. B. Anal. Chem. **29**, 60 (1957).
10. BROOKSBY, J. B. The technique of complement fixation in foot-and-mouth disease research. A.R.C. Rept. Ser. London, No. 12 (1952).
11. WRIGHT, N. W. and STACE-SMITH, R. To be published.
12. ENGLANDER, S. W. and EPSTEIN, H. T. Arch. Biochem. Biophys. **68**, 144 (1957).
13. GINOZA, W., ATKINSON, E. D., and WILDMAN, S. G. Science, **119**, 269 (1954).
14. SIEGAL, A. and WILDMAN, S. G. Phytopathology, **44**, 277 (1954).
15. PIRIE, N. W. J. Biol. Chem. **63**, 316 (1956).
16. MATTHEWS, R. E. F. and SMITH, J. O. Nature, **180**, 375 (1957).
17. PIRIE, N. W. Exptl. Cell Research, (Suppl.) **1**, 193 (1949).
18. PIRIE, N. W. Advances in Virus Research, **4**, 159 (1957).

Can. J. Chem. Downloaded from www.nrcresearchpress.com by 190.90.36.8 on 09/04/12
For personal use only.

Can. J. Chem. Downloaded from www.nrcresearchpress.com by 190.90.36.8 on 09/04/12
For personal use only.

THE N- AND C-TERMINAL END GROUPS OF HAIR KERATIN[1]

M. F. KERR AND C. GODIN

ABSTRACT

The N-terminal and the C-terminal residues of human and horse hair and partially reduced hair have been determined. Aspartic acid, glutamic acid, glycine, serine, threonine, alanine, and valine were identified as N-terminal groups. Aspartic acid, glutamic acid, glycine, serine, threonine, and alanine were identified as C-terminal groups. These are the same N-terminal and C-terminal amino acids as have been found previously for wool and feather keratin.

INTRODUCTION

The purpose of the following work was to establish a procedure which would serve to differentiate among the hair keratins of different species of animals, including man. At present a visual microscopic procedure is used in practically all forensic work involving hair. For most cases this is sufficient, particularly if negative results will suffice. In some cases, however, the microscope is simply inadequate in providing the information required by the examiner.

Recently, the N-terminal and the C-terminal residues of wool keratin were determined (1, 2, 3, 4, 5, 6). Complex mixtures of end groups were found and it was hoped that some qualitative differences could be established between the hair keratins of different species using these methods. This paper reports the identification of N-terminal and C-terminal residues in human and horse hair.

EXPERIMENTAL

Hair.—The human hair was obtained from the "N" Division, R.C.M.P. Barracks, and was exclusively male. The horse hair was obtained from the "N" Division, R.C.M.P. Stables, and was exclusively tail hair. To degrease the hair it was extracted in a Soxhlet for 2 hours each with acetone and ether and then air-dried. Finely ground hair was obtained by grinding the hair in liquid nitrogen in a porcelain mortar.

Dinitrophenylation.—Finely ground hair (0.5 g) was suspended in water (12 ml) containing sodium bicarbonate (0.5 g). Ethanol (25 ml) containing 1-fluoro-2,4-dinitrobenzene (FDNB) (0.86 g) was added and the mixture was shaken for 48 hours at 40° C (2). The hair was then isolated by filtration, washed with water, alcohol, and ether. When partly reduced keratin was dinitrophenylated, the mixture was first extracted with ether, then acidified. The insoluble dinitrophenyl-proteins (DNP-proteins) were centrifuged down and washed with water, alcohol, and ether.

Hydrazinolysis.—The method described by Niu and Fraenkel-Conrat (7) was used.

Hydrolysis.—The DNP-proteins were hydrolyzed in 6 *N* HCl in sealed tubes for 24 hours at 100° C.

Chromatography.—The DNP-amino acids were spotted on Whatman paper No. 3 MM buffered at pH 6. The chromatograms were developed with *tert*-amyl alcohol saturated with pH 6 phthalate buffer (8). Each spot obtained was run again after elution from the paper. The same paper was used for the second run but the phthalate buffer alone was used as solvent. In the buffer alone the R_f values are different from those obtained in *tert*-amyl alcohol.

Reduction.—Hair keratin was partly reduced with sodium thioglycolate (9). Hair (0.5 g) was suspended in water (25 ml) containing sodium hydroxide (4 g). Thioglycolic

[1]*Manuscript received August 15, 1958.*
Contribution from the Department of Chemistry, Faculty of Science, University of Ottawa, Ottawa, Ontario.

acid (2.5 ml) was added. The mixture was shaken at room temperature for a given period of time (3 to 5 hours). The residue was then filtered off and the keratin precipitated by careful acidification with acetic acid or dilute hydrochloric acid. The acidification was followed with a pH meter; a first protein fraction (black solid) came out between pH 8 and pH 7 and a second fraction (white solid) between pH 4 and pH 1.

RESULTS

Hair.—The N-terminal amino acids obtained from human and horse hair by the dinitrophenyl method were aspartic acid, glutamic acid, glycine, serine, threonine, alanine, and valine. Using the hydrazinolysis method for the determination of C-terminal groups in proteins, six C-terminal residues were detected in human and horse hair. They were identified by paper chromatography after transformation into DNP-derivatives. They were shown to be aspartic acid, glutamic acid, glycine, serine, threonine, and alanine.

Partly Reduced Keratin.—Treatment with alkaline thioglycolate for 3 hours transforms keratin into a protein mixture containing 25% of its sulphur as cysteine (9). When the reduction was allowed to proceed for 3 to 5 hours, the protein fractions obtained by acidification to pH 8–7 and pH 4–1 had the same N-terminal and C-terminal groups as intact hair.

DISCUSSION

Human hair and horse hair have the same seven N-terminal groups and the same six C-terminal groups. The same amino acids are also found as N-terminal and C-terminal residues of wool keratin (1–6). The same seven N-terminal groups have also been found recently in feather keratin (10). No attempt was made to do a quantitative estimation of end groups because it was shown recently that the results of quantitative determination in wool are not very reliable (4), at least not reliable enough to establish species differences with certitude. Crude wool keratin was also shown recently to have the same N-terminal groups as intact wool (4). It is therefore not surprising that partly reduced hair keratin has the same N-terminal and C-terminal groups as intact hair.

As no qualitative differences are found between keratin terminal groups in four species —man, horse, sheep, and fowl—this method was not investigated any further as a means of distinguishing between the hair keratins of different species.

REFERENCES

1. BLACKBURN, S. Biochem. J. **47**, 443 (1950).
2. MIDDLEBROOK, W. R. Biochim. et Biophys. Acta, **7**, 547 (1951).
3. ALEXANDER, P. and SMITH, L. F. Proc. Intern. Wool Textile Research Conf. Australia, Vol. B, p. B-56 (1956).
4. THOMPSON, E. O. P. Australian J. Biol. Sci. **10**, 225 (1957).
5. BLACKBURN, S. and LEE, G. R. J. Textile Inst. **45**, T487 (1954).
6. BRADBURY, J. H. Biochem. J. **68**, 482 (1958).
7. NIU, C-I. and FRAENKEL-CONRAT, H. J. Am. Chem. Soc. **77**, 5882 (1955).
8. BLACKBURN, S. and LOWTHER, A. G. Biochem. J. **48**, 126 (1951).
9. GODDARD, D. R. and MICHAELIS, L. J. Biol. Chem. **112**, 361 (1935).
10. WOODIN, A. M. Biochem. J. **63**, 576 (1956).

Can. J. Chem. Downloaded from www.nrcresearchpress.com by 190.90.36.8 on 09/04/12
For personal use only.

Can. J. Chem. Downloaded from www.nrcresearchpress.com by 190.90.36.8 on 09/04/12
For personal use only.

A NOTE ON THE ELECTRICAL CONDUCTANCES OF DIELECTRIC FLUIDS IN ULTRASONIC FIELDS[1]

N. BERKOWITZ

ABSTRACT

The electrical conductances of ethyl bromide, *n*-propyl bromide, *n*-butyl bromide, methanol, and ethanol in ultrasonic fields have been measured at frequencies between 250 kc/s and 2 Mc/s and intensities between 0.7 and 24 w/cm^2. Measurements were made at room temperature, using a simple d-c. technique. It is shown that a *simple* transient increase in conductance, such as has previously been observed by Seidl, may be confined to unassociated fluids and that it can occasionally give way to a much more complex—and not as yet fully understood—behavior pattern.

When a dielectric liquid (such as hexane or toluene) is placed in an ultrasonic field, a marked transient change in its electrical conductance K is induced. As soon as irradiation is begun, a sharp (and often virtually instantaneous) rise in K, followed by a relatively slow approach to a new equilibrium conductance, is observed; and when the acoustic field is removed, K will more or less rapidly return to its original value (1, 2). The plot of K vs. time t (at constant frequency f and intensity I) will, in other words, take the form illustrated in Fig. 1. Meyer (1) has interpreted these phenomena by assuming transfer of adsorbed impurities from the electrodes into the liquid, while Seidl (2), working with toluene, hexane, and carbon tetrachloride, rejects Meyer's explanation and postulates, instead, an acoustic splitting of "complex ions" and a consequent increase either in the number or in the mobility of the charge carriers.

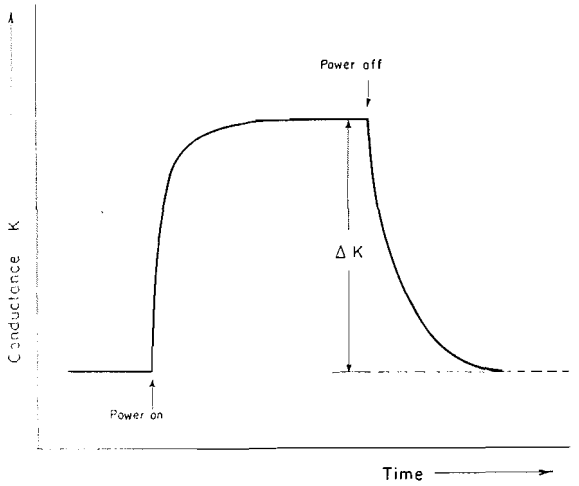

FIG. 1. General variation of conductance with time of irradiation (after Seidl).

Measurements made in this laboratory tend, broadly, to support Seidl's thesis: desorption of impurities—or a simple temperature effect that would accrue from acoustic heating of the liquid under test— appear quite insufficient to account for the experimental observations (and, indeed, to be generally irreconcilable with them). Both processes are, for instance, inconsistent with the very rapid initial rise in K and with its almost equally

[1]*Manuscript received September 4, 1958.*
Contribution No. 74 from the Research Council of Alberta, Edmonton, Alberta.

rapid fall when the ultrasonic field is switched off; and ΔK is always far greater than can be accounted for by the relatively small temperature rise in the test fluid during irradiation (cf. Seidl). On the other hand, the available evidence now suggests that "complex ion" splitting represents only one of several phenomena. If the range of fluids under examination is extended, and if measurements of K are made at several frequencies and intensities, seemingly more complex changes than those exemplified by Fig. 1 are occasionally recorded. Pronounced differences can, in particular, be noted in the responses of associated and unassociated liquids; and under certain conditions, ultrasonic irradiation appears to cause a *fall* rather than an increase in the conductance.* The purpose of this note is to report data illustrating these statements.

In the study here under review, a Mullard E.7562 generator, coupled to an oscillating ($\sim$15 cm^2) quartz crystal mounted in a sealed transducer housing, was used to produce ultrasonic waves in the frequency range 250 kc/s to 2 Mc/s. Maximum intensities of the tuned beams varied from about 2.3 w/cm^2 at 250 kc/s to nearly 35 w/cm^2 at 2 Mc/s. The conductivity cell was blown of thin pyrex glass and fitted with two platinum plate electrodes disposed at 90° to the acoustic wave front; a 1.5-volt potential was applied to these electrodes from a (frequently checked) dry cell. Resistances were measured by connecting cell and battery in series to a Leeds & Northrup d-c. bridge and a Pye "Scalamp" galvanometer. No attempt was made to determine the cell constant and

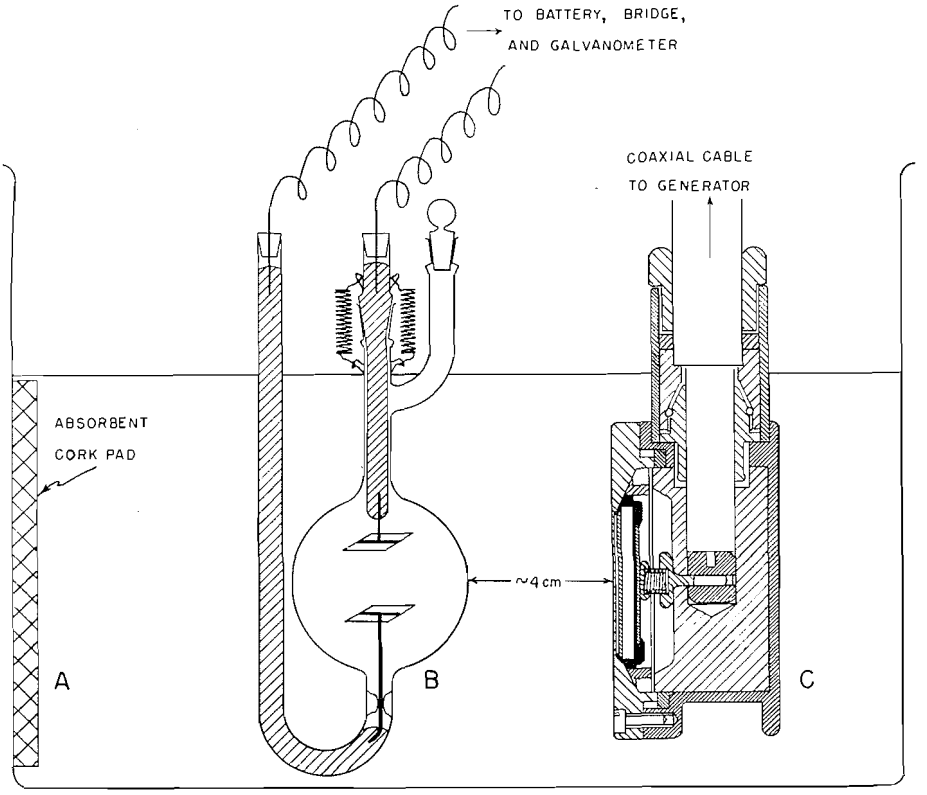

FIG. 2. Diagram of apparatus (not to scale):
A: constant-temperature bath; B: conductivity cell; C: transducer.

**It should be noted that this phenomenon further militates against attributing the observed change in K—or any substantial part of this change—to a temperature rise in the liquid under test.*

Can. J. Chem. Downloaded from www.nrcresearchpress.com by 190.90.36.8 on 09/04/12
For personal use only.

to convert the measured resistances to absolute resistivities; and similarly, no attempt was made, at this time, to investigate the variation of the measured response with the cell/crystal distance. Since large changes in K during ultrasonic irradiation did not apparently require a particularly critical adjustment of the assembly (or, for that matter, a critical design of the cell), it was deemed adequate to select an arbitrary cell/crystal distance (*ca.* 4 cm) and to maintain this constant throughout the investigations. Spurious conductance changes (such as might arise from impurities) were minimized by employing pure liquids and by conditioning the cell for several hours with the particular liquid under test. (The conditioning aliquot was removed and the cell freshly filled immediately prior to a measurement.) Further, in order to eliminate back e.m.f.'s, measurements of K in the ultrasonic field were only begun after the external potential had been applied to the test sample for at least 30 minutes and the conductance had attained a constant value. Both cell and transducer were immersed in a constant-temperature bath controlled to within $\pm 0.02°$ C. The assembly is shown diagrammatically in Fig. 2.

Liquids chosen for study were (*a*) a homologous series of unassociated fluids (comprising ethyl, *n*-propyl, and *n*-butyl bromide, all obtained from the Matheson Company Inc. with "reagent grade" purity), and (*b*) two highly associated fluids (methyl and ethyl alcohol).* The latter were purified by careful drying and subsequent double redistillation. In the case of (*a*), K was always measured at $25 \pm 0.02°$ C and in the case of (*b*), at $35 \pm 0.02°$ C. In the diagrams shown below, all experimental data are expressed as conductances (in reciprocal ohms). The degree of reproducibility can be gauged from the duplicates that are shown in several instances.

Plots of K/t for the three unassociated dielectrics (EtBr, *n*-PrBr, *n*-BuBr) are reproduced in Figs. 3 and 4. They follow closely upon the course of Seidl's curves (cf. Fig. 1)—a course here designated as Type A—but they differ from them in some quantitative aspects. Thus, at $f = 250$ kc/s and $I = 2.3$ w/cm², ΔK is in all three instances of the order of 10% (as compared with 31% and 47% reported by Seidl for CCl_4 and hexane respectively); and the return of K to its initial value after the field has been switched off occurs over a rather shorter period (*ca.* 5 minutes as compared with 20 minutes for

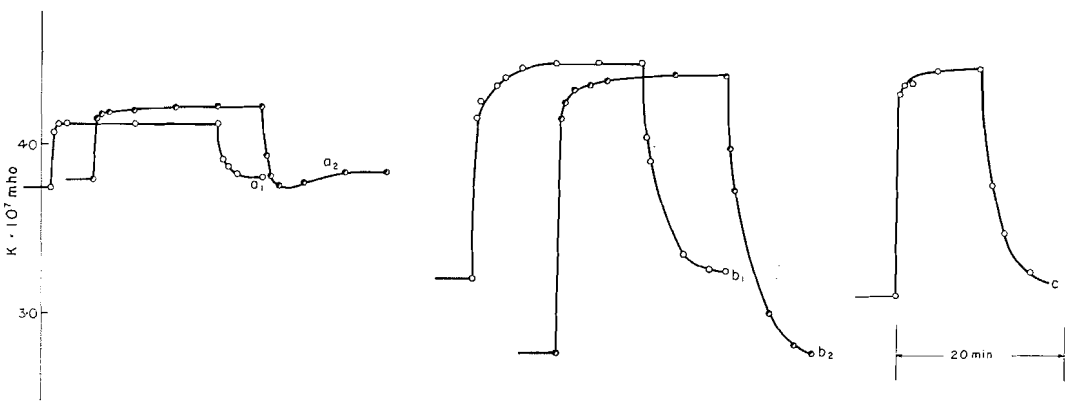

FIG. 3. a_1, a_2: Ethyl bromide; $f = 250$ kc/s, $I \sim 2.3$ w/cm².
b_1, b_2: Ethyl bromide; $f = 1$ Mc/s, $I \sim 12.4$ w/cm².
c: Ethyl bromide; $f = 2$ Mc/s, $I \sim 24$ w/cm².

**Because Seidl concentrated on non-polar or very weakly polar dielectrics, attention in the present study was focused upon relatively strongly polar ones.*

Can. J. Chem. Downloaded from www.nrcresearchpress.com by 190.90.36.8 on 09/04/12
For personal use only.

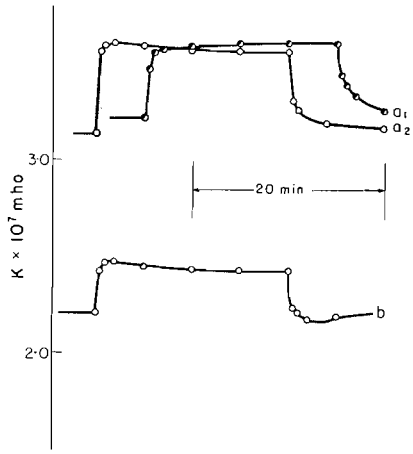

FIG. 4. a_1, a_2: *n*-Propyl bromide; f = 250 kc/s, $I \sim 2.3$ w/cm^2.
b: *n*-Butyl bromide; f = 250 kc/s, $I \sim 2.3$ w/cm^2.

CCl_4). These differences, however, are almost certainly merely a consequence of different experimental conditions. For example, the rate of fall in K after termination of irradiation will depend upon the rate of cooling of the liquid to bath temperature and upon acoustic reverberation within the cell; and ΔK itself may be expected to depend upon the frequency and/or intensity (i.e. upon parameters not mentioned in Seidl's paper). This latter dependence is, in fact, clearly shown in Fig. 3: for ethyl bromide, ΔK increases from roughly 10% at f = 250 kc/s and I = 2.3 w/cm^2 to nearly 50% at f = 1 Mc/s and I = 12.4 w/cm^2. The fact that no further increase in ΔK is observed when irradiating at f = 2 Mc/s and I = 24 w/cm^2 suggests, however, that there is a more or less definite limiting value that cannot be appreciably exceeded. In Seidl's terms, it may correspond to *complete* splitting of complex ions and, hence, to maximum mobility of the resultant simple charge carriers. Significantly, ΔK was unaffected by molecular size or by the extent of cavitation (which could be varied by dissolving variable quantities of pure nitrogen in the outgassed liquid).

In the case of the two alcohols, however, much more profound departures from Seidl's data are noted. With methanol, the general behavior is still reminiscent of that of the bromides; but ΔK at 250 kc/s and I = 2.3 w/cm^2 now amounts to nearly 50% (instead of 10% as recorded with the bromides under the same conditions), and K tends to *fall* slightly after rapid attainment of its maximum value (cf. Fig. 5—a form designated as Type B). It should here be pointed out that this fall cannot be associated with a back e.m.f., since termination of the irradiation is accompanied by a rapid return of the conductance *to its original value, not to a lower one.* This is particularly well exemplified by curve d of Fig. 5; the same curve, incidentally, suggests that ΔK_{max} lies close to 50% reached at f = 250 kc/s, I = 2.3 w/cm^2.

Finally, with ethanol, neither Type A nor Type B K/t curves are found. At f = 250 kc/s and $I < 1$ w/cm^2 as well as at f = 1 Mc/s and I = 12.4 w/cm^2, K *falls* under the influence of ultrasonic irradiation ($-\Delta K$ amounting to about 9 and 15% respectively); at f = 1 Mc/s, recovery of K requires inordinately long periods of time (25–30 minutes); and an upward change of the conductance during irradiation is only observed at f = 250 kc/s and I = 1.4 and 2.3 w/cm^2. Even in this range, the *initial* response to irradiation is a reduction (cf. Figs. 6 and 7).

Can. J. Chem. Downloaded from www.nrcresearchpress.com by 190.90.36.8 on 09/04/12
For personal use only.

Can. J. Chem. Downloaded from www.nrcresearchpress.com by 190.90.36.8 on 09/04/12
For personal use only.

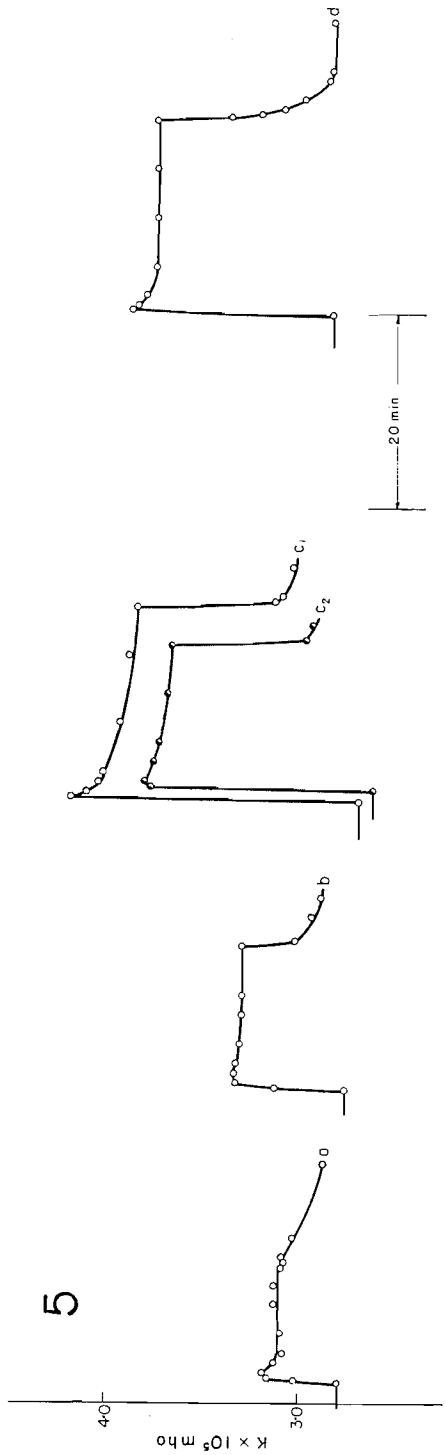

FIG. 5. *a*: Methanol; $f = 250$ kc/s, $I \sim 0.7$ w/cm².
b: Methanol; $f = 250$ kc/s, $I \sim 1.4$ w/cm².
c_1, c_2: Methanol; $f = 250$ kc/s, $I \sim 2.3$ w/cm².
d: Methanol; $f = 1$ Mc/s, $I \sim 12.4$ w/cm².

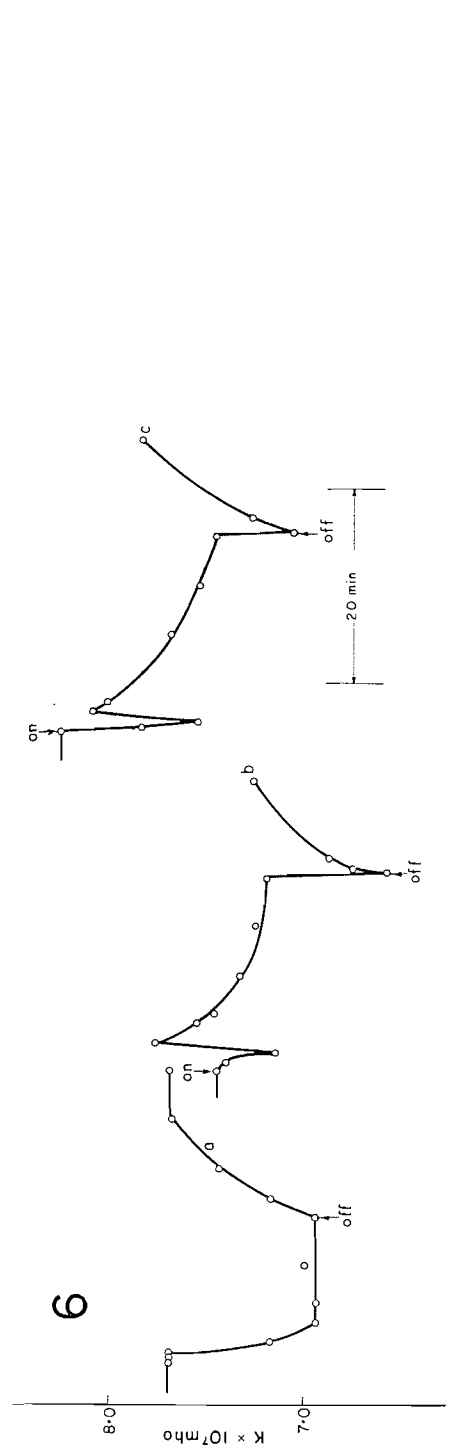

FIG. 6. *a*: Ethanol; $f = 250$ kc/s, $I \sim 0.7$ w/cm².
b: Ethanol; $f = 250$ kc/s, $I \sim 1.4$ w/cm².
c: Ethanol; $f = 250$ kc/s, $I \sim 2.3$ w/cm².

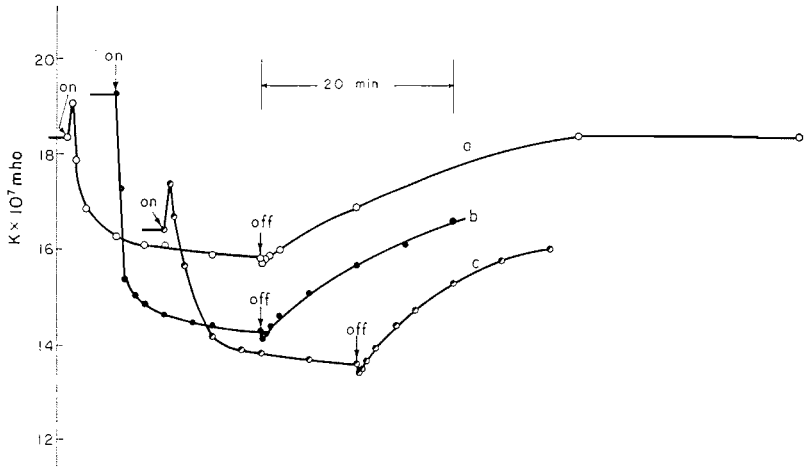

FIG. 7. *a*, *b*, *c*: Ethanol; $f = 1$ Mc/s, $I \sim 12.4$ cm².

To account for the observations made with methanol, only a slight modification of Seidl's hypothesis appears to be necessary: if the initial upward change of K is once again (as in the case of unassociated fluids) ascribed to disruption of complex ions (or better, to disruption of associated complexes), the subsequent slight fall of the conductance can be attributed to the re-establishment of some form of equilibrium between associated and non-associated charge carriers. But in the case of ethyl alcohol, the experimental data indicate a much more complex pattern of events. The nature of these events remains, at this stage, necessarily speculative and it is therefore not proposed to discuss them here. Two notable features of the K/t curves obtained at $f = 250$ kc/s and $I = 1.4$–2.3 w/cm² (Fig. 6, curves *b* and *c*) might, however, usefully be noted. First, the rise in conductance after the 2nd or 3rd minute of irradiation was in all cases accompanied by a sudden onset of cavitation. As long as the liquid was not cavitating, K continued to fall towards an equilibrium value similar to that shown in Fig. 6*a*.* Secondly, the form of curve (excluding the initial portion) is strongly reminiscent of the dielectric relaxation

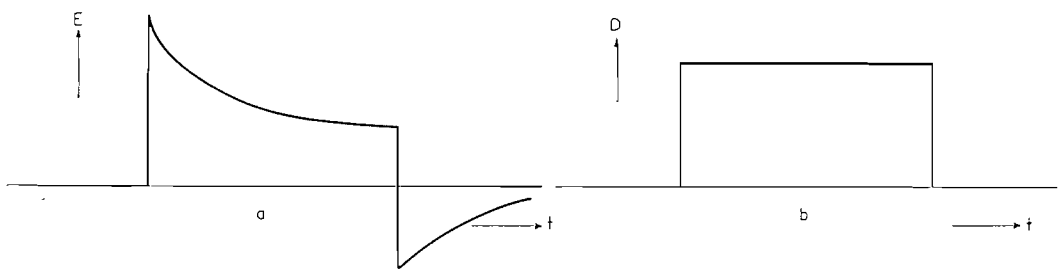

FIG. 8. Dielectric relaxation under prescribed D (after Böttcher).
a: Variation of electrical field with time.
b: Variation of dielectric displacement with time.

**In the case of the bromides and methyl alcohol, there was no apparent connection between an upward change of K and cavitation. For example, at f = 250 kc/s and I = 0.75 w/cm², the conductance of methanol increased despite complete absence of visible cavitation; and with the bromides, ΔK was found to be independent of the extent of cavitation. In the light of these observations, one is tempted to suggest that cavitation (insofar as it can occur at all) and an upward change in the conductance are two events following upon a single cause, e.g. an energy build-up in the liquid to a critical threshold value.*

Can. J. Chem. Downloaded from www.nrcresearchpress.com by 190.90.36.8 on 09/04/12
For personal use only.

curves discussed by Böttcher (3); the particular case considered by him involves a polar dielectric between the plates of an ideal condenser to which a uniform static field is applied and in which one is concerned with the time variation of the resultant electrical field E. (This variation, and the corresponding variation of the dielectric displacement D, are shown as curves a and b in Fig. 8.)

REFERENCES

1. MEYER, M. Z. Physik, **102**, 279 (1936).
2. SEIDL, F. Z. Physik, **116**, 359 (1940).
3. BÖTTCHER, C. J. F. Discussions Faraday Soc. No. **23**, 7 (1957).

Can. J. Chem. Downloaded from www.nrcresearchpress.com by 190.90.36.8 on 09/04/12
For personal use only.

Can. J. Chem. Downloaded from www.nrcresearchpress.com by 190.90.36.8 on 09/04/12
For personal use only.

DETERMINATION OF URANIUM IN FLOTATION CONCENTRATES AND IN LEACH LIQUORS BY X-RAY FLUORESCENCE[1]

G. L. SMITHSON, R. L. EAGER, AND A. B. VANCLEAVE

ABSTRACT

X-Ray fluorescence has been applied to the analysis of flotation concentrates obtained from pegmatitic uranium ores occurring in Northern Saskatchewan. Approximate uranium analyses can be obtained by direct measurement on flotation concentrates but more accurate results are obtained by using an internal standard such as strontium or yttrium. The time required for an analysis, as compared to that of conventional chemical or fluorimetric methods, is considerably reduced and flotation pilot plant operations can therefore be more effectively controlled. The method has been extended to include the analysis of sulphate leach liquors obtained from the leaching of pegmatitic ores and their flotation concentrates. Organic phases obtained in liquid – liquid extraction studies can also be rapidly analyzed for uranium by X-ray fluorescence.

INTRODUCTION

The application of X-ray fluorescence to quantitative analysis for uranium has been the subject of studies by Cope (1), Pish and Huffman (2), and Kehl and Russell (3). It has generally been found desirable to use internal standards such as strontium, molybdenum, yttrium, or bromine to avoid matrix effects. Claisse (4) has suggested a fusion method by which accurate X-ray fluorescence analysis can be done without an internal standard. The fusion method involves dilution of the sample with the flux, thus decreasing the limit of detection.

The authors have been interested in developing rapid and reasonably accurate methods for the determination of uranium in flotation concentrates collected from the low grade pegmatitic ores of Northern Saskatchewan (5). Uranium analyses on sulphate leach liquors and on aqueous and other liquid phases resulting from liquid – liquid extraction studies are also of interest. The conventional chemical methods and the widely used fluorimetric method (6) of uranium analysis are very time consuming and of little value in the control of a flotation pilot plant. The possibility of applying X-ray fluorescence to this problem has therefore been investigated.

EXPERIMENTAL

Equipment

A General Electric XRD-5D/F X-ray spectrometer equipped with a Machlett AEG 50 tungsten target tube, a lithium fluoride crystal, a 0.010-inch Soller slit, and a No. 2 SPG (Krypton) proportional counter tube was used. The X-ray tube was operated at 50 KVP and 50 ma. In charting spectra the following settings were normally employed: scanning speed 0.2 deg/min; chart speed 6 in./hr; time constant 8; full-scale pen deflections of 200, 1000, or 2000 c.p.s. Bakelite sample holders with $22 \times 22 \times 3$ mm recesses were used for solid samples.

The grinding and mixing of solid samples was done in a motor-driven mullite mortar and pestle.

[1]*Manuscript received July 14, 1958.*
Contribution from the Department of Chemistry, University of Saskatchewan, Saskatoon, Saskatchewan. Based on a paper presented at the 7th Annual Conference on Industrial Applications of X-Ray Analysis, Denver, August 13–15, 1958.

ANALYSIS OF FLOTATION CONCENTRATES WITHOUT AN INTERNAL STANDARD

Since the matrix minerals and the average particle size in the flotation concentrate from a particular pegmatitic ore were believed to be reasonably uniform, an attempt was made to apply X-ray fluorescence analysis to the concentrates without any pretreatment other than drying. Typical results are shown by the lower line in Fig. 1 in which the intensity of the U L_{α_1} line (as determined from chart recording) is shown plotted against the per cent of U_3O_8 (as determined fluorimetrically (6)) in the sample. The positions of the straight lines in Fig. 1 were determined by the method of least squares. The scatter

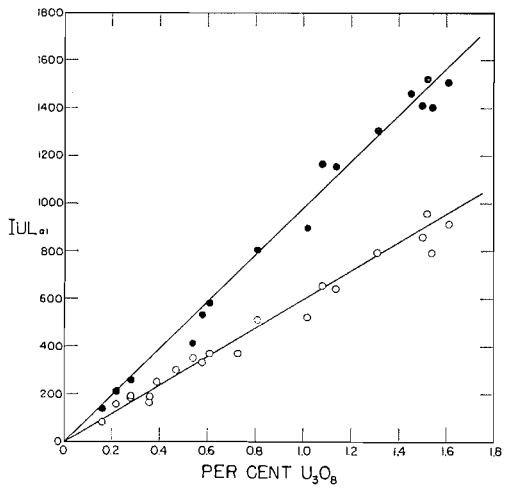

FIG. 1. Calibrations for the determination of U_3O_8 in flotation concentrates without using an internal standard.

○ Dry samples direct from flotation plant.
● Dry samples from flotation plant ground for 30 minutes in a mechanical mortar.

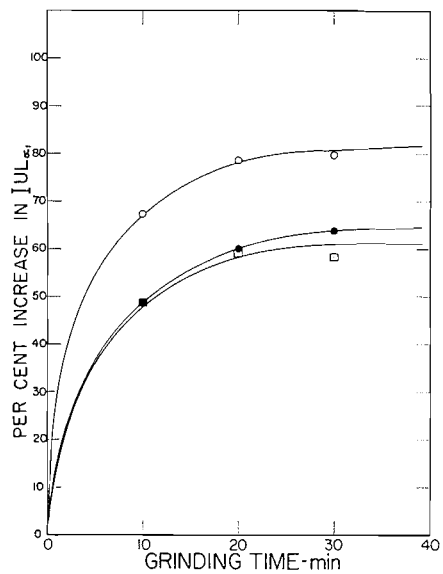

FIG. 2. The effect of mortar grinding time on the intensity of the U L_{α_1} line in three samples of flotation concentrate.

Can. J. Chem. Downloaded from www.nrcresearchpress.com by 190.90.36.8 on 09/04/12
For personal use only.

of the experimental points about the lower line is partly due to errors inherent in both the fluorimetric and X-ray fluorescence methods, and partly due to variations in particle size of the samples. Some measure of the effect of particle size variation is shown by the results given in Figs. 1 and 2. The intensity of the U L_{α_1} line was observed to increase as the particle size was reduced,* finally reaching a constant level after about 30 minutes of grinding of the sample in a mortar. The top line in Fig. 1 could be used as a calibration curve to determine the per cent U_3O_8 in flotation concentrates from the particular ore used, provided that the particle size of the samples had been sufficiently reduced either in the grinding circuit of the pilot plant or by subsequent treatment in a mortar. Calibrations lying anywhere between the two lines shown in Fig. 1 could be obtained for the particular ore depending on the degree of comminution of the sample. Standards would have to be set up for each ore for a particular set of grinding conditions. Obviously, this would not be a very satisfactory procedure if a number of ores were being treated under a variety of pilot plant conditions. However, if a large number of analyses were required on flotation concentrates from a given ore, and the grinding circuit remained unchanged, it would be possible to apply X-ray fluorescence methods directly to the concentrate samples without further preparation. The results obtained would not be as reliable as those that can be obtained by employing a suitable internal standard. The main advantage would be in obtaining an approximate result in the minimum of time.

The per cent deviation from the mean intensity of the U L_{α_1} line produced by removing samples from the sample holder and repacking them, varied from 0.2 to 2.4%. Such fluctuations are considered to be within the accuracy of the X-ray technique.

ANALYSIS OF FLOTATION CONCENTRATES USING AN INTERNAL STANDARD

Uranium Determination

If uranium analyses of flotation concentrates collected by a variety of methods or of ores from a variety of sources are required, the addition of a suitable internal standard is desirable. Since no significant amounts of strontium have been detected in the Saskatchewan pegmatites under study, it has been convenient to use it as an internal standard for solid samples.

The procedure adopted for adding the internal standard to solid samples is as follows:

(*a*) A 3-g sample of dry flotation concentrate is poured into a watch glass to form a cone-shaped mass.

(*b*) A crater is formed in the cone by pressing the bottom of a small test tube down on the apex of the cone.

(*c*) One milliliter of absolute ethanol is added to the crater. (The dry flotation concentrates are hydrophobic. The ethanol facilitates the spreading of the aqueous solution of the standard through the sample.)

(*d*) One milliliter of aqueous $Sr(NO_3)_2$ solution containing 10 mg of Sr per milliliter is added to the crater.

(*e*) The sample is dried for 30 minutes under a heat lamp, transferred to the mullite mortar, and ground for 30 minutes.

A portion of the sample prepared as above is packed into a sample holder and the significant part of the X-ray spectrum either recorded or determined by setting the spectrogoniometer at 2θ angles as listed in Table I and counting for 100 seconds. The background count at the position of the peak is interpolated from the background counts on either side of the peak.

**The original flotation concentrates were approximately 90% minus 270 mesh. Grinding for 30 minutes reduces the sample to approximately 90% minus 400 mesh.*

Can. J. Chem. Downloaded from www.nrcresearchpress.com by 190.90.36.8 on 09/04/12
For personal use only.

TABLE I
2θ Angle settings for LiF crystal

	Desired constituent						Internal standard						
	U			Fe			Sr		Y			Br	
Matrix	B.G.[a]	P.[b]	B.G.	B.G.	P.	B.G.	B.G.	P.	B.G.	P.	B.G.	P.	B.G.
Solid		26.14	27.10	55.00	57.50	60.00	24.60	25.18					
Aqueous solution	25.40	26.14	27.40	55.00	57.50	60.00			23.20	23.82	24.40		
Aqueous solution / Organic solution	25.30	26.14	29.00									29.96	34.50

[a]B.G.—Background count.
[b]P.—Peak position.

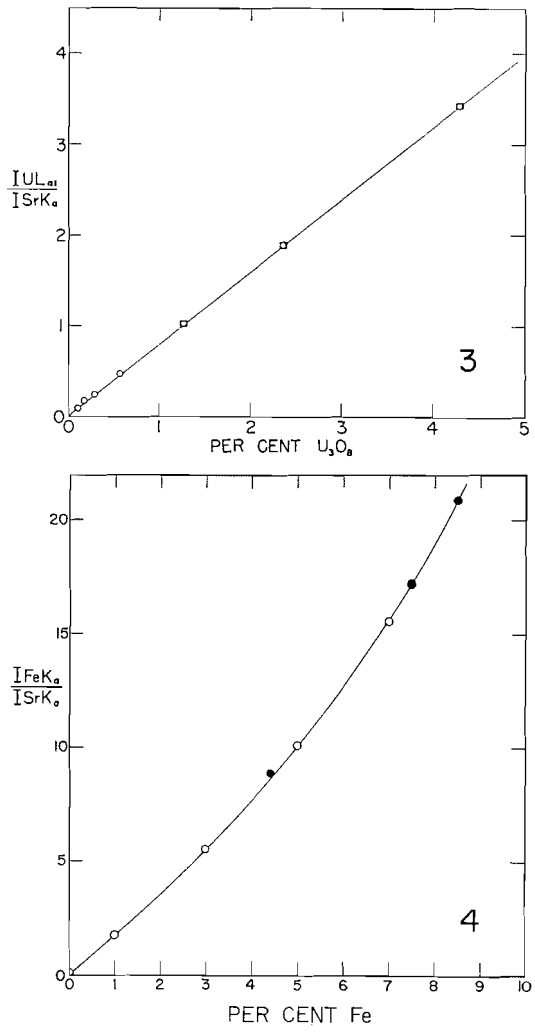

FIG. 3. Calibration for the determination of U_3O_8 in solids with strontium as internal standard. ○Chart-recording method. □Direct-count method.
FIG. 4. Calibration for the approximate determination of iron in solids by reference to strontium internal standard. ○Synthetic mixtures. ●Analyzed flotation concentrates.

Can. J. Chem. Downloaded from www.nrcresearchpress.com by 190.90.36.8 on 09/04/12
For personal use only.

Can. J. Chem. Downloaded from www.nrcresearchpress.com by 190.90.36.8 on 09/04/12
For personal use only.

The samples used for calibration (Fig. 3) were obtained from the Department of Mines and Resources, Ottawa, and the New Brunswick Laboratory of A.E.C., New Brunswick, N.J., together with two samples analyzed chemically (7) by the authors. Although these samples contained a variety of uranium minerals in differing matrices, the experimental points, whether determined from chart recordings or by counting at the specified angles, occur within experimental error on the straight line shown in Fig. 3. Although this method of analysis requires more time than would be the case if no internal standard was used, it yields more accurate and reliable results. Using the chart-recording technique, a single operator can analyze about 24 samples in an 8-hour day. Since samples of flotation concentrate can be fairly rapidly dried, analytical results can be transmitted to the pilot plant operator much more rapidly than is the case when the ultraviolet fluorimetric method is used.

The reproducibility of the method of using strontium as an internal standard was tested by repeating the procedure for adding the standard on 10 separate portions of a given sample. The ratio $I(\text{U } L_{\alpha_1})/I(\text{Sr } K_\alpha)$ was determined for each preparation both from the chart recording and by counting at fixed positions. The mean intensity ratios and the standard deviations were 0.649 ± 0.015 and 0.670 ± 0.020 for the direct-count and chart-recording methods respectively. The standard deviations for the two methods indicate an overlap in the ratio values. As expected, the results calculated from chart recordings are less precise than those obtained by direct counting.

Table II shows a comparison of analytical results on three flotation concentrate samples as determined by chemical analysis, fluorimetric analysis, and by X-ray fluorescence analysis using strontium as an internal standard. The agreement between the results for the three methods is well within their estimated limits of accuracy. The approximate relative time required for an analysis by each of these methods was estimated on the assumption that a single operator worked full time on a routine basis.

TABLE II

Comparison of results from different analytical methods

	% U_3O_8		
Sample	Chemical	Fluorimetric	X-Ray fluorescence
F 18 C_1	0.91	0.97	0.89
F 22 C_1	1.56	1.60	1.61
F 23 C_1	2.15	2.19	2.13
Approx. relative time required for analysis	5	2.5	1
Estimated max. % error	±2	±10	±5

Iron Determination

There is a tendency for acid-consuming minerals, such as iron oxides and other minerals containing iron, to be collected along with uranium minerals in the flotation of pegmatitic ores (5). A knowledge of the approximate iron content of uranium ore flotation concentrates is therefore useful in assessing the value of various collectors and systems of flotation. A good estimate of the iron content of these flotation concentrates can be made by referring the intensity of the Fe K_α line to that of the internal standard used to determine the uranium content. A calibration curve used for this purpose is shown in Fig. 4.

The samples used for calibration were (*a*) synthetic mixtures prepared by mixing iron ores of known iron content with quartz and (*b*) flotation concentrates which had been chemically analyzed for their iron content by the authors. The failure of the calibration curve to go through the origin is due to the occurrence of a small peak for this element inherent in the X-ray equipment (see also Fig. 6).

ANALYSIS OF SULPHATE LEACH LIQUORS

Uranium Determination

The X-ray fluorescence technique has also been applied to the analysis of pregnant leach solutions resulting from the leaching of uranium ores or their flotation concentrates with sulphuric acid. The design of the sample holder for liquids is similar to that described by Pish and Huffman (2) except that a polyethylene washer is used and the cell is covered with a piece of 0.0005-inch mylar film. It has been found necessary to replace the mylar film each time that the sample is changed to avoid effects due to uranium adsorption. Liquids are transferred to and from the sample holder by means of a hypodermic syringe equipped with a curved-tip stainless steel needle.

Although strontium is a convenient internal standard to use with solid samples, it is not suitable for use with solutions which contain sulphate ions. An alternative standard, yttrium, has been found to be quite satisfactory for use with sulphate leach liquors. The pegmatitic ores under investigation contain only trace amounts of rare earths and there is no evidence for the presence of yttrium in the ore or sulphate leach solutions. In the event that significant amounts of rare earths were present in the ore, another internal standard such as bromine could be selected. The calibration for the determination of uranium in aqueous solution shown in Fig. 5 was set up by diluting a standard solution of uranyl nitrate and using yttrium nitrate as the internal standard. Aqueous solution samples are prepared for analysis by adding 0.50 ml of stock yttrium nitrate solution (10 mg of yttrium per milliliter) to a 10-ml volumetric flask and diluting to volume with the solution containing dissolved uranium. Relative intensities determined from chart recordings and by direct counting (see Table II for spectrometer settings) were found to agree within estimated experimental error.

The greater precision of the direct-counting method, as compared to that of the chart-recording method of determining relative intensities for samples in the same concentration range, is shown in Table III. The data in Table III also indicate the decrease in precision that occurs in the chart-recording method when the concentration of U_3O_8 in the sample drops below 1 mg/ml. The per cent standard deviation of the intensity ratio determined by direct count for samples containing more than 1 mg/ml of U_3O_8 would undoubtedly be less than the $\pm 2.2\%$ shown for the chart-recording method. Concentrations as low as 0.1 mg U_3O_8 per milliliter can readily be determined by this method.

TABLE III

Comparison of percentage standard deviations in $I(\mathrm{U}\ L_{\alpha_1})/I(\mathrm{Y}\ K_\alpha)$ determined by chart-recording and by direct-counting methods

Method	No. determinations	Concn. range U_3O_8 in mg/ml	% Standard deviation
Chart record	30	1.0–10	±2.2
Chart record	15	0.5–1.0	±10.9
Direct count	15	0.5–1.0	±3.8

Can. J. Chem. Downloaded from www.nrcresearchpress.com by 190.90.36.8 on 09/04/12
For personal use only.

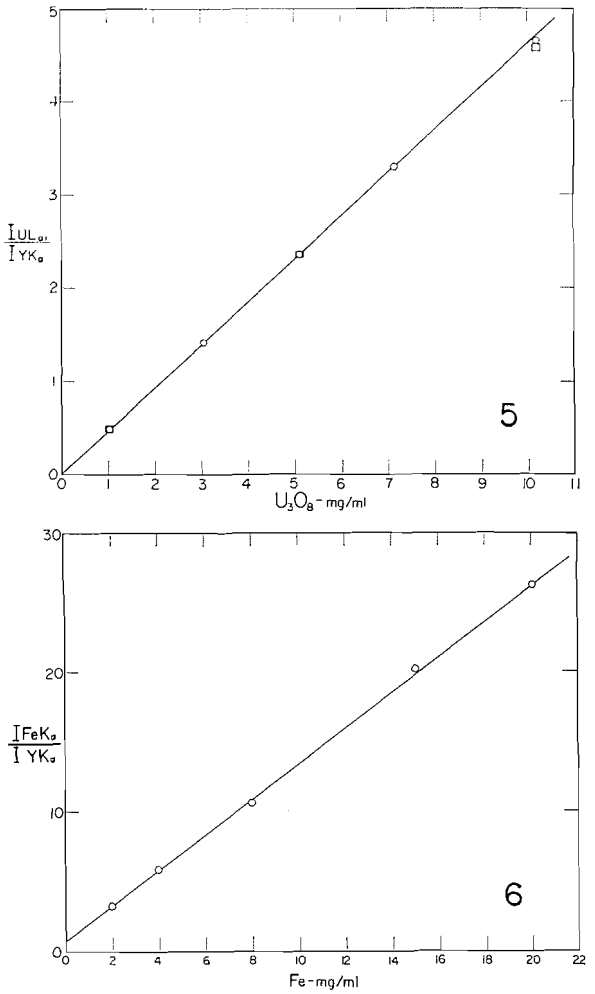

FIG. 5. Calibration for the determination of U_3O_8 in aqueous solutions using yttrium as an internal standard. ○Direct-count method. □Chart-recording method.
FIG. 6. Calibration for the approximate determination of dissolved iron in aqueous solutions by reference to yttrium internal standard.

No special precautions were taken to provide for additional heat exchangers to prevent temperature changes in the liquid samples during irradiation.

Since the concentration of dissolved iron in sulphate leach liquors varies considerably, the effect of adding varying amounts of iron on the observed $I(\text{U } L_{\alpha_1})/I(\text{Y } K_\alpha)$ ratio was studied. Experiments were done in which the iron content of the solutions was varied from 2 to 20 mg/ml. Although the intensities of both the U L_{α_1} and Y K_α lines were decreased as the iron concentration in the solution was increased, the ratio of their intensities was found to be constant within experimental error. This analytical method for uranium can therefore be applied to the analysis of pregnant leach liquors with confidence.

Iron Determination

It is often useful to have at least an approximate idea of the dissolved iron content

Can. J. Chem. Downloaded from www.nrcresearchpress.com by 190.90.36.8 on 09/04/12
For personal use only.

in uranium ore leach liquors. Yttrium would not normally be used as an internal standard for iron because of the considerable difference in the wave lengths of their K_α lines. However, since yttrium is already present in the sample for the uranium analysis, a good approximation of the iron content can be made by reference to it. An example of a calibration curve used for such determinations is shown in Fig. 6 (see comment regarding Fig. 4).

Determination of Uranium in an Organic Solvent

In the course of liquid – liquid extraction studies of the recovery of uranium from pregnant leach solutions, many uranium analyses of both aqueous and organic phases are required. Although the ultraviolet fluorimetric method of uranium analysis is usually the most satisfactory one to use in determining the normally small concentrations of uranium remaining in the aqueous phase, it is often cumbersome and inaccurate when applied to the loaded organic phase. If the fluorimetric method is used for the analysis of the organic phase it is generally necessary to back-extract the uranium to an aqueous phase (8), a step which often reduces the accuracy of the determination. An X-ray fluorescence analysis method applied directly to the loaded organic phase does not suffer from this difficulty. Since inorganic substances such as strontium and yttrium are generally not very soluble in the organic liquids that extract uranium, some other internal standard has to be chosen. Bromine in the form of bromobenzene has been suggested for this purpose (2).

Calibrations for the use of bromine as an internal standard are shown in Fig. 7 for both aqueous solutions of uranyl sulphate and for uranium in 0.1 *M* solutions of tri(iso)-octyl amine in kerosene containing 2.5 volume per cent of *n*-decyl alcohol. The calibration for aqueous solutions shown in Fig. 7 was obtained by adding 0.50 ml of sodium bromide solution (10 mg Br per milliliter) to a 10-ml volumetric flask and diluting to volume with standard uranyl sulphate solution. The organic solution calibration was obtained by successively extracting 50 ml of standard uranyl sulphate solution (pH adjusted to 1.5 with sulphuric acid) with five 20-ml portions of a 0.1 *M* solution of tri(iso)octyl amine in kerosene containing 2.5 volume per cent of *n*-decyl alcohol. (A fluorimetric analysis of the raffinate showed that at least 99.4% of the uranium had

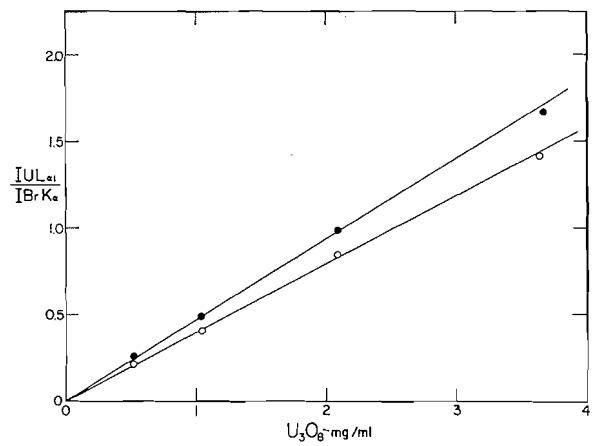

FIG. 7. Calibrations for the determination of U_3O_8 in aqueous and kerosene solutions with bromine as internal standard.
●Aqueous solutions. ○0.1 *M* tri(iso)octyl amine in kerosene solution.

Can. J. Chem. Downloaded from www.nrcresearchpress.com by 190.90.36.8 on 09/04/12
For personal use only.

been extracted to the organic phase.) The organic extracts were combined and a 9.5-ml aliquot taken for analysis along with 0.50 ml of a solution of analyzed bromobenzene in kerosene (10 mg Br per milliliter). As long as the concentration of dissolved uranium (expressed as U_3O_8 equivalent) exceeds 0.1 mg/ml, this method of analyzing aqueous or organic phases is very satisfactory and requires much less time than other standard analytical methods. However, it is necessary to have a calibration for each organic diluent used, as the reflection of X-rays is dependent on the density of the medium (9).

CONCLUSIONS

X-Ray fluorescence analysis greatly reduces the time required for the analysis of flotation concentrates accumulating from pilot plant studies on uranium ores. It is possible to do uranium analyses directly on concentrate samples from a given ore that has been subjected to a standard treatment but, if reliable and more accurate results are required, the addition of an internal standard such as strontium or yttrium and further comminution of the sample is necessary. An approximate analysis for iron in an ore or concentrate can be made by reference to the internal standard used for uranium. The lowest concentration of uranium that can conveniently be determined by X-ray fluorescence analysis of solids is about 0.02% U_3O_8.

Uranium analyses and approximate iron analyses can also very conveniently be done on sulphate leach liquors containing uranium by X-ray fluorescence with reference to a yttrium internal standard. The use of bromine as an internal standard for the determination of uranium in organic solvents is quite satisfactory. The low limit for the accurate determination of uranium in solution is about 0.1 mg of U_3O_8 per milliliter.

X-Ray fluorescence could probably readily be adapted to continuous control analysis in commercial uranium mills.

ACKNOWLEDGMENTS

Financial assistance provided by the Saskatchewan Research Council is gratefully acknowledged. The authors are indebted to Dr. Brad Gunn for the ultraviolet fluorimetric analyses.

REFERENCES

1. Cope, J. H. Norelco Reptr. **3**, 41 (1956).
2. Pish, G. and Huffman, A. A. Anal. Chem. **27**, 1875 (1955).
3. Kehl, L. W. and Russel, R. G. Anal. Chem. **28**, 1350 (1956).
4. Claisse, F. Quebec Dept. of Mines, Prelim. Rept. No. **327** (1956).
5. VanCleave, A. B. and Eager, R. L. Proc. Second Intern. Conf. Peaceful Uses Atomic Energy, A/CONF. 15/P/230 (1958).
6. Centanni, F. A., Ross, A. M., and De Sesa, M. A. Anal. Chem. **28**, 1651 (1956).
7. New Brunswick Laboratory. Manual of analytical methods for the determination of uranium and thorium in their ores. 15 (1955).
8. Thompson, R. B. M.Sc. Thesis, University of Saskatchewan. 1957.
9. Kokotailo, G. T. and Damon, G. F. Anal. Chem. **25**, 1185 (1953).

Can. J. Chem. Downloaded from www.nrcresearchpress.com by 190.90.36.8 on 09/04/12
For personal use only.

Can. J. Chem. Downloaded from www.nrcresearchpress.com by 190.90.36.8 on 09/04/12
For personal use only.

URONIC ACIDS FROM WHITE SPRUCE (PICEA GLAUCA (MOENCH) VOSS)[1]

G. A. ADAMS

ABSTRACT

Acid hydrolysis of extractive-free white spruce wood produced a number of neutral and acidic sugars and oligosaccharides. The acidic components were isolated and three of these were shown to be 4-*O*-methyl-D-glucuronic acid, 2-*O*-(4-*O*-methyl-α-D-glucopyranosyluronic acid)-D-xylose, and tentatively *O*-(4-*O*-methyl-α-D-glucopyranosyluronic acid)-(1 → 2)-*O*-β-D-xylopyranosyl-(1 → 4)-D-xylopyranose.

Investigations of the hemicelluloses of white spruce (*Picea glauca*) have yielded an arabogalactan (1) and a glucomannan (2). Since neither of these fractions contained more than a trace of uronic acids, it seemed likely that the acid components were associated with the xylan portion of the wood. The present communication is concerned with the composition and identification of three uronic acid components isolated from spruce wood by partial hydrolysis.

The uronic acids were obtained by acid hydrolysis of extractive-free white spruce wood and separated from the neutral sugars by adsorption on an anion exchange resin. Further separation of the recovered uronic acid components yielded several fractions of which three (I, II, and III) were identified.

Chromatographic evidence, methoxyl content, and equivalent weight tentatively identified fraction I as 4-*O*-methyl-D-glucuronic acid. Conversion of the acid to its methyl ester methyl glycoside and reduction with lithium aluminum hydride yielded 4-*O*-methyl-D-glucose, which was characterized as crystalline 4-*O*-methyl-D-glucose phenylosazone.

Hydrolysis of fraction II and chromatographic examination of the hydrolyzate indicated the presence of D-xylose and 4-*O*-methyl-D-glucuronic acid. Reduction of the ester glycoside gave the corresponding disaccharide glycoside which on hydrolysis yielded crystalline D-xylose and 4-*O*-methyl-D-glucose, the latter being identified as its crystalline phenylosazone. The point of attachment of the 4-*O*-methyl-D-glucuronic acid to the D-xylose residue was determined by methylation studies. The aldobiouronic acid methyl ester, methyl glycoside, was converted to methyl-*O*-(4-*O*-methyl-D-glucopyranosyl)-D-xyloside by reduction with lithium aluminum hydride and the product was then fully methylated. On hydrolysis it yielded 3,4-di-*O*-methyl-D-xylose and 2,3,4,6-tetra-*O*-methyl-D-glucose thus proving that the acid was attached glycosidically to $C_{(2)}$ of the xylose residue. Recent evidence has established that the glycosidic bond in this aldobiouronic acid is in the α configuration (3). These findings showed that the aldobiouronic acid was 2-*O*-(4-*O*-methyl-α-D-glucopyranosyluronic acid)-D-xylopyranose.

The aldotriouronic acid (fraction III) was composed of 4-*O*-methyl-D-glucuronic acid and D-xylose and had $[\alpha]_D^{25}$ +59°. It could not be obtained in crystalline form. The attachment of the 4-*O*-methyl-D-glucuronic acid and the xylose units to one another was determined by methylation studies. The aldotriouronic acid was converted to its corresponding methyl ester methyl glycoside by treatment with 1% methanolic hydrogen chloride at room temperature. Reduction with lithium aluminum hydride provided the

[1]*Manuscript received September 11, 1958.*
Contribution from the Division of Applied Biology, National Research Council, Ottawa, Canada.
Issued as N.R.C. No. 4970.

glycoside of the trisaccharide which was methylated with methyl iodide and silver oxide. Hydrolysis of the fully methylated trisaccharide yielded approximately equimolecular quantities of 2,3,4,6-tetra-*O*-methyl-D-glucose, 2,3-di-*O*-methyl-D-xylose, and 3,4-di-*O*-methyl-D-xylose. The lower rotation of the aldotriouronic acid (+59°) as compared to that of the aldobiouronic acid (+97°) indicated that the xylobiose moiety in the former had a negative rotation and its glycosidic linkage was β. The foregoing findings established the aldotriouronic acid tentatively as *O*-(4-*O*-methyl-α-D-glucopyranosyluronic acid)-(1 → 2)-*O*-β-D-xylopyranosyl-(1 → 4)-D-xylopyranose.

The aldobiouronic acid, 2-*O*-(4-*O*-methyl-α-D-glucopyranosyluronic acid)-D-xylose, is the most common uronic component of wood. Its presence was first suggested in oak wood (4) and in 1952 it was identified in aspen wood (5). Since that time it has been found in all woods examined for it including both coniferous (6–13) and deciduous species (14–21).

Aldotriouronic acids containing 4-*O*-methyl-D-glucuronic acid and D-xylose have been isolated from aspen wood (17) in crystalline form and from Monterey pine (22), although the structures have not been reported. The aldotriouronic acid, *O*-(4-*O*-methyl-α-D-glucopyranosyluronic acid)-(1 → 2)-*O*-β-D-xylopyranosyl-(1 → 4)-D-xylose, has been obtained in crystalline form from western hemlock (23) and jute (24). The present aldotriouronic acid of white spruce, although not obtained in crystalline form, has a chemical structure identical with the crystalline uronic acids of western hemlock and jute.

It was pointed out in an earlier publication (25) that the presence of a methyl ether substituent on $C_{(4)}$ of the glucuronic acid is associated with glycosidic attachment to $C_{(2)}$ of the xylose unit. Recently Brasch and Wise have isolated 3-*O*-α-(4-*O*-methyl-D-glucuronosyl)-D-xylose from Monterey pine (13) and have suggested that it may be a component of other woods; however, careful examination of the hydrolyzate from white spruce has not revealed the presence of this component.

EXPERIMENTAL

All specific rotations were equilibrium values unless otherwise stated and melting points are corrected.

Paper Chromatography

Chromatographic separations were carried out by the descending method on Whatman No. 1 paper using the following solvents: (A) ethyl acetate: pyridine: water (2:1:2); (B) ethyl acetate: acetic acid: formic acid: water (19: 3: 1: 4); and (C) ethanol: benzene: water (47: 200: 15). A 3% solution of *p*-anisidine hydrochloride in ethanol was used as the spray reagent.

Preparation of Uronic Acids

White spruce wood (*Picea glauca* (Moench) Voss) was reduced to shavings and rendered extractive-free as previously described (26). The wood (500 g) was heated with 0.5 *N* sulphuric acid (7000 ml) at a temperature of 94° C until the reducing power became constant (9 hours). The hot solution of sugars and sugar acids was recovered by filtration through a sintered glass filter (porosity C) and the wood residue was washed free of acid. The hydrolyzate and washings were brought to pH 6.0 by careful addition of barium hydroxide and barium carbonate. The barium sulphate was removed by filtration and the solution and washings were passed through a column of Amberlite IR-120 resin to remove cations. The uronic acid components were then absorbed on a column of Dowex 1-X^4 (acetate form) (30×180 mm). The column was washed with water until the eluate gave a negative anthrone test for sugars. Electrophoretic examination of the

Can. J. Chem. Downloaded from www.nrcresearchpress.com by 190.90.36.8 on 09/04/12
For personal use only.

Can. J. Chem. Downloaded from www.nrcresearchpress.com by 190.90.36.8 on 09/04/12
For personal use only.

washings on paper in 0.025 *N* sodium bicarbonate solution showed no trace of uronic acids. The uronic acid components were eluted from the column by 0.1 *N* formic acid and were collected by an automatic fraction collector in 200 tubes (13 ml in each tube). Chromatographic examination of the recovered fractions in solvent B showed that only minor separation of four major components had been achieved. The major fraction (tubes 41–80) contained 74% of the material put on the column. Further separation of this fraction was carried out on a cellulose column (30 mm × 450 mm) using solvent B. Four main fractions were obtained having R_x values (movement relative to that of xylose) as follows: 0.49, 0.64, 0.93, 1.16. Paper chromatographic examination (solvent B) showed that one fraction (R_x 0.49) was a mixture of two components. The eluting solvent was partly removed by evaporation at 40° C under reduced pressure and the aqueous solution of the residual uronic acid extracted thoroughly with ether to remove formic acid. Freeze drying of the aqueous solution yielded the uronic acids as white porous solids. Three fractions having the following properties were recovered: fraction I (0.222 g); R_x 1.16 (solvent B); $[\alpha]_D^{25}$ +48.6°; methoxyl 14.9; acid equivalent 205 (calculated for $C_7H_{12}O_7$, methoxyl 14.9%; acid equivalent 208). Fraction II (0.816 g); R_x 0.93 (solvent B); $[\alpha]_D^{25}$ +97°; methoxyl 9.4%; acid equivalent 340 (calculated for $C_{12}H_{20}O_{11}$, methoxyl 9.1%; acid equivalent 340). Fraction III (0.988 g); R_x 0.64 (solvent B); $[\alpha]_D^{25}$ +59°; methoxyl 6.1%; acid equivalent 510 (calculated for $C_{17}H_{28}O_{15}$, methoxyl 6.54%; acid equivalent 472).

Hydrolysis Products of Uronic Acid Fractions

Samples of fractions II and III (approximately 10 mg each) were heated in sealed tubes with 4 ml of methanolic hydrogen chloride (8%) for 10 hours at 80° C. After removal of solvent, hydrolysis was continued with *N* hydrochloric acid for 12 hours at 100° C. Chromatograms of the hydrolyzates in solvent A and B showed the presence of D-xylose and 4-*O*-methyl-D-glucuronic acid. On the basis of chromatographic comparison in solvent B with a known reference, fraction I was identified tentatively as 4-*O*-methyl-D-glucuronic acid.

Examination of the Uronic Acid Fractions

4-O-Methyl-D-glucuronic Acid (Fraction I)

The acid (113 mg) was converted to its methyl ester methyl glycoside by heating in a sealed glass tube with 15 ml of methanolic hydrogen chloride (3%) for 10 hours at 80° C. The product (123 mg) was dissolved in dry tetrahydrofuran (25 ml) and the solution was added dropwise over a period of 1 hour to a stirred suspension of lithium aluminum hydride (500 mg) in tetrahydrofuran (25 ml). The reaction mixture was refluxed gently for 1 hour, cooled, and the unused lithium aluminum hydride was decomposed by addition of ethyl acetate and finally water. After filtration, concentration, and deionization by Amberlite IR-120 and Amberlite IR-4B the glycoside of the monosaccharide was recovered (112 mg). Hydrolysis by 0.5 *N* hydrochloric acid (6 ml) in a sealed glass tube at 100° C for 8 hours yielded 4-*O*-methyl-D-glucose, as shown by chromatographic examination of the neutralized hydrolyzate in solvent A.

The phenylosazone of 4-*O*-methyl-D-glucose was prepared by heating the sugar (88 mg) with water (2.0 ml), acetic acid (0.3 ml), and phenylhydrazine (0.5 ml) for 1 hour at 90° C. The recovered 4-*O*-methyl-D-glucose phenylosazone was recrystallized from benzene and had a m.p. and mixed m.p. of 158–159° C (27).

2-O-(4-O-Methyl-α-D-glucopyranosyluronic Acid)-D-xylose (Fraction II)

Identification of the constituents of the aldobiouronic acid was made as follows: the aldobiouronic acid (370 mg) was converted to the methyl ester methyl glycoside (390

mg) and reduced by lithium aluminum hydride to the glycoside of its corresponding disaccharide (398 mg) by the methods described above. Hydrolysis with 0.5 *N* hydrochloric acid yielded a syrup (383 mg) which on chromatographic examination in solvent A was found to contain D-xylose and 4-*O*-methyl-D-glucose. A portion of the mixture (250 mg) was separated on a Celite column (28) (35 mm × 160 mm) using butanol saturated with water as the eluting solvent. Xylose (89 mg) was obtained in crystalline form and on recrystallization from methanol had a m.p. and mixed m.p. of 142–143° and $[\alpha]_D^{25}$ +19.2° (*c*, 1.7% in water). The syrupy 4-*O*-methyl-D-glucose (115 mg), $[\alpha]_D^{25}$ +60.1 (*c*, 2.3% in water) methoxyl 15.6% (calculated for $C_7H_{14}O_6$, methoxyl 16.0%), was converted to its crystalline phenylosazone. The 4-*O*-methyl-D-glucose phenylosazone on recrystallization from 25% aqueous acetone solution had a m.p. of 158–159° C.

Conversion of Aldobiouronic Acid to Disaccharide

The aldobiouronic acid (896 mg) was converted to its methyl glycoside methyl ester by refluxing with 2% methanolic hydrogen chloride (30 ml) for 8 hours. The methyl ester methyl glycoside (924 mg) in tetrahydrofuran solution (25 ml) was reduced by lithium aluminum hydride (1 g) to the glycoside of the neutral disaccharide (842 mg) $[\alpha]_D^{25}$ +95° (*c*, 1.29% in water).

Methylation of the Glycoside of 4-O-Methyl-D-glucosyl-D-xylose

The disaccharide (842 mg) was dissolved in 20% sodium hydroxide (10 ml) and methylated by the simultaneous dropwise addition of 45% sodium hydroxide and dimethyl sulphate 30 ml; two additional methylations were carried out prior to the recovery of the product. The reaction mixture was heated at 95° for 1 hour, cooled, acidified with sulphuric acid to pH 5.0, and extracted with chloroform. Evaporation of the chloroform yielded a syrup (805 mg). The infrared spectrum of this product indicated that a small amount of free hydroxyl groups was still present. One methylation with Purdie's reagents, methyl iodide (25 ml) and silver oxide (10 g), yielded a syrup (798 mg) having no free hydroxyl groups as shown by its infrared spectrum. Anal. Calc. for $C_{18}H_{34}O_{10}$: OCH_3, 52.9%. Found: OCH_3, 51.9%.

Hydrolysis of Methyl-2-O-(2,3,4,6-tetra-O-methyl-D-glucopyranosyl)-3,4-di-O-methyl-D-xyloside and Recovery of Methylated Sugars

The methylated disaccharide (798 mg) was dissolved in 8% methanolic hydrogen chloride (25 ml) and refluxed gently for 18 hours. Solvent was removed and the hydrolysis was continued in 0.5 *N* hydrochloric acid (20 ml) for 9 hours at 100° C. The hydrolyzate was neutralized with silver carbonate, deionized by Amberlite IR-120 resin and Amberlite IR-4B resin, and concentrated *in vacuo* to a clear syrup (584 mg). Chromatographic examination of the syrup in solvent C revealed two spots similar in mobility and color reaction to 3,4-di-*O*-methyl-D-xylose and 2,3,4,6-tetra-*O*-methyl-D-glucose. The sugars were separated on a Celite column (30 mm × 350 mm) using butanol saturated with water to give 3,4-di-*O*-methyl-D-xylose (120 mg) and 2,3,4,6-tetra-*O*-methyl-D-glucose (281 mg).

Identification of 3,4-Di-O-methyl-D-xylose

The clear syrup had $[\alpha]_D^{25}$ +21±1° (*c*, 1.0% in water); methoxyl content calculated for $C_7H_{14}O_5$: 34.8%; found: OCH_3, 34.8%. Chromatographic examination in solvent C showed that the syrup had the same R_g value (0.38) as 3,4-di-*O*-methyl-D-xylose and was easily distinguished from the 2,3- and 2,4-isomers (R_g values 0.31 and 0.27 respectively). Electrophoresis (29) in borate buffer using the same reference sugars showed

Can. J. Chem. Downloaded from www.nrcresearchpress.com by 190.90.36.8 on 09/04/12
For personal use only.

Can. J. Chem. Downloaded from www.nrcresearchpress.com by 190.90.36.8 on 09/04/12
For personal use only.

that the unknown sugar had the same mobility as 3,4-di-*O*-methyl-D-xylose. The sugar (71 mg) in water (1.5 ml) containing barium carbonate (65 mg) was oxidized in the dark with bromine (0.6 ml) for 48 hours. The bromine was removed by aeration, and the solution was extracted continuously with chloroform for 48 hours. The syrup which was recovered from the chloroform extract was distilled, boiling point (bath temp.) 120–150° (0.02–0.018 mm), and on seeding with 3,4-di-*O*-methyl-D-xylono-δ-lactone, crystallization occurred. Recrystallization from ether solution to which a few drops of hexane were added yielded 3,4-di-*O*-methyl-D-xylono-δ-lactone, m.p. and mixed m.p. 66–67° C, $[\alpha]_D^{25}$ $-22°\pm1°$ (*c*, 1.0 in water) (30).

Identification of 2,3,4,6-Tetra-O-methyl-D-glucose

The clear syrup recovered from the Celite column crystallized on seeding with 2,3,4,6-tetra-*O*-methyl-D-glucose. Recrystallization from ether – petroleum ether solution gave needles having m.p. and mixed m.p. 94–96° C and $[\alpha]_D^{25}$ $+84°\pm2°$ (*c*, 1.07 in water). A methanolic solution of the sugar (52 mg) was refluxed with aniline (25.4 mg) for 2 hours to give crystalline 2,3,4,6-tetra-*O*-methyl-*N*-phenyl-D-glucosylamine which on recrystallization from hexane had m.p. and mixed m.p. 134–136° C, $[\alpha]_D^{25}$ $+239°\pm1°$ (*c*, 1% in chloroform) (31).

Characterization of O-4-O-Methyl-α-D-glucopyranosyluronic Acid-(1 → 2)-O-β-D-xylopyranosyl-(1 → 4)-D-xylose (Fraction III)

Attempts to crystallize the aldotriouronic acid were unsuccessful. The acid (500 mg) was converted to its methyl glycoside methyl ester by reacting with 1% methanolic chloride (10 ml) at room temperature. Within 5 hours the specific rotation had become constant and the solution no longer reduced Fehling's solution. Chromatographic examination in solvent C showed only one component and hence no hydrolysis had occurred. The methyl ester methyl glycoside (481 mg) was reacted with diazomethane in methanol solution to assure esterification of all carboxyl groups. Reduction with lithium aluminum hydride in tetrahydrofuran solution yielded the glycoside of the neutral trisaccharide (493 mg).

Methylation of Methyl[O-4-O-methyl-α-D-glucopyranosyl-(1 → 2)-O-β-D-xylopyranosyl-(1 → 4)]-D-xyloside

The trisaccharide (493 mg) was dissolved in methanol (10 ml) and methylated with methyl iodide (30 ml) and silver oxide (6 g) by refluxing 20 hours. After the third methylation the product was completely soluble in methyl iodide. Five methylations yielded a brownish syrup (315 mg) having no free hydroxyl groups as shown by its infrared spectrum. Anal. Calc. for $C_{25}H_{46}O_{14}$: OCH_3, 48.9. Found: OCH_3, 46.8; $[\alpha]_D^{25}$ $+52.9°$ (*c*, 1% in methanol).

Hydrolysis of Methyl[O-2,3,4,6-tetra-O-methyl-α-D-glucopyranosyl-(1 → 2)-O-β-3,4-di-O-methyl-D-xylosyl-(1 → 4)]-2,3-di-O-methyl-D-xyloside

The methylated trisaccharide (300 mg) was dissolved in 8% methanolic hydrogen chloride and refluxed for 12 hours; after removal of the solvents, the hydrolysis was completed by heating in 0.5 *N* hydrochloric acid for 8 hours. Recovery after neutralization with Amberlite IR-4B yielded a clear syrup (230 mg). Chromatographic examination in solvent C showed the presence of three sugars which corresponded in color reaction and rate of movement to authentic samples of 2,3-di-*O*-methyl-D-xylose, 3,4-di-*O*-methyl-D-xylose, and 2,3,4,6-tetra-*O*-methyl-D-glucose. The methylated sugars were separated on sheets of Whatman No. 1 filter paper using solvent C. Elution of the paper

strips with methanol yielded solutions of the crude syrups which were filtered and then dried to constant weight. Yields: 2,3,4,6-tetra-*O*-methyl-D-glucose, 69.8 mg; 3,4-di-*O*-methyl-D-xylose, 48.3 mg; and 2,3-di-*O*-methyl-D-xylose, 42.6 mg.

Identification of Component Sugars

*3,4-Di-O-methyl-*D*-xylose.*—The colorless syrup had $[\alpha]_D^{25}$ +22.2° (*c*, 1.20% in methanol) and the R_g values in solvent C were identical with those of an authentic sample of 3,4-di-*O*-methyl-D-xylose. Anal. Calc. for $C_7H_{14}O_5$: OCH_3, 34.8. Found: OCH_3, 34.4. Bromine oxidation as described above yielded crystalline 3,4-di-*O*-methyl-D-xylono-δ-lactone, m.p. 66–67° C, $[\alpha]_D^{25}$ −21° (*c*, 1% in water).

*2,3-Di-O-methyl-*D*-xylose.*—This sugar had $[\alpha]_D^{25}$ +20.8° (*c*, 1.06% in methanol). Anal. Calc. for $C_7H_{14}O_5$: OCH_3, 34.8. Found: OCH_3, 34.6. The R_g value in solvent C was identical with that of 2,3-di-*O*-methyl-D-xylose. Conversion to the anilide provided crystalline 2,3-di-*O*-methyl-*N*-phenyl-D-xylosylamine, m.p. and mixed m.p. 123–124° C and $[\alpha]_D^{25}$ +188 (*c*, 0.5% in ethyl acetate) (32).

*2,3,4,6-Tetra-O-methyl-*D*-glucose.*—The rate of movement of this sugar on paper strips in solvent C was the same as that of an authentic sample of 2,3,4,6-tetra-*O*-methyl-D-glucose. Refluxing with aniline in methanolic solution provided the characteristic crystalline 2,3,4,6-tetra-*O*-methyl-*N*-phenyl-D-glycosylamine which on recrystallization from hexane had a m.p. and mixed m.p. of 134–136° C, $[\alpha]_D^{25}$ +235±1° (*c*, 1.1% in chloroform).

ACKNOWLEDGMENT

The author acknowledges with thanks the valuable technical assistance of A. E. Castagne throughout the course of this study.

REFERENCES

1. Adams, G. A. Can. J. Chem. **36**, 755 (1958).
2. Timell, T. E. and Tyminski, A. Tappi, **40**, 519 (1957).
3. Gorin, P. A. J. and Perlin, A. S. Can. J. Chem. **36**, 999 (1958).
4. O'Dwyer, M. H. Biochem. J. **28**, 2116 (1934).
5. Jones, J. K. N. and Wise, L. E. J. Chem. Soc. 2750 (1952).
6. Gorrod, A. R. N. and Jones, J. K. N. J. Chem. Soc. 2522 (1954).
7. Ball, D. H., Jones, J. K. N., Nicholson, W. H., and Painter, T. J. Tappi, **39**, 438 (1956).
8. Jones, J. K. N. and Painter, T. J. J. Chem. Soc. 669 (1957).
9. Aspinall, G. O. and McKay, J. E. J. Chem. Soc. 1059 (1958).
10. Dutton, G. G. S. and Smith, F. J. Am. Chem. Soc. **78**, 2505 (1957).
11. Hamilton, J. K. and Thompson, N. S. J. Am. Chem. Soc. **79**, 6464 (1957).
12. Aspinall, G. O. and Carter, M. E. J. Chem. Soc. 3744 (1956).
13. Brasch, D. J. and Wise, L. E. Tappi, **39**, 768 (1956).
14. Gillham, J. K. and Timell, T. E. Can. J. Chem. **36**, 410 (1958).
15. Jones, J. K. N. and Wise, L. E. J. Chem. Soc. 2750, 3389 (1952).
16. Jones, J. K. N., Merler, E., and Wise, L. E. Can. J. Chem. **35**, 634 (1956).
17. Milks, J. E. and Purves, C. B. J. Am. Chem. Soc. **78**, 3738 (1956).
18. Aspinall, G. O., Hirst, E. L., and Mahomed, R. S. J. Chem. Soc. 1734 (1954).
19. Adams, G. A. Can. J. Chem. **35**, 556 (1957).
20. Glaudemans, C. P. J. and Timell, T. E. J. Am. Chem. Soc. **80**, 941 (1958).
21. Saarnio, J., Wathem, K., and Gustafsson, C. Acta Chem. Scand. **8**, 825 (1954).
22. Brasch, D. J. and Wise, G. E. Tappi, **39**, 581 (1956).
23. Hamilton, J. K. and Thompson, N. S. J. Am. Chem. Soc. **79**, 6464 (1957).
24. Srivastava, H. C. and Adams, G. A. (In press).
25. Adams, G. A. and Bishop, C. T. J. Am. Chem. Soc. **78**, 2842 (1956).
26. Adams, G. A. Tappi, **40**, 721 (1957).
27. Smith, F. J. Chem. Soc. 2646 (1951).
28. Lemieux, R. U., Bishop, C. T., and Pelletier, G. E. Can. J. Chem. **34**, 1365 (1956).
29. Consden, R. and Stanier, W. M. Nature, **169**, 783 (1952).
30. James, S. P. and Smith, F. J. Chem. Soc. 739 (1945).
31. Irvine, J. C. and Moodie, A. M. J. Chem. Soc. **93**, 95 (1908).
32. Ehrenthal, I., Rafique, M. C., and Smith, F. J. Am. Chem. Soc. **74**, 1341 (1952).

Can. J. Chem. Downloaded from www.nrcresearchpress.com by 190.90.36.8 on 09/04/12
For personal use only.

Can. J. Chem. Downloaded from www.nrcresearchpress.com by 190.90.36.8 on 09/04/12
For personal use only.

PHOTOCHEMICAL SEPARATION OF MERCURY ISOTOPES

II. THE REACTION OF $Hg^{202}6(^3P_1)$ ATOMS, PHOTOEXCITED IN NATURAL MERCURY VAPOR, WITH WATER VAPOR AND OTHER HgO-FORMING SUBSTRATES[1]

R. PERTEL[2] AND H. E. GUNNING[3]

ABSTRACT

An investigation has been made of the reaction of $Hg^{202}(^3P_1)$ atoms, photoexcited in natural mercury vapor, with several HgO-forming substrates, including water vapor, nitrous oxide, and oxygen. The reactions were carried out under flow conditions at room temperature. Emphasis has been placed on the Hg^{202} content of the HgO product. Enrichment in Hg^{202} would be evidence of the primary formation of a mercury compound.

In the reactions with nitrous oxide and oxygen, it was found that the HgO product contained the normal abundance of Hg^{202}. With water vapor, a product containing up to 35% Hg^{202} was obtained, compared to the normal abundance of 29.8%. The addition of 1,3-butadiene to the water vapor substrate was found to have a marked effect on the enrichment in Hg^{202} in the HgO product. A product containing 85% Hg^{202} was recovered when the substrate contained 21 mole % of added butadiene. A systematic study of the effect of butadiene concentration on the enrichment reaction showed that the Hg^{202} content remains constant for butadiene concentrations exceeding approximately 10 mole %. The water–butadiene reaction is recommended as a simple method for preparing Hg^{202} from natural mercury.

The factors influencing the enrichment process are discussed, together with the significance of the results with respect to the mechanisms of decomposition of the molecules studied.

INTRODUCTION

In the mercury-$6(^3P_1)$-photosensitized decomposition of certain gaseous oxygen-containing compounds, HgO is formed as a product of the reaction. Important among such substrates are water vapor, oxygen, and nitrous oxide. Through the technique of monoisotopic photosensitization, it is possible to obtain information on the extent to which a mercury compound is formed in the primary process. Thus, in the water reaction, if a single isotope specie, Hg^{i}, is photoexcited in the natural mercury vapor (Hg^{N}) present in the reaction cell, it is possible to distinguish between primary processes of the type:

$$Hg^{i}6(^3P_1) + HOH \rightarrow Hg^{i}OH + H \quad [1]$$

and

$$Hg^{i}6(^3P_1) + HOH \rightarrow H + OH + Hg^{i}6(^1S_0), \quad [2]$$

since reaction [1] could lead to the formation of an HgO enriched in the exciting isotope.

The reaction of $Hg^{198}6(^3P_1)$ atoms, in Hg^{N}, with HOH–N_2 mixtures has been studied previously (1). The HgO was found to contain 15% Hg^{198}, compared to the natural abundance of 10.0%. The photoexcitation of $Hg^{198}6(^3P_1)$ atoms in Hg^{N} is complicated by the juxtaposition of the 201*b* of Hg^{201} in the h.f.s. of Hg^{N}. Some excitation of $Hg^{201}6(^3P_1)$ atoms in Hg^{N} would be expected in irradiation with an Hg^{198} source. The experimental and theoretical aspects of the photoexcitation of single mercury isotopes in Hg^{N} has been discussed in an earlier study (2).

Zellikoff, Aschenbrand, and Wyckoff (3) have made a preliminary study of the reaction of $Hg^{202}6(^3P_1)$ atoms, in Hg^{N}, with HOH–N_2 mixtures. At low substrate pressures the HgO product was found to contain 35% Hg^{202}, compared to the natural abundance of 29.8%.

In the present investigation, major emphasis has been placed on the reaction of $Hg^{202}6(^3P_1)$ atoms with water vapor. Certain of our preliminary findings have already

[1]*Manuscript received August 29, 1958.*
Joint contribution from the Department of Chemistry, Illinois Institute of Technology, Chicago 16, Illinois, and the Department of Chemistry, University of Alberta, Edmonton, Alberta. This work was supported in part by the U.S. Atomic Energy Commission under Contract AT(11-1)-43. This support is gratefully acknowledged.
[2]*Present address: Department of Chemistry, University of California, Los Angeles 24, California.*
[3]*Present address: Department of Chemistry, University of Alberta, Edmonton, Alberta.*

been published (4, 5). Experimental conditions have been sought which yield maximum enrichment in Hg^{202} in the HgO product of the reaction. In addition to the information on reaction mechanism which can be obtained from such a study, it was hoped that the reaction could be developed into a simple method for proliferating mercury isotopes.

Preliminary data are also reported on the reaction of $Hg^{202}6(^3P_1)$ atoms with O_2 and N_2O, in order to assess the importance of primary HgO formation in these reactions.

The details of the investigation follow.

EXPERIMENTAL

The reactions were carried out under flow conditions, at room temperature, in a high-vacuum system. The reaction cell consisted of a 5-coil helix, fashioned of 12 mm O.D. optical quartz. The cell was attached to the flow system by standard tapers. For the light source, a quartz electrodeless discharge was used, 8 mm O.D., 150 mm in length, containing a few milligrams of 98.3% Hg^{202}. The discharge was sustained with a Baird Microwave Exciter, operating at a wavelength of 12.2 cm. The lamp was maintained at 25.0° C by being enclosed in a jacket of Vycor 7910 glass, through which thermostatted distilled water was circulated. The lamp-water jacket assembly was axially disposed within the coils of the spiral reaction cell. The microwave reflector was placed a few centimeters from the reaction cell.

Flow rates were measured with calibrated, U-shaped manometers containing dibutyl phthalate. The flow rates were expressed in milliliters per minute at 25° C and 760 mm pressure. Hoke high-vacuum needle valves served to control the flow rate.

Efficient mercury vapor saturation of the substrate gases was achieved by allowing the gases to pass through an operating, umbrella-type, mercury diffusion pump. The partial pressure of mercury vapor in the gas stream was controlled by circulating thermostatted water through the jacket of the mercury diffusion pump.

Small Emil Greiner vernier manometers were used to measure pressures in the reaction zone.

In the water reaction, difficulty was encountered in maintaining a constant pressure of water vapor under flow conditions. This problem was partially solved by installing a water reflux assembly with two 60-cm Graham Coil condensers in series, with a spray trap at the top of the reflux unit, connecting to the flow system. The vapor pressure of water in the stream was controlled by circulating water from a thermostat through the condenser jackets.

The gases used were the highest purity grades obtainable from the Mathieson Company. The nitrous oxide and butadiene were further purified by trap-to-trap distillation. When gas mixtures were used, the mole ratio was controlled by separate flow control units. Samples of the gas mixtures were analyzed by low temperature distillation.

The HgO deposits were removed from the cell by solution in hydrochloric acid. The mercury was recovered from the neutralized solution by deposition on gold wire. The fraction of Hg^{202} in the recovered mercury was determined, by Resonance Radiation Absorbiometry. The method has been described elsewhere (6).

RESULTS

Calibration of Isotope Analysis Unit

The analytical unit was repeatedly calibrated, during the course of the investigation, by determining the absorption of the radiation from the Hg^{202} source by a sample of

Can. J. Chem. Downloaded from www.nrcresearchpress.com by 190.90.36.8 on 09/04/12
For personal use only.

Hg^N in the absorption cell. Aminco, style F, calibrated, fused quartz absorption cells with path length of 0.1003 cm were used throughout the study. The temperature of the Hg^N in the absorption cell was varied from 10° C to 40° C in the calibration runs. The mercury vapor pressure data used were those of Busey and Giauque (7), as in the original investigation on the analytical method (6). The natural abundance of Hg^{202} was taken to be 29.80% (8). The validity of the calibration is dependent upon the shape of the emission line from the Hg^{202} source. There must be negligible overlap of the emission line on absorption contours adjacent to that of Hg^{202}. In order to check this point, AEC-enriched samples, containing up to 98.5% Hg^{202}, were analyzed, using the afore-mentioned method of calibration. The deviation from the mass spectrometric values on the samples did not exceed 2%.

Nitrous Oxide

Data obtained over the pressure range 2–102 mm are shown in Table I. For these runs the mean percentage of Hg^{202} in the oxide is 29.8±0.9%. These data would suggest that HgO is not formed in the primary process in the nitrous oxide reaction. It should be emphasized, however, that failure to find enrichment in the exciting isotope in the HgO is not unequivocal proof that primary formation of HgO is absent. This matter will be discussed in a later section of this paper.

TABLE I

Hg^{202} enrichment in the HgO product of the reaction of $Hg^{202}6(^3P_1)$ atoms in Hg^N with nitrous oxide under flow conditions

Pressure, mm	Temp., °C	Flow rate ml/min at 25° and 760 mm	% Hg^{202} in HgO
2.2	29	80	29.0
21.1	34	47.2	30.3
26.0	28	36	29.3
100	30	50	28.8
102	29	—	31.6
		Average	29.8±0.9

At reaction pressures less than one millimeter the apparent percentage of Hg^{202} in the HgO product was found to vary from 21.5% to 27.8%. The most reasonable explanation of these subnormal values is that there was insufficient mercury from the HgO product to achieve equilibrium vapor pressure in the absorption cell. The product yield was observed to be small at low pressures, owing, presumably, to incomplete quenching.

Oxygen

The enrichment data for dry oxygen and oxygen–nitrogen mixtures are shown in Table II. Copious HgO formation was observed at all pressures studied. No problem was therefore encountered in obtaining sufficient material for analysis.

From the data in Table II, it is apparent that there is no evidence for Hg^{202} enrichment in the HgO product of the reaction of $Hg^{202}6(^3P_1)$ with oxygen and oxygen–nitrogen mixtures. The mean value of 30.2±1.2 can be considered, within the experimental error, as normal abundance. There is, therefore, no evidence for primary HgO formation from these data.

Can. J. Chem. Downloaded from www.nrcresearchpress.com by 190.90.36.8 on 09/04/12
For personal use only.

TABLE II

Hg^{202} enrichment in the HgO product of the reaction of $Hg^{202}6(^3P_1)$ atoms in Hg^N with oxygen and oxygen–nitrogen mixtures

Pressure, mm	Temp., ° C	Comp. mole % O_2	Comp. mole % N_2	Flow rate ml/min at 25° and 760 mm	% Hg^{202} in HgO
6.8	30	100	0	22.8	30.1
14.7	30	100	0	36.8	29.7
23.0	28	100	0	140.8	30.3
24.6	32	100	0	74.5	31.5
0.015	27	21	79	—	31.9
9.5	28	24.2	75.8	26.2	31.3
13.7	30	30.6	69.4	43.3	28.6
14.8	27	51.4	48.6	63.3	28.1
				Average	30.2±1.2

Water Vapor

In the initial work on the reaction of water vapor with $Hg^{202}6(^3P_1)$ atoms, a number of exploratory runs were made in order to test various hypotheses, and to confirm the findings of the previous study (3). In all runs, the total pressure was kept low, in order to avoid broadening effects in absorption (2).

In these preliminary runs, the flow rates varied appreciably during the course of a run, and the rates given are averaged values. Both nitrogen and helium were used as carrier gases, in order to ascertain whether the ability of nitrogen to induce $6(^3P_0)$ atom formation in mercury would be significant in the enrichment process.

Several runs were made in which gases were added to suppress the secondary formation of Hg^NO. Thus NO was added to combine with free oxygen atoms, since the latter are capable of forming Hg^NO with the Hg^N in the gas stream.

Isobutane was used as the carrier gas in one series, as a possible method of reducing the concentration of H atoms and OH radicals in the reaction zone, by abstraction reactions of the type:

$$H + C_4H_{10} \rightarrow H_2 + C_4H_9, \quad [3]$$

$$OH + C_4H_{10} \rightarrow HOH + C_4H_9. \quad [4]$$

Unfortunately the addition of isobutane to the stream resulted in a rapid reduction of the HgO product to Hg, and hence insufficient product was recovered for analysis.

Data representative of a large number of runs are given in Table III.

TABLE III

Hg^{202} enrichment in the HgO product of the reaction of $Hg^{202}6(^3P_1)$ atoms in Hg^N with water vapor

Pressure, mm	Temp., ° C	Comp. mole % HOH	Comp. mole % Carrier	Flow rate ml/min at 25° C and 760 mm	% Hg^{202} in HgO
8.9	28	100	0	20	34.7
10.2	26	100	0	15	32.1
11.4	29	50	50 (He)	33	31.3
13.3	33	50	50 (N_2)	42	33.5
15.4	32	50	50 (N_2)	53	30.7
9.0	26	28	72*	24	30.3

*Carrier gas contained 29% N_2 and 43% NO.

Can. J. Chem. Downloaded from www.nrcresearchpress.com by 190.90.36.8 on 09/04/12
For personal use only.

As can be seen from Table III, the percentage of Hg^{202} in the HgO product varied from 30–35%. Carrier gases were not found to play an advantageous role. Later in this paper data will be presented which suggest that the variation in the isotopic abundance of Hg^{202} in the HgO product is intimately associated with the method of recovering mercury from the product. Our findings at this stage of the investigation were in general agreement with those of Zelikoff, Aschenbrand, and Wyckoff (3).

Since it appeared probable that the enrichment in Hg^{202} arose from the formation of $Hg^{202}OH$, from reaction [1] the failure to obtain pure $Hg^{202}O$ could be due to the secondary formation of $Hg^{N}OH$ by interaction of OH radicals formed in [2], with the Hg^{N} always present in the reaction zone:

$$Hg^{N} + OH + M \rightarrow Hg^{N}OH + M. \quad [5]$$

It is conceivable that reaction [1] is the only primary process under which conditions the degradation of the $Hg^{202}OH$ could arise from exchange reactions of the type:

$$Hg^{202}OH + Hg^{N} \rightarrow Hg^{N}OH + Hg^{202}. \quad [6]$$

Butadiene would be expected to react rapidly with OH radicals, and also possibly with $Hg^{202}OH$, since the latter should have free-radical character. Studies were therefore undertaken with water–butadiene mixtures as a possible means for suppressing the isotopically degradative reactions [5] and [6]. The remarkable effect of the addition of butadiene to the reaction stream is shown in Table IV for runs of 90-minute duration.

From Table IV, it can be seen that the addition of butadiene to the gas stream has resulted in a marked increase in the Hg^{202} content of the HgO product. During these runs, it was observed that a thin film of polymer formed on the walls of the spiral cell. The mercury-6($^3P_1$)-sensitized decomposition of 1,3-butadiene was investigated by Gunning and Steacie (9). These authors showed that butadiene does not polymerize under flow conditions, since free radicals are not formed in the primary process. The presence of butadiene polymer would therefore be evidence, in our study, of the formation of free radicals in the water decomposition.

TABLE IV

Hg^{202} enrichment in the HgO product of the reaction of $Hg^{202}6(^3P_1)$ atoms in Hg^{N} with water vapor – 1,3-butadiene mixtures

Pressure, mm	Temp., ° C	Comp. mole % HOH	Comp. mole % C_4H_6	Flow rate ml/min at 25° C and 760 mm	% Hg^{202} in HgO
5.3	25	96	4	12.2	78
5.1	25	94	6	21.8	84
9.8	30	93	7	51.5	72
8.5	24	93	7	22.4	75
8.4	27	79	21	34.8	85
17.1	28	75	25	69.7	70
8.5	28	46	54	45.3	66
8.6	24		~100*	21.5	32.5
11.7	27	45	10†	60.8	75

*There may have been a trace of moisture in the butadiene.
†45% Nitrogen added, 45-minute exposure.

In a reaction of this type, there are many variables which require systematic study: i.e. flow rate, pressure, reaction temperature, water-to-butadiene ratio, product-recovery methods, etc. These studies will form the basis of further investigations. In the apparatus

Can. J. Chem. Downloaded from www.nrcresearchpress.com by 190.90.36.8 on 09/04/12
For personal use only.

used in this study, it was difficult to vary flow rate and reaction pressure independently. A series of runs of 120-minute duration were carried out, however, in which the reaction pressure was held constant at 3.7 ± 1.0 mm at low flow rates, while the water-to-butadiene ratio was varied. The results of these runs are summarized in Table V.

From Table V it can be seen that at constant pressure, low flow rate, and butadiene concentrations exceeding 10 mole %, the percentage of Hg^{202} appears to reach a constant value, independent of butadiene concentration, of $75 \pm 3\%$. A major experimental difficulty in this investigation was the maintenance of a constant partial pressure of water vapor over the course of a run. In obtaining the data for Table V, great care was taken to maintain a constant pressure of water vapor during each run. This accounts, in large measure, for the greater consistency in the enrichment values obtained, in comparison with those given in Table IV. Furthermore, in comparing the data of Tables IV and V, it should be borne in mind that the former are values for runs of 90-minute duration, while the latter are for runs of 120-minute duration. In general, it was found that prolonging the exposure time decreased the enrichment.

TABLE V

Hg^{202} enrichment in the HgO product of the reaction of $Hg^{202}6(^3P_1)$ atoms of Hg^N with water vapor – 1,3-butadiene mixtures as a function of the butadiene concentration (Total pressure 3.7 ± 1.0 mm)

Temp.	Comp. mole % HOH	Comp. mole % C_4H_6	Flow rate ml/min at 25° C and 760 mm	% Hg^{202} in HgO
27	96	4	10.6	58
25	93.5	6.5	7.7	72
27	90	10	8.5	77
25	87.5	12.5	8.6	76
32	86	14	16.2	64
24	79	21	12.2	63
27	73	27	11.0	73
25	71.5	28.5	7.5	77
20	48.1	51.9	5.3	76

A variable which was appreciated relatively late in the investigation was the degradative effect of product-recovery techniques on the percentage of Hg^{202} in the recovered mercury. In an earlier paper (5), data were presented which showed that Hg^{202++} ions will be isotopically degraded when the solution is in contact with a globule of Hg^N. The exchange occurs presumably between dissolved Hg^N and Hg^{202++}. The $Hg^{202}O$ deposited in the reaction cell has chemisorbed upon it a layer of Hg^N. This adsorbed layer is extremely difficult to remove. A number of experiments were performed in which the cell, after reaction, was exhaustively evacuated through a trap containing liquid nitrogen, in an attempt to drive off the adsorbed Hg^N. This procedure had little effect upon the percentage of Hg^{202} in the product.

The kinetics of the exchange reaction between dissolved Hg^N and Hg^{202++} ion will require detailed study. It is fairly clear, however, at this stage, that the rate of exchange decreases with decreasing concentration of the hydrochloric acid used to dissolve the HgO from the reaction cell. The effect of acid concentration is illustrated by the following data: three runs were made with a substrate containing $5.5 \pm 1.5\%$ butadiene. Acid concentrations of 12.0 *M*, 6.0 *M*, and 2.5 *M* were used in recovering the HgO product. The analyses of the recovered mercury samples gave, for the percentage of Hg^{202}, 72, 78,

Can. J. Chem. Downloaded from www.nrcresearchpress.com by 190.90.36.8 on 09/04/12
For personal use only.

and 84 respectively. There appeared to be little effect on the Hg^{202} enrichment when acid concentrations less than 2.5 *M* were employed. For the runs reported in Table V, 0.16 *M* hydrochloric acid was used to dissolve the HgO product from the cell.

DISCUSSION

Nitrous Oxide and Oxygen Reactions

The failure to obtain an HgO product, enriched in Hg^{202}, in the nitrous oxide and oxygen reactions, would suggest that a mercury compound is not formed in the primary process. However, even with the pure water vapor reaction, the enrichment is small, butadiene being required to suppress the isotopically degradative processes operative. The oxygen and nitrous oxide reactions will require further study, in the presence of free-radical acceptor addends, before unequivocal statements can be made concerning the primary formation of mercury compounds.

Water Vapor Reaction

As a positive result of this investigation, it has been shown that in the flow reaction between $Hg^{202}6(^3P_1)$ atoms in Hg^N and mixtures of water vapor and 1,3-butadiene, the HgO product of the reaction is highly enriched in Hg^{202}. The reaction recommends itself as a simple method for preparing Hg^{202} from natural mercury.

In the reaction with pure water vapor, the Hg^{202} content of the HgO product was not found to exceed 35%, in agreement with an earlier study (3). From the kinetic standpoint, it can be conservatively stated that some fraction of the primary interaction between $Hg^{202}6(^3P_1)$ atoms and HOH molecules leads to the formation of a mercury compound. The role of butadiene in increasing the Hg^{202} content of the oxide can be explained, at this stage of our knowledge, on two bases:

(*a*) There are two primary processes—reactions [1] and [2]. The butadiene serves to clean up OH radicals, formed in [2], thereby suppressing the formation of Hg^NO by reaction [5].

(*b*) Reaction [1] is the only primary process operative and the failure to obtain pure $Hg^{202}O$, from water substrate alone, is attributable to exchange reactions, similar to [6], occurring in the gas phase or on the wall. Here the butadiene could suppress exchange degradation by combining with the quasi-free radical $Hg^{202}OH$.

It should be pointed out that $Hg^{202}OH$ is not necessarily the initial mercury compound formed. The primary step could be

$$Hg^{202}6(^3P_1) + HOH \rightarrow Hg^{202}H + OH. \qquad [7]$$

The unstable species HgH has been adduced many times to explain the preference of Hg $6(^3P_1)$ atoms for C–H bond scission in hydrocarbon reactions. The problem has been thoroughly discussed by Steacie (10). The low heat of formation of HgH (8.5 kcal) would argue against its surviving sufficiently long to form a stable product in the water reaction.

Investigations are now in progress in the laboratories of one of us (H.E.G.) which should yield further information on the kinetics of the water reaction. In addition to systematic studies of the effects of the various reaction parameters on the Hg^{202} content of the HgO product, the quantum yield of $Hg^{202}O$ formation is being investigated. Quantum yield measurements are difficult in water vapor – butadiene mixtures, owing to the high quenching cross section of butadiene. The situation is further complicated by the fact that water vapor converts Hg $6(^3P_1)$ atoms to the $6(^3P_0)$ state at least as efficiently

Can. J. Chem. Downloaded from www.nrcresearchpress.com by 190.90.36.8 on 09/04/12
For personal use only.

as nitrogen. Finally, information is being obtained on the nature of the polymer formed in the reaction with water–butadiene mixtures. The presence of Hg–C bonds in the polymer would be evidence of interaction of butadiene with mercurial free radicals.

REFERENCES

1. BILLINGS, B. H., HITCHCOCK, W. J., and ZELIKOFF, M. J. Chem. Phys. **21**, 1762 (1953).
2. OSBORNE, K. R., MCDONALD, C. C., and GUNNING, H. E. J. Chem. Phys. **26**, 124 (1957).
3. ZELIKOFF, M., ASCHENBRAND, L. M., and WYCKOFF, P. H. J. Chem. Phys. **21**, 376 (1953).
4. PERTEL, R. and GUNNING, H. E. J. Chem. Phys. **26**, 219 (1957).
5. GUNNING, H. E. Can. J. Chem. **36**, 89 (1958).
6. OSBORN, K. R. and GUNNING, H. E. J. Opt. Soc. Am. **45**, 552 (1955).
7. BUSEY, R. H. and GIAUQUE, W. F. J. Am. Chem. Soc. **75**, 806 (1953).
8. NIER, A. O. Phys. Rev. **79**, 450 (1950).
9. GUNNING, H. E. and STEACIE, E. W. R. J. Chem. Phys. **12**, 484 (1944).
10. STEACIE, E. W. R. Atomic and free radical reactions. Reinhold Publishing Corp., New York. 1954. pp. 414 ff.

Can. J. Chem. Downloaded from www.nrcresearchpress.com by 190.90.36.8 on 09/04/12
For personal use only.

Can. J. Chem. Downloaded from www.nrcresearchpress.com by 190.90.36.8 on 09/04/12
For personal use only.

FUSED HETEROCYCLICS

PART III. SYNTHESIS OF QUINOLINO-(2′:3′:3:4)-QUINOLINE[1]

RAGINI ANET[2]

ABSTRACT

Quinolino-(2′:3′:3:4)-quinoline has been synthesized from 3-aminoquinoline-4-carboxylic acid via 4′-hydroxyquinolino-(2′:3′:3:4)-quinoline.

Quinolinoquinolines containing fused pyridine rings were of interest in connection with the structure of calycanine (1). In Part II of this series (2) the synthesis of quinolino-(2:3:3′:2′)-quinoline was reported. The synthesis of an angular isomer, quinolino-(2′:3′:3:4)-quinoline, is now described.

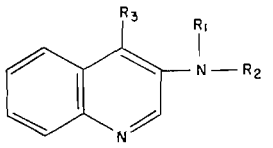

I, $R_1 = R_2 = H$; $R_3 = COOH$
II, $R_1 = Ph$; $R_2 = H$; $R_3 = COOH$
III, $R_1 = R_2 = Ph$; $R_3 = COOH$
IV, $R_1 = Ph$; $R_2 = R_3 = H$
V, $R_1 = R_2 = Ph$; $R_3 = H$

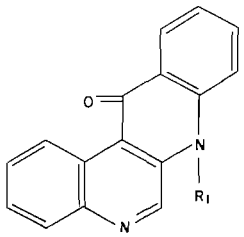

VII, $R_1 = Ph$

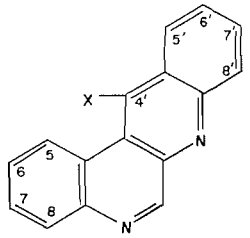

VI, X = OH
VIII, X = Cl

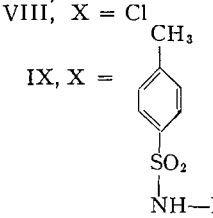

IX, X =

X, X = H

Although the base itself (X) has not been synthesized previously, 4′-hydroxy derivatives with substituents in the 2-, 6′-, 7′-, and 8′-positions have been prepared by the cyclization of appropriately substituted 3-arylaminoquinoline-4-carboxylic acids (3, 4, and 5). This method, in its essentials, was followed for the synthesis of 4′-hydroxyquinolino-(2′:3′:3:4)-quinoline.

The preparation of 3-phenylaminoquinoline-4-carboxylic acid (II) was carried out by the extension of the arylation reaction described in Part II (2). When 3-aminoquinoline-4-carboxylic acid (I) (6) was treated with iodobenzene and copper catalyst, a mixture of 3-phenylamino- and 3-(diphenylamino)-quinoline-4-carboxylic acids (II and III respectively) was obtained. As in the case of the corresponding quinaldine acid (2), the monosubstituted acid could not be obtained exclusively. The acids were separated by fractional crystallization and decarboxylated to the corresponding bases 3-phenylamino- and 3-(diphenylamino)-quinolines (IV and V), which were characterized as their picrates.

The mixture of acids obtained in the arylation reaction was cyclized with phosphoryl

[1]*Manuscript received September 5, 1958.*
Contribution from the Dyson–Perrins Laboratory, Oxford. This work was carried out as a part of the D.Phil. Thesis of the author, Oxford University, 1952.
[2]*nee Phadké. Present address: c/o Dr. F. A. L. Anet, Department of Chemistry, University of Ottawa.*

chloride, and the intermediate chloro derivatives hydrolyzed to give 4′-hydroxyquinolino-(2′:3′:3:4)-quinoline (VI) and 4′-keto-1′-phenyldihydroquinolino-(2′:3′:3:4)-quinoline (VII). The cyclized products were separated readily as they had markedly different solubilities in organic solvents. The 4′-hydroxy derivative (VI) gave a typical acridone-like fluorescence in presence of alkali (7) and was characterized as its picrate; whereas the 4′-keto compound was non-fluorescent and did not give any crystalline salts.

The reduction of the 4′-hydroxy derivative to the unsubstituted quinolinoquinoline with zinc dust did not prove successful. However, by using the method of Albert and Royer (8) for the conversion of acridone into acridine, the desired compound (X) was obtained. The 4′-hydroxy derivative (VI) was refluxed with phosphoryl chloride to give the 4′-chloro compound (VII) which was sensitive to hydrolysis with acid, but could be stored satisfactorily over potassium hydroxide *in vacuo*. It was characterized as the picrate. On treatment of the chloro derivative with *p*-toluenesulphonylhydrazide (8) in chloroform, the 4′-*p*-tosylhydrazidoquinolino-(2′:3′:3:4)-quinoline (IX) was obtained as the hydrochloride. Attempts to prepare the free base from its hydrochloride were unsuccessful and led to considerable decomposition. It was found that the reaction of the chloro derivative with *p*-tosylhydrazide was slower than in the case of the acridine derivative (8). The 4′-hydrazido hydrochloride was treated with 1 *N* sodium hydroxide in ethylene glycol to give a mixture of the 4′-hydroxy derivative (VI) and the desired quinolino-(2′:3′:3:4)-quinoline (X) which were readily separated by chromatography over alumina. The quinolinoquinoline crystallized from methanol in cream-colored needles m.p. 179°–180° C. Its ultraviolet absorption spectrum is recorded in Fig. 1.

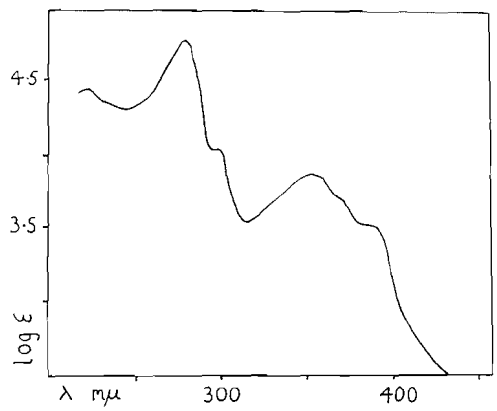

FIG. 1. Ultraviolet absorption spectrum of quinolino-(2′:3′:3:4)-quinoline in methanol.

EXPERIMENTAL

All melting points are uncorrected. Analyses by Drs. Weiler and Strauss, Oxford.

3-Phenylaminoquinoline-4-carboxylic Acid (II)

3-Aminoquinoline-4-carboxylic acid (I, 6.35 g) (6), 10 g (7.35 ml) iodobenzene, 9 g anhydrous potassium carbonate, and 0.8 g copper catalyst (Naturkupfer C) were refluxed in a mixture of 20 ml benzyl alcohol and 40 ml cyclohexanol for 3 hours with strict exclusion of moisture. The reaction mixture was cooled, diluted with 50 ml water, and steam-distilled to remove the alcohols. The solution was filtered hot into dilute acetic acid and allowed to stand at room temperature for 6–8 hours. The orange precipitate (9.2 g, m.p. 224°–232° C, with decomposition) was dried, and crystallized from a 1:1 mixture

Can. J. Chem. Downloaded from www.nrcresearchpress.com by 190.90.36.8 on 09/04/12
For personal use only.

of chloroform–methanol. Lemon-yellow feathery needles of the 3-phenylamino acid (II), m.p. 243°–244° C (decomp.), were obtained after several crystallizations. Found: C, 72.1; H, 4.8; N, 10.9. Calc. for $C_{16}H_{12}N_2O_2$: C, 72.7; H, 4.5; N, 10.6%. The acid was sparingly soluble in water, benzene, ether, and alcohol. Its solutions in alkali were colorless.

3-Phenylaminoquinoline (IV)

The acid (II, 1.2 g) was heated at 250° C for 1 hour. The acid melted with decomposition and after the first few minutes, some of the base started to sublime into the air condenser attached to the flask. After decarboxylation was complete, the contents of the flask were allowed to cool and were extracted with methanolic hydrochloric acid. The acid solution was poured into an excess of aqueous potassium hydroxide, and the aqueous solution extracted with ether. Evaporation of the ether extract after charcoal treatment gave an oil (0.9 g), which solidified on refrigeration. Crystallization from dilute methanol gave the base (IV) as needles, m.p. 121°–123° C. Found: C, 81.9; H, 5.45; N, 12.4. Calc. for $C_{15}H_{12}N_2$: C, 81.8; H, 5.45; N, 12.4%. The base was very soluble in organic solvents and its solutions exhibited a strong blue fluorescence in ultraviolet light.

The *picrate* prepared in methanol gave orange needles, m.p. 189°–190° C with decomposition. Found: N, 15.4. Calc. for $C_{21}H_{15}N_5O_7$: N, 15.6%.

3-(Diphenylamino)-quinoline-4-carboxylic Acid (III)

A suspension of 1.5 g of 3-amino acid (I) in 25 ml benzyl alcohol was refluxed with 2.0 g anhydrous potassium carbonate, 0.2 g. Naturkupfer C and 2.3 g (1.7 ml) iodobenzene for 6 hours. The reaction was worked up as in the case of the 3-phenylamino acid (II) described above when 1.95 g of a bright yellow solid, m.p. 255°–264° C, was obtained. This was washed with acetone and crystallized from chloroform–methanol in stout yellow rods, m.p. 270°–272° C with decomposition. Found: C, 77.5; H, 4.8; N, 8.1. Calc. for $C_{22}H_{16}N_2O_2$: C, 77.6; H, 4.8; N, 8.2%. The acid was sparingly soluble in most organic solvents but was readily soluble in aqueous alkali to give colorless solutions. It was insoluble in dilute mineral acids but dissolved in concentrated hydrochloric acid on prolonged boiling.

3-(Diphenylamino)-quinoline (V)

The acid (III, 1.5 g) was decarboxylated at 270° C for 1 hour. On working up the reaction as in the case of the 3-phenylamino compound (IV), an oil (1.0 g), solidifying on refrigeration was obtained (m.p. 155°–164° C with previous softening). Repeated crystallizations from dilute methanol or other organic solvents failed to raise the melting point and the base was therefore purified by sublimation at 180° C under reduced pressure (20 mm). Crystallization of the sublimate from dilute methanol gave colorless needles, m.p. 162°–164° C. Found: C, 84.7; H, 5.4; N, 9.7. Calc. for $C_{21}H_{16}N_2$: C, 85.1; H, 5.4; N, 9.4%. The base was very soluble in organic solvents to give yellowish solutions with a vivid blue fluorescence.

The *picrate* prepared from equimolecular quantities of the base and picric acid in benzene–methanol formed orange needles, m.p. 205°–206° C with decomposition. Found: C, 61.9; H, 3.7; N, 13.6. Calc. for $C_{27}H_{19}N_5O_7$: C, 61.7; H, 3.7; N, 13.3%.

4′-Hydroxyquinolino-(2′:3′:3:4)-quinoline (VI)

Five grams of the crude 3-phenylamino acid (II) were refluxed with 12.5 ml phosphoryl chloride under anhydrous conditions. A vigorous reaction set in at 60°–65° C and heating was interrupted till it was over. The refluxing was continued for 90 minutes the bath temperature being maintained at 110–120° C. Phosphoryl chloride was removed under

Can. J. Chem. Downloaded from www.nrcresearchpress.com by 190.90.36.8 on 09/04/12
For personal use only.

reduced pressure, care being taken that the bath temperature did not exceed 100° C. The dark residue, after removal of the acid chloride, was heated on the steam bath with 300 ml 1 *N* hydrochloric acid for 2 hours, filtered, and poured into excess ammonium hydroxide. After 16 hours at room temperature the dark solid was filtered, dried, and extracted with hot chloroform to remove the 4′-keto compound (vide infra) formed from the disubstituted acid (III). The residue was extracted with hot ethanol (charcoal) and the 4′-hydroxy derivative obtained by evaporation of the ethanol was crystallized from dilute acetic acid in yellow needles, m.p. 360° C. Found (sample dried at 100° C under 2 mm): C, 72.9; H, 4.6. Calc. for $C_{16}H_{10}N_2.H_2O$: C, 72.7; H, 4.5. Found (sample dried at 250° C under 0.5 mm): C, 74.9; H, 4.6. Calc. for $C_{16}H_{10}N_2O.H_2O$: C, 75.0; H, 4.3%. Attempts to remove the last 0.5 molecule of water of crystallization were unsuccessful even after repeated sublimation and extensive drying. The 4′-hydroxy compound was sparingly soluble in ether, benzene, and chloroform but readily so in ethanol and ethyl acetate. Its alcoholic solutions were non-fluorescent but gave a vivid green fluorescence in presence of a pellet of potassium hydroxide.

The *picrate* formed by refluxing (VI) with picric acid in ethanol for 4 hours gave needles, m.p. 255°–258° C. Found: C, 55.9; H, 3.1; N, 14.8. Calc. for $C_{22}H_{13}N_5O_8$: C, 55.6; H, 2.7; N, 14.8%.

4′-Keto-1′-phenyldihydroquinolino-(2′:3′:3:4)-quinoline (VII)

Diphenylamino acid (III, 0.8 g) was refluxed with 5 ml phosphoryl chloride and the reaction worked up as above. The 4′-keto derivative (VII) was obtained from the chloroform extract as a dark solid (0.6 g). Treatment with charcoal and crystallization from methanol gave pale yellow needles, m.p. 282°–284° C. Found: C, 81.8; H, 4.4; N, 8.7. Calc. for $C_{22}H_{14}N_2O$: C, 82.0; H, 4.4; N, 8.7%.

4′-Chloroquinolino-(2′:3′:3:4)-quinoline (VIII)

4′-Hydroxy compound (VI, 1.5 g) was refluxed with 20 ml phosphoryl chloride under anhydrous conditions for 6 hours. After removal of the acid chloride under reduced pressure, the orange-colored solid was added to a vigorously stirred 5% aqueous ammonium hydroxide containing crushed ice. The solution was kept alkaline to phenolphthalein by adding more ammonia if necessary. After 30 minutes the solution was centrifuged and the cream-colored solid dried in a vacuum desiccator over potassium hydroxide. Extraction of the dry solid with benzene containing a pellet of potassium hydroxide gave the 4′-chloro compound which crystallized from petroleum ether (b.p. 40°–60° C) in colorless prismatic needles, m.p. 191°–192° C. Found: C, 73.0; H, 3.8; Cl, 13.1. Calc. for $C_{16}H_9N_2Cl$: C, 72.6; H, 3.4; Cl, 13.4%.

The *picrate* formed in benzene gave orange needles, m.p. 209°–210° C with decomposition. Found: C, 54.0; H, 2.6. Calc. for $C_{22}H_{12}N_5O_7Cl$: C, 53.5; H, 2.4%.

4′-p-Tosylhydrazidoquinolino-(2′:3′:3:4)-quinoline Hydrochloride (IX)

The 4′-chloro compound (VIII, 0.18 g) was dissolved in the minimum quantity of chloroform and added to a saturated solution of 0.17 g *p*-tosylhydrazide (8) in the same solvent. After 48 hours at room temperature, the solution turned pale yellow but no solid separated. The chloroform was removed on the steam bath and fresh chloroform added to the reaction mixture which was left at room temperature for a further 72 hours. (It was found that a fast stream of hydrogen chloride when passed through the solution after the initial 48 hours gave the hydrochloride of (VIII) in one experiment.) After the completion of the reaction, the red solid was filtered from the chloroform, dried, and

Can. J. Chem. Downloaded from www.nrcresearchpress.com by 190.90.36.8 on 09/04/12
For personal use only.

crystallized from methanol containing a drop of hydrochloric acid in red needles which did not melt but decomposed at 320° C. Found: C, 61.5; H, 4.2. Calc. for $C_{23}H_{19}N_4SO_2Cl$: C, 61.3; H, 4.2%.

Quinolino-(2′:3′:3:4)-quinoline (X)

One half gram of (IX) was heated on the steam bath with 10 ml 1 *N* sodium hydroxide in ethylene glycol (4 g sodium hydroxide dissolved in a mixture of 70 ml ethylene glycol and 30 ml water) for 3 hours. The solution turned crimson and lumps of a precipitate were formed which were broken up from time to time with a glass rod. Evolution of gas began after the first few minutes and continued for 2 hours, when the solution became clear. It was then diluted with 20 ml water and refrigerated overnight. The flocculent precipitate that had separated was filtered after 24 hours, taken up in 1 *N* hydrochloric acid, and reprecipitated with ammonia. The base was taken up in ethyl acetate and chromatographed over alumina, when the quinolinoquinoline (X) separated as a strongly fluorescent band in ultraviolet light. Elution with ethyl acetate gave (X) which crystallized from methanol in needles, m.p. 179°–180° C. Found: C, 83.1; H, 4.5. Calc. for $C_{16}H_{10}N_2$: C, 83.5; H, 4.4%. The base was readily soluble in ethyl acetate, alcohol chloroform, and ether. It dissolved in mineral acids to give non-fluorescent solutions

ACKNOWLEDGMENTS

The author is indebted to Sir Robert Robinson, for his advice and encouragement and to the University of Bombay for a Sir Mangaldas Nathubhai Scholarship.

REFERENCES

1. ROBINSON, R. and TEUBER, H. J. Chem. & Ind. 783 (1954).
2. ANET, R. Can. J. Chem. **36**, 1449 (1958).
3. DIESBACH, H. DE and MOSER, E. Helv. Chim. Acta, **20**, 132 (1937).
4. DIESBACH, H. DE and KLEMENT, O. Helv. Chim. Acta, **24**, 166 (1941).
5. COLONNA, M. and DAL MONTE-CASONI, D. Gazz. chim. ital. **78**, 793 (1948).
6. COLONNA, M. Boll. sci. fac. chim. ind. univ. Bologna, 89 (1941); Chem. Abstr. **37**, 3096 (1943).
7. ALBERT, A. The acridines. Edward Arnold & Co., London. 1951.
8. ALBERT, A. and ROYER, R. J. Chem. Soc. 1148 (1949).

Can. J. Chem. Downloaded from www.nrcresearchpress.com by 190.90.36.8 on 09/04/12
For personal use only.

Can. J. Chem. Downloaded from www.nrcresearchpress.com by 190.90.36.8 on 09/04/12
For personal use only.

THE INTERACTION OF FRIEDEL–CRAFTS CATALYSTS WITH ORGANIC MOLECULES

I. THE CH_3COCl:$AlCl_3$ SYSTEM[1]

DENYS COOK[2]

ABSTRACT

An infrared study of the liquid complex of aluminum chloride with acetyl chloride has been undertaken. The results indicate that the pure liquid complex is not a simple mixture, but consists of (1) the donor–acceptor complex $CH_3\underset{\displaystyle Cl}{\underset{|}{C}}{=}O \ldots AlCl_3$ and (2) the ions $[CH_3CO]^+$ and $[AlCl_4]^-$. A solution of the liquid complex in a solvent of high dielectric constant like nitrobenzene ($\epsilon = 36.1$) contains both these species, but in a low dielectric constant solvent like chloroform ($\epsilon = 5.05$) only (1) is present. The carbon–chlorine bond in (1) is modified. The mechanism of Friedel–Crafts ketone synthesis is briefly examined in the light of these results.

A variety of metallic halides have been used as catalysts in the Friedel–Crafts ketone synthesis. The most widely used of these is $AlCl_3$, but others, such as BF_3, $AlBr_3$, $SbCl_3$, $SbCl_5$, $FeCl_3$, $TiCl_4$, $SnCl_4$, and $ZnCl_2$ etc., have all been used. All these halides have in common the function of Lewis acids, due either to electron deficiency, or to hybridization changes to give complex ions.

Numerous examples exist in the literature of complexes formed from such Lewis acids and various donors. The characteristics of the donor molecule are usually those of well-directed lone-pair electrons. Thus compounds like R_2O, $R_2C{=}O$, RCN, R_3N, RNO_2 etc. can all form more or less stable complexes with Lewis acids, the electron deficiency of the latter being satisfied by sharing the lone-pair electrons of the donor group. Some of the Lewis acids can function as acceptors in a slightly different way. Thus NaCl and $AlCl_3$ form the compound $NaAlCl_4$, which has been shown to consist of Na^+ and $[AlCl_4]^-$ ions (1, 2).

The presence of two functional groups in an acyl halide, namely a carbonyl donor group and an ionizable chlorine atom, suggests that two types of intermediates may be possible in the Friedel–Crafts ketone synthesis: (*a*) the ions $[CH_3CO]^+$ and $[AlCl_4]^-$, and (*b*) the donor–acceptor complex formed between the carbonyl–oxygen lone-pair electrons and the vacant orbital of the $AlCl_3$, as suggested by Pfeiffer (3). An extension of (*b*) proposed by Dilthey (4) involved loss of a Cl^- from the donor–acceptor complex to give a complex ion.

It is the purpose of this paper, from the spectroscopic evidence presented, to show that the donor–acceptor complex as in (*b*) is present in solution in solvents of low dielectric constant, but that in the pure complex or in its solution in solvents of high dielectric constant ions such as in (*a*) are present as well as the donor–acceptor complex.

After the experimental work described here was completed, two papers by Susz and Wuhrmann (5, 6) appeared on the infrared spectra of the complexes CH_3COF:BF_3 and CH_3COCl:$AlCl_3$. These gave the first clear indication of the presence of the $[CH_3CO]^+$ ion. The present work corroborates their findings but important differences exist which are detailed below.

[1]*Manuscript received August 28, 1958.*
Contribution from the Spectroscopy Laboratory, The Dow Chemical Company, Midland, Michigan.
[2]*Present address: Exploratory Research Laboratory, Dow Chemical of Canada, Limited, Sarnia, Ontario, Canada.*

Can. J. Chem. Downloaded from www.nrcresearchpress.com by 190.90.36.8 on 09/04/12
For personal use only.

EXPERIMENTAL

Aluminum chloride was purified by vacuum sublimation of reagent grade $AlCl_3$ in the apparatus shown in Fig. 1*a*. The $AlCl_3$ was sublimed from the bulb to the cold finger and then transferred to the seal-off tube with continuous pumping. A known quantity, 4.729 g, was then transferred to the reaction tube (which had been flamed and then cooled with dry nitrogen) in Fig. 1*b* which was sealed off as quickly as possible. The molar equivalent of CH_3COCl, 2.77 g, was distilled onto the $AlCl_3$ at liquid nitrogen temperatures. On warming to room temperature the $AlCl_3$ gradually went into solution, though slight heat was necessary to make the last traces dissolve, giving a homogeneous light brown solution. Excessive heat which would favor decomposition was avoided. Even so some slight decomposition occurred as HCl was found in the gas phase. Infrared examination of the gas phase showed the evolved gases to be chiefly HCl and CH_3COCl, and mass spectrometry confirmed this but also indicated the presence of further unidentified fragments of mass 45, 60, 73, and 87. The total volume of gas evolved was computed from the pressure and an estimate of the volume of the apparatus. Assuming only the two components mentioned above to be significant, the weight of these products lost from the reaction tube was 0.072 g HCl and 0.157 g CH_3COCl. These represent maximum values, since the unidentified products would lower these figures.

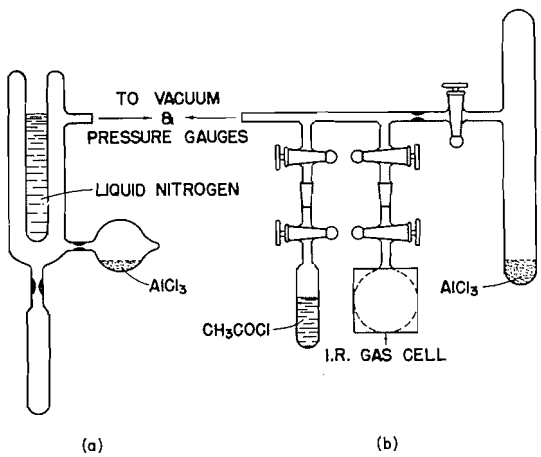

FIG. 1. (*a*) $AlCl_3$ sublimation apparatus. (*b*) Apparatus for preparation of complex.

The reaction tube was transferred to a dry box which contained a bed of silica gel, and which had been well flushed with dry nitrogen for a few hours before. After it had been left standing for at least two hours in the dry box the reaction tube was opened, and the various cells made up for spectroscopic analysis.

A double beam rock salt spectrometer was used to record the spectra in the region of 4000 cm^{-1} to 625 cm^{-1}. From 625 cm^{-1} to 350 cm^{-1} a modified Perkin–Elmer 12C spectrometer with CsBr optics was used. The standard bands in a thin film of polystyrene were used for calibration.

RESULTS

The principal bands of the various spectra are shown in Table I together with those of pure acetyl chloride. Figure 2 shows the spectrum of the pure liquid complex.

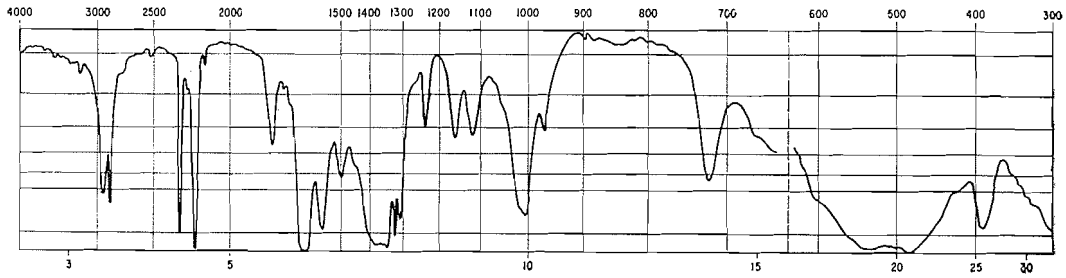

FIG. 2. Spectrum of pure liquid complex. Capillary film between NaCl plates.

TABLE I

Principal bands in the spectra

Assignment	CH_3COCl*	$CH_3COCl:AlCl_3$		$CH_3COCl:AlCl_3$ in solution in:		
		This work	Susz and Wuhrmann	$C_6H_5NO_2$†	$CHCl_3$‡	CS_2‡
ν CH_3, a''	3012 w§	2941 m	2950 m			
ν CH_3, a'	2960	2874 m				
ν $[CH_3CO]^+$		2307 s	2305 vs			
		2203 vs	2200 w, sh	2193 vs		
ν C=O, a'	1808 vs	1779 m		1805 vs	1793 w	1802 w
				1681 m		
ν C=O ... $AlCl_3$		1637 vs	1639 m	1642 vs	1660 m	
					1613 m	
		1567 s	1560 w		1558 w	
δ CH_3, a''	1433 m	1497 s	1485 m		1479 m	
δ CH_3, a''?	1418 m					
δ CH_3, a'	1370 s	1379 s, b			1389 w	
	1357 s	1348 s			1340 w	
		1321 s	1312 s			
		1305 s				
		1236 m				
		1159 m	1154 w		1156 m	
		1117 m				
		1018 m, sh				
ν C—C, a'	1103 vs	1006 s	1000 vs		1099 w	1095 w
δ CH_3, a''?	1028 s					
δ CH_3, a'	952 vs	969 m			952 w	952 vw
		716 m	719 s			
		662 m, sh				
		649 m			625 m	
ν C—X, a'	539 s					
		540 s, b			540 s	
		485 s, b	500 s		500 m	
δ C—X, a'	436 s					
or		390 s			370 s	
δ CCO, a'	352 m					

obscured by solvent

*These values agree well with those of J. C. Evans and H. J. Bernstein, Can. J. Chem. **34**, 1083 (1956), whose notation is followed.
†About 0.5 cc liquid complex in about 5 cc $C_6H_5NO_2$.
‡Saturated solution.
§w = weak, m = medium, s = strong, v = very, b = broad, sh = shoulder.

DISCUSSION

The strongest band in the spectrum of the pure liquid complex is at 1637 cm^{-1}. On account of its intensity it is likely that this is a carbonyl group vibration, and it seems logical to assign this band to the C=O vibration in the complex I:

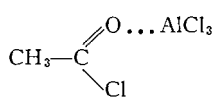

I

Can. J. Chem. Downloaded from www.nrcresearchpress.com by 190.90.36.8 on 09/04/12
For personal use only.

Since $\nu_{C=O}$ for acetyl chloride is 1807 cm^{-1} in the liquid, this band in the complex is lowered by 170 cm^{-1}. Shifts in $\nu_{C=O}$ of comparable magnitude have been observed by Susz and Cooke (7) in the equimolar complex of benzophenone and $AlCl_3$. In the complex $\nu_{C=O}$ was 1525 cm^{-1} and in pure benzophenone it was 1650 cm^{-1}, a shift of 125 cm^{-1}.

Susz and Wuhrmann tentatively assigned the 1639 cm^{-1} band to the C=C vibration in $CH_2{=}C(Cl){-}O{-}AlCl_2$ which they thought might have been present in small amounts in their complex, and the 1567 cm^{-1} band to the perturbed carbonyl vibration. The high intensity of the 1637 cm^{-1} band would seem to rule out this interpretation, since such a C=C vibration would be expected to be quite weak. It is much more likely that their band at 1639 cm^{-1} was due to a small amount of the complex I which could very well have been present in their complex.

Two strong bands are located at 2307 cm^{-1} and 2203 cm^{-1}. These two bands are in the region of triple bond stretching frequencies and their presence in the spectrum is of unusual interest. They constitute the grounds for suspecting the presence of the ion $[CH_3CO]^+$ in the complex. This ion should be linear (it is isoelectronic with CH_3CN). Variations in carbonyl stretching frequencies are due, in part, to the electronegativity of the group, or groups, attached to the carbonyl group (8). The positive charge on the carbon atom of the carbonyl group should have a very strong electron-withdrawing effect. This would, therefore, raise the carbonyl frequency by a large amount. The band at 2307 cm^{-1} is thought to be compatible with such a structure. Alternatively the structure may be described in terms of resonance, where the actual structure is a hybrid of the forms $CH_3C^+{=}O$ and $CH_3C{\equiv}O^+$. The bond order of the carbonyl group would be between 2 and 3, and the carbonyl frequency much higher than an ordinary ketone.

This is in harmony with the findings of Susz and Wuhrmann (5), who observed a very strong band at 2305 cm^{-1}. In contrast, the band at 2200 cm^{-1}, which they report to be of weak intensity, is very strong. This band could have two possible causes. It may be due to the complex ion II, as proposed by Dilthey, or an ion pair of the form III

$[CH_3CO]^+ \ldots AlCl_3$

II

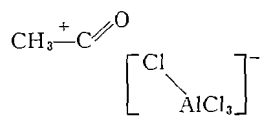

III

in which there is little interaction between the Cl atom and the central C atom. In support of II the lowering of $\nu_{C=O}$ from 2307 cm^{-1} in $[CH_3CO]^+$ to 2203 cm^{-1} in $[CH_3CO]^+ \ldots AlCl_3$ seems to be in accord with other data on the lowering of $\nu_{C=O}$ of carbonyl compounds in complexes with strong Lewis acids. However, it might be argued that III seems more probable, since the cation $[CH_3CO]^+$, by virtue of its electron deficiency, might not be able to form a donor–acceptor complex with a Lewis acid. Evidence presented later in this paper tends to support III as a better interpretation of the 2203 cm^{-1} band.

The main differences between the spectra of Susz and Wuhrmann and the present work can be ascribed to the different physical state of the respective complexes. Susz and Wuhrmann worked exclusively with the solid complex, whereas the complex reported here was a viscous liquid. The solid would be disposed to allow the maximum contribution from the ionic species, but in the liquid state such long-range order would break down leading to the presence of both the ions $[CH_3CO]^+$ and $[AlCl_4]^-$, and the donor–acceptor complex I, with the latter probably predominating.

Can. J. Chem. Downloaded from www.nrcresearchpress.com by 190.90.36.8 on 09/04/12
For personal use only.

The band at 2941 cm^{-1} is assigned to the antisymmetrical CH stretching frequency, the other sharp band at 2874 cm^{-1} being the symmetrical CH stretching vibration. The lowered CH_3 stretching frequencies in the complex, 2941 and 2874 cm^{-1} (compared with 3012 and 2960 cm^{-1} in acetyl chloride), are compatible with the ionic structure $[CH_3CO]^+$, since hyperconjugation ($H^+CH_2{=}C{=}O$ etc.) in the ion should produce such shifts. Two strong bands 1379 cm^{-1} and 1348 cm^{-1} are probably associated with the CH deformation frequencies of the CH_3—C group.

In the low frequency region one significant feature emerges. This is the disappearance of the bands at 436 cm^{-1} and 593 cm^{-1} associated with the C—Cl bond. The formation of the ion $[CH_3CO]^+$ would naturally result in the absence of these bands. However, the formation of the complex I would modify them. Three alternatives can be considered: (1) In the complex I all the group frequencies may be altered so that, even though the C—Cl bond still has the same force constant, its frequency is shifted. (2) The force constant is increased leading to a band at higher frequency. (3) The force constant is lowered leading to a lower frequency. Of these (2) can be ruled out, since there is no band in this region of sufficient intensity to be considered a C—Cl fundamental. Since many of the other bands are found in approximately the proper region this would tend to discount (1), and leave (3) as the probable reason for the disappearance of the two bands. Since the low frequency cutoff of CsBr is about 320 to 350 cm^{-1} it is not possible to observe bands with lower frequencies.

If the cation $[CH_3CO]^+$ is present then there should be signs in the spectrum of $[AlCl_4]^-$. Little is known of the spectroscopic behavior of this anion in the infrared. Gerding and co-workers (2) have investigated some systems containing $AlCl_3$ by Raman spectroscopy. In the system $Na^+ + [AlCl_4]^-$ they found the following frequencies: $\nu_1 = 349$, $\nu_2 = 146$, $\nu_3 = 575$, and $\nu_4 = 180$ cm^{-1}. For liquid $NO^+ + [AlCl_4]^-$ they found $\nu_1 = 349$, $\nu_2 = 136$, $\nu_3 = 450$–539 very broad, $\nu_4 = 182$ cm. However, for solid $NO^+ + [AlCl_4]^-$ ν_3 seemed to be a composite band with peaks at 460, 470, and 549 cm^{-1}. Of these Raman frequencies only ν_3, and ν_4 should be infrared active, and because of wavelength limitations only ν_3 visible.

In the CH_3COCl: $AlCl_3$ complex two broad strong bands at 485 and 540 cm^{-1} are observed. It is not possible to ascribe these to any specific vibration, but their presence suggests the structures $[AlCl_4]^-$ or $Cl_3Al\ldots O$. The spectrum of $AlCl_3$ dissolved in acetone contains these bands and here the complex can only be formed between the O lone-pair electrons and the $AlCl_3$.

Preliminary experiments had indicated the presence of the 2203 cm^{-1} band in mixtures prepared without taking extensive precautions to exclude air. This band at 2203 cm^{-1} was at that time thought to be due to the $[CH_3CO]^+$ ion, but the possibility remained that it could be due to a ketene-like structure, possibly as a result of dehydrohalogenation of the acyl halide. Ketenes have bands considerably higher in frequency than ordinary carbonyl bands. On account of the volatility of such compounds (ketene b.p. −56° C) it would be expected that some of it should be present in the vapor phase. However, no bands in the appropriate region were found in the infrared spectrum of the evolved vapors, nor did analysis by mass spectrometer reveal any ketene. The possibility of any ketene-like compound being present in the liquid complex is therefore very remote.

The behavior of the complex alone should be compared with the results obtained by dissolving the complex in various solvents. Frequently nitrobenzene is used as solvent in Friedel–Crafts ketone synthesis. The bands in the spectrum of the complex in nitrobenzene, in which it dissolves completely to give a yellow solution, are shown in Table I.

Can. J. Chem. Downloaded from www.nrcresearchpress.com by 190.90.36.8 on 09/04/12
For personal use only.

Some similarities exist between these bands and those of the complex alone. The band at 2193 cm^{-1} (cf. 2203 cm^{-1} in the pure complex) is present, as is the band at 1642 cm^{-1} (cf. 1637 cm^{-1} in the pure complex). The band at 1805 cm^{-1} is more intense than that (1779 cm^{-1}) in the pure complex. The band at 2307 cm^{-1} has completely disappeared. These changes can be explained by a partial dissociation of the complex I to give essentially free CH_3COCl (the band at 1805 cm^{-1}). The $AlCl_3$ released can interact with the excess nitrobenzene (to form the complex $C_6H_5NO_2.AlCl_3$ which is soluble in excess nitrobenzene), or complex with the $[CH_3CO]^+$. The former seems more likely, since it is probable that nitrobenzene is a better donor than the $[CH_3CO]^+$ ion. The absence of the 2307 cm^{-1} band and the strong 2193 cm^{-1} band suggests that the $[CH_3CO]^+$ is present as the ion pair III.

The liquid complex is only slightly soluble in $CHCl_3$. Most of it remains as an oily layer at the bottom of the tube, but the $CHCl_3$ layer turns a pink color which gradually fades with time. Table I lists the bands observed in the latter layer. Apart from the chloroform bands the strongest band is at 1660 cm^{-1}. It is assumed that this is the same band as that at 1637 cm^{-1} in the complex and in $C_6H_5NO_2$ solution. This band is apparently doubled with another subsidiary peak at 1613 cm^{-1}. The weaker band at 1793 cm^{-1} is undoubtedly due to CH_3COCl interacting with $CHCl_3$. It is significant that no bands are observed in the 4.5 μ region. The two bands at 436 cm^{-1} and 493 cm^{-1} associated with the C—Cl bond in CH_3COCl are either weak or absent, while those at 500 and 540 cm^{-1} are due to the complex I, as observed earlier.

In solution in CS_2 the only bands present are reasonably well accounted for by CH_3COCl.

The foregoing provides strong evidence that the pure complex contains the $[CH_3CO]^+$ ion, which is currently accepted as being an intermediate in the Friedel–Crafts ketone synthesis. In solvents of high dielectric constant like nitrobenzene ($\epsilon = 36.1$) the same conclusion holds. In solvents of low dielectric constant like chloroform ($\epsilon = 5.05$) no ions have been detected *in solution*, and the CH_3COCl and $AlCl_3$ exist in the form of the donor–acceptor complex I. In this complex the C—Cl bond is thought to be weakened. This would have the effect of lowering the activation energy of the reaction between the complex and an aromatic hydrocarbon to form a ketone, and facilitate reaction. Two important experimental conditions would be fulfilled on this view. Firstly, the yield of ketone would be proportional to the amount of $AlCl_3$ used, and secondly, the $AlCl_3$ would be complexed with the carbonyl group throughout the reaction. It should be reiterated, however, that the pure liquid complex is not completely soluble in $CHCl_3$, but forms a lower insoluble layer. Reaction at the surface of this layer could still take place via an ionic intermediate.

REFERENCES

1. BAENZIGER, N. C. Acta. Cryst. **4**, 216 (1951).
2. GERDING, H. and HOUTGRAAF, H. Rec. trav. chim. **72**, 21 (1953).
3. PFEIFFER, P. Organische molekulverbindungen. 2nd ed. von Ferdinard Enke. 1927. p. 409.
4. DILTHEY, W. Ber. **71**, 1350 (1938).
5. SUSZ, B. P. and WUHRMANN, J. J. Helv. Chim. Acta, **40**, 722 (1957).
6. SUSZ, B. P. and WUHRMANN, J. J. Helv. Chim. Acta, **40**, 971 (1957).
7. SUSZ, B. P. and COOKE, I. Helv. Chim. Acta, **37**, 1273 (1954).
8. COOK, D. J. Am. Chem. Soc. **80**, 49 (1958).

Can. J. Chem. Downloaded from www.nrcresearchpress.com by 190.90.36.8 on 09/04/12
For personal use only.

Can. J. Chem. Downloaded from www.nrcresearchpress.com by 190.90.36.8 on 09/04/12
For personal use only.

THE ADSORPTION OF KRYPTON ON GRAPHITE ABOVE AND BELOW THE TRIPLE POINT[1]

H. L. McDermot and B. E. Lawton

ABSTRACT

The adsorption of krypton on graphite has been measured above and below its Triple Point. Above the Triple Point, a smooth isotherm was found which showed two types of hysteresis. In contrast, the isotherm measured below the Triple Point displayed two discontinuities. The surface area of this graphite measured by means of the krypton isotherm was found to be in agreement with that previously measured by nitrogen adsorption.

INTRODUCTION

The adsorption of krypton by artificial graphite has been studied as part of a program directed toward a study of these graphites. The adsorption of krypton by a substance closely related to graphite (P33 carbon black graphitized at 2700° C) has been studied by Singleton and Halsey (10); Amberg, Spencer, and Beebe (1); Clark (4); and Ross and Winkler (9). In every instance stepwise isotherms were obtained at 77° K. The reversibility of the isotherm was demonstrated by Clark. Heats of adsorption measured by Amberg, Spencer, and Beebe were found to show a maximum at a coverage close to the monolayer. A second smaller maximum coincided with the completion of the second layer. The stepwise isotherms, coupled with the heat curve, are strong evidence that the surface of this graphitized black was homogeneous. Ross and Winkler conducted measurements down to low pressures and presented isotherms which displayed discontinuities characteristic of two-dimensional phase changes. They made measurements at 77° and 90° K and showed that the vertical discontinuity signifying two-dimensional liquefactions occurred at 77° but not at 90° K. The two-dimensional critical temperature was estimated to be 82° K. The measurements reported here were undertaken to investigate further the rather unusual hysteresis effects reported previously for artificial graphites manufactured by Acheson Co. Previous papers in this series (6, 7) have presented evidence of two types of hysteresis occurring on the adsorption of oxygen, nitrogen, and argon (6, 7) by artificial graphites at liquid air temperatures. These measurements have now been extended to krypton and sulphur dioxide (8). Those with krypton were done above and below the Triple Point. Two types of hysteresis have been reported with the artificial graphites: the normal type of hysteresis due to pores occurring at high relative pressures and a second type extending down to low relative pressures which has been termed "swelling hysteresis". This type of hysteresis has also been demonstrated for the adsorption of nitrogen by the carbon black "Spheron 6" at 77° K and for the adsorption of diethyl ether by charcoal (2, 7).

EXPERIMENTAL AND RESULTS

The graphite used in these experiments was a purified Acheson graphite designated by us as GF-3. Its properties have been given before (7, 11).

The krypton was obtained from the Matheson Co. and used without further purification.

Isotherms were measured at 119° K and 78° K. Before each isotherm was measured, the sample was evacuated for at least 12 hours at 200° C. The isotherm at 119° K was

[1]*Manuscript received July 31, 1958.*
Contribution from the Defence Research Chemical Laboratories, Ottawa, Canada.
Issued as D.R.C.L. Report No. 288.

Can. J. Chem. Downloaded from www.nrcresearchpress.com by 190.90.36.8 on 09/04/12
For personal use only.

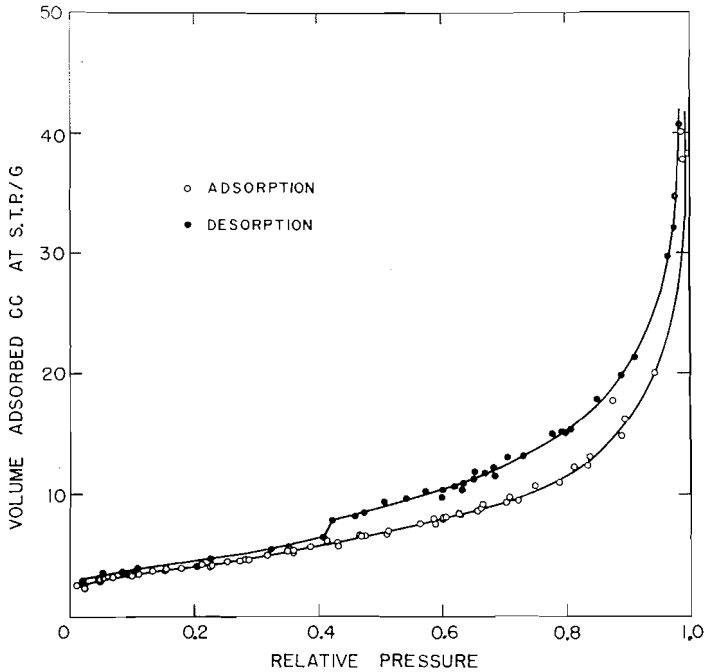

FIG. 1. The adsorption of krypton by graphite at 119° K.

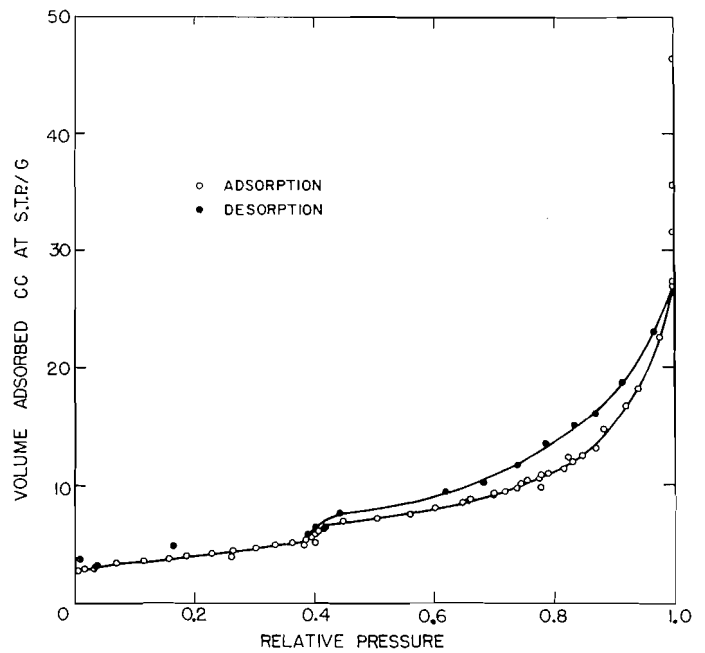

FIG. 2. The adsorption of krypton by graphite at 78° K.

measured with a standard volumetric adsorption apparatus. The constant-temperature bath consisted of Dewar flask containing Freon 12, which was cooled externally by a liquid nitrogen bath and heated internally by means of a nichrome heater. Control was effected by means of a krypton vapor pressure thermometer. The temperature was maintained at 119.4° K to better than a tenth of a degree. The isotherm at 78° K was measured using an open bath of liquid nitrogen. Pressures were measured by means of a McLeod gauge. Low pressures were corrected for thermal transpiration by the formula of Liang (5).

The isotherms at 119° and 78° K are presented in Figs. 1 and 2 respectively. It is clear that the isotherm at 119° K is smooth and displays pore hysteresis and swelling hysteresis. Although swelling hysteresis was observed above the Triple Point of krypton, it was found impossible to demonstrate it at 78° K, below the Triple Point, owing to difficulties in desorption at low pressures. The few points obtained by warming the sample were not conclusive. The 78° K isotherm is presented because it gives evidence of two discontinuities for adsorption on a heterogeneous surface in contrast to those discussed in the Introduction which were observed with a homogeneous carbon surface. One discontinuity observed at a relative pressure of 0.4 is shown in Fig. 2, while the second found at a pressure of 1.7 μ is shown in Fig. 3.

DISCUSSION

The hysteresis loop shown in Fig. 1 is similar in shape to those previously reported for argon, oxygen, and nitrogen (6). It is interesting that the isotherm resembles closely the argon isotherm (6) on another artificial graphite despite the fact that the diameter of the krypton is about 17% greater than that of the argon. Figure 2 gives the isotherm

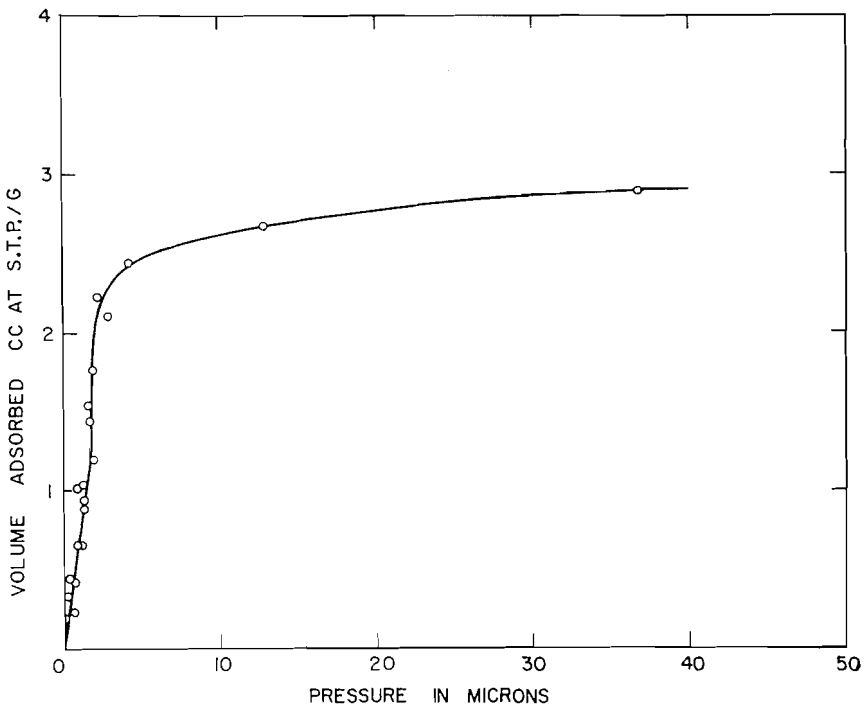

FIG. 3. The adsorption of krypton by graphite at 78° K (low pressure region).

Can. J. Chem. Downloaded from www.nrcresearchpress.com by 190.90.36.8 on 09/04/12
For personal use only.

at 78° K below the Triple Point of krypton. The isotherm is quite different from that measured above the Triple Point. The hysteresis loop is differently shaped and it shows a marked discontinuity at a relative pressure of 0.4. A second discontinuity shown in Fig. 3 was found at a pressure of 1.7 μ. This type of discontinuity, which is generally interpreted as a two-dimensional condensation, is usually seen only with homogeneous surfaces. The surface of this graphite is known to be heterogeneous (11), hence this phenomenon can be explained in these terms only if one postulates that the surface contains homogeneous regions of widely different surface energies. Thus it might be imagined that two-dimensional condensation occurs on a homogeneous region of high surface energy, while little adsorption occurs at other sites. The second discontinuity occurs at the completion of two monolayers. It may conceivably signal the point at which a solid lattice starts to form in the pores.

The surface area of the graphite was estimated from the isotherm at 78° K using the B.E.T. equation and the value of 19.5 Å^2 (3) for the area of the krypton molecule. The area was found to be 17.4 m^2/g, in good agreement with the area of 18.4 m^2/g previously reported (6) using nitrogen as the adsorbate.

REFERENCES

1. AMBERG, C. H., SPENCER, W. B., and BEEBE, R. A. Can. J. Chem. **33**, 305 (1955).
2. ARNELL, J. C. and McDERMOT, H. L. Proc. Second Intern. Congr. Surface Activity, **II**, 113 (1957).
3. BEEBE, R. A., BECKWITH, J. B., and HONIG, J. M. J. Am. Chem. Soc. **67**, 1554 (1945).
4. CLARK, H. J. Phys. Chem. **59**, 1068 (1955).
5. LIANG, S. J. Appl. Phys. **22**, 148 (1951).
6. McDERMOT, H. L. and ARNELL, J. C. Can. J. Chem. **33**, 913 (1955).
7. McDERMOT, H. L. and LAWTON, B. E. Can. J. Chem. **34**, 769 (1956).
8. McDERMOT, H. L. Unpublished.
9. ROSS, S. and WINKLER, W. J. Colloid Sci. **10**, 330 (1955).
10. SINGLETON, J. H. and HALSEY, C. D. J. Phys. Chem. **58**, 1011 (1954).
11. WILSON, L. G. and McDERMOT, H. L. Can. J. Chem. **35**, 15 (1957).

Can. J. Chem. Downloaded from www.nrcresearchpress.com by 190.90.36.8 on 09/04/12
For personal use only.

Can. J. Chem. Downloaded from www.nrcresearchpress.com by 190.90.36.8 on 09/04/12
For personal use only.

FORMATION OF AN ORGANOCHROMIUM COMPOUND IN THE REDUCTION OF CHLOROFORM BY CHROMOUS PERCHLORATE[1]

F. A. L. ANET

ABSTRACT

The reduction of chloroform by chromous perchlorate in aqueous solution gave chloropentaaquochromium(III) perchlorate and dichloromethylpentaaquochromium(III) perchlorate in equimolecular amounts.

Anet and Leblanc (1) reported that the reduction of benzyl chloride by chromous perchlorate gave an organochromium ion of the structure $Cr(H_2O)_5CH_2Ph^{++}$(I). This method of preparing organochromium compounds could not be extended to simple alkyl halides for these were resistant to reduction under the conditions used. Other halides, e.g. phenacyl chloride, were reduced (1), but did not give organometallic compounds. The present communication deals with the formation of an organochromium compound in the reduction of chloroform by chromous perchlorate.

Whereas methyl chloride and methylene chloride were not reduced by chromous perchlorate at room temperature, chloroform was reduced in a few minutes, and carbon tetrachloride in a few seconds. In both cases where reduction took place, as observed by a change in color from blue (Cr^{++}) to red, it was immediately apparent that the chromous ion was not being oxidized solely to either $Cr(H_2O)_6^{+++}$ (pale blue-violet) or $Cr(H_2O)_5Cl^{++}$ (green), or to a mixture of the two ions. The red solution obtained from carbon tetrachloride decomposed to a green solution in a few seconds, and was not examined further. However, the red solution obtained in the reduction of (excess) chloroform appeared to be unchanged after a few hours, even in the presence of air. The products in this solution were therefore investigated.

The solution, which was actually grayish-red in color, contained no free chloride ion, for addition of silver nitrate did not give a precipitate. Since it was suspected that there was more than one chromium species present, separation of the components from the red solution by extraction with butanol was tried. This failed, although the procedure had been successful (1) in separating the products from the reduction of benzyl chloride. A separation into two components was achieved by ion-exchange chromatography of the solution on Dowex 50-X4 resin and elution with *M* perchloric acid. The first fraction eluted was green in color and its visible absorption spectrum and reactions showed that it contained the ion $Cr(H_2O)_5Cl^{++}$. The second fraction was pinkish-red and appeared to contain only a single colored ion, as shown by the constancy of its absorption spectrum (λ_{max} 395 mμ and 510 mμ) as it was being eluted. Analysis of this fraction (*vide infra*) showed that the color was due to an organochromium ion of the structure $Cr(H_2O)_5CHCl_2^{++}$.

The method of analysis previously (1) used with I was not applicable, as no reaction took place on addition of mercuric chloride to the red fraction. When the red fraction was heated, chloride ions were liberated and a reducing solution was produced. Accordingly, it was heated with silver perchlorate and potassium permanganate. Silver chloride was precipitated along with manganese dioxide, but addition of hydrogen peroxide left only the former, which was collected and weighed. The carbon dioxide which was evolved during the oxidation was swept out by nitrogen and determined as barium

[1]*Manuscript received September 8, 1958.*
Contribution from the Department of Chemistry, University of Ottawa, Ottawa, Canada.

Can. J. Chem. Downloaded from www.nrcresearchpress.com by 190.90.36.8 on 09/04/12
For personal use only.

carbonate. Finally, chromium was determined spectrophotometrically in the solution left after filtration of the silver chloride. These results gave a ratio of Cr: C: Cl very close to 1: 1: 2. The amount of potassium permanganate consumed was determined in separate experiments and corresponded to the oxidation of $Cr(H_2O)_5CHCl_2^{++}$ to Cr^{+++}, Cl^-, H_2O, and CO_2.

The position of elution of the red fraction strongly suggested that the colored ion had two positive charges, for King and Dismukes (2) have found that the minimum concentrations of perchloric acid required to easily elute chromium species of charges +1, +2, and +3 from Dowex 50 resin are 0.1 *M*, 1 *M*, and 5 *M* respectively.

The amounts of chromium present in the green and red fractions above were equal, and accounted for all the chromous perchlorate used in the reduction.

These results can be explained most simply if the red fraction contains the ion $Cr(H_2O)_5CHCl_2^{++}$(II), analogous in structure to $Cr(H_2O)_5CH_2Ph^{++}$ obtained from benzyl chloride (1), and formed as follows:

$$CHCl_3 + 2Cr^{++} + 10H_2O \rightarrow Cr(H_2O)_5Cl^{++} + Cr(H_2O)_5CHCl_2^{++}.$$

The ion II may be described as an octahedral complex of chromium(III) with five water molecules and the dichloromethyl anion as ligands. The stability of this organochromium ion, like that of I, is due to the substitution-inertness of chromium(III) complexes (3). Thus the chromium–carbon bond behaves like a covalent bond with little polar character.

The reactions of II were rather different from those of I previously studied (1). Whereas I underwent decomposition on heating to give bibenzyl, presumably via benzyl radicals, II did not give tetrachloroethane, or its reduction product, dichloroethylene (since chromous ions would be formed as well). Instead, chloride ions were liberated but no volatile organic compound was formed. This reaction is at present under investigation. Unlike I, II did not react with oxygen, sulphur dioxide, or mercuric chloride, nor was it reduced by hydrogen in the presence of a palladium catalyst. Attempts to obtain sparingly soluble salts of II were not successful.

Taube and Myers (4) have found that chromous perchlorate reduced $Co(NH_3)_5Cl^{++}$ as follows:

$$Co(NH_3)_5Cl^{++} + Cr^{++} + 5H_2O \rightarrow Cr(H_2O)_5Cl^{++} + Co^{++} + 5NH_3.$$

In this one-electron reduction, no free chloride ion was liberated, and it was shown that the reduction took place by direct transfer of a chlorine atom from cobalt to chromium. If it is assumed that the first step in the reduction of chloroform proceeds in a similar fashion, with transfer of a chlorine atom from carbon to chromium, then dichloromethyl radicals will be formed,

$$CHCl_3 + Cr^{++} + 5H_2O \rightarrow Cr(H_2O)_5Cl^{++} + \cdot CHCl_2.$$

These radicals can either dimerize or react with chromous ion to give an organochromium ion as follows:

$$\cdot CHCl_2 + Cr^{++} + 5H_2O \rightarrow Cr(H_2O)_5CHCl_2^{++}.$$

If this reaction is fast, no dimerization will take place.

Thus the mechanism is consistent with the observed facts that no chloride ion was produced and that an equal amount of II and $Cr(H_2O)_5Cl^{++}$ were formed.* It is also

**It was stated in our communication (1) on the reduction of benzyl chloride with chromous perchlorate that the inorganic chromium species formed were* $Cr(H_2O)_5^{+++}$ *(mainly) and* $Cr(H_2O)_5Cl^{++}$. *It seems, however, that the* $Cr(H_2O)_6^{+++}$ *was formed as a result of the decomposition of* $Cr(H_2O)_5CH_2Ph^{++}$, *for under suitable conditions we have now found that no chloride ion is liberated during the reduction.*

in agreement with the fact that carbon tetrachloride was reduced most easily and methyl chloride least easily, for it is known (5) that chlorine substitution stabilizes the methyl free radical. Further work on the mechanism of these reductions is in progress.

EXPERIMENTAL

Preparation of Chromous Perchlorate Solution

Chromous perchlorate was prepared by the electrolytic reduction of chromic perchlorate containing perchloric acid at a mercury cathode. A carbon anode separated from the cathode by a porous porcelain pot was used. The chromic perchlorate was prepared (6) by reduction of reagent grade chromium trioxide with formic acid in dilute perchloric acid and was recrystallized from a small amount of dilute perchloric acid. The reagent was prepared, stored, and used under an atmosphere of nitrogen, purified by bubbling through two solutions of chromous chloride containing amalgamated zinc followed by a water wash. As found recently by Schug and King (6), this reagent is stable for some months, unlike that prepared by zinc–amalgam reduction. Various strengths of the reagent from 0.2 *M* to 0.5 *M* Cr^{++} in perchloric acid of concentration 0.2 *M* to 1 *M* were prepared.

Reduction of Chloroform with Chromous Perchlorate

Water (1 l) was freed of oxygen and then shaken with chloroform (10 ml). Chromous perchlorate (500 ml, 0.2 *M*) solution was added in an atmosphere of nitrogen and the solution allowed to stand 2 to 3 hours at room temperature. The grayish-red solution gave no precipitate with silver nitrate solution at room temperature. A portion (100 ml) of this solution was placed on a column (15 cm × 2 cm) of Dowex 50-X4 (200–400 mesh) in the hydrogen form and the column eluted with *M* perchloric acid at the rate of 1–2 drops per second. A green fraction (100 ml) was soon eluted, followed by a colorless solution (150 ml), and then by a red fraction (110 ml). The green fraction had the same visible absorption as described for $Cr(H_2O)_5Cl^{++}$ by Elving and Zemel (7). It gave no precipitate with silver nitrate in the cold, but on heating, silver chloride was gradually precipitated leaving a bluish-violet solution of $Cr(H_2O)_6^{+++}$. The chromium content of the green fraction was determined by direct spectrophotometric measurement in a 1-cm cell, taking $\epsilon = 17.8$ for $Cr(H_2O)_5Cl^{++}$ at λ_{max} 605 mμ (7).

Analysis of Dichloromethylpentaaquochromium(III) Perchlorate Solution

For analysis a quantity of the red fraction above was heated to boiling for 5 minutes with excess (about twofold) of silver perchlorate and potassium permanganate solutions. The cooled solution was treated with hydrogen peroxide to dissolve the manganese dioxide, and the silver chloride filtered off on a sintered glass crucible. The filtrate was made up to a definite volume and its absorbance at 575 mμ measured in a 5-cm cell. For $Cr(H_2O)_6^{+++}$ ϵ was taken as 13.9 at λ_{max} 575 mμ (7). The consumption of potassium permanganate was determined in separate experiments carried out as above except that instead of adding hydrogen peroxide a known quantity of ferrous ammonium sulphate was added, sufficient to react with the excess potassium permanganate and manganese dioxide. The excess ferrous salt was then back-titrated with 0.1 *N* $KMnO_4$.

A number of analyses were carried out on samples from the same reduction and from different reductions; a typical value obtained for the Cr: C: Cl ratio was 1.00: 1.02: 2.06.

Reactions of Dichloromethylpentaaquochromium(III) Perchlorate Solutions

Solutions in dilute perchloric acid were stable for several hours at room temperature,

Can. J. Chem. Downloaded from www.nrcresearchpress.com by 190.90.36.8 on 09/04/12
For personal use only.

and many days at 0°. When the solutions were heated the red color gradually disappeared and the solution became greenish-blue and contained large amounts of chloride ion.

REFERENCES

1. ANET, F. A. L. and LEBLANC, E. J. Am. Chem. Soc. **79**, 2649 (1957).
2. KING, E. L. and DISMUKES, E. B. J. Am. Chem. Soc. **74**, 1674 (1952).
3. TAUBE, H. Chem. Revs. **50**, 69 (1952).
4. TAUBE, H. and MYERS, H. J. Am. Chem. Soc. **76**, 2103 (1954).
5. STEACIE, E. W. R. Atomic and free radical reactions. Vol. 1. 2nd ed. Reinhold Publishing Corporation, New York. 1954. p. 96.
6. SCHUG, K. and KING, E. L. J. Am. Chem. Soc. **80**, 1089 (1958).
7. ELVING, P. J. and ZEMEL, F. J. Am. Chem. Soc. **79**, 1281 (1957).

Can. J. Chem. Downloaded from www.nrcresearchpress.com by 190.90.36.8 on 09/04/12
For personal use only.

Can. J. Chem. Downloaded from www.nrcresearchpress.com by 190.90.36.8 on 09/04/12
For personal use only.

THE KINETICS OF THE DECAY OF NITROGEN ATOMS AS DETERMINED FROM CHEMICAL MEASUREMENTS OF ATOM CONCENTRATIONS AS A FUNCTION OF PRESSURE[1]

ROGER KELLY[2] AND C. A. WINKLER

ABSTRACT

A method is described for studying both the surface and homogeneous decay of N atoms in which the atom concentration reaching a reaction vessel after a period of decay is measured as a function of pressure by HCN production from ethylene or ethane under conditions of complete consumption of the atoms and complete initial dissociation of the nitrogen. The results indicated that the surface decay proceeded by a first-order mechanism between 55° C and 400° C, with the collision efficiency for an Na_2HPO_4 surface essentially constant at 2.75×10^{-4}. The activation energy of surface decay was 1.0 kcal mole^{-1} and the concentration of surface species 1.9×10^{14} cm^{-2}. It was concluded that the surface decay probably leads directly to molecules in the ground state.

Depending on the temperature and whether or not N_2 and N were considered equivalent as third bodies, the rate constant of the homogeneous decay varied from 1.09×10^{-33} to 13.2×10^{-33} cc^2 molecule^{-2} sec^{-1}. The homogeneous decay therefore appears to have a positive temperature coefficient and to be of only secondary importance below about 2 mm pressure under the prevailing conditions. The similarity of *one-half* the rate constant of homogeneous decay at 25° C (0.55×10^{-33} to 0.97×10^{-33}) to the rate constant of afterglow emission obtained by Berkowitz *et al.* (2×10^{-33}) suggests that *all* homogeneous decay gives rise to afterglow via the $^5\Sigma$ state.

Of the numerous studies on atom decay that have been published, perhaps the most conclusive have been those of Smith (1) and Linnett and Marsden (2, 3) on the surface decay of H and O atoms respectively. In both cases, atom concentrations in a side arm attached to a discharge tube were measured with a thermocouple probe. Since complications due to flow were eliminated, the mathematical analysis of the results was fairly simple, and it was possible to show that first-order surface decay with a collision efficiency in the range 10^{-3} to 10^{-5} was the dominant mode of decay at the pressures and temperatures used. The homogeneous decay of H atoms has also received considerable attention (e.g. 4).

Studies on the decay of active nitrogen and therefore on the recombination of the N(^4S) atoms which are its major constituent (5, 6) have, on the other hand, generally been qualitative. In fact, the only rate constant for N atom decay that has apparently been published is that for the emission of afterglow in homogeneous decay (6), while, in the case of the surface decay, even the order itself has not been settled beyond question. The main facts known about N atoms are thus the following. They decay in part on surfaces and in part homogeneously (7). The surface decay is nonluminous, i.e. the afterglow does not intensify in the neighborhood of surfaces (7), and probably first-order (7, 8, 9). Part or all of the homogeneous decay is accompanied by the emission of yellow-orange afterglow (7), the intensity of which is proportional to [active nitrogen]^2 [inert gas] (10, 6). (The work cited did *not* determine whether the inert gas could include the active nitrogen itself.) The rate constant of afterglow emission is 2×10^{-33} cc^2 molecule^{-2} sec^{-1} (6) and the mechanism probably involves an $N_2(^5\Sigma)$ intermediary (6, 11).

The present work was undertaken to confirm the order of the surface decay of N atoms, and to obtain rate constants for both the surface and homogeneous decay.

[1]*Manuscript received July 16, 1958.*
Contribution from the Department of Chemistry, McGill University, Montreal, Quebec, with financial assistance from the National Research Council of Canada.
[2]*Holder of National Research Council Studentships 1956–57, 1957–58. Present address: Atomic Energy of Canada Ltd., Chalk River, Ontario.*

Can. J. Chem. Downloaded from www.nrcresearchpress.com by 190.90.36.8 on 09/04/12
For personal use only.

EXPERIMENTAL

Choice of Method

The measurement of N atom concentrations is complicated by the fact that, though active nitrogen contains the ^4S atom as a major constituent, there is still a possibility that excited molecules are present (12, 13, 14, 15, 16), if only in low vibrational levels of the ground state. Virtually any excited form would, of course, be deactivated on a metal surface (14), so that measurements of the activity using a thermocouple probe (cf. 1, 2, 3) would be of uncertain significance. On the other hand, the production of HCN from ethylene under conditions of complete consumption ("cleanup") of active nitrogen (high ethylene flowrates and elevated temperatures), a mode of measurement frequently used in past work (e.g. 17, 18), would likely reflect the *atom* concentration alone owing to the high activation energy to be expected in most reactions involving excited nitrogen molecules (13).[3] HCN production also has the advantages that it is not subject to mechanical failure and, since negligibly small quantities of other nitrogen-containing compounds are formed (20, 21), it provides an absolute value of the atom concentration. Production of HCN from ethylene was therefore chosen to measure the N atom concentration and the results were checked using ethane.

Apparatus

The use of chemical measurement of the atom concentrations meant that a fast-flow system of the type employed by Winkler and co-workers (see, in particular, 21, 22, 23) rather than the much simpler diffusion system of Smith (1) or static system of Rayleigh (7) had to be used (Fig. 1).

Dry, oxygen-free nitrogen[4] at atmospheric pressure was introduced at A and passed through a needle reduction valve B and a capillary flowmeter C. In the discharge tube D the nitrogen was subjected to a rapid condensed discharge. (Internal electrodes which had been machined from solid aluminum were used. They were about 60 cm apart, and were each 7.0 cm long, 1.8 cm O.D., and 7/16 inch I.D.; two setscrews were used to affix them to lengths of 0.060-inch diameter tungsten wire.) The resulting atom-containing mixture was then passed through a tube E, which will be called the "decay tube". In most of the work the decay tube had a volume of 281 cc, a length of 31.7 cm, and an I.D. of 3.36 cm (see, however, series 2). The large volume served to increase the time of decay and therefore (i) to lower the N atom concentration sufficiently, even under conditions of complete initial dissociation, for cleanup to be readily achieved, and (ii) to make the effect of dissociation on the decay time less marked (Appendix C). The large diameter served (i) to reduce the pressure gradient in the decay tube (Appendix A), and (ii) to reduce the rate constant of surface decay. A cylindrical, electrically heated furnace was built around the decay tube to determine the effects of temperature on the rate constants. At the lower end of the decay tube was a constriction 2.0 cm long and 0.60 cm I.D. which served (i) to terminate the region of decay sharply and independently of pressure (i.e. the reaction flame was invariably located just below the constriction), (ii) to enable independent heating and poisoning of the decay tube and reaction vessel, and (iii) to prevent back-diffusion of the reactant from the reaction vessel. The decay tube was followed by a 300-cc spherical reaction vessel F into which the reactant could be injected

[3]*Direct evidence to this effect appears to have been obtained in a study of the reaction of active nitrogen with nitric oxide (19). However, even if the excited molecules could react to give* HCN, *such* HCN *production would be automatically eliminated by the use of limiting slopes as described in a following section, provided the excited molecules were formed only by homogeneous atom decay.*

[4]*The method of purification is that described in references (21) and (23) rather than (22), i.e. passing the nitrogen over heated copper and through a liquid-air trap.*

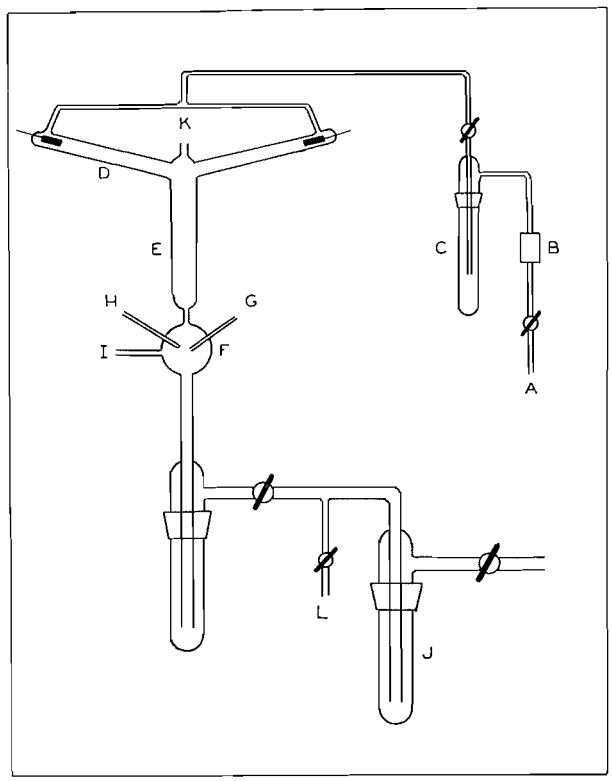

FIG. 1. Apparatus.

through jet G. (The arrangement for metering in the reactants has been described elsewhere (21).) The reaction vessel was surrounded by a second furnace, the temperature of which was measured by a thermocouple in the well H; a McLeod gauge was attached at I. From the reaction vessel the gas mixture was led through a trap J surrounded by liquid air, and thence to a pump. The Wrede gauge outlet K was present only during the experiments of series 4.

In the majority of the experiments the discharge tube, decay tube, and reaction vessel were poisoned by drawing up a 20% aqueous solution of Na_2HPO_4. This poison was used, rather than the more efficient HPO_3, since it did not react with ammonia and was unusually stable and reproducible. In a few experiments of series 6 the poison on the reaction vessel alone was changed to KCl; however, KCl could not be used in the discharge tube nor on any heated surface, since the active nitrogen then reacted with it, creating an intense reddish-orange glow.

Power was supplied from a 220-v a-c. source, transformed first with a 2400-w, 220-v variac and then with an 1897-w, 110 → 4820-v transformer, and finally rectified with two Raytheon 866A tubes in parallel. The weakest element in the circuit was the variac, which burned out several times. For most of the work the secondary circuit had a resistance of 1250 ohms and a capacitance of either 4 μf (for pressures <1.7 mm) or 2 μf (for pressures >1.7 mm, <4 mm). If the variac were adjusted to give a flashrate of 60 per second (except in the pressure range 1.2 to 1.7 mm, when 30 to 40 per second was adequate), complete dissociation of the nitrogen could be brought about. (This is treated in detail in a following section.)

Can. J. Chem. Downloaded from www.nrcresearchpress.com by 190.90.36.8 on 09/04/12
For personal use only.

HCN production was determined by titrating the recovered HCN with $AgNO_3$ (24) after it had been distilled at $-23°$ C from the trap (previously coated with solid CCl_4) into a removable unit attached at L and containing about 15 cc of frozen water (cf. 25). A sufficient amount of product to enable convenient analysis was generally obtained with reaction times of 100 seconds.

THEORY

To derive decay equations, i.e. equations which will relate the atom concentrations measured in the reaction vessel to the rate constants for decay, it is necessary to know the rate-controlling step in each mode of decay. These steps may be summarized as follows:

radiative decay $\quad N + N \rightarrow N_2 + h\nu,$

homogeneous decay $\quad N + N + M \xrightarrow{k_2} N_2^* + M,$

where M is a third body and N_2^* an unspecified excited molecule;

first-order surface decay $\quad N + N \cdot \text{surface} \xrightarrow{k_1} N_2 + \text{surface},$

and *second-order surface decay* $\quad N + N + \text{surface} \xrightarrow{k_3} N_2 + \text{surface}.$

The constants k_1, k_2, and k_3 will be defined to give the rate of atom destruction directly, without a factor of two.

Before proceeding further it will be necessary to introduce certain simplifications. Radiative decay will be neglected altogether, in general because stabilizing radiation is seldom observed in the recombination of atoms and free radicals, in particular because the nitrogen afterglow, which might be identified with such radiation, is neither continuous (26, p. 400) nor diffuse (26, p. 414), and obeys termolecular kinetics. For homogeneous decay only extreme cases of third-body efficiency will be treated. In the one case, which in the present work turns out to correspond to a lower limit of k_2, N_2 and N will be considered to be equivalent as third bodies for N atom recombination, so that [M] becomes simply the total observed pressure P. In the other, which corresponds to an upper limit of k_2, the efficiency of N as a third body will be considered to be much less than that of N_2, so that [M] becomes $(P-[N])$.[5] The two orders of surface decay will be assumed to be mutually exclusive. In terms of the mechanisms of surface decay to be discussed later this situation should prevail at temperatures or atom concentrations where the number per cm^2 of surface species (C_s in equation [10]) either approaches its maximum (i.e. monolayer) value to yield first-order surface decay, or becomes proportional to the atom concentration, corresponding to second-order surface decay.

Depending on the order of the surface decay and the relative efficiencies of N_2 and N as third bodies, four differential equations of decay are thus possible:

$$[1] \qquad d[N]/dt = -k_1[N] - k_2[N]^2 P,$$

$$[2] \qquad = -k_1[N] - k_2[N]^2 (P - [N]),$$

$$[3] \qquad = -k_3[N]^2 - k_2[N]^2 P,$$

$$[4] \qquad = -k_3[N]^2 - k_2[N]^2 (P - [N]).$$

[5] *In the event that evidence was obtained that the efficiency of* N *was greater than that of* N_2, *the case where* [M] = [N] *would have to be considered instead. This case cannot, of course, be eliminated a priori, since according to the mechanism of homogeneous decay proposed by Berkowitz et al. (6) the main function of the third body is to induce an electronic transition.*

Can. J. Chem. Downloaded from www.nrcresearchpress.com by 190.90.36.8 on 09/04/12
For personal use only.

The significance of each is obvious. If $[N]_0$ is the value of [N] at $t = 0$, the solutions of equations [1] and [3] are, respectively,

$$P/[N] = e^{k_1 t}P/[N]_0 + (e^{k_1 t}-1)k_2P^2/k_1 \quad [5]$$

and

$$1/[N]-1/[N]_0 = (k_3+k_2P)t. \quad [6]$$

Though an exact solution to equation [2] can also be obtained, it is not readily used for interpreting experimental data unless $[N]_0 = P$ and $[N] \ll P$. Then

$$\ln P/[N]-k_1t \approx (k_2P/\sqrt{q})\ln\frac{1+k_2P/\sqrt{q}}{1-k_2P/\sqrt{q}},$$

where $q = k_2^2P^2+4k_1k_2$. If, in addition, $k_2P \ll 2\sqrt{k_1k_2}$, an even simpler form arises,

$$1/(\ln P/[N]-k_1t) \approx \tfrac{1}{2}+2k_1/k_2P^2. \quad [7]$$

Equation [7] is obviously valid only at low pressures and also requires a prior knowledge of k_1t obtained from equation [5]. Since the surface decay will be shown to be first order, equation [4] will not be further considered except to note that at not too low pressures its solution reduces to equation [6].

In interpreting experimental data in terms of equations [5] to [7], the data obtained at low pressures must be weighted more heavily than those at high pressures. For example, in plots of $P/[N]$ versus P^2, the limiting slopes as $P \rightarrow 0$ would be derived rather than slopes of best fit. The reasons are the following: (i) Equations [1] to [7] actually presume a number of conditions respecting diffusion, the time of decay, etc., such that the equations are more valid at low pressures (see Appendix A). (ii) Equation [7] is *inherently* valid only at low pressures. (iii) If excited molecules are present, there is a possibility that their reactivity will be superimposed upon that of the atoms; however, if they are formed only by the homogeneous decay of the atoms, their concentration necessarily falls off rapidly as the pressure is decreased.

Though equations [5] to [7] can in general be applied to studies in which any one of $[N]_0$, time, or pressure is varied, pressure variation alone is used in the present work. However, it is then necessary that the initial dissociation be complete, i.e. $[N]_0 = P$, since otherwise $[N]_0$ becomes an unknown function of P. Additional reasons why complete dissociation is desirable are that a precise control of the flashrate is then not necessary, equation [7] is inherently valid only under such conditions, and it becomes possible to distinguish unambiguously the different orders of surface decay simply by comparing the low-pressure asymptote of a graph of [N] versus P with the line corresponding to the maximum possible atom flowrate, i.e. $2[N_2]$ versus P. The asymptote would coincide with this line if the surface decay were second order, but would have a much reduced slope (Pe^{-k_1t}) if it were first order. These relations hold irrespective of the relative efficiencies of N_2 and N as third bodies. (While the striking feature of Smith's method was a similar clear-cut distinction of reaction order, it should be pointed out that the present method, in contrast to that of Smith, enables the evaluation of rate constants for homogeneous decay. It is not sufficiently sensitive, however, to determine the relative efficiencies of N_2 and N as third bodies.)

An additional relation that will be required is that for obtaining the collision efficiency or "recombination coefficient" from a rate constant for first-order surface decay. For a cylindrical decay tube of radius r_0 it is given by (27)

$$\gamma = (2r_0/\bar{c})(k_1/2), \quad [8]$$

Can. J. Chem. Downloaded from www.nrcresearchpress.com by 190.90.36.8 on 09/04/12
For personal use only.

where $\bar{c}$ is the mean kinetic velocity. If γ is known, the activation energy of surface decay (E_1) and the number per cm^2 of surface species (C_s) can also be obtained using absolute rate theory (28, 27):

[9] $$E_1 = -Rd(\ln \gamma T)/d(1/T)$$

and

[10] $$C_s = 2\pi mkT\gamma/h^2 e^{-E_1/RT},$$

where T is the absolute temperature and k the Boltzmann constant. Equations [9] and [10] should be valid for any mechanism of surface decay which assumes an *immobile* surface layer.

The use of $k_1/2$ rather than k_1 in equation [8] represents a departure from the original treatment (27), but is likely more correct. Thus, considering a given surface site, each instance of decay will be followed by an instance of surface-layer formation. Since dissociation or bond stretching are not involved in the formation of a surface layer of atoms, the activation energy should be zero (28) and the process correspondingly rapid. The result is that the observed rate of decay will be double that due to the activated process described by equations [8] to [10]. Conversely, the use of an uncorrected rate constant in equation [8] as in previous publications (e.g. 1, 2, 3, 27) would make γ *high* by a factor of two.

RESULTS

Conditions of Cleanup

A cleanup of N atoms is achieved only at high reactant flowrates and above a certain temperature. For the reactants used in the present work the minimum temperatures (about 300° C) were readily obtained from published data (21). Since minimum flowrates, on the other hand, depend on the atom concentration, on the reaction temperature, and on factors peculiar to each apparatus, the results of past work could not be used. It was therefore necessary to determine, at a series of atom concentrations, the minimum flowrate applicable with each reactant and reaction temperature. The data obtained in these preliminary experiments will not be given, though it will be understood that in all experiments to be described plateau flowrates of reactant were used.

Extent of Initial Dissociation

The first four series of experiments were designed to determine if complete initial dissociation, i.e. $[N]_0 = P$, could be brought about without overtaxing the electronic components. In all cases the decay tube and reaction vessel were unheated. In *series 1* the amount of HCN formed from ethylene at 0.80 mm pressure and a capacitance of 4 μf was determined as a function of primary voltage (variac setting) and thence flashrate. Discharge was observed to start at 35 v, while the HCN production remained constant from 45 to 70 v.

The apparatus used in *series 2* differed in having a much smaller decay tube: 14.0 by 1.55 cm, volume = 26 cc. Accordingly, the time of decay was much shortened and the data should have indicated more directly the variation of $[N]_0$. However, a cleanup of N atoms was difficult to achieve, so that the destruction of ammonia, which is apparently due to excited molecules present in the active nitrogen in small amounts (12, 13, 16), was measured instead. (The amount of ammonia destroyed was determined as the difference between pressure–volume measurements of the amount drawn from the storage vessel and the amount recovered.) The results, obtained as a function of pressure, primary voltage,

Can. J. Chem. Downloaded from www.nrcresearchpress.com by 190.90.36.8 on 09/04/12
For personal use only.

and capacitance are given in Fig. 2A. It is seen that, as the pressure was increased, the ammonia destruction at each primary voltage and capacitance at first followed a common curve, but finally dropped below as the flashrate decreased to zero. No energy expenditure would bring the reactivity above this common curve.

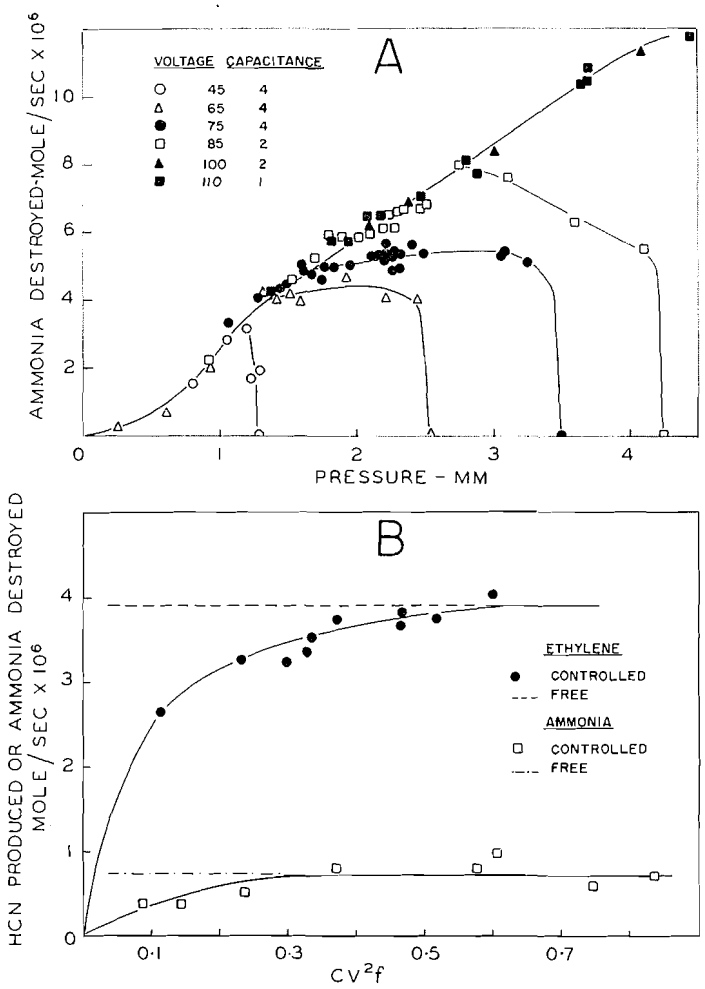

FIG. 2A. Series 2. Ammonia destruction as a function of pressure, primary voltage, and capacitance (μf).
FIG. 2B. Series 3. HCN production from ethylene and ammonia destruction as functions of CV^2f and the nature of the discharge.

In *series 3* a more precise energy variation study was conducted at 1.4 mm pressure with the flashrate electronically controlled.[6] The exact amount of energy expended in terms of CV^2f, where C is the capacitance, V the primary voltage, and f the flashrate, could thus be determined. As in series 1 and 2, the reactivities of ethylene and ammonia were readily made independent of energy expenditure (Fig. 2B), and it will be noted that the values then corresponded to those obtained at a similar pressure but under the conditions of series 5 and 6, viz. free discharge and with the circuit described earlier.

[6]*A General Electric FG105 thyratron was incorporated into the high-voltage circuit, a 90-v dry cell being sufficient to keep it non-conducting. The flashrate could then be controlled by shorting out the dry cell with a variable speed, motor-driven, rotary spark gap.*

Can. J. Chem. Downloaded from www.nrcresearchpress.com by 190.90.36.8 on 09/04/12
For personal use only.

Can. J. Chem. Downloaded from www.nrcresearchpress.com by 190.90.36.8 on 09/04/12
For personal use only.

The observation in the preceding series that reactivities could be made independent of energy expenditure indicates, of course, either that the desired condition of complete initial dissociation was achieved, or else that an equilibrium condition of partial dissociation occurred. Accordingly, in *series 4* a Wrede gauge made of sintered glass (Fisher filter stick of fine porosity) was attached to the discharge tube as indicated in Fig. 1 (K), and then connected to a differential manometer consisting of a nearly horizontal U-tube filled with diffusion-pump oil. The manometer was calibrated against a McLeod gauge. However, some difficulty was encountered using the Wrede gauge, since each reading required at least 20 minutes before the manometer was steady, so that, by the time several readings had been made at the high energy expenditures used, the discharge tube became contaminated with material from the electrodes (cf. 2, p. 496) and $[N]_0/P$ values in the range 0.15 to 0.20 were the highest that could be obtained. In an attempt to counteract this contamination, ethane was injected into the nitrogen stream at a point prior to the discharge tube for a few seconds at the beginning of each experiment. The polymeric material which would be laid down on the walls was expected to restore the apparatus to a condition more nearly like that during normal experiments, and greatly increased $[N]_0/P$ values (in the range 0.55 to 0.60) were in fact observed.

In interpreting the gauge measurements, it must be borne in mind that they represent the *average* atom concentrations in the discharge tube, not those at the instant of discharge. The observed $[N]_0/P$ values should therefore be compared with the maximum average values obtainable at the flashrates used, i.e. with

$$\overline{[N]_0/P} = 1/t \int_0^t ([N]/P)\, dt.$$

Expressing $[N]/P$ in terms of equation [5], and substituting $P = 1.4$ mm (the pressure at which most of the gauge measurements were made), $k_1 = 17.2$, $k_2 = 1.77$ (rate constants applicable at 400° C, from Table II), it is possible to show that the values of $\overline{[N]_0/P}$ corresponding to flashrates of 60 and 30 per second are 0.85 and 0.73. If k_1 is doubled, the values for the same flashrates are 0.70 and 0.58. It is therefore evident that, while the $\overline{[N]_0/P}$ values calculated for high flashrates and for normal values of k_1 are slightly in excess of the gauge measurements, the effect of a moderate increase in the rate constant of surface decay k_1, such as would result if the discharge tube were contaminated from the electrodes, is sufficient to make the values agree quite closely. Complete initial dissociation therefore appears to have been achieved (cf. Armstrong and Winkler (29)). (The $\overline{[N]_0/P}$ values given above are of incidental interest in that they indicate the upper limits of active nitrogen concentration that can be obtained at a given flashrate by shortening the decay tube or increasing the flowrate.)

With the information available in series 1 to 4, the minimum energy expenditures which bring about complete initial dissociation at a given pressure can, in principle, be determined. However, a general statement of conditions which give adequate, but otherwise unspecified, energy expenditures is sufficient for the present purposes: see description of circuit. All subsequent experiments will be understood to be conducted under these conditions.

HCN *Production as a Function of Pressure*

The actual study of the decay of N atoms was now undertaken. With the furnace on the reaction vessel set for about 350° C and the decay tube either unheated (average temperature = 55° C; *series 5*) or at 400° C[7] (*series 6*), the HCN production from ethylene

[7]*When the decay tube was at 400° C it was not necessary to heat the reaction vessel to achieve maximum reactivity with ethylene. This was not true, however, with ethane.*

and ethane was determined as a function of pressure (Fig. 3). The maximum possible N atom flowrates, obtained from the observed relation between nitrogen flowrate and pressure by doubling the flowrate values to take dissociation into account, are also indicated in Fig. 3. The experimental values for the two series were obtained in random order so that any differences would be real and not due to permanent changes in the glass or poison. In some of the experiments of series 6 the poison on the reaction vessel alone was changed to KCl. The fact that the low-pressure asymptotes of the curves for HCN production lead to a pressure slightly greater than zero (0.15 mm) probably has no great significance, since a similar property is evident in the relation between nitrogen flowrate and pressure.

The main conclusions to be drawn from Fig. 3 are the following:

(i) Since the amounts of HCN formed from ethylene and ethane coincide at all pressures investigated, a complete cleanup of N atoms rather than fortuitously similar reactivities *without cleanup* is proved.

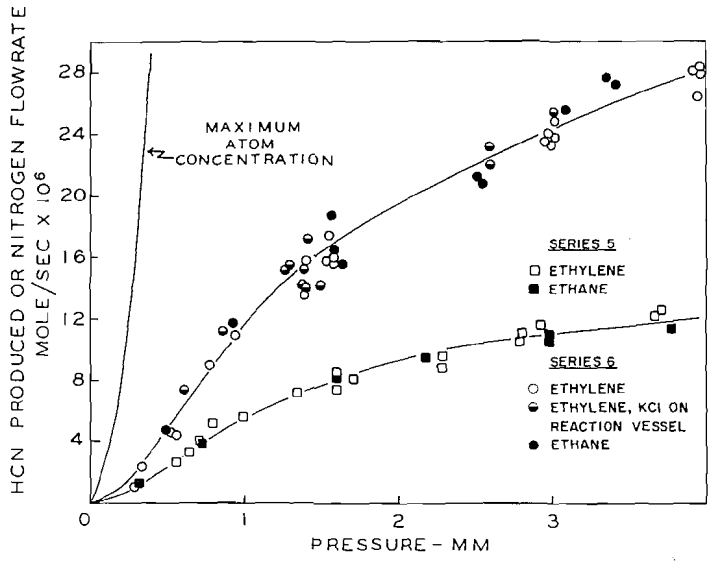

FIG. 3. Series 5 and 6. HCN production from ethylene and ethane as a function of pressure at elevated temperatures.

(ii) Since the use of KCl on the reaction vessel has no effect on the results, surface effects may be assumed absent unless, as is unlikely, KCl and Na_2HPO_4 happen to have equivalent poisoning qualities. The absence of surface effects further confirms that cleanup was achieved.

(iii) Heating the decay tube greatly increases the number of N atoms which reach the reaction vessel, though, since the rate constants for decay will be shown to *increase* with temperature, this effect must be due solely to a decreased time of decay (cf. equation [15]).

(iv) Since the low-pressure asymptotes of the curves for HCN production do not coincide with the line giving the maximum possible atom flowrate, the surface decay is shown to be first order and the relevant decay equations are therefore [5] and [7].

(v) The curves for HCN production diverge only slightly from their low-pressure asymptotes up to 2 mm pressure. Surface decay is therefore more important than

Can. J. Chem. Downloaded from www.nrcresearchpress.com by 190.90.36.8 on 09/04/12
For personal use only.

homogeneous decay in this pressure region, at least with the poison used and for the given diameter of decay tube.

It was also shown in experiments which will not be described here (*series 7*) that the effect of temperature on decay varies continuously without maxima between the temperatures used in series 5 and 6. All conclusions on N atom decay may therefore be generalized over this range. Such a generalization would not otherwise follow, since, as seen in the H atom study of Smith (1) and in several instances cited by Shuler and Laidler (27, p. 1215), the surface collision efficiency may maximize under certain conditions.

Calculations

As a first step in fitting the data of series 5 and 6 to the relevant decay equations [5] and [7], it was necessary to convert the observed HCN flowrates into partial pressures. This was done by means of the empirical relation between nitrogen flowrate and pressure (part of which is shown in Fig. 3, though with a factor of two), with a suitable correction for dissociation. These relations are discussed in Appendix B and lead to equation [14]. Values of $P/[N]$ calculated from the data of series 5 and 6 by means of this equation are included in Table I.

TABLE I

Data used for the calculation of the rate constants for N atom decay

Pressure, mm	[N] = HCN μm/sec$\times 10^6$ (from Fig. 3)	Conversion factor μm/sec $\leftrightarrow$ mm (from eq. [14])	$P/[N]$	$1/(\ln P/[N]-k_1t)$
		Temperature of decay tube: 55° C		
0.5	2.3	.0233	9.32	24.
1.0	5.4	.0190	9.74	11.6
1.5	7.7	.0180	10.8	5.26
2.0	9.3	.0176	12.2	3.22
2.5	10.3	.0174	13.95	2.25
3.0	11.0	.0173	15.75	1.76
3.5	11.6	.0172	17.55	1.48
4.0	12.2	.0172	19.1	1.32
		Temperature of decay tube: 400° C		
0.5	4.6	.0223	4.87	23.
1.0	11.6	.0180	4.79	37.
1.5	16.0	.0171	5.48	6.21
2.0	19.4	.0168	6.14	3.64
2.5	22.2	.0167	6.73	2.72
3.0	24.4	.0166	7.40	2.17
3.5	26.4	.0166	7.97	1.87
4.0	28.0	.0166	8.59	1.64

To obtain k_1, the lower limits of k_2, and certain related quantities, plots of $P/[N]$ versus P^2 in accordance with equation [5] were now made (Figs. 4A and 4B). From the intercepts of the limiting slopes as $P \rightarrow 0$, i.e. e^{k_1t} (note that the factor $P/[N]_0$ drops out under conditions of complete initial dissociation), the quantity k_1t was obtained, with k_1 following from equation [17] as derived in Appendix C. The lower limits of k_2 could then be obtained from the limiting slopes themselves, i.e.

$$d(P/[N])/dP^2 = (e^{k_1t}-1)k_2/k_1,$$

and values for the collision efficiency (γ), activation energy of surface decay (E_1), and number per cm^2 of surface species (C_s) from equations [8], [9], and [10] respectively.

Can. J. Chem. Downloaded from www.nrcresearchpress.com by 190.90.36.8 on 09/04/12
For personal use only.

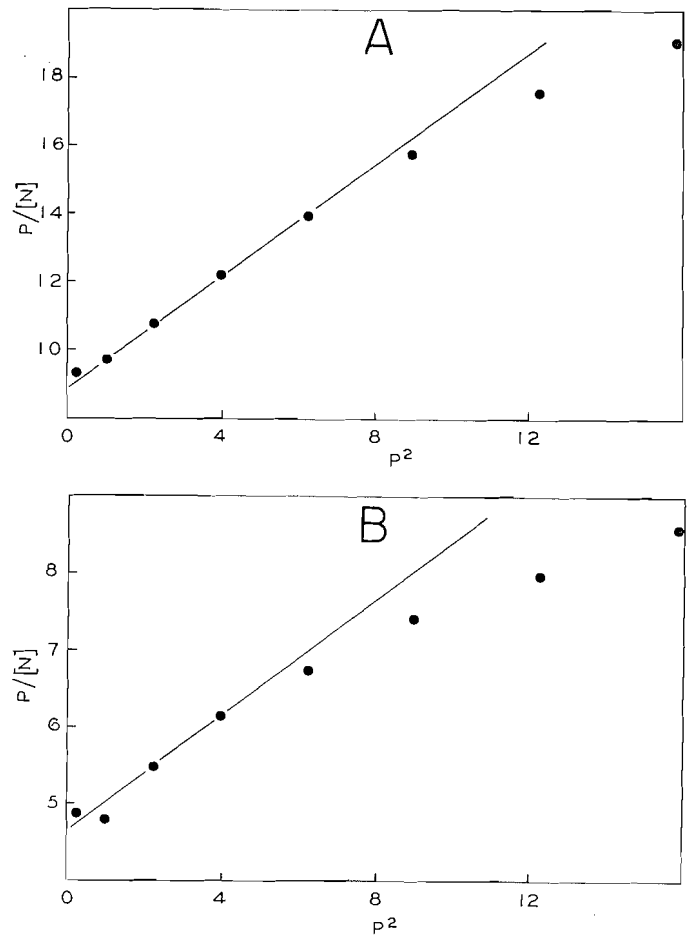

FIG. 4A. Analysis of the data of series 5 in accordance with equation [5]. (Intercept = 8.9, limiting slope = 0.82 mm^{-2}.)
FIG. 4B. Analysis of the data of series 6 in accordance with equation [5]. (Intercept = 4.65, limiting slope = 0.375 mm^{-2}.)

Finally, to obtain the upper limits of k_2, plots of $1/(\ln P/[\mathrm{N}]-k_1t)$ versus $1/P^2$ in accordance with equation [7] were made (Fig. 4C). (Values of $1/(\ln P/[\mathrm{N}]-k_1t)$ were included in Table I.) The upper limits of k_2 followed from the slopes of the lines joining the point $(0, \frac{1}{2})$ with *high* values of $1/P^2$, i.e.

$$\frac{d(1/(\ln P/[\mathrm{N}]-k_1t))}{d(1/P^2)} = 2k_1/k_2.$$

The values for the various quantities that were derived are given in Table II.

To evaluate exactly the relative importance of homogeneous and surface decay *under the prevailing conditions*, the following relation was used: mean ratio of homogeneous to surface decay =

$$1/P\int_0^P (k_2/k_1)P[\mathrm{N}]d[\mathrm{N}] = k_2P^2/2k_1.$$

Can. J. Chem. Downloaded from www.nrcresearchpress.com by 190.90.36.8 on 09/04/12
For personal use only.

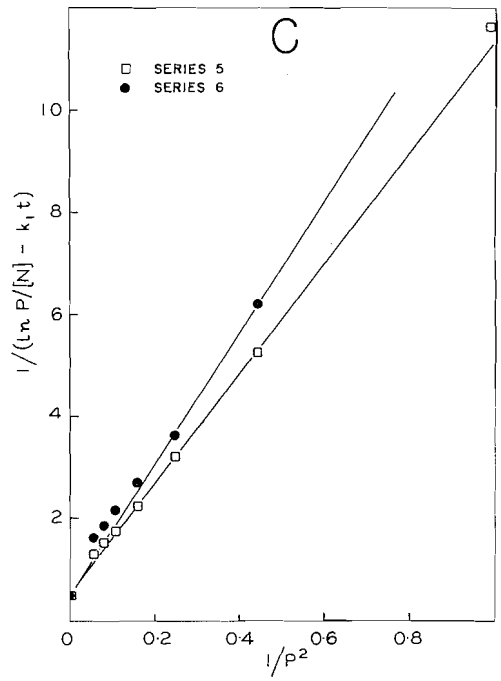

FIG. 4C. Analysis of the data of series 5 and 6 in accordance with equation [7]. (Limiting slopes = 10.90 mm² [series 5], 12.60 mm² [series 6].)

Using $k_1 = 11.1$ and $k_2 = 1.15$ this expression yields 0.052 at 1 mm and 0.83 at 4 mm. The previous conclusion is therefore confirmed that homogeneous decay is of secondary importance below about 2 mm pressure *under the prevailing conditions.*

TABLE II

The rate constants for N atom decay and related quantities

Quantity*	Value at 55° C	Value at 400° C
$k_1 t$	2.19	1.54
k_1	11.1 sec^{-1}	17.2 sec^{-1}
γ	2.65×10^{-4}	2.86×10^{-4}
k_2 (lower limit)	1.15 A	1.77 A
	1.32×10^{-33} B	8.6×10^{-33} B
k_2 (upper limit)	2.04 A	2.73 A
	2.35×10^{-33} B	13.2×10^{-33} B
E_1	1.0 kcal $mole^{-1}$	
C_s	1.9×10^{14} cm^{-2}	

*k_1, γ, E_1, and C_s apply only to surfaces coated with Na_2HPO_4. The units of k_2 are abbreviated as follows: A $\equiv$ $mm^{-2}\,sec^{-1}$, B $\equiv$ cc^2 $molecule^{-2}\,sec^{-1}$. Values for k_2, obtained from those at 55° C by usiug 298° K in the factor to convert mm^{-2} to cc^2 $molecule^{-2}$, are as follows: $>1.09\times10^{-33}$ B, $<1.94\times10^{-33}$ B.

DISCUSSION

The Decay of N, H, *and* O *Atoms*

The present work has confirmed that the surface decay of N atoms follows first-order kinetics. While this result was anticipated, it is perhaps significant that close similarities

Can. J. Chem. Downloaded from www.nrcresearchpress.com by 190.90.36.8 on 09/04/12
For personal use only.

exist in the behavior of N, H, and O atoms. All exhibit first- rather than second-order surface decay with collision efficiencies (γ) in the range 10^{-3} to 10^{-5}, activation energies (E_1) in the range 1 to 2 kcal mole^{-1}, and values of 10^{14} to 10^{15} cm^{-2} for the concentration of surface species (C_s).[8] It would therefore be expected that the mechanism of the surface decay of N atoms would be the adsorption mechanism which has been so successful in explaining the behavior of H atoms (27). This mechanism proposes that the gas-phase atoms recombine with a layer of atoms adsorbed on the surface (8, 9, 27, 28), the order of the process depending on whether the surface layer is complete or concentration dependent. However, Linnett and Marsden (2, 3) have pointed out that at room temperature O atoms are only weakly adsorbed on glass. To explain the first-order decay they therefore suggested a slightly different mechanism according to which the gas-phase O atoms combine directly with the structural oxygen of the glass or poison, with water of hydration, or with a surface layer of oxide. This mechanism would give second-order kinetics only at temperatures sufficiently high to decompose the surface compound, i.e. at temperatures well in excess of the "desorption" temperature.

Since there seems to be no information available on the adsorption of N atoms on Na_2HPO_4 or related solids, it is not possible to decide with certainty whether the surface layer responsible for the surface decay consisted of adsorbed atoms or a true surface compound (a nitride or nitrate). However, whatever the origin of the layer, it evidently remains intact even at 400° C so that it was valid to assume, in deriving equations [1] to [7], that the two orders of surface decay were not competitive. Furthermore, as stated before, the decision does affect the validity of equations [8] to [10].

The homogeneous decay of N and H atoms is perhaps less comparable than the surface decay, since the rate constants for N atoms (Table II) appear to be an order of magnitude smaller than those for H atoms (Amdur's values of 30×10^{-33} to 61×10^{-33} (4) are typical of a number of H atom studies), in spite of the greater diameter of nitrogen. However, the difference is probably adequately explained by the steric factor shown by Berkowitz *et al.* (6) to be associated with the transition $N_2(^5\Sigma) + M \rightarrow N_2(B^3\Pi) + M$.

A positive temperature coefficient was observed for the rate constant of N atom homogeneous decay. This was unexpected in view of Rayleigh's (10) observation of a negative temperature coefficient in measurements of afterglow intensity between the temperature of liquid air and 100° C, and it is therefore possible that the results of the present work were subject to a large, systematic error. Perhaps the most likely source of such an error lies in the assumption of complete initial dissociation, since, had $[N]_0/P$ steadily decreased as pressure was increased, the effect would have been easily mistakable for a pressure-dependent mode of decay; however, no pressure dependence in $[N]_0/P$ was observed in the Wrede gauge measurements of series 4. The positive temperature coefficient therefore appears to be real. If the positive temperature coefficient observed by Robinson and Amdur (30) in the decay of H atoms could be attributed not only to the surface decay, but also to the homogeneous decay, the present results for N atoms could be considered to have good precedent.

Details of the Decay Mechanisms

To good approximation, a ^4S atom can combine only into $^1\Sigma_g^+$, $^3\Sigma_u^+$, $^5\Sigma_g^+$, and $^7\Sigma_u^+$ molecular states (6). For nitrogen, the $^7\Sigma$ state is probably higher than the ^4S dissociation

[8]*For* H *atoms the values of* E_1 *and* C_s *are:* $E_1 = 0.9$ *(30),* $C_s = 1.35\times10^{15}$ *(31, 32, 27), where* E_1 *applies only to dry surfaces (27). The corresponding values for* O *atoms can be calculated from the data of Linnett and Marsden as given in Table I of ref. (2) (Fig. 8 of this reference could not be used as it appears to have an error in the ordinate):* $\gamma = (1.2/2)\times10^{-4}$ *at 17° C,* $\gamma = (3.56/2)\times10^{-4}$ *at 400° C. Hence* $E_1 = 2.0$, $C_s = 2.7\times10^{14}$. *The introduction of a factor of two was justified in an earlier section.*

Can. J. Chem. Downloaded from www.nrcresearchpress.com by 190.90.36.8 on 09/04/12
For personal use only.

energy, while the $^5\Sigma$ state is believed to be the precursor of the afterglow (6, 11). Therefore, since it has been observed both by Rayleigh (7) and in the present work[9] that the afterglow intensity remains unchanged in the neighborhood of various surfaces, the *final* molecules formed in surface decay must be in the $A^3\Sigma$ or ground states. A further decision between these two states could perhaps best be made if the long-lived $A^3\Sigma$ molecules (14) could be shown absent from active nitrogen, or, if present, formed only from homogeneous atom decay. Such information is not available, but it is significant that the surface layer responsible for the surface decay remained intact at 400° C. That is, the *transition* molecules formed in surface decay probably exist briefly in close association with the wall, so that complete deactivation to low vibrational levels of the ground state should occur before the molecules separate. It is therefore suggested that the following mechanism accounts for *all* the surface decay (cf. 27):

$$\begin{aligned} N(^4S) + \text{surface} &\rightarrow N(^xS)\cdot\text{surface}, \\ N(^4S) + N(^xS)\cdot\text{surface} &\xrightarrow{k_1} N_2(^y\Sigma)\cdot\text{surface}, \\ &\rightarrow N_2(^1\Sigma)\cdot\text{surface}, \\ &\rightarrow N_2(^1\Sigma) + \text{surface}, \end{aligned}$$

where x and y cannot be specified with certainty due to the proximity of a surface, and $N_2(^y\Sigma)\cdot$ and $N_2(^1\Sigma)\cdot$ are transition molecules.

With homogeneous decay there exists a similar choice of paths and it was, in fact, considered by Berkowitz *et al.* (6) that recombination into the $^5\Sigma$ state with subsequent afterglow emission accounted for only part of the decay. This conclusion was based on a comparison of the rate constant of afterglow emission (2×10^{-33}) with the rate constant for a three-body collision process ($\sim10^{-32}$). However, comparing the former with *one-half*[10] the rate constant of homogeneous decay at 25° C as obtained in the present work (0.55×10^{-33} to 0.97×10^{-33}), it appears that *all* homogeneous decay must give rise to afterglow via the $^5\Sigma$ state, since the constants are essentially equal. This conclusion would be unaltered even if the afterglow constant were *high* by a factor of two or three, so that the following mechanism, which is identical with that proposed by Berkowitz *et al.* (6), may be tentatively assumed to account for *all* the homogeneous decay:[11]

$$\left.\begin{aligned} 2N(^4S) + M &\rightleftharpoons N_2(^5\Sigma) + M \\ N_2(^5\Sigma) + M &\longrightarrow N_2(B^3\Pi) + M \end{aligned}\right\} k_2$$

$$N_2(B^3\Pi) \rightarrow N_2(A^3\Sigma) + h\nu$$

$$N_2(A^3\Sigma) \rightarrow ?.$$

The last step will be considered further in a subsequent paper.

REFERENCES

1. SMITH, W. V. J. Chem. Phys. **11**, 110 (1943).
2. LINNETT, J. W. and MARSDEN, D. G. H. Proc. Roy. Soc. A, **234**, 489 (1956).
3. LINNETT, J. W. and MARSDEN, D. G. H. Proc. Roy. Soc. A, **234**, 504 (1956).
4. AMDUR, I. J. Am. Chem. Soc. **60**, 2347 (1938).
5. JACKSON, D. S. and SCHIFF, H. I. J. Chem. Phys. **23**, 2333 (1955).
6. BERKOWITZ, J., CHUPKA, W. A., and KISTIAKOWSKY, G. B. J. Chem. Phys. **25**, 457 (1956).
7. RAYLEIGH, LORD. Proc. Roy. Soc. A, **151**, 567 (1935).

[9]*The apparatus used was constructed by Dr. A. Fontijn of this Department. It had a window suitable for observing reaction flames.*

[10]*The factor of two arises since two atoms disappear for each photon emitted.*

[11]*Actually, Berkowitz et al. show that this mechanism requires a negative temperature coefficient. A discrepancy therefore exists which must be satisfactorily explained before the mechanism can be adopted without reservation.*

Can. J. Chem. Downloaded from www.nrcresearchpress.com by 190.90.36.8 on 09/04/12
For personal use only.

8. BUBEN, N. and SHEKHTER, A. Acta Physicochim. U.R.S.S. **10**, 371 (1939).
9. SHEKHTER, A. Acta Physicochim. U.R.S.S. **10**, 379 (1939).
10. RAYLEIGH, LORD. Proc. Roy. Soc. A, **176**, 1 (1940).
11. KISTIAKOWSKY, G. B. and WARNECK, P. J. Chem. Phys. **27**, 1417 (1957).
12. FREEMAN, G. R. and WINKLER, C. A. J. Phys. Chem. **59**, 371 (1955).
13. EVANS, H. G. V. and WINKLER, C. A. Can. J. Chem. **34**, 1217 (1956).
14. LICHTEN, W. J. Chem. Phys. **26**, 306 (1957).
15. KAUFMAN, F. and KELSO, J. R. J. Chem. Phys. **28**, 510 (1958).
16. KISTIAKOWSKY, G. B. and VOLPI, G. G. J. Chem. Phys. **28**, 665 (1958).
17. FORST, W., EVANS, H. G. V., and WINKLER, C. A. J. Phys. Chem. **61**, 320 (1957).
18. WILES, D. M. and WINKLER, C. A. Can. J. Chem. **35**, 1298 (1957).
19. VERBEKE, G. J. O. Ph.D. Thesis, McGill University, Montreal, Quebec. 1958.
20. VERSTEEG, J. and WINKLER, C. A. Can. J. Chem. **31**, 1 (1953).
21. GARTAGANIS, P. A. and WINKLER, C. A. Can. J. Chem. **34**, 1457 (1956).
22. GREENBLATT, J. H. and WINKLER, C. A. Can. J. Research, B, **27**, 721 (1949).
23. BLADES, H. and WINKLER, C. A. Can. J. Chem. **29**, 1022 (1951).
24. KOLTHOFF, I. M. and SANDELL, E. B. Textbook of quantitative inorganic analysis. Revised ed. Macmillan & Co., Ltd., London. 1948.
25. ONYSZCHUK, M., BREITMAN, L., and WINKLER, C. A. Can. J. Chem. **32**, 351 (1954).
26. HERZBERG, G. Spectra of diatomic molecules. 2nd ed. D. Van Nostrand Company, Inc., New York. 1950.
27. SHULER, K. E. and LAIDLER, K. J. J. Chem. Phys. **17**, 1212 (1949).
28. LAIDLER, K. J. J. Phys. Chem. **53**, 712 (1949).
29. ARMSTRONG, D. A. and WINKLER, C. A. J. Phys. Chem. **60**, 1100 (1956).
30. ROBINSON, A. L. and AMDUR, I. J. Am. Chem. Soc. **55**, 2615 (1933).
31. JOHNSON, M. C. Trans. Faraday Soc. **28**, 162 (1932).
32. LANGMUIR, I. J. Chem. Soc. 511 (1940).
33. STEINER, W. Trans. Faraday Soc. **31**, 623 (1935).
34. STEINER, W. Trans. Faraday Soc. **31**, 962 (1935).
35. BRONWELL, A. Advanced mathematics in physics and engineering. McGraw-Hill Book Co., Inc., New York. 1953.

APPENDIX A

Assumptions in the Decay Equations

The decay equations assume a number of simplifying conditions beyond the basic ones already discussed. The use of a time-independent pressure, P, requires that there be no significant pressure gradient in the decay tube whether due to flow, heating, or dissociation (valid at all pressures). The use of plots extending over a range of pressure requires that the molar flowrate of nitrogen vary directly with pressure, for only then will the linear velocity of the gas and thence the time of decay (at least in the absence of dissociation) be pressure independent (see Fig. 3; the validity increases with pressure). The effect of dissociation on the time of decay must also be pressure independent (see Appendix C; valid only at low pressures or large decay times). The use of an average temperature for the decay tube in calculating the time of decay (Appendix C) assumes that the temperature of the decay tube is uniform (valid, in particular at higher temperatures). The decay tube must be of uniform diameter so that k_1 and k_3 will be constant.

Axial diffusion, i.e. diffusion in the direction of flow, must transport an insignificant amount of mass compared with the flow. This is borne out by the following calculation: the maximum contribution by diffusion to the flow occurs initially when, at 55° C and a pressure of 2 mm, and with $[N]_0 = P$, it amounts to

$$-D\partial[N]/\partial t \cdot \partial t/\partial x \cdot \pi r_0^2 = 6.6\ \mu m/sec,$$

where $D = \bar{c}\lambda/3$, λ is the mean free path, $-\partial[N]/\partial t = (k_1P + k_2P^3)(n\mu/P)$, $n\mu$ is the number of micromoles per cubic centimeter at a pressure P, $\partial t/\partial x = t_0/2 \times 31.7$, t_0 is given by equation [15], 2 is a factor to take dissociation into account, and 31.7 is the length of the decay tube. Since the flow under the same conditions is 218 μm/sec (from equation [11]), diffusion can be neglected.[12] This would not necessarily be true at very

[12]*Steiner (33) has made a similar calculation to determine if diffusion could be neglected.*

Can. J. Chem. Downloaded from www.nrcresearchpress.com by 190.90.36.8 on 09/04/12
For personal use only.

high pressures owing to the greater value of $\partial[N]/\partial t$. Radial diffusion, on the other hand, must eliminate any radial concentration gradient (see Appendix D; valid at low pressures and high temperatures).

APPENDIX B

Conversion of Flowrates to Partial Pressures

It was found that above about 0.30 mm the relation between nitrogen flowrate and pressure (cf. Fig. 3) was approximately linear and could therefore be represented simply by

$$[N_2]_{\mu m/sec} = 59.0(P-0.15), \quad [11]$$

where μm/sec is the abbreviation for micromoles per second and P is in millimeters. The temperature at which the measurements were made was 25 to 30° C. Neglecting the effect of dissociation, a relation applicable to N atoms formed in the nitrogen stream follows as

$$[N]_{\mu m/sec} = 59.0([N]_{mm}/P)(P-0.15). \quad [12]$$

However, equation [12] must be corrected for the fact that with the apparatus used, dissociation brought about an increased flowrate rather than an increased pressure such that (cf. 33)

$$\text{flowrate} \propto \frac{P}{P-[N]_{mm}/2}. \quad [13]$$

Substituting for $[N]_{mm}$ in equation [13] the approximate value $[N]_{\mu m/sec}/59.0$ obtained from equation [12], and then using the result as a correction factor for equation [12], one obtains the desired relation:

$$[N]_{mm} \approx \frac{[N]_{\mu m/sec}(P-[N]_{\mu m/sec}/118)}{59.0(P-0.15)}. \quad [14]$$

APPENDIX C

The Time of Decay

The volume flowrate can be derived directly from equation [11] and has an average value of 1006 cc sec^{-1} at 25° C and in the region 1 to 3 mm pressure. It therefore follows that the average time of flow through the 281 cc decay tube, provided the nitrogen is undissociated, is

$$t_0 = 0.279\times 298/T \text{ sec}, \quad [15]$$

where T is the average temperature of the decay tube in ° K. The increased flowrates arising from dissociation will reduce the time, so that it is necessary to find a relation between t_0 and the true time of decay t. Let x be distance measured along the decay tube, x_0 the length of the decay tube, and v_0 the linear flowrate in the absence of dissociation. Then, if there is no dissociation, $x_0/v_0 = t_0$, while if there *is* dissociation (cf. equation [13]),

$$dx/dt = v_0/(1-[N]/2P). \quad [16]$$

Neglecting homogeneous decay, the substitution $[N] \approx Pe^{-k_1 t}$ can now be made and equation [16] integrated, so that, on equating the two expressions for x_0/v_0, one obtains

$$k_1 \approx \frac{k_1 t+\ln 2-\frac{1}{2}e^{-k_1 t}}{t_0}. \quad [17]$$

Equation [17] is necessarily valid only at low pressures (when homogeneous decay is of secondary importance) or at large decay times (when the entire effect of dissociation becomes less marked).

Can. J. Chem. Downloaded from www.nrcresearchpress.com by 190.90.36.8 on 09/04/12
For personal use only.

Can. J. Chem. Downloaded from www.nrcresearchpress.com by 190.90.36.8 on 09/04/12
For personal use only.

APPENDIX D

Radial Diffusion

As a result of surface decay it is inevitable that a radial concentration gradient, however slight, will exist, and that the surface decay will therefore be self-inhibiting. However, such an effect has in the past generally been treated with such a rigid application of Fick's laws that a simple method of correcting for radial diffusion has apparently not been obtained (cf. 34). Since the formal approach involves assigning variability to the "shape" of the gradient, it was natural to try an approach in which a constant "shape" was used, in particular a *linear* gradient such that, as seen along a diameter of the system, it appears as an inverted "V".[13] A simple expression for the effect of radial diffusion when the surface decay is first order is then readily obtained.

Equating the rate of decay to the rate of diffusion towards the walls in the manner indicated by Steiner (34), one obtains

$$2\times\bar{c}[\mathrm{N}]'\gamma/4 = -D\partial[\mathrm{N}]/\partial r = (\bar{c}\lambda/3r_0)([\mathrm{N}]''-[\mathrm{N}]'), \qquad [18]$$

where [N]′ is the atom concentration at the surface of the decay tube, [N]″ is the concentration at the center of the decay tube, and r is the variable corresponding to r_0. The necessity of the factor of two on the left side was indicated in an earlier section. It is readily shown that the average atom concentration in a *cylindrical* system, $\overline{[\mathrm{N}]}$, is related to [N]′ and [N]″ by

$$\overline{[\mathrm{N}]} = \tfrac{1}{3}[\mathrm{N}]''+\tfrac{2}{3}[\mathrm{N}]'. \qquad [19]$$

Combining equations [18] and [19],

$$[\mathrm{N}]' = \overline{[\mathrm{N}]}/(1+\gamma r_0/2\lambda),$$

where the term $(1+\gamma r_0/2\lambda)$ is the desired correction for radial diffusion. The rate constant for surface decay is therefore more correctly given by

$$k_1' = k_1/(1+\gamma r_0/2\lambda) = k_1/(1+\alpha P),$$

where k_1 is given by equation [8] and (assuming $\sigma = 3.84\times10^{-8}$ cm) $\alpha = 3.16\times10^4\gamma r_0/T$ mm^{-1}.

If similar arguments are applied to a *spherical* system, where

$$\overline{[\mathrm{N}]} = \tfrac{1}{4}[\mathrm{N}]''+\tfrac{3}{4}[\mathrm{N}]',$$

then $\alpha = 3\gamma r_0/8\lambda = 2.37\times10^4\gamma r_0/T$ mm^{-1}. It can be proved that, provided $\alpha P \ll 1$, no correction is necessary to k_2 in either a cylindrical or spherical system.

The treatment given is general and can be applied to experimental situations other than the present, e.g. static systems. However, it may not be valid for a short-lived species formed in the *interior* of a system, since a very marked pressure effect would be expected if the time for diffusion to the walls were comparable to the life of the species. As far as the present work is concerned, since α would amount to only 0.043 mm^{-1} (for $r_0 = 1.68$ cm, $\gamma = 2.65\times10^{-4}$, $T = 328°$ K), the correction for radial diffusion can be neglected, at least at the lower pressures.

[13] *A gradient of this sort appears to have theoretical justification, since it represents the limiting case as Dt gets large, i.e. it applies at high temperatures, low pressures, or when decay is slow. (That a decreasing rate of decay is very approximately equivalent to an increasing value of Dt is evident from the fact that there is no gradient in the absence of decay.) Compare the exact expression for radial diffusion in a cylinder (35, p. 272).*

Can. J. Chem. Downloaded from www.nrcresearchpress.com by 190.90.36.8 on 09/04/12
For personal use only.

RADIOLYSIS OF TETRACHLOROETHYLENE[1]

J. W. SUTHERLAND AND J. W. T. SPINKS

ABSTRACT

When tetrachloroethylene is irradiated with Co^{60} gamma rays in the presence of oxygen or air, the main products are trichloroacetyl chloride, phosgene, and oxalyl chloride. The reaction is a chain reaction. Possible reaction mechanisms are discussed.

INTRODUCTION

Tetrachloroethylene, when irradiated in a two-phase aqueous system or when irradiated with a soluble pH indicator dye, liberates acidic products. The acid yields are high (G_{H^+} values up to 6000), suggesting that a chain mechanism is operative (1, 2). Chain reactions, although highly sensitive, are often greatly influenced by dose rate, temperature, and the presence of trace impurities. In addition, this particular reaction proceeds to some degree under the influence of light (3, 4). These complicating factors, undesirable in chemical dosimetry, can be effectively removed and in some cases totally suppressed by the addition of stabilizing reagents such as ethyl alcohol, resorcinol, and thymol. Although the sensitivity of the system to radiation is thereby markedly reduced (G value about 30), the use of stabilizers has made it possible to use tetrachloroethylene dosimeters which can register doses in the range, 1.0 to 10^6 r and which show excellent reproducibility (1).

The purpose of this study is to arrive at a more fundamental understanding of the chain mechanism in this sytem and to see whether further study of it would be useful in interpreting some of the processes occurring when ionizing radiation interacts with matter, e.g., in providing evidence of track effects (5).

EXPERIMENTAL

Reagent grade Kodak Eastman tetrachloroethylene, stabilized by the addition of 0.5% ethyl alcohol, was used as starting material. The alcohol can be removed by repeated water extractions or by fractional distillation. Pure tetrachloroethylene is prone to decompose under the influence of light and oxygen (3, 4), and thus a large sample of pure material cannot be prepared and stored for any length of time. Since this necessitates preparation of alcohol-free reagent immediately prior to each irradiation run, the following procedure was adopted.

Approximately 50 ml of reagent grade tetrachloroethylene (ethyl alcohol stabilized) was shaken with $CaCl_2$, filtered, and fractionally distilled. The middle fraction, b.p. 120–121° C, was used. Samples which had been treated for 24 hours and 3 days, respectively, were equally sensitive to radiation. Samples which had been extracted for periods of 2 and 12 hours were found less radiation sensitive.

The system irradiated, unless stated otherwise, was a 3-ml sample of pure tetrachloroethylene overlayered with 2 ml of water which had been distilled from alkaline permanganate and then redistilled from an alkaline suspension of manganous hydroxide. Samples were irradiated in glass-stoppered Pyrex tubes (12×100 mm), with gamma radiation from either a 1-curie or a 1000-curie Co^{60} source (6). After irradiation the solution was transferred to a 10-ml Erlenmeyer flask, and two 1-ml portions of wash water added. The acids liberated were titrated against standard base (NaOH) using a

[1]*Manuscript received June 20, 1958.*
Contribution from the Department of Chemistry, University of Saskatchewan, Saskatoon, Saskatchewan.

microburette and a 0.1% solution of chlorophenol red as indicator. Samples were titrated to the same color as a blank (pH about 6), which had received identical treatment except for irradiation.

Irradiations were carried out at room temperature.

Dose rates were measured with a ferrous sulphate dosimeter ($G_{Fe^{+++}} = 15.5$) (7).

Infrared spectra were recorded with a Perkin–Elmer double beam infrared spectrophotometer.

RESULTS

In general, titration of the acids formed on irradiation was difficult owing to a pronounced postradiation effect which, however, apparently decreased in magnitude the less acid there was liberated. For example, there was no measurable postradiation effect with a 0.3% hexylresorcinol stabilized, air-equilibrated system (Table I).

TABLE I

Irradiation of air-equilibrated tetrachloroethylene stabilized with 0.3% by weight hexylresorcinol

(Samples, 3 ml stabilized tetrachloroethylene overlayered with 2 ml water; temp., 25° C; mean dose rate = 10 r/minute.)

Dose, kr	Time between irradiation and titration (minutes)	Acid yield, meq $\times 10^{-3}$ per ml	Acid yield, meq $\times 10^{-6}$ per ml TCE per r	G_H^+ values*
9.22	30	0.20	0.0216	15.1
9.10	50	0.195	0.0214	15.0
9.83	100	0.203	0.0214	15.0
9.55	230	0.207	0.0216	15.1
9.55	325	0.207	0.0216	15.1
10.3	440	0.220	0.0223	15.6
				15.2±0.2

*G values are calculated on the basis that only the energy absorbed by the tetrachloroethylene phase is responsible for the chemical reactions. The factor for converting column 4 to column 5 is 703.

However, with a more sensitive system, e.g., using tetrachloroethylene which had been freed from alcohol and saturated with oxygen prior to irradiation, complete extraction of acid products was more difficult (Table II).

Preliminary experiments were also done in air-equilibrated tetrachloroethylene–water systems. In such systems, reproducibility was apparently achieved by periodic shaking

TABLE II

Irradiation of purified tetrachloroethylene saturated with oxygen

(Samples, 3 ml purified tetrachloroethylene ($CaCl_2$ extracted for 24 hours, redistilled) saturated with O_2 prior to irradiation. Acidic products extracted with H_2O after irradiation. Temp., 25° C; mean dose rate, 10 r/minute.)

Dose, r	Acid yield at various postreaction times in meq $\times 10^{-3}$/ml TCE				Total yield		
	25 hr	29 hr	47 hr	52 hr	Meq $\times 10^{-3}$ per ml	Meq $\times 10^{-6}$ per ml per r	G_H^+ values
160	0.042				0.042	0.26	180
323	0.120				0.120	0.34	240
640	12.00	2.85	4.20	0.59	19.60	30.10	21,100
960	19.20	2.77	2.46	0.36	24.80	25.00	17,500
1300	20.30	1.75	2.28	0.22	24.60	19.00	13,300
1620	—	20.7	1.27	0.16	22.10	13.60	9,500

Can. J. Chem. Downloaded from www.nrcresearchpress.com by 190.90.36.8 on 09/04/12
For personal use only.

of samples during a 24-hour period before titration. It was also noted that if the samples were titrated immediately following irradiation, a sharp end-point color was reached which rapidly changed to the acidic color on standing. When the sample was left to stand without stirring, an acid aqueous layer formed at the interface of the water and tetrachloroethylene phase. This behavior occurred whether the system was left in the dark or not. Identical treatment of the blank showed no such behavior, even on exposure to sunlight. When bromocresol purple indicator was used, some of the indicator (chlorophenol red is insoluble in the tetrachloroethylene layer) dissolved in the tetrachloroethylene phase and showed a persistently acid reaction. The addition of hexylresorcinol, subsequent to irradiation (even in large amounts), had no inhibiting effect on this behavior, although it would presumably prevent decomposition under the influence of light and temperature. The more acid liberated, the more difficult it was to reach a stable end point. Shaking the solution or stirring it more vigorously produced more acid in the aqueous layer. Samples overlayered with different amounts of water gave similar acid yields.

When water saturated with tetrachloroethylene was irradiated, no detectable acid was liberated in the dose range being studied (0–2000 r).

These observations suggest that the continued acid production after irradiation is a result of gradual extraction of acidic products from the tetrachloroethylene phase, rather than a continuation of a chemical decomposition of the tetrachloroethylene.

Variation of Acid Yield with Absorbed Dose

Experimental data are summarized in Figs. 1, 2, and 3. Data for Fig. 1 were obtained for tetrachloroethylene which had been extracted for about 24 hours with $CaCl_2$ and redistilled before irradiation.

A series of runs at different dose rates was made with a sample of air-equilibrated tetrachloroethylene which had been left for a month overlayered with water. The water was separated, the tetrachloroethylene dried with $CaCl_2$ and redistilled. The results are shown in Figs. 2 and 3.

It is evident that we are now dealing with a more sensitive system. In samples where the tetrachloroethylene was overlayered with water the same limiting value of acid liberated was obtained, viz., about 4 meq $\times 10^{-3}$/ml, but this value was reached at

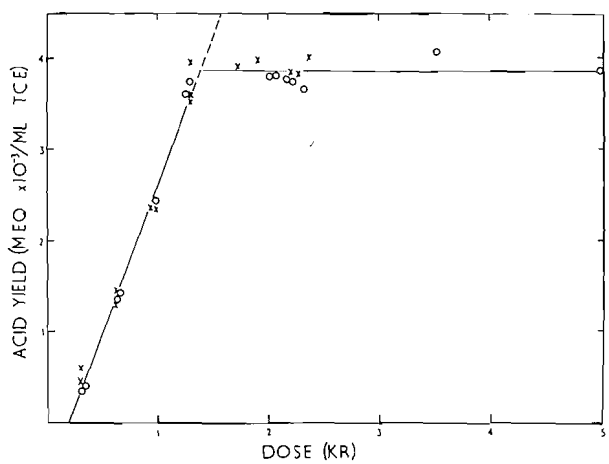

FIG. 1. Acid yield as a function of absorbed dose. Tetrachloroethylene extracted 24 hours with calcium chloride and redistilled. Samples consisted of 3 ml of tetrachloroethylene overlayered with 2 ml of water and air equilibrated. Temperature, 25° C; dose rate, 10 r per minute.

Can. J. Chem. Downloaded from www.nrcresearchpress.com by 190.90.36.8 on 09/04/12
For personal use only.

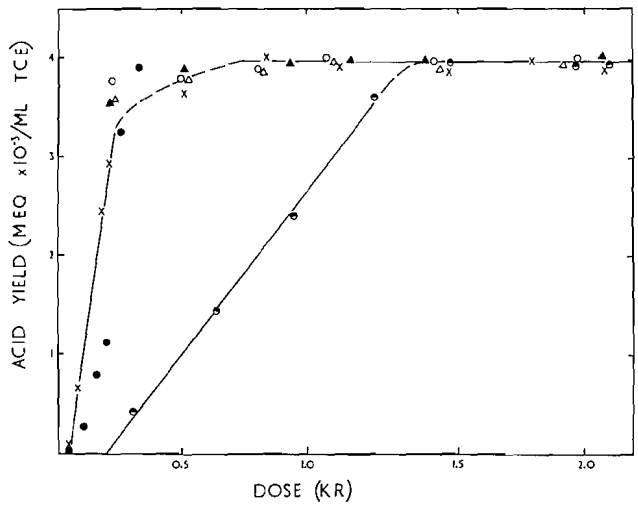

FIG. 2. Acid yield as a function of adsorbed dose.
◓Tetrachloroethylene extracted with $CaCl_2$ for 24 hours and redistilled. Dose rate 10 r per minute.
△, ▲, ○, ●, × Tetrachloroethylene extracted with water for about one month, dried, and redistilled.
● 2.67 r/min; ▲ 10.r/min; ○ 13.0 r/min; △ 26.6 r/min; × 41.9 r/min. All samples were 3 ml of tetrachloroethylene overlayered with 2 ml of water and air equilibrated.

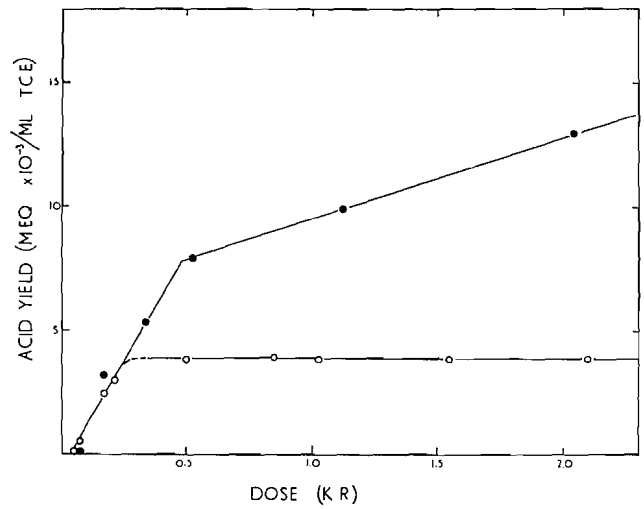

FIG. 3. Acid yield versus absorbed dose. Tetrachloroethylene extracted with water for about one month. Dose rate, 41.9 r/min. Temperature, 28° C.
● Samples were 3 ml of air-equilibrated tetrachloroethylene; 2 ml water added after irradiation.
○ Samples were 3 ml of air-equilibrated tetrachloroethylene overlayered with 2 ml of water.

lower doses of the order of 200 r (cf. Fig. 1, 1.4 kr). The probable explanation for the increased rate is that traces of alcohol left by the $CaCl_2$ method of purification were removed from the system by the water, thus making it more radiation sensitive. The G values are extremely high, e.g., at 41.3 r/minute G_{H^+} is of the order 12,600, over the initial range of absorbed dose.

Figure 3 shows a comparison of the acid yields obtained when tetrachloroethylene alone and tetrachloroethylene overlayered with water, both systems being air equilibrated, are irradiated. When tetrachloroethylene alone is irradiated, there is no limiting value to acid production though the rate of reaction changes after a time. The change in slope

Can. J. Chem. Downloaded from www.nrcresearchpress.com by 190.90.36.8 on 09/04/12
For personal use only.

is attributed to progressive exhaustion of the original oxygen present in the solution followed by diffusion of the oxygen from the gas phase into the tetrachloroethylene. This is extremely slow when the tetrachloroethylene is overlayered with water but is fast enough to support an appreciable rate of reaction when the tetrachloroethylene is in direct contact with air.

The induction period is reduced to about 50 r for the more highly purified tetrachloroethylene system.

Studies on the Effect of Oxygen

It is seen that the same limiting value of acid produced is reached in all systems overlayered with water despite their differing sensitivities. These observations suggest that an oxidation reaction is occurring in the tetrachloroethylene phase, the extent of the reaction being determined by the oxygen content of the tetrachloroethylene phase layer. This view was supported by the results of experiments in which the system was flushed, (*a*) with N_2, and (*b*) with oxygen, prior to irradiation. (See Table III.)

TABLE III

Effect on acid yield of flushing system with oxygen or nitrogen prior to irradiation

(Samples, 3 ml of tetrachloroethylene overlayered with 2 ml H_2O; dose rate, 10 r/minute; temp., 25° C.)

Pretreatment	Dose, kr	Acid yield, meq $\times 10^{-6}$ per r per ml	G_{H^+} values
(*a*) Tetrachloroethylene purified by $CaCl_2$ extraction (24 hours), followed by distillation			
Air-saturated	2.17	1.80	1270
	2.16	1.85	1300
N_2-flushed	2.18	0.0038	2.7
	2.12	0.0036	2.7
O_2-flushed	2.15	8.75	6150
	2.10	8.90	6250
(*b*) Ethyl alcohol stabilized tetrachloroethylene (0.5% EtOH)			
Air-saturated	16.8	0.190	133
	21.0	0.160	112
N_2-flushed	6.9	0.0049	3.4
	7.1	0.0057	4.0

From Fig. 3, the limiting amount of acid produced in an air-saturated sample is 3.94 meq $\times 10^{-3}$ per ml, i.e., 23.7×10^{17} hydrogen ions per milliliter of TCE.

In a subsequent section, the analysis of the radiation products is described. From this, it appears that 2 molecules of acid are formed from each molecule of acid chloride formed, and that the percentages of $(COCl)_2$, $COCl_2$, and CCl_3—COCl are 3–4%, 37–38%, and 59%, respectively.

Hence, 11.85×10^{17} molecules of acid chloride are formed per milliliter of TCE, and using the percentage analysis figures, the total number of acid chloride molecules liberated per milliliter of tetrachloroethylene is 0.35×10^{17} molecules $(COCl)_2 + 4.5 \times 10^{17}$ molecules of $COCl_2$ and 7.0×10^{17} molecules CCl_3COCl.

Therefore, the total number of oxygen molecules required to produce the products is 6.1×10^{17}.

No value for the oxygen content of an air-saturated solution of tetrachloroethylene is available in the literature. However, values for various related compounds, given in International Critical Tables (8), are tabulated below:

Can. J. Chem. Downloaded from www.nrcresearchpress.com by 190.90.36.8 on 09/04/12
For personal use only.

Compound	No. oxygen molecules per milliliter of air-saturated compound
CCl_4	1.2×10^{18}
$CHCl_3$	1.1×10^{18}
$C_2H_2Cl_4$	5.5×10^{17}
C_2Cl_4	4.8×10^{17}

together with a value for C_2Cl_4 obtained in a preliminary experiment done in these laboratories. It is in line with the values reported for similar compounds.

The above evidence suggests that the observed break in Figs. 1, 2, and 3 is due to oxygen depletion and that the radiolysis of tetrachloroethylene is essentially an oxidation reaction.

Identification of Reaction Products

Fifty milliliters of purified tetrachloroethylene was irradiated with gamma rays, a slow stream of oxygen being bubbled through to promote the yield of product. The solution was given a dose of about 10^3 r.

The irradiated solution had a pungent odor. On distillation the first 0.5–1 ml distilled at about 118° C (fraction 1). The bulk (fraction 2) distilled at 120–121° C, the boiling point of TCE, and retained to some extent the pungent odor. A residue of about 0.2 ml of a higher boiling fraction (fraction 3) remained. An attempt to find its boiling point resulted in some decomposition.

Infrared spectra were measured of pure tetrachloroethylene, irradiated tetrachloroethylene, and fractions 1, 2, and 3.

Irradiated tetrachloroethylene showed an additional band of low intensity at 1800 cm^{-1}, characteristic of the C=O of an acid chloride (9). Fraction 1 gave a sharper, much enhanced, band at 1810 cm^{-1} and also a strong band at 830 cm^{-1}, the C–Cl region of an acid chloride. In addition, a weak band appeared at 1650 cm^{-1}, which was tentatively ascribed to a C=C linkage. The spectrum of fraction 3 was identified as that of a trichloroacetic acid – tetrachloroethylene mixture.

It was concluded that the main chemical reaction taking place on irradiation of an oxygen–tetrachloroethylene solution was an oxidation to acid chlorides. Part of the acid chloride has been hydrolyzed to trichloroacetic acid, presumably by traces of H_2O which may have been present in the O_2 supply. One of the acid chlorides is trichloroacetyl chloride.

In order to identify any other acid chlorides which may have been present, 50 ml of irradiated tetrachloroethylene was reacted with excess primary amine and the reaction products isolated and identified as far as possible by comparing their melting points and infrared spectra with those of specimens of pure compounds. The method used for the working up of the products of reaction with aniline is shown in Table IV.

The compounds isolated from the reaction in this manner of aniline and *p*-toluidine respectively were aniline hydrochloride, trichloroacetanilide, N,N′-diphenylurea, oxanilide, and the corresponding *p*-toluidine derivatives. Unidentified derivatives of aniline and *p*-toluidine having m.p.'s of 137 and 179° C, respectively, were also obtained. The data available suggest that they were derived from the same compound. For the aniline derivative, empirical formula $C_{16}H_{14-16}N_2O$, infrared spectra indicates N—H, C—H aromatic, C=N, a monosubstituted phenyl —X, a carbonyl linkage 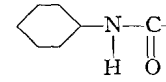 ·Cl is absent.

Can. J. Chem. Downloaded from www.nrcresearchpress.com by 190.90.36.8 on 09/04/12
For personal use only.

TABLE IV

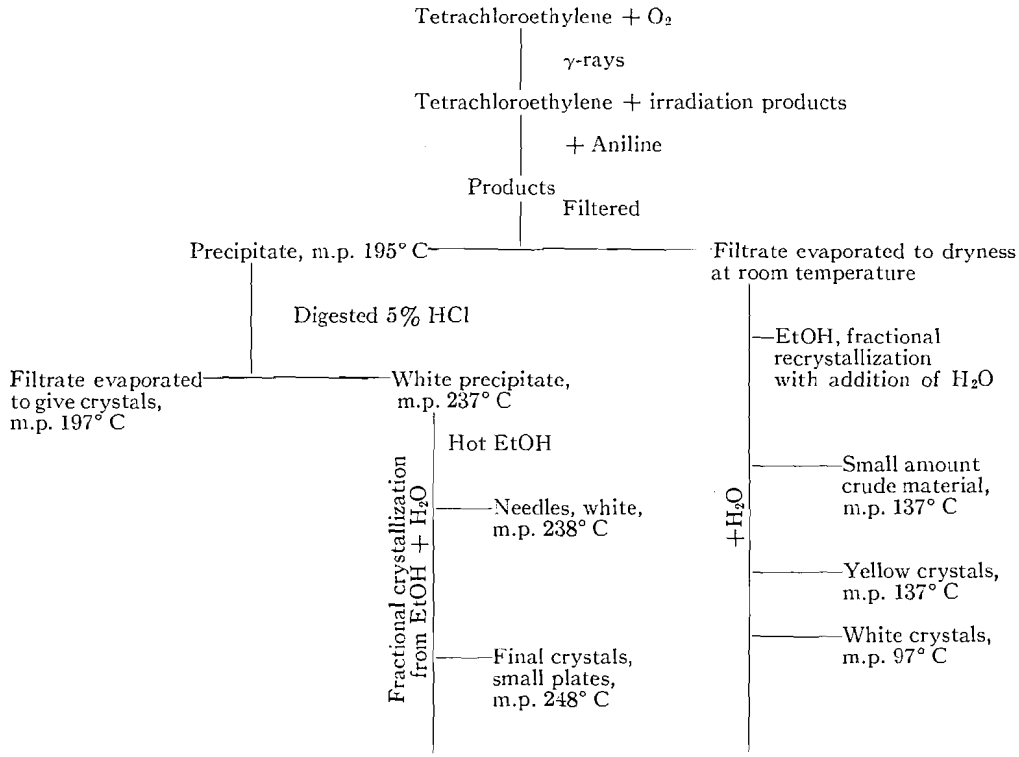

One possible formula* is: 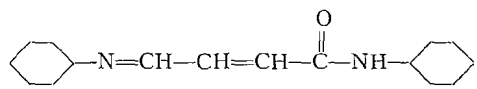
and it is probable that the precursor is a 4-carbon molecule formed in the radiation reaction.

Identification of Acids Formed on Hydrolysis

The irradiated solution was extracted with water and the water phase separated and evaporated to dryness at room temperature. Crystals were obtained, m.p. 54° C (trichloroacetic acid, m.p. 57–58° C). Evaporation must be at a low temperature, since in hot water or basic solution (10) trichloroacetic acid decomposes in the manner, $CCl_3COOH \rightarrow CO_2 + CHCl_3$.

The crystals, on being shaken with concentrated aqueous ammonia containing Cu_2Cl_2, gave a dark blue color instantly. This is characteristic of trichloroacetic acid (10), though similar behavior is exhibited by dichloroacetic acid. Aqueous hydrolysis of $COCl_2$ and $(COCl)_2$ yields only hydrochloric acid (10). No oxalic acid is formed, although vapor-phase hydrolysis of $(COCl)_2$ is said to yield some.

$$COCl_2 + H_2O \rightarrow CO_2 + 2HCl,$$
$$(COCl)_2 + H_2O \rightarrow CO + 2HCl + CO_2.$$

Quantitative Determination of Products

The three main reactions which yield acidic products in the irradiation of TCE are:

**Suggested by Dr. R. A. Abramovitch.*

Can. J. Chem. Downloaded from www.nrcresearchpress.com by 190.90.36.8 on 09/04/12
For personal use only.

$$CCl_3C(=O)Cl + H_2O \rightarrow CCl_3COOH + HCl, \quad [1]$$

$$COCl_2 + H_2O \rightarrow CO_2 + 2HCl, \quad [2]$$

$$(COCl)_2 + H_2O \rightarrow CO + CO_2 + 2HCl. \quad [3]$$

About 30 ml of TCE + 5 ml H_2O (to trap the phosgene) were irradiated for 3 days. A stream of oxygen was bubbled through during the irradiation. The irradiated mixture was extracted three times with water (about 30-ml portions each time) over a period of 24 hours. The water layer was separated and its acid content determined by titrating 5-ml samples with standard alkali to pH 4 using screened methyl orange as indicator. The chloride content of the sample was estimated by titration of 5-ml samples, which had been neutralized by NaOH (phenolphthalein as indicator), with standard $AgNO_3$ solution using dichlorofluorescein as an indicator. The amount of HCl expressed as a percentage of the total acid was 70.5. Hence:

acidity due to $CCl_3COOH = 29.5\%$,
acidity due to $CCl_3COCl = 59\%$,
acidity due to $COCl_2 + (COCl)_2 = 41\%$.

Since CCl_3COCl, $COCl_2$, and $(COCl)_2$ all yield 2 molecules of acid per molecule of acid chloride, the percentages of the acid chloride formed in the irradiation of TCE are 59% CCl_3COCl and 41% ($COCl_2$ + $(COCl)_2$).

Determination of $COCl_2$ *and* $(COCl)_2$ *Content*

Since these two compounds behave very similarly chemically, it is difficult to estimate the composition of a mixture of them by chemical means. However, under experimental conditions phosgene ($COCl_2$) is a gas, b.p. 8° C, and oxalyl chloride a liquid, b.p. 62° C, and therefore the mixture should be readily separable by refluxing. Approximately 30 ml of TCE was irradiated, with O_2 bubbling through, for 5 days. Ten milliliters of solution was refluxed for 2 hours to distill off the phosgene, the remaining acid chlorides hydrolyzed, and the percentage chloride of the total acid content determined. The value obtained was 51.4%. A second sample, which was refluxed for 45 minutes, gave 52.0%. Taking the HCl content of the solution as 52%, then 96% of the acidity is due to hydrolysis of CCl_3COCl and 4% due to oxalyl chloride. Hence, since originally a sample of irradiated TCE contained 59% trichloroacetyl chloride, the true percentage of oxalyl chloride in a sample of irradiated TCE is $59/96 \times 4 = 3\%$. While no great accuracy is claimed for this figure it does indicate that oxalyl chloride is found in relatively small amounts and that the main reaction products are: CCl_3COCl (59%), $COCl_2$ (37–38%), and $(COCl)_2$ (3–4%). An implicit assumption in these calculations has been that the same fraction of each acid chloride is formed irrespective of dose received.

DISCUSSION

G Values

G_{H^+} values were calculated, assuming that acidic products are formed only as the result of energy absorbed by the tetrachloroethylene phase.

At the water–tetrachloroethylene interface there may be some reaction by H and OH radicals from the radiolysis of water. These reactions may lead to acidic products, but such reactions will probably not produce long chains, and in these circumstances their effect will be negligible.

Can. J. Chem. Downloaded from www.nrcresearchpress.com by 190.90.36.8 on 09/04/12
For personal use only.

Because of the influence of oxygen depletion in the solution, and the presence of an apparent induction period, G values are taken from the slopes of the straight lines in Fig. 2. From the analysis figures found for the relative amounts of CCl_3COCl (59%), $COCl_2$ (39%), and $(COCl)_2$ (3%), the following G values can be calculated (Table V).

TABLE V

Tetrachloroethylene extracted with $CaCl_2$ and H_2O

(Samples, 3 ml air-equilibrated tetrachloroethylene overlayered with 2 ml water)

(*a*) Tetrachloroethylene extracted with $CaCl_2$ (24 hours) redistilled	(*b*) Tetrachloroethylene extracted with H_2O (about one month), dried over $CaCl_2$, and redistilled
$G_{(H^+)} = 2250$	$G_{(H^+)} = 12{,}600$
G (acid chloride) = 1125	G (acid chloride) = 6300
G (CCl_3COCl) = 660	G (CCl_3COCl) = 3700
G ($COCl_2$) = 430	G ($COCl_2$) = 2400
G ($(COCl)_2$) = 34	G ($(COCl)_2$) = 190
G (C_2Cl_4) = 910	G (C_2Cl_4) = 5000
G (O_2) = 570	G (O_2) = 3240

One question arises which the present experimental data cannot settle, viz., is the production of oxalyl chloride a primary oxidation product or is it a secondary product resulting from radiolysis of CCl_3COCl or $COCl_2$?

The large G $(COCl)_2$ value, 190, suggests that $(COCl)_2$ is a primary oxidation product. (N.B. In these calculations of G values we have assumed that we can extrapolate analysis data from a sample which had been given a dose of 1000 kr with O_2 bubbling to the dose range being studied, viz., about 1 kr.) The final concentration of acid chloride reached in the 1000-kr run was 0.16 molar $\equiv$ 4.3% conversion on a mole basis.

Radical Yields

Radical yields G_R for several organic liquids have been measured. Chapiro *et al.* (11) find values of G_R for CCl_4 and $CHCl_3$ of about 70 and 60, respectively, using the D.P.P.H. method. Schulte (12), using tagged Cl_2 in CCl_4, finds a value for G_R as $\lesssim 3.5$.

If we assume that G_R for C_2Cl_4 is between 60 and 3.5, and assume each radical initiates a chain reaction leading to acidic products (see later this section) approximate values for kinetic chain lengths can be derived, e.g., for systems (*a*) and (*b*) Table V. We have: $G_{H^+} = 2250$, kinetic chain length between 34 and 650; $G_{H^+} = 12600$, kinetic chain length between 210 and 3600.

Tetrachloroethylene Dosimeters

The radiation reaction in a tetrachloroethylene air-equilibrated solution has been shown to be an oxidation reaction, and there will be a limiting value to the dose which can be measured by a dosimeter consisting of tetrachloroethylene overlayered with water. From our results this limiting value will correspond to a maximum value of 3.94 meq $\times 10^{-3}$ per ml TCE of acid liberated. A typical value for the rate of acid production in a stabilized two-phase tetrachloroethylene dosimeter is 0.05 meq $\times 10^{-6}$ per ml per r (1). Hence, for a system of this particular sensitivity, one would expect that for doses greater than 80 kr, this system would lose its sensitivity (provided no oxygen has diffused into the tetrachloroethylene phase during irradiation).

Our work emphasizes the observation by Taplin (1) that, after exposure of the dosimeter, vigorous shaking over a period of time is required to bring about complete extraction of acidic products.

Can. J. Chem. Downloaded from www.nrcresearchpress.com by 190.90.36.8 on 09/04/12
For personal use only.

Can. J. Chem. Downloaded from www.nrcresearchpress.com by 190.90.36.8 on 09/04/12
For personal use only.

Effect of Stabilizers

Certain reagents, notably alcohols and phenols, retard the radiation-induced reaction (1). Bailey (3, 4) has found that the photochemical oxidation of perchloroethylene is accelerated by I_2, slightly retarded by quinol, fairly well retarded by butyl-α-isobutyl alcohols, turpentine, benzaldehyde, resorcinol, naphthols, napthylamine, and sulphur, and well retarded by alcohol, ether, thymol, *o*-toluidine, sodium thiosulphate, and thiourea. He observes that in certain cases, e.g., quinol, benzaldehyde, resorcinol, diphenylamine, napthylamine, and the naphthols, the retarding agent caused development of color. This is interesting, since such reactions might be easily followed spectrophotometrically and might help in elucidating the chain propagating reactions or in development of a method of finding the radical yield in tetrachloroethylene.

Oxidation Reaction

The main reactions occurring in the radiolysis of tetrachloroethylene can be summarized thus:

$$C_2Cl_4 + \tfrac{1}{2}O_2 \rightarrow CCl_3COCl, \qquad [a]$$

$$C_2Cl_4 + O_2 \rightarrow 2COCl_2, \qquad [b]$$

$$C_2Cl_4 + O_2 \rightarrow (COCl)_2 + 2Cl. \qquad [c]$$

Reaction [*c*] is non-stoichiometric, there being a loss of 2 atoms of chlorine. This may appear in the system as molecular Cl_2 or C_2Cl_6. Such compounds have not been looked for, but other workers (13) have detected molecular Cl_2.

Reaction Mechanism

In the present system the oxygen concentration is about 0.002 molal and if it is assumed that the ease of ionization of O_2 and C_2Cl_4 is about the same, and that there is no preferential transfer of ionization or excitation energy to the O_2 molecules, then ionization and excitation will be mainly confined to the C_2Cl_4 molecules.

Both ionic and molecular species will be in a variety of excited states. The nature of the secondary processes ultimately leading to chemical reaction is still obscure, although theoretical evidence has been advanced showing that in a liquid charge neutralization occurs before the ions can react chemically (14, 15, 16). Ion molecule type reactions have also been proposed. Iodine scavenger studies (17) have shown that molecular decomposition processes occur in organic systems.

However, the chain characteristics of the oxidation reactions are such that initiation and propagation must be by free radicals. Molecular products can be assumed to be of negligible importance. These radicals probably arise from dissociation of excited molecules.

Because of its simplicity, changes in the excited tetrachloroethylene molecule are limited to rather few possibilities, e.g.

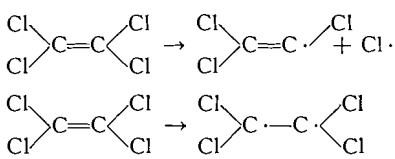

The formation of a diradical will be energetically more improbable, and hence as a result of the primary act we would anticipate the production of Cl· and C_2Cl_3· radicals.

Can. J. Chem. Downloaded from www.nrcresearchpress.com by 190.90.36.8 on 09/04/12
For personal use only.

Important in any radiation scheme is the spatial distribution of such radicals. Chapiro (5) has recently discussed the distribution of free radicals and is of the opinion that the over-all spatial distribution of free radicals is similar but not identical with the distribution of the ions.

In the radiolysis of C_2Cl_4, Cl and C_2Cl_3 radicals will be produced. Some of these radicals will recombine and react with each other yielding molecular products, possibly Cl_2 and C_4Cl_6 (hexachlorobutadiene). The yield of these products will be influenced by the rate of diffusion of radicals, the velocity constants of their reactions, and the presence and efficacy of any scavenger molecules present.

It is interesting to note that in a N_2-saturated system a value of G_{H^+} of $\backsim 4$ was obtained (Table III), whether pure tetrachloroethylene or stabilized tetrachloroethylene was used.

Thus we would anticipate that, in a tetrachloroethylene solution overlayered with water, acids will continue to be produced after exhaustion of the dissolved oxygen. However, the rate will be so low that it is not measurable under our conditions up to an absorbed dose of 20 kr.

With gamma radiation, where the clusters are widely separated, there will be little chance of radical–radical reactions from different tracks, and hence there will be a finite number of radicals escaping into the solvent from the clusters for a fixed amount of radiation absorbed.

These radicals can then interact with solvent molecules, C_2Cl_4, and solute molecules, O_2. The ensuing reactions will again be governed by: (*a*) rate of diffusion of radicals, (*b*) velocity constants of the reaction, and (*c*) concentration of solute and solvent molecules.

Pertinent to this work are the studies by Schumacher (18, 19) and co-workers, and Dickinson and co-workers (20, 21, 22) on the photochemical chlorine sensitized oxidation of tetrachloroethylene. The products of the oxidation reaction, isolated by them, were CCl_3COCl and $COCl_2$. The reaction was studied in the gas phase and in CCl_4 as solvent (21). Dickinson and Leermakers (20, 21) show that the products of oxidation, CCl_3COCl and $COCl_2$, undergo little or no further oxidation on prolonged exposure to light. In CCl_4 solution the rate of oxidation of C_2Cl_4 is independent of $[O_2]$ (provided the latter is not too low), proportional to the first power of the light intensity, and dependent on the chlorine concentration but only to the extent that the amount of chlorine affects the rate of energy absorption. The reaction rate varies to some extent with the tetrachloroethylene concentration and the temperature. A quantum yield of 1–2.5 moles of C_2Cl_4 oxidized per einstein is found.

In the gas phase (22), the rate of reaction has no strong dependence on the partial pressures of Cl_2, O_2, and C_2Cl_4. However, the reaction is much faster and quantum yields of 200–500 were found.

Schumacher (19) has also studied this reaction in the vapor phase and finds that approximately 80% of tetrachloroethylene is converted to CCl_3COCl and 20% to $COCl_2$, in agreement with Dickinson's figures. The phosgene content of the reaction product slowly increases with temperature. The over-all temperature coefficient is unity and the total pressure has little effect on the rate of reaction. The addition of alcohol strongly retards the reaction. With pure tetrachloroethylene he finds a quantum efficiency of 230 molecules of tetrachloroethylene per quantum at a temperature of 60° C and at 100 mm Cl_2, 200 mm O_2, and an absorbed intensity of 1.6×10^{12} hv/sec cc.

Possible Reaction Mechanisms in the Radiolysis of Air-equilibrated Tetrachloroethylene

From the foregoing one can postulate that the following chain mechanism is occurring in our system:

Initiation	$C_2Cl_4 \rightsquigarrow Cl + C_2Cl_3\cdot$	[1]
Propagation (I)	$Cl + C_2Cl_4 \rightarrow C_2Cl_5\cdot$	[2]
	$C_2Cl_5\cdot + O_2 \rightarrow C_2Cl_4O_2\cdot$	[3]
	$C_2Cl_5O_2\cdot \rightarrow CCl_3COCl + ClO$	[4*a*]
	or $\rightarrow 2COCl_2 + Cl$	[4*b*]
	$ClO + C_2Cl_4 \rightarrow CCl_2COCl + Cl$	[5*a*]
	or $\rightarrow COCl_2 + CCl_3\cdot$	[5*b*]
	$CCl_3\cdot + O_2 \rightarrow CCl_3O_2\cdot$	[6]
	$CCl_3O_2\cdot \rightarrow COCl_2 + Cl$	[7]
Propagation (II)	$C_2Cl_3\cdot + O_2 \rightarrow C_2Cl_3O_2\cdot$	[8]
	$C_2Cl_3O_2\cdot \rightarrow COCl_2 + COCl\cdot$	[9*a*]
	or $\rightarrow (COCl)_2 + Cl$	[9*b*]
	$COCl\cdot + C_2Cl_4 \rightarrow COCl_2 + C_2Cl_3\cdot$	[10]

Chain termination is probably by mutual destruction of radicals. Propagation step [2] can account for increased phosgene to trichloroacetyl chloride ratio found in the radiolysis reaction.

Other equally plausible mechanisms can be advanced based on the formation of epoxides (23, 24) or of the ClOO radical (cf. (25)). Further work in the absence of oxygen and using E.P.R. techniques might help to establish the mechanism.

ACKNOWLEDGMENT

Grateful acknowledgment is made to the National Research Council of Canada for the award of a Postdoctorate Fellowship to one of us (J.W.S.).

REFERENCES

1. Taplin, G. V. Radiation dosimetry. *Edited by* G. J. Hine and G. L. Brownell. Academic Press Inc., New York. 1956. Chap. 8.
2. Sigoloff, S. C. Nucleonics, **16** (No. 10), 54 (1956).
3. Bailey, K. C. J. Chem. Soc. 767 (1939).
4. Bailey, K. C. and Hickson, W. S. E. J. Chem. Soc. 145 (1941).
5. Chapiro, A. Radiation Research, **6**, 11 (1957).
6. Hummel, R. W., Van Cleave, A. B., and Spinks, J. W. T. Can. J. Chem. **31**, 1203 (1953).
7. Weiss, J., Allen, A. O., and Scharz, H. A. Intern. Conf. Peaceful Uses Atomic Energy, **14**, 179 (1956).
8. International Critical Tables. Vol. 3. McGraw-Hill Book Co., Inc., New York. 1928.
9. Bellamy, J. J. The infra-red spectra of complex molecules. Methuen & Co. Ltd., London. 1954.
10. Huntress, E. M. Organic chlorine compounds. John Wiley & Sons, Inc., New York. 1950.
11. Prevot-Bernas, A., Chapiro, A., Counsin, C., Laidler, T., and Magat, M. Discussions Faraday Soc. **12**, 98, 129 (1952).
12. Schulte, J. W. J. Am. Chem. Soc. **79**, 4643 (1957).
13. Schulte, J. W., Suttle, J. F., and Wilhelm, R. J. Am. Chem. Soc. **75**, 2222 (1953).
14. Collinson, E. and Swallow, A. J. Chem. Revs. **56**, 471 (1956).
15. Burton, M., Magee, J. L., and Samuel, A. H. J. Chem. Phys. **20**, 760 (1952).
16. Samuel, A. H. and Magee, J. L. J. Chem. Phys. **21**, 1080 (1953).
17. McCauley, C. E. and Schuler, R. H. J. Am. Chem. Soc. **79**, 4008 (1957).
18. Schumacher, H. J. Z. Elektrochem. **42**, 522 (1936).
19. Schott, C. and Schumacher, H. J. Z. physik. Chem. B, **49**, 107 (1941); Chem. Abstr. **38**, 3551 (1944).
20. Dickinson, R. C. and Leermakers, J. A. J. Am. Chem. Soc. **54**, 3852 (1932).
21. Dickinson, R. C. and Leermakers, J. A. J. Am. Chem. Soc. **54**, 4648 (1932).
22. Dickinson, R. C. and Carrico, J. L. J. Am. Chem. Soc. **56**, 1473 (1934).
23. Mayo, F. R., Miller, A. A., and Russel, G. A. J. Am. Chem. Soc. In press.
24. Twigg, G. H. Chem. Eng. Sci. Suppl. **3**, 5 (1954).
25. Porter, G. and Wright, F. J. Discussions Faraday Soc. **14**, 23 (1953).

Can. J. Chem. Downloaded from www.nrcresearchpress.com by 190.90.36.8 on 09/04/12
For personal use only.

Can. J. Chem. Downloaded from www.nrcresearchpress.com by 190.90.36.8 on 09/04/12
For personal use only.

THE HEAT AND ENTROPY OF ASSOCIATION OF THE COMPLEX IONS FORMED BY EDTA WITH THE LANTHANIDE ELEMENTS IN AQUEOUS SOLUTION[1]

R. H. Betts and Olive F. Dahlinger

ABSTRACT

A radio tracer method has been used to measure the heat and entropy of association of all the lanthanide ions (except promethium) with the chelating agent EDTA. Entropy terms are largely responsible for the remarkable stability of these complex ions. The results suggest, but do not prove, that a change in configuration of the complex occurs after gadolinium (element 64).

INTRODUCTION

All of the trivalent lanthanide ions in aqueous solution form very robust 1:1 complexes with the chelating agent ethylenediamine tetraacetic acid (EDTA). Wheelwright *et al.* (1) found the association constant K for the complex in 0.1 M potassium chloride to increase with atomic number, rising from 5×10^{14} for lanthanum (element 57) to 1.2×10^{19} for lutetium (element 71). The *average* difference between association constants for successive members of this group is 2.4. However a "plateau" occurs in the region Eu–Gd, for which $K_{Eu} = 4.9\times10^{16}$ and $K_{Gd} = 5\times10^{16}$. Beyond gadolinium, the interval between the association constants opens out again.

These authors suggest, as an explanation for this plateau, that the progressively smaller radii of the lanthanide ions in the series from La to Lu imposes increasing steric hindrance on the interaction between EDTA and the ion; they also suggest that for the series La to Gd, EDTA exerts its maximum chelating effect, all six groups (four carboxyls and two amino nitrogens) being co-ordinated to the metal ion. After Gd, only five of the chelating groups can fit around the central ion, leaving 1 molecule of water still attached. The evidence of Moeller *et al.* (2), however, suggests that Nd^{3+} is probably penta-co-ordinated by EDTA rather than 6 co-ordinated. A change in co-ordination after Gd would then be from penta-co-ordination to tetra-co-ordination, rather than from 6- to 5- as proposed by Wheelwright.

If such changes in co-ordination occurred, then on the basis of Cobble's discussion of the entropy of complex ions (3), one might expect significant differences in the entropy of formation of the complex ions of the two groups. The only experimental information available relating to the heat and entropy changes in these systems is given in an earlier paper from this laboratory (4). It was shown there that the difference in the heats of reaction for the systems

$$La^{3+} + X^{-4} \leftrightharpoons LaX^{-} \qquad [1]$$

and

$$Nd^{3+} + X^{-4} \leftrightharpoons NdX^{-} \qquad [2]$$

was zero (X^{-4} represents the fully ionized form of EDTA). Moreover, the differences in the entropies of formation of LaX^{-} and NdX^{-} appeared to be satisfactorily related to the differences in the partial molal entropies of the hydrated cations.

[1]*Manuscript received September 18, 1958.*
Contribution from the Research Chemistry Branch, Atomic Energy of Canada Limited, Chalk River, Ontario. Issued as A.E.C.L. No. 720.

The present paper records the application of a radiochemical technique, described in ref. 4, to measurements of the relative stability, as a function of temperature, of the complex ions of EDTA with all the lanthanide elements except element 61. The object of the measurements was to provide further quantitative data on those factors which determine differences in stability among the members of this group of elements. In particular, heat and entropy changes which occur on formation of the complexes have been evaluated. The results also provide an independent confirmation of earlier isothermal measurements of the stability of these complex ions (1).

The method used depends on measurement of the position of equilibrium in the system:

$$R_1X^- + R_2^{3+} \leftrightharpoons R_2X^- + R_1^{3+} \qquad [3]$$

where R_1 and R_2 represent different lanthanides. The equilibrium constant $K_{1,2}$ for reaction [3] is

$$K_{1,2} = (R_2X^-)(R_1^{3+})/(R_1X^-)(R_2^{3+}).$$

The association constant K_1 for formation of the complex ion R_1X^- may be written as:

$$K_1 = (R_1X^-)/(R_1^{3+})(X^{-4})$$

corresponding to the equilibrium:

$$R_1^{3+} + X^{-4} \leftrightharpoons R_1X^-.$$

A similar relation can be written for the association constant K_2 for the formation of R_2X^-. Clearly, $K_{1,2} = K_2/K_1$; measurement of the position of equilibrium in reaction [3] gives therefore the *ratio* of the stability constants for the formation of the two complex ions concerned. Similarly, the thermodynamic quantities $\Delta F^\circ_{1,2}$, $\Delta H^\circ_{1,2}$, and $\Delta S^\circ_{1,2}$ of reaction [3] are simply related to the corresponding quantities for the formation of the complex ions. Thus, for element 1:

$$\Delta F^\circ_1 = -RT \ln K_1 = \Delta H^\circ_1 - T\Delta S^\circ_1;$$

for the element 2:

$$\Delta F^\circ_2 = -RT \ln K_2 = \Delta H^\circ_2 - T\Delta S^\circ_2,$$

$$\Delta F^\circ_{1,2} = -RT \ln K_{1,2} = -RT \ln K_2/K_1 = (\Delta H^\circ_2 - \Delta H^\circ_1) - T(\Delta S^\circ_2 - \Delta S^\circ_1),$$

whence

$$\Delta F^\circ_{1,2} = \Delta F^\circ_2 - \Delta F^\circ_1,$$
$$\Delta H^\circ_{1,2} = \Delta H^\circ_2 - \Delta H^\circ_1,$$

and

$$\Delta S^\circ_{1,2} = \Delta S^\circ_2 - \Delta S^\circ_1.$$

Evidently the enthalpy and free energy of formation for a single lanthanide–EDTA system can be calculated from the equilibria including two lanthanides, provided these quantities are available for one of them. The results in this paper have been normalized using the value of $-21{,}890$ calories, for ΔF_{Nd}, from the results of Wheelwright *et al.* (1). Their value was measured at 20° C, but has been adjusted to 25° using $\Delta H_{Nd} = -800$ cal/mole, a value obtained in this present work. For our single normalizing value of ΔH, we are indebted to Dr. R. W. Attree of these laboratories. Using a Tian–Calvet calorimeter recently described (5) reaction [1] above was found to be exothermic, $\Delta H_{La} = -800 \pm 20$ cal per mole. As will be seen below the discussion of the results depends primarily on the *differences* among the lanthanides, so that errors associated with the normalizing values ΔF_{Nd} and ΔH_{La} will have no serious consequences.

Can. J. Chem. Downloaded from www.nrcresearchpress.com by 190.90.36.8 on 09/04/12
For personal use only.

Can. J. Chem. Downloaded from www.nrcresearchpress.com by 190.90.36.8 on 09/04/12
For personal use only.

EXPERIMENTAL

Materials

The lanthanide chlorides, with the exception of cerium, were prepared by dissolving a weighed amount of oven-dried (110° C) oxide in a slight excess of hydrochloric acid. The excess acid was removed by several evaporations to near dryness, after which the material was made up to a known volume in water. The oxide formula was taken to be R_2O_3 for all of the lanthanides except for praeseodymium (Pr_6O_{11}) and terbium (Tb_4O_7). Cerium chloride was prepared by dissolving CeO_2 in a mixture of sulphuric acid and hydrogen peroxide. The trivalent hydroxide was then precipitated with ammonia, washed several times, and then redissolved in hydrochloric acid. The resulting solution was taken to near dryness several times, and finally dissolved in a known volume of water.

The oxides of La, Pr, Nd, Sm, Eu, Gd, Tb, Ho, Er, and Tm were purchased from Lindsay Chemical; the analyses supplied indicated a chemical purity of 99.8% or better. The cerium was Johnson–Matthey "spec-pure" CeO_2. Dy, Yb, and Lu were provided as 99.8% pure oxides by courtesy of the Ames Laboratory of the U.S.A.E.C.

The solutions prepared in this way were used, except for Nd, without further standardization. The Nd stock solution was standardized by titrating aliquots with versene (the disodium salt of EDTA) in the presence of calcium, using eriochrome black T as an indicator for the end point. This method, which is adopted from a procedure described by Cheng *et al.* (6), uses calcium carbonate as a primary standard.

EDTA was purified by recrystallization of the acid H_4X from a water solution of the disodium salt. The insoluble acid was washed, dried at 105° C, and samples assayed in the presence of excess calcium chloride by titration with standard sodium hydroxide. The pH was monitored with a Beckman model G glass electrode assembly. An aqueous stock solution of EDTA, fully neutralized with potassium hydroxide, was prepared from this purified and standardized material.

The radio tracers used in the analytical scheme (see below) were 11.6-day Nd^{147}, $Yb^{169,175}$ (30-day and 4.2-day), and 72-day Tb^{160}. These were prepared by neutron irradiation in the NRX reactor of the corresponding pure oxides. The steps taken to establish the radiochemical purity of the neodymium and ytterbium activities have been described previously (4, 7). The radioactive decay of Tb^{160} was followed for 7 months (three half-lives) and showed no indication of extraneous radio nuclides. A half-life of 72.8±0.1 days was observed. Values of 72.3-day (8) and 73.0-day (9) have been recorded in the literature.

Procedure

Solutions for which equilibrium measurements were made were 0.10 *M* in potassium chloride and 0.01 *M* in ammonium acetate. The KCl was added to maintain the solutions at constant ionic strength, and also to make the results directly comparable with those of Wheelwright *et al.* (1). Ammonium acetate was added to ensure that all comparable experiments were made at the same pH (5.3±0.1). Doubly distilled water was used throughout this investigation.

Solutions were prepared containing known amounts of two lanthanides, together with a known concentration of K_4X. Conditions were so chosen that the concentration of the chelating agent (2×10^{-4} *M*) was never more than 50% of the sum of the concentrations of the two lanthanides present ($4-12\times10^{-4}$ *M*). Under these conditions, all of the EDTA was present at equilibrium either as R_1X^- or R_2X^-; the concentrations of the species H_4X, H_3X^-, .../X^{-4} etc. being negligible in comparison.

TABLE I
Summary of equilibrium constants at various temperatures

Lanthanide pair	0°	25.7°	35.2°	ΔH, cal/mole	$K_{25°}$
	Series A. Comparisons with terbium				
(TbX)(Sm)/(Tb)(SmX)	4.25	6.53	7.08		
	4.20	6.20	6.59	+2300	6.16±0.10
	4.38	6.43	6.93	(130)	
(TbX)(Eu)/(Tb)(EuX)	3.34	4.36	4.57	+1660	4.51±0.10
	3.43	4.74	5.04	(190)	
	3.66	4.80	5.06		
(TbX)(Gd)/(Tb)(GdX)	2.38	3.64	2.97		
	2.80	3.29	3.45	+1070	3.15±0.13
	2.72	3.18	3.17	(330)	
(TbX)(Dy)/(Tb)(DyX)	.344	.326	.355	0	
	.320	.338	.326	(190)	0.344±.008
	.351	.366	.360		
(TbX)(Ho)/(Tb)(HoX)	.175	.186	.183		
	.183	.190	.200	+250	
	.180	.190	.182	(120)	.187±.003
(TbX)(Er)/(Tb)(ErX)	.083	.084	.090		
	.090	.092	.091	0	
	.090	.088	.085	(150)	0.088±.002
	Series B. Comparisons with neodymium				
(NdX)(La)/(Nd)(LaX)	7.4*	7.2*	7.2*	0	7.2±0.1
(NdX)(Ce)/(Nd)(CeX)	4.16	3.78	3.92	−330	
	4.31	4.11	3.86	(140)	4.01±0.06
	(4.62)	4.05	4.10		
(NdX)(Pr)/(Nd)(PrX)	1.96	1.84	2.00		
	1.99	1.91	1.91	0	
	(2.24)	2.04	1.97	(150)	1.95±0.03
(NdX)(Sm)/(Nd)(SmX)	.332	.342	.332		
	.327	.335	.335	0	
	(.309)	.326	.336	(60)	0.333±0.002
	Series C. Comparisons with ytterbium				
(YbX)(Ho)/(Yb)(HoX)	7.69	8.28	8.50		
	8.29	8.34	8.37	+230	
	(9.16)	8.29	8.25	(100)	8.28±0.09
(YbX)(Er)/(Yb)(ErX)	4.66	4.56	4.72		
	4.96	4.50	4.57	−340	
	4.85	4.20	4.36	(160)	4.54±0.09
(YbX)(Tm)/(Yb)(TmX)	2.37	2.23	2.28		
	2.43	2.14	2.21	−360	
	2.32	2.14	2.19	(110)	2.23±0.03
(YbX)(Lu)/(Yb)(LuX)	.634	.703	.755		
	.672	.709	.771	+680	
	.655	.692	.772	(110)	.720±.010

Values of the equilibrium constants enclosed in parentheses were not used in the calculations. The probable errors in the ΔH values in column five are indicated by parentheses.
*Data for the La–Nd system from ref. 4.

The appropriate tracer was prepared as an aqueous solution of RCl_3, and added to each equilibrium solution concurrently with the other components of the systems.

Three aliquots were taken from each solution, one of which was allowed to reach equilibrium at 0° C, the second at 25.7° C, and the third at 35.2° C. After equilibrium had been reached (as judged by analysis on successive days*), three samples for each

**In some cases, particularly those involving the heavier lanthanides at 0° C, equilibrium was attained only after several weeks. This is not unexpected, since earlier work (4) has shown that the rate of dissociation of* RX^{-} *ions in aqueous solution at pH 5.3 is very slow.*

Can. J. Chem. Downloaded from www.nrcresearchpress.com by 190.90.36.8 on 09/04/12
For personal use only.

temperature were taken for determination of the position of equilibrium (see below). Each lanthanide pair was studied at three different values of the ratio R_1Cl_3/R_2Cl_3 (1:1, 2.5:1, and 5:1), so that in all nine measurements of the position of equilibrium (three sets in triplicate) were obtained at each temperature for each pair of elements examined. Altogether about 300 such measurements were made in the present study.

The pH of the equilibrium systems was measured in every case, and was found to be 5.3 ± 0.1.

The position of equilibrium in each system was calculated from the distribution of a radioactive tracer for one of the lanthanide ions between the forms R^{3+}_{aq} and RX^{-}. The cationic form is held quantitatively on a short Dowex 50 cation resin column, while the form RX^{-}, being anionic, passes through to the effluent. The relative amounts of the element R in the anionic or cationic form were calculated from the radioactivity in the effluent relative to that in the original solution. Further details of this technique, and of the methods of radioassay used are given in ref. 4.

Tb^{160} was used in the first series of experiments, in which the lanthanides Sm, Eu, Gd, Dy, Ho, and Er were compared with Tb. Nd^{147} was used in the second series, in which Nd was compared with La, Ce, Pr, and Sm. $Yb^{169,175}$ was used as the tracer in the last series, involving comparisons of Ho, Er, Tm, and Lu with Yb.

TABLE II

Comparison of association constants for formation of lanthanide–EDTA complex ions

$T = 25.0°$ C $\qquad\qquad$ $\mu = 0.1$ (KCl)

R	This work	Ref. 1	R	This work	Ref. 1
La	1.56×10^{15}	0.51×10^{15}	Tb	207×10^{15}	190×10^{15}
Ce	2.79	2.4	Dy	602	390
Pr	5.74	5.5	Ho	1107	500
Nd	(11.2)	(11.2)	Er	2350	1000
Sm	33.6	35	Tm	4450	4100
Eu	45.9	49	Yb	9920	5000
Gd	65.7	50	Lu	13800	12000

RESULTS

The experimental results are summarized in Table I. The first column in the table identifies the lanthanide pair, and defines the form of the equilibrium constant. The second, third, and fourth columns list the experimental values at 0° C, 25.7° C, and 35.2° C, respectively, of the equilibrium constant defined in column one. Three values for each temperature are recorded, and represent the results of separate experiments for different concentration ratios of the lanthanide pair. The fifth column gives the value of the enthalpy change (ΔH) for the equilibrium. These values of ΔH are calculated in each case by a least squares fit of the data to the relation:

$$\log K = -(\Delta H/2.303\,RT) + \text{constant}. \qquad [4]$$

Least squares analyses were also used to calculate the probable errors in the ΔH terms; the appropriate uncertainties are given in parentheses in column 5. The final column gives the value of K at 25.0° C, calculated from the appropriate form of equation [4] above. The probable errors indicated for K in this column were also calculated by least squares analyses.

Can. J. Chem. Downloaded from www.nrcresearchpress.com by 190.90.36.8 on 09/04/12
For personal use only.

Thermodynamic Quantities for Each Lanthanide–EDTA System

The results of Table I have been normalized to yield values for changes in the free energy ($\Delta F°$), entropy ($\Delta S°$), and enthalpy ($\Delta H°$) involved for each lanthanide–EDTA system.

(*a*) *Normalization of the $\Delta F°$ Terms*

The value of 1.12×10^{16} for the equilibrium constant for the NdX–Nd system at 25° C has been taken from the work of Wheelwright *et al.* (1). Thus the value of K_{La}, from the results in Table I, is therefore

$$1.12\times10^{16}/7.2 = 1.56\times10^{15},$$

while that for K_{Sm} is

$$1.12\times10^{16}/0.333 = 3.36\times10^{16}.$$

The result for Tb is then calculated from that for Sm, and the values for Eu, Gd, Dy, Ho, and Er are then calculated relative to Tb. The value for K_{Yb} is calculated by comparison with both K_{Ho} and K_{Er} and finally the values of K_{Tm} and K_{Lu} are calculated relative to that of K_{Yb}. The results of these comparisons are shown in Table II. Column two of Table III gives the same results expressed in calories per mole at 25.0° C. The free energy change $\Delta F°$ has been calculated from the relation $\Delta F° = -RT \ln K$.

(*b*) *Normalization of the $\Delta H°$ Terms*

The reaction: $La^{3+} + X^{-4} \leftrightharpoons LaX^{-}$ is found to be exothermic (see Introduction) and $\Delta H_{La} = -800$ cal per mole. The equilibrium constant for the La–Nd system is independent of temperature and therefore ΔH_{Nd} is also -800 cal per mole. Equilibria in the systems Nd–Pr and Nd–Sm are also temperature independent, and this implies that $\Delta H_{La} = \Delta H_{Pr} = \Delta H_{Nd} = \Delta H_{Sm} = -800$ cal per mole.

The value of ΔH for the Tb–Sm system is $+2300$ cal per mole, which leads to a value of $+1500$ cal per mole for the Tb system. (See the appropriate equations in the Introduction, where $\Delta H°_2 = -800$ cal, $\Delta H°_{1,2} = +2300$ cal, and $\Delta H°_1 = (2300-800) = +1500$ cal per mole.)

Proceeding in this way, the value of ΔH for each lanthanide–EDTA system was calculated; the results are listed in column three of Table III.

TABLE III

Thermodynamic quantities for the formation of lanthanide–EDTA complex ions at 25° C

Lanthanide	$\Delta F°$, cal/mole	$\Delta H°$, cal/mole	$\Delta S°$, cal/mole/° C
La	−20,720	− 800*	66.8
Ce	−21,070	− 470	69.1
Pr	−21,490	− 800	69.4
Nd	−21,890*	− 800	70.7
Sm	−22,540	− 800	72.9
Eu	−22,720	− 160	75.7
Gd	−22,940	+ 430	78.4
Tb	−23,620	+1500	84.3
Dy	−24,250	+1500	86.3
Ho	−24,610	+1250	86.7
Er	−25,060	+1500	89.1
Tm	−25,440	+1580	90.6
Yb	−25,910	+1320	91.3
Lu	−26,110	+ 640	89.7

*Normalizing values (see text).

Can. J. Chem. Downloaded from www.nrcresearchpress.com by 190.90.36.8 on 09/04/12
For personal use only.

The entropy change accompanying complex formation was calculated directly from the relation

$$\Delta F^\circ = \Delta H^\circ - T\Delta S^\circ, \text{ for } T = 298.1^\circ \text{ K.}$$

These values are given in column four of Table III.

Precision of the Derived Results

Table I shows that the probable error in the enthalpy change for each lanthanide pair lies between 60 and 330 calories, the average uncertainty in this quantity being ±150 calories. The equilibrium constants listed in Table I appear to be precise to ±2%. However, the method of intercomparison used to deduce the thermodynamic quantities for each lanthanide–EDTA system inevitably causes a carry-over and multiplication of these errors. Assuming a coefficient of variation of ±2% in every ratio given in Table I, then (relative to K_{Nd}, for which no error need be assigned) K_{Sm} is in doubt by ±3%, as are the values for K_{La}, K_{Ce}, and K_{Pr}. The Tb value relative to K_{Sm} is precise to ±2%, but relative to K_{Nd}, it is precise to $\sqrt{(3^2+2^2)} \cong \pm 4\%$. The further stages of intercomparison give rise to a maximum uncertainty in the values of K_{Lu} and K_{Tm}, *relative to* K_{Nd}, of ±6%.

The uncertainty in ΔF°, relative to ΔF° for Nd, then varies from ±10 cal per mole for La, to ±35 cal per mole for Lu and Tm.

The uncertainty of ±150 cal per mole for each value of ΔH listed in Table I leads in a similar way to a maximum uncertainty of ±370 cal for ΔH°_{Lu}, again relative to the value of −800 cal per mole for the normalizing value of ΔH°_{La}. The relative uncertainty between ΔH values for adjacent lanthanides is about ±210 cal per mole.

These errors in both ΔF° and ΔH° are reflected in the precision of the ΔS° terms; the values for this quantity listed in the last column of Table III are thought to be precise to ±2.0 e.u.

DISCUSSION

A comparison of the present results at 25° C with those of Wheelwright *et al.* (1) is shown in Table II. The two sets of data have been normalized to give agreement at K_{Nd}. In addition, the earlier results have been adjusted to 25° C from 20° C, using the appropriate ΔH values listed in Table III. The largest adjustments required (5.7%) are in the K values for Tb to Yb, inclusive.

The errors quoted for the K values in ref. 1 vary from a minimum of ±15%, in the region from La to Sm, and gradually increase to reach ±250% at Lu. Generally speaking, with the possible exception of the values for K_{La}, the two sets of data are in reasonable agreement. However, the present results are thought to be considerably more precise than the previously published measurements.

The results in Table III show very clearly that the remarkable stability of these complex ions is due almost entirely to the large increase in the entropy of the system when the complex is formed. The differences in stability among the complex ions are also in large measure due to the entropy terms, although in some cases, both ΔH and ΔS terms contribute appreciably in this respect.

The results in Table III may be used, with reservations, to calculate the *relative* partial molal entropies of the complex ions themselves. For this purpose it is convenient to consider the relation between the observed entropy change, ΔS°, and the conventional partial molal entropies, $\bar{S}^\circ$, of the species concerned. Thus for the reaction:

Can. J. Chem. Downloaded from www.nrcresearchpress.com by 190.90.36.8 on 09/04/12
For personal use only.

$$R^{3+}_{aq} + X^{-4} \rightleftharpoons RX^{-}$$

$$\Delta S^\circ = \bar{S}^\circ_{RX^-} - \bar{S}^\circ_{R^{3+}} - \bar{S}^\circ_{X^{-4}},$$

and

[5] $$(\Delta S^\circ + \bar{S}^\circ_{R^{3+}}) = \bar{S}^\circ_{RX^-} - \bar{S}^\circ_{X^{-4}}.$$

For a series of lanthanide–EDTA systems, the left hand side of equation [5] provides a *relative* measure of $\bar{S}^\circ_{RX^-}$, since the term $\bar{S}^\circ_{X^{-4}}$ is common. To make such comparisons, it is necessary to know the appropriate value of $\bar{S}^\circ_{R^{3+}}$, in addition to the experimental quantity ΔS°. Unfortunately, no experimentally based values of $\bar{S}^\circ_{R^{3+}}$ are available, and it is necessary to calculate these quantities for semiempirical formulae.

The two most generally accepted equations for calculation of $\bar{S}^\circ$ terms for aqueous ions are due to Powell and Latimer (10) and, more recently, to Laidler (11). Both equations provide a good fit to a large assembly of experimental information. In the following, both formulae are used to calculate the partial molal entropies of the lanthanide cations. The fundamental parameter required by both equations is the radius of the ion. The recent measurements of Dauben and Templeton (12) are particularly suitable in this connection, since as these authors observe, the radii have been estimated with sufficient precision to permit meaningful comparison of the properties of the lanthanides which depend on this parameter.

Table IV summarizes the results of these calculations. The data in columns 2 and 3 depend on the Powell–Latimer equation, while the last two columns are derived from the Laidler equation. The latter treatment gives results for $\bar{S}^\circ$ which are slightly more

TABLE IV

Relative partial molal entropy of the complex ions RX^-

	Ref. 10		Ref. 11	
R	$-\bar{S}^\circ_{R^{3+}}$	$(\Delta S^\circ + \bar{S}^\circ_{R^{3+}})$	$-\bar{S}^\circ_{R^{3+}}$	$(\Delta S^\circ + \bar{S}^\circ_{R^{3+}})$
La	34.7	32.1	39.2	27.6
Ce	36.3	32.8	41.3	27.8
Pr	37.5	31.9	43.0	26.4
Nd	38.5	32.2	44.5	26.2
Sm	40.3	32.6	47.1	25.8
Eu	41.1	34.6	48.4	27.3
Gd	41.8	36.6	49.5	28.9
Tb	42.7	41.6	50.9	33.4
Dy	43.6	42.7	52.3	34.0
Ho	44.5	42.2	53.8	32.9
Er	45.3	43.8	55.2	33.9
Tm	46.1	44.5	56.5	34.1
Yb	46.8	44.5	57.7	33.6
Lu	47.5	42.2	58.8	30.9

Values of ΔS° from Table III.
Units are cal/mole/° C at 25° C.

negative than the corresponding values calculated from ref. (10). However, the results for either equation, when combined with the experimental entropy change ΔS° shown in Table III, gives results which are qualitatively compatible.

The relative entropy of the complex ion RX^- (as expressed by the quantity $(\Delta S^\circ + \bar{S}^\circ_{R^{3+}})$ in Table IV) is essentially constant for the lanthanides La to Gd; after Gd, a second group of constant values is apparent, which differ significantly from the first group. A quantitative statement of this result is shown in Table V.

Can. J. Chem. Downloaded from www.nrcresearchpress.com by 190.90.36.8 on 09/04/12
For personal use only.

TABLE V

Average values for the relative entropies of the complex ions RX^-

	$(\Delta S^\circ + \bar{S}^\circ_{R^{3+}})$ cal/mole/° C	
Elements	Ref. 10	Ref. 11
La to Gd	33.3±1.4	27.1±0.9
Tb to Lu	43.1±1.1	33.3±0.7
Difference	9.8±1.8	6.2±1.1

The difference between the entropies of the complex ions of the two groups is from 6 to 10 e.u., depending on which equation is used to evaluate the terms in $\bar{S}^\circ_{R^{3+}}$. The constancy of the values in each group is particularly striking; in only two cases (Lu and Gd) does an individual value of $(\Delta S^\circ + \bar{S}^\circ_{R^{3+}})$ differ from the average value of the subgroup by more than the estimated uncertainty attached to the quantity ΔS°.

Clearly, the results shown in Table V depend very critically on the validity of the calculations of the terms in $\bar{S}^\circ_{R^{3+}}$. In this connection, no allowance has been made for possible contributions to the entropy of the lanthanide ions arising from the term $R \ln p$, when p is the multiplicity of the ground state of the ion (10). These reservations must be borne in mind during the discussion which follows.

The entropy of a simple hydrated ion is determined primarily by its charge and radius, while the entropies of complex ions have additional contributions arising from structural factors (3). The constancy of the entropies within each of the two groups of complex ions (La to Gd, and Tb to Lu) would therefore appear to indicate the close similarity in structure and radius of the individual ions comprising each subgroup. Moreover, the trend with atomic number that is evident in the terms $\bar{S}_{R^{3+}}$ has largely disappeared when the corresponding ions RX^- are compared. This is thought to be a consequence of the reduction of charge (from +3 to −1); in addition the ionic charge is spread over a relatively large structure. The radius of the individual ions RX^- in each subgroup appears to be determined mainly by the EDTA part of the ion and the slight differences in the radii of the central ion are evidently smoothed out. As a result, the lanthanide contraction, the effect of which is evident in the entropies of the hydrated ions, is no longer reflected in the individual members of each subgroup of the complex ions.

On the other hand, the entropies of the two groups of complex ions differ by 6 to 10 e.u. An unreasonably large change in the radius would have to be postulated to account for a change of this magnitude in the entropy of a singly charged ion in solution. It appears likely therefore that a change in configuration occurs after Gd, as suggested by Wheelwright *et al.* (1). However, it is not possible from entropy considerations alone to state with precision the exact nature of the structural changes that may be involved. The following comments must therefore be considered as speculative, and are put forward to indicate that reasonable changes in structure will account for the observed entropy differences.

If the central ion is co-ordinated to five chelating groups in the EDTA molecule (2), then one of the nitrogen atoms participates in two 5-membered rings in the chelate structure. One ring involves the sequence N–C–C–N–R, and the other N–C–C–O–R. The opening of this N–R bond gives rise to a tetra-co-ordinate structure, and would lead to an entropy gain of ∽28 e.u. (14 e.u. for each ring involved (3)). The co-ordination

Can. J. Chem. Downloaded from www.nrcresearchpress.com by 190.90.36.8 on 09/04/12
For personal use only.

position freed on the central ion would then be occupied by a water molecule, leading to an entropy decrease of ∽17 e.u. (3). The net result is that the entropy of the less highly organized complex would be approximately $28-17=11$ e.u. more positive than that of the fully co-ordinated species, in reasonable agreement with the experimental result.

SUMMARY AND CONCLUSION

The complex ions formed by the lanthanide ions with EDTA owe their exceptional stability to the large positive increase in entropy which occurs when the complex ion is formed. Two subgroups (La to Gd, and Tb to Lu) can be distinguished on the basis of the entropy changes involved. The differences between the two subgroups can be accounted for by plausible changes in the structure of the complex ions of the two groups. Within each subgroup, the differences in the partial molal entropy of the hydrated ions account very largely for the successive gradation in the association constants. The partial molal entropies of the individual complex ions is constant within experimental error in each of the two groups.

ACKNOWLEDGMENTS

We are indebted to Dr. R. W. Attree of A.E.C.L. for calorimetric measurements of the heat of association of lanthanum ion with EDTA. Samples of pure Dy_2O_3 and Yb_2O_3 were provided by courtesy of the Ames Laboratory of the U.S.A.E.C.

REFERENCES

1. WHEELWRIGHT, E. J., SPEDDING, F. H., and SCHWARZENBACH, G. J. Am. Chem. Soc. **75**, 4196 (1953).
2. MOELLER, T., MOSS, F. A. J., and MARSHALL, R. H. J. Am. Chem. Soc. **77**, 3182 (1955).
3. COBBLE, J. W. J. Chem. Phys. **21**, 1451 (1953).
4. BETTS, R. H., DAHLINGER, O. F., and MUNRO, D. M. UNESCO Conf. on Radioisotopes, Paris, Sept. 1957. The Pergamon Press, Ltd., London. 1958. Paper No. 212.
5. ATTREE, R. W., CUSHING, R. L., LADD, J. A., and PIERONI, J. J. Rev. Sci. Instr. **29**, 491 (1958).
6. CHENG, K. L., KURTZ, T., and BRAY, R. H. Anal. Chem. **24**, 1640 (1952).
7. BETTS, R. H., DAHLINGER, O. F., and MUNRO, D. M. Can. J. Phys. **36**, 73 (1958).
8. KESHISHIAN, V., KRUSE, H. W., KLOTZ, R. J., and FOWLER, C. M. Phys. Rev. **96**, 1050 (1954).
9. THIRY, H. Bull. soc. roy. sci. Liège, **26**, 29 (1957).
10. POWELL, R. E. and LATIMER, W. M. J. Chem. Phys. **19**, 1139 (1951).
11. LAIDLER, K. J. Can. J. Chem. **34**, 1107 (1956).
12. TEMPLETON, D. H. and DAUBEN, C. H. J. Am. Chem. Soc. **76**, 5237 (1954).

Can. J. Chem. Downloaded from www.nrcresearchpress.com by 190.90.36.8 on 09/04/12
For personal use only.

Can. J. Chem. Downloaded from www.nrcresearchpress.com by 190.90.36.8 on 09/04/12
For personal use only.

ISOMERIC 5-(SUBSTITUTED)AMINOTHIATRIAZOLE AND 1-SUBSTITUTED-TETRAZOLINETHIONES[1]

EUGENE LIEBER[2] AND J. RAMACHANDRAN

ABSTRACT

The reaction of organic isothiocyanates with sodium azide in ethanol and water has been investigated. Water is shown to be the more advantageous solvent for this reaction giving higher yields and initially purer 1-substituted-tetrazoline-5-thiones. A series of these latter compounds was made by this procedure. The yield of product appears to be dependent on the electrical properties of the substituent of the isothiocyanate, the yields decreasing as the electron-donating properties increase. A series of new 4-substituted-thiosemicarbazides has been prepared and converted by diazotization to the corresponding 5-(substituted)amino-thiatriazoles. A theory to account for the differences in the mode of reaction of hydrazoic acid and azide ion is presented and discussed. The basic conversion of 5-(substituted)amino-thiatriazoles to 1-substituted-tetrazolinethiones may involve a simple dearrangement–rearrangement mechanism complicated by side reactions. A summary of known isomeric 5-(substituted)aminothiatriazoles and 1-substituted-tetrazolinethiones is presented.

INTRODUCTION

Recently, Lieber, Pillai, and Hites (1) have shown that the reaction of 4-substituted-thiosemicarbazides (I) as well as the reaction of alkyl- or aryl-isothiocyanates (II), with hydrazoic acid, leads to identical 5-(substituted)amino-1,2,3,4-thiatriazoles (III). Oliveri-Mandala (2) had previously assigned a thiocarbamyl azide structure (V) to the reaction product of compound II with hydrazoic acid. The resolution of this problem is similar to that discussed by Lieber and co-workers (3, 4) for the reaction of azide ion with carbon disulphide, which was shown to be thiatriazolinethione (VI), rather than the

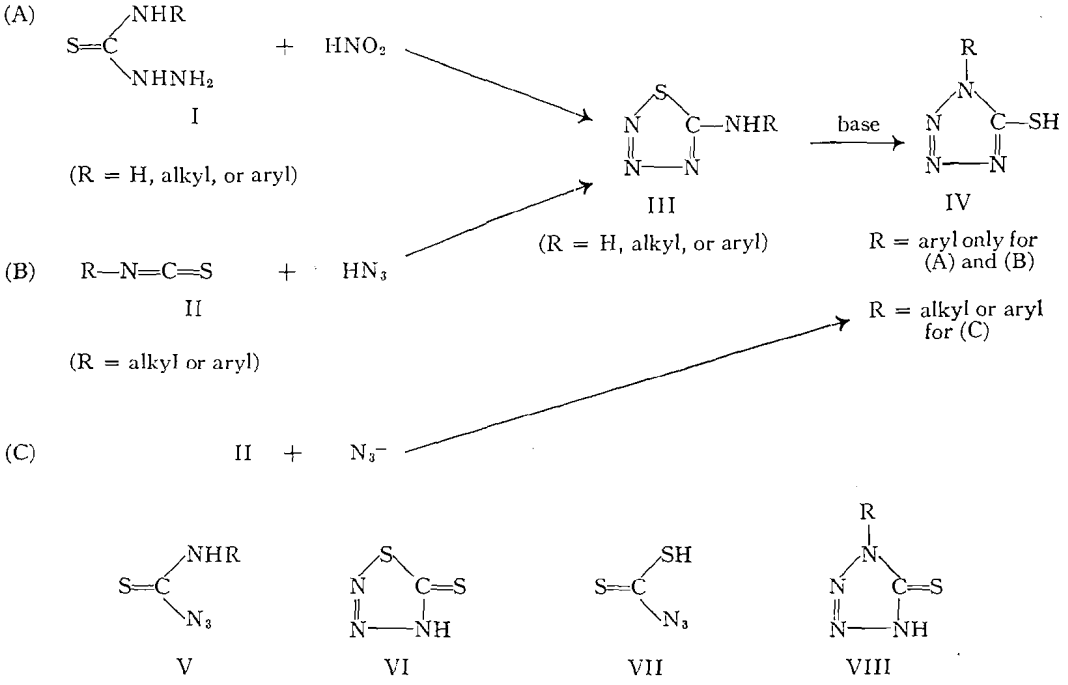

[1]*Manuscript received August 18, 1958.*
Contribution from the Department of Chemistry of DePaul University, Chicago, Illinois.
[2]*To whom all requests for additional information should be addressed.*

Can. J. Chem. Downloaded from www.nrcresearchpress.com by 190.90.36.8 on 09/04/12
For personal use only.

acyclic azidodithiocarbonic acid (VII) (5). On the other hand, Stolle (6) had previously shown that the reaction of azide ion (sodium azide) with II leads to the formation of 1-substituted-tetrazole-5-thiols (IV, R = alkyl or aryl), the end products of the reaction (B) (isomerization of III with base for R = aryl substituents only (1)). More recently, Lieber and co-workers (7) have shown, by infrared absorption spectroscopy, that IV exists in the *thione form*, VIII, and, hence, is more properly termed 1-substituted-tetrazolinethiones. The interesting divergence in the mode of reaction of hydrazoic acid and azide ion, as illustrated by (B) and (C), prompted an investigation of the effect of solvent on the behavior of azide ion with organic isothiocyanates, since it was considered that the type of product produced, III or IV, would be dependent on the reactive intermediates involved, which in turn would be influenced by the solvent used. The influence of solvent should be particularly noted for azide ion owing to its initially charged character, in contrast to hydrazoic acid. Stolle (6) carried out the reaction with azide ion in boiling ethanol, whereas Oliveri-Mandala (2) used an ethereal solution of hydrazoic acid. Lieber and co-workers (1) showed that the reaction with hydrazoic acid can be carried out equally well in either ethanol or water, reaction (B), the 5-(substituted) amino-1,2,3,4-thiatriazole (III) being obtained in each case, and identical with the initial product of reaction (A).

The present communication relates to a study of reaction (C), particularly with the effect of solvents on the yields and purity of the reaction product,[3] IV, and extends the number of isomeric 5-(substituted)aminothiatriazoles, III, reported previously (1).

EXPERIMENTAL[4, 5]

Organic isothiocyanates, RNCS.—The organic isothiocyanates described previously (1) were used in the present study. Additional isothiocyanates prepared were R = *p*-nitrophenyl-; 2,4-dichlorophenyl-; *p*-dimethylaminophenyl-; and *p*-fluorophenyl-; by the reaction of the corresponding amine hydrochloride with thiophosgene.[6] The *p*-fluorophenylamine was made by the sequence: *p*-nitraniline; *p*-nitrophenyl diazonium fluoborate (8) (yield 90%, m.p. 156° (decomp.)); *p*-nitrofluorobenzene (8) (yield 33%, m.p. 27°); *p*-fluoroaniline (9) (yield 45%, b.p. 182–187° at 748 mm). The following data gives in sequence R, % yield, m.p. or b.p., and references: *p*-nitrophenyl, 90, m.p. 113° (10); 2,4-dichlorophenyl, 94, m.p. 39–40° (11); *p*-dimethylaminophenyl, 90, m.p. 70° (12); *p*-fluorophenyl, 63, b.p. 222–226° at 740 mm (10).

4-Substituted-thiosemicarbazides (Table I).—These were prepared as previously described (1). With the exception of the *p*-fluorophenyl-derivative, all of the 4-substituted-thiosemicarbazides described in Table I are new compounds. The melting point of the *p*-fluorophenyl-derivative obtained in this research does not agree with that previously reported. While a well-defined white crystalline product was obtained for the *p*-dimethylaminophenyl-derivative, an acceptable analysis could not be obtained, although its diazotization (see below, Table II) gave a correctly defined thiatriazole.

Syntheses of thiatriazoles (Table II).—These were prepared by suspending the 4-substituted-thiosemicarbazide in 10% hydrochloric acid and diazotizing according to the method described by Lieber and co-workers (1). The resulting precipitates were purified by recrystallization from aqueous acetone.

[3]*A preliminary report on a study of reaction (C) using water as a solvent in comparison with ethanol has been presented by Lieber, E. and Ramachandran, J. Chem. & Ind. 461 (1958).*
[4]*All melting points are uncorrected and were determined on a Fisher-Johns block.*
[5]*Microanalyses by Dr. C. Weiler and Dr. F. B. Strauss, Oxford, England.*
[6]*Supplied by Rapter Laboratories, Chicago, Illinois.*

Can. J. Chem. Downloaded from www.nrcresearchpress.com by 190.90.36.8 on 09/04/12
For personal use only.

TABLE I

4-Substituted-thiosemicarbazides and benzylidene derivatives

R =	% Yield	M.p., ° C[a]	Formula	% C		% H		% N		% S	
				Calc.	Found	Calc.	Found	Calc.	Found	Calc.	Found
			RNHC(S)NHNH$_2$								
4-$O_2NC_6H_4$[b]	90	190	$C_7H_8N_4O_2S$	39.62	39.58	3.77	3.50	26.41	26.80	15.09	14.91
2,4-$Cl_2C_6H_3$[b,c]	95	174	$C_7H_7Cl_2N_3S$	35.59	35.56	3.00	3.20	17.79	17.40	13.56	13.40
4-FC_6H_5	84	177–178[d]	$C_7H_8FN_3S$	45.38	45.31	4.38	4.50	22.68	22.20		
4-$(CH_3)_2NC_6H_4$[e]	100	192	$C_9H_{14}N_4S$	51.40	57.23	6.71	6.97	26.64	21.90	15.25	14.2
			RNHC(S)NHN=CHC$_6$H$_5$								
4-$O_2NC_6H_4$[b]	93	215–216	$C_{14}H_{12}N_4O_2S$	56.00	55.76	4.00	4.02	18.67	18.80	10.67	10.57
2,4-$Cl_2C_6H_3$[b,f]	—	218	$C_{14}H_{11}Cl_2N_3S$	51.85	51.82	3.40	3.19	12.96	12.90	9.87	9.22
4-FC_6H_5[b]	—	195–196	$C_{14}H_{12}FN_3S$					15.39	15.20		

NOTES: [a]With decomposition. [b]New compounds. [c]Calc.: Cl, 30.09. Found: Cl, 30.40. [d]BuvHoi (13) reports a melting point of 189°. [e]This is a new compound; the analysis represents the best obtainable after repeated purifications and analysis. [f]Calc.: Cl, 21.91. Found: Cl, 21.90.

TABLE II

5-Arylamino-1,2,3,4-thiatriazoles

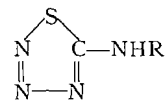

R =	% Yield	M.p., ° C	Formula	Analysis							
				% C		% H		% N		% S	
				Calc.	Found	Calc.	Found	Calc.	Found	Calc.	Found
4-$NO_2C_6H_4$*	90	152–153	$C_7H_5N_5O_2S$	37.67	37.71	2.24	2.31	31.39	31.20	14.35	14.40
2,4-$Cl_2C_6H_3$*[a]	85	140	$C_7H_4Cl_2N_4S$	34.01	34.17	1.62	1.83	22.68	22.20	12.95	13.15
4-FC_6H_4*	75	127–128	$C_7H_5FN_4S$	42.86	42.41	2.51	2.71	28.57	28.90	16.32	16.40
4-$(CH_3)_2NC_6H_4$	88	140	$C_9H_{11}N_5S$	48.85	48.95	5.01	4.74	31.65	32.00	14.49	14.45

[a]Calculated: Cl, 28.75%. Found: Cl, 29.00%.
*New compound.

Can. J. Chem. Downloaded from www.nrcresearchpress.com by 190.90.36.8 on 09/04/12
For personal use only.

TABLE III

1-Substituted tetrazoline-5-thiones

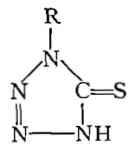

R =	% Yield	M.p., °C Found	M.p., °C Rept.	Formula	Analysis % C Calc.	% C Found	% H Calc.	% H Found	% N Calc.	% N Found	% S Calc.	% S Found
C_6H_6[a]	96	150	150									
2,4-$Cl_2C_6H_3$*[a,b]	97	130–131	—	$C_7H_4Cl_2N_4S$	34.01	34.09	1.62	1.56	22.68	22.78	12.95	12.91
2-$CH_3C_6H_4$[a]	92	123	123									
4-$CH_3C_6H_4$[a]	82	153	150									
4-$NO_2C_6H_4$*[a]	80	148	—	$C_7H_5N_5O_2S$	37.67	37.65	2.24	2.34	31.39	31.40	14.35	14.35
4-FC_6H_4*[a]	78	154–155	—	$C_7H_5FN_4S$	42.86	42.89	2.55	2.61	28.57	28.20	16.33	16.10
4-$(CH_3)_2NC_6H_4$*[a]	73	180	—	$C_9H_{11}N_5S$	48.87	48.90	4.98	5.07	31.75	31.40	14.47	14.46
$C_6H_5CH_2$[c]	48	144	144									
CH_3[c,e]	52	125–126	126	$C_2H_4N_4S$	20.68	20.84	3.47	3.43	48.24	48.20	27.61	27.80
C_2H_5*[c,e]	46	50	—	$C_3H_6N_4S$	27.68	27.80	4.65	4.52	43.04	43.50	24.63	24.50
CH_2=CH—CH_2[d,e]	88	69	69	$C_4H_6N_4S$							22.55	22.30

*New compound. [a]Refluxed for 6 hours. [b]Calculated for $C_7H_4Cl_2N_4S$: Cl, 28.75%. Found: Cl, 28.80%. [c]Refluxed for 8 hours. [d]Stirred at room temperature for 3 hours. [e]Worked up by alternate procedure.

1-Substituted-tetrazoline-5-thiones (*Table III*).—The following general procedure was adopted. A mixture of 0.05 mole of the isothiocyanate and 0.075 mole of sodium azide dissolved in 100 cc of water was refluxed for a period ranging from 4 to 8 hours. The mixture was then cooled and filtered from any insoluble material present. The filtrate was then extracted twice with ether to remove any unreacted isothiocyanate present. The aqueous layer was cooled and acidified with concentrated hydrochloric acid to pH 3 (Congo red paper end point). If the product precipitated out at this stage (as was usually the case), it was filtered and washed with water. An alternative procedure (designated in Table III by the superscript [e]) was employed if the product did not precipitate subsequent to acidifying to Congo red paper. The acidified solution was extracted with ether and the ether extract washed with a little ice-cold water. The ether extract was then dried, filtered from the drying agent, and the ether carefully removed on a steam bath. The product which remains as a residue was purified. The purification was effected in the case of the 1-aryl tetrazoline-5-thiones by recrystallization from ethanol and a mixture of chloroform and petroleum ether was employed in the case of the 1-alkyl derivatives.

The reaction of n-heptyl isothiocyanate and n-butyl isothiocyanate with sodium azide.—The products obtained were oils which decomposed on distillation and consequently could not be purified. In the case of the *n*-heptyl isothiocyanate, 70% of the isothiocyanate was recovered unchanged after refluxing for 10 hours. In the reaction of *n*-butyl isothiocyanate with sodium azide, 50% of the isothiocyanate was recovered after refluxing for 10 hours.

The reaction of sodium azide with p-nitrophenyl isothiocyanate.—An insoluble orange-red precipitate was obtained. This was found to melt at 172–174°. The melting point identified the substance to be 1,3-di-(*p*-nitrophenyl)-thiourea:

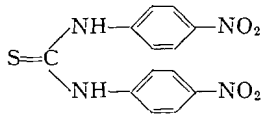

as the reported (15) m.p. is 175°.

The reaction of phenyl isothiocyanate with sodium azide.—This reaction was studied under different conditions. The results are summarized in Table IV, where the experimental conditions are also given.

Reaction of 5-methylamino-1,2,3,4-thiatriazole with sodium azide.—Sodium azide, 2.6 g (0.04 mole), dissolved in 100 cc of water was refluxed with 2 g (0.02 mole) of 5-methylamino-1,2,3,4-thiatriazole for 4 hours. The reaction mixture was cooled and the yellow

TABLE IV
Reaction of sodium azide with phenyl isothiocyanate in different solvents

Solvent	No. moles of sodium azide used	Time of refluxing (hours)	Yield of 1-phenyl tetrazoline-5-thione (%)	Melting point of crude product (° C)
95% Ethanol[b]	1.5	7	60	140–143
50% Ethanol	1.5	4	68	146–148
Water	1.5	4	96	150[a]
Water	1.0	4	88	150[a]

[a]The melting point of pure 1-phenyl tetrazoline-5-thione is 150° C.

Can. J. Chem. Downloaded from www.nrcresearchpress.com by 190.90.36.8 on 09/04/12
For personal use only.

material that had precipitated was filtered. The filtrate was acidified, extracted with ether, washed, and dried. The ether was then removed by distillation and the white crystalline residue washed with petroleum ether and filtered. Yield, 0.3 g (15%), m.p. 124–126°; no depression of mixed melting point with an authentic (1) sample of 1-methyltetrazoline-5-thione.

DISCUSSION

Water was used as the solvent for the synthesis of the 1-substituted-tetrazoline-5-thiones summarized in Table III. It will be noted that the yield of product is approximately doubled as one proceeds from the 1-alkyl- to the 1-aryl-derivatives. This trend in yield suggests that resonance interaction is important for the activation of the organic isothiocyanate. This is reasonable, since competitive conjugation is possible in the isothiocyanates as indicated below:

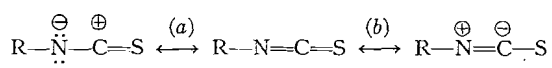

When R is an aryl group resonance interaction by process (*a*) is predominant, facilitating the creation of an electron-deficient carbon atom; whereas if R is an alkyl group resonance interaction by process (*a*) is inhibited and activation is then probably achieved by process (*b*). It is evident that this latter activation will be considerably less than in process (*a*), primarily as a result of the smaller difference in electronegativities of carbon and sulphur and, secondly, because of the electron-releasing properties of alkyl groups. The reaction may be considered as a nucleophilic attack of the azide ion on the electron-deficient carbon atom of the isothiocyano-group, followed by ring closure to the tetrazole by donating of electrons to an electron-deficient nitrogen atom of the azido-moiety. This suggests two conceivable pathways by which the reaction may proceed on this basis, the driving force being the considerable resonance stabilization of the tetrazolinethione anion, (1). While thus far only the activation of the isothiocyanate has been discussed, it must be considered that the activation of the azide ion is also an important step in the process. The observation that the yields and purity of 1-substituted-tetrazoline-5-thiones are improved considerably when the solvent is changed from alcohol to water suggests that the activation of the azide ion is of importance. While the solvent thus appears to be of considerable importance, the interpretation of the data is made difficult by the occurrence of side reactions.

The propensity of hydrazoic acid or azide ion to react with reagents leading to the formation of tetrazoles or 1,2,3-triazoles (16) necessitates the concept of a reactive intermediate for the azido-moiety which departs from the rigid linearity of this group in order that ring closure be effected. This concept suggests the necessity for the activation of the azide ion by the following processes:

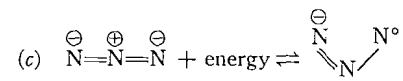

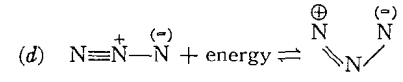

Can. J. Chem. Downloaded from www.nrcresearchpress.com by 190.90.36.8 on 09/04/12
For personal use only.

The advantage of this theory is that the activated structures produced by either (*c*) or (*d*) (or both) is not restricted by any criterion of linearity. The departure from linearity can be assumed to take place after the initial attack of the azide ion. On the other hand there is a great deal of attraction to the alternative assumption that *both the isothiocyano- and azido-moieties are activated prior to condensation.* This latter assumption then leads to the process in which the tetrazole ring is the result of a simple neutralization of charges, illustrated for one case as follows:

X

Similar reactive intermediates to that of X can be considered for the other resonance forms of the isothiocyano- and azido-groups.

The trend in the yields of the 1-aryl tetrazoline-5-thiones also lends support to the idea that resonance interaction of the isothiocyano group with the aromatic ring influences the activation of the isothiocyanate. Thus, the dimethylamino-, fluoro-, and methyl-groups in the para position of the aryl ring lower the yields (Table III) to a small extent, since the resonance interaction, in these cases, tends to suppress activation of the isothiocyano group by process (*a*), with probably increase of process (*b*). On the other hand, ortho substituents in the aromatic ring of the isothiocyanate increases the yields to a small extent probably because of steric inhibition of resonance. The above considerations lead to the expectation that the maximum yield of 1-substituted-tetrazoline-5-thione would be obtained by reaction of *p*-nitrophenyl isothiocyanate owing to the relatively greater electron-withdrawing ability of the nitro group. The apparent fall in yield is due to a side reaction involving the hydrolysis of the isothiocyanate to *p*-nitraniline, which is subsequently converted to 1,3-di(*p*-nitrophenyl)-thiourea. Dyson and Browne (10) have demonstrated that the solvolytic (in ethanol) attack on substituted-aryl-isothiocyanates increases as the electron-withdrawing ability of the substituent increases. This factor readily explains the lower yields of 1-substituted-tetrazoline-5-thiones when ethanol is used as solvent (Table IV), where as in water the solvolytic attack is reduced *owing to a higher degree of activation of the azide ion in water as contrasted with ethanol.*

The difference in the types of products formed when hydrazoic acid is used remains to be explained. It is suggested that the tetrazole ring closure is blocked as a result of the protonation of the organic isothiocyanate due to an initial acid–base reaction:

$$RNCS + HN_3 \rightarrow (R{-}NH{-}\overset{+}{C}{=}S)N_3^-.$$

The subsequent step involving a neutralization of charges which may be indicated as follows:

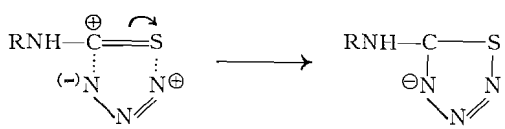

XI

Can. J. Chem. Downloaded from www.nrcresearchpress.com by 190.90.36.8 on 09/04/12
For personal use only.

the protonation of the nitrogen preventing ring closure at that point, since such a ring closure would produce a *high energy* form of the isomeric structure:

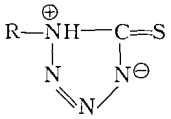

The process thus proceeds by a path producing the product of minimum energy, the anion XI.

In the previous investigation (1) on the chemistry of 5-(substituted)amino-1,2,3,4-thiatriazoles, it was noted that their isomerization with base to give the 1-substituted-tetrazoline-5-thione could be effected only with the 5-arylaminothiatriazoles (III, R = aryl). The yields in this reaction ranged from 22 to 37% and 1,3-diaryl thioureas were formed as by-products. Azide ion was identified among the degradation products. Organic isothiocyanates were also identified (either *per se* or as the 1,3-diaryl thiourea). The present investigation accordingly suggests that the mechanism of the base isomerization of III to IV may simply involve a dearrangement–rearrangement:

$$\text{III} \rightarrow \text{RNCS} + N_3^- \rightarrow \text{IV}.$$

However, the speculations are complicated by the observations (1) that III simultaneously undergoes an internal oxidation–reduction to form elemental sulphur, nitrogen, and cyanamid derivatives. The observation that a 15% yield of 1-methyltetrazoline-5-thione (IV, R = CH_3) was obtained by refluxing 5-methylamino-1,2,3,4-thiatriazole with sodium azide is of considerable interest in that it suggests that the yields obtained in the base isomerization of III to IV is dependent upon the base strength. The latter factor will determine the rate at which the isothiocyanate *undergoes hydrolysis rather than recombination* to IV.[7] It is also interesting to note that when *n*-heptyl isothiocyanate was refluxed with sodium azide in water, 75% of the isothiocyanate was recovered unchanged after 10 hours. The apparent inertness of *n*-heptyl isothiocyanate to react with azide ion[8] may be accounted for by a too high electron density on the carbon of the isothiocyano group due to the electron-donating character of the heptyl radical. Under the same conditions, 50% of *n*-butyl isothiocyanate was recovered unchanged.

A summary of the known isomeric 5-(substituted)amino-1,2,3,4-thiatriazoles and 1-substituted-tetrazoline-5-thiones are presented in Table V together with their uncorrected melting points. It is unlikely that a correlation can be found, since both types of structures are thermally unstable. It is interesting to note that a third structural isomer can be readily made by the reaction of organic thiocyanates with azide ion, in which 5-mercaptotetrazoles are formed (17):

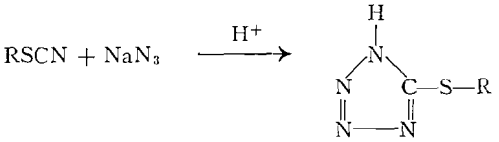

[7]*In unpublished data from the authors' laboratory, III (R = C_6H_5) (1 mole) was refluxed for 30 minutes in aqueous media with 2 mole proportion of the respective bases: (a) sodium carbonate; (b) sodium bicarbonate; (c) ammonium hydroxide; and (d) sodium acetate. The data following represents the percentage yields of IV (R = C_6H_5) and 1,3-diphenyl thiourea isolated: (a) (44) (20); (b) (58) (4); (c) (25) (62); (d) (7) (none). In only the latter case, 80% of unchanged III (R = C_6H_5) was recovered. This phase of the investigation is being continued.*

[8]*Further unpublished work from the authors' laboratory has found that attempts to base isomerize III (R = n-(C_7H_{15}) yields only n-heptyl isothiocyanate, azide ion, and n-heptyl urea; the latter product offering evidence for the internal oxidation–reduction disruption of the molecule.*

Can. J. Chem. Downloaded from www.nrcresearchpress.com by 190.90.36.8 on 09/04/12
For personal use only.

This reaction is under investigation and will be subsequently reported upon.

TABLE V

Summary of isomeric 5-(substituted)aminothiatriazoles and 1-substituted-tetrazoline-5-thiones

R=	Melting point, °C: 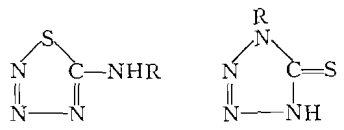	Melting point, °C:
CH_3	93–96	125–126
C_2H_5	66–67	50
n-C_4H_9	40–41	oil[b]
n-C_7H_{15}	75–75.5	oil[b]
CH_2=$CHCH_2$	53–53.5	69
$C_6H_5CH_2$	80.5–81	144
C_6H_5	142–143	150
2-$CH_3C_6H_4$	114–115	121–123
4-$CH_3C_6H_4$	142–144	153
4-ClC_6H_4	147–148	156–157
2,4-ClC_6H_3	140	130–131
4-FC_6H_4	127–128	154–155
4-$O_2NC_6H_4$	152–153	148
4-$(CH_3)_2NC_6H_4$	140	180
$(CH_3)_2$[a]	49–51	—

NOTE: [a]5-Dimethylamino-1,2,3,4-thiatriazole.
[b]Composition as yet unconfirmed.

ACKNOWLEDGMENTS

The authors gratefully acknowledge the receipt of research grants from the Eli Lilly Company, Indianapolis, Indiana, and the Frederick Gardner Cottrell Program of the Research Corporation, New York, New York, which made this study possible.

REFERENCES

1. LIEBER, E., PILLAI, C. N., and HITES, R. D. Can. J. Chem. **35**, 832 (1957).
2. OLIVERI-MANDALA, E. Gazz. chim. ital. **43**, I, 304 (1913); **44**, I, 670 (1914); **51**, II, 195 (1921).
3. LIEBER, E., PILLAI, C. N., RAMACHANDRAN, J., and HITES, R. D. J. Org. Chem. **22**, 1750 (1957).
4. LIEBER, E., OFTEDAHL, E., GRENDA, S., and HITES, R. D. Chem. & Ind. 893 (1958).
5. AUDRIETH, L. F. Chem. Revs. **15**, 169 (1934).
6. STOLLE, R. (*a*) J. prakt. Chem. **124**, 261 (1930); (*b*) J. prakt. Chem. **133**, 60 (1932); (*c*) Ber. **63**, 670 (1930).
7. LIEBER, E., RAO, C. N. R., PILLAI, C. N., RAMACHANDRAN, J., and HITES, R. D. Can. J. Chem. **36**, 801 (1958).
8. SCHIEMANN, G. and PILLERSKY, R. Ber. **62**, 3040 (1929).
9. WILKINSON, J. H. and FINAR, I. L. J. Chem. Soc. 759 (1947).
10. DYSON, G. M. and BROWNE, D. W. J. Chem. Soc. 3285 (1931).
11. DYSON, G. M., GEORGE, H. J., and HUNTER, R. F. J. Chem. Soc. 3041 (1926).
12. DYSON, G. M., GEORGE, H. J., and HUNTER, R. F. J. Chem. Soc. 442 (1927).
13. BUV-HOI, No. Ph., XUONO, No. D., and NAM, No. H. J. Chem. Soc. 2160 (1956).
14. KENDALL, J. D. U. S. Patent No. 2,386,869. Oct. 16, 1945; C. A. **40**, 611.
15. DYSON, G. M. J. Chem. Soc. 174 (1934).
16. (*a*) BENSON, F. R. and SAVELL, W. L. Chem. Revs. **46**, 1 (1950). (*b*) BENSON, F. R. Chem. Revs. **41**, 1 (1947). (*c*) HUISGEN, R. and UGI, I. Chem. Ber. **90**, 2914 (1957). (*d*) UGI, I. and HUISGEN, R. Chem. Ber. **91**, 531 (1958).
17. FINNEGAN, W. G., HENRY, R. A., and LOFQUIST, R. J. Am. Chem. Soc. **80**, 3908 (1958).

Can. J. Chem. Downloaded from www.nrcresearchpress.com by 190.90.36.8 on 09/04/12
For personal use only.

Can. J. Chem. Downloaded from www.nrcresearchpress.com by 190.90.36.8 on 09/04/12
For personal use only.

THE CONDENSATION OF 3-AMINO-5-PYRAZOLONES WITH ALDEHYDES SYNTHESES OF 5-PYRAZOLONOGUANIDINES[1]

PAUL E. GAGNON, JEAN L. BOIVIN,[2] AND JOSEPH ZAUHAR[3]

ABSTRACT

3-Amino-5-pyrazolones did not react with guanidine in aqueous solution, but with aldehydes in the presence of piperidine, the amino group was removed in some cases. 5-Pyrazolonoguanidines were synthesized by the direct fusion of 3-amino-5-pyrazolones and dicyandiamide. The infrared spectra of the pyrazolone derivatives prepared are briefly discussed.

INTRODUCTION

Previous investigations by Nencki and Sieber (1) have shown that the amino function of α-amino acids could interreact with guanidine carbonate to yield guanidoaliphatic acids. It was expected that 3-amino-5-pyrazolones (2, 3, 4, 5, 6, 7) and 3-amino-1-phenyl-5-pyrazolone (8) would behave similarly towards guanidine or guanidine carbonate when heated in aqueous solution. However, in all the experiments made, the starting materials were recovered, no evidence of condensation being detected. This was attributed to the prototropic shift occurring in 3-amino-5-pyrazolones and its 4-substituted derivatives which can exhibit 10 possible tautomeric structures (5) of which configurations I, II, and III contribute to their stability towards guanidine.

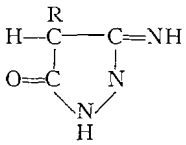

I

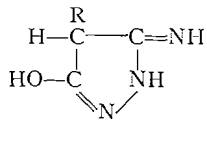

II

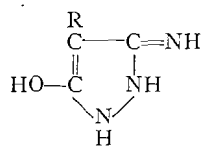

III

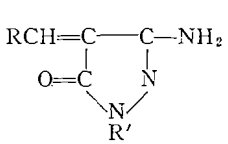

IV

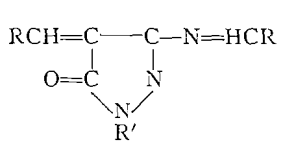

V

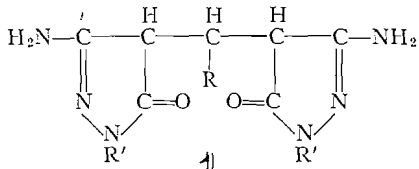

VII

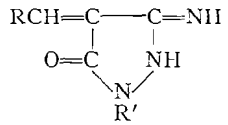

IV*a*

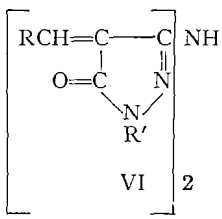

VI 2

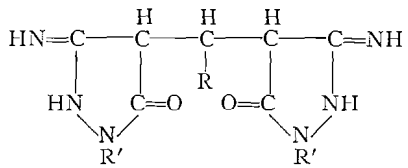

VII*a*

[1]*Manuscript received July 24, 1958.*
Contribution from the Department of Chemistry, Laval University, Quebec, Que. This paper constitutes part of a thesis submitted to the Graduate School, Laval University, in partial fulfillment of the requirements for the degree of Doctor of Science.
[2]*Canadian Armament Research and Development Establishment, Valcartier, Quebec.*
[3]*Graduate student, holder of National Research Council of Canada Studentships in 1956–58.*

Since the amino group of 3-amino-5-pyrazolones did not react with guanidine, the behavior of pyrazolones towards aldehydes was studied in order to determine the stability of the amino groups.

Theoretically, condensation between 3-amino-5-pyrazolones and aldehydes in a basic medium would be expected to yield pyrazolones IV, IV*a*, V, VI, VII, and VII*a*.

In formula IV the amino group is stabilized by the tautomeric form IV*a* and consequently, no reaction would be expected. Configuration V would result from the condensation of 1 mole of pyrazolone and 2 moles of aldehydes. The formation of a Schiff base in position 3 would give evidence of the existence of a free amino group. If 3-amino-5-pyrazolones reacted with 1 mole of aldehyde, 1 mole of ammonia being liberated in the process, pyrazolone VI would be formed. This type of condensation would justify the existence of a free amino group in position 3, the condensation occurring in a similar manner with α-amino acids and guanidine. Graham, Reckhow, and Weissberger (9) have shown that such a condensation was possible between 3-amino-1-phenyl-5-pyrazolone and ethylamine. A mixture of 3-ethylamino-1-phenyl-5-pyrazolone and 3,3-imino-bis(1-phenyl-5-pyrazolone) was obtained, the latter being the principal product of the reaction. Condensation of type VII would indicate that the stability of the amino group is probably due to the prototropic shift giving the tautomeric form VII*a*.

RESULTS AND DISCUSSION

3-Amino-5-pyrazolone, Benzaldehyde, and Phenylacetaldehyde

When a mixture of benzaldehyde and 3-amino-5-pyrazolone, in a molar ratio of 3 : 1 respectively, was refluxed in the presence of piperidine, the reaction proceeded according to the following equation:

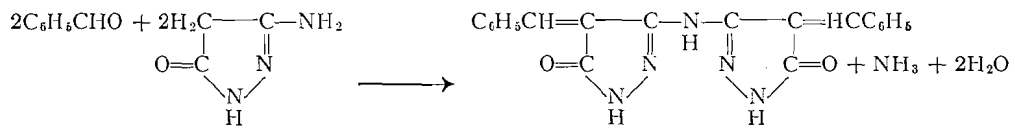

The compound isolated was slightly soluble in bases, insoluble in acids, and gave a negative test with ferric chloride, indicating no actual or potential enolic group.

With phenylacetaldehyde under similar conditions, the reaction was quite different. The amino group was not eliminated but reacted with the aldehyde.

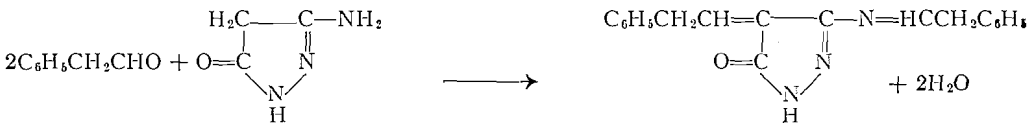

The compound which was isolated indicated that an active amino group, similar to those of primary amines, was present in position 3.

3-Amino-1-phenyl-5-pyrazolone and Aldehydes

3-Amino-1-phenyl-5-pyrazolone was also condensed with five aldehydes under similar conditions as in the foregoing experiments. The results obtained are recorded in Table I. Acetaldehyde condensed with only the methylene group of the pyrazolone and similar results were obtained with propionaldehyde indicating that under the above conditions,

Can. J. Chem. Downloaded from www.nrcresearchpress.com by 190.90.36.8 on 09/04/12
For personal use only.

the amino group was not reactive. Previous investigations by Knorr (10) have shown that 3-methyl-1-phenyl-5-pyrazolone, when treated with sodium ethylate, was not transformed into the corresponding hydroxy compound. However, in the present work, when the propylidene derivative was treated with sodium and ethyl alcohol, not only the corresponding hydroxy compound was formed but also ammonia was evolved to yield 3,3′-imino-bis(4-propylidene-1-phenyl-5-pyrazalin-5-ol).

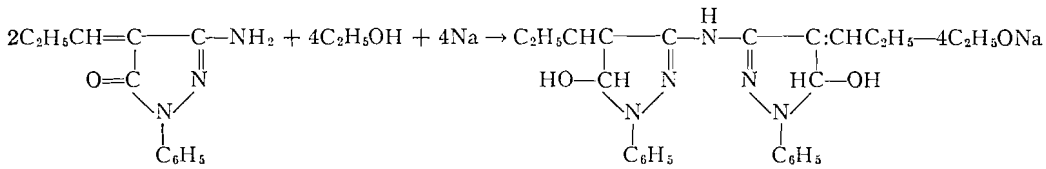

The equation indicates that the amino and not the imino structure of the pyrazolone was the predominant tautomeric form, the amino group being susceptible to elimination, *n*-valeraldehyde, on the other hand, condensed with both the methylene and the amino group. According to the elemental analyses and molecular weight determinations, both a monomer and a dimer having the same empirical formula $C_{19}H_{25}ON_3$ were isolated.

When benzaldehyde and the pyrazolone were condensed in a solution of benzene without piperidine, reaction occurred only with the methylene group. No ammonia was eliminated and the compound formed could be reduced to the corresponding pyrazalin-5-ol. On the other hand, in the presence of piperidine, benzaldehyde condensed with the methylene group and 1 mole of ammonia was eliminated from 2 moles of the intermediate product to yield 3,3′-imino-bis(4-benzylidene-1-phenyl-5-pyrazolone). A dimer with the same empirical formula, $C_{32}H_{23}O_2N_5$, was also isolated. With *p*-methoxybenzaldehyde in the presence of piperidine, condensation occurred with the methylene group, and 1 mole of ammonia was eliminated from 2 moles of the intermediate to give 3,3′-imino-bis(4-*p*-methoxybenzylidene-1-phenyl-5-pyrazolone). The corresponding pyrazalin-5-ol was easily obtained by reduction with sodium and ethyl alcohol. All the above compounds gave negative tests with ferric chloride, indicating the absence of an enolic group. No evidence for compounds having the structure VII could be found in the present work.

The condensation products of 3-amino-5-pyrazolones with aldehydes clearly indicate that the amino group in position 3 does not always exhibit the same stability and can be removed in some cases under appropriate conditions.

5-Pyrazolonoguanidines

4-Butyl-, 4-amyl-, and 4-benzyl-3-amino-5-pyrazolones, when heated with dicyandiamide, yielded the corresponding 5-pyrazolonoguanidines. For instance, 4-butyl-3-amino-5-pyrazolone and dicyandiamide heated at 150° C yielded 4-butyl-5-pyrazolonoguanidine. The biguanide intermediate probably formed at 150° C decomposed to the 5-pyrazolonoguanidine.

The guanidine derivative isolated was soluble in acids and bases and gave a positive test with ferric chloride for an enolic structure.

With 4-amyl-3-amino-5-pyrazolone, the reaction was carried at 180° C, since fusion was complete at a much higher temperature than in the case of 4-butyl-3-amino-5-pyrazolone. The reaction took place through the formation of a biguanide intermediate which decomposed at 180° C to give N,N′-bis(4-amyl-5-pyrazolono)-guanidine and ammonia. With 4-benzyl-3-amino-5-pyrazolone, the result was similar to that obtained with 4-amyl-3-amino-5-pyrazolone. The above compounds were soluble in bases and insoluble in acids and gave a positive test with ferric chloride.

Can. J. Chem. Downloaded from www.nrcresearchpress.com by 190.90.36.8 on 09/04/12
For personal use only.

Can. J. Chem. Downloaded from www.nrcresearchpress.com by 190.90.36.8 on 09/04/12
For personal use only.

TABLE I

3-Amino-1-phenyl-5-pyrazolone and aldehydes

Aldehydes RCHO R =	Products	Solvent	M.p., °C	Yield	Formula	Molecular weight Calc.	Molecular weight Found (Rast)	Analysis Calc. C	Calc. H	Calc. N	Found C	Found H	Found N	Solubility Acids	Solubility Bases
CH_3—	$CH_3CH{:}C(OC{-}N(C_6H_5){-}N){=}C{-}NH_2$	Ethanol	225–226	95.7	$C_{11}H_{11}ON_3$	201	184 and 215	65.53	5.47	20.80	65.1	5.6	20.5	Slight	Insoluble
C_2H_5—	$C_2H_5CH{:}C(OC{-}N(C_6H_5){-}N){=}C{-}NH_2$	Ethanol	184–186	56.1	$C_{12}H_{13}ON_3$	215	232 and 256	67.00	6.10	19.60	67.2	6.0	19.0	Slight	Insoluble
C_4H_9—	$C_4H_9CH{:}C(OC{-}N(C_6H_5){-}N){=}C{-}N{:}CH{-}C_4H_9$	Methanol or benzene	165–167	51.0	$C_{19}H_{25}ON_3$	311	301 and 319	73.30	8.04	13.41	73.5	7.9	13.2	Insoluble	Insoluble
	+ Dimer	Ethanol	241–243	18.0	$(C_{19}H_{25}ON_3)_2$	622	604 and 670	73.30	8.04	13.41	73.6	8.2	13.1	Insoluble	Insoluble
C_6H_5—	$C_6H_5CH{:}C(OC{-}N(C_6H_5){-}N){=}C{-}NH_2$	Methanol	231–233	84.5	$C_{16}H_{13}ON_3$	263	256 and 261	72.98	4.98	15.96	70.8	5.1	16.0	Slight	Insoluble
C_6H_5—	$(C_6H_5CH{:}C(OC{-}N(C_6H_5){-}N){=}C)_2{=}NH$	Dioxane	242–244	34.1	$C_{32}H_{23}O_2N_5$	509	Insoluble in camphor	75.42	4.54	13.75	75.9	5.0	13.6	Insoluble	Insoluble
	+ Dimer	Methanol	260–261	17.2	$(C_{32}H_{23}O_2N_5)_2$	1018	940 and 1050	75.42	4.54	13.75	75.8	4.7	13.4	Insoluble	Insoluble
$C_6H_4(OCH_3)$—	$(C_6H_4(OCH_3)CH{:}C(OC{-}N(C_6H_5){-}N){=}C)_2{=}NH$	Acetic acid	253–254	89.1	$C_{34}H_{27}O_4N_5$	569	Insoluble in camphor	71.69	4.77	12.29	71.7	5.2	11.7	Insoluble	Insoluble

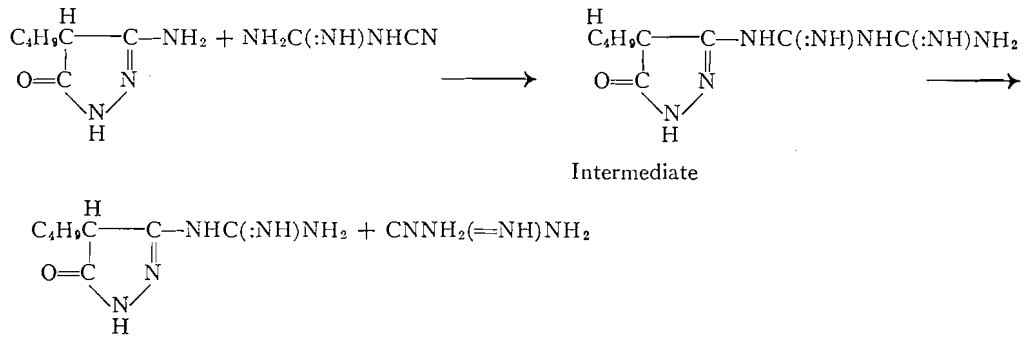

Infrared Absorption Spectra

The infrared absorption spectra were obtained with a Perkin–Elmer Model 21, double beam self-recording spectrophotometer and the bands corresponding to the 16 compounds studied are recorded in Table II. With most of the pyrazolones investigated, three absorption bands at 3400, 3300, and 3100 wave numbers were obtained and are attributed to the NH stretching vibrations of these compounds. However, these absorption bands are absent in the spectra of 4-phenylethylidene-3-iminophenyl-ethylidene-5-pyrazolone and 4-pentylidene-3-iminopentylidene-1-phenyl-5-pyrazolone where the

TABLE II

Infrared absorption spectra

Compound No.	Absorption bands in wave numbers										
1		3300	3225	1710	1690	1610	1590	1490		725	695
2						1600	1555		763	715	700
3		3300	3150		1680	1630	1590	1490	755	715	690
4	3400	3300	3150		1680	1625	1590	1490	760	710	685
5		3300			1670		1580	1480	760	740	685
6					1670	1600	1585	1500	760	720	690
7			3100	1700	1670	1620	1585	1500	750	720	690
8	3400	3300	3100		1680	1605	1550	1480	745	720	700
9	3400	3300	3100		1680	1600	1550	1480	750		700
10			3150		1690	1620	1585	1480	750	720	690
11		3250		1700	1680	1620	1590	1490	750	725	695
12			3150		1670	1600	1590	1490	750	720	685
13		3270	3110		1685	1600	1585	1490	750	720	690
14	3400	3270	3100		1640		1580	1490	760	720	690
15		3280	3100		1620				760	720	685
16	3300	3280	3100		1610			1490	760	720	695

1. 3,3′-Imino-bis(4-benzylidene-5-pyrazolone).
2. 4-Phenylethylidene-3-iminophenylethylidene-5-pyrazolone.
3. 4-Ethylidene-3-amino-1-phenyl-5-pyrazolone.
4. 4-Propylidene-3-amino-1-phenyl-5-pyrazolone.
5. 3,3′-Imino-bis(4-propylidene-1-phenyl-5-hydroxypyrazolone).
6. 4-Pentylidene-3-iminopentylidene-1-phenyl-5-pyrazolone.
7. Dimer of 4-pentylidene-3-iminopentylidene-1-phenyl-5-pyrazolone.
8. 4-Benzylidene-3-amino-1-phenyl-5-pyrazolone.
9. 4-Benzylidene-3-amino-1-phenyl-5-pyrazalin-5-ol.
10. 3,3′-Imino-bis(4-benzylidene-1-phenyl-5-pyrazolone).
11. Dimer of 3,3′-imino-bis(4-benzylidene-1-phenyl-5-pyrazolone).
12. 3,3′-Imino-bis(4-*p*-methoxybenzylidene-1-phenyl-5-pyrazolone).
13. 3,3′-Imino-bis(4-*p*-methoxybenzylidene-1-phenyl-5-pyrazalin-5-ol).
14. (4-Butyl-5-pyrazolono)-guanidine.
15. N,N′-bis(4-amyl-5-pyrazolono)-guanidine.
16. N,N′-bis(4-benzyl-5-pyrazolono)-guanidine.

Can. J. Chem. Downloaded from www.nrcresearchpress.com by 190.90.36.8 on 09/04/12
For personal use only.

hydrogen has been substituted by a benzyl and butyl group respectively. The ketonic function was exhibited in the range of 1620 to 1690 wave numbers by all the compounds but the spectra of 3,3′-imino-bis(4-propylidene-1-phenyl-5-pyrazalin-5-ol) and 3,3′-imino-bis(4-*p*-methoxybenzylidene-1-phenyl-5-pyrazalin-5-ol) failed to show their hydroxyl function.

An analogy found in these spectra and attributed to the over-all molecule is the three absorption bands in the range of 750 to 720 and 690 wave numbers.

EXPERIMENTAL*

3-Amino-5-pyrazolone and Benzaldehyde

3,3′-Imino-bis(4-benzylidene-5-pyrazolone).—Benzaldehyde (0.56 mole) was introduced into a flask containing cooled ethanol (200 ml), piperidine (4 ml), and 3-amino-5-pyrazolone (0.20 mole) and the resulting mixture refluxed. 3-Amino-5-pyrazolone slowly passed into solution, during which time ammonia was liberated, and after refluxing for 24 hours, the reaction was complete. The resulting reddish-brown solution was then filtered, the filtrate was evaporated to one-half of its original volume, and left to stand in a cool place. The white product which separated from the solution after it had been left standing for 24 hours was filtered, washed with ethanol, and dried. The compound 3,3′-imino-bis(4-benzylidene-5-pyrazolone) was recrystallized from ethanol. It was insoluble in acids and slightly soluble in bases and gave a negative test with ferric chloride, m.p. 252–253° C. Yield, 17%. Calc. for $C_{20}H_{15}O_2N_5$: C, 67.20; H, 4.23; N, 19.60%. Found: C, 67.6; H, 4.1; N, 19.3%.

3-Amino-5-pyrazolone and Phenylacetaldehyde

4-Phenylethylidene-3-iminophenylethylidene-5-pyrazolone.—To a cooled mixture of 3-amino-5-pyrazolone (0.20 mole) in ethanol (715 ml) and piperidine (4 ml), phenylacetaldehyde (50%, 134.4 g, 0.56 mole) was slowly added, and the mixture refluxed for 24 hours and treated as in the preceding experiment. A white solid separated from the concentrated solution when it was left standing. The crude product was filtered, washed with ethanol, and dried. 4-Phenylethylidene-3-iminophenylethylidene-5-pyrazolone, which crystallized from methanol in plate-like crystals, was insoluble in acids and slightly soluble in bases. It gave a negative test with ferric chloride and could not be reduced with sodium in ethanol, m.p. 264–266° C. Yield, 30%. Calc. for $C_{19}H_{17}ON_3$: C, 75.21; H, 5.65; N, 13.85%. Found: C, 75.7; H, 5.4; N, 13.9%.

3-Amino-1-phenyl-5-pyrazolone and Aldehydes

3-Amino-1-phenyl-5-pyrazolone.—To a cooled mixture of aldehyde (0.14 mole), ethanol (50 ml), and piperidine (2 ml) was added 3-amino-1-phenyl-5-pyrazolone (0.06 mole). The mixture was refluxed for 24 hours and the alcoholic solution was then evaporated under reduced pressure to one-half of its original volume, and upon cooling, the crude material separated from the solution. The products isolated together with their recrystallizing solvents, melting points, yields, molecular weights, analyses, and solubility tests are given in Table I. All the compounds isolated gave negative tests with ferric chloride.

Benzaldehyde

4-Benzylidene-3-amino-1-phenyl-5-pyrazolone. To a cooled solution of benzaldehyde (0.34 mole) in benzene (800 ml) was added 3-amino-1-phenyl-5-pyrazolone (0.11 mole).

**All melting points are uncorrected.*

Can. J. Chem. Downloaded from www.nrcresearchpress.com by 190.90.36.8 on 09/04/12
For personal use only.

The reaction mixture was refluxed for 24 hours, after which time a white solid precipitated from the solution. The product was cooled, filtered, and washed with ethanol. The crude product was extracted with methanol (375 ml), the extract was filtered and evaporated to one-half of its original volume, and then left to crystallize overnight in the refrigerator. 4-Benzylidene-3-amino-1-phenyl-5-pyrazolone crystallized out in clustered colorless needles. The compound was soluble in hot ethanol, soluble in acids, and insoluble in bases. No coloration was obtained with ferric chloride, m.p. 231–233° C. Yield, 85%. Calc. for $C_{16}H_{13}ON_3$: C, 72.98; H, 4.98%. Found: C, 72.8; H, 5.1; N, 16.0%.

Reduction of 5-Pyrazolones with Sodium and Absolute Ethanol

3,3′-Imino-bis(4-propylidene-1-phenyl-5-hydroxypyrazolone).—A suspension of 4-propylidene-3-amino-1-phenyl-5-pyrazolone (0.01 mole) in absolute ethanol was prepared in a 3-necked flask fitted with a condenser. To the mixture were added clean pieces of sodium (0.07 mole) at such a rate that vigorous refluxing was continuous. The mixture was then refluxed for 1½ hours to assure that all the sodium had reacted, and during this time, ammonia was evolved. The ethanol was then removed by evaporation under reduced pressure. The resulting yellow sludge was dissolved in water (40 ml) and the solution filtered. The filtrate was neutralized with acetic acid (50%), whereupon a red amorphous product precipitated immediately. The reduced compound, 3,3′-imino-bis(4-propylidene-1-phenyl-5-pyrazalin-5-ol), was separated by filtration, washed with water, and dried. The crude product crystallized from methanol in red cubical crystals. 3,3′-Imino-bis(4-propylidene-1-phenyl-5-pyrazolone) was found insoluble in water, acids, and ether, and slightly soluble in bases. A negative test was obtained with ferric chloride, m.p. 215–217° C. Yield, 82%. Calc. for $C_{24}H_{27}O_2N_5$: C, 69.0; H, 6.52; N, 16.78%. Found: C, 70.0; H, 6.4; N, 16.6%.

4-Benzylidene-3-amino-1-phenyl-5-pyrazalin-5-ol. — 4-Benzylidene-3-amino-1-phenyl-5-pyrazolone (0.01 mole) in absolute ethanol (125 ml) was reduced with sodium (0.17 mole) as in the foregoing experiment. The reduced compound, 4-benzylidene-3-amino-1-phenyl-5-pyrazalin-5-ol, was recrystallized from methanol and isolated as colorless needles; it was soluble in acids and bases and insoluble in ether. A negative test was obtained with ferric chloride; the compound had a tendency to decompose in air, m.p. 197–199° C. Yield, 58%. Calc. for $C_{16}H_{15}ON_3$: C, 72.43; H, 5.70; N, 15.84%. Found: C, 72.0; H, 5.2; N, 15.2%.

3,3′-Imino-bis(4-p-methoxybenzylidene-1-phenyl-5-pyrazalin-5-ol.—A suspension of 3,3′-imino-bis(4-*p*-methoxybenzylidene-1-phenyl-5-pyrazolone (0.02 mole) and ethanol (300 ml) was treated with sodium (0.38 mole) so that refluxing was continuous and the reaction mixture was then treated as in the preceding experiments. The crude product obtained recrystallized from benzene gave a colorless compound, m.p. 170–172° C. Yield, 38%. Calc. for $C_{34}H_{31}O_4N_5$: C, 71.19; H, 5.45; N, 12.21%. Found: C, 70.5; H, 5.6; N, 11.8%.

5-Pyrazolonoguanidines

N,N′-bis(4-substituted-5-pyrazolono)-guanidines. — 4-Substituted-3-amino-5-pyrazolone (0.03 mole) was fused with dicyandiamide (0.02 mole), with stirring. The mixture began to melt at 90° C, during which time a slight exothermic reaction occurred and ammonia was liberated. The temperature of the melt was then raised to 180° C and kept there for 3 hours. The molten mass was then cooled, extracted with ethanol, and precipitated with a large quantity of water. The guanidine derivative was then recrystallized several times from an ethanol–water mixture. The compound was soluble in acetone and bases,

Can. J. Chem. Downloaded from www.nrcresearchpress.com by 190.90.36.8 on 09/04/12
For personal use only.

and insoluble in acids. A positive test for an enolic group was obtained with ferric chloride. The guanidine derivatives isolated were: N,N′-bis(4-amyl-5-pyrazolono)-guanidine, m.p. 197–199° C. Yield, 86%. Calc. for $C_{17}H_{29}O_2N_7$: C, 56.20; H, 7.99; N, 27.0%. Found: C, 55.9; H, 7.8; N, 27.4%. Molecular weight: Calc. 363. Found (Rast method): 382 and 395. N,N′-bis(4-benzyl-5-pyrazolono)-guanidine, m.p. 258–261° C. Yield, 75%. Calc. for $C_{21}H_{21}O_2N_7$: C, 62.53; H, 5.21; N, 24.30%. Found: C, 62.3; H, 5.0; N, 23.6%. Molecular weight: Calc. 403. Found (Rast method): 419 and 427.

4-Butyl-5-pyrazolonoguanidine.—4-Butyl-3-amino-5-pyrazolone (0.03 mole) was fused with dicyandiamide (0.02 mole), with stirring. The mixture began to melt at 85° C, and the temperature was slowly raised to 150° C and held at that temperature for 3 hours. The melt was then treated as in the preceding experiments. The crude 4-butyl-5-pyrazolonoguanidine was then recrystallized from an ethanol–water mixture. The compound was soluble in acetone, acids, and bases and gave a positive test with ferric chloride, m.p. 239–241° C. Yield, 57%. Calc. for $C_8H_{15}ON_5$: C, 48.73; H, 7.61; N, 35.53%. Found: C, 48.4; H, 7.6; N, 35.5%. Molecular weight: Calc. 197. Found (Rast method): 210 and 221.

REFERENCES

1. NENCKI, M. and SIEBER, N. J. prakt. Chem. **17**, 478 (1878).
2. CONRAD, M. and ZART, M. Ber. **39**, 2282 (1906).
3. HEPNER, B. and FAJERSZTEJN, S. Bull. soc. chim. France, **4**, 854 (1937).
4. GAGNON, P. E., SAVARD, K., GAUDRY, R., and RICHARDSON, M. Can. J. Research, B, **25**, 28 (1947).
5. GAGNON, P. E., BOIVIN, J. L., and JONES, R. N. Can. J. Research, B, **27**, 190 (1949).
6. GAGNON, P. E., BOIVIN, J. L., and GIGUÈRE, J. Can. J. Chem. **29**, 328 (1951).
7. GAGNON, P. E., NOLIN, B., and JONES, R. N. Can. J. Chem. **29**, 843 (1951).
8. WEISSBERGER, A. and PORTER, H. D. J. Am. Chem. Soc. **64**, 2133 (1942).
9. GRAHAM, B., RECKHOW, W., and WEISSBERGER, A. J. Am. Chem. Soc. **76**, 3993 (1954).
10. KNORR, L. Ann. **238**, 147 (1887).

Can. J. Chem. Downloaded from www.nrcresearchpress.com by 190.90.36.8 on 09/04/12
For personal use only.

Can. J. Chem. Downloaded from www.nrcresearchpress.com by 190.90.36.8 on 09/04/12
For personal use only.

NOTES

SYNTHESIS OF ALKYL 1-PHENYL-5-CHLORO-1,2,3-TRIAZOLE-4-CARBOXYLATE

EUGENE LIEBER,* T. S. CHAO, AND C. N. R. RAO

INTRODUCTION

The ability to exchange the chlorine in position 5 of the *vic*-triazoles by nucleophilic substitution makes it a desirable intermediate in synthetic work in this field. Dimroth (1), and later Dutt (2), reported on the preparation of I and II by the reaction of the esters of 1-phenyl-5-hydroxy-1,2,3-triazole-4-carboxylate (3), III, with phosphorus pentachloride and by the diazotization of the hydrochloride of the ester of 1-phenyl-5-amino-1,2,3-triazole-4-carboxylate (1), IV; in the latter synthesis Dimroth (1) gave no details of procedure nor yield of product. The phosphorus method is also sketchily described, the literature (1, 2) implying that it

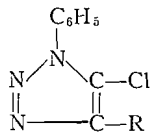

I (R = $CO_2C_2H_5$)
II (R = CO_2CH_3)

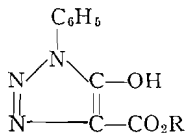

III (R = CH_3; or, C_2H_5)

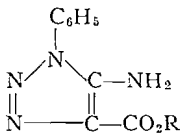

IV (R = CH_3; or, C_2H_5)

merely involves heating IV and phosphorus pentachloride together. In our hands the yields obtained with the phosphorus pentachloride method were found to be dependent on the care taken to maintain anhydrous conditions and the rates of phosphorus pentachloride addition. As triazoles of the general structure I and II were required for previous studies (4, 5, 6), detailed experimental procedures were worked out starting from the intermediates III and IV and are reported upon in the present communication. The diazotization procedure offers an advantage in that the required intermediate IV can be made more easily and in higher yields than III (4) and in turn gives comparable conversions to the required 5-chloro-compounds (I, II). The experimental section presents typical preparations involving both the phosphorus pentachloride and diazotization methods, respectively.

EXPERIMENTAL†,‡

Methyl 1-Phenyl-5-chloro-1,2,3-triazole-4-carboxylate (II)

Phosphorus pentachloride procedure.—A 500-ml, 3-necked flask was equipped with a stirrer and a reflux condenser. To the third neck was connected a 125-ml Erlenmeyer flask connected by a short piece of $\frac{1}{2}$-in.-diameter Tygon tubing through 16 mm glass tubing from the necks of the Erlenmeyer flask and reaction flask respectively. The Tygon connector was of sufficient length to permit the Erlenmeyer flask to rest on its bottom when not in use as described below. The complete setup was flame-dried and cooled to room temperature under a nitrogen atmosphere. The reaction flask was then charged with 65.7 g (0.3 mole) of *methyl 1-phenyl-5-hydroxy-1,2,3-triazole-4-carboxylate* (II, R = CH_3) (3), which had been dried in a vacuum desiccator over Drierite for 2 days.

*To whom all inquiries for additional information should be addressed.
†Melting points were taken on a Fisher–Johns heating block and are corrected.
‡Microanalyses by Dr. C. Weiler and Dr. F. B. Strauss, Oxford, England.

Seventy-four grams (0.33 mole) of PCl_5 was placed in the Erlenmeyer flask. The reaction flask was heated in a water bath to 70° and kept at 65–70° during the reaction. By raising the Erlenmeyer flask containing the PCl_5 to a slightly inverted position and gently tapping its wall, PCl_5 was caused to flow slowly and intermittently into the reaction flask. The progress of the reaction was indicated by the HCl evolution and was controlled accordingly, completing the addition of PCl_5 in about 90 minutes, after which time the reaction mixture was heated in a gently boiling water bath for 4 hours in order to complete the reaction. After being cooled to room temperature the system was connected to a water pump through a $CaCl_2$ tower and a dry-ice trap. The dissolved HCl was first removed, after which the $POCl_3$ was distilled off at 31–32° at 47 mm. The last traces of $POCl_3$ were removed by distilling at 1–2 mm, using a well-protected oil pump. The residue solidified into a brown mass while being stirred with a glass rod. The suspension was poured into 500 ml of water and filtered. The solid was suction dried and weighed 44 g, m.p. 80–82°. The filtrate was separated into two layers. The ether layer was washed with water, dried, and evaporated under vacuum recovering 4 g additional product. Purification was effected by recrystallization from methanol; yield, 41 g (57.4%), white needles, m.p. 87° (1). Anal. Calc. for $C_{10}H_8ClN_3O_2$: C, 50.52; H, 3.40; N, 17.70; Cl, 14.92. Found: C, 50.57; H, 3.48; N, 17.60; Cl, 14.82. The mother liquor was in the form of a dark red thick oil which failed to crystallize.

Ethyl 1-Phenyl-5-chloro-1,2,3-triazole-4-carboxylate (I)

Diazotization procedure.—A mixture of 250 ml of absolute ethanol and 23.2 g (0.1 mole) of *ethyl 1-phenyl-5-amino-1,2,3-triazole-4-carboxylate* (1, 4) was placed in a 1-l. 3-necked flask equipped with a stirrer, dropping funnel, and a gas inlet tube, all exits were protected with drying tubes. The mixture was cooled to 0–5° with stirring, whereupon a slow stream of *dry* HCl gas was slowly bubbled through the mixture until the suspended solid went into solution. Seventeen grams (0.1 mole) of freshly prepared isoamyl nitrite (7) was then added rapidly and the reactants stirred at 0–5° for 48 hours. It was then poured into 500 ml of ice water with vigorous stirring. A fine orange-colored precipitate was obtained. It was filtered, suction dried, and dissolved in 50 ml of boiling methanol. After evaporation *in vacuo*, 12 g (47%) of deeply yellow-colored needle-like crystals was obtained. Recrystallization from methanol containing a small amount of water gave pale yellow needles, m.p. 79°. Dutt (2) reported a m.p. 80–81°. Anal. Calc. for $C_{11}H_{10}ClN_3O_2$: C, 52.50; H, 4.01; Cl, 14.09; N, 16.70. Found: C, 52.24; H, 4.10; Cl, 13.90; N, 17.00. The mother liquor, after evaporation of all of the solvent, gave about five grams of a red viscous oil which could not be crystallized.

ACKNOWLEDGMENTS

The authors gratefully acknowledge grants-in-aid from the Research Corporation, New York, N.Y., and the Eli Lilly Company, Indianapolis, Indiana, which made this study possible. We are also indebted to C. N. Pillai and J. Ramachandran for aid in checking the procedures described.

1. Dimroth, O. Ann. **364**, 183 (1909).
2. Dutt, P. K. J. Chem. Soc. 265 (1923).
3. Dimroth, O. Ann. **335**, 1 (1904).
4. Lieber, E., Chao, T. S., and Rao, C. N. R. J. Org. Chem. **22**, 654 (1957).
5. Lieber, E., Rao, C. N. R., and Chao, T. S. J. Am. Chem. Soc. **79**, 5962 (1957).
6. Lieber, E., Rao, C. N. R., and Chao, T. S. Current Sci. (India), **26**, 14 (1957).
7. Noyes, W. A. Org. Syntheses, Coll. Vol. II, 109 (1943).

Received September 15, 1958.
Department of Chemistry,
DePaul University,
Chicago 14, Illinois, U.S.A.

Can. J. Chem. Downloaded from www.nrcresearchpress.com by 190.90.36.8 on 09/04/12
For personal use only.

Can. J. Chem. Downloaded from www.nrcresearchpress.com by 190.90.36.8 on 09/04/12
For personal use only.

Symposium on Charge Transfer Processes

A REPORT ON A SYMPOSIUM HELD BY THE PHYSICAL CHEMISTRY DIVISION OF THE CHEMICAL INSTITUTE OF CANADA[1]

B. E. Conway

INTRODUCTION

A symposium on Charge Transfer Processes both in the homogeneous solution phase and at electrode interfaces was held at the Chemistry Department of the University of Toronto on 4th and 5th September, 1958. The meeting was sponsored by the Chemical Institute of Canada, supported by the National Research Council, and organized under the chairmanship of B. E. Conway (University of Ottawa). Twenty-seven invited papers were presented, the majority of which had been preprinted and circulated to participants prior to the meeting. The sessions were devoted to ten-minute presentations of these papers together with periods of discussion on related groups of papers. A number of the invited papers are being published in the present issue of the Canadian Journal of Chemistry. In this paper a general account of the meeting is given together with reports on the main matters which arose in discussion and the conclusions arising therefrom.

Although individual papers on some aspects of Charge Transfer Processes have been presented at various meetings in North America and Europe, it is some time since a meeting specifically on this topic has been held. The last general meetings held specifically on electrochemical charge transfer processes were the Faraday Society Discussion in 1947 and the Bunsengesellschaft meeting at Goslar in 1951. Since these meetings, there have been considerable advances made in the field both in homogeneous and heterogeneous processes. In the present symposium an attempt was made to bring together contributions from those interested in homogeneous and also heterogeneous processes, since similar problems are encountered in both of these types of charge transfer processes; thus, the degree of solvent reorganization which occurs in the charge transfer step, the nature of the electron transfer process, specific effects of aquo- and non-aquo-ligand interaction with the ions involved are problems common to both the fields of homogeneous and heterogeneous processes. For the latter type of reactions, adsorption of reactants and solvent, the effect of electrode field on the reaction kinetics and adsorption of reactants and the electronic character of the metal (e.g. *s*, *p*, or *d*-band character) must also be considered. Papers were therefore also invited on adsorption at electrodes and the nature of the double layer at electrode interfaces. The somewhat specialized fields of so-called "charge-transfer spectra" and "charge-transfer complexes" were considered to be outside the scope of the present meeting.

HOMOGENEOUS PROCESSES

Despite their familiarity in classical inorganic solution chemistry, the detailed mechanism of a number of apparently simple redox reactions involving simple and complex inorganic ions has not until relatively recently been examined or understood. The first four papers of the symposium dealt with theoretical and experimental results obtained with such systems.

[1]*Manuscript received July 10, 1958.*
Contribution from the Department of Chemistry, University of Ottawa, Ottawa, Canada.

Can. J. Chem. Downloaded from www.nrcresearchpress.com by 190.90.36.8 on 09/04/12
For personal use only.

Electron Transfer Reactions between Ions in Solution

H. Taube (University of Chicago), in giving the opening paper on "Bridging and Simple Ligand Effects in Electron Transfer Reactions", stressed the role of changes which must occur in the co-ordination sphere of the ions when the transfer of the electron(s) occurs. Two types of transition states are to be distinguished: (i) the outer sphere activated complex in which both of the ions concerned in the redox reaction are relatively inert to ligand substitution (e.g. as determined by isotopic exchange experiments) and in which the inner co-ordination spheres hence cannot suffer appreciable interpenetration; (ii) the bridged activated complex in which a ligand, often anionic, is shared between the metal ions, so that a change in the first co-ordination sphere of at least one of the partners of the redox pair must occur. Examples of redox pairs involved in the first type of reaction are $Fe(CN)_6^{-3,-4}$, $IrCl_6^{-2,-3}$, $Mo(CN)_8^{-3,-4}$, $Fe(dipy)_3^{+3,+2}$, $Os(o\text{-phen})_3^{+3,+2}$, $MnO_4^{-1,-2}$; in the second type of case the redox reaction between $(NH_3)_5CoCl^{++}$ with Cr^{++} was discussed. $CrCl^{++}$ is formed as a product and not $Cr(H_2O)_6^{+++}$ in this reaction, thus suggesting that a Cr—Cl bond is involved in the activated state. A variety of other anions which may take part in the formation of bridged transition states were listed, and kinetic data were presented in cases involving reactions between Cr^{++} and Cr(III) complexes. The role of conjugation when organic ligands are involved in the reaction between Cr^{++} and Co(III) complexes was examined. It was pointed out that, although the reaction mechanisms are known in a number of selected cases, the subject of inorganic redox reactions must be regarded as still being in an unsatisfactory state of development so long as relatively common reactions such as those between Fe^{++}–Fe^{+++} and Fe^{++} and Ce(IV) are not understood with regard to their detailed mechanism.

In regard to the Fe^{++}–Fe^{+++} case, K. J. Laidler (University of Ottawa) presented some interesting theoretical considerations concerning the mechanism and free energy of activation of this reaction. The reaction between Fe^{++} and Fe^{+++} was considered to be diffusion controlled, the approach of the ions being hindered by their electrostatic repulsion, which was estimated taking into account the dielectric saturation in the solvent near to the ions. As the ions are brought together the electrostatic repulsion rapidly increases but the probability of electron tunneling between the ions increases at the same time. An optimum separation of the ions exists for which the redox reaction has a maximum rate or minimum free energy of activation $\Delta G^{\ddagger}$. The value of $\Delta G^{\ddagger}$ calculated is in good agreement with that derived from experimental data.

The applicability of the Franck–Condon principle to the electron transfer and solvent redistribution which occurs in electron transfer reactions such as that between Fe^{++}–Fe^{+++} ions, was vigorously discussed by R. A. Marcus (Brooklyn Polytechnic Institute) and K. J. Laidler. It was felt that since the electron transfer must occur by a relatively rapid tunneling step, the solvent distribution about the ions could be regarded as essentially remaining static during the electron transfer. This is what had been assumed in the calculations.

The principle of equivalence change in redox systems was dealt with in a paper by J. Halpern (University of British Columbia). A number of oxidizing and reducing reagents are known where stable oxidation states differ by two electron equivalents, e.g. Tl(I)–Tl(III); Sn(II)–Sn(IV). The mechanism of the reactions in which such redox pairs react with 1-equivalent reductants or oxidants, e.g. Fe(II)–Fe(III) or Ce(III)–Ce(IV), is of interest. The principle of equivalence change (Schaffer (1)) states that such reactions are generally slow compared with analogous reactions between 1-equivalent reductants

and 1-equivalent oxidants or between 2:2 equivalent systems. The equivalence principle was examined by Halpern with reference to the kinetics of three types of reaction: (i) electron transfer reactions between two metal ions; (ii) oxidation of metal ions by molecular oxygen; and (iii) reduction of metal ions by molecular hydrogen. It was concluded that the principle has only limited applicability to the reactions studied and that other factors are involved in determining the kinetics, viz. formation of intermediate complexes between the oxidant and reductant, participation of chain reactions. Some reactions are complicated in that they proceed by simultaneous bimolecular and termolecular paths, the latter being favored by lower activation energies.

A general theoretical paper by R. A. Marcus (Brooklyn Polytechnic Institute) "On the Theory of Electrochemical and Chemical Electron Transfer Processes" brought together some of the problems common to the fields of homogeneous and heterogeneous charge transfer reactions. The solvent configuration about the reacting ions was considered gradually to change during the reaction to a configuration characteristic of the final state of the reaction; at the same time the electronic configuration was regarded as undergoing a corresponding change, following the molecular redistribution adiabatically. This view was disputed by K. J. Laidler, who regarded the electron tunneling as fast and preceding the molecular rearrangement of the solvent. The role of image forces in heterogeneous reactions was given some qualitative examination in the light of recent calculations of Sachs and Dexter (2). It must be pointed out, however, that a problem of some magnitude still exists. Thus in electrode processes and in ionic adsorption, it appears that the effect of the image potential is surprisingly small; thus the absence of any significant specific adsorption of NaF and of simple cations at the electrocapillary maximum of Hg is unexpected. In the double layer the water molecules in the first coordination sphere about the ions will have a low dielectric constant (cf. (6); see (3), and K. J. Laidler, this symposium), so that the image potential might be expected to be not less than three or four kilocalories. It was pointed out by R. A. Marcus that the attraction of the ions to the interface may lower the entropy of solvation of the ions. However, this would not be in the direction which would cancel the effect of the electrostatic image interaction. It appears that this matter requires some further examination.

Proton Transfer Reactions

In recent years, considerable interest has been shown in the mechanism of proton transport in solutions and in hydrogen bonded solids. Two papers concerning this topic were presented: one on the "Limiting Conductance of Lyonium and Lyate Ions" by M. Kilpatrick (Illinois Institute of Technology) and the second on "Some Considerations on the Role of Proton Tunneling in Certain Charge Transfer Processes" by B. E. Conway (University of Ottawa). M. Kilpatrick presented data for the ratio of equivalent conductances of HCl–DCl mixtures to that of KCl in H_2O–D_2O solutions and also for the ratio of conductance of $HClO_4$–$KClO_4$ and HCl–KCl in H_2O–H_2O_2 and H_2O–CH_3OH mixtures, respectively. In H_2O–H_2O_2 solutions the anomalous proton conductance is partially eliminated; in H_2O–D_2O mixtures it is diminished at intermediate concentrations of D_2O. Preferential solvation effects are important in determining the anomalous proton conductance in solutions of acids in mixed solvents. The conductance behavior of a number of interesting non-aqueous systems was discussed.

The conductance of solid D_2O had been measured under conditions of rigorous purification by B. E. Conway in order to obtain an estimate of the isotopic ratio of equivalent conductance of H^+/D^+ in their respective pure ices. A value of about 1.6 was obtained for this ratio. The proton tunneling theory previously given (4) was re-examined using

Can. J. Chem. Downloaded from www.nrcresearchpress.com by 190.90.36.8 on 09/04/12
For personal use only.

a quantal energy distribution and it was shown that an isotopic ratio of conductance of H^+ to that of D^+ in H_2O and D_2O ices, respectively, of 1.1 could be derived and a better value of the absolute mobility of H^+ in H_2O ice obtained. Classically, an isotopic ratio of conductance in the ices should be about nine.

The electrochemical behavior which would arise if proton tunneling occurred at electrodes was also examined and criteria were proposed for recognition of the effect. At intermediate overpotentials the Tafel equation is still obeyed but has an anomalously high slope which is dependent upon the isotopic mass. High separation factors do not necessarily arise in H^+/D^+ tunneling. Values comparable with those deduced classically (*ca.* 3 to 10) should arise at moderate cathodic overpotentials. It was pointed out that except in ice, the proton tunneling mechanism is not unambiguously demonstrable experimentally yet is theoretically indicated in a number of reactions. R. A. Marcus suggested that this could be because energy levels in initial and final states of the reaction were not available at comparable energies except in the case of proton transfer in ice where the initial and final states of the reaction are identical. J. E. B. Randles (University of Birmingham) pointed out that in the case examined by B. E. Conway for electrodes, some suitable levels should become available as the electrode potential was varied. Similarly, B. E. Conway referred to the *o*, *p*-hydrogen conversion case as one where the necessary levels should be available yet proton tunneling was not clearly indicated as the mechanism (5) of this reaction.

HETEROGENEOUS PROCESSES

Electrolytic Metal Deposition

Three papers on metal deposition were presented. The first by J. O'M. Bockris and W. Mehl (University of Pennsylvania) was concerned with the determination of the rate-determining step(s) in the electrolytic deposition of silver. A galvanostatic method had been employed in which the overpotential build-up lines at constant current density were interpreted with the aid of kinetic equations deduced for various limiting conditions corresponding to (i) slow ionic transfer of Ag^+ to the metal surface; (ii) comparably slow transfer and surface diffusion of adsorbed ions or atoms; and (iii) slow surface diffusion alone. The results indicated that path (iii) was rate-determining at low current densities whilst (i) was rate determining at high current densities. A useful comparison of expressions used in crystal growth from the vapor phase, with corresponding ones arising in electrolytic metal deposition was presented.

The kind of information which can be deduced from a study of radioisotope exchange reactions between ions and their corresponding metals was examined by C. V. King (New York University). The roles of the exchange current, adsorption of ions, local cell electrolysis and corrosion, and self-diffusion in the metal were discussed. It was shown that, in general, the exchange current cannot unambiguously be measured by the radiotracer method unless conditions are unusually favorable. Some results were presented which demonstrated the importance of internal self-diffusion as a factor to which too little attention had been paid in previous work.

The mechanism of growth of electrolytic metal whiskers was described by D. A. Vermilyea (General Electric Company) in terms of the theory of crystal growth. Incorporation of organic additives into the growing whiskers was likely and poisoning of the non-growing crystal faces was indicated below a certain critical current density, i_c. An estimate of i_c made theoretically was in quite good agreement with that found experimentally for silver whisker formation from $AgNO_3$ solutions.

Some discussion of these papers centered around the question of the nature of the

Can. J. Chem. Downloaded from www.nrcresearchpress.com by 190.90.36.8 on 09/04/12
For personal use only.

adsorbed entity resulting from the first ionic transfer stage in metal deposition and the mechanism by which a whisker begins its growth from a non-dendritic surface. It is probable that the adsorbed species which undergo surface diffusion across planar crystal faces to growing edges are not completely neutral atoms. Some appreciable ionic character in the bond between the adsorbed species and the bulk metal is probably preserved, e.g. as with H atoms adsorbed at metals where the surface dipole moment is considerable. Ionic transfer directly from the double layer to growing edges or kinks is unlikely as is indicated theoretically (6) on general energetic grounds.

The Hydrogen Evolution Reaction

Three papers were read on various aspects of the cathodic hydrogen evolution reaction. D. J. G. Ives (Birkbeck College, University of London) described some anomalies in the behavior of gold electrodes with respect to rest potentials and kinetics of the hydrogen evolution reaction, when the electrodes had been thermally deactivated at 800° C. The rest potentials were positive and overpotentials increased during polarization. The behavior was similar to that observed with poisoned platinum electrodes. The desorption of adsorbed H as molecule ions through the mechanisms

$$H_{ads} + H^+_{aq} \rightarrow H_2{}^+_{aq} \text{ (acid solutions)}$$

and

$$H_{ads} + H_2O_{aq} \rightarrow H_2{}^+_{aq} + OH^- \text{ (alkaline solution)}$$

was considered. It was shown that such processes are energetically not unlikely if it can be assumed that $H_2{}^+$ has a heat of hydration of at least -221 kcal mole^{-1}. The molecular dimensions and electron distribution in $H_2{}^+$ are not inconsistent with such a solvation energy. The desorption mechanism involving $H_2{}^+$ was suggested as a possible explanation for "reduction at a distance" claimed by Kobosew and Nekrassov (7) and again demonstrated by Poltorak (8). It was suggested that H_2 molecule production could occur in the solution by dissociation and recombination of the H atoms with liberation of the protons. Protons from the solution would thus only be involved as "carriers" in this desorption and H_2 production mechanism.

Electrolytic hydrogen production at single and polycrystalline silver electrodes was considered by A. Antoniou and F. E. W. Wetmore (University of Toronto), who reported new experimental data over a range of temperatures for polarization of silver in 1 M H_2SO_{4aq}. Tafel lines having an inflection were observed thus confirming qualitatively the previous work on silver (9); the Tafel slopes were approximately 0.059 (i.e., $2.3RT/F$) and 0.112 (i.e., 2.3 $(2RT/F)$). The apparent heat of activation was 18.8 kcal for low current densities and 14.3 kcal mole^{-1} for higher current densities. The lower slope of 0.059 could be explained in terms of slow surface migration of H atoms to recombination sites or on the basis of a first order H atom recombination step (10). At high current densities $\nu/\beta = 1$ (where ν is the stoichiometric number and β the symmetry factor taken as 0.5) so that a slow H^+ ion discharge reaction is indicated as the rate-determining step. It was pointed out by R. Parsons (University of Bristol) in discussion that a previous explanation (11) of the change of slope in terms of the change of the ψ_1* potential, as the electrode potential passes through the potential of zero charge of the metal, could not explain the magnitude of the change of Tafel slope observed. B. E. Conway emphasized that a similar effect would also be expected at other metals, e.g. Pb, Cu, Ni, where the potential of zero charge is within the range of potentials accessible in cathodic overpotential studies. The fact that inflections in Tafel lines are not observed for these

*ψ_1 *is the potential of the outer Helmholtz plane.*

Can. J. Chem. Downloaded from www.nrcresearchpress.com by 190.90.36.8 on 09/04/12
For personal use only.

metals lends support to Parson's comment. Moreover, it is only for silver that the potential of zero charge is positive to the hydrogen reversible potential, i.e. outside the range of cathodic overpotentials examined. The somewhat unique polarization behavior of silver therefore appears to reflect a genuine change of rate-determining mechanism with change of electrode potential (see also (12)).

The nature of the Pd–H system and the mechanism of hydrogen transport through the metal have been problems of interest for some years. Technological interest in these phenomena has arisen on account of the effect of dissolved H on the mechanical properties of certain metals, e.g. iron. S. Schuldiner and J. P. Hoare (U.S. Naval Research Laboratory) reported some interesting experiments on the transport of hydrogen through Pd and Pt bielectrodes and through Pd-clad electrodes in the form of sandwiches with the Pd as the outside metal. Studies were made by measuring the current–potential or potential behavior on both sides of diaphragm electrodes. Transport of hydrogen in an *atom* concentration gradient (i.e. using the β-phase of the Pd–H system) occurs with Pd and Pd-clad Fe only. Under a proton concentration gradient, hydrogen transfer occurs readily through Pd but not through Pt unless this is sandwiched between Pd. Transfer also occurs through sandwiched Fe. No transport of hydrogen either as protons or atoms occurs through Au or Ni. The latter result is surprising and occasioned some discussion, since under other conditions Ni dissolves hydrogen and the time variation of overpotential at Ni in ultrapurified solutions is believed to be due to uptake of H into the metal with consequent change in the electronic properties of the metal.

Other Electrochemical Reduction Processes

Three papers were devoted to heterogeneous reduction reactions other than those involved in the deposition of metals or hydrogen. J. E. B. Randles (University of Birmingham) described methods of calculating kinetic parameters of fairly fast redox reactions, from current potential curves obtained with rotating electrodes or stationary electrodes in stirred solutions or with dropping mercury electrodes. A comparison between the results obtained by means of the steady state current–potential relationship and by a-c. impedance measurements for the V^{2+}/V^{3+} reaction at the dropping mercury electrode was made. Satisfactory agreement between the kinetic parameters obtained by means of the two methods is found if in the interpretation of the current–potential curves due allowance is made for concentration polarization effects. This was achieved in the case of the expanding mercury drop at which the slow V^{++}/V^{+++} electrochemical reaction was occurring, by using Koutecky's analysis of the diffusion problem for this case. A mathematical and numerical analysis was given.

In the case of the reduction of chloraquo–Cr(III) ions at the dropping mercury electrode, P. J. Elving (University of Michigan) and B. Zemel (Shell Development) showed that the polarographic waves for Cr(III) species in various concentrations of perchloric acid, hydrochloric acid, and neutral salts were best interpreted by assuming two concurrent mechanisms for the electron transfer process: (i) the direct transfer of an electron to the Cr(III) ion from the electrode at the interface of the drop and (ii) the transfer of an electron to the Cr(III) ion from a Cr(II) ion produced at the interface. Only in the case of $[CrCl_2(H_2O)_4]^+$ ions in 12 *M* HCl is the direct electron transfer mechanism dominant.

Some problems in electrochemical reduction and cathodic preparation of certain organic compounds of pharmacological and biochemical interest were discussed by M. J. Allen (C.I.B.A. Pharmaceutical Products) and apparatus used in controlled potential electrolysis was described.

Can. J. Chem. Downloaded from www.nrcresearchpress.com by 190.90.36.8 on 09/04/12
For personal use only.

Can. J. Chem. Downloaded from www.nrcresearchpress.com by 190.90.36.8 on 09/04/12
For personal use only.

Anodic Electrode Processes

The development of the field of anodic processes has in general lagged behind that of cathodic processes mainly on account of the greater complexity of problems involved. This is due, for example, to the variety of surface oxide species which can be formed anodically on certain metals, the resistance of the surface films, and the time variation of electrode potential during formation of the films and during oxygen evolution on them. Two papers were given on the anodic passivation of iron; in the first paper by Snavely and Hackerman (University of Texas) a study of passivation at iron was made by determining the charge corresponding to the amount of iron dissolved in solution compared with the charge required to reach passivation in an anodic polarization of the iron. The number of coulombs found to be involved in the formation of the passive layer corresponding to a film of Fe_2O_3 15 Å thick if the electrode surface were planar was 0.002 cm^{-2}. A Flade arrest is not observed in anodic decay traces unless a potential of at least 1.2 v (E_H) is reached during the anodic charging. The passive layer is thus probably incomplete below this potential. The charge corresponding to the Flade arrest is equivalent to only about 10% of the passive layer.

The mechanism of formation and the properties of passive films on iron were discussed by M. Cohen (National Research Council). The reactions of water with iron under the following conditions were described: in the absence of oxygen and additives; in the absence of oxygen but in the presence of additives (oxidizing anions, e.g. nitrite, chromate, tungstate, molybdate); in the presence of oxygen; in the presence of oxygen plus oxidizing ions; and in the presence of oxygen and non-oxidizing buffering ions. Film-stripping techniques have shown that the films are mainly anhydrous ferric oxides. The thickness and chemical nature of the films formed under various conditions were reported.

L. Young (British Columbia Research Council) considered the growth of anodic oxide films, mainly from a theoretical standpoint; a number of models were considered for the formation and growth of oxide films. The roles of movement by metal ions, by oxygen, by lattice vacancies or interstitial ions, and the creation of defects by the applied field were examined.

Electrochemical processes at the nickel – nickel oxide electrode were examined by B. E. Conway and P. Bourgault (University of Ottawa) particularly with respect to the mechanism of the self-discharge and oxygen evolution which occurs on open circuit after charging the electrode. The open-circuit decay occurs by mixed anodic and cathodic processes, the rates of which are limited by the rate of evolution of oxygen at anodic sites. The potential on open circuit is determined by the quasi-equilibrium between the reduced and oxidized forms of the nickel oxide present at a given potential, the rate constants of the redox reactions between these species being large compared with that of the oxygen evolution process. Rates of self-discharge were determined as a function of KOH and H_2O activity and it was shown that two consecutive processes were involved in the decay, one having a Tafel slope of 2.3 $\frac{2}{3}(RT/F)$ and the other 2.3 $\frac{2}{5}(RT/F)$ (or 2.3 $\frac{1}{3}(RT/F)$). The rate of the process which was more dependent upon potential was also more dependent on KOH activity. The rates of both processes were increased by increasing KOH activity but decreased by increasing H_2O activity thus confirming the rate-controlling process as the oxygen evolution reaction. Mechanisms of anodic oxygen evolution which could explain the experimental results were proposed. In discussion of these papers, R. Parsons pointed out that under the limiting conditions for which rate laws for complex anodic processes have been previously calculated by the Christiansen method (13), this method was not in fact always necessary, since the same results could be obtained by

use of a simpler direct procedure using "quasi-equilibrium" steady-state concentrations of reacting intermediates for steps prior to the rate-determining step in a series of consecutive reactions.

Adsorption at Electrode Interfaces and the Double Layer

The last six papers of the symposium were concerned with the properties of the double layer and with adsorption in relation to electrode processes. In a paper by A. Frumkin *et al.* (Academy of Sciences, Moscow) some interesting effects of specifically adsorbed anions on the rate of electroreduction of $S_2O_8^{-2}$ ions at the negatively charged mercury electrode were reported. At a given potential and for a given cation the rate of reduction is increased in the order $Cl^- < Br^- < I^-$. The acceleration of the electroreduction, e.g. by I^-, depends on the nature of the cation, increasing in the sequence $Na^+ < K^+ < Cs^+$. It is concluded that the ψ_1 potential which determines, in part, the kinetics of the reaction is a fluctuating one influenced locally by the proximity of cations and anions, and is not the usually considered average ψ_1 potential in the double layer. In this way the specific effect of cations can be explained. The adsorption of anions at the negatively charged mercury electrode depends to a considerable extent on the formation of cationic "bridges".

Some general considerations on the correlation between the double-layer structure and electrode kinetics were presented by M. Breiter and P. Delahay (Louisiana State University). Experimental results on the reduction of IO_3^-, CH_3NO_2, and discharge of $[Cd(CN)_4]^{2-}$ were considered in terms of the double-layer structure and specific adsorption at the electrode. R. S. Hansen (Iowa State College) described some results on the frequency dependence of the double-layer capacity at mercury and deduced relaxation times, τ, for the water in the double layer as low as 10^{-2} seconds. Since this was very much higher than τ values for H_2O bound in ice (10^{-6} seconds) it was felt that the results and their interpretation might require further examination. R. Parsons presented a rigorous thermodynamic analysis for calculation of heats and entropies of adsorption of ionic species from electrocapillary data obtained at various temperatures, and showed results for adsorption of KI at mercury. E. Blomgren and J. O'M. Bockris (University of Pennsylvania) described electrocapillary data obtained for adsorption of HCl and aromatic amine hydrochlorides at mercury and deduced the components of charge in the double layer as a function of electrode potential. J. M. Los and C. K. Tompkins (University of New Brunswick) reported results obtained for the adsorption of methylene blue on mercury, determined by allowing many drops of mercury to come into equilibrium with the solution, and then to fall off into a common pool in a separate vessel, the solution in which was subsequently analyzed. The adsorption followed a Langmuir type of isotherm. B. E. Conway and R. G. Barradas in discussion reported some determinations of adsorption of organic ions and molecules at *solid* metal electrodes of Cu, Ni, and Ag using a direct spectrophotometric method. Isosteric heats of adsorption had been derived for acridine in aqueous solution at copper.

ACKNOWLEDGMENTS

The author would like to take this opportunity of acknowledging the assistance he has received from Professor F. E. W. Wetmore of the University of Toronto and Dr. R. J. Cvetanović, National Research Council, in the organization of the meeting and in the technical production of the preprints of the papers. The author and the Chemical Institute of Canada are much indebted to the National Research Council for providing technical facilities for the preprinting of the papers presented at the meeting.

Can. J. Chem. Downloaded from www.nrcresearchpress.com by 190.90.36.8 on 09/04/12
For personal use only.

REFERENCES

1. SHAFFER, P. A. J. Am. Chem. Soc. **55**, 2169 (1933). J. Phys. Chem. **40**, 1021 (1936).
2. SACHS, R. G. and DEXTER, D. L. J. Appl. Phys. **21**, 1304 (1950).
3. WEBB, J. C. J. Am. Chem. Soc. **48**, 2589 (1926).
4. CONWAY, B. E., BOCKRIS, J. O'M., and LINTON, H. J. Chem. Phys. **24**, 834 (1956).
5. BELL, R. P. Proc. Roy. Soc. (London), A, **139**, 466 (1933).
6. CONWAY, B. E. and BOCKRIS, J. O'M. Proc. Roy. Soc. (London) (In press).
7. KOBOSEW, N. V. and NEKRASSOV, N. I. Z. Elektrochem. **36**, 529 (1930).
8. POLTORAK, O. M. Zhur. Fiz. Khim. **27**, 599 (1953).
9. BOCKRIS, J. O'M. and CONWAY, B. E. Trans. Faraday Soc. **48**, 724 (1952).
10. LAIDLER, K. J. J. Phys. & Colloid Chem. **53**, 712 (1949).
11. BOCKRIS, J. O'M., AMMAR, I. A., and HUQ, A. K. J. Phys. Chem. **61**, 879 (1957).
12. CONWAY, B. E. and BOURGAULT, P. L. Can. J. Chem. **37** (1959) (This issue).
13. BOCKRIS, J. O'M. J. Chem. Phys. **24**, 817 (1956).

Can. J. Chem. Downloaded from www.nrcresearchpress.com by 190.90.36.8 on 09/04/12
For personal use only.

Can. J. Chem. Downloaded from www.nrcresearchpress.com by 190.90.36.8 on 09/04/12
For personal use only.

BRIDGING AND NON-BRIDGING LIGAND EFFECTS IN REDOX REACTIONS OF METAL IONS[1]

HENRY TAUBE

In this paper we shall be concerned with a description of the processes which are involved in the transfer of an electron from one metal ion center to another in solution, emphasizing in the description the changes in the first co-ordination spheres. Two distinct types of activated complexes have been characterized for these reactions, which throughout this article will be called the "outer sphere" activated complex and the "bridged" activated complex. In the outer sphere activated complex, the number and identity of the groups comprising the first co-ordination sphere remains unaltered on electron transfer; in the bridged activated complex, a common group is shared by the metal ions, so that a change in the first co-ordination sphere of at least one of the partners accompanies the formation of the activated complex. Other types of activated complexes have been suggested for redox reactions of metal ions, but for none of the others has as direct a demonstration of the characteristic features been possible as for the two which have been described above. This remark applies also to the hydrogen atom transfer formulation (1, 2, 3) (or its variations) according to which it is proposed that the redox process is brought about by the transfer of a hydrogen atom from the first co-ordination sphere of a hydrated reducing cation to that of the oxidizing cation. Although such a mechanism may apply in some cases, there is no proof that it operates in the systems for which it has been proposed.

A property of the ions in the system undergoing reaction which is significant in determining the reaction mechanism, and in permitting classification of the reaction type, is the ease with which they undergo substitution. Only when certain conditions are fulfilled with respect to the substitution lability of the redox partners has it been possible to draw fairly definite conclusions as to the nature of the activated complexes. The majority of the systems do not meet the rather special requirements which the substitution labilities compared to rates of electron transfer must fulfill, and for them the evidence as to mechanism type thus far advanced remains indirect.

The differences in the activated complexes recognized by the classification which has been made are not trivial. It is obvious that for the outer sphere types, the readjustments which accompany electron transfer may take place largely in the solvent and in the ion atmospheres. Such effects exist outside the first co-ordination sphere also for bridged activated complexes, although in certain cases they may be much reduced in intensity, but in addition, important chemistry in the first co-ordination spheres must be recognized as taking place. For reactions involving activated complexes which differ so markedly in structure as the two outlined, it is difficult at the present stage of development to propose a single simple theory of reaction rates which embraces both. Rather, it appears essential first to delineate experimentally each type of mechanism, and to try to assess the importance of the factors that affect the rate by each kind of reaction path. In this area as in others concerned with reaction mechanisms, it is in general not a question of either/or, and contributions to the over-all rate by rival paths must in general be acknowledged.

[1]*Manuscript received July 18, 1958.*
Contribution from the Department of Chemistry, University of Chicago, Chicago 37, Illinois. This paper was presented at the Symposium on Charge Transfer Processes held at the University of Toronto, Toronto, Ontario, September 4 and 5, 1958.

The emphasis which is placed on the bridged activated complex in this paper in no sense implies that this kind of mechanism is considered more important—in fact, the development of the subject will show that definite proof of the operation of the mechanism involving bridged activated complexes is restricted thus far to only a small number of different central cations. However, the mechanisms involving the bridged activated complex have associated with them interesting chemistry in large variety, and are worthy of consideration for their own sake, so that no apology for the present lack of generality is due. Further, it is likely that the most fruitful way to attack the systems which do not readily lend themselves to direct tests of mechanism will be from ground thoroughly prepared by understanding systems of known mechanisms.

A brief outline of observations and problems in the field of mechanisms involving outer sphere activated complexes is offered, and following this, a more detailed discussion of the bridged activated complex.

THE OUTER SPHERE ACTIVATED COMPLEX

In many redox reactions, reactant and product complex ions are substitution inert, or at least submit to substitution much less rapidly than to electron transfer. If in addition the species concerned are co-ordinatively saturated, it can reasonably be supposed that there is no interpenetration of the co-ordination spheres on electron transfer. The conclusion that an outer sphere activated complex operates for such systems is for the most part based on evidence no more direct than that outlined, yet some of the systems in question are so extremely inert to substitution that there is little doubt that an outer sphere activated complex is all that is accessible to the systems. Thus redox reactions or exchange reactions involving only species drawn from among the following and their like: $Fe(CN)_6^{-3,-4}$, $IrCl_6^{-2,-3}$, $Mo(CN)_8^{-3,-4}$, $Fe(dip)_3^{+3,+2}$, $Os(o\text{-phen})_3^{+3,+2}$, $MnO_4^{-1,-2}$ almost certainly take place without interpenetration of, or dislocations in, the first co-ordination spheres of the reactant ions. Substitution in the first co-ordination spheres of these ions is slow (for the manganese oxy-ions, this is true only in alkaline solution), and it is doubtful that any useful labilization of the ligands takes place on close approach of the reactants (this is particularly true when the products resulting on electron transfer are also substitution inert). For the MnO_4^-–$MnO_4^=$ electron exchange reaction, which is the one which has been most thoroughly studied (4), it is known that the co-ordination spheres are not disrupted on electron transfer. This follows from Symons' observation (5) that the reduction of MnO_4^- to $MnO_4^=$ in alkaline solution takes place preserving the oxygen-isotopic composition of the complex ions.

It is a feature of all the systems mentioned above that not only is the co-ordination sphere not reorganized on electron transfer, but in fact there is little change in the dimensions of the molecules when the indicated change in electronic charge takes place. For these systems, electron exchange takes place rapidly (specific rates at 25° of the order of 10^{-3} $mole^{-1}$ sec^{-1} and higher) (6). Whether the conditions that the geometry remains unchanged when electron transfer takes place is sufficient to ensure that the process be rapid is not at all certain, however. The ions referred to are also of such nature that the *d* electrons are probably not localized on the central metal ions, and for them, Marcus's (7) assumption that they be considered conducting spheres may well be justified. However, for a pair of fully ammonated ions, which then present a shell of protons on their exterior and which satisfy the geometric requirements, the rates may well be slower by several powers of 10. Such a system may be hard to find, for the property of the ligands which brings *d* electrons to the exterior of the complex ion is also the property that ensures that little change in dimensions takes place on electron transfer.

Can. J. Chem. Downloaded from www.nrcresearchpress.com by 190.90.36.8 on 09/04/12
For personal use only.

Can. J. Chem. Downloaded from www.nrcresearchpress.com by 190.90.36.8 on 09/04/12
For personal use only.

It is by no means a necessary condition for the operation of the outer sphere mechanism that there be little change in dimensions of the ions, for if the ligands are chosen to be unfavorable to the formation of the bridged activated complex, electron transfer through the intact co-ordination spheres may still be the easier route to products. Thus the electron exchange between $Co(en)_3^{++}$ and $Co(en)_3^{+++}$ (8) presumably must occur by the outer sphere mechanism, for although $Co(en)_3^{++}$ is substitution labile, $Co(en)_3^{+++}$ is not, and the groups on the co-ordinated nitrogens prevent the formation of a bridged activated complex. The $Co(en)_3^{++}$–$Co(en)_3^{+++}$ reaction is much slower ($k \sim 10^{-3}$ $mole^{-1}$ sec^{-1} at 25°) than the others of this class mentioned above. This is a result in part at least of the cost in energy for making the substantial change in the dimensions of the ions prior to electron transfer, which is necessary to bring about the matching of the energy of the electron at the two sites. As already mentioned, the difference in specific properties of en as compared to *o*-phen, for example, may also be a factor but it is impossible at the present time to evaluate its importance.

Some of the features of interest in the reactions which proceed by outer sphere activated complexes have been referred to already, as for example, the influence on the rates of the geometrical requirements and the properties of the ligands. Of interest also are the dielectric properties of the reaction medium, which are dealt with in Marcus's theory (9), and salt effects, which are delineated partially in the experiments by Sheppard and Wahl (4). An important problem which remains to be settled is the average separation of the ions in the activated complexes for electron transfer: the experimental solution of this problem is by no means obvious.

THE BRIDGED ACTIVATED COMPLEX

Introduction

For a system in which the oxidizing agent is substitution inert, the reducing agent is labile to substitution, but the product formed on its oxidation is inert to substitution, a direct demonstration of a bridged structure for the activated complex can be made by simple analysis of reaction products. The significance of the conditions imposed on the substitution properties is most easily developed by using a specific example. The reaction of $(NH_3)_5CoCl^{++}$ with Cr^{++} has been found to take place forming as product not $Cr(H_2O)_6^{+++}$ but $CrCl^{++}$ (9) (in addition to Co^{++} and NH_4^+ as other products). Cr^{+++} is very slow to undergo substitution, thus $CrCl^{++}$ can not have been formed from Cr^{+++} and Cl^-. This conclusion is reinforced by repeating the experiment in the presence of radioactive Cl^-; it is found that substantially no radioactivity gets into the $CrCl^{++}$ (10). The formation of $CrCl^{++}$ proves a Cr–Cl bond in the activated complex; the property of the oxidizing agent $Co(NH_3)_5Cl^{++}$ as being substitution inert ensures that a Co–Cl bond is maintained, and the property of $Cr^{++}{}_{aq}$ as being substitution labile provides for the formation of the bridged structure.

Most of the work in this field has been done with Co(III) complexes as oxidizing agents and $Cr^{++}{}_{aq}$ as reducing agent. $Cr^{++}{}_{aq}$ appears to be unique among the pure aquo-ions under ordinary conditions in having the combination of properties required to establish the operation of the bridged activated complex. If interest is not restricted to pure aquo-ions, Co(II) can also be mentioned as a reducing agent which can be similarly exploited. In the presence of NH_3 and numerous other ligands, Co(II), although itself labile to substitution, becomes substitution inert on oxidation. As oxidizing agents that lend themselves to the type of experiment outlined, we have a wider choice, including most Co(III) complexes, Cr(III) complexes, Pt(IV) complexes (though here a complication enters because the stable product is 2 e^- removed), Ir(IV) complexes, Ru(IV)

Can. J. Chem. Downloaded from www.nrcresearchpress.com by 190.90.36.8 on 09/04/12
For personal use only.

complexes, and some complexes of Fe(III). It is possible that at lower temperatures, such as become accessible when CH_3OH is solvent, many more oxidizing agents and reducing agents will show the necessary relation of rates of substitution to rate of electron transfer to make a direct test of mechanism possible for them. Before these general remarks are concluded, attention should be drawn explicitly to the remarkable feature of inorganic cations that a change in oxidation number by one unit can cause enormous changes in substitution lability. Thus, the replacement of water in $Cr(H_2O)_6^{+++}$ by solvent water takes place at 25° with a half time of the order of 30 hours. The similar exchange for $Cr^{++}{}_{aq}$ is so rapid that it has not been measured and $t_{\frac{1}{2}}$ is likely of the order of 10^{-5} seconds. To add interest to the situation, Cr(IV) is again probably very labile to substitution (12, 13).

For the remainder of this section, experimental results on features of the bridged activated complex will be presented, and any discussion of the implications of these observations for other systems will be deferred.

Variety of Bridging Groups

Complexes of the type $(NH_3)_5Co^{III}L$ can be prepared with a great variety of ligands L. Experiments using oxidizing agents of this class and Cr^{++} as reducing agent have demonstrated group transfer from Co to Cr for L = F^-, Cl^-, Br^-, I^-, CNS^-, N_3^-, $SO_4^=$, $PO_4^{\equiv}$, $P_2O_7^{\equiv}$, and a variety of carboxylic acids, results for which will be discussed in some detail in the next subsection. Of special interest are experiments on the transfer of H_2O and OH^-, as relating to redox reactions of aquo-cations. A definitive result has been obtained for L = OH^-, showing that transfer is complete for this ion; the experiments with L = H_2O are inconclusive but some transfer at least by this path is indicated (14). With L = NO_3^-, net transfer to chromium is not observed. Many of the ligands mentioned have also been shown to transfer when Cr(III) complexes act as oxidizing agents (15).

Relative Rates for Various Bridging Groups

A rate comparison which has an obvious qualitative interpretation is that for the reactions of Cr^{++} with $Co(NH_3)_6^{+++}$ and with $Co(NH_3)_5OH_2^{+++}$, the reaction with the aquo-ion is more rapid by a factor of at least one hundred. The significant difference between the two oxidizing agents is that only with the aquo-ion is a pair of electrons exposed to make a bridged complex readily accessible. The totally ammonated complex may in fact react by making use of an outer sphere activated complex.

Other rate comparisons which will be offered are somewhat more subtle. Thus it is not obvious what progression in rates should be observed for the series of halo complexes. Kinetic experiments on reactions of the two types

$$(NH_3)_5Cr\ X^{++} + Cr^{++} + 5H^+ = Cr^{++} + 5NH_4 + Cr^{++}$$

and

$$(H_2O)_5Cr^*\ X^{++} + Cr^{++} = Cr^{*++} + (H_2O)_5Cr\ X^{++}$$

agree that rates increase progressively from X = F^- to X = I^-. It should be noted that in each class of reaction, the rates are first order in chromic complex, first order in chromic ion, and independent of (H^+). The data for these reactions and other similar ones are summarized in Table I.

A comparison of special interest displayed in this table is that of the rate of reaction of Cr^{++} with CrN_3^{++} and $CrNCS^{++}$. Ball and King (15) make the point that attack by Cr^{++} at the atom bearing the Cr^{+++} is impossible for steric reasons, and that attack

TABLE I

The rates of reaction of Cr^{++} with various Cr(III) complexes

Oxidant	k, mole^{-1} sec^{-1}	Temp.	$\Delta H^{\ddagger}$	$\Delta S^{\ddagger}$	Ref.
CrF^{++}	2.6×10^{-2}	27	13.7	−20	15
$CrCl^{++}$	8.3 ± 2, 9.1 ± 1	0	—	—	16, 15
$CrBr^{++}$	>60	0	—	—	15
$CrNCS^{++}$	1.8×10^{-4}	27	—	—	15
CrN_3^{++}	>1.2	0	—	—	15
$(NH_3)_5CrF^{++}$	2.7×10^{-4}	25	13.4	−30	17
$(NH_3)_5CrCl^{++}$	5.1×10^{-2}	25	11.1	−23	17
$(NH_3)_5CrBr^{++}$	3.2×10^{-1}	25	8.5	−33	17
$(NH_3)_5CrI^{++}$	5.5 ± 1.5	25	—	—	17
t-$CrCl_2^+$	$\sim2\times10^3$	25	—	—	10

takes place at the remote end of the ligand. The slower rate for NCS^- compared to N_3^- can be attributed to this, that remote attack by Cr^{++} on NCS^- forms products different from the reactants, and in a less stable form, so that the energy requirements of the over-all process must be added to the pure kinetic requirements in determining the rate.

The results of experiments done by Sebera and Taube (18) on carboxylic acids as electron mediators are summarized in Table II. These experiments are still in progress, and a large number of experiments of obvious interest still remain to be done.

TABLE II

Carboxylic acids as electron mediators in the reaction of $(NH_3)_5Co^{III}$ L with Cr^{++} (μ = 1.00, 25° C)

L	k, mole^{-1} sec^{-1}	$\Delta H^{\ddagger}$	$\Delta S^{\ddagger}$	Ref.
$CH_3CO_2^-$	0.15			19
$CH_3(CH_2)_2CO_2^-$	0.08			19
$CH_3CH{=}CHCO_2^-$	0.18			19
$HO_2CCH_2CH_2CO_2^-$	0.19	3.0	−50	18
$^-O_2CCH_2CH_2CO_2^-$	1			18
Trans-$HO_2CCH{=}CHCO_2^-$	1.13	7.5	−33	18
Cis-$HO_2CCH{=}CHCO_2^-$	>200			18
o-Phthalic	0.076	5.1	−47	18
m-Phthalic	0.093	2.6	−56	18
p-Phthalic	~40			18
Oxalate	>200			19

One comparison of interest is that of the rate for fumaric acid as ligand with that for succinic acid. The latter reacts at a specific rate much like those at which monocarboxylic acids react. Thus for all of this group including succinic acid attack by Cr^{++} at the carboxyl adjacent to the Co(III) is indicated. To explain the higher rate for fumaric acid it is suggested that when it is the bridging group, attack by Cr^{++} takes place at the end remote from the Co(III). This mechanism is possible because fumarate can offer a conjugated system of double bonds for electron transfer. The higher rates come about because the Cr^{++} is not required to approach as closely to the Co(III) center as is the case when succinate is bridging group. An extraordinary result, not included in the table, and consistent with this interpretation is that the rate of electron transfer when fumaric acid is bridging group, is strongly accelerated by acid. The function of the additional proton may be to improve the conjugation between the Co(III) and Cr(II) centers.

Can. J. Chem. Downloaded from www.nrcresearchpress.com by 190.90.36.8 on 09/04/12
For personal use only.

By associating with the carbonyl oxygen adjacent to Co(III), it brings about the necessary redistribution of the electrons, as indicated in the formulation below of the activated complex.

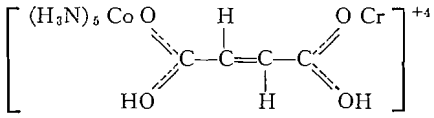

These general conclusions are supported by the observations made with the isomers of phthalic acid. Conjugation is not possible for the ortho or meta acid (but for different reasons) and the rates are slow. For the para isomer conjugation is possible and the rates are very high; furthermore, with this isomer but not the others, acceleration by acid is observed.

The high rate for the maleate complex is not understood by the considerations outlined thus far. The maleate complex reacts more rapidly than does the fumarate complex, although the geometry prevents effective conjugation, and it reacts much more rapidly than the *o*-phthalic complex which has similar geometry. An hypothesis which is reasonable in the light of these comparisons and which furthermore accommodates the observations that of all the ligands mentioned maleate is the most easily reduced by Cr^{++} is that when maleate is the ligand we are dealing not with electron transfer *through* the ligand, but *to* the ligand. A similar mechanism may operate for oxalate, which is also easily reduced by Cr^{++}. Isotopic fractionation experiments can differentiate the mechanisms proposed on the one hand for fumarate and on the other for maleate, but these have not been done, and they will in fact be rather difficult to do.

The Reaction of $(NH_3)_5CoOH_2^{+++}$ *with* Cr^{++}

This reaction is especially featured because of its relation to the important class of redox reactions between aquo-ions. It differs from most other reactions of its class in admitting much more incisive tests of mechanism than are usually possible. One of these which provided proof that reaction takes place by transfer of oxygen has already been mentioned.

In common with other redox reactions of aquo-cations which have been studied, the reaction in acidic medium proceeds by two parallel paths differing in the dependence on (H^+). The rate law for this reaction may be represented by the equation:

$$-d(Cr^{++})/dt = k_1(Cr^{++})[(NH_3)_5CoH_2O^{+++}]+k_2'(Cr^{++})[(NH_3)_5CrOH_2^{+++}]/(H^+)$$

The kinetic data on this system, including experiments with D_2O as solvent are shown in Table III (20). It should be noted that the second term on the right of the equation above can be cast in the equivalent form:

$$k_2(Cr^{++})[(NH_3)_5CoOH^{++}],$$

where $k_2 = k_2'/K_D$ and K_D is a dissociation constant of $(NH_3)_5CoOH_2^{+++}$ under the specific experimental conditions (21).

TABLE III

Kinetics of the reaction of Cr^{++} with $(NH_3)_5CoOH_2^{+++}$ (at $\mu = 1.0$, temp. 20° second as unit of time)

Solvent	k_1	k_2'	k_2	E_1	E_2	$\Delta S_1^{\ddagger}$	$\Delta S_2^{\ddagger}$
H_2O	0.50	1.58	1.5×10^6	3.3	4.8	−48	−15
D_2O	0.13	0.40					

Can. J. Chem. Downloaded from www.nrcresearchpress.com by 190.90.36.8 on 09/04/12
For personal use only.

Can. J. Chem. Downloaded from www.nrcresearchpress.com by 190.90.36.8 on 09/04/12
For personal use only.

Of interest in the kinetic data is the large change in specific rate caused by the loss of the proton from the aquo-ion, and the low values of the activation energies. These points will not be developed further here, but should not be dismissed without mentioning that a case for the existence, not merely of a binuclear activated complex, but of a binuclear intermediate can be based on the low values of E observed here and in other cases as well. Of significance equal to that of the oxygen-tracer experiments are experiments on oxygen-isotope fractionation in the reaction (14). These experiments have shown that $(NH_3)_5CoO^{16}H^{++}$ reacts more rapidly than the ion having O^{18} in the OH group by a factor of 1.03_5. This is a relatively large kinetic oxygen isotope effect, and it shows that the Co–O bond is greatly weakened in the activated complex. Thus the OH^- is not to be regarded merely as a means of binding Co(III) and Cr(II) together, but in fact an important event in the transfer of the electron is the stretching of the Co–OH bond, and presumably the simultaneous shortening of the Cr–OH bond. The question of other bond dislocations in the activated complex will be dealt with in the next subsection.

The measurement of the effect on the rate of electron transfer caused by the change from H_2O to D_2O as solvent has been suggested as a means of distinguishing the "hydrogen atom transfer" mechanism from other mechanisms. The significance of the H_2O–D_2O experiments in the present system is that they test the magnitude of the effect for a reaction which does not involve hydrogen atom transfer, but which by one path at least proceeds by transfer of OH. The remarkable result is that a large H–D isotope effect is found, a decrease in k_1 and k_2' of almost a factor of 4 in changing from H_2O to D_2O as solvent. The effect on k_2' must be factored into the effect on k_2 and K_D. The H_2O–D_2O effect on K_D has been measured as 1.5 (21) (K_D in H_2O compared to K_D in D_2O), thus a healthy kinetic isotope effect in k_2 of 2.6 is still left. The origin of this large isotope effect is in the hydrogen-containing bridging group (the specific rate for the reaction $(NH_3)_5CrCl^{++} + Cr^{++}$ decreases by only a factor of 1.3 in changing to D_2O as solvent). It means presumably that the H–O bond is substantially stretched in the activated complex. Possibly the complex adopts a linear arrangement of Co–O–Cr centers, and the p-electrons of oxygen are used to contribute to the bonding. The two paths for the reaction may be quite similar except that when the aquo-ion reacts, both hydrogens in water are removed in the activated complex, but when the hydroxy complex reacts, one is removed by an equilibrium process preceding the rate-controlling step and one in the activated complex. Rather similar H–D isotope effects are to be expected on this basis, as is observed.

Effects of Non-bridging Ligands

This important subject will be dealt with only briefly, because little in the way of systematic work on this feature of these reactions has been done. The existence of important ligand effects, short of bridging ligand effects is, of course, to be expected and is easily demonstrated. Thus, when the reaction of $(NH_3)_5CoOH_2^{+++}$ with Cr^{++} proceeds in the presence of pyrophosphate ion, it takes place much more rapidly than when pyrophosphate is omitted, and pyrophosphate is incorporated into the chromic product (19). The inertia of the Co(III) complex to substitution ensures that the pyrophosphate does not act as a bridging group, yet it does get into the activated complex, presumably by replacing water molecules on Cr^{++}. That a bridging group is involved is proved by the experiment using $(NH_3)_6CoCl^{++}$ as oxidizing agent. When this is done, both Cl and pyrophosphate are incorporated into the chromic complex.

Groups differ widely also in their capacity to influence rates in non-bridging positions.

Pyrophosphate, $SO_4^=$, and Cl^- decrease in effect in this order; the effect of Cl^- is so small that in 0.1 *M* solution, its influence on the rate of the reaction of $(NH_3)_5$ to OH_2^{+++} with Cr^{++} is not detected.

The non-bridging ligand effects can conveniently be studied by working with a series of Co(III) complexes containing a common bridging group. Such studies have not been carried far, and only a single problem in this field has been given some attention. Orgel (22) has discussed the reaction of Cr^{++} with Co(III) complexes, and has suggested that the electron gained by Co(III) is accommodated in the d_{z^2} orbital. This orbital is made available by removing not only the bridging ligand from the cobalt, but also the group *trans* to it. This interesting suggestion finds support in the observation that *trans* $Co(en)_2Cl_2^+$ is reduced *more* rapidly by $V^{++}{}_{aq}$ or $Fe^{++}{}_{aq}$ than is the *cis* form (23). It has been tested by observing the fractionation of nitrogen in NH_3 when *cis-* and *trans-* $NH_3(en)_2CoCl^{++}$ react with Cr^{++}. These experiments have shown (24) that there is no significant N-isotope fractionation either when NH_3 is *cis* or when it is *trans* to the Cl bridging group. This experimental result, if sustained, would show that the principal bond dislocations of the Co(III) center take place at the bridging group and would suggest that the primary product of the reaction is a penta-co-ordinated Co(III) complex which retains the configuration of the parent complex, but which has in place of the bridging group a single electron. The result cannot be considered general even for all Co(III) complexes and the ion $NH_3(dip)_2CoCl^{++}$ might in fact show a strong *trans* effect on electron transfer.

CONCLUSION

Not all aspects of interest in the field of reactions proceeding by the bridged activated complex have been discussed nor even referred to, but perhaps a sufficient number of results were reviewed to indicate the nature of the problems and the nature of the experiments which can be done to elucidate mechanisms. Most of the techniques used unfortunately do not apply to the redox reactions of ions when both partners are substitution labile. However much is written concerning the outer sphere and bridged activated complexes the subject of redox reactions of metal ions remains in an unsatisfactory state when a reaction as much studied as the Fe^{++}–Fe^{+++} electron exchange is not understood nor a reaction as much applied as the Fe^{++}–Ce(IV) reaction. It is to be hoped that experimental techniques will be introduced which will yield conclusions for these systems as direct as some of those possible for specially selected systems. Failing to discover such techniques an indirect attack must be used, to develop thoroughly an understanding of the field in which mechanisms can be established, to develop the experimental observations in the field of the labile systems, and to bring to bear on these observations the principles which have been established for systems of known mechanisms.

An illustration of this kind of approach which will serve better perhaps to expose its limitations than to reveal its capacities is the following: from the fact that Cl^- does not markedly accelerate the reaction of $(NH_3)_5CoOH_2^{+++}$ with Cr^{++}, that $CrCl^{++}$ is not formed in this reaction, and that Cl^- does markedly accelerate the reaction of Fe^{+++} with Cr^{++} forming $CrCl^{++}$, we argue that in the activated complex for the latter process both Fe^{+++} and Cr^{++} make a bond to Cl^- (i.e., the difference in the kinetic behavior of the two systems is understood by invoking the difference in substitution lability of the two oxidizing agents). Thus the reaction of Fe^{+++} with Cr^{++} accelerated by a variety of ligands can be brought into the field of the bridged activated complexes. There is a close similarity (9) of the rates at which Fe^{++} reacts with Fe(III) complexes to the rates at

Can. J. Chem. Downloaded from www.nrcresearchpress.com by 190.90.36.8 on 09/04/12
For personal use only.

which Cr^{++} reacts with the same complexes and therefore similar mechanisms are indicated. These considerations thus lead to the conclusion that the Fe^{++}–Fe(III) exchange reactions also proceed by bridged activated complexes. Considerations of this kind are hardly satisfactory however, because they do not expose the contributions of minor, but nevertheless interesting, rival paths, nor is a sufficiently convincing case for the mechanism by the major paths made.

A field for experiment which may improve our understanding of the redox process under discussion is in the reactions of reducing agents having differing electronic structures with a series of substitution-inert complexes. Thus, some interesting conclusions are indicated by results recently obtained (23) using V^{++} as reducing agent when these results are considered in the context of those already obtained with Cr^{++}. A large number of Co(III) complexes show the same order of reactivity with V^{++} as they do with Cr^{++}, but the contrast in rates is much less. The reaction of $(NH_3)_5CoOH_2^{+++}$ is abnormally rapid, however, and shows some unusual salt effects. We believe at present that V^{++} reacts by both kinds of mechanism. When a suitable bridging group is present, the bridged activated complex is still formed. But when the aquo-ion or the hexammino-ion is used the outer sphere activated complex predominates as providing the reaction path. The differences in V^{++} and Cr^{++} are to be understood as resulting from the differences in electronic structure, V^{++} having only the three lower lying *d*-orbitals populated but Cr^{++} having one electron more. Eu^{++} will also be of interest in these studies as will Fe^{++} (its reactivity can be enormously increased by suitable complexing).

Another area which promises to be fruitful is the reduction of Co(III) and, if possible, Cr(III) complexes by reaction through outer sphere activated complexes. This can be done by using $Cr(dip)_3^{++}$ or $V(dip)_3^{++}$ as reducing agent. The reaction of $Co(NH_3)_6^{+++}$ with $Cr(dip)_3^{++}$ in fact proceeds so rapidly that we (23) have not succeeded in measuring its rate, in marked contrast to the slow rate when $Cr^{++}{}_{aq}$ is used. Rate comparison for the same series of Co(III) complex being reduced by both mechanisms should prove to be very instructive, and instructive also in comparison with rates of reduction of the same complexes at electrodes.

REFERENCES

1. Dodson, R. W. and Davidson, N. J. Phys. Chem. **56**, 866 (1952).
2. Hudis, J. and Dodson, R. W. J. Am. Chem. Soc. **78**, 911 (1956).
3. Reynolds, W. L. and Lumry, R. W. J. Chem. Phys. **23**, 2460 (1955).
4. Sheppard, J. C. and Wahl, A. C. J. Am. Chem. Soc. **79**, 1020 (1957).
5. Symons, M. C. R. J. Chem. Soc. 3676 (1954).
6. Wahl, A. C. and Deck, C. D. J. Am. Chem. Soc. **76**, 4054 (1954). Eichler, B. and Wahl, A. C. J. Am. Chem. Soc. **80**, 4145 (1958). George, P. and Irvine, D. H. J. Chem. Soc. 587 (1954).
7. Marcus, R. A. J. Chem. Phys. **24**, 966 (1956).
8. Lewis, W. B., Coryell, C. D., and Irvine, J. J. Chem. Soc. Suppl. Issue, **2**, S386 (1949).
9. Taube, H., Myers, H., and Rich, R. L. J. Am. Chem. Soc. **75**, 4118 (1953).
10. Taube, H. and Myers, H. J. Am. Chem. Soc. **76**, 2103 (1954).
11. Hunt, J. P. and Taube, H. J. Chem. Phys. **19**, 602 (1951).
12. Taube, H. Chem. Revs. **50**, 69 (1952).
13. Ogard, A. E. and Taube, H. J. Phys. Chem. **62**, 357 (1958).
14. Murmann, R. K., Taube, H., and Posey, F. A. J. Am. Chem. Soc. **79**, 262 (1957).
15. Ball, D. L. and King, E. L. J. Am. Chem. Soc. **80**, 1091 (1958).
16. Taube, H. and King, B. L. J. Am. Chem. Soc. **76**, 4053 (1954).
17. Ogard, A. E. and Taube, H. J. Am. Chem. Soc. **80**, 1084 (1958).
18. Sebera, D. R. and Taube, H. To be published.
19. Taube, H. J. Am. Chem. Soc. **77**, 4481 (1955).
20. Zwickel, A. and Taube, H. To be published.
21. Bearcroft, D. J. and Taube, H. To be published.
22. Orgel, L. E. Inst. intern. chim. Solvay, X^e Conseil chim. 289 (1956).
23. Zwickel, A. and Taube, H. Unpublished observations.
24. Schug, K. and Taube, H. These results should be regarded as tentative. The experiments reported are of good quality but further checking is necessary before the result is published.

Can. J. Chem. Downloaded from www.nrcresearchpress.com by 190.90.36.8 on 09/04/12
For personal use only.

Can. J. Chem. Downloaded from www.nrcresearchpress.com by 190.90.36.8 on 09/04/12
For personal use only.

SOME THEORETICAL ASPECTS OF ELECTRON-TRANSFER PROCESSES IN AQUEOUS SOLUTION[1]

KEITH J. LAIDLER

ABSTRACT

A theoretical treatment has been developed for the rates of electron-transfer reactions in aqueous solution, with particular reference to the ferric–ferrous system. The reactions are considered to be diffusion-controlled processes, the approach of the ions being hindered by the electrostatic repulsion between them. Calculations have been made of the free energy of the diffusion process and for the repulsion, account being taken of the variation in dielectric constant with the electric field. The form of the potential-energy barrier between the ions is calculated for various separations, and the transmission coefficient calculated using the quantum-mechanical expression corresponding to a rectangular barrier. The total free energy of activation for the reaction, which is the sum of the contributions due to diffusion, repulsion, and tunnelling, is found to pass through a minimum at a separation of about 4 Å. The calculated free energy of activation for the reaction is 15.4 kcal, in good agreement with the experimental value of 16.8 kcal. The energy and entropy of activation for the reaction are also briefly discussed.

INTRODUCTION

During the past few years a considerable number of kinetic studies have been concerned with electron-transfer processes between ions in different valency states. A well-known process of this type is that between ferric and ferrous ions in aqueous solution,

$$Fe^{++} + Fe^{+++} \rightarrow Fe^{+++} + Fe^{++}.$$

Although many complexities exist, the evidence indicates that in some cases these reactions occur by a simple transfer of an electron from one ion to another. This is possibly true of the ferric–ferrous reaction, and Silverman and Dodson (1) have determined values of 9.9 kcal and -25 e.u. for the energy and entropy of activation of the process.

This paper is concerned with the theory of simple electron-transfer reactions, and for the most part deals quantitatively with the factors influencing the rate of the Fe^{++}–Fe^{+++} reaction. Several previous theoretical discussions of these reactions have been presented, notably by Libby (2), Weiss (3), Eyring and co-workers (4, 5), and by Marcus (6*e*). In the case of the latter two treatments, an attempt was made to calculate the free energies of activation (ΔF^*) of a number of reactions, including the Fe^{++}–Fe^{+++} one. The quantitative agreement with experiment was not, however, completely satisfactory. The experimental ΔF^* for the Fe^{++}–Fe^{+++} system is 16.8 kcal at 25° C: Eyring *et al.* obtain agreement only by arbitrarily adding a term of 8.1 kcal, while Marcus (6*a*) calculated a value of 9.8 kcal.* It has appeared to the present writer that this lack of good agreement could be attributed to failure to take into consideration certain important factors which must influence the rate. In particular it would seem that neither Eyring nor Marcus treated in sufficient detail the collisions (or, more correctly, *encounters*) between the reacting ions.

In the present work an attempt has been made to bring about some improvement, particularly with respect to the two points noted above. If in the present paper a somewhat critical view appears to have been taken of the preceding theoretical treatments

[1]*Manuscript received May 23, 1958.*
Contribution from the Department of Chemistry, University of Ottawa, Ottawa, Canada. This paper was presented at the Symposium on Charge Transfer Processes held at the University of Toronto, Toronto, Ontario, September 4 and 5, 1958.

**In a later paper (6b) Marcus quotes a calculated value of 18 kcal, but details are not given.*

this has been done entirely to clarify the main points, and not to deprecate the earlier work which contains many valuable features and upon which the present work relies very heavily.

THE FREQUENCY OF IONIC ENCOUNTERS

In what follows it will be concluded, on the basis of the experimental evidence, that there does occur a direct transfer of an electron from the ferric to the ferrous ion. The electron-transfer process will be seen later to occur by quantum-mechanical tunnelling, and is much more probable when the ions are close together. The very close approach of the ions is obviously rendered unlikely by the electrostatic repulsions. A compromise is therefore struck, the most likely transfers occurring (as will be seen) when the ions are about 4 Å apart.

In the treatment of Eyring *et al.* (4) the rate of encounter has been taken as equal to the term $\mathbf{k}T/h$ multiplied by the factor $\exp(-\Delta F^*_{rep}/RT)$, where ΔF^*_{rep} is the free energy of repulsion between the two ions. This, however, cannot be correct, since it does not take proper account of the variation in the frequency of encounter with the separation of the ions, σ, in the activated state. The distance σ does appear in the ΔF^*_{rep} term, but it should also appear in the pre-exponential term; quite apart from electrostatic effects an encounter with a large σ is intrinsically more probable than one with a small σ, and intuitively one would expect the pre-exponential term to be proportional to σ.

A more satisfactory treatment of the frequency with which the ions come within a distance of σ of one another is provided by the theory of diffusion-controlled reactions, a theory that has been developed to explain the coagulation of colloids (7, 8), the rates of quenching of fluorescence in solution (9), and more recently the rates of certain enzyme-catalyzed reactions (10). The theory is briefly as follows. According to Smoluchowski (7), in the absence of electrostatic interactions the frequency of approach of two molecules to within a distance of σ cm is given by

$$Z = 2\pi(D_1+D_2)n_1n_2\sigma, \qquad [1]$$

where n_1 and n_2 are the numbers of the two types of molecules in unit volume and D_1 and D_2 are the diffusion constants. Bradley (11), however, argues that Smoluchowski's equation is too large by a factor of 12, and instead proposes

$$Z = \tfrac{1}{6}\pi(D_1+D_2)n_1n_2\sigma. \qquad [2]$$

This expression is equivalent to the following expression for the rate constant:

$$k = \tfrac{1}{6}(\pi N/1000)D_{12}\sigma \text{ liter mole}^{-1} \text{ sec}^{-1}, \qquad [3]$$

where $D_{12} = D_1+D_2$. The above equations are arrived at by integration of the appropriate differential equations for diffusion.

When the reacting species are ions the electrostatic interactions have to be taken into account in the setting up of the differential equations. This has been done by Debye (9), who found that the reaction rate in the case of a free energy of repulsion equal to ΔF^{**}_{rep} must now be divided by the integral

$$1/f = \sigma \int_\sigma^\infty \Delta F^{**}_{rep}/kT \, \frac{dr}{r^2}. \qquad [4]$$

The repulsive free energy is given for the case of constant dielectric constant ϵ by

Can. J. Chem. Downloaded from www.nrcresearchpress.com by 190.90.36.8 on 09/04/12
For personal use only.

$$\Delta F^{**}_{rep} = z_1 z_2 e^2/\epsilon k T r, \quad [5]$$

where e is the electronic charge and z_1 and z_2 the valencies of the ions. When ϵ is independent of σ the reciprocal of the integral becomes

$$f = (z_1 z_2 e^2/\epsilon k T \sigma)(e^{z_1 z_2 e^2/\epsilon k T \sigma} - 1)^{-1}. \quad [6]$$

When z_1 and z_2 are of the same sign, as for the reactions under consideration, the exponential term is always much larger than unity, so that

$$f = (z_1 z_2 e^2/\epsilon k T \sigma)\ e^{-z_1 z_2 e^2/\epsilon k T \sigma} \quad [7]$$

$$= (\Delta F^{**}_{rep}/kT)\ e^{-\Delta F^{**}_{rep}/kT}. \quad [8]$$

The expression for the rate constant for the encounter is therefore

$$k_{enc} = \tfrac{1}{6}(\pi N/1000)\ D_{12}\sigma\ (\Delta F^{**}_{rep}/kT)\ e^{-\Delta F^{**}_{rep}/kT} \quad [9]$$

with ΔF^{**}_{rep} given by eq. [5].

Since the experimental results are usually quoted in terms of a conventional free energy of activation, defined by

$$k = (\mathbf{k}T/h)\ e^{-\Delta F^{*}_{exp}/RT}, \quad [10]$$

it is convenient to express k_{enc} in the same form, namely as

$$k_{enc} = (\mathbf{k}T/h)\ e^{-\Delta F^{*}_{diff}/RT}\ e^{-\Delta F^{*}_{rep}/RT}, \quad [11]$$

where ΔF^{*}_{diff} relates to the diffusion process only and ΔF^{*}_{rep} to the repulsive term f. The term ΔF^{*}_{diff} depends slightly upon the value taken for D_{12}. There is not a large variation in the diffusion constants for ions, and a value of 1.2×10^5 cm^2 sec^{-1} has been taken as typical of the diffusion constant of ions such as Fe^{++} and Fe^{+++}. With $D = 2.4 \times 10^5$ it is then readily calculated that at a temperature of 25.0° C,

$$\Delta F^{*}_{diff} = 1.358 \log_{10} 8.203\times10^4/\sigma. \quad [12]$$

In the same way it is found that since

$$e^{-\Delta F^{*}_{rep}/RT} = (\Delta F^{**}_{rep}/RT)\ e^{-\Delta F^{**}_{rep}/RT}, \quad [13]$$

$$\Delta F^{*}_{rep} = \Delta F^{**}_{rep} - 2.303RT \log_{10} \Delta F^{**}_{rep}/RT. \quad [14]$$

THE FREE ENERGY OF ACTIVATION DUE TO ELECTROSTATIC REPULSION

The exact treatment of electrostatic repulsion presents a problem of very considerable difficulty. If the solvent were a continuous dielectric having a dielectric constant ϵ that is independent of the field strength, the free energy ΔF^{**}_{rep} corresponding to a separation of σ would be given by eq. [5] with r equal to σ; ΔF^{*}_{rep} could then be readily calculated using eq. [14]. The true ΔF^{*}_{rep} values are, however, at all distances somewhat greater than calculated in this way, since the dielectric constant in the neighborhood of the ions is actually less than the macroscopic value. This effect has a significant effect on the calculated free energies of activation, as will be seen later.

The dielectric behavior of water in the near neighborhood of ions has recently been treated by Laidler and Pegis (12), whose work will now be extended to give an approximate treatment of electrostatic repulsive energies. According to Kirkwood (13), Booth (14), and Grahame (15) the variation of the differential dielectric constant ϵ_d with the field strength E is given extremely closely by the expression

Can. J. Chem. Downloaded from www.nrcresearchpress.com by 190.90.36.8 on 09/04/12
For personal use only.

[15] $$\epsilon_d = dD/dE = [(\epsilon_0 - n^2)/(1+bE^2)] + n^2,$$

where D is the electric displacement, ϵ_0 the dielectric constant at zero field strength (taken as 78.5 for water at 25.0° C), n is the optical refractive index ($n^2 = 1.78$), and b is a quantity the value of which is given by Booth's theory. In the present calculations a value of 1.08×10^{-8} e.s.u.$^{-2}$ has been taken for b, since this value agrees closely with Booth's theory and with the experimental results obtained by Malsch (16).

Equation [15] integrates to

[16] $$D = n^2E + [(\epsilon_0 - n^2)/b^{\frac{1}{2}}] \tan^{-1} b^{\frac{1}{2}}E$$

and since the electric displacement D at a distance r from an ion of valency z is ze/r^2 we have

[17] $$n^2E + [(\epsilon_0 - n^2)/b^{\frac{1}{2}}] \tan^{-1} b^{\frac{1}{2}}E = ze/r^2.$$

Although E cannot be expressed explicitly as a function of r, eq. [17] can be used to prepare curves showing the variation; such curves are shown in Fig. 1 for $z = 1$, 2, 3, and 4. By interpolation, values of E can therefore be obtained corresponding to various values of r, and eq. [15] can then be used to calculate the differential dielectric constant at various distances from the ion. Such plots are shown in Fig. 2, from which it is seen that for a ferric ion, for example, the dielectric constant has the low value of 1.78 up to a distance of about 3 Å, after which the value rises fairly steeply. Even at a distance of 10 Å, however, the value is significantly below the limiting value of 78.5.

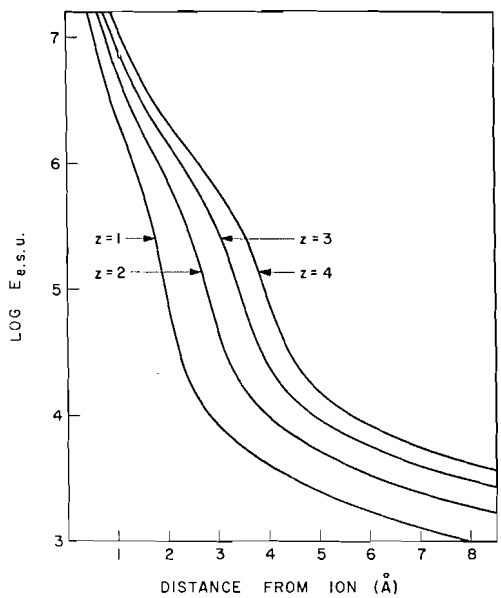

FIG. 1. Plots of the logarithm of the field strength, in electrostatic units (dynes), against the distance from the ion, for ions of valencies equal to 1, 2, 3, and 4.

The difficulty of calculating the repulsive free energy between two ions such as the ferric and ferrous ions arises from the fact that each ion produces a field, so that there is a considerable superposition of fields when the ions are close together. This superposition affects the dielectric constant, which in turn affects the individual fields. There appears

Can. J. Chem. Downloaded from www.nrcresearchpress.com by 190.90.36.8 on 09/04/12
For personal use only.

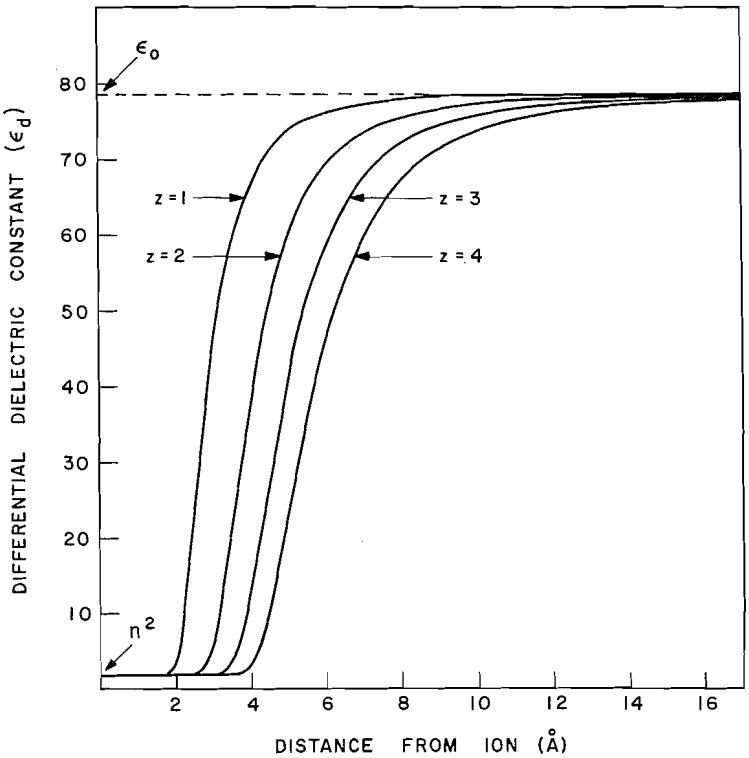

FIG. 2. Plots of the differential dielectric constant against the distance from the ion, for ions of valencies equal to 1, 2, 3, and 4.

to be no simple way of treating this problem, and the only exact procedure seems to be to bring the ions together in a vacuum and then to calculate the energy residing in the dielectric. Mathematically this problem has so far proved intractable and a simpler procedure has therefore been employed.

The method adopted was to calculate the field at a distance r from the ferric ion, and to assume that the force acting on the ferrous ion is equal to this field multiplied by the charge on the ferrous ion. This procedure would, of course, be strictly correct if instead of the ferrous ion one were considering a test charge sufficiently small as not to affect the field of the ferric ion. Owing to the mutual interference of fields there will, however, be some error in the case of a large charge such as the ferrous ion. The procedure employed will, however, undoubtedly give a repulsive energy that is a significantly better approximation than that given by assuming the dielectric constant to be 78.5, and will probably not be far from the truth.

The procedure used is as follows. From the $z = 3$ curve in Fig. 1 it is possible to evaluate numerically the area under the curve from $r = \infty$ to r equal to any desired value σ. This area is a measure of the work required to bring a unit charge from infinity to σ. Multiplication by the charge on the ferrous ion then gives a value for the work, i.e. of ΔF^{**}_{rep}, required to bring the ferrous ion from infinity to a distance of σ. Figure 3 shows another plot of E against σ, and also gives ΔF^{**}_{rep} plotted against σ. Included on the figure are the curves that are calculated on the assumption that there is no dielectric saturation, i.e. that ϵ remains 78.5 at all distances. The difference between the two cases is seen to be negligible at distances greater than about 5 Å, but to be extremely

Can. J. Chem. Downloaded from www.nrcresearchpress.com by 190.90.36.8 on 09/04/12
For personal use only.

great at smaller distances. Neglect of the saturation effect would therefore lead to considerable error, in that the ions would be permitted to approach much more closely than they are actually able to do.

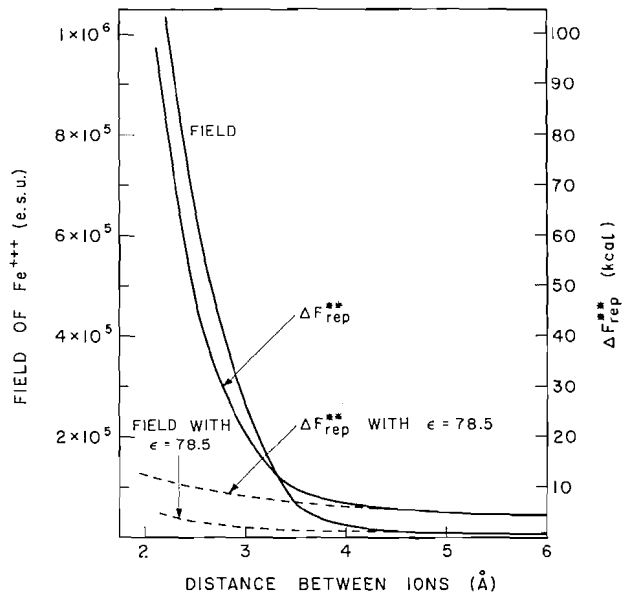

FIG. 3. Plots of the field due to a ferric ion (left-hand scale), and of the free energy of repulsion between a ferric ion and a ferrous ion (right-hand scale) against the distance. The dotted curves are calculated on the assumption of a dielectric constant of 78.5, the full curves for a dielectric constant that varies with field strength according to equation [15].

QUANTUM-MECHANICAL TUNNELLING

Inspection of Fig. 3 shows that the two ions cannot approach to within a distance of 3 Å without a considerable expenditure of free energy. Calculations of the work of electron transfer show that except at distances shorter than 3 Å the energy barrier for the transfer of an electron is more than 200 kcal in height. It therefore follows that the transfer must occur by quantum-mechanical tunnelling, and it is readily found that for the types of energy barriers involved the tunnelling rates are sufficiently large to permit reaction to proceed by this mechanism.

The first problem is the calculation of the potential-energy barrier. Here the main point that must be taken into consideration is that the rates of electron tunnelling are so large that there is insufficient time for the reorganization of neighboring solvent molecules. In other words, after the electron has left the ferrous ion the surrounding solvent molecules remain oriented in the same manner even though the ion has now become a ferric ion. The field around the newly formed ferric ion must therefore be calculated on the basis of a charge of $3e$ on the ion, but with a ferrous-type ionic atmosphere. This can simply be done by calculating the field due to a ferrous ion in its ferrous-type atmosphere and multiplying the result by 3/2.

The calculations of the barriers have therefore been carried out in this way, and the assumption of superposition of fields has again been made. The procedure has been to calculate, using the methods of the preceding section, the field round the newly formed ferric ion, with its ferrous-like atmosphere, and also that round the ferric ion

Can. J. Chem. Downloaded from www.nrcresearchpress.com by 190.90.36.8 on 09/04/12
For personal use only.

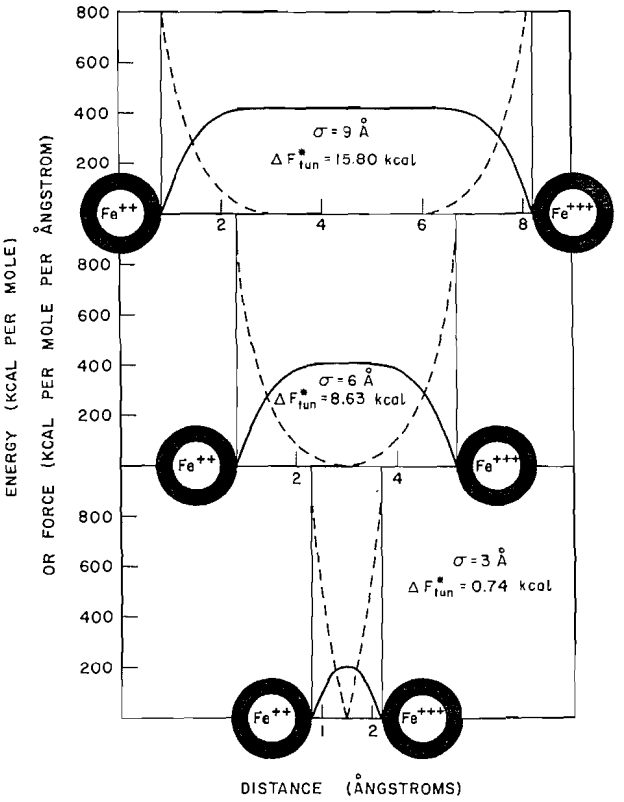

FIG. 4. Plots of force between ferric and ferrous ions against their separation (dotted curves) and of the potential-energy barrier (full curves). The ferric ion produced when the electron leaves the ferrous ion is in a ferrous-like atmosphere; this causes a slight asymmetry in the potential-energy barriers.

which the electron is approaching; this has a normal ferric-type atmosphere. For a given value of σ the two fields can be superimposed, and a curve can therefore be plotted for the force on the electron at various positions. By graphical integration the energy can then be calculated, and the barrier plotted. Figure 4 shows, for separations of 3, 6, and 9 Å, the plots of force and energy. In making these calculations the radius of the ferric ion was taken as 0.8375 Å, which is the crystal radius of 0.67 Å multiplied by the factor 1.25, as suggested by Couture and Laidler (17) and by Laidler and Pegis (12). It is to be noted that the energy curves in Fig. 4 rise and fall fairly steeply; this is because, during the first and last parts of its progress, the electron is moving through a region where the dielectric constant is small and where the forces are therefore strong.

The expression for the probability of tunnelling takes simple forms for barriers that are triangular or rectangular. The barriers for the present system are closer to rectangles than to triangles, and the approximation will be made of treating them as rectangular; the transmission coefficient is then (18)

[18] $$\kappa = 4e^{-2\gamma a}[2\alpha\gamma/(\alpha^2+\gamma^2)]^2,$$

where

[19] $$\alpha = 2\pi\sqrt{(2mW)/h}$$

and

[20] $$\gamma = 2\pi\sqrt{[2m(V_0-W)]/h},$$

Can. J. Chem. Downloaded from www.nrcresearchpress.com by 190.90.36.8 on 09/04/12
For personal use only.

m is the mass of the electron, V_0 the height of the barrier, and W is the kinetic energy of the electron prior to tunnelling. Following Marcus, Zwolinski, and Eyring (4) a value of 77.18 kcal per mole has been taken for W.

The values of κ calculated for the three separations of 3 Å, 6 Å, and 9 Å are shown in Fig. 4. The transmission coefficient can formally be expressed as

$$\kappa = e^{-\Delta F^*_{tun} F/RT}, \quad [21]$$

and the ΔF^*_{tun} values calculated in this way are shown in Fig. 4; additional values are included in Table I.

TABLE I

Free energies of activation for the Fe^{++}–Fe^{+++} exchange at various ionic separations

Separation (Å)	ΔF^{**}_{rep}	ΔF^*_{rep}	ΔF^*_{diff}	ΔF^*_{tun}	ΔF^*_{calc}
2.5	48.34	45.73	6.20	0.11	52.04
3.0	20.70	18.60	6.02	0.74	25.36
3.5	9.65	8.00	6.00	2.40	16.40
4.0	6.88	5.43	5.80	3.60	14.83
4.5	5.64	4.30	5.75	4.85	14.90
5.0	5.07	3.80	5.71	6.10	15.60
6.0	4.23	3.07	5.61	8.63	17.31
7.0	3.62	2.55	5.50	11.00	19.05
8.0	3.17	2.18	5.40	13.40	20.98
9.0	2.81	1.89	5.38	15.80	23.07

Weighed average of ΔF^*_{calc} = 15.4 kcal.

THE OVER-ALL FREE ENERGY OF ACTIVATION

The results of the various calculations are summarized in Table I for a range of values of σ. Included in this table are the ΔF^*_{diff} values calculated using eq. [12], the ΔF^*_{rep} values calculated using eq. [14] from the ΔF^{**}_{rep} values shown in Fig. 3, and the ΔF^*_{tun} values calculated in the manner described in the preceding section. Since according to the definitions of the three quantities the over-all rate of reaction corresponding to a given σ is given by

$$k = (\mathbf{k}T/h)\, e^{-\Delta F^*_{diff}/RT}\, e^{-\Delta F^*_{rep}/RT}\, e^{-\Delta F^*_{tun}/RT}, \quad [22]$$

the calculated ΔF^*_{calc} is the sum of ΔF^*_{diff}, ΔF^*_{rep}, and ΔF^*_{tun}, and is shown in the last column of the table. The values are shown plotted against σ in Fig. 5.

It is seen from the plot of ΔF^*_{calc} that the value passes through a minimum of about 14.8 kcal at a separation of about 4 Å. This value does not, however, quite represent the over-all free energy of activation, which will actually be a value averaged over all values of σ. The average ΔF^*_{calc} is given by

$$\Delta F^*_{calc} = \frac{\int_{14.8}^{\infty} \Delta F^*_{calc}\, e^{-\Delta F^*_{calc}/RT}\, d\Delta F^*_{calc}}{\int_{14.8}^{\infty} e^{-\Delta F^*_{calc}/RT}\, d\Delta F^*_{calc}}, \quad [23]$$

the value of which is found to be 15.4 kcal.

In view of the approximation involved, particularly in the treatment of the superposition of fields, the agreement between this calculated value and the experimental value of 16.8 kcal is quite satisfactory. The agreement is much better than that given by earlier treatments, a fact that is to be attributed to the following factors:

Can. J. Chem. Downloaded from www.nrcresearchpress.com by 190.90.36.8 on 09/04/12
For personal use only.

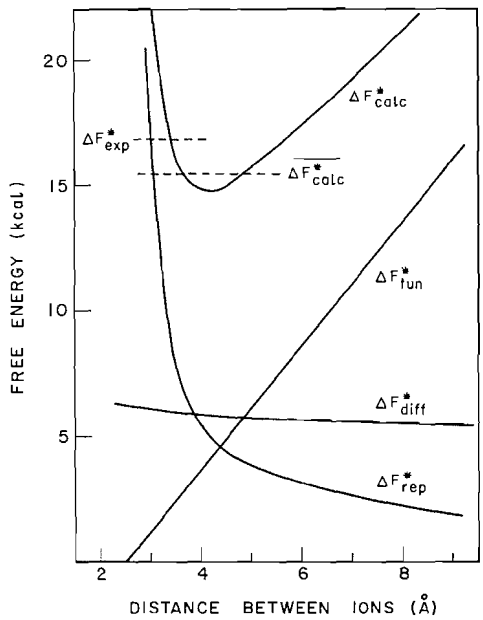

FIG. 5. Plots of the various free-energy terms against the distance between the ions. The upper curve represents the sum of the three contributions, and the lower horizontal line shows the calculated weighted-average free energy of activation, to be compared with the observed value shown by the upper horizontal line.

(1) The present treatment of the reaction as a diffusion-controlled one. The value of ΔF^*_{diff} at 4 Å is seen to have a value of nearly 6 kcal; no corresponding term appears in the earlier treatments.

(2) The more careful consideration devoted, in the present work, to the effects of dielectric saturation. Neglect of these effects allows the ions to approach much more closely than 4 Å, and the resulting ΔF^*_{calc} is less by more than a kilocalorie.

The reason that the present treatment gives a value of ΔF^*_{calc} that is too low is probably due to the fact that the treatment of repulsive effects somewhat underestimates the value of ΔF^*_{rep}. It does not seem likely that the calculated values of ΔF^*_{diff} and ΔF^*_{tun} can be much in error. It is to be noted that the present way of looking at the problem, particularly of treating the energy barriers, leaves no place for the "rearrangement" free energy considered by Eyring *et al.*, this factor having been included in the present treatment of the repulsive energy and the potential-energy barrier.

ENERGIES AND ENTROPIES OF ACTIVATION

The calculation of energies and entropies of activation is always more difficult than that of free energies of activation, since the energies and entropies depend in a more intimate way on the various structural factors. It is, however, of interest to see to what extent the present treatment offers an interpretation of the experimental values of $E = 9.9$ kcal and $\Delta S^* = -25$ e.u. We will consider separately the three terms involved, namely diffusion, tunnelling, and repulsion. Since the average ΔF^* corresponds approximately to a value of σ equal to 5.0 Å, the figures to be quoted below will be related to this separation.

Activation energies for the viscous flow of water (19) and for diffusion processes in water (20) are usually close to 4.0 kcal at 25° C. Since at $\sigma = 5.0$ Å, $\Delta F^*_{\text{diff}} = 5.7$ kcal, it follows that $\Delta S^*_{\text{diff}} = -5.7$ e.u.

Can. J. Chem. Downloaded from www.nrcresearchpress.com by 190.90.36.8 on 09/04/12
For personal use only.

The transmission coefficient is proportional to $\exp[k(V_0-W)^{\frac{1}{2}}]$ and V_0 and W are practically temperature independent (since most of the work of transferring the electron is done through the dielectrically saturated layer). The free energy of activation for tunnelling, equal to 6.1 kcal, therefore corresponds entirely to an apparent entropy of activation, so that

$$E_{tun} = 0 \text{ and } \Delta S^*_{tun} = -20.3 \text{ e.u.}$$

Since the heats and entropies for repulsion are very difficult to estimate in a reliable manner they have been obtained by difference, and are shown as starred values in the table below:

	ΔF^*	E	ΔS^*
Diffusion	5.7	4.0	−5.7
Tunnelling	6.1	0	−20.3
Repulsion	5.0*	5.9*	3.0*,†
Experimental values	16.8	9.9	−25

†The apparent discrepancy in the ΔS^* values is due to the fact that in the calculation of ΔS^*_{exp} the pre-exponential factor is taken as $e\mathrm{k}T/h$ rather than $\mathrm{k}T/h$.

The very elementary theory of the entropy of activation for repulsion, with $\epsilon = 78.5$ and $\partial \ln \epsilon/\partial T = -0.0046$, gives,

$$\Delta S^*_{rep} = -18.8(z_1z_2/\sigma) = -22.6 \text{ e.u.},$$

which is very far from the derived value of 3.0 e.u. The entropy of activation will, however, be very markedly increased when there is initially almost complete saturation in the vicinity of both of the reacting ions. It is found, for example, that entropies of activation for reactions between ions of the same sign are frequently larger than predicted by the elementary theory. The reason for these effects may well be that, in order for the ions to approach closely, water molecules must be "unfrozen"; such a process will require energy and will result in an increase in entropy.

REFERENCES

1. SILVERMAN, J. and DODSON, R. W. J. Phys. Chem. **56**, 846 (1952).
2. LIBBY, W. F. J. Phys. Chem. **56**, 863 (1952).
3. WEISS, J. Proc. Roy. Soc. A, **222**, 128 (1954).
4. MARCUS, R. J., ZWOLINSKI, B. J., and EYRING, H. J. Phys. Chem. **58**, 432 (1954).
5. ZWOLINSKI, B. J., MARCUS, R. J., and EYRING, H. Chem. Revs. **55**, 157 (1955).
6. MARCUS, R. A. (*a*) J. Chem. Phys. **26**, 867 (1957). (*b*) Trans. N.Y. Acad. Sci. **19**, 423 (1957).
7. SMOLUCHOWSKI, M. V. Z. physik. Chem. **92**, 129 (1917).
8. VERWEY, E. J. and OVERBEEK, J. Th. G. Theory of the stability of lyophobic colloids. Elsevier Press, Inc., N.Y. 1948.
9. DEBYE, P. Trans. Electrochem. Soc. **82**, 265 (1942).
10. ALBERTY, R. A. and HAMMES, G. G. J. Phys. Chem. **62**, 154 (1958).
11. BRADLEY, R. S. Trans. Chem. Soc. 1910 (1934).
12. LAIDLER, K. J. and PEGIS, C. Proc. Roy. Soc. A, **241**, 80 (1957).
13. KIRKWOOD, J. G. J. Chem. Phys. **7**, 911 (1939).
14. BOOTH, F. J. Chem. Phys. **19**, 391, 1327, 1615 (1951).
15. GRAHAME, D. C. J. Chem. Phys. **21**, 1054 (1953).
16. MALSCH, J. Physik. Z. **29**, 770 (1928); **30**, 837 (1929).
17. COUTURE, A. M. and LAIDLER, K. J. Can. J. Chem. **34**, 1209 (1956).
18. MOTT, N. F. and SNEDDON, I. N. Wave mechanics and its applications. The Clarendon Press, Oxford. 1948. pp. 15–17.
19. EWELL, R. H. and EYRING, H. J. Chem. Phys. **5**, 726 (1937).
20. SCHEFFER, J. D. R. and SCHEFFER, F. E. C. Proc. Acad. Sci. Amsterdam, **19**, 148 (1916).

Can. J. Chem. Downloaded from www.nrcresearchpress.com by 190.90.36.8 on 09/04/12
For personal use only.

Can. J. Chem. Downloaded from www.nrcresearchpress.com by 190.90.36.8 on 09/04/12
For personal use only.

THE PRINCIPLE OF EQUIVALENCE CHANGE IN OXIDATION–REDUCTION REACTIONS[1]

J. HALPERN

ABSTRACT

The principle of equivalence change predicts that oxidation–reduction reactions between 1-equivalent oxidants and 2-equivalent reductants (or vice versa) will, in general, be slow, since they must proceed either through termolecular paths or through the formation of unstable intermediates. In this paper, the kinetics and mechanisms of a number of reactions of this type are examined and an attempt is made to assess the validity of the considerations on which this principle is based. Among the reactions considered are (1) electron transfer between metal ions; (2) oxidation of metal ions by oxygen; and (3) reduction of metal ions by hydrogen. In each of these cases it is found that the principle of equivalence change has only limited validity and that a number of other factors are important in determining the relative rates and mechanisms of reactions of different equivalence type. Among these are the formation of stabilized intermediate complexes between oxidant and reductant and the possibility of unstable intermediates acting as carriers in chain reactions. In reactions of thallium(I) or thallium(III) with 1-equivalent metal ions, thallium(II) is formed as an intermediate. Some of these reactions are not as slow as expected, apparently because of favorable entropies of activation. Several of the reactions examined proceed simultaneously through bimolecular and termolecular paths, the latter being favored because of lower activation energies.

INTRODUCTION

A large number of oxidizing and reducing agents are known whose stable oxidation states differ by two electron equivalents (e.g., Tl(I)–Tl(III), Sn(II)–Sn(IV), H_2–$2H^+$, O_2–H_2O_2) and the question arises of how these react with 1-equivalent reductants or oxidants (e.g., Fe(II)–Fe(III), Ce(III)–Ce(IV), etc.). The principle of equivalence change, due to Shaffer (1, 2, 3), states that such reactions are, in general, slow compared to reactions between 1-equivalent oxidants and 1-equivalent reductants or between 2-equivalent oxidants and 2-equivalent reductants. This principle can be interpreted in the following way: Two general types of mechanisms can be conceived for a reaction between a 1-equivalent reductant, A, with stable oxidation states N and N+1, and a 2-equivalent oxidant, B, with stable oxidation states N and N+2.

$$\text{I} \quad \left\{ \begin{array}{l} \xrightarrow{\text{slow}} \\ 2A^N + B^{N+2} \longrightarrow 2A^{N+1} + B^N \end{array} \right.$$

$$\text{II} \quad \left\{ \begin{array}{l} \left. \begin{array}{l} \xrightarrow{\text{slow}} \\ A^N + B^{N+2} \longrightarrow A^{N+1} + B^{N+1} \\ \xrightarrow{\text{fast}} \\ A^N + B^{N+1} \longrightarrow A^{N+1} + B^N \end{array} \right\} (a) \\ \text{or} \\ \left. \begin{array}{l} \xrightarrow{\text{slow}} \\ A^N + B^{N+2} \longrightarrow A^{N+2} + B^N \\ \xrightarrow{\text{fast}} \\ A^N + A^{N+2} \longrightarrow 2A^{N+1} \end{array} \right\} (b) \end{array} \right.$$

[1]*Manuscipt received July 5, 1958.*
Contribution from the Department of Chemistry, University of British Columbia, Vancouver, B.C. This paper was presented at the Symposium on Charge Transfer Processes held at the University of Toronto, Toronto, Ontario, September 4 and 5, 1958.

It is anticipated that reactions proceeding by the first type of mechanism will be slow because they involve a termolecular step, while reactions of the second type will be slow because of the high activation energy associated with the formation of the unstable intermediate, B^{N+1} or A^{N+2}. It also follows that such reactions should be susceptible to catalysis by species, X, which have three oxidation states, N, N+1, and N+2, with suitably disposed potentials through a mechanism of the type:

III
$$\begin{cases} A^N + X^{N+2} \longrightarrow A^{N+1} + X^{N+1} \\ A^N + X^{N+1} \longrightarrow A^{N+1} + X^N \\ X^N + B^{N+2} \longrightarrow X^{N+2} + B^N \end{cases}$$

Recent studies on the kinetics and mechanisms of a variety of inorganic oxidation–reduction reactions make possible for the first time a detailed assessment of the validity of these considerations. This is attempted in the present paper with particular reference to three relatively simple types of reactions, (1) electron transfer between metal ions; (2) oxidation of metal ions by molecular oxygen; and (3) reduction of metal ions by molecular hydrogen. The principles which emerge from a consideration of these systems appear capable of extension to reactions of more complex species.

1-EQUIVALENT AND 2-EQUIVALENT OXIDANTS AND REDUCTANTS

The inherent tendencies of different oxidizing agents to undergo 1-equivalent or 2-equivalent reduction are revealed by differences in the products that are obtained when they react with certain reducing agents, notably hydrazine (4, 5) and sulphurous acid (6). In the case of sulphurous acid, 1-equivalent oxidation favors the formation of dithionate, while 2-equivalent oxidation results exclusively in the formation of sulphate, according to the mechanisms:

$$SO_3^{2-} \xrightarrow{-e} SO_3^- \longrightarrow \tfrac{1}{2}S_2O_6^{2-},$$

$$SO_3^{2-} \xrightarrow{-2e} SO_3(SO_4^{2-}).$$

The following classification of oxidants, due to Higginson and Marshall (6), is based on this criterion:

1-Equivalent	2-Equivalent	1,2-Equivalent
Ce(IV)	Tl(III)	$Cr_2O_7^{2-}$
Co(III)	H_2O_2	MnO_4^-
Fe(III)	I_2, Br_2, Cl_2	$PtCl_6^{4-}$
Mn(III)	IO_3^-, BrO_3^-	VO_2^+
OH	BrO^-, ClO^-	

Many oxidants can be unambiguously classified as being of the 1- or 2-equivalent type; a few which give intermediate stoichiometry are denoted as 1,2-equivalent.

The occurrence of 2-equivalent steps in oxidation–reduction reactions is now well recognized and Michaelis's hypothesis that all such reactions proceed by successive univalent steps (7) must be considered as without general validity. This conclusion is relevant to the present discussion, since this hypothesis, if valid, would remove the most obvious basis for the principle of equivalence change.

Can. J. Chem. Downloaded from www.nrcresearchpress.com by 190.90.36.8 on 09/04/12
For personal use only.

Can. J. Chem. Downloaded from www.nrcresearchpress.com by 190.90.36.8 on 09/04/12
For personal use only.

ELECTRON-TRANSFER REACTIONS BETWEEN METAL IONS

A significant test of the principle of equivalence change should be provided by comparing the kinetics of an oxidation–reduction reaction between a 1-equivalent and a 2-equivalent metal ion, with the kinetics of the isotopic exchange reactions between the two valence states of each ion. The data summarized in Table I permit three such comparisons, i.e., for the Fe^{2+}–Tl^{3+}, Tl^{+}–Co^{3+}, and Tl^{+}–Ce^{4+} reactions.

TABLE I

Electron-transfer reactions between metal ions

Reaction	Equivalence type	k (25°), 1 mole^{-1} sec^{-1}	E, kcal	$\Delta S^{\ddagger}$ e.u.	Reference
Fe^{2+}–Fe^{3+}	1–1	4	9.9	−25	8
Co^{2+}–Co^{3+}	1–1	0.75(0°)	—	—	9
Ce^{3+}–Ce^{4+}	1–1	2×10^{-2}	7.7	−40	10
Tl^{+}–Tl^{3+}	2–2	4×10^{-6}	17.6	−21	11
Fe^{2+}–Tl^{3+}	1–2	2×10^{-2}	18	−7	12
Tl^{+}–Co^{3+}	2–1	3×10^{-3}	26.4	+22	13
Tl^{+}–Ce^{4+}	2–1	Very slow	—	—	14

Both the Fe^{2+}–Tl^{3+} and Tl^{+}–Co^{3+} reactions have been shown to proceed through type II mechanisms, involving one-electron transfer steps with the formation of Tl(II) as an intermediate (13, 15). In line with the principle of equivalence change, the activation energy of each of these reactions appears to be higher than the activation energies of both the corresponding isotopic electron-exchange reactions; presumably this reflects the formation of the unstable Tl(II) species. However, the rates of these reactions are not lower than, but in both cases intermediate between, those of the corresponding exchange reactions, i.e., $k_{Tl^{+}-Tl^{3+}} < k_{Fe^{2+}-Tl^{3+}} < k_{Fe^{2+}-Fe^{3+}}$. This is because in each case the mixed reaction is favored by a more positive entropy of activation.

Until data are obtained for more systems, it is not possible to conclude whether this is a general feature of such reactions, but there are grounds for anticipating that this may prove to be the case. These are provided by the recognition that one of the principal contributing factors to the instability of intermediate valence states of metal ions in solution is a low hydration energy; usually this is because the ion is "abnormally" large having, as in the case of Tl^{2+}, only a single electron in its outer shell. However, for the same reason the entropy of hydration of the ion will tend to be more positive than those of stable ions of similar charge (e.g., Tl^{2+} vs. Hg^{2+}). A reaction involving the formation of such an ion would therefore be expected to require considerable energy but to be favored by an abnormally positive entropy. If, as often tends to be the case, the charge distribution of the activated complex approaches that of the products, a similar trend would be reflected in the energies and entropies of activation.

The increase in entropy of activation (relative to the exchange reactions) is more pronounced for the Tl^{+}–Co^{3+}, than for the Fe^{2+}–Tl^{3+} reaction, and this may be due to the influence of an additional factor. The rate-determining step of this reaction,

$$Tl^{+} + Co^{3+} \longrightarrow Tl^{2+} + Co^{2+}$$

involves a change in the ionic charges in the direction of charge equalization (more uniform spreading out of the charge). This is generally accompanied by a decrease in the electrostriction of the surrounding solvent and hence by an increase in entropy. The entropy of activation should also be shifted toward more positive values. This effect should not be apparent in the Fe^{2+}–Tl^{3+} reaction, whose rate-determining step,

$$Fe^{2+} + Tl^{3+} \longrightarrow Fe^{3+} + Tl^{2+}$$

involves no change in charge type, nor in the isotopic exchange reactions which are, of course, symmetrical.

In contrast to the other two systems and more clearly in line with the principle of equivalence change, the Tl^{+}–Ce^{4+} reaction appears to be much slower than either the Tl^{+}–Tl^{3+} or Ce^{3+}–Ce^{4+} exchange reaction. It is not possible to draw any detailed conclusions from this, since there is some uncertainty about the mechanism of oxidation of Tl^{+} by Ce^{4+}. Preliminary kinetic measurements (14) suggest that this proceeds not by direct reaction between the ions but by a mechanism, such as

$$CeOH^{3+} \rightleftharpoons Ce^{3+} + OH,$$
$$Tl^{+} + OH \rightarrow Tl^{2+} + OH^{-},$$
$$Tl^{2+} + Ce^{4+} \rightarrow Tl^{2+} + Ce^{3+}.$$

The possibility that the first step of this mechanism also constitutes a path of Ce^{3+}–Ce^{4+} exchange cannot be dismissed.

Catalysis of the Tl^{+}–Ce^{4+} reaction by Mn^{2+} (1) and by halide ions (16) has been reported and attributed to a type III mechanism.

The above reactions have been discussed without reference to the question of whether they occur by actual electron transfer between the metal ions or by some other mechanism, e.g., H-atom transfer between the hydration shells of the ions. There is still some uncertainty about this question (17), but the considerations which have been invoked here would be applicable in either case.

OXIDATION OF METAL IONS BY MOLECULAR OXYGEN

The first stable reduction product of oxygen is hydrogen peroxide, and it can therefore be considered as a 2-equivalent oxidizing agent. Kinetic data for the oxidation of several metal ions by oxygen are summarized in Table II.

TABLE II
Oxidation of metal ions by oxygen

Reaction	Kinetics	E (kcal)	$\Delta S^{\ddagger}$ (e.u.)	Reference
Fe(II) → Fe(III)	$k[O_2][Fe(II)]^2$	17.4	−15	18
Pu(III) → Pu(IV)	$k[O_2][Pu(III)]^2$	19	+11.2*	19
V(III) → V(IV)	$k[O_2][V(III)]$	20.1	+6†	20
U(IV) → U(VI)	$k[O_2][U(IV)]$	22	—	21

*The high apparent entropy of activation may be due to considerable charge neutralization in the activated complex, since the kinetics suggest that 2–3 sulphate ions participate in the rate-determining step.

†Calculated on the assumption that the reacting species is VOH^{2+}; this is suggested by the pH dependence of the rate.

Fe(II) is a 1-equivalent reductant and its oxidation by oxygen, as evidenced by the third-order kinetics, appears to proceed by a type I mechanism. This is also the case for the oxidation of Pu(III) to Pu(IV), despite the fact that the +5 state of Pu is relatively stable and hence a 2-equivalent oxidation of Pu(III) is feasible. On the other hand, the oxidation of V(III) to V(IV) is a second-order reaction and probably proceeds by a type II mechanism; possible intermediates are V(V) and HO_2. This reaction is very susceptible to catalysis by cupric salts, probably through a mechanism of the type

$$V(III) + Cu(II) \xrightarrow{\text{slow}} V(IV) + Cu(I),$$
$$Cu(I) + O_2 \xrightarrow{\text{fast}} Cu(II).$$

Can. J. Chem. Downloaded from www.nrcresearchpress.com by 190.90.36.8 on 09/04/12
For personal use only.

It is of interest that the activation energies for the oxidation of these three metal ions are similar.

Despite the fact that U(IV) is a 2-equivalent reductant, its oxidation to U(VI) by O_2 is not accomplished in a single 2-equivalent step. It has been shown (21) that this reaction occurs by a chain mechanism involving the 1-equivalent steps

$$U(V) + O_2 \rightarrow U(VI) + HO_2,$$

$$U(IV) + HO_2 \rightarrow U(V) + H_2O_2.$$

This mechanism involves the formation of the unstable intermediates HO_2 and U(V), but is favored over the direct 2-equivalent oxidation, because of the "amplification factor" introduced by the chain reaction. While this also applies to a number of other reactions between 2-equivalent oxidants and reductants (e.g., the oxidation of $SO_3^=$ by O_2) these do not include any examples of reaction between two metal ions. Thus, the Tl(I)–Tl(III) exchange and the oxidation of U(IV) by Tl(III) (22), which could, in principle, occur by analogous mechanisms, appear to be simple bimolecular reactions.

REDUCTION OF METAL IONS BY MOLECULAR HYDROGEN

Molecular hydrogen reacts homogeneously with a number of metal ions in aqueous solution, reducing them to metallic form or to compounds of lower valence (23). The kinetics of the primary steps in these reactions are summarized in Table III.

TABLE III

Reduction of metal ions by hydrogen

Ion	Kinetics	E (kcal)	$\Delta S^{\ddagger}$ (e.u.)	Reference
Cu^{2+}	$k[H_2][Cu^{2+}]$	26.6	−10	24
Hg^{2+}	$k[H_2][Hg^{2+}]$	18.1	−12	25
Hg_2^{2+}	$k[H_2][Hg_2^{2+}]$	20.4	−10	25
Ag^+ (I)	$k[H_2][Ag^+]$	24.0	−6	26
Ag^+ (II)	$k[H_2][Ag^+]^2$	14.7	−25	26
MnO_4^-	$k[H_2][MnO_4^-]$	14.7	−17	27
$Ag^+ + MnO_4^-$*	$k[H_2][Ag^+][MnO_4^-]$	9.3	−26	27

*Ag^+—Catalyzed reaction between MnO_4^- and H_2.

Since the formation of H atoms (or H_2^+ ions) in aqueous solution is energetically very unfavorable, hydrogen might be expected to behave as a 2-equivalent reductant in these reactions.

The reactions of hydrogen with Hg^{++}, Hg_2^{++}, and MnO_4^- are consistent with this. For example, the mechanism of the reduction of Hg^{2+} to Hg_2^{2+} is probably

$$Hg^{2+} + H_2 \xrightarrow{\text{slow}} Hg + 2H^+,$$

$$Hg + Hg^{2+} \xrightarrow{\text{fast}} Hg_2^{2+}.$$

This mechanism is plausible on energetic as well as kinetic grounds, since the proposed rate-determining step, in which a Hg atom is formed, is exothermic by 27 kcal (23). Similar considerations apply to the reduction of Hg_2^{2+} and of MnO_4^-. In each of these cases the rate-determining step appears to be a 2-equivalent reduction, leading to the formation of Hg_2 and Mn(V), respectively, as intermediates.

Can. J. Chem. Downloaded from www.nrcresearchpress.com by 190.90.36.8 on 09/04/12
For personal use only.

From the standpoint of the principle of equivalence change, the homogeneous bimolecular reactions of H_2 with Cu^{2+} and with Ag^+ are, however, surprising. Cu^{2+} is a 1-equivalent oxidant and either type II mechanism would involve a rate-determining step

$$Cu^{2+} + H_2 \rightarrow Cu^+ + H^+ + H \qquad (\Delta H^\circ \sim 54 \text{ kcal})$$

or

$$Cu^{2+} + H_2 \rightarrow Cu + 2H^+ \qquad (\Delta H^\circ \sim 66 \text{ kcal}),$$

which is energetically inconsistent with the observed activation energy of 26 kcal. The mechanism of the reduction of Cu^{2+} to Cu^+ by H_2 has actually been shown (28) to be

$$Cu^{2+} + H_2 \overset{k}{\rightleftharpoons} CuH^+ + H^+,$$

$$CuH^+ + Cu^{2+} \rightarrow 2Cu^+ + H^+.$$

It is thus apparent that in reactions such as this, where the oxidant and reductant form an intermediate complex which is stabilized by covalent bonding, the principle of equivalence change offers little guidance as to the probable kinetics and mechanism.

The reduction of Ag^+ by H_2 also appears to proceed through the formation of covalently bonded hydride intermediates. It is of interest that two paths are observed for this reaction, in which the rate-determining steps involve the heterolytic and homolytic splitting of hydrogen, respectively,

$$Ag^+ + H_2 \rightarrow AgH + H^+,$$

$$2Ag^+ + H_2 \rightarrow 2AgH^+.$$

Despite the fact that the latter reaction is termolecular, it is favored relative to the alternative bimolecular path, by its lower activation energy (14.7 vs. 24 kcal) and predominates at lower temperatures. Similarly the marked susceptibility of the reduction of MnO_4^- by H_2, to catalysis by Ag^+, is due to a termolecular rate-determining step,

$$Ag^+ + MnO_4^- + H_2 \rightarrow AgH + MnO_4^{2-} + H^+,$$

which competes with the bimolecular uncatalyzed reaction because of its lower activation energy (9.3 vs. 14.7 kcal).

These observations prompt some comment on the question of the relative probabilities of bimolecular and termolecular reactions in general. Some measure of this is provided by the difference in entropy of activation for the two types of processes. In solution, this difference is normally only about 10 e.u., corresponding to a factor of about 100 in the rate constant. This is the equivalent of a difference in activation energy of only about 3000 cal at 25°. Even at reactant concentrations as low as 0.001 M an activation energy difference of about 7000 cal will equalize the rates. Since variations of activation energy of this order, even among closely related reactions in solution, are fairly common the widespread emphasis which is encountered in the literature on kinetics on the improbability of termolecular reactions is somewhat misleading. This is particularly relevant to reactions of the type considered here, in which the presence of alternative bimolecular and termolecular paths (the latter having a lower activation energy) is an intrinsic feature.

REFERENCES

1. SHAFFER, P. A. J. Am. Chem. Soc. **55**, 2169 (1933); J. Phys. Chem. **40**, 1021 (1936); Cold Spring Harbor Symposia Quant. Biol. **1**, 50 (1939).
2. REMICK, A. E. J. Am. Chem. Soc. **69**, 94 (1947).
3. WESTHEIMER, F. H. *In* The mechanism of enzyme action. *Edited by* W. D. McElroy and B. Glass. John Hopkins Press, Baltimore, Md. 1954. p. 321.
4. KIRK, R. E. and BROWNE, A. W. J. Am. Chem. Soc. **50**, 337 (1928).

Can. J. Chem. Downloaded from www.nrcresearchpress.com by 190.90.36.8 on 09/04/12
For personal use only.

5. HIGGINSON, W. C. E., SUTTON, D., and WRIGHT, P. J. Chem. Soc. 282, 1402 (1953); 1551 (1955).
6. HIGGINSON, W. C. E. and MARSHALL, J. W. J. Chem. Soc. 447 (1958).
7. MICHAELIS, L. Trans. Electrochem. Soc. **71**, 107 (1937); Cold Spring Harbor Symposia Quant. Biol. **7**, 33 (1939).
8. SILVERMAN, J. and DODSON, R. W. J. Phys. Chem. **56**, 846 (1952).
9. BONNER, N. A. and HUNT, J. P. J. Am. Chem. Soc. **74**, 1866 (1952).
10. GRYDER, J. W. and DODSON, R. W. J. Am. Chem. Soc. **73**, 2890 (1951).
11. PRESTWOOD, R. and WAHL, A. C. J. Am. Chem. Soc. **71**, 3137 (1949).
12. JOHNSON, C. E. J. Am. Chem. Soc. **74**, 959 (1952).
13. ASHURST, K. G. and HIGGINSON, W. C. E. J. Chem. Soc. 343 (1956).
14. ARMSTRONG, A. M. and HALPERN, J. Unpublished results.
15. ASHURST, K. G. and HIGGINSON, W. C. E. J. Chem. Soc. 3044 (1953).
16. DUKE, F. R. and BORCHERS, C. E. J. Am. Chem. Soc. **75**, 5186 (1955).
17. BASOLO, F. and PEARSON, R. G. *In* Mechanisms of inorganic reactions. Chap. 8. John Wiley & Sons, Inc., New York. 1958.
18. GEORGE, P. J. Chem. Soc. 4349 (1954).
19. BAKER, F. B. and NELSON, T. W. J. Phys. Chem. **61**, 381 (1957).
20. RAMSEY, J. B., SUGIMOTO, R., and DEVORKIN, H. J. Am. Chem. Soc. **63**, 3480 (1941).
21. HALPERN, J. and SMITH, J. G. Can. J. Chem. **34**, 1419 (1956).
22. HARKNESS, A. and HALPERN, J. Unpublished results.
23. HALPERN, J. Quart. Revs. **10**, 463 (1956); Advances in Catalysis, **9**, 302 (1957).
24. PETERS, E. and HALPERN, J. J. Phys. Chem. **59**, 793 (1955).
25. KORINEK, G. J. and HALPERN, J. J. Phys. Chem. **60**, 285 (1956).
26. WEBSTER, A. H. and HALPERN, J. J. Phys. Chem. **61**, 1239, 1245 (1957).
27. WEBSTER, A. H. and HALPERN, J. Trans. Faraday Soc. **53**, 51 (1957).
28. HALPERN, J., MACGREGOR, E. R., and PETERS, E. J. Phys. Chem. **60**, 1455 (1956).

Can. J. Chem. Downloaded from www.nrcresearchpress.com by 190.90.36.8 on 09/04/12
For personal use only.

Can. J. Chem. Downloaded from www.nrcresearchpress.com by 190.90.36.8 on 09/04/12
For personal use only.

ON THE THEORY OF ELECTROCHEMICAL AND CHEMICAL ELECTRON TRANSFER PROCESSES[1]

R. A. MARCUS

ABSTRACT

Kinetic studies of simple electron transfer systems in solution and at electrodes have revealed a number of interesting and simplifying features. The chemical reactions also represent one of the very few cases in kinetics where it has been possible to make reasonable calculations of the absolute rate constant without introducing adjustable parameters or arbitrary assumptions. Because of their comparative simplicity, these processes also serve as a useful kinetic tool for investigating ion–solvent–electrode interactions.

In the present paper the writer's recent theoretical investigations are summarized and used to interpret data obtained from both solution and electrode studies. Various phenomena are discussed in the light of this theory and several predictions of behavior are made. The topics considered include effects of changing the overpotential or the standard free energy of reaction, the ionic structure, temperature, salt concentration, solvent, and electrode material. Both the parallelism between chemical and electrochemical transfers and the role played by the electrostatic image in the latter case are discussed. A classification of reactants is employed throughout, based in part on differences in the theoretical treatment.

INTRODUCTION

In 1952 Libby (19) interpreted the behavior of some isotopic exchange electron transfer reactions in terms of the Franck–Condon principle, a suggestion which served to stimulate much further experimental and theoretical work. About the same time, Randles (31) discussed the rates of simple electron transfer electrode processes in terms of related concepts. This work was followed several years later by Rudolph J. Marcus, Zwolinski, and Eyring's investigation of an electron tunnelling mechanism for electron transfer (28) and by Taube's evidence that a bridge-activated complex may serve as an intermediate in some cases (38). Each of these stimulating contributions was qualitative (19, 31, 38) or semiempirical in nature (28).

More recently the writer has formulated a quantitative theory of electron transfers in solution (20) and at electrodes (26). It is free from arbitrary assumptions and adjustable parameters. In its present form it was devised for *simple* electron transfer reactions in which no rupture or formation of chemical bonds occurs in the transfer step.

THEORY

The basic assumption of the theory is that only a weak electronic interaction of the two reacting species is required for a simple electron transfer process to occur. The reactants may be ions or molecules and, in the electrode system, the electrode and an ion or molecule. Several deductions may be made quantum mechanically from this basic assumption:

(1) The electronic configuration and therefore the charge distribution of the activated complex are inordinately sensitive to the atomic configuration of the medium (as well as to that of the reactants). In this respect and in its consequent mode of treatment it is apparently unique among activated complexes, but it has much in common with the "polaron" (30), the *F*-center (30), and the "solvated electron".

(2) During the course of a reactive encounter, the atomic configuration of the entire

[1]*Manuscript received July 6, 1958.*
Contribution from the Department of Chemistry, Polytechnic Institute of Brooklyn, Brooklyn 1, N.Y. This paper was presented at the Symposium on Charge Transfer Processes held at the University of Toronto, Toronto, Ontario, September 4 and 5, 1958.

system gradually changes from one characteristic of the reactants to one characteristic of the products. At the same time the electronic configuration undergoes a corresponding change, following this atomic configurational change adiabatically (27).

(3) As in any reaction, the activated complex can possess one of many possible atomic configurations of positions and momenta, but in the present case the configuration must satisfy a severe energy restriction (20). In *this* atomic configuration, a hypothetical system possessing the electronic wave function (and therefore the ionic charges) of the reactants must have the same energy as that of a hypothetical system possessing the electronic wave function of the products in the same configuration.

An infinite number of atomic configurations can satisfy this energy condition, but only a group of these contribute to the macroscopic or "thermodynamic" properties of the activated complex, namely those which minimize its free energy of formation from the reactants.

In setting up an expression for the reaction rate, the atomic configuration of the system outside the co-ordination shell of each reactant was treated as forming a continuous dielectric medium (20, 26). The configuration of the co-ordination shells themselves was expressed in terms of structural properties such as bond force constants and lengths, using statistical mechanics (22). Special methods involving "nonequilibrium" electrostatic considerations were developed for solving the minimization of free-energy problem subject to the energy restriction (21, 25). The group of atomic configurations constituting the activated complex could not be in electrostatic equilibrium with both hypothetical charge distributions at the same time.

On the basis of theoretical considerations it seems appropriate to classify the reactants somewhat loosely into three groups. Class I consists of those species for which the co-ordination shell of the oxidized form has essentially the same interatomic distances as does that of the reduced form. Class II consists of those in which the bonds of one form have become slightly stretched or compressed compared with the other form. Class III consists of those in which large stretching or compression has occurred.

Examples of Class I include (35) MnO_4^-–MnO_4^{-2} and probably $Fe(CN)_6^{-3}$–$Fe(CN)_6^{-4}$. Examples of Class II include many hydrated metal cations such as $Fe(H_2O)_6^{+3}$–$Fe(H_2O)_6^{+2}$, and those of Class III include (3, 6) $Co(NH_3)_6^{+3}$–$Co(NH_3)_6^{+2}$ and $Cr(H_2O)_6^{+3}$–$Cr(H_2O)_6^{+2}$.

The equations given below were derived for reactants of Class I. Some modifications appropriate to the other classes are noted.

THEORETICAL EQUATIONS

Using as a reaction co-ordinate either a solvent polarization co-ordinate or a movement of either reacting ion relative to the solvent, the following relation can be deduced for both solution and electrode–electron transfer rate constants (20, 26):

$$k = A' e^{-\Delta F^*/RT} \qquad [1]$$

where ΔF^* is defined below and where A' is of the order of 10^{15} cc mole^{-1} sec^{-1} and 5×10^4 cm sec^{-1} for solution and electrode processes, respectively.* Defining the activation energy, E_a, in the usual way as $-\partial \ln k/\partial(1/RT)$ and neglecting the minor temperature dependence of A' we find:

**The exact value of A' is under current study. It depends both on the detailed nature of the reaction co-ordinate and on the value of the collision frequency of two uncharged species. Derivations of a high value (10, 20) for the bimolecular collision frequency in solution can be shown to be overestimates for the system under consideration.*

Can. J. Chem. Downloaded from www.nrcresearchpress.com by 190.90.36.8 on 09/04/12
For personal use only.

[2] $$k = A\, e^{-E_a/RT}$$

where

[3] $$E_a = \Delta F^* + T\Delta S^*$$

[4] $$A = A'\, e^{\Delta S^*/RT}$$

[5] $$\Delta S^* = -\partial \Delta F^*/\partial T.$$

ΔF^* represents the change in free energy of ion–ion and ion–solvent interactions accompanying the formation of the activated complex from the reactants:

solution

[6] $$\Delta F^* = w^* + m^2\lambda$$

[7] $$-(2m+1)\lambda = \Delta F^0 + w - w^*$$

electrode

[8] $$\Delta F^* = w^* + m^2\lambda/2$$

[9] $$-(2m+1)\lambda/2 = -ne\eta_a + w - w^*$$

[10] $$\lambda = n^2e^2(1/a - 1/r)\,(1/D_{op} - 1/D_s).$$

The following symbols are employed in these equations:

w^*, w = Work required to bring the two reactants together and the two products together, respectively, from infinity to the positions they would occupy in the activated complex. For the electrode system, w^* and w denote the work required to transport the reactant and the product to the electrode, respectively.

m, λ = Defined by equations [7], [9], and [10].

n = Number of electrons transferred from one reactant to the other (i.e., from a reactant to the electrode, for the electrode case).

e = Unit of electronic charge.

a = Ionic radius (including region occupied by co-ordination shell). If the radii of the two ionic reactants differ, and have values a_1 and a_2, then $2/a = (1/a_1)+(1/a_2)$.

r = Interionic distance in the activated complex or, for the electrode case, twice the distance from the electrode to the center of the ion.

D_{op} = Square of the refractive index.

D_s = Static dielectric constant.

$\Delta F^\circ = -RT \ln K$, K being the equilibrium constant for the reaction at the given salt concentration. ΔF° will be called the "standard" free energy of reaction.

η_a = Activation overpotential (zero for equilibrium at the given salt concentration).

INTERPRETATION OF THE EQUATIONS

Experimentally, various properties of the electron transfer rate constants of both processes can be measured: their dependence on standard free energy or activation overpotential; their dependence on ionic structure; the extent of parallelism between both rate constants for a series of reactants; the frequency factor and activation energy; the dependence of rate constants on added salts, on the solvent medium, and on the electrode material and surface contamination. The equations will be examined with these features in mind.

The theoretical equations of the two processes are closely related. Typically in each

Can. J. Chem. Downloaded from www.nrcresearchpress.com by 190.90.36.8 on 09/04/12
For personal use only.

case, ΔF^* decreases with increasing a, decreasing ne, decreasing r, increasing D_{op}, decreasing D_s (except for the latter's effect, more important perhaps, on w^* and w), and increasingly negative ΔF° or $-ne\,\eta_a$. This behavior has a simple physical interpretation related to the ease with which the energy restriction discussed earlier can be satisfied (23, 24).

For example, ion–solvent interactions decrease with increasing ionic radius a, so that there would be a smaller energy difference between the two hypothetical charge distributions in the original atomic configuration of the reactants and therefore a smaller reorganization would be needed to equalize the two energies. Similarly, the smaller the charge transferred, ne, or the smaller the distance between the reactants (or between the ion and its electrostatic image in the electrode), the less the medium can discriminate energywise between the two hypothetical charge distributions and therefore the less the reorganization needed for energy equalization. A larger optical dielectric constant, D_{op}, serves to partially neutralize the electrostatic fields of the charges and therefore to reduce their energy difference for a given atomic configuration. The more D_s approaches D_{op}, the smaller the dipolar contribution to the electrical polarization of the medium and the less the necessary rearrangement of the atoms (at least for zero ΔF° or zero η_a).

The RHS of equations [7] and [9] has an interesting interpretation. The effective driving force of the reaction is not really the free energy difference (ΔF° or $-ne\,\eta_a$) between reactants and products when the reacting species are far apart but rather when they are in the positions they occupy in the activated complex. These quantities are simply the $\Delta F^\circ+w-w^*$ and $-ne\,\eta_a+w-w^*$ of equations [7] and [9]. By lowering the free energy of the final state of the system relative to that of the initial state, these terms reduce the amount of necessary reorganization of atomic configuration of the initial state in order to satisfy the energy restriction (24).

One difference between the two sets of equations is that λ in equations [6] and [7] for the homogeneous system has become $\lambda/2$ for the electrode system. This difference can be attributed to the absence of one half of the dielectric medium in the electrode case. (Effectively, the charge is transferred from the ion to its electrostatic image, and the metal surface bisects the line drawn between the two.)

The theoretical expressions for ΔF^* and ΔS^* of Classes II and III naturally would contain additional terms. Interesting suggestions concerning these classes have been made by several groups (e.g., 1, 3, 6, 9, 14, 29).

INTERPRETATION OF THE DATA

The data will be discussed from the point of view of the various factors influencing the reaction rate.

"Standard" Free Energy Change or Activation Overpotential

The influence of this factor alone on the rate constant, holding the other factors essentially constant, is more easily investigated for the electrode process. When w and w^* are sufficiently small, it can be deduced from equations [1], [8], and [9] that the transfer coefficient—$\partial \ln k/\partial (ne\,\eta_a)$—is 0.5, a value found in a number of simple electron transfer processes (11, 14, 33). Complexation of the reacting species with added salt can change this coefficient (11) but equation [8] does not apply to such systems.

The quantitative effect of ΔF° on the homogeneous bimolecular rate constants has been measured experimentally for some nonspherical reactants (4, 5). While ion–solvent interactions in these systems (oxidation of hydroquinone-like compounds) were not as simple as assumed in equation [6] and an atom transfer mechanism could not be ruled out, reasonable agreement with the experimental rate constants was found (24).

Can. J. Chem. Downloaded from www.nrcresearchpress.com by 190.90.36.8 on 09/04/12
For personal use only.

Can. J. Chem. Downloaded from www.nrcresearchpress.com by 190.90.36.8 on 09/04/12
For personal use only.

Ionic Structure

The effect of ion size on the rates of homogeneous reactions is most conveniently studied using isotopic exchange reactions whose reactants merely exchange their charges, for then ΔF° and w^*-w are both zero, and m of equation [6] is simply $\frac{1}{2}$. The factor of ion size has been extensively investigated by Wahl and co-workers (8, 35, 39, 40). The rates of large ions, probably of Class I, were found to be much larger than those of the smaller ions, $MnO_4^{-1,-2}$ and $Fe(CN)_6^{-3,-4}$. Again, the latter two systems had comparable rates in spite of the greater Coulombic repulsion in the second case, perhaps because of the larger size of the iron cyanide ion (4.5 vs. 2.9 Å). Rather good agreement was obtained between experimental and calculated rate constants using the theoretical equations, taking into consideration the absence of adjustable parameters (16).

The cobalt–nitrogen bonded complexes probably are members of Class III (3, 6) and the rates are therefore extremely slow. The marked increase in rate (3, 18) in the sequence $Co(NH_3)_6^{+3,+2}$, $Co(en)_3^{+3,+2}$, and $Co(phen)_3^{+3,+2}$ may be partly a reflection of increasing ionic size, and partly a reflection of ligand field (29) effects.

The ferrous–ferric system is probably of Class II, and its rate (36) is correspondingly much less than that of the MnO_4^- or $Fe(CN)_6^{-3}$ systems. Nevertheless, its rate greatly exceeds that (1) of $Cr(H_2O)_6^{+3,+2}$, a probable member of Class III (3). Reasonable agreement between calculated and experimental results for the $Fe(H_2O)_6^{+3,+2}$ was found by adapting the theory to Class II reactants (22). Thus far, there is no experimental evidence which definitely establishes either an electron or an atom transfer mechanism for these homogeneous isotopic exchange reactions of hydrated cations. The general parallelism of various rates in the two processes discussed below suggests, however, a common electron transfer mechanism.

Parallelism Between Rates in Solution and at Electrodes

When similar mechanisms are operative, the theoretical equations suggest a close parallelism between the rates of the two processes, particularly when ΔF° and η_a are zero and the work terms are small. The parallelism becomes very close, therefore, when the rates of isotopic exchange reactions are compared with the corresponding electrochemical exchange currents.

The distance of closest approach for the electrode case will depend on the surface contamination and on the strength of metal–solvent binding. Let us write, therefore, $r = 2a+2b$ for this system and $r = 2a$ for the homogeneous system. When the work terms are negligible, we obtain

$$\Delta F^*_{\text{solution}} = \lambda_s^2/4,\ \Delta F^*_{\text{electrode}} = \lambda_e^2/8 \qquad [11]$$

where

$$\lambda_e/\lambda_s = (1+2b/a)/(1+b/a). \qquad [12]$$

The chemical and electrochemical electron transfer rates of the systems (3, 32, 36, 39) $Cr(H_2O)_6^{+3,+2}$, $Fe(H_2O)_6^{+3,+2}$, and $Fe(CN)_6^{-3,-4}$ both increase in the order given as do those of the systems (15, 16, 18) $Co(NH_3)_6^{+3,+2}$ and $Co(en)_3^{+3,+2}$. The absolute rates of various electrochemical processes (32) are in the general range expected from the values of the chemical rate constants, but further work is desirable, both theoretically on Class II and Class III systems as well as experimentally on salt effects and hydrolysis effects.

Frequency Factor and Activation Energy

While some application (24) of the theory has been made to the hydroquinone oxidations referred to earlier, the frequency factors, A, of the simpler isotopic exchange

reactions have been much more revealing. For the latter systems, ΔF^* equals $w^*+\lambda/4$. Correspondingly, ΔS^* is the sum of two terms. The first, $-\partial w^*/\partial T$, is the usual entropy change which results when two ions are brought together. The second, $-(d\lambda/dT)/4$, is the entropy of formation of the "nonequilibrium" atomic configurations from the equilibrium ones at the same r in order to satisfy the energy restriction. Its value may be computed from equation [10]. It proves to be very small for reactants of Class I.

Application of the theoretical equations to Class I reactants by the writer led to good agreement between experimental and calculated frequency factors for the $MnO_4^{-1,-2}$ system and (within a factor of 50) for the $Fe(CN)_6^{-3,-4}$ system, the latter system having an extremely small frequency factor (40).† These results suggest that the probability of adiabatic reaction may be of the order of unity, at least for these systems. The frequency factors of Class I reactants provide the most direct measure of this probability factor.

Many of the hydrated metal cations, which are mainly of Class II, tend to hydrolyze and form other complexes easily. In a careful investigation Silverman and Dodson (36) unravelled the rate constant of the $Fe^{+3,+2}$ system from those involving $FeOH^{+2}$ and others. The frequency factor was very small. If $-\partial w^*/\partial T$ is fairly small at the high ionic strengths (high acidity) needed to minimize hydrolysis, this low A-value indicates an additional negative contribution to ΔS^*.

Recently, Baker, Basolo, and Neumann (3) have reported a most interesting result of a very high frequency factor, 5×10^{16} cc mole^{-1} sec^{-1}, for a Class III system, $Co(phen)_3^{+3,+2}$. One simple extension of the present theory for Class I systems to those of Class III can provide an explanation of this possible behavior if the following reaction has an appreciably positive entropy change:

$$Co(phen)_3^{+3}+M(phen)_3^{+2} = Co(phen)_3^{+2}+M(phen)_3^{+3},$$

where $M(phen)_3^{+2}$ is some reactant of Class I or II, such as $Fe(phen)_3^{+2}$. No entropy data appear to have been reported for this process. A similarly high frequency factor has been reported for another Class III system (2*a*), $Cr(H_2O)_6^{+3,+2}$, but this reaction may be complicated by hydrolysis effects.

The frequency factors of the electrochemical systems have not been measured in the same detail. However, in a recent study, Randles and Somerton (32) found them to be typically in the range 3×10^2 to 3×10^4 cm sec^{-1}. The reactants were primarily hydrated metal cations and so were mostly of Class II. In one system, $Cr(CN)_6^{-3,-4}$, a rather low frequency factor (10 cm sec^{-1}) was found. The electrostatic repulsion between ion and electrode was estimated to be large for this system, and the low A-value was attributed to a small transition probability factor because of the increased r. However, we see from equation [10] that there is also an image term present. This term would tend to favor small r's. An alternative explanation for the A-value could be given on the basis of the usual sign of $-\partial w^*/\partial T$. When two reactants of like sign approach each other, the enhanced electrostatic field polarizes the solvent more strongly and causes a negative ΔS^*. A different region for testing the appropriateness of assuming simple Coulombic interactions and their consequent effects on ΔS^* is suggested in the concluding section.

Activation energies for several electrochemical electron transfers have been measured (32). While these results cannot be precisely compared with those of the isotopic exchange reactions (36, 40), partly because there was no detailed examination of hydrolysis and

†*The data were extrapolated to infinite dilution, taking cognizance of the comparative insensitivity of the theoretical activation energy to salt effects.*

Can. J. Chem. Downloaded from www.nrcresearchpress.com by 190.90.36.8 on 09/04/12
For personal use only.

salt effects, the results tentatively indicate the activation energies of the electrode reactions to be more than one-half those of the corresponding exchange processes. Should this result prove to be generally true (at least for Class I and Class II reactants) one possible interpretation would be that the distance between the ion in the activated complex and its electrical image exceeds twice the ionic radius (cf. equations [10] and [11]). An independent, approximate estimate of this distance may be obtainable from an experiment suggested in the concluding section.

Salt Effects

Using a rough model for ionic interactions the w and w^* terms were calculated by the writer for several Class I reactions and compared with the data of Wahl and co-workers (35, 40). Fair agreement was obtained using no adjustable parameters.

No detailed study of salt effects for simple electron transfers at electrodes appears to have been reported. Therefore it is not yet possible to adequately test the usual assumption (one not made here) that the work required to transport an ion from the body of the solution to the electrode, w^* or w, equals the ionic charge multiplied by the difference of potential at the initial and final positions of the ion, these potentials being computed in the absence of the ion. This assumption is clearly valid when the ionic charge is so small that it does not perturb the configuration of the remaining ions. It is also clearly invalid at the point of zero electrode charge. At this point, the work term estimated on the basis of the above assumption is zero, whereas it actually equals the free energy of interaction of the ion with the image. For infinite dilution, the latter term is $-q^2/2D_s r$, q being the ionic charge, while for dilute salt solutions, an approximate (unpublished) estimate of it is $(-q^2/2D_s r)\exp(-\kappa r)$, κ being the usual Debye κ.

Solvent Effects

Solvent effects for simple electron transfers will occur, according to the theory, whenever there is a change in dielectric constant, refractive index, ionic radius, or standard free energy of reaction. Changes in composition of the co-ordination shell, which may include the solvent, naturally alter a, $\Delta F°$, and the ease of intramolecular compression or stretching. In addition, there are effects which were not incorporated in the theory, effects such as changes in ion-pairing, selective solvation of solvent mixtures, and a change of the mechanism itself. A possible example of selective solvation (7) has been described (2).

Heavy water has been used as a solvent in several studies (e.g., 13, 37). Hudis and Dodson (13) have demonstrated the importance, when hydrolyzed species and other complexes are present, of determining the various equilibrium constants so that meaningful electron transfer rate constants for the different species can be obtained and solvent effects evaluated. The rate constant for $Fe^{+3,+2}$ was smaller by a factor of 2 in D_2O (13), while that of $NpO_2^{+2,+1}$ was smaller by a somewhat smaller factor (37). A qualitative interpretation of the solvent effects can be given in terms of atom transfer (13, 37) or electron transfer (23) theories. Thus far, however, comparative studies in the two solvents do not permit either mechanism to be distinguished from the other. This situation results from the fact that ions have different solvation energies in the two media (17), so that water does not behave as an inert solvent.

The rate of the $Co(NH_3)_6^{+3,+2}$ reaction appears to be faster in liquid ammonia (12) than in water, where it was immeasurably slow (18). The activation energy was high, being in the range found for two other Class III compounds (2*a*, 3). Possible explanations

Can. J. Chem. Downloaded from www.nrcresearchpress.com by 190.90.36.8 on 09/04/12
For personal use only.

for the solvent effect include a change of mechanism, such as a dissociation (12) or possibly a hydrolyzed intermediate, $Co(NH_3)_5NH_2^{+2}$. However, the effect of pH on the reaction rate is not known.

Effects of Electrode Material

A dependence of rate constant on electrode material will occur if there is any change in surface contamination (32) and possible metal–solvent binding, or if electrode charge density at a given η_a changes sufficiently to alter w^* or w. The rate constants measured for one system with several solid electrodes underwent no great variation (within a factor of 10) but were much smaller than that found for a mercury electrode (32).

The Image Force Law and Its Implications

The role of the electrostatic image has been generally ignored in electrochemical theories. A recent investigation (34) of the quantum limitations of the image force law for a vacuum is reassuring. It has been applied by the writer to dielectric media and to electrochemical theory.

The effect of this image is to partially neutralize the field of the ion and to reduce, thereby, the configurational rearrangement free energy needed to satisfy the energy restriction. It is noteworthy that its calculated effect remains, even at salt concentrations sufficiently large as to make w^* and w negligible. This is because it is impossible for the ionic atmosphere in the activated complex to neutralize the ion–image interactions of the two different hypothetical charge distributions at the same time. A compromise configuration results. A similar behavior exists in the homogeneous case, where the $1/r$ term remains even if w^* and w are zero.

At the point of zero electrode charge there is a net, shielded Coulombic attraction between the ion and its image, which is quite large for very dilute solutions. According to the theory a positive ΔS^* would result, since the attraction lowers the entropy of the solvation. A measurement of the frequency factor in this region would permit a determination of this ΔS^*.

If this prediction is verified for Class I reactants, it will be interesting to compare ΔS^* with the theoretical estimates.

ACKNOWLEDGMENTS

The writer is pleased to acknowledge the support of this research by the Office of Naval Research and by the National Science Foundation.

REFERENCES

1. ADAMSON, A. W. and VORRES, K. S. J. Inorg. & Nuclear Chem. **3**, 206 (1956).
2. AMIS, E. S. J. Chem. Phys. **26**, 880 (1957).
2*a*. ANDERSON, A. and BONNER, N. A. J. Am. Chem. Soc. **78**, 3826 (1954).
3. BAKER, B. R., BASOLO, F., and NEUMANN, H. M. Paper presented at the Symposium on Mechanisms of Inorganic Reactions in Solution. Northwestern University, Chicago, Ill. 1958.
4. BAXENDALE, J. H. and HARDY, H. R. Trans. Faraday Soc. **50**, 808 (1954).
5. BAXENDALE, J. H. and LEWIN, S. Trans. Faraday Soc. **42**, 126 (1946).
6. BROWN, H. C. J. Phys. Chem. **56**, 868 (1952).
7. COHEN, D., SULLIVAN, J. C., AMIS, E. S., and HINDMAN, J. C. J. Am. Chem. Soc. **78**, 1543 (1956).
8. EICHLER, E. and WAHL, A. C. Private communication.
9. FRIEDMAN, H. L., HUNT, J. P., PLANE, R. A., and TAUBE, H. J. Am. Chem. Soc. **73**, 4028 (1951).
10. FROST, A. A. and PEARSON, R. G. Kinetics and mechanism. John Wiley & Sons. Inc., New York. 1953. p. 118.
11. GERISCHER, H. Z. Elektrochem. **54**, 366 (1950).
12. GROSSMAN, J. J. and GARNER, C. S. J. Chem. Phys. **28**, 268 (1958).
13. HUDIS, J. and DODSON, R. W. J. Am. Chem. Soc. **78**, 1911 (1956).
14. HUSH, N. S. J. Chem. Phys. **28**, 962 (1958).
15. LAITINEN, H. A. and GRIEB, M. W. J. Am. Chem. Soc. **77**, 5201 (1954).

Can. J. Chem. Downloaded from www.nrcresearchpress.com by 190.90.36.8 on 09/04/12
For personal use only.

16. LAITINEN, H. A. and KIVALO, P. J. Am. Chem. Soc. **75**, 2198 (1953).
17. LANGE, E. and MARTIN, J. Z. Elektrochem. **42**, 662 (1936).
18. LEWIS, W. B., CORYELL, C. D., and IRVINE, J. W. J. Chem. Soc., Suppl. Issue, **2**, S386 (1949).
19. LIBBY, W. F. J. Phys. Chem. **56**, 863 (1952).
20. MARCUS, R. A. J. Chem. Phys. **24**, 966 (1956).
21. MARCUS, R. A. J. Chem. Phys. **24**, 979 (1956).
22. MARCUS, R. A. Paper presented at the Southeast Chemical Conference, American Chemical Society, Memphis, Tenn. 1956; cf. Trans. N.Y. Acad. Sci. **19**, 423 (1957).
23. MARCUS, R. A. J. Chem. Phys. **26**, 867 (1957).
24. MARCUS, R. A. J. Chem. Phys. **26**, 872 (1957).
25. MARCUS, R. A. O.N.R. Technical Report No. 11, Project NR-051-331 (1957).
26. MARCUS, R. A. O.N.R. Technical Report No. 12, Project NR-051-331 (1957). Paper presented at 132nd National Meeting of the American Chemical Society, New York City, N.Y. 1957.
27. MARCUS, R. A. Unpublished lectures. 1957.
28. MARCUS, R. J., ZWOLINSKI, B. J., and EYRING, H. J. Phys. Chem. **58**, 432 (1952).
29. ORGEL, L. E. Report to X^e Inst. intern. Chim. Solvay, Conseil chim. 289 (1956).
30. PEKAR, S. I. Untersuchungen über die Elektronentheorie der Kristalle, Akademische Verlagsgesellschaft M.B.H., Berlin. 1953.
31. RANDLES, J. E. B. Trans. Faraday Soc. **48**, 828 (1952).
32. RANDLES, J. E. B. and SOMERTON, K. W. Trans. Faraday Soc. **48**, 937 (1952).
33. RUBIN, H. and COLLINS, F. C. J. Phys. Chem. **58**, 958 (1954).
34. SACHS, R. G. and DEXTER, D. L. J. Appl. Phys. **21**, 1304 (1950).
35. SHEPPARD, J. C. and WAHL, A. C. J. Am. Chem. Soc. **79**, 1020 (1957).
36. SILVERMAN, J. and DODSON, R. W. J. Phys. Chem. **56**, 846 (1952).
37. SULLIVAN, J. C., COHEN, D., and HINDMAN, J. C. J. Am. Chem. Soc. **79**, 3672 (1957).
38. TAUBE, H. and MYERS, H. J. Am. Chem. Soc. **76**, 2103 (1954).
39. WAHL, A. C. and DECK, C. P. J. Am. Chem. Soc. **76**, 4054 (1954).
40. WAHL, A. C. Private communication.

Can. J. Chem. Downloaded from www.nrcresearchpress.com by 190.90.36.8 on 09/04/12
For personal use only.

Can. J. Chem. Downloaded from www.nrcresearchpress.com by 190.90.36.8 on 09/04/12
For personal use only.

ON THE EQUIVALENT REDOX POTENTIAL OF AQUEOUS SOLUTIONS UNDER IONIZING RADIATION[1]

I. H. S. Henderson, E. G. Lovering, R. L. Haines, and E. J. Casey

ABSTRACT

A study of the electrochemical behavior of aqueous solutions irradiated by Co^{60} γ- and 50–300-kv X-rays is being carried out. Results are presented which show that aqueous solutions of various electrolytes over a pH range of 0.0 to 14.0 attain a steady-state potential under irradiation.

This steady-state potential, whose existence was postulated by Dainton and Collinson (who called it the equivalent redox potential), has been determined to be −0.85 v with respect to a hydrogen electrode in the same solution. This value is a property of water and is independent of pH, solute, temperature and radiation energy, and intensity within the ranges investigated.

Electrodes under irradiation sometimes show potentials different from the potential of the bulk electrolyte. This is considered to be a result of selective adsorption of one or more primary or secondary radiation products. These transient phenomena depend upon source intensity and solute concentration and disappear when irradiation is stopped.

INTRODUCTION

There is much indirect evidence that among the primary products formed during gamma- or X-irradiation of water and aqueous solutions are hydrogen atoms and hydroxyl radicals. These species undergo further reaction to produce hydrogen molecules and hydrogen peroxide as well as oxidation or reduction products which are characteristic of the solute. Ions such as ceric, iodate, nitrate, and permanganate are reduced; while others, such as ferrous, iodide, nitrite, sulphite, and oxalate are oxidized. Allen (1) suggested that prolonged irradiation should lead ultimately to an equilibrium concentration ratio of a redox system. This idea was further developed by Dainton and Collinson (2), who proposed in 1950 that a solution under irradiation attained an equivalent redox potential (ERP) when the rate of oxidation equalled the rate of reduction in the solution. This ERP was assumed to be a characteristic of the solvent and hence independent of the nature and, within limits, the amount of solute. From a consideration of the normal electrode potentials of a number of systems whose behavior under irradiation had been investigated, Dainton and Collinson estimated the ERP for X-, γ-, and α-irradiation to be in the neighborhood of −0.95 v, and that increasing acidity displaced the ERP to even more negative values and that there was an increasing tendency toward oxidation in acid media. These authors argued further that, since on thermodynamic grounds the potential expected from an equimolar solution of H and OH would be somewhat positive, there was a possibility that the highly oxidizing species OH^+ was also present. Its fate was suggested to be $OH^+ + OH^- = H_2O_2$. (Hydrogen molecule ions may also be present as secondary intermediate products.) The effect of oxygen on the ERP was not considered in detail, but from work of Amphlett (3) on ferrous *o*-phenothroline they suggested (2) that the effect of oxygen, and hence HO_2, on the ERP was small.

A survey of the literature reveals that there have been few attempts to follow the course of radiation-induced chemical reactions by measurement of the potential changes in solution during and after irradiation. Veselovsky (4) has reviewed some of his own and other Russian work in this field, and has concluded that the concept of the equivalent

[1]*Manuscript received September 19, 1958.*
Contribution from Defence Research Chemical Laboratories, Ottawa, Canada. Issued as D.R.C.L. Report No. 292. This paper was presented at the Symposium on Charge Transfer Processes held at the University of Toronto, Toronto, Ontario, September 4 and 5, 1958.

redox potential was invalid because it ignored the kinetic behavior of electrochemical processes determining the steady-state potentials of the solution. His argument was based essentially on the observations that (*a*) platinum electrodes in γ-irradiated aqueous solutions of sulphuric acid, particularly in the presence of oxalate, showed a potential corresponding to that of the hydrogen electrode and (*b*) that electrodes such as a silver electrode in oxygen-saturated solution showed potentials approaching that of the oxygen electrode and in oxygen-free solutions showed a potential from 0.5 to 0.6 v more noble than a hydrogen electrode in the same solution. Under his conditions, the steady-state potentials measured were those due to individual radical species in the presence of excess oxidizing or reducing agent, and hence these observations have no direct bearing on the Dainton–Collinson ERP concept, which referred to the steady state obtained when the rates of oxidation and reduction processes in the bulk solution were equal.

Mendvedovsky *et al.* (5) used platinum electrodes in irradiated solutions of 0.8 *N* sulphuric acid containing ferrous and ferric sulphates to follow potential changes in the solution. Ferrous sulphate was oxidized during irradiation until the ratio of ferrous sulphate to ferric sulphate was steady at approximately 0.02. Similar results were obtained in perchloric acid solution and it was concluded that the potential measured was a property only of the final ratio of ferric ion to ferrous ion, and not a direct effect of radiation on the electrodes.

In a recent technical note, Clark (6) has reported the effect of Co^{60} γ-irradiation on the potential behavior of platinum and stainless steel electrodes in 0.1 *N* sulphuric acid under atmospheres of hydrogen, nitrogen, and air. Measurements were made at 85° C using Ag/Ag_2SO_4 reference electrodes. Under irradiation, the Pt electrode potential rapidly approached the hydrogen potential. When irradiation was interrupted, the potential decreased to -0.85 v with respect to the hydrogen electrode. In an experiment carried out under hydrogen, a trace of potassium bromide was added to the electrolyte. The electrode continued to show the hydrogen potential until the hydrogen flow was interrupted, after which the potential of the solution decreased to approximately -0.78 v with respect to the hydrogen electrode in the same solution. When irradiation was discontinued, the potential decreased further to at least -0.82 v.

Because of the apparent uncertainty (3) concerning the existence and the properties of the ERP, it was decided that part of our study of the electrochemical properties of aqueous solutions under irradiation should include an investigation of this concept.

EXPERIMENTAL METHOD

Glass cells containing test solutions were irradiated using a 300-curie Co^{60} source at a distance of approximately 20 cm, or using a 50- to 300-kv, 3-kw X-ray machine. The maximum energies absorbed were approximately 6×10^{13} ev cm^{-3} sec^{-1} and 6×10^{14} ev cm^{-3} sec^{-1} respectively. Each cell had appropriate electrode assemblies so that the potential of the solution could be followed during irradiation.

Potentials were measured using a General Radio type 1230A Electrometer-Amplifier with input resistance settings of 10^{10} ohms or higher.

The solutions were made up using conductivity water and reagent grade chemicals. The acid used was redistilled reagent grade sulphuric acid. Supporting electrolyte solutions for certain experiments were pre-electrolyzed under an argon atmosphere after being placed in the cells. A small weighed amount of "redox indicator" reagent was added directly to the electrolyte in the test flasks. The materials used for this purpose were potassium iodide, potassium iodate, iron, thallium, and cerous sulphate at concentrations of 10^{-4} to 10^{-3} molar.

Can. J. Chem. Downloaded from www.nrcresearchpress.com by 190.90.36.8 on 09/04/12
For personal use only.

Argon was deoxygenated by passage over Cu at 700° C and Ti at 800–900° C in a purification train. Stirring was achieved either by magnetic stirrers rotated at about 300 r.p.m., or by vibrating stirrers operated by 60 cycle a-c. Irradiations were carried out at room temperature.

Figure 1 is the photograph of a 100-ml cell which was a round bottom flask having a number of ground glass outlets through which were inserted reference electrodes, polarizing electrodes, and gas inlet tubes. The internal indicator electrode was a piece of Pt gauze, and the external reference was Hg/Hg_2SO_4 for cells containing sulphuric acid as supporting electrolyte, $Pb/PbSO_4$ for cells containing sodium sulphate with $pH < 10$, and Hg/HgO for solutions with $pH > 10$. The reference electrodes were connected to the cell solutions by salt bridges filled with supporting electrolyte of the same concentration as in the reference electrode and cell. The data of Hamer (7) and Harned and Hamer (8) were used to determine the potentials of the Hg/Hg_2SO_4 and $Pb/PbSO_4$

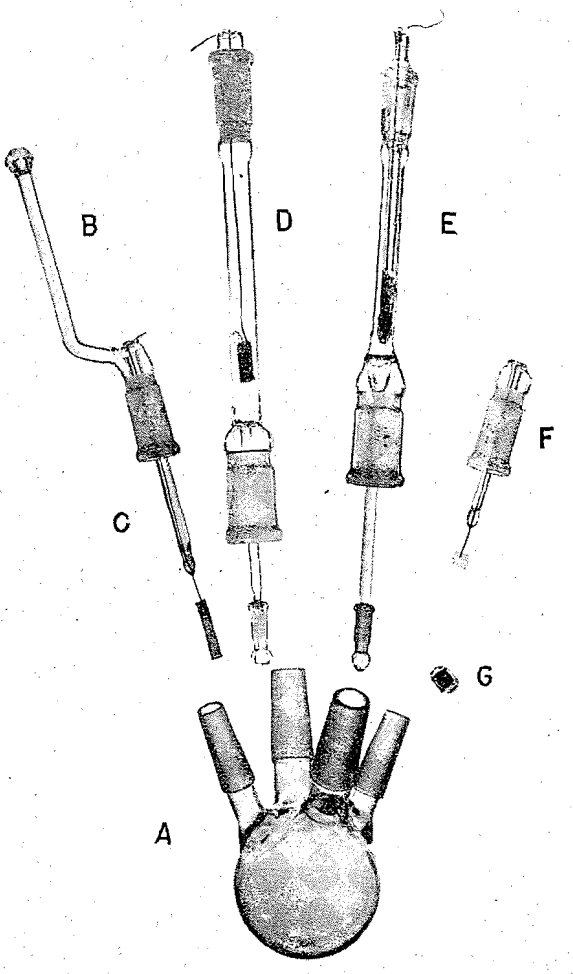

FIG. 1. Photograph of cell. A—100-ml cell; B—argon inlet; C—internal polarizing electrode; D—external polarizing electrode; E—reference electrode (Hg/Hg_2SO_4); F—internal reference electrode (Pt); G—magnetic stirring bar.

Can. J. Chem. Downloaded from www.nrcresearchpress.com by 190.90.36.8 on 09/04/12
For personal use only.

electrodes, and that of Akerlof and Bender (10) for the Hg/HgO electrode in alkaline solutions. The potential of each electrode was checked periodically against a hydrogen electrode in the same solution.

RESULTS AND DISCUSSION

The Steady State ERP

Under the experimental conditions of the present work, radiation had no effect on the reference electrodes, probably because (*a*) the concentration changes brought about by irradiation were small by comparison with the amount of redox material in the reference electrodes, and (*b*) the reference electrodes were exposed to radiation of much lower intensity than that experienced by the test cells.

The iodine redox indicator system in sulphuric acid, sodium sulphate, and potassium hydroxide was found to be the most convenient in the present work over the pH range investigated because of the absence of insoluble products at high pH.

In general, each electrolyte when irradiated showed a definite and reproducible potential, whose value (referred to the normal hydrogen electrode) was to a first approximation a function only of the hydrogen ion activity of the electrolyte, and was independent of the supporting electrolyte and indicator redox system. However, in several cases to be discussed later, transient potential behavior occurred during the first few minutes of the irradiation or after irradiation was stopped. In the iodine-containing electrolytes these transients were found to be the smallest. They were absent at high pH, but were present at low pH in sufficient degree to introduce an uncertainty of ± 0.03 v in the values of the ERP.

Table I gives the final steady-state values obtained during irradiation of several

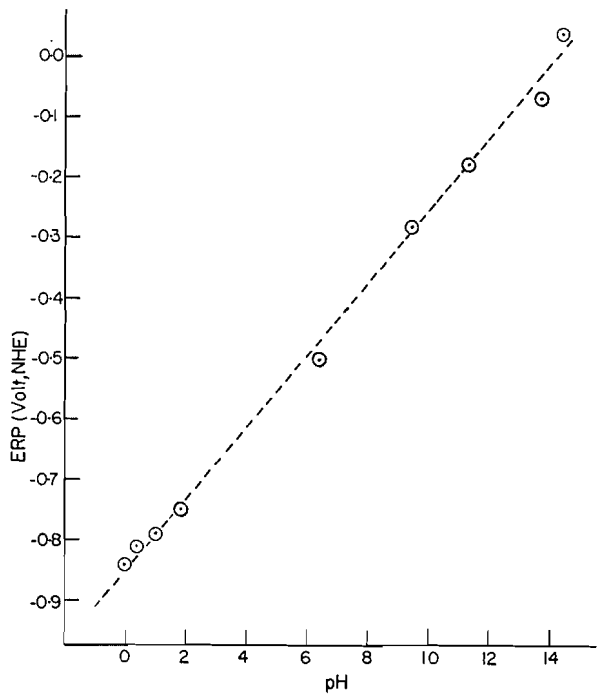

FIG. 2. Plot of equivalent redox potential referred to normal hydrogen electrode vs. pH. Slope of line 0.059 v/pH unit.

Can. J. Chem. Downloaded from www.nrcresearchpress.com by 190.90.36.8 on 09/04/12
For personal use only.

Can. J. Chem. Downloaded from www.nrcresearchpress.com by 190.90.36.8 on 09/04/12
For personal use only.

TABLE I

Equivalent redox potential of several electrolytes under ionizing X-radiation

Solution No.	Indicator conc., moles/liter	Carrier electrolyte and conc.	Reference type	ERP vs. ref.* (measured)	pH (measured)	ERP vs. H_2†	ERP vs. NHE (calc.)
1	KI(10^{-4} *M*)	H_2SO_4(1.0 *M*)	Hg/Hg_2SO_4	−0.17	−0.13	−0.84	−0.84
2	$Ce_2(SO_4)_3$(10^{-3} *M*)	H_2SO_4(0.5 *M*)	Hg/Hg_2SO_4	−0.14	0.37	−0.83	−0.81
3	Tl(10^{-4} *M*)	H_2SO_4(0.5 *M*)	Hg/Hg_2SO_4	−0.17	0.37	−0.86	−0.84
4	None added	H_2SO_4(0.4 *M*)	Hg/Hg_2SO_4	−0.14	0.50	−0.83	−0.81
5	Fe(5×10^{-4} *M*)	H_2SO_4(0.4 *M*)	Hg/Hg_2SO_4	−0.18	0.50	−0.87	−0.85
6	KI(10^{-3} *M*)	H_2SO_4(0.4 *M*)	Hg/Hg_2SO_4	−0.14	0.50	−0.87	−0.81
7	As_2O_3(10^{-3} *M*)	H_2SO_4(0.4 *M*)	Hg/Hg_2SO_4	−0.14	0.50	−0.83	−0.81
8	KIO_3(6×10^{-4} *M*)	H_2SO_4(0.1 *M*)	$Pb/PbSO_4$	−1.09	0.90	−0.85	−0.77
9	KI(2.5×10^{-4} *M*)	H_2SO_4(0.1 *M*)	Hg/Hg_2SO_4	−0.09	0.90	−0.85	−0.77
10	KI(5×10^{-4} *M*)	H_2SO_4(0.01 *M*)	Hg/Hg_2SO_4	−0.07	2.09	−0.86	−0.75
11	KI(5×10^{-4} *M*)	KCl(0.2 *M* with Na-K-phosphates	H_2/H^+	−0.876	6.4	−0.876	−0.50
12	KI(5×10^{-4} *M*)	Na_2SO_4(1.0 *M*)	$Pb/PbSO_4$	−0.63	9.47	−0.84	−0.28
13	KI(8×10^{-4} *M*)	Na_2SO_4(0.01 *M*)	$Pb/PbSO_4$	−0.48	11.35	−0.85	−0.18
14	$Ce_2(SO_4)_3$(10^{-4} *M*)	KOH(1.0 *M*)	Hg/HgO	−0.03	13.9	−0.89	−0.065
15	KI(10^{-4} *M*)	NaOH(1.4 *M*)	H_2/H^+	−0.879	—	−0.879	—
16	KI(5×10^{-4} *M*)	$HC_2H_3O_2$(0.2 *M*)	$Hg/Hg_2(C_2H_3O_2)_2$		Extensive transients		No steady value
17	Fe(10^{-3} *M*)	HNO_3(1.0 *M*)	H_2/H^+		No steady value		

*Minus signs are used when ERP is the more noble electrode.

†Hydrogen electrode in the same solution.

electrolytes. The values for solutions containing iodine and iron are listed as measured; thallium, cerium, and pure acid values listed have been corrected for transient potential behavior. The mean values at each pH are plotted in Fig. 2 as ERP (referred to the normal hydrogen electrode, NHE) vs. pH with a line of calculated slope 0.059 drawn through the points. Hence, the value of the ERP was consistently 0.85 v more noble than the hydrogen electrode in the same solution or 0.38 v less noble than the oxygen electrode.

The steady-state values were found to be independent of the intensity and maximum energy of the radiation within the limits of the available equipment.

The Approach to the ERP

The steady-state potentials obtained in these experiments were attained after a period of irradiation which varied with (*a*) redox indicator concentration, (*b*) source intensity, and (*c*) the number of coulombs by which the system had been oxidized or reduced away from the ERP prior to irradiation.

Figure 3, a plot of potential vs. time for iodine in 1.0 *M* sulphuric acid, shows the typical behavior of solutions in approaching the steady-state value. In the example shown, the solution was reduced with respect to the ERP before irradiation began. The effect of the radiation was to oxidize the solution to a potential of −0.84 v. The value remained constant when the irradiation was stopped, as shown by the regions labelled "open-circuit". After the solution had been oxidized with respect to the ERP by passage of current, irradiation reduced the solution until it again showed a potential of −0.84 v.

The redox reactions taking place as the system approached the ERP were followed by continuous measurement of potential during the irradiation, but the experimental conditions reported here were not conducive to a straightforward analysis of the reaction kinetics. The type of curve obtained for *E* vs. time was a function of redox indicator concentration, the standard electrode potential of the redox system, and the intensity

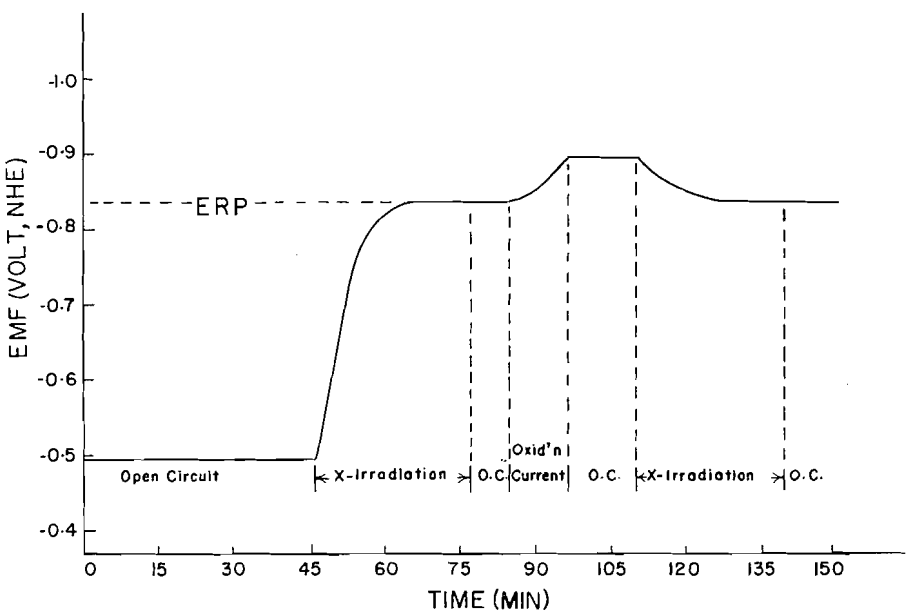

FIG. 3. Potential vs. time curve showing approach to steady state during irradiation for solution (i) reduced and (ii) oxidized with respect to the steady-state value.

Can. J. Chem. Downloaded from www.nrcresearchpress.com by 190.90.36.8 on 09/04/12
For personal use only.

and energy of the radiation. The presence of trace impurities such as oxygen had a marked effect on the shape of the potential–time curves. The same steady-state value (within ± 0.005 v for a given solution) was reached whether the solution had been previously oxidized or reduced with respect to the steady-state value, and the potential remained constant for a period of minutes to hours after irradiation ceased. In this respect the results differed from those of Clark (6). However, ERP's estimated from his results at 85° are in good agreement with the present results at 25° C. This indicates that there is no marked temperature coefficient for the ERP, a result consistent with the behavior of free radical reactions.

The potentials listed in Table I as ERP values were not characteristic of the electrode metal under irradiation. In general, the potentials shown by the electrode when a steady state had been attained during irradiation did not change on interruption of the irradiation, and fresh Pt or Au electrodes inserted into the cell after irradiation showed the same potentials as the irradiated electrodes. In one experiment, carried out in potassium hydroxide solution, in which cerium oxides were deposited on a nickel electrode, both the nickel electrode and a platinum electrode in the same solution attained the same steady-state potential. It appeared that prolonged irradiation of platinum electrodes in sulphuric acid solution made the electrode more noble by as much as 0.03 v with respect to a fresh platinum electrode. This effect was not reproducible. Whenever it was observed, the ERP value was taken as the potential shown by fresh electrodes, since the irradiated electrodes after a cleaning in hot concentrated nitric acid solution and flaming to yellow heat showed the same potential as did the fresh electrodes. (This could not be attributed to an overvoltage effect on the electrodes because for all measurements the input resistance of the electrometer was at least 10^{10} ohms, whereas polarization was not observed unless the electrometer input resistance was less than 10^7 ohms.)

Transient Phenomena

With carefully pre-electrolyzed and deoxygenated strong acids containing iodide, a change in the potential of the indicator electrode to a value different from that of the bulk electrolyte was observed when irradiation began. Upon cessation of irradiation the potential quickly (within 3 minutes) assumed the potential of the electrolyte. This phenomenon could be attributed to the preferential adsorption of hydrogen atoms on the platinum electrode which made the electrode show a potential more "hydrogen-like" than the potential of the solution during irradiation. This effect, which was reproducible, was more pronounced with greater source intensities and in the absence of solutes with which hydrogen atoms could react before becoming adsorbed on the electrode. It is interesting to note that, since oxygen is an effective trap for hydrogen atoms via the formation of HO_2, the effect was not observed unless great care was taken to exclude oxygen, or at least until sufficient energy had been absorbed by the solutions to remove oxygen as HO_2. The transient potential behavior observed by Clark (6), obtained with much higher γ-intensities than used in the present work, could also be interpreted as due to hydrogen atom or hydrogen molecule adsorption, even in experiments carried out in cells exposed to the air, since it is probable that the radiation intensity was high enough for hydrogen atoms to remove oxygen from the system as HO_2 more rapidly than oxygen could redissolve in the solution. When there was sufficient oxygen present to react with all the hydrogen atoms during irradiation, platinum electrodes showed a transient potential a few millivolts more noble than that of the solution. This effect was attributable in part to the action of HO_2 radicals on the electrode, and confirms an observation made by Veselovsky.

Can. J. Chem. Downloaded from www.nrcresearchpress.com by 190.90.36.8 on 09/04/12
For personal use only.

In the present work, the indicator ions were usually present in sufficient concentration to be potential determining at and near the ERP; that is, the hydrogen or hydrogen atom concentration was not great enough to produce a direct effect on the potential of the platinum electrode. Attempts to measure the ERP of ultrapure water or sulphuric acid would be expected to show transient potentials during irradiation, even though irradiation leads to a steady-state hydrogen peroxide concentration (9), because of the relatively large adsorbability of hydrogen atoms on the platinum surface. Thus Zalkind *et al.* (11), during irradiation of oxygen-free solutions of acid and alkali, have observed potentials as high as 0.95 v between platinum and gold electrodes in the same solution. The effect was attributed to the selective adsorption of hydrogen on platinum and hydroxyl radicals on gold.

General Considerations

The relationship between ERP and the hydrogen and oxygen electrodes indicates that this potential is a characteristic of water and its hydrogen ion concentration only, and is not affected by source intensity or energy. Thus the results of the present investigation are in general agreement with the theory proposed by Dainton and Collinson, and demonstrate its essential correctness, although their estimated value for the ERP (−0.95 v) is more noble by about 0.1 v than the experimental value reported here. In agreement with Dainton and Collinson, it is not anticipated that the ERP of solutions exposed to α- or β-radiation would be very different from the value observed for γ- and X-radiation. However, if α- and β-emitters were present in the solution during measurement, it is expected that the very high local radical density produced would give rise to even larger transient effects than those observed with γ- and X-rays.

The ERP may be expected to change from the value of −0.85 v reported here when the activity of the water is appreciably decreased. In this case the ERP would be a function of the solute and its concentration. The ERP may also be expected to be a function of the ratio of the volume of solution to the area of catalytic surface for combination of radicals, since this would interfere with the steady-state radical concentrations (cf. ref. 4 concerning production of hydrogen peroxide during irradiation of suspensions of zinc oxide).

Veselovsky has pointed out that the application of electrochemical techniques can be a useful tool in the study of a number of problems in radiation chemistry. As an example of this, he has estimated the influence of oxalate on the rate of production of hydrogen atoms (the "G" value) during irradiation of aqueous sulphuric acid. The results which have been obtained in the present work indicate that solvent and solute effects on both the "G" values for primary and secondary products and on the ERP, as well as the influence of radiation on solids (electrodes) in contact with aqueous solution, may also be investigated electrochemically. The major advantage of these techniques over other kinetic methods employed in radiation chemistry is that they permit the investigator to follow and to monitor continuously the chemical changes taking place during irradiation.

REFERENCES

1. ALLEN, A. O. J. Phys. & Colloid Chem. **52**, 479 (1948).
2. DAINTON, F. S. and COLLINSON, E. Ann. Rev. Phys. Chem. **2**, 99 (1951).
3. AMPHLETT, C. B. Nature, **165**, 977 (1950); **171**, 690 (1953); Trans. Faraday Soc., Radiation Chem. 144 (1952).
4. VESELOVSKY, V. I. Proc. Intern. Conf. Peaceful Uses Atomic Energy, Geneva, **7**, 599 (1956). ZALKIND, Ts.I. and VESELOVSKY, V.I. Sbornik Rabot Radiatsionnoi Khim, Akad. Nauk, S.S.S.R. 66 (1955).
5. MENDVEDOVSKY, V. I., BAKH, N. A., and ZHURAVSKAYA, E. V. Sbornik Rabot Radiatsionnoi Khim, Akad. Nauk, S.S.S.R. 71 (1955).
6. CLARK, W. E. J. Electrochem. Soc. **105**, 483 (1958).

Can. J. Chem. Downloaded from www.nrcresearchpress.com by 190.90.36.8 on 09/04/12
For personal use only.

7. HAMER, W. J. J. Am. Chem. Soc. **57**, 9 (1935).
8. HARNED, H. S. and HAMER, W. J. J. Am. Chem. Soc. **57**, 33 (1935).
9. HOCHANADEL, C. J. J. Phys. Chem. **56**, 587 (1952). See also ref. 4.
10. AKERLOF, G. C. and BENDER, P. J. Am. Chem. Soc. **70**, 2366 (1948).
11. ZALKIND, Ts.I., VESELOVSKY, V. I., and GOCHALIEV, G. Z. All-union Conference on the Application of Radioactive and Stable Isotopes and Radiation in the National Economy and Science, Session on Radiation Chemistry. Moscow, March 25 to April 2, 1957.

Can. J. Chem. Downloaded from www.nrcresearchpress.com by 190.90.36.8 on 09/04/12
For personal use only.

Can. J. Chem. Downloaded from www.nrcresearchpress.com by 190.90.36.8 on 09/04/12
For personal use only.

LIMITING CONDUCTANCE OF LYONIUM AND LYATE IONS[1]

MARTIN KILPATRICK

ABSTRACT

The problem of proton mobility has been considered in H_2O–CH_3OH, H_2O–D_2O, and H_2O–H_2O_2 solvents from the current viewpoint of the mechanism of proton mobility for aqueous solutions. Mixed solvents are more complicated in that one must consider the relative basicity and acidity of the species competing for the protons. It is concluded that for dilute solutions of $HClO_4$, where water is replaced by hydrogen peroxide, the decrease in equivalent conductance relative to that of KCl in the same solvent mixture is due to the partial elimination of the proton transfer process.

For highly acidic non-aqueous solvents of high dielectric constants such as HF, HCN, and HCOOH, the problem of the weakness of the usual "strong" acids of aqueous solution makes a direct determination of the limiting equivalent conductances difficult. In the case of anhydrous hydrogen fluoride the available experimental evidence indicates that the limiting conductance of the lyonium ion is approximately the same as that of the potassium ion but the lyate ion has a higher limiting conductance than other stable anions.

The higher proton mobility in ice leads one to expect that hydrogen-bonded systems may be found where the conductivity may approach that of electronic semiconductors.

In a paper presented before the 111th meeting of the Electrochemical Society in May, 1957, and to be published elsewhere (1), the author showed that the limiting equivalent conductance of perchloric acid relative to that of potassium perchlorate decreased as the water was replaced by hydrogen peroxide. The experimental results (2) are presented in Fig. 1 together with some more recent results (3) for 0.01 *M* HCl relative to 0.01 *M* KCl when water is replaced by methyl alcohol and some earlier work on the replacement of H_2O by D_2O (4). The conclusion was drawn that the change in structure of the solvent decreased the conductance by proton transfer.

Thomas and Maass (5) offer an alternative explanation on the basis of the reduction of the number of ions in the solution owing to a decrease in the degree of dissociation of the acid. They confirm the experimental results of Shanley *et al.* (2) for sulphuric acid and report additional data for HNO_3 and HF in H_2O–H_2O_2 mixtures at higher concentrations of acid.

The generally accepted view for water is that in addition to 1 water molecule associated with the proton there are 3 molecules of water hydrogen bonded to the hydroxonium ion (6). This cluster forms the inner hydration shell with an outer shell held more loosely by hydrogen bonding. The inner-shell hydrogen bonds are strengthened by dipole interaction and will be less subject to disorder from thermal motion. Within the inner sphere, proton jumps take place readily while transfer of protons beyond this depends on reorientation of the water molecules. From the fact that the number of hydrogen bonds decreases with increasing temperature while the extra mobility increases, Krogh-Moe (7) concludes that the rate cannot be proportional to the mean number of hydrogen bonds. That the model is only a qualitative one has been pointed by Samoilov (8), who points out that the tetrahedral arrangement in ice is partially washed out by the thermal motion. The X-ray diffraction studies show the number of nearest neighbors to be 4.6 at 30° (9).

A mixed solvent will be more complex than a solvent composed of one species and one must deal with strong electrolytes and consider at least three effects. The two solvent

[1]*Manuscript received July 5, 1958.*
Contribution from the Department of Chemistry, Illinois Institute of Technology, Chicago, Illinois. This paper was presented at the Symposium on Charge Transfer Processes held at the University of Toronto, Toronto, Ontario, September 4 and 5, 1958.

species will compete for the proton to form the lyonium ion; there will also be competition for the inner hydration sphere and orientation of both species at the periphery of the inner hydration shell. For low mole fractions of alcohol, the lyonium ions will be hydronium ions and we might conclude that the interference with the proton transfer process occurs first in the outer hydration zone. As the mole fraction of alcohol increases, some water is replaced by alcohol in the inner zone and the lyonium ions are partially alcohol-solvated protons. The increase beyond 90% alcohol is due to proton transfers via alcohol molecules. In this case HCl does show indications of being a weak acid in alcohol but this is not true of perchloric acid.

In the case of the replacement of water by hydrogen peroxide, while it is true that acids become weaker due to the more acidic nature of hydrogen peroxide, perchloric acid at low concentration is a strong electrolyte (10) and at the high dielectric constant of the solvent there should not be ion pairs. The first effect should be in the outer shell and at very high mole fractions of H_2O_2 the lyonium ion will become protons solvated with H_2O_2. It is not impossible that in pure anhydrous H_2O_2 we might have chain transfer via proton jumps between H_2O_2 molecules but these will have to be practically in the absence of water. In other words the curve in Fig. 1 may rise steeply beyond 99%.

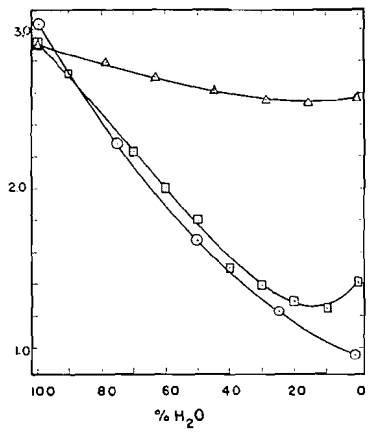

FIG. 1. Ratio of equivalent conductances:
△ H_2O-D_2O; $\Lambda^{\cdot 01}_{HCl+DCl}/\Lambda^{\cdot 01}_{KCl}$
○ $H_2O-H_2O_2$; $\Lambda^{\circ}_{HClO_4}/\Lambda^{\circ}_{KClO_4}$
□ H_2O-CH_3OH; $\Lambda^{\cdot 01}_{HCl}/\Lambda^{\cdot 01}_{KCl}$

In the case of the H_2O–D_2O mixtures the D_2O will have a good fraction of the protons at equal mole fractions but even here the non-linearity above the viscosity effect shows that there is some interference in the proton and deuteron transfers. The fraction of protons on H_2O and D_2O could be determined by nuclear magnetic resonance measurements.

Figure 2 shows the ratio of $\Lambda^{\circ}_{KOH}/\Lambda^{\circ}_{KCl}$ for water peroxide solvents and $\Lambda_{KOH}/\Lambda_{KCl}$ at 0.01 molar concentration for water – methyl alcohol. Here the curves are quite different, the addition of methyl alcohol decreasing the proton transfer via the water molecule and showing no appreciable minimum, although there are methoxide ions present at the high alcohol side (11). In the case of hydrogen peroxide – water solvents the hydroxyl ions react with the hydrogen peroxide to form hydroperoxide ions and the lyate ions, hydroxyl and hydroperoxide have both water and hydrogen peroxide in the inner solvation shell.

Can. J. Chem. Downloaded from www.nrcresearchpress.com by 190.90.36.8 on 09/04/12
For personal use only.

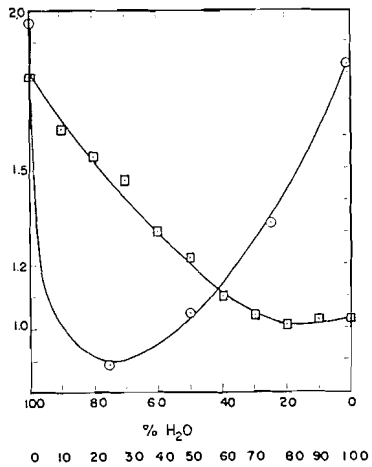

FIG. 2. Ratio of equivalent conductances:
○ H_2O—H_2O_2; $\Lambda^\circ_{KOH}/\Lambda^\circ_{KClO_4}$
□ H_2O-CH_3OH; $\Lambda^{\cdot 01}_{KOH}/\Lambda^{\cdot 01}_{KCl}$

The ratio $\Lambda^\circ_{HCl}/\Lambda^\circ_{KCl}$ from the data of Barak and Hartley (12) at 25° C gives 0.98 instead of 1.03 (Fig. 2); so we conclude there is no minimum in the curve and there is no increase in the limiting conductance of the methoxide ion in methyl alcohol. Gurney (13) explains this fact by pointing out that although proton jumps do take place, that owing to the removal of the dipole moment on addition of a proton, such proton jumps take place equally well in the direction of the field as against the field.

LIMITING EQUIVALENT CONDUCTANCES IN NON-AQUEOUS SOLUTIONS

In ammonia the lyonium and lyate ions are the ammonium and amide ions.

$$NH_3 + NH_3 \rightleftharpoons NH_4^+ + NH_2^-$$

The ions show no abnormal electrical mobility and Gurney (13) accepts the Hückel explanation on the basis that the ammonium ion has no dipole moment. There is no experimental evidence for abnormal limiting conductance in the solvents hydrazine, pyridine, hydroxylamine, and other amines.

In the highly acidic solvents both the sulphuric acid cation and anion show abnormal conductance (13). In anhydrous hydrogen fluoride the fluoride ion has been shown to have a higher mobility than the borofluoride and antimony hexafluoride ions but there is no evidence that the solvated proton shows abnormal electrical conductance (14). The problem in determining the limiting conductance in this solvent is that the strong acids of aqueous solution are weak electrolytes in anhydrous hydrogen fluoride.

The measurements were based on the fluoride ion accepting property of antimony pentafluoride to form the stable SbF_6^- anion. Conductance measurements showed Na^+ SbF_6^- to be a strong electrolyte and the equivalent conductance of $H_2{}^+F$ SbF_6^- was shown to be less than that of the sodium salt, leading to the conclusion that $l^\circ_{H_2{}^+F} < l^\circ_{Na^+}$. The success of these experiments depended on the exclusion of water, as H_2O would compete with HF for the protons and SbF_6^- would be converted to an hydroxy acid (15). If these experiments are reliable we have a case where the anion of the solvent may be chain conducting but the cation has no abnormal conductance.

Liquid hydrogen cyanide is another high dielectric solvent where the "strong" acids of aqueous solution are weak. Other cations and anions show equivalent conductances

Can. J. Chem. Downloaded from www.nrcresearchpress.com by 190.90.36.8 on 09/04/12
For personal use only.

which are three or four times higher than the corresponding ions in water (16). The problem of the limiting conductance of the lyonium ion could probably be attacked in analogous fashion to that used for HF. The ion product is 2×10^{-19} (17), and reasoning by analogy from aqueous solution (18) the $[Cu(CN)_2]^-$ anion is quite stable.

$$\begin{array}{l} HCN + HCN \rightleftharpoons H^+\cdot HCN + CN^- \\ \qquad\qquad\qquad\qquad\quad + \\ \qquad\qquad\qquad\qquad\quad CuCN \\ \qquad\qquad\qquad\qquad\quad \downarrow \\ \qquad\qquad\qquad\qquad\quad [Cu(CN)_2]^- \end{array}$$

A comparison of $\Lambda°$ for $NaCu(CN)_2$ and $\Lambda°$ for a solution of CuCN in anhydrous hydrocyanic acid should decide the ratio $l°_{H^+}/l°_{Na^+}$. Mercuric cyanide might be more suitable than cuprous cyanide provided it was sufficiently soluble. The solubilities of non-ionic cyanides in anhydrous hydrocyanic acid are not accurately known. There is no evidence of abnormal conductance of lyonium or lyate ions in acetonitrile.

The carboxylic acids with the exception of formic acids are solvents of low dielectric constant. Potentiometric studies in formic acid (dielectric constant 58 at 16° C) (19) indicate the "strong" acids of water are weak electrolytes. Like sulphuric acid, the autoprotolysis of formic acid is so high that the solvent conductance makes conductivity studies of acids difficult to interpret (20). Formamide (21) and dimethyl formamide (22) are high dielectric solvents but show no abnormal conductance.

PROTON CONDUCTANCE IN SOLIDS

Bjerrum (23) reviews the dielectric properties and conductance of ice and calculates the energy of activation for proton jumps to be 2.5 kcal for $H_3{}^+O$ and 4.7 kcal for HO^-, which corresponds to an over-all E for the equivalent conductance of 3.1 at 0° which is lower than the experimental value. More recent measurements (24) for polycrystalline ice yield a value of 3.9 kcal at $-15°$ C compared to Bjerrum's calculated value of 2.5. These calculations are based on equivalent conductances $\Lambda° = 298$ with $l°_{H^+} = 215$ and $l°_{HO^-} = 83$ at 0° C. Very recently Conway and Bockris (25) emphasized that the conclusions of Bradley (26) and Owston (27) based on specific conductance are on an unsound basis and they recomputed the absolute mobilities and concluded the rate-determining step in ice is proton tunneling but in water the rate-determining step is controlled by the rotation of the water molecules. This conclusion brings their findings into qualitative agreement with the earlier results of Eigen (28), who determined experimentally both the ion product and the proton mobility. Eigen finds that the protonic mobility is appreciably higher in ice than in water but that a small amount of fluoride markedly reduces the conductivity. Ice crystallized from a solution of caesium fluoride has been found to have H–F incorporated in the lattice (29). Certain polyhydric alcohols show a marked change in conductivity with temperature below their melting points and a proton transfer, and molecular rotation mechanism has been proposed (30).

The structures of HF and HCN (31, 32) in the solid state are both known to be linear chains but no conductance measurements have been reported on the solids. The high proton mobility in ice indicates that H—O···H bonds are involved but this phenomenon should also apply to H—N···H bonds.

Polyvalent metal ions form polynuclear complexes in aqueous solution, and the structures are often held together by oxygen or hydrogen bridges (33). In the corrosion of metals the nature of the solid films is similar to the species found in solution, and proton

Can. J. Chem. Downloaded from www.nrcresearchpress.com by 190.90.36.8 on 09/04/12
For personal use only.

mobility along the hydrogen bonds may be the rate-determining step. There have also been some studies of the conductance of hydrocarbon films (34) which indicate that some organic compounds are semiconducting.

ACKNOWLEDGMENT

This research was supported in part by a grant from the Petroleum Research Fund administered by the American Chemical Society. Grateful acknowledgment is hereby made to the donors of said fund.

REFERENCES

1. KILPATRICK, M. J. Electrochem. Soc. **104**, 73C (1957).
2. SHANLEY, E. S., ROTH, E. W., NICHOLS, G. M., and KILPATRICK, M. J. Am. Chem. Soc. **78**, 5190 (1956).
3. ERDY-GRUZ, T., KUGLER, E., and REICH, A. Acta Chim. Acad. Sci. Hung. **13**, 439 (1958).
4. BAKER, W. M. and LAMER, V. K. J. Chem. Phys. **3**, 406 (1935).
5. THOMAS, D. K. and MAASS, O. Can. J. Chem. **36**, 744 (1958).
6. ACKERMAN, T. Discussions Faraday Soc. **24**, 180 (1957).
7. KROGH-MOE, J. Acta Chem. Scand. **10**, 331 (1956).
8. SAMOILOV, O. YA. Zhur. Fiz. Khim. **3**, 537 (1957).
9. MORGAN, J. and WARREN, B. E. J. Chem. Phys. **6**, 666 (1938).
10. MITCHELL, A. G. and WYNNE-JONES, W. F. K. Trans. Faraday Soc. **51**, 1690 (1955).
11. KOSKIKALLIO, J. Suomen Kemistilehti, B, **30**, 111 (1957).
12. BARAK, M. and HARTLEY, H. Z. physik. Chem. **165**, 290 (1933).
13. GURNEY, R. W. Ionic processes in solution. McGraw-Hill Book Co., Inc., New York and London. 1953. p. 77.
14. KILPATRICK, M. and LEWIS, T. J. J. Am. Chem. Soc. **78**, 5186 (1956).
15. SCHREWELIUS, N. Dissertation. Stockholm. 1943.
16. COATES, J. E. and TAYLOR, E. G. J. Chem. Soc. 1245, 1495 (1936).
17. JANDER, G. and GRUTTNER, B. Chem. Ber. **81**, 102 (1948).
18. VLADIMIROVA, M. G. and KALOVSKII, I. A. Zhur. Priklad. Khim. **23**, 580 (1950).
19. SHKODIN, A. M., IZMAILOV, N. A., and DZYUBA, N. P. J. Gen. Chem. U.S.S.R. **23**, 25 (1953).
20. HAMMETT, L. P. and DIETZ, N., JR. J. Am. Chem. Soc. **52**, 4795 (1930).
21. DAWSON, L. R., NEWHALL, T. M., and MCCREARY, W. J. J. Am. Chem. Soc. **76**, 6024 (1954).
22. DAWSON, L. R., GOLBEN, M., LEADER, G. R., and ZIMMERMAN, H. K., JR. J. Electrochem. Soc. **99**, 28 (1952).
23. BJERRUM, N. Kgl. Danske Videnskab. Selskab, Mat. fys. Medd. **27**, No. 1, 56 (1951).
24. SPERNOL, A. Z. Elektrochem. **59**, 31 (1955).
25. CONWAY, B. E. and BOCKRIS, J. O'M. J. Chem. Phys. **28**, 354 (1958).
26. BRADLEY, R. S. Trans. Faraday Soc. **53**, 687 (1957).
27. OWSTON, P. G. Quart. Revs. **5**, 344 (1951).
28. EIGEN, M. J. Electrochem. Soc. **104**, 72C (1957).
29. BRILL, R. and ENDER, H. Nature, **176**, 925 (1955).
30. KAKUICHI, Y. Research Inst. Appl. Elec., Hokkaido Univ., Monograph Ser. **4**, 75 (1954).
31. DULMAGE, W. S. and LIPSCOMB, W. N. Acta Cryst. **4**, 330 (1954).
32. HORNIG, D. F. Discussions Faraday Soc. **9**, 115 (1950).
33. BIEDERMAN, G., KILPATRICK, M., POKRAS, L., and SILLÉN, L. G. Acta Chem. Scand. **10**, 1327 (1956).
34. NORTHRUP, D. C. and SIMPSON, O. Proc. Roy. Soc. (London), A, **234**, 124 (1956).

Can. J. Chem. Downloaded from www.nrcresearchpress.com by 190.90.36.8 on 09/04/12
For personal use only.

Can. J. Chem. Downloaded from www.nrcresearchpress.com by 190.90.36.8 on 09/04/12
For personal use only.

SOME CONSIDERATIONS ON THE ROLE OF PROTON TUNNELING IN CERTAIN CHARGE TRANSFER PROCESSES[1]

B. E. CONWAY

ABSTRACT

Quantum mechanical tunneling of H atoms in certain reactions can have a rate comparable with that of the corresponding classical reaction. Proton tunneling appears to be the mechanism of proton transport in ice. Further studies of this mechanism have been made by determination of the a-c. and d-c. conductance of D_2O (and H_2O) ice under rigorous conditions of purification. Pre-electrolysis techniques have been applied to the ultrapurification of the D_2O and H_2O used for the conductance determinations. Isotopic ratios of conductance in solid H_2O and D_2O are obtained and discussed in terms of the mechanism of H^+ or D^+ transport in the solid and liquid substances. The theory of proton tunneling previously given is improved by using a quantal distribution function in the calculation of tunneling rates and better agreement with experiment is then obtained. The theoretical isotopic ratio of conductances by the tunneling mechanism in the ices is similar to that found experimentally and smaller than that predicted classically.

Since the proton tunneling theory is quantitatively successful in the case of conductance of ice, its examination for other electrochemical processes involving H is necessary. A favorable case for investigation is the electrochemical hydrogen evolution reaction for which the barrier height for tunneling can be varied. Tunneling probabilities are calculated for proton and deuteron discharge at mercury from acid solutions using the theory of Eckart. At intermediate overpotentials the Tafel equation is still obeyed; at low overpotentials a linear current–potential relation is found as in the classical theory. H/D separation factors are calculated for the tunneling mechanism and it is shown that at intermediate and high overpotentials, tunneling leads to values of the separation factor comparable with those deduced classically. Only at low electrochemical rates of H or D production are high separation factors predicted. The tunneling mechanism, however, is distinguishable from the classical mechanism by a new criterion: the Tafel slopes for the tunneling process would be considerably larger (0.2–0.3) than those arising classically (0.12) for a simple discharge mechanism assuming a symmetry factor of 0.5. It is concluded that in certain cases proton tunneling may occur simultaneously with the classical reaction in electrochemical proton discharge and lead to anomalous Tafel '*b*' values which are sometimes observed experimentally.

INTRODUCTION

The possibility of quantum mechanical effects arising from tunneling was recognized by Wigner (1) and Bell (2) as a factor to be considered in the kinetics of chemical reactions involving H or D. Several attempts to find experimental support for this effect have been made and some evidence has been given for quantum mechanical tunneling of H ions or atoms in the following reactions: (i) the ortho-para hydrogen conversion (2, 3); (ii) the rate-determining proton transfer step in the bromination of 2-carbethoxy-cyclopentanone (4); and (iii) in the proton conductance of water and ice (5, 6). In the latter case, the tunneling process is the only one which can account for the high mobility of protons in ice. In the first two cases it appears that only participation of the quantum mechanical process in the net reaction occurs, i.e., quantum and classical processes can occur at comparable rates. However, in proton mobility in ice and water, the quantum mechanical process appears to be considerably faster and hence preferred, although in *liquid* water the over-all rate is limited by water dipole rotation (5).

Further tests of the quantum mechanical mechanism should be possible in the case of conductance of ice by determination of the specific conductance, and hence mobility, of deuterons in heavy ice. Measurements of the specific conductance of ice prepared from 99.8% D_2O have been carried out and estimates of the ionic mobility of D^+ in D_2O ice are made.

[1]*Manuscript received June 29, 1958.*
Contribution from the Department of Chemistry, University of Ottawa, Ottawa, Ontario. This paper was presented at the Symposium on Charge Transfer Processes held at the University of Toronto, Toronto, Ontario, September 4 and 5, 1958.

Tunneling effects in heterogeneous proton transfer reactions, e.g., in the electrolytic hydrogen evolution reaction may be expected, since in the case of the proton transfer conductance of water and ice such effects occur. The electrochemical kinetic behavior, which would arise if quantum mechanical penetration of the potential barrier at an electrode took place, is deduced and criteria for recognition of the effect are presented.

EXPERIMENTAL

Conductance determinations have been made on D_2O ice (and H_2O ice) and the corresponding liquids by the a-c. and d-c. methods. Alternating-current measurements were made by means of a shielded Wheatstone bridge with capacitative and ohmic components; the a-c. source was a Hewlett–Packard precision oscillator. Direct-current measurements were made on the same bridge but with only ohmic components using a Leeds and Northrup galvanometer of sensitivity 4.5×10^{-9} amp/mm. The cell is shown in Fig. 1 and was mounted in a heavy brass cylinder in order to provide electromagnetic shielding and a region of thermal inertia around the cell. Palladium electrodes were used (cf. 7). The apparatus was maintained at various temperatures constant to 0.05° C in a refrigerated thermostat.

Water was distilled five times: (i) from a Barnstead still; (ii) from alkaline permanganate; (iii) through a column of glass beads heated to 450° C, through which hydrogen

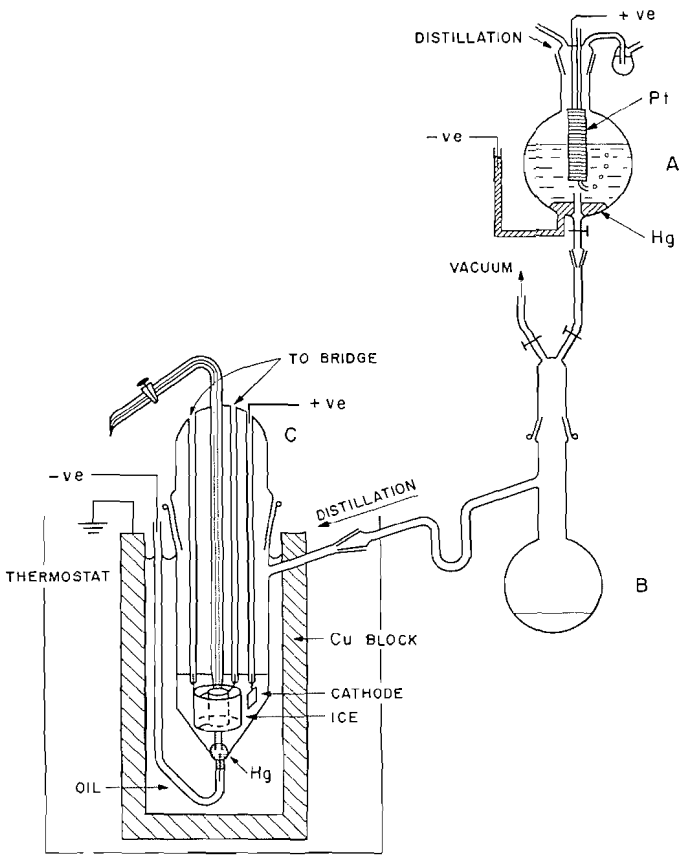

FIG. 1. D_2O distillation, purification, and conductance apparatus.

Can. J. Chem. Downloaded from www.nrcresearchpress.com by 190.90.36.8 on 09/04/12
For personal use only.

Can. J. Chem. Downloaded from www.nrcresearchpress.com by 190.90.36.8 on 09/04/12
For personal use only.

(free from CO_2 and purified by passage through two liquid air traps) was passed; (iv) again in H_2 in another vessel; and (v) in a fused silica still *in vacuo* under conditions of smooth evaporation from a still water surface. Fifteen milliliters of water was then passed over into the silica conductance vessel in order to wash it and then removed through a capillary tube. Further distillation was then carried out *in vacuo* and another 15 ml of water passed into the cell. This water was then frozen by dipping the lower end of the cell into a bath at $-20°$ C (cf. 7). After several freezing and melting cycles *in vacuo*, ice as clear as liquid water was obtained and no flaws, cracks, or bubbles were visible. After clear ice was obtained, the cell was placed in the thermostat and allowed to stand for some days in order to anneal the ice. Melting, evacuation, and freezing cycles were continued until no further change in conductance occurred.

In previous determinations (7, 8) of the conductance of ice, the conductance of the water used for the preparation of the ice was about fifty times that (9) corresponding to the equilibrium concentrations of H_3O^+ and OH^- ions. The significance of the conductance values thus determined may hence be somewhat limited, since the impurities present in the water may, particularly if acidic, contribute to the conductance in the ice. At the same time, the impurities, if slightly soluble in the ice, create defects in the crystal which could change the behavior of the ice. Such impurities have, for example, a marked effect on the dielectric properties of ice (10).

In the present work, electrolytic purification of the water using a mercury cathode has been carried out, in addition to multiple distillation. Electrolytic purification of "pure solvents" was first used in conductance studies by Jaffé (11) and Schroeder (12), who found that considerable diminution of conductance of ordinarily purified solvents could be achieved by this procedure. Water from stage (iii) (see above) was distilled from stage (iv) into the vessel A in Fig. 1, containing mercury which had been anodically purified, dried, and redistilled in a Hewlett still. After 48 hours' electrolysis at 500 v with the mercury cathodic, the liquid was run out into the silica vessel B. Stage (v) distillation was then carried out. A further electrolysis could be carried out at the mercury drop in the cell C (Fig. 1), but this made no significant difference to the specific conductance of the water prior to freezing, which was between 3 and 5 $\times 10^{-7}$ mho cm^{-1}.

Deuterium oxide (99.8%) was purified by distillation, as above, using steps (iv) with N_2 to (v) and subjected to electrolytic purification as described; measurements were made as in the case of water.

Determinations of the cell constant were made at $25.00 \pm 0.02°$ C by means of the Jones and Bradshaw (13) standard solutions of KCl. The resistance of the empty cell under vacuum, and that of the leads in the circuit, was about 100 times greater than that of the cell containing ice, and could only be measured with difficulty.

RESULTS

After several cycles of freezing and melting *in vacuo* the resistance of the D_2O ice reached an approximately constant value. The value was checked by melting the ice and returning the liquid to the silica still and repeating the operation. The a-c. resistance (1000 c.p.s.) measured at $-2.0°$ C varied between 2.30×10^6 and 2.74×10^6, whilst the corresponding d-c. values varied from 16.4×10^6 to 19.6×10^6 ohms. The cell constant was 24.8 so that the specific conductances (κ) were $1.6 \pm 0.5 \times 10^{-8}$ mho cm^{-1} for 1000 c.p.s. a-c. and $2.2 \pm 0.6 \times 10^{-9}$ mho cm^{-1} for d-c. The corresponding values for H_2O ice were $3.5 \pm 0.5 \times 10^{-8}$ and $5.2 \pm 0.7 \times 10^{-9}$ mho cm^{-1}. The latter value falls near to that given by Bradley (7) for H_2O ice at $-2.0°$ C viz. $10^{-8.24}$ mho cm^{-1}. There is some spread in the

present results but it is comparable with that (0.14 in $\log_{10} \kappa$) found in previous determinations (7). The determinations reported here lead to an isotopic ratio of specific conductance of $\kappa_{H_2O\ ice}/\kappa_{D_2O\ ice} = 2.2$ for a-c. measurements (1000 c.p.s.) and 2.4 for for d-c. measurements.

The a-c. values of conductance are frequency dependent as shown in Fig. 2. The d-c. measurements are time dependent as found previously with H_2O ice (7, 14). The values at "zero time" are recorded above and a typical time dependence is shown in Fig. 3; the effect probably arises from build-up of a space charge near the electrodes when the field is applied. This is probably the cause of the frequency dependence of the a-c. conductance and with this in mind we have plotted in Fig. 2 the a-c. conductance as a function of the square root of the reciprocal frequency; the relationship is not, however, linear, as might be expected if there were a concentration polarization of charge carriers when the field was applied. More complex effects are probably involved. Consideration of the significance of the results will therefore be limited to the "zero time" d-c. values.

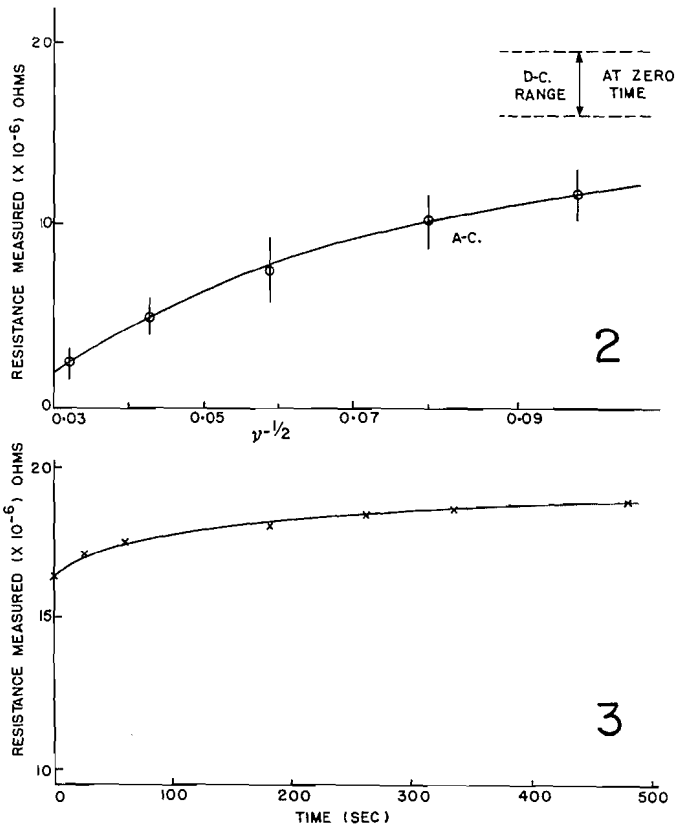

FIG. 2. Comparison of a-c. and d-c. resistance of D_2O ice.
FIG. 3. Typical time variation of d-c. resistance of D_2O ice.

DISCUSSION

1. Proton and Deuteron Mobility and Tunneling in Ice

The above measurements on specific conductance cannot be directly interpreted in terms of ionic mobility and hence of ionic transport mechanisms until values (cf. 15) of

Can. J. Chem. Downloaded from www.nrcresearchpress.com by 190.90.36.8 on 09/04/12
For personal use only.

the concentration of D_3O^+ and OD^- ions in the ice are available. In H_2O ice the concentration of the corresponding protium species is known (15) and leads to a proton mobility of 1.9×10^{-1} cm^2 sec^{-1} v^{-1}. The theoretical rate of quantum mechanical tunneling of protons in an unperturbed ice structure (i.e., with all H bonds linear and no librational motion) has been calculated (5, 6) using the theory of Eckart (16) for the permeability and a value of 7×10^{-1} cm^2 sec^{-1} v^{-1} for the tunneling rate has been obtained. In the theory previously given (5) we have used, following Bell (2), the expression

$$N = \frac{N_0}{kT}\int_0^\infty P_w\, e^{-w/kT}dw \qquad [1]$$

in order to calculate the integral tunneling probability, where N is the number of penetrations of the barrier out of N_0 presentations of the particle at the barrier per second, w is the total energy of the particle, and P_w is the quantum mechanical tunneling probability for the particle of energy w, calculated from the theory of Eckart (16). For the OH bond, the vibrational half quantum is about 5 kcal mole^{-1}, so that it would be more correct to use a quantal distribution rather than the classical distribution function in equation [1]. Quantally, the total tunneling rate should then be written

$$N = N_0\,\frac{\sum_0^\infty (P_w.p\, e^{-(n+\frac{1}{2})h\nu_0/kT})}{\sum_0^\infty p.\, e^{-(n+\frac{1}{2})h\nu_0/kT}}, \qquad [2]$$

where n is the vibrational quantum number, ν_0 the ground state vibrational frequency of the OH or OD bond in H_3O^+ or D_3O^+, and p is the quantum weight assumed equal to unity. Since for the OH or OD vibration, $h\nu_0 \gg kT$, the value of N is closely approximated by the value of the *r.h.s* of equation [1] for $n = 0$, other terms contributing negligibly. If we identify N_0 with the frequency of presentations of the particle H or D at the barrier (cf. 2), the rate of tunneling between an H_3O^+ ion and a favorably oriented H_2O molecule follows from the theory previously given as

$$v = \nu\delta\,\frac{\phi_z}{kT}\,\frac{\sum_0^\infty (P_w.p.\, e^{-(n+\frac{1}{2})h\nu_0/kT})}{\sum_0^\infty p.\, e^{-(n+\frac{1}{2})h\nu_0/kT}}. \qquad [3]$$

When $n = 0$ and the particles predominantly approach the barrier with an energy $\frac{1}{2}h\nu_0$, P_w has the values 0.87 for H and 0.60 for D. In equation [3], ν is stretching frequency of the OH or OD bond in H_3O^+ or D_3O^+ undergoing dissociation, δ is the distance (2.8 Å) the proton is transferred per jump, and ϕ_z is the mean change of electrical energy of the particle per jump when unit field is applied; it has the value 1.53×10^{-20} erg (5). In an unperturbed structure with all OH$\cdots$O hydrogen bonds stationary and colinear, v would give the proton mobility. However, the ice is thermally perturbed in so far as each molecule executes librational oscillations in the lattice. Following the argument of Bernal and Fowler (17), the proton transfer rate will be modified from that given by v on account of the necessity that each OH bond be in a suitable orientation to that of the $2p_z$ partially hybridized lone pair orbitals on the oxygen atom of a neighboring water molecule, before transfer can occur. We have previously shown (5) that orientations*

**The orientation requirement discussed here is not the same as the reorientation involved when a proton migrates through liquid water. The molecules in ice are already the "correct way round" for proton transfer to occur, but their librative oscillations restrict proton tunneling since favorable mutual orientations of neighbors in their librational excursions only occur part of the time (17).*

Can. J. Chem. Downloaded from www.nrcresearchpress.com by 190.90.36.8 on 09/04/12
For personal use only.

of H_3O^+ and neighboring H_2O molecules, mutually favorable for proton transfer by tunneling, occur with a probability of about $\frac{1}{9}$. Owing to the lower zero point librational energy of D_2O in D_2O ice, the librational excursions in the deuterium case will be smaller and the molecule will spend more of its time in orientations favorable to D^+ transfer. This is equivalent to the situation in liquid D_2O, which has a more ordered structure on account of the lower librational zero point energy than in liquid water. Calculations show that in the case of deuteron transfer in D_2O ice the probability factor for mutually favorable orientations is about $\frac{1}{7}$. Using these factors, the mobilities of H^+ and D^+ in their respective ices may now be calculated from equation [3], taking $\nu_{OH} = 1.12\times10^{14}$ sec^{-1} and $\nu_{OD} = (1.12/\sqrt{2})\times10^{14}$ sec^{-1}. The mobilities, u, are then

$$u_{H^+} = 0.11 \text{ and } u_{D^+} = 0.07 \text{ cm}^2 \text{ sec}^{-1} \text{ v}^{-1}.$$

From considerations based on the experimental value of the over-all specific conductance, u_{H^+} in H_2O–ice has been deduced as 0.19 cm^2 sec^{-1} v^{-1} (6). Use of the quantal distribution in equation [2] thus gives better agreement with experiment than that given by the semiclassical equation [1].

The mobility ratio for the H^+ and D^+ isotopic ions calculated from equation [1] is 6.1. That from equation [3] is only 1.6, i.e., near to that (1.4) for rate-determining rotation of H_2O or D_2O dipoles (5). However, although the isotopic ratios of conductance are now similar for the two mechanisms, the large increase of mobility on going from aqueous acid solutions to pure ice can only be explained in terms of a *transition* from rate-determining dipole rotation (in water) to rate-determining proton tunneling in ice. The dependence of anomalous mobility in alcoholic solutions on the length of the hydrocarbon function (5) has in any case confirmed the dipole rotational mechanism in the case of acid solutions.

It is now of interest to examine if the theory is consistent with the experimental data on the conductance of the heavy ice. We can only make mechanistic interpretations of the results if we can obtain the *mobility* from the experimental conductance. At the present time, we can only proceed further by making the not unreasonable assumption that the *ratio* of ionic products in H_2O ice and D_2O ice is the same as the corresponding ratio for liquid H_2O and D_2O, viz. (at 25° C) $1\times10^{-14} : 0.2\times10^{-14}$ (18). Some indication that this assumption is not unjustifiable is given by the following considerations: the difference of the heat of ionization of D_2O and H_2O is 0.94 kcal $mole^{-1}$ (19), and it is readily seen that this figure can account for the difference of the ionization constant to within 10%, so that isotopic entropy differences are not significant in determining the *ratio* of ionization constants of D_2O and H_2O. The difference of heat of ionization arises from the different zero-point energies of the species involved. In ice the same situation should hold and the ratio of ionization constants in H_2O and D_2O ices should be approximately equal to the corresponding ratio for the liquid phases if only heat terms are involved.

In ice at $-10°$ C, the concentration of protons is 5×10^{-11} g ion $l.^{-1}$ (15, 6). If we take the ratio of ionization constants as $1\times10^{-14}/0.2\times10^{-14}$ for H_2O and D_2O, the ratio of proton to deuteron concentrations in H_2O ice and D_2O ice, respectively, will be $(1/0.2)^{\frac{1}{2}}$ i.e., 2.23 : 1. The experimental isotopic d-c. conductance ratio is 5.2/2.2 i.e., 2.35. Hence the ratio of *mobilities** of H^+ and D^+ in their respective ices is about 1.1. The theoretical calculations predict a ratio of 1.6. This must be considered a satisfactory agreement in

**The transport numbers of* H^+ *in* H_2O *and* D^+ *in* D_2O *are approximately equal (viz. 0.64 and 0.66 respectively; see (6) and (34)).*

Can. J. Chem. Downloaded from www.nrcresearchpress.com by 190.90.36.8 on 09/04/12
For personal use only.

view of the several assumptions made. The measurements clearly support the tunneling mechanism both for protons and deuterons in ice. The classical mechanism predicts much lower mobilities (5) and an isotopic ratio of mobilities having the approximate value exp. $(\Delta_{D-H}\frac{1}{2}h\nu_0)/kT$ i.e., about 9, which is not observed experimentally. In the case of mobilities of H^+ and D^+ in ice, the isotopic ratio of tunneling rates is hence actually less than that predicted classically. This is contrary to what has usually been supposed for tunneling mechanisms.

2. Proton Tunneling at Electrodes

The quantitative success of the proton tunneling theory (5, 6) in the case of proton conductance in ice suggests that proton tunneling can participate in certain reactions as is also indicated in other cases (2, 4, 20). It is therefore of interest to examine the theory in relation to other electrochemical processes involving proton transfer.

Quantum mechanical effects in electrode processes were first considered by Gurney in 1932 (21) with respect to electrons. Bawn and Ogden (22) suggested that tunneling of protons and deuterons might explain the H/D electrolytic separation factors (s) at various metals and they deduced a value of s for tunneling of about 100. Such a value was experimentally observed by Appelby and Ogden (23) but has never been confirmed (24). On the basis of the theoretical calculations and the more usually observed values of s (from 3 to 10), it has generally been regarded that tunneling could not participate to any important extent in the cathodic hydrogen evolution reaction. However, the calculations of Bawn and Ogden were made on a basis which was not relevant to the case under consideration; thus the barrier widths which were assumed (1.5, 2.0, and 3.0 Å) are too large and no consideration of the effect of applied potential, which modifies the height of the potential energy barrier and hence the probability of tunneling, was made. For the proton transfer reaction

$$H_3O^+ + M + e \rightarrow H_2O + MH_{ads},$$

e.g., at a mercury electrode, the barrier height at the potential of zero charge is about 18 kcal mole^{-1} (25). The barrier width is calculated (cf. 25, 26) from the OH bond length in the hydroxonium ion, the radius of the hydroxonium ion (assumed approximately equal to that of water), and the HgH bond length (27). The width is found (25) to be between 0.55 and 0.50 Å. Such a width is consistent with the probable thickness of the double layer at mercury in acid solutions. For the calculation of the above figures, the "width" is taken to be the distance of the proton about to be discharged in the H_3O^+ ion from the position of the H atom adsorbed on the electrode surface. A barrier of width of 0.50–0.55 Å leads to a theoretical (25) classical heat of activation similar to that observed experimentally (28). The barrier width assumed by Bawn and Ogden is thus about four times too large and, since the tunneling probability is very sensitive to dimensional parameters of the barrier, the value of s calculated is likely to be in error. It is therefore desirable to calculate the tunneling probabilities for protons and deuterons for the more realistic barrier dimensions given above and as a function of electrode potential.

A barrier having a form similar to that arising from the intersection of two Morse curves may be expressed by the function

$$[4] \qquad V_{(x)} = Ae^{2\pi x/l}/(1+e^{2\pi x/l}) + Be^{2\pi x/l}/(1+e^{2\pi x/l})^2,$$

where $V_{(x)}$ is the potential energy at a distance x along the reaction co-ordinate for a barrier having a width of $2l$, A is the difference of potential energy between the final and initial states, and B is $4E^{\ddagger}$, where $E^{\ddagger}$ is the energy of activation, i.e., the value of V at the maximum of the curve, referred to $V = 0$ at $x = -l$.

Can. J. Chem. Downloaded from www.nrcresearchpress.com by 190.90.36.8 on 09/04/12
For personal use only.

The solution of the Schroedinger equation when $V_{(x)}$ is given by equation [4] leads (16) to the permeability or probability of tunneling, P_w, as

$$[5] \qquad P_w = \frac{\cosh 2\pi(\alpha+\beta)-\cosh 2\pi(\alpha-\beta)}{\cosh 2\pi(\alpha+\beta)+\cosh \pi\frac{(B-c)^{\frac{1}{2}}}{c}},$$

where $c = h^2/2ml^2$, $\alpha = l/h(2mw)^{\frac{1}{2}}$, $\beta = l/h[2m(w-A)]^{\frac{1}{2}}$, m is the mass of the particle undergoing tunneling, and h is Planck's constant. w is the total energy of the particle approaching the barrier. The total number of particles penetrating the barrier per second is then given (2) by equations [1] or [2].

For tunneling at the mercury electrode interface we place $E^{\ddagger}$ equal to $E_0{}^{\ddagger}+\beta\Delta\phi F$, where β is the symmetry factor taken equal to 0.5, $\Delta\phi$ the rational electrode potential, and $E_0{}^{\ddagger}$ is the heat of activation at the potential of zero charge (i.e., about 18 kcal mole^{-1}); $2l$ is taken as 0.5 Å and m values are those for H and D ions. The probable value of A for proton transfer at the potential of zero charge is -2.5 kcal mole^{-1} (25). The value of A for deuteron transfer from H_2DO^+ ions differs from that for proton transfer by 1.1 kcal mole^{-1}, on account of isotopic differences of (i) OH and OD bond dissociation energies, (ii) heats of hydration, (iii) H and D ionization potentials, and (iv) heats of adsorption at mercury, as discussed by Conway (29) in calculations of the classical values of s for various reaction mechanisms. $E_0{}^{\ddagger}$ for deuteron transfer is 1.8 kcal larger than that for proton transfer (29). For various values of $\Delta\phi$, A becomes $A_0+\Delta\phi F$, where A_0 is the change of potential energy in the reaction at the potential of zero charge. The values of w in P_w and in the exponential in equation [1] are also changed to $w' = (w+\Delta\phi.F)$ for various values of w and $\Delta\phi$. P_w is then evaluated for a range of values of w' from 0.2×10^{-14} to 100×10^{-14} erg molecule^{-1} and the integral tunneling probability is obtained from equation [1]. The tunneling functions $P_{w'}\,e^{-w'/kT}$, from which N is evaluated, are shown in Figs. 4, 5, and 6 for five electrode potentials, three temperatures, and for the isotopes ${}_1^1H$ and ${}_1^2D$. In distinction to tunneling through a nuclear potential energy barrier, proton and deuteron tunneling rates are temperature dependent, since the distribution of energies of particles approaching the barrier is temperature dependent and the permeability for a given impact is a function of the total energy of the particle. The apparent energy of activation for a given barrier height is, however, lower than the corresponding classical value (2).

For the electrochemical reaction considered, the main points of interest are the dependence of the tunneling rate upon electrode potential and upon isotopic mass. It is seen from Fig. 7 that the dependence of tunneling probability upon isotopic mass is potential dependent. The values of the separation factor defined by

$$s = (C_D/C_H)_{soln}\cdot v_H/v_D,$$

where C refers to isotopic concentrations in the solution and v_H/v_D is the ratio of rates of discharge of the isotopic ions, may be calculated from the tunneling probabilities together with the ratio of concentrations of H_3O^+ and H_2DO^+ (e.g., in 0.1 N aqueous acid solutions) and the isotopic abundance ratio (30). $a_{H_3O^+}/a_{H_2DO^+}$ has been calculated previously (29) for this case and has a value of 2.6×10^2 in 0.1 N acid solution. Values of s, as a function of electrode potential, are given in Table I.

The separation factor calculated classically is almost independent of potential and has a value of 2.9 (29) for proton discharge at mercury (the experimental value is 3.1 ± 0.2). In isotopic separation work involving the usual analysis of evolved gases, current densities of at least 10^{-3} amp cm^{-2} are required in order to obtain workable rates of gas evolution.

Can. J. Chem. Downloaded from www.nrcresearchpress.com by 190.90.36.8 on 09/04/12
For personal use only.

Can. J. Chem. Downloaded from www.nrcresearchpress.com by 190.90.36.8 on 09/04/12
For personal use only.

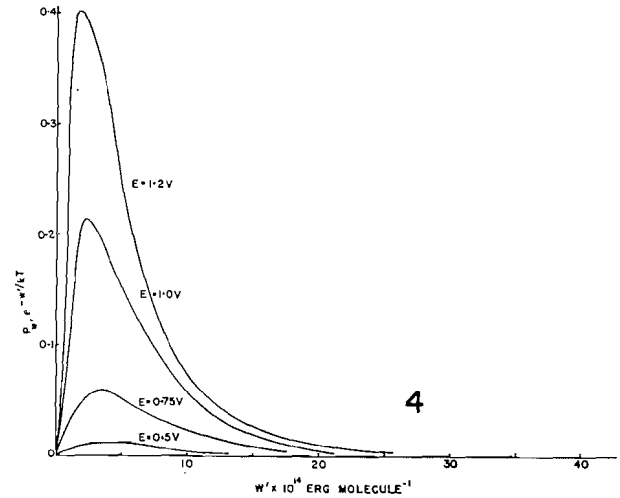

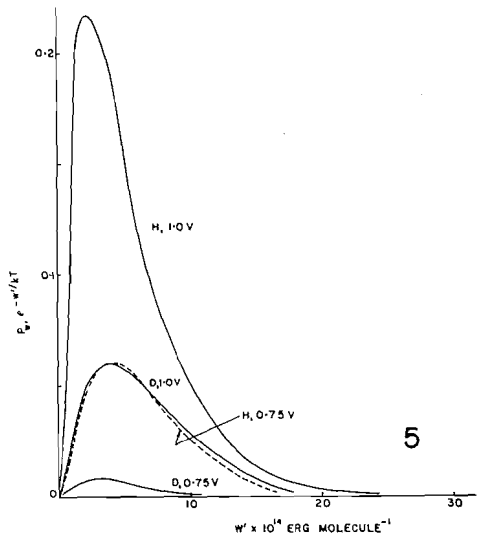

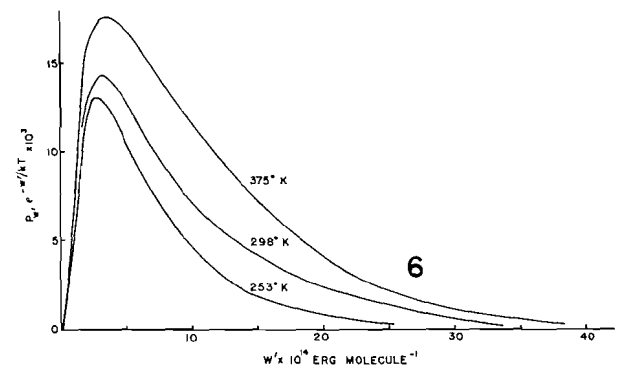

FIG. 4. Potential dependence of the tunneling function (for H at 298° K).
FIG. 5. Isotopic dependence of the tunneling function at 298° K.
FIG. 6. Temperature dependence of the tunneling function (for H at $E = 0.5$ v).

TABLE I

Isotopic separation factors arising if proton or deuteron tunneling occurs

$\Delta\phi$ v	0	0.25	0.50	0.75
s	12.40	5.0	1.6	0.7

The electrode potential at mercury is hence about -1 v (with respect to a hydrogen electrode in the same solution) for such a rate of evolution of gases. The value of s arising from the tunneling mechanism (Table I) is then comparable in magnitude with that calculated for classical transfer. The high values previously predicted (22) are misleading, since the relevant barrier dimensions were not used. Tunneling cannot therefore be excluded as a possible process in electrolytic proton transfer by reference to values of the separation factor, previously indicated as very high if tunneling occurred.

It is possible, however, to propose a new criterion for occurrence of tunneling in electrochemical proton transfer. Fig. 7 shows the logarithm of the integral tunneling probability (to which the electrochemical proton transfer rate is proportional) as a function of electrode potential for proton and deuteron transfer at mercury.

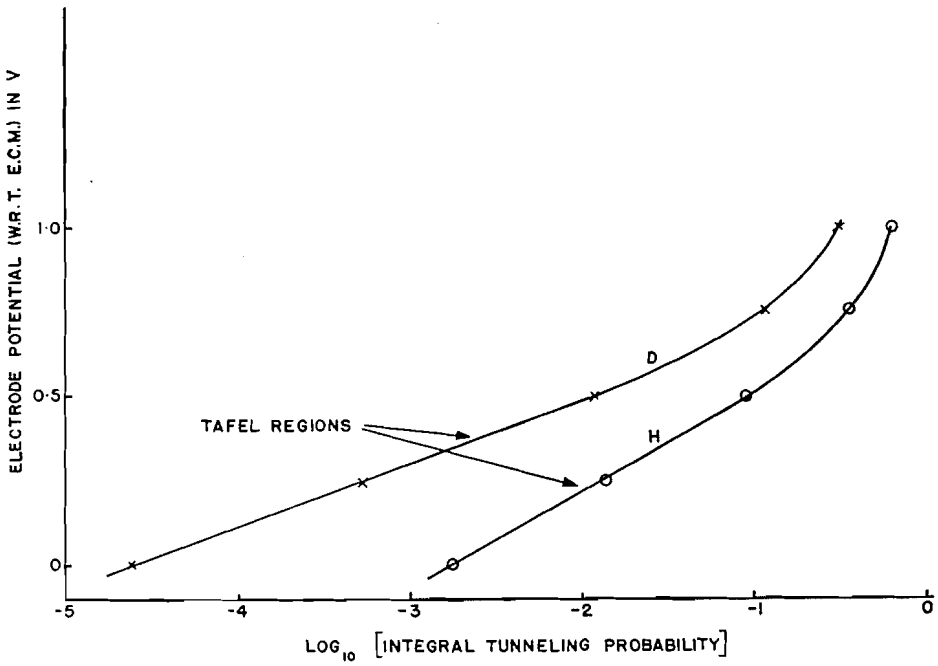

FIG. 7. Tunneling probability and electrode potential.

At intermediate electrode potentials, a linear $\Delta\phi$ – log (rate) law is obeyed, i.e., the Tafel equation holds as in classical proton transfer at an electrode. At very low overpotentials Ohm's law is obeyed (5) and hence a linear $\Delta\phi$ – (rate) law is followed, again as in the classical theory. At high electrode potentials there is some tendency for the tunneling rate to approach a limiting value. In the potential range where the behavior is approximated by the Tafel equation, the slope of the $\Delta\phi$ – log (rate) relationship (Fig. 7) has, however, a value of about 0.25 for proton discharge and 0.17 for deuteron discharge. The

Can. J. Chem. Downloaded from www.nrcresearchpress.com by 190.90.36.8 on 09/04/12
For personal use only.

values of these slopes would hence be diagnostic for tunneling transfer, since slopes as high as this do not follow from any mechanism yet proposed for the hydrogen evolution reaction assuming the symmetry factor to be about 0.5. In impure solutions, e.g., at Pb or Hg electrodes, Tafel slopes as high as 0.3 have been observed (33), which are difficult to explain on any of the previously discussed mechanisms (32) of the hydrogen evolution reaction unless unusual values of the symmetry factor are assumed. In impure solutions, the normal barrier height is probably raised as a result of poisoning of adsorption sites for H. Under these conditions the relative participation of proton tunneling compared with classical proton transfer may be enhanced, and hence higher Tafel slopes could arise; some participation of tunneling in the hydrogen evolution reaction at rhodium may account for the anomalous continuously increasing Tafel slope, with increasing overpotential observed for this metal (33). As in the generalized calculations of Bell (2), the tunneling probability calculated here for electrochemical proton transfer is actually larger than the corresponding classical probability, particularly at high cathodic potentials. Use of a quantal distribution in equation [1] instead of the classical one does not materially change the anomaly. In all proton transfer reactions hitherto considered with respect to quantum mechanical effects, only for the case of proton transfer in ice where the potential energy barrier is much lower than in the present case, is the expected tunneling rate actually observed. In the present, and in other cases examined by Bell (2, 4, 20), the experimental kinetic behavior indicates that participation of the classical process in relation to the quantal one is unexpectedly high and constitutes an anomaly of some theoretical interest. Participation of the tunneling process should be more easily observed in relation to the classical process at low temperatures, e.g., in cathodic hydrogen evolution from alcoholic HCl at $-110°$ C. Experiments are in progress to examine this possibility.

ACKNOWLEDGMENT

The author is indebted to the National Research Council for a grant in aid of this and related work.

REFERENCES

1. WIGNER, E. Z. physik. Chem. B, **19**, 203 (1933).
2. BELL, R. P. Proc. Roy. Soc. (London), A, **139**, 466 (1933).
3. PELZER, H. and WIGNER, E. Z. physik. Chem. B, **15**, 445 (1932).
4. BELL, R. P., FENDLEY, J. A., and HULETT, J. R. Proc. Roy. Soc. (London), A, **235**, 453 (1950).
5. CONWAY, B. E., BOCKRIS, J. O'M., and LINTON, H. J. Chem. Phys. **24**, 834 (1956).
6. CONWAY, B. E. and BOCKRIS, J. O'M. J. Chem. Phys. **28**, 354 (1958).
7. BRADLEY, R. S. Trans. Faraday Soc. **53**, 687 (1957).
8. JOHNSTONE, M. Proc. Trans. Nova Scotian Inst. Sci. **13**, 126 (1912).
9. KOHLRAUSCH, F. and HEYDWEILER, A. Z. physik. Chem. **14**, 317 (1894).
10. SMYTHE, C. P. and HITCHCOCK, J. J. Am. Chem. Soc. **54**, 4631 (1932).
11. JAFFÉ, G. Ann. Phys. **28**, 326 (1909).
12. SCHROEDER, J. Ann. Phys. **29**, 125 (1909).
13. JONES, G. and BRADSHAW, B. C. J. Am. Chem. Soc. **55**, 1780 (1933).
14. GRÄNICHER, H. C., JACCARD, C., SCHERRER, P., and STEINMANN, A. Discussions Faraday Soc. **23**, 50 (1957).
15. EIGEN, M. and MAEYER, L. Z. Elektrochem. **60**, 1037 (1956).
16. ECKART, C. Phys. Rev. **35**, 1303 (1930).
17. BERNAL, J. D. and FOWLER, R. H. J. Chem. Phys. **1**, 515 (1933).
18. ABEL, E., BRATU, E., and REDLICH, O. Z. physik. Chem. **173**, 353 (1935).
19. LANGE, E. Z. Elektrochem. **44**, 43 (1938).
20. BELL, R. P. Proc. Roy. Soc. (London), A, **148**, 241 (1935).
21. GURNEY, R. W. Proc. Roy. Soc. (London), A, **134**, 137 (1932).
22. BAWN, C. E. H. and OGDEN, G. Trans. Faraday Soc. **30**, 432 (1934).
23. APPELBY, M. P. and OGDEN, G. J. Chem. Soc. 163 (1936).
24. WALTON, M. F. and WOLFENDON, J. H. Trans. Faraday Soc. **34**, 436 (1938).

Can. J. Chem. Downloaded from www.nrcresearchpress.com by 190.90.36.8 on 09/04/12
For personal use only.

25. PARSONS, R. and BOCKRIS, J. O'M. Trans. Faraday Soc. **47**, 914 (1951).
26. CONWAY, B. E., BOCKRIS, J. O'M., and LOVROCEK, B. Proc. Comité intern. thermodynam. et cinét. electrochim. 207 (1954).
27. HERZBERG, G. Molecular spectra and molecular structure. Vol. I. D. Van Nostrand Company, Inc., New York. 1950. p. 501.
28. BOCKRIS, J. O'M. and PARSONS, R. Trans. Faraday Soc. **45**, 916 (1949).
29. CONWAY, B. E. Proc. Roy. Soc. (London), A, **247**, 400 (1958).
30. MATTAUCH, J. Nuclear physics tables. Interscience Publishers, Inc., New York. 1946.
31. PENTLAND, N., BOCKRIS, J. O'M., and SHELDON, E. J. Electrochem. Soc. **104**, 182 (1957).
32. BOCKRIS, J. O'M. Modern aspects of electrochemistry. Academic Press, Inc., New York. 1954. Chap. IV.
33. HICKLING, A. and SALT, F. W. Trans. Faraday Soc. **36**, 1226 (1940). See also BOCKRIS, J. O'M. and CONWAY, B. E. Trans. Faraday Soc. **45**, 989 (1949).
34. GIERER, A. Z. Naturforsch. **5**, 581 (1950).

Can. J. Chem. Downloaded from www.nrcresearchpress.com by 190.90.36.8 on 09/04/12
For personal use only.

Can. J. Chem. Downloaded from www.nrcresearchpress.com by 190.90.36.8 on 09/04/12
For personal use only.

ON THE MECHANISM OF ELECTROLYTIC DEPOSITION AND DISSOLUTION OF SILVER[1]

WOLFGANG MEHL AND JOHN O'M. BOCKRIS

INTRODUCTION

The mechanism of crystal growth has been an object of study for many years. Beginning with Gibbs (1), major contributions have been made by Volmer (2), Kossel (3), Stranski (4), Becker and Döring (5), Frenkel (6), and Frank (7). From this work it was concluded that the first step in crystal growth is "adsorption" on the surface, whereafter "adatoms" (2) diffuse to steps and along steps to kinks, where they are incorporated into the lattice, after which repetition of these steps ("repeatable step") brings about the incorporation of a kink atom into the lattice (cf. Fig. 1 and Conway and Bockris (21)).

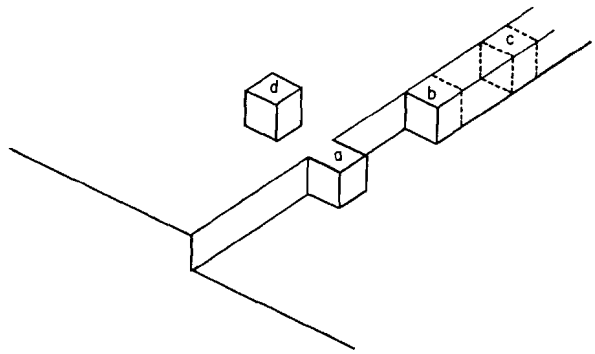

FIG. 1. Schematic view of metal–solution interface depicting (*a*) atom at edge, (*b*) kink, (*c*) atom in edge, (*d*) adion.

After all the stepped surfaces have been used up, two-dimensional nucleation was expected in the earlier theory (1, 2, 3, 4, 5, 6) to occur on surfaces of low index, which implied that some degree of supersaturation was necessary for the continuation of the growth process. Experiments show, however, that usually crystals can grow indefinitely without a large degree of supersaturation of the surface. This discrepancy arises because the model for crystal growth, sketched above, applies to the growth of a perfect crystal, but most real crystals contain imperfections which provide the steps necessary for growth.

Frank *et al.* (7) have studied the influence of imperfections, mainly screw dislocations, on the growth mechanism. Screw dislocations were found to provide a practically inexhaustible source of steps which turn at higher supersaturations into spirals, forming growth pyramids on the surface.

The equations deduced by Frank (7, 8) can also be used for a discussion of electrolytic crystal growth if the parameters are appropriately changed, but it is necessary to keep in mind that the energetic properties of a metal surface in contact with an electrolytic solution differ essentially from those of a surface in contact with its vapor. Thus, in a solution there exists at the metal surface an electrical double layer, with a field strength of about 10^7 v cm^{-1}; ions from the solution phase are adsorbed on the surface, etc. (13).

[1]*Manuscript received July 23, 1958.*
Contribution from the John Harrison Laboratories, University of Pennsylvania, Philadelphia, U.S.A. This paper was presented at the Symposium on Charge Transfer Processes held at the University of Toronto, Toronto, Ontario, September 4 and 5, 1958.

Can. J. Chem. Downloaded from www.nrcresearchpress.com by 190.90.36.8 on 09/04/12
For personal use only.

For electrolytic crystal growth an important difference to growth of crystals from the gas phase is also that an activation energy has to be overcome to make it possible for the metal ions to cross the electrical double layer and to strip off the solvation sheath (21).

It is the electric field at the metal–solution interface which gives rise to two possible extreme idealizations for models of electrolytic crystal growth (9).

In model A nearly all the electrode surface is active for the process of transferring ions from the solution to the electrode (transfer reaction). The particles on the surface carry probably a partial charge and are therefore best termed adions (21). The consecutive process to that of transfer is surface diffusion of adions to the growth positions on the surface, the final step being incorporation of adions into the lattice. In addition, at higher concentration of adions, nucleation on the surface may occur.

In model B the ions from the solution transfer directly to growing points on the surface (active centers).

Little informative work has been hitherto possible on electrolytic crystal growth, mainly because of experimental difficulties. Metal surfaces readily adsorb impurities, possibly at the active centers important for the crystal growth process. Because of this sensitivity to impurities, one of the main experimental difficulties in such work is keeping a small metal area (of the order of 0.01–1 sq. cm in area) in contact with solution but free of adsorbed impurities. A further intrinsic difficulty is that of carrying out significant measurements whilst the electrode surface remains essentially constant, i.e., observations of the rate of the reaction of a given potential must be made rapidly.

Because of these experimental difficulties only qualitative discussions of electrolytic crystal growth have been possible until now (9, 10). But experiences gained in the preparation of electrodes for studies of the hydrogen evolution reaction (11) and in the development of improved electronic measuring techniques (12) seemed to make worth while an experimental study of the kinetics of electrolytic metal deposition and dissolution.

At silver electrodes, Gerischer *et al.* (14) observed a deviation from the current–potential relationship to be expected if a rate-determining transfer reaction occurs (a similar observation was recorded by Mattson (15) for copper deposition on copper). These workers found that the exchange current for the system Ag/Ag^+ is independent of the concentration of silver ions in the solutions which appeared to indicate a rate-determining crystallization process for the over-all metal deposition.* Kaischew and co-workers (16) showed by microscopic studies that growth spirals are formed on the silver surface during deposition, thus supporting the applicability of Frank's theory of crystal growth by means of dislocation to electrolytic crystal growth.

It is the aim of the present work to find out: (1) which is the general path (i.e. that of model A or η model B) by which the ions pass from their initial state of hydration in the solution to their final state in the lattice and vice versa, and (2) which step in this path is rate-determining under given sets of conditions.

METHOD OF INVESTIGATION: THE GALVANOSTATIC METHOD

1. Introduction

In the study of the mechanism of crystal growth from the gas phase, the rate of crystal growth is studied as a function of the degree of supersaturation of the vapor. The corresponding measurement here is that of the rate of growth as a function of potential.

**Gerischer has also recently carried out, independently of the present workers, potentiostatic (24) and galvanostatic (25) measurements on silver dissolution, and comes to conclusions similar to those described here (cf. Mehl and Bockris (28)). Different i_0 values recorded in the work of this author, compared with those recorded here, depend upon the quite different methods of preparation of the electrode surfaces used.*

If one tries to obtain this i–η relationship under conditions of long-time (minutes) polarization, changes of the electrode surface with time due to the deposition or dissolution process itself, or adsorption of residual impurities, even from highly purified solutions, may make interpretation difficult. Consequently, short-time (milliseconds) polarization is preferable, and the galvanostatic (constant current) method (17) was chosen for the present investigation. Another advantage of this method compared with long-time measurements is that it enables additional evidence concerning the deposition mechanism to be obtained from the potential–time function.

The electrodes are in contact with the solution for minutes (between the time the protecting bulb around the electrodes is broken and that at which the sweep is taken). Therefore, extreme purification of solutions was carried out.

2. Double Layer Charging and Transfer

If a constant current density, i, is switched onto an electrode, this current divides itself into two components. The first one, i_C, is used for charging the electrical double layer at the electrode–solution interface; the second part, i_F, brings about transfer of ions across the double layer from the solution to the electrode surface. The current density, i_C, rapidly decreases with time, during the galvanostatic charging process, which means that i_F increases with time, because

$$i = i_C + i_F \qquad [1]$$

is constant. If i_F is controlled exclusively by the transfer reaction, then:*

$$i = Cd\eta/dt + i_0(e^{-\beta\eta\, zF/RT} - e^{(1-\beta)\eta\, zF/RT}), \qquad [2]$$

where C = the double layer capacity; i_0 = the exchange current density for the transfer controlled reaction; $0 < \beta < 1$; R, T, and F have their usual significance; and z is the valency of the cation in solution.

A general solution of this equation with the assumption that the double layer capacity is independent of potential was given by Rojter, Juza, and Polujan (17). The η–t relationship thus obtained is complicated and therefore difficult to verify by experiment. For small overpotentials, $\alpha\eta\ zF/RT < 1$, and the solution of equation [2] is, again assuming C independent of potential,

$$\eta_t = \eta_\infty(1 - e^{-t/\tau_1}) \qquad [3]$$

with η_∞ = steady state overpotential,

$$\tau = (RT/zFi_0)C. \qquad [4]$$

Equation [3] is only an approximation as the double layer capacity changes during the charging process with time so that an exact separation of i_F and i_C is not possible (18). This means that for the analysis of electrode reactions with help of the $\eta(t)$ functions, only such reactions are detectable which have a relaxation time of $\tau > \tau_1$.

3. Electrolytic Resistance of Solution

The ohmic potential drop between reference electrode and measurement electrode can easily be determined because it appears in the $\eta(t)$ function as a jump parallel to the potential axis (see Fig. 5).

**It is assumed that the maximum supply of ions from the bulk of the solution to the double layer (by diffusion and electrolytic transport) far exceeds that required for deposition.*

Can. J. Chem. Downloaded from www.nrcresearchpress.com by 190.90.36.8 on 09/04/12
For personal use only.

4. Transfer and Surface Diffusion of Ions

In the following considerations, constant Faradaic current ($t \gg \tau_1$) is assumed. If the surface diffusion coefficient for adions on the metal surface is sufficiently small, so that this process is important for the rate of the over-all process, the surface concentration of adions increases during polarization to a value above that of the surface concentration corresponding to equilibrium, and becomes less than this value during dissolution. In this section the discussion will be limited to the consideration of low overpotential, i.e., a small degree of supersaturation.

Assuming that the adions cause only a small reduction of the free surface area for the transfer reaction and neglecting concentration polarization in the solution, the potential–time function is:

$$[5] \qquad (i_F)_t = i_0[e^{-\beta\eta_t\, zF/RT} - (c_{\eta(t)}/c_0)\, e^{(1-\beta)\eta_t\, zF/RT}]$$

where c_0 is the concentration of adions at equilibrium and $c_{\eta(t)}$ is the concentration of adions at a time t when the overpotential has reached a value of η. For $\eta < RT/\alpha\, zF$ and neglecting second-order terms, one obtains, by expansion of [5] and rearrangement,

$$[6] \qquad -\eta_t = (RT/zF)\ (i/i_0) + (RT/zF)\ (\Delta c_{\eta(t)}/c_0),$$

where

$$\Delta c_{\eta(t)} = c_{\eta(t)} - c_0.$$

Hence, η depends in this case both on i_0 for the transfer reaction and the "concentration overpotential due to surface diffusion".

It is necessary to express $c_{\eta(t)}$ as a function of i and t. Now:

$$[7] \qquad dc/dt = (i_F/zF) - v,$$

where v is the average of the surface diffusion flux of the adions during their passage from the point at which they are transferred to the metal surface and that at which they meet a crystal building point.

Surface diffusion on metal crystals has been dealt with thoroughly by Frank *et al.* (7) and applied to electrolytic deposition by Vermilyea (10). The present results are consistent with the simple assumption (for $|\eta| \leqslant 5$ mv) that the surface diffusion flux is proportional to the surface supersaturation, $[(c_{\eta(t)}/c_0) - 1]$. Hence:

$$[8] \qquad v = v_0[(c_{\eta(t)}/c_0) - 1]$$

assuming that, near to kinks, the adion concentration remains at equilibrium value, c_0, whilst on crystal planes, where the metal ions are regarded as first being transferred from the solution to the metal surface, the mean surface concentration of adions is $c_{\eta(t)}$. Substituting [8] into [7] and integrating yields

$$[9] \qquad \frac{c_{\eta(t)} - c_0}{c_0} = \frac{\Delta c}{c_0} = \frac{i_F}{zFv_0}(1 - e^{-t/\tau_2})$$

$$[10] \qquad \tau_2 = c_0/v_0.$$

Thus, the steady state value of the increased concentration of adions over that expected for pure transfer control is given ($t = \infty$) by:

$$[11] \qquad \Delta c/c_0 = i_F/zFv_0.$$

With [9] and [6] the $\eta(t)$ function at small overpotentials, with both surface diffusion

Can. J. Chem. Downloaded from www.nrcresearchpress.com by 190.90.36.8 on 09/04/12
For personal use only.

and transfer of ions across the double layer as influencing the value of η_t, and for time $t > \tau_1$, becomes:

$$[12] \qquad -\eta_{(t)} = \frac{RT}{zF}\left[\frac{i_F}{i_0}+\frac{i_F}{v_0 zF}\left(1-e^{-(v_0/c_0)\,t}\right)\right].$$

For times t, for which $\tau_1 < t < \tau_2$ and with $\tau_2 = c_0/v_0$, from [12]

$$[13a] \qquad -\eta_{(t)} = \frac{RT}{zF}\left(\frac{i_F}{i_0}+\frac{i_F}{c_0 zF}\,t\right)$$

and

$$[13b] \qquad \frac{d\eta_t}{dt} = \frac{RT}{z^2F^2}\,\frac{i_F}{c_0}$$

5. Current–Potential Relations in the Steady State

(*a*) *Transfer is rate-determining.*—The i–η function will then be controlled by:

$$[14] \qquad i_F = i_0(e^{-\beta\eta\, zF/RT} - e^{(1-\beta)\eta\, Fz/RT}).$$

The adion concentration is at its equilibrium value and therefore surface coverage can be neglected (6).

(*b*) *Transfer and surface diffusion control the role of the over-all reaction.*—With [12] and [11] we get

$$[15]^* \qquad i_F = \frac{e^{-zF\eta/RT}-1}{(1/i_0)\,e^{-(1-\beta)\eta\, zF/RT} + 1/zFv_0}.$$

(*c*) *Surface diffusion is rate-determining.*—For

$$zFv_0 < i_0\, e^{(1-\beta)\eta\, zF/RT}$$

there follows,

$$[16] \qquad i_F = zFv_0(e^{-\eta\, zF/RT}-1).$$

Equations [15] and [16] have been derived under the assumption that v_0 is overpotential-independent. Theoretical work by Frank *et al.* (7) shows, however, that this assumption is incorrect; v_0 increases with increasingly negative overpotential (cf. Discussion).

EXPERIMENTAL

1. Galvanostatic Arrangement (Fig. 2)

The potential source consisted of dry batteries, e.m.f. 90–200 v. Precision resistors (I.R.C.) are represented by R and were arranged in 10 steps, from 1 kilohm to 6.2 meg. The letter O represents a Tektronix oscilloscope, type 531, with type 53/54D plug-in preamplifier. The potential–time curves were photographed with an Exakta camera having a 50-mm lens. Projection of the 35-mm film was made with an enlargement of about ten times to obtain numerical η–t curves. The switch S contained a Western Electric relay, type 175, having a rise time of about 10^{-7} sec[22].

2. Treatment of Solution and Electrodes

The solution was made from A.R. $HClO_4$, which was distilled three times *in vacuo*, the last distillation being into a burette leading directly to the cell. The water was distilled

**Equation [15] is valid only under conditions such that the surface coverage with adions is sufficiently low to yield negligible hindrance to the transfer of ions from the solution. In fact, if v_0 is sufficiently low a surface coverage could build up and the first term in [5] should be preceded by a term of the type $1-\theta_\eta/1-\theta_0$, where θ_η is the surface coverage at overpotential η. A limiting current could then ensue at sufficiently high overpotentials. But this case is unlikely because of nucleation and a possible increase of v_0 with increasing overpotential.*

Can. J. Chem. Downloaded from www.nrcresearchpress.com by 190.90.36.8 on 09/04/12
For personal use only.

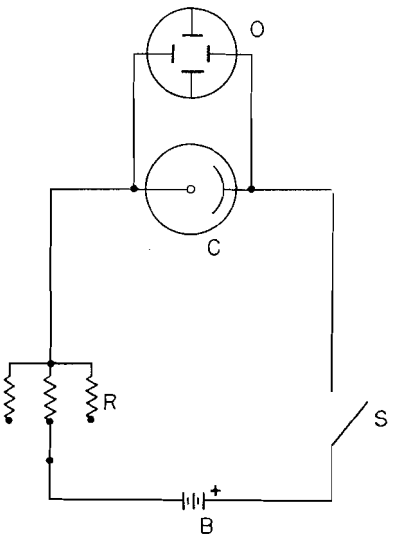

FIG. 2. Galvanostatic arrangement:
B: battery, 90 v; C: measuring cell; O: oscilloscope; S: switch; and R: resistances.

several times and had a final conductance of about 10^{-7} mho cm^{-1}. The $AgClO_4$ ("pure" grade) was recrystallized twice outside the system and twice inside and then introduced into a special cell in which it was subjected to pre-electrolysis for about twenty-four hours with alternating current density of about 3×10^{-1} amp cm^{-2}. The solution was vigorously stirred with carefully purified nitrogen gas, the cathode was of silver, the anode of platinum (vigorous stirring prevented silver needles from growing through the closed tap between cathode and anode compartments).*

The electrodes were prepared by heating a thin (spectroscopically pure) silver wire (0.5 mm diameter) in an atmosphere of purified hydrogen in a quartz tube. A spherical shape was attained by partial melting. Finally, the electrode was sealed in a glass bulb containing only hydrogen, or helium, and the bulb was broken in the solution shortly before measurement. A detailed description of this procedure has been published (19). This method of preparing electrodes is similar in nature to "thermal etching", which has been studied experimentally and theoretically by several authors (20). During the heating process a rearrangement of surface atoms of the polycrystalline surface occurs, to produce facets with simple crystallographic indices; grain boundaries occur as grooves. As the electrodes are being cooled down in a hydrogen stream (high heat conductivity), a relatively high thermal stress would appear in the metal, producing a high concentration of dislocations.

Electron micrographs were taken of the electrodes prepared in this way. They show etch pits with a density of about 10^7 per sq. cm (Fig. 3). According to Hirth and Pound (26, 27), these may be interpreted as due to dislocations with a screw component normal to the surface. Occasionally electrodes indicate surface films of unknown origin (possibly connected with accidental contact between the hot metal and the glass tube during electrode preparation) and results from such electrodes were not further examined.

Other experimental conditions, particularly with regard to purification of gases, etc., were as already described (29).

**The exterior of the pre-electrolysis cell was coated black to exclude light effects. The measurements were carried out under conditions of minimum illumination.*

Can. J. Chem. Downloaded from www.nrcresearchpress.com by 190.90.36.8 on 09/04/12
For personal use only.

Can. J. Chem. Downloaded from www.nrcresearchpress.com by 190.90.36.8 on 09/04/12
For personal use only.

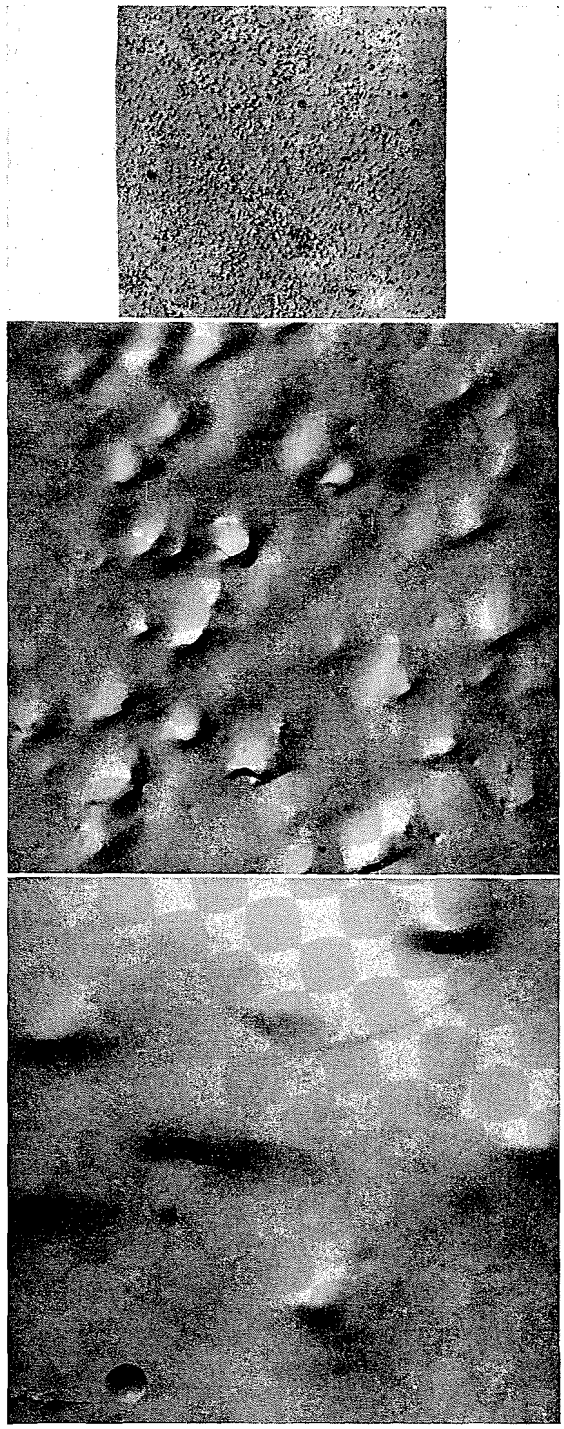

FIG. 3. Electromicrographs of polycrystalline thermally etched silver surfaces.*
(*a*) Etch pits due to dislocation sites
Magnification 4000 ×
Magnification 33000 ×
Magnification 78000 ×
*For footnote see following page.

FIG. 3. Electromicrographs of polycrystalline thermally etched silver surfaces.*
(*b*) Grain boundary with precipitate
Magnification 13000 ×
Magnification 33000 ×

*SiO *replicas the contact side of which was shadowed with tungsten oxide. The work was carried out by H. G. Wilsdorf to whom the authors' thanks are due.*

3. Procedure

After one of the four electrodes in the cell had been lowered by means of a sliding fit joint into the solution, the glass bulb surrounding it was broken and the electrode adjusted until it was inside a platinum gauze basket which acted as counterelectrode. The outside resistance R (Fig. 2) was set at a value appropriate for the given current density, and a current impulse given to the electrode. By means of the switch S (22) (Fig. 2) the impulse was restricted to an amount of electricity not more than 10^{-4} coulombs cm^{-2} (i.e., the amount to cover about 1 geometric cm^2). The resulting potential–time curve was photographed.

Such photographs were made at some ten current densities (over the range 3×10^{-4} to 8×10^{-1} amp/cm^2) for each electrode and in each run a maximum of four electrodes were examined. Measurements were made at a variety of concentrations between 10^{-2} and 10^{-1} moles $l.^{-1}$ so that concentration polarization could be avoided. At the end of a series of measurements with increasing current density, some sweeps at lowest current densities were repeated and results, closely similar to those taken earlier, found.

Can. J. Chem. Downloaded from www.nrcresearchpress.com by 190.90.36.8 on 09/04/12
For personal use only.

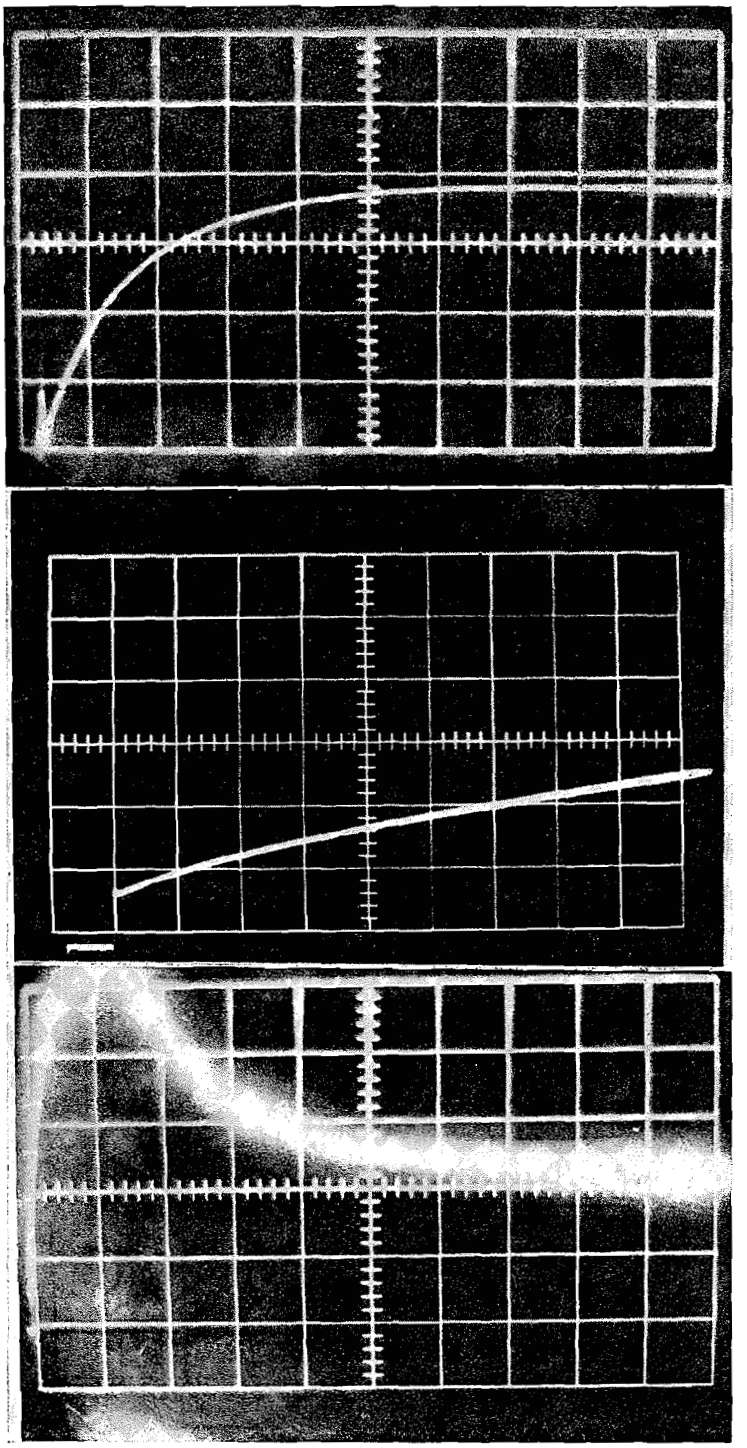

FIG. 4. (*Top*) Charging curve at low current density: ($AgClO_4$): 2×10^{-1} mole/l.; $i = 2$ ma cm^{-2}; units: t—axis, 2 msec, η—axis, 1 mv.
FIG. 5. (*Center*) Charging of electrical double layer: $i = 2.5$ ma/cm^2; $t = 10^{-4}$ sec; $\eta = 2$ mv.
FIG. 6. (*Bottom*) Superpolarization: $i = 500$ ma/cm^2; units: $t = 5\times10^{-3}$ sec; η: 30 mv.

Can. J. Chem. Downloaded from www.nrcresearchpress.com by 190.90.36.8 on 09/04/12
For personal use only.

4. Results

Figure 4 shows a typical potential–time curve for the current density 2 ma cm^{-2} at a concentration of 0.2 *N* $AgClO_4$ in 1 *N* $HClO_4$ for cathodic polarization. Similar results were obtained for anodic polarization. In Fig. 5, a typical η–t relationship for short times is shown. Figure 6 shows a typical η–t curve measured in unpurified solution, which exhibits the phenomenon of superpolarization.

Figure 7 shows a typical plot of the log i–η_∞ relation for cathodic and anodic polarization, and Fig. 8 a typical linear relation of i to η_∞ at low current densities.

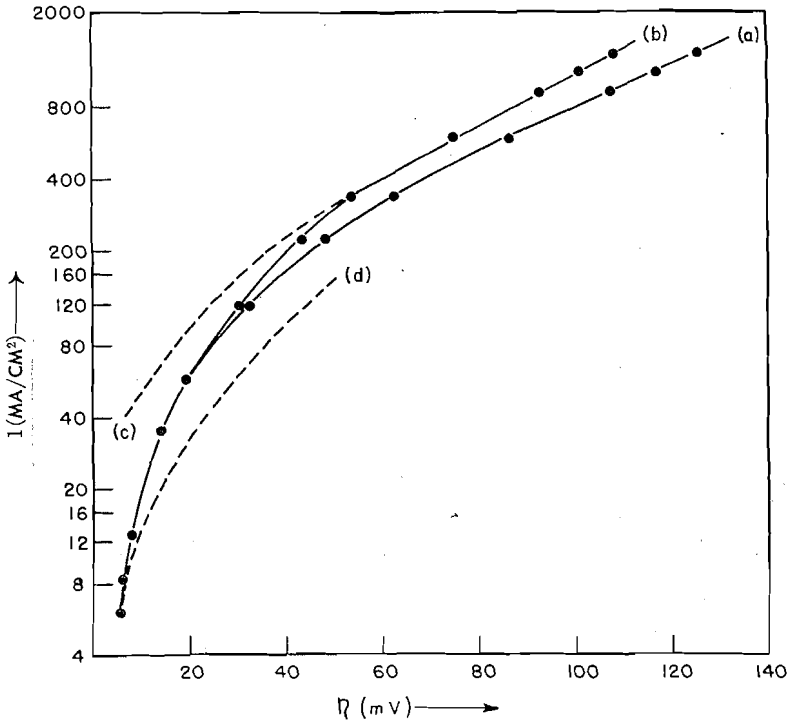

FIG. 7. Log i–η plot for deposition (*a*), dissolution (*b*).
$c_{AgClO_4} = 2\times10^{-1}$ mole/l.
(*c*) Represents (- - - -) slow transfer reaction.
(*d*) Represents (- - - -) simple diffusion theory.

DISCUSSION

1. Potential–Time Curves

At very short times the current flowing during build-up of potential is used almost exclusively for the charging of the double layer, the capacity of which is therefore given (in the linear $\eta_{(t)}$–t region) by:

$$C = it/\eta_{(t)}. \qquad [17]$$

This linear η–t relationship can be expected for times limiting low value of t. With a double-layer capacity of about 20 μ *F* cm^{-2}, RT/zFi_0) = 2 ohm cm^2 and allowing a roughness factor 2, the linear relationship can be expected for times of about $t < 10^{-4}$ second, when $\eta < RT/zF$. In fact, a linear relationship was observed for more than 10^{-3} second with a slope which according to [17] would give an impossible value of 500

Can. J. Chem. Downloaded from www.nrcresearchpress.com by 190.90.36.8 on 09/04/12
For personal use only.

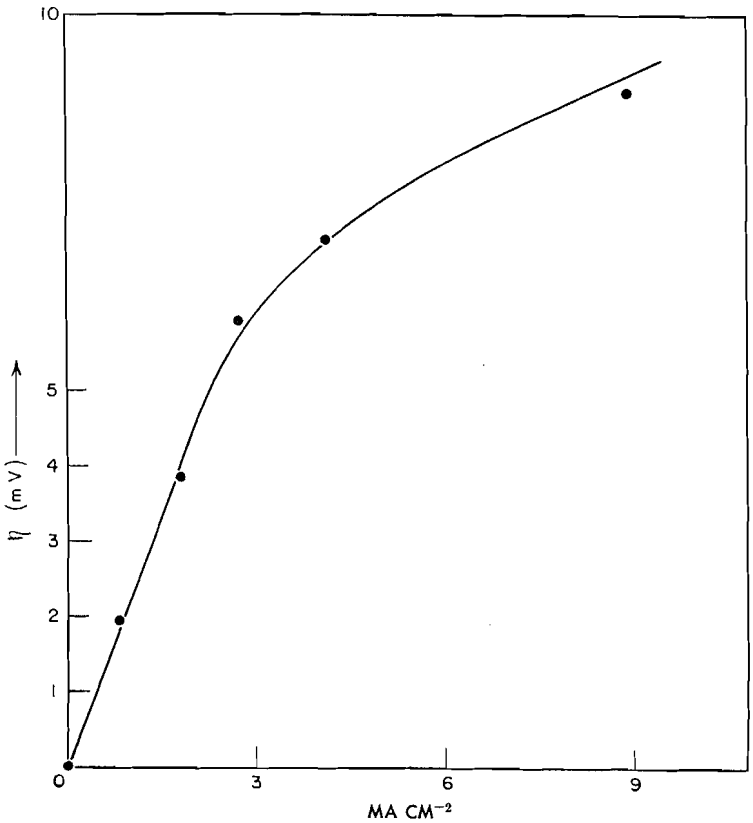

FIG. 8. i–η plot for low current densities. $(AgClO_4) = 2.10^{-1}$ mole $l.^{-1}$.

μ F/cm^2 for the double-layer capacity. Similarly, if the transfer step alone were rate-determining, equation [3] shows that the steady state overpotential should be reached at a time of about

$$t = 4\,(RT/zFi_0)C \qquad [18]$$

for $\eta < RT/zF$. The actually observed values for this time are more than ten times larger than those predicted.

This slow rise time may be interpreted in terms of the build-up of an adsorption layer of adions, as shown in the next section.*

2. Potential–Time Relation and the Role of Surface Diffusion

From [13]:

$$\eta_{(t)} - \eta_\infty = \frac{RT}{zF}\frac{i_F}{zFv_0}\,e^{-(v_0/c_0)t}. \qquad [19]$$

Also, from [12]:

$$\eta_{t=0} = \frac{RT}{zF}\frac{i_F}{i_0} \qquad [20]$$

and

**A slow reaction in the solution cannot be responsible for this behavior because during deposition of metals upon amalgams, behavior may be satisfactorily interpreted in terms of rate-controlling transfer (23).*

Can. J. Chem. Downloaded from www.nrcresearchpress.com by 190.90.36.8 on 09/04/12
For personal use only.

[21] $$\eta_{t=0} - \eta_\infty = \frac{RT}{zF}\frac{i_F}{zFv_0}.$$

Further, from [12]:

[22] $$\eta_\infty = \frac{RT}{zF}\left(\frac{i_F}{i_0} + \frac{i_F}{zFv_0}\right).$$

Note that in the above equations the double-layer charging has been neglected; they are therefore valid only for times much greater than the rise time of the transfer reaction, i.e., in the systems reported on here, about 10^{-4} seconds (also, it has been assumed that $|\eta| < 5$ mv).

According to [19] $\eta_{t=0}$ can be got by extrapolating a plot of log $(\eta_t - \eta_{st})$ against t to $t = 0$ (Fig. 9).* The value for i_0 obtained this way [22] can be compared with values obtained by the independent method of extrapolating the linear part of η–log i relation to $\eta = 0$. The values agree to about $\pm 30\%$. If one takes into consideration that the accuracy with which the potential can be determined is $\pm 5\%$ and the overpotential due to transfer (at $|\eta| \leqslant 5$ mv) is about 10% of the total overvoltage, the agreement between the i_0 values obtained in these two independent ways is satisfactory. This agreement confirms the interpretation of the slow rise time of the η–t curve on the basis of slow surface diffusion of adions.

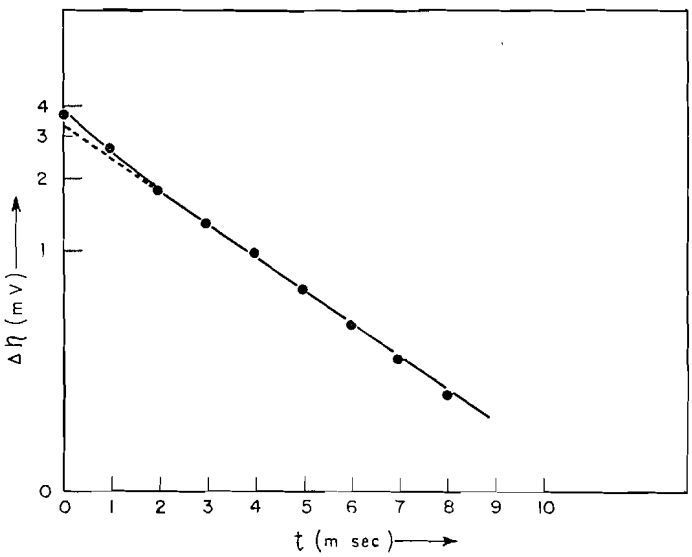

FIG. 9. Separation of total polarization into diffusion and transfer polarization by extrapolation of galvanostatic $\eta(t)$ curves (for parameters, see Fig. 4).

Table I gives values of i_0 obtained by the extrapolation of the Tafel line.† With the known values of i_0, [22] allows the calculation of v_0, values of which are shown in Table I.

3. Concentration of Adions at the Reversible Potential

From [19] we get:

**The* $\eta_{t=0}$ *referred to is a quantity susceptible only to calculation upon a model such as that suggested. It signifies the potential of the electrode during charging with respect to the corresponding electrode, under conditions such that the double-layer charging is terminated, but before the surface diffusion has had time to affect the concentration of adions over that corresponding to the reversible potential. Correspondingly,* $\eta_{t=0}$ *depends only upon* i_0*, and not upon* v_0*.*

†*The* i_0 *values for deposition and dissolution agree well; values of* β *are almost the same* ($\simeq 0.50$) *for each process.*

Can. J. Chem. Downloaded from www.nrcresearchpress.com by 190.90.36.8 on 09/04/12
For personal use only.

[23] $$(d/dt)\ln(\eta_t-\eta_\infty) = -v_0/c_0.$$

From [23] (with v_0 from [21]) and from [13*a*] directly, the concentration of adions at the reversible potential may be calculated. Both methods lead to the same results. The values obtained this way are presented in Table I.

TABLE I

$AgClO_4$ mole/liter	i_0 amp cm^2	zFv_0 amp/cm^2	c_0 mole/apparent cm^2
2.0×10^{-1}	0.10	1.2×10^{-2}	8×10^{-10}
1.3×10^{-1}	0.08	1.0×10^{-2}	2×10^{-9}
1.0×10^{-1}	0.07	1.4×10^{-2}	4×10^{-10}
0.8×10^{-1}	0.07	1.2×10^{-2}	3×10^{-9}
0.8×10^{-1}	0.07	1.6×10^{-2}	6×10^{-10}
0.6×10^{-1}	0.06	1.2×10^{-2}	1×10^{-9}
0.6×10^{-1}	0.06	1.1×10^{-2}	8×10^{-10}
0.4×10^{-1}	0.05	1.2×10^{-2}	1×10^{-9}
0.2×10^{-1}	0.04	1.5×10^{-2}	6×10^{-10}
0.1×10^{-1}	0.03	1.1×10^{-2}	5×10^{-10}

4. Current–Potential Relation

With the aid of values of v_0 and i_0 calculated as described above, it is possible to evaluate the theoretical η–i and η – log i relations for the steady state. These are compared with experiment in Fig. 7.

5. Mechanism of Deposition and Dissolution

As Fig. 7 shows, for silver deposition and dissolution for electrodes prepared by thermal etching, surface diffusion of adions is the principal rate-determining step at low overpotentials, and at high overpotentials the transfer of ions from the solution to the electrode is the rate-determining step. As v_0 does not depend upon the concentration of silver ions in solution (see Table I), the concentration dependence of i_0 is given by:

$$\partial \ln i_0/\partial \ln \alpha_{Ag} = \beta.$$

It can be predicted from the values for i_0 and v_0 (Table I) that the above statement concerning rate control will be valid down to Ag^+ concentrations of about 10^{-4} to 10^{-5} mole $l.^{-1}$. At lower concentrations than these, the transfer step will be rate-controlling at all current densities (for the type of silver surfaces used in the present study).

The path determined for this fundamental example of simple metal deposition corresponds therefore more closely to model A rather than model B (see above).

The transition from rate-determining surface diffusion to rate-determining transfer is due to the decrease of the average distance between growing lines (and hence increase of v_0) with increasing overpotential. The dependence of v_0 upon potential has not yet been subject to a satisfactory theoretical treatment. Provisionally, the following empirical equation may be suggested: $v_0(\eta) = v_0\, e^{-\eta\, zF/RT}$, whereupon the complete course of the i–η relation can thus be described by the equation:

[24] $$i = \frac{e^{-\eta\, zF/RT}-1}{(1/i_0)\, e^{-(1-\beta)\eta\, zF/RT} + (1/v_0zF)\, e^{zF\eta/RT}}.$$

For higher overpotentials (24) gives:

[25] $$i = \frac{e^{-\eta\, zF/RT}-1}{(1/i_0)\, e^{-(1-\beta)\eta\, zF/RT}},$$

and for low cathodic overvoltages:

[26] $$i = zFv_0\, e^{-\eta\, zF/RT}(e^{-zF\,\eta/RT}-1).$$

Can. J. Chem. Downloaded from www.nrcresearchpress.com by 190.90.36.8 on 09/04/12
For personal use only.

Correspondingly, for crystal growth from the vapor phase, a linear dependence of the rate of growth upon the degree of supersaturation has been found at higher supersaturations (linear law), and a parabolic dependence upon supersaturation at low supersaturations (cf. Frank *et al.* (7)).

The "critical overpotential", which separates the linear and the parabolic law, depends on the ratio i_0/zFv_0 and thus upon the concentration of Ag^+ ions in solution (upon which i_0 depends).

It should be noted here that a perfect parabolic law, viz.,

$$i = k(e^{-zF\,\eta/RT}-1)^2$$

(where k is a constant) can only be expected for a single dislocation and a function such as that reported here for distribution of dislocations on the crystal surface.

6. Equilibrium Concentration of Adions

The equilibrium concentration of adatoms c_{ad} for the system metal–vapor can easily be calculated. With an energy of vaporization for silver of about 65 kcal, it is found that the equilibrium concentration of adions during electrochemical deposition is very much higher than the equilibrium concentration of adatoms during deposition from the vapor phase.

7. Superpolarization

This phenomenon (Fig. 6) occurs at higher overvoltages, 100 mv, and is difficult to study experimentally because of its poor reproducibility. Superpolarization was observed almost exclusively for solutions which had not been well purified so that the phenomenon might well be one of "over-shoot" (24) due to supersaturation of the surface with adions. Vermilyea (10) has discussed this type of phenomenon in terms of dislocation theory (7).

APPENDIX

Certain Terms Used in Electrochemical Crystal Growth Compared with Those Used in Crystal Growth from the Vapor Phase

Burton, Cabrera, and Frank (7) define supersaturation in the vapor by

[1*] $$\sigma = \alpha-1; \quad \alpha = p/p_0,$$

where p is the actual vapor pressure and p_0 the saturation value. The supersaturation of adsorbed molecules on the surface is defined by,

[2*] $$\sigma_s = \alpha_s-1; \quad \alpha_s = c_s/c_0$$

where c_s and c_0 are the actual and equilibrium concentration of adsorbed molecules respectively.

The "current" from the vapor to the surface is written as

[3*] $$j = (\alpha-\alpha_s)c_0/\tau_s,$$

where τ_s is the mean life of an adsorbed atom on the surface defined by

[4*] $$\tau_s = \frac{1}{\nu}\exp(W'_s/RT)$$

where W' = evaporation energy from the surface to the vapor, and ν = frequency factor. In the present theory, the current from the solution to the surface is written (cf. 5) as:

[5*] $$i = (e^{-zF\,\eta/RT}-c_s/c_0)i_0\,e^{(1-\beta)\eta\,zF/RT}.$$

Can. J. Chem. Downloaded from www.nrcresearchpress.com by 190.90.36.8 on 09/04/12
For personal use only.

Comparison of [3*] and [5*] yields the following analogies:

Comparison of expressions used in crystal growth from vapor phase and by electrolytic means

	Burton, Cabrera, and Frank (7) (vapor phase)	This paper (electrolytic)
Supersaturation in the vapor (solution)	p/p_0-1	$e^{-zF\eta/RT}-1$
Supersaturation on the surface	c_s/c_0-1	c_s/c_0^0-1
Mean lifetime of adsorbed molecules	τ_s	$(c_0/i_0)\,e^{-(1-\alpha)z\eta F/RT}$

REFERENCES

1. GIBBS, J. W. Collected works. Longmans, Green & Co., Ltd., London. 1928.
2. VOLMER, M. Kinetik der Phasenbildung. Verlag von Theodor Steinkopff, Dresden und Leipzig. 1939.
3. KOSSEL, W. O. Nachr. Ges. Wiss. Göttingen, 135 (1927).
4. STRANSKI, J. N. Z. physik. Chem. **136**, 259 (1928).
5. BECKER, R. and DÖRING, W. Ann. Physik, Leipzig, **24**, 719 (1935).
6. FRENKEL, I. J. Phys. Chem. (U.S.S.R), **9**, 392 (1945).
7. FRANK, F. C. Discussions Faraday Soc. **5**, 48, 67 (1949). CABRERA, N. and BURTON, W. K. Discussions Faraday Soc. **5**, 33, 40 (1949). BURTON, W. K., CABRERA, N., and FRANK, F. C. Nature, **163**, 398 (1949). BURTON, W. K., CABRERA, N., and FRANK, F. C. Phil. Trans. Roy. Soc. London, A, **243**, 299 (1951). FRANK, F. C. Phil. Mag. **41**, 200 (1950).
8. FORTY, A. J. and FRANK, F. C. Proc. Roy. Soc. A, **217**, 262 (1953).
9. FISCHER, H. Elektrolytische Abscheidung und Elektrokristallisation von Metallen. Springer-Verlag, Berlin. 1954.
10. VERMILYEA, D. A. J. Chem. Phys. **25**, 1254 (1956).
11. BOCKRIS, J. O'M. and CONWAY, B. E. J. Sci. Instr. **25**, No. 8, 283 (1948).
12. DELAHAY, P. New instrumental methods in electrochemistry. Interscience Publishers, Inc., New York. 1954.
13. PARSONS, R. Modern aspects of electrochemistry. *Edited by* J. O'M. Bockris. Academic Press, Inc., New York. 1954. Chap. IV.
14. GERISCHER, H. and VIELSTICH, W. Z. Elektrochem. **56**, 380 (1952). GERISCHER, H. and VIELSTICH, W. Comité intern. thermodynam. et cinét. électrochim. IV, Réunion. (1952). GERISCHER, H. and TISCHER, R. P. Z. Elektrochem. **58**, 819 (1954).
15. MATTSON, E. and LINDSTROM, R. Comité intern. thermodynam. et cinét. électrochim. VI, Réunion. Poitiers. (1954).
16. KAISCHEW, R., MUTAFTSCHIEW, B., and NENOW, D. Z. physik. Chem. **205**, 341 (1956).
17. ROJTER, W. A., JUZA, W. A., and POLUJAN, E. S. Acta Physicochim. U.R.S.S. **10**, 389, 845 (1939).
18. BOCKRIS, J. O'M., MEHL, W., CONWAY, B. E., and YOUNG, L. J. Chem. Phys. **25**, 776 (1956).
19. CONWAY, B. E., BOCKRIS, J. O'M., and MEHL, W. J. Sci. Instr. **33**, 400 (1956).
20. GWATHMEY, A. T. and BENTON, A. F. J. Chem. Phys. **8**, 431 (1940). CHALMERS, B., KING, R., and SHUTTLEWORTH, R. Proc. Roy. Soc. (London), A, **193**, 465 (1948). MULLINS, W. J. Appl. Phys. **28**, 333 (1957).
21. BOCKRIS, J. O'M. and CONWAY, B. E. Proc. Roy. Soc. (1958) (In press).
22. MEHL, W., DEVANATHAN, M. A. V., and BOCKRIS, J. O'M. Rev. Sci. Instr. **29**, 180 (1958).
23. RANDLES, J. E. B. and SOMERTON, K. W. Trans. Faraday Soc. **48**, 951 (1952).
24. GERISCHER, H. and TISCHER, R. P. Z. Elektrochem. **61**, 1159 (1957).
25. GERISCHER, H. Private communication.
26. HIRTH, I. P. and POUND, M. G. Acta Met. **6**, 1958.
27. HIRTH, I. P. and POUND, M. G. Meeting of AIME. New York. 1958.
28. MEHL, W. and BOCKRIS, J. O'M. J. Chem. Phys. **27**, 818 (1957).
29. BOCKRIS, J. O'M. and CONWAY, B. E. J. Chem. Phys. **28**, 707 (1958).

Can. J. Chem. Downloaded from www.nrcresearchpress.com by 190.90.36.8 on 09/04/12
For personal use only.

Can. J. Chem. Downloaded from www.nrcresearchpress.com by 190.90.36.8 on 09/04/12
For personal use only.

EXCHANGE BETWEEN METALS AND THEIR IONS IN SOLUTION[1]

CECIL V. KING AND NANCY E. MCKINNEY

ABSTRACT

The mechanisms by which a metal specimen can acquire radioactivity when immersed in a tracer solution of its own ions are discussed. Consideration is given to the roles of exchange current, adsorption, local cell electrolysis, corrosion, and self-diffusion within the metal. It is shown that exchange current cannot be measured by the tracer method unless conditions are unusually favorable, and that too little attention has been paid to the role of internal diffusion. Some experimental results with silver are presented and the importance of internal diffusion is shown.

INTRODUCTION

A great many articles dealing with metal – metal ion exchange have been published, but the interpretation of experimental results is not entirely satisfactory. The role of diffusion within the metal has been especially puzzling. It is the purpose of this paper to discuss some of the pertinent factors in exchange and to indicate their relative importance. New experimental work with silver is used for illustration.

Exchange Current

A kinetic interpretation of the Nernst equation for "electrode potential"

$$E = RT \ln P/p$$

or its modern equivalent, implies a continual exchange between ions in solution and ions or atoms within the metal phase. The equilibrium exchange rate, when expressed in electrical units, is known as the exchange current i_0. Direct proof of exchange is possible through the use of radioisotopes as tracers, but the tracer method can measure i_0 only under conditions probably never attainable in practice.

1. Assume one face of a metal single crystal to be immersed in a solution of its own ions (with tracer), and that there is no corrosion, no adsorption or electrical double layer formation involving the salt, no local cell electrolysis, no internal diffusion, and no temporary depletion of tracer in the solution next the interface. Exchange can then take place with only one atomic layer on the metal surface, and the rate of activity pickup, extrapolated to zero time, will give the exchange current. Or, an expression could be found for the rate of attainment of radioactive equilibrium, from which the specific exchange rate could be calculated. A value of $i_0 = 5 \times 10^{-8}$ amp/cm^2 corresponds to exchange of about one atomic layer per hour, but since much re-exchange would occur, radioactive pickup would continue for several hours. For silver, i_0 is reported to be about 10^{-3} amp/cm^2 (1), and radioactive equilibrium with the surface layer should require only a second or two. This has been found to be the case (2), but the actual rate has not been measured.

2. Exchange current could be measured with the same conditions as above except that self-diffusion in the metal should be much faster than exchange. Nearly all the active atoms entering the surface would diffuse inward rather than re-exchange, and the rate of pickup would give i_0 directly.

The fact is that conditions are never as simple as those discussed above.

[1]*Manuscript received July 3, 1958.*
Contribution from the Department of Chemistry, New York University, New York, N.Y. This paper was presented at the Symposium on Charge Transfer Processes held at the University of Toronto, Toronto, Ontario, September 4 and 5, 1958.

Adsorption

Assuming no internal diffusion, but that salt can be firmly adsorbed (through primary attachment of either cation or anion), the rate of attainment of equilibrium could depend on both i_0 and the kinetics of adsorption. In the case of silver–silver salts it is known that adsorption–desorption is a slow process, both from classical and from tracer studies (3, 4). Little is known about adsorption of their own salts on active metals.

If internal diffusion plays a role, then adsorption changes the surface concentration and the activity gradient in the surface layers.

Corrosion

If corrosion products are soluble, the rate and amount of activity pickup by the metal will depend on the exchange current, and whether internal penetration is faster than the metal dissolution. The extreme case has been investigated by dissolving the metal anodically. Matsuura (5) found that the activity acquired by a zinc anode corresponded to about three apparent atomic layers of complete exchange, independent of current density. Gerischer and Tischer found similar results with silver (2). This indicates only that surface exchange is rapid compared to internal diffusion.

If corrosion products are insoluble, activity may be acquired by exchange with the metal and the corrosion products, or by precipitation and adsorption from solution. An extreme case has been found with iron (unpublished results in this laboratory); internal diffusion is inappreciable, i_0 is very small, and there is little activity pickup unless corrosion is quite evident.

Local Cell Electrolysis

There is reason to believe that potential differences, which can cause metal to dissolve at one spot while deposition occurs at another, become negligible after a few hours of immersion. Certain faces of copper single crystals, immersed in $CuSO_4$ solution, undergo recrystallization and the potentials approach an equilibrium value (6). Silver specimens used in exchange experiments have been pre-equilibrated in non-radioactive solutions for periods up to several months (2, 7). Gerischer and Vielstich found no further effect after 24 hours.

Local cell electrolysis which results in solid corrosion products is another matter. The solution becomes alkaline at local cathodes, and radioactive metal can be precipitated as hydrous oxide without any actual exchange. Zinc acquires far more active zinc ion in the presence of air than from deaerated solution, even before an oxide film is visible.

Internal Diffusion

Assuming that corrosion and local cell electrolysis can be eliminated or minimized, then continuing activity pickup, which corresponds to more than adsorption or double layer formation plus complete exchange in one atomic layer, must be due to internal diffusion. Internal diffusion was considered by Gerischer, Vielstich, and Tischer (2) in their work with silver, but was discounted because the calculated diffusion coefficient was several powers of 10 higher than expected. Matsuura (5) found the same difficulty in the case of zinc. We believe that the discrepancies are due to lack of knowledge of the true surface concentration of the diffusing species. The solutions used generally have a concentration of 10^{-4}–10^{-5} moles/cm^3, while the metal contains about 0.1 g-atom/cm^3. Adsorption of a fraction of a monolayer results in a surface concentration much greater than in solution. Adsorption on silver depends on the anion, and can amount to several tenths of a monolayer (8).

Can. J. Chem. Downloaded from www.nrcresearchpress.com by 190.90.36.8 on 09/04/12
For personal use only.

In polycrystalline metals grain-boundary diffusion is generally much greater at lower temperatures than lattice diffusion, even though the area of exposed grain boundaries is only a small fraction of the total. Self-diffusion in metals is usually measured by milling thin layers from the surface, after diffusion has taken place from an electrodeposited layer; the activity in each layer is then determined. In diffusion experiments at room temperature much thinner layers must be removed by dissolution in a suitable etching solution.

DIFFUSION EQUATIONS

In the experiments discussed below, it is assumed that the tracer has a constant concentration at the metal surface, which is not strictly true until adsorption equilibrium is reached. This is not the same as in dry diffusion from an electrodeposited layer, where the surface concentration decreases with time. There are two methods of relating the activity pickup and the diffusion coefficient: (1) the total pickup is a function of time, and (2) the activity per unit volume at a given penetration depth after a given time is a function of depth. The equations are analogous to those for heat conduction and are discussed in books on that subject and on diffusion in solids (9); the solutions for *homogeneous* diffusion with the boundary conditions assumed here are described in detail by Darken and Gurry (10).

Total Activity as Function of Time

The activity flux per unit area at the surface (a measure of the number of atoms entering and leaving the metal) is given by:

$$da/dt = a_0 D^{\frac{1}{2}} (\Pi\, t)^{-\frac{1}{2}}, \quad [1]$$

where D is the diffusion coefficient (assumed constant). Integration gives

$$a_t = 2a_0 \Pi^{-\frac{1}{2}}\, (Dt)^{\frac{1}{2}}, \quad [2]$$

where a_t is the total activity acquired at time t. This equation is given by Gerischer and Vielstich (2) with the addition of a constant term for the initial rapidly acquired surface activity. If adsorption is slow as it is with silver, or if the surface changes in any way, the surface concentration represented by a_0 will not be constant.

Distribution of Activity in Depth

For homogeneous diffusion with constant a_0, the activity a_x at a given penetration distance x, after a fixed time t, is given, per unit area, by

$$a_x = a_0[1 - \mathrm{erf}\; x/(4Dt)^{\frac{1}{2}}], \quad [3]$$

where erf refers to the error function. If x can be made small enough and t large enough compared to D, it is convenient to use the expansion

$$\mathrm{erf(y)} = \frac{2}{\Pi^{\frac{1}{2}}}\left(\mathrm{y} - \frac{\mathrm{y}^3}{3} + \frac{\mathrm{y}^5}{5\times 2!} - \cdots\right) \quad [4]$$

and to neglect the higher terms. This gives

$$a_x = a_0 - a_0 x(\Pi\, Dt)^{-\frac{1}{2}}. \quad [5]$$

If thin layers can be etched from a specimen, the activity per milligram (for example) should be linear with x, or if self-absorption of radiation is negligible, the activity remaining on the specimen should be linear with x. This equation has never been tested so far as we know. Diffusion from a thin deposited layer requires that ln a_x be linear with x^2.

Can. J. Chem. Downloaded from www.nrcresearchpress.com by 190.90.36.8 on 09/04/12
For personal use only.

Grain-boundary Diffusion

Most of the work on exchange from solution has been done with polycrystalline metal specimens. There is no independent theory of grain-boundary diffusion, which is presumably most important at room temperature. Probably equation [2] should apply with an area term depending on grain size inserted. In diffusion from electrodeposited layers, $\ln a_x$ is linear with x rather than x^2.

An analysis of the relation between the grain-boundary diffusion coefficient D_b and the volume or lattice diffusion coefficient D_v has been made by Fisher (11), through the analogy with heat flow into thin metal sheets imbedded in a semi-insulating medium. His expression may be put in the following form:

$$[6] \qquad D_b = 2D_v^{\frac{1}{2}}(\log e)^2/\delta(d \log a_x/dx)^2 \, (\Pi t)^{\frac{1}{2}},$$

where e is the logarithm base, δ is the grain-boundary thickness. The equation requires that $\log a_x$ be linear with x, as is found in practice.

EXPERIMENTS WITH SILVER

Disks of 99.8% silver, of 5.56 cm² area (both sides), were prepared from commercial rolled sheet. Half of the disks were washed in alcohol–ether, immersed for 1 minute in 0.5 *M* KCN to remove surface compounds, washed, and stored in 0.5 *M* $AgNO_3$ (inactive) for 1 year. The other disks were annealed at about 700° C for several hours, cooled slowly, etched for 1 minute in dilute $KCN–H_2O_2$, washed, and stored in 0.5 *M* $AgNO_3$ for 8 months. The annealed disks were visibly crystalline and noticeably roughened.

All exchange experiments were carried out in 0.5 *M* $AgNO_3$ containing Ag^{110} as tracer. Measurement of activity pickup and conversion of counts per minute to gram atoms per cm² or apparent atomic layers (of complete exchange) were done in the usual manner.

Disturbing the Specimens

In previous work it has been found that frequent removal of silver coupons for washing and counting results in much more activity pickup than if they are undisturbed for an equal immersion time. This has been ascribed to removal of adsorbed salt from the surface (4, 7) or possibly to slight cold-working of the surface by handling (12). It is now certain that hot-water washing increases the internal diffusion which is obviously responsible for most of the pickup.

Several disks were immersed in the active 0.5 *M* $AgNO_3$ for periods up to 98 days. Some were removed frequently, washed in cold water, and counted, and these were found to acquire more activity than others which were counted only near the end of the period. The effect of washing in hot water is shown below.

Activity vs. Time

Twelve cold-rolled disks were taken from the storage solution, six were blotted, and six were washed in boiling water. All were immersed in active 0.5 *M* $AgNO_3$ and kept at room temperature (near 25° C). One of each group was removed each 10 days, washed, and counted. A group of 12 annealed disks was treated in the same way. The activity acquired was plotted vs. the square root of time, as shown in Figs. 1 and 2, as a test of equation [2]. The initial blotting or washing made no apparent difference.

While the points are quite scattered, especially in Fig. 2, it is not inappropriate to draw the straight lines shown, with intercepts of about one day. Gerischer and Tischer have shown that a similar plot, examined over a period of 9 days at 25° C, shows curvature upward during this time, with an intercept at zero time of about three apparent atomic

Can. J. Chem. Downloaded from www.nrcresearchpress.com by 190.90.36.8 on 09/04/12
For personal use only.

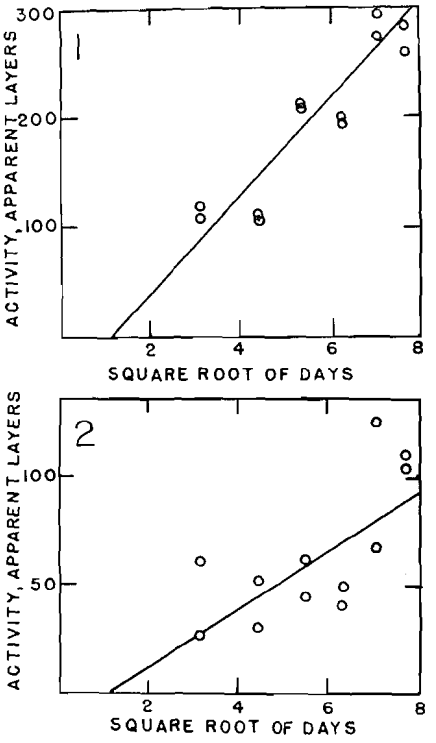

FIG. 1. Cold-rolled disks.
FIG. 2. Annealed disks.

layers (the activity acquired in a few seconds). The upward curvature could be due to two factors: (*a*) the slow establishment of adsorption equilibrium, and (*b*) diffusion along grain boundaries offers a continually expanding area from which lattice diffusion can take place.

Slopes of the straight lines of Figs. 1 and 2 may be inserted in equation [2] to calculate D. Apparent atomic layers are converted to gram atoms/cm^2 by multiplying by 19.9 $\times 10^{-10}$, and $a_0 = 5 \times 10^{-4}$ moles/cm^3, the solution concentration. This gives

$$\text{cold-rolled coupons:} \quad D = 2.0 \times 10^{-13} \text{ cm}^2/\text{sec};$$
$$\text{annealed coupons:} \quad D = 1.8 \times 10^{-14} \text{ cm}^2/\text{sec}.$$

It is probable that the cold-rolled silver has a larger grain-boundary area and volume than the annealed silver (or its equivalent in broken grains and imperfections) so that this "apparent" diffusion coefficient is larger.

Hoffman and Turnbull (13) have measured both lattice and grain-boundary diffusion in silver in the range 375–500° C by the dry method. For the latter they give the equation

$$D_b = 0.03 \exp(-20200/RT) \text{ cm}^2/\text{sec}.$$

Extrapolation to 25° C gives $D_b = 4 \times 10^{-17}$ cm^2/sec. If a_0 were taken as concentrations corresponding to 0.3 and 0.1 atomic layers of adsorbed ion respectively, this value for D would be obtained in the above calculations. Since the roughness factors of the coupons are unknown, and grain size is certainly a factor, further consideration is unwarranted.

Can. J. Chem. Downloaded from www.nrcresearchpress.com by 190.90.36.8 on 09/04/12
For personal use only.

Activity vs. Penetration Depth

Although exchange has been reported in most of the literature, in terms of apparent atomic layers of complete exchange, it is evident that exchange occurs to much greater depths. On etching silver coupons which had been immersed for a long time, activity was found to have penetrated as far as 2×10^{-4} cm (about 9000 atomic layers). A solution was prepared which is believed to dissolve silver uniformly: equal parts of (*a*) 0.5 g KCN in 150 ml water, and (*b*) 0.9 ml 30% H_2O_2 in 150 ml water.* A 2-minute etch in this mixture dissolved about 0.8 mg from one of the silver disks (840 layers). The disks were weighed after each etch and comparison was made with the total weight loss after a series of etches.

Four cold-rolled and four annealed coupons were immersed in active 0.5 *M* $AgNO_3$ and used in testing equation [6]. The results of the etching process are shown in Figs. 3 and 4, where log of activity remaining after each etch is plotted vs. weight lost. The history of

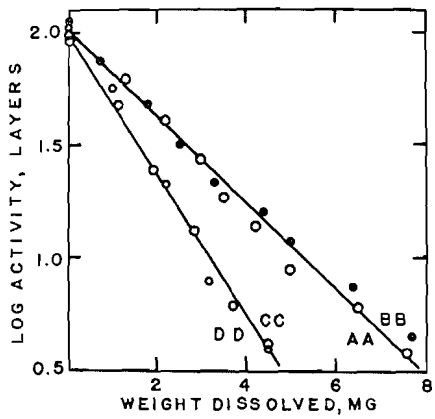

FIG. 3. Cold-rolled disks.

the disks follows: AA and BB were removed from solution three times, washed in boiling water, counted, and reimmersed; they were washed in boiling water at the end of the period (19 and 23 days); CC and DD were immersed for 20 days, washed in cold water, and stored in a desiccator for 18 days before etching; EE and FF were immersed for 50 days and etched immediately; GG was immersed for 20 days and stored for 30 days; HH was immersed 40 days and stored 10 days before etching. Evidently storage makes little difference, although the surface activity must decrease somewhat by diffusion inward; but washing in hot water is equivalent to using a higher temperature throughout.

The difference between the cold-rolled and the annealed specimens is striking. In the latter case 50–60% of the activity was removed in the first 0.8-mg etch. The grain area exposed to the solution is large, the grain-boundary area small, so that a larger part of the diffusion follows a different law. In any case the slopes of the lines drawn in Fig. 4 were used to calculate D_b.

The value of D_v used was taken from the work of Slifkin, Lazarus, and Tomizuka (14), who made measurements over a wider temperature range than Hoffman and Turnbull. Their equation for the temperature coefficient is:

$$D_v = 0.724 \exp(-45500/RT) \text{ cm}^2/\text{sec}$$

**The best evidence we have that this solution does etch the silver uniformly is the linearity of the plots in Fig. 3.*

Can. J. Chem. Downloaded from www.nrcresearchpress.com by 190.90.36.8 on 09/04/12
For personal use only.

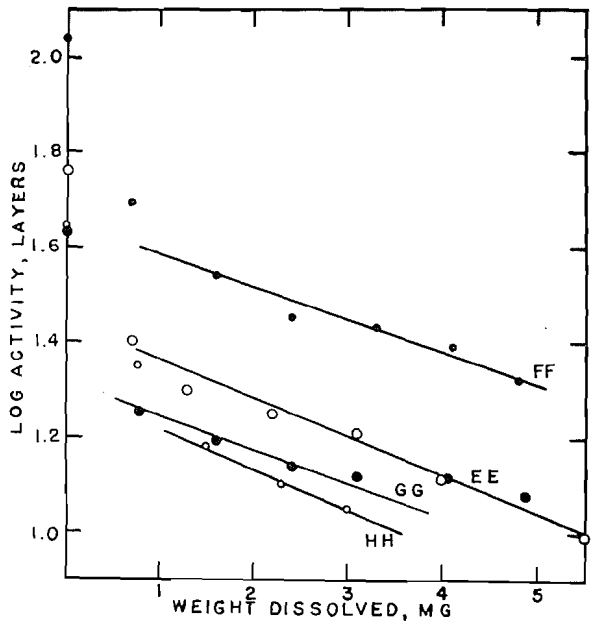

FIG. 4. Annealed disks.

from which $D_v = 4.4\times10^{-34}$ cm²/sec at 25° C. Fisher (11) suggested that δ, the grain-boundary thickness, be taken as 5×10^{-8} cm, and all other workers have used this figure. Inserting numerical values in equation [6], we obtain

$$D_b = 9\times10^{-11}/(\text{slope})^2 t^{\frac{1}{2}} \text{ cm}^2/\text{sec}.$$

In calculating the slope ($= d \log a_x/dx$), mg silver is multiplied by 1.7×10^{-5} to convert to centimeters for the disks used. The results are given in Table I.

TABLE I

Grain-boundary diffusion coefficients from the Fisher equation

Cold-rolled disks	(Diff. time, sec)$^{\frac{1}{2}}$	Slope $\times10^{-4}$ cm^{-1}	$D_b \times10^{21}$ cm²/sec
AA	1280	1.13	0.55
BB	1420	1.13	0.49
CC	1810	1.84	0.15
DD	1810	1.84	0.15
Annealed disks			
EE	2080	0.48	1.9
FF	2080	0.40	2.7
GG	2080	0.42	2.4
HH	2080	0.48	1.9

DISCUSSION

The fact that the values of D_b in Table I are 4 to 5 orders of magnitude smaller than that calculated from the high-temperature experiments, viz. 4×10^{-17} cm²/sec, is not surprising in view of the uncertain extrapolations and other factors. If D_v at 25° C is taken from the temperature-coefficient equation of Hoffman and Turnbull, our values of D_b become about 10^{-24} cm²/sec. The important thing is that continuing exchange *does*

Can. J. Chem. Downloaded from www.nrcresearchpress.com by 190.90.36.8 on 09/04/12
For personal use only.

depend on internal diffusion and that measurements *can* be made at room temperature. Gerischer and Tischer commented that the distribution of activity in depth would be useful to know, but that penetration was too shallow for successful measurements. We believe that the etching technique overcomes the difficulty.

Experiments with silver have the advantage that corrosion can be neglected. Similar experiments have been carried out in this laboratory with zinc and cadmium, in solutions which minimize corrosion; they will be described elsewhere. Plots of a_t vs. $t^{\frac{1}{2}}$ curve upward in the initial immersion period as with silver, and D is larger than D_b calculated from dry-diffusion work in the literature. The Fisher method again gives values which are smaller.

Work with single crystals is indicated, and is under way. Since the amount of adsorption on silver is known, equation [2] should apply directly if the surface area can be controlled. With the etching technique it should be possible to apply equation [3] in some form.

ACKNOWLEDGMENT

This report was in part made possible through assistance from the U.S. Army Office of Ordnance Research.

REFERENCES

1. VIELSTICH, W. and GERISCHER, H. Z. physik. Chem. **4**, 10 (1955).
2. GERISCHER, H. and VIELSTICH, W. Z. Elektrochem. **56**, 380 (1952). GERISCHER, H. and TISCHER, R. P. Z. Elektrochem. **58**, 819 (1954).
3. PROSKURNIN, M. and FRUMKIN, A. Z. physik. Chem. A, **155**, 29 (1931).
4. KING, C. V. and LEVY, B. J. Phys. Chem. **59**, 910 (1955).
5. MATSUURA, N. Sci. Papers Coll. Gen. Educ., Univ. Tokyo, **5**, 97 (1955).
6. TRAGERT, W. E. and ROBERTSON, W. D. J. Electrochem. Soc. **102**, 86 (1955).
7. KING, C. V. and SIMONSEN, A. J. Electrochem. Soc. **104**, 194 (1957).
8. KING, C. V. and SCHOCHET, R. K. J. Phys. Chem. **57**, 895 (1953).
9. CARSLAW, H. S. and JAEGER, J. C. Conduction of heat in solids. Oxford University Press, London. 1948. BARRER, R. M. Diffusion in and through solids. Cambridge University Press, London. 1951.
10. DARKEN, L. S. and GURRY, R. W. Physical chemistry of metals. McGraw-Hill Book Co., Inc., New York. 1953. Chap. 18.
11. FISHER, J. C. J. Appl. Phys. **22**, 74 (1951).
12. TINGLEY, I. I., HENDERSON, I. H. S., and COFFIN, C. C. Can. J. Chem. **34**, 14 (1956).
13. HOFFMAN, R. E. and TURNBULL, D. J. Appl. Phys. **22**, 634 (1951).
14. SLIFKIN, L., LAZARUS, D., and TOMIZUKA, T. J. Appl. Phys. **23**, 1032 (1952).

Can. J. Chem. Downloaded from www.nrcresearchpress.com by 190.90.36.8 on 09/04/12
For personal use only.

Can. J. Chem. Downloaded from www.nrcresearchpress.com by 190.90.36.8 on 09/04/12
For personal use only.

SOME ABNORMAL HYDROGEN ELECTRODE REACTIONS

D. J. G. IVES

ABSTRACT

A brief account is given of experiments in which gold electrodes, as a result of thermal deactivation in hydrogen, change from a state in which their behavior in relation to the hydrogen evolution reaction is normal to a state characterized by high positive rest potentials, greatly enhanced overpotentials which increase progressively during current flow, and which decay slowly on open circuit, generating potential–time curves which resemble desorption isotherms.

Conclusions based on these phenomena are supported by the results of experiments with poisoned platinum electrodes, which not only behave similarly but are also shown to retain reducing power for a limited time on open circuit.

It is suggested that electrodeposited hydrogen atoms may sometimes evaporate from an electrode into solution by a mechanism involving the participation of molecule-ions. A recent theoretical treatment of hydrogen overpotential can be extended to allow for the occurrence of such a final reaction step.

Hydrogen overpotential measurements have been made (1) using gold electrodes in the apparatus illustrated in Fig. 1, into which pre-electrolyzed, decinormal hydrochloric acid was delivered by pressure of hydrogen. Further pre-electrolysis of the solution was conducted by means of the ancillary gold electrode in compartment B. The gold test electrode in compartment A, arranged for even distribution of current over the whole of its surface, was supplied by a rapid flow of solution normal to each face by the powerful

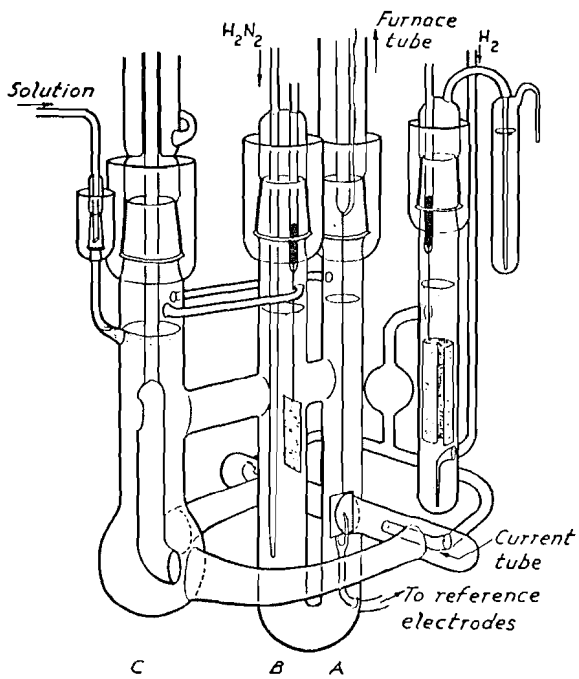

FIG. 1.

[1]*Manuscript received July 10, 1958.*
Contribution from the Department of Chemistry, Birkbeck College, University of London, London, England. This paper was presented at the Symposium on Charge Transfer Processes held at the University of Toronto, Toronto, Ontario, September 4 and 5, 1958.

centrifugal stirrer C. Except at the highest current densities, all hydrogen produced in the electrode reaction was removed in the dissolved state. Other features of the apparatus are self-explanatory and permit the stringent precautions known to be essential in hydrogen overpotential work to be observed.

Gold electrodes, cleaned by normal chemical methods, showed zero rest potentials with respect to a reversible hydrogen electrode in the same solution. On cathodic polarization, they gave rise to Tafel plots typified by Fig. 2. These plots show slopes consistent with rate-limitation by slow discharge, except where decreasing cathodic polarization allows the back-reaction to assume increasing significance; that the occurrence of a back-reaction must be entertained is shown by, *inter alia*, the effect of sweeping out the cell solution with nitrogen instead of hydrogen.

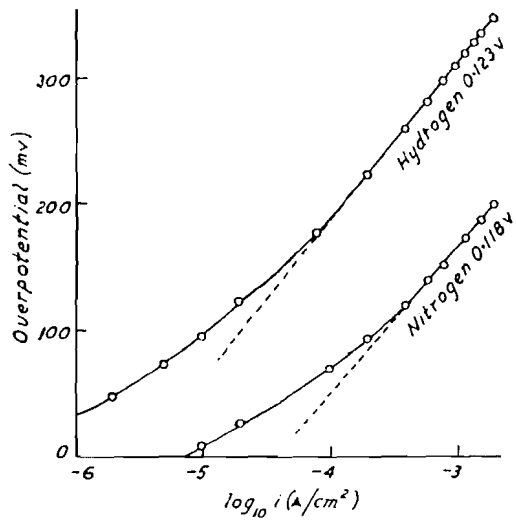

FIG. 2.

This behavior is reasonably normal. The main interest of these experiments arises from the results of withdrawing such a normal electrode from the solution into a silica furnace tube, forming an integral part of the apparatus, and subjecting it to prolonged annealing in hydrogen at temperatures falling from 800° C. On restoration of the cooled electrode to the same solution, its properties were found to be radically changed. It showed a rest potential of about +400 mv, complete insensitivity under all conditions to substitution of nitrogen for hydrogen passing through the cell solution, and greatly enhanced cathodic overpotentials which increased steadily with time and generated curved Tafel plots of varying, but excessively high, gradients. The behavior of the electrode on open circuit after cathodization was even more remarkable. On breaking the polarizing circuit, the negative potential of the electrode fell rapidly and linearly with log time to a value between −150 and −200 mv. From this point, the potential decayed more slowly, passing through zero in its progress to the original resting value of +400 mv. These changes were slow enough to allow some study to be made of the state of the electrode both before and after its potential passed through zero. Thus, connection via a microammeter to a reversible hydrogen electrode in the same solution caused anodic current to flow at the gold electrode whilst its potential was still negative, but cathodic current passed spontaneously under these same conditions when the gold electrode had attained

Can. J. Chem. Downloaded from www.nrcresearchpress.com by 190.90.36.8 on 09/04/12
For personal use only.

positive potentials. In both cases stirring enhanced the current flow, and in both cases the potentials recovered from their displacements towards zero after disconnection. It is thus clearly shown that the potentials through which the electrode passes after cathodic treatment are very well defined, decisively determined by the physical or chemical state of the electrode at each instant. In turn, each state of the electrode must be a function of the stage reached in a slow reaction leading to the final resting state.

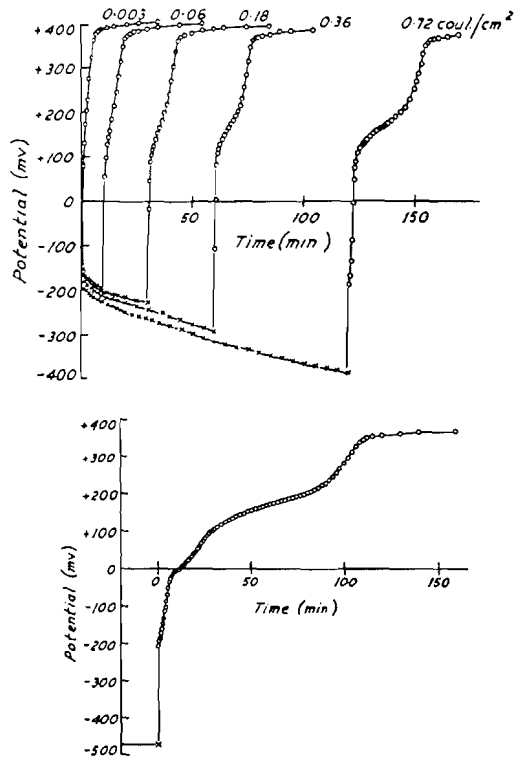

FIG. 3.

Two further facts assist in identifying this reaction. For a given constant current density of cathodization, the course of the open-circuit potential decay which follows depends systematically upon the duration of cathodization. This is illustrated in Fig. 3, where the results of six polarizations at 100 μa cm^{-2} are shown (in the last of these the growth of overpotential, during the cathodization period of 6 hours, is omitted). The form of the open-circuit potential–time curve depends strongly upon the current density in the preceding cathodization *up to a certain current density*, above which there is no such dependence. This is illustrated in Fig. 4, which shows the potential changes following 6-hour cathodizations at three current densities. Attention is drawn to the substantial identity of the curve relating to 20 μa cm^{-2} with that for 100 μa cm^{-2} in Fig. 3. It is believed that this effect is really due to the attainment during polarization of an electrode potential exceeding about -300 mv, when the subsequent potential decay curve assumes the same inflected form, which, for a given electrode, is remarkably reproducible.

There can be little doubt that the main effects of the heat treatment of the gold in hydrogen are the promotion of crystal growth (confirmed by microscopical examination)

Can. J. Chem. Downloaded from www.nrcresearchpress.com by 190.90.36.8 on 09/04/12
For personal use only.

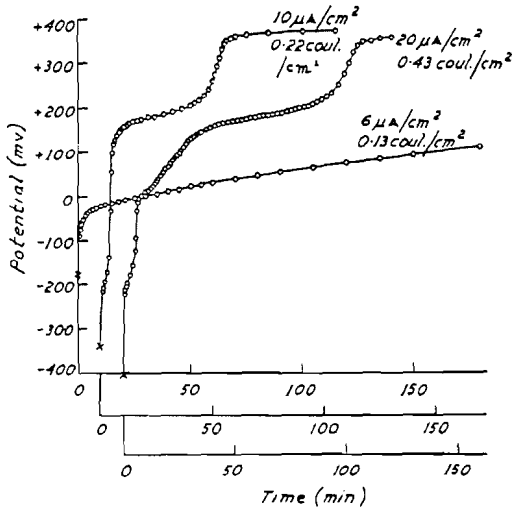

FIG. 4.

and the "burning-out" of catalytically active centers. Certainly, the gold becomes quite indifferent to its gaseous surroundings and is no longer capable of atomizing molecular hydrogen. It follows that it can no longer catalyze the recombination of hydrogen atoms.

The behavior of this thermally deactivated gold as a substrate for the hydrogen evolution reaction is only intelligible in terms of the progressive accumulation of electromotive material during cathodization, and the only material which presents itself is atomic hydrogen. The conclusion is reached that annealed gold forms a "non-equilibrium hydrogen electrode" at which cathodically generated hydrogen atoms pile up and are unable to escape by any *facile* mechanism: combination, evaporation, electrochemical desorption, or ionization. All of the partial processes which are mobile at the reversible hydrogen electrode have become strongly hindered, so that the electrode potential cannot at any stage be determined by a Nernst relation.

In terms of this hypothesis, the sequence of events during cathodization and afterwards is pictured as follows. Hydrogen atoms accumulate at the surface of the electrode at a rate determined by the current density and, normally, the processes by which they leave the surface increase in rate until a steady kinetic state is established. But when these processes are very slow, then at all but the lowest current densities, the accumulation of atoms may become extensive and lead to progressive changes in the properties of the electrode surface, perhaps by the burning-out or saturation of the few remaining active centers. If there is an upper limit to rate of dissipation of hydrogen atoms, not dependent upon potential, *and not kinetically linked with the discharge process*, there will clearly be a critical rate of discharge. For rates of discharge less than this, a kinetic steady state may be established; for higher rates, the accumulation of atoms may proceed unchecked and lead to progressive saturation. Since rate of discharge is a function of electrode potential, this is consistent with the observation that the attainment of a critical potential has a profound effect upon subsequent electrode behavior. The slow and prolonged growth of overpotential, and the dependence of open-circuit potential decay upon the time for which cathodization is continued, coupled with its independence of the current density of cathodization above a certain minimum, strongly suggest that hydrogen atoms penetrate the gold lattice. Gold does not dissolve hydrogen from the

Can. J. Chem. Downloaded from www.nrcresearchpress.com by 190.90.36.8 on 09/04/12
For personal use only.

molecular gas phase, but it has recently been shown (2) that an evaporated film of gold takes up gaseous hydrogen atoms quite rapidly; it is believed that a gold cathode which is incapable of catalyzing atom recombination will do the same. If this bulk penetration of the gold can be accepted, then the inflected potential decay curves have a more than superficial relationship to the desorption isotherms (as of hydrogen from palladium) which they so strikingly resemble.

These conclusions have been supported in more detail elsewhere (1), and further discussion must give way to an attempt to meet the obvious demand to demonstrate the alleged heavy, slowly dispersing accumulations of hydrogen atoms at such inactive electrodes.

This has been done with the aid of poisoned platinum electrodes (3) in an apparatus illustrated in Fig. 5, which is largely self-explanatory. The hemispherical platinum "microelectrode" C, cathodized in 0.001 *N* hydrochloric acid by means of the very large hydrogen electrode A, could be depressed at will against a sintered glass "target" F, which carried a deposit of tungsten trioxide, and through which the cell solution was

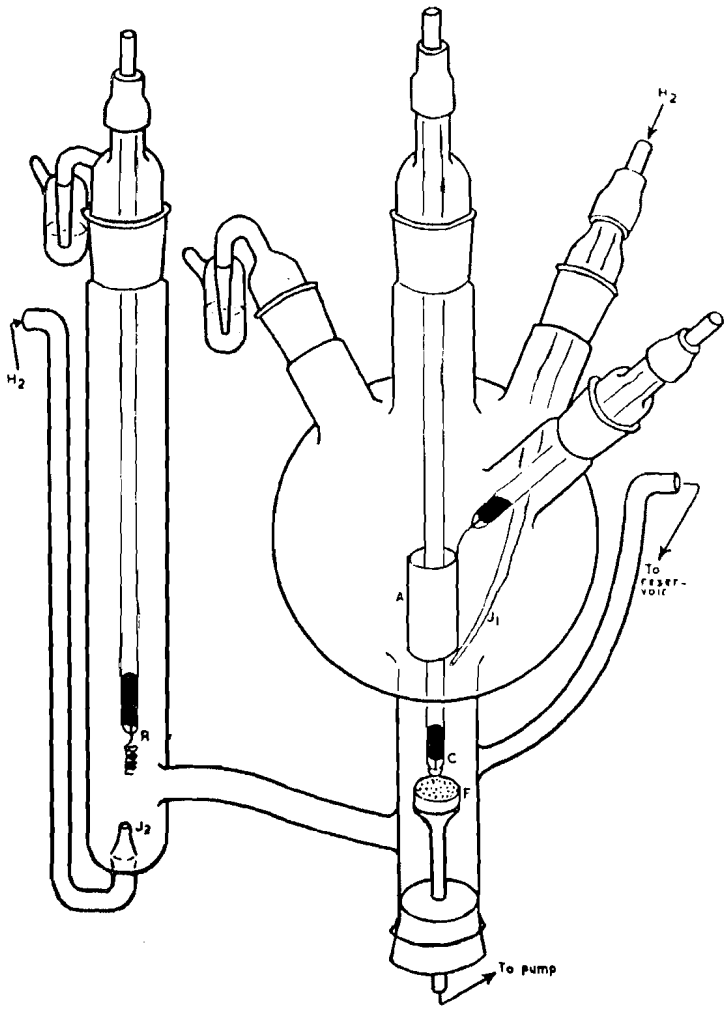

FIG. 5.

Can. J. Chem. Downloaded from www.nrcresearchpress.com by 190.90.36.8 on 09/04/12
For personal use only.

continuously drawn. Since poisoned systems were to be studied, rigorous techniques were not employed and the electrodes were studied in three states: (1) ostensibly unpoisoned, (2) poisoned by an electrodeposition of mercury, and (3) additionally poisoned by 10^{-5} mole l^{-1} of mercuric chloride in the cell solution.

The electrodes showed positive rest potentials increasing from 350 to 625 mv with increasing degrees of poisoning (adventitious and deliberate), and very high and erratic overpotentials during cathodic polarization, rising to tens of volts at the maximum current density of about 125 ma cm^{-2}. Even under these extreme conditions, involving blackening and disruption of the electrode surface, the overpotentials remained strongly influenced by poisoning. After cathodization, the negative electrode potentials decayed in a slow and inflected way on open circuit. Provided that a limiting current density had been exceeded in the preceding cathodization, the potential–time curves showed arrests, of length roughly proportional to current density and duration of cathodization; some examples of these curves are shown in Fig. 6.

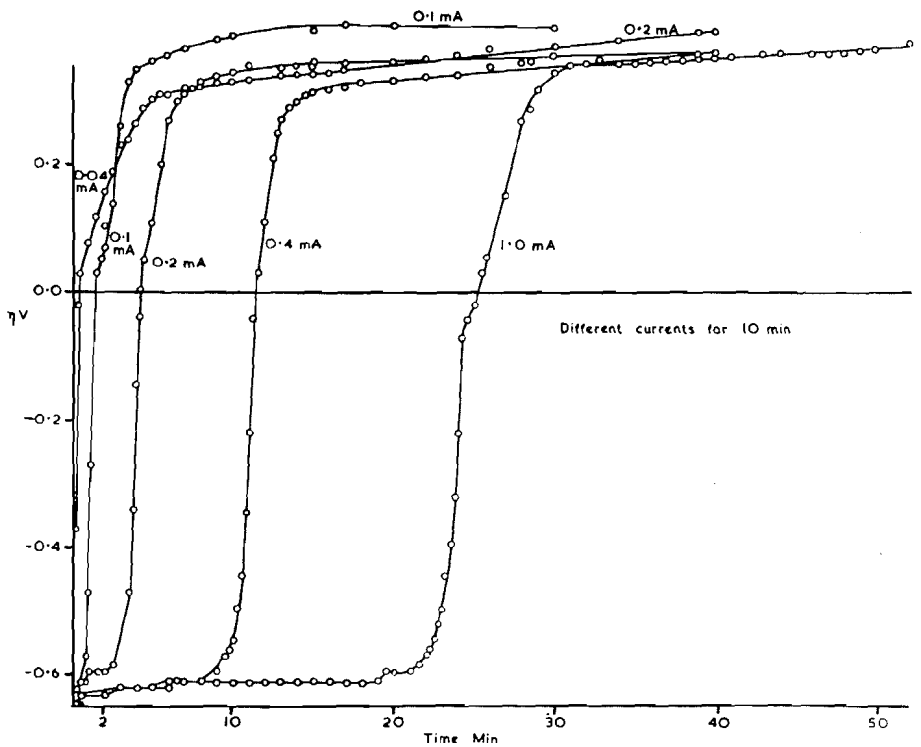

FIG. 6.

A closer correspondence to the behavior of the annealed gold electrodes could hardly be expected, and there can be little doubt that very similar phenomena are involved in the two cases. It was now possible, however, to carry out a chemical test for the presence of a cathodic product with reducing properties, by bringing the cathode into contact with the tungsten trioxide target. Contact established during current flow produced an immediate imprint of tungsten blue, no doubt owing to electronic conduction. For the unpoisoned electrodes, this property vanished instantly the circuit was broken, but it was retained on open circuit by the poisoned electrodes to an extent systematically

Can. J. Chem. Downloaded from www.nrcresearchpress.com by 190.90.36.8 on 09/04/12
For personal use only.

related to the duration and current density of cathodization and the degree of poisoning. It was possible to follow the decay of reducing power with time in an approximate way by producing imprints in a standardized manner, and by assessing their depth of color in terms of an arbitrary scale of "color numbers" having a maximum of 10 set by an imprint produced during current flow. It is hoped in due course to improve upon the *ad hoc* device used in this preliminary work. For a standard time of cathodization of 30 minutes at a uniform current density of 25 ma cm^{-2}, the results shown in the following table were obtained.

TABLE I

	Electrode state (2)		Electrode state (3)	
Decay interval	Potential on making contact, mv	Color No.	Potential on making contact, mv.	Color No.
3 seconds	−646	8	−646	10
10 seconds	−646	7	−646	10
30 seconds	−596	4	—	—
1 minute	−546	3	−621	9
5 minutes	−509	2	−621	5
10 minutes	+79	1	−496	3
30 minutes	+159	0	−483	1

It is evident that the residual reducing power was not directly linked with electrode potential, and was in fact often retained when this potential had become positive. It is suggested that these experiments support the conclusion previously drawn.

It may be that this work has some importance as a basis for the view that consideration of the hydrogen evolution reaction has perhaps been too closely confined within the narrow framework of but three reaction steps succinctly denoted by the names Volmer, Tafel, Horiuti (VTH), one or other of which, it is almost universally assumed, must be rate-limiting. One is still invited to accept the gullet-sticking conclusion that at platinum electrodes atom recombination is very fast but is rate-limiting, whilst at mercury it is very slow but is not rate-limiting. The work of the Knorr school (4) has shown the weakness of much of the evidence relating to low overpotential metals and has strongly reinforced the inverse relation established by Bonhöffer (5) between overpotential and catalytic power. This relation has been discounted (6) on the basis of work by Schechter (7) which does not, in the author's view, have any relevance. The fact remains that for eight common metals the sequence of increasing overpotential is the same as the sequence of decreasing catalytic activity, and the chance that these two sequences should occur *un*related to each other is about 1 in 1.6×10^9. But it was the assumption that this obvious relationship required the rate-limiting step in the hydrogen evolution reaction to be atom recombination that was false.

The evidence that slow discharge is rate-controlling at mercury electrodes is strong, but there is no satisfactory evidence at all about the subsequent stages of the reaction at this metal (8, 9). The elegant potentiostatic experiments of Gerischer and Mehl (9) suggest that the mercury surface is bare of hydrogen atoms. What then happens to the atoms that are deposited? It must be admitted that the present position is not altogether satisfactory.

Reconsideration of the work of Kobosew and Nekrassow (10) appears to be desirable for two reasons. A relation was established between hydrogen overpotential at horizontally disposed electrodes of various metals and the degree of reduction of tungsten

Can. J. Chem. Downloaded from www.nrcresearchpress.com by 190.90.36.8 on 09/04/12
For personal use only.

trioxide suspended in the electrolyte above the electrodes. The interpretation of this in terms of atomic hydrogen was attacked by the Frumkin school (11), but the resulting polemical exchanges have, in the author's view, been resolved by Poltorak (12), who has convincingly demonstrated "reduction at a distance" (of about 0.5 μ) from a high overpotential cathode, as well as retention of reducing power after cathodization. The present work confirms the latter result, and invites more serious attention to the views of Kobosew. In the earlier paper with Nekrassow (10), he considered both penetration into the metal phase and free evaporation into solution as possible fates for electrodeposited hydrogen atoms, and first introduced, in a rather generalized form, what is now known as electrochemical desorption and generally associated with the name of Horiuti. He has maintained his views for over twenty years, and his quite recent "adsorption theory of hydrogen overpotential" (13), in spite of certain weaknesses, very adequately explains the opposite effects of poisons on the catalytic and "electrocatalytic" activities of metals.

It appears that more attention is now being given to the role of adsorbed hydrogen atoms in relation to hydrogen overpotential, and one of the most satisfactory discussions is due to Gerischer (14), although still largely confined within the VTH framework. The suggestion is made that his treatment could be extended along the following lines.

There is no lack of evidence that hydrogen atoms can exist in solution for a finite time and no reason to suppose that, generated at an electrode, they need be in equilibrium with the gas phase, need be potential-determining according to a Nernst relation, or are unable ever to leave the electrode by evaporating into the solution. Developments in radiation chemistry have established the molecule-ion, H_2^+, as an intermediate of frequent occurrence, and it is suggested that it may well be concerned in an evaporative process. Coulson has recently emphasized (15) that this entity, one sixth of the size of the hydrogen atom, has its single electron almost exclusively located in regions between the nuclei. The protons are therefore substantially unscreened from the outside, so that the molecule-ion may be expected to behave as if it were two halves of a proton separated by about 1 Å. In this case, its considerable bond energy of 61 kcal mole^{-1} might be expected to be supplemented in aqueous solution by a hydration energy of the same order of magnitude as that of the proton itself (282 kcal g-atom^{-1}). An upper limit to this hydration energy of 255 kcal mole^{-1} has in fact been calculated (16), and it can be shown that a lower limit of 221 kcal mole^{-1} is needed to make the reaction $H + H^+_{hydr.} = H_2^+{}_{hydr.}$ exothermic. It is considered to be very likely that the hydration energy lies between these limits, or is at least large enough to make the hydrogen molecule-ion an entity very frequently to be reckoned with in aqueous solution in any reaction ostensibly involving hydrogen atoms.

If this can be accepted, a ready means can be seen for the desorption of hydrogen atoms from an electrode at which the absorption energy is not too great. What happens to these atoms when they have diffused, as molecule-ions, some few Angstroms from the electrode surface ceases to be a part of the electrochemical problem! In alkaline solutions, the alternative reaction $H + H_2O = H_2^+{}_{hydr.} + OH^-_{hydr.}$ may well operate, for it does not seem to be unduly disfavored energetically. Gerischer's calculations may be adapted to this suggestion and, assuming that the standard free energy of hydration of the molecule ion is 50 kcal mole^{-1} less negative than that of the proton, they indicate that for an adsorption energy of hydrogen atoms less than about 30 kcal g-atom^{-1}, an evaporative process involving molecule-ions might well follow a rate-limiting discharge step. It seems appropriate to suggest the name "Kobosew step" for this final stage, which is thought to be operative for high overpotential metals such as mercury.

Can. J. Chem. Downloaded from www.nrcresearchpress.com by 190.90.36.8 on 09/04/12
For personal use only.

It is undeniable that the molecule-ion must be a participant, however transitory, in the Horiuti (electrochemical desorption) step. It is therefore tempting to envisage a transition state which could break down in two ways, according to whether desorption or electron transfer were the easier.

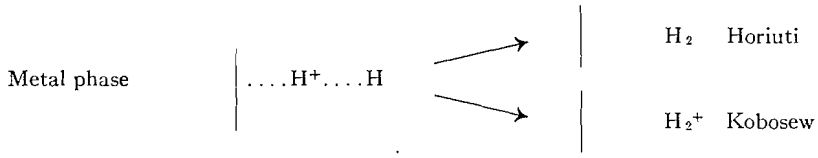

It is clear that the distinction between various proposed mechanisms for the hydrogen evolution reaction depends upon the sequence of acts of discharge, combination, and desorption. The suggestion is now made, in a provocative rather than a didactic spirit, that the usual assumption that desorption must be preceded by, or coupled with, completion of discharge of all the ions involved is not necessarily true.

REFERENCES

1. IVES, D. J. G. and SWAROOPA, S. J. Chem. Soc. 3489 (1955).
2. TOMPKINS, F. C. Private communication.
3. GUTT, W. and IVES, D. J. G. Proc. Chem. Soc. (London), 344 (1957).
4. KNORR, C. A. Z. Elektrochem. **59**, 647 (1955).
5. BONHÖFFER, K. F. Z. physik. Chem. **113**, 199 (1924); Naturwiss. **6**, 219 (1927).
6. BOCKRIS, J. O'M. J. Electrochem. Soc. **99**, 366C (1952).
7. SCHECHTER, A. Acta Physicochim. U.R.S.S. **10**, 379 (1939).
8. FRUMKIN, A. Acta Physicochim. U.R.S.S. **18**, 23 (1943).
9. GERISCHER, H. and MEHL, W. Z. Elektrochem. **59**, 1049 (1955).
10. KOBOSEW, N. I. and NEKRASSOW, N. Z. Elektrochem. **36**, 529 (1930).
11. BAGOTSKY, V. S. and JOFA, Z. A. Compt. rend. acad. sci. U.R.S.S. **53**, 439 (1946). FRUMKIN, A. N., JOFA, Z. A., and BAGOTSKY, V. S. Zhur. Fiz. Khim. **25**, 1117 (1951).
12. POLTORAK, O. M. Zhur. Fiz. Khim. **27**, 599 (1953).
13. KOBOSEW, N. I. Zhur. Fiz. Khim. **26**, 112 (1952).
14. GERISCHER, H. Z. physik. Chem. (Frankfurt), **8**, 137 (1956).
15. COULSON, C. A. J. Chem. Soc. 778 (1956).
16. RIGG, T., STEIN, G., and WEISS, J. Proc. Roy. Soc. (London), A, **211**, 375 (1952). RIGG, T. and WEISS, J. J. Chem. Phys. **20**, 1194 (1952).

Can. J. Chem. Downloaded from www.nrcresearchpress.com by 190.90.36.8 on 09/04/12
For personal use only.

Can. J. Chem. Downloaded from www.nrcresearchpress.com by 190.90.36.8 on 09/04/12
For personal use only.

CATHODIC POLARIZATION OF SILVER IN SULPHURIC ACID[1]

A. A. Antoniou and F. E. W. Wetmore

ABSTRACT

The hydrogen overpotential on fine silver cathodes has been determined from 2 to 35° and over a current density range from 0.03 to 2000 μa cm^{-2}. Two Tafel slopes were observed, RT/F at low currents, $2RT/F$ at high currents. The stoichiometric number was found to be one and the symmetry factor one-half at low currents. The heat of activation changed from 18.8 kcal at low currents to 14.3 at high currents.

EXPERIMENTAL METHODS

The silver cathodes were of high purity (less than 0.001% impurity) and in the form of single crystal and polycrystalline slabs. After being electropolished the metal was held in a hot hydrogen atmosphere for a few days; a small amount of silver was removed by gentle anodizing. Electrodes so treated were more consistent in their behavior than those not strongly hydrogenated; the latter gave high Tafel slopes, as mentioned by Frumkin (3). Teflon containers exposed only one surface of the slab (110 or 111 plane of the single crystals), of area about 3.5 cm^2.

The anode and the Luggin probe were both hydrogen electrodes. A platinum electrode used for pre-electrolysis could be swung out of the solution when not required. In all the experiments the electrolyte was molar H_2SO_4, made up from triply-distilled reagents. All parts of the cell were maintained under a slightly positive pressure of purified hydrogen.

The cells were mounted in an air bath kept within 0.1° of the desired temperature. A danger in lesser control lies in the variation of the temperature of the probe electrode, which usually has a small heat capacity.

Polarizing currents were kept constant by an electronic regulator. Potential difference between probe and cathode was imposed on a direct-coupled amplifier having an input resistance of 10^{10} ohms; the output could be coupled to either a potentiometer or one of three recording devices. For slow changes an Esterline-Angus recorder (0.5 sec) was convenient; for more rapid changes a Kipp galvanometer (0.01 sec) and drum camera were used; a direct-coupled oscilloscope and fixed camera were used for fast changes. In order that transient fluctuations associated with mechanical contacts could be avoided, rapid build-ups and decays were initiated by a thyratron switch.

RESULTS

Rest-potential

The potential E_r to which the electrode decays after removal of the polarizing current can give information about the purity of the system. The most likely contaminant is oxygen. Experiment has shown that oxygen promotes the corrosion of silver and thus the rest-potential can be viewed as an indicator of the silver ion activity or the equivalent effective concentration of oxygen. For the conditions used here, and at 25°, the partial pressure of oxygen above the electrolyte would correspond to

$$\log p_{O_2}(\text{atm}) = 68E_r - 84.$$

[1]*Manuscript received July 12, 1958.*
Contribution from the Department of Chemistry, University of Toronto, Toronto 5, Ontario. This paper was presented at the Symposium on Charge Transfer Processes held at the University of Toronto, Toronto, Ontario, September 4 and 5, 1958.

In most of the experiments E_r lay in the range 0.35 to 0.45 volt positive, but in several was substantially less positive. For example, in a particular series the decays occurred within minutes to zero potential and after 8 hours to only 17 mv positive.

Overpotential–Current Relationships

The Tafel plot was found to consist of two distinct linear portions, as exemplified in Fig. 1. Table I gives the slopes, the exchange current densities, and the potential of intersection of the pairs of lines.

The low current slope corresponded closely to RT/F until the electrode had been polarized and allowed to decay many times. The slope then increased, as the time sequences show. It was evident from examination of electrodes used over long periods that some silver had dissolved and been redeposited; a change in the surface was apparent.

TABLE I

Overpotential–current relationships

Date	Temp., °C	Tafel B = 2.3b	i_0, μa cm^{-2}	Tafel B = 2.3b	i_0, μa cm^{-2}	Intersection, mv
			Cell 1, 110 face no. 1			
4.9	25	0.057	0.20			
7.9	15	0.058	0.12			
10.9	34.5	0.056	0.26			
11.9	5.5	0.057	0.026			
26.9	12	0.063	0.21			
30.9	2.5	0.066	0.041	0.122	0.72	180
2.10	2.5	0.075	0.029	0.120	0.35	220
3.10	10	0.073	0.038	0.120	0.43	195
4.10	20	0.067	0.049	0.125	0.93	187
5.10	30	0.065	0.10	0.121	1.6	180
7.10	2	0.081	0.017	0.120	0.11	220
9.10	20	0.074	0.043	0.120	0.49	210
9.11	20	0.095	0.12			
			Cell 3, polycrystalline face			
5.12	20	0.060	0.33	0.112	6.0	160
14.12	20	0.061	0.24	0.111	3.6	160
21.12	7	0.063	0.045	0.115	1.2	200
			Cell 2, 111 face			
8.12	20	0.060	0.24	0.109	4.2	166
14.12	20	0.060	0.36	0.115	6.3	156
			Cell 1, 110 face no. 2			
7.3	26.5	0.069	0.044	0.121	1.2	195
8.3	13.4	0.073	0.012	0.121	0.38	220
11.3	26	0.068	0.044	0.120	1.3	220
12.3	14	0.073	0.012	0.114	0.24	260
19.3	14.5	0.081	0.031	0.116	0.28	250
			Cell 3, 111 face			
30.3	25.5	0.060	0.20	0.117	6.7	190
31.3	25.5	0.058	0.25	0.117	9.4	175
1.4	13	0.058	0.097	0.110	3.3	190
3.4	2	0.061	0.079	0.109	1.6	180
4.4	1.4	0.061	0.042	0.111	1.7	192
5.4	14	0.058	0.10	0.114	3.9	188
6.4	28.3	0.054	0.19	0.120	10.0	178
7.4	27.9	0.052	0.19			
8.4	13	0.055	0.076			
10.4	2.5	0.060	0.039			
18.4	3.7	0.063	0.033	0.107	1.1	220
24.5	5.	0.083	0.030			
7.6	4.4	0.079	0.021			
9.6	4.5	0.080	0.024			
11.6	6.7	0.091	0.054			

Can. J. Chem. Downloaded from www.nrcresearchpress.com by 190.90.36.8 on 09/04/12
For personal use only.

The high current slope remained at approximately $2RT/F$ throughout the experiments.

The change from one slope to the other occurred over a small range of current and potential in any particular run. The average potential of intersection was 196 ± 20 mv. The current density of intersection, like the exchange current densities associated with the two linear portions of the Tafel curve, showed considerable scatter, but for each electrode showed a systematic change with temperature. It is clear that these current parameters depend not only on the temperature, but also on the effective surface area, as evidenced by variation of the capacitance of the electrode in the same sense as the variation in i_0.

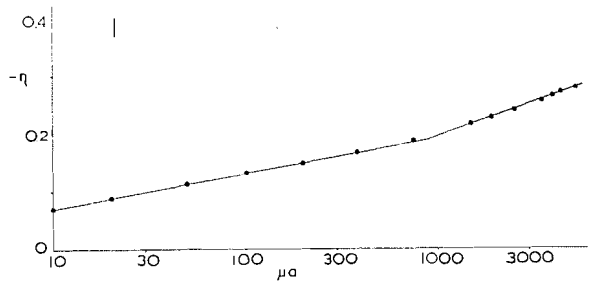

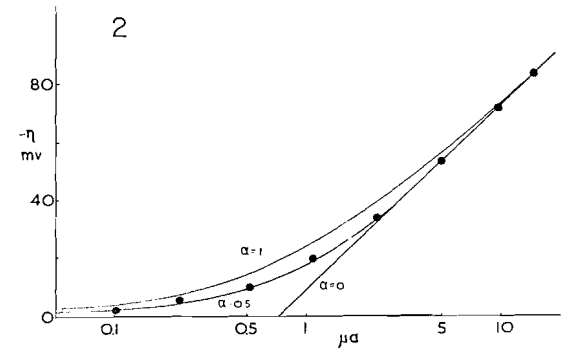

FIG. 1. Typical overpotential–current relationship.
FIG. 2. Low current overpotential–current plot.

Symmetry Factor and Stoichiometric Number

The dots of Fig. 2 show the relationship of the overpotential and the current found when decay occurred to zero potential (oxygen practically absent). The bend from linearity indicates clearly that omission of a term for reverse current makes Tafel's equation (shown by the line marked $\alpha = 0$) unsuitable for the range of current below about $10i_0$. Figure 3 shows the plot of the expression

$$i = 2i_0 . \sinh(-\eta/b)$$

proposed earlier (4) as an improvement over Tafel's expression, but premised on symmetry of energy division ($\alpha = 0.5$).

The curves of Fig. 2 express the equations

$$\begin{aligned}
&\text{(asymmetric, } \alpha = 1) \quad i = i_0[\exp(-36.6\eta) - 1] \\
&\text{(symmetric, } \alpha = 0.5) \quad i = i_0[\exp(-36.6\eta) - \exp(36.6\eta)] \\
&\qquad\qquad\qquad\qquad = 2i_0 . \sinh(-36.6\eta) \\
&\text{(asymmetric, } \alpha = 0) \quad i = i_0 \exp(-36.6\eta)
\end{aligned}$$

Can. J. Chem. Downloaded from www.nrcresearchpress.com by 190.90.36.8 on 09/04/12
For personal use only.

in which the factor 36.6 is the value of $1/b$ found from consideration of the whole range of current below the change of slope of the Tafel plot. The curve indicating symmetry is in close agreement with experiment.

The stoichiometric number has been defined (5) at high overpotentials by

$$\nu = \alpha nFb/RT$$

and at low overpotentials by

$$\nu = -(nFi_0/RT)(\partial\eta/\partial i)_{\eta\to 0}.$$

As $$\eta \to 0, \sinh(-\eta/b) \to -\eta/b$$

and $$-\partial(\eta/b)/\partial i \to \partial \sinh(-\eta/b)/\partial i = 1/2i_0.$$

Hence $\nu = nFb/2RT$, which is simply the first definition with $\alpha = 0.5$.

Since at low currents b was found to be RT/F and α to be 0.5, the corresponding value of ν is $n/2 = 1$. Owing to the change in slope of the Tafel plot, it is not possible to determine the values of α and ν separately at high currents; all that can be said is that $\nu/\alpha = 4$, to agree with $b = 2RT/F$.

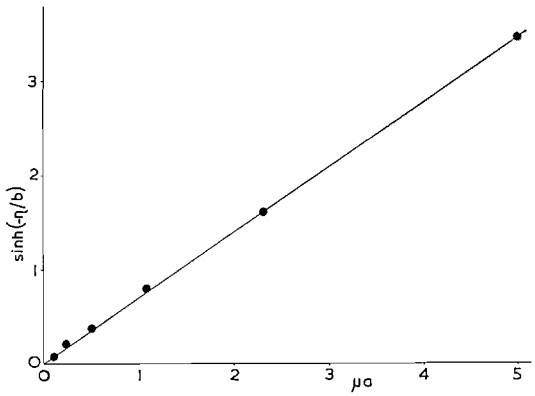

FIG. 3. Linear function plot.

Temperature Dependence of Overpotential

On varying the temperature at constant current and confirming that the overpotential did return to its original value when the original temperature was re-established, the data of Table II were found.

Diffusion of Hydrogen in Silver

In order to determine whether hydrogen diffuses appreciably through silver, an experiment was carried out with a thin silver foil separating two portions of electrolyte. While one face was polarized at 3 ma cm^{-2}, a probe on the other face showed no change of potential.

Build-up and Decay Curves

The change of potential during polarization and in decay was examined, but not as intensively as the steady state overpotential. There are a few points which may merit mention.

At constant charging current the potential build-up was linear with time and then bent off smoothly to the constant value of overpotential, usually taking longer to reach a steady state than would be expected from the simple expression for build-up (4), and sometimes showing a slight drop after the rapid part of the build-up. In some runs, in

Can. J. Chem. Downloaded from www.nrcresearchpress.com by 190.90.36.8 on 09/04/12
For personal use only.

TABLE II

Variation of overpotential with temperature

c.d. μa cm^{-2}	Temp. range, ° C	$\Delta\eta/\Delta T$, mv deg^{-1}	Tafel B	ΔH, kcal mole^{-1}	No. of determinations
		Cell 2, polycrystalline			
12.5	13.4–25.7	−2.54	0.060	16.7	2
	5.9–13.4	−3.0	0.060	18.3	1
25	13.0–25.5	−2.7	0.060	17.7	2
	6.2–13.0	−3.0	0.060	18.3	1
125	13–25	−3.8	0.116	12.8	3
	7–13	(−5.5)	0.112	(18.6)	1 (not precise)
250	13–25	−4.2	0.116	14.3	8
	7–13	−4.1	0.112	13.6	8
		Cell 2, 111 face			
15.6	13.4–25.7	−3.1	0.060	20.2	2
	5.9–13.4	−3.2	0.060	19.5	1
31.2	13.0–25.5	−3.1	0.060	20.2	2
	6.2–13.0	−3.3	0.060	20.2	1
156	13–25	−4.3	0.116	14.6	4
	7–13	−4.15	0.112	13.6	3
312	13–25	−4.7	0.116	15.9	7
	7–13	−4.3	0.112	13.9	6

Average ΔH, weighted for number of determinations:
low currents, 18.8; high currents, 14.3.

which oxygen was known to be present, the initial part of the curve was sigmoid, as would be expected. The apparent capacitance was usually high at very low polarizing currents; capacitances determined through analysis of decay curves did not generally show this same behavior.

Most decays showed linearity of potential in $\log(t+\theta)$ when θ was chosen appropriately (4), but this was not always so for the highest currents. Decay curves taken with the oscilloscope did not show linearity of the potential with time, even initially.

DISCUSSION

Bockris and Conway (2) and Bockris, Ammar, and Huq (1) studied the overpotential on silver in various concentrations of HCl at room temperature. Their results are compared with those found in this work:

	B–C			B–A–H		A–W
	0.1	1.0	5.0	0.1	0.4 *N* HCl	2 *N* H_2SO_4
B, low i	0.09	0.06	0.07	0.057	0.058	0.059
B, high i	0.12	0.13	0.12	0.097	0.101	0.116
Potential of intersection	0.27	0.19	0.28	0.07	0.15	0.20

The present work supports the existence of two distinct Tafel slopes, agrees with the low current slope of B–A–H and the low current stoichiometric number unity, adds that the value of α at low currents is 0.5, and shows a high current slope of $2RT/F$, which lies between the earlier sets. The present work shows that there is a rise in the low current slope as the electrode is worked and that this change may be related to the surface condition; there is no evidence that the change is caused by surface contamination.

Bockris and Conway attributed the existence of two slopes to a phenomenon related to the adsorption of H_3O^+ on the electrode and suggested that the mechanism is probably slow discharge followed by combination.

Can. J. Chem. Downloaded from www.nrcresearchpress.com by 190.90.36.8 on 09/04/12
For personal use only.

Bockris, Ammar, and Huq pointed out that the low current slope, RT/F, cannot be explained in terms of simple interpretation of mechanisms already proposed, except by assumption of unrealistic values of α. In order to account for the slope they proposed two explanations. The first of these involves migration of H on the metal surface; they considered it unsatisfactory for silver. Their second and preferred explanation is based on the nearness of the overpotential to the electrocapillary maximum potential and leads to the conclusion that the slope of the Tafel plot can depend on the electrode potential and have the value $2RT/F$ as a maximum. They concluded that electrochemical desorption is the slow step throughout, but did not offer proof that $\nu = 1$ at high currents.

These earlier reports were not in agreement on the low current slope, the high current slope, the variation of the low current slope with concentration, or the potential of intersection. From the second study (B–A–H) there is no indication that the low current slope varies with concentration and it is striking that the present work, at higher acid concentration, shows practically the same value. The considerable variation in the potential of intersection, even in the same solution (0.1 N HCl), raises doubt about the validity of the second explanation (B–A–H) for the change in slope.

Both the sharpness of the break in the Tafel curve and the discontinuity of the heat of activation in going from low to high current point to a change in the nature of the rate-determining step as the current is increased. At high current a slow discharge step with $\alpha = 0.5$ would lead appropriately to $\nu = 2$ and $b = 2RT/F$. At low current $\nu = 1$, which rules out the discharge process as the rate-determining step. The slope, $b = RT/F$, could be attributed to slow surface migration or to another process which is first order with respect to H.

The authors gratefully acknowledge financial support from the National Research Council through Grant A 412.

REFERENCES

1. Bockris, J. O'M., Ammar, I. A., and Huq, A. K. J. Phys. Chem. **61**, 879 (1957).
2. Bockris, J. O'M. and Conway, B. E. Trans. Faraday Soc. **48**, 724 (1952).
3. Frumkin, A. Discussions Faraday Soc. **1**, 57 (1947).
4. Morley, H. B. and Wetmore, F. E. W. Can. J. Chem. **34**, 359 (1956).
5. Parsons, R. Trans. Faraday Soc. **47**, 1332 (1951).

Can. J. Chem. Downloaded from www.nrcresearchpress.com by 190.90.36.8 on 09/04/12
For personal use only.

Can. J. Chem. Downloaded from www.nrcresearchpress.com by 190.90.36.8 on 09/04/12
For personal use only.

TRANSPORT OF HYDROGEN THROUGH PALLADIUM-CLAD ELECTRODES

SIGMUND SCHULDINER AND JAMES P. HOARE[2]

ABSTRACT

Electrochemical polarization studies of the transport of hydrogen through Pd, Pt, Pd-clad Pt, Au, Ni, and Fe were conducted under conditions of a concentration gradient of either atoms or protons. Transport of hydrogen through an atom concentration gradient was found for Pd and Pd-clad Fe only. Under a proton concentration gradient, protons migrated readily through Pd, but their transfer through Pt was immeasurable unless the Pt was sandwiched between Pd. Transfer of protons through Fe sandwiched between Pd was also found. Hydrogen atoms evidently did not dissolve to a significant extent in Pt, but if protons are introduced from Pd-clad to Pt they can, under the proper conditions, migrate through Pt. The solution and diffusion of hydrogen atoms and also the migration of protons occurred in Fe. Transport of hydrogen, in any form, through Au and Ni was not detected. Considering the electronic configuration of these metals, it was reasonable that proton migration through Au was negligible; however, it was surprising that protons did not migrate through Ni. Reasons for this anomaly are suggested.

INTRODUCTION

Investigations of the diffusion of atomic hydrogen and deuterium through a β–Pd diaphragm (1, 2, 3) and the migration of protons and deuterons through an α–Pd bielectrode (3, 4) have been reported from the laboratory. For the β–Pd diaphragm a concentration gradient of atomic hydrogen in the palladium cathode arises, whereas for the α–Pd bielectrode there is a migration of protons through the metal under a proton concentration gradient caused by the difference in the electrochemical affinities of the reactions on the cathode and anode sides of the bielectrode.

It was felt that an investigation of the solution and transfer of hydrogen through such metals as Pt, Au, Ni, and Fe could be accomplished by a series of experiments in which these metals would be clad with palladium. The reasons for cladding these metals were twofold. Firstly, by controlling the phase of the palladium–hydrogen alloy (α or β), investigations of the transfer of hydrogen through metals clad with the palladium under conditions of a concentration gradient of either atoms or protons were possible. Secondly, by sandwiching such metals as iron and nickel with palladium, their solution in acid media was prevented. Since the rate of transport of hydrogen through the metals studied was presumably in all cases much slower than for the palladium, the rate would be controlled by these metals. The species of hydrogen which came into contact with these metals at the Pd–metal interface could be controlled also, since the palladium was their only source of hydrogen.

It was also the purpose of this work to try to relate the electronic configuration of the metals studied with the solubility and transfer of hydrogen through them.

EXPERIMENTAL

The experimental techniques and the cell used were the same as reported in references (1, 2, 3, 4). The solution was in all cases highly purified 2 N sulphuric acid. The metal membranes were prepared by cladding the metals on one and/or both sides with palladium. This was done by covering layers of clean metals with sheet titanium, heating red hot with an acetylene torch, and running through a steel roll press with cold rolls. The titanium sheets were then stripped off and the surfaces of the bimetallic sheets were

[1]*Manuscript received June 12, 1958.*
Contribution from the U.S. Naval Research Laboratory, Washington 25, D.C. This paper was presented at the Symposium on Charge Transfer Processes held at the University of Toronto, Toronto, Ontario, September 4 and 5, 1958.
[2]*Present address: Ford Scientific Laboratory, Ford Motor Company, Dearborn, Michigan.*

polished with metallographic paper, followed by cleaning in concentrated nitric acid.

The metal foils used in preparation of the bimetallic specimens were 99.7% palladium, 0.004 inch; 99.99% nickel, 0.002 inch; mild steel, 0.004 inch; 99.97% gold, 0.010 inch; and 99.99% platinum, 0.005 inch thick. The following bimetallic specimens were prepared: Pd: Au, 0.006 inch; Pd: Pt, 0.006 inch; Pd: Pt: Pd, 0.010 inch; Pd: Au: Pd, 0.009 inch; Pd:Ni:Pd, 0.006 inch; and Pd: Fe: Pd, 0.006 inch thick.

For the experiments in which the bimetallic foils were used as cathode diaphragms, purified hydrogen was bubbled through the solutions in both compartments on each side of the diaphragm. The reference electrodes used in each compartment were Pt/H_2 electrodes. The potential drop due to solution resistance on the cathode side was determined simultaneously with the pseudocapacitance test for electrode cleanliness on each side of the membrane by the current interrupter technique (5, 6).

For the experiments in which the bimetallic foils were used as bielectrodes, after the pre-electrolysis and surface activation procedure was finished, solution resistance and cleanliness of electrodes were determined. Then purified hydrogen was bubbled only through the solution in the compartment on the cathode side of the bielectrode, and purified helium was bubbled through the solution in the compartment on the anode side of the bielectrode. When the anode side of the bielectrode consisted of palladium, hydrogen dissolved in this part of the foil was removed by anodic polarization. The removal of hydrogen was indicated by following the anodic charging curve and observing when the anodic potential was several hundred millivolts positive to the potential plateau which resulted from the dissolved hydrogen. This anodic charging was repeated several times at successively reduced applied current densities to assure the removal of most of the hydrogen from the anode side of the bielectrode. The overvoltages on the hydrogen-saturated cathode side were determined against a Pt/H_2 electrode in the same solution. The overvoltages on the helium-stirred anode side were determined against a $(Pd–H)_\alpha/H^+$ electrode (7) in the same solution.

In addition to the experiments with the above materials, pure palladium and pure platinum bielectrodes were compared. These experiments were conducted with hydrogen bubbling through both compartments.

The ambient temperature was $30 \pm 2°$ C. The apparent exposed area of all the electrodes was 0.14 cm^2.

COMPARISON OF A PLATINUM WITH A PALLADIUM BIELECTRODE

A comparison of the overvoltage on a platinum bielectrode with that on a palladium bielectrode of the same dimensions is shown in Fig. 1. Since the catalytic activity of α-palladium is not far removed from that of platinum (4, 8), these curves show the strong influence of the rate of proton migration through the palladium bielectrode. It was previously shown (2) that atomic hydrogen does not diffuse through a platinum diaphragm with a clean surface. Also, a comparison of the anodic polarization curve of the platinum bielectrode, shown in Fig. 1, with the anodic polarization curve for a simple platinum anode indicates that there is not a significant amount of proton migration through the platinum bielectrode. It should be noted that in Fig. 1 the ordinate is given in terms of η', where η' is defined as the difference in potential between the open circuit, reversible electrode potential compared to the polarized electrode potential of the same metal/solution system. This means that the overvoltages on the platinum bielectrode were against a Pt/H_2 electrode in the same solution, and that the overvoltages on the palladium bielectrode were against a $(Pd–H)_\alpha/H^+$ electrode in the same solution.

Can. J. Chem. Downloaded from www.nrcresearchpress.com by 190.90.36.8 on 09/04/12
For personal use only.

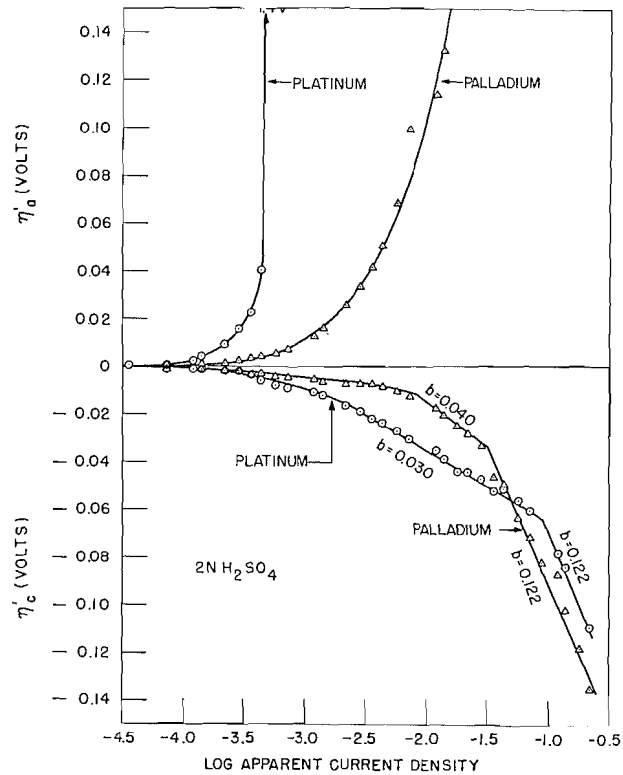

FIG. 1. Comparison of the hydrogen overvoltage on Pd and Pt bielectrodes. Pd and Pt overvoltage values are vs. $(Pd–H)_\alpha/H^+$ and Pt/H_2 reference electrodes, respectively.

In the low current density range the atomic hydrogen concentration on both sides of the palladium bielectrode changes little, while that on the platinum is rapidly changing. This largely accounts for the difference in overvoltage between the two metals. As the current density is increased on both the platinum and palladium cathode sides, there is a change to a Tafel b-slope of 0.12. In the current density range in which the b-slope on the cathode side is 0.12, most of the anodic reaction on the anode sides of these metal bielectrodes goes into the production of oxygen. As was indicated in previous work (4), it is believed that this change in Tafel slope is caused by the poisoning of the cathode surfaces by oxygen which migrates from the anode side. Kalish and Burshtein (9) have shown that oxygen can diffuse from the interior to the surface of platinum at room temperature. Previous work done at this laboratory (5, 10) has indicated that cathodically polarized platinum in strong sulphuric acid solutions will maintain a Tafel slope of 0.03 to current densities well beyond the value at which the change in slope from 0.03 to 0.12 takes place for the Pt curve in Fig. 1.* Thus for both the platinum and the palladium

**The limiting diffusion current density, i_L, for hydrogen ions in 2 N sulphuric acid solution can be approximated by the equation:*

$$\eta_c = 0.059 \log [(i_L - i)/i_L].$$

Using the data for the platinum cathode shown in Fig. 1, at an overvoltage of −0.06 v, the current density is equal to 0.100 amp/cm². Applying these values of η_c and i to the above equation, i_L is equal to about 2.8 amp/cm². Thus the limiting diffusion current density is well beyond the value at which the change in slope from 0.03 to 0.12 takes place for the Pt *curve in Fig. 1.*

Can. J. Chem. Downloaded from www.nrcresearchpress.com by 190.90.36.8 on 09/04/12
For personal use only.

cathode sides of their respective bielectrodes there is a change in the rate-controlling step from the catalytic combination or electrochemical desorption to a slow hydronium ion discharge. This change takes place at current densities well below the limiting current densities for hydronium ion depletion in the concentration layer on the solution side of the electrodes.

It should be noted that the previous work of the authors on the mechanism of the hydrogen-producing reactions on platinum (5, 10) and palladium (11) have also indicated a change in Tafel slope from 0.03 or 0.04 to 0.12. For these systems it was shown that at the current density at which the change in slope took place there was a depletion of hydronium ions at the interface, and the change in slope was interpreted to mean a change to a slow discharge of water to atomic hydrogen as the rate-controlling step. In other words, in the case of a simple platinum or palladium cathode, the change in slope to 0.12 occurs at a concentration limiting current density because there are not enough hydronium ions at the interface to support the applied current flow. In the case of the cathode side of a platinum or palladium bielectrode, the change in slope appears to be caused by the poisoning of the catalytic surface with oxygen.

Figure 1 further shows that the change in Tafel slope to 0.12 occurs at a significantly lower current density for palladium than for platinum. This is either because the solubility of oxygen in palladium is higher than in platinum or the effects of poisoning by oxygen is much greater for palladium. This is confirmed by the results shown in Fig. 2. Here both electrodes were anodized at 10 ma for a period of 45 minutes. The circuit was broken and both electrodes were allowed to come to their reversible potentials in hydrogen-saturated sulphuric acid solution. As the curves show, the time required for the palladium to reach its open-circuit, steady-state potential was about three times longer than that for the platinum electrode. This was either because the palladium dissolved more oxygen, which took a longer time to remove because of a slow rate of diffusion of the oxygen from the interior to the surface or, if only an equivalent surface layer of oxygen or oxide was formed by both metals, the rate of reduction of the oxygen by hydrogen was slower on the palladium surface. There is also the possibility that these effects are operating simultaneously.

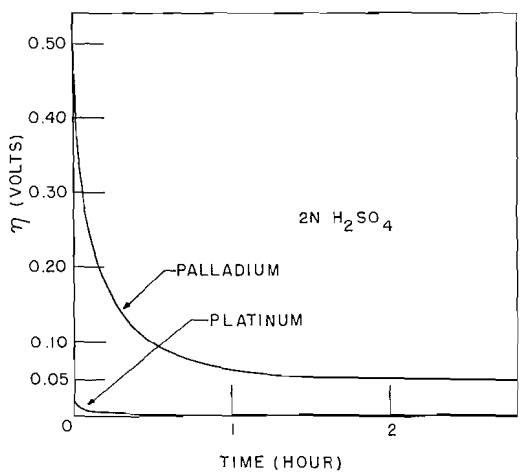

FIG. 2. Comparative rates of reaching reversible, open-circuit potentials on Pd and Pt after anodic polarization. Pt/H_2 reference electrode.

Can. J. Chem. Downloaded from www.nrcresearchpress.com by 190.90.36.8 on 09/04/12
For personal use only.

Can. J. Chem. Downloaded from www.nrcresearchpress.com by 190.90.36.8 on 09/04/12
For personal use only.

NOBLE METAL ELECTRODES CLAD WITH PALLADIUM ON ONE SIDE

Cathode overvoltage curves for Pd: Pt, Pt: Pd, Pd: Au, and Au: Pd* diaphragms shown in Fig. 3 indicate that in each case the metal exposed to the solution on the polarization, η_p, side of the cell determined the hydrogen-producing mechanism. The absence of overvoltage effects on the diffusion, η_d, sides indicated that hydrogen did not diffuse through any of these combinations.

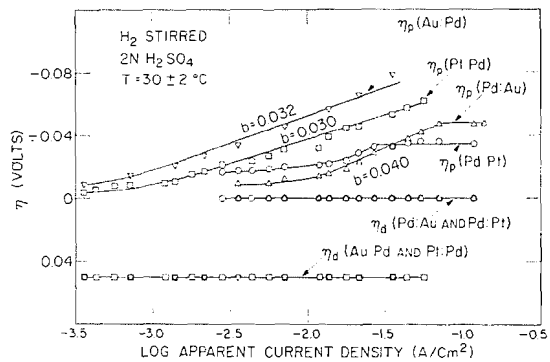

FIG. 3. Hydrogen overvoltage on polarization and diffusion surfaces of Au and Pt cathode-diaphragms clad on only one side with Pd. Pt/H_2 reference electrode.

In order to determine if protons could migrate through the same palladium-clad noble metal combinations, the electrodes were treated as bielectrodes. On the cathode side of these bielectrodes, the solution was stirred with hydrogen, whereas on the anode side the solution was stirred with helium. By this technique the possibility of the oxidation of molecular hydrogen on the anode side was eliminated and, if hydrogen did migrate through the bielectrode, a depolarization effect should be evident on the anode side. Figure 4 shows the results of these experiments. Because of the complete polarization of the anode curves it can be concluded that proton migration through these metal combinations does not occur significantly. The change from the lower to the 0.12 slope on the cathode overvoltage curves can be interpreted, as above, as due to the migration of oxygen from the anode to the cathode sides with the consequent poisoning of the cathode surface.

METALS SANDWICHED BETWEEN PALLADIUM

Hydrogen overvoltage, η_p, curves for Pd: Fe: Pd, Pd: Ni: Pd, Pd: Au: Pd, and Pd: Pt: Pd cathode diaphragms are shown in Fig. 5. The curves for the polarization sides of the diaphragms are similar to those for palladium (11). As expected, the metal in

**Throughout this paper the order of metal foils clad together will be signified by their arrangement from left to right. For the cathode diffusion diaphragms this order will represent the following arrangement in the two-compartment cell:*

polarization side: diffusion side.

For example, Pd: Pt means that the palladium was on the polarization side and the platinum was on the diffusion side of the diaphragm. Pd: Pt: Pd means that palladium was on both the polarization and diffusion sides and that platinum was sandwiched in-between. For the bielectrodes, the order from left to right will represent the following arrangement in the two-compartment cell:

cathode: anode.

For example, Pd: Pt means that the palladium was on the cathode side of the bielectrode and the platinum was on the anode side. Pd: Pt: Pd means that palladium was on both the cathode and anode sides and that platinum was sandwiched in-between.

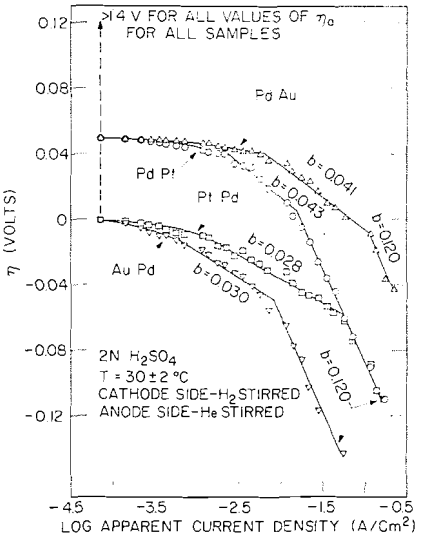

FIG. 4. Hydrogen overvoltage on Au and Pt bielectrodes clad on only one side with Pd. Pt/H_2 reference electrode on cathode side; $(Pd\text{-}H)_\alpha/H^+$ reference electrode on anode side.

the interior does not appear to influence the shape of the overvoltage curves. The differences in the i_0 values and the potentials for the plateaus for these curves are undoubtedly due primarily to the variation in the amount of cold working of each of these sandwiches (2).

Figure 5 shows the diffusion overvoltage, η_d, for the various metal sandwiches. Only for the case of the iron sandwich was there evidence of a significant amount of hydrogen diffusion through the diaphragm. In all cases the potential on the diffusion side at open circuit was equal to 0.05 v. This showed that during the cathodic charging of the palladium with hydrogen on the polarization side not enough hydrogen diffused through the metal in the center to charge the diffusion side to the β-phase. Hence on the polarization sides of these sandwiches the palladium was charged with hydrogen to the β-phase, and on the diffusion side the palladium was in the α-phase. Previous work by the authors (1, 2) has indicated that atomic hydrogen does diffuse through β-palladium. The results shown in Fig. 5 indicate that atomic hydrogen can diffuse through iron also, but not through nickel, platinum, or gold.

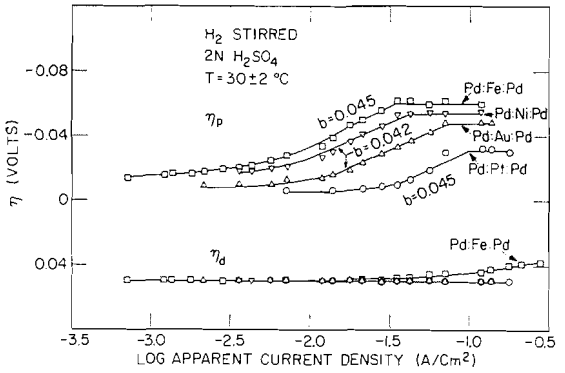

FIG. 5. Hydrogen overvoltage on polarization and diffusion surfaces of cathode-diaphragms consisting of Au, Pt, Ni, and Fe clad on both sides with Pd. Pt/H_2 reference electrode.

Can. J. Chem. Downloaded from www.nrcresearchpress.com by 190.90.36.8 on 09/04/12
For personal use only.

The metal sandwiches treated as bielectrodes gave the cathodic overvoltage, η_c, curves shown in Fig. 6. These curves are similar to those found for α-palladium bielectrodes (4). The separation of these curves arises from a complicated combination of conditions which include the migration of protons through the membrane, differences in cold working of the sandwiches, area differences, and the rate of oxygen diffusion from the anodic side. Since the primary purpose of this work was to determine the migration of protons through metals other than palladium, a determination of the effects of each of these factors was not made.

The anodic overvoltage, η_a, curves for this series of sandwiches is shown in Fig. 7. In

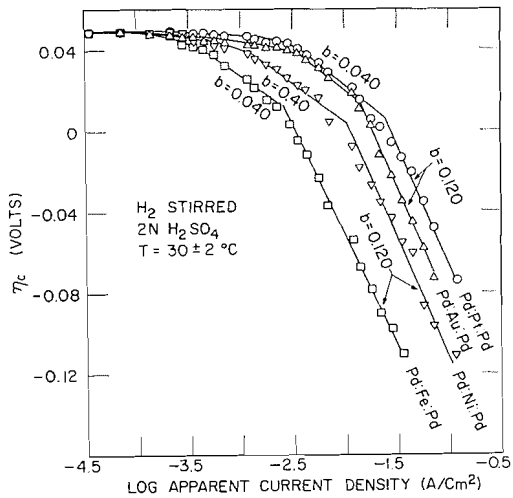

FIG. 6. Hydrogen overvoltage on the cathode surfaces of bielectrodes consisting of Au, Pt, Ni, and Fe clad on both sides with Pd. Pt/H_2 reference electrode.

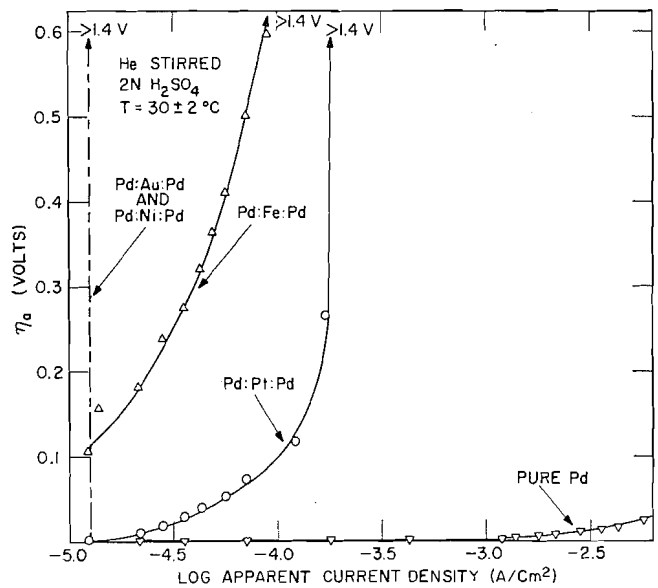

FIG. 7. Hydrogen overvoltage on the anode surfaces of bielectrodes consisting of Au, Pt, Ni, and Fe clad on both sides with Pd. $(Pd\text{-}H)_\alpha/H^+$ reference electrode.

Can. J. Chem. Downloaded from www.nrcresearchpress.com by 190.90.36.8 on 09/04/12
For personal use only.

order to determine the magnitude of the migration of protons through the membranes, the anode was stirred with helium. Hence any depolarization effects on this side would be due to the hydrogen which had migrated from the cathode side. As can be seen in Fig. 7, the platinum sandwich showed the most marked depolarization effect. The iron sandwich showed a depolarization effect also; however, neither gold nor nickel showed any evidence of proton migration through the bielectrode. In Fig. 7 is shown also part of the anodic polarization curve for a pure palladium bielectrode in the same solution (a more complete curve under these conditions is shown in ref. (3)). The comparison of the pure palladium with the platinum and iron sandwiches emphasizes the great differences in rate of proton migration through these specimens.

DISCUSSION

Previous work (1, 2) has shown that when a palladium diaphragm which separates two bodies of solution is made a cathode, hydrogen will be generated on the polarization side. Part of this hydrogen will dissolve in the palladium to form the β-phase. Further solution of hydrogen will set up a concentration gradient of atomic hydrogen* across the diaphragm and the atoms diffusing through the metal will cause an overvoltage effect, η_d, on the diffusion side. When palladium on the cathode side of a bimetallic diaphragm is charged with hydrogen in excess of the β-phase (H/Pd > 0.6), atomic hydrogen will exist in its interior. If this atomic hydrogen can diffuse through Pt, Au, Fe, or Ni clad to palladium, then its effect should be evident as an atomic concentration overvoltage. Such an effect was only found for the Pd : Fe : Pd sandwich and this indicated that atomic hydrogen did diffuse through steel.

If a pure palladium membrane is arranged as a bielectrode, the palladium will be maintained in the α-phase because hydrogen will be removed from the anode side as fast as it will dissolve in the metal on the cathode side (4). It has been shown that this hydrogen migrates through the palladium as protons. Low current density experiments in which the bimetallic membranes were used as bielectrodes would give evidence of the transfer of protons through the metals. If hydrogen, owing to the difference in the electrochemical affinities of the reaction on the cathode and anode sides, migrates through the bielectrode the palladium on the cathode side is maintained in the α-phase and atomic hydrogen virtually does not exist in its interior. Evidence of proton migration through the non-palladium metal would be shown by lowered anodic overvoltages, η_a.

The experimental results with platinum and gold clad on only one side with palladium showed that when the palladium was on the cathode side of the bielectrode there was no evidence of proton diffusion through the membrane. Similarly when the platinum or gold was on the cathode side, proton migration did not occur. However, for the steel and platinum sandwiches there was definite evidence of proton migration through these metals. In the case of platinum there apparently was no proton migration through the Pd: Pt combination because at low current densities the hydrogen would merely dissolve in the palladium until it was charged to the β-phase. The solution or removal of the hydrogen atoms on the Pd–cathode side was evidently much more rapid than the oxidation of hydrogen atoms on the Pt–anode side. The small effect of current density on cathodic overvoltage in the low current density range shown in Fig. 4 is indicative of the charging of the palladium with hydrogen. For the case of the sandwich Pd: Pt: Pd, proton migration through the bielectrode occurred, since, in the low density range, the

**Electrons from these atoms can be considered to occupy the* H *1s-band rather than the* Pd *4d-band. These electrons in excess of the amount required to fill the d-band of* Pd *move in a band which is characteristic of the proton lattice.*

Can. J. Chem. Downloaded from www.nrcresearchpress.com by 190.90.36.8 on 09/04/12
For personal use only.

rate of removal of hydrogen atoms from the palladium cathode side would evidently be the same as the rate of oxidation of hydrogen atoms on the palladium anode side.

Proton migration through palladium, iron, and platinum bielectrodes can be explained on the basis of the holes in the *d*-bands of these metals. When the hydrogen atom formed on the surface of α–Pd enters the interior of the metal, it donates its electron to the *d*-band of the palladium and the proton exists in an interstitial position in the Pd lattice. In order for the proton to exist in the platinum or steel lattice, an electron must accompany it, so that electrical neutrality may be maintained. Both platinum and iron have holes in their *d*-bands so that the addition of electrons will not increase the total energy significantly, since the density of levels in the *d*-bands of these metals is very large. Hence protons can exist in and migrate through the interior of these metals. On the other hand, gold has a filled *d*-band and electrons would have to enter the 6*s*-band. Since the density of levels in the *s*-band is very low this would require a large increase in energy. As a result, under the experimental conditions used, protons do not migrate through gold.

From this viewpoint it is expected that protons should migrate through nickel. The experimental evidence does not support this, even at current densities as low as 10^{-7} amp/cm^2. A partial explanation may lie in the fact that the holes in the *d*-band of Ni are completely polarized in one spin direction (12), which is not the case for Pd, Pt, or Fe. Since electrons can enter only one half of the *d*-band in Ni but can enter both halves in Pd, Pt, or Fe, the energy for the solution of the same amount of hydrogen will be increased much more in the case of Ni than in the other metals. This, of course, assumes that for these metals the density of levels is nearly the same for the 3*d*-, 4*d*-, and 5*d*-band. This extra energy appears to be prohibitive to the solution of hydrogen as protons in nickel to an appreciable extent. However, other effects such as differences in solvation energy of the proton may be more important.

CONCLUSIONS

For the β–Pd cathode of a Pd : Pt or Pd : Pt : Pd diaphragm where there is an atomic hydrogen gradient and hydrogen can diffuse through the palladium, diffusion through the platinum was not detected. This indicates that under an atomic hydrogen concentration gradient alone hydrogen atoms will not dissolve in platinum. In the case where a concentration gradient of protons exists across a bielectrode of platinum sandwiched between palladium, protons will migrate through. In this case the protons already exist in the palladium in contact with the platinum. Hence, as is also shown in the case of the Pt : Pd bielectrode, the *s*-electron of a hydrogen atom does not enter the *d*-band of platinum spontaneously.

A similar argument can be used for the Pd : Fe : Pd bielectrode. However, for this combination there is some atomic hydrogen diffusion through the steel if a concentration gradient and the *s*-electrons of hydrogen atoms can enter the *d*-band of iron spontaneously.

It can be concluded that, under the experimental conditions used, hydrogen can dissolve and migrate only as protons through platinum, whereas it can either migrate as protons or diffuse as atoms through iron or palladium. Neither protons nor hydrogen atoms can be transported through gold or nickel.

ACKNOWLEDGMENTS

The authors are indebted to Drs. J. C. White and G. W. Castellan, of the Electrochemistry Branch, Chemistry Division, and to Dr. A. I. Schindler, of the Metallurgy Division of the U. S. Naval Research Laboratory, for suggestions and advice during the course of this work.

Can. J. Chem. Downloaded from www.nrcresearchpress.com by 190.90.36.8 on 09/04/12
For personal use only.

REFERENCES

1. SCHULDINER, S. and HOARE, J. P. J. Electrochem. Soc. **103**, 178 (1956).
2. HOARE, J. P. and SCHULDINER, S. J. Electrochem. Soc. **103**, 237 (1956).
3. SCHULDINER, S. and HOARE, J. P. J. Electrochem. Soc. **105**, 278 (1958).
4. HOARE, J. P. and SCHULDINER, S. J. Electrochem. Soc. **104**, 564 (1957).
5. SCHULDINER, S. J. Electrochem. Soc. **99**, 488 (1952).
6. SCHULDINER, S. and HOARE, J. P. J. Chem. Phys. **26**, 1771 (1957).
7. SCHULDINER, S., CASTELLAN, G. W., and HOARE, J. P. J. Chem. Phys. **28**, 16 (1958).
8. SCHULDINER, S. and HOARE, J. P. International colloquium on reference electrodes and structure of the double layer. Paris. October, 1956.
9. KALISH, T. V. and BURSHTEIN, R. K. Doklady Akad. Nauk, S.S.S.R. **88**, 863 (1953).
10. SCHULDINER, S. J. Electrochem. Soc. **101**, 426 (1954).
11. HOARE, J. P. and SCHULDINER, S. J. Electrochem. Soc. **102**, 485 (1955).
12. BOZORTH, R. M. Ferromagnetism. D. Van Nostrand Company, Inc., New York. 1951. Figs. 10–17.

Can. J. Chem. Downloaded from www.nrcresearchpress.com by 190.90.36.8 on 09/04/12
For personal use only.

Can. J. Chem. Downloaded from www.nrcresearchpress.com by 190.90.36.8 on 09/04/12
For personal use only.

THE DETERMINATION OF KINETIC PARAMETERS OF REDOX REACTIONS FROM CURRENT–POTENTIAL CURVES[1]

J. E. B. Randles

ABSTRACT

Methods are suggested for calculating kinetic parameters of moderately rapid redox reactions from current–potential curves obtained with (*a*) rotating electrodes or stationary electrodes in stirred solutions, (*b*) dropping mercury electrodes. Experimental results for the V^{2+}/V^{3+} reaction at a dropping mercury electrode are presented and compared with a-c. impedance measurements on the same system. It is found that there is a good agreement between the kinetic parameters obtained by the two methods when the current–potential curves are interpreted with the aid of Koutecký's theory of diffusion to a dropping mercury electrode.

INTRODUCTION

In the investigation of the kinetics of moderately rapid electrode reactions by means of the steady-state current–potential relationship, the necessity of taking account of concentration polarization has been recognized for a long time and a number of theoretical treatments have appeared (1). However, no very satisfactory method of deriving the kinetic parameters for such reactions from the current–potential data has emerged. Simple plots of η (overpotential) against log i are still commonly used (2), although this is of little value in the region of the reversible potential or when concentration polarization becomes predominant. Frequently very little of the graph approximates to a straight line. Similar remarks apply to the utilization of current–potential curves obtained with a dropping mercury electrode (D.M.E.) when the deviation from the ideal reversible curve is not large.

For reactions too rapid to be satisfactorily investigated by d-c. polarization in the steady state, or quasi steady state (D.M.E.), relaxation methods are employed.* Of these, measurements of the a-c. impedance of an electrode is probably the most useful. The range of application (in terms of rate of electrode reaction) of this method overlaps with that of the d-c. polarization methods and it is of interest to compare the kinetic parameters obtained by the two types of method for the same electrode reaction. This comparison promises to be of most interest when the D.M.E. is used, for two reasons: (*a*) the reproducibility of the electrode makes an accurate comparison possible, (*b*) there remains some uncertainty in the theory of the current–potential relationship for this electrode which such a comparison may resolve.

The present paper has two purposes: first to present what the author regards as the most convenient method of calculating kinetic parameters of moderately rapid electrode reactions from current–potential curves, and secondly to compare results so obtained with a D.M.E. with the results of a-c. impedance measurements. The reaction selected for this purpose is the V^{2+}/V^{3+} reaction.

Calculation of Kinetic Parameters From Current–Potential Curves

We shall consider a simple electrode reaction of first order in both the cathodic and anodic directions which may be written

[1]*Manuscript received July 5, 1958.*
Contribution from the University of Birmingham, Birmingham, England. This paper was presented at the Symposium on Charge Transfer Processes held at the University of Toronto, Toronto, Ontario, September 4 and 5, 1958.

For reviews of these, and other, methods with their ranges of application, see Gerischer, H. Z. Elektrochem.* **59, *604 (1955), Grahame, D. C. Ann. Rev. Phys. Chem.* **6**, *337 (1955), and Delahay, P. Ann. Rev. Phys. Chem.* **8**, *229 (1957).*

[1] $$(1)+ne^- \rightleftharpoons (2).$$

Substances (1) and (2) are both present in the electrolyte solution or, if the electrode is mercury, (2) may be a metal dissolved in the mercury. Any other molecules such as H_2O or complexing ions which may take part in the reaction are assumed to be present in such large excess that the reaction remains pseudounimolecular in both directions. The modification of the treatment given below to the case when (2) is the metal of the electrode can easily be made.

In practice, free diffusion of ions unaccompanied by migration is ensured by the presence of an excess of an indifferent electrolyte, and this also results in the substances (1) and (2) having activity coefficients independent of their own concentrations. Hence the Nernst equation for the potential E^r, of a reversible electrode becomes

[2] $$E^r = E_f^\circ + (RT/nF) \ln(C_1^\circ/C_2^\circ)$$

where C_1° and C_2° are the bulk concentration of (1) and (2) and E_f° is the 'formal' potential (for $C_1^\circ = C_2^\circ$). Further, if k_1^r and k_2^r are the rate constants of the forward (left to right) and reverse directions of reaction [1] at the equilibrium potential E^r, then

[3] $$k_1^r C_1^\circ = k_2^r C_2^\circ.$$

Hence it is easily seen that for two potentials of the electrode E^r and $E^{r\prime}$ (corresponding to different ratios of C_1° to C_2°),

[4] $$E^r - E^{r\prime} = (RT/nF) \ln(k_2^r/k_1^r)\ (k_1^{r\prime}/k_2^{r\prime}).$$

For a particular system, having given bulk concentrations C_1° and C_2°, we shall denote by k_1^r and k_2^r the rate constants at the equilibrium potential and by k_1 and k_2 the rate constants at any other potential E, thus

[5] $$E - E_r = \eta = (RT/nF)\ \ln(k_2/k_1)\ (k_1^r/k_2^r)$$

or,

[6] $$k_2/k_1 = (k_2^r/k_1^r) \exp nf\eta$$

where F/RT is abbreviated to f, and η is the overpotential of the electrode.

Steady-state Diffusion

For steady-state diffusion, using a rotating electrode or stationary electrode in a stirred solution, the Nernst layer treatment of diffusion leads to

[7] $$i = nFD_1(C_1^\circ - C_1)/\delta = nFD_2(C_2 - C_2^\circ)/\delta$$

where i is the cathodic current density, C_1 and C_2 are the concentrations of (1) and (2) at the electrode surface, D_1 and D_2 are diffusion coefficients, and δ is the thickness of the Nernst layer. Thus, if i_1 and i_2 respectively are the limiting cathodic and anodic diffusion currents (both given positive sign),

[8] $$i_1 = nFD_1C_1^\circ/\delta, \qquad i_2 = nFD_2C_2^\circ/\delta.$$

From [7] and [8]

[9] $$C_1/C_1^\circ = (i_1 - i)/i_1, \qquad C_2/C_2^\circ = (i_2 + i)/i_2.$$

The net current density is also given by

Can. J. Chem. Downloaded from www.nrcresearchpress.com by 190.90.36.8 on 09/04/12
For personal use only.

[10] $$i = nF(k_1C_1 - k_2C_2)$$

which, using [9], [3], and [6] becomes

[11] $$i = nFk_1\,C_1^\circ\left[\frac{i_1-i}{i_1} - \left(\frac{i_2+i}{i_2}\right)\exp nf\eta\right].$$

By rearrangement we have

[12] $$-\log_{10} nFk_1\,C_1^\circ = \log_{10}\left[\left(\frac{1}{i}-\frac{1}{i_1}\right) - \left(\frac{1}{i}+\frac{1}{i_2}\right)\exp nf\eta\right].$$

Thus, by plotting the right hand side of [12] against $nf\eta$ a nearly straight line should be obtained.

The slope at any point

[13] $$d(\log_{10} k_1)/d(nf\eta) = -\alpha/2.303$$

gives the cathodic transfer coefficient, α, and the intercept at $nf\eta = 0$ is $\log_{10}(nFC_1^\circ k_1^r)$.

It is advantageous to use $[nf\eta + \ln(C_1^\circ/C_2^\circ)]$ instead of $nf\eta$ as abscissa, since, from equation [2],

$$nf\eta + \ln(C_1^\circ/C_2^\circ) = nf(E-E^r) + nf(E^r-E_f^\circ) = nf(E-E_f^\circ)$$

and this quantity depends only on the potential of the electrode relative to the solution. If also $\log_{10} nFC_1^\circ$ is added to the right hand side of equation [12] before plotting as ordinate, the graphs obtained for any value of C_1° and C_2° should coincide, and the intercept on the axis $nf\eta + \ln(C_1^\circ/C_2^\circ) = 0$ is now $\log_{10} k_s$ where k_s is the standard rate constant of the reaction.*

Dropping Mercury Electrode

The theory of diffusion to a dropping mercury electrode is complicated both by the growth of the drop surface and by the fact that the surface is not planar but spherical. The mathematical difficulties are such that all attempts at an exact solution of the diffusion equations have assumed the electrode reaction to be first order in both directions, as we have already done. A solution of the diffusion equation for an expanding mercury drop electrode and an electrode process involving a slow chemical step was first obtained by Koutecký and Brdička (3). More detailed solutions, specifically for the case of a slow electrochemical step have been given by Smutek (4), Kambara and Tachi (5), and Delahay (6). These workers solved the diffusion equation first for a stationary plane electrode, obtaining expressions for the current density equivalent to

[14] $$i = nF(k_1C_1^\circ - k_2C_2^\circ)\exp Q^2t\ \mathrm{erfc}\ Qt^{\frac{1}{2}},$$

where

[15] $$Q = (k_1D_1^{-\frac{1}{2}} + k_2D_2^{-\frac{1}{2}}),$$

t is the time from the start of the electrolysis, and erfc denotes the complementary error function. This result, for a plane electrode, has to be modified in order to give the current at a dropping mercury electrode. Smutek, and Kambara and Tachi, simply multiplied the whole expression [14] by the area of the drop, while Delahay multiplied also by the Ilkovič (7) factor $(7/3)^{\frac{1}{2}}$. The use of the Ilkovič factor for an expanding drop is certainly

*$k_s = k_1^r = k_2^r$ *when* $C_1^\circ = C_2^\circ$, *see Randles, J. E. B. Discussions Faraday Soc.* **1**, *11 (1947) and Delahay, P. New instrumental methods in electrochemistry. Interscience Publishers, Inc., New York. 1954. Chap. 7.*

Can. J. Chem. Downloaded from www.nrcresearchpress.com by 190.90.36.8 on 09/04/12
For personal use only.

necessary but a consideration of the origin of this factor* shows that the continuous lateral expansion of the diffusion layer, by reducing its thickness, has the same effect as multiplying the diffusion coefficients by 7/3. Thus the correct way of introducing the Ilkovič factor appears to be to redefine Q thus

$$Q = (3/7)^{\frac{1}{2}}(k_1 D_1^{-\frac{1}{2}} + k_2 D_2^{-\frac{1}{2}}). \quad [16]$$

This procedure is supported by the fact that it leads to the correct result for the extreme cases, i.e. very slow or very fast electrode reactions, while multiplication of the whole expression [14] by $(7/3)^{\frac{1}{2}}$ leads to an incorrect result for very slow reactions.

An approach distinct from the above was made by Koutecký (18), who solved a diffusion equation appropriate to an expanding electrode but still neglected the curvature of the surface. His results are expressed in terms of a variable χ which is equivalent to $2Qt^{\frac{1}{2}}$ where Q is given by [16]. In later work (9) Koutecký and Cížek have included the effect of the curvature of the surface. Expression [14] and Koutecký's results can be applied with equal ease to the interpretation of polarographic current–potential curves.

It is probably more accurate experimentally, when using a dropping electrode, to measure the instantaneous current at maximum drop size than to measure the average current. Therefore the method of interpreting current–potential curves will be developed for currents measured at maximum drop size. Only minor changes are needed in order to apply it to average currents.

From equation [14] the current at time τ from the start of a new drop (τ = drop life) is given by

$$i_\tau = nFA(k_1 C_1^\circ - k_2 C_2^\circ) \exp Q^2\tau \operatorname{erfc} Q\tau^{\frac{1}{2}}, \quad [17]$$

where A is the surface area of the drop at maximum drop size. Using expressions [3] and [6] which are still valid, [17] becomes

$$i_\tau = nFA\ k_1 C_1^\circ(1 - \exp nf\eta) \exp Q^2\tau \operatorname{erfc} Q\tau^{\frac{1}{2}}. \quad [18]$$

Now if we denote by i_{τ_1} and i_{τ_2} the limiting cathodic and anodic diffusion currents at maximum drop size, then provided that τ is the same for both

$$i_{\tau_1}/i_{\tau_2} = C_1^\circ D_1^{\frac{1}{2}}/C_2^\circ D_2^{\frac{1}{2}}. \quad [19]$$

Also, with the aid of equations [3], [6], and [19] and using the abbreviation

$$i_{\tau_1}/i_{\tau_2} = r \quad [20]$$

expression [16] becomes

$$Q = (3/7)^{\frac{1}{2}}\ k_1 D_1^{-\frac{1}{2}}(1 + r \exp nf\eta). \quad [21]$$

Finally, by using [21] to substitute for k_1 in [18] we reach the equation

$$i_\tau = nFA\ C_1^\circ \left(\frac{7D_1}{3\pi\tau}\right)^{\frac{1}{2}} \left[\frac{1 - \exp nf\eta}{1 + r \exp nf\eta}\right] \theta(Q\tau^{\frac{1}{2}}) \quad [22]$$

where

$$\theta(Q\tau^{\frac{1}{2}}) = \pi^{\frac{1}{2}} Q\tau^{\frac{1}{2}} \exp Q^2\tau \operatorname{erfc} Q\tau^{\frac{1}{2}}. \quad [23]$$

The function $\theta(Q\tau^{\frac{1}{2}})$ has the property of approaching unity as $Q\tau^{\frac{1}{2}} \to \infty$, i.e. for very rapid electrode reactions. Expression [22] may therefore be written

$$i_\tau = i_{\tau\infty}\, \theta(Q\tau^{\frac{1}{2}}) \quad [24]$$

*See Stackelberg, M.v. *Z. Elektrochem.* **45**, 466 (1939).

Can. J. Chem. Downloaded from www.nrcresearchpress.com by 190.90.36.8 on 09/04/12
For personal use only.

where $i_{\tau\infty}$ is the value of i_τ for an infinitely rapid electrode reaction at the same value of η (i.e. k_1/k_2 unchanged but k_1 and $k_2 \rightarrow \infty$). Values of the function $\theta(\chi)$ for a series of values of χ are tabulated in Milner's Polarography (Longmans, Green & Co., Inc., New York and Toronto. 1957. Table 4.1). Koutecký expressed his results in a similar form

$$i_\tau = i_{\tau\infty}F(\chi) \qquad [25]$$

where $\chi = 2Q\tau^{\frac{1}{2}}$, and he tabulates (10) $F(\chi)$. This table is reproduced by Delahay, P' New instrumental methods in electrochemistry. Interscience Publishers Inc., New York. 1954. Table 4.1.

In order to use equation [24] or [25] it is necessary to find $i_{\tau\infty}$. It is given by [22] with $\theta(Q_\tau^{\frac{1}{2}}) = 1$, and may be expressed in terms of either limiting diffusion current. In terms of the cathodic current, i_{τ_1},

$$i_{\tau\infty} = i_{\tau_1}\left(\frac{1-\exp nf\eta}{1+r\exp nf\eta}\right).$$

The calculation of $i_{\tau\infty}$ from this expression for each case is laborious and a sufficiently accurate and much simpler method is as follows. The current i_τ measured at a series of overpotentials is expressed as a fraction of $\frac{1}{2}(i_{\tau_1}+i_{\tau_2})$ (both limiting currents being given positive sign) and plotted against $nf\eta$. Figure 1 shows a typical curve. On this scale the $i_{\tau\infty}$ curve is that of $\tanh -nf\eta/2$ drawn between the limiting current lines and cutting the experimental curve at the point of zero current (see Fig. 1). A template may be used to draw this curve on standard squared graph paper. The results described below were obtained by using a 'Perspex' template on which the full extent of the current axis (i.e. from $\tanh -\infty = -1$ to $\tanh +\infty = +1$) = 20 cm, and one unit on the $nf\eta$ axis = 2.5 cm. The accuracy of the experimental current measurement would justify a somewhat larger scale.

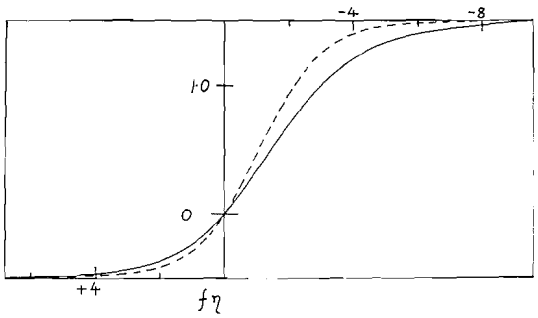

FIG. 1. Full curve: experimental $2i_\tau/(i_{\tau_1}+i_{\tau_2})$.
Broken curve: $i_{\tau\infty}$.
Cathodic current plotted above the zero current axis.

The ratio $i_\tau/i_{\tau\infty}$ is calculated from the two curves at a series of values of $nf\eta$ corresponding (for reasons which will be apparent later) to selected values of $(nf\eta + \ln r)$. These selected values ranged from -5.2 to $+5.2$ in steps of 0.4, in the calculations to be described below. The fraction $i_\tau/i_{\tau\infty}$ is equal to $F(\chi)$ or $\theta(\chi/2)$ and the next step is therefore to read off the corresponding value of $\log(\chi/2)$ from a graph of $F(\chi)$ or $\theta(\chi/2)$ against $\log(\chi/2)$. From equation [22],

$$\log \chi/2 = \log Q\tau^{\frac{1}{2}} = \log(3/7)^{\frac{1}{2}}k_1D_1^{-\frac{1}{2}}\tau^{\frac{1}{2}}[1+\exp(nf\eta + \ln r)]$$

or

$$\log \chi/2 - \log[1+\exp(nf\eta + \ln r)] = \log_{10}(3\tau/7D_1)^{\frac{1}{2}}k_1. \qquad [26]$$

Can. J. Chem. Downloaded from www.nrcresearchpress.com by 190.90.36.8 on 09/04/12
For personal use only.

The left hand side of [26] is calculated with the aid of a previously prepared table of values of $\log[1+\exp(nf\eta + \ln r)]$ for the selected values of $(nf\eta + \ln r)$, and is plotted against $(nf\eta + \ln r)$. Since

$$r = i_{r_1}/i_{r_2} = C_1^\circ D_1^{\frac{1}{2}}/C_2^\circ D_2^{\frac{1}{2}}.$$

Therefore

[27] $$(nf\eta + \ln r) = nf(E - E_f^\circ) + \tfrac{1}{2} \ln D_1/D_2.$$

Equation [27] shows that the abscissa $(nf\eta + \ln r)$ depends on the potential of the electrode relative to the solution but is independent of C_1°/C_2°. Thus the graphs obtained for any values of C_1° and C_2° should coincide. The slope at any point is

[28] $$d \log_{10} k_1/d(nf\eta) = -\alpha/2.303$$

and the intercept with the line $(nf\eta + \ln r) = \frac{1}{2} \ln D_1/D_2$ has the value $\log_{10}(3\tau/7D_1)^{\frac{1}{2}} k_s$.

As will be shown later, these graphs can be compared directly with the results of a-c. measurements.

EXPERIMENTAL

Materials

Solutions were made up in water redistilled in an all-glass still. Perchloric and sulphuric acids were distilled under reduced pressure. A stock solution of VO^{++} in perchloric acid solution was prepared from Analar ammonium vanadate by reduction with SO_2 and boiling out the excess. The solution therefore contained a little $SO_4^=$ and NH_4^+. The final reduction to a mixture of V^{2+} and V^{3+} was carried out in the electrolysis cell.

Apparatus

The dropping electrode consisted of a short length of capillary tube of 0.045 mm bore, sealed at one end to a length of 1-mm bore tubing which was connected to a mercury reservoir by silicone tubing. The lower end of the capillary was blown out to a small bulb which was drawn to a fine thin-walled tube and cut to a square end (i.d. $\sim$ 0.05 mm, o.d. $\sim$ 0.15 mm, at the tip). This ensures the minimum possible shielding of the mercury drop by the end of the capillary. The dropping electrode was inserted through a ground joint in the cap of the electrolysis cell which also carried an inlet for purified hydrogen, a tube closed by a sintered-glass plug and containing an auxilliary platinum electrode, and a J tube containing mercury which served as a reversible reference electrode. Mercury was introduced into the electrolysis cell from a connection at the lower end. The final reduction of the VO^{++} to a mixture of V^{2+} and V^{3+} was carried out cathodically at the large mercury pool stirred by a stream of hydrogen and with the platinum electrode as anode. The mercury pool also served as second electrode in the d-c. polarization measurements and in the a-c. impedance measurements. The whole electrolysis vessel was surrounded by a thermostatic water jacket.

In the d-c. polarization measurements the current at maximum drop size was measured directly by means of calibrated Cambridge 'spot' galvanometer, internal resistance 50 ohms, of period 2 seconds, slightly under damped. The drop time of the capillary was mechanically controlled at 6.0 seconds (natural drop time $\sim$9 seconds). The overpotential was measured between the dropping electrode and the stationary mercury electrode in the J tube. The ohmic potential drop due to the resistance of the capillary and the electrolyte (about 50 ohms) was never greater than 0.3 mv, and was neglected. The capacity current at maximum drop size was also negligible.

Can. J. Chem. Downloaded from www.nrcresearchpress.com by 190.90.36.8 on 09/04/12
For personal use only.

The a-c. impedance measurements were carried out by means of an improved version of an apparatus already described (11), details of which will appear in a later publication.

RESULTS AND DISCUSSION

Figure 1 shows an experimental current–potential curve for V^{2+}/V^{3+} in 1 M H_2SO together with the i_∞ curve. The temperature was 15.3° C, the total vanadium concentration 0.003 M, and the ratio of the cathodic to anodic limiting currents ($= i_{\tau_1}/i_{\tau_2} = r$) was 3.05. Corresponding curves were obtained for the same solution but with $r = 1.06$ and 0.187 respectively. The left hand side of equation [26] calculated for each of the three curves is plotted against ($nf\eta + \ln r$) in the lower part of Fig. 2 using Koutecký's values (10) of $F(\chi)$ modified by his correction for spherical diffusion (see below). The good agreement between the three sets of points is typical of what is obtained if the difference between i_τ and $i_{\tau\infty}$ is as great as, or greater than, that shown in Fig. 1. In the upper part of Fig. 2 are three sets of points calculated from the current–potential curve for $r = 1.06$. The lowest set (⊙) was obtained by equating $i_\tau/i_{\tau\infty}$ to $\theta(\chi/2)$ (equation [23]). The next set (×) was obtained using Koutecký's tabulated values of $F(\chi)$ and the uppermost set (+) by using $F(\chi)$ corrected for spherical diffusion. This correction has been calculated by Koutecký and Cížek (9) and takes the form $\xi.H_c(\chi)$ where ξ depends on the drop time, rate of flow of mercury, and diffusion coefficients of the reactants, and $H_c(\chi)$ is a function

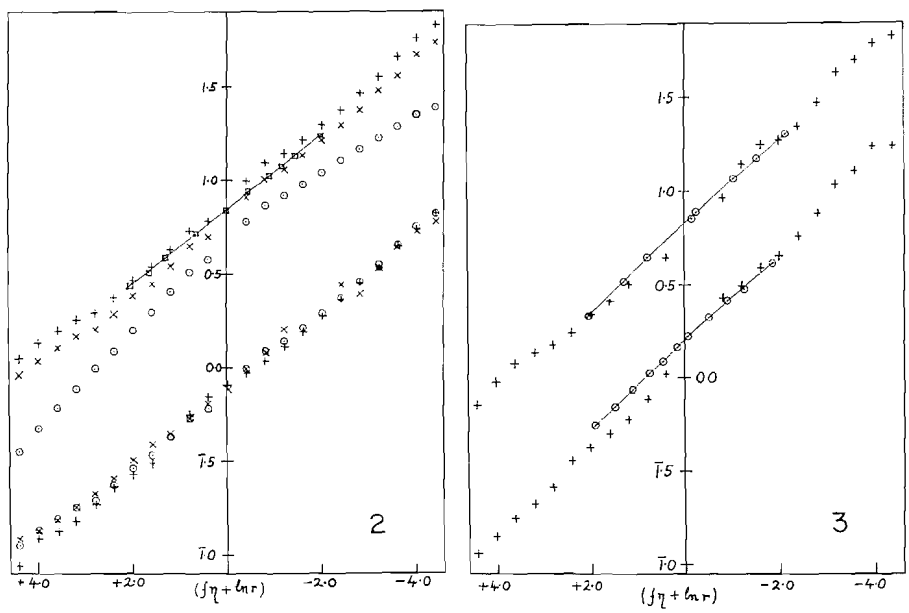

FIG. 2. V^{2+}/V^{3+} in 1 M H_2SO_4, 15.3° C, L.H.S. of equation [26] plotted as ordinate.
Lower part: $i_\tau/i_{\tau\infty} = F(\chi)$ corrected for spherical diffusion.
+ — $r = 3.05$; ⊙ — $r = 1.06$; × — $r = 0.181$.
Upper part: (all points shifted upwards one unit on ordinate scale) $r = 1.06$.
⊙ — $i_\tau/i_{\tau\infty} = \theta(\chi/2)$; × — $i_\tau/i_{\tau\infty} = F(\chi)$.
+ — $i_\tau/i_{\tau\infty} = F(\chi)$ corr. for spherical diffusion.
⊡ — from a-c. impedance.

FIG. 3. V^{2+}/V^{3+} in 1 M $HClO_4$.
+ — L.H.S. of equation [26] plotted as ordinate.
⊙ — From a-c. impedance.
Lower part: 14.2° C.
Upper part: 25° C (points shifted upwards by 0.5 unit).

Can. J. Chem. Downloaded from www.nrcresearchpress.com by 190.90.36.8 on 09/04/12
For personal use only.

of χ which they tabulate. The correction is easily applied by drawing a curve of $F(\chi)-\xi.H_c(\chi)$ against $\log(\chi/2)$, ξ being constant for a given system if τ is constant, and in the present case $\xi = 0.191$. The fourth set of points (⊡) in the upper part of Fig. 2 was obtained from the a-c. impedance of the same electrode in the same solution but with the total vanadium concentration raised to 0.009 M to improve the accuracy of the measurements. Impedance measurements were made for a range of values of r. The activation resistance,* R_a, of the electrode is related to the exchange current i_0 by

$$(nFR_a)^{-1} = i_0 = nFA' k_1{}^r C_1{}^\circ = nFA' k_2{}^r C_2{}^\circ$$

where A' is the area of the drop at the time of the impedance measurement. In practice this measurement was made when the age of the drop was 0.9τ so that the ratio of A' to the maximum area is $(0.9)^{\frac{2}{3}}$. It is thence easily deduced that

[29] $$-\log[nF(0.9)^{\frac{2}{3}}\pi^{\frac{1}{2}}R_a i_{\tau_1}] = \log(3\tau/7D_1)^{\frac{1}{2}}k_1{}^r.$$

The right hand side (R.H.S.) of [29] is identical with the R.H.S. of [26], and hence the L.H.S. of [29] is plotted as the fourth set of points (⊡) in the upper part of Fig. 2. The other points which agree best with this set are those calculated with the use of Koutecký's $F(\chi)$ corrected for spherical diffusion; the improved agreement resulting from the inclusion of this correction is often more marked than in this example. It is evident that the use of $\theta(\chi/2)$ would give an erroneously low value of the rate constant. None of the lines from the current–potential curves are very straight but those calculated by means of $F(\chi)$ are straighter than those calculated by means of $\theta(\chi/2)$.

In Fig. 3 points calculated from current–potential curves using $F(\chi)$ corrected for spherical diffusion are compared with those calculated from a-c. impedance measurements, for V^{2+}/V^{3+} in 1 M $HClO_4$ at 14.2° C and 25.0° C respectively. There is again good agreement. In both cases the ratio i_{τ_1}/i_{τ_2} was near unity so that the points from the current–potential curves are absent or very uncertain at small values of $(nf\eta + \ln r)$. In Fig. 4 the data from a-c. impedance measurements are plotted on a larger scale. The

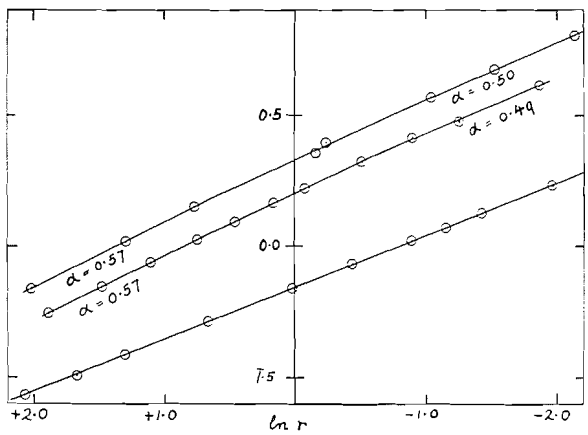

FIG. 4. L.H.S. of equation [29] plotted as ordinate.
V^{2+}/V^{3+} in: (upper line) 1 M $HClO_4$, 25° C; (middle line) 1 M $HClO_4$, 14.2° C; (lowest line) 1 M H_2SO_4, 15.3° C.

*R_a *is equivalent to* $R_r - 1/\omega C_r$ *of earlier papers (Randles, J. E. B. Discussions Faraday Soc.* **1**, *11 (1947).), to* R_D *of Gerischer, H. (Z. physik. Chem.* **198**, *286 (1951).), and to* θ *of Grahame, D. C. (J. Electrochem. Soc.* **99**, *370C (1952).). It was calculated by a method similar to that previously described (Laitinen, H. A. and Randles, J. E. B. Trans. Faraday Soc.* **51**, *54 (1954).).*

Can. J. Chem. Downloaded from www.nrcresearchpress.com by 190.90.36.8 on 09/04/12
For personal use only.

points for the sulphuric acid base solution at 15.3° C give a straight line corresponding to $\alpha = 0.455$ and $k_s = 1.39 \times 10^{-3}$ cm sec^{-1}. Those for the perchloric acid base solution give slightly curved lines corresponding to α decreasing from 0.57 to 0.50 (25° C) and from 0.57 to 0.49 (14.2° C) with increasing cathodic potential. However, the evidence is as yet insufficient to confirm that this represents a genuine change in α. The values of k_s are 2.20×10^{-3} and 3.64×10^{-3} cm sec^{-1} respectively corresponding to $\Delta H^{\neq} = 7.6$ kcal.

It is concluded from the above results that reliable values of the rate constants and transfer coefficients of redox reactions may be calculated from the current–potential curves obtained with a dropping mercury electrode by means of the Koutecký function $F(\chi)$ corrected for spherical diffusion. With the author's present equipment the method can give an accuracy in the rate constant of $\pm 5\%$ when $k_s \sim 1 \times 10^{-3}$ cm sec^{-1} decreasing to $\pm 30\%$ when $k_s \backsim 5 \times 10^{-3}$ cm sec^{-1}. As k_s decreases, the accuracy improves to about $\pm 3\%$, and for $k_s < 2 \times 10^{-4}$ cm sec^{-1} the d-c. polarization method is preferred to the a-c. impedance method, since the accuracy of the latter falls off as k_s decreases below 1×10^{-3} cm sec^{-1}. A disadvantage of the dropping mercury electrode is the occurrence in some circumstances of the interfacial stirring which causes polarographic 'maxima'. This becomes more marked with an increased rate of mercury flow and shorter drop time, which otherwise would be advantageous for measurements on the more rapid reactions.

REFERENCES

1. Essin, O. and Loschkarev, M. A. Acta Physicochim. U.R.S.S. **10**, 513 (1939). Essin, O. Acta Physicochim. U.R.S.S. **13**, 429 (1942). Petrocelli, J. V. J. Electrochem. Soc. **98**, 187 (1951). Lewarcowitz, E. J. chim. phys. **49**, 557, 564, 573 (1952). Delahay, P. New instrumental methods in electrochemistry. Interscience Publishers, Inc., New York. 1954. Chap. 9.
2. Tobias, C. W., Eisenberg, M., and Wilke, C. R. J. Electrochem. Soc. **101**, 306 (1954). Stern, M. J. Electrochem. Soc. **104**, 559 (1957).
3. Koutecký, J. and Brdička, R. Collection Czechoslov. Chem. Communs. **12**, 337 (1947).
4. Smutek, M. Chem. Listy, **45**, 241 (1951); Collection Czechoslov. Chem. Communs. **18**, 171 (1953).
5. Kambara, T. and Tachi, I. Bull. Chem. Soc. Japan, **25**, 135 (1952).
6. Delahay, P. J. Am. Chem. Soc. **75**, 1430 (1953).
7. Ilkovič, D. Collection Czechoslov. Chem. Communs. **6**, 498 (1934); J. chim. phys. **35**, 129 (1938).
8. Koutecký, J. Collection Czechoslov. Chem. Communs. **18**, 597 (1953).
9. Koutecký, J. and Cífžek, J. Collection Czechoslov. Chem. Communs. **21**, 836 (1956).
10. Koutecký, J. Chem. Listy, **47**, 323 (1953). See also ref. 8, p. 607.
11. Randles, J. E. B. Trans. Faraday Soc. **50**, 1246 (1954).

Can. J. Chem. Downloaded from www.nrcresearchpress.com by 190.90.36.8 on 09/04/12
For personal use only.

Can. J. Chem. Downloaded from www.nrcresearchpress.com by 190.90.36.8 on 09/04/12
For personal use only.

MECHANISMS OF REDUCTION OF CHLOROAQUOCHROMIUM(III) IONS IN ACID MEDIA[1]

PHILIP J. ELVING AND BERNARD ZEMEL

ABSTRACT

The polarographic behavior of the hexaaquochromium(III) and dichlorotetraaquochromium(III) ions was observed in the absence of maxima suppressors, and in the presence of various concentrations of perchloric acid, hydrochloric acid, and neutral salt. The polarographic waves obtained for each Cr(III) species in the different media were analyzed by plotting the function $\log[i/(i_d-i)]$ vs. E; the plots generally consist of two straight lines intersecting at about the half-wave potential and can best be explained by assuming two different concurrent mechanisms for the electron transfer process: the direct transfer of an electron to the Cr(III) ion from the electrode at the mercury–solution interface, and the transfer of an electron to Cr(III) from a Cr(II) ion produced at that interface. Only for the dichlorotetraaquochromium(III) ion in 12 M HCl does the direct transfer process appear to be dominant. Polarography of Cr(III) in the latter medium before and after reaction with the medium shows no change in $E_{\frac{1}{2}}$ corresponding to the shift observed in the ultraviolet spectra; this is accounted for by the "catalytic" degradation, i.e., the loss of chloride of the higher chloro complexes due to the rapid anion transfer mechanism for the electron transfer process between halo Cr(III) and Cr(II) ions.

The literature (1) on the polarographic reduction of Cr(III) to Cr(II) indicates the variability of the half-wave potential, $E_{\frac{1}{2}}$, with the natures of the Cr(III) species and of the background electrolyte.

In 0.1 M potassium chloride $E_{\frac{1}{2}}$ of -0.91 v has been reported for the "aged" solution (1*a*, *f*). Two waves ($E_{\frac{1}{2}} \simeq -0.61$, -0.88 v) were found for the "fresh" green chromic chloride in 0.4 M KCl; the height of the first wave decreased with time and the second increased equivalently (1*b*). In saturated calcium chloride solution, $E_{\frac{1}{2}}$ was reported at -0.55 v (1*e*); however, other workers (1*g*) described two waves of $E_{\frac{1}{2}}$ equal to -0.57 and -0.87 v. With time, the wave at -0.57 v increased in height and that at -0.87 showed an equivalent decrease; on heating to 100° C, the second wave disappeared and reappeared only on dilution. An $E_{\frac{1}{2}}$ of -1.04 v was reported for the violet chromic sulphate and $E_{\frac{1}{2}}$ of -1.25 v for the "green" form in 1.0 M K_2SO_4 (1*h*).

All results reported in the previous paragraph involved the addition of varying amounts of gelatin as a maximum suppressor. Unfortunately, gelatin tends to shift $E_{\frac{1}{2}}$ and to change the wave shape. The extent of these effects is a function of the gelatin concentration and of the type and concentration of background electrolyte (1*e*). The mechanism of maximum suppression is not well understood and, while use of a maximum suppressor may make measurement of a wave easier, its presence generally introduces unknown complications into the electrode process.

In the present study, the polarographic behavior of the two commonly occurring forms of Cr(III), the violet hexaaquo and the dark green dichlorotetraaquo ions, has been investigated in various media in the absence of any maxima suppressor; the Cr(III) concentrations used were low enough that maxima did not interfere. The experimental conditions were such as to permit definite knowledge of the Cr(III) species present, e.g., the supporting electrolytes were usually sufficiently high in acid concentration so as to inhibit formation of hydroxo and condensed species.

[1]*Manuscript received July 8, 1958.*
Contribution from the Department of Chemistry, University of Michigan, Ann Arbor, Michigan. This paper was presented at the Symposium on Charge Transfer Processes held at the University of Toronto, Toronto, Ontario, September 4 and 5, 1958.

Can. J. Chem. Downloaded from www.nrcresearchpress.com by 190.90.36.8 on 09/04/12
For personal use only.

DISCUSSION OF OBSERVED POLAROGRAPHIC BEHAVIOR

Selected data to illustrate the discussion are given in Table I.

TABLE I

Half-wave potential and wave slope data for reduction of Cr(III) to Cr(II)

Original species added	Background electrolyte	$-E_{\frac{1}{2}}$ v	Slope of log plot* Before $E_{\frac{1}{2}}$ mv†	Slope of log plot* After $E_{\frac{1}{2}}$ mv†
$[Cr(H_2O)_6]^{+3}$	0.1 *M* $HClO_4$	0.80	73 (0.81)	66 (0.89)
	0.5 *M* $HClO_4$	0.85	76 (0.78)	79 (0.75)
	1.0 *M* $HClO_4$	0.91	86 (0.69)	102 (0.58)
	1.5 *M* $HClO_4$	0.92	89 (0.66)	116 (0.51)
	0.1 *M* $HClO_4$+1.9 *M* $NaClO_4$	0.89	78 (0.76)	128 (0.48)
	1.9 *M* $NaClO_4$			
$[CrCl_2(H_2O)_4]^+$	0.1 *M* KCl	0.57	118 (0.50)	129 (0.46)
	0.1 *M* HCl	0.55	107 (0.55)	107 (0.55)
	1.0 *M* $HClO_4$	0.53	139 (0.43)	180 (0.33)
	12 *M* HCl‡	0.63	54 (1.10)	60 (0.98)
	12 *M* HCl§	0.63	53 (1.11)	69 (0.86)

*Slope for the plot of $\log[i/(i_d-i)]$ vs. E.
†Value in parentheses corresponds to the slope in millivolts divided into 59.1 mv, i.e., equals the alpha term of equation [2].
‡Data obtained 5 minutes after dissolution of dichlorotetraaquochromium(III) chloride.
§Data obtained after equilibrium was reached.

Hexaaquochromium(III) Ion

The polarography of $[Cr(H_2O)_6]^{+3}$ was investigated using 0.1 to 1.5 *M* perchloric acid as background electrolyte; in 0.1 *M* acid the ionic strength was varied by the addition of $NaClO_4$ to an ionic strength of two.

$E_{\frac{1}{2}}$ shifts considerably with the nature and concentration of the background electrolyte. At higher $HClO_4$ concentrations, the hydrogen discharge is superposed on the first (III $\rightarrow$ II) wave, making it somewhat difficult to evaluate. The waves become increasingly more drawn out with increasing $HClO_4$ concentration and ionic strength; $E_{\frac{1}{2}}$ decreases from -0.80 v in 0.1 *M* $HClO_4$ to -0.91 in 1.0 *M* $HClO_4$; this may be due at least in part to an ionic strength effect, since increasing ionic strength at 0.1 *M* $HClO_4$ shifts $E_{\frac{1}{2}}$ from -0.80 to -0.89 v. Maxima appear when the Cr(III) concentration exceeds 0.8 m*M* in 0.10 *M* $HClO_4$. Polarograms for 0.1 to 5.0 m*M* Cr(III) solutions indicate that above 0.5 m*M* $E_{\frac{1}{2}}$ becomes slightly more negative with increase in chromium concentration; there is little change below 0.5 m*M*.

The polarograms were analyzed by plotting $\log[i/(i_d-i)]$ vs. E; $E_{\frac{1}{2}}$, given by intersection of the plot with the zero log axis, was generally identical with that obtained from the polarographic curve by geometrical plotting to within a few millivolts. The plots are unsymmetrical and may best be represented as two straight lines intersecting at or near $E_{\frac{1}{2}}$. The asymmetry increases with both ionic strength and acidity as the slope of the section above the zero log axis decreases more, relatively, than the section preceding $E_{\frac{1}{2}}$. At higher $HClO_4$ concentrations, presence of the hydrogen wave causes a small uncertainty in the i_d value; the value of $E_{\frac{1}{2}}$ is, however, relatively insensitive to this error, the principal effect being a small curvature at high i values.

Dichlorotetraaquochromium(III) Ion

$[Cr(H_2O)_4Cl_2]^+$ was studied in potassium chloride, hydrochloric acid, and perchloric acid solutions. These were prepared immediately before use by dissolving the anhydrous

salt, $[Cr(H_2O)_4Cl_2]Cl$, in a solution containing the proper amount of background electrolyte, and then diluting to the desired concentration. Delay in using the solutions, particularly in perchlorate media, results in a long, ill-defined wave extending to the hydrogen discharge.

As in the case of the hexaaquo ion, the polarographic waves show relatively large shifts in $E_{\frac{1}{2}}$ with changes in concentration and type of supporting electrolyte. The wave shapes are particularly sensitive to the medium used and are considerably more drawn out than in the case for the corresponding $[Cr(H_2O)_6]^{+3}$ waves. Log plots show these waves to be unsymmetrical about $E_{\frac{1}{2}}$ and representable by two intersecting lines.

Chromium(III) in 12 M Hydrochloric Acid

When either the hexaaquo or dichlorotetraaquochromium(III) ions are dissolved in concentrated hydrochloric acid, a slow reaction occurs, as evidenced by a change in the color of the solution. The absorption spectrum, when equilibrium has been established, is independent of the starting material (2). It is, therefore, of considerable interest to observe the effect of this "leveling" process on the polarographic reduction of the species present in solution.

The reaction between the Cr(III) species and 12 *M* hydrochloric acid, which results in the formation of $[Cr(H_2O)_3Cl_3]^0$, proceeds sufficiently slowly that the polarographic wave obtained within the first 10 minutes after dissolution is merely that for the Cr(III) species added (the wave for the hexaaquo species before appreciable reaction has taken place is cloaked by the hydrogen wave and cannot be deciphered). The wave obtained after equilibrium has been established is then that due to the equilibrium species of Cr(III) in 12 *M* hydrochloric acid. The waves obtained for either case had an $E_{\frac{1}{2}}$ of -0.60 v, although the wave for the former case appears better formed; the difference in the two waves is best illustrated by the log plot. The Cr(III) to Cr(II) reduction wave for the species present before appreciable reaction has occurred is more symmetrical and its slope is nearer that predicted for a reversible reduction where n equals 1. After reaction with the medium, the wave becomes more asymmetric about $E_{\frac{1}{2}}$; the slope of the section positive to $E_{\frac{1}{2}}$ remains unchanged and that at potentials more negative than $E_{\frac{1}{2}}$ changes.

MECHANISMS OF THE CHROMIUM(III) REDUCTION

In general, ions of the so-called transition groups of the Periodic Table yield irreversible polarographic waves; consequently, their polarography cannot always be straightforwardly interpreted.

For a reversible polarographic wave for reduction of a soluble species to a soluble product, the relationship between current and potential is given by

$$E_{d.e.} = E_{\frac{1}{2}} - [RT/nF] \ln[i/(i_d - i)]. \quad [1]$$

For irreversible waves, the same thermodynamic considerations as apply to a reversible wave still hold, but the potential depends also on the rates of the various processes occurring at the mercury drop. By definition, $E_{\frac{1}{2}}$ still is given by the value of $E_{d.e.}$ at the point where $i = i_d/2$, but the simple Heyrovsky–Ilkovic expression of equation [1] no longer holds. Theoretical treatments of the irreversible polarographic wave have been developed (3). The complexity of the process, however, is such that simplifying assumptions must be made and the problem is still far from solved. In the classic treatment developed by Eyring and co-workers (3*b*), the following equation was obtained by assuming that the properties of an irreversible wave are determined by the rates of diffusion and of electrochemical reduction,

Can. J. Chem. Downloaded from www.nrcresearchpress.com by 190.90.36.8 on 09/04/12
For personal use only.

$$E = E_{\frac{1}{2}} - [RT/\alpha nF] \ln[i/(i_d - i)], \quad [2]$$

where α is the transfer coefficient such that the fraction α of the electrode potential favors the reduction at the cathode, and the fraction $(1-\alpha)$ of the potential applies to the reverse process.

If the plot of the log term of equation [2] vs. E is composed of two or more straight-line segments instead of just one straight line, a number of interpretations concerning the electrode processes involved is possible, e.g., the segments are due to successive electrode processes which, although they merge into one wave, have sufficiently different αn product values to produce slope changes in the log i plot (4). Another possibility is that the slope change is due to different, perhaps even concurrent, mechanisms for the electron transfer process with one mechanism predominating in the early part of the wave and the other predominating in the later development of the wave. Other explanations of such multisegmented slopes are possible (5).

Hexaaquo Ion

For the Cr(III)–(II) reduction, $n = 1$, and the slope of the log plot then gives the value for $2.303RT/\alpha F$, i.e., $0.0591/\alpha$ at 25°. The fact that two values for α are obtained from a single polarographic wave for the hexaaquo ion in perchloric acid media may then be interpreted as indicating two different electron transfer processes. The known reactions of the Cr(III)–Cr(II) system lend considerable support to the notions that these consist of the direct transfer of an electron to the Cr(III) species from the electrode at the solution–electrode interface and a second process involving an electron transfer reaction between Cr(III) and Cr(II).

There is evidence for the occurrence of the latter process; an electron exchange

$$Cr^*(III) + Cr(II) = Cr^*(II) + Cr(III) \quad [3]$$

occurs in 1 M perchloric acid with a rate constant of 0.0073 liter mole^{-1} min^{-1} at 25° C (6*a*). The specific rate of the Cr(III)–Cr(II) electron exchange is likely 0.028 liter mole^{-1} min^{-1} with a water molecule probably being the bridging group in the activated complex (6*b*). Equation [3], which omits ligands, is therefore a simplified statement of the reaction, since water and hydrogen ions are also involved.

When the polarographic reduction of Cr(III) begins, the Cr(II) concentration in the diffusion layer is negligible, and the Cr(III) is presumably reduced at the electrode interface. As reduction proceeds, the Cr(II) concentration at the interface increases and, at $E_{\frac{1}{2}}$, is essentially equal to that of Cr(III). At potentials more negative than $E_{\frac{1}{2}}$, the [Cr(II)]/[Cr(III)] ratio becomes increasingly greater and there is an increased probability that, instead of the entering Cr(III) being reduced directly at the electrode interface, it may be reduced by a Cr(II) ion at the interface or diffusing from the interface into the diffusion layer. A Cr(II) ion at the mercury–solution interface may thus serve as the electron transfer agent between the incoming Cr(III) ion and the electrode, acquiring another electron from the electrode after it has become a Cr(III) species. The latter electron transfer process may occur before the newly formed Cr(II) ion diffuses away from the original Cr(II) ion, which is fixed at the interface, or possibly even during the electron transfer process between fixed Cr(II) and incoming Cr(III).

In extending the reaction summarized in equation [3] to a reaction which may occur at an electrode interface, the difficulty must be recognized of defining the activated complex concerned, which may or may not involve a water molecule as a bridging group and unknown hydrogen ion dependence.

If the electrolysis of an ion at an electrode is assumed to involve at least two stages

Can. J. Chem. Downloaded from www.nrcresearchpress.com by 190.90.36.8 on 09/04/12
For personal use only.

i.e., transfer of the solvated ion from the bulk of the solution to the electrode surface (with more or less loss of the hydration sheath) and subsequent combination of the adsorbed ion with an electron provided by the electrode (7), it is possible that the secondary process outlined in the previous paragraphs, in which the Cr(III) species is already oriented at the interface for the electron transfer process, would have a lower transfer coefficient than the normal direct reduction, so that qualitatively one may account for the two slopes found in the log slope.

If the transfer coefficient is defined as that fraction of the potential "required" to transform an ion from a solution environment to that of the electrode interface, then it is true that the closer an ion is to the interface environment, the lower is the transfer coefficient. It therefore follows that, if a Cr*(II) formed at this surface is oxidized to Cr*(III) by an incoming Cr(III) ion, we have in effect transformed a Cr(III) ion from a position Cr to Cr*, i.e., closer to the interface, so that part of the transformation occurs under this "exchange potential", and only part is facilitated by an applied potential. Consequently the *total* process must have a lower transfer coefficient than one in which there are no exchanges between Cr(III) and Cr*(II).

In order not to have a lower transfer coefficient for the case of Cr(III)–Cr*(II) position exchange, one would have to assume a completely quantum-like jump from solution environment to surface environment without an intermediate state, which seems highly unlikely. To have a higher transfer coefficient would require a new mechanism, e.g., introduction of other ions.

Dichlorotetraaquo Ion

The polarography of the dichlorotetraaquochromium(III) species follows the same general pattern as that observed for the hexaaquo ion. The waves are considerably more drawn out and occur at more positive $E_{\frac{1}{2}}$ values; the log plots show the same asymmetry. However, the situation is complicated by the fact that the Cr(III)–Cr(II) exchange in the chloro complexes is accomplished by an anion transfer mechanism (8), which, omitting complexed water, may be written as

$$Cr^*Cl_2^+ + Cr(II) = Cr^*(II) + CrCl^{++} + Cl^- \quad [4]$$

Consequently, one must deal with an alteration in the complex ions as well as with multiple electron transfer processes and space charge effects. Under these circumstances, it is difficult to arrive at any consistent picture without knowing considerably more than is now known about these processes.

One point which should be noted concerning the anion transfer mechanism of equation [4] is the "catalytic" degradation of the higher chloro complexes by the Cr(II) formed in the reduction. The specific rate constant (8) for the reaction of equation [4] at 2° C is 10^4 liters mole^{-1} min^{-1}. It is reasonable to suppose that, in view of the greater lability of the chloride ligands in the higher Cr(III) complexes, the rate for the comparable process for these complexes would be considerably higher. It is then not surprising that $E_{\frac{1}{2}}$ for $[Cr(H_2O)_4Cl_2]^+$ in 12 *M* hydrochloric acid solution is the same before and after the reaction with the hydrochloric acid, since this catalytic degradation would tend to "level" the complexity of the species involved. Ultraviolet absorption indicates the Cr(III) species finally formed in 12 *M* HCl to be the trichlorotriaquochromium(III).

EXPERIMENTAL

Preparation, purification, and analysis of the various chromium(III) salts have been described (2). Sodium perchlorate was obtained as a solution of known molarity by titration of sodium hydroxide with a perchloric acid solution.

Can. J. Chem. Downloaded from www.nrcresearchpress.com by 190.90.36.8 on 09/04/12
For personal use only.

A Sargent Model XXI Polarograph and a Leeds & Northrup Model E Electro-Chemograph were used in conjunction with a jacketed H-cell (9), maintained at 25±0.1° C, which contained a saturated calomel electrode (S.C.E.) in one arm, separated by a sintered glass disk and KCl–agar plug from the working arm. After runs in perchlorate media, the cell was thoroughly flushed with warm distilled water to remove any precipitated potassium perchlorate from the region near the glass disk.

All $E_{\frac{1}{2}}$ data are referred to the S.C.E.; the iR drop in the cell system was negligible. Some runs were made against a mercury pool electrode in order to ascertain the effect of the agar–KCl bridge; the results were similar to those obtained against the S.C.E.

Oxygen was removed from the test solutions by purging with water-pumped nitrogen which was first deoxygenated by passage through an acid Cr(II) sulphate solution and then equilibrated by passage through some of the test solution; suitable traps were included to prevent contamination. In solutions of high acidity, it was necessary to deoxygenate for extended periods of time before introducing mercury; otherwise, oxygen waves interfered with the polarograms. No maximum suppressors were added.

In order to observe the polarographic wave of the Cr(III) species in 12 M hydrochloric acid before appreciable reaction has taken place, the following procedure was adopted: concentrated hydrochloric acid was placed in the polarographic cell; nitrogen was bubbled through the solution for about 30 minutes; dry $[Cr(H_2O)_4Cl_2]Cl$ or $[Cr(H_2O)_6]Cl_3$, which had been flushed with nitrogen, was then introduced into the solution under a nitrogen cover; the resulting solution was deoxygenated for another 5 to 7 minutes; the polarogram was then taken.

The polarogram of the Cr(III) species existing in 12 M HCl when equilibrium is attained was observed by first dissolving the chromic chloride in the 12 M acid (the form of the complex is immaterial), warming to 90° C to hasten equilibrium, then cooling to room temperature, transferring to the polarographic cell, sweeping with nitrogen for about an hour (from spectrophotometric evidence, reaction is complete within this time), and then taking the polarogram.

ACKNOWLEDGMENT

The authors wish to thank the Atomic Energy Commission, which helped support the work described.

REFERENCES

1. (*a*) DAMASSIEUX, M. and HEYROVSKY, J. J. chim. phys. **26**, 219 (1929). (*b*) HAMM, R. E. and SHULL, C. M. J. Am. Chem. Soc. **73**, 1240 (1951). (*c*) KALOUSEK, M. Collection Czechoslov. Chem. Communs. **11**, 592 (1939). (*d*) KOLTHOFF, I. M. and LINGANE, J. J. Polarography. Vol. II. 2nd ed. Interscience Publishers, Inc., New York. 1952. (*e*) PECSOK, R. L. and LINGANE, J. J. J. Am. Chem. Soc. **72**, 189 (1950). (*f*) PRAJZLER, J. Collection Czechoslov. Chem. Communs. **3**, 406 (1931). (*g*) REYNOLDS, G. F., SHALGOSKY, H. I., and WEBBER, T. J. Anal. Chim. Acta, **8**, 564 (1953). (*h*) WILLIS, J. B. J. Proc. Roy. Soc. N. S. Wales, **78**, 239 (1946).
2. ELVING, P. J. and ZEMEL, B. J. Am. Chem. Soc. **79**, 1281 (1957).
3. (*a*) DELAHAY, P. New instrumental methods in electrochemistry. Interscience Publishers, Inc., New York. 1954. (*b*) EYRING, H., MARKER, L., and KWOH, T. C. J. Phys. & Colloid Chem. **53**, 1453 (1949). (*c*) KOUTECKY, J. Collection Czechoslov. Chem. Communs. **18**, 597 (1953).
4. ELVING, P. J. and OLSON, E. C. J. Am. Chem. Soc. **79**, 2697 (1957).
5. LAITINEN, H. A., OLDHAM, K. B., and ZIEGLER, W. A. J. Am. Chem. Soc. **75**, 3048 (1953).
6. (*a*) ANDERSON, A. and BONNER, N. A. J. Am. Chem. Soc. **76**, 3826 (1954). (*b*) PLANE, R. A. and TAUBE, H. J. Phys. Chem. **56**, 37 (1952).
7. GLASSTONE, S., LAIDLER, K. J., and EYRING, H. The theory of rate processes. McGraw-Hill Book Co., Inc., New York. 1941. pp. 575–577.
8. TAUBE, H. and MEYERS, H. J. Am. Chem. Soc. **76**, 2103 (1954).
9. KOMYATHY, J. C., MALLOY, F., and ELVING, P. J. Anal. Chem. **24**, 431 (1952).

Can. J. Chem. Downloaded from www.nrcresearchpress.com by 190.90.36.8 on 09/04/12
For personal use only.

Can. J. Chem. Downloaded from www.nrcresearchpress.com by 190.90.36.8 on 09/04/12
For personal use only.

THE INFLUENCE OF SURFACE ACTIVE ANIONS ON THE ELECTROREDUCTION OF THE PERSULPHATE ANION AT NEGATIVE POTENTIALS[1]

A. Frumkin, N. Nikolajeva-Fedorovich, and R. Ivanova

The dependence of the kinetics of electrode processes on the surface layer structure has recently been the subject of a series of investigations. This dependence is especially pronounced if the electrode surface and the reacting particle have charges of the same sign, as in the case of anion electroreduction on a negatively charged surface (1, 2, 3, 4, 5). The phenomena observed under these conditions might be understood if we assume that the rate of the electrode reaction depends not only on the electrode potential, ϕ, but on the potential in that point of the double layer where the center of the particle in the transition state of the reaction is situated too. This local ψ_1-potential value is influenced by the cation which is the nearest neighbor of the reacting anion (5, 6, 7, 8, 9), and might be markedly different from the average potential, $\bar{\psi}_1$, at a distance from the electrode equal to the radius of the reacting particle. The rate of the electrode process depends therefore not only on the interaction between the charge of the anion with the charges on the metal surface, but on its interaction with the charge of the neighboring cation, which facilitates its approach to the negatively charged surface as well. In this sense we can use the concept of the formation of cationic bridges between the negatively charged surface and the reacting anion (Fig. 1). We shall not discuss here the question of the role played by the adjacent cation in the elementary act of the electron transfer itself.

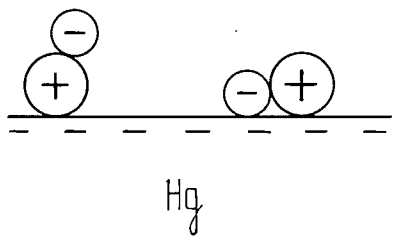

Fig. 1. Schematic representation of the adsorption of anions on a negatively charged metallic surface. The decrease of the absolute value of the negative charge of the mercury surface on anion adsorption shows that the configuration represented to the right is the preponderant one.

The object of this communication is to describe some characteristic features of the electroreduction of the $S_2O_8^{2-}$ anion, which might be considered as an example of the dependence of the kinetics of this reaction upon the details of the double layer structure.

Kalish and Frumkin found that the rate of the persulphate electroreduction on positively charged mercury strongly decreases in the presence of surface active anions (10). Thus, the half-wave potential of this reaction is *ca.* 0.6 v more negative in *N* KBr than in *N* Na_2SO_4. Qualitatively, this can be easily accounted for by the building up of a negative ψ_1-potential, when Br^- anions are adsorbed on mercury, which decreases the surface concentration of the $S_2O_8^{2-}$ ions (and shifts the effective potential difference

[1]*Manuscript received July 24, 1958.*
Contribution from the Institute of Electrochemistry, Academy of Sciences, Moscow, U.S.S.R. This paper was presented at the Symposium on Charge Transfer Processes held at the University of Toronto, Toronto, Ontario, September 4 and 5, 1958.

ϕ–ψ_1 between the electrode surface and the center of the reacting particle in an unfavorable direction too). However, a quantitative comparison of the rates of the process at different potentials shows that the decrease of the reaction velocity caused by the negative ψ_1-potential at equal $\bar{\psi}_1$-values is smaller when the ψ_1-potential arises from a specific anion adsorption than in the case of a negative ψ_1-potential build-up in the neighborhood of a negatively charged metal surface, which attracts cations by coulombic forces only, that is in a double layer with a "normal" structure. Although a quantitative explanation of this discrepancy cannot be given at the present moment, it is probable that the discrepancy is connected with the difference between the average and the local (effective) ψ_1-potential values. In an electric field with localized negative charges, which arise from the specific adsorption of anions, the distribution of the potential parallel to the electrode surface must be much more inhomogeneous than in a "normal" double layer with negative electrical charges smeared on the equipotential metal surface.

Kalish and Frumkin came to another, somewhat unexpected, conclusion. They found that with a negatively charged surface at potentials at which the repulsion between the electrode and the reacting anion manifests itself and a minimum on the current–voltage curve is observed, the sequence of the action of halogen anions is reversed. Thus, when 10^{-4} N $K_2S_2O_8$ is reduced in the presence of potassium halogenides at a concentration of 10^{-2} N, the current strength increases in the sequence $Cl^- < Br^- < I^-$. The small adsorption of anions which occurs on a negatively charged surface therefore exerts on the kinetics of the process an influence opposite to that observed in the case of their strong adsorption on a positively charged surface. The cause of this inversion has not been completely elucidated until now and we shall not consider it here in detail.*

Differential capacity measurements as well as determinations of the zero-charge potential in solutions of fluorides, chlorides, and iodides of sodium, potassium, and cesium showed that the adsorption of surface active anions on a negatively charged surface is strongly influenced by the nature of the cations (8, 11). Thus, the increase of the differential capacity at negative potentials and the shift of the zero charge potential to more negative values is much more pronounced in the case of a transition from a CsCl solution to a CsI solution of equal concentration than in the case of a transition from a NaCl solution to a NaI solution. Apparently, the adsorption of anions on a negatively charged mercury depends to a large extent on the formation of cationic bridges, although, as follows from other considerations, the $\bar{\psi}_1$-potential in the cationic Helmholtz layer is also more positive in the presence of Cs^+ cations than in the presence of Na^+ cations.

On comparing these results with those obtained earlier by Kalish and Frumkin, the conclusion could be drawn that the acceleration of the $S_2O_8^{2-}$ electroreduction by iodide ions described in (10) must depend on the nature of the cation, increasing in the sequence $Na^+ < K^+ < Cs^+$. To check this conclusion some measurements with a dropping electrode were carried out. Current–voltage curves obtained with 2.10^{-4} N solutions of $K_2S_2O_8$ in the presence of fluorides, chlorides, bromides, and iodides of sodium, potassium,

**At any rate, an effect of that kind would be impossible, if the average ψ-potential would determine the rate, as the specific adsorption of anions will always cause a shift of ψ_1 to more negative values, and must therefore decrease the reaction rate. It appears that by taking into account the inhomogeneity of the potential distribution in the double layer in the case of specific anion adsorption and the decrease of the absolute value of the negative charge of the metal surface, caused by the appearance of this double layer, it can be understood that local ψ_1-potential values (in points lying sufficiently far from adsorbed anions) at a given Φ might be, in fact, more positive in this case than in a "normal" double layer. In the paper of Kalish and Frumkin a schematic picture of the double layer was given with the purpose of explaining the kinetic effects observed, but a more detailed consideration showed that this scheme is incorrect and must be abandoned.*

Can. J. Chem. Downloaded from www.nrcresearchpress.com by 190.90.36.8 on 09/04/12
For personal use only.

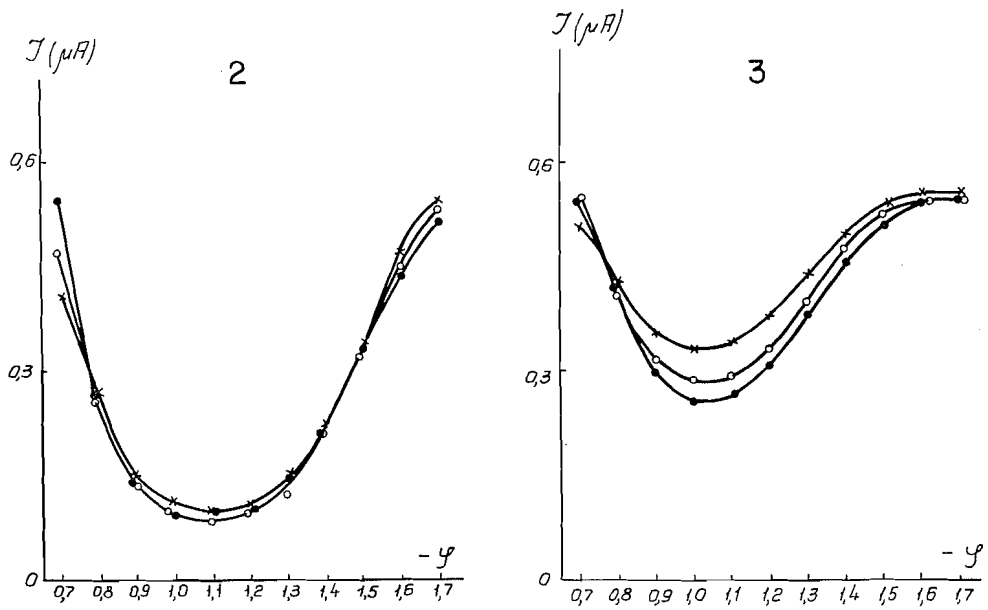

FIG. 2. Current–voltage curves for the electroreduction of 2.10^{-4} N $K_2S_2O_8$ in the presence of sodium salts. ● 10^{-2} N NaF; ○ 10^{-2} N NaCl; × 10^{-2} N NaI.

FIG. 3. Current–voltage curves for the electroreduction of 2.10^{-4} N $K_2S_2O_8$ in the presence of potassium salts. ● 10^{-2} N KCl; ○ 10^{-2} N KBr; × 10^{-2} N KI.

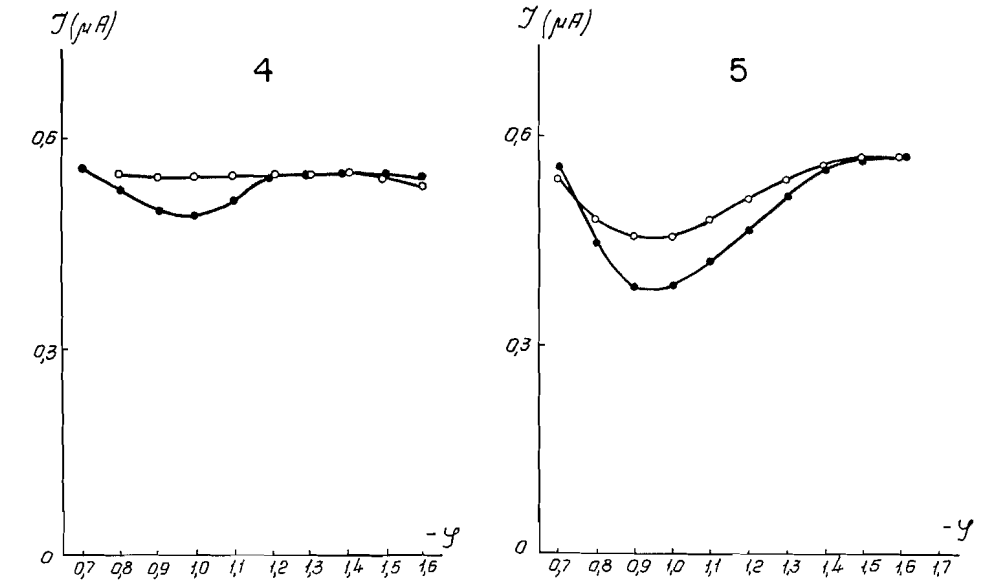

FIG. 4. Current–voltage curves for the electroreductions of 2.10^{-4} N $K_2S_2O_8$ in the presence of cesium salts. ● 10^{-2} N CsCl; ○ 10^{-2} N CsI.

FIG. 5. Current–voltage curves for the electroreduction of 2.10^{-4} N $K_2S_2O_8$ in the presence of cesium. ● 5.10^{-3} N CsCl; ○ 5.10^{-3} N CsI.

Can. J. Chem. Downloaded from www.nrcresearchpress.com by 190.90.36.8 on 09/04/12
For personal use only.

and cesium in a 10^{-2} N concentration are given on Figs. 2, 3, 4, and 5. The potentials are referred to a N.C.E. The parts of the current–voltage curves corresponding to potentials more positive than the zero-charge potential, which are deformed by a polarographic maximum of the first kind, have been omitted throughout. No difference between the current strength $\bar{J}$ in the presence of F^- and Cl^- can be observed within the limits of experimental error in sodium salts solutions (Fig. 2); the transition to a sodium iodide solution causes an increase of the reaction rate amounting to some 20%. On substituting K^+ for Na^+ we observe a marked increase of the velocity of the reaction (Fig. 3), which was already discussed in earlier papers (3, 8, 12) (primary cationic effect); at the same time the difference between the rates in the presence of different anions strongly increases. Thus on transition from 10^{-2} N KCl to 10^{-2} N KI the quantity $\bar{J}/(\bar{J}_d-\bar{J})$ increases *ca.* 1.6 times. In the presence of 10^{-2} N CsI (Fig. 4) the rate of the $S_2O_8^{2-}$ electroreduction on negatively charged mercury becomes so large that the minimum on the current–voltage curve disappears altogether. In order to obtain a quantitative estimate of the I^- anion efficiency in the presence of Cs^+, we have carried out measurements with 5.10^{-3} N solutions of CsCl and CsI. The quantity $\bar{J}/(\bar{J}_d-\bar{J})$ increases in this case on transition from Cl^- to I^- approximately twice* (Fig. 5). The experiments thus confirm the expected dependence of the influence of surface active anions on the rate of the $S_2O_8^{2-}$ electroreduction at negatively charged mercury on the nature of the cation.

REFERENCES

1. KRJUKOVA, T. Compt. rend. acad. sci. U.R.S.S. **65**, 57 (1949).
2. FRUMKIN, A. and FLORIANOVICH, G. M. Compt. rend. acad. sci. U.R.S.S. **80**, 907 (1951); J. Phys. Chem. (U.S.S.R.), **29**, 1827 (1955).
3. FRUMKIN, A. Z. Elektrochem. **59**, 807 (1955).
4. FRUMKIN, A. Proc. Second Congr. Surface Activity (London), **III**, 58 (1957).
5. FRUMKIN, A. and NIKOLAJEVA-FEDOROVICH, N. J. Chem. Phys. **26**, 1552 (1957).
6. FRUMKIN, A. Actualités sci. et ind. **373** (1936).
7. FRUMKIN, A. Proc. Acad. Sci. U.S.S.R., Sect. Chem. (English Translation), 1429 (1957).
8. FRUMKIN, A. and NIKOLAJEVA-FEDOROVICH, N. Vestnik Moskov. Univ. Chem. Ser. 169 (1957).
9. FRUMKIN, A. Trans. Faraday Soc. (In press).
10. KALISH, A. and FRUMKIN, A. J. Phys. Chem. (U.S.S.R.), **28**, 1473 (1954).
11. FRUMKIN, A., DAMASKIN, A., and NIKOLAJEVA-FEDOROVICH, N. Compt. rend. acad. sci. U.R.S.S. **115**, 751 (1957); **121**, 129 (1958).
12. ZEZULA, I. Chem. Listy, **47**, 492, 969 (1953).

**At a potential $\phi = 0.75$ v the current strength is always somewhat smaller in the presence of I^- as in the presence of Cl^-. This effect is caused by the superposition of the current of the anodic dissolution of mercury on the current of the $S_2O_8^{2-}$ electroreduction. The former becomes noticeable in iodide solutions at the given potential on account of complex formation with mercury.*

Can. J. Chem. Downloaded from www.nrcresearchpress.com by 190.90.36.8 on 09/04/12
For personal use only.

Can. J. Chem. Downloaded from www.nrcresearchpress.com by 190.90.36.8 on 09/04/12
For personal use only.

CATHODIC ORGANIC PROCESSES[1]

M. J. ALLEN

The investigation of cathodic organic processes has been handicapped by two factors: the physical chemist who is qualified to indulge in this work but who feels organic systems too complex to ever be decipherable, and the organic chemist who being aware of the complexity of his medium is generally fearful of a pair of wires, a voltmeter, ammeter, and the other physical accessories, both real and mathematical, required to accomplish an electrochemical investigation. Thus investigations of this type have been left to those too few physical–organic chemists who understand the underlying physical principles and who are not overcome by the thought of working with an organic system.

As the organic electrochemist deals mainly with irreversible systems he must be content with a more empirical approach than his colleagues the inorganic electrochemists, who can readily obtain the potential of their system by application of the thermodynamic expression for a reversible electrochemical reaction:

$$E = E - RT/nF \ln(\mathrm{Ox})/(\mathrm{Red}).$$

The organic electrochemist is at a further disadvantage in that his reactions usually cannot be studied in purely aqueous systems and he must be concerned with the possible side reactions associated with the medium and/or the temperature used in the experiment. However, despite these difficulties, many problems involving cathodic processes have been more readily solved by use of a methodical approach which I admit is somewhat empirical, but still superior to a grossly haphazard attack on the problem which generally results in discouraging negative results. I should like to illustrate my point by a brief discussion followed by a few examples.

The first concern in the performance of a cathodic process is the choice of a medium which will serve as a suitable solvent for the organic compound, and still when mixed with an electrolyte offer as low a resistance as possible to the passage of an electric current. These conditions are far superior to the use of an excellent electrolyte medium but a poor solvent medium. The consequence of the latter is that one has essentially a suspension of the organic compound in the catholyte which leads to low process efficiency. Within this category also lies the choice of electrode material, and the current density or reference potential required to achieve the desired end result. Constant current density electrolysis is suitable so long as it is used in conjunction with an electrode whose potential is such that it will give the desired reduction product and will not further reduce this product. Under these circumstances it must be remembered that maximum efficiency is impossible, for as the depolarizer (the organic compound being reduced) diminishes in concentration as a result of the cathodic process, the limiting reaction current should also diminish. Generally a polarographic or voltammetric investigation prior to a mass electrolysis study will give the desired information as to the optimum reference potential to use when controlled potential electrolysis is being considered, or the ideal electrode material to consider for the process. When controlled potential conditions are to be used the electrode material is generally not a problem as one chooses a high overpotential electrode such as mercury or lead and adjusts its reductive ability by the potential at the electrode

[1]*Manuscript received July 3, 1958.*
Contribution from the Research Department, CIBA Pharmaceutical Products Inc., Summit, New Jersey, U.S.A. This paper was presented at the Symposium on Charge Transfer Processes held at the University of Toronto, Toronto, Ontario, September 4 and 5, 1958.

surface vs. a standard reference electrode. When using constant current density conditions, one can obtain an arbitrary focal point for initial experimentation by application of the limiting current equation, i.e. $L_i = 0.0223DCn$ in which D is the diffusion coefficient, C the concentration of the organic species in g-moles per liter, and n the number of electrons exchanged in the process. By performing experiments at multiples or fractions of this arbitrary calculated limiting reaction current, and by examination of the reaction products, one can then choose those constant current density conditions which will yield maximum results.

Having decided on the aforementioned conditions the next item is the choice of a cell to be used for the actual experiment. Beyond the fact that the electrolysis cell consists of a cathode, anode, a low porosity membrane to separate the catholyte from the anolyte, a stirrer, a thermometer, and a reference electrode if controlled potential conditions are to be employed, the investigator may permit free reign to his imagination in the design of these cells. Two such cells are illustrated in Figs. 1 and 2.

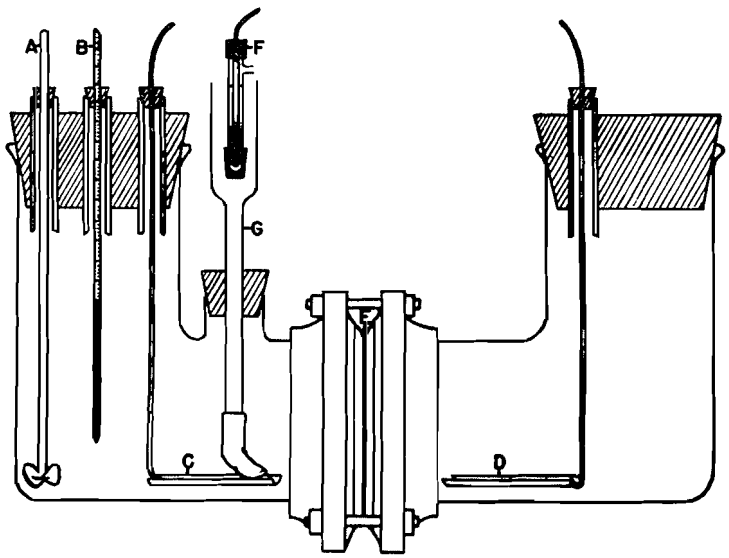

FIG. 1. Electrolysis cell for solid type electrode. A, stirrer; B, thermometer; C, lead cathode; D, platinum, lead, nickel, or stainless steel anode; E, gasketed ion-exchange or cellophane membrane; F, reference electrode; G, salt bridge.

Last but by no means the least important item in performing the electrolysis is the electrical equipment required for this operation. A simple circuit will consist of a variable d-c. voltage supply, a voltmeter, ammeter, and if one desires to investigate the possibilities of controlled potential conditions a reference electrode, and a vacuum tube voltmeter. Such a simple circuit is described in Fig. 3.

The literature, of course, abounds with descriptions of devices for automatic controlled potential electrolysis (1). Each of these devices has its respective advantages and disadvantages. The prime prerequisite for an instrument which is to be used for organic electrochemical investigations is that it have an output of approximately 10 amp and 60 v. The circuit of an apparatus of this type recently designed in our laboratories is illustrated in Figs. 4 and 5.

Can. J. Chem. Downloaded from www.nrcresearchpress.com by 190.90.36.8 on 09/04/12
For personal use only.

Can. J. Chem. Downloaded from www.nrcresearchpress.com by 190.90.36.8 on 09/04/12
For personal use only.

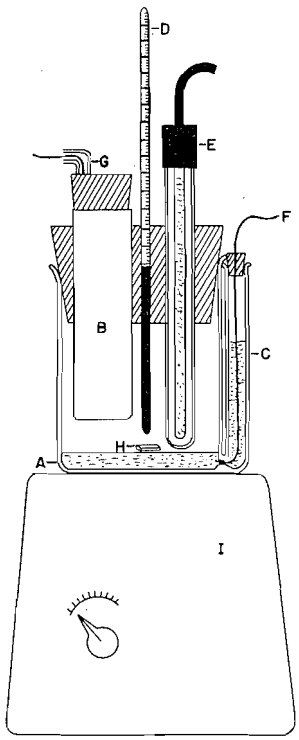

FIG. 2. Electrolysis cell for mercury cathode. A, pyrex beaker; B, porous porcelain membrane (Alundum); C, side-arm contact to the mercury pool consisting of a piece of glass tubing through which is sealed a piece of platinum wire; D, thermometer; E, reference electrode; F, cathode lead wire; G, nitrogen inlet and outlet tubes (for removal of peroxides from anode compartment); H, glass-covered magnetic bar; I, magnetic stirrer.

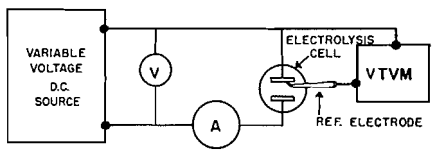

FIG. 3. Simple electrolysis circuit.

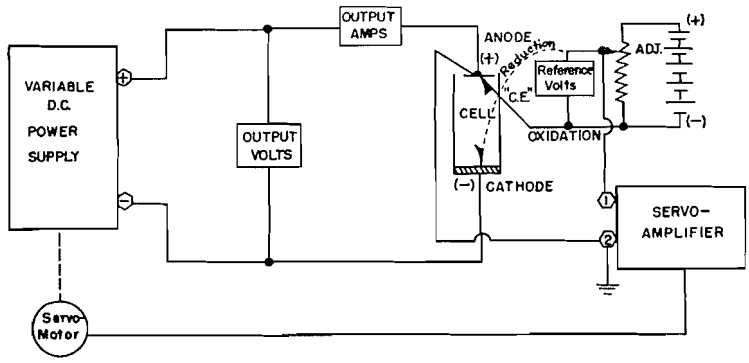

FIG. 4. Function diagram—Redox-o-trol Mark IV.

Can. J. Chem. Downloaded from www.nrcresearchpress.com by 190.90.36.8 on 09/04/12
For personal use only.

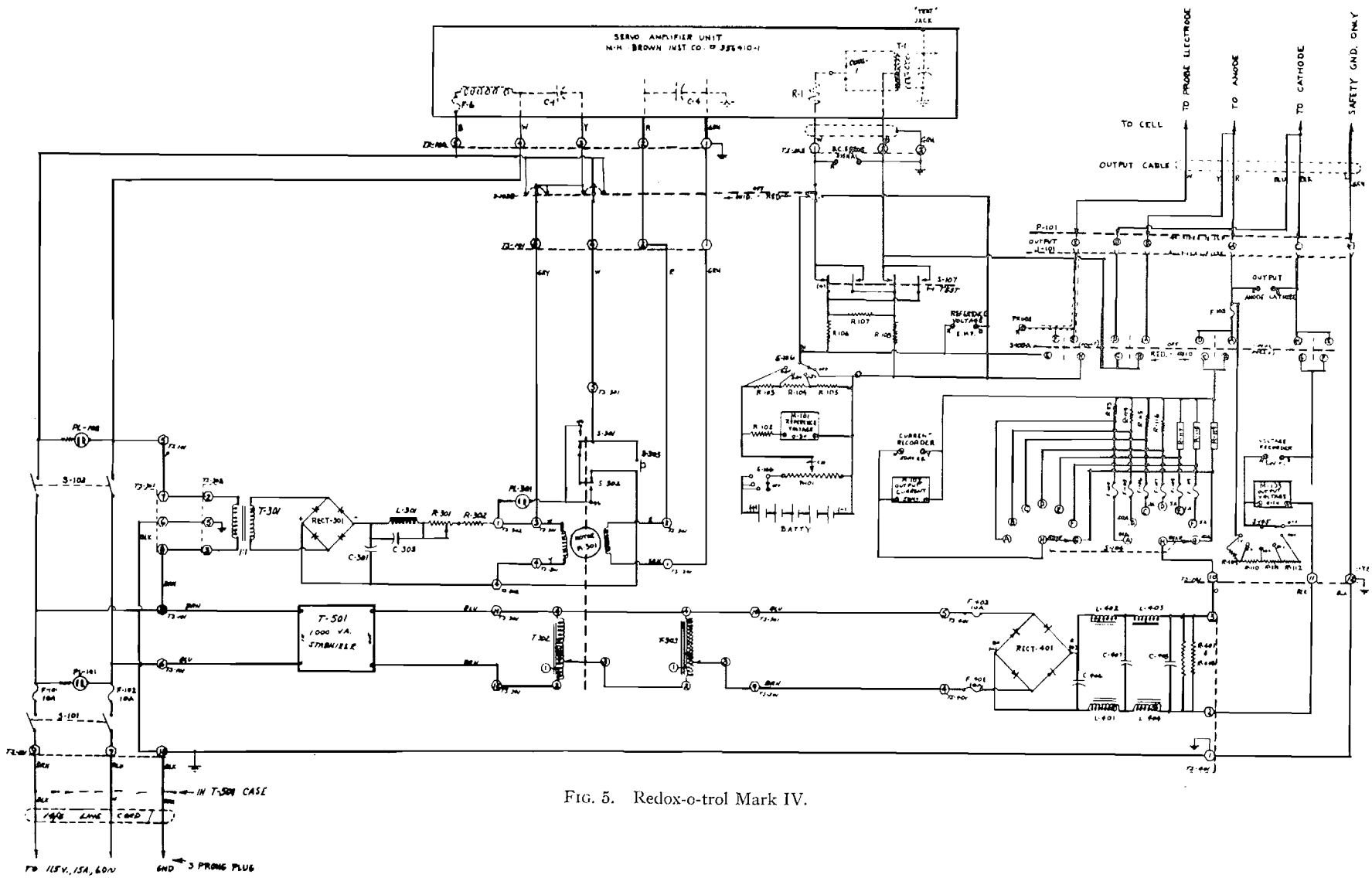

FIG. 5. Redox-o-trol Mark IV.

Components list:

Amplifier	M.H.-Brown No. 356410-1	
*Conv.-1	M.H.-Brown No. 75829-1 (Part of above)	
*M-301	M.H.-Brown No. 76750-3	
Capacitors		
C-1, 4	1.0 mf, 600 v (Part of Brown Amplifier)	
C-301	20 mf, 250 v Sprague TVL-1509	
C-302	0.5 mf, 600 v Sprague No. BP-506	
*C-406	500 mf, 125 v, d-c. Mallory No. NP1255	
*C-407, 408	1000 mf, 150 v, d-c. Mallory No. HC-15010	
Fuses		
*F-6	1/2 amp Slo-Blo	3 AG (Part of amplifier)
*F-101, 102, 103	10 amp	3 AG Little-Fuse No. 314010
*F-104	1/100 amp	8 AG " " No. 361010
*F-105	1/16 amp	8 AG " " No. 361062
*F-106	1/8 amp	8 AG " " No. 361125
*F-107	1/2 amp	8 AG " " No. 361500
*F-108	1 amp	8 AG " " No. 361001
*F-109	5 amp	8 AG " " No. 361005
F-401, 402	10 amp 250 v	(Renewable links) Chase-Shawmutt "Shurlag" No. 1007
Connectors		
J-101	No. AN-3102A-18-125 Amphenol Co.	
P-101	No. AN-3108A-18-12P Amphenol Co.	
All other Jacks	"5 Way" Binding Posts—H. H. Smith No. 257, or Johnson No. 108-900 Series.	
Chokes		
L-301	8 Hys., 40 ma, Stancor No. C-1333	
L-401, 402, 403, 404	Special .04 Hys., 2 ohms, 10 amp (Virgina Electronics Products Company, Bethesda, Maryland)	

Lamps

PL-101 115 v, Neon, Clear Jewel, NE 51 Bulb, Dial Company No. 91408-930
PL-102 115 v, Neon, Yellow Jewel, NE 51 Bulb, Dial Company No. 91408-936
PL-301 115 v, Neon, Red Jewel, NE 51 Bulb, Dial Company No. 91408-931

Resistors	
R-1	47 kohm, 10%, 1/2 W. Carbon IRC No. BTS
R-101	1000 ohm, Potentiometer, 4 w, W.W., Mallory No. MIMPK
R-102, 103	3 kohm, 1%, 1/2 w, W. W., IRC No. WW3J
R-104, 105	1.5 kohm, 1%, 1/2 w, W. W., IRC No. WW3J
R-106, 108	10 kohm, 10%, 1/2 w, Carbon IRC BTS
R-107	2 ohm, 10%, 1/2 w, Carbon IRC BTS
R-109	4 kohm, 1%, 1/2 w, W. W., IRC No. WW3J
R-110	5 kohm, 1%, 1/2 w, W. W., IRC No. WW3J
R-111	40 kohm, 1%, 1/2 w, W. W., IRC No. WW3J
R-112	50 kohm, 1%, 1/2 w, W. W., IRC No. WW3J
R-113	25 ohm, 1/2% (consists of four 100 ohm selected W.W.)
R-114	1/2 ohm, 1% (made of 1.0, 1%, and 0.2, 1% IRC No. WW3J)
R-115	.545 ohm, 1%, 1/2 w, W. W. IRC No. WW3J
R-116	.102 ohm, 1%, 1/2 w, W. W. IRC No. WW3J
R-117	SHUNT 1.0 amp, 50 mv Westinghouse No. 936938
R-118	SHUNT 5.0 amp, 50 mv Westinghouse No. 724755
R-119	SHUNT 10.0 amp, 50 mv Westinghouse No. 724756
R-301	5000 ohm Adj., 10 w, Ohmite No. 1033
R-302	2500 ohm, 5 w, Ohmite "Brown Devil"
R-401, 402	3000 ohm, 20%, 10 w, Ohmite "Brown Devil"
Rectifiers	
RECT-301	Four (4) 75 ma, 115 v Federal No. 1003A
RECT-401	10 amp, 100 v, Full Wave Bridge, Sarkes No. D35
Switches	
S-101	D.P.S.T. 15 amp, 250 v, Toggle, C-H No. 7561
S-102	D.P.S.T. 12 amp, 250 v, Toggle, C-H No. 7565
S-103A	4.P., 3 Pos. 10 amp, 250 v, Electro-Switch Corporation
S-103B	4.P., 3 Pos. Centralab No. 2515 (Note: S-103A and 103B are ganged to operate together)
S-104	2.P., 7 Pos., 10 amp, 250 v, Electro-Switch Corporation
S-105	1.P., 6 Pos., 10 amp, 250 v, General Electric Company
S-106	2 Pole, 5 Pos. Centralab No. 1405

Can. J. Chem. Downloaded from www.nrcresearchpress.com by 190.90.36.8 on 09/04/12
For personal use only.

R-107	4 Pole, 3 Pos. Lever Switch, Switchcraft No. 6038
S-301, 302	S.P.D.T. 10 amp, 115 v, Roller Arm, Microswitch No. BZ-2RW22-A2
S-303	P.B. (open) 5 amp, 115 v, Grayhill No. 4001
Batteries	
*Five (5) required	Mercury Cells (1.34 to 1.4 v) Mallory No. RM-12-R RCA No. VS313
Meters	
M-101	3 volts d-c., 1000 ohms/volt, 2%, Triplett No. 420
M-102	50 mv., d-c. (10 amp scale), 2%, Triplett No. 420
M-103	1 volt d-c., 1000 volt ohms, 2%, Triplett No. 420
Transformers	
T-301	Isolation, 115 v to 115 v, Triad No. N-51X
T-302	Variable Voltage, "Variac", General Radio No. V-10
T-303	Variable Voltage, "Variac", General Radio No. V-20H
T-501	Stabilizer, 1000 va, Sola No. 20–13–210

Notes:

5 inside ⬡ TS-301 denotes 5th terminal, 1st strip, 300 series unit.

A or 2 inside ○ denotes terminal number on particular component.
Unit series numbers are servo amp unit.
100 series numbers are control chassis and panel.
200 series numbers are monitor panel.
300 series numbers are variac chassis and panel.
400 series numbers are rectifier chassis and panel.
500 series numbers are stabilizers.

**Indicates recommended spare part item.*

Essentially this instrument consists of a d-c. power rectifier, the magnitude of whose output is controlled by a motor-driven rheostat on the a-c. side of the power supply. The rheostat receives its activating signal from the amplifier, which in turn receives its signal from the cathode in conjunction with the reference electrode. In Fig. 6 will be seen the front and rear views of the instrument mentioned.

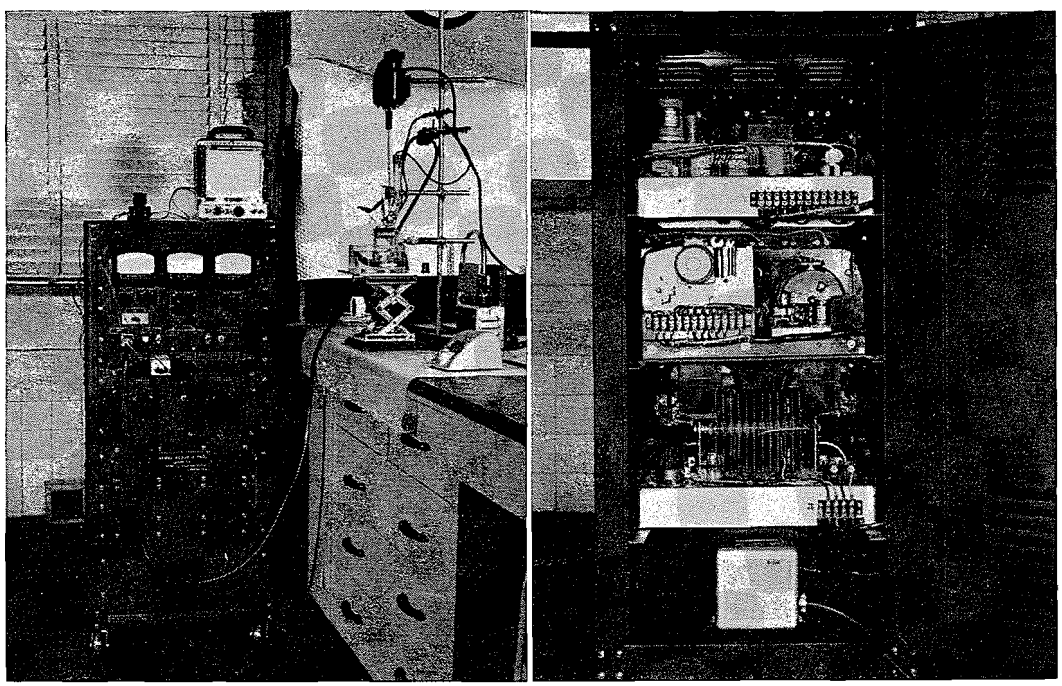

FIG. 6. Redox-o-trol Mark IV: left, front view; right, rear view.

Can. J. Chem. Downloaded from www.nrcresearchpress.com by 190.90.36.8 on 09/04/12
For personal use only.

The ammeter of this instrument has seven ranges of 100 divisions each, so that one can obtain a minimum of 0.01 amp to a maximum of 10 amp full scale. The voltmeter indicating total applied voltage has a range of 1 volt to 100 volts full scale. Reference potentials as high as 3 volts can be imposed from a separate voltage supply. In addition the instrument is also suitable for oxidations under controlled potential conditions as well as constant current density electrolysis by the use of a suitable resistor built into the instrument.

I shall now briefly illustrate by a few examples the approach generally taken in the solution of a problem. The first example involves the cathodic reduction of 3,4,5,6-tetrachloro-N-(2-dimethylaminoethyl)phthalimide (I) to the fully reduced isoindoline (IV), an intermediate in the preparation of a potent ganglionic blocking agent used in the treatment of hypertension.

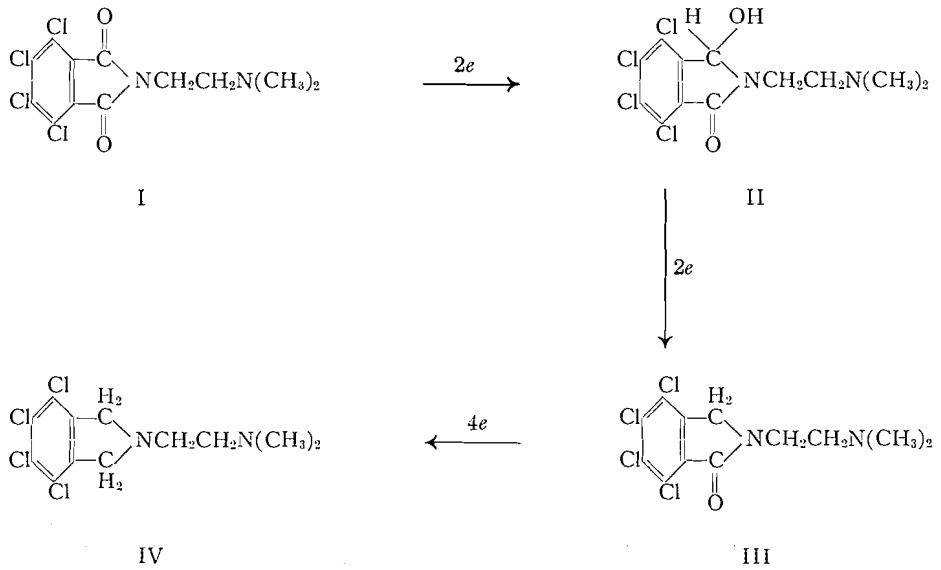

Previous investigators in their studies on phthalimides found that in an aqueous sulphuric acid medium at a copper cathode the phthalimide underwent a 2-electron change to yield the hydroxyphthalimidine. The use of a lead electrode yielded the fully reduced isoindoline via an 8-electron change (a). This indicated that in our case a lead electrode would be the most desirable one to use. It was obvious that the media used in the past which gave a suspension of the starting material accounted, together with the reported excessive current densities, for the low current efficiencies obtained. Therefore, as we in the solution of our particular problem desired improved efficiency, we firstly had to choose a medium which would enable us to perform our reactions on a solution, and secondly determine the optimum current density for the reactions. The former was solved by using an aqueous acetic sulphuric acid medium. By application of the limiting current equation in which D was 0.6 cm^2 day^{-1} and C, 0.2435 g-moles/liter we found our arbitrary current density to be 0.0493 amp/cm^2 when corrected for an electrolysis temperature of 50°. As the process at best was not too efficient we found it necessary to run the reaction twice the theoretical time in order to obtain suitable yields.

The results obtained using multiples and fractions thereof are illustrated in Table I.

Can. J. Chem. Downloaded from www.nrcresearchpress.com by 190.90.36.8 on 09/04/12
For personal use only.

TABLE I

Effect of current density on yield of isoindoline

Current density (amp/cm²)	% yield isoindoline	% current efficiency
0.1950	39.6	19.8
↑ 0.1540	52.0	26.0
0.1190	53.9	27.0
H_2 0.0770	56.4	28.2
0.0493	91.1	45.6
0.0243	90.5	45.2

At current densities of 0.0770 amp/cm² and higher, considerable gas evolution was observed initially and throughout the course of the electrolysis which accounted to a great extent for the low current efficiency. Also in these experiments a considerable amount of partially reduced tetrachlorophthalimidine (III) was isolated from the reaction mixture. Use of the two lower current densities resulted in practically no gas evolution until approximately 1.25 times the theoretical current had been passed. In these cases, if there was any partially reduced tetrachlorophthalimidine (III), its quantity was too small to be detected. Thus we see that even the empirical use of an exact physical equation can be useful as an arbitrary focal point for a beginning.

In order to demonstrate the value of controlled potential electrolysis in obtaining maximum current efficiency an experiment was performed using a lead cathode previously treated by Tafel's method and a catholyte, the same as used in previous experiments, consisting of 6.5 g of the tetrachlorophthalimide (I) dissolved in a solution of 30 ml glacial acetic acid, 36 ml distilled water, and 90 ml concentrated sulphuric acid. The anolyte consisted of a solution of 9 ml concentrated sulphuric acid in 66 ml distilled water. At a reference potential of −1.10 v vs. S.C.E. previously determined from a voltammetric curve, the initial current density was 0.0589 amp/cm². After 80 minutes the current plateaued at a current density of 0.0143 amp/cm². From the area under the current vs. time curve the total number of coulombs passed was 15,280. The desired tetrachloroisoindoline (IV) was isolated from the catholyte in a 84.3% yield with a 77.7% current efficiency. Thus we see in this instance the advantage of the use of controlled potential in obtaining greater current efficiency than obtained under constant current density conditions.

Of interest is an experiment performed at a potential of −0.68 v vs. S.C.E. The initial current density was 0.0189 amp/cm². After 70 minutes the current plateaued at 0.0107 amp/cm². From the catholyte was isolated 4,5,6,7-tetrachloro-2-(2-dimethylaminoethyl)-3-hydroxyphthalimidine (II) in 86% yield. Thus we also see here another advantage of controlled potential electrolysis, i.e. the selective reduction of a particular group in a molecule containing more than one reducible center.

I shall now illustrate another type approach to the solution of an electrochemical problem. Perhaps a brief history of the general problem might be of interest at this point. Some years ago in the course of studying the electrochemical mechanism of bimolecular reductions, one of the compounds studied was *p*-aminoacetophenone (V). The pinacol, 2,3-bis-(*p*-aminophenyl)-2,3-butanediol (VI), obtained from this ketone by cathodic bimolecular reduction was found to be an active anti-estrogen. Further pursuit of the biological aspects of the problem indicated that the animals under test with this compound tended toward demonstration of other biological responses. However, perhaps

Can. J. Chem. Downloaded from www.nrcresearchpress.com by 190.90.36.8 on 09/04/12
For personal use only.

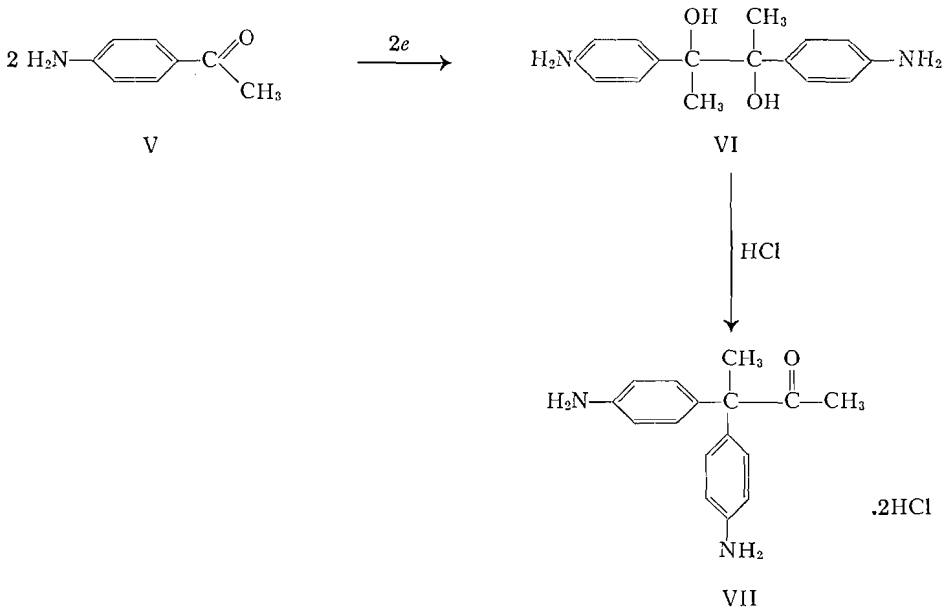

V VI VII

because of the lack of proper bodily reagents the animal could not quite accomplish the necessary transformation. Therefore it was decided to perform a pinacol–pinacone type reaction which resulted in the compound 3,3-di(*p*-aminophenyl)-butanone-2-dihydrochloride (VII), commonly referred to as Amphenone and which was found to have interesting adrenal inhibiting effects (3). Unfortunately, however, despite the widespread use of this compound its undesirable side effect precluded general usefulness for this drug. This naturally led us to search for more specific adrenal inhibitory compounds in the Amphenone series. One of the compounds which seemed interesting, but only moderately active, was the pinacol of 3-acetylpyridine (4). This pinacol (VIII) upon being subjected to a pinacol–pinacone type rearrangement gave, as the major product, 2-methyl-1,2-bis-(3-pyridyl)-1-propanone (IX) (5), which has been found to be a potent adrenocortical inhibitor (6).

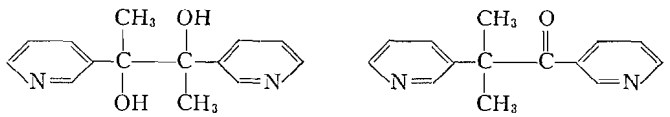

VIII IX

To return to the electrochemical aspects of this problem I should mention that the acidic medium used in the previously reported preparation of the pinacol of 3-acetylpyridine (4) made isolation of the desired pinacol extremely difficult. Therefore it became necessary for us to find a practical medium for this preparation. As a result of our previous experience it was decided that a basic medium of some type was probably desirable. Preliminary investigations in this direction indicated a solution of potassium acetate in aqueous ethanol at reflux temperature (82.5° C) to be a suitable medium. Analysis of the voltammetric curve indicated two processes occurring, the first at a potential of −1.5 to −1.64 v vs. S.C.E. and the other at a potential of −2.0 to −2.2 v vs. S.C.E.

Can. J. Chem. Downloaded from www.nrcresearchpress.com by 190.90.36.8 on 09/04/12
For personal use only.

As it has been demonstrated by other investigators (7) that pyridine can be fully reduced to piperidine under high potential conditions, it was decided that probably the lower potentials represented the bimolecular reduction to the pinacol. This was confirmed by controlled potential electrolysis at −1.6 v vs. S.C.E. It was further decided to determine the effect of constant current density on yield and efficiency using the calculated current density of 0.378 amp/cm². This electrolysis was run for approximately 1.75 times theory and a plot made of reference potential vs. time. The results are shown in Fig. 7.

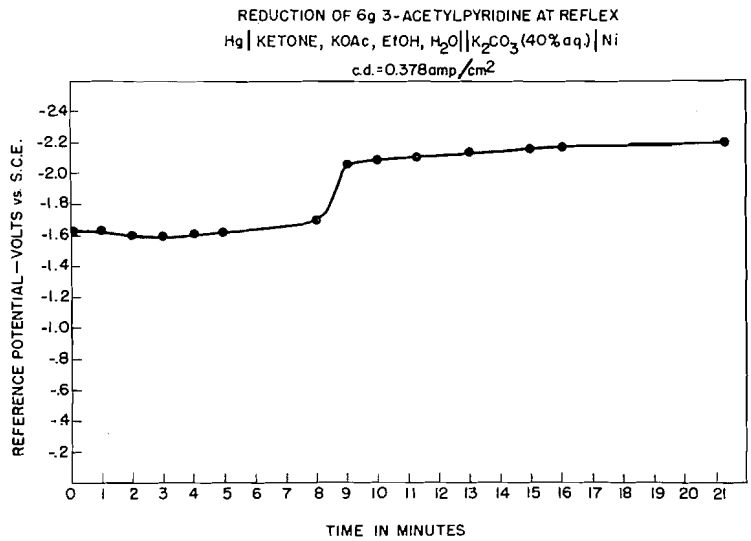

FIG. 7. Reference potential vs. time curve for reduction of 3-acetylpyridine at constant current density.

From this curve it can be seen that at 6 minutes (65.3% of theoretical time) the potential begins to rapidly increase from −1.6 v to −2.05 v vs. S.C.E. At 12.25 minutes (theoretical time) the potential is already at the point known to give a secondary product. It was difficult to isolate more than a small quantity of the desired pinacol from this experiment. Experiments performed for the theoretical time (12.25 minutes) gave satisfactory yields and current efficiencies. In order to try to approach results obtained at controlled potential, experiments were performed using a higher current density for approximately 49% of the theoretical time and then lowering the current density to another fixed value with the object of maintaining the reference potential throughout the course of the electrolysis at −1.5 to −1.64 v vs. S.C.E. This gave yields and current efficiencies approaching that obtained under controlled potential conditions. Finally, as it was observed that the pinacol began to precipitate during the reaction using the original aqueous ethanolic potassium acetate medium, and as it was thought that in so doing the precipitate might occlude the electrode surface and thus prevent maximum efficiency, the alcohol content of the medium was increased with the net result being an increase in yield and efficiency. The results of the various mentioned experiments are tabulated in Table II.

It has been the objective in this presentation to illustrate that it is possible without strict mathematical treatment to arrive at information which can give the organic chemist the desired results. If we few investigators in the field of electroorganic chemistry can reduce the subject from an art to a science as we are rapidly doing it may be in time

Can. J. Chem. Downloaded from www.nrcresearchpress.com by 190.90.36.8 on 09/04/12
For personal use only.

TABLE II

Catholyte	Mode of operation	% yield	% current efficiency
Ketone, 6 g EtOH, 25 ml KOAc, 15 g H_2O, 17 ml	Reference potential −1.6 v vs. S.C.E. 0.408 to 0.051 amp/cm²	58.3	61.4
	0.378 amp/cm² 6 minutes 0.2034 amp/cm² 11.6 minutes 1 × theory	52.0	52.0
	0.378 amp/cm² 1 × theory	43.1	43.1
Ketone, 6 g EtOH, 35 ml KOAc, 15 g H_2O, 17 ml	Reference potential −1.6 v vs. S.C.E. 0.403 to 0.029 amp/cm²	68.3	80.3
	0.378 amp/cm² 6 minutes 0.2034 amp/cm² 11.6 minutes 1 × theory	60.2	60.2

NOTE: The anolyte in the above experiments consisted of 40% K_2CO_3.

that organic chemists will begin to look upon the electrochemical technique as a vital tool in his armentarium of reagents. The future lies in the hands of those physical and organic chemists who choose to collaborate to achieve this common goal.

REFERENCES

1. ALLEN, M. J. Organic electrode processes. Reinhold Publishing Corp., New York. 1958.
2. SPÄTH, E. and BREUSCH, F. Monatsh. **50**, 349 (1928). SAKURAI, B. Bull. Chem. Soc. Japan, **5**, 184 (1930); **7**, 155 (1932). CLEMO, G. R., RAPER, R., and TENNISWOOD, C. R. S. J. Chem. Soc. 429 (1931). COOK, E. W. and FRANCE, W. G. J. Phys. Chem. **36**, 2383 (1932).
3. ALLEN, M. J. and CORWIN, A. H. J. Am. Chem. Soc. **72**, 114, 117 (1950). ALLEN, M. J., HERTZ, R., and TULLNER, W. W. Proc. Soc. Exptl. Biol. Med. **74**, 632 (1950). HERTZ, R., ALLEN, M. J., and TULLNER, W. W. Proc. Soc. Exptl. Biol. Med. **75**, 627 (1950). HERTZ, R., TULLNER, W. W., and ALLEN, M. J. Proc. Soc. Exptl. Biol. Med. **77**, 480 (1951). HERTZ, R., ALLEN, M. J., TULLNER, W. W., and WESTFALL, B. B. Proc. Soc. Exptl. Biol. Med. **79**, 42 (1952). THORN, G. W. *et al.* New Engl. J. Med. **254**, 547 (1956). RENOLD, A. E. *et al.* New Engl. J. Med. **256**, 16 (1957). BENCZE, W. L. and ALLEN, M. J. J. Org. Chem. **22**, 352 (1957).
4. ALLEN, M. J. J. Org. Chem. **15**, 435 (1950).
5. ALLEN, M. J. and BENCZE, W. L. Unpublished results.
6. CHART, J. J., SHEPPARD, H., ALLEN, M. J., BENCZE, W. L., and GAUNT, R. Experientia, **14**, 151 (1958).

Can. J. Chem. Downloaded from www.nrcresearchpress.com by 190.90.36.8 on 09/04/12
For personal use only.

Can. J. Chem. Downloaded from www.nrcresearchpress.com by 190.90.36.8 on 09/04/12
For personal use only.

THE ANODIC PASSIVATION OF IRON[1]

EARL S. SNAVELY, JR. AND NORMAN HACKERMAN

ABSTRACT

A study was made of the anodic passivation of iron in solutions of 0.1 *M* sodium sulphate at a pH of 3.0. A mass balance of iron equivalent to coulombs required for passivation and iron found in solution after passivation showed that approximately 0.002 coulomb/cm² is involved in the passive layer. A Flade arrest does not appear in decay traces of anodic potential unless a potential of at least 1.2 v (E_H) is achieved on charging the electrode, indicating incomplete coverage by the passive layer below 1.2 v. Partial cathodic reduction followed by anodic reformation of the passive layer at the Flade arrest showed that the first charging current involved in reformation is highly efficient even when as much as 70% of the Flade arrest is reduced. These results support the view that only a fraction of the passive layer is represented by coulombs involved in the Flade arrest and that after partial reduction the remainder of the passive layer disintegrates spontaneously. Addition of chelating agents to the electrolyte has an adverse effect on passivation by chelation of ferrous ion.

INTRODUCTION

Experimental conditions necessary to achieve passivity of iron are well known; however, the nature of the passive layer is less familiar and has been the subject of many recent investigations. The theories which have been advanced can, in general, be divided into categories of oxide film theories and adsorption theories. The former are concerned with an iron oxide, rich in oxygen and hydrated, which requires specific conditions to form in such a manner as to give a high degree of protection to the base metal. The adsorption theories maintain that passivity is the result of adsorption of chemical species such as hydroxyl ions or molecular and atomic oxygen. Films of either type, oxide or adsorbed, can be similar once formed because of migration of iron atoms or ions through the passive film, and their chief difference lies in their means of formation. An oxide film formed by anodic polarization requires nucleation and lateral growth with a necessary consumption of coulombs, while an adsorbed film forms rapidly and completely on a properly prepared surface.

This paper presents the results of experiments to determine the quantity of electricity involved in the formation of a passive layer by anodic treatment. Other results concerning the phenomena observed on cathodic reduction of the passive layer are presented.

EXPERIMENTS

The iron electrodes used in all experiments were made from stock supplied by the Armco Steel Corporation and were reported to be 99.9% Fe containing 0.04% copper, 0.01% carbon, and traces of manganese, phosphorus, and silicon.

Circular coupons about 3.5 cm in diameter were vacuum-annealed and mounted in bakelite so that one face of the iron disk was exposed. This face was ground flush with the bakelite by means of a surface grinder and polished with 4/0 emery paper. The bakelite–iron junction at the periphery of the electrode, as well as all exposed bakelite, was covered with clean Ucilon or Glyptal to prevent imbibition of solution.

Electrical connection to the iron was accomplished by a tapped hole in the bakelite through which a metal rod could be screwed against the iron. The metal rod was protected with Myva wax.

[1]*Manuscript received July 10, 1958.*
Contribution from the Department of Chemistry, University of Texas, Austin, Texas. This paper was presented at the Symposium on Charge Transfer Processes held at the University of Toronto, Toronto, Ontario, September 4 and 5, 1958.

All solutions were 0.1 M in Na_2SO_4. They were made from recrystallized salt and triple-distilled water and adjusted to a pH of 3.0 with c.p. H_2SO_4.

The polarization cell was a Pyrex vessel equipped with a large platinum electrode and a fritted gas-dispersion tube through which helium was bubbled to rid the cell and its contents of oxygen. The helium was purified by passage through a tube filled with hot copper followed by a drying tube containing $Mg(ClO_4)_2$. The cell and the electrical circuit are shown in Fig. 1.

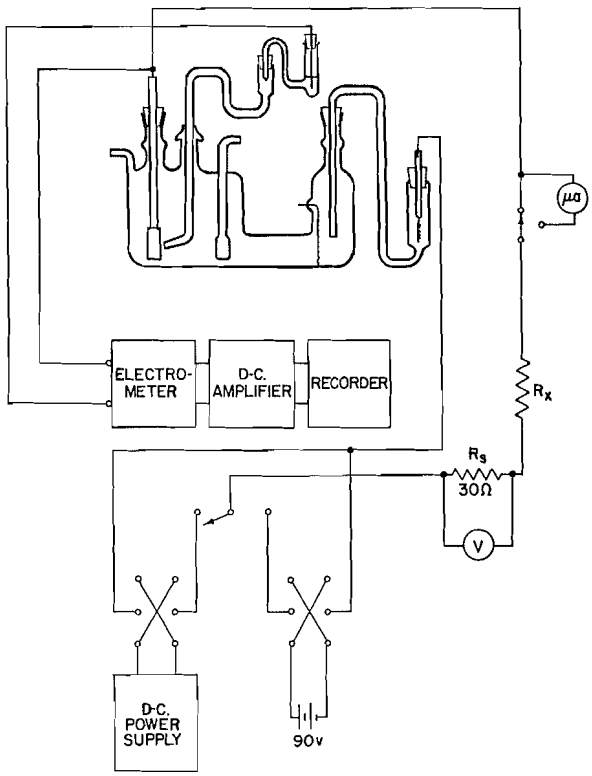

FIG. 1. Passivation cell and circuit.

Potential measurements were made with reference to a Hg, Hg_2SO_4 electrode. All potentials reported here are given with respect to the standard hydrogen electrode. The surface of the electrode is treated as a projected area and results are presented on that basis.

As shown in Fig. 1, the potential measuring circuit consisted of a Keithley Model 210 electrometer having an input impedance of 10^{14} ohms. The output of the electrometer supplied a d-c. amplifier which drove a Brush Recorder equipped for chart speeds of 25, 10, and 5 cm/second.

Analytical Experiments

To determine the amount of electricity required to passivate iron, a material balance was made on the amount of iron actually present in the cell solution after passivation was achieved and the amount of iron equivalent to the coulombs passed during the passivating process.

Can. J. Chem. Downloaded from www.nrcresearchpress.com by 190.90.36.8 on 09/04/12
For personal use only.

In these experiments the cleaned electrode was placed in the cell about 3 inches above the solution, while the latter was degassed by bubbling He. The iron was then lowered into the solution under an applied cathodic current of 12.5 ma/cm² to prevent corrosion. The recorder was then set on high speed and when the electrode had been in the cell solution 15 seconds an anodic current of 50 to 70 ma/cm² was applied. This passivated the iron and the electrode was then withdrawn from the cell while still passive and while oxygen was being evolved. The exact volume of solution was determined by weighing the cell, and the concentration of iron was then measured by the *o*-phenanthroline method. Cell solution in which iron had been only cathodically treated was used as a blank.

In these experiments the potential changes during passivation were recorded as shown in Fig. 2. The number of coulombs required for passivation was calculated from the constant current applied and the time interval from point A to the reversible oxygen potential or point B. This interval was used for reasons which are pointed out later.

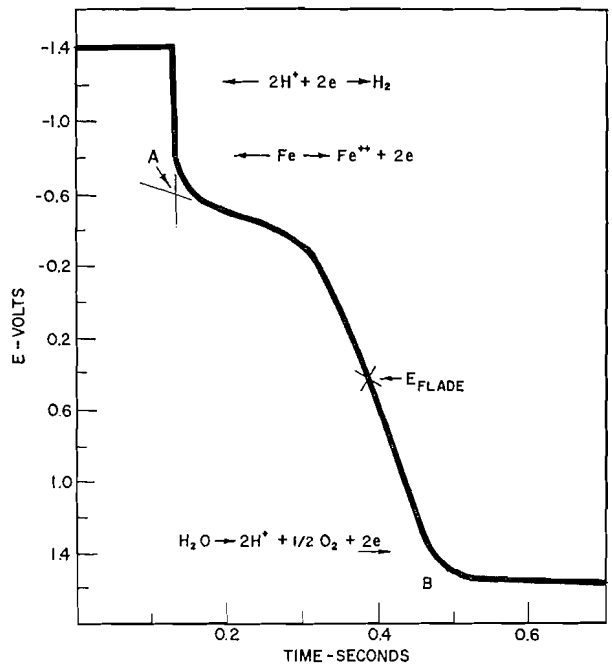

FIG. 2. Typical passivating curve.

Typical results for these analytical experiments are shown in Table I. The column titled "Equivalent Fe^{++}" gives the amount of ferrous ion equivalent to the coulombs passed during passivation. The next column lists the amount of ferrous ion which was found in the cell solution after passivation. The average of all values in the last column of Table I yields a value of 1 γ of Fe or 0.003 coulombs, which approaches the value reported by Kabanov (1). This is the amount of ferrous ion, as coulombs in the passivating process, in excess over the amount of iron determined in solution and per square centimeter of electrode surface. The results have an average deviation of 0.25 γ or about 30%.

The value of 0.003 coulomb/cm² required for passivation is far in excess of the quantity of electricity which is observed at the Flade region on reduction of the passive layer. For example, reduction of the passive layer in the 3.0 pH 0.1 *M* Na_2SO_4 solution at 14.5 μa/cm² requires 0.00016 coulomb/cm³ or less than $\frac{1}{10}$ that required for passivation. It

Can. J. Chem. Downloaded from www.nrcresearchpress.com by 190.90.36.8 on 09/04/12
For personal use only.

TABLE I

Excess coulombic iron at the reversible oxygen potential

Anodic c.d. (ma/cm²)	Time to rev. O_2 potential	Coulombs $\times 10^3$/cm²	Equivalent Fe^{++} (γ/cm²)	Fe^{++} det'd. (γ/cm²)	Excess coulombic Fe^{++} (γ/cm²)
71.6	0.20	14.3	4.1	3.2	0.9
53.0	0.23	12.2	3.5	2.5	1.0
53.0	0.22	11.7	3.4	2.9	0.5
54.0	0.20	10.8	3.1	2.6	0.5
51.9	0.21	10.9	3.2	2.8	0.4
53.5	0.22	11.8	3.4	2.7	0.7
54.8	0.22	12.1	3.5	3.1	0.4
46.3	0.24	11.1	3.2	2.7	0.5
46.3	0.24	11.1	3.2	2.8	0.4
45.3	0.40	18.1	5.2	2.6	2.6
46.3	0.26	12.1	3.5	2.1	1.4
46.3	0.26	12.1	3.5	2.8	0.7
40.2	0.43	17.3	5.0	2.5	2.5
40.6	0.32	13.0	3.8	2.6	1.2
				Average	0.98

is known that the iron passive layer is anodic to iron, and exposure of bare iron during the reduction process most certainly increases local cell action which leads to spontaneous decay of the passive layer (2).

To determine the extent to which the passive layer could be reduced without exposing iron, the current efficiency for formation of the passive layer was determined. This was done by repeatedly reducing and reforming the passive layer until a constant value for the number of coulombs involved at the Flade region was obtained. Care was taken to apply anodic current just at the end of the arrest so that excessive currents would not be required for repassivation. When a constant value was obtained, a small reducing current was applied until a fraction of the Flade arrest was passed. The current was then reversed and a small anodic current applied for a short period. The current was reversed again and reduction allowed to proceed until the end of the arrest was reached. The difference between the constant coulomb numbers necessary to pass through the Flade region, and the number of coulombs initially passed cathodically gives the charge remaining in the surface at any point in the region.

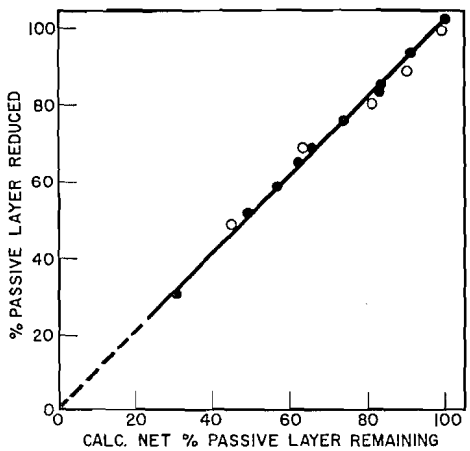

FIG. 3. Relative anodic current efficiencies at Flade arrest.
● 0.1 *M* Na_2SO_4, pH 3.0; ○ 0.1 *M* Na_2SO_4, pH 3.0, 0.05% *o*-phenanthroline.

Can. J. Chem. Downloaded from www.nrcresearchpress.com by 190.90.36.8 on 09/04/12
For personal use only.

For a 100% efficient anodic current the number of coulombs actually required to pass the remainder of the arrest should be greater by an amount equal to the number of coulombs added anodically after the initial reduction. Figure 3 shows the results of an experiment in which 14.5 $\mu c/cm^2$ was added to the passive layer after various fractions of the arrest had been passed. The curve clearly shows the anodic current to be highly efficient up to a reduction of 70% of the Flade region. The open circles of Fig. 3 are results of the same experiment in which 0.05% *o*-phenanthroline was added to the cell solution. This treatment had no effect on efficiency of the anodic current.

Figure 4 shows the effect of additions of *o*-phenanthroline on the time required to achieve passivity when the passive layer is completely reduced. Presumably *o*-phenanthroline increases the time required for passivation due to chelation of the ferrous ions which are necessary to achieve the high potentials required for passivity (3). The high potentials are the result of precipitation of ferrous hydroxide on a ferrous salt. A cleaned coupon was used for each point of Fig. 4 so that equivalent roughness factors were involved for each passivation. Since 0.003 coulomb/cm^2 are involved in a formed passive layer but only 0.00016 coulomb/cm^2 are involved in the Flade region, the Flade region should be evident on reduction *only* if the passive layer is about 90% complete. If the Flade arrest is considered to involve a 1-electron process and passivation a 3-electron process, then the arrest should appear only if the passive layer is about 70% complete.

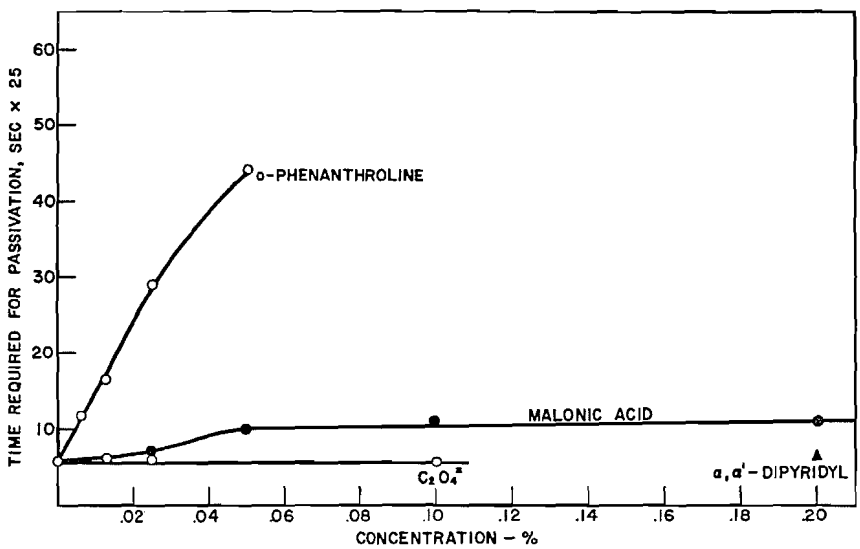

FIG. 4. Concentration chelating agent versus time required for passivation.

Additional evidence that the Flade region represents only a fraction of the passive layer is shown by the results in Fig. 5. This curve was obtained by plotting the anodic coulombs required to attain the reversible oxygen potential versus the fraction of Flade region achieved by cathodic reduction. When approximately 95% of the Flade region was passed passivity could no longer be attained by an anodic current of 14.5 $\mu a/cm^2$. When about 70% of the Flade region was passed the time required to reach the reversible oxygen potential increased, indicating that some iron was exposed and that local cell current began to increase. The flat portion of the curve in Fig. 5 is in accordance with the view that the thickness of the passive layer is proportional to the anodic potential

Can. J. Chem. Downloaded from www.nrcresearchpress.com by 190.90.36.8 on 09/04/12
For personal use only.

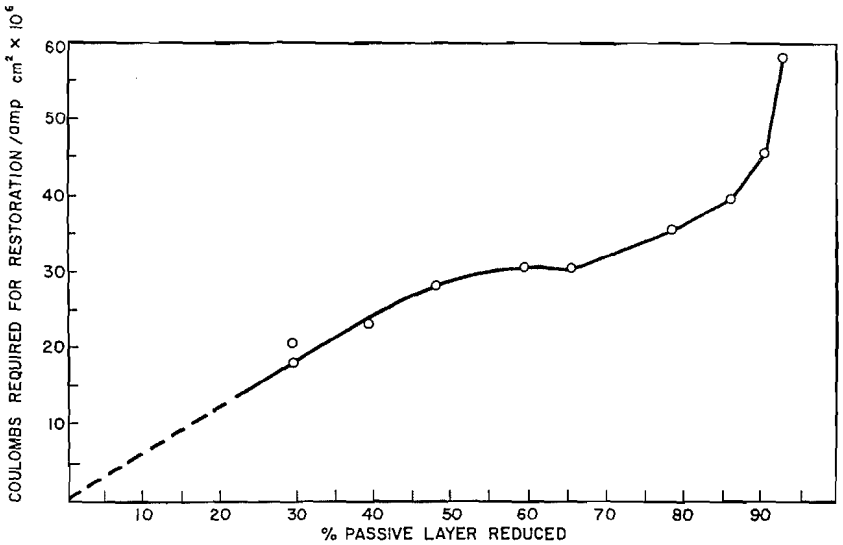

FIG. 5. Restoration of passive layer. Anodic c.d. = 12.9 μa/cm^2; cathodic c.d. = 14.2 μa/cm^2.

achieved. If only a small part of the passive layer is reduced at the Flade region, then a nearly constant number of coulombs is required to attain the oxygen potential after various fractions of the arrest have been passed. In these experiments the total number of coulombs involved in the arrest was calculated from the time at which the current was made cathodic to the end of the flat portion. For the low currents used, concentration polarization was very small and any resistance drop at the electrode surface was not detectable.

In constant current experiments such as these, the only arrest which appears in the charging curve is found at a potential corresponding to the Fe, Fe^{++} potential. Even if the Flade region represents the formation potential of the passive layer it is not surprising that a detectable arrest does not appear in this region during charging because of the high current involved. For example, the results of the previously described analytical experiments yielded a value of 0.003/cm^2 for the coulombs involved in the passive layer. For a passivating current of 70 ma/cm^2 only 1/35 second is required to pass 0.003 coulomb/cm^2 and, since some of the passive layer forms at potentials more anodic than that of the Flade region, only a portion of this short time would be involved in this arrest. To determine the potential at which a nearly complete passive layer had formed, the charging current was interrupted at various times and the potential then achieved was allowed to undergo open-circuit decay. Figure 6 shows the results of this experiment and indicates that a potential near the reversible oxygen potential must be achieved before a complete passive layer is formed. The Flade arrest on decay is visible only in the lower two charts where the potential achieved was 1.4 v. This result is in agreement with calculations made with the figures reported in Table I. Calculation of the time required, at the anodic current density employed, to account for all iron found in solution after passivation yields an average value corresponding to the achievement of 1.2 v. These results indicate that iron dissolution slows appreciably only on attainment of potentials more anodic than the Flade region.

To determine if the excess iron in solution after passivation was due to local cell action or if iron dissolution is necessary to achieve passivation, several chelating agents were

Can. J. Chem. Downloaded from www.nrcresearchpress.com by 190.90.36.8 on 09/04/12
For personal use only.

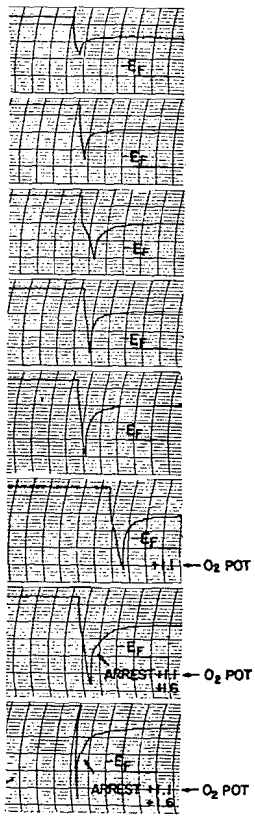

FIG. 6. Appearance of the Flade arrest in open-circuit decay. Anodic c.d. = 70.0 ma/cm²; chart speed = 2.5 cm/second.

added to the cell solution prior to passivation. These included *o*-phenanthroline, malonic acid, and α, α'-bipyridyl. As shown in Fig. 4 none had a significant effect except *o*-phenanthroline. In the first case the time required to achieve passivation is proportional to the *o*-phenanthroline concentration. The instability constant of the ferrous–*o*-phenanthroline complex is very small, i.e., approximately 10^{-21}. As pointed out by a previous experiment, additions of *o*-phenanthroline to the cell solution after the passive layer was formed had no effect on its reduction or reformation from a partially reduced state. Thus, oxidation of the chelating agent does not play a major role in the increased consumption of electricity during the passivating process. Apparently at least a portion of the iron dissolved in the anodic treatment of iron is necessary to achieve passivity.

DISCUSSION

Suitable corrections must be applied to the results of the analytical experiments in order to arrive at an exact figure for the coulombs involved in formation of the passive layer. Presence of hydrogen in the metal has an inhibiting effect on passivity as shown by others (4). Introduction of hydrogen by the initial cathodic treatment may be responsible for instability of the passive layer at potentials more cathodic than the oxygen potential during the passivating process. Also, the number of coulombs involved in competing electrode processes such as oxidation of ferrous ion or ferrous hydroxide is

Can. J. Chem. Downloaded from www.nrcresearchpress.com by 190.90.36.8 on 09/04/12
For personal use only.

not known; however, the absence of arrests in the charging curve indicates that they do not take place to any notable extent. It was not possible to remove the iron electrode from the cell solution at the instant passivity was achieved and it is quite likely that the coupon, even though passive, corroded slightly, contributing to the amount of iron in solution, thereby making the results too small. Also, open-circuit decay of the electrode potential during the charging process indicates that some growth of the passive layer takes place after the beginning of oxygen evolution so that the number of coulombs involved in a complete passive layer is slightly larger than that obtained in the analytical experiments. If the Flade region represents only 10% of the passive layer as concluded from other experiments presented here, then growth of the passive layer above the oxygen potential should add this amount to the 0.003 coulombs obtained from the analytical experiments.

A complete passive layer is very stable and passivity in acid solutions can be maintained by anodic currents of less than 1 $\mu a/cm^2$ (5). Very few changes are involved at the Flade region on cathodic reduction of a passive layer maintained by such a low current. These results indicate that passivity can be achieved by less than a monolayer. The monolayer is probably composed of sorbed ions and dipoles held in place by appreciable force fields. An alternative explanation is the stabilization of a primary passive film by an adsorbed species (6). The role of adsorption in maintaining passivity is indicated by the rapid potential changes associated with the application of small currents at the Flade region, the absence of effect of a chelating agent on current efficiencies at the Flade region, and the small number of coulombs involved in formation of a passive layer.

CONCLUSIONS

Anodic dissolution of iron at a rapid rate is necessary to achieve passivity, and passivity can be deferred or prevented by the addition of a suitable chelating agent. Approximately 0.003 coulomb/cm^2 is involved in the passive layer; this amount of electricity is equivalent to a thickness of 15 Å of Fe_2O_3 based on projected areas. Coulombs involved at the Flade region represent only 10% of the passive layer and the remainder decays spontaneously when iron is exposed. Small anodic currents applied at the Flade region are completely efficient, indicating absence of local cell action and a passive film consisting of at least a monolayer.

ACKNOWLEDGMENTS

This work was supported in some part by the Office of Naval Research under Contract No. 375(02), and in some part by a Welch Foundation Grant.

REFERENCES

1. KABANOV, B. Discussions Faraday Soc. **1**, 259 (1947).
2. BONHOEFFER, K. F. Corrosion, **11**, No. 7, 32 (1955).
3. EVANS, U. R. Metallic corrosion, passivity and protection. Edward Arnold & Co., London. 1948. p. 51.
4. UHLIG, H. H., CARR, N. E., and SCHNEIDER, P. H. Trans. Electrochem. Soc. **79**, 111 (1941).
5. WADE, W. H. and HACKERMAN, N. Trans. Faraday Soc. **53**, 1636 (1957).
6. HACKERMAN, N. Z. Elektrochem. **61**, 632 (1958).

Can. J. Chem. Downloaded from www.nrcresearchpress.com by 190.90.36.8 on 09/04/12
For personal use only.

Can. J. Chem. Downloaded from www.nrcresearchpress.com by 190.90.36.8 on 09/04/12
For personal use only.

THE THEORY OF FORMATION OF HIGH RESISTANCE ANODIC OXIDE FILMS[1]

L. YOUNG

ABSTRACT

Various models are considered for the growth of anodic oxide films (metal ions mobile). In general, a transition is expected, as the thickness of the film is increased, from control by the metal/oxide interface (Cabrera and Mott) with very thin films to control by the movement of ions through the body of the film (Verwey), with the concentration of mobile ions taking up the value (p, say) which gives electroneutrality. The field strength only varies with thickness in the transition region of thickness. Dewald's theory is the special case of p zero, which gives a field increasing continuously to infinite thickness. The high field production of Frenkel defects (with the vacant cation sites immobile and the interstitial ions mobile) as postulated by Bean, Fisher, and Vermilyea, and a slight mobility of oxygen ions are two processes which would allow p to vary with the field strength, and which would, therefore, give rise to "overshoot" in the transients in the field strength which occur when the applied current is suddenly changed. However, if the field strength is sufficiently great to produce Frenkel defects it would be expected to be sufficiently great to cause the vacancies to be mobile. This case is considered. Finally, it is noted that in an amorphous oxide it is difficult to maintain a distinction between lattice and interstitial ions, and, in fact, a range of site energies and jump distances would be expected. Some of the observed features (including "overshoot", and Tafel slope anomalies) of the kinetics for tantalum may, therefore, be due simply to the fact that the oxide is amorphous.

INTRODUCTION

This paper is concerned with developing the consequences of various models intended to represent the formation of the high ionic resistance type of anodic film in order to find crucial differences for experimental test. This type of film is formed on tantalum and niobium in most electrolytes and on aluminum, titanium, zirconium, hafnium, tungsten, uranium, silicon, germanium, and other metals or intermetallic compounds in certain electrolytes. It is distinguished from the type of anodic film used in storage batteries by the characteristic that electric field strengths of the order of 10^6 v cm^{-1} are produced in the oxide by anodic polarization, the resulting current being predominantly ionic. Part of the interest in the formation process lies in the connection with the formation of oxide films by reaction with oxygen ("tarnishing reaction"). The essential difference between the two processes is that in anodic oxidation only ions need cross the film for growth to occur,* but in the tarnishing reaction electrons must also move, since otherwise macroscopic separation of large electric charges would occur. In effect, the electrical circuit is closed within the oxide in the tarnishing reaction and externally in the anodic reaction. This means that the anodic kinetics should in principle be easier to interpret, in that there is no question, as there is in some tarnishing reactions (1), as to whether the ionic or the electronic current is rate determining. The anodic system is easier to investigate experimentally, since it has an extra degree of freedom: at a given temperature and concentration of reactants the rate of formation may still be varied (and, in fact, exactly controlled) by controlling the current through the oxide. In practice, it is only

[1]*Manuscript received July 8, 1958.*
Contribution from the British Columbia Research Council, University of British Columbia, Vancouver, B.C. This paper was presented at the Symposium on Charge Transfer Processes held at the University of Toronto, Toronto, Ontario, September 4 and 5, 1958.

**A "leakage" current is usually observed. This is due partly to an electronic current through the oxide and partly to ionic discharge in pores. However, this current has invariably been tacitly assumed to be independent of (that is, in parallel with) the ionic current, though, admittedly, ultraviolet irradiation, which would be expected to produce only an electronic current, also causes film growth.*

possible to discuss in a very provisional way whether a given metal behaves like a given model, since the experimental data are very restricted, and, even with the metals—tantalum, niobium, and zirconium—which have been at all extensively investigated, are incomplete or in dispute.

Basic Equations for the Ionic Current

All present theories treat ionic movement using models which are strictly applicable only to crystalline material. Thus they assume that either vacant anion or cation sites, or interstitial ions, are mobile, and that one vacancy or interstitial ion is exactly equivalent to another. Now, at least as far as X-ray diffraction is concerned, this type of film is normally amorphous. (Crystalline films can be produced, but detailed kinetic studies have not been made.) In an amorphous solid, it would seem difficult to make a distinction between interstitial and lattice ions. In fact, it may be necessary to abandon this distinction, and to consider the oxide as consisting of two random lattices (oxygen and metal), probably with a large concentration of vacancies in each lattice. There will be a distribution of mobilities because of the varying local environment of each ion. In other words, a given ion will encounter a range of jump distances and activation energies along its path through the oxide. Against this argument, there is, of course, the point that, even in an apparently amorphous lattice, there will be some degree of local order. For example, the detailed structures of tantalum and niobium pentoxide have not been worked out, but, if the structure reported (2) for one form of vanadium pentoxide is any guide, the lattice of the amorphous oxide may consist essentially of oxygen tetrahedra randomly linked to neighboring tetrahedra at an average of three points and with an average of one metal ion per tetrahedron.

The conventional equations, which are used to describe the ionic movement, apply only to either a few ions moving in a large number of empty sites, or a few vacancies moving in a nearly full lattice. This is because no allowance is made for the possibility that one carrier may block the path of another. It seems quite possible that this assumption of a very low concentration of the mobile species may fail. In particular, some theories postulate an exponential variation of carrier concentration with the field strength, with a large value appearing at accessible fields.

The same equations have been used to describe the movement both of interstitial ions and of vacant lattice sites. They were first applied to anodic oxide films by Verwey (3), who was, as it happens, considering specifically the movement of aluminum ions in the spinel structure γ-alumina, which has a large concentration of vacant cation sites at electroneutrality when the oxygen lattice is full. The conventional assumption is that the current at a given point x may be written

$$[1] \qquad i = 2anv \exp -(W-qaE)/kT - 2a[n+2a(\partial n/\partial x)]v \exp -(W+qaE)/kT,$$

where a = (mean) half jump distance for the ions, n = concentration of ions, v = vibration frequency of ions, W = activation energy at zero field, q = charge on the ions, and E = the field strength. The first term refers to the ions moving with the field, and the second term refers to ions moving against the field. The magnitudes of W and aq are such that, for the range of currents which is experimentally accessible at present, the second term is negligible (high field approximation). The concentration gradient needed to give a diffusion current comparable with the migration term is so large as to have little physical significance. The remaining term

Can. J. Chem. Downloaded from www.nrcresearchpress.com by 190.90.36.8 on 09/04/12
For personal use only.

[2] $$i = 2an\nu \exp -(W-qaE)/kT$$

gives a relation between field strength and current density which is of the form

$$i = i_0 \exp \beta E.$$

The kinetic expressions 1 and 2 apply to an ion vibrating in simple harmonic motion in one dimension with a frequency ν, so that the chance of acquiring sufficient energy to jump the barrier on a given vibration is given by the Boltzmann factor. This treatment is, of course, an oversimplification. In particular, one would expect that success in jumping the barrier would depend on the correct phase relation with the vibration of neighboring atoms, and, perhaps, on sufficiently great amplitudes of their vibration. Unfortunately, even to allow for the accumulation of a critical energy in several degrees of freedom leads to cumbersome expressions, and still does not represent much greater correspondence with reality. The significance of ν and the possibilities of multiple jumps have been discussed recently by Ubbelohde (4) for ordinary diffusion. Multiple jumps are more likely in the present systems, since the ion continues to gain energy from the field so long as it moves. The transition state theory either provides the same final expressions by a more circuitous route, or leaves one with expressions, involving free energies and activity coefficients of imprecisely defined transition states, and these expressions, though of great generality, are not very amenable to experimental verification.

We have so far formulated equations for the ionic current at a point where the concentration of ions and the field strength are specified. A complete account of a given model is obtained when it is determined how these two quantities vary through the thickness of the oxide.

The present discussion will be chiefly restricted to the model in which metal ions carry most of the current. The alternative single carrier model in which oxygen ions carry most of the current gives analogous equations when treated using the conventional equations, but the two models differ in that adsorption effects may occur at the oxide/solution interface and structural effects (discussed below) may occur at the metal/oxide interface.

The discussion is confined to the rather idealized case that pores and fissures are not present in the oxide.

Interface Control

The interfaces were first taken into account by Mott and Cabrera (5), who considered (apparently intuitively) that the first barrier which metal ions have to surmount to enter the film will be higher than subsequent barriers encountered during passage through the film. The passage over this first barrier was treated in the same way as the jumps over the barriers within the film, but with the vital difference that the concentration of metal ions facing the barrier was assumed to be a constant, determined by the concentration of metal ions on the metal surface. Space charge was neglected so that the field strength was assumed to be constant through the film. The current over the entrance barrier is given by

[3] $$i = m_s\nu_s \exp -(W'-qa'E)/kT,$$

where m_s = surface concentration of metal ions, ν_s = their vibration frequency, W' = activation energy required to jump the first barrier with zero field, and a' = the half jump distance for this barrier. The concentration n_0 say of ions within the oxide adjusts itself so that the current given by 2 is equal to that given by 3, giving

Can. J. Chem. Downloaded from www.nrcresearchpress.com by 190.90.36.8 on 09/04/12
For personal use only.

$$[4] \qquad n_0 = \frac{(m_s\nu_s)^{a/a'}}{2a\nu} \exp\left(\frac{W - aW'/a'}{kT}\right) \cdot i^{1-a/a'}.$$

The kinetics are therefore determined by the entrance barrier. We may attempt to generalize the conditions under which the entrance barrier controls the kinetics. The required conditions are that space charge be negligible and that no upper limit be placed on n_0. The kinetics will then be controlled by the first barrier at which the backwards current is negligible (6). We introduce here an important parameter, the concentration (p, say) of mobile ions in the electrically neutral oxide. Apart from the improbable case that $n_0 \doteq p$, both n_0 and p must be small or the film must be very thin if the space charge is to be negligible. n_0 is certainly small in the original model, in which the first barrier is higher than later barriers. The significance of "small" will be clarified later.

Metal Ions Mobile, Space Charge Due to These Only

The theory proposed by Cabrera and Mott predicts that the Tafel slope $\partial E/\partial \log i$ is given by kT/qa', so that it should be proportional to the absolute temperature. This was reported not to be the case with tantalum (7, 6), niobium (8), and zirconium (9, 10), though it should be noted that the details of the behavior of tantalum as reported in recent investigations do not agree (6, 11, 12). Dewald (13) showed that an almost temperature-independent Tafel slope could appear if, as he claimed to be the case, the mobile metal ions were the only source of space charge. Actually, this assumption must be regarded as being made because it gives simple equations rather than because it would be expected to be true, as may be seen by putting it in the form that the concentration of the mobile ion near the interface given by 4 is assumed to be much greater than the critical value p which corresponds to electroneutrality. Poisson's equation gives

$$[5] \qquad \partial E/\partial x = 4\pi\, nq/\epsilon,$$

where ϵ is the dielectric constant of the oxide. The continuity equation for the current is

$$[6] \qquad \partial i/\partial x = \partial n/\partial t,$$

where t = time. Dewald puts $\partial i/\partial x = 0$. (The final result that $n(x)$ is not a function of the total thickness is derived directly from this initial assumption.) From [1] to [6], after two integrations,

$$[7] \qquad E = \frac{1}{\beta'} \log[i/m_s\nu_s \exp(-W'/kT)] + \frac{1}{\beta} \log(1 + \beta 4\pi\, qn_0x/\epsilon),$$

where

$$\beta = qa/kT \qquad \text{and} \qquad \beta' = qa'/kT.$$

This model exhibits a Tafel slope nearly independent of temperature over a certain region of temperature provided that certain conditions are fulfilled. Essentially, the space charge due to the ions causes a transition from control by the entrance barrier to control by the barriers within the oxide. However, the model also gives a field strength increasing with thickness. This has not been observed with tantalum or niobium though it is difficult to be sure that the small amount of variation required by the theory is absent. For example, the data given by Vermilyea (11, 14) for tantalum are inconclusive, because the ionic current was not shown to be constant, variations of surface area with thickness had not been shown to be absent, and the capacity had not been shown to measure thickness to the required accuracy. Some of these difficulties have been removed in subsequent work (15). When the integral rather than the differential field strength is

Can. J. Chem. Downloaded from www.nrcresearchpress.com by 190.90.36.8 on 09/04/12
For personal use only.

considered, a certain degree of uncertainty is caused by our lack of knowledge of the inner potential differences between phases of different chemical composition. This point is not always recognized. The uncertainty may be conservatively reckoned as corresponding to about one volt, i.e. 1% in the field strength at 100 volts overpotential, and proportionately more for thinner films.

It may be noted that when (below) we introduce the more realistic assumption that the concentration of ions p corresponding to electroneutrality is not negligible, the transition occurs between Cabrera and Mott's case and Verwey's case (control by movement of metal ions through the electrically neutral oxide) with the field strength independent of thickness except in the transition region.

Dewald (12) has recently shown that his model—when treated using the conventional equations—does not predict the "overshoot" which is observed in the transients in the field strength when the current is suddenly changed. This would invalidate its application to tantalum and niobium. However, Willis, Adams, and van Rysselberghe (9) have suggested that these transients could be due to the sluggish opening and closing of growth spirals, which, effectively, is equivalent to a variation of m_s.

The evidence is thus fairly conclusively against the application of this model to tantalum and niobium, either with $p = 0$ (Dewald) or with p constant and not zero. By contrast, recent work (10) has shown that zirconium in addition to Tafel slope variations exhibits a marked increase in field strength with thickness, and fails to exhibit the overshoot in the transients, in agreement with the predicted behavior for $p \ll n_0$.

The effect that, with a non-zero concentration of carriers, the next site in the path of a given carrier may be already occupied may be allowed for by multiplying the right of (2) and (3) by $(1-n/N)$, where N is the total concentration of available sites. Variations of vibration frequencies and of the activation energies would remain to be taken into account. This modification introduces considerable complication, but does not explain the transients.

Field Production of Frenkel Defects

Bean, Fisher, and Vermilyea (16) have proposed for tantalum pentoxide films that Frenkel defects (lattice vacancy plus interstitial ion) are produced in the metal lattice by the high fields. They assume *ad hoc* that the interstitial ions are mobile and the vacancies are immobile. The idea that the field might produce lattice defects was considered as improbable in older work on conventional ionic conduction (17), but the greater field strengths in the present systems make it more feasible. In view of the amorphous nature of the oxide it can only represent an approximation to a real process. These authors appear to assume that the defect-producing process directly determines the concentration of interstitial ions. A more correct view is that the process creates a certain concentration of immobile negative space charge (associated with the vacant cation sites), and that any control of the concentration of mobile metal ions is due to this, in the way which is discussed in the next section.

Bean, Fisher, and Vermilyea postulated in addition that there is a quite sudden transition with increasing field strength in the half barrier width for the production of interstitial ions.* This gave an explanation for the sudden change from a half barrier width of 2.4 Å to one of 4.8 Å which Vermilyea (11) found in his second investigation of the kinetics. They seem to envisage that several barriers are taken at one jump,

**Unless the maxima and minima in the potential energy curve of an ion in transit are mirror images there will, of course, be a second-order variation of the half jump distance with field strength. Further sources of gradual variation of "a" with field strength are discussed later.*

Can. J. Chem. Downloaded from www.nrcresearchpress.com by 190.90.36.8 on 09/04/12
For personal use only.

though this is not stated explicitly. There is some disagreement on the experimental issues, and Dewald (12) has suggested that Vermilyea allowed insufficient time for the transients to decay. The present author's results (unpublished) suggest that the (apparent) jump distance (derived in a similar way) does vary with the field, but that there is no evidence for any sudden transition from a value a to $2a$. As a result of the variation of "a" with E, $(\partial E/\partial \log i)_E$ varies correctly with temperature, but $(\partial E/\partial \log i)_t$ is almost independent of temperature.

Both Vermilyea (18) and Dewald (12) have shown that this model can give "overshoot". The essential reason for this is that the concentration of carriers lags behind the field when the current is suddenly changed. More precisely, the concentration of negative charge (and hence the concentration of mobile ions) increases sluggishly with the field strength. The treatments given by these authors are, of course, not exact because they assume $n = p$ at all times.

Production of Frenkel Defects with Both Vacancies and Interstitial Ions Mobile

It seems reasonable to assume that if the field strength is sufficiently great to pull a lattice ion out of its position and place it in an interstitial position, it should also be able to move a lattice ion to an adjacent empty site. The assumption made by Bean, Fisher, and Vermilyea that vacant cation sites are immobile seems, therefore, inconsistent with the assumption of the creation of Frenkel defects. The more consistent model in which the vacancies are allowed to be mobile gives some interesting limiting cases. The equation for the rate of change of vacancy concentration at a given point acquires an extra term and becomes (in the form used by Dewald (12) in considering Bean, Fisher, and Vermilyea's model),

$$\partial m/\partial t = \partial i_m/\partial x + (N_0 - m)\gamma'' \exp -(W'' - Eqa'')/kT - i\sigma_m,$$

where m = concentration of vacancies; i_m = vacancy current (in ions); N_0 = total concentration of lattice sites; W'', ν'', and a'' the activation energy at zero field, vibration frequency, and half jump distance for the production of a Frenkel defect; and σ_m is the cross section for the capture of an interstitial ion by a vacancy. i_m is given by a term of the usual type.

If vacancies are not produced at the interface, $i_m(x = 0) = 0$. If the mobility of vacancies is sufficiently great with respect to their rate of production, their concentration falls to zero throughout. If not, m varies with x, and the field varies with thickness.

If vacancies are produced at the metal interface, as well as in the oxide, both constant and varying m and field are possible, according to the parameters, and the interface partly controls the kinetics over the range of fields where the vacancy current is important.

The Model in which Metal Ions Move in a Uniform Immobile Negative Space Charge

The significance of this model has been indicated in previous sections. We consider an immobile, uniform negative space charge given by $-pq$ where q is the charge on the *metal* ion. Poisson's equation is now

$$\partial E/\partial x = 4\pi\, q(n - p)/\epsilon,$$

where n, as before, is the concentration of metal ions. Using the continuity equation

$$\partial i/\partial x = 0$$

we obtain

$$(\partial n/\partial x) + n\beta(\partial E/\partial x) = 0.$$

Can. J. Chem. Downloaded from www.nrcresearchpress.com by 190.90.36.8 on 09/04/12
For personal use only.

After integrating as in Dewald's theory, we obtain

$$[8] \qquad n = p/\{1-(1-p/n_0)\exp(-\beta 4\pi\, qpx/\epsilon)\}$$

and, after a second integration,

$$[9] \qquad E = E_0+\frac{1}{\beta}\log\{[n_0-(n_0-p)\exp(-\beta 4\pi\, qpx/\epsilon)]/p\}$$

where n_0 and E_0 are the values of n and E at $x = 0$, and are given by equations [4] and [3] respectively.

For large x, the field is given by

$$[10] \qquad E = E_0+(1/\beta)\log(n_0/p).$$

On substituting for E_0,

$$[11] \qquad E = \frac{1}{\beta}\{\log(i/2a\nu\, p)+W/kT\}.$$

The field then becomes independent of the interface and is determined by whatever determines p. This is the result which Verwey (3), Bean, Fisher, and Vermilyea (16), and Dewald (12) assume implicitly or, in Dewald's case, explicitly, to apply at all x. The validity of their assumption depends on p/n_0 and on the value of p, since this controls the characteristic length l (say) $= \epsilon/\beta 4\pi\, qp$ in equation [8]. For $l \simeq 10$ Å, $p \simeq 10^{21}$ metal ion equivalents per cm^3, assuming a typical value for a in $\beta = qa/kT$ of 3 Å. The total concentration of metal ions in the oxide is $2\rho L/M \simeq 10^{22}$, where ρ = density, L = Avogadro's number, and M = the molecular weight of the oxide. Thus for $l \simeq 10$ Å, a fraction of the order of 1 in 10 ions must be mobile and so on. In the theory of Bean, Fisher, and Vermilyea p varies exponentially with the field, so that it appears that at low fields when p is small, the space charge region should become important, and the assumption of no net space should break down. At high fields p will become rather large. In contrast with Dewald's model, the concentration of mobile metal ions may either fall below or rise above the value corresponding to electroneutrality. The possibility of the net space charge being either positive or negative means that the field strength in the interfacial region may either rise or fall in passing from the interfacial region towards the center of the oxide.

Consequences of the Amorphous Nature of the Oxide

It has been noted that in the amorphous oxide one would expect a range of types of site. Thus as the field is increased an increasing proportion of sites will stop acting as traps for the mobile ions. In particular, sites which have a short "a" for the exit of ions will become active as the contribution of the field (qaE) increases. The effect is, therefore, that p is expected to increase with the field strength so that "overshoot" will occur and in addition, changes in "a" and W with field strength are to be expected. The experimental observation of these features may need no further explanation than the fact that the oxide is amorphous. However, another source of variation in "a" with field strength is due to the obvious but never-mentioned fact that jumps occur in a cone of solid angle along the field direction. This cone will open as the field increases. The expectation that n and "a" change instantaneously with field strength seems to invalidate Vermilyea's method of obtaining "a" by transient studies (18), in which "a" is assumed to be independent of field strength.

Can. J. Chem. Downloaded from www.nrcresearchpress.com by 190.90.36.8 on 09/04/12
For personal use only.

Both Ions Mobile

It appears fairly certain that for the usual experimental conditions most of the current is carried through the films on tantalum and niobium by metal ions (19, 20). However, this does not exclude the occurrence of a slight mobility of oxygen ions, and this could be important because it provides another mechanism causing the concentration of negative ions (and hence p) to vary sluggishly with the field strength.

The steady-state condition is discussed first.

It is assumed that the oxygen ion current may be described by an equation of the same form as that which is used to describe the metal ion current. The limitations in this assumption have already been discussed. The subscripts + and − refer to metal and to oxygen ions, respectively. The current is now given as a charge flow rather than as ion flow:

$$i_+ = q_+ 2a_+n_+\nu_+ \exp(-W_+/kT) \exp \beta_+E,$$

where

[12] $$\beta_+ = q_+a_+/kT,$$

and similarly (with i_- and q_- as positive quantities)

[13] $$\begin{aligned} i_- &= q_- 2a_-n_-\nu_- \exp(-W_-/kT) \exp \beta_-E, \\ &= q_+ 2a_-p\nu_- \exp(-W_-/kT) \exp \beta_-E. \end{aligned}$$

As before, Poisson's equation gives

[14] $$\partial E/\partial x = 4\pi\, q_+(n-p)/\epsilon.$$

In the steady state, the continuity equation becomes

[15] $$(\partial i_+/\partial x) = (\partial i_-/\partial x) = 0.$$

Hence from [12] to [15],

[16] $$n_+ = n_+{}^0 \exp -\beta_+(E-E^0)$$

and

[17] $$p = p^0 \exp -\beta_-(E-E^0),$$

where n^0, p^0, and E^0 refer to values at $x = 0$.
From [14], [16], and [17]

[18] $$x = \int_0^x dE/\{(4\pi\, q/\epsilon)(n_+{}^0 \exp -\beta_+(E-E^0) - p \exp -\beta_-(E-E^0)\}.$$

Since $q_+ = 5e$ and $q_- = 2e$ it is probable that for tantalum $\beta_+ > \beta_-$. Hence, if the space charge near the metal is negative, so that E decreases with increasing x, both n_+ and n_- will increase with x, but n_+ will increase more rapidly, so that eventually the space charge must fall to zero. Conversely, if the space charge is initially positive, then the field at first increases, both n_+ and n_- decrease with distance but n_+ decreases more than n_- so that the space charge eventually becomes very small. Thus for large x we have n_+, n_-, and the field strength all constant. The model behaves essentially the same as that with p constant throughout the film. The difference is that p is determined by the field strength in the outer part of the oxide, since this field strength determines the rate of entry of negative ions into the oxide, and their rate of movement through the oxide.

The reaction at the oxide/solution interface by which O″ enters the oxide must be

Can. J. Chem. Downloaded from www.nrcresearchpress.com by 190.90.36.8 on 09/04/12
For personal use only.

essentially $H_2O = O''(\text{oxide}) + 2H^+$. The experimental data for tantalum show (1) that the kinetics are independent of the pH and of the electrolyte in dilute aqueous solutions, but (2) that the kinetics are affected by a variation of composition large enough to vary the activity of the H_2O species.

The entry of O'' may be described using equations similar in form to those used to describe the entry of metal ions at the other interface:

$$\begin{aligned} i_-(D) &= q_- m_l \nu_l \exp(-W_l/kT) \exp \beta_l E \\ &= q_- 2a_- n_-(D)\ \nu_- \exp(-W_-/kT) \exp \beta_-/kT, \end{aligned}$$

in which D = thickness of oxide, the subscript l refers to the oxide/solution boundary, and the field across the oxide/solution boundary is put equal to the field just inside the oxide. Hence,

$$n_-(D) = \frac{m_l \nu_l}{2a_- \nu_-} \exp\left(\frac{W_- - W_l}{kT}\right) \exp\left(\frac{Eq_-(a_l - a_-}{kT}\right).$$

The measured current is nearly equal to the metal ion current from equation [12] with n_+ put equal to $p(D)$.

$$i_+ = q_- 2a_+ \nu_+ \left(\frac{m_l \nu_l}{2a_- \nu_-}\right) \exp\left(\frac{W_- - W_l - W_+}{kT}\right) \exp E(\beta_+ + \beta_l - \beta_-).$$

This model has the peculiar characteristic that the kinetics are controlled by the metal/oxide interface when the film is very thin and space charge effects are negligible, and by migration through the oxide (with the concentration of mobile ions controlled by the oxide/solution interface) when the film is thick enough for space charge effects to have isolated the bulk of the film from the effects of the metal/oxide interface.

The mathematics of the non-steady state are complex, and only a qualitative discussion will be attempted.

The concentration of oxygen ions will either increase or decrease with increasing $E(D)$ according to whether β_l is greater or smaller than β_-. The first case will be assumed. Since it is assumed that the metal ions are far more mobile than oxygen ions, the metal ion distribution at each stage will be nearly in the steady-state condition appropriate to the instantaneous distribution of negatively charged ions. Suppose that after the system has come to a steady state at an applied current $I_1 \simeq i_+$, the current is suddenly increased to a new value I_2. The average field will first rise to a new value given by equation [11] with almost the same value of p as existed before I was increased. The process is that of charging a condenser with a leakage given by $i = i_0 \exp \beta E$, where $E \simeq V/D$. If V = voltage across the condenser of capacity C,

$$I(t) = CdV/dt + i_0 \exp(\beta V/D),$$

where $$I(t) = I_1 \text{ for } t \leqslant 0 \text{ and } I = I_2 \text{ for } t > 0,$$

we obtain $$I_2 t = (DC/\beta) \log\{(1 - I_2/I_1)/[1 - I_2/i_0 \exp(\beta V/D)]\}.$$

The time t for the condenser to charge up to a given fraction of its final charge is inversely proportional to the current density and independent of D.

As the field in the oxide increases, the rate of entry of oxygen ions also increases. As the concentration of oxygen ions builds up the field decreases and levels out at the new steady-state value. The decay of the overshoot should depend on the thickness of oxide, since the decay involves the movement across the oxide of something in the nature of a step function

Can. J. Chem. Downloaded from www.nrcresearchpress.com by 190.90.36.8 on 09/04/12
For personal use only.

in the concentration of both ions, and the velocity of movement will tend to be independent of thickness. According to Dewald (12), with tantalum the decay does not depend on the thickness, so that the above model would appear (if our qualitative treatment is correct) not to apply to this metal.

Structural Effects at the Metal/Oxide Interface

Each time that a metal ion leaves the metal to enter the oxide it leaves a vacancy in the metal lattice and some degree of local misfit. This may cause the outer two or three layers of metal to become effectively amorphous. The effect will depend on the current density, since the diffusion within the metal surface will tend to repair the damage. The degree of directional bonding within the metal, and the presence of impurities will also affect this process. When the disarrangement is present, it will tend to remove the differences between the kinetics on different crystal faces that might be expected when the Cabrera–Mott theory applies.

SUMMARY

A great many different special cases are possible—movement by metal or oxygen, vacancies or interstitial ions, creation of defects by the field, interfacial barriers important or not important according to the relative values of various parameters, and so on. A few essential principles may, however, be formulated. In the first place, for metal ion movement the metal/oxide interface will control the kinetics unless sufficient space charge can accumulate near this interface to permit the field strength at the boundary to differ appreciably from the field strength further into the oxide. If the interface is, so to speak, isolated by space charge effects, the concentration of carriers in the main body of the film is controlled by whatever determines the net space charge density due to the non-mobile species. The field production of Frenkel defects, the movement of oxygen ions, and the range of sites due to the amorphous nature of the oxide could cause this background charge to vary with the field strength. When the background charge varies with the field strength, it becomes possible to have "overshoot" in the field transients. Variation of jump distance and hence of Tafel slope with field strength may be due to the variation of sites to be expected in an amorphous oxide, and to the fact that jumps occur at greater angles to the field direction as the field strength increases.

This work was supported by the Defence Research Board of Canada.

REFERENCES

1. Uhlig, H. U. Acta Met. **4**, 541 (1956).
2. Ketelaar, J. A. A. Nature, **137**, 316 (1936).
3. Verwey, E. J. W. Physica, **2**, 1059 (1935).
4. Ubbelohde, A. R. Discussions Faraday Soc. **23**, 128 1957.
5. Cabrera, N. and Mott, N. F. Repts. Progr. in Phys. **12**, 163 (1948–1949).
6. Jacobs, P. W. M., Bray, A. R., and Young, L. Proc. Phys. Soc. **71**, 405 (1958).
7. Vermilyea, D. A. Acta Met. **1**, 282 (1956).
8. Young, L. Trans. Faraday Soc. **52**, 502 (1956).
9. Willis, G. C., Adams, G. B., and van Rysselberghe, P. Private communication. (1958).
10. Young, L. Unpublished.
11. Vermilyea, D. A. J. Electrochem. Soc. **102**, 655 (1955).
12. Dewald, J. F. Phys. and Chem. Solids, **2**, 55 (1957).
13. Dewald, J. F. J. Electrochem. Soc. **102**, 1 (1955).
14. Vermilyea, D. A. J. Electrochem. Soc. **104**, 140 (1957).
15. Young, L. Proc. Roy. Soc. A, **244**, 41 (1958).
16. Bean, C. P., Fisher, J. C., and Vermilyea, D. A. Phys. Rev. **101**, 551 (1956).
17. Tompkins, F. C. and Jacobs, P. W. M. Quart. Revs. **6**, 238 (1952).
18. Vermilyea, D. A. J. Electrochem. Soc. **104**, 427 (1957).
19. Vermilyea, D. A. Acta Met. **2**, 482 (1954).
20. Young, L. Trans. Faraday Soc. **53**, 841 (1957).

Can. J. Chem. Downloaded from www.nrcresearchpress.com by 190.90.36.8 on 09/04/12
For personal use only.

Can. J. Chem. Downloaded from www.nrcresearchpress.com by 190.90.36.8 on 09/04/12
For personal use only.

THE FORMATION AND PROPERTIES OF PASSIVE FILMS ON IRON[1]

MORRIS COHEN

ABSTRACT

A unified mechanism for the formation of passive films on iron in aqueous solutions is presented. The effects of water, oxygen, and oxidizing and non-oxidizing ions are considered. The γ-Fe_2O_3 film is formed first by the oxidation of water-formed magnetite and further thickening of the film takes place by the oxidation of diffusing Fe^{++} ion at the water surface of the oxide film. The main force leading to diffusion is the field set up by the adsorbed negative ion and the positive Fe^{++} ions at the surface of the metal. Some of the properties of the protective γ-Fe_2O_3 film and factors leading to its destruction are discussed.

When iron is exposed to aqueous solutions containing certain oxidizing ions such as chromate or nitrite, or buffering agents and oxygen, it becomes passive. Electron diffraction measurements and film stripping experiments indicate that the iron is covered by a thin film, composed mainly of γ-Fe_2O_3 (1, 2).

Although much has been published concerning the behavior and possible physical and chemical structure of these passive films on iron (3, 4, 5), very little data has been presented or possible mechanisms proposed to account for the formation of the films.

Since the behavior of passive films on iron is much the same, independent of the solution in which they are formed, there is probably a common general mechanism of formation. In this paper such a mechanism for the formation process and composition of passive films is developed and used to explain the build-up and break-down of the films.

1. Reactions of Iron with Water

(a) In the Absence of Oxygen

This reaction has been reviewed recently by V. J. Linnenbom (6). At room temperature he found evidence for ferrous hydroxide only. At higher temperatures some Fe_3O_4 was also found. In earlier work Schikorr (7) reports that $Fe(OH)_2$ converted slowly to magnetite at room temperature but this was not confirmed by Linnenbom. It is thermodynamically possible for iron to react with water to form either $Fe(OH)_2$ or Fe_3O_4.

When film-free iron is exposed to water, in all probability a film is formed which separates the iron from the water. If this film is formed by a heterogeneous reaction between the iron and the water then the composition of the film will probably approximate that of an anhydrous oxide. FeO is not stable below a temperature of 500° C, so that the most likely film is Fe_3O_4. This persists as a very thin film and the iron remains bright and silvery in appearance.

The rate of reaction of iron with oxygen-free water is very slow, of the order of 20 $\mu g/cm^2$ in 5 days (3). This rate is about the same in the presence of chloride ion. The reaction rate corresponds to the reaction of 56 Å of metal/day or a current of $2\times10^{-1}/\mu a\ cm^2$. The potential of the specimen, which corresponds to the equilibrium potential of iron in a saturated solution of $Fe(OH)_2$, indicates high hydrogen polarization. The mechanism of the reaction is probably that of diffusion of both Fe^{++} and electrons through a thin magnetite film of the order of 1 or 2 unit cells (8–16 Å) thick with the

[1]*Manuscript received July 10, 1958.*
Contribution from the Division of Applied Chemistry, National Research Council, Ottawa. This paper was presented at the Symposium on Charge Transfer Processes held at the University of Toronto, Toronto, Ontario, September 4 and 5, 1958.
Issued as N.R.C. No. 4982.

rate of the reaction being controlled by the rate of formation of hydrogen. The very thin film of magnetite acts as a separator rather than a diffusion barrier and is stabilized by being in contact with the metal.

The reactions can be expressed as:

$$Fe \longrightarrow Fe^{++} + 2e,$$

$$\frac{2e + 2H_2O \longrightarrow 2OH^- + H_2}{Fe + 2H_2O \longrightarrow Fe(OH)_2 + H_2}.$$

The rapidly formed magnetite film is formed by the reaction:

$$3Fe + 4H_2O \longrightarrow Fe_3O_4 + 4H_2.$$

The magnetite thickens and becomes visible at higher temperatures or by the addition of certain other chemicals—that is when the rate of the reaction of $Fe^{++} \longrightarrow Fe_3O_4$ in contrast to $Fe^{++} \longrightarrow Fe^{++}$ hydrated is increased.

A diagram of the reactions of iron in oxygen-free water is shown in Fig. 1.

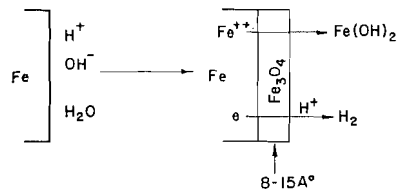

FIG. 1. Development of steady-state corrosion of iron in water. A thin film of magnetite is formed by direct reaction with water. Reaction continues by diffusion of ferrous ion into the solution and hydrogen formation.

(b) Absence of Oxygen but Presence of Oxidizing Anions

Four oxidizing ions—namely nitrite, chromate, molybdate, and tungstate—have been found to form films on iron in oxygen-free water. Of these, chromate forms a passive film at the lowest concentration. This film is of the order of 50–75 Å thick and contains both γ-Fe_2O_3 and Cr_2O_3 (8).

With nitrite solutions, at low concentrations thick films of Fe_3O_4 are formed. When the concentration of nitrite is increased to about 0.1 *N* a thin film of γ-Fe_2O_3, possibly containing some γ-FeO(OH), is formed (1).

Of the four oxidizing inhibitors the strongest oxidizing agent with respect to ferrous ion in neutral solution is chromate. The others react relatively slowly. All four inhibitors are poor cathodic depolarizers: nitrite ion is not reduced when exposed to cathodically polarized iron, while the reaction rate of iron with water, which is controlled by cathodic depolarization, is the same irrespective of the presence of low concentrations of molybdate and tungstate (3).

As in the presence of water alone, the instantaneous surface reaction of film-free iron is a heterogeneous one to form Fe_3O_4. Adsorption of the oxidizing anions on the films during the formation of the film leads to further oxidation to γ-Fe_2O_3. In the case of the chromate ion, where the reduction product is insoluble Cr_2O_3, this leads to the build-up of a film containing both Cr_2O_3 and γ-Fe_2O_3 in a ratio of about 1:3. The amount of chromium found in the film would correspond to a film about 50–75 Å thick (8).

In the case of nitrite the reduction products are soluble and at sufficiently high concentrations a film consisting mainly of γ-Fe_2O_3 is formed. At low concentrations (0.001 *N*) magnetite films of sufficient thickness to be visible are formed (9).

Can. J. Chem. Downloaded from www.nrcresearchpress.com by 190.90.36.8 on 09/04/12
For personal use only.

With molybdate and tungstate visible magnetite films are also formed. However, if the iron is made anodic, γ-Fe_2O_3 films of a protective nature are formed. This may be due to an increase in oxidation rate by the discharge of hydroxyl ion to form oxygen and/or discharge of the anions at the metal oxide – solution interface.

This order of efficiency of the formation of passive films is probably related to the oxidizing power of the anions with respect to the oxidation of Fe^{++} to Fe^{+++}. The reaction of chromate ion with ferrous ion is very rapid, while that of nitrite, molybdate, and tungstate is relatively slow.

The γ-Fe_2O_3 which forms the main part of all the passive films is formed as the film grows. The first formed unit cell of Fe_3O_4 is oxidized to γ-Fe_2O_3 and further diffusion of Fe^{++} takes place through this γ-Fe_2O_3 film. The ferrous ion which reaches the oxide–solution interface is oxidized to ferric ion by the adsorbed oxidizing agent, thus leading to further thickening of the film. Although there is no direct contact between the iron and the solution the iron is oxidized to Fe^{++} by water in that the electrons are neutralized by H^+. The main force responsible for the diffusion of Fe^{++} through the γ-Fe_2O_3 is supplied by the electrostatic attraction between the adsorbed negative anion and positive metal ions in the lattice. This force is sufficient to allow a film of about 50–75 Å thick to form. The geometry of these reactions is shown in Fig. 2.

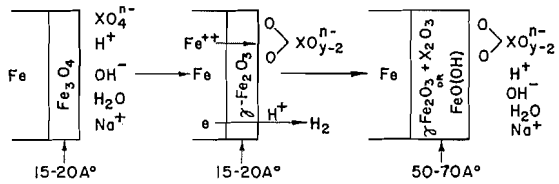

FIG. 2. Conversion of Fe_3O_4 to γ-Fe_2O_3 and further thickening of γ-Fe_2O_3 to form passive film. The attractive force between the anion and Fe^{++} depends on charge and thickness.

If the concentration of the passivating oxidizing agent is too low, oxidation of the ferrous ion takes place to magnetite only and a proportion of ferrous ion escapes into the solution. The magnetite film thickens considerably, probably because the cationic diffusion rate through magnetite is greater than that through γ-Fe_2O_3.

A number of oxidizing anions such as permanganate do not form passive films on iron. This could be due to either the physical nature of the reduction product and/or their ability to depolarize the cathodic reaction. The former is probably the more important in that a gelatinous reduction product interferes with the growth of the protective passive film. Because of depolarization of the hydrogen formation reaction some oxidizing anions may act as corrosion accelerators rather than passivating agents.

(*c*) *Presence of Oxygen*

Iron reacts rapidly with dry oxygen at room temperature to form a film of γ-Fe_2O_3 15–20 Å thick (10). At this thickness the reaction essentially ceases. If iron is exposed to water saturated with oxygen at normal pressures and temperatures the reaction continues at a relatively constant rate, the main products of the reaction being hydrated ferric oxides. If the specimen becomes covered with hydrated reaction product, so that there is a decrease in the oxygen concentration at the oxide–precipitate interface, visible films of magnetite are formed. The corrosion rate is very much higher than the rate in oxygen-free water, being of the order of 1.3 mg/cm^2 5 days or 13 μa/cm^2, or 65 times the rate in oxygen-free water.

Can. J. Chem. Downloaded from www.nrcresearchpress.com by 190.90.36.8 on 09/04/12
For personal use only.

Can. J. Chem. Downloaded from www.nrcresearchpress.com by 190.90.36.8 on 09/04/12
For personal use only.

The initial reaction is the formation of a thin layer of magnetite as in the case of oxygen-free water. This thin layer of magnetite can then be oxidized to γ-Fe_2O_3 by reaction with adsorbed oxygen. At room temperature and pressure the solubility of oxygen in water is only 8 parts per million and owing to incomplete coverage by oxygen both the rate of oxidation to γ-Fe_2O_3 and further thickening of the γ-Fe_2O_3 film is slow. Fe^{++} ions continue to diffuse through the oxide into the solution where they are oxidized by dissolved oxygen to FeO(OH). These hydrated oxides are precipitated on the metal surface and form a diffusion barrier for the movement of oxygen to the metal surface. As in the case of the oxidizing anions, the lowered concentration of oxygen at the metal oxide – solution interface allows further growth of magnetite but does not oxidize the magnetite to γ-Fe_2O_3. The precipitate, being laid down unevenly, will tend to allow the formation of separate anodic and cathodic areas on the surface and the over-all corrosion current is sufficiently high and the pH sufficiently low to cathodically reduce any already formed γ-Fe_2O_3 (11). The above sequence of formation of Fe_3O_4, etc., will then be repeated. As well as oxidizing magnetite to γ-Fe_2O_3 the oxygen can also react with $(e + H^+)$ to form OH^- ions. This both accelerates the rate of corrosion and, at the normally low concentrations of oxygen in the solution, decreases the per cent of the surface area covered by oxygen. This lowered coverage leads to a decreased probability of the formation of a protective γ-Fe_2O_3 film.

At sufficiently high concentrations of oxygen it is possible to obtain protective passive films. This is related to a more rapid replenishment of the cathodically removed oxygen which leads to γ-Fe_2O_3 film growth rather than corrosion. The formation of a protective film thicker than 15–20 Å may be due in part to the field set up by the adsorption of some OH^- ions.

(*d*) *Presence of Oxygen and Oxidizing Ion*

In general the presence of oxygen decreases the concentration of oxidizing anion required to give passivity. Because of the presence of the anion the film still thickens to 50–75 Å. The main function of the oxygen in the case of the nitrite, molybdate, and tungstate is probably the oxidation to γ-Fe_2O_3 of some of the magnetite formed by the oxidation of ferrous ion by the anion.

(*e*) *Presence of Oxygen and Non-oxidizing Buffering Ion*

Iron is passive in air-saturated solutions containing relatively high concentrations of alkaline buffering agents such as Na_2CO_3, Na_3PO_4, and C_6H_5COONa. The passive film is mainly composed of γ-Fe_2O_3 with some hydrated oxide, and in the case of the phosphate, hydrated ferric phosphate (12). Most of the hydrated material appears to be located in rather thick inclusions which protrude above the oxide film (9). The salts would appear to serve two purposes. Firstly adsorption of the negative ion, by increasing the field strength across the oxide, leads to a sufficient thickening of the γ-Fe_2O_3 film formed by the reaction of O_2 with Fe_3O_4 to prevent further diffusion of iron ions. Secondly, where the film has not thickened, so that Fe^{++} ions continue to escape into the solution, the anodic pores are kept on the basic side. This decreases the rate of cathodic reduction and consequent thinning of the adjacent oxide. Since diffusion of ferrous ions through the porous precipitated plug of hydrated material is probably more rapid than through the oxide the plugs grow relatively thick before the reaction stops.

2. Reactions in the Presence of the Air-formed Film

As mentioned above, the air-formed film is γ-Fe_2O_3 of the order of 20 Å thick. In the presence of the passivating agent this film thickens, by the formation of more γ-Fe_2O_3

and possibly other hydrated products. Under borderline passivating conditions some of the film may be removed by cathodic reduction and either new film or plugs are formed in the manner outlined above.

3. Effect of an Applied Current

If the iron is made cathodic the γ-Fe_2O_3 film is reduced. At low cathodic current densities corrosion continues, probably through a layer of magnetite. At higher cathodic currents corrosion essentially ceases, probably with some redeposition of iron.

At low anodic currents the corrosion of iron is increased. At higher current densities passivity is often observed. This can be explained by a combination of the suppression of the cathodic reaction with its possibility of cathodic reduction of the γ-Fe_2O_3 and the direct discharge of oxygen on the metal surface. Because of the high overvoltage for oxygen evolution the equivalent pressure of oxygen at the metal surface is high and conditions for the formation of γ-Fe_2O_3 favorable. Oxidizing ions such as tungstate and molybdate will also be discharged at the anodic areas with a similar effect of apparent increased activity.

4. Properties of the Passive Film

Passive films have been stripped from iron by both chemical (13) and electrochemical (14) dissolution of the underlying metal. They are found to be mainly anhydrous γ-Fe_2O_3. They are chemically inert and dissolve in acid only with difficulty. The hydrated parts of the film are less inert than the anhydrous oxide. The film may be cathodically reduced to Fe^{++} ion which, at neutral and low pH's, is quite soluble. The film is a relatively good electronic conductor but a poor cationic conductor and the growth of the film appears to be controlled by the rate of cationic conduction.

The breakdown of the passive film probably takes place through the breakdown of pores in the anhydrous oxide film. Electron microscope and diffraction studies indicate that most of the passive films have discontinuities in the anhydrous oxide films which contain the less inert hydrated ferric oxides or other insoluble ferric salts. Diffusion of the solution through these rather porous precipitated plugs leads to the formation of acidity in the pores—particularly in the presence of such ions as chloride or sulphate. The ferric salts can be removed by the formation of soluble complexes with many ions. The combination of anodic current and acid conditions leads to undermining or cathodic reduction of the protective γ-Fe_2O_3 film.

It is rather surprising that there is such a large difference in the cationic diffusion properties of magnetite and γ-Fe_2O_3 as indicated by possible thicknesses of the two types of film. It is generally assumed that γ-Fe_2O_3 has essentially the Fe_3O_4 structure with cation vacancies (15). The diffraction patterns of the two oxides are very similar. The two oxides, however, behave quite differently chemically. Fe_3O_4 dissolves in acid very easily, while γ-Fe_2O_3 dissolves only with difficulty. On cathodic reduction γ-Fe_2O_3 is reduced completely to the ferrous state with high current efficiency, while magnetite is reduced with difficulty and very low current efficiency. In some X-ray diffraction studies in this laboratory it has been found that γ-Fe_2O_3 produced in several ways has d-values greater than 6 Å as well as two lines which do not appear in the Fe_3O_4 patterns. This would point to a somewhat different kind of ordered structure and may account for the different chemical and diffusional behaviors of the two oxides. This would also indicate that some recrystallization takes place in the conversion of Fe_3O_4 to γ-Fe_2O_3.

A second factor which may contribute to a difference in the growth rate and hence final thickness of the two oxides could be a difference in the rate of transfer of Fe^{++} ions

Can. J. Chem. Downloaded from www.nrcresearchpress.com by 190.90.36.8 on 09/04/12
For personal use only.

across the metal–oxide interface. This would be partly related to a difference in the crystallographic arrangement of the oxides on the metal. Thin films of Fe_3O_4 show preferred orientation on iron, while γ-Fe_2O_3 films do not. The bulk of evidence shows that γ-Fe_2O_3, the main constituent of the passive film, is an inert material which in passivating solutions grows to a maximum thickness of 50–75 Å.

REFERENCES

1. COHEN, M. J. Phys. Chem. **56**, 451 (1952).
2. MAYNE, J. E. O. and PRYOR, M. J. J. Chem. Soc. 1831 (1949).
3. PRYOR, M. J. and COHEN, M. J. Electrochem. Soc. **100**, 203 (1953).
4. WADE, W. H. and HACKERMAN, N. Trans. Faraday Soc. **53**, 1636 (1957).
5. HOAR, T. P. and EVANS, U. R. J. Electrochem. Soc. **99**, 212 (1952).
6. LINNENBOM, V. J. J. Electrochem. Soc. **105**, 322 (1958).
7. SCHIKORR, G. Z. anorg. u. allgem. Chem. **212**, 33 (1933).
8. COHEN, M. and BECK, A. F. Z. Elektrochem. (In press).
9. MELLORS, G. W., COHEN, M., and BECK, A. F. J. Electrochem. Soc. **105**, 332 (1958).
10. GULBRANSEN, E. A. J. Electrochem. Soc. **81**, 327, 1942.
11. OSWIN, H. G. and COHEN, M. J. Electrochem. Soc. **104**, 9 (1957).
12. PRYOR, M. J., COHEN, M., and BROWN, F. J. Electrochem. Soc. **99**, 542 (1952).
13. VERNON, W. H. J., WORMWELL, F., and NURSE, J. T. J. Chem. Soc. 621 (1939).
14. EVANS, U. R. Nature, **126**, 130 (1930).
15. WELLS, A. F. Structural inorganic chemistry. Oxford University Press, London. 1950. p. 381.

Can. J. Chem. Downloaded from www.nrcresearchpress.com by 190.90.36.8 on 09/04/12
For personal use only.

Can. J. Chem. Downloaded from www.nrcresearchpress.com by 190.90.36.8 on 09/04/12
For personal use only.

THE ELECTROCHEMICAL BEHAVIOR OF THE NICKEL – NICKEL OXIDE ELECTRODE

PART I. KINETICS OF SELF-DISCHARGE[1]

B. E. Conway and P. L. Bourgault

ABSTRACT

The nickel – nickel oxide electrode forms the positive plate in the charged nickel–cadmium battery. After "charging" the electrode to a chemical state represented by the non-structural formula NiO_x, where x can vary from about 1.4 to 1.8 depending on the current density and temperature, loss of oxygen and a fall of potential on open circuit occurs. In the present work this "self-discharge" effect has been examined by study of (i) the rate of decay of e.m.f. on open circuit, (ii) rate of oxygen evolution on open circuit, (iii) the electrochemical capacity of the electrode, and (iv) the build-up or charging curves for the electrode. The decay behavior has been studied in aqueous KOH solutions from 0.0015 to 15 *M*. Tafel slopes are obtained from the plots of e.m.f. vs. log (time of decay), and abrupt changes occur at certain electrode potentials which indicate changes of rate-determining mechanism in the self-discharge process. The slopes observed are interpreted in terms of a new scheme of consecutive reactions for anodic oxygen evolution by deducing, by means of the Christiansen method, the relevant Tafel slopes. It is shown that the scheme proposed uniquely accounts for the experimental behavior and that the change of mechanism observed in the self-discharge can only be explained if two consecutive and not alternative processes are involved. The dependence of the rates of self-discharge upon OH^- ion and water activity is deduced and the significance of these results is discussed.

INTRODUCTION

Interest in the behavior of the nickel – nickel oxide electrode arises from its use as the positive plate in the nickel–cadmium and nickel–iron batteries; at the same time, study of the system affords further insight into the fundamental kinetics of anodic processes, which in the case of the nickel system are complex owing to the existence of several possible oxidation states of the metal in corresponding hydrated oxides (1, 2). One of the features of interest is the loss of charge of the nickel oxide electrode when it is left standing in pure alkaline solution on open circuit. The loss of charge is accompanied by oxygen evolution and decay of e.m.f. of the electrode (e.g., measured with respect to the Hg/HgO electrode in the same solution). Hitherto, studies of the kinetics of decay have not been made rigorously and only somewhat arbitrary rate measurements have been obtained (i) by determining the total time required for the e.m.f. of the electrode to decay over about 0.6 v (3), and (ii) by determining the *total* volume of oxygen liberated from an electrode at the end of a period of 13 hours (4). Since it is clear that over the potential range studied (3) more than one process is involved in the decay, because the e.m.f.–time curve passes through an inflection, and since in the oxygen evolution process (4) the rate of oxygen evolution depends on the electrode potential, it must be concluded that the kinetic significance of "rates" measured by these procedures is unclear. Furthermore, the "rates" of self-discharge thus measured by these two procedures are found to be dependent in *opposite* senses upon the KOH or water activities in the solutions used. In the present work we have therefore attempted to make a more rigorous kinetic analysis of the self-discharge process by obtaining the decay of e.m.f. as a function of the theoretically significant *logarithm* of the time of decay, and relating this to the volume of

[1]*Manuscript received July 1, 1958.*
Contribution from the Department of Chemistry, University of Ottawa, Ottawa, Ontario. This paper was presented at the Symposium on Charge Transfer Processes held at the University of Toronto, Toronto, Ontario, September 4 and 5, 1958.

oxygen evolved, measured frequently during an over-all period of 10^5 to 10^6 seconds. Electrochemical capacities of the electrodes studied are obtained by several different methods involving the kinetics of the decay and charging processes.

EXPERIMENTAL

Electrodes

The electrodes used were similar to those utilized in the nickel–cadmium battery. Porous sintered pure nickel plaques having an average pore size of 1 μ (5) were impregnated under vacuum with a saturated solution of cobalt-free nickel nitrate prepared by recrystallization from A.C.S. analytical reagent grade material. The nickel hydroxide, $Ni(OH)_2$, was then precipitated in the sinter by immersion in 20% aqueous KOH solution purified as described below. The electrodes were then treated cathodically as described previously (6) and then washed in 10 changes of conductance water. The electrodes were finally charged anodically in the experimental solution (see below) until oxygen evolution occurred. The weight of oxide formed in the electrode was determined from the difference of the weights of the dry unimpregnated sinter and the oxide-impregnated one after drying at 80° C; under these conditions the oxide in the sinter is $Ni(OH)_2$. From this weight, the theoretical electrochemical capacity for a given degree of subsequent oxidation can be calculated.

Solutions

Conductance water was redistilled in CO_2-free nitrogen passed through liquid air traps containing charcoal. The steam was passed up a column of hard glass chips heated to 450° C. The water was then condensed into a second distillation vessel from which it was redistilled into a vessel containing solid A.C.S. analytical reagent grade KOH. This vessel was provided with a sintered glass bottom for filtering, and suitable exit and entry tubes for gas and solution. The KOH solution thus prepared was then recrystallized by immersion of the vessel in a refrigerated bath at −20° C; the mother liquor was forced out of the tube leaving crystals of the dihydrate of KOH. Further water was then distilled on to the recrystallized KOH from the second distillation stage. The solution thus obtained was then used to prepare potassium amalgam which was then reacted with more of the redistilled water until a suitable concentration of aqueous KOH was obtained. This solution was then passed into the experimental cell where it was pre-electrolyzed with a nickel anode, purified oxygen being bubbled through the solution. The pre-electrolysis current of 10^{-2} amp per apparent cm^2 was passed for 12 hours between the nickel anode and a charged nickel – nickel oxide electrode as cathode. This procedure was adopted in order that no hydrogen could be evolved cathodically and diffuse subsequently to the experimental charged nickel electrode, which might thereby be depolarized. Experiments were also made, in order to simulate battery conditions, in ordinarily purified solutions, i.e., without KOH regeneration by means of potassium amalgam. These experiments were carried out mainly in the higher range of concentrations of KOH as used in the nickel battery.

Cells

In dilute solutions ($< 0.1\ N$) it was found that use of the usual two-limb cell (7) with reference electrode and Luggin capillary lead to non-uniform charging* of the electrode, owing to asymmetry of the position of the electrode with regard to current

*By "charging" we signify the process of conversion of the initially precipitated $Ni(OH)_2$ to the non-stoichiometric higher hydrated oxide often referred to as nickel peroxide or NiO_2.

Can. J. Chem. Downloaded from www.nrcresearchpress.com by 190.90.36.8 on 09/04/12
For personal use only.

lines from the cathode. In order to overcome this difficulty, e.m.f. and oxygen volume measurements were made on electrodes charged in the cell shown in Fig. 1. The apparatus consisted in a central anodic compartment provided with two Hg/HgO reference electrodes and Luggin capillaries. The test electrode was situated at the center of two conical side limbs each communicating with a charged nickel – nickel oxide electrode used as a cathode. The field in which the test electrode was charged was thus relatively uniform, and uniform oxidation on both sides of the electrode was observed to occur. For stronger solutions it was found that an ordinary two-compartment cell with reference electrode and Luggin capillary could be satisfactorily used.

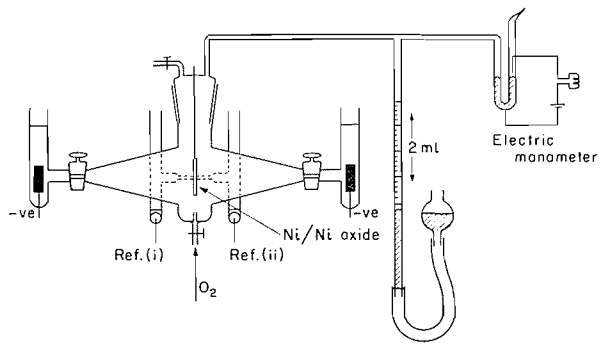

FIG. 1. Uniform field cell for oxygen evolution measurements.

Measurements of Oxygen Evolution

The rates of oxygen evolution on open circuit were measured after termination of charging, by closing off the cathode compartment by means of a stopcock, closing off the oxygen supply used for stirring the solution, and allowing the system to come into communication with a 2-ml gas pipette calibrated in 0.01-ml marks, readable to 0.003 ml and connected to a variable head of mercury. The pipette was also joined to one side of a constant-pressure manometer with an electrical device capable of indicating constancy of pressure to 0.2 mm Hg. Capillary tubing was used between the cell, the pipette, and the manometer in order to minimize dead space, which was about 7 ml; in oxygen volume measurements the cell was filled, within a few milliliters, up to the top of the glass cap. The oxygen volume could be measured to 0.003 ml. The whole apparatus was maintained in an air thermostat at 25° C constant to 0.05° C. The total oxygen volumes measured over periods of 2 to 3 days were from 2 to 5 ml. Volumes above 2 ml were determined as follows: 2 ml were initially collected and measured up to a certain time; the cell was closed off and the mercury brought back up to the zero volume mark, the 2 ml being rejected out of another stopcock. Communication was then remade to the cell and further oxygen collected; the total volume at various times was then calculated. Volumes were corrected to n.t.p. allowing for the vapor pressure of water over the various solutions used (8).

Electrical Measurements

Potential measurements were made by means of a high impedance Doran pH-millivoltmeter and in some cases with a Tinsley potentiometer. Direct-current charging curves were obtained by manual potentiometric measurements and also in some cases by means of a high impedance recording electronic potentiometer. Short period e.m.f. decay curves were obtained by means of a Hewlett–Packard cathode ray oscillograph.

Can. J. Chem. Downloaded from www.nrcresearchpress.com by 190.90.36.8 on 09/04/12
For personal use only.

In these measurements in dilute solutions (< 0.01 N), a flow technique was used (flow rates up to 15 ml sec^{-1} past the electrode could be attained in a 2-cm diameter cell) in order to eliminate concentration polarization effects which otherwise influence the open-circuit decay behavior in the most dilute solutions during the first several seconds of decay.

RESULTS

Electromotive force decay curves were obtained at 25° C for the charged nickel – nickel oxide electrode at the following concentrations: 0.0015, 0.015, 0.145, 0.93, 2.9, 7.0, 9.4, and 14.6 M, and are shown in Figs. 2, 4, and 5, where the e.m.f. is plotted (see below) against logarithmic time plus a correction factor θ which is the time required for the electrode to decay from infinite positive potential to the potential at zero time, i.e., at the moment of beginning of the open-circuit decay measurements. Figures 3 and 6 show the corresponding oxygen volume measurements obtained at various times and plotted against the corresponding values of e.m.f. Figure 3 shows the dependence of volume of oxygen evolved in 7.1 M KOH solutions as a function of logarithmic time. At other

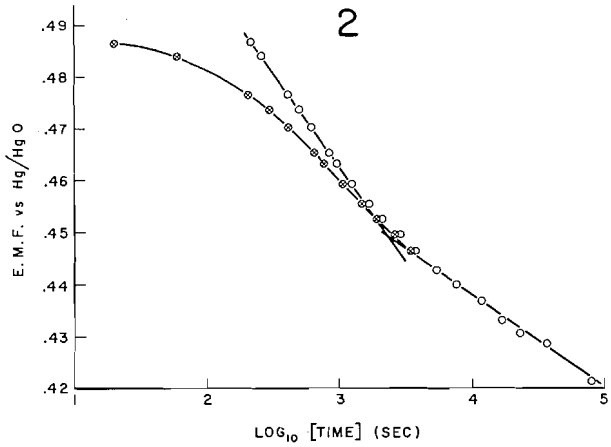

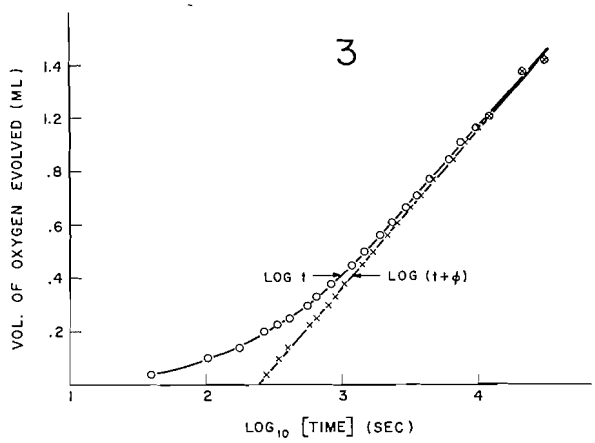

FIG. 2. Typical e.m.f. – log (time) relationship in 0.72 M KOH showing θ correction and corresponding electrode capacity.

FIG. 3. Oxygen evolution as a function of log (time) or log (time $+\phi$) where ϕ is analogous to θ in Fig. 2.

Can. J. Chem. Downloaded from www.nrcresearchpress.com by 190.90.36.8 on 09/04/12
For personal use only.

concentrations the oxygen evolution rates follow from the data in the Figs. 4 and 6. The decay curves show two linear regions having different Tafel slopes; the upper region has a slope of 0.039 ± 0.003 whilst that of the lower region is 0.021 ± 0.002. These values closely correspond, at 25° C, with Tafel slopes having values of 2.3 ($2RT/3F$) and 2.3 ($2RT/5F$), respectively, although the lower slope observed could correspond to the value 2.3 $RT/3F$. It is seen that the potential or time at which the change of slope occurs depends markedly upon the concentration of the KOH (Figs. 4, 5). The e.m.f. at the inflection point of the e.m.f. – log (time) lines is shown in Fig. 7 as a function of KOH concentration.

DISCUSSION

The results show that the self-discharge process occurs on open circuit with change of e.m.f. of the electrode and simultaneous evolution of oxygen. The self-discharge must hence proceed by an electrochemical mechanism analogous to that of corrosion, i.e., anodic and cathodic reactions are occurring simultaneously at a mixed potential. Usually either the cathodic or the anodic process is rate-determining and a potential corresponding to the rate of one or other of the processes, whichever is the faster, is set up. We have, therefore, to decide from the observed kinetics: (*a*) whether the anodic or the cathodic type of process is rate-determining and (*b*) having established this, what individual mechanism(s) in the net anodic or cathodic process determines its rate.

For an ordinary metal electrode for which the activation polarization behavior can be represented by the Tafel equation, it follows quite generally (9) that the decay of e.m.f. is logarithmic in the time of decay measured from the moment of cessation of the polarizing current. This relationship holds over wide ranges of time, except at very short times after interrupting the polarizing current or near the reversible potential for the process concerned. It has been shown (10) that the e.m.f., E, depends on the time of decay, t, according to

$$[1] \qquad dE/dt = -\frac{b}{2.303} \Big/ (t+\theta),$$

where b is the slope of the Tafel equation for the rate-determining process in decay and θ is as defined above, assuming a constant double-layer capacity. The integral form of equation [1] is

$$[2] \qquad E = E' - b \log (t+\theta),$$

where E' is the initial potential at $t = 0$ plus $b \log \theta$. E is thus logarithmic in $(t+\theta)$. θ can then be evaluated semiempirically from the e.m.f. – log (time) plots as that value of time which when added to the time, t, gives an initially linear e.m.f. – log $(t+\theta)$ plot, collinear with the relationship directly observed at higher times, e.g., for $t > ca.\ 10\ \theta$. When θ has been evaluated as above, the capacitance C of the double layer at the electrode can be obtained from

$$[3] \qquad \theta = \frac{b}{2.303} C/i,$$

where i is the polarizing current passing at the moment of commencement of the decay.

It may be expected that the decay of e.m.f. of the nickel oxide electrode should be analogous to that for the discharge of the double-layer condenser at a polarized metal electrode, except that the capacitance involved probably has a different origin and order of magnitude. We have therefore plotted the decay of e.m.f. as a function of log t and log

Can. J. Chem. Downloaded from www.nrcresearchpress.com by 190.90.36.8 on 09/04/12
For personal use only.

Can. J. Chem. Downloaded from www.nrcresearchpress.com by 190.90.36.8 on 09/04/12
For personal use only.

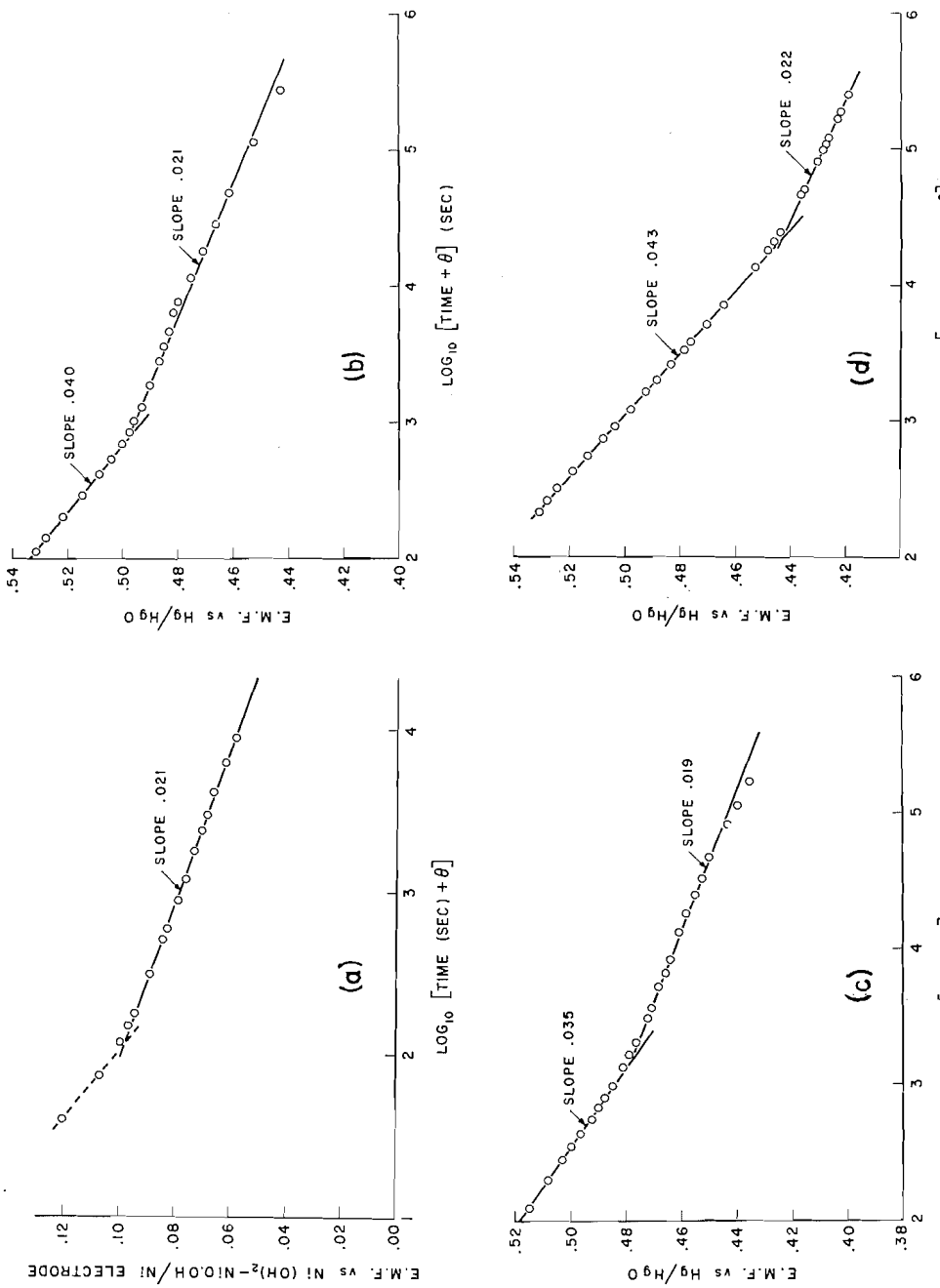

FIG. 4. Electromotive force decay lines at four low KOH concentrations. (*a*) 0.0015 *M*; (*b*) 0.015 *M*; (*c*) 0.145 *M*; (*d*) 0.93 *M*.

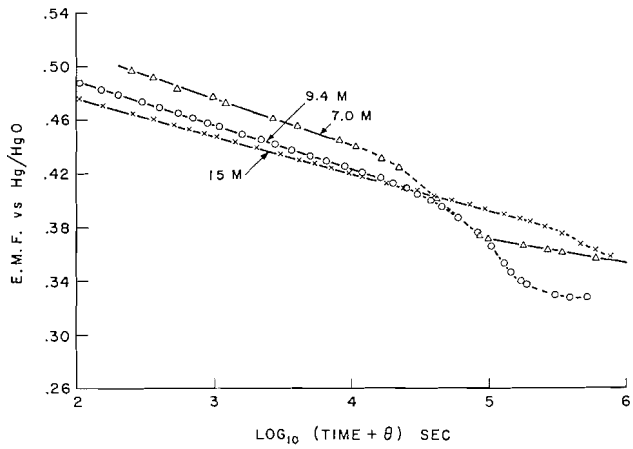

FIG. 5. Electromotive force decay lines at high KOH concentrations.

$(t+\theta)$ in Fig. 2 (see also Figs. 4 and 5) for the electrode in 0.72 M KOH. The plots of log t and log $(t+\theta)$ are identical beyond about $10^{3.4}$ seconds. A unique value of θ exists, which gives the theoretically expected linear behavior; its value for 0.72 M KOH in Fig. 2 is 200 seconds. In this figure it is clear that there are two linear–logarithmic regions and it must be emphasized that in this and other cases (see Fig. 4), no value of θ can be found which gives a *single* straight line for the e.m.f. – log (time) plots except in the one case of the behavior in 15 M KOH solution (Fig. 5). Any arbitrariness in the value of θ derived semiempirically and any consequent uncertainty in the slope of the decay line can be avoided by plotting the e.m.f., E, as a function of log Δt for constant decrements of E during decay intervals Δt. Tafel b values, the same as these calculated semi-empirically, are obtained. (We are indebted to Dr. R. Parsons for this suggestion.) The e.m.f. – log $(t+\theta)$ lines shown in Fig. 4 and Fig. 5, for a wide range of concentrations from 0.0015 to 15 M, indicate a complex behavior in which more than one rate-determining mechanism in the self-discharge is involved. The slopes of the e.m.f. – log (time) line (see Figs. 4 and 5) have the values given in Table I and are characteristic of several steps in processes previously discussed (11) for the anodic evolution of oxygen. The higher slope of 0.038 is also found in direct polarization measurements (12).

The plots of oxygen evolved during decay as a function of e.m.f. shown in Fig. 6 also

TABLE I

Tafel slopes observed in the decay of e.m.f. of the nickel oxide electrode

Concn. of KOH	Mean slope in high potential region	Mean slope in low potential region	No. runs
14.6	0.028±0.0005	—	3
9.4	0.032±0.0005	—	2
9.0	0.032±0.001	—	2
7.1	0.038±0.0002	0.020±0.0003	9
2.9	0.034	0.016	1
0.93	0.040±0.0003	0.023±0.0005	4
0.327	0.038	0.019	1
0.145	0.037±0.0015	0.024±0.0004	2
0.077	0.040	0.021	1
0.015	0.039±0.002	0.020±0.000	2
0.0015	0.040±0.002	0.023±0.002	2

Can. J. Chem. Downloaded from www.nrcresearchpress.com by 190.90.36.8 on 09/04/12
For personal use only.

Can. J. Chem. Downloaded from www.nrcresearchpress.com by 190.90.36.8 on 09/04/12
For personal use only.

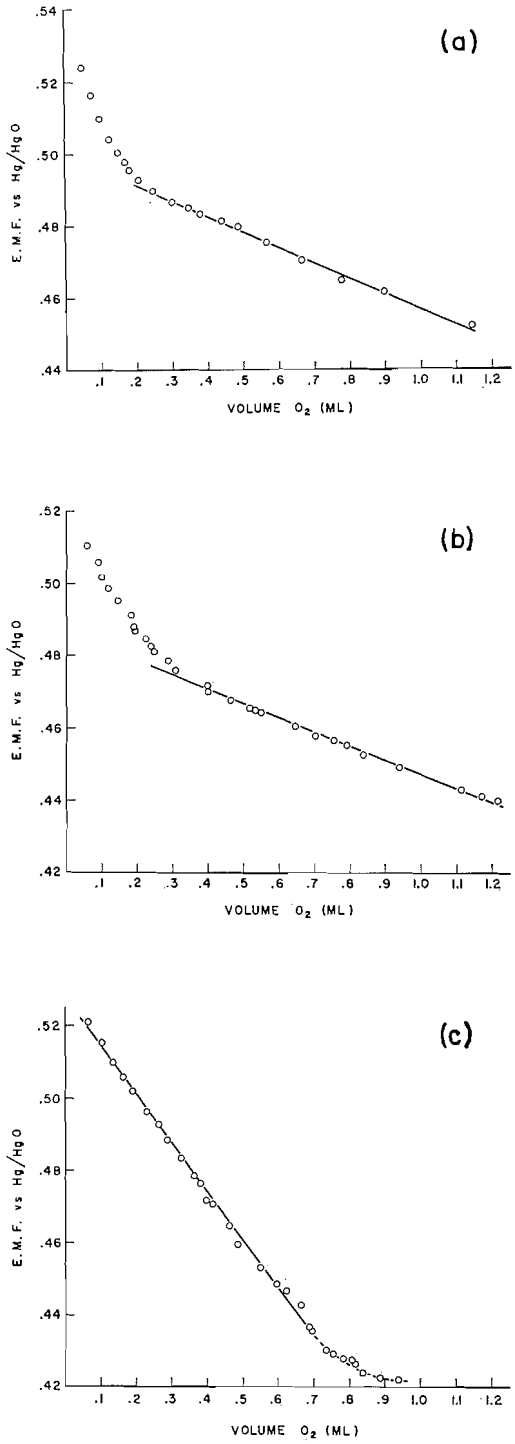

FIG. 6. Volumes of oxygen evolved on open circuit as a function of e.m.f. during decay. (*a*) 0.015 *M* KOH; (*b*) 0.145 *M* KOH; (*c*) 0.93 *M* KOH.

indicate changes of the potential-determining species during the self-discharge process. Thermodynamic investigations of this aspect of the behavior of the electrodes are in progress. It is apparent that both in the e.m.f. decay and in the corresponding oxygen evolution behavior, the process which comes in at later times (or lower e.m.f.'s) is more dependent upon KOH activity than the first process at earlier times. The first process, however, gives Tafel slopes of 0.038 in dilute solution but in the strongest solutions the value changes to 0.029.

Evaluation of Rates of Self-discharge

Comparison of the rates of the two processes at high and low e.m.f.'s can be made if we can obtain a measure of the exchange currents for these processes.

(*i*) *From E.M.F. Decay*

The rate of decay of the e.m.f., E, is given (10) by

$$[4] \qquad dE/dt = -\frac{i_0}{C}10^{\eta/b},$$

where i_0 is the exchange current for the rate-determining process in decay, C is the electrochemical capacity involved, η the oxygen overpotential,* and b the Tafel slope for the decay process obtained from the e.m.f. – log (time) plots. The values of η can be obtained from the values of e.m.f. experimentally measured with respect to the Hg/HgO electrode, since the reversible oxygen electrode is at 0.303 v more positive than the Hg/HgO electrode and its e.m.f. depends upon OH^- ion activity in the same way as does that of the Hg/HgO electrode.

From the logarithmic e.m.f. decay lines (Figs. 4, 5), we can obtain dE/d log (time) $(= -b)$; hence for a time t of decay required for the electrode to reach an overpotential η_t, equation [4] gives

$$[5] \qquad i_0 = -C\frac{dE}{dt}10^{-\eta/b} = \frac{Cb}{2.3t}10^{-\eta_t/b}.$$

The exchange current, and hence rate of self-discharge at any potential, is determined by the reciprocal of the time required to reach a given potential during decay.

From Figs. 4 and 5, values of t for various solutions can be obtained for chosen constant e.m.f. values and i_0 evaluated. The rates of self-discharge measured by $1/t_\eta$, for constant η, are shown in Fig. 8 for the range of concentrations studied and for the upper region of the decay lines. It is clear from Fig. 8 that the process at high positive potentials is much less dependent upon KOH activity than that at low potentials; at long times or low potentials the rate of self-discharge is approximately proportional to $(a_{OH^-})^2$; at shorter times or higher potentials the rate is proportional to a power of a_{OH^-} between $\frac{1}{2}$ and $\frac{1}{3}$.

(*ii*) *From Oxygen Evolution on Self-discharge*

From Figs. 2 and 6, the oxygen evolution rate, dV_{O_2}/dt, can be obtained from the slopes of the oxygen volume – e.m.f. lines and those of the e.m.f. – log (time) lines, since

$$[6] \qquad \frac{dV_{O_2}}{dt} = \left(\frac{dE}{dt}\right)\Big/\left(\frac{dE}{dV_{O_2}}\right) = \frac{1}{2.3t}\cdot\frac{dE}{d\log t}\Big/\frac{dE}{dV_{O_2}},$$

where t is again the time required to reach a given e.m.f. during oxygen evolution resulting from the self-discharge.† dV_{O_2}/dt can now be expressed as the anodic current, i_a, in

*We are here assuming that anodic processes are rate-determining in the self-discharge. That this is so, is indicated by the dependence of the rates upon OH^- and H_2O activity discussed below.

†dV_{O_2}/dt can, of course, be obtained directly by taking tangents to the oxygen volume – time curve; this procedure gives similar results to those obtained by means of equation [6], using appropriate values of the time, t.

Can. J. Chem. Downloaded from www.nrcresearchpress.com by 190.90.36.8 on 09/04/12
For personal use only.

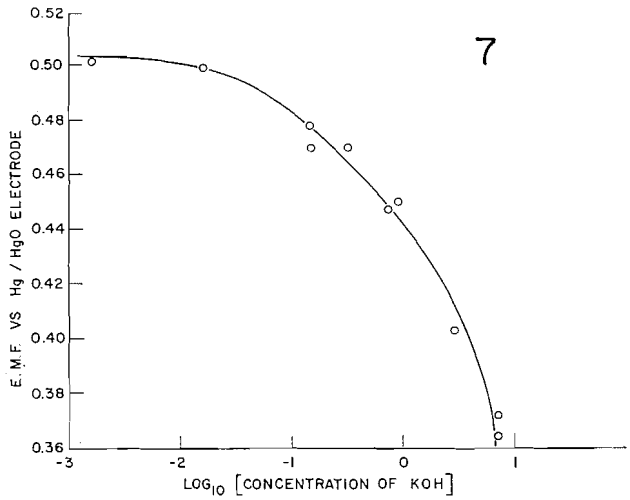

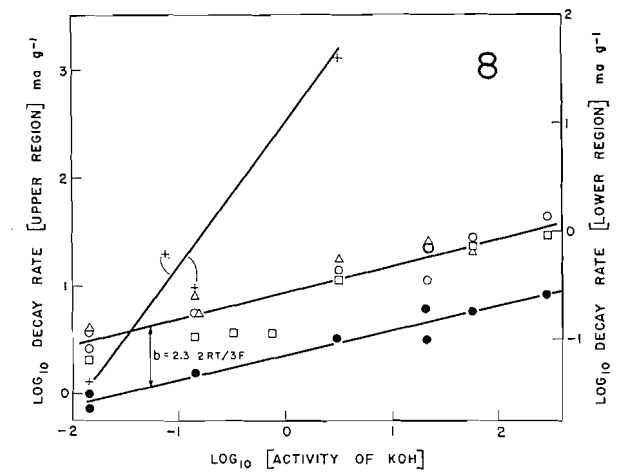

FIG. 7. Electromotive force at the inflection point in decay as a function of KOH concentration.
FIG. 8. Self-discharge rates from oxygen volume and e.m.f.–time measurements as a function of KOH activity; rates for high and low potential regions are shown.
+ Lower potential region, from $(1/2.3t)\ (dE/d\ \log\ t)/(dE/dV_{O_2})$. $E = 0.44$ v.
○ Upper potential region, from $(1/2.3t)\ (dE/d\ \log\ t)/(dE/dV_{O_2})$. $E = 0.48$ v.
□ Upper potential region, from $Cb/2.3t$. $E = 0.48$ v.
△ Upper potential region, from dV_{O_2}/dt. $E = 0.48$ v.
● Upper potential region, from $(1/2.3t)\ (dE/d\ \log\ t)/(dE/dV_{O_2})$. $E = 0.46$ v.

self-discharge at the oxygen overpotential η, since $4F$ are required to evolve 22.4 l. of oxygen gas. Since the Tafel slope is found directly from the e.m.f. – log (time) plots, i_0 may readily be evaluated from the value of i_a at any suitable potential. The rates of self-discharge for the upper and lower potential regions may be expressed as current per unit weight of active material ($Ni(OH)_2$) in the electrode. Values thus calculated are also shown in Fig. 8 as a function of KOH activity and for two electrode potentials; the dependence of the rates of self-discharge (from oxygen evolution measurements) upon KOH activity for the two regions is seen to be similar to that calculated for e.m.f. decay rates, as would be expected.

Can. J. Chem. Downloaded from www.nrcresearchpress.com by 190.90.36.8 on 09/04/12
For personal use only.

Can. J. Chem. Downloaded from www.nrcresearchpress.com by 190.90.36.8 on 09/04/12
For personal use only.

(iii) Values of Exchange Current

From the above considerations, the values of i_0 for the self-discharge process, expressed with respect to unit weight of active material, are then obtained and are given in Table II for unit activity of KOH in solution. Agreement between the values obtained by the two methods is satisfactory and as good as the reproducibility usually obtained in other kinds of electrode–kinetic measurements (13). Owing to the nature of the impregnated electrodes, it is not possible to specify the total real interfacial area exposed to the solution; hence i_0 values cannot be stated in the usual way, i.e., in amperes per square centimeter. An upper estimate may, however, be made of the area available per gram of active material. The electrodes consist of sintered particles having a size of about 1 μ with 80% free space between them (5). If we regard the particles as spherical for the purposes of the calculation of the order of magnitude of the real accessible area, a value of 6000 cm^2 per cm^3 of sinter may be calculated. An electrode plate 3 in. $\times$ 1.0 in. $\times$ 0.04 in. can be impregnated with about 1 g of $Ni(OH)_2$; we can then calculate that there are about 10^4 cm^2 per gram of oxide. i_0 values per cm^2 are then about 10^{-11} and 10^{-13} amp cm^{-2} for the process occurring in the upper and lower potential regions, respectively. The main interest in the present determinations of i_0 and the rates of self-discharge is not their absolute magnitude but their *relative* values, which indicate that the process appearing at lower potentials has a lower electrochemical rate constant than that at higher potentials; the rate of the slower process is also more affected by electrode potential and by OH^- ion concentration than is that of the process occurring at more positive potentials.

TABLE II

Rates of self-discharge (i_0) at the reversible oxygen potential

Method	From e.m.f. decay	From O_2 evolution
Upper potential region	11.8×10^{-8} a.g.$^{-1}$	7.0×10^{-8} a.g.$^{-1}$
Lower potential region	3.5×10^{-10} a.g.$^{-1}$	4.3×10^{-10} a.g.$^{-1}$

Electrode Capacity

The electrochemical capacity involved in the self-discharge processes may be calculated in three ways: (i) from the θ correction in the determination of decay of e.m.f. using equation [3], (ii) from the volume of oxygen evolved as a function of e.m.f., i.e., from dV_{O_2}/dE, and (iii) from studies of d-c. charging on electrodes at which the self-discharge had virtually terminated (i.e. on electrodes still having a degree of oxidation approximately represented by the formula $NiO_{1.5}$). Values of electrode capacity obtained by the various methods are listed in Table III together with the ratios of "active" oxygen to nickel measured from the total charge which can be withdrawn from the electrode through an external circuit. From the active oxygen – nickel ratios in column 3 of Table III it is seen that the electrode is oxidized to the formal state $NiO_{1.57}$ in the strongest solution and to a smaller extent in more dilute solutions. The degrees of oxidation achieved with the present type of electrodes are thus somewhat less than that found by Wynne-Jones *et al.* (2, 3) for oxide films formed directly on nickel electrodes. The capacitance values calculated from θ, and oxygen evolution in the initial part of the decay are comparable as expected, since θ refers to this decay region. At longer times, the lower decay region (Fig. 2) gives higher capacities indicating that a different process

TABLE III

Electrode capacity and charge

Concn. of KOH, *M*	No. of results averaged	Active oxygen/nickel	Capacity, farads/equiv. $\times 10^{-3}$			
			From θ	O_2/e.m.f. I	O_2/e.m.f. II	D-c. charging
14.6	3	0.57	17.8	21	41	—
9.4	2	0.51	26	32	64.6	—
7.0	8	0.48	33.4	41	62.5	—
2.9	1	0.45	31.9	39.5	70.3	37
0.93	4	0.43	47.5	57	—	39
0.145	2	0.39	25.1	44	170	25
0.015	2	0.36	21	33	140	20

Notes: (i) In columns 5 and 6, I and II signify the upper and lower regions, respectively, of oxygen evolution shown in Fig. 6.
(ii) Direct-current charging capacities in column 7 are given for the *initial* build-up of potential. At higher potentials in stronger solutions a more complex behavior is observed (Fig. 9).

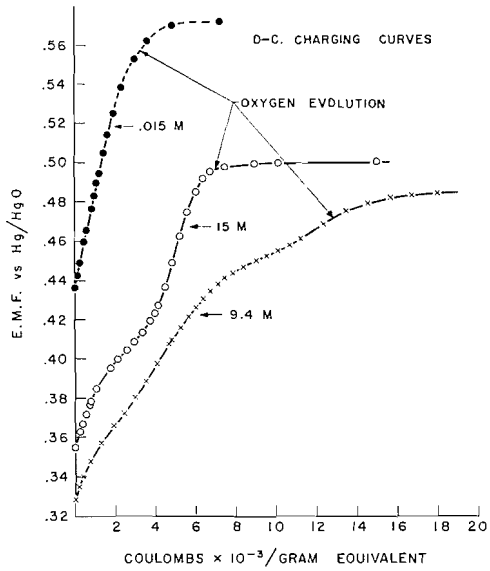

FIG. 9. Direct-current charging curves for the nickel oxide electrode at three KOH concentrations.

is probably involved. The d-c. charging capacities for dilute solutions are recorded for comparison.

Reaction Mechanisms in the Self-discharge Process

The electrode capacities measured under various conditions, including those from the θ constant in e.m.f. decay, are clearly several orders of magnitude too large to be identifiable with the interfacial double-layer capacity of the electrode. However, the kinetics of the discharge process are formally analogous to those observed (9) for decay of e.m.f. of a polarized electrode through discharge of the double-layer condenser. A mechanism must therefore be proposed whereby the active material in the bulk of the electrode can be involved in self-discharge and be electrically accessible to the solution, yet the kinetics of the process can be formally similar to those observed in the discharge

Can. J. Chem. Downloaded from www.nrcresearchpress.com by 190.90.36.8 on 09/04/12
For personal use only.

of the double-layer condenser on open circuit. The following general scheme involving a mixed Ni^{III} and Ni^{IV} non-stoichiometric hydrated oxide lattice* (1, 3, 14) meets these requirements:

$$Ni^{4+}.2O^{--}_{(surface)} + OH^- \rightarrow Ni^{4+}.2O^{--}_{(surface)} + OH_{(ads)} + e_{(lattice)} \quad [7]$$

$$Ni^{4+}.2O^{--}_{(surface)} + e_{(lattice)} \xrightarrow{\text{electron transfer}} Ni^{3+}.2O^{--}_{(surface)} \quad [8]$$

$$Ni^{3+}.2O^{--}_{(surface)} + H_2O \xrightarrow{\text{proton transfer}} Ni^{3+}.O^{--}.OH^-. \quad [9]$$

If there is electronic and protonic mobility in the lattice (3), $Ni^{4+}.2O^{--}$ can be regenerated in the surface of the oxide, since we can then write

$$Ni^{3+}.O^{--}.OH^-_{(surface)} + Ni^{4+}.2O^{--}_{(bulk)} \xrightarrow{e,\ H^+} Ni^{4+}.2O^{--}_{(surface)} + Ni^{3+}.O^{--}.OH^-_{(bulk)}. \quad [10]$$

Process [7] can then continue to occur by discharge of OH^- ions in the double layer until all Ni^{4+} is converted to Ni^{3+}; similar self-discharge of the $Ni^{3+}.O^{--}.OH^-$ phase to $Ni^{++}.2OH^-$ could also occur if the potential of the electrode remained positive to that of the reversible oxygen electrode.† Oxygen evolution through process [7] then proceeds by the *over-all* reaction

$$2OH_{(ads)} \longrightarrow H_2O + \tfrac{1}{2}O_2. \quad [11]$$

The rate-determining step in the anodic oxygen evolution process [7] with [11] is discussed below. Processes [8] and [10] involve electron shifts in the lattice and are likely to be very fast. The self-discharge rates are *increased* substantially by increasing KOH activity (Figs. 8, 9); hence process [9] is unlikely to be rate-determining, since with increasing KOH activity from 0 to 15 *M*, the water activity *falls* from unity to about 0.2 (8). Some step in the anodic oxygen evolution process in self-discharge is therefore rate-determining (cf. p. 300).

Rate-determining Steps in the Anodic Process

Two processes are likely to be involved, since two distinct slopes in the decay lines and in the e.m.f. – oxygen evolution plots are found (Figs. 2, 4, 5). These processes could be either consecutive or alternative; the one which is observed at lower electrode potentials has an exchange current of about 4×10^{-10} a.g^{-1} and a Tafel *b* value of about 0.021, whilst the other, observed at higher potentials, has an exchange current of about 9×10^{-8} a.g^{-1} and a Tafel *b* value of about 0.038. Since for two consecutive reactions, the slower determines the rate of the over-all reaction, whilst for two alternative reactions, it is the faster which predominates and hence kinetically characterizes the reaction, it follows from the above values of i_0 and *b* for the two processes concerned that they are *consecutive*. We therefore have to find a scheme of consecutive reactions which give amongst other possible slopes two leading to values of the Tafel *b* constant of 0.038 (2.3 $2RT/3F$) and

The constitution of the highest oxide of nickel is still under dispute (2, 15). It may be a peroxide of Ni^{II}(15) but this is hardly likely in view of the fact that the better characterized compound, β–NiO.OH, is formed as the electrode is charged, the highest state of oxidation being subsequently reached upon "overcharge". The higher oxides appear to be electrically conducting (2) otherwise the oxide electrode in the battery could hardly function in the necessary "reversible" manner. Such electronic conductivity would not be expected in a true peroxide lattice containing only Ni^{II} ions. In other kinds of compound the Ni^{IV} state is known to exist (16, 17).

†*In the studies of Wynne-Jones (3) on the nickel oxide electrode it appears that self-discharge occurred down to a potential of about zero volts with respect to the Hg/HgO electrode, i.e., 0.3 v negative to the oxygen reversible potential. In the present experiments the self-discharge of the electrode never continued below the reversible oxygen potential even after a period of a month. If depolarizers are, however, present, e.g., hydrogen, then further discharge can occur to lower potentials.*

Can. J. Chem. Downloaded from www.nrcresearchpress.com by 190.90.36.8 on 09/04/12
For personal use only.

0.021 (2.3 $RT/3F$ and 2.3 $2RT/5F$ are both close to the experimental value). Inspection of the schemes given by Bockris (11) and Hackerman (18) shows that none gives both slopes in the *same* reaction scheme; but in different schemes (i.e., alternative pathways) processes leading to one or other of these slopes occur (11). We may examine, however, the following consecutive reaction schemes for anodic oxygen evolution, which have not previously been considered:

$$M + OH^- \rightarrow MOH + e, \quad [12]$$

$$MOH + OH^- \rightarrow MO + H_2O + e, \quad [13]$$

$$MO + MOH \rightarrow MHO_2, \quad [14]$$

$$MHO_2 + MOH \rightarrow M + H_2O + O_2; \quad [15]$$

here M signifies the electronically conducting bulk oxide phase rather than the base metal as previously considered (11), since the electrochemical oxygen evolution occurs at the surface of the oxide (19) rather than at that of the metal. The present treatment differs only from previous approaches in that we regard the transient radical species as adsorbed at the oxide–solution interphase rather than at the metal–solution interphase. At the same time, the OH^- ion being discharged may be adsorbed (see 18 and below).

For the series of consecutive reactions [12] to [15], the rates v are given by

$$\begin{aligned}
v_{12} &= k_{12}\, C_{OH^-}(1 - k'\, C_{MOH} - k''\, C_{MO}) e^{\Delta\phi F/2RT},\\
v_{-12} &= k_{-12}\, C_{MOH}\, e^{-\Delta\phi F/2RT},\\
v_{13} &= k_{13}\, C_{MOH}\, C_{OH^-}\, e^{\Delta\phi F/2RT},\\
v_{-13} &= k_{-13}\, C_{MO}\, e^{-\Delta\phi F/2RT},\\
v_{14} &= k_{14}\, C_{MOH}\, C_{MO},\\
v_{-14} &= k_{-14}\, C_{MHO_2},\\
v_{15} &= k_{15}\, C_{MHO_2}\, C_{MOH},
\end{aligned}$$

where C_{OH^-} is the concentration of hydroxyl ions in the double layer and $\Delta\phi$ is the potential difference between the electrode and the outer Helmholtz layer, k' and k'' are constants relating fractional surface coverage by intermediates to their surface concentrations (or activities). The symmetry factor for the charge-transfer steps is taken as 0.5 (cf. 13). In order to obtain the Tafel slopes for various rate-determining steps in the above scheme, we calculate the Christiansen coefficients w for each step as

$$\begin{aligned}
w_{12} &= k_{12}\, C_{OH^-}\, e^{\Delta\phi F/2RT},\\
w_{-12} &= k_{12}k'\, C_{OH^-}\, e^{\Delta\phi F/2RT} + k_{12}k''\, C_{OH^-}{}^2\, K_{13}\, e^{3\Delta\phi F/2RT} + k_{-12}\, e^{-\Delta\phi F/2RT},
\end{aligned}$$

if C_{MOH} and C_{MO} are both appreciable, i.e., if [14] is rate-determining; or as

$$w_{-12} = k_{12}k'\, C_{OH^-}\, e^{\Delta\phi F/2RT} + k_{-12}\, e^{-\Delta\phi F/2RT},$$

if only C_{MOH} is appreciable, i.e., if [13] is rate-determining. K_{13} is the quasi-equilibrium constant for [13] in the steady state if [14] is rate-determining. Other w values are

$$\begin{aligned}
w_{13} &= k_{13}\, C_{OH^-}\, e^{\Delta\phi F/2RT},\\
w_{-13} &= k_{-13}\, e^{-\Delta\phi F/2RT},\\
w_{14} &= k_{14}\, C_{MOH},\\
w_{-14} &= k_{-14},
\end{aligned}$$

and

$$w_{15} = k_{15}\, C_{MOH}.$$

Can. J. Chem. Downloaded from www.nrcresearchpress.com by 190.90.36.8 on 09/04/12
For personal use only.

If step [13] is rate-determining, the over-all velocity is then

$$v = \frac{k_{12}k_{13}\, C_{OH^-}{}^2\, e^{\Delta\phi F/RT}}{k_{12}k'\, C_{OH^-}\, e^{\Delta\phi F/2RT} + k_{-12}\, e^{\Delta\phi F/2RT}},$$

which at relatively low potentials gives

[16] $$v = K_{12}k_{13}\, C_{OH^-}{}^2\, e^{3\Delta\phi F/2RT};$$

and if [14] is rate-determining, and at relatively low potentials

[17] $$v = K_{12}{}^2K_{13}k_{14}\, C_{OH^-}{}^3\, e^{3\Delta\phi F/RT}$$

where K_{13} is the quasi-equilibrium constant for [13] when [14] is rate-determining. Equations [16] and [17] give the Tafel b constants as

$$b_{13} = 2.3\ (2RT/3F) \text{ and } b_{14} = 2.3RT/3F.$$

For [12] as the rate-determining step, b has the usual value of 2.3 $(2RT/F)$. The slopes for the decay in the low potential region could also be close to the value 2.3 $(2RT/5F)$ which differs from 2.3 $RT/3F$ by only 4 mv. The scheme in equations [12] to [15] could be modified by changing process [14] to a charge-transfer reaction as follows:

$$M + OH^- \rightarrow MOH + e, \quad [12]$$

$$MOH + OH^- \rightarrow MO + H_2O + e, \quad [13]$$

$$MO + OH^- \rightarrow MHO_2 + e, \quad [14a]$$

$$MHO_2 + MOH \rightarrow M + H_2O + O_2. \quad [15]$$

The mathematical analysis then gives the Tafel slope for process [14a], if it were rate-determining, as $b = 2.3\ (2RT/5F)$, with b for process [13] still as 2.3 $(2RT/3F)$.

The schemes in equations [12] to [15] through [14] or [14a] are the only ones which can be formulated (cf. 13, 21) in which there are *two consecutive* steps in a single reaction path having Tafel slopes in agreement with those observed in the present work, and from which the correct *sequence* of slopes (viz. 0.038 at higher potentials followed by 0.021 at lower potentials, if [14] becomes rate-determining) can be deduced. The reactions in either of the schemes [12] to [15] hence appear to offer a satisfactory explanation of the experimental results at present available. Distinction between [14] and [14a] as mechanisms for the low potential process must await a rather more accurate determination of the slopes. With decreasing electrode potential on decay, [14] can tend to become slower than [13], and hence rate-determining, since the rate of [14] is more strongly dependent $(e^{3\Delta\phi F/RT})$ on potential than of that of [13].

In very strong solutions the Tafel slope for the high potential process changes towards the value 0.029; this could occur (11, 18) if recombination desorption of adsorbed OH radicals replaced the discharge process indicated in reaction [13].

In the absence of excess electrolyte, e.g., K_2SO_4, not participating in the discharge reaction, all mechanisms should lead to rates independent of activity of OH^- ions (11). In the present work, however, the observed rates of both steps in the self-discharge are increased with increasing KOH activity. This effect probably arises from specific adsorption of OH^- ions on the surface of the polar oxide lattice, as has been indicated in the case of anodic processes at the iron electrode (18).

ACKNOWLEDGMENTS

One of us (P.L.B.) is indebted to the Consolidated Mining and Smelting Company for the award of a Cominco Fellowship.

Can. J. Chem. Downloaded from www.nrcresearchpress.com by 190.90.36.8 on 09/04/12
For personal use only.

Support for this work from the Defence Research Board, Department of National Defence (Canada), on Grant No. 5480-12 is gratefully acknowledged.

REFERENCES

1. GLEMSER, O. and EINERHAND, J. Z. anorg. Chem. **261**, 26 (1950).
2. BRIGGS, G. W. D. and WYNNE-JONES, W. F. K. Trans. Faraday Soc. **52**, 1272 (1956).
3. JONES, E. and WYNNE-JONES, W. F. K. Trans. Faraday Soc. **52**, 1260 (1956).
4. PITMAN, A. L. and WORK, G. W. Naval Research Lab. Rept. 4844 (1956); 4845 (1956).
5. CASEY, E. J., BOURGAULT, P. L., and LAKE, P. E. Can. J. Technol. **34**, 95 (1956).
6. FLEISCHER, A. Trans. Electrochem. Soc. **94**, 289 (1948).
7. AZZAM, A. M., BOCKRIS, J. O'M., CONWAY, B. E., and ROSENBERG, H. Trans. Faraday Soc. **46**, 918 (1950).
8. AKERLOF, G. C. and BENDER, P. J. Am. Chem. Soc. **70**, 2366 (1948).
9. ARMSTRONG, G. and BUTLER, J. A. V. Trans. Faraday Soc. **29**, 1261 (1933).
10. MORLEY, H. B. and WETMORE, F. E. W. Can. J. Chem. **34**, 359 (1956).
11. BOCKRIS, J. O'M. J. Chem. Phys. **24**, 817 (1956).
12. ELINA, C. M., BORISOVA, T. K., and ZALKIND, T. I. Zhur. Fiz. Khim. **28**, 785 (1953).
13. BOCKRIS, J. O'M. and POTTER, E. C. J. Chem. Phys. **20**, 614 (1952).
14. FOERSTER, F. Z. Elektrochem. **13**, 414 (1907); **14**, 17 (1908). ZEDNER, J. Z. Elektrochem. **11**, 809 (1905); **12**, 463 (1906).
15. SIDGWICK, N. V. Chemical elements and their compounds. Vol. II. Oxford University Press, London. 1950. p. 1451.
16. KLEMM, W. Angew. Chem. **66**, 468 (1954). BESSON, J. Compt. rend. **222** (No. 7), 390 (1946).
17. BESSON, J. Compt. rend. **220** (No. 7), 320 (1945).
18. WADE, W. H. and HACKERMAN, N. Trans. Faraday Soc. **53**, 1636 (1957).
19. KUCHINSKII, E. and ERSCHLER, B. V. Zhur. Fiz. Khim. **14**, 985 (1940).

Can. J. Chem. Downloaded from www.nrcresearchpress.com by 190.90.36.8 on 09/04/12
For personal use only.

Can. J. Chem. Downloaded from www.nrcresearchpress.com by 190.90.36.8 on 09/04/12
For personal use only.

THERMODYNAMICS OF ADSORPTION IN IONIC SYSTEMS[1]

ROGER PARSONS

1. INTRODUCTION

Recently we have made measurements of the electrocapillary curve of mercury in aqueous solutions of potassium iodide at different temperatures (1). The object of this work was to increase our knowledge of the behavior of specifically adsorbed ions by determining the heat of adsorption. In the interpretation of these results, we drew an analogy between the mercury-solution system and the adsorption of a gas on a condensed phase. This enabled us to use the equations developed by Everett (2) for the calculation of the thermodynamic functions accompanying the adsorption process. A similar analogy has been used by Pethica (3) and his co-workers in considering adsorption of long-chain compounds at the air–solution interphase.

In the present paper we attempt to develop the thermodynamics of interphases between two phases containing charged particles in order to find out to what extent this analogy is justified.

2. THE COMPOSITION TERM IN THE CHARACTERISTIC EQUATION

The total differential of the energy (E) of any phase of c components is given by

$$[1] \qquad dE = TdS - pdV + \sum_{i=1}^{i=c} \mu_i \, dn_i$$

where T, p, S, and V are the temperature, pressure, entropy, and volume of the phase, and n_i is the number of moles of species i whose chemical potential in the phase is μ_i. For a plane interphase the corresponding equation is

$$[2] \qquad dE^\sigma = TdS^\sigma - pdV^\sigma + \gamma dA + \sum_{i=1}^{i=c} \mu_i \, dm_i,$$

where γ is the interfacial tension, A the area of the interphase, and m_i the number of moles of i in the interphase. We regard the interphase as a region of finite thickness comprising all the inhomogeneous region between the two phases (4).

Similar equations may be written for the other thermodynamic potentials, but at present we wish to concentrate attention on their common feature: the term

$$[3] \qquad \sum_{i=1}^{i=c} \mu_i \, dm_i.$$

For an ionic interphase the summation over all components is subject to the restriction that the interphase as a whole must remain electrically neutral. This condition may readily be incorporated in expression [3] so that [2] remains a complete differential. The form of expression [3] then, however, depends upon the nature of the interphase. For a perfectly non-polarizable interphase in which there is chemical equilibrium of one or more ionic species throughout the interphase, we may simply redefine our system in terms of $c-1$ components, each of which is a neutral complex of ions, i.e., a 'salt molecule'.

Thus, in the interphase between a zinc amalgam and an aqueous solution of zinc

[1]*Manuscript received June 29, 1958.*
Contribution from the Department of Physical and Inorganic Chemistry, The University, Bristol, England. This paper was presented at the Symposium on Charge Transfer Processes held at the University of Toronto, Toronto, Ontario, September 4 and 5, 1958.

chloride containing hydrochloric acid, there are six components which may be chosen as: Zn^{++}, Cl^-, H^+, H_2O, Hg^+, and e. For the total differential, we may choose the five $\mu\, dm$ terms corresponding to $ZnCl_2$, HCl, H_2O, Zn, and Hg. The electroneutrality condition is then automatically satisfied. The thermodynamics of such an interphase is then precisely of the same form as that for an interphase consisting of non-ionic components only (5).

On the other hand, this form is not obtained for an interphase in which there is no ionic equilibrium between one side of it and the other, such as in the perfectly polarized electrode. In order to study such an electrode it is necessary to combine it with a second electrode, which for thermodynamic convenience is reversible to one of the ions present in the interphase of the perfectly polarized electrode. The independent components can then be chosen, as before, as 'salt molecules', of which there will be $c-2$, leaving two ionic species, one on either side of the interphase. It is usually convenient to choose electrons as one of these, since one phase is normally a metal. The amount of each of these species in the interphase is then proportional to the charge on either side of the interphase (and may be positive or negative). Thus, we may write

$$z_{c-1}F\, m_{c-1} = Q^\alpha \qquad [4]$$

and

$$z_cF\, m_c = Q^\beta, \qquad [5]$$

where the $(c-1)$th component of valency z_{c-1} is left on the side of the interphase adjoining phase α and the cth on that adjoining phase β. Q^α is the electrical charge on the α side of the interphase and Q^β that on the β side. Since the interphase as a whole is electrically neutral,

$$Q^\alpha + Q^\beta = 0. \qquad [6]$$

Thus, for a perfectly polarized electrode the sum [3] becomes

$$\left(\frac{\bar{\mu}_{c-1}}{z_{c-1}} - \frac{\bar{\mu}_c}{z_c}\right)\frac{dQ^\alpha}{F} + \sum_{i=1}^{i=c-2} \mu_i\, dm_i. \qquad [7]$$

We note, by comparing the expression [3] for perfectly polarized and non-polarized electrodes, that for each the electroneutrality condition results in the loss of one degree of freedom.

It is convenient to express the coefficient of dQ^α in [7] in terms of more readily accessible quantities. It is here that the second electrode plays its part, since (if α is the metallic phase) we can find a relation between $\bar{\mu}_c$ and the electrochemical potential of the electrons in the reversible electrode. In general this coefficient, which we abbreviate as ϵ, is related to the measured e.m.f. E between these two electrodes through a constant K;

$$\left(\frac{\bar{\mu}_{c-1}}{z_{c-1}} - \frac{\bar{\mu}_c}{z_c}\right)\frac{1}{F} = \epsilon = E + K, \qquad [8]$$

where K is a sum of chemical potentials of neutral substances. For example, in the cell

$$\mathrm{Hg'} \mid \underset{(\mathrm{sat})}{\mathrm{Hg_2Cl_2}} \mid \mathrm{BaCl_2,\ HCl,\ H_2O} \mid {}^{\sigma} \mid \mathrm{Hg''} \qquad [9]$$

we have six components in the interphase: Ba^{++}, H^+, Cl^-, H_2O, Hg^+, and e^-. One choice of independent components would be $BaCl_2$, HCl, H_2O, Hg with Cl^-, and e^- regarded as constituting the charge. The constant K in [8] thus becomes

Can. J. Chem. Downloaded from www.nrcresearchpress.com by 190.90.36.8 on 09/04/12
For personal use only.

[10] $$K = \frac{\mu_{Hg} - \mu_{HgCl}}{(-1)F}.$$

3. CHARACTERISTIC EQUATIONS

In view of equations 2.7 and 2.8 we can write the analogue of 2.1 for a perfectly polarized electrode as

[1] $$dE^\sigma = TdS^\sigma - PdV^\sigma + \gamma dA + \epsilon dQ^\alpha + \sum_{i=1}^{i=c-2} \mu_i dm_i.$$

From equation [1] we may derive in the usual way complete differentials for the other characteristic thermodynamic potentials H^σ, F^σ, and G^σ. It has been pointed out by Guggenheim and by Everett (2) that, unlike a bulk phase, which has these four characteristic equations, a surface phase has eight. The additional four are defined in terms of the thermodynamic potentials $\mathfrak{E}$, $\mathfrak{H}$, $\mathfrak{F}$, and $\mathfrak{G}$ which are defined by equations such as*

[2] $$\begin{aligned} \mathfrak{E} &= E^\sigma - \gamma A, \\ &\vdots \quad\quad \vdots \\ \mathfrak{G} &= G^\sigma - \gamma A. \end{aligned}$$

The presence of the electrical energy term ϵdQ^α in the characteristic equation for a perfectly polarized electrode means that the number of characteristic equations is doubled again, since we can write equations for the thermodynamic potentials E_e, H_e, F_e, G_e, $\mathfrak{E}_e$, $\mathfrak{H}_e$, $\mathfrak{F}_e$, and $\mathfrak{G}_e$ which are defined by equations such as

[3] $$\begin{aligned} E_e &= E^\sigma - \epsilon Q^\alpha \\ &\vdots \quad\quad \vdots \\ \mathfrak{G}_e &= \mathfrak{G} - \epsilon Q^\alpha. \end{aligned}$$

For example,

[4] $$d\mathfrak{G}_e = -S^\sigma dT + V^\sigma dp - Ad\gamma - Q^\alpha d\epsilon + \sum_{i=1}^{i=c-2} \mu_i dm_i.$$

We may contrast [4] with the characteristic equations for the perfectly non-polarized electrode, since for the latter there is no term in Q^α and ϵ. Consequently, there are only eight characteristic equations which are the same as for a non-ionic interphase. The same is true if we restrict consideration of a perfectly polarized electrode to the condition $Q^\alpha = 0$ (the point of zero charge), since again the Q^α, ϵ term vanishes. This may be regarded as the state of affairs at an air–solution interphase.

4. HEATS OF ADSORPTION

It follows from Section 3 that just as there are four different heats of adsorption for a gas on a solid, there will be eight if the interphase is perfectly polarized. There is, however, a further complication due to the fact that we are necessarily dealing with a system of more than one adsorbed component. In dealing with a one-component system, Everett (2) was able to consider the adsorbed phase as a pure component and effectively to use in place of 3.1

[1] $$dE^\sigma = TdS^\sigma - PdV^\sigma + \gamma dA, \text{ etc.}$$

**To avoid confusion it must be noted that the quantities represented by 'German' capitals without subscripts are the same as those for which Everett (2) used 'Script' capitals.*

Can. J. Chem. Downloaded from www.nrcresearchpress.com by 190.90.36.8 on 09/04/12
For personal use only.

From equations of this type, we obtain heats of adsorption in two classes: at constant surface pressure and at constant amount adsorbed. There are no exact analogues for a multicomponent system.

We consider as an example the heat of adsorption related to 4.4. By cross-differentiating, we obtain

$$[2] \qquad \left(\frac{\partial \mu_j}{\partial T}\right)_{m_i,p,\gamma,\epsilon} = -\left(\frac{\partial S}{\partial m_j}\right)_{T,p,\gamma,\epsilon,m_i \neq m_j}.$$

Solving for dS the characteristic equation for $\mathfrak{H}_e$ and differentiating with respect to m_j while keeping T, p, γ, ϵ, and the other m_i constant, we obtain

$$[3] \qquad \left(\frac{\partial S}{\partial m_j}\right)_{T,p,\gamma,\epsilon,m_i \neq m_j} = \frac{1}{T}\left[\left(\frac{\partial \mathfrak{H}_e}{\partial m_j}\right)_{T,p,\gamma,\epsilon,m_i \neq m_j} - \mu_j\right],$$

whence

$$[4] \qquad \left[\frac{\partial(\mu_j/T)}{\partial T}\right]_{m_i,p,\gamma,\epsilon} = -\frac{\bar{\mathfrak{H}}_e}{T^2},$$

where $\bar{\mathfrak{H}}_{e,j} = (\partial \mathfrak{H}_e/\partial m_j)_{T,p,\gamma,\epsilon,m_i \neq m_j}$ is the interfacial partial molar electrochemical heat content of species j. The Clausius–Clapeyron equation is obtained from [4] by subtracting the corresponding equation for j in its standard state in the bulk phase. A complete analysis (which is too lengthy to present here) shows that all the Clausius–Clapeyron equations involve differentiating the chemical potential with respect to temperature at constant surface composition* and so all the corresponding heats are 'isosteric', although they differ according to which of three other pairs of variables are kept constant: (p,V), (γ,A), and (Q,ϵ). It must be emphasized that this conclusion applies to any type of interphase. Thus, it is only when we have a rather complete knowledge of the interfacial composition that we can determine heats of adsorption by means of the Clausius–Clapeyron equations.

5. THE GIBBS–DUHEM EQUATION

We can obtain the interfacial analogue of the Gibbs–Duhem equation from any of the characteristic equations by the usual methods

$$[1] \qquad S^\sigma dT - V^\sigma dp + A d\gamma + Q\alpha d\epsilon + \sum_{i=1}^{i=c-2} m_i d\mu_i = 0.$$

This equation is well known as the basic electrocapillary equation (6). However, there is one feature by which [1] differs from the equation normally employed: the term $Qd\epsilon$. This is usually written with the cell e.m.f. E in place of ϵ. These quantities are related by 2.8 and it is clear that while $d\epsilon$ can be equated to dE at constant temperature (cf. 2.10), this assumption is not correct where temperature variations are to be considered.

It is possible to eliminate two variables from [1] by taking into account the Gibbs–Duhem equations for the adjoining phases. We write these in the form:

$$[2] \qquad d\mu_1 = -\frac{S^\alpha}{n_1^\alpha} dT + \frac{V^\alpha}{n_1^\alpha} dp - \sum_{i \neq 1} \frac{n_i^\alpha}{n_1^\alpha} d\mu_i,$$

$$[3] \qquad d\mu_2 = -\frac{S^\beta}{n_2^\beta} dT + \frac{V^\beta}{n_2^\beta} - \sum_{i \neq 2} \frac{n_i^\beta}{n_2^\beta} d\mu_i,$$

**We have ignored here the effect of the neighboring phases on the number of degrees of freedom in equations like 3.4. For a perfectly polarized electrode this reduces the number of independent composition variables by two.*

Can. J. Chem. Downloaded from www.nrcresearchpress.com by 190.90.36.8 on 09/04/12
For personal use only.

and substitute in [1] the values of $d\mu_1$ and $d\mu_2$ the changes in the chemical potentials of the reference substances 1 and 2. If at the same time we divide through equation [1] by the area of the interphase A, we obtain:

$$[4] \qquad sdT-vdp+d\gamma+qd\epsilon+\sum_{i=3}^{i=c-2}\Gamma_i d\mu_i = 0,$$

where

$$[5] \qquad s = \left(S^\sigma-\frac{m_1}{n_1^\alpha}S^\alpha-\frac{m_2}{n_2^\beta}S^\beta\right)\Big/ A,$$

$$[6] \qquad v = \left(V^\sigma-\frac{m_1}{n_1^\alpha}V^\alpha-\frac{m_2}{n_2^\beta}V^\beta\right)\Big/ A,$$

$$[7] \qquad q = Q^\alpha/A,$$

$$[8] \qquad \Gamma_i = \left(m_i-\frac{m_1}{n_1^\alpha}n_i^\alpha\right)\Big/ A,$$

or

$$[9] \qquad \left(m_i-\frac{m_2}{n_2^\beta}n_i^\beta\right)\Big/ A.$$

It is frequently convenient to consider the adsorption of one substance taking as a starting point the system in the absence of this substance at the same T, p, ϵ, and μ_i for other components. If we consider the adsorption of component 3, then for the base system, equation [4] becomes

$$[10] \qquad s^\circ dT-v^\circ dp+d\gamma^\circ+q^\circ d\epsilon+\sum_{i=4}^{i=c-2}\Gamma_i^\circ d\mu_i = 0.$$

Subtracting [4] from [10], we obtain

$$[11] \qquad (s^\circ-s)dT-(v^\circ-v)dp+d\pi+(q^\circ-q)d\epsilon+\sum_{i=4}^{i=c-2}(\Gamma_i^\circ-\Gamma_i)d\mu_i-\Gamma_3 d\mu_3 = 0,$$

where $\pi = \gamma^\circ-\gamma$ is the surface pressure associated with component 3. We can use [11] to calculate the effect of component 3 on various properties of the interphase, e.g.,

$$[12] \qquad (\partial\pi/\partial\mu_3)_{T,p,\epsilon,\mu_i\neq\mu_3} = \Gamma_3,$$

$$[13] \qquad (\partial\pi/\partial T)_{p,\epsilon,\mu_i} = s-s^\circ,$$

$$[14] \qquad (\partial\mu_3/\partial T)_{p,\pi,\epsilon,\mu_i\neq\mu_3} = -(s-s^\circ)/\Gamma_3,$$

etc.

6. CHANGE OF VARIABLE TO ξ

In previous work we have argued that it is useful to consider changes in the composition of the interphase of a perfectly polarized electrode at a constant value of q. For convenience in calculation we have defined a new variable

$$[1] \qquad \xi = \gamma+qE.$$

However, it is evident from the foregoing that when temperature variation is to be considered, a better definition would be

$$[2] \qquad \xi = \gamma+q\epsilon.$$

Can. J. Chem. Downloaded from www.nrcresearchpress.com by 190.90.36.8 on 09/04/12
For personal use only.

Equation 5.4 then becomes

$$[3] \qquad sdT - vdp + d\xi - \epsilon dq + \sum_{i=3}^{i=c-2} \Gamma_i d\mu_i,$$

and the analogue of 4.11, if we consider introducing component 3 to the base system, this time keeping q and not ϵ constant, is

$$[4] \qquad (s^\circ - s)dT - (v^\circ - v)dp + d\Phi + (\epsilon^\circ - \epsilon)dq + \sum_{i=4}^{i=c-2} (\Gamma_i^\circ - \Gamma_i)d\mu_i - \Gamma_3 d\mu_3 = 0,$$

where

$$\Phi = \xi^\circ - \xi.$$

Again we can calculate the effect of component 3 on various properties of the interphase and obtain analogues of 5.12, 5.13, 5.14, etc.

$$[5] \qquad (\partial\Phi/\partial\mu_3)_{T,p,q,\mu_i \neq \mu_3} = \Gamma_3,$$

$$[6] \qquad (\partial\Phi/\partial T)_{p,q,\mu_i} = s - s^\circ,$$

$$[7] \qquad (\partial\mu_3/\partial T)_{p,\Phi,q,\mu_i \neq \mu_3} = -(s - s^\circ)/\Gamma_3.$$

Thus, we find that the same quantities may be calculated by two different routes. It is also evident that there is no advantage in principle in using [4] rather than 5.11, since the same quantities may be obtained from either. However, there may be practical advantages in a particular problem which would lead one to use one equation rather than the other.

It may be remarked here that our previous use of [1] in calculations from electrocapillary curves at different temperatures, which is incorrect in principle, has in fact led to no error because even with temperature varying

$$[8] \qquad E^\circ - E = \epsilon^\circ - \epsilon$$

and we have used equations based on equation [4] in which only $\epsilon^\circ - \epsilon$ appears.

7. APPLICATION TO EXPERIMENT

The systems used up to now consist of an aqueous electrolyte CA in contact either with air (3) or with mercury (1). Provided that the electrolyte has no tendency to hydrolyze so that the effect of the ionization of water may be neglected, the terms under the summation sign in 5.11 and 6.4 vanish. We identify component 3 with the electrolyte CA. Under these conditions 5.14 reduces, for the air–solution interphase to

$$[1] \qquad (\partial\mu_{CA}/\partial T)_{p,\pi} = -(s - s^\circ)/\Gamma_{CA},$$

while 6.7 for the mercury–solution interphase becomes

$$[2] \qquad (\partial\mu_{CA}/\partial T)_{p,\Phi,q} = -(s - s^\circ)/\Gamma_{CA}.$$

[1] and [2] are identical if $q = 0$, so that we need only consider [2]. The so-called integral or isotensile heats of adsorption, which have been obtained for these interphases, have been calculated from the expression

$$[3] \qquad \left[\frac{\partial(\mu_{CA} - \mu_{CA}^\circ)/T}{\partial T}\right]_{p,\Phi,q} = -\frac{\Delta h}{T^2}$$

where μ_{CA}° is the standard chemical potential of CA and

$$[4] \qquad \Delta h = h - H_{CA}^\circ.$$

Can. J. Chem. Downloaded from www.nrcresearchpress.com by 190.90.36.8 on 09/04/12
For personal use only.

H_{CA}° is the heat content of CA in its standard state. Since it is well known that

$$[5] \qquad \left[\frac{\partial(\mu_{CA}^{\circ}/T)}{T}\right]_p = -\frac{H_{CA}^{\circ}}{T^2}$$

we need only investigate the meaning of the remaining part of [3] involving μ_{CA} and h. From [2] it follows that

$$[6] \qquad \left[\frac{\partial(\mu_{CA}/T)}{\partial T}\right]_{p,\Phi,q} = -\frac{1}{T^2}\left\{\frac{T(s-s^{\circ})}{\Gamma_{CA}}+\mu_{CA}\right\} = -\frac{h}{T^2}.$$

It is evident from [6] that h is none of the thermodynamic potentials defined above. Therefore, in general, the heat of adsorption obtained from [3] has no simple significance. However, if it is assumed that the change in the interfacial entropy when CA is adsorbed can be ascribed entirely to CA and also that it is a linear function of the amount adsorbed, then we can put

$$[7] \qquad \frac{s-s^{\circ}}{\Gamma_{CA}} = \left(\frac{\partial S\sigma}{\partial m_{CA}}\right)_{T,p},$$

and

$$[8] \qquad h = \bar{H}\sigma = \bar{\mathfrak{H}} = \bar{H}_e = \bar{\mathfrak{H}}_e,$$

i.e., the distinction between the various partial heat contents of the adsorbed phase vanishes. Thus, under these rather specialized conditions Δh has a satisfactory interpretation in terms of the change of a thermodynamic potential. For other conditions it would seem preferable to calculate the change in entropy of the interphase from 5.7 or 6.6 first, before attempting an interpretation in terms of a model.

On the other hand the isosteric heat of adsorption can be calculated from the rate of change of chemical potential with respect to temperature, if as well as the surface composition, one of each of the conjugate pairs of variables (γ,A), (q,ϵ) is kept constant (cf. 4.4). These conditions can be attained in practice, but if the surface concentration is obtained from interfacial tension measurements it is difficult to obtain accurate results.

Results of measurements of the Hg/KI(aq) system have previously been presented (1) in the form of curves of $-\Delta h$ and $[(s-s^{\circ})-\bar{S}_{KI}^{\circ}]/\Gamma_{KI}$ against Γ_{KI}, although they were originally interpreted as isotensile heat and differential entropy curves. At higher coverages it was found that the entropy was approximately independent of coverage. In this region, it follows from the above that the heats of adsorption are simply differences of heat content in the two states. At lower coverages the interpretation is more complex; consequently, it appears that no thermodynamic error has been made in the discussion of these results except at the low coverages.

A further important result of the above analysis is that the thermodynamic quantities, in particular the entropy, can be calculated for any point on the electrocapillary curve, whereas the previous method was in practice limited to the region of a negative charge on the mercury surface. We hope to present some of these results for specifically adsorbed systems in the near future.

REFERENCES

1. ANDERSON, W. and PARSONS, R. Proc. 2nd Intern. Congr. Surface Activity, **III**, 45 (1957).
2. EVERETT, D. H. Trans. Faraday Soc. **46**, 453 (1950).
3. ANDERSON, P. J. and PETHICA, B. A. Trans. Faraday Soc. **52**, 1080 (1956). BETTS, J. J. and PETHICA, B.A. Proc. 2nd Intern. Congr. Surface Activity, **I**, 152 (1957).
4. GUGGENHEIM, E. A. Trans. Faraday Soc. **36**, 397 (1940).
5. GUGGENHEIM, E. A. Thermodynamics. North-Holland Pub. Co., Amsterdam. 1949. p. 326.
6. PARSONS, R. Modern aspects of electrochemistry. *Edited by* Bockris, J. O'M. Butterworth Scientific Publications, London. 1954. Chap. III.

Can. J. Chem. Downloaded from www.nrcresearchpress.com by 190.90.36.8 on 09/04/12
For personal use only.

Can. J. Chem. Downloaded from www.nrcresearchpress.com by 190.90.36.8 on 09/04/12
For personal use only.

THE ADSORPTION OF METHYLENE BLUE ON A POSITIVELY CHARGED MERCURY SURFACE[1]

J. M. Los and C. K. Tompkins

ABSTRACT

Direct measurement of the surface concentration Γ of methylene blue, adsorbed from a phosphate buffer solution onto an ideally polarized mercury electrode, has produced a Langmuir-type isotherm. The maximum value of Γ, Γ_m, was found to be dependent on the potential applied (E). Surface tension measurements showed that the rate-controlling process is not diffusion, but, presumably, the exchange of methylene blue cation (MB^+) with phosphate ions. A model for this process has been proposed. This allowed the calculation of the rate constant of adsorption (k_a) from the surface tension values as a function of time ($k_a \sim 5\times10^{-5}$ cm/sec; $dk_a/dE \sim 30\times10^{-5}$). There is some evidence for the occurrence of a consecutive process, most likely the combination of adsorbed MB^+ to dimers.

INTRODUCTION

It is well known that the presence of organic substances that will adsorb on mercury may change the characteristics of polarographic current–voltage waves of depolarizers. Even "reversible" waves can be affected. Much less is known about the effect on half-wave potential and limiting current that inorganic ions, mostly anions, may have. This problem should become interesting when the depolarizer is a big organic molecule, if it has to occupy a relatively large area of the electrode surface before electron transfer can take place. Alternatively, no adsorption of the compound may be needed for the latter, if only the electrons could be transferred by way of the Helmholtz part of the double layer. It is, therefore, of interest to find a compound which adsorbs more slowly than is required for reversibility (the rate constant of the electrode reaction at the latter's standard potential must be at least 10^{-2} cm sec^{-1} (1)). The experimental correlation between adsorption and reduction should thus enable one to decide upon the above-mentioned question of the mode of electron transfer.

The present paper will be concerned with an approach to this problem, namely a study of the kinetic parameters of adsorption of the compound methylene blue (MB^+Cl^-) on an ideally polarized mercury electrode, the solution being buffered by phosphate ($C_{HPO_4^=} = 0.05$; $C_{H_2PO_4^-} = 0.05$ moles/liter; pH is about 7).

The range of potentials available for ideal polarization is rather narrow. A polarogram shows that this range lies between anodic mercury dissolution, starting at +0.2 v (due to insolubility of Hg_2HPO_4, not of Hg_2Cl_2) and methylene blue reduction ($E_{\frac{1}{2}} \sim -0.2$ v; actually there is a small prewave, which, according to Brdicka (2), is due to the strong adsorption of reduced or leuco methylene blue). It was desirable to do measurements at more than one potential. The work presented here was done at −0.024 and +0.076 v (with respect to S.C.E.), i.e., 0.1 v apart.

MEASUREMENTS

Two types of measurements were performed, at 25° C.

(*1*) *Direct measurement of the surface concentration (excess) of methylene blue.*—This was achieved by means of an apparatus based on the principle of allowing the surface of many successive mercury drops at constant potential, to come to equilibrium with the

[1]*Manuscript received July 10, 1958.*
Contribution from the Department of Chemistry, University of New Brunswick, Fredericton, New Brunswick. This paper was presented at the Symposium on Charge Transfer Processes held at the University of Toronto, Toronto, Ontario, September 4 and 5, 1958.

surrounding methylene blue solution before the drops are dislodged and separated from the solution (together with their adhering double layer). Finally all unite and reject their skins of solution into a common pool. The concentration difference between this collected solution and the original one is then directly related to the actual surface excess. Although the essential features of this apparatus have been described previously (3), a few additional remarks need to be made concerning its operation (see Experimental Section).

(*2*) *Measurements of the surface tension by the drop-weight method, as a function of time, potential, and concentration.*—Craxford and McKay (4) have shown that this method yields values as precise as the capillary electrometer. Surface tension and surface concentration are, of course, related to each other by the Gibbs adsorption equation,

$$[1] \qquad d\gamma = -\sum_i \Gamma_i d\mu_i^{\alpha} - qdE,$$

where α is the solution phase. This equation may only be applied if equilibrium has been attained.

RESULTS

The experimental points of Fig. 1, which shows the results of the surface concentration (Γ) measurements, bear out that we have a Langmuir-type isotherm. Each point is an average of three to six measurements. This number was taken in order to test for differences with change in radius of the mercury drops, curvature of the solution–nitrogen interface, and drop time. Values of the latter around 3.6, 25, and 50 seconds were usually taken. Taking into account that the average deviation of a single measurement from the mean value was about 3–5%, no dependence on drop radius and interface curvature could be established. Apparently, at the lowest concentrations ($c \sim 10^{-8}$ moles/cm^3) the influence of the drop time has made itself felt (see Fig. 1). These particular points have, therefore, not been included in the least-square evaluation of the straight line.

Results of the surface tension (γ) measurements have been given as γ vs. t plots for five different concentrations in Fig. 2A (for -0.024 v) and Fig. 3A (for $+0.076$ v).

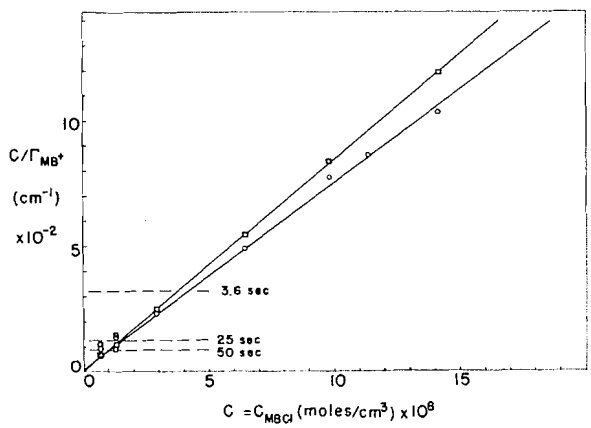

FIG. 1. The constants of the lines $c/\Gamma = a + bc$ are:
Lower line at -0.024 v: $b = (7.40 \pm 0.11) \times 10^9$ cm^2/mole; $a = 10 \pm 9$ cm^{-1}.
Upper line at $+0.076$ v: $b = (8.37 \pm 0.03) \times 10^9$ cm^2/mole; $a = 5 \pm 2$ cm^{-1}.
(Deviations are probable errors.) For broken lines see text.

Can. J. Chem. Downloaded from www.nrcresearchpress.com by 190.90.36.8 on 09/04/12
For personal use only.

Can. J. Chem. Downloaded from www.nrcresearchpress.com by 190.90.36.8 on 09/04/12
For personal use only.

DISCUSSION

Surface Concentration Measurements

At first glance (Fig. 1) these measurements seem to provide ample proof that equilibrium with the solution has been approached quite closely, except for the low concentration points with drop time around 3.6 seconds. Since the c/Γ vs. c lines go nearly through the origin (according to the surface tension measurements even more so than indicated by the intercept (a) values in the caption to Fig. 1), the isotherm must have a very steep ascending branch and for all concentrations measured Γ_e should be closely equal to Γ_m (Γ_e is the equilibrium value, Γ_m is the maximum value of the surface concentration). This means that the minimum time necessary to reach equilibrium may be calculated from the Ilkovic equation (5),

$$\Gamma_t = \frac{6}{7}(7/3)^{\frac{1}{2}}(D^{\frac{1}{2}}t^{\frac{1}{2}}/\pi^{\frac{1}{2}})c\ , \qquad [2]$$

where Γ_t is the maximum possible surface concentration at time t and D is the diffusion coefficient, here taken as 5×10^{-6} cm^2 sec^{-1}. The c/Γ_t values calculated from equation [2] for the drop times 3.6, 25, and 50 seconds, respectively, have been indicated in Fig. 1 by three horizontal broken lines. Measured points could not have reached equilibrium within 3.6, etc., seconds if they should fall below the corresponding line, and the reverse of this statement is approximately true as well. Whereas the low concentration points *included* in the calculation of the line had been taken at drop times 25 or 50 seconds, the corresponding 3.6-second points should have been at the level of the upper line. Of course, stirring of the solution by the falling drop invalidates equation [2] and speeds up the diffusion process. Such points, however, are of no value, since the potential of a falling drop changes rapidly if equilibrium has not been attained before it is released from the electrode.*

However, the surface tension measurements show clearly that a much slower process than diffusion must be rate-controlling, since γ continues to decrease for c/Γ values much in excess of the critical c/Γ values indicated by the horizontal lines in Fig. 1. From the analysis of the γ vs. t plots it follows that Γ_e would apply for drop times of 50 seconds and $c > 10\times10^{-8}$ moles/cm^3. The isotherm lines in Fig. 1 must therefore have the correct slope, while their intercepts could hardly be less within experimental error. Again considering the fact that the 3.6-second points are much lower than they should be, it follows that a mechanism other than stirring must be operating while the drops fall, so as to accelerate the surface adsorption.

Since $b = 1/\Gamma_m$ it follows that Γ_m (-0.024 v) $= 1.35\times10^{-10}$ and Γ_m ($+0.076$ v) $= 1.20\times10^{-10}$ moles/cm^2. These values have a precision of about 1%, and are in the sequence expected: the phosphate ions, in particular HPO_4^-, are more strongly held and the ions MB^+ more strongly repelled by the surface at the higher potential.

The Γ_m values correspond to an area/molecule of 1.22 Å^2 at -0.024 v and 1.39 Å^2 at $+0.076$ v, which values indicate that there is still phosphate left on the surface at "complete" coverage with MB^+. (A value of 90 Å^2 would probably be closer to the true area of a molecule.)

**The apparatus constructed by Kalousek and Blahnik (6), which is quite analogous to ours, has rapid dropping combined with a very long path of the drops through the solution. In principle, this long path should not be necessary.*

Surface Tension Measurements

Gibb's adsorption equation does not apply to non-equilibrium cases, such as the γ vs. t plots of Figs. 2A and 3A. In order to find the change of γ with time we must treat the adsorption layer as a separate phase (σ), theoretically in equilibrium with the surrounding solution (α) at infinite time only. For the surface phase then, we have at constant potential,

$$[3] \qquad d\gamma = -\sum_i \Gamma_i d\mu_i^{\sigma},$$

Γ_i being the surface concentration of species i and $\Gamma_i = \Gamma_i\ (t,c,E)$.

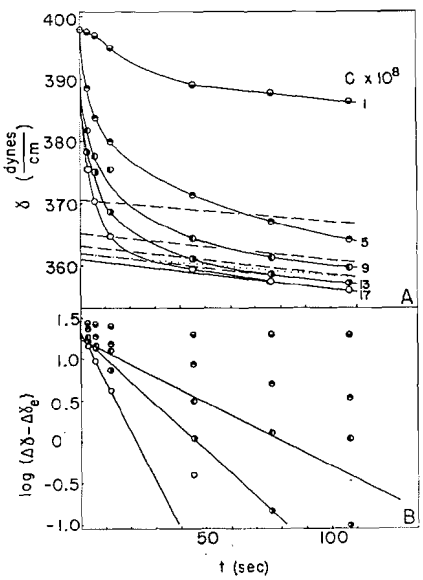

FIG. 2. A. γ vs. t plots for -0.024 v (S.C.E.). For broken and dotted lines see text.
B. Plot of points from 2A according to equation [12].

We now shall postulate the following model:

(*a*) If σ is considered as an ordinary phase, only differing from the latter in its property of surface tension, we may write,

$$[4] \qquad \mu_i^{\sigma} = \mu_i^{\sigma,0} + R^*T \ln \Gamma_i/\Gamma_{i,e},$$

where

$$[5] \qquad \mu_i^{\sigma,0} = \mu_i^{\alpha,0} + RT \ln a_{i,e}.$$

Equation [5] assures that $\mu_i^{\sigma} = \mu_i^{\alpha}$ for $\Gamma_i = \Gamma_{i,e}$. It can be shown quite generally that $R^* = Rd \ln a_i/d \ln \Gamma_i$. As a first approximation R^* will be taken as independent of Γ_i.

(*b*) Chloride ions do not adsorb in significant quantity. The only species entering into equation [3] is MB^+. Although these cations are known to dimerize to some extent in solution (the dimer concentration is about 1.2×10^{-8} at a total concentration of 10^{-7} moles/cm^3 (7)), we shall assume monomers (M) only.

(*c*) The rate of reaching equilibrium at the surface is entirely determined by the interchange of MB^+ with phosphate ions. Consequently, the volume concentration of

Can. J. Chem. Downloaded from www.nrcresearchpress.com by 190.90.36.8 on 09/04/12
For personal use only.

MB^+ is constant up to the surface ($c_M = c$) and the equilibrium to be established is

$$M^\alpha \underset{k_d}{\overset{k_a}{\rightleftharpoons}} M^\sigma.$$

(*d*) A Langmuir-type isotherm applies to the adsorption of M, as suggested by Fig. 1,

[6] $$c/\Gamma_e = a+bc,$$

where

$$a = a'/\Gamma_m = k_d/k_a\Gamma_m$$

and

$$b = 1/\Gamma_m.$$

(*e*) No surface activity coefficients will be considered. Constant ionic strength of the solution α does not guarantee the same in the surface phase.

(*f*) Expansion of the mercury drops, as used in the drop-weight method, will be neglected in the first analysis.

From (*a*), equation [4], we obtain

[7] $$d\mu_M{}^\sigma = R^*T\, d \ln \Gamma_M.$$

Substitution of equation [7] into equation [3] gives, considering (*b*) and (*c*),

[8] $$d\gamma = -R^*T\, d\Gamma_M.$$

Now we must find $\Gamma_M(t)$. According to (*c*),

$$\left(\frac{\partial \Gamma_M}{\partial t}\right)_{E,c} = k_a c(1-\theta) - k_d\theta.$$

Putting $\theta = \Gamma_M/\Gamma_m$, and substituting equation [6],

$$\left(\frac{\partial \Gamma_M}{\partial t}\right)_{E,c} = k_a c\left(1-\frac{\Gamma_M}{\Gamma_{M,e}}\right).$$

Upon integration:

[9] $$\Gamma_M = \Gamma_{M,e}(1-e^{-k_a c t/\Gamma_{M,e}}).$$

Now, substituting equation [9] into equation [8] and integrating:

[10] $$\Delta\gamma = -R^*T\Gamma_{M,e}(1-e^{-k_a c t/\Gamma_{M,e}}).$$

For $t \to \infty$, $\Delta\gamma \to \Delta\gamma_e$, and this establishes

[11] $$R^*T = -\Delta\gamma_e/\Gamma_e.$$

From equation [10] and equation [11] we derive,

[12] $$\log(\Delta\gamma - \Delta\gamma_e) = \log(-\Delta\gamma_e) - (k_a c/2.303\ \Gamma_e)t.$$

The surface tension falls off very rapidly at first, especially for the higher concentrations, but then it appears to decrease at a uniform rate. Rough calculations may show that this descent is too large to be caused by our postulate (*f*). We suggest that there may be a secondary process, slow compared with the one treated above. As a matter of fact, if we plot equation [12] as a straight line plot (Figs. 2B and 3B), we find that the best straight line can be obtained by correcting the experimental points of Figs. 2A and 3A

Can. J. Chem. Downloaded from www.nrcresearchpress.com by 190.90.36.8 on 09/04/12
For personal use only.

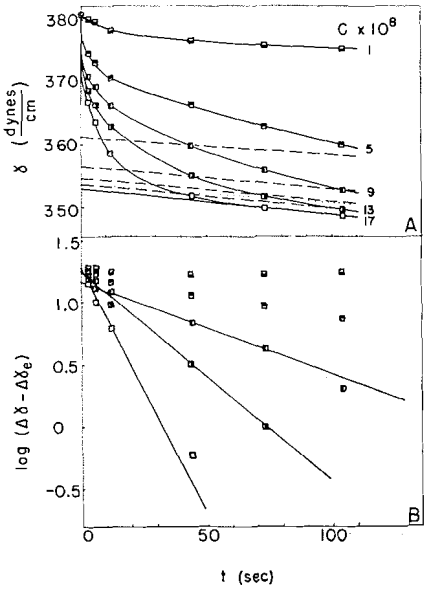

FIG. 3. A. γ vs. t plots for +0.076 v (S.C.E.). For broken and dotted lines see text.
B. Plot of points from 3A according to equation [12].

for this secondary process as indicated for the γ vs. t lines of $c = 17\times10^{-8}$. The extrapolation to $t = 0$ is not quite legitimate (see below), but this should not cause a large error. If one does not wish to admit that a consecutive process occurs, no correction is then made and $(\Delta\gamma_e) <$ smallest $\Delta\gamma$ measured. A plot according to equation [12] was found to deviate very much from a straight line in that case.

The following model would seem most logical in dealing with this secondary process:

(i) Dimers are produced on the surface in either one of two ways:

$$2\,M^\sigma \rightleftharpoons D^\sigma \text{ (homogeneous) or } M^\alpha + M^\sigma \rightleftharpoons D^\sigma \text{ (heterogeneous).}$$

(ii) This process is so slow with respect to the first one, that at times $t > t_1$, the equilibrium under (c) remains established.

(iii) Analogous to equation [4] we have,

$$\mu^\sigma{}_D = \mu_D{}^{\sigma,0} + R^*T \ln \Gamma_D/\Gamma_{D,e}, \qquad [13]$$

where

$$\mu_D{}^{\sigma,0} = 2\mu_M{}^{\sigma,0}.$$

Also, the postulates (b), (e), and (f) remain relevant.

The significance of (ii) and (e) is that $\Gamma_M = \Gamma_{M,e}$ and $\mu_M{}^\sigma = \mu_M{}^\alpha$, ($d\ \mu_M{}^\sigma = 0$) for constant c and E, so that equation [3] now becomes

$$\begin{aligned} d\gamma &= -\Gamma_D\, d\mu_D{}^\sigma \\ &= -R^*T\, d\Gamma_D \text{ (postulate (iii)).} \end{aligned} \qquad [14]$$

For the processes mentioned under (i) we obtain, respectively,

$$d\Gamma_D = k_2\Gamma_{M,e}{}^2\, dt, \qquad [15]$$

or

$$d\Gamma_D = k_2'\, \Gamma_{M,e} c\, dt. \qquad [16]$$

Can. J. Chem. Downloaded from www.nrcresearchpress.com by 190.90.36.8 on 09/04/12
For personal use only.

Note that these processes are pseudo-zeroth order for $t > t_1$. Substitution of equation [16] and equation [11] into equation [14] finally gives

$$\left(\frac{\partial\gamma}{\partial t}\right)_{c,E} = -k_2\Delta\gamma_e\Gamma_{M,e}, \qquad [17]$$

if the process is homogeneous. Alternatively, substituting equation [16] instead of equation [15], we obtain

$$(\partial\gamma/\partial t)_{c,E} = -k_2'\Delta\gamma_e c, \qquad [18]$$

if the process is heterogeneous ($\Delta\gamma_e$ is the equilibrium value for the first process).

In Figs. 2A and 3A we have assumed that the correct slope is given by the solid straight line through the lowest two points of $c = 17\times10^{-8}$. Since

$$\Delta\gamma_e = -\frac{RT}{b}\ln\frac{a+bc}{a} \qquad [19]$$

(substituting equation [6] into equation [1]), values of a may be calculated if the b values, previously given, are substituted. This yields

$$a(-0.024\text{ v}) = 0.02 \quad \text{and} \quad a(+0.076\text{ v}) = 0.11\text{ cm}^{-1}.$$

These a values should be free from the systematic error to which the pair obtained from the surface concentration measurements was subjected, although the precision is certainly very poor in both cases.

The other (broken) straight lines in Figs. 2A and 3A have been calculated: their intercepts from [19] and their slopes from [17] (the ratio of the slopes of a broken and a solid line equals the ratio of the corresponding $\Delta\gamma_e$ values, $\Gamma_{M,e} \cong \Gamma_m$). By doing this we see from Figs. 2A and 3A that the points of longest drop time for $c = 13\times10^{-8}$ may have reached equilibrium with the monomer, but none of the other points have.

If, on the other hand, equation [18] had been used for the calculation of the same slopes, the latter would have been much larger (i.e., less negative; see dotted line for $c = 13\times10^{-8}$) and certain experimental points would have fallen below the dotted lines, which makes no physical sense. Of course more experimental points are needed to establish the conclusion definitely, but pending the production of this evidence, we tentatively conclude that the dimerization process—if it occurs at all, i.e., if our second model is correct—must be the *homogeneous* one.

The straight-line plots of Figs. 2B and 3B according to equation [12] have intercepts ($\log - \Delta\gamma_e$) which are somewhat less than the ones calculated from the $\Delta\gamma_e$ values of Figs. 2A and 3A. Also, the k_a values calculated from the slopes seem to increase somewhat with concentration causing the rather large individual deviations in the values quoted below. Taking the straight lines for the three highest concentrations for each potential, these values of k_a are:

$$k_a(-0.024\text{ v}) = (7.5\pm2.5)\ 10^{-5}\text{ cm sec}^{-1},$$
$$k_a(+0.076\text{ v}) = (4.2\pm1.8)\ 10^{-5}\text{ cm sec}^{-1}.$$

The lower concentrations cannot be expected to follow equation [12], especially at small values of the drop time; their γ values must be high because of diffusion control, as is clearly shown in the figures.

The k_a values given above certainly would agree with the anticipated trend: higher for the smaller potential. It would seem, then, that methylene blue is a compound which might show irreversible features in its polarographic current–voltage wave (see Introduction).

Can. J. Chem. Downloaded from www.nrcresearchpress.com by 190.90.36.8 on 09/04/12
For personal use only.

Values of $k_d = a\Gamma_m k_d$ are necessarily extremely inaccurate, but if the a values obtained from the surface tension measurements are used, these values are:

$$k_d(-0.024 \text{ v}) = 2\times10^{-15} \quad \text{and} \quad k_d(+0.076 \text{ v}) = 6\times10^{-16} \text{ mole cm}^{-2} \text{ sec}^{-1}.$$

EXPERIMENTAL

Surface Concentration Measurements

Reference will be made to Fig. 1 of ref. 3 throughout this section, which deals with further details on the operation of the apparatus used. The three sections, A, B, and C, which fit together with wide ground-glass joints, are assembled and the whole apparatus is placed in the thermostated water bath, as indicated in Fig. 1 (3). The connection to the Erlenmeyer flask outside the bath is made by way of a three-way stopcock (just above section A). The syphon (c) has a polyethylene section for flexibility. Connected to and vertically above the stopcock is a pear-shaped vessel, not shown. The Erlenmeyer flask contains sufficient solution to fill all the "dropping section" B, the siphon, and the flask itself to a height of about 1 cm. Before transferring the solution, the latter and the remainder of the glass apparatus are thoroughly washed with oxygen-free nitrogen by manipulating a set of stopcocks (not shown) in such a way that the nitrogen will pass through the tubular section in downward and upward directions alternatingly (the "head" A contains an extra outlet tube with stopcock, not shown). All but a small volume of the solution is next forced into the pear-shaped vessel above the apparatus, from which it can then flow into section B by gravity and extra nitrogen pressure. Simultaneously, a rather powerful stream of nitrogen is passed upward through capillary d in order to prevent any solution from entering this capillary. Both stopcocks above A are then closed and the nitrogen is shut off. The nitrogen overpressure in the small gas pocket above the solution in B will now force the solution downward into the capillary if the overpressure in C is slowly released through a stopcock on the side tube. Since the solution should not flow past the flare e it is necessary to open, simultaneously and carefully, the three-way stopcock toward the Erlenmeyer flask. The latter has been lowered a small distance to facilitate the operation, but after the solution has reached the flare e, it is raised till the surface of the solution in it is at the level of the bottom of the flare. It must be noticed that such a siphon is stable over a few (4–8) millimeters distance only, by virtue of the fact that the changing radius of the flare provides a balancing force of capillary "rise". Without the flare, the siphon would be completely unstable. An equally important function of the flare is that it allows the individual mercury drops to pass through the interface without difficulty.

The reference electrode ($Pt/Hg/Hg_2HPO_4/HPO_4^=, H_2PO_4^-$) had a fairly large mercury surface. It was filled to the top and then sealed, so that no liquid could flow into the methylene blue solution through the sintered glass disk. Its potential (+0.3105 v at 25° C with respect to S.C.E.) never changed more than a few ten thousandths of a volt throughout its period of use (many months).

The surface concentration, Γ_{MB^+}, is simply related to the concentration difference, Δc, between c_{MB^+} in the solution collected and the average in the dropping section B (before and after the period of dropping) by the equation

$$\Gamma_{MB^+} = v\Delta c/4\pi r^2_{Hg},$$

where Γ_{MB^+} is in moles/cm^2 and Δc in moles/cm^3. The volume of solution entrained per drop (v) is found from the total volume of solution collected (determined by weighing) over the total number of mercury drops (calculated from the drop time, which was

Can. J. Chem. Downloaded from www.nrcresearchpress.com by 190.90.36.8 on 09/04/12
For personal use only.

usually quite constant, and the total duration of dropping), and the radius per drop (r_{Hg}) from the total weight of mercury collected. In order to collect 4 ml of solution in the tube f, ten to twenty thousand drops were required, depending on the radius of the dropping electrode and on the curvature of the solution–nitrogen interface at the flare (the more the interface was bulging downward, the larger v). There was no danger that part of the double layer should be stripped off when the mercury drops pierced the interface, since the value of v corresponds to a thickness of the entrained layer of 0.01 mm or so.

The determination of Δc was done with a Beckman D.U. spectrophotometer. At 620 mμ there is a strong absorption shoulder, but unfortunately Beer's law is known not to be obeyed (8), so before and after each analysis a calibration curve was determined by plotting $-\Delta \log T/\Delta c$ vs. Δc for four other methylene blue solutions, made at the same time as the solution used in the experiment.

Three runs could be done simultaneously in the same bath.

Surface Tension Measurements

These were generally performed under the same circumstances as described under "Surface Concentration Measurements". The mercury drops were collected in a little cup below the dropping electrode, from where they could be removed by suction without opening the apparatus. A 20-cm long capillary, diameter of bore ~50 μ, could be used for the measurements up to 120 seconds drop time, without putting in any constrictions. This is a much longer drop time than the Poiseuille equation would give. It is known (9) that solution can penetrate between mercury and a glass wall and that at certain heights in the capillary this film of solution can become quite thick, so as to form a natural constriction somewhere along the tube. Drop times are not very constant this way, but the results are just as reproducible as those of short drop times.

Materials

The methylene blue (Merck, reagent grade) was recrystallized from alcohol and dried *in vacuo* (not in an oven, because of slight decomposition at 110° C). The sodium phosphate salts were recrystallized from water and dried *in vacuo* over P_2O_5. Water redistilled from a quartz still was used throughout.

REFERENCES

1. DELAHAY, P. J. Am. Chem. Soc. **75**, 1430 (1953).
2. BRDICKA, R. Collection Czechoslov. Chem. Communs. **12**, 522 (1947).
3. LOS, J. M. and TOMPKINS, C. K. J. Chem. Phys. **24**, 630 (1956).
4. CRAXFORD, S. R. and MCKAY, H. A. C. J. Phys. Chem. **39**, 545 (1935).
5. DELAHAY, P. and TRACHTENBERG, I. J. Am. Chem. Soc. **79**, 2355 (1957).
6. KALOUSEK, M. and BLAHNIK, R. Collection Czechoslov. Chem. Communs. **20**, 782 (1955).
7. VETTER, K. J. and BARDELEBEN, J. Z. Elektrochem. **61**, 135 (1957).
8. MICHAELIS, L. J. Phys. & Colloid Chem. **54**, 1 (1950).
9. JOHNSTON, R. J. and UBBELOHDE, A. R. Proc. Roy. Soc. (London), A, **206**, 275 (1951).

Can. J. Chem. Downloaded from www.nrcresearchpress.com by 190.90.36.8 on 09/04/12
For personal use only.

Can. J. Chem. Downloaded from www.nrcresearchpress.com by 190.90.36.8 on 09/04/12
For personal use only.

Canadian Journal of Chemistry

Issued by THE NATIONAL RESEARCH COUNCIL OF CANADA

VOLUME 37 FEBRUARY 1959 NUMBER 2

ω-HALOALKYL AND ω-AMINOALKYL SULPHIDES

CLEAVAGE OF THE ALKYL–SULPHUR BOND[1]

MARSHALL KULKA

ABSTRACT

In the homologous series of *p*-chlorophenyl ω-chloroalkyl sulphides (I), the first and second members reacted abnormally with amines to yield 1,ω-bis(*p*-chlorophenylmercapto)alkanes (II). The fourth member of the series reacted normally to produce 4-aminobutyl *p*-chlorophenyl sulphide (III). The formation of II is explained on the basis of an alkyl–sulphur bond cleavage. The members of the *p*-chlorobenzyl series (VI) in general reacted with amines to form the expected aminoalkyl sulphides (VII). However, the *p*-chlorobenzyl chloroalkyl sulphides (VI) were thermally labile and decomposed to *p*-chlorobenzyl chloride and a sulphur component. A cyclic sulphur component originated from VI whose chloroalkyl carbon chain was 4, 5, or 6. The thermal degradation of VI is explained through a sulphonium salt cleavage.

INTRODUCTION

It has been recently shown that *p*-chlorophenyl chloromethyl sulphide (I, $n = 1$) can undergo an unusual bimolecular reaction to form 2,8-dichloro-6H,12H-dibenzo(*b*,*f*)-1,5-dithiocin (1). Now another anomalous reaction of I has been discovered and is the subject

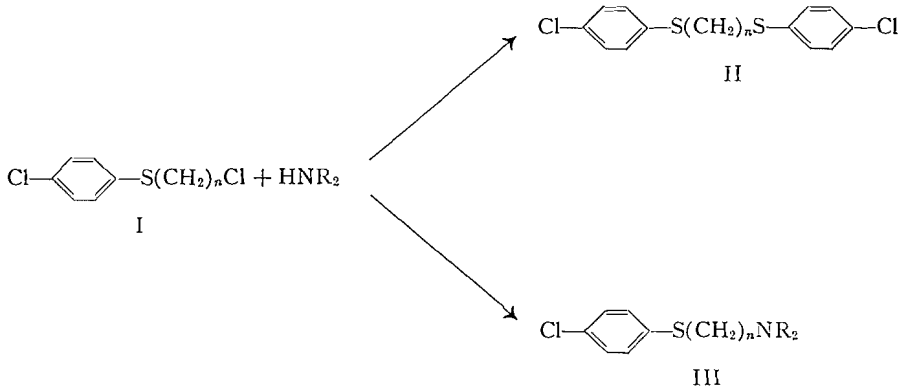

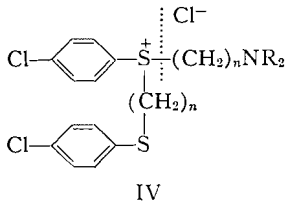

IV

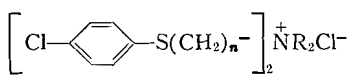

V

[1]*Manuscript received September 18, 1958.*
Contribution from the Dominion Rubber Company Limited Research Laboratories, Guelph, Ontario.

of this paper. When I (n = 1) was heated with ammonia, di-n-butylamine, or t-butylamine, the expected aminomethyl, p-chlorophenyl sulphide (III, n = 1), was not obtained. Instead, bis(p-chlorophenylmercapto)methane (II, n = 1) was the product.

On treatment of higher members of the homologous series of I with amines, it was found the 2-chloroethyl p-chlorophenyl sulphide (I, n = 2) also reacted abnormally in boiling di-n-butylamine to form 1,2-bis(p-chlorophenylmercapto)ethane (II, n = 2). However, when the temperature of the reaction was lowered to about 120° the only product was N,N-di-n-butylaminoethyl p-chlorophenyl sulphide (III, n = 2). Normal reaction only was indicated with higher members of the homologous series, since p-chlorophenyl 4-chlorobutyl sulphide (I, n = 4) with boiling di-n-butylamine gave p-chlorophenyl 4-di-n-butylaminobutyl sulphide (III, n = 4) in high yield. In this connection it was interesting to note that III (n = 2 and 4) forms a hydrochloride which is soluble in benzene and which distills readily without decomposition.

Any mechanism which attempts to explain the formation of II from I must take into account the observation that neither I nor III thermally decomposed to II, but that an equimolecular mixture of I and III on heating at 180° yielded II. This observation suggests two possible intermediates in the mechanism of the reaction, the sulphonium salt IV and the quaternary ammonium salt V, each of which could arise by the reaction of I with III. The dissociation of the sulphonium salt IV (indicated by the dotted line) would lead to II and chloroalkylamine. However, evidence is against this sulphonium salt mechanism since phenyl sulphides in general resist sulphonium chloride formation.

The formation of II (n = 1 and 2) from I might be attributed to a side reaction of I with p-chlorothiophenol in the presence of the amine. p-Chlorothiophenol could arise through an alkyl–sulphur bond cleavage of the quaternary ammonium salt V of I and III. A similar alkyl–sulphur bond cleavage has been experienced previously in the hydrazinolysis of β-p-chlorophenylmercapto-ethyl N,N-dimethyldithiocarbamate to p-chlorothiophenol (2).

The alkyl–sulphur bond in compounds of the benzyl series VI, unlike that of the phenyl series I, appeared to resist amine cleavage. Thus in the reaction of p-chlorobenzyl ω-chloroalkyl sulphides (VI) with amines only the normal products, VII, were formed and little if any of the neutral sulphides VIII could be detected.

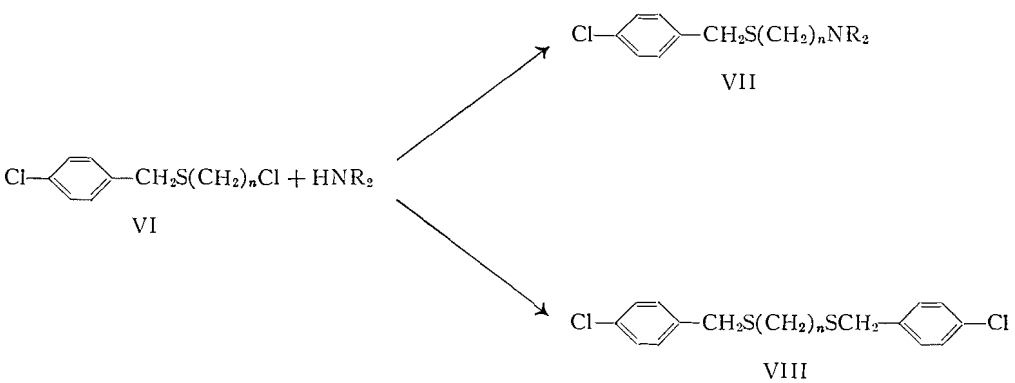

However, an alkyl–sulphur bond cleavage of a different nature was encountered in this series. It was found that the p-chlorobenzyl ω-haloalkyl sulphides (VI) were thermally

Can. J. Chem. Downloaded from www.nrcresearchpress.com by 190.90.36.8 on 09/04/12
For personal use only.

labile (unlike the members of the phenyl series I) and cleaved to *p*-chlorobenzyl chloride and a sulphur component. ω-Bromoalkyl *p*-chlorobenzyl sulphides were even more sensitive to heat and yielded *p*-chlorobenzyl bromide.

The lower members of the series VI could be distilled *in vacuo* with little if any decomposition but the higher members (n = 4 and 5) were too labile. Thus vacuum distillation of IX (Y = 0), IX (Y = CH_2), IX (Y = S), and IX (Y = 0) yielded *p*-chlorobenzyl chloride (XI) in each case together with tetrahydrothiophene (XII, Y = 0) (not isolated),

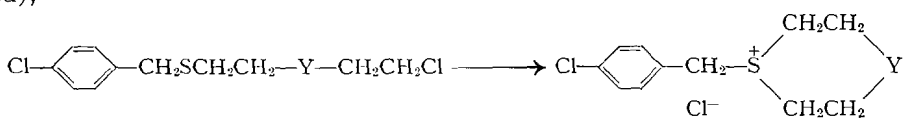

IX X

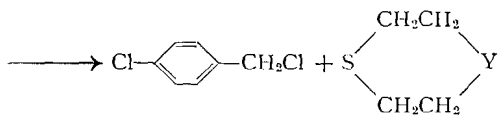

XI XII

pentamethylene sulphide (XII, Y = CH_2), 1,4-dithiane (XII, Y = S), and 1,4-oxathiane (XII, Y = 0) respectively. An attempt to prepare 4-bromo-2-butenyl *p*-chlorobenzyl sulphide from *p*-chlorobenzyl mercaptan and 1,4-dibromo-2-butene resulted in a mixture of *p*-chlorobenzyl bromide and a malodorous liquid which was probably dihydrothiophene.

The explanation for these reactions must involve sulphonium salt formation. Thus intramolecular sulphonium salt cyclization of IX could occur to form the ring X, which by dissociation would yield *p*-chlorobenzyl chloride (XI) and the cyclic sulphur compound (XII). Similar alkyl–sulphur bond cleavages with and without cyclizations have been reported by other workers (3, 4, 5). Bell, Bennett, and Hock (3) showed that mustard gas when heated at 180° yielded *p*-dithiane and ethylene dichloride. They proposed a mechanism for this reaction which consisted of both intermolecular and intramolecular sulphonium salt formation followed by dissociation.

An interesting example is provided of an alkyl–sulphur bond cleavage which must involve a seven-membered sulphonium salt ring (XIV). Thus when 2-β-chloroethoxy-5-methylbenzyl *p*-chlorobenzyl sulphide (XIII) was slowly distilled at 11 mm pressure, a

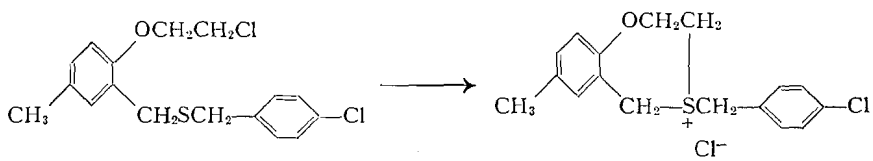

XIII XIV

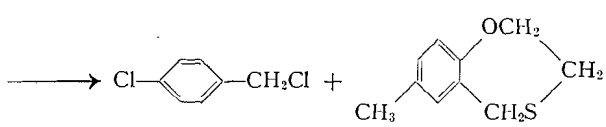

XI XV

Can. J. Chem. Downloaded from www.nrcresearchpress.com by 190.90.36.8 on 09/04/12
For personal use only.

mixture of low-boiling compounds was obtained. These compounds proved to be *p*-chlorobenzyl chloride (XI) and 2,3-dihydro-7-methylbenzo(*f*)-1,4-oxathiepin (XV) (6).

EXPERIMENTAL

Bis(p-chlorophenylmercapto)methane (II, $n = 1$) *from p-Chlorophenyl Chloromethyl Sulphide* (I, $n = 1$)

To *p*-chlorophenyl chloromethyl sulphide (7) (20 g) was added *t*-butylamine (40 ml) and the solution was heated under reflux for 4 hours. The precipitated *t*-butylamine hydrochloride was filtered off from the cooled reaction mixture and the filtrate freed of excess *t*-butylamine by distillation. The residue was dissolved in benzene, the solution washed with water, and the solvent removed. The residue distilled at 160–162° (0.5 mm) and the distillate (12 g or 77%) when crystallized from methanol melted at 42–43° alone or in admixture with bis(*p*-chlorophenylmercapto)methane (8).

In another experiment *p*-chlorophenyl chloromethyl sulphide was heated in a sealed bomb with excess liquid ammonia at 50–55° for 15 hours. This yielded only bis(*p*-chlorophenylmercapto)methane.

1,2-Bis(p-chlorophenylmercapto)ethane (II, $n = 2$) *from p-Chlorophenyl 2-Chloroethyl Sulphide* (I, $n = 2$)

A solution of *p*-chlorophenyl 2-chloroethyl sulphide (20 g) and di-*n*-butylamine (40 ml) was heated under reflux for 5 hours. The excess di-*n*-butylamine was removed *in vacuo* and the residue was crystallized from methanol. The white prisms (9 g) melted at 92–93° and did not depress the melting point of 1,2-bis(*p*-chlorophenylmercapto)ethane (9).

In another experiment *p*-chlorophenyl 2-chloroethyl sulphide was heated in a sealed bomb with methylamine at 140° for 6 hours. The product was 1,2-bis(*p*-chlorophenylmercapto)ethane.

2-(Di-n-butylamino)ethyl p-Chlorophenyl Sulphide (III, $n = 2$, R = C_4H_9)

A solution of *p*-chlorophenyl 2-chloroethyl sulphide (50 g) and di-*n*-butylamine (100 ml) was heated at 115–125° for 18 hours. The excess di-*n*-butylamine was removed *in vacuo*, the residue dissolved in benzene, and the solution washed with dilute hydrochloric acid. The benzene was removed and the residue distilled yielding a very viscous distillate (52 g) boiling at 160° (0.5 mm). When it was rubbed and warmed, it solidified and the white solid melted at 86–88°. This proved to be the hydrochloride of 2-(di-*n*-butylamino)-ethyl *p*-chlorophenyl sulphide (it is rather unusual that an amine salt should distill and be soluble in benzene). Anal. Calc. for $C_{16}H_{27}NCl_2S$: C, 57.14; H, 8.03. Found: C, 56.68; H, 7.79.

The free base was liberated from the hydrochloride by dissolving the latter in benzene and shaking with aqueous sodium hydroxide. 2-(Di-*n*-butylamino)ethyl *p*-chlorophenyl sulphide boiled at 137–140° (0.5 mm), $n_D^{20} = 1.5350$ and remained a colorless mobile liquid. Anal. Calc. for $C_{16}H_{26}NClS$: C, 64.11; H, 8.68. Found: C, 63.58, 63.27; H, 8.34, 8.52.

In another experiment when *p*-chlorophenyl 2-chloroethyl sulphide was heated with di-*n*-butylamine at 130–150° for 5 hours, a mixture of 2-(di-*n*-butylamino)ethyl *p*-chlorophenyl sulphide and 1,2-bis(*p*-chlorophenylmercapto)ethane was obtained.

4-(Di-n-butylamino)butyl p-Chlorophenyl Sulphide (III, $n = 4$, R = C_4H_9)

A solution of *p*-chlorophenyl 4-chlorobutyl sulphide (1) (17 g) and di-*n*-butylamine

Can. J. Chem. Downloaded from www.nrcresearchpress.com by 190.90.36.8 on 09/04/12
For personal use only.

Can. J. Chem. Downloaded from www.nrcresearchpress.com by 190.90.36.8 on 09/04/12
For personal use only.

(50 ml) was heated under reflux for 5 hours. The excess amine was removed *in vacuo*, the residue was dissolved in benzene, and the solution washed with aqueous sodium hydroxide and with water. Removal of the solvent and distillation of the residue yielded a colorless liquid (18 g), b.p. = 155° (0.5 mm); $n_D^{22} = 1.5288$. Anal. Calc. for $C_{18}H_{30}NClS$: C, 65.95; H, 9.16. Found: C, 65.43; H, 8.98.

2-(Diethylamino)ethyl p-Chlorophenyl Sulphide (III, $n = 2$, R = C_2H_5)

A solution of *p*-chlorophenyl 2-chloroethyl sulphide (20 g) and 98% diethylamine (35 ml) was heated at 120–130° in a sealed bomb for 6 hours. The product which was worked up as above boiled at 163–165° (11 mm); $n_D^{22} = 1.5535$. The yield was 12 g. Anal. Calc. for $C_{12}H_{18}NClS$: C, 59.14; H, 7.39. Found: C, 58.81, 59.25; H, 7.53, 7.50.

2-Aminoethyl p-Chlorophenyl Sulphide (III, $n = 2$, R = H)

To a solution of sodium hydroxide (10 g) in water (100 ml) was added *p*-chlorothiophenol (16 g) and 2-bromoethylamine hydrobromide (20 g) in water (30 ml). The resulting solution was heated on the steam bath for ½ hour and the precipitated oil was extracted with benzene. The benzene solution was washed with water, the solvent removed, and the residue distilled, b.p. = 152° (11 mm); $n_D^{25} = 1.6025$. The yield was 15 g. Anal. Calc. for $C_8H_{10}NClS$: C, 51.20; H, 5.33. Found: C, 50.27, 50.87; H, 5.25, 5.31.

2-Aminoethyl Pentachlorophenyl Sulphide

This was prepared in 60% yield from pentachlorobenzenethiol and 2-bromoethylamine hydrobromide as above. The white prisms crystallized from benzene – petroleum ether and melted at 89–90°. Anal. Calc. for $C_8H_6NCl_5S$: C, 29.46; H, 1.81. Found: C, 30.17, 29.81; H, 2.23, 2.12.

p-Chlorobenzyl 2-(Di-n-butylamino)ethyl Sulphide (VII, $n = 2$, R = C_4H_9)

A solution of *p*-chlorobenzyl 2-chloroethyl sulphide (9) (20 g) and di-*n*-butylamine (40 ml) was heated under reflux for 3 hours. The excess amine was removed *in vacuo*, the residue dissolved in benzene and washed with water. The solvent was removed and the residue fractionally distilled. The first fraction consisted of low-boiling material. The second fraction (7 g), which boiled at 137–140° (0.5 mm); $n_D^{27} = 1.5320$, was the required *p*-chlorobenzyl 2-(di-*n*-butylamino)ethyl sulphide. Anal. Calc. for $C_{17}H_{28}NClS$: C, 65.07; H, 8.93. Found: C, 65.26; H, 8.75.

The third fraction (3 g) boiled at 180–210° (0.5 mm) and the distillate on crystallization from methanol yielded white prisms (1.2 g) which melted at 74–76° alone or in admixture with 1,2-bis(*p*-chlorobenzylmercapto)ethane (9).

Pyrolysis of p-Chlorobenzyl 5-Chloropentyl Sulphide (VI, $n = 5$)

The crude *p*-chlorobenzyl 5-chloropentyl sulphide (40 g) (see below) was distilled at 12 mm first, and the distillate was then fractionated.

Fraction 1 consisted of 9 g of colorless malodorous liquid boiling at 140°; $n_D^{20} = 1.5060$. These properties agree with those of pentamethylene sulphide (10, 11). When a portion of fraction 1 was dissolved in acetic acid and treated with 30% hydrogen peroxide, pentamethylene sulphone (12), m.p. 96–97°, was formed.

Fraction 2 consisted of 19 g of colorless lachrymatory liquid; $n_D^{20} = 1.5560$ boiling at 87–89° (11 mm). It solidified on cooling and melted at 29°. Recrystallization from petroleum ether yielded long white needles melting at 29–30° alone or in admixture with *p*-chlorobenzyl chloride.

Pyrolysis of p-Chlorobenzyl 4-Chlorobutyl Sulphide (VI, $n = 4$)

Crude *p*-chlorobenzyl 4-chlorobutyl sulphide was prepared and pyrolyzed as above. *p*-Chlorobenzyl chloride was obtained in 74% yield but no tetrahydrothiophene could be isolated.

Pyrolysis of p-Chlorobenzyl 4-Bromo-2-butenyl Sulphide

To a stirred solution of potassium hydroxide (11 g) in methanol (200 ml) and *p*-chlorobenzyl mercaptan (30 g), cooled to 0°, was added a chilled solution of 1,4-dibromo-2-butene (100 g) in benzene (100 ml). The reaction mixture was stirred with cooling at 5–10° for 1 hour. The precipitated potassium bromide was filtered off and the solvents were removed from the filtrate. The residue was dissolved in benzene, the solution washed with water, and the solvent removed. The residue was distilled at 11 mm and the distillate then fractionated. Fraction 1 was a colorless malodorous liquid boiling at 40–60° (11 mm) and was probably dihydrothiophene. Fraction 2, boiling at 60–95° (11 mm), consisted mainly of 1,4-dibromo-2-butene. Fraction 3 (14 g) boiled at 95–102° (11 mm) and on crystallization from methanol yielded white needles melting at 49–50° alone or in admixture with *p*-chlorobenzyl bromide (13).

β-p-Chlorobenzylmercaptoethyl 2-Hydroxyethyl Sulphide

To a solution of potassium hydroxide (6 g) in methanol (100 ml) was added 2-mercaptoethanol (9 ml) and *p*-chlorobenzyl 2-chloroethyl sulphide (9) (20 g). The resulting solution was heated under reflux for 2 hours and then the methanol distilled off. The residual oil was extracted with benzene, the solution washed with water, and the solvent removed. The residue distilled at 175–178 (0.5 mm) yielding 19 g of a colorless liquid, $n_D^{26} = 1.5992$. Anal. Calc. for $C_{11}H_{15}OClS_2$: C, 50.28; H, 5.71. Found: C, 50.59; H, 5.82.

β-o-Chlorobenzylmercaptoethyl 2-Hydroxyethyl Sulphide

This was prepared in 87% yield from *o*-chlorobenzyl 2-chloroethyl sulphide as above, b.p. = 170–175° (0.5 mm); $n_D^{22} = 1.6020$. Anal. Calc. for $C_{11}H_{15}OClS_2$: C, 50.28; H, 5.71. Found: C, 50.55; H, 5.76.

Pyrolysis of β-p-(IX, Y = S) *and β-o-Chlorobenzylmercaptoethyl 2-Chloroethyl Sulphide*

A solution of *β-o*-chlorobenzylmercaptoethyl 2-hydroxyethyl sulphide (30 g), benzene (100 ml), and thionyl chloride (12 ml) was heated under reflux for 2 hours. The benzene and excess thionyl chloride were removed *in vacuo* and the residue was slowly distilled at 11 mm. The distillate was cooled and the white malodorous precipitate (6 g) filtered, washed with cold methanol, and dried. It sublimed readily and melted at 111–112°. This was *p*-dithiane (14).

The filtrate on distillation yielded *o*-chlorobenzyl chloride.

When *β-p*-chlorobenzylmercaptoethyl 2-hydroxyethyl sulphide was converted to the 2-chloroethyl derivative IX, (Y = S) with thionyl chloride and treated as above, a separable mixture of *p*-dithiane and *p*-chlorobenzyl chloride was obtained.

Pyrolysis of β-p-Chlorobenzylmercaptoethyl 2-Chloroethyl Ether (IX, Y = 0)

β-p-Chlorobenzylmercaptoethyl 2-chloroethyl ether (10 g) (see below) was heated at 160–170° for 7 hours. A malodorous liquid (3 g) distilled into the receiver which on redistillation boiled at 147–150°; $n_D^{22} = 1.5070$. The properties of this compound are in agreement with those given for 1,4-oxathiane (15, 16).

The residue on distillation yielded 5 g of *p*-chlorobenzyl chloride.

Can. J. Chem. Downloaded from www.nrcresearchpress.com by 190.90.36.8 on 09/04/12
For personal use only.

Pyrolysis of 2-β-Chloroethoxy-5-methylbenzyl p-Chlorobenzyl Sulphide (XIII)

To a solution of potassium hydroxide (5 g) in methanol (100 ml) was added *p*-chlorobenzyl mercaptan (11 g) and 2-β-chloroethoxy-5-methylbenzyl chloride (6) (15 g) in that order. The resulting reaction mixture was heated under reflux for 15 minutes. The methanol was removed, the residue dissolved in benzene, the solution washed with water, and the solvent removed. The residue was distilled slowly at 11 mm pressure up to 200° and the distillate was fractionated. Fraction 1 (5 g) which boiled at 80–135° (11 mm) was treated with thiourea in ethanol. The resulting isothiuronium salt melted at 205–207° and did not depress the melting point of the isothiuronium salt of *p*-chlorobenzyl chloride. Fraction 2 (9 g) boiled at 135–150° (11 mm) and when crystallized from methanol yielded white prisms melting at 45–46° alone or in admixture with 2,3-dihydro-7-methylbenzo(*f*)-1,4-oxathiepin (XV) (6).

Preparation of ω-Chloroalkyl Sulphides

These were prepared by the method used for 2-chloroethyl aryl and aralkyl sulphides previously described (9).

(*a*) *p-Chlorobenzyl 3-chloropropyl sulphide* (VI, $n = 3$) was obtained in 87% yield from 1,3-dichloropropane and *p*-chlorobenzyl mercaptan, b.p. = 115–118 (0.5 mm); $n_D^{22} = 1.5720$. Anal. Calc. for $C_{10}H_{12}Cl_2S$: C, 51.06; H, 5.10. Found: C, 50.63, 50.91; H, 4.89, 4.64.

(*b*) *p-Chlorobenzyl 3-bromopropyl sulphide* was prepared in 60% yield from 1,3-dibromopropane and *p*-chlorobenzyl mercaptan, b.p. = 120–125° (0.5 mm); $n_D^{22} = 1.5884$. Anal. Calc. for $C_{10}H_{12}ClBrS$: C, 42.93; H, 4.29. Found: C, 42.21, 42.27; H, 3.39, 3.50.

(*c*) *p-Chlorobenzyl 2-bromoethyl sulphide* could not be prepared in pure form because pyrolysis occurred during distillation to form *p*-chlorobenzyl bromide.

(*d*) *n-Amyl 4-chlorobutyl sulphide* was prepared in 20% yield from *n*-amyl mercaptan and 1,4-dichlorobutane, b.p. = 120–130° (11 mm); $n_D^{23} = 1.4775$. Anal. Calc. for $C_9H_{19}ClS$: C, 55.53; H, 9.76. Found: C, 56.33, 56.74; H, 9.75, 9.84.

(*e*) *β-p-Chlorobenzylmercaptoethyl 2-chloroethyl ether* (IX, Y = 0) was prepared in 75% yield from *p*-chlorobenzyl mercaptan and excess β,β′-dichloroethyl ether, b.p. = 137–140° (0.5 mm); $n_D^{22} = 1.5618$. Anal. Calc. for $C_{11}H_{14}OCl_2S$: C, 49.81; H, 5.28. Found: C, 49.94, 49.82; H, 5.08, 5.12.

(*f*) *p-Chlorobenzyl 5-chloropentyl sulphide* (VI, $n = 5$) was prepared from *p*-chlorobenzyl mercaptan and 1,5-dichloropentane (17). No attempt was made to distill the crude product because it pyrolyzed very readily.

(*g*) *Crude p-chlorobenzyl 4-chlorobutyl sulphide* (VI, $n = 4$) was prepared similarly.

o-Chlorobenzyl 2-Hydroxyethyl Sulphide

To a stirred mixture of sodium hydroxide (70 g) in 2-mercaptoethanol (200 ml) and benzene (200 ml) was added, over ½ hour, a solution of *o*-chlorobenzyl chloride (250 g) in benzene (150 ml). The reaction mixture boiled vigorously. It was heated under reflux for 2 hours, washed with water, the solvent removed, and the residue distilled, b.p. = 175–178° (11 mm); $n_D^{20} = 1.5832$. The yield was 293 g. Anal. Calc. for $C_9H_{11}OClS$: C, 53.33; H, 5.43. Found: C, 53.73; H, 5.58.

o-Chlorobenzyl 2-Chloroethyl Sulphide

To a stirred solution of *o*-chlorobenzyl 2-hydroxyethyl sulphide (200 g) in benzene (250 ml) was added, over ½ hour, thionyl chloride (125 g) with cooling. The reaction

Can. J. Chem. Downloaded from www.nrcresearchpress.com by 190.90.36.8 on 09/04/12
For personal use only.

mixture was heated under reflux for 1 hour, the solvent removed, and the residual oil distilled, b.p. = 155–158° (11 mm); n_D^{23} = 1.5827. The yield was 190 g. Anal. Calc. for $C_9H_{10}Cl_2S$: C, 48.87; H, 4.52. Found: C, 48.76; H, 4.05.

β-p-t-Butylphenoxyethyl 2-Hydroxyethyl Sulphide

This was prepared in 90% yield from *p-t*-butylphenyl 2-chloroethyl ether and 2-mercaptoethanol in the same way as was *o*-chlorobenzyl 2-hydroxyethyl sulphide above. The colorless liquid boiled at 205–210° (11 mm); n_D^{23} = 1.5410. Anal. Calc. for $C_{14}H_{22}O_2S$: C, 66.14; H, 8.66. Found: C, 65.49; H, 8.86.

β-p-t-Butylphenoxyethyl 2-Chloroethyl Sulphide

This was prepared in 94% yield by treatment of *β-p-t*-butylphenoxyethyl 2-hydroxyethyl sulphide with thionyl chloride. It distilled at 145–148° (0.5 mm) as a colorless liquid, n_D^{22} = 1.5400. Anal. Calc. for $C_{14}H_{21}OClS$: C, 61.65; H, 7.70. Found: C, 61.83; H, 7.79.

Preparation of the Aminoalkyl Sulphides

These were prepared by the same method as was (*a*).

(*a*) *p-Chlorobenzyl 2-aminoethyl sulphide* (VII, $n = 2$, R = H) was prepared by the addition of liquid ammonia (about 100 ml) to 30 g *p*-chlorobenzyl 2-chloroethyl sulphide cooled by dry ice, and the reaction mixture was sealed in a hydrogenation bomb and heated at 135–140° for 6 hours. The excess ammonia was allowed to evaporate, the residue treated with aqueous sodium hydroxide and extracted with benzene. The benzene solution was washed with water, the solvent removed, and the residue distilled. Most of it (20 g) distilled at 103–105° (0.2 mm) as a colorless liquid; n_D^{25} = 1.5850. Anal. Calc. for $C_9H_{12}NClS$: C, 53.59; H, 5.95. Found: C, 52.83, 53.01; H, 5.83, 6.02. The residue from the distillation on treatment with hydrochloric acid and crystallization from methanol yielded 3 g of bis(*β-p*-chlorobenzylmercaptoethyl)amine hydrochloride melting at 140–141°. Anal. Calc. for $C_{18}H_{21}NCl_2S_2$: C, 51.07; H, 5.20. Found: C, 51.22, 51.32; H, 5.26, 5.36.

(*b*) *o-Chlorobenzyl 2-aminoethyl sulphide* was prepared from *o*-chlorobenzyl 2-chloroethyl sulphide in 76% yield. The almost colorless liquid boiled at 160–165° (13 mm); n_D^{24} = 1.5862. Anal. Calc. for $C_9H_{12}NClS$: C, 53.59; H, 5.95. Found: C, 53.86, 53.38; H, 5.56, 5.93.

(*c*) *β-p-Chlorobenzylmercaptoethyl 2-aminoethyl ether* was prepared from *β-p*-chlorobenzylmercaptoethyl 2-chloroethyl ether in 45% yield. It distilled as a colorless liquid boiling at 135–137° (0.5 mm); n_D^{22} = 1.5640. Anal. Calc. for $C_{11}H_{16}NOClS$: C, 53.77; H, 6.42. Found: C, 53.68, 52.97; H, 6.25, 6.21.

(*d*) *p-Chlorobenzyl 5-aminopentyl sulphide* (VII, $n = 5$, R = H) was prepared in 25% yield from crude *p*-chlorobenzyl 5-chloropentyl sulphide. It distilled at 145–150° (0.5 mm); n_D^{25} = 1.5580. Anal. Calc. for $C_{12}H_{18}NClS$: C, 59.14; H, 7.39. Found: C, 58.94, 59.41; H, 7.10, 7.14.

(*e*) *p-Chlorobenzyl 3-amino-2-hydroxypropyl sulphide* was prepared from *p*-chlorobenzyl 3-chloro-2-hydroxypropyl sulphide (9) in 68% yield. It distilled at 170–175° (0.5 mm) and crystallized from ether containing a little methanol as white prisms which melted at 85–86°. Anal. Calc. for $C_{10}H_{14}NOClS$: C, 51.84; H, 6.04. Found: C, 51.96; H, 5.80. The residue from the distillation crystallized from methanol to yield bis(1-*p*-chlorobenzylmercapto-2-hydroxypropyl)amine melting at 97–100°. Anal. Calc. for $C_{20}H_{25}NO_2Cl_2S_2$: C, 53.81; H, 5.60. Found: C, 54.25, 53.85; H, 5.47, 5.31.

Can. J. Chem. Downloaded from www.nrcresearchpress.com by 190.90.36.8 on 09/04/12
For personal use only.

(*f*) *p-Chlorobenzyl 3-aminopropyl sulphide* (VII, $n = 3$, R = H) was prepared from *p*-chlorobenzyl 3-chloropropyl sulphide in 67% yield. It distilled as a colorless liquid with b.p. = 112–115° (0.5 mm); $n_D^{22} = 1.5754$. Anal. Calc. for $C_{10}H_{14}NClS$: C, 55.68; H, 6.49. Found: C, 54.91, 55.13; H, 6.47, 5.99.

(*g*) *n-Amyl 4-aminobutyl sulphide* was prepared from *n*-amyl 4-chlorobutyl sulphide in 42% yield. It distilled as a colorless liquid with b.p. = 112° (11 mm); $n_D^{23} = 1.4790$. Anal. Calc. for $C_9H_{21}NS$: C, 61.71; H, 12.00. Found: C, 60.99, 61.17; H, 11.91, 12.17.

(*h*) *n-Dodecyl 2-aminoethyl sulphide* was prepared from *n*-dodecyl 2-chloroethyl sulphide (18) in 50% yield. It distilled as a yellow liquid with b.p. = 120–123° (0.5 mm); $n_D^{23} = 1.4755$. Anal. Calc. for $C_{14}H_{31}NS$: C, 68.57; H, 12.65. Found: C, 68.56, 68.76; H, 12.21, 12.62.

(*i*) *β-p-t-Butylphenoxyethyl 2-aminoethyl sulphide* was prepared from *β-p-t*-butylphenoxyethyl 2-chloroethyl sulphide in 73% yield. It distilled as an almost colorless liquid with b.p. = 138–140° (0.5 mm); $n_D^{24} = 1.5400$. Anal. Calc. for $C_{14}H_{23}NOS$: C, 66.40; H, 9.09. Found: C, 66.44; H, 9.16.

REFERENCES

1. KULKA, M. Can. J. Chem. **36**, 750 (1958).
2. KULKA, M. Can. J. Chem. **34**, 1093 (1956).
3. BELL, E. V., BENNETT, G. M., and HOCK, A. L. J. Chem. Soc. 1803 (1927).
4. FUSON, R. C. and ZIEGLER, J. B. J. Org. Chem. **11**, 510 (1946).
5. MEADOW, J. R. and REID, E. E. J. Am. Chem. Soc. **56**, 2177 (1934).
6. KULKA, M. Can. J. Chem. **33**, 1442 (1955).
7. SCHERER, O. and FINK, K. German Pat. No. 845,511 (1952); Chem. Abstr. **47**, 5442 (1953).
8. FAITH, H. E. J. Am. Chem. Soc. **72**, 837 (1950).
9. KULKA, M. and VAN STRYK, F. Can. J. Chem. **35**, 519 (1957).
10. NAYLOR, R. F. J. Chem. Soc. 1106 (1947).
11. YUŘEV, Yu. K., PERVOVA, E. YA., and SAZONOVA, V. A. J. Gen. Chem. (U.S.S.R.) **9**, 590 (1939); Chem. Abstr. **33**, 7779 (1939).
12. BIRCH, S. F. and FIDLER, F. A. Brit. Pat. No. 654,464 (1951); Chem. Abstr. **46**, 3573 (1952).
13. BAKER, J. W. J. Chem. Soc. 1448 (1936).
14. FUSON, R. C., LIPSCOMB, R. D., MCKUSICK, B. C., and REED, L. J. J. Org. Chem. **11**, 513 (1946).
15. CLARKE, H. T. J. Chem. Soc. **101**, 1806 (1912).
16. JOHNSON, D. A. J. Chem. Soc. 1530 (1933).
17. PUMMERER, R. and SCHÖNAMSGRUBER, M. Ber. B, **72**, 1834 (1939).
18. FINKE, J. K. U.S. Pat. No. 2,598,640 (1952); Chem. Abstr. **47**, 2199 (1953).

Can. J. Chem, Downloaded from www.nrcresearchpress.com by 190.90.36.8 on 09/04/12
For personal use only.

Can. J. Chem. Downloaded from www.nrcresearchpress.com by 190.90.36.8 on 09/04/12
For personal use only.

THE STUDY OF HYDROGEN BONDING AND RELATED PHENOMENA BY ULTRAVIOLET LIGHT ABSORPTION

PART II. THE EFFECT OF SOLVENT–SOLUTE INTERACTIONS ON THE INTERMOLECULAR HYDROGEN BOND IN BENZOIC ACIDS[1]

W. F. Forbes and A. R. Knight

ABSTRACT

The concentration dependence of some electronic absorption bands, which has previously been ascribed to intermolecular hydrogen bonding, is reinvestigated. The concentration dependences are compared for a number of substituted benzoic acids in inert solvents, and in solvent mixtures containing various amounts of ether. The results are discussed in terms of current theories of hydrogen bonding.

INTRODUCTION

In Part I (1) of this series it was found convenient to classify environmental influences affecting ultraviolet absorption spectra as follows: (i) intermolecular hydrogen bonding acting between solute molecules only; (ii) intermolecular hydrogen bonding acting between solute and solvent molecules; and (iii) solvent–solute interactions which do not involve hydrogen bonding.

The first of these effects was shown in Part I to be qualitatively susceptible to spectral analysis, and the concentration dependence of the electronic spectra of benzoic acids in cyclohexane media was ascribed to intermolecular hydrogen bonding. The next aim was to obtain quantitative relations between absorption spectra and solution concentrations for these and other substituted benzoic acids. It was then found that a number of substituted benzoic acids were not sufficiently soluble in cyclohexane to permit the determination of the concentration dependence of their spectra, and ether had to be added in order to obtain solution. The characteristic concentration dependence was still obtained under these conditions, but the question arose whether addition of ether affects the dimeric hydrogen bond, or whether addition of small amounts of ether does not unduly disturb the spectral effect associated with the formation of the dimeric hydrogen bond. In order to decide, the spectra of a number of cyclohexane-soluble benzoic acids were determined in cyclohexane and in solvent mixtures containing various proportions of cyclohexane and ether.

EXPERIMENTAL

The ultraviolet absorption spectra were determined as previously described in this series (1). For each compound the concentration dependence was determined at least in duplicate. A considerable extension of the concentration range was achieved by using progressively more concentrated solutions in the solvent cell instead of pure solvents. By using solutions of biphenyl in cyclohexane, which do not show any appreciable concentration dependence, it was shown that this modification does not introduce any additional errors.* By extremely careful manipulation, ϵ_{max} values could be measured with a precision estimated to be $\pm 2\%$ or better, and the day-to-day reproducibility was also well within this margin. Results are listed in Figs. 2, 3, 4, and 5 where the vertical brackets indicate the $\pm 2\%$ reproducibility.

[1]*Manuscript received September 15, 1958.*
Contribution from the Memorial University of Newfoundland, St. John's, Newfoundland.
**We are indebted to Dr. O. H. Wheeler for suggesting this modification to us.*

Solvent mixtures were prepared by mixing together the corresponding volume percentages. The cyclohexane used was Fisher Certified Reagent, spectroanalyzed, and the ethyl ether used was Eastman white label, spectrograde. No evidence was found to indicate the presence of traces of acids or base in the solvents. The benzoic acids were purified by standard methods and carefully dried. Elemental analyses showed the absence of any appreciable amounts of water of crystallization in the benzoic acids. For example, *p*-toluic acid analyzed for C, 70.7% (calc. C, 70.6%), whereas $C_8H_8O_2.H_2O$ requires C, 62.3%.

THE EFFECT OF ADDITION OF ETHER ON THE O–H---O BOND IN BENZOIC ACID DIMERS

The absorption spectrum of benzoic acid in cyclohexane solution at different concentrations is shown in Fig. 1.

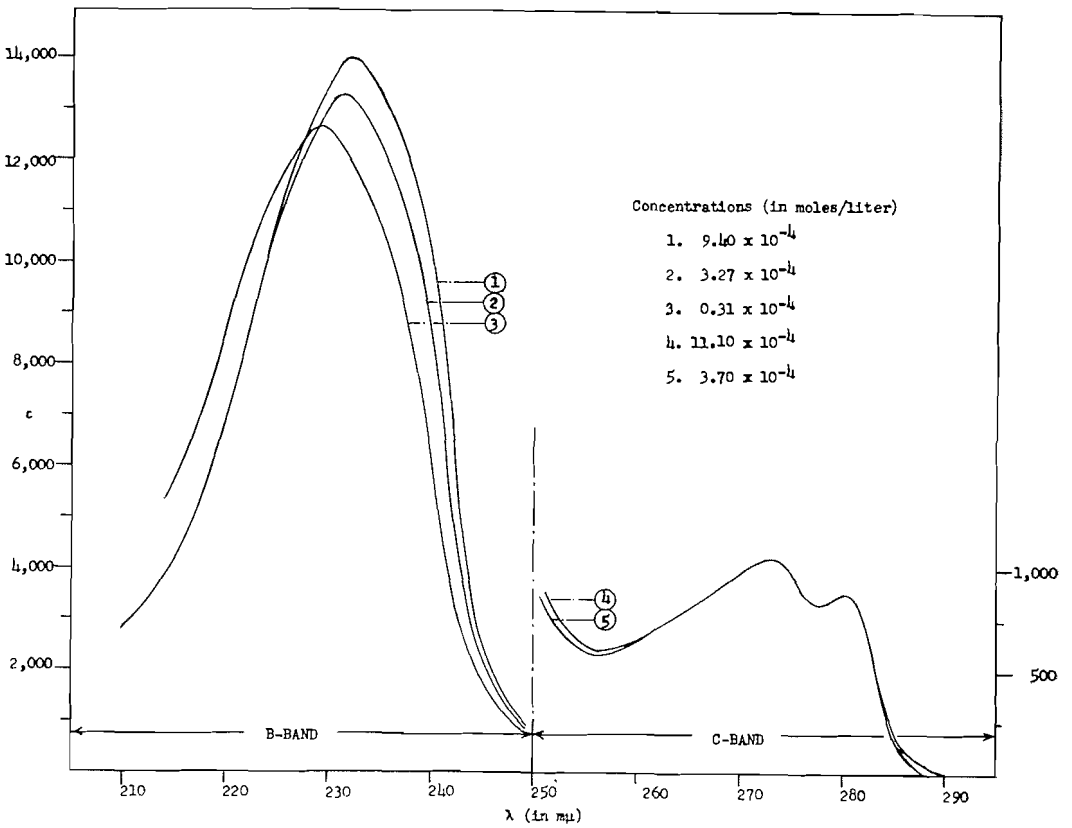

FIG. 1. The effect of concentration on the ultraviolet absorption spectrum of benzoic acid in cyclohexane solution. The description of the absorption bands as *B*- and *C*-bands follows the nomenclature adopted in Part I (1, cf. also ref. 2).

The following observations lead us to ascribe this concentration dependence to intermolecular hydrogen bonding between solute molecules, that is, to dimerization as shown in I:

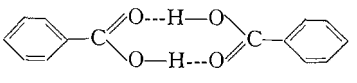

I

Can. J. Chem. Downloaded from www.nrcresearchpress.com by 190.90.36.8 on 09/04/12
For personal use only.

(i) A similar concentration dependence is not observed for a number of other molecules within the investigated concentration range (1).

(ii) The concentration dependence practically disappears for methyl benzoate (1, 3). Hence, the hydroxyl group is necessary.

(iii) The concentration dependence for benzoic acid relates with the supposed dimerization of benzoic acids at concentrations similar to those of the present investigation (cf. refs. 4, 5).

(iv) Addition of ether decreases the concentration dependence (see Figs. 2, 3, 4, and 5).

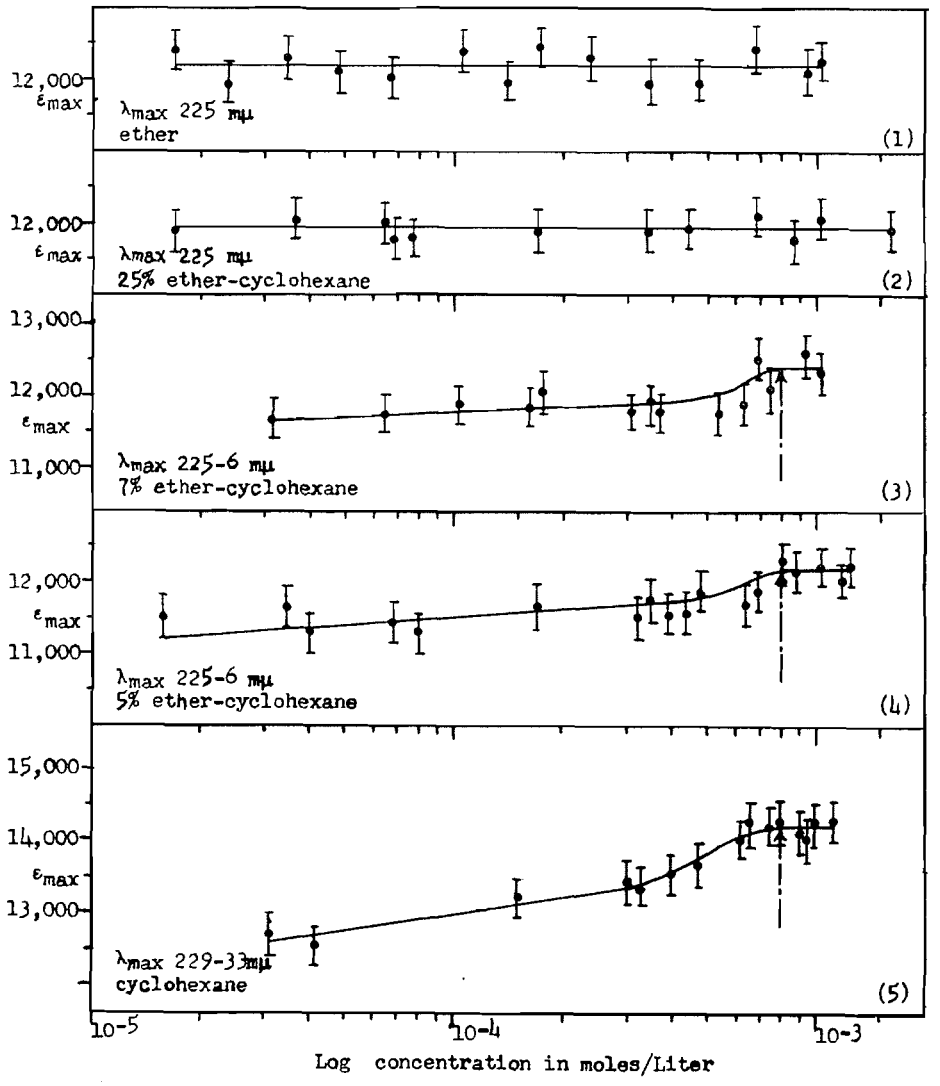

FIG. 2. The variation of ϵ_{max} on changing the concentration of acid for benzoic acid in (1) ether solution, (2) cyclohexane solution containing 25% ether, (3) cyclohexane solution containing 7% ether, (4) cyclohexane solution containing 5% ether, and (5) cyclohexane solution. In this and subsequent figures the lower λ_{max} value shown indicates the maximal wavelength at the smallest concentration, and the higher λ_{max} value indicates the maximal wavelength at the largest concentration. In this way, for example in Fig. 2 for benzoic acid in cyclohexane solution, λ_{max} 229 mμ represents the maximal wavelength for the most dilute solution.

Can. J. Chem. Downloaded from www.nrcresearchpress.com by 190.90.36.8 on 09/04/12
For personal use only.

Can. J. Chem. Downloaded from www.nrcresearchpress.com by 190.90.36.8 on 09/04/12
For personal use only.

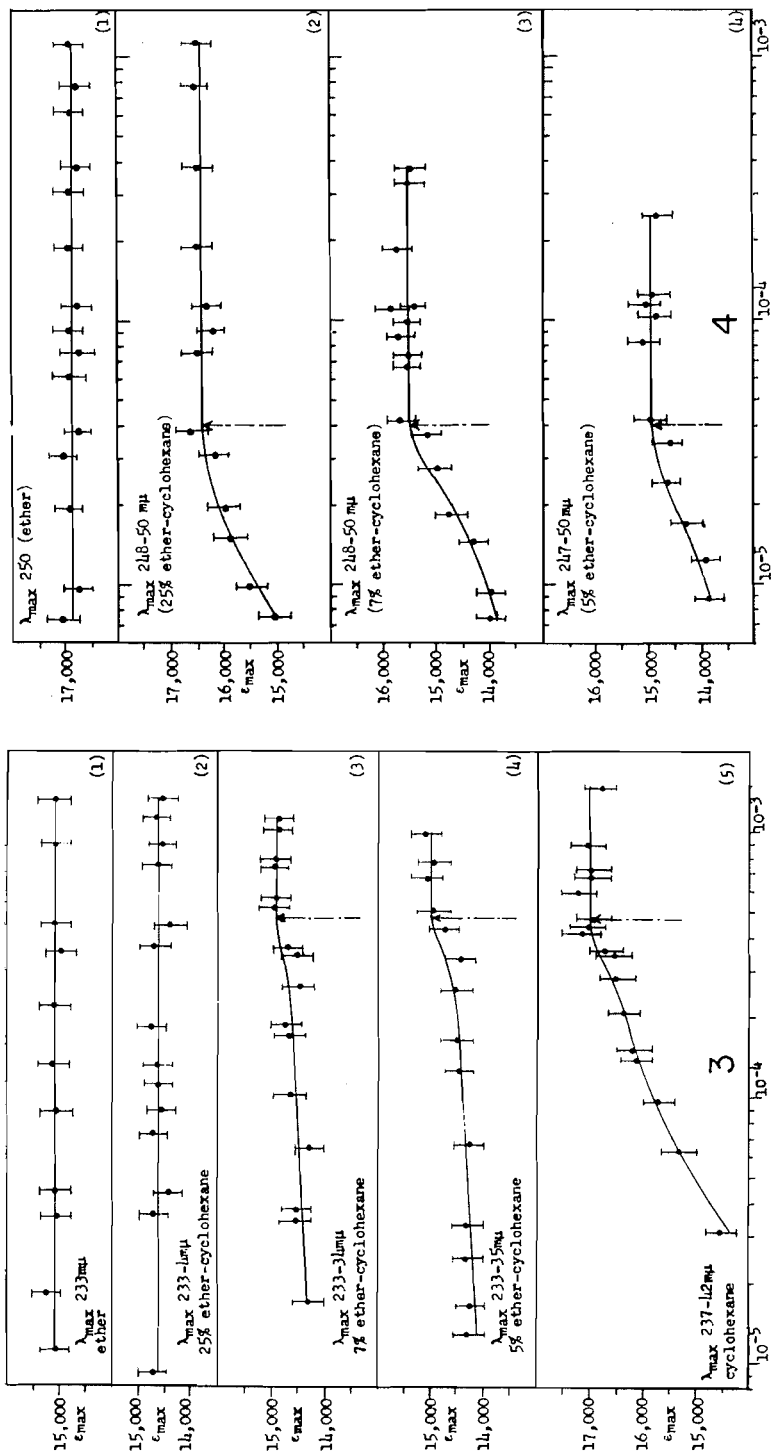

FIG. 3. The variation of ϵ_{max} on changing the concentration of acid for *p*-toluic acid in (1) ether solution, (2) cyclohexane solution containing 25% ether, (3) cyclohexane solution containing 7% ether, (4) cyclohexane solution containing 5% ether, and (5) cyclohexane solution.

FIG. 4. The variation of ϵ_{max} on changing the concentration of acid for *p*-hydroxybenzoic acid in (1) ether solution, (2) cyclohexane solution containing 25% ether, (3) cyclohexane solution containing 7% ether, and (4) cyclohexane solution containing 5% ether.

This indicates a competitive intermolecular hydrogen bonding, and hence indirectly suggests solute–solute hydrogen bonding as an explanation of the observed concentration dependence.

(v) Intramolecular hydrogen bonding in salicylic acid apparently reduces the strength of the dimeric hydrogen bond (cf. Figs. 2 and 5, and subsequent discussion). Since various forms of hydrogen bonding would be expected to compete with each other, this again indicates that association is responsible for the observed concentration dependence (cf. ref. 6).

Figure 1 also shows that the shape of both *B*- and *C*-bands remains approximately similar on changing the solute concentration; similar curves are also obtained for the substituted benzoic acids on changing the concentration. Consequently, maximal molecular extinction coefficients (ϵ_{max}) are used as a first approximation to measure the actual absorption intensities. Figure 2 shows the observed changes in ϵ_{max} with solute concentration for benzoic acid in cyclohexane solution and in various cyclohexane–ether solvent mixtures.

Figure 2 shows that it is possible to determine the concentration above which the values of ϵ_{max} become approximately independent of concentration changes. These values, as shown in Figs. 2, 3, 4, and 5 by vertical arrows, are assumed to represent the concentrations below which the particular benzoic acids exist appreciably in the monomeric form. Figure 2 also shows that in ether solution no concentration dependence is observed. On the other hand, in cyclohexane solution containing 5% of ether, a concentration dependence is observed, and generally, in solutions containing intermediate percentages of ether, intermediate concentration dependences are observed.

It also follows from the argument set out in the previous paragraph, that the *lower* the concentration at which a particular benzoic acid begins to exist appreciably in the monomeric form, the *stronger* will be the dimeric hydrogen bond. Figures 3 and 4 show

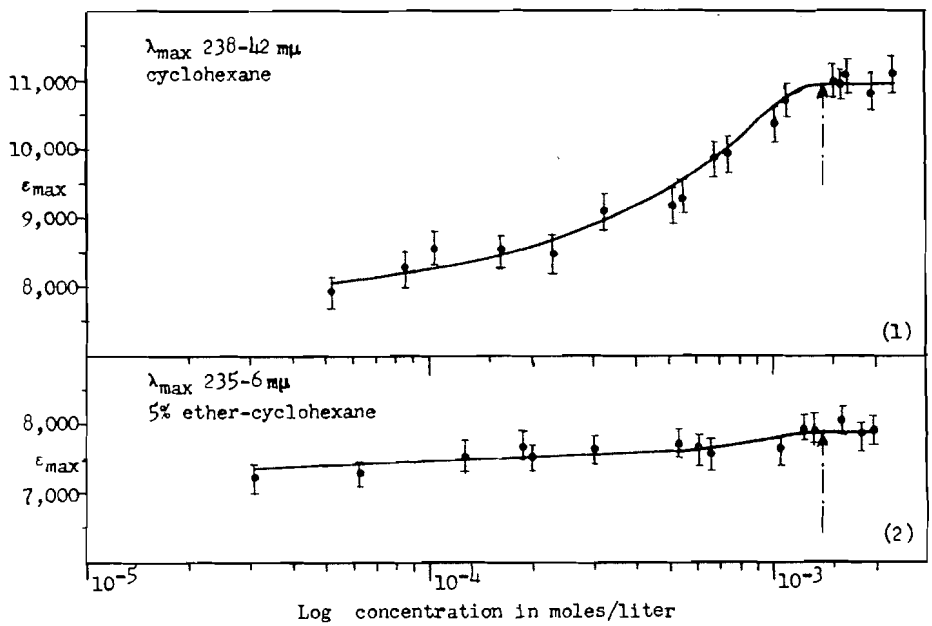

FIG. 5. The variation of ϵ_{max} on changing the concentration of acid for salicyclic acid in (1) cyclohexane, (2) cyclohexane solution containing 5% ether.

Can. J. Chem. Downloaded from www.nrcresearchpress.com by 190.90.36.8 on 09/04/12
For personal use only.

that a *p*-methyl- or a *p*-hydroxyl-group in benzoic acid apparently has this effect of strengthening the dimeric hydrogen bond, and the *p*-hydroxyl group appears to be more effective than the *p*-methyl group. Further, for *p*-hydroxybenzoic acid the concentration dependence, ascribed to intermolecular hydrogen bonding, is readily discernible in 25% ether (see Fig. 4), whereas for benzoic and *p*-toluic acid no concentration dependence could be observed under those conditions (see Figs. 2 and 3).

The effect of solute concentration on the maximal extinction coefficient of salicylic acid is shown in Fig. 5. Figure 5 indicates that the intramolecular hydrogen bond in salicylic acid decreases the strength of the dimeric hydrogen bond in this acid, compared with benzoic acid or *p*-hydroxybenzoic acid. On addition of 5% of ether to the solution of salicylic acid in cyclohexane the concentration dependence is only recognized with difficulty, whereas under similar conditions the concentration dependence in benzoic acid may readily be discerned (see Figs. 2 and 5).

DISCUSSION

Three conclusions may be reached from the data. First, the vertical arrows in Figs. 2, 3, 4, and 5, indicating the appearance of monomeric forms, occur at approximately the same concentration, irrespective of whether a small amount of ether has been added to the solvent or not. Hence in comparing the relative strengths of the dimeric hydrogen bond for substituted benzoic acids by this method, *the concentration dependence may be determined either in cyclohexane or in cyclohexane containing small amounts of ether.* This allows the extension of the comparison to benzoic acids which are only slightly soluble in cyclohexane; applications of this extension will be reported in Part III of this series.

Secondly, as expected (cf. ref. 4), for the four benzoic acids studied, *the dimeric hydrogen bond is stronger than any competing intermolecular hydrogen bonding occurring between benzoic acid and ether molecules.* This follows because if hydrogen-bonded forms of type II were to compete with dimeric forms of type I and if in addition the intermolecular

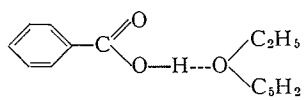

II

hydrogen bond in II were stronger than the bond in I, structures of type II would be formed preferentially. It would then be inconceivable that the very small amounts of benzoic acid present in cyclohexane solution, containing relatively large amounts of ether, would have the opportunity to dimerize to any appreciable extent. However, dimerization occurs, and hence the initial conclusion follows.

Notwithstanding the conclusion deduced in the previous paragraph, the spectra of the three benzoic acids in 100% ether are believed to correspond to the spectra of monomeric forms. We arrive at this conclusion thus: the absence of concentration dependence in 100% ether suggests that there is present predominantly only one molecular species of acid. At the same time, there is no evidence that, for example, in benzoic acid dimerization predominates below an acid concentration of *ca.* 8×10^{-4} moles/l. (see Fig. 2). Hence the absorption in the concentration region below 8×10^{-4} moles/l. can hardly correspond to dimer absorption, and consequently, since only one acid species is believed to be present, this is assumed to be a monomeric species. A satisfactory way to account for these two, apparently contradictory, observations—that is, that the dimeric hydrogen

Can. J. Chem. Downloaded from www.nrcresearchpress.com by 190.90.36.8 on 09/04/12
For personal use only.

bond is stronger than the ether – benzoic acid linkage while at the same time the observed spectra are frequently ascribed to ether – benzoic acid hydrogen-bonded complexes—is to postulate that *neither the dimeric hydrogen bond between benzoic acid molecules nor the intermolecular hydrogen bond between acid and ether molecules represents a stable hydrogen-bonded complex under the conditions of the experiment.* That is, it is assumed that both intermolecular bonds are continuously formed, broken, and re-formed; and the characteristic spectral effect, ascribed to intermolecular hydrogen bonding, will only be observed if bond formation occurs sufficiently often or if the bond formed is sufficiently strong. According to this view benzoic acid molecules, in solution containing large amounts of ether, are sufficiently surrounded by ether molecules so that the spectral effect, ascribed to dimerization, is no longer observed. According to this view also, a stronger dimeric hydrogen bond, as has been postulated in *p*-hydroxybenzoic acid compared with benzoic acid, would be anticipated to require a greater ether concentration to obscure the concentration dependence ascribed to dimerization; whereas a weaker dimeric hydrogen bond, as has been postulated in salicylic acid, would be anticipated to require a smaller ether concentration to achieve the same effect. That these predictions are borne out is indicated from Figs. 2, 4, and 5. Finally, the hypothesis receives indirect support from the work of Coggeshall and Lang (7), who showed the absence of spectral changes for solutions of phenol or aniline at different temperatures, although the temperature change was quite adequate to destroy any hydrogen-bonded complexes. They conclude that for these compounds spectral differences between solutions in polar and non-polar solvents do not depend on stable hydrogen-bonded complexes.

ACKNOWLEDGMENTS

The authors are pleased to acknowledge the assistance of Miss V. M. Walsh and Mr. J. F. Templeton in some of the preliminary work, and they are indebted to Mr. J. C. Dearden for a number of valuable discussions.

The major part of this work was carried out under a contract between the Fisheries Research Board of Canada and the Memorial University of Newfoundland. Preliminary studies were supported from grants of the National Research Council of Canada and the Research Corporation of New York.

REFERENCES

1. FORBES, W. F. and TEMPLETON, J. F. Can. J. Chem. **36**, 180 (1958).
2. FORBES, W. F., MUELLER, W. A., RALPH, A. S., and TEMPLETON, J. F. Can. J. Chem. **35**, 1049 (1957).
3. UNGNADE, H. E. and LAMB, R. W. J. Am. Chem. Soc. **74**, 3789 (1952).
4. JONES, R. N. and SANDORFY, C. *In* Chemical applications of spectroscopy. *Edited by* W. West. Interscience Publishers, Inc., New York. 1956. p. 426.
5. BANEWICZ, J. J., REED, C. W., and LEVITCH, M. E. J. Am. Chem. Soc. **79**, 2693 (1957).
6. SIMOVA, P. D. and SKORCHEV, B. Izvest. Bulgar. Akad. Nauk., Otdel. Fiz.-Mat. i Tekh. Nauki Ser. Fiz. **4**, 47 (1954); Chem. Abstr. **50**, 6923 (1956).
7. COGGESHALL, N. D. and LANG, E. M. J. Am. Chem. Soc. **70**, 3283 (1948).

Can. J. Chem. Downloaded from www.nrcresearchpress.com by 190.90.36.8 on 09/04/12
For personal use only.

THE QUENCHING OF POTASSIUM RESONANCE RADIATION BY HYDROCARBONS[1]

E. A. CHERNIAK[2] AND W. M. SMITH

ABSTRACT

The quenching of the resonance radiation of potassium by some unsaturated and saturated hydrocarbons has been examined at 67° C. The behavior was found to be almost identical with that previously observed with sodium, the saturated hydrocarbons quenching to a negligible extent, the unsaturated hydrocarbons exhibiting cross sections with potassium not significantly different from those exhibited towards sodium.

INTRODUCTION

An examination of the quenching of excited potassium ($4^2P \rightarrow 4^2S$) by hydrogen and deuterium was described in an earlier publication (1). We report here on an extension of the measurements to quenching by some saturated and unsaturated hydrocarbons, work undertaken with a view to obtaining information about the comparative behavior of the various excited alkali metals.

METHOD

The method used to measure the cross sections for the quenching process was the same as that described before (1) except that pyrex resonance vessels were used during all measurements. The features of the method are as follows. Potassium atoms in the 4^2P state are produced at constant rate by irradiation of potassium vapor in a resonance vessel by a filtered beam from a G.E. K-1 lamp. The intensity of the "resonance radiation" (due to return of the excited atoms to the 4^2S state) is estimated in the presence and in the absence of quenching gas. The ratio of these intensities is known as the quenching ratio Q and its values for various pressures of quenching gas are the primary data from which a cross section σ^2 may be estimated (1). Also required is the mean life of a 4^2P potassium atom, and we have taken Stephenson's value 2.71×10^{-8} seconds (2). All measurements were made at $66.7 \pm 0.4°$ C.

MATERIALS

Potassium was purified and introduced into the quenching vessels in the manner described previously (1).

Methane was prepared by the reduction of ethanolic methyl iodide by a zinc–copper couple (3). The gas was passed through fuming sulphuric acid, and potassium hydroxide solution, and was collected for intermediate storage over water in an aspirator bottle. This gas was then passed through a dry-ice trap, fractionally distilled with the aid of liquid air, and dried over potassium before final storage.

Propane was Phillips Research Grade hydrocarbon.

Ethene was from two sources. One sample was Matheson C.P. grade. The other was made by dehydrating ethanol with freshly prepared pyrophosphoric acid (4). The impure ethene was then dried and fractionally distilled as was the methane.

The butenes were Phillips Research Grade hydrocarbons.

[1]*Manuscript received September 26, 1958.*
Contribution from the Department of Chemistry, Queen's University, Kingston, Ontario.
[2]*Holder of a National Research Council Bursary, 1955–56. Present address: Department of Chemistry, University of Leeds, England.*

Can. J. Chem. Downloaded from www.nrcresearchpress.com by 190.90.36.8 on 09/04/12
For personal use only.

RESULTS

It was found that the unsaturated hydrocarbons quench strongly, and that the saturated hydrocarbons quench to an almost negligible extent. Data for the unsaturated hydrocarbons are summarized in Figs. 1 and 2 as plots of $1/Q$ against pressure. These data are in reasonable accord with the Stern-Volmer relation (a linear relation between $1/Q$ and pressure). On the other hand, the saturated hydrocarbons methane and propane led to a significant increase rather than a decrease in the intensity of the resonance radiation. At a pressure of 5 mm of mercury the quenching ratios were 1.03 and 1.10 respectively. Apparently these gases were leading to an increase in the rate of production

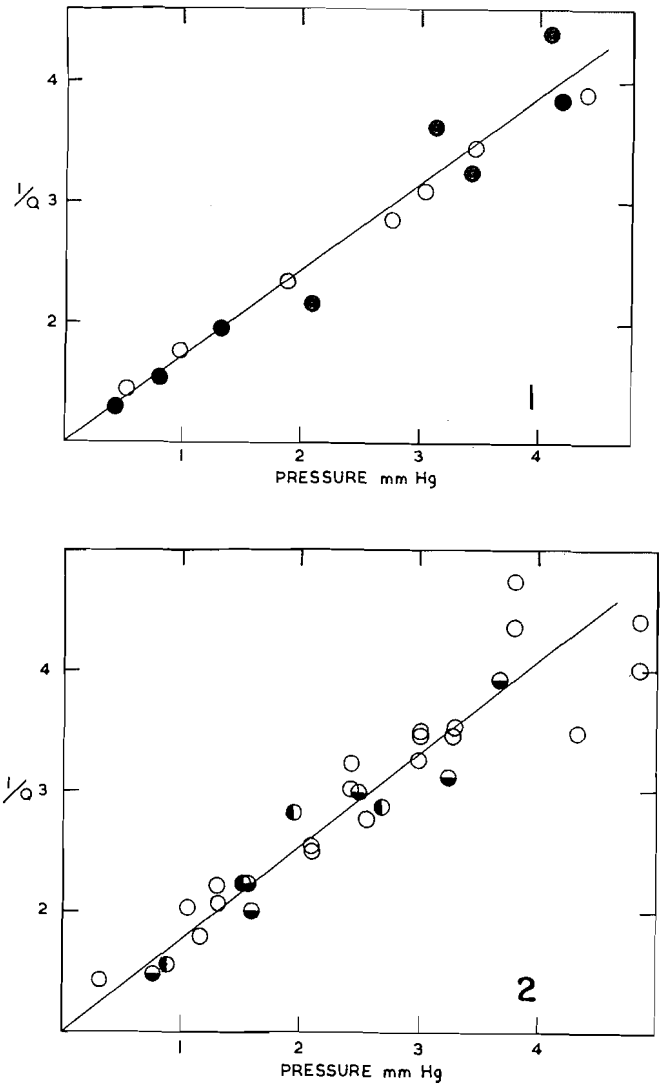

FIG. 1. Plot of $1/Q$ against pressure of ethene.
● Ethene from ethanol. ○ Ethene (Matheson C.P.).
FIG. 2. Plot of $1/Q$ against pressure for the butenes.
○ Butene-1. ◒ *trans*-Butene-2. ◐ *cis*-Butene-2.

Can. J. Chem. Downloaded from www.nrcresearchpress.com by 190.90.36.8 on 09/04/12
For personal use only.

of excited potassium atoms, probably through broadening of the absorption line of the potassium vapor. It is not possible to estimate quenching cross sections for methane and propane from these data, but they must be very small.

Cross sections (σ^2) for quenching by the unsaturated hydrocarbons estimated from the data summarized in Figs. 1 and 2 are given in Table I, along with previously reported values for the quenching of excited potassium by hydrogen (1), and the quenching of excited sodium (5) by all those substances whose behavior with potassium are recorded.

TABLE I

Quenching cross sections ($cm^2 \times 10^{16}$)

Gas	With potassium	With sodium
Ethene	44	44[a]
Butene-1	57	58[a]
cis-Butene-2	57	
trans-Butene-2	57	58[a]
Hydrogen	1.56[b]	7.4[a]

[a]From ref. 5.
[b]From ref. 1.

The cross sections were estimated from values of the slopes of the plots of $1/Q$ against pressure, the effects of added gas on the rate of production of excited atoms being ignored. We do not have data which would enable corrections to be made for this effect, but the fact that methane and propane do apparently increase the absorption suggests that the true values of $1/Q$ and σ^2 for the unsaturated hydrocarbons may be a little greater than recorded in the table. The data for the different butenes have been grouped together in determining a single slope and a single cross section.

DISCUSSION

The hydrocarbons which were investigated exhibit quenching characteristics towards excited potassium (4^2P) which are almost identical with those exhibited by the same gases towards sodium (3^2P) in spite of the difference in the excitation energies of the two metals. On the other hand hydrogen was previously found to exhibit significantly different behavior with the two metals (1).

The data for the saturated and unsaturated hydrocarbons indicate that it is the unsaturated center which is decisive in controlling quenching efficiency. As has been pointed out by Laidler (6) there is no excited singlet level in the alkenes low enough to be excited by either alkali atoms in the ^2P state. It follows that the electronic state of the hydrocarbons does not change in a quenching encounter, and that the electronic excitation energy of potassium is transferred directly into vibrational and rotational.

Theories developed by Laidler (7) and Magee and Ri (8) for processes involving degradation of electronic excitation energy of the excited alkali metals to vibrational and translational suggest that quenching occurs with high cross section only when the excited atom, and quenching molecule, are held in association for periods much in excess of the time of a normal collision, the magnitude of the quenching cross section depending on the probability of change of electronic state during the lifetime of the complex as well as on the cross section for complex formation. No attempt was made to estimate the probability of change of electronic state, and it was assumed that it approached unity unless the rotational energy was unduly high. Magee and Ri's treatment of quenching

Can. J. Chem. Downloaded from www.nrcresearchpress.com by 190.90.36.8 on 09/04/12
For personal use only.

of the excited alkali metals by hydrogen led to such a picture, and also to the prediction that potassium would be quenched by hydrogen less effectively than sodium, essentially because the smaller stability of the complex involving potassium implied a smaller cross section for the association reaction yielding the complex.

The large values of the quenching cross sections for processes involving the alkenes suggest that the probability of change in electronic state approaches unity, and along with the nearly identical values exhibited by a given alkene with both alkali metals, could be taken to imply that the interactions leading to complex formation are very similar. However, cross sections for complex formation considerably in excess of the values implied by atomic radii appear possible, particularly where there are strong ionic contributions to the interaction and it may be that the cross sections for complex formation are somewhat greater than the admittedly large values noted for quenching and that the probabilities of electronic transition are appreciably less than unity. If this were so, the increase in quenching cross sections with increasing molecular weight of the alkene might be due in part to an associated increase in the probability of electronic transition during the lifetime of the complex. It would be enlightening in this connection to have independent means, experimental or theoretical, for estimating the cross sections for complex formation between the alkenes and excited alkali metals in the gas phase.

ACKNOWLEDGMENT

This work was supported by a grant from the Committee on Scientific Research of Queen's University.

REFERENCES

1. SMITH, W. M., STEWART, J. A., and TAYLOR, G. W. Can. J. Chem. **32**, 961 (1954).
2. STEPHENSON, G. Nature, **167**, 112 (1951).
3. GLADSTONE, J. H. and TRIBE, A. J. Chem. Soc. **45**, 154 (1884).
4. MICHELS, A., DE GRUYTER, J., and NIELSON, F. Physica, **III**, 346 (1936).
5. NORRISH, R. G. W. and SMITH, W. M. Proc. Roy. Soc. (London), A, **176**, 295 (1940).
6. LAIDLER, K. J. The chemical kinetics of excited states. Oxford University Press. 1955. p. 104.
7. LAIDLER, K. J. J. Chem. Phys. **10**, 34 (1942).
8. MAGEE, J. L. and RI, T. J. Chem. Phys. **9**, 638 (1941).

Can. J. Chem. Downloaded from www.nrcresearchpress.com by 190.90.36.8 on 09/04/12
For personal use only.

Can. J. Chem. Downloaded from www.nrcresearchpress.com by 190.90.36.8 on 09/04/12
For personal use only.

BROMINATION OF STEROID 20-KETALS[1]

ARTHUR A. AMOS AND P. ZIEGLER

ABSTRACT

Bromination of 3α,12α-diacetoxypregnan-20-one ethylene ketal provided in good yield the corresponding 21-monobromo compound. This product, on acid hydrolysis and subsequent acetolysis, gave the known 3α,12α,21-triacetoxypregnan-20-one. Acid hydrolysis of the bromoketal, followed by Faworsky rearrangement, led to 3α,12α-diacetoxy-17α-methyletiocholanic acid methyl ester.

In order to prepare 11-keto steroids from the readily available 3α,12α-diacetoxypregnan-20-one (I*b*), it had been planned to apply the elegant Glaxo procedure (1, 2) to 3α-acetoxy-12,20-diketopregnane 20-ethylene ketal (VIII*b*), obtained from I. However, when VIII*b* was treated with varying amounts of bromine in methylene chloride at low temperature and in the presence of calcium oxide, the reaction products consisted of mixtures of brominated 20-keto steroids. At no time could VIII*b* be brominated exclusively at C-11; it was apparent that, during the reactions, the ketal group was removed and that bromine also had been substituted at C-17 and/or C-21. It had been observed before (3) that 3β-acetoxy-12,20-diketoallopregnane 12-ethylene ketal could be brominated at C-17, but only with simultaneous hydrolysis of the 12-ketal group. As will be seen later on, 3α,12α-diacetoxypregnan-20-one ethylene ketal (II*b*) could be brominated, under the same conditions as described above, to the corresponding 21-bromoketal (III); this reaction had no effect on the ketal group which remained intact. It is therefore assumed that α-monobromination of the ketal II*b* proceeded by a free radical mechanism during which the substitution of bromine at C-21 and the formation of hydrogen bromide took place without preliminary or concurrent formation of hydrogen ions. The hydrogen bromide did not dissociate rapidly in methylene chloride and the protons that did form were immediately taken up by the calcium oxide. On the other hand, α-brominations of ketones proceed via the enol form of the ketone by an ionic mechanism, during which protons as such are believed to be transferred. In the bromination of VIII*b*, enolization of the 12-keto group and subsequent bromination at C-11 probably produced hydrogen ions in proximity of the 20-ketal group, which then rapidly decomposed. The liberated 20-keto steroid then reacted with more bromine at C-17 and C-21.

Very little information is available on the bromination of ketals. Sapogenins react with bromine in the spiroketal side chain at C-23 giving compounds in which the bromine atom is in the α-position to the potential carbonyl group (4). Similarly, aliphatic acetals react with bromine (5, 6, 7) or N-bromosuccinimide (8) to yield the corresponding α-bromoacetals. An indication that steroidal 3-ketals react with bromine at C-4 has been reported (9). When 3α,12α-diacetoxypregnan-20-one ethylene ketal (II*b*) was brominated, only 1 mole of bromine was taken up, and there was obtained 70–80% of a crystalline monobromo derivative. This compound did not exhibit a ketone band in the ultraviolet region, and it was therefore assumed that the 20-ketal structure had remained unchanged during bromination; elemental analyses indicated structure III or the corresponding 17-bromo isomer. The latter formulation was at first preferred mainly because the reaction of 3α,12α-diacetoxypregnan-20-one (I*b*) with 1 mole of bromine has been reported (10) to provide predominantly the 17-bromo derivative of I*b*. This is in agreement with other

[1]*Manuscript received September 8, 1958.*
Contribution from the Research and Development Laboratories of Canada Packers Ltd., Toronto, Ontario.

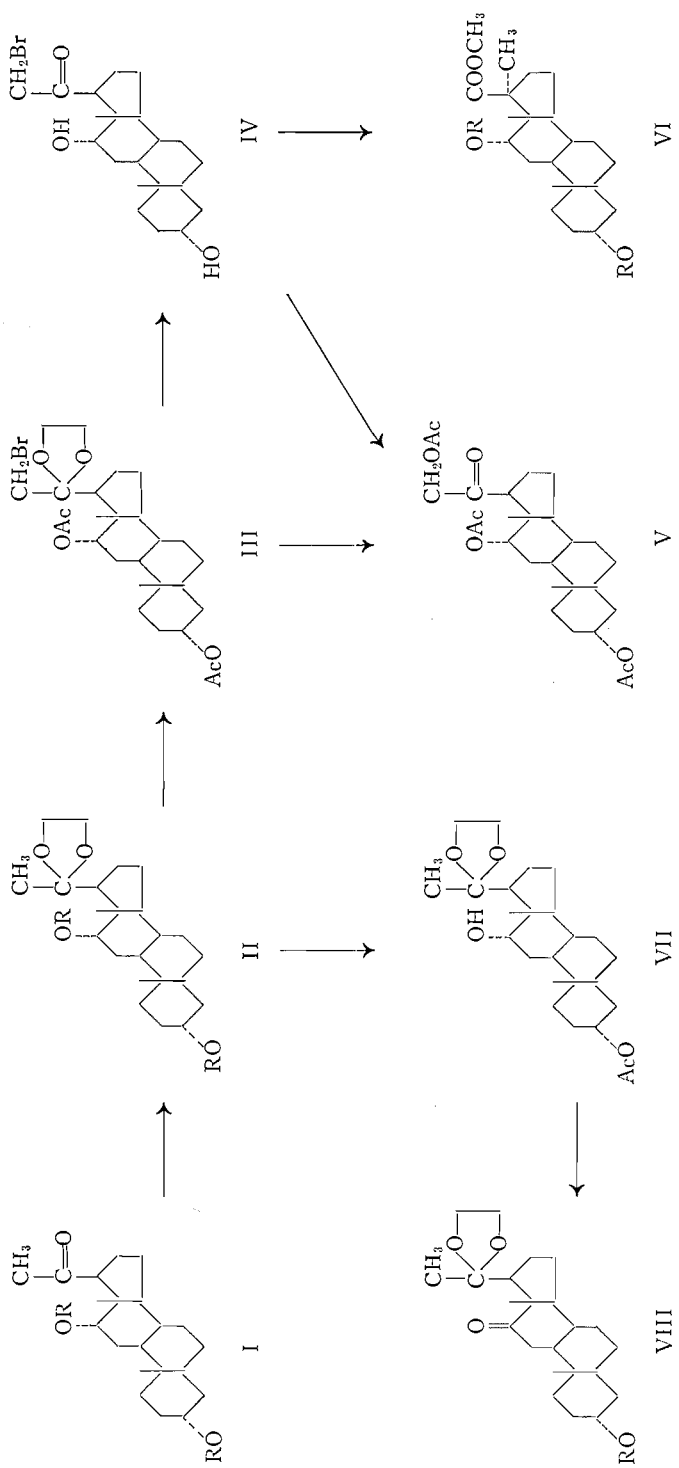

Can. J. Chem. Downloaded from www.nrcresearchpress.com by 190.90.36.8 on 09/04/12
For personal use only.

Can. J. Chem. Downloaded from www.nrcresearchpress.com by 190.90.36.8 on 09/04/12
For personal use only.

data (11, 12) which indicate that 20-keto steroids with equimolar amounts of bromine provide the related 17-bromo compounds. The bromoketal III was then found to yield, after treatment with 80% acetic acid and subsequent acetolysis, the known (13) 3α,12α,21-triacetoxypregnan-20-one (V); this clearly proved that the bromine atom in III was attached to C-21, and that compounds I*b* and II*b* react in a different manner towards bromine.

The bromoketal III was then converted quantitatively, by vigorous acid hydrolysis, to the bromoketone IV; carbon and hydrogen analyses for this compound did not correspond to the assigned empirical formula, a finding which had been made previously (13) when IV was obtained by an entirely different route. This discrepancy was ascribed to partial decompositon during recrystallization. The identity of IV was verified by its conversion to V by acetolysis and acetylation. As expected, the bromoketone IV underwent a Faworsky rearrangement upon mild alkaline treatment to afford, after acetylation, the known (10, 14) methyl 3α,12α-diacetoxy-17α-methyletiocholanate (VI*b*). This type of rearrangement has been described both in the case of 17- and 21-halogenated 20-keto steroids (15).

Preliminary results show that ketals, closely related to II*b* but which lack the 12α-acetoxy group, cannot be monobrominated at C-21 in good yield. Thus 3α-acetoxypregnan-20-one ethylene ketal with equimolar amounts of bromine yields a dibromoketal of as yet unknown constitution.

EXPERIMENTAL*

3α,12α-Diacetoxypregnan-20-one Ethylene Ketal (II*b*)

Compound I*b* (10 g) and *p*-toluenesulphonic acid (0.25 g), dissolved in a mixture of dry benzene (150 ml) and ethylene glycol (20 ml), were stirred and refluxed for 16 hours. During this time 1.05 ml of water was collected in a Dean-Stark trap. The reaction mixture was then neutralized by addition of sodium bicarbonate (2.2 g), the solvents were evaporated *in vacuo*, and the residue was taken up in water and ether. The ether extract, after being washed with water, dried over sodium sulphate, and evaporated, provided the crude products (10.8 g) which crystallized readily from methanol to yield 8.75 g (80%) of crystals, m.p. 141–142°. One crystallization from ether–hexane and three from methanol gave pure II*b*, m.p. 145–146° and $[\alpha]_D^{25}$ +124.2° (*c*, 0.512, ethanol). Anal. Calc. for $C_{27}H_{42}O_6$: C, 70.09; H, 9.15; O, 20.77. Found: C, 69.79; H, 9.21; O, 21.00.

3α,12α-Dihydroxypregnan-20-one Ethylene Ketal (II*a*)

The diacetoxyketal II*b* (10 g) was saponified by refluxing for 17 hours with potassium hydroxide (10 g), water (5 ml), and ethanol (95 ml). The solution was cooled to 20°, poured into water (600 ml), and the gummy mixture was stirred for ½ hour. The solid was then filtered off, washed with water, and dried to yield 8.05 g (98.5%) of product, m.p. 157–158°. After three recrystallizations from ether, this material had m.p. 157–159° but did not give satisfactory elemental analyses. It was dissolved in benzene, the solvent was distilled off, and the residue was crystallized twice from ether–iso-octane to give m.p. 146.5–148° and $[\alpha]_D^{25}$ +82.8° (*c*, 0.528, ethanol). Anal. Calc. for $C_{23}H_{38}O_4$: C, 72.97; H, 10.12. Found: C, 73.19, 73.10; H, 10.36, 10.28.

3α-Acetoxy-12α-hydroxypregnan-20-one Ethylene Ketal (VII)

Compound II*a* (2 g) was acetylated at 25° with pyridine (1.35 ml) and acetic anhydride (0.81 ml). After 20 hours the solution was diluted with water and ether, the solvent

**Microanalyses were kindly performed by Mr. E. Thommen, Basel, Switzerland.*

extract was washed several times with water, dried, and evaporated. The residue (2.4 g) crystallized from ether–hexane to provide 1.55 g (70%) of product, m.p. 154–156°. Three recrystallizations from methanol gave pure VII, m.p. 163–164° and $[\alpha]_D^{25}$ +72° (*c*, 0.541, ethanol). Anal. Calc. for $C_{25}H_{40}O_5$: C, 71.39; H, 9.59; O, 19.02. Found: C, 71.46; H, 9.74; O, 19.22.

3α-Acetoxy-12,20-diketopregnane 20-Ethylene Ketal (VIII*b*)

Compound VII (3 g) in *t*-butanol (45 ml) and pyridine (1.35 ml) was oxidized with N-bromosuccinimide (2.47 g) at 20° under constant stirring. After 6 hours the orange-red solution was poured into water (200 ml), the mixture was stirred briefly, then refrigerated overnight. The solid was filtered off, washed with dilute sodium sulphite solution and then with water. The dry material (3 g), m.p. 195–200°, was crystallized first from ethyl acetate, then from ether to afford VIII*b*, m.p. 226–228° and $[\alpha]_D^{25}$ +111.8° (*c*, 0.214, ethanol). Anal. Calc. for $C_{25}H_{38}O_5$: C, 71.73; H, 9.15; O, 19.11. Found: C, 71.85, 71.92; H, 9.35, 9.27; O, 19.02.

3α-Hydroxy-12,20-diketopregnane 20-Ethylene Ketal (VIII*a*)

Saponification of VIII*b* by refluxing with methanolic potassium hydroxide and subsequent isolation by precipitation with water, afforded quantitatively crude VIII*a*, m.p. 166–168°. Several recrystallizations from ethyl acetate gave the analytical specimen, m.p. 171–172° and $[\alpha]_D^{25}$ +105.5° (*c*, 0.679, ethanol). Anal. Calc. for $C_{23}H_{36}O_4$: C, 73.36; H, 9.64. Found: C, 73.30, 73.40; H, 9.81, 9.78.

Bromination of 3α-Acetoxy-12,20-diketopregnane 20-Ethylene Ketal (VIII*b*)

The reactions were carried out in methylene chloride at 0° to −10° in the presence of calcium oxide. With stirring, 1–4 molar equivalents of bromine was added within 10–20 minutes, whereupon the mixtures were poured into dilute sodium bicarbonate solution. The organic solvent extracts were then washed with water, dried, and evaporated to a residue.

Using 1, 2.4, 3, or 4 molar equivalents of bromine and resorting to fractional crystallization of the crude reaction products, two compounds could be isolated. The first of these had m.p. 210–213° (decomp.), $[\alpha]_D^{25}$ −19.1° (*c*, 0.404, chloroform), and contained 42.64% C, 4.31% H, and 42.6% Br. On refluxing with 80% acetic acid, the material remained unchanged which indicated that the ketal group was hydrolyzed during bromination. The same product, having m.p. 212–215° (decomp.) and $[\alpha]_D^{25}$ −19.2° (*c*, 0.414, chloroform), was also obtained when 3α-acetoxypregnan-12,20-dione was brominated under similar conditions. The second compound, isolated in only small amounts, had m.p. 200–202° (decomp.) and $[\alpha]_D^{25}$ −31.8° (*c*, 0.432, chloroform). Since monobromination of VIII*b* at C-11 could not be effected, these experiments were discontinued.

3α,12α-Diacetoxy-21-bromopregnan-20-one Ethylene Ketal (III)

To a solution of II*b* (10 g) in methylene chloride (170 ml) there was added calcium oxide (4.35 g), and the mixture was cooled to −10°. With constant stirring, a solution of bromine (4.66 g; 1.34 molar equivalents) in methylene chloride (30 ml) was added dropwise and, after ½ hour, the red mixture was poured into water (150 ml) containing sodium bicarbonate (8 g). The organic solvent extract was washed with sodium thiosulphate solution, then with water, dried over sodium sulphate, and evaporated. Crystallization of the residue (12.6 g) from aqueous methanol provided 8.2 g (74%) of product, m.p. 138–140°. Repeated recrystallization from methanol gave pure III, m.p. 145–147° and $[\alpha]_D^{25}$ +100.7° (*c*, 0.35, ethanol). Anal. Calc. for $C_{27}H_{41}O_6Br$: C, 59.88; H, 7.63; Br, 14.76. Found: C, 59.91, 59.78; H, 7.60, 7.71; Br, 14.80.

Can. J. Chem. Downloaded from www.nrcresearchpress.com by 190.90.36.8 on 09/04/12
For personal use only.

3α,12α-Dihydroxy-21-bromopregnan-20-one (IV)

Compound III (6 g) was refluxed for 1¼ hours with methanol (60 ml) and concentrated hydrochloric acid (3 ml). Dilution with water (100 ml) produced a precipitate which was filtered off, washed with water, and dried; the solid (4 g; 94%), m.p. 147–150°, was crystallized once from aqueous methanol and twice from ether to afford a sample for analysis, m.p. 147–150°, $[\alpha]_D^{25}$ +151° (*c*, 0.284, chloroform). Anal. Calc. for $C_{21}H_{33}O_3Br$: C, 61.01; H, 8.05. Found: C, 64.74, 64.43; H, 8.56, 8.88. This compound has been reported (13) to have m.p. 148–150°, $[\alpha]_D^{25}$ +148.5° (*c*, 0.793, chloroform), and giving the following analyses: C, 64.57; H, 8.85; Br, 17.54.

3α,12α,21-Triacetoxypregnan-20-one (V)

(*a*) *From* III.—The bromoketal III (2.5 g) was heated on the steam bath for 2¼ hours with 80% acetic acid (65 ml) in order to hydrolyze the ketal grouping. After addition of water, the products were extracted with ether, the ether extract was washed with dilute sodium bicarbonate and then with water. The residue (2.3 g) from evaporation of solvent was refluxed for 16 hours with potassium acetate (9.2 g), potassium iodide (35 mg), acetic acid (1.4 ml), and acetone (138 ml). After the mixture had been cooled the salts were filtered off, the filtrate was evaporated to a small volume, and the residue was taken up in ether and water. From the ether extract a gum (2.3 g) was obtained, which crystallized from ether–hexane to yield 0.89 g of material, m.p. 143–148°. Four recrystallizations gave pure V, m.p. 151–152° and $[\alpha]_D^{25}$ +151.7° (*c*, 0.23, acetone). Anal. Calc. for $C_{27}H_{40}O_7$: C, 68.04; H, 8.46. Found: C, 68.16, 68.24; H, 8.33, 8.37. This compound was reported (13) to have m.p. 153–153.5° and $[\alpha]_D^{25}$ +159.5° (*c*, 1.03, acetone).

(*b*) *From* IV.—Compound IV (100 mg) was refluxed for 17 hours with freshly fused potassium acetate (200 mg), potassium iodide (5 mg), acetic acid (0.25 ml), and acetone (10 ml). The cooled solution was diluted with water, extracted with ether, and the solvent extract was washed and dried. Acetylation of the residue (90 mg) with pyridine (2.5 ml) and acetic anhydride (5 ml) at 25° for 18 hours, followed by solvent extraction of the products and working up in the usual manner, yielded a gum which crystallized from ether–hexane. There was obtained 81 mg (71.5%) of V, m.p. 148–152°, giving no depression in melting point on admixture with a sample of V obtained in the previous experiment.

3α,12α-Diacetoxy-17α-methyletiocholanic Acid Methyl Ester (VI*b*)

Compound IV (1 g) was dissolved in methanol (75 ml), a solution of sodium hydroxide (0.8 g) in water (25 ml) was added, and the resulting solution was kept at 25° for 20 hours. After neutralization of the alkali with acetic acid (1.2 ml), most of the methanol was evaporated, and the products were taken up in ether and water. The solvent extract, after having been washed with water, dried, and evaporated, provided a residue (0.95 g); this was acetylated at 20° with pyridine (2.5 ml) and acetic anhydride (5 ml) to afford, subsequent to the usual work-up, 1.08 g of material which failed to crystallize. Chromatography on alumina finally yielded 0.15 g of crystals, m.p. 160–162°, eluted from the column with benzene–hexane (2:3 and 3:2). One recrystallization from hexane gave pure VI*b*, m.p. 163–164° and $[\alpha]_D^{25}$ +121.9° (*c*, 0.305, chloroform). This compound has been reported (10, 14) to have m.p. 161–161.5°, 163–165°, and $[\alpha]_D^{25}$ +117.4° (*c*, 0.78, chloroform).

3α,12α-Dihydroxy-17α-methyletiocholanic Acid Methyl Ester (VI*a*)

Saponification of VI*b* (100 mg) with 5% methanolic potassium hydroxide (10 ml) for 4 hours at reflux temperature and precipitation of the product by addition of water

Can. J. Chem. Downloaded from www.nrcresearchpress.com by 190.90.36.8 on 09/04/12
For personal use only.

(40 ml) gave crude VI*a* (80 mg), having double m.p. 95–100° and 155–156°. This was crystallized from ether–hexane to yield the pure compound, m.p. 155–157° and $[\alpha]_D^{25}$ +51.1° (*c*, 0.351, chloroform). The literature (10) reports m.p. 152–152.5° and $[\alpha]_D^{22}$ +42.3° (*c*, 0.79, chloroform).

REFERENCES

1. CHAPMAN, J. H., ELKS, J., and WYMAN, L. J. Chem. & Ind. 603 (1955).
2. ROTHMAN, E. S. and WALL, M. E. J. Am. Chem. Soc. **79**, 3228 (1957).
3. CALLOW, R. K. and JAMES, V. H. T. J. Chem. Soc. 4744 (1956).
4. WALL, M. E. and JONES, H. W. J. Am. Chem. Soc. **79**, 3222 (1957).
5. HARTUNG, W. H. and ADKINS, H. J. Am. Chem. Soc. **49**, 2517 (1927).
6. MCELVAIN, S. M. and WALTERS, P. M. J. Am. Chem. Soc. **64**, 1963 (1942).
7. ALEXANDER, E. R. J. Am. Chem. Soc. **70**, 2592 (1948).
8. MARVELL, E. N. and JONCICH, M. J. J. Am. Chem. Soc. **73**, 973 (1951).
9. OLIVETO, E. P., SMITH, H. Q., GEROLD, C., WEBER, L., RAUSSER, R., and HERSHBERG, E. B. J. Am. Chem. Soc. **77**, 2224 (1955).
10. ENGEL, CH. R., JENNINGS, K. F., and JUST, G. J. Am. Chem. Soc. **78**, 6153 (1956).
11. ENGEL, CH. R. J. Am. Chem. Soc. **78**, 4727 (1956).
12. WENDLER, N. L., GRABER, R. P., and HAZEN, G. G. Tetrahedron, **3**, 144 (1958).
13. MEYSTRE, CH. and WETTSTEIN, A. Helv. Chim. Acta, **30**, 1037 (1947).
14. KOECHLIN, B. and REICHSTEIN, T. Helv. Chim. Acta, **27**, 549 (1944).
15. HEUSSER, H., BERIGER, E., and ENGEL, CH. R. Helv. Chim. Acta, **37**, 2166 (1954).

Can. J. Chem. Downloaded from www.nrcresearchpress.com by 190.90.36.8 on 09/04/12
For personal use only.

Can. J. Chem. Downloaded from www.nrcresearchpress.com by 190.90.36.8 on 09/04/12
For personal use only.

STERIC INHIBITION OF RESONANCE

I. 9-NITROANTHRACENE AND 9,10-DINITROANTHRACENE[1]

JAMES TROTTER[2]

ABSTRACT

Detailed X-ray analyses of the crystal structures of 9-nitroanthracene and 9,10-dinitroanthracene have shown that the nitro groups are tilted out of the planes of the aromatic rings by 84.7° in the nitro derivative and 63.7° in the dinitro. The decreases in resonance interaction resulting from these deviations from coplanarity have been correlated with the characteristic vibration frequencies of the nitro groups.

INTRODUCTION

Examination of some of the physical properties of the nitro and acetyl derivatives of durene and mesitylene suggests that the steric effect of the methyl groups prevents the attainment of a completely coplanar configuration, and reduces the resonance interaction between the aromatic π-electrons and the substituent nitro and acetyl groups. Consideration of Raman and infrared frequencies, dipole moments, ultraviolet spectra, acid-base strengths, and rates of reaction indicates a great amount of inhibition of resonance in this type of molecule (1). Few direct measurements of the deviations from coplanarity have been made however.

Huse and Powell (2) have investigated the crystal structure of picryl iodide (I) by X-ray diffraction methods; their results indicate that the para-nitro group is coplanar with the benzene nucleus and, owing to resonance with ionic structures (II), the para C–N bond length (1.35 Å) is much shorter than the normal single bond distance, but the planes of the ortho-nitro groups are approximately at right angles to the benzene ring, there is no resonance with the aromatic π-electrons, and the ortho C–N bond length (1.45 Å) corresponds closely to the single bond distance. The molecular geometry and dimensions have not been determined very accurately, however, owing to the presence of the heavy iodine atom.

Francel (3) has investigated the infrared spectra of five ortho-substituted nitrobenzenes in the solid state using polarized radiation. The polarization of the absorption band arising from the asymmetric NO_2 stretching vibration in *o*-nitrobromobenzene indicates that the nitro group is rotated well out of the plane of the benzene ring owing to the steric effect of the bromine atom, and is probably almost perpendicular to the ring. The polarization of the bands in the corresponding chloro derivative is assumed to indicate a smaller angle between the benzene ring and the nitro group, which would be expected because of the difference in the van der Waals radii of chlorine and bromine. Again, however, no accurate measure of the deviation from coplanarity has been possible.

The present investigations, which are confined chiefly to nitro derivatives, were undertaken to obtain accurate measurements of the tilts of the planes of the substituent groups out of the aromatic planes, using X-ray diffraction methods, and to correlate these values with the reduction in resonance interaction, the bond lengths in the molecules, the infrared frequencies, dipole moments, and other physical data.

[1]*Manuscript received October 8, 1958.*
Contribution from the Division of Pure Physics, National Research Council, Ottawa, Canada.
Issued as N.R.C. 5002.
[2]*National Research Council Postdoctorate Fellow.*

Such steric effects and resonance inhibition should be observable also in 9- and 9,10-substituted anthracenes, where the environments of the substituent groups are very similar to those in durene and mesitylene derivatives. Contributions to the ground state of the 9-nitroanthracene molecule from structures such as III and IV would be greatest when the nitro group is coplanar with the anthracene nucleus, but this involves distances which are much less than the usual van der Waals separations, between the oxygen atoms and the hydrogen atoms bonded to carbons 1 and 8. It would be expected that the strain due to this 'overcrowding' would be relieved by rotation of the nitro group about the C–N bond. Jones (4, 5) has examined the ultraviolet spectra of certain 9,10-diarylanthracenes, and observes that the introduction of phenyl groups, for example, at positions 9 and 10 causes very little change in the anthracene spectrum, and indeed methyl groups actually produce a greater displacement towards longer wavelengths. He concludes that the phenyl groups are hindered to such an extent that they probably lie more or less perpendicular to the main plane of the anthracene nucleus.

The infrared spectra of 9-nitroanthracene and 9,10-dinitroanthracene have now been measured, and the characteristic nitro group vibration frequencies have been correlated with the angles between the planes of the nitro groups and the anthracene nuclei. These angles have been determined by accurate X-ray analyses of the crystalline materials. Extension of these investigations to durene and mesitylene derivatives will be described in subsequent communications.

EXPERIMENTAL

Preparation and Purification of Materials

Commercial 9-nitroanthracene was purified by chromatography on alumina and crystallization from petroleum ether, giving yellow crystals melting at 146°. From this material 9,10-dinitroanthracene was prepared by nitration with nitric acid in acetic anhydride, and then purified by chromatography and crystallization, giving yellow crystals, melting point 310°. Crystals of each substance grown by slow crystallization from petroleum ether were suitable for the X-ray examinations.

Infrared Spectra

The spectra measured (Fig. 1) were those of 1 mg of the pure solids dispersed in potassium bromide disks of thickness 1 mm and weighing 400 mg as observed with a Perkin–Elmer model 21 infrared spectrophotometer with a rock salt prism. The peak positions of the NO_2 symmetrical stretching frequencies in the region of 1370 cm^{-1} were more accurately determined using a Perkin–Elmer spectrometer model 12C, but these more accurate values agreed closely with the previously measured frequencies.

X-Ray Analyses

Crystals of 9-nitroanthracene are monoclinic with four molecules in a unit cell of dimensions $a = 7.49$, $b = 13.77$, $c = 11.44$ Å, $\beta = 115°11'$, space group $P2_1/a$. The structure was determined from projections along the three principal crystallographic axes. The nitro group is very markedly tilted out of the plane of the anthracene nucleus about the C–N bond, the angle between the planes of the aromatic ring and of the nitro group being 84.7°. Figure 2 shows a projection of the structure along the c-axis; the individual atoms are not separately resolved in this projection, but the large deviation from coplanarity is well illustrated.

9,10-Dinitroanthracene is triclinic with one molecule in a unit cell of dimensions $a = 3.95$, $b = 8.68$, $c = 8.76$ Å, $\alpha = 106°46'$, $\beta = 98°59'$, $\gamma = 98°01'$, space group

Can. J. Chem. Downloaded from www.nrcresearchpress.com by 190.90.36.8 on 09/04/12
For personal use only.

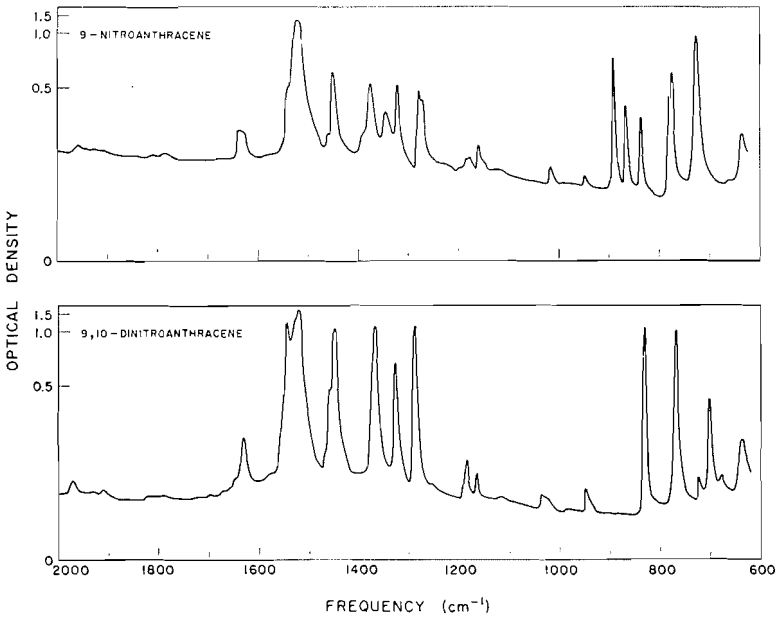

FIG. 1. Infrared spectra.

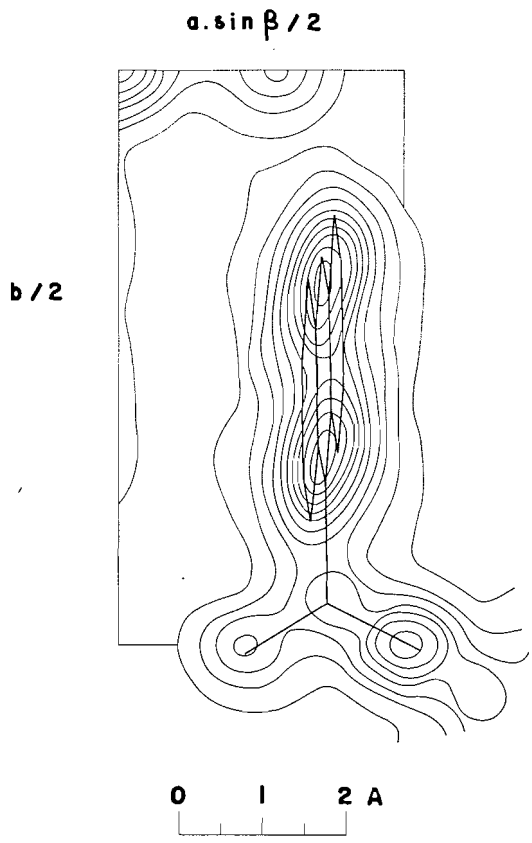

FIG. 2. Projection of the structure of 9-nitroanthracene along the *c*-axis, showing the tilt of the nitro group.

Can. J. Chem. Downloaded from www.nrcresearchpress.com by 190.90.36.8 on 09/04/12
For personal use only.

$P\bar{1}$. In the projection along the short a-axis all the atoms are very well resolved. Figure 3 shows a projection of the structure along the b-axis, in which the resolution of the individual atoms is not so good, but which shows very clearly the tilt of the nitro groups. The molecule is centrosymmetrical and the angle between the planes of a nitro group and the aromatic nucleus is in this case 63.7°. This deviation from planarity is just sufficient to increase the separations between the oxygen atoms and neighboring carbon and hydrogen atoms to the normal van der Waals distances. Full details of the crystal structure analyses are published elsewhere (6, 7).

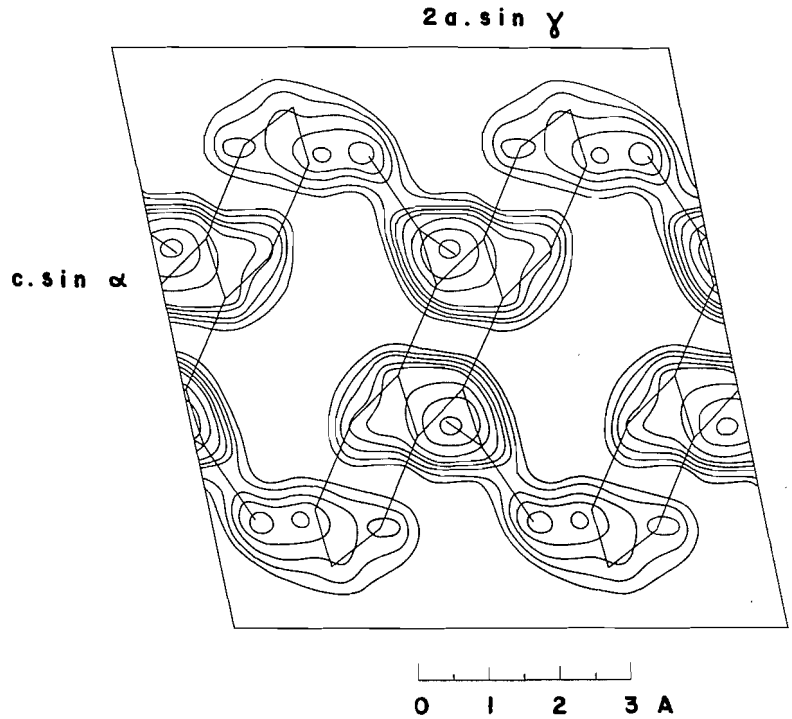

FIG. 3. Projection of the 9,10-dinitroanthracene structure along the b-axis, showing the nitro-group tilts.

DISCUSSION

The spectra of 9-nitroanthracene and 9,10-dinitroanthracene in the range 2000 cm^{-1} to 600 cm^{-1} are shown in Fig. 1, and the peak positions and intensities of the absorption bands are listed in Table I. The maxima at 1374 cm^{-1} in 9-nitroanthracene and at 1367 cm^{-1} in 9,10-dinitroanthracene can be assigned to the NO_2 symmetrical stretching vibrations, the intensity of the absorption in the dinitro compound being about double that in the mononitro derivative. The NO_2 asymmetrical stretching vibrations cannot be assigned quite so unambiguously. In 9,10-dinitroanthracene there are bands of about equal intensity at 1519 cm^{-1} and 1542 cm^{-1}, while in the 9-nitro there is a band at 1519 cm^{-1} corresponding in intensity to that of the dinitro derivative and a shoulder at 1540 cm^{-1} of about half this intensity, and on this basis the bands around 1540 cm^{-1} have been assigned to the NO_2 asymmetrical stretching vibrations.

The C–N stretching frequency in nitromethane (8) is at 918 cm^{-1}, although it is at rather lower frequencies in the higher nitroparaffins (at 804 cm^{-1} in 1-nitropropane for

Can. J. Chem. Downloaded from www.nrcresearchpress.com by 190.90.36.8 on 09/04/12
For personal use only.

TABLE I

Frequencies and intensities of absorption bands

9-Nitroanthracene		9,10-Dinitroanthracene		
Frequency (cm^{-1})	Intensity	Frequency (cm^{-1})	Intensity	Vibration
1623–1639	w	1631	w	C=C (conjugated) stretching
1540	m (sh)	1542	s	NO_2 asymmetrical stretching
1519	s	1519	s	C=C (conjugated) stretching
1458	w	1458	m (sh)	
1449	m	1447	s	
1374	m	1367	s	NO_2 symmetrical stretching
1344	w→m			
1322	m	1327	m	
1279	m	1288	s	
1271	m			
1186	w (sh)	1190	w (sh)	
1179	w	1186	w	
1159	w	1166	w	Characteristic anthracene bands
1017	w	1023–1037	w	
949	w	949	w	
890	s			C_{10}—H out-of-plane vibration
866	m			
836	m	831	s	C—N stretching
778	m (sh)			
773	s	768	s	
724	s	724	w	Characteristic anthracene band
		702	m	
		678	w	
637	m	639	m	NO_2 symmetrical bending

example), while in aromatic nitro compounds (9) it is at 849 cm^{-1}. The absorption maxima at 836 cm^{-1} and 831 cm^{-1} in the meso-nitroanthracenes can be assigned to the C–N stretching vibrations. The strong absorption at 890 cm^{-1} in the mononitro derivative, which is not observed in the dinitro, corresponds to the C_{10}–H out-of-plane vibration.

In Table II the characteristic nitro group frequencies in 9-nitroanthracene and 9,10-dinitroanthracene are compared with those in nitromethane and those in typical aromatic nitro compounds (9). In aromatic nitro compounds contributions from ionic structures of type V lead to a decrease in the force constant of the N–O bonds and a consequent decrease in the NO_2 symmetrical and asymmetrical stretching frequencies (1349 cm^{-1} and 1518 cm^{-1}) compared with non-conjugated nitro compounds (1377 cm^{-1} and 1586 cm^{-1} in nitromethane). The frequency of the NO_2 symmetrical stretching vibration in 9-nitroanthracene is much higher than in nitrobenzene, and nearly equal to the frequency in nitromethane, corresponding to a negligible amount of resonance interaction between the nitro group and the anthracene nucleus. In 9,10-dinitroanthracene the band is at 1367 cm^{-1}, indicating a very marked reduction in resonance interaction compared with nitrobenzene, but also suggesting that the resonance is not inhibited to such an extent as in the 9-nitro derivative.

These frequencies are in accord with the tilts of the nitro groups out of the aromatic planes, which are given in the final column of Table II. The tilt has been assumed to be zero in nitrobenzene, although this is not quite certain; X-ray crystal analyses of *p*-dinitrobenzene for example have shown that the nitro group is tilted 9°25′ out of the plane of the benzene ring in this molecule (10). Resonance interaction is at a maximum in nitrobenzene (corresponding to $\theta = 0°$) and zero in nitromethane (corresponding effectively to $\theta = 90°$). The frequencies of the NO_2 symmetrical stretching vibrations indicate that resonance between aromatic rings and nitro groups is almost completely inhibited

Can. J. Chem. Downloaded from www.nrcresearchpress.com by 190.90.36.8 on 09/04/12
For personal use only.

TABLE II

Characteristic nitro-group frequencies (cm^{-1}) and deviations from coplanarity

Molecule	NO_2 stretching		C–N stretching	NO_2 tilt (θ in degrees)
	Symmetrical	Asymmetrical		
Nitromethane	1377	1586	918	90
9-Nitroanthracene	1374	1540	836	84.7
9,10-Dinitroanthracene	1367	1542	831	63.7
Aroamtic nitro compounds	1349	1518	849	0

in 9-nitroanthracene ($\theta = 85°$) and inhibited to a large extent in 9,10-dinitroanthracene ($\theta = 64°$). The NO_2 asymmetrical stretching vibrations in 9-nitro and 9,10-dinitroanthracene are also in accord with resonance inhibition, although quantitatively the agreement is not so good.

Resonance inhibition decreases the weight of ionic structures such as III and IV, and the resulting decrease in the force constant of the C–N bond should lead to lower frequencies for the C–N stretching vibration in 9-nitroanthracene and 9,10-dinitro-

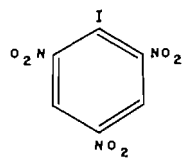

I

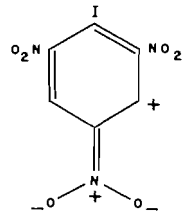

II

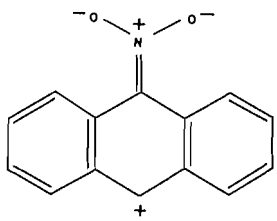

III

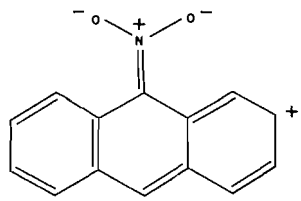

IV

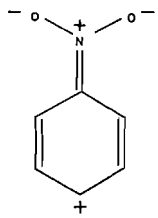

V

Can. J. Chem. Downloaded from www.nrcresearchpress.com by 190.90.36.8 on 09/04/12
For personal use only.

anthracene than in nitrobenzene, in agreement with the observed frequencies. The C–N stretching frequency in nitromethane would then appear to be anomalous, but the higher frequency in this case is not unexpected as the carbon atom can vibrate more freely than those in the more rigid aromatic molecules.

The characteristic NO_2 vibration frequencies in meso-nitroanthracenes then indicate a marked inhibition of the resonance interaction between the nitro groups and the aromatic π-electrons, in complete agreement with the effect which would be predicted from a measure of the tilts of the nitro groups out of the aromatic planes. For the NO_2 symmetrical stretching frequencies the results would appear to be semiquantitative, but this is probably fortuitous, since only qualitative agreement is obtained with the other characteristic vibrations. Only qualitative agreement is to be expected of course, since the nitro-group frequencies are not entirely independent of the remainder of the molecule, and small frequency variations are observed among quite similar aromatic molecules where no steric effects are involved. Quantitative information concerning the resonance interaction may be obtained from an examination of the bond lengths in these molecules, since structures of types III and IV would impart a considerable amount of double bond character to the C–N bond, reduce the double bond character of the N–O bonds, and also influence the bond lengths in the aromatic rings. Discussion of these quantitative relations obtainable from a study of the bond length variations will be given in later communications.

ACKNOWLEDGMENTS

The author wishes to thank Dr. W. G. Schneider for samples of 9-nitroanthracene and 9,10-dinitroanthracene, and Mr. R. Lauzon for recording the infrared spectra.

REFERENCES

1. WHELAND, G. W. Resonance in organic chemistry. John Wiley & Sons, Inc., New York. 1955.
2. HUSE, G. and POWELL, H. M. J. Chem. Soc. 1398 (1940).
3. FRANCEL, R. J. J. Am. Chem. Soc. 74, 1265 (1952).
4. JONES, R. N. J. Am. Chem. Soc. **67**, 2127 (1945).
5. JONES, R. N. Chem. Revs. **41**, 353 (1947).
6. TROTTER, J. Acta Cryst. **11**, 564 (1958).
7. TROTTER, J. Acta Cryst. (In press).
8. SMITH, D. C., PAN, C., and NIELSEN, J. R. J. Chem. Phys. **18**, 706 (1950).
9. RANDLE, R. R. and WHIFFEN, D. H. J. Chem. Soc. 4153 (1952).
10. ABRAHAMS, S. C. Acta Cryst. **3**, 194 (1950).

Can. J. Chem. Downloaded from www.nrcresearchpress.com by 190.90.36.8 on 09/04/12
For personal use only.

Can. J. Chem. Downloaded from www.nrcresearchpress.com by 190.90.36.8 on 09/04/12
For personal use only.

THE SYNTHESIS OF 4-*O*-β-D-GALACTOSYL-D-GLUCOSE (LACTOSE)[1]

E. J. C. CURTIS AND J. K. N. JONES

ABSTRACT

4-*O*-β-D-Galactosyl-D-glucose (lactose) has been synthesized using a modification of the Koenigs–Knorr reaction.

INTRODUCTION

4-*O*-β-D-Galactosyl-D-glucose (lactose) occurs in all mammalian milk to the extent of about 5%. It has also been reported in the long-styled pollen of forsythia flowers. It was prepared in 1942 by Haskins, Hann, and Hudson (1) from epilactose (4-*O*-β-D-galactosyl-D-mannose), but has not previously been synthesized directly.

One of the most useful methods of disaccharide synthesis is that due to Koenigs and Knorr (2). They prepared tetra-*O*-acetyl-α-D-glucopyranosyl-bromide and found that this, in the presence of silver carbonate or dry pyridine, reacted with methanol to form methyl-β-D-glucopyranoside. The reaction—essentially the elimination of hydrogen halide between a glycosyl halide and a hydroxyl group—was adapted for disaccharide synthesis by Helferich (3) and by Hudson (4). They allowed the acetobrom sugar to react with a suitably substituted sugar derivative in a dry inert medium in the presence of silver carbonate or silver oxide. With modern refinements—use of "Drierite" as drying agent and small amounts of iodine as catalyst—good yields can be obtained in the case of $1 \rightarrow 6$ linked hexose disaccharides, where a primary hydroxyl group is involved. However, up to the present only small yields have been obtained in the case of disaccharides where a secondary hydroxyl group is involved. This is due to the lesser reactivity of the secondary hydroxyl group and to steric hindrance by the alcohol component due to the presence of the hemiacetal ring and the substituent groups. It was thought that this second factor might be lessened—and thus greater yields obtained—by the use of an open-chain sugar derivative as the alcohol reactant. Here the accessibility of the hydroxyl group is much greater than in the corresponding ring compound.

In the present work 2,3-5,6-di-*O*-isopropylidene-D-glucose diethyl acetal was condensed with acetobrom-D-galactose under standard Koenigs–Knorr conditions (5). The reaction mixture was boiled with sodium hydroxide solution to remove acetyl groups from the product and to destroy excess acetobrom-galactose, cooled, and deionized. Hydrolysis of isopropylidene and acetal groups was carried out with hot dilute acetic acid. The resulting mixture of mono- and di-saccharides was separated by charcoal- and paper-chromatography. Lactose was obtained crystalline in 35% yield, which is well in excess of the yields usually obtained from Koenigs–Knorr syntheses where a secondary hydroxyl group is involved. Two other disaccharide fractions were obtained in small yield. These have not been completely identified but presumably result from isomers of 2,3-5,6-di-*O*-isopropylidene-D-glucose diethyl acetal. These are inevitably present in small amount as a result of the method of preparation of this compound (via a mercaptal mixture (8) consisting mainly of the 2,3-5,6-di-*O*-isopropylidene derivative).

EXPERIMENTAL

Optical rotations were measured in water at 21°±2° C. The following solvent systems (v/v) were used to separate sugars on paper chromatograms: (A) ethyl acetate: acetic acid: formic acid: water, 18:3:1:4; (B) *n*-butanol:ethanol: water, 3:1:1. Sugars were

[1]*Manuscript received August 11, 1958.*
Contribution from the Department of Chemistry, Queen's University, Kingston, Ontario.

detected with the *p*-anisidine hydrochloride spray (6). Solutions were concentrated under reduced pressure at 40° C.

D-*Glucose Diethyl Thioacetal* (*Ref. 7*)

D-Glucose (60 g), ice-cold ethanethiol (60 ml), and ice-cold concentrated hydrochloric acid (60 ml) were shaken together in a stoppered flask, and left at room temperature. After 3 hours the material had formed a crystalline mass. Methanol (*ca.* 300 ml) was added and sufficient lead carbonate to neutralize the solution, which was then filtered and the precipitate washed with boiling methanol. The crude product crystallized from the filtrate on cooling and was recrystallized from methanol. Yield: 62 g (65%), m.p. 119–120° C.

Di-O-isopropylidene-D-*glucose Diethyl Thioacetal* (*Ref. 8*)

Glucose diethyl thioacetal (36 g) was added to a mixture of dry acetone (350 ml) and concentrated sulphuric acid (8.5 g) and the resulting solution was left at room temperature for 72 hours. The solution was neutralized with a solution of barium hydroxide in methanol, and filtered. The filtrate was evaporated to a pale yellow mobile syrup. Yield: 35 g.

Di-O-isopropylidene-D-*glucose Diethyl Acetal*

The method used was similar to that employed by Wolfrom *et al.* (9) in the preparation of D-galactose diethyl acetal pentaacetate. Di-*O*-isopropylidene-D-glucose diethyl thioacetal (40 g), mercuric oxide (80 g), and lead carbonate (20 g) were added to dry ethanol (400 ml) and the solution heated to 70–80° C while it was being stirred. A solution of mercuric chloride (176 g) in dry ethanol (300 ml) was then added and the solution stirred for 5 hours at 70–80° C with occasional addition of mercuric oxide. The solution was filtered hot and the precipitate washed with hot ethanol. The filtrate was evaporated to a small volume and then diluted with chloroform (400 ml). This chloroform solution was extracted with water until chloride-free and dried over Drierite. Filtration and subsequent evaporation yielded a syrup (30 g), which was purified by distillation, a fraction (22 g) being collected with b.p. 130–140° C at 0.05 mm.

Condensation of Di-O-isopropylidene-D-*glucose Diethyl Acetal with Acetobromo*-D-*galactose*

Di-*O*-isopropylidene-D-glucose diethyl acetal (15 g, 0.0449 mole) was dissolved in dry, alcohol-free chloroform (200 ml) and to the solution were added Drierite (20 g), silver oxide (20 g), and glass beads (35 g). The solution was shaken in the dark. After 4 hours acetobrom-D-galactose (46 g, 0.112 mole) in dry, alcohol-free chloroform (150 ml) and iodine (1 g) were added and the shaking continued. After 42 hours a test for ionizable bromine was negative. The solution was filtered, evaporated to a syrup, and dissolved in a solution of sodium hydroxide (20 g) in methanol (400 ml). This was heated under reflux for 3.5 hours, cooled, and de-cationized on Amberlite IR-120 resin in the cold. The acidic eluate was heated at 65° C for 1 hour in order to hydrolyze isopropylidene and acetal groups, and then de-ionized by passage through a column of Duolite A-4 resin. Concentration of the eluate yielded a syrup (20 g) which was shown by paper chromatography to consist, in addition to glucose and galactose, of a main fraction with R_{gal} 0.45 (solvent A) and 0.28 (solvent B) and two much smaller spots running slightly in front of, and behind, this spot.

A portion of the syrup (8.1 g) was fractionated on a column of Darco charcoal (4×5 cm) (10). Elution with water removed all the monosaccharide and in the final stages a faint trace of the slower-moving components: subsequent elution with ethanol/water (5:95) removed the bulk of the slower-moving components (2.9 g). This latter syrup

Can. J. Chem. Downloaded from www.nrcresearchpress.com by 190.90.36.8 on 09/04/12
For personal use only.

was dissolved in a little moist methanol, nucleated with authentic lactose, and the solvent allowed to evaporate at room temperature. Part of the material crystallized, 1.8 g being obtained. It was recrystallized from moist methanol and was found chromatographically to be a single substance indistinguishable from lactose. Hydrolysis yielded galactose and glucose in equal amounts. It had m.p. 201–202° C undepressed by admixture with an authentic specimen of lactose monohydrate, and $[\alpha]_D$ +86.3 (5 min) → +58.1° (16 hr). The infrared spectra of the material and of authentic lactose monohydrate were identical. Calculated for $C_{12}H_{22}O_{11}.H_2O$: C, 40.00%; H, 6.67%. Found: C, 40.19%; H, 6.82%.

Part of the syrup which failed to crystallize (0.6 g) was separated on filter paper (Whatman No. 3 MM). A further quantity of lactose (0.20 g) was obtained in addition to two other fractions: I (51.2 mg) and II (49.9 mg). Fraction I had R_{gal} 0.33 (solvent A) and 0.15 (solvent B) while II had R_{gal} 0.47 (solvent A) and 0.32 (solvent B). Both fractions yielded galactose and glucose in equal amounts on hydrolysis.

Periodate Oxidation of Fractions I and II

Portions of fractions I and II were oxidized with aqueous sodium metaperiodate solution using standard procedures. The periodate uptake was estimated by the method of Neumüller and Vasseur (11) and the formic acid liberation by that of Andrews *et al.* (12).

The molar periodate consumptions per mole of disaccharide were as follows: fraction I, 3.90 (after 25 min), 4.44 (1 hr), 4.75 (3.5 hr), and 4.83 (22 hr); fraction II, 2.35 (0.5 hr), 2.84 (1 hr), 3.08 (4 hr), and 3.56 (22 hr). The molar productions of formic acid were: fraction I, 3.77 (after 40 min), 4.29 (1.5 hr), 4.92 (4 hr), and 5.34 (22.5 hr); fraction II, 1.01 (40 min), 1.25 (1.5 hr), 1.41 (4 hr), and 2.12 (22.5 hr). Extrapolation of the flat part of the curve to zero time gave values of: fraction I, periodate uptake = 4.78 moles per mole of sugar, formic acid production = 4.41 moles per mole; fraction II, periodate uptake = 2.95 moles per mole sugar, formic acid production = 1.17 moles per mole.

The figures for fraction I are difficult to interpret. The large amount of formic acid could not have come from any normal type of sugar and it may be that this fraction is a mixture of disaccharide and some other material. The figures for fraction II—where the slope of the flat part of the periodate and formic acid curves indicates that over-oxidation was taking place—are those to be expected of a 1 → 3 linked hexopyranose disaccharide. Crystalline derivatives of fractions I and II have not yet been obtained.

ACKNOWLEDGMENTS

The authors are indebted to the National Research Council for a grant. One of them (E.J.C.C.) thanks Queen's University for the award of a fellowship.

REFERENCES

1. Haskins, W. T., Hann, R. M., and Hudson, C. S. J. Am. Chem. Soc. **64**, 1852 (1942).
2. Koenigs, W. and Knorr, E. Ber. **34**, 957 (1901).
3. Helferich, B. Advances in carbohydrate chemistry. Vol. 3. Academic Press, Inc., New York. 1948. p. 79.
4. Knauf, A. E., Hann, R. M., and Hudson, C. S. J. Am. Chem. Soc. **63**, 1447 (1941).
5. Evans, W. L., Reynolds, D. D., and Talley, E. A. Advances in carbohydrate chemistry. Vol. 6. Academic Press, Inc., New York. 1951. p. 27.
6. Hough, L., Jones, J. K. N., and Wadman, W. H. J. Chem. Soc. 1702 (1950).
7. Hough, L. and Taylor, T. J. J. Chem. Soc. 1212 (1955).
8. Munro, J. and Percival, E. G. V. J. Chem. Soc. 873 (1935).
9. Wolfrom, M. L., Tanghe, L. T., George, R. W., and Waisbrot, S. W. J. Am. Chem. Soc. **60**, 132 (1938).
10. Andrews, P., Hough, L., and Powell, D. B. Chem. & Ind. 658 (1956).
11. Neumüller, G. and Vasseur, E. Arkiv Kemi, **2**, 235 (1953).
12. Andrews, P., Hough, L., and Jones, J. K. N. J. Chem. Soc. 806 (1954).

Can. J. Chem. Downloaded from www.nrcresearchpress.com by 190.90.36.8 on 09/04/12
For personal use only.

Can. J. Chem. Downloaded from www.nrcresearchpress.com by 190.90.36.8 on 09/04/12
For personal use only.

THE INFRARED SPECTRA OF SOME CYCLIC MALONATES[1]

R. A. ABRAMOVITCH

ABSTRACT

The infrared spectra of isopropylidene malonate and some of its derivatives have been examined and compared with those of open-chain malonate esters and of 5,5-dimethylcyclohexane-1,3-dione. Two bands in the carbonyl stretching region are attributed to vibrational coupling of the carbonyl groups in the cyclic esters. There is no evidence that isopropylidene malonate exists in the enolic form either in the solid state or in chloroform solution. This cyclic ester structure for "Meldrum's acid" is thus confirmed.

In an investigation of the infrared spectra of a number of malonate esters it was shown (1) that most of them exhibited two ester carbonyl stretching bands, and that these were not due to enolization and conjugate chelation, or to association. It was not possible, at that stage, to decide whether these double carbonyl bands were due to vibrational coupling or to rotational isomerism, or yet perhaps to another still unknown cause.

It was of interest to determine whether, in the absence of the possibility of rotational isomerism, two ester carbonyl groups beta- to each other could undergo vibrational coupling. For this purpose the spectra of isopropylidene malonate and some of its derivatives have been examined, since apart from ethylene glycolyl malonate (2) (which is not unambiguously characterized), no other simple cyclic esters of malonic acid seem to be known. Vibrational coupling does not appear to have been observed in cyclic 6-membered β-diketones: here, enolization with intermolecular chelation has been reported (3). The carbonyl groupings, which are beta- to each other, in cyclic anhydrides are known to undergo coupling (4), and it has recently been suggested that this type of interaction also occurs in substituted isatoic anhydrides (5) though in this case the carbonyl groups are different in nature and one would have expected each to exhibit its own stretching frequency.

Isopropylidene malonate (I) poses an interesting structural problem which was largely clarified by the work of Davidson and Bernhard (6). The cyclic ester, also known as "Meldrum's acid", is prepared by the action of acetone on malonic acid in a cold acetic anhydride – sulphuric acid medium, and was originally attributed the structure of β,β-dimethyl-β-propiolactone-α-carboxylic acid (II). On the basis of chemical evidence Davidson and Bernhard were able to suggest structure (I) for the product and structure (III) for the dimethylated derivative.

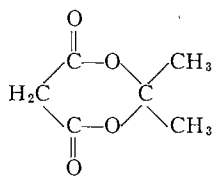

(I)

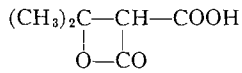

(II)

They compared the reactions of the cyclic ester with those of 5,5-dimethylcyclohexane-1,3-dione (IV) and attributed the acidity of the ester (pK_a 5.1) to enolization (($I \rightleftarrows V$) in the same way as the acidity of 5,5-dimethylcyclohexane-1,3-dione (pK_a 5.2) is

[1]*Manuscript received September 22, 1958.*
Contribution from the Chemistry Department, University of Saskatchewan, Saskatoon, Saskatchewan.

Can. J. Chem. Vol. 37 (1959)

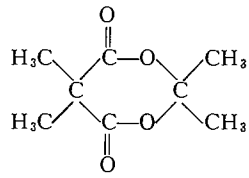

(III)

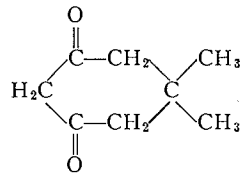

(IV)

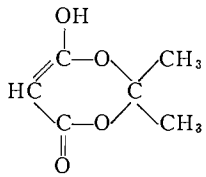

(V)

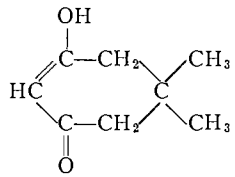

(VI)

attributed to a similar enolization (IV $\rightleftarrows$ VI). In fact, the dione (IV) is 95% in the enolic form in water solution (7). On the other hand, isopropylidene dimethylmalonate, which cannot exist in an enolic form, exhibits no acidic properties (6). It should be pointed out, however, that diethyl malonate itself is not enolized to any appreciable extent ((1), and references cited therein).

EXPERIMENTAL

Isopropylidene malonate and isopropylidene dimethylmalonate were prepared by the method of Davidson and Bernhard (6). Isopropylidene malonate could be recrystallized either from acetone–water, or more conveniently from water or anhydrous carbon tetrachloride giving needles, m.p. 96°. 5,5-Dimethylcyclohexane-1,3-dione had m.p. 147–148.5°.

Isopropylidene ethylmalonate.—To a suspension of ethylmalonic acid (6.6 g) in acetic anhydride (6 ml) was added concentrated sulphuric acid (0.2 ml) with stirring. Most of the solid dissolved. Acetone (4 ml) was added dropwise to the suspension kept at 20–25° and the resulting solution was kept in the refrigerator overnight. The solid which separated was filtered and washed repeatedly with ice water, and the filtrate and washings combined to give a further amount of isopropylidene ethylmalonate. The product (6.09 g), m.p. 108–109° (depressed to 86–88° on admixture with ethylmalonic acid, m.p. 111°), was recrystallized from distilled water giving long, colorless needles, m.p. 108–109°. Found: C, 55.5; H, 7.1. Calc. for $C_8H_{12}O_4$: C, 55.8; H, 7.0.

Isopropylidene deuteromalonate.—An attempt to replace the reactive hydrogen atoms by sodium (with sodium ethoxide) followed by evaporation to dryness and treatment with D_2O, as in the case of diethyl ethylmalonate (1), only led to hydrolysis of the cyclic ester. Exchange of the active hydrogens of isopropylidene malonate took place readily when the compound was recrystallized from 99.9% deuterium oxide; seven such recrystallizations gave the deuterated ester as flat needles, m.p. 93–94°.

Infrared spectra.—A Perkin–Elmer model 21 double beam spectrophotometer with sodium chloride optics was used. The chloroform used for the solution spectra was AnalaR grade, dried and redistilled before use. The solution cell thickness was 0.028 mm and the concentrations were in the range of 20–22 mg/ml. Carbon tetrachloride was also of AnalaR grade and was dried before use.

Can. J. Chem. Downloaded from www.nrcresearchpress.com by 190.90.36.8 on 09/04/12
For personal use only.

Compound	Nujol mull			Chloroform solution		
	$\nu_{C=O}$ cm^{-1}	Mean value	$\Delta\nu_{C=O}$ cm^{-1}	$\nu_{C=O}$ cm^{-1}	Mean value	$\Delta\nu_{C=O}$ cm^{-1}
Isopropylidene malonate	1785, 1753	1769	32	1778, 1749	1763	29
Isopropylidene deutero-malonate	1778 (br), 1740 (br)	1759	38	1782, 1745	1763	37
Isopropylidene ethylmalonate	1777, 1737	1757	40	1783, 1747	1765	36
Isopropylidene dimethyl-malonate	1780 (br), 1745 (br)	1758	35	1770, 1735 1787, 1749*	1753 1768	35 38
5,5-Dimethylcyclohexane-1,3-dione	1612 (br)	—	—	1733, 1710, 1612 (br)	—	—
Diethyl malonate (1)	1760, 1742†	1751	22	1761, 1742	1752	19

br = Broad band.
*Carbon tetrachloride solution.
†Liquid film.

RESULTS

The 3–5 μ region.—5,5-Dimethylcyclohexane-1,3-dione is the only compound which shows OH stretching absorption in that region: in the solid state a very broad band is observed at 2505 cm^{-1} with a shoulder at 2380 cm^{-1}. These bands are attributed to the enolic OH group, which is strongly intermolecularly bonded. The intensities of these bands are decreased considerably in dilute chloroform solution and vanish altogether at high dilution. Isopropylidene deuteromalonate exhibits a band at 2155 cm^{-1} (Nujol mull) attributed to the CD_2 vibration, indicating that at least a large proportion of the active hydrogen atoms have been exchanged for deuterium; if only one of the two hydrogen atoms had been replaced no appreciable band corresponding to the tertiary C—D stretching mode would have been observed (1). None of the other compounds examined showed any O—H stretching bands either in the solid state or in chloroform solution.

The 5–6 μ region.—The cyclic malonates exhibited two bands in this region above 1730 cm^{-1} whether in the solid state or in solution. In the solid state 5,5-dimethylcyclohexane-1,3-dione exhibited only a single broad band at 1612 cm^{-1}, whereas in dilute chloroform solution three bands were observed at 1733 (m), 1710 (s), and 1612 cm^{-1} (s) (broad). Bellamy and Beecher (8) reported bands at 1733, 1706, and 1603 cm^{-1} which they attributed to the keto, free enol, and intermolecularly chelated forms respectively. Though the positions of the double maxima of the cyclic malonates are altered on going from the solid state to the solutions, or, in the case of isopropylidene dimethylmalonate on changing from a chloroform solution to a carbon tetrachloride solution, $\Delta\nu_{C=O}$ for each individual compound remains approximately the same. The effect of deuteration does not change the mean of the positions of the two bands of isopropylidene malonate in chloroform solution though the positions of the bands themselves are altered, as is also $\Delta\nu_{C=O}$ (which becomes closer to that of isopropylidene dimethylmalonate).

DISCUSSION

Structure (II) for "Meldrum's acid" is eliminated owing to absence of the broad peaks characteristic of the carboxyl group in the 3–4 μ region, as well as of a band at around 1700 cm^{-1}. It is clear, however, that neither in the solid state nor in chloroform solution is isopropylidene malonate (I) enolized to any appreciable extent. This is shown by the absence of any O—H stretching bands, whether bonded or unbonded, by the absence of a definite band corresponding to an α,β-unsaturated ester carbonyl group as would be present in the free enol, as well as by the non-appearance of a band corre-

Can. J. Chem. Downloaded from www.nrcresearchpress.com by 190.90.36.8 on 09/04/12
For personal use only.

sponding to a chelated ester carbonyl group. Also, since isopropylidene dimethylmalonate shows two bands above 1730 cm^{-1} these cannot be due to an equilibrium between keto and enol forms. The possibility that the two bands are due to different conformations of the 6-membered ring is rendered very unlikely by the fact that in isopropylidene dimethylmalonate there would be large 1,4-interactions in the boat form (VII).

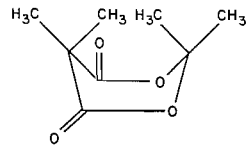

(VII)

Vibrational coupling is, therefore, the most logical answer. The fact that vibrational coupling can occur in cyclic malonates where rotational isomerism is not possible does not, however, mean that this is necessarily the explanation for the appearance of two ester carbonyl bands in open-chain malonates; all it does show is that coupling can occur between suitably situated ester carbonyl groups beta- to each other. The acidity of isopropylidene malonate must be due to the ease with which it undergoes enolization *in the presence of base.*

The difference in behavior between malonates and β-diketones is interesting. The greater degree of enolization of β-diketones has been attributed to the larger —M effect of the acyl group over that of the ester group (9) as well as in the added stabilization due to internal hydrogen bonding of the enol form (10). The cyclic β-diketone 5,5-dimethylcyclohexane-1,3-dione is enolized to an even larger extent than acetylacetone and this may be due to greater steric ease of intermolecular hydrogen bonding between two molecules of the enol existing in semichair conformations. It is tempting, therefore, to suggest that, since cyclic malonates are not enolized to any appreciable extent in the solid state or in solution whereas 5,5-dimethylcyclohexane-1,3-dione is almost completely enolized and intermolecularly chelated in the solid state, ketonic carbonyl groups have a greater tendency to undergo hydrogen bonding than similarly situated ester carbonyl groups. This could be rationalized if it were assumed that ease of hydrogen bonding in such cases depended among other things on the availability of electrons at the oxygen atom, since in ketones the alkyl group has a +I effect whereas in ester groups the alkoxyl group has a −I effect.

Some comments may also be made about the two bands at 1733 and 1710 cm^{-1} in the spectrum of 5,5-dimethylcyclohexane-1,3-dione in chloroform solution, which were previously observed by Bellamy and Beecher (8) at 1733 and 1706 cm^{-1}, and which they attributed to the unenolized keto form and to the free enol respectively. These authors observed that the band at 1603 cm^{-1}, due to the intermolecularly chelated form, vanished on great dilution owing to the breaking of the intermolecular hydrogen bonds, as expected. They found, however, that the 1710 cm^{-1} band also vanished at very high dilutions; they suggested that this band was due to the free enol form and that at these high dilutions in non-polar solvents the compound existed only in the keto form. If, after breaking the intermolecular hydrogen bonds by solution in chloroform, the free enol form were stable in that solvent it is difficult to see why further dilution with the same solvent should have rendered this form less stable. On the other hand, it is not stated whether after dilution a proportionally greater cell thickness was used in the

Can. J. Chem. Downloaded from www.nrcresearchpress.com by 190.90.36.8 on 09/04/12
For personal use only.

measurements. It may be possible that the two bands at 1733 and 1710 cm^{-1} are again due to vibrational coupling of the two unenolized carbonyl groups. A 6-membered ring ketone normally absorbs at *ca.* 1720–1710 cm^{-1} (though this might conceivably be raised to 1733 cm^{-1} if a strongly electron-attracting substituent is attached to the α-carbon atom as is the case here); an α,β-unsaturated 6-membered ring ketone, on the other hand, might be expected to absorb below 1700 cm^{-1} (11). The position of the two bands observed would fit in with the trend of one band being above, the other below, the common frequency in cases where vibrational coupling occurs (12).

ACKNOWLEDGMENTS

The author wishes to thank Dr. L. C. Leitch for a generous gift of deuterium oxide and the National Research Council for a grant-in-aid of this research. Useful discussions with Drs. J. M. Pepper and R. A. Heacock are gratefully acknowledged.

REFERENCES

1. ABRAMOVITCH, R. A. Can. J. Chem. **36**, 151 (1958).
2. TILICHEEV, M. D. J. Russ. Phys.-Chem. Soc. **58**, 447 (1927).
3. RASMUSSEN, R. S., TUNNICLIFF, D. D., and BRATTAIN, R. R. J. Am. Chem. Soc. **71**, 1068 (1949).
4. THOMPSON, H. W. J. Chem. Soc. 328 (1948).
5. O'SULLIVAN, D. G. and SADLER, P. W. J. Chem. Soc. 2916 (1957).
6. DAVIDSON, D. and BERNHARD, S. A. J. Am. Chem. Soc. **70**, 3426 (1948).
7. SCHWARZENBACH, G. and FELDER, E. Helv. Chim. Acta, **27**, 1044 (1944).
8. BELLAMY, L. J. and BEECHER, L. J. Chem. Soc. 4487 (1954).
9. INGOLD, C. K. Structure and mechanism in organic chemistry. Bell & Sons, Ltd., London. 1953. p. 555.
10. HINE, J. Physical organic chemistry. McGraw-Hill Book Co., Inc., New York. 1956. p. 233.
11. JONES, R. N., HUMPHRIES, P., and DOBRINER, K. J. Am. Chem. Soc. **72**, 956 (1950).
12. JONES, R. N. and SANDORFY, C. Techniques of organic chemistry. Vol. IX. Chemical applications of spectroscopy. Interscience Publishers, Inc., London. 1956. p. 495.

Can. J. Chem. Downloaded from www.nrcresearchpress.com by 190.90.36.8 on 09/04/12
For personal use only.

Can. J. Chem. Downloaded from www.nrcresearchpress.com by 190.90.36.8 on 09/04/12
For personal use only.

PERACETIC ACID OXIDATION OF HALOGENATED AZOBENZENES[1]

PAUL E. GAGNON AND BRIAN T. NEWBOLD[2]

ABSTRACT

A series of dihalogenated and five tetrachloroazobenzenes were oxidized to the corresponding azoxy compounds by means of 30% hydrogen peroxide in glacial acetic acid, the reaction being carried out at about 60–70° C, for 24 hours.

As expected, the yields, in general, obtained from azobenzenes containing substituents in the 2,2′-positions were lower than those from compounds having substituents in the 3,3′- and 4,4′-positions, which gave very good results.

INTRODUCTION

One of the most useful methods for the preparation of azoxybenzenes is the reduction of the appropriate nitrobenzene with a suitable reagent. However, azoxy compounds have also been obtained by oxidation of amines by means of peracids. For example, aniline when oxidized with an equimolar quantity of perbenzoic acid (1), or with peracetic acid (2), gave rise to azoxybenzene. D'Ans and Kneip (2) stated that primary amines can give rise to azo and azoxy compounds when treated with concentrated peracids under various conditions. Later, Greenspan (3) obtained a much better yield, 85%, of azoxybenzene from aniline by oxidation with 45% peracetic acid.

A third method of obtaining azoxybenzenes is the oxidation of the corresponding azobenzenes. For instance, azobenzene gave azoxybenzene when treated with an acetic acid solution of chromic acid in a sealed tube at 150–250° C (4) and 4,4′-dinitroazoxybenzene was obtained from the azo compound by the action of fuming nitric acid at room temperature (5).

The direct oxidation of azobenzenes to azoxybenzenes by means of organic peracids has been a subject of interest for many years. Angeli and others (6, 7, 8, 9) studied this reaction. For example, when azobenzene was treated for several days with peracetic acid, made by combining glacial acetic acid with 30% hydrogen peroxide, azoxybenzene was obtained (6). In a review (10), Swern states that this reaction proceeds readily under mild conditions and quantitative yields are frequently obtained, and he lists the azoxybenzenes prepared by this method up to 1949. In recent work, azobenzene was also oxidized by perbenzoic acid (11).

There are some examples of peracid oxidation of halogenated azobenzenes mentioned in the literature. For instance, 4-bromo-, 4,4′-dibromo-, and 2-bromo-4-nitro-azobenzene have been oxidized to the corresponding azoxy compounds by 30% hydrogen peroxide in glacial acetic acid (12, 13). Badger *et al.* (14) recently oxidized 3-bromo-, 4-bromo-, and 4-chloro-azobenzene with perbenzoic acid. However, only one dichloroazobenzene, namely, the 4,4′-derivative, has been oxidized to the azoxy compound by means of peracetic acid (15). Recently (16), 3,3′- and 4,4′-difluoroazoxybenzenes were prepared from the azo compounds by oxidation with peracetic acid using the method of Angeli.

The main object of the present work was to oxidize a series of dihalogenated and tetrachloroazobenzenes to the corresponding azoxy derivatives by means of 30% hydrogen peroxide in glacial acetic acid and to compare the yields obtained.

[1]*Manuscript received August 22, 1958.*
Contribution from the Department of Chemistry, Laval University, Quebec, Que., and St. Joseph's University, Moncton, New Brunswick.
[2]*Head of the Department of Chemistry, St. Joseph's University, Moncton, New Brunswick.*

Can. J. Chem. Downloaded from www.nrcresearchpress.com by 190.90.36.8 on 09/04/12
For personal use only.

THEORETICAL PART

In the present work, many oxidations of dihalogenated azobenzenes were carried out using 30% hydrogen peroxide in glacial acetic acid. The manner in which the hydrogen peroxide was added to the solution of the azo compound was found to be important. The best results were obtained when most of the hydrogen peroxide was added regularly in small portions during the first 2 hours. The solubility of the azobenzene in glacial acetic acid was of considerable importance. It was found that the azobenzenes which were very soluble were the most easily oxidized. The time of the reaction was also critical, for instance, when the period of heating at 60–70° C was only a few hours, the yields of the azoxy derivatives were low. Therefore, the period of heating for the oxidations described in this work was extended to 24 hours.

The experimental conditions for the best yields of the dihalogenated azoxybenzenes are given in Table I. It is seen that only a low yield, 28%, of 2,2′-dichloroazoxybenzene was obtained, and that almost half of the starting material was recovered. It is evident that 2,2′-dichloroazobenzene was quite stable to oxidation with peracetic acid. Bigelow *et al.* (17) found that 4-amino-azobenzene was very difficult to oxidize, there being incomplete oxidation even after 6 days of refluxing in 30% hydrogen peroxide. In the present work, however, very good yields of 3,3′- and 4,4′dichloroazoxybenzene were obtained.

TABLE I

Oxidation of halogenated azobenzenes

Azobenzenes	Amount, g	30% H_2O_2, ml	CH_3COOH, ml	Temp., °C	Azoxy compound Yield, %	M.p., °C	Lit. m.p., °C		Starting material rec., %
				Dihalogenated azobenzenes					
2,2′-Dichloro-	2.000	41	150	60–70	28	56	56	(23)	47
3,3′-Dichloro-	2.000	41	200	62–75	93	98–99	97	(24)	Nil
4,4′-Dichloro-	0.512	31	200	60–82	89	154–155	155–156	(21)	"
2,2′-Dibromo-	0.232	10	50	63–66	13	112–113	114	(25)	"
3,3′-Dibromo-	0.300	10	50	64–65	Quant.	111–112	111.5	(26)	"
4,4′-Dibromo-	0.202	16	100	65–68	Quant.	171–171.5	172	(27)	"
3,3′-Diiodo-	0.200	10	100	62–67	96	116–117	117–118	(20)	"
				Tetrachloroazobenzenes					
2,2′;3,3′-Tetrachloro-	0.042	20	150	66–70	71	136–138	—	*	Nil
2,2′;4,4′- "	0.098	30	100	65–67	26	128–129	130.5	(20)	72
2,2′;5,5′- "	0.088	35	100	65–68	25	145–146	147	(28)	75
3,3′;4,4′- "	0.160	22	150	62–68	98	137.5–138.5	137–138	(29)	Nil
3,3′;5,5′- "	0.095	20	150	61–70	71	172–173	171–172	(30)	"

*2,2′;3,3′-Tetrachloroazoxybenzene also prepared from 2,2-dichloronitrobenzene using dextrose in alkaline medium was pale yellow, m.p. 138–138.5° C. Yield, 2%. Anal. calc. for $C_{12}H_6N_2OCl_4$: Cl, 42.20%. Found: Cl, 41.22%.

By contrast, the yield of 2,2′-dibromoazoxybenzene was low, 13%, and there was apparently considerable complete oxidation, there being no recovery of unreacted starting material. Bigelow *et al.* (17) showed that both 4-nitro-4′-hydroxyazobenzene and 4-hydroxyazobenzene were completely oxidized to carbon dioxide and nitrogen by prolonged refluxing with 30% hydrogen peroxide. Quantitative yields of 3,3′- and 4,4′-dibromoazoxybenzene were obtained in the present study. As shown in Table I, the yield of 3,3′-diiodoazoxybenzene was very good, but here again, in some experiments, considerable decomposition occurred.

As far as we know, there are no instances of oxidation of tetrachloroazobenzenes with

peracetic acid that have been recorded in the literature. In the present work, five tetrachloroazoxybenzenes were prepared from the azo compounds by oxidation with 30% hydrogen peroxide in glacial acetic acid. The solubility of the tetrachloroazobenzene in glacial acetic acid, the manner in which the hydrogen peroxide was added, and the time of heating were of importance.

The experimental conditions and best results are given in Table I. It is seen that the yield of 2,2′;3,3′-tetrachloroazoxybenzene, which is described for the first time, was 71%, whereas the yields of 2,2′;4,4′- and 2,2′;5,5′-tetrachloroazoxybenzene were only 26 and 25% respectively. By comparison, both 3,3′;4,4′- and 3,3′;5,5′-tetrachloroazobenzene gave good yields of the azoxy derivatives.

In general, it may be said that oxidation of halogenated azobenzenes with peracetic acid is a good method for the preparation of azoxybenzene derivatives having no substituents in the 2,2′-positions.

EXPERIMENTAL PART*

Preparation of Halogenated Azobenzenes

The halogenated azobenzenes were prepared from the corresponding nitrobenzenes by standard methods given in the literature. For example, 4,4′-dichloroazobenzene was made by reducing 4-chloronitrobenzene with magnesium and absolute methanol (18). In the case of 3,3′;4,4′-tetrachloroazobenzene, the azoxy compound (19) was reduced with zinc dust and sodium hydroxide, followed by oxidation in air, as previously described (20).

Peracetic Acid Oxidation

The procedure followed was essentially the same in every case; therefore the preparation of only one compound needs to be described in detail.

4,4′-Dichloroazobenzene (0.512 g) was dissolved in glacial acetic acid (200 ml) at 80° C, and then 30% hydrogen peroxide (2 ml) was added. Further additions of 30% hydrogen peroxide (2 ml) were made every 15 minutes during the first 2 hours, when a further 5 ml was added. The heating was continued at about 65° C, then after 3 hours, 3 ml of 30% hydrogen peroxide was added. To complete the reaction, after 19 and 20 hours 2- and 5-ml portions of hydrogen peroxide, respectively, were added. Heating was continued until the 24-hour period was over, the solution being then allowed to cool to room temperature. The original orange color had changed to pale yellow. The solution was poured into an excess of water (300 ml) and a pale yellow product separated out. It was washed with water and dried. Crude yield, 89%. The 4,4′-dichloroazoxybenzene was recrystallized several times from ethanol as pale yellow needles, m.p. 154–155° C, alone or with an authentic sample (lit. m.p. 155–156° C (21)).

In some cases, the aqueous filtrate, obtained after precipitation with water and filtration, yielded a small amount of product after standing in a refrigerator. In some experiments, precipitation took place after several portions of hydrogen peroxide had been added and glacial acetic acid was used to restore the solution. In cases where there was incomplete oxidation, that is, where a mixture of azoxy compound and starting material was obtained, separation was achieved either by crystallization or chromatography. The latter method was used particularly for the separation of products obtained from the oxidation of the tetrachloroazobenzenes. The chromatography was carried out with columns containing a (4:1) mixture of salicylic acid – celite as absorbant. The celite was celite 535. The products were placed on the column in ligroin solution and

**All melting points are uncorrected.*

Can. J. Chem. Downloaded from www.nrcresearchpress.com by 190.90.36.8 on 09/04/12
For personal use only.

development was carried out with ligroin (b.p. 66–75° C). Elution was achieved with 95% ethanol. The azoxy compound was absorbed high on the column as a yellow band and the starting material (orange band) moved down to the bottom or was passed into the filtrate. The products separated by chromatography were further purified by recrystallizations from ethanol. In order to verify the oxidation method used in the present work, azobenzene was employed as a reference compound. Azobenzene (2 g), glacial acetic acid (50 ml), 30% hydrogen peroxide (18 ml) were heated at 65° C for 24 hours. The crude yield of azoxybenzene was 83%: m.p. 35–36° C, alone or with an authentic sample (lit. m.p. 35.5–36.5° C (22)).

The experimental details and results for all the halogenated azoxybenzenes prepared are given in Table I.

ACKNOWLEDGMENT

The authors wish to express their sincere thanks to Dr. Karl F. Keirstead, who gave them some halogenated azo- and azoxy-benzene samples.

REFERENCES

1. PRILESCHAJEW, N. Ber. **42**, 4811 (1909).
2. D'ANS, J. and KNEIP, A. Ber. **48**, 1136 (1915).
3. GREENSPAN, F. P. Ind. Eng. Chem. **39**, 847 (1947).
4. PETRIEW, H. Ber. **6**, 557 (1873).
5. WEINER, A. and STIASMY, E. Ber. 3263 (1899).
6. ANGELI, A. Atti accad. nazl. Lincei, **19** [I], 793 (1910).
7. ANGELI, A. and ALESSANDRI, L. Atti accad. nazl. Lincei, **20** [I], 896 (1911).
8. ANGELI, A. Gazz. chim. ital. **46** (2), 67 (1916).
9. BIGIAVI, D. and SABATELLI, V. Gazz. chim. ital. **57**, 559 (1927).
10. SWERN, D. Chem. Revs. **45**, 1 (1949).
11. BADGER, G. M., BUTTERY, R. C., and LEWIS, G. E. J. Chem. Soc. 2143 (1953).
12. ANGELI, A. and VALORI, B. Atti. accad. nazl. Lincei, **21** [I], 155 (1912).
13. BIGIAVI, D., ALBANESE, C., and POGGI, I. Gazz. chim. ital. **61**, 392 (1931).
14. BADGER, G. M., BUTTERY, R. C., and LEWIS, G. E. J. Chem. Soc. 2147 (1953).
15. BURNS, J., MCCOMBIE, H., and SCARBOROUGH, H. A. J. Chem. Soc. 2928 (1928).
16. GORE, P. H. and WHEELER, O. H. J. Am. Chem. Soc. **78**, 2160 (1956).
17. BIGELOW, H. E., HOLDER, C. H., and LINTON, E. P. Can. J. Research, B, **19**, 132 (1941).
18. KEIRSTEAD, K. F. Can. J. Chem. **31**, 1064 (1953).
19. GAUDRY, R. and KEIRSTEAD, K. F. Can. J. Research, B, **27**, 893 (1949).
20. GAUDRY, R. and KEIRSTEAD, K. F. Can. J. Research, B, **27**, 900 (1949).
21. HEUMANN, K. Ber. **5**, 911 (1872).
22. BIGELOW, H. E. and PALMER, A. Org. Syntheses, Collective Vol. **II**, 57 (1943).
23. BRAND, K. J. prakt. Chem. **67**, 145 (1903).
24. LAUBENHEIMER, A. Ber. **8**, 1623 (1875).
25. ZECHMEISTER, L. and ROM, P. Ann. **468**, 117 (1928).
26. GABRIEL, S. Ber. **9**, 1405 (1876).
27. FARROW, M. D. and INGOLD, C. K. J. Chem. Soc. 2543 (1924).
28. DE CRAUW, T. Rec. trav. chim. **50**, 782 (1931).
29. DAINS, F. B. and KENYON, W. O. J. Am. Chem. Soc. **52**, 2357 (1931).
30. BEILSTEIN, F. and KURBATOW, A. Ann. **197**, 84 (1879).

Can. J. Chem. Downloaded from www.nrcresearchpress.com by 190.90.36.8 on 09/04/12
For personal use only.

Can. J. Chem. Downloaded from www.nrcresearchpress.com by 190.90.36.8 on 09/04/12
For personal use only.

A NEW SPECTROPHOTOMETRIC PROCEDURE FOR PLATINUM WITH TIN (II) CHLORIDE[1]

S. S. Berman and E. C. Goodhue

ABSTRACT

A spectrophotometric procedure has been developed for microgram quantities of platinum utilizing an absorption peak at 310 mμ formed when platinum salts react with tin (II) chloride. The method offers a 5-fold increase in sensitivity over the conventional platinum – tin (II) chloride procedure. Several factors influencing the intensity and stability of the absorbing species, whose nature is unknown, are described. Palladium and rhodium produce gross interferences, but small quantities of iridium, iron, copper, and chromium can be tolerated. The procedure is applicable to fumed sulphuric acid solutions of platinum and to solutions of platinum in nitric acid. The recommended concentration range is 0.4 to 6 p.p.m. when measurements are made in 1.0-cm cells.

INTRODUCTION

Tin (II) chloride has long enjoyed wide use as a satisfactory colorimetric reagent for platinum. The earliest reported application was in 1921 by Davis (1). Several workers have since investigated this reagent (2, 3, 4, 5, 6, 7), the most extensive report being produced by Ayres and Meyer (4). In spite of its relatively low sensitivity tin (II) chloride has been preferred in many laboratories because it offered a wide freedom from interference and range of applicability. Two other reagents have also found a wide use. These are potassium iodide (3) and *p*-nitrosodimethylaniline (8). The potassium iodide procedure is less sensitive than that involving tin (II) chloride and suffers gross interferences. The *p*-nitrosodimethylaniline method is the most sensitive procedure for platinum published to date. It is fairly tolerant to the presence of some base metals but is not applicable to solutions of platinum in sulphuric acid and the conditions for the development of the colored species must be followed rather rigorously. (The diacetoimidoplatinum method of Barkovskiĭ and Kul'berg (9) has been reported in Chemical Abstracts (10) to be applicable to platinum concentrations "varying between 25 and 90 μg per liter". However, a study of the original paper has shown that this should have read "250 to 900 μg per ml".)

A comparison of the sensitivities of some of the usefully developed spectrophotometric procedures for platinum is given in Table I.

Ayres and Meyer (4) in their examination of the tin (II) chloride procedure (absorption maximum at 403 mμ) noted the existence of a second absorption peak at about 310 mμ

TABLE I

Sensitivity of spectrophotometric methods for platinum

Method	Molar absorptivity
Thiosemicarbazide (13)	2.46
Diacetoimidoplatinum (9)	2.4×10^2
Potassium iodide (3)	6.05×10^3
Tin (II) chloride (403 mμ) (4)	7.83×10^3
Hexachloroplatinate (14)	8.40×10^3
Phenylthiosemicarbazide (15)	1.35×10^4
Tin (II) chloride (310 mμ)	3.95×10^4
p-Nitrosodimethylaniline (8)	5.29×10^4

[1]*Manuscript received August 25, 1958.*
Contribution from the Division of Applied Chemistry, National Research Council, Ottawa, Canada. Issued as N.R.C. No. 5008.

but stated that the absorption of the reagent blank was so great below 325 mμ as to render this peak unsuitable for use. The authors have succeeded in establishing conditions whereby this absorption peak can be used as the basis for a precise and sensitive determination of platinum. This was done primarily by a gross reduction in the quantity of tin (II) chloride used to produce the absorbing species, and the addition of sulphuric and perchloric acids to stabilize the species and affect a hypsochromic shift in the absorption band due to the tin (II) chloride reagent. A spectral curve (A) of a solution containing 3.92 p.p.m. of platinum treated by the procedure described below is shown in Fig. 1. The absorbance at 310 mμ is five times that at 403 mμ, and the spectral curve (B) of the reagent blank against water shows that the absorbance of the blank is quite low at 310 mμ.

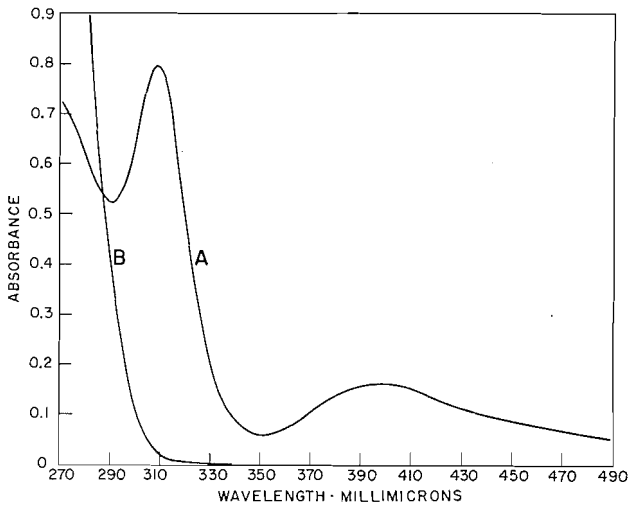

FIG. 1. A: Spectral curve of a solution containing 3.92 p.p.m. platinum against a reagent blank.
B: Spectral curve of the reagent blank against water.

EXPERIMENTAL

Apparatus and Solutions

Absorption measurements were made with a Beckman Model DU quartz spectrophotometer equipped with a hydrogen lamp source and matched 1.00-cm quartz cells. Spectral curves and some studies of the stability of the absorbing species under various conditions were made with a Beckman Model DK-1 recording spectrophotometer.

A standard platinum solution was prepared by dissolving pure platinum sponge in aqua regia, evaporating several times to dryness with hydrochloric acid, and then dissolving the residue and diluting with 0.1 *M* hydrochloric acid. The solution was standardized by precipitation with 4-phenylthiosemicarbazide (11). A 5-ml aliquot of this solution was diluted to 1000 ml with 0.1 *M* hydrochloric acid. The resulting solution contained 9.80 μg of platinum per milliliter of solution.

The reagent was a 2% w/v solution of tin (II) chloride dihydrate in 1.5 *M* hydrochloric acid. The reagent was prepared by dissolving the tin (II) chloride in concentrated hydrochloric acid and then diluting the solution with water.

All chemicals used were of analytical reagent grade.

Can. J. Chem. Downloaded from www.nrcresearchpress.com by 190.90.36.8 on 09/04/12
For personal use only.

Can. J. Chem. Downloaded from www.nrcresearchpress.com by 190.90.36.8 on 09/04/12
For personal use only.

DEVELOPMENT OF THE METHOD

Preliminary experiments using 5-ml aliquots of the dilute stock platinum solution, 5 ml of concentrated hydrochloric acid, and 2 ml of the reagent solution diluted to 25 ml with water, showed that a stable absorption peak was produced at 310 mμ. The absorbance of the reagent blank measured against water was 0.080. A slit width of about 0.3 mm was required when making measurements on the platinum solutions against a reagent blank.

However, very erratic results were obtained when the stock solution was treated in any way prior to the development of the color in an effort to simulate an actual sample in practice (e.g. boiling with hydrochloric acid, addition of sulphuric acid). Furthermore, it was found that in all these cases the absorption species was not stable, tending to fade rather rapidly, the rate of fading being proportional to the amount of light to which the sample was subjected. The addition of perchloric acid to the system prior to the addition of the reagent succeeded in stabilizing the color but did not increase the precision.

It was found that very precise results could be obtained, regardless of prior treatment of the platinum solution, if sulphuric acid was added and the solution heated to expel all volatile acids (care being taken not to fume the sample).

THE REAGENT

There was no difference in the absorbance produced when 1, 2, or 4 ml of reagent were used. However, 0.5 ml of reagent was insufficient to produce maximum absorbance. In order to keep the absorbance of the reagent blank at 310 mμ at a minimum, 2 ml was chosen as the optimum quantity.

Some experiments were carried out in which the hydrochloric acid concentration of the reagent was 3 *M* instead of 1.5 *M*. This difference in acid concentration had no apparent effect on the absorbance of the resulting solutions.

Low results were sometimes obtained when the color was developed with reagent solution that was one or two days old. It is therefore recommended that fresh reagent solution be prepared daily.

EFFECT OF PERCHLORIC ACID

The addition of concentrated perchloric acid (70–72%) had the effect of stabilizing the system. Solutions which contained no perchloric acid faded quickly, especially when exposed to light.

Some experiments were carried out in which the solutions were entirely shielded from light. The rate of fading was much less in these cases but still too fast to produce reliable results. The same phenomenon was noticed by one of the authors (S.S.B.) in the development of a similar spectrophotometric procedure for rhodium with tin (II) bromide (12). In this case perchloric acid also stabilized the system.

No differences in absorbance were apparent when quantities of concentrated perchloric acid ranging from 5 to 10 ml were used. Five milliliters was chosen as the optimum amount.

When 5 ml of concentrated perchloric acid was used the yellow color of the solution developed totally within a few minutes of the addition of the reagent. The absorbance was stable for at least 4 hours and decreased by only a few per cent in 18 hours.

Another effect of the addition of perchloric acid was to produce a hypsochromic shift in the absorption band due to the tin (II) chloride reagent. The absorbance of the reagent blank containing 5 ml of perchloric acid measured against water at 310 mμ

was 0.020. Slit widths of only about 0.13 mm were required when making absorbance measurements against reagent blanks.

EFFECT OF SULPHURIC ACID

After the preliminary experiments it was evident that all platinum solutions would have to be pretreated in some manner in order to convert the platinum to some species which would react favorably with the tin (II) chloride reagent.

Boiling with hydrochloric acid and with aqua regia were tried unsuccessfully.

It was found, however, that if sulphuric acid and hydrochloric acid were added to the platinum solution and the solution heated, but not fumed, until all the hydrochloric acid was evolved, quite reproducible results could be obtained regardless of the previous history of the sample.

Quantities of concentrated sulphuric acid ranging from 5 to 10 ml produced no differences in the absorbance of replicate samples. Six milliliters was chosen as the optimum value as less than 5 ml proved to be inadequate (low results being obtained) and there is always the danger of losing some acid by fuming.

Fumed samples generally gave low results unless the precaution was taken of adding several milliliters of concentrated hydrochloric acid again and boiling until the volatile acid had been expelled.

Several samples which were fumed quite strongly and then treated with hydrochloric acid as described above gave excellent results.

RECOMMENDED PROCEDURE

Transfer the solution containing the platinum to a small beaker. Add 6 ml of concentrated sulphuric acid and 5 ml of concentrated hydrochloric acid. Cover and boil the solution gently on a hot plate until all the hydrochloric acid is expelled taking care not to bring the solution to fumes of sulphuric acid. Cool and transfer the sulphuric acid solution to a 25-ml volumetric flask with a small quantity of water. Add 5 ml of concentrated perchloric acid followed by 2.0 ml of the reagent. Dilute to volume with water and mix thoroughly. Measure the absorbance at 310 mμ using a reagent blank for comparison.

PRECISION ATTAINABLE

The mean absorbance of 12 replicate samples each containing 49.0 μg of platinum in a final volume of 25 ml was 0.397. The mean deviation of these results was 0.002 or 0.5%.

ADHERENCE TO BEER'S LAW

The solutions adhered to Beer's law throughout the whole range of concentrations tested, which was from 0.4 to 6 p.p.m. This is demonstrated in Table II.

A solution containing 0.078 p.p.m. of platinum was prepared and the absorbance measured in 5-cm quartz cells. The absorbance was 0.080 giving an absorbance to

TABLE II

Adherence to Beer's law

P.P.M. Pt (C)	Absorbance (A)	Ratio A/C
0.392	0.081	0.206
1.18	0.240	0.202
1.96	0.397	0.201
3.92	0.796	0.202
5.88	1.190	0.201

Can. J. Chem. Downloaded from www.nrcresearchpress.com by 190.90.36.8 on 09/04/12
For personal use only.

concentration ratio (when corrected for the longer path length) of 0.204. This agreed very well with the ratios obtained for the more concentrated solutions and indicated that the procedure was quite applicable for these small quantities of platinum.

The recommended range for this procedure is 0.4 to 6 p.p.m. when measurements are made in 1-cm cells, and 0.08 to 1.2 p.p.m. when measurements are made in 5-cm cells.

INTERFERENCES

Gross quantities of nitric acid can be tolerated as this acid is expelled along with the hydrochloric acid in the pretreatment of the sample.

Several metals commonly associated with platinum were tested to ascertain their effect on the procedure. The results of these tests are shown in Table III. In each case the metal was added prior to the sulphuric acid – hydrochloric acid treatment of the sample.

TABLE III

Effect of diverse metals on 49.0 μg Pt

Metal added	Absorbance
—	0.397
47.8 μg Pd^{++}	0.741
45.4 μg Ir^{++++}	0.410
49.9 μg Rh^{+++}	0.890
1.0 mg Cu^{++}	0.410
1.0 mg Ni^{++}	0.355
1.0 mg Fe^{+++}	0.406
1.0 mg Cr^{+++}	0.399

It is apparent that small quantities (up to 1 mg) of chromium, iron, and copper and equivalent amounts of iridium produce a maximum error of 3% in the estimation of platinum.

EFFECT OF USING A TUNGSTEN LAMP AND COREX CELLS

All the work reported above was done using a hydrogen lamp source and quartz cells, since 310 mμ is beyond the recommended limit (320 mμ) for Corex-glass cells. Since many laboratories do not have an ultraviolet accessory it was decided to test the procedure using a tungsten lamp source and Corex-glass cells. It was found that measurements could be made quite conveniently, the only effect being the increase in slit width from 0.13 to 0.34 mm due to the loss of energy at this wavelength.

REFERENCES

1. Davis, C. W. U.S. Bur. Mines, Tech. papers, 270 (1921).
2. Wölbling, H. Ber. **67**, 773 (1934).
3. Sandell, E. B. Colorimetric determination of traces of metals. Interscience Publishers Inc., New York. 2nd ed. 1950.
4. Ayres, G. H. and Meyer, A. S. Anal. Chem. **23**, 299 (1951).
5. Ayres, G. H. Anal. Chem. **25**, 1622 (1953).
6. Meyer, A. S. and Ayres, G. H. J. Am. Chem. Soc. **77**, 2671 (1955).
7. Milner, O. I. and Shipman, G. F. Anal. Chem. **27**, 1476 (1955).
8. Kirkland, J. J. and Yoe, J. H. Anal. Chem. **26**, 1340 (1954).
9. Barkovskiĭ, V. F. and Kul'berg, L. M. Izvest. Sektora Platiny i Drug. Blagorod. Metal., Inst. Obschei i Neorg. Khim., Akad. Nauk S.S.S.R. **29**, 141 (1955).
10. Chemical Abstracts, **50**, 9932 (1956).
11. Fraser, J. G. M.A. Thesis, University of Toronto, Toronto, Ontario, Canada. 1951.
12. Berman, S. S. and Ironside, R. Can. J. Chem. **36**, 1151 (1958).
13. De Trecco, D. R. Rev. asoc. Bioquím. arg. **15**, 355 (1951).
14. Kirkland, J. J. and Yoe, J. H. Anal. Chim. Acta, **9**, 441 (1953).
15. Komatsu, S. and Oonishi, K. J. Chem. Soc. Japan, Pure Chem. Sect. **76**, 661 (1955).

Can. J. Chem. Downloaded from www.nrcresearchpress.com by 190.90.36.8 on 09/04/12
For personal use only.

Can. J. Chem. Downloaded from www.nrcresearchpress.com by 190.90.36.8 on 09/04/12
For personal use only.

MICROCALORIMETRY OF ADSORPTION OF WATER VAPOR ON LEAD DI-IODIDE[1]

HENRY M. PAPÉE[2]

ABSTRACT

Using a microcalorimeter of the Calvet type, measurements of the total heat of adsorption of water vapor on microcrystals of lead di-iodide have been made. By comparing the results obtained with those relating to the kinetic process of surface sintering by water vapor, heats for the process of sintering were calculated. The same sintering characteristics were found for preheated and unheated samples, but it was found that the heated product adsorbs more water than the original salt. Qualitative experiments on lead mono-iodide show a different pattern of heat evolution with time, and the over-all process requires more water to reach completion than in the case of di-iodide. The heats evolved are much greater, probably partly due to the reaction of water with the surface.

INTRODUCTION

The activity of lead iodide crystals towards ice nucleation and cloud precipitation (1, 2, 3, 4, 5) has recently resulted in studies with the object of gaining insight into the mechanism of the process. Much information was obtained by Birstein (6), who studied the process using conventional adsorption techniques and established that a considerable number of layers of water molecules can be formed on lead iodide particles. A study of the phenomenon by use of microcalorimetry was attempted in this laboratory under a U.S.A.F. contract, with the object of directly measuring the energies of the steps involved.

EXPERIMENTAL

Apparatus

A microcalorimeter of the Tian–Calvet type was used, and the general pattern of the experimentation followed closely that used recently in this laboratory for the study of the process of adsorption of water vapor on sodium chloride microcrystals (7).

Reagents

Pure lead di-iodide of large specific surface areas was prepared by a method previously described, and the specific areas of the product were changed, when required, by heating (8).

Procedure

Three series of experiments* were carried out as follows:

Series 1.—In this series of measurements, the microcalorimetry was carried out using different amounts of salt originating from a batch product of an initial surface area of 2.05 m^2/g. The original material was never heated above 25° C.

Series 2.—The work was done on samples of different specific surface areas. These were obtained by heating the original product under vacuum.

Series 3.—Two measurements were carried out on samples of lead mono-iodide. This product was obtained from the di-iodide by thermal decomposition at 240° C under dry nitrogen and at atmospheric pressure. The product obtained in this way had been outgassed by pumping it to a high vacuum for several days at 25° C.

[1]*Manuscript received August 28, 1958.*
Contribution of the Department of Chemistry, University of Ottawa, Canada.
[2]*Present address: Division of Applied Chemistry, National Research Council, Ottawa, Canada.*
**All calorimetry experiments were carried out at the pressure of water vapor at 25° C. Every experiment lasted 24 hours and was performed at 25.00° C.*

Can. J. Chem. Downloaded from www.nrcresearchpress.com by 190.90.36.8 on 09/04/12
For personal use only.

RESULTS

The admission of water vapor into the cell containing lead iodide leads to a pattern of heat evolution with time, such as the one shown in Fig. 1. The process is slow and takes several hours to finish. Since it is to be expected that an initial fast process of adsorption will be followed by a slow process of sintering of the surface, and since the kinetic aspect of this second phenomenon is known, heats corresponding to both processes can be estimated graphically from the experimental curves.

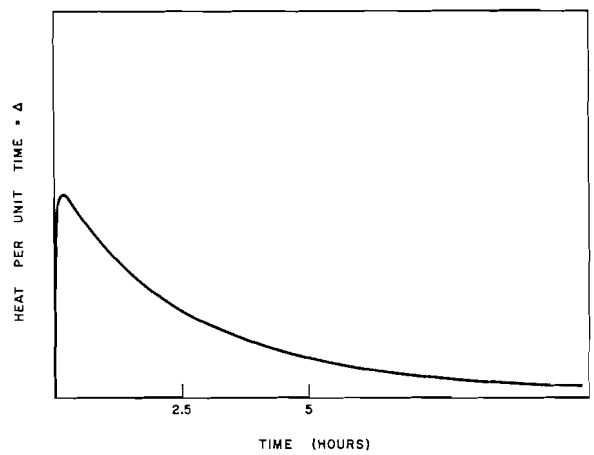

FIG. 1. Schematic plot of rate of heat evolution against time.

The decrease of lead iodide surface with time upon hydration has been shown previously (8) to follow a first-order pattern according to the equation

$$[1] \qquad \log(S-S_\infty) = -0.245t+A.$$

The symbols used in this paper are:

S: specific surface in meters^2 per gram, at time t,
t: time in hours,
S_0: initial specific surface of the product,
S_∞: specific surface of the product after long exposure to water vapor,
Q: heat of sintering,
A, a, b: constants,
w: weight of salt used in experiment,
Δ: deviation of galvanometer, approximately equal to (rate of heat evolution) $\times$ (proportionality constant).*

1st Series

The values of S_0 and S_∞ in this series were determined by B.E.T. nitrogen adsorption, and were $S_0 = 2.05$ and $S_\infty = 0.82$. Constant A of equation [1] is therefore $A = 0.090$ and

$$[2] \qquad S-S_\infty = \exp\{2.303(-0.245t+0.090)\}.$$

The process of heat evolution representative of the sintering of the crystalline surface under exposure to water vapor will follow the general equation

**Because of the slowness of the process this approximation is very good.*

$$[3] \qquad \frac{dQ}{dt} = a\left(w\frac{d(S-S_\infty)}{dt}\right) = b\Delta\,.$$

Substituting eq. [2] in [3] and taking logarithms

$$[4] \qquad \log\Delta = \log((-a/b)0.564)+\log w-0.245t+0.090$$

or

$$[4'] \qquad \log\Delta = \log w-0.245t+K$$

in which the constant K contains all constants of eq. [4].

Figure 2 shows a series of calorimetric heat evolution curves in logarithmic form and represents examples of patterns obtained when working with different amounts of substance. The dotted line through the origin represents a line of gradient -0.245, which was obtained by measuring the kinetics of sintering by B.E.T. nitrogen estimation of surfaces at different times. Good agreement between the two methods can be seen.

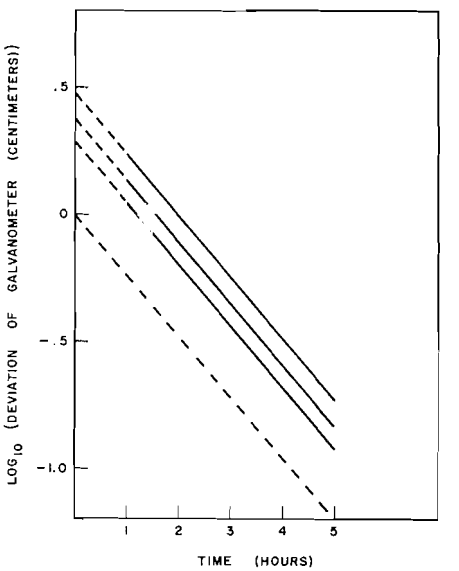

FIG. 2. Plot of decimal logarithm of rate of heat evolution against time, in microcalorimetry salt container. The lines represent experiments with different weights of the product. The dotted line gives the slope of the process as obtained by other means, and using B.E.T. surface measurements.

It was noticed that the curves become linear after about 30 minutes, initial irregularities being partly due to the heat of adsorption which superposes itself on the heat of sintering of the surface. Furthermore, for rapid initial heat evolution, the expression for Δ is no longer accurate enough (see also ref. 9). Because of this, the curves are shown after the first hour has elapsed, by which time they obey with good approximation the law of eq. [1].

Extrapolating the plots to zero time, the hypothetic value of the parameter Δ at the start of the process can be obtained. Under such conditions eq. [4'] becomes

$$[4''] \qquad [\log\Delta]_{t=0} = \log w+K.$$

Thus constant K can be obtained. Based on 9 experimental values it is found to be:

Can. J. Chem. Downloaded from www.nrcresearchpress.com by 190.90.36.8 on 09/04/12
For personal use only.

$$K = -0.08 \pm 0.02.$$

Substitution of the value for K in eq. [4′] gives, for unit weight of salt,

[4‴] $$\Delta = 10^{(-0.245t-0.08)}.$$

Taking the calibration coefficients of the instrument into account, and integrating eq. [4‴] between zero and infinite time, the value of 0.084 ± 0.006 cal/g is obtained, and corresponds to the sintering of the surface of 1 g of lead di-iodide from 2.05 to 0.82 m^2/g.*

The over-all heat of the process is obtained by planimetric integration of the recorded curves. The results obtained are shown in Fig. 3. The heat evolved by 1 g of di-iodide when put in contact with water vapor is given by the slope of the line and is found to be 0.179 ± 0.007 cal.

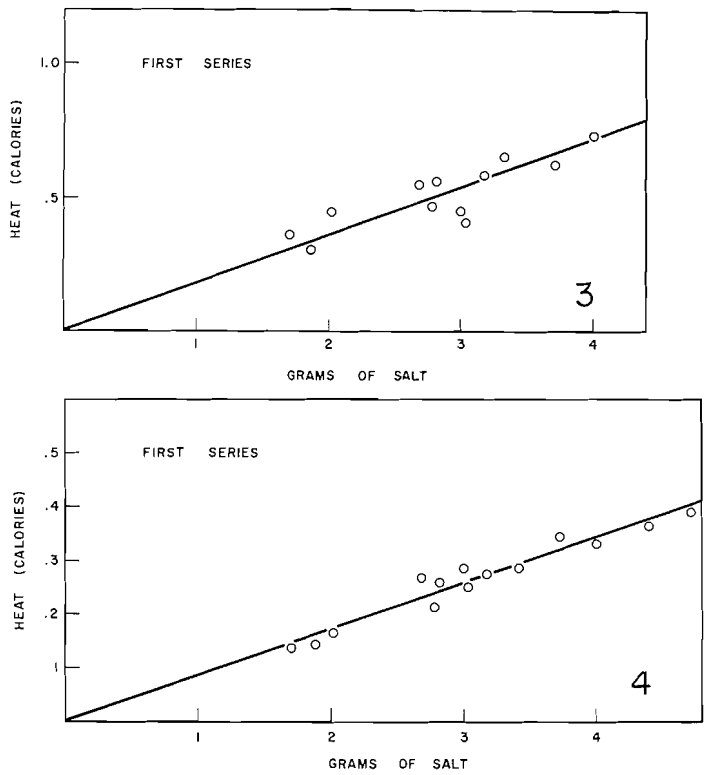

FIG. 3. Plot of over-all heat obtained by planimetric integration of areas under curves recorded, for cell in which salt was contained, against weight of salt.
FIG. 4. Plot of heat absorbed in cell from which water was evaporating, against weight of salt.

The evaporation of water necessary to induce the process described above was followed simultaneously, and the recorded curves showed rapid initial evaporation of water, but this was of short duration and only very small amounts of water evaporated per unit time after several hours. No relationship between kinetics of sintering and the amount of water used could be established. The heats of evaporation of water were therefore estimated by planimetric integration of the area obtained experimentally, and the

The values quoted in the present paper are 'thermochemical' calories, equal to 4.1840 joules. The instrument was calibrated electrically.

Can. J. Chem. Downloaded from www.nrcresearchpress.com by 190.90.36.8 on 09/04/12
For personal use only.

results representing the over-all process are shown in Fig. 4. The slope of the line gives the heat of evaporation of water required for the process of adsorption on, and sintering of, the salt, and is 0.086 ± 0.002 cal/g.

Since the specific surface of the salt is equal to 0.82 m^2/g, at the end of the process, the amount of the water adsorbed by unit surface will be deduced from the heat absorbed and the latent heat of evaporation of water. The heat of evaporation of the amount of water used in the process just discussed is

$$(0.086 \pm 0.002)/0.82 = 0.105 \pm 0.0024 \text{ cal/m}^2$$

and assuming 10.6 $Å^2$ for the area occupied by a water molecule, the coverage is calculated to be 0.68 ± 0.02 layers.

*2nd Series**

Since samples of different initial surface areas were used in this case, eq. [1] will become

$$[5] \qquad (S - S_\infty) = (S_0 - S_\infty) \exp(-0.5642t),$$

which after substitution in eq. [3] becomes on taking logarithms

$$[6] \qquad \log \Delta = -0.245t + \log\{w(S_0 - S_\infty)\} + K$$

where K is constant.

Experiments were performed on 4 batches of salt, each of which was heated for 24 hours, to a different temperature. The specific areas of the products were determined by B.E.T. nitrogen adsorption both before exposure to water vapor and after long periods of exposure. Plots of ($\log \Delta$) against time were found to follow linear patterns of the type previously discussed and the gradients of the lines were the same as before. From these K is obtained following the method previously described. Seven separate runs give $K = -0.25 \pm 0.03$. This shows that sintering of lead di-iodide crystals that were moderately heated under vacuum by exposure to water vapor proceeds along a pattern similar to that of unheated salt. Substitution of the calculated value of K in eq. [6] leads after rearrangement and integration of Δ between zero and infinite time to a value of 0.056 ± 0.006 cal and represents the heat that is developed when 1 g of

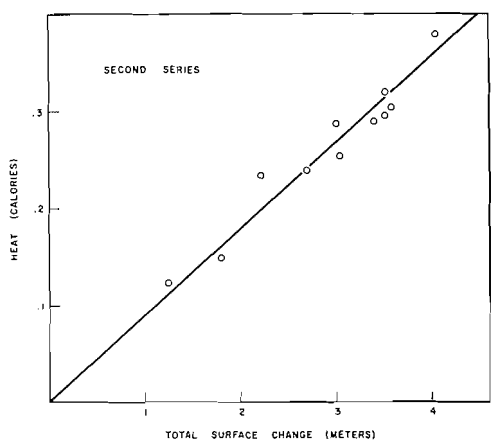

FIG. 5. Plot of over-all heat obtained by planimetric integration of areas under curves recorded for cell in which salt was contained, against $w(S_0 - S_\infty)$.

**Salt sintered by heat under vacuum in the range between 50 and 150° C.*

Can. J. Chem. Downloaded from www.nrcresearchpress.com by 190.90.36.8 on 09/04/12
For personal use only.

salt sinters by 1 m². Planimetric integration of the over-all phenomenon leads to results shown in Fig. 5, where the heat obtained is plotted against $w(S_0-S_\infty)$. The over-all heat that is evolved when the total surface changes by 1 meter is obtained from the slope of the line, and is 0.089 ± 0.002 cal.

As in the previous series, the heats of evaporation of water required to induce the phenomena described above were estimated by planimetric integration of the over-all areas under the curve. In contrast to Series 1, the phenomenon seemed to last longer, and the rate of heat evolution after 24 hours, although very small, could still be detected, and was fairly constant over the last 10 hours. However, no counterpart of this could be detected in the salt container. The heats are given in Fig. 6, which shows furthermore that the amount of water used in the process is a function not of the surface change but of the final surface S_∞.

The slope of the line gives the heat per unit surface, and is in this case 0.278 ± 0.004 cal/m² and the corresponding coverage is 1.79 ± 0.03 layers.

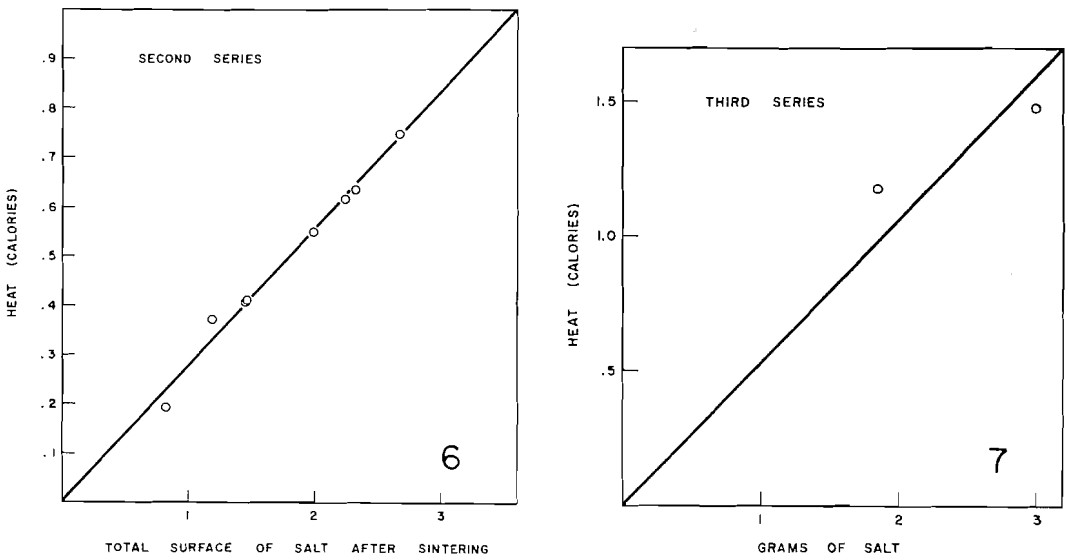

FIG. 6. Plot of heat absorbed in cell from which water was evaporating against product of weight of salt multiplied by its surface area after hydration.
FIG. 7. Plot of over-all heat evolved in salt container against weight of salt.

3rd Series

Although the conversion of the lead di-iodide by heating at 240° under dry nitrogen gave a mono-iodide 98.6% pure, it is not certain whether the subsequent outgassing in vacuum at 25° C liberated completely the surface of the product from elementary iodine which must have certainly been adsorbed there. The results reported in this series are therefore to be considered only as a by-product of the main experimentation, and are reported for the purpose of a tentative comparison with the previous data. Furthermore, the preparation of lead iodide for cloud-seeding experiments (cf. refs. 1, 2, 3, 4, 5) must invariably result in partial alteration of the salt (8). It is thought therefore that a brief discussion of the results obtained in this series is justified, since it might be helpful towards further studies of the subject.

Can. J. Chem. Downloaded from www.nrcresearchpress.com by 190.90.36.8 on 09/04/12
For personal use only.

Two runs were made on samples originating from the same batch. This consisted of salt of specific surface area of 0.84_5 m²/g. No determinations were made of the surface after hydration.

Plots of [log Δ] against time in both cases gave straight lines of gradients -0.12_2 hours^{-1}.

Heats evolved in the salt cell were estimated planimetrically and are plotted in Fig. 7 against the weight of salt. The line was fixed through the origin, and its gradient is 0.53 ± 0.06 cal/g.

Finally, the heat absorbed in the water container is given in Fig. 8 as a function of the amount of salt on which adsorption was carried out. The slope of the line is 0.31 ± 0.08 cal/g $= 0.4 \pm 0.1$ cal/m². This corresponds to the amount of water required to form 2.4 ± 0.61 layers.

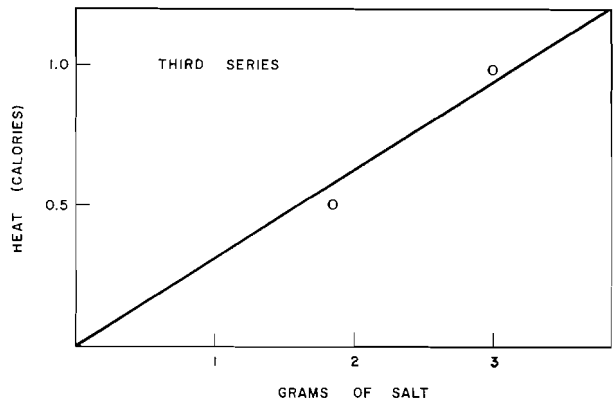

FIG. 8. Plot of heat absorbed in cell from which water was evaporating, against weight of salt.

DISCUSSION

The results obtained are summarized in the table.

Series	Nature of salt	Heat of sintering of surface under exposure to water vapor, cal/m²	Total heat measured, cal/m²	Heat of evaporation of water, cal/m² of sintered salt	Water coverage layers
1	PbI_2 salt handled only at temperatures below 25° C	0.068 ± 0.005	0.145 ± 0.006	0.105 ± 0.002	0.68 ± 0.02
2	PbI_2 salt heated between 50 and 150° C before adsorption measurements	0.056 ± 0.006	0.089 ± 0.002	0.278 ± 0.004	1.79 ± 0.03
3	PbI obtained from PbI_2 by thermal decomposition		0.53 ± 0.06	0.31 ± 0.08	2.4 ± 0.6

It can be seen that for PbI_2 no difference in the kinetic pattern of sintering of the surface by exposure to water vapor takes place, whether the surface was moderately heated or not, since the rate plots obey the same law. As expected, this is different in case of lead mono-iodide, although the general pattern probably remains of the first order with respect to surface.

Can. J. Chem. Downloaded from www.nrcresearchpress.com by 190.90.36.8 on 09/04/12
For personal use only.

In the case of preheated samples, the results are slightly lower than in the case of samples that were handled at room temperature. It is interesting to note, however, that the product which has been 'activated' by heat adsorbs a considerably larger amount of water than a non-activated salt. Since the heat evolved in the salt container in the first two series of experiments does not indicate condensation of water on the surface, or chemical reaction such as hydrolysis etc., this result can be tentatively interpreted in terms of 'electrostriction' of water molecules around charges appearing in the original area of imperfections induced by heat, after the surface is placed in contact with water vapor. Detailed analysis of the absorption of heat in the water container with time is indicative of a similar pattern. It can be seen that the rate drops almost to zero after a few hours, and then gradually slightly increases. A slow downward trend of the rate is observed again after about 20 hours, but a small process of heat absorption can be detected in most cases even after the period of 24 hours. If similar mechanism occurs in the case of silver iodide, which, like lead iodide is known to be an excellent ice-nucleating agent, the time lag (10) in formation of ice crystals after injection into supercooled water vapor might tentatively be explained along these lines.

The heat evolved in the salt container is much larger in the case of lead mono-iodide, than in the case of the previous series. Although the amount of water used in the process is also larger it does not explain the difference between the values obtained and those related to the process occurring on lead di-iodide. The result points therefore to

(i) a different heat of sintering of the surface of the product; and/or,
(ii) condensation of water on the surface; and/or,
(iii) hydrolysis of the salt.

The number of water layers on the surface is found to be very small in comparison with the measurements of Birstein (6) and the heats obtained, although of the same order of magnitude, are lower than his isosteric data. This might be due to one or both of the following factors:

(i) Small leaks in our calorimetry system, which would reduce the number of layers adsorbed.
(ii) Small temperature differences between the source of water vapor and the salt in Birstein's system. Calibration evidence points in our case to a thermal stability of the apparatus to within 10^{-5} degrees centigrade over long time periods.

Since all of our experiments were performed in the same system, and without disturbing the apparatus, it is thought that experimental abnormalities would show up in individual cases, and major leaks would be therefore easily detected. No sign of this was found during the experimentation. Furthermore, as implied previously, the process does not appear to be controlled by diffusion of H_2O. Because of this controversy, however, it appears that the relative behavior towards adsorption of water vapor of the three products under study is of more immediate significance than the direct data obtained.

ACKNOWLEDGMENTS

The author is indebted to Drs. G. C. Benson, J. A. Morrison, and A. R. Blake of the National Research Council for many helpful discussions, and to Professor K. J. Laidler of this Department for reading the manuscript and his interest in this project. The work was performed under a contract between the U.S. Air Force Cambridge Research Center, and the University of Ottawa.

Can. J. Chem. Downloaded from www.nrcresearchpress.com by 190.90.36.8 on 09/04/12
For personal use only.

REFERENCES

1. SCHAEFER, V. J. J. Meteorol. **11**, 417 (1954).
2. HASLER, C. L. and SPALDING, G. R. Artificial stimulation of rain (Symposium). Pergamon Press, New York. 1957. p. 369.
3. BIRSTEIN, S. J. and ANDERSON, C. E. J. Meteorol. **12**, 68 (1954).
4. PRUPPACHER, H. R. and SÄNGER, R. Z. angew. Math u. Phys. **VI**, 407 (1955).
5. FUKUTA, N. J. Meteorol. **15**, 17 (1958).
6. BIRSTEIN, S. J. Geophys. Research Paper No. 32 (1954).
7. PAPÉE, H. M. and LAIDLER, K. J. Can. J. Chem. **36**, 1338 (1958).
8. PAPÉE, H. M. Can. J. Chem. **36**, 1443 (1958).
9. CALVET, E. and PRAT, H. Microcalorimetric, applications physiques et biologiques. Masson et Cie, Paris. 1956. p. 66.
10. VONNEGUT, B. Chem. Revs. **44**, 277. (1949).

Can. J. Chem. Downloaded from www.nrcresearchpress.com by 190.90.36.8 on 09/04/12
For personal use only.

Can. J. Chem. Downloaded from www.nrcresearchpress.com by 190.90.36.8 on 09/04/12
For personal use only.

POTATO X VIRUS

PART III. LIGHT SCATTERING STUDIES[1]

M. E. REICHMANN

ABSTRACT

Light scattering studies were made on a non-aggregated potato X virus preparation. The data are consistent with a cylindrical model 5400 Å long having a molecular weight of 35×10^6. The weight average length of 4700 Å was determined from the high angle measurements. The low value of the weight average length, as compared with the length of the most frequent particle from electron microscopy, is interpreted in terms of a slight tendency to aggregate side-by-side. The insignificant extent of this aggregation is demonstrated by a direct evaluation of the weight average diameter. The value of 109 Å obtained is only 9% higher than the number average diameter reported in the literature.

INTRODUCTION

The spontaneous end-to-end aggregation of potato X virus in the process of purification has been the main obstacle in physicochemical studies of its properties in solution. The molecular weight of this virus has not been previously determined. The value of 37.5×10^6 used by Niu *et al.* (1) from data of Bode and Kohler (2) does not appear in the original paper, and was probably calculated from the electron microscope dimensions. These dimensions have now been corrected by Bode and Paul (3). Loring estimated the molecular weight to be 26×10^6 from sedimentation and viscosity measurements (4). Assuming a cylindrical shape, Loring also derived the dimensions of the virus particle as being 98 Å in diameter and 4330 Å in length.

From flow-birefringence studies on the virus in untreated tobacco sap and from a partially fractionated preparation, we reported a particle length of 5400–6200 Å (5).

The diameter of the dry virus particle has been determined from electron micrographs as 160 Å (6) and 100 Å (7). More recently, the length of the most probable particle has been given as 5000–5250 Å, and the diameter of 100 Å was confirmed (3).

In a previous publication, we reported a method for preparing purified, non-aggregated potato X virus from tobacco sap (8). The availability of this method facilitated further studies of the properties of the virus in solution, which are the subject of this paper.

MATERIAL AND METHODS

The method of virus preparation used in these studies has been described (8). Virus concentrations were determined by nitrogen analysis and checked by measurements of optical density at 260 mμ in 0.1 phosphate buffer pH 5.7 (8).

The angular distribution of the intensity of scattered light was measured in a Brice–Phoenix Universal Light Scattering Photometer manufactured by Phoenix Precision Instrument Co., Philadelphia, Penn. (9), using the cylindrical cell furnished with the instrument. The symmetry of the envelope of the cell was checked with a fluorescein solution and the cell was calibrated with a Ludox solution (10, 11). Reflectance corrections (12, 13) were made as described in other publications (10, 11). Dust-free solvents were obtained by filtration through a U.F. sintered-glass filter. Dust was removed from the virus solution by centrifuging the stock solutions in a Servall centrifuge at $15{,}000\times g$ for 30 minutes. A small amount of virus was precipitated under these conditions. Light

[1]*Manuscript received September 22, 1958.*
Contribution No. 6, Chemistry Division, Science Service, Canada Department of Agriculture Research Laboratory, Vancouver, B.C.

scattering measurements were therefore also made on solutions that were centrifuged 20 and 60 minutes. Within the error of the experiment the same data were obtained, indicating that no fractionation of the virus material had taken place. Although the light scattering measurements were made at room temperature, the virus stock solution was kept in the cold. The manner in which dilutions were made has been described (14).

The specific refractive index increment, dn/dc, was determined with a Brice–Speiser differential refractometer (15). As mentioned previously (8), the non-aggregated virus was insoluble in water in the absence of electrolytes. Errors can be anticipated in refractive index increments determined in the presence of electrolytes as a result of differences in electrolyte concentrations between dialyzate and solvent due to the Donnan term. It was therefore preferable to measure the refractive index increment of an aggregated preparation obtained by 5 cycles of high and low speed centrifugation in distilled water. The dn/dc value found was 0.189 ± 0.004.

THEORETICAL CONSIDERATIONS

The relationship between the angular distribution of the intensity of scattered light and the molecular parameters in the case of rigid rods has been discussed (16). It has been shown that the weight average molecular weight and the z average length can be determined provided that the parameter $x^2 = (2L\pi/\lambda' \sin \theta/2)^2$ does not exceed 15 in the low angle range of measurements. Table I gives the values of x and x^2, for a monodisperse rod whose length L is 5000 Å, in the angular range $\theta = 30°$–$90°$ at a wave length $\lambda' = 3280$ Å ($= 4360$ Å/1.33). Between the angles 30° and 50°, x^2 is smaller than 15 and Kc/R_θ should be linear in $\sin^2 \theta/2$. In the case of a polydisperse system with a number average length of 5000 Å, the downward curvature will set in at lower angles, depending on the width of the distribution function (17). It should, however, be possible to determine the z average length and the weight average molecular weight of potato X virus, provided only that the polydispersity is not too great.

TABLE I

Theoretical values of the parameter x (see text) for angles at which light scattering measurements were made. Monodisperse rigid rods 5000 Å long. Wave length (4360/1.33) Å

θ	x	x^2
30°	2.50	6.25
35°	2.90	8.40
40°	3.30	10.90
45°	3.70	13.70
50°	4.10	16.80
60°	4.80	23.00
70°	5.50	30.25
80°	6.20	38.45
90°	6.80	46.25

From the asymptotic value of Kc/F_θ vs. $\sin \theta/2$, the number average length and molecular weight can be determined (18, 19, 20). In addition, if the weight average molecular weight is known, the weight average length can also be evaluated (16). The approximations made in the theoretical treatment require that $x > 2$. As can be seen from Table I this condition is fulfilled for a monodisperse particle 5000 Å long over the

Can. J. Chem. Downloaded from www.nrcresearchpress.com by 190.90.36.8 on 09/04/12
For personal use only.

entire range of angles tabulated. In the case of polydispersity the smaller particles may contribute significantly to the scattering and cause a deviation from linearity at low angles.

RESULTS AND DISCUSSION

Figures 1 and 2 represent typical Zimm plots of the angular distribution of the intensity of light scattered by four different virus concentrations in 0.1 M potassium chloride and 0.005 M sodium citrate, respectively. The plots are practically linear between 30° and 50°, and the weight average molecular weight and z average length were determined from the intercept and slope respectively. To check the reproducibility of the purification procedure three different virus preparations were investigated. The molecular weights were $34–36\times10^6$ and the length was 5300–5500 Å. Within the error of the experiment, the data in 0.005 M sodium citrate were the same as in 0.1 M potassium chloride. Therefore, no change in shape occurred, although the net charge on the virus particles increased as indicated by the increase of the second virial coefficient. The rigidity of the virus particle, as demonstrated previously by flow-birefringence measurements (5), was thus confirmed.

Figure 3 represents a plot of $(Kc/R_\theta)_{c=0}$ vs. sin $\theta/2$ corresponding to the data in Fig. 1. The linear relationship was followed. The slope of the regression line corresponds to

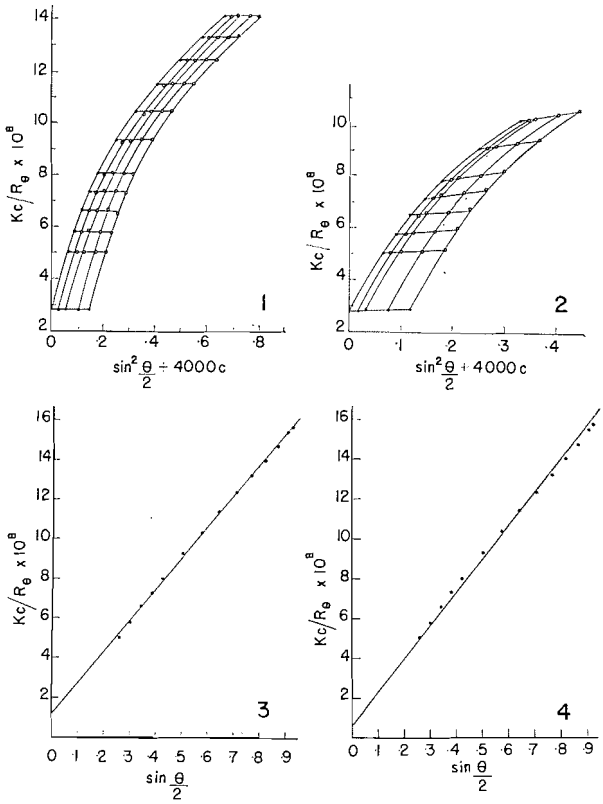

FIG. 1. Typical Zimm plot of light scattering data of potato X virus in 0.1 M potassium chloride.
FIG. 2. Typical Zimm plot of light scattering data of potato X virus in 0.005 M sodium citrate.
FIG. 3. The angular distribution of the intensity of scattered light from potato X virus solutions in 0.1 M potassium chloride as a function of sin $\theta/2$. Virus concentration was extrapolated to zero. Solid line is regression line: $(Kc/R_\theta)_{c=0} = (0.12+1.60 \sin \theta/2)\times10^{-7}$.
FIG. 4. Same data as in Fig. 3. Solid line is regression line with average slope 1.675×10^{-7} (see text).

Can. J. Chem. Downloaded from www.nrcresearchpress.com by 190.90.36.8 on 09/04/12
For personal use only.

1.60×10^{-7}. Taking the weight average molecular weight from Fig. 1 as 35.7×10^6 a weight average length of 4700 Å was calculated. From the best fit of the experimental values of $1/P$ vs. $\sin^2\theta/2$ with a theoretical curve at high angles, the value of 4800 Å was derived. As could be anticipated (16) this value is very close to the weight average length.

The uncertainty in the determination of number averages has been discussed (16). This can be illustrated with the data in Fig. 3. From the intercept and slope of the straight line in Fig. 3 the following number averages were derived: molecular weight 17×10^6, length 2200 Å. Obviously these data are unreasonably low. A more reasonable value can be obtained in the following manner. Taking the best straight lines through the points between 30° and 60° and between 90° and 135° separately, an average slope of 1.675×10^{-7} can be evaluated. Using this as the slope, the regression line through all the points will be given by $(Kc/R_\theta)_{c=0} = (0.063+1.675\sin\theta/2)\times10^{-7}$ (Fig. 4). The number average molecular weight and length from this line would be 32×10^6 and 4400 Å respectively. It should be noticed that while the slope has been changed by 5%, the molecular parameters increased by a factor of two. On the other hand the weight average length from Fig. 4 would be 4900 Å, not very different from the value derived from Fig. 3.

It was somewhat surprising that the weight average length was found to be lower than the most probable particle length as determined from electron microscopy. Inspection of light scattering data on tobacco mosaic virus will show that a similar discrepancy can also be found there (21, 22). We have pointed out that this can be anticipated in the case of polydispersity in thickness (16). The low value of the number average length could therefore be interpreted as indicating a tendency for side-to-side aggregation. The extent of this aggregation can be estimated by evaluating the radius of the cylinder, rather than the weight average length, from the slope in Fig. 3. The particle width determined from this slope should be independent of the distribution of length (19) and if the shape is known, can be determined unambiguously. Assuming a cylindrical shape the weight average radius is given by (16): $\sqrt{(r^2)_w} = \sqrt{4/\pi\rho N\lambda'\times(\text{slope})} = 54.5$ Å giving a diameter of 109 Å. This is only 9% higher than the number average value determined with the electron microscope.

The difference between the weight average and z average length, a measure of the total polydispersity, was relatively small (15%). We would therefore anticipate a sharp distribution function of lengths in our preparation.*

Assuming a cylinder 5100 Å long, 100 Å in diameter (3), with a partial specific volume of 0.73 ml/g (23), the predicted molecular weight is 33×10^6, in good agreement with the light scattering data. The value of 26×10^6 calculated by Loring (4) can be considered only as a rough estimate. The sedimentation constant and viscosity on which this estimate was based were determined at finite concentrations and the viscosity was measured at relatively high gradients (Ostwald Viscometer). From what is known about the dependence of the sedimentation constant on concentration and the viscosity on gradient in the case of large elongated particles, it is obvious that both values must have been too low. This is also apparent from the particle length derived from these data, which is 4330 Å.†

Finally, it should be mentioned that as in the case of tobacco mosaic virus (21), the

*A comparison with a uniform tobacco mosaic virus preparation can be made (21, 22). The difference in length determined from high values of $1/P$ and from the limiting slope of this function was 10%. In our potato X virus preparation the difference was 13% (4800 Å and 5460 Å).

†We have also determined the molecular weight from sedimentation–diffusion measurements. Because of the very slow rate of diffusion, the diffusion constant could not be determined accurately. We found, however, that at low virus concentrations the boundary remained Gaussian over a period of 8 days in the Spinco electrophoresis–diffusion apparatus. We obtained $D_{20} = 3.2\times10^{-8}$. The molecular weight obtained from this value and $S_{20} = 117.8\times10^{-13}$ (8) was 33×10^6.

Can. J. Chem. Downloaded from www.nrcresearchpress.com by 190.90.36.8 on 09/04/12
For personal use only.

light scattering particle length of potato X virus is significantly lower than the hydrodynamic length determined from flow birefringence (5). The inadequacy of the ellipsoid of revolution to represent a cylinder has been discussed in detail (21). Since the same considerations apply in the case of potato X virus, a similar discrepancy between the light scattering and flow-birefringence length can be anticipated.

REFERENCES

1. NIU, C. I., SHORE, V., and KNIGHT, C. A. Virology, **6**, 226 (1958).
2. BODE, O. and KOHLER, E. Naturforsch, **76**, 598 (1952).
3. BODE, O. and PAUL, H. L. Biochim. et Biophys. Acta, **16**, 343 (1955).
4. LORING, H. S. J. Biol. Chem. **126**, 455 (1938).
5. REICHMANN, M. E. Can. J. Chem. **36**, 1603 (1958).
6. TAKAHASHI, N. W. and RAWLINS, T. E. Am. J. Botany, **33**, 740 (1946).
7. KLECZKOWSKI, A. and NIXON, H. L. J. Gen. Microbiol. **4**, 220 (1950).
8. REICHMANN, M. E. Can. J. Chem. **37**, 4 (1959).
9. BRICE, B., HALVER, M., and SPEISER, R. J. Opt. Soc. Am. **40**, 768 (1950).
10. HOLTZER, A. M., BENOIT, H., and DOTY, P. J. Phys. Chem. **58**, 624 (1954).
11. BOEDTKER, H. and DOTY, P. J. Phys. Chem. **58**, 968 (1954).
12. SHEFFER, H. and HYDE, J. C. Can. J. Chem. **30**, 817 (1952).
13. OTH, A., OTH, J., and DESREUX, V. J. Polymer Sci. **10**, 551 (1953).
14. REICHMANN, M. E., BUNCE, B. H., and DOTY, P. J. Polymer Sci. **10**, 109 (1953).
15. BRICE, B. and HALVER, M. J. Opt. Soc. Am. **41**, 1033 (1951).
16. REICHMANN, M. E. Can. J. Chem. **37** (1959) (In press).
17. GOLDSTEIN, M. J. Chem. Phys. **21**, 1255 (1953).
18. HOLTZER, A. M. J. Polymer Sci. **17**, 432 (1955).
19. CASASSA, E. F. J. Chem. Phys. **23**, 596 (1955).
20. STACEY, K. A. Light scattering in physical chemistry. Butterworth Scientific Publications, London. 1956.
21. BOEDTKER, H. and SIMMONS, N. S. J. Am. Chem. Soc. **80**, 2550 (1958).
22. HALL, C. E. J. Am. Chem. Soc. **80**, 2556 (1958).
23. LAUFFER, M. A. and CARTWRIGHT, T. E. Arch. Biochem. Biophys. **38**, 371 (1952).

Can. J. Chem. Downloaded from www.nrcresearchpress.com by 190.90.36.8 on 09/04/12
For personal use only.

Can. J. Chem. Downloaded from www.nrcresearchpress.com by 190.90.36.8 on 09/04/12
For personal use only.

FREE RADICALS BY MASS SPECTROMETRY

XV. THE MERCURY-PHOTOSENSITIZED DECOMPOSITION OF FORMIC ACID, ACETIC ACID, AND METHYL FORMATE[1]

P. KEBARLE[2] AND F. P. LOSSING

ABSTRACT

The $Hg(^3P_1)$ photosensitized decomposition of formic acid proceeds by two intramolecular rearrangement reactions, leading respectively to H_2O and CO, and to H_2 and CO_2. No free radicals are produced. The decomposition reactions of methyl formate and of acetic acid proceed predominantly by the formation of free radicals, but intramolecular rearrangements also occur to a significant extent. For both these latter compounds the evidence suggests the occurrence of two modes of dissociation into free radicals:

$$RC(=O)—OR' + Hg^* \rightarrow RC(=O) + OR' + Hg$$

$$RC(=O)—OR' + Hg^* \rightarrow R + C(=O)—OR' + Hg.$$

No evidence for the alternative mode of dissociation

$$RC(=O)—OR' + Hg^* \rightarrow RC(=O)—O + R' + Hg$$

was found.

INTRODUCTION

In the photolytic decomposition of molecules of the type RCOOR′, several types of primary steps appear to occur. A bond rupture to give two free radicals may occur at one of several bonds, and an intramolecular shift of a hydrogen atom to give two molecular products appears to be also an important mode of decomposition.

The simplest molecule of the RCOOR′ type, formic acid, has been examined both by direct photolysis and by mercury photosensitization. Ramsperger and Porter (1) found that in the region 2260 Å – 2500 Å two molecular rearrangements occurred:

$$HCOOH + h\nu \rightarrow CO + H_2O\ (64\%), \quad [1]$$

$$HCOOH + h\nu \rightarrow CO_2 + H_2\ (36\%). \quad [2]$$

Reaction [1] accounted for 64% of the molecules reacted, and reaction [2] accounted for the remainder.

Bates and Taylor (2) examined the mercury-photosensitized decomposition at 2537 Å and found a similar situation:

$$Hg^* + HCOOH \rightarrow Hg + CO + H_2O\ (76\%), \quad [3]$$

$$Hg^* + HCOOH \rightarrow Hg + CO_2 + H_2\ (24\%). \quad [4]$$

The same products were found by Herr and Noyes (3). A more comprehensive examination of the direct photolysis over the region 1900–2540 Å was made by Gorin and Taylor (4). They found the ratio of reaction [1] to reaction [2] to vary with wavelength, shorter wavelengths and higher temperatures favoring reaction [2]. Molecules of the dimeric

[1]*Manuscript received September 16, 1958.*
Contribution from the Division of Pure Chemistry, National Research Council, Ottawa, Canada.
Issued as N.R.C. No. 5012.
[2]*National Research Council of Canada Postdoctorate Fellow 1956–58.*

form of formic acid $(HCOOH)_2$ decomposed solely into CO_2 and H_2 at all wavelengths used. From experiments with parahydrogen the authors concluded that a primary split

$$HCOOH + h\nu \rightarrow H + COOH \quad [5]$$

did not occur to any significant extent. A similar conclusion was reached by Burton (5), who found that antimony mirrors were not removed in the direct photolysis. The only evidence for a free radical mode of dissociation comes from the observations of Terenin (6) of the OH radical in emission during photolysis.

The next simplest molecules of the RCOOR′ type are methyl formate, $HCOOCH_3$, and acetic acid, CH_3COOH. Very little data is available on the photodecomposition of methyl formate. Ausloos (7) found the photolysis of liquid methyl formate to yield CH_4, CO_2, CO, and H_2 as products. No runs on gaseous methyl formate were reported.

The photolysis of CH_3COOH was examined by Burton (8), who, on the basis of mirror removal experiments, rejected the primary split

$$CH_3COOH + h\nu \rightarrow CH_3 + COOH \quad [6]$$

in favor of the process

$$CH_3COOH + h\nu \rightarrow CH_3COO + H. \quad [7]$$

No CH_3 radicals or radicals such as CH_3CO which would decompose to form CH_3 could be detected. A molecular process

$$CH_3COOH + h\nu \rightarrow CH_4 + CO_2 \quad [8]$$

was reported by Farkas and Wansbrough-Jones (9). A recent investigation of the photolysis by Ausloos and Steacie (10) using deuterium labelling provides good evidence that reaction [8] occurs to the extent of about 10%. Three other primary processes were possible, reactions [6], [7], and a split into acetyl and hydroxyl radicals:

$$CH_3COOH \rightarrow CH_3CO + OH. \quad [9]$$

From the behavior with temperature, it was evident that dimers $(CH_3COOH)_2$ played no part in the primary process.

EXPERIMENTAL

The reactor and mercury lamp have been described in previous publications (11, 12). A new ion source, similar in some respects to that used by Leger in a rapid-scan mass spectrometer (13), was constructed for this work and is shown in Fig. 1. It possessed a number of features designed to improve the sensitivity of detection for oxygenated radicals. The plates of the source were rectangular in shape, 2 in. long by $\frac{5}{8}$ in. wide. The side walls of the ionization chamber facing the orifice and the pumping lead consisted only of tungsten mesh screen of high transparency (> 90%). Owing to the open construction of the ionization chamber relatively little obstruction was placed in the flight path of a molecule from the orifice to the pumping lead, and the proportion of radicals ionized after colliding with surfaces should consequently be much less than in the design used previously. Although this feature is probably of little advantage for radicals which are not reactive toward metal surfaces, such as the alkyl radicals (14), it might be expected that oxygenated radicals are more sensitive to such collisions. A further advantage, that fewer molecules are able to enter the analyzer tube, permitted a higher differential pressure to be maintained between the ionization chamber and the analyzer tube. A rough estimate based on the ratio of the pressures in the pumping leads in the two designs indicated a four- or five-fold improvement in this ratio.

Can. J. Chem. Downloaded from www.nrcresearchpress.com by 190.90.36.8 on 09/04/12
For personal use only.

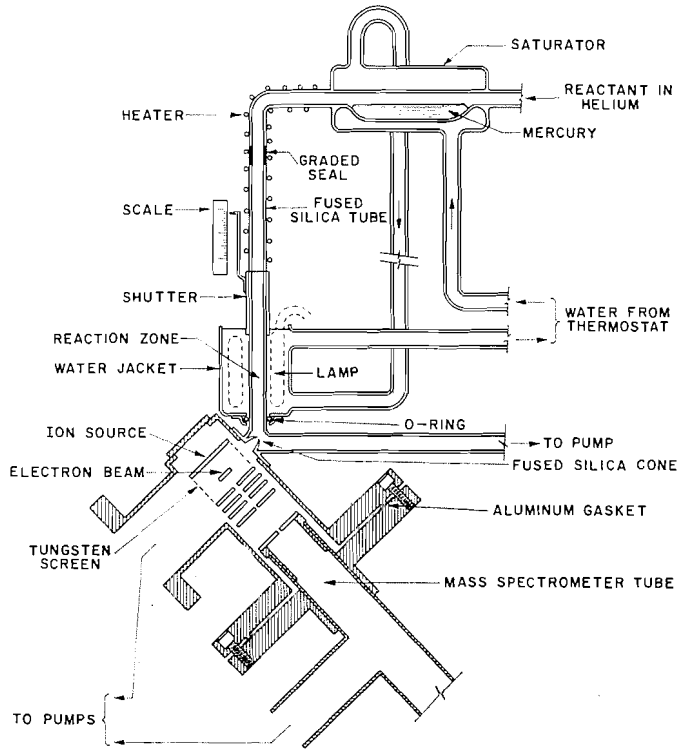

FIG. 1. Diagram of photochemical reactor and mass spectrometer ion source.

MATERIALS

The formic acid, methyl formate, and acetic acid were samples of commercial grades of high purity which were carefully degassed before using. The deuterated methyl formate and acetic acid were kindly supplied by Dr. L. C. Leitch.

RESULTS AND DISCUSSION

Before discussing the results in detail, it will not be amiss to point out some differences in reaction conditions between the reactor used in this work and those used in conventional photochemical experiments. In previous investigations using the same apparatus a number of compounds were found to decompose by a primary split into free radicals. In all these cases no evidence was found for the occurrence of reactions between free radicals and the parent compound. The reason for this is easily understood. Such abstraction reactions require an activation energy of 8–10 kcal/mole while radical combination and disproportionation reactions require considerably less, probably 0–1 kcal/mole. At 55° C the rate constant for abstraction reactions is consequently only 10^{-5} to 10^{-6} as large as for radical–radical reactions. In conventional photochemical systems this large factor is counterbalanced by the very small steady-state concentration of radicals relative to the parent compounds, and an abstraction reaction may consequently be of great importance. In the reactor used in this work the situation is quite different. For example, in the mercury-photosensitized decomposition of acetone (12) the concentration of methyl radicals was about $\frac{1}{10}$ of the concentration of acetone during most of the contact time. With such relatively high concentrations of radicals, radical–radical interactions will be

Can. J. Chem. Downloaded from www.nrcresearchpress.com by 190.90.36.8 on 09/04/12
For personal use only.

at least 10^4 times faster than reactions of radicals with the parent compound, and the formation of radicals or other products by such reactions can be neglected.

The situation is similar in many respects to that produced in the flash photolysis experiments of Khan, Norrish, and Porter (15) in which radical–radical reactions were considered to predominate. It is of interest to note that in the flash experiments the average decomposition was about 1% for a flash duration of about 10^{-4} second. No chains were found to participate and the entire decomposition resulted from the primary act. In the present system the extent of decomposition was 10–20% of the parent compound in a time of 10^{-3} second. The rates of radical production and consequently the ratio of concentrations of radicals and parent compound in the two reaction systems are, therefore, of about the same order.

A further consequence of the high concentration of radicals in the present experiments is the possibility of reaction of a radical with an excited mercury atom, leading to dissociation of the radical. Such reactions had to be postulated for allyl radicals (11) and for acetyl radicals (12) to explain the formation of certain products.

Formic Acid

In the mercury photosensitized decomposition of formic acid vapor, only four products were found: CO, H_2O, CO_2, and H_2. No free radicals could be detected. The amounts of products formed at two partial pressures of formic acid, and at various positions of the shutter (i.e. various exposure times) are given in Table I. Some difficulties were encountered in measuring the sensitivity coefficients for formic acid and for water, on account of the absorption effects of the glass surfaces in the sample line, and the mass balances of the products are therefore somewhat different from 100%. The analysis of formic acid and of the products at short exposure times were quite uncertain since only small changes in the composition were produced. The amounts of HCOOH decomposed and of products formed are shown in Figs. 2 and 3, as a function of the exposure time. It is evident that within the experimental error $\phi_{CO} = \phi_{H_2O}$ and $\phi_{CO_2} = \phi_{H_2}$. The equality of these pairs of products and the lack of variation with exposure time indicates that the only modes of decomposition are the two intramolecular rearrangement reactions found in earlier work, reactions [3] and [4]. From the present data the ratio of occurrence of these two reactions is about $\phi_3/\phi_4 \approx 70/30$. This ratio is slightly different from the

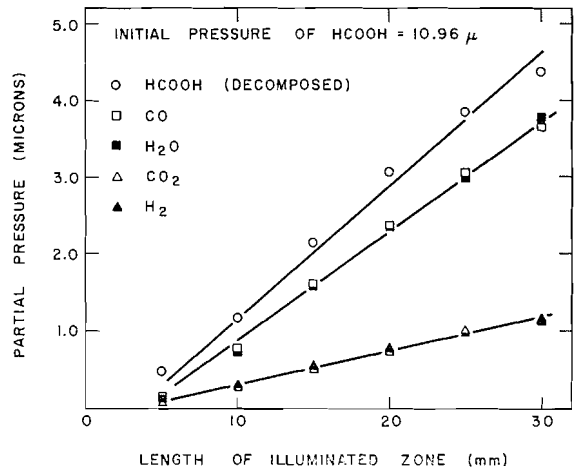

FIG. 2. Products from mercury-photosensitized decompositon of formic acid vapor.

Can. J. Chem. Downloaded from www.nrcresearchpress.com by 190.90.36.8 on 09/04/12
For personal use only.

ratio 76–24 found by Bates and Taylor, but in view of the uncertainty in the analysis of HCOOH and H_2O in the present work it is not entirely certain that the difference is significant. The present work does, however, confirm the view that a dissociation into free radicals or into an atom and a free radical occurs to a very small extent or not at all.

TABLE I

Decomposition of formic acid

Length of illuminated zone (mm)	Formic acid (μ) present		Formic acid decomposed		Products (μ)				Mass balance (%) for:			$CO_2 + H_2$
	Lamp off	Lamp on	μ	%	CO	H_2O	CO_2	H_2	C	O	H	$CO + H_2O$
5	10.96	10.48	0.48	4.38	0.14	0.13	0.10	0.06	(50)	(49)	(40)	(0.59)
10	10.96	9.79	1.17	10.7	0.77	0.71	0.25	0.27	87	85	84	0.35
15	10.96	8.83	2.13	19.4	1.58	1.56	0.50	0.51	98	97	97	0.32
20	10.96	7.90	3.06	27.9	2.37	2.36	0.73	0.79	102	101	103	0.32
25	10.96	7.12	3.84	35.0	3.09	2.96	1.00	0.99	107	105	103	0.33
30	10.96	6.59	4.37	39.9	3.65	3.78	1.14	1.19	110	100	114	0.31
5	25.84	25.47	0.37	1.43	0.23	0.22	0.08	0.04	(71)	(70)	(59)	(0.27)
10	25.84	24.54	1.30	5.03	1.05	1.03	0.34	0.30	107	106	102	0.31
15	25.84	23.23	2.61	10.1	2.09	2.16	0.60	0.62	103	104	107	0.29
20	25.84	21.76	4.08	15.8	3.11	3.25	0.92	0.94	98.8	100	103	0.29
25	25.84	20.32	5.52	21.4	4.26	4.48	1.16	1.31	98.2	100	105	0.28
30	25.84	19.27	6.57	25.4	5.16	5.55	1.38	1.58	99.5	103	109	0.28

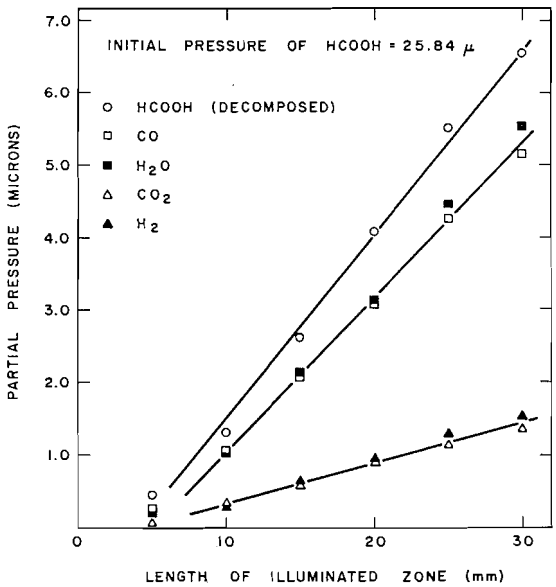

FIG. 3. Products from mercury-photosensitized decomposition of formic acid vapor.

Methyl Formate

The distribution of products formed by the mercury-photosensitized decomposition of methyl formate with different lengths of illuminated zone are given in Table II. In addition to these products very small amounts of methyl acetate and dimethyl ether were also produced. Two other minor products could be detected only by their parent peaks at mass 58 and mass 62. A search for free radicals was made using initial pressures

Can. J. Chem. Downloaded from www.nrcresearchpress.com by 190.90.36.8 on 09/04/12
For personal use only.

Can. J. Chem. Downloaded from www.nrcresearchpress.com by 190.90.36.8 on 09/04/12
For personal use only.

TABLE II

Decomposition of methyl formate

Length of illuminated zone (mm)	Methyl formate (μ) present		Methyl formate decomposed		Products (μ)							Mass balance (%) for:		
	Lamp off	Lamp on	μ	%	CO_2	CH_3OH	C_2H_6	CH_2O	CO	CH_4	H_2	O	C	H
5	19.87	19.21	.66	3.32	.070	$.04_1$	$.01_1$	$.06_9$	$.23_4$	$.01_5$	$.15_7$	36.7	34.2	28.1
10	19.87	18.43	1.44	7.25	$.14_1$	$.42_0$	$.02_9$	$.19_4$	$.65_4$	$.04_0$	$.46_2$	53.4	52.2	66.3
15	19.87	17.97	1.90	9.56	$.23_7$	$.94_1$	$.04_7$	$.39_9$	1.32	$.07_9$	$.68_7$	82.8	81.2	86.2
20	19.87	17.34	2.53	12.73	$.33_1$	1.18_7	$.07_8$	$.56_6$	1.86	$.11_7$	$.92_4$	84.5	83.4	85.6
25	19.87	16.54	3.33	16.76	$.44_1$	1.54_5	$.10_0$	$.69_4$	2.23	$.14_0$	1.22	80.3	78.9	83.9
30	19.87	16.00	3.87	19.48	$.49_0$	1.81_1	$.12_7$	$.83_3$	2.80	$.18_6$	1.41	83.1	82.5	85.6

of methyl formate two or three times higher than in the quantitative experiments. Using low electron energies, at which only parent ions should be formed, the peaks at mass 15, 29, 31, and 59 were found to increase when the lamp was on. These mass numbers correspond to the parent ions of CH_3, CHO, CH_3O, and $COOCH_3$ radicals. The presence of these radicals is also indicated by the formation of a number of products which evidently arise from the corresponding radical–radical interactions. Ethane undoubtedly was formed by the combination of two methyl radicals, the dimethyl ether from the combination of a methyl and a methoxy radical, and the methyl acetate from the combination of a methyl and a $COOCH_3$ radical. The unidentified peaks at mass 58 and mass 62 might be the parent peaks of glyoxal, the dimer of CHO radical, and dimethyl peroxide, the dimer of CH_3O, but a positive identification could not be made.

In order to obtain a further confirmation for some of these findings a separate experiment was carried out in which mercury dimethyl was added to the helium stream carrying the methyl formate. With the lamp on, a small additional increase in the peaks at mass 74 and mass 43 was observed. The increased portions of these peaks had a ratio mass 74/mass 43 = 0.15. The ratio of these peaks in the mass spectrum of methyl acetate measured in a separate experiment was 0.18. An increase was also observed for the mass 46 and 45 peaks, in the ratio mass 46/mass 45 = 0.34. The ratio for dimethyl ether measured separately was 0.40. Although the agreement is somewhat approximate, there can be little doubt that the corresponding increases in the peaks were caused by the formation of methyl acetate and dimethyl ether by reaction of $COOCH_3$ and OCH_3 radicals with the additional CH_3 radicals provided by the decomposition of mercury dimethyl.

The presence of the CH_3O and HCO radicals indicate that the following primary step must occur:

$$Hg^* + HCOOCH_3 \rightarrow Hg + HCO + OCH_3. \qquad [10]$$

The presence of the $COOCH_3$ radical suggests the occurrence of a second primary dissociation process:

$$Hg^* + HCOOCH_3 \rightarrow Hg + H + COOCH_3. \qquad [11]$$

The formation of the $COOCH_3$ radical by a primary step, and not by abstraction of a H atom from methyl formate by one of the radicals produced in reaction [10] depends on the validity of the discussion given above concerning the occurrence of radical–substrate reactions.

The presence of methyl radicals might result from a third primary mode of dissociation:

$$Hg^* + HCOOCH_3 \rightarrow Hg + HCOO + CH_3. \qquad [12]$$

It is not necessary, however, to postulate this reaction since the dissociation of the $COOCH_3$ radical by the reaction:

$$COOCH_3 \rightarrow CO_2 + CH_3 \qquad [13]$$

might be expected to be quite rapid at 55° C. Although the strength of the COO—CH_3 bond is unknown, it can be shown from thermochemical data that it cannot be very strong. From the relation

$$D(H—COOCH_3) + D(COO—CH_3) = \Delta H_f(H) + \Delta H_f(CH_3) + \Delta H_f(CO_2) - \Delta H_f(HCOOCH_3)$$

and standard thermochemical data, the sum of the two bonds is 73.6 kcal/mole. Since it might be expected that the C—H bond alone must be nearly this strong, D(COO—CH_3)

Can. J. Chem. Downloaded from www.nrcresearchpress.com by 190.90.36.8 on 09/04/12
For personal use only.

must be certainly not greater than 10–15 kcal/mole. It is rather surprising that the $COOCH_3$ radical could be detected at all in the present experiments.*

The quantitative data given in Table II were obtained from the mass spectra of the products in the reaction stream taken with 50-v electrons. After subtracting the contributions of the stable reaction products from the mass spectra, a small residual peak remained for mass 59, and somewhat larger ones for mass 31, 29, and 15. It is probable that these peaks were caused by the presence of the $COOCH_3$, CH_3O, CHO, and CH_3 free radicals. Since the mass spectrum of the CH_3O radical is not known, its contribution to the mass 15 peak could not be evaluated. Thus the concentration of the CH_3 radical, which is the only one whose sensitivity coefficient is known, could not be determined. The mass balances given in Table II therefore do not include free radical contributions. Contributions from the minor products methyl acetate, dimethyl ether, and the tentatively identified methyl peroxide and glyoxal are also not included.

Two approximate relations between the amounts of the various products given in Table II can be seen:

$$[CO] \approx [CH_3OH] + [CH_2O] \qquad \text{I}$$

$$[CO_2] \approx [CH_4] + [C_2H_6]. \qquad \text{II}$$

TABLE III

Product balances—methyl formate

Length of illuminated zone (mm)	Methyl formate		Products (μ)			
	Initial pressure (μ)	% Decomposed	[CO]	$[CH_3OH + CH_2O]$	$[CO_2]$	$[2\,C_2H_6 + CH_4]$*
20	19.87	12.73	1.86	1.75	.331	.273
25	19.87	16.76	2.23	2.24	.441	.340
30	19.87	19.48	2.80	2.64	.490	.440

*This sum should include $[CH_3]$, which could not be measured.

Numerical values for these product balances are given in Table III. Product balance I can be related to the primary reaction [10] if it is assumed that all of the HCO radicals produced by [10] are converted to CO by subsequent reactions, and that essentially all the CH_3O radicals disproportionate to CH_3OH and CH_2O. Similarly, product balance II will hold provided that essentially all the $COOCH_3$ radicals produced by reaction [11] are converted by subsequent reactions to CO_2, C_2H_6, and CH_4. A reaction mechanism fulfilling the requirements of product balances I and II is given below:

$$Hg^* + HCOOCH_3 \rightarrow Hg + HCO + OCH_3 \qquad [10]$$

$$Hg^* + HCOOCH_3 \rightarrow Hg + H + COOCH_3 \qquad [11]$$

$$COOCH_3 \rightarrow CO_2 + CH_3 \qquad [13]$$

$$Hg^* + OCH_3 \rightarrow Hg + H + CH_2O \qquad [14]$$

$$Hg^* + HCO \rightarrow Hg + H + CO \qquad [15]$$

$$2CH_3O \rightarrow CH_3OH + CH_2O \qquad [16]$$

$$2HCO \rightarrow H_2 + 2CO \qquad [17]$$

**Some further support for the instability of* $COOCH_3$ *is given by a comparison with the* CH_3CO *radical. From the relation:*

$$D(H—COCH_3) + D(CO—CH_3) = \Delta H_f(H) + \Delta H_f(CH_3) + \Delta H_f(CO) - \Delta H_f(CH_3CHO)$$

the sum of the two bonds is 97.5 kcal/mole. If, as might reasonably be expected, $D(H—COCH_3)$ *is not much less than* $D(H—COOCH_3)$ *it is evident that* $D(COO—CH_3)$ *is significantly weaker than* $D(CO—CH_3)$.

Can. J. Chem. Downloaded from www.nrcresearchpress.com by 190.90.36.8 on 09/04/12
For personal use only.

$$CH_3O + HCO \rightarrow CH_3OH + CO \quad [18]$$

$$CH_3O + HCO \rightarrow 2CH_2O \quad [19]$$

$$H + CH_3O \rightarrow CH_2O + H_2 \quad [20]$$

$$H + HCO \rightarrow CO + H_2 \quad [21]$$

$$CH_3 + CH_3O \rightarrow CH_4 + CH_2O \quad [22]$$

$$CH_3 + HCO \rightarrow CH_4 + CO \quad [23]$$

$$2CH_3 \rightarrow C_2H_6 \quad [24]$$

The evidence for reactions [10], [11], and [13] has been discussed. It is evident that with at least four free radicals, H atoms, and excited mercury atoms present as reactive species it is not possible to distinguish between alternative methods of producing many of the secondary products. The reactions listed above are all probable ones, but other modes of radical–radical interaction may, of course, occur. Reactions [14] and [15], for which there is no direct evidence, were included on the basis of previous work on the decomposition of acetone (12), using the same apparatus, in which the formation of ketene could only be explained by the reaction of acetyl radicals with excited mercury atoms. Reactions [16] to [23] are radical disproportionation steps, all of which may not be active in the mechanism. However, since products of radical combination, with the exception of ethane, were found only in minute amounts, it is to be expected that disproportionation reactions must account for the largest part of the products found.

In the preceding discussion the possibility of a dissociation involving an intramolecular rearrangement was not considered. It is clear that product balance I will still hold if part of the decomposition proceeds by the reaction

$$Hg^* + HCOOCH_3 \rightarrow Hg + CH_3OH + CO \quad [25]$$

since for every CO molecule one CH_3OH molecule is also produced. Similarly, product balance II will be obeyed if the intramolecular rearrangement

$$Hg^* + HCOOCH_3 \rightarrow Hg + CH_4 + CO_2 \quad [26]$$

is one of the primary reactions. These are analogous to reactions [3] and [4] respectively, as found to occur in the decomposition of formic acid. In order to establish whether methyl formate decomposes partly by reaction [25] some experiments were carried out using mixtures of $HCOOCH_3$ and $DCOOCD_3$. The total pressure of the two isomers in the helium stream was kept approximately equal to the pressure of methyl formate used in the previous experiments. In a series of runs, the mole fraction of deuterated methyl formate was varied from unity to almost zero. For each composition the amount of CD_3OD formed and the percentage of decomposition of $DCOOCD_3$ were measured. In these experiments the length of the illuminated zone was 30 mm. The results are summarized in Table IV. A plot of the ratio CD_3OD formed/$DCOOCD_3$ decomposed versus the mole fraction of $DCOOCD_3$ is shown in Fig. 4. If CD_3OD were formed entirely by the intramolecular rearrangement reaction [25], the ratio would not be affected by the addition of $HCOOCH_3$. Conversely, if CD_3OD were formed entirely by a free radical process, the ratio should approach zero as the mole fraction of $DCOOCD_3$ approaches zero. The observed dependence shows an intermediate behavior indicating the participation of both a molecular and a free radical process. The ratio obtained by extrapolation is approximately 0.12. Thus about 12% of the methyl formate decomposes by the rearrangement reaction [25]. In the experiments with $HCOOCH_3$ reported in Table II (for a 30-mm illuminated zone) the yield of CO was 72.4% of the methyl formate

Can. J. Chem. Downloaded from www.nrcresearchpress.com by 190.90.36.8 on 09/04/12
For personal use only.

decomposed. Since the yield of CO represents the fraction of methyl formate decomposing by reactions [10] and [25], it follows that the methyl formate decomposing by reaction [10] alone is approximately $72.4-12.0 = 60.4\%$.

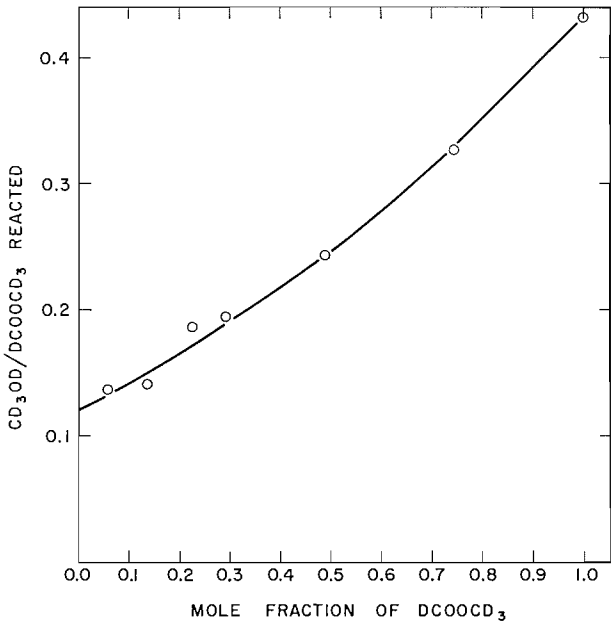

FIG. 4. Formation of CD_3OD in $DCOOCD_3$–$HCOOCH_3$ mixtures.

TABLE IV

CD_3OD Production in $DCOOCD_3$–$HCOOCH_3$ mixtures

$DCOOCD_3$ (μ), initial	$HCOOCH_3$ (μ), initial	Mole fraction $DCOOCD_3$	$DCOOCD_3$ decomposed		CD_3OD formed	CD_3OD formed
			μ	%	(μ)	$DCOOCD_3$ decomposed
1.21	19.6	.058	.226	18.7	.031	.137
2.64	16.7	.136	.516	19.5	.073	.141
4.89	16.7	.226	.909	18.6	.170	.187
6.94	16.7	.293	1.37	19.7	.266	.194
8.48	8.8	.490	1.81	21.3	.440	.243
14.97	5.1	.747	2.96	19.8	.968	.327
20.93	0.0	1.00	4.05	19.3	1.75	.432

Similarly, the methyl formate decomposing by reactions [11] and [26] should be equal to the yield of CO_2, that is 12.7% (Table II). Assuming that all the methane is formed by reaction [26] an upper limit for the participation of this reaction would be given by the methane yield, which is 4.8%. Since methane could also be formed by reactions [22] and [23], it is probable that the true extent for the occurrence of reaction [26] is much smaller than 4.8%, and possibly zero.

Acetic Acid

The yields of products obtained in the mercury-photosensitized decomposition of acetic acid are given in Table V. The full intensity of the lamp was used in this experiment by withdrawing the shutter completely out of the reaction zone. The principal

Can. J. Chem. Downloaded from www.nrcresearchpress.com by 190.90.36.8 on 09/04/12
For personal use only.

products were water, carbon dioxide, ketene, methane, ethane, methyl radicals, and acetone. The formation of a polymeric substance on the walls of the reactor, which was visible as a brown stain after several minutes' exposure, may account for the deficiency in the mass balances given in Table V. This deposit may result from the polymerization of the ketene formed in the reaction. In the mercury-photosensitized reaction of acetone (12) in which ketene was a product, a similar deposit was formed.

TABLE V

Decomposition of acetic acid

Acetic acid (μ) present		Acetic acid decomposed		Products (μ)								Mass balance (%) for:		
Lamp off	Lamp on	μ	%	CO_2	CO	C_2H_6	H_2O	CH_4	CH_3	Acetone	Ketene	O	C	H
7.35	6.12	1.23	16.7	0.461	0.260	0.224	0.654	0.231	0.073	0.015	0.292	87.7	87	91.6

Using electrons of low energy, the only radical which could be detected was methyl. However, the formation of acetone as a product can be explained only by the presence of acetyl radicals, which must have been present in concentrations too low to detect. Addition of mercury dimethyl to the reaction stream caused an increase in the amount of acetone formed, thus confirming the presence of CH_3CO radicals. The presence of CH_3CO radicals, together with the formation of substantial amounts of water, indicates that the following step must occur:

$$Hg^* + CH_3COOH \rightarrow Hg + CH_3CO + OH. \quad [27]$$

Although the CH_3 radicals detected might arise by dissociation of CH_3CO, the presence of large amounts of CO_2 together with the fact that the yield of CO is not nearly twice the yield of ethane indicates that a second primary process, in which CH_3 radical and a radical ultimately forming CO_2 are produced, must occur: one possibility is that this reaction is the following:

$$Hg^* + CH_3COOH \rightarrow Hg + CH_3 + COOH. \quad [28]$$

CO_2 would then be formed by the decomposition of the COOH radical as follows:

$$COOH \rightarrow CO_2 + H. \quad [29]$$

Reaction [29] appears to be a much more probable mode of dissociation of COOH than the more frequently proposed dissociation into CO and OH, since $\Delta H_f(CO_2)+\Delta H_f(H)$ is some 25 kcal/mole less than $\Delta H_f(CO)+\Delta H_f(OH)$. A difference in dissociation energy of this magnitude between the O—O and O—H bonds in COOH should be sufficient to ensure that COOH dissociates mainly by reaction [29]. However, an alternative primary decomposition step

$$Hg^* + CH_3COOH \rightarrow Hg + CH_3COO + H \quad [30]$$

would ultimately form CH_3 and CO_2 by dissociation. Reaction [30] was proposed by Burton (8) and by Ausloos and Steacie (10) as the primary dissociation step in the direct photolysis. A search for the $CH_3C\dot{O}O$ radical, using low electron energies, showed no indication of its presence. In experiments in which mercury dimethyl was added to the reaction stream, no sign of methyl acetate, the combination product of $CH_3C\dot{O}O$ and CH_3, could be found. It must be concluded that either the $CH_3C\dot{O}O$ radical was not formed in appreciable amounts, or alternatively that this radical has an extremely short lifetime at 55° C. (Care should be taken to distinguish between this radical, $CH_3C\dot{O}O$, and the isomeric radical $\dot{C}OOCH_3$ produced from methyl formate.) Since four

Can. J. Chem. Downloaded from www.nrcresearchpress.com by 190.90.36.8 on 09/04/12
For personal use only.

radical products can result from these primary steps, 10 radical recombination products are possible. Two of these lead to re-formation of acetic acid. A search was made for the parent peaks of the other eight, but aside from acetone and ethane no other recombination products could be detected. The observed products must then arise mainly by radical decomposition and disproportionation reactions. The following set of reactions appear probable:

$$COOH \rightarrow CO_2 + H \quad [29]$$

$$Hg^* + COOH \rightarrow Hg + CO_2 + H \quad [31]$$

$$CH_3CO \rightarrow CH_3 + CO \quad [32]$$

$$Hg^* + CH_3CO \rightarrow Hg + CH_2{=}CO + H \quad [33]$$

$$COOH + CH_3 \rightarrow CH_4 + CO_2 \quad [34]$$

$$COOH + OH \rightarrow H_2O + CO_2 \quad [35]$$

$$2CH_3 \rightarrow C_2H_6 \quad [24]$$

$$CH_3 + COCH_3 \rightarrow CH_3COCH_3. \quad [36]$$

Reactions [29] and [32] could be either thermal decompositions or decompositions of excited radicals produced in the primary splits. Reactions [31] and [33] have been assumed on the basis of previous experience with the apparatus as discussed above. Reactions [34] and [35] are plausible disproportionation reactions, and reactions [24] and [36] account for the formation of ethane and acetone.

These reactions lead to a number of relations between the yields of various products which can be compared with the analytical results. There are two modes of formation of methyl radicals, the primary reaction [28] and the decomposition reaction [32]. Since all the COOH produced by reaction [28] is evidently converted to CO_2 by subsequent reactions, the sum of the yields of CO and CO_2 should equal the total amount of methyl formed, that is:

$$[CO] + [CO_2] = [CH_3] + [CH_4] + 2[C_2H_6] + [CH_3COCH_3].$$

From Table V $[CO] + [CO_2] = 0.752\ \mu$, and the total methyl yield is $0.721\ \mu$, in reasonable agreement. The OH radicals produced by the primary step [27] are evidently all converted to H_2O. The quantity of H_2O should then be equal to the sum of the products derived from CH_3CO radicals, i.e.

$$[H_2O] = [CH_2{=}CO] + [CO] + [CH_3COCH_3].$$

From Table V, $[H_2O] = 0.65\ \mu$ and the sum of the acetyl products is 0.57. If allowance is made for the fact that some ketene may have polymerized, this agreement is reasonably close.

However, these two product balances would also apply if part of the primary decomposition occurred by one or both of the intramolecular rearrangement steps:

$$Hg^* + CH_3COOH \rightarrow Hg + CH_4 + CO_2, \quad [37]$$

$$Hg^* + CH_3COOH \rightarrow Hg + H_2O + CH_2{=}CO. \quad [38]$$

In order to determine the extent to which these reactions occur, an attempt was made to carry out experiments with CD_3COOD–CH_3COOH mixtures similar to those with deuterated methyl formate. It was found that the acidic hydrogen and deuterium atoms exchanged so rapidly in the reaction system that useful experiments with mixtures could not be carried out. It is possible, however, to set upper limits to the extent of

Can. J. Chem. Downloaded from www.nrcresearchpress.com by 190.90.36.8 on 09/04/12
For personal use only.

these reactions from an examination of the data in Table V. The proportion of acetic acid decomposing by reactions [28] and [37] should be given by the yield of CO_2, that is, 37.5%. On the assumption that all the methane was produced by reaction [37], the upper limit for the occurrence of this reaction is 18.8%, and a lower limit for sum of reactions [28] and [30] is 37.5% − 18.8%, i.e. 18.7%. Since methane could also be produced by reaction [34] the actual extent was probably significantly less. The proportion of acetic acid decomposing by the primary reactions [27] and [38] should be given by the yield of H_2O, that is, 53%. On the assumption that all the ketene was formed by reaction [38], this reaction accounted for 23.7%, and a lower limit for reaction [27] would be 29.3%. The approximate extent of the various primary processes can be summarized as follows:

$$Hg^* + CH_3COOH \rightarrow Hg + CH_3CO + OH \quad \sim 29\% \quad [27]$$

$$\rightarrow \begin{cases} Hg + CH_3 + COOH \\ Hg + CH_3COO + H \end{cases} \sim 18\% \quad \begin{cases} [28] \\ [30] \end{cases}$$

$$\rightarrow Hg + CH_4 + CO_2 \quad \sim 19\% \quad [37]$$

$$\rightarrow Hg + H_2O + CH_2{=}CO \sim 24\%. \quad [38]$$

CONCLUSION

It is evident that the modes of mercury-photosensitized decomposition of compounds of the type $R\overset{\overset{O}{\|}}{C}OR'$ do not by any means conform to a pattern. It is quite surprising that although HCOOH decomposes solely by molecular rearrangement reactions, methyl formate and acetic acid decompose predominantly by a split into free radicals. Two parallels in behavior can, however, be observed. In all three compounds the molecular rearrangement involving the transfer of a hydrogen atom to the oxygen atom of the hydroxy- or methoxy-group occurs with a greater probability than other molecular rearrangements. This reaction may be visualized as follows for the three compounds:

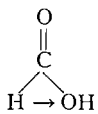

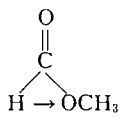

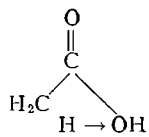

Secondly, in methyl formate and acetic acid the present experiments indicate that the predominating mode of dissociation into free radicals is the recation:

$$R\overset{\overset{O}{\|}}{C}OR' \rightarrow R\overset{\overset{O}{\|}}{C} + OR'. \quad [39]$$

Of secondary importance is the reaction:

$$R\overset{\overset{O}{\|}}{C}OR' \rightarrow R + \overset{\overset{O}{\|}}{C}OR'. \quad [40]$$

It may be noted further that when R is H, reaction [39] is much faster than [40], but when R′ is H the difference in rate is much smaller.

It is evident from the tables that the amount of formic acid decomposed is considerably greater than the amounts of methyl formate and acetic acid decomposed in an equal time under the same conditions. Provided that the quenching cross sections of the three compounds are not greatly different, it appears that the formic acid molecule

Can. J. Chem. Downloaded from www.nrcresearchpress.com by 190.90.36.8 on 09/04/12
For personal use only.

possesses a much greater facility for molecular rearrangements than do methyl formate or acetic acid. The lack of a free radical mode of decomposition for formic acid is therefore probably a consequence of the rapidity with which molecular rearrangements can occur. On the basis of structural considerations it is not clear why formic acid and methyl formate should differ so greatly in this respect.

REFERENCES

1. RAMSPERGER, H. C. and PORTER, C. W. J. Am. Chem. Soc. **48**, 1267 (1926).
2. BATES, J. R. and TAYLOR, H. S. J. Am. Chem. Soc. **49**, 2438 (1927).
3. HERR, D. S. and NOYES, W. A., JR. J. Am. Chem. Soc. **50**, 2345 (1928).
4. GORIN, E. and TAYLOR, H. S. J. Am. Chem. Soc. **56**, 2042 (1934).
5. BURTON, M. J. Am. Chem. Soc. **58**, 1155 (1936).
6. TERENIN, A. Acta Physicochim. U.R.S.S. **3**, 181 (1935).
7. AUSLOOS, P. Can. J. Chem. **36**, 383 (1958).
8. BURTON, M. J. Am. Chem. Soc. **58**, 1644 (1936).
9. FARKAS, L. and WANSBROUGH-JONES, O. H. Z. physik. Chem. B, **18**, 124 (1932).
10. AUSLOOS, P. and STEACIE, E. W. R. Can. J. Chem. **33**, 1530 (1955).
11. LOSSING, F. P., MARSDEN, D. G. H., and FARMER, J. B. Can. J. Chem. **34**, 701 (1956).
12. LOSSING, F. P. Can. J. Chem. **35**, 305 (1957).
13. LÉGER, E. G. Can. J. Phys. **33**, 74 (1955).
14. FABIAN, D. J. and ROBERTSON, A. J. B. Trans. Faraday Soc. **53**, 363 (1957).
15. KHAN, M. A., NORRISH, R. G. W., and PORTER, G. Proc. Roy. Soc. A, **219**, 312 (1953).

Can. J. Chem. Downloaded from www.nrcresearchpress.com by 190.90.36.8 on 09/04/12
For personal use only.

Can. J. Chem. Downloaded from www.nrcresearchpress.com by 190.90.36.8 on 09/04/12
For personal use only.

DÉRIVÉS DU TRIMÉTHYL-1,8,8 BICYCLO[3,2,1]OCTANE

III. SYNTHÈSE DES TRIMÉTHYL-1,8,8 BICYCLO[3,2,1]OCTANOLS-2α ET -2β ET DES TRIMÉTHYL-5,8,8 BICYCLO[3,2,1]OCTANOLS-2α ET -2β[1]

H. Favre, M. Lefebvre[2] et (en partie) J-C. Richer[3]

RÉSUMÉ

Le (+)-triméthyl-1,8,8 bicyclo[3,2,1]octanol-2α et le (+)-triméthyl-5,8,8 bicyclo[3,2,1]-octanol-2α ont été préparés en réduisant par le sodium et l'alcool le (−)-homocamphre et le (+)-homoépicamphre respectivement. L'hydrogénation catalytique de ces cétones par le platine dans l'acide acétique conduit au (−)-triméthyl-1,8,8 bicyclo[3,2,1]octanol-2β et au (+)-triméthyl-5,8,8 bicyclo[3,2,1]octanol-2β respectivement. Les rendements stériques de ces opérations sont supérieurs à 90%. Les configurations ont été attribuées à la suite de l'analyse des modes de formation, des pouvoirs rotatoires et des vitesses d'oxydation chromique des alcools.

Nous rapportons dans ce mémoire des travaux relatifs à la réduction du (−)-homocamphre (I) et du (+)-homoépicamphre (II)[4] et à la détermination de la configuration de chacun des 4 alcools[5] (III–VI) obtenus. L'obtention des alcools stériquement purs n'offre pas de grandes difficultés. Pour chaque cétone la réduction par le sodium et l'éthanol conduit en prépondérance à l'un des épimères (alcool au sodium), tandis que l'autre s'obtient facilement par l'hydrogénation catalytique sur platine dans l'acide acétique (alcool au platine). Après chaque réduction, l'alcool brut fut transformé en *p*-nitrobenzoate; ce dérivé fut cristallisé jusqu'à point de fusion et pouvoir rotatoire constants, puis saponifié. Les quatre alcools obtenus de cette manière (Tableau I) sont

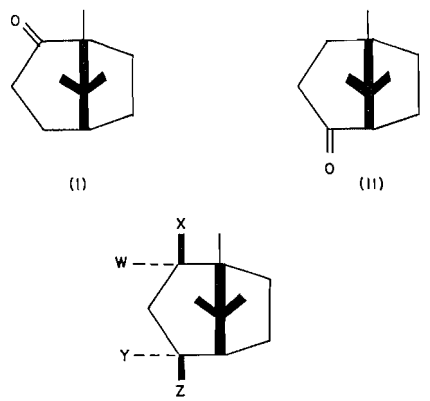

III.	W = OH; X,Y,Z = H	Triméthyl-1,8,8 bicyclo[3,2,1]octanol-2α
IV.	X = OH; W,Y,Z = H	Triméthyl-1,8,8 bicyclo[3,2,1]octanol-2β
V.	Y = OH; W,X,Z = H	Triméthyl-5,8,8 bicyclo[3,2,1]octanol-2α
VI.	Z = OH; W,X,Y = H	Triméthyl-5,8,8 bicyclo[3,2,1]octanol-2β

[1]*Manuscrit reçu le 27 août, 1958.*
Contribution du Département de Chimie de l'Université de Montréal, Montréal, P.Q.; elle est tirée du mémoire de maîtrise de M. Lefebvre et de la thèse de doctorat de J-C. Richer.
[2]*Boursier de l'Office de Recherches Scientifiques de la Province de Québec, 1955–1956. Adresse actuelle: Shawinigan Chemicals Ltd., Shawinigan, P.Q.*
[3]*Boursier du Conseil National de Recherches du Canada, 1954–1958. Adresse actuelle: Dept. of Chemistry, University of Notre Dame, Notre Dame, Ind.*
[4]*Pour la préparation de ces cétones, voir (1, 2).*
[5]*La nomenclature est celle en vigueur pour les dérivés du nortropane (aza-8 bicyclo[3,2,1]octane) et les composés apparentés (3). Les formules spatiales III A–VI A et III B–VI B représentées plus loin sont équivalentes aux formules III–VI.*

stériquement purs à la chromatographie sur alumine; chacun donne naissance à un *p*-nitrobenzoate en tous points semblable à celui qui servit à la purification. Chaque alcool fut oxydé par l'acide chromique en homocamphre ou en homoépicamphre, suivant son origine. Il convient de relever que les alcools épimères ne donnent pas de dépression de point de fusion en mélange, alors que leurs dérivés (esters) mentionnés plus haut en donnent. Une observation semblable avait été faite pour les cétones I et II (1).

TABLEAU I

Description des alcools III–VI

Alcools	P.f.	Rendements en alcools	Rendements stériques	$[\alpha]_D$*
Alcool au sodium III	212°	97%	94%	+17.9°±2.0°
Alcool au platine IV	234–235°	93%	90–95%	−29.2°±2.0°
Alcool au sodium V	166°	94%	92%	+35.9°±2.0°
Alcool au platine VI	206°	87%	97%	+43.9°±2.0°

*Benzène.

Le succès de la réduction catalytique dépend de la position du groupe méthyle pontal (position 1 ou 5) par rapport au groupe carbonyle à réduire. Ainsi l'homoépicamphre est aisément réduit par le platine dans l'acide acétique glacial et tout aussi aisément par le platine ou le nickel de Raney dans l'alcool (sans pression et 25°). L'homocamphre, dont le groupe carbonyle est adjacent au méthyle pontal, n'est réduit à une vitesse appréciable que par le platine dans l'acide acétique. Lorsque la réduction a lieu, le rendement stérique est toujours supérieur à 90%. La réduction par le sodium et l'éthanol procède sans difficultés: les rendements en alcools et les rendements stériques sont les mêmes pour la réduction de l'homocamphre et de l'homoépicamphre. Les rendements stériques (Tableau I) ont été déterminés par l'analyse du pouvoir rotatoire des alcools bruts; celui de la réduction de l'homocamphre au platine a dû être estimé, car l'alcool brut contenait des traces de cétone décelées par spectroscopie infrarouge.

Pour déterminer les configurations et les conformations respectives des quatre alcools III à VI, nous avons appliqué plusieurs méthodes. Celles qui font appel aux modes de formation des alcools, à leurs rotations moléculaires et à leurs vitesses d'oxydation chromique seront discutées ici. Les réactions d'élimination des groupes —OH et de leurs esters feront l'objet de mémoires séparés en raison de leur complexité.

Nous appliquerons en premier lieu la méthode des rotations moléculaires de Bose et Chaterjee (4). La règle stipule que si les configurations absolues de deux composés alicycliques épimères peuvent être ramenées aux configurations VII et VIII, l'épimère VII sera plus dextrogyre que l'épimère VIII, pour autant que L, M, S et T représentent l'ordre décroissant de l'encombrement stérique des substituants ou des parties de la molécule adjacents au carbone asymétrique.

Comme la configuration absolue de l'homocamphre (I) et de l'homoépicamphre (II)

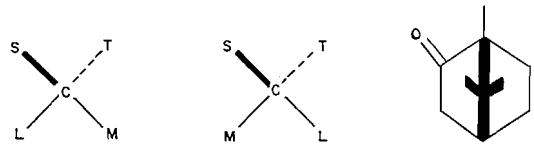

(VII) (VIII) (IX)

Can. J. Chem. Downloaded from www.nrcresearchpress.com by 190.90.36.8 on 09/04/12
For personal use only.

est connue avec certitude—puisque ces cétones sont dérivées (1, 2) du (+)-camphre (configuration absolue (5, 6), formule IX) par un procédé qui ne saurait provoquer d'inversion de configuration—nous pouvons connaître L et M pour les quatre alcools III à VI en question; L est l'atome de pont et M le groupe méthylène en position 3. En posant: —OH = S et —H = T, nous arrivons aux configurations suivantes:

Série de l'homocamphre: l'alcool au sodium, plus dextrogyre que l'alcool au platine, reçoit la configuration VII et par suite, la formule III. L'alcool au platine sera IV.

Série de l'homoépicamphre: l'alcool au platine, étant le plus dextrogyre, reçoit la configuration VII, donc VI. L'alcool au sodium sera V.

En fait, les formules III à VI peuvent être transposées en formules spatiales, qui se rattachent à deux conformations que nous appelons A et B.

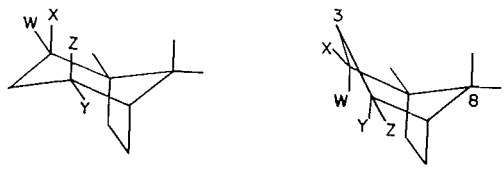

I A	W,X = = O (cétone); Y,Z = —H	I B
II A	Y,Z = = O (cétone); W,X = —H	II B
III A	W = —OH; X,Y,Z = —H	III B
IV A	X = —OH; W,Y,Z = —H	IV B
V A	Y = —OH; W,X,Z = —H	V B
VI A	Z = —OH; W,X,Y = —H	VI B

La conformation B (cyclohexanique bateau) est certainement moins stable que la conformation A (cyclohexanique chaise), en raison principalement de l'interférence prononcée du groupe méthyle en position 8 (flagpole, *fp*) avec l'hydrogène (*fp*) en position 3. Nous avançons ceci en tenant compte de l'analogie qui existe entre les dérivés du triméthyl-1,8,8 bicyclo[3,2,1]octane et les verbanones. Bose a montré (7) que la *cis*-verbanone réagit sous sa conformation X C (analogue à I A et II A) plutôt que X D (analogue à I B et II B); voir aussi (8). Bose laisse toutefois ouverte la question de savoir si le néoisoverbanol a la conformation XI C ou XI D, XI C pouvant être défavorisée en raison des trois substituants axiaux.

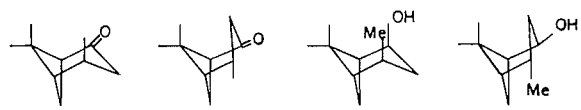

X C X D XI C XI D

Nous ne retenons ainsi pour l'homocamphre (I) et l'homoépicamphre (II) que les conformations I A et II A respectivement, où le groupe carbonyle à réduire se présente comme celui d'une cyclohexanone chaise. De nombreux exemples supportent le fait que la réduction d'un groupe carbonyle par le sodium et l'alcool engendre un groupe —OH équatorial. Les hydroxyles des deux alcools au sodium seraient ainsi équatoriaux et leurs configurations α. Les alcools au platine seraient par conséquent les alcools axiaux, de configuration β, ce qui est conforme à ce que l'on sait de l'hydrogénation catalytique qui conduit, dans des conditions expérimentales ne favorisant pas une isomérisation, à la fixation de l'hydrogène sur le côté le plus dégagé de la molécule: généralement le groupe—OH est axial. Pour de nombreuses références, voir (7, 9, 10, 11, 12).

Can. J. Chem. Downloaded from www.nrcresearchpress.com by 190.90.36.8 on 09/04/12
For personal use only.

TABLEAU II
Vitesses d'oxydation chromique et fréquences de vibration C—O des alcools III à VI

Alcools	Vitesses d'oxydation relatives à celle du cyclohexanol	Fréquences de vibration* C—O, cm^{-1}
Cyclohexanol	1	
Alcool au sodium III	5.7	1044 (f), 1033 (f), 1013 (F)
Alcool au platine IV	111.8	1029 (F), 1005 (F)
Alcool au sodium V	6.5	1038 (F)
Alcool au platine VI	125.0	1044 (F)

*Mesurées dans le sulfure de carbone. (F) signifie bande forte, (f) bande plus faible.

À la suite des premiers travaux de Vavon (13) concernant la vitesse de l'oxydation chromique des alcools secondaires en cétones, Barton (14, 15) a fait remarquer que les groupes —OH axiaux étaient oxydés plus rapidement que les hydroxyles équatoriaux. Schreiber et Eschenmoser (16) ont interprété ce fait en termes d'interactions entre atomes non liés et de décompression stérique lors du passage des esters chromiques aux cétones, la décompression stérique, par suite la vitesse d'oxydation, étant plus grande pour une conformation axiale, plus comprimée qu'une conformation équatoriale.

Les résultats[6] rapportés au Tableau II montrent que les deux alcools au platine sont oxydés environ 20 fois plus rapidement que les deux alcools au sodium; ces résultats sont donc bien en accord avec les conformations IV A et VI A pour les alcools au platine (groupes —OH axiaux) et avec les conformations III A et V A pour les alcools au sodium (groupes —OH équatoriaux).

En définitive, l'analyse des modes de formation des alcools III à VI, de leurs pouvoirs rotatoires et de leurs vitesses d'oxydation chromique, contribue à former un faisceau d'indices favorables à l'interprétation suivante: les alcools sont formés à partir des cétones de conformation A (I A et II A, cyclohexanique chaise) et existent sous cette conformation en tant qu'alcools axiaux (IV A et VI A, alcools au platine) et alcools équatoriaux (III A et V A, alcools au sodium).

Nous rapportons au Tableau II les fréquences des vibrations C—O des quatre alcools III à VI; nous les avons mesurées dans le but de les comparer aux valeurs moyennes déduites par Cole, Jones et Dobriner (17) pour les alcools stéroides axiaux (996–1036 cm^{-1}) et équatoriaux (1038–1044 cm^{-1}). Les alcools III et IV issus de l'homocamphre montrent plusieurs bandes et il n'est pas possible d'en choisir une plutôt que l'autre pour appliquer la règle. L'inversion observée pour les triméthyl-5,8,8 bicyclo[3,2,1]-octanols-2α et -2β (V et VI) n'est donc plus significative et ne saurait être retenue pour invalider les conclusions tirées plus haut au sujet de la conformation de ces alcools.

PARTIE EXPÉRIMENTALE[7]

L'homocamphre utilisé dans les sections 1 et 2 a été préparé selon (1).

1. Triméthyl-1,8,8 bicyclo[3,2,1]octanol-2β (IV)

1.1. Préparation de l'alcool brut

(*a*) On procède à l'hydrogénation préalable de 100 mg de PtO_2 dans 10 ml d'acide acétique glacial, puis à l'hydrogénation proprement dite de 2.0 g d'homocamphre dissous

[6]*Nous avons choisi la valeur arbitraire de 1 pour le cyclohexanol; on pourra ainsi rapprocher les vitesses d'oxydation des alcools III à VI de celles données par Schreiber et Eschenmoser pour divers cholestanols (16).*

[7]*Les points de fusion (p.f.) ont été déterminés dans des tubes capillaires dans un bloc chauffé électriquement et en utilisant un thermomètre étalonné avec les standards du Bureau des Standards de Washington. Les spectres infrarouges ont été mesurés à l'aide d'un spectromètre "Perkin–Elmer" modèle 112, à simple faisceau et parcours double, prisme* NaCl. *Les analyses carbone–hydrogène sont de Geller Laboratories, Hackensack, N.J.; celles d'azote sont de M. Lefebvre. Les valeurs des pouvoirs rotatoires* $[\alpha]_D$ *sont à* $\pm 2°$ *près.*

Can. J. Chem. Downloaded from www.nrcresearchpress.com by 190.90.36.8 on 09/04/12
For personal use only.

dans 30 ml d'acide acétique glacial. Il y a absorption de 235 ml d'hydrogène en $4\frac{1}{2}$ h (calculé pour $1H_2$: 245 ml; 748 mm, 23°). On reprend le tout par de l'éther, extrait l'acide acétique par des lavages avec une solution aqueuse de soude caustique à 10%. Après les lavages habituels jusqu'à neutralité, séchage et évaporation de l'éther, le résidu est sublimé pour donner 1.89 g (93%) d'alcool brut, p.f. 235°; $[\alpha]_D^{23} = -32.4°$ ($c = 3.93$; benzène).

(*b*) En 8 heures, il n'y eut aucune absorption lorsque 5 g d'homocamphre furent agités en atmosphère d'hydrogène en présence de 5 g de nickel de Raney dans 50 ml d'éthanol 95% et 10 ml de solution alcoolique de soude 10%. De même, en 1 heure, aucune absorption d'hydrogène n'eut lieu ne présence de platine dans l'éthanol 95%.

1.2. Purification de l'alcool brut

L'alcool brut (3.8 g) est chauffé à l'ébullition à reflux durant 2 heures dans 30 ml de pyridine sèche avec 6.5 g de chlorure de *p*-nitrobenzoyle. Après refroidissement, on précipite l'ester par addition d'eau. Le solide est essoré et repris dans de l'éther. On lave (HCl 10%, NaOH 10% puis eau). On sèche, évapore le solvant et cristallise le résidu dans du méthanol jusqu'à point de fusion et pouvoir rotatoire constants. On a 6.5 g (91%) de *p*-nitrobenzoate p.f. 123–124°, $[\alpha]_D^{23} = -96.6°$ ($c = 3.97$; benzène). On en saponifie 4.0 g par chauffage à reflux durant 2 heures avec 4.0 g de NaOH dans 25 ml d'éthanol et 25 ml d'eau. On isole à la manière habituelle 1.3 g de triméthyl-1,8,8 bicyclo[3,2,1]-octanol-2β régénéré. Cet alcool régénéré (2.050 g) est adsorbé sur 60 g d'alumine Merck pour chromatographie. Des élutions de 100 ml chacune ont donné:

(A) Fractions 1–14, éther de pétrole, p.é. 30–40°, 0.685 g, p.f. 234–235°, $[\alpha]_D^{23} = -29.2°$;

(B) Fractions 15–24, éther de pétrole–benzène 1–1, 1.140 g, p.f. 234–235°, $[\alpha]_D^{23} = -28.7°$;

(C) Fractions 25–26, benzène, 0.139 g, p.f. 233–234°, $[\alpha]_D^{23} = -26.4°$. Pour $[\alpha]_D^{23}$: $c = 4.0$; benzène.

Un échantillon de triméthyl-1,8,8 bicyclo[3,2,1]octanol-2β a été sublimé pour l'analyse; p.f. 234–235°, $[\alpha]_D^{23} = -29.2°$ ($c = 4.0$; benzène). Calculé pour $C_{11}H_{20}O$: C, 78.51; H, 11.98%. Trouvé: C, 78.33; H, 12.06%. Spectre infrarouge: bandes à 1029 et 1005 cm^{-1} (CS_2/0.03 *M*).

1.3 p-Nitrobenzoate

L'alcool pur (350 mg) et 420 mg de chlorure de *p*-nitrobenzoyle sont chauffés à reflux durant 2 heures dans 5 ml de pyridine sèche. On isole à la manière habituelle 489 mg de *p*-nitrobenzoate, paillettes incolores, p.f. 125° (éthanol 95%), $[\alpha]_D^{23} = -84.5°$ ($c = 4$; chloroforme). Calculé pour $C_{18}H_{23}O_4N$: C, 68.12; H, 7.30; N, 4.41%. Trouvé: C, 68.19; H, 7.55; N, 4.35%.

1.4. Oxydation chromique

L'alcool (360 mg) et 150 mg d'anhydride chromique sont dissous dans 10 ml d'acide acétique glacial. La solution s'échauffe un peu. On abandonne à température de la pièce pendant 3 heures. On ajoute ensuite 30 ml d'eau et neutralise avec du bicarbonate de sodium (solution aqueuse à 10%). On extrait à l'éther et isole à la manière habituelle 353 mg de cétone brute que l'on traite par 423 mg de dinitro-2,4 phénylhydrazine en solution dans 8 ml de méthanol contenant 4% d'acide chlorhydrique conc. On obtient, après une précipitation lente, 641 mg de dinitro-2,4 phénylhydrazone brute que l'on cristallise dans l'acide acétique glacial. On retrouve 452 mg de dinitro-2,4 phénylhydrazone d'homocamphre, p.f. 238–239° seule ou en mélange avec un échantillon de dinitro-2,4 phénylhydrazone d'homocamphre authentique (1).

Can. J. Chem. Downloaded from www.nrcresearchpress.com by 190.90.36.8 on 09/04/12
For personal use only.

Can. J. Chem. Downloaded from www.nrcresearchpress.com by 190.90.36.8 on 09/04/12
For personal use only.

2. Triméthyl-1,8,8 bicyclo[3,2,1]octanol-2α (III)

2.1. Préparation de l'alcool brut

Dans un ballon à trois tubulures surmonté d'un agitateur mécanique et d'un réfrigérant, on introduit 9.6 g (0.057 mole) d'homocamphre et 150 ml d'alcool isobutylique. On porte à l'ébullition et ajoute, par portions de 0.5 g environ, 15.0 g (0.65 mole) de sodium. Après l'addition, on chauffe encore 5 heures à reflux, avec agitation. On ajoute de l'eau (30 ml) et distille sous vide. On retrouve 9.36 g (après sublimation) d'alcool brut, à odeur camphrée, p.f. 208–216°, $[\alpha]_D^{23} = +15.1°$ ($c = 4.0$; benzène). Rendement: 97%.

Un essai semblable effectué à partir de 4.0 g d'homocamphre dans 100 ml d'éthanol anhydre et 8 g de sodium a donné 3.9 g (97%) d'alcool brut, après sublimation, p.f. 207.5–209.5°, $[\alpha]_D^{23} = +14.6°$ ($c = 4.00$; benzène).

2.2. Purification de l'alcool brut (Mode opératoire 1.2)

Le *p*-nitrobenzoate brut fond à 127–128°, $[\alpha]_D^{23} = +32.9°$ ($c = 4.00$; benzène). Il est saponifié et donne l'alcool régénéré, p.f. 212–213°, $[\alpha]_D^{23} = +16.5°$ ($c = 4.12$; benzène), qui est chromatographié sur alumine; trois fractions principales sont recueillies:

(A) 29%, éther de pétrole–benzène 4–1 (p.é. 30–40°), p.f. 213–215°, $[\alpha]_D^{23} = +15.7°$;

(B) 40%, éther de pétrole–benzène 1–1, p.f. 212°, $[\alpha]_D^{23} = +17.3°$;

(C) 27%, benzène, p.f. 212°, $[\alpha]_D^{23} = +17.9°$. (Pour tous les pouvoirs rotatoires: $c = 4.00$; benzène.)

La fraction (C) fut analysée. Calculé pour $C_{11}H_{20}O$: C, 78.51; H, 11.98%. Trouvé: C, 78.43; H, 12.08%. Le point de fusion de mélange avec l'alcool épimère p.f. 234–235° (voir section 1.2) est de 216.5–220°. Spectre infrarouge: bandes à 1013, 1033 et 1044 cm^{-1} (CS_2/0.03 *M*).

2.3. p-Nitrobenzoate (Préparation, voir 1.3)

Aiguilles incolores (méthanol), p.f. 127–128°, $[\alpha]_D^{23} = +35.0°$ ($c = 4$; chloroforme). Calculé pour $C_{18}H_{23}O_4N$: C, 68.12; H, 7.30; N, 4.41%. Trouvé: C, 68.45, 68.03; H, 7.11, 7.31; N, 4.42%.

2.4. Oxydation chromique (Mode opératoire, voir 1.4)

La dinitro-2,4 phénylhydrazone obtenue fond à 238–238.5° seule et 237–239° en mélange avec la dinitro-2,4 phénylhydrazone de l'homocamphre (1).

3. Triméthyl-5,8,8 bicyclo[3,2,1]octanol-2β (VI)

3.1. Préparation de l'alcool brut

(*a*) L'homoépicamphre (5.0 g) dissous dans 50 ml d'éthanol 95% est hydrogéné en présence de 5.0 g de nickel de Raney et 10 ml d'une solution alcoolique de NaOH à 5%. En 24 heures, il y a absorption de 725 ml d'hydrogène (calculé pour $1H_2$: 729 ml; 760 mm, 23°). On essore le catalyseur, évapore le filtrat, on reprend le résidu par de l'éther. Après les lavages habituels, on sèche et évapore l'éther; le résidu est sublimé: 4.72 g d'alcool brut (93%), p.f. 207–208.5°, $[\alpha]_D^{23} = +42.8°$ ($c = 4.04$; benzène).

(*b*) L'homoépicamphre (2 g) est hydrogéné en présence de 60 mg de PtO_2, hydrogéné au préalable, dans 40 ml d'acide acétique glacial. Au bout de 3 heures, l'hydrogénation est terminée; absorption: 285 ml (calculé pour $1H_2$: 296 ml; 748 mm, 23°). On essore le catalyseur, reprend la solution par de l'éther, que l'on lave avec une solution aqueuse de NaOH 10%. On extrait à la manière habituelle 1.76 g (87%) d'alcool brut (sublimé), p.f. 205–206°, $[\alpha]_D^{23} = +43.4°$ ($c = 4.0$; benzène).

3.2. Purification de l'alcool brut

Le *p*-nitrobenzoate se présente sous forme de paillettes après cristallisation dans l'éthanol. Il fond à 137–138°, $[\alpha]_D^{23} = +78.5°$ ($c = 4$; chloroforme). Calculé pour

$C_{18}H_{23}O_4N$: C, 68.12; H, 7.30; N, 4.41%. Trouvé: C, 68.24; H, 7.31; N, 4.39%. Après saponification, on retrouve un triméthyl-5,8,8 bicyclo[3,2,1]octanol-2β (VI) homogène à la chromatographie sur alumine: p.f. 206°; $[\alpha]_D^{23} = +43.9°$ ($c = 4.0$; benzène). Calculé pour $C_{11}H_{20}O$: C, 78.51; H, 11.98%. Trouvé: C, 78.27; H, 11.81%. Spectre infrarouge: bande à 1044 cm^{-1} (CS_2/0.03 *M*).

3.3. Oxydation chromique

L'alcool (504 mg) donne 659 mg de dinitro-2,4 phénylhydrazone d'homoépicamphre, p.f. 178–178.5°, seule ou en mélange avec la dinitro-2,4 phénylhydrazone de l'homoépicamphre (1).

4. Triméthyl-5,8,8 bicyclo[3,2,1]octanol-2α (V)

4.1. Préparation de l'alcool brut

Selon le mode opératoire 2.1, 12 g d'homoépicamphre sont réduits par 20 g de sodium dans 200 ml d'éthanol anhydre. On obtient 11.3 g (94%) d'alcool brut sublimé, p.f. 172–173°, $[\alpha]_D^{23} = +36.4°$ ($c = 4.03$; benzène).

4.2. Purification de l'alcool brut (Mode opératoire 1.2)

Le *p*-nitrobenzoate pur fond à 120°, $[\alpha]_D^{23} = +24.5°$ ($c = 4$; chloroforme). Calculé pour $C_{18}H_{23}O_4N$: C, 68.12; H, 7.30; N, 4.41%. Trouvé: C, 68.28; H, 7.39; N, 4.33%. Après saponification, on retrouve un triméthyl-5,8,8 bicyclo[3,2,1]octanol-2α (V) homogène, p.f. 166°, $[\alpha]_D^{23} = +35.9°$ ($c = 4.0$; benzène). Calculé pour $C_{11}H_{20}O$: C, 78.51; H, 11.98%. Trouvé: C, 78.25; H, 11.82%. Le p.f. de cet alcool avec l'épimère p.f. 206° (alcool VI, section 3.2) est de 179–185°. Spectre infrarouge: bande forte à 1038 cm^{-1} (CS_2/0.03 *M*).

4.3. Oxydation chromique (Mode opératoire, voir 1.4)

L'alcool V (504 mg) donne 632 mg de dinitro-2,4 phénylhydrazone d'homoépicamphre, p.f. 177.5°, seule ou en mélange avec la dinitro-2,4 phénylhydrazone de l'homoépicamphre (1).

5. Mesures des vitesses d'oxydation chromique

La mesure de la disparition de l'acide chromique se fait dans un spectrophotomètre Beckman DK1, ajusté à la longueur d'onde de 3500 Å. Une courbe de calibration de la densité optique des solutions de CrO_3, à cette longueur d'onde, a d'abord été tracée en fonction de la concentration. La vitesse d'oxydation a ensuite été mesurée grâce à la variation de la densité optique de la solution en fonctions du temps.

À partir d'une solution mère d'acide acétique aqueux à 90.9% (volume/volume) maintenue à température constante (24.9°±0.1°), on prépare: (*a*) une solution de CrO_3 environ 1.05×10^{-3} *M* que l'on place dans le bain à température constante; (*b*) une solution contenant les alcools à oxyder; cette solution est préparée juste avant l'oxydation. Au temps zéro, on mélange rapidement les solutions (*a*) et (*b*) de manière à obtenir environ 50 ml en tout; on en remplit une cellule en quartz que l'on place dans la chambre de mesures d'un spectrophotomètre Beckman DK1; ces diverses opérations prennent de 20 à 30 secondes depuis le temps zéro. La technique varie ensuite un peu, selon la rapidité de l'oxydation: (1) pour les oxydations lentes, allant jusqu'à 60 minutes, on conserve la solution contenant l'alcool et le CrO_3 dans le bain à température constante; on en prélève des échantillons de temps en temps, que l'on place dans la chambre de mesures du spectrophotomètre et dont on mesure la densité optique; on assure ainsi l'uniformité de la température au cours de l'expérience; (2) pour les oxydations rapides, ne dépassant pas 5 minutes, tous les points de la courbe sont enregistrés automatiquement sur le papier qui se déroule sans interruption; comme la température de la chambre de mesures du spectrophotomètre est voisine de 25°, les variations de température sont négligeables.

Can. J. Chem. Downloaded from www.nrcresearchpress.com by 190.90.36.8 on 09/04/12
For personal use only.

Les résultats et les données expérimentales sont rapportés au Tableau III. La vitesse $v = -d\ CrO_3/dt$ a été déterminée par la méthode graphique et les valeurs de v données sont les valeurs de la vitesse extrapolée au temps zéro.

TABLEAU III

Détail des déterminations des vitesses d'oxydation chromique

Alcools	Concentrations molaires des alcools	Concentrations molaires en CrO_3	$v = -d\ CrO_3/dt$ mole×litre^{-1}×min^{-1}
Cyclohexanol	7.136×10^{-4}	10.22×10^{-4}	2.80×10^{-6} (lente)
Alcool au sodium III	7.162×10^{-4}	10.85×10^{-4}	16.0×10^{-6} (lente)
Alcool au platine IV	7.013×10^{-4}	10.76×10^{-4}	330.0×10^{-6} (rapide)
Alcool au sodium V	7.108×10^{-4}	10.76×10^{-4}	18.4×10^{-6} (lente)
Alcool au platine VI	7.111×10^{-4}	10.77×10^{-4}	350.0×10^{-6} (rapide)

REMERCIEMENTS

Nous remercions le Conseil National de Recherches du Canada de son aide financière (subvention de recherche, H.F., et bourse d'études, J-C.R.) et l'Office de Recherches Scientifiques de la Province de Québec d'une bourse d'études, M.L.

BIBLIOGRAPHIE

1. Favre, H., Marinier, B. et Richer, J-C. Can. J. Chem. **34**, 1329 (1956).
2. Favre, H. et Marinier, B. Can. J. Chem. **35**, 278 (1957).
3. Fodor, G. et Nador, K. J. Chem. Soc. 721 (1953).
4. Bose, A. K. Résumé des communications. Tome II. XVIe Congrès international de Chimie pure et appliquée, Paris. juillet 1957. page 141.
5. Fredga, A. et Miettinen, T. K. Acta Chem. Scand. **1**, 371 (1947).
6. Freudenberg, K. et Lwowski, W. Ann. **587**, 213 (1954).
7. Bose, A. K. J. Org. Chem. **20**, 1003 (1955).
8. Kergomard, A. et Geneix, M.Th. Bull. soc. chim. France, (5), 397 (1958).
9. Bose, A. K. J. Org. Chem. **20**, 1010 (1955).
10. Naves, Y.-R. Bull. soc. chim. France, (5), 1020 (1956).
11. Wicker, R. J. J. Chem. Soc. 2165 (1956).
12. Dauben, W. G., Blanz, E. J., Jr., Jiu, J. et Micheli, R. A. J. Am. Chem. Soc. **78**, 3752 (1956).
13. Vavon, G. et Zaremba, C. Bull. soc. chim. France, **49** (4), 1853 (1931).
14. Barton, D. H. R. Experientia, **6**, 316 (1950).
15. Barton, D. H. R. J. Chem. Soc. 1027 (1953).
16. Schreiber, J. et Eschenmoser, A. Helv. Chim. Acta, **38**, 1529 (1955).
17. Cole, A. R. H., Jones, R. N. et Dobriner, K. J. Am. Chem. Soc. **74**, 5571 (1952).

Can. J. Chem. Downloaded from www.nrcresearchpress.com by 190.90.36.8 on 09/04/12
For personal use only.

Can. J. Chem. Downloaded from www.nrcresearchpress.com by 190.90.36.8 on 09/04/12
For personal use only.

DÉRIVÉS DU TRIMÉTHYL-1,8,8 BICYCLO[3,2,1]OCTANE

IV. DÉTERMINATION DES CONFIGURATIONS DES DEUX DIMÉTHYL-5,5 CYCLOHEXANEDIOLS-1,3[1]

H. Favre et J-C. Richer[2]

RÉSUMÉ

À la suite de l'analyse des modes de formation et des vitesses d'oxydation chromique des diméthyl-5,5 cyclohexanediols-1,3, les auteurs attribuent la configuration *cis* au diol p.f. 149–151° et la configuration *trans* à l'isomère p.f. 106–107.5°.

Au cours de l'étude de la réduction catalytique de la triméthyl-1,8,8 bicyclo[3,2,1]-octanedione-2,4 (I) (1) nous avons utilisé le dimédon (II) comme substance modèle. Nous avons obtenu avec un rendement de 95% un seul des deux diméthyl-5,5 cyclo-

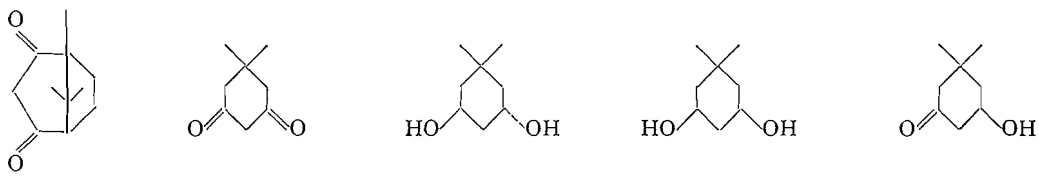

I II III IV V

hexanediols-1,3 stéréoisomères (p.f. 106–107.5°, III), en opérant à pression atmosphérique et à 25°, en présence de nickel de Raney dans l'éthanol. Les deux diméthyl-5,5 cyclohexanediols-1,3 sont connus à la suite de réductions chimiques ou catalytiques (Tableau I); à notre connaissance, leurs configurations respectives, *cis* et *trans*, ne le sont pas; ce travail a pour but de les déterminer.

TABLEAU I

Réductions du dimédon conduisant aux diméthyl-3,3 cyclohexanediols-1,3

Conditions expérimentales	P.f. et rendements en diméthyl-5,5 cyclohexanediols-1,3	Autres produits de réduction	Références
Ni Raney, 150–200 at., 125°	102–104°+146° (80%)	Diméthyl-3,3 cyclohexanol-1 (3.8%)	(2)
Ni Raney, 100 at., 180°	146°	Diméthyl-3,3 cyclohexanol-1 (75%)	(3)
Ni Raney, 748 mm, 23°, $+CHCl_3$	106–107.5° (95%)		Ce travail
Sodium-éthanol	147° (63–68%)	Diméthyl-3,3 cyclohexanol-1 (7%)	(4)
$LiAlH_4$	102–103.2°+147.6–148° (4%)	Diméthyl-5,5 cyclohexène-2 ol-1 (62%)	(5)

Nous avancerons d'abord quelques considérations concernant le mécanisme de l'hydrogénation catalytique. Dans tous nos essais, l'hydrogénation prenait fin après absorption de deux moles d'hydrogène. En interrompant la réaction après fixation d'une

[1]*Manuscrit reçu le 27 août, 1958.*
Contribution du Département de Chimie de l'Université de Montréal, Montréal, P.Q. Ce mémoire est tiré de la thèse de doctorat de J-C. Richer; il fut présenté au 41e Congrès annuel de l'Institut de chimie du Canada à Toronto, les 26–28 mai, 1958.
[2]*Boursier du Conseil national de Recherches du Canada, 1954–1958. Adresse actuelle: Department of Chemistry, University of Notre Dame, Notre Dame, Ind.*

mole d'hydrogène seulement, nous avons pu mettre en évidence la présence de la diméthyl-5,5 cyclohexanolone-3,1 (V) dans le milieu, à côté du dimédon non réduit et du diol III. En pratique, nous avons isolé le produit de déshydratation du β-cétol V, la diméthyl-5,5 cyclohexène-2 one-1. Cette formation de β-cétol était connue pour la réduction de nombreuses β-dicétones aliphatiques (6). Nous l'avons montrée pour étayer notre raisonnement. Nous formulons ainsi la réaction d'hydrogénation: la réduction catalytique du dimédon conduit d'abord à la diméthyl-5,5 cyclohexanolone-3,1 (V) qui se détache du catalyseur pour s'y fixer à nouveau et se faire réduire en diol. La configuration du diol obtenu dépendra de la conformation du β-cétol V, si aucune isomérisation n'a lieu. Il y a alors une analogie entre la réduction de ce β-cétol et celle de la triméthyl-3,3,5 cyclohexanone-1 (VI A) étudiée en détail par Wicker (7, 8, 9). Cet auteur a montré que dans des conditions douces (température basse, peu de catalyseur alcalin susceptible de provoquer des isomérisations), la cétone VI conduisait principalement à l'alcool *trans* VII (88% de *trans* pour 12% de *cis*); la triméthyl-3,3,5 cyclohexanone serait réduite sous la conformation VI A de préférence à VI B à cause de l'interférence des deux groupes méthyle axiaux 3 et 5; la fixation de l'hydrogène se fait de façon à donner l'alcool axial.

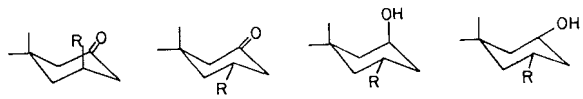

V B R = OH V A R = OH III R = OH IV R = OH
VI B R = CH_3 VI A R = CH_3 VII R = CH_3 VIII R = CH_3

Ainsi, la conformation V A, préférée à V B pour la diméthyl-5,5 cyclohexanolone-3,1,[3] conduira au diol III *trans*, groupes —OH *a*—*e*, à la condition qu'il n'y ait pas d'isomérisation consécutive à la formation du diol. Nous avons mis en oeuvre un nickel de Raney traité par du chloroforme. Cornubert et ses collaborateurs (12, 13, 14, 15) ont montré que le chloroforme et d'autres composés organiques halogénés abaissaient considérablement l'aptitude du nickel de Raney à réduire les groupes carbonyle; l'explication donnée est que le chloroforme engendre avec le nickel de l'acide chlorhydrique qui neutralise la soude fixée par le catalyseur. Comme nous n'avons pas utilisé les quantités prescrites par Cornubert pour contraindre le nickel et l'empêcher de réduire les groupes carbonyle, mais seulement des quantités modérées n'empêchant pas la réduction, nous pensons que notre nickel s'approchait de la neutralité et puisque nous n'avons opéré ni sous pression ni à température élevée, une isomérisation n'était plus à craindre et une configuration *trans* (III) se justifie pour le diol p.f. 106–107.5°. Le diol p.f. 149–151° est alors le diol *cis*.

Nous avons tenté de corroborer ces configurations par deux méthodes:

1. La résolution en antipodes optiques qui fait de l'isomère dédoublable l'isomère *trans*. Nous avons réussi à préparer le bi-phtalate acide de l'isomère p.f. 106–107.5° (*trans*, donc dédoublable, selon nos considérations antérieures), mais nous n'avons pu en cristalliser les sels de strychnine ou de brucine.

2. L'étude infrarouge des ponts hydrogène internes, à la manière de Kuhn (16), qui a montré que le cyclohexanediol-1,3 *cis*, en solution 0.005 *M* dans le tétrachlorure de carbone, présente deux bandes, 3619 et 3544 cm^{-1}, attribuées respectivement aux groupes —OH libres et —OH liés par un pont hydrogène; l'isomère *trans* ne présente qu'une

[3]*Dans son exposé sur la prééminence des formes équatoriales, Cornubert (10) démontre que le diméthyl-3,3 cyclohexanol existe sous la forme* —OH *équatorial. Eliel et Lukach (36) arrivent à la même conclusion. Nous trouvons dans ces travaux la justification de notre avancé.*

Can. J. Chem. Downloaded from www.nrcresearchpress.com by 190.90.36.8 on 09/04/12
For personal use only.

bande, 3620 cm^{-1}, la distance séparant les hydroxyles axial et équatorial ne permettant pas la formation d'un pont hydrogène interne. Cette méthode est inappliquable au cas des diméthyl-5,5 cyclohexanols-1 *cis* et *trans*, car les deux isomères ne montrent qu'une bande: 3621 cm^{-1} pour l'isomère p.f. 149–151° et 3627 cm^{-1} pour l'isomère p.f. 106–107.5°.

Nous nous sommes alors tournés vers l'étude cinétique de l'oxydation chromique des deux diols III et IV, en nous inspirant des travaux de Vavon (17) et de Winstein (11) (indiquant que les alcools cyclohexaniques axiaux s'oxydent plus rapidement que les alcools équatoriaux (18, 19)), et de Schreiber et Eschenmoser (20) (montrant que la vitesse d'oxydation est proportionnelle à la compression stérique du système; en particulier, qu'un groupe méthyle axial porté par un carbone en β de celui qui porte le groupe —OH augmente considérablement la vitesse de l'oxydation de l'alcool axial, celle de l'alcool équatorial étant sensiblement la même que s'il n'y avait pas le groupe méthyle: cas des cholestanols-2α et -2β, et -3α et -3β).

Nous avons ainsi commencé par mesurer les vitesses d'oxydation des cyclohexanediols-1,2, -1,3 et -1,4 *cis* et *trans* dont les configurations sont bien connues. Les résultats (Tableau II) appellent les commentaires suivants: (*a*) les diols-1,2 *cis*, -1,3 *trans* et -1,4 *cis* s'oxydent plus rapidement que leur isomère *trans*, *cis* et *trans* respectif; (*b*) les diols qui s'oxydent plus rapidement présentent nécessairement un groupe —OH axial et l'autre équatorial; nous en concluons que les diols qui s'oxydent plus lentement le font sous leur conformation diéquatoriale et non diaxiale.

TABLEAU II

Vitesses d'oxydation chromique des cyclohexanediols

Alcools*	Conformations†	Concentrations molaires en alcool	Concentrations molaires en CrO_3	$v = -d CrO_3/dt$‡ mole $\times litre^{-1} \times min^{-1}$
Cyclohexanol	$a+e$	7.136×10^{-4}	10.22×10^{-4}	2.8×10^{-6}
Cyclohexanediol-1,2 *cis* (21)	$a-e$	3.542×10^{-4}	10.70×10^{-4}	5.00×10^{-6}
Cyclohexanediol-1,2 *trans* (22, 23)	$e-e$ $a-a$	3.585×10^{-4}	10.70×10^{-4}	1.68×10^{-6}
Cyclohexanediol-1,3 *cis* (24)	$e-e$ $a-a$	3.585×10^{-4}	10.60×10^{-4}	1.76×10^{-6}
Cyclohexanediol-1,3 *trans* (25, 26)	$a-e$	3.539×10^{-4}	10.60×10^{-4}	3.4×10^{-6}
Cyclohexanediol-1,4 *cis* (27, 28, 29, 30, 31, 32)	$a-e$	3.558×10^{-4}	10.60×10^{-4}	2.12×10^{-6}
Cyclohexanediol-1,4 *trans* (27, 33, 34)	$e-e$ $a-a$	3.553×10^{-4}	10.60×10^{-4}	1.72×10^{-6}
Diméthyl-5,5 cyclohexanediol-1,3 *cis*, p.f. 149–151° IV	$e-e$ $a-a$	3.555×10^{-4}	10.60×10^{-4}	2.4×10^{-6}
Diméthyl-5,5 cyclohexanediol-1,3 *trans*, p.f. 106–107.5° III	$a-e$	3.542×10^{-4}	10.60×10^{-4}	20.00×10^{-6}

*On trouve à la suite des diols les références bibliographiques concernant leurs configurations et leurs modes de préparation. Les points de fusion de ces diols sont identiques à ceux décrits dans la littérature.

†Pour les conformations du cyclohexanol, voir (10, 11).

‡Acide acétique aqueux, 90.9% (v/v); $t = 24.9° \pm 0.1°$.

Il est clair que ces résultats sont essentiellement approchés. Winstein (11) considère que la réaction d'oxydation est la résultante de plusieurs réactions ayant des vitesses distinctes: (*a*) estérification (réaction d'équilibre, rapide); (*b*) formation de la cétone (réaction lente); (*c*) réactions secondaires, par exemple oxydation de la cétone formée (vitesses inconnues). Dans le cas des diols-1,3 qui nous intéressent, ces réactions secondaires peuvent être extrêmement complexes; les β-cétols issus des diols-1,3 *cis* et *trans*

Can. J. Chem. Downloaded from www.nrcresearchpress.com by 190.90.36.8 on 09/04/12
For personal use only.

pouvant (*a*) s'oxyder en dicétone, susceptible elle-même d'être oxydée, (*b*) se déshydrater en cétone α,β-éthylénique, aussi oxydable. De toute façon, nous avons déterminé la vitesse d'oxydation d'une manière simple, en extrapolant graphiquement au temps zéro les vitesses données par l'équation $v = -d\ CrO_3/dt$, et nous ne tirerons de la comparaison des vitesses d'oxydation que des renseignements qualitatifs, d'autant plus que nous prenons pour acquis que l'acide chromique oxydera l'un et l'autre des groupes hydroxyle,[4] ce qui rend toute étude quantitative prématurée. Les cyclohexanediols-1,3, dont l'isomère *trans* s'oxyde 1.9 fois plus rapidement que l'isomère *cis*, nous serviront de point de comparaison pour interpréter les résultats de l'oxydation des diméthyl-5,5 cyclohexanediols-1,3 (III et IV). De ces derniers, l'isomère p.f. 106–107.5° s'oxyde 8.3 fois plus rapidement que l'isomère p.f. 149–151°. Nous interprétons ceci en faisant du premier de ces diols l'isomère *trans*, $a-e$, et du deuxième le diol *cis*, oxidé sous sa forme $e-e$. Nous retrouvons non seulement la différence attendue entre les vitesses d'oxydation, mais encore une accélération notoire de la vitesse du diol diméthylé *trans* (III) par rapport à celle du cyclohexanediol-1,3 *trans*, bien en accord avec la présence d'un groupe méthyle axial sur le carbone en β de celui qui porte le groupe —OH axial. Les configurations déduites de l'oxydation chromique sont donc les mêmes que celles tirées plus haut du mécanisme de l'hydrogénation catalytique.

PARTIE EXPÉRIMENTALE[5]

Le dimédon mis en oeuvre a été cristallisé plusieurs fois dans l'éthanol 95%; il fond à 149–150°.

1. Réduction du dimédon en diméthyl-5,5 cyclohexanediol-1,3 trans (III)

Le dimédon (7.28 g) dissous dans 150 ml d'éthanol 95% est introduit dans un ballon à hydrogéner contenant 7.5 g de nickel de Raney; (préparation voir (37)); on ajoute 50 mg de chloroforme (sous forme d'une solution alcool-chloroforme 90–10) et secoue en atmosphère d'hydrogène. Au bout de 42 heures, la réaction s'arrête d'elle-même. On essore le catalyseur, le lave avec un peu de méthanol, évapore le filtrat à pression ordinaire, puis sous vide de 11 mm. Le résidu est repris par de l'éther et lavé avec une solution aqueuse de NaOH 10% puis à l'eau. On sèche sur sulfate de sodim, évapore l'éther et chromatographie le résidu, dissous dans du benzène, sur 100 g d'alumine Merck pour chromatographie; 300 ml de benzène éluent 3.5 g de composés en partie cristallisés, puis 700 ml de benzène éluent 0.209 g de diol p.f. 105–107°; finalement, 350 ml de méthanol éluent 3.7 g de diol p.f. 106–108°. La fraction partiellement cristalline est reprise dans de l'éther de pétrole et adsorbée sur 100 g d'alumine; l'élution par 600 ml de chloroforme donne 0.256 g de liquide brun, puis 300 ml de méthanol éluent 3.2 g de diol p.f. 106–108°. Le diméthyl-5,5 cyclohexanol pur fond à 106–107.5°, après cristallisation dans l'éther. Calculé pour $C_8H_{16}O_2$: C, 66.63; H, 11.18%. Trouvé: C, 66.99; H, 11.06. Le rendement en diol brut est de 95%.

Si l'on ajoute des quantités de chloroforme représentant 7.5, 14 ou 25% de la quantité de nickel de Raney, il n'y a pas d'absorption d'hydrogène.

[4]*Gallagher et Long (35) ont bien démontré ce fait en étudiant l'oxydation chromique de l'ester méthylique de l'acide cholique; bien que réagissant avec des vitesses différentes, les trois groupes* —OH *sont oxydés, et l'oxydation préférentielle de l'hydroxyle en position 7 ne se fait qu'avec un rendement de 40%.*

[5]*Les points de fusion ont été déterminés en tubes capillaires, le thermomètre étant étalonné avec des substances provenant du Bureau des Standards de Washington. Les spectres infrarouges ont été mesurés à l'aide d'un spectrophotomètre "Perkin–Elmer", modèle 112, à simple passage et double faisceau, optique* LiF.

Can. J. Chem. Downloaded from www.nrcresearchpress.com by 190.90.36.8 on 09/04/12
For personal use only.

2. Hydrogénation interrompue: préparation de la diméthyl-5,5 cyclohexène-2 one-1

Le dimédon (5.27 g) est hydrogéné dans 80 ml d'éthanol contenant 90 mg de chloroforme, en présence de 4.5 g de nickel de Raney, jusqu'à fixation de 1.02 mole d'hydrogène; la réaction est interrompue, le catalyseur essoré et lavé avec du méthanol, le filtrat évaporé; le résidu est entraîné par de la vapeur d'eau après adjonction de 50 ml carbonate de sodium (sol. aqueuse 10%). On examine séparément le distillat et les eaux alcalines.

(*A*) *Le distillat.*—Il est saturé par du chlorure de sodium et extrait à l'éther. Les solutions éthérées de plusieurs extractions sont réunies, séchées et évaporées; le résidu est traité par de l'acétate de semicarbazide dans du méthanol. On recueille 125 mg de semicarbazone de diméthyl-5,5 cyclohexène-2 one-1, p.f. 191–192.5° (méthanol) seule ou en mélange avec une semicarbazone de diméthyl-5,5 cyclohexène-2 one-1. Analyse: calculé pour $C_9H_{15}ON_3$: N, 23.19%. Trouvé: N, 23.35%.

(*B*) *Des eaux alcalines.*—On extrait par l'éther le diméthyl-5,5 cyclohexanediol-1,3, p.f. brut 101–103° (1.7 g) et après adjonction d'acide chlorhydrique, le dimédon qui n'a pas réagi (2.1 g).

3. Détermination des vitesses d'oxydation chromique

Le mode opératoire est celui décrit en détail dans la partie III de cette série (37) et les résultats sont rapportés au Tableau II. Les composés ont été préparés selon les travaux antérieurs dont référence est faite au Tableau II.

REMERCIEMENTS

Nous remercions le Conseil National de Recherches du Canada d'une subvention de recherche (H.F.) et d'une bourse d'études (J-C.R.).

BIBLIOGRAPHIE

1. Favre, H. et Richer, J-C. Can. J. Chem. **37**, 417 (1959).
2. Sprague, J. M. et Adkins, H. J. Am. Chem. Soc. **56**, 2669 (1934).
3. Henshall, T. J. Soc. Chem. Ind. London, **62**, 127 (1943).
4. Crossley, A. W. et Renouf, N. J. Chem. Soc. 602 (1915).
5. Dreiding, A. S. et Hartmann, J. A. J. Am. Chem. Soc. **75**, 3723 (1953).
6. Stutsman, P. S. et Adkins, H. J. Am. Chem. Soc. **61**, 3303 (1939).
7. Peppiat, E. G. et Wicker, R. J. Chem. & Ind. 747 (1955).
8. Peppiat, E. G. et Wicker, R. J. J. Chem. Soc. 3122 (1955).
9. Wicker, R. J. J. Chem. Soc. 2165 (1956).
10. Cornubert, R. Bull. soc. chim. France, (5) 996 (1956).
11. Winstein, S. et Holness, N. J. J. Am. Chem. Soc. **77**, 5562 (1955).
12. Cornubert, R. et Kaziz, C. Bull. soc. chim. France, (5) 410 (1952).
13. Cornubert, R. et Phélisse, J. Bull. soc. chim. France, (5) 403 (1952).
14. Cornubert, R. et Réal, M. Bull. soc. chim. France, (5) 407 (1952).
15. Cornubert, R. et Thomas, P. Bull. soc. chim. France, (5) 524 (1954).
16. Kuhn, L. P. J. Am. Chem. Soc. **74**, 2492 (1952).
17. Vavon, G. et Zaremba, C. Bull. soc. chim. France, 1853 (1931).
18. Barton, D. H. R. Experientia, **6**, 316 (1950).
19. Barton, D. H. R. J. Chem. Soc. 1027 (1953).
20. Schreiber, J. et Eschenmoser, A. Helv. Chim. Acta, **38**, 1529 (1955).
21. Clarke, M. F. et Owen, L. N. J. Chem. Soc. 315 (1949).
22. Derx, H. G. Rec. trav. chim. 41, 312 (1922).
23. Brown, J. B., Henbest, H. B. et Jones, E. R. H. J. Chem. Soc. 3634 (1950).
24. Rigby, W. J. Chem. Soc. 1586 (1949).
25. Rigby, W. J. Chem. Soc. 1588 (1949).
26. Clarke, M. F. et Owen, L. N. J. Chem. Soc. 2103 (1950).
27. Grewe, R., Lorenzen, W. et Vining, L. Chem. Ber. **87**, 793 (1954).
28. Willstatter, R. et Lessing, R. Ber. **34**, 506 (1901).
29. Rothstein, B. Ann. chim. **14**, 461 (1930).
30. Olberg, R. C., Pines, H. et Ipatieff, V. N. J. Am. Chem. Soc. **66**, 1096 (1944).
31. Owen, L. N. et Robins, P. A. J. Chem. Soc. 320 (1949).
32. White, J. N. Z. Krist. **80**, 5 (1931).

Can. J. Chem. Downloaded from www.nrcresearchpress.com by 190.90.36.8 on 09/04/12
For personal use only.

33. PERRINE, T. D. et WHITE, W. C. J. Am. Chem. Soc. **69**, 1542 (1947).
34. COOPS, J., DIENSKE, J. W. et SMIT, W. M. Rec. trav. chim. **57**, 637 (1938).
35. GALLAGHER, T. F. et LONG, W. P. J. Biol. Chem. **147**, 131 (1943).
36. ELIEL, E. L. et LUKACH, C. A. J. Am. Chem. Soc. **79**, 5986 (1957).
37. FAVRE, H., LEFEBVRE, M. et RICHER, J-C. Can. J. Chem. **37**, 403 (1959).

Can. J. Chem. Downloaded from www.nrcresearchpress.com by 190.90.36.8 on 09/04/12
For personal use only.

Can. J. Chem. Downloaded from www.nrcresearchpress.com by 190.90.36.8 on 09/04/12
For personal use only.

DÉRIVÉS DU TRIMÉTHYL-1,8,8 BICYCLO[3,2,1]OCTANE

V. RÉDUCTIONS CATALYTIQUE ET CHIMIQUE DE LA TRIMÉTHYL-1,8,8 BICYCLO[3,2,1]OCTANEDIONE-2,4[1]

H. FAVRE ET J-C. RICHER[2]

RÉSUMÉ

Les auteurs montrent que la triméthyl-1,8,8 bicyclo[3,2,1]octanedione-2,4 est réduite: en triméthyl-1,8,8 bicyclo[3,2,1]octanediol-2β,4β en présence de nickel de Raney et de soude caustique; en triméthyl-1,8,8 bicyclo[3,2,1]octène-3 one-2, ou directement en homocamphre, en présence de nickel de Raney et de très petites quantités de chloroforme, par l'intermédiaire de la triméthyl-1,8,8 bicyclo[3,2,1]octanol-4β one-2; en un mélange de triméthyl-1,8,8 bicyclo[3,2,1]octanediols-2α,4α; -2α,4β et probablement -2β,4α par le sodium dans l'éthanol. Les configurations des diols furent assignées à la suite de l'analyse de leurs modes de formation, de leurs vitesses d'oxydation chromique et des rotations moléculaires de leurs di-*p*-nitrobenzoates.

Rupe et Frey (1) ont hydrogéné la triméthyl-1,8,8 bicyclo[3,2,1]octanedione-2,4 (I) en présence d'un catalyseur de nickel dans l'éthanol aqueux à 50%. A température de 60–70° et sous pression de 90 atmosphères, ils ont obtenu un composé p.f. 276–279° qui n'a pas été étudié, et qui est décrit simplement comme un "dimère". A température et à pression ordinaires, en présence de carbonate de sodium, ces auteurs ont obtenu la triméthyl-1,8,8 bicyclo[3,2,1]octène-3 one-2 (III) avec un rendement de 87.5%; le β-cétol II est postulé comme intermédiaire.

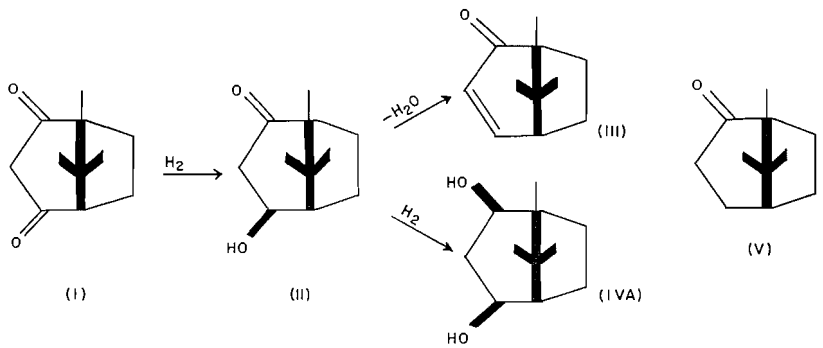

En reprenant les essais du Rupe et Frey, dans le but d'obtenir de l'homocamphre, nous n'avons obtenu que peu ou pas du tout de la cétone α,β-éthylénique III, mais principalement un composé p.f. 279–284°; nous utilisions un catalyseur de nickel de Raney (dans leur mémoire, Rupe et Frey n'indiquent ni la nature ni le mode de préparation de leur nickel). Après avoir caractérisé le composé inconnu, p.f. 279–284°, comme un des 4 triméthyl-1,8,8 bicyclo[3,2,1]octanediols-2,4 stéréoisomères (nous montrons plus loin dans cet article que c'est l'isomère 2β,4β (IV A) répondant à la formule $C_{11}H_{20}O_2$, donnant un di-*p*-nitrobenzoate bien cristallisé, p.f. 213–215°), nous nous sommes attachés à préciser les conditions opératoires pouvant conduire fidèlement soit au diol IV A, soit à la cétone α,β-éthylénique III. On trouve au Tableau I les résultats de cette étude.

Les hydrogénations ont été effectuées dans des conditions contrôlées, le nickel de

[1]*Manuscrit reçu le 27 août, 1958.*
Contribution du Département de Chimie de l'Université de Montréal, Montréal, P.Q. Ce mémoire est tiré de la thèse de doctorat de J-C. Richer.
[2]*Boursier du Conseil National de Recherches du Canada, 1954–1958. Adresse actuelle: Department of Chemistry, University of Notre Dame, Notre Dame, Ind.*

TABLEAU I

Hydrogénations catalytiques de la triméthyl-1,8,8 bicyclo[3,2,1]octanedione-2,4

No. d'ordre	Poids de cétone	Poids de nickel	Adjonction*	H_2 absorbé†	Temps d'absorption	Produits‡
1	12.5 g	12.0 g	0.5 mole NaOH	1.00 mole	25 heures	47% Dicétone I 35% Diol IV A 5.6% Cétones
2	10 g	12 g	1 mole NaOH	0.22 mole	25 heures	91% Dicétone I 5% Diol IV A 2% Cétones
3	5.0	5 g	1.5% Chloroforme	1.02 mole	20 heures	Environ 94% de β-cétol II (selon hydrogénation No. 4)
4	9.85 g	5 g	1.5% Chloroforme	0.97 mole	25 heures	2% Dicétone I 94% Cétone non saturée III
5	20.0 g	12 g	(*a*) 0.9% Chloroforme (*b*) 1 mole NaOH	1.03 mole 0.78 mole	20 heures 30 minutes	92% Homocamphre V 5% Diol IV A
6	5.0 g	3 g	(*a*) Nil (*b*) 1 mole NaOH	1.07 mole 0.72 mole	22 heures 45 minutes	82% Homocamphre V 12% Diol IV A

*La quantité de soude ajoutée est exprimée en mole par mole de dicétone I. Le pourcentage de chloroforme est relatif au poids de nickel de Raney mis en oeuvre.

†Exprimé en mole par mole de dicétone I.

‡Cétones = fractions cétoniques pouvant contenir de l'homocamphre et de la triméthyl-1,8,8 bicyclo[3,2,1]octène-3 one-2 (III) et peut-être d'autres cétones.

Raney mis en oeuvre étant l'objet d'une attention particulière: il fut préparé à partir d'un alliage AN 50 selon le mode décrit dans la partie expérimentale, et fut utilisé rapidement après sa préparation; des échantillons vieux de quelques semaines ne permettent pas de reproduire les résultats.

Delépine et Horeau (2) ont montré que l'activité réductrice du nickel de Raney envers les cétones et l'acétylacétone était accrue par des adjonctions de petites quantités de soude caustique au milieu, tandis que Cornubert et ses collaborateurs (3, 4, 5, 6, 7) ont rapporté l'influence inhibitrice du chloroforme et d'autres dérivés organiques halogénés sur la réduction des groupes carbonyle. Nous nous sommes inspirés de ces observations pour choisir les agents appelés à modifier l'activité du nickel de Raney et à rendre ce catalyseur spécifique et fidèle.

L'addition de soude caustique favorise nettement la formation du diol IV A (essai 1, Tableau I); les rendements en diols dépendent directement de la quantité de soude introduite, car le sel sodé de la dicétone n'est pas réduit comme le montre l'essai 2 (Tableau I).

L'addition massive de chloroforme inhibe complètement la réduction (voir réduction du dimédon (8)); par contre, l'adjonction de quantités ne dépassant pas 2%[3] du poids du catalyseur mis en oeuvre permet la réduction du carbonyle en position 4 et inhibe avec satisfaction celle du carbonyle en position 2. Ce mode opératoire nous a permis d'obtenir:

(1) Le β-cétol intermédiaire II (hydrogénation 3) en évaporant avec précaution le solvant débarrassé du catalyseur lorsque la réduction s'arrête d'elle-même après absorption de 1.0 mole d'hydrogène; ce β-cétol est un composé très instable, p.f. 249–250°,

[3]*Nous avons adopté les termes suivants: nickel "ordinaire", pour le nickel utilisé tel que préparé selon notre méthode; nickel "modéré", lorsque le nickel "ordinaire" est traité par des quantités de chloroforme ne dépassant pas 2% de son poids. Cornubert appelle nickel "contraint" le nickel inapte à réduire les groupes carbonyle.*

Can. J. Chem. Downloaded from www.nrcresearchpress.com by 190.90.36.8 on 09/04/12
For personal use only.

spectre infrarouge, bandes à 3455 (—OH) et 1705 (C = 0) cm^{-1}, perdant facilement une molécule d'eau par sublimation ou par entraînement à la vapeur d'eau.

(2) La triméthyl-1,8,8 bicyclo[3,2,1]octène-3 one-2 (III) (hydrogénation 4) avec un rendement de 94% (9, 1).

(3) L'homocamphre (V). Dans ce cas (hydrogénation 5), après absorption d'une mole d'hydrogène et arrêt spontané de la réaction, on introduit dans le milieu réactionnel une mole de soude caustique en solution dans l'éthanol 95%. Il se produit un échauffement de la solution avec élimination d'une molécule d'eau du β-cétol II; l'absorption d'hydrogène reprend aussitôt, et bien que l'absorption ne corresponde alors qu'à 0.78 mole d'hydrogène, on isole l'homocamphre (V) avec un rendement de 94%. Cet homocamphre est très pur et son mode de préparation est le plus simple de tous ceux décrits jusqu'ici (9). L'hydrogénation 6 présente un certain intérêt; elle fut réalisée avec un nickel de Raney "ordinaire" (sans adjonction de soude ou de chloroforme); elle démontre clairement l'influence inhibitrice du chloroforme sur la réduction du carbonyle en position 2 (cf. hydrogénation 5). Elle montre aussi que l'adjonction de soude doit se faire au début de l'hydrogénation si l'on veut obtenir un bon rendement en diol IV A (comme dans l'hydrogénation 1). L'emploi du nickel de Raney "ordinaire" reste cependent fort aléatoire: de nombreux essais ont donné des quantités variables du diol IV A et de la cétone α,β-éthylénique III. Ces essais peu intéressants en raison du manque de fidélité du catalyseur ne sont pas rapportés dans ce mémoire.

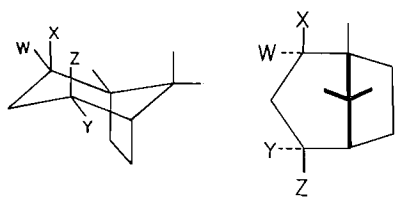

IV A X,Z = OH; W,Y = H
IV B W,Y = OH; X,Z = H
IV C X,Y = OH; W,Z = H
IV D W,Z = OH; X,Y = H

VI X = OH; W,Y,Z = H
VII W = OH; X,Y,Z = H
VIII Y = OH; W,X,Z = H
IX Z = OH; W,X,Y = H

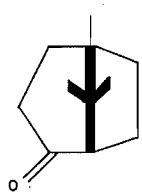

X

Les produits de la réduction de la dicétone I par le sodium dans l'éthanol ont été séparés en produit acide (dicétone I de départ non entrée en réaction) 58.1% et en composés neutres, 39.9%, qu'une chromatographie sur alumine a séparés en:

(1) 4.1% d'un solide jaune non étudié;

(2) 5.5% d'un solide incolore, p.f. 171–173°, $[\alpha]_D^{23} = +23.6°$, correspondant à la formule $C_{11}H_{20}O$. Ce résultat d'analyse et la facilité avec laquelle ce solide s'élue de l'alumine indiquent qu'il doit être un mélange des monoalcools VI–IX;

(3) 20.4% d'un solide incolore, p.f. 250–255°, $[\alpha]_D^{23} = +7.2°$ donnant un di-*p*-nitrobenzoate p.f. 211–212.5°, $[\alpha]_D^{23} = +70.0°$ dont on tire par saponification le diol IV D, p.f. 237–239°, $[\alpha]_D^{23} = -9.0°$;

Can. J. Chem. Downloaded from www.nrcresearchpress.com by 190.90.36.8 on 09/04/12
For personal use only.

(4) 68.4% de diol IV B, p.f. 234–236°, $[\alpha]_D^{23} = +32.7°$, dont le di-*p*-nitrobenzoate fond à 221–224°, $[\alpha]_D^{23} = +37°$.

Nous avons en main trois des quatre triméthyl-1,8,8 bicyclo[3,2,1]octanediols-2,4 stéréoisomères; nous les considérons comme stériquement purs; leurs di-*p*-nitrobenzoates donnent des dépressions de point de fusion en mélange. À la suite de l'analyse de leurs modes de formation, de l'application à leurs di-*p*-nitrobenzoates de la méthode des différences de rotation moléculaire et de leurs vitesses d'oxydation chromique, nous leur avons attribué les configurations suivantes:

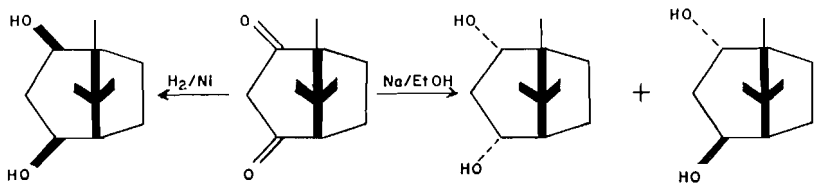

IV A p.f. 279–284° | I | IV B p.f. 234–236° | IV D p.f. 237–239°

Nous pensons aussi avoir en main un mélange des diols IV D et IV C dont le p.f. est de 250–255° (réduction chimique, fraction 3 brute), car le comportement chromatographique de ce mélange semble montrer que l'isomère IV D, qui le constitue en partie, n'est pas accompagné des diols IV A et IV B.

Nous examinerons dans l'ordre les modes de formation, la méthode des différences des rotations moléculaires et les vitesses d'oxydation des diols.

L'hydrogénation catalytique de la triméthyl-1,8,8 bicyclo[3,2,1]octanedione-2,4 (I) est stéréospécifique. Elle rappelle les hydrogénations de l'homocamphre (V) et de l'homoépicamphre (X) qui conduisent aux monols VI et IX de configuration β, —OH axial (10). Il semble raisonnable d'attribuer la configuration -4β au β-cétol intermédiaire (II) et d'envisager que la réduction du groupe C = 0 de ce cétol conduira comme celle de l'homocamphre à un groupe —OH axial. Le diol qui se formera sera ainsi diaxial ou -2β,4β (IV A)[4]; ceci est vrai pour autant qu'il n'y ait pas d'isomérisation des groupes —OH axiaux en groupes équatoriaux; nous voyons l'absence de toute isomérisation dans le fait que nous avons obtenu (voir mémoire antérieur (10)) le même rendement stérique en alcool axial au cours de la réduction de l'homoépicamphre, en mettant en oeuvre le platine dans l'acide acétique et le nickel de Raney en présence de soude.

Nous avançons également par analogie que le diol p.f. 234–236° qui se forme en quantité prépondérante lors de la réduction par le sodium et l'éthanol est le diol-2α,4α (IV B), puisque l'homocamphre (V) et l'homoépicamphre (X) engendrent principalement les monols de configuration α (VII et VIII)(10).

L'examen des rotations moléculaires des di-*p*-nitrobenzoates donne les conclusions suivantes. Utilisant la valeur $[M]_D = +24°$ pour la rotation moléculaire du triméthyl-1,8,8 bicyclo[3,2,1]octane[5] et les valeurs des rotations moléculaires des *p*-nitrobenzoates des triméthyl-1,8,8 et -5,8,8 bicyclo[3,2,1]octanols-2α et -2β décrites dans la partie III de cette série (10), nous pouvons calculer[6] les valeurs des rotations moléculaires des di-*p*-nitrobenzoates des quatre diols (voir Tableau II).

Nous remarquons alors une correspondance convenable entre les valeurs calculées

[4]*Nous ne retenons que la conformation "cyclohexane chaise" pour les diols-2,4 du triméthyl-1,8,8 bicyclo [3,2,1]octane; voir (10).*

[5]*Travaux de notre laboratoire non-publiés. Cet hydrocarbure a été préparé à partir du (+) camphre, sans inversion de configuration.*

[6]*Nous trouvons une justification de cette manière de procéder dans les travaux de Striebel et Tamm (11).*

Can. J. Chem. Downloaded from www.nrcresearchpress.com by 190.90.36.8 on 09/04/12
For personal use only.

Can. J. Chem. Downloaded from www.nrcresearchpress.com by 190.90.36.8 on 09/04/12
For personal use only.

TABLEAU II

Rotations moléculaires des *p*-nitrobenzoates des monols VI–IX et des di-*p*-nitrobenzoates des diols IV A – IV D

Composés	$[M]_D$ Observées			$[M]_D$ Calc.
	p-Nitrobenzoates	Di-*p*-nitrobenzoates	Δ (O-*p*-Nitrobenzoyle)	Di-*p*-nitrobenzoates
Triméthyl-1,8,8 bicyclo[3,2,1]octane	+24°±3°			
Triméthyl-1,8,8 bicyclo[3,2,1]octanol-2β (VI)	−268°±6°		−292°±9°	
Triméthyl-1,8,8 bicyclo[3,2,1]octanol-2α (VII)	+106°±6°		+82°±9°	
Triméthyl-5,8,8 bicyclo[3,2,1]octanol-2β (IX)	+249°±6°		+225°±9°	
Triméthyl-5,8,8 bicyclo[3,2,1]octanol-2α (VIII)	+78°±6°		+54°±9°	
Triméthyl-1,8,8 bicyclo[3,2,1]octanediol-2β,4β (IV A) (catalytique)		+20°±10°		−43°±15°
octanediol-2β,4α (IV C)				−214°±15°
octanediol-2α,4β (IV D) (Na + EtOH)		+339°±10°		+331°±15°
octanediol-2α,4α (IV B) (Na + EtOH)		+178°±10°		+160°±15°

TABLEAU III

Vitesses d'oxydation chromique comparées des monols et des diols dans les positions 2 et 4 du triméthyl-1,8,8 bicyclo[3,2,1]octane

Composés	Conformations des groupes OH	Concentrations molaires en monol ou diol	Concentrations molaires en CrO_3	$v = -d\ CrO_3/dt$* mole×litre^{-1}×min^{-1}
Triméthyl-1,8,8 bicyclo[3,2,1]octanol-2β (VI)	*a*	7.013×10^{-4}	10.76×10^{-4}	330×10^{-6}
octanol-2α (VII)	*e*	7.162×10^{-4}	10.85×10^{-4}	10×10^{-6}
Triméthyl-5,8,8 bicyclo[3,2,1]octanol-2β (IX)	*a*	7.111×10^{-4}	10.77×10^{-4}	350×10^{-6}
octanol-2α (VIII)	*e*	7.108×10^{-4}	10.76×10^{-4}	18.4×10^{-6}
Triméthyl-1,8,8 bicyclo[3,2,1]octane diol-2β,4β (IV A)	*a*−*a*	3.557×10^{-4}	10.66×10^{-4}	300×10^{-6}
diol-2α,4α (IV B)	*e*−*e*	3.550×10^{-4}	10.58×10^{-4}	12×10^{-6}
diol-2α,4β (IV D)	*a*−*e*	3.550×10^{-4}	10.67×10^{-4}	120×10^{-6}
Mélange, p.f. 250–255°, $[\alpha]_D^{23} = +7.2°$		3.550×10^{-4}	10.69×10^{-4}	110×10^{-6}

*Dans l'acide acétique aqueux 90.9% (v/v); $t = 24.9°\pm0.1°$.

et observées si nous faisons du diol p.f. 234–236° le diol diéquatorial (IV B) et du diol p.f. 237–239° l'isomère 2α,4β (équatorial en 2 et axial en 4) (IV D). La correspondance est encore bonne si l'isomère p.f. 279–284° (catalytique) est le diol-2β,4β (IV A); la différence s'explique par un effet de voisinage.

Finalement, l'étude des vitesses d'oxydation chromique (Tableau III) donne les résultats suivants. Avec Lefebvre (10), nous avons montré que les monols axiaux VI et IX s'oxydent par l'acide chromique plus rapidement que les monols équatoriaux VII et VIII. Nous avons montré également (8) que le cyclohexanediol-1,3 *trans* ($a-e$) s'oxyde plus rapidement que l'isomère *cis* (oxydé sous sa forme $e-e$); malgré son caractère empirique, la méthode est applicable à l'étude des diols-1,3. En l'appliquant à l'élucidation des configurations des diols IV qui font l'object de cette étude, nous n'avions plus affaire à des cyclohexanes convertibles, mais à un système rigide. Théoriquement, donc, nous pouvons prévoir que les diols IV A à IV D se diviseront en trois groupes: (1) diol $a-a$; (2) diol $e-e$ et (3) les deux diols $a-e$ —et que ces trois groupes s'oxyderont avec des vitesses différentes, respectivement grande, petite et moyenne; nous admettons que les deux groupes hydroxyle[7] des diols s'oxydent l'un aussi bien que l'autre.

On remarque (Tableau III) que l'accord est bon, compte tenu de la réduction en concentration molaire des diols, entre les valeurs des monols VI–IX et des 2 diols IV A et IV B et que les configurations assignées sont les mêmes que celles déduites plus haut des modes de formation et des pouvoirs rotatoires. Le diol qui s'oxyde avec la vitesse intermédiaire aura l'un de ses groupes axial et l'autre équatorial; son di-*p*-nitrobenzoate, par son pouvoir rotatoire, en fait le diol-2α,4β (IV D) (voir plus haut).

Nous avons oxydé également le mélange des diols p.f. 250–255°; sa vitesse, semblable à celle du diol axial-équatorial, -2α,4β, nous fait supposer que ce mélange est formé des diols-2α,4β et -2β,4α, comme le comportement chromatographique nous l'avait fait supposer plus haut.

Nous avons mesuré[8] le spectre infrarouge du diol diaxial dans le but de voir à la manière de Kuhn (14) si les groupes —OH pouvaient former un pont hydrogène intramoléculaire; nous n'avons trouvé qu'une bande dans la région caractéristique, à 3630 cm^{-1}; le diol diéquatorial présente également une seule bande à 3627 cm^{-1}.

Nous en concluons que le groupe méthyle axial ne permet pas la formation d'un pont hydrogène intramoléculaire; un tel pont se serait manifesté par une bande de fréquence plus basse que 3630 cm^{-1}. Rappelons qu'un pont hydrogène intramoléculaire ne se forme pas chez le diméthyl-5,5 cyclohexanediol-1,3 *cis* (8). Ces faits nous amènent à considérer un point qui a retenu tout particulièrement notre attention au cours de ce travail. Alors que l'homocamphre n'est pas hydrogénable par le nickel de Raney en présence de soude caustique (10), l'hydroxy-4 homocamphre (II) l'est. La seule explication que nous puissions offrir est que dans l'hydroxy-cétone, l'interaction OH—CH_3 diaxiale modifie la conformation cyclohexanique chaise du squelette au point de rendre l'hydrogénation du groupe cétonique suffisamment rapide pour devenir effective. Nous tentons actuellement de démontrer jusqu'où peut aller cette déformation de conformation dont le stade ultime serait une forme cyclohexanique bateau (voir le IIIe mémoire de cette série (10)).

PARTIE EXPÉRIMENTALE[9]

La (−) triméthyl-1,8,8 bicyclo[3,2,1]octanedione-2,4 (I) a été préparée selon (1, 9).

[7]*L'oxydation chromique de l'acide cholique justifie cet avancé (8, 12).*

[8]*Optique* LiF.

[9]*Les points de fusion (p.f.) ont été déterminés en tubes capillaires, le thermomètre étant étalonné avec des substances de p.f. connu (Bureau des Standards de Washington). Les spectres infrarouges ont été mesurés à l'aide d'un spectromètre Perkin–Elmer, modèle 112, à simple faisceau et parcours double (sauf indication contraire, prisme* NaCl). *Les analyses sont de Geller Laboratories, Hackensack, et de W. Manser, Herrliberg.*

Can. J. Chem. Downloaded from www.nrcresearchpress.com by 190.90.36.8 on 09/04/12
For personal use only.

Can. J. Chem. Downloaded from www.nrcresearchpress.com by 190.90.36.8 on 09/04/12
For personal use only.

1. Hydrogénation catalytiques

Préparation du nickel de Raney

L'alliage AN 50 (50 g) est ajouté par petites portions à 800 ml de soude caustique 20% à température de 0°–5°. Après l'addition, le tout est chauffé sur un bain-marie durant deux heures. La solution de soude est décantée et remplacée par 400 ml de solution fraîche. Le chauffage au bain-marie est continué pendant une heure. Par décantations successives, le nickel est lavé 20 fois avec l'eau du robinet (portions de 800 ml), trois fois avec de l'éthanol 95% distillé dans un appareil de verre Pyrex. Le catalyseur est conservé dans de l'éthanol 95%.

Nous décrivons les essais dans l'ordre donné au Tableau I (partie théorique).

Hydrogénation No. 1—Nickel de Raney + soude caustique: obtention du triméthyl-1,8,8 bicyclo[3,2,1]octanediol-2β,4β IV A

La dicétone I (12.5 g, 0.0694 mole) et 1.39 g de NaOH (0.0348 mole) en solution dans 150 ml d'éthanol 95% sont hydrogénés en présence de 12.0 g de nickel de Raney. En 25 heures, il y a absorption de 1720 ml d'hydrogène (calculé pour $1H_2$: 1710 ml, pour 750 mm et 23°). Le catalyseur est essoré; la solution alcoolique est évaporée et le résidu soumis à l'action de la vapeur d'eau.

La fraction volatile, extraite à l'éther, représente 700 mg (5.6%); il s'agit de cétones qui n'ont pas été étudiées.

La solution alcaline qui contient les composés non volatils est extraite par de l'éther, puis acidifiée par HCl (rouge Congo); une extraction au chloroforme permet de retrouver 5.9 g de dicétone (47%) qui n'a pas réagi. La solution éthérée contient les composés neutres dont on retire par chromatographie sur alumine et élution par le chloroforme 81% de triméthyl-1,8,8 bicyclo[3,2,1]octanediol-2β,4β (IV A) très pur; les fractions éluées par le benzène et le mélange benzène-chloroforme 1-1, précédant l'élution par le chloroforme pur, n'ont pas été étudiées. Le diol pur présente les constantes suivantes: p.f. 279–284°, $[\alpha]_D^{22} = -17.4°$ ($c = 4.09$; éthanol/95%).

Calculé pour $C_{11}H_{20}O_2$: C, 71.69; H, 10.94%. Trouvé: C, 71.87; H, 10.94%. En chauffant le diol avec du chlorure de *p*-nitrobenzoyle dans de la pyridine sèche le di-*p*-nitrobenzoate précipite sous forme d'aiguilles qui se transforment en paillettes par cristallisation dans le chloroforme-éthanol: p.f. 213–215°, $[\alpha]_D^{23} = +4.16°$ ($c = 2.97$; chloroforme). Calculé pour $C_{25}H_{26}O_8N_2$: C, 62.23; H, 5.43; N, 5.81%. Trouvé: C, 62.34; H, 5.46; N, 5.52, 5.80%. Poids moléculaire du di-*p*-nitrobenzoate, déterminé dans le camphre, 432; valeur théorique: 482.

Hydrogénation No. 2—Nickel de Raney + soude caustique

Si l'on hydrogène 10.0 g de dicétone I (0.055 mole) en présence de 2.22 g de NaOH (0.055 mole) et de 12 g de nickel de Raney, dans 85 ml d'éthanol 95%, en 25 heures, il y a absorption de 310 ml d'hydrogène. On retrouve, selon le mode opératoire de l'hydrogénation No. 1, 91% de cétone qui n'a pas réagi, 5% de diol IV A brut p.f. 267–276° et 2% de cétones (non étudiées).

Hydrogénation No. 3—Nickel de Raney + chloroforme: obtention de la triméthyl-1,8,8 bicyclo[3,2,1]octanol-4β one-2 (II)

Dans un ballon à hydrogéner on introduit 5.022 g de dicétone I, 50 ml d'éthanol 95% et 5 g de nickel de Raney; on ajoute alors 0.75 ml d'une solution éthanolique de chloroforme à 10% (soit 75 mg de chloroforme) et on procède à l'hydrogénation. En 20 heures il y a fixation de 710 ml d'hydrogène (calculé pour $1H_2$: 698 ml; 774 mm et 26°). On essore le catalyseur et sépare la solution alcoolique en deux portions égales.

La première portion est évaporée sur un bain-marie; le résidu est rendu alcalin et

entrainé à la vapeur d'eau; on recueille la triméthyl-1,8,8 bicyclo[3,2,1]octène-3 one-2 p.f. 174–176° (pour la caractérisation de ce composé voir (9) et dans ce travail l'hydrogénation No. 4).

La deuxième portion est évaporée à 25°, puis séchée sous vide poussé à cette température. La triméthyl-1,8,8 bicyclo[3,2,1]octanol-4β one-2 se présente sous la forme d'un solide incolore et amorphe, p.f. 249–250°. L'analyse centésimale est satisfaisante en raison des conditions rudimentaires d'isolement du composé: calculé pour $C_{11}H_{18}O_2$: C, 72.52; H, 9.96%. Trouvé: C, 71.05; H, 9.85%. Ce β-cétol perd une molécule d'eau si on le sublime; les fractions de tête de la sublimation fondent à 180–182° et leur spectre infrarouge présente une bande à 1678 cm^{-1}, caractéristique d'une cétone α,β-éthylénique. Les fractions de queue de la sublimation fondent à 242–244°: leur spectre infrarouge montre la présence du groupe —OH (3455 cm^{-1}) et de la cétone saturée (1705 cm^{-1}), dans le Nujol.

Hydrogénation No. 4—Nickel de Raney + chloroforme: obtention de la triméthyl-1,8,8 bicyclo[3,2,1]octène-3 one-2 (III)

La dicétone I (9.854 g) est hydrogénée, en présence de 5 g de nickel de Raney modéré par adjonction de 0.7 ml d'une solution de chloroforme-éthanol 10–90, dans 100 ml d'éthanol 95%. En 25 heures il y a absorption de 1265 ml d'hydrogène (calculé pour $1H_2$: 1300 ml; 745 mm et 25°). On essore le catalyseur, distille l'alcool à pression ordinaire, ajoute 100 ml d'une solution de Na_2CO_3 10% au résidu et entraîne à la vapeur d'eau. Le solide qui est entraîné est repris par de l'éther qui après séchage est évaporé. Le résidu (8.22 g, 94%) est sublimé. La triméthyl-1,8,8 bicyclo[3,2,1]octène-3 one-2 (III) fond à 176.5–178°, $[\alpha]_D^{23} = -54.9°$ ($c = 3.93$; benzène). Calculé pour $C_{11}H_{16}O$: C, 80.44; H, 9.82%. Trouvé: C, 80.37; H, 9.84%. La dinitro-2,4 phénylhydrazone fond à 191–192.5°. L'homocamphre qui résulte de la réduction de la double liaison fond à 191–191.5°, $[\alpha]_D^{23} = -111.4°$ ($c = 4.32$; benzène). Pour fins de comparaison, voir (9, 1). Les composés non volatils avec la vapeur d'eau ont été séparés en: (*a*) triméthyl-1,8,8 bicyclo[3,2,1]-octanediol-2β,4β (IV A), p.f. 280–281.5° (rendement 4%); (*b*) dicétone I qui n'a pas réagi (2%).

Hydrogénation No. 5—Nickel de Raney + chloroforme: obtention de l'homocamphre

La dicétone I (20 g) est hydrogénée dans 200 ml d'éthanol 95%, en présence de 12 g de nickel de Raney modéré par adjonction de 1.08 ml d'une solution à 10% de chloroforme dans l'éthanol 95% (soit 108 mg de chloroforme). En 20 heures il se fixe 2825 ml d'hydrogène (calculé pour $1H_2$: 2750 ml; 749 mm et 23°). Lorsque l'absorption s'arrête, on indroduit dans le milieu 44.4 ml d'une solution à 10% de NaOH dans l'éthanol 95% (1 mole de NaOH par mole de dicétone I). Il y a dégagement de chaleur et le tout, remis en présence d'hydrogène, absorbe alors 2140 ml d'hydrogène en 30 minutes. On essore le catalyseur, évapore lentement l'éthanol du filtrat à travers une colonne de Widmer. Le résidu est repris dans de l'éther qui est séché sur sulfate de sodium et évaporé (colonne de Widmer). L'homocamphre brut pèse 17.92 g. On le chromatographie sur alumine Merck pour chromatographie. Pour 41 g on utilise 300 g d'alumine; l'élution par 2250 ml de benzène donne 38.54 g d'homocamphre pur, p.f. 191–192°, $[\alpha]_D^{23} = -112.2°$ ($c = 2.97$; benzène) et 2.22 g de triméthyl-1,8,8 bicyclo[3,2,1]octanediol-2β,4β (IV A), p.f. 275–280°.

Hydrogénation No. 6—Nickel de Raney sans adjonction

La dicétone I (5.0 g; 0.0275 mole) est hydrogénée dans 50 ml d'éthanol 95% en présence de 3 g de nickel de Raney. En 22 heures il se fixe 740 ml d'hydrogène (calculé pour $1H_2$:

Can. J. Chem. Downloaded from www.nrcresearchpress.com by 190.90.36.8 on 09/04/12
For personal use only.

686 ml; 754 mm et 25°). Ce temps écoulé, on introduit dans le milieu 1.11 g de NaOH (0.0227 mole) sous forme d'une solution alcoolique) et l'on reprend l'hydrogénation. Il y a alors absorption de 495 ml d'hydrogène. On essore le catalyseur, évapore l'alcool du filtrat, reprend par de l'éther que l'on sèche sur sulfate de sodium anhydre. On recueille après distillation de l'éther 4.458 g de composés neutres que l'on chromatographie sur 130 g d'alumine Merck pour chromatographie. L'élution par 600 ml de benzène donne 3.658 g d'homocamphre, $[\alpha]_D^{23} = -114°$ ($c = 4.95$; éthanol); 40 mg sont élués ensuite des mélanges benzène-chloroforme; le triméthyl-1,8,8 bicyclo[3,2,1]octanediol-2β,4β (IV A) est finalement élué par 300 ml de méthanol: 517 mg, p.f. 276–280°.

2. Réduction chimique (sodium et éthanol) de la dicétone I

À une solution de 20.78 g (0.1156 mole) de dicétone I dans 500 ml d'éthanol anhydre, on ajoute par petites portions 36 g (1.564 mole) de sodium. Lorsque le sodium a fini de réagir, on ajoute 40 ml d'eau et distille l'éthanol à travers une colonne de Widmer. Le résidu est repris par de l'eau et extrait par du chloroforme. Les fractions chloroformiques réunies sont séchées sur du sulfate de sodium et évaporées à travers une colonne de Widmer: on recueille 8.455 g de composés neutres, que l'on met en suspension dans 850 ml d'un mélange benzène-chloroforme 1-1 et que l'on introduit dans un tube à chromatographie contenant 250 g d'alumine Merck pour chromatographie. La partie insoluble du mélange se trouve reposer au sommet de la colonne d'alumine; on procède alors à l'élution par des portions de 850 ml de solvant.

Chromatographie I

Fractions	Eluant	Quantité éluée	P.f.
1	Benz-chlor 1-1	0.025 g	
2	Benz-chlor 1-2	0.225 g	
3	Benz-chlor 1-4	0.738 g	184–186°
4	Chloroforme	1.034 g	265–267°
5	Chloroforme	1.260 g	235–238°
6–12	Chloroforme	5.175 g	236–238°

Les fractions 6–12 sont sublimées et constituent le triméthyl-1,8,8 bicyclo[3,2,1]-octanediol-2α,4α (IV B), p.f. 234–236°, $[\alpha]_D^{23} = +32.7°$ ($c = 3.82$; éthanol 95%). Calculé pour $C_{11}H_{20}O_2$: C, 71.69; H, 10.94%. Trouvé: C, 71.49; H, 10.80%. On en prépare un di-*p*-nitrobenzoate, p.f. 221–224°, $[\alpha]_D^{23} = +37.0°$ ($c = 2.91$; chloroforme). Calculé pour $C_{25}H_{26}O_8N_2$: C, 62.23; H, 5.43; N, 5.81%. Trouvé: C, 62.37; H, 5.38; N, 5.67%.

Les fractions 3, 4 et 5 de la chromatographie I sont mises en solution dans 300 ml de benzène et adsorbées sur 90 g d'alumine. L'élution par des portions de 300 ml de solvent donne:

Chromatographie II

Fractions	Eluant	Quantité éluée	Caractéristiques
1–2	Benzène	0.085 g	
3–5	Benz-chlor Jusqu'à 1-1	0.438 g	$[\alpha]_D^{23} = +22.1°$ ($c = 3.6$; benz)
6–12	Benz-chlor 1-1	1.265 g	$[\alpha]_D^{23} = +8.36°$ ($c = 3.7$; EtOH)
13–17	Benz-chlor Jusqu'à 1-9	0.410 g	$[\alpha]_D^{23} = +4.93°$ ($c = 3.5$; EtOH)
18–21	Chloroforme	0.373 g	$[\alpha]_D^{23} = +34.2°$ ($c = 4$; EtOH)
22–23	Chloroforme	0.156 g	$[\alpha]_D^{23} = +36.9°$ ($c = 3.4$; EtOH)
24	Chloroforme	0.057 g	

Can. J. Chem. Downloaded from www.nrcresearchpress.com by 190.90.36.8 on 09/04/12
For personal use only.

Les fractions 3–5 de la chromatographie II sont sublimées: p.f. 171–173°, $[\alpha]_D^{23} = +23.6°$ ($c = 3.6$; benzène). Calculé pour $C_{11}H_{20}O$: C, 78.51; H, 11.98%. Trouvé: C, 78.56; H, 11.95%. Il s'agit d'un mélange de triméthyl-1,8,8 et -5,8,8 bicyclo[3,2,1]-octanols-2α et -2β (VI–IX) qui n'a pas été étudié plus à fond.

Les fractions 6–12 sont réunies et sublimées: p.f. 250–255°, $[\alpha]_D^{23} = +7.2°$($c = 4.2$; EtOH). Calculé pour $C_{11}H_{20}O_2$: C, 71.69; H, 10.94%. Trouvé: C, 71.57; H, 11.07%. On en prépare un di-*p*-nitrobenzoate brut, qui après 8 cristallisations dans le nitrométhane fond à 211–212.5°, $[\alpha]_D^{23} = +70.0°$($c = 2$; chloroforme). Calculé pour $C_{25}H_{26}O_8N_2$: C, 62.23; H, 5.43; N, 5.81%. Trouvé: C, 62.24; H, 5.42; N, 5.91%. Il s'agit du di-*p*-nitrobenzoate du triméthyl-1,8,8 bicyclo[3,2,1]octanediol-2α,4β. Une fraction (432 mg) légèrement moins pure de cet ester a été saponifiée par 500 mg de NaOH dans 20 ml d'éthanol et 5 ml d'eau par chauffage à reflux durant 3 heures. Le triméthyl-1,8,8 bicyclo[3,2,1]octanol-2α,4β (IV D) fut isolé à la manière habituelle; après chromatographie sur alumine et sublimation (152 mg) il fondait à 237–239°, $[\alpha]_D^{23} = -9.0°$ ($c = 1.4$; éthanol 95%).

3. Vitesses d'oxydation chromique

Elles ont été déterminées selon le mode opératoire décrit dans la partie III de cette série (8) et sont rapportées au Tableau III (partie théorique).

REMERCIEMENTS

Nous remercions le Conseil National de Recherches du Canada de son aide financière: subvention de recherche (H.F.), et bourse d'études (J-C. Richer). Nous remercions également M. le Professeur C. Sandorfy de son aide dans l'étude des spectres infrarouges.

BIBLIOGRAPHIE

1. Rupe, H. et Frey, C. Helv. Chim. Acta, **27**, 627 (1944).
2. Delépine, M. et Horeau, A. Bull. soc. chim. France, **4** (5), 31 (1937).
3. Cornubert, R. et Phélisse, J. Bull. soc. chim. France, **19** (5), 403 (1952).
4. Cornubert, R. et Réal, M. Bull. soc. chim. France, **19** (5), 407 (1952).
5. Cornubert, R. et Kaziz, C. Bull. soc. chim. France, **19** (5), 410 (1952).
6. Cornubert, R. et Eggert, H. G. Bull. soc. chim. France, 522 (1954).
7. Cornubert, R. et Thomas, P. Bull. soc. chim. France, 524 (1954).
8. Favre, H. et Richer, J-C. Can. J. Chem. **37**, 411 (1959).
9. Favre, H., Marinier, B. et Richer, J-C. Can. J. Chem. **34**, 1329 (1956).
10. Favre, H., Lefebvre, M. et Richer, J-C. Can. J. Chem. **37**, 403 (1959).
11. Striebel, P. et Tamm, Ch. Helv. Chim. Acta, **37**, 1094 (1954).
12. Gallagner, T. F. et Long, W. P. J. Biol. Chem. **147**, 131 (1943).
13. Schreiber, J. et Eschenmoser, A. Helv. Chim. Acta, **38**, 1529 (1955).
14. Kuhn, L. P. J. Am. Chem. Soc. **74**, 2492 (1952).

Can. J. Chem. Downloaded from www.nrcresearchpress.com by 190.90.36.8 on 09/04/12
For personal use only.

Can. J. Chem. Downloaded from www.nrcresearchpress.com by 190.90.36.8 on 09/04/12
For personal use only.

A NEW MOLECULAR REARRANGEMENT

IV. FURTHER OBSERVATIONS ON THE CHEMISTRY OF 1-NITRO-2,3,5,6-TETRAHYDRO-1(H)-IMIDAZ(1,2-a)IMIDAZOLE AND 1-(β-CHLOROETHYL)-2-IMIDAZOLIDONE[1]

A. F. McKay and M.-E. Kreling

ABSTRACT

Chlorination of 1-(β-hydroxyethyl)-2-nitriminoimidazolidine gives a mixture of 1-(β-chloroethyl)-2-nitriminoimidazolidine and 1-nitro-2,3,5,6-tetrahydro-1(H)-imidaz(1,2-a)imidazole hydrochloride. The other products, 1-(β-aminoethyl)-3-nitro-2-imidazolidone hydrochloride and 1-(β-nitraminoethyl)-2-imidazolidone, isolated during the original study of the chlorination of 1-(β-hydroxyethyl)-2-nitriminoimidazolidine are formed by the action of ethanol on 1-nitro-2,3,5,6-tetrahydro-1(H)-imidaz(1,2-a)imidazole hydrochloride. Amines add to 1-nitro-2,3,5,6-tetrahydro-1(H)-imidaz(1,2-a)imidazole nitrate to give the corresponding 1-(β-nitraminoethyl)-2-substituted amino-2-imidazoline nitrates. These reactions and the aminolysis of 1-(β-chloroethyl)-2-imidazolidone are described in detail.

INTRODUCTION

The present work was directed to a comparison of the chemical properties of 1-(β-chloroethyl)-2-nitroguanidine (1) with 1-(β-chloroethyl)-2-nitriminoimidazolidine (2) and to an attempt to find an explanation for the origin of the products isolated from the reaction of thionyl chloride with 1-(β-hydroxyethyl)-2-nitriminoimidazolidine (2).

The cyclization of 1-(β-chloroethyl)-2-nitroguanidine to 1-nitro-2-iminoimidazolidine hydrochloride (or its tautomer, 1-nitro-2-amino-2-imidazolinium chloride) was described first in 1950 (1). This cyclization occurred at the melting point of the compound or it could be effected by heating the compound with an inert solvent. A carbonium ion mechanism was suggested (3, 4) for this cyclization reaction but it was noted that this suggestion was premature owing to the absence of kinetic data. Later the kinetic data were supplied by the work of Boyars, Sager, and Skolnik (5). They found that the relative rates of cyclization of the 1-β-substituted-2-nitroguanidines were 1-β-bromoethyl- > 1-β-chloroethyl- > 1-β-nitroxyethyl-. These relative rates of reaction are in agreement with the bond energies for C–Br, C–Cl, C–O covalent links which would be expected in a carbonium ion mechanism. However, since the rate of cyclization of 1-(β-nitroxyethyl)-2-nitroguanidine was greater than the cyclization rate of 1-(β-nitroxypropyl)-2-nitroguanidine, an internal Sn_2 mechanism rather than a carbonium ion mechanism was favored. Further evidence for the internal Sn_2 mechanism was established by a demonstration (6) of the lack of salt effect on the cyclization rate. Thus the cyclization of 1-(β-chloroethyl)-2-nitroguanidine is considered to occur by a backside approach of the nitrimino group to the substituted side chain as follows:

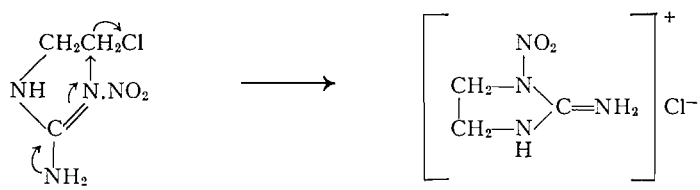

[1]*Manuscript received May 14, 1958.*
Contribution No. 21 from the L. G. Ryan Research Laboratories of Monsanto Canada Limited, Montreal, Quebec.

If cyclization of 1-(β-chloroethyl)-2-nitriminoimidazolidine to 1-nitro-2,3,5,6-tetrahydro-1(H)-imidaz(1,2-a)imidazole hydrochloride occurred in a similar manner, it would provide an explanation for some of the products obtained in the reactions (2, 7) of the former compound.

DISCUSSION

A study of the chemical properties of 1-(β-chloroethyl)-2-imidazolidone (III), 1-(β-aminoethyl)-3-nitro-2-imidazolidone hydrochloride (V), and 1-(β-nitraminoethyl)-2-imidazolidone (VI) obtained (2) from the reaction of thionyl chloride with 1-(β-hydroxyethyl)-2-nitriminoimidazolidine has indicated that the origin of these products may be represented as shown in Chart I. The mechanism for the chlorination of 1-(β-hydroxyethyl)-2-nitriminoimidazolidine (I) to 1-(β-chloroethyl)-2-nitriminoimidazolidine (III) is assumed to be similar to that suggested (8) for the chlorination of alcohols with thionyl chloride.

CHART I

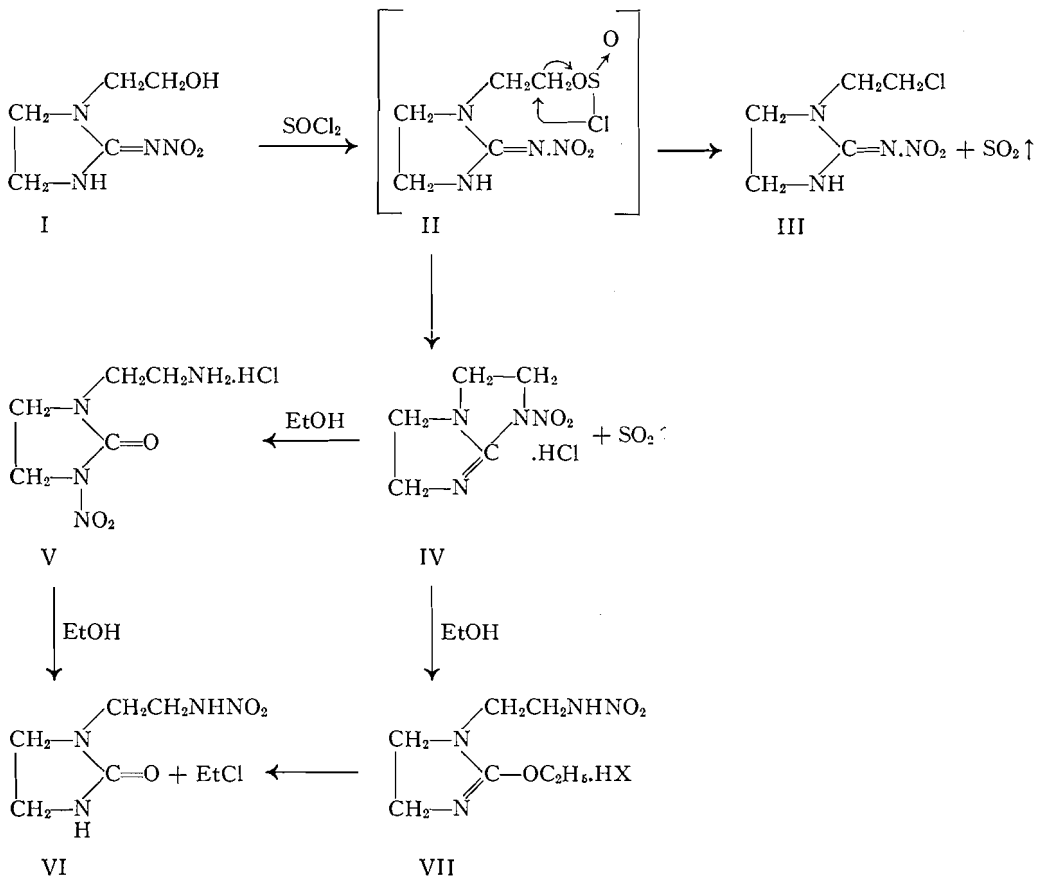

Since 1-(β-chloroethyl)-2-nitriminoimidazolidine (III) was recovered unchanged in 90% yield after it was heated under reflux for 4 hours in benzene containing dry hydrogen chloride and thionyl chloride, it cannot be considered the precursor of 1-nitro-2,3,5,6-tetrahydro-1(H)-imidaz(1,2-a)imidazole hydrochloride (IV) or 1-(β-aminoethyl)-3-nitro-2-imidazolidone hydrochloride (V). We could find no evidence for the cyclization of 1-(β-chloroethyl)-2-nitriminoimidazolidine (III) under the conditions (1) used successfully in the cyclization of 1-(β-chloroethyl)-2-nitroguanidine. Thus the bicyclic compound

Can. J. Chem. Downloaded from www.nrcresearchpress.com by 190.90.36.8 on 09/04/12
For personal use only.

IV would have to arise from II or an active intermediate in the chlorination of I to III.

1-Nitro-2,3,5,6-tetrahydro-1(H)-imidaz(1,2-a)imidazole nitrate was converted into 1-(β-aminoethyl)-3-nitro-2-imidazolidone hydrochloride by heating with moist benzene containing hydrogen chloride. Therefore the bicyclic compound (IV) could give rise to 1-(β-aminoethyl)-3-nitro-2-imidazolidone hydrochloride (V). Moreover, 1-(β-nitraminoethyl)-2-imidazolidone (VI) also must arise from one of the products of the thionyl chloride reaction during their isolation because primary nitramines are unstable in the presence of acid chlorides even under anhydrous conditions (9, 10, 11, 12, 13, 14, 15). It has been shown that both 1-nitro-2,3,5,6-tetrahydro-1(H)-imidaz(1,2-a)imidazole nitrate (16) and 1-(β-aminoethyl)-3-nitro-2-imidazolidone nitrate (7) on refluxing with ethanol give good yields of 1-(β-nitraminoethyl)-2-imidazolidone (VI). 1-Nitro-2,3,5,6-tetrahydro-1(H)-imidaz(1,2-a)imidazole nitrate in the presence of warm ethanol (50° C) gives a new compound whose analysis and properties agree with the structure, 1-(β-nitraminoethyl)-2-ethoxy-2-imidazolinium nitrate (VII, X = NO_3). The latter compound VII on heating under reflux in absolute ethanol is converted in good yield into 1-(β-nitraminoethyl)-2-imidazolidone (VI). On heating 1-(β-aminoethyl)-3-nitro-2-imidazolidone hydrochloride (V) with ethanol, ethyl chloride forms and the unstable free base rearranges to the more stable compound (VI).

When 1-nitro-2,3,5,6-tetrahydro-1(H)-imidaz(1,2-a)imidazole nitrate was heated in benzene containing hydrogen chloride and thionyl chloride it was converted into 1-nitro-2,3,5,6-tetrahydro-1(H)-imidaz(1,2-a)imidazole hydrochloride. Thus the hydrochloride salt of the bicyclic compound (IV) is stable under the conditions previously (2) used in the chlorination of 1-(β-hydroxyethyl)-2-nitriminoimidazolidine. Since both the 1-(β-chloroethyl)-2-nitriminoimidazolidine and the bicyclic compound IV are stable under these conditions, a method was developed for their isolation from the reaction of 1-(β-hydroxyethyl)-2-nitriminoimidazolidine with thionyl chloride. The crude crystalline product from the chlorination reaction was washed with water leaving behind the water insoluble 1-(β-chloroethyl)-2-nitriminoimidazolidine (59% yield). The aqueous filtrate on treatment with aqueous picric acid solution gave a crystalline picrate of 1-nitro-2,3,5,6-tetrahydro-1(H)-imidaz(1,2-a)imidazole (41% yield). It is now apparent that the products produced directly in the reaction of 1-(β-hydroxyethyl)-2-nitriminoimidazolidine with thionyl chloride are 1-(β-chloroethyl)-2-nitriminoimidazolidine (III) and 1-nitro-2,3,5,6-tetrahydro-1(H)-imidaz(1,2-a)imidazole hydrochloride (IV). The other products, 1-(β-aminoethyl)-3-nitro-2-imidazolidone hydrochloride and 1-(β-nitraminoethyl)-2-imidazolidone, isolated during the original (2) study of this chlorination reaction, were formed by the reaction of the bicyclic compound with ethanol.

1-(β-Chloroethyl)-2-nitriminoimidazolidine (III) has been converted (7) into 1-(β-nitraminoethyl)-2-benzylamino-2-imidazolinium chloride (VIII) by heating with benzylamine in the presence of water.

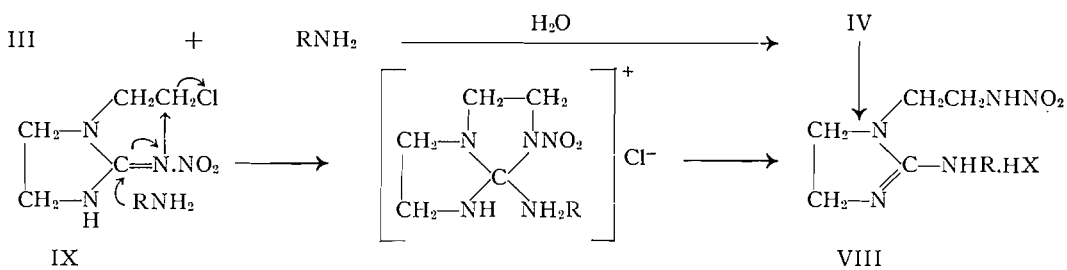

Can. J. Chem. Downloaded from www.nrcresearchpress.com by 190.90.36.8 on 09/04/12
For personal use only.

A carbonium ion mechanism giving a bicyclic intermediate was suggested for this reaction. On the basis of this proposal it was considered that 1-nitro-2,3,5,6-tetrahydro-1(H)-imidaz(1,2-a)imidazole might provide a more favorable starting material for the preparation of 1-(β-nitraminoethyl)-2-substituted amino-2-imidazoline salts (VIII). This proved to be the case and the compounds prepared by this method are described in Table I. However the successful use of a proposed bicyclic intermediate in a reaction does not provide unequivocal proof of its importance in the reaction mechanism. The concerted mechanism with ring opening (IX → VIII) offers an equally plausible mechanism for this reaction.

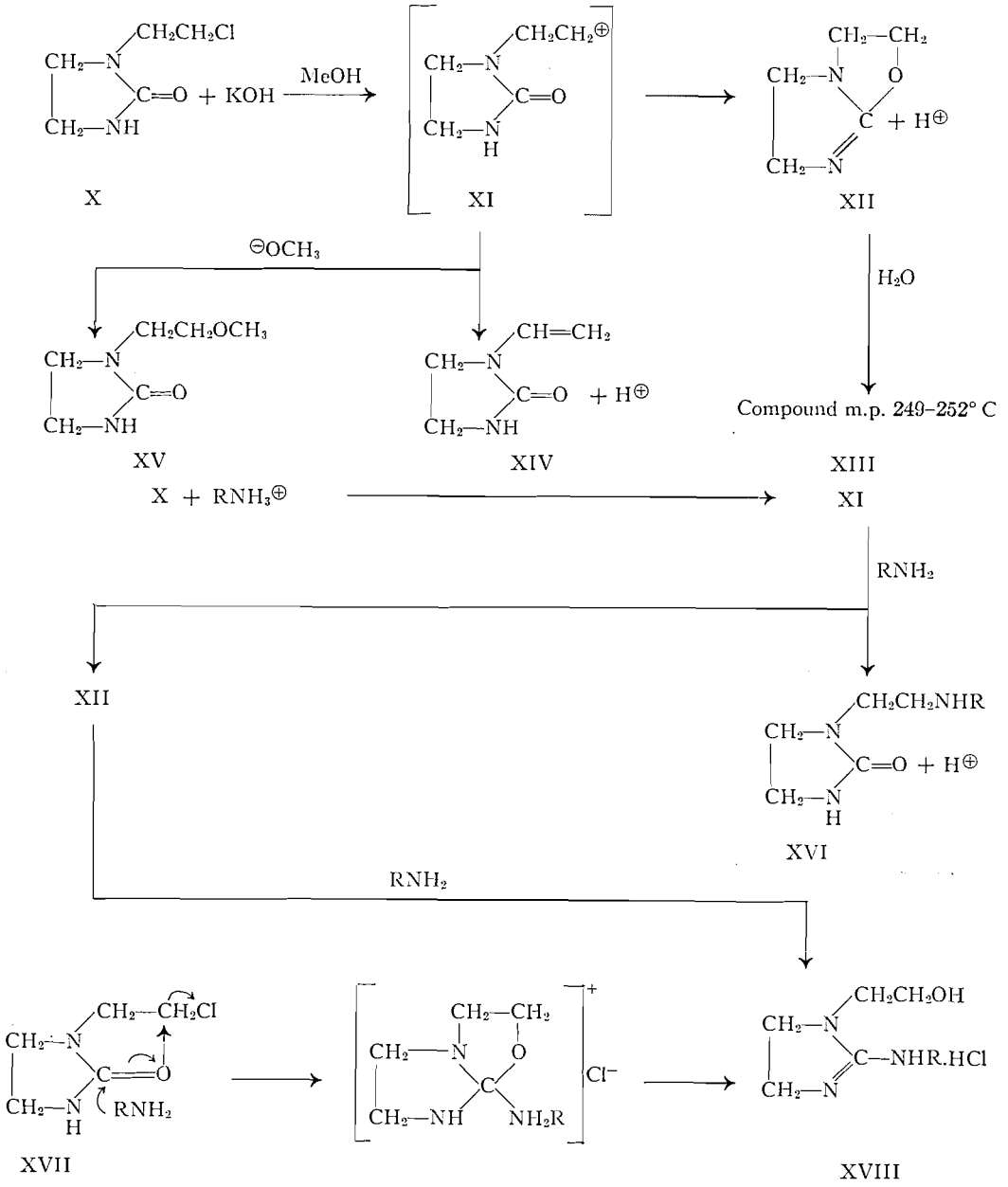

Can. J. Chem. Downloaded from www.nrcresearchpress.com by 190.90.36.8 on 09/04/12
For personal use only.

Can. J. Chem. Downloaded from www.nrcresearchpress.com by 190.90.36.8 on 09/04/12
For personal use only.

A further study was made of the reaction between methanolic potassium hydroxide and 1-(β-chloroethyl)-2-imidazolidone (X). This reaction gives several products, which is considered typical (17) of reactions involving carbonium ion intermediates. However, the number of products produced in a reaction involving a carbonium ion intermediate depend to some extent on the concentration of reactants and reaction conditions. The products identified from the reaction of 1-(β-chloroethyl)-2-imidazolidone with methanolic potassium hydroxide were Δ^7-1-oxa-4,7-diazabicyclo(3.3.0)octene (XII), 1(-β-methoxyethyl)-2-imidazolidone (XV), and 1-vinyl-2-imidazolidone (XIV).

Freshly distilled samples of Δ^7-1-oxa-4,7-diazabicyclo(3.3.0)octene (XII) on standing deposited crystals (XIII), which melted at 249–252° C. It appears that the bicyclic compound is converted slowly into the latter compound by absorbed moisture. Δ^7-1-Oxa-4,7-diazabicyclo(3.3.0)octene (XII) was considered (18) a possible intermediate in the formation of 1-(β-hydroxyethyl)-2-iminoimidazolidine (or its tautomer, 1-(β-hydroxyethyl)-2-amino-2-imidazoline) from 1-(β-chloroethyl)-2-imidazolidone (X). The bicyclic compound XII could arise from a carbonium ion intermediate (XI). This intermediate XI would also explain the formation of 1-(β-aminoethyl)-2-imidazolidone in the reaction of X with ammonia. If, however, we considered the concerted mechanism with ring opening (XVII → XVIII) for the formation of 1-(β-hydroxyethyl)-2-amino-2-imidazoline (XVIII, R = H) from the reaction of ammonia with XI, then another mechanism[2] must be operative in this reaction to produce the second product 1-(β-aminoethyl)-2-imidazolidone (XVI, R = H).

Δ^7-1-Oxa-4,7-diazabicyclo(3.3.0)octene (XII) on treatment with benzylamine gave 1-(β-hydroxyethyl)-2-benzylamino-2-imidazoline (XVIII, R = benzyl).

EXPERIMENTAL[3]

1-(β-Nitraminoethyl)-2-ethoxy-2-imidazolinium Nitrate

A freshly prepared sample of 1-nitro-2,3,5,6-tetrahydro-1(H)-imidaz(1,2-a)imidazole nitrate (7) (10 g, 0.046 mole) was dissolved in absolute ethanol (500 ml) at 50° C. Although this solution was cooled immediately in freezing mixture only 2.2 g (22%) of 1-nitro-2,3,5,6-tetrahydro-1(H)-imidaz(1,2-a)imidazole nitrate (m.p. 149–151° C with decomposition) was recovered. After the filtrate was concentrated to a volume of 200 ml, a second crystalline compound (m.p. 116–119° C with decomposition) was obtained, yield 5.1 g (42%). The melting point was raised to 124–125.5° C with decomposition by one crystallization from ethanol–ether (2:1) solution. Anal. Calc. for $C_7H_{15}N_5O_6$: C, 31.70; H, 5.70; N, 26.42%. Found: C, 31.90; H, 5.75; N, 26.41%.

1-(β-Nitraminoethyl)-2-imidazolidone from 1-(β-Nitraminoethyl)-2-ethoxy-2-imidazolinium Nitrate

1-(β-Nitraminoethyl)-2-ethoxy-2-imidazolinium nitrate (215 mg, 0.81 mm) was heated under reflux in absolute ethanol (5 ml) for 2 hours. Removal of the ethanol *in vacuo* gave a crystalline product melting at 176–180° C with decomposition. One crystallization from absolute ethanol (7 ml) raised the melting point to 180–182.5° C with decomposition, yield 133 mg (94%). A mixture melting point determination with a known sample of 1-(β-nitraminoethyl)-2-imidazolidone (7) was not depressed.

[2]*The Referee has suggested that the reaction between ammonia and 1-(β-chloroethyl)-2-imidazolidone represents a competition between* Sn_2 *and elimination reactions. This is certainly a possibility.*

[3]*All melting points are uncorrected. Microanalyses were performed by Micro-Tech Laboratories, Skokie, Illinois.*

Can. J. Chem. Downloaded from www.nrcresearchpress.com by 190.90.36.8 on 09/04/12
For personal use only.

TABLE I

1-(β-Nitraminoethyl)-2-substituted amino-2-imidazolines

Substituents	Yield, %	m.p. °C	Formula	C Calc.	C Found	H Calc.	H Found	N Calc.	N Found
Benzyl	86.4	115.5–116.5	$C_{12}H_{18}N_6O_5$*	44.17	43.90	5.56	5.54	25.76	25.75
	78.0	151.5–152.5	$C_{18}H_{20}N_8O_9$†	43.90	43.86	4.09	4.27	22.76	22.42
Phenyl	90.4	139–140	$C_{17}H_{18}N_8O_9$†	42.68	42.81	3.79	4.08	23.42	23.15
p-Methoxyphenyl	96.4	118.5–120‡	$C_{12}H_{18}N_6O_6$*	42.10	42.49	5.30	5.47	24.55	24.26
	78.0	121–122	$C_{18}H_{20}N_8O_{10}$†	42.52	42.69	3.97	4.18	22.04	22.35
p-Ethoxyphenyl	81.8	125.5–127‡	$C_{13}H_{20}N_6O_6$*	43.82	43.76	5.66	5.80	23.58	23.58
p-Hydroxyphenyl	80.6	189.5–190.5‡	$C_{11}H_{16}N_6O_6$*	40.24	40.40	4.91	5.13	25.60	25.57
5-(1-Hydroxynaphthyl)	32.3	198.5–199.5‡	$C_{15}H_{18}N_6O_6$*	47.61	47.50	4.79	5.15	22.21	21.89

*Nitrate salt. †Picrate. ‡Melts with decomposition.

1-(β-Nitraminoethyl)-2-substituted Amino-2-imidazolines

The properties of the 1-(β-nitraminoethyl)-2-substituted amino-2-imidazoline salts prepared by the reaction of amines with 1-nitro-2,3,5,6-tetrahydro-1(H)-imidaz(1,2-a)-imidazole nitrate are described in Table I. Since the conditions for these reactions are very similar, only the preparation of 1-(β-nitraminoethyl)-2-(*p*-anisidino)-2-imidazoline nitrate is described below in detail.

1-Nitro-2,3,5,6-tetrahydro-1(H)-imidaz(1,2-a)imidazole nitrate (657.5 mg, 0.003 mole) and *p*-anisidine (369 mg, 0.003 mole) in absolute ethanol (8 ml) were heated under reflux for 3 hours. After removal of the solvent *in vacuo*, a hard gum was obtained, yield 1.025 g (100%). Trituration with acetone gave 984 mg (96%) of crystalline product melting at 115–118° C with decomposition. Four crystallizations from ethanol–ether (5:3) solution raised the melting point to 118.5–120° C with decomposition.

An oily picrate, which crystallized slowly on standing in the refrigerator for 2 weeks, was obtained in the usual way from water in 78% yield. Two recrystallizations from water raised the melting point from 120 to 122° C to a constant value of 121–122° C.

Stability of 1-(β-Chloroethyl)-2-nitriminoimidazolidine

1-(β-Chloroethyl)-2-nitriminoimidazolidine (235 mg) in absolute ethanol (7 ml) was heated under reflux for 7 hours. The solution on cooling deposited crystals melting at 142–144° C with decomposition, yield 178 mg (76%). The crystals were identified as unchanged starting material by a mixed melting point determination.

1-(β-Chloroethyl)-2-nitriminoimidazolidine (188 mg) was also recovered in 90% yield after it was refluxed for 4 hours in a benzene solution containing dry hydrogen chloride (200 mg) and thionyl chloride (150 mg).

1-(β-Aminoethyl)-3-nitro-2-imidazolidone Nitrate from 1-Nitro-2,3,5,6-tetrahydro-1(H)-imidaz(1,2-a)imidazole Nitrate

1-Nitro-2,3,5,6-tetrahydro-1(H)-imidaz(1,2-a)imidazole nitrate (1 g, 0.0046 mole) in benzene (50 cc) saturated with hydrogen chloride was heated under reflux for 8.5 hours. After the solvent was decanted from the insoluble oil (0.76 g) the oil was triturated with warm (40° C) ethanol. The crystals (m.p. 155–159° C with decomposition) were recovered by filtration, yield 0.36 g (38%). The crystals were purified by solution in water and precipitation with ethanol. The pure product melted at 160.5° C with decomposition alone and on admixture with a known (7) sample of 1-(β-aminoethyl)-3-nitro-2-imidazolidone nitrate.

The picrate (m.p. 198° C decomposition) was prepared in the usual manner from water. It did not depress the melting point of a known (7) sample of the picrate of 1-(β-aminoethyl)-3-nitro-2-imidazolidone.

Stability of 1-Nitro-2,3,5,6-tetrahydro-1(H)-imidaz(1,2-a)imidazole Hydrochloride in Benzene – Thionyl Chloride Medium

Thionyl chloride (5 ml) was added to dry benzene (15 ml) and then 1-nitro-2,3,5,6-tetrahydro-1(H)-imidaz(1,2-a)imidazole nitrate (0.57 g, 0.0026 mole) was added portionwise at room temperature. A vigorous reaction occurred and brown fumes were evolved. Although the reaction was complete in 15 minutes, the solution was held at 55° C for a further 6 hours. At the end of this time the solution was cooled and the crystalline precipitate was recovered by filtration, yield 0.49 g (98% based on 1-nitro-2,3,5,6-tetrahydro-1(H)-imidaz(1,2-a)imidazole hydrochloride). The melting point was raised from 130–135° C with decomposition to 137–139° C with decomposition by solution in ethanol

Can. J. Chem. Downloaded from www.nrcresearchpress.com by 190.90.36.8 on 09/04/12
For personal use only.

at room temperature and precipitation with ether. This sample gave low chlorine values on analysis so it was characterized as its picrate.

The picrate was formed in 50% yield in the usual manner from aqueous solution. It melted at 150–151° C alone and on admixture with a known (16) sample of 1-nitro-2,3,5,6-tetrahydro-1(H)-imidaz(1,2-a)imidazole picrate.

Chlorination of 1-(β-Hydroxyethyl)-2-nitriminoimidazolidine

1-(β-Hydroxyethyl)-2-nitriminoimidazolidine (2, 19) (1.74 g, 0.01 mole) was chlorinated with thionyl chloride in benzene under the conditions previously (2) described. At the end of the reaction period the crystalline starting material had been transformed into a colorless oil which crystallized after a small amount of benzene had been evaporated *in vacuo* at 50° C. The hygroscopic crystals were collected by filtration and dried *in vacuo*, yield 1.87 g (98%). A sample (0.74 g) of the crude product was suspended in water. The water insoluble crystalline product (m.p. 142–143° C) was collected by filtration and dried, yield 0.44 g (59%). A mixed melting point determination with a known (2) sample of 1-(β-chloroethyl)-2-nitriminoimidazolidine (m.p. 142.5–143.5° C) gave no depression.

The filtrate from 1-(β-chloroethyl)-2-nitriminoimidazolidine on treatment with aqueous picric acid yielded a crystalline picrate (m.p. 150–151.5° C). A mixture melting point with a known sample of 1-nitro-2,3,5,6-tetrahydro-1(H)-imidaz(1,2-a)imidazole picrate (m.p. 151° C) was not depressed.

The yield of picrate was 306 mg. Since pure 1-nitro-2,3,5,6-tetrahydro-1(H)-imidaz-(1,2-a)imidazole hydrochloride under the same conditions gives a 50% yield of picrate, this yield of picrate corresponds to the presence of 304 mg (41%) of bicyclic hydrochloride.

Δ^7-1-Oxa-4,7-diazabicyclo(3.3.0)octene

A methanolic solution of potassium hydroxide (533 ml of 1.69 *N* solution) was added dropwise over a period of 1.5 hours to a solution of 1-(β-chloroethyl)-2-imidazolidone (18) (133 g, 0.9 mole) in absolute methanol (300 ml). This reaction mixture was heated under reflux for 5 hours after which it was worked up as previously (18) described. The volume of the final chloroform solution was 265 ml. A portion (29.4 ml) of the chloroform extract on evaporation gave 11.9 g of yellowish oil. This oil on treatment with aqueous picric acid solution yielded 6.7 g (18.5%) of crude (m.p. 134–138° C) Δ^7-1-oxa-4,7-diazabicyclo(3.3.0)octene picrate. One crystallization from acetone–ether (3:1) solution raised the melting point to 145–146.5° C. This picrate did not depress the melting point of a known (18) sample of Δ^7-1-oxa-4,7-diazabicyclo(3.3.0)octene picrate (m.p. 144.5–145.5° C).

The residual oil (21.8 g) from another portion (55 ml) of the chloroform extract was distilled *in vacuo*. The following four fractions were obtained: (1) 1.69 g of crystals (b.p. 78–80° C/0.07 mm), (2) 0.9 g of liquid containing some crystals (b.p. 82–88° C/0.06 mm), (3) 2.18 g of turbid liquid (b.p. 92–95° C/0.06 mm), and (4) 15.26 g of a low melting crystalline material (b.p. 98–100° C/0.06 mm).

A small sample of fraction 1 on treatment with a saturated aqueous picric acid solution gave Δ^7-1-oxa-4,7-diazabicyclo(3.3.0)octene picrate (m.p. 145–146° C) in 86% yield. Two samples (1.3 g) of Δ^7-1-oxa-4,7-diazabicyclo(3.3.0)octene (both samples originally contained 86–87% bicyclic compound by picrate analyses), which had been standing for 2 weeks, were combined and redistilled *in vacuo*. It was noted that most of the originally low melting solid had been converted into a high melting solid which was no longer distillable. Only 0.3 g (b.p. 76–78° C/0.07 mm) of distillate was obtained. This small

Can. J. Chem. Downloaded from www.nrcresearchpress.com by 190.90.36.8 on 09/04/12
For personal use only.

sample of Δ^7-1-oxa-4,7-diazabicyclo(3.3.0)octene was redistilled for analysis. Anal. Calc. for $C_5H_8N_2O$: C, 53.55; H, 7.19; N, 24.99%. Found: C, 53.25; H, 7.09; N, 24.63%.

The residue from the distillation of bicyclic compound was crystallized from chloroform–hexane solution, yield 0.35 g (27% by weight). The melting point was increased from 237–241° C to 249–252° C by two crystallizations from chloroform–hexane solution. Anal. Calc. for $C_{10}H_{18}N_4O_3$: C, 49.57; H, 7.49; N, 23.13%. Found: C, 49.90; H, 7.38; N, 23.45%.

Iodometric titrations of fractions 3 and 4 indicated that they contained 58.7 and 50.8% respectively of the 1-vinyl-2-imidazolidone compound. Fractions 3 and 4 on treatment with dinitrophenylhydrazine in acid solution gave 56% and 47.2% yields respectively of the dinitrophenylhydrazone of acetaldehyde. The dinitrophenylhydrazone melted at 151–152° C with sintering at 149° C after several crystallizations from aqueous methanol. Anal. Calc. for $C_8H_8N_4O_4$: C, 42.86; H, 3.60; N, 24.99%. Found: C, 43.32; H, 3.51; N, 25.13%. The formation of the dinitrophenylhydrazone of acetaldehyde from fractions 3 and 4 agrees with the observation of Reppe (20) that vinyl groups attached to nitrogen are split off as acetaldehyde under the influence of weak acids.

Reaction of Δ^7-1-Oxa-4,7-diazabicyclo(3.3.0)octene with Benzylamine

Benzylamine (0.086 g, 0.008 mole) was added to Δ^7-1-oxa-4,7-diazabicyclo(3.3.0)-octene (0.09 g, 0.008 mole) in absolute ethanol (5 ml). The mixture was allowed to stand at room temperature overnight after which it was evaporated to dryness *in vacuo* at 40° C. A pink-colored semicrystalline oil was obtained, yield 120 mg.

A portion (40 mg) of this oil on treatment with aqueous picric acid solution gave a 68% yield of crystalline picrate (m.p. 116–119° C). Crystallization from ethanol raised the melting point to 122.5° C. This picrate did not depress the melting point of a known sample of 1-(β-hydroxyethyl)-2-benzylamino-2-imidazoline picrate (21).

REFERENCES

1. McKay, A. F. and Milks, J. E. J. Am. Chem. Soc. **72**, 1616 (1950).
2. McKay, A. F. and Gilpin, J. R. J. Am. Chem. Soc. **78**, 486 (1956).
3. McKay, A. F. and Braun, R. O. J. Org. Chem. **16**, 1829 (1951).
4. McKay, A. F. Chem. Revs. **51**, 301 (1952).
5. Boyars, C., Sager, W. F., and Skolnik, S. J. Am. Chem. Soc. **78**, 4590 (1956).
6. Boyars, C., Cary, H., and Stark, V. J. Org. Chem. **22**, 716 (1957).
7. McKay, A. F., Hatton, W. G., and Braun, R. O. J. Am. Chem. Soc. **78**, 6144 (1956).
8. Cowdrey, W. A., Hughes, E. D., Ingold, C. K., Masterman, S., and Scott, A. D. J. Chem. Soc. 1267 (1937).
9. Hall, R. H., McKay, A. F., and Wright, G. F. J. Am. Chem. Soc. **73**, 2205 (1951).
10. McKay, A. F. and Hatton, W. G. J. Am. Chem. Soc. **75**, 963 (1953).
11. McKay, A. F., Hatton, W. G., and Taylor, G. W. J. Am. Chem. Soc. **75**, 1120 (1953).
12. McKay, A. F. J. Am. Chem. Soc. **77**, 1057 (1955).
13. Barrott, J., Denton, I. N., and Lamberton, A. H. J. Chem. Soc. 1998 (1953).
14. Denton, I. N. and Lamberton, A. H. J. Chem. Soc. 1655 (1955).
15. Bruck, P., Denton, I. N., and Lamberton, A. H. J. Chem. Soc. 921 (1956).
16. McKay, A. F., Kreling, M.-E., Paris, G. Y., Braun, R. O., and Whittingham, D. J. Can. J. Chem. **35**, 843 (1957).
17. Burton, H. and Praill, P. F. G. Quart. Revs. (London), **6**, 302 (1952).
18. McKay, A. F., Paris, G. Y., and Kreling, M.-E. J. Am. Chem. Soc. **79**, 5276 (1957).
19. McKay, A. F., Bryce, J. R. G., and Rivington, D. E. Can. J. Chem. **29**, 382 (1951).
20. Reppe, W. Ann. **601**, 208 (1956).
21. McKay, A. F. and Vavasour, G. R. Can. J. Chem. **32**, 59 (1954).

Can. J. Chem. Downloaded from www.nrcresearchpress.com by 190.90.36.8 on 09/04/12
For personal use only.

Can. J. Chem. Downloaded from www.nrcresearchpress.com by 190.90.36.8 on 09/04/12
For personal use only.

CO-ORDINATION COMPOUNDS OF NICKEL(II)

PART I. THE SPECTRA OF SALICYLALDIMINE DERIVATIVES OF NICKEL(II) IN SOME ORGANIC SOLVENTS[1]

H. C. Clark and R. J. O'Brien

ABSTRACT

Measurements of the ultraviolet and visible absorption spectra of bis-N-methyl-salicylaldimine nickel(II) and its 5-chloro and 5-bromo derivatives in benzene, chloroform, carbon tetrachloride, and cyclohexane solutions at temperatures between 15° and 45° C are reported. The results confirm the occurrence of a temperature dependent equilibrium between dia- and para-magnetic forms. The nature of the paramagnetic form is discussed in terms of the recent developments of the ligand field theory. The effect on the equilibrium of substitution of chlorine or bromine in the five position of the salicylaldehyde molecule is also discussed.

INTRODUCTION

The co-ordination compounds formed between nickel and various salicylaldimines are generally highly colored, diamagnetic solids with square planar configurations. Willis and Mellor (1) found that the addition to these complexes of organic solvents such as pyridine, dioxan, benzene, and chloroform caused changes to paramagnetism, magnetic moments of between 1 and 3 Bohr magneton being observed at room temperature. These magnetic moments are independent of concentration, but measurements over a wide temperature range have shown (2, 3) that in many of these solutions, a temperature dependent equilibrium occurs between dia- and para-magnetic forms, the latter being favored at low temperatures. The paramagnetic species may be (1) octahedral with two co-ordination sites occupied by solvent molecules, (2) tetrahedral, or (3) square planar but with unpaired electrons. Tetrahedral nickel(II) complexes, although long postulated theoretically, have only recently been isolated (4) and the existence of such complexes in solution now seems more probable. Square planar paramagnetic complexes can be predicted only from ligand field theory and have not been isolated as yet.

Later work on the absorption spectra of nickel–salicylaldimine complexes in organic solvents (5) generally supported the magnetic evidence of a temperature dependent equilibrium between dia- and para-magnetic forms, but there were several important exceptions. Further spectral measurements as reported below, and also by Sacconi, Paoletti, and Del Re (6) provide assistance in explaining these exceptional cases.

EXPERIMENTAL

The complexes were prepared by the method described previously (3, 7) in which bis-salicylaldehyde nickel(II) or its 5-chloro or 5-bromo derivative was gradually added to a saturated alcoholic solution of methylamine. It was interesting to note that in the early stages of the preparation, when a large excess of methylamine was present, a light green flocculent precipitate was formed. As more of the salicylaldehyde complex was added, this precipitate was converted to the more familiar, dark green crystals of the desired product. This light green precipitate is possibly an octahedral nickel complex containing two methylamine molecules linked directly to the nickel atom. In the presence of larger amounts of bis-salicylaldehyde nickel(II), these two molecules are readily lost. The final dark green products were recrystallized from either chloroform or carbon

[1]*Manuscript received October 2, 1958.*
Contribution from the Chemistry Department, University of British Columbia, Vancouver 8, B.C.

tetrachloride, and identities of the new compounds confirmed by determinations of the nickel content by precipitation with dimethylglyoxime.

Bis-N-methyl-5-chloro-salicylaldimine nickel(II): Found: Ni, 14.76. Calc. for Ni-$(C_8H_7ONCl)_2$ 14.84%.

Bis-N-methyl-5-bromo-salicylaldimine nickel(II): Found: Ni, 12.25. Calc. for Ni-$(C_8H_7ONBr)_2$ 12.11%.

All solvents used were carefully dried and purified by standard procedures. The spectral measurements were made with a Cary recording spectrophotometer, model 14, with 10-mm sample cells. These cells were contained in a thermostated tank which was controlled to ±0.5° at 15°, 25°, 35°, or 45° C. The following tables (I and II) give values of the molecular extinction coefficients at the above temperatures, in chloroform, benzene, carbon tetrachloride, cyclohexane, and ethyl alcohol.

The tables in many cases show a slight decrease in the extinction coefficient with

TABLE I

Molecular extinction coefficients for the 325 mμ bands

Compound	Solvent	Concentration (molar)	15°	25°	35°	45°
Bis-N-methylsalicyl-aldimine nickel(II)	Chloroform	4.89×10^{-3}	9940	9910	9780	9670
	Benzene	1.11×10^{-2}	9210	8850	8790	8650
	Carbon tetrachloride	3.41×10^{-3}	9670	9520	9430	9060
	Cyclohexane					
Bis-N-methyl-5-chlorosalicylaldimine nickel(II)	Chloroform	5.66×10^{-4}	9770	9740	9740	9500
	Benzene	3.64×10^{-4}	8950	8870	8770	8680
	Carbon tetrachloride	8.11×10^{-4}	7950	7800	7830	7800
	Cyclohexane	1.01×10^{-4}	7810	7840	8000	7940
Bis-N-methyl-5-bromosalicylaldimine nickel(II)	Chloroform	3.05×10^{-3}	8960	8970	9070	9390
	Benzene	2.31×10^{-3}	8880	8880	9060	9060
	Carbon tetrachloride	9.09×10^{-4}	8250	8250	7900	8090
	Cyclohexane	6.48×10^{-5} (approx.)	6940	6940	6630	6700
Molecular extinction coefficients for the 415 mμ bands						
Bis-N-methylsalicyl-aldimine nickel(II)	Chloroform	1.96×10^{-4}	3990	4010	4020	4030
	Benzene	1.78×10^{-4}	4280	4220	4170	4130
	Carbon tetrachloride	1.36×10^{-4}	4230	4170	4110	4070
	Cyclohexane					
Bis-N-methyl-5-chlorosalicylaldimine nickel(II)	Chloroform	2.25×10^{-4}	3690	3690	3700	3700
	Benzene	1.82×10^{-4}	4070	4070	4020	3990
	Carbon tetrachloride	1.62×10^{-4}	3050	3080	3130	3200
	Cyclohexane	1.01×10^{-4}	3370	3380	3520	3520
Bis-N-methyl-5-bromosalicylaldimine nickel(II)	Chloroform	1.22×10^{-4}	3090	3130	3250	3350
	Benzene	2.31×10^{-3}	3660	3680	3720	3720
	Carbon tetrachloride	3.64×10^{-5}	3380	3380	3350	3350
	Cyclohexane	6.48×10^{-5}	2140	2240	2240	2140
Molecular extinction coefficients for the 620 mμ bands						
Bis-N-methylsalicyl-aldimine nickel(II)	Chloroform	1.84×10^{-2}	58.1	61.2	65.5	68.5
	Benzene	1.25×10^{-2}	64.6	67.2	68.9	69.5
	Carbon tetrachloride	3.41×10^{-3}	74.9	76.3	77.7	78.4
Bis-N-methyl-5-chlorosalicylaldimine nickel(II)	Chloroform	6.50×10^{-3}	49.3	60.9	69.7	75.7
	Benzene	2.54×10^{-3}	78.0	94.3	110.0	124.0
	Carbon tetrachloride	8.11×10^{-4}	81.4	91.2	94.5	97.3
Bis-N-methyl-5-bromosalicylaldimine nickel(II)	Chloroform	3.05×10^{-3}	71.2	78.0	83.3	86.6
	Benzene	1.93×10^{-3}	75.7	79.3	81.3	
	Carbon tetrachloride	9.09×10^{-4}	105.0	110.0	114.0	117.0

Can. J. Chem. Downloaded from www.nrcresearchpress.com by 190.90.36.8 on 09/04/12
For personal use only.

TABLE II

Molecular extinction coefficients of ethyl alcohol solutions

Compound	Concentration (molar)	max (mμ)	15°	25°	35°	45°
Bis-N-methylsalicylaldimine nickel(II)	3.53×10^{-5}	325	6515	6660	6855	7050
		378	4530	4250	3995	3770
		410	2550	2775	2890	3005
Bis-N-methyl-5-chlorosalicylaldimine nickel(II)	1.60×10^{-4}	325	3560	4120	4570	5070
		378	8480	7580	6840	6100
		410	2440	2580	2910	3010
Bis-N-methyl-5-bromosalicylaldimine nickel(II)	8.00×10^{-5}	325	3630	4000	4570	4640
		378	8000	7300	6660	5970
		410	2290	2560	2690	2880

increasing temperature. This is attributed to the change in concentration that is due to the expansion of the solvent, and a suitable correction would show the extinction coefficient to remain constant.

DISCUSSION

It should first be pointed out that these results differ from those of Sacconi *et al.* (6), who found a slight temperature variation in the intensities of the 325 mμ and 415 mμ bands of bis-N-methylsalicylaldimine nickel(II) in benzene solution. The present results are, however, in good agreement with others previously reported (5). Sacconi also reported that the "620 mμ" band is actually located at 615 mμ in chloroform, 630 mμ in dioxan, and 635 mμ in benzene. We could find no definite indication of such a shift.

The temperature dependent equilibrium observed both magnetically and spectrophotometrically in solutions of these complexes is unusual, and has otherwise been observed only in solutions of bis-formylcamphorethylenediimine nickel(II) (8). The addition to a planar nickel complex of an organic solvent may produce one of several effects: (*a*) the co-ordination of two solvent molecules to the nickel atom to form an octahedral, or more accurately, tetragonal paramagnetic complex; (*b*) conversion to a tetrahedral configuration; (*c*) a reduction in the splitting of the 3*d* energy levels by the ligand to produce a square planar, paramagnetic complex. Solvation of the resultant complex is possible in all cases and must be carefully distinguished from co-ordination occurring only in case (*a*). The first effect will be expected in basic solvents such as pyridine; thus bis-N-methyl-salicylaldimine nickel(II) forms a stable paramagnetic dipyridine adduct. Conversion to a tetrahedral configuration may possibly occur when the intermolecular forces of the crystalline solid are removed by the addition of a non-co-ordinating solvent such as cyclohexane, thus allowing the isolated molecule to assume the shape of lowest potential energy (9). The energy difference between the planar and tetrahedral configurations must be small allowing a thermal equilibrium; at low temperatures the more stable tetrahedral form will predominate, while at higher temperatures, where thermal distortion of the complex molecule becomes appreciable, the diamagnetic planar form will exist. Hence, in agreement with observation, the magnetic moment will decrease with increasing temperature. Alternatively, the removal of intermolecular crystalline forces may merely reduce the splitting of the 3*d* levels so that it is energetically preferable for the electrons to remain unpaired. However, it is less easy to determine the cause of this transition, as compared with the planar–tetrahedral change. That diamagnetism may be peculiar to the solid state, and that the change to paramagnetism

Can. J. Chem. Downloaded from www.nrcresearchpress.com by 190.90.36.8 on 09/04/12
For personal use only.

may occur in the absence of a solvent, is further shown by the observation that certain nickel–salicylaldimine complexes are paramagnetic in the molten state (10). In particular, the transition to paramagnetism of bis-N-methyl-salicylaldimine nickel(II) above 180° has been interpreted (11) as being due to the formation of a polymeric octahedral complex, but these results can with equal validity be interpreted as resulting from either effect (*b*) or effect (*c*) discussed above.

Previously (5) the relationships between the magnetic and spectral properties of nickel–salicylaldimine complexes in pyridine, alcohol, and dioxan solutions have been discussed. In these cases, octahedral paramagnetic adducts appear to be formed. This paper is concerned with the spectra of the benzene, methylbenzene, chloroform, carbon tetrachloride, and cyclohexane solutions. These spectra consist of four bands located at approximately 270 mμ, 325 mμ, 415 mμ, and 620 mμ, and in many cases a "shoulder" in the 360–370 mμ region is also apparent. The first of these bands at 270 mμ is produced by a transition in the benzenoid ring of the salicylaldehyde molecule (12). Similarly, the 325 mμ band must result from internal transitions within the conjugated system of the free ligand since it also occurs in the spectra of the free organic ligands. The band at 415 mμ is observed only in the spectra of the complexes, and from its high intensity must be considered a charge transfer band due to electron transfer in the new conjugated system present only in the complex.

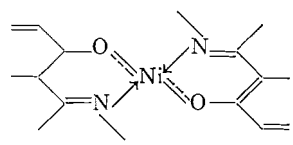

The fourth band at 620 mμ (for which $\log \epsilon < 2$) is due to a so-called "forbidden" *d–d* transition of the nickel atom.

Bis-N-methylsalicylaldimine nickel(II) has been shown to exist in pyridine solution as the tetragonal dipyridine adduct, which shows absorption at 270 mμ and 378 mμ. After allowance is made for the shift of up to 20 mμ to longer wavelengths which is observed in all these pyridine solutions, the latter of these two bands may be considered the enhancement of the "shoulder" at 360–370 mμ. Certainly, high intensities of this band are characteristic of an octahedral configuration of these complexes. Also, in appropriate cases where an equilibrium between diamagnetic and paramagnetic forms occurs, its intensity is related in an inverse manner to the intensities of the 325 mμ and 415 mμ band. The relative intensities of these three bands may therefore allow conclusions to be drawn concerning the extent of solvent–solute interaction. The ethyl alcohol solution of this nickel complex absorbs at 325 mμ, 378 mμ, and 415 mμ, and the effect of increasing temperature is to increase the intensity of the first and last of these bands at the expense of the 378 mμ band. Hence, a temperature-dependent equilibrium exists in this solution between a diamagnetic planar form characterized by the 325 and 415 mμ bands, and a paramagnetic tetragonal species characterized by the 378 mμ band, since there is clearly sufficient interaction between the complex and the solvent to greatly enhance this last charge transfer band. It also may be noted that the spectra of the 5-chloro and 5-bromo derivatives show that the equilibrium has shifted in favor of the paramagnetic species. For the dioxan solution of this complex, the bands at 325 mμ and 410 mμ show only very small changes with temperature, and

Can. J. Chem. Downloaded from www.nrcresearchpress.com by 190.90.36.8 on 09/04/12
For personal use only.

only a slight shoulder is apparent at 360 mμ. Hence solute–solvent interaction is weak and any resultant tetragonal product must retain its fifth and sixth groups very weakly.

For solutions in benzene, the methylbenzenes, and chloroform, magnetic measurements again showed the occurrence of an equilibrium, but absorption bands are apparent only at 325 mμ and 415 mμ, and the intensities of these bands are temperature independent. Hence in these solvents, there can be no strong interaction between solvent and solute, since there is no enhancement of the 360–370 mμ charge transfer band. The paramagnetic form must therefore be either tetrahedral or square planar (paramagnetic). Basolo and Matoush (8) have previously concluded that the paramagnetic form of bis-formylcamphorethylenediimine nickel(II) in methyl benzene solutions is tetrahedral, since no direct correlation could be found between the magnetic susceptibilities of these solutions and the base strengths of the solvents. Whatever the configuration of the paramagnetic form, it is remarkable that there are no changes in the charge transfer bands, since the change from dia- to para-magnetism must result from changes in the splittings of the 3*d* levels and these levels are almost certainly involved in several of the charge transfer processes.

From the present results, similar conclusions regarding the configuration of the paramagnetic form may now be drawn for solutions in carbon tetrachloride and cyclohexane, for solutions of the 5-chloro derivative in benzene, chloroform, carbon tetrachloride, and cyclohexane, and of the 5-bromo derivative in carbon tetrachloride and cyclohexane. In all these solutions, the 325 mμ and 415 mμ bands are unaffected by temperature changes, so that solvent–solute interaction must be negligibly weak, and again the paramagnetic form can only be four-co-ordinated. A list of the solvents arranged in order of decreasing effect on these charge transfer bands further supports this deduction regarding the nature of the paramagnetic form, the order being pyridine > alcohol > dioxane > benzene > chloroform ~ methylbenzenes ~ carbon tetrachloride ~ cyclohexane. This order is that of decreasing basic strength, or decreasing co-ordinative ability of these solvents.

Since the 620 mμ band results from forbidden *d–d* transitions and is hence directly concerned with the configuration of the 3*d* electrons of the nickel atom, a direct relationship must exist between the intensity of this band and the concentration of the paramagnetic form. The above results show that without exception, the 620 mμ band increases in intensity with increasing temperature as compared with the observed decrease in magnetic moment. Unfortunately, the solubilities in cyclohexane were too low for accurate measurement of the optical densities in this region. It is noticeable that the intensity changes are much greater in certain cases than in others; thus the intensity of the 620 mμ band of the benzene solution of the 5-chloro compound shows much greater changes than that of the carbon tetrachloride solution. This is probably due to the fact that in this latter solvent the equilibrium lies very much more on the diamagnetic side, so that much smaller changes in the extinction coefficient can occur.

The effect of varying the solvents in the order of decreasing co-ordinative power is thus to change the configuration of the paramagnetic form from almost regularly octahedral for pyridine solutions, through more tetragonal configurations in alcohol and dioxan solutions, to either tetrahedral or planar paramagnetic configurations in chloroform, carbon tetrachloride, and cyclohexane. It is not reasonable to conclude that in these latter solvents, solvent interaction with the complex molecule is strong enough to produce paramagnetism (and hence a tetragonal configuration) and yet on the other hand, is so weak that the charge transfer bands are not affected. For such non-co-ordinating

Can. J. Chem. Downloaded from www.nrcresearchpress.com by 190.90.36.8 on 09/04/12
For personal use only.

solvents as carbon tetrachloride and cyclohexane, the resultant paramagnetic product can contain no solvent molecules and hence can only be tetrahedral or square planar. The point in the above solvent series at which co-ordination of solvent molecules ceases is difficult to determine, and may depend on the balance between the co-ordinating power of the solvent, and the tendency of the complex molecule to attain a more energetically favorable configuration. Certainly in pyridine, ethyl alcohol, and probably in dioxan, these salicylaldimine complexes form tetragonal species, while in carbon tetrachloride and cyclohexane no co-ordination of solvent molecules occurs.

Assignment of the 620 mμ band is best made in terms of ligand field theory. The splittings of the 3*d* energy levels for different geometries of the ligand field are shown below together with the arrangement within these levels of the eight 3*d* electrons of the nickel(II) atom.

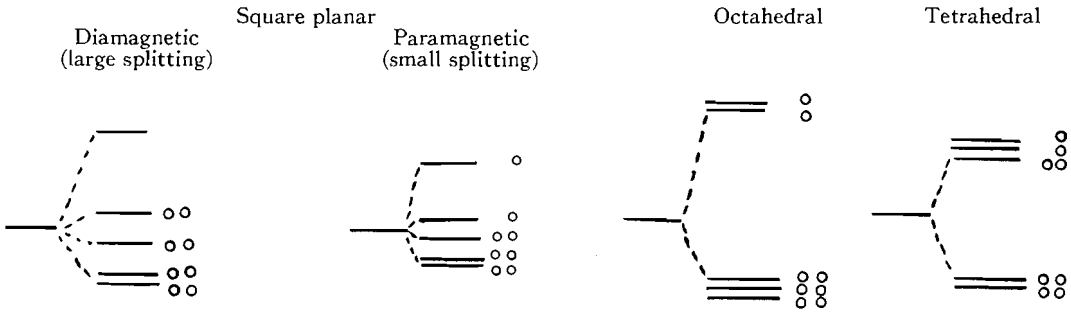

Hence, for the planar configurations, three "forbidden" *d–d* transitions are possible, which may be named ω_1, ω_2, and ω_3 according to the scheme of Belford, Calvin, and Belford (13). Only one transition is possible for the tetrahedral form, although the removal of the degeneracy of the upper triplet as a result of the Jahn–Teller effect will produce several transitions which differ only very slightly in energy content. For an octahedral form, only one transition is possible since the Jahn–Teller effect does not apply. Analysis of a typical 620 mμ band (Fig. 1) shows that after allowance is made

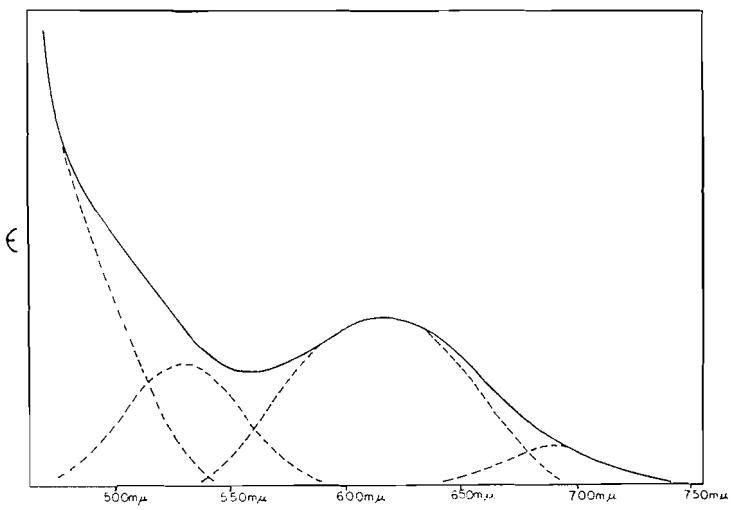

FIG. 1.

Can. J. Chem. Downloaded from www.nrcresearchpress.com by 190.90.36.8 on 09/04/12
For personal use only.

for the tail of the intense 415 mμ band, there remains a broad asymmetric peak which may be separated into three gaussian components. This closely resembles the spectra of planar copper complexes in the 650 mμ band region (13). Moreover, this 620 mμ band is also observed in ethyl alcohol solutions for which the paramagnetic form is tetragonal, while for pyridine solutions there is no absorption band in 600–650 mμ region. Hence this 620 mμ band must be produced by the diamagnetic complex, and as the proportion of this form increases with increasing temperature the intensity of this band will also increase in agreement with observation.

Sacconi, Paoletti, and Del Re (6) have previously suggested that the paramagnetic forms in these non-co-ordinating solvents are of the "outer" sp^3d type, this being the valence bond description of paramagnetic square planar complexes. This conclusion is based on the observation that bis-N-alkyl-salicylaldimine – nickel(II) complexes in benzene and dioxan solutions at 25° have a very low, almost zero, dipole moment; hence the paramagnetic form must still be planar. However, magnetic measurements (3) have shown that at this temperature and in these solvents, more than half of the complex is already in the diamagnetic planar form which has a zero moment. Thus, bis-N-methyl-salicylaldimine nickel(II) exists in benzene solution at 25° to the extent of 64% in the diamagnetic, trans-planar form. Hence, assuming a tetrahedral nickel(II) complex to have a moment of approximately 5 D, the observed value of 1 to 2 D is to be expected and may still be consistent with a tetrahedral configuration of the paramagnetic form. Moreover, if as suggested above, the paramagnetic form in dioxan is actually tetragonal, with two trans-solvent molecules, the dipole moment will in any case be zero. Only in solvents such as chloroform, carbon tetrachloride, and cyclohexane and at low temperatures, can an appreciable dipole moment be expected. Such measurements are now in progress, and it is hoped the results will make it possible to distinguish between tetrahedral and square planar paramagnetic forms.

These present results also show the effect on the equilibrium of differences in the solvent, and also differences in the complex itself. From a consideration of the intensity of the 620 mμ band at say 15°, it would appear that the proportion of diamagnetic form increases as the solvent is changed from chloroform to benzene to carbon tetrachloride, although this effect is less apparent at higher temperatures. The spectra of the alcohol solutions shows the effect of substitution on the aromatic ring. The halogen atom, substituted in the five position and acting through the conjugated system of the Schiff's base, will reduce the donor properties of the nitrogen atom. In other words, the ligand field strength will be reduced, thus facilitating the formation of a species in which the electrons remain unpaired. Thus the spectra of the alcohol solutions show that the intensity of the 378 mμ band which is characteristic of the tetragonal form is markedly greater for the 5-chloro and 5-bromo derivatives. The secondary effect of increased acidity of the phenolic group by this substitution is apparently of secondary importance to the reduced donor properties of the nitrogen atom in determining the strength of the ligand field.

Further substituted derivatives are being examined to determine more extensively the factors which control the equilibrium.

ACKNOWLEDGMENTS

The authors thank Dr. T. N. Waters of A.E.R.E., Harwell, England, and Dr. J. Halpern for much valuable discussion and advice.

Can. J. Chem. Downloaded from www.nrcresearchpress.com by 190.90.36.8 on 09/04/12
For personal use only.

REFERENCES

1. WILLIS, J. B. and MELLOR, D. P. J. Am. Chem. Soc. **69**, 1237 (1947).
2. FUJII, S. and SUMITANI, M. Sci. Repts. Research Insts., Tohoku Univ., Ser. I, **37**, 49 (1953).
3. CLARK, H. C. and ODELL, A. L. J. Chem. Soc. 3431 (1955).
4. VENANZI, L. M. J. Chem. Soc. 719 (1958).
5. CLARK, H. C. and ODELL, A. L. J. Chem. Soc. 520 (1956).
6. SACCONI, L., PAOLETTI, P., and DEL RE, G. J. Am. Chem. Soc. **79**, 4062 (1957).
7. PFEIFFER, P. Ann. **503**, 84 (1933).
8. BASOLO, F. and MATOUSH, W. R. J. Am. Chem. Soc. **75**, 5663 (1953).
9. NYHOLM, R. S. Chem. Revs. **53**, 263 (1953).
10. SACCONI, L., CINI, R., and MAGGIO, F. J. Am. Chem. Soc. **79**, 3933 (1957).
11. SACCONI, L., PAOLETTI, P., and CINI, R. J. Am. Chem. Soc. **80**, 3583 (1958).
12. LEMON, H. W. J. Am. Chem. Soc. **69**, 2998 (1947).
13. BELFORD, R. L., CALVIN, M., and BELFORD, G. J. Chem. Phys. **26**, 1165 (1957).

NOTE ADDED IN PROOF: Since this paper was submitted, Maki (J. Chem. Phys. **29**, 1129 (1958)) has made a more elegant assignment of the spectra of bis-N-methylsalicylaldimine nickel(II), as a solid and in pyridine and chloroform solutions. The conclusion is reached that for a complex with this *trans*-planar symmetry, only a small axial perturbation is sufficient to cause a change from dia- to para-magnetism. However, the charge transfer bands are not mentioned and from the above results it would seem more a matter of definition to determine whether the small axial perturbation produced by a solvent such as carbon tetrachloride can be termed "co-ordination", or whether it is sufficient to term the product a para-magnetic planar complex. Maki's work is certainly opposed to any possibility of tetrahedral configurations.

Can. J. Chem. Downloaded from www.nrcresearchpress.com by 190.90.36.8 on 09/04/12
For personal use only.

Can. J. Chem. Downloaded from www.nrcresearchpress.com by 190.90.36.8 on 09/04/12
For personal use only.

THE REACTIVITY OF CELLULOSE

III. THE NITRATION OF COTTON LINTERS ALTERNATELY WETTED WITH WATER AT VARIOUS TEMPERATURES AND DRIED, AND THE PROBABLE DISTRIBUTION OF THE NITRATE GROUPS[1,2]

T. P. YIN[3] AND R. K. BROWN

ABSTRACT

Cotton linters alternately wetted at 0° or 25° and dried show progressively greater ease of nitration paralleling the number of wetting–drying cycles. The reverse is found to be true for linters wetted at 50°, 75°, or 100°. Analysis of the data obtained from lead tetraacetate oxidation of the nitrates favors the depressive concept of nitration and indicates that the observed changes in reactivity occasioned by the wetting–drying treatments are largely due to greater alterations in the accessibility of the primary rather than the secondary hydroxyl groups.

INTRODUCTION

It is known that the physical treatment and moisture history of cellulose has a definite effect upon its reactivity (1, 2, 3). Highly swollen cotton linters nitrate to a significantly greater extent than do the same linters "collapsed" by drying from a water-soaked state (3). Furthermore, repeated experiments have shown that dewaxed cotton linters, alternately wetted with water at 25° and dried, exhibit a small increase in accessibility to thallous ethylate in ether, to a nitration mixture of sulphuric acid, nitric acid, and water, and to deuterium exchange with heavy water (4, 5). Thus the extent of reaction and doubtless the distribution of the reacted hydroxyl groups are determined to some extent by the treatment the cellulose has received prior to reaction.

The present work attempts to gain more information concerning the effects of the wetting–drying process on the reaction proclivities of the primary and secondary hyrodxyl groups of cellulose as well as to verify and extend the observation that linters wetted at 80° and dried become *less* rather than *more* reactive (5).

Accordingly, cotton linters were repeatedly subjected to alternate wetting and drying cycles, the wetting temperature ranging from 0° to 100°. The dried samples were nitrated and the nitrates examined by lead tetraacetate oxidation for glycol content. The data from the nitration and oxidation reactions were analyzed and certain conclusions made concerning the probable course of the nitration reaction.

EXPERIMENTAL

Preparation of the Cotton Linters

High grade cotton linters[4] were dewaxed (5) and air-dried. A quantity of the dried linters was divided into five 20- to 30-gram portions, each one of which was given 15 cycles of alternate wetting and drying, the wetting temperatures being, for the five portions respectively, 0° (a mixture of ice and water), 25°, 50°, 75°, and 100° (wet steam). Each wetting involved immersion of the linters in water at the specified temperature for a 3-hour period while the mixture was occasionally stirred. The 100° wetting was

[1]*Manuscript received September 15, 1958.*
Contribution from the Department of Chemistry, University of Alberta, Edmonton, Alberta, Canada. This paper was presented in part at the Fourth Regional Conference of the Chemical Institute of Canada at Winnipeg, Manitoba, on September 4–6, 1958.
[2]*Taken in part from the thesis submitted by T. P. Yin in partial fulfillment of the requirements for the degree of M.Sc.*
[3]*Present address: Department of Chemistry, University of Wisconsin, Madison, Wis., U.S.A.*
[4]*Generously donated by the Hercules Powder Company.*

Can. J. Chem. Downloaded from www.nrcresearchpress.com by 190.90.36.8 on 09/04/12
For personal use only.

accomplished by passing wet steam (at 100°) through a mass of loosely packed linters held in a wide tube with smaller openings at either end. The water was then separated from the linters by mild suction and the moist fibers spread out to dry in air. This preliminary drying was followed by one of greater intensity with phosphorus pentoxide as previously described (5). A sample (1.5–2 g) was retained while the bulk of the linters was again wetted and dried. In this way a number of samples of linters were obtained and all were kept in a large desiccator over phosphoric anhydride for 2 weeks before further treatment.

Nitration of the Dried Cotton Linters

Standard tables (6, 7) facilitated the preparation of a nitration mixture which would produce 10–11% nitrogen in the cellulose nitrate. A quantity of this reagent, sufficient for the whole series of experiments, was kept in a refrigerator and found to maintain its strength. The details of the nitration followed the published directions (3, 4) but with the modification that during the ½-hour nitration, the linters and mixed acid were constantly though gently stirred to facilitate diffusion of the liquid.

Nitrogen Estimation

Analysis for nitrogen by the Du Pont semimicronitrometer (8) followed the procedure adopted previously (5).

Lead Tetraacetate Oxidations

Glacial acetic acid was freed from aldehyde by heating for 3 hours under reflux with chromic anhydride (2.5 g per liter of acid) added in small quantities at suitable intervals to avoid violent reaction. The acid was then fractionated in an all-glass apparatus.

Acetic anhydride was purified by fractionation.

The nitrocellulose (0.5 g corrected for moisture absorption) was weighed to 4 figures in a capped weighing bottle and transferred to a 200-ml glass-stoppered volumetric flask. The sample was covered with 125 ml purified anhydrous ethyl acetate (9) and slowly dissolved by agitation in a mechanical shaker for 2–3 days. Fifty milliliters of 0.1 *N* lead tetraacetate (10) in glacial acetic acid was added followed by enough ethyl acetate to bring the total volume to the 200-ml mark. The flask was well shaken again and placed in a constant temperature bath at 25°±0.1°. Two blanks were prepared simultaneously and duplicate runs were made for each sample.

Consumption of lead tetraacetate by the cellulose nitrate was followed by amperometric titration (11) with 0.02 *N* sodium thiosulphate added from a microburette. The

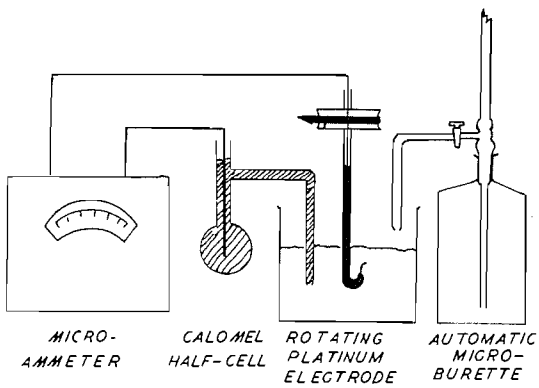

FIG. 1. Amperometric titration apparatus for the lead tetraacetate analyses.

apparatus is shown in Fig. 1 and consists of a rotating platinum electrode operating at 60 r.p.m., a saturated calomel half-cell, and a microammeter connected to the two electrodes. At suitable intervals the volumetric flasks were removed from the bath and briskly shaken. Suspended, undissolved material, if any, was allowed to settle and then a 10-ml aliquot was pipetted into 30 ml of potassium iodide – sodium acetate solution (12) in a 300-ml electrolysis beaker. The pipette was flushed with 10 ml of pure ethyl acetate and the washings added to the beaker. This is important, since the viscosity of the solutions of the cellulose nitrate in ethyl acetate varies with the nitrogen content of the nitrates producing variable delivery from the pipette. After the addition of 100 ml of distilled water the contents of the beaker was titrated with the two electrodes well-immersed in the liquid. The course of the titration was followed by the

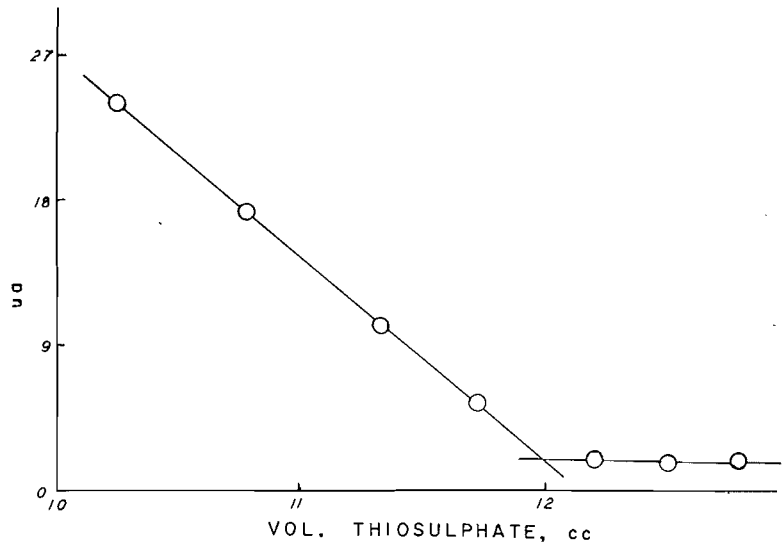

FIG. 2. Sample titration graph using the amperometric method.

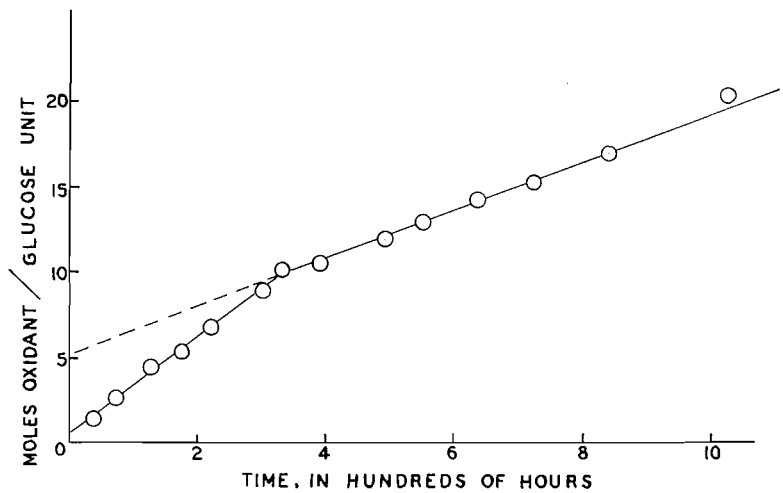

FIG. 3. Lead tetraacetate oxidation of the nitrate obtained from cotton linters which had received eleven cycles of immersion in water at 25° followed by drying.

Can. J. Chem. Downloaded from www.nrcresearchpress.com by 190.90.36.8 on 09/04/12
For personal use only.

scale readings of the microammeter. Usually 6–7 readings were recorded, three or four before and three after the equivalence point. This point was determined by plotting the volume of thiosulphate against the corresponding microammeter readings. A typical plot is shown in Fig. 2. Consumption of oxidant is expressed as the difference in titrations between blank and sample, and calculated as moles of oxidant consumed per glucose unit. One can add starch indicator to act as a visual check on the end point, but since the iodine is absorbed by the cellulose and the ethyl acetate layer, colorimetric end points are not reliable.

RESULTS AND DISCUSSION

Table I contains the data obtained from duplicate or triplicate nitrometer nitrogen analyses of the five series of nitrates. For convenience, the degree of substitution (D)[5] per glucose unit is listed along with the percentage of nitrogen. In addition the nitrogen analyses for the dewaxed but unwetted linters, nitrated by the same stock mixture, are noted in the same table. The decreased nitratability occasioned by one wetting at 0° or 25° (e.g. from 10.36% N to 10.20% N or 10.29% N) has been observed before (4, 5) and ascribed to a general collapse of the accessible cellulose from the partly swollen state which might have been attained during the dewaxing process. However, a similar single wetting–drying treatment at the higher temperatures (50°–100°) either maintains the same state or produces more reactive linters as in the case of the 75° series (an increase from 10.36% N to 10.63% N).

Examination of the data in Table I shows unmistakably that linters repeatedly wetted at 0° or 25° show enhanced nitration while those wetted at 50°, 75°, or 100° become less inclined to react as the number of wetting–drying cycles is increased. The differences are small, but several repetitions of this work show that the trend, though not the figures, is quite reproducible. The division between increasing and decreasing ease of nitration occurs somewhere in the region of 25° to 50°.

It should also be noted that the greatest over-all enhancement of reactivity caused by the wetting processes is found in the 0° series (0.41% N increase), while the most marked change in reactivity due to the first wetting is found in the 75° series (0.27% N increase). These observations *may* be significant.

Furthermore, of the five series of treated linters, only that exposed to steam at 100° gave a product which was non-uniform in physical appearance. It was somewhat more brittle and contained many small "nodules" which no doubt gave rise to the greater variability observed in the nitrogen analyses of the nitrates. At least three analyses were made on each nitrate of the 100° series in order to obtain a reasonable average value for the nitrogen content. These observations and the figures for the 100° series in Table I suggest that linters wetted by steam at 100° and dried, in addition to becoming less homogeneous, suffer a general reduction of accessibility to a technical nitration mixture.

The lead tetraacetate oxidations of the nitrates of these five series were carried out with the same stock solutions of the tetraacetate in acetic acid (normality, 0.0969). Although the nitrates in the ethyl acetate – acetic acid gave transparent, gel-like solutions, they were considered suitable for reaction and apparently presented no difficulties during the oxidations. Analyses were made by amperometric titration, since in several trials it was found that even though the blue-violet coloration of the starch–iodine complex disappeared, indicating complete reaction of the iodine with thiosulphate, the thin

[5]*The usual abbreviation is* D.S. *Here* D *is used for the sake of brevity.*

Can. J. Chem. Downloaded from www.nrcresearchpress.com by 190.90.36.8 on 09/04/12
For personal use only.

Can. J. Chem. Downloaded from www.nrcresearchpress.com by 190.90.36.8 on 09/04/12
For personal use only.

TABLE I

Nitrogen analyses (% N)[b] and degree of substitution (D)[c] of nitrocelluloses

No. of[a] wetting–drying cycles	0° Series		25° Series		50° Series		75° Series		100° Series	
	% N	D	% N	D	% N	D	% N	D	% N	D
1	10.20	1.76	10.29	1.78	10.41	1.81	10.63	1.87	10.30	1.79
3	10.49	1.83	10.54	1.85	10.29	1.78	10.52	1.84	10.29	1.78
5	10.46	1.83	10.39	1.81	10.22	1.76	10.49	1.83	10.24	1.77
7	10.51	1.84	10.44	1.82	—	—	—	—	10.25	1.77
9	10.54	1.85	10.46	1.83	—	—	—	—	10.20	1.76
11	10.59	1.86	10.51	1.84	—	—	—	—	10.19	1.76
13	10.63	1.87	10.53	1.84	—	—	—	—	10.22	1.76
15	10.61	1.87	10.52	1.84	—	—	—	—	10.16	1.75
0			10.36	1.80						

[a]Each wetting consisted of 3-hour immersion in water at the specified temperature, followed first by air-drying, then thorough drying over P_2O_5 under vacuum. The 100° series was exposed to wet steam at 100° for the 3-hour period.

[b]Average of duplicate or triplicate Dupont nitrometer analyses generally agreeing very well. Those for the 100° series gave somewhat poorer reproducibility, hence the percentage of nitrogen values shown are the averages of *at least three* analyses per sample.

[c]Obtained from the relation: (D×atomic wt. nitrogen)/(submolar wt. of cellulose) = $14D/(162.2-45D)$ = %N /100.

TABLE II

Comparison of glycol content (G) of cellulose nitrates with their unnitrated hydroxyl content (F)

Wetting–drying cycle	0° Series		25° Series		50° Series		75° Series		100° Series	
	G[a]	F[b]	G[a]	F[b]	G[a]	F[b]	G[a]	F[b]	G[a]	F[b]
1	0.057	1.24	0.045	1.22	0.039	1.19	0.052	1.13	0.049	1.21
5	0.050	1.17	0.052	1.19	0.043	1.24	0.053	1.17	0.050	1.23
11	0.049	1.14	0.055	1.16	—	—	—	—	0.051	1.24
15	0.047	1.13	0.058	1.16	—	—	—	—	0.051	1.25
0	0.033	1.20							0	

[a]Moles of 2,3-glycol per glucose unit as measured by consumption of lead tetraacetate in moles per anhydroglucose unit.

[b]Total unnitrated hydroxyl content per anhydroglucose unit obtained from the degree of nitrate substitution D (Table I) subtracted from 3, the number of hydroxyl groups per anhydroglucose unit in cellulose.

organic layer of ethyl acetate still showed a faint yellow color of iodine. The starch was used, if at all, only as a visual aid for the determination of the approaching end point, and the exact equivalence point obtained amperometrically.

The consumption of lead tetraacetate by cellulose nitrate should reach a maximum when all free glycol groups in the anhydroglucose unit have reacted. However, in the present work, consumption continued to rise in all cases even after a period of 1200 hours. This phenomenon has been reported by other workers (12, 13). The glycol estimation, however, was obtained in the usual manner by extrapolation of the slower reaction curve to zero time. Figure 3 is typical of the results obtained in all cases and shows that a definite and unambiguous break occurs in the line. Duplicates were generally in very good agreement. The break in the oxidation curve usually occurred at about 300 hours. Confidence that the break did indicate completion of the glycol oxidation was obtained from the observation that cellulose trinitrate under similar conditions showed no evidence of oxidation (14).

Table II summarizes the oxidation data for the samples of nitrocelluloses from the five series of linters. It is unfortunate that for the series 50° and 75° only two sets of values are available. This was unavoidable at the time, since a choice was necessary because only a limited number of oxidations could be carried on simultaneously. Nevertheless, the information in Table II reveals that lead tetraacetate consumption (and therefore glycol content), *decreases* in the 0° series, but *increases* for the 50°, 75°, and 100° groups with the number of cycles. Since the capacity for reaction with the nitration mixture employed was found to follow the directly opposite trend in these four cases, one infers that the augmented ease of reaction for the 0° linters is at least partly due to *greater accessibility and reactivity* of the secondary hydroxyl units, whereas the lowered nitratability for the 50°–100° series is due, in part, to the *diminishing accessibility and reactivity* of the secondary hydroxyl groups developed by the repeated wetting and drying.

Cyclic treatment at 25°, however, yields linters whose accessibility to nitration, *and* glycol content of the resulting nitrate, increases with the number of wettings. One must infer, therefore, that the rising nitration is due to the greater availability of the primary hydroxyl groups, outweighing the fall in accessibility of those on carbons 2 and 3 of the glucose unit.

The region of 25° in wetting temperature appears to constitute a dividing line between high and low temperature wetting effects, the former increases while the latter decreases the accessibility of the secondary hydroxyl groups to technical nitration.

It is also to be noted that the glycol content of the unwetted but dewaxed and nitrated linters is lower than that of any of the singly wetted and dried samples, even though the nitrogen content exceeds that found for the 0° and 25° series.

In attempting to understand the causes of the changes in reactivity noted above and the resulting distribution of reacted hydroxyl groups, one must consider both the kinetics and the nature of the nitration reaction. Since the over-all rate of nitration is fairly rapid and the reaction is essentially complete within 10 minutes (15), the $\frac{1}{2}$-hour allowed for the nitration should give ample time for the equilibrium to be well established for both primary and secondary hydroxyl groups. Thus the differences in reaction rates between these two types of hydroxyls should not be a determining factor in the distribution of the reacted positions. It is true, however, that reaction at one hydroxyl of the glycol pair might somehow inhibit reaction at the second hydroxyl of the pair. What seems to be important is the position of equilibrium and the accessibility of the hydroxyl groups in determining the extent of reaction and the distribution of affected sites.

Because the nitration mixture is of constant composition, the equilibrium position

Can. J. Chem. Downloaded from www.nrcresearchpress.com by 190.90.36.8 on 09/04/12
For personal use only.

Can. J. Chem. Downloaded from www.nrcresearchpress.com by 190.90.36.8 on 09/04/12
For personal use only.

reached (16) at the completion of the reaction should be the same in all cases. Two factors might interfere with the attainment of this equilibrium. The first is the "bound water" content in the linters. Previous work (5) has shown that a series of linters wetted at 25° shows progressively greater water content, measured by Karl Fischer titration, as the number of cycles of wetting and drying increase. A stock nitration mixture should then, upon reaching equilibrium, have a slightly larger water content for the more frequently wetted and dried linters than is found in the case of the singly wetted and dried sample. The extent of nitration determined by the final composition of the nitration solution (16) should then be less. But, since the reverse was found true (5), small differences in the "bound water" content do not cause the regular variation in nitratability observed. The second factor, that of diffusion of the reagent to the reaction site, probably involving reaction with more resistant "hydrogen bonded" hydroxyls, appears to be important, since it has been shown that extension of the reaction time of nitration from 30 to 90 minutes obliterated the differences observed (5).

Some assistance in the clarification of this problem might be gained by a consideration of the three proposed concepts of the manner in which nitration occurs in the cellulose fiber. The most popular one, the *homogeneous* or *permutoid* method, considers that the fibrous structure of the cellulose is sufficiently swollen by the reaction environment that all portions of the macromolecule are uniformly exposed to the reagent and the hydroxyl groups are randomly substituted. This method is also referred to in this paper as the *random* method. The *heterogeneous* concept considers that the readily accessible regions of the fiber are extensively substituted and the hydrophobic shell so formed hinders the progress of the reagent to the interior of the micelles. There is thus produced a nitrate in which the glucose units are either completely substituted or entirely unsubstituted. The third concept of interest is termed the *depressive* method wherein a permutoid-like reaction occurs. The C_6 hydroxyl reacts without difficulty but substitution at either the C_2 or C_3 hydroxyl depresses the reactivity of the remaining member of the glycol pair (13, 17, 18).

Considerable evidence is available which discounts the heterogeneous viewpoint (18). The homogeneous or permutoid (random) theory agrees with a large mass of information available (18). However, the depressive mode of reaction has been postulated to account for the observation that in partly xanthated cellulose, the xanthate groups occupy the C_3 and C_6 but not the C_2 position (19), and the same concept may explain the presence of approximately half the nitrate groups in the primary position with the other half "distributed between" the two available secondary positions in cellulose nitrates containing from 2.5% to 7.5% nitrogen (20).

Expressions may be obtained for the coincidence of glycol groups for these three concepts of nitration and have been used in conjunction with data from tosylation, iodination, and oxidation experiments to estimate the probable distribution of substituents between the three available hydroxyl groups of cellulose (12, 13, 17, 21).

Setting H equal to the total molar value of the secondary hydroxyl groups unnitrated, and X as the concentration of the unreacted C_2 hydroxyl per anhydroglucose unit, the probability of glycol occurrence based on the assumption of random or homogeneous nitration is $(X)(H-X)$ whose value is maximum when $X = H-X = H/2$. Thus $H^2/4$ estimates the glycol occurrence. The depressive concept, permitting in the ideal case reaction at only one of either the C_2 or C_3 hydroxyls, would exhibit the presence of glycol only when the total degree of substitution in the secondary positions falls below one hydroxyl per glucose unit. The probability for glycol occurrence is then $[(H-X)+X]-1$

Can. J. Chem. Downloaded from www.nrcresearchpress.com by 190.90.36.8 on 09/04/12
For personal use only.

TABLE III

Total number of reacted (nitrated) secondary (2−H) and primary (D−2+H) hydroxyl groups per glucose unit in the nitrate

Based on assumption of:	No. of cycles	0° Series		25° Series		50° Series		75° Series		100° Series	
		Secondary	Primary	Secondary	Primary	Secondary	Primary	Secondary	Primary	Secondary	Primary
A. Random substitution	1	1.52	0.24	1.58	0.20	1.61	0.20	1.54	0.33	1.56	0.23
	5	1.55	0.28	1.54	0.27	1.59	0.17	1.54	0.29	1.55	0.22
	11	1.56	0.30	1.53	0.31	—	—	—	—	1.55	0.21
	15	1.57	0.30	1.52	0.32	—	—	—	—	1.55	0.20
	0	1.64	0.16	—	—	—	—	—	—	—	—
Over-all change*		+0.05	+0.06	−0.06	+0.12	−0.02	−0.03	0.00	−0.04	−0.01	−0.03
B. Depressed substitution	1	0.94	0.82	0.96	0.83	0.96	0.85	0.95	0.92	0.95	0.84
	5	0.95	0.88	0.95	0.86	0.96	0.80	0.95	0.88	0.95	0.82
	11	0.95	0.91	0.95	0.90	—	—	—	—	0.95	0.81
	15	0.95	0.92	0.94	0.90	—	—	—	—	0.95	0.80
	0	0.97	0.83	—	—	—	—	—	—	—	—
Over-all change*		+0.01	+0.10	−0.02	+0.07	0.00	−0.05	0.00	−0.04	0.00	−0.04
C. Heterogeneous substitution	1	1.89	−0.13	1.91	−0.13	1.92	−0.11	1.89	−0.02	1.90	−0.11
	5	1.90	−0.07	1.90	−0.09	1.91	−0.15	1.89	−0.06	1.90	−0.13
	11	1.90	−0.04	1.89	−0.05	—	—	—	—	1.90	−0.14
	15	1.91	−0.04	1.88	−0.04	—	—	—	—	1.90	−0.15
	0	1.93	−0.13	—	—	—	—	—	—	—	—
Over-all change*		+0.02		−0.03		−0.01		0.00		0.00	

* + indicates increase; − indicates decrease in extent of nitration.

or H−1. Finally, the heterogeneous viewpoint allows either 100% glycol or 0% glycol per glucose unit and the estimate for glycol occurrence is obviously H/2 if it occurs at all.

Equating in turn these three expressions to the glycol content measured by lead tetraacetate oxidations, one obtains a figure for H representing the probable occurrence of *unreacted* secondary hydroxyl groups for each of the three modes of nitration. By subtracting this value from the total unnitrated hydroxyl content (F) per glucose unit (Table II), one arrives at probable values for unreacted primary hydroxyls (F−H). From this can be obtained the probable extent of nitration of the primary and secondary positions. For example, the equation for the sample isolated after one wetting–drying cycle at 0° is $0.057 = H^2/4$, or H/2 or H−1, according to the three assumptions, yielding values for the unnitrated secondary hydroxyl groups of H = 0.48, 1.06, and 0.11, respectively. Subtraction from the total amount of unnitrated hydroxyl groups (F in Table II) then gives values for the primary hydroxyl group as (1.24−0.48) = 0.76, etc. The probable extent of nitration in the two secondary positions is then (2−0.48) or 1.52, and that in the single primary position (1−0.76) or 0.24. All the nitrate substitutions calculated on the three assumptions are recorded in Table III.

The negative values for primary nitration shown in the lower section of Table III immediately eliminate heterogeneous nitration as a reasonable process. The figures for the probable reaction on the basis of random substitution suggest that the secondary positions react to a five- to seven-fold greater extent than do the primary positions. However, many examples can be quoted from the literature which clearly show that the primary hydroxyl in cellulose reacts more readily than do the secondary hydroxyl groups (22). In view of this, and the implication in the concept of random substitution that all hydroxyls are equally exposed to reaction and at equilibrium the extent of their reaction should be roughly the same, one would not expect this great preponderance of secondary over primary positions esterified. On the other hand, the depressive type of reaction, if permutoid-like, might be expected to yield after equilibrium is attained, a nitrate with the primary, and one of the two secondary positions more or less equally affected. This agrees with the analysis of the oxidation data on the basis of the depressive reaction theory. The observation by Murray and Purves (20) that half the nitrate groups in a nitrocellulose containing less than 8% nitrogen are found in the primary position lends support to the acceptance of the depressive permutoid-like reaction process as a reasonable mode for nitration. Although the homogeneous concept is favored for esterifications and etherifications in general, the suggestion has been made that nitration may not follow the course of most esterifications (23).

A further conclusion can be drawn from the data in Table III. The over-all change in primary and secondary nitrate substitution was obtained by subtracting the value after the first wetting–drying cycle from that obtained after the last, e.g. 1.57–1.52 or +0.05, in the case of the secondary nitrates in the 0° series assuming random substitution. The figures reveal that, except in the case of the 50° series, the differences in ease of nitration observed are largely due to the two- to three-fold greater change in reactivity of the primary over the secondary hydroxyl groups.

ACKNOWLEDGMENTS

The authors express their appreciation for the financial support given to this project by the National Research Council of Canada. One of us, T. P. Yin, wishes to thank the Shell Oil Company for the award of a scholarship which permitted him to carry out this work.

Can. J. Chem. Downloaded from www.nrcresearchpress.com by 190.90.36.8 on 09/04/12
For personal use only.

REFERENCES

1. JAYME, G. Cellulosechemie, **21**, 73 (1943).
2. SCHUR, M. O. and HOOS, B. G. Ind. Eng. Chem. **29**, 26 (1937).
3. BROWN, R. K. and PURVES, C. B. Pulp & Paper Mag. Can. **48** (6), 100 (1947).
4. ROSENTHAL, A. and BROWN, R. K. Pulp & Paper Mag. Can. **51** (6), 99 (1950).
5. BRICKMAN, W. J., DUNFORD, H. B., TORY, E. M., MORRISON, J. L., and BROWN, R. K. Can. J. Chem. **31**, 550 (1953).
6. DOREE, C. The methods of cellulose chemistry. Chapman & Hall, Ltd., London. 1933. p. 223.
7. OTT, E. and SPURLIN, H. M. *Editors* Cellulose and cellulose derivatives. Interscience Publishers, Inc., New York, 1954. pp. 718–722.
8. ELVING, P. T. and MCELROY, W. R. Ind. Eng. Chem. Anal. Ed. **14**, 84 (1942).
9. FIESER, L. E. Experiments in organic chemistry. 3rd ed. D. C. Heath & Co., New York. 1955, p. 287.
10. WALTON, H. F. Inorganic preparations. Prentice-Hall, Inc., New York. 1953. p. 138.
11. EWING, G. W. Instrumental methods of chemical analysis. McGraw-Hill Book Co., Inc., New York. 1954. p. 80.
12. CRAMER, F. B., HOCKETT, R. C., and PURVES, C. B. J. Am. Chem. Soc. **61**, 3463 (1939).
13. MAHONEY, J. F. and PURVES, C. B. J. Am. Chem. Soc. **64**, 9 (1942).
14. BROWN, R. K. Thesis submitted to the Faculty of Graduate Studies at McGill University, Montreal, Quebec. 1946. p. 102.
15. OTT, E. and SPURLIN, H. M. *Editors* Cellulose and Cellulose derivatives. Interscience Publishers, Inc., New York. 1954. pp. 722–723.
16. OTT, E. and SPURLIN, H. M. *Editors* Cellulose and cellulose derivatives. Interscience Publishers, Inc., New York. 1954. p. 730.
17. HONEYMAN, J. J. Chem. Soc. 168 (1947).
18. OTT, E. and SPURLIN, H. M. *Editors* Cellulose and cellulose derivatives. Interscience Publishers, Inc., New York. 1954. pp. 733–736.
19. SWAN, E. P. and PURVES, C. B. Can. J. Chem. **35**, 1522 (1957).
20. MURRAY, G. E. and PURVES, C. B. J. Am. Chem. Soc. **62**, 3194 (1940).
21. SPURLIN, H. M. J. Am. Chem. Soc. **61**, 2222 (1939).
22. CRAMER, F. B. and PURVES, C. B. J. Am. Chem. Soc. **61**, 3458 (1939).
23. TIMELL, T. E. Chem. Eng. News, 4036 (1955).

Can. J. Chem. Downloaded from www.nrcresearchpress.com by 190.90.36.8 on 09/04/12
For personal use only.

Can. J. Chem. Downloaded from www.nrcresearchpress.com by 190.90.36.8 on 09/04/12
For personal use only.

THE DETERMINATION OF ATOMIC RATIOS IN THE URANIUM–OXYGEN SYSTEM BY A THERMOGRAVIMETRIC METHOD[1]

L. G. STONHILL

ABSTRACT

A description is given of a thermogravimetric oxidation–reduction method for determining U–O ratios, especially suited to oxygen-sensitive materials of undetermined purity, and equally applicable to pure stoichiometric and non-stoichiometric oxides and their mixtures with each other and with uranium metal.

Provided that no uncombined base metals other than uranium, and no oxidizable or reducible matter other than its oxides, are present, it is not essential to know the detailed composition of the sample, since the assay is based on interconversion of the stoichiometric oxides UO_2 and U_3O_8 within that sample.

Incidental advantages of this method are: the avoidance of manipulation of the sample during the determination, precise reaction control, and immediate recording of the completion or otherwise of the required reaction.

INTRODUCTION

One of the chief characteristics of the uranium–oxygen system is the extent to which excess oxygen can be absorbed into the crystal lattice to form non-stoichiometric oxides. By far the most important of the oxides which has this ability is the dioxide, UO_2, often termed "brown oxide". In view of its function as an intermediate in the production of the metal, and being itself a potentially valuable reactor fuel, a knowledge of its exact U–O atomic ratio is often necessary. Current research into new methods of production has extended this need to materials, such as freshly precipitated oxide, which are extremely sensitive to oxidation by exposure to air and may contain inert impurities besides a large percentage of water.

It appeared likely that thermogravimetry offered a solution to the problems connected with this type of product, and would also provide a convenient general method for U–O ratios. A controlled-atmosphere apparatus (1) incorporating a Stanton milligram recording thermobalance was used in the investigation: the advantages of exact control over reaction conditions and a visible continuous record of the weight changes associated with a reaction make it possible to carry out a complete analytical operation within the assembly, thereby avoiding excessive manipulation of sensitive samples.

The standard chemical methods for determining atomic ratios, namely oxidation to U_3O_8 (2) or reduction to UO_2 (3), have been evaluated and refined by Bright *et al.* (4): these latter investigators point out the necessity of preparation and weighing in an oxygen-free atmosphere and recommend the use of an argon-filled dry box for these operations. Assumptions are usually made that the material under investigation contains only uranium oxide after a preliminary heat treatment to drive off water, etc. Though justifiable with familiar samples, such assumptions could not be made in the case of unusual products, and preliminary assays of material subject to aging should be avoided. The method to be described postulates only that oxidizable and reducible matter other than uranium and its oxides shall be absent, and uses interconversion of stoichiometric UO_2 and U_3O_8 as an internal standard on which to base the assay.

Composition of Oxides UO_x

The empirical formula UO_x may represent a homogeneous oxide species or, alternatively, a mixture of various oxidation states from UO_3 down to the uncombined metal.

[1]*Manuscript received September 30, 1958.*
Contribution from the Metallurgical Laboratories, Eldorado Mining and Refining Ltd., Ottawa, Canada.

Thus, UO may be the true monoxide, or mixed uranium metal and other oxides, and partial reduction of UO_3 with hydrogen results in a product $UO_{2.x}$ containing UO_3, U_3O_8, and the dioxide, as evinced by its behavior in the thermobalance and also by analysis (5). The importance of these alternative possibilities in the development of a general procedure for determining formulae will be considered below.

Thermogravimetric Behavior of Uranium Oxides

In view of the preceding observations it will be clear that a knowledge of the behavior of uranium in various oxidation states towards heat, and oxidizing and reducing atmospheres, is required. Figure 1 shows the effect of these factors on the pure oxides and also on the metal. Between UO_2 and U_3O_8 several phases have been detected by X-ray study: these tend to disproportionate on being heated (6), presumably without loss of oxygen from the system (7).

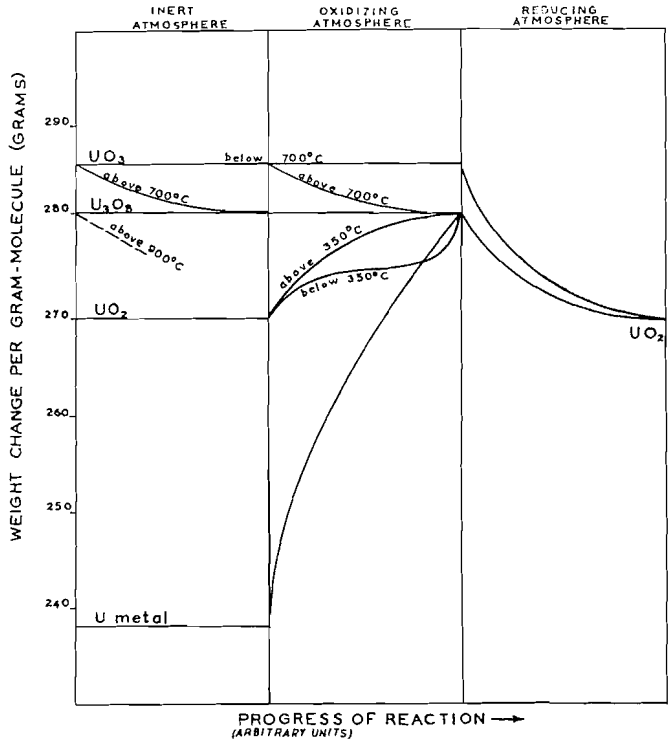

FIG. 1. Behavior of uranium and its principal oxides in various environments (temperatures approximate).

In the case of mixtures, the observed behavior depends on circumstances: in an inert atmosphere UO_3 will oxidize UO_2 with little or no evolution of oxygen until the rest of the uranium has been converted to U_3O_8; but if the material be oxidized by heating gradually in air from cold, the UO_3, which is unaffected by such treatment, will decompose on reaching a temperature of about 700° C, and the material will undergo a loss in weight.

The experimental observations on which Fig. 1 is based show (*a*) that for complete conversion of the uranium of any mixture to pure U_3O_8, it should be heated to 800° C to constant weight in air to ensure decomposition of UO_3, then cooled somewhat to compensate for a tendency of U_3O_8 to lose oxygen at that temperature; (*b*) that for

Can. J. Chem. Downloaded from www.nrcresearchpress.com by 190.90.36.8 on 09/04/12
For personal use only.

similarly complete reduction to UO_2, temperature is not a critical factor but can be chosen so as to give a suitable reaction velocity; (*c*) that to ensure decomposition of hydrates, particularly of UO_3, and to volatilize traces of nitric acid, preliminary heating to at least 550° C is advisable.

Derivation of U–O *Molecular Formulae*

Suppose that a sample contains oxygen combined with uranium to an extent giving a general formula UO_x, and that the following reactions are made to occur in such a way that the whole of the uranium present is converted to the appropriate stoichiometric compound, either UO_2 or U_3O_8, thus

$$UO_x \rightarrow U_3O_8 \rightarrow UO_2,$$

or alternatively

$$UO_x \rightarrow UO_2 \rightarrow U_3O_8.$$

The weight changes accompanying these reactions can be obtained directly from the thermogravimetric record. For any given weight of uranium, let these weights be *a*, *b*, and *c* as shown diagrammatically:

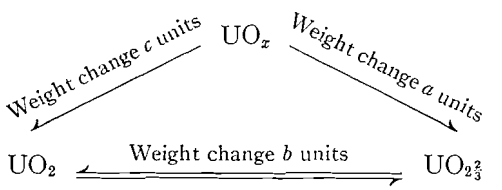

The weight change in each reaction step will be proportional to the amount of uranium taking part (a constant, *k*) and the change in its level of oxidation: therefore, for the conversion UO_x to U_3O_8 to UO_2:

$$a = k(2\tfrac{2}{3}-x)$$

and

$$b = k(2\tfrac{2}{3}-2),$$

therefore

$$a/b = (2\tfrac{2}{3}-x)/\tfrac{2}{3} = 4-(3x/2).$$

Similarly for the alternative route UO_x to UO_2 to U_3O_8:

$$c = k(x-2)$$

therefore

$$c/b = (3x/2)-3.$$

Obviously the value of *x* is obtainable from either of these reaction cycles independently of the actual sample weight employed. In practice, however, several limiting possibilities should be distinguished.

Case *a*: $$2\tfrac{2}{3} < x \leqslant 3.$$

This arises when oxygen is present beyond the proportion required to give U_3O_8, and, therefore, presumably the material contains some UO_3. When the material is heated in air there will be a net *loss* in weight owing to the decomposition of this UO_3, but the general equations deduced above still apply.

Case *b*: $$x = 2\tfrac{2}{3}.$$

Can. J. Chem. Downloaded from www.nrcresearchpress.com by 190.90.36.8 on 09/04/12
For personal use only.

Stoichiometric U_3O_8 is of course not further oxidizable by heating in air, but net weight changes associated with reduction followed by reoxidation will be equal.

Case *c*: $2 < x < 2\frac{2}{3}$.

This covers the range of oxides usually met. Either sequence of reactions may be employed.

Case *d*: $x = 2$.

The true dioxide is not often encountered, since, once it has been exposed to air, an excess of oxygen is always present (3), but it could be simulated by a mixture of metal with other oxides.

Case *e*: $0 \leqslant x < 2$.

In this case metal is most probably present in view of the uncertainties surrounding the monoxide UO (8, 9). Only the procedure involving a preliminary oxidation is applicable, as explained below.

Material Containing Uranium Metal

The presence of uncombined uranium metal invalidates the use of the equation derived above for reduction followed by oxidation, since the supposition that the whole of the uranium present takes part in the full cycle of reaction would not be true. However, the alternative preliminary oxidation procedure would be reliable, because the metal begins to oxidize at about 400° C (depending on its state of subdivision) and gives a final product of U_3O_8 in the same way as the oxides.

Samples containing uranium metal show a gain in weight during initial heating in nitrogen (see method, below) owing to nitride formation. On the admission of air, this nitride is converted to oxide.

ANALYTICAL PROCEDURE

Air is first displaced from the reaction chamber of the thermobalance by passing in oxygen-free nitrogen for about 10 minutes at a rate of 1 l. per minute. A sample of the material under test, weighing approximately 10 g (or, in the case of precipitated oxide, sufficient to contain that weight of UO_2), is then placed in the sample holder and the furnace lowered into position.

The material is thereby protected from oxidation, and may be subsequently balanced; the tare weight being known, this gives the weight of sample actually taken. Nitrogen is fed into the seal compartment at a rate of 0.75 l. per minute and the exhaust system, calibrated for an extraction rate of 1.5 l. per minute, set in operation.

The furnace is then heated to 600° C and held at this temperature until the sample has maintained a constant weight for about 5 minutes. If reduction is to be employed, the nitrogen flow rate is reduced to 0.25 l. per minute and 0.75 l. per minute hydrogen added to the gas stream; if oxidation, then the seal nitrogen flow is cut off and the gas input line disconnected to allow the entry of air. For faster oxidation a mixture of air and oxygen may be introduced. During this oxidation the furnace temperature is allowed to rise to 900° C, by which time the reaction should be complete (it is not essential to reach this temperature in the reduction stage—cooling can be commenced when reaction ceases) and the furnace is allowed to cool back to 600° C.

The reaction chamber is next purged with nitrogen under the same conditions used at the start of the operation; after 10 minutes the weight change accompanying the reaction

Can. J. Chem. Downloaded from www.nrcresearchpress.com by 190.90.36.8 on 09/04/12
For personal use only.

may be noted. The reverse operation, either reduction or oxidation, can then be carried out, and on its completion the standard conditions of nitrogen flush and temperature are restored so that each weight change is measured under as nearly as possible identical conditions, thereby avoiding spurious changes due to buoyancy, etc. The uranium–oxygen ratio is calculated from the formulae deduced above. Incidentally it is worth noting that the thermogravimetric record, by showing the actual weight change involved in the interconversion of UO_2 and U_3O_8, gives data from which the total uranium content of the sample may be calculated.

Certain special problems require a slight modification of the above procedure; thus, if a loss on ignition determination is to be carried out, the furnace temperature is initially raised to the necessary extent, then brought back to 600° C. Any weight loss commencing near 700° C would then require especial notice if the presence of UO_3 were possible. In the case of samples containing uranium metal, argon is used as the flushing gas in place of nitrogen.

RESULTS

A sample of U_3O_8 (99.9% pure) used as a reference standard in these laboratories was employed in the evaluation of the reduction–oxidation technique. In five consecutive runs the number of oxygen atoms per uranium atom was found to be 2.669, 2.672, 2.665, 2.665, and 2.668, giving an average value close to 2.668 compared with a theoretical 2.667 for 100% pure U_3O_8. It therefore appears that a good degree of accuracy is obtainable.

In order to test the procedure through both possible reaction cycles, and over a wide range of sample types, a number of materials which could be met in practice were taken. These are listed in Table I, together with the results obtained.

TABLE I

Atomic ratios obtained by the thermogravimetric procedure

Material	Atoms of oxygen per atom of uranium as determined by: Oxidation followed by reduction	Reduction followed by oxidation
UO_3 (technical)	3.003	3.005
UO_3 (partly reduced with hydrogen):		
Sample *a**	2.873	2.878
b	2.412	2.410
c	2.277	2.274
d	2.147	2.150
e	2.082	2.083
f	2.035	2.038
UO†	0.99	Not applicable
U (metal, 99.4% pure)	0.008	Not applicable

*Microscopic examination shows presence of UO_3.

†Prepared by oxidizing uranium metal in the thermobalance, followed by cooling in argon. Microscopic examination shows presence of uncombined metal.

The data recorded above indicate that the present method can be used over the full range U to UO_3 with an accuracy suitable for all practical purposes.

DISCUSSION

The need for caution in applying the method in the presence of uranium metal has already been noted, and the absence of oxidizable or reducible foreign matter presupposed.

Can. J. Chem. Downloaded from www.nrcresearchpress.com by 190.90.36.8 on 09/04/12
For personal use only.

Apart from independent tests, these complications would normally manifest themselves in inconsistent results if both oxidation and reduction procedures were to be applied to the same material, and this might be used as a distinguishing criterion. Substantial quantities of free metals other than uranium, oxides of transitional metals, and certain compounds of uranium apart from the oxides would be expected to interfere.

From the point of view of accuracy this method compares favorably with earlier procedures with which, according to Bright (4), the number of oxygen atoms per atom of uranium can be determined to a precision of ± 0.005.

In conclusion, it is suggested that the general procedure is adaptable to the study of other metal–oxygen systems, as, for example, those involving molybdenum and tungsten, lead, etc., for which comparable reaction schemes might be devised.

REFERENCES

1. STONHILL, L. G. J. Inorg. & Nuclear Chem. To be published.
2. RODDEN, C. J. Analytical chemistry of the Manhattan project. 1st ed. McGraw-Hill Book Co., Inc., New York. 1950. p. 46.
3. ROBERTS, L. E. J. and HARPER, E. A. The determination of oxygen in uranium oxides. Atomic Energy Research Establ., Gt. Brit. A.E.R.E. C/R 885 (1952).
4. BRIGHT, N. F. H., RIPLEY, L. G., ROWLAND, J. F., and LAKE, R. H. Department of Mines & Technical Surveys, Mines Branch (Canada), MD-207 (1956).
5. STONHILL, L. G. Can. J. Chem. **36**, 1487 (1958).
6. ALBERMAN, K. B. and ANDERSON, J. S. J. Chem. Soc. 303 (1949).
7. ROBERTS, L. E. J. Uranium dioxide as a fuel element. Atomic Energy Research Establ., Gt. Brit. A.E.R.E. C/M 268, 2 (1956).
8. WILLIAMS, J. and WESTMACOTT, K. H. Atomic Energy Research Establ., Gt. Brit. A.E.R.E. M/R 1235 (1953).
9. VAUGHAN, D. A., MELTON, C. W., and GERDS, A. F. Battelle Memorial Institute, B.M.I. Rept. 1175 (1957).

Can. J. Chem. Downloaded from www.nrcresearchpress.com by 190.90.36.8 on 09/04/12
For personal use only.

Can. J. Chem. Downloaded from www.nrcresearchpress.com by 190.90.36.8 on 09/04/12
For personal use only.

ORBITAL CONSTRUCTIONS AND ELECTRON POPULATIONS IN THE TRANSITION ELEMENTS[1]

W. R. TROST

ABSTRACT

Orbital constructions and electron populations for the bands in the transition elements have been worked out. With the assumption of uniform density of states in delocalized bands among nearest neighbors, it is possible to predict correctly the lattice elected by the elements. Manganese and iron are exceptions. Numerical values for electron populations in the several *s*, *p*, *d*, and hybrid bands, including their bonding, antibonding, and non-bonding levels, are obtained.

INTRODUCTION

Though molecular orbitals were first proposed for metals by Bloch (1) in 1928, the orbital constructions and hence the electron populations for the bands in metals, particularly for the transition metals, are still lacking. In simple cases, such as the alkali metals, detailed calculations of the binding energy have been made and reasonable agreement with experimentally determined binding energies obtained (2). Even in the case of atoms with one valence electron, however, the definition in space of the atomic orbitals comprising the bands is missing. In the more complicated case of the transition metals, where up to 12 valence electrons and 9 atomic orbitals are to be counted for each atom, the binding energy calculations are more difficult, and the problem of locating the orbitals and electrons is also more complex. It is perhaps correct to say that as yet no general success has been met with here. Indeed in many cases, as a simplification, the *d* orbitals have been ignored. It is true that Pauling counted *d* electrons when he proposed metallic valences for the transition metals (3). However, the spatial constructions and the electron populations of the bands were not offered. Indeed, precisely because of a general lack of emphasis on the directive properties of the orbitals it has not been possible up till now to answer the simple structural question, "Why should a particular metal have one lattice rather than another?"

It would seem that a solution to the problem is implicit in the molecular orbital theory, particularly in view of recent developments in the ligand-field theory (4), and the work of Jaffe (5) and of Craig, Maccoll, Nyholm, Orgel, and Sutton (6, 7) on orbital pairs.

THE TRANSITION METALS

In the transition metals nine orbitals (one *ns*, three *np*, and five $(n-1)d$) are to be counted for each atom. To make a metal it is necessary to locate in space the nine orbitals of each of an infinite number of atoms in such a way that the orientations and the overlaps of every orbital become specified. The orbital constructions are to place the nuclei on lattice points. At the same time, through the overlap property, the orbital interactions that stabilize the lattice are established.

The number of valence electrons in the transition elements varies from 3 (s^2d^1) to 12 (s^2d^{10}). As bonding, antibonding, and non-bonding bands are, in general, to be expected from the orbital constructions, the net binding energy and hence the stability of the lattice will also be a reflection of the changing electron populations in these bands. It therefore becomes necessary to classify the energy levels of the several bonding, antibonding, and non-bonding bands, relative to each other, so that the valence electrons

[1]*Manuscript received July 31, 1958.*
Contribution from the Chemistry Department, Dalhousie University, Halifax, Nova Scotia.

can be placed and the populations in the bands calculated. That is, electron density and orbital overlap both become criteria for lattice stability.

THE ORBITAL CONSTRUCTIONS OF THE BANDS

The overlaps and symmetry relationships as between pairs of s, p, and d orbitals have been worked out in detail by several authors (5, 6, 7) and are summarized in Fig. 1. Removal of the restriction that the number of orbitals in overlap be limited to two permits more closely packed assemblies of these orbitals to be sought. When all orbitals have been so arranged, and consideration given to the numbers of electrons involved, lattice systems that reproduce the metallic lattices are obtained. The d, p, and hybrid orbitals become the orbitals that determine structure. The spherical s orbital, having no directional dependence, offers no choice between alternative close-packed structures. The results are summarized in Table I.

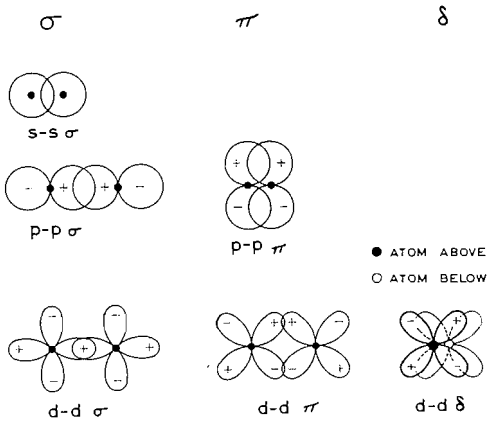

FIG. 1. Overlaps among orbital pairs.

TABLE I

Lattice systems and orbital assignments

Structure type	Orbital type	
	Bonding	Antibonding
1. *bcc*		
Nearest neighbors	s, p^3, $d\epsilon$	s'
Next to nearest	$d\gamma$	
2. *hcp*		
Nearest neighbors	s, d^5p, p^2 (or) sp^2, d^5p (or) sd^4p, p^2	
Next to nearest	d_z	d_z'
3. *ccp*		
Nearest neighbors	s, p^3, $d\epsilon$	$d\epsilon'$
Next to nearest	$d\gamma$	$d\gamma'$
4. Distorted *hcp*		
Nearest neighbors	sp^2, p	

1. *The p Orbitals*

The shape and the degeneracy of the orbitals provides a basis for choosing among alternative close-packed schemes. The p orbital construction shown in Fig. 2, in which each p orbital overlaps eight others, has three advantages. The arrangement can be

Can. J. Chem. Downloaded from www.nrcresearchpress.com by 190.90.36.8 on 09/04/12
For personal use only.

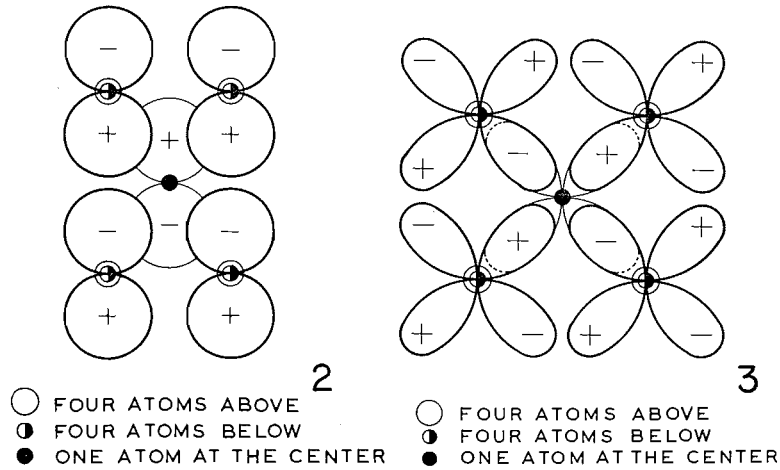

FIG. 2. The body-centered cubic p band.
FIG. 3. The body-centered cubic $d\epsilon$ band.

indefinitely and smoothly expanded, as more orbitals are added, to produce an indefinitely large and perfect body-centered cube. The arrangement has a threefold degeneracy, as the three mutually perpendicular directions are equivalent with $p_x(p_x)_8 = p_y(p_y)_8 = p_z(p_z)_8$. That is, the three p orbitals on each atom overlap the corresponding orbitals on the adjacent eight atoms in the same way. Finally, as an assurance that the overlap factor for the arrangement is favorable, the distance between the axes of the overlapping lobes is 0.81 the internuclear distance.

The result is that what will be called the *bcc* p band has cubic symmetry, is perfectly degenerate in the three p orbitals, is delocalized over all atoms in the lattice, and constitutes a close-packed assembly of p orbitals.

2. The d Orbitals

Turning to the d orbitals, it at once becomes evident that the degeneracy of the subshell cannot be retained in metallic bonding unless hybridization occurs, as all d orbitals cannot achieve the same overlap at the same time in any one lattice. The symmetry relationships for space-packing, however, separate the subshell into two groups of orbitals, the diagonal (d_{xy}, d_{xz}, d_{yz}) and the axial ($d_{x^2-y^2}$, d_{z^2}). Two different close-packed structures are possible for the diagonal orbitals. In the first of these, shown in Fig. 3, one orbital overlaps eight others. This configuration has the merit that each diagonal orbital becomes identically engaged, so that $d_{xy}(d_{xy})_8 = d_{xz}(d_{xz})_8 = d_{yz}(d_{yz})_8$, thereby preserving the degeneracy of the three orbitals and establishing a body-centered cubic lattice. In it the d band is delocalized over all atoms. The interlobar distance,[2] in this construction, is 0.58 the internuclear distance, a favorable feature for overlaps that is at least partly counterbalanced by the manner of approach of the orbitals. This is through the thickness of the lobes, much as in the d–$d\delta$ bonding of Fig. 1, which is not in the direction of maximum extension. The band will be called the *bcc* $d\epsilon$ band to conform with usage in the ligand-field theory (4). (The $d\epsilon$ level has also been called t_{2g} and γ^5.) The two remaining orbitals, $d_{x^2-y^2}$ and d_{z^2}, constitute the $d\gamma$ level.

A second way to close-pack d orbitals, shown in Fig. 4, places four orbitals around a central one. When the 3 diagonal orbitals on a central atom are so engaged, 12 atoms

[2]*The interlobar distance is the distance between the principal axes of the lobes.*

Can. J. Chem. Downloaded from www.nrcresearchpress.com by 190.90.36.8 on 09/04/12
For personal use only.

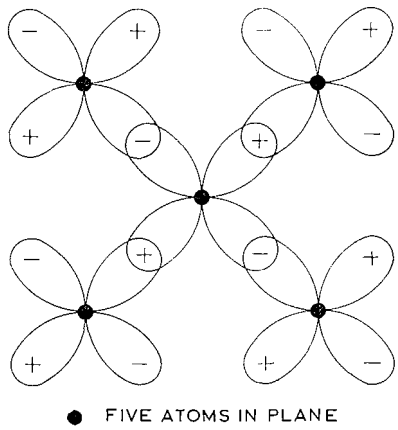

FIG. 4. The cubic close-packed $d\epsilon$ band.

surround the central one, in a cubic close-packed arrangement. That is, $d_{xy}(d_{xy})_4 = d_{xz}(d_{xz})_4 = d_{yz}(d_{yz})_4$, so the cubic close-packed $d\epsilon$ band, like the body-centered cubic $d\epsilon$ band, has cubic symmetry and is delocalized over all atoms. In each arrangement (i.e. *bcc* $d\epsilon$ and *ccp* $d\epsilon$) 2 *d* orbitals are still to be located. In both lattices, the direction of maximum extension of the $d\gamma$ orbitals ($d_{x^2-y^2}$, d_{z^2}) is identical with an octahedral arrangement of next nearest neighbors. The distance between the next nearest neighbors, as compared to the nearest neighbor distance, is 1.15 in *bcc* and 1.42 in *ccp*. In orbital constructions like that of Fig. 4 (for $d_{x^2-y^2}$, d_{z^2} has its maximum extension on the z-axis) these internuclear distances enable *bcc* $d\gamma$ to make a substantial minor contribution to the bonding,[3] whereas *ccp* $d\gamma$ is virtually non-bonding. The *bcc* $d\gamma$ will therefore support *bcc* $d\epsilon$ when fewer than five *d* electrons are present, but will weaken *bcc* $d\epsilon$ when more than five electrons are present. In the latter case, as antibonding levels in *bcc* $d\gamma$ become occupied, the cubic close-packed lattice with a *ccp* $d\epsilon$ band becomes preferred.

3. Hybrid Orbitals

Two hybrid orbital constructions lead to close-packed lattices. One of these applies to ground states between d^3 and d^7, which is just the gap left when orbital constructions based on the $d\epsilon$–$d\gamma$ split are employed. The second hybrid construction becomes relevant when the *d* subshell becomes non-bonding, as in s^2d^{10}.

The only hybrid sets that use four and five *d* orbitals and lead to close-packed structures are sd^4p and d^5p. In both of these 1×6 configurations, the bonding directions are towards the corners of a trigonal prism (8). When a set of identical atoms in this state are brought together a hexagonal close-packed lattice results, in which each atom is bonded to 6 neighbors through localized bonds, but is equidistant from 12, as shown in Fig. 5. The orbitals remaining after sd^4p or d^5p is chosen are accordingly to be placed with reference to the *hcp* system.

The last arrangement to be described is an sp^2 construction. The packing of sp^2 orbitals as in Fig. 6 sets up close-packed layers of atoms. The layers are bonded to each other

[3]*In view of the somewhat different shapes of the 2 orbitals it is possible that* $d\gamma$ *is not perfectly degenerate. A detailed analysis shows, however, that these orbitals also have small overlaps with nearest neighbors (the overlaps are small because of the orientations and shapes of the orbitals) that tend to make the two bonding functions equivalent. Therefore, although the band cannot be considered solely a next nearest neighbor band, it is possibly correct to describe it as a weakly bonding band with twofold degeneracy. It is also assumed in ligand-field theory (4) that* d_{z^2} *and* $d_{x^2-y^2}$ *remain degenerate in the* $d\gamma$ *level.*

Can. J. Chem. Downloaded from www.nrcresearchpress.com by 190.90.36.8 on 09/04/12
For personal use only.

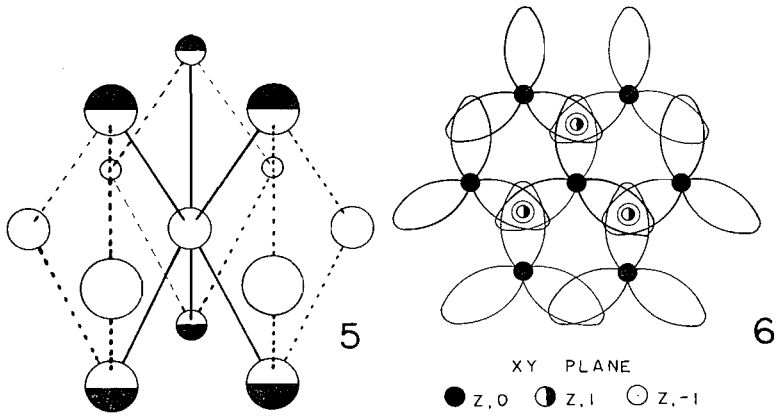

FIG. 5. The hexagonal close-packed hybrid band (sd^4p or d^5p).
FIG. 6. The distorted hexagonal close-packed sp^2 band.

through the p_z orbital, which provides a $p_z(p_z)_6$ band, and by a perpendicular delocalization in the three-center sp^2 molecular orbitals. A distorted hexagonal close-packed lattice appears, with six nearest neighbors in a layer, and three more distant ones above and three below. The electron cloud of the p_z band extends over the lattice but contains regularly spaced vacancies that have a definite shape. The superimposed sp^2 molecular orbitals through delocalization attain the shape of an endlessly repeated hour glass, with the thin part of the electron cloud between the layers and the thick part in the layer. The sp^2 band consists of an indefinite array of these, in parallel extension in a 1×6 packing, with each endless hour glass precisely occupying a vacancy in the electron cloud of the p_z band.

THE ATOMIC ORBITAL ENERGY LEVELS

An explanation of the properties of the transition metals should take account of both the spatial and the energy level properties of the orbitals. The foregoing consideration of the spatial problem gave rise to specific band systems with orbital constructions requiring one or another of four lattices, the body-centered cubic, the hexagonal close-packed, the cubic close-packed, and the distorted hexagonal close-packed. The energy level problem involves a consideration of both the atomic and molecular orbital energy levels. Complications arise here because of the likelihood that these levels change as the d subshell fills; as the principal quantum number varies; and in the molecular orbitals, as the band systems change. The atomic orbitals will be dealt with first.

An inspection of the ground states of the transition elements shows that the energy level of the $(n-1)d$ orbitals, which at first is above that of the ns orbital, as in s^2d^0, changes value until it is the stabler orbital, as in s^0d^9 and s^0d^{10}. This cannot be thought of as simply a regular increase in the stability of the d orbital as the d subshell fills, for energy is also contributed to the system in a non-linear way. Because of a lower electrostatic repulsive energy and a more favorable exchange energy among single electrons with parallel spins, states with the maximum number of singly filled orbitals are favored, as is well known from Hund's rule (4). As the magnitude of this energy term depends directly on the number of singly filled states, the d orbitals will be stabilized by increasing amounts as the number of valence electrons increases from one to six. Such a change is shown in the ground states of these atoms.

Can. J. Chem. Downloaded from www.nrcresearchpress.com by 190.90.36.8 on 09/04/12
For personal use only.

Valence electrons	Ground states
1	s^1d^0
2	s^2d^0
3	s^2d^1
4	s^2d^2
5	s^2d^3, s^1d^4
6	s^2d^4, s^1d^5

The number of single electrons, and hence the magnitude of the exchange energy contribution, must necessarily diminish upon the addition of further electrons. This will make the d levels fall more slowly after the six-electron atom than before it. However, the linear factor, associated with the increasing positive charge on the nucleus, still persists. The d levels are stabilized more than s because the $(n-1)d$ electrons are on the average closer to the nucleus than the ns. The d levels are therefore more directly affected by the increasing electrostatic field of the nucleus. At the same time, the $(n-1)d$ electrons intervene between the nucleus and the spherical electron cloud of the ns orbital. A screening effect occurs that tends to make the s electrons somewhat unresponsive to an increase in the charge on the nucleus. Both affects foresay a steadily increasing relative stability in the d orbitals as the subshell fills. This can also be seen in the ground states of the elements.

Valence electrons	Ground states
7	s^2d^5, s^1d^6
8	s^2d^6, s^1d^7
9	s^2d^7, s^1d^8, s^0d^9
10	s^2d^8, s^1d^9, s^0d^{10}
11	s^1d^{10}
12	s^2d^{10}

It is to be noticed that the d levels are unambiguously below the s level for the first time in the ground state, s^0d^9.

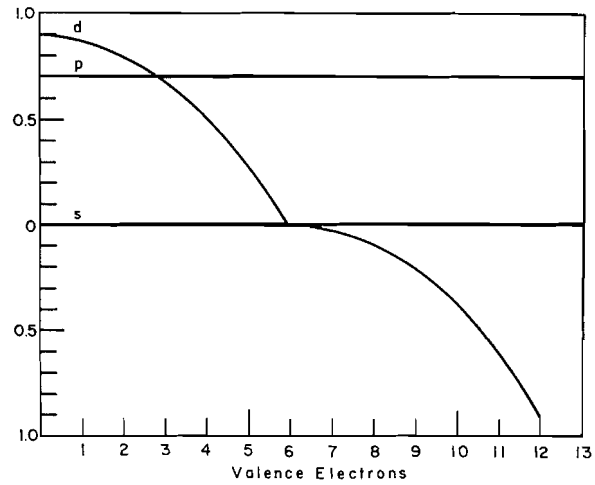

FIG. 7. Atomic orbital energy levels.

Can. J. Chem. Downloaded from www.nrcresearchpress.com by 190.90.36.8 on 09/04/12
For personal use only.

When the effects of filling the subshell are combined with the stabilizing property of single electrons in the subshell, a two-part curve as in Fig. 7 is forecast, which shows the change in the relative values of the energy levels as the number of valence electrons increases. When Fig. 7 was drawn, it was assumed that the d passes through the s level at six valence electrons (s^1d^5), and that d is just below p at three valence electrons (s^2d^1). As a simplification the two parts of the d curve were drawn to repeat each other.[4]

THE METALLIC BANDS

For an adequate description of the bands in a metal, in addition to the energy levels of the atomic orbitals and the orbital construction of the bands, it is necessary to know the binding energy and the density of states in the molecular orbitals that comprise the bands. Delocalized, localized, antibonding, and non-bonding bands are to be considered.

TABLE II

Electron populations in the bands of the transition elements

Element		Band populations							
		Bonding							
Valence electrons	Lattice system	s band	p band*	$d\epsilon$ band	$d\gamma$ or d_z band†	hybrid bands‡	Anti-bonding bands§	Non-bonding bands‖	Valence, net-bonding electrons
1	*bcc*	0.775	0.225						1.0
3	*bcc*	1.00	0.96	1.02			0.02		2.96
4	*bcc*	1.00	1.02	1.69	0.24		0.05		3.90
5	*bcc*	1.00	0.92	2.18	0.90				5.00
6	*bcc*	0.92	0.66	2.76	1.68				6.00
6	*hcp*	0.12				5.88			6.00
7	*hcp*		0.37		0.63	6.0			7.00
8	*hcp*		0.50		1.0	6.0	0.50		7.00
9	*ccp*	0.97	0.81	3.0	2.0		2.21		4.57
10	*ccp*	0.99	0.89	3.0			1.12	4.0	3.76
11	*ccp*	1.0	1.00	3.0			2.00	4.0	3.00
12	dis. *hcp*		0.33			1.67		10.0	2.00

*Threefold degeneracy in cubic lattices; twofold in *hcp*; onefold in distorted *hcp*.
†$d\gamma$ and d_z are next nearest neighbor bands in cubic and hexagonal systems respectively.
‡sd^4p for 6 electrons; d^5p for 7 and 8; sp^2 for 12.
§s' for 3 and 4 valence electrons; d_z' for 8; $d\epsilon'$ and $d\gamma'$ for 9 (see Fig. 9).
‖$d\gamma$ for 10 and 11 valence electrons; d^{10} for 12.

1. The Delocalized Bands

Bands in which electrons are delocalized over all atoms have been constructed from s, p, and d orbitals and, with a more limited delocalization, from sp^2 orbitals. These delocalized bands are specific cases satisfying the principal conditions for the classic Bloch molecular orbitals (1). The width of the bands, which is the separation between the lowest and the highest state in the band, and the level of the lowest lying state are to be obtained.

[4]*It is to be noted that Fig. 7 has been drawn independently of the principal quantum number. The assumption that the relative levels of the ns, np, and (n−1)d atomic orbitals are independent of n is certainly not correct. Figure 7 therefore becomes an average curve that need not be precisely correct for any element. The electron population values in Table II depend on Fig. 7 and therefore contain a substantial probable error. They are given to three significant figures, however, as this helps to keep the adding neat.*

Can. J. Chem. Downloaded from www.nrcresearchpress.com by 190.90.36.8 on 09/04/12
For personal use only.

Can. J. Chem. Downloaded from www.nrcresearchpress.com by 190.90.36.8 on 09/04/12
For personal use only.

It is convenient, though not entirely correct (see later for a rule of thumb), to assume that the density of states is uniform in delocalized bands made up of overlaps from among nearest neighbors. The phenomena of width in the band arises from the delocalization property. As the wave function for each electron extends over all nuclei incorporated in the delocalized wave function, and as no two electrons can be identical, successive electrons must lie in states that are distinguishable in the energy parameter. Consequently the density of states has a relation to the effectiveness of the delocalization property. In the multiple overlaps encountered in the prescribed orbital constructions, delocalization is measured by both the number of overlaps an orbital has, and by the magnitude of the overlap volume. The bands made up from orbitals in close-packed arrangements can be expected to be somewhat similar in both these regards. For the d orbitals it may be recalled that delocalized bands were found among both nearest neighbors (*bcc* $d\epsilon$ and *ccp* $d\epsilon$) and next nearest neighbors (*bcc* $d\gamma$ and *ccp* $d\gamma$). In these cases of nearest and next nearest neighbor bands, both the density of states and the binding energy must vary, with internuclear distance as the most direct parameter.

In detailed calculations (2) for the alkali metals it has been shown that both s and p states are populated in Li and Na. As there is only one valence electron in these metals it is necessary to conclude that upper states in the s band lie above lower states in the p band. Using the assumption of uniform density of states and remembering the threefold degeneracy of the *bcc* p band, an electron population chart as in Fig. 8 can at once be drawn. The separation between the s and p band heads, which is the only independent adjustment, has been arbitrarily chosen so that the s and p band populations become 0.775 and 0.225 electrons respectively.[5] Counting the degeneracy, this amounts to 0.775 and 0.075 electrons per orbital for the s and p orbitals respectively. This arbitrary decision is not unimportant. For it, along with the assumption of uniform density of states, at once defines the energy separation between s and p atomic orbitals in units of the width of a nearest neighbor delocalized band. This can be seen by comparing the ordinates of Figs. 7 and 8. Specific population figures did not appear in the calculations for the alkali metals referred to above. Pauling (9) has used the value 0.1 for the p orbital population in Li. A somewhat larger value was chosen here in the expectation that the energy separation between the atomic orbitals decreases as the principal quantum number increases. Such a trend would require a more important p orbital participation in the heavier alkali metals than in Li.

2. The Localized Bands

Band systems that retain more than a threefold degeneracy in the d orbitals set up an hexagonal close-packed lattice. In this lattice, both the d^4sp and d^5p hybrid configurations gave rise to orbital-pair overlaps between nearest neighbors, with the result that the bonding electrons became localized on pairs of nuclei. As in the ordinary convention for electron-pair covalent bonds, these spatially independent states are here assumed to be without appreciable effect on each other. That is, all such states exist at the same energy level. For purposes of definiteness, the discrete energy levels of the d^5p and of the sd^4p bands have been taken from the weighted average of the energy levels of the band heads of the delocalized s, p, and d bands. The decision, in so far as its correctness is concerned, could affect electron population calculations only in the case of one modification of the six-electron atom, Table II.

It should perhaps be mentioned that in another hybrid construction, that of the sp^2

[5]*See footnote 4.*

configuration in a distorted hexagonal close-packed lattice, a localization property also appears when the electron population is equal to or in excess of 0.66 electrons per orbital. Then bonding electron pairs can be associated with nuclear triads. The electron population was less than 0.66 per orbital in the 12 (or 2) valence electron atoms considered here.

3. The Antibonding and the Non-bonding Bands

The antibonding bands are identified with the corresponding bonding bands through the assumption of uniform density of states, and through the requirement that the binding energies of the bonding and antibonding states be equal and opposite. For electron population purposes, the bonding and antibonding bands then become a single

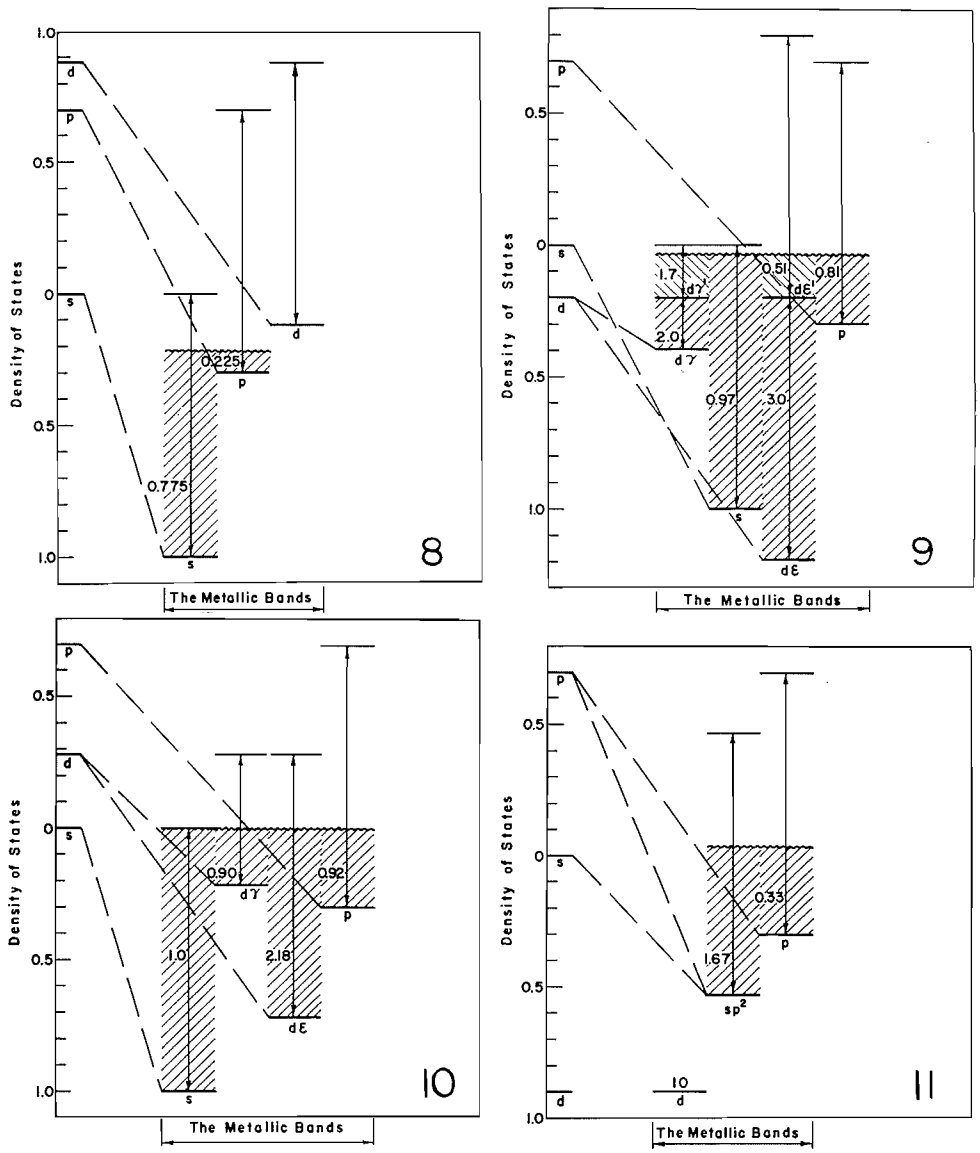

FIG. 8. Electron population chart for 1-electron atoms.
FIG. 9. Electron population chart for 9-electron atoms.
FIG. 10. Electron population chart for 5-electron atoms.
FIG. 11. Electron population chart for 12-electron atoms.

Can. J. Chem. Downloaded from www.nrcresearchpress.com by 190.90.36.8 on 09/04/12
For personal use only.

system of uniformly separated states, divided into equivalent bonding and antibonding portions by the energy level of the (non-bonding) atomic orbital. This can be seen in the electron population chart, Fig. 9, where bonding ($d\epsilon$, $d\gamma$) and antibonding ($d\epsilon'$, $d\gamma'$) bands are shown.

The symmetrical disposition of the bonding and antibonding states about the level of the non-bonding atomic orbital includes two variations that have a general significance. One points up the distinction to be made between nearest and next nearest neighbor bands; the other corresponds with a transition from localized to delocalized bands. Either the binding energy can decrease, which tends to compress the bonding and antibonding bands into a narrower region about the non-bonding level; or, if a decrease in delocalization occurs, both bonding and antibonding bands are compressed away from the non-bonding level towards their own lower and upper states, respectively. In each of these cases, the density of states is altered, though in the same way in both bonding and antibonding bands.

The next nearest neighbor bands, *bcc* $d\gamma$, *ccp* $d\gamma$, and *hcp* d_z, with internuclear distances of 1.15, 1.41, and 1.62 respectively, provide an example in which binding energies progressively decrease, compared to nearest neighbor bands like *bcc* $d\epsilon$ and *ccp* $d\epsilon$ where the internuclear distance is unity. In view of the proximity (overlap) there is a decrease in the resonance integral. The density of states must therefore necessarily increase as the internuclear distance increases conceivably until, when the internuclear distance is large enough, the atomic orbital is non-bonding and single states are achieved. By associating the levels of the band heads with the internuclear distance,[6] the density of states in *bcc* $d\gamma$ becomes twice, in *ccp* $d\gamma$ 5, and in *hcp* d_z 10 times that in nearest neighbor bands. As *bcc* $d\gamma'$ attains no antibonding population, for the lattice becomes unstable before antibonding electrons appear, the decision affects antibonding electron populations only in the eight and nine valence electron elements. The first antibonding electrons are absorbed by *hcp* d_z' and *ccp* $d\gamma'$. Once these bands are filled, creating in conjunction with *hcp* d_z or *ccp* $d\gamma$ the equivalent of one or two filled non-bonding d orbitals respectively, the question of the density of states in bands with different binding energies no longer affects the population figures.

A change in the delocalization factor may also occur more gradually than is implied in the assumption of the two extremes of delocalized and localized bonds. This is already indicated in the appearance of orbital constructions in which single orbitals overlap varying numbers of others (as for example eight in *bcc* $d\epsilon$, six in the distorted *hcp* p band, and four in *ccp* $d\epsilon$, compared with one in a localized bond) while still retaining the delocalized property. If delocalization were subject to such a continuous diminishment, its effect on the electron population figures would be real, though small, and found mostly in the 8-, 9-, and 10-electron atoms. If, for example, *ccp* $d\epsilon$ and *ccp* $d\epsilon'$ (because of the four co-ordination in their orbital constructions) were to some extent compressed away from the non-bonding level while *bcc* $d\epsilon$ and *bcc* $d\epsilon'$ (with eight co-ordination) were not, minor changes in the population of the antibonding *ccp* $d\epsilon'$ would result. The largest effect occurs when the *ccp* $d\epsilon'$ band is just beginning to be occupied, as in atoms with nine valence electrons, the correction tending to eliminate itself as more electrons are added.

The antibonding levels associated with the localized bonding orbitals achieve no significant population. It is therefore not necessary to specify them closely at this time.

THE FOUR LATTICES

The methods that have been outlined assume to predict both the lattice a transition

[6]*Approximately inversely proportional to the third power of the internuclear distance.*

Can. J. Chem. Downloaded from www.nrcresearchpress.com by 190.90.36.8 on 09/04/12
For personal use only.

element elects, and the electron population of the bands in that lattice. The predicted and the known lattices can be compared at once. Experimental values for electron populations are, however, not available, so the validity of the calculated populations cannot be properly assessed. In what follows a few words will be said about each metallic lattice.

1. The Body-centered Cubic Lattice

The band system for the body-centered cubic lattice consists of an s band, a p band (Fig. 1), and two d bands. The *bcc* $d\epsilon$ band has threefold degeneracy, and begins at a lower level than the *bcc* $d\gamma$ band which is a next nearest neighbor band, with twofold degeneracy.

In atoms with one valence electron, the electron population is confined to the s and p bands, Fig. 8. With an increase in the number of valence electrons, not only must more electrons be placed, but the energy level of the d orbitals falls relative to the s and p as shown in Fig. 7. In atoms with five valence electrons, the d orbitals may be fairly said to dominate the structure, holding 3.08 of the five electrons, Table II and Fig. 10. The important changes that occur in the band system as the valence electron count increases from three to six are the disappearance of a small antibonding population, a regular increase in the $d\epsilon$ population, and a relatively more rapid increase of the electron density in the $d\gamma$ band. These features combine to give the lattice its limited stability range.

It is evident that in any band system the upper levels make a smaller contribution to the binding energy than do the lower states. Moreover, in systems in which the band pattern changes because of changes in the symmetry of the orbital constructions, it follows that maximum binding energy and consequently a stable lattice corresponds with those constructions that provide a maximum population in the low-lying states. It is suggested as a rule of thumb for these multiple overlap systems that a stable lattice corresponds with an electron density of $2/m$ in the bonding orbitals. Here m is the number of lobes (not orbitals) in mutual overlap.

The rule of thumb may have some validity as a delocalization factor, though it is not in this sense that it will be applied. It is taken as a generalization of the delocalization observed in lone pairs and covalent bonds where m, the number of lobes that overlap, is 1 and 2 respectively, the electron density is 2 and 1 as is in each case required by the rule of thumb. In application to the multiple overlap systems, with m equal to 5 in the p band, 3 in the *bcc* $d\epsilon$ band, and 2 in the *ccp* $d\epsilon$ band, the rule of thumb electron densities become 0.4, 0.66, and 1.0 respectively. In so far as it has significance as a delocalization factor, the rule of thumb implies that the density of states in the respective bands differs in such a way as to make their lattice constructions stable, compared to alternate arrangements, at the prescribed electron density. If this is the case, the rule of thumb describes a limitation to the assumption of uniform density of states in the delocalized bands. It will actually be used, however, in a rather more rough and ready sense than this in what follows. In any event it should be noted that the rule of thumb does not apply, as an indicator of lattice stability, to the s orbitals, for this band does not determine structure.

Both the *bcc* $d\epsilon$ and the *ccp* $d\epsilon$ orbital constructions can be applied to atoms with three, four, five, or six valence electrons. The differences in the electron population charts for the two lattice systems, at any rate under the present assumptions, are entirely due to the difference, not in *bcc* $d\epsilon$ and *ccp* $d\epsilon$, but in *bcc* $d\gamma$ and *ccp* $d\gamma$. As *bcc* $d\gamma$ (at 1.15 the internuclear distance) provides more binding energy than *ccp* $d\gamma$ (at 1.41 the internuclear distance) the *bcc* $d\gamma$ band begins at a lower level. The effect of this is to increase the total number of d electrons lying at low and intermediate levels in the *bcc* bands, as compared with *ccp*, where the uppermost energy levels would have to be occupied as well. The concentration of electrons in the stabler states occurs whenever the *bcc* $d\gamma$

Can. J. Chem. Downloaded from www.nrcresearchpress.com by 190.90.36.8 on 09/04/12
For personal use only.

band shows a population, which is in the four-, five-, and six-valence electron atoms, Table II. Consequently, the *bcc* lattice can be chosen over the *ccp* lattice unambiguously only for the four-, five-, and six-electron atoms. The over-all result is that the *bcc* $d\gamma$ band keeps the electron density of the *bcc* $d\epsilon$ band in the vicinity of 0.66, which is the rule of thumb density for *bcc d* (0.34, 0.56, 0.73, and 0.92 are the calculated values for the three-, four-, five-, and six-electron atoms respectively). The electron density in the *p* band is also close to the 'best' value, 0.4, except in the six-electron atom (0.32, 0.34, 0.31, and 0.22 in the three-, four-, five-, and six-electron atoms respectively).

There is no $d\gamma$ population in the three-electron atom. It is therefore not possible to make a choice between the *bcc* and *ccp* lattices for this element on the proffered grounds. Moreover, the antibonding population appearing when *bcc* is elected (Table II) and the relatively small *d* population, together indicate that the band system for the three-electron atom is apt to be different in detail from those of the other transitional elements. However, a close-packed metal can evidently be obtained.

A *d* band population of 4.54 electrons is calculated for the *bcc* system for the six-electron atom. Of this, 1.68 electrons are in the relatively weakly binding $d\gamma$ band. The result is that at this stage a concentration of electrons is beginning to build up in the less stable upper levels of the *d* band. This is to be expected as the principal *d* band has only threefold degeneracy, and at least four *d* electrons are available for bond formation. Instability features are also shown in the deviation of the *p* and *d* electron densities from the rule of thumb values. However, when the alternate band system for the six-electron atom, which employs a hexagonal close-packed lattice, is charted, an instability feature also appears in it. The d^5p band, a system of localized electrons, is incompletely occupied, Table II. It is therefore necessary to predict that an atom with six valence electrons will show two forms, one with a *bcc*, the other with an *hcp* lattice. The predictions therefore are that transition elements with four, five, and six valence electrons have a *bcc* lattice, as is in fact the case for βTi, βZr, V, Cb, Ta, αCr, Mo, and αW.

2. The Hexagonal Close-packed Lattice

The hexagonal close-packed lattice emerges as a consistent choice for elements with six, seven, or eight valence electrons, although the band systems that establish the lattice are subject to minor variations within this group. With both sd^4p and d^5p providing trigonal hybrids, either configuration will establish an *hcp* lattice. The difference between the two will therefore be small depending for the most part on whether an *s* band (with d^5p) or a d_z band (with sd^4p) is to be found in the lattice. The *p* band is doubly degenerate in either case, though a third alternative, that of a delocalized sp^2 band (in connection with d^5p), is also possible. These three alternatives correspond to rather slight changes in the over-all electron population picture, being confined to minor variations in the electron density and direction dependence property of the conductivity bands. In no case is the lattice affected, at any rate with respect to its classification as *hcp*. The electron population calculations, Table II, were made for d^5p in the case of the six-electron atoms, and for sd^4p for the seven- and eight-electron atoms.

In addition to the appearance of localized bonds, an important antibonding population also appears for the first time in this group of elements. The precise value of this population depends on the level selected for the d_z band which, like *bcc* $d\gamma$ and *ccp* $d\gamma$, is a next nearest neighbor band. The distance in d_z is 1.6 the nearest neighbor distance, so that the band would be expected to be less effective than either of the $d\gamma'$. The antibonding population is confined to the *d* orbitals and, under the assumptions used, is not quite equivalent to having an electron pair in a non-bonding d_{z^2} orbital in the eight-electron atom. In the latter case, the net-bonding electrons would be lowered from 7.0 to

Can. J. Chem. Downloaded from www.nrcresearchpress.com by 190.90.36.8 on 09/04/12
For personal use only.

6.0. The prediction of an *hcp* lattice for the six-, seven-, and eight-electron atoms is borne out in the elements Mo, Tc, Re, Ru, and Os. Manganese and iron are exceptions and will be referred to again.

3. The Cubic Close-packed Lattice

Atoms with 9, 10, and 11 valence electrons satisfy the conditions for the *ccp* band system, Fig. 9. The transformation to the *ccp* lattice occurs when an extra electron is added to the *hcp* system. The ninth electron, going into the antibonding *d* levels of the *hcp* system would produce the near equivalent of two filled non-bonding *d* orbitals in that system. As a result, neither d^5p nor sd^4p can be constructed, and the *hcp* lattice is destroyed. At 9 electrons in the *ccp* system the $d\gamma$ band is nearly non-bonding, and becomes so at 10 electrons. The *ccp* $d\epsilon$ remains, and with an electron density of one electron per orbital provides the *d* orbital contribution to the binding energy and determines the structure.

The antibonding levels that are occupied as electrons are added to the *ccp* system are altogether in the *d* orbitals, with the increase for the most part to be found in the triply degenerate *ccp* $d\epsilon'$ band. That is to say, the bonding *s* and *p* and the antibonding *d* levels have approximately the same energy throughout this triad. The over-all result, going from 9 to 11 electrons in the *ccp* system, is to steadily diminish the net contribution of the *d* orbitals to the binding energy and the lattice. At 12 electrons the *d* orbitals have become altogether non-bonding, with 3 electrons in $d\epsilon'$ balancing 3 electrons in $d\epsilon$. Counting the non-bonding $d\gamma$, the non-bonding $d\epsilon$ now restore a fivefold degeneracy to the *d* orbitals. That is to say, at 12 electrons, the *d* subshell has become a part of the inner core. The prediction of a cubic close-packed lattice for 9-, 10-, and 11-electron atoms is observed without exception in these elements, namely Co, Rh, Ir, Ni, Pd, Pt, Cu, Ag, Au. The fact that αCo is *hcp* will be mentioned again.

4. The Distorted Hexagonal Close-packed Lattice

As described above, the 12-electron atom (speaking in valence terms) becomes a 2-electron atom, as the *d* levels are fully occupied and non-bonding. The band system projected for the 12-electron atom, Fig. 11, is therefore in principle also applicable to the 2-electron elements, Be and Mg. The only differences to be expected are those that can be associated with the principal quantum number. This band system is, however, incompatible with the two-electron elements, Ca, Ba, and Sr. These elements have vacant *d* levels, which by taking electrons away from the sp^2, *p* bands, permit quite different electron distributions and orbital constructions. It is therefore correct to predict a distorted hexagonal close-packed lattice for Be, Mg, Zn, and Cd, as is observed. It is also correct to predict that Ca, Ba, and Sr will not have the same distorted *hcp* lattice. (Ca, Sr, and Ba have cubic lattices.)

DISCUSSION

When the antibonding population is subtracted from the bonding population a figure giving the net number of bonding electrons is obtained, Table II. As this number sums up only the electron populations of the several bands, and as the properties and electron dependencies of the bands differ, the number of net-bonding electrons by no means shows all the significances of the band systems. For example, if the property of plasticity were to be judged from changes in overlap accompanying nuclear displacements that do not alter internuclear distances, the *s* band would be plastic, the *d* bands hard. Moreover, as the character of the overlaps are different in the different *d* bands, the band populations do not always correctly evaluate the relative magnitude of even so specific

Can. J. Chem. Downloaded from www.nrcresearchpress.com by 190.90.36.8 on 09/04/12
For personal use only.

a property. As another example, the p band has consistently the lowest ionization potential and the lowest electron density (about 0.33 electrons per orbital) and may for these reasons be principally responsible for the properties of conductivity and paramagnetism in these metals. Nevertheless, other delocalized bands may on occasion also make important contributions to these two properties, as for example the d bands in the five-electron atoms.

In a more general way as well numbers for net-bonding electrons have less significance than the itemized list of their parts. This arises from the condition that in band systems electrons occupy successive levels and do not therefore all make the same contribution to the binding energy. This is possibly of most importance when the antibonding levels are just beginning to be occupied (the seven-, eight-, and nine-electron atoms). As the lowest levels of both bonding and antibonding bands are filled first, the net contribution to the binding energy of a bonding and antibonding band exactly cancel only when both bands are fully occupied. When the antibonding band is not completely full, it still cancels out a numerically equivalent population. To be correct from the binding energy point of view, however, the upper more weakly binding states in the bonding band are the ones to be selected. That is, the stablest states remain and give a binding energy contribution that is underemphasized in a number that by implication describes average electrons.

Whatever their deficiencies, it is nevertheless these numbers for net-bonding electrons that have the simplest correspondence with the concept of a numerical valence. They are therefore to be compared with the metallic valences proposed by Pauling (3) for the transition elements.

Valence electrons	1	2	3	4	5	6	7	8	9	10	11	12
Pauling's valence	1	2	3	4	5	6	6	6	6	6	5.5	4.5
Net-bonding electrons	1	2	3	3.9	5	6	7	7	4.6	3.8	3.0	2.0
Integral valence	1	2	3	4	5	6	7	6	5	4	3	2

It is evident that agreement is good until elements with an important antibonding population are encountered. In atoms with seven and eight valence electrons, the very weakly binding d_z band is being occupied. As it holds 0.6 and 1.0 binding electrons in the two elements respectively, the number 7 rather overestimates the effective situation. Also, in the atoms with 9 and 10 valence electrons, rather more than a justifiable weight is given to the antibonding population in $ccp\ d\epsilon'$, as has been mentioned. This cannot have a greater effect than to provide values for an 'average' valence of 5.0 and 4.0 for these elements respectively. In brief, that is, the concept of an integral valence can in fact be justified as a reasonable approximation to the net-bonding electron values, as shown above. Even with such adjustments to average values, a significant departure from the metallic valences proposed by Pauling for atoms with 9, 10, 11, and 12 valence electrons still remains. As additional support for the net-bonding electron values presented in this paper, their correspondence with conventional chemical valences for these elements may be pointed out. Moreover, the physical and chemical relationships that are evident in the series of elements, Be, Mg, Zn, and Cd strongly suggest divalent atoms throughout.

Lattice structures and band populations are the predictions made in this paper. Factual comparisons are possible for the lattices, but band populations have not yet been measured. Even in the comparison that is possible some ambiguity remains. For it is conceivable that a specific lattice and particularly a close-packed one can be set up from more than one set of orbital constructions, as was indicated in the case of the hexagonal

Can. J. Chem. Downloaded from www.nrcresearchpress.com by 190.90.36.8 on 09/04/12
For personal use only.

close-packed lattice. Agreement with respect to the lattice does not, therefore, necessarily prove the correctness of the orbital constructions. The corollary is also ambiguous. If a lattice is incorrectly predicted for one member of a family, it does not necessarily follow that the orbital constructions are wrong for the other members, though they must of course be wrong in the specific case.

Of the 30 transition elements, the lattices of Mn and Fe (and Hg) were incorrectly forecast. This deviation from expectations corresponds with the appearance of the property of ferromagnetism in the transition elements and may therefore have a somewhat special significance. The assumption, implied by the application of the population figures to all elements in a subgroup, that the relative levels of the ns, np, and $(n-1)d$ atomic orbitals are independent of n is certainly not altogether correct. A general expectation is that the separations become smaller as n becomes larger. Secondly, the overlaps in the n type and $(n-1)$ type bands are apt to have different magnitudes, even among near neighbors. This has a direct bearing on the binding energies and also on the density of states if the bands are delocalized. It is known that the ratio of the radii of the $(n-1)$ to the n shell has its smallest values in the first transitional period, and in that period the minimum occurs at Fe. Taken together, these two factors, the decreasing separation between the atomic orbital energy levels and the increasing relative radius of the $(n-1)d$-orbitals as n increases, imply that the $(n-1)d$ orbitals become consistently more important to the binding energy with larger values of the principal quantum number. This accounts for the singular observation that the melting and boiling points of transition metals (with 4 to 10 valence electrons) invariably increase, while the melting and boiling points of non-transitional metals invariably decrease, with increases in n (atoms with 3 and 11 valence electrons are intermediate in this respect: Zn, Cd, and Hg fall into the non-transitional group with Be and Mg).

As it happens, the impact of what might be called these n-type variations have their maximum effect precisely at the elements Mn, Fe, and Co. Moreover, as the antibonding d bands are here just beginning to be occupied, the disposition of bonding and antibonding electrons will, at the same time, be most responsive to these changes. That is, both the cause and the response to the cause are maximal at Mn, Fe, and Co, among the transition elements. The problem becomes therefore to relocate the orbitals in these elements as specific cases (Fe has four lattices; Mn, three; and Co, two) and discover thereby, in the particular instances of αFe and αCo, the location and properties of the ferromagnetic orbitals, presumably resident in the $(n-1)d$ band.

ACKNOWLEDGMENTS

The author would like to thank the Department of Mines and the University of Toronto for their accommodations during a Sabbatical Year. Special thanks are due Professor Maurice Lister, who was kind enough to read the manuscript in draft form.

REFERENCES

1. Bloch, P. Z. Physik. **52**, 555 (1928).
2. Brooks, H. Theory of alloy phases. Am. Soc. Metals, Cleveland. 1956. pp. 199–220.
3. Pauling, L. Theory of alloy phases. Am. Soc. Metals, Cleveland. 1956. pp. 220–242.
4. Griffith, J. S. and Orgel, L. E. Quart. Revs. **10**, 381 (1957).
5. Jaffe, H. H. J. Phys. Chem. **58**, 185 (1954).
6. Craig, D. P., Maccoll, A., Nyholm, R. S., Orgel, L. E., and Sutton, L. E. J. Chem. Soc. 332 (1954).
7. Craig, D. P., Maccoll, A., Nyholm, R. S., Orgel, L. E., and Sutton, L. E. J. Chem. Soc. 354 (1954).
8. Kimball, G. E. J. Chem. Phys. **8**, 188 (1940).
9. Pauling, L. Proc. Roy. Soc. A, **196**, 343 (1949).

Can. J. Chem. Downloaded from www.nrcresearchpress.com by 190.90.36.8 on 09/04/12
For personal use only.

Can. J. Chem. Downloaded from www.nrcresearchpress.com by 190.90.36.8 on 09/04/12
For personal use only.

THE KINETICS OF THE EVOLUTION AND DISSOLUTION OF HYDROGEN AT ELECTRODES[1]

J. O'M. Bockris and H. Mauser

INTRODUCTION

The kinetics of the electrolytic evolution of hydrogen at electrodes have been treated previously only in an approximate way (Frumkin (1) and Bockris and Potter (2)); or upon the assumption that only one step influences the reaction rate (Parsons (3)); or without regard to H coverage (Vetter (4)). In the work reported here, a rigorous treatment of the kinetics of two probable paths for cathodic and anodic reactions of hydrogen at electrodes is developed, with attention to the evaluation of quantities which are open to experimentation and have values specific to certain reaction mechanisms.

GENERAL

The concept of a rate-determining step for a given path in electrode kinetics is regarded as follows. General equations are deduced for the velocity of the given reaction by way of a chosen path, and the current density at the electrode for a given overpotential can thence be expressed as a function of a number of electrochemical rate constants characteristic of steps within the path. Relations among these rate constants are then found which lead to a current density which depends, at constant overpotential, only upon *one* rate constant, k_p. The relations among the rate constants which give rise to this special case are then regarded as the condition for the over-all reaction to have a rate-determining step, p.

The conditions to provide a given rate-determining step can be deduced in terms of chemical (potential-independent) rate constants, or two types of electrochemical (potential-dependent) rate constants.

Thus,

$$\bar{k}_p = k_p \, e^{\pm \beta \Delta\phi \; zF/RT} \qquad [1]$$

where $\bar{k}_p$ is the electrochemical rate constant for a reaction involving the transfer of a charge z at a current density (c.d.) of i, $0 < \beta < 1$, $\Delta\phi$ is the Galvani p.d. between metal and solution; and k_p is the corresponding chemical rate constant. The reversible electrochemical rate constant is then

$$\bar{k}_{p,R} = k_p \, e^{\pm \beta \Delta\phi_R \; zF/RT} \qquad [2]$$

i.e., it is the value of $\bar{k}_p$ at the reversible potential.

Then,

$$\bar{k}_p = \bar{k}_{p,R} \, e^{\pm \beta \eta \; zF/RT} \qquad [3]$$

where η is the overpotential associated with the c.d., i.

A. Reaction Paths Considered

Likely paths for the hydrogen evolution reaction have been discussed (Bockris (5) and Breiter (6)). Here, the kinetics of only the two most probable paths will be considered; they differ only by the reaction in which hydrogen is desorbed.

[1]*Manuscript received September 6, 1958.*
Contribution from the John Harrison Laboratory of Chemistry, University of Pennsylvania, Philadelphia, Pennsylvania, U.S.A. This paper was prepared for presentation at the Symposium on Charge Transfer Processes held at the University of Toronto, Toronto, Ontario, September 4 and 5, 1958 (see Can. J. Chem. **37**, *120 (1959)).*

(*i*) *The Electrochemical Desorption Path* (*Kobosew and Nekrassow, 1930*)

Protons are discharged onto free sites* on the metal surface. The resulting chemisorbed hydrogen is desorbed to form a hydrogen molecule upon discharge onto it of a further proton. Conversely, hydrogen molecules adsorb on the electrode surface to form one adsorbed hydrogen atom and a proton in solution, the latter also being formed by the dissolution of chemisorbed hydrogen atoms.

(*ii*) *The Hydrogen Atom Combination Desorption Path* (*Tafel, 1903*)

Protons are discharged onto free sites. The resulting chemisorbed hydrogen atoms combine to form molecules. In dissolution, hydrogen molecules adsorb dissociatively on free sites on the electrode surface, each molecule forming two chemisorbed atoms. These dissolve, forming protons in solution.

The common step in both paths of the evolution reaction is the discharge of protons (Smits (7), Bowden and Rideal (8), Baars (9), and Erdey-Grúz and Volmer (10)). Proton discharge may occur either from hydroxonium ions or from water, the latter source of protons being probable only in alkaline solutions (Parsons and Bockris (11) and Poltorak (12)).

Each of the above-mentioned steps may become the rate-controlling step in either hydrogen evolution or dissolution. Because of the dependence of electrochemical rate constants upon potential, the rate-determining step may change with current density for a given electrode–solution system.

The following assumptions are made. (i) The systems considered have reached a stationary state. (ii) The symmetry factors (cf. Bockris (13)) involved in various charge-transfer partial reactions have the same value. (iii) H is chemisorbed on the electrode surface (and does not dissolve into the metal at an appreciable rate). (iv) There is no lack of supply of ions in solution to the electrode.

B. The Electrochemical Desorption Path

(*i*) *General Equations*

The reactions are

$$[4] \qquad H^+ + e_0^- \underset{-1}{\overset{1}{\rightleftharpoons}} MH$$

$$[5] \qquad H^+ + MH + e_0^- \underset{-2}{\overset{2}{\rightleftharpoons}} H_2$$

where MH represents hydrogen atoms, chemisorbed on the metal surface.

Assuming a Langmuir isotherm,†

$$[6] \qquad v_1 = k_1(1-k'c_H)c_{H^+}\, e^{-\beta\Delta\phi\, F/RT}$$

$$[7] \qquad v_{-1} = k_{-1}c_H\, e^{(1-\beta)\Delta\phi\, F/RT}$$

$$[8] \qquad v_2 = k_2c_Hc_{H^+}\, e^{-\beta\Delta\phi\, F/RT}$$

$$[9] \qquad v_{-2} = k_{-2}p_{H_2}(1-k'c_H)\, e^{(1-\beta)\Delta\phi\, F/RT}$$

where k' is a constant, such that $k'c_H$ is the fraction of surface covered with chemisorbed

**Free sites means here those not already occupied by hydrogen atoms.*

†If a logarithmic, and not a Langmuir, isotherm were used, a different general expression for the over-all current density would be obtained. However, the results at limitingly low, and limitingly high, degrees of surface coverage would be almost the same as those obtained here; and it is these limiting conditions which are most commonly needed in the use of relations between current density and, e.g., potential, as criteria of mechanisms.

Can. J. Chem. Downloaded from www.nrcresearchpress.com by 190.90.36.8 on 09/04/12
For personal use only.

H at a given c.d., c_{H^+} is the hydroxonium ion concentration in the Helmholtz double layer; and other terms are as already defined.

In the steady state, the over-all velocity, v, is given by

[10] $$v = v_1 - v_{-1} = v_2 - v_{-2}.$$

Eliminating c_H and remembering that the current density is related to v by

[11] $$i = 2F\,v/\nu$$

where ν is the stoichiometric number,

[12] $$i = \frac{2F}{\nu}\,\frac{\bar{k}_{1,R}\bar{k}_{2,R}c^2_{H^+}\,e^{-2\beta\eta\,F/RT} - \bar{k}_{-1,R}k_{-2,R}p_{H_2}\,e^{2(1-\beta)\eta\,F/RT}}{c_{H^+}(\bar{k}_{2,R}+\bar{k}_{1,R}k')\,e^{-\beta\eta\,F/RT} + (\bar{k}_{-1,R}+\bar{k}_{-2,R}k'p_{H_2})\,e^{(1-\beta)\eta\,F/RT}}.$$

Equation [12] shows that i is positive ("cathodic") if $\eta < 0$, negative ("anodic") if $\eta > 0$.

If $i = 0$, $\eta = 0$; then [11] yields

[13] $$e^{\Delta\phi_R\,F/RT} = \sqrt{K_1K_2(c^2_{H^+}/p_{H_2})}$$

where $K_1 = k_1/k_{-1}$ and $K_2 = k_2/k_{-2}$. Equation [13] is a form of the Nernst equation, i.e., confirms [12].

(ii) Cathodic Tafel Region

By the "Tafel region" is meant that region of the current density – potential relation for which $i = Ae^{B\eta}$ where A and B are constants. From [12] and for a net cathodic current density, two limiting cases give Tafel relations, i.e., if

[14] $$(\bar{k}_{2,R}+\bar{k}_{1,R}k')c_{H^+}\,e^{-\beta\eta\,F/RT} \gg (\bar{k}_{-1,R}+\bar{k}_{-2,R}k'p_{H_2})\,e^{(1-\beta)\eta\,F/RT}$$

then,

[15] $$i = 2F\,\frac{\bar{k}_{1,R}\bar{k}_{2,R}c_{H^+}}{\bar{k}_{2,R}+\bar{k}_{1,R}k'}\,e^{-\beta\eta\,F/RT}.$$

But if

[16] $$(\bar{k}_{-1,R}+\bar{k}_{-2,R}k'p_{H_2})\,e^{(1-\beta)\eta\,F/RT} \gg (\bar{k}_{2,R}+\bar{k}_{1,R}k')c_{H^+}\,e^{-\beta\eta\,F/RT}$$

then,

[17] $$i = 2F\,\frac{\bar{k}_{1,R}\bar{k}_{2,R}c^2_{H^+}}{\bar{k}_{-1,R}+\bar{k}_{-2,R}k'p_{H_2}}\,e^{-(1+\beta)\eta\,F/RT}.$$

By virtue of its form, [16] cannot be applicable at large negative overpotentials, when it must go over into [14]. Remembering that the cathodic Tafel region occurs only for $\beta\eta\,F/RT > 1$, the necessary relation among the rate constants for the occurrence of [17] is

[18] $$(\bar{k}_{-1,R}+\bar{k}_{-2,R}k'p_{H_2}) > (\bar{k}_{2,R}+\bar{k}_{1,R}k')c_{H^+}\,e^2.$$

(iii) Anodic Tafel Region

From [12], with condition [14]:

[19] $$i = -2F\,\frac{\bar{k}_{-1,R}\bar{k}_{-2,R}p_{H_2}}{(\bar{k}_{2,R}+\bar{k}_{1,R}k')c_{H^+}}\,e^{(2-\beta)\eta\,F/RT}$$

Or, with condition [16], [12] becomes:

[20] $$i = -2F\,\frac{\bar{k}_{-1,R}\bar{k}_{-2,R}p_{H_2}}{\bar{k}_{-1,R}+\bar{k}_{-2,R}k'p_{H_2}}\,e^{(1-\beta)\eta\,F/RT}.$$

Can. J. Chem. Downloaded from www.nrcresearchpress.com by 190.90.36.8 on 09/04/12
For personal use only.

Equation [19], as a consequence of the form of [14], can be applicable only at lower positive values of the overpotential. The condition for it to occur at any potential in an anodic Tafel region,

$$[21] \qquad (\bar{k}_{2,R}+\bar{k}_{1,R}k')c_{H^+} > (\bar{k}_{-1,R}+\bar{k}_{-2,R}k'p_{H_2})\, e^2.$$

(iv) "Reversible" Region

By the "reversible region" is meant the range of overpotentials for which the expansion of $e^{\pm\alpha\eta\, F/RT}$ can be written as $1\pm\alpha\eta\, F/RT$ to an accuracy not less than that corresponding to the experimental measurement of η.

Applying this condition to [12]:

$$[22] \qquad i = -4F\frac{\bar{k}_{1,R}\bar{k}_{2,R}c^2_{H^+}\,\eta F/RT}{(\bar{k}_{2,R}+\bar{k}_{1,R}k')c_{H^+}+(\bar{k}_{-1,R}+\bar{k}_{-2,R}k'p_{H_2})}$$

and

$$[23] \qquad \bar{k}_{1,R}\bar{k}_{2,R}c^2_{H^+} = \bar{k}_{-1,R}\bar{k}_{-2,R}p_{H_2}.$$

(v) Coverage of Electrode with Adsorbed Atomic Hydrogen

The explicit expression for c_H follows from [10], utilizing [6]–[9], as

$$[24] \qquad c_H = \frac{\bar{k}_{1,R}c_{H^+}\, e^{-\beta\eta\, F/RT}+\bar{k}_{-2,R}p_{H_2}\, e^{(1-\beta)\eta\, F/RT}}{(\bar{k}_{1,R}k'+\bar{k}_{2,R})c_{H^+}\, e^{-\beta\eta\, F/RT}+(\bar{k}_{-1,R}+\bar{k}_{-2,R}k'p_{H_2})\, e^{(1-\beta)\eta\, F/RT}}.$$

Defining the degree of surface coverage at an overpotential η, θ_η, as

$$[25] \qquad \theta_\eta = k'c_H,$$

two limiting values for the Tafel regions follow from [24] and [25] as:

$$[26] \qquad (\theta_\eta)_c = \bar{k}_{1,R}k'/(\bar{k}_{1,R}k'+\bar{k}_2),$$

$$[27] \qquad (\theta_\eta)_a = \bar{k}_{-2,R}k'p_{H_2}/(\bar{k}_{-1,R}+\bar{k}_{-2,R}p_{H_2}k').$$

(vi) Influence of Concentration of Hydrogen Ions in Solution and Hydrogen Pressure in the Tafel Regions

The pH effects are known (Frumkin (15), Parsons (3), Bockris and Potter (5), and Bockris and Watson (14)).

The effect of hydrogen pressure on overpotential may be calculated in terms of the coefficient $\left(\frac{\partial\eta}{\partial \ln p_{H_2}}\right)_i$.

In the cathodic region, they follow from [15], for the condition [14]. Thence,

$$[28] \qquad \left(\frac{\partial\eta}{\partial \ln p_{H_2}}\right)_i = \frac{RT}{2F}.$$

If [16] applies, [17] gives:

$$[29] \qquad \left(\frac{\partial\eta}{\partial \ln p_{H_2}}\right)_i = \frac{RT}{2F}-\frac{RT}{(1+\beta)F}\left(\frac{k_{-2}k'p_{H_2}}{k_{-1}+k_{-2}k'p_{H_2}}\right).$$

In the anodic region, condition [14], resulting in [19], gives

$$[30] \qquad \left(\frac{\partial\eta}{\partial \ln p_{H_2}}\right)_i = -\frac{RT}{2F}\frac{\beta}{2-\beta}$$

whereas [16] and [20] give:

$$[31] \qquad \left(\frac{\partial\eta}{\partial \ln p_{H_2}}\right)_i = -\frac{RT}{(1-\beta)F}\left(\frac{1+\beta}{2}-\frac{k_{-2}k'p_{H_2}}{k_{-1}+k_{-2}p_{H_2}}\right).$$

Can. J. Chem. Downloaded from www.nrcresearchpress.com by 190.90.36.8 on 09/04/12
For personal use only.

(vii) Limiting Cases for the Electrochemical Path

The general equations for the electrochemical desorption path (cf. page 476) give rise to two general divisions, depending upon whether [14] or [16] is applicable. In the following tables, limiting values are given for the Tafel equation, degree of coverage with atomic hydrogen, and pressure coefficient of overpotential at constant current density, on the further assumption that the heights of the energy barriers in the successive reactions differ by an amount greater than about 3 kcal mole^{-1}.

C. The Atomic Hydrogen Desorption Mechanism

1. General Equations

The reactions are:

[32] $$H^+ + e_0^- \underset{-1}{\overset{1}{\rightleftharpoons}} MH,$$

[33] $$MH + MH \underset{-2}{\overset{2}{\rightleftharpoons}} H_2 + 2M.$$

Hence,

[6] $$v_1 = k_1(1-k'c_H)c_{H^+}\, e^{-\beta\Delta\phi\ F/RT}$$

[7] $$v_{-1} = k_{-1}c_H\, e^{(1-\beta)\Delta\phi\ F/RT}$$

[34] $$v_2 = k_2 c_H^2$$

[35] $$v_{-2} = k_{-2}(1-k'c_H)^2 p_{H_2}.$$

In the steady state:

[36] $$2(v_1-v_{-1}) = v_2-v_{-2} = v.$$

From [6], [7], [34], [35], and [36]

[37] $$\frac{1}{4}\left(\frac{k_2}{k'^2}-k_{-2}p_{H_2}\right)\left(\frac{i}{2F}\right)^2-\left(\bar{k}^2_{1,R}c^2_{H^+}\, e^{-2\beta\eta\ F/RT}+\frac{\bar{k}_{1,R}k_2}{k'^2}c_{H^+}\, e^{-\beta\eta\ F/RT}\right.$$
$$\left.+2\frac{\bar{k}_{1,R}\bar{k}_{-1,R}}{k'}c_{H^+}\, e^{(1-2\beta)\eta\ F/RT}\right.$$
$$\left.+k_{-2}p_{H_2}\frac{\bar{k}_{-1,R}}{k'}\, e^{(1-\beta)\eta\ F/RT}+\frac{\bar{k}^2_{-1,R}}{k'^2}\, e^{2(1-\beta)\eta\ F/RT}\right)\frac{i}{2F}$$
$$+\bar{k}^2_{1,R}\frac{k_2}{k'^2}c_{H^+}\, e^{-2\beta\eta\ F/RT}-\frac{\bar{k}^2_{1,R}}{k'^2}k_{-2}p_{H_2}\, e^{2(1-\beta)\eta\ F/RT} = 0.$$

From [37], with the condition $i = 0$ ($\eta = 0$), the first two terms vanish, whence, with [1] and [2],

[38] $$e^{\Delta\phi_R\ F/RT} = K_1K_2^{\frac{1}{2}}(c_{H^+}/\sqrt{p_{H_2}})$$

where $K_1 = k_1/k_{-1}$, $K_2 = k_2/k_{-2}$, the equilibrium constants of the partial reaction [32] and [33].

Also, from [37], with $\eta = 0$,

[39] $$\bar{k}^2_{1,R}k_2c^2_{H^+} = \bar{k}^2_{-1,R}k_{-2}p_{H_2}.$$

Can. J. Chem. Downloaded from www.nrcresearchpress.com by 190.90.36.8 on 09/04/12
For personal use only.

2. General Solution for Current Density (Cathodic and Anodic Currents)

From [37]:

$$\frac{i}{2F}=\frac{2}{(k_2/k'^2)-k_{-2}p_{H_2}}\left\{\left(\bar{k}^2_{1,R}c_{H^+}\,e^{-2\beta\eta\,F/RT}+\frac{\bar{k}_{1,R}k_2}{k'^2}c_{H^+}\,e^{-\beta\eta\,F/RT}\right.\right.$$
$$\left.+2\,\frac{\bar{k}_{-1,R}\bar{k}_{1,R}}{k'}c_{H^+}\,e^{(1-2\beta)\eta\,F/RT}+\frac{\bar{k}_{-1,R}k_2}{k'}p_{H_2}\,e^{(1-\beta)\eta\,F/RT}+\frac{\bar{k}^2_{-1,R}}{k'^2}\,e^{2(1-\beta)\eta\,F/RT}\right)(+)$$
$$\left(\bar{k}^4_{1,R}c^4_{H^+}\,e^{-4\beta\,F/RT}+2\,\frac{\bar{k}^3_{1,R}k_2}{k'^2}c^3_{H^+}\,e^{-3\beta\eta\,F/RT}+\frac{\bar{k}^2_{1,R}k_2k_{-2}}{k'^2}c^2_{H^+}p_{H_2}\,e^{-2\beta\eta\,F/RT}\right.$$
$$+4\frac{\bar{k}^3_{1,R}\bar{k}_{-1,R}}{k'}c_{H^+}\,e^{(1-4\beta)\eta\,F/RT}$$
[40] $$+2\,\frac{\bar{k}^2_{1,R}\bar{k}_{-1,R}}{k'}c^2_{H^+}\left(k_{-2}p_{H_2}+2\,\frac{k_2}{k'^2}\right)e^{(1-3\beta)\eta\,F/RT}+2\,\frac{\bar{k}_{1,R}\bar{k}_{-1,R}k_2k_{-2}}{k'^3}c_{H^+}p_{H_2}\,e^{(1-2\beta)\eta\,F/RT}$$
$$+6\,\frac{\bar{k}^2_{1,R}\bar{k}_{-1,R}}{k'^2}c^2_{H^+}\,e^{(2-4\beta)\eta\,F/RT}$$
$$+2\,\frac{\bar{k}^2_{-1,R}\bar{k}_{1,R}}{k'^2}c_{H^+}(k_2+k_{-2}p_{H_2})\,e^{(2-3\beta)\eta\,F/RT}+4\,\frac{k_{1,R}\bar{k}^3_{-1,R}}{k'^2}c_{H^+}\,e^{(3-4\beta)\eta\,F/RT}$$
$$+\frac{\bar{k}_{-1,R}k_2k_{-2}p_{H_2}}{k'^4}\,e^{2(1-\beta)\eta\,F/RT}$$
$$\left.\left.+2\,\frac{\bar{k}^3_{-1,R}}{k'^2}k_{-2}p_{H_2}\,e^{3(1-\beta)\eta\,F/RT}+\frac{\bar{k}^4_{-1,R}}{k'^4}\,e^{4(1-\beta)\eta\,F/RT}\right)^{\frac{1}{2}}\right\}.$$

In [40], the minus sign before the last bracket is taken; for, then, with $-\eta$, i is positive; and, if η is positive, i is negative, i.e., the signs of the i values change with the sign of η, in accordance with physical sense. If the plus sign is taken, i has the same sign, independently of the signs of η, i.e., the solution is unreal.

To obtain Tafel equations from [39], we rearrange the expression in such a way that a simple assumption regarding the predominance of one term over all others can result in expressions with only one potential dependent term.

3. Special Case of Equation [40] for $\bar{k}^4_{1,R}c^4_{H^+}e^{-4\beta\eta\,F/RT}$ Predominating in the Square Root Term (Cathodic and Anodic Case)

With this condition,

$$\frac{i}{2F}=\frac{2}{(k_2/k'^2)-k_{-2}p_{H_2}}\left\{\left(\bar{k}^2_{1,R}c^2_{H^+}\,e^{-2\beta\eta\,F/RT}+\frac{\bar{k}_{1,R}k_2}{k'^2}c_{H^+}\,e^{-\beta\eta\,F/RT}\right.\right.$$
$$\left.+2\,\frac{k_{-1,R}k_{1,R}}{k'}c_{H^+}\,e^{(1-2\beta)\eta\,F/RT}+\frac{\bar{k}_{-1,R}k_{-2}}{k'}p_{H_2}\,e^{(1-\beta)\eta\,F/RT}+\frac{\bar{k}^2_{-1}}{k'^2}\,e^{2(1-\beta)\eta\,F/RT}\right)$$
$$-\bar{k}^2_{1,R}c^2_{H^+}\,e^{-2\beta\eta\,F/RT}\left(1+\frac{2k_2}{k'^2\bar{k}_{1,R}c_{H^+}}\,e^{\beta\eta\,F/RT}+\frac{k_2}{k'^2}\,\frac{k_{-2}p_{H_2}}{\bar{k}^2_{1,R}c_{H^+}}\,e^{2\beta\eta\,F/RT}+4\,\frac{\bar{k}_{-1,R}}{k'\bar{k}_{1,R}c_{H^+}}\,e^{\eta\,F/RT}\right.$$
$$+\frac{2\bar{k}_{-1,R}(k_{-2}p_{H_2}+k_2/k'^2)}{k'\bar{k}_{1,R}c_{H^+}}\,e^{(1-\beta)\eta\,F/RT}+\frac{2\bar{k}_{-1,R}k_2k_{-2}p_{H_2}}{k'^3}\,e^{(1+2\beta)\eta\,F/RT}$$
[41] $$+6\,\frac{\bar{k}^2_{-1,R}}{k'^2\bar{k}^2_{1,R}c^2_{H^+}}\,e^{2\eta\,F/RT}$$
$$+\frac{2\bar{k}^2_{-1,R}(k_2/k'^2+2k_{-2}p_{H_2})}{k'^2\bar{k}^3_{1,R}c^3_{H^+}}\,e^{(2+\beta)\eta\,F/RT}+4\,\frac{\bar{k}^3_{-1,R}}{k'^3\bar{k}^3_{1,R}c^3_{H^+}}\,e^{3\eta\,F/RT}$$
$$\left.+\frac{\bar{k}^2_{-1,R}}{k'^4}\,\frac{k_2k_{-2}p_{H_2}}{\bar{k}^4_{1,R}c^4_{H^+}}\,e^{2(1+\beta)\eta\,F/RT}\right.$$

Can. J. Chem. Downloaded from www.nrcresearchpress.com by 190.90.36.8 on 09/04/12
For personal use only.

$$+\frac{2\bar{k}^3_{-1,R}}{k'^3}\frac{k_{-2}p_{H_2}}{\bar{k}^4_{1,R}c^4_{H^+}}e^{(3+\beta)\eta F/RT}+\frac{\bar{k}^4_{-1,R}}{\bar{k}^4_{1,R}}\frac{1}{k'^4c^4_{H^+}}e^{4\eta F/RT}\Bigg)^{\frac{1}{2}}\Bigg\}.$$

If the square root term of equation [41] is expanded, it is necessary to continue the expansion to the fourth term, otherwise the terms from the root term cancel with the terms before the square root. Utilizing the fact that all the terms in the square root after the first are $\ll 1$, then one obtains:

[42] $$\frac{k_2}{k'^2\bar{k}_{1,R}c_{H^+}} \ll e^{-\beta\eta F/RT}$$

[43] $$\frac{k_{-2}p_{H_2}}{\bar{k}_{1,R}c_{H^+}} \ll e^{-\beta\eta F/RT}$$

[44] $$\frac{\bar{k}_{-1,R}}{k'\bar{k}_{1,R}c_{H^+}} \ll e^{-\eta F/RT},$$

or, utilizing [39], [44] becomes:

$$k_2/k'^2\, k_{-2}\, p_{H2} \ll e^{-2\eta F/RT}.$$

These conditions, in [41], yield:

[45] $$i = 2F(k_2/k'^2)(1-e^{2\eta F/RT}).$$

Equation [45] expresses the net current under cathodic or anodic overpotential when the condition [42], [43], and [44] applies. Limiting conditions of this equation will be considered below.

4. Special Case of [40] for which $\bar{k}^2_{1,R}c^2_{H^+}(k_2k_{-2}/k'^2)p_{H_2}\ e^{-2\beta\eta F/RT}$ *Predominates in the Square Root Term*

Applying this condition to [40] one obtains:

[46] $$k'^2\bar{k}_{1,R}\,c_{H^+}/k_2 \ll e^{\beta\eta F/RT},$$

[47] $$\bar{k}_{1,R}c_{H^+}/(k_{-2}\,p_{H_2}) \ll e^{\beta\eta F/RT}.$$

Then, in [41]:

[48] $$i = 4F\,\bar{k}_{1,R}c_{H^+}\frac{1-[k'^2(k_{-2}p_{H_2}/k_2)]^{\frac{1}{2}}}{1-k'^2(k_{-2}p_{H_2}/k_2)}e^{-\beta\eta F/RT}.$$

5. Special Case of [40] for which $(\bar{k}^2_{-1,R}/k'^4)/k_2k_{-2}p_{H_2}\ e^{2(1-\beta)\eta F/RT}$ *Predominates in Square Root Term*

Applying this condition to [40] one obtains:

[49] $$k'\bar{k}_{-1,R}/k_2 \ll e^{-(1-\beta)\eta F/RT}$$

[50] $$\bar{k}_{-1,R}/(k'k_{-2}p_{H_2}) \ll e^{-(1-\beta)\eta F/RT}.$$

Then, from [41]:

[51] $$i = 4F\frac{\bar{k}_{-1,R}}{k'}\frac{1-(k_2/k'^2k_{-2}p_{H_2})^{\frac{1}{2}}}{1-(k_2/k'^2k_{-2}p_{H_2})}e^{(1-\beta)\eta F/RT}.$$

6. Special Case for which $(\bar{k}_{-1,R}/k'^4)\ e^{4(1-\beta)\eta F/RT}$ *Predominates in Square Root Term*

Application of this condition to equation [40] necessitates expansion of the square root term to four terms. The resulting conditions are:

[52] $$k'k_{-2}p_{H_2}/\bar{k}_{-1,R} \ll e^{(1-\beta)\eta F/RT},$$

[53] $$k_2/k'\bar{k}_{-1,R} \ll e^{(1-\beta)\eta F/RT},$$

[54] $$k'\bar{k}_{1,R}c_{H^+}/\bar{k}_{-1,R} \ll e^{\eta F/RT}.$$

Can. J. Chem. Downloaded from www.nrcresearchpress.com by 190.90.36.8 on 09/04/12
For personal use only.

Or, utilizing [39], [54] becomes:

$$[55] \qquad k'^2 k_{-2} p_{H_2}/k_2 \ll e^{-2\eta\, F/RT}.$$

With these conditions in [40], one obtains:

$$[56] \qquad i = 2F\, k_{-2} p_{H_2}(e^{-2\eta\, F/RT} - 1).$$

7. Reversible Region

Near the reversible potential, i in [37] is limitingly small. This implies that the term in i^2 in [37] will be negligible compared with that in i. Correspondingly, η will be limitingly small. In this equation we expand the e function to the first term only in the i term (of [37]) and to the second term in the term independent of i (the first term vanishing). One obtains:

$$[57] \qquad i = -(4\eta\, F^2/RT) \Big/ \left(\frac{1}{\bar{k}_{1,R} c_{H^+}} + \frac{k'^2}{k_2} + \frac{2\bar{k}_{-1,R} k'}{\bar{k}_{1,R} k_2 c_{H^+}} + \frac{k'}{\bar{k}_{-1,R}} + \frac{1}{k_{-2} p_{H_2}}\right).$$

Then, with [39],

$$[58] \qquad i = -(4\eta\, F^2/RT) \Big/ \left[\frac{1}{\bar{k}_{1,R} c_{H^+}} + \left(\frac{k'}{\sqrt{k_2}} + \frac{1}{\sqrt{(k_{-2} p_{H_2})}}\right)^2 + \frac{k'}{\bar{k}_{-1,R}}\right].$$

Several limiting conditions can be derived for equation [58] by regarding Figs. 1, 2, 3, and 6 (cf. Tables). Thus, from Fig. 1, $\bar{k}_{1,R}$ is the smallest rate constant so that:

$$[59] \qquad i = -4\bar{k}_{1,R}\, c_{H^+}(F^2/RT)\eta.$$

From Fig. 2, $\bar{k}_{-1,R}$ is the smallest rate constant and thus gives

$$[60] \qquad i = -4(\bar{k}_{-1,R}/k')(F^2/RT)\eta.$$

From Fig. 3, k_{-2} is the smallest rate constant and therefore

$$[61] \qquad i = -4\, k_{-2}\, p_{H_2}\, (F^2/RT)\eta.$$

From Fig. 6, k_2 is the smallest rate constant and therefore

$$[62] \qquad i = -4\, \frac{k_2}{k'^2}\, \frac{F}{RT}\, \eta.$$

The pH and p_{H_2} dependence of these current densities in the reversible region may be noted as an aid to diagnostic evaluation of mechanism.

8. Coverage at the Equilibrium Potential

From [34] and [35],

$$[63] \qquad v_2 = v_{-2}.$$

Hence:

$$[64] \qquad \theta = \sqrt{\left(\frac{k_{-2} p_{H_2} k'^2}{k_2}\right)} \Big/ 1 + \sqrt{\left(\frac{k_{-2} p_{H_2} k'^2}{k_2}\right)}.$$

9. Coverage in the Tafel Region

From [6] and [7] and

$$[65] \qquad \tfrac{1}{2} v = v_1 - v_{-1}$$

$$[66] \qquad c_H = \frac{1}{k'}\, \frac{\bar{k}_{1,R} c_{H^+}\, e^{-\beta\eta\, F/RT} - (v/2)}{\bar{k}_{1,R} c_{H^+}\, e^{-\beta\eta\, F/RT} + (\bar{k}_{-1,R}/k')\, e^{(1-\beta)\eta\, F/RT}}.$$

Can. J. Chem. Downloaded from www.nrcresearchpress.com by 190.90.36.8 on 09/04/12
For personal use only.

From [34] and [35], with: $v = v_2 - v_{-2}$

$$[67] \qquad c_H = \frac{1}{k'}\left[-\frac{k_{-2}p_{H_2}}{k_2/k'^2 - k_{-2}p_{H_2}} + \sqrt{\left(\frac{k_{-2}p_{H_2}k_2}{k'^2[(k_2/k') - k_{-2}p_{H_2}]^2} + \frac{v}{k_2/k'^2 - k_{-2}p_{H_2}}\right)}\right].$$

10. Limiting Cases for the Catalytic Desorption Mechanism

The equations derived in sections 5 and 6 are based upon certain mathematical restrictions, and, with these limitations, apply to both cathodic and anodic polarization. If further restrictions in regard to the relative values of the constants in equations [48] and [51] are taken into account, the simple limiting cases (equivalent to the existence of a predominant rate-determining step) shown in Tables V and VI arise.

DISCUSSION

The characteristic quantities given in Tables I, II, III, and IV allow a complete distinction to be made between (*a*) the electrochemical and catalytic desorption paths, and (*b*) the energy–distance profiles and thus the rate-determining step. The distinguishing criteria are summarized in Table V.

The use of these criteria is clearly restricted to the assumption that only either the electrochemical or catalytic desorption mechanisms occurs, and that the surface H atoms block part of the surface for the discharge of H^+ ions.

The Tafel equations deduced for various limiting conditions in Tables I–IV may be divided into two groups:

1. Those equations which have the form: current density = charge factors × equilibrium constant of reaction *before* the r.d.s. × rate constant of the r.d.s. × concentration factor × a potential factor.

In this type of equation there is agreement with the formulation of consecutive reactions proposed by Eyring (16) which implies that the free energy of activation of the over-all reaction is the difference in free energy between the initial state and the activated state of the rate-determining reaction.

2. Those equations which have the form: current density = charge factor × rate constant of r.d.s. and equilibrium constant of reaction *following* the r.d.s. × concentration factor* × potential factor.

In this latter type of relation, the only rate constant (apart from those which make up the equilibrium constants) is that for the step from the initial state of the over-all reaction to the state of highest energy in consecutive reactions, and, in this formal sense, the rate-determining step is consistent with the definition made by Eyring *et al.* (16) for the rate-determining step in consecutive reactions. However, consider, for example, (Table III) the expression

$$i = 4F\frac{\bar{k}_{1,R}}{k'}c_{H^+}\sqrt{\left(\frac{k_2}{k_{-2}p_{H_2}}\right)}\,e^{-\beta\eta F/RT}$$

with [39]:

$$i = 4F\frac{\bar{k}_{-1,R}}{k'}\,e^{-\beta\eta F/RT}.$$

Thus, in such expressions, the energy barrier which determines the over-all reaction rate is that between the energy of the surface-adsorbed H atom and the state of highest energy in the system. (In such cases, the surface of the electrode is highly covered.)

**Except in the case of equations containing k_{-1}, when no concentration factor occurs in the form of the relation given.*

Can. J. Chem. Downloaded from www.nrcresearchpress.com by 190.90.36.8 on 09/04/12
For personal use only.

Can. J. Chem. Downloaded from www.nrcresearchpress.com by 190.90.36.8 on 09/04/12
For personal use only.

TABLE I

The electrochemical desorption reaction under cathodic conditions

Relations among the constants	[14] or [16] applicable	Tafel eq.	Coverage	$\left(\frac{\partial\eta}{\partial \ln p_{H_2}}\right)_i$	Energy barrier
$\frac{\bar{k}_{2,R}}{k'}c_{H^+} > \frac{\bar{k}_{-1,R}}{k'} > \bar{k}_{-2,R} > \bar{k}_{1,R}c_{H^+}$ and $\frac{\bar{k}_{2,R}}{k'}c_{H^+} > \bar{k}_{-2,R}p_{H_2} > \frac{\bar{k}_{-1,R}}{k'} > \bar{k}_{1,R}c_{H^+}$	[14]	$i = 2F\bar{k}_1 c_{H^+} e^{-\beta\eta F/RT}$	$(c_H)_0 \to 0$ $(c_H) \to 0$	$\frac{RT}{2F}$	$E(A)c$
$\bar{k}_{-2,R}p_{H_2} > \frac{\bar{k}_{2,R}c_{H^+}}{k'} > \bar{k}_{1,R}c_{H^+} > \frac{\bar{k}_{-1,R}}{k'}$ and $\bar{k}_{-2,R}p_{H_2} > \bar{k}_{1,R}c_{H^+} > \frac{\bar{k}_{2,R}c_{H^+}}{k'} > \frac{\bar{k}_{-1,R}}{k'}$	[16]	$i = 2F\bar{k}_{1,R}\frac{\bar{k}_{2,R}}{k'\bar{k}_{-2,R}}c^2_{H^+} e^{-(1+\beta)\eta F/RT}$	$(c_H)_0 \to \frac{1}{k'}$ $(c_H) \to \frac{1}{k'}$	$-\frac{RT}{2F}\frac{1-\beta}{1+\beta}$	$E(B)c$
$\frac{\bar{k}_{-1,R}}{k'} > \frac{\bar{k}_{2,R}c_{H^+}}{k'} > \bar{k}_{1,R}c_{H^+} > \bar{k}_{-2,R}p_{H_2}$ and $\frac{\bar{k}_{-1,R}}{k'} > \bar{k}_{1,R}c_{H^+} > \frac{\bar{k}_{2,R}c_{H^+}}{k'} > \bar{k}_{-2,R}p_{H_2}$	[16]	$i = 2F\frac{\bar{k}_{1,R}}{\bar{k}_{-1,R}}k_{2,R}c^2_{H^+} e^{-(1+\beta)\eta F/RT}$	$(c_H)_0 \to 0$ $(c_H) \to 0$	$\frac{RT}{2F}$	$E(C)c$
$\bar{k}_{1,R}c_{H^+} > \frac{\bar{k}_{-1,R}}{k'} > \bar{k}_{-2,R}p_{H_2} > \bar{k}_{2,R}c_{H^+}$ and $\bar{k}_{1,R}c_{H^+} > \bar{k}_{-2,R}p_{H_2} > \frac{\bar{k}_{-1,R}}{k'} > \frac{\bar{k}_{2,R}c_{H^+}}{k'}$	[14]	$i = 2F\frac{\bar{k}_{2,R}}{k'}c_{H^+} e^{-\beta\eta F/RT}$	$(c_H)_0 \to \frac{1}{k'}$ $(c_H) \to \frac{1}{k'}$	$\frac{RT}{2F}$	$E(D)c$

TABLE II

The electrochemical desorption reaction under anodic conditions

Relations among the constants	[14] or [16] applicable	Tafel eq.	Coverage	$\left(\frac{\partial\eta}{\partial \ln p_{H_2}}\right)_i$	Energy barrier
$\frac{\bar{k}_{2,R}}{k'}c_{H^+} > \frac{\bar{k}_{-1,R}}{k'} > \bar{k}_{-2,R}p_{H_2} > \bar{k}_{1,R}c_{H^+}$ and $\frac{\bar{k}_{2,R}}{k'}c_{H^+} > \bar{k}_{-2,R}p_{H_2} > \frac{\bar{k}_{-1,R}}{k'} > \bar{k}_{1,R}c_{H^+}$	[14]	$i = -2F\bar{k}_{-1,R}\frac{\bar{k}_{-2,R}p_{H_2}}{\bar{k}_{2,R}c_{H^+}} e^{(2-\beta)\eta F/RT}$	$(c_H)_0 \to 0$ $(c_H) \to 0$	$-\frac{RT}{2F}\frac{\beta}{2-\beta}$	$E(A)a$
$\bar{k}_{-2,R}p_{H_2} > \frac{\bar{k}_{2,R}}{k'}c_{H^+} > \bar{k}_{1,R}c_{H^+} > \frac{\bar{k}_{-1,R}}{k'}$ and $\bar{k}_{-2,R}p_{H_2} > \bar{k}_{1,R}c_{H^+} > \frac{\bar{k}_{2,R}}{k'}c_{H^+} > \frac{\bar{k}_{-1,R}}{k'}$	[16]	$i = -2F\frac{\bar{k}_{-1,R}}{k'} e^{(1-\beta)\eta F/RT}$	$(c_H)_0 \to \frac{1}{k'}$ $(c_H) \to \frac{1}{k'}$	$\frac{RT}{2F}$	$E(B)a$
$\frac{\bar{k}_{-1,R}}{k'} > \frac{\bar{k}_{2,R}}{k'}c_{H^+} > \bar{k}_{1,R}c_{H^+} > \bar{k}_{-2,R}p_{H_2}$ and $\frac{\bar{k}_{-1,R}}{k'} > \bar{k}_{1,R}c_{H^+} > \frac{\bar{k}_{2,R}}{k'}c_{H^+} > \bar{k}_{-2,R}p_{H_2}$	[16]	$i = -2F\bar{k}_{-2,R}p_{H_2} e^{(1-\beta)\eta F/RT}$	$(c_H)_0 \to 0$ $(c_H) \to 0$	$-\frac{RT}{2F}\frac{1+\beta}{1-\beta}$	$E(C)a$
$\bar{k}_{1,R}c_{H^+} > \frac{\bar{k}_{-1,R}}{k'} > \bar{k}_{-2,R}p_{H_2} > \frac{\bar{k}_{2,R}c_{H^+}}{k'}$ and $\bar{k}_{1,R}c_{H^+} > \bar{k}_{-2,R}p_{H_2} > \frac{\bar{k}_{-1,R}}{k'} > \frac{\bar{k}_{2,R}c_{H^+}}{k'}$	[14]	$i = -2F\bar{k}_{-2,R}\frac{\bar{k}_{-1,R}p_{H_2}}{\bar{k}_{1,R}k'c_{H^+}} e^{(2-\beta)\eta F/RT}$	$(c_H)_0 \to \frac{1}{k'}$ $(c_H) \to \frac{1}{k'}$	$-\frac{RT}{2F}\frac{\beta}{2-\beta}$	$E(D)a$

Can. J. Chem. Downloaded from www.nrcresearchpress.com by 190.90.36.8 on 09/04/12
For personal use only.

TABLE III

The catalytic desorption mechanism under cathodic conditions

Relations among the constants	From general equation	Tafel eq.	Coverage	$\left(\frac{\partial\eta}{\partial \ln p_{H_2}}\right)_i$	Energy diagram
$\frac{k_2}{k'^2\bar{k}_{1,R}c_{H^+}} \ll e^{-\beta\eta F/RT}$ $\frac{k_{-2}p_{H_2}}{\bar{k}_{1,R}c_{H^+}} \ll e^{-\beta\eta F/RT}$ $\frac{k_{-1,R}}{k'\bar{k}_{1,R}c_{H^+}} = \sqrt{\left(\frac{k_2}{k'^2k_{-2}p_{H_2}}\right)} \ll e^{-\eta F/RT}$	[41]	$i = 2F\frac{k_2}{k'^2}$	$(c_H) \to \frac{1}{k'}$	—	—
$\frac{\bar{k}_{1,R}c_{H^+}k'^2}{k_2} \ll e^{\beta\eta F/RT}$ $\frac{\bar{k}_{1,R}c_{H^+}}{k_{-2}p_{H_2}} \ll e^{\beta\eta F/RT}$ $\frac{k_{-2}p_{H_2}k'^2}{k_2} \ll 1$	[48]	$i = 4F\bar{k}_{1,R}c_{H^+}e^{-\beta\eta F/RT}$	$(c_H)_0 \to 0$ $(c_H) \to 0$	$\frac{RT}{2F}$	 $T(A)c$
$\frac{\bar{k}_{1,R}c_{H^+}k'^2}{k_2} \ll e^{\beta\eta F/RT}$ $\frac{\bar{k}_{1,R}c_{H^+}}{k_{-2}p_{H_2}} \ll e^{\beta\eta F/RT}$ $\frac{k_2}{k_{-2}p_{H_2}k'^2} \ll 1$	[48]	$i = 4F\frac{k_{1,R}c_{H^+}}{k'}\sqrt{\left(\frac{k_2}{k_{-2}p_{H_2}}\right)}e^{-\beta\eta F/RT}$	$(c_H)_0 \to \frac{1}{k'}$ $(c_H) \to \frac{1}{k'}$	$-\frac{RT}{2F}\frac{1-\beta}{\beta}$	 $T(B)c$
$\frac{\bar{k}_{1,R}c_{H^+}k'}{\bar{k}_{-1,R}} = \sqrt{\left(\frac{k_{-2}p_{H_2}k'^2}{k_2}\right)} \ll e^{\eta F/RT}$ $\frac{k_{-2}p_{H_2}k'}{\bar{k}_{-1,R}} \ll e^{(1-\beta)\eta F/RT}$ $\frac{k_2}{\bar{k}_{-1,R}k'} \ll e^{(1-\beta)\eta F/RT}$	[56]	$i = 2F\frac{\bar{k}^2_{1,R}k_2c^2_{H^+}}{\bar{k}^2_{-1}}e^{-2\eta F/RT}$	$(c_H)_0 \to 0$ $(c_H) \to 0$	$\frac{RT}{2F}$	 $T(C)c$

Can. J. Chem. Downloaded from www.nrcresearchpress.com by 190.90.36.8 on 09/04/12
For personal use only.

TABLE IV

The hydrogen desorption mechanism under anodic conditions

Relations among the constants	From general equation	Tafel eq.	Coverage	$\left(\frac{\partial\eta}{\partial \ln p_{H_2}}\right)_t$	Energy diagram
$\frac{k_{-2}p_{H_2}k'}{\bar{k}_{-1,R}} \ll e^{(1-\beta)\eta\ F/RT}$ $\frac{k_2}{\bar{k}_{-1,R}k'} \ll e^{(1-\beta)\eta\ F/RT}$ $\frac{\bar{k}_{1,R}c_{H^+}+k'}{\bar{k}_{-1,R}} = \sqrt{\left(\frac{k_{-2}p_{H_2}k'^2}{k_2}\right)} \ll e^{\eta\ F/RT}$	[56]	$i = -2Fk_{-2}p_{H_2}$	—	—	—
$\frac{\bar{k}_{-1,R}k'}{k_2} \ll e^{-(1-\beta)\eta\ F/RT}$ $\frac{\bar{k}_{-1,R}}{k_{-2}p_{H_2}k'} \ll e^{-(1-\beta)\eta\ F/RT}$ $\frac{k_2}{k'^2k_{-2}p_{H_2}} \ll 1$	[48]	$i = -4F\frac{\bar{k}_{-1,R}}{k'}e^{(1-\beta)\eta\ F/RT}$	$(c_H)_0 \to \frac{1}{k'}$ $(c_H) \to \frac{1}{k'}$	$\frac{RT}{2F}$	$T(B)a$
$\frac{k_{-1,R}k'}{k_2} \ll e^{-(1-\beta)\eta\ F/RT}$ $\frac{k_{-1,R}}{k_{-2}p_{H_2}k'} \ll e^{-(1-\beta)\eta\ F/RT}$ $\frac{k'^2k_{-2}p_{H_2}}{k_2} \ll 1$	[48]	$i = -4F\bar{k}_{-1,R}\sqrt{\left(\frac{k_{-2}p_{H_2}}{k_2}\right)}e^{(1-\beta)\eta\ F/RT}$	$(c_H)_0 \to 0$ $(c_H) \to 0$	$-\frac{RT}{2F}\frac{\beta}{1-\beta}$	$T(A)a$
$\frac{k_2}{\bar{k}_{1,R}k'^2c_{H^+}} \ll e^{-\beta\eta\ F/RT}$ $\frac{k_{-2}p_{H_2}}{\bar{k}_{1,R}c_{H^+}} \ll e^{-\beta\eta\ F/RT}$ $\frac{\bar{k}_{-1,R}}{k'\bar{k}_{-1,R}c_{H^+}} = \frac{1}{k'}\sqrt{\left(\frac{k_2}{k_{-2}p_{H_2}}\right)} \ll e^{-\eta\ F/RT}$	[41]	$i = -2Fk_{-2}p_{H_2}\frac{\bar{k}^2_{-1,R}}{\bar{k}_{1,R}c_{H^+}+k'^2}e^{2\eta\ F/RT}$	$(c_H)_0 \to \frac{1}{k'}$ $(c_H) \to \frac{1}{k'}$	0	$T(D)a$

For the above general kinetics of the h.e.r., it is possible to calculate an expression for the stoichiometric number, ν (Horiuti and Ikusima (17)), namely:

[68] $$\nu = \frac{2\, i_0 F}{RT}\left(\frac{\partial \eta}{\partial i}\right)_{\eta \to 0}.$$

In the limiting cases where a r.d.s. appears (except those leading to a limiting current density), as assumed in Tables I–IV, simple values of ν, namely, those of 1 or 2, are obtained. These values are shown in Table VI.

TABLE V

Distinguishing criteria in catalytic and electrochemical desorption paths

Energy profile (cf., Tables I–IV)	Tafel slope		Coverage (high region)		Pressure effect	
	Cathodic	Anodic	Cathodic	Anodic	Cathodic	Anodic
Electrochemical A	β	$2-\beta$	0	0	$\frac{RT}{2F}$	$-\frac{RT}{2F}\frac{\beta}{2-\beta}$
Catalytic A	β	$1-\beta$	0	0	$\frac{RT}{2F}$	$-\frac{RT}{2F}\frac{\beta}{1-\beta}$
Electrochemical B	$1+\beta$	$1-\beta$	$\frac{1}{k'}$	$\frac{1}{k'}$	$-\frac{RT}{2F}\frac{1-\beta}{1+\beta}$	$\frac{RT}{2F}$
Catalytic B	β	$1-\beta$	$\frac{1}{k'}$	$\frac{1}{k'}$	$-\frac{RT}{2F}\frac{1-\beta}{\beta}$	$\frac{RT}{2F}$
Electrochemical C	$1+\beta$	$1-\beta$	0	0	$\frac{RT}{2F}$	$-\frac{RT}{2F}\frac{1+\beta}{1-\beta}$
Catalytic C	2	0	0	0	$\frac{RT}{2F}$	–
Electrochemical D	β	$2-\beta$	$\frac{1}{k'}$	$\frac{1}{k'}$	$\frac{RT}{2F}$	$-\frac{RT}{2F}\frac{\beta}{2-\beta}$
Catalytic D	0	2	$\frac{1}{k'}$	$\frac{1}{k'}$	–	0

A, B, C, D are the types of energy profiles drawn in Tables I, II, III, and IV.

TABLE VI

Values of the stoichiometric number

Electrochemical A	1
Catalytic A	2
Electrochemical B	1
Catalytic B	2
Electrochemical C	1
Catalytic C	1
Electrochemical D	1
Catalytic D	1

Thus, the values of ν enable a distinction to be made between the catalytic desorption mechanism A or B with rate-determining discharge step and the corresponding electrochemical desorption step. This distinction is of particular use because these steps have the same Tafel slopes.

It may be noted that the appropriate value of i_0 which should be substituted into [68] is that measured very near to the reversible potential. In practice it is usual to substitute the value of i_0 obtained from an extrapolation of the Tafel line. If use of this

Can. J. Chem. Downloaded from www.nrcresearchpress.com by 190.90.36.8 on 09/04/12
For personal use only.

i_0 value gives simple values of ν, the existence of the same mechanism in the region of the reversible potential, as that which occurs in the Tafel region, is confirmed (for experimental values, see Pentland, Bockris, and Sheldon (18)).

Vetter (4) stated that it was not possible to apply a determination of ν to distinguish between a rate-determining discharge mechanism (catalytic path) and a rate-determining electrochemical desorption (electrochemical path), without independent knowledge of other kinetic characteristics of the reaction occurring in a given case. He purported to show that indefinite values of ν could arise from such an attempt. However, values of ν differing from the integral values of Table VI arise only in the absence of the simple limiting conditions given in Tables I–IV, whereupon no single rate-determining step awaits identification and ν (which concerns a rate-determining step) has no simple meaning. If a simple integral value of ν is obtained from an application of [68], its use in the evaluation of a rate-determining step is possible (Table VI).

ACKNOWLEDGMENTS

The authors are indebted to the University of Pennsylvania for a Fellowship to H.M. and to the Yardney Electric Company for other financial assistance.

REFERENCES

1. FRUMKIN, A. N. Acta Physicochim. **7**, 474 (1937).
2. BOCKRIS, J. O'M. and POTTER, E. C. J. Electrochem. Soc. **99**, 169 (1952).
3. PARSONS, R. Trans. Faraday Soc. **47**, 1332 (1951).
4. VETTER, K. J. Z. Elektrochem. **59**, 435 (1955).
5. BOCKRIS, J. O'M. Modern aspects of electrochemistry. Butterworths Scientific Publications, London. 1954. p. 200.
6. BREITER, M. Habilitationsschrift. Munich. 1956.
7. SMITS, A. The theory of allotropy. Longmans, Green and Co., Ltd., London. 1922. p. 115.
8. BOWDEN, P. and RIDEAL, E. Proc. Roy. Soc. (London), A, **120**, 59, 80 (1928).
9. BAARS, M. Sitzber. Ges. Beförder. ges. Naturw. Marburg, **63**, 213 (1928).
10. ERDEY-GRÚZ, T. and VOLMER, M. Z. physik. Chem. **150**, 203 (1930).
11. PARSONS, R. and BOCKRIS, J. O'M. Trans. Faraday Soc. **47**, 914 (1951).
12. POLTORAK, O. M. Zhur. Fiz. Khim. **28**, 1845 (1954).
13. BOCKRIS, J. O'M. Modern aspects of electrochemistry. Butterworths Scientific Publications, London. 1954. p. 187.
14. BOCKRIS, J. O'M. and WATSON, R. G. H. J. chim. phys. **49**, 41 (1952).
15. FRUMKIN, A. N. Z. physik. Chem. **164**, 121 (1933).
16. GLASSTONE, S., LAIDLER, K. J., and EYRING, H. The theory of rate processes. McGraw-Hill Book Co., Inc., New York. 1941. p. 100. Bockris, J. O'M. Modern aspects of electrochemistry. Butterworths Scientific Publications, London. 1954. p. 181.
17. HORIUTI, J. and IKUSIMA, M. Proc. Imp. Acad. (Tokyo), **15**, 39 (1939).
18. PENTLAND, N., BOCKRIS, J. O'M., and SHELDON, E. J. Electrochem. Soc. **104**, 182 (1957).

Can. J. Chem. Downloaded from www.nrcresearchpress.com by 190.90.36.8 on 09/04/12
For personal use only.

Can. J. Chem. Downloaded from www.nrcresearchpress.com by 190.90.36.8 on 09/04/12
For personal use only.

INTERPRETATION OF LIGHT SCATTERING DATA OBTAINED FROM SOLUTIONS OF LARGE ROD-LIKE PARTICLES

M. E. REICHMANN

It has been shown that the number average molecular weight and particle size can be evaluated from the angular distribution of the intensity of scattered light in addition to the customary weight average molecular weight and z average particle size (1, 2, 3). An evaluation of two different averages is useful inasmuch as it provides an idea as to the width of the distribution function. It is the purpose of this note to show that although sound in theory, the evaluation of the number averages of rods is extremely inaccurate in practice.

Qualitative information concerning the width of the distribution can also be gained from an evaluation of both the z average and weight average particle size. It will be demonstrated that the latter can be determined in a more reliable way than the number average.

In all the derivations the assumption has been made of a one-to-one correspondence between polydispersity in molecular weight and length. As pointed out by Rice in the case of random coils, such a correspondence would not exist if the system was polydisperse in stiffness (4). An equivalent situation may arise in rigid rods if there was polydispersity in thickness. In this case it will be shown that the weight average length as determined from experimental data will be underestimated.

The correlation between the angular distribution of the intensity of scattered light and the molecular parameters is given by the following expression:

$$[1] \qquad Kc/R_\theta = (1/M_w P)+2Bc$$

(c = concentration in g/ml, R_θ = Rayleigh's ratio at angle θ, M_w = weight average molecular weight, B = second virial coefficient, and $K = 2\pi^2 n_0^2 (dn/dc)^2/N\lambda^4$, n_0 = refractive index of solvent, dn/dc = refractive index increment of solution, N = Avogadro's number, and λ = wave length in vacuum).

For rigid rods the function P is given by:

$$[2] \qquad P = \int_0^x \frac{\sin w}{w}\, dw - \left(\frac{\sin x}{x}\right)^2$$

$x = (2\pi/\lambda')\, L \sin \theta/2$ ($\lambda' = \lambda/n$, L = length of rod).

When x is small $1/P$ can be expressed by the first two terms of a power series (5):

$$[3] \qquad 1/P = 1+x_z^2/9$$

$$[4] \qquad (Kc/R_\theta)_{c=0} = \frac{1}{M_w}(1+x_z^2/9) \qquad (x_z = z \text{ average of } x).$$

Figure 1 demonstrates that this approximation represents the $1/P$ function in the range of $x^2 = 0$–3, and that the error in the evaluation of the limiting slope and intercept is not too large up to $x^2 = 15$. It requires therefore a distribution function with a negligible fraction of particles for which $x^2 > 15$.

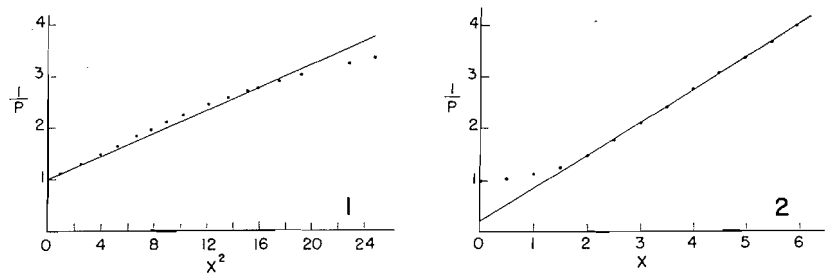

FIG. 1. Reciprocal of particle scattering function vs. x^2 (see text). Solid line was derived from approximation for small values of x.
FIG. 2. Reciprocal of particle scattering function vs. x (see text). Solid line was derived from approximation for large values of x.

When x is large P can be approximated by the following equation (1):

$$P = (\pi/2x_w)\ (1-1/\pi x_n) \qquad [5]$$

$$1/P = (2x_w/\pi)\ (1+1/\pi x_n+1/\pi^2 x_n^2+\ldots) \qquad [5a]$$

neglecting higher terms and introducing $x_w/x_n = M_w/M_n$

$$\frac{1}{P} = \frac{M_w}{M_n}\left(\frac{2}{\pi^2}+\frac{2x_n}{\pi}\right) \qquad [5b]$$

$$\frac{1}{PM_w} = \left(\frac{Kc}{R_\theta}\right)_{c=0} = \frac{1}{M_n}\left(\frac{2}{\pi^2}+\frac{2x_n}{\pi}\right). \qquad [5c]$$

In Fig. 2, $1/P$ for monodisperse rods ($M_w/M_n = 1$) is plotted as a function of x. The line is given by equation [5b]. As Fig. 2 indicates, equation [5b] is a good approximation provided $x > 2$.

Equation [5c] has been suggested as a basis for the evaluation of the number average molecular weight and length. Let us consider the expression in the brackets in [5c]. The value of the first term is 0.203. For $x > 2$ the second term will be larger than 1.30. Therefore the slope of $(Kc/R_\theta)_{c=0}$ versus $\sin\theta/2$ will be larger than an order of magnitude compared to the intercept. An average error of 3% in the slope will introduce an error of 30% or larger in the intercept, and since both M_n and L_n can only be evaluated with the aid of the intercept, this will also be the uncertainty in their determination.

Moreover, by neglecting the higher terms in [5a] the intercept is seriously affected. Remembering that it is the second term in the brackets that determines the intercept one can see that when $x = 2$ the third term will be 16% of the second, and with $x = 6$ the contribution of the third term will be 5% of the second term. Therefore, the intercept evaluated from experimental data will be too high, leading to too low values of the number average parameters.

Since the slope of $(Kc/R_\theta)_{c=0}$ vs. $\sin\theta/2$ can be evaluated with some precision, it would be useful to investigate whether independent information can be obtained from the slope alone. Introducing into [5c] $1/M_n = x_w/M_w x_n$ we obtain:

$$(Kc/R_\theta)_{c=0} = 2L_w/\pi^2 M_w L_n+(4L_w/M_w\lambda')\ \sin\theta/2. \qquad [6]$$

This is the equation derived by Casassa (6). M_w can be evaluated from the intercept of $(Kc/R_\theta)_{c=0}$ vs. $\sin^2\theta/2$ and thus the weight average length can be obtained from the slope of equation [6].

Can. J. Chem. Downloaded from www.nrcresearchpress.com by 190.90.36.8 on 09/04/12
For personal use only.

In the case of polydispersity in the thickness of the rod, the weight average molecular weight, as determined from the intercept of $(Kc/R_\theta)_{c=0}$ vs. $\sin^2 \theta/2$, will be given for a cylinder of radius r by:

$$M_w = \rho\pi N(r^2)_w L_w$$

whereas in the case of uniform thickness

$$M_w = \rho\pi N r^2 L_w' \qquad (\rho = \text{particle density}).$$

The slopes in equation [6] will be $4/\rho\pi N\lambda'(r^2)_w$ and $4/\rho\pi N\lambda' r^2$ respectively. Except in the case of a net side-to-side dissociation, $(r^2)_w > r^2$ resulting in the underestimation of the weight average length.

This can also be expressed in a different way. To preserve the one-to-one correspondence between molecular weight and length, we can formally replace the fluctuation in thickness by an equivalent fluctuation in length. A greater polydispersity in length than in the case of uniform thickness results. Rice has shown that any increase in polydispersity in length leads to a sharper downward curvature of $1/P$ vs. $\sin^2 \theta/2$ (4). The values of $1/P$ at high angles, and the particle length calculated from these values, would be consequently underestimated. Polydispersity in thickness can therefore be considered as the rod equivalent of polydispersity in stiffness in coils (4).

It is sometimes customary to examine polydispersity by comparing the particle length derived from the limiting slope of $1/P$ vs. $\sin^2 \theta/2$ (L_z), with the particle length derived from the best fit of the experimental data with a theoretical curve at high angles (7). It can be shown that the latter particle length will be very close to the weight average length, provided only that the distribution is not very wide. This follows from equation [5*a*]. Neglecting higher terms:

$$[7] \qquad 1/P = 2x_w/\pi^2 x_n + 2x_w/\pi$$

and the explicit $1/P$ function reduces when x is large to:

$$[7a] \qquad 1/P = 2/\pi^2 + 2x/\pi = 0.20 + 2x/\pi.$$

If x is large, $2x/\pi$ practically determines the value of $1/P$. The same applies to [7] provided x_w/x_n is not very large compared to one. Thus the x determined from the theoretical curve will be very close to x_w.

In a recent publication, light scattering data on tobacco mosaic virus have been reported (7). The particle size was determined from the limiting slope and from the best fit at high angles of the $1/P$ vs. $\sin^2 \theta/2$ curve. The small difference between these two values (10%), was taken as evidence in favor of a narrow distribution. What has been done in effect was a comparison between L_z and L_w. It is somewhat surprising that the length determined from high angle measurements (2900 Å) was lower than the length of the most frequent particle (3000 Å), as determined with the electron microscope. A similar discrepancy was obtained in our laboratory on potato X virus (see preceding article). These discrepancies resulted probably from polydispersity in thickness, as discussed above. The 10% difference would be a measure of the total polydispersity. In view of this it is not surprising that the distribution function of length in tobacco mosaic virus as obtained from electron microscope data was extremely sharp (8).

1. HOLTZER, A. M. J. Polymer Sci. **17**, 432 (1955).
2. BENOIT, H. J. Polymer Sci. **11**, 507 (1953).
3. BENOIT, H., HOLTZER, A. M., and DOTY, P. J. Phys. Chem. **58**, 635 (1954).

Can. J. Chem. Downloaded from www.nrcresearchpress.com by 190.90.36.8 on 09/04/12
For personal use only.

4. RICE, S. A. J. Polymer Sci. **16**, 94 (1955).
5. ZIMM, B. J. Chem. Phys. **16**, 1099 (1948).
6. CASASSA, E. F. J. Chem. Phys. **23**, 596 (1955).
7. BOEDTKER, H. and SIMMONS, N. S. J. Am. Chem. Soc. **80**, 2550 (1958).
8. HALL, C. E. J. Am. Chem. Soc. **80**, 2556 (1958).

RECEIVED SEPTEMBER 22, 1958.
CONTRIBUTION NO. 7, CHEMISTRY DIVISION, SCIENCE SERVICE,
CANADA DEPARTMENT OF AGRICULTURE RESEARCH LABORATORY,
VANCOUVER, B.C.

Can. J. Chem. Downloaded from www.nrcresearchpress.com by 190.90.36.8 on 09/04/12
For personal use only.

THE DIELECTRIC CONSTANT AND DIPOLE MOMENT OF 1,3-DIOXANE[1]

R. WALKER[2] AND D. W. DAVIDSON

In contrast to 1,4-dioxane, which has been extensively investigated, neither the dielectric constant nor the dipole moment of 1,3-dioxane has been previously measured, although the dipole moment has been recently calculated (1). The present note reports the static dielectric constants of liquid and solid 1,3-dioxane and the dipole moment as measured in cyclohexane and benzene solutions.

EXPERIMENTAL METHODS

1,3-Dioxane was prepared from 1,3-propanediol and paraformaldehyde by essentially the method of Clarke (2), followed by distillation in a Todd still over calcium oxide and a second distillation over calcium hydride. Boiling point (757 mm) 104.9–105.1° (corr.), n_D^{25} 1.4171. The water content, estimated by the Fischer method, was 0.013% and the absence of significant quantities of hydroxyl- and carbonyl-containing impurities was shown by the infrared spectrum. Gas chromatographic analyses showed only a trace (less than 0.3%) of volatile impurities, except for one sample.

Solvents were dried by refluxing over calcium hydride, followed by distillation. Benzene, after 84 hours of refluxing, had a water content of less than 0.001%.

Dielectric measurements on the liquid and solid were made by a method previously described (3). Dipole moment determinations were made at 25.0° C with a cell of 37 $\mu\mu$f capacitance using a substitution method which involved a number of reiterations to increase the total capacitance measured. For the most dilute solutions 20 reiterations were made.

Refractive indices were measured at 25.0° C with an Abbé Refractometer.

RESULTS AND DISCUSSION

The dielectric constant is shown as a function of temperature in Fig. 1. The melting point is indicated by the break in the curve at −44° C. In the liquid there is no dependence of dielectric constant (ϵ') on frequency up to at least 500 kc/sec. In the solid there is some dispersion of ϵ' over a temperature range extending a few degrees below the melting point where the points in the figure refer to measurements made at 10 kc/sec. At higher frequencies the curve shows less curvature before the melting point is reached.

Between the melting point and 25° C the static dielectric constant values for the liquid may be represented by

$$\epsilon_0 = -5.29_5 + 5.62_3 \times 10^3/T$$

with an average deviation of ±0.2%.

[1]*Issued as N.R.C. No. 5019.*
[2]*Present address: Department of Chemistry, The University, Hull, England.*

4. RICE, S. A. J. Polymer Sci. **16**, 94 (1955).
5. ZIMM, B. J. Chem. Phys. **16**, 1099 (1948).
6. CASASSA, E. F. J. Chem. Phys. **23**, 596 (1955).
7. BOEDTKER, H. and SIMMONS, N. S. J. Am. Chem. Soc. **80**, 2550 (1958).
8. HALL, C. E. J. Am. Chem. Soc. **80**, 2556 (1958).

RECEIVED SEPTEMBER 22, 1958.
CONTRIBUTION NO. 7, CHEMISTRY DIVISION, SCIENCE SERVICE,
CANADA DEPARTMENT OF AGRICULTURE RESEARCH LABORATORY,
VANCOUVER, B.C.

Can. J. Chem. Downloaded from www.nrcresearchpress.com by 190.90.36.8 on 09/04/12
For personal use only.

THE DIELECTRIC CONSTANT AND DIPOLE MOMENT OF 1,3-DIOXANE[1]

R. WALKER[2] AND D. W. DAVIDSON

In contrast to 1,4-dioxane, which has been extensively investigated, neither the dielectric constant nor the dipole moment of 1,3-dioxane has been previously measured, although the dipole moment has been recently calculated (1). The present note reports the static dielectric constants of liquid and solid 1,3-dioxane and the dipole moment as measured in cyclohexane and benzene solutions.

EXPERIMENTAL METHODS

1,3-Dioxane was prepared from 1,3-propanediol and paraformaldehyde by essentially the method of Clarke (2), followed by distillation in a Todd still over calcium oxide and a second distillation over calcium hydride. Boiling point (757 mm) 104.9–105.1° (corr.), n_D^{25} 1.4171. The water content, estimated by the Fischer method, was 0.013% and the absence of significant quantities of hydroxyl- and carbonyl-containing impurities was shown by the infrared spectrum. Gas chromatographic analyses showed only a trace (less than 0.3%) of volatile impurities, except for one sample.

Solvents were dried by refluxing over calcium hydride, followed by distillation. Benzene, after 84 hours of refluxing, had a water content of less than 0.001%.

Dielectric measurements on the liquid and solid were made by a method previously described (3). Dipole moment determinations were made at 25.0° C with a cell of 37 $\mu\mu$f capacitance using a substitution method which involved a number of reiterations to increase the total capacitance measured. For the most dilute solutions 20 reiterations were made.

Refractive indices were measured at 25.0° C with an Abbé Refractometer.

RESULTS AND DISCUSSION

The dielectric constant is shown as a function of temperature in Fig. 1. The melting point is indicated by the break in the curve at −44° C. In the liquid there is no dependence of dielectric constant (ϵ') on frequency up to at least 500 kc/sec. In the solid there is some dispersion of ϵ' over a temperature range extending a few degrees below the melting point where the points in the figure refer to measurements made at 10 kc/sec. At higher frequencies the curve shows less curvature before the melting point is reached.

Between the melting point and 25° C the static dielectric constant values for the liquid may be represented by

$$\epsilon_0 = -5.29_5 + 5.62_3 \times 10^3/T$$

with an average deviation of ±0.2%.

[1]*Issued as N.R.C. No. 5019.*
[2]*Present address: Department of Chemistry, The University, Hull, England.*

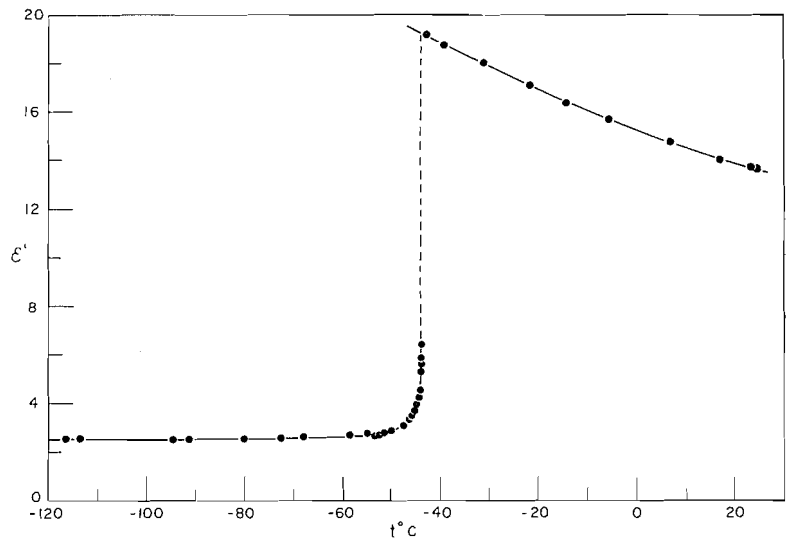

FIG. 1.

The dielectric results provide no evidence of the existence of more than one solid phase, although the possibility of a transition between two non-polar forms which do not differ greatly in density is not excluded. The value of ϵ_0 ($\sim$2.6) in the solid is about that to be expected for the square of the refractive index and shows the absence of any appreciable rotational polarization. 1,4-Dioxane exhibits a solid–solid transition some 11° below the melting point (4).

Figure 2 is a plot of Δ/w vs. w for the cyclohexane and benzene solutions. Here $\Delta = (\epsilon-\epsilon_1)-(n^2-n_1^2)$ and w is the weight fraction of dioxane. The dipole moment was calculated from

$$\mu^2 = \frac{27kT}{4\pi N_A}\frac{M}{(\epsilon_1+2)^2 d_1}\cdot\left(\frac{\Delta}{w}\right)_0$$

in which ϵ_1 and d_1 refer to the solvent and $(\Delta/w)_0$ to the value extrapolated to $w = 0$.

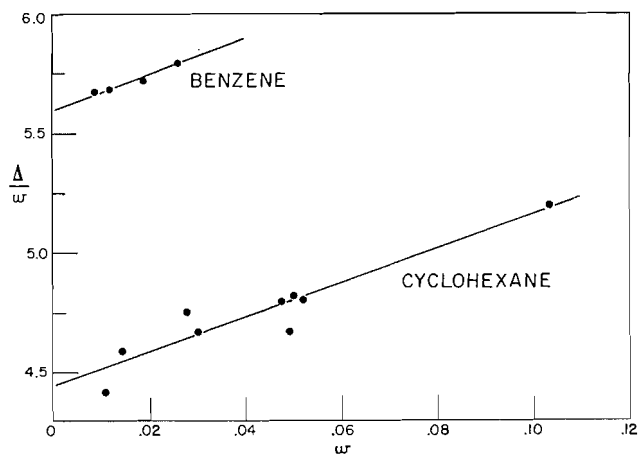

FIG. 2.

Can. J. Chem. Downloaded from www.nrcresearchpress.com by 190.90.36.8 on 09/04/12
For personal use only.

As pointed out by Guggenheim (5), a least squares treatment of a quantity like Δ/w as a function of concentration weighs too heavily the less accurate data at low concentrations. Consequently we have fitted the data by least squares to the equations

$$\epsilon - \epsilon_1 = \alpha w + \beta w^2$$

$$n^2 - n_1^2 = \gamma w + \delta w^2$$

and obtained $(\Delta/w)_0$ as $(\alpha - \gamma)$. The straight lines in Fig. 2 result from this treatment.

The dipole moments obtained are 2.14_5 D from the solutions in cyclohexane and 2.13_4 D for those in benzene, with an over-all accuracy estimated at ± 0.03 D.

By the use of the Onsager equation (6) an "effective" dipole moment for the undiluted dioxane may be calculated from the dielectric constant of the liquid. At 25° C, μ (Onsager) = 2.55 D, a value which is practically independent of temperature. The difference between the Onsager moment and the dilute solution moments implies a considerable correlation between the moments of neighboring molecules in the liquid.

The value of the dipole moment calculated by Le Fèvre, Le Fèvre, and Smith (1), for the purpose of establishing the configuration of dimethylene pentaerythritol, was 1.86_5 D. Our measured values are sufficiently close to this figure not to change these workers' conclusion that the two 1,3-dioxane rings having ring atom 5 in common are most likely both in the chair configuration.

The difference between the moment of 1,3-dioxane and that of 2-methyl-1,3-dioxane (1.89 D in benzene (7)) is probably primarily due to the effect of the methyl group in making the ring flatter and the OCO angle larger. The calculation of the moment of 1,3-dioxane referred to above (1) made use of an assumed moment for the C–O–C group of 1.25 D, which is one experimental value of the dipole moment of dimethyl ether. However, in general the C–O–C group appears to have a higher moment in cyclic ethers, the dipole moment of pentamethylene oxide, for example, being 1.87 D (8). In addition, the presence of two C–O–C groups in the ring will change the charge distribution in such a way as to reduce the effective dipole moment associated with each.

To the extent that the contribution of C–H bond moments is negligible, there is no difference between the dipole moments of the chair and boat forms of 1,3-dioxane. Some indirect evidence, however, for the predominance of the chair form is afforded by the magnitude of the difference between μ (Onsager) and μ (solution), which is unusually large for a liquid in which hydrogen bonding is absent (6). Figure 3 illustrates what are perhaps the most favorable relative positions for neighboring molecules, along with the directions of their dipole moments. In each configuration the dipole moment lies in the plane of symmetry of the molecule and each molecule is represented by its projection on this plane. It is evident that complexes of the type shown for the chair configuration, in which neighboring molecules have their moments parallel to one another, will lead to an effective dipole moment considerably higher than that of an isolated molecule. For

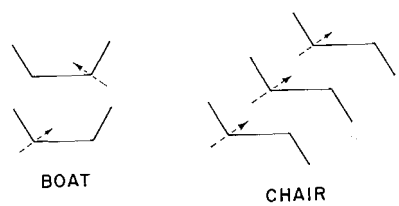

FIG. 3. "Favored" packing of molecules in 1,3-dioxane. Dipole moments are drawn through projections of O atoms on the planes of symmetry.

Can. J. Chem. Downloaded from www.nrcresearchpress.com by 190.90.36.8 on 09/04/12
For personal use only.

vertically stacked boat molecules, on the other hand, adjacent molecules have only a small (~1 D) vertical component of moment in common.

ACKNOWLEDGMENTS

We are indebted to R. Ironside and M. E. Bednas for Fischer, infrared, and gas chromatographic analyses, and to Mrs. G. Wheeler for technical assistance.

1. Le Fèvre, C. G., Le Fèvre, R. J. W., and Smith, M. R. J. Chem. Soc. 16 (1958).
2. Clarke, H. T. J. Chem. Soc. **103**, 1788 (1912).
3. Davidson, D. W. Can. J. Chem. **35**, 458 (1957).
4. Jacobs, C. J. and Parks, G. S. J. Am. Chem. Soc. **56**, 1513 (1934).
5. Guggenheim, E. A. Trans. Faraday Soc. **47**, 573 (1951).
6. Böttcher, C. J. F. Theory of electric polarization. Elsevier Pub. Co., Inc., Amsterdam. 1952. p. 323.
7. Otto, M. M. J. Am. Chem. Soc. **59**, 1590 (1937).
8. Allen, J. S. and Hibbert, H. J. Am. Chem. Soc. **56**, 1398 (1934).

Received October 19, 1958.
Division of Applied Chemistry,
National Research Council of Canada,
Ottawa, Canada.

ON THE CONSTITUTION OF 2-KETO-L-GULONIC ACID

N. J. Gaspar* and J. M. Los

In the course of a polarographic investigation of 2-keto-L-gulonic acid (1) the following constitutional features were observed.

In aqueous solution the compound exists in the free acid lactol form as proposed by Reichstein and Grüssner (2), in equilibrium with an extremely small concentration of the free keto acid. The solid state can be either a free keto acid or the corresponding lactone. The latter crystallizes from a solution either of high viscosity or of high ionic strength. Sometimes mixtures of the two solid forms were obtained. Each form was invariably found to contain one molecule of water of crystallization.

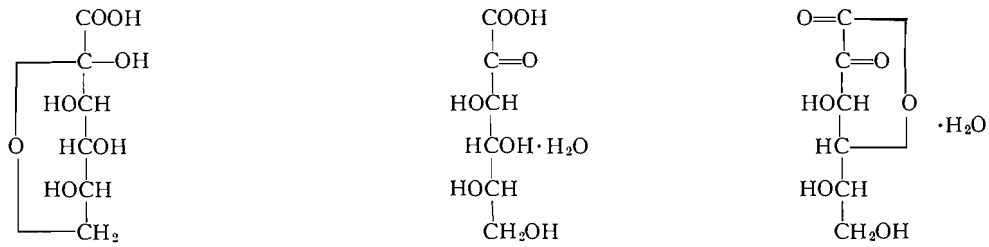

free acid lactol in solution | free keto acid in solid state | lactone

The lactone is, of course, the keto tautomer of L-ascorbic acid.

The solid 2-keto-L-gulonic acid was made by the method of Reichstein and Grüssner (2): 20 g of diacetone-2-keto-L-gulonic acid were dissolved in 200 ml of distilled water. The solution was heated to boiling and was allowed to stand over a boiling water bath for 45 minutes. The water was then evaporated *in vacuo* till a sirup remained. We found

Holder of a National Research Council of Canada Studentship.

Can. J. Chem. Downloaded from www.nrcresearchpress.com by 190.90.36.8 on 09/04/12
For personal use only.

vertically stacked boat molecules, on the other hand, adjacent molecules have only a small (~1 D) vertical component of moment in common.

ACKNOWLEDGMENTS

We are indebted to R. Ironside and M. E. Bednas for Fischer, infrared, and gas chromatographic analyses, and to Mrs. G. Wheeler for technical assistance.

1. Le Fèvre, C. G., Le Fèvre, R. J. W., and Smith, M. R. J. Chem. Soc. 16 (1958).
2. Clarke, H. T. J. Chem. Soc. **103**, 1788 (1912).
3. Davidson, D. W. Can. J. Chem. **35**, 458 (1957).
4. Jacobs, C. J. and Parks, G. S. J. Am. Chem. Soc. **56**, 1513 (1934).
5. Guggenheim, E. A. Trans. Faraday Soc. **47**, 573 (1951).
6. Böttcher, C. J. F. Theory of electric polarization. Elsevier Pub. Co., Inc., Amsterdam. 1952. p. 323.
7. Otto, M. M. J. Am. Chem. Soc. **59**, 1590 (1937).
8. Allen, J. S. and Hibbert, H. J. Am. Chem. Soc. **56**, 1398 (1934).

Received October 19, 1958.
Division of Applied Chemistry,
National Research Council of Canada,
Ottawa, Canada.

ON THE CONSTITUTION OF 2-KETO-L-GULONIC ACID

N. J. Gaspar* and J. M. Los

In the course of a polarographic investigation of 2-keto-L-gulonic acid (1) the following constitutional features were observed.

In aqueous solution the compound exists in the free acid lactol form as proposed by Reichstein and Grüssner (2), in equilibrium with an extremely small concentration of the free keto acid. The solid state can be either a free keto acid or the corresponding lactone. The latter crystallizes from a solution either of high viscosity or of high ionic strength. Sometimes mixtures of the two solid forms were obtained. Each form was invariably found to contain one molecule of water of crystallization.

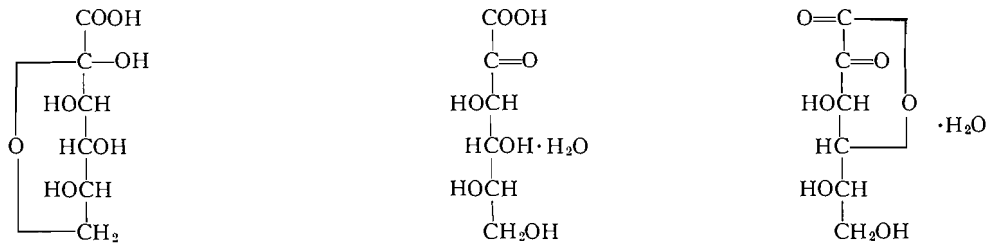

free acid lactol in solution | free keto acid in solid state | lactone

The lactone is, of course, the keto tautomer of L-ascorbic acid.

The solid 2-keto-L-gulonic acid was made by the method of Reichstein and Grüssner (2): 20 g of diacetone-2-keto-L-gulonic acid were dissolved in 200 ml of distilled water. The solution was heated to boiling and was allowed to stand over a boiling water bath for 45 minutes. The water was then evaporated *in vacuo* till a sirup remained. We found

Holder of a National Research Council of Canada Studentship.

Can. J. Chem. Downloaded from www.nrcresearchpress.com by 190.90.36.8 on 09/04/12
For personal use only.

that crystallization from a low-viscosity solution yielded a different substance from that crystallizing at high viscosity. At intermediate viscosity, mixtures of these two would form.

This conclusion was drawn primarily from the results of alkalimetric titration: the product from low-viscosity solution was found to be 99.9% pure if its molecular weight was assumed to be 212, i.e. that of the free acid plus one molecule of water of crystallization. The substance obtained from the high-viscosity solution showed the same degree of purity if its molecular weight was put at 194. This could mean either that the water of crystallization does not appear in the latter case, or that the lactone ring has closed during crystallization.

Heating of the higher molecular weight compound at 50° *in vacuo* for a few hours also produced the compound of molecular weight 194, the loss of weight corresponding to exactly one molecule of water.

The decision as to the nature of the lower molecular weight compound could be made on the basis of the infrared spectra of both solid compounds (Fig. 1). The spectra were taken from KBr pellets (about 1.5 mg of solid in 400 mg of KBr) with a Perkin–Elmer Model 21 spectrophotometer. The product of molecular weight 212 has a strong adsorption peak at 5.75 μ, characteristic of the carbonyl stretching band and much like the corresponding peak of pyruvic acid at 5.73 μ. The product of molecular weight 194, however, shows a peak at 5.67 μ, which is typical of a lactone. Therefore it is concluded that the water is lost in the closing of the lactone ring and not by giving up water of crystallization (the slight adsorption around 6.10 μ seems characteristic of free water).

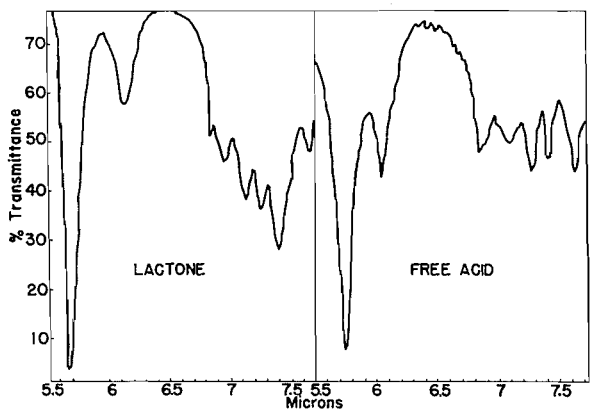

FIG. 1.

It is not likely that either of the two solid forms contains a lactol ring. Molecular models may show that the lactone cannot have a cyclohemiacetal ring as well. The most favorable case is a very strained double-ring structure obtained when the pyranose lactol has the boat conformation and the OH groups on C_2 and C_3 are *cis* to one another. Furthermore, it is not likely that a lactol ring exists in the solid free acid either: (*a*) the C=O adsorption peak at 5.75 μ is very large, (*b*) the above-mentioned transition of this free acid into the lactone form would probably require a total rearrangement within the crystal.

Both solid forms dissolve in water as the free acid, predominantly with a cyclohemiacetal ring. However, equilibrium with the free keto acid must exist, as borne out

Can. J. Chem. Downloaded from www.nrcresearchpress.com by 190.90.36.8 on 09/04/12
For personal use only.

by the completely rate-controlled current–voltage wave at the dropping mercury electrode (1). The ionization constant ($K = f\pm(c_{H^+}c_{A^-}/c_{HA})$) is 2.86×10^{-3} at 25° C and ionic strength 0.7 (1).

When KBr pellets were made not by mixing of the solid with KBr but by quickly freezing a solution of the free acid containing a high concentration of KBr, and then removing the water by freeze-drying, the lactone form was invariably produced.

In order to decide whether this is due to the high KBr concentration or to the lower temperature, the following experiment was carried out.

Two identical samples of the lactone (15 mg each) were dissolved in 10 ml of water. To one of these, 4 g of KBr was added. Each solution was then rapidly frozen in a dry ice – acetone mixture and the ice was sublimed *in vacuo*. The sample to which no KBr had been added was then mixed with 4 g of the latter. Identical pellets were made. The spectra showed clearly that the sample containing the KBr in solution had crystallized in the lactone form, the other as the free keto acid (in spite of the fact that it had its starting point in the solid lactone). We may therefore conclude that in the case of the first sample most of the water had been tied up as water of hydration of the K^+ and Br^- ions, lowering the activity of the water to such an extent that only the lactone could crystallize, just as if the crystallization had taken place from a very viscous solution.

Our thanks go to the National Research Council for financial assistance and to Merck and Company, Montreal, for providing the diacetone 2-keto-L-gulonic acid.

1. Los, J. M. and Gaspar, N. J. To be published.
2. Reichstein, T. and Grüssner, A. Helv. Chim. Acta, **17**, 311 (1934).

Received August 25, 1958.
Department of Chemistry,
University of New Brunswick,
Fredericton, New Brunswick.

ISOLATION OF OLIGOSACCHARIDES IN IMPROVED YIELD BY THE ENZYMATIC DEGRADATION OF POLYSACCHARIDES

T. J. Painter[1]

Theoretical considerations originating with Kuhn (1) predict that, for random degradation of a uniform linear macromolecule, the yield of the n-membered fragment is given by $n\alpha^2(1-\alpha)^{n-1}$, where α is the degree of scission. The maximum possible yield of the fragment is then $n[2/(n+1)]^2[(n-1)/(n+1)]^{n-1}$, and occurs when $\alpha = 2/(n+1)$. Further calculation shows that the maximum possible yield of dimer plus trimer occurs when $\alpha = 0.59$, and amounts to 46%.

In the hydrolysis or acetolysis of polysaccharides, lack of randomness in the degradation usually results in considerably lower yields, and study of the literature shows that the combined yield of di- and tri-saccharides has seldom exceeded 35% by weight of the total hydrolyzate. Apart from the wastage of material, examination of the oligosaccharides obtained in these cases would reveal only the dominant structural features of the parent polysaccharide. In addition, misleading artifacts may arise from the recombination (reversion) of simple sugars, although in the case of acetolysis this effect appears to be minimized (2).

[1]*Harold Hibbert Memorial Fellow, McGill University, Montreal, Quebec, 1957–58.*

Can. J. Chem. Downloaded from www.nrcresearchpress.com by 190.90.36.8 on 09/04/12
For personal use only.

by the completely rate-controlled current–voltage wave at the dropping mercury electrode (1). The ionization constant ($K = f\pm(c_{H^+}c_{A^-}/c_{HA})$) is 2.86×10^{-3} at 25° C and ionic strength 0.7 (1).

When KBr pellets were made not by mixing of the solid with KBr but by quickly freezing a solution of the free acid containing a high concentration of KBr, and then removing the water by freeze-drying, the lactone form was invariably produced.

In order to decide whether this is due to the high KBr concentration or to the lower temperature, the following experiment was carried out.

Two identical samples of the lactone (15 mg each) were dissolved in 10 ml of water. To one of these, 4 g of KBr was added. Each solution was then rapidly frozen in a dry ice – acetone mixture and the ice was sublimed *in vacuo*. The sample to which no KBr had been added was then mixed with 4 g of the latter. Identical pellets were made. The spectra showed clearly that the sample containing the KBr in solution had crystallized in the lactone form, the other as the free keto acid (in spite of the fact that it had its starting point in the solid lactone). We may therefore conclude that in the case of the first sample most of the water had been tied up as water of hydration of the K^+ and Br^- ions, lowering the activity of the water to such an extent that only the lactone could crystallize, just as if the crystallization had taken place from a very viscous solution.

Our thanks go to the National Research Council for financial assistance and to Merck and Company, Montreal, for providing the diacetone 2-keto-L-gulonic acid.

1. Los, J. M. and Gaspar, N. J. To be published.
2. Reichstein, T. and Grüssner, A. Helv. Chim. Acta, **17**, 311 (1934).

Received August 25, 1958.
Department of Chemistry,
University of New Brunswick,
Fredericton, New Brunswick.

ISOLATION OF OLIGOSACCHARIDES IN IMPROVED YIELD BY THE ENZYMATIC DEGRADATION OF POLYSACCHARIDES

T. J. Painter[1]

Theoretical considerations originating with Kuhn (1) predict that, for random degradation of a uniform linear macromolecule, the yield of the n-membered fragment is given by $n\alpha^2(1-\alpha)^{n-1}$, where α is the degree of scission. The maximum possible yield of the fragment is then $n[2/(n+1)]^2[(n-1)/(n+1)]^{n-1}$, and occurs when $\alpha = 2/(n+1)$. Further calculation shows that the maximum possible yield of dimer plus trimer occurs when $\alpha = 0.59$, and amounts to 46%.

In the hydrolysis or acetolysis of polysaccharides, lack of randomness in the degradation usually results in considerably lower yields, and study of the literature shows that the combined yield of di- and tri-saccharides has seldom exceeded 35% by weight of the total hydrolyzate. Apart from the wastage of material, examination of the oligosaccharides obtained in these cases would reveal only the dominant structural features of the parent polysaccharide. In addition, misleading artifacts may arise from the recombination (reversion) of simple sugars, although in the case of acetolysis this effect appears to be minimized (2).

[1]*Harold Hibbert Memorial Fellow, McGill University, Montreal, Quebec, 1957–58.*

Can. J. Chem. Downloaded from www.nrcresearchpress.com by 190.90.36.8 on 09/04/12
For personal use only.

Can. J. Chem. Downloaded from www.nrcresearchpress.com by 190.90.36.8 on 09/04/12
For personal use only.

As Kuhn pointed out, these yields can be considerably increased if the oligosaccharides, once formed, are protected in some way from further degradation. Cellobiose octaacetate, for example, is partly protected by crystallization during the acetolysis of cellulose, and yields of over 40% are not uncommon (3). When completely protected, the maximum yield of n-mer in a random degradation would be $2/(n+1)$, and the maximum yield of dimer plus trimer, if both were protected, would be 83.3%.

This note suggests a possible method of protection in which the lower oligosaccharides are continuously removed from the system by dialysis. To achieve this, it is clear that neither the catalyst, nor any saccharides higher than those desired, should be dialyzable and that the former should not attack the membrane. These conditions were met quite closely by using some fungal hemicellulases and pectinases* in conjunction with a cellophane membrane (4).

Aqueous solutions of a series of polysaccharides, together with the enzyme preparation, were enclosed in cellophane dialysis bags which were large enough to permit a 100% increase in volume of the solution, such as would arise through osmosis. The bags were placed in beakers containing relatively large volumes of water, maintained at 37° C. At intervals, the dialyzates were replaced with fresh water until no further carbohydrate material was removed from the reaction mixture. The combined dialyzates in each case were concentrated to yield syrupy mixtures of sugars, which were shown by paper chromatography to contain large amounts of di-, tri-, tetra-, and higher saccharides, in addition to monosaccharides.

Quantitative experiments were carried out with the four polysaccharides listed in Table I. Each was used in conjunction with a purified hemicellulase preparation, which effected rapid and nearly complete (80–95%) conversion into dialyzable material, while having little effect on the cellophane membrane. The sugars obtained in each case were weighed and then adsorbed on small charcoal columns. The monosaccharide components were selectively eluted and weighed, and the weights of the oligosaccharides were assumed to be represented by the difference.

TABLE I

Recovery of oligosaccharides from polysaccharides

Polysaccharide	Sample* (g)	Saccharides in dialyzate†			
		Total (g)	Mono- (g)	Oligo-‡ (g)	Oligo- (%)
Galactoglucomannan§	0.49	0.44	0.16	0.28	64
Galactoglucomannan‖	0.46	0.43	0.26	0.17	39
Arabogalactan‖	0.50	0.48	0.23	0.25	52
4-*O*-Methylglucuronoxylan¶	0.51	0.43	0.30	0.13	30

*Solution or suspension in water (40 ml), plus 1% w/v hemicellulase in water (10 ml).
†Dialyzates (1 l.) replaced by water every 8 hours for 24 hours, then combined.
‡From columns 3 and 4 by difference.
§From wood of loblolly pine (*Pinus taeda* Linn.) (5).
‖From inner bark of white spruce (*Picea glauca* (Moench) Voss) (6).
¶From wood of white birch (*Betula papyrifera* Marsh.) (7).

These figures provide merely an approximate indication of the possible general usefulness of the method. The yield of oligomers in a particular case will, of course, be greatly dependent upon the nature of the polymer and the enzyme preparation used, as well as conditions of temperature, pH, and concentration. It will also be dependent upon the

Obtained from the Nutritional Biochemicals Corporation, Cleveland, Ohio.

dimensions of the dialysis vessel in which hydrolysis is carried out, and the rate at which the dialyzate is replaced by fresh water. A more detailed investigation of the optimum conditions for the partial hydrolysis of a number of polysaccharides is now in progress, and an apparatus has been constructed which provides for continuous replacement of the dialyzate, automatic collection of the oligosaccharides, and the use of suitable buffer solutions. It is also intended to construct a dialysis vessel such that the area of membrane for a given volume of reaction mixture is greatly increased, in order to facilitate rapid diffusion of the oligosaccharides.

The author wishes to thank Professor C. B. Purves for his kind interest in this work, and the National Research Council for financial assistance.

1. KUHN, W. Ber. B, **63**, 1503 (1930).
2. SMITH, F. and SRIVASTAVA, H. C. J. Am. Chem. Soc. **78**, 1404 (1956).
3. BRAUN, G. *In* Organic syntheses, Coll. Vol. **II**, 122 (1943).
4. JONES, J. K. N., MERLER, E., and WISE, L. E. Can. J. Chem. **35**, 634 (1957).
5. JONES, J. K. N. and PAINTER, T. J. J. Chem. Soc. 669 (1957).
6. PAINTER, T. J. Forthcoming publication.
7. GLAUDEMANS, C. P. J. and TIMELL, T. E. J. Am. Chem. Soc. **80**, 941, 1209 (1958).

RECEIVED OCTOBER 21, 1958.
McGILL UNIVERSITY AND
PULP AND PAPER RESEARCH INSTITUTE OF CANADA,
MONTREAL, QUEBEC.

5-*O*-β-D-GALACTOFURANOSYL-D-GALACTOSE FROM GALACTOCARALOSE*

P. A. J. GORIN AND J. F. T. SPENCER

Galactocaralose, a polysaccharide formed by *Penicillium charlesii* G. Smith in Raulin-Thom medium has been shown to contain D-anhydrogalactofuranose units linked 1,5 linearly to a chain length of 9–10 units as indicated by the methylation (1, 2) technique. Its $[\alpha]_{5780}$ (−84°) suggested strongly that the galactose units have the β-configuration.

In the present work partial acid hydrolysis of galactocaralose, which contained smaller amounts of the more acid-stable mannocaralose, produced, as shown by paper chromatography, a homologous series of oligosaccharides. The mixture was fractionated on a cellulose column (3) and materials which appeared to be galactose (4.5%), galactobiose (1.8%), galactotriose (1.4%), galactotetraose (0.4%), and galactopentaose (0.8%) were obtained.

The galactobiose contained a furanose non-reducing end unit, since the sugar was rapidly hydrolyzed with 0.01 *N* sulphuric acid at 100° C (4). Only D-galactose was formed as shown by paper chromatographic examination and by preparation of the 1-methyl 1-phenylhydrazone derivative (5). Treatment of the disaccharide with excess lead tetraacetate in acetic acid resulted in nearly 2 moles of oxidant being consumed at a moderately rapid rate which ruled out 2-, 3-, and probably 4-substitution, and suggested that the glycosidic linkage was either 1,5 or 1,6 (6). A crystalline galactobiitol, obtained by sodium borohydride reduction (7) of the aldose, consumed in 2 minutes 4 molar equivalents of sodium periodate with concomitant release of 2 moles of formic acid; in a separate experiment 2 moles of formaldehyde were formed on sodium periodate oxidation. More prolonged treatment of the polyol resulted in overoxidation probably

*Issued as N.R.C. No. 5022.

Can. J. Chem. Downloaded from www.nrcresearchpress.com by 190.90.36.8 on 09/04/12
For personal use only.

dimensions of the dialysis vessel in which hydrolysis is carried out, and the rate at which the dialyzate is replaced by fresh water. A more detailed investigation of the optimum conditions for the partial hydrolysis of a number of polysaccharides is now in progress, and an apparatus has been constructed which provides for continuous replacement of the dialyzate, automatic collection of the oligosaccharides, and the use of suitable buffer solutions. It is also intended to construct a dialysis vessel such that the area of membrane for a given volume of reaction mixture is greatly increased, in order to facilitate rapid diffusion of the oligosaccharides.

The author wishes to thank Professor C. B. Purves for his kind interest in this work, and the National Research Council for financial assistance.

1. KUHN, W. Ber. B, **63**, 1503 (1930).
2. SMITH, F. and SRIVASTAVA, H. C. J. Am. Chem. Soc. **78**, 1404 (1956).
3. BRAUN, G. *In* Organic syntheses, Coll. Vol. **II**, 122 (1943).
4. JONES, J. K. N., MERLER, E., and WISE, L. E. Can. J. Chem. **35**, 634 (1957).
5. JONES, J. K. N. and PAINTER, T. J. J. Chem. Soc. 669 (1957).
6. PAINTER, T. J. Forthcoming publication.
7. GLAUDEMANS, C. P. J. and TIMELL, T. E. J. Am. Chem. Soc. **80**, 941, 1209 (1958).

RECEIVED OCTOBER 21, 1958.
McGILL UNIVERSITY AND
PULP AND PAPER RESEARCH INSTITUTE OF CANADA,
MONTREAL, QUEBEC.

5-*O*-β-D-GALACTOFURANOSYL-D-GALACTOSE FROM GALACTOCARALOSE*

P. A. J. GORIN AND J. F. T. SPENCER

Galactocaralose, a polysaccharide formed by *Penicillium charlesii* G. Smith in Raulin-Thom medium has been shown to contain D-anhydrogalactofuranose units linked 1,5 linearly to a chain length of 9–10 units as indicated by the methylation (1, 2) technique. Its $[\alpha]_{5780}$ (−84°) suggested strongly that the galactose units have the β-configuration.

In the present work partial acid hydrolysis of galactocaralose, which contained smaller amounts of the more acid-stable mannocaralose, produced, as shown by paper chromatography, a homologous series of oligosaccharides. The mixture was fractionated on a cellulose column (3) and materials which appeared to be galactose (4.5%), galactobiose (1.8%), galactotriose (1.4%), galactotetraose (0.4%), and galactopentaose (0.8%) were obtained.

The galactobiose contained a furanose non-reducing end unit, since the sugar was rapidly hydrolyzed with 0.01 *N* sulphuric acid at 100° C (4). Only D-galactose was formed as shown by paper chromatographic examination and by preparation of the 1-methyl 1-phenylhydrazone derivative (5). Treatment of the disaccharide with excess lead tetraacetate in acetic acid resulted in nearly 2 moles of oxidant being consumed at a moderately rapid rate which ruled out 2-, 3-, and probably 4-substitution, and suggested that the glycosidic linkage was either 1,5 or 1,6 (6). A crystalline galactobiitol, obtained by sodium borohydride reduction (7) of the aldose, consumed in 2 minutes 4 molar equivalents of sodium periodate with concomitant release of 2 moles of formic acid; in a separate experiment 2 moles of formaldehyde were formed on sodium periodate oxidation. More prolonged treatment of the polyol resulted in overoxidation probably

*Issued as N.R.C. No. 5022.

Can. J. Chem. Downloaded from www.nrcresearchpress.com by 190.90.36.8 on 09/04/12
For personal use only.

due to attack of the 2,3-*trans*-glycol of the anhydrogalactofuranose unit. Thus the only reasonable structure for the reducing disaccharide is the hitherto undescribed 5-*O*-D-galactofuranosyl-D-galactose, which complements the methylation data obtained from the original polysaccharide.

In agreement with the oxidation data, treatment of the galactobiitol with excess sodium periodate followed by sodium borohydride reduction gave a sirupy arabofuranosyl glycerol ($[\alpha]_D$ −129°). The latter, which gave an amorphous penta-*p*-nitrobenzoate, yielded arabinose and glycerol on acid hydrolysis and consumed 1 molar equivalent of sodium periodate which accords with the values expected from 2-*O*-L-arabofuranosyl glycerol. The configuration of the glycosidic linkage is deduced to be α by isorotational considerations mentioned later. It has been shown that in many glycopyranosyl-polyols the open-chain glycols are attacked preferentially by lead tetraacetate in acetic acid (8, 9). However, *trans* α-glycols in 5-membered ring systems may be oxidized relatively quickly with lead tetraacetate, and aqueous sodium periodate is a more specific oxidizing agent (10) for the required purpose. Based on Hudson's rules of isorotation (11), which have been used in the methyl glycopyranosyl and the glycopyranosyl glycerol series of sugars (8, 12), the specific rotation of 2-*O*-α-L-arabofuranosyl glycerol is calculated to be −108° using the following values: (*a*) 2-*O*-α-D-galactopyranosyl-glycerol, $[\alpha]_D$ +165° (13); (*b*) methyl-α-D-galactopyranoside·H_2O, $[\alpha]_D$ +179° (14); (*c*) methyl-α-D-arabofuranoside, $[\alpha]_D$ +123° (15).

EXPERIMENTAL

Optical rotations were measured at 27° C and evaporations done at 40° C. Solvents for paper chromatographic separations were ethyl acetate – acetic acid – water (9:2:2 v/v) for reducing oligosaccharides and butanol–ethanol–water (40:11:19 v/v) for other carbohydrates. *p*-Anisidine hydrochloride (16) was used as spray reagent for reducing and ammoniacal silver nitrate (17) for non-reducing sugars. R_{Gal} and R_{Rh} denote distances travelled by sugars on paper chromatograms compared to galactose and rhamnose, respectively.

Galactobiose from Galactocaralose

Trial hydrolyses of galactocaralose under a variety of pH's from 1 to 4 at 75° C for 18 hours (cf. the conditions of Andrews, Hough, and Powell (18) for partial hydrolysis of beet araban) showed that pH 2.2 gave the optimum yield of galactobiose (R_{Gal} 0.9), as judged from paper chromatograms. Therefore, galactocaralose (30.0 g), obtained by fermentation of Raulin-Thom medium by *Penicillium charlesii*, was dissolved in water (2 l.) and brought to pH 2.2 with sulphuric acid. After heating at 75° C for 18 hours the solution was neutralized ($BaCO_3$), filtered, and evaporated to a small volume which was added to excess methanol. The methanol-soluble material gave, on a paper chromatogram, a sugar corresponding to galactose and also four other slower moving yellow spots. The mixture of what appeared to be a homologous series of oligosaccharides was fractionated on a cellulose column. Ethyl acetate – acetic acid – water (9:2:2 v/v) eluted galactose (1.50 g); a 9:3:3 mixture gave galactobiose (0.55 g) then galactotriose (0.42 g) and a 9:4:4 mixture galactotetraose (0.12 g) and galactopentaose (0.24 g).

5-O-D-Galactofuranosyl-D-galactose

The sirupy material which appeared to be a galactobiose (19 mg), $[\alpha]_D$ −65° (*c*, 3.8 H_2O), was hydrolyzed as a 1% solution in 0.01 *N* sulphuric acid at 100° C. The specific rotation was −20° after 45 minutes, +5° (90 minutes), and +70° (16 hours; constant

Can. J. Chem. Downloaded from www.nrcresearchpress.com by 190.90.36.8 on 09/04/12
For personal use only.

value). The product was neutralized ($BaCO_3$), filtered, and evaporated to a sirup (17 mg) which corresponded to galactose on a paper chromatogram and was converted to its 1-methyl 1-phenylhydrazone (13 mg), m.p. and mixed m.p. 179° C, which had an X-ray diffraction pattern identical with known material.

The above galactobiose (18.8 mg) was oxidized with 4 moles per mole of lead tetra-acetate in acetic acid (10 cc) containing water (0.5 cc). The oxidant uptake was 1.5, 1.6, 1.8, 1.9, and 2.2 moles after 2, 5, 15, 30, and 1260 minutes, respectively.

*5-O-*D*-Galactofuranosyl-*D*-galactitol*

The galactobiose (188 mg) was reduced by treatment with sodium borohydride (75 mg) in water (10 cc) for 3 hours. The solution was treated with excess acetic acid, followed by Amberlite IR120, and then evaporated to a crust which was repeatedly dissolved in methanol and evaporated. The product, which had R_{Gal} 0.6, crystallized and was recrystallized from methanol–ethanol. Yield 89 mg, m.p. 149–151° C, and $[\alpha]_D$ −65° (*c*, 0.9 H_2O). Calculated for $C_{12}H_{24}O_{11}$: C, 41.9%; H, 7.0%. Found: C, 41.8%; H, 7.2%. The polyol (15.0 mg in 10 cc water) was oxidized with 0.1 *M* sodium periodate (10 cc). After 2.5, 5, 7.5, and 10 minutes, 4.0, 4.3, 4.2, and 4.4 moles per mole of oxidant were consumed and 1.8 and 1.9 moles of formic acid produced after 2 and 7.5 minutes, respectively. About 0.5 moles of formic acid existed in each case as formate ester, as shown by titration with alkali. When a solution of the polyol (113γ) in 0.02 *M* sodium periodate (2.5 cc) was estimated for formaldehyde by the chromotropic acid method 2.1, 1.9, 2.0 moles per mole were produced after 2.5, 5, and 15 minutes, respectively.

*2-O-*L*-Arabofuranosyl-glycerol*

The galactobiitol (89 mg) was oxidized with aqueous sodium periodate (6 molar equivalents; 10 cc) for 1 minute and the solution then added to a suspension of Amberlite IR120 and Dowex-1 in water. The resin was filtered off and to the filtrate sodium borohydride (50 mg) was added. The solution was evaporated to a small volume and the mixture was worked up as in the previous sodium borohydride reduction. The sirupy derivative (41 mg) had R_{Rh} 0.95 and was purified on a cellulose column using *n*-butanol as solvent to give a material which had $[\alpha]_D$ −129° (*c*, 1.0 H_2O) and produced arabinose and glycerol on acid hydrolysis. The disaccharide consumed 0.96 moles per mole of sodium periodate after 1 hour, the specific rotation of the solution becoming constant after 30 minutes.

The purified glycerol derivative (19 mg) was heated for 30 minutes at 80° C in pyridine (2 cc) containing *p*-nitrobenzoyl chloride (0.20 g). The mixture was added to aqueous sodium bicarbonate and after this mixture was shaken for 30 minutes the precipitate was filtered off and reprecipitated twice from ethyl acetate with petroleum ether (b.p. 30–60° C). Yield, 62 mg. The powder had m.p. 88–92° and $[\alpha]_D$ 0° (*c*, 1.1 2,4-lutidine). Calculated for $C_{44}H_{31}O_{22}N_5$: C, 53.8%; H, 3.2%. Found: C, 53.2%; H, 3.5%.

The authors wish to thank Mr. J. A. Baignee and Mr. M. Mazurek for microanalytical determinations and Miss S. Lubin and Mr. N. Gardner for technical assistance.

1. Clutterbuck, P. W., Haworth, W. N., Raistrick, H., Smith, G., and Stacey, M. Biochem. J. **28**, 94 (1934).
2. Haworth, W. N., Raistrick, H., and Stacey, M. Biochem. J. **31**, 640 (1937).
3. Hough, L., Jones, J. K. N., and Wadman, W. H. J. Chem. Soc. 2511 (1949).
4. Haworth, W. N. Ber. A, **61**, 50 (1932).
5. Lobry de Bruyn, C. A. and van Ekenstein, W. A. Rec. trav. chim. **15**, 226 (1896).
6. Charlson, A. J. and Perlin, A. S. Can. J. Chem. **34**, 1200 (1956).

Can. J. Chem. Downloaded from www.nrcresearchpress.com by 190.90.36.8 on 09/04/12
For personal use only.

7. WOLFROM, M. L. and WOOD, H. B. J. Am. Chem. Soc. **73**, 2933 (1951).
8. CHARLSON, A. J., GORIN, P. A. J., and PERLIN, A. S. Can. J. Chem. **34**, 1811 (1956).
9. GORIN, P. A. J. and PERLIN, A. S. Can. J. Chem. **35**, 262 (1957).
10. MITRA, A. K. and PERLIN, A. S. Unpublished results.
11. HUDSON, C. S. J. Am. Chem. Soc. **38**, 1566 (1916).
12. CHARLSON, A. J., GORIN, P. A. J., and PERLIN, A. S. Can. J. Chem. **35**, 365 (1957).
13. PUTMAN, E. W. and HASSID, W. Z. J. Am. Chem. Soc. **76**, 2221 (1954).
14. DALE, J. K. and HUDSON, C. S. J. Am. Chem. Soc. **52**, 2536 (1930).
15. MONTGOMERY, E. and HUDSON, C. S. J. Am. Chem. Soc. **59**, 992 (1937).
16. HOUGH, L., JONES, J. K. N., and WADMAN, W. H. J. Chem. Soc. 1702 (1950).
17. PARTRIDGE, S. M. Nature, **158**, 270 (1946).
18. ANDREWS, P., HOUGH, L., and POWELL, D. B. Chem. & Ind. (London), 658 (1956).

RECEIVED SEPTEMBER 29, 1958.
NATIONAL RESEARCH COUNCIL OF CANADA,
PRAIRIE REGIONAL LABORATORY,
SASKATOON, SASKATCHEWAN.

Can. J. Chem. Downloaded from www.nrcresearchpress.com by 190.90.36.8 on 09/04/12
For personal use only.

THE CONDENSATION OF 1-PHENYL-2-PROPANONE WITH AROMATIC ALDEHYDES

R. A. ABRAMOVITCH AND A. OBACH

In connection with some other work it was necessary to determine whether, in the condensation of 1-phenyl-2-propanone (I) with aromatic aldehydes in the presence of piperidine, reaction took place at the methylene or at the ω-methyl group. If condensation took place at the methylene group the geometrical configuration would have to be determined, whereas the *trans*-isomer would be expected if reaction took place at the methyl group.

Previous work (1, 2, 3) had indicated that in the presence of aqueous alkali reaction took place at the methyl group

$$\underset{\text{(I)}}{C_6H_5{-}CH_2{-}CO{-}CH_3} + Ar{-}CHO \xrightarrow{OH^-} C_6H_5{-}CH_2{-}CO{-}CH{=}CHAr$$

whereas under acidic conditions reaction took place at the methylene group

$$C_6H_5{-}CH_2{-}CO{-}CH_3 + ArCHO \xrightarrow{H^+} C_6H_5{-}\underset{\underset{\underset{\text{(II)}}{Ar{-}C{-}H}}{\|}}{C}{-}CO{-}CH_3$$

Dickinson (4) reported that, with piperidine as a catalyst, salicylaldehyde reacted with 1-phenyl-2-propanone at the methyl group. In a reinvestigation of Dickinson's work Heilbron and Irving showed that condensation had actually taken place at the methylene group, but the geometry of the product was not established (5).

The condensation of 1-phenyl-2-propanone with benzaldehyde in the presence of piperidine and *n*-heptoic acid gave *cis*-1,2-diphenyl-1-butene-3-one (II; Ar=C_6H_5), whose structure and configuration were established by the fact that it reacted with sodium hypochlorite to give *cis*-α-phenylcinnamic acid (*cis*- with respect to the phenyl groups). The absence of a band for *trans*- CH=CH at 970 cm^{-1} in the infrared confirmed that condensation had not taken place at the terminal methyl group. The condensation with *m*-nitrobenzaldehyde similarly gave *cis*-1-*m*-nitrophenyl-2-phenyl-1-butene-3-one, which reacted with hypochlorite to give *cis*-1-*m*-nitrophenylcinnamic acid. The reaction of phenylpropanone with *o*-nitrobenzaldehyde, on the other hand, did not proceed as easily and only a 22% yield of *cis*-1-*o*-nitrophenyl-2-phenyl-1-butene-3-one was obtained

7. WOLFROM, M. L. and WOOD, H. B. J. Am. Chem. Soc. **73**, 2933 (1951).
8. CHARLSON, A. J., GORIN, P. A. J., and PERLIN, A. S. Can. J. Chem. **34**, 1811 (1956).
9. GORIN, P. A. J. and PERLIN, A. S. Can. J. Chem. **35**, 262 (1957).
10. MITRA, A. K. and PERLIN, A. S. Unpublished results.
11. HUDSON, C. S. J. Am. Chem. Soc. **38**, 1566 (1916).
12. CHARLSON, A. J., GORIN, P. A. J., and PERLIN, A. S. Can. J. Chem. **35**, 365 (1957).
13. PUTMAN, E. W. and HASSID, W. Z. J. Am. Chem. Soc. **76**, 2221 (1954).
14. DALE, J. K. and HUDSON, C. S. J. Am. Chem. Soc. **52**, 2536 (1930).
15. MONTGOMERY, E. and HUDSON, C. S. J. Am. Chem. Soc. **59**, 992 (1937).
16. HOUGH, L., JONES, J. K. N., and WADMAN, W. H. J. Chem. Soc. 1702 (1950).
17. PARTRIDGE, S. M. Nature, **158**, 270 (1946).
18. ANDREWS, P., HOUGH, L., and POWELL, D. B. Chem. & Ind. (London), 658 (1956).

RECEIVED SEPTEMBER 29, 1958.
NATIONAL RESEARCH COUNCIL OF CANADA,
PRAIRIE REGIONAL LABORATORY,
SASKATOON, SASKATCHEWAN.

Can. J. Chem. Downloaded from www.nrcresearchpress.com by 190.90.36.8 on 09/04/12
For personal use only.

THE CONDENSATION OF 1-PHENYL-2-PROPANONE WITH AROMATIC ALDEHYDES

R. A. ABRAMOVITCH AND A. OBACH

In connection with some other work it was necessary to determine whether, in the condensation of 1-phenyl-2-propanone (I) with aromatic aldehydes in the presence of piperidine, reaction took place at the methylene or at the ω-methyl group. If condensation took place at the methylene group the geometrical configuration would have to be determined, whereas the *trans*-isomer would be expected if reaction took place at the methyl group.

Previous work (1, 2, 3) had indicated that in the presence of aqueous alkali reaction took place at the methyl group

$$\underset{\text{(I)}}{C_6H_5{-}CH_2{-}CO{-}CH_3} + Ar{-}CHO \xrightarrow{OH^-} C_6H_5{-}CH_2{-}CO{-}CH{=}CHAr$$

whereas under acidic conditions reaction took place at the methylene group

$$C_6H_5{-}CH_2{-}CO{-}CH_3 + ArCHO \xrightarrow{H^+} C_6H_5{-}\underset{\underset{\underset{\text{(II)}}{Ar{-}C{-}H}}{\|}}{C}{-}CO{-}CH_3$$

Dickinson (4) reported that, with piperidine as a catalyst, salicylaldehyde reacted with 1-phenyl-2-propanone at the methyl group. In a reinvestigation of Dickinson's work Heilbron and Irving showed that condensation had actually taken place at the methylene group, but the geometry of the product was not established (5).

The condensation of 1-phenyl-2-propanone with benzaldehyde in the presence of piperidine and *n*-heptoic acid gave *cis*-1,2-diphenyl-1-butene-3-one (II; Ar=C_6H_5), whose structure and configuration were established by the fact that it reacted with sodium hypochlorite to give *cis*-α-phenylcinnamic acid (*cis*- with respect to the phenyl groups). The absence of a band for *trans*- CH=CH at 970 cm^{-1} in the infrared confirmed that condensation had not taken place at the terminal methyl group. The condensation with *m*-nitrobenzaldehyde similarly gave *cis*-1-*m*-nitrophenyl-2-phenyl-1-butene-3-one, which reacted with hypochlorite to give *cis*-1-*m*-nitrophenylcinnamic acid. The reaction of phenylpropanone with *o*-nitrobenzaldehyde, on the other hand, did not proceed as easily and only a 22% yield of *cis*-1-*o*-nitrophenyl-2-phenyl-1-butene-3-one was obtained

under the conditions used in the previous condensations. This ketone was obtained as an oil and was best analyzed as its 2,4-dinitrophenylhydrazone. Its structure and configuration were established by the reaction with sodium hypochlorite which gave *cis*-1-*o*-nitrophenylcinnamic acid. Although the ketone gave a positive iodoform reaction no cinnamic acid could be isolated by this method.

EXPERIMENTAL

1,2-Diphenyl-1-butene-3-one

1-Phenyl-2-propanone (12.09 g) and benzaldehyde (5.76 g) were dissolved in benzene (70 ml), and piperidine (6 drops) and *n*-heptoic acid (3 drops) were added. The mixture was boiled under reflux for 24 hours using a Dean–Stark water separator to remove the water azeotropically. Most of the benzene was then evaporated and the residue steam-distilled. The residual oil solidified in the refrigerator overnight; the solid was filtered off and recrystallized from aqueous ethanol giving 1,2-diphenyl-1-butene-3-one (52.7% yield), m.p. 54–55°. Goldschmiedt and Knöpfer (1) give m.p. 53–54° for this compound. Infrared spectrum (Nujol mull) (main peaks only): 1655 (s) (α,β-unsaturated C=O), 1618 (m) (C=C), 1598 (w) (phenyl), 793 (w), 752 (m), 722 (m), 696 (s), and 685 cm^{-1} (s).

The product (0.108 g) was treated with sodium hypochlorite (2 ml) (prepared by dissolving sodium hydroxide (4 g) in water (10 ml) and passing chlorine gas (2 g) through this solution at 0°), heated to 90°, and the flask stoppered and shaken vigorously. Heating at 90° and shaking was continued for ½ hour, water being added after 15 minutes to dissolve the solid which separated on cooling. The solution was filtered and the cold filtrate acidified with gaseous sulphur dioxide. The acid which precipitated was filtered and recrystallized from aqueous ethanol to give *cis*-α-phenylcinnamic acid (54% yield), m.p. 169.5–170.5°. Stoermer and Voht give m.p. 172° for this compound (6).

1-m-Nitrophenyl-2-phenyl-1-butene-3-one

This was prepared similarly from *m*-nitrobenzaldehyde (7.04 g) and 1-phenyl-2-propanone (12.034 g). It crystallized from aqueous ethanol as yellow prisms (57.2% yield), m.p. 79–80°. Calc. for $C_{16}H_{13}O_3N$: C, 71.90; H, 4.90. Found: C, 72.15; H, 4.83. Infrared spectrum (Nujol mull) (main peaks only): 1660 (s), 1625 (w), 1602 (w), 1532 (s) ($-NO_2$), 826 (m), 819 (m), 728 (m), 703 cm^{-1} (s).

Oxidation of the ketone with sodium hypochlorite gave *cis*-α-*m*-nitrophenylcinnamic acid, m.p. 178–180°. Bakunin (7) gives m.p. 181–182° for this acid.

1-o-Nitrophenyl-2-phenyl-1-butene-3-one

The residue, after steam distillation of the product of condensation of *o*-nitrobenzaldehyde (7.0 g) and 1-phenyl-2-propanone (12.06 g), was extracted repeatedly with ether, the dried ($MgSO_4$) extract was evaporated, and the residual oil distilled under vacuum, the fraction b.p. 142–180° at 0.5 mm being collected (21.8% yield). This was redistilled (b.p. 180–186° at 0.6 mm) giving the nitroketone as an orange-red oil (12.8% based on *o*-nitrobenzaldehyde). Infrared spectrum (liquid film) (main peaks only): 1685 (s), 1618 (m), 1585 (m), 1535 (s), 1505 (w), 865 (m), 790 (w), 755 (m), 720 (s), 700 (s), and 675 cm^{-1} (w). The 2,4-dinitrophenylhydrazone crystallized from an ethyl acetate – ethanol mixture in red prisms, m.p. 188–189°. Calc. for $C_{22}H_{17}O_6N_5$: C, 59.06; H, 3.80. Found: C, 59.32; H, 3.75.

With sodium hypochlorite the ketone gave *cis*-*o*-nitrophenylcinnamic acid, m.p. 193–194°. With sodium hypoiodite, iodoform, m.p. 115–118°, was obtained but the cinnamic acid could not be isolated. The melting point of the acid as reported in the literature (8) is 193–195°.

Can. J. Chem. Downloaded from www.nrcresearchpress.com by 190.90.36.8 on 09/04/12
For personal use only.

1. GOLDSCHMIEDT, G. and KNÖPFER, G. Monatsh. **18**, 437 (1897).
2. GOLDSCHMIEDT, G. and KRCZMAR, H. Monatsh. **22**, 659 (1901).
3. HARRIES, C. and MÜLLER, G. H. Ber. **35**, 966 (1902).
4. DICKINSON, R. J. Chem. Soc. 2234 (1926).
5. HEILBRON, I. M. and IRVING, F. J. Chem. Soc. 975 (1929).
6. STOERMER, R. and VOHT, G. Ann. **409**, 36 (1915).
7. BAKUNIN, M. Gazzetta chim. ital. **25**, 137 (1895).
8. PSCHORR, R. Ber. **29**, 496 (1896).

RECEIVED SEPTEMBER 17, 1958.
DEPARTMENT OF CHEMISTRY,
UNIVERSITY OF SASKATCHEWAN,
SASKATOON, SASKATCHEWAN.

Can. J. Chem. Downloaded from www.nrcresearchpress.com by 190.90.36.8 on 09/04/12
For personal use only.

CYCLIZATION OF 1,3-BIS-(β-CHLOROETHYL)-UREA*

M.-E. KRELING AND A. F. MCKAY

It was found that the double melting point property of 2-(β-chloroethylamino)-2-oxazoline hydrochloride (II*a*) is associated with its conversion in the molten state into 1,3-bis-(β-chloroethyl)-urea (I*a*). Although 2-(β-chloroethylamino)-2-oxazoline hydrobromide (II*b*) does not exhibit a double melting point, it also rearranges in the molten state to the corresponding urea (I*b*).

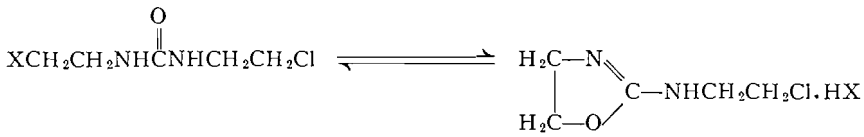

I*a*, X = Cl
b, X = Br

II*a*, X = Cl
b, X = Br

1-(β-Bromoethyl)-3-(β-chloroethyl)-urea and 1,3-bis-(β-chloroethyl)-urea on heating in water cyclized respectively to the hydrobromide and hydrochloride salts of 2-(β-chloroethylamino)-2-oxazoline. The conversion of 1-(β-bromoethyl)-3-(β-chloroethyl)-urea into the hydrobromide salt II*b* rather than the hydrochloride salt of 2-(β-bromoethylamino)-2-oxazoline can be attributed to the lower bond energy of the C–Br linkage in comparison with the C–Cl linkage.

EXPERIMENTAL†

1,3-Bis-(β-chloroethyl)-urea

1,3-Bis-(β-chloroethyl)-urea (m.p. 126.5–128° C) was prepared in 61.2% yield by the method of Bestian (1). A mixture melting point determination with a known (2) sample of 1,3-bis-(β-chloroethyl)-urea gave no depression.

2-(β-Chloroethylamino)-2-oxazoline Hydrochloride

1,3-Bis-(β-chloroethyl)-urea (20 g, 0.1 mole) in water (50 ml) was heated under reflux for 1 hour. After the clear solution was evaporated to dryness *in vacuo*, crystals were obtained, yield 20 g (100%). These crystals melted at 103–104° C, resolidified and remelted at 121–123° C. Three crystallizations from absolute ethanol–ether (1 : 1) solution raised the melting points to 107–109° C and 125–127° C. Anal. Calc. for $C_5H_{10}Cl_2N_2O$:

**Issued as Report No. 22 from the L. G. Ryan Research Laboratories, Monsanto Canada Limited, Ville LaSalle, Quebec.*

†*All melting points are uncorrected. The microanalyses were determined by Micro-Tech Laboratories, Skokie, Ill., and Schwartzkopf Microanalytical Laboratory, Woodside, N. Y.*

1. GOLDSCHMIEDT, G. and KNÖPFER, G. Monatsh. **18**, 437 (1897).
2. GOLDSCHMIEDT, G. and KRCZMAR, H. Monatsh. **22**, 659 (1901).
3. HARRIES, C. and MÜLLER, G. H. Ber. **35**, 966 (1902).
4. DICKINSON, R. J. Chem. Soc. 2234 (1926).
5. HEILBRON, I. M. and IRVING, F. J. Chem. Soc. 975 (1929).
6. STOERMER, R. and VOHT, G. Ann. **409**, 36 (1915).
7. BAKUNIN, M. Gazzetta chim. ital. **25**, 137 (1895).
8. PSCHORR, R. Ber. **29**, 496 (1896).

RECEIVED SEPTEMBER 17, 1958.
DEPARTMENT OF CHEMISTRY,
UNIVERSITY OF SASKATCHEWAN,
SASKATOON, SASKATCHEWAN.

Can. J. Chem. Downloaded from www.nrcresearchpress.com by 190.90.36.8 on 09/04/12
For personal use only.

CYCLIZATION OF 1,3-BIS-(β-CHLOROETHYL)-UREA*

M.-E. KRELING AND A. F. MCKAY

It was found that the double melting point property of 2-(β-chloroethylamino)-2-oxazoline hydrochloride (II*a*) is associated with its conversion in the molten state into 1,3-bis-(β-chloroethyl)-urea (I*a*). Although 2-(β-chloroethylamino)-2-oxazoline hydrobromide (II*b*) does not exhibit a double melting point, it also rearranges in the molten state to the corresponding urea (I*b*).

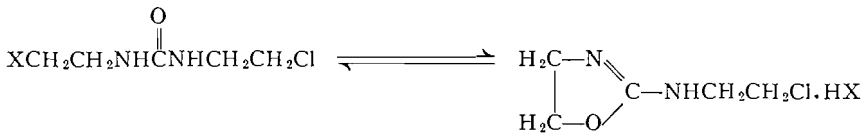

I*a*, X = Cl
b, X = Br

II*a*, X = Cl
b, X = Br

1-(β-Bromoethyl)-3-(β-chloroethyl)-urea and 1,3-bis-(β-chloroethyl)-urea on heating in water cyclized respectively to the hydrobromide and hydrochloride salts of 2-(β-chloroethylamino)-2-oxazoline. The conversion of 1-(β-bromoethyl)-3-(β-chloroethyl)-urea into the hydrobromide salt II*b* rather than the hydrochloride salt of 2-(β-bromoethylamino)-2-oxazoline can be attributed to the lower bond energy of the C–Br linkage in comparison with the C–Cl linkage.

EXPERIMENTAL†

1,3-Bis-(β-chloroethyl)-urea

1,3-Bis-(β-chloroethyl)-urea (m.p. 126.5–128° C) was prepared in 61.2% yield by the method of Bestian (1). A mixture melting point determination with a known (2) sample of 1,3-bis-(β-chloroethyl)-urea gave no depression.

2-(β-Chloroethylamino)-2-oxazoline Hydrochloride

1,3-Bis-(β-chloroethyl)-urea (20 g, 0.1 mole) in water (50 ml) was heated under reflux for 1 hour. After the clear solution was evaporated to dryness *in vacuo*, crystals were obtained, yield 20 g (100%). These crystals melted at 103–104° C, resolidified and remelted at 121–123° C. Three crystallizations from absolute ethanol–ether (1 : 1) solution raised the melting points to 107–109° C and 125–127° C. Anal. Calc. for $C_5H_{10}Cl_2N_2O$:

**Issued as Report No. 22 from the L. G. Ryan Research Laboratories, Monsanto Canada Limited, Ville LaSalle, Quebec.*

†*All melting points are uncorrected. The microanalyses were determined by Micro-Tech Laboratories, Skokie, Ill., and Schwartzkopf Microanalytical Laboratory, Woodside, N. Y.*

C, 32.45; H, 5.45; Cl, 38.32; N, 15.14%. Found: C, 32.77; H, 5.37; Cl, 37.86; N, 14.96%.

A picrate (m.p. 192–194° C) was formed in the usual manner from water. The product was identified by a mixture melting point determination with a known (2) sample of 2-(β-chloroethylamino)-2-oxazoline picrate (m.p. 193–194° C).

A sample of 2-(β-chloroethylamino)-2-oxazoline hydrochloride (m.p. 107–109° C and 125–127° C) was held in the molten state for 1 minute. The molten mass crystallized immediately on cooling and the crystals melted sharply at 125–127° C. These crystals no longer gave a picrate and they did not depress the melting point of a known sample of 1,3-bis-(β-chloroethyl)-urea.

2-(β-Chloroethylamino)-2-oxazoline hydrochloride (9.25 g, 0.05 mole) in absolute methanol (180 ml) was passed through a column of Amberlite IRA-400 resin (150 ml in the hydroxyl form). The column was washed with the same volume of methanol and the eluate and washings were evaporated to dryness *in vacuo* under nitrogen. The residual crystalline mass melted at 81–84° C, yield 7.43 g (100%). These crystals of 2-(β-chloroethylamino)-2-oxazoline were very soluble in water, alcohol, and acetone. Three crystallizations from acetone–hexane solution raised the melting point to 84–86° C. Anal. Calc. for $C_5H_9ClN_2O$: C, 40.40; H, 6.10; Cl, 23.85; N, 18.85%. Found: C, 39.78; H, 6.35; Cl, 23.50; N, 18.52%.

2-(β-Chloroethylamino)-2-oxazoline Hydrobromide

Gaseous hydrogen bromide was passed into a solution of 2-(β-chloroethylamino)-2-oxazoline (841 mg, 0.005 mole) in water (10 ml) until a pH of 3 was obtained. The solution was evaporated *in vacuo* at 45° C and the resulting oil crystallized on standing in a vacuum desiccator overnight, yield 1.3 g (100%). Crystallization from ethanol–ether solution gave a constant melting point of 118.5–119.5° C. Anal. Calc. for $C_5H_{10}BrClN_2O$: C, 26.17; H, 4.39; halogen, 50.27; N, 12.21%. Found: C, 26.41; H, 4.26; halogen, 49.88; N, 11.77%.

A sample of 2-(β-chloroethylamino)-2-oxazoline hydrobromide in water was converted into its picrate (m.p. 193–194° C) in 95% yield in the usual manner.

1-(β-Bromoethyl)-3-(β-chloroethyl)-urea

1-(β-Chloroethylamino)-2-oxazoline hydrobromide (76 mg, 0.00033 mole) was heated for 15 minutes in dry *o*-xylene (3 ml) to 130–140° C (temperature of the oil bath). The mixture upon cooling deposited crystals, which were collected by filtration; yield, 42 mg (55.3%). Crystallization from warm (50° C) ethanol–ether solution raised the melting point from 108.5–110° C to 109–111° C. Anal. Calc. for $C_5H_{10}BrClN_2O$: C, 26.17; H, 4.39; halogen, 50.27; N, 12.21%. Found: C, 26.02; H, 4.35; halogen, 50.30; N, 12.01%.

Cyclization of 1-(β-Bromoethyl)-3-(β-chloroethyl)-urea

1-(β-Bromoethyl)-3-(β-chloroethyl)-urea (80 mg) in water (2 ml) was heated for approximately 1 hour at 70–80° C until a clear solution was obtained. The clear solution on treatment with aqueous picric acid solution gave a 93.5% yield of 2-(β-chloroethylamino)-2-oxazoline picrate (193–194° C) which was identified by a mixed melting point determination.

1. Bestian, H. Ann. **566**, 210 (1950).
2. McKay, A. F., Weinberg, M. A., Picard, J. P., Hatton, W. G., Bedard, M., and Rooney, H. E. J. Am. Chem. Soc. **76**, 6371 (1954).

Received September 8, 1958.
L. G. Ryan Research Laboratories,
Monsanto Canada Limited,
Ville LaSalle, Quebec.

Can. J. Chem. Downloaded from www.nrcresearchpress.com by 190.90.36.8 on 09/04/12
For personal use only.

Can. J. Chem. Downloaded from www.nrcresearchpress.com by 190.90.36.8 on 09/04/12
For personal use only.

Canadian Journal of Chemistry

Issued by THE NATIONAL RESEARCH COUNCIL OF CANADA

VOLUME 37 MARCH 1959 NUMBER 3

A PROPOSED STRUCTURE FOR CHLOROPHYLL *d*[1]

A. S. HOLT AND H. V. MORLEY[2]

ABSTRACT

Treatment of chlorophyll *a* or methyl chlorophyllide *a* with potassium permanganate effected oxidation of the 2-vinyl group without concomitant oxidation of the cyclopentanone ring. One of the products obtained was of especial interest because its visible absorption spectrum was identical with that of a previously known, but chemically uncharacterized, pigment—chlorophyll *d*. The preparation and identification of this oxidation product as 2-desvinyl-2-formyl-chlorophyll-*a* is given and its probable identity with chlorophyll *d* is discussed in detail.

Chlorophyll *d* is a pigment which has been reported to occur in a number of species of the Rhodophyceae, a group which contains chlorophyll *a* but, at most, only traces of chlorophyll *b* (1, 2). It was first isolated and described by Manning and Strain in 1943 (2). Recently Smith and Benitez (3) obtained chromatographically pure samples and calculated the specific absorption curve by determining the magnesium content and by assuming the molecular weight to be that of chlorophyll *a* (see Fig. 1). To date its chemical constitution has not been determined nor has any useful function been ascribed to it, although there have been speculations that it may be responsible for the anomalous action spectra of photosynthesis and chlorophyll fluorescence in red algae (1).

The present work arose from some observations made in connection with studies on the allomerization of chlorophyll *a*. When the phase test intermediate of chlorophyll *a*, in acetone containing base, was treated with dilute permanganate, it was oxidized immediately. Examination with a visual spectroscope showed a "red" absorption maximum at about 675 mμ, which was characteristic of Mg-purpurin-18 (4). However, when base was omitted a gradual but different spectral change occurred; two new "red" maxima appeared at about 650 and 685 mμ. When the mixture was chromatographed, there were, besides a minor zone of unchanged chlorophyll *a*, three new zones. The pigments were designated as fractions A, B, and C, in the relative order of their position on the column, fraction C being uppermost. Each fraction gave a positive phase test which indicated that allomerization had not occurred. Most interesting was fraction A which had visible absorption spectra in methanol and in ether which were identical with those published for chlorophyll *d* (2, 3). The present communication describes fraction A and evidence to indicate that it is similar to and probably identical with chlorophyll *d*. Fractions B and C will be discussed in a subsequent communication.

The change in spectrum obtained when fraction A in isopropanol was treated with methanolic magnesium methoxide (4) is given in Fig. 2. Enhanced absorption in the

[1]*Manuscript received November 14, 1958.*
Contribution from the Division of Applied Biology, National Research Council, Ottawa, Canada.
Issued as N.R.C No. 5038.
[2]*N.R.C. Postdoctorate Fellow, 1957–58.*

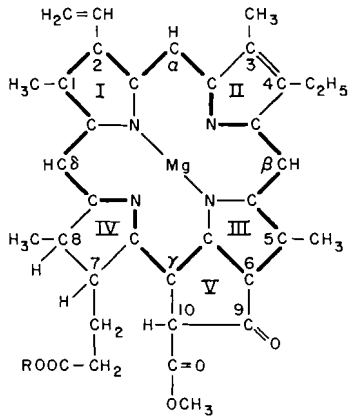

COMPOUND	R	Mg
CHLOROPHYLLIDE	H	+
PHEOPHORBIDE	H	−
CHLOROPHYLL	$C_{20}H_{39}$	+
PHEOPHYTIN	$C_{20}H_{39}$	−
METHYL CHLOROPHYLLIDE	CH_3	+
METHYL PHEOPHORBIDE	CH_3	−

b COMPOUNDS: $3-CH_3$ IS REPLACED BY CHO
"PYRO" COMPOUNDS: $10-CO_2CH_3$ IS REPLACED BY H
"MESO" COMPOUNDS: $2-CH=CH_2$ IS REPLACED BY C_2H_5
CHLORIN E_6 – TRIMETHYL ESTER: $R=CH_3$, RING V IS REPLACED BY $\gamma-CH_2CO_2CH_3$ AND $6-CO_2CH_3$

FIG. 1. Structure of chlorophyll *a* and its derivatives.

"green" and decreased absorption in the "red" are characteristic of phase-test-positive pigment (5). When aqueous or methanolic KOH was added to a pyridine or dimethylformamide solution, the intermediate was more strikingly reddish to the eye than when magnesium methoxide was added, but was far less stable.

The positive phase test indicated that ring V of this product was intact. Thus, the remaining likely sites of oxidation were the vinyl group of ring I and the hydrogen atoms at positions 7 and 8 of ring IV. The appearance of an infrared absorption band at 1675 cm^{-1} in the spectrum of the magnesium-free derivative indicated that oxidation of the vinyl group had probably occurred (Fig. 3, curve 2). On comparing the infrared spectrum with that of pheophytin *b*, it seemed likely that the extra band was due to a conjugated aldehyde group (6). Treatment with small quantities of sodium borohydride (7) yielded a product whose spectrum no longer contained the band at 1675 cm^{-1} (Fig. 3, curve 4). This compound gave a positive phase test, and possessed a visible absorption spectrum which was, for all practical purposes, identical with that of meso-methyl pheophorbide *a* (8). Such a result was consistent only with the assumption that oxidation of the hydrogen atoms at positions 7 and 8 had not occurred, since replacement of these

Can. J. Chem. Downloaded from www.nrcresearchpress.com by 190.90.36.8 on 09/04/12
For personal use only.

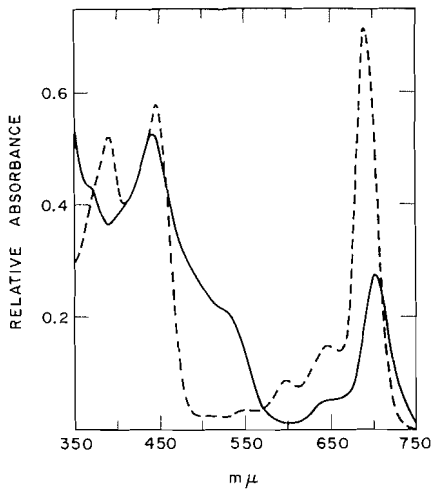

FIG. 2. Visible absorption spectra of fraction A in isopropanol plus and minus methanolic $Mg(OCH_3)_2$. Dashes: isopropanol alone. Solid line: an equal concentration of pigment in a 1:5 mixture of methanolic $Mg(OCH_3)_2$ (*ca.* 20 mg of Mg per milliliter of stock solution) in isopropanol. Air atmosphere.

in meso-methyl pyropheophorbide *a* by hydroxyl groups causes the "red" maximum to shift from 658 to 667 mμ (9).

Previously, Fischer and Walter (10) had carried out studies on the oxidation of the vinyl group of magnesium-free derivatives of chlorophyll *a* using permanganate in aqueous pyridine. These workers stated that owing to the activating influence of the 10-carbomethoxy group, oxidation yielded purpurins and left the vinyl group intact. To avoid this they chose chlorin-e_6-trimethyl ester and methyl pyropheophorbide *a* as starting materials. The 2-desvinyl-2-formyl derivatives were the only compounds isolated which possessed a conjugated carbonyl group. The 2-desvinyl-2-formyl structure of fraction A and its methyl derivative (prepared from methyl chlorophyllide *a*) was confirmed when their chlorin-e_6-trimethyl esters were shown to be identical with the known compound 2-desvinyl-2-formyl-chlorin-e_6-trimethyl ester (10). The absorption of this compound in the double bond stretching region is given in Fig. 3, curve 3, and clearly shows the ester (1725 cm^{-1}) and formyl (1673 cm^{-1}) bands. The oxime was also prepared and its spectrum was found to be identical with that reported earlier (10).

The formation of the 2-desvinyl-2-formyl derivative under the conditions described was in disagreement with the results of Fischer and Walter. These workers found only the 7,8-dihydroxy derivative when aqueous acetone was used as the solvent. Another disagreement was that while the spectrum of the magnesium-free derivative of fraction A agreed well with that given for 2-desvinyl-2-formyl-methyl pheophorbide *a* (prepared by ring closure of the 2-desvinyl-2-formyl-chlorin-e_6-trimethyl ester), that of the product obtained by introducing magnesium into the pheophorbide did not agree with the spectrum of fraction A. It was reported, however, that when magnesium was removed the resulting spectrum was shifted to the "blue" relative to that of the original pheophorbide. It was thought that this product may have resulted from a secondary reaction at the 2-position.

Having shown that fraction A was a 2-desvinyl-2-formyl derivative of chlorophyll *a*, it remained to show its relationship to chlorophyll *d*. Excellent agreement of the visible absorption spectra of fraction A and its magnesium-free derivative with those of chlorophyll *d* and pheophytin *d* in ether (3) are shown in Figs. 4 and 5. Fraction A

Can. J. Chem. Downloaded from www.nrcresearchpress.com by 190.90.36.8 on 09/04/12
For personal use only.

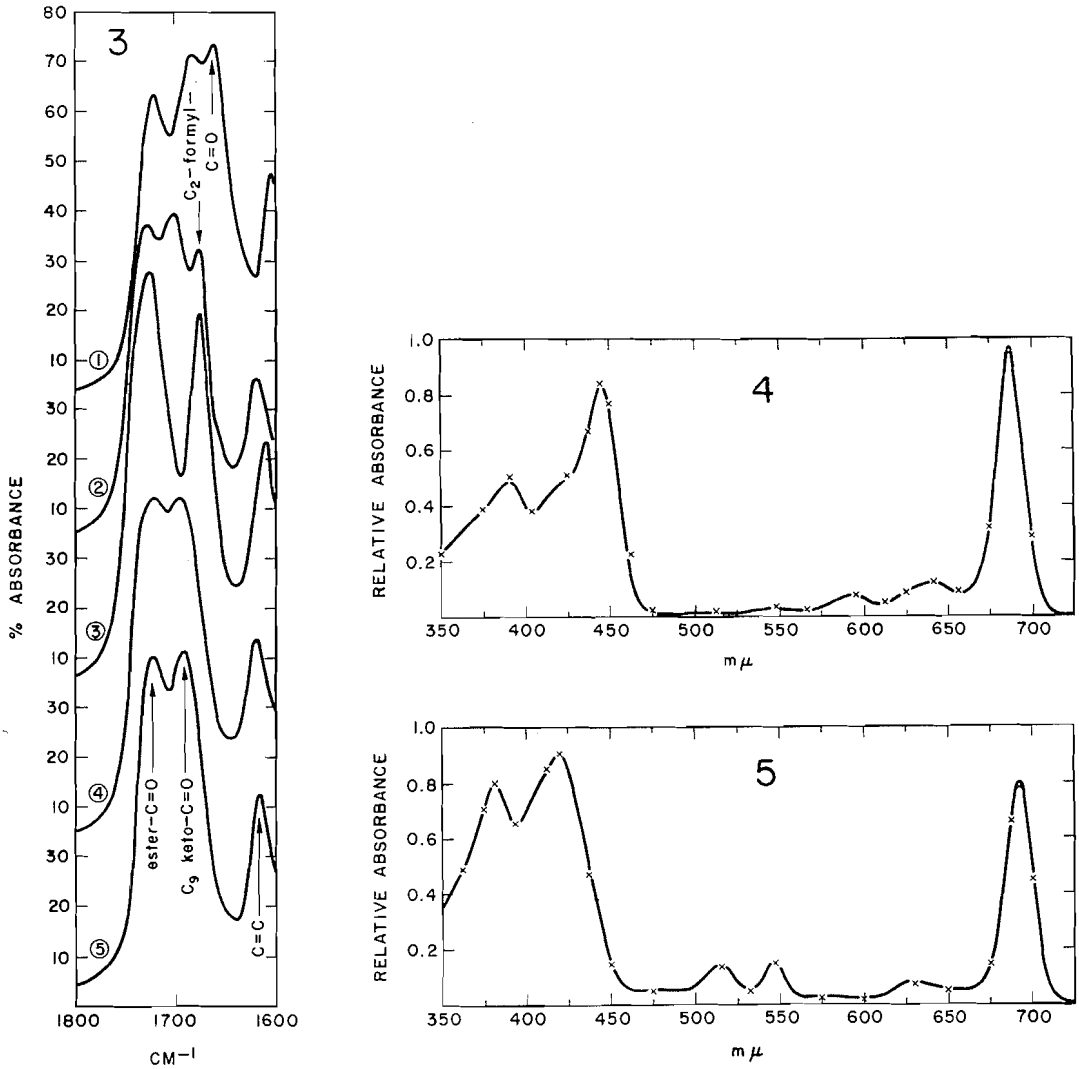

FIG. 3. Double bond stretching region of the infrared absorption spectra of fraction A and its derivatives in chloroform. (1) Fraction A or 2-desvinyl-2-formyl-chlorophyll-*a*. (2) 2-Desvinyl-2-formyl-pheophytin-*a*. (3) 2-Desvinyl-2-formyl-chlorin-e_6-trimethyl ester. (4) 2-Desvinyl-2-hydroxymethyl-pheophytin-*a*. (5) 2-Desvinyl-2-formyl-pheophytin-*a*-2-dimethyl acetal. Concentration *ca.* 5% (w/v).

FIG. 4. Visible absorption spectrum of 2-desvinyl-2-formyl-chlorophyll-*a* in ether (solid line) compared with published spectrum of chlorophyll *d* (3) (indicated by crosses). The spectra were adjusted to make "blue" maxima equal.

FIG. 5. Visible absorption spectrum of 2-desvinyl-2-formyl-pheophytin-*a* in ether (solid line) compared with published spectrum for pheophytin *d* (3) (indicated by crosses). The spectra were adjusted to make the "blue" maxima equal.

appeared to be identical with chlorophyll *d* in all respects. The most significant similarity was the ready interconversion of the magnesium-free derivative and a product whose properties corresponded to those of a so-called isomer of pheophytin *d*, namely, isopheophytin *d*. This product has now been shown to be the dimethyl acetal derivative; it was formed readily in the presence of methanolic hydrogen chloride, the reagent used by Manning and Strain (2) to convert chlorophyll *d* into pheophytin *d*. Total conversion back to the 2-formyl compound is effected by extracting the acetal from ether into aqueous HCl, as shown in Fig. 6. Formation of the acetal of fraction A was

Can. J. Chem. Downloaded from www.nrcresearchpress.com by 190.90.36.8 on 09/04/12
For personal use only.

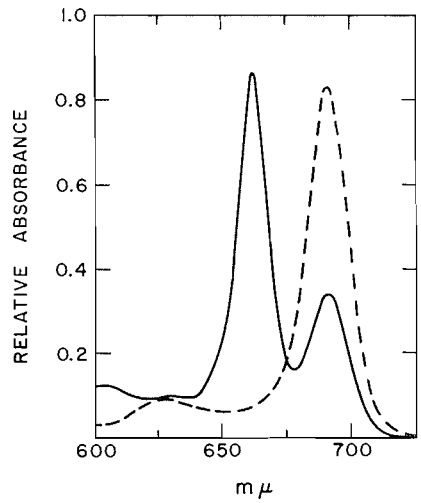

FIG. 6. Visible absorption curve of a mixture of 2-desvinyl-2-formyl-pheophorbide-*a* methyl ester in ether and its dimethyl acetal derivative. Solid line: after 1 minute exposure of the 2-formyl compound to 4.9% (w/w) methanolic HCl. Dashes: after extraction of the pigment into 20% (w/w) aqueous HCl and its transfer back into ether.

followed spectrophotometrically in methanol containing ammonium chloride (11) and resulted in an equilibrium mixture. Since the acetal of the 2-formyl-chlorin-e_6 derivative was always present in the mother liquor after crystallization, it would appear that it was formed in methanol, even in the absence of hydrochloric acid. From these findings it seems that absorption curves of 2-formyl derivatives of chlorophyll *a* should be measured in non-hydroxylic solvents, e.g. ether, to ensure that no contamination with the acetal occurs. Figure 3, curve 5, shows the double bond stretching region of the infrared absorption curve of the acetal. The carbonyl absorption band of the 2-formyl group is missing.

Although formation of the acetal of methyl pheophorbide *b* has been observed using orthoformic ester (12), it was not formed in detectable quantities in methanolic hydrogen chloride even after 24 hours. This difference in the behavior of the formyl groups at positions 2 and 3 is but one example of the non-equivalence of these positions in the phorbide nucleus. Other examples, still involving the formyl group, are as follows: (1) the carbonyl absorption band of the 2-formyl group of fraction A in chloroform absorbs at 1662 cm^{-1} (Fig. 3, curve 1), whereas that of chlorophyll *b* absorbs at 1655 cm^{-1} (6); and (2) introduction of a formyl group at position 2 of meso-methyl pheophorbide *a* causes a "red" shift and has little effect on the hydrochloric acid number, whereas its introduction at position 3 causes a "blue" shift and an increase of five in the acid number (8, 13). (The hydrochloric acid number is the percentage strength acid (w/w) which extracts about two-thirds of the pigment from an equal volume of ether solution (14).)

The probable effect of permanganate on the double bond of the phytol chain has not been mentioned. Oxidation at this point would not have affected the visible absorption spectrum but would have altered the chromatographic behavior. The product(s) formed would have been expected to be strongly adsorbed at the top of a sugar column. To test the effect of the presence of one hydroxyl group in the molecule the 2-hydroxymethyl derivative was prepared and co-chromatographed with a mixture of fraction A and chlorophylls *b* and *b'*, using the method described by Manning and Strain (2). Five zones were observed, the topmost being the firmly bound 2-hydroxy compound; further

Can. J. Chem. Downloaded from www.nrcresearchpress.com by 190.90.36.8 on 09/04/12
For personal use only.

down the column was the band of chlorophyll *b*, followed closely by fraction A and chlorophyll *b'*. The lowest band was well separated and was probably fraction A' (the "red" maximum in ether was at 687 mμ, as compared with 686 mμ for fraction A). The chromatographic properties of fraction A were identical with those described for chlorophyll *d* (2) making it likely that the phytol group was intact, and that fraction A and chlorophyll *d* are identical. Further support for this view is the fact that the specific absorption coefficient of the "red" absorption maximum was found to be in reasonable agreement with the value given by Smith and Benitez (3).

Unfortunately chlorophyll *d* was apparently absent from the three species of red algae which were made available to us. This was not unexpected, since conclusive demonstration of the occurrence of chlorophyll *d* in all 18 species tested by Manning and Strain (2) is lacking. *Chondrus crispus* and *Gigartina stellata* were collected fresh in the vicinity of Halifax, Nova Scotia, and were shipped immediately via air mail in iced containers. Upon their delivery, which was about eight to twelve hours later, the samples were extracted using published methods. *Rhodocorton rothii* was collected on the coast of Ireland and was delivered, in a moist condition, several days after its collection. No special storage conditions were maintained during transit. A further check upon the presence of chlorophyll *d* was the treatment of all chlorophyll pigment with aqueous hydrochloric acid to decompose any of the dimethyl acetal derivative which might have been formed from the use of methanol during extraction. It seems improbable that the condition of the first two species of red algae could have deteriorated during shipment to the extent that chlorophyll *d* was destroyed *in vivo* prior to their arrival. It is believed, however, that the successful re-isolation of chlorophyll *d*, perhaps from the original sources which were collected on the Pacific Coast of the United States of America (2, 3), will show this pigment to be a 2-desvinyl-2-formyl derivative of chlorophyll *a*.

EXPERIMENTAL

All solvents were reagent grade and were, with the exception of acetone, used without further purification. Acetone was refluxed with a slight excess of $KMnO_4$ and distilled over anhydrous K_2CO_3. Chlorophyll *a* and methyl chlorophyllide *a* were prepared as given previously (15, 16). Chlorin-e_6-trimethyl ester was prepared from chlorophyll *a* by mild hydrolysis in boiling 2% (w/v) methanolic KOH for 15 minutes, and subsequent isolation and treatment according to previous methods (17). Visible absorption spectra were measured on a Cary Recording Spectrophotometer, Model 11M; infrared absorption spectra were measured on a Perkin–Elmer Model 21, Double Beam Recording Infrared Spectrophotometer.

2-Desvinyl-2-formyl-chlorophyll-a

Chlorophyll *a* (1 g) dissolved in purified acetone (300 ml) was oxidized with freshly prepared aqueous potassium permanganate (3% w/v). About 18 ml were added in 3-ml portions with stirring during 1 hour. Samples were removed at 10-minute intervals and transferred into ether, and the course of the reaction followed spectrophotometrically. When the ratio of absorbance at 650 mμ to that at 687 mμ reached *ca.* 2.5, the mixture was poured into a large volume of ether and the manganese dioxide was removed by filtration. The filtrate was well washed with water and extracted three times with aqueous potassium hydroxide (0.5 *N*), which removed a small quantity of acidic products. After several washes with distilled water, the ether solution was evaporated to dryness under vacuum. The pigment was adsorbed on a powdered sucrose column from 1 l. of 50% (v/v) ether – petroleum ether (b.p. 30–60° C). Five hundred milliliters of 10% ether plus 5% isopropanol in petroleum ether removed unchanged chlorophyll *a* and fraction A

Can. J. Chem. Downloaded from www.nrcresearchpress.com by 190.90.36.8 on 09/04/12
For personal use only.

Can. J. Chem. Downloaded from www.nrcresearchpress.com by 190.90.36.8 on 09/04/12
For personal use only.

together, and left fractions B and C adhering to the column. Chlorophyll *a* and fraction A were separated later using 0.5% isopropanol in petroleum ether. Chlorophyll *a* passed into the suction flask ahead of fraction A. Fraction A was re-chromatographed and traces of impurities were removed by successive treatments with 50, 75, and 90% benzene in petroleum ether, followed by 0.5 and 1.0% isopropanol – petroleum ether mixtures. The yield was about 100 mg.

Prolonging the oxidation increased the yield of acidic products with concomitant decrease in the yields of fractions A, B, and C. No significant decrease in the ratio of absorbance at 687 to 650 mμ was noted, however.

2-Desvinyl-2-formyl-chlorophyllide-a Methyl Ester

Methyl chlorophyllide *a* (170 mg) was oxidized, and fractions corresponding to those designated above were isolated as follows: A and B were separated from C by passing the pigment dissolved in 60% $CHCl_3$ – petroleum ether mixture through a sugar column. A and B and a small amount of methyl chlorophyllide *a* passed into the suction flask. The mixture was dried and adsorbed on a fresh column from 25% $CHCl_3$ in petroleum ether and treated with 3.5% isopropanol in petroleum ether. Fraction A passed into the flask after methyl chlorophyllide *a*. It was then re-chromatographed and treated with 0.75% isopropanol plus 20% $CHCl_3$ in petroleum ether. The acid number of the magnesium-free derivative was 16.5.

2-Desvinyl-2-formyl-chlorin-e_6-trimethyl Ester

This was prepared as a reference compound by oxidation of chlorin-e_6-trimethyl ester using the method given for chlorophyll *a*. The product was isolated by the method of Fischer and Walter (10). It was also prepared by oxidation of chlorophyll *a* (0.7 g), and subsequent hydrolysis in methanolic KOH. After the transfer of the pigment mixture into ether, 15% HCl (w/v) was used to extract all pigment no longer containing phytol. This acid-extractable fraction was then esterified with diazomethane in ether. Extraction of the ether solution with 2% HCl removed the chlorin-e_6-trimethyl ester derivative of fraction C, while 5% HCl removed most of that of fraction B. The pigment remaining in the ether was evaporated to dryness and adsorbed on a powdered sugar column from 15% chloroform in petroleum ether, and treated with 10% $CHCl_3$ plus 0.7% isopropanol in petroleum ether. The sugar column was extruded and the main zone of pigment was isolated and extracted with ether. The ether solution was well washed with distilled water and evaporated to dryness. The product was crystallized from methanol containing a trace of acetone. The precipitate was removed and washed well with pentane. Two further crystallizations yielded long needles, m.p. 222–223° C. Found: C, 67.5; H, 6.15. Calculated for $C_{36}H_{40}O_7N_4$: C, 67.5; H, 6.25%.

The same compound was prepared by oxidation of methyl chlorophyllide *a* using appropriate variations of the above procedure. A mixed melting point of the products obtained from the three starting materials showed no depression. The visible absorption spectra were identical. Absorption maxima in ether: I, 691; II, 632; III, 575; IV, 545; V, 509; VI, *ca.* 480; VII, 414 mμ. Relative absorbancies: VII > I > V > IV > II > VI > III.

The oxime derivative was prepared as given by Fischer and Walter (10). Absorption maxima in ether: I, 671; II, 617; III, 564; IV, 534; V, 501; VI, 403 mμ. Relative absorbancies: VI > I > V > IV > II > III.

2-Desvinyl-2-formyl-pheophorbide-a Dimethyl Acetal Methyl Ester

The methyl ester of fraction A was dissolved in a small volume of 5% (w/w) methanolic

HCl. After 1 minute, the pigment was transferred into ether by dilution with distilled water. The pigment was evaporated to dryness after removal of acid, and adsorbed on a sucrose column from 1% pyridine in petroleum ether. The column was developed by 0.5% isopropanol in petroleum ether, and the main zone of pigment was removed after extrusion of the sugar. Absorption maxima in ether: I, 664; II, 634; III, 607; IV, 558; V, 534; VI, 505; VII, 471; VIII, 406 mμ. Relative absorbancies: VIII > I > VI = V > III > II > IV > VII.

2-Desvinyl-2-hydroxymethyl-pheophytin-a

2-Desvinyl-2-formyl-chlorophyll-*a* (5 mg) in methanol (20 ml) was treated with sodium borohydride (5 mg). After 2 minutes the "red" absorption maximum shifted from about 690 mμ to about 660 mμ. The mixture was poured into ether and was well shaken with aqueous 0.5% potassium acid phosphate, and with distilled water. The solution was evaporated to dryness and the pigment was adsorbed on sucrose from 100% benzene. The column was developed with 2% isopropanol in petroleum ether. Pigment in the main zone was isolated and magnesium was removed by dilute aqueous HCl in acetone. Absorption maxima in ether: I, 660; II, 630; III, 603; IV, 556; V, 533; VI, 503; VII, 490 mμ. Relative absorbancies: I > VI > V > III > VII > II > IV.

Determination of Magnesium Content of Fraction A

The magnesium content in 50 ml of an ether solution was determined by the method of Smith and Benitez (3). Absorbance per cm at 687 mμ: 6.60. Slope of the calibration curve at 540 mμ: 0.266 absorbance units per cm per 0.108 mg of magnesium. Absorbance of unknown at 540 mμ: 0.185, equivalent to 0.076 mg of magnesium. Weight of fraction A per 50 ml calculated using the specific absorption coefficient of Smith and Benitez: 2.99 mg. Weight calculated from magnesium determination assuming molecular weight of 895: 2.81 mg. Calculated extinction coefficient: 117.8; Smith and Benitez: 110.4 for chlorophyll *d*.

ACKNOWLEDGMENTS

The authors are very grateful to Miss C. I. MacFarlane of the Nova Scotia Research Foundation for having sent the samples of *Chondrus* and *Gigartina*, and to Dr. M. B. Allen of the Kaiser Foundation, Berkeley, California, for having sent the sample of *Rhodocorton*. Infrared absorption spectra were measured by Mr. F. Rollin. Technical assistance was provided by Mr. E. Versteeg.

REFERENCES

1. Rabinowitch, E. I. Photosynthesis. Vol. II. Pt. 2. Interscience Publishers, Inc., New York. 1956.
2. Manning, W. M. and Strain, H. H. J. Biol. Chem. **151**, 1 (1943).
3. Smith, J. H. C. and Benitez, A. Modern methods of plant analysis. Vol. IV. Springer-Verlag, Berlin. 1955. pp. 142–196.
4. Holt, A. S. Can. J. Biochem. Physiol. **36**, 439 (1958).
5. Weller, A. J. Am. Chem. Soc. **76**, 5819 (1954).
6. Holt, A. S. and Jacobs, E. E. Plant Physiol. **30**, 553 (1955).
7. Holt, A. S. To be published.
8. Fischer, H. and Lakatos, E. Ann. **506**, 123 (1933).
9. Fischer, H. and Lautsch, W. Ann. **528**, 247 (1937).
10. Fischer, H. and Walter, H. Ann. **549**, 44 (1941).
11. Haworth, R. D. and Lapworth, A. J. Chem. Soc. 79 (1922).
12. Fischer, H., Breitner, S., Hendschel, A., and Nüssler, L. Ann. **503**, 1 (1933).
13. Fischer, H., Lakatos, E., and Schnell, J. Ann. **509**, 201 (1934).
14. Willstätter, R. and Stoll, A. Untersuchungen über Chlorophyll. J. Springer, Berlin. 1913.
15. Holt, A. S. and Jacobs, E. E. Am. J. Botany, **41**, 710 (1954).
16. Jacobs, E. E., Vatter, A., and Holt, A. S. Arch. Biochem. and Biophys. **53**, 228 (1954).
17. Fischer, H. and Orth, H. Chemie des pyrroles. Vol. II. Pt. 2. Leipzig. 1940.

Can. J. Chem. Downloaded from www.nrcresearchpress.com by 190.90.36.8 on 09/04/12
For personal use only.

Can. J. Chem. Downloaded from www.nrcresearchpress.com by 190.90.36.8 on 09/04/12
For personal use only.

A MASS SPECTROMETER WITH A LOW-TEMPERATURE IONIZATION CHAMBER

TO STUDY HETEROGENEOUS REACTIONS OF ATOMS AND FREE RADICALS: EXAMPLE, IODINE ATOMS[1]

L. P. BLANCHARD[2] AND P. LE GOFF

ABSTRACT

The main features of a mass spectrometer in which the ionization chamber can be cooled in a controlled way to the temperature of liquid nitrogen are given. Atoms or free radicals, formed in a heterogeneous quartz reactor that can be heated to 1000° C, effuse through a small hole in the wall of this reactor and enter directly into the ionization chamber. With this instrument it is possible to study the various ways in which unstable particles disappear during collisions on a metallic surface maintained at low and controlled temperatures.

The collision efficiency "*b*" of iodine atoms to form iodine molecules was found to vary between 1.7×10^{-3} and 4×10^{-3} on a surface at a temperature between +40° C and −25° C. Between −25° C and −60° C, the atoms are condensed at the same time as the iodine molecules; at lower temperatures, they are more "volatile" than iodine molecules, most of them colliding on the molecules of condensed iodine without reacting.

INTRODUCTION

In recent years an increasing number of workers have been focusing their attention on the study of atoms and free radicals trapped on surfaces maintained at liquid nitrogen or helium temperatures, but little attention has been paid to the trapping process itself.

A special mass spectrometer was designed and constructed in Nancy to study the primary process that takes place when a free radical collides with a surface at a controlled low temperature. Four possibilities must be considered in this process:

(1) that the radicals are adsorbed and trapped in the free state without undergoing any transformation;

(2) that the radicals are adsorbed on the surface but interreact to form stable molecules which immediately freeze to the surface;

(3) that the radicals are adsorbed and react as in (2) but form volatile products that leave the surface;

(4) that the radicals undergo elastic collisions with the cooled surface, while stable products are formed elsewhere by secondary reactions.

It has been reported that when the temperature of a surface on which radicals have been trapped is allowed to rise slowly, a point is reached where the radicals regain sufficient mobility to react and form stable molecules, giving off heat and sometimes light. The instrument mentioned above has been designed to study the mechanism of such reactions, since with it, it is possible to analyze directly the unstable as well as the stable products formed during the recombination–desorption process.

Operating Principle of the Instrument (See Fig. 1)

The ionization chamber of the mass spectrometer was machined out of a block of non-magnetic stainless steel that is mounted in such a way that its temperature can be lowered in a controlled manner to that of liquid nitrogen. The particles contained in a molecular jet coming from a nearby reactor are admitted to the ionization chamber through a slit "A_2" cut in one of the side walls. The present reactor is a quartz tube,

[1]*Manuscript received November 7, 1958.*
Contribution from l'École Nationale Supérieure des Industries Chimiques, Université de Nancy, France.
[2]*Postdoctorate Fellow of the National Research Council of Canada. Present address: Département de Génie Chimique, Université Laval, Quebec, Canada.*

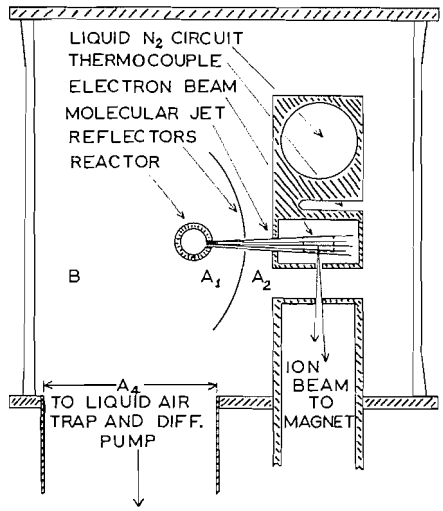

FIG. 1. Schematic diagram of the ion source. The ion source unit and the reactor are shown at a scale six times that of the bell jar enclosure.

3 mm i.d., that can be heated to 1000° C. This tube located 8 mm away from the ionization chamber contains a small orifice "A_1" through which effuse the gases of the molecular jet. The ion source and reactor assembly are located within a large bell jar, which is evacuated by a 600-liter-per-second mercury diffusion pump, and liquid-nitrogen trap.

The metallic block which contains the ionization chamber has no physical contact with the neighboring parts of the ion source: the filament (made of 0.258 mm carbon rod) is mounted on one of the pole pieces of the source magnet, while the other pole piece serves as the electron trap. Contrary to usual mass spectrometer technique, the ion source is grounded through the copper tubes of the liquid nitrogen circuit and the ion acceleration potential is applied to the magnet analyzer tube. Electrical insulation of the tube from the rest of the vacuum envelope is maintained by mineral-free synthetic rubber *o*-rings at the vacuum seals and teflon sheet elsewhere.

After deviation in the magnetic field the ion beam falls on the first copper–beryllium dynode of a 12-stage Allen-type ion–electron multiplier. The outcoming signal is fed to the vertical amplifier of a cathode ray oscilloscope. Fast scanning of the mass spectrum can be carried out by modulation of the magnet current (10 sweeps/second) or the ion acceleration potential (100 sweeps/second).

Flow and Pressure of Gases in the Ionization Chamber

A fraction of the molecular stream leaving the reactor enters directly into the ionization chamber while the complementary fraction diffuses into the bell jar.

Under usual operating conditions the following pressures are observed in the instrument: 1×10^{-2} mm Hg in the reactor, 1.1×10^{-4} mm Hg in the ionization chamber, and 1.6×10^{-5} mm Hg in the bell jar. Using the method previously described (2) for the statistical study of the fate of every molecule, an expression was found for the molecular concentration in that region of the chamber where the ionizing electron beam crosses the molecular stream. In the case of a condensable gas, with the reactor and the ion source both at room temperature, this expression is composed of two terms: one (amounting to 14% of the total concentration) which represents the "equivalent jet concentration", i.e. the molecules that have come directly from the reactor and have *not yet*

Can. J. Chem. Downloaded from www.nrcresearchpress.com by 190.90.36.8 on 09/04/12
For personal use only.

collided with the chamber walls; the second (the remaining 86%) which corresponds to the molecules homogeneously distributed throughout the chamber and undergoing an average number of 102 collisions with the walls before leaving by a "collision" with one of the four slits.

If "b" is the probability that the particle will disappear at every collision with the walls, then the concentration C in the ionizing region is given by the following expression:

$$\frac{C}{C_0} = 0.14 + 0.86\left(\frac{T_r}{T_c}\right)^{\frac{1}{2}} \frac{(1-b)}{(1+101b)}$$

where T_r and T_c are respectively the temperatures of the reactor and of the ionization chamber and C_0 is the concentration in the case where $T_r = T_c$ and $b = 0$.

EXPERIMENTAL RESULTS

Experiments were carried out using mixtures of iodine vapor and argon, the argon serving as internal standard.

1. Spectrum of Iodine at Low Temperatures

When iodine vapor is introduced at a constant flow rate into the source through the reactor maintained at room temperature, i.e. +40° C, and the chamber is progressively cooled to lower temperatures, the following results are observed:

(*a*) *Between +40° C and −45° C* the reading of an ionization gauge located in the bell jar is constant; the I_2^+ peak decreases from 5.7 to 2.2 while the I^+ peak remains essentially constant at 1.4.* This is in fact the variation with temperature of the cracking pattern of iodine molecules.

(*b*) *Between −45° C and −70° C* the vapor pressure of iodine passes from 1×10^{-4} to approximately 1×10^{-6} mm Hg. Effectively the reading from the ionization gauge decreases and the I_2^+ and I^+ peaks fall to about 6% of their values at room temperature. It must be concluded that the condensation probability of iodine molecules on the walls varies gradually from zero to one in this temperature range.

(*c*) *Below −70° C* the condensation probability is equal to one. The remaining ionic intensities are constant and correspond to the molecules arriving in the jet directly from the reactor.

2. Dissociation of Iodine into Atoms

When the reactor is heated to 697° C, the ionization chamber being maintained at +40° C, the I_2^+ peak is observed to fall to 32% of its initial value, while the intensity of the I^+ peak remains constant. From thermodynamic data it can be assumed that the iodine molecules passing through the reactor are totally dissociated into atoms. Thus the iodine molecules observed would come solely from recombination reactions on the walls. The probability of recombination of an iodine atom at every collision has been calculated to be: 1.7×10^{-3}.

3. Freezing Experiments with Iodine Atoms and Molecules

When the ionization chamber is slowly cooled, the reactor being maintained at 697° C, the I_2^+ and I^+ peak intensities vary in a manner completely different from that observed when the reactor is at 40° C.

At first, the I_2^+ peak decreases slowly from 1.8 at +40° C to 1.6 at −40° C, then sharply to 0.3 at −70° C. The I^+ peak, on the other hand, increases from 1.2 to 1.5

*I_2^+ *and* I^+ *peak intensities are expressed as the ratio of the peak height to that of argon at each temperature.*

Can. J. Chem. Downloaded from www.nrcresearchpress.com by 190.90.36.8 on 09/04/12
For personal use only.

then decreases slowly to a value of 0.6. The fundamental difference from the first case resides in the fact that the I^+ peak maintains an appreciable intensity below $-70°$ C.

A detailed analysis of the various low temperature mass spectra has been given elsewhere (1), however the essential points of the method are as follows:

(1) The mass spectrometric sensitivity and cracking pattern of iodine having been obtained in the first experiment, the concentration of molecules at each temperature of the present case can be evaluated.

(2) By subtracting from the total I^+ peak measured that part due to the dissociative ionization of iodine molecules, the intensity of the I^+ peak due to iodine atoms is thus obtained at each temperature.

(3) By means of an iodine material balance in the ionization chamber and the assumption that the mass spectrometric sensitivity for I^+ coming from iodine atoms is constant, the concentration of these atoms in the ionization chamber at every temperature is obtained.

The experimental results are as follows (refer to Fig. 2):

(1) When the temperature drops from $+40°$ C to $-30°$ C, the iodine atom concentration decreases slowly, the collision efficiency for the recombination of iodine atoms increasing from 1.7×10^{-3} to about 4×10^{-3}.

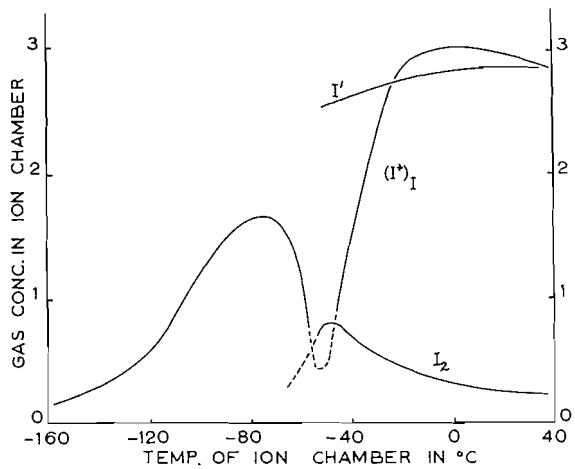

FIG. 2. Concentration variations of atomic and molecular iodine in the ionization chamber when this chamber is being cooled. Reactor at 697° C. The unit of concentration used on this graph corresponds to a pressure of 5×10^{-4} mm Hg at $+40°$ C.

(2) From $-30°$ C, the iodine atom concentration decreases sharply: iodine atoms disappear readily when they collide with the walls, *without* giving molecules which would desorb from the surface. However, it is not possible to distinguish whether the atoms are condensed in a free state within the matrix of the molecules condensing simultaneously, or whether the atoms recombine beforehand to form molecules that are immediately frozen out.

(3) When the temperature is lowered further, the iodine atom concentration presents a new maximum between $-70°$ C and $-80°$ C which would indicate that the majority of these atoms rebound from the layer of condensed iodine molecules without recombining or condensing.

Can. J. Chem. Downloaded from www.nrcresearchpress.com by 190.90.36.8 on 09/04/12
For personal use only.

4. Defrosting Experiments

A film of iodine was condensed on the walls of the chamber:

(1) by cooling the chamber gradually, and later

(2) by introducing the vapor into a precooled source at −195° C.

Defrosting experiments showed no particular characteristics; iodine molecules alone were desorbed at the same rate and at the same temperature regardless of the reactor temperature during the freezing process.

The work described here was carried out in the laboratories of Professor M. Letort, to whom the authors are indebted for the facilities placed at their disposal. One of us (L.P.B.) wishes to thank the National Research Council of Canada for a Postdoctorate Overseas Fellowship.

REFERENCES

1. Conference on Mass Spectrometry in London, England, September, 1958.
2. Le Goff, P. J. chim. phys. **53**, 359 (1956).

Can. J. Chem. Downloaded from www.nrcresearchpress.com by 190.90.36.8 on 09/04/12
For personal use only.

Can. J. Chem. Downloaded from www.nrcresearchpress.com by 190.90.36.8 on 09/04/12
For personal use only.

THE DEHYDRATION OF UREA, BENZAMIDE, AND PHENYLUREA BY THIONYL CHLORIDE IN THE PRESENCE OF AMMONIA[1]

PAUL E. GAGNON, JEAN L. BOIVIN,[2] AND JOHN H. DICKSON[3]

ABSTRACT

The decomposition of thionyl chloride in the presence of ammonia was found to give sulphur, ammonium sulphate, and ammonium sulphamate besides ammonium chloride. Heating urea and the reaction products of thionyl chloride and ammonia under pressure yielded guanidine hydrochloride and melamine, under different conditions of temperature, time, and pressure. Under similar conditions, benzamide was transformed into benzonitrile, and phenylurea into aniline or aniline black and diphenylurea, guanidine being absent.

INTRODUCTION

Guanidine has been synthesized from urea using various dehydrating agents, such as sulphur trioxide (1), sulphur dioxide (2), ammonium sulphamate (1), aluminum metal, or aluminum chloride (3) in the presence of ammonia or ammonium salts. In all cases, the highest yields of guanidine were obtained when the reaction was carried out under pressure (4). Since thionyl chloride is a good dehydrating agent, which reacts with water giving sulphur dioxide and hydrochloric acid, it is of interest to study its potentiality with respect to the dehydration of urea, benzamide, and phenylurea.

As the formation of guanidine is considered as an ammoniation of cyanamide, which in turn is produced by dehydration of urea:

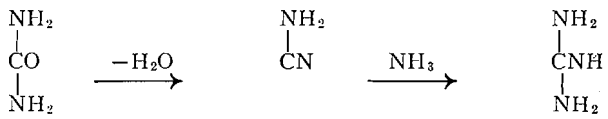

there is an indication that guanidine would be unstable if thionyl chloride reacted alone with urea. It is known that ammonium salts or ammonia under pressure stabilize the molecule, and the effect of both will be necessary at high temperatures to prevent its decomposition into melamine (5).

Preliminary experiments carried out by heating, in a pressure vessel, urea, thionyl chloride, and ammonia which had been frozen separately in liquid air proved to be hazardous and unreliable. Therefore, to study the dehydrating properties of thionyl chloride with respect to urea and benzamide, a solution of thionyl chloride in anhydrous benzene was treated with an excess of ammonia. The yellow solid was collected and dried over calcium chloride and used without further purification. It will be called a thionyl chloride – ammonia complex since it is an ill-defined material (6, 7, 8, 9).

Thermal Stability of the Thionyl Chloride – Ammonia Complex

Since the synthesis of guanidine is best carried out under pressure, the thermal stability of the thionyl chloride – ammonia complex was studied under various conditions of temperature and pressure. It was observed that sulphur, ammonium sulphate, and ammonium sulphamate were the reaction products obtained, besides the normally

[1]*Manuscript received June 4, 1958.*

Contribution from the Department of Chemistry, Laval University, Quebec, Que., with financial assistance from the Defence Research Board of Canada. This paper constitutes part of a thesis submitted to the Graduate School, Laval University, in partial fulfillment of the requirements for the degree of Doctor of Science.

[2]*Defence Research Board, C.A.R.D.E., Valcartier, Que.*

[3]*Graduate student, holder of a Shell Oil Co. of Canada Ltd. Scholarship in 1957–58, Laval University, Quebec, Que.*

present ammonium chloride under different conditions. At atmospheric pressure over a range of temperature of 150–325° C, the yield of sulphur was nearly constant to 7.5% and there was an increase of ammonium sulphate from 0.9% at 150° C to 7.5% at 300° C and a decrease to 5.2% at 325° C, as shown in Table I. Ammonium sulphamate was obtained in maximum yield at 250° C, which decreased from 12.6 to 3.1% at 325° C.

Under an ammonia pressure of 100 and 300 p.s.i., the results were similar, but it was observed that ammonium sulphate was present in larger quantities from 275 until 350° C.

TABLE I

Decomposition products of the thionyl chloride – ammonia complex at atmospheric pressure

Temp., °C	% Composition of solid products			
	S	NH_4Cl	$(NH_4)_2SO_4$	$NH_2SO_3NH_4$
150	7.2	65.7	0.9	8.2
175	7.2	64.4	1.3	9.2
200	7.3	64.7	1.1	10.8
225	7.8	65.2	1.3	11.9
250	7.8	64.1	2.1	12.6
275	7.8	65.7	3.9	11.9
300	7.5	61.8	7.5	4.2
325	7.3	62.4	5.2	3.1

Guanidine from Urea and Thionyl Chloride – Ammonia Complex

As ammonium sulphamate is present in the decomposition products of the complex, it is expected that it could transform urea into guanidine (1). The reaction of the thionyl chloride – ammonia complex with urea was studied under various conditions of temperature, pressure, time, and ratio of reactants.

The method used consisted of mixing thoroughly urea with the dry thionyl chloride – ammonia complex and heating the mixture under normal pressure or under ammonia pressure in the autoclave. The reaction products were analyzed for sulphur, ammonium sulphate, ammonium sulphamate, guanidine, and melamine. Results are given in Table II for the reaction under 300 p.s.i. for a 30-minute period of heating.

TABLE II

Guanidine formation at 300 p.s.i. pressure for a 30-minute period of heating

Temp., °C	% Composition of reaction products				
	S	$(NH_4)_2SO_4$	$NH_2SO_3NH_4$	$H_2NC(NH)NH_2$	$C_3H_6N_6$
150	6.8	2.0	4.9	—	—
175	6.9	0.6	6.4	—	—
200	7.2	1.2	4.7	—	—
225	7.6	3.8	4.5	—	—
250	7.6	28.6	3.5	19.4	2.8
275	6.9	38.0	2.3	33.8	3.9
300	5.8	38.5	2.5	35.1	4.1
325	5.7	23.5	2.1	31.2	4.5
350	5.6	7.5	1.3	17.5	3.7

At atmospheric pressure, urea was transformed into guanidine between 225° C and 250° C. The conversion of urea into guanidine reached a maximum at 275° C and then fell off sharply at higher temperatures so that no guanidine was found when the experiment was carried out above 325° C. The fact that melamine was found in place of

Can. J. Chem. Downloaded from www.nrcresearchpress.com by 190.90.36.8 on 09/04/12
For personal use only.

guanidine at the higher temperatures indicates that the guanidine decomposed into cyanamide which trimerized into melamine. Ammonia pressure had a stabilizing effect, and the yield of guanidine was increased from 17 to 35% at 275–300° C when the pressure was either 100 or 300 p.s.i.

In the solid products, sulphur was present to a practically constant proportion of about 7.0% which, however, decreased with increasing temperatures to 5.6%. Ammonium sulphate increased proportionally with the amount of guanidine formed while the ammonium sulphamate content decreased.

With different ratios of urea at a temperature of 275° C and an ammonia pressure of 300 p.s.i., the yield of sulphur was practically constant and the production of ammonium sulphate varied directly with increasing quantity of urea used, whereas the yield of ammonium sulphamate varied inversely with the urea. When the reaction time was limited to 30 minutes, the yield of sulphur was about 7%. Between 60 and 150 minutes, it fell to 5%, but with longer periods of heating it decreased sharply and was less than 1% after 210 minutes. The proportion of ammonium sulphate in the reaction products remained constant for heating periods longer than 60 minutes. Although ammonium sulphate decomposed at temperatures above 300° C (10) during a reaction time of 30 minutes, it was quite stable at 275° C, even when heated for periods up to 3½ hours. Only traces of ammonium sulphamate were found in the reaction products under these conditions.

Guanidine and ammonium sulphate increased continuously with the reaction time up to a maximum yield of about 44%, and further heating had no apparent effect. The increase in the reaction time was unfavorable for the formation of melamine and the yield was reduced from 14.4% after 60 minutes to 10.5% after 210 minutes.

Benzonitrile from the Thionyl Chloride – Ammonia Complex and Benzamide

Since the thionyl chloride – ammonia complex was a dehydrating agent by way of the formation, on heating, of ammonium sulphamate, amides should be converted into the corresponding nitriles (11, 12). By heating the thionyl chloride – ammonia complex and benzamide under pressure, benzonitrile was obtained in only 5% yield at 175° C and more was formed as the temperature was increased until a maximum yield of 57.4% was reached at 325° C. The production of ammonium sulphate increased to a maximum of about 30% at 275° C and then decreased with increasing temperatures. A maximum yield of ammonium sulphamate was obtained at 150° C, but decreased continuously with the increase in temperature.

Products of the Reaction of Phenylurea with the Thionyl Chloride – Ammonia Complex

The reaction of the thionyl chloride – ammonia complex with phenylurea at different pressures led to a mixture of salts where aniline was present at the lower temperatures and aniline black at temperatures above 250° C. When the experiments were performed at atmospheric pressure, the highest yield of ammonium sulphate obtained was about 4% whereas the quantity of ammonium sulphamate for temperatures above 200° C was much lower. The yield of aniline, constant up to a temperature of 275° C, increased slightly at higher temperatures and was accompanied by an increase in the pressure.

An ammonia pressure of 100 p.s.i. gave rise to larger amounts of ammonium sulphamate at 150° C which decreased as the temperature was raised. Again fairly large amounts of aniline black were present up to 300° C. The ammonia pressure caused an increase in the yield of ammonium sulphate and a much higher yield of aniline which, however, decreased from 63.3% at 150° C to 22.0% at 325° C, while that of ammonium sulphate increased from 0.2% at 150° C to 7.9% at 325° C.

Can. J. Chem. Downloaded from www.nrcresearchpress.com by 190.90.36.8 on 09/04/12
For personal use only.

A higher ammonia pressure of 300 p.s.i. favored the production of larger quantities of ammonium sulphate, the maximum yields being obtained at 200° and 275° C. Higher temperatures led to reduced yields. Ammonium sulphamate production was highest at the lower temperatures although the amount was a good deal lower. The maximum yield of aniline, 63.3%, was also obtained at the lower temperatures. Ammonia pressure stabilized aniline particularly at the higher temperatures where the minimum yield was found to be about 37%.

Also diphenylurea was obtained between 150 and 250° C at 300 p.s.i., in yields varying from 0.1 to 4.0%, depending on the temperature used. At pressure lower than 300 p.s.i., diphenylurea could not be isolated.

DISCUSSION OF RESULTS

The ill-defined thionyl chloride – ammonia complex was decomposed at ordinary pressure or under an ammonia pressure into sulphur, ammonium sulphate, and ammonium sulphamate. While it is difficult to account specifically for all these products, this behavior should be similar to that of sulphur dioxide and ammonia which give, by heating under pressure, ammonium sulphamate and sulphur and no ammonium sulphate (2). The fact that ammonium sulphate is present indicates that a similar oxidoreduction has taken place where ammonia reduced the chloro derivative of sulphur dioxide into sulphur giving water, which then hydrolyzed part of ammonium sulphamate into ammonium sulphate.

When urea is present, the mechanism of formation of the products sulphur, ammonium sulphate, ammonium sulphamate, guanidine, and melamine is easily explained by reactions similar to the synthesis of guanidine from urea, sulphur dioxide, and ammonia (2). In this case, urea is dehydrated into cyanamide and ammonolyzed into guanidine. Guanidine is present in the actual synthesis as the hydrochloride because of the greater solubility of this salt in liquid ammonia than the sulphamate salt, whereas guanidine sulphate is completely insoluble (5).

When monophenylurea was heated with ammonium sulphamate, aniline, guanidine, and cyanuric acid were produced (12). On heating thionyl chloride and ammonia with monophenylurea, ammonium chloride, sulphate, sulphamate, aniline, aniline black, and diphenylurea were formed. It was assumed that monophenylurea underwent ammonolysis to give urea and aniline, and also diphenylurea. It is well known that aniline, in the presence of an oxidizing agent, forms a polymer, or better a variety of polymers, grouped together under the generic name of aniline blacks, the exact constitution of which is still unknown; since free sulphur was absent, it was concluded that it had oxidized the aniline to form aniline black, sulphur being transformed into hydrogen sulphide.

The absence of urea or guanidine derivatives in the reaction products was explained by the inhibition of hydrogen sulphide to form ammonium sulphamate from the chloro derivative of sulphur dioxide.

EXPERIMENTAL

Thionyl Chloride – Ammonia Complex

Thionyl chloride (20.0 g) was added to a 1-l. flask containing anhydrous benzene (400 ml), and anhydrous ammonia was bubbled through the solution until there was no further evolution of heat. The light yellow solid which precipitated out was separated by filtration on a Büchner funnel, washed with anhydrous benzene, and dried in a vacuum desiccator over calcium chloride (yield, 30.4 g).

The dried yellow starting material (8.0 g) was added to the removable Pyrex glass

Can. J. Chem. Downloaded from www.nrcresearchpress.com by 190.90.36.8 on 09/04/12
For personal use only.

liner of a pressure vessel which had a volume of 183 ml without the liner, and 108 ml with the liner in place. The liner was fitted with a glass wool plug, and air was displaced by the evaporation of several drops of liquid ammonia in the autoclave. The reaction vessel was then heated at the desired temperature for 30 minutes, removed from the heating jacket, and cooled rapidly.

The solid products were analyzed for sulphur, ammonium chloride, sulphate, and sulphamate (2). Ammonium sulphamate was extracted from the mixture by means of absolute alcohol in which it is slightly soluble and recrystallized to give a melting point of 131° C, which was not depressed by admixing an authentic sample.

Since it would be impracticable to give all the results obtained, the data were omitted.

Thionyl Chloride – Ammonia Complex and Urea

The yellow starting material (5.5 g), made from thionyl chloride and ammonia, and urea (3.0 g, 0.05 mole) were intimately mixed and heated as in the above method. The products were analyzed for sulphur, ammonium sulphate, ammonium sulphamate, guanidine hydrochloride, and melamine (2). Guanidine hydrochloride was isolated by absolute ethanol extraction of the dried products and recrystallized from a mixture of alcohol and acetone. It had a melting point of 184–185° C, which was not depressed by mixing with an authentic sample.

Reaction with Benzamide

The yellow starting material (5.5 g) was added to a glass liner containing benzamide (6.1 g, 0.06 mole, m.p. 130° C) which had been recrystallized. The two solid compounds were then thoroughly mixed and heated in the autoclave and cooled overnight. Caution was exercised in reducing the internal pressure to atmospheric pressure since benzonitrile could be entrained out.

Benzonitrile was determined by extraction with ether and weighing the residue. It boiled at 188–191° C and gave benzoic acid, m.p. 121° C, by hydrolysis with alcoholic sodium hydroxide. The residue which was insoluble in ether was analyzed for ammonium sulphate and sulphamate (2).

Reaction with Monophenylurea

The yellow starting material (5.5 g) and monophenylurea (6.8 g, 0.05 mole) were placed in a Pyrex liner, thoroughly mixed together, and heated in the autoclave. The solid products were analyzed for aniline, ammonium sulphate, ammonium sulphamate, and diphenylurea by extraction or precipitation with barium chloride (2).

REFERENCES

1. MACKAY, J. S. U.S. Pat. No. 2,515,244. July 18, 1950.
2. BOIVIN, J. L. Can. J. Chem. **34**, 827 (1956).
3. SANDER, F. Ger. Pat. No. 527,237. Jan. 1, 1928.
4. BLAIR, J. S. J. Am. Chem. Soc. **48**, 87 (1926).
5. BOIVIN, J. L. Can. J. Chem. **33**, 1467 (1955).
6. SCHIFF, H. Ann. 102 (1857).
7. MICHAELIS, A. Z. Chem. (2), **6**, 460 (1870).
8. EPHRAIM, F. and PIATROWSKI, H. Ber. **44**, 379 (1911).
9. SCHENK, P. W. Ber. **75**, 94 (1942).
10. SMITH, W. J. Soc. Chem. Ind. (London), **14**, 629 (1895); **15**, 3 (1896).
11. BOIVIN, J. L. Can. J. Chem. **28**, 671 (1950).
12. GAGNON, P. E., BOIVIN, J. L., and HAGGART, C. Can. J. Chem. **34**, 1662 (1956).

Can. J. Chem. Downloaded from www.nrcresearchpress.com by 190.90.36.8 on 09/04/12
For personal use only.

Can. J. Chem. Downloaded from www.nrcresearchpress.com by 190.90.36.8 on 09/04/12
For personal use only.

DIALKYL PHOSPHOROISOTHIOCYANATIDATES[1]

MARSHALL KULKA

ABSTRACT

An improved method for the preparation of dialkyl phosphoroisothiocyanatidates (II) is given. These compounds (II) are labile and decompose under the influence of heat and catalysts to the corresponding alkyl thiocyanates (III). In the presence of water they hydrolyze to dialkyl hydrogenphosphates (VI) in high yield. A series of thiourea derivatives (VII) has been prepared from II and amines.

Some discrepancies have appeared in the literature regarding diethyl phosphoroisothiocyanatidate (1). The compound is referred to as a thiocyanate by some workers (2, 3, 4), and isothiocyanate by others (5, 6). There has also been a lack of harmony in regard to its properties and preparation. Saunders *et al.* (2) first reported that when diethyl phosphorochloridate (I) was heated under gentle reflux with potassium thiocyanate, diethyl phosphorothiocyanatidate boiling at 40° (13 mm) was obtained. Kosolapoff (7) pointed out that this boiling point was too low and when the English workers (3) re-examined the reaction, they found that it proceeded at room temperature to form diethyl phosphorothiocyanatidate in 50% yield boiling at 80–82° (1 mm). Other workers have employed acetone (5) and methyl ethyl ketone (4) as solvent but without improvement in yield.

Recently (5, 6) it was pointed out that the higher-boiling reaction product of I and potassium thiocyanate reacted readily with amines to form thiourea derivatives. This indicated that the product is diethyl phosphoroisothiocyanatidate (II) and not a thiocyanate. It can be assumed that II arises through a thiocyanate–isothiocyanate rearrangement which in phosphorus compounds would be expected to take place with ease.

Dialkyl phosphoroisothiocyanatidates (II) were required as intermediates in connection with a synthetic program of insecticides. For this reason a study of the preparation and properties of II was undertaken. It was found that the compound (II) could be readily prepared and in excellent yield by merely stirring a solution of I in dry benzene with ammonium thiocyanate at 20°, followed by washing with cold brine solution, drying, and cautiously distilling.

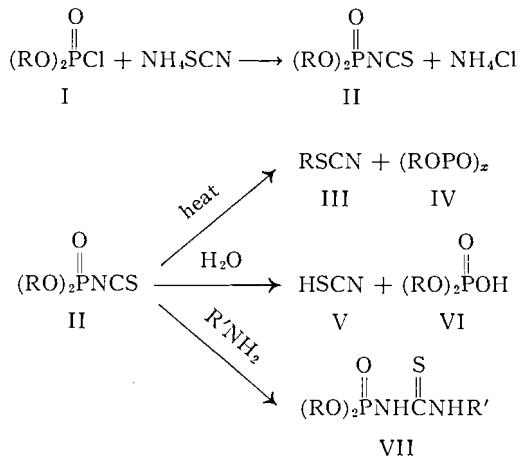

[1]*Manuscript received November 10, 1958.*
Contribution from the Dominion Rubber Company Limited, Research Laboratories, Guelph, Ontario.

Can. J. Chem. Downloaded from www.nrcresearchpress.com by 190.90.36.8 on 09/04/12
For personal use only.

Diethyl phosphoroisothiocyanatidate (II) is a labile compound. Under the influence of heat it decomposed to a low-boiling material which appeared to be the same as that obtained by the original workers (2) and mistaken for II. The decomposition occurred very rapidly at 150°, more slowly in refluxing benzene or methyl ethyl ketone, and was catalyzed by traces of ammonium or potassium thiocyanate. The low-boiling phosphorus-free decomposition product did not react with amines but on heating with aqueous alcoholic alkali yielded diethyl disulphide and sodium cyanide, a reaction which is characteristic of alkyl thiocyanates. After an examination of the physical properties it was concluded that the decomposition product of II was ethyl thiocyanate (III, R = ethyl). In the same way di-*n*-butyl phosphoroisothiocyanatidate (II, R = *n*-butyl) on heating alone or in the presence of ammonium thiocyanate decomposed to butyl thiocyanate III, (R = *n*-butyl) and presumably butyl metaphosphate (IV).

It will be seen that II is both an anhydride and an isothiocyanate presenting at least two sites for attack. With warm water II did not react like a typical isothiocyanate. Instead hydrolysis occurred to form thiocyanic acid (V) and dialkyl hydrogenphosphate (VI) in high yield. This makes an excellent preparative method for VI. Primary amines attacked II at the isothiocyanate site to form dialkyl phosphorylthioureas shown in Tables I and II.

TABLE I

N^1-Diethylphosphoryl-N^2-substituted thioureas

$$(C_2H_5O)_2\overset{\overset{O}{\|}}{P}NH\overset{\overset{S}{\|}}{C}NHR$$

R =	Prepared from:	M.p., °C	Method of prep.	Yield, %	Analyses, N Calc.	Found
Phenyl (5)	Aniline	107–108	A	77	9.70	9.63
p-Chlorophenyl	*p*-Chloroaniline	129–130	B	91	8.68	9.14
3,4-Dimethoxyphenyl	3,4-Dimethoxyaniline	124–125	B	52	8.04	8.08
β-Naphthyl	β-Naphthylamine	117–118	B	60	8.28	8.50
2,4-Dichlorobenzyl	2,4-Dichlorobenzylamine	133–134	A	86	7.55	7.45
Cyclohexyl	Cyclohexylamine	84–85	A	90	9.52	9.67
Phenylethyl	Phenethylamine	80–81	A	48	8.86	8.57
β-Pentachloroanilinoethyl	N-2-Aminoethylpentachloroaniline	134–135	B	55	C, 30.99 H, 3.37	C, 30.59 H, 3.57
β-*p*-Chlorophenylmercaptoethyl	*p*-Chlorophenyl 2-aminoethyl sulphide	85–86	A	45	7.32	7.56
3-Indolylethyl	Tryptamine	134–136	C	37	11.83	11.65
Octadecyl	Stearylamine	62–63	A	57	6.04	5.84

TABLE II

Bis(dialkylphosphorylthioureas)

$$(C_2H_5O)_2\overset{\overset{O}{\|}}{P}NH\overset{\overset{S}{\|}}{C}NH - X - NH\overset{\overset{S}{\|}}{C}NH\overset{\overset{O}{\|}}{P}(OC_2H_5)_2$$

X =	Prepared from:	M.p., °C	Method of prep.	Yield, %	Analyses, N Calc.	Found
1,2-Ethylene	Ethylenediamine	149–150	A	50	C, 32.00 H, 6.22	C, 32.50 H, 6.47
p-Phenylene	*p*-Phenylenediamine	144–145 decomp.	C	85	11.25	11.42
o-Phenylene	*o*-Phenylenediamine	137–138 decomp.	C	55	11.25	11.18
4-Methyl-1,3-phenylene	4-Methyl-1,3-phenylenediamine	145–146	C	62	10.92	10.79
4,4′-Diphenylmethane	4,4′-Diaminodiphenylmethane	142–143	C	50	9.50	9.82
1,5-Naphthalene	1,5-Diaminonaphthalene	163–166 decomp.	C	48	10.22	10.15

Can. J. Chem. Downloaded from www.nrcresearchpress.com by 190.90.36.8 on 09/04/12
For personal use only.

EXPERIMENTAL

Diethyl Phosphoroisothiocyanatidate (II, R = Ethyl)

To a stirred and cooled solution of diethyl phosphorochloridate (150 g) in dry benzene (100 ml) was added ammonium thiocyanate (75 g), and the reaction mixture was stirred at 15–20° for 5 hours. Then benzene (300 ml) was added and the reaction mixture quickly washed with cold dilute sodium chloride solution until the washings were no more acid to litmus. The benzene solution was dried over sodium sulphate, the solvent removed under slightly reduced pressure, and the colorless residual liquid distilled applying only steam heat, b.p. (1 mm) = 88°, $n_D^{23} = 1.4772$. The yield of the colorless liquid was 155 g or 91%. The pure product also distilled at 112–113° (12 mm). In a cool dark place it could be kept for several months.

Di-n-butyl Phosphoroisothiocyanatidate (II, R = Butyl)

This was prepared from di-*n*-butyl phosphorochloridate (I, R = butyl) and ammonium thiocyanate in 65% yield according to the procedure described above. The colorless liquid boiled at 104–105° (0.1 mm) and the pure product distilled at 153–155° (12 mm) with only slight decomposition, $n_D^{20} = 1.4728$. An attempt to analyze this compound for carbon and hydrogen gave erratic results as is usually the experience with phosphorus compounds.

n-Butyl Thiocyanate (III, R = Butyl)

(*a*) *From di-n-butyl phosphorochloridate.*—A reaction mixture of di-*n*-butyl phosphorochloridate (50 g), ammonium thiocyanate (30 g), and dry benzene (50 ml) was stirred and heated under reflux for 5 hours. The cooled reaction mixture was washed with water, the solvent removed, and the residue distilled, b.p. (12 mm) = 64°, $n_D^{20} = 1.4640$. The yield was 26 g. On redistillation this liquid boiled at 184–185°. These properties are identical with those of butyl thiocyanate reported in the literature (8). Anal. Calc. for C_5H_9NS: C, 52.17; H, 7.82. Found: C, 52.15; H, 7.95. The colorless odoriferous liquid contained nitrogen and sulphur but no phosphorus or chlorine, and when boiled with aqueous alcoholic potassium hydroxide yielded dibutyl disulphide and sodium cyanide.

(*b*) *Directly from di-n-butyl phosphoroisothiocyanatidate.*—A reaction mixture of di-*n*-butyl phosphoroisothiocyanatidate (14 g), dry benzene (50 ml), and ammonium thiocyanate (1 g) was heated under reflux for 3 hours, cooled, and filtered. The solvent was removed from the filtrate and the residue distilled. There was obtained two fractions, one consisting of butyl thiocyanate (5 g) and the other unchanged starting material (4 g).

Ethyl Thiocyanate

This compound boiling at 140–143° with $n_D^{25} = 1.4615$ was obtained in 85% yield as a colorless odoriferous liquid from diethyl phosphorochloridate in a manner similar to that described in section (*a*) for butyl thiocyanate and also directly from diethyl phosphoroisothiocyanatidate. The properties of this compound were identical with those of ethyl thiocyanate reported in the literature (9).

Diethyl Hydrogenphosphate (VI, R = Ethyl)

A mixture of diethyl phosphoroisothiocyanatidate (II, R = ethyl) (70 g) and water (350 ml) was heated on the steam bath with occasional swirling for 15 minutes. The aqueous thiocyanic acid was removed under slightly reduced pressure from the resulting clear solution and the residual liquid distilled, b.p. (0.2 mm) = 130–135°, $n_D^{24} = 1.4162$. These properties agree with those of diethyl hydrogenphosphate reported in the literature (10). The yield was 49 g or 89%.

A small portion of the diethyl hydrogenphosphate in alcohol solution when treated with a strong aqueous solution of lead acetate yielded white needles of the lead salt of VI (R = ethyl) which melted at 183–184°; lit. m.p. 180° (7).

Preparation of the N^1-Dialkylphosphoryl-N^2-substituted Thioureas

Method A.—Diethyl phosphoroisothiocyanatidate (II) (1 mole) was added dropwise with cooling and stirring to the amine (1 mole), the temperature being kept below 50°. The reaction product which solidified was crystallized from methanol or aqueous methanol.

Method B.—This method was essentially the same as method A except that dry benzene was used as solvent for the amine and the product usually crystallized from the benzene solution on cooling.

Method C.—This method was essentially the same as method A except that acetone was employed as solvent for the amine and the product usually crystallized from the acetone solution on cooling.

N^1-Di-n-butylphosphoryl-N^2-p-chlorophenylthiourea (VII, R = *n*-Butyl, R′ = *p*-Chlorophenyl)

This was prepared in 58% yield from di-*n*-butyl phosphoroisothiocyanatidate and *p*-chloroaniline by method B. It melted at 65–66° after crystallization from aqueous methanol. Anal. Calc. for $C_{15}H_{24}N_2O_3ClPS$: N, 7.39. Found: N, 6.94, 6.85.

$N^1,N^{1'}$-(1,4-Phenylene)-$N^2,N^{2'}$-bis(di-n-butylphosphorylthiourea)

This was prepared in 72% yield by method C from *p*-phenylenediamine and di-*n*-butyl phosphoroisothiocyanatidate. The white solid melted at 149–150°. Anal. Calc. for $C_{24}H_{44}N_4O_6P_2S_2$: N, 9.18. Found: N, 8.85.

N^1-Diethylphosphoryl-N^2,N^2-diethylthiourea

This was prepared in 65% yield by method A from diethyl phosphoroisothiocyanatidate and diethylamine. The white product when crystallized by dissolving in acetone and cooling in dry ice melted at 70–72°. When exposed to moist air it liquefied to an acidic product. Anal. Calc. for $C_9H_{21}N_2O_3PS$: N, 10.45. Found: N, 10.19, 10.56.

REFERENCES

1. American Chemical Society Official Reports. Chem. Eng. News, **30**, 4515 (1952).
2. Saunders, B. C., Stacey, G. J., Wild, F., and Wilding, I. G. E. J. Chem. Soc. 699 (1948).
3. Cook, H. G., Ilett, J. D., Saunders, B. C., Stacey, G. J., Watson, H. G., Wilding, I. G. E., and Woodcock, S. J. J. Chem. Soc. 2921 (1949).
4. McIvor, R. A., McCarthy, G. D., and Grant, G. A. Can. J. Chem. **34**, 1819 (1956).
5. Levchenko, E. S. and Zhmurova, I. N. Ukrain. Khim. Zhur. **22**, 623 (1956); Chem. Abstr. **51**, 5719 (1957).
6. Michalski, J. and Wieczorkowski, J. Roczniki Chem. **31**, 585 (1957); Chem. Abstr. **52**, 5283 (1958).
7. Kosolapoff, G. M. Organophosphorus compounds. John Wiley & Sons, Inc., New York. 1950. p. 242.
8. Kaufman, R. J. and Adams, R. J. Am. Chem. Soc. **45**, 1744 (1923).
9. Hawthorne, J. J. Chem. Soc. **89**, 563 (1906).
10. Toy, A. D. P. J. Am. Chem. Soc. **70**, 3882 (1948).

Can. J. Chem. Downloaded from www.nrcresearchpress.com by 190.90.36.8 on 09/04/12
For personal use only.

Can. J. Chem. Downloaded from www.nrcresearchpress.com by 190.90.36.8 on 09/04/12
For personal use only.

REACTIONS OF OXYGEN ACTIVATED BY ELECTRICAL DISCHARGE WITH BUTENE-1

J. M. S. Jarvie and R. J. Cvetanović

ABSTRACT

Reactions of oxygen activated by electrical discharge with butene-1 have been studied in a "spherical diffusion" reaction zone. When small concentrations of oxygen are passed through the discharge tube in helium as the carrier gas, and the concentration of butene-1 in the reaction zone is sufficiently high, the observed products are entirely explainable by an interaction of the ground-state oxygen atoms with butene-1. With large deviations from these conditions considerable complexities arise, and under some conditions α-butylene ozonide and its decomposition products become important and the products are then explainable without any significant participation of oxygen atoms in the process.

INTRODUCTION

The number of methods available for the production of oxygen atoms in the laboratory is limited. One of the earliest methods employed for the production of oxygen atoms was the gaseous electrical discharge in oxygen molecules (1). The other methods frequently used are the mercury-photosensitized decomposition of nitrous oxide and the photodecomposition of nitrogen dioxide, and both these methods have been used extensively in this laboratory to study reactions of oxygen atoms. With the use of the nitrous oxide technique the main features of the reactions of oxygen atoms with olefins have now been established (2). In the present work one of the olefin reactions with oxygen atoms produced by electrical discharge was studied in order to compare this method for producing oxygen atoms with the nitrous oxide and the nitrogen dioxide methods. The relatively simple reaction of oxygen atoms with butene-1 was chosen for this purpose. An experimental arrangement incorporating the usual features of a "diffusion flame technique" (3, 4) was adopted in order to minimize any tendency for the occurrence of surface reactions, and to find out at the same time whether the application of the Garvin–Kistiakowsky "Temperature Pattern Method" (5) for the determination of rate constants is suitable for this reaction.

In the reaction of oxygen atoms with butene-1, two principal products are formed, α-butylene oxide and *n*-butyraldehyde, together with smaller amounts of methyl ethyl ketone and traces of some other compounds (2). The addition products possess excess energy when formed because of the high heats of reaction and decompose if not deactivated collisionally. This fragmentation is essentially suppressed at a pressure of about 10 mm (6) and the course of the reaction is then relatively simple. In the present work, on the other hand, considerable complexities are observed, especially under certain conditions. At the same time the electrical discharge technique is widely used to generate oxygen atoms and study their reactions. It is therefore essential to emphasize its potentially complex character. The latter is due to several factors. The technique is restricted to relatively quite low pressures, and as a result the concentration of the primary reactant is also low so that secondary attacks by oxygen atoms on the products may and indeed very frequently do take place. Also, when "hot" products are formed in the primary step, as is the case in the addition of oxygen atoms to olefins, they will tend to decompose

[1]*Manuscript received September 29, 1958.*
Contribution from the Division of Applied Chemistry, National Research Council, Ottawa, Canada. Issued as N.R.C. No. 5035.
[2]*National Research Council Postdoctorate Fellow 1956–57. Present address: Jackson Laboratory, Organic Chemicals Department, E. I. du Pont de Nemours and Company, Wilmington, Delaware, U.S.A.*

into free radicals at the low pressures, leading thus to further secondary reactions. An additional potential disadvantage of the low pressures is the difficulty of establishing whether any surface reactions occur. (In the present work any surface reactions in the reaction zone have been disregarded: it is likely that at least under some experimental conditions employed they are unimportant.) Another factor contributing to the observed complexities is the frequent presence, in addition to oxygen atoms, of other reactive or potentially reactive species, including here excess molecular oxygen when present. The object of the present work is to illustrate on the example of a reaction, the mechanism of which has been previously established by more convenient methods, some of the complexities which may be encountered in the application of the electrical discharge technique. The discussion of the obtained results is consequently more extensive than would be otherwise justifiable in view of its largely qualitative character.

EXPERIMENTAL

Apparatus

The apparatus used was an all-glass flow system. The gas flows were controlled by capillaries and needle valves (Edwards and Co.) with a constant pressure head. The pressure in the reactor was varied by means of internal capillaries of various dimensions. Helium and oxygen were passed through a liquid nitrogen trap before the discharge to remove any grease or mercury vapor in the gases, as these gave inconsistent results due to coating of the surface of the discharge tube (a quartz tube, 10 mm i.d.). An electrodeless discharge was used at microwave frequencies, supplied from a Raytheon Diatherm unit with the use of a 90% power output. The two probes were of copper wire, each a $\frac{1}{4}$ wavelength. These were placed at a distance of 22 cm from the nozzle through which the gases were discharged into a wide pyrex tube in which the reaction was carried out. The nozzle projected some distance into the reaction zone and had an orifice 0.5 mm in diameter. Butene-1 was introduced directly into the wide tube, but at a point below the nozzle to assure uniform distribution before the reaction zone was reached.

The products were frozen out in two liquid nitrogen traps and were transferred to a LeRoy still (7) at $-120°$ C and fractionated to obtain the products free of unreacted butene-1 and of any products of equal or greater volatility.

Attempts were made to measure the concentration of oxygen atoms at the nozzle by measuring the heat of recombination on a hot platinum wire, on a hot platinum wire coated with either silver or cobalt, and a silver-plated glass tip probe. It was found that all these methods gave inconsistent results so the direct measurement of the oxygen atom concentration was abandoned.

Materials

Research grade butene-1 (Phillips Petroleum Co.) was transferred to a storage volume at liquid nitrogen temperature and degassed at dry ice temperature. This was repeated several times until a pressure of 10^{-5} mm Hg was obtained.

Oxygen (People's Gas Co., Ottawa) was used without further purification. In some of the experiments extra-dry and pure oxygen (Matheson Co.) was used and it was found that the results obtained were identical with those obtained with the ordinary cylinder oxygen.

Helium (Air Reduction Co.) was passed through a liquid nitrogen trap to remove any water and was used without any further purification.

Analysis of Products

The products of the reaction after the removal of the unreacted butene-1 and of any products of equal or greater volatility in the low-temperature fractionation still

Can. J. Chem. Downloaded from www.nrcresearchpress.com by 190.90.36.8 on 09/04/12
For personal use only.

were passed through a gas–liquid chromotographic (GLC) column. The GLC apparatus used was modelled on that used by Callear and Cvetanović (8). The column consisted of 7.5-ft glass tubing (4 mm i.d.) packed with glass spheres passing 270 mesh with dinonyl phthalate as the liquid phase (4 g of dinonyl phthalate per 100 g of glass spheres). The column was maintained at room temperature. For some analyses a high resolution 50-ft column of $\frac{1}{4}$-in. copper tubing was used. It contained, as the stationary phase, 40 g of tricresyl phosphate per 100 g of firebrick (30–60 mesh). The products eluted from the column could be collected at liquid nitrogen temperature, and thus analyzed also by infrared and mass spectrometer.

The products of the reaction identified by these means were propionaldehyde, acetaldehyde, methyl alcohol, ethyl alcohol, *n*-butyraldehyde, α-butylene oxide, methyl ethyl ketone, and α-butylene ozonide. A sample of α-butylene ozonide was kindly prepared by Dr. T. Vrbaški using the method of Harries (9, 10).

RESULTS

The reaction of butene-1 with oxygen atoms produced by microwave discharge was found to be more complex than the corresponding reaction with oxygen atoms formed by mercury-photosensitized decomposition of nitrous oxide (2) or by photolysis of nitrogen dioxide (6). In the last two reactions *n*-butyraldehyde, α-butylene oxide, and small amounts of methyl ethyl ketone, acetaldehyde, and propionaldehyde are formed. In the present case, in addition to these compounds, ethanol and methanol and under certain conditions α-butylene ozonide and formaldehyde are also produced, and propionaldehyde is frequently formed in large amounts.

In order to obtain some insight into the mechanism of formation of these products, the pressure of butene-1, oxygen, and helium and the total pressure were varied.

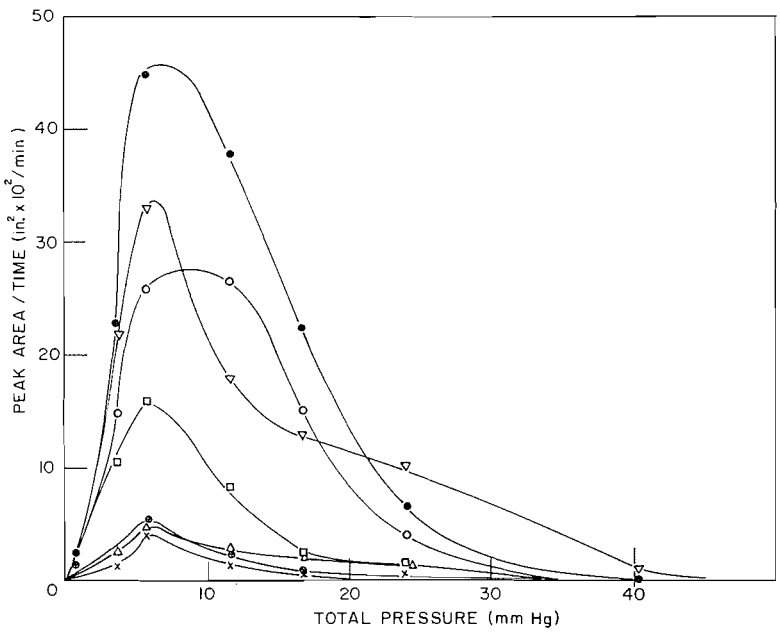

FIG. 1. Variation in the amounts of products formed per unit time with total pressure at low butene-1 flow. Oxygen flow 2.54 ml/min, helium flow 54.0 ml/min, butene-1 flow 0.75 ml/min: × methanol, △ methyl ethyl ketone, ⊕ acetaldehyde, □ ethanol, ○ *n*-butyraldehyde, ▽ propionaldehyde, ● α-butylene oxide.

Can. J. Chem. Downloaded from www.nrcresearchpress.com by 190.90.36.8 on 09/04/12
For personal use only.

Variation of Total Pressure

The total pressure was varied from 0 to 40 mm for both high and low butene-1 flows, using constant flows of the reactants in each case. In Fig. 1, the results obtained for the amounts of the products formed (measured as peak area per unit time from the GLC data) as a function of total pressure are shown for low butene-1 flow (0.75 ml/min). The main products are α–butylene oxide, propionaldehyde, ethanol, and *n*-butyraldehyde with smaller amounts of methyl ethyl ketone, acetaldehyde, and methanol. All the products show maxima at around 6.5 mm. It is understandable that there would be, at low pressure, a decrease in the amounts of the products formed due to recombination of the oxygen atoms on the walls of the discharge tube. However, at high pressure there was a gradual decrease in the amounts of products until at 40 mm there were essentially no products detectable on GLC. It was noted that during this gradual decrease the light intensity of the discharge appeared to decrease also. The light intensity of the discharge was therefore measured as a function of the pressure and it was found that the photocell readings showed a similar decrease to that observed above. Since the light intensity probably parallels in an approximate and qualitative manner the amount of dissociation of the molecules into atoms, it would appear that as the pressure is increased the energy available for dissociation of the molecules is reduced.

The experiments with high butene-1 flow (40 ml/min) showed the same general trends as found for low butene-1 flow and the maxima in the amounts of products were again at around 6 mm (Fig. 2). There was, however, an important difference: the amount of propanal formed remained in this case quite small, while it is one of the major products at low butene-1 flow.

Variation of Oxygen: Helium Ratio

The ratio of oxygen to helium was varied at constant pressure (3.5 mm) and constant butene-1 flow (0.75 ml/min). A plot of percentage oxygen against peak area of the products per unit time is shown in Fig. 3. The results obtained showed the same trends as before, with α-butylene oxide, propionaldehyde, *n*-butyraldehyde, and ethanol as the main products and smaller amounts of acetaldehyde, methyl ethyl ketone, and methanol. Up to about 7% oxygen there was an increase in the peak areas of each of the products, but as the percentage oxygen was still further increased (and at the same time the percentage of helium was correspondingly decreased) there was a general decrease in the amounts of the products. Since this is observed with all the products, it would appear that this effect is concerned with the initial formation of the oxygen atoms in the discharge. A possible explanation of this effect is that the efficiency of oxygen for the capture of electrons is less than that of helium, so that at high oxygen percentages the concentration of oxygen atoms is reduced.

Variation of Oxygen in the Absence of Helium

The flow of oxygen was varied from 0.80 ml/min to 25.6 ml/min in the absence of helium at a constant butene-1 flow (0.75 ml/min). The total pressure for this range of oxygen flows varied from 0.19 mm to 2.60 mm. Since the butene-1 flow was small compared to the oxygen flow, the total pressure was essentially the partial pressure of oxygen. Under these conditions it was found that the results were not reproducible. However, it was possible to note certain trends in the results. As the pressure of oxygen increased, there was an increase in the amounts of α-butylene oxide, propionaldehyde, and a small increase in the amount of acetaldehyde and methyl ethyl ketone, while amounts of ethanol and methanol decreased. Under these conditions, however, *n*-butyraldehyde was not found in the products.

Can. J. Chem. Downloaded from www.nrcresearchpress.com by 190.90.36.8 on 09/04/12
For personal use only.

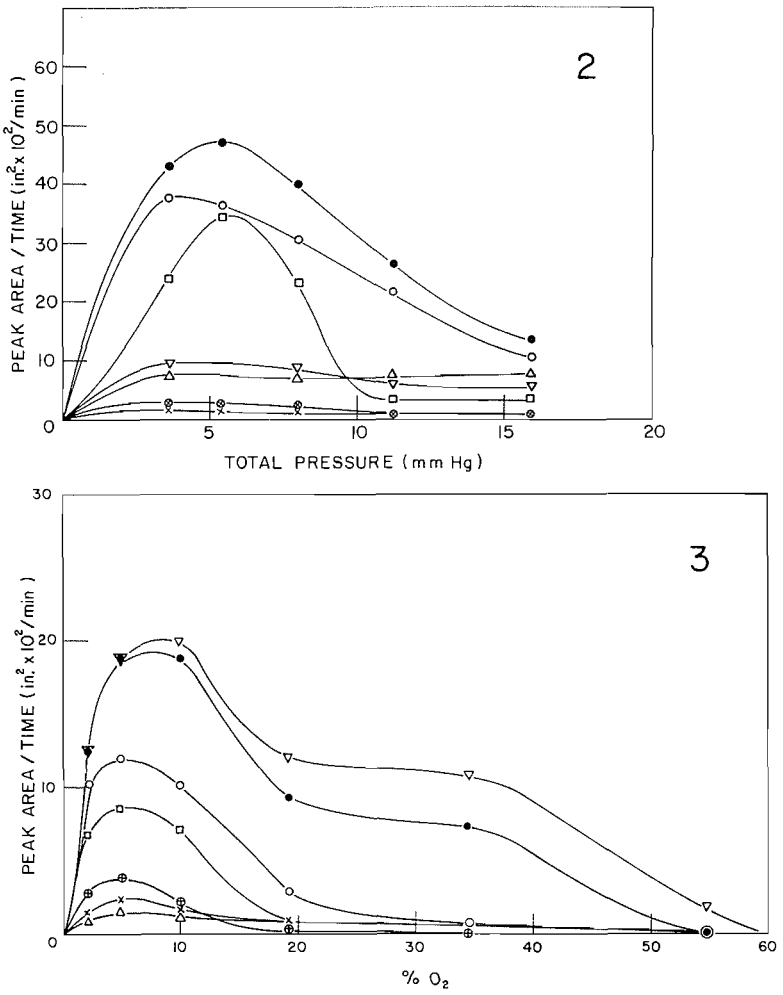

FIG. 2. Variation in the amounts of products formed per unit time with total pressure at high butene-1 flow. Oxygen flow 2.54 ml/min, helium flow 54.0 ml/min, butene-1 flow 40.1 ml/min: × methanol, △ methyl ethyl ketone, ⊗ acetaldehyde, □ ethanol, ○ *n*-butyraldehyde, ▽ propionaldehyde, ● α-butylene oxide.

FIG. 3. Plot of per cent oxygen in discharge gas against the amount of product formed per unit time. Total pressure 3.4 mm, butene flow 0.75 ml/min: × methanol, △ methyl ethyl ketone, ⊕ acetaldehyde, □ ethanol, ○ *n*-butyraldehyde, ▽ propionaldehyde, ● α-butylene oxide.

In all these experiments it was noted that a large diffuse GLC peak appeared at an elution time of about 200 minutes. This peak was collected and analyzed by infrared and mass spectra. It was found to be identical with a synthetic sample of α-butylene ozonide. Some observations on the stability and the manner of decomposition of a synthetic sample of α-butylene ozonide suggested that this compound was probably the main initial product in these experiments. It was probably formed directly from ozone and butene-1 while α-butylene oxide, acetaldehyde, and methyl ethyl ketone were formed in the course of the same reaction or together with propionaldehyde in the subsequent decomposition of the α-butylene ozonide. The absence of *n*-butyraldehyde suggested that a reaction of oxygen atoms with butene-1 was unimportant under these conditions.

Can. J. Chem. Downloaded from www.nrcresearchpress.com by 190.90.36.8 on 09/04/12
For personal use only.

Variation of Oxygen in the Presence of Helium

The partial pressure of oxygen was varied at constant total pressure (3.5 mm), constant helium flow (54.0 ml/min), and constant butene-1 flow (0.75 ml/min). The results obtained have been plotted in Fig. 4. Below 0.05 mm it was not possible to observe any products, perhaps because the small amounts of oxygen atoms formed recombined before they reached the nozzle. Above this pressure there was a steep increase in the amount of products to a maximum, and at higher partial pressures of oxygen there was a gradual decline in the amount of products formed. As was found above, propionaldehyde, α-butylene oxide, n-butyraldehyde, and ethanol were the main products with smaller amounts of acetaldehyde, methanol, and methyl ethyl ketone.

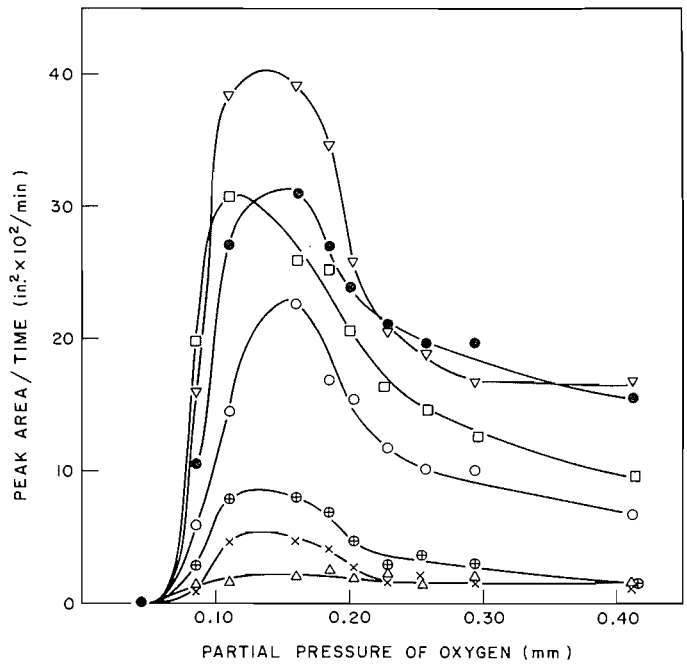

FIG. 4. Plot of oxygen pressure against the amount of products formed per unit time. Butene-1 flow 0.75 ml/min, helium flow 54.0 ml/min, total pressure 3.5 mm: × methanol, △ methyl ethyl ketone, ⊕ acetaldehyde, □ ethanol, ○ n-butyraldehyde, ▽ propionaldehyde, ● α-butylene oxide.

Variation of Butene-1

The flow rate of butene-1 was varied from 0.56 ml/min to 40 ml/min at constant flows of helium (54.0 ml/min) and oxygen (2.54 ml/min) and constant pressure (3.5 mm). A plot of the partial pressure of butene-1 against the GLC peak area per unit time is shown in Fig. 5. It is apparent from this graph that the compounds formed fall into two classes. The first class of compounds (α-butylene oxide, n-butyraldehyde, ethanol, and methyl ethyl ketone) show a steady rise in the amount formed at lower partial pressures of butene-1 and finally reach a constant value, while with the second class (propionaldehyde, acetaldehyde, and methanol) after an initial sharp increase in the amounts formed there is a gradual decrease to constant values. In order to determine whether these effects were due to a change in the discharge intensity, photocell readings were taken of the light intensities of the discharge and it was found that these remained

Can. J. Chem. Downloaded from www.nrcresearchpress.com by 190.90.36.8 on 09/04/12
For personal use only.

constant. Thus, under these conditions the change in the amount of product formed is directly connected with the partial pressure of butene-1. At very low butene-1 flow (0.56 ml/min) a relatively large amount of water was formed, probably due to secondary attack on the compounds initially formed by excess oxygen atoms. This effect was not noted at higher concentrations of butene-1.

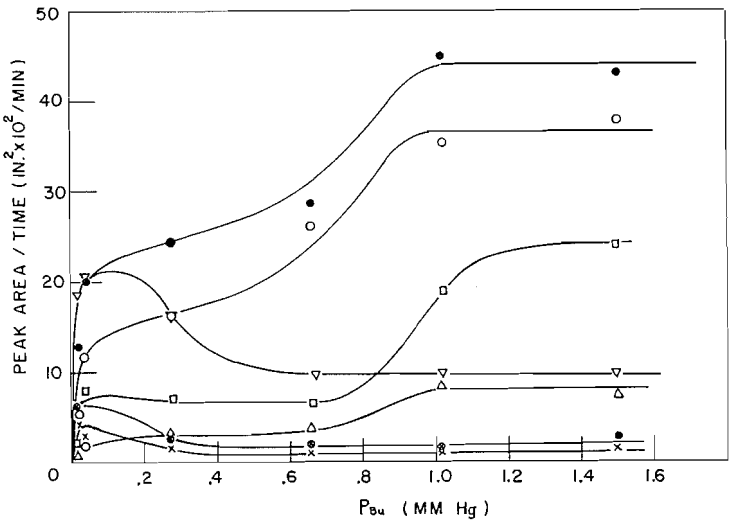

FIG. 5. Plot of butene-1 pressure against the amount of products formed per unit time. Total pressure 3.5 mm, oxygen flow 2.54 ml/min, helium flow 54 ml/min: × methanol, △ methyl ethyl ketone, ⊗ acetaldehyde, □ ethanol, ○ *n*-butyraldehyde, ▽ propionaldehyde, ● α-butylene oxide.

DISCUSSION

Since discharge is passed through oxygen and helium some distance from the nozzle, it is convenient to treat the reactions occurring in the discharge tube separately from those occurring at the nozzle, i.e. in the reaction zone where butene-1 is present as well.

The proposed reactions which are likely to occur in the discharge tube are the following:

$$\mathrm{He} + e \rightarrow \mathrm{He}^* \qquad [\phi_1]$$

$$\mathrm{O_2} + e \rightarrow 2\mathrm{O} \qquad [\phi_2]$$

$$\mathrm{O_2} + e \rightarrow \mathrm{O_2}^* \qquad [\phi_3]$$

$$\mathrm{He}^* + \mathrm{O_2} \rightarrow 2\mathrm{O} + \mathrm{He} \qquad [\mathrm{I}]$$

$$\mathrm{He}^* + \mathrm{O_2} \rightarrow \mathrm{O_2}^* + \mathrm{He} \qquad [\mathrm{II}]$$

$$\mathrm{He}^* + \mathrm{He} \rightarrow 2\mathrm{He} \qquad [\mathrm{III}a]$$

$$\mathrm{O_2}^* + \mathrm{He} \rightarrow \mathrm{O_2} + \mathrm{He} \qquad [\mathrm{III}b]$$

$$\mathrm{O} + \mathrm{O} + \mathrm{W} \rightarrow \mathrm{O_2} + \mathrm{W} \qquad [\mathrm{IV}]$$

$$\mathrm{O} + \mathrm{O} + \mathrm{M} \rightarrow \mathrm{O_2}^* + \mathrm{M} \qquad [\mathrm{V}]$$

$$\mathrm{O} + \mathrm{O_2}^* + \mathrm{M} \rightarrow \mathrm{O_3} + \mathrm{M} \qquad [\mathrm{VI}]$$

$$\mathrm{O} + \mathrm{O_2} + \mathrm{M} \rightarrow \mathrm{O_3} + \mathrm{M} \qquad [\mathrm{VII}]$$

$$\mathrm{O} + \mathrm{O_3} \rightarrow 2\mathrm{O_2}. \qquad [\mathrm{VIII}]$$

Reaction $[\phi_1]$ is probably the initiation reaction in the discharge since the efficiency for electron capture is greater in the case of helium than oxygen. When no helium is

Can. J. Chem. Downloaded from www.nrcresearchpress.com by 190.90.36.8 on 09/04/12
For personal use only.

present, reactions [ϕ_2] and [ϕ_3] take place giving oxygen atoms and excited oxygen molecules. Reactions [*I*] and [II] form oxygen atoms and excited oxygen molecules by transfer of energy from the excited helium. The quenching of the excited helium and excited oxygen are shown in reactions [III*a*] and [III*b*]. Reactions [IV] and [V] recombine oxygen molecules by third-body collision with the wall and other molecules, respectively. To account for the formation of ozone, reactions [VI] and [VII] are proposed. Reaction [VIII] re-forms oxygen molecules by the attack of oxygen atoms on ozone.

Of the products formed in the discharge tube the only ones which may reach the nozzle and eventually react with butene-1 in the reaction zone are: oxygen atoms, ozone, and excited oxygen molecules.

The general mechanism of reaction of oxygen atoms with butene-1 is as follows (2):

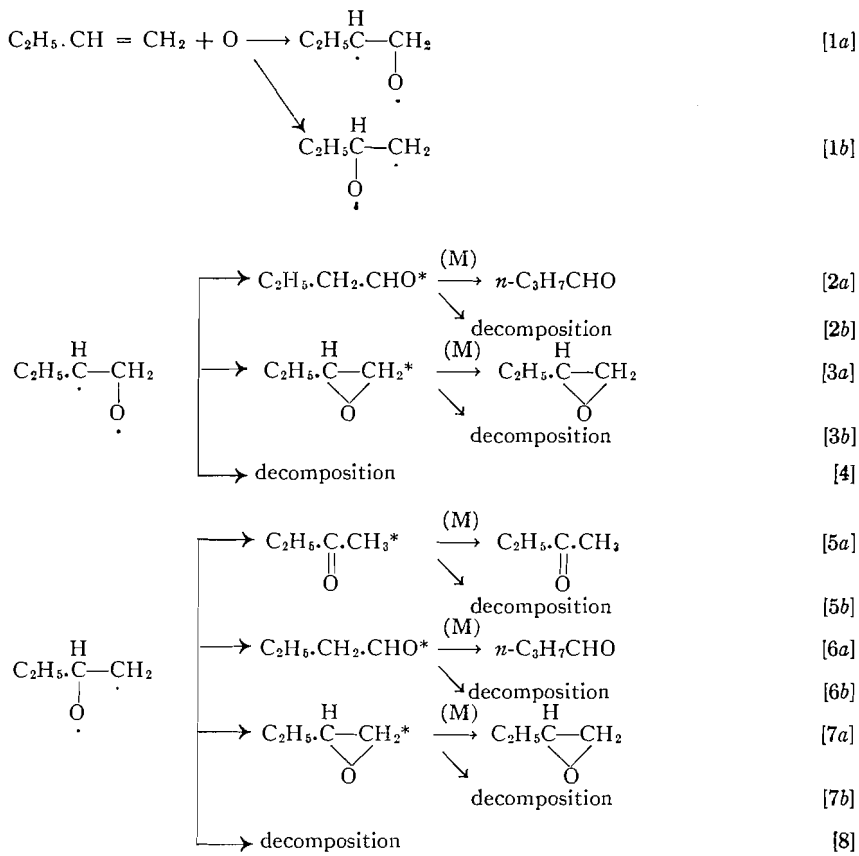

[1*a*] [1*b*] [2*a*] [2*b*] [3*a*] [3*b*] [4] [5*a*] [5*b*] [6*a*] [6*b*] [7*a*] [7*b*] [8]

where [1*a*], addition to the less substituted carbon atom of the double bond, largely predominates over [1*b*] so that considerably more n-C_3H_7CHO is formed than $C_2H_5.CO.CH_3$. There is reason to believe that pressure-independent decomposition processes, reactions [4] and [8], are not very important in this reaction (2). At pressures higher than about 10 to 30 mm the collisional deactivations in [2*a*], [3*a*], [5*a*], [6*a*], and [7*a*] are essentially complete, so that the main products are α-butene oxide, n-butyraldehyde, and a smaller amount of methyl ethyl ketone. In addition to these, even at the higher pressures, very small amounts of acetaldehyde and propionaldehyde are also

Can. J. Chem. Downloaded from www.nrcresearchpress.com by 190.90.36.8 on 09/04/12
For personal use only.

formed (2, 6) and the mechanism of their formation is not yet known, although they may be due then to some pressure-independent fragmentation. At lower pressures the pressure-independent fragmentation processes begin to be of importance, especially so below about 10 mm. This leads to an increase in the amounts of acetaldehyde and propionaldehyde and to a decrease in the addition products (α-butene oxide, n-butyraldehyde, and methyl ethyl ketone) (6).

Disregarding for the moment methanol and ethanol, which are observed in the present work in addition to the above compounds, it is evident that under conditions of the experiments plotted in Fig. 5 (total pressure 3.5 mm, helium to oxygen ratio approximately 20) and when the partial pressure of butene-1 is sufficiently high the products formed are within the limits of experimental accuracy, quantitatively, such as would be expected to be formed in the reaction of the ground state oxygen atoms with butene-1 at the actual total pressure (3.5 mm). At such a low total pressure the pressure-dependent fragmentation is quite important and appreciable amounts of free C_2H_5 radicals and smaller amounts of free CH_3 radicals could be expected to be produced. The formation of ethanol and methanol is then explained by the interaction of these free radicals with the molecular oxygen present, as is frequently observed. Thus, in the reaction of butene-2 with oxygen atoms from the mercury-photosensitized decomposition of N_2O, the relatively large amounts of free CH_3 radicals form large amounts of methanol when some molecular oxygen is added (2). The same reaction with oxygen atoms from photolysis of NO_2 gives large amounts of CH_3NO_3 and CH_3NO_2 instead (11), because of the presence of excess NO_2. In the reaction of butene-1 with oxygen atoms from NO_2 photolysis some $C_2H_5NO_3$ has indeed been identified, suggesting the presence of free C_2H_5 radicals (the elution time of $C_2H_5NO_2$ is considerably larger than that of $C_2H_5NO_3$ and $C_2H_5NO_2$ would, therefore, not be observed in small amounts at the GLC column temperature used) (6). Similarly in the isobutene reaction very small amounts of CH_3NO_3 and CH_3NO_2 are found, suggesting formation of some free CH_3 radicals, as would be expected in this case. All this supports the proposed explanation for the formation of ethanol and methanol in the present work. The absence of these two compounds in the same reaction with oxygen atoms formed from N_2O, even when molecular oxygen is present (2), is explained by the much higher total pressures used and the consequent suppression of the pressure dependent fragmentation. In the NO_2 work, the excess NO_2 acted as free radical scavenger as already indicated, so that even at low pressures no alcohols were detected.

As the butene-1 pressure is decreased in Fig. 5, ethanol and the direct oxygen atom addition products, α-butene oxide, n-butyraldehyde, and methyl ethyl ketone, begin to decrease while propionaldehyde, acetaldehyde, and methanol increase. This suggests that under conditions of these experiments butene-1 pressure has to be relatively quite high before secondary processes are suppressed and that propionaldehyde, acetaldehyde, and methanol result at least to a large extent from secondary processes, especially so propionaldehyde. The trend in ethanol is consistent with the mechanism of its formation suggested in the preceding paragraph. It shows at the same time that the effect of decreasing butene pressure is not due (at least not predominantly so) to a decreasing efficiency of the gaseous mixture for collisional deactivation as butene concentration is lowered, since the trend in ethanol would be expected then to be the same as that of propionaldehyde, acetaldehyde, and methanol.

The foregoing explanations are supported by the difference in the composition of the

Can. J. Chem. Downloaded from www.nrcresearchpress.com by 190.90.36.8 on 09/04/12
For personal use only.

products at various pressures for a low and a high butene flow as shown in Figs. 1 and 2, respectively. In this case again, propionaldehyde, acetaldehyde, and methanol are much smaller, especially so propionaldehyde, at the high butene flow.

Relatively high butene-1 pressures necessary to suppress secondary processes even when the partial pressure of oxygen is small, as in Fig. 5, would seem to preclude quantitative use of the Garvin–Kistiakowsky's Temperature Pattern Method for this reaction, at least under conditions of the present experiments. At small butene-1 pressures, such as would be anticipated to be necessary in order not to confine the reaction to a very small region around the nozzle, considerable complexities arise. The results of the experiments at such low partial pressures of butene are shown in Figs. 1, 3, and 4. The observed complexities are difficult to explain in detail, but are likely to be of general occurrence under certain experimental conditions and may seriously affect both quantitative and qualitative studies of oxygen atom reactions. For this reason a discussion of these results may be in order.

The reasons for the general trend in the amounts of products formed with varying pressure, as shown in Fig. 1, have already been discussed. The gaseous mixture in these experiments consisted mainly of helium which is probably not too efficient as a collisional deactivator and there are no drastic changes in the character of the products formed. At higher pressure the relative increase in propionaldehyde is conspicuous. This is probably due to the simultaneous increase in the partial pressure of oxygen (the composition of the gases was kept constant while the pressure was varied). The effect of the increasing concentration of oxygen is shown better in Figs. 3 and 4. Here again the reasons for the general decline in the amounts of products formed as oxygen concentration is increased have already been discussed. Attention should now be focussed on the variation in the relative amounts of the products, and it is evident that at higher percentages of oxygen in the mixture propionaldehyde becomes relatively more important while *n*-butanal and ethanol tend to be suppressed. Roughly similar trend was observed when oxygen pressure was varied in the absence of helium. As the oxygen pressure was increased from 0.2 to 2.6 mm the amounts of α-butylene oxide and propionaldehyde increased, ethanol decreased, and *n*-butyraldehyde was not found in the products under these conditions. In these last experiments, however, the reproducibility was poor and also α-butylene ozonide was identified as an important product. This compound is unstable and the lack of reproducibility was almost certainly largely due to the varying extent of its decomposition.

The formation of α-butylene ozonide suggests an important participation of ozone in the process under these conditions. When ozone reacts at room temperature with butene-1 in the gas phase (in the presence of excess oxygen) propionaldehyde and formaldehyde appear to be the main products (12). The largely increased formation of propionaldehyde at low butene-1 and larger oxygen concentrations is probably due to this reaction. In agreement with this, under these conditions large amounts of polymerized formaldehyde were found in the liquid nitrogen trap for the collection of the products, from where samples of the polymer were directly withdrawn for qualitative identification.

The manner in which ozone is formed is uncertain. There are two general possibilities: it may be formed in and after the discharge but predominantly before the gases reach the nozzle, or it may result from the reactions which take place after the stream of gas containing oxygen atoms meets butene-1 in the reaction zone. The first possibility depends on the efficiency of reaction [VII] which competes with [VIII] and with the reverse

Can. J. Chem. Downloaded from www.nrcresearchpress.com by 190.90.36.8 on 09/04/12
For personal use only.

of [VII]. Depending on the pressure of the gas and its efficiency as the "third body", a certain steady-state concentration of ozone should establish itself. It is not possible at present to predict with certainty whether this concentration should in a particular case be negligible compared with the concentration of oxygen atoms. The problem has been recently discussed by Herron and Schiff (13), who could not detect ozone mass spectrometrically in oxygen subjected to electrical discharge, although calculations based on literature values of rate constants of the above reactions (but for a different "third body") suggested detectable steady-state concentrations of ozone. Such calculated steady-state concentrations of ozone would be of the correct order of magnitude to be of importance under conditions of some of the present experiments.

The established formation of α-butylene ozonide cannot be regarded as a proof that ozone results directly from the discharge, since it may be, perhaps, equally well formed in the reaction zone. It is well known that under certain conditions in the atmosphere (and these conditions were simulated in the laboratory) ozone is formed in a chain reaction following an initial interaction of oxygen atoms with hydrocarbons (14). The detailed mechanism of this chain process is not known, although it appears reasonably certain that it involves initially an interaction of free radicals with molecular oxygen to form a hydroperoxy free radical. The latter, perhaps, reacts with another molecule of oxygen to give ozone. In agreement with these views it was possible to initiate ozone formation by generating free radicals in an oxygen atmosphere (14). Similar conditions can be readily envisaged in some of the experiments in the present work. Hydroperoxy radicals appear to be able also to react in some instances directly with olefins to form epoxides (15). It is evident then that explanations can be suggested for the results of some experiments in the present work, in particular to explain the formation of the ozonide, propanal, and the epoxide and the significant absence of *n*-butanal, as outlined before, without assuming any significant participation of oxygen atoms in the process (except, perhaps, in the initiation stage). Further substantial progress has to be made in this general field before a more reliable and quantitative discussion can be undertaken.

Substantial quantities of excited molecules of oxygen have been detected (13) mass spectrometrically in oxygen subjected to electrical discharge, the excited state being probably the $^1\Delta_g$ electronic state. What effect, if any, such molecules would have on butene-1 is not known. The increased formation of propanal at lower butene-1 concentrations, as shown in Fig. 5, cannot be due to excited molecules of oxygen since in this case no suppression with increasing butene-1 pressure would be expected. Under conditions of these experiments (low oxygen concentration in helium) no evidence was detected for any significant reaction of eventually present excited oxygen molecules with butene-1. Whether such molecules play a role in the experiments in which the concentration of oxygen in the discharge tube is large cannot be said at present because it is not possible to treat the results in a quantitative manner.

In conclusion, it ought to be stressed that the present work shows that under appropriate conditions oxygen atoms produced from molecular oxygen by electrical discharge lead to the same type of reaction as obtained with ground state oxygen atoms produced by mercury-photosensitized decomposition of nitrous oxide or by photolysis of nitrogen dioxide. The observed differences are understandable in view of the low over-all pressures and the excess molecular oxygen present. At the same time, considerable caution has to be exercised in the choice of the appropriate conditions when this technique is employed in order to avoid secondary processes which can sometimes completely mask the primary reactions of the oxygen atoms.

Can. J. Chem. Downloaded from www.nrcresearchpress.com by 190.90.36.8 on 09/04/12
For personal use only.

ACKNOWLEDGMENTS

The authors wish to acknowledge the assistance of Dr. A. W. Tickner for mass spectrometer analyses, Mr. J. Waterman for the building of the electronic equipment, and Dr. T. Vrbaški for the preparation of α-butylene ozonide.

REFERENCES

1. HARTECK, P. and KOPSCH, U. Z. physik. Chem. B, **12**, 327 (1937).
2. CVETANOVIĆ, R. J. J. Chem. Phys. **25**, 376 (1956); Can. J. Chem. **36**, 623 (1958).
3. HARTEL, H. V. and POLYANI, M. Z. physik. Chem. B, **11**, 97 (1930).
4. HELLER, W. Trans. Faraday Soc. **33**, 1556 (1937).
5. GARVIN, D. and KISTIAKOWSKY, G. B. J. Chem. Phys. **20**, 105 (1952).
6. SATO, S. and CVETANOVIĆ, R. J. Can. J. Chem. **36**, 970 (1958).
7. LE ROY, D. J. Can. J. Research, B, **28**, 492 (1950).
8. CALLEAR, A. B. and CVETANOVIĆ, R. J. Can. J. Chem. **33**, 1256 (1955).
9. HARRIES, C. and HAEFFNER, K. Ber. **41**, 3098 (1908).
10. HARRIES, C. and KOETSCHAU, R. Ber. **42**, 3305 (1909).
11. SATO, S. and CVETANOVIĆ, R. J. Can. J. Chem. **36**, 1668 (1958).
12. VRBAŠKI, T. and CVETANOVIĆ, R. J. Preliminary results.
13. HERRON, J. T. and SCHIFF, H. I. Can. J. Chem. **36**, 1159 (1958).
14. HAAGEN-SMIT, A. J. and FOX, M. M. Ind. Eng. Chem. **48**, 1484 (1956). HAAGEN-SMIT, A. J., BRADLEY, C. E., and FOX, M. M. Proceedings of the Second National Air Pollution Symposium. Pasadena, Calif. 1952. p. 54.
15. MAYO, F. R. J. Am. Chem. Soc. **80**, 2465 (1958).

Can. J. Chem. Downloaded from www.nrcresearchpress.com by 190.90.36.8 on 09/04/12
For personal use only.

Can. J. Chem. Downloaded from www.nrcresearchpress.com by 190.90.36.8 on 09/04/12
For personal use only.

PREPARATION OF 1,5-DIPHENYLNAPHTHALENE[1]

A. S. BAILEY[2]

ABSTRACT

The transformation of 1,5-dioxodecalin into 1,5-diphenylnaphthalene is described.

1-Phenylnaphthalene does not form solid complexes with the usual complexing agents (1) but has been found to form a complex with benzotrifuroxan (2). It was of interest, therefore, to prepare 1,5-diphenylnaphthalene and examine its complex-forming abilities. After this work was completed a synthesis of the hydrocarbon was reported in the literature (3).

It is stated (3) that treatment of 1,5-dioxodecalin (I, mixture of isomers) with phenylmagnesium bromide gives the glycol (III, m.p. 233–249°) in 33% yield. Under these conditions and using the pure *trans*-diketone (I) the only crystalline material isolated

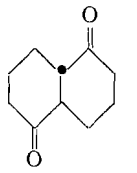

I

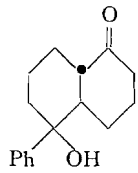

II

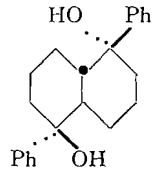

III

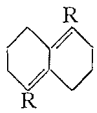

IV

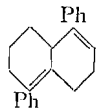

V

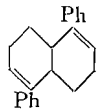

VI

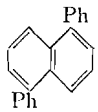

VII

R.CH=CH.CH=CH.R

VIII

was the monoadduct (II, yield 45%), none of the glycol being formed. However, treatment of the diketone (I) with lithium phenyl gave an excellent yield of 1,5-dihydroxy-1,5-diphenyldecahydronaphthalene (III, m.p. 275–277°). The material appeared to be homogeneous and it most probably has structure (III) with the two phenyl groups equatorial. This is the most stable isomer, having the larger groups equatorial, and its formation is likely to be favored by "steric approach control" (4).

Buchta and co-workers dehydrated the glycol (m.p. 233–249°) with potassium hydrogen sulphate, affording an olefin (m.p. 117–119°, 22% yield) to which structure (IV, R = Ph) was assigned without any supporting evidence (3). By dehydrating the pure glycol (III) with formic acid, an olefin (m.p. 179–182°) has now been obtained which may have structure (IV, R = Ph), (V), or (VI); the ultraviolet spectrum of the olefin

[1]*Manuscript received October 7, 1958.*
Contribution from the Dyson Perrins Laboratory, South Parks Road, Oxford, England.
[2]*Address during 1958–59, Royal Military College, Kingston, Ontario.*

showed λ_{max} 235 mμ (ϵ 19,300); λ_{inflex} 284 mμ (ϵ 6020); the absorption then steadily decreased (at 310 mμ, ϵ = 2400). Styrene has two absorption bands (λ_{max} 244 mμ, ϵ 12,000 and λ_{max} 282 mμ, ϵ 450) and the ultraviolet spectrum of 1-phenylcyclohexene contains only a single band (λ_{max} 247 mμ, ϵ 12,940) (5). Compounds having structures (V) or (VI) would be expected to show absorption of this type, the value of ϵ being smaller than 24,000 because of the non-coplanarity of the phenyl and reduced napththalene rings (6). This evidence suggests that the olefin obtained in this work is the conjugated diene (IV, R = Ph). The ultraviolet spectrum of (IV, R = Ph) indicates that the benzene and hexahydronaphthalene rings in this compound must be non-coplanar, since 1,4-diphenylbutadiene (VIII, R = Ph) has λ_{max} 328 mμ, ϵ 41,000 (5).

The corresponding diketone (IV, R = CO.CH_3) (7) has an absorption band at 295 mμ whose intensity (ϵ = 9020) is only one third of that of the open-chain analogue (VIII, R = $COCH_3$) which has λ_{max} 272 mμ (ϵ 31,000) and λ_{max} 279 mμ (ϵ 32,000) (8).

Dehydrogenation of the hexahydro compound using palladium–charcoal gave 1,5-diphenylnaphthalene (VII) in 80% yield as compared with the 20% obtained using sulphur (3). The ultraviolet spectra of 1-phenylnaphthalene and 1,5-diphenylnaphthalene are very similar, indicating non-coplanarity of the benzene and naphthalene rings.

EXPERIMENTAL

Ultraviolet spectra were determined in ethanol solution; infrared spectra measured in Nujol mulls unless otherwise indicated. All melting points are uncorrected.

1-Hydroxy-5-oxo-1-phenyldecahydronaphthalene (II)

To a solution of phenylmagnesium bromide (magnesium 3 g, bromobenzene 20 cc) in ether (50 cc) was added *trans*-1,5-dioxodecalin (5 g, m.p. 160°) (9) in benzene (100 cc) and the mixture refluxed and stirred for 5 hours. Next day water and saturated ammonium chloride solution were added, the aqueous layer extracted with benzene, the combined organic layers dried (magnesium sulphate), and the solvents removed. The semisolid residue was triturated with petroleum ether (10 cc, b.p. 60–80°) and then crystallized from benzene (25 cc) giving a solid (3.3 g, 45%) of m.p. 150–155°. Crystallization from benzene and then from methanol gave 1-hydroxy-5-oxo-1-phenyldecahydronaphthalene, colorless plates, m.p. 163–164° (mixed m.p. with starting material, 130–145°). Found: C, 78.4; H, 8.1%. Calc. for $C_{16}H_{20}O_2$: C, 78.7; H, 8.2%. Ultraviolet spectrum: λ_{max} 205 mμ (ϵ 9620); λ_{max} 251 mμ (ϵ 205); λ_{max} 257 mμ (ϵ 246); λ_{max} 263 mμ (ϵ 204); λ_{max} 266 mμ (ϵ 161). Infrared spectrum contained bands at 3390 cm^{-1} (OH); 1686 cm^{-1} (CO); 1600 cm^{-1} (ar. CC). The *2,4-dinitrophenylhydrazone* formed orange-colored needles (from acetic acid), m.p. 207–209°. Found: C, 62.2; H, 5.6; N, 13.4%. Calc. for $C_{22}H_{24}O_5N_4$: C, 62.3; H, 5.7; N, 13.2%. The *semicarbazone* crystallized from 2-methoxyethanol as colorless prisms, m.p. 253–255°. Found: C, 67.2; H, 7.9; N, 13.3%. Calc. for $C_{17}H_{23}N_3O_2$: C, 67.7; H, 7.7; N, 13.9%. A solution of the carbinol (1 g) in formic acid (10 cc) was refluxed for 30 minutes, the solution cooled, diluted with water, and the mixture extracted with ether. The ethereal extracts were washed with sodium carbonate solution, dried (magnesium sulphate), and the solvent removed, giving an oil whose ultraviolet absorption λ_{max} 240 mμ (ϵ 11,100) indicated that the double bond formed was conjugated with the benzene nucleus; but the infrared spectrum of the oil (natural film) contained two carbonyl bands (1710 and 1665 cm^{-1}) indicating the presence of some $\alpha\beta$-unsaturated ketone. The benzene mother liquors from the Grignard reaction were evaporated giving an oil which did not crystallize and whose infrared spectrum contained bands at 3370

Can. J. Chem. Downloaded from www.nrcresearchpress.com by 190.90.36.8 on 09/04/12
For personal use only.

cm^{-1}, 1692 cm^{-1}, and 1595 cm^{-1}. A portion of this oil was dehydrated with formic acid, the product isolated in the usual way and distilled up to 250° (oil bath) at 0.01 mm. The infrared spectrum of the resulting glass contained intense carbonyl bands (1715 and 1645 cm^{-1}) indicating absence of the glycol (III) in the original preparation. Ultraviolet spectrum of the glass: λ_{max} 237 mμ (ε 11,100).

1,5-Dihydroxy-1,5-diphenyldecahydronaphthalene (III)

Trans-1,5-dioxodecalin (5 g) in warm benzene (70 cc) was added dropwise to a solution of lithium phenyl prepared from lithium (1.7 g), bromobenzene (19 g), and ether (50 cc). The mixture was then stirred and boiled under nitrogen for 10 hours. Next day water and ammonium chloride solution were added, the suspension stirred for 2 hours, the solid collected, washed well with water, and dried (8.4 g, 87%), m.p. 250–255°. The glycol crystallized from 2-ethoxyethanol as colorless, hexagonal plates, m.p. 275–277°. Found: C, 81.7; H, 7.8%. Calc. for $C_{22}H_{26}O_2$: C, 82.0; H, 8.1%. Ultraviolet spectrum: λ_{max} 207 mμ (ε 21,080), λ_{max} 252 mμ (ε 417), λ_{max} 257 mμ (ε 487), λ_{max} 260 mμ (ε 417), λ_{max} 263 mμ (ε 368), λ_{max} 266 mμ (ε 278). The infrared spectrum contained bands at 3472 cm^{-1} (OH) and 1605 cm^{-1} (ar. CC).

1,5-Diphenylnaphthalene (VII)

The finely powdered glycol (2 g) was added to formic acid (25 cc) and the suspension heated under reflux (oil bath, 140°) for 30 minutes. Hot dimethylformamide (25 cc) was added, the solution boiled for 5 minutes, allowed to cool, the solid which separated collected, and washed with a little ethanol (1.3 g, 73%). After crystallization from acetic acid the product had m.p. 167–172°; crystallization from benzene gave a specimen of m.p. 179–182°. Found: C, 92.2; H, 7.3. Calc. for $C_{22}H_{22}$: C, 92.3; H, 7.7%. Ultraviolet spectrum: λ_{max} 235 mμ (ε 19,300), λ_{inflex} 284 mμ (ε 6020). Infrared spectrum 1597 cm^{-1} (ar. CC). The 1,5-diphenylhexahydronaphthalene (1.2 g) was mixed with 30% palladium–charcoal (0.2 g) (10) and heated (metal bath) at 240° for 30 minutes, the temperature of the bath was then raised to 300° (30 minutes), and finally to 330° (30 minutes), a slow stream of hydrogen being passed through the apparatus. The cold solid was extracted exhaustively with chloroform, the extracts evaporated, and the residue crystallized from benzene (0.94 g, 80%, m.p. 220–223°). 1,5-Diphenylnaphthalene formed colorless needles (from benzene) m.p. 223–224°, reported (3) m.p. 220–222°. Found: C, 94.2; H, 5.55. Calc. for $C_{22}H_{16}$: C, 94.3; H, 5.7%. Ultraviolet spectrum: λ_{max} 228 mμ (ε 48,200), λ_{max} 297 mμ (ε 14,200). The hydrocarbon did not give a solid complex with either 2,4,7-trinitrofluorenone or with benzotrifuroxan.

REFERENCES

1. FRIEDEL, R. A., ORCHIN, M., and REGGEL, L. J. Am. Chem. Soc. **70**, 199 (1948). ORCHIN, M. and FRIEDEL, R. A. J. Am. Chem. Soc. **71**, 3002 (1949).
2. BAILEY, A. S. and CASE, J. R. Tetrahedron, **3**, 113 (1958).
3. BUCHTA, E., VATES, H., and KNOPP, H. Chem. Ber. **91**, 228 (1958).
4. DAUBEN, W. G., BLANZ, E. J., JR., JIU, J., and MICHELI, R. A. J. Am. Chem. Soc. **78**, 3752 (1956).
5. BRAUDE, E. A. Ann. Repts. on Progr. Chem. (Chem. Soc. London), **42**, 105 (1945). ELIEL, E. L., MCCOY, J. W., and PRICE, C. C. J. Org. Chem. **22**, 1533 (1957). MIXER, R. Y. and YOUNG, W. G. J. Am. Chem. Soc. **78**, 3379 (1956).
6. BRAUDE, E. A. and NACHOD, F. C. Determination of organic structures by physical methods. Academic Press, Inc., New York. 1955. Chap. 4. KLYNE, W. Progress in stereochemistry I. Butterworth Scientific Publications, London. 1954. p. 126.
7. INHOFFEN, H. H. and KATH, J. Chem. Ber. **87**, 1589 (1954).
8. AHMAD, R., SONDHEIMER, F., WEEDON, B. C. L., and WOODS, R. J. J. Chem. Soc. 4089 (1952).
9. JOHNSON, W. S., GUTSCHE, C. D., and BANERJEE, D. K. J. Am. Chem. Soc. **73**, 5464 (1951).
10. LINSTEAD, R. P. and THOMAS, S. L. S. J. Chem. Soc. 1127 (1940).

Can. J. Chem. Downloaded from www.nrcresearchpress.com by 190.90.36.8 on 09/04/12
For personal use only.

Can. J. Chem. Downloaded from www.nrcresearchpress.com by 190.90.36.8 on 09/04/12
For personal use only.

THE ADSORPTION OF HYDROGEN ON RUTHENIUM–ALUMINA[1]

M. J. D. Low and H. A. Taylor

ABSTRACT

The rate of adsorption of hydrogen on $Ru–Al_2O_3$ has been studied at four temperatures from 100 to 257° C at pressures from 15 to 80 cm DBP. The Elovich parameters α and a for these data have been calculated and their temperature and pressure dependencies found. It is shown that, regardless of temperature, the amount adsorbed at a given time and the parameters α and $\log a\alpha$ show a dependence on the initial pressure which is different above and below 25 cm DBP indicating different types of adsorption. The temperature dependencies yield an energy of activation for the initial rate of the high pressure chemisorption of 17.7 kcal $mole^{-1}$ which is independent of the pressure. Similar E values below 25 cm increase with a decrease in pressure. Four runs showed a very slow nitrogen adsorption on the same surface, raising the question of an enhancement of the adsorption of one gas by traces of another.

The elementary state of our knowledge of chemisorption and the lack of complete correlation with such physical factors as surface geometry or work function suggests that more attention be given to the chemical factors involved, such as the chemical reactions which may occur at surfaces contributing to chemisorption. It is obvious that, since the classical treatment of experimental data has not provided this information, new treatments and new techniques are necessary. The authors (1) have recently attempted this in a study of the chemisorption of hydrogen on nickel–kieselguhr. A variation, not hitherto observed, in the type of adsorption dependent on the initial gas pressure, independent of temperature, was discovered. That this effect is not peculiar to the nickel–hydrogen system is shown in the present study and in others which will be reported later. The accounting for the effect was given in the earlier paper. No repetition, here, is necessary, since the results presented speak for themselves.

EXPERIMENTAL

The adsorbent used was a commercial $Ru \cdot Al_2O_3$ hydrogenation catalyst weighing 15.82 g.[2] It consisted of 1.25 cm extruded Al_2O_3 pellets with 0.5% Ru on the surface and was placed in a Vycor tube in the constant-volume adsorption system described previously, in which the pressure changes during adsorption were read on a dibutyl phthalate (DBP) manometer. After 10 hours of evacuation at 500° C the pressure in the system was below 10^{-6} mm, the catalyst maintaining its original black color. Pure hydrogen was introduced and remained for 10 minutes at 500° C and 60 cm DBP pressure, followed by evacuation at the same temperature for 2 hours. This procedure was repeated six times. After the first treatment the catalyst turned grey and remained so until exposure to air occurred at the end of all the experiments, when it resumed its original color. A final treatment with hydrogen at 500° C and 30 cm Hg pressure was made for 2 hours. It was found that, after this treatment and after subsequent experiments, a pressure of less than 10^{-6} mm Hg could be attained by evacuating at 500° C for about 6 hours. A standard evacuation time of 10 hours at 500° C was adopted. The hydrogen was purified by diffusion through heated palladium thimbles. The catalyst was maintained at constant temperature by means of vapor baths.

The chemisorption rate data were treated using the Elovich equation (2),

$$dq/dt = a \exp(-\alpha q),$$

[1]*Manuscript received November 6, 1958.*
Contribution from the Nichols Laboratory, New York University, New York 53, New York, U.S.A.
[2]*Purchased from Baker and Co. Inc., Lot No. 1979. The support is* γ–Al_2O_3.

where q is the amount adsorbed in time t, a is the initial rate, and α, a constant. For large values of $a\alpha$ the integrated equation has the form (3),

$$q_{nt}-q_{mt} = (2.3/\alpha)\log(n/m),$$

where q_{nt} and q_{mt} are the volumes of gas at n.t.p. adsorbed at times nt and mt, n and m being integers. When, as in the present study, the values of $a\alpha$ are large, the closeness of approach to constancy of $(q_{nt}-q_{mt})$ for successive values of mt serves as a much more satisfactory test of the applicability of the Elovich equation than is ever possible by a linearity of a $q-\log t$ plot. Values of α are then readily obtained from the differences $(q_{nt}-q_{mt})$, and a can be calculated from the Elovich equation and the experimental points.

RESULTS

The experimental conditions of pressure and temperature and the calculated constant of the rate equations for the runs performed are summarized in Table I. The experiments were performed in the order shown in column 1. The temperature of the adsorbent T and the calculated initial pressure P_i are shown in columns 2 and 3. Column 4 lists the mean α value calculated as mentioned, and in column 5 are the average deviations in per cent of the α values found during the run. Column 6 lists the values of $\log a\alpha$ with their average deviation in per cent in column 7. Column 8 shows the initial rates, a, and column 9 the values of q_1, the calculated amount adsorbed at $t = 1$ minute.

Plots of q against $\log t$ were linear in all cases. The precision with which the Elovich constants can reproduce the experimental data is shown in Table II for two typical runs by a comparison of q_{obs} with q_{calc} calculated from the relation: $q = (2.3/\alpha)\log(1+a\alpha t)$.

TABLE I

Run	T, °C	P_i, cm DBP	α	% dev.	$\log a\alpha$	% dev.	$a = x \cdot 10^n$		q_1
							x	n	
1103	100	78.4	6.4	9	8.03	0.2	1.7	7	2.87
1104	100	65.1	7.5	7	8.85	0.5	9.4	7	2.71
1105	100	48.8	8.2	2	9.81	0.2	7.9	8	2.77
1107	257	79.9	12.5	8	15.10	0.3	1.0	14	2.78
1108	257	33.1	14.5	5	15.40	0.2	1.7	14	2.45
1109	257	66.1	13.7	4	15.76	0.3	4.2	14	2.65
1110	257	49.4	14.6	4	16.10	0.8	8.6	15	2.54
1111	257	16.4	23.3	4	21.72	0.2	2.3	20	2.15
1112	257	32.7	15.0	3	15.91	0.1	5.4	14	2.43
1113	257	24.2	17.7	2	17.84	0.1	3.9	16	2.32
1114	100	31.8	8.4	5	8.84	0.4	9.0	7	2.44
1115	100	24.2	10.1	6	10.48	0.5	3.0	9	2.39
1116	100	16.1	10.6	11	10.04	0.7	1.0	9	2.18
1117	100	16.2	10.6	12	9.97	0.6	8.9	8	2.16
1118	100	65.8	7.3	6	8.84	0.3	9.5	7	2.78
1119	200	17.6	20.4	2	20.09	0.05	6.0	18	2.27
1120	200	66.3	12.2	5	14.20	0.1	1.3	13	2.67
1121	200	49.5	12.8	3	14.67	0.2	3.7	13	2.63
1123	200	78.8	12.2	4	14.49	0.1	2.5	13	2.74
1125	200	33.0	14.3	8	15.35	0.3	1.6	14	2.47
1127	200	24.5	14.8	6	15.74	0.3	3.7	14	2.44
1128	147	79.0	8.9	4	10.83	0.2	7.6	9	2.80
1132	147	48.8	10.2	3	11.52	0.2	3.3	10	2.60
1134	147	79.0	9.5	6	11.22	0.2	1.8	10	2.73
1136	147	16.0	14.7	12	13.89	0.6	5.3	12	2.17
1137	147	32.2	10.5	6	11.15	0.4	1.3	10	2.45
1138	147	24.5	11.5	7	11.76	0.6	5.0	10	2.35

Can. J. Chem. Downloaded from www.nrcresearchpress.com by 190.90.36.8 on 09/04/12
For personal use only.

TABLE II
Comparison of q_{obs} and q_{calc}

Min.	Run 1103, $T = 100°$ C, $P_i = 78.4$ cm DBP			Run 1108, $T = 257°$ C, $P_i = 33.1$ cm DBP		
	P	q_{obs}	q_{calc}	P	q_{obs}	q_{calc}
0	93.03	0	0	39.05	0	0
0.5	64.50	2.70	2.77	—	—	—
1.0	63.72	2.85	2.88	19.50	2.45	2.45
1.5	63.35	2.92	2.94	—	—	—
2.0	63.03	2.99	2.98	19.20	2.51	2.50
2.5	62.83	3.02	3.01	—	—	—
3.0	62.67	3.05	3.02	19.08	2.53	2.52
3.5	62.55	3.07	3.07	—	—	—
4.0	62.45	3.10	3.09	18.95	2.55	2.54
4.5	62.35	3.12	3.11	—	—	—
5.0	62.26	3.13	3.13	18.90	2.56	2.56
6.0	—	—	—	18.84	2.57	2.57
7.0	—	—	—	18.79	2.58	2.58
7.5	61.94	3.19	3.19	—	—	—
8.0	—	—	—	18.74	2.59	2.59
9.0	—	—	—	18.70	2.60	2.60
10	61.70	3.24	3.23	18.68	2.60	2.61
15	61.40	3.30	3.30	18.50	2.63	2.64
20	61.18	3.34	3.34	18.41	2.65	2.66
25	61.01	3.38	3.36	18.30	2.67	2.67
30	60.87	3.40	3.38	18.24	2.68	2.68
35	60.75	3.42	3.43	18.15	2.70	2.69
40	60.66	3.44	3.45	18.10	2.70	2.70
50	60.52	3.47	3.48	18.01	2.72	2.72
60	60.38	3.49	3.51	17.95	2.73	2.73
70	—	—	—	17.87	2.75	2.74
80	60.19	3.51	3.56	17.81	2.76	2.75
90	—	—	—	17.80	2.76	2.76
100	60.00	3.55	3.59	17.73	2.77	2.77

Temperature and Pressure Dependencies of a and α

Inspection of Table I shows that a variety of initial pressures were used at each of four temperatures. Although these initial pressures were not identical at all temperatures they are close enough for comparative purposes. Each group of runs at nearly identical initial pressures could be used to determine the temperature dependence of a parameter, while from each group of runs at the same temperature a pressure dependence could be derived.

α–T, P Relations

Figure 1 shows plots of α values against $1/T$ for the five pressures approximating 15, 25, 30, 50, 65, and 80 cm DBP. The linearity of these plots suggested the representation of the α–T relation in the form $\alpha = u + w/T$. Since the slopes of the plots are not equivalent, the parameters u and w must be functions of the initial pressure. Plotting the values of u and w as a function of P_i as in Fig. 2, it becomes apparent that a change of slope occurs in the pressure range 25–27 cm DBP. This has been taken as a dividing mark and points at pressures above 25 cm have been taken in one group, points below 25 cm in another group, a linear dependence of u and w on P_i being assumed. In the high pressure range these dependencies are given numerically by the equations:

$$u = 33.26 - 0.0678\ P_i$$
$$w = -8710 + 10.02\ P_i$$

while at low pressures:

$$u = 90.40 - 2.322\ P_i$$
$$w = -29018 + 823.3\ P_i$$

using a least-squares method where justified by the number of points involved.

Can. J. Chem. Downloaded from www.nrcresearchpress.com by 190.90.36.8 on 09/04/12
For personal use only.

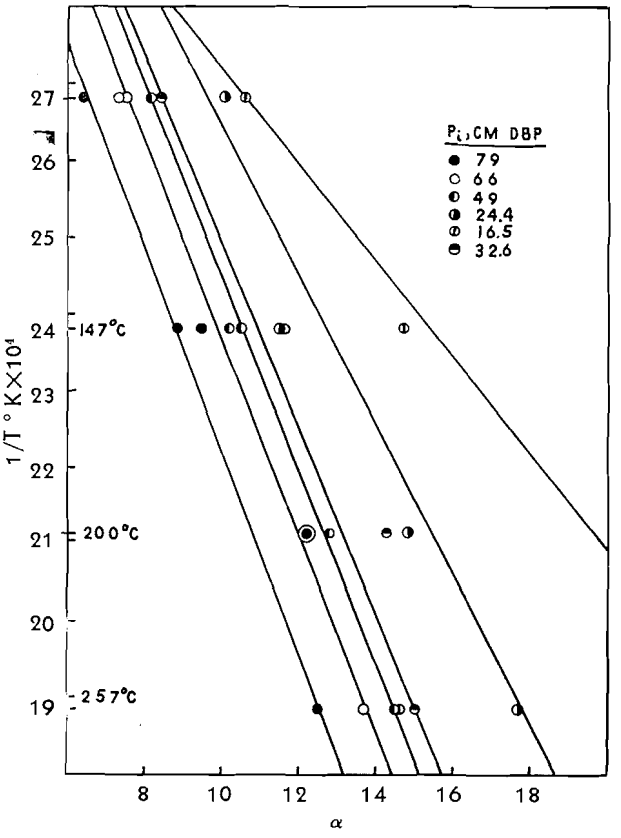

FIG. 1. Variation of α with temperature at different pressures.

log $a\alpha$–T, P Relation

In a similar manner $\log a\alpha$ is found to be linear in $1/T$ and is expressible by the equation:

$$\log a\alpha = r + s/T.$$

The terms r and s are found to be pressure dependent and show a similar linear dependence above and below 30 cm to that found for α. The following equations give the numerical dependencies:

high pressure: $r = 35.05 - 0.0456\ P_i$
$-s = 9513 - 10.52\ P_i$
low pressure: $r = 85.96 - 2.03\ P_i$
$-s = 28421 - 7585\ P_i$.

The change in the pressure dependence of both α and $\log a\alpha$ in the neighborhood of 25 cm is also reflected in the actual volumes of gas adsorbed at a given time q_t, when considered as a function of the initial pressure, P_i. Figure 3 illustrates this at 257° C where q_t values for 2, 10, and 100 minutes are plotted as a function of P_i. In each case there is an abrupt change of slope around 25 cm. Plots at the other temperatures show a similar effect at the same pressure irrespective of the temperature. Again, it was shown previously (1) that the energy of activation E as conventionally calculated may be related to the quantities represented here as w and s by the relation, $E = Rwq - sR$,

Can. J. Chem. Downloaded from www.nrcresearchpress.com by 190.90.36.8 on 09/04/12
For personal use only.

Can. J. Chem. Downloaded from www.nrcresearchpress.com by 190.90.36.8 on 09/04/12
For personal use only.

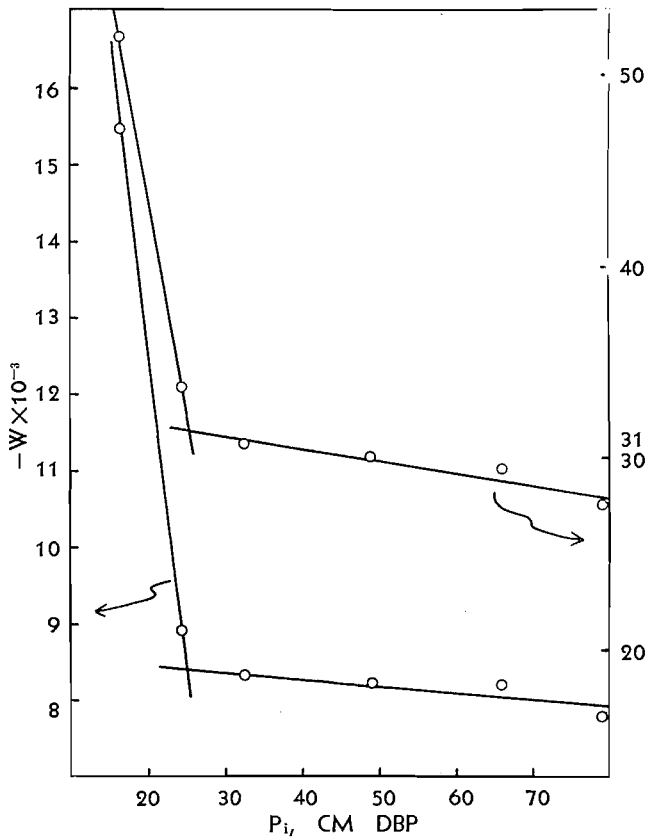

FIG. 2. Variation of w and u with initial pressure.

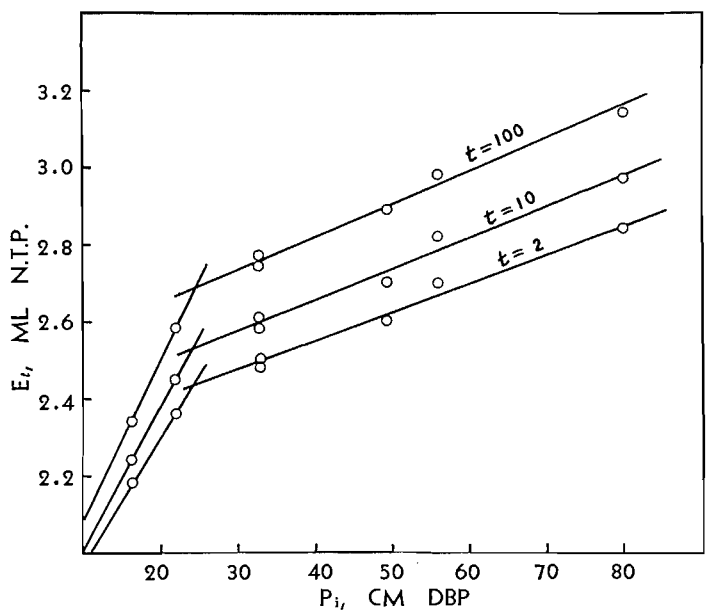

FIG. 3. Variation of q_t with initial pressure.

where R is the gas constant. Table III presents these various values in kcal/mole for the several initial pressures. Figure 4 shows the variation of $(-sR)$ as a function of the initial pressure. Although there is some scatter to the points there is distinct evidence of a change in pressure dependence around 25 cm. From the previous relation it is seen that $(-sR)$ is a measure of the energy of activation, E, at $q = 0$. It is essentially an extrapolated value for E at the beginning of the slow adsorption. In Fig. 5 are plotted values of J as a function of the initial pressure, derived by expressing the temperature dependence of the initial rates, a, by the relation, $\ln a = I + J/T$. If the initial rate of the slow adsorption, a, is Arrhenian, its energy of activation, E_a, should be given by $E_a = -JR$, where R is the gas constant. The similarity of Figs. 4 and 5 showing the change in slope at the same pressure, with an apparent independence of pressure above the break, becomes quantitative in the high pressure range. From Fig. 4 the high pressure value of $E_{q=0}$ is 17.7 kcal/mole. From Fig. 5 the high pressure value of J is -8800 yielding E_a as 17.6 kcal/mole. The agreement of these two values of E is, of course, necessary and only indicates consistency in the alternative treatments, on the one hand of a alone, on the other, of α and $a\alpha$. The agreement, nevertheless, provides some confirmation of the form of the temperature dependencies of α and $a\alpha$ used. The independence of initial pressure on the part of $E_{q=0}$ above 25 cm DBP contrasts with the marked dependence below 25 cm. This in itself is significant that two different adsorption processes are involved.

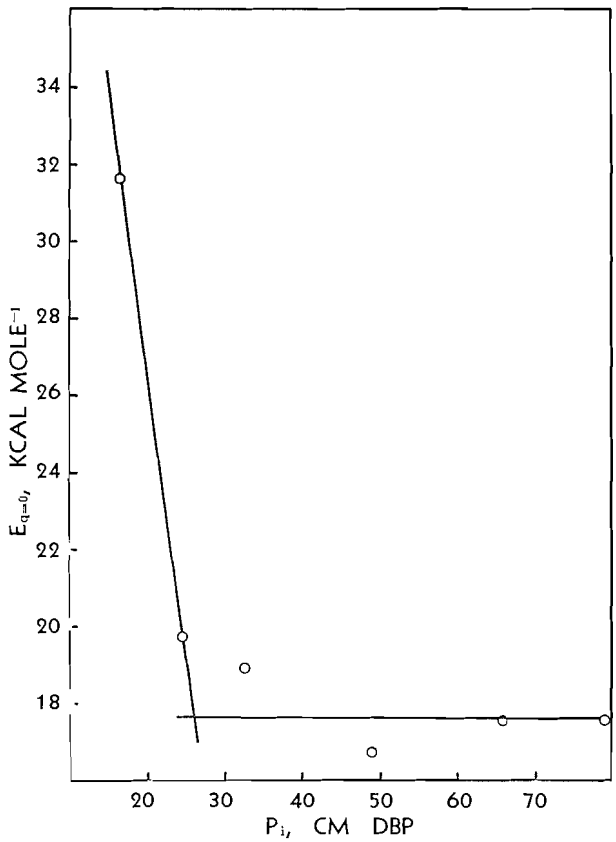

FIG. 4. Variation of activation energy with initial pressure.

Can. J. Chem. Downloaded from www.nrcresearchpress.com by 190.90.36.8 on 09/04/12
For personal use only.

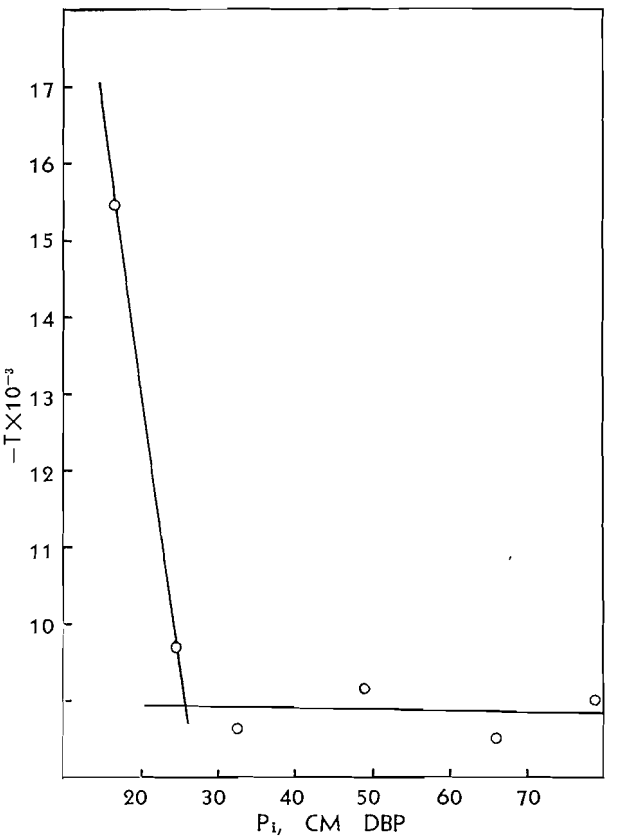

FIG. 5. Variation of J with initial pressure.

TABLE III

Data for activation energy

P_i	$-w$	$-s$	$-Rw$	$-sR$	$s/w = q_{E=0}$
79	7789	8836	15.48	17.56	1.13
66	8220	8880	16.33	17.64	1.08
49	8234	8432	16.36	16.75	1.02
32.6	8325	9518	16.54	18.91	1.14
24.4	8929	9914	17.74	19.70	1.11
16.5	15433	15906	30.67	31.61	1.03

Although E is positive for $q = 0$, it may be seen from Table III that as adsorption proceeds, E will rapidly become negative. As pointed out previously, therefore, E has no significance when calculated from values taken during the course of adsorption and its apparent variation during adsorption is no valid argument for "surface heterogeneity". It should be pointed out that in the present study, as in the earlier study on nickel, the temperature range covered corresponds to a decreasing total adsorption with increasing temperature. This may be seen from Fig. 6, which plots the amounts adsorbed after 100 minutes for the different temperatures and initial pressures. Although these are not strictly saturation values for the surface, so very little more gas is adsorbed after 100 minutes that they approximate saturation values. Thus in run 1134, 3.23 ml

Can. J. Chem. Downloaded from www.nrcresearchpress.com by 190.90.36.8 on 09/04/12
For personal use only.

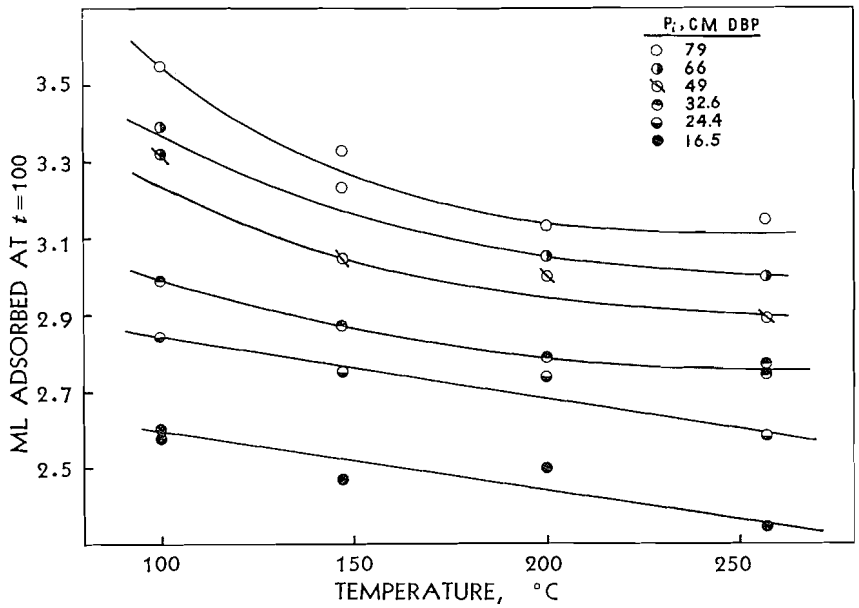

FIG. 6. Variation of the amounts adsorbed after 100 minutes with temperature at different initial pressures.

are adsorbed at 100 minutes, and 3.35 ml at 975 minutes. In run 1136 whereas 2.47 ml are adsorbed at 100 minutes only 2.60 ml are adsorbed at 1710 minutes. There is every indication at each pressure studied that the total adsorption is diminishing with increasing temperature. This contrasts with the classical studies of the variation of energy of activation of adsorption with coverage wherein the temperature range studied was restricted to regions in which the isobars increased with increasing temperature. It is not inconceivable that the well-known variation of the equilibrium amount adsorbed as a function of temperature, initially high at low temperature, decreasing to a minimum, rising to a maximum, and decreasing steadily thereafter as the temperature is increased, may simply reflect changes in the values of α associated with changes in the adsorption process.

Nitrogen Adsorption

At the conclusion of the experiments with hydrogen four exploratory runs were made using nitrogen. At 100° C and 257° C a definite but very slow adsorption of nitrogen was found to occur. The data are shown graphically in Fig. 7. Owing to the slow adsorption, the precision of the experiments was very poor and further investigation was abandoned. The results obtained, nevertheless, appear to confirm the views expressed by Amano and Taylor (4) that ruthenium should be included in group A of Trapnell's (5) classification as capable of adsorbing nitrogen. However, Trapnell's classification was intended for the pure metal films and may not apply to commercial catalyst preparations. Amano and Taylor found that in each initial run with each catalyst where there had been no previous contact with ammonia there was an anomaly in the rate of ammonia decomposition. Further, "between individual runs the catalyst was reduced for 2 hours at 450° C in hydrogen. After each such reduction the rate of decomposition rose gradually." The parallel situation in the present work with ruthenium after long use for hydrogen adsorption and possibly containing traces of unremoved hydrogen with

Can. J. Chem. Downloaded from www.nrcresearchpress.com by 190.90.36.8 on 09/04/12
For personal use only.

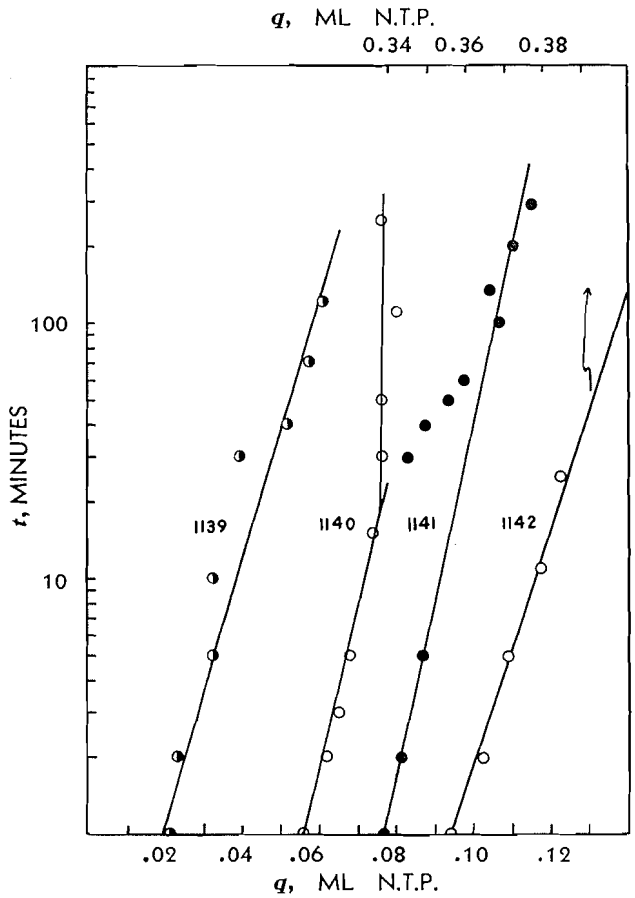

FIG. 7. Adsorption of nitrogen. 1139: P_i = 59.8 cm; 257° C; 1140: P_i = 73.1 cm; 257° C (displaced by +0.02 ml); 1141: P_i = 35.7 cm; 257° C (displaced by +0.04 ml); 1142: P_i = 59.4 cm; 100° C.

that of Amano and Taylor with a purposeful hydrogen treatment is obvious. It suggests that the small nitrogen adsorption may be facilitated by the presence of hydrogen. A similar effect was found by Gundry (6), who observed no nitrogen adsorption on clean nickel films but a small nitrogen adsorption in the presence of traces of hydrogen. The conclusion is obvious that the presence of hydrogen can create sites for nitrogen adsorption that are not already present on the clean metal or which nitrogen cannot make for itself. Considerable further study of the effects of traces of one gas on the adsorption of another, not alone from the point of view of poisoning but particularly for the possibility of enhancement of adsorption, is necessary for a complete understanding of the functions of the gas and the surface in chemisorption.

REFERENCES

1. LEIBOWITZ, L., LOW, M. J. D., and TAYLOR, H. A. J. Phys. Chem. **62**, 471 (1958).
2. TAYLOR, H. A. and THON, N. J. Am. Chem. Soc. **74**, 4169 (1952).
3. SARMOUSAKIS, J. N. and LOW, M. J. D. J. Chem. Phys. **25**, 178 (1956).
4. AMANO, A. and TAYLOR, H. J. Am. Chem. Soc. **76**, 4201 (1954).
5. TRAPNELL, B. M. W. Proc. Roy. Soc. A, **218**, 566 (1953).
6. GUNDRY, P. M. Private communication.

Can. J. Chem. Downloaded from www.nrcresearchpress.com by 190.90.36.8 on 09/04/12
For personal use only.

Can. J. Chem. Downloaded from www.nrcresearchpress.com by 190.90.36.8 on 09/04/12
For personal use only.

VIBRATIONAL SPECTRA OF NAPHTHALENE-d_0, -α-d_4, AND -d_8 MOLECULES[1]

S. S. MITRA[2] AND H. J. BERNSTEIN

ABSTRACT

The infrared and Raman spectra of the naphthalene-α-d_4 molecule have been obtained. The spectra of the d_0 molecule have also been repeated and for the most part previous measurements have been confirmed. Together with the literature data for the naphthalene-d_8 molecule, a complete assignment has been presented for all three molecules. It is recognized that the assignment is not definitive, although satisfactory agreement with the requirements of the band polarizations and contours, as well as product and sum rules, has been obtained. The calculated and observed values for the heat capacity and entropy are also in good agreement.

1. INTRODUCTION

A large amount of experimental work has been reported on the vibrational spectra of naphthalene and naphthalene-d_8 molecules. The present position has been summarized in three recent communications (1, 2, 3) (henceforth referred to as I, II, and III respectively), along with the presentation of three independent sets of assignments. Manneback (4) has given a theoretical discussion of the planar skeletal vibrations of the molecule. Calculations of vibrational frequencies using force constants transferred from benzene have been given by Brandmüller and Schmid (5) for the symmetrical A_g class, and by Scully and Whiffen (6) for the out-of-plane vibrations, A_u, B_{1u}, B_{2g}, and B_{3g}.

In the present investigation we have obtained the infrared[3] and Raman spectra of the intermediate α-d_4 compound, and along with the data on the d_0 and d_8 molecules, a complete assignment for all the three molecules has been attempted. Additional bands not used as fundamentals have been explained as combination tones.

2. EXPERIMENTAL

The photoelectrically recorded spectra of naphthalene and α-naphthalene-d_4[4] were obtained using a White Raman grating spectrometer (8). Mass spectrometric analysis of the d_4 sample gives its composition as 0.8, 10.6, 8.4, 70.4, 8.9, and 1.0%, respectively, for the $1D$, $2D$, $3D$, $4D$, $5D$, and $6D$ molecules. The Raman spectra are shown in Figs. 1 and 2.

The infrared spectra of the two compounds were measured on a Perkin–Elmer Model 12C double pass spectrometer equipped with CsBr, NaCl, and LiF optics. The infrared spectra were recorded for solutions in CS_2 and CCl_4 (about 1 M by volume). Comparison with a spectrum of a less pure sample of the α-d_4 compound enabled us to eliminate some of the bands not belonging to the d_4 molecule. The infrared spectra are shown in Figs. 3 and 4. The experimental data are tabulated in Table I.

The Raman and infrared data of Lippincott and O'Reilly (1) and Luther *et al.* (3) were used for the d_8 compound, except for the CsBr region where the spectrum has been carefully re-examined for reasons given in Section 4.

[1]*Manuscript received November 21, 1958.*
Contribution from the Division of Pure Chemistry, National Research Council, Ottawa, Canada. Issued as N.R.C. No. 5050.
[2]*N.R.C. Postdoctorate Research Fellow 1957–.*
[3]*Bayer and O'Reilly (7) have reported a few infrared bands of the α-d_4 compound in the region 700 cm^{-1} to 900 cm^{-1}, which are in agreement with our observations.*
[4]*We are greatly indebted to Dr. L. Leitch, who prepared this compound.*

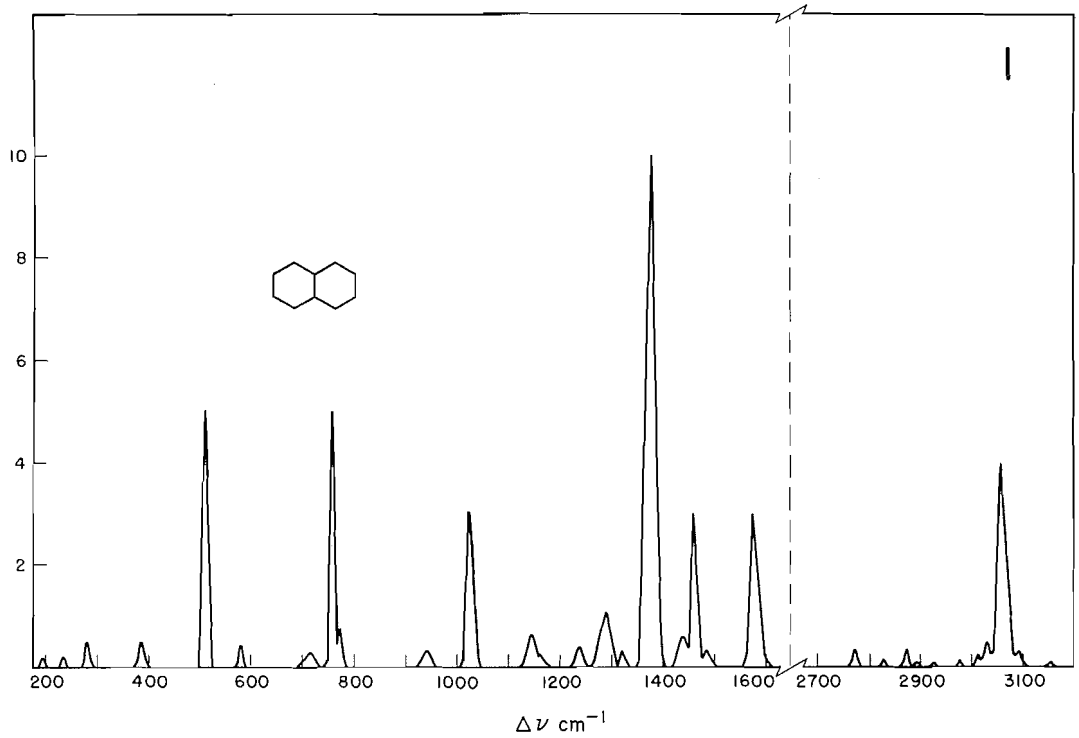

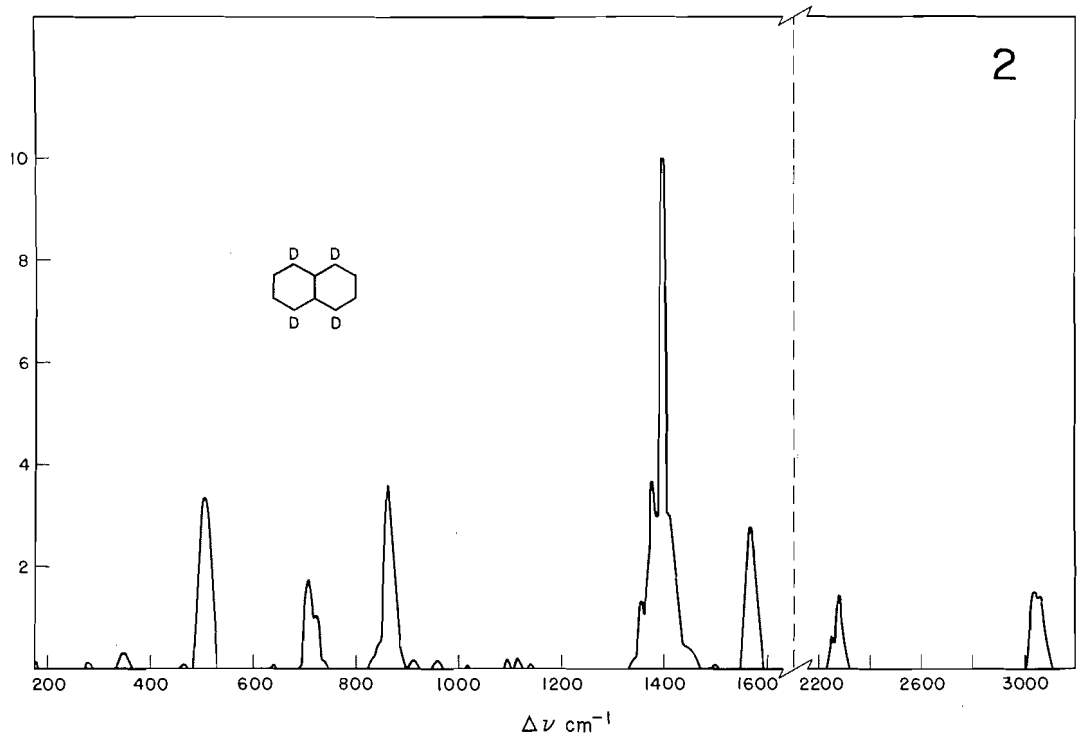

FIG. 1. Raman spectrum of naphthalene (liquid, *ca.* 90° C).
FIG. 2. Raman spectrum of naphthalene-α-d_4 (liquid, *ca.* 90° C).

Can. J. Chem. Downloaded from www.nrcresearchpress.com by 190.90.36.8 on 09/04/12
For personal use only.

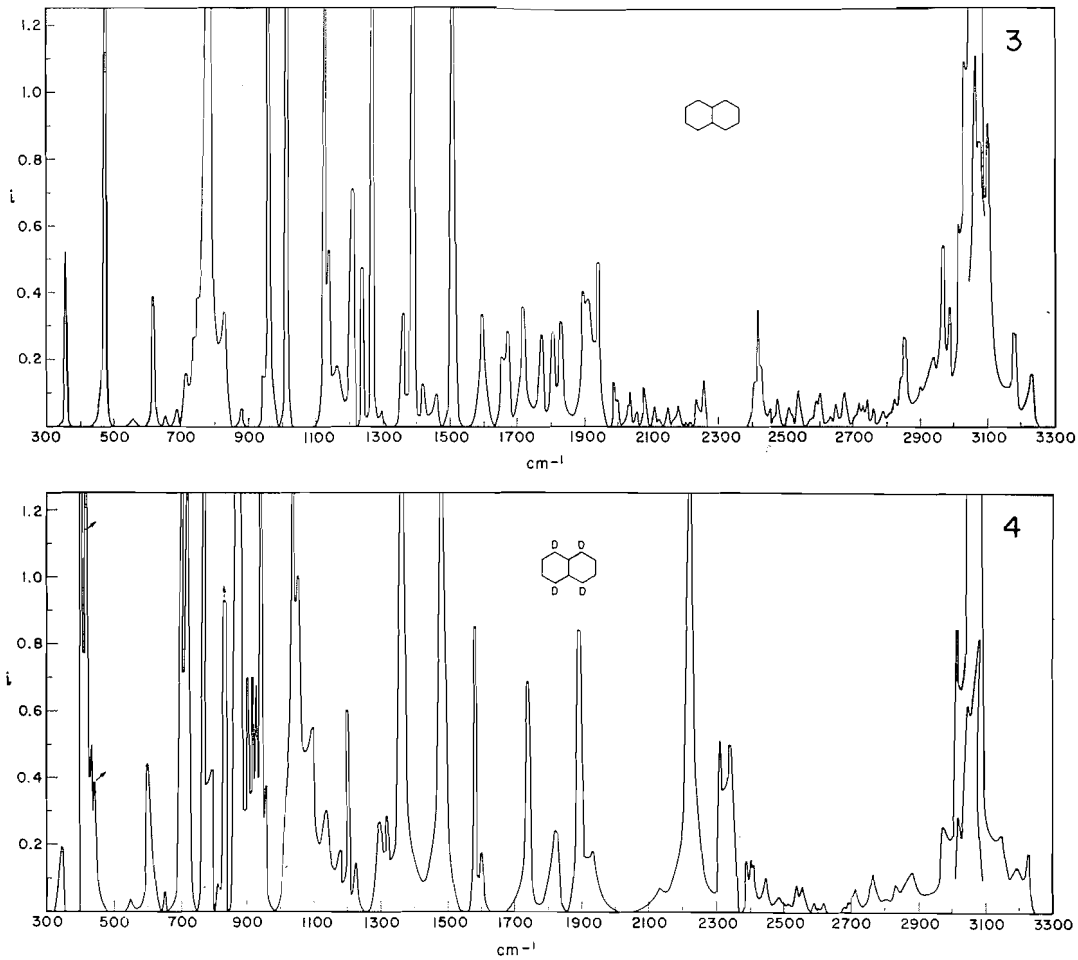

FIG. 3. Infrared spectrum of naphthalene in solution. 300 cm^{-1} to 700 cm^{-1}: solution in CCl_4 (CsBr prism); 700 cm^{-1} to 850 cm^{-1}: solution in CS_2 (NaCl prism); 850 cm^{-1} to 2000 cm^{-1}: solution in CCl_4 (NaCl prism); 2000 cm^{-1} to 3300 cm^{-1}: solution in CCl_4 (LiF prism). Intensities have been calculated for a 1 M solution and 1 mm path length except for the region 2000 cm^{-1} to 3300 cm^{-1} where the path length is 2.7 mm.

FIG. 4. Infrared spectrum of naphthalene-α-d_4 in solution. Conditions are the same as in Fig. 3. Intensities are calculated for a 1 M solution and 1 mm path length as usual, except for the region 2300 cm^{-1} to 3300 cm^{-1} where the path length is 2.7 mm. The arrows indicate bands due to the presence of other isotopically substituted species.

3. DISCUSSION

All three molecules belong to the D_{2h} point group. Each has 48 fundamental modes of vibration, of which 24 are Raman active, 20 infrared active, and 4 are completely inactive. Since the center of symmetry is a symmetry element of the D_{2h} point group, the mutual exclusion principle holds. In assigning the fundamentals the following points have been kept in mind.

(i) The frequencies of a particular mode in the three molecules should be in the order $d_0 > d_4 > d_8$.

(ii) The frequencies should lie in the spectral regions characteristic of the different types of vibrations, and should be consistent with the isotope ratio (R) associated with the type of vibration (1).

Can. J. Chem. Downloaded from www.nrcresearchpress.com by 190.90.36.8 on 09/04/12
For personal use only.

TABLE I

Infrared and Raman frequencies of naphthalene-d_0, -α-d_4, and -d_8 in cm^{-1}

Naphthalene		Naphthalene-α-d_4		Naphthalene-d_8 infrared†	Naphthalene		Naphthalene-α-d_4		Naphthalene-d_8 infrared†
Infrared	Raman*	Infrared	Raman*		Infrared	Raman*	Infrared	Raman*	
359(1)	195(0.5)	338(0.5)	183(0.5)	328(0.5)	1458(0)	2978(0.5)	1318(0.5)	1569(6)d?	
476(3)	285(1)d	407(8)	280(0.5)	404(5)	1506(4)	3012(0.5)	1362(5)	2252(3)	
562(0)	386(1)d	435(1)	350(1)	542(0)	1592(0.7)	3031(1)	1480(4)	2276(5)	
618(1)	512(10)p	557(0)	467(0)	594(2)	1652(0)	3060(8)p	1581(2)	3045(5)	
655(0)	585(1)d	602(1)	505(7)p	626(10)	1669(0.5)	3092(0.5)	1601(0.5)	3063(5)	
689(0)	717(0.5)	654(0)	639(0)		1715(0.7)	3154(0)	1738(1)		
717(0)	758(10)p	710(5)	710(5)p		1770(0.5)		1822(0.5)		
739(0)	770(1.5)	729(7)	721(1)p		1804(0.5)		1888(1.5)		
753(0)	943(0.5)	775(4)	737(0.5)		1830(0.5)		1931(0.5)		
782(20)	1025(6)p	793(1)	828(0.5)		1896(0.8)		2132(0)		
825(0.5)	1145(1)d	823(0)	844(1)d		1908(0.8)		2217(2)		
877(0)	1158(0.5)	874(20)	864(7)p		1939(1)		2260(4)		
943(0)	1239(1)	905(1.5)	908(0.5)p		2256(0)		2268(1)		
958(5)	1320(0.5)	917(1.5)	958(0.5)d		2414(0.5)		2278(1)		
1011(5)	1376(20)p	929(1.5)	1020(0?)		2851(0.5)		2295(0)		
1128(4)	1438(1)d	942(4)	1095(0.5)		2968(1)		2308(0.5)		
1138(1)	1460(6)p	957(0.5)	1114(0.5)		2987(0.8)		2338(0)		
1163(0)	1483(0.5)d	1038(3)	1140(0?)		3010(0.5)		3014(1)		
1210(1.5)	1577(6)p	1051(0.5)	1341(0.5)		3027(1)		3046(4)		
1238(1)	1624(0)	1098(0.5)	1355(1)d		3060(10)		3076(5)		
1267(4)	2774(0.5)	1137(0.5)	1379(3)d?		3076(4)				
1295(0)	2828(0)	1178(0.5)	1397(20)p		3098(1)				
1361(0.5)	2874(0.5)	1199(1)	1410(1)d?		3180(0.5)				
1387(4)	2894(0)	1214(0.5)	1451(1)d		3230(0.5)				
1419(0)	2928(0)	1296(0.5)	1497(0)						

*p = polarized, d = depolarized.

†For rest of the infrared and Raman data on naphthalene-d_8 see ref. 1.

(iii) The Teller–Redlich product rule should be obeyed.

(iv) The frequency sum rules (9, 10) should be obeyed. In this particular case the application of these rules means for a particular symmetry class

$$\Sigma\nu(d_4) = (\Sigma\nu(d_0)+\Sigma\nu(d_8))/2$$

and

$$\Sigma\nu^2(d_4) = (\Sigma\nu^2(d_0)+\Sigma\nu^2(d_8))/2.$$

The assignment should be consistent with:

(v) the polarization of the Raman lines in the molten phase, and with the polarization of the infrared bands of single crystal samples (for this point see refs. 1, 2, 3; and also Person, Pimentel, and Schnepp (11); and Pimentel, McClellan, Person, and Schnepp (12));

(vi) the contours of the infrared bands in the gaseous phase (3, 11);

(vii) the intensity of the bands;

(viii) the calculations of Brandmüller and Schmid (5), and Scully and Whiffen (6);

(ix) the trends calculated by Manneback (4) for the skeletal modes; that is, the frequencies should be in the following increasing order:

$$A_gB_{3u}A_gB_{3u}\ldots.$$

$$B_{2u}B_{3u}B_{2u}B_{3u}\ldots$$

$$A_gB_{1g}A_gB_{1g}\ldots.$$

$$B_{2u}B_{1g}B_{2u}B_{1g}\ldots;$$

Can. J. Chem. Downloaded from www.nrcresearchpress.com by 190.90.36.8 on 09/04/12
For personal use only.

(x) the experimental values of the heat capacity and entropy of gaseous naphthalene.

As we do not possess any single crystal or gas phase infrared spectra of the d_4 compound, for assigning the infrared modes of this molecule, criteria (v) in part and (vi) could not be used. Criterion (x) could be used only for the d_0 compound, since no experimental data on the thermodynamic properties of the d_4 and d_8 compounds exist.

4. INFRARED ASSIGNMENT

The band polarization measurements in the solids, and band contours in the gas phase spectra, decide unambiguously the species of many bands. The intensity and position aid in identifying the bands with particular vibrations. Our infrared assignments do not differ very much from those of McClellan and Pimentel (2). The bands for the intermediate d_4 molecule have been selected chiefly from intensity considerations and requirements of the product rule ratio and sum rules.

B_{1u} Class

McClellan and Pimentel's assignment of the four B_{1u} fundamentals for the d_0 and d_8 compounds is in complete agreement with Scully and Whiffen's predictions. We have accepted this assignment and have tried to choose four reasonable intermediate frequencies for the d_4 compound. From intensity considerations the band at 874 cm^{-1} is the only possibility for ν_{22}. In the case of ν_{23}, there are three strong bands of the d_4 molecule with frequencies intermediate between 782 cm^{-1} (d_0) and 626 cm^{-1} (d_8). A Fermi resonance has been assumed to occur between the pair at 729 cm^{-1} and 775 cm^{-1}, and the band at 710 cm^{-1} is considered to be a combination. A rough center-of-gravity calculation predicts the position of the unperturbed bands at 740 cm^{-1}. One of these is assigned as ν_{23} and the other a combination band of species B_{1u}. As the band at 407 cm^{-1} of the d_4 molecule is the strongest in that vicinity, it had to be selected as ν_{24}. However, if one accepts the reported (1) value of 408 cm^{-1} for the fundamental of the d_8 molecule, the criterion (i) of Section 3 is obviously violated. This suggested that a re-examination of the d_8 spectrum in this region would be worthwhile, and indeed, the position was measured at 404 cm^{-1} instead of 408 cm^{-1}. As no data below 300 cm^{-1} are available for the d_4 and d_8 compounds, values of 172 cm^{-1} and 163 cm^{-1} are estimated for the ν_{25} fundamental in these molecules.

B_{2u} Class

For the B_{2u} species our choice of ν_{31} (CC stretch) for the d_8 molecule is different from that in II. The chief criticism of the choice of the 1440 cm^{-1} band in II is that it is not observed in solution spectra of d_8, whereas the corresponding 1592 cm^{-1} band of the d_0 compound is a relatively strong band. Instead, we have chosen the fairly strong 1540 cm^{-1} band as ν_{31} in the d_8 compound. In I, the band at 1540 cm^{-1} has also been used instead of 1440 cm^{-1}. With reasonable choices for the CH and CD valence modes, the complete B_{2u} assignment is consistent with product and sum rules.

B_{3u} Class

Our assignment for the B_{3u} class differs from that of II only in two places, ν_{45} and ν_{47}. Instead of their 1143, 905 cm^{-1} pair for the ν_{45} mode in the d_0 and d_8 molecules we have preferred the 1210, 946 cm^{-1} pair. The chief reason is that the 1210 cm^{-1} band is stronger than the band in the 1140 cm^{-1} region of our spectrum of the d_0 compound in solution. For the ν_{47} mode we have chosen the 877, 756 cm^{-1} pair instead of the pair 742, 680 cm^{-1} adopted in II. Although both the 877 cm^{-1} and 742 cm^{-1} bands are observed in

Can. J. Chem. Downloaded from www.nrcresearchpress.com by 190.90.36.8 on 09/04/12
For personal use only.

solution, only the former is observed in the gas phase. Moreover, according to Person, Pimental, and Schnepp (11) the best choice of symmetry class for the 877 cm^{-1} band is unambiguously B_{3u}, whereas that for the 742 cm^{-1} band is either B_{1u} or B_{3u}. Further the 680 cm^{-1} band is not observed in solution spectra of the d_8 compound but the band at 756 cm^{-1} is. This assignment thus coincides with I. Our assignments of the CH and CD valence modes are essentially similar to those of II.

5. ASSIGNMENT OF RAMAN FREQUENCIES

A_g Class

For assigning the Raman active A_g modes Brandmüller and Schmid's theoretical calculations are a good guide. All the intense and polarized bands observed in the Raman spectra are included in this class. Our assignment does not differ essentially from II. Corresponding strong and polarized bands of the d_4 compound could be identified and were assigned to the A_g species. Instead of the 1240, 1006 cm^{-1} pair we have preferred that at 1158, 929 cm^{-1} for one of the CH and CD bending modes in the d_0 and d_8 molecules. As neither of the bands (1240 or 1158 cm^{-1}) are polarized, one cannot have an unambiguous choice. Lippincott and O'Reilly's argument in favor of Fermi resonance between the two strong bands at 1379 cm^{-1} and 1460 cm^{-1} in the d_0 molecule has been accepted. Our estimated position for the unperturbed band, however, is 1405 cm^{-1} instead of their value of 1393 cm^{-1}, because the corresponding band of the d_4 compound is situated at 1397 cm^{-1}. Moreover, a rough center-of-gravity calculation with the observed intensities of the two bands in question also requires a higher value.

B_{1g} Class

Following II, the 1624, 1573 cm^{-1} pair has been assigned to the CC stretching frequency ν_{16}; but as we have not observed any corresponding line in the d_4 molecule, a value of 1610 cm^{-1} has been estimated for this mode in the intermediate compound. Since in our Raman spectrum of the d_0 compound no line has been observed at 1586 cm^{-1}, it has not been included in the present assignment. Instead, the 1483, 1451, 1408 cm^{-1} system has been chosen as the ν_{17} CC stretching mode in the d_0, d_4, and d_8 molecules respectively. Moreover, the 1451 cm^{-1} band of the d_4 compound clearly shows depolarization. Of the two CH in-plane deformation modes ν_{18} and ν_{20}, ν_{18} has been assigned as in II. A corresponding line at 1410 cm^{-1} was observed for the intermediate compound, which appears to be depolarized. In the case of ν_{20}, the 1145 cm^{-1} line of the d_0 molecule (being clearly a depolarized line) has been retained in the B_{1g} symmetry class as in II, but for its counterpart in the d_8 molecule we have used 829 cm^{-1} instead of 929 cm^{-1}, since the latter has already been included in our A_g symmetry class. The former choice has also been adopted in I. For the ν_{20} band of the intermediate compound, the 844 cm^{-1} band has been selected, which is depolarized and also has an isotope ratio value (R) of the right order. For the two in-plane distortion modes (ν_{19} and ν_{21}) there is no specific criterion for selection, excepting for Manneback's rule $A_g < B_{1g}$ for all skeletal modes. For the ν_{21} vibration, the 585 cm^{-1} line has been preferred to 611 cm^{-1} as chosen by II, because the latter was not observed in this work for the d_0 molecule; furthermore, the 585 cm^{-1} line is clearly depolarized. As we have not been able to detect any corresponding line in the d_4 molecule, an estimated value of 582 cm^{-1} has been used. The 569 cm^{-1} band seems to be the corresponding frequency in the d_8 molecule. Thus the assignment for the ν_{21} mode completely agrees with that of I. We have also adopted their selection of a rather high frequency for the ν_{19} mode. Thus for this mode the line at 1320 cm^{-1} has been chosen for the d_0 molecule, with its counterpart at 1295 cm^{-1} in d_8. As no line has

Can. J. Chem. Downloaded from www.nrcresearchpress.com by 190.90.36.8 on 09/04/12
For personal use only.

been observed in the d_4 molecule in this region, a frequency of 1309 cm^{-1} has been estimated. After the selection of the CH and CD valence modes for the A_g class, the rest of the observed bands in these regions have been used in the B_{1g} class. As we do not have enough CD stretching lines in the d_8 molecule, an estimated frequency of 2220 cm^{-1} was used instead of using the 2257 cm^{-1} line twice (once in A_g and once in B_{1g}, as done in II).

Out-of-plane Modes (Raman)

For the out-of-plane deformation modes, calculations of vibration frequencies have been made by Scully and Whiffen (6). On the basis of their calculations for the d_0 and d_8 molecules it is not difficult to select the intermediate d_4 frequencies having proper intensity and obeying the sum and product rules. The major discrepancy of such an assignment is that the calculated thermodynamic functions for the d_0 compound show large deviations from the observed ones. On the other hand, McClellan and Pimentel's (11) assignment gives very good agreement between the calculated and experimental values of the thermodynamic properties, but is completely inconsistent with Scully and Whiffen's calculations. We have tried to present an assignment which gives reasonable agreement with the thermodynamic properties, and at the same time does not violate grossly Scully and Whiffen's predictions.

Agreement of calculated values of thermodynamic functions with the observed ones requires a low frequency line (preferably 195 cm^{-1}) to be included among the fundamentals. This has been done by II. In addition to this, a skeletal normal co-ordinate treatment requires that the lowest out-of-plane frequencies have the order $B_{1u} < B_{2g}$

TABLE II

The fundamental vibration frequencies for naphthalene-d_0, -α-d_4, and -d_8; (assignment A)

Species	Freq. No.	Type of vibration	$C_{10}H_8$, cm^{-1}	$C_{10}H_4D_4$ (1-4-5-8), cm^{-1}	$C_{10}D_8$, cm^{-1}	Species	Freq. No.	Type of vibration	$C_{10}H_8$, cm^{-1}	$C_{10}H_4D_4$ (1-4-5-8), cm^{-1}	$C_{10}D_8$, cm^{-1}
A_g (∥)	1	CH stretching	3060	3045	2268		25	Wing-wagging	176	172e	163e
	2	CH stretching	3031	2276	2257	B_{2g} (⊥)	26	CH bending	1239	1114	1006
	3	CC stretching	1577	1569	1548		27	CH bending	717	639	541
	4	CC stretching	1405*	1397	1380		28	Skeletal bending	195	183	180
	5	CH bending	1158	1095	929	B_{2u} (∥)	29	CH stretching	3060	3046	2299
	6	CC stretching	1025	908	862		30	CH stretching	3027	2260	2259
	7	CH bending	943	864	777		31	CC stretching	1592	1581	1540
	8	Skeletal breathing	758	710	694		32	CC stretching	1387	1362	1260
	9	Skeletal distortion	512	505	491		33	CH bending	1267	1199	1039
A_u (⊥)	10	CH bending	915				34	CH bending	1128	929	886
	11	CH bending	730				35	Skeletal distortion	618	602	594
	12	Skeletal distortion	698?				36	Skeletal distortion	359	338	328
	13	Skeletal distortion	400e			B_{3g} (⊥)	37	CH bending	1099	958	875
B_{1g} (∥)	14	CH stretching	3092	3063	2302		38	CH bending	874	828	752
	15	CH stretching	2978	2252	2220e		39	Skeletal bending	770	737	671
	16	CC stretching	1624	1610e	1573		40	Skeletal bending	285	280	270
	17	CC stretching	1483	1451	1408	B_{3u} (∥)	41	CH stretching	3076	3076	2323†
	18	CH bending	1438	1410	1170		42	CH stretching	2987	2278	2278
	19	Skeletal distortion	1320	1309e	1295		43	CC stretching	1715	1601	1562
	20	CH bending	1145	844	829		44	CC stretching	1506	1480	1403
	21	Skeletal distortion	585	582e	569		45	CH bending	1210	1038	946
B_{1u} (⊥)	22	CH bending	958	874	791		46	CH bending	1011	942	831
	23	CH bending	782	740*	626		47	Skeletal distortion	877	823	756
	24	Skeletal bending	476	407	404		48	Skeletal distortion	562	557	542

*Denotes the estimated unperturbed position of a fundamental that is affected by Fermi resonance.
e Estimated value.
†Band observed in solid phase only.

Can. J. Chem. Downloaded from www.nrcresearchpress.com by 190.90.36.8 on 09/04/12
For personal use only.

$< B_{3g}$. Thus the present assignment of the non-planar deformation frequencies (B_{2g} and B_{3g}) has been chiefly based on the following facts: (1) inclusion of the 195 cm^{-1} band as a fundamental, (2) consistency with the trend indicated by Scully and Whiffen's calculations, (3) consistency with the inequality $B_{1u} < B_{2g} < B_{3g}$ for the lowest frequencies, and finally, (4) utilization of those few Raman bands left over, i.e. not used as A_g or B_{1g} modes. Final assignments given in Table II satisfy product and sum rule requirements also. One weak point of this assignment is that it has included two frequencies 874 cm^{-1} and 1099 cm^{-1} for the d_0 molecule, which we have not observed. As we are not left with any other bands to be used for this purpose we have used the data of Lippincott and O'Reilly (I) and Luther *et al.* (III). For the d_4 molecule all the lines have been recorded by us. And for the d_8 molecule, as usual, we have used the data of I.

6. A_u MODES

Finally we are left with the selection of four A_u fundamentals, which are inactive in both infrared and Raman. Very little basis exists for their selection. The bands which have been observed in the infrared spectra of the solid but not in gas or solution can be chosen for this species because, presumably, the selection rules for a free molecule could break down in the crystal field. In II, this procedure has also been followed, but as all frequencies chosen are greater than those calculated by Scully and Whiffen, we preferred to make a new choice, not inconsistent with the trends indicated by the calculations. Lines at 915 cm^{-1} and 730 cm^{-1} have been selected on the above basis (i.e., observed in solid phase only). The line at 698 cm^{-1} has been reported for solid naphthalene by Person, Pimentel, and Schnepp (11), and not in solution, but as it has also been observed by them in the gas phase, there is some doubt as to its assignment as an A_u mode. Luther *et al.*, however, have not observed this band in the gas phase. The last frequency selected at 400 cm^{-1} is just a guess, made by all the previous workers (I, II, and III) also. No attempt has been made to assign the A_u modes of the other two molecules.

The assignment of all the fundamentals is presented in Table II. The observed and calculated product rule ratios and $\Sigma\nu$ and $\Sigma\nu^2$ values are recorded in Table III.

TABLE III

Product rule ratio and $\Sigma\nu$ and $\Sigma\nu^2$ values for the naphthalene-d_0, -α-d_4, and -d_8 molecules

	$\Pi\frac{\nu(d_4)}{\nu(d_0)}$		$\Pi\frac{\nu(d_8)}{\nu(d_0)}$		$\Sigma\nu(d_4)\times10^{-3}$ cm^{-1}		$\Sigma\nu^2(d_4)\times10^{-6}$ cm^{-2}	
Species	Obs.	Calc.	Obs.	Calc.	Obs.	Calc.	Obs.	Calc.
A_g	0.524	0.500	0.260	0.250	12.369	12.338	22.395	22.300
A_u		0.707		0.500				
B_{1g}	0.518	0.514	0.287	0.268	12.521	12.516	23.904	23.735
B_{1u}	0.721	0.718	0.519	0.515	2.193	2.188	1.507	1.497
B_{2g}	0.751	0.712	0.566	0.531	1.936	1.939	1.683	1.712
B_{2u}	0.518	0.508	0.278	0.258	11.317	11.321	21.518	21.523
B_{3g}	0.781	0.760	0.568	0.546	2.803	2.798	2.225	2.250
B_{3u}	0.518	0.508	0.261	0.258	11.795	11.793	22.357	22.305

7. THERMODYNAMIC PROPERTIES

The heat capacity and entropy of naphthalene-d_0 have been calculated at 451.0° K and 522.7° K using the above assignments. The formulas and physical constants published by the A.P.I. Research Project 44 (13) have been used in these calculations. The calculated values are compared with the experimental ones due to Barrow and

Can. J. Chem. Downloaded from www.nrcresearchpress.com by 190.90.36.8 on 09/04/12
For personal use only.

McClellan (14) in Table IV. The agreement is not significant however, due to the uncertainty in the value of the lowest A_u frequency.

TABLE IV

Comparison of the experimental and calculated values of the heat capacity and entropy of naphthalene

Temp., °K	$C_p°$, cal/deg-mole			$S°$, cal/deg-mole		
	Expt.	Calc. assign. A	Calc. assign. B	Expt.	Calc. assign. A	Calc. assign. B
451.0	48.18±0.48	48.23	48.02	96.85±0.44	96.88	96.75
522.7	54.17±0.54	54.36	54.15	104.41±0.44	104.45	104.28

TABLE V

Combination bands

Infrared, cm^{-1}	Assignment	Raman, cm^{-1}	Assignment
	Naphthalene-d_0		
655	$\nu_{24}+\nu_{28}=671$ (B_{3u})	386	$2\nu_{28}=390$ (A_g)
689	$\nu_9+\nu_{25}=688$ (B_{1u})	2774	$\nu_{16}+\nu_5=2782$ (B_{1g})
717	?	2828	$(\nu_{39}+\nu_{24})+\nu_{31}=2838$ (A_g)
739 B_{1u} or B_{3u}	$\nu_{37}-\nu_{36}=740$ (B_{1u})	2874	$\nu_4+\nu_{17}=2888$ (B_{1g})
753 B_{1u}	$\nu_{48}+\nu_{28}=757$ (B_{1u})	2894	$\nu_3+\nu_{19}=2897$ (B_{1g})
825 B_{1u}	?	2928	$(\nu_{23}+\nu_5)+\nu_{34}=2935$ (B_{3g})
943	$\nu_{21}+\nu_{36}=944$ (B_{3u})	3012	$2\nu_{44}=3012$ (A_g)
1138 B_{3u}	$\nu_{22}+\nu_{28}=1153$ (B_{3u})	3154	$2\nu_3=3154$ (A_g)
1163	$\nu_{39}+\nu_{18}=1170$ (B_{3u})		
1238 B_{2u}	$\nu_{39}+\nu_{24}=1246$ (B_{2u})		
1295	$\nu_{23}+\nu_9=1294$ (B_{1u})		
1361 B_{3u}	$\nu_{47}+\nu_9=1389$ (B_{3u})		
1419	$\nu_7+\nu_{24}=1419$ (B_{1u})		
1458	$\nu_{22}+\nu_9=1470$ (B_{1u})		
1652	$\nu_{23}+\nu_{38}=1656$ (B_{2u})		
1669	$\nu_{19}+\nu_{36}=1679$ (B_{3u})		
1770	$\nu_{33}+\nu_9=1779$ (B_{2u})		
1804	$\nu_{23}+\nu_6=1807$ (B_{1u})		
1830	$\nu_{17}+\nu_{36}=1842$ (B_{3u})		
1896	$\nu_9+\nu_{32}=1899$ (B_{2u})		
1908	$\nu_{18}+\nu_{24}=1914$ (B_{2u})		
1939	$\nu_{23}+\nu_5=1940$ (B_{1u})		
2256	$\nu_5+\nu_{44}=2264$ (B_{3u})		
2414	$\nu_{46}+\nu_4=2416$ (B_{3u})		
2851	$\nu_{20}+\nu_{43}=2860$ (B_{2u})		
2968	$(\nu_{23}+\nu_{38})+\nu_{19}=2976$ (B_{3u})		
3010	$\nu_{32}+\nu_{16}=3011$ (B_{3u})		
3098	$(\nu_{28}+\nu_6)+\nu_5=3098$ (B_{1u})		
3180	$2\nu_{44}+\nu_{25}=3188$ (B_{1u})		
3230	$\nu_1+\nu_{25}=3236$ (B_{1u})		
	Naphthalene-α-d_4		
435	Impurity ?	350	$2\nu_{28}=366$ (A_g)
654	$\nu_{38}-\nu_{25}=656$ (B_{2u})	467	$\nu_{28}+\nu_{40}=463$ (B_{1g})
710	$\nu_{10}-\nu_{28}=$? (B_{2u}); Impurity ?	721	$\nu_{48}+\nu_{25}=729$ (B_{2g})
740*	$\nu_{48}+\nu_{28}=740$ (B_{1u})	1020	$\nu_{20}+\nu_{28}=1027$ (B_{3g})
793	$\nu_4-\nu_{35}=795$ (B_{2u})	1140	$\nu_{27}+\nu_9=1144$ (B_{2g})
905	$\nu_{39}+\nu_{25}=909$ (B_{2u})	1341	$\nu_{27}+\nu_5=1349$ (B_{2g})
917	$\nu_{21}+\nu_{36}=920$ (B_{3u})	1355	$\nu_{40}+\nu_5=1375$ (B_{3g})?
957	Impurity ?	1379	$\nu_{48}+\nu_{47}=1380$ (A_g)
1051	$\nu_9+\nu_{48}=1062$ (B_{3u})	1497	$\nu_7+\nu_{27}=1503$ (B_{2g})

Infrared, cm^{-1}	Assignment	Raman, cm^{-1}	Assignment
	Naphthalene-α-d_4 (*continued*)		
1098	$\nu_{43}-\nu_9=1096$ (B_{3u})		
1137	$\nu_{43}+\nu_{21}=1139$ (B_{2u})		
1178	$\nu_{20}+\nu_{36}=1182$ (B_{3u})		
1214	$\nu_{34}+\nu_{40}=1219$ (B_{1u})		
1296	$\nu_{36}+\nu_{37}=1296$ (B_{1u})		
1318	$\nu_9+\nu_{47}=1328$ (B_{3u})		
1738	$\nu_7+\nu_{22}=1738$ (B_{1u})		
1822	$\nu_{37}+\nu_{22}=1832$ (B_{2u})		
1888	$\nu_{37}+\nu_{34}=1887$ (B_{1u})		
1931	$\nu_{39}+\nu_{33}=1936$ (B_{1u})		
2132	$\nu_{45}+\nu_5=2133$ (B_{3u})		
2217	$\nu_7+\nu_{32}=2226$ (B_{2u})		
2268	$\nu_{22}+\nu_4=2271$ (B_{1u})		
2295	$(\nu_{20}+\nu_{36})+\nu_{26}=2296$ (B_{1u})		
2308	$\nu_{43}+\nu_8=2311$ (B_{3u})		
2338	$\nu_7+\nu_{44}=2344$ (B_{3u})		
3014	$\nu_{18}+\nu_{43}=3011$ (B_{2u})		
	Naphthalene-d_8†		
721	$\nu_{28}+\nu_{48}=722$ (B_{1u})	346‡	$2\nu_{28}=354$ (A_g)
738 B_{2u}	?	1120	$\nu_{19}-\nu_{28}=1115$ (B_{3g})
819 B_{1u} or B_{3u}	?	1219	$\nu_{23}+\nu_{35}=1220$ (B_{3g})
837 B_{3u} ?	$\nu_4-\nu_{48}=838$ (B_{3u})	1437	$\nu_{37}+\nu_{21}=1444$ (B_{2g})
879 B_{2u} ?	$\nu_{23}-\nu_{40}=896$ (B_{2u})	2780	$\nu_{17}+\nu_4=2788$ (B_{1g})
905	$\nu_{38}+\nu_{25}=915$ (B_{2u})		
1087	$\nu_5+\nu_{25}=1092$ (B_{1u})		
1172	$\nu_7+\nu_{24}=1181$ (B_{1u})		
1193 B_{2u}	$\nu_6+\nu_{36}=1190$ (B_{2u})		
1214 B_{2u} / 1228 B_{2u}	$\nu_3-\nu_{36}=1220$ (B_{2u})		
1292	$\nu_{39}+\nu_{23}=1297$ (B_{2u})		
1311 B_{2u}	$\nu_{21}+\nu_{48}=1325$ (B_{2u})		
1330	$\nu_5+\nu_{24}=1333$ (B_{1u})		
1418 B_{2u}	?		
1626 B_{2u}	$(\nu_{35}+\nu_{23})+\nu_{24}=1624$ (B_{2u})		
2101	$\nu_{27}+\nu_{43}=2103$ (B_{1u})		
2149	$(\nu_{19}-\nu_{28})+\nu_{33}=2154$ (B_{1u})		
2431	$\nu_3+\nu_{34}=2434$ (B_{2u})		
2861	$\nu_{29}+\nu_{21}=2868$ (B_{3u})		
3152	$\nu_1+\nu_{31}=3154$ (B_{2u})		

*Denotes the estimated unperturbed position of a fundamental that is affected by Fermi resonance.

†Data from ref. 1.

‡From ref. 3.

Can. J. Chem. Downloaded from www.nrcresearchpress.com by 190.90.36.8 on 09/04/12
For personal use only.

Can. J. Chem. Downloaded from www.nrcresearchpress.com by 190.90.36.8 on 09/04/12
For personal use only.

8. COMBINATION BANDS

Most of the infrared and Raman bands of the three compounds not used as fundamentals have been explained as combination bands. The assignment is consistent with the known symmetry established in some cases from the infrared solid data (11). The assignments are presented in Table V.

9. AN ALTERNATIVE ASSIGNMENT (B)

An alternative assignment of fundamentals is possible, which obeys all the necessary criteria mentioned above. This assignment differs from that given above (assignment A) only in a few respects. These are pointed out in Table VI. The essential difference is the inclusion of the 386, 350, 339 cm^{-1} system as an out-of-plane Raman mode and assigning the 195, 183, 180 cm^{-1} system to the A_u species. The calculated thermodynamic properties using this alternative assignment (B) are also included in Table IV.

TABLE VI
Alternative assignment (B) of some of the fundamentals

Species	Freq. No.	$C_{10}H_8$, cm^{-1}	$C_{10}H_4D_4$ (1-4-5-8), cm^{-1}	$C_{10}D_8$, cm^{-1}
A_g	ν_5	1239	1140	1006
A_u	ν_{10}	1094		
	ν_{11}	842		
	ν_{12}	730		
	ν_{13}	195		
B_{2g}	ν_{26}	1158	958	875
	ν_{28}	285	280	270
B_{3g}	ν_{37}	1099	1020	929
	ν_{40}	386	350	339

The chief drawbacks of this assignment are: firstly, the vibration frequency at 195 cm^{-1} has to be used as an A_u mode, although it is observed in the Raman spectrum. It is quite unlikely that an A_u mode will become Raman active in the molten state in violation of the selection rule, although Scully and Whiffen (6) in their assignment of the A_u class have assumed such violation. Secondly, two of the d_4 Raman bands at 1020 cm^{-1} and 1140 cm^{-1} used here, are very weak and rather doubtful. The only advantage of this assignment over the previous one (A) presented in this communication is that the numerical deviations from Scully and Whiffen's calculated frequencies for the out-of-plane modes are reduced.

REFERENCES

1. Lippincott, E. R. and O'Reilly, E. J. J. Chem. Phys. **23**, 238 (1955).
2. McClellan, A. L. and Pimentel, G. C. J. Chem. Phys. **23**, 245 (1955).
3. Luther, H., Feldmann, K., and Hampel, B. Z. Elektrochem. **59**, 1008 (1955). Luther, H., Brandes, G., Günzler, H., and Hampel, B. Z. Elektrochem. **59**, 1012 (1955).
4. Manneback, C. J. chim. phys. **46**, 49 (1949).
5. Brandmüller, J. and Schmid, E. Z. Physik, **144**, 428 (1956).
6. Scully, D. B. and Whiffen, D. H. J. Mol. Spectroscopy, **1**, 257 (1957).
7. Bayer, R. W. and O'Reilly, E. J. J. Phys. Chem. **62**, 504 (1958).
8. White, J. U., Alpert, N., and DeBell, A. G. J. Opt. Soc. Am. **45**, 154 (1955).
9. Bernstein, H. J. and Pullin, A. D. E. J. Chem. Phys. **21**, 2188 (1953).
10. Decius, J. C. and Wilson, E. B. J. Chem. Phys. **19**, 1409 (1951). Sverdlov, L. M. Doklady Akad. Nauk S.S.S.R. **78**, 1115 (1951).
11. Person, W. B., Pimentel, G. C., and Schnepp, O. J. Chem. Phys. **23**, 230 (1955).
12. Pimentel, G. C., McClellan, A. L., Person, W. B., and Schnepp, O. J. Chem. Phys. **23**, 234 (1955).
13. Selected Values of Properties of Hydrocarbons. Circular of the National Bureau of Standards. C461. U.S. Govt. Printing Office, Washington, D.C. 1947.
14. Barrow, G. M. and McClellan, A. L. J. Am. Chem. Soc. **73**, 573 (1951).

Can. J. Chem. Downloaded from www.nrcresearchpress.com by 190.90.36.8 on 09/04/12
For personal use only.

ULTRAVIOLET ABSORPTION SPECTRA AND ACIDITIES OF ISOMERIC THIATRIAZOLE AND TETRAZOLE DERIVATIVES[1]

EUGENE LIEBER,[2] J. RAMACHANDRAN, C. N. R. RAO, AND C. N. PILLAI

ABSTRACT

The ultraviolet absorption spectra of 5-(substituted)amino-1,2,3,4-thiatriazoles and the corresponding isomeric 1-substituted-tetrazoline-5-thiones have been studied. The spectra and the dipole moments of the 5-(substituted)amino-1,2,3,4-thiatriazoles eliminate the possibility of meso-ionic structures for these compounds. The dipole moments of 5-amino-, 5-methylamino-, and 5-dimethylamino-1,2,3,4-thiatriazole were all high but approximately of the same value (5.77 to 5.84 D). This suggests that the amino thiatriazoles are best represented by conventional covalent structures with significant ionic resonance contributions. The thiatriazole ring system exhibits a characteristic absorption maximum at 250–255 mμ and an electron-withdrawing effect approximately equal to the tetrazolyl ring system. The tetrazolinethionolyl ring system is similarly electron-withdrawing. The relative acidities of the 1-substituted-tetrazoline-5-thiones and the 5-alkylmercaptotetrazoles have also been studied and the results support the observations made on the basis of their ultraviolet absorption spectra.

INTRODUCTION

In recent communications, Lieber and co-workers (1, 2) reported upon the formation and chemistry of 5-(substituted)amino-1,2,3,4-thiatriazoles, I, and the corresponding isomeric 1-substituted-tetrazoline-5-thiones, II (R^2 = H). 5-Amino-1,2,3,4-thiatriazole[3]

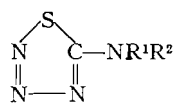

I

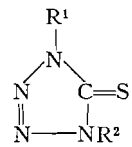

II

(1, 3, 4) (I, R^1 = R^2 = H) has a high melting point (128–130°, decomp.), a well-defined crystalline character, and is easily soluble in water. In general, the crystalline character and relatively high melting points extend to the 5-(substituted)amino-1,2,3,4-thiatriazoles (I, R^1 = (substituted)aryl; R^2 = H) and the corresponding isomeric 1-substituted-tetrazoline-5-thiones (II, R^1 = (substituted)aryl; R^2 = H) (1). This behavior has been explained by the proposal (1) that compounds of structure I (R^2 = H) exist as a tautomeric mixture probably in zwitterion form, the latter being best expressed as a meso-ionic structure,[4] III (R^3 = H):

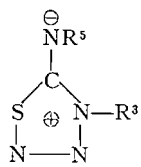

III

[1]*Manuscript received August 26, 1958.*
Contribution from the Department of Chemistry of De Paul University, Chicago, Illinois.
[2]*To whom all requests for reprints and additional information should be addressed.*
[3]*Nomenclature and ring number system from A. M. Patterson and L. T. Cappel, The ring index, Reinhold Publishing Corp., New York. 1940.*
[4]*A study of all the possible tautomeric structures, charged and uncharged, shows that the proton of 5-(substituted)-amino-1,2,3,4-thiatrazoles,* I (R^1 = *alkyl, aryl, or hydrogen,* R^2 = H), *could appear on all the nitrogen atoms present. It is represented on the nitrogen in position 3 in order to bring out its analogy to other meso-ionic structures.*

The 5-(substituted)arylamino-1,2,3,4-thiatriazoles (I, R^1 = substituted aryl; R^2 = H) undergo a facile isomerization in basic media to tetrazole derivatives which are found to be moderately strong acids (1). These latter compounds are also capable of tautomerism, of which structure IV (R^2 = H) is of principal interest due to the formation of the thiol-grouping. Recently, Lieber and co-workers (5) have demonstrated by a study of their infrared absorption spectra that the substances are thiones of structures II and V. The 5-(substituted)mercapto-tetrazoles (IV, R^1 = H; R^2 = alkyl, alkaryl, or aryl) are also of considerable interest in that they are isomeric with structures I and II. Two members of IV, namely, 5-methylmercaptotetrazole (IV, R^1 = H; R^2 = CH_3)

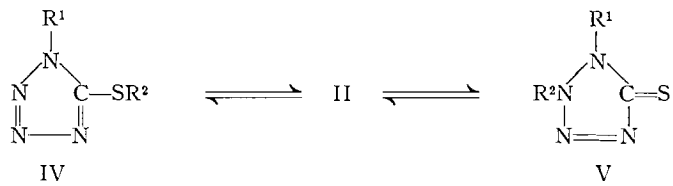

and 5-benzylmercaptotetrazole (IV, R^1 = H; R^2 = $C_6H_5CH_2$), are included in the present investigation. These derivatives are also acids. The present communication reports on the ultraviolet absorption spectra of the isomeric structures I, II, and IV and also the comparative acidities in order to gain an insight into the structural problems pointed out above.

EXPERIMENTAL

Compounds.—The 5-(substituted)amino-1,2,3,4-thiatriazoles (I, R^1 = H or CH_3; R^2 = substituent) and the 1-substituted-tetrazolinethiones (II, R^2 = H) were prepared by methods described elsewhere (1, 2, 3). 5-Methylmercaptotetrazole, IV (R^1 = H; R^2 = CH_3), m.p. 152° (uncorr.), was prepared by the method of Freund and Paradies (6). 5-Benzylmercaptotetrazole, IV (R^1 = H; R^2 = $C_6H_5CH_2$), m.p. 138–138.5° (uncorr.); anal. calc. for $C_8H_8N_4S$: S, 16.68; found: S, 16.75; this compound was prepared by essentially the same procedure by diazotization of S-benzyl isothiosemicarbazide hydrochloride and recrystallization from aqueous ethanol.

Spectroscopy.—A Beckman, Model DU, spectrophotometer and a Cary recording spectrophotometer were used for all the measurements. The wavelengths are recorded in mμ and the intensities in terms of logarithms of the molar extinction coefficients.

Comparative acidities.—The apparent dissociation constants of II (R^2 = H) and IV (R^2 = CH_3 and $C_6H_5CH_2$ respectively) were determined by potentiometric titration in 50% ethanol using a precalibrated photovolt pH meter. Standardization of the apparatus was accomplished with a series of substituted benzoic acids having reported pK_a's in the range encountered in the present investigation. It was found that differences in apparent dissociation constants as low as 0.1 pK_a units were reproducible.

Dielectric constant measurements.—The dielectric constant measurements were made in purified dioxan essentially as described in the literature (7).

RESULTS AND DISCUSSION

5-(Substituted)amino-1,2,3,4-thiatriazoles

The ultraviolet absorption data are summarized in Table I with a few typical absorption spectral curves shown in Fig. 1. 5-Amino-1,2,3,4-thiatriazole (I, R^1 = R^2 = H) shows

Can. J. Chem. Downloaded from www.nrcresearchpress.com by 190.90.36.8 on 09/04/12
For personal use only.

a strong absorption band at 267 mμ and the introduction of a saturated substituent causes a prominent bathochromic shift. Baker and co-workers (8, 9) during their investigation of cyclic meso-ionic compounds found that sydnones which contained no

TABLE I

Ultraviolet absorption spectra of 5-(substituted)amino-1,2,3,4-thiatriazoles[b] (I)

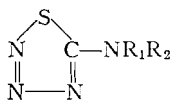

		log ε		log ε		log ε	
R_1	R_2	λ_{max}	max	λ_{max}	max	λ_{max}	max
H	H	250[a]	3.51	267	3.68	—	—
CH_3	H	255[a]	—	274	—	—	—
n-C_4H_9	H	255[a]	3.65	276	3.84	—	—
n-C_7H_{15}	H	255[a]	3.68	277	3.99	—	—
$C_6H_5CH_2$	H	255[a]	3.62	275	3.85	—	—
CH_3	CH_3	255[a]	3.40	279	3.79	—	—
C_6H_5	H	241	3.91	285[a]	3.91	302	4.03
4-$CH_3C_6H_4$	H	242	3.96	290[a]	3.97	305	4.03
4-ClC_6H_4	H	246	3.98	293	4.07	306[a]	4.03
4-$CH_3OC_6H_4$	H	243	3.98	298	4.04	311[a]	3.99
4-$N(CH_3)_2C_6H_4$	H	261.5	4.18	—	—	322.5	4.06
4-$NO_2C_6H_4$	H	222	—	—	—	335	—

[a]Appears as a shoulder.
[b]All measurements in ethanolic solution of pH 7.5.

other conjugated system showed a well-defined absorption maximum around 292 mμ in the ultraviolet region. They explained this by the suggestion that the sydnone ring possessed aromatic character and was a hybrid of a large number of contributing forms. Henry, Finnegan, and Lieber (10) found that 1,3-dialkyl-5-aminotetrazoles, VI, have a characteristic absorption band between 254 and 258 mμ, whereas the usual substituted tetrazoles containing no other conjugated system have been reported to show only end absorption (11, 12). On this basis a structure of the type VI was proposed. Baker and Ollis (9) have suggested that meso-ionic structures be represented so that the sydnone ring becomes positively charged so as to emphasize its aromatic nature. This is shown by structure VII, which does not imply that a complete negative charge is resident

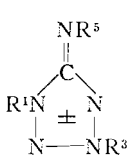

VI

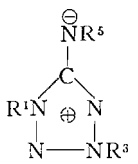

VII

$R^5 = H$
$R^1 = R^3 = alkyl$

upon the exocyclic nitrogen atom. The difficulty of representing such structures is recognized (9), although the attempted exclusion of structures which can be represented satisfactorily[5] by any one covalent or polar structure might exclude compounds which

[5]*This was recognized by Baker and Ollis (9), who pointed out that "the inevitable ambiguity here is the word satisfactory".*

Can. J. Chem. Downloaded from www.nrcresearchpress.com by 190.90.36.8 on 09/04/12
For personal use only.

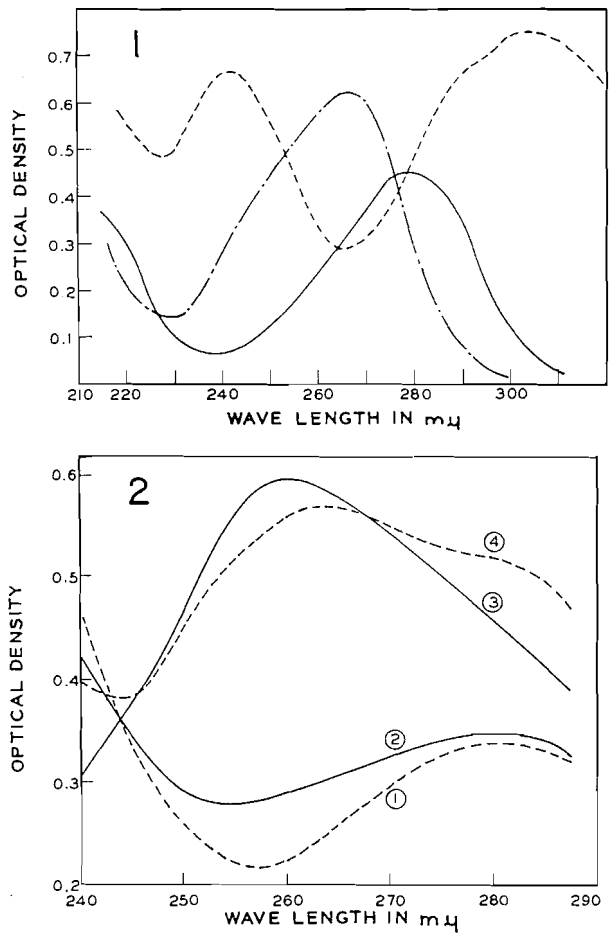

FIG. 1. Ultraviolet absorption spectra of 5-(substituted)amino-1,2,3,4-thiatriazoles:
– – – – – 5-*p*-tolylamino;
– · – · – · 5-amino;
———— 5-dimethylamino.

FIG. 2. Ultraviolet absorption spectra of 1-phenyl tetrazoline-5-thione (II, $R^2 = H$; $R^1 = C_6H_5$) in solvents of varying pH:
(1) 0.1 *N* NaOH;
(2) pH 7.5;
(3) 0.1 *N* HCl;
(4) 95% ethanol.

are, indeed, meso-ionic. Thus, Henry, Finnegan, and Lieber (10) found that, surprisingly, 2-methyl-5-alkylaminotetrazoles, VIII, which have been considered to possess the tetrazole ring system with normal covalent bonds, appear to exist principally in meso-ionic form, IX, since their ultraviolet absorption spectra are very similar to those for the 1,3-dialkyl-5-iminotetrazoles (structures VI or VII). The introduction of a methyl group

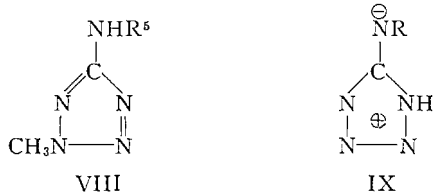

VIII IX

Can. J. Chem. Downloaded from www.nrcresearchpress.com by 190.90.36.8 on 09/04/12
For personal use only.

into the 5-amino position of either 1- or 2-methyl-5-aminotetrazole effects a bathochromic shift in the absorption maximum (10). The above ideas have been supported by the X-ray analysis of the hydrobromide of 1,3-dimethyl-5-iminotetrazole (13), and a modified 3-dimensional Fourier synthesis (14) has demonstrated unambiguously that the structures are cyclic meso-ionic. In their survey of known meso-ionic compounds Baker and Ollis (9) present structures which bear a close analogy to that of structure III proposed in this communication. Two such structures X and XI are shown below in comparison with structure III (*vide ut supra*).[6] Accordingly, the ultraviolet absorption data (Table I) and the analogies discussed above may appear to support a meso-ionic structure for the

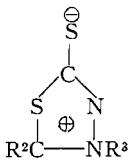

X

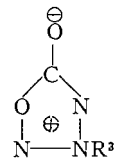

XI

5-(substituted)amino-1,2,3,4-thiatriazoles (III).

Baker and Ollis (9) have defined a meso-ionic compound as a 5- or possibly 6-membered heterocyclic compound which cannot be satisfactorily represented by any one covalent or polar structure and possesses a sextet of electrons in association with all the atoms comprising the ring. The ring bears a fractional positive charge balanced by a corresponding negative charge located on a covalently attached atom or group of atoms. The 5-(substituted)amino-1,2,3,4-thiatriazoles can be represented as meso-ionic structures III (R^3 = H). However, a conclusive assignment of meso-ionic structure in these compounds is not possible on the basis of the ultraviolet spectra, since the dimethylamino derivative (I, $R^1 = R^2 = CH_3$) *in which no tautomerism is possible* also shows the same characteristic absorptions. For this reason the dipole moments of 5-amino- (I, $R^1 = R^2$ = H); 5-methylamino- (I, R^1 = H; $R^2 = CH_3$); and 5-dimethylamino-1,2,3,4-thiatriazole (I, $R^1 = R^2 = CH_3$), respectively, were determined. Although it has been demonstrated by Kaufman and co-workers (7) that this measurement does not provide a sound basis for the assignment of meso-ionic structures, it was felt that it could contribute to a clearer picture of the thiatriazole ring system. Further, if structures I (R^1 = H) are meso-ionic there would be a significant difference in the dipole moments of the 5-(monosubstituted)amino- and 5-(disubstituted)amino-1,2,3,4-thiatriazoles. The dipole moments obtained are summarized below:

Compound I		
R^1	R^2	μ (Debye units)
H	H	5.77
H	CH_3	5.72
CH_3	CH_3	5.84

While the dipole moments are large they are all approximately the same. It is therefore suggested that 5-amino-1,2,3,4-thiatriazole and its derivatives are best represented by

[6]*Recent investigations (15, 16) in progress in this laboratory have revealed that substances formerly considered to be derivatives of azidodithiocarbonic acid,* $N_3C(S)SH$, *are in reality derivatives of 1,2,3,4-thiatriazoline-5-thione, the simplest members of which has a relatively high decomposition point and is nicely crystalline. Its structure should be closely related to* XI (R^3 = H) *replacing the oxygens by sulphur.*

Can. J. Chem. Downloaded from www.nrcresearchpress.com by 190.90.36.8 on 09/04/12
For personal use only.

conventional covalent structures and that the ultraviolet absorption spectral characteristics are due to the interaction of the thiatriazole nucleus with the substituent in the 5-position. Unfortunately, the dipole moment data do not provide the direction of the moment in these compounds.[7] The thiatriazole ring contains three nitrogen atoms (positions 2, 3, and 4) which are sp^2 hybridized and which should induce a large concentration of negative charge away from the ring and the substituent in the 5-position. The ultraviolet absorption data supports this suggestion.

From the data in Table I, it can be seen that all of the 5-alkyl substituted derivatives exhibit a shoulder at 255 mμ and an absorption band around 275 mμ. Since the unsubstituted compound (I, $R^1 = R^2 = H$) also exhibits a shoulder at 250 mμ, it is considered that this 250–255 mμ absorption is characteristic of the 1,2,3,4-thiatriazole ring system:

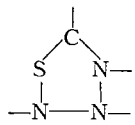

The major absorption bands at the longer wavelength are caused by the interaction of the amino or the substituted group with the heterocyclic nucleus. It will also be noted from Table I that there is very little change in the position of this maximum with different alkyl substituents including the benzyl group in the 5-amino position. Table I also shows that all of the 5-arylamino-1,2,3,4-thiatriazoles studied (I, $R^1 = H$; R^2 = aryl) show a distinct peak in the vicinity of 242 mμ, probably due to the thiatriazole nucleus. Also indicated are a shoulder and a peak at longer wavelengths probably due to the interaction of the aromatic ring with the heterocyclic nucleus. Analogies with the ultraviolet absorption spectra of 5-(substituted)amino tetrazoles (17) and substituted amino-1,2,3-triazoles (18) can be made. The 5-arylamino-1,2,3,4-thiatriazoles (I, $R^1 = H$; R^2 = aryl) may also be considered as substituted benzenes, XII. The position of the absorption maxima of the compounds represented by structure XII depends markedly

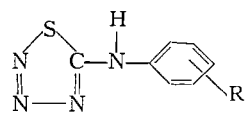

XII

on the nature of the substituent R on the aromatic ring, the λ_{max} increasing approximately in proportion to the electron-donating power of the substituent. This proportionality indicates that the grouping XIII is an electron-withdrawing group, capable of appreciable resonance interaction. Recently, Rao (19) has correlated the ultraviolet absorption spectra of meta- and para-disubstituted benzenes with reactivities and resonance parameters (20). The correlation of the wavelength displacements with the reactivities and

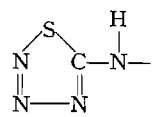

XIII

[7] *An investigation on an extended series of appropriate structures* I ($R^1 = H$; R^2 = *substituted aryl*) *to determine the direction of this moment is in progress and will be reported upon in a separate communication.*

Can. J. Chem. Downloaded from www.nrcresearchpress.com by 190.90.36.8 on 09/04/12
For personal use only.

resonance parameters indicate that the electron-withdrawing ability of XIII by resonance interaction is of the same order of magnitude as that of the 5-aminotetrazolyl group:

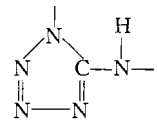

This is surprising in view of the somewhat smaller electronegativity value for sulphur over that of nitrogen (21).

Accordingly, from the above discussion it is concluded that the ultraviolet absorption data and the dipole moments reported are due to hybridization effects (22) and the contribution of ionic resonance structures XIV and XV. The case here is similar to that reported by Kaufman and co-workers (7) for 1-ethyltetrazole, XVI, which has a higher moment (5.46 D) than the meso-ionic compound 1,3-dimethyl-5-iminotetrazole (4.02 D) (VI, $R^5 = H$; $R^1 = R^3 = CH_3$). In the case of XVI the moment is directed with the

XIV XV

XVI XVII

negative pole away from the carbon atom in the ring, the high dipole moment probably due to the hybridization effects of the 2, 3, and 4 ring nitrogens and resonance contributions of ionic structures (7). In the case of 1,3-dimethyl-5-imino-tetrazole (VI, $R^5 = H$; $R^1 = R^3 = CH_3$; XVII), the moment is directed with the negative pole towards the exocyclic nitrogen at the 5-position, the lower value of the moment being the results of the hybridization effect of the nitrogen in position-2 in the ring of XVII, which results in a concentration of negative charge away from the exocyclic nitrogen atom and the ring.

1-Substituted Tetrazoline-5-thiones

The ultraviolet absorption spectral data obtained with the 1-(substituted)phenyl-tetrazoline-5-thiones (II, $R^2 = H$; $R^1 =$ aryl) are summarized in Table II. Considering these compounds as substituted benzene, represented by the structure XVIII, it will be noted (Table II) that the compounds display primary absorption bands in the region 217–254 mμ, which can be ascribed to the primary bands of the substituted benzene (19).

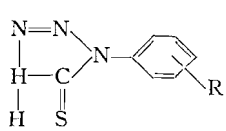

XVIII

Can. J. Chem. Downloaded from www.nrcresearchpress.com by 190.90.36.8 on 09/04/12
For personal use only.

This primary absorption maximum varies in proportion to the electron-donating power of the substituents on the 1-phenyl group. Thus, a bathochromic shift in the absorption maximum is observed with substitution by groups capable of donating electrons by resonance interaction. This effect is appreciable in the case of the *p*-dimethylamino derivative (XVIII, R = 4-$(CH_3)_2N$) which exhibits the primary band at 254 mμ. From the

TABLE II

Ultraviolet absorption spectra of 1-substituted tetrazoline-5-thiones

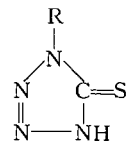

R	λ_{max}	log ϵ_{max}	λ_{max}	log ϵ_{max}	λ_{max}	log ϵ_{max}	In 0.1 *N* NaOH in 95% ethanol λ_{max}
C_6H_5	217.5	4.19	262	3.85	280[a]	3.81	280
2-$CH_3C_6H_4$	—	—	253	3.98	271[a]	3.71	—
2-$CH_3OC_6H_4$	217	4.53	254	4.43	274[a]	4.23	—
4-FC_6H_4	219	4.12	262	3.91	282[a]	3.79	—
4-$CH_3C_6H_4$	220	4.50	262.5	4.18	282[a]	4.10	278
4-$CH_3OC_6H_4$	229	4.14	264	3.98	280[a]	3.91	274
4-ClC_6H_4	226	4.22	263.5	3.77	288[a]	3.79	—
2,4-$Cl_2C_6H_3$	222[a]	4.27	250[a]	3.96	281[a]	3.61	—
4-$(CH_3)_2NC_6H_4$	254	4.31	295	4.22	—	—	308[a]
4-$NO_2C_6H_4$	—	—	252	4.32	332.5	3.91	—
$C_6H_5CH_2$	—	—	248	4.09	—	—	—
CH_3	—	—	245	4.13	—	—	245

[a]Appears as a shoulder.

correlation of Rao (19), it is found that the 1-tetrazoline thionyl group, XIX, is electron withdrawing in nature of about the same order of magnitude as the 5-amino-tetrazolyl group and the 5-amino-1,2,3,4-thiatriazole group (XIII).

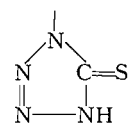

XIX

In addition to the primary band of the substituted benzene, the 1-aryl-tetrazoline-5-thiones (XVIII), in general, exhibit another absorption maximum between 252 and 295 mμ and a shoulder between 270 and 288 mμ (Table II). The absorption maximum is considered to be due to the acid XVIII and the shoulder as being due to the anion XX. No definite assignments seem to be possible in the case of the 1-(*p*-nitro)phenyl derivative (XVIII, R = 4-O_2N—C_6H_4), probably due to the absorption of the nitro group itself.

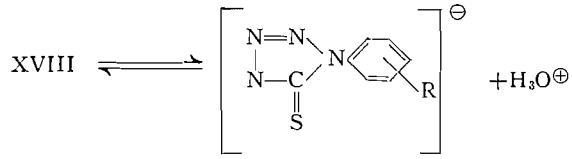

XX

Can. J. Chem. Downloaded from www.nrcresearchpress.com by 190.90.36.8 on 09/04/12
For personal use only.

In Fig. 2 are shown the absorption spectra of 1-phenyl-tetrazoline-5-thione (II, $R^2 = H$; $R^1 = C_6H_5$) in solvents of different pH. In 95% ethanol, the bands due to the undissociated acid and the anion are observed at 262 and 280 mμ respectively. In 0.1 *N* hydrochloric acid, however, the 262 mμ band appears as a strong peak and the shoulder at 280 mμ disappears. In 0.1 *N* sodium hydroxide solution, the shoulder at 280 mμ assigned to the anion becomes a peak and the 262 mμ band is absent. From Fig. 2 it can be seen that the compound is almost completely dissociated even in a buffer of pH 7.5. The absorption spectra further indicates that the anion is considerably resonance stabilized, since the anions absorb at higher wavelengths than the undissociated acids. Table II also lists the absorption maxima of some of the 1-substituted tetrazoline-5-thiones (II, $R^2 = H$) in 0.1 *N* sodium hydroxide in 95% ethanol. From the data in Table II it is seen that the 1-alkyl-derivatives exhibit only one absorption maximum at lower wavelengths than the 1-alkyl-derivatives. Further, the anion of 1-methyltetrazoline-5-thione (II, $R^2 = H$; $R^1 = CH_3$) absorbs at the same wavelength as the undissociated acid. This suggests that there is little or negligible extra resonance stabilization of the anion in the alkyl derivatives.

A study of the apparent dissociation constants of the 1-substituted tetrazoline-5-thiones (II, $R^2 = H$) summarized in Table III seems to support the observations based on the ultraviolet spectra regarding the electrical effects of the substituents in this system (R in XVIII). A plot of the pK_a values of the 1-substituted phenyltetrazoline-5-thiones

TABLE III

Apparent dissociation constants of 1-substituted tetrazoline-5-thiones (Temperature, 25±2° C)

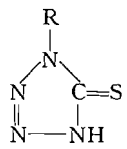

R	pK_a[a]
4-$NO_2C_6H_4$	3.36
2,4-$Cl_2C_6H_3$	3.41
4-FC_6H_4	3.61
4-ClC_6H_4	3.62
2-$CH_3C_6H_4$	3.62
C_6H_5	3.65
2-$CH_3OC_6H_4$	3.74
4-$CH_3C_6H_4$	3.75
4-$CH_3OC_6H_4$	3.78
$C_6H_5CH_2$	3.80
C_2H_5	3.85
CH_3	3.86
CH_2=CH—CH_2	3.91
4-$(CH_3)_2N$—C_6H_4	4.09

[a]Mean of three independent determinations.

(XVIII) against the Hammett sigma (σ) values for groups (23) is reasonably linear as shown in Fig. 3. The slope of this line, the rho value (ρ), is smaller than the rho values for the 5-(substituted)phenylamino-4-phenyl-1,2,3-triazoles and the 5-(substituted)-phenylaminotetrazoles (24, 25). This indicates a smaller magnitude of the electrical effects of the substituents in the tetrazolinethione system (XIX). It is, however, interesting to note (Table III) that while the pK_a of the aryl derivatives varies between 3.36

Can. J. Chem. Downloaded from www.nrcresearchpress.com by 190.90.36.8 on 09/04/12
For personal use only.

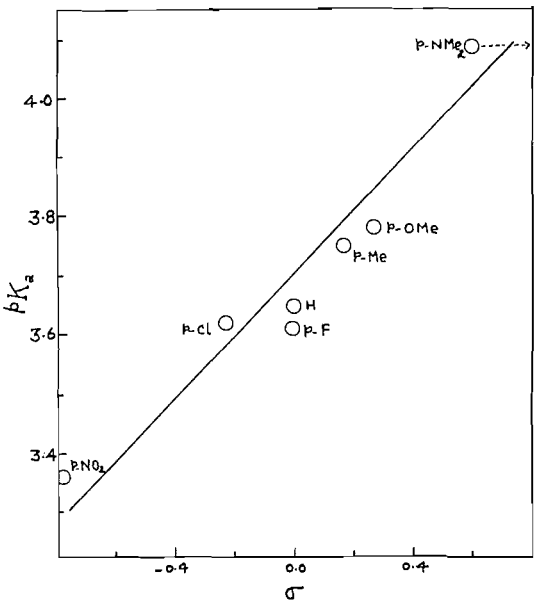

FIG. 3. pK_a of 1-substituted tetrazoline-5-thiones versus Hammet sigma (σ) values for groups.

and 4.09, the alkyl derivatives possess pK_a values between 3.80 and 3.91. In 1-(*p*-dimethylamino)phenyltetrazoline-5-thione (XVIII, R = 4-$(CH_3)_2N$) where there is strong complimentary substitution, the displacement of the primary benzene band in the ultraviolet spectrum is greatest as is also the effect on the acidity. The 2-methyl, 2-methoxy, and 2,4-dichlorophenyl derivatives exhibit the ultraviolet absorption bands (Table II) at wavelengths lower than the corresponding para isomers. The ortho derivatives also show slight increase in acidity from the para derivatives (Table III). Such behavior may be due to steric effects of the ortho substituents (26, 28). The possibility of intramolecular hydrogen bonding cannot be excluded in the case of the ortho-anisyl derivative (XVIII, R = 2-$CH_3OC_6H_4$). The band displacement exhibited by the *p*-fluorophenyl derivative (XVIII, R = 4-FC_6H_4) is too small to be accounted for on the basis of the proposed resonance parameter of -0.44 (20) for the *p*-fluoro group. A lower resonance parameter of the order of -0.10 seems more reasonable (26, 27).

TABLE IV

Apparent dissociation constants of 5-(substituted)mercapto tetrazoles
(Temperature, 25±2° C)

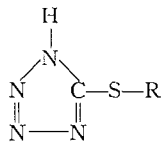

R	pK_a[a]
CH_3	4.07
$C_6H_5CH_2$	3.94

[a]Mean of three independent measurements.

Can. J. Chem. Downloaded from www.nrcresearchpress.com by 190.90.36.8 on 09/04/12
For personal use only.

The 5-alkyl mercaptotetrazoles (IV, $R^1 = H$; R^2 = alkyl)[8] are weaker acids (Table IV) compared to the corresponding 1-substituted tetrazoline-5-thiones (II, $R^2 = H$). The ultraviolet absorption of 5-alkyl mercaptotetrazoles (Table V) are similar to the derivatives of tetrazole (17) rather than those of the tetrazoline-5-thiones. Since there is no conjugating group in the 5-position, these mercapto derivatives absorb at lower wavelengths. Further, the ultraviolet absorption spectrum of the 5-methylmercapto derivative (IV, $R^1 = H$; $R^2 = CH_3$) in alkaline solution shows little extra resonance stabilization of the anion.

TABLE V

Ultraviolet absorption spectra of 5-substituted mercapto tetrazoles

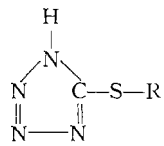

			In 0.1 *N* sodium hydroxide in 95% ethanol
R	λ_{max}	log ϵ	λ_{max}
CH_3	230[a]	3.52	235[a]
$C_6H_5CH_2$	220[a]	4.05	—

[a]Appears as a shoulder.

ACKNOWLEDGMENT

The authors gratefully acknowledge grants-in-aid from the Frederick Gardner Cottrell Program of the Research Corporation, New York, N.Y., and the Lilly Research Laboratories, Eli Lilly and Company, Indianapolis, Indiana, which made this study possible.

REFERENCES

1. LIEBER, E., PILLAI, C. N., and HITES, R. D. Can. J. Chem. **35**, 832 (1957).
2. LIEBER, E. and RAMACHANDRAN, J. Can. J. Chem. **37**, 101 (1959).
3. LIEBER, E., OFTEDAHL, E., PILLAI, C. N., and HITES, R. D. J. Org. Chem. **22**, 441 (1957).
4. FREUND, M. and SCHANDER, A. Ber. **29**, 2500 (1896).
5. LIEBER, E., RAO, C. N. R., PILLAI, C. N., RAMACHANDRAN, J., and HITES, R. D. Can. J. Chem. **36**, 801 (1958).
6. FREUND, M. and PARADIES, T. Ber. **34**, 3110 (1910).
7. KAUFMAN, M. H., ERNSBERGER, F. M., and MCEWEN, W. S. J. Am. Chem. Soc. **78**, 4197 (1956).
8. BAKER, W., OLLIS, W. D., and POOLE, V. D. J. Chem. Soc. 307 (1949).
9. BAKER, W. and OLLIS, W. D. Quart. Revs. **11**, 15 (1957).
10. HENRY, R. A., FINNEGAN, W. G., and LIEBER, E. J. Am. Chem. Soc. **76**, 2894 (1954).
11. ELPERN, B. and NACHOLD, F. C. J. Am. Chem. Soc. **72**, 3379 (1950).
12. ELPERN, B. J. Am. Chem. Soc. **75**, 661 (1953).
13. BRYDEN, J. H., HENRY, R. A., FINNEGAN, W. G., BOSCHAN, R. H., MCEWAN, W. S., and VAN DOLAH, R. W. J. Am. Chem. Soc. **75**, 4863 (1953).
14. BRYDEN, J. H. Acta Cryst. **8**, 211 (1955); **9**, 874 (1956); **10**, 148 (1958).
15. LIEBER, E., PILLAI, C. N., RAMACHANDRAN, J., and HITES, R. D. J. Org. Chem. **22**, 1750 (1957).
16. LIEBER, E., OFTEDAHL, E., GRENDA, S., and HITES, R. D. Chem. & Ind. 893 (1958).
17. LIEBER, E., RAO, C. N. R., and PILLAI, C. N. Current Sci. (India), **26**, 167 (1957).
18. LIEBER, E., RAO, C. N. R., and CHAO, T. S. Spectrochim. Acta, **10**, 250 (1958).
19. RAO, C. N. R. Chem. & Ind. 666 (1957); 1239 (1957).
20. TAFT, R. W., JR. *In* Steric effects in organic chemistry. *Edited by* M. S. Newman. John Wiley & Son, Inc., New York. 1956. Chap. 13.
21. HINE, J. Physical organic chemistry. McGraw-Hill Book Company, New York. 1956. p. 7.

[8]*The* C=S *and the* —N—C=S *frequencies are not apparent in these compounds as in the 1-substituted-tetrazoline-5-thiones*, II ($R^2 = H$), (*5*).

Can. J. Chem. Downloaded from www.nrcresearchpress.com by 190.90.36.8 on 09/04/12
For personal use only.

22. COULSON, C. A. Valence. Oxford University Press. 1952.
23. JAFFE, H. H. Chem. Revs. **53**, 191 (1953).
24. LIEBER, E., RAO, C. N. R., CHAO, T. S., and RAMACHANDRAN, J. J. Org. Chem. (1959).
25. HENRY, R. A., FINNEGAN, W. G., and LIEBER, E. J. Am. Chem. Soc. **76**, 88 (1954).
26. JONES, R. N., FORBES, W. F., and MUELLER, W. A. Can. J. Chem. **35**, 504 (1957).
27. RAO, C. N. R. J. Sci. Ind. Research (India), **17** (In press) (1958).
28. HERBST, R. M. and WILSON, K. R. J. Org. Chem. **22**, 1142 (1957).

Can. J. Chem. Downloaded from www.nrcresearchpress.com by 190.90.36.8 on 09/04/12
For personal use only.

THE CHARACTERIZATION OF TRI-*O*-TOSYL SUCROSE[1]

P. D. Bragg and J. K. N. Jones

ABSTRACT

Tri-*O*-tosyl sucrose was synthesized by the action of *p*-tolylsulphonyl chloride upon sucrose in pyridine, and the tosyl groups were shown by methylation to be mainly (84%) located on the three primary hydroxyl groups.

INTRODUCTION

Hockett and Zief (1) prepared sulphonyl esters of sucrose by reaction with methane sulphonyl (mesyl) chloride or *p*-tolyl-sulphonyl (tosyl) chloride in pyridine solution. Although none of the products were isolated in crystalline form, analytical values were recorded for the tri-*O*- and octa-*O*-mesyl and tosyl sucrose derivatives. Tosyl and mesyl compounds undergo a large number of important reactions (2) so thorough characterization of the trisubstituted sucrose was considered to be desirable.

Tri-*O*-tosyl sucrose was prepared by Hockett and Zief's method (1). Complete methylation to tri-*O*-tosyl-penta-*O*-methyl sucrose was obtained by a single treatment with methyl iodide and silver oxide in dimethylformamide solution (3). Detosylation and subsequent hydrolysis gave a mixture of tri-*O*-methyl glucose, di-*O*-methyl fructose, and di-*O*-methyl glucose. A small amount (5%) of tri-*O*-methyl fructose was also present.

The methyl ethers of glucose were characterized by conversion to 2,3,4-tri-*O*-methyl-*N*-phenyl-D-glucosylamine and 2,4-di-*O*-methyl-*N*-*p*-nitrophenyl-D-glucosylamine respectively.

The di-*O*-methyl fructose was chromatographically identical with 3,4-di-*O*-methyl fructose. The measured rotation was lower than the quoted value (4) but this was probably due to the presence of an optically inactive impurity derived from the filter paper on which the sugar was fractionated. The identity of the fructose methyl ether was confirmed as 3,4-di-*O*-methyl-D-fructofuranose by periodic acid oxidation followed by bromine oxidation to dimethylsuccinic acid and the isolation of crystalline (−)-D-dimethoxysuccinamide formed by the action of ammonia on the methyl ester (5).

The isolation of 2,4-di-*O*-methyl-D-glucose from the hydrolysis mixture suggests that some undermethylation had occurred. In glucose the hydroxyl group at $C_{(3)}$ is less reactive than that at $C_{(2)}$, $C_{(4)}$, or $C_{(6)}$ (9), and 2,4-di-*O*-methyl glucose would result from undermethylation.

This sugar might arise through the formation of a 3,6-anhydro ring on the glucose residue of sucrose during methylation. But no 2,4-di-*O*-methyl-D-glucose was formed from methyl 2,4-di-*O*-methyl-3,6-anhydro α-D-glucoside when the latter was submitted to the conditions of hydrolysis used for the methylated sucrose derivative. The infrared spectrum of the methylated sucrose showed that hydroxyl groups were absent. However, it has been observed in these laboratories that incompletely methylated polysaccharides which had been submitted to the Kuhn methylation procedure in dimethylformamide (3) gave an infrared spectrum without hydroxyl peaks, and yet gave amounts of sugars which indicated that methylation was incomplete. This phenomenon is as yet unexplained.

The tri-*O*-tosyl sucrose consisted mainly therefore of 6,1[1],6[1]-tri-*O*-tosyl sucrose. This

[1]*Manuscript received November 10, 1958.*
Contribution from the Department of Chemistry, Queen's University, Kingston, Ontario.

Can. J. Chem. Downloaded from www.nrcresearchpress.com by 190.90.36.8 on 09/04/12
For personal use only.

result is in agreement with the results of Lemieux and Barrette (6), who found that the trianhydro sucrose derived from the above compound was different from that obtained from 4,1^1,6^1-tri-*O*-tosyl sucrose, which had been prepared from 2,3,6,3^1,4^1-penta-*O*-acetyl sucrose (7). This structure is also supported by the isolation of a sirupy di-iodo-di-deoxy-mono-*O*-tosyl sucrose pentaacetate from the action of sodium iodide (8) on tri-*O*-tosyl sucrose pentaacetate. The iodine atoms are probably located on the $C_{(6)}$ of both fructose and glucose moieties, the tosyl group on fructose-$C_{(1)}$ remaining unsubstituted. In agreement with this, Lemieux and Barrette (6) obtained only a mono-iodo derivative from 4,1^1,6^1-tri-*O*-tosyl sucrose.

It is probable that the tri-*O*-tosyl sucrose is not pure. However the high yield (89%) of di-iodo-di-deoxy-mono-*O*-tosyl sucrose pentaacetate (analysis indicates 94% purity) that was prepared from it shows that at least 84% of the preparation must have tosyl groups on $C_{(6)}$ and $C_{(6^1)}$. Since no other tri-*O*-methyl glucoses were found, which would be the case if other tri-*O*-tosyl sucroses were present, the preparation is probably purer than the above figure. The chromatography solvent used (*n*-butanol : ethanol : water, 3 : 1 : 1) resolved 2,3,4-tri-*O*-methyl-D-glucose (R_f 0.62) from 2,3,6-tri-*O*-methyl- (R_f 0.59) and 3,4,6-tri-*O*-methyl-D-glucose (R_f 0.58). Complete separation from 2,4,6-tri-*O*-methyl-D-glucose (R_f 0.61) was not obtained but since tosylation at $C_{(3)}$ of sucrose is unlikely (9) it is probable that this methylated sugar was not present.

Reduction of 6,1^1,6^1-tri-*O*-tosyl sucrose with lithium aluminum hydride gave 6,6^1-dideoxy sucrose (cf. 6), which was cleaved by invertase to 6-deoxy-D-glucose and D-rhamnoketose.

EXPERIMENTAL

Paper chromatograms were developed in the solvent system: *n*-butanol : ethanol : water (3 : 1 : 1). Reducing sugars were detected by *p*-anisidine hydrochloride and a resorcinol spray reagent was used for the specific detection of ketoses (10). Melting points are uncorrected and were determined on a Kofler microheating stage.

Tri-O-tosyl Sucrose

This was prepared by Hockett and Zief's method (1) and had $[\alpha]_D^{17}$ +41.3° (*c*, 2.06 in chloroform). Anal. Calc. for $C_{33}H_{40}O_{17}S_3$: S, 11.9%. Found: S, 11.5%.

Methylation of Tri-O-tosyl Sucrose

Tri-*O*-tosyl sucrose (7.3 g), dried over phosphoric oxide, was dissolved in dimethylformamide (120 ml), which had been distilled from barium oxide, and methyl iodide (45 ml). Silver oxide (45 g) was added portionwise with vigorous stirring, the temperature was not permitted to rise above 35°. After 7 hours, the mixture was filtered, the precipitate was washed with dimethylformamide (2×50 ml), and then chloroform (50 ml), and the combined liquids were poured into 1% aqueous sodium cyanide (500 ml). The aqueous layer was shaken with chloroform, which was then added to the chloroform layer and the combined solutions were washed well with water, dried (sodium carbonate), and concentrated to a sirup (5.33 g) $[\alpha]_D^{24}$ +49.5° (*c*, 4.05 in chloroform). The product showed no hydroxyl peaks in its infrared spectrum. Anal. Calc. for $C_{38}H_{50}O_{17}S_3$: OMe, 17.8%. Found: OMe, 20.7%. The high value for methoxyl suggests contamination of the product with dimethylformamide.

Detosylation of the Methylated Sucrose

The sirup (5.2 g) in 85% aqueous methanol (200 ml) was stirred with 4% sodium amalgam (125 g) for 18 hours. After filtration and neutralization with solid carbon

Can. J. Chem. Downloaded from www.nrcresearchpress.com by 190.90.36.8 on 09/04/12
For personal use only.

dioxide, the solution was concentrated to a solid which was extracted with boiling chloroform (3×150 ml). The extract afforded a sirup (2.6 g) which on concentration did not give a solution in water or 50% aqueous ethanol sufficiently clear for optical rotation measurements.

Hydrolysis and Separation of the Methyl Sugars

The methylated sucrose (2.6 g) was hydrolyzed with 0.01 *N* sulphuric acid (150 ml) at 100° for 1½ hours. After neutralization the resulting mixture (2.4 g) was examined on paper chromatograms. With *p*-anisidine, tri-*O*-methyl glucose (R_f 0.62), di-*O*-methyl fructose (R_f 0.52), and di-*O*-methyl glucose (R_f 0.48) were detected. The resorcinol spray showed the presence of a small amount of a further component, tri-*O*-methyl fructose, having an identical R_f value to the tri-*O*-methyl glucose which previously masked it.

The mixture of sugars was fractionated on a cellulose column (30×3 cm) using methyl ethyl ketone : water azeotrope as solvent (7). A complete separation of the component sugars was not obtained so the fractions were combined to give a tri-*O*-methyl hexose fraction (0.75 g) and a di-*O*-methyl hexose fraction (1.2 g).

The tri-*O*-methyl hexose fraction was dissolved in 0.35% methanolic hydrogen chloride (25 ml) and the rotation was followed until equilibrium was reached (22 hours). After neutralization with silver oxide and removal of the silver ions with hydrogen sulphide, tri-*O*-methyl glucose (R_f 0.65) was separated on sheet paper chromatograms from a small amount of tri-*O*-methyl methyl fructofuranoside. The di-*O*-methyl hexose fraction was similarly fractionated into di-*O*-methyl glucose (R_f 0.49) and di-*O*-methyl methyl fructofuranoside (R_f 0.66).

Characterization of the Methyl Sugars

Tri-*O*-methyl hexose (280 mg) was refluxed with redistilled aniline (110 mg) in ethanol (10 ml). Removal of the ethanol under reduced pressure initiated crystallization. After recrystallization from ether – light petroleum (60–80°), the colorless needles had m.p. and mixed m.p. 144°–146° with authentic 2,3,4-tri-*O*-methyl-*N*-phenyl-D-glucosylamine. Anal. Calc. for $C_{15}H_{23}O_5N$: OMe, 31.3%. Found: OMe, 30.9%.

The di-*O*-methyl hexose (202 mg), having $[\alpha]_D$ +54° (*c*, 2.0 in water), was refluxed for 3 hours with *p*-nitroaniline (164 mg) in ethanol (5.5 ml) and acetic acid (5 drops). The reaction mixture was concentrated to a smaller volume and cooled to 5°. The light-brown precipitate was washed with ethanol and recrystallized as pale yellow crystals from ethyl acetate, m.p. 251°, $[\alpha]_D^{24}$ −250° (*c*, 0.38 in pyridine). Anal. Calc. for $C_{14}H_{20}O_7N_2$: OMe, 18.9%. Found: OMe, 19.9%. 2,4-Di-*O*-methyl-*N*-*p*-nitrophenyl-D-glucosylamine has m.p. 250°–251° $[\alpha]_D$ −252° (pyridine) (11).

The di-*O*-methyl methyl fructofuranoside was hydrolyzed (0.05 *N* H_2SO_4; 2 hours; 100°) to yield di-*O*-methyl-D-fructose (0.57 g), $[\alpha]_D$ −45° (*c*, 2.64 in water). Anal. Calc. for $C_8H_{16}O_6$: OMe, 29.7%. Found: OMe, 28.3%. Di-*O*-methyl fructose (160 mg) in 1.15 *M* periodic acid (5 ml) was kept at 25° for 3 days. The solution was freed from iodine by extraction with carbon tetrachloride. Barium chloride (0.5 g) and excess barium carbonate were added, and after filtration, enough bromine was added to give a saturated solution. After 2 days, excess bromine was removed by aeration, hydrobromic acid by lead carbonate, and lead ions with hydrogen sulphide. The solution was filtered and the filtrate was concentrated to a solid which was then refluxed overnight with 4% methanolic hydrogen chloride. Excess hydrogen chloride was removed with lead carbonate, as above, and the filtrate was concentrated to a solid. Chloroform extraction of the solid and

Can. J. Chem. Downloaded from www.nrcresearchpress.com by 190.90.36.8 on 09/04/12
For personal use only.

subsequent evaporation of the solvent yielded a sirup (40 mg) which was dissolved in methanolic ammonia (3 ml) and kept at 0°. After 6 days, white crystals (15 mg) of (−)-D-di-methoxysuccinamide were deposited, $[\alpha]_D$ −94° (*c*, 0.60 in water), m.p. and mixed m.p. 275° (capillary tube) with authentic (−)-D-dimethoxysuccinamide. The compound showed maxima in the infrared at 3330 (s), 3150 (s), 2910 (w), 1637 (s), 1425 (s), 1341 (m), 1314 (w), 1210 (m), 1193 (m), 1139 (m), 1100 (s), 1023 (m), 881 (m), 825 (w), 805 (m), 705 (m) cm^{-1} and gave an identical infrared spectrum to authentic (−)-D-dimethoxysuccinamide.

Reaction of Sodium Iodide with Tri-O-tosyl Sucrose

Tri-*O*-tosyl sucrose pentaacetate (2.0 g) was heated at 110° for 2 hours with sodium iodide (5 g) in acetone (5 ml). The reaction mixture was poured into chloroform and after filtration was washed well with water containing sodium thiosulphate (5%) and sodium hydrogen carbonate (5%). After drying ($CaCl_2$), concentration of the chloroform extract gave sirupy mono-*O*-tosyl-di-iodo-di-deoxy sucrose pentaacetate (1.7 g) $[\alpha]_D^{19}$ +40° (*c*, 3.8 in chloroform). Anal. Calc. for $C_{39}H_{36}O_{16}I_2S$: I, 26.5%. Found: I, 24.9%.

Reduction of Tri-O-tosyl Sucrose

Tri-*O*-tosyl sucrose was reduced (10 hours) with $LiAlH_4$ at the boiling point of tetrahydrofuran. Following destruction of excess hydride with moist ethyl acetate and deionization of the solution with ion-exchange resin, 6,6^1-dideoxy sucrose was isolated as a chromatographically homogeneous, crisp solid (R_f 0.32), $[\alpha]_D^{19}$ +49.7° (*c*, 1.27 in water). Anal. Calc. for $C_{12}H_{22}O_9$: CMe, 9.7%. Found: CMe, 9.2%.

Dideoxy sucrose was completely hydrolyzed by invertase (48 hours) to give two compounds which cochromatographed with authentic rhamnoketose and 6-deoxy glucose.

ACKNOWLEDGMENT

The authors wish to thank the Sugar Research Foundation, Inc., for a grant.

REFERENCES

1. HOCKETT, R. C. and ZIEF, M. J. Am. Chem. Soc. **72**, 1839 (1950).
2. TIPSON, R. S. *In* Advances in carbohydrate chemistry. Vol. 8. Academic Press, Inc., New York. 1953.
3. KUHN, R., LOW, I., and TRISCHMANN, H. Ber. **88**, 1492 (1955).
4. HIRST, E. L., MITCHELL, W. E. A., PERCIVAL, E. E., and PERCIVAL, E. G. V. J. Chem. Soc. 3170 (1953).
5. ARNI, P. C. and PERCIVAL, E. G. V. J. Chem. Soc. 1822 (1951).
6. LEMIEUX, R. U. and BARRETTE, J. P. J. Am. Chem. Soc. **80**, 2243 (1958).
7. MCKEOWN, G. G., SERENIUS, R. S. E., and HAYWARD, L. D. Can. J. Chem. **35**, 28 (1957).
8. FINKELSTEIN, F. Ber. **43**, 1528 (1910).
9. SUGIHARA, J. M. *In* Advances in carbohydrate chemistry. Vol. 8. Academic Press, Inc., New York. 1953.
10. HOUGH, L., JONES, J. K. N., and WADMAN, W. H. J. Chem. Soc. 796 (1952).
11. VAN CLEVE, J. W. and SCHAFFER, W. C. J. Am. Chem. Soc. **77**, 5341 (1955).

Can. J. Chem. Downloaded from www.nrcresearchpress.com by 190.90.36.8 on 09/04/12
For personal use only.

Can. J. Chem. Downloaded from www.nrcresearchpress.com by 190.90.36.8 on 09/04/12
For personal use only.

MASS SPECTROMETRIC STUDY OF THE REACTIONS OF SOME HYDROCARBONS WITH ACTIVE NITROGEN[1]

JOHN T. HERRON, J. L. FRANKLIN,[2] AND PAUL BRADT

ABSTRACT

The reactions of active nitrogen with acetylene, ethylene, and propylene have been studied in a flow system using a mass spectrometer to analyze the products continuously. Certain features of the mass spectra of the products can be explained on the basis of cyano radical replacement reactions.

Winkler and his co-workers have studied the reactions of active nitrogen with acetylene (1), ethylene (2), and propylene (3), in addition to a large number of other compounds (4). The major product containing nitrogen, aside from small amounts of cyanogen, was HCN. In the case of the acetylene reaction an additional product was found in the form of a polymer, containing about 32% nitrogen.

We have made a mass spectrometric study of these reactions, using a flow system. The nitrogen atoms were produced by passing a stream of nitrogen gas at from 1 to 5 mm pressure through a 2450 Mc electrodeless discharge. The atom concentration as measured by gas titration with NO (5) was of the order of 2 mole %. The reactor was made of 10-mm i.d. glass tubing. Hydrocarbons were added to the system through an inlet located about 20 cm ahead of a small glass leak through which the gas stream was continuously sampled and analyzed by a mass spectrometer. With linear flow rates of the order of 1 meter/second, the time for the gas to pass from the hydrocarbon gas inlet to the sampling leak was about 0.02 second.

This type of experimental arrangement does not permit observation of any but very long-lived free radicals. Since the reaction flames themselves extended only a few centimeters from the reactant inlet, it seems reasonably certain that our analytical results refer only to stable products.

In general our results are very similar to those of Winkler and co-workers. However, several new features were observed. For acetylene we found the major product to be HCN, along with smaller amounts of $(CN)_2$, as indicated by their peaks at m/e 27 and

TABLE I

Observed mass spectra

Reactant, m/e	C_2H_2	C_3H_4	C_2H_4	C_3H_6
50	22	100	30	100
51	100	380	100	270
53	—	—	100	370
62	—	—	—	—
63	—	34	—	40
64	—	74	—	70
65	—	100	—	70
66	—	—	—	40
67	—	—	—	100

[1]*Manuscript received November 10, 1958.*
Contribution from the Mass Spectrometry Section, National Bureau of Standards, U.S. Department of Commerce, Washington, D.C. This research was performed under the National Bureau of Standards' Free Radical Research Program, supported by the Department of the Army.
[2]*Guest Scientist on leave from Humble Oil and Refining Company. Present address: Humble Oil and Refining Company, Baytown, Texas.*

52 respectively. In addition, however, there were peaks at m/e 50 and 51, but no peaks at higher masses. Similarly, for methyl acetylene, there were peaks at m/e 50, 51, and m/e 63, 64, 65, but again none at higher masses. The relative magnitudes of the ion currents are shown in Table I. The m/e 52 peak has been omitted.

In the case of the acetylene reaction, the absence of peaks at masses greater than m/e 52 (C_2N_2) makes it difficult to conceive of the m/e 51 peak being due to anything other than C_3HN which we feel certain is cyanoacetylene. The mass 50 peak is probably C_2CN^+ from C_2HCN. It is not diacetylene, since other peaks from the mass spectrum of diacetylene were absent.

Similarly the mass 65 peak probably corresponds to the methyl cyanoacetylene ion, $CH_3C_2CN^+$, the ions of mass 64 and 63 would represent the loss of one and two hydrogens from the parent molecule. Of course, the peaks at 63, 64, 65 could also be attributed to propargyl cyanide, though we think this less likely.

It is difficult to account for these products other than through direct replacement of a hydrogen by a cyano radical. Since diacetylene is not found in either reaction, it seems certain that the C_2H radical does not play an important part. Hence we cannot account for the cyanoacetylene as resulting from the reaction

$$CN + C_2H \rightarrow C_2HCN.$$

Furthermore, the methylacetylene reaction leads to the formation of considerably more cyanoacetylene than methyl cyanoacetylene as is shown in Table II. The absence of a peak at m/e 78 in the products of reaction with methylacetylene shows that the C_3H_3 radical probably plays very little part in the reaction and thus suggests that recombination of this radical with CN is not responsible for the C_3H_3CN observed.

TABLE II

Per cent of N in products for typical experiments

Product reactant	NH_3	HCN	C_3HN	C_2N_2	C_3H_3N	C_4H_3N	C_4H_5N
C_2H_2	13	62	7	18			
C_3H_4	6	75	6	12	?	1	
C_2H_4	<1	97	<1	2	<1		
C_3H_6	?	>78	<4	12	5		1

We consider the most plausible set of reactions to be:

$$CN + C_2H_2 \rightarrow C_2HCN + H \qquad \Delta H^* = -12$$
$$CN + CH_3C_2H \rightarrow C_2HCN + CH_3 \qquad \Delta H = -22$$
$$\rightarrow CH_3C_2CN + H \qquad \Delta H = -12$$
$$\rightarrow CH_2CNC_2H + H \qquad \Delta H = -7$$

Table II gives the per cent of the total nitrogen in each product. The actual numerical values are necessarily somewhat crude, inasmuch as we had no way of determining the relative sensitivities of the various products. In addition the formation of brown deposits on the walls of the reactor largely negates any attempt at exact analyses.

Nevertheless, it can be seen that the proportion of products containing the cyano radical is quite high, i.e. of the order of 25%. This would seem to argue that the cyano radical plays a rather important part in these reactions. It is interesting to note that

*Kcal/mole, estimated from group equivalent values (ref. 6).

Can. J. Chem. Downloaded from www.nrcresearchpress.com by 190.90.36.8 on 09/04/12
For personal use only.

in the case of the acetylene reaction, as the flow rate of acetylene is increased, the amount of cyanogen increases quite steeply, and then falls off again as conditions approach complete consumption of the active nitrogen (1). The cyanogen is presumably produced by the recombination of CN radicals.

With the olefins studied, the major product containing nitrogen was again HCN, which accounted for 97% of the nitrogen in the ethylene reaction, and more than 78% in the propylene reaction. The later reaction also yielded appreciable amounts of cyanogen.

Although the mass spectra over the range of masses 50–70 show several interesting features, it would be unwise to draw overly firm conclusions from them, since the peaks are quite small. The spectra are shown in Table I.

With ethylene the largest peaks were at masses 51, 52, and 53 with a series of smaller peaks extending to mass 56. The peak at mass 52 can be attributed at least in part to cyanogen, while that at mass 53 can be attributed to C_3H_3N, which could be cyanoethylene. The peaks at 50, 51 may be due in part to cyanoacetylene, since acetylene is a product of this reaction (2). As can be seen from Table II the proportion of nitrogen in products other than HCN is very small.

In the case of propylene, however, this may not be the case. Propylene gave a series of peaks from masses 50 to 58, and from 63 to 67, the two largest being at 52 and 53. The series at 63 to 67 is probably due to C_4H_5N, which may be either propenyl cyanide, isopropenyl cyanide, allyl cyanide, or a mixture of them. The peak at mass 53 may be cyanoethylene.

By analogy with the corresponding acetylene reactions, the following reactions can be written to describe the olefin reactions:

$$\begin{aligned}
CN + C_2H_4 &\rightarrow C_2H_3CN + H && \Delta H \text{ (ref. 6)} = -10\\
CN + CH_3C_2H_3 &\rightarrow C_2H_3CN + CH_3 && \Delta H = -22\\
&\rightarrow CH_3C(CN)CH_2 + H && \Delta H = -11\\
&\rightarrow CH_3C_2H_2CN + H && \Delta H = -8\\
&\rightarrow CH_2(CN)CHCH_2 + H && \Delta H = -7
\end{aligned}$$

Unfortunately, we were unable to obtain samples of pure cyanoacetylene or methyl cyanoacetylene in order to compare mass spectra. We have obtained the mass spectra of the three possible C_4H_5N products. They are very similar, and have approximately the spectra m/e 67:66:65:64:63; 100:35:6:20:7. In view of the presence of a large m/e 53 peak, the discrepancy in the spectra from m/e 65 to 63 may be due to the presence of a C_3H_4 component.

It is of interest that ammonia was produced in the reactions with both acetylenes and with ethylene,* although it was not detected in the propylene reaction (Table II). Very approximately, the amount of ammonia produced increased with the proportion of cyano containing products. We are unable to propose a mechanism for this formation of ammonia. It might come about by successive recombination of N atoms, which are relatively abundant, with H atoms, but this is purely speculative.

The complete mechanism for the reaction of N atoms with the lower acetylenes and olefins is certainly very complex and we have made no effort to determine it. We do think that the evidence points to the importance of the CN radical in the reaction and strongly suggests that it forms several important products by displacement reactions at one of the carbons of the double or triple bond.

**In agreement with an earlier observation on the ethylene reaction by J. T. Herron and H. I. Schiff (1955, unpublished).*

Can. J. Chem. Downloaded from www.nrcresearchpress.com by 190.90.36.8 on 09/04/12
For personal use only.

REFERENCES

1. VERSTEEG, J. and WINKLER, C. A. Can. J. Chem. **31**, 129 (1953).
2. VERSTEEG, J. and WINKLER, C. A. Can. J. Chem. **31**, 1 (1953).
3. TRICK, G. S. and WINKLER, C. A. Can. J. Chem. **30**, 915 (1952).
4. EVANS, H. G. V., FREEMAN, G. R., and WINKLER, C. A. Can. J. Chem. **34**, 1271 (1956).
5. HERRON, J. T., FRANKLIN, J. L., DIBELER, V. H., and BRADT, P. J. Chem. Phys. **29**, 230 (1958).
6. FRANKLIN, J. L. Ind. Eng. Chem. **41**, 1070 (1949).

Can. J. Chem. Downloaded from www.nrcresearchpress.com by 190.90.36.8 on 09/04/12
For personal use only.

Can. J. Chem. Downloaded from www.nrcresearchpress.com by 190.90.36.8 on 09/04/12
For personal use only.

THE METAL-CATALYZED DECOMPOSITION OF NITROUS OXIDE (I). DECOMPOSITION ON PURE SILVER, SILVER–GOLD, AND SILVER–CALCIUM ALLOYS[1]

KENNETH E. HAYES[2]

ABSTRACT

The decomposition of nitrous oxide on silver, a silver – 1.14% gold alloy, and a series of silver–calcium alloys has been studied. On all of these catalysts the *initial rate* of decomposition is proportional to the nitrous oxide pressure. The activation energy for pure metals, including platinum and gold, is proportional to the work function. For the silver–calcium alloys the activation energy falls rapidly with increasing calcium content, suggesting that the work function of these alloys falls with increasing calcium content.

INTRODUCTION

This investigation was undertaken as part of a larger program concerned with the silver-catalyzed oxidation of ethylene. For many years this laboratory has been interested in the direct oxidation of ethylene to ethylene oxide using silver–calcium alloys as catalysts (1, 2). However, although a great amount of work has been reported in this field, certain ambiguities remain. It was hoped that the investigation of a comparatively simple reaction, such as the decomposition of nitrous oxide, would prove fruitful in establishing an unequivocal mechanism of the silver-catalyzed oxidation of ethylene.

Although the catalytic decomposition of nitrous oxide by semiconductors has claimed the attention of many workers, comparatively little has been done with metallic catalysts. To date the only metals to have been investigated are platinum (3), gold (4), silver (5), and nickel (6), and even for these, activation energies have been reported only for the first two.

The investigation of Suhrmann (7) on the effect of nitrous oxide on the resistance of transparent nickel films (8) and on the photoelectric emission of platinum surfaces (9) shows that nitrous oxide is probably chemisorbed on metals as N_2O^-, the rate determining step in the decomposition then being the adsorption of nitrous oxide, followed by a fast thermal dissociation of nitrogen from the adsorption complex. If this is correct, then the activation energy for the decomposition should be proportional to the work function of the catalyst.

EXPERIMENTAL

Apparatus

The apparatus used was a conventional high-vacuum system. The reactor was a wire wound Pyrex glass tube, 35 mm O.D. and approximately 30 cm long. At one end of this tube was a 29/42 female standard taper joint, for ease in changing catalysts; the matching male joint had a 6-mm thermocouple well running through the center, this tube ending in the center of the reactor, and bent at such an angle so as to be within the catalyst mass when the catalyst was installed. An all-glass centrifugal circulating pump, a 1-liter ballast flask, and a mercury manometer completed the reactor circuit. U-tubes filled with silver turnings were inserted between the reactor and the manometer, and also

[1]*Manuscript received September 15, 1958.*
Contribution from the Division of Applied Chemistry, National Research Council, Ottawa, Canada.
Issued as N.R.C. No. 5060.
[2]*National Research Council Postdoctoral Fellow 1954–56. Assistant Research Officer 1956–58. Present address: Chemistry Department, Dalhousie University, Halifax, N.S.*

between the reactor and inlet to the vacuum system, to prevent contamination of the catalysts by mercury. The temperature of the reactor was held to within ±2° C by a Bristol controller. Catalyst powders were contained in a Pyrex glass boat placed in the center of the reactor. When foils were used as catalysts these were wrapped around the center thermocouple well.

Nitrous Oxide

The nitrous oxide was supplied by the Matheson Company and had a nominal purity of 98%. It was purified in the conventional manner by a triple sublimation/distillation, always discarding the first and last fractions.

The Catalyst

1. The pure silver catalyst was prepared as a foil (10 feet×0.625 in.×0.002 in.) from a vacuum melted, chill cast ingot, the silver had been purified by a triple-electrolysis of Mint-Grade silver, and had a purity of 99.998% as found by spectrographic analysis. This catalyst weighed 37.000 g.

2. The silver–gold alloy foil was prepared in a similar manner to the pure silver foil, i.e. the metals were melted together in a small induction furnace, chill cast under vacuum, and rolled. The gold, which again had been purified by repeated electrolysis, analyzed as 99.9995% Au. The foil contained 1.14% Au. The catalyst was of the same thickness and width as for No. 1, two lengths were used in the experiments to give weights of 28.500 and 40.000 g.

3. The silver–calcium alloys were prepared from an 8.5% calcium in silver master alloy. Some 50–60 g of 60–200 mesh alloy were held in steam at from 200–350° C for from 1–8 hours. After cooling, the alloy was then subjected to the following leaching schedule: (*a*) soak in cold 20% acetic acid for 10 minutes, (*b*) wash well in distilled water, (*c*) repeat (*a*), (*d*) repeat (*b*), (*e*) boil in 20% acetic acid for 30 minutes, (*f*) repeat (*b*), (*g*) boil in 20% acetic acid for 60 minutes, (*h*) repeat (*b*), (*i*) boil in distilled water for 30 minutes, (*j*) drain and dry, resieve the catalyst, retaining only the 60–200 mesh size, and send sample to analysis. By varying the temperature of the steam, and/or the steaming time, a series of catalysts was prepared with residual calcium contents varying from 0.11% to 1.70%.

Experimental Technique

A sample of the catalyst powder was weighed out accurately and put into the reactor as described, the reactor was closed, using a sulphur-free mass-spectrometer wax[3] to seal the 29/42 joint together, the necessary glass blowing was then done, and the catalyst evacuated, by mercury pump, at 500° C for 19–20 hours. This treatment was sufficient to remove any adsorbed gases, such as water, oxygen, or carbon dioxide that had been picked up during storage. Experiments were always performed to check on the reaction kinetics before the activation energy runs, by making observations at constant temperature and different initial pressures. Activation energy runs were always made using the bracketing technique.

RESULTS AND DISCUSSION

For all of the catalysts studied, the *initial rate* law is given by:

$$[1] \qquad \frac{-dP_{N_2O}}{dt} = kP_{N_2O}.$$

[3]*Manufactured by Robert R. Austin, Box 374E, Pasadena 8, California, U.S.A.*

Can. J. Chem. Downloaded from www.nrcresearchpress.com by 190.90.36.8 on 09/04/12
For personal use only.

This is illustrated in Fig. 1, which gives typical results for a plot of initial rate (cm/min) against initial nitrous oxide pressure. Steacie and Folkins (5) have shown that, on silver catalysts, the over-all rate of the decomposition is given by:

$$[2] \qquad \frac{-dP_{N_2O}}{dt} = \frac{kP_{N_2O}}{1+bP_{O_2}},$$

the integrated form of [2] is:

$$[3] \qquad k = \frac{(1+ab)}{t} \ln [a/(a-x)] - \frac{bx}{t},$$

where a is the initial nitrous oxide pressure and x is the amount of nitrous oxide that has reacted after time t. Following Steacie and Folkins we may write

$$\frac{1}{t} \ln \frac{a}{(a-x)} = K_m,$$

and $x/t = V$. A plot of K_m against V will then give a straight line if equation [2] is correct. Although this investigation deals in the main with initial rates, an indication that equation [2] is correct is illustrated in Figs. 2 and 3, which give the raw data for the decomposition on pure silver foil at 793° K and the K_m–V plot for the same data. The fall from linearity of the last points for the low pressure experiment is probably due to the reaction becoming diffusion controlled, the extent of reaction having taken place exceeding 95%.

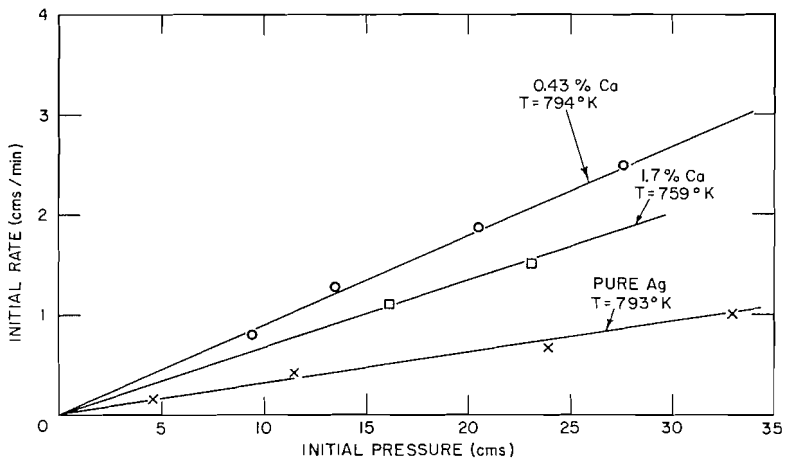

FIG. 1. Dependence of initial rate on N_2O pressure.

In Fig. 4 a plot of $-\log k$ against $1/T$ is given (where k is the initial rate constant per gram of catalyst) for most of the catalysts that were used. Not all of the results are shown for the sake of clarity. The values of the activation energies were obtained by the method of Least Mean Squares, which gave at the same time the values of the logarithm of the pre-exponential factor, A.

In Fig. 5, a composite plot of activation energy against work function, and activation energy against calcium content in silver, is shown. The activation energies obtained by Hinschelwood and Pritchard for platinum and gold are included for completeness. The point for Ag – 1.14% Au is placed on the E–ϕ line quite arbitrarily, being defined solely by the value of E.

Can. J. Chem. Downloaded from www.nrcresearchpress.com by 190.90.36.8 on 09/04/12
For personal use only.

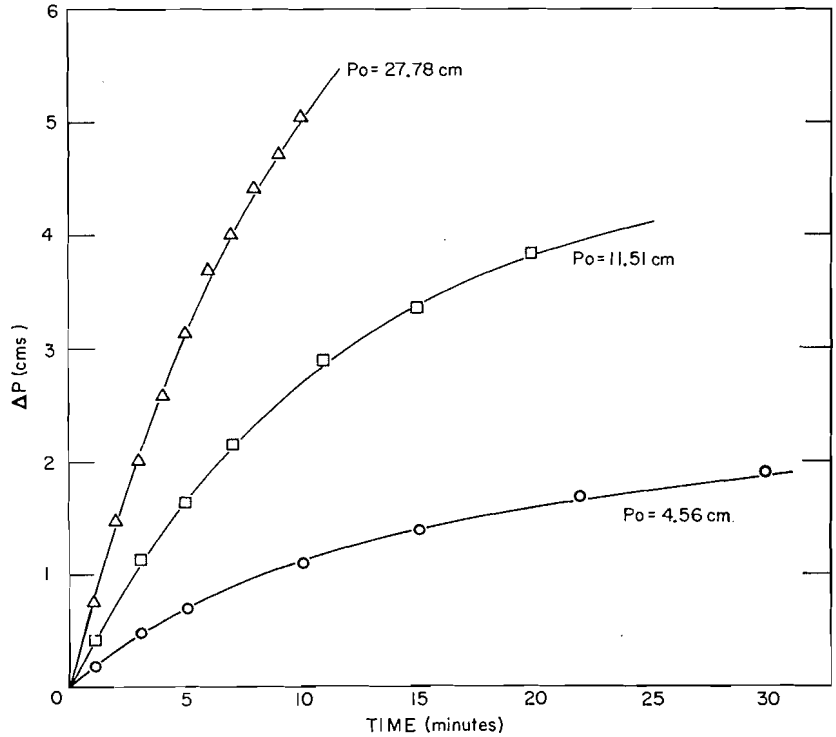

FIG. 2. Decomposition of N_2O on pure Ag at 793° K.

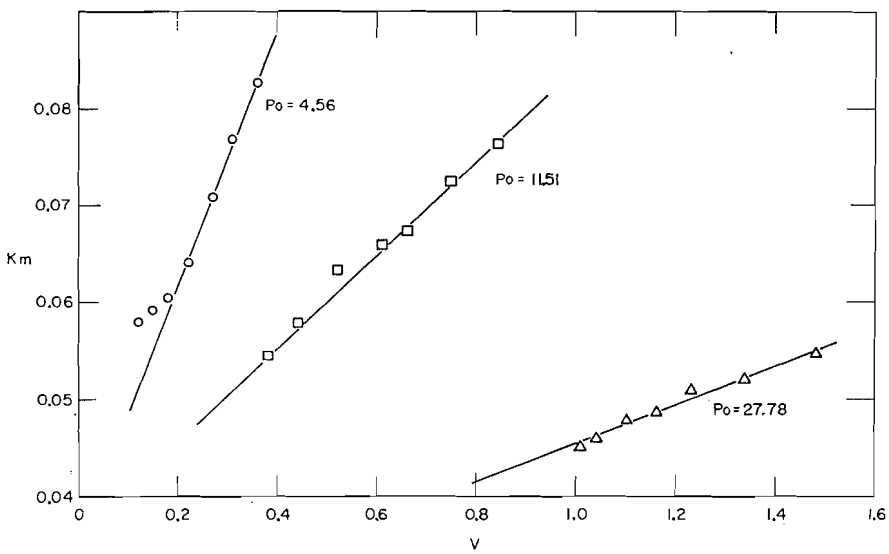

FIG. 3. The data of Fig. 2, plotted according to equation [3].

Can. J. Chem. Downloaded from www.nrcresearchpress.com by 190.90.36.8 on 09/04/12
For personal use only.

Can. J. Chem. Downloaded from www.nrcresearchpress.com by 190.90.36.8 on 09/04/12
For personal use only.

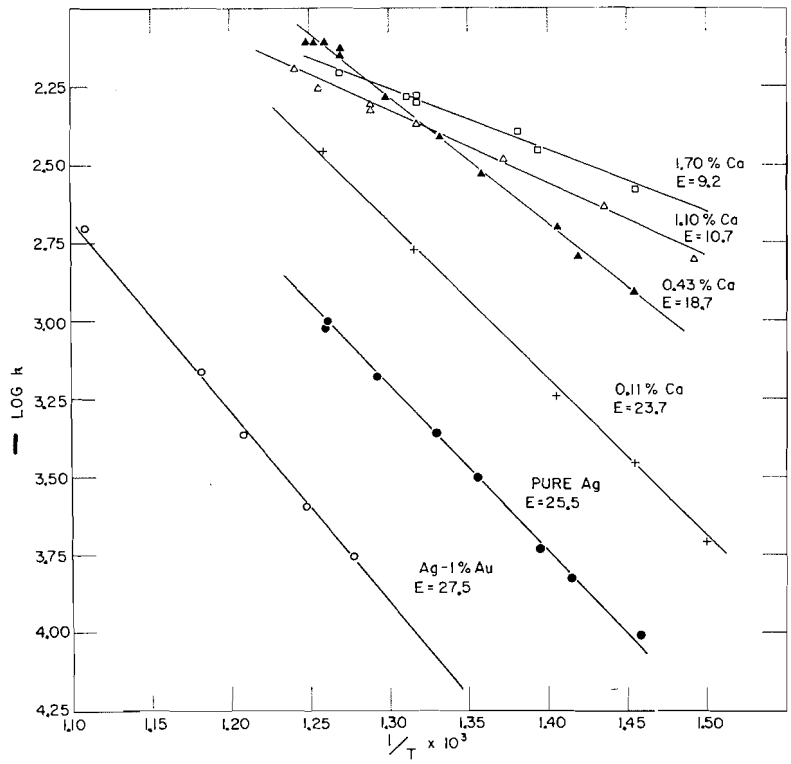

FIG. 4. Arrhenius plot for the various catalysts.

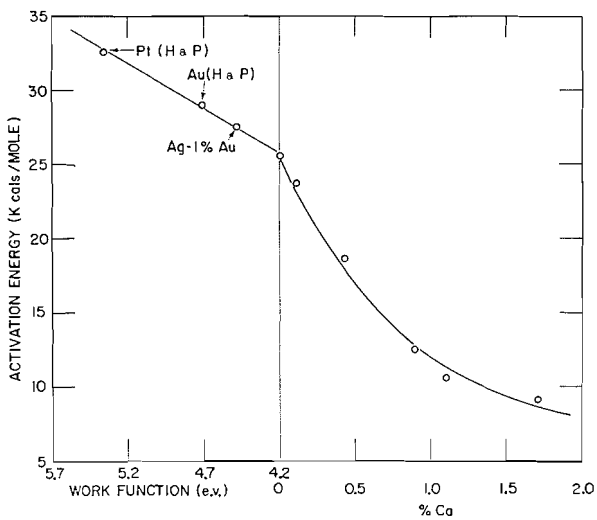

FIG. 5. The relationship between activation energy and work function for pure metals, and between activation energy and calcium content for Ca–Ag alloys.

From the linear relationship between E and ϕ it may be concluded that the rate determining step in the decomposition involves an electron transfer from the catalyst to the adsorbed gas. In this case, there are two possible mechanisms: (1) that the rate determining step is the adsorption of N_2O as N_2O^-,

$$N_2O + e \overset{\text{r.d.s.}}{\rightleftharpoons} N_2O^- \qquad [4a]$$

$$N_2O^- \underset{\text{fast}}{\longrightarrow} N_2 + O^- \qquad [4b]$$

or (2) that the r.d.s. is the dissociative chemisorption of nitrous oxide

$$e + N_2O \overset{\text{r.d.s.}}{\longrightarrow} N_2 + O^-. \qquad [5]$$

Although the present work is unable to distinguish between these two mechanisms, it is clear that the removal of adsorbed oxygen, either by the reaction between two adsorbed O^- ions, or between O^- and gaseous N_2O, cannot be the rate determining step, as either of these two reactions involves the donation of electrons back to the catalyst. Such a requirement would lead to the expectation of finding that the activation energy decreased with increasing work function, in opposition to the observed facts. It is hoped that a projected study of the adsorption characteristics of nitrous oxide on these catalysts, together with a detailed examination of the over-all reaction rate will be able to settle the mechanism of the reaction more definitely.

From Fig. 4 and the right-hand side of Fig. 5, it is seen that residual calcium has a marked effect both on the specific activity of the catalysts and on the activation energy. On the basic postulate that the activation energy is proportional to the work function, it is apparent from Fig. 5 that the role of calcium in the Ca–Ag alloys is to lower the work function, and hence enhance the N_2O decomposition. In view of the well-known role of alkaline earths in governing emission from oxide covered cathodes (10), this result is not surprising.

Figure 6 shows the compensation effect that was obtained with the Ag–Ca alloys. A possible explanation for this effect is that these alloys are truly heterogeneous, even on the macroscale. The values of Ca % of Fig. 5 refer to catalyst samples of 60–200 mesh, and for several samples of the same catalyst the Ca analysis was reproducible to 1% or better. However, an analysis of various mesh sizes for the same catalyst showed that the calcium content was strongly dependent on the degree of subdivision of the catalyst.

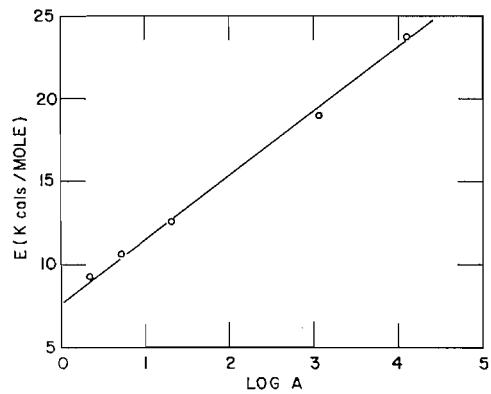

FIG. 6. The compensation effect for Ca–Ag alloys.

Can. J. Chem. Downloaded from www.nrcresearchpress.com by 190.90.36.8 on 09/04/12
For personal use only.

Three samples of one catalyst gave the following result: (1) average mesh size 80, Ca % = 0.69; (2) A.M.S. 100, Ca % = 0.53; (3) A.M.S. 150, Ca % = 0.22. It therefore follows that the activation energies found for the Ag–Ca alloys are probably only approximations, good over only a small temperature range; more detailed and accurate values of k extending over a much larger temperature range might be expected to produce log $k - 1/T$ plots with definite curvatures.

ACKNOWLEDGMENTS

The author is indebted to Drs. W. A. Alexander and W. G. Henry of the Metallurgy Section for assistance in the catalyst preparation.

REFERENCES

1. CAMBRON, A. and MCKIM, F. L. W. U. S. Patent No. 2,562,857 (1951); Can. Patent No. 475,366 (1951).
2. ORZECHOWSKI, A. and MACCORMACK, K. E. Can. J. Chem. **32**, 388, 415, 432, 443 (1954).
3. HINSHELWOOD, C. N. and PRICHARD, C. R. J. Chem. Soc. **127**, 327 (1925).
4. HINSHELWOOD, C. N. and PRICHARD, C. R. Proc. Roy. Soc. (London), A, **108**, 211 (1925).
5. STEACIE, E. W. R. and FOLKINS, H. O. Can. J. Research, B, **15**, 237 (1937).
6. HEDVALL, J. A., HEDIN, R., and PERSSON, O. Z. physik. Chem. B, **27**, 196 (1934).
7. ADVANCES IN CATALYSIS. Vol. VII. Academic Press Inc., New York. 1955. p. 303 ff.
8. SUHRMANN, R. and SCHULZ, K. Z. physik. Chem. (N.F.) **1**, 69 (1954).
9. SUHRMANN, R. and SACHTLOS, W. Z. Naturforsch. **9a**, 14 (1954).
10. BOER, J. H. DE. Electron emission and adsorption phenomena. Cambridge University Press, London. 1935. p. 339 ff.

Can. J. Chem. Downloaded from www.nrcresearchpress.com by 190.90.36.8 on 09/04/12
For personal use only.

Can. J. Chem. Downloaded from www.nrcresearchpress.com by 190.90.36.8 on 09/04/12
For personal use only.

THE BROMINATION OF URACIL AND THYMINE DERIVATIVES[1]

A. M. MOORE[2] AND SHENA M. ANDERSON[2]

ABSTRACT

The bromination of 1,3-dimethyluracil, uracil, and thymine and of the nucleosides and nucleotides of the latter two compounds has been followed potentiometrically and spectrophotometrically. The results indicate that all the compounds except uracil react initially with 1 mole of bromine to form 5-bromo-6-hydroxy-hydropyrimidine derivatives. If the resulting compound still has a hydrogen at position 5 it may undergo dehydration on heating or with acid catalysis to form the corresponding 5-bromopyrimidine, which is then capable of further reaction with bromine. Uracil itself appears first to undergo substitution to 5-bromouracil, and then both the uracil and 5-bromouracil are brominated together to yield ultimately 5,5-dibromo-6-hydroxyhydrouracil.

INTRODUCTION

The study of the chemical changes induced by ultraviolet light in the uracil and cytosine components of nucleic acids has led to the recognition that the initial products of reaction in aqueous systems belong to the class of 6-hydroxy-hydropyrimidines (8, 9, 10, 12). This finding has led, in turn, to new interest in the 5-bromo-6-hydroxyhydrouracils and related compounds both as intermediates in the synthesis of the irradiation products and as chemical analogues of such products.

A recent report by Wang (11) has shed a good deal of light on the bromination reactions of uracil and 1,3-dimethyluracil. Our own studies reported here have included these compounds but have also been extended to the nucleosides and nucleotides of uracil and thymine.

EXPERIMENTAL

The spectrophotometric measurements were made with a Beckman Model DK2 Recording Spectrophotometer. Except where otherwise noted the spectroscopic changes during bromination were determined by adding 10^{-2} M bromine water a few microliters at a time to 10^{-4} M pyrimidine solutions. The small dilution involved has been neglected.

For the potentiometric titrations a platinum and a saturated calomel electrode were used in conjunction with a Leeds and Northrup Student Potentiometer in the earlier experiments, and with a Radiometer Titrator in the later ones. A small beaker equipped with a magnetic stirrer and held at room temperature (22–24° C) was charged with a measured volume of 10^{-2} M solution of the pyrimidine compound in acetate buffer and, with continuous rapid stirring, the potential was measured after successive additions of standard bromine water (approximately 10^{-2} M). The bromine was dispensed from a small automatic burette with blackened reservoir. To minimize the effect of a rather rapid initial drift in potential the measurements were all made 1 minute after each addition of bromine. Corresponding measurements using the same volume of buffer in place of the pyrimidine solution were used to determine a blank correction.

The uracil, uridine, uridylic acid, and thymine were obtained from Nutritional Biochemicals Corp., the thymidine from California Biochemical Research Corp. The uracil was recrystallized twice from water and dried at room temperature *in vacuo*. 1,3-Dimethyluracil was prepared from it by the method of Davidson and Baudisch (2) and was

[1]*Manuscript received December 5, 1958.*
Contribution from Atomic Energy of Canada Limited, Chalk River, Ontario.
Issued as A.E.C.L. No. 761.
[2]*Biology Division, Atomic Energy of Canada Limited.*

recrystallized from 95% ethanol (m.p. 122° C; ϵ = 8600 at 266 mμ). The rest of the compounds were used as received after checking that the molecular extinctions and other characteristics of their absorption spectra were in satisfactory agreement with published values (1).

RESULTS

1,3-Dimethyluracil

Potentiometric titration (Fig. 1) indicated that any excess bromine beyond 1 mole per mole of dimethyluracil remained in solution as free bromine. This finding was supported by the spectrophotometric measurements (Fig. 2) which demonstrated that 1 mole of bromine was sufficient to eliminate completely the absorption band at 266 mμ. The absorption curves throughout the reaction exhibited isosbestic points at 215 and 245 mμ, thus pointing to a quantitative conversion of 1,3-dimethyluracil to 5-bromo-6-hydroxy-1,3-dimethyluracil. If, after the addition of 1 mole of bromine, the solution was heated at 100° C or if it was acidified to pH 1 (HCl) the spectrum underwent further progressive change, with a new isosbestic point at 254 mμ, to yield finally and quantitatively 5-bromo-1,3-dimethyluracil (ϵ_{max} = 8000 at 283 mμ; ϵ_{min} = 1290 at 245 mμ; m.p. 181° C) (cf. curve 5, Fig. 2).

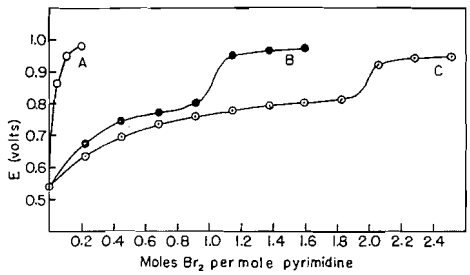

FIG. 1. Potentiometric titrations with bromine water (0.01 *M*). The pyrimidines (0.01 *M*) were dissolved in 0.1 *M* acetate buffer, pH 4.76. A—Buffer blank; B—1,3-dimethyluracil; C—uracil.

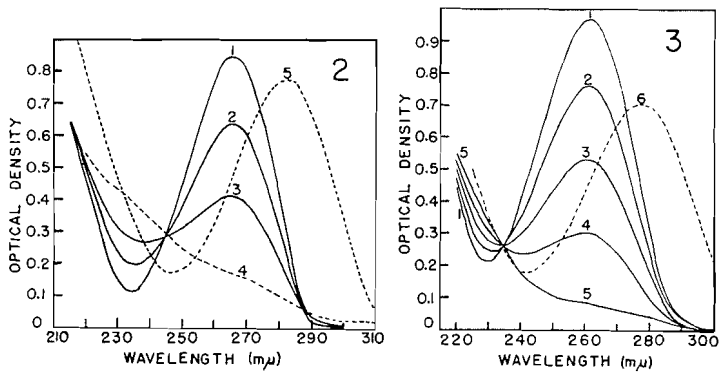

FIG. 2. Bromination of 1,3-dimethyluracil (10^{-4} *M*; in water). Curves 1–4 respectively represent spectra obtained after adding zero, 0.27, 0.54, and 0.98 moles of Br_2 per mole of 1,3-dimethyluracil. Curve 5 is the spectrum obtained upon adding 1 molecular equivalent of bromine and heating for 15 minutes at 100° C after acidification to pH 1 with concentrated HCl.

FIG. 3. Bromination of uridylic acid (10^{-4} *M*; in water). Curves 1–5 respectively represent spectra obtained after adding zero, 0.25, 0.50, 0.75, and 1.0 mole of Br_2 per mole of uridylic acid. Curve 6 shows the result of adding 1 molecular equivalent of Br_2 and then heating for 10 minutes at 100° C before reading the spectrum.

Can. J. Chem. Downloaded from www.nrcresearchpress.com by 190.90.36.8 on 09/04/12
For personal use only.

Can. J. Chem. Downloaded from www.nrcresearchpress.com by 190.90.36.8 on 09/04/12
For personal use only.

Uridine and Uridylic Acid

These behaved similarly and will be considered together. Both compounds lost their 262 mμ absorption band on addition of 1 molecular equivalent of bromine, the transformation exhibiting isosbestic points at 234 and 291 mμ in both cases. An experiment with uridylic acid is illustrated in Fig. 3.

To follow the titration of these compounds with bromine two procedures were employed. At a concentration of 10^{-4} *M* the optical density at 260 mμ was found to decrease linearly with the amount of added bromine to a limiting value corresponding to the absorbance of the product; thereafter the density remained constant. The limiting density was reached in the case of uridine at 0.97 and in the case of uridylic acid at 0.99 moles of bromine per mole of pyrimidine.

In the second procedure, by using concentrations of the order of 10^{-3} *M* for both the bromine and the pyrimidines it was possible to observe the appearance of the absorption band at 390 mμ due to free bromine when the end point was reached. At this wavelength the optical density was constant (nearly zero) up to the end point and then rose rapidly as extra bromine was added. The end point occurred for uridine at 1.01 and for uridylic acid at 0.95 moles bromine per mole of pyrimidine.

In the case of uridylic acid an argentimetric titration (potentiometric) of the free bromide ion at the end point verified that 1 mole of bromine while eliminating the absorption band at 262 mμ yielded 1 equivalent of bromine.

When the brominated solution of uridylic acid was heated at 100° C the spectrum developed a new maximum at 278 mμ and minimum at 242 mμ as dehydration gave rise to 5-bromouridylic acid. (Compare ϵ_{max} 279 mμ, ϵ_{min} 244 mμ for the deoxyribonucleotide of 5-bromouracil in 0.1 *N* HCl (3).)

Uracil

The spectral changes accompanying the reaction of bromine with uracil in 0.1 molar acetate buffer (pH 4.7) are illustrated in Fig. 4. Two moles of bromine were required to eliminate the absorption maximum at 259 mμ. Although, at that wavelength the absorbance decreased progressively as bromine was added, the situation was quite

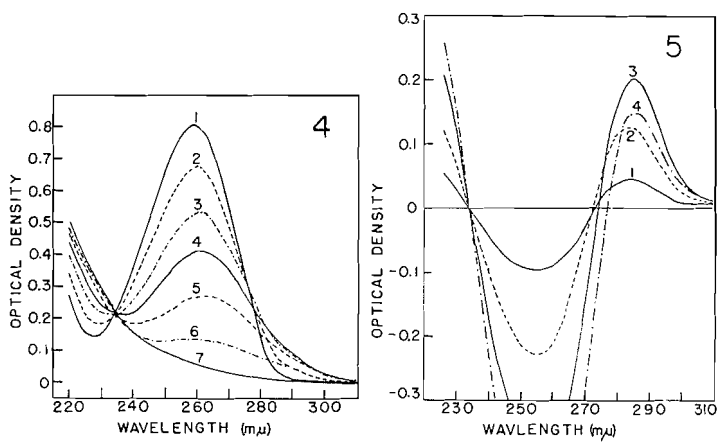

FIG. 4. Bromination of uracil (10^{-4} *M*; in 0.1 *M* acetate buffer, pH 4.7). Curves 1–7 respectively show the spectra obtained upon adding zero, 0.32, 0.64, 0.96, 1.28, 1.60, and 1.92 moles of Br_2 per mole of uracil.

FIG. 5. Differential spectra obtained by placing 10^{-4} *M* uracil in both the sample and reference cuvettes of the spectrophotometer and then recording the spectrum after successive additions of Br_2 to the sample cuvette. Curves 1–4 respectively represent 0.41, 0.84, 1.44, and 1.85 moles of Br_2 per mole of uracil.

different at 280 mμ. Here the absorbance first increased to a maximum and then decreased again as more bromine was added. The changes during the first part of the reaction can be more clearly understood by examining the differential spectra (Fig. 5).

The form of the absorption curves suggested that 5-bromouracil (λ_{max} = 276 mμ) was being produced as an intermediate and that it reacted eventually with more bromine to yield 5,5-dibromo-6-hydroxyhydrouracil. In such an event presumably the 5-bromouracil would increase in amount initially to the point at which it would be reacting with bromine at the same rate as the residual uracil and then, as the uracil was used up, the reaction of the 5-bromouracil would predominate. If this were true one might expect that if one added 5-bromouracil to the uracil initially, in sufficient quantity, the absorption curves during the bromination would not exhibit the preliminary increase in the region of 280 mμ. A series of mixtures of the two compounds was studied in this way and this was indeed the finding. Figure 6 gives one example in which 5-bromouracil was added initially to the sample to a concentration of 0.55×10^{-4} *M*. The same amount of 5-bromouracil was added to the reference cell so that its contribution to the absorption curve was cancelled out. The changes during bromination thus appeared as the simple removal of uracil and its conversion to 5,5-dibromo-6-hydroxyhydrouracil, the known final product.

The results of the potentiometric titration with bromine, included in Fig. 2, were in agreement with the spectrophotometric measurements in indicating no end point until 2 moles of bromine had been added per mole of uracil.

Thymine

The family of absorption curves obtained for the bromination of thymine exhibited 2 isosbestic points (at 223 and 233.5 mμ) corresponding to a mole for mole conversion of thymine to 5-bromo-6-hydroxyhydrothymine. The elimination of the absorption band required approximately 1 mole of bromine. As the thymine was found chromatographically to contain several per cent of uracil as impurity quantitative study was not pursued further in this case.

Thymidine

The spectral changes during the bromination of thymidine resembled those for thymine but with isosbestic points at 225.5 and 236 mμ (Fig. 8). The absorption band at 265 mμ was eliminated by 1.07 moles of bromine per mole of thymidine. The rate of reaction was lower than in the case of the uracil derivatives so that some minutes were required for it to go to completion. A 10-minute reaction time was employed in the experiments reported here. The effect of heating the brominated thymidine solution is shown in the final curve of Fig. 8.

Reaction of Uracil with 5,5-Dibromo-6-hydroxyhydrouracil

As an aid in interpreting the results of the uracil bromination experiments the following reaction has been investigated: 0.112 g uracil (0.001 mole) and 0.288 g of 5,5-dibromo-6-hydroxyhydrouracil (0.001 mole) were dissolved in 10 ml of 1 *N* HCl at 100° C and the solution was kept in the steam bath at 100° C. Samples were withdrawn from time to time and the absorption spectra recorded after diluting 1:1000 with water. The results are illustrated in Fig. 7. It should be pointed out that, after about 30 minutes, 5-bromouracil began to crystallize from the solution, so that its concentration remained constant from then on. At the times the samples were taken aliquots were also removed for chromatography on paper along with markers of uracil, 5-bromouracil, and 5,5-dibromo-6-hydroxyhydrouracil. The paper chromatogram was developed with *n*-butanol saturated

Can. J. Chem. Downloaded from www.nrcresearchpress.com by 190.90.36.8 on 09/04/12
For personal use only.

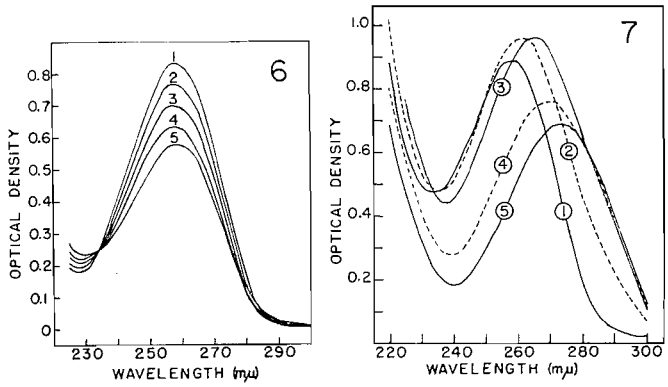

FIG. 6. Bromination of a mixture of uracil (10^{-4} M) and 5-bromouracil (0.55×10^{-4} M). Curves 1–4 correspond respectively to zero, 0.125, 0.25, 0.375, and 0.50 moles of Br_2 per mole of pyrimidine. A solution of 5-bromouracil (0.55×10^{-4} M) was used as a reference in the spectrophotometer.

FIG. 7. Bromination of uracil by means of 5,5-dibromo-6-hydroxyhydrouracil. Curves 1–5 show the spectra obtained for samples withdrawn at 3 minutes, 1 hour, 2 hours, 4 hours, and 24 hours respectively.

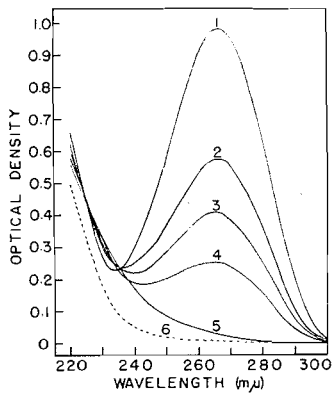

FIG. 8. Bromination of thymidine (10^{-4} M). Curves 1–5 respectively correspond to addition of zero 0.47, 0.65, 0.84, and 1.21 moles of Br_2 per mole of thymidine. Curve 6 shows the effect of heating at 100° C for 10 minutes after adding 1.21 molecular equivalents of Br_2.

with water and the spots located by the ultraviolet print method. The formation of 5-bromouracil (R_f 0.48) and the disappearance of both uracil (R_f 0.31) and 5,5-dibromo-6-hydroxyhydrouracil (R_f 0.62) during the reaction was clearly evident (Fig. 9).

DISCUSSION

The results of these studies lead to the conclusion that the reaction of dilute solutions ($\leqslant10^{-2}$ M) of uridine, uridylic acid, and 1,3-dimethyluracil with bromine water may be summarized:

[1]

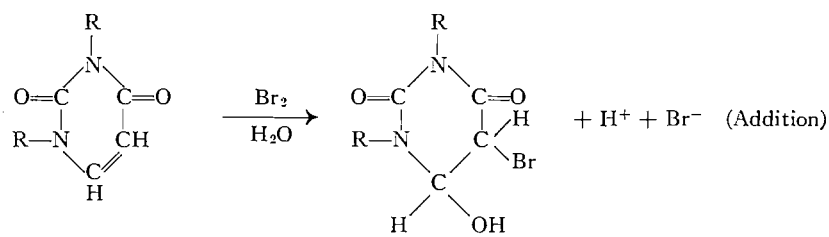

Can. J. Chem. Downloaded from www.nrcresearchpress.com by 190.90.36.8 on 09/04/12
For personal use only.

[2] 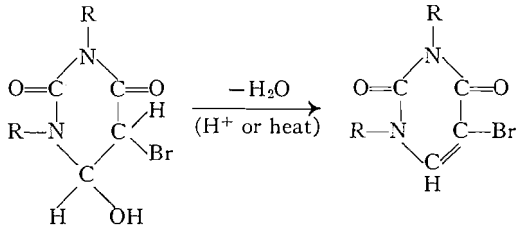

(Dehydration)

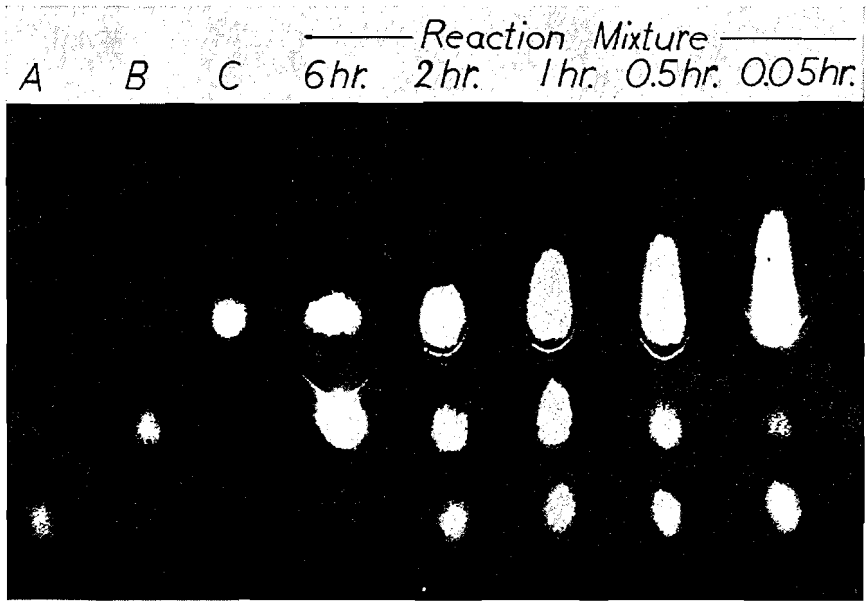

FIG. 9. Paper chromatogram showing reaction of uracil with 5,5-dibromo-6-hydroxyhydrouracil. Origin at top. Lanes A, B, and C represent markers (0.01 ml) of 5,5-dibromo-6-hydroxyhydrouracil (0.1 *M*), 5-bromouracil (10^{-2} *M*), and uracil (10^{-2} *M*) respectively. Solvent: *n*-butanol saturated with water. The narrow arc preceding some of the uracil spots is due to the presence of HCl in the reaction mixture.

The products of reaction [1], all 5-monobromo-6-hydroxyhydrouracil derivatives, are moderately stable compounds which, however, lose water on heating or, with acid catalysis, at room temperature to yield nearly quantitatively the corresponding 5-bromouracil derivative. Both reactions are readily observed spectrophotometrically, the first leading to elimination of the original absorption band in the 260–265 mμ region, the second producing a new band in the vicinity of 280 mμ. Unless reaction [2] is promoted the uptake of bromine stops when 1 mole has reacted. In the case of uridylic acid it was shown that 1 equivalent of bromide ion was produced at this stage.

Thymine and thymidine undergo the first of the foregoing reactions but the products, lacking any hydrogen on position 5, are not capable of the subsequent dehydration. Instead, on heating in weakly acid solution they react in a manner that leads to a marked decrease in ultraviolet absorption at all wavelengths <280 mμ. This change is probably attributable to opening of the pyrimidine ring but we have made no attempt to isolate the products.

The foregoing interpretation is in general agreement with the conclusions of Wang (11) based on his study of the bromination of 1,3-dimethyluracil.

Can. J. Chem. Downloaded from www.nrcresearchpress.com by 190.90.36.8 on 09/04/12
For personal use only.

The case of uracil itself we have found to be rather more complicated than Wang's interpretation would indicate. The potentiometric titration gave no end point until 2 moles of bromine had been added per mole of uracil (Fig. 1) and 2 moles of bromine were required to eliminate the absorption band at 259 mμ (Fig. 4). The picture is further complicated by the transient appearance of what appears to be 5-bromouracil during the bromination.

This is the behavior that one would expect of a reaction proceeding as follows:

[3] 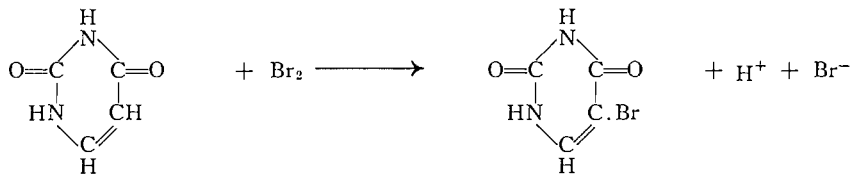

[4] 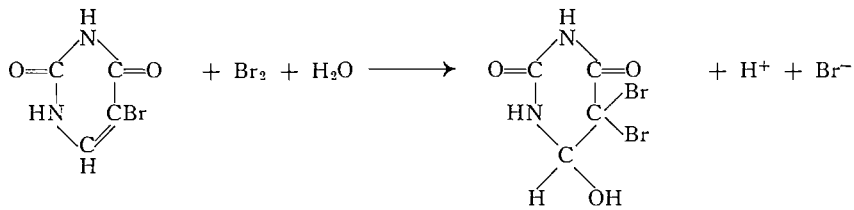

If we represent the instantaneous concentrations of bromine, uracil, 5-bromouracil, and 5,5-dibromo-6-hydroxyhydrouracil at time t by s, x, y, and z respectively then we may write for these reactions the following equations in which the subscript zero implies initial concentration:

$$-dx/dt = k_1xs, \quad [5]$$

$$dy/dt = k_1xs - k_2ys, \quad [6]$$

$$dz/dt = k_2ys, \quad [7]$$

$$-ds/dt = k_1xs + k_2ys, \quad [8]$$

$$x_0 = x+y+z, \quad [9]$$

$$s_0 = s+y+2z. \quad [10]$$

An analytical solution of these equations does not yield the values of y and z in a convenient explicit form, but it has been possible, with the aid of a Datatron electronic digital computer, to calculate the final concentrations of x, y, and z for values of s_0 from zero to $2x_0$ and for values of $\kappa = k_2/k_1$ ranging from 0.5 to 2.0. Using these concentrations together with the known molecular extinctions of the three organic compounds the corresponding absorption spectra have been calculated for $\kappa = 2$ and are plotted in Fig. 10 for comparison with the experimental curves (Fig. 4). The general agreement is very good. The variation of the curves is not sufficiently sensitive to κ to make this a good way of estimating this constant, but an estimate may be obtained from the experimental results. From equation [6] it is evident that when uracil and 5-bromouracil are both reacting with bromine in such a way that $dy/dt = 0$, $k_1xs = k_2ys$ and $\kappa = k_2/k_1 = x/y$. Thus by brominating various initial mixtures of uracil and 5-bromouracil and determining the ratio at which $dy/dt = 0$ one may estimate κ. This is easily done, since,

Can. J. Chem. Downloaded from www.nrcresearchpress.com by 190.90.36.8 on 09/04/12
For personal use only.

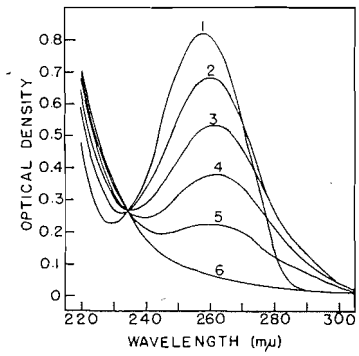

FIG. 10. Calculated curves for the bromination of uracil (10^{-4} M) by mechanism proposed in text, assuming $\kappa = 2$, and amounts of Br_2 ranging from zero to 2 molecular equivalents in 5 equal steps.

of the various components of the reaction mixture, only the 5-bromouracil contributes appreciably to the optical density at 282 mμ. The initial density change, ΔD_{282}, for a fixed amount of added bromine (0.1 mole) is nearly a linear function of the initial uracil:bromouracil ratio, and interpolation to $\Delta D_{282} = 0$ yields $\kappa = 1.7$. The reactions [3] and [4] are so rapid that direct estimation of k_1 and k_2 was not feasible.

The foregoing is not the only possible mechanism for the bromination of uracil that might be considered. An alternative would be the route suggested by reactions [1] and [2] followed by reaction of the 5-bromouracil thus formed with a second mole of bromine. Qualitatively this would explain the formation of 5-bromouracil and the over-all consumption of 2 moles of bromine.

Unfortunately for this hypothesis the dehydration of the 5-bromo-6-hydroxyhydrouracils is quite a slow reaction at room temperature and near neutral pH's, whereas the over-all bromination (2 moles) as observed during the present experiments is very rapid—too fast to measure by our technique. For all the uracil derivatives which we have investigated, the dehydration of the 5-bromo-6-hydroxyhydrouracil derivative is markedly slower than the dehydration of the corresponding 6-hydroxyhydrouracil derivative. Now the dehydration of 6-hydroxyhydrouracil itself at pH 5 and 20° C has a half life of about 19 hours (7) so that one would expect 5-bromo-6-hydroxyhydrouracil to have a half life of at least this magnitude under these conditions.

We must conclude that this can not be the mechanism by which the 5-bromouracil is formed and that, in contrast with the 1-substituted uracils which react by the mechanism cited in reactions [1] and [2], uracil itself first undergoes substitution at position 5 and only then enters into reactions [1] and [2].

One further point deserves comment here. It has been stated in the literature that uracil solutions treated with 1 molecular equivalent of bromine and subsequently heated give quantitative yields of 5-bromouracil (11). Our findings indicate that, before heating, such solutions contain 5,5-dibromo-6-hydroxyhydrouracil, 5-bromouracil, and uracil in roughly comparable amounts. How then can one explain the reported high yield of 5-bromouracil?

We suggest that the explanation lies in the fact that one of the two bromine atoms of 5,5-dibromo-6-hydroxyhydrouracil is capable of acting as a brominating agent. Hilbert and Jansen (4) observed that warm aqueous solutions of the compound liberated iodine from potassium iodide, and Johnson *et al.* (5, 6) showed that under similar conditions it oxidized thiourea and brominated malonic acid. In each case the dibromo-compound

Can. J. Chem. Downloaded from www.nrcresearchpress.com by 190.90.36.8 on 09/04/12
For personal use only.

itself was reduced to 5-bromouracil. In the present instance the residual uracil is presumably brominated on heating, at the expense of the 5,5-dibromo-6-hydroxyhydrouracil so that 5-bromouracil is the sole product.

In the usual preparation of 5-bromouracil, one evaporates to dryness a brominated solution of uracil which is strongly acid (HBr). Our study of the reaction between uracil and 5,5-dibromo-6-hydroxyhydrouracil under similar conditions of acidity and temperature showed that 5-bromouracil is formed in good yield at the expense of both reagents. With an initial concentration of 10^{-4} M for each compound the reaction was too slow to follow conveniently but at 0.1 M concentration, as reported here, the reaction proceeded at an easily measurable rate. Evaporation of a reaction mixture would provide ideal conditions for complete reaction. We believe that this mechanism provides the solution of the apparent discrepancy between our findings and those of Wang (11). On the other hand, this reaction is evidently much too slow to necessitate its inclusion along with reactions [3] and [4] in describing the kinetics of bromination of dilute (10^{-4} M) solutions of uracil at room temperature.

ACKNOWLEDGMENT

The authors gratefully acknowledge their indebtedness to Dr. J. M. Kennedy of the Theoretical Physics Branch, Atomic Energy of Canada Limited, for programming and carrying out the computations, the results of which are reported in the foregoing pages.

REFERENCES

1. CHARGAFF, E. and DAVIDSON, J. N. The nucleic acids. Vol. 1. Academic Press, Inc., New York. 1955. p. 502 ff.
2. DAVIDSON, D. and BAUDISCH, O. J. Am. Chem. Soc. **48**, 2379 (1926).
3. DUNN, D. B. and SMITH, J. D. Biochem. J. **67**, 494 (1957).
4. HILBERT, G. E. and JANSEN, E. F. J. Am. Chem. Soc. **56**, 134 (1934).
5. JOHNSON, T. B. J. Am. Chem. Soc. **62**, 2269 (1940).
6. JOHNSON, T. B. and WINTON, M. G. J. Am. Chem. Soc. **63**, 2379 (1941).
7. MOORE, A. M. and THOMSON, C. H. *In* Progress in radiobiology. *Edited by* Mitchell, J. J., Holmes, B. E., and Smith, C. L. Oliver and Boyd, Edinburgh. 1956. p. 75 ff.
8. MOORE, A. M. and THOMSON, C. H. Can. J. Chem. **35**, 163 (1957).
9. MOORE, A. M. Can. J. Chem. **36**, 281 (1958).
10. WANG, S. Y., APICELLA, M., and STONE, B. R. J. Am. Chem. Soc. **78**, 4180 (1956).
11. WANG, S. Y. Nature, **180**, 91 (1957).
12. WIERZCHOWSKI, K. L. and SHUGAR, D. Biochim. et Biophys. Acta, **25**, 355 (1957).

Can. J. Chem. Downloaded from www.nrcresearchpress.com by 190.90.36.8 on 09/04/12
For personal use only.

Can. J. Chem. Downloaded from www.nrcresearchpress.com by 190.90.36.8 on 09/04/12
For personal use only.

PRESSURE AND TEMPERATURE EFFECTS ON THE KINETICS OF THE ALKALINE FADING OF ORGANIC DYES IN AQUEOUS SOLUTION[1]

DAVID T. Y. CHEN AND KEITH J. LAIDLER

ABSTRACT

The rates of the alkaline fading of bromphenol blue, phenolphthalein, crystal violet, and malachite green have been studied from atmospheric pressure to 16,000 pounds per square inch. The rates for phenolphthalein and malachite green were also measured over a range of temperatures in order to determine the activation energies and entropies. The reactions went essentially to completion with the exception of the fading of phenolphthalein, for which the effects of temperature and pressure on the back reaction and equilibrium constant were also studied. No effect of pressure was found for the fading of crystal violet, but the reactions of the other three dyes were accelerated by pressure, so that there are negative volumes of activation. These are correlated with the entropies of activation and are interpreted in terms of the reaction mechanisms.

INTRODUCTION

Previous work (1, 2, 3, 4) has shown that for a number of reactions in aqueous solution the effects of pressure may be interpreted in terms of the electrostriction of the solvent around ions and dipoles. The present investigation consists of a study of reactions involving the attack by a hydroxide ion on large organic dye molecules. These reactions are of such a nature that electrostriction effects are not as powerful as in many of the previous reactions studied, so that structural effects are expected to play a part in determining the influence of pressure. Since the reactions chosen are structurally similar to one another, but are quite different electrically, they provide a useful means of separating the two effects. The dyes used were bromphenol blue, phenolphthalein, crystal violet, and malachite green, and of these the first two are negatively charged and the second two positively charged.

The kinetics of the alkaline fading of bromphenol blue were first studied under atmospheric pressure by Panepinto and Kilpatrick (5) and by Amis and La Mer (6). The results of these workers led to the following proposed mechanism, which was suggested by Amis and La Mer:

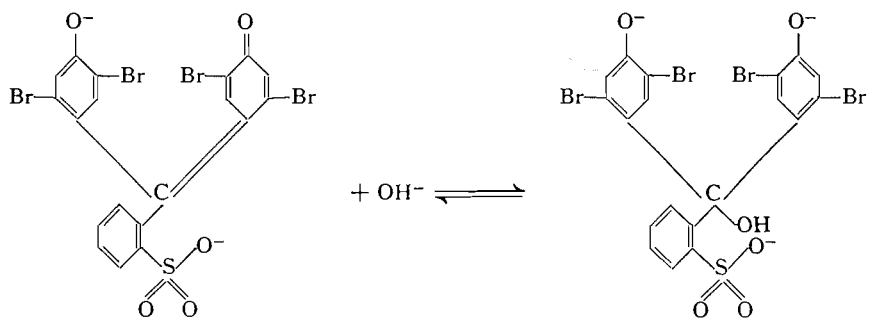

Quinoid form (blue) Carbinol form (colorless)

The reaction went to completion.

The alkaline fading of phenolphthalein was studied by Kober and Marshall (7), Biddle

[1]*Manuscript received November 20, 1958.*
Contribution from the Department of Chemistry, University of Ottawa, Ottawa, Canada.

Can. J. Chem. Vol. 37 (1959)

and Porter (8), Lund (9), Wygaerts and Eeckhout (10), and by Barnes and La Mer (11). The mechanism of the reaction can be represented by the following equations:

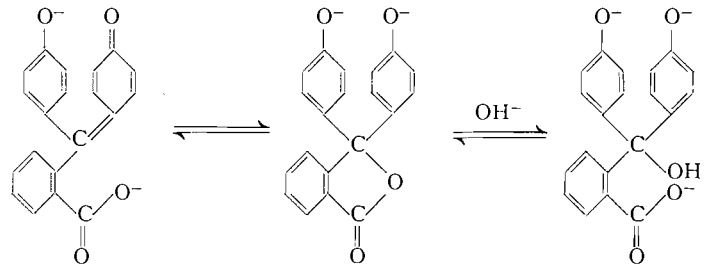

Quinoid form (red) Lactone form Carbinol form (colorless)

The reaction does not go to completion, and in our investigation the kinetics have been investigated in both directions over a range of temperatures and pressures.

The kinetics at atmospheric pressure of the fading of crystal violet in alkaline solution was studied by Biddle and Porter (8), Hockberg and La Mer (12), Goldacre and Phillips (13), and in great detail by Turgeon and La Mer (14). The reaction goes essentially to completion, and again involves the formation of a carbinol, as indicated below:

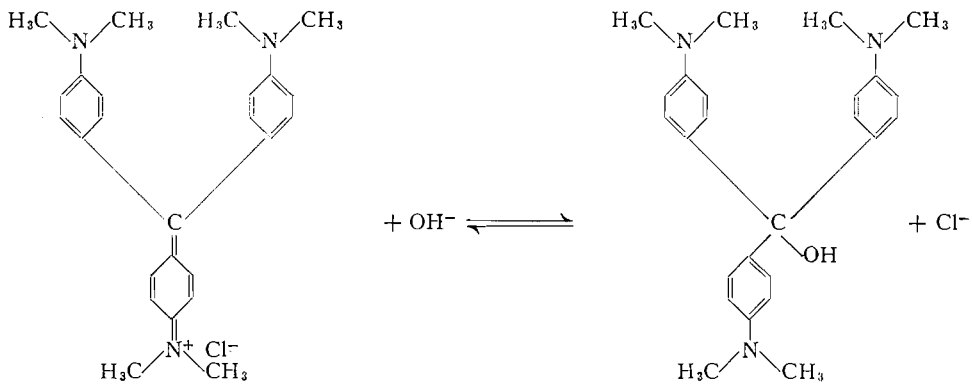

Quinoid form (violet) Carbinol form (colorless)

Very little work has previously been done on the fading of malachite green, which proceeds according to the equation:

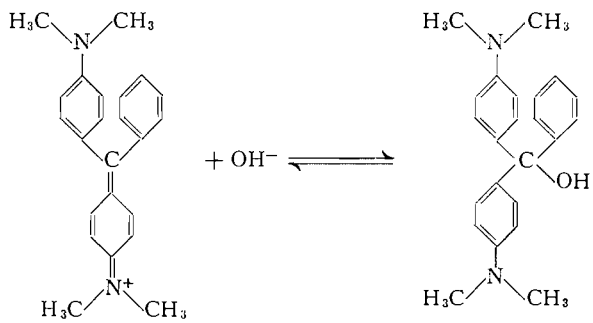

Quinoid form (green) Carbinol form (colorless)

Can. J. Chem. Downloaded from www.nrcresearchpress.com by 190.90.36.8 on 09/04/12
For personal use only.

In 1909 Sidgwick and Moore (15) made a few rate measurements, and Goldacre and Phillips (13) later made some studies in buffered solutions of pH 7.9.

It is to be seen that the four reactions may be represented schematically by the following equations:

$$(\text{B.P.B.})^- + \text{OH}^- \leftrightarrows (\text{B.P.B.})^{=}\text{OH}$$
$$(\text{P.P.})^- + \text{OH}^- \leftrightarrows (\text{P.P.})^{=}\text{OH}$$
$$(\text{C.V.})^+ + \text{OH}^- \leftrightarrows (\text{C.V.})\text{OH}$$
$$(\text{M.G.})^+ + \text{OH}^- \rightleftarrows (\text{M.G.})\text{OH}$$

The first two are reactions between ions of the same sign, the last two between ions of opposite sign. If electrostatic effects alone were important the first two reactions would therefore be expected to involve a decrease in volume during the activation process, and to be accelerated by pressure. The last two reactions, on the other hand, should involve an increase in volume and should be retarded by pressure. The results below show that these anticipations are realized in the first two cases, but that the third reaction is unaffected by pressure. The fourth reaction is accelerated by pressure. These results may be due to the fact that the charges do not approach very closely in the formation of the activated complex, and that structural effects are important.

EXPERIMENTAL PROCEDURE

Materials

The bromphenol blue used in the investigation was an Eastman Organics product. A stock solution was prepared by dissolving the dye in absolute ethanol, adding 0.01 *M* sodium hydroxide to convert it to the monosodium salt, evaporating the resulting solution in vacuum to dryness, and diluting with water to 1 liter. The phenolphthalein used was a C.P. grade Fisher product, and it was recrystallized three times from absolute methanol. The crystal violet used was an Anachemia Chemicals Ltd. product, and was purified by precipitating it as the carbinol, dissolving in hydrochloric acid, and recrystallizing the chloride twice; the crystals were dried in a vacuum desiccator. The malachite green used was a Fisher Scientific Company product (M-73), and was found by analysis to have the composition $2[C_{23}H_{25}N_2]C_2H_2O_4 + C_2H_2O_4$ (mol. wt. 926.90). It was purified by recrystallizing it twice from water.

High-pressure Technique

The high-pressure technique used has been described in detail in a previous paper (4) in which a diagram of the apparatus is shown. In brief, the pressure vessel is designed so that the solutions are separated by mercury from the oil used in the rest of the apparatus, and so that samples can be introduced and withdrawn within a short period of time.

Kinetic Procedure

Since the sodium hydroxide was in all cases in excess of the dye, the reactions in the case of bromphenol blue, crystal violet, and malachite green were simple first-order reactions. The phenolphthalein reaction, on the other hand, had to be treated as consisting of opposing first-order reactions.

The first-order rate constants for the bromphenol blue reaction were obtained by plotting the logarithm of the photometric density L against the time and determining the slopes. The kinetic runs were carried out using a mixture that was 2×10^{-5} *M* in bromphenol blue and 0.2 *M* in sodium hydroxide. Five-milliliter samples were taken at

Can. J. Chem. Downloaded from www.nrcresearchpress.com by 190.90.36.8 on 09/04/12
For personal use only.

intervals of about 1500 seconds and delivered into a colorimeter tube containing 5 ml of water. The photometric densities of the solution were determined in an Evelyn photoelectric colorimeter using filter 565; the Lambert–Beer law was found to be obeyed by the dye solutions.

Since the phenolphthalein fading is reversible the mechanism must be represented as

$$(\text{P.P.})^{=} + \text{OH}^- \underset{k_{-1}}{\overset{k_1}{\rightleftharpoons}} (\text{P.P.})^{\equiv}\text{OH}.$$

The rate of disappearance of the dye is therefore given by

$$[1] \qquad -\frac{d[(\text{P.P.})^{=}]}{dt} = k_1[(\text{P.P.})^{=}][\text{OH}^-] - k_{-1}[(\text{P.P.})^{\equiv}\text{OH}],$$

where k_1 is the second-order rate constant for the forward reaction and k_{-1} is the first-order rate constant for the reverse reaction. Since $[\text{OH}^-]$ is practically constant we can combine it with k_1 to form a pseudo-first-order constant k_1', the resulting equation being

$$[2] \qquad -\frac{d[(\text{P.P.})^{=}]}{dt} = k_1'[(\text{P.P.})^{=}] - k_{-1}[(\text{P.P.})^{\equiv}\text{OH}].$$

The behavior is therefore that of reversible first-order reactions, which obey the kinetic law

$$[3] \qquad k_1' + k_{-1} = \frac{2.303}{t} \log \frac{c_e}{c_e - c}.$$

Here c_e is the equilibrium concentration of the carbinol form of phenolphthalein, and c is the concentration of the carbinol form at any time t. Let c_r be the total concentration of phenolphthalein, c_e' the equilibrium concentration of the pink form of phenolphthalein, and c' the concentration of the pink form at any time t. Then since

$$[4] \qquad c_e = c_r - c_e'$$

and

$$[5] \qquad c = c_r - c',$$

equation [3] becomes

$$[6] \qquad k_1' + k_{-1} = \frac{2.303}{t} \log \frac{c_r - c_e'}{c' - c_e'}.$$

The absorption of light by the substance was found to obey the Lambert–Beer law, and the concentration of the colored substance is therefore directly proportional to the photometric density L according to the expression

$$[7] \qquad c' = L/K_1.$$

Here K_1 is the calibration constant whose value depends on the nature of the colored substance and the characteristics of the filter used. L is the photometric density, equal to $\log (I_0/I)$, where I_0 is the intensity of the incident light and I that of the transmitted light. Equation [6] therefore becomes

$$[8] \qquad k_1' + k_{-1} = \frac{2.303}{t} \log \frac{L_r - L_e}{L - L_e},$$

Can. J. Chem. Downloaded from www.nrcresearchpress.com by 190.90.36.8 on 09/04/12
For personal use only.

where L_e is the photometric density of the solution at equilibrium, L_τ is the photometric density of the solution when all its phenolphthalein is in the pink form, and L that at any time t. L_τ and L_e are constants. From equation [8] it can be seen that a plot of $\log (L-L_e)$ against the time should result in a straight line with a slope equal to

$$-\frac{k_1'+k_{-1}}{2.303},$$

so that the value of the combined rate constant $(k_1'+k_{-1})$ can be calculated. The individual rate constants k_1 and k_{-1} can be found from the equilibrium constant K, which is equal to k_1/k_{-1}. If $(k_1'+k_{-1})$ is called k_c then

$$[9] \qquad k_1 = \frac{k_1'}{[OH^-]} = \frac{k_c-k_{-1}}{[OH^-]} = \frac{k_c-k_1/K}{[OH^-]}.$$

From this

$$[10] \qquad k_1 = \frac{k_c}{[OH^-]+(1/K)}$$

so that

$$[11] \qquad k_{-1} = k_c-k_1'.$$

The kinetic runs with phenolphthalein were carried out using a solution that was 1.00×10^{-5} M in phenolphthalein and 0.01 M in sodium hydroxide. Ten-milliliter samples were taken at about 2000-second intervals and the photometric densities of the samples were determined in the Evelyn photoelectric colorimeter using filter 540 (the absorption maximum is at 550 μ). The photometric density at equilibrium was determined in each case by allowing the reaction mixture to remain under the experimental conditions for at least 24 hours. The value of the combined rate constant k_c was determined by plotting $\log (L-L_e)$ against the time.

The procedure with crystal violet was similar to that with bromphenol blue. The dye shows an adsorption maximum at 590 μ and the best filter was No. 565. The Lambert–Beer law was again obeyed. The kinetic runs were carried out in a mixture that was 5.0×10^{-6} M in dye and 2.0×10^{-3} M in sodium hydroxide. Samples were withdrawn at intervals of about 900 seconds and the photometric densities L determined using the colorimeter. The values of $\log L$ were plotted against the time, and straight lines obtained in each case. The apparent first-order rate constants were calculated from the slopes of the lines.

The kinetic procedure with malachite green was similar to that with crystal violet. The solutions used were 0.0004 N in NaOH and 0.00002 M in malachite green. Owing to the much lower concentration of NaOH used the solutions were protected from CO_2 with a soda-lime tube. For runs under pressure, 40 ml each of the reacting solution were mixed and introduced into the pressure vessel. Ten-milliliter samples were taken at about 1000-second intervals and the photometric density measured as before using filter No. 565. In each case the logarithms of the photometric densities were plotted against the time.

EXPERIMENTAL RESULTS

Bromphenol Blue

Rate constants for the bromphenol blue reaction were determined at a temperature of 25.0° C and at pressures varying from atmospheric to 16,000 pounds per square inch. Typical plots of $\log L$ against time are shown in Fig. 1, and the rate constants,

Can. J. Chem. Downloaded from www.nrcresearchpress.com by 190.90.36.8 on 09/04/12
For personal use only.

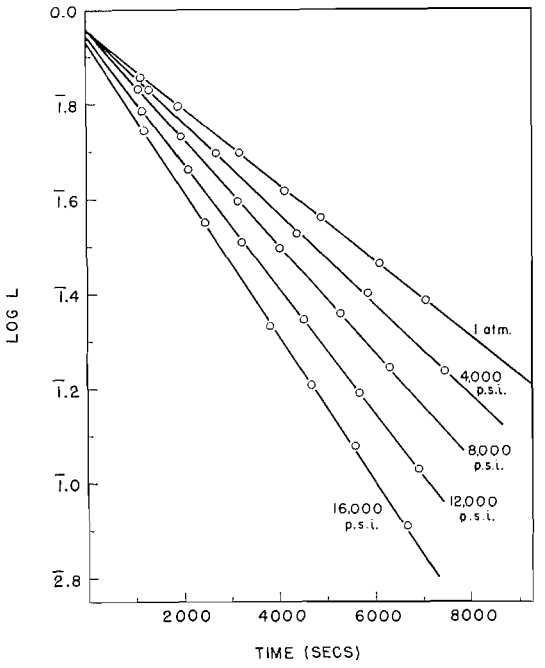

FIG. 1. Plots of log L against time for the fading of bromphenol blue at various pressures.

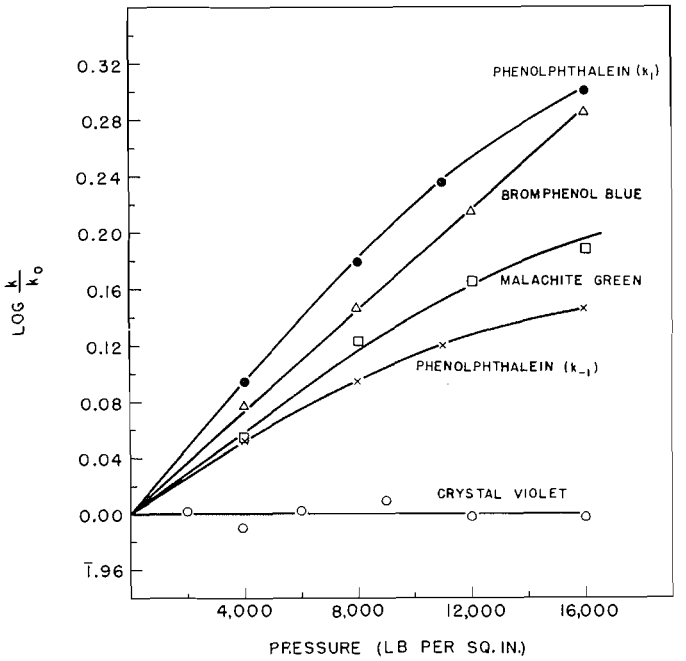

FIG. 2. Van't Hoff plots of the logarithms of k/k_0 against the hydrostatic pressure.

obtained from the slopes, are listed in Table I; k_1' represents the apparent first-order rate constant and k_1 the second-order rate constant. Figure 2 includes a plot of log k/k_0 against the pressure for this reaction. The relationship is seen to be quite linear, and the

Can. J. Chem. Downloaded from www.nrcresearchpress.com by 190.90.36.8 on 09/04/12
For personal use only.

slope of the line corresponds to a volume of activation of -14.9 cc per mole. The energy of activation for the reaction was determined by Amis and La Mer (6), and the results at zero ionic strength are

$$\Delta S^* = -13.34 \text{ calories per degree per mole},$$
$$E = 12.2 \text{ kcal per mole},$$
$$A = 2.04 \times 10^{10} \text{ liters per mole per second}.$$

TABLE I

Summary of results for the alkaline fading of bromphenol blue ($T = 25.0°$ C)

P (lb/in.^{2})	k_1' (sec^{-1})	k_1 (M^{-1} sec^{-1})	k/k_0	log k/k_0
14.7	0.0001860	0.0009298	1	0
4000	0.0002226	0.001113	1.197	0.0781
8000	0.0002609	0.001305	1.404	0.1473
12000	0.0003056	0.001528	1.643	0.2156
16000	0.0003588	0.001794	1.929	0.2853

$\Delta V^* = -14.90$ cc/mole.

Phenolphthalein

Since an activation energy for the phenolphthalein reaction had not previously been determined, the rates of the reaction in both directions were measured over a range of temperatures. From the slopes of plots of log $(L-L_e)$ against time, the values of $k_1'+k_{-1}$ can be calculated, and the results are included in Table II. By allowing the mixtures to

TABLE II

Rate and equilibrium constants for the fading of phenolphthalein at various temperatures

Temperature (° C)	$k_1'+k_{-1}$ (sec^{-1})	K (M^{-1})	k_1' (sec^{-1})	k_1 (M^{-1} sec^{-1})	k_{-1} (sec^{-1})
9.7	0.0000412	74.0	0.0000262	0.00262	0.0000151
20.0	0.0000960	86.9	0.0000446	0.00446	0.0000513
25.0	0.000143	66.7	0.0000572	0.00572	0.0000858
34.6	0.000311	41.8	0.0000917	0.00917	0.000219

$\Delta H = -9.97$ kcal/mole. $\Delta F = -2.49$ kcal/mole.
$E_1 = 8.59$ kcal/mole. $\Delta S_1^* = -41.94$ cal/deg-mole. $A_1 = 1.14 \times 10^4$ M^{-1} sec^{-1}.
$E_{-1} = 18.47$ kcal/mole. $\Delta S_{-1}^* = -17.12$ cal/deg-mole. $A_{-1} = 3.06 \times 10^9$ sec^{-1}.

stand for over 24 hours at the four temperatures the equilibrium constants were determined, and are also shown in the table. The separated values of k_1' and k_{-1} are also shown and from k_1' the values of k_1 are calculated, and are shown in the table. Figure 3 shows a van't Hoff plot of the logarithm of the equilibrium constant against the reciprocal of the absolute temperature, and it is seen that a straight line is obtained. The thermodynamical values obtained from this plot are as follows:

$$\Delta H = -9.97 \text{ kcal per mole},$$
$$\Delta F = -2.49 \text{ kcal per mole},$$
$$\Delta S = -25.1 \text{ cal mole}^{-1} \text{ deg}^{-1}.$$

Figures 4 and 5 show plots of log k_1 against $1/T$ and of log k_{-1} against $1/T$. The Arrhenius law is seen to be obeyed accurately, and the frequency factors and energies and entropies of activation obtained are:

Can. J. Chem. Downloaded from www.nrcresearchpress.com by 190.90.36.8 on 09/04/12
For personal use only.

$$E_1 = 8.59 \text{ kcal per mole},$$
$$A_1 = 1.14\times10^4 \text{ liters mole}^{-1} \text{ sec}^{-1},$$
$$\Delta S_1^* = -41.49 \text{ cal mole}^{-1} \text{ deg}^{-1},$$
$$E_{-1} = 18.47 \text{ kcal per mole},$$
$$A_{-1} = 3.06\times10^9 \text{ sec}^{-1},$$
$$\Delta S_{-1}^* = -17.12 \text{ cal mole}^{-1} \text{ deg}^{-1}.$$

Table III shows the results obtained at 25.0° C and at the various pressures employed. Figure 6 shows a plot of the logarithm of the equilibrium constant against the pressure and from the slope of the straight line a value of ΔV of 8.7 cc per mole was calculated. The plots of the logarithms of k_1 and k_{-1} against the pressure are included in Fig. 2, and from the initial slopes values of −19.7 and −11.0 cc per mole are calculated for the volumes of activation for the forward and reverse reactions.

TABLE III

Rate and equilibrium constants for the fading of phenolphthalein, at various pressures (T = 25.0° C)

P (p.s.i.)	$k_1'+k_{-1}$ (sec^{-1})	K (liters mole^{-1})	k_1' (sec^{-1})	k_1 (liters mole^{-1} sec^{-1})	k_{-1} (sec^{-1})	k_1/k_0	k_{-1}/k_0
14.7	0.000143	66.7	0.0000572	0.00572	0.0000858	1	1
4000	0.000168	73.6	0.0000712	0.00712	0.0000967	1.245	1.127
8000	0.000193	81.2	0.0000865	0.00865	0.000107	1.512	1.241
11000	0.000212	87.3	0.0000986	0.00986	0.000113	1.724	1.317
16000	0.000232	98.0	0.000115	0.0115	0.000120	1.993	1.398

$\Delta V_1^* = -19.66$ cc/mole.
$\Delta V_{-1}^* = -10.98$ cc/mole.
$\Delta V = -8.68$ cc/mole.

Crystal Violet

Rate constants for the fading of crystal violet were measured at a temperature of 25.0° C and at pressures varying from atmospheric to 16,000 lb per sq. in. The results are summarized in Table IV, which shows the apparent first-order constants k_1' and the true second-order constants k_1 obtained by dividing k_1' by the concentration of hydroxide ions.

TABLE IV

Summary of results for the alkaline fading of crystal violet (T = 25.0° C)

P (p.s.i.)	k_1' (sec^{-1})	k_1 (liters mole^{-1} sec^{-1})	k_1/k_0	log k_1/k_0
14.7	0.000520	0.260	1	0
2000	0.000522	0.261	1.004	$\underline{0}.0017$
4000	0.000509	0.255	0.981	$\overline{1}.9917$
6000	0.000522	0.261	1.004	0.0017
9000	0.000532	0.266	1.023	$\underline{0}.0098$
12000	0.000518	0.259	0.996	$\overline{1}.9983$
16000	0.000518	0.259	0.996	$\overline{1}.9983$

$\Delta V^* = 0$.

Pressure is seen to have essentially no effect on the rates, a conclusion that is verified by the plot shown in Fig. 2.

The results obtained by Turgeon and La Mer (14) at atmospheric pressure are, at an ionic strength of 0.0011 M,

Can. J. Chem. Downloaded from www.nrcresearchpress.com by 190.90.36.8 on 09/04/12
For personal use only.

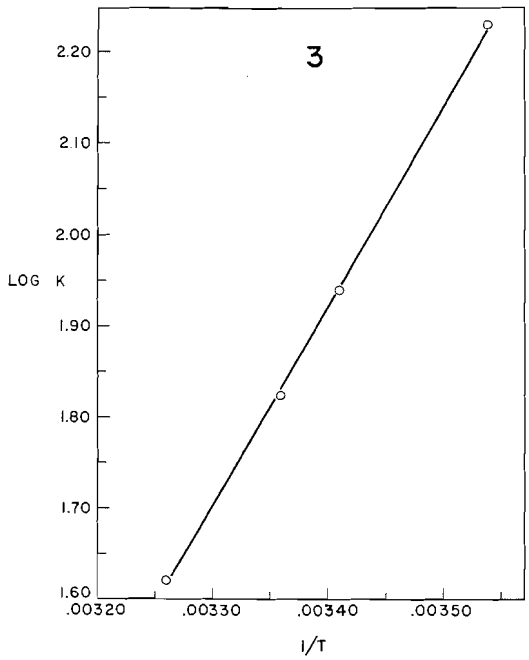

FIG. 3. Plot of the logarithm of the equilibrium constant against $1/T$, for the fading of phenolphthalein.

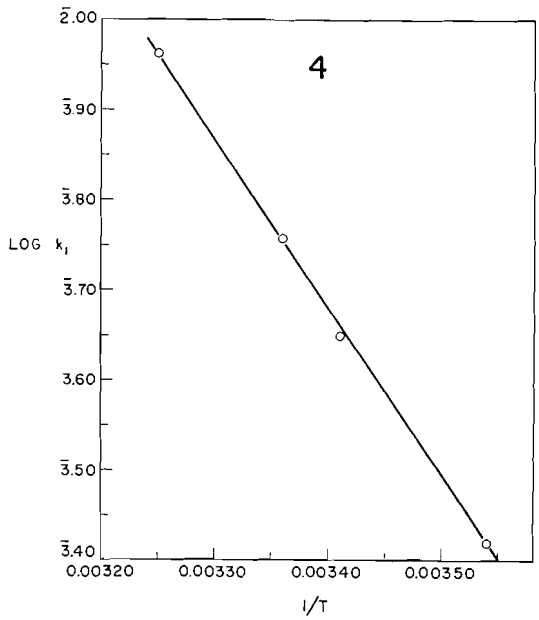

FIG. 4. Plot of log k_1 against $1/T$, for the fading of phenolphthalein.

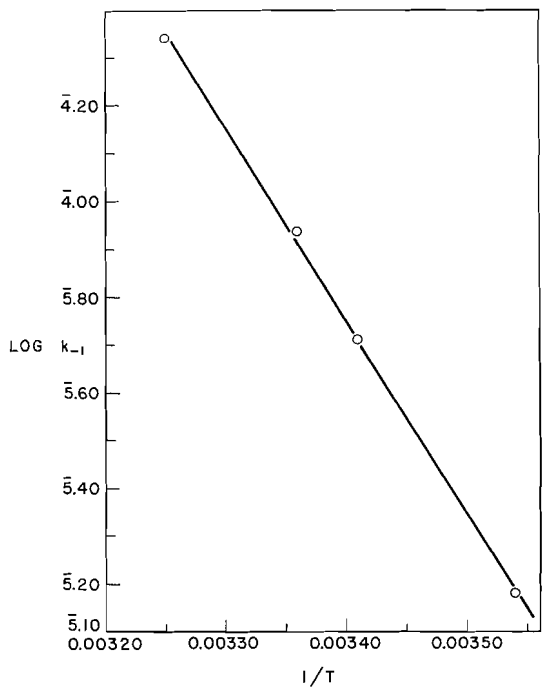

FIG. 5. Plot of log k_{-1} against $1/T$, for the fading of phenolphthalein.

Can. J. Chem. Downloaded from www.nrcresearchpress.com by 190.90.36.8 on 09/04/12
For personal use only.

Can. J. Chem. Downloaded from www.nrcresearchpress.com by 190.90.36.8 on 09/04/12
For personal use only.

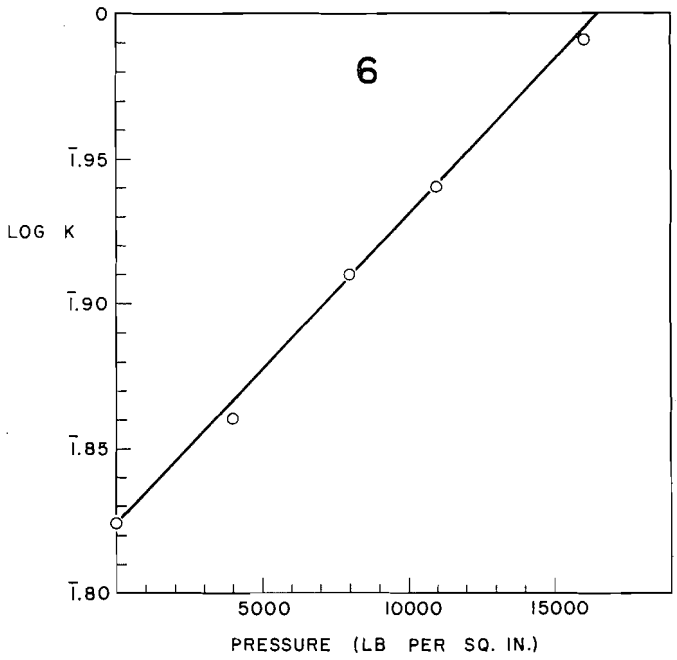

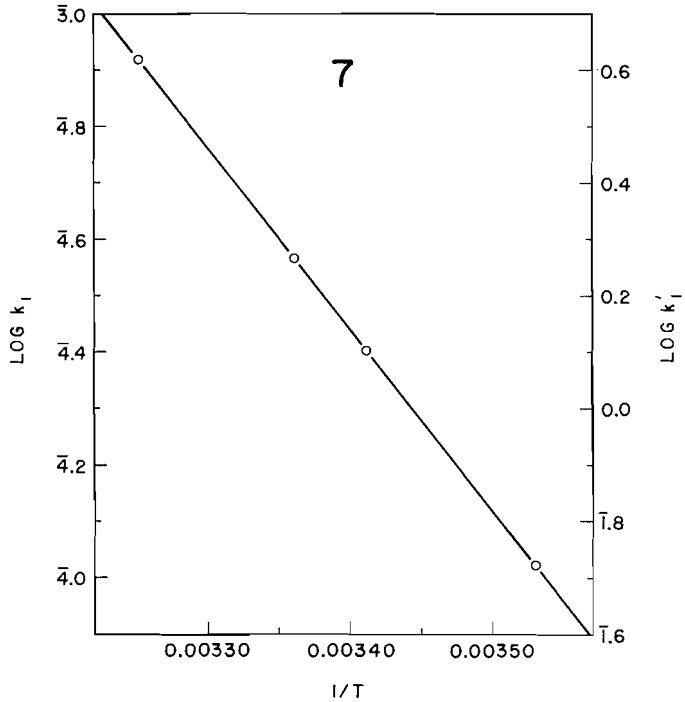

FIG. 6. Plot of log K against the pressure, for the fading of phenolphthalein.
FIG. 7. Plot of log k_1 against $1/T$ for the fading of malachite green.

$$E = 15.1 \text{ kcal mole}^{-1},$$
$$A = 3.13 \times 10^{10}\ M^{-1} \text{ sec}^{-1},$$
$$\Delta S^* = -12.3 \text{ cal deg}^{-1} \text{ mole}^{-1}.$$

Malachite Green

Rate constants under atmospheric pressure and at the various temperatures employed are summarized in Table V, in which k_1' represents the apparent first-order rate constant

TABLE V

Summary of results for the alkaline fading of malachite green under atmospheric pressure

Temperature (° C)	k_1' (sec^{-1})	k_1 ($M^{-1}\,\text{sec}^{-1}$)
10.2	0.0001053	0.5265
20.0	0.0002533	1.267
25.0	0.0003684	1.842
34.9	0.0008291	4.146

E = 14.65 kcal/mole.
$A = 1.023 \times 10^{11}\ M^{-1}\,\text{sec}^{-1}$.
$\Delta S^* = -10.15$ e.u.

and k_1 the true second-order rate constant. The corresponding Arrhenius plot is shown in Fig. 7. The energy of activation, frequency factor, and entropy of activation obtained are:

$$E = 14.65 \text{ kcal mole}^{-1},$$
$$A = 1.023 \times 10^{11}\ M^{-1} \text{ sec}^{-1},$$
$$\Delta S^* = -10.15 \text{ e.u.}$$

Table VI shows the rate constants obtained at 25.0° C and under various pressures. The corresponding van't Hoff plot is included in Fig. 2; the curve is seen to be not linear. From the slope at the lower pressures we calculate a volume of activation of −12.0 cc per mole.

TABLE VI

Summary of results for the alkaline fading of malachite green (T = 25.0° C)

P (p.s.i.)	k_1' (sec^{-1})	k_1 ($M^{-1}\,\text{sec}^{-1}$)	k_1/k_0
14.7	0.0004789	2.395	1
4000	0.0005422	2.711	1.132
8000	0.0006358	3.179	1.327
12000	0.0007014	3.507	1.464
16000	0.0007384	3.692	1.542

$\Delta V^* = -12.0$ cc/mole.

DISCUSSION

Comparison with Previous Work

It is difficult to compare the rate constants obtained in the present investigation with those obtained by previous workers, owing to the different conditions employed. The following comparisons may, however, be of interest.

For bromphenol blue the value of the rate constant obtained at 25.0° C and 1 atm pressure was 0.000932 $M^{-1}\,\text{sec}^{-1}$. Extrapolation of Amis and La Mer's (6) results to the same ionic strength (0.2 M) gives 0.000854 $M^{-1}\,\text{sec}^{-1}$.

Can. J. Chem. Downloaded from www.nrcresearchpress.com by 190.90.36.8 on 09/04/12
For personal use only.

For the fading of phenolphthalein the present values of K, k_1, and k_{-1} at 25° C and 1 atm pressure are as shown below:

$$K = 65.25\ M^{-1},$$
$$k_1 = 0.00572\ M^{-1}\ \text{sec}^{-1},$$
$$k_{-1} = 0.0000858\ \text{sec}^{-1}.$$

The values obtained by Barnes and La Mer (11) under the same conditions are:

$$K = 66.70\ M^{-1},$$
$$k_1 = 0.00634\ M^{-1}\ \text{sec}^{-1},$$
$$k_{-1} = 0.0000972\ \text{sec}^{-1}.$$

For crystal violet the value of k_1 obtained in the present work was 0.260 M^{-1} sec^{-1} at 25.0° C. The value of Turgeon and La Mer (14), corrected to the same ionic strength, was 0.256 M^{-1} sec^{-1}. It was found that for this reaction there was some catalysis by the mercury in contact with the solution in the case of the work done in the high pressure vessel; the rate constant in the absence of mercury was 0.207 M^{-1} sec^{-1}.

On the whole the agreement between the results of the present work and those of the previous workers is quite satisfactory.

Significance of the ΔV^* Values

The ΔV^* values obtained in the present investigation are listed in the last column of Table VII, which also gives the values of E, A, and ΔS^*. Also included in this table are the data for a number of other reactions; the last four are in solvents other than pure water.

TABLE VII

Summary of data for reactions in aqueous solution

Reaction	E (kcal)	A	ΔS^* (e.u.)	ΔV^* (cc per mole)	Ref.
Bromphenol blue + OH^-	12.2	2.0×10^{10}	−13.3	−14.9	Present work
Phenolphthalein + OH^- (k_1)	8.6	1.1×10^{4}	−41.9	−19.7	Present work
Phenolphthalein + OH^- (k_{-1})	18.5	3.1×10^{9}	−17.1	−10.6	Present work
Crystal violet + OH^-	15.1	3.1×10^{10}	−12.3	0.0	Present work
Malachite green + OH^-	14.7	1.0×10^{11}	−10.2	−12.0	Present work
Methyl acetate + OH^-	12.0	9.3×10^{7}	−24.1	− 9.9	4
Ethyl acetate + OH^-	11.6	3.2×10^{7}	−26.2	− 8.8	4
Acetamide + OH^-	14.2	9.5×10^{5}	−33.5	−14.2	4
Propionamide + OH^-	14.6	1.5×10^{6}	−32.6	−16.9	4
CH_2BrCOO^- + $S_2O_3^=$	13.3	1.6×10^{9}	−17.0	− 4.8	2
CH_2ClCOO^- + OH^-	22.7	5.7×10^{10}	−11.6	− 6.1	16, 17, 18
$CH_2BrCOOCH_3$ + $S_2O_3^=$	17.2	1.0×10^{14}	− 5.7	+ 3.2	2
$Co(NH_3)_5Br^{++}$ + OH^-	23.6	5.0×10^{17}	21.7	8.5	2
$(CH_3)(C_2H_5)(C_6H_5)(C_6H_5CH_2)N^+Br^-\rightarrow$ $(CH_3)(C_6H_5)(C_6H_5CH_2)N + C_2H_5Br$	29.7	3.1×10^{16}	14.9	3.3	17, 18
$C_2H_5O^-$ + $C_2H_5I \rightarrow C_2H_5OC_2H_5$ + I^-	20.7	2.1×10^{11}	− 9.7	− 4.1	16, 18, 19
$C_6H_5CCl_3 \rightarrow C_6H_5CCl_2^+ + Cl^-$	15.0	3.5×10^{5}	−35.0	−14.5	1, 2
$C_5H_5N + C_2H_5I \rightarrow C_5H_5N^+(C_2H_5)I^-$	14.4	3.6×10^{5}	−35.4	−15.8	18, 19

Figure 8 shows a plot of ΔV^* against ΔS^* for all of the reactions listed in Table VII. As previously shown (4), there is a fairly good correlation between the values, although the reactions studied in the present work show greater deviations than do the other reactions. This is presumably due to the fact that structural factors are playing a more important role. When electrostatic interactions are predominant a correlation is expected, for reasons discussed in a previous paper (3), but structural effects may introduce deviations.

Can. J. Chem. Downloaded from www.nrcresearchpress.com by 190.90.36.8 on 09/04/12
For personal use only.

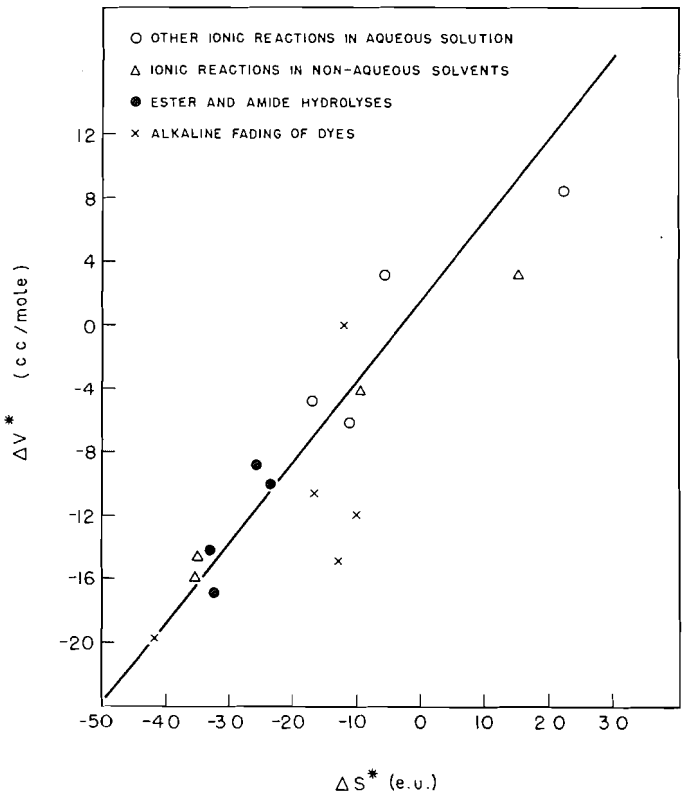

FIG. 8. Plot of ΔV^* against ΔS^* for a number of reactions.

The values of ΔV^* obtained in the present investigation will now be discussed with reference to the mechanisms. The negative volumes of activation obtained for the fading of bromphenol blue and of phenolphthalein are consistent with the fact that there is an approach of charges of the same sign. However, since the hydroxide ion approaches the uncharged central carbon atom, a strong electrostatic effect is not to be expected. It therefore seems likely that structural effects contribute, and some evidence with regard to this is referred to below.

With crystal violet there is no volume of activation in spite of the approach of ions of opposite sign. The hydroxide ion, however, attacks the central carbon atom which is separated by several Ångstroms from the three nitrogen atoms which share the positive charge. Electrostriction effects are therefore unimportant, and the zero value of ΔV^* suggests that there is no volume change due to structural effects.

This conclusion gives the clue to the negative volumes of activation found with the other three fading reactions. The crystal violet ion is the only one of the four investigated in which the three benzene rings lie in a plane. This arises because the resonance involving the quinoid forms of the rings can occur with all three rings.* In the case of bromphenol blue, phenolphthalein, and malachite green only two of the three rings can be involved

**Spectroscopic results (20) have in fact indicated that, owing to repulsion between hydrogen atoms on neighboring rings, the crystal violet ion is not quite planar but that the three rings are twisted slightly out of the plane. This is not found with malachite green and other molecules in which one ring does not enter into the resonance and is therefore out of the plane of the other two rings.*

Can. J. Chem. Downloaded from www.nrcresearchpress.com by 190.90.36.8 on 09/04/12
For personal use only.

in such resonance. The third ring may therefore be twisted out of the plane of the rest of the molecule, and the molecule may occupy a somewhat greater volume relative to the carbinol form.

The suggestion is therefore that in the bromphenol blue, phenolphthalein, and malachite green reactions the quinoid forms of the dyes may structurally be somewhat larger (relative to the carbinol forms) than in crystal violet, so that the fading reaction involves a decrease in volume. In the bromphenol blue and phenolphthalein reactions there may also be small contributions from electrostriction effects; these, however, will be unimportant for malachite green for the same reason as for crystal violet.

REFERENCES

1. BUCHANAN, J. and HAMANN, S. D. Trans. Faraday Soc. **49**, 1425 (1953).
2. BURRIS, C. T. and LAIDLER, K. J. Trans. Faraday Soc. **51**, 1497 (1955).
3. LAIDLER, K. J. Discussions Faraday Soc. **22**, 88 (1956).
4. LAIDLER, K. J. and CHEN, D. T. Y. Trans. Faraday Soc. **54**, 1026 (1958).
5. PANEPINTO, F. W. and KILPATRICK, M. J. Am. Chem. Soc. **59**, 1871 (1937).
6. AMIS, E. S. and LA MER, V. K. J. Am. Chem. Soc. **61**, 905 (1939).
7. KOBER, P. A. and MARSHALL, J. T. J. Am. Chem. Soc. **33**, 59 (1911).
8. BIDDLE, H. C. and PORTER, C. W. J. Am. Chem. Soc. **37**, 1571 (1915).
9. LUND, H. J. Chem. Soc. 1844 (1930).
10. WYGAERTS, M. and EECKHOUT, J. Natuurw. Tijdschr. **17**, 163 (1935).
11. BARNES, M. D. and LA MER, V. K. J. Am. Chem. Soc. **64**, 2312 (1942).
12. HOCKBERG, S. and LA MER, V. K. J. Am. Chem. Soc. **63**, 3110 (1941).
13. GOLDACRE, R. S. and PHILLIPS, J. N. J. Chem. Soc. 1724 (1949).
14. TURGEON, J. C. and LA MER, V. K. J. Am. Chem. Soc. **74**, 9588 (1952).
15. SIDGWICK, N. V. and MOORE, T. S. J. Chem. Soc. **95**, 889 (1909).
16. PERRIN, M. W. Trans. Faraday Soc. **34**, 144 (1938).
17. WILLIAMS, E. W., PERRIN, M. W., and GIBSON, R. C. Proc. Roy. Soc. A, **154**, 684 (1936).
18. MOELWYN-HUGHES, E. A. The kinetics of reactions in solution. Clarendon Press, Oxford. 1947. p. 324.
19. GIBSON, R. C., FAWCETT, E. W., and PERRIN, M. W. Proc. Roy. Soc. A, **150**, 223 (1935).
20. LEWIS, G. N., MAGEL, T. T., and LIPKIN, D. J. Am. Chem. Soc. **64**, 1774 (1942).

Can. J. Chem. Downloaded from www.nrcresearchpress.com by 190.90.36.8 on 09/04/12
For personal use only.

Can. J. Chem. Downloaded from www.nrcresearchpress.com by 190.90.36.8 on 09/04/12
For personal use only.

SOME OBSERVATIONS ON THE THEORY OF DIELECTRIC RELAXATION IN ASSOCIATED LIQUIDS[1]

B. E. CONWAY

ABSTRACT

The theory of absolute reaction rates is examined for the case of relaxation in associated polar liquids where the activation process is probably an excitation of a librational motion to one of complete rotation over a rotational potential energy barrier. The rotational barriers in water are calculated using the point-charge model of the water quadrupole and the effect of thermal bond bending is examined. The experimental heats of activation for dielectric relaxation in water and deuterium oxide are discussed and their temperature dependence examined; the heat capacity change for rotational activation is derived. Isotopic effects in the heats of activation, the relaxation times, and frequency factors are discussed. A qualitative explanation is sought for the homogeneity of relaxation times in water; rotation of water molecules in the fields of the hydroxonium and hydroxide ions present in water may account for the narrow distribution of relaxation times observed experimentally. This mechanism is shown to be consistent with other theoretically derived quantities and with the mechanism of proton mobility in water. A different mechanism is indicated in ice, where the proton concentration is lower, but in ice containing extra protons, the mechanism probably reverts to that existing in water.

INTRODUCTION

Although it appears that a number of substances, e.g. H_2S, hydrogen halides, N_2, O_2, CH_4, and certain ammonium salts exhibit rotation–libration transitions (1) as indicated by changes of the specific heat (2, 3) and dielectric constant (4, 5) over a relatively narrow range of temperatures, a free rotation model for treatment of dielectric relaxation behavior is in general inapplicable to more polar associated condensed phases, e.g. water and the alcohols. In such systems the molecules execute librational oscillations rather than rotational motion except upon activation when a temporary libration–rotation transition is indicated, the frequency of which is inversely related to the relaxation time as determined from dielectric dispersion or absorption conductance studies. In the theory of absolute reaction rates as applied to ordinary chemical reactions, the passage of the reacting particle over the potential-energy barrier has been regarded as a transition of one vibrational mode into a linear translational one along the reaction co-ordinate. Extraction of the partition function for this motion from the total partition function for the activated state, followed by multiplication by the classical average linear velocity of the particle along the reaction co-ordinate, leads to the familiar rate expression for the rate constant of the process. It has usually been assumed (6, 7) without proof that the same expression holds for a libration–rotation activation in dielectric relaxation. It is of interest to show that a formal treatment of rotational instead of the translational activation leads to the same absolute rate equation.

For an activation of, for example, a diatomic molecule A from librational to complete rotational motion we may write the equilibrium constant $K^{\ddagger}$ for the quasi-equilibrium between activated and initial states as

$$K^{\ddagger} = (F_A{}^{\ddagger}/F_A)\, e^{-E_0/RT}.$$

Extracting the partition function for the rotational motion arising from the activation gives

$$K^{\ddagger} = (F_A{}^{\ddagger\prime}/F_A)(1/\sigma)(8\pi^3 IkT/h^2)^{\frac{1}{2}}\, e^{-E_0/RT}, \qquad [1]$$

[1]*Manuscript received June 4, 1958.*
Contribution from the Department of Chemistry, University of Ottawa, Ottawa, Canada.

where $F^{\pm}$ is the total partition function for the activated state and F_A that for the initial state; E_0 is the energy of activation at 0° K and $F^{\pm\prime}$ differs from $F_A{}^{\pm}$ since one librational mode has been converted to one of free rotation in the activated state; σ is the Ehrenfest symmetry factor. If the molecule has a moment of inertia I, its classical rotational kinetic energy in one degree of freedom is $\frac{1}{2}I\omega^2$ if ω is the angular velocity. The average angular velocity $\bar{\omega}$ is hence $(kT/2\pi I)^{\frac{1}{2}}$, whence the corresponding average effective circular frequency $\bar{\nu}$ for σ-fold symmetry is

$$\bar{\nu} = \sigma\bar{\omega}/2\pi = \sigma(kT/8\pi^3 I)^{\frac{1}{2}}. \qquad [2]$$

By analogy with the procedure for activation in a linear vibrating bond, we now multiply $K^{\pm}$ by $\bar{\nu}$ to obtain the rate constant $\mathbf{k}$. Then from [1] and [2]

$$\mathbf{k} = 1/\tau = (kT/h)(F_A{}^{\pm\prime}/F_A)\, e^{-E_0/RT} \qquad [3]$$

where τ is the relaxation time. The expression is thus of the same form as for bond-stretching activation in ordinary chemical reactions.

HEAT OF ACTIVATION AND ITS TEMPERATURE DEPENDENCE

Heats of activation for dielectric relaxation processes may be obtained by determination of the temperature dependence of the critical wavelength at which dispersion of the dielectric constant occurs. In water and deuterium oxide, the heat of activation determined in this way shows a marked apparent dependence upon temperature. The plot of the logarithm of the experimental relaxation times (τ)* against $1/T$ is non-linear and apparent heats of activation, $\Delta H^{\circ\pm}$, derived by taking tangents at various temperatures on this plot, decrease with increasing temperature. Arrhenius plots based on the data for water collected by Smyth (8) and on the measurements of Collie, Hasted, and Ritson (9) for water and heavy water are shown in Fig. 1. The temperature dependence of the heat of activation found in the dielectric relaxation measurements parallels that

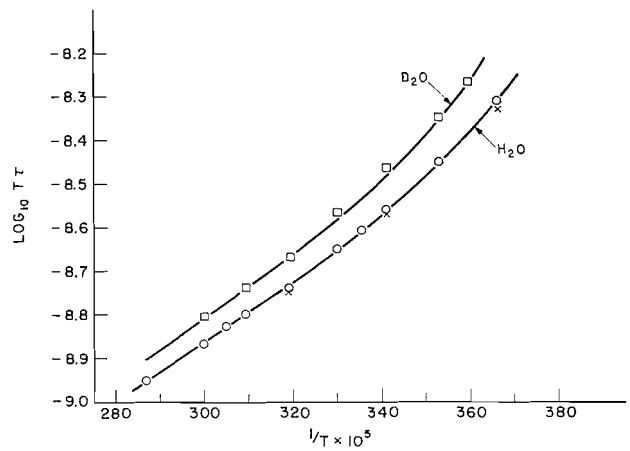

FIG. 1. Arrhenius plots for dielectric relaxation times for water and deuterium oxide.
○ Data for H_2O based on values of Smyth (8).
× Data for H_2O based on individual values of Collie, Hasted, and Ritson (9).
□ Data for D_2O based on values of Collie, Hasted, and Ritson (9).

From the form of the rate equation, it is clear that it is the log of $T\tau$ which should be plotted in order to obtain the heat of activation. Although log τ itself is often plotted (11, 12), the data for water appear to be of sufficient accuracy to justify plotting log $T\tau$. This has been done in Fig. 1.

Can. J. Chem. Downloaded from www.nrcresearchpress.com by 190.90.36.8 on 09/04/12
For personal use only.

found for the viscosity of water and for proton mobility in aqueous acid solutions, which process has a rate controlled by the frequency of rotation of water molecules (10). The non-linearity of the Arrhenius plots could arise from a temperature dependence of $\Delta H^{\circ\ddagger}$ and of the entropy of activation, $\Delta S^{\circ\ddagger}$, usually regarded as constant. If $\Delta H^{\circ\ddagger}$ varies with temperature, it is because there is a finite difference of heat capacity, $\Delta C_p^{\ddagger}$, between molecules in the activated state and those in the initial state of the relaxation process. $\Delta C_p^{\ddagger}$ can be evaluated as follows and hence the true dependence of $\Delta H^{\circ\ddagger}$ and $\Delta S^{\circ\ddagger}$ upon temperature, calculated. We may write [3] in the form

$$\mathbf{k} = 1/\tau = (kT/h)\, e^{-\Delta G^{\circ\ddagger}/RT}, \qquad [4]$$

where $\Delta G^{\circ\ddagger}$ is the standard free energy of activation corresponding to $\Delta H^{\circ\ddagger}$ and $\Delta S^{\circ\ddagger}$. With $K^{\ddagger}$ as defined above, it follows from equation [4] that

$$K^{\ddagger} = (1/\tau)(h/kT).$$

Following the treatment of Everett and Wynne-Jones (13), we may obtain $\Delta C_p^{\ddagger}$ from knowledge of pairs of $K^{\ddagger}$ values at various pairs of temperatures, since by applying the treatment of Everett and Wynne-Jones to the activation equilibrium constant $K^{\ddagger}$, it may be shown in general that for pairs of results 1,2 at different temperatures

$$\frac{\Delta_{1,2}(T \ln K^{\ddagger})}{\Delta_{1,2}T} = \frac{\Delta C_p^{\ddagger}}{R}\cdot\frac{\Delta_{1,2}(T \ln T)}{\Delta_{1,2}T} + B, \qquad [5]$$

where $B = (\Delta S_0^{\circ\ddagger} - \Delta C_p^{\ddagger})/R$. The slope of the line obtained by plotting $\Delta_{1,2}(T \ln K^{\ddagger})/\Delta_{1,2}(T)$ versus $\Delta_{1,2}(T \ln T)/\Delta_{1,2}(T)$ then gives $\Delta C_p^{\ddagger}/R$. $K^{\ddagger}$ values are calculated from the data given by Smyth (8) and Collie, Hasted, and Ritson (9), and terms in the equation [5] are plotted in Fig. 2 from which $\Delta C_p^{\ddagger}$ for water and deuterium oxide may be calculated as -33.2 cal $^{\circ}$ C^{-1} mole^{-1}. Isotopic differences in $\Delta C_p^{\ddagger}$ cannot be detected within the accuracy of the derivation of $\Delta C_p^{\ddagger}$, since the calculation requires high accuracy in the initial data, because a second derivative of the relaxation times with respect to temperature is, in effect, being calculated. The results shown in Figs. 2 and 3 speak well for the accuracy of the data on the relaxation times, since satisfactory lines are obtained in the $\Delta C_p^{\ddagger}$ plot (Fig. 2) and there is very little spread amongst the points through which the lines in Fig. 3 have been drawn.

If $\Delta C_p^{\ddagger}$ is independent of temperature,

$$\ln K^{\ddagger} = \frac{A}{T} + \frac{\Delta C_p^{\ddagger}}{R} \ln T + B, \qquad [6]$$

where A $= \Delta H_0^{\circ\ddagger}/R$ and B is another constant. $\Delta H_0^{\circ\ddagger}$, the heat of activation at the absolute zero (if water remained a liquid down to this temperature), can be derived from Fig. 3 using equation [6]. The values of $\Delta H_0^{\circ\ddagger}$ calculated from slopes of the two lines in Fig. 3 are significantly different, viz. 13.7 kcal g mole^{-1} for water and 14.0 kcal g mole^{-1} for deuterium oxide. Values of $\Delta H^{\circ\ddagger}$ at other temperatures can be derived together with $\Delta G^{\circ\ddagger}$ and $\Delta S^{\circ\ddagger}$ using equation [4] and the data for the relaxation times (8, 9). The thermodynamic data for the activation process are summarized in Table I for one temperature and several results of interest may be pointed out. Firstly the value of $\Delta C_p^{\ddagger}$ is surprising as it is large and negative and similar to that found, for example, in the ionization of acids. $\Delta S^{\circ\ddagger}$ on the other hand is positive but it follows from the data given that it becomes less positive as the temperature is raised. Qualitatively, this is as

Can. J. Chem. Downloaded from www.nrcresearchpress.com by 190.90.36.8 on 09/04/12
For personal use only.

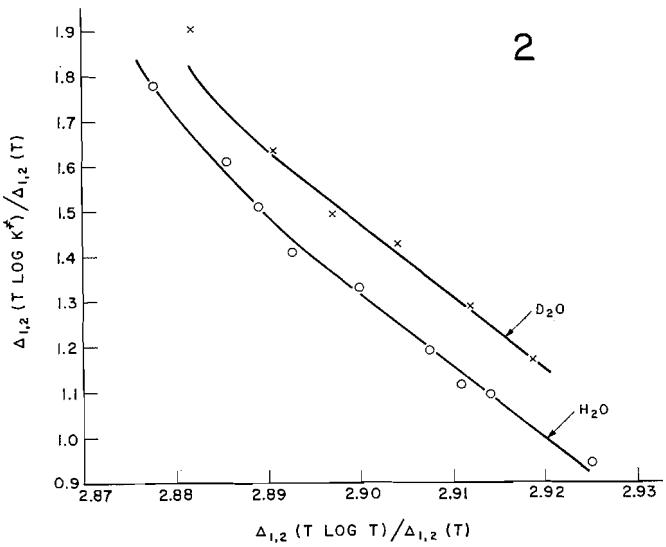

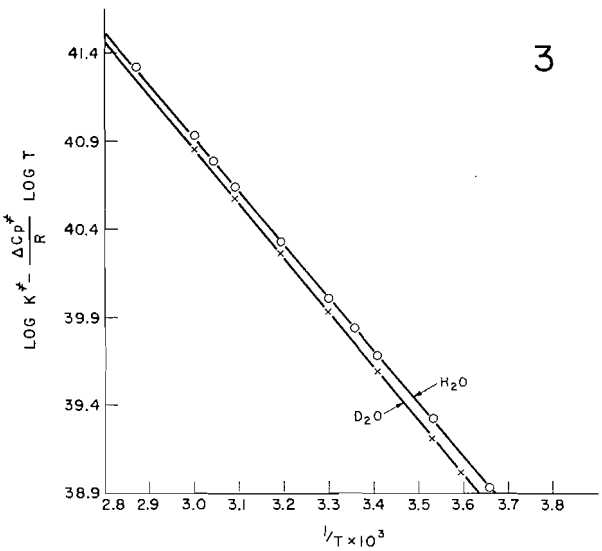

FIG. 2. Wynne-Jones plots for $\Delta C_p^{\neq}$ for H_2O and D_2O.
FIG. 3. Wynne-Jones plots for $\Delta H_0^{\circ\neq}$ for H_2O and D_2O.

expected, for reasons which are discussed below. However, the difference of sign between $\Delta C_p^{\neq}$ and $\Delta S^{\circ\neq}$ is difficult to account for but may be connected with long-range structure breaking (29) in the water. Similar anomalous differences between the signs of ΔC_p and ΔS° values for ionization of bases in water are known (13) and are connected with structure breaking (32).

$\Delta H^{\circ\neq}$ diminishes with increasing temperature since $\Delta C_p^{\neq}$ is negative. It has been considered (14, 15) that increase of temperature causes increasing breakage of H bonds in water. If this were so, the decrease of $\Delta H^{\circ\neq}$ with increase of temperature would be readily accounted for, since with increasing breakage of H bonds, fewer would have to

Can. J. Chem. Downloaded from www.nrcresearchpress.com by 190.90.36.8 on 09/04/12
For personal use only.

be broken in the activation step. However, thermodynamic considerations (cf. 16) preclude the possibility that any significant proportion of H bonds are broken even near the boiling point. This is confirmed by the fact that the latent heat of vaporization of water at the boiling point is still close to the energy required to break four half-hydrogen bonds per molecule, each having the usually accepted (16, 17) dissociation energy of about 5–6 kcal mole^{-1}. The structural change in water which occurs through the melting point and at higher temperatures is best regarded as resulting from the "bending" (16) of the O—H---O bonds rather than from their dissociation; on the basis of such a model the temperature dependence of the dielectric constant has been quantitatively deduced (16) and the change of radial distribution function with temperature accounted for. It is of interest to apply this model in order to examine the effect of bond-bending upon the activation energy for rotation of a water molecule in water.

TABLE I

Thermodynamic data for the activation process in dielectric relaxation in water and deuterium oxide

	$\Delta H_0°\neq$ kcal mole^{-1}	$\Delta S°\neq$ (10° C) cal ° C^{-1} mole^{-1}	$\Delta G°\neq$ (10° C) kcal mole^{-1}	$\Delta C_p\neq$ cal °C^{-1} mole^{-1}
Water	13.7	6.6	2.42	−33
Deuterium oxide	14.0	7.4	2.54	−33

THE ROTATIONAL POTENTIAL ENERGY BARRIER

The H bond in water can be regarded (16) to a satisfactory approximation as arising from the sum of a number of electrostatic interactions between point charges in each OH bond dipole and the two partially hybridized unshared pairs of electrons on the oxygen atoms of neighboring water molecules. Due to hybridization, these unshared pairs have a strong directional character (16, 18) and act as localized centers of negative charge. The electrostatic model for the hydrogen bond has been shown to be adequate (19) except for extreme vibrational excursions of the H atom or for very short bonds where covalent canonical forms become important. For water, the electrostatic model provides a satisfactory basis for calculation of bulk dielectric properties of the substance (16, 20). It will therefore be applied here in order to examine the features of the potential energy barrier for a water molecule rotating in the field of its nearest neighbors whose orientations have been thermally perturbed from the average orientations existing in ice. As a basis for the calculation, an idealized 4-co-ordinated structure is assumed such as exists to a first approximation in ice and to an important extent (21) in liquid water near the melting point. The rotational potential barriers for motions about the bond XY and the dipole axis of the water molecule shown in Fig. 4 in a thermally unperturbed structure have already been calculated by Conway *et al.* (10). The method used may be adapted for calculation of the rotational barrier when one or more bonds are bent and there is thermal perturbation of the ideal structure. Reference is made to Fig. 5 where XYZ is the water molecule undergoing rotation, for example about the axis XY. The choice of the mode of rotation is somewhat arbitrary but the one assumed here and in the previous calculations, (10), involves least breakage of hydrogen bonds and may therefore be the preferred motion; other modes, e.g., the axial spin mode previously examined in connection with proton mobility (10), cannot lead to a change of dielectric polarization of the water upon application of a field and is hence not considered here.

In the hydrogen bond YZW, point charges are assumed to be localized as in the model

Can. J. Chem. Downloaded from www.nrcresearchpress.com by 190.90.36.8 on 09/04/12
For personal use only.

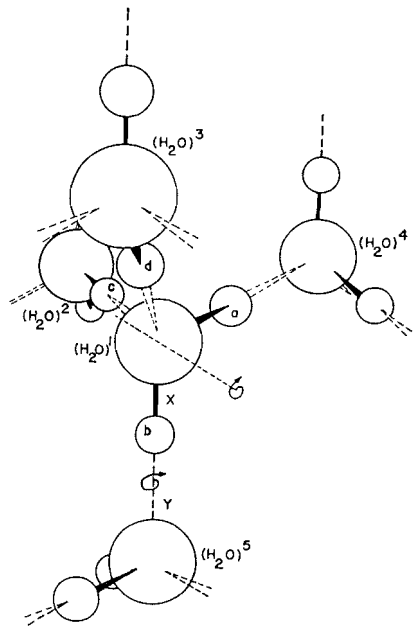

FIG. 4. The situation of a water molecule H_2O^1 amongst tetrahedrally co-ordinated neighbors showing the possible modes of rotation about H bond XY through H atom b, or axially; the latter mode involves breaking of all four bonds through H atoms a, b, c, and d.

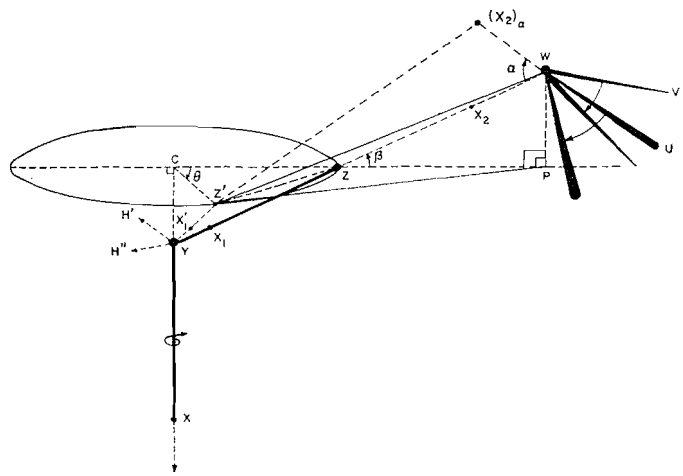

FIG. 5. Model for calculation (cf. 10) of the rotational potential energy barrier for a water molecule in water as a function of the angle of rotation, θ, and the angle α, of disorientation or bond bending of bonds with nearest neighbors.

given by Lennard-Jones and Pople (16). The energy of the hydrogen bond YZW is then calculated as a function of the angle, θ, of rotation of the bond YZ from its equilibrium position, as previously carried out (10) but now for various degrees of bond-bending determined, for example, by the degree of disorientation, α, of the directed lone pair of electrons X_2 in the hydrogen bond YZW, or of the OH bond. For any position of Z (e.g. at Z'), the distance WZ' or X_2Z' may be computed and the energy of electrostatic

Can. J. Chem. Downloaded from www.nrcresearchpress.com by 190.90.36.8 on 09/04/12
For personal use only.

interaction between the two electronic charges at W and X_2, and the one at the proton at Z' (16), can be calculated (16). The other four electrostatic interactions (16) leading to the total interaction energy in the bond are calculated similarly for various values of θ. It can be shown (10) that

$$(WZ')^2 = 4(CZ')\ (\sin^2\theta/2)\ [CZ'+ZW\cos\beta]+(ZW)^2 \qquad [7]$$

and similar expressions may be obtained for the other distances required, e.g., WX_1', X_2Z', X_2X_1'. As the molecule XYZ is rotated, lone-pair electrons directed towards other hydrogen atoms H′ and H″ (not shown in Fig. 5) also suffer rotation. The energy of the two hydrogen bonds involving these orbitals are calculated as a function of θ by equations similar in form to that of [7].

When the orbital directed from W to X_2 is oriented by an angle, α, from the colinear configuration YX_1ZX_2W, X_2Z' and other similar distances may be calculated trigonometrically, since it may be shown that

$$(X_2Z')^2 = (ZW)^2+(WX_2)^2-2(ZW).(WX_2)\cos\alpha+4(CZ')\sin^2\theta/2.[CZ'+ZW\cos\beta]. \qquad [8]$$

The form of this equation is general, so that other distances may be calculated, e.g. X_2X_1' as a function of θ and α; alternatively the molecule XYZ in Fig. 5, and hence the bond YZ may be considered oriented and the barrier for rotation of the molecule UVW about UW or VW calculated.

In order to examine the *form* of the dependence of the height of the rotational barrier for a given water molecule upon the angle α, calculations have been carried out for four values of α from 0° to 90° and for six values of θ from 0° to 100°. It must be emphasized that only a very small fraction of molecules will be thermally disoriented to angles as large as 90°. A greater number will be thermally disoriented at lower values of α. However, a rotation of a given molecule will involve bending or temporary breaking of bonds with neighbors and this will also facilitate the rotation of the neighbors themselves. Thus, those molecules which do rotate, would preferentially tend to do so at regions of the liquid where there is already a transient thermal disorientation. The process of activation is therefore probably best regarded as a somewhat co-operative one involving the participation of other molecules as well as the one which actually "rotates".

Each H bond has six component coulombic interactions and the resulting 144 interactions for the range of angles considered enables the electrostatic potential energy of the representative water molecule to be calculated as a function of θ and α for various assumed conformations of the structure; for example one, two, three, or four bonds to nearest neighbors may be considered to be disoriented. The total energy of the representative water molecule is calculated by summing the relevant individual partial coulombic interactions as described previously (10). Examples of the effect of bond bending on the rotational barrier are shown in Figs. 6 and 7. As a given molecule rotates in an ideal ice-like structure the molecule successively passes through the configurations shown as projections in Fig. 8. Unless the structure is perturbed, it is clear that any rotation must always lead to states of higher energy, since repulsive interactions will occur either between pairs of OH bonds or between the unshared-pair orbitals as they come into opposition as shown in Fig. 8. This leads to maxima at 120° and 240° in the rotational barrier as shown in Fig. 6. The energy of repulsion which arises when two OH bonds are in opposition is diminished if there is some bending of the H bonds, as shown by the result in Fig. 6; one of the most important qualitative effects of thermal bending is seen to be the diminution of the energy of this repulsive interaction. That such an

Can. J. Chem. Downloaded from www.nrcresearchpress.com by 190.90.36.8 on 09/04/12
For personal use only.

Can. J. Chem. Downloaded from www.nrcresearchpress.com by 190.90.36.8 on 09/04/12
For personal use only.

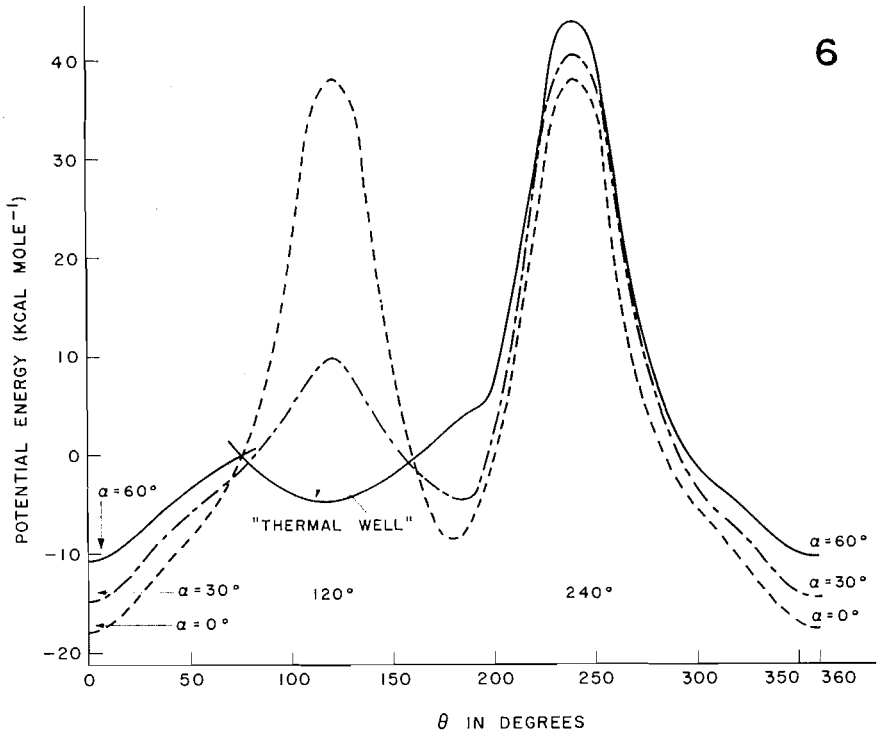

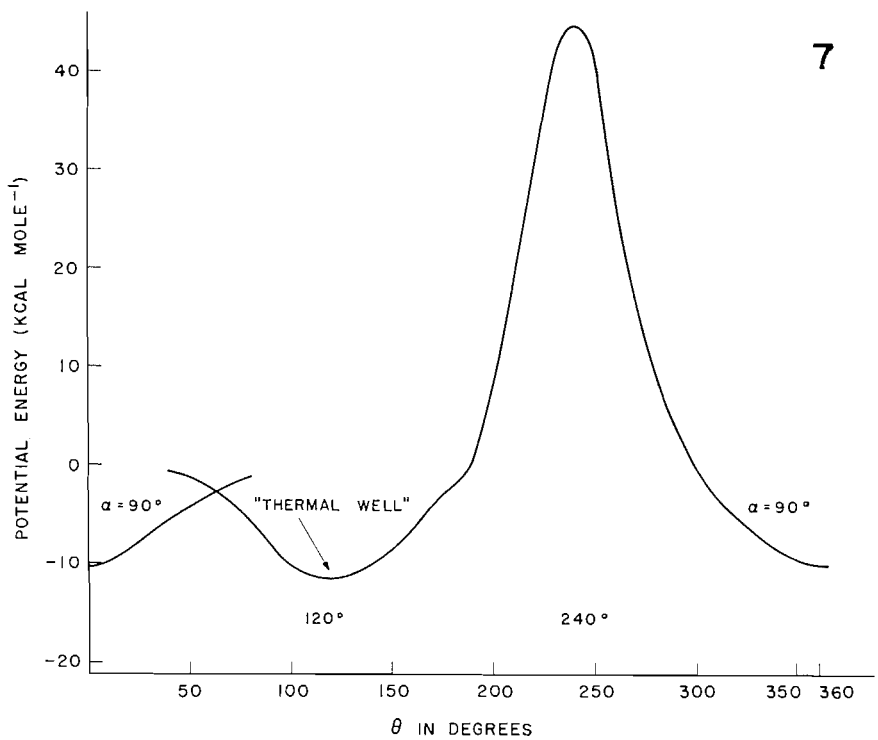

FIG. 6. The electrostatic potential energy barriers for rotation of a water molecule in water as a function of θ and α (α = 0, 30, and 60°).
FIG. 7. The potential energy barrier as in Fig. 6, but for α = 90°.

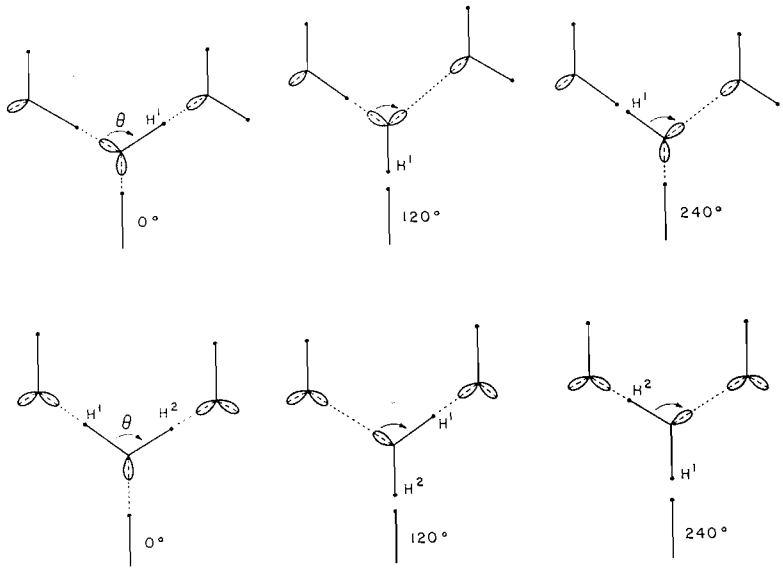

FIG. 8. Projections of configurations passed through by a water molecule rotating about one OH....O bond in water.

(i) Upper series: rotation about OH....O
(ii) Lower series: rotation about O....HO

H^1 and H^2 are H atoms in the representative H_2O molecule undergoing rotation.

interaction may be of importance in the experimental relaxation behavior in ice is indicated by the fact that the heat of activation for relaxation in ice is 13.2 kcal $mole^{-1}$, i.e., significantly larger than the energy necessary (viz. the heat of sublimation) completely to break all four "half"-hydrogen bonds per water molecule in ice. In liquid water, where $\Delta H^{\circ\ddagger}$ is between 2 and 5 kcal $mole^{-1}$ over the temperature range 0–75° C, this effect must be almost absent, Figs. 6 and 7 show that if the degree of bending is sufficient, the repulsive interaction, for example at 120° of rotation, is eliminated and in fact replaced by one of attraction. Under these conditions a new potential energy minimum occurs other than that at the initial state (0°) and at the intermediate state (180°) of the rotation. We may identify minima of this kind with the transient "thermal wells" postulated by Garton (22) to explain the dielectric behavior of polar liquids. We have, of course, only considered some special cases where one bond to a nearest neighbor water molecule is bent or disoriented. Qualitatively similar effects arise if two or more bonds are simultaneously bent; however, such a situation will be statistically less probable than that in which fewer bonds to a given water molecule are bent.

From Figs. 6 and 7, it is clear that the barrier for rotation of a given water molecule can be considerably lowered by thermal bending of bonds or "disorientation" of neighboring molecules and hence the dependence of $\Delta H^{\ddagger}$ upon temperature qualitatively explained. In so far as disorientation of molecules other than the given one is involved, the rotation process is a co-operative one.

An alternative explanation for the temperature dependence of the thermodynamic parameters for dielectric relaxation in water may be sought in terms of the hole-theory of liquids (23); thus Schellman (24) has suggested that defects (missing bonds) in the ice structure are propagated in the rotational process, and a similar effect could occur in water. Rotation at defect sites will certainly require less energy of activation and this may be demonstrated by calculating the rotational barrier for such sites, as shown in

Can. J. Chem. Downloaded from www.nrcresearchpress.com by 190.90.36.8 on 09/04/12
For personal use only.

Fig. 9. This approach is equivalent to assuming that a significant number of hydrogen bonds are completely dissociated in water and ice; whilst this is thermodynamically unlikely (16), metastable crystal imperfections in ice may, however, provide the necessary sites for rotation in that case (33).

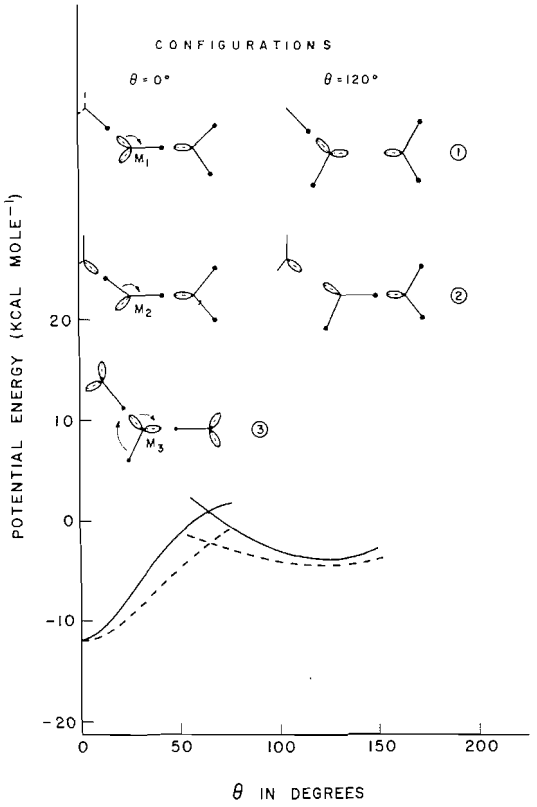

FIG. 9. The rotational potential energy barrier from 0 to 120° for a water molecule M in ice at a bond vacancy site where there are only three H bonds to the representative molecule. Projections of three situations are shown: (1) rotation about the OH. . . . O bond (dotted line); (2) rotation about the O. . . . HO bond (solid line). The configurations at $\theta = 0°$ (initial state) and $\theta = 120°$ (final state) are indicated; (3) rotation in this configuration can only lead to OH bonds in opposition with a resultant increase of potential energy with no minimum as in Fig. 6 for $\alpha = 0$.

FREQUENCY FACTORS

Since $\Delta H_0^{\circ\ddagger}$ has been evaluated for relaxation in water and deuterium oxide, we can use equation [3] as a basis for comparison of experimental and theoretical frequency factors.

If the potential energy function for libration is of the form $V = V_0 \cos\theta$, and three modes of restricted rotation are possible in the initial state, F_A in equation [3] may be written (27)

$$F_A = \frac{8\pi^2(8\pi^3 I_1 I_2 I_3 k^3 T^3)^{\frac{1}{2}}}{h^3} \frac{\sinh(V_0/kT)}{V_0/kT} F_v \cdot F_t, \qquad [9]$$

where F_v is the product of partition functions for the internal vibrations in the bonds of the molecule and F_t the total translational partition function. The cosine potential function will only be applicable if the internal field is uniform. This, however, is unlikely

Can. J. Chem. Downloaded from www.nrcresearchpress.com by 190.90.36.8 on 09/04/12
For personal use only.

for the short range interactions considered above. Inspection of the minima near $\theta = 0$ in the rotational potential energy diagrams indicates (Fig. 6) that the potential function near the minima is more accurately represented by $V = \frac{1}{2}K\theta^2$, where K is the force constant for the restricted rotation, so that (cf. 28) F_A is then given by

$$F_A = \left[1-\exp\left(\frac{-h\nu_1}{kT}\right)\right]^{-1}\cdot\left[1-\exp\left(\frac{-h\nu_2}{kT}\right)\right]^{-1}\cdot\left[1-\exp\left(\frac{-h\nu_3}{kT}\right)\right]^{-1}\cdot F_v\cdot F_t, \qquad [10]$$

where ν_1, ν_2, and ν_3 are the three frequencies of restricted rotation corresponding to the normal modes of rotation of an unhindered non-linear triatomic molecule. In equation [1], $F_A^{\ddagger\prime}$ differs from F_A only on account of the conversion of one mode of libration to one of (temporary) free rotation.

Hence*

$$\mathbf{k} = \frac{kT}{h}\cdot\frac{1}{\left[1-\exp\left(\frac{-h\nu_3}{kT}\right)\right]^{-1}}\cdot e^{-E_0/RT} \qquad [11]$$

if the librational mode designated as 3 is the one which becomes a free rotational motion in the activation step. The frequency ν_3 may be estimated from the rotational potential energy function. Figure 10 shows the dependence of the energy of a water molecule in water (in the thermally unperturbed structure) upon θ^2 in degrees. The slope of the line in Fig. 10 calculated in terms of erg molecule^{-1} and radians gives $K = 2.1\times10^{-12}$. Now for the simple harmonic libration of type 3,

$$\nu_3 = 1/2\pi(K_3/I_3)^{\frac{1}{2}} \qquad [12]$$

and taking I_3 as 1.9×10^{-40} g cm^2 (37), gives $\bar{\nu}_3 = 550$ cm^{-1}. This is in satisfactory agreement with the value of the frequency of hindered rotation ($\bar{\nu} = 570$ cm^{-1}) calculated by a different method from Morse functions by Cross *et al.* (14). The value falls in the

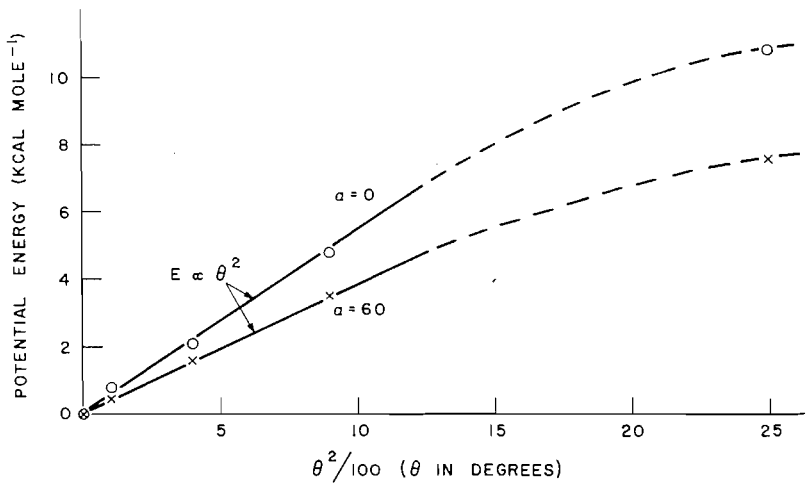

FIG. 10. Plot of potential energy vs. square of angle, θ, of rotation for low values of θ, and two values of α, showing the effect of bond bending on the force constant K.

**This involves the assumption that the other two librational modes maintain the same frequencies during the rotational motion. Whilst this is probably true only as a first approximation, the results which follow for the ratio of frequency factors for relaxation in H_2O and D_2O ice confirm the general correctness of the assumption, at least in the case of ice.*

Can. J. Chem. Downloaded from www.nrcresearchpress.com by 190.90.36.8 on 09/04/12
For personal use only.

middle of the infrared band in water ascribed to "hindered rotation" (14). The above calculation is based on the rotational potential energy function for the unperturbed structure, i.e., with no bond-bending; this is justified by the fact that the majority of the molecules observed spectroscopically will be in states corresponding to a relatively unperturbed structure, since perturbed molecules will be distributed as $e^{-E/RT}$, where E is the energy involved in causing a perturbation. Lower values of $\bar{\nu}_3$ result when perturbed structures (i.e. α in Fig. 5 differs from zero) are considered, since then K_3 is less, as shown for example in Fig. 10. We may now evaluate the apparent frequency factor in equation [11], whereupon

$$\mathbf{k} = (kT/h)\ (0.93)\ e^{-E_0/RT} = 5.8\times10^{12}\ e^{-E_0/RT}. \qquad [13]$$

Direct comparison of this frequency factor with those obtained experimentally near room temperature is complicated by the large temperature dependence of the experimental heat of activation found at room temperature for relaxation in water.

In a condensed phase, E_0 and $\Delta H_0^{\circ\ddagger}$ are almost identical (35) but differ from the experimentally measured activation energy, $E^{\ddagger}$, according to

$$E^{\ddagger} = E_0+\Delta C_p{}^{\ddagger}T+RT. \qquad [14]$$

The experimental behavior is represented by

$$1/\tau = Ae^{-E^{\ddagger}/RT} = [(ekT/h)\ e^{\Delta S_0{}^{\ddagger}/R}]\ e^{-E^{\ddagger}/RT}. \qquad [15]$$

In order to compare the experimental frequency factor in [15] with that arising theoretically in [13], we convert [13] into a form comparable with [15] by eliminating E_0 in [13] using equation [14], so that both equations involve $E^{\ddagger}$. Hence

$$k = 5.8\times10^{12}e.\ e^{\Delta C_p{}^{\ddagger}/R}\ e^{-E^{\ddagger}/RT} \qquad [16]$$

and the frequency factor A is then $5.8\times10^{12}\ e.\ e^{\Delta C_p{}^{\ddagger}/R}$. At 20° C, A is 3×10^{14} sec^{-1}, whilst the apparent frequency factor from [16], to be compared with the experimental value, is 6×10^{5} sec^{-1} using the value of $\Delta C_p{}^{\ddagger}$ derived above. It is clear that the simple model in which a loose libration becomes a complete rotation does not account adequately for the experimental frequency factor which is much higher than that deduced theoretically with the above model; accordingly an alternative mechanism must be sought (see below). Further insight into the molecular processes occurring in the activation step may be obtained by considering isotopic effects in water and ice.

ISOTOPIC EFFECTS

In ice, the ratio of frequency factors for the relaxation rates, $1/\tau$, in H_2O and D_2O is (29) 1.45. The libration frequencies for any pair of corresponding modes of libration in ordinary and heavy ice will be in the ratio (see equation 12)

$$\nu_{H_2O}/\nu_{D_2O} = (2)^{\frac{1}{2}},$$

since the force constants for the libration of the isotopic molecules are approximately the same. The $\sqrt{2}$ factor is also confirmed by the experimental infrared data for water (14). Equation [11] then gives the ratio of frequency factors for the relaxation in ice and D_2O ice as 1.1 if the libration frequencies are such that $h\nu_3 > kT$. The experimental ratio is close to $\sqrt{2}$. This suggests that the libration which becomes a rotation in the relaxation process is a looser one than those predominating in the normal ice structure, since then, if $h\nu_3 < kT$, equation [11] indicates that the isotopic ratio of frequency factors becomes

Can. J. Chem. Downloaded from www.nrcresearchpress.com by 190.90.36.8 on 09/04/12
For personal use only.

$\sqrt{2}$. This value could be accounted for if the relaxation process in ice only occurs at sites where there is a considerable perturbation of the structure, e.g. at crystal defects or imperfections (33) or holes, where one or more of the normal four hydrogen bonds is absent or where two H atoms are in opposition in a given bond. The librational potential energy well for a molecule at a bond-vacancy site will then be less deep (Fig. 9) and the librational frequency of the molecule would be correspondingly less. Sufficiently loose librations ($\nu_3 < kT/h$) to account for the isotopic factor of $\sqrt{2}$ must have frequencies less than about 210 cm^{-1}. Such a mode of motion is, in fact, known in ice (14) near this frequency.

In liquid water the situation is different. From the data in Table I, the entropy of activation, e.g., at 30° C for D_2O is 5.1 and that for H_2O at the same temperature is 4.4 cal ° C^{-1} $mole^{-1}$. The ratio of experimental frequency factors for H_2O and D_2O at 30° C is hence $\exp[-0.7/R] \doteqdot 1/\sqrt{2}$, i.e. in the *opposite direction* to that found with ice. Qualitatively the higher positive entropy of activation found for the relaxation rate in D_2O than in H_2O follows from the greater degree of order which exists in liquid D_2O (14) than in water owing to the greater apparent* strength of "deuterium-bonds" than that of hydrogen bonds. In the rotation of the D_2O molecule from its initial state of libration more entropy is gained than in water, since the initial state is more regular in D_2O. The apparent strength of the "deuterium bond" in D_2O is some 0.23 kcal $mole^{-1}$ greater than that of the hydrogen bond in water, as may be deduced from the heats of sublimation of D_2O and H_2O (12,631 and 12,170 cal $mole^{-1}$ respectively (30)); hence in D_2O there will be less thermal perturbation of the structure by bond-bending than in H_2O. The origin of this isotopic difference in the heats of sublimation has been explained by Eucken (31). The greater interaction energy between D_2O molecules in heavy water than between H_2O molecules in ordinary water also accounts for the consistently higher value (about 0.3 kcal) of $\Delta H^{\circ\ddagger}$ (Table I) for the relaxation rate in D_2O than in H_2O, since more energy is required rotationally to displace a D_2O molecule than an H_2O molecule. The higher value of $\Delta H^{\circ\ddagger}$ leads to an isotopic effect on the relaxation rate opposite in direction to that arising from the difference in frequency factors. Thus at 30° C, the ratio of the terms containing the heats of activation for rotation of H_2O and D_2O is $(e^{-3650/RT})/(e^{-3970/RT})$, i.e. 1.71. The ratio of the relaxation rates is hence

$$(1/\tau_{H_2O})/(1/\tau_{D_2O}) = 0.7 \times 1.71, \text{ i.e. } 1.20.$$

At 30° C, comparison of the actual values of τ (8) for D_2O and H_2O gives $\tau_{D_2O}/\tau_{H_2O} = 1.22$.

Positive values of $\Delta S^{\circ\ddagger}$ which are found (Table I) for the relaxation process in water may be contrasted with the negative ones found for more complex molecules, e.g., permitol (36). However, it is not difficult to see that the rotation of large and complex molecules such as the chlorinated diphenyls may well require more co-operative (and hence less probable) reorientation by neighboring molecules than is the case for rotation of a water molecule in water. Furthermore, an important qualitative difference between these cases is that the water is already a relatively highly ordered structure (21), whilst there is no evidence that a similar structure exists in permitol. Any thermal perturbations, such as those involved in the reorientation of a molecule, may not unreasonably be supposed to lead locally to more disordered configurations in the quasi-crystalline water structure. That this is likely is indicated by the positive values of $\Delta S^{\ddagger}$ which become more positive with decreasing temperature (see the data in Table I). Such a

*This effect arises (34) from the lower zero-point librational energies of the deuterium analogue than those of water.

Can. J. Chem. Downloaded from www.nrcresearchpress.com by 190.90.36.8 on 09/04/12
For personal use only.

trend of the $\Delta S^{\ddagger}$ values would not be unexpected in the case of water, since the degree of quasi-crystalline structure in the liquid increases with decrease of temperature so that the initial state of the relaxation process can become relatively more ordered, i.e., have a lower entropy. A more quantitative evaluation of the frequency factors for the rotation process in liquid water and deuterium oxide must await a more detailed knowledge of the structure of water and how it depends on temperature.

PROTON MOBILITY IN WATER AND ICE, AND THE ROTATION MECHANISM

We have shown previously (10, 26) in calculations of the proton mobility in aqueous solutions, that above a certain critical concentration of about 10^{-6} M in H_3O^+ ions, there is a sufficient flux of protons that virtually all rotations of solvent molecules which occur do so in the fields of each newly produced H_3O^+ ion as the latter is formed from an antecedent H_3O^+ ion by rapid proton tunneling (10) to an adjacent water molecule already reoriented in the immediately preceding proton jump event. Whilst the actual concentration of H_3O^+ and OH^- ions is small (10^{-7} g ion $l.^{-1}$ at 25° C, of each ion), they can indirectly affect a large number of water molecules.

The rotation rate, which is observed in dielectric dispersion experiments, may therefore correspond to rotation of water molecules in the fields of the H_3O^+ (and/or OH^-) ions, as the protons arrive at various sites during their motion throughout the liquid. Such a mechanism is consistent with a number of aspects of the relaxation behavior.

Rotation of water molecules adjacent to the H_3O^+ ions may account for the apparent lack of any significant distribution of relaxation times in water; thus, it has consistently been observed that the dispersion behavior can be treated in terms of a single* relaxation time, which suggests that the rotations occur in a relatively reproducible environment, e.g. adjacent to and in the strong orienting fields of the ions. On the other hand, random thermal bond bending in "non-ionic" environments in the bulk water structure might be expected to lead to a distribution of heats of activation for rotation, and hence of the corresponding relaxation times.

In support of these views, it may be noted that the heat of activation for rotation in water (3–5 kcal $mole^{-1}$) is considerably less than that required to break four hydrogen bonds even in a partially thermally perturbed structure of water. The rotation process in the field of the new H_3O^+ ion upon arrival of a proton at a given water molecule will have a lower heat of activation (cf. 10) than that for rotation in the bulk of the solvent, since the energy of interaction (*ca.* 15 kcal $mole^{-1}$) of the water dipole with the ion assists the rotation process. When molecules are rotated near the ion out of their normal average orientations in the 4-co-ordinated water structure, a multiplicative effect can originate, since rotation of one molecule causes temporary opposition of OH bonds between nearest neighbors (i.e., there are "bonds" doubly occupied by H atoms as shown in Fig. 8); this facilitates rotation of a neighboring molecule by repulsion in the doubly occupied "bonds". This effect will enhance the probability of rotation and could account for the experimentally observed greater probability of rotation than that calculated for simple thermal reorientation on the basis of librational partition functions as from equations [13] and [16].

In ice, the different isotopic effects from those in water and the much greater heat of activation suggest a different mechanism for the rotational process. We have shown previously (26) that on account of the lower proton concentration in ice, the proton

**Some heterogeneity may still be present but not apparent in the Cole and Cole plot. This, for example, is shown with mixtures (36) in certain ranges of concentration.*

Can. J. Chem. Downloaded from www.nrcresearchpress.com by 190.90.36.8 on 09/04/12
For personal use only.

mobility in ice is no longer limited in its rate (as it is in water) by the rotation of water molecules in the fields of H_3O^+ ions, the rotation process occurring predominantly amongst neighboring water molecules in the absence of ionic fields. The observed heat of activation for the relaxation is then about 13 kcal mole^{-1} (29, 33) as expected (see Figs. 6, 9) for thermal reorientation.

The self-consistency of the proposed change of mechanism may be checked by calculating the relative probabilities of relaxation by the field-induced mechanism, (I), and the thermal reorientation mechanism, (II). Process I can be regarded as a pseudo-unimolecular reaction involving H_3O^+ and H_2O while II is to be regarded as unimolecular involving only H_2O. $\Delta H^{\circ\ddagger}$ for I is 3.9 kcal mole^{-1} at 25° C (see Table I) and $\Delta H^{\circ\ddagger}$ for II is 13.3 kcal mole^{-1} (29). The relative probability R that rotations will occur in unit volume and time by process I or by II is given approximately by

$$R = 3\times10^{14}\, a_{H_3O^+}\times 4\, \exp[-3900/RT]/1.8\times10^{-15}\times55.5\, \exp[-13300/RT] \quad [17]$$

and is unity when $a_{H_3O^+}$ is about 10^{-5} g ion l.$^{-1}$. In equation [17], the figures 3×10^{14} and 1.8×10^{15} are the experimental frequency factors for rotation in water and ice, respectively, and the factor 4 allows for the fact that each H_3O^+ ion influences the orientation of four nearest neighbor water molecules. The mechanism of rotation would hence tend to become predominantly II as C_{H^+} is decreased much below about 10^{-5} g ion l.$^{-1}$ (as in ice) and mainly I in more acidic solutions ($a_{H_3O^+} > 10^{-5}$ g ion l.$^{-1}$). Comparable contributions from both mechanisms would occur at proton concentrations of the order of magnitude of 10^{-5} g ion l.$^{-1}$. This concentration, at which a change of mechanism for rotation is predicted, is of a similar order of magnitude as that for which the change of mechanism for proton mobility is indicated (26).

Upon addition of extra protons to the ice by the formation of solid solutions with an acid we should expect a change of mechanism of proton mobility back to that (viz. rate-determining rotation of water molecules in the field of H_3O^+ ions) which occurs in water (10), and a corresponding drop of the heat of activation for rotation of the water molecule as discussed above. In ice containing traces of HF this is actually found (33) and the experimentally observed heat of activation for relaxation drops from 13 kcal mole^{-1} in pure ice to about 5 kcal mole^{-1} in HF–ice, a value very close to that for liquid water at 0° C (Table I). It therefore appears that the mechanisms for relaxation in pure ice and water differ on account of the different orders of concentration of ions in these phases, the critical concentration of H_3O^+ or OH^- ions for the change of mechanisms both of proton mobility (26) and dielectric relaxation, being about 10^{-6} to 10^{-7} mole l.$^{-1}$. Although protons are present in ice, it appears that they do not participate significantly in the relaxation process unless they are present above the critical concentration (10, 26). Below this concentration the rotation of the molecules can occur at non-ionic defect sites. This conclusion is supported by the work of Gränicher *et al.* (33). The proton polarization mechanism of Latimer (25) appears to be applicable only when the ice contains extra protons (33).

In pure liquid methanol where the proton concentration is very much lower than in ice or water, it is experimentally found (12, 36) that the frequency factor for relaxation is about 2.5×10^{12} (36) and $\Delta C_p^{\ddagger}$ is very small or zero within the experimental accuracy of the results (12). Theoretically, using [13], a value of the order 10^{13} is expected if the mechanism is one of rotation amongst other methanol molecules and not in the fields of ions. These values are in much better agreement than in the case of water considered above and give a further indication that in liquid water a simple rotation process amongst

Can. J. Chem. Downloaded from www.nrcresearchpress.com by 190.90.36.8 on 09/04/12
For personal use only.

other water molecules is unlikely to be the mechanism of relaxation. The isotopic ratio of relaxation frequencies in MeOH and MeOD appears to be about $(2)^{\frac{1}{2}}$ (12), within the experimental uncertainties, as expected from [13] if the librational mode becoming a rotation upon activation, is a loose one, and is consistent with a non-ionic mechanism. This is also the ratio found for ice, for which the non-ionic mechanism is indicated.

ACKNOWLEDGMENT

The author is indebted to Dr. D. W. Davidson for making available some results on the relaxation behavior of MeOH and MeOD prior to their publication.

REFERENCES

1. Pauling, L. Phys. Rev. **36**, 430 (1930).
2. Giauque, W. F. and Wiebe, R. J. Am. Chem. Soc. **50**, 101, 2193 (1928); **51**, 1441 (1929).
3. Clusius, K. Z. Elektrochem. **39**, 528 (1933).
4. Smyth, C. P. and Hitchcock, C. S. J. Am. Chem. Soc. **56**, 1084 (1934).
5. Cone, R. M., Denison, G. H., and Kemp, J. D. J. Am. Chem. Soc. **53**, 1278 (1931).
6. Stearn, A. E. and Eyring, H. J. Chem. Phys. **7**, 113 (1937).
7. Kauzmann, W. Revs. Mod. Phys. **14**, 12 (1942).
8. Smyth, C. P. Dielectric behavior and molecular structure. McGraw-Hill Book Co., Inc., New York. 1955.
9. Collie, C. H., Hasted, J. B., and Ritson, D. M. Proc. Phys. Soc. (London), **60**, 145 (1948).
10. Conway, B. E., Bockris, J. O'M., and Linton, H. J. Chem. Phys. **24**, 834 (1956).
11. Hennelley, E. J., Heston, W. M., and Smyth, C. P. J. Am. Chem. Soc. **70**, 4102 (1948).
12. Davidson, D. W. Can. J. Chem. **35**, 458 (1957).
13. Everett, D. H. and Wynne-Jones, W. F. K. Trans. Faraday Soc. **35**, 1380 (1939).
14. Cross, P. C., Burnham, J., and Leighton, P. A. J. Am. Chem. Soc. **59**, 1134 (1957).
15. Ewell, R. H. and Eyring, H. J. Chem. Phys. **5**, 726 (1937).
16. Lennard-Jones, J. and Pople, J. A. Proc. Roy. Soc. (London), A, **205**, 155, 163 (1951).
17. Coulson, C. A. Valence. Oxford University Press, London. 1953.
18. Schneider, W. G. J. Chem. Phys. **23**, 26 (1955).
19. Coulson, C. A. and Danielsson, U. Arkiv Fysik, **8**, 239, 245 (1954).
20. Powles, J. G. J. Chem. Phys. **20**, 1302 (1952).
21. Bernal, J. D. and Fowler, R. H. J. Chem. Phys. **1**, 515 (1933).
22. Garton, C. G. Trans. Faraday Soc. A, **42**, 56 (1946).
23. Frenkel, J. Kinetic theory of liquids. Oxford University Press, London. 1946.
24. Schellman, J. A. Ph.D. Thesis, Princeton University. 1951.
25. Latimer, W. M. Chem. Revs. **44**, 59 (1949).
26. Conway, B. E. and Bockris, J. O'M. J. Chem. Phys. **28**, 354 (1958).
27. Fowler, R. H. Statistical mechanics. Cambridge University Press, London. 1936.
28. Eley, D. D. and Evans, M. G. Trans. Faraday Soc. **34**, 1093 (1938).
29. Auty, R. P. and Cole, R. H. J. Chem. Phys. **20**, 1309 (1952).
30. Bartholemé, E. and Clusius, K. Z. physik. Chem. B, **28**, 167 (1935).
31. Eucken, A. Nachr. Akad. Wiss. Göttingen, Math-phys. Kl. Biol. physiol. chem. Abt. 1 (1949).
32. Frank, H. C. and Wen, W. Y. Discussions Faraday Soc. Preprint No. 11 (1958) (In press).
33. Gränicher, H., Jaccard, C., Scherrer, P., and Steinmann, A. Discussions Faraday Soc. **23**, 50 (1957).
34. Whalley, E. Trans. Faraday Soc. **53**, 1578 (1957).
35. Glasstone, S., Laidler, K. J., and Eyring, H. The theory of rate processes. McGraw-Hill Book Co., Inc., New York. 1941.
36. Denney, D. J. and Cole, R. H. J. Chem. Phys. **23**, 1767 (1955).
37. Moelwyn Hughes, E. A. Physical chemistry. Cambridge University Press, London. 1947.

Can. J. Chem. Downloaded from www.nrcresearchpress.com by 190.90.36.8 on 09/04/12
For personal use only.

Can. J. Chem. Downloaded from www.nrcresearchpress.com by 190.90.36.8 on 09/04/12
For personal use only.

NOTES

PREPARATION AND CHEMISTRY OF TRANS 1-CYANO-4-CHLORO-2-BUTENE

CL. DAESSLE, E. J. TARLTON, AND A. F. MCKAY

Trans 1-cyano-4-chloro-2-butene (III) and 1-cyano-2-chloro-3-butene (II) were prepared by the addition of butadiene to a complex of aluminum chloride and cyanogen chloride in nitromethane. Cowen (1) previously used this complex to add cyanogen

$$\underset{\text{I}}{CH_2{=}CH{-}CH{=}CH_2} + CNCl \xrightarrow{AlCl_3} \underset{\text{II}}{CH_2{=}CH{-}CHClCH_2CN} + \underset{\text{III}}{CH_2ClCH{=}CHCH_2CN}$$

chloride to monoolefins. Both 1-cyano-4-chloro-2-butene (III) and 1-cyano-2-chloro-3-butene (II) were converted in liquid ammonia into 1-cyano-1,3-butadiene. The former compound also gave 1-cyano-1,3-butadiene on treatment with hexamethylenetetramine. The known 1,4-dicyano-2-butene (2, 3, 4) was prepared by the reaction of sodium cyanide with 1-cyano-4-chloro-2-butene in the presence of cuprous chloride.

3-Carbethoxy-7-cyano-5-hepten-2-one was prepared by condensation of ethyl acetoacetate with 1-cyano-4-chloro-2-butene in the presence of sodium ethylate. Similar reaction with diethyl malonate gave ethyl 2-carbethoxy-6-cyano-4-hexenoate (12.6% yield), identified by its conversion to pimelic acid through subsequent hydrogenation, hydrolysis, and decarboxylation (5).

The main bands of the infrared absorption spectra of these nitrile derivatives are listed in Table I. The assignments agree with those reported by Bellamy (6). 1-Cyano-4-chloro-2-butene, 1,4-dicyano-2-butene, and 3-carbethoxy-7-cyano-5-hepten-2-one display a strong absorption band at 968–972 cm^{-1} characteristic of CH out-of-plane

TABLE I

Infrared absorption bands of nitrile derivatives

	C—H stretching	C≡N stretching	C—H in-plane deformations	C—H out-of-plane deformations	Other bands
$CNCH_2CH{=}CHCH_2Cl$	3040, 2960, 2930, 2850	2270 (m)	1412, 1441	968 (s), 936 (w), 909 (w)	688
$CNCH_2CH{=}CH{-}CH_2CN$		2265 (m) 2230 (sh)	1416 (s)	972 (s), 912 (m)	
$CN{-}CH{=}CH{-}CH{=}CH_2$	3120, 3080, 3000, 2950, 2925, 2860	2235 (s)		1004 (m), 966 (sh), 958 (sh), 933 (m)	1623 (C=C) (m) 1593 (m), 1530
$CNCH_2CHClCH{=}CH_2$	3080, 2965, 2930, 2875	2270 (m)	1414	986 (s), 955 (sh), 938 (s), 909 (sh)	700 (s), 1530
$CH_3C(O)CH(COOEt)$-$CH_2CH{=}CHCH_2CN$	2970, 2930 (sh)	2270 (m→w)	1418, 1460	970 (m→s), 926 (vw), 906 (vw)	677 (s), 1733 (ester) (s), 1719 (carbonyl) (s), 1623 (C=C) (m)

s, Strong; m, medium; w, weak; and vw, very weak absorption bands; sh, shoulder on stronger absorption bands.

deformation for a trans —CH=CH— group. 1-Cyano-1,3-butadiene and 1-cyano-2-chloro-2-butene have absorption bands at 1004 cm^{-1} and 986 cm^{-1}, respectively, which are associated with the CH out-of-plane deformations of the vinyl group. 1-Cyano-1,3-butadiene also has an absorption band at 966 cm^{-1}, since it also contains the —CH=CH— grouping. The absorption spectrum of 1,4-dicyano-2-butene was determined in Nujol mull so the C—H stretching vibrations are not recorded in Table I.

EXPERIMENTAL[1]

Cyanogen Chloride

Cyanogen chloride was prepared as a clear, colorless liquid in 70% yield by the method of Barnett *et al.* (7).

Addition of Cyanogen Chloride to Butadiene

Cyanogen chloride (52 ml, 1.0 mole) was vaporized into a mixture of anhydrous aluminum chloride (133.5 g, 1.0 mole) in nitromethane (100 ml) cooled to −5° C. Butadiene (27 l., 1.1 mole) was led in under the surface of this reaction mixture over a period of 3 hours. Strong cooling was required to maintain the temperature between 0 and 5° C. After the addition of the butadiene, the reaction mixture was poured into ice and water, and acidified with dilute hydrochloric acid solution. This acidified mixture was extracted with ether, the ether was removed by evaporation, and the residue was distilled *in vacuo*. The following fractions were obtained: (1) liquid b.p. 90–95° C at 15 mm, yield 25 g; (2) yellow liquid b.p. 100–105° C at 15 mm, yield 12.5 g; and (3) liquid b.p. 100–150° C at 2–3 mm, yield 3.5 g. Redistillation *in vacuo* using a Vigreux column gave 16.5 g (14.3%) of 1-cyano-2-chloro-3-butene (b.p. 74–76° C at 13 mm, n_D^{25} 1.45837) and 19 g (16.4%) of 1-cyano-4-chloro-2-butene (b.p. 105–107° C at 13 mm, 67–68° C at 1.5 mm, n_D^{25} 1.47330, d_4^{25} 1.087, M_R calc. 29.44, found 29.85). 1-Cyano-2-chloro-3-butene, anal. calc. for C_5H_6ClN: C, 52.05; H, 5.23; Cl, 30.70; N, 12.12%. Found: C, 51.94; H, 5.27; Cl, 30.02; N, 12.54%. 1-Cyano-4-chloro-2-butene, anal. calc. for C_5H_6ClN: C, 52.05; H, 5.23; Cl, 30.70; N, 12.12%. Found: C, 51.86; H, 5.41; Cl, 30.34; N, 12.41%. The physical constants reported by Prichard and Whitman (8) for 1-cyano-4-chloro-2-butene are b.p. 44–46° C at 0.3 mm and n_D^{25} 1.4735.

In other experiments where the amount of aluminum chloride was reduced to 0.1 mole or replaced by antimony pentachloride, only resinous products were obtained. In the presence of zinc chloride (ethereal solution), cyanogen chloride and butadiene failed to react.

1-Cyano-1,3-butadiene

Method A.—1-Cyano-4-chloro-2-butene (4.8 g, 0.042 mole) was dissolved in liquid ammonia (80 ml) and the solution was allowed to stand for 3 hours. After the ammonia had evaporated from the reaction mixture, the residue was extracted with ether. The liquid residue from the ether extract was fractionally distilled *in vacuo*. The main fraction (b.p. 56–58° C at 42 mm; n_D^{25} 1.4892) was 1-cyano-1,3-butadiene, yield 2.4 g (75%). Anal. Calc. for C_5H_5N: C, 75.91; H, 6.37; N, 17.70%. Found: C, 75.61; H, 6.37; N, 18.18%. The physical constants of 1-cyano-1,3-butadiene are reported by Snyder and Poos (9) to be b.p. 49.5–53° C at 31 mm, n_D^{20} 1.4852–1.4895.

Method B.—1-Cyano-2-chloro-3-butene (4.8 g, 0.042 mole) on treatment with liquid

[1]*All melting points and boiling points are uncorrected. Microanalyses by Micro-Tech Laboratories, Skokie, Ill.*

Can. J. Chem. Downloaded from www.nrcresearchpress.com by 190.90.36.8 on 09/04/12
For personal use only.

ammonia under the conditions described in method A gave a 72% yield of 1-cyano-1,3-butadiene (b.p. 56–58° C at 43 mm). This product was identified by its infrared spectrum and analysis.

Method C.—1-Cyano-4-chloro-2-butene (5.6 g, 0.05 mole) was added to hexamethylenetetramine (7 g, 0.05 mole) in chloroform (50 ml) and the reaction mixture was heated under reflux for 18 hours. After the reaction mixture cooled to room temperature, the precipitated hexamethylenetetramine hydrochloride was removed by filtration. The filtrate was evaporated to remove chloroform and the residue was filtered free from solid. Fractional distillation of the filtrate gave 1.5 g (45%) of 1-cyano-1,3-butadiene (b.p. 75° C at 70 mm). This product was identified by a comparison of its infrared spectrum and physical properties with 1-cyano-1,3-butadiene prepared by method B.

1,4-Dicyano-2-butene

1-Cyano-4-chloro-2-butene (3.42 g, 0.03 mole) was added over a period of 1 hour to a refluxing suspension of sodium cyanide (1.5 g, 0.03 mole) and cuprous chloride (0.12 g) in acetonitrile (8.4 g) under an atmosphere of nitrogen. The reaction mixture was refluxed for a further period of 48 hours after which the hot mixture was filtered and the filter cake was washed with hot acetonitrile. The combined filtrate and washings were evaporated and the crystalline residue was dissolved in methanol. This methanol solution on cooling deposited crystals (m.p. 74–76° C), yield 1.2 g (35%). The reported melting points of 1,4-dicyano-2-butene are 75–77° C (4) and 74° C (2).

3-Carbethoxy-7-cyano-5-hepten-2-one

A solution of ethyl acetoacetate (6.3 g, 0.045 mole) and sodium metal (1.05 g, 0.045 mole) in ethanol (23 ml) was treated dropwise (cooling) with 1-cyano-4-chloro-2-butene (5.2 g, 0.045 mole), and the reaction was allowed to proceed at room temperature overnight. The precipitated sodium chloride was removed by filtration and the filtrate was evaporated *in vacuo*. Dilution of the residue with water (20 ml) followed by ether extraction gave a crude oil, which was distilled *in vacuo* to give 2.5 g (26.6%) of 3-carbethoxy-7-cyano-5-hepten-2-one (b.p. 134–136° C at 0.6 mm, n_D^{25} 1.4592, d_4^{25} 1.078). Anal. Calc. for $C_{11}H_{15}NO_3$: C, 63.11; H, 7.22; N, 6.69%. Found: C, 63.27; H, 7.12; N, 7.06%.

ACKNOWLEDGMENT

The infrared absorption spectra were determined by Dr. C. Sandorfy of the Department of Chemistry, University of Montreal, Montreal, Quebec.

1. COWEN, F. M. J. Org. Chem. **20**, 287 (1955).
2. KURTZ, P. Ann. **572**, 23 (1951).
3. CASS, O. W. and ROGERS, A. O. U.S. Patent No. 2,342,101; Chem. Abstr. **38**, 4622 (1944).
4. IMPERIAL CHEMICAL INDUSTRIES LTD. Brit. Patent No. 647,420; Chem. Abstr. **45**, 7139 (1951).
5. CHARLISH, J. L., DAVIS, W. H., and ROSE, J. D. J. Chem. Soc. 232 (1948).
6. BELLAMY, L. J. The infrared spectra of complex molecules. Methuen & Co., London. 1954.
7. BARNETT, H. W., DAVIS, R. G., and GRAHAM, R. P. Can. J. Research, B, **25**, 289 (1947).
8. PRICHARD, W. W. and WHITMAN, G. M. U.S. Patent No. 2,524,833; Chem. Abstr. **45**, 1618 (1951).
9. SNYDER, H. R. and POOS, G. I. J. Am. Chem. Soc. **71**, 1055 (1949).

RECEIVED SEPTEMBER 9, 1958.
REPORT NO. 23,
L. G. RYAN RESEARCH LABORATORIES,
MONSANTO CANADA LIMITED,
VILLE LASALLE, QUEBEC.

Can. J. Chem. Downloaded from www.nrcresearchpress.com by 190.90.36.8 on 09/04/12
For personal use only.

Can. J. Chem. Downloaded from www.nrcresearchpress.com by 190.90.36.8 on 09/04/12
For personal use only.

INFRARED SPECTRUM OF CRYSTALLINE H_2S_2

NUMAN ZENGIN[1] AND PAUL A. GIGUÈRE

Wilson and Badger (1) have measured the infrared spectrum of gaseous hydrogen persulphide, H_2S_2, while Fehér and his co-workers (2, 3) have studied the Raman spectrum of the liquid. However, no structural investigation of the crystal, either by X-ray diffraction or spectroscopy, has been reported yet. The infrared spectrum of that solid is of some interest in view of the close analogy of the molecule with hydrogen peroxide, on the one hand, and the absence of hydrogen bonding, on the other hand.

The sample of H_2S_2 used for the present work was prepared after the method of Butler and Maass (4). Three successive fractional distillations were sufficient to yield a clear, colorless liquid, free from higher polysulphides. All traces of water were removed by collecting the distillate over P_2O_5. The final product seemed very stable when kept at dry-ice temperature in a Pyrex flask previously treated with gaseous HCl. No analyses were carried out since the purity of the persulphide was confirmed by the absence from its spectra of any absorption due to H_2S. As a further precaution the measurements were always made on freshly distilled samples. Clear, transparent films of the solid were easily obtained by deposition of the vapor on disks of NaCl or CsI cooled to liquid-air temperature in a conventional absorption cell. From the amount of liquid used and the surface of the salt disk and its metal support, the thickness of the crystalline films was estimated of the order of 10 microns. The infrared absorption was measured over the range 290 to 5000 cm^{-1} with a Perkin–Elmer, Model 12-C spectrometer using prisms of NaCl, KBr, and CsBr.

The various bands observed are shown in Fig. 1 and the frequency of the maxima are listed in Table I along with those of the gas and the Raman shifts of the liquid. As could be expected from the weakness of the intermolecular forces, the vibrational frequencies of the free molecule change very little in the condensed phases. For the same

TABLE I

Frequency of the bands in the infrared spectra of crystalline H_2S_2

Gas, cm^{-1}	Liquid, cm^{-1}	Solid, cm^{-1}	Intensity	Assignment
	509	501	w.	ν_3
		518	v.w.	
		814	w.	$\nu_6 - \nu_T$
		857	v.w.	
		868	v.s.	ν_2 or ν_6
875		881	v.w.	
897	882	890	v.s.	ν_6
		940	v.w.	$\nu_6 + \nu_T$
		1070	m.	$\nu_6 + \nu_4$?
		2380	v.w.	$\nu_5 - \nu_R$
2557		2480	v.s.	ν_5
	2509	2495	s.	ν_1 ?
		2590	w.	$\nu_5 + \nu_R$
		2930	v.w.	
3065		2960	w.	$\nu_3 + \nu_5$
		2995	v.w.	
3400		3345	m.	$\nu_5 + \nu_6$
5007		4840	v.w.	$\nu_1 + \nu_5$

[1]*Postdoctorate Fellow of the National Research Council, Ottawa, Canada. Present address: University of Ankara, Faculty of Science, Ankara, Turkey.*

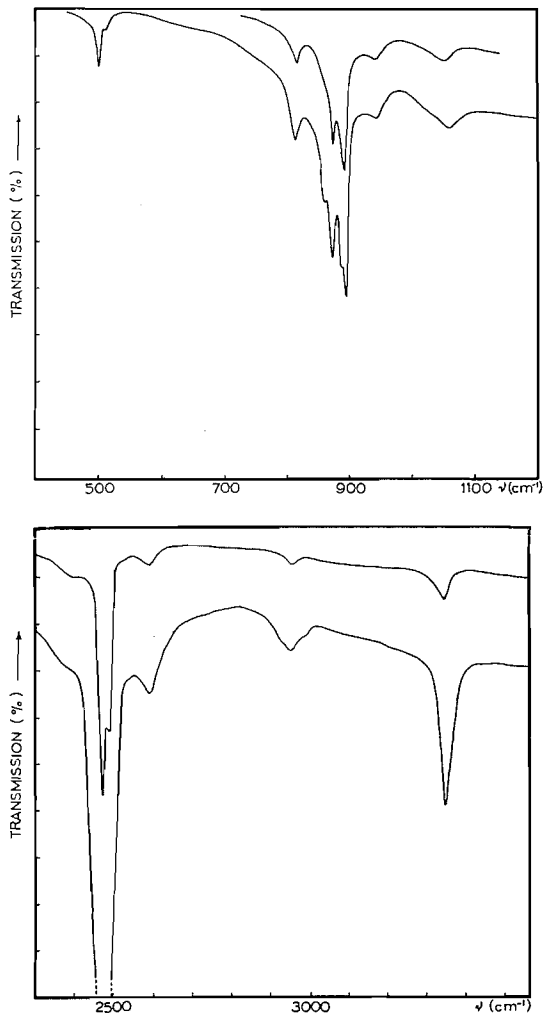

FIG. 1. Infrared absorption spectra of crystalline H_2S_2, for two films of different thickness.

reason the H_2S_2 bands are much sharper than those of its oxygen analogue, H_2O_2 (5). Apart from ν_3, the S–S stretching vibration at 501 cm^{-1}, the S–H stretching and bending fundamentals give rise to regions of strong absorption near 2500 and 880 cm^{-1} respectively. Because the crystal structure of H_2S_2 is unknown the various peaks in these two bands cannot be assigned unambiguously. Tentatively the pair of strong lines at 890 and 868 cm^{-1} may be ascribed to the asymmetric (ν_6) and the symmetric (ν_2) bending modes although they could also be two components of the former mode. The very weak shoulders at 10 cm^{-1} on the low-frequency side of the two main peaks, visible only in the thickest samples, might conceivably belong to the isotopic molecules $HS^{32}S^{34}H$ (natural abundance about 4%). They show roughly the same relative intensity as some of the isotopic bands of SO_2 (6). Sum–difference combinations of the bending frequencies with a lattice vibration of some 65–70 cm^{-1} give rise to the weak satellites at 814 and 940 cm^{-1}. Another combination band at 1070 cm^{-1} involves, no doubt, ν_6 and a frequency of the order of 200 cm^{-1}. This is of the right magnitude for ν_4, the torsional frequency,

Can. J. Chem. Downloaded from www.nrcresearchpress.com by 190.90.36.8 on 09/04/12
For personal use only.

which has not been detected yet. It must be added, however, that it could also fit one of the libration frequencies of the H_2S_2 molecule, namely that about the S–S axis. As in the case of H_2O_2 (7) these two frequencies are expected to lie fairly close together. Naturally the corresponding frequencies are very much higher in solid H_2O_2 (about 650 cm^{-1}) on account of the strong hydrogen bonds. The strongest lines at 2480 and 2495 cm^{-1} also show sum–difference combinations with a lattice frequency of about 110–120 cm^{-1}. Finally the overtone bands at 2960, 3345, and 4840 cm^{-1} are assigned after the corresponding vapor bands (1).

1. WILSON, M. K. and BADGER, R. M. J. Chem. Phys. **17**, 1232 (1949).
2. FEHÉR, F. and BAUDLER, M. Z. Elektrochem. **47**, 844 (1941).
3. FEHÉR, F., LANE, W., and WINKHAUS, G. Z. anorg. Chem. **288**, 113 (1956).
4. BUTLER, K. H. and MAASS, O. J. Am. Chem. Soc. **52**, 2184 (1930).
5. BAIN, O. and GIGUÈRE, P. A. Can. J. Chem. **33**, 527 (1955).
6. REDING, F. P. and HORNIG, D. F. J. Chem. Phys. **27**, 1024 (1957).
7. GIGUÈRE, P. A. and HARVEY, K. B. J. Mol. Spectroscopy. In press.

RECEIVED NOVEMBER 26, 1958.
DEPARTMENT OF CHEMISTRY,
LAVAL UNIVERSITY,
QUEBEC, QUE.

ELECTRON SPIN RESONANCE ABSORPTION SPECTRUM OF PUMMERER'S OXYGEN RADICAL

J. B. FARMER, Y. MATSUNAGA,* AND C. A. MCDOWELL

Though dehydro-hydroxy-binaphthylene-oxide (I) was prepared as early as 1914 by Pummerer and Frankfurter and reported to dissociate nearly completely into free radicals in dilute benzene solution (1), no magnetic measurements have been done on this compound.

The electron spin resonance absorption spectra of dehydro-oxy-binaphthylene-oxide (I), and binaphthyl-bis-peroxy-binaphthylene-oxide (II) in benzene and pyridine solutions, were examined at room temperature at a frequency of 9 k Mc/s, in a high-resolution high-sensitivity electron spin resonance spectrometer constructed in this department (7). The resonance spectrum shown in Fig. 1 was found in both cases and attributed to the existence of the free radical (III). The reddish-violet solution of this free radical is somewhat sensitive toward oxygen, but for these measurements it was unnecessary to handle it in vacuum or in an inert atmosphere.

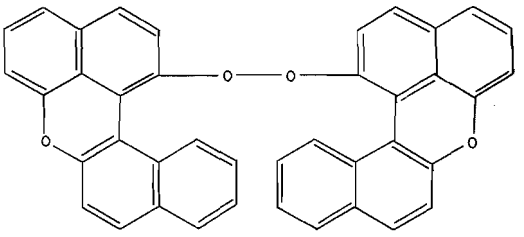

(I)

*N.R.C. Postdoctoral Fellow 1957–.

Can. J. Chem. Downloaded from www.nrcresearchpress.com by 190.90.36.8 on 09/04/12
For personal use only.

which has not been detected yet. It must be added, however, that it could also fit one of the libration frequencies of the H_2S_2 molecule, namely that about the S–S axis. As in the case of H_2O_2 (7) these two frequencies are expected to lie fairly close together. Naturally the corresponding frequencies are very much higher in solid H_2O_2 (about 650 cm^{-1}) on account of the strong hydrogen bonds. The strongest lines at 2480 and 2495 cm^{-1} also show sum–difference combinations with a lattice frequency of about 110–120 cm^{-1}. Finally the overtone bands at 2960, 3345, and 4840 cm^{-1} are assigned after the corresponding vapor bands (1).

1. WILSON, M. K. and BADGER, R. M. J. Chem. Phys. **17**, 1232 (1949).
2. FEHÉR, F. and BAUDLER, M. Z. Elektrochem. **47**, 844 (1941).
3. FEHÉR, F., LANE, W., and WINKHAUS, G. Z. anorg. Chem. **288**, 113 (1956).
4. BUTLER, K. H. and MAASS, O. J. Am. Chem. Soc. **52**, 2184 (1930).
5. BAIN, O. and GIGUÈRE, P. A. Can. J. Chem. **33**, 527 (1955).
6. REDING, F. P. and HORNIG, D. F. J. Chem. Phys. **27**, 1024 (1957).
7. GIGUÈRE, P. A. and HARVEY, K. B. J. Mol. Spectroscopy. In press.

RECEIVED NOVEMBER 26, 1958.
DEPARTMENT OF CHEMISTRY,
LAVAL UNIVERSITY,
QUEBEC, QUE.

ELECTRON SPIN RESONANCE ABSORPTION SPECTRUM OF PUMMERER'S OXYGEN RADICAL

J. B. FARMER, Y. MATSUNAGA,* AND C. A. MCDOWELL

Though dehydro-hydroxy-binaphthylene-oxide (I) was prepared as early as 1914 by Pummerer and Frankfurter and reported to dissociate nearly completely into free radicals in dilute benzene solution (1), no magnetic measurements have been done on this compound.

The electron spin resonance absorption spectra of dehydro-oxy-binaphthylene-oxide (I), and binaphthyl-bis-peroxy-binaphthylene-oxide (II) in benzene and pyridine solutions, were examined at room temperature at a frequency of 9 k Mc/s, in a high-resolution high-sensitivity electron spin resonance spectrometer constructed in this department (7). The resonance spectrum shown in Fig. 1 was found in both cases and attributed to the existence of the free radical (III). The reddish-violet solution of this free radical is somewhat sensitive toward oxygen, but for these measurements it was unnecessary to handle it in vacuum or in an inert atmosphere.

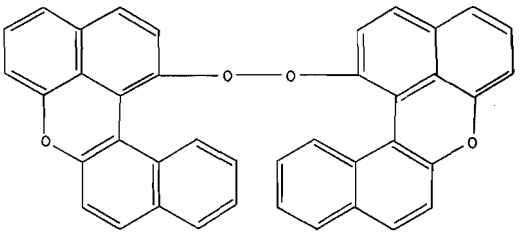

(I)

*N.R.C. Postdoctoral Fellow 1957–.

Can. J. Chem. Downloaded from www.nrcresearchpress.com by 190.90.36.8 on 09/04/12
For personal use only.

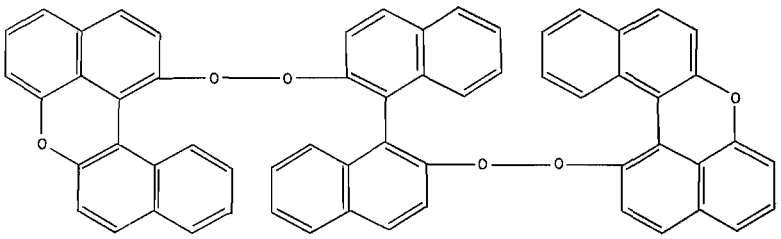

(II)

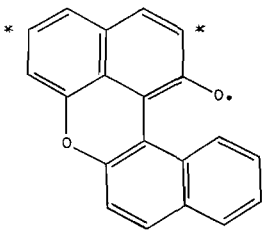

(III)

Dehydro-hydroxy-binaphthylene-oxide (I) and binaphthyl-bis-peroxy-binaphthylene-oxide (II) were prepared by the methods given in refs. 1 and 2, respectively.

The spectra of the two compounds in benzene or pyridine consist of three equally-spaced lines with a separation of 2.5 oersteds. The center of spectrum of Pummerer's radical is located 0.50 oersted lower in field than that of diphenyl-picryl-hydrazyl. If we take the g-value of the latter as 2.0036 (3), the value for Pummerer's radical is approximately 2.0039.

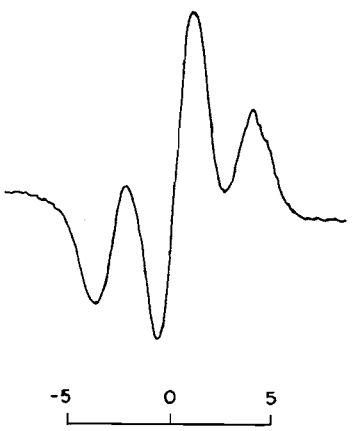

FIG. 1. Electron spin resonance absorption spectrum of Pummerer's oxygen radical.

Can. J. Chem. Downloaded from www.nrcresearchpress.com by 190.90.36.8 on 09/04/12
For personal use only.

As the compounds (I) and (II) give the same resonance spectrum, it appears that the middle part of the compound (II) does not form a biradical in the process of dissociation, or the lifetime of the radical formed is too short to be detected.

The number of lines in Fig. 1 shows that only two protons among eleven in Pummerer's radical can interact with the unpaired electron. It is suggested that the radical is highly distorted by steric hindrance and the distribution of the unpaired electron is restricted to the naphthalene nucleus to which the peroxide oxygen atom is attached. By the simple LCAO-MO method, the density of the frontier electrons, i.e., the electrons in the highest occupied energy level, in β-substituted naphthalene was calculated by Fukui *et al.* (4). Based on their result, the protons which contribute to the hyperfine splitting can be assigned to those attached to the starred carbon atoms in (III). The same conclusion can be obtained by consideration of the following resonance structures:

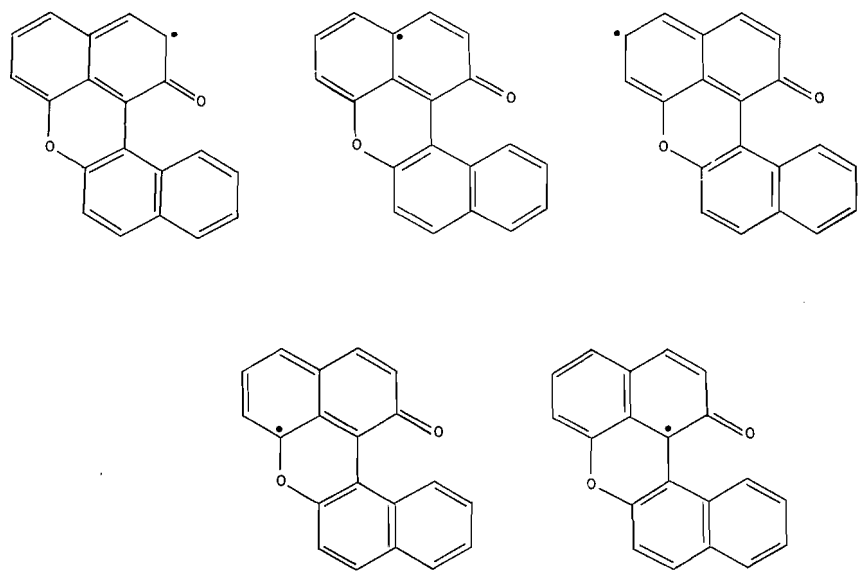

If we assume that the unpaired electron density on each carbon atom in Pummerer's radical is given by one half of the frontier-electron density in β-substituted naphthalene, the constant Q in the relation $a_j = Q \cdot \rho_j$ (5) is about 42 in the present case. This value seems to be of the correct order.

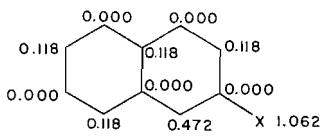

FIG. 2. Density of frontier electrons after Fukui *et al.* (Assumed $\alpha_x = \alpha_c$, $\beta_{cx} = \beta_{ar}$.)

The anomalous stability of Pummerer's radical may be due, in part, to conjugation between the naphthalene nucleus and the attached oxygen atom. However, the main reason is probably that the bulky substituent protects the oxygen atom from any reaction, as in the case of 2,4,6-tri-tert-butyl-1-phenoxyl (6).

We wish to thank the National Research Council and the Defence Research Board for grants in aid of this work.

Can. J. Chem. Downloaded from www.nrcresearchpress.com by 190.90.36.8 on 09/04/12
For personal use only.

1. PUMMERER, R. and FRANKFURTER, F. Ber. **47**, 1472 (1914).
2. PUMMERER, R. and RIECHE, A. Ber. **59**, 2161 (1926).
3. HOLDEN, A. N., YAGER, W. A., and MERRITT, F. R. J. Chem. Phys. **19**, 1319 (1951).
4. FUKUI, K., YONEZAWA, T., NAGATA, C., and SHINGU, H. J. Chem. Phys. **22**, 1433 (1954).
5. MCCONNELL, H. M. J. Chem. Phys. **24**, 632 (1956).
6. MÜLLER, E. and LEY, K. Chem. Ber. **87**, 922 (1954).
7. CORFIELD, W., FARMER, J. B., HORSFIELD, A., and MCDOWELL, C. A. To be published.

RECEIVED NOVEMBER 24, 1958.
DEPARTMENT OF CHEMISTRY,
UNIVERSITY OF BRITISH COLUMBIA,
VANCOUVER 8, BRITISH COLUMBIA.

Can. J. Chem. Downloaded from www.nrcresearchpress.com by 190.90.36.8 on 09/04/12
For personal use only.

THE ADSORPTION OF SULPHUR DIOXIDE BY GRAPHITE*

H. L. MCDERMOT AND B. E. LAWTON

INTRODUCTION

The adsorption of sulphur dioxide by a number of carbon blacks and graphite has been studied by Beebe and Dell (1). The carbon blacks used were Spheron 6 and a number of samples of Spheron 6 which had been deoxygenated at successively higher temperatures. A very pure graphite whose properties have already been described (4) was used. It was found that the untreated Spheron 6 with about 4% of oxygen on its surface adsorbed about seven times more sulphur dioxide than the samples from which virtually all the oxygen had been removed. It was also found that Spheron 6 which had been deoxygenated and graphitized at 2700° C displayed a similar isotherm to that of pure graphite. Thus it was concluded that the adsorption of sulphur dioxide provided a sensitive method for the detection of chemisorbed oxygen. It is likely that this conclusion can be extended to all polar groups on the surface. In the work reported here the adsorption of sulphur dioxide by artificial graphites was undertaken as a part of the program to study these carbons. Isotherms were measured to test for the presence of chemisorbed oxygen and to ascertain whether the hysteresis effects reported with non-polar gases on these graphites also existed for sulphur dioxide. Finally, isotherms were measured at a number of temperatures to study the temperature dependence of the branches of the hysteresis loop.

EXPERIMENTAL AND RESULTS

The graphites used in these experiments were two Acheson graphites designated by us as GF-3 and GF-5. Their properties have been given before (3, 5).

The sulphur dioxide was obtained from the Matheson Company and used without further purification.

Isotherms were measured at four temperatures for each graphite: at 236.6°, 244.5°, 256.8°, and 273.2° K for GF-3; and at 244.3°, 253.8°, 261.5°, and 273.2° K for GF-5. Adsorption was measured by means of a simple volumetric adsorption apparatus. A Dewar flask full of cracked ice and water was used for the isotherms at 273.2° K. For the lower temperatures, the bath was cooled by pumping liquid nitrogen through a copper coil. Two bath fluids were used: a 50 : 50 mixture of water and ethylene glycol, and a 65 : 35 mixture of chloroform and carbon tetrachloride. The bath was agitated by an electric stirrer and regulated by a sulphur dioxide vapor pressure thermometer. Before each isotherm, the sample was evacuated for at least 12 hours at 200° C.

Issued as D.R.C.L. Report No. 297.

1. PUMMERER, R. and FRANKFURTER, F. Ber. **47**, 1472 (1914).
2. PUMMERER, R. and RIECHE, A. Ber. **59**, 2161 (1926).
3. HOLDEN, A. N., YAGER, W. A., and MERRITT, F. R. J. Chem. Phys. **19**, 1319 (1951).
4. FUKUI, K., YONEZAWA, T., NAGATA, C., and SHINGU, H. J. Chem. Phys. **22**, 1433 (1954).
5. MCCONNELL, H. M. J. Chem. Phys. **24**, 632 (1956).
6. MÜLLER, E. and LEY, K. Chem. Ber. **87**, 922 (1954).
7. CORFIELD, W., FARMER, J. B., HORSFIELD, A., and MCDOWELL, C. A. To be published.

RECEIVED NOVEMBER 24, 1958.
DEPARTMENT OF CHEMISTRY,
UNIVERSITY OF BRITISH COLUMBIA,
VANCOUVER 8, BRITISH COLUMBIA.

Can. J. Chem. Downloaded from www.nrcresearchpress.com by 190.90.36.8 on 09/04/12
For personal use only.

THE ADSORPTION OF SULPHUR DIOXIDE BY GRAPHITE*

H. L. MCDERMOT AND B. E. LAWTON

INTRODUCTION

The adsorption of sulphur dioxide by a number of carbon blacks and graphite has been studied by Beebe and Dell (1). The carbon blacks used were Spheron 6 and a number of samples of Spheron 6 which had been deoxygenated at successively higher temperatures. A very pure graphite whose properties have already been described (4) was used. It was found that the untreated Spheron 6 with about 4% of oxygen on its surface adsorbed about seven times more sulphur dioxide than the samples from which virtually all the oxygen had been removed. It was also found that Spheron 6 which had been deoxygenated and graphitized at 2700° C displayed a similar isotherm to that of pure graphite. Thus it was concluded that the adsorption of sulphur dioxide provided a sensitive method for the detection of chemisorbed oxygen. It is likely that this conclusion can be extended to all polar groups on the surface. In the work reported here the adsorption of sulphur dioxide by artificial graphites was undertaken as a part of the program to study these carbons. Isotherms were measured to test for the presence of chemisorbed oxygen and to ascertain whether the hysteresis effects reported with non-polar gases on these graphites also existed for sulphur dioxide. Finally, isotherms were measured at a number of temperatures to study the temperature dependence of the branches of the hysteresis loop.

EXPERIMENTAL AND RESULTS

The graphites used in these experiments were two Acheson graphites designated by us as GF-3 and GF-5. Their properties have been given before (3, 5).

The sulphur dioxide was obtained from the Matheson Company and used without further purification.

Isotherms were measured at four temperatures for each graphite: at 236.6°, 244.5°, 256.8°, and 273.2° K for GF-3; and at 244.3°, 253.8°, 261.5°, and 273.2° K for GF-5. Adsorption was measured by means of a simple volumetric adsorption apparatus. A Dewar flask full of cracked ice and water was used for the isotherms at 273.2° K. For the lower temperatures, the bath was cooled by pumping liquid nitrogen through a copper coil. Two bath fluids were used: a 50 : 50 mixture of water and ethylene glycol, and a 65 : 35 mixture of chloroform and carbon tetrachloride. The bath was agitated by an electric stirrer and regulated by a sulphur dioxide vapor pressure thermometer. Before each isotherm, the sample was evacuated for at least 12 hours at 200° C.

Issued as D.R.C.L. Report No. 297.

Can. J. Chem. Downloaded from www.nrcresearchpress.com by 190.90.36.8 on 09/04/12
For personal use only.

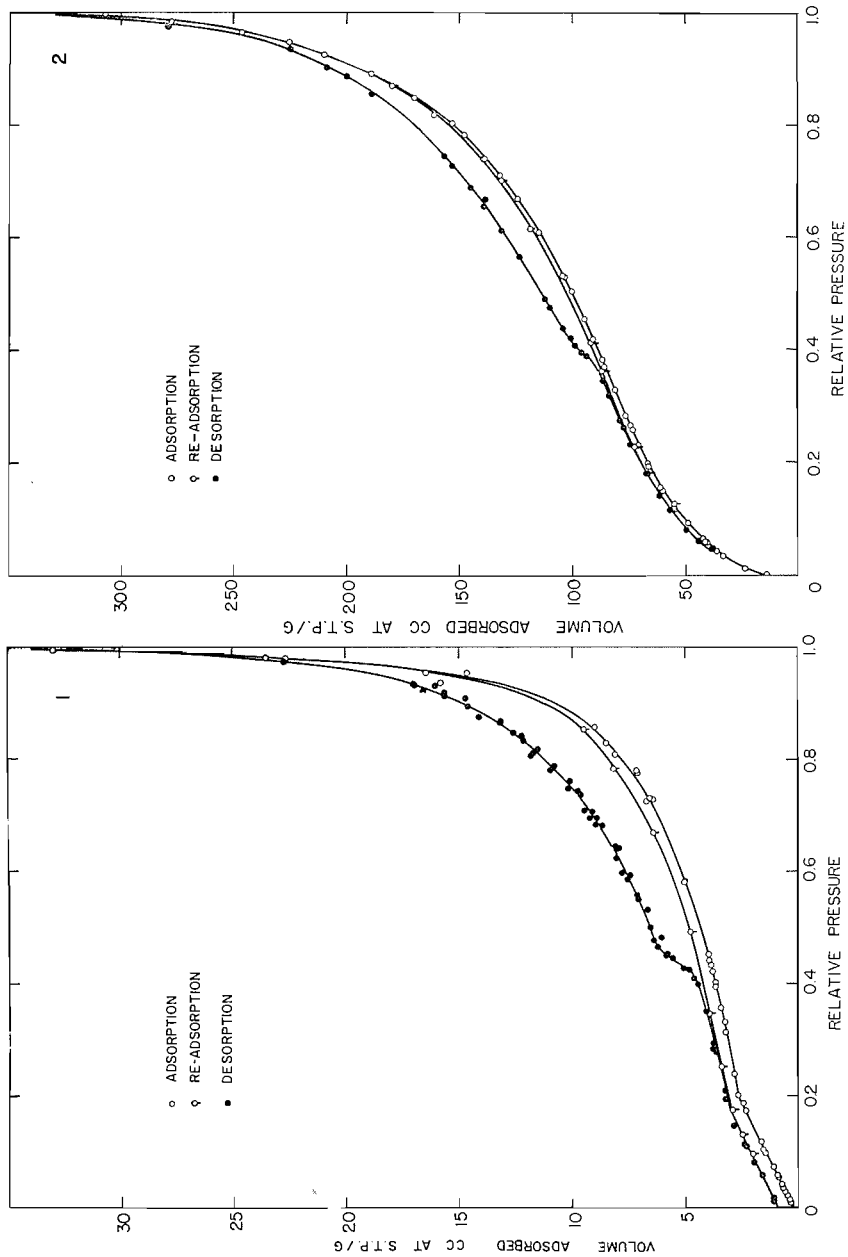

FIG. 1. The adsorption of sulphur dioxide by GF-3 at 256.8° K.
FIG. 2. The adsorption of sulphur dioxide by GF-5 at 253.8° K.

Two typical isotherms are presented in Figs. 1 and 2. Figure 1 shows the isotherm of sulphur dioxide adsorbed on GF-3 at 256.8° K. Figure 2 depicts the isotherm for GF-5 at 253.8° K. It is interesting to note that the isotherm in Fig. 1 shows a sharp break at a relative pressure of about 0.2. This break, which was characteristic of the isotherms measured with GF-3, was absent in those measured with GF-5.

DISCUSSION

The low adsorption of sulphur dioxide by these graphites is indicative of their lack of chemisorbed oxygen. This point is illustrated by Fig. 3, which compares the adsorption of sulphur dioxide by GF-3 and GF-5 with the data of Beebe and Dell (1) for a deoxygenated carbon black and a very pure graphite. All four carbons adsorb sulphur dioxide to about the same degree. It has been demonstrated that smooth isotherms such as have been observed with these graphites for the adsorption of nitrogen and argon are indicative of heterogeneous surfaces (2). The graphites contain little ash and the data given here show the absence of chemisorbed oxygen, hence the heterogeneity must be of the topographic type.

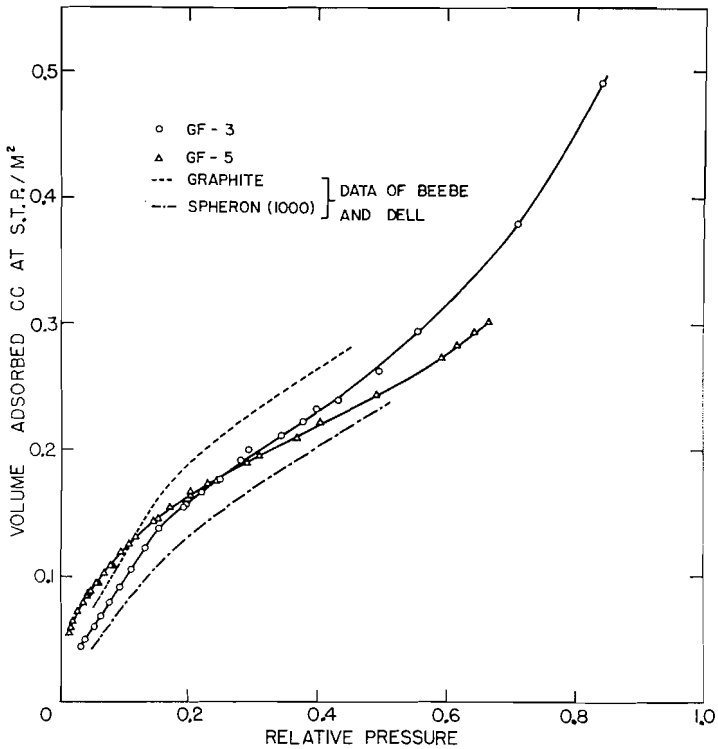

FIG. 3. A comparison of the adsorption of sulphur dioxide by three graphites and a deoxygenated carbon black.

Figures 1 and 2 show that isotherms of both of these graphites give evidence of what we have called "swelling" type hysteresis as well as the normal hysteresis caused by the presence of pores. The "swelling" type hysteresis manifests itself as a second curve just above the initial adsorption curve extending from low to high relative pressures. Isosteric heats have been calculated from both of these curves using data from all four

Can. J. Chem. Downloaded from www.nrcresearchpress.com by 190.90.36.8 on 09/04/12
For personal use only.

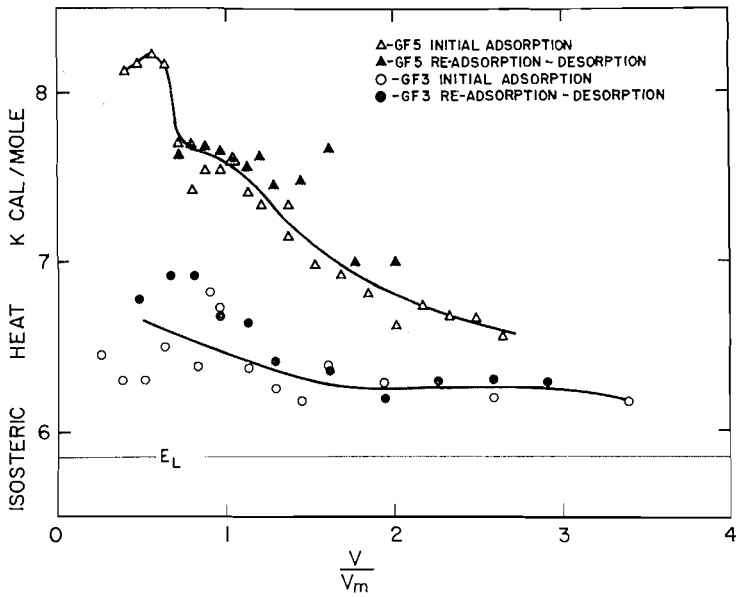

FIG. 4. Isosteric heats for the adsorption of sulphur dioxide by GF-3 and GF-5.

temperatures. These heats presented in Fig. 4 show values well above the heat of liquefaction of sulphur dioxide. Within the experimental error, no difference could be discerned between heats calculated from the initial adsorption curves and those calculated from the desorption and readsorption curves. Thus no heat effect can be detected in this way which could be attributed to swelling of the graphite crystallites. Possibly the method is too rough to measure the heats involved.

REFERENCES

1. BEEBE, R. A. and DELL, R. M. J. Phys. Chem. **59**, 746 (1955).
2. BEEBE, R. A. and YOUNG, D. M. J. Phys. Chem. **58**, 93 (1954).
3. MCDERMOT, H. L. and LAWTON, B. E. Can. J. Chem. **34**, 769 (1956).
4. PIERCE, C., SMITH, R. N., WILEY, J. W., and CORDES, H. J. Am. Chem. Soc. **73**, 4551 (1951).
5. WILSON, L. G. and MCDERMOT, H. L. Can. J. Chem. **35**, 15 (1957).

RECEIVED SEPTEMBER 12, 1958.
DEFENCE RESEARCH CHEMICAL LABORATORIES,
DEFENCE RESEARCH BOARD,
OTTAWA, CANADA.

Can. J. Chem. Downloaded from www.nrcresearchpress.com by 190.90.36.8 on 09/04/12
For personal use only.

Can. J. Chem. Downloaded from www.nrcresearchpress.com by 190.90.36.8 on 09/04/12
For personal use only.

Canadian Journal of Chemistry

Issued by THE NATIONAL RESEARCH COUNCIL OF CANADA

VOLUME 37 APRIL 1959 NUMBER 4

THE REACTION OF ACTIVE NITROGEN WITH HYDROGEN BROMIDE[1]

H. B. DUNFORD AND BERNADINE E. MELANSON

ABSTRACT

The reaction of active nitrogen with hydrogen bromide was found to produce bromine and ammonium bromide as the main products, along with traces of compounds tentatively identified as bromamine, NH_2Br, and bromimine, $NHBr_2$. Hydrogen abstraction from hydrogen bromide by nitrogen atoms, imine and amine radicals can account for ammonia formation. Considerable catalysis of nitrogen atom recombination by hydrogen bromide appears to occur. A resonance transfer of the electronic energy responsible for the nitrogen afterglow to bromine with a resultant bromine emission spectrum is proposed to account for the orange reaction flame.

INTRODUCTION

In an early study Willey and Rideal (1) attributed the reactivity of active nitrogen in its reaction with hydrogen bromide to excited nitrogen molecules. However, Ewart and Rodebush (2) believed that the reactivity was due entirely to atomic nitrogen. The present paper reports the results of a more extensive investigation of the reaction.

EXPERIMENTAL

Hydrogen bromide was produced by burning the mixture obtained by bubbling cylinder hydrogen through Baker's C. P. bromine (3) which was kept at room temperature. The resultant hydrogen bromide and excess hydrogen were passed through a trap cooled with a dry ice – acetone mixture to remove moisture, and the hydrogen bromide was retained in a second trap cooled with liquid air. It was stored for use after a single bulb-to-bulb distillation.

The nitrogen was activated by a condensed discharge and was reacted with the hydrogen bromide in a fast flow system. Details of the type of apparatus have been described elsewhere (4, 5). In the present system the flow rate of molecular nitrogen was 3.64×10^{-5} mole per second at a pressure of 0.8 mm of mercury. Reaction time was 0.2 second. Condensable gases obtained as reaction products were retained in traps cooled with liquid air and analyzed after fractionation in a LeRoy still (6). The rate of salt deposition from the reaction of active nitrogen with hydrogen bromide was determined in a special series of experiments in which the salt was washed from the system with distilled water and titrated for bromide ion. The washing process eventually removed some of the metaphosphoric acid used to poison the flow system, so that when products condensable in liquid air were being analyzed, the salt was removed from the system by

[1]*Manuscript received October 7, 1958.*
A joint contribution from the Departments of Chemistry, Dalhousie University, Halifax, N.S., and the University of Alberta, Edmonton, Alberta. Based on a paper presented at the 41st Annual Conference and Exhibition of the Chemical Institute of Canada, Toronto, May 26–28, 1958.

reaction with active nitrogen. In a few experiments, products of the reaction of active nitrogen with salt were retained for analysis by placing liquid air around the second trap in the flow system.

Bromine and various mixtures of bromine – hydrogen bromide and hydrogen – hydrogen bromide were also reacted with active nitrogen. Flow rates of hydrogen and hydrogen bromide were each determined by conventional pressure–volume–time measurements. Liquid bromine was stored in a cylindrical container which was immersed in an ice–water mixture. Bromine vapor from the container was pumped through various sizes of calibrated flowmeters.

The maximum yield of hydrogen cyanide obtained from the reaction of active nitrogen with ethylene was also determined at room temperature and at 340° in order to determine the flow rate of atomic nitrogen (4). In two experiments ethylene was fed into a reaction vessel which had previously been coated with ammonium bromide.

RESULTS

The Reaction of Active Nitrogen with Hydrogen Bromide

At 80° C the reaction of active nitrogen with hydrogen bromide produced an orange flame and effectively quenched the nitrogen afterglow. As was observed earlier (2), the flame consisted of bands in the 590–600 mμ region. At 380°, the typical active nitrogen afterglow could be observed emerging from the reaction vessel at all but the highest rates of hydrogen bromide input; about two inches below the reaction vessel the afterglow was replaced by the orange flame.

A salt deposit formed on the walls of the reaction vessel in experiments conducted at 80° C. At higher temperatures, it formed only on the walls of the tubing connecting the reaction vessel to the first liquid air trap. Kjeldahl determinations and Volhard titrations indicated a 1.01:1.00 ratio (±0.01) of ammonium to bromide ions. Tests for hydrazine hydrobromide (7) were negative as were tests for oxidizing agents with potassium iodide. It was therefore concluded, in agreement with the findings of Ewart and Rodebush, that the salt was pure ammonium bromide.

The volatile products of the reaction of active nitrogen with hydrogen bromide, which were separated on the LeRoy still, were as follows. Hydrogen bromide was removed by distillation at −135° C. The rate of its recovery was determined by pressure–volume measurements and by titration with standard alkali solution. A small amount of product (A) was recovered at −90° C. Crude measurements indicated that its vapor pressure obeyed the equation $\log p_{mm} = -1.7\times10^3/T+9.0$ over the pressure range 0.01 to 0.4 mm. The material was white in the solid state, gave a negative Nessler test, and liberated iodine when warmed with frozen potassium iodide solution. Its rate of formation was of the order of 10^{-8} mole per second. Bromine was distilled at 50° C and trapped on frozen potassium iodide solution. The iodine liberated upon warming was titrated with standard thiosulphate solution. A trace of material (B) was removed after the distillation of bromine. It was white when frozen and had a vapor pressure, measured over the range 0.01 to 0.05 mm, comparable to that of hydrazine (8). However, it gave a negative test with salicylaldehyde (7). Furthermore, any hydrazine which might have been formed might be expected to react with excess hydrogen bromide to form hydrazine hydrobromide. It is proposed tentatively that A and B are bromamine, NH_2Br, and bromimine, $NHBr_2$, respectively. Neither compound has been isolated before, although the preparation of ether solutions of NH_2Br and $NHBr_2$ has been reported (9).

The rates of formation of bromine and ammonium bromide at various flow rates of

Can. J. Chem. Downloaded from www.nrcresearchpress.com by 190.90.36.8 on 09/04/12
For personal use only.

hydrogen bromide are shown in Figs. 1 and 2, respectively. The maximum rate of recovery of hydrogen cyanide from the reaction of active nitrogen with ethylene at 80° C was 8.0×10^{-6} mole per second, and this was unaffected by the presence of ammonium bromide in the reaction vessel; at 340° it was 9.0×10^{-6} mole per second.[2] Since the rate of hydrogen cyanide recovery from the reaction of active nitrogen with ethylene becomes constant above 250°, the latter figure is used as an indication of the atomic nitrogen flow rate at all temperatures.

The Reaction of Active Nitrogen with Ammonium Bromide

The flame of the reaction of active nitrogen with ammonium bromide, as observed with a pocket spectroscope, was the same as that obtained in the corresponding hydrogen bromide flame. As the salt with its orange flame was slowly swept along the flow system

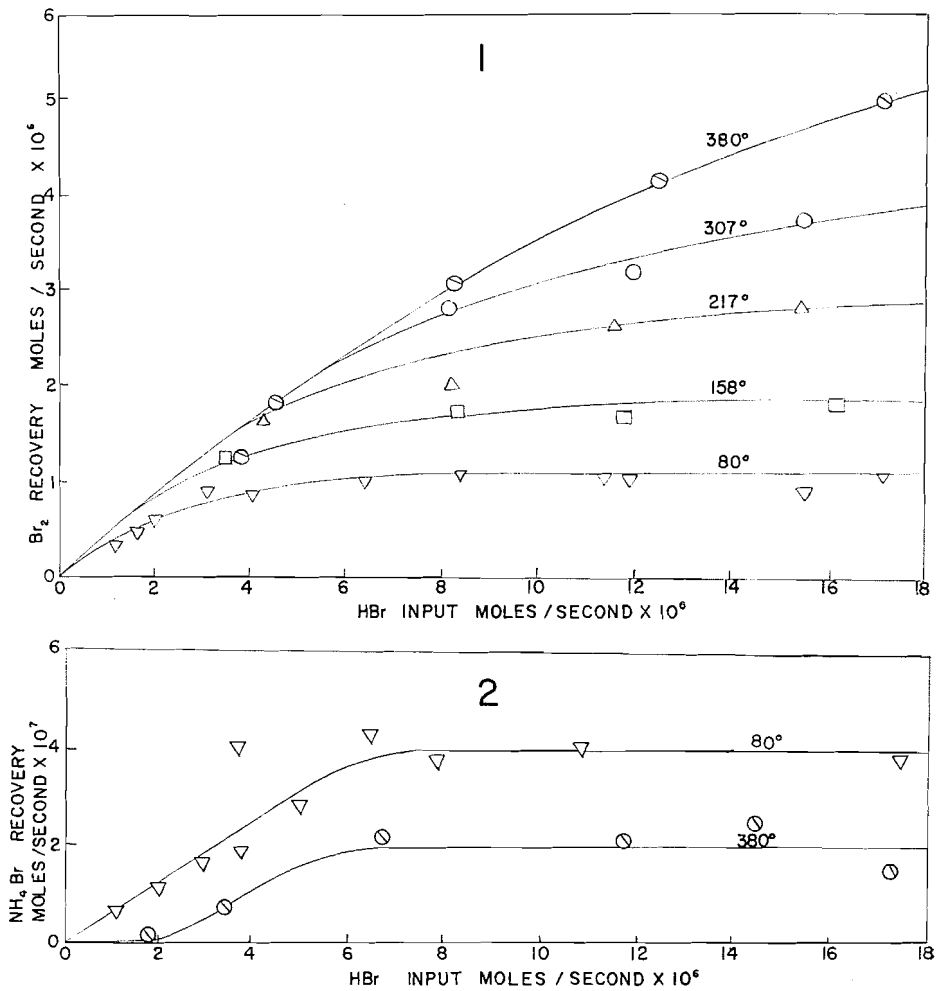

FIGS. 1 and 2.

[2]*Larger temperature coefficients from room temperature to 250° for the rate of hydrogen cyanide production from the reaction of active nitrogen with ethylene have been observed in faster flow systems (10).*

Can. J. Chem. Downloaded from www.nrcresearchpress.com by 190.90.36.8 on 09/04/12
For personal use only.

a blue glow gradually developed between the nitrogen afterglow and the orange emission. The blue glow, as observed spectroscopically, appeared as a continuum with its long wave length edge at approximately 510 mμ. In a typical experiment active nitrogen was reacted for 1 hour with 1.5×10^{-4} mole of ammonium bromide which had previously been deposited in the reaction vessel. All but a trace of the salt was destroyed and 4.2×10^{-5} mole of hydrogen bromide, 5.5×10^{-5} mole of bromine, and a trace of compound B were recovered.

The Reactions of Active Nitrogen with Bromine and Hydrogen – Hydrogen Bromide and Bromine – Hydrogen Bromide Mixtures

When bromine was fed into the active nitrogen stream no product was recovered except molecular bromine (1). However, the same orange band as that observed in the flame of active nitrogen reactions with hydrogen bromide and ammonium bromide was observed in the flame produced by the interaction of active nitrogen and bromine. Furthermore, when the input of bromine was stopped, but the flow of active nitrogen was continued, the same blue continuum, as observed in the reaction of active nitrogen with ammonium bromide was produced as the orange flame retreated rapidly.

The results of the combined additions of bromine – hydrogen bromide and hydrogen – hydrogen bromide mixtures are summarized in Fig. 3.

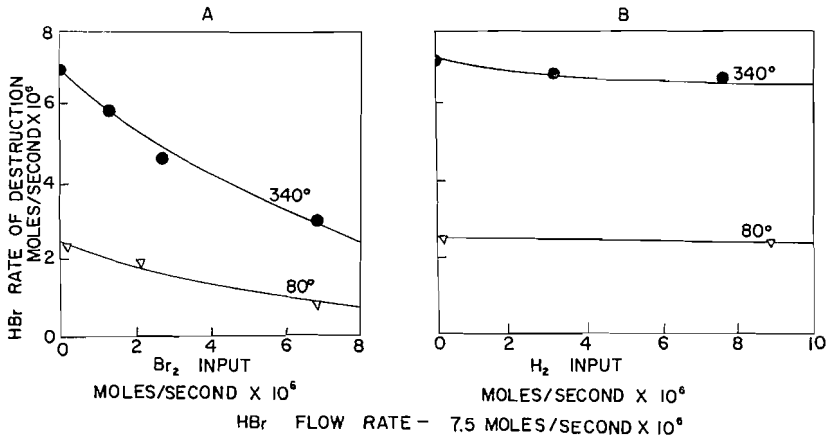

FIG. 3.

DISCUSSION

The mechanism of ammonium bromide formation proposed by Ewart and Rodebush, with added thermochemical data,[3] is as follows:

$$N + HBr \rightarrow NH + Br + 1 \text{ kcal}, \quad [1]$$

$$NH + HBr \rightarrow NH_2 + Br + 1 \text{ kcal}, \quad [2]$$

$$NH_2 + HBr \rightarrow NH_3 + Br + 17 \text{ kcal}, \quad [3]$$

[3] *All heats of reaction are calculated from the following data:*
D_{H-Br} = *87 kcal*, D_{H-H} = *104 kcal*, D_{Br-Br} = *46 kcal—Selected values of chemical thermodynamic properties. National Bureau of Standards, Washington, D.C. 1950.*
D_{N-H} = *88 kcal—Pannetier, G. and Gaydon, A. G. J. chim. phys.* **48**, *221 (1951).*
D_{NH_2-H} = *104 kcal—Swarcz, M. Chem. Revs.* **47**, *75 (1950).*
D_{N_2} = *225 kcal—Hendrie, J. M. J. Chem. Phys.* **22**, *1503 (1954).*
ΔH_f NH_3 = *11 kcal—Handbook of chemistry and physics.*
ΔH_{sublt} NH_4Br = *44 kcal—Smits, A. and deLange, W. J. Chem. Soc. 2936 (1928).*

Can. J. Chem. Downloaded from www.nrcresearchpress.com by 190.90.36.8 on 09/04/12
For personal use only.

$$NH_3 + HBr \rightarrow NH_4Br + 44 \text{ kcal}, \quad [4]$$

$$2Br + M \rightarrow Br_2 + M + 46 \text{ kcal}. \quad [5]$$

There is ample evidence that atomic nitrogen is present in active nitrogen and that it is chemically reactive (11). However, if reactions [1–5] were the only ones occurring then the optimum rate of recovery of ammonium bromide would be equal to the flow rate of atomic nitrogen, and the rate of molecular bromine formation would be 1.5 times as great. Actually, the maximum recovery rates of ammonium bromide and bromine obtained at 80° C are, respectively, only 1/22 and 1/9 as great as the available supply of atomic nitrogen, as indicated by the maximum recovery of hydrogen cyanide from ethylene. At 380° the yield of ammonium bromide is still lower and the bromine recovery has climbed to 5/9 the amount of atomic nitrogen available.

Reactions of the type:

$$2NH \rightarrow N_2 + H_2 + 153 \text{ kcal}, \quad [6]$$

$$2NH_2 \rightarrow N_2 + 2H_2 + 81 \text{ kcal}, \quad [7]$$

$$N + NH \rightarrow N_2 + H + 137 \text{ kcal}, \quad [8]$$

$$N + NH_2 \rightarrow N_2 + 2H + 49 \text{ kcal}, \quad [9]$$

would have the effect of a reduction in the yields of bromine and ammonium bromide. Reaction [9], which is spin allowed for three out of every eight collisions, would be favored over the more exothermic reaction

$$N + NH_2 \rightarrow N_2 + H_2 + 153 \text{ kcal},$$

which is spin disallowed. Reactions [6–9] inclusive presumably would have very low activation energies and might occur more rapidly on the wall, since they are all free radical or atomic reactions.

However, even if every imine radical were destroyed in [8], the yield of bromine would still be too large, namely one-quarter of the available supply of atomic nitrogen. Only the possible fate of atomic hydrogen formed in [8] and [9] might reconcile the above mechanism with the experimental observations.

Atomic hydrogen, if formed, might be expected to recombine

$$2H + M \rightarrow H_2 + M + 104 \text{ kcal} \quad [10]$$

or to undergo one of the following reactions:

$$H + HBr \rightarrow H_2 + Br + 17 \text{ kcal}, \quad [11]$$

$$H + Br_2 \rightarrow HBr + Br + 41 \text{ kcal}, \quad [12]$$

$$H + Br + M \rightarrow HBr + M + 87 \text{ kcal}. \quad [13]$$

Both reactions [12] and [13] would decrease the yield of bromine. The ratio k_{12}/k_{11} is known to be about 10 over a considerable temperature range (12). Since both [11] and [12] are extremely rapid, they might be expected to consume most of the available atomic hydrogen before it could reach the reaction vessel wall.

Two rather serious objections can be raised to the mechanism outlined in [1–13]. First, an increase in the flow rate of hydrogen bromide should increase the rate of bromine formation through [1–3] and [11], yet plateaus in bromine production are observed at the two lowest temperatures at which the reaction was studied.

Second, if the above mechanism is to account for the low rate of recovery of bromine at 80°, then [8–9] followed by [12] must be remarkably efficient processes. The slope of the curve in Fig. 3A would indicate that if [12] is extensive in the present system, its

Can. J. Chem. Downloaded from www.nrcresearchpress.com by 190.90.36.8 on 09/04/12
For personal use only.

effect is largely offset by [11]; cf. the effect of added chlorine on the rate of destruction of hydrogen chloride observed by Wiles and Winkler (10). Furthermore the existence of excess active nitrogen at high flow rates of hydrogen bromide at high temperatures is not compatible with the postulate of extensive occurrence of [8–9] in the present system.

In the reaction of active nitrogen with hydrogen chloride, where hydrogen abstraction by atomic nitrogen is prohibitive energetically at lower temperatures, the initiation steps were assumed to be

$$N + HCl \rightarrow [H\text{–}Cl\text{–}N],$$
$$N + [H\text{–}Cl\text{–}N] \rightarrow N_2 + H + Cl.$$

If the corresponding initial steps occurred in the present system, then ammonia formation would proceed through the reactions

$$N + H + M \rightarrow NH + M, \qquad [14]$$
$$NH + H_2 \rightarrow NH_3, \qquad [15]$$

as first proposed by Steiner (13).

A qualitative comparison of other reactions involving atomic hydrogen in the reaction of active nitrogen with hydrogen chloride and in the present system may be of interest. In the former system considerable quantities of atomic hydrogen are liberated and largely removed through the reactions

$$H + HCl \rightarrow H_2 + Cl,$$
$$H + Cl_2 \rightarrow HCl + Cl,$$

which have activation energies of 5 and 3 kcal, respectively. In the present system, the corresponding reactions [11] and [12] both have activation energies of 2 kcal or less, and so removal of hydrogen atoms is even more rapid. Since no ammonia is formed through [14–15] in the reaction of active nitrogen with hydrogen chloride, it might appear even less likely in the present system, where the steady state concentration of atomic hydrogen is even lower. A more convincing argument perhaps is the fact that if the reactions

$$N + HBr \rightarrow [H\text{–}Br\text{–}N], \qquad [1a]$$
$$N + [H\text{–}Br\text{–}N] \rightarrow N_2 + H + Br, \qquad [16a]$$

which would be the principle source of atomic hydrogen, were predominant at 80°, then the yield of molecular bromine would be one-quarter of the available supply of atomic nitrogen, provided, as appears to be the case, that the net regeneration of hydrogen bromide from atomic hydrogen reactions is not of prime significance at 80°.

A mechanism which would appear to account for most features of the reaction satisfactorily is [1*a*] followed by

$$[H\text{–}Br\text{–}N] \rightarrow NH + Br, \qquad [1b]$$
$$N + [H\text{–}Br\text{–}N] \rightarrow N_2 + HBr. \qquad [16b]$$

Ammonia formation could proceed through [2–3].

If [16*b*] is predominant at 80°, an increase in the flow rate of hydrogen bromide would mainly increase the rate of nitrogen atom recombination. Hence the plateau in the rate of bromine production can be explained. At higher temperatures, if [1*b*] becomes increasingly important, then the temperature coefficient for bromine production, and its increased sensitivity to hydrogen bromide flow rate with increased temperature, can be

Can. J. Chem. Downloaded from www.nrcresearchpress.com by 190.90.36.8 on 09/04/12
For personal use only.

Can. J. Chem. Downloaded from www.nrcresearchpress.com by 190.90.36.8 on 09/04/12
For personal use only.

explained. It is thus not necessary to attach prime importance to reactions [6–13] in the present system.

Whether the substance which catalyzes the recombination of atomic nitrogen will be decomposed is dependent on the fraction of the recombination energy which is transmitted to the remainder of the complex. For a hydrogen bromide complex, it would appear that this fraction is less than the ratio of the bond dissociation energies of hydrogen bromide and nitrogen, namely 87/225, or 0.39, provided that the hydrogen bromide remains in its electronic ground state. For a hydrogen chloride complex, the fraction must have a minimum value of 0.46. The difference might be attributed to the relative sizes of the p orbitals of chlorine and bromine, the latter being too large to facilitate formation of a strongly bonded complex with atomic nitrogen.

There remains the problem of why the yield of ammonium bromide decreases with increasing temperature. Because of the appreciable sublimation pressure of ammonium bromide at higher temperatures (one atmosphere at 396° C), the occurrence of [4] is prevented in a hot reaction vessel. Ammonia, which at 80° would be removed rapidly from the flow system by [4], could, to a large measure, be destroyed by reaction with active nitrogen at higher temperatures. The rapid rate of reaction of active nitrogen with ammonia, even in competition with the reaction of active nitrogen with ethylene, introduced as a second reactant, has been demonstrated previously (14).

Because the bands in the 590–600 mμ region are produced as a result of the interaction of active nitrogen and pure bromine, it would appear that bromine, produced in the reactions of active nitrogen with hydrogen bromide and ammonium bromide, respectively, is responsible for the emission of the same orange band in the latter two reactions.

Ewart and Rodebush originally proposed that the transfer of two vibrational quanta from the $B\ ^3\Pi_g$ state of nitrogen to a ground state molecule of hydrogen bromide, followed by a modified $B\ ^3\Pi_g \rightarrow A\ ^3\Sigma_u^+$ transition in the active nitrogen as the cause of the orange flame. This appeared plausible as the appropriate vibrational energy spacings of the B state of nitrogen are roughly double those of the ground state of hydrogen bromide, and the selection rule for the transfer of vibrational quanta states that $v = \pm 1$ or ± 2. However, if the interaction of active nitrogen and bromine is responsible for the orange band, then an explanation in terms of a modified nitrogen afterglow is not possible, since the vibrational energy spacings of the ground state of bromine differ by a factor of approximately nine from those of the B state of nitrogen (15).

Transitions between the ground state of bromine, $X\ ^1\Sigma_g^+$, and the state $B\ ^3\Pi_{0u}^+$ are known in both emission and absorption. A careful plot of the potential functions of both states shows that the energy corresponding to the transition from the first vibrational level of the X state of bromine to the 15th, 16th, and 17th levels of the B state matches exactly the energy emitted in the first positive bands of active nitrogen. The transition does not violate the Franck–Condon principle; furthermore, an appreciable fraction of ground state bromine molecules have $v = 1$ at 80° C. Such a resonance transfer is much more likely to occur when the energy matching is exact (16). The return transitions $15' \rightarrow 2''$, $16' \rightarrow 2''$, and $17' \rightarrow 2''$ could account for the orange emission. Transitions to the zero vibrational level of the ground state would violate the Franck–Condon principle.[4] That the emission occurs in such a selective wave length region might indicate that

[4]*The referee has pointed out the apparent violation of spin conservation in the energy transfer process proposed above. However, the* $^3\Pi$–$^1\Sigma$ *transition in the halogens appears identical with a* $^1\Sigma$–$^1\Sigma$ *transition (17). No real significance can be attached to the S and* Λ *quantum numbers, but only to* Ω *for the excited state of bromine.*

quenching of the B state bromine molecules occurs in the present system more rapidly than the exchange of vibrational quanta among B state molecules of bromine. The quenching of the B state of iodine and bromine by various gases by an induced predissociation mechanism has been observed by various authors (15).

The blue emission continuum corresponds to that observed for the two-body recombination of $^2P_{3/2}$ and $^2P_{1/2}$ bromine atoms followed by a $B \rightarrow X$ transition. The source of excited bromine atoms is not clear. Furthermore the probability of the two-body atom recombination occurring is very slight, but it appears to provide the only readily available explanation of the blue glow. The two-body recombination of atoms has been observed spectroscopically for the halogens at high temperatures (18) and for tellurium vapor in an intense discharge (19).

ACKNOWLEDGMENTS

This project was supported financially by the National Research Council. One of us (B.E.M.) is also indebted to Canadian Industries Limited for a Fellowship and to N.R.C. for a Studentship.

REFERENCES

1. WILLEY, E. J. B. and RIDEAL, E. K. J. Chem. Soc. 669 (1927).
2. EWART, R. H. and RODEBUSH, W. R. J. Am. Chem. Soc. **56**, 97 (1934).
3. ORGANIC SYNTHESES. Vol. XV. John Wiley & Sons, Inc., New York. 1935. p. 35.
4. GREENBLATT, J. and WINKLER, C. A. Can. J. Research, B, **27**, 721 (1949).
5. BLADES, H. and WINKLER, C. A. Can. J. Chem. **30**, 915 (1952).
6. LEROY, D. J. Can. J. Research, B, **28**, 492 (1950).
7. FEIGL, F. Spot tests. Nordemann Publishing Co., New York. 1939. p. 155.
8. HANDBOOK OF CHEMISTRY AND PHYSICS. Chemical Rubber Publishing Co., Cleveland. 1957.
9. COLEMAN, G. H., YAGER, C. B., and SOROOS, H. J. Am. Chem. Soc. **56**, 965 (1934).
10. WILES, D. M. and WINKLER, C. A. Can. J. Chem. **35**, 1298 (1957).
11. EVANS, H. G. V. and WINKLER, C. A. Can. J. Chem. **34**, 1217 (1956).
12. LAIDLER, K. J. Chemical kinetics. McGraw-Hill Book Company. 1950.
13. STEINER, W. Z. Elektrochem. **36**, 807 (1930).
14. FREEMAN, G. R. and WINKLER, C. A. J. Phys. Chem. **59**, 371 (1955).
15. HERZBERG, G. Spectra of diatomic molecules. 2nd ed. D. Van Nostrand Co., New York. 1950.
16. LAIDLER, K. J. The chemical kinetics of excited states. Oxford. 1955.
17. MULLIKEN, R. A. Rev. Modern Phys. **4**, 1 (1932).
18. KONDRATJEW, V. and LEIPUNSKY, A. Trans. Faraday Soc. **25**, 736 (1929).
19. ROMPE, R. Z. Physik, **101**, 214 (1936).

Can. J. Chem. Downloaded from www.nrcresearchpress.com by 190.90.36.8 on 09/04/12
For personal use only.

Can. J. Chem. Downloaded from www.nrcresearchpress.com by 196.1.178.254 on 09/04/12
For personal use only.

MEASUREMENT OF Ni^{63} WITH A 2π PROPORTIONAL COUNTER[1]

J. R. MacEwan,[2] J. U. MacEwan, and L. Yaffe

ABSTRACT

Measurement of Ni^{63}, a β^- emitter with very low maximum energy, is described. External absorption curves were determined in aluminum and a range 8.5 ± 0.5 mg/cm^2 was found. This corresponds to a maximum energy of the β radiation of 72.7 ± 2.5 kev, in reasonably good agreement with values obtained by other methods. Self-absorption curves of electrolytically deposited samples were obtained and attempts made to compare these with the theoretical predictions of Gora and Hickey.

A. INTRODUCTION

An investigation of the counting characteristics of Ni^{63}, a nuclide emitting 67-kev beta rays, was undertaken, since few precise 2π counting studies have been made in this energy range. Self-absorption measurements with Ni^{63} are particularly interesting because Gora and Hickey's (1) theoretical expressions for self-absorption in wide-angle geometries have yet to be verified for use with nuclides emitting soft beta radiation. Their general expression for self-absorption is an integrated form of equation [1], which corrects for the extra distance a particle emitted at an angle θ to a normal on the source mount surface must travel before reaching the surface.

$$[1] \qquad A(x, \theta) = \frac{a_0 \cos\theta}{k}\left(1 - e^{-\frac{kx}{\cos\theta}}\right)$$

where $A(x, \theta)$ is the detected activity of particles emitted at an angle θ from a source of thickness x, consisting of material of specific activity a_0, and k is the absorption coefficient. They have refined this treatment further to include the case where a fraction, p, of the particles incident on the source mount are scattered back towards the active volume of the counter, but were unable to include the effects of self- and back-scattering in the source. This relationship was very successfully applied by them to their results for self-absorption of C^{14} in narrow- and wide-angle geometries.

In addition, a measurement of the range of Ni^{63} beta particles in aluminum was made because it provides a check on this method for determination of maximum energies in this range as compared with beta spectrometer and other proportional counter studies.

B. EXPERIMENTAL TECHNIQUES AND RESULTS

Tracer Purification and Source Preparation

The active material used in this investigation was prepared by the irradiation of spectrographically pure nickel in the Brookhaven reactor in a position where the flux was predominantly thermal. A gamma-emitting impurity, identified as Co^{58} by scintillation spectrometry, was found. This was presumably produced by the reaction $Ni^{58}(n,p)$-Co^{58}. The cobalt was removed by dissolving the nickel in 9 *M* HCl and eluting the resulting solution through an anion exchange column (2). One passage through the column was sufficient to effect a complete separation, with the cobalt being retained on the resin.

[1]*Manuscript received October 30, 1958.*
Contribution from the Radiochemistry Laboratory, Department of Chemistry, and the Department of Metallurgy, McGill University, Montreal, Que., with financial assistance from the National Research Council, Atomic Energy Control Board, and the Defence Research Board.
[2]*Present address: Fuel Development Branch, Atomic Energy of Canada Limited, Chalk River, Ontario.*

Can. J. Chem. Downloaded from www.nrcresearchpress.com by 196.1.178.254 on 09/04/12
For personal use only.

The resulting solution was evaporated to dryness and the nickel chloride was dissolved in an ammonia – ammonium sulphate electrolysis solution. The resulting electrolyte had a nickel concentration of 0.03 moles per liter. All sources used for measurement in this investigation were prepared by electroplating nickel from aliquots of this stock solution onto copper planchets 1 in. in diameter, to give deposits 0.70 in. in diameter. Plating was carried out in rotating anode plating cells at a current density of 20 ma/cm^2. The rotational speed and anode shape were adjusted until extremely uniform deposits were obtained.

The sources were counted on an internal source proportional counter (AEP CFIS 2) with a 2π geometry. An AEP 1448 amplifier-discriminator unit, a Marconi AEP scale of 1000, and a Dynatron power supply P200A comprised the associated electronic equipment. The counter gas was C.P. methane, dried over silica gel. The long, flat plateaux (approximately 400 v long and with slopes of 0.5% per 100 v) and general stability of this equipment ensured that any small observed variations in counting rate were due solely to counting statistics. Coincidence loss corrections were made for all sources wherever necessary. The calibration curve for this correction was obtained using a multiple source technique (3).

External Absorption Curve

When an aluminum foil is placed over the source in an internal source counter, the chamber is effectively converted into an end window counter. Unless the foil is in intimate contact with the source, besides the reduction in counting rate caused by absorption in the absorber, further reductions are caused by absorption in the methane trapped between the foil and source and also by scattering of beta particles at the foil surface. It was found that these latter effects could be eliminated by laminating the aluminum absorbers onto the source with a thin layer of plastic adhesive, in this case a solution of VYNS resin in cyclohexanone. For the thinnest foils employed, the weight of aluminum was 0.23 mg/cm^2 and that of plastic about 0.06 mg/cm^2. With thicker aluminum foils the ratio of aluminum to plastic increased accordingly, and in this investigation the absorbers were considered to consist solely of aluminum. Aluminum foils with mass thicknesses of 0.23, 0.66, and 1.90 mg/cm^2 were laminated singly and in various combinations onto the source to cover the range of absorbers used, 0 to 13.5 mg/cm^2. In most cases sufficient counts were obtained at each absorber thickness to give satisfactory statistics, but in those instances where a small number of counts were obtained the accuracy of the plotted values is indicated in the usual manner.

Self-absorption Curve

To investigate the phenomenon of self-absorption of Ni^{63}, a series of active sources was prepared by electrodeposition. All sources were prepared from material of the same specific activity. The range of source thicknesses investigated varied from 0.05 to 4.50 mg/cm^2. Weights of the deposits were determined on a five-place balance sensitive to 0.005 mg. The deposits were checked for circular symmetry by measuring across several diameters and the mass thickness of the source calculated using the mean of these diameters. All observed counting rates were corrected to correspond to the same area of active surface—a correction $\leqslant 1.5\%$. Sufficient counts were obtained in all cases so that the statistical variation was negligible.

C. RESULTS AND DISCUSSION

External Absorption Curve

Results for the absorption of radiation in aluminum are plotted in Fig. 1. The measured

counting rates are a composite of the detected radiation from Ni^{59} ($\sim 0.02\%$) which decays by K-electron capture with the emission of a Co $K\alpha$ X-ray (4), and of Ni^{63}, which decays by emission of a 70-kev beta particle (4, 9). The low activity component has a half-thickness of 9.0 mg/cm^2. This value is in agreement with that given in X-ray tables for the absorption of Co $K\alpha$ X-rays of 9.4 mg/cm^2 and serves to identify this component as Ni^{59}. The absence of a gamma-ray background indicates that the anion exchange separation completely removed the radioactive impurity, Co^{58}. The absorption curve for the soft component, the Ni^{63} radiation, was obtained in the usual manner by deducting the Ni^{59} background from the total activity, as shown in Fig. 1. The value for the range of Ni^{63} in these experiments is estimated to be 8.5 ± 0.5 mg/cm^2. A 'visual method' of estimating the range from the absorption curve was employed, since a suitable standard is as yet not available in this energy range for a Feather analysis (5). Values of 0.52_3 mg/cm^2 and 1.33 cm^2/mg were found respectively for the half-thickness and absorption coefficient of Ni^{63} beta radiation. (Since the curve is very close to a true exponential, these values can be used over most of the range.)

The value of the range found in this work for Ni^{63} is greater than that given by Wilson and Curran (6) of 6.0 mg/cm^2 and by Brosi *et al.* (4) of 6.6 mg/cm^2. However, as the individual measurements made to determine the external absorption curve can be accurately reproduced, there is no reason to suspect this new value. It is difficult to assess the accuracy of Wilson and Curran's result, as they failed to publish an absorption

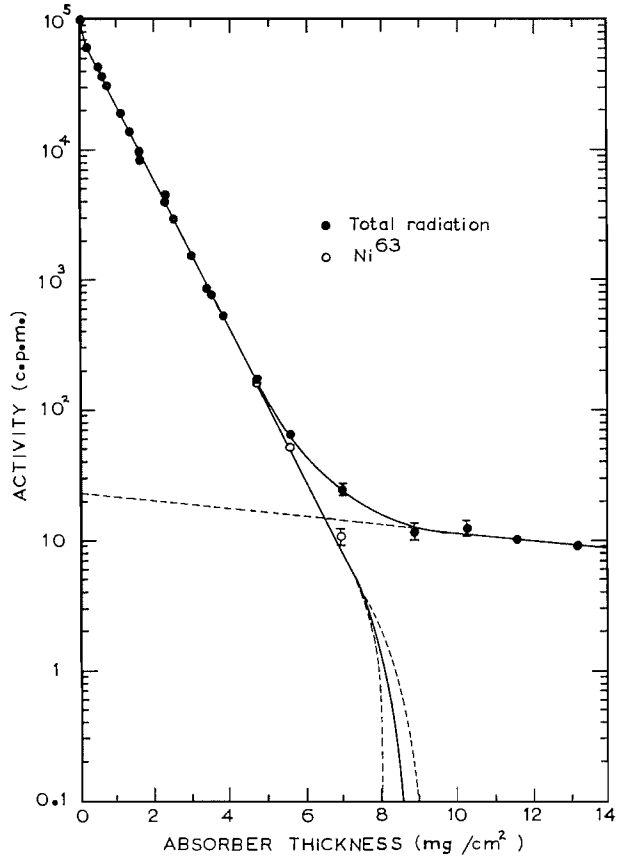

FIG. 1. Absorption curve for Ni^{63} in aluminum.

Can. J. Chem. Downloaded from www.nrcresearchpress.com by 196.1.178.254 on 09/04/12
For personal use only.

curve. Brosi *et al.* determined their range value using a Feather plot. Unfortunately they do not state which nuclide was used as a standard in the range determination. As they followed the absorption of Ni^{63} over only three decades of activity, the use of a standard having an energy spectrum different from Ni^{63} could result in an appreciable error in the estimated range. Furthermore, examination of their absorption curve shows that they did not completely eliminate the scattering phenomenon which occurs when the first absorber is placed over the source. This could also account for their low value for the range.

There are many empirical and semiempirical expressions for relating the maximum energy of a beta-ray spectrum to the observed range of these particles in aluminum. However, only Glendenin's range–energy curve (7) and Libby's range–energy relation (8) are recommended for use below 100 kev. The maximum energy of Ni^{63} beta particles obtained from these relations, using the range value found in this work, are 72.5 ± 2.5 and 72.9 ± 2.5 kev respectively.

This value is slightly higher than a recent value of 67.0 ± 0.5 kev by Preiss, Fink, and Robinson (9) but is considered to be reasonably good agreement, bearing in mind the method used. This presents additional justification for this fairly rapid, seemingly rough method and further verification of the range–energy formulae quoted above.

Self-absorption Curve

The results of the self-absorption measurements are summarized in the data plotted in Fig. 2. For convenience, the apparent specific activity, rather than the actual specific activity, of each source was plotted against the mass thickness of deposit. The apparent specific activity of the active material was arbitrarily taken as unity to simplify the comparison of these results with Gora and Hickey's theoretical expression. The experimental results are nearly identical with those obtained in a 2π geometry by Schweitzer, Stein, and Nehls (10).

In Fig. 3, three separate curves are drawn representing Gora and Hickey's theoretical self-absorption expression corresponding to values of the back-scattering factor, p, of

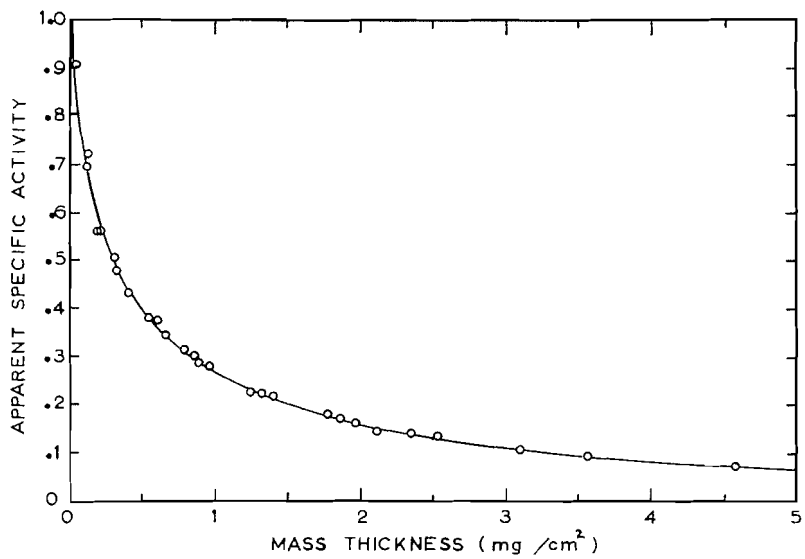

FIG. 2. Self-absorption curve for Ni^{63} in nickel—apparent specific activity plot.

Can. J. Chem. Downloaded from www.nrcresearchpress.com by 196.1.178.254 on 09/04/12
For personal use only.

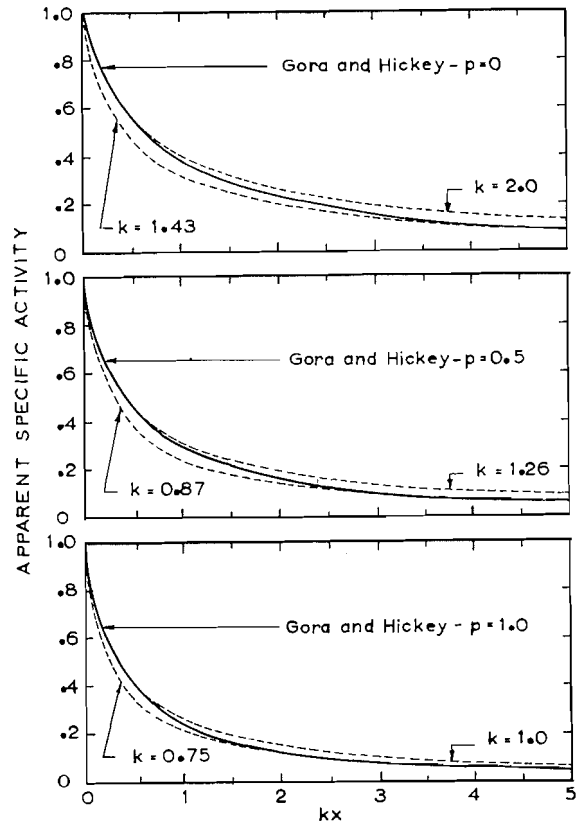

FIG. 3. A comparison of self-absorption of Ni^{63} with the theoretical curves by Gora and Hickey. Experimental data for Ni^{63} taken from Fig. 2 and shown as dotted lines for various values of R.

0.0, 0.5, and 1.0. These correspond to the respective cases where either none, half, or all the emitted particles incident on the source mount are scattered back towards the active volume of the counter. If Gora and Hickey's expression is an adequate description of the processes occurring in a source and mount, then it should be possible to make the experimental results coincide with the theoretical curve by proper selection of the back-scattering factor, p, and the absorption coefficient, k. By selecting various values of k, consistent with various parts of the experimentally determined absorption curve, it was attempted to correlate the self-absorption results shown in Fig. 2 with the theoretical curves in Fig. 3. It is apparent that the experimental results for Ni^{63} self-absorption are not consistent with the theoretical expressions. As can be observed, the correlation is improved when a correction is made for source mount back-scattering, with better correlation for the hypothetical case $p = 1.0$ than for $p = 0.5$. From this it may be concluded that for low energy beta-emitters the effects arising from self-scattering and back-scattering are important enough to invalidate any description of self-absorption in a 2π system which ignores these processes. Similar results have been obtained in conditions where 4π 'geometry' prevails (11).

When a value of the mass absorption coefficient, k, is selected to make the theoretical and experimental curves coincide for large source thicknesses, it is observed that the experimentally determined apparent specific activity decreases more rapidly than that

Can. J. Chem. Downloaded from www.nrcresearchpress.com by 196.1.178.254 on 09/04/12
For personal use only.

predicted theoretically. This suggests that the back-scattering processes in the source degrades the energy of the scattered particle, so that it is more easily absorbed in the overlying layers of atoms in the source. This is in agreement with the experimental work of Pate and Yaffe (11), who also suggest that the effect is more marked for wide-angle geometries. In addition, their results show that the back-scattering factor, p, for an infinitely thick source mount increases with decreasing energy of the beta emitter. This probably accounts for the fact that Gora and Hickey could successfully interpret their results for self-absorption of C^{14} (β^-, 0.154 Mev), while the results for Ni^{63} are inconsistent with their equations.

ACKNOWLEDGMENTS

The authors wish to express their gratitude to the Defence Research Board, the Atomic Energy Control Board, and the National Research Council for grants-in-aid.

REFERENCES

1. Gora, E. K. and Hickey, F. C. Anal. Chem. **26**, 1158 (1954).
2. Moore, G. E. and Kraus, K. A. J. Am. Chem. Soc. **73**, 9 (1951); **74**, 843 (1952).
3. Pate, B. D. and Yaffe, L. Can. J. Chem. **33**, 610 (1955).
4. Brosi, A. R., Borkowski, C. J., Conn, E. E., and Greiss, J. C., Jr. Phys. Rev. **81**, 391 (1951).
5. Feather, N. Proc. Cambridge Phil. Soc. **34**, 599 (1938).
6. Wilson, H. W. and Curran, S. C. Phil. Mag. **40**, 631 (1949).
7. Glendenin, L. E. Nucleonics, **2**, 12 (1948).
8. Libby, W. F. Anal. Chem. **19**, 2 (1947).
9. Preiss, I. L., Fink, R. W., and Robinson, B. L. J. Inorg. & Nuclear Chem. **4**, 233 (1957).
10. Schweitzer, G. K., Stein, B. R., and Nehls, J. W. J. Phys. Chem. **56**, 692 (1952).
11. Pate, B. D. and Yaffe, L. Can. J. Chem. **33**, 1656 (1955).

Can. J. Chem. Downloaded from www.nrcresearchpress.com by 196.1.178.254 on 09/04/12
For personal use only.

Can. J. Chem. Downloaded from www.nrcresearchpress.com by 186.233.112.2 on 09/04/12
For personal use only.

THE REACTIONS OF ACTIVE NITROGEN WITH ACETYLENE, METHYLACETYLENE, AND DIMETHYLACETYLENE[1]

A. SCHAVO[2] AND C. A. WINKLER

ABSTRACT

Hydrogen cyanide was the main nitrogen-containing product of all three reactions, but whereas only about one-half the available active nitrogen was converted to product in the acetylene reaction, the conversion by methyl- and dimethyl-acetylene was substantially complete. A faster-than-linear increase of HCN production with acetylene flow rate was observed at low flow rates. Similar behavior was just perceptible in the corresponding curve for methylacetylene, while no observable inflection was present with dimethylacetylene. Polymer formation was pronounced with acetylene, less so with methylacetylene, and practically absent with dimethylacetylene. Small amounts of cyanogen resulted from all three reactions, while condensable hydrocarbons were obtained in significant yields from the methyl- and dimethyl-acetylene reactions only at higher flow rates of the alkynes.

In a previous investigation (1) of the reaction of active nitrogen with acetylene, the products were found to be HCN, C_2N_2, CH_4, and H_2, together with a nitrogen-containing polymer. The conversion of active nitrogen to HCN appeared to be only about one-half that observed under optimal conditions in similar reactions with saturated and olefinic hydrocarbons. Since it was of interest to determine whether the relatively low extent of HCN formation from acetylene was characteristic of the acetylene structure, the reactions of active nitrogen with methyl- and dimethyl-acetylene have now been investigated. At the same time, some additional information was obtained about the reaction of acetylene itself.

EXPERIMENTAL

The apparatus, purification of reactants, experimental procedures, and analytical methods were similar in all essential respects to those used in previous investigations (for references, see (2)). Hydrogen cyanide and cyanogen were analyzed by titration methods, other condensable products by low temperature distillation, and non-condensable products with a mass spectrometer. A solution of ammonium hydroxide (2 *M*) was found to be effective for removing polymer from the wall of the reaction vessel, presumably because it attacked the metaphosphoric acid with which the wall was poisoned.

The flow rate of active nitrogen was estimated from the rate of production of hydrogen cyanide from ethylene at 300° C to be approximately 12 micromoles/second (3, 4).

RESULTS AND DISCUSSION

There were some rather interesting differences for the three reactions. Figure 1 shows the yields of HCN, and Fig. 2A those of C_2N_2, at different flow rates of the reactants. The relative rates of HCN production at lower flow rates, particularly from 0 to about 5 micromoles per second, were in the order acetylene < methylacetylene < dimethylacetylene. On the other hand, in the same flow rate range, the rate of production of HCN from acetylene showed a rather pronounced "induction" effect, i.e. it increased

[1]*Manuscript received November 12, 1958.*
Contribution from the Physical Chemistry Laboratory, McGill University, with financial assistance from the National Research Council of Canada.
[2]*Holder of C.I.L. Fellowship.*

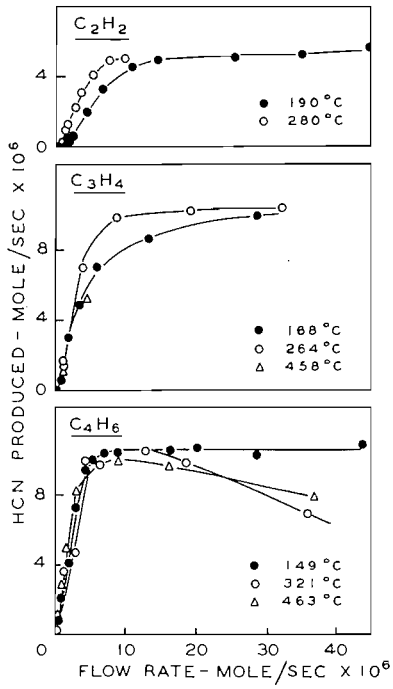

FIG. 1. Dependence of hydrogen cyanide production on the flow rates of the hydrocarbons in the reactions of active nitrogen with acetylene, methylacetylene, and dimethylacetylene.

rather markedly with flow rate, whereas similar behavior was much less evident for methylacetylene and not apparent at all in the results for dimethylacetylene. When the ratio of the rate of HCN production to flow rate of reactant is plotted against flow rate, as in Fig. 2B, the linear increase in this ratio for acetylene and possibly also for methylacetylene at the lower flow rate indicates quadratic dependence of HCN production on flow rate of hydrocarbon in this region. A similar conclusion is not possible for dimethylacetylene, although it is conceivable that it might hold for flow rates below those experimentally accessible in the present study.

Marked differences were observed also in the maximum extents to which active nitrogen could be converted to HCN in the three reactions. With acetylene, this conversion never exceeded about one-half the available active nitrogen,[3] while maximum production of HCN from methyl- and dimethyl-acetylene appeared to correspond roughly to the flow rate of active nitrogen in the system.

The yield of cyanogen was observed previously to pass through a maximum with increased flow rate of acetylene itself (1), but the same did not appear to be true with the other two acetylenes (Fig. 2A). Further, although small but significant yields of hydrogen and methane were obtained from the reaction of acetylene with active nitrogen, mass spectrometric examination showed not more than traces of these products in the non-condensables from the reaction with methylacetylene. In the reaction of dimethylacetylene, small amounts of methane (2×10^{-7} mole/second) were found only at high flow rates.

[3]*Independent experiments with acetylene in this laboratory by Mr. George have confirmed this observation for temperatures up to 400° C.*

Can. J. Chem. Downloaded from www.nrcresearchpress.com by 186.233.112.2 on 09/04/12
For personal use only.

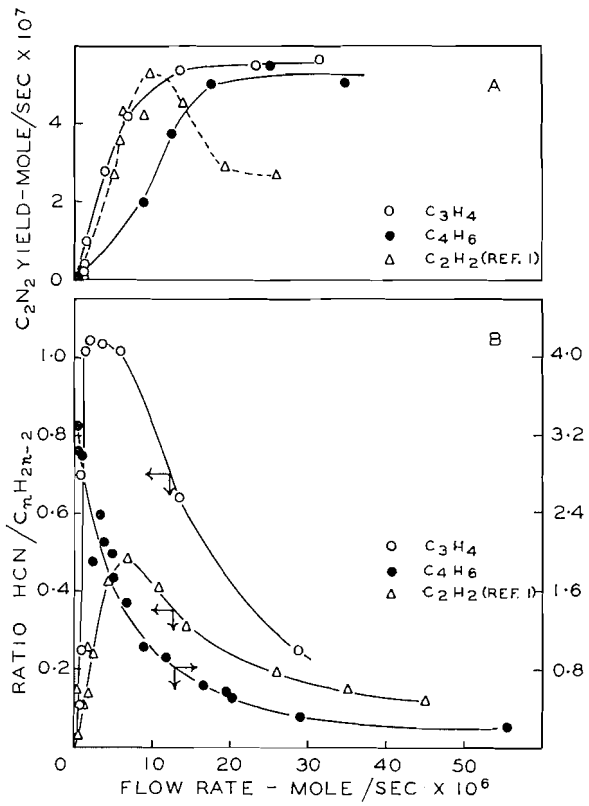

FIG. 2. A. Dependence of cyanogen production on the flow rates of the hydrocarbons in the reactions of active nitrogen with acetylene, methylacetylene, and dimethylacetylene.
B. Relation between ratio HCN/hydrocarbon and the flow rates of the hydrocarbons in the reactions of active nitrogen with acetylene, methylacetylene, and dimethylacetylene.

Other hydrocarbons were not found in more than trace amounts in the condensable products from the methyl- and dimethyl-acetylene reactions at lower flow rates. However, when the flow rates had been increased to about 10 to 20 micromoles/second, the methylacetylene reaction yielded C_2H_2 (1.7×10^{-7} mole/second), C_3H_6 (3×10^{-7} mole/second), and C_4H_8 (8×10^{-6} mole/second), while the dimethylacetylene reaction yielded C_2H_2 (1.8×10^{-7} mole/second), C_2H_6 (8×10^{-8} mole/second), C_3H_6 (2×10^{-6} mole/second), and a C_5 fraction (8×10^{-6} mole/second).

Polymer yields from the acetylene and methylacetylene reactions are shown in Table I. The amount of polymer from the reaction of dimethylacetylene was too small for quantitative estimation. Analyses of the polymers[4] showed their composition to be somewhat similar from the two reactions, with roughly 65% carbon, 27% nitrogen, and 7% hydrogen. However, the composition of the polymer probably has limited significance, since it seems likely that it would be subject to considerable variability as a result of attack by free radicals, active nitrogen, hydrogen atoms, and the parent hydrocarbon. They were all insoluble in the common solvents and were attacked only slowly by a mixture (equal volumes) of concentrated nitric and sulphuric acids.

[4]*We are indebted for these analyses to Dr. Léo Marion, Director, Division of Pure Chemistry, National Research Council, Ottawa.*

Can. J. Chem. Downloaded from www.nrcresearchpress.com by 186.233.112.2 on 09/04/12
For personal use only.

TABLE I

Yields of polymer from the reactions of acetylene and methylacetylene with active nitrogen

Acetylene		Methylacetylene	
Flow rate (mole/sec×10⁶)	Polymer yield (g/sec×10⁶)	Flow rate (mole/sec×10⁶)	Polymer yield (g/sec×10⁶)
7.6	128	1.4	22
11.0	98	6.7	65
		16.1	50

In the previous paper (1) it was suggested that HCN was produced in the acetylene – atomic nitrogen reaction by

$$C_2H_2 + N \rightarrow C_2H_2N \rightarrow HCN + CH. \quad [1]$$

However, this reaction would be endothermic and correspondingly doubtful if, as now seems likely (2), the heat of sublimation of graphite must be taken to be at least 170 kcal/mole. An alternative, which suffers no similar difficulty, would be to assume a relatively long-lived complex such that HCN might be formed by further reactions of the type

$$C_2H_2N + N \rightarrow 2HCN \quad [2]$$

$$\rightarrow 2CN + H_2 \quad [3]$$

$$2C_2H_2N \rightarrow HCN + CH \equiv C - CN + H_2 \quad [4][5]$$

$$\rightarrow HCN + H + CN + C_2H_2. \quad [5]$$

Such bimolecular processes would explain the observed greater-than-linear dependence of HCN yield on C_2H_2 flow rate at low flow rates of acetylene.

Reaction [4] is an interesting possibility, since it seems reasonable that the unsaturated nitrile should polymerize rapidly, hence account not only for formation of polymer with about the composition observed, but perhaps also for the reaction of not more than about one-half the available active nitrogen to form HCN.

The higher conversions of active nitrogen to HCN by methyl- and dimethyl-acetylene may be explained if the corresponding complexes were comparatively unstable and predominantly suffered decomposition similar to reaction [1], i.e. reactions such as:

methylacetylene:

$$C_3H_4 + N \rightarrow C_3H_4N \rightarrow HCN + C_2H_3 \quad [6]$$

$$\rightarrow HCN + C_2H_2 + H \quad [7]$$

$$\rightarrow CN + C_2H_2 + H_2, \quad [8]$$

dimethylacetylene:

$$C_4H_6 + N \rightarrow C_4H_6N \rightarrow HCN + C_3H_5 \quad [9]$$

$$\rightarrow HCN + C_3H_4 + H \quad [10]$$

$$\rightarrow HCN + C_2H_2 + CH_3 \quad [11]$$

$$\rightarrow CN + C_3H_6. \quad [12]$$

[5] *A product of mass 51, thought to be cyanoacetylene, has been observed in a mass spectrometric study of the reaction between active nitrogen and acetylene. (Private communication from Dr. J. L. Franklin, Humble Oil and Refining Company, while working at the National Bureau of Standards, Washington.)*

Can. J. Chem. Downloaded from www.nrcresearchpress.com by 186.233.112.2 on 09/04/12
For personal use only.

It is possible that polymer is formed in the methylacetylene reaction mainly by polymerization of $CH_3C \equiv C-CN$, which may be produced in a reaction similar to reaction [4]. The absence of polymer in the dimethylacetylene reaction may be ascribed to greater instability of the dimethylacetylene – nitrogen atom complex, which would not favor such a reaction.

Any radicals resulting from the foregoing reactions (e.g. C_2H_3, C_3H_5) would be expected to react rapidly with active nitrogen.

$$C_2H_3 + N \rightarrow HCN + CH_2 \quad [13]$$

$$\rightarrow CN + CH_3, \text{ etc.} \quad [14]$$

$$C_3H_5 + N \rightarrow HCN + C_2H_3 + H, \text{ etc.} \quad [15]$$

The amount of HCN formed from acetylene – nitrogen atom complexes by reactions such as [2], [4], and [5] would almost certainly be limited by interaction of the complexes or their reaction with nitrogen atoms to regenerate molecular nitrogen and the parent hydrocarbon or CH radicals. Reaction of the complex with acetylene to form polymer would also decrease the extent to which HCN may be produced. An upper limit of about one-half the active nitrogen converted to HCN is therefore not surprising, even if reaction [4] does not occur.

The absence of methane in the products from methyl- and dimethyl-acetylene is readily explained if the single carbon free radicals produced in these reactions, e.g. CH_3 and CH_2, are rapidly consumed by active nitrogen. The production of methane during the acetylene reaction suggests, therefore, that the single carbon free radical from this reaction, presumably the CH radical, is not rapidly attacked by active nitrogen. This might mean that the reaction

$$CH + N \rightarrow HCN$$

requires a three-body collision, while the corresponding reaction to form CN + H is not favored.

Cyanogen production in all three reactions is probably by recombination of CN radicals. Since the cyanogen yield from acetylene passes through a maximum, while that from the other two reactions increases steadily with flow rate of hydrocarbon, the CN radicals are probably produced directly by decomposition of the methyl- and dimethyl-acetylene complexes (e.g. reactions [8] and [12]), but indirectly from acetylene complexes by further nitrogen atom attack or interaction of complexes as in reactions [3] or [5].

The presence, in the products, of small amounts of hydrocarbons, such as C_2H_6 and C_3H_6, and the larger amounts of C_4H_8 and C_5 fraction at higher flow rates of methyl- and dimethyl-acetylene, indicate that H atom and free radical reactions occurred under these conditions. However, there would seem to be little point in attempting to detail these, since they probably bear little relation to the nitrogen reactions which are of principal concern.

It might be noted that the production of as much as 3.3 moles HCN per mole dimethyl-acetylene requires hydrogen rearrangement in the complex. Similar behavior has been indicated by the results for some other reactions of active nitrogen with hydrocarbons (2).

REFERENCES

1. VERSTEEG, J. and WINKLER, C. A. Can. J. Chem. **31**, 129 (1953).
2. EVANS, H. G. V., FREEMAN, G. R., and WINKLER, C. A. Can. J. Chem. **34**, 1271 (1956).
3. FORST, W., EVANS, H. G. V., and WINKLER, C. A. J. Phys. Chem. **61**, 320 (1957).
4. WILES, D. M. and WINKLER, C. A. J. Phys. Chem. **61**, 902 (1957).

Can. J. Chem. Downloaded from www.nrcresearchpress.com by 186.233.112.2 on 09/04/12
For personal use only.

SOME YIELDS IN THERMAL NEUTRON FISSION OF U^{233} AND Pu^{239} [1]

ROSALIE M. BARTHOLOMEW, J. S. MARTIN,[2] AND A. P. BAERG

ABSTRACT

Relative yields of Sr^{89}, Sr^{91}, Ba^{139}, Ba^{140}, and La^{141} have been measured for U^{233} and Pu^{239} thermal neutron fission. Ion exchange separations and 4π beta-counting methods were used. The following relative values were obtained for the nuclides as listed: 1.05, 1.00, 1.00, 1, and 1.10 in U^{233} fission and 0.301, 0.431, 1.07, 1, and 1.01 in Pu^{239} fission.

INTRODUCTION

Although the mass distribution of the products of U^{235} fission has been well studied and yields accurately determined for most masses, relatively few accurate measurements have been made for the fission of the nuclides U^{233} and Pu^{239}. Radiochemical studies of the fission of U^{233} have been reported by Grummitt and Wilkinson (9) in 1948 and by Steinberg *et al.* (16) in the same year. Papers reporting earlier radiochemical studies of Pu^{239} fission have been summarized by Steinberg and Freedman (13). All of the radiochemical data, with revised values for U^{233} fission yields, together with some more recent relative mass spectrometric measurements have been summarized by Steinberg and Glendenin in 1955 (14).

Mass spectrometric relative yield measurements in U^{233} fission have been reported for the isotopes of xenon, cesium, and krypton (6) and the isotopes of zirconium, molybdenum, and ruthenium (15). Similar relative values for Pu^{239} fission have been obtained for the isotopes of xenon by Fleming and Thode (5) and for the isotopes of cerium, neodymium, and cesium by Krizhansky *et al.* (11).

Absolute mass spectrometric yields for some nuclides have been obtained by the isotope dilution technique. In Pu^{239} fission preliminary values have been reported for cesium, cerium, neodymium, and samarium isotopes by Wiles *et al.* (17). Absolute values for the isotopes of neodymium and cerium are reported for U^{233} fission by Kukavadze *et al.* (12).

All of the data, both radiochemical and mass spectrometric, reported to 1958 have recently been evaluated and summarized by Katcoff (10). The radiochemical data were obtained using end-window Geiger counters and the values have an accuracy of 10–20% (14). The mass spectrometric yields have a relative accuracy, in most cases, of 1–2% and absolute values are usually accurate to 3–5% (14).

During the 1958 International Conference on the Peaceful Uses of Atomic Energy, further data have become available. These include radiochemical measurements of the heavy rare earths in Pu^{239} fission (4), absolute mass spectrometric yields for Cs^{133}, Xe^{135}, Nd^{143}, Sm^{149}, and Sm^{151} for both U^{233} and Pu^{239} fission (3), and for the isotopes of Xe and Kr in Pu^{239} fission (7). Anikina *et al.* (1) have reported absolute yields for isotopes of Sr, Cs, Ba, Ce, Nd, and Sm for U^{233} and Pu^{239} fission. They have also obtained yields of La^{139} and Eu^{153} for U^{233} fission and of Pr^{141} for fission of U^{233} and Pu^{239} using mass spectrometric methods requiring the comparison of integrated ion currents.

We have recently used improved radiochemical methods (2) to measure relative yields of Sr^{89}, Sr^{91}, Ba^{139}, Ba^{140}, and La^{141} in U^{235} fission with a reliability believed comparable

[1]*Manuscript received December 2, 1958.*
Contribution from the Chemistry and Metallurgy Division, Research Chemistry Branch, Atomic Energy of Canada Limited, Chalk River, Ontario.
Issued as A.E.C.L. No. 764.
[2]*Present address: Columbia University, New York, N.Y., U.S.A.*

Can. J. Chem. Downloaded from www.nrcresearchpress.com by 186.233.112.2 on 09/04/12
For personal use only.

with that achieved by mass spectrometric techniques. Except for the mass 91 chain the cumulative yields of these masses can better be obtained by radiochemical determination of the nuclides listed and the purpose of this work was to extend the measurements already made for U^{235} fission to fission of U^{233} and Pu^{239}.

EXPERIMENTAL

Except for several minor modifications, the procedure used for the relative yield measurements here was the same as that reported earlier (2). In the work with U^{235} relatively large samples (10 to 50 mg) of natural uranium were irradiated as the oxides in the Chalk River NRX reactor. In the present experiments with U^{233} and Pu^{239}, however, samples of about 100 μg only were sealed in quartz for the irradiations. Under these conditions it was found that up to 50% of the fission fragments were embedded in the quartz and not recovered in the subsequent dissolution. As a consequence of partial segregation of the products arising from differences in fragment ranges, very significant errors in the relative yield values were observed, even for adjacent masses. To avoid these errors from the loss of fission fragments, the fissile material was deposited as the nitrate solution on a pure iron oxide matrix (50 mg) to serve as a fragment catcher in the quartz tube. The samples were dried and heated to the oxide before sealing.

Following irradiation, the samples were crushed and dissolved in aqua regia containing small quantities (about 50 μg each) of suitable carriers, then dried, and taken up in 9 N hydrochloric acid. This solution was passed through an anion column to remove the Pu^{239} or U^{233} and iron together with various anionic fission products. The cations in the effluent, predominantly the alkali metals, alkaline earths and rare earths, were subsequently adsorbed on a cation column and the various species separated by elution with ammonium α-hydroxyisobutyrate. Details of the separation procedures and 4π beta-counting methods have been given in ref. 2. All yield calculations were based on half-lives as quoted in the same reference.

In the absolute beta counting of Sr^{89} and Y^{91} small corrections (usually less than 1%) were made for the presence of 27.7-year Sr^{90} and its 64.8-hour Y^{90} daughter. To make these corrections it was assumed that the ratio of yields Sr^{90}/Sr^{89} is 1 for U^{233} fission and 1.5 for Pu^{239} fission, while the Sr^{91}/Sr^{90} yield ratio was assumed to be 1 for U^{233} and 0.9 for Pu^{239} fission.

RESULTS AND DISCUSSION

The relative yield values obtained are listed in Table I, each set of experiments being divided into two groups: one for the Ba^{139}/Ba^{140} ratios and the other for the ratios of Sr^{89}, Sr^{91}, and La^{141} to Ba^{140}. In Table II the values of Table I have been combined and converted to absolute values on the basis of selected yields for mass 140 as given by Katcoff (10). The errors quoted reflect only the precision of the values given in Table I. Included for comparison in Table II are the relevant yields quoted in refs. 10 and 14.

U^{233}

In U^{233} fission the value of 5.60% for the yield of Ba^{140} corresponds to that of Ce^{140} determined mass spectrometrically by Kukavadze *et al.* (12). We make the reasonable assumption that the yields of Ce^{140} and Ba^{140} are equivalent. With this assumption our results for Sr^{89} and Sr^{91} are somewhat lower than those reported for these masses in ref. 14. The Zr^{91} yield of ref. 14 is based on relative mass spectrometric data fitted together with the aid of earlier radiochemical yields for Sr^{89}, Zr^{95}, Mo^{99}, and Ru^{103} to give a yield curve for the light mass group (15). The discrepancies with the present

Can. J. Chem. Downloaded from www.nrcresearchpress.com by 186.233.112.2 on 09/04/12
For personal use only.

TABLE I

Relative yields in thermal neutron fission of U^{233} and Pu^{239}

	Expt.	Ba^{140}	Ba^{139}	La^{141}	Sr^{89}	Sr^{91}
U^{233}	1	1	1.00_4			
	2	1	0.99_5			
	3	1	0.99_7			
	4	1	0.99_9			
	5	1		1.10_7	1.04_6	0.99_7
	6	1		1.10_8	1.07_8	1.02_2
	7	1		1.08_7	1.01_9	0.99_4
	8	1		1.10_7	1.05_1	0.99_6
Pu^{239}	1	1	1.06_8			
	2	1	1.07_9			
	3	1	1.06_0			
	4	1	1.07_0			
	5	1		1.00_4	0.29_1	0.41_7
	6	1		0.99_3	0.30_6	0.43_3
	7	1		1.02_3	0.31_0	0.43_8
	8	1		1.03_2	0.29_7	0.43_8

TABLE II

Yields normalized to selected values for Ba^{140}

	Ba^{140}	Ba^{139}	La^{141}	Sr^{89}	Sr^{91}
U^{233}	5.60	5.59	6.17	5.87	5.61
Standard deviation		0.02	0.05	0.12	0.06
Data of ref. 14*	5.6 Ce^{140}			6.1	6.09 Zr^{91}
Pu^{239}	5.68	6.07	5.75	1.71	2.45
Standard deviation		0.04	0.09	0.04	0.05
Data of ref. 10	5.68	5.7	5.2 Ce^{141}	1.9	2.4 Y^{91} 3.0%

*The original data, based on 6.0% for Ba^{140} (16), are renormalized to 5.6% for this nuclide.

results are, however, probably within the associated errors.

Anikina *et al.* (1) have reported values of 5.91 and 5.57% respectively for La^{139} and Pr^{141}. These values are based on mass spectrometer integrated ion currents and are to be compared with 5.59 and 6.17% respectively for Ba^{139} and La^{141} relative to 5.6% for Ba^{140}. The differences are greater than the quoted errors allow and no explanation for the discrepancies is obvious.

Pu^{239}

In Pu^{239} fission the yield of Ba^{140} given by Steinberg and Glendenin (14) was 5.36%. This value was increased to 5.68% by Katcoff (10) to make the total yields 100% each for the light and heavy groups. The preliminary mass spectrometric values of Wiles *et al.* (17) indicate a yield of 7.36% for Ce^{140}. On the other hand, Krizhansky *et al.* (11) have made relative measurements of the cerium isotopes which agree well with those of Wiles *et al.* except at mass 140. Accepting the absolute values of Wiles *et al.* for masses other than Ce^{140} and combining these with the relative values of Krizhansky *et al.*, the Ce^{140} absolute yield becomes 5.63%, which agrees well with that selected by Katcoff for Ba^{140}.

The yields of Ba^{139}, Ce^{141}, Sr^{89}, and Sr^{91} quoted in ref. 10 are from the data of Steinberg *et al.* (13, 14) normalized to a value of 5.68% for Ba^{140}. Comparison of these yields with those obtained here shows agreement within the experimental errors. The integral mass spectrographic value of 6.02% for Pr^{141} given by Anikina *et al.* (1) is greater than the value (5.75%) we obtained for La^{141}. The difference is larger than the quoted errors

Can. J. Chem. Downloaded from www.nrcresearchpress.com by 186.233.112.2 on 09/04/12
For personal use only.

and also larger than could reasonably be attributed to independent formation of Ce^{141}. The value for Sr^{91} found here is in good agreement with that of ref. 10. There is, however, a large difference between it and the values for Y^{91} (10, 14) implying a high independent yield for the latter. The difference seems excessive but may possibly arise from a short-lived isomeric state in Sr^{91} which feeds Y^{91}. Evidence for such chain branching has already been given by Grummitt and Milton (8) for U^{235} fission.

REFERENCES

1. Anikina, M. P., Aron, R. M., Gorshov, V. K., Ivanov, R. N., Krizhansky, L. M., Kukavadze, G. M., Mourin, A. N., Reformatsky, I. A., and Ershler, B. V. Second United Nations International Conference on the Peaceful Uses of Atomic Energy, Paper No. 2040 (1958).
2. Baerg, A. P. and Bartholomew, R. M. Can. J. Chem. **35**, 980 (1957).
3. Bidinosti, D. R., Fickel, H. R., and Tomlinson, R. H. Second United Nations International Conference on the Peaceful Uses of Atomic Energy, Paper No. 201 (1958).
4. Bunney, L. R., Scadden, E. M., Abriam, J. O., and Ballou, N. E. Second United Nations International Conference on the Peaceful Uses of Atomic Energy, Paper No. 644 (1958).
5. Fleming, W. H. and Thode, H. G. Can. J. Chem. **34**, 193 (1956).
6. Fleming, W. H., Tomlinson, R. H., and Thode, H. G. Can. J. Phys. **32**, 522 (1954).
7. Fritze, K., McMullen, C. C., and Thode, H. G. Second United Nations International Conference on the Peaceful Uses of Atomic Energy, Paper No. 187, rev. 1 (1958).
8. Grummitt, W. E. and Milton, G. M. J. Inorg. Nucl. Chem. **5**, 93 (1957).
9. Grummitt, W. E. and Wilkinson, G. Nature, **161**, 520 (1948).
10. Katcoff, S. Nucleonics, **16**, 78 (1958).
11. Krizhansky, L. M., Maly, Y., Murin, A. N., and Preobrazhensky, B. K. Soviet J. Atomic Energy, **2**, 334 (1957).
12. Kukavadze, G. M., Anikina, M. P., Goldin, L. L., and Ershler, B. V. Conference of the Academy of Sciences of the U.S.S.R. on the Peaceful Uses of Atomic Energy (English translation), p. 125 (July 1955).
13. Steinberg, E. P. and Freedman, M. S. National Nuclear Energy Series, Div. IV. Vol. 9. McGraw-Hill Book Company, Inc., New York. 1951. Paper 219.
14. Steinberg, E. P. and Glendenin, L. E. International Conference on the Peaceful Uses of Atomic Energy. Vol. 7. United Nations, New York. 1956. p. 614.
15. Steinberg, E. P., Glendenin, L. E., Inghram, M. G., and Hayden, R. J. Phys. Rev. **95**, 867 (1954).
16. Steinberg, E. P., Seiler, J. A., Goldstein, A., and Dudley, A. U.S. Atomic Energy Comm. Rept. MDDC-1632 (1948).
17. Wiles, D. M., Petruska, J. A., and Tomlinson, R. H. Can. J. Chem. **34**, 227 (1956).

Can. J. Chem. Downloaded from www.nrcresearchpress.com by 186.233.112.2 on 09/04/12
For personal use only.

Can. J. Chem. Downloaded from www.nrcresearchpress.com by 190.90.36.8 on 09/04/12
For personal use only.

PROTONATION OF THE CARBONYL GROUP

II. THE BASICITIES OF SUBSTITUTED BENZALDEHYDES[1]

K. YATES[2] AND ROSS STEWART

ABSTRACT

The basicities of seven meta- and para-substituted benzaldehydes have been determined by a spectrophotometric method in sulphuric acid media. The simple Hammett relation does not hold for these bases but a good correlation exists between pK_{BH^+} and σ^+. The effects of substitution on the wavelengths of maximal ultraviolet absorption in benzaldehyde are compared with those in acetophenone.

The basicity of *o*-tolualdehyde was determined in an attempt to estimate the steric effects of ortho substitution. The effects of symmetrical trisubstitution on the basicity of benzaldehyde and acetophenone are compared and discussed.

INTRODUCTION

In connection with studies of the protonation of ketones reported previously (1) and of carboxylic acids to be reported soon, we have determined the effects of ring substitution on the basicity of benzaldehydes. In determining the strengths of these very weak bases we have again followed the approach used by Hammett in his classical investigations (2) utilizing the concept of the H_0 acidity function. This has the advantage of yielding basicity values which are absolute in so far as they are based on dilute aqueous solution as the standard state. Pratt and Matsuda (3) determined relative basicities of some oxygen-containing organic bases in benzene solution by their effect on acid catalyzed reactions. Gordy and Stanford (4) have also determined relative basicities of similar compounds by a spectroscopic method. Wepster (5) has used a number of physical and chemical properties to determine base strengths of substituted nitrobenzenes.

EXPERIMENTAL

Commercially available benzaldehydes were purified either by vacuum distillation under a small positive pressure of nitrogen or by several recrystallizations. *o*-Tolualdehyde was prepared from *o*-bromotoluene by the method of Smith and Nichols (6). (B.p. 89°/22 mm, $n_D^{24} = 1.5410$. Lit. b.p. 72°/6 mm, and $n_D^{25} = 1.5430$ (7).) Stock solutions of these compounds in the range 10^{-2}–10^{-3} molar were titrated against standard alkali immediately after use and found to be free of the corresponding benzoic acids.

Sulphuric acids of various concentrations were prepared by dilution of Fisher C.P. reagent grade sulphuric acid (95.0% min.). Further solutions up to 99.9% were prepared by mixing the above with 30% fuming sulphuric acid (Baker & Adamson Reagent). Determination of the H_0 values of these acids and the preparation of suitably absorbing solutions of the aldehydes in them is described in Part I of this series.

The extinction coefficients of these solutions at various concentrations of sulphuric acid were determined at two wavelengths with quartz cells of 1 cm path length using a Beckman Model DU Spectrophotometer, whose cell compartment was maintained at 25±0.1° by means of thermospacers. The sulphuric acids were tested for optical clarity in the regions used and a solvent blank of the same concentration as that containing the aldehyde was used. Ultraviolet absorption spectra of the aldehydes in 44.0% and

[1]*Manuscript received November 12, 1958.*
Contribution from the Department of Chemistry, University of British Columbia, Vancouver.
[2]*Holder of N.R.C. studentships, 1957–59.*

95.5% acids measured with a Cary Model 14 Recording Spectrophotometer were used to locate the wavelengths of maximal absorption of the unprotonated (λ_u) and protonated (λ_i) forms. These are listed in Table I.

TABLE I

Absorption spectra of substituted benzaldehydes

	In 44.0% H_2SO_4			In 95.5% H_2SO_4		
Substituent	λ_{max} (mμ)	log ϵ_{max}	$\Delta\lambda_u$ (mμ)	λ_{max} (mμ)	log ϵ_{max}	$\Delta\lambda_i$ (mμ)
m-Chloro	250	3.89	−1	297	4.16	1
p-Chloro	263	4.18	12	316	4.37	20
p-Nitro	270	4.13	19	282	4.25	−14
p-Methoxy	290	3.87	39	344	4.23	48
Hydrogen	251	4.08	0	296	4.36	0
o-Methyl	260	4.26	9	302	4.48	6
m-Methyl	258	4.03	7	301	4.27	5
p-Methyl	264	4.14	13	313	4.43	17

The pK_{BH^+} values were determined by the method of Davis and Geissman (8) as follows: The extinction coefficients $\epsilon(\lambda_u)$ and $\epsilon(\lambda_i)$ of the two species were measured in at least 12 different concentrations of acid. The function $[\epsilon(\lambda_i)-\epsilon(\lambda_u)]$ which is linearly related to the fraction ionized was plotted against H_0. At the inflection point of this curve it can be shown that the fraction ionized equals the fraction un-ionized, hence $\log (c_{BH^+}/c_B) = 0$ and $H_0 = pK_{BH^+}$. In all cases a sigmoid titration type curve was obtained and the inflection point taken as the mid-point of the "straight" portion. The results of a typical determination are shown in Fig. 1. The advantages and limitations of the method are discussed by the above authors. In cases where λ_i is very close to λ_u or where $\epsilon(\lambda_i) \gg \epsilon(\lambda_u)$ we have found that smooth curves cannot be obtained. The method fails for *m*-nitrobenzaldehyde and the second decimal in the pK_{BH^+} value of the *p*-nitro isomer is of doubtful significance.

Because of the possibility of chemical change other than protonation occurring in the strongly acid solutions the absorption spectra of the aldehydes in 95.5% acid were repeated after 1 hour's standing. They were found to undergo no appreciable change and on subsequent dilution the spectra reproduced closely those of control solutions in dilute acid. The possibility of sulphonation in very high concentrations is not serious, since this region is not in a critical part of the curve. However, to minimize any such effects all measurements used in determining pK_{BH^+} were taken as rapidly as possible after the addition of the acids.

RESULTS AND DISCUSSION

Effects of Meta and Para Substitution on Basicity

The values of pK_{BH^+} for the substituted benzaldehydes are listed in Table I and are plotted as a function of σ (9), the Hammett substituent constant in Fig. 2. It can be seen that the correlation is rather poor even if only meta and para substituents are considered (open circles). The 2,4,6-substituted compounds (closed circles) will be discussed in a later section. The four points through which the dotted line is drawn represent those substituents which are not able to supply electrons to the positively charged conjugate acid by direct resonance with the group and hence are expected to obey the Hammett equation (10),

$$\log (K/K_H) = \rho\sigma.$$

Can. J. Chem. Downloaded from www.nrcresearchpress.com by 190.90.36.8 on 09/04/12
For personal use only.

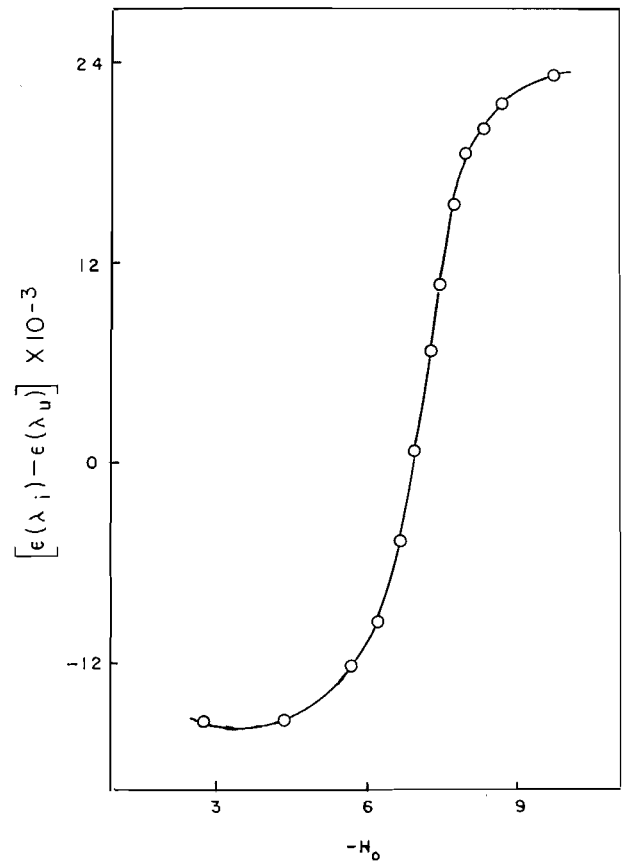

FIG. 1. The function $[\epsilon(\lambda_i)-\epsilon(\lambda_u)]\times10^{-3}$ plotted against $-H_0$ for *p*-chlorobenzaldehyde.

The other three points represent para substituents which are able to do this owing to contributions from structures like II.

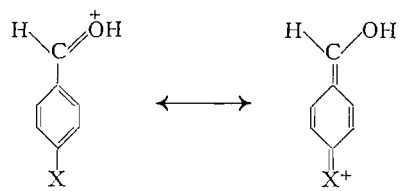

I II

The latter substituents thus give higher basicities than their σ values predict owing to increased stabilization of the conjugate acid.

Several investigators (11) have noted that substituents such as *p*-methoxy are able to stabilize carbonium ions to a much greater extent than is indicated by their σ values, and σ^+ values have been derived (12) for groups which are able to supply electrons for use in reactions where a positive charge is developed in conjugation with the group. Figure 3 shows a plot of pK_{BH^+} of the same seven compounds against σ^+. A good linear correlation ($r = 0.994$) now exists for both meta and para points.

Can. J. Chem. Downloaded from www.nrcresearchpress.com by 190.90.36.8 on 09/04/12
For personal use only.

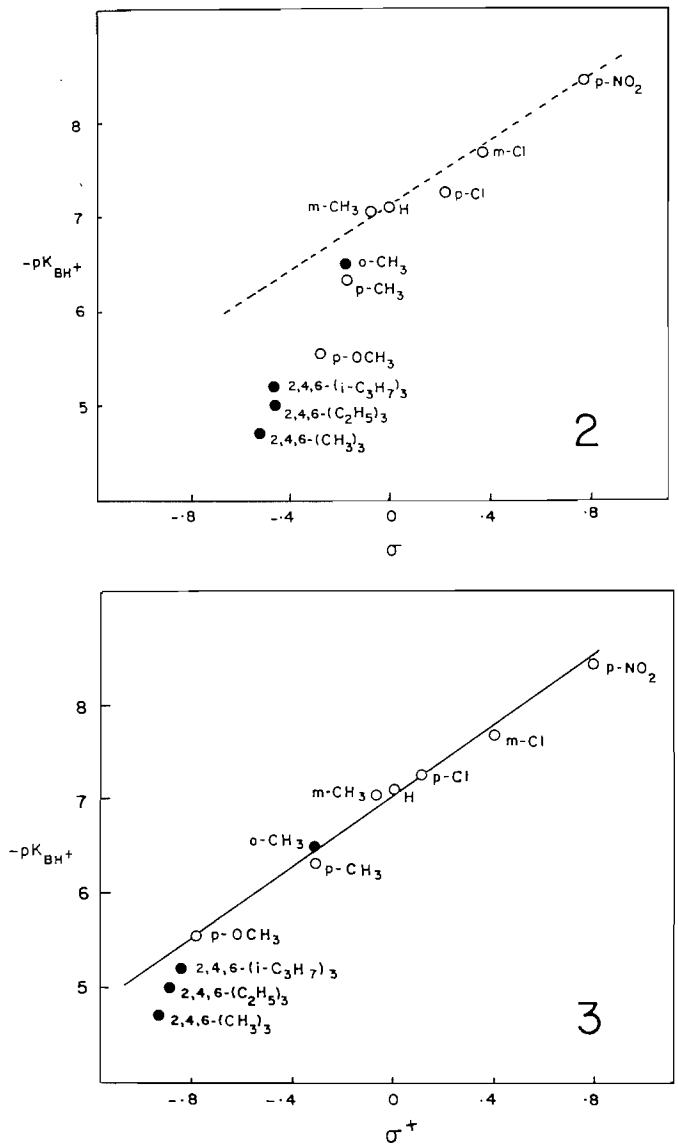

FIG. 2. $-pK_{BH^+}$ for substituted benzaldehydes plotted against Hammett's σ constants.
FIG. 3. $-pK_{BH^+}$ for substituted benzaldehydes plotted against Brown's σ^+ constants.

As might be expected these results are very similar to those obtained with substituted acetophenones (1) in which similar resonance effects are possible. However, two points of difference arise. In the case of the ketones the basicity of the *p*-methoxy group was found to be lower than that predicted by the σ^+ value. Similar deviations for alkoxy groups have been noted by other workers (13). The above deviation was explained on the basis that solvent–solute hydrogen-bonding for such groups should be particularly strong in sulphuric acid with a consequent increase in σ^+, thus lowering the basicity. The point for the analogous *p*-methoxybenzaldehyde, however, falls on a good straight line through all the other points. This is surprising, since the solvent effects discussed

Can. J. Chem. Downloaded from www.nrcresearchpress.com by 190.90.36.8 on 09/04/12
For personal use only.

previously (1) should be at least as strong for benzaldehydes. The possibility of protonation occurring at the methoxy rather than the formyl group was considered but rejected for two reasons:

1. The spectral changes of *p*-methoxybenzaldehyde in sulphuric acid parallel those of other benzaldehydes and acetophenones, i.e. a pronounced red shift on protonation. If protonation occurred preferentially at the methoxy group the change would be expected to be in the opposite direction as in the case of anilines which undergo a blue shift on protonation (14).

2. The evidence of other workers (3, 4) indicates that alkyl aryl ethers are considerably less basic than aromatic aldehydes and ketones. This difference should be even more pronounced where there is an electron-withdrawing formyl group para to the alkoxyl group as shown below:

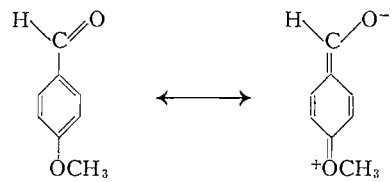

III IV

The second point of difference between the two series is the magnitude of the reaction constant. The ρ value obtained from the meta and para points in Fig. 3 is 1.85 (least squares calculations used throughout), whereas the value for acetophenones is 2.17 (neglecting the point for *p*-methoxy). The larger ρ for the acetophenone series compared to the benzaldehyde series suggests that the charge is more localized on the ketone carbon atom of the former than on the aldehyde carbon of the latter (15). A similar effect occurs in the solvolysis of α-phenylethyl chloride compared to the benzyl compound (16).[3] The greater localization of charge in the cases of the ketone conjugate acid and the α-phenylethyl carbonium ion can be rationalized in terms of steric hindrance of the methyl group to solvation in the cations.

Effects of Substitution on the Ultraviolet Spectra

Forbes *et al.* (17) have shown in a recent series of papers that para substitution of benzaldehydes produces displacements of the wavelength of maximum absorption (π–π^* transitions) relative to that of the parent compound. These displacements are directly related to those produced by similar substitution in nitrobenzenes and acetophenones and it was suggested that this proportionality is primarily due to the similarity of resonance effects on the transition energies in all three types of compounds. In Figs. 4*a* and 4*b* the wavelength displacements produced by the introduction of substituents in benzaldehyde ($\Delta\lambda_u$) and its conjugate acid ($\Delta\lambda_l$) are taken from Table I and plotted against the corresponding values for acetophenones. Since most of Forbes' measurements were taken in neutral solvents, it is interesting to see that a good correlation ($r = 0.981$) still exists for the unprotonated forms (Fig. 4*a*). Despite the large change in medium the slope of the line (0.88) is close to that observed by Forbes, although the wavelength shifts appear to be more pronounced in 44.0% sulphuric acid. This indicates that, although medium effects on the spectra are rather large, they are similar for both types of carbonyl compound.

An equally good correlation ($r = 0.984$) is found for the conjugate acids (Fig. 4*b*,

[3]*We are grateful to the referee for drawing this to our attention.*

Can. J. Chem. Downloaded from www.nrcresearchpress.com by 190.90.36.8 on 09/04/12
For personal use only.

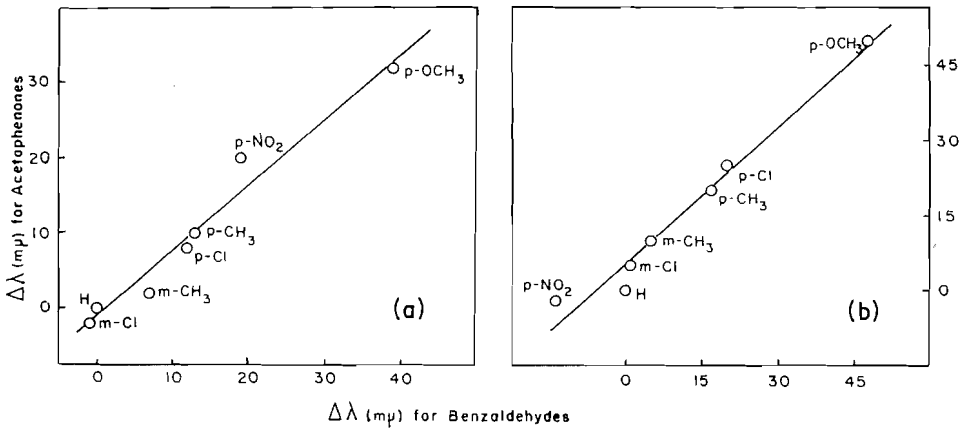

FIG. 4. Wavelength displacements of the principal ultraviolet band obtained on introducing substituents (*a*) into acetophenone and benzaldehyde and (*b*) in the conjugate acids of acetophenone and benzaldehyde.

slope = 0.90) and the displacements are now in the approximate order of the ability of the groups to donate electrons by resonance. The fact that the slopes of the lines in Figs. 4*a* and 4*b* are approximately unity indicates that resonance is of comparable importance in the acetophenone and benzaldehyde series being possibly slightly more important in the latter case. A further indication of this is the fact that those groups which can donate electrons by resonance (*p*-methoxy, *p*-methyl, *p*-chloro) produce *a slightly larger* increase in basicity when substituted in benzaldehyde than when substituted in acetophenone. This is despite the greater over-all ρ for the acetophenones.

Steric Effects of Alkyl Groups

It is interesting to compare the effect of methyl substitution in different positions on the basicities of benzaldehydes as shown in Table II and Figs. 2 and 3. It is apparent that ortho methyl substitution produces an increase in basicity roughly comparable to para substitution. Symmetrical trimethyl substitution as in 2,4,6-trimethylbenzaldehyde results in a greatly enhanced basicity as shown in Fig. 3, where we have assumed the sigma value for 2,4,6-trialkyl substitution to be $\Sigma\sigma^+$ para (21). The extent of deviation of the three alkyl groups ($CH_3 > C_2H_5 > i\text{-}C_3H_7$) is in the order of decreasing size possibly reflecting decreasing extents of steric hindrance to solvation of the cations. If the latter effect was unimportant the three points would all presumably deviate even farther from the straight line.

TABLE II

pK_{BH^+} values of substituted benzaldehydes

Substituent	$-pK_{BH^+}$	Substituent constants*	
		σ	σ^+
m-Chloro	7.68	0.373	0.399
p-Chloro	7.26	0.227	0.114
p-Nitro	8.45	0.778	0.790
p-Methoxy	5.54	−0.268	−0.778
Hydrogen	7.10	0.0	0.0
o-Methyl	6.50	—	—
m-Methyl	7.06	−0.069	−0.066
p-Methyl	6.32	−0.170	−0.311
2,4,6-Trimethyl†	4.7	—	—
2,4,6-Triethyl†	5.0	—	—
2,4,6-Triisopropyl†	5.2	—	—

*Refs. 9 and 12.
†Ref. 22.

Can. J. Chem. Downloaded from www.nrcresearchpress.com by 190.90.36.8 on 09/04/12
For personal use only.

Braude and Sondheimer (18) among others (19) have used changes in electronic spectra and dipole moments to estimate the steric effects of two ortho methyl groups on the coplanarity of the carbonyl group and the benzene ring for both benzaldehydes and acetophenones. Their results as shown in Table III indicated a mean rotation of about 15–20° for 2,4,6-trimethylbenzaldehyde. (The amount of π orbital overlap is reduced by an amount which varies as $\cos^2 \theta$ (20).) The process studied by Braude and Sondheimer in evaluating the extent of steric interference was the absorption of a photon to give the excited state crudely represented by VI. The oxygen atom as a result of bearing an increased negative charge should be larger than the oxygen atom in V.

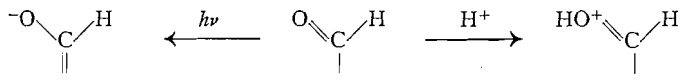

VI V VII

The protonation reaction on the other hand results in a positively charged oxygen atom as in VII which should be smaller than the oxygen in V, smaller at least in the direction at right angles to the O—H bond axis. The greater degree of coplanarity thus allowed the conjugate acid compared to the neutral aldehyde and the consequent increased resonance with the ring may explain the enhanced basicity of 2,4,6-trimethylbenzaldehyde.

TABLE III

Steric effects of 2,4,6-trimethyl substitution in benzaldehyde and acetophenone (18)

Compound	θ_ϵ*	θ_μ†	μ_{obs} (D)	μ_{calc} (D)	pK_{BH^+}	
Benzaldehyde	0°	0°	2.92	2.92	−7.1	
2,4,6-Trimethylbenzaldehyde	22°	15°	2.96	2.99	−4.7	(22)
Acetophenone	0°	0°	2.96	2.96	−6.15	(1, 22)
2,4,6-Trimethylacetophenone	63°	62°	2.81	3.03	−7.9	(22)

*Mean interplanar angle calculated from ratio of observed ϵ of K band to that expected in a uniplanar system (Braude and Sondheimer (18)).

†Mean interplanar angle calculated from observed dipole moment data (18).

It is interesting to compare the effects of similar substitution on the basicity of acetophenone. Table III shows that the observed dipole moment of 2,4,6-trimethylacetophenone is much lower than the calculated value and approaches the value for saturated ketones (μ = 2.75 D for acetone (18)) unlike mesitaldehyde whose observed dipole moment is close to the calculated value. This indicates that the contribution of dipolar resonance structures such as VIII is greatly reduced by steric inhibition. This is due to the bulky acetyl methyl which overlaps the ortho groups much more than does the

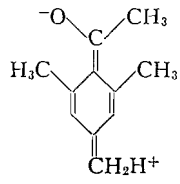

VIII

carbonyl oxygen. In support of this the mean interplanar angle θ calculated from ultra-

Can. J. Chem. Downloaded from www.nrcresearchpress.com by 190.90.36.8 on 09/04/12
For personal use only.

violet spectra is 63°. This should result in drastic reduction of π-orbital overlap involving the carbonyl group and the ring. In agreement with this the basicity of 2,4,6-trimethylacetophenone (22) is found to be 1.75 log units less than the parent compound, whereas the inductive effects alone of three methyl groups would normally be expected to increase the basicity. The shrinking of the carbonyl group as a result of protonation, which we discussed above as an explanation for the enhanced basicity of 2,4,6-trimethylbenzaldehyde, is not an important factor in the case of the ketones. Here it is the ketone methyl which is largely responsible for the steric repulsions rather than the carbonyl group as for the aldehydes.

ACKNOWLEDGMENT

The financial aid of the National Research Council is gratefully acknowledged.

REFERENCES

1. STEWART, R. and YATES, K. J. Am. Chem. Soc. **80**, 6355 (1958).
2. FLEXSER, L. A., HAMMETT, L. P., and DINGWALL, A. J. Am. Chem. Soc. **57**, 2103 (1935). FLEXSER, L. A. and HAMMETT, L. P. J. Am. Chem. Soc. **60**, 885 (1938). HAMMETT, L. P. and DEYRUP, A. J. J. Am. Chem. Soc. **54**, 2721 (1932).
3. PRATT, E. F. and MATSUDA, K. J. Am. Chem. Soc. **75**, 3739 (1935).
4. GORDY, W. and STANFORD, S. C. J. Chem. Phys. **8**, 170 (1940).
5. WEPSTER, B. M. Rec. trav. chim. **76**, 335, 337 (1957).
6. SMITH, L. J. and NICHOLS, J. J. Org. Chem. **6**, 489 (1941).
7. HASS, H. B. and BENDER, M. L. Org. Syntheses, **30**, 99 (1950).
8. DAVIS, C. T. and GEISSMAN, T. A. J. Am. Chem. Soc. **76**, 3507 (1954).
9. JAFFE, H. H. Chem. Revs. **53**, 191 (1953).
10. HAMMETT, L. P. Physical organic chemistry. McGraw-Hill Book Company, Inc., New York. 1940. Chap. VII.
11. PEARSON, D. E., BAXTER, J. F., and MARTIN, C. J. J. Org. Chem. **17**, 1511 (1952). KOCHI, J. K. and HAMMOND, G. S. J. Am. Chem. Soc. **75**, 3445 (1953). JARUZELSKI, J. J., DENO, N. C., and SCHREISHEIM, A. J. Org. Chem. **19**, 155 (1954).
12. DENO, N. C. and EVANS, W. L. J. Am. Chem. Soc. **79**, 5804 (1957). BROWN, H. C. and OKAMOTO, Y. J. Am. Chem. Soc. **80**, 4979 (1958).
13. BROWN, H. C. and OKAMOTO, Y. J. Am. Chem. Soc. **79**, 1913 (1957). See also WILES, L. A. Chem. Revs. **56**, 329 (1956).
14. MATSEN, F. A. *In* Chemical applications of spectroscopy. *Edited by* A. Weissberger. Interscience Publishers Ltd., London. 1956. p. 671.
15. TAFT, R. W. and LEWIS, I. C. J. Am. Chem. Soc. **80**, 2436 (1958).
16. BERLINER, E. and SHIEH, N. J. Am. Chem. Soc. **79**, 3849 (1957).
17. FORBES, W. F. Can. J. Chem. **36**, 1350 (1958). DEARDEN, J. C. and FORBES, W. F. Can. J. Chem. **36**, 1362 (1958). FORBES, W. F. and LECKIE, I. R. Can. J. Chem. **36**, 1371 (1958).
18. BRAUDE, E. A. and SONDHEIMER, F. J. Chem. Soc. 3754 (1955).
19. KADESH, R. G. and WELLER, S. W. J. Am. Chem. Soc. **63**, 1310 (1941). KLEVENS, H. B. and PLATT, J. R. J. Am. Chem. Soc. **71**, 1714 (1949). BRAUDE, E. A., SONDHEIMER, F., and FORBES, W. F. Nature, **173**, 117 (1954).
20. COULSON, C. A. Conference on quantum mechanical methods in valence theory. U.S. Government Printing Office. 1951. p. 47.
21. TAFT, R. W. *In* Steric effects in organic chemistry. *Edited by* M. S. Newman. John Wiley & Sons, Inc., New York. 1956. p. 577 ff.
22. PAUL, M. A. and LONG, F. A. Chem. Revs. **57**, 1 (1957). SCHUBERT, W. M. and ZAHLER, R. E. J. Am. Chem. Soc. **76**, 1 (1954).

Can. J. Chem. Downloaded from www.nrcresearchpress.com by 190.90.36.8 on 09/04/12
For personal use only.

THE REACTION OF METHYL RADICALS WITH FORMALDEHYDE[1]

S. TOBY[2] AND K. O. KUTSCHKE

ABSTRACT

Azomethane was photolyzed in the presence of up to 30 mole per cent formaldehyde and formaldehyde-d_2 at temperatures from 80° C to 180° C. The value of the activation energy for the abstraction reaction with methyl radicals was found to be 6.2 kcal mole^{-1} for CH_2O and 7.9 kcal mole^{-1} for CD_2O. The results indicated that the formyl radical was stable over the temperature range studied.

INTRODUCTION

This work was undertaken to provide data on a reaction which is of considerable interest in mechanisms of oxidation. Kodama and Takezaki (1) have reacted methyl radicals, produced by the thermal decomposition of azomethane at 310° C, with formaldehyde. They cite a value of 5.63 kcal per mole for the activation energy of the abstraction reaction; however, very little experimental data was given. It seemed desirable to investigate this reaction more fully.

EXPERIMENTAL

The methyl radicals were produced by photolysis of azomethane (2) using standard photochemical procedures. The optical system consisted of a Hanovia S-500 medium pressure mercury arc, two quartz lenses which produced an approximately parallel beam of light, and a Corning 5860 filter used with two filters of clear Pyrex glass. This combination gave radiation at approximately 3660 Å with an intensity of about 10^{14} quanta cm^{-3} sec^{-1} (using azomethane as an actinometer). A photocell was used to measure relative absorption.

The reaction cell was a cylindrical quartz vessel of volume 189 cm^3 connected to a magnetic stirrer, two Wood's alloy cutoffs (3), and a quartz spiral manometer. The whole was situated in an insulated box, the temperature of which could be kept constant within 1° C up to 200° C. Experiments were done at temperatures from 80° C (below which formaldehyde readily polymerizes) to 180° C (above which azomethane decomposes thermally).

The thermostatted section of the apparatus was connected to a conventional gas analysis system. After an experiment the non-condensable products were passed through a solid nitrogen trap into a gas burette via a small mercury diffusion pump backed by a Toepler pump. Carbon monoxide was oxidized over cupric oxide at 260° C and measured as carbon dioxide. The remaining mixture of nitrogen and methane was analyzed mass spectrometrically. Ethane was distilled through a Ward still at −180° C and its purity checked by the mass spectrometer.

Azomethane, supplied by Dr. L. C. Leitch of these laboratories, was distilled *in vacuo*, the center fraction being retained. Mass spectrometric analysis detected no impurity. Formaldehyde monomer was prepared by repeated distillation of α-polyoxymethylene (4), the only impurity being a trace of CO_2. The formaldehyde was stored at liquid nitrogen temperature. Illumination of pure formaldehyde produced less than 0.01% photodecomposition in a time comparable to the normal experiment. There was no detectable dark reaction between formaldehyde and azomethane.

[1]*Manuscript received December 8, 1958.*
Contribution from the Division of Pure Chemistry, National Research Council, Ottawa, Canada.
Issued as N.R.C. No. 5085.
[2]*National Research Council of Canada Postdoctorate Fellow 1955–1957. Present address: Department of Chemistry, Rutgers University, New Brunswick, N.J., U.S.A.*

Can. J. Chem. Downloaded from www.nrcresearchpress.com by 190.90.36.8 on 09/04/12
For personal use only.

Formaldehyde-d_2, supplied by Dr. L. C. Leitch (5), contained 99.4% atom per cent deuterium. In the case of runs using formaldehyde-d_2, methanes-d_0 and -d_1 were formed. It was confirmed that there was no deuterium exchange when the non-condensables were left in the CuO furnace for an hour.

Up to 5% of the azomethane was decomposed, and up to 2% of the formaldehyde was allowed to react. The azomethane concentration was kept at approximately two millimoles per liter corresponding to pressures of about 50 mm. The light intensity was not intentionally varied, but two arcs which had a difference of 20% in their output were used.

RESULTS AND DISCUSSION

The results of experiments with CH_2O are given in Table I and with CD_2O in Table II. They are consistent with the following reaction scheme:

$$CH_3N_2CH_3 \xrightarrow{h\nu} 2CH_3 + N_2, \quad [0]$$

$$2CH_3 \rightarrow C_2H_6, \quad [1]$$

$$CH_3 + CH_3N_2CH_3 \rightarrow CH_4 + CH_2N_2CH_3, \quad [2]$$

$$CH_3 + CH_2O \rightarrow CH_4 + CHO, \quad [3]$$

$$CH_3 + CHO \rightarrow CH_4 + CO. \quad [4]$$

TABLE I

Photolysis of mixtures of azomethane and formaldehyde

T, ° K	[Azo] moles/liter $\times 10^4$	[CH_2O] moles/liter $\times 10^4$	Time, sec.	Absorption, %	Rate $\times 10^{10}$ moles liter^{-1} sec^{-1} N_2	CH_4	C_2H_6	CO	$R_{CO}/\{R^{\frac{1}{2}}_{C_2H_6}[CH_2O]\}$, $l^{\frac{1}{2}}M^{-\frac{1}{2}}s^{-\frac{1}{2}}$
357.5	19.4	0.871	3600	16.0	72.3	19.2	26.3	5.2	0.12
357	18.7	1.03	7200	15	74.0	22.1	20.1	6.7	0.14$_5$
358	19.1	1.21	4500	18	70.2	22.3	27.1	8.3	0.13
357	20.4	2.58	4500	17.9	75.0	33.7	25.2	15.6	0.12
356.5	19.6	4.34	3600	17	96.1	54.9	28.0	29.4	0.13
363	23.4	1.57	5460	19.5	90.1	30.4	18.8	9.7	0.14
366	19.0	0.942	3600	17	73.4	23.5	14.9	7.1	0.19$_5$
371	20.1	4.78	3600	18	102	82.4	20.4	38.7	0.18
390	19.4	0.415	3300	17.9	83.2	25.6	7.2	3.5	0.32
389.5	19.9	0.819	2520	18	87.4	30.1	6.1	6.5	0.32
390	20.1	0.976	3600	17	107	46.0	18.2	11.2	0.27
389	21.7	1.08	5400	18.4	90.1	34.8	8.8	7.6	0.24
389	19.8	1.84	3060	17.7	83.4	43.1	7.2	15.1	0.31
389.5	19.1	2.24	3660	18.4	88.7	40.0	7.6	15.4	0.25
389	20.8	3.70	3900	18	80.5	55.7	9.7	26.9	0.23$_5$
387	20.2	4.37	4200	17	102	75.5	11.3	36.6	0.25
389	19.6	8.80	4200	17.3	101	99.8	7.3	60.1	0.25
389	19.1	12.7	3600	16.5	100	112	4.7	74.1	0.27
409	21.6	1.76	7200	20	76.6	42.0	3.7	12.0	0.36
412	23.1	1.37	4560	20.2	84.7	41.2	2.6	10.3	0.47
425.5	19.3	1.11	7380	15.2	72.3	45.1	2.2	16.3	0.52
432	22.8	1.26	3480	20.6	92.4	46.5	1.8	10.8	0.70
432.5	22.0	1.24	3600	20.7	92.4	47.7	1.7	11.2	0.69$_5$
457.5	17.6	1.15	7200	17.3	77.6	47.9	1.0	10.1	0.86
456.5	21.5	1.37	2460	20.6	92.9	51.0	1.5	11.1	0.65$_5$
452.5	20.2	7.88	3600	19.4	114	121	1.6	67.4	0.68
450.5	20.8	7.93	5400	20.5	112	121	0.81	65.0	0.91
452	20.2	10.1	3600	19.7	110	137	0.76	78.9	0.90
451	20.6	11.3	4200	20	111	150	0.85	86.1	0.83

Can. J. Chem. Downloaded from www.nrcresearchpress.com by 190.90.36.8 on 09/04/12
For personal use only.

TABLE II

Photolysis of mixtures of azomethane and formaldehyde-d_2

T, °K	[Azo] moles/-liter $\times 10^4$	[CD_2O] moles/-liter $\times 10^4$	Time of run, sec.	Absorption, %	Rate $\times 10^{10}$ moles liter^{-1} sec^{-1} N_2	CH_4	CH_3D	C_2H_6	CO	$R_{CH_4}/\{R^{\frac{1}{2}}_{C_2H_6}[Azo]\}$, $l^{\frac{1}{2}}M^{-\frac{1}{2}}s^{-\frac{1}{2}}$	R_{CH_3D}/R_{CO}	$\{R_{CH_3D}-R_{CO}\}/\{R^{\frac{1}{2}}_{C_2H_6}[CD_2O]\}$, $l^{\frac{1}{2}}M^{-\frac{1}{2}}s^{-\frac{1}{2}}\times 10^2$	$\{R_{CH_3D}-R_{CO}[Azo]\}/R_{CH_4}[CD_2O]$
350.5	21.9	1.48	4200	19	117	14.0	2.0	54.9	0.96	0.00866	2.1	0.97	1.1
361	18.8	0.58	3900	15	107	16.8	0.7	44.7	0.3	0.0133	2	1.1	0.8
362	20.0	2.09	4200	17.3	108	17.3	3.5	38.8	1.5	0.0139	2.3	1.5	1.1
362.5	19.4	2.40	3900	18	107	16.6	4.0	42.1	1.8	0.0132	2.1	1.4	1.1
360.5	20.3	4.13	4200	17.5	103	19.9	7.9	42.9	3.3	0.0150	2.4	1.7	1.1
357.5	21.6	8.03	3600	19.5	108	21.6	14.7	42.6	6.7	0.0154	2.2	1.5	0.99
359	21.7	8.12	3500	19	110	21.4	14.6	42.8	6.9	0.0150	2.1	1.5	0.96
374.5	19.7	1.58	4500	16.7	113	22.1	3.6	32.3	1.5	0.0198	2.3	2.3	1.2
387	18.5	1.79	5100	17	103	24.2	4.8	22.4	1.8	0.0278	2.7	3.6	1.3
405.5	19.3	1.02	5400	17.5	109	32.9	3.0	12.6	1.3	0.0481	2.4	4.8	0.98
401	19.6	1.13	5460	16.9	110	31.3	3.3	11.1	1.4	0.0478	2.3	4.8	1.0
402.5	20.3	2.07	5400	18.2	113	31.5	6.1	12.9	2.4	0.0432	2.5	5.0	1.1$_5$
401	20.3	3.34	4500	19	109	39.0	12.8	12	4.1	0.055	3.1	7.2	1.4
403	19.6	7.16	4800	18	110	36.0	24.9	12.7	9.1	0.0517	2.7	6.2	1.2
403	19.9	9.24	3600	18.9	118	34.5	30.2	11.9	12.0	0.0504	2.5	5.7	1.1
425.5	18.5	1.15	5580	17.1	106	38.3	34.2	5.0	1.5	0.0929	2.2	7.4	0.79
453.5	18.4	0.68	6600	17.4	113	50.2	2.0	2.7	1.0	0.168	2.4	11	0.6
454	18.7	1.22	7200	17	116	52.1	3.9	2.8	1.9	0.167	2.6	12	0.7
453	17.7	1.79	5400	18	111	46.4	6.4	2.5	2.6	0.166	2.4	13.5	0.82
452.5	17.9	5.50	6300	18	115	47.0	22.2	2.5	8.7	0.165	2.5$_5$	15.5	0.94
452.5	18.3	9.43	7500	19	119	45.3	35.8	2.6	14.6	0.157	2.4$_5$	14	0.91
452.5	18.1	11.4	5400	19.4	120	44.5	43.4	2.6	18.2	0.152	2.4	14	0.95

Some experiments were performed in which azomethane was photolyzed alone. In this case

$$\frac{k_2}{k_1^{\frac{1}{2}}} = \frac{R_{CH_4}}{R^{\frac{1}{2}}_{C_2H_6}[Azo]}.$$

This same rate expression holds when CD_2O was present, since all methane formed in reaction [2] is undeuterated. A plot of log $k_2/k_1^{\frac{1}{2}}$ against the reciprocal of the absolute temperature is shown in Fig. 1. The presence of up to 30 mole % CD_2O is seen to have no effect on the value of log $k_2/k_1^{\frac{1}{2}}$. The slope of the best straight line through the points leads to a value of 8.4 ± 0.3 kcal mole^{-1} for E_2, assuming E_1 is zero. This differs from the value of 7.6 obtained by Jones and Steacie (2) and 7.3 by Ausloos and Steacie (6) but agrees with the value obtained by Wenger (7).

A conventional treatment of the results gives

$$\frac{k_3}{k_1^{\frac{1}{2}}} = \left(\frac{R_{CH_4}-R_{CO}}{R^{\frac{1}{2}}_{C_2H_6}} - \frac{k_2}{k_1^{\frac{1}{2}}}[Azo]\right)\frac{1}{[CH_2O]}.$$

The results obtained were not sufficiently accurate to use this expression, since it involves the difference between two quantities which, in this case, are of similar magnitude. The CH_2O results may be treated by assuming a steady state of formyl radical concentration. In this case

$$\frac{k_3}{k_1^{\frac{1}{2}}} = \frac{R_{CO}}{R^{\frac{1}{2}}_{C_2H_6}[CH_2O]}.$$

Can. J. Chem. Downloaded from www.nrcresearchpress.com by 190.90.36.8 on 09/04/12
For personal use only.

This rate expression is approximately constant at constant temperature with up to 30-fold changes in CH_2O concentration, as shown in Table I. A plot of log $k_3/k_1^{\frac{1}{2}}$ against $1/T$ is given in Fig. 2 and the least mean square line is given by

$$k_3/k_1^{\frac{1}{2}} = 780 \exp[-(6200 \pm 300)/RT] \text{ (mole liter}^{-1})^{-\frac{1}{2}} \text{ sec}^{-\frac{1}{2}}.$$

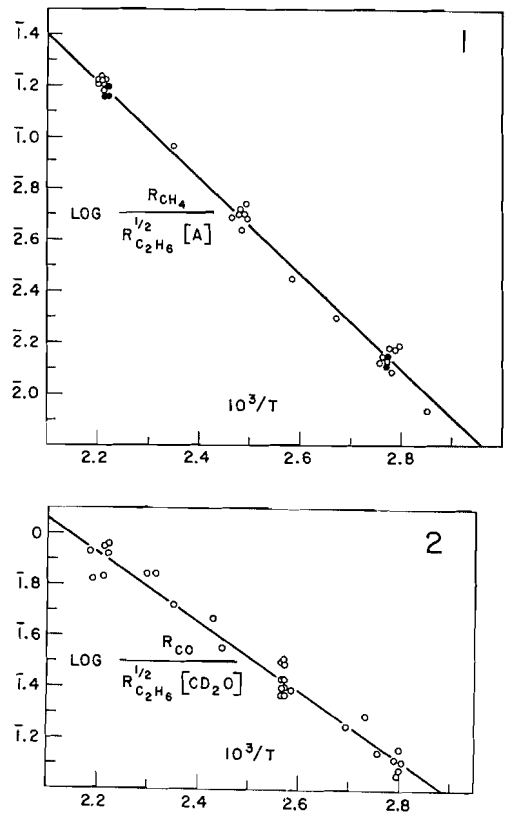

FIG. 1. Arrhenius plot for the reaction $CH_3 + CH_3N_2CH_3$: ● azomethane alone, ○ variable amounts CD_2O present; see text.
FIG. 2. Abstraction of hydrogen from CH_3O by methyl radicals.

The only published result with which this may be compared is the value of 5.63 kcal mole^{-1} for E_3 given by Kodama and Takezaki (1).

In the case of the CD_2O experiments the rate equations give directly

$$\frac{k_3'}{k_1^{\frac{1}{2}}} = \frac{R_{CH_3D} - R_{CO}}{R^{\frac{1}{2}}_{C_2H_6}[CD_2O]}$$

and

$$\frac{k_3'}{k_2} = \frac{R_{CH_3D} - R_{CO}}{R_{CH_4}} \frac{[Azo]}{[CD_2O]}.$$

These expressions are plotted in Fig. 3 and give

$$k_3'/k_1^{\frac{1}{2}} = 960 \exp[-(7900 \pm 300)/RT] \text{ (mole/liter)}^{-\frac{1}{2}} \text{ sec}^{-\frac{1}{2}}$$

and

$$k_3'/k_2 = 0.48 \exp(590 \pm 300/RT) \text{ (mole/liter)}^{-\frac{1}{2}} \text{ sec}^{-\frac{1}{2}}$$

Can. J. Chem. Downloaded from www.nrcresearchpress.com by 190.90.36.8 on 09/04/12
For personal use only.

respectively. From Fig. 1

$$k_2/k_1^{\frac{1}{2}} = 1700 \exp[-(8400\pm300)/RT] \text{ (mole/liter)}^{-\frac{1}{2}} \text{ sec}^{-\frac{1}{2}},$$

hence

$$k_3'/k_1^{\frac{1}{2}} = 810 \exp[-(7800\pm400)/RT] \text{ (mole/liter)}^{-\frac{1}{2}} \text{ sec}^{-\frac{1}{2}},$$

in satisfactory agreement with the former value. The values $E_3 = 6.2$, $E_3' = 7.9$ kcal mole^{-1} may be compared with the corresponding activation energies for the abstraction reaction with acetaldehyde and acetaldehyde-*d* as found by Ausloos and Steacie (8). They obtained $E = 6.8$, $E' = 7.9$ kcal mole^{-1} for the corresponding reactions.

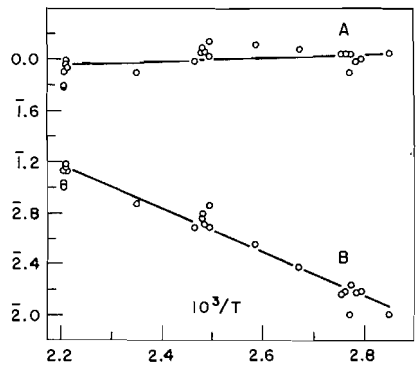

FIG. 3. Abstraction of deuterium from CD_2O by methyl radicals: A: $\log\{(R_{CH_3D}-R_{CO})/R_{CH_4}[CD_2O]\}$ vs. $10^3/T$; B: $\log\{(R_{CH_3D}-R_{CO})/R^{\frac{1}{2}}_{C_2H_6}[CD_2O]\}$ vs. $10^3/T$.

In Fig. 4 the amounts of the products of the CD_2O experiments are plotted as a function of CD_2O concentration. It can be seen that the amount of CH_3D and CO formed increases linearly with CD_2O concentration. There is, however, no corresponding decrease

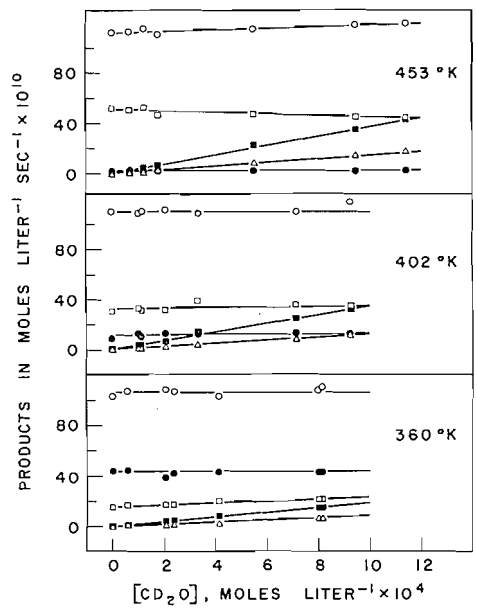

FIG. 4. Products of CD_2O experiments as functions of formaldehyde-d_2 concentration: ○ N_2, ● C_2H_6, □ CH_4, ■ CH_3D, △ CO.

Can. J. Chem. Downloaded from www.nrcresearchpress.com by 190.90.36.8 on 09/04/12
For personal use only.

in the amounts of CH_4 and C_2H_6 formed. Since the amount of azomethane photolyzed shows no appreciable increase with CD_2O (as shown by the N_2 formed), the source of the extra methyl radicals is not apparent. It is possible that fewer addition products of CH_3 + azomethane were formed in the presence of CD_2O but this could not be verified. The corresponding graph for the CH_2O runs is not given, since the light intensity was not constant. However, it may be seen from Table I that the increase in CH_4 and CO production at constant temperature has no corresponding decrease in C_2H_6 production.

Other Fates for the Formyl Radical

The addition reaction corresponding to the disproportionation reaction [4] is

$$CH_3 + CHO \rightarrow CH_3CHO. \qquad [5]$$

No acetaldehyde was found by mass spectrometric analysis of the products, however. If any acetaldehyde were formed it seemed likely that it would copolymerize with the excess CH_2O. The residues from several runs were therefore collected and tested with Leys reagent, which will detect 0.1% acetaldehyde in CH_2O solution (9). The tests were negative and from this it can be inferred that reaction [4] occurs at least four times as fast as reaction [5] under the conditions studied.

For the CD_2O experiments $k_5'/k_4' = R_{CH_3D}/R_{CO} - 2$. The value of R_{CH_3D}/R_{CO} is reasonably constant with CD_2O concentration and with temperature as shown in Table II. The results give $k_5'/k_4' \simeq 0.4$. These findings agree with those of Lossing (10), who found that reaction [4] was much faster than reaction [5] at 55° C.

No hydrogen was found in the products. This does not rule out the occurrence of

$$CHO \rightarrow CO + H \qquad [6]$$

because any H formed would probably undergo addition rather than abstraction reactions with azomethane, since CH_3 adds to azomethane approximately five times as fast as it abstracts from it in the temperature range employed (2). Reaction [6] is thought not to have occurred, however, for the following reasons.

In the CD_2O experiments it was found that the CH_3D/CO ratio was approximately 2.4 regardless of temperature or CD_2O concentration. E_6 is at least 12 kcal mole^{-1} (11), which is undoubtedly much higher than E_3 or E_4. If an appreciable fraction of the carbon monoxide were formed by reaction [6] then it would be expected that the CH_3D/CO ratio would decrease as the temperature increased, and this is not in accordance with the results obtained. Hence reaction [6] is slow up to at least 180° C.

Other possible fates for the formyl radical were

$$2CHO \rightarrow (CHO)_2, \qquad [7]$$

$$2CHO \rightarrow CO + CH_2O. \qquad [8]$$

The residues of several experiments were collected and analyzed mass spectrometrically for glyoxal with negative results, ruling out the appreciable occurrence of reaction [7] in the system studied. Reaction [8] could not be directly checked, however; its occurrence would not be in accordance with the rate law found.

ACKNOWLEDGMENTS

The authors wish to thank Dr. E. W. R. Steacie for his interest in this work and Miss Bernice Thornton and Mrs. K. O. Kutschke for the mass spectrometer analyses.

Can. J. Chem. Downloaded from www.nrcresearchpress.com by 190.90.36.8 on 09/04/12
For personal use only.

REFERENCES

1. KODAMA, S. and TAKEZAKI, Y. J. Chem. Soc. Japan, **73**, 13 (1952).
2. JONES, M. H. and STEACIE, E. W. R. J. Chem. Phys. **21**, 1018 (1953).
3. TOBY, S. and KUTSCHKE, K. O. Rev. Sci. Instr. **28**, 470 (1957).
4. STAUDINGER, H. *et al.* Ber. **64**, 398 (1931).
5. BANNARD, R. A., MORSE, A. T., and LEITCH, L. C. Can. J. Chem. **31**, 351 (1953).
6. AUSLOOS, P. and STEACIE, E. W. R. Can. J. Chem. **32**, 593 (1954).
7. WENGER, F. and KUTSCHKE, K. O. To be published.
8. AUSLOOS, P. and STEACIE, E. W. R. Can. J. Chem. **33**, 31 (1955).
9. WALKER, J. F. Formaldehyde. 2nd ed. Reinhold Publishing Corp., New York. 1953.
10. LOSSING, F. P. Can. J. Chem. **35**, 305 (1957).
11. CALVERT, J. G. J. Phys. Chem. **61**, 1206 (1957).

Can. J. Chem. Downloaded from www.nrcresearchpress.com by 190.90.36.8 on 09/04/12
For personal use only.

Can. J. Chem. Downloaded from www.nrcresearchpress.com by 196.1.178.254 on 09/04/12
For personal use only.

THE STABLE ALKYLATION PRODUCTS OF ORGANONITROSOHYDROXYLAMINES[1]

M. V. George, R. W. Kierstead, and George F Wright

ABSTRACT

The stable alkylation products of alkyl and aryl nitrosohydroxylamines seem to exist in a hitherto unknown structure, the diimide dioxide linkage. The alternative possibility is the alkyl diazotate monoxide structure, but the latter cannot account for the pure methane evolved when the substances are treated with methyl halide Grignard reagent. The principal products of this reaction with Grignard reagents are diimide monoxides formed subsequently by addition of an equivalent of reagent with elimination of the original alkoxy group as its magnesium salt. Nitration of N-methyl-N′-phenyldiimide dioxide shows that in salt-forming media (nitric–sulphuric) the N_2O_2R group is electrically negative, but dipole moment studies show that it is highly degenerate. This resonance stabilization is not unexpected in view of the high stability of the diimide dioxides in acidic media.

The first nitrosohydroxylamines were prepared (1) by reaction of nitric oxide with substances containing an active methylene group in presence of ethanolic sodium hydroxide. Typical is the reaction with acetone which may be postulated as follows:

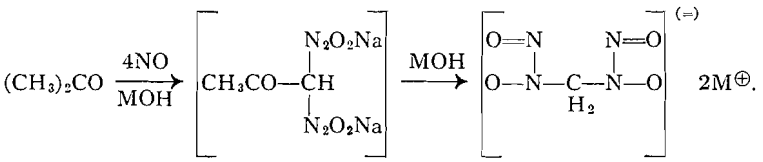

I

The second, more orthodox, method of preparation involved the nitrosation of an arylhydroxylamine (2), and led to the preparation of salts such as ammonium phenylnitrosohydroxylaminate (cupferron). The free acids are rather unstable.

When the silver salts of these nitrosohydroxylamines (II, M = Ag) are treated with alkyl iodides two products, designated α and β, are formed. The β isomers may be desig-

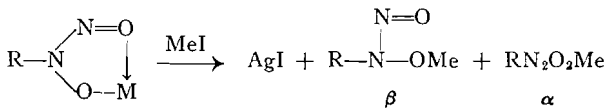

II

nated as the nitroso derivatives of hydroxylamine O-ethers, since they give a positive Liebermann test and some may be synthesized by nitrosation of the O-alkylhydroxylamines (3, 4).

The structure of the α derivative was not proved. Hantzsch (5) suggested structures III or IV while Bamberger and Ekecrantz (6) suggested either IV or V. To this list may be added VI, although it is in conflict with one structure proposed for nitroso dimers (7, 8, 9, 10, 11).

There are two claims that nitroso dimers are best represented by structure VI or charge-distorted modification of it. An X-ray diffraction study (8) of tribromonitroso-

[1]*Manuscript received October 14, 1958.*
Contribution from the Chemistry Department, University of Toronto, Toronto, Ontario.

Can. J. Chem. Vol. 37 (1959)

benzene has been interpreted in terms of a central plane containing two nitrogen and two oxygen atoms, but it is doubtful whether this definition is justified when six bromine atoms are present. A more specific claim (10) that the *cis* and *trans* isomers of VI (R = Me) have been isolated may be interpreted in terms of polymorphism. Moreover, there is no convincing reason to expect that substances having structure VI would show the instability characteristic of nitroso, carboxylic, or peroxidic dimers. For these reasons we prefer to exclude VI for consideration as a nitroso dimer, and to include it among the possible structures of the α-alkylated nitrosohydroxylamines.

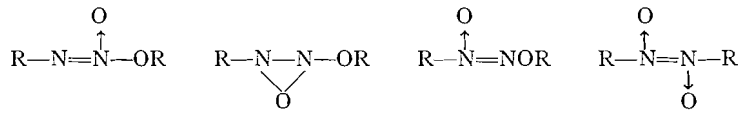

III IV V VI

In view of present knowledge structure III is inadmissable because it may clearly be assigned to isonitramines (12). The postulation of structures IV or V is justified by the observation (13) that basic hydrolysis of the methyl derivative of phenylnitrosohydroxylamine regenerates the salt (II, M = Na or K). We have extended this observation by hydrolysis of the dimethyl α derivative of the salt I using hydrazine as the basic reagent. Subsequent precipitation by use of sodium or barium hydroxide yields the appropriate salt of I rather than of methylene dinitramine (14).

Thus hydrolytic evidence favors IV or V rather than III, but it should be noted that VI is not excluded by this criterion since the alkylazoxy linkage is known to react with alkalis (15). The principal evidence favoring IV and V in contrast to VI has been presented by Bamberger (6, 13), who reduced methyl phenylnitrosohydroxylaminate and its *p*-bromo analogue. Reduction with zinc and acetic acid was said to give diazonium salts, while neutral reduction with aluminum amalgam gave the methyl ester of benzenediazotic acid. However, identification seems to have been accomplished only by odor and color tests. Only when the reduction was alkaline (4% sodium amalgam) was phenylhydrazine or its *p*-bromo analogue characterized in favor of structures IV and V rather than VI. But alkaline conditions also would yield sodium phenylnitrosohydroxylaminate by hydrolysis. Since this salt is easily reduced to phenylhydrazine, Bamberger's argument is not entirely convincing.

In order to evaluate further the criterion of reduction for a choice between structures IV, V, and VI we have applied alternative reducing agents to the methyl derivative of phenylnitrosohydroxylamine. We have found, like Bamberger, that the substance is fairly resistant. It is practically unchanged by reagents like titanous chloride in acetic anhydride, aqueous sodium bisulphite, aqueous sodium arsenite, and aqueous (47%) hydriodic acid, although a 4% yield of aniline was obtained from the latter reaction. A 24% yield of aniline was obtained, together with unchanged reagent and unidentifiable material, by catalytic reduction with platinum. But also, the alkaline reagent, sodium hydrosulphite, gave a 4% yield of phenylhydrazine together with a 65% recovery of the original substance. In fact the only reduction which might support Bamberger's contention for IV and V is that with lithium aluminum hydride which gives a 40% yield of phenylhydrazine. However, the latter reductant must be considered together with Grignard reagents which it resembles in its behavior.

Treatment of the methyl α derivative from phenylnitrosohydroxylamine with methyl halide Grignard reagent by the Kohler modification of the Zerewitinoff analysis (16)

Can. J. Chem. Downloaded from www.nrcresearchpress.com by 196.1.178.254 on 09/04/12
For personal use only.

shows that one equivalent of pure methane is liberated easily. Enough may be collected at room temperature for demonstration of an uncontaminated infrared spectrum. The analysis shows also that 1.5 equivalents of Grignard reagent are added during the process. Since it has been shown that the isolable reaction product is fixed as its magnesium salt (and therefore cannot easily undergo further reaction), the evidence for active hydrogen would seem to exclude IV or V as possible structures, but not VI with its methylene group adjacent to an azoxy linkage. Accordingly VI (R = C_6H_5, R′ = Me) is now designated for the α derivative of phenylnitrosohydroxylamine, and it is named N-phenyl-N′-methyldiimide dioxide.*

When methylphenyldiimide dioxide (VII, R = H) is treated with an excess of bromotoluene Grignard reagent in ethyl ether the significant product is N-4-tolyl-N′-phenyldiimide N′-oxide (17) (XII, R′ is *p*-tolyl). When an excess of VII is used to ensure complete consumption of the Grignard reagent both methanol and toluene (IX, R′ = tolyl) can be isolated. On the basis of this information the reaction may be formulated as follows:

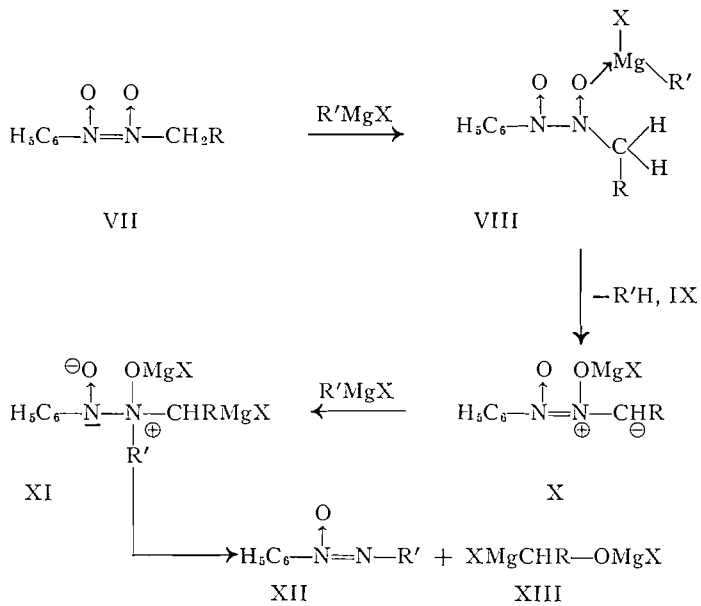

Although either of the oxide linkages might be expected to co-ordinate with the Grignard reagent only the co-ordination shown in VIII would seem to be propitious for elimination of R′H, IX. The remaining dipolar fragment, X, should then co-ordinate and add Grignard reagent to give XI, from which XIII (R = H) (finally leading to methanol) and XII would be produced. It is noteworthy that none of the isomeric N′-4-tolyl-N-phenyldiimide N′-oxide (the structure of which was proved (17) by facile bromination in the phenyl substituent) was found among the reaction products.

**It has become evident that the nomenclature of azo and azoxy compounds is inadequate for communication among chemists. A revision has been suggested (15), but this in turn cannot be used to describe structures such as VI. Consequently we suggest that azo compounds be designated by the Chemical Abstracts classification, N,N′-diimide* (R—N=N—R′), *that azoxy compounds be called diimide oxides (or monoxides), and that substances with structures corresponding to VI be called diimide dioxides. For example the α- and β-4-chlorophenylazoxybenzenes would be renamed N-phenyl-N′-[4-chlorophenyl]diimide N-oxide and N′-oxide respectively. From this adaptation of amine oxide nomenclature it becomes simple to describe the unsymmetrical azo and azoxy compounds as well as our diimide dioxides.*

Can. J. Chem. Downloaded from www.nrcresearchpress.com by 196.1.178.254 on 09/04/12
For personal use only.

Can. J. Chem. Downloaded from www.nrcresearchpress.com by 196.1.178.254 on 09/04/12
For personal use only.

When an otherwise comparable experiment is carried out by use of methyl chloride Grignard reagent the isolable product, besides unchanged VII, would then be designated as N-methyl-N′-phenyldiimide N′-oxide. This oily product (XII, R′ = Me) has been characterized by analysis and by reaction with lithium aluminum hydride which converts it to the previously known N-methyl-N′-phenyldiimide. The structure of XII (R′ = Me) is assigned principally by analogy with XII (R′ = tolyl), but also it might be expected that the structure isomeric with XII (in which the amine oxide group is vicinal to the methylene group) would liberate methane from methyl halide Grignard reagent. Actually the product (XII, R′ = Me) was very sluggish in this respect and only 0.3 equivalent could be discovered under the forced conditions of pyridine solvent at 100° C.

The yield of XII is always low (when R′ = Me, 14%) and this circumstance is not unexpected in view of the known reactivity of N-oxides toward Grignard reagents. For example the free N-oxide group in VIII would be expected to oxidize Grignard reagent, leading to reduction products. Presumably such reactions would be slower than the series shown as VII → XIII. In order, then, to rationalize the low yields of diimide monoxides from the dioxides in terms of side reactions with the Grignard reagent we have chosen an especially difficult example. The addition of N-methyl-N′-phenyldiimide dioxide to an equivalent of benzyl chloride Grignard reagent in diethyl ether gives a yield not exceeding 7% of the monoxide. About 40% of the diimide dioxide is recovered indicating that much of VIII or X does not react further, and that some of the Grignard reagent is consumed in reactions not included in the formulation VII → XIII. The recovery of at least 7% of a derivative of benzaldehyde from the remaining complex mixture indicates that reduction of the monoxide has occurred subsequent to its formation.

$$C_6H_5N_2OCH_2C_6H_5 \xrightarrow{RMgX} ROMgX$$

$$+$$

$$H_5C_6{-}\overset{H}{\overset{|}{C}}{=}N{-}N{-}C_6H_5 \xleftarrow{\text{rearr.}} H_5C_6{-}N_2{-}CH_2{-}C_6H_5$$

This latter reaction seems to be a significant one because reversal of addition (Grignard reagent into diimide dioxide) only raises the monoxide yield to 10%. However, threefold dilution under the latter conditions raises this yield to 14%. Moreover, equivalent addition into a tube containing a downward-pitched screw which conveys its contents into a dry-ice bath within 1 minute, Fig. 1, raises the final yield of diimide monoxide to 20%. It would appear from these experiments that low yield of diimide monoxide is partly due to reaction of XI (or some XII formed in the system before hydrolysis) with Grignard reagent. This conclusion is not vitiated by the 25% yield to be obtained when benzyl chloride Grignard reagent in diethyl ether is added slowly to the whole of N-methyl-N′-phenyldiimide in dioxane. It may be expected that the dibenzylmagnesium which remains in solution after precipitation of magnesium halides is less reactive toward XI or XII than is the whole Grignard reagent.

There are contradictions in the literature with respect to the structure that we have assigned to XII (R′ = benzyl). The diimide monoxide produced by this reaction has also been obtained by the peracid oxidation of benzaldehyde phenylhydrazone, XIV (18). Of the three possible structures which may be written, Bergmann *et al.* favored the epoxy arrangement XVII; but later two independent groups of workers favored the

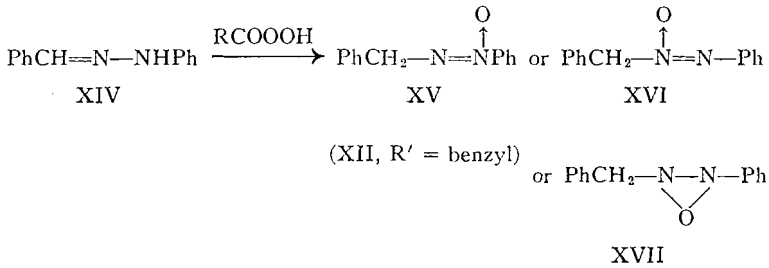

structure N-benzyl-N′-phenyldiimide N-oxide, XVI. One group (19) based its contention on bromination to N-benzyl-N′-*p*-bromophenyldiimide N-oxide, but a repetition (20) of this bromination was unsuccessful. The other group (21) approved XVI because a reaction of XIV with ethyl chloride Grignard reagent yielded diphenylamidine, XIX, but their argument is unconvincing. Indeed the formation of XIX may be explained at least as well on the basis of XV.

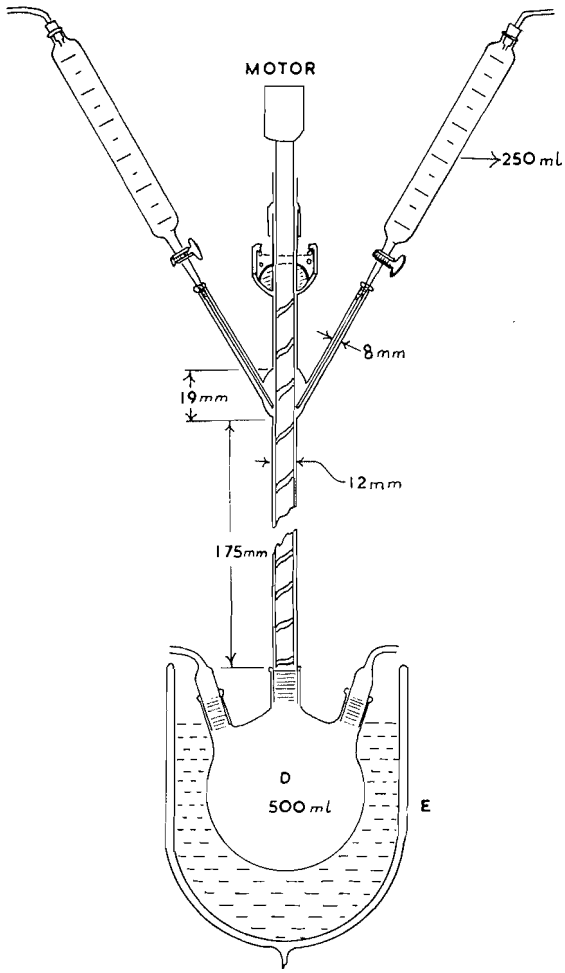

FIG. 1.

Can. J. Chem. Downloaded from www.nrcresearchpress.com by 196.1.178.254 on 09/04/12
For personal use only.

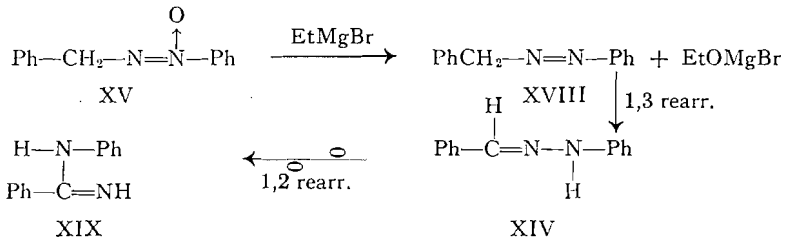

As may be seen by this formulation the reduction of XV → XIX is accomplished by the oxidation of Grignard reagent. By contrast the mechanism of Witkop and Kissman does not include the necessary oxidation step. On the other hand their mechanism does include reactions involving active hydrogen, although Witkop and Kissman searched for and could not find ethane. Lack of evidence for active hydrogen under normal conditions of Grignard treatment is confirmed by our results, although we did observe the formation of gas indicative of active hydrogen under forcing conditions (i.e. with prolonged reaction at 100° C when N-methylmorpholine was used as the reaction medium). This behavior is not unexpected when substances like XVIII, XIV, and XIX are present. For example acetone anil can be made to show the presence of active hydrogen (22). In summary it may be said that neither Pausacker nor Witkop and their co-workers have any real evidence for designation of XVI as the structure for the peroxidation product of benzaldehyde phenylhydrazone.

Actually this conclusion was drawn some years ago (19) by Lythgoe and his co-workers after preparation of both 4-chlorobenzylphenyldiimide monoxides by peroxidation of 4-chlorobenzylphenyldiimide. The product corresponding to XV was geoisomerized to the peroxidation product of 4-chlorobenzaldehyde. Also this chloro analogue of XV was brominated to give the 3-bromo-4-chlorobenzyl analogue, whereas the peroxidation product corresponding with XVI was brominated to give N-4-chlorobenzyl-N′-4-bromophenyldiimide N′-oxide.

Thus by the standard proof (17) Lythgoe and his co-workers have demonstrated the structure (XV) as the product that we obtain from phenylmethyldiimide dioxide and benzyl chloride Grignard reagent. This demonstration is not vitiated by the possibility that a modernized version of structure XVII may also explain part of the experiments of Lythgoe and his co-workers.

The behavior of Grignard reagents with N-methyl-N′-phenyldiimide dioxides provides an explanation for the action of lithium aluminum hydride in terms of the reaction sequence VII → XII inclusive, where the metal hydride replaces Grignard reagent. Moreover the heterogeneous reductants mentioned by Bamberger should behave as metal hydrides and also give N-phenyldiimide N-oxide (XII, R′ = H) initially, which ultimately would be reduced to the phenylhydrazine that eventually is obtained.

It should be noted that the nomenclature devised for diimide dioxides does not imply that characteristic properties may be specified for this group alone. In all instances at least one alkyl group must be attached to a nitrogen and no diimide dioxide has been prepared in which both organic groups attached to nitrogen are aromatic. For example an attempt to oxidize 4,4′-dichlorodiphenyldiimide to the dioxide with boiling 40% nitric acid leads only to 4,4-dichloronitrodiphenyldiimide oxide (23). On the other hand both organic groups attached to nitrogens may be aliphatic. Traube (1) prepared N,N′-methylene-bis-[N-methyldiimide]tetroxide and the ethyl homologue by treatment of the silver salt of methylene-bis-nitrosohydroxylamine (I) with the alkyl iodides. We have

Can. J. Chem. Downloaded from www.nrcresearchpress.com by 196.1.178.254 on 09/04/12
For personal use only.

prepared the 2-chloroethyl analogue (XX) by the same method taking advantage of the unusual stability of these substances toward prolonged boiling with 70% nitric acid in order to destroy the unstable isomer, di-2-chloroethyl methylene-bis-nitrosohydroxylaminate (XXI). We have also prepared methylene-bis-[methyldiimide]tetroxide and its

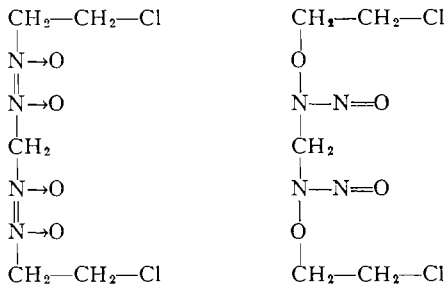

XX XXI

ethyl analogue by treatment of the sodium or ammonium salt of I with dialkyl sulphate but in this event the nitroso isomers corresponding with XXI evidently are destroyed *in situ*, since the tetroxides corresponding with XX are isolated in a pure state.

The chemical reactions of these aliphatic diimides have been examined by use of methylene-bis-[methyldiimide]tetroxide but they are not very informative. Pyrolysis gives methanol, nitrous oxide, and carbon, while alkaline hydrolysis gives formic acid, methanol, and nitrous acid. Treatment with bromobenzene Grignard reagent gives a small yield of benzophenone phenylhydrazone. On the other hand treatment with methyl iodide Grignard reagent under analytical conditions (Soltys machine) shows that reaction in isoamyl ether is limited to evolution of gas indicative of two equivalents of active hydrogen. A precipitate is formed immediately, which accounts for the fact that only 0.1 equivalent of Grignard reagent is found additionally to be consumed in the system.

The infrared spectra through the 1600–600 cm^{-1} range have been determined for a series of diimide dioxides, the monoxides derived from them, some oxime methyl ethers, and some methyl isonitramines (III). These spectra are shown in Table I. Among this limited number of examples two bands may be assigned tentatively to the motion of the diimide dioxide linkage. The first of these is a weak to medium absorption at 1194–1210 cm^{-1}, while the other is a consistently strong band at 995–1018 cm^{-1}. These bands are not observed among the other candidates of Table I. On the other hand the spectra of diimide dioxides are noticeably transparent in the 1000–700 cm^{-1} range whereas the O-ethers and the isonitramines show considerable absorption in this region. Although such spectral evidence cannot of itself be considered to be definitive, it does seem to confirm the chemical evidence that structure VI, and not III, IV, or V, is correct for α methylation derivatives of nitrosohydroxylamines.

The behavior of the alkyldiimide dioxide linkage as an aromatic substituent is of interest. Despite the inertness of this diimide dioxide linkage it may be displaced by forced bromination, and 4-bromonitrobenzene is obtained when N-methyl-N′-4-nitrophenyldiimide dioxide is treated in this manner. The oxidizing action of the alkyldiimide dioxide linkage may be involved, since N-methyl-N′-4-nitrophenyldiimide dioxide may be converted in part to nitrobenzene by prolonged reflux in ethanol. This reduction finds its counterpart in the oxidation of the ethanol to acetaldehyde.

Can. J. Chem. Downloaded from www.nrcresearchpress.com by 196.1.178.254 on 09/04/12
For personal use only.

Can. J. Chem. Downloaded from www.nrcresearchpress.com by 196.1.178.254 on 09/04/12
For personal use only.

TABLE I

Infrared spectra in the 1600–600 cm^{-1} region as liquids (L), solutions in carbon disulphide and carbon tetrachloride (S), in Nujol mulls (M), or in potassium bromide pellets (P)

Substance	Method																					
N-Methyl-N′-phenyldiimide dioxide	L	1590 W		1475 S	1430 S	1312 M	1294 M	1197 M		1100 M		1042 S	1014 S					795 S				
N-Methyl-N′-4-chlorophenyl-diimide dioxide	S			1486 S	1464 S	1308 M		1200 M		1095 S		1050 S	1015 S									
N-Benzyl-N′-phenyldiimide dioxide	S	1595 W		1472 S	1430 S	1305 W	1290 W	1210 W		1095 W		1036 S	1008 S									
N-N′-Dibenzyldiimide dioxide	S	1600 W		1486 S	1438 S	1325 M	1285 S	1210 W				1034 S	1018 S									
N-Methylene-bis-(N′-methyl-diimide) dioxide	M		1515 M	1482 S	1428 S	1315 M	1292 S	1205 M		1086 S		1040 S	995 S					795 S				
N-Methylene-bis-(N′-ethyl diimide) dioxide	M		1515 M	1482 S	1428 S	1315 M	1286 S	1194 M		1086 S		1040 S	1008 S					784 M				
N-Methylene-bis-(β-chloro-ethyldiimide) dioxide	M		1520 M	1488 S	1430 S	1320 W	1280 S	1194 M		1085 S		1032 S	1018 S					783 M				
N-Methyl-N′-phenyldiimide N′-monoxide	L	1605 M	1495 S	1452 M	1425 M	1320 S	1308 S		1160 W	1108 W	1070 M	1025 S		926 M				775 S		688 S		
N,N′-Diphenyldiimide monoxide	L	1595 W	1478 S	1455 M	1440 S	1330 S	1300 S		1164 M	1096 W	1072 M	1025 M		925 M				762 S		682 S		
N-Phenyl-N′-tolyldiimide N-monoxide	L	1605 M	1495 S	1458 M	1440 S	1325 M	1294 S		1165 M	1096 W	1070 M	1022 M		925 W				771 S		685 S		
N-Phenyl-N′-tolyldiimide N′-monoxide	L	1600 M	1500 S	1460 S	1447 S	1330 M	1295 M		1165 M	1098 W	1075 W	1027 W		922 W				763 S		684 S		
N-Benzyl-N′-tolyldiimide N′-monoxide	P	1602 M	1470 S	1440 M	1430 S	1310 S	1298 S		1170 W		1064 M	1022 M		918 M				775 S		680 S		
Benzophenone oxime O-methyl ether[a]	L	1595 W	1570 W	1498 M	1450 S	1428 W		1307 M		1168 M		1054 S	1032 S	1001 W		918 W			845 W	772 S	738 W	693 S
syn-Benzaldoxime O-methyl ether[b]	L	1600 M	1589 W	1493 W	1450 M	1427 W		1312 M		1169 M		1055 S	1030 M	1002 W		919 S			845 M	757 S	747 S	692 S
Benzophenone oxime N-methyl ether[a]	S			1490 M	1440 S					1169 M			1033 W	1001 W								704 M
Diisopropyl isonitramine	L		1550 S		1470 M		1388 M	1330 M	1239 S	1177 W	1142 M				963 M	920 S	906 S					702 M
Di-*n*-propyl isonitramine	L		1558 S		1472 M	1432 M	1382 W	1338 M	1239 S		1145 VW			1005 W	947 S		890 W					699 M
Di-*n*-butyl isonitramine	L		1555 S		1465 M	1432 M	1379 W	1344 M	1240 S	1162 VW	1145 W			1005 W	959 M	942 M	887 M					695 M

[a]Prepared according to Semper, L. and Lechertadt, L. Ber. 51, 928 (1918).
[b]Prepared according to Aurvens, K. V. and Otters, B. Ber. B, 57, 446 (1924).

The dissimilarity of the diimide dioxide linkage with that of the monoxides may be observed by nitration of N-methyl-N′-phenyldiimide dioxide. It is well known (24) that aromatic diimide monoxides are slowly nitrated, and almost not at all in the aromatic ring adjacent to the N → O linkage. However when substitution in this NO-adjacent ring does occur the group enters in the meta position (25). By contrast N-methyl-N′-phenyldiimide dioxide is nitrated rapidly in nitric – sulphuric acid mixture. As would be expected from this rapidity the 58% yield of this rapid nitration is predominantly (81%) the para isomer. Only 7% is found as the meta isomer and 12% as the ortho isomer.

The meta isomer could not be hydrogenolized satisfactorily to metanitroaniline but its positional isomerism seems to be proved by the tin – hydrochloric acid reductions of the ortho and para isomers to ortho- and para-nitroaniline respectively. Moreover the para isomer may be reduced to the amine which can be diazotized and then converted to N-methyl-N′-4-chlorophenyldiimide dioxide. This compound has been synthesized (2) from 4-chlorophenylnitrosohydroxylamine.

The crystallography of this 4-chloro analogue has been examined carefully in connection with a single crystal study now in progress. Incidental to this study it has been found that this typical diimide dioxide is monomeric. It has also been found that, unlike nitramines (26), the "atom polarization" of N-methyl-N′-4-chlorophenyldiimide dioxide is normal in the sense that it amounts to only a few per cent of the total (P_{E+A}) distortion polarization in a weak electric field. However the orientation polarization seems to present an anomaly.

From the formal structural representation of the diimide dioxide linkage one may draw an analogy with the nitro group. The dipole moment studies (Table II) might at

TABLE II

Electrical polarizations of some diimide dioxides in benzene at 20±0.05° C

Diimide dioxide	Polarization values				Solid dielectric			
	α	β (neg.)	P_T, cc	R_D, cc	d_4^{20}	ϵ	P_{E+A}, cc	μ, Debyes
N-Methyl-N′-phenyl	8.03	.307	267	42.8[a]				3.26
N-Methyl-N′-(4-nitrophenyl)	7.23	.437	309	50.1[a]	1.465[c]	2.815	50.7	3.50
N-Methyl-N′-(2-nitrophenyl)	15.47	.424	614	47.9[a]				5.19
N-Methyl-N′-(3-nitrophenyl)	8.11	.424	342	48.1[a]				3.74
N-Methyl-N′-(4-chlorophenyl)	4.55	.397	200	46.3[b]	1.470[c]	3.020	50.9	2.69
				48.6[a]	1.470[d]			
N-Benzyl-N′-phenyl	5.72	.317	299		1.392[c]	2.780	61.0	3.36
N-Benzyl-N′-benzyl	4.60	.315	267		1.292[c]	2.834	71.1	3.05
N′,N′-Methylene-bis-N-methyl[e]	11.36	.228	342	37.9[b]				3.80

[a]Extrapolated n_0^{20} of solutions. [b]Calc. for $n_\alpha+n_\beta+n_\gamma/3$ of solid. [c]Air displacement. [d]Flotation in zinc chloride. [e]Dioxane used instead of benzene as solvent.

first inspection seem to confirm this analogy. This $N_2O_2CH_3$ group might then be assigned the group moment 3.26 D, negative with respect to hydrogen, just as the nitro group moment is 4.0 D, negative according to the orientation polarization of nitrobenzene. Actually the observed moment (3.74 D) of N-methyl-N′-3-nitrophenyldiimide dioxide is approximate to the value calculated from $\mu_{resultant} = (m_1^2+m_2^2+2m_1m_2 \cos\theta)^{\frac{1}{2}} = 3.69$ D, where m_1 and m_2 are the group moments of $N_2O_2CH_3$ and NO_2, and θ is 120° C. However the calculated value for N-methyl-N′-4-nitrophenyl diimide dioxide (0.74 D) is widely divergent from the observed moment of 3.50 D. Likewise, a calculation

Can. J. Chem. Downloaded from www.nrcresearchpress.com by 196.1.178.254 on 09/04/12
For personal use only.

of moment for N-methyl-N′-2-nitrophenyldiimide dioxide (θ = 60° C) gives μ = 6.29 D which is considerably higher than the observed value (5.19 D). A comparable discrepancy is found for N-methyl-N′-4-chlorophenyldiimide dioxide which shows a moment of 2.64 D, about one Debye greater than that expected by calculation.

If one reconsiders the $N_2O_2CH_3$ group in respect of these discrepancies it is apparent that a simple analogy with the nitro group is not valid, and this distinction may be seen in the geometry of the group. One may depict *cis* and *trans* forms and would expect distinct physical and chemical differences. However, the variation in structure probably is more subtle than can be expressed by this simple geometry.

cis *trans*

It would appear from the results of Table II that the group moment of the diimide dioxide group is subject to wide variation depending on the substituents that may be attached to it. This variation is best explained in terms of N–N bond rotation, in which the anharmonicity is a function of the group substituent to the diimide dioxide linkage. Of course this concept conflicts with the orthodox doubly bonded diimide structure, but it is doubtful that the diimide dioxides should assume such a structure. Indeed, it would appear that the adjacent positive charge of a diimide dioxide structure such as XXII is somewhat anomalous and is better explained as a resonance hybrid of XXIII*a* and *b*.

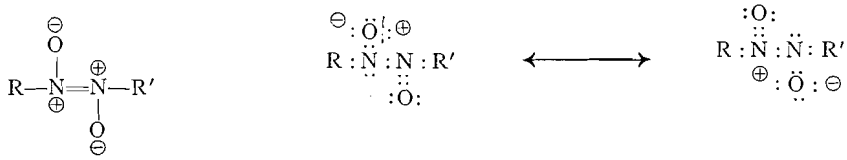

XXII XXIII*a* XXIII*b*

The resonance formulation is not intended to depict *trans* planarity; indeed the rotameric conformation of XXIII is thought to account for the apparent anomalies among the nitro and chloro derivatives described above. Certainly the conformation is not *trans* as shown in XXIII because in this event the electric moment of N,N′-dibenzyldiimide dioxide would be zero instead of 3.05 D (Table II).

The authors are grateful to Messrs. Myers and Bedard, Canadian Armament Research and Development Establishment, for the determinations of infrared absorption. They acknowledge extensive financial aid from the Defence Research Board of Canada.

EXPERIMENTAL*

N-Methyl-N′-phenyldiimide Dioxide

To a mixture of cupferron (160 g, 0.6 mole) and sodium bicarbonate (140 g, 1 mole) in 1160 ml of water was added 210 g (1 mole) of dimethyl sulphate during 7 hours with stirring. Cooling with a water bath was necessary. After 15 subsequent hours of stirring

Melting points have been corrected against appropriate standards (Can. J. Technol. **34, 89 (1956)). X-Ray diffraction patterns are recorded, using* CuK_α (Ni *filtered) radiation, in Ångstroms at relative intensities* $[I/I_1]$.

Can. J. Chem. Downloaded from www.nrcresearchpress.com by 196.1.178.254 on 09/04/12
For personal use only.

at 20° C the deep-red system was extracted with a total of 1500 ml of diethyl ether. This extract, dried with calcium chloride, was distilled finally at 0.5 mm to yield 119 g of oil, b.p. 98–100° C, which partially solidified. This product was diluted by addition with $\frac{1}{2}$ volume of petroleum ether, b.p. 40–60° C, then cooled, and finally filtered. The solid was crystallized from 3.5 l. of petroleum ether (b.p. 40–60° C) and cooled to give 94 g, m.p. 37.5–39° C (60%). A similar recrystallization raised the melting point to 39.5–40.5° C. Absorption in the ultraviolet region showed λ_{max} at 262 mμ; E_{max} 10,690. The X-ray diffraction pattern was [10] 3.48; [9] 4.78; [7] 4.14; [6] 7.16; [5] 4.17; [4] 6.58; [3] 3.13; [2] 2.89, 3.38; [1] 5.19, 3.17, 3.09, 2.85, 2.61.

When this substance was heated to 100° C with 85% sulphuric acid or chlorosulphonic acid it was recovered unchanged. Likewise it was unaffected by 6 hours' treatment with acetic anhydride at 200° C.

Hydrazine Phenylnitrosohydroxylaminate

A mixture of 4.56 g (0.03 mole) of N-methyl-N′-phenyldiimide dioxide and 3.0 g (0.06 mole) of 100% hydrazine hydrate was refluxed for 17 hours, then cooled, and diluted with 15 ml of absolute ethanol. Several crystal crops totalling 3.40 g (66%, m.p. 127–128° C) were combined and crystallized from 90 ml of absolute ethanol, 2.61 g (51%) of the salt, m.p. 127–128° C (decomp.); recrystallized, m.p. 128.5–129° C. Calc. for $C_6H_{10}O_2N_4$: C, 42.3; H, 5.92; N, 32.9. Found: C, 42.3; H, 6.02; N, 33.8. Acidification of 0.25 g in 3 ml of water by 3 ml of 12% hydrochloric acid gave 1.6 g (77%), m.p. 56.5–58° C, of phenylnitrosohydroxylamine. After crystallization from 5 ml of petroleum ether (b.p. 40–60° C) the product, m.p. 58–59° C, was characterized by mixture melting point. The presence of hydrazine was demonstrated by treatment of the salt with aqueous picric acid. The hydrazine picrate melted at 182–183° C.

Reduction of N-Methyl-N′-phenyldiimide Dioxide

(*a*) *Catalytic reduction.*—A solution of 3.8 g (0.025 mole) in 50 ml of absolute ethanol with Adams catalyst absorbed 2 moles of hydrogen and then yielded aniline, b.p. 180–184° C (756 mm), which was characterized as acetanilide, 0.43 g, 24%, m.p. 112–114° C. Also 12% of the original dioxide was recovered unchanged.

(*b*) *By hydriodic acid.*—After 2 days' reflux of 1.0 g (0.0066 mole) in 3 ml of 47% hydriodic acid, 0.76 g (76%) of the original dioxide was recovered unchanged. An ether extract of the remainder was treated with oxalic acid in ether to give 4.6 mg (0.25%) of aniline oxalate, m.p. and m.m.p. 153.5–155.5° C.

(*c*) *By sodium hydrosulphite.*—A mixture of 0.99 g (0.0065 mole) in 8 ml of ethanol and 6.8 g (0.039 mole) of sodium hydrosulphite in 20 ml of water was heated with stirring at 80° C for 45 minutes. Extraction with diethyl ether yielded 65% of the unchanged starting material. The aqueous–alcoholic solution was concentrated under reduced pressure and the residue was extracted by ether to give 90 mg of oil. Treatment with picric acid yielded 104 mg (4.7%) of crude phenylhydrazine picrate, m.p. 135–137° C, which was crystallized from benzene, m.p. and m.m.p. 145.5° C.

(*d*) *By lithium aluminum hydride.*—A solution of 0.99 g (0.0065 mole) in 25 ml of dry ether was added to a solution of 0.813 g (0.0215 mole) of lithium aluminum hydride in 25 ml of the same diethyl ether with stirring during 20 minutes at 20° C. After a subsequent 30-minute stirring time the system was treated with 5 ml of 10% aqueous sodium hydroxide and then extracted with ether to yield 0.4 g of an oil. Distillation at 125–130° C (18 mm) gave 0.23 g (40%) of phenylhydrazine, characterized by conversion to *p*-chlorobenzaldehyde phenylhydrazone, m.p. and m.m.p. 125–126° C.

Can. J. Chem. Downloaded from www.nrcresearchpress.com by 196.1.178.254 on 09/04/12
For personal use only.

Bromination of N-Methyl-N′-phenyldiimide Dioxide

A mixture of N-methyl-N′-phenyldiimide dioxide (3.04 g, 0.02 mole) with 8 g (0.05 mole) of bromine in 10 ml of carbon disulphide was refluxed with 150 mg of iron filings for 15 hours. Subsequent steam distillation (4 l.) yielded 1.06 g, m.p. 68.5–71.5° C, which was crystallized from 7 ml of ethanol, and 0.48 g (6.1%, m.p. 89.8–90.8° C) of crude 1,2,3,5-tetrabromobenzene, crystallized further from ethyl acetate, m.p. 99–99.7° C. Calc. for $C_6H_2Br_4$: C, 18.3; H, 0.51. Found: C, 18.3; H, 0.73. Chloroform extraction of the steam distillation residue gave 0.51 g, m.p. 219–220° C, crystallized from dioxane, m.p. 221.6–221.9° C. This substance was not identified. Calc. for $C_7H_3Br_4$: C, 21.7; H, 0.75. Found: C, 21.1; H, 0.75.

N-Methyl-N′-4-nitrophenyldiimide Dioxide

To a chilled solution of 10.6 ml (0.26 mole) of 99% nitric acid and 45.3 ml (0.846 mole) of 100% sulphuric acid was added 19.8 g (0.13 mole) of N-methyl-N′-phenyldiimide dioxide during 15 minutes with constant stirring at 0° C. After a short time of warming to room temperature the system was poured into 400 g of crushed ice. Filtration removed 25.5 g which was twice crystallized from carbon tetrachloride to yield 12 g (47%) of the para–nitro derivative, m.p. 152–153° C. Calc. for $C_7H_7N_3O_4$: C, 42.6; H, 3.58; N, 21.3. Found: C, 42.7; H, 3.33; N, 20.8. The X-ray diffraction pattern was [10] 3.18; [8] 7.76, 7.49; [6] 4.69; [5] 5.04; [3] 3.68, 3.52; [2] 11.1; [1] 2.31; [0.5] 2.16. The ultraviolet absorption in ethanol gave λ_{max} at 243 mμ, 330 mμ with E_{max} 10,970 and 567 respectively. The substance was recovered unchanged after 12 hours at 200° C with acetic anhydride.

An unsuccessful attempt was made to prepare this compound by peroxidation of methyl 4-nitrobenzenediazotate (27). This ester was prepared via the silver salt from 4-nitrobenzenediazonium sulphate by Bamberger's method but the 2 g obtained from 6.9 g of *p*-nitroaniline was used without characterization because of its tendency toward decomposition. The orange-yellow solid (0.011 mole) was mixed with 15 ml of acetic acid and 9 ml of 30% hydrogen peroxide and kept at 0° C for 12 hours, then at 25° C for 2 days. Upon treatment with 150 ml of water and extraction with ether 1.11 g of red-brown solid was obtained upon evaporation. This solid was developed on a chromatoplate (28) (prepared from 80% silica gel and 20% plaster of Paris at 120° C) together with *p*-nitrophenol and also N-methyl-N′-4-nitrophenyldiimide dioxide. The developer was 18:1 benzene–acetone. By means of a sulphuric – nitric acid spray (95:5) only *p*-nitrophenol and not the diimide dioxide could be detected.

A mixture of 2.51 g (0.013 mole) of N-methyl-N′-4-nitrophenyldiimide dioxide and 9.2 g (0.078 atom) of granulated tin was treated with 18.8 ml (0.188 mole) of concentrated hydrochloric acid during 25 minutes. After 40 minutes of reflux the system was cooled and treated with 20 g of sodium hydroxide in 40 ml of water and then steam-distilled. From the distillate was obtained 0.89 g, m.p. 135–140° C, of *p*-phenylenediamine which was crystallized from benzene, m.p. and m.m.p. 139–140° C, 0.3 g (22%).

N-Methyl-N′-4-aminophenyldiimide Dioxide

A mixture of the para–nitro derivative (0.97 g, 0.0049 mole) and 15 ml of hydroiodic acid (sp. gr. 1.5) was heated under reflux for 15 minutes. After 12 hours at 20° C the system was diluted with 20 ml of water to precipitate 0.25 g (26%) of unchanged starting material, m.p. 152–153° C, after crystallization from carbon tetrachloride.

The amine (0.19 g, m.p. 171–172.5° C, 23%) was precipitated by addition of alkali to pH 8. It was crystallized from ethanol (95%), m.p. 176.5–176.8° C. The X-ray diffraction

Can. J. Chem. Downloaded from www.nrcresearchpress.com by 196.1.178.254 on 09/04/12
For personal use only.

pattern was [10] 4.81; [9] 3.51; [7] 4.25; [5] 3.47; [4] 7.56, 3.03; [2] 6.58, 5.86, 5.26, 2.05; [1] 2.93, 2.61. Calc. for $C_7H_9N_3O_2$: C, 50.3; H, 5.43; N, 25.1. Found: C, 50.7; H, 5.35; N, 25.5.

4-Chlorophenylhydroxylamine (2)

To a refluxing system comprised of 180 g (1.14 mole) of 4-chloronitrobenzene in 1200 ml of ethanol and 24 g (0.45 mole) of ammonium chloride in 300 ml of water was added 300 g (4.6 atom) of zinc dust in 10-g lots. One-minute periods of addition and stirring were alternated with 1-minute periods of reflux until the color of the reaction mixture passed its lightest stage of brown and began once more to darken. The residual zinc dust was quickly filtered hot. Steam distillation of the filtrate gave 50 g (30.5%), m.p. 83–83.5° C.

N-Methyl-N′-4-chlorophenyldiimide Dioxide

(*a*) *From N-Methyl-N′-4-aminophenyldiimide dioxide.*—To a suspension of N-methyl-N′-4-aminophenyldiimide dioxide (100 mg, 0.006 mole) in 0.8 ml of concentrated hydrochloric acid plus 0.5 ml of water at 0° C was slowly added a solution of 50 mg of sodium nitrite in 0.3 ml of water. To the orange-yellow reaction mixture at 0° C was then added 90 mg of cupric chloride in 0.75 ml of concentrated hydrochloric acid during 20 minutes. The system was then slowly warmed to 20° C and subsequently heated at 60° C for 10 minutes. When the mixture was cooled 60 mg (54%) of N-methyl-N′-4-chlorophenyldiimide dioxide separated, m.p. 70–71° C. After crystallization from petroleum ether (b.p. 40–60° C) a mixture melting point (71–72° C) with an authentic specimen (2) was not depressed. The X-ray diffraction pattern was [10] 5.34; [9] 3.52; [8] 3.36; [6] 3.71; [5] 4.36; [4] 4.92; [3] 6.28; [2] 2.19, 1.91; [1] 6.51, 2.94, 2.59, 2.51, 2.44, 2.22.

(*b*) *From 4-chlorophenylhydroxylamine.*—A solution of 50 g (0.348 mole) of 4-chlorophenylhydroxylamine in 335 ml of ethanol was acidified (2) with 135 ml of 2 *N* hydrochloric acid and the stirred system was held at 5° C. Then 24.6 g (0.356 mole) of sodium nitrite in saturated aqueous solution was added during 30 minutes. The precipitate was filtered off, washed with water, and, partially dried, was suspended in a solution of 80.5 g (0.761 mole) of sodium bicarbonate in 935 ml of water. The stirred suspension was treated with 45 ml (0.475 mole) of methyl sulphate. After 40 minutes the system was chilled and filtered. The crude product (54 g) was dissolved in a minimum of boiling ethanol. The hot filtrate was chilled to remove 4-chlorophenyl-bis-diimide (9.4 g, 23.9%). The filtrate was steam-distilled and 17.5 g (m.p. 69–70° C, 27%) of N-methyl-N′-4-chlorophenyldiimide dioxide was obtained from the ether extract of the distillate. After crystallization from petroleum ether (b.p. 40–60° C) it melted at 73.1–74.6° C. Rod-shaped crystals suitable for X-ray diffraction studies were obtained from *p*-cymene; they cleaved well along (100), (001), and (102).

The refractive indices were measured by the crushed crystal immersion method (29) as α, 1.49, about 10° C from (010), while β is 1.67 along (001), and γ is 1.78 about 20° C from (100). The density by flotation in aqueous zinc chloride at 29° C is 1.476, while by the air-displacement method (30) it is 1.470. Calculations of the polarization (from $\alpha+\beta+\gamma$ divided by 3) gave 46.2 cc in contrast to 50.9 cc obtained from $\epsilon = 3.020$ by dielectric constant measurement of the pelleted solid (31).

Zero level Weissenberg photographs of crystals mounted on the *b*-axis (in capsules because of sublimation) were carried out with CuK_α radiation giving constants: $a = 17.20 \pm 0.04$ Å, $b = 3.91 \pm 0.01$ Å, and $c = 13.11 \pm 0.04$ Å of a monoclinic cell with $\beta = 108.0 \pm 0.2°$ C. Since this corresponds with a cell volume of $(838$ Å$)^3$ and the molecular volume

Can. J. Chem. Downloaded from www.nrcresearchpress.com by 196.1.178.254 on 09/04/12
For personal use only.

is calculated as (210 Å)^3 there are four molecules per unit cell. Molecular weight by the Rast method was determined at 190 (calc., 186.6).

Examination of Weissenberg photographs showed no extinctions on (*hkl*), but (*oko*) reflections were found only when $k = 2n$ and (*hol*) reflections only when $l = 2n$. The space group is therefore assigned at $P2_{1/c}$. Structure factors have been determined (32).

p-Chloroaniline

Although N-methyl-N′-4-chlorophenyldiimide dioxide was unaffected by hydriodic acid at 100° C for 30 minutes, reduction was effected in a mixture of 0.56 g (0.003 mole) of the substance with 2.14 g (0.018 atom) of granulated tin to which 3.7 ml (0.095 mole) of concentrated hydrochloric acid was added during 3 minutes. Subsequently the system was maintained at 90–100° C for 30 minutes and at 20° C for 12 hours. After treatment with 6 g of sodium hydroxide in 6 ml of water the system was ether-extracted. Evaporation of the extract left 105 mg, m.p. 60–68° C, which was crystallized from petroleum ether (b.p. 40–60° C), 50 mg (13%) of *p*-chloroaniline characterized by m.p. and m.m.p. of 68.5–70° C.

4-Nitrobromobenzene

A system comprised of 0.98 g (0.005 mole) of N-methyl-N′-4-nitrophenyldiimide dioxide, 1.6 g (0.01 mole) of bromine, 100 mg of iron filings, and 5 ml of carbon disulphide was refluxed for 3 hours and then steam-distilled. The cooled distillate (220 ml) yielded 0.14 g, m.p. 67.6–69.5° C, of crude 4-nitrobromobenzene which was crystallized from ethanol, m.p. 113–115° C, 90 mg (9%), and then from commercial hexane, m.p. and m.m.p. 122.7–123.3° C.

Nitrobenzene

When a solution of N-methyl-N′-4-nitrophenyldiimide dioxide (2.56 g, 0.013 mole) in 50 ml of 95% ethanol was refluxed for 41 hours the cooled system precipitated 1.31 g (51%) of starting material, m.p. 152–153.5° C. Distillation of the filtrate gave 0.26 g of an oil, b.p. 78° C (10 mm), which on redistillation was shown to be nitrobenzene (0.23 g, 14%, b.p. 208–212° C at 756 mm, n_D^{20} 1.55256, m.p. and m.m.p. 6–7° C).

In an experiment, identical except for the addition of 0.1 g of concentrated sulphuric acid and for a 120-hour reflux, only 13% of starting material was recovered and 48% of nitrobenzene was obtained. Additionally a precipitate was formed in a trap containing acid – alcoholic 2,4-dinitrophenylhydrazine solution which surmounted the reflux condenser. This was proved by mixture melting point to be acetaldehyde 2,4-dinitrophenylhydrazone, m.p. 162–164° C.

N-Methyl-N′-3-nitrophenyldiimide Dioxide

The mother liquor (1100 ml) from which the N-methyl-N′-4-nitrophenyldiimide dioxide was removed (see above) was concentrated to a volume of 250 ml and then cooled to give 5.2 g, m.p. 103–111° C. A second crop (1.18 g, m.p. 108–113° C) was obtained by concentrating the filtrate and then eluting it on a Doucil column (1 in. × 14 in.) by means of 450 ml of 1:1 Commercial hexane – carbon tetrachloride. The combined eluates gave 6.38 g which was crystallized from 400 ml of benzene, 1.04 g (4%) of N-methyl-N′-3-nitrophenyldiimide dioxide, m.p. 128–132° C. Recrystallization from methanol raised this melting point to 133–134° C. Calc. for $C_7H_7N_3O_4$: C, 42.6; H, 3.58; N, 21.3. Found: C, 42.3; H, 3.50; N, 21.4. The X-ray diffraction pattern was [10] 3.23; [3] 7.86; [2] 4.65; [1] 4.25, 3.94, 3.70; [0.5] 6.10, 5.27. The ultraviolet absorption in ethanol at 23° C showed λ_{max} at 254 Å with E_{max} 15,350.

Can. J. Chem. Downloaded from www.nrcresearchpress.com by 196.1.178.254 on 09/04/12
For personal use only.

Can. J. Chem. Downloaded from www.nrcresearchpress.com by 196.1.178.254 on 09/04/12
For personal use only.

N-Methyl-N′-2-nitrophenyldiimide Dioxide

The eluted Doucil column (see above) was further eluted, now with carbon tetrachloride (450 ml) and then with chloroform (400 ml). These eluates gave 2.22 g, m.p. 52–60° C, and 0.55 g, m.p. 62–66° C, respectively. The combination was crystallized from a 1:1 mixture of benzene and petroleum ether (b.p. 40–60° C), 1.9 g 7.4%, m.p. 60–64° C. A similar recrystallization raised this melting point to 66.5–67.3° C. Calc. for $C_7H_7N_3O_4$: C, 42.6; H, 3.58; N, 21.3. Found: C, 42.3; H, 3.67; N, 20.9. The X-ray diffraction pattern was [10] 4.13, 3.52; [9] 7.79; [8] 5.81, 4.87, 3.87, 3.39; [6] 5.21, 2.54; [5] 4.64; [4] 3.05; [1] 7.08, 6.44. The ultraviolet absorption in ethanol at 23° C was λ_{max} 258, 289 Å with E_{max} 10,830 and 9,415 respectively.

A system comprised of 100 mg (0.0005 mole) of this isomer with 0.37 g (0.0031 atom) of granulated tin and 0.75 ml of concentrated hydrochloric acid was refluxed for 40 minutes. The cooled system, treated with 1.2 g of sodium hydroxide in 8 ml of water was ether extracted. The extract contained 35 mg, m.p. 93–97° C. This was crystallized from benzene, m.p. 100–101° C (14 mg, 26%), and then was characterized by m.p. and m.m.p. (100–102° C) as orthophenylenediamine.

N,N′-Dibenzyldiimide Dioxide

This substance was prepared in 38% yield, m.p. 58–59° C, from N-benzylhydroxylamine (33) by the previously reported procedure (3). The X-ray diffraction pattern was [10] 4.53; [8] 4.10; [7] 3.16; [6] 5.38, 4.71; [5] 3.96, 3.10; [4] 2.36; [3] 2.60; [2] 7.0; [1] 2.24, 2.91, 3.29, 3.58.

A 4% solution in benzene showed bands with the following per cent transmission (% *T*) at the recorded frequency in cm^{-1}: (89) 494, (90) 555, (86) 601, (51) 710, (66) 741, (91) 835.

N-Benzyl-N′-phenyldiimide Dioxide

To a solution of sodium ethoxide (1.38 g Na in 50 ml of absolute ethanol, 0.06 mole) was slowly added 9.3 g (0.06 mole) of cupferron. After further addition of 7.59 g (0.06 mole) of freshly distilled benzyl chloride the system was refluxed for 210 minutes. Removal of the solvent under reduced pressure left a brown residue which was extracted by diethyl ether. The evaporated extract was crystallized from a hexane–ether mixture, 2.28 g (16.7%), m.p. 80–81° C. Calc. for $C_{13}H_{12}N_2O_2$: C, 68.4; H, 5.31; N, 12.3. Found: C, 68.6; H, 5.42; N, 12.2. The X-ray diffraction pattern was [10] 4.25; [9] 5.75; [8] 3.90; [7] 4.60, 4.73; [6] 4.10; [5] 3.55, 3.17; [4] 5.06; [3] 3.26, 2.36; [2] 3.38, 3.44, 3.03; [1] 2.93.

Action of Grignard Reagents on Diimide Dioxides

(*a*) *In the Soltys apparatus.*—N-Methyl-N′-phenyldiimide dioxide was studied by the reported procedure (34) in isoamyl ether with methyl iodide Grignard reagent in the same solvent which was distilled from sodium and then from methyl iodide Grignard reagent under nitrogen. The system evolved gas at 25° C but in order to complete the reaction it was heated by boiling water bath for 10 minutes prior to and 10 minutes after the addition of aniline. The active hydrogen was found to be 0.88 and 1.01 equivalent for two determinations in which "addition" of reagent was 1.66 and 1.59 equivalent. In a separate determination the gas was collected before the addition of aniline and was shown to be methane, free from ethane, by infrared absorption in a gas cell with potassium bromide windows: 3205 (W), 2916 (M), 2814 (S), 2786 (S), 1341 (M), 1328 (M), 1290 (S), 1258 (M), 1023 (M) cm^{-1}. Under comparable conditions the gas from N-methyl-N′-phenyldiimide N′-monoxide did not appear to be evolved at 25° C, and at 100° C it did not exceed 0.3 equivalent, although pyridine was the solvent. N,N′-Dibenzyldiimide

Can. J. Chem. Downloaded from www.nrcresearchpress.com by 196.1.178.254 on 09/04/12
For personal use only.

dioxide (9) in isoamyl ether medium showed 0.7 active hydrogen and 0.3 equivalent of Grignard addition. In the better solubilizing medium, N-methylmorpholine, the active hydrogen was 1.5 and the equivalent of Grignard addition was 1.9. The gas evolved was proved by infrared absorption to be only methane. A simple Zerewitinoff determination in pyridine (finally at 100° C) gave 0.4 active hydrogen. N-Benzyl-N′-phenyldiimide dioxide in isoamyl ether medium showed 0.5 active hydrogen and 0.7 equivalent of Grignard addition, whereas the determination in N-methylmorpholine showed 1.9 equivalent each of hydrogen and Grignard addition. The gas evolved was entirely methane (infrared). A Zerewitinoff determination in pyridine at 100° C showed 0.2 equivalent of active hydrogen.

(*b*) *N,N′-Diphenyldiimide monoxide.*—An ether solution (265 ml, 0.1 *N*, 0.027 mole) of bromobenzene Grignard reagent was added slowly to a solution of N-methyl-N′-phenyldiimide dioxide (2.6 g, 0.0172 mole) in 50 ml of diethyl ether during 150 minutes with constant stirring. Subsequently the system was treated with 100 ml of saturated ammonium sulphate. The ether phase was steam-distilled (0.93 g of unidentified oil in the distillate) and the residue was extracted by diethyl ether. Distillation of this red extract gave a 0.69-g fraction, b.p. 80–120° C (0.6 mm), and a 1.18-g fraction, b.p. 115–130° C (0.6 mm). The latter fraction, crystallized from 4 ml of petroleum ether (b.p. 40–60° C) gave 0.58 g, m.p. 34.5–35.5° C (17%), of diphenyldiimide monoxide identified by mixture melting point (35–36° C) after recrystallization from 4 ml of methanol.

(*c*) *N-Methyl-N′-phenyldiimide N′-oxide.*—Methyl chloride Grignard reagent (185 ml, 0.21 *N*, 0.0389 mole) was added slowly to a stirred solution of 4.2 g (0.0276 mole) of N-methyl-N′-phenyldiimide dioxide in 50 ml of diethyl ether during 3 hours at 20° C. After subsequent decomposition by means of 100 ml of saturated ammonium sulphate a deep-red solid (37 mg, m.p. 126–127° C decomp.) separated from the ether layer. This unidentified solid melted at 140.5° C after crystallization from benzene (60.8% C, 3.70% H). The ether layer was steam-distilled. Ether extraction of the steam distillate removed 2 g of a yellow oil, the higher boiling fraction of which (b.p. 106° C at 1 mm) was 14% of unchanged starting material, m.p. 37–39° C, while the lower boiling fraction gave 0.90 g (b.p. 90–106° C at 16 mm). Crystallization from petroleum ether, b.p. 40–60° C, gave 0.54 g (14%) of N-methyl-N′-phenyldiimide N′-monoxide, m.p. −3 to 0° C. Two similar crystallizations raised this melting point to 6.5–8.5° C, n_D^{20} 1.556. Calc. for $C_7H_8N_2O$: C, 61.7; H, 5.85; N, 20.6. Found: C, 61.9; H, 6.18; N, 20.7. The brown viscous residue from steam distillation (1.27 g) was not identified.

(*d*) *N-Methyl-N′-phenyldiimide.*—To a stirred solution of 180 mg (0.0047 mole) of lithium aluminum hydride in 10 ml of absolute diethyl ether was added 180 mg (0.0013 mole) of N-methyl-N′-phenyldiimide N′-monoxide during 10 minutes. After 35 minutes of subsequent stirring 1 ml of water was added and the system was filtered. The ether extract of the filtrate, dried over magnesium sulphate, was mixed with 3 ml of ether containing 180 mg of anhydrous oxalic acid to give 95 mg, m.p. 138–139° C, of crude methylphenyldiimide oxalate. Two crystallizations from absolute ethanol gave 36 mg (13%), m.p. 145–146° C, which did not depress the melting point of an authentic specimen (35, 36).

(*e*) *N-4-Tolyl-N′-phenyldiimide N′-monoxide.*—To a solution of 3.8 g (0.025 mole) of N-methyl-N′-phenyldiimide dioxide in 50 ml of dry diethyl ether was slowly added during 4 hours at 25° C 200 ml of 0.185 *N* *p*-bromotoluene Grignard reagent (0.037 mole). Then 100 ml of saturated aqueous ammonium chloride solution was added. Evaporation of the separated non-aqueous layer left a red liquid which was steam-distilled. Ether

Can. J. Chem. Downloaded from www.nrcresearchpress.com by 196.1.178.254 on 09/04/12
For personal use only.

extraction of the distillate (250 ml) gave 60 mg of *p,p'*-bitolyl. Ether extraction of the steam distillation residue gave 4.75 g of oil which was distilled, the first fraction (b.p. 100–120° C, 0.5 mm) of which was more bitolyl (total 0.21 g, 6%) identified after methanol crystallization by m.p. and m.m.p., 118–119° C. The higher boiling fraction (2.85 g, b.p. 120–150° C at 0.5 mm) was crystallized from methanol, 2.23 g, m.p. 42–48° C. Two further crystallizations raised the melting point to 50–51° C (1.67 g, 31.5%), and a mixture melting point with an authentic specimen (17) was not depressed. The X-ray powder diagram was [10] 4.35; [9] 3.72; [8] 4.62; [7] 7.49; [6] 3.05; [5] 6.52; [4] 3.15; [3] 5.27; entirely identical with that of the authentic sample but appreciably different from that of N-4-tolyl-N'-phenyldiimide N-monoxide, also prepared by Bigiavi and Sabatelli, [10] 4.67; [9] 3.95; [8] 3.34; [7] 9.34; [6] 3.65; [5] 4.17; [4] 5.34; [3] 5.65; [2] 4.98; [1] 3.49. In a separate experiment the mixture of 0.048 mole of *p*-bromotoluene Grignard reagent and 0.032 mole of the diimide dioxide reacted for 2 hours at 20° C. A Gilman test 1 (37) for excess Grignard reagent was then negative. The red oil obtained after hydrolysis was dried and distilled through a 10-plate column to give 2.04 g, b.p. 40–70° C (756 mm), and 1.65 g, b.p. 70–115° C (756 mm), as well as 5.34 g, b.p. 100–140° C at 10 mm. The first fraction was redistilled, 0.44 g (43%), b.p. 50–60° C, and identified as methanol by its *p*-nitrobenzoate, m.p. and m.m.p. 95–96° C. The second fraction was redistilled, b.p. 100–110° C (756 mm), 0.43 g (12% as toluene) which was converted to 2,4,6-trinitrotoluene, m.p. and m.m.p. 80–81° C for characterization.

(*f*) *N-Benzyl-N'-phenyldiimide N'-oxide.*—The best preparation involved the addition of 100 ml of 0.2 *N* benzyl chloride Grignard reagent in diethyl ether (0.02 mole) to a dioxane solution of N-methyl-N'-phenyldiimide dioxide (1.53 g, 0.01 mole in 50 ml) during 90 minutes. Then 25 ml of saturated aqueous ammonium chloride was added. The white solid which separated was filtered off and its quantity was augmented by chilling the non-aqueous layer at 0° C for 12 hours, 0.54 g (25%) as N-benzyl-N'-phenyldiimide N'-monoxide, m.p. 198–199° C decomp. This melting point was not depressed by admixture with a sample prepared according to Lynch and Pausacker (19). Moreover the X-ray diffraction patterns were identical: [10] 3.90; [9] 5.60; [8] 4.40; [7] 8.98; [6] 4.20; [5] 4.82; [4] 5.40; [3] 3.44; [2] 10.3; [1] 3.66. Calc. for $C_{13}H_{12}N_2O$: C, 73.6; H, 5.70; N, 13.2. Found: C, 73.8; H, 5.34; N, 13.2.

Preparations in diethyl ether alone were less successful. The yield by adding Grignard reagent to an equimolar amount of the diimide dioxide in 65 ml of ether was 10%, which was lowered to 7% by reversing the order of addition, while threefold dilution with consequent longer addition time gave 14% yield. The best yield in diethyl ether (20%) was obtained by adding equivalent amounts at equivalent concentrations of the reagents from two burettes into a tube in which a downward pitched screw conveyed the mixture to a dry-ice-cooled trap within 1 minute of the time of introduction.

The other products of these reactions are of interest. The red oil remaining after evaporation of the filtered non-aqueous part of the hydrolyzate showed at least 6 constituents when examined on a chromatoplate (28). Column chromatography of the red oil on alumina (100–150 mesh activated at 150° C for 10 hours) eluted by benzene gave 3.18 g which was rechromatographed similarly to give 2.74 g that yielded 0.51 g (19%) of bibenzyl (m.p. and m.m.p. 51–52° C) by crystallization from methanol. The methanolic filtrate on treatment with 2,4-dinitrophenylhydrazine reagent gave 0.58 g (m.p. 227–228° C, 7%) of crude benzaldehyde 2,4-dinitrophenylhydrazone, identified by m.p. and m.m.p. (234–236° C) after crystallization from benzene.

Elution of the alumina columns by chloroform gave a liquid (1.99 g) which was crystal-

lized from petroleum ether (b.p. 40–60° C) to give unchanged starting material, m.p. 38–39° C, 1.85 g, 40%, characterized by mixture melting point.

A modification of the preparation of N-benzyl-N′-phenyldiimide N′-oxide was made by filtration of the reaction system. To a stirred solution of 6.1 g (0.04 mole) of N-methyl-N′-phenyldiimide dioxide in 50 ml of absolute diethyl ether was added 0.06 mole of benzyl chloride Grignard reagent (300 ml, 0.2 *N*) during 2 hours. The system was filtered under nitrogen to remove the white precipitate from the ultimately red solution. Hydrolysis of this filtrate by addition of 50 ml of saturated aqueous ammonium chloride gave 3.6 g of viscous oil after drying and evaporation of the ether. Treatment of this oil with 15 ml of hexane precipitated 0.1 g (1.2%) of N-benzyl-N′-phenyldiimide N′-oxide, m.p. 198–199° C after crystallization from toluene, authenticated like the main bulk of this product by mixture melting point and infrared spectra.

The hexane-soluble portion of the oil was chromatographed on alumina to yield by hexane elution 0.6 g (10%) of unchanged methylphenyldiimide dioxide (m.p. 38–39° C) and then by carbon tetrachloride elution 0.1 g (1.3%, m.p. 154–155° C after crystallization from cyclohexane) of benzaldehyde phenylhydrazone, authenticated by mixture melting point and infrared spectra.

The white precipitate from the reaction system was hydrolyzed by treatment with 75 ml of saturated aqueous ammonium chloride. The ether extract of the hydrolyzate, evaporated and then dissolved in hot toluene, yielded 1.2 g (14%) of N-benzyl-N′-phenyldiimide N′-oxide, m.p. 198–199° C. Evaporation of the mother liquors left 4.5 g of unidentified red oil.

Solvolysis of N-Benzyl-N′-phenyldiimide N′-Monoxide

A mixture of 0.5 g (0.00236 mole) of the monoxide and 5 ml of glacial acetic acid (13) was gently refluxed for 15 minutes and then poured into 25 g of crushed ice. The system, neutralized by addition of sodium bicarbonate, was ether-extracted. Evaporation left an oil (0.76 g) from which 0.28 g (42%) of benzaldehyde 2,4-dinitrophenylhydrazone (m.p. and m.m.p. 235–236° C) was isolated by treatment with 2,4-dinitrophenylhydrazine reagent.

Analysis of N-Benzyl-N′-phenyldiimide N′-Monoxide in the Soltys Machine

By the technique used for analysis of methylphenyldiimide dioxide the N-benzyl-N′-phenyldiimide N′-monoxide did not react at all at room temperature; at 100° C it yielded only 0.5 active hydrogen and 0.7 equivalent of addition. Consequently the isoamyl ether was replaced by N-methylmorpholine (dried over solid potassium hydroxide, then barium oxide, and distilled under nitrogen, b.p. 136–136.5° C). In this reaction medium 1.9 equivalent of active hydrogen and 1.9 equivalent of addition were observed, after 20 minutes at 100° C. No gas was evolved at 25° C. A Zerewitinoff determination at 100° C in pyridine showed 0.3 equivalent of active hydrogen.

N′,N′-Methylene-bis-[N-ethyldiimide]tetroxide

A solution of 45 g (0.294 mole) of monoammonium methylene-bis-nitrosohydroxylaminate (1) in 140 ml of 8% aqua ammonia was stirred during 24 hours while 88.5 ml (0.675 mole) of diethyl sulphate was added gradually, the pH being maintained at 8 by addition of more ammonia. The precipitate which was filtered off weighed 8.2 g, m.p. 145° C, after it was dried and washed with chloroform. This 15% molar yield of ammonium N-ethyl-N′-diimidomethylnitrosohydroxylaminate dioxide could be purified by rapid solution in 40 ml of water at 70° C, followed by quick cooling to avoid decom-

Can. J. Chem. Downloaded from www.nrcresearchpress.com by 196.1.178.254 on 09/04/12
For personal use only.

position with evolution of colorless gas. The recovery was 41% of that added, m.p. 150.1–150.6° C decomp., but a second crop, m.p. 149° C, could be obtained by dilution of the liquors with ethanol. Calc. for $C_3H_{11}N_5O_4$: C, 19.8; H, 6.13; N, 38.6. Found: C, 19.9; H, 6.40; N, 38.1.

The reaction liquor from which the ammonium salt precipitated was treated during 7 hours with 50 ml of diethyl sulphate and sufficient ammonia to maintain the pH at 8. The clear solution was then extracted three times with chloroform and these extracts were vacuum evaporated to leave 10 g of gummy solid which was treated with 10 ml of 68% nitric acid. After the strenuous evolution of nitrogen oxides had ceased the hot solution was cooled and neutralized by strong alkali. The crystals (4.4 g, m.p. 75.8–76.3° C) were N′,N′-methylene-bis-[N-ethyldiimide]tetroxide.

This compound also was obtained when 2.96 g (0.014 mole) of the ammonium salt described above was dissolved in 10 ml of water with 12 ml of 10% aqueous sodium hydroxide (0.03 mole) and was treated during 24 hours with 3.9 ml (0.03 mole) of diethyl sulphate. The product (1.3 g) was crystallized from 95% ethanol (1.5 ml per g) 0.68 g, m.p. 78.9° C. More of the same compound was obtained (0.4 g) by concentration of the mother liquors followed by fume-off with hot nitric acid. Calc. for $C_5H_{12}N_4O_4$: N, 29.2. Found: N, 29.6.

The methyl analogue was prepared in the same manner but with less complication because the ammonium salt did not precipitate. Consequently a 33% yield, m.p. 136° C, could be obtained within one day. The X-ray diffraction diagram was [10] 5.88; [9] 3.87; [8] 3.80; [7] 3.12; [6] 3.58; [5] 5.21; [4] 2.60; [3] 3.23; [2] 3.96, 3.35; [1] 2.40, 2.32, 2.36.

N,N′-Methylene-bis-methyldiimide tetroxide, m.p. 136° C, may be crystallized from 70% nitric acid in which it is quite stable, even during several hours at the boiling point of this medium. The density at 20° C of the solid substance is 1.368 (flotation) in comparison with 1.378 calculated from the following X-ray data. The crystal is orthorhombic pyramidal with $a = 14.38 \pm 0.04$ Å, $b = 15.16 \pm 0.04$ Å, $c = 7.16 \pm 0.02$ Å when crystallized from benzene. Reflections (Weissenberg) are found in (*hkl*) only when $h+k$, $k+l$, and $l+h$ are even; in (*hol*) only when $h = 2n$, $l = 2n$, and $h+l = 4n$; in (*okl*) only when $k = 2n$, $l = 2n$, and $k+l = 4n$. Hence the space group is $C_{2\gamma}^{19}(F_{ddm})$. There will be eight molecules per unit cell with a twofold molecular symmetry axis. Since the volume of the unit cell is 1561 Å^3, the total number of electrons is 688. The absorption coefficient for CuK_α radiation is thus 12.6 cm^{-1}.

The crystals are twinned parallel to the *b*-axis and are strongly piezoelectric, indicating lack of centrosymmetry. The refractive indices measured by the crushed crystal technique are $\alpha = 1.38$, $\beta = 1.445$, $\gamma = 1.48$, so $\alpha+\beta+\gamma/3 = 1.44$. A tentative orientation was chosen and structure factors were determined (38).

N,N′-Methylene-bis-[N-β-chloroethyldiimide]tetroxide

A suspension of 2.23 g (0.0146 mole) of monoammonium methylene-bis-nitrosohydroxylaminate in 50 ml of water was treated with water until solution was complete. To this solution was added 4.96 g (0.0202 mole) of silver nitrate in 25 ml of water. The silver salt was filtered off, washed twice with water, and thrice with absolute ethanol. It was then suspended in 30 ml of absolute ethanol and 5.55 g (0.029 mole) of 1-chloro-2-iodoethane was added. After 5 days the silver iodide was filtered off and washed with absolute ethanol. Evaporation of the filtrate left 2.16 g which was treated with 2 ml of 68% nitric acid to destroy the nitroso compounds. After the strenuous reaction had subsided the system was diluted with water and the crystals were filtered off, 1.20 g

Can. J. Chem. Downloaded from www.nrcresearchpress.com by 196.1.178.254 on 09/04/12
For personal use only.

(37%), m.p. 87.8–89.5° C, not raised by crystallization from ethanol (5 ml per g). Calc. for $C_5H_{10}N_4O_4Cl_2$: N, 21.4. Found: N, 21.8.

Bromobenzene Grignard Reagent with Methylene-bis-[methyldiimide]tetroxide

Into 75 ml (0.1375 mole) of bromobenzene Grignard reagent under nitrogen at 0° C was added 3.28 g (0.02 mole) of the powdered tetroxide during 30 minutes with strong gas evolution. The brownish-red system was filtered to remove a gummy mass from which, after hydrolysis, 0.50 g (15%) of the tetroxide was recovered by decomposition of the remainder with 70% nitric acid, m.m.p. 134° C. The filtered reaction mixture was hydrolyzed by 12% hydrochloric acid and the dried non-aqueous layer was distilled, finally at 130° C (20 mm) to remove 2.02 g of biphenyl. Continuation gave a distillate, b.p. 140–240° C (9 mm), which was dissolved in 4 ml of ethanol, 0.71 g, m.p. 126–130° C. This 13% yield of benzophenone phenylhydrazone was twice crystallized from ethanol, m.p. 133–133.5° C, not depressed by admixture with the authentic compound.

Pyrolysis of Methylene-bis-[methyldiimide]tetroxide

The substance decomposed smoothly when 4.92 g (0.03 mole) was heated during 2 hours at 210–220° C. After 15 minutes at 245° C the distillate was converted by means of *p*-nitrobenzoyl chloride to 1.68 g (89%) of the methyl ester. The pyrolysis residue (0.32 g, 93%) was carbon. Analysis of the evolved gas showed that 86% was nitrous oxide.

Qualitative and Quantitative Tests with Methylene-bis-[methyldiimide]tetroxide

A Barger–Rast molecular weight determination in camphor was 163, calc. 164. The substance was unaltered by treatment with acid hydrogen peroxide during 7 hours, and it did not react after 12 hours in methanol with sodium borohydride, but a vigorous reaction occurred with lithium aluminum hydride. However, no products could be isolated from the latter reaction. No reaction occurred with benzaldehyde, *p*-nitrobenzaldehyde, cyclohexanone, urea, but a vigorous reaction occurred with hot phenylhydrazine. No recognizable product was obtained. The alkaline hydrolysis of the tetroxide yielded methanol, formic acid, nitrous acid, and perhaps some hydrogen cyanide either with 30% aqueous sodium hydroxide or with sodium ethoxide.

The active hydrogen determination was carried out in the Soltys machine by the prescribed procedure (34) in isoamyl ether for 20 minutes at 100° C, but it was observed that a precipitate formed immediately upon addition of the reagent and a red solution was formed which faded upon heating. The active hydrogen was found to be 1.9 equivalent. The amount of Grignard reagent which underwent an addition reaction was only 0.1 equivalent, undoubtedly due to the insolubility of the original precipitate from which methane was evolved.

Electrical Polarization Studies

Dielectric constants and specific volumes of either benzene or (in one instance) dioxane solution were carried out as described previously (39, 40) and calculations were made by the method of Halverstadt and Kumler (41). The distortion polarization was determined either from refractive index, additive refractions, or by direct determination with the solid substance (31). Densities were determined by an air-displacement method (30) or by flotation. The results are shown in Table II.

Infrared Spectra

The spectra have been obtained with a Perkin–Elmer 21 spectrometer by Messrs. Bedard and Myers of Canadian Armament Research and Development Establishment,

Can. J. Chem. Downloaded from www.nrcresearchpress.com by 196.1.178.254 on 09/04/12
For personal use only.

Quebec, Que., to whom we are indebted. The samples were studied as Nujol mull (M), as solutions in carbon tetrachloride and carbon disulphide (S), or, whenever possible, as liquids (L) and these notations are made in Table I, where the principal wave numbers in the significant range are recorded.

REFERENCES

1. TRAUBE, W. Ann. **300**, 81 (1898).
2. BAMBERGER, E. and BAUDISCH, O. Ber. **42**, 358 (1909).
3. BEHREND, R. and KÖNIG, E. Ann. **263**, 218 (1891).
4. LINDER, R. Ann. **275**, 133 (1893).
5. HANTZSCH, A. Ber. **31**, 177 (1898).
6. BAMBERGER, E. and EKECRANTZ, T. Ber. **29**, 2412 (1896).
7. HAMNICK, D. U., NEW, R. G. A., and SUTTON, L. E. J. Chem. Soc. 742 (1932).
8. FENIMORE, CH. P. J. Am. Chem. Soc. **72**, 3226 (1950).
9. DARWIN, C. and HODGKIN, D. C. Nature, **166**, 827 (1950).
10. GOWENLOCK, B. G. and TROTMAN, J. J. Chem. Soc. 4190 (1955).
11. SMITH, J. W. J. Chem. Soc. 1124 (1957).
12. KINGDON, W. R. and WRIGHT, G. F. J. Am. Chem. Soc. **72**, 1030 (1950).
13. BAMBERGER, E. Ber. **31**, 574 (1898).
14. LAMBERTON, A. H. Quart. Revs. **V**, 75 (1951).
15. LANGLEY, B. W., LYTHGOE, B., and RAYNER, L. S. J. Chem. Soc. 4191 (1952).
16. KOHLER, E. P., STONE, J. F., and FUSON, R. C. J. Am. Chem. Soc. **49**, 3181 (1927).
17. BIGIAVI, D. and SABATELLI, V. Gazz. chim. ital. **57**, 557 (1927).
18. BERGMANN, M., ULPTZ, R., and WITTE, CH. Ber. **56**, 679 (1923).
19. LYNCH, B. M. and PAUSACKER, K. H. J. Chem. Soc. **3**, 2517 (1953).
20. BROUGH, J. N., LYTHGOE, B., and WATERHOUSE, P. J. Chem. Soc. **4**, 4069 (1954).
21. WITKOP, B. and KISSMAN, H. M. J. Am. Chem. Soc. **75**, 1975 (1953).
22. SHORT, W. F. and WATT, J. S. J. Chem. Soc. **2**, 2293 (1930).
23. CALM, A. and HEUMANN, K. Ber. **13**, 1185 (1880).
24. BIGELOW, L. Chem. Revs. **9**, 117 (1931).
25. VALORI, B. Atti. accad. Lincei, **22**, II, 125 (1913).
26. GEORGE, M. V. and WRIGHT, G. F. J. Am. Chem. Soc. **80**, 1200 (1958).
27. BAMBERGER, E. Ber. **28**, 225 (1895).
28. ALLENTOFF, N. and WRIGHT, G. F. Can. J. Chem. **35**, 900 (1957).
29. BUNN, C. W. Chemical crystallography. Oxford University Press, London. 1946. p. 63.
30. GEORGE, M. V. and WRIGHT, G. F. Can. J. Chem. **36**, 189 (1958).
31. MEREDITH, C. C., WESTLAND, L., and WRIGHT, G. F. J. Am. Chem. Soc. **79**, 2385 (1957).
32. DONOVAN, R. G. M.A. Thesis, University of Toronto. 1954.
33. JONES, L. W. and SNEED, M. C. J. Am. Chem. Soc. **39**, 674 (1917).
34. ORGANIC ANALYSES. Vol. I. Interscience Publishers, Inc., New York. 1953. p. 155.
35. KNORR, L. Ber. **39**, 3265 (1906).
36. KNORR, L. and WEIDEL, A. Ber. **42**, 3523 (1909).
37. GILMAN, H. and SCHULZE, F. J. Am. Chem. Soc. **47**, 2002 (1925).
38. BINNIE, W. P. Defence Research Board Postdoctoral Research Report (available from G. F Wright by request).
39. MEREDITH, C. C. and WRIGHT, G. F. Can. J. Technol. **33**, 182 (1955).
40. SIPOS, J. C., SAWATZKY, H., and WRIGHT, G. F. J. Am. Chem. Soc. **77**, 2759 (1955).
41. HALVERSTADT, I. F. and KUMLER, W. D. J. Am. Chem. Soc. **64**, 2988 (1942).

Can. J. Chem. Downloaded from www.nrcresearchpress.com by 196.1.178.254 on 09/04/12
For personal use only.

Can. J. Chem. Downloaded from www.nrcresearchpress.com by 190.90.36.8 on 09/04/12
For personal use only.

THE ELECTRONIC STATES OF *CIS*- AND *TRANS*-ACETYLENE[1]

H. HOWARD AND G. W. KING

ABSTRACT

The electronic energy levels of *cis*- and *trans*-bent planar centrosymmetric acetylene molecules, with $\angle CCH = 120°$ and $r_{CC} = 1.383$ Å, have been calculated by the LCAO/-ASMO/CI procedure. The lowest energy state that can spectroscopically combine with the linear ground state is found to be of symmetry class A_u belonging to the *trans*-bent molecule and to lie at 4.58 ev above the ground state. This compares favorably with the experimentally observed electronic transition of lowest energy which is of type $(^1A_u - ^1\Sigma_g^+)$ and at 5.24 ev. The lowest-energy allowed transition to a *cis*-bent state of these dimensions is at 9.39 ev, and hence this may not form part of the unanalyzed system of bands in the 2000–1500 Å region, as has been suggested. However, a transition to a *trans*-bent state of type $(^1B_u - ^1\Sigma_g^+)$ is predicted to fall in this region. The energies of other electronic states are discussed in relation to the observed absorption systems of acetylene.

INTRODUCTION

The molecular orbitals method has been successful in predicting the geometry and energy of electronic states of simple and highly symmetric molecules. Such orbitals are commonly constructed by linear combination of appropriate atomic orbitals (LCAO/MO method). Qualitative, empirical extensions to more complex systems have been made in which the stereochemistries of electronically excited molecular states are also considered; in papers on this subject by Walsh (1) and Mulliken (2) the acetylene molecule is considered in some detail as an example. It is known experimentally (3, 4) that the absorption bands of acetylene in the 2400–2000 Å region are due to a transition from a linear ground state of $^1\Sigma_g^+$ symmetry, with $r_{CC} = 1.202$ Å, to a *trans*-bent planar excited state of A_u electronic symmetry (point group C_{2h}) with $r_{CC} = 1.383$ Å and $\angle CCH = 120°$. Thus the excited molecule resembles an ethylene molecule with two *trans* hydrogen atoms missing.

We report, in this paper, the results of calculations of the electronic energy levels of *cis*- and *trans*-bent planar acetylene molecules, belonging to symmetry point groups C_{2v} and C_{2h} respectively, both with the same carbon–carbon bond length as in the A_u state above and with 120° carbon–hydrogen bond angles. Insofar as the approximations which it has been necessary to make are valid, the calculations reveal patterns of energy levels that are helpful in identifying further optical transitions involving bent excited states and which enable comparisons to be made with the predictions of Walsh and Mulliken. Ross (5) has already calculated the energy levels of the linear molecule by a similar method, and by using his values a comparison can be made between the experimental and theoretical energy of the $(^1A_u - ^1\Sigma_g^+)$ transition. This is of especial interest, since the latter quantity is a difference in energies obtained from independent calculations on two models of quite different geometry and electronic structure, and hence this provides a stringent test of the accuracy of these methods of calculation.

THEORY

The basic LCAO/MO procedure is well known (see 6, 7) and is presented in outline here to illustrate its application to this problem.

We consider specifically N of the electrons in a molecule; these may be all the electrons

[1]*Manuscript received December 22, 1958.*
Contribution from the Burke Chemical Laboratories, Hamilton College, McMaster University, Hamilton, Ontario.

or a certain fraction of these, called "valence electrons" which are significantly disturbed by light absorption or change in geometry. An orthonormal set of single-electron molecular wave functions $\phi_\nu(\mathbf{r}_\nu)$ are constructed, $\mathbf{r}_\nu$ being the position vector of the νth electron. 2^N possible determinantal antisymmetrized product (ASMO) wave functions, each satisfying the Pauli principle, can be constructed for the N-electron system. These have the normalized form.

$$\Phi_p = (N!)^{-\frac{1}{2}} |\phi_0(q_0)\ \phi_1(q_1) \ldots\ldots \phi_N(q_N)| \quad [1]$$

where only terms in the leading diagonal are written between bars. q_ν is a scalar product of $\mathbf{r}_\nu$ with basic spin vectors α or β.

Suitable linear combinations of the functions [1] can be classed as eigenfunctions of the squared spin angular momentum operator S^2;

$$\Omega^S = \sum_{q,p} a_{q,p}\, \Phi_p^S \quad [2]$$

where the a's are coefficients.

The total Hamiltonian operator H for the N-electron system may be written

$$H = H^\circ + \sum_{\nu \neq \mu}^{N} e^2/r_{\nu\mu} \quad [3]$$

where

$$H^\circ = \sum_{\nu=1}^{N} H^\circ_\nu(\mathbf{r}_\nu),$$

$H^\circ_\nu(\mathbf{r}_\nu)$ being the single-electron operator for the νth electron in a potential field due to the nuclei plus non-valence electrons, and the second term in [3] represents the inter-electronic repulsion between the valence electrons. We seek the best approximations to the eigenvalues E_k of H in the variational form

$$\int \Psi_k^{S*} H\, \Psi_k^S\, d\tau \quad [4]$$

for the lowest energy state and states orthogonal to this, where in general the Ψ_k are combinations of the linearly independent AP Ω^S; in practice a finite number m of these are taken in each combination.

$$\Psi_k^S = \sum_m b_{km}\, \Omega_m^S. \quad [5]$$

The MOs ϕ_i are each generally formed by linear combination of some n AOs,

$$\phi_i = \sum_n c_{in}\chi_n. \quad [6]$$

The LCAO/SCF method (8) is an iterative process for evaluating [4]; the coefficients c_{in} in [6] and an effective Hamiltonian H^* in [4] are varied to minimize the energy, subject to retaining orthonormality of the MOs. This method is most readily applied when Ψ_k consists of a single AP Φ_p, such as in ground-state closed-shell molecular configurations; it gives a good approximation to the best MOs for such states.

In the alternative LCAO/MO/CI procedure used here, approximate MOs are constructed from analytic AOs in equation [6], and the best Ψ_k of type [5] determined variationally. Large determinantal secular equations are obtained, which can generally be factored into blocks along the leading diagonal if the molecule has symmetry and the

Can. J. Chem. Downloaded from www.nrcresearchpress.com by 190.90.36.8 on 09/04/12
For personal use only.

ϕ_t are constructed so as to transform like irreducible representations of the appropriate symmetry point group.

The single-electron form of H° in [3] and the orthogonality of the ASMO Φ_p in [1] lead to elements of type

$$E_l' = \int \Omega_l^{S*} H \, \Omega_l^S \, d\tau \qquad [7]$$

along the principal diagonals of the secular determinants; these are first approximations to the eigenvalues of H, and the simple LCAO/MO treatment consists in evaluating these. The E_l' are necessarily approximate because the ASMO functions employed are, in general, only approximations to exact wave functions. This is corrected by introducing Configuration Interaction (CI), this term being applied when the off-diagonal elements of the secular determinants, of form

$$\int \Omega_l^{S*} \left| \sum_{\nu \neq \mu}^{N} e^2/r_{\nu\mu} \right| \Omega_m^S \, d\tau, \qquad [8]$$

are evaluated and the eigenvalues of H are obtained by solution of the full secular determinants.

The integrals [7] and [8] can all be evaluated by standard methods (9).

APPLICATION TO ACETYLENE

In linear acetylene, six electrons constitute the carbon–carbon bond; excitations of either one or two of these give rise to the energetically low excited states (5). In the approximation used here, the corresponding set of six electrons in the *cis*- and *trans*-bent molecules were taken as valence electrons. Of the remaining eight, the carbon 1*s*-electrons were taken merely to screen their respective nuclei, reducing the net charge to $+4e$; the hydrogen atoms and their electrons were neglected (see (5) for comments on the validity of this approximation; a similar justification should apply here). Exchange and repulsion effects between the valence electrons and those contributed by each carbon atom to a carbon–hydrogen bond were included in the calculation.

Apart even from non-planar states of acetylene, there are an infinite possible number of geometrical configurations for planar states, with different combinations of bond lengths and angles. The only geometric data available for a bent state are those for the *trans*-bent A_u state (3, 4) and were used as a basis for our calculations. In both the *cis*- and *trans*-bent models, the carbon–carbon bond length was taken as 1.383 Å, and sp^2-hybridized carbon atomic orbitals were used in forming the molecular orbitals, the hydrogen atoms being formally attached at C–C–H angles of 120°. The use of these specific dimensions does not restrict the applicability of the results as much as would appear at first sight, since what is essentially a 3-electron carbon–carbon bond in the A_u state, similar to that found in benzene, recurs in other excited configurations. In any case, for other electronic states with different actual dimensions, these calculations give excitation energies to such vibronic energy levels as have approximately the dimensions used here, in accordance with the Franck–Condon principle.

Real, normalized Slater AOs were used for the carbon $n = 2$ atomic orbitals, of form:

$$\begin{aligned} a_s &= (\delta^5/3\pi)^{\frac{1}{2}} r_a \exp(-\delta r_a) \\ \left.\begin{aligned} a_x &= \\ a_y &= \\ a_z &= \end{aligned}\right\} & (\delta^5/\pi)^{\frac{1}{2}} r_a \exp(-\delta r_a) \left\{\begin{aligned} x_a \\ y_a \\ z_a \end{aligned}\right. \end{aligned}$$

Can. J. Chem. Downloaded from www.nrcresearchpress.com by 190.90.36.8 on 09/04/12
For personal use only.

centered on each of the carbon atoms a and b. The z-axes on each atom projected towards each other, and the x-axes were perpendicular to the molecular plane. δ was assigned the value 1.59.

The a_s Slater function is nodeless; a better form for the $2s$ orbital is one that is orthogonal to the corresponding $1s$ orbital;

$$a_s^\circ = (a_s - 0.21284\, a_{1s})/0.9771.$$

This form was used in evaluating all mononuclear integrals in which the $2s$ orbital occurred, for which it gives significantly improved values. The sp^2-hybridized AOs were:

$$\chi_1 = (3)^{-\frac{1}{2}}(a_s + 2^{\frac{1}{2}}a_z) \qquad \chi_2 = (3)^{-\frac{1}{2}}(b_s + 2^{\frac{1}{2}}b_z)$$
$$\chi_3 = a_x \qquad \chi_4 = b_x$$
$$\chi_5 = 3^{-\frac{1}{2}}a_s - 6^{-\frac{1}{2}}a_z - 2^{-\frac{1}{2}}a_y \qquad \chi_6 = 3^{-\frac{1}{2}}b_s - 6^{-\frac{1}{2}}b_z \mp 2^{-\frac{1}{2}}b_y$$
$$\chi_7 = 3^{-\frac{1}{2}}a_s - 6^{-\frac{1}{2}}a_z - 2^{-\frac{1}{2}}a_y \qquad \chi_8 = 3^{-\frac{1}{2}}b_s - 6^{-\frac{1}{2}}b_z \pm 2^{-\frac{1}{2}}b_y$$

where the orbitals χ_7 and χ_8 were taken as pointing towards the hydrogen atoms, the upper and lower signs referring to *trans-* and *cis*-states respectively. The sets of LCAO/MOs constructed from these AOs which span the irreducible representations of point groups C_{2h} and C_{2v} are shown in Table I, together with their appropriate symmetry representations.† The N_i are normalizing factors.

TABLE I

LCAO/MOs for *cis-* and *trans*-bent acetylene

MO	Description	Symmetry classification C_{2v}	Symmetry classification C_{2h}
$\phi_0 = (2N_0)^{-\frac{1}{2}}(\chi_1+\chi_2)$	$(\sigma_g.2sp^2)$	a_1	a_g
$\phi_1 = (2N_1)^{-\frac{1}{2}}(\chi_3+\chi_4)$	$(\pi_u.2p)$	b_2	a_u
$\phi_2 = (2N_2)^{-\frac{1}{2}}(\chi_5-\chi_6)$	$(2sp^2)$	b_1	b_u
$\phi_3 = (2N_3)^{-\frac{1}{2}}(\chi_5+\chi_6)$	$(2sp^2)$	a_1	a_g
$\phi_4 = (2N_4)^{-\frac{1}{2}}(\chi_3-\chi_4)$	$(\pi_g.2p)$	a_2	b_g
$\phi_5 = (2N_5)^{-\frac{1}{2}}(\chi_1-\chi_2)$	$(\sigma_u.2sp^2)$	b_1	b_u

ϕ_3^* (*cis*) $= 1.0005(\phi_3 - 0.09602\,\phi_0)$.
ϕ_3^* (*trans*) $= 1.0061(\phi_3 - 0.10972\,\phi_0)$.
ϕ_5^* (*cis*) $= 1.0481(\phi_5 + 0.29939\,\phi_2)$.
ϕ_5^* (*trans*) $= 1.03628(\phi_5 + 0.26228\,\phi_2)$.

The MOs ϕ_0 and ϕ_3, also ϕ_2 and ϕ_5, belong to the same symmetry species in both *cis-* and *trans*-models and are not orthogonal to each other. Properly orthogonal forms of ϕ_3 and ϕ_5 are shown starred at the bottom of Table I. The lack of orthogonality between ϕ_0 and ϕ_3 is small, and could be ignored in many parts of the calculation; but the orthogonalized forms of ϕ_3 were used, for example, in calculating the orbital energies ϵ_3 described below. The orthogonalized ϕ_5^* orbitals were used throughout in evaluating integrals. The description in the table indicates the AOs from which the MOs are formed, and also the corresponding MOs of the linear molecule. This description will be retained for convenience in discussing ϕ_3^* and ϕ_5^* orbitals.

AP wave functions were constructed in determinantal form [1] from these MOs by the principles outlined in the previous section: these could be classified according to the

†*Detailed character tables, tables of direct products, and correlations between representations of these groups for acetylene are given in reference (3), p. 2711. Walsh (1) makes a slightly different classification of the C_{2v} species: as a result his symmetry species b_1 and b_2 are interchanged with respect to these used here. Where Walsh's conclusions are mentioned (see discussion, later) his symbols are changed to accord with the definitions used here, which appear more generally accepted in the literature: see (10).*

Can. J. Chem. Downloaded from www.nrcresearchpress.com by 190.90.36.8 on 09/04/12
For personal use only.

symmetry of the occupied MOs under the appropriate point groups. Only combinations corresponding to singlet states were used as Ω functions [2]. Then the integrals [4] break down into sums of integrals over electrons in MOs, of form

$$\text{"Orbital Energy"} \quad \epsilon_a = \int \phi_a^*(\nu)[H^\circ_\nu(\mathbf{r}_\nu)]\phi_a(\nu)\, d\tau_\nu$$

$$\zeta_{bd}^{ac} = \iint \phi_a^*(\nu)\,\phi_b^*(\mu)[e^2/r_{\nu\mu}]\phi_c(\nu)\,\phi_d(\mu)\, d\tau_\nu\, d\tau_\mu.$$

The former type of integral only arises in evaluation of the diagonal elements of the determinants. The latter type can be expanded into sums of integrals over AOs. These were evaluated independently from the tables of Kotani (11) and Kopineck (12) by five-point Lagrangian interpolation, the separate values being in excellent agreement. Certain mononuclear integrals were obtained from formulae given by Barnett and Coulson (13) and Roothan (14).

The orbital energy integrals ϵ_a require special mention. Their evaluation is discussed in detail by Ross (5) in an appendix to his paper. The operator involved can be split into two parts,

$$H^\circ_\nu = T^\circ_\nu + U^\circ_\nu.$$

U°_ν is the potential energy operator for the νth electron and contains terms representing nuclear attraction and exchange and repulsion with the carbon–hydrogen bond electrons. The evaluation of integrals over this operator is straightforward, since each integral splits up into a sum of integrals over AOs, and these are all to be found in the tables referred to above. However, as Ross shows, it is not easy to get satisfactory values for integrals involving the kinetic energy operator T°_ν when analytic Slater atomic orbitals are used, even when these are in properly orthogonalized form. Here we did not explicitly evaluate the kinetic energy integrals, but took the kinetic energies of 2*s*- and 2*p*-electrons to be equal in Slater AOs. Such an assumption is merely the most reasonable one to make in the circumstances; it is admitted that a different choice of kinetic energies could alter the final energy levels by some 2- or 3-electron volts. However, it enabled immediate comparison to be made with the results of Ross for the linear molecule; and since in this comparison only differences in energies are involved, there is some cancellation of such errors in the same direction as may be introduced by our assumption.

For each of the four symmetry classes of both *cis*- and *trans*-acetylene the necessary matrix elements were calculated between the ground state and between all excited states which differed in configuration from the ground state in the assignment of either one or two electrons, and which had energies lying, in first approximation, within approximately 50 ev of the ground state. The calculations were pursued in duplicate, by each author, to minimize error. Eight large determinantal equations were obtained, of orders ranging between 10 and 14. The lower roots of these were obtained using a Bendix D-15G digital computer, for which a subroutine for evaluating matrices by diagonalization was available. The computer was programmed to substitute series of possible values for the roots in the equations and evaluate the resultant matrices. Graphical interpolation gave the roots as values where the matrix equalled zero. While mathematically inelegant, this method can be recommended for speed and simplicity.

RESULTS

The calculated energies of the lower electronic states of *cis*- and *trans*-bent acetylene are given in Tables II and III. All values are relative to the energy of the ground $^1\Sigma_g^+$

Can. J. Chem. Downloaded from www.nrcresearchpress.com by 190.90.36.8 on 09/04/12
For personal use only.

state of the linear molecule, obtained by recalculation from the figures of Ross.* The energies "no CI" and "CI" are relative to Ross' corresponding 6-electron calculation results. Allowance has been made for the change in nuclear repulsion energy in going from the linear to the bent carbon–carbon nuclear separation.

TABLE II

Calculated energy levels for *trans*-bent acetylene

Symmetry	Configuration	Energy levels	
		No CI	CI
A_u	$(a_g\sigma_g 2sp^2)^2(a_u\pi_u 2p)(b_u 2sp^2)^2(a_g 2sp^2)$	4.77	4.58 ev
A_g	$(a_g\sigma_g 2sp^2)^2(a_u\pi_u 2p)^2(b_u 2sp^2)^2$	4.83	4.65
B_u	$(a_g\sigma_g 2sp^2)^2(a_u\pi_u 2p)^2(b_u 2sp^2)(a_g 2sp^2)$	14.18	6.70
A_g	$(a_g\sigma_g 2sp^2)^2(b_u 2sp^2)^2(a_g 2sp^2)^2$	6.46	8.12
B_g	$(a_g\sigma_g 2sp^2)^2(a_u\pi_u 2p)(b_u 2sp^2)(a_g 2sp^2)^2$	8.31	9.02
A_u	$(a_g\sigma_g 2sp^2)^2(a_u\pi_u 2p)^2(b_u 2sp^2)(b_g\pi_g 2p)$	11.92	10.81
A_g	$(a_g\sigma_g 2sp^2)^2(a_u\pi_u 2p)^2(a_g 2sp^2)^2$	11.48	11.63
B_g	$(a_g\sigma_g 2sp^2)^2(a_u\pi_u 2p)^2(a_g 2sp^2)(b_g\pi_g 2p)$	15.08	14.53
B_u	$(a_g\sigma_g 2sp^2)^2(a_u\pi_u 2p)(b_u 2sp^2)^2(b_g\pi_g 2p)$	16.69	18.78

TABLE III

Calculated energy levels for *cis*-bent acetylene

Symmetry	Configuration	Energy levels	
		No CI	CI
A_1	$(a_1\sigma_g 2sp^2)^2(b_2\pi_u 2p)^2(a_1 2sp^2)^2$	7.33	7.23 ev
B_1	$(a_1\sigma_g 2sp^2)^2(b_2\pi_u 2p)^2(b_1 2sp^2)(a_1 2sp^2)$	16.31	9.39
B_2	$(a_1\sigma_g 2sp^2)^2(b_2\pi_u 2p)(b_1 2sp^2)^2(a_1 2sp^2)$	12.65	10.24
A_2	$(a_1\sigma_g 2sp^2)^2(b_2\pi_u 2p)(b_1 2sp^2)(a_1 2sp^2)^2$	10.67	11.63
A_1	$(a_1\sigma_g 2sp^2)^2(b_1 2sp^2)^2(a_1 2sp^2)^2$	12.80	11.71
A_2	$(a_1\sigma_g 2sp^2)^2(b_2\pi_u 2p)^2(a_1 2sp^2)(a_2\pi_g 2p)$	12.91	14.32
A_1	$(a_1\sigma_g 2sp^2)^2(b_2\pi_u 2p)^2(b_1 2sp^2)^2$	13.85	14.93
B_2	$(a_1\sigma_g 2sp^2)^2(b_2\pi_u 2p)^2(b_1 2sp^2)(a_2\pi_g 2p)$	16.29	15.44
B_1	$(a_1\sigma_g 2sp^2)(b_2\pi_u 2p)^2(b_1 2sp^2)(a_1 2sp^2)^2$	20.87	22.23

In general, the off-diagonal elements in the secular determinants are small compared to the E_i'; consequently, single configurations [2] dominate in most excited states after applying CI, and the simple MO description in the tables for the electronic states can be retained. Extensive configurational mixing does occur in the lowest electronic states of B_1 and B_u symmetry, leading to considerable depression of energy after CI. Here the MO description is not accurate but is retained for convenience.

The treatment only gives approximate energies for higher electronic states of a given symmetry class, but these could be readily calculated from the secular determinants, and some are included in the tables. The results are shown graphically in Fig. 1, which also shows the lower linear state energy levels calculated by Ross. The left-hand side shows the levels before, and the right-hand side after, CI is applied.

Experimentally, the lowest energy transition observed in absorption for gaseous acetylene is that mentioned in the Introduction, a $(^1A_u - {}^1\Sigma_g^+)$ transition at 5.24 ev (3, 4). The calculated energy of 4.58 ev compares favorably with this; furthermore, these calculations agree that a ^1A_u *trans*-bent state is the lowest to which transition is allowed from the ground state. The MO description for this ^1A_u state agrees with that predicted by

We thank Dr. Ross for correspondence about this.

Can. J. Chem. Downloaded from www.nrcresearchpress.com by 190.90.36.8 on 09/04/12
For personal use only.

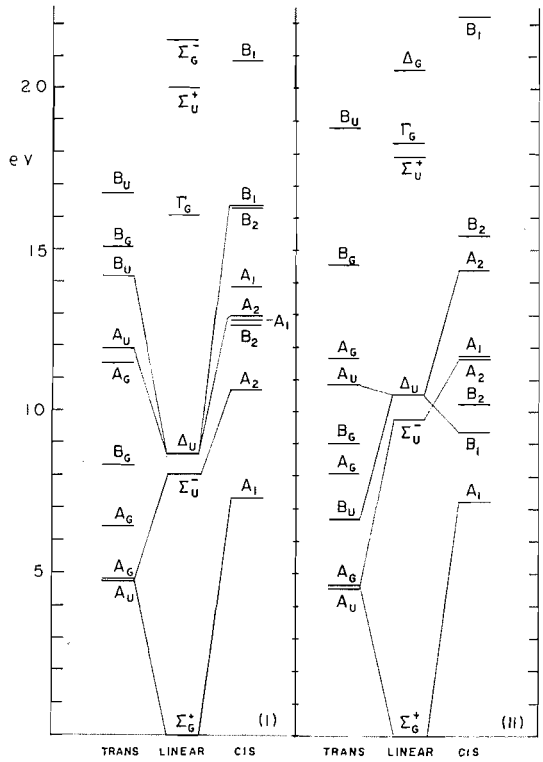

FIG. 1. Energy levels for bent and linear acetylene (i) before CI, (ii) after CI. Correlations are shown here between the lower energy states.

Ingold and King (3) from general valency arguments, by Walsh (1) from MO correlation diagrams, and by Mulliken (2) from analogy with the electronically similar nitrogen and carbon monoxide molecules. However, Walsh correlates this state with a linear Δ_u state; Fig. 1 shows correlation with a linear Σ_u^- state, which is lower in energy than Δ_u according to Ross; this order is preferred by Mulliken.

Acetylene exhibits complex absorption in the 2000–1550 Å region, which is especially intense and of different appearance below 1725 Å (15), indicating the presence of an additional electronic transition here. The bands in this region have not been analyzed: however, Wilkinson (16) has found that discrete absorption bands in the 1520–1280 Å region can be assigned to two Rydberg transitions and two transitions to excited states called *B* and *C*, both of the latter lying some 9.2 ev above the ground state and being *trans*-bent, their band structure being similar to that for the $(^1A_u{-}^1\Sigma_g^+)$ transition mentioned above. There is also some evidence that state *C* is planar and state *B* nonplanar.

Electronic transitions from the ground state to planar, *trans*-bent A_u and B_u states are allowed; the former being a perpendicular-type transition, the latter possessing both perpendicular and parallel components. The calculated $(^1B_u{-}^1\Sigma_g^+)$ transition energy is 6.70 ev; this would correspond to absorption in the 2000–1550 Å region. Wilkinson, following Mulliken's predictions of a ^1B_u state at 8.6 ev, discusses its identification with his '*B*' state, but finds an insufficiency of parallel bands in the spectrum to justify this assignment. We suggest that the $(^1B_u{-}^1\Sigma_g^+)$ transition is responsible for the strong

Can. J. Chem. Downloaded from www.nrcresearchpress.com by 190.90.36.8 on 09/04/12
For personal use only.

absorption around 1725 Å, and that much of the absorption around 2000–1800 Å is due to the tail of the lowest (^1A_u–$^1\Sigma_g^+$) transition, which, on Franck–Condon grounds, has an intensity maximum in this region. It is possible that Wilkinson's state *B* may correlate with some planar state which cannot formally combine with the ground state, such as the A_g state at 8.1 ev; when this is bent out of plane (coming under symmetry class '*A*' of the C_2 point group) it can combine with the ground state in a perpendicular-type transition. However, the observed high absorption coefficient does mitigate this possibility. The lowest allowed transition to a *cis*-state is calculated to be ($^1B_1$–$^1\Sigma_g^+$)* at 9.4 ev, and although it must be remembered that this figure does not necessarily correspond to the electronic origin of a transition, it is rather high to be used to explain the 2000–1550 Å absorption as due to transition to a *cis*-state.

ACKNOWLEDGMENTS

We are most grateful to Professor D. P. Craig of University College, London, for helpful correspondence on this problem. We are also indebted to the National Research Council for financial support.

REFERENCES

1. WALSH, A. D. J. Chem. Soc. 2288 (1953).
2. MULLIKEN, R. S. Can. J. Chem. **36**, 10 (1958).
3. INGOLD, C. K. and KING, G. W. J. Chem. Soc. 2708 (1953).
4. INNES, K. K. J. Chem. Phys. **22**, 863 (1954).
5. ROSS, I. G. Trans. Faraday Soc. **48**, 973 (1952).
6. MULLIKEN, R. S. J. chim. phys. **46**, 497 (1949).
7. CRAIG, D. P. Proc. Roy. Soc. A, **200**, 474 (1950).
8. ROOTHAN, C. C. J. Revs. Modern Phys. **23**, 69 (1951).
9. CONDON, E. U. and SHORTLEY, G. H. The theory of atomic spectra. Cambridge University Press, London. 1935.
10. HERZBERG, G. Infrared and Raman spectra of polyatomic molecules. D. Van Nostrand Company, Inc., New York. 1945.
11. KOTANI, M., AYAO, A., EIICHI, I., and TOSAKU, K. Tables of molecular integrals. Maruzen Company, Ltd., Tokyo. 1955.
12. KOPINECK, H. J. Z. Naturforsch. **5a**, 420 (1950); **6a**, 177 (1951).
13. BARNETT, M. P. and COULSON, C. A. Trans. Roy. Soc. A, **243**, 221 (1951).
14. ROOTHAN, C. C. J. J. Chem. Phys. **19**, 1445 (1951).
15. PRICE, W. C. and WALSH, A. D. Trans. Faraday Soc. **41**, 381 (1945).
16. WILKINSON, P. G. J. Mol. Spectroscopy, **2**, 387 (1958).

**See previous footnote about the symmetry species of cis-bent states.*

Can. J. Chem. Downloaded from www.nrcresearchpress.com by 190.90.36.8 on 09/04/12
For personal use only.

Can. J. Chem. Downloaded from www.nrcresearchpress.com by 190.90.36.8 on 09/04/12
For personal use only.

QUANTITATIVE GAS CHROMATOGRAPHY OF REACTION PRODUCTS FROM THE CATALYTIC OXIDATION OF ETHYLENE[1]

C. H. AMBERG, E. ECHIGOYA,[2] AND D. KULAWIC

ABSTRACT

A simple two-stage gas chromatograph is described which employs only one detector for both effluent streams. It was designed specifically for the routine quantitative analysis of mixtures of ethylene oxide, carbon dioxide, and ethylene in the presence of water vapor and a large excess of air, and for concentrations down to 0.2% by volume of individual components.

INTRODUCTION

The routine quantitative analysis of products from the catalytic oxidation of ethylene is of considerable interest in this laboratory for operations both on the bench and pilot plant scale. It was desirable, in particular, to evolve a method by which both the selectivity of the catalyst and the total conversion of ethylene could be computed exclusively from the analytical data furnished by one gas sample. The indirect titration methods frequently employed for the analysis of ethylene oxide and carbon dioxide (following absorption in Lubatti's reagent and sodium hydroxide, respectively) have disadvantages in that they are not suitable for low gas concentrations and in that two separate gas samples have to be collected. Moreover, information about two components only is thus obtained.

A two-stage gas chromatographic apparatus has been constructed which is able to analyze quantitatively the amounts of ethylene oxide, carbon dioxide, and ethylene in a 10-cc sample of moist air. Analysis on a single column and at invariant temperatures has not proved feasible, chiefly because of the generally high retention time of ethylene oxide and water relative to that of air, carbon dioxide, and ethylene.

EXPERIMENTAL

Apparatus

The apparatus was modelled on that of Simmons and Snyder (1) in which two chromatographic columns could be run alternately in series and in parallel. The flow scheme in the present instance was rearranged so as to enable the effluent from both columns to be detected by one thermal conductivity cell only (see Fig. 1). Column lengths and flow rates were adjusted so that peaks passing through opposite sides of the cell K would not interfere with each other. By reversing the polarity of the bridge output at appropriate times, all recorded peaks were made to point in the same direction.

The columns were made of $\frac{1}{4}$-in. coiled copper tubing. Column 1 was 15 ft long and packed with 32.8 g of *n*-octadecane supported on Celite 545 in the ratio 40:100 w/w. The Celite had been size-graded by flotation as described by James and Martin (2). Celite is to be preferred to firebrick, because it was found to cause less tailing of the ethylene oxide bands. Column 2, 7.5 ft in length, was packed with 27.1 g of 35- to 80-mesh silica gel (Davison No. 12).

Helium was used as the carrier gas at an inlet pressure of 31 p.s.i.g.; it was first led through a silica gel drying column. Both streams were vented to the atmosphere at the rate of 90 cc/min as measured by the soap film method. The accuracy of these measure-

[1]*Manuscript received November 20, 1958.*
Contribution from the Division of Applied Chemistry, National Research Council, Ottawa, Canada. Issued as N.R.C. No. 5084.
[2]*National Research Council Postdoctorate Fellow 1957–1959.*

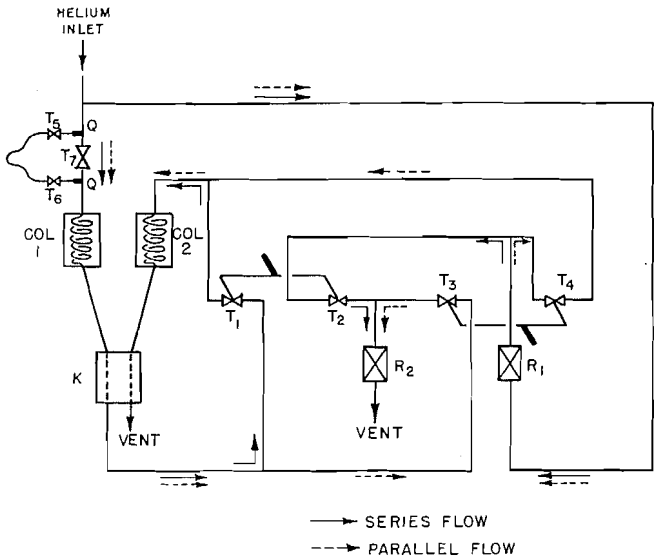

FIG. 1. Schematic flow diagram.

ments was ±0.5%. However, to adjust the dummy flow resistances, needle valves R_1 and R_2 (1), it was found more expedient to employ a Fisher and Porter Flowrator. This resulted in possible 1–2% differences in flow rate between the two streams, still sufficient to give a base line change of no more than 10 μv on changing the flow pattern from series to parallel flow.

A thermal conductivity cell (Gow-Mac Co., Model 9285) served as the detector, K, in conjunction with a recording potentiometer that could be attenuated from 20 mv to 1 mv full scale deflection. A bridge current of 200±0.2 ma was maintained with a 6-v lead storage battery.

The assembly also included Hoke toggle valves T_1 to T_4, which were joined by handles as indicated by the "double pole switches" in Fig. 1. This facilitated the instantaneous change of flow pattern.

Samples were introduced by means of a calibrated 10-cc doser. This consisted of a ¼-in. copper U-tube furnished with toggle valves T_5 and T_6, and a pair of bayonet fittings (Crawford Co., Swagelok), which enabled the doser to be inserted into the gas stream across bypass valve T_7.

The whole unit with the exception of the doser was constructed to fit into a water bath, 1 ft deep by 1 ft in diameter; this was thermoregulated at 30±0.05° C. Figure 2 gives a general view of the apparatus. Temperature and pressure regulating devices are not shown. Additional needle valves, not included in Fig. 1, simply serve to isolate the unit during shutdown. The two glass fittings at the vents on the left can be connected to flowmeters; a Flowrator is shown in position in one of them.

Procedure

To analyze a sample, the doser is evacuated and then flushed with reactor gas. Before insertion, the open ends at T_5 and T_6 must be pumped free of sample, since the calibrated volume is contained between T_5 and T_6. The introduction of an additional volume of air is of no consequence, but the volume of atmospheric carbon dioxide contained therein appears as a positive intercept on the peak height axis of the calibration curve (*v.i.*).

Can. J. Chem. Downloaded from www.nrcresearchpress.com by 190.90.36.8 on 09/04/12
For personal use only.

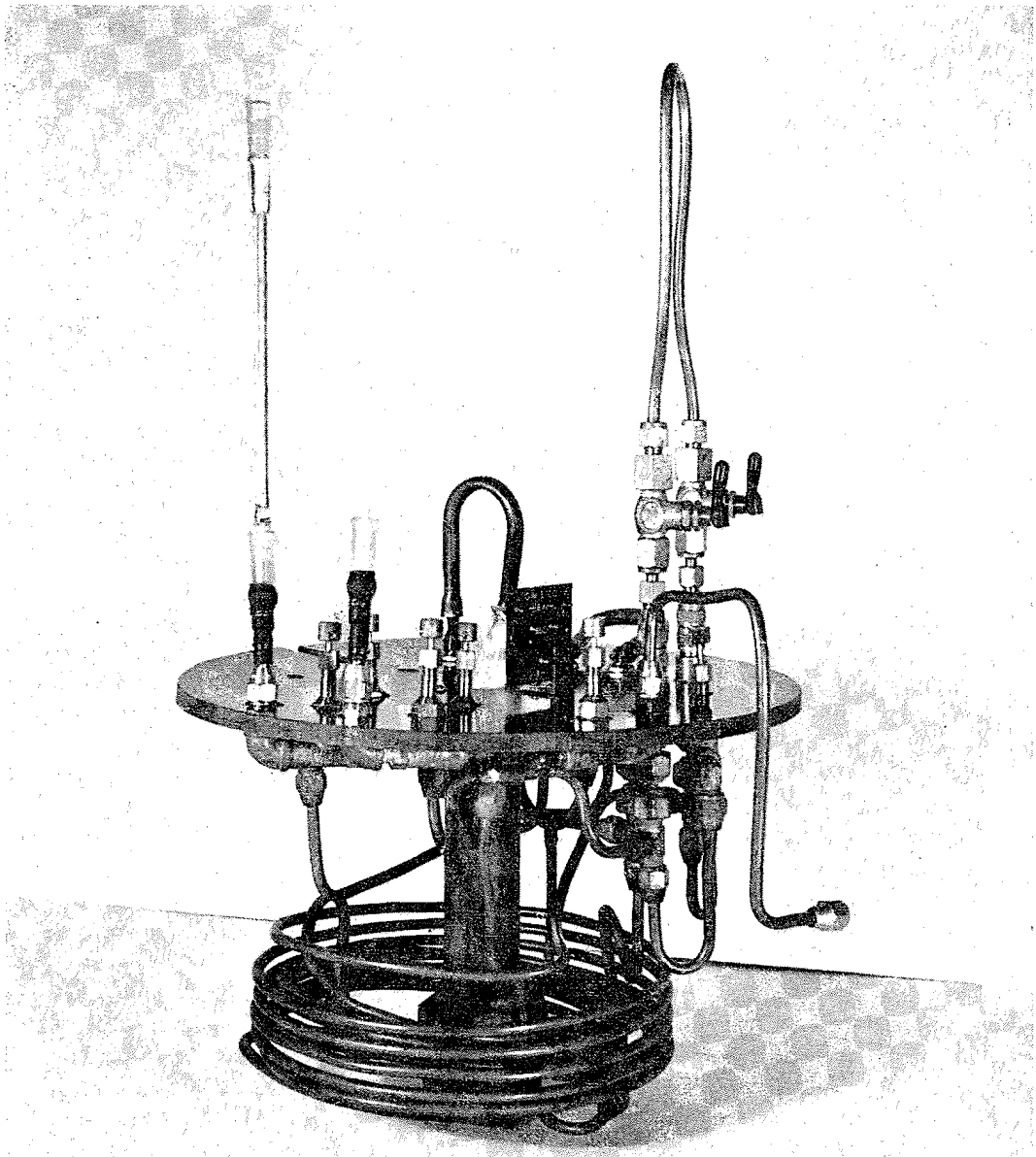

FIG. 2. View of the apparatus.

The sample is introduced with the instrument set for series flow. After 5.5 minutes the flow pattern is switched to parallel flow. At this point ethylene oxide and water are still partitioning in column 1, while carbon dioxide and ethylene are partitioning in column 2, the air having already passed through both columns and out to atmosphere.

Ethylene oxide is now recorded. It is followed by a clearly delineated water front. No

Can. J. Chem. Downloaded from www.nrcresearchpress.com by 190.90.36.8 on 09/04/12
For personal use only.

attempt was made to evaluate water quantitatively because of poor and irreproducible peak formation. Both vapors are vented without entering the silica gel column; this is an essential step, since they would otherwise contaminate the gel.

After reversal of the polarity of the bridge output, carbon dioxide and ethylene elute from column 2 and are recorded. Under the conditions indicated it takes 25 minutes to complete a run.

Calibrations

Calibrations were performed with the separate gases by means of four open-ended pipettes ranging from 0.078 to 0.72 cc in volume. These consisted of different lengths of 2-mm steel tubing soldered onto hypodermic syringe needles. They were flushed with the gas to be calibrated, closed at one end with a finger, and inserted into the evacuated doser through a rubber serum cap. Finally, air was allowed to flush the remaining gas into the doser. Corrections to normal pressure and a convenient standard temperature had to be applied.

This relatively simple method has not been used before to our knowledge; we feel, therefore, that its reliability merits discussion in some detail. Table I shows the results of calculating the best straight line by the method of least squares. The precision of the slopes and intercepts was calculated at the 95% confidence level.

TABLE I

Linear calibrations (peak height vs. gas volume)

Gas	Approx. sensitivity, moles/mv $\times 10^6$	Confidence limit,* ±%	Intercept, cc	Confidence limit,* ±cc
C_2H_4O	4	0.4	0.0038	0.0018
CO_2	8	0.8	−0.014	0.0037
C_2H_4	11	0.6	0.0012	0.0027

*At the 95% level.

The two main sources of error during calibration are probably loss by diffusion from the needle during transfer and loss through incomplete transfer into the calibrated part of the doser. The first of these was calculated to be about 0.001 cc/sec, 1 second being the approximate maximum time of transfer. The other factor was of the same order of magnitude or less, as established by separate experiments.

Loss errors of this type to some extent invalidate the use of the method of least squares which is based on random distribution of errors. For this reason the calibration line for ethylene oxide was recalculated using highest values only. This changed the value of the slope by less than one part in 10^4 and reduced the intercept by 0.001 cc, neither change being significant.

It is possible that all calibration lines were slightly curved (3), the degree of curvature being reflected in part by the confidence limits in Table I. For ethylene oxide and ethylene satisfactory results were obtained by assuming linear relationships and by drawing a parallel line through the origin, i.e. assuming the intercepts to be due to calibration losses only. For ethylene, at any rate, a zero intercept fell within the calculated limits.

The curvature of the carbon dioxide line was somewhat more marked. Also, the negative intercept was too large to be accounted for by atmospheric carbon dioxide alone. Hence, a calibration curve was obtained graphically and fitted by a quadratic equation. The resulting intercept of −0.0036 cc agreed closely with blank determinations using atmospheric air. The final curve had to be corrected for the atmospheric carbon

Can. J. Chem. Downloaded from www.nrcresearchpress.com by 190.90.36.8 on 09/04/12
For personal use only.

dioxide contained in the calibrated volume of the doser.

Calibrations were frequently checked using one pipette only. After a shutdown, 3–5% drifts in the slopes towards equilibrium values were found over as much as a 2-day period, after which sensitivities remained steady within 1%.

The instrument has been in use for approximately seven months with its original columns, during which time over 1000 runs have been carried out. It was found beneficial to purge the columns every 6–8 weeks at 50–60° C for several hours. Although there is some uncertainty regarding the initial period, no significant deterioration has been observed over the past 5 months. Variations in the final sensitivity value, once stability had been reached after a new start, were found to be about ±3%.

Performance

The best way to evaluate the accuracy of the apparatus was to analyze synthetic mixtures of ethylene oxide, carbon dioxide, and ethylene. A conventional B.E.T. apparatus was used to measure out the gas volumes into a 1-l. calibrated bulb. Air was admitted at atmospheric pressure and the mixture displaced from the bulb by mercury.

Table II shows a series of such tests in the order in which they were carried out. It is believed that deviations here were due to experimental errors in measuring out the gas mixtures at least as much as they were due to fluctuations in the analyzer. This is borne out by the following observations.

(1) Agreement was excellent where only one gas was handled. With increasing experience this was equally true for two gases, but some deviations occurred when three gases were involved.

(2) To exclude any possibility of mutual interference, separate tests were made during calibrations with a pipette. No sign of interference was discovered. Therefore, although no unambiguous standard was available with an accuracy known to be substantially higher than that expected of the analyzer, we estimate an approximate accuracy of ±5%, where the gas concentrations are in the 0.2 to 0.3% region. This will improve to at least ±2% for concentrations of 1% and higher.

TABLE II

Analysis of synthetic mixtures

Calculated from pressure–volume data, % by volume			Gas chromatographic analysis, % by volume		
C_2H_4O	CO_2	C_2H_4	C_2H_4O	CO_2	C_2H_4
0.57	—	—	0.57	—	—
1.20	—	—	1.20	—	—
—	—	2.21	—	—	2.24
1.02	2.17	3.32	1.09	2.17	3.34
0.48	1.52	2.53	0.50	1.46	2.52
0.64	1.24	2.37	0.61	1.28	2.41
0.85	1.33	—	0.84	1.40	—
—	1.20	—	—	1.20	—
1.09	1.20	2.54	1.11	1.20	2.57
0.92	1.15	2.64	0.89	1.20	2.68
—	—	2.41	—	—	2.42
—	—	2.38	—	—	2.38
0.55	0.60	4.55	0.59	0.52	4.57
0.61	0.72	4.87	0.63	0.72	4.97
0.64	0.65	4.93	0.63	0.69	5.02
—	0.30*	—	—	0.30	—
0.31	0.34*	—	0.31	0.35	—
0.36	0.35*	—	0.37	0.37	—

*Atmospheric carbon dioxide removed from air. Correction of 0.035% was applied in all other cases.

Can. J. Chem. Downloaded from www.nrcresearchpress.com by 190.90.36.8 on 09/04/12
For personal use only.

Finally, inspection of Table III will give some indication of the precision of the apparatus in the analysis of reactor gas. To make this as unbiased a selection as possible, *all* the results of an arbitrary, continuous 30-day period are given for those cases where more than one analysis had been carried out for a given set of reaction parameters. Each of the nine runs shown was done on the same bench reactor under different conditions. It should be noted that most of the ethylene oxide concentrations in the table are near the lower limit considered practicable for our instrument in its present form.

TABLE III

Analysis of the products from a bench reactor

Run	Interval between samples, hours	% Composition		
		C_2H_4O	CO_2	C_2H_4
A	0	0.26	0.36	4.32
	1	0.26	0.37	4.38
B	0	0.53	0.96	3.82
	2	0.59	1.03	3.71
	2	0.53	0.90	3.87
C	0	0.22	0.32	2.52
	2	0.22	0.34	2.46
	1	0.23	0.33	2.49
D	0	0.17	0.29	2.73
	19	0.16	0.26	2.72
E	0	0.27	0.40	4.42
	2.5	0.26	0.41	4.49
F	0	0.26	0.36	5.60
	1	0.24	0.35	5.56
G	0	0.26	0.46	5.94
	1	0.26	0.44	6.00
	17	0.25	0.39	6.01
H	0	0.25	0.41	4.41
	18	0.24	0.42	4.38
I	0	0.28	0.52	2.50
	18	0.31	0.52	2.56

Again, it is difficult to assign responsibility for the fluctuations in the results. Undoubtedly some are due to variations in reactor conditions, as is suspected, for instance, in run G. At any rate, they allow approximate outside limits of repeatability to be estimated. These limits are at least equal to, and probably somewhat better than, the expected limits of accuracy specified above.

ACKNOWLEDGMENT

The authors wish to thank Mr. W. Thayer for valuable help in the construction of the apparatus and, in particular, for suggesting the use of bayonet fittings for sample introduction.

REFERENCES

1. SIMMONS, M. C. and SNYDER, L. R. Anal. Chem. **30**, 32 (1958).
2. JAMES, A. T. and MARTIN, A. J. P. Biochem. J. **50**, 679 (1951).
3. KEULEMANS, A. I. M., KWANTES, A., and RIJNDERS, G. W. A. Anal. Chim. Acta, **16**, 29 (1957).

Can. J. Chem. Downloaded from www.nrcresearchpress.com by 190.90.36.8 on 09/04/12
For personal use only.

Can. J. Chem. Downloaded from www.nrcresearchpress.com by 196.1.178.254 on 09/04/12
For personal use only.

THE SURFACE ENERGY OF TOBERMORITE[1]

STEPHEN BRUNAUER, D. L. KANTRO, AND C. H. WEISE

ABSTRACT

The total surface energy (or surface enthalpy) of a calcium silicate hydrate, tobermorite, having the composition of $Ca_3Si_2O_7 \cdot 2H_2O$, was determined at 23.5° C. The tobermorite was obtained from the room-temperature hydration of tricalcium silicate, Ca_3SiO_5, or β-dicalcium silicate, β-Ca_2SiO_4, two of the most important constituents of portland cements. The hydration reactions were carried out in three different ways, and 14 preparations were obtained. For each preparation the heats of solution in a mixture of nitric acid and hydrofluoric acid were measured at 23.5° C, and the surface areas were determined by the B.E.T. method, using water vapor at 25° C as the adsorbate. The cross-sectional area of the adsorbed water molecule was taken to be 11.4 Å^2. The surface energy of tobermorite at 23.5° C was found to be 386 ± 20 ergs/cm^2. It is close to the geometric mean of the surface energies of calcium hydroxide and hydrous amorphous silica, previously reported.

Nitrogen adsorption did not measure the true surface area of most tobermorite preparations. This was indicated by negative surface energy values in a number of instances.

INTRODUCTION

Tricalcium silicate and β-dicalcium silicate are two of the most important constituents of portland cement, together making up about three-fourths of a portland cement by weight. In experiments reported earlier (4, 5, 8) the two silicates were hydrated at room temperature by three methods: (*a*) in a small steel ball mill, (*b*) in paste form, and (*c*) in a polyethylene bottle rotated on a wheel. The stoichiometry of the hydration of β-dicalcium silicate by all three methods was represented by the equation

$$2\beta\text{-}Ca_2SiO_4 + 4H_2O = Ca_3Si_2O_7 \cdot 3H_2O + Ca(OH)_2 \quad [1]$$

and the stoichiometry of the hydration of tricalcium silicate by methods (*b*) and (*c*) was represented by the equation

$$2Ca_3SiO_5 + 6H_2O = Ca_3Si_2O_7 \cdot 3H_2O + 3Ca(OH)_2. \quad [2]$$

The same calcium silicate hydrate, tobermorite, was produced in all five cases. Only the ball-mill hydration of tricalcium silicate produced a different calcium silicate hydrate, afwillite (4), which is not discussed in the present paper but will be discussed in a future publication.

Among the three methods of hydration, method (*b*) is of especial importance, because it attempts to simulate the hydration of portland cement in concrete and mortar. In paste hydration, both tricalcium silicate and dicalcium silicate produce tobermorite, and there is ample evidence that in the hydration of portland cements both silicates produce tobermorite. In all probability, the properties of concrete and mortar are determined to a greater extent by the properties of tobermorite than by the properties of any of their other constituents.

Although in the above reactions the calcium silicates were mixed with distilled water, lime saturation was established at an early stage of hydration, after which the reaction proceeded in a saturated calcium hydroxide solution. Under these conditions, the calcium silicate hydrate obtained was the high-lime end member of a series of hydrates designated by Taylor (13) as calcium silicate hydrate (I) or CSH (I). Because of the similarity of this hydrate to the natural mineral tobermorite (12), in the earlier papers (4, 5, 8) it was called tobermorite and, in the absence of general agreement on nomenclature, that

[1]*Manuscript received December 15, 1958.*
Contribution from the Research and Development Laboratories, Portland Cement Association, Skokie, Illinois.

name will be retained here. Bernal (3) proposed the structural formula $Ca_2[SiO_2(OH)_2]_2$-$[Ca(OH)_2]$ for this compound.

The natural mineral tobermorite and some of its synthetic varieties are well crystallized substances, but the tobermorite obtained in the room-temperature hydration of tricalcium silicate or β-dicalcium silicate was poorly crystallized, exhibiting only three X-ray diffraction lines (8). The tobermorite was also very finely divided; its specific surface area in the 14 preparations used in the present experiments ranged from 244 to 376 meters^2/g. Because of the colloidal nature of the hydrate, its equilibrium water vapor pressure varied with water content in a continuous rather than stepwise manner. At a vapor pressure of 8×10^{-3} mm of mercury the water content was about 2.8 moles, at 5×10^{-4} mm it was about 2.1 moles per mole of tobermorite.

The method used for the determination of surface energy (or, more strictly, surface enthalpy) was similar to that used for the determination of the surface enthalpies of amorphous silica and hydrous amorphous silica (10); namely, the heat-of-solution method. Heats of solution at three different concentrations, water content, and surface area were measured for each preparation, and the composition was determined by chemical and X-ray analysis. From these data, the heat of solution, water content, and surface area of the tobermorite were calculated. The results were then subjected to a least squares analysis to evaluate the surface energy and other parameters.

EXPERIMENTAL

Materials

The preparation of tricalcium silicate was described in an earlier paper (7), and that of β-dicalcium silicate in another (11). The analyses of the two silicates were given in the latter paper.

Details of the three methods of hydration were also given in earlier papers; one described ball-mill hydration (4), another paste hydration (5), and a third one hydration in the polyethylene bottle (8). All hydrations were carried out in a constant-temperature room, kept at 23.5±0.5° C. The hydration products were dried either at a vapor pressure of 5×10^{-4} mm of mercury (the vapor pressure of ice at −78° C) or at 8×10^{-3} mm of mercury (the equilibrium pressure of $Mg(ClO_4)_2\cdot2H_2O$ and $Mg(ClO_4)_2\cdot4H_2O$). The methods of drying were described in previous papers (4, 7).

Fourteen preparations (batches) were made, as shown in Table I. C-17 and C-18

TABLE I

Hydration of calcium silicates

Batch designation	Calcium silicate	Method of hydration	Time of hydration	Vapor pressure of drying
C-17	Ca_3SiO_5	Paste	17 months	5×10^{-4}
C-18	Ca_3SiO_5	Paste	17 months	8×10^{-3}
C-23	β-Ca_2SiO_4	Paste	17 months	5×10^{-4}
C-24	β-Ca_2SiO_4	Paste	17 months	8×10^{-3}
D-28	β-Ca_2SiO_4	Ball-mill	46 days	5×10^{-4}
D-35	Ca_3SiO_5	Bottle	47 days	5×10^{-4}
D-40	β-Ca_2SiO_4	Bottle	162 days	5×10^{-4}
D-42	Ca_3SiO_5	Bottle	49 days	5×10^{-4}
D-43	Ca_3SiO_5	Bottle	49 days	8×10^{-3}
D-47	β-Ca_2SiO_4	Ball-mill	63 days	5×10^{-4}
D-49	Ca_3SiO_5	Bottle	49 days	5×10^{-4}
D-50	Ca_3SiO_5	Bottle	49 days	5×10^{-4}
D-51	β-Ca_2SiO_4	Ball-mill	47 days	5×10^{-4}
D-52	β-Ca_2SiO_4	Ball-mill	64 days	5×10^{-4}

Can. J. Chem. Downloaded from www.nrcresearchpress.com by 196.1.178.254 on 09/04/12
For personal use only.

were the same paste divided into two parts, one part dried at 5×10^{-4}, the other at 8×10^{-3} mm pressure. The same was true of C-23 and C-24. D-42 and D-43 were also the same preparation; however, when the slurry was divided into two parts, a slight separation of the constituents occurred, as evidenced by chemical analysis.

Each batch was analyzed for calcium oxide, silicon dioxide, aluminum oxide, carbon dioxide, and loss on ignition, with results shown in Table II, columns 2 to 6. The magnesium oxide, sodium oxide, sulphur trioxide, and boric oxide contents were assumed to be the same as in the unhydrated calcium silicates. The methods of analysis used were reported before (7).

TABLE II

Analyses of hydration products* (ignited weight basis)

1 Batch No.	2 CaO	3 SiO_2	4 Al_2O_3	5 Ignition loss	6 CO_2	7 Other analyses
	%	%	%	%	%	
C-17	72.92	25.98	0.07	20.48	0.35	
C-18	72.92	25.98	0.07	23.22	0.50	
C-23	64.45	34.22	0.12	11.54	0.26	30.65% β-Ca_2SiO_4
C-24	64.45	34.22	0.12	13.60	0.32	30.65% β-Ca_2SiO_4
D-28	63.19	33.95	0.15	16.53	0.40	1.01% Fe, 0.06% FeO, 0.41% Fe_2O_3
D-35	72.53	26.41	0.12	19.09	0.14	3.73% Ca_3SiO_5
D-40	64.26	34.48	0.08	11.70	0.40	30.75% β-Ca_2SiO_4
D-42	73.93	25.15	0.09	20.42	0.12	3.06% Ca_3SiO_5
D-43	72.80	26.66	0.10	22.17	0.11	3.06% Ca_3SiO_5
D-47	62.43	33.41	0.11	17.48	0.59	1.93% Fe, 0.05% FeO, 0.03% Fe_2O_3
D-49	71.15	28.11	0.12	18.92	0.26	3.42% Ca_3SiO_5
D-50	72.79	26.02	0.14	19.76	0.14	3.99% Ca_3SiO_5
D-51	62.75	33.36	0.11	16.78	0.37	1.72% Fe, 0.34% FeO, 0.14% Fe_2O_3
D-52	63.22	33.51	0.11	18.10	0.38	1.31% Fe, 0.16% FeO, 0.12% Fe_2O_3

*All Ca_3SiO_5 preparations contained 0.23% MgO and 0.08% Na_2SO_4, and all β-Ca_2SiO_4 preparations 0.22% MgO, 0.06% Na_2SO_4, and 0.53% B_2O_3.

Because in the ball-mill hydration of dicalcium silicate some iron was rubbed off the steel balls, the ball-mill batches were analyzed for free, ferrous, and ferric iron. The method used was a modification of that proposed by Wesly (14). The results are shown in Table II, column 7.

Eight of the batches contained some unhydrated tricalcium silicate or dicalcium silicate. The amounts of these were determined by X-ray quantitative analysis, using magnesium hydroxide as an internal standard, as described before (8). The results are shown in Table II, column 7.

All the analytical results in Table II are given on ignited weight basis; i.e., the sum of the component oxides of the *ignited* batch is taken as 100%. The composition of each batch was calculated, with the results shown in Table III. The excess water, given in column 6, is the water in the tobermorite in excess of two molecules per molecule. Thus, the composition of the tobermorite in C-17 was $Ca_3Si_2O_7.2.08H_2O$, in C-18 it was $Ca_3Si_2O_7.2.79H_2O$.

Measurements

The method of determination of the heats of solution was described before (10, 11). Three sample weights were used: approximately 0.7, 1.0, and 1.3 g. The calorimeter acid was a mixture of 8 ml of 49.4% hydrofluoric acid with sufficient 2 *N* nitric acid added to make the total weight 420 g.

The surface areas were measured by the B.E.T. method (6), using water vapor and

Can. J. Chem. Downloaded from www.nrcresearchpress.com by 196.1.178.254 on 09/04/12
For personal use only.

TABLE III

Compositions of the hydration products (ignited weight basis)*

1 Batch No.	2 $Ca_3Al_2O_6 \cdot 6H_2O$	3 $CaCO_3$	4 $Ca(OH)_2$	5 $Ca_3Si_2O_7 \cdot 2H_2O$	6 Excess H_2O
	%	%	%	%	%
C-17	0.27	0.80	47.87	70.67	0.46
C-18	0.27	1.14	47.62	70.67	3.11
C-23	0.45	0.59	14.62	63.91	0.00
C-24	0.45	0.73	14.52	63.91	2.02
D-28	0.56	0.91	19.77	92.07	0.37
D-35	0.45	0.32	44.92	69.14	0.12
D-40	0.29	0.91	13.70	64.52	0.21
D-42	0.34	0.27	49.55	66.08	0.71
D-43	0.38	0.25	45.04	69.89	3.14
D-47	0.41	1.34	19.69	91.39	1.32
D-49	0.45	0.59	39.74	73.73	0.58
D-50	0.52	0.32	45.90	67.96	0.66
D-51	0.41	0.84	20.49	90.80	0.70
D-52	0.41	0.86	20.82	91.20	1.89

*The composition of each batch also includes the data of Table II, column 7, which were not repeated in this table. However, Fe_2O_3 is in the form of $Fe_2O_3 \cdot H_2O$ under the drying conditions employed. In addition, all Ca_3SiO_5 preparations contained 0.33% $Mg(OH)_2$ and 0.08% Na_2SO_4, and all β-Ca_2SiO_4 preparations 0.32% $Mg(OH)_2$, 0.06% Na_2SO_4, and 0.94% H_3BO_3.

nitrogen as adsorbates. Water vapor adsorption was measured gravimetrically at 25° C and nitrogen adsorption volumetrically at −195.8° C.

RESULTS

The heats of solution of the seven batches of hydrated tricalcium silicate are given in Table IV, and those of the seven batches of hydrated β-dicalcium silicate in Table V. From each heat value, the heat of solution of tobermorite was calculated by correcting for the heats of solution of the other substances present in the batch. The heats of solution of tricalcium aluminate hexahydrate, calcium carbonate, magnesium hydroxide, and boric acid were given in an earlier paper (7), and those of tricalcium silicate, β-dicalcium silicate, and sodium sulphate in another (11). The heats of solution of free iron, ferrous oxide, and ferric oxide monohydrate in the nitric acid – hydrofluoric acid mixture were found to be 1450, 360, and 255 cal/g, respectively. The 1.0- and 1.3-g samples of ball-mill hydrated β-dicalcium silicate usually contained some undissolved ferric oxide at the end of the calorimetric runs. Appropriate corrections were made for this in the calculations.

The heats of solution of 0.2, 0.3, 0.4, 0.5, 0.7, and 0.9 g of calcium hydroxide in the acid mixture were found to be 439.1, 437.3, 435.6, 435.6, 441.3, and 447.3 cal/g, respectively. Each value is the average of four to seven determinations. The results can be represented by two intersecting straight lines. The increase in heat of solution at higher concentrations is caused by the precipitation of calcium fluoride (11).

In the calculation of the heat of solution of tobermorite, it was assumed that the heats of solution of the constituents of the hydration products were additive. The correction for the deviation from additivity will be discussed later.

The specific surface areas of the 14 batches of hydration products are shown in Table VI. The adsorption area of a nitrogen molecule was taken to be 16.2 Å^2, and that of a water molecule 11.4 Å^2. The reasons for adopting the latter value were given in an earlier paper (8). Only the areas obtained by water vapor adsorption were used, for reasons to be discussed later.

Can. J. Chem. Downloaded from www.nrcresearchpress.com by 196.1.178.254 on 09/04/12
For personal use only.

TABLE IV

Heats of solution of tricalcium silicate hydration products

Weight, g	Heat of solution, cal/g	Weight, g	Heat of solution, cal/g	Weight, g	Heat of solution, cal/g
C-17		D-35			
0.6812	461.07	0.7113	474.21	1.2916	450.91
0.7101	459.49	0.7162	475.53	1.2972	449.57
0.7513	461.59			1.3052	452.75
		1.0109	473.89	1.3118	451.55
1.0226	460.66	1.0178	476.01	D-49	
1.0274	459.65	1.0270	474.74	0.7022	476.93
1.0299	460.10			0.7034	472.10
		1.3350	476.04	0.7072	476.11
1.3069	461.21	1.3556	475.93	0.7102	473.44
1.3285	461.90	D-42		0.7209	475.88
C-18		0.6862	470.44		
0.6950	445.87	0.6950	466.06	0.9852	475.28
0.6980	446.54	0.7354	466.27	1.0090	473.21
0.7042	443.72			1.0136	474.08
0.7236	443.90	0.9952	468.20	1.0502	472.92
0.7258	436.84	1.0024	469.45		
0.7366	440.86	1.0478	466.93	1.3000	473.51
				1.3016	473.29
1.0086	442.60	1.3008	467.55	1.3086	473.82
1.0118	440.93	1.3152	467.32	1.3162	473.05
1.0232	441.88	1.3264	468.16	D-50	
1.0294	442.53	D-43		0.6958	470.26
1.0358	441.65	0.6844	449.97	0.7055	470.36
		0.6950	449.67	0.7166	469.70
1.2834	443.49	0.7258	447.93		
1.2966	440.88	0.7427	451.86	0.9960	470.01
1.3052	442.78			0.9986	469.85
1.3332	441.92	0.9920	449.46	1.0013	470.62
1.3369	441.98	0.9980	451.21		
1.3448	440.58	1.0178	450.89	1.3000	470.13
		1.0298	450.48	1.3065	469.47

In the calculation of the specific surface area of tobermorite from the specific surface area of the hydration products, it was assumed that all of the surface resided in tobermorite. The error introduced by this approximation was negligible except possibly for the ball-mill hydrated dicalcium silicate batches. Because of the prolonged grinding, in these batches about 2% of the total surface area was contributed by calcium hydroxide. Nevertheless, no attempt was made to correct the area, for two reasons. In the first place, a reliable determination of the surface area of the calcium hydroxide could not be made (8). In the second place, the slight error introduced by overestimating the tobermorite surface was partly compensated by a simultaneous overestimation of the heat of solution of tobermorite. This was because not only the surface area but also the surface energy of calcium hydroxide was neglected. As will be seen later, the results obtained for the four ball-mill hydrated batches agreed very well with those obtained for the 10 other batches.

DISCUSSION

Analysis of Data

After the heat of solution, the specific surface area, and the water content of the tobermorite in each sample of each batch were calculated, the data were subjected to a least squares analysis, similar to that described in an earlier paper (10). The main

Can. J. Chem. Downloaded from www.nrcresearchpress.com by 196.1.178.254 on 09/04/12
For personal use only.

TABLE V

Heats of solution of β-dicalcium silicate hydration products

Weight, g	Heat of solution, cal/g	Weight, g	Heat of solution, cal/g	Weight, g	Heat of solution, cal/g	Weight, g	Heat of solution, cal/g
C-23		1.0158	480.19	1.0070	492.86		
0.6900	497.33	1.1656	477.79	1.0114	491.34	0.9918	475.82
0.6999	497.82			1.0150	493.72	0.9924	479.82
0.7006	497.99	1.2812	478.36	1.0250	491.93	1.0000	477.63
0.7160	495.56	1.2954	478.95			1.0022	476.85
0.7390	497.27	1.3056	480.26	1.3018	492.78	1.0106	475.96
		1.3059	481.86	1.3148	495.30		
0.9996	497.05	1.3072	479.73	1.3244	496.04	1.2984	477.18
1.0164	495.02	D-28		1.3267	493.99	1.3003	477.66
1.0221	495.49	0.6386	475.87	1.3267	494.44	1.3076	481.11
1.0291	494.94	0.6752	475.21	D-47		1.3204	476.12
1.0371	494.95	0.8326	475.00	0.6976	472.36	D-52	
		0.9648	474.83	0.6994	474.22	0.7004	465.63
1.3152	496.05			0.7166	474.36	0.7054	464.64
1.3216	495.55	1.3136	474.77			0.7134	465.10
1.3224	495.98	1.4196	475.23	0.9950	469.85	0.7138	461.94
1.3242	497.13	1.5233	473.70	1.0086	470.91		
1.3442	498.84	D-40		1.0128	470.67	0.9996	463.07
C-24		0.6853	498.12			1.0036	463.53
0.6214	479.91	0.7162	495.60	1.2964	469.51	1.0040	464.35
0.6716	479.77	0.7344	493.20	1.3084	470.29	1.0074	463.14
0.7032	480.55	0.7374	491.60	D-51		1.0092	462.73
0.7154	480.92	0.7384	492.00	0.6978	478.31		
0.7158	479.50	0.7531	494.60	0.7012	481.14	1.2994	461.49
				0.7036	477.77	1.3034	461.20
1.0074	479.79	1.0039	494.45	0.7088	479.35	1.3108	461.38
1.0092	478.47	1.0053	490.27	0.7138	480.06	1.3280	460.67

difference was that an additional parameter was used in the present treatment, to correct for the non-additivity of the heats of solution.

In an investigation of the heat of decomposition of tricalcium silicate into β-dicalcium silicate and calcium oxide (11), it was found that the heat of solution of an equimolar mixture of β-dicalcium silicate and calcium oxide in the acid mixture was not equal to the sum of the heats of solution of the two components dissolved individually. A similar non-additivity was expected and found for the heats of solution of tobermorite

TABLE VI

Specific surface areas of hydration products

Batch No.	By water adsorption (meters²/g)	By nitrogen adsorption (meters²/g)
C-17	171.5, 172.7	76.6
C-18	135.7	44.3
C-23	170.8, 172.3	35.8
C-24	134.5	
D-28	220.7, 221.4, 212.7, 210.0	217.4, 222.0
D-35	214.6, 214.6, 220.7, 223.7	119.2, 123.4
D-40	174.9, 176.9, 173.8, 174.6	95.0, 86.1
D-42	191.0, 191.7	85.4
D-43	167.6	
D-47	191.0, 191.7, 188.7, 189.8	144.6
D-49	233.3, 232.9, 227.2, 222.2	
D-50	196.7, 198.6, 202.4, 199.7	
D-51	220.3, 219.2, 224.1, 222.6	
D-52	197.1, 192.0	

Can. J. Chem. Downloaded from www.nrcresearchpress.com by 196.1.178.254 on 09/04/12
For personal use only.

and calcium hydroxide. Since a separate determination of this effect would have been extremely laborious, it was evaluated from the data of the present experiments as a parameter in the least squares calculations.

The parameters were evaluated from the experimental data in three different ways. The heats of solution were determined at three sample weights, 0.7, 1.0, and 1.3 g; and in the first evaluation, the data obtained for each weight were treated separately. The three equations employed were of the form

$$[3] \qquad H_{ijk}+w_jh-A_j\epsilon_s-c_jX_k = H_k$$

where H_{ijk} is the heat of solution, in cal/g of $Ca_3Si_2O_7\cdot 2H_2O$, of the ith sample of the jth batch, having weight k;

w_j is the "excess water" content of the jth batch (Table III, column 6) in g/g of $Ca_3Si_2O_7\cdot 2H_2O$;

h is the average heat evolved, in cal/g of water, when $Ca_3Si_2O_7\cdot 2H_2O$ reacts with water to form a tobermorite of higher water content;

A_j is the average specific surface area of the jth batch in meters^2/g of $Ca_3Si_2O_7\cdot 2H_2O$;

ϵ_s is the average surface energy (or surface enthalpy) of $Ca_3Si_2O_7\cdot 2H_2O$ in cal/-meters^2;

c_j is the total calcium oxide in the hydration products in the jth batch, in g/g of $Ca_3Si_2O_7\cdot 2H_2O$;

X_k is the non-additivity correction factor for a sample having weight k, expressed in cal/g of calcium oxide; and

H_k is the heat of solution, in cal/g of $Ca_3Si_2O_7\cdot 2H_2O$, of a sample of weight k, having zero surface and zero excess water.

The term c_jX_k is the correction to the heat of solution of tobermorite, caused by non-additivity of the heats of solution of the hydration products. The value of c_j is approximately 1 for all hydrated tricalcium silicate batches and approximately 2/3 for all hydrated dicalcium silicate batches.

A least squares analysis of the data led to the results shown in Table VII, columns 2 and 3. Actually, three values were obtained for each of the parameters h, ϵ_s, and X (one for each sample weight), and the values given in column 2 are the weighted means of the three values.

TABLE VII

Results of least squares analyses

1	2	3	4	5	6	7
	Individual weight		Five-parameter		Six-parameter	
Parameter	Weighted mean	Standard error	Weighted mean	Standard error	Weighted mean	Standard error
$H_{0.7}$ (cal/g of $Ca_3Si_2O_7\cdot 2H_2O$)	455.5	4.0	453.7	1.2	450.9	1.1
$H_{1.0}$ (cal/g of $Ca_3Si_2O_7\cdot 2H_2O$)	448.7	3.1	446.9	1.1	450.3	1.1
$H_{1.3}$ (cal/g of $Ca_3Si_2O_7\cdot 2H_2O$)	451.0	2.0	452.1	1.2	451.5	1.1
X (cal/g of CaO)	10.6	1.8			11.1	1.2
h (cal/g of H_2O)	420.4	14.9	419.0	9.7	422.2	9.9
ϵ_s (cal/meters^2)	0.0927	0.0072	0.0929	0.0036	0.0914	0.0048
ϵ_s (ergs/cm^2)	388	30	389	15	383	20

The values of X for the 0.7-, 1.0-, and 1.3-g samples were found to be 7.2 ± 4.6, 14.6 ± 3.6, and 9.8 ± 2.4 cal/g of calcium oxide, respectively. In the second evaluation

Can. J. Chem. Downloaded from www.nrcresearchpress.com by 196.1.178.254 on 09/04/12
For personal use only.

of the parameters, the heat of solution of tobermorite was recalculated for each sample, using the appropriate values of c and X for correction. The equation then was of the form

[4] $$H'_{ijk}+w_j h - A_j \epsilon_s = H_k$$

where $H'_{ijk} = H_{ijk} - c_j X_k$. All terms in eq. [4] have the same meaning as in eq. [3]. In the second evaluation, the data for all weights were used together. The results for the five parameters are given in Table VII, columns 4 and 5.

As the data in the previous paragraph show, the errors in $X_{0.7}$, $X_{1.0}$, and $X_{1.3}$ are so large that, actually, the three parameters may be equal. In the third evaluation it was assumed that the parameter X was the same for all three weights. The equation used was of the form of eq. [3]; the data for all weights were used together, and six parameters were calculated. The results are shown in Table VII, columns 6 and 7.

The values of the parameters, and even of the standard errors, obtained in the five- and six-parameter calculations are very close to each other. There is little to choose between them; consequently, the mean value estimates are probably as good as any that can be obtained from the present data.

The Surface Energy of Tobermorite

1. The surface energy of tobermorite obtained in the room temperature hydration of tricalcium silicate or β-dicalcium silicate and having a composition of $Ca_3Si_2O_7 \cdot 2H_2O$ is 386 ± 20 ergs/cm^2 at 23.5° C. The qualification in this statement as to the source of tobermorite is probably essential. It was stated in the Introduction that the tobermorite obtained in the room-temperature hydration of the two calcium silicates was a poorly crystallized substance exhibiting only three X-ray diffraction lines. Better crystallized tobermorites of the same composition can be prepared in a variety of ways, and their surface energies may be different from the value reported here.

The surface energy value of 386 ergs/cm^2 is intermediate between the surface energies of calcium hydroxide and hydrous amorphous silica (silanol), 1180 and 129 ergs/cm^2, respectively (9, 10). This was expected, for two reasons: the calcium silicate hydrate is chemically intermediate between calcium hydroxide and hydrous silica, and it is also intermediate structurally. The calcium hydroxide consisted of nearly perfect crystals (9), the hydrous silica was completely amorphous (10), and the tobermorite was very poorly crystallized. Actually, the surface energy of tobermorite is very close to the geometric mean of the surface energies of calcium hydroxide and hydrous amorphous silica.

The standard error of 20 ergs/cm^2 is an estimate of the precision of the experimental measurements and not of the accuracy of the surface energy value. The least squares analysis evaluates the random errors but not the systematic errors. For example, if the area of an adsorbed water molecule, 11.4 Å^2, is in error by 5%, the surface energy value is also in error by 5%, from this factor alone.

2. To present a clearer picture of the consistency of the results, in Fig. 1 the variation of the heat of solution of $Ca_3Si_2O_7 \cdot 2H_2O$ with specific surface area is shown for the 1.0-g samples. The average heat of solution of the tobermorite in each preparation was calculated, and the results were corrected (1) for the excess water by using $h = 420$ cal/g of water, and (2) for non-additivity by using $X = 11.1$ cal/g of calcium oxide (Table VII). C-17 and C-18 had the same specific surface area; the arrows in the figure indicate which point belongs to which preparation. The same is true of C-23 and C-24, and D-42 and D-43.

Can. J. Chem. Downloaded from www.nrcresearchpress.com by 196.1.178.254 on 09/04/12
For personal use only.

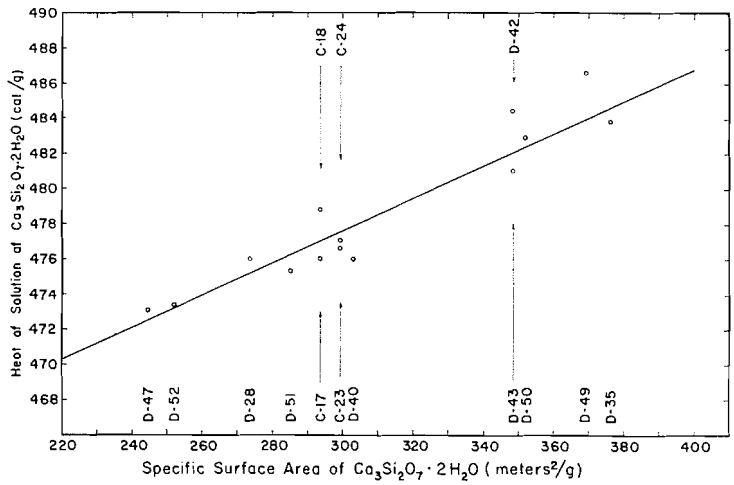

FIG. 1. Variation of the heat of solution of $Ca_3Si_2O_7 \cdot 2H_2O$ with specific surface area for 1.0-g samples.

The straight line drawn in Fig. 1 is a theoretical curve, based on $H_{1.0} = 450$ cal/g of $Ca_3Si_2O_7 \cdot 2H_2O$, and $\epsilon_s = 0.092$ cal/meters². Although the points are scattered, the line appears to be a good representation of the results. Similar data for the 0.7-g samples show somewhat more scatter and those for the 1.3-g samples somewhat less. The point that falls farthest from the straight line is 2.6 cal/g too high (D-49). Such deviations may come about by slight differences in the body structure or somewhat greater differences in surface structure. (The 2.6 cal/g is 0.58% of the heat of solution of the body of tobermorite, and 7.6% of the energy of the surface of the tobermorite in D-49.) However, probably, the real reason is random variation caused by accumulation of the errors in all measurements. This is seen from the results for the pairs C-17 and C-18, and D-42 and D-43. Each of these pairs was a single preparation divided into two parts and dried at different vapor pressures (Table I). As Fig. 1 shows, the difference between the heats of solutions is 2.8 cal/g for the first pair and 3.4 cal/g for the second, the drier preparation giving the lower value for the first pair, and the higher value for the second.

As Fig. 1 shows, only 4 of the 14 preparations had heats of solution deviating from the theoretical value by more than 1.0 cal/g. The average of the absolute values of the deviations is 1.1 cal/g. This corresponds to 0.24% of the heat of solution of the body of tobermorite or to 3.8% of the surface energy. Thus, even if all variation in the heat of solution is ascribed to variation in body structure, or in surface structure, the conclusion is that *both the body structure and the surface structure of tobermorite are highly reproducible.* The different starting materials (tricalcium silicate and β-dicalcium silicate) and the different methods of hydration (ball-mill, paste, bottle) produced a tobermorite of the same body structure and the same surface structure. The method of preparation, however, appears to have an effect on the specific surface area. Tobermorite obtained in ball-mill hydration seems to have the smallest specific surface, and that produced in bottle hydration, the largest.

There is no variation of ϵ_s with specific surface area within the experimental error. Similar result was obtained by Benson and co-workers (1, 2) for sodium chloride. The areas of their samples varied from 1 to 50 meters²/g.

3. The tobermorite formed in the room-temperature hydration of tricalcium silicate

Can. J. Chem. Downloaded from www.nrcresearchpress.com by 196.1.178.254 on 09/04/12
For personal use only.

Can. J. Chem. Downloaded from www.nrcresearchpress.com by 196.1.178.254 on 09/04/12
For personal use only.

or β-dicalcium silicate has probably three molecules of water of hydration per molecule, rather than two (5, 8). It would be of considerable interest to know the surface energy of $Ca_3Si_2O_7 \cdot 3H_2O$, but the difficulties in its experimental determination would be very great. This is because the binding energies of combined water and adsorbed water overlap. At a water vapor pressure of 8×10^{-3} mm of mercury, tobermorite contains 2.8 moles of water per mole, of which 2.54 moles are combined water and 0.26 moles adsorbed water (8). At a higher vapor pressure, tobermorite would contain more combined water and more adsorbed water.

A rough estimate of the surface energy of $Ca_3Si_2O_7 \cdot 3H_2O$ can be made on the basis of the following considerations. Tobermorite is a layer crystal, like the clay minerals. At a vapor pressure of 5×10^{-4} mm of mercury, it contains two moles of combined water per mole, and the distance between the layers is 9.3 Å. At a vapor pressure of 8×10^{-3} mm the distance between the layers is 10.4 Å, indicating that the third mole of combined water, or at least a part of it, is between the layers. On the other hand, in the surface area determinations water vapor does not penetrate between the layers; it measures the external surface areas of the tobermorite crystallites (8). If *all* of the third mole of combined water were between the layers, the surface energy of $Ca_3Si_2O_7 \cdot 3H_2O$ would be only slightly different from that of $Ca_3Si_2O_7 \cdot 2H_2O$.

The opposite extreme would be if all of the third mole of combined water were on the surface. In earlier work, it was found that the surface energy of calcium hydroxide was 130 ergs/cm^2 lower than that of calcium oxide (9), and the energy of the surface of hydrous amorphous silica (silanol) was 130 ergs/cm^2 lower than that of amorphous silica (siloxane) (10). It seems, therefore, reasonable to assume that a mole of combined water on the surface of $Ca_3Si_2O_7 \cdot 2H_2O$ would lower the surface energy by about 130 ergs/cm^2.

It follows from the above considerations that *the surface energy of tobermorite having a composition of* $Ca_3Si_2O_7 \cdot 3H_2O$ *falls in the range 320±70 ergs/cm^2, and probably it is not far from the upper limit of the range.*

4. The tobermorite crystallites are very thin sheets. The dimensions of the sheets are of the order of several thousand Angstrom units, the thickness is only two or three unit cells (20 to 30 Å). It was shown in an earlier work (8) that the specific surface area can be calculated from crystal structure and density data. If the sheets are all two unit cells thick, the area should be 377 meters^2/g, and if they are all three unit cells thick, it should be 251 meters^2/g.

On the basis of water vapor adsorption, the specific surface area of the tobermorite in D-47 is 244 and that in D-35 is 376 meters^2/g (Fig. 1). All other area values fall between these limits. Thus, the indication from the water adsorption results is that all tobermorite crystallites are two or three unit cells thick; and the indication from the crystallographic data is that water adsorption measures the true surface of tobermorite.

In contrast with this, with one exception (D-28), nitrogen adsorption indicates smaller specific surface areas (Table VI), ranging down to 21% of the area measured by water (C-23). That nitrogen does not measure the true surface of tobermorite can be seen from the following considerations. As Fig. 1 shows, the heat of solution of the tobermorite in D-35 is about 8 cal/g larger than that of the tobermorite in D-28, but the surface area of the former is only about half as large, as measured by nitrogen adsorption (Table VI). This would indicate a *negative* surface energy, an absurdity. Several other pairs of preparations would, likewise, lead to negative surface energy values.

The probable explanation for the low nitrogen areas is that aggregation of the tober-

morite crystallites, or rolling of the sheets, or both together prevent nitrogen molecules from reaching some parts of the surface that are accessible to water molecules.

The Heat of Hydration, h

1. The heat evolved when $Ca_3Si_2O_7 \cdot 2H_2O$ reacts with liquid water at 23.5° C to form a hydrate of higher water content was evaluated from data on preparations ranging in water content from 2.0 to 2.8 moles per mole of tobermorite. It was stated before that of the 2.8 moles, 2.54 moles were chemically combined and 0.26 moles were adsorbed water. The latter value corresponds to a surface coverage of about 18%. The fact that at 8×10^{-3} mm vapor pressure this adsorbed water remains on the surface indicates that the free energy of binding of the 0.26 moles of adsorbed and 0.54 moles of combined water to $Ca_3Si_2O_7 \cdot 2H_2O$ is the same. It seems a fair approximation to assume that the heat of binding is, likewise, the same. Thus, the value of $h = 420$ cal/g of water is probably a good value for the heat of hydration, especially since 11 of the 14 preparations were dried at 5×10^{-4} mm pressure, at which the amount of adsorbed water is negligible.

If it is assumed that the heat of hydration of $Ca_3Si_2O_7 \cdot 2H_2O$ is the same for the uptake of the entire additional mole of water, it follows that

$$Ca_3Si_2O_7 \cdot 2H_2O(c) + H_2O(1) = Ca_3Si_2O_7 \cdot 3H_2O(c), \quad \Delta H_{296.6} = -7600 \text{ cal.} \qquad [5]$$

The value of ΔH was rounded off to the nearest 100 cal. The heat evolved is intermediate between the heat of hydration of calcium oxide to calcium hydroxide, 15,620 cal (9), and the heat of hydration of siloxane to silanol, 4660 cal (10).

2. The heat of solution of $Ca_3Si_2O_7 \cdot 3H_2O$ having zero surface can be calculated from the data of Table VII. For 0.7-, 1.0-, and 1.3-g samples it is 406.4, 402.9, and 405.9 cal/g of $Ca_3Si_2O_7 \cdot 3H_2O$, respectively.

ACKNOWLEDGMENTS

The authors are greatly indebted to Dr. Paul Seligmann for deriving the complicated statistical equations, to Dr. Fred Ordway for valuable discussion of the paper, to Messrs. E. E. Pressler and E. LaBonde for most of the analytical data, and to Miss Edith Turtle for most of the X-ray data.

REFERENCES

1. BENSON, G. C. and BENSON, G. W. Can. J. Chem. **33**, 232 (1955).
2. BENSON, G. C., SCHREIBER, H. P., and VAN ZEGGEREN, F. Can. J. Chem. **34**, 1553 (1956).
3. BERNAL, J. D. Proceedings of the Third International Symposium on the Chemistry of Cement. London. 1952. p. 216.
4. BRUNAUER, S., COPELAND, L. E., and BRAGG, R. H. J. Phys. Chem. **60**, 112 (1956).
5. BRUNAUER, S., COPELAND, L. E., and BRAGG, R. H. J. Phys. Chem. **60**, 116 (1956).
6. BRUNAUER, S., EMMETT, P. H., and TELLER, E. J. Am. Chem. Soc. **60**, 309 (1938).
7. BRUNAUER, S., HAYES, J. C., and HASS, W. E. J. Phys. Chem. **58**, 279 (1954).
8. BRUNAUER, S., KANTRO, D. L., and COPELAND, L. E. J. Am. Chem. Soc. **80**, 761 (1958).
9. BRUNAUER, S., KANTRO, D. L., and WEISE, C. H. Can. J. Chem. **34**, 729 (1956).
10. BRUNAUER, S., KANTRO, D. L., and WEISE, C. H. Can. J. Chem. **34**, 1483 (1956).
11. BRUNAUER, S., KANTRO, D. L., and WEISE, C. H. J. Phys. Chem. **60**, 771 (1956).
12. CLARINGBULL, G. F. and HEY, M. H. Mineral. Mag. **29**, 960 (1952).
13. TAYLOR, H. F. W. J. Chem. Soc. 3682 (1950).
14. WESLY, W. Chemiker-Ztg. **68**, 106 (1944).

Can. J. Chem. Downloaded from www.nrcresearchpress.com by 196.1.178.254 on 09/04/12
For personal use only.

Can. J. Chem. Downloaded from www.nrcresearchpress.com by 186.233.112.2 on 09/04/12
For personal use only.

THE OXIDATION OF SOME TERMINAL-SUBSTITUTED POLYHYDRIC ALCOHOLS BY ACETOBACTER SUBOXYDANS[1]

L. HOUGH,[2] J. K. N. JONES, AND D. L. MITCHELL

ABSTRACT

Various terminal-substituted pentitols and hexitols, which possessed either the L-*lyxo*- or the D-*ribo*-configuration at the three contiguous carbon atoms adjacent to the terminal carbon atom, were oxidized to ketoses by *Acetobacter suboxydans*. The terminal hydroxyl group of the polyol was replaced by -H, -*O*Me, -*S*Et, and -*O*Ac groups; several 1,1-dithioacetal derivatives of aldoses were also tested. The preparation of 1-*O*-acetyl-DL-galactitol, 1-deoxy-1-*S*-ethyl-D-arabitol, and 6-deoxy-6-*S*-ethyl-L-sorbose are described. 6-Deoxy-6-*S*-ethyl-L-sorbose was prepared by the microbiological oxidation of 1-deoxy-1-*S*-ethyl-D-glucitol.

INTRODUCTION

The oxidation of unsubstituted sugar alcohols by proliferating cells of *Acetobacter suboxydans* has resulted in the formulation of the Bertrand–Hudson rule for oxidations occurring within the pH range of 5–6.5 (1, 2). Thus a polyol with the D-*erythro* configuration (I) is oxidized mainly at the secondary alcohol group adjacent to the terminal primary alcohol to give a ketose (II). Many examples of this reaction have been reported (3, 4, 5, 6, 7, 8). More recently, cell-free extracts have been used for the oxidation of some polyols in an alkaline environment (optimum pH 7.8), although the reaction is less specific since polyols possessing either the L-*threo*- (III) or D-*erythro*- (I) configurations were utilized (9).

Investigation of the microbiological oxidation of various ω-deoxy-sugar alcohols at pH 5–6.5 has shown that ω(*n*)-deoxy-polyols with the D-*erythro* configuration at the carbon atoms (*n*-2) and (*n*-3) (where *n* equals the number of carbons in the chain) (e.g. VI and VII) gave copper reducing products even when the favorable D-*erythro* configuration was absent at the other end of the chain (10, 11). This configuration is present in L-fucitol (6-deoxy-L-galactitol) (IV), which has been shown to be oxidized at carbon 4 to give 1-deoxy-D-*xylo*-3-hexulose (L-fuco-4-ketose) (V). Hudson, Stewart, and Richtmyer reconciled this evidence with the known specificity of the organism by suggesting that the secondary alcohol at carbon 5 of 6-deoxy-L-galactitol (IV), which can be considered as a *C*-methyl derivative of a pentitol, serves at the enzyme surface in a capacity similar to the primary alcohol of an unsubstituted acyclic polyol. We have investigated the specificity of this microbiological oxidation with a view to the preparation of 3-hexuloses and 3-pentuloses.

A limited number of polyols which possess the favorable D-*ribo*- (VI) or L-*lyxo*- (VII) configuration adjacent to a substituent other than hydroxyl at the terminal carbon atom have been tested as substrates for *A. suboxydans* and some gave reducing products. The substituents included a hydrogen atom (ω-deoxy), ω-*O*-methyl, ω-deoxy-ω-*S*-ethyl, and an ω-*O*-acetyl group. All of the unbranched polyols except 1-deoxy-1-*S*-ethyl-L-arabitol were oxidized to reducing products, which unlike the polyols gave bright yellow or orange spots with *p*-anisidine hydrochloride on paper chromatograms. Similar color reactions were reported for 2-*O*-methyl-3-hexuloses (12) and more commonly for 2-hexuloses (13). Although 1-deoxy-L-arabitol (5-deoxy-L-lyxitol) was oxidized by *A. suboxydans*

[1]*Manuscript received December 9, 1958.*
Contribution from the Department of Chemistry, Queen's University, Kingston, Ontario, and the Department of Organic Chemistry, The University, Bristol 8, England.
[2]*Present address: Department of Organic Chemistry, The University, Bristol 8, England.*

(11) to give a reducing product that resulted in a typical ketose reaction with *p*-anisidine hydrochloride, the substitution of a thioethyl group for a hydrogen atom at carbon-1 in this molecule completely inhibited the oxidation. However, in the cases of 6-deoxy-L-galactitol and 6-deoxy-6-*S*-ethyl-L-galactitol, both substrates yielded reducing compounds in moderate yields. Terminal-branched polyols like diethyldithioacetals (aldose mercaptals) were also tested but they did not appear to be oxidized by *A. suboxydans*, thus supporting the observations of Hudson (1) and Iselin (14).

Estimates of the amounts of reducing sugars formed from the oxidation of various substrates by *A. suboxydans* were made by copper-reduction measurements on aliquots taken from the culture medium at various times during incubation. However, this determination was found to be unsatisfactory when the substrate contained sulphur and unexpectedly high reducing values were obtained; ω-deoxy-ω-thioethyl polyols and dithioacetals reduced the copper reagent when tested in control solutions. An approximate reducing value was obtained by subtracting a 'control reducing value' from the reducing value of the medium which was being tested for biochemical oxidation. The reducing values reported by Bollenback and Underkofler for sugar dithioacetals, when they were used as substrates for *A. suboxydans*, were most likely due to the oxidation of the sulphur atom(s) by the copper reagent (11).

The finding that 6-substituted derivatives of L-galactitol, such as 6-deoxy-L-galactitol (L-fucitol), 1,6-dideoxy-L-galactitol (1,6-dideoxy dulcitol (10)), and 6-deoxy-6-*S*-ethyl-L-galactitol were oxidized by *A. suboxydans* prompted an investigation of the preparation and oxidation of similar derivatives. Two possible synthetic routes to 3-hexuloses might use either L-galactose or DL-galactitol (dulcitol) as starting compounds.

Preferential esterification of the primary alcohol group at carbon 6 of D-galactose and D-glucose has been accomplished by Duff (15, 16) using 50% acetic acid at 100° C. Acetylation of DL-galactitol under slightly modified conditions followed by chromatography on charcoal (25) yielded a crystalline monoacetate as the major product. Periodate

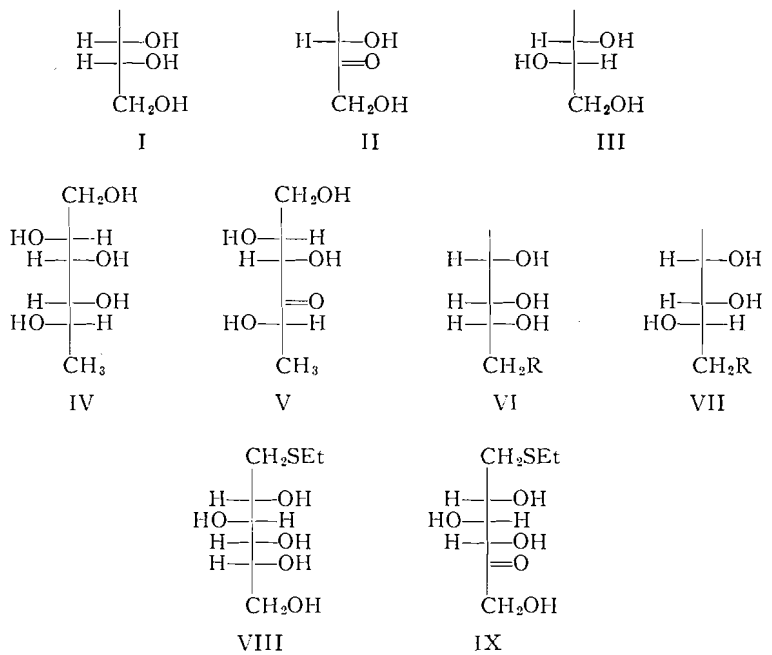

Can. J. Chem. Downloaded from www.nrcresearchpress.com by 186.233.112.2 on 09/04/12
For personal use only.

oxidation experiments revealed that esterification had taken place at one of the primary alcohol groups, and the compound was therefore identified as 1-*O*-acetyl-DL-galactitol (6-*O*-acetyl-DL-galactitol). Since only one-half of the DL-galactitol derivative, the D-isomer (i.e. 6-*O*-acetyl-L-galactitol), can be utilized by *A. suboxydans*, a lower copper reducing value would be anticipated from this substrate than from an L-isomer, such as 6-deoxy-L-galactitol, and this has been verified experimentally.

The oxidation product of 1-deoxy-1-*S*-ethyl-D-glucitol (VIII) has been identified conclusively as 6-deoxy-6-*S*-ethyl-L-sorbose (IX), since after conversion to the 2,3-*O*-isopropylidene derivative, reductive desulphurization gave 6-deoxy-L-sorbose which was characterized as the derived phenylosazone.

At the present time, structural studies are in progress on the products formed by oxidation with *A. suboxydans* of 6-deoxy-6-*S*-ethyl-L-galactitol and 1-*O*-acetyl-DL-galactitol. From the known specificity of the microorganism, these products are probably derivatives of 3-hexuloses.

EXPERIMENTAL

Solutions were concentrated under reduced pressure (*ca.* 15 mm). Optical rotations were determined in water at 23°±3° C unless otherwise stated. Paper chromatography was carried out by the descending method (17) on Whatman No. 1 filter paper using the following solvent systems (v:v): (*a*) ethyl acetate – acetic acid – water (9:2:2); (*b*) ethyl acetate – acetic acid – formic acid – water (18:3:1:4); (*c*) butan-1-ol–ethanol–water (40:11:19); and (*d*) butan-1-ol–pyridine–water (10:3:3). Paper electrophoresis was carried out on Whatman No. 3 filter paper impregnated with 0.05 *M* borate buffer (pH 9.2 at 1800 volts for 1.5 hours). Reducing compounds were detected on paper chromatograms and paper electrophoretograms by the *p*-anisidine hydrochloride reagent (13). Non-reducing compounds were detected on paper chromatograms with an alkaline silver nitrate reagent (18) and on paper electrophoretograms by 3% (w:v) lead tetra-acetate in absolute benzene (19). The rate of movement on paper chromatograms is quoted relative to that of rhamnose (R_{Rh} value). On paper electrophoretograms the mobilities are quoted relative to that of D-glucose (M_G value), and are corrected for endosmosis from the rate of movement of tetra-*O*-methyl-D-glucose relative to the D-glucose standard.

Acetobacter suboxydans (A.T.C.C. No. 621) was kindly supplied by Dr. N. K. Richtmyer. The stock culture was grown on agar slopes on a medium consisting of sorbitol (5%, w:v), yeast extract (0.5% w:v),* and potassium dihydrogen phosphate (0.05% w:v) (10). The substituted polyols under examination (Table II) were made up as a broth containing the polyol (1–3%, accurately weighed), yeast extract (0.5% w:v), potassium dihydrogen phosphate (0.05% w:v), and were fortified with sorbitol (0.1% w:v). Control solutions, made up in duplicate, contained the above constituents except the substituted polyol. The solutions (10 ml) in 75-ml conical flasks were autoclaved (15 p.s.i., 20 minutes), cooled to room temperature, and inoculated with a 72 hours' culture of *A. suboxydans* grown on sorbitol (1 drop). The flasks were stored without agitation at 27° C.

At intervals, an aliquot sample (*ca.* 2 ml) was removed from the medium with a sterile pipette and a little examined directly on paper chromatograms and paper electrophoretograms. The remainder (1 ml) was deproteinized and the reducing power estimated using Somogyi's microcopper reagent (20). Solutions of the sulphur-containing polyols

**Difco Laboratories Inc., Detroit, Michigan, U.S.A.*

Can. J. Chem. Downloaded from www.nrcresearchpress.com by 186.233.112.2 on 09/04/12
For personal use only.

Can. J. Chem. Downloaded from www.nrcresearchpress.com by 186.233.112.2 on 09/04/12
For personal use only.

were made up to identical concentration for copper-reduction estimation. The reducing values of the two control solutions were then subtracted from the reducing value of the medium containing the sulphur-containing polyols under biochemical test. The reducing values are quoted in moles of reducing sugar (calculated as L-sorbose)/100 moles of polyol.

The results are shown in Table II. The 1,1-diethyldithioacetals of D-arabinose, D-glucose, D-galactose, and the 1,1-dibenzyldithioacetal of D-arabinose were not oxidized by *A. suboxydans* as revealed by the copper-reducing power of the culture medium and the absence of any products on paper chromatograms.

Preparation of Substrates

2-Amino-2-deoxy-D-glucitol and 2-acetamido-2-deoxy-D-glucitol were prepared by borohydride-reduction of the respective aldoses according to the method of Bragg and Hough (21). 5-Deoxy-D-ribitol and 5-*O*-methyl-D-ribitol were prepared from D-ribono-1→4-lactone (22). 1-Deoxy-1-*S*-ethyl-polyols were prepared from the corresponding aldose diethyldithioacetals by partial desulphurization with aged Raney nickel (23).

1-Deoxy-1-S-ethyl-D-arabitol

D-Arabinose diethyldithioacetal (3.0 g) was partially desulphurized (23) to yield 57% of product melting at 124–125° C, and with $|\alpha|_D^{28}$ 13°±1° (*c*, 1.1). Anal. Calc. for $C_7H_{16}O_4S$: C, 42.8; H, 8.2; S, 16.3. Found: C, 43.1; H, 8.2; S, 16.7.

1-Deoxy-1-S-ethyl-D-arabitol Tetraacetate

1-Deoxy-1-*S*-ethyl-D-arabitol was acetylated with acetic anhydride in pyridine. The product crystallized when it was poured into a slurry of chipped ice and water, and it was collected by filtration. Recrystallization from aqueous ethanol yielded flakes that melted at 58° C, and with a $|\alpha|_D$ 38°±4° (*c*, 1.3, chloroform). Anal. Calc. for $C_{15}H_{24}O_8S$: C, 49.4; H, 6.6; S, 8.8. Found: C, 49.8; H, 6.8; S, 8.2.

1-O-Acetyl-DL-galactitol (6-O-Acetyl-DL-galactitol, 1-O-Acetyl-dulcitol)

Dulcitol (100 g) was heated under reflux with 50% acetic acid (100 ml) for 36 hours at 80° C (15, 16). Upon cooling, most of the unreacted dulcitol was recovered by filtration and the soluble acetates were obtained as a white residue upon removal of the solvent. Paper chromatographic examination of the residue indicated at least four constituents which had R_{Rh} values of 0.96, 1.23 (major constituent), 1.90, and 2.22 (solvent *a*). The mixture (55 g) was fractionated on a short charcoal column (10×12 cm) of Ultrasorb S.C.* 120–240 (24, 25). Elution was then carried out stepwise with successive fractions (3 liters) of water, and 1.5, 3, 5, 8, 12.5, and 25% ethanol; the major constituent was found in the 8% ethanol fraction. This fraction was filtered, deionized with Amberlite resins (IR-120 (H) and IR-400 (carbonate)) at 5° C, and concentrated to dryness. The product (18 g—low yield due to an accident) after recrystallization from ethanol melted at 131–133° C and possessed a strong adsorption peak in the infrared at ν_{max} 1745 cm^{-1} (nujol). Sorbitol hexaacetate gave an absorption peak at ν_{max} 1748 cm^{-1} and D-glucose diethyldithioacetal possessed a double-peaked adsorption at ν_{max} 1730 and ν_{max} 1750 cm^{-1}. Anal. Calc. for $C_8H_{16}O_7$: C, 42.9; H, 7.2; OAc, 19.2. Found: C, 43.0; H, 7.1; OAc, 19.7.

Structural Determination by Periodate Oxidation Experiments

Oxidations were carried out in the dark at 18° C.

**British Carbo Norit Union Ltd., West Thurrock, Gray's, Essex, England.*

The sample (23 mg) was dissolved in water (21 ml) containing 0.3 *M* sodium metaperiodate solution (4 ml). At intervals, aliquots (2 ml) were withdrawn for either the determination of periodate consumption or the estimation of formic acid liberated (26). Formaldehyde was estimated on aliquots that were diluted 10-fold prior to the estimation (27).

TABLE I

The periodate oxidation of 1-*O*-acetyl-DL-galactitol

Hours	0.08	0.25	0.5	2.25	4.0	28
Periodate uptake*	3.7	3.9	3.9	4.0	4.0	
Formic acid*		2.9		2.8		2.8
Formaldehyde*	0.95		0.95		0.95	

*Moles/mole of 1-*O*-acetyl-DL-galactitol.

*6-Deoxy-6-S-ethyl-*L*-sorbose Phenylosazone*

A culture medium containing 1-deoxy-1-*S*-ethyl-D-glucitol was oxidized for 10 days with *A. suboxydans*. A portion of the solution was deproteinized, deionized with Amberlite resins (IR-120 (H) and IR-4B (OH)), and concentrated to a syrup. The components were separated by paper chromatography (Whatman 3MM) in the usual way (solvent *c*). Some of the syrupy ketose (18 mg) was dissolved in a mixture of phenylhydrazine (0.1 ml), acetic acid (0.1 ml), and water (0.5 ml), and heated in a water bath at 70° C for 3 hours. The phenylosazone (18 mg) was washed first with water, followed by benzene, and was finally recrystallized from aqueous ethanol to give a product melting at 185–190° C. Anal. Calc. for $C_{20}H_{26}N_4O_3S$: C, 59.7; H, 6.5; N, 13.9. Found: C, 59.6; H, 6.5; N, 13.7.

*Reductive Desulphurization to 6-Deoxy-*L*-sorbose (via the O-Isopropylidene Derivative)*

A solution of 6-deoxy-6-*S*-ethyl-L-sorbose (0.20 g) in acetone (20 ml) containing concentrated hydrochloric acid (0.2 ml) was shaken at room temperature for 2.5 hours

TABLE II

Substrates			Products						
			Copper-reducing power (days)						
	R_{Rh}[a]	M_G[b]	3	5	6	14	21	R_{Rh}[a,d]	M_G[d]
5-Deoxy-D-ribitol	1.2	0.75	81.5[c]	—	91	72	—	1.7 (Y)[f]	0.89
5-Deoxy-L-lyxitol	1.2	0.83	—	—	—	—	—	1.6 (Y)	0.89
6-Deoxy-L-galactitol (L-fucitol)	1.1	0.95	17.6	—	38	—	50	1.3 (Y)	0.80
5-*O*-Methyl-D-ribitol	1.3	0.72	6.7	—	15.4	22.9	24.4	1.8 (Y)	0.81
6-*O*-Acetyl-DL-galactitol	1.2	—	—	26	—	21.8	—	1.6[g](Y)	—
2-Amino-2-deoxy-D-glucitol	—	—	—	6.9	—	6.9	—	Nil	—
2-Acetamido-2-deoxy-D-glucitol	0.82	—	51	—	—	57	—	0.75 (Y)	—
1-Deoxy-1-*S*-ethyl derivative of:									
-D-Glucitol	1.6	—	19	—	87	116	116	2.1 (Y)	—
-L-Arabitol	1.8	0.85	—	—	—	—	—	Nil	—
-D-Arabitol	1.8	0.83	71	—	75	82	92	2.6 (O)[e]	0.84
-D-Galactitol	1.6	0.84	16	—	24	27	31	2.1 (Y)	0.88

[a]Solvent (*b*) detected with silver nitrate – sodium hydroxide reagent.
[b]Detected with lead tetraacetate reagent.
[c]Moles of reducing substance/100 moles of substrate.
[d]Detected with *p*-anisidine hydrochloride reagent.
[e]Orange color with *p*-anisidine hydrochloride (O).
[f]Yellow color with *p*-anisidine hydrochloride (Y).
[g]Detected with resorcinol reagent (13).

Can. J. Chem. Downloaded from www.nrcresearchpress.com by 186.233.112.2 on 09/04/12
For personal use only.

followed by neutralization with silver carbonate. The filtrate was concentrated to a syrup which was non-reducing and moved on paper chromatograms at a rate considerably faster than the original ketose. The *O*-isopropylidene derivative (0.12 g) was dissolved in ethanol containing freshly prepared Raney nickel W-2 catalyst (6 ml settled volume) (28) and was heated under reflux for 4 hours. After cooling and filtering free of nickel, a syrup (97 mg) was obtained which had $|\alpha|_D$ 18°±2° (*c*, 1.2, ethanol). (Lit. for 2,3-*O*-isopropylidene-L-sorbose $|\alpha|_D$ 17.9° (29).)

A solution of the syrupy *O*-isopropylidene compound (61 mg) was dissolved in a mixture of phenylhydrazine (0.1 ml), acetic acid (0.1 ml), and water (2 ml), and heated in a water bath at 70° C for 3 hours. The phenylosazone which crystallized from the solution during heating was collected by filtration and washed with cold water followed by ether. Its melting point (175–180° C) was not depressed when admixed with an authentic specimen prepared from 6-deoxy-L-sorbose (30). (Lit. melting point 183–185° C (29) and 168–172° C (9).) The infrared adsorption spectra of the derived and authentic specimens were identical over the frequency range of 600–4000 cm^{-1}.

ACKNOWLEDGMENTS

The authors wish to thank Dr. N. K. Richtmyer of the National Institute of Arthritis and Metabolic Diseases, National Institute of Health, Bethesda, Maryland, for cultures, and Mr. D. J. Anderson for a specimen of sorbitol hexaacetate. One of us (D.L.M.) thanks the Ontario Research Foundation for a scholarship.

REFERENCES

1. Hann, R. M., Tilden, E. B., and Hudson, C. S. J. Am. Chem. Soc. **60**, 1201 (1938).
2. Bertrand, G. Ann. chim. **3** (8), 209, 287 (1904).
3. Whistler, R. L. and Underkofler, L. A. J. Am. Chem. Soc. **60**, 2507 (1938).
4. Bosshard, W. and Richstein, T. Helv. Chim. Acta, **18**, 959 (1935).
5. Stewart, L. C., Richtmyer, N. K., and Hudson, C. S. J. Am. Chem. Soc. **71**, 3532 (1949).
6. Pratt, J. W., Richtmyer, N. K., and Hudson, C. S. J. Am. Chem. Soc. **74**, 2210 (1952).
7. Stewart, L. C., Richtmyer, N. K., and Hudson, C. S. J. Am. Chem. Soc. **74**, 2206 (1952).
8. Pratt, J. W. and Richtmyer, N. K. J. Am. Chem. Soc. **77**, 6326 (1955).
9. Arcus, A. C. and Edson, N. L. Biochem. J. **64**, 385 (1956).
10. Richtmyer, N. K., Stewart, L. C., and Hudson, C. S. J. Am. Chem. Soc. **72**, 4934 (1950).
11. Bollenback, G. N. and Underkofler, L. A. J. Am. Chem. Soc. **72**, 741 (1950).
12. Jones, J. K. N. J. Am. Chem. Soc. **78**, 2855 (1956).
13. Hough, L., Jones, J. K. N., and Wadman, W. H. J. Chem. Soc. 1702 (1950).
14. Iselin, B. J. Biol. Chem. **175**, 997 (1948).
15. Duff, R. B. J. Chem. Soc. 4730 (1957).
16. Duff, R. B. Biochem. J. **70**, 515 (1958).
17. Partridge, S. M. Biochem. J. **42**, 238 (1948).
18. Trevelyan, W. E., Proctor, D. P., and Harrison, J. S. Nature, **166**, 444 (1950).
19. Buchanan, J. G., Dekker, C. A., and Long, A. G. J. Chem. Soc. 3162 (1950).
20. Somogyi, M. J. Biol. Chem. **160**, 61, 69 (1945).
21. Bragg, P. D. and Hough, L. J. Chem. Soc. 4347 (1957).
22. Hough, L., Jones, J. K. N., and Mitchell, D. L. Can. J. Chem. **36**, 1720 (1958).
23. Jones, J. K. N. and Mitchell, D. L. Can. J. Chem. **36**, 206 (1958).
24. Hughes, R. C. and Whelan, W. J. Chem. & Ind. 884 (1958).
25. Andrews, P., Hough, L., and Powell, D. B. Chem. & Ind. 658 (1956).
26. Hough, L., Taylor, T. J., Thomas, G. H. S., and Woods, B. M. J. Chem. Soc. 1212 (1958).
27. O'Dea, J. F. and Gibbons, R. A. Biochem. J. **55**, 580 (1953).
28. Organic syntheses. Vol. 21. John Wiley & Sons, Inc., New York. 1941. p. 15.
29. Müller, H. and Reichstein, T. Helv. Chim. Acta, **21**, 263, 1023 (1938).
30. Hough, L. and Jones, J. K. N. J. Chem. Soc. 4052 (1952).

Can. J. Chem. Downloaded from www.nrcresearchpress.com by 186.233.112.2 on 09/04/12
For personal use only.

Can. J. Chem. Downloaded from www.nrcresearchpress.com by 190.90.36.8 on 09/04/12
For personal use only.

MYCOCHRYSONE

I. ISOLATION, PROPERTIES, AND PRELIMINARY CHARACTERIZATION[1]

G. READ,[2] P. SHU,[3] L. C. VINING, AND R. H. HASKINS

ABSTRACT

Mycochrysone, an orange-red crystalline pigment, has been isolated from in vitro cultures of an inoperculate discomycetous fungus. It possesses quinonoid properties and forms a monoquinoxaline derivative. At least two phenolic or enolic groups are present, one of which is in the *peri* position to a quinone carbonyl. Reduction of the pigment with a zinc dust – zinc chloride mixture gives perylene, together with some hydroperylenes. The pigment shows limited antibiotic activity.

An inoperculate discomycete, designated PRL 1252, which was isolated from a diseased *Pinus sylvestris* seedling, produces an orange-red pigment when grown in vitro on an agar-solidified nutrient medium. The mold probably cannot be identified accurately until its sexual stage is discovered in nature and the organism, for the present, remains unnamed (9). For this reason it is not possible to follow the customary practice of naming the pigment after the species designation and the name "mycochrysone" has therefore been chosen. Cultures grown on a Difco potato dextrose agar were found to give the best yields of pigment, which appeared as sheaves of bright orange needles in the mycelial exudate and in the surrounding medium.

When pigment yield appeared optimal by visual inspection, the cultures were harvested, freeze-dried, and defatted with petroleum ether. The extract yielded a pale yellow thermolabile oil with an infrared spectrum characteristic of a triglyceride ester. The pigment was extracted from the residue by repeated leaching with chloroform at room temperature in the dark, since in solution it is thermolabile and photosensitive. The extracts, upon careful concentration, gave an orange-red microcrystalline solid in a yield of 4% of the total dry weight of mycelium and agar. Paper chromatographic examination suggested that the pigment contained only a single component. Recrystallization from hot solvents usually resulted in gel formation but analytically pure samples, which decomposed slowly when heated above 180° C, were obtained by concentrating cold chloroform solutions as in the initial extraction. Recrystallization by concentrating cold ethereal solutions frequently gave a dimorphic form as short orange-brown rods which decomposed slowly above 200° C and which could be converted to the orange-red modification by recrystallization from chloroform.

Mycochrysone was found to inhibit the two Gram-positive bacteria *Bacillus subtilis* and *Staphylococcus aureus* but showed no activity against a typical Gram-negative bacterium (*Escherichia coli*), a yeast (*Candida albicans*), or a filamentous fungus (*Penicillium roqueforti*).

Determinations of molecular weight by the Rast method were unsatisfactory owing to decomposition of the pigment, but a value of 370 was obtained by isothermal distillation (4). This was in good agreement with values of 358 and 367 for the reduction equivalent obtained by measuring hydrogen uptake over palladized asbestos. Tests for

[1]*Manuscript received January 2, 1959.*
Contribution from the National Research Council of Canada, Prairie Regional Laboratory, Saskatoon, Saskatchewan.
Issued as N.R.C. No. 5080.
[2]*National Research Council of Canada Postdoctorate Fellow, 1957–1959.*
[3]*Present address: Biochemical Research Section, Lederle Laboratories Division, American Cyanamid Company, Pearl River, New York.*

nitrogen, halogens, and sulphur were negative, and elemental analyses best fitted a formula of $C_{20}H_{14}O_7$. No C- or O-methyl groups were detected; a Zerewitinoff determination corresponded to 2.66 active hydrogens per mole.

In concentrated sulphuric acid, a deep blue solution was formed. Dilution with water precipitated an amorphous dark red solid, distinct from the original pigment, which could not be crystallized and appeared heterogeneous when chromatographed on paper. A similar product was deposited after a few minutes from the orange-red solution given by the pigment in cold concentrated hydrochloric acid, or on warming an alcoholic solution with dilute mineral acid. Since no reducing sugars could be detected after the latter treatment, the pigment is not a simple glycoside. Mycochrysone dissolved readily in aqueous alkali to form a purple solution. It could be recovered unchanged when precipitated with acetic acid after a short interval in sodium bicarbonate but above pH 9 degradation was rapid. Prolonged exposure in solution to even slightly alkaline conditions (pH 7.2) caused extensive decomposition. The product formed was heterogeneous and has not been investigated further.

Solutions of mycochrysone were reduced by sodium hydrosulphite or zinc and dilute acid. The uptake of 1 mole of hydrogen over palladium catalyst was rapid and when the leuco compound so formed was reoxidized by exposure to air, the original pigment was regenerated. The recovery was not quantitative. This readily reversible reduction, together with positive ethylenediamine and indole tests (11), indicates that a quinone group is present. With titanium trichloride a methanolic solution of mycochrysone gave a violet color which faded to a violet-brown; in methanol containing pyridine a red-brown color was obtained after shaking and subsequently a brown precipitate formed. Such reactions are shown by 1,2-quinones and by 1,4-quinones with a hydroxyl group in either the 2-position or *peri* to one of the quinone carbonyls (17). An inconclusive Craven test (7) was obtained, but the purple and brown color with boroacetic anhydride and ferric chloride, respectively, provide evidence for a *peri*-hydroxyl group in the chromophore. The boroacetate derivative could not be isolated, and it appeared to be degraded when allowed to stand in the reaction medium. With methanolic lead acetate the pigment formed a purple precipitate, suggesting that a second, more acidic group is also present. This is supported by the solubility in bicarbonate, a property not associated with chelated *peri*-hydroxyl groups. Although an accurate pK value for this group could not be obtained because of the instability of the pigment in alkali, the pH of a solution in 80% methanol after rapid neutralization with 0.5 moles of alkali was 7.75. Since this would represent a minimum value for the pK_1 of the most acidic hydroxyl, the group is too weakly ionized to be a 2-hydroxy-1,4-quinone but must be activated to some extent. Brockmann and Muxfeldt (3) report a pK of 4.65 and 4.8 for lawsone and despeptidoactinomycin, respectively, in 50% dimethylformamide, while Schwarzenbach and Suter (13) give pK's of 2.73 and 5.18 for 2,5-dihydroxybenzoquinone in water. Under very mild conditions the pigment gave a yellow-brown quinoxaline, $C_{26}H_{18}O_5N_2$, decomposing above 229° C. Considered with the absence of a strongly dissociated acidic group in the molecule the ease with which this reaction occurred suggested that an *o*-quinone, and not a 2-hydroxy group adjacent to a quinonoid carbonyl, was present.

Zinc dust reduction gave only traces of volatile material. Better yields were achieved by fusion with zinc dust in a zinc chloride – sodium chloride eutectic mixture (6). The products were partially separated by chromatography on alumina and the major fraction found to be perylene, obtained in a yield of 13%. A second component with a typical phenanthrene absorption spectrum was shown to be identical with an authentic sample

Can. J. Chem. Downloaded from www.nrcresearchpress.com by 190.90.36.8 on 09/04/12
For personal use only.

of hexahydroperylene. This ultraviolet evidence has been used previously by Hua-chih and Conrad-Billroth (10) to show that the hydroperylene has structure I but the fact appears to have been overlooked in more recent publications (5, 19). The remaining component was a volatile oil with an ultraviolet spectrum characteristic of a highly substituted naphthalene. During the preparation of authentic hexahydroperylene considerable amounts of a volatile by-product with very similar spectral properties were obtained. Analyses indicate a formula $C_{20}H_{22}$, and considering its origin there is little doubt that this is a hitherto unreported decahydroperylene. Since the bathochromic displacement of the absorption spectrum is considerably greater than that of a 1,8-disubstituted naphthalene, the compound is assigned the structure II, and it is clear that, contrary to the report of Zinke and Benndorf (18), products intermediate between octa- and tetradeca-hydroperylene are formed. Since these hydroperylenes are readily obtained from perylene by reduction, no significance is attached to their presence in the product from zinc dust fusion of the pigment. Moreover, the formation of perylene by this treatment does not restrict the carbon skeleton of the pigment to that of perylene, for under these conditions derivatives of 1,1′-dinaphthyl would also be expected to give a fully condensed ring hydrocarbon (12, 14). The possibility of naphthalene derivatives dimerizing is more remote, although, under the experimental conditions used, β-naphthoquinone did give a trace of perylene. The absence of an aromatic central ring in a perylene skeleton is suggested by the failure to obtain mellitic acid upon oxidation of the pigment with concentrated nitric acid (8).

On the basis of the above facts, the partial structure III is proposed for mycochrysone. This accommodates all of the carbon atoms and suggests a close structural relationship between the pigment and 4,9-dihydroxyperylene-3,10-quinone, isolated by Anderson and Murray from the fruiting bodies of the fungus *Daldinia concentrica* (1).

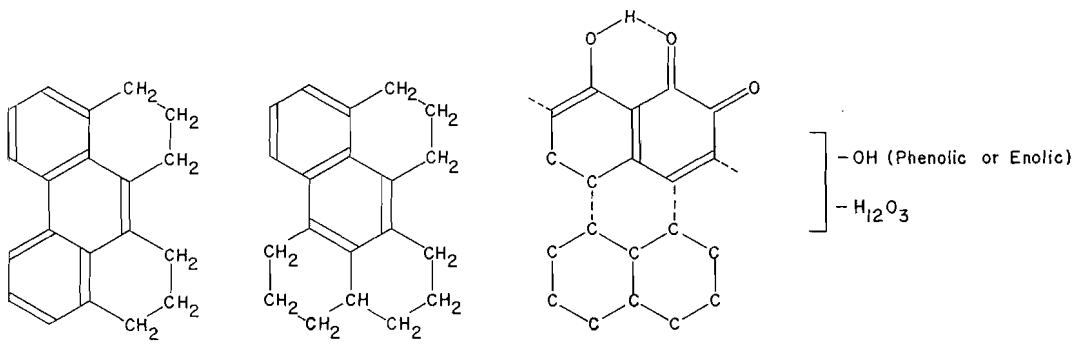

(I) (II) (III)

EXPERIMENTAL

Production

Petri dishes (9 cm diameter) containing potato dextrose agar (Difco) were inoculated at 5 to 8 well-separated points with blocks (*ca.* 0.5 cm cube) of agar and mycelium from 7-day-old cultures. Incubation was carried out for 7 days at 28° C, followed by 14 days at room temperature (20–25° C). Crystals of the pigment appeared among the dark mycelium after 7 to 10 days. On suitable liquid media, in shaken flasks, growth of the organism was more rapid and profuse, but under these conditions no mycochrysone could be detected.

Can. J. Chem. Downloaded from www.nrcresearchpress.com by 190.90.36.8 on 09/04/12
For personal use only.

Isolation

The freeze-dried mycelium and agar (143 g) from 160 plates were macerated in a Waring blendor with petroleum ether (1 liter) and the mixture kept for 12 hours at room temperature before filtering. The solvent was then evaporated to give a pale yellow oil (1.7 g) which decomposed on attempted distillation at 90° C at 0.05 mm.

Analar chloroform (3 liters) was added to the residue and the suspension was kept in the dark for 3 days at room temperature. The orange solution was filtered and concentrated to about 700 ml on a rotary evaporator to precipitate the pigment as orange microcrystalline needles. The extraction was repeated and the filtrate was added to the initial concentrate and again evaporated to about 700 ml. After the mixture had been left to stand at 4° C overnight the product (4.27 g) was filtered off and dried (100° C, high vacuum). On treatment of the residual mycelium and agar with a further 6 liters of chloroform in two extractions, as above, an additional 1.48 g of pigment was obtained.

Prepared in this way the pigment gave a single zone (R_f 0.60) when examined by circular chromatography on formamide-treated paper with chloroform as mobile phase. It was considered sufficiently pure for most experiments. After two crystallizations from chloroform by the same technique used in the initial isolation, the pigment decomposed slowly above 180° C. Found: C, 65.31, 65.67, 65.74; H, 3.82, 4.08, 3.68; active hydrogen (Zerewitinoff) 0.72%; no nitrogen, halogen, methoxy, or terminal methyl. Calculated for $C_{20}H_{14}O_7$: C, 65.57; H, 3.85; 3 active hydrogens, 0.82%. Ultraviolet absorption in ethanol λ_{max} 236, 307, and 438 mμ; log ϵ 4.50, 3.62, and 3.78, respectively.

The purified pigment was soluble in methanol, ethanol, and acetone, fairly soluble in benzene, chloroform, ether, and water, but insoluble in petroleum ether or carbon disulphide.

Quinoxaline

o-Phenylenediamine (200 mg) in ethanol (15 ml) was added to a solution of the pigment (100 mg) in hot ethanol (25 ml) and the reactants refluxed for 15 minutes. The quinoxaline separated after a few minutes as brown prisms, decomposing slowly above 223° C. Two recrystallizations from ether gave the product as yellow-brown prisms decomposing slowly above 229° C. Found: C, 71.11; H, 3.87; N, 6.05%. Calculated for $C_{26}H_{18}O_5N_2$: C, 71.22; H, 4.14; N, 6.39%.

Attempts to prepare analytical samples of this derivative from methanolic solutions invariably gave a product with a lower decomposition point (from 210° C). Such samples gave lower values on analysis for C, H, and N, and it is concluded that under these conditions a small amount of oxidative degradation takes place.

When a methanolic solution containing mycochrysone and an excess of *o*-phenylenediamine, or an ethereal solution of the reactants together with anhydrous sodium sulphate, was kept for 12 hours at room temperature (2), it was shown by paper chromatography using formamide-treated paper and benzene as mobile phase that mycochrysone (R_f 0.05) had been completely converted to the quinoxaline (R_f 0.50).

Molecular Weight Determinations

Isothermal distillation in acetone solution at 45° C using cholesterol as a standard gave a value of 370 for the molecular weight. The experiment was carried out in the dark. Microhydrogenations using 5% palladium–asbestos catalyst in ethanol at room temperature and atmospheric pressure showed a rapid uptake of hydrogen corresponding to reduction equivalents of 358 and 367. Under these conditions a further slow reduction took place.

Can. J. Chem. Downloaded from www.nrcresearchpress.com by 190.90.36.8 on 09/04/12
For personal use only.

Antibiotic Properties

Activity against bacteria and fungi was tested using the streak-dilution assay (15) on Waksman's glucose-broth supplemented agar (16). A stock solution containing 1 mg/ml of mycochrysone was prepared in 50% aqueous ethanol. Subsequent dilutions were made in sterile distilled water and aliquots of the suspension were mixed immediately with the cooled but still molten agar to give a range of final concentrations. Suspensions of the test organisms were streaked over the surface of the agar plates. *Staphylococcus aureus* v. *pyogenes* (PRL M2), *Bacillus subtilis* (PRL R2), *Escherichia coli* (PRL B44), and *Candida albicans* (ATCC 10231) were incubated at 37° C. Complete suppression of growth was obtained with the *Staphylococcus* at 5 μg/ml and with the *Bacillus* at 15 μg/ml. The remainder of the organisms and *Penicillium roqueforti* (PRL 1763), which was incubated at 28° C, were not inhibited at the highest concentrations tested (100 μg/ml). Controls included in the assay demonstrated that inhibition was not due to solvent toxicity.

Zinc Chloride – Zinc Dust Fusion (Typical Run)

A stirred solution of mycochrysone (49 mg) in acetone (5 ml) and zinc dust (1 g) was evaporated to dryness by an air stream so that a fine precipitate of the pigment adhering to the zinc was obtained.

Zinc dust (3.5 g) was stirred into a melt of zinc chloride (4.0 g) and sodium chloride (0.8 g). On cooling, the mass was broken up, ground into a fine powder, and divided into two equal portions. One was intimately mixed with the pigment-coated zinc and added in equal portions to five small test tubes. The second half of the melt was divided similarly, placed on top of the first layer, and tamped firmly down.

The reactants were heated at 210° C for 4 minutes and subsequently at 310° C for 5 minutes. The froth formed on top of the melts during the heating was dispersed with glass rods. On cooling, the zinc and zinc chloride were dissolved in hot, dilute hydrochloric acid. The aqueous suspension was extracted with benzene (4×100 ml) and the extract evaporated to dryness, redissolved in petroleum ether – benzene (95:5), and chromatographed on a column (7×1.5 cm) of alkaline alumina (Brockmann Grade I). Two fluorescent fractions were collected, the first eluted with petroleum ether – benzene (95:5), and the second with petroleum ether – benzene (50:50). The second fraction was evaporated to dryness and sublimed in high vacuum to give perylene (4.4 mg, 13%), m.p. 272–274° C, undepressed on admixture with an authentic sample. Found: C, 95.44; H, 4.85%. Calc. for $C_{20}H_{12}$: C, 95.21; H, 4.79%.

The first fraction was found to contain a mixture of an oil and a solid. The products from several fusions were combined and sublimed. The solid fraction was separated from the oil by trituration with petroleum ether and purified by a further sublimation (110° C at 0.01 mm). The compound, m.p. 176–182° C (softening at 168° C), gave ultraviolet and infrared spectra indistinguishable from an authentic sample of hexahydroperylene (m.p. 178–184° C), and the melting point on admixing the two compounds showed no depression.

β-Naphthoquinone (50 mg) under the same conditions gave perylene (0.14 mg, 0.35%).

Decahydroperylene

Perylene (100 mg) was reduced in a benzene and alcohol solution with sodium (1 g). The conditions differed from those employed by Zinke and Benndorf (19) only in that the reaction was completed in 45 minutes. Chromatography of the product on a column (8×1.4 cm) of cationotropic alumina (Brockmann Grade I) gave the following fractions:

Can. J. Chem. Downloaded from www.nrcresearchpress.com by 190.90.36.8 on 09/04/12
For personal use only.

(*a*) Petroleum ether eluate. Colorless oil (b.p. 110° C at 0.02 mm) (59 mg). Found: C, 91.44; H, 8.39%. Calc. for $C_{20}H_{22}$: C, 91.55; H, 8.45%. Ultraviolet absorption spectrum shows λ_{max} 240, 265, 274, and 299 mμ; log ϵ 4.52, 3.38, 3.41, and 3.40, respectively.

(*b*) Petroleum ether – benzene (98:2) octahydroperylene (8 mg).

(*c*) Petroleum ether – benzene (95:5) hexahydroperylene (7 mg), m.p. 178–184° C.

ACKNOWLEDGMENTS

The authors wish to express their appreciation to Dr. O. Vaartaja, Forest Pathology Laboratory, Canada Department of Agriculture, Saskatoon, Saskatchewan, for the culture of the fungus under study which was received February 12, 1953, and to Dr. W. A. Taber of this laboratory for determining the antimicrobial activity of mycochrysone.

REFERENCES

1. ANDERSON, J. M. and MURRAY, J. Chem. & Ind. 376 (1956).
2. ANSLOW, W. K. and RAISTRICK, H. Biochem. J. **32**, 687 (1938).
3. BROCKMANN, H. and MUXFELDT, H. Chem. Ber. **89**, 1379 (1956).
4. CHILDS, C. E. Anal. Chem. **26**, 1963 (1954).
5. CLAR, E. Aromatische Kohlenwasserstoffe. Springer-Verlag. 1952. p. 284.
6. CLAR, E. Chem. Ber. **72**, 1645 (1939).
7. CRAVEN, R. J. Chem. Soc. 1605 (1931).
8. DUEWELL, H., JOHNSON, A. W., MACDONALD, S. F., and TODD, A. R. J. Chem. Soc. 485 (1950).
9. HASKINS, R. H., SHU, P., and VINING, L. C. Paper presented before the Botanical and Mycological Societies of America at Storrs, Connecticut. 1956.
10. HUA-CHIH, C. and CONRAD-BILLROTH, H. Z. physik. Chem. **20**, 333 (1933).
11. KARIUS, H. and MAPSTONE, G. E. Chem. & Ind. 266 (1956).
12. MARSCHALK, C. Bull. soc. chim. [4] **43**, 1388 (1928).
13. SCHWARZENBACH, G. and SUTER, H. Helv. Chim. Acta, **24**, 617 (1941).
14. THOMAS, D. G. and NATHAN, A. H. J. Am. Chem. Soc. **70**, 331 (1948).
15. WAKSMAN, S. A. and REILLY, H. C. Ind. Eng. Chem., Anal. Ed. **17**, 556 (1945).
16. WAKSMAN, S. A. The actinomycetes. Chronica Botanica Co., Waltham, Mass. 1950. p. 195.
17. WEYGAND, F. and CSENDES, E. Chem. Ber. **85**, 45 (1952).
18. ZINKE, A. and BENNDORF, O. Monatsh. Chem. **59**, 241 (1932).
19. ZINKE, A. and BENNDORF, O. Monatsh. Chem. **64**, 87 (1934).

Can. J. Chem. Downloaded from www.nrcresearchpress.com by 190.90.36.8 on 09/04/12
For personal use only.

Can. J. Chem. Downloaded from www.nrcresearchpress.com by 190.90.36.8 on 09/04/12
For personal use only.

THEORY OF THE TRANSIENT PHASE IN AN ENZYME SYSTEM INVOLVING TWO ENZYME–SUBSTRATE COMPLEXES

THE CASE OF THE FORMATION OF PRODUCTS FROM THE FIRST COMPLEX[1]

LUDOVIC OUELLET[2] AND JAMES A. STEWART[3]

ABSTRACT

A theoretical treatment is worked out for the kinetic scheme

$$\begin{matrix} E + S \rightleftarrows ES_1 \rightarrow ES_2 + P_1 \\ ES_2 \rightarrow E + P_2 \end{matrix}$$

in which the concentration of P_1 is followed. The steady-state and transient phase equations are obtained subject to the condition that the substrate concentration is greatly in excess of the enzyme concentration. The conditions under which evidence in favor of this mechanism can be obtained from experimental data are discussed. Under certain conditions, the weight of the enzyme corresponding to one active site can be determined. Methods for the evaluation of the different constants are described.

INTRODUCTION

The description of the transient phase of an enzyme–substrate system in cases involving one enzyme–substrate complex or two consecutive enzyme–substrate complexes with products appearing as a result of the decomposition of the last complex has been given previously (1, 2). In certain cases, such as the hydrolysis of esters by chymotrypsin (3) or by trypsin (4), there are indications that the release of products involves two steps, one for the release of the alcohol and one for the release of the acid. Following the rate of appearance of the first-appearing product is often possible (if the alcohol is a phenol, for example, and can be determined colorimetrically), and could provide additional useful information on the mechanism of the reaction. The purpose of this paper will be to discuss such a case in more detail than has been done previously (5).

THEORY

Let us consider the system

$$\underset{e_0-y_1-y_2}{E} + \underset{s_0}{S} \underset{k_{-1}}{\overset{k_1}{\rightleftharpoons}} \underset{y_1}{ES_1} \xrightarrow{k_2} \underset{y_2}{ES_2} + \underset{p_1}{P_1}$$

$$\underset{y_2}{ES_2} \xrightarrow{k_3} E + \underset{p_2}{P_2}.$$

In most cases the concentration of the substrate s_0 is much larger than the concentration of the enzyme e_0, so that s_0 can be considered constant during the transient phase. The following differential equations describe the system:

$$[1] \qquad \dot{y}_1 = k_1 s_0 (e_0 - y_1 - y_2) - (k_{-1} + k_2) y_1,$$

$$[2] \qquad \dot{y}_2 = k_2 y_1 - k_3 y_2,$$

[1]*Manuscript received August 22, 1958.*
Contribution from the Chemistry Department, the University of Ottawa, Ottawa, Canada.
[2]*Present address: Université Laval, Quebec, Canada.*
[3]*Present address: Laboratories of the Food and Drug Directorate, Department of National Health and Welfare, Ottawa, Canada.*

[3] $$\dot{p}_1 = k_2 y_1,$$

[4] $$\dot{p}_2 = k_3 y_2.$$

Steady State

The steady state equations are obtained by setting $\dot{y}_1$ and $\dot{y}_2$ equal to zero. This leads to

[5] $$\dot{p}_1 = \dot{p}_2 = \frac{k_1 k_2 k_3 e_0 s_0}{k_1 s_0 (k_2 + k_3) + k_3 (k_{-1} + k_2)}$$

which can be reduced to the following classical form of Michaelis and Menten (6)

[6] $$\dot{p}_1 = \frac{V s_0}{K'_m + s_0}$$

where V, the maximum rate is given by

[7] $$V = \frac{k_2 k_3 e_0}{k_2 + k_3}$$

and K'_m, the experimental Michaelis constant is

[8] $$K'_m = \frac{k_3}{k_2 + k_3} \frac{k_{-1} + k_2}{k_1}.$$

It should be noticed that if $k_3 \gg k_2$, the complex ES_2 exists only in very small amounts and the steady state description of the system is given by

[9] $$V = k_2 e_0$$

[10] $$K'_m = (k_{-1} + k_2)/k_1 = K_m$$

corresponding to the case of a single complex.

Transient Phase

Eliminating y_2 between equations [1] and [2] leads to

[11] $$\ddot{y}_1 + (k_1 s_0 + k_{-1} + k_2 + k_3)\dot{y}_1 + [k_1 s_0 (k_2 + k_3) + k_3 (k_{-1} + k_2)] y_1 - k_1 k_3 e_0 s_0 = 0,$$

which can be written as

[12] $$\ddot{y}_1 + P\dot{y}_1 + Q y_1 - R = 0.$$

It has been shown previously (2) that the case $P^2 - 4Q < 0$, leading to periodic solutions, is not particularly interesting because the period is longer than the transient phase. In the cases where $P^2 - 4Q > 0$, the solution of equation [12] is

[13] $$y_1 = (R/Q) + M e^{Ft} + N e^{Gt}$$

where

[14] $$F = \tfrac{1}{2}[-P + \sqrt{(P^2 - 4Q)}]$$

[15] $$G = \tfrac{1}{2}[-P - \sqrt{(P^2 - 4Q)}]$$

and M and N are constants to be determined from the boundary conditions that at time zero, $y_1 = 0$ and $\dot{y}_1 = k_1 e_0 s_0$.

This leads to the following values for M and N

[16] $$M = -(R/Q) \frac{k_3 G + Q}{k_3 (G - F)},$$

Can. J. Chem. Downloaded from www.nrcresearchpress.com by 190.90.36.8 on 09/04/12
For personal use only.

[17] $$N = (R/Q)\frac{k_3F+Q}{k_3(G-F)}.$$

Inserting the value of y_1 into equation [3] and integrating one obtains for the value of p_1 as a function of time

[18] $$p_1 = \frac{k_2Rt}{Q}+\frac{k_2M}{F}(e^{Ft}-1)+\frac{k_2N}{G}(e^{Gt}-1).$$

When t is sufficiently large, so that the terms e^{Ft} and e^{Gt} become negligible (F and G are always negative),

[19] $$p_1 = \frac{k_2Rt}{Q}-\frac{k_2M}{F}-\frac{k_2N}{G}.$$

It is evident that equation [19] is the proper integrated form of equation [5] for an open system in which s_0 is maintained constant.

A qualitative plot of the function represented by equation [18] is shown in Fig. 1. The initial exponential rise is due to the term $(k_2N/G)(e^{Gt}-1)$ of the expression. The approach to steady state, with decreasing rate is due to $(k_2M/F)(e^{Ft}-1)$. The relative magnitudes of these two terms depend on the relative magnitudes of F and G. As all the quantities involved are positive, G will usually be larger than F, and e^{Gt} will approach 0 more rapidly than e^{Ft}, whilst the coefficient of e^{Gt} containing F/G will be smaller than the coefficient of e^{Ft} containing G/F. This condition suggests that the e^{Ft} term will be easier to detect, experimentally, than the e^{Gt} term.

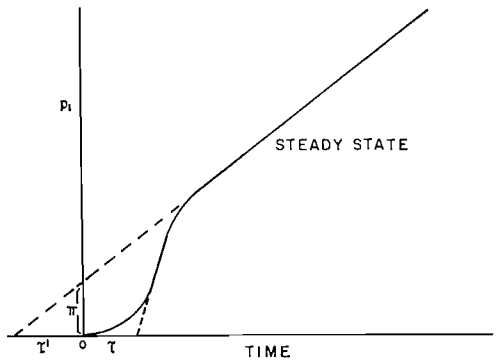

FIG. 1. Schematic plot of amount of product 1 (p_1) against time, in the general case.

The straight line obtained after steady state conditions have prevailed introduces, when extrapolated to the axes, two quantities that can be measured: τ', the intercept on the time axis, and π, the intercept of the p_1 axis.

From equation [19], which describes the steady state condition of the system, τ' can be obtained by making $p_1 = 0$, and solving for t. After substitution of the proper quantities for R, Q, M, N, and F, τ' becomes

[20] $$\tau' = \frac{k_3^2-k_1k_2s_0}{k_1k_3(k_2+k_3)(s_0+K'_m)}.$$

Two extreme cases regarding the relative magnitudes of k_2 and k_3 will be considered. In the first case, if $k_3 \gg k_2$, corresponding to only a fleeting existence of the complex ES_2, equation [20] reduces to

Can. J. Chem. Downloaded from www.nrcresearchpress.com by 190.90.36.8 on 09/04/12
For personal use only.

[21] $$\tau' = 1/k_1(s_0+K_m) - k_2 s_0/k_3^2(s_0+K_m).$$

The first part of this expression is identical with that obtained in the case where only one complex is formed (1). The second part could be considered a correction term the magnitude of which depends on the relative magnitudes of $k_1 s_0$, k_2, and k_3.

In the second extreme case where $k_2 \gg k_3$, τ' becomes

[22] $$\tau' = -s_0/k_3(s_0+K'_m) + k_3/k_1 k_2(s_0+K'_m).$$

In the second term of equation [22], k_3/k_2 is small by hypothesis. On the other hand, $1/k_1(s_0+K'_m)$ is usually very small (3). At any rate, it could be measured from the true induction period, τ, if it is not small (see Fig. 1, and equation [37]). In the cases where an induction period cannot be detected, the influence of the second term of equation [22] on τ' is negligible, as it is k_3/k_2 times an undetectably small quantity. Under those conditions, τ' becomes

[23] $$\tau' = -s_0/k_3(s_0+K'_m).$$

If enough data are available to plot $1/\tau'$ against $1/s_0$, the intercept on the $1/\tau'$ axis of the straight line obtained would give $-k_3$. The slope of the straight line obtained is K'_m, the experimental Michaelis constant obtained under steady state conditions. Since a value for $k_3 e_0$ can readily be obtained from the steady state rate of the reaction, under the condition that $k_2 \gg k_3$ (see equation [7]), a value for the concentration of the enzyme e_0 can be calculated, in moles per liter, the units of p_1. In the case of pure enzymes, e_0 can be measured directly in grams per unit volume, and one can calculate the number of grams of enzyme reacting with 1 mole of substrate to form the complex ES_2. This would give the number of active sites per molecule of enzyme if the molecular weight of the enzyme was known from other methods.

Similar information could, of course, be obtained from the intercept on the p_1 axis. According to equation [19] the extrapolated value of p_1 at $t = 0$ is

[24] $$\pi = [k_2^2 e_0 s_0^2/(k_2+k_3)^2(s_0+K'_m)^2] - k_2 k_3^2 e_0 s_0/[k_1(k_2+k_3)^2(s_0+K'_m)^2].$$

In the case $k_3 \gg k_2$, π could become negative, depending on the relative magnitudes of k_2 and $k_1 s_0$. At best it is small compared to e_0.

In the case, $k_2 \gg k_3$, π becomes

[25] $$\pi = e_0 s_0^2/(s_0+K'_m)^2 - k_3^2 e_0 s_0/k_1 k_2(s_0+K'_m)^2.$$

The second term of this expression becomes negligible unless $k_1 s_0 \ll k_3$, a somewhat improbable situation, as k_1 is usually unmeasurably large. With the condition that $k_2 \gg k_3$, π then reduces to

[26] $$\pi = e_0 s_0^2/(s_0+K'_m)^2.$$

At high concentrations of substrate, compared to K'_m, the ratio $s_0^2/(s_0+K'_m)^2$ becomes practically equal to 1 and

[27] $$\pi = e_0.$$

Hartley and Kilby (7) have reported that the extrapolation of the concentration of *p*-nitrophenol produced during the hydrolysis of *p*-nitrophenol acetate by chymotrypsin to zero time gives the molar concentration of the enzyme. Such an observation could be interpreted as evidence that chymotrypsin has but one active site.

At low concentrations of substrate compared to K'_m, similar considerations lead to somewhat more complex results that will not be discussed.

Can. J. Chem. Downloaded from www.nrcresearchpress.com by 190.90.36.8 on 09/04/12
For personal use only.

Can. J. Chem. Downloaded from www.nrcresearchpress.com by 190.90.36.8 on 09/04/12
For personal use only.

Equations [24] and [25] indicate that the intercept on the p_1 axis is very small unless k_3 is much smaller than k_2 and $k_1 s_0$. Unless these conditions are fulfilled, equation [18] is hardly of any use as the steady state is approached very rapidly and the influence of the exponential part is very small. For these reasons, a discussion of equation [18] will be limited to the cases where k_2 and $k_1 s_0$ are larger than k_3. Under these conditions

[28] $$P = k_1(s_0+K_m)$$

[29] $$Q = k_1 k_2(s_0+K'_m)$$

where K_m and K'_m are described as

[30] $$K_m = (k_1+k_2)/k_1$$

[31] $$K'_m = k_3 K_m/k_2.$$

The series development of $\sqrt{(P^2-4Q)}$ leads to

[32] $$F = -\frac{k_2(s_0+K'_m)}{s_0+K_m} - \cdots$$

[33] $$G = -k_1(s_0+K_m)+k_2(s_0+K'_m)/(s_0+K_m) - \cdots$$

A further simplification can be obtained in F and G if experimental conditions are so chosen that s_0 is much larger than K'_m. The conditions $k_2 \gg k_3$ and equation [31] imply that such conditions could be realized and still have s_0 of a magnitude comparable to K_m. This leaves

[34] $$F = -\frac{k_2 s_0}{s_0+K_m} - \cdots$$

[35] $$G = -k_1(s_0+K_m)+k_2 s_0/(s_0+K_m) - \cdots$$

Under these conditions equation [18] becomes

[36] $$p_1 = \pi+k_3 e_0 t+k_2(M/F)\exp[-k_2 s_0/(s_0+K_m)]t + k_2(N/G)\exp[-k_1(s_0+K_m)+k_2 s_0/(s_0+K_m)]t.$$

At the very beginning of the reaction, the second exponential will have a retarding effect on the appearance of the product P_1. Figure 2 is a theoretical plot of p_1 as a function of time according to equation [18]. It is obtained by assuming that $s_0 \gg K_m$ and assigning values of 100, 10, and 1 to $k_1 s_0$, k_2, and k_3 respectively. Under these conditions $F = -11.3$ and $G = -99.8$, which justifies, in part, the assumption that under the present conditions F and G can be approximated to the values given by equations [34] and [35].

The short induction period indicated in Fig. 2 can be calculated by expanding $\exp[(-k_2 s_0/(s_0+K_m)]t$ in series and taking the first two terms only, since t is small at the beginning of the reaction. The extrapolation to $p_1 = 0$ of the curve obtained when $\exp[-k_1(s_0+K_m)]t$ is negligibly small gives

[37] $$\tau = 1/k_1(s_0+K_m).$$

In cases where both a measurable π, interpreted according to equation [25], and a measurable τ, interpreted according to equation [37] appear, values for both k_1 and k_2 can be obtained. Such cases are unknown, as far as we know. In the known cases where the mechanism described here could apply, the induction period is unmeasurably small (3). Such behavior implies that $\exp(Gt)$ is unmeasurably small even at the beginning of the reaction. Under such conditions, equation [35] becomes, assuming $k_2 \gg k_3$,

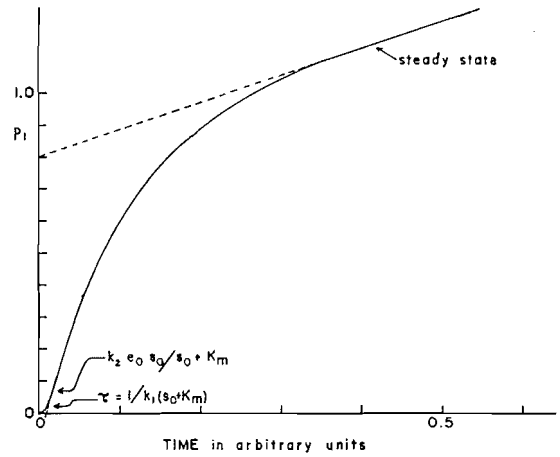

FIG. 2. Theoretical plot of p_1 as a function of time assuming $s_0 \gg K_m$ and $k_1 s_0 = 100$, $k_2 = 10$, $k_3 = 1$ $k_{-1} = 0.1$. The ordinate p_1 is in enzyme concentration units.

$$[38] \qquad p_1 = e_0 + k_3 e_0 t - e_0 \exp[-k_2 s_0/(s_0 + K_m)]t.$$

If a physical property proportional to p_1 can be measured, k_2 and K_m can be evaluated from the values of $k_2 s_0/(s_0 - K_m)$ at different concentrations of substrate, using the Guggenheim technique (8).

At the beginning of the reaction, the series development of the exponential part of equation [38] would give a good approximation of the function. From equation [38], one can then describe the initial rate of production of the first appearing product, P_1, by,

$$[39] \qquad p_1 = [k_3 + k_2 s_0/(s_0 + K_m)]e_0 t.$$

The smaller k_3 becomes, compared to k_2, the better the approximation. Values for k_2 and K_m can be obtained from initial rate data using the ordinary techniques of enzyme kinetics (9). In so doing, one assumes that the concentration ES_1 is in a steady state right at the beginning of the reaction while the concentration of ES_2 reaches a steady state sometime later.

RÉSUMÉ

Une discussion théorique de la cinétique, dans le cas de réactions enzymatiques, d'une réaction du type

$$E + S \rightleftharpoons ES_1 \rightarrow ES_2 + P_1$$
$$ES_2 \rightarrow E + P_2$$

est présentée. Différentes situations expérimentales sont analysées en termes des simplifications qu'elles apportent et des renseignements qu'elles donnent sur le système. L'analyse du système permet de justifier la détermination des constantes cinétiques et en certains cas de donner une approximation de la masse de l'enzyme par site actif, si le mécanisme proposé ci-haut est appuyé par des données expérimentales suffisantes.

ACKNOWLEDGMENTS

We wish to acknowledge with thanks the continued financial support from the National

Can. J. Chem. Downloaded from www.nrcresearchpress.com by 190.90.36.8 on 09/04/12
For personal use only.

Research Council of Canada. We are indebted to Mr. G. E. Pelletier, who suggested several modifications to the present text.

REFERENCES

1. LAIDLER, K. J. Can. J. Chem. **33**, 1614 (1955).
2. OUELLET, L. and LAIDLER, K. J. Can. J. Chem. **34**, 146 (1956).
3. HARTLEY, B. S. and KILBY, B. A. Biochem. J. **50**, 672 (1952).
4. STEWART, J. A. and OUELLET, L. Can. J. Chem. **37**, 751 (1959).
5. GUTFREUND, H. and STURTEVANT, J. M. Biochem. J. **63**, 656 (1956).
6. MICHAELIS, L. and MENTEN, M. L. Biochem. Z. **49**, 333 (1913).
7. HARTLEY, B. S. and KILBY, B. A. Biochem. J. **65**, 288 (1954).
8. GUGGENHEIM, E. A. Phil. Mag. **2**, 538 (1926).
9. LINEWEAVER, H. and BURK, D. J. Am. Chem. Soc. **56**, 658 (1934).

Can. J. Chem. Downloaded from www.nrcresearchpress.com by 190.90.36.8 on 09/04/12
For personal use only.

Can. J. Chem. Downloaded from www.nrcresearchpress.com by 196.1.178.254 on 09/04/12
For personal use only.

A STOPPED-FLOW MIXING DEVICE FOR THE SPECTROPHOTOMETRIC STUDY OF RAPID REACTIONS[1]

JAMES A. STEWART[2] AND LUDOVIC OUELLET[3]

ABSTRACT

A simplified stopped-flow mixing device, which has been adapted to a Beckman DU spectrophotometer, is described. Removable storage syringes are used to inject the required solutions into the apparatus, while the operations of filling the reaction syringes, mixing the reactants, or standardization are achieved with T-bore stopcocks. Provision has been made in the design for interchangeable mixing chambers and observation cells. The temperature is controlled by circulating water through a suitable enclosure surrounding the reaction syringes. A zero-suppression method has been devised to record the extent of reaction.

The transient phase kinetics of several enzyme systems has been described from the experimental and theoretical point of view by Chance (1, 2, 3, 4, 5, 6, 7, 8), Beers (9, 10, 11), Gutfreund (12, 13, 14, 15, 16), and Laidler (16, 17). This type of investigation, which provides useful information not obtainable from steady state kinetics, has not been fully utilized probably because of the complex experimental technique. Therefore, this paper will attempt to develop a simplified technique for the study of transient phase kinetics employing the stopped-flow apparatus along the lines of other workers (1, 4, 5, 6, 11, 18, 19, 20, 21).

APPARATUS

A block diagram of the apparatus is shown in Fig. 1. A Beckman Model DU spectro-

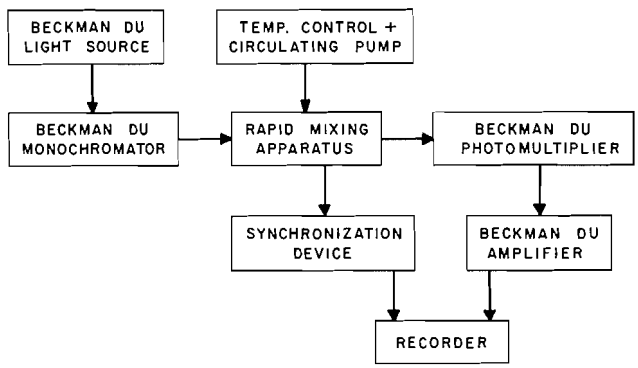

FIG. 1. Block diagram of the apparatus.

photometer equipped with a photomultiplier attachment and recording adapter (#5800) was used. The time constant of the circuit was decreased by altering the load resistance on the photomultiplier cell from 22 meg and 0.01 μf to 0.68 meg and 0.002 μf. The 510-ohm output resistor of the Beckman recording adapter was replaced with a 750-ohm potentiometer, so that the output impedance or sensitivity could be varied.

[1]*Manuscript received August 22, 1958.*
Contribution from the Department of Chemistry, University of Ottawa, Canada.
[2]*Present address: Laboratories of the Food and Drug Directorate, Department of National Health and Welfare, Ottawa, Canada.*
[3]*Present address: Department of Chemistry, Laval University, Quebec, Quebec.*

Stopped-flow Mixing Apparatus

The stopped-flow method was originally conceived by Chance (1) for the rapid mixing of enzyme and substrate. The apparatus to be described is in principle the same, but such features as a plunger-release mechanism, standardization, temperature control, magnetic stopcock at the outlet, the use of rubber "O" ring seals, removable storage syringes, and interchangeable observation tubes and mixing chambers have been added for greater ease in operation and construction.

The details of the apparatus, which is illustrated in Fig. 2, are as follows. The 1-ml

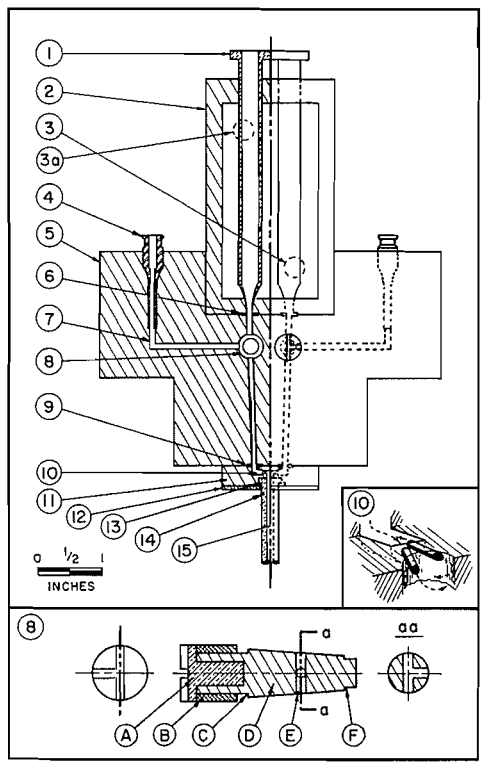

FIG. 2. The stopped-flow mixing apparatus.

reaction syringes "1" are held in the plexiglass enclosure "2" which acts as a constant-temperature bath, fitted with water inlet "3" and outlet "3*A*". The reaction syringes are filled from removable storage syringes located on hypodermic needles "4" embedded in the plexiglass section "5". The lower insert in Fig. 2 gives the details of the T-bore plug of the stopcock "8", which connects the veins "7" from storage syringe to reaction syringe, reaction syringe to mixing chamber, or storage syringe to mixing chamber. The T-slotted head of brass core "*A*" is positioned to coincide with T-bore "*E*" to aid in the alignment of the bore with the veins. An aluminum sleeve "*B*" secures the plexiglass plug "*D*" to brass core "*A*". External leakage of liquid is prevented by rubber "O" ring seals located at "*C*" and "*F*", which are held in position by pressure plates (not illustrated).

A three-dimensional sketch of the mixing chamber "10" is shown in the right-hand insert of Fig. 2. Here, each reactant enters through a pair of 0.5-mm jets that are located

Can. J. Chem. Downloaded from www.nrcresearchpress.com by 196.1.178.254 on 09/04/12
For personal use only.

between the tangent and diameter of the chamber and diagonal to each other (19). The mixed reactants pass into the observation cell "15" where the change in absorbance is measured photoelectrically. The present 2-mm observation cell is constructed of plexiglass, but provision has been made in the design for the use of quartz or pyrex observation tubes. These will be sealed in the plexiglass block "11" by a rubber O ring and pressure plate "12".

The plexiglass sections "2", "5", and "11" are fastened together with vertical screws,

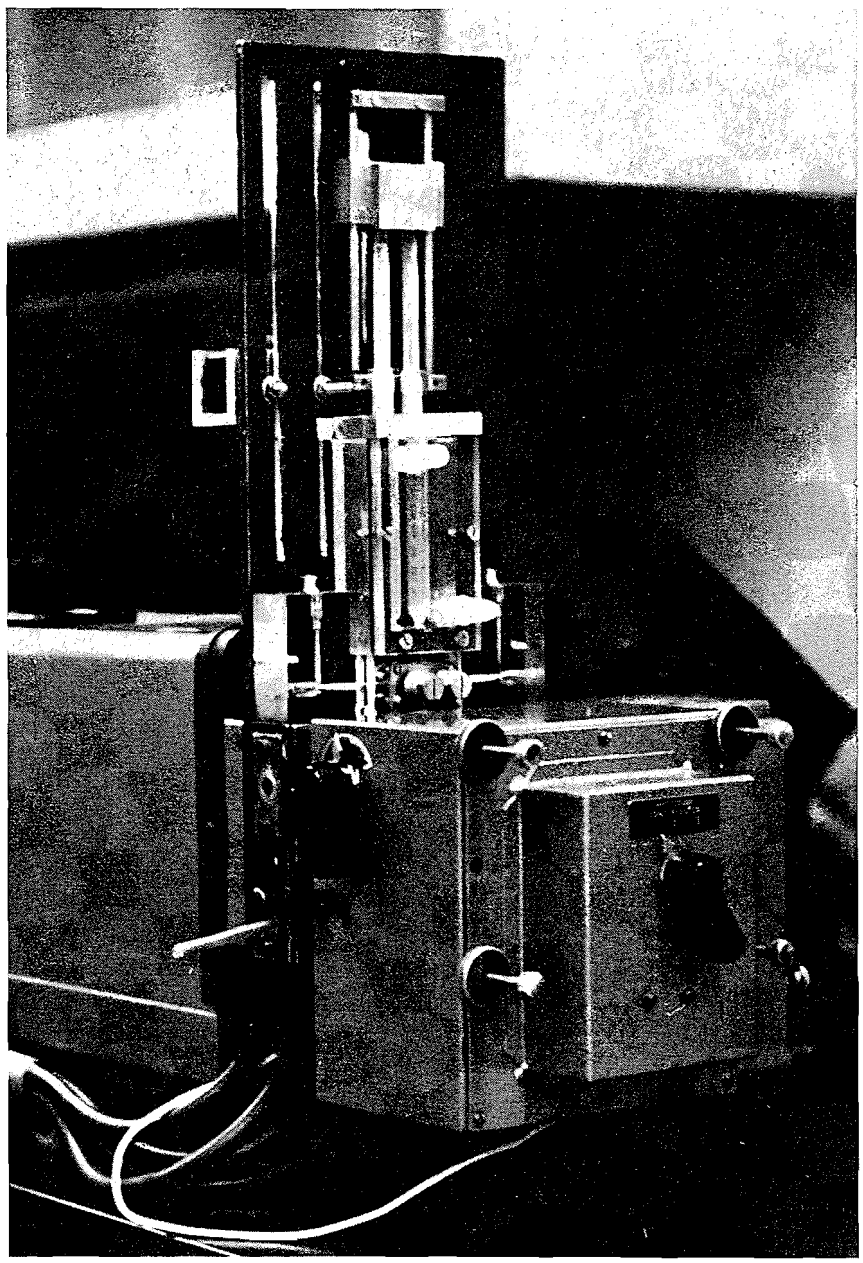

FIG. 3. The stopped-flow apparatus mounted in the Beckman DU.

Can. J. Chem. Downloaded from www.nrcresearchpress.com by 196.1.178.254 on 09/04/12
For personal use only.

and external leakage at the joins is prevented by rubber "O" ring seals at "6" and "9". The apparatus is attached to an aluminum plate which replaces the cell compartment of a Beckman DU spectrophotometer as illustrated in Fig. 3. This aluminum plate also supports the plunger and synchronization mechanism.

Plunger Holder and Release Mechanism

Equal portions of two reactants are driven manually from the reaction syringes into the observation cell by the mechanism shown in Fig. 4. A track consisting of two vertical rods carries a brass block that drives the plungers. A plunger-release plate restrains the

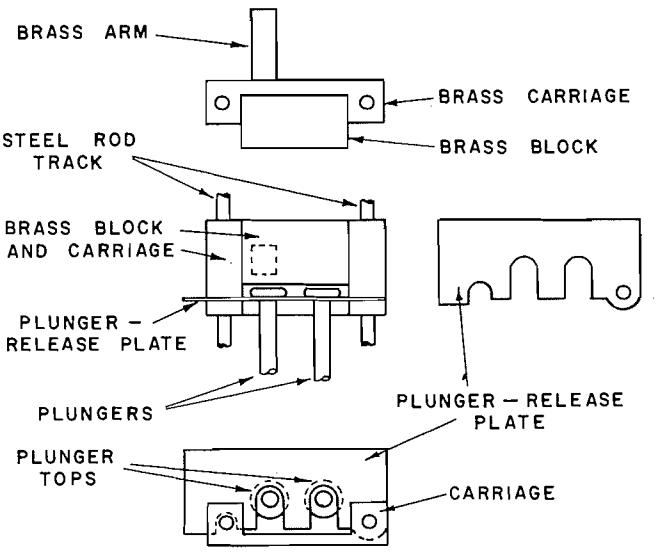

FIG. 4. The plunger holder and release mechanism.

downward motion of the plungers, and is hinged to one side of the track so that the plungers may be freed. This allows the reaction syringes to be filled by pressure from the storage syringes, or the plungers to be removed for the elimination of residual air by completely filling the syringes.

Synchronization Mechanism

The synchronization mechanism in Fig. 5 is used to synchronize the events of stopped

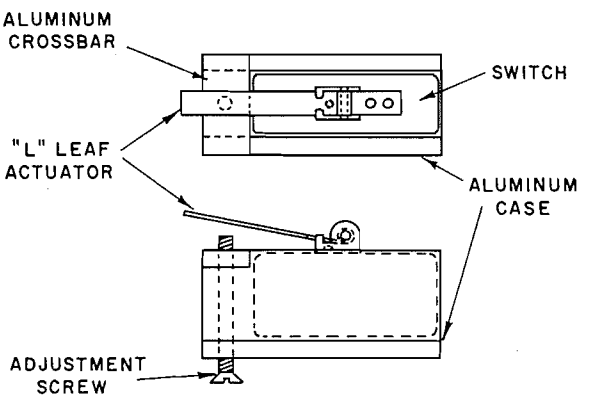

FIG. 5. The synchronization mechanism.

Can. J. Chem. Downloaded from www.nrcresearchpress.com by 196.1.178.254 on 09/04/12
For personal use only.

flow and the beginning of recording. This is accomplished by a brass arm on the carriage of the plunger mechanism (Fig. 4), which actuates the "L" leaf of a snap-action switch when it reaches the crossbar of the case surrounding the switch (Fig. 5). Synchronization is adjusted by a screw located in this cross bar.

In the "on" position the switch applies an electrical potential to initiate the sweep circuit of a cathode-ray oscillograph, the chart drive of a pen recorder, or the operation of a time-marker device. In the case where more than one potential is to be synchronized a fast acting four-pole-double-throw relay is incorporated in the circuit.

Temperature Control

Water from a thermostated bath capable of control to $\pm 0.1°$ C is circulated through the enclosure around the reaction syringes, Beckman thermospacers, and the lamp housing of the spectrophotometer.

Recorders

The cathode-ray oscillograph, the pen oscillograph, and the high-speed strip-chart recorder are all suitable for studying rapid reactions, each having its own particular advantage. The cathode-ray oscillograph is useful when a response of <0.01 second is required, while the pen oscillograph could be recommended above this range because of the direct-writing feature. In the case of certain reactions, which have been studied in this laboratory, the high-speed strip-chart recorder with a response of 0.25 second for a 10-inch deflection was found to be sufficient.

MODE OF OPERATION

Reactants kept in a constant temperature bath are transferred to the reaction syringes by means of suitable storage syringes. The reaction is recorded by manually driving the plunger mechanism, which forces the reactants into the mixing chamber and the observation cell. When the flow stops, a synchronized recorder produces the reaction trace.

The following zero suppression method was found to achieve the sensitivity required by the stopped-flow technique (5). With the phototube shutter closed (0% transmittance) the output voltage of the recording adapter is given an arbitrary value (300 mv available) using the suppression and dark current adjustments. The phototube shutter is then opened, and the slit of the monochromator varied until this output is zero. The latter may be chosen to correspond to 100% transmittance or a convenient percentage reaction with an appropriate standard solution in the observation cell. The first procedure is used when the reactants are colorless but the products colored, while the second is adapted to follow the disappearance of colored reactants.

APPLICATION

The apparatus described has been employed in a kinetic study of the enzymatic hydrolysis of *p*-nitrophenyl acetate with trypsin and is the subject of a subsequent paper (22). The stopped-flow method, however, has been used in a similar instance for the study of *p*-nitrophenyl acetate hydrolysis with chymotrypsin (15). Therefore, it was convenient to repeat part of this work as a check on technique.

Hydrolysis of p-Nitrophenyl Acetate with Chymotrypsin

Theoretical.—Measurements of the rate of appearance of *p*-nitrophenol at small values of t have been employed for this chymotrypsin system to evaluate F given in the relationship,

Can. J. Chem. Downloaded from www.nrcresearchpress.com by 196.1.178.254 on 09/04/12
For personal use only.

[1] $$P_1 = k'_3\, e_{0t} + e_0\,(1-\exp Ft) \qquad \text{(ref. 23)}$$

where P_1 is the concentration of *p*-nitrophenol, k'_3 is the apparent rate constant for deacetylation of enzyme, e_0 is the initial concentration of enzyme, t is the time, and $-F$ is the quantity to be determined. If equation [1] is treated as suggested by Guggenheim (24) the result is

[2] $$\log|r_1+r_3-2r_2| = \log \text{constant} + (Ft_1/2.303) \qquad \text{(ref. 15)}$$

where r_1, r_2, and r_3 are readings directly proportional to P_1 taken at the times t_1, $t_1+\Delta t$, and $t_1+2\Delta t$, respectively. Therefore, F can be determined from the slope of a plot of $\log|r_1+r_3-2r_2|$ against t_1.

EXPERIMENTAL

Enzyme.—Twice crystallized chymotrypsin (salt-free) was purchased from the Mann Research Laboratories, Inc., New York.

Substrate.—*p*-Nitrophenyl acetate was synthesized according to the method of Chattaway (25), and recrystallized from an ethanol–water solution m.p. 78–79°.

Buffers.—The appropriate buffered solutions were prepared from monosodium and disodium phosphate so that the reaction solutions contained 0.05 *M* phosphate.

Solvent.—To improve the solubility of the substrate 20% (v/v) isopropyl alcohol was used.

RESULTS

Figure 6 gives the Guggenheim plot for the reaction trace in Fig. 7 that was recorded

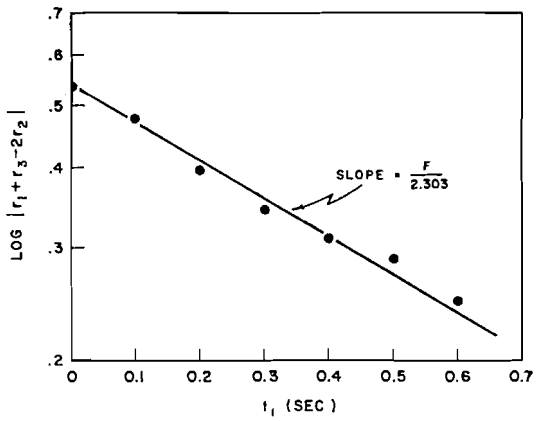

FIG. 6. A Guggenheim plot of the reaction trace for the chymotrypsin–NPA system.

TABLE I

The value of F obtained with different types of recorders for $S_0 = 5\times10^{-3}$ *M* at pH 7.8 and 25° C

Type of recorder	$-F$
Pen oscillograph (Brush BL201)	1.30 (15)
Pen oscillograph (Brush BL202)	1.33±0.07
Cathode-ray oscillograph (DuMont 403)	1.37±0.12
Strip-chart (Brown, Quarter Second)	1.35±0.08
Mean	1.34
Standard deviation	±0.02

Can. J. Chem. Downloaded from www.nrcresearchpress.com by 196.1.178.254 on 09/04/12
For personal use only.

with a high-speed strip-chart recorder. The same reaction was also recorded with a pen oscillograph and cathode-ray oscillograph equipped with a Polaroid Land camera. The values for F obtained from these records are listed in Table I along with the result estimated from the work reported previously. The mean result for a substrate concentration of 5×10^{-3} M and a pH 7.8 at 25° C is 1.34 ± 0.02. This is within the limit of error expected of the stopped-flow method.

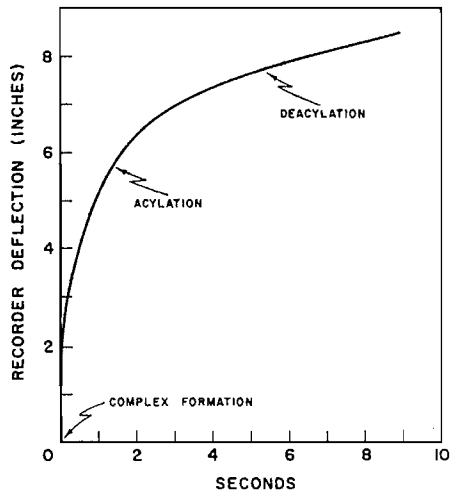

FIG. 7. A typical reaction trace recorded with a Brown "Quarter Second" recorder for 1 mg/ml chymotrypsin and 5×10^{-3} M NPA at pH 7.8.

ACKNOWLEDGMENTS

The authors are indebted to the National Research Council of Canada for a grant in aid of this work. We are grateful to Professor K. J. Laidler for his advice and interest in this research and to Mr. F. Giacobbi, who constructed many parts of the apparatus.

REFERENCES

1. CHANCE, B. J. Franklin Inst. **229**, 455, 613, 737 (1940).
2. CHANCE, B. J. Biol. Chem. **151**, 533 (1943).
3. CHANCE, B. Acta Chem. Scand. **1**, 236 (1947).
4. CHANCE, B. Biochem. J. **46**, 387 (1950).
5. CHANCE, B. Rev. Sci. Instr. **22**, 619 (1951).
6. CHANCE, B. Rapid reactions. *In* A. WEISSBERGER, *Editor*. Technique of organic chemistry. Vol. VIII. Interscience Publishers, Inc., New York. 1953. p. 690.
7. CHANCE, B., GREENSTEIN, D. S., and ROUGHTON, F. J. W. Arch. Biochem. Biophys. **37**, 311 (1952).
8. CHANCE, B. Arch. Biochem. Biophys. **71**, 130 (1957).
9. BEERS, R. F. and SIZER, I. W. J. Phys. Chem. **57**, 290 (1953).
10. BEERS, R. F. J. Phys. Chem. **58**, 197 (1954).
11. BEERS, R. F. Biochem. J. **62**, 492 (1956).
12. ROUGHTON, F. J. W. Discussions Faraday Soc. **17**, 116 (1954).
13. GUTFREUND, H. Discussions Faraday Soc. **20**, 167 (1955).
14. GUTFREUND, H. Trans. Faraday Soc. **51**, 441 (1955).
15. GUTFREUND, H. and STURTEVANT, J. M. Biochem. J. **63**, 656 (1956).
16. LAIDLER, K. J. Can. J. Chem. **33**, 1614 (1955).
17. OUELLET, L. and LAIDLER, K. J. Can. J. Chem. **34**, 146 (1956).
18. HARTRIDGE, H. and ROUGHTON, F. J. W. Proc. Roy. Soc. A, **104**, 376 (1923).
19. ROUGHTON, F. J. W. Rapid reactions. *In* A. WEISSBERGER, *Editor*. Technique of organic chemistry. Vol. VIII. Interscience Publishers, Inc., New York. 1953. p. 669.
20. GIBSON, Q. H. and ROUGHTON, F. J. W. Proc. Roy. Soc. B, **143**, 310 (1955).
21. SIRS, J. A. Trans. Faraday Soc. **54**, 201, 207 (1958).
22. STEWART, J. A. and OUELLET, L. Can. J. Chem. **37**, 751 (1959).
23. OUELLET, L. and STEWART, J. A. Can. J. Chem. **37**, 737 (1959).
24. GUGGENHEIM, E. A. Phil. Mag. **2**, 538 (1926).
25. CHATTAWAY, F. D. J. Chem. Soc. **134**, 2495 (1931).

Can. J. Chem. Downloaded from www.nrcresearchpress.com by 196.1.178.254 on 09/04/12
For personal use only.

Can. J. Chem. Downloaded from www.nrcresearchpress.com by 196.1.178.254 on 09/04/12
For personal use only.

THE TRYPSIN CATALYZED HYDROLYSIS OF *p*-NITROPHENYL ACETATE[1, 2]

JAMES A. STEWART[3] AND LUDOVIC OUELLET[4]

ABSTRACT

The hydrolysis of *p*-nitrophenyl acetate (NPA) by trypsin has been investigated in the early stage of the reaction using stopped-flow techniques. The influence of pH on the initial rate suggests competitive inhibition of the active site of the enzyme by hydrogen ions. The dissociation constant of the enzyme obtained from the kinetics of this reaction ($pK = 6.9$) indicates possible catalysis by an amino group or an imidazole group of the enzyme. Lysine methyl ester as an analogue of the enzyme catalyzes the hydrolysis of NPA under similar experimental conditions. The results are described in terms of an assumed mechanism and the nature of the catalytic site is discussed.

Hartley and Kilby (1, 2) first reported that the enzyme chymotrypsin was capable of catalyzing the hydrolysis of *p*-nitrophenyl acetate (NPA). From their results they concluded that the mechanism consisted of three distinct stages. The first stage is extremely rapid and concerns the combination of enzyme with substrate, the second stage is moderately rapid and involves the liberation of phenol and the acetylation of the enzyme, while the last stage, which is slow, liberates acetate with the consequent regeneration of enzyme.

Gutfreund and Sturtevant (3), employing stopped-flow techniques, showed that the rate constant for acetylation (second stage) of chymotrypsin with NPA was pH independent. This is contrary to their results for dinitrophenyl acetate (4) and the results of other workers (5) who report pH dependence.

The purpose of our investigation into the mechanism of trypsin catalyzed hydrolysis of NPA is mainly to clarify the problem as to whether or not the rate constant related to acetylation is pH independent, and compare the suggested mechanism with a mechanism recently proposed by Cunningham (6). His scheme, which emphasizes the hydroxyl group of a serine residue as primary site rather than the imidazolyl group of histidine, satisfies the available experimental evidence (7). However, when trypsin (8) or chymotrypsin (9) are treated with DFP^{32} (diisopropyl fluorophosphate) no histidine residue occurs in the vicinity of the phosphorylated serine, so that we would like to present some evidence that an amino group other than the imidazolyl might function as part of the catalytic site.

EXPERIMENTAL

Twice crystallized trypsin (salt-free) was obtained from the Mann Research Laboratories Inc., New York. The substrate *p*-nitrophenyl acetate was synthesized as described by Chattaway (10). All reactions were carried out in 20% (v/v) isopropyl alcohol at 25° C with 0.025 *M* phosphate as buffer. The pH values quoted refer to the buffer and were measured in the absence of alcohol, but in the presence of enzyme, using a Beckman Model G pH meter.

The rapid acetylation reaction was studied employing the stopped-flow apparatus

[1]*Manuscript received August 22, 1958.*
Contribution from the Department of Chemistry, University of Ottawa, Ottawa, and the Laboratories of the Food and Drug Directorate, Department of National Health and Welfare, Ottawa, Canada.
[2]*Presented at the Chemical Institute of Canada Conference, Toronto, May 1958.*
[3]*Present address: Laboratories of the Food and Drug Directorate, Department of National Health and Welfare, Ottawa, Canada.*
[4]*Present address: Department of Chemistry, Laval University, Quebec, Que.*

described previously (11), while the slow deacetylation reaction was followed with a Cary Model 11 spectrophotometer using the differential technique. The data were treated according to the suggested mechanism by the theoretical method outlined in a preceding paper (12).

RESULTS AND DISCUSSION

Effect of pH on Acetylation

The initial rapid production of *p*-nitrophenol, corresponding to the formation of acetyl-trypsin was recorded at several substrate and hydrogen-ion concentrations. The constant F (12) was then calculated from the reaction trace using the Guggenheim technique (13). A typical Lineweaver–Burk plot (14) of some of the results is given in Fig. 1, where the extrapolation of $1/F$ at infinite substrate concentration yields the same value for $1/k_2$ at two widely separated pH values. The fact that seven such plots between pH 6.2 and 7.8 produced the same result for $1/k_2$ strongly suggests competitive inhibition by hydrogen-ions. The same result, though not elucidated as competitive inhibition, was obtained with chymotrypsin (3). Similar to the usual Michaelis–Menten treatment, the slopes obtained from the Lineweaver–Burk plot in Fig. 1 involve K_m/k_2. According to Laidler (15), the variation of K_m/k_2 with pH provides the dissociation constants of the groups which comprise the active site of the enzyme. It should also be pointed out, as has been done previously (3), that should the three-step mechanism be general for other enzyme systems, then the standard Michaelis constant may consist of a rather large number of constants.

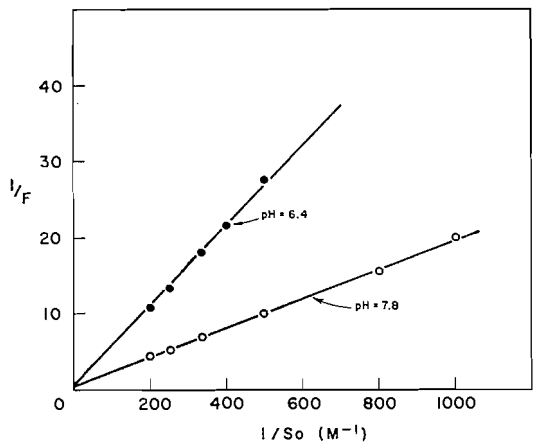

FIG. 1. A Lineweaver–Burk plot of the hydrolysis of NPA by trypsin (1 mg/ml) at pH 6.4 and 7.8.

The results given in Fig. 1 can be explained if we assume that hydrogen-ion competitively inhibits the initial combination of enzyme and substrate. With this in mind, the scheme for acetylation becomes,

$$(a) \qquad E + H^+ \underset{k_{-4}}{\overset{k_4}{\rightleftharpoons}} EH^+$$

$$(b) \qquad E + S \underset{k_{-1}}{\overset{k_1}{\rightleftharpoons}} ES_1$$

Can. J. Chem. Downloaded from www.nrcresearchpress.com by 196.1.178.254 on 09/04/12
For personal use only.

Can. J. Chem. Downloaded from www.nrcresearchpress.com by 196.1.178.254 on 09/04/12
For personal use only.

(*c*) $$ES_1 \xrightarrow{k_2} ES_2 + P_1$$

where E is the active form and EH^+ the inactive form of the enzyme, S is the substrate, ES_1 is the Michaelis complex, ES_2 is the acetylated enzyme, P_1 is the phenol, and k_1, k_{-1}, k_2, k_4, and k_{-4} are the appropriate rate constants. When this scheme is treated theoretically (12) and the effect of hydrogen-ion taken into account (15, 16, 17) $-F$, the quantity to be determined, formulates to

[1] $$F = -\frac{(k_2+k'_3)\,s_0+k'_3K'_m}{s_0+[(k'_3+k_2+k_{-1})/k_1](Ka+[H])/Ka}$$

when $k_2 \gg k'_3$

[2] $$F = -\frac{k_2 s_0}{s_0+K'_m}$$

where

[3] $$K'_m = K_m\left(\frac{Ka+[H]}{Ka}\right)$$

[4] $$K_m = \frac{k_2+k_{-1}}{k_1}$$

and

[5] $$Ka = k_{-4}/k_4.$$

Equation [2] may be also written as,

[6] $$-\frac{1}{F} = \frac{1}{k_2}+\frac{1}{s_0}\left(\frac{K_m}{k_2}+[H]\frac{K_m}{Ka\,k_2}\right).$$

Figure 2 was obtained by plotting the slopes of equation [6] against [H]. The resultant dissociation constant $Ka = 1.4\times10^{-7}$, which is related to the active site of the enzyme, was calculated from the intercept K_m/k_2 and the slope $K_m/k_2\,Ka$.

Equation [2] may be rearranged in still another fashion,

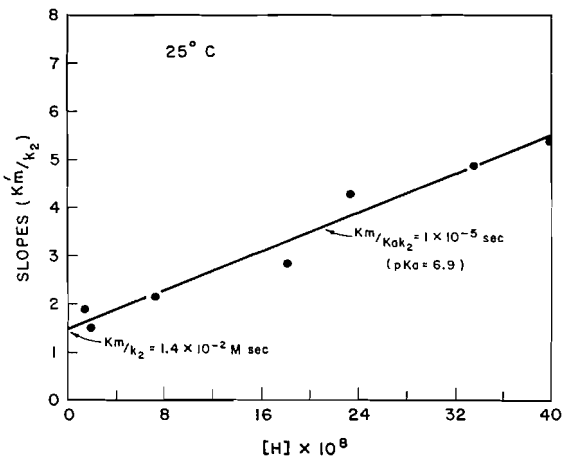

FIG. 2. The determination of K_m/k_2 and $K_m/Ka\,k_2$ for the trypsin–NPA system, from a plot of slopes against $[H^+]$.

[7] $$-\frac{1}{F}=\left(\frac{1}{k_2}+\frac{1}{s_0}\frac{K_m}{k_2}\right)+[\mathrm{H}]\frac{K_m}{s_0 Ka\, k_2}.$$

The constants k_2 and K_m were evaluated by plotting the intercepts of equation [7] against $1/s_0$, as illustrated in Fig. 3. The rate constant of acetylation $k_2 = 1.5\ \mathrm{sec}^{-1}$ was estimated from the intercept $1/k_2$, which allowed a Michaelis constant $K_m = 2.1 \times 10^{-2}\ M$ to be determined from K_m/k_2, the slope of the line.

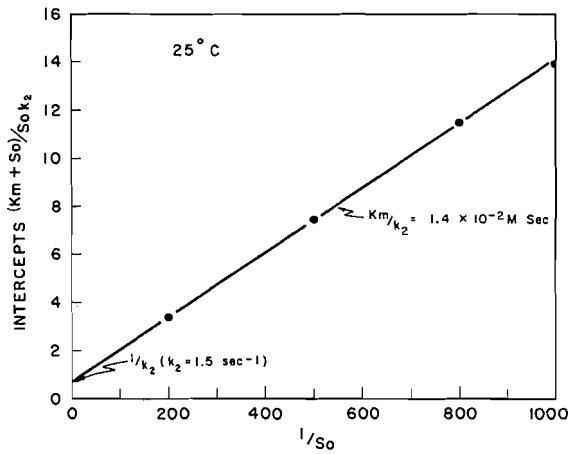

FIG. 3. The estimation of $1/k_2$ and K_m/k_2 by means of a plot of intercepts versus s_0, for trypsin catalyzed hydrolysis of NPA.

The results for k_2, Ka, and K_m are included in Table I, where the constants for trypsin and chymotrypsin are compared.

TABLE I

Kinetic constants for the enzymatic hydrolysis of *p*-nitrophenyl acetate

Constant	Trypsin	Chymotrypsin*
k_2 (sec^{-1})	1.5	3.1
K_m (M)	2.1×10^{-2}	6.8×10^{-3}
pK_a	6.9	6.6
pK'_a	7.0	7.3†
k_3 (sec^{-1})	0.013	0.025

*Calculated from the results of Gutfreund, H. and Sturtevant, J. M. Biochem. J. **63**, 656 (1956).

†6.8 for ester hydrolysis (ref. 5).

Effect of pH on Deacetylation

The reactions which represent deacetylation are:

(*d*) $$\mathrm{ES_2} \xrightarrow{k_3} \mathrm{E}+\mathrm{P_2}$$

(*e*) $$\mathrm{ES_2}+\mathrm{H^+} \underset{k_{-5}}{\overset{k_5}{\rightleftharpoons}} \mathrm{ES_2H^+}$$

where ES_2 is the unstable form and ES_2H^+ the stable form of the acetylated enzyme, P_2 is acetate, and k_3, k_5, and k_{-5} the appropriate rate constants. When t is large the rate is

Can. J. Chem. Downloaded from www.nrcresearchpress.com by 196.1.178.254 on 09/04/12
For personal use only.

[8] $$\dot{p}_1 = \dot{p}_2 = k'_3\, e_0 \text{ (refs. 3, 10)},$$

where

[9] $$k'_3 = k_3\left(\frac{Ka'}{Ka'+[\mathrm{H}]}\right)$$

and

[10] $$Ka' = k_{-5}/k_5.$$

The slow deacetylation reaction was studied spectrophotometrically by following the phenol produced after the rapid acetylation reaction had subsided. The results were conveniently corrected for the spontaneous hydrolysis of NPA by placing the reaction solution in the sample cell and the same solution less enzyme in the reference cell of a double beam spectrophotometer, and recording the difference in absorbance. The reaction was started by introducing equal portions of NPA simultaneously into both cells with hypodermic syringes. The necessary corrections were then applied to the records to take into account that the fraction of colored species of *p*-nitrophenol, i.e. $pK_a = 7.15$ (18), varies with pH.

In the above manner the rates at different hydrogen-ion concentrations, which are plotted as the reciprocal rate against [H] in Fig. 4, were obtained. This plot gives a dissociation constant $Ka' = 1\times10^{-7}$ for acetylated trypsin and compares favorably with the constant Ka, concerned with the active site. The rate constant for deacetylation, $k_3 = 1.3\times10^{-2}$ sec^{-1}, was determined from the intercept of Fig. 4; the extinction coefficient of *p*-nitrophenol was taken as 1.8×10^4 (19), and the molecular weight of trypsin as 21,000 (20).

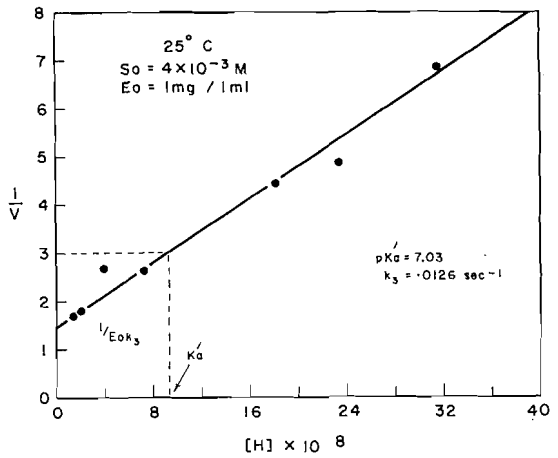

FIG. 4. A plot of the reciprocal rate of liberation of *p*-nitrophenol against $[H^+]$, for the determination of k_3e_0 and Ka' in the catalyzed hydrolysis of NPA by trypsin.

Mechanism of Hydrolysis

When the effect of proton inhibition is introduced, the result suggests a mechanism similar to that proposed by Cunningham (6). Quite different from former mechanisms his scheme advocates the hydroxyl group as primary site, rather than the imidazolyl which is now thought to be secondary. To facilitate a comparison of the two mechanisms those stages which correspond to reactions (*a*) to (*e*) are represented in the scheme outlined in Fig. 5. As our present experimental method does not detect the acyl-transfer

Can. J. Chem. Downloaded from www.nrcresearchpress.com by 196.1.178.254 on 09/04/12
For personal use only.

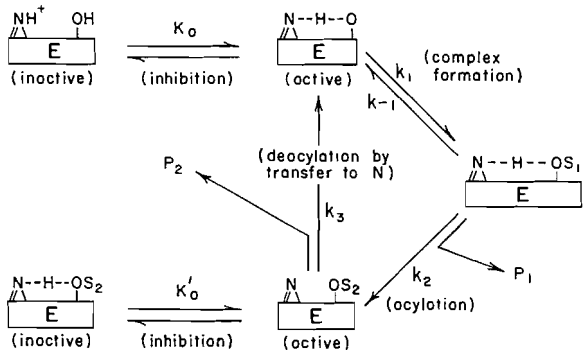

FIG. 5. The mechanism of enzymatic ester hydrolysis.

reaction, the absence of this transfer is the main difference in the two schemes. Thus, the rate constant k_3 for deacetylation is a composite constant involving two stages: the transfer of acetyl to nitrogen and its subsequent release.

In the scheme as shown in Fig. 5 the enzyme is inactive to complex formation unless a proton is released from the active site, and explains why inhibition is competitive rather than non-competitive. On examination of equation [1] it is seen that under certain conditions competitive inhibition may not be realized. This is especially true when the rate constants of acetylation and deacetylation are of the same order of magnitude. A Lineweaver–Burk plot of the data will not produce a straight line with constant intercept, and competitive inhibition may appear to be non-competitive.

The initial point of attack of substrate is the hydroxyl group of serine where the complex undergoes partial decomposition, releasing phenol. The hydroxyl group becomes acetylated, but before deacetylation can proceed there must be a transfer of the acetyl group to the nitrogen. The stability of certain acylated enzymes at low pH has been reported (5, 21, 22). This can be explained on the basis that transfer from the hydroxyl only takes place at higher pH values where the nitrogen does not have the inhibiting hydrogen intact. Therefore, proton inhibition at the deacylation stage accounts for this inactivity and stability of acetyltrypsin and chymotrypsin below a pH of 5 to 6.

A similar approach may be used to explain inhibition by certain organophosphorus compounds. For instance, in the case of DFP the hydroxyl group of a serine residue in the enzyme is phosphorylated, but transfer of this phosphoryl group to the nitrogen is difficult, resulting in an inactive enzyme.

Nature of the Catalytic Site

Tracer experiments show that DIP^{32} (diisopropyl phosphate) is attached to the hydroxyl group of a serine residue and no histidine (imidazole) occurs in the vicinity (8, 9). However, Westheimer (23) presents in detail the necessary orientation of the active site of chymotrypsin that enables the imidazolyl and hydroxyl groups to come together by folding. Also, spectrophotometric evidence has been published to show that acetyl-imidazolyl is an intermediate when acetyl-chymotrypsin decomposes (7).

The lack of histidine in the neighborhood of DIP^{32}–serine, and the differences in the pK values and the degree of activity of trypsin and chymotrypsin (see Table I) has led us to postulate that other groups might also function in partnership with the hydroxyl group to constitute an active site. As for model hydrolysis (24) the facts present the possibility that the basicity of the nitrogen containing group of the active site may

Can. J. Chem. Downloaded from www.nrcresearchpress.com by 196.1.178.254 on 09/04/12
For personal use only.

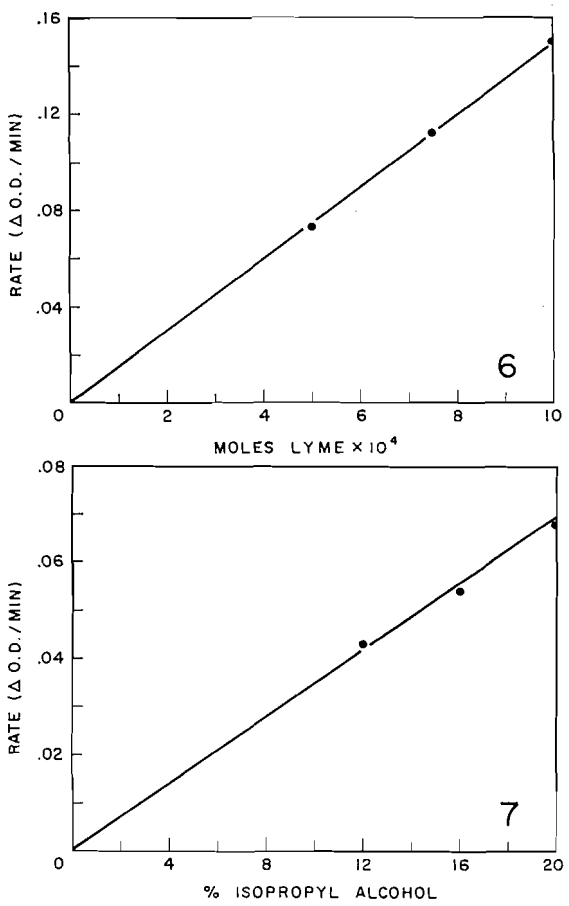

FIG. 6. The effect of LYME on the rate of hydrolysis of NPA in the presence of 20% (v/v) isopropyl alcohol.

FIG. 7. The effect of isopropyl alcohol on the rate of hydrolysis of NPA in the presence of 4×10^{-4} *M* LYME.

be the important factor. Since the pK of a free α-amino group in an ester is in the neighborhood of the pK for the active site of trypsin, lysine methyl ester (LYME) was tested and found to influence the rate of hydrolysis of NPA under conditions comparable to enzymatic hydrolysis. This effect is demonstrated in Fig. 6, where the rate of hydrolysis of NPA is proportional to the amino acid concentration. The same result was obtained by varying the isopropyl alcohol concentration and is given in Fig. 7. These results show that the aliphatic hydroxyl and amino groups could play a significant part in the constitution of an enzymatic site. Further evidence to support this hypothesis can be secured from the literature. Hartley and Kilby (2) have reported that the phenolic hydroxyl and the aliphatic amino groups may act as acceptors of the acetyl group. The work of Balls and co-workers reveals that chymotrypsin mediates the transfer of acetyl to ethanol (22) or trimethylacetyl to *n*-butanol (25), illustrating the importance of hydroxyl; while the significance of an amino group is shown by the transfer of acetyl from chymotrypsin to hydroxylamine (22) and the fact that certain monoacylated chymotrypsin derivatives are reactivated by tyrosine ethyl ester (25). Also, Wagner-Jauregg and Hackley (26) discovered during an investigation of the model hydrolysis

Can. J. Chem. Downloaded from www.nrcresearchpress.com by 196.1.178.254 on 09/04/12
For personal use only.

of organophosphorus inhibitors that certain amino and hydroxyl substituted pyridines, and such compounds as catechol, increased the rate of hydrolysis as compared to pyridine.

Finally, some results were obtained by infrared spectroscopy using the KBr-pellet technique which indicate the α-amino group is acetylated when NPA is allowed to hydrolyze in the presence of tyrosine ethyl ester (TYEE). From the infrared spectra in Fig. 8 it is seen that both acetyl-TYEE and the system of NPA hydrolyzed in the presence of TYEE possess appreciable absorbance at 1660 cm^{-1}, while TYEE and hydrolyzed NPA do not; thereby disclosing that tyrosine ethyl ester is acetylated during the hydrolysis of NPA.

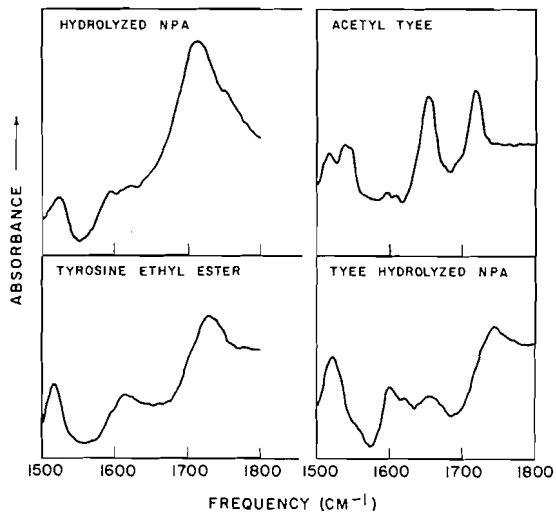

FIG. 8. The infrared spectra of freeze-dried solutions of hydrolyzed NPA, TYEE, acetyl-TYEE, and NPA hydrolyzed in the presence of TYEE; each containing 20% (v/v) isopropyl alcohol and 0.05 *M* phosphate pH 7.8.

CONCLUSIONS

The rate constant related to the acetylation stage during the trypsin or chymotrypsin catalyzed hydrolysis of NPA appears to be pH independent. The mechanism implied by the result is in agreement with the postulated mechanism of Cunningham. There is some degree of suggestion that this three-step scheme might be general, and in the instance of other enzyme systems the Michaelis constant may be a composite of a larger number of constants than formerly anticipated. Even though it has been shown that hydroxyl groups and amino groups influence the rate of hydrolysis of NPA, further investigations will be required before definitely establishing the nature of their relationship to enzymatic hydrolysis. This is particularly true in the case of the free α-amino group. Although the pK of this group in an ester and possibly a peptide would be in agreement with the pK reported for the active site of trypsin, free α-amino groups are believed to exist only in the terminal residues of proteins.

ACKNOWLEDGMENT

We wish to thank the National Research Council of Canada for their financial support of a portion of this research.

Can. J. Chem. Downloaded from www.nrcresearchpress.com by 196.1.178.254 on 09/04/12
For personal use only.

REFERENCES

1. HARTLEY, B. S. and KILBY, B. A. Biochem. J. **50**, 672 (1952).
2. HARTLEY, B. S. and KILBY, B. A. Biochem. J. **56**, 288 (1954).
3. GUTFREUND, H. and STURTEVANT, J. M. Biochem. J. **63**, 656 (1956).
4. GUTFREUND, H. and STURTEVANT, J. M. Proc. Natl. Acad. Sci. **42**, 719 (1956).
5. DIXON, G. H. and NEURATH, H. J. Biol. Chem. **225**, 1049 (1957).
6. CUNNINGHAM, L. W. Science, **125**, 1145 (1957).
7. DIXON, G. H. and NEURATH, H. J. Am. Chem. Soc. **79**, 4558 (1957).
8. DIXON, G. H., KAUFFMAN, D. L., and NEURATH, H. J. Am. Chem. Soc. **80**, 1260 (1958).
9. SCHAFFER, N. K., SIMET, L., HARSHMAN, S., ENGLE, R. R., and DRISKO, R. W. J. Biol. Chem. **225**, 197 (1957).
10. CHATTAWAY, F. D. J. Chem. Soc. **134**, 2495 (1931).
11. STEWART, J. A. and OUELLET, L. Can. J. Chem. **37**, 744 (1959).
12. OUELLET, L. and STEWART, J. A. Can. J. Chem. **37**, 737 (1959).
13. GUGGENHEIM, E. A. Phil. Mag. **2**, 538 (1926).
14. LINEWEAVER, H. and BURK, D. J. Am. Chem. Soc. **56**, 658 (1934).
15. LAIDLER, K. J. Trans. Faraday Soc. **51**, 550 (1955).
16. LAIDLER, K. J. Trans. Faraday Soc. **51**, 528 (1955).
17. LAIDLER, K. J. Trans. Faraday Soc. **51**, 540 (1955).
18. ROBINSON, R. A. and BIGGS, A. I. Trans. Faraday Soc. **51**, 901 (1955).
19. BIGGS, A. I. Trans. Faraday Soc. **50**, 800 (1954).
20. SEDLACEK, B. and BARTL, P. Chem. Listy, **49**, 996 (1955).
21. BALLS, A. K. and ALDRICH, F. L. Proc. Natl. Acad. Sci. **41**, 190 (1955).
22. BALLS, A. K. and WOOD, H. N. J. Biol. Chem. **219**, 245 (1956).
23. WESTHEIMER, F. H. Proc. Natl. Acad. Sci. **43**, 969 (1957).
24. BRUICE, T. C. and SCHMIR, G. L. J. Am. Chem. Soc. **79**, 1663 (1957).
25. MCDONALD, C. E. and BALLS, A. K. J. Biol. Chem. **227**, 727 (1957).
26. WAGNER-JAUREGG, P. and HACKLEY, B. E. J. Am. Chem. Soc. **75**, 2125 (1953).

Can. J. Chem. Downloaded from www.nrcresearchpress.com by 196.1.178.254 on 09/04/12
For personal use only.

Can. J. Chem. Downloaded from www.nrcresearchpress.com by 190.90.36.8 on 09/04/12
For personal use only.

THE STEREOCHEMISTRY OF THE PIMARIC ACIDS[1,2]

O. E. EDWARDS AND R. HOWE[3]

ABSTRACT

Isodextropimaric and dextropimaric acids have been shown to have the same stereochemistry at C_1, C_{11}, and C_{12}, but to be epimeric at C_7. A critical survey is made of the present evidence with regard to the stereochemistry at C_{13} in these acids. Preliminary experiments on the action of formic acid on isodextropimaric acid are reported.

In view of the current interest in the stereochemistry of the tetracarbocyclic diterpenes, e.g. rimuene (2, 3), phyllocladene (3, 4, 5, 6), mirene (3, 7), steviol (6, 8), cafestol (6, 9, 10) and gibberellic acid (11), and also the tetracarbocyclic diterpene alkaloids, e.g. the *Garrya* alkaloids (6, 10, 12), atisine (13), and ajaconine (14), the question of whether their close relatives, the pimaric acids, belonged to one steric group became of outstanding interest.

While the skeleton I (R_1 = vinyl; R_2 = methyl) and stereochemistry at C_1, C_{11}, and C_{12} of dextropimaric acid have been well established (15, 16), the stereochemistry at C_7 and C_{13} has remained in doubt. Isodextropimaric acid, which occurs with dextropimaric acid in the oleoresin of *Pinus palustris* (17), has been shown to have the same basic skeleton as dextropimaric acid by Harris and Sanderson (18). However, their

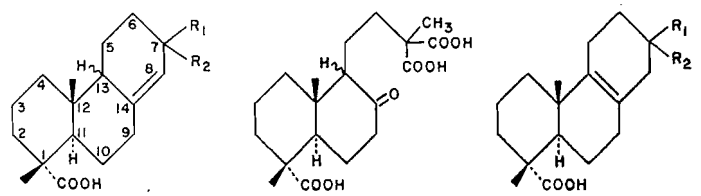

I II III

degradation products were optically inactive and the possibility existed that epimerization at the asymmetric center adjacent to the carbonyl group of the keto-tricarboxylic acid II might have taken place (3). Hence the only safe conclusion which may be drawn from their experiments is that isodextropimaric acid is identical at C_1, C_{11}, and C_{12} to dextropimaric acid, or bears an over-all mirror image relation to it at these centers.

The evidence presented below establishes that the two acids are identical at C_1, C_{11}, and C_{12}, and that they are epimeric at C_7 as originally suggested by Harris and Sanderson (18) on equivocal evidence, but allows no certain conclusion about the stereochemistry at C_{13}. Since our preliminary communication (1), Wenkert and Chamberlin (19), and Green, Harris, and Whalley (20) have announced the same and further conclusions (see below for a critical discussion).

As a preliminary to our work it was necessary to re-examine the properties of the dihydro- and tetrahydro-derivatives of both acids, because of the conflicting data in the literature. The vinyl double bond in both acids was readily reduced in the presence

[1]*Manuscript received December 16, 1958.*
Contribution from the Division of Pure Chemistry, National Research Council, Ottawa, Canada. Issued as N.R.C. No. 5097.
[2]*A preliminary report of some of this work was published earlier (ref. 1).*
[3]*National Research Council of Canada Postdoctoral Fellow. Present address: Research Laboratory, I.C.I. Pharmaceutical Division, Fulshaw Hall, Alderly Rd., Wilmslow, Manchester, England.*

Can. J. Chem. Downloaded from www.nrcresearchpress.com by 190.90.36.8 on 09/04/12
For personal use only.

of presaturated palladized charcoal. Dihydroisodextropimaric acid was purified by chromatography on silica gel and recrystallization of its cyclohexylamine salt. It melted at 173–175° and had $[\alpha]_D$ −7°. (The literature values are m.p. 173–175°, $[\alpha]_D$ ±0° (EtOH) (18) and m.p. 173.5°, $[\alpha]_D$ −16° (chloroform–acetone, 1 : 1) (21).) The dihydrodextropimaric acid was isolated directly from Staybelite Resin by a modification[4] of the method of Hasselstrom and Bogert (22). It melted at 243–245° and had $[\alpha]_D$ +22°. The infrared spectrum of both acids (nujol mull) contained medium bands at 825 cm^{-1}, corresponding to the trisubstituted double bonds.

Dihydroisodextropimaric acid slowly took up 0.76 mole of hydrogen over Adams' catalyst in acetic acid giving a product with $[\alpha]_D$ +30°. This took up a further 0.27 mole of hydrogen in the presence of fresh catalyst. The tetrahydro-acid had m.p. 172–173° and $[\alpha]_D$ +24° (EtOH), +21° ($CHCl_3$). Ukita *et al.* (23) report a melting point of 172–172.5° (no rotation).

A similar hydrogenation of dihydrodextropimaric acid gave tetrahydrodextropimaric acid, m.p. 238–240°, $[\alpha]_D$ +18°, in agreement with Ruzicka *et al.* (24), who report a melting point of 236–237° (no rotation). Le-Van-Thoi and Ourgaud (25) report a melting point of 198° with $[\alpha]_J$ +55° for tetrahydrodextropimaric acid. This appears to be a mixture of Δ^{13}-dihydrodextropimaric acid (see below) and the tetrahydro-acid which we now report. (Their analytical figures fit $C_{20}H_{32}O_2$ rather than $C_{20}H_{34}O_2$.) When dihydrodextropimaric acid was allowed to absorb 0.25 mole of hydrogen the total product melted at 193–197° and had $[\alpha]_D$ +53° in excellent agreement with their product. On complete reduction this mixture gave pure tetrahydro-acid, m.p. 238–240°, $[\alpha]_D$ +19°.

In order to compare the asymmetry at C_7, methods were sought for eliminating or rendering identical the asymmetry at C_{13} in dextro- and isodextro-pimaric acids and their derivatives. The action of strong acids on the pimaric acids could possibly cyclize the diene to a tetracarbocyclic system, isomerize the nuclear double bond to the Δ^{13}-position, produce γ- and δ-lactones (e.g. IV and V), and convert the C_7-substituents to an isopropylidene group. In the isodextropimaric acid series, conditions have been found for producing all these changes except the cyclization of the diene system.

The easiest method of destroying the asymmetry at C_{13} appeared to be by isomerizing the $\Delta^{8,14}$-ethylenic bond to the Δ^{13}-position. When isodextropimaric acid was refluxed with *p*-toluenesulphonic acid in dry dioxane, the desired migration was slowly brought about,[5] but it was found to be a poor preparative method. The cleanest method of isomerizing the $\Delta^{8,14}$ double bond to the Δ^{13}-position was found to be by the action of hydrogen chloride in chloroform. The method was first applied to the dihydro-acids (I; R_1 = ethyl; R_2 = methyl) in order to prevent complicating reactions due to the vinyl group.

Dihydrodextropimaric acid (I; R_1 = ethyl; R_2 = methyl) and dihydroisodextropimaric acid (I; R_1 = methyl; R_2 = ethyl) were converted by hydrogen chloride in chloroform to their Δ^{13}-isomers (III), m.p. 181.3°, $[\alpha]_D$ +73°, and m.p. 107–108°, $[\alpha]_D$ +76.7° respectively. The infrared spectra of the products lacked the 825 cm^{-1} band characteristic of the starting materials and together with the hydrogenation evidence presented below leads to the Δ^{13}-assignment for the double bond.

Hydrogenation of Δ^{13}-dihydrodextropimaric acid in acetic acid with Adams' catalyst gave the same tetrahydrodextropimaric acid as reported above, m.p. 238–240°,

[4]*We cordially thank Dr. T. H. Sanderson, of Hercules Research Center, for the resin and for kindly furnishing details of the isolation method.*

[5]*We thank Dr. D. K. R. Stewart for characterizing the isodextropimaric acid, and for preliminary experiments on the isomerization with p-toluenesulphonic acid.*

$[\alpha]_D$ +19° as the only product. Similar conditions converted Δ^{13}-dihydroisodextropimaric acid to the same tetrahydroisodextropimaric acid as reported above, m.p. 172–173°, $[\alpha]_D$ +21°. Since dihydrodextropimaric acid is recovered unchanged after refluxing with glacial acetic acid for 5 hours, the possibility of group migration or skeletal rearrangement may be precluded in both the hydrogenation experiments and during the hydrogen chloride – chloroform treatment of the dihydro-acids.

It was reported above that the intermediate product isolated during the reduction of dihydroisodextropimaric acid had a rotation which was more positive than either the starting material or the final product. This provided a valuable clue that hydrogenation was accompanied by double-bond migration to give the Δ^{13}-dihydro-acid of high positive rotation and less facile reducibility. An interpretation of Le-Van-Thoi and Ourgaud's results was also afforded. We attempted, but found that it was not possible, to obtain pure Δ^{13}-dihydrodextropimaric acid from dihydrodextropimaric acid by isomerization on the catalyst surface; conditions favoring isomerization also brought about some reduction.

Dextropimaric acid has usually been considered to be stable to mineral acids (16), although Vesterburg (26) obtained some evidence that isomerization did occur when an ethereal solution of the acid was saturated with hydrogen chloride. Ruzicka and Balas (27) report the formation of three monohydrochlorides by long treatment of dextropimaric acid with acetic acid saturated with hydrogen chloride. When dextropimaric acid in chloroform was saturated with hydrogen chloride we found that the only product was the expected Δ^{13}-isomer, m.p. 131–132°, $[\alpha]_D$ +70°. The infrared spectrum revealed that the vinyl group had remained intact, while the trisubstituted ethylenic bond peak (825 cm^{-1}) had disappeared. Selective reduction of the vinyl group of the new Δ^{13}-acid gave the Δ^{13}-dihydrodextropimaric acid, m.p. 181–182°, $[\alpha]_D$ +75° reported above. Application of the hydrogen chloride method of isomerization to isodextropimaric acid, m.p. 162–164°, $[\alpha]_D$ ±0° produced the Δ^{13}-isomer, m.p. 106–107°, $[\alpha]_D$ +113°, the infrared spectrum showing peaks due to a vinyl group but none due to a trisubstituted ethylenic bond. Selective reduction of the vinyl group of the new Δ^{13}-acid gave Δ^{13}-dihydrodextropimaric acid, m.p. 107–108°, $[\alpha]_D$ +73° reported above.

Since our preliminary report of this work was published (1), Green, Harris, and Whalley (20) have reported Δ^{13}-isodextropimaric acid as having m.p. 118° and $[\alpha]_D$ +58°. Their isomerization appears to have been only partial, since we have prepared a synthetic mixture (*ca.* 1:1) of isodextropimaric acid and Δ^{13}-isodextropimaric acid having $[\alpha]_D$ +58° and found it to have m.p. 118–121°. In view of this the Δ^{13}-dihydroisodextropimaric acid which they report would also seem to be a mixture. Molecular rotation correlations based on the figures may well be meaningless.

We now turn our attention to the lactones produced by more vigorous acid treatment of the dihydrodextro- and dihydroisodextro-pimaric acids. Δ^{13}-Dihydrodextropimaric acid with concentrated sulphuric acid at −5° C gave the known γ-lactone (28) (IV; R_1

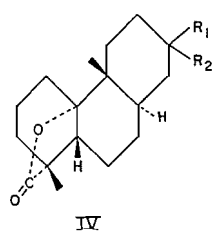

IV

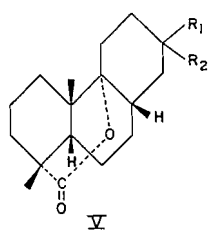

V

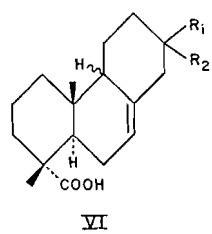

VI

Can. J. Chem. Downloaded from www.nrcresearchpress.com by 190.90.36.8 on 09/04/12
For personal use only.

= ethyl; R_2 = methyl) m.p. and mixed m.p. 100°, $[\alpha]_D$ −15°, which was also obtained from dihydrodextropimaric acid. Similar conditions converted both dihydroisodextro and Δ^{13}-dihydroisodextropimaric acid to a new γ-lactone (IV; R_1 = methyl; R_2 = ethyl) m.p. 105–106°, $[\alpha]_D$ −9°. More vigorous acid treatment, i.e. concentrated sulphuric acid at 25° C converted the γ-lactone of dihydroisodextropimaric acid to a new δ-lactone (V; R_1 = methyl; R_2 = ethyl) m.p. 72–73°, $[\alpha]_D$ −40°, which could also be obtained directly from dihydroisodextropimaric acid under similar conditions. This δ-lactone differed from the known δ-lactone (28) (V; R_1 = ethyl; R_2 = methyl) from dihydrodextropimaric acid, m.p. 142°, $[\alpha]_J$ −45°. In one experiment, the action of *p*-toluenesulphonic acid on isodextropimaric acid in dioxane solution produced a new γ-lactone IV (R_1 = methyl; R_2 = vinyl), m.p. 128–130°, $[\alpha]_D$ −1° in very poor yield.

The fact that dihydrodextropimaric and dihydroisodextropimaric acids give different Δ^{13}-derivatives, γ-lactones, and δ-lactones proves conclusively that the acids are epimeric at C_7. The correspondence of ΔM_D on going from the Δ^{13}-dihydro-acids to the γ-lactones (−268° and −260° respectively) firmly indicates the *identical* stereochemistry at C_1, C_{11}, and C_{12} in both acids. The comparable rotational change on the transformation of Δ^{13}-dihydroabietic acid (III; R_1 = isopropyl; R_2 = H) to a γ-lactone (29) (IV; R_1 = isopropyl; R_2 = H) (ΔM_D −398°) provides additional proof that the stereochemistry of ring A of the pimaric acids is correctly shown in I.

Ukita and Tsumita (21) report the isolation from the fruits of *Juniperus japonica* of isodextropimaric acid and also a new pimaric acid, m.p. 162.5–165°, $[\alpha]_D$ −8.9°, which gives tetrahydroisodextropimaric acid, m.p. 172–173° on complete hydrogenation. This new acid cannot have the Δ^{13}-structure (III; R_1 = methyl; R_2 = vinyl) which they assign to it (23), since its properties are distinct from those of Δ^{13}-isodextropimaric acid (m.p. 106–107°, $[\alpha]_D$ +113°) reported here. Through the great kindness of Professor Ukita we have been able to make further observations on this new acid. Treatment of Ukita's acid in chloroform with hydrogen chloride converted it to Δ^{13}-isodextropimaric acid, m.p. 105–107°, $[\alpha]_D$ +110°, identical with that reported above. We conclude that Ukita's acid[6] may be $\Delta^{9,14}$-isodextropimaric acid (VI; R_1 = methyl; R_2 = vinyl) or its 13-epimer. The key compound (VII; R_1 = methyl; R_2 = ethyl) in Ukita's proof of structure was derived from the corresponding allyl alcohol, which must have arisen by

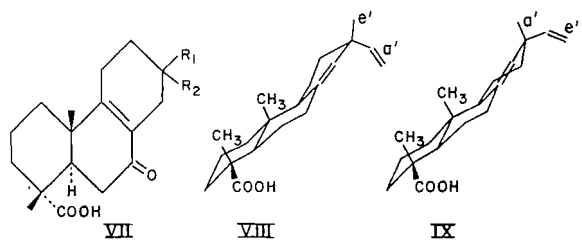

VII VIII IX

allylic oxidation and double bond migration during selenium dioxide oxidation of VI (R_1 = methyl; R_2 = ethyl). Fieser (30) has reported several examples of bond migration concomitant with selenium dioxide oxidations. The infrared spectrum of Ukita's acid has peaks at 1410, 1000, and 910 cm^{-1}, characteristic of a vinyl group, but shows only a shoulder at 825 cm^{-1} due to the trisubstituted ethylenic bond. However, the corre-

[6]*The naming of Ukita's acid will be deferred until the stereochemistry at C_{13} is known, when it can be named so as to indicate its relationship to isodextropimaric acid.*

Can. J. Chem. Downloaded from www.nrcresearchpress.com by 190.90.36.8 on 09/04/12
For personal use only.

Can. J. Chem. Downloaded from www.nrcresearchpress.com by 190.90.36.8 on 09/04/12
For personal use only.

sponding dihydro-acid with the vinyl group reduced, m.p. 154–157°, $[\alpha]_D$ +18° shows the expected trisubstituted ethylenic bond peak at 825 cm^{-1}.

The change in molecular rotation on reduction of the Δ^{13}-ethylenic bond of Δ^{13}-dihydrodextropimaric and Δ^{13}-dihydroisodextropimaric acid (ΔM_D −182° and −175° respectively) indicates that hydrogenation has taken place in the same stereospecific sense in both cases. Models indicate that approach of a catalyst surface will be much more facile from the α-face, regardless of the C_7 orientation. Assuming *cis*-addition of hydrogen, this leads to a structure for the tetrahydro-acids having the C_{13} and C_{14} hydrogen atoms α-orientated. It is interesting to note that ΔM_D for the conversion of rimuene to tetrahydro-rimuene (2) (+65°) agrees better with the ΔM_D for the similar change in the isodextropimaric acid series (+72°) rather than that in the dextropimaric acid series (−199°).

Having shown that dextropimaric and isodextropimaric acid are epimeric at C_7, it remains to decide the actual stereochemistry at C_7 for each acid and to elucidate the stereochemistry at C_{13}. Wenkert and Chamberlin (19) have studied the infrared spectra of the equilibrium mixtures of γ- and δ-lactones derived from dihydrodextropimaric and dihydroisodextropimaric acids. From the percentages of γ- and δ-lactones (5±0.6% and 95±0.6%) and (3.6±0.8% and 96.4±0.8%) respectively in each equilibrium mixture, they reach the conclusion that in dextropimaric acid the vinyl group is β-orientated, and therefore in isodextropimaric acid it must be α-orientated. This result is independent of the stereochemistry at C_{13}. However, in view of the very small observed difference in the percentages of the γ- and δ-lactones in each equilibrium mixture and the intrinsic difficulty in obtaining high precision in quantitative infrared spectrophotometry, it seems to us that one should be cautious in accepting these conclusions.

From surface tension measurements, Bruun (31, 32) had previously reached the same conclusion concerning the stereochemistry at C_7 in these acids but had tacitly assumed that the C_{13} hydrogen atom is α-orientated in both acids. This seems a reasonable assumption in view of the closeness of the collapse areas for dextropimaric and the abietic acids (44.2 → 44.6 sq. Å), and isodextropimaric (43.6 sq. Å).[7] However since Bruun ignored the effect of the $\Delta^{8,14}$-ethylenic bond on the conformation of ring C (VIII and IX), his conclusions with regard to the stereochemistry at C_7 based on the film balance studies and on the intensities of absorption due to the vinyl group in the infrared (34, 35) are not necessarily correct. Furthermore, following a recent mass spectrometric study of the resin acids, Bruun, Ryhage, and Stenhagen (36) have reached the conclusion that dextropimaric and isodextropimaric acids are epimeric at C_{13} in opposition to the conclusion indicated on the basis of the film balance work.

Green, Harris, and Whalley (20), following a method reported earlier by us, agree that dextropimaric and isodextropimaric acid are epimeric at C_7 and without giving any details conclude that they are probably also epimeric at C_{13}. In dextropimaric acid, they consider that the C_{13}-hydrogen atom is α-orientated, i.e., *trans*- to the C_{12} methyl group, because dextropimaric acid is said to be stable to mineral acids. We have already shown, however, that dihydrodextropimaric acid is readily isomerized by hydrogen chloride in chloroform, and now report that dextropimaric acid behaves in a similar manner.

In view of the above uncertainties, we consider that the stereochemistry at C_{13} remains unproved for dextropimaric and isodextropimaric acids.

[7]*While no close analogue is available a somewhat comparable change of molecular shape to that involved in changing from a 13α- to a 13β-hydrogen atom in the pimaric acids is found in the cholestanol → coprostanol transformation (33). Here the effect is to increase the collapse area by ca. 3 sq.* Å.

We have simultaneously measured the amount of migration in a given time of the $\Delta^{8,14}$-ethylenic bond of dihydrodextropimaric and dihydroisodextropimaric acid catalyzed by mineral acid. The conditions were not sufficiently reproducible from run to run to give the same values for any given time interval but for every run carried out dihydroisodextropimaric acid was found to isomerize faster than dihydrodextropimaric acid as shown by the representative values given in the table.

	% of Δ^{13}-isomer formed	
Time (min.)	Dihydrodextropimaric acid	Dihydroisodextropimaric acid
3	11	25
6	23	39
10	40	52
15	38	45
20	48	58
40	79	82
100	86	88

These results could point to a difference in stereochemistry at C_{13} in the two acids, but may also be a measure of the effect of the differing stereochemistry at C_7, i.e., a quasi-equatorial ethyl group becoming equatorial after migration would act as an additional driving force whereas a quasi-axial group becoming axial after migration would retard the process.

We are at present engaged in converting the vinyl group of both dextropimaric and isodextropimaric acid to a methyl group in order to eliminate the asymmetry at C_7, and thereby establish whether or not dextropimaric and isodextropimaric acid have similar or dissimilar stereochemistry at C_{13}.

Some preliminary observations have been made on the action of formic acid on isodextropimaric acid, under conditions which cyclize rimuene (X) to isophyllocladene (37) (XI). No acidic product was isolated from the reaction. The products characterized

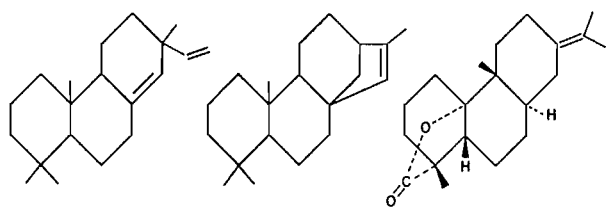

X XI XII

are an unsaturated γ-lactone of probable structure (XII), a hydrocarbon $C_{19}H_{29}$, clearly formed by decarboxylation of the β-γ-unsaturated acid which is intermediate in the formation of the γ-lactone XII, and also the known hydroxy-γ-lactone previously obtained (38) by the action of concentrated sulphuric acid on dextropimaric acid at $-30°$ C. The γ-lactone (XII), m.p. 109.5–111°, $[\alpha]_D$ $-54°$, showed no absorption in the infrared at 825 cm^{-1} characteristic of a trisubstituted ethylenic bond, and when it was hydrogenated in acetic acid with Adams' catalyst, it formed the known saturated γ-lactone (IV; R_1 = isopropyl; R_2 = hydrogen) which may be obtained from any of the dihydroabietic acids by the action of concentrated sulphuric acid at $-5°$ (39, 40). In order to obtain a reference sample of this γ-lactone, neoabietic acid was partially hydrogenated in ethanol solution using palladized charcoal (30%). A-Dihydroabietic

Can. J. Chem. Downloaded from www.nrcresearchpress.com by 190.90.36.8 on 09/04/12
For personal use only.

acid (29, 41), m.p. 149°, $[\alpha]_D$ +43°, was isolated in 25% yield and was converted by concentrated sulphuric acid at −5° into the γ-lactone IV (R_1 = isopropyl; R_2 = hydrogen). On similar treatment, the non-crystalline material from the hydrogenation afforded the same γ-lactone.

EXPERIMENTAL

Unless otherwise stated rotations were determined in absolute ethanol, and infrared spectra were determined on nujol mulls using a Perkin–Elmer model 21 double beam spectrophotometer.

Isodextropimaric Acid

WW pine gum rosin was converted to its 2-methyl-2-amino-1,3-propanediol salt in 2-butanone and the sparingly soluble salt of neoabietic acid collected (42). The mother liquors on concentration gave several crops of salt with low rotation. After three recrystallizations from 2-butanone this salt melted at 184–187° with slight preliminary sintering. The acid was liberated from the salt and recrystallized twice, giving a sample melting at 159–162° and having $[\alpha]_D$ −2±1° (*c*, 3.36). This was reconverted to the aminopropanediol salt, which after two recrystallizations melted at 184–187° after sintering slightly at 180°. The acid liberated from this had m.p. 160–163° and $[\alpha]_D$ 0° (*c*, 2.1). It did not depress an authentic specimen of isodextropimaric acid very kindly provided by Mr. R. V. Lawrence. It gave a methyl ester with diazomethane which crystallized from methanol as glistening plates, m.p. 61.5–62.5°.

Partial Hydrogenation of Isodextropimaric Acid

A solution of isodextropimaric acid (600 mg) in ethanol (25 ml) was hydrogenated in the presence of prereduced palladized charcoal catalyst (30%; 125 mg). Hydrogen (48 ml) was rapidly absorbed during 2 minutes, after which time absorption ceased abruptly. Calc. for 1 mole, 49 ml. The total product $[\alpha]_D$ −2° (*c*, 1.26; $CHCl_3$) was adsorbed on silica gel (15 g) and eluted with 50-ml portions of light petroleum – benzene (1:1) to give seven fractions as gums. Fractions 2 → 5 inclusive had similar rotations ($[\alpha]_D$ −4°) and were combined and recrystallized from methanol to give dihydroisodextropimaric acid as stout needles, m.p. 173–175° (450 mg), $[\alpha]_D$ −7° (*c*, 1.11), $[\alpha]_D$ −5° (*c*, 1.1; $CHCl_3$). Found: C, 78.61; H, 10.32. Calc. for $C_{20}H_{32}O_2$ (304): C, 78.94; H, 10.52. Infrared spectrum 1698 cm^{-1} (—COOH); 825 cm^{-1} (trisubstituted double bond).

The dihydro-acid (200 mg) in acetone was treated with cyclohexylamine (66 mg) in acetone to form the salt. After four recrystallizations from acetone the salt formed soft needles m.p. 203–206° (too insoluble for determination of rotation). Found: C, 77.56; H, 10.72. Calc. for $C_{21}H_{44}NO_2$ (402): C, 77.62; H, 10.95. The dihydro-acid regenerated from the pure salt had m.p. 173–175°, $[\alpha]_D$ −5° (*c*, 1.27; $CHCl_3$). The methyl ester formed plates m.p. 75° from methanol–water, $[\alpha]_D$ −5° (*c*, 2.01). Found: C, 78.89; H, 10.35. Calc. for $C_{21}H_{34}O_2$ (318): C, 79.25; H, 10.69.

Hydrogenation of Dihydroisodextropimaric Acid

A solution of dihydrodextropimaric acid (100 mg) in acetic acid (20 ml) was hydrogenated in the presence of Adams' catalyst (75 mg); 0.76 moles of hydrogen were absorbed in 24 hours. The total product, thrown out of methanol solution by water had m.p. 158–161°, $[\alpha]_D$ +30° (*c*, 0.96; $CHCl_3$) and showed some unsaturation with tetranitromethane. The total product in acetic acid (20 ml) was rehydrogenated using 125 mg of the catalyst. In 12 hours 0.27 moles of hydrogen were absorbed. The total product, thrown out of methanol solution by water, formed needles m.p. 163–167°, $[\alpha]_D$ +19°

Can. J. Chem. Downloaded from www.nrcresearchpress.com by 190.90.36.8 on 09/04/12
For personal use only.

(c, 1.15; $CHCl_3$). Chromatography on silica gel (3 g) using benzene as eluting solvent gave tetrahydroisodextropimaric acid as needles m.p. 172–173° (73 mg) from methanol–water, $[\alpha]_D$ +24° (c, 0.9), $[\alpha]_D$ +21° (c, 0.95; $CHCl_3$). Found: C, 78.46; H, 11.25. Calc. for $C_{20}H_{34}O_2$ (306): C, 78.37; H, 11.18%. Infrared spectrum 1700 cm^{-1} (—COOH). The methyl ester formed needles m.p. 68–69° from methanol–water, $[\alpha]_D$ +18° (c, 0.86). Found: C, 78.67; H, 11.08. Calc. for $C_{21}H_{36}O_2$ (320): C, 78.75; H, 11.26%.

Hydrogenation of Dihydrodextropimaric Acid

A solution of dihydrodextropimaric acid (117 mg) in acetic acid (35 ml) was added to Adams' catalyst (200 mg) which had been freshly reduced in acetic acid (5 ml). One mole of hydrogen was absorbed in 20 hours. The catalyst was removed by filtration and the acetic acid evaporated under reduced pressure. The crude product with m.p. 218–223° and $[\alpha]_D$ +20° (c, 1.13) was twice recrystallized from methanol to give tetrahydrodextropimaric acid as needles m.p. 238–240° (100 mg), $[\alpha]_D$ +18° (c, 1.1). Found: C, 78.41; H, 11.09. Calc. for $C_{20}H_{34}O_2$ (306): C, 78.37; H, 11.18%. Infrared spectrum 1699 cm^{-1} (—COOH).

Isomerization of Dihydrodextropimaric Acid on the Surface of a Catalyst

(*a*) A solution of dihydrodextropimaric acid (100 mg) in acetic acid (30 ml) was added to Adams' catalyst (20 mg) which had been freshly reduced in acetic acid (5 ml). One mole of hydrogen was absorbed in 20 hours. The crude product $[\alpha]_D$ +30° (c, 1.05) was recrystallized three times from methanol to give tetrahydrodextropimaric acid as needles m.p. and mixed m.p. 238–240° (60 mg), $[\alpha]_D$ +18° (c, 0.98). The mother liquors gave plates m.p. 177–180° (28 mg), $[\alpha]_D$ +39° (c, 0.86). A similar experiment to the above was carried out but without prereduction of the catalyst. The crude product with $[\alpha]_D$ +27° (c, 0.98) gave tetrahydrodextropimaric acid (65 mg) m.p. and mixed m.p. 238–240°, $[\alpha]_D$ +18° (c, 1.08), and also some plates m.p. 177–180° (20 mg), $[\alpha]_D$ +39° (c, 0.86). The material (45 mg) m.p. 177–180° obtained from the mother liquors of the above reductions was dissolved in acetic acid (30 ml) and added to Adams' catalyst (90 mg) which had been freshly reduced in acetic acid (5 ml). Two milliliters of hydrogen was absorbed in 20 hours. The total product $[\alpha]_D$ +17° (c, 0.74) was recrystallized from methanol to give tetrahydrodextropimaric acid as needles m.p. and mixed m.p. 238–240° (37 mg), $[\alpha]_D$ +18° (c, 1.0).

(*b*) A solution of dihydrodextropimaric acid (100 mg) in acetic acid (25 ml) was added to Adams' catalyst (20 mg) which had been freshly reduced in acetic acid (5 ml). Hydrogenation was allowed to proceed for 100 minutes after which time 1.9 ml of hydrogen had been absorbed. Calc. for 1 mole, 8.2 ml. The catalyst was removed by filtration and the acetic acid evaporated to give a solid m.p. 188–191°, $[\alpha]_D$ +54° (c, 1.17). When thrown out of methanol solution by water the total product formed prisms m.p. 193–197°, $[\alpha]_D$ +53° (c, 1.17). The constants of this material are approximately those m.p. 198°, $[\alpha]_J$ +55° reported by Le-Van-Thoi and Ourgaud (25) for tetrahydrodextropimaric acid. The above material m.p. 193–197° (63 mg) in acetic acid (20 ml) was added to Adams' catalyst (150 mg) freshly reduced in acetic acid (5 ml). Five milliliters of hydrogen was absorbed overnight. The crude product, $[\alpha]_D$ +20° (c, 0.92), was recrystallized twice from methanol to give tetrahydrodextropimaric acid as needles, m.p. and mixed m.p. 238–240° (48 mg), $[\alpha]_D$ +19° (c, 0.87).

(*c*) A solution of dihydrodextropimaric acid (100 mg) in acetic acid (25 ml) was added to Adams' catalyst (20 mg) which had been freshly reduced in acetic acid (5 ml). The mixture was shaken briefly once every minute for 1 hour under hydrogen. There was

Can. J. Chem. Downloaded from www.nrcresearchpress.com by 190.90.36.8 on 09/04/12
For personal use only.

no uptake of hydrogen and the starting material was recovered virtually unchanged, m.p. and mixed m.p. 240–242°, $[\alpha]_D$ +25° (*c*, 0.77).

(*d*) The above experiment was repeated except that this time the mixture was shaken briskly for 22 hours under nitrogen, after first reducing the catalyst in hydrogen. Starting material was recovered, m.p. and mixed m.p. 240–242°, $[\alpha]_D$ +21° (*c*, 1.06).

Isomerization of Isodextropimaric Acid Using p-Toluenesulphonic Acid

Isodextropimaric acid (440 mg) in dry dioxane (30 ml) was refluxed with *p*-toluenesulphonic acid (100 mg) under nitrogen for 4 hours and then allowed to stand overnight. The dioxane was evaporated, the viscous residue dissolved in chloroform, and washed free from *p*-toluenesulphonic acid using water. Evaporation of the dried chloroform solution gave a yellow gum $[\alpha]_D$ +82° (*c*, 2.05; $CHCl_3$). The gum was dissolved in ether and extracted with aqueous potassium carbonate, the carbonate soluble part being recovered by the addition of dilute hydrochloric acid. The acidic gum so obtained was adsorbed on a silica gel column (7.5 g) and eluted with benzene (50-ml portions) to give eight fractions. Fractions $2 \rightarrow 6$ inclusive in acetone gave solid when cooled to −10°. The solid was recrystallized four times from acetone–water to give Δ^{13}-isodextropimaric acid as clusters of prisms, m.p. 105–106° (105 mg), $[\alpha]_D$ +94° (*c*, 1.14; $CHCl_3$). Found: C, 79.74; H, 9.75. Calc. for $C_{20}H_{30}O_2$ (302): C, 79.49; H, 9.93. Infrared spectrum 1694 cm^{-1} (—COOH); 1413 cm^{-1}, and 908 cm^{-1} (vinyl group).

Several repetitions of this experiment under similar or slightly different conditions gave products having rotations between +45° and +55° from which it was not found possible to obtain pure Δ^{13}-isodextropimaric acid by either chromatography or fractional crystallization of the free acid or its cyclohexylamine or 2-aminopropan-1,3-diol salts. A better preparative method is given below.

Isomerization of Dihydrodextropimaric Acid Using Hydrogen Chloride

Dry hydrogen chloride was passed into a solution of dihydrodextropimaric acid (400 mg) in dry chloroform (50 ml) at −5° C for 4 hours. The chloroform solution was washed free from mineral acid with water and then dried (Na_2SO_4) and evaporated to give a gum (390 mg), $[\alpha]_D$ +75° (*c*, 0.95) which solidified. After five recrystallizations from methanol, Δ^{13}-dihydrodextropimaric acid formed plates, m.p. 182–183° (305 mg), $[\alpha]_D$ +73° (*c*, 1.00). Found: C, 79.05; H, 10.35. Calc. for $C_{20}H_{32}O_2$ (304): C, 78.94; H, 10.52. Infrared spectrum 1696 cm^{-1} (—COOH); no ethylenic absorption.

Isomerization of Dihydroisodextropimaric Acid Using Hydrogen Chloride

Dry hydrogen chloride was passed into a solution of dihydroisodextropimaric acid (210 mg) in dry chloroform (12 ml) at −5° C for 4 hours. The chloroform solution was extracted with aqueous potassium carbonate. The aqueous extract on acidification gave an acid gum (170 mg) $[\alpha]_D$ +74° (*c*, 1.03; $CHCl_3$). The gum was adsorbed on silica gel (4 g) and eluted with 30-ml portions of light petroleum – benzene (1:1) to give 10 fractions. Fractions $2 \rightarrow 8$ inclusive were combined and recrystallized three times from acetone–water to give Δ^{13}-dihydroisodextropimaric acid as needles, m.p. 107–108° (130 mg) $[\alpha]_D$ +76° (*c*, 0.92), $[\alpha]_D$ +74° (*c*, 0.99; $CHCl_3$). Found: C, 78.96; H, 10.41. Calc. for $C_{20}H_{32}O_2$ (304): C, 78.94; H, 10.52. Infrared spectrum 1696 cm^{-1} (—COOH); no ethylenic absorption. The methyl ester was a colorless oil, b.p. 130–135° at 2×10^{-2} mm, $[\alpha]_D$ +56° (*c*, 1.04). Found: C, 79.13; H, 10.58. Calc. for $C_{21}H_{34}O_2$ (318): C, 79.25; H, 10.69.

Rate of Isomerization Experiments

Twenty-five milligrams of each dihydropimaric acid in a finely powdered state were

Can. J. Chem. Downloaded from www.nrcresearchpress.com by 190.90.36.8 on 09/04/12
For personal use only.

simultaneously dissolved in 7-cc portions of ethanol-free dry chloroform previously saturated with hydrogen chloride at 0°. Dry hydrogen chloride was bubbled through the solutions maintained at 0°. Reaction time was measured from the time of complete solution. The reaction was quenched by three water washes, and the chloroform solution dried and evaporated. Rotations were done in ethanol on the total product. The results of a series of runs are summarized in the table.

Hydrogenation of Δ^{13}-Dihydrodextropimaric Acid

A solution of Δ^{13}-dihydrodextropimaric acid (83 mg) in acetic acid (16 ml) was hydrogenated in the presence of Adams' catalyst (166 mg); 1.07 moles of hydrogen were absorbed in 17 hours. The catalyst was removed by filtration and then the solvent was evaporated under reduced pressure. The product was dissolved in ether, washed with water, and dried. Evaporation of the ether gave a solid product (80 mg) $[\alpha]_D$ +17° (*c*, 1.15). The product was adsorbed on silica gel (2.5 g) and eluted with benzene–ether (19:1) in 20-ml portions to give four fractions. Fraction 1 had $[\alpha]_D$ +18° (*c*, 0.84) and fraction 4 had $[\alpha]_D$ +19° (*c*, 0.9). The four fractions were combined and recrystallized four times from methanol–water to give tetrahydrodextropimaric acid as needles, m.p. and mixed m.p. 238–240° (66 mg), $[\alpha]_D$ +19° (*c*, 0.84), identical with that obtained above.

Hydrogenation of Δ^{13}-Dihydroisodextropimaric Acid

A solution of Δ^{13}-dihydroisodextropimaric acid (100 mg) in acetic acid (20 ml) was hydrogenated in the presence of Adams' catalyst (200 mg); 1.05 moles of hydrogen were absorbed in 17 hours. The catalyst was removed by filtration and the solvent was evaporated under reduced pressure. The product was dissolved in ether, washed with water, and dried. The total product, thrown out of methanol solution by means of water, formed needles, m.p. 165–168°, $[\alpha]_D$ +21° (*c*, 1.11; $CHCl_3$) and gave no coloration with tetranitromethane. Chromatography on silica gel (3 g) and elution with benzene gave tetrahydroisodextropimaric acid, m.p. and mixed m.p. 172–173° (89 mg), $[\alpha]_D$ +21° (*c*, 1.07; $CHCl_3$), identical with that obtained above.

Isomerization of Dextropimaric Acid Using Hydrogen Chloride

Dry hydrogen chloride was passed into a solution of dextropimaric acid (100 mg) in dry chloroform (30 ml) at −5° C for 4 hours. The chloroform solution was washed free from mineral acid with water and then dried and evaporated to give a gum (95 mg), $[\alpha]_D$ +69° (*c*, 0.76). The gum was adsorbed on silica and eluted with 20-ml portions of benzene – light petroleum (3:2) to give 10 fractions. Fractions $2 \rightarrow 8$ inclusive had rotations between +69° and +71° and were combined to give Δ^{13}-dextropimaric acid as prisms, m.p. 131–132° (55 mg) from methanol–water, $[\alpha]_D$ +70° (*c*, 0.94). Found: C, 79.34; H, 9.97. Calc. for $C_{20}H_{30}O_2$ (302): C, 79.49; H, 9.93. Infrared spectrum 1697 cm^{-1} (—COOH); 1408 cm^{-1}, 995 cm^{-1}, and 908 cm^{-1} (vinyl group).

Partial Hydrogenation of Δ^{13}-Dextropimaric Acid

Δ^{13}-Dextropimaric acid (26.4 mg) in ethanol (7 ml) was hydrogenated in the presence of palladized charcoal catalyst (30%) (10 mg). Hydrogen (2.14 ml) was absorbed in 8 minutes after which time absorption ceased abruptly. Calc. for 1 mole, 2.15 ml. The total product $[\alpha]_D$ +75° (*c*, 0.85) was recrystallized three times from methanol–water to give Δ^{13}-dihydrodextropimaric acid as plates, m.p. and mixed m.p. 181–182°, $[\alpha]_D$ +75° (*c*, 0.94).

Isomerization of Isodextropimaric Acid Using Hydrogen Chloride

Dry hydrogen chloride was passed into a solution of isodextropimaric acid (1.4 g) in

Can. J. Chem. Downloaded from www.nrcresearchpress.com by 190.90.36.8 on 09/04/12
For personal use only.

dry chloroform (30 ml) at −5° C for 4 hours. The chloroform solution was washed free from mineral acid with water and then dried and evaporated to give a gum (1.36 g), $[\alpha]_D$ +91° (*c*, 1.0; $CHCl_3$). The gum was adsorbed on silica gel (30 g) and eluted with 50-ml portions of light petroleum – benzene (1:1) to give nine fractions as gums. Fractions 1 → 6 inclusive had rotations between +92° and +89° and were combined (0.97 g). After six recrystallizations from acetone–water, Δ^{13}-isodextropimaric acid was obtained as clusters of prisms, m.p. 106–107° (0.6 g), $[\alpha]_D$ +113° (*c*, 0.88), $[\alpha]_D$ +96° (*c*, 1.34; $CHCl_3$). Found: C, 79.29; H, 9.74. Calc. for $C_{20}H_{30}O_2$ (302): C, 79.49; H, 9.93. A further crop of 470 mg, m.p. 104–106°, was obtained from the residues. The methyl ester formed flattened needles, m.p. 70–71° from methanol–water, $[\alpha]_D$ +118° (*c*, 0.82). Found: C, 79.75; H, 9.95. Calc. for $C_{21}H_{32}O_2$ (316): C, 79.75; H, 10.13.

Partial Hydrogenation of Δ^{13}-Isodextropimaric Acid

Δ^{13}-Isodextropimaric acid (304 mg) in ethanol (20 ml) was hydrogenated in the presence of palladized charcoal catalyst (30%) (150 mg). Hydrogen (23.9 ml) was rapidly absorbed during 2 minutes, after which time absorption ceased abruptly. Calc. for 1 mole, 24.3 ml. The total product, $[\alpha]_D$ +68° (*c*, 1.32; $CHCl_3$) was adsorbed on silica gel (7.5 g) and eluted with 50-ml portions of light petroleum – benzene (1:1) to give seven fractions. Fractions 2 → 6 inclusive were combined and recrystallized three times from acetone–water to give Δ^{13}-dihydroisodextropimaric acid as needles, m.p. and mixed m.p. 107–108° (225 mg), $[\alpha]_D$ +73° (*c*, 0.99; $CHCl_3$).

γ-Lactone of Dihydrodextropimaric Acid

(*a*) *From dihydrodextropimaric acid.*—Dihydrodextropimaric acid (400 mg) was added gradually during 15 minutes to sulphuric acid (2.5 ml, d = 1.84) cooled to −5° C. After 1 hour the reaction mixture was worked up as described previously to give a neutral gum (380 mg), $[\alpha]_D$ −20° (*c*, 1.22), which solidified. The gum was adsorbed on silica gel (10 g) and eluted with 30-ml portions of benzene–ether (19:1) to give six fractions. Fractions 1 → 4 inclusive, when precipitated from methanol solution by water, formed plate-like crystals. These were combined and recrystallized from methanol–water to give the γ-lactone of dihydrodextropimaric acid as plates, m.p. 100°, $[\alpha]_D$ −15° (*c*, 1.17). Found: C, 78.66; H, 10.35. Calc. for $C_{20}H_{32}O_2$ (304): C, 78.94; H, 10.52. Infrared spectrum 1763 cm^{-1} (γ-lactone). Le-Van-Thoi and Ourgaud (28) report m.p. 100° $[\alpha]_j$ −17° (EtOH). The melting point was depressed to 97° on admixture with the γ-lactone of dihydroisodextropimaric acid.

(*b*) *From Δ^{13}-dihydrodextropimaric acid.*—Δ^{13}-Dihydroisodextropimaric acid (100 mg) was added gradually during 15 minutes to sulphuric acid (1 ml, d = 1.84) cooled to −5° C. After 1 hour the reaction mixture was worked up as described previously to give a neutral gum (98 mg), $[\alpha]_D$ −22° (*c*, 1.26), which crystallized on seeding. The product was adsorbed on silica gel (2.5 g) and eluted with benzene–ether (19:1) in 30-ml portions to give seven fractions. Fractions 1 → 5 inclusive were combined and recrystallized from methanol–water to give the γ-lactone of dihydrodextropimaric acid as plates, m.p. and mixed m.p. 100° (58 mg), $[\alpha]_D$ −15° (*c*, 1.07).

γ-Lactone of Dihydroisodextropimaric Acid

(*a*) *From dihydroisodextropimaric acid.*—Dihydroisodextropimaric acid (400 mg) was added gradually during 15 minutes to sulphuric acid (2.5 ml, d = 1.84) cooled to −5° C in a mixture of ice and salt. After being kept at −5° C for 1 hour the reaction mixture was decomposed by being poured into water containing chopped ice. The organic material

Can. J. Chem. Downloaded from www.nrcresearchpress.com by 190.90.36.8 on 09/04/12
For personal use only.

Can. J. Chem. Downloaded from www.nrcresearchpress.com by 190.90.36.8 on 09/04/12
For personal use only.

was extracted with ether and the extract washed with water to remove mineral acid. The ether extract was then washed with aqueous potassium carbonate (10%) to remove acidic material. The ether extract was washed with water, dried (Na_2SO_4), and evaporated to give a neutral gum (380 mg), $[\alpha]_D$ −19° (*c*, 1.1). The gum was adsorbed on silica gel (10 g) and eluted with 30-ml portions of benzene to give seven fractions. Fractions 1 → 4 inclusive, which when thrown out of methanol solution by water formed plate-like crystals, were combined and recrystallized from methanol–water to give the γ-lactone as plates, m.p. 105–106° (250 mg), $[\alpha]_D$ −90° (*c*, 1.59). Found: C, 78.57; H, 10.47. Calc. for $C_{20}H_{32}O_2$ (304): C, 78.94; H, 10.52. Infrared spectrum 1770 cm^{-1} (γ-lactone).

(*b*) *From Δ^{13}-dihydroisodextropimaric acid.*—Δ^{13}-Dihydroisodextropimaric acid (80 mg) was added gradually during 15 minutes to sulphuric acid (0.6 ml, d = 1.84) cooled to −5° C in a mixture of ice and salt. After being kept at −5° C for 1 hour the reaction mixture was worked up as described above to give a neutral gum (79 mg), $[\alpha]_D$ −18° (*c*, 1.01). The gum was adsorbed on silica gel (3 g) and eluted with benzene. The first fractions were recrystallized from methanol–water to give the γ-lactone as plates, m.p. and mixed m.p. 105–106° (43 mg), $[\alpha]_D$ −8° (*c*, 1.06).

δ-Lactone of Dihydroisodextropimaric Acid

(*a*) *From dihydroisodextropimaric acid.*—Dihydroisodextropimaric acid (170 mg) was added gradually during 15 minutes to sulphuric acid (3 ml, d = 1.84) at room temperature (23° C). After 5 hours the reaction mixture was poured into water containing chopped ice. The organic material was extracted with ether and washed with water to remove mineral acid. The ether extract was then washed with aqueous potassium carbonate (10%) to remove acidic material. The ether extract was washed with water, dried (Na_2SO_4), and evaporated to give a neutral gum (168 mg), $[\alpha]_D$ −31° (*c*, 1.14). The gum was adsorbed on silica gel (4 g) and eluted with 30-ml portions of benzene to give eight fractions. Fractions 4 → 8 inclusive, which when thrown out of methanol solution by water formed plate-like crystals, were combined and recrystallized from methanol–water to give the δ-lactone as plates, m.p. 74–75° (70 mg), $[\alpha]_D$ −40° (*c*, 0.93). Found: C, 79.05; H, 10.49. Calc. for $C_{20}H_{32}O_2$ (304): C, 78.94; H, 10.52. Infrared spectrum 1720 cm^{-1} (δ-lactone). A further crop of plates, m.p. 72–74° (30 mg) was obtained from the mother liquors.

(*b*) *From the γ-lactone.*—The γ-lactone (80 mg) was gradually added during 15 minutes to sulphuric acid (2 ml, d = 1.84) at room temperature (23° C). After 5 hours the lactonic material was isolated as described above to give a colorless gum (80 mg), $[\alpha]_D$ −29° (*c*, 0.93), which solidified on seeding. The total product was adsorbed on silica gel (2 g) and eluted with benzene in 30-ml portions to give four fractions. The last two fractions were combined and recrystallized from methanol–water to give the δ-lactone as plates, m.p. and mixed m.p. 73–74° (40 mg) $[\alpha]_D$ −39° (*c*, 0.97).

Isomerization of Ukita's Acid Using Hydrogen Chloride

Dry hydrogen chloride was passed into a solution of Ukita's acid (20 mg) in dry chloroform (15 ml) at −5° for 4 hours. The chloroform solution was washed free from mineral acid with water, and then dried, and evaporated to give a colorless gum (19 mg), $[\alpha]_D$ +108° (*c*, 0.79), which was twice recrystallized from acetone–water to give Δ^{13}-isodextropimaric acid as stout prisms (15 mg), m.p. and mixed m.p. 105–107°, $[\alpha]_D$ +110° (*c*, 1.08).

Partial Hydrogenation of Ukita's Acid

A solution of Ukita's acid (15.5 mg) in ethanol (7 ml) was hydrogenated in the presence

of pre-reduced palladized charcoal catalyst (30%, 3 mg); 1 mole of hydrogen (1.25 ml) was absorbed during 8 minutes and then absorption ceased. The crude product, m.p. 148–152° was recrystallized five times from methanol–water to give the dihydro-acid as prisms, m.p. 154–157° (9.4 mg), $[\alpha]_D$ +18° (*c*, 0.72). Found: C, 78.96; H, 10.31. Calc. for $C_{20}H_{32}O_2$ (304): C, 78.94; H, 10.52. Infrared spectrum 1700 cm^{-1} (—COOH); 825 cm^{-1} (trisubstituted double bond).

γ-Lactone of Isodextropimaric Acid

Isodextropimaric acid (200 mg) in dry dioxane (20 ml) was refluxed under nitrogen with *p*-toluenesulphonic acid (1 g) for 4 hours and then allowed to stand overnight. The dioxane was evaporated off and the viscous residue taken up in ether. Extraction of the ether solution with aqueous potassium carbonate (10%) gave only 15 mg of acidic material which was not further investigated. The ether layer was washed with water and dried (Na_2SO_4). On evaporation of the ether a neutral gum (180 mg), $[\alpha]_D$ −18° (*c*, 1.24), was obtained. The product was adsorbed on silica (4 g) and eluted with benzene in 20-ml portions to give five fractions. Fractions 4 and 5 gave some solid material with methanol–water and after several recrystallizations from methanol–water, the γ-lactone of isodextropimaric acid formed plates, m.p. 128–130° (15 mg), $[\alpha]_D$ −1° (*c*, 0.84). Found: C, 79.59; H, 9.90. Calc. for $C_{20}H_{30}O_2$ (302): C, 79.49; H, 9.93. Infrared spectrum: 1770 cm^{-1} (γ-lactone); 1480 cm^{-1}, 1000 cm^{-1}, 910 cm^{-1} (vinyl group).

Treatment of Isodextropimaric Acid with Formic Acid

Isodextropimaric acid (500 mg) was refluxed for 60 hours with formic acid (90%, 75 ml). The formic acid was evaporated under reduced pressure. Globules of oil which steam-distilled over were isolated by extracting the neutralized distillate with ether, and proved to be a mobile hydrocarbon (84 mg), $[\alpha]_D$ +4° (*c*, 0.79). The distillation residue was dissolved in ether and washed free from formic acid with water. The dried ether extract gave a brown gum (385 mg), $[\alpha]_D$ +18° (*c*, 1.5) on evaporation. Infrared spectrum ($CHCl_3$) 3520 cm^{-1} (—OH), 1780 cm^{-1} (γ-lactone), 1730 cm^{-1} (δ-lactone); absence of carboxyl and vinyl groups. The product was split into the following fractions by chromatography on neutral alumina (Grade IV, 10 g).

A. Hexane (20 ml) readily eluted a mobile hydrocarbon fraction (38 mg).

B. Hexane (200 ml) gave 10 fractions, $[\alpha]_D$ −43° to −34° which were combined (137 mg).

C. Benzene and chloroform eluted further fractions as gums (210 mg).

To fraction C was added material (60 mg) from the mother liquors of the recrystallization of fraction B. Further chromatography of this material on neutral alumina (Grade II, 5 g) gave the following fractions.

D. Hexane (100 ml) eluted material which crystallized from methanol–water (125 mg) $[\alpha]_D$ −28° (*c*, 0.98).

E. Benzene eluted non-crystalline material.

F. Benzene–chloroform (3:1) eluted material (25 mg), m.p. 170–172°, which crystallized spontaneously on evaporation of the solvent.

Investigation of the Fractions

A. The hydrocarbon fraction was combined with that from the steam distillate and warmed with aqueous sodium hydroxide (10%). The hydrocarbon, recovered by ether extraction, was dissolved in hexane and percolated through alumina. The hydrocarbon distilled as a colorless mobile oil, b.p. 90° at 0.05 mm, n_D^{24} 1.5125, $[\alpha]_D$ +6° (*c*, 1.09). Found: C, 88.21; H, 12.10. Calc. for $C_{19}H_{30}$: C, 88.30; H, 11.70.

Can. J. Chem. Downloaded from www.nrcresearchpress.com by 190.90.36.8 on 09/04/12
For personal use only.

B. The combined material (137 mg) was recrystallized twice from methanol–water and then four times from methanol to afford prisms, m.p. 109.5–111° (70 mg), $[\alpha]_D$ −52° (*c*, 0.97). Found: C, 79.12; H, 9.60. Calc. for $C_{20}H_{30}O_2$ (302): C, 79.49; H, 9.93. Infrared spectrum 1762 cm^{-1} (γ-lactone); no bands for ethylenic bonds.

When the above γ-lactone (24.4 mg) in acetic acid (6 ml) was hydrogenated in the presence of Adams' catalyst (10 mg), 0.96 mole of hydrogen was absorbed in 1 hour. The crystalline product, recrystallized from methanol–water afforded prisms, m.p. 131–132°, $[\alpha]_D$ −5° (*c*, 0.8). Found: C, 78.78; H, 10.32. Calc. for $C_{20}H_{32}O_2$ (304): C, 78.94; H, 10.52. This material is identical (mixed m.p. 131–132°) with the known γ-lactone obtained from any of the dihydroabietic acids (see below).

D. Fraction D was recrystallized from methanol–water to give a further crop of γ-lactone, m.p. 109.5–111° (47 mg).

E. No solid material could be isolated from this fraction.

F. Recrystallization of this fraction from methanol gave needles, m.p. 179–180°, $[\alpha]_D$ −6° (*c*, 0.9). Found: C, 75.08; H, 9.83. Calc. for $C_{20}H_{32}O_3$ (320): C, 74.96; H, 10.06. Infrared spectrum: 3548 cm^{-1} (—OH), 1764 cm^{-1} (γ-lactone). This is clearly the known hydroxy-γ-lactone from dextropimaric acid (38).

Partial Hydrogenation of Neoabietic Acid

Neoabietic acid (1.035 g) in ethanol (40 ml) in the presence of palladized charcoal (30%, 200 mg) rapidly absorbed 1.07 moles of hydrogen in 11 minutes, after which time absorption became comparatively slow. The ultraviolet spectrum of the product $[\alpha]_D$ +26° (*c*, 1.2) showed the presence of less than 1% of neoabietic acid. Chromatography on silica gel using hexane as eluting solvent gave 14 fractions. Fractions 1 → 6 having rotations ranging from +12° to +25° were combined (530 mg). Fractions 7 → 14 of $[\alpha]_D$ +37° gave A-dihydroabietic acid (29) on crystallization from methanol–water (98 mg), m.p. 149°, $[\alpha]_D$ +43° (*c*, 1.03). Found: C, 78.66; H, 10.27. Calc. for $C_{30}H_{32}O_2$ (304): C, 78.94; H, 10.52. Infrared spectrum: 1697 cm^{-1} (—COOH); 826 cm^{-1} (trisubstituted double bond).

Fractions 1 → 6, together with material (340 mg) from the mother liquors of the recrystallization of fractions 7 → 14, were converted to the piperidine salt and recrystallized from acetone. Two crops of the least soluble material, $[\alpha]_D$ +31° (*c*, 1.5) and $[\alpha]_D$ +27° (*c*, 0.9), were combined (350 mg) and reconverted to acid, $[\alpha]_D$ +35° (*c*, 0.94). Recrystallization from methanol–water afforded a further crop of A-dihydroabietic acid as needles (165 mg), m.p. 147–148°, $[\alpha]_D$ +39° (*c*, 0.99). The more soluble piperidine salt gave acid (580 mg), $[\alpha]_D$ +19° (*c*, 1.0).

γ-Lactone of A-Dihydroabietic Acid

A-Dihydroabietic acid (165 mg) was added gradually during 15 minutes to sulphuric acid (1 ml, d = 1.84) cooled to −5°. After 1 hour the reaction mixture was worked up as in the previous examples to give neutral material which crystallized spontaneously. Chromatography on alumina (Grade III, neutral) using hexane as eluting solvent gave the γ-lactone as prisms, m.p. 132°, $[\alpha]_D$ −4° (*c*, 1.04). Found: C, 78.96; H, 10.35. Calc. for $C_{20}H_{32}O_2$ (304): C, 78.94; H, 10.52. Infrared spectrum: 1758 cm^{-1} (γ-lactone).

The non-crystalline dihydroneoabietic acid $[\alpha]_D$ +19° afforded the same γ-lactone on similar treatment.

ACKNOWLEDGMENTS

We are indebted to Mr. R. V. Lawrence for a supply of pine gum and rosin, and

Can. J. Chem. Downloaded from www.nrcresearchpress.com by 190.90.36.8 on 09/04/12
For personal use only.

valuable advice on the isolation of the acids, and to Dr. T. F. Sanderson for a generous sample of dextropimaric acid, a gift of Staybelite resin, and valuable advice. We wish to thank Mr. A. Knoll for technical assistance, Mr. H. Seguin for the analyses, and Mr. R. Lauzon for determining the infrared absorption spectra.

REFERENCES

1. EDWARDS, O. E. and HOWE, R. Chem. & Ind. 629 (1958).
2. BRIGGS, L. H., CAIN, B. F., and WILMSHURST, J. K. Chem. & Ind. 599 (1958).
3. WENKERT, E. Chem. & Ind. 282 (1955).
4. BRANDT, C. W. New Zealand J. Sci. Technol. B, **34**, 46 (1952).
5. BOTTOMLEY, W., COLE, A. R. H., and WHITE, D. E. J. Chem. Soc. 2624 (1955).
6. DJERASSI, C., RINIKER, R., and RINIKER, B. J. Am. Chem. Soc. **78**, 6362 (1956).
7. BRIGGS, L. H., CAWLEY, R. W., LOE, J. A., and TAYLOR, W. I. J. Chem. Soc. 955 (1950).
8. MOSETTIG, E. and NES, W. R. J. Org. Chem. **20**, 884 (1955).
9. HAWORTH, R. D. and JOHNSTONE, R. A. W. J. Chem. Soc. 1492 (1957).
10. DJERASSI, C., CAIS, M., and MITSCHER, L. A. J. Am. Chem. Soc. **80**, 246 (1958).
11. CROSS, B. E., GROVE, J. F., MACMILLAN, J., and MULHOLLAND, T. P. C. Proc. Chem. Soc. 221 (1958).
12. WIESNER, K., ARMSTRONG, R., BARTLETT, M. F., and EDWARDS, J. A. J. Am. Chem. Soc. **76**, 6068 (1954).
13. DVORNIK, D. and EDWARDS, O. E. Chem. & Ind. 623 (1958).
14. DVORNIK, D. and EDWARDS, O. E. Proc. Chem. Soc. 280 (1958).
15. RUZICKA, L., DE GRAAFF, G. B. R., GOLDBERG, M. W., and FRANK, B. Helv. Chim. Acta, **15**, 915 (1932).
16. SIMONSEN, J. and BARTON, D. H. R. The terpenes. Vol. III. Cambridge University Press. 1952. p. 448.
17. HARRIS, G. C. and SANDERSON, T. F. J. Am. Chem. Soc. **70**, 2079 (1948).
18. HARRIS, G. C. and SANDERSON, T. F. J. Am. Chem. Soc. **70**, 2081 (1948).
19. WENKERT, E. and CHAMBERLIN, J. W. J. Am. Chem. Soc. **80**, 2912 (1958).
20. GREEN, B., HARRIS, A., and WHALLEY, W. B. Chem. & Ind. 1084 (1958).
21. UKITA and TSUMITA. J. Pharm. Soc. Japan, **72**, 1324 (1952).
22. HASSELSTROM, T. and BOGERT, M. T. J. Am. Chem. Soc. **57**, 2118 (1935).
23. UKITA, TSUMITA, and UTSUGI. Pharm. Bull. Japan, **3**, 441 (1955).
24. RUZICKA, L., HUYSER, H. W., and SEIDEL, C. F. Rec. trav. chim. **47**, 363 (1928).
25. LE-VAN-THOI and OURGAUD, J. Bull. soc. chim. France, 205 (1956).
26. VESTERBERG, K. A. Ber. **19**, 2167 (1886).
27. RUZICKA, L. and BALAS, F. Ann. **460**, 202 (1928).
28. LE-VAN-THOI and OURGAUD, J. Bull. soc. chim. France, 202 (1956).
29. VELLUZ, L., MULLER, G., PETIT, A., and MATHIEU, J. Bull. soc. chim. France, 401 (1954).
30. FIESER, L. F. J. Am. Chem. Soc. **75**, 4395 (1953).
31. BRUUN, H. H. Acta Acad. Aboensis, Math. et Phys. **19**(3), 7 (1954).
32. BRUUN, H. H. Finska Kemistsamfundets Medd. **63**, 22 (1954).
33. ADAM, N. K., ASKEW, F. A., and DANIELLI, J. F. Biochem. J. **29**, 1786 (1935).
34. BRUUN, H. H. Paperi ja Puu, **38**, 577 (1956).
35. BRUUN, H. H. Paperi ja Puu, **39**, 221 (1957).
36. BRUUN, H. H., RYAGE, R., and STENHAGEN, E. Acta Chem. Scand. **12**, 789 (1958).
37. BRANDT, C. W. New Zealand J. Sci. Technol. **20**, 8 (1938).
38. FLECK, E. E. and PALKIN, S. J. Am. Chem. Soc. **62**, 2044 (1940).
39. BARTON, D. H. R. Chem. & Ind. 638 (1948).
40. SUBLUSKEY, L. A. and SANDERSON, T. F. J. Am. Chem. Soc. **76**, 3512 (1954).
41. LOMBARD, R. and EBELIN, J. Bull. soc. chim. France, 930 (1953).
42. LOEBLICH, V. M. and LAWRENCE, R. V. J. Org. Chem. **21**, 610 (1956).

Can. J. Chem. Downloaded from www.nrcresearchpress.com by 190.90.36.8 on 09/04/12
For personal use only.

Can. J. Chem. Downloaded from www.nrcresearchpress.com by 196.1.178.254 on 09/04/12
For personal use only.

APPLICATIONS OF PROTON MAGNETIC RESONANCE SPECTRA IN FATTY ACID CHEMISTRY[1]

C. Y. Hopkins and H. J. Bernstein

ABSTRACT

An introductory study has been made of the proton magnetic resonance spectra of fatty acids, fatty acid esters, and natural glyceride oils. Characteristic signals were recorded for the hydrogens of such groupings as hydroxy, acetoxy, and epoxy; isolated, conjugated, and methylene-interrupted double bonds; and others. Examples are given of the application of this technique in identifying the fatty acids of natural glyceride oils. Semiquantitative estimations are shown to be feasible. Evidence for Nunn's formula for sterculic acid is discussed on the basis of the spectra of the acid and its derivatives.

Proton magnetic resonance measurements provide a new method of distinguishing certain groupings in fatty acid molecules. This preliminary study indicates that the method is of value in determining the structure of fatty acids and their derivatives and in estimating in a roughly quantitative manner the proportions of certain fatty acids in mixtures. Quantitative estimation is applicable in some degree to single mixed glycerides and to natural oils, which are mainly mixtures of mixed glycerides.

Small amounts of impurities are not likely to interfere, since components constituting less than 5% of the sample do not usually give a measurable signal.

In the present work measurements were made with a Varian V-4300 NMR spectrometer operating at a frequency of 40 Mc/s and equipped with a Varian Field Stabilizer. Each sample was dissolved in chloroform at sufficiently high concentration to give signals of moderate intensity. Some of the oxygenated acids were used at maximum solubility. Usually 0.2 to 0.5 g of sample was dissolved in 0.5 to 1.0 ml of chloroform. The sample tube was 5 mm o.d. and was set spinning by a jet of nitrogen.

Chemical shifts were measured from the dissolved chloroform signal or that of the long-chain CH_2 signal by the well-known side-band technique. All chemical shifts were referred to the long-chain CH_2 signal, the signals at lower applied field having negative values. All figures are displayed with applied magnetic field increasing toward the right.

MATERIALS

Oleic acid, methyl oleate, and methyl linoleate were prepared from natural oils by fractional distillation of the esters followed by low-temperature crystallization. 9,10-Diacetoxystearic acid was made by acetylating the pure dihydroxy acid. 12,13-Dihydroxyoleic acid was prepared from the seed oil of *Vernonia colorata* by Gunstone's procedure (1). Commercial ethyl ricinoleate was purified by low-temperature crystallization.

Vernonia oil and *Sterculia* oil were extracted in the laboratory from seed of *Vernonia colorata* and *Sterculia foetida* respectively. The other oils and the lauric acid were commercial products. Methyl 10,12-octadecadienoate was kindly supplied by Dr. O. S. Privett.

Sterculic acid was made by cold saponification of *Sterculia* oil, followed by repeated crystallization from acetone at low temperature. It was hydrogenated with palladium

[1]*Manuscript received December 16, 1958.*
Contribution from the Division of Pure Chemistry, National Research Council, Ottawa, Canada.
Issued as N.R.C. No. 5093.

catalyst. 9,11-Diketononadecanoic acid, m.p. 59–60°, was obtained by controlled oxidation of sterculic acid.

RESULTS AND DISCUSSION

Typical spectra are shown in Fig. 1. The saturated acid, lauric, shows the signals common to all fatty acids. The groupings and the position of the corresponding signals were as follows (parts per million): terminal CH_3, +0.43; CH_2 groups of the chain, 0; CH_2 adjacent (α) to the carboxyl group, −1.0. The position of the signal for the carboxy hydrogen (offscale to low field) is strongly affected by the degree of dilution and is not shown.

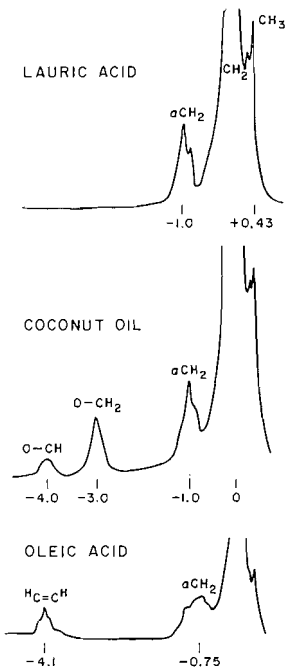

FIG. 1. Proton resonance spectra of a saturated acid, a highly saturated oil, and a monounsaturated acid. The signal for the acid proton is offscale to the left.

Coconut oil, consisting mainly of glycerides of saturated acids, shows the signals for terminal CH_3, CH_2 chain, and αCH_2, and also for the glyceryl residue.* The two $O-\overset{|}{C}H_2$ groups of the glyceryl radical appeared at −3.0 p.p.m. with intensity 4 (four protons) and the $O-\overset{|}{C}H$ at −4.0 p.p.m. with intensity 1.

Oleic acid produced a signal at −4.1 p.p.m. characteristic of the monounsaturated grouping CH=CH. The CH_2 groups adjacent to the double bond carbons contribute to the intensity of the signal at −0.75 p.p.m.

Double Bond Unsaturation

Characteristic signals for the various types of double bond groupings were observed. Those for simple monoenes, 1,4-dienes, and conjugated dienes are shown in Fig. 2.

**The identification of these signals followed by comparison with the spectrum of glyceryl triacetate.*

Can. J. Chem. Downloaded from www.nrcresearchpress.com by 196.1.178.254 on 09/04/12
For personal use only.

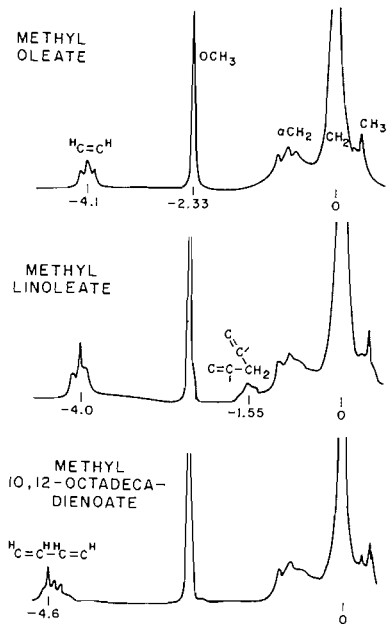

FIG. 2. Proton resonance spectra of methyl esters of a monoenoic acid, a non-conjugated dienoic acid, and a conjugated dienoic acid.

The CH_3 of the ester group in these compounds gave a sharp peak at -2.32 to -2.35 p.p.m. In the 1,4-diene, methyl linoleate, the signal at -1.55 p.p.m. for the CH_2 of the divinyl methane grouping has half the intensity of the signal for the two CH=CH groups, since the latter contain a total of four protons. In the 1,3-diene, methyl 10,12-octadecadienoate, the effect of conjugation on the ethylenic protons is to shift the signal to low field (-4.6 p.p.m.). The divinyl methane signal has disappeared.

Hydroxy- and Keto-acids

The —CHOH group in hydroxy acids is recognized by two signals, one for each hydrogen, at different frequencies (Fig. 3). Thus 12,13-dihydroxyoleic acid, in addition to the usual peaks shown by oleic acid, gave a signal at -2.2 p.p.m. due to the —CH—O groups. The position of the —OH signal varies with concentration (8), and is observed here at -4.8 p.p.m. In these experiments the concentration was not standardized. Accordingly, the —OH signal appeared at -1.2 p.p.m. in ethyl ricinoleate. The quartet and triplet characteristics of the ethyl group of the ethyl ester are clearly observed.

The spectrum of 9,11-diketononadecanoic acid indicates that enolization has taken place to a large extent. A diketone enolizes according to the mechanism:

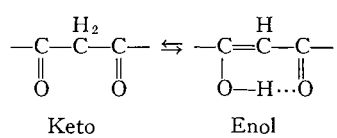

Keto Enol

The hydrogen-bonded signal of the enol form has been found in acetylacetone to appear at very low field (2). The signal at -4.1 p.p.m. corresponds to the C=CH group in the enol form and that at about -2.1 p.p.m. to the CH_2 group of the keto form. This

Can. J. Chem. Downloaded from www.nrcresearchpress.com by 196.1.178.254 on 09/04/12
For personal use only.

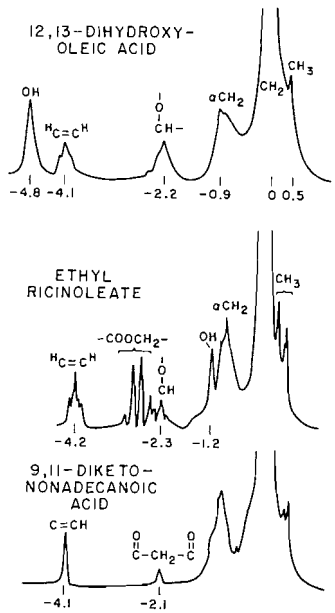

FIG. 3. Proton resonance spectra of compounds having hydroxy- and keto-groups.

is 2 p.p.m. to high field of the C=CH signal in acetylacetone also (2). From the relative areas under these signals (~1:3) the ratio of keto to enol concentration is about 1:6.

Epoxy Acids and Epoxy Oils

The epoxy group $-\underset{H}{\overset{O}{C}}-\underset{H}{C}-$ in the long-chain fatty acids produced a signal at −1.55 to −1.7 p.p.m. This has been shown in 9,10-epoxystearic acid and 12,13-epoxyoleic acid (3), and in 9,10,12,13-diepoxystearic acid.

Certain natural oils are known to contain 12,13-epoxyoleic acid as glyceride. However, detection of the epoxy group in these oils is complicated by the fact that linoleate is usually present and gives a signal at approximately the same position in the field. Thus the seed oil of *Vernonia colorata*, in which the fatty acids are approximately 70% epoxyoleic and 15% linoleic, gave a signal in the region of −1.65 p.p.m. which is due to the summation of the signals due to the epoxy group protons and the diene-activated CH_2 of the 1,4-dienoic acid (A, Fig. 4).

To resolve this difficulty, the oil was acetylated, thereby converting the epoxy group to diacetoxy. The residual intensity at −1.75 p.p.m. is due then to the contribution of the CH_2 group of the 1,4-diene, (B, Fig. 4). The acetylated oil produced a new signal at −2.3 p.p.m., attributed to the hydrogens adjacent to the acetyl groups. 9,10-Diacetoxystearic acid gave a signal at approximately the same position, −2.4 p.p.m. The triplet structure (spacing of 6.2 c/s) is probably due to spin–spin coupling with the hydrogens of the adjacent CH_2 group. The hydrogens of the two acetyl groups produced two sharp peaks in the vicinity of −0.8 p.p.m.

This acetylation procedure seems useful in detecting or confirming the presence of epoxy acids in natural oils where the amount exceeds 5% of the total acids.

Can. J. Chem. Downloaded from www.nrcresearchpress.com by 196.1.178.254 on 09/04/12
For personal use only.

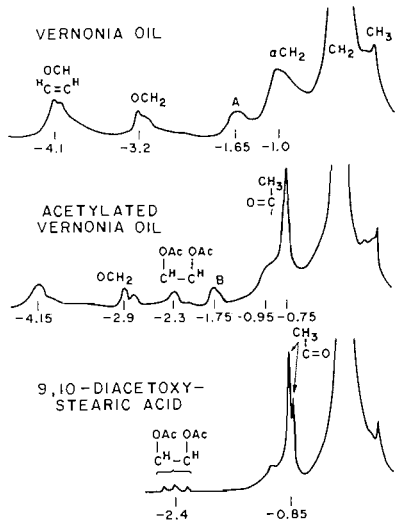

FIG. 4. Proton resonance spectra of an epoxy-acid oil, showing the effect of acetylation, and a simple diacetoxy acid.

Examination of Natural Fatty Oils

It is evident from the foregoing data that useful information on the components of natural glyceride oils can be obtained from proton magnetic resonance absorption measurements. The presence of free carboxyl, hydroxy, 1,4-diene, conjugated double bonds, and isolated double bonds can usually be determined by inspection of the spectra. By converting the oil to methyl esters and determining the spectrum of the mixed esters, the glycerol signals are eliminated and no longer interfere with the signal of the isolated double bonds.

Confirmation of the presence of the OH group can be obtained by acetylating, whereby the product gives a new signal due to the acetoxy group. Similarly, oils having a 1,4-diene grouping can be isomerized to the conjugated form, producing a new signal which is readily identified.

Quantitative applications are also possible. The intensity of a given signal is directly proportional to the number of protons contributing to it. By comparing the areas of peaks in the same spectrum, estimates can be made of the relative proportions of certain groupings in the sample. The glyceryl radical provides a useful internal reference standard for such calculations in examining the oils. Its signal A at -3.0 p.p.m. (Fig. 5) is due to the two —OCH groups and thus represents four protons. Its signal B at -4.0 (—OCH) represents only one proton.

On this basis, one can calculate the ratios of saturated: monoene: diene fatty acids in ordinary glyceride oils composed of these three types of acids. The degree of precision is of the order of ± 5 units %.

In the spectrum for cocoa butter (Fig. 5), the absence of a signal in the region of -1.55 p.p.m. shows that there is little or no 1,4-diene (actually about 2% of linoleate is present), so that for purposes of calculation the component acids are regarded as consisting of saturated and monoenoic acids. If the acid residues were entirely monoenoic the ratio of the area of B to the total area of A would be 7:4 ($3 \times$ CH=CH+OCH: $2 \times OCH_2$) since there would be three molecules of monoenoic acid to one of glycerol. The component

Can. J. Chem. Downloaded from www.nrcresearchpress.com by 196.1.178.254 on 09/04/12
For personal use only.

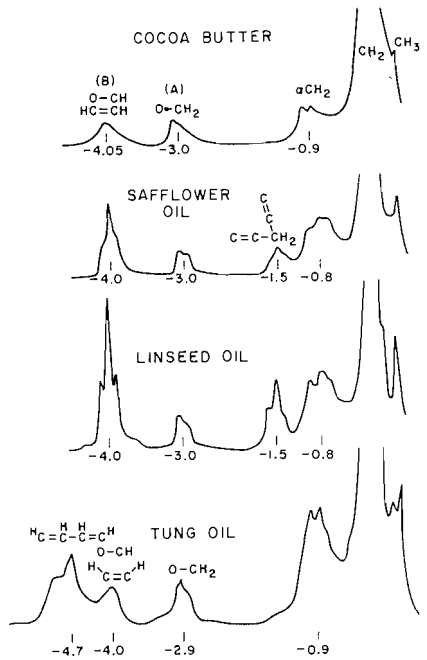

FIG. 5. Proton resonance spectra of typical oils. The increasing degree of unsaturation in the first three oils is indicated by the ratio of the areas of the B and A signals. In tung oil the total unsaturation is indicated by the peaks at −4.0 and −4.7 p.p.m.

of B due to the OCH group is one-quarter of the area of the A signal (one proton/four protons). Therefore, deducting one-quarter of the area of A from B gives the area due to the CH=CH groups. If the acids were entirely monoenoic, the ratio of this area to A would be 6:4. By actual measurement, the ratio was found to be about 2.4:4, hence the ratio of monounsaturated acids to total acids is about $(2.4 \div 6) : 1 = 0.4 : 1$ in this sample.

By extending this procedure to include the diene signal at −1.55 p.p.m., the ratios of saturated:monoene:diene in cottonseed or similar oils can be estimated. Similarly the proportion of conjugated acid, e.g. in tung oil, can be estimated by comparing the areas of the glyceryl signal and the signal at −4.7 p.p.m. In the curve for tung oil, the signal at −4.0 p.p.m. represents the non-conjugated ethylenic groups of oleic and linoleic acids present in the oil, in conjunction with the O—CH— glycerol signal.

cis- and trans-Groupings

Two pairs of *cis–trans* isomeric compounds were examined, viz. oleic and elaidic acids, and *cis-* and *trans*-9,10-epoxystearic acid. 12,13-Epoxyoleic acid, prepared by the action of peracetic acid on linoleic acid, was also compared with *Vernonia colorata* oil, which contains *cis*-12,13-epoxyoleic acid as glyceride. The difference in the positions of the double bond signals and the epoxy group signals in these pairs of compounds was not great enough to be significant. However, the possibility of a significant difference between *cis-* and *trans*-groupings under more exactly controlled conditions is not excluded.

Constitution of Sterculic Acid

The spectra of sterculic acid and some of its derivatives were examined to obtain evidence for the structure of the acid, which has been in dispute (4, 5).*

**Shortly after our work was completed, the proton resonance spectrum of sterculic acid was reported by Rinehart, Nilsson, and Whaley (6).*

Can. J. Chem. Downloaded from www.nrcresearchpress.com by 196.1.178.254 on 09/04/12
For personal use only.

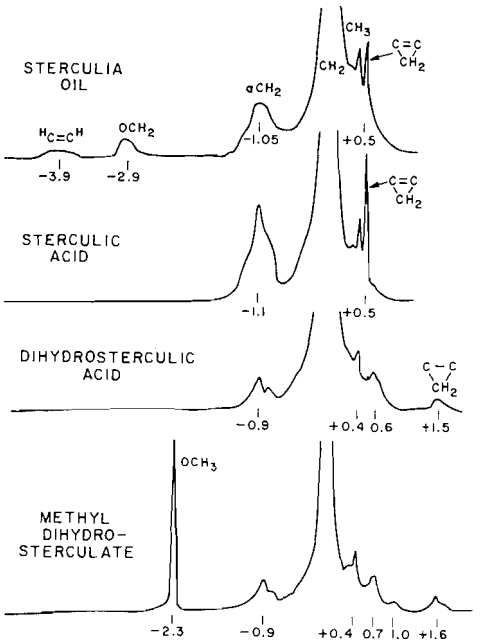

FIG. 6. Proton resonance spectra of *Sterculia* oil, sterculic acid, and two derivatives. The signal of the CH_2 group of the cyclopropane ring is at +1.5 p.p.m.

In our experiments, *Sterculia foetida* oil showed a signal of low intensity at −3.9 p.p.m. attributable to the unsaturated linkages of the small percentage of ordinary unsaturated acids in the glycerides. Sterculic acid itself, prepared by cold saponification of the oil and crystallization of the acids at low temperature, gave no signal in the region expected for isolated double bonds. Hence the proposed formula (5)

$$CH_3(CH_2)_5CH\text{—}CH\text{—}CH{=}CH(CH_2)_7COOH$$
$$\qquad\qquad\quad \diagdown\ \diagup$$
$$\qquad\qquad\quad CH_2$$

I

is judged to be incorrect. Absence of the signal for the CH_2 group of the cyclopropane ring in the region of +1.5 p.p.m. is further evidence for the rejection of formula I.

The signal at +0.5 p.p.m., attributed by Rinehart and co-workers (6) to the cyclopropene ring of Nunn's formula

$$CH_3(CH_2)_7C{=}C\text{—}(CH_2)_7COOH,$$
$$\qquad\qquad\quad \diagdown\ \diagup$$
$$\qquad\qquad\quad CH_2$$

II

can scarcely be regarded as positive proof of structure II until the position of this signal has been confirmed by examining model compounds of similar structure. However, hydrogenation of sterculic acid to dihydrosterculic acid undoubtedly gives a cyclopropane ring, as confirmed by synthesis (7) and the magnetic resonance spectrum of dihydrosterculic acid (Fig. 6) gives a signal at 1.5 p.p.m., which is characteristic of the CH_2 group in a cyclopropane ring.* Since this signal is absent in the spectrum of sterculic acid,

**Unpublished results (H.J.B.).*

Can. J. Chem. Downloaded from www.nrcresearchpress.com by 196.1.178.254 on 09/04/12
For personal use only.

formula I is clearly inadmissible and the NMR evidence strongly supports formula II. The spectra of dihydrosterculic acid and its methyl ester were identical except for the carboxy and ester signals respectively. The signal at 0.7 p.p.m. has not been positively identified but is possibly associated with the CH groups of the cyclopropane ring.

ACKNOWLEDGMENT

We wish to acknowledge the assistance of J. R. Nicholson in obtaining the NMR spectra.

REFERENCES

1. GUNSTONE, F. D. J. Chem. Soc. (London), 1611 (1954).
2. JARRET, H. S., SADLER, M. S., and SHOOLERY, J. N. J. Chem. Phys. **21**, 2092 (1953).
3. CHISHOLM, M. J. and HOPKINS, C. Y. Can. J. Chem. **35**, 358 (1957).
4. NUNN, J. R. J. Chem. Soc. 313 (1952).
5. VARMA, J. P., NATH, B., and AGGARWAL, J. S. Nature, **175**, 84 (1955).
6. RINEHART, K. L., JR., NILSSON, W. A., and WHALEY, H. A. J. Am. Chem. Soc. **80**, 503 (1958).
7. HOFMANN, K., OROCHENA, S. F., and YOHO, C. W. J. Am. Chem. Soc. **79**, 3608 (1957).
8. COHEN, A. D. and REID, C. J. Chem. Phys. **25**, 790 (1956).

Can. J. Chem. Downloaded from www.nrcresearchpress.com by 196.1.178.254 on 09/04/12
For personal use only.

Can. J. Chem. Downloaded from www.nrcresearchpress.com by 190.90.36.8 on 09/04/12
For personal use only.

EFFECT OF PRESSURE ON THE SPONTANEOUS AND THE BASE-CATALYZED HYDROLYSES OF EPOXIDES[1]

J. KOSKIKALLIO[2] AND E. WHALLEY

ABSTRACT

The effect of pressures up to 3000 atm on the spontaneous and the base-catalyzed hydrolyses of ethylene and propylene oxides has been determined. It is that expected from the accepted mechanisms. The volumes of activation of ion–molecule reactions that probably occur without major change in polarity are reviewed. For all reactions that have been studied so far in which a C–O bond is formed the volumes of activation are about -5 to -10 cm^3 mole^{-1}.

1. INTRODUCTION

Epoxides hydrolyze spontaneously and by acid and base catalysis (1, 2, 3). We have already described (4) the effect of pressure on the acid-catalyzed reaction, and in this paper the effect of pressure on the base-catalyzed and the spontaneous hydrolyses is described.

2. EXPERIMENTAL METHODS

The epoxides, the pressure technique, and the method of analysis for epoxide were as described in a previous paper (4). At 1 atm, 5-ml sealed ampoules were used for the rate measurements. The concentration of epoxide was about 0.1 *M* at the start of each run. About seven samples were taken during each run.

Spontaneous hydrolysis.—The rates of hydrolysis in a buffer solution containing 0.001-*M* 2,4,6-trimethylpyridine and 0.0015-*M* 2,4,6-trimethylpyridinium perchlorate (3) (pH 7.3) were taken to be the rates of the spontaneous hydrolysis. There was a difference of only a few per cent between the rates in the buffer and in pure water.

Alkaline hydrolysis.—The alkali was carbonate-free sodium hydroxide and was usually about 0.01 *M*. The first-order rate constant k is given by

$$k = k_0 + k_b c_{OH^-},$$

where k_0 and k_a are the rate constants for the spontaneous and the base-catalyzed reactions and c_{OH^-} is the concentration of hydroxyl ion at the temperature and pressure of the experiment. The calculation of k_b is straightforward. The compression and thermal expansion of the solution were assumed to be the same as those of pure water (5).

3. RESULTS

The experimental rate constants for the spontaneous hydrolysis of ethylene and propylene oxides are given in Table I and those for the base-catalyzed hydrolysis of ethylene oxide are given in Table II. Previous measurements at 1 atm are given for comparison; the agreement is good.

The rate constants at 1 atm for the spontaneous hydrolysis were fitted graphically to the Arrhenius equation, and the Arrhenius energy E_A and the enthalpy $\Delta H^{\ddagger}$ and entropy $\Delta S^{\ddagger}$ of activation were obtained. We found:

[1]*Manuscript received December 19, 1958.*
Contribution from the Division of Applied Chemistry, National Research Council, Ottawa, Canada.
Issued as N.R.C. No. 5070.
[2]*N.R.C. Postdoctorate Fellow 1957–58. Present address: Department of Chemistry, University of Helsinki, Helsinki, Finland.*

$$E_A = 19.5 \pm \sim .2 \text{ kcal mole}^{-1},$$

$$\Delta H^{\ddagger} = 18.9 \pm \sim .2 \text{ kcal mole}^{-1},$$

and

$$\Delta S^{\ddagger} = -23.6 \pm \sim .6 \text{ cal deg}^{-1} \text{ mole}^{-1},$$

the errors being estimated. Our value of E_A agrees well with Lichtenstein and Twigg's (2), 19.0±.3 kcal mole^{-1}.

TABLE I

Spontaneous hydrolysis of ethylene and propylene oxides

			$10^6 k_0$/sec^{-1}		
Oxide	Temp.	p/atm	This work	Ref. (1)	Ref. (3)
Ethylene	20° C	1	(0.332)*	0.413	0.36
	25° C	1	0.58		
		1000	1.07		
		2000	1.71		
		3000	2.58		
	60° C	1	19.2		
		500	27.2		
		1000	36.6		
		2000	59.1		
		3000	86.5		
	70° C	1	43.9	43.1	
		1000	86.3		
		2000	135		
		3000	206		
Propylene	25° C	1	0.69		
		3000	3.32		
	60° C	1	21.1		
		3000	95.2		

*The value in parentheses is extrapolated using the Arrhenius equation.

TABLE II

Base-catalyzed hydrolysis of ethylene oxide at 60° C

		$10^3 k_b$/l. mole^{-1} sec^{-1}	
p/atm	c_{OH^-}/mole l.$^{-1}$	This work	Ref. (2)
1	0.0102	2.76	(2.79)*
1	0.0195	2.81	
1	0.0390	2.84	
500	0.0097	3.19	
1000	0.0102	3.64	
1000	0.0196	3.58	
2000	0.0102	4.31	
2000	0.0196	4.56	
3000	0.0098	5.71	
3000	0.0106	5.33	

*The value in parentheses is interpolated.

The rate constants as a function of pressure at constant temperature for both the spontaneous and the base-catalyzed hydrolyses are shown in Fig. 1. The volumes of activation at 1 atm were obtained graphically; values found were, for the spontaneous hydrolysis,

Can. J. Chem. Downloaded from www.nrcresearchpress.com by 190.90.36.8 on 09/04/12
For personal use only.

at 25° C $\Delta V^{\ddagger} = -15.9 \pm \sim 1$ cm^3 mole^{-1},

at 60° C $\Delta V^{\ddagger} = -18.9 \pm \sim 1$ cm^3 mole^{-1},

and

at 70° C $\Delta V^{\ddagger} = -19.9 \pm \sim 1$ cm^3 mole^{-1};

for the base-catalyzed hydrolysis

at 60° C $\Delta V^{\ddagger} = -7.0 \pm \sim 1$ cm^3 mole^{-1}.

The errors are estimated.

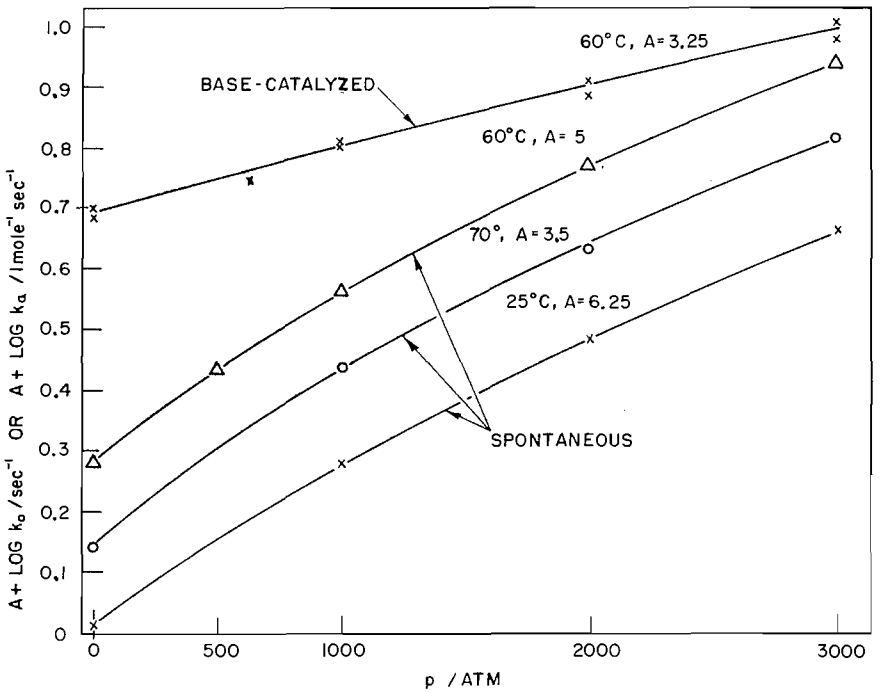

FIG. 1. Effect of pressure on the spontaneous and the base-catalyzed hydrolyses of ethylene oxide.

4. DISCUSSION

Spontaneous Hydrolysis

The volume of activation for the spontaneous hydrolysis of ethylene oxide at 60° C is $-18.9 \pm \sim 1$ cm^3 mole^{-1}. The mechanism is very likely to be (6)

[4.1] $$H_2O + \begin{matrix} H_2C \\ | \\ H_2C \end{matrix}\!\!>\!O \xrightarrow{\text{slow}} H_2O^+\!-\!CH_2 \,|\, H_2C\!-\!O^- \xrightarrow{\text{fast}} \begin{matrix} CH_2OH \\ | \\ CH_2OH \end{matrix}$$

There are two effects causing a decrease of volume when the transition state is formed, the conversion of a van der Waals' interaction between water and epoxide into a partial valence bond, and the increased electrostriction of the solvent due to the separation of charges in the transition state (7). The contribution of valence-formation to the volume-decrease will presumably be similar to that in similar reactions in which no major change of electrostriction is expected. We show below that the contribution of valence-formation to the volume of activation is expected to be about -5 to -10 cm^3 mole^{-1}. The con-

Can. J. Chem. Downloaded from www.nrcresearchpress.com by 190.90.36.8 on 09/04/12
For personal use only.

tribution of valence-formation in reaction [4.1] is, therefore, likely to be about $\frac{1}{3}$ to $\frac{1}{2}$ of the total volume of activation; the remaining $\frac{2}{3}$ to $\frac{1}{2}$ is presumably due to electrostriction of the solvent.

Although the volume of activation for the spontaneous hydrolysis of propylene oxide cannot be calculated for lack of data, it is of the same order of magnitude as that for ethylene oxide, and is presumably the sum of similar contributions.

A volume of activation can be divided into an enthalpy effect and an entropy effect thus

$$\Delta V^{\ddagger} = (\partial \Delta H^{\ddagger}/\partial p)_T - T(\partial \Delta S^{\ddagger}/\partial p)_T. \qquad [4.2]$$

Using the relations

$$(\partial \Delta S^{\ddagger}/\partial p)_T = -(\partial \Delta V^{\ddagger}/\partial T)_p, \qquad [4.3]$$

$$(\partial \Delta H^{\ddagger}/\partial p)_T = -T^2 [\partial(\Delta V^{\ddagger}/T)/\partial T]_p, \qquad [4.4]$$

we find from our measurements that

$$\partial \Delta H^{\ddagger}/\partial p = 19 \pm \sim 10 \text{ cm}^3 \text{ mole}^{-1} \text{ at } 25\text{–}70^\circ \text{ C and 1 atm},$$
$$T\partial \Delta S^{\ddagger}/\partial p = 38 \pm \sim 10 \text{ cm}^3 \text{ mole}^{-1} \text{ at } 25\text{–}70^\circ \text{ C and 1 atm}.$$

Thus both the enthalpy and the entropy of activation increase as the pressure is increased, the entropy term dominating the enthalpy term and determining the sign of $\Delta V^{\ddagger}$. Similar reactions, in which charges are created in the transition state, behave similarly (8, 9, 10).

Base-catalyzed Hydrolysis

The volume of activation for the base-catalyzed hydrolysis at 60° C is $-7.0 \pm \sim 1$ cm^3 mole^{-1}. The mechanism of the reaction is

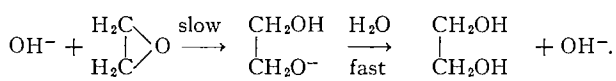

There are two contributions to the volume of activation, the formation of a new partial valence bond between oxygen and carbon and the extension of an existing C–O bond in the epoxide, and the decreased electrostriction of the solvent due to the dispersion of the negative charge between two oxygen atoms thus

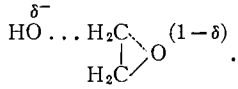

The value, -7.0 cm^3 mole^{-1}, is presumably the sum of these effects.

It is important to establish the sum of these effects for a number of similar reactions for the following reason. In a bimolecular reaction between a molecule and an ion the main contributors to the volume of activation are valence-formation and charge-dispersion as described above and electrostriction of the solvent due to newly separated charges. If the loss of volume due to valence-formation and charge-dispersion can be estimated then it should be possible to determine whether a major separation of charge occurs in the transition state. Laidler and Chen (11) have done this by assuming that the loss in volume due to valence formation is unimportant. We now examine the available evidence on the volumes of activation of ion–molecule reactions. The volume of activation will probably not depend strongly upon whether the ion is positively or negatively

Can. J. Chem. Downloaded from www.nrcresearchpress.com by 190.90.36.8 on 09/04/12
For personal use only.

charged. In order to reduce the possibility of increased polarity in the transition state we will omit reactions that occur near a highly polarizable group such as a carbonyl group. The available information on the volumes of activation of such reactions is summarized in Table III. For some of the reactions only rough rate constants were obtained; for example, David and Hamann (15) claim an accuracy no greater than 30% in the rate constants. It is worthwhile to include these only because there are so few data at present and even rough values are better than none.

TABLE III

Volumes of activation of reactions that probably occur without major change in polarity

Reaction	Solvent	Temperature	$\Delta V^{\ddagger}$/cm^3 mole^{-1}	Ref.
$C_2H_4O + OH^- \rightarrow C_2H_4(OH)O^-$	H_2O	60° C	$-7\pm\sim1$	This work
$C_2H_4O + H_3O^+ \rightarrow C_2H_4(OH)O^+H_2$	H_2O	0° C	$-5.9\pm\sim1$	4
		15° C	$-7.4\pm\sim1$	4
		25° C	$-7.9\pm\sim1$	4
		40° C	$-8.9\pm\sim1.3$	4
$CH_3.C_2H_3O + H_3O^+ \rightarrow CH_3C_2H_3(OH)O^+H_2$	H_2O	0° C	$-8.4\pm\sim1.3$	4
$(CH_3)_2.C_2H_2O + H_3O^+ \rightarrow (CH_3)_2C_2H_4(OH)O^+H_2$	H_2O	0° C	$-9.2\pm\sim1.7$	4
$(C_2H_5)_2O + H_3O^+ \rightarrow C_2H_5O^+H_2 + C_2H_5OH$	H_2O	161.2° C	$-8.5\pm\sim2$	12
$CH_3Br + \begin{cases} OH^- \\ OC_2H_5^- \end{cases} \rightarrow \begin{cases} CH_3OH \\ CH_3OC_2H_5 \end{cases} + Br^-$	'80%' C_2H_5OH in water	0° C	~-7	13*
			~-8	14*
$C_2H_5Br + OCH_3^- \rightarrow C_2H_5OCH_3 + Br^-$	CH_3OH	30° C	~-9	13*
$C_2H_5I + OC_2H_5^- \rightarrow (C_2H_5)_2O + I^-$	C_2H_5OH	30° C	~-5	8*
$CH_2ClCO_2^- + OH^- \rightarrow CH_2(OH)CO_2^- + Cl^-$	H_2O	40° C	$-8.2\pm\sim2$	15*
		60° C	$-6.6\pm\sim2$	15*
		80° C	$-9.4\pm\sim2$	15*
n-$C_3H_7Br + Br^{82-} \rightarrow n$-$C_3H_7Br^{82} + Br^-$	'90%' C_2H_5OH in H_2O	19° C	~-12	16
n-$C_3H_7I + I^{131-} \rightarrow n$-$C_3H_7I^{131} + I^-$	,,	,,	~-13	16

*The values of $\Delta V^{\ddagger}$ cited were obtained graphically from data in the reference.

All the reactions in Table III except the halogen-exchange reactions result in the formation of a bond between carbon and oxygen. The loss of volume is about -5 to -10 cm^3 mole^{-1}. It seems reasonable to conclude, therefore, on the basis of present evidence that the volume of activation of ion–molecule reactions in which a C–O bond is formed and in which no major increase in the polarity occurs is about -5 to -10 cm^3 mole^{-1}.

REFERENCES

1. Bronsted, J. N., Kilpatrick, M., and Kilpatrick, M. J. Am. Chem. Soc. **51**, 428 (1929).
2. Lichtenstein, J. and Twigg, G. H. Trans. Faraday Soc. **44**, 905 (1948).
3. Long, F. A., Pritchard, J. D., and Stafford, F. E. J. Am. Chem. Soc. **78**, 2663, 2667 (1956).
4. Koskikallio, J. and Whalley, E. Trans. Faraday Soc. **55**, (1959) (In press).
5. Bridgman, P. W. Proc. Am. Acad. Arts Sci. **48**, 309 (1912).
6. Ingold, C. K. Structure and mechanism in organic chemistry. Cornell Univ. Press, Ithaca, N.Y. 1953. p. 343.
7. Hamann, S. D. Physico-chemical effects of pressure. Butterworth Scientific Publications, London. 1957. Chap. 9.
8. Gibson, R. O., Fawcett, E. W., and Perrin, M. W. Proc. Roy. Soc. A, **150**, 223 (1935).
9. Weale, K. E. Discussions Faraday Soc. **22**, 122 (1956).
10. Perrin, M. W. and Williams, E. G. Proc. Roy. Soc. A, **159**, 162 (1937).
11. Laidler, K. J. and Chen, D. Trans. Faraday Soc. **54**, 1026 (1958).
12. Koskikallio, J. and Whalley, E. Can. J. Chem. **37**, 788 (1959).
13. David, H. G. and Hamann, S. D. Trans. Faraday Soc. **50**, 1188 (1954).
14. Strauss, W. Australian J. Chem. **10**, 38 (1957).
15. Williams, E. G., Perrin, M. W., and Gibson, R. O. Proc. Roy. Soc. A, **154**, 684 (1936).
16. Gonikberg, M. G., Miller, V. B., Neĭman, M. B., D'yachkovskiĭ, F. S., Lickhtenshteĭn, G. I., and Opekunov, A. A. Zhur. Fiz. Khim. **30**, 784 (1956).

Can. J. Chem. Downloaded from www.nrcresearchpress.com by 190.90.36.8 on 09/04/12
For personal use only.

Can. J. Chem. Downloaded from www.nrcresearchpress.com by 190.90.36.8 on 09/04/12
For personal use only.

PRESSURE EFFECT AND MECHANISM IN ACID CATALYSIS

IV. THE HYDROLYSIS OF DIETHYL ETHER[1]

J. KOSKIKALLIO[2] AND E. WHALLEY

ABSTRACT

The acid-catalyzed hydrolysis of diethyl ether has been measured in the temperature range 120–160° C at low acid concentrations; the entropy of activation is $-9.0\pm\sim2.5$ cal deg^{-1} mole^{-1}. The effect of pressures up to 3000 atm has been measured at 161.2° C; the volume of activation at 1 atm is $-8.5\pm\sim2$ cm^3 mole^{-1}. These two results show that the slow step is bimolecular. The rate in concentrated acids was measured at 119° C; the rate was much more nearly proportional to the acidity function h_0 than to concentration of acid. This is contrary to the predictions of the Zucker–Hammett hypothesis, which is therefore not valid for the hydrolysis of diethyl ether.

1. INTRODUCTION

Diethyl ether hydrolyzes to ethanol by acid catalysis (see ref. 1 for review). The reaction is presumed to involve a pre-equilibrium proton-transfer to the ether though there is no compelling evidence for this. Two possible slow steps are the unimolecular decomposition of the conjugate acid (A-1 mechanism)

$$R_2OH^+ \rightarrow R^+ + ROH, \qquad [1.1]$$

or its bimolecular substitution (A-2 mechanism)

$$H_2O + R_2O^+H \rightarrow RO^+H_2 + ROH. \qquad [1.2]$$

There is no firm evidence about which mechanism is followed, though Long and Paul (2) have noted that the entropies of activation calculated from the measurements of Skrabal and Zahorka (3) are positive and say that this suggests that the mechanism for primary and secondary ethers is A-1. It was shown in Part I of this series of papers (4) that there are no grounds for thinking that entropies of activation of A-2 reactions cannot be positive, and consequently, the conclusion of Long and Paul is not valid.

It has been shown (4, 5, 6) that the A-1 and A-2 mechanisms can be distinguished by measuring reaction rates under pressure, and in this paper the technique is applied to the hydrolysis of diethyl ether. The measurements of Skrabal and Zahorka (3) of the hydrolysis of diethyl ether catalyzed by 0.5-*M* *p*-toluenesulphonic acid indicate a rapid variation with temperature of the Arrhenius energy and of the entropy of activation, and rates over a temperature range have been measured in an attempt to verify this. Measurements of the rates over a range of acid concentrations have been made in order to examine the validity of the Zucker–Hammett hypothesis.

2. EXPERIMENTAL METHODS

Because the rates of hydrolysis are slow it is necessary to measure them at fairly high temperatures, and the range 120–160° C has been used. Because ether is very volatile and not very soluble in water it is most important to avoid having a vapor-space above the reaction mixture in order to avoid loss of reactant from the solution. Consequently, all reported rate measurements were done in such a way that there was no

[1]*Manuscript received December 19, 1958.*
Contribution from the Division of Applied Chemistry, National Research Council, Ottawa.
Issued as N.R.C. No. 5092.
[2]*National Research Council Postdoctorate Fellow, 1957–58. Present address: Chemistry Department, University of Helsinki, Helsinki, Finland.*

vapor-space. Some rate measurements were made using sealed ampoules as reactors, and vapor was present. The apparent rate constants were badly reproducible and were only a fraction of those obtained as described below, in which there was no vapor-space above the solution.

All reagents used were of analytical quality. The usual catalyst was perchloric acid in concentrations up to 5.65 *M*. A few runs were done with sulphuric acid and hydrochloric acid as catalysts.

High-pressure Technique

The high-pressure equipment was essentially that used in previous work (5), except that the acid solution at the high temperature needed (up to 160° C) reacted with stainless steel so that stainless-steel tubing could not be used to connect the hypodermic syringe to the valve. Consequently, a batch method was used. The reactors were 10-cm³ hypodermic syringes that had the outlets sealed off and the pistons sawn off short. The reaction mixture was thus in contact with glass only. The tubes were placed in the pressure vessel, which was then closed and placed in the thermostat, and the pressure was applied. After a suitable reaction time, which was usually 1 day or more, the vessel was cooled and opened and the three samples were analyzed. There was no evidence of oil entering the reactor or of solution leaving it. The heating of the pressure vessel after it was introduced into the bath had a half life of about 4 minutes as determined from the change in pressure in the closed system. In calculating the reaction time 20 minutes were allowed for warming.

Analysis

The rate of the reaction was followed by analyzing the ethanol produced by oxidizing it to acetic acid with potassium dichromate and sulphuric acid. Five milliliters of the reaction mixture, which was initially about 0.05 *M* in diethyl ether, were put into a mixture containing 3 ml of 96% sulphuric acid and 5 ml of potassium dichromate solution which contained about 50% excess over that required for the oxidation. The mixture was thermostated at 50° C for 20 minutes and then about 100 cm³ of distilled water and 10 cm³ of 0.1-*M* potassium iodide solution were added. The iodine liberated was titrated with 0.4-*N* sodium thiosulphate. The difference between the titer and that of a blank is proportional to the amount of ethanol present in the sample. During the oxidation of the ethanol the ether present is also slowly oxidized. When the unhydrolyzed diethyl ether solution was analyzed by the above method about 4% of the diethyl ether was oxidized; in partly hydrolyzed samples the amount of oxidation was proportionately less. A correction for this was applied to the ethanol analyses. If the sample contained much acid then less sulphuric acid was added when the sample was analyzed in order not to increase the rate of oxidation of ether and thus the correction needed.

The amount of ether initially present in the solution was found by completely oxidizing the ether to acetic acid with potassium dichromate. For this purpose samples of the solution were mixed with the potassium dichromate solution and sulphuric acid and kept in sealed ampoules in a thermostat at 99° C for 1–2 days. When a solution of acetic acid, potassium dichromate, and sulphuric acid, in the same concentrations as above was heated at 99° C for 10 days no oxidation occurred. The amount of ether found by analysis agreed with the amount calculated from the weight of ether in the sample. The 0.05-*M* solution of ether in water was also completely hydrolyzed by heating with 5.7-*M* sulphuric acid for 22 hours at 120°. The amount of ethanol found in this sample agreed within about 2% with the amount found by direct oxidation of ether.

Can. J. Chem. Downloaded from www.nrcresearchpress.com by 190.90.36.8 on 09/04/12
For personal use only.

Can. J. Chem. Downloaded from www.nrcresearchpress.com by 190.90.36.8 on 09/04/12
For personal use only.

3. RESULTS

The first-order rate constants k were calculated from the results of two analyses for ethanol. Those obtained from runs at different reaction times agreed within about 10%. The second-order constants k_a for runs with dilute acid were corrected for compression and thermal expansion of the solution by extrapolating the densities of water obtained from the literature (7); the correction factors are given in Table I. The second-order constants agreed within about 10%, and those for dilute acids are summarized in Table I. The first-order constants for concentrated solutions of acids are summarized in Table II. The accuracy is probably about 10%.

TABLE I

The second-order rate constants for the hydrolysis of diethyl ether catalyzed by perchloric acid

Temp.	p/atm	c_{HClO_4}/mole l.$^{-1}$	$(\rho_{20°,1\ atm})/\rho_{t,p}$*	$10^6 k_a$/l. mole^{-1} sec^{-1}
119.2°	50	0.198	1.06	1.46
130.4°	50	0.198	1.07	4.36
140.8°	50	0.198	1.08	10.8
151.8°	50	0.198	1.09	26.2
161.2°	50	0.0495	1.10	74
161.2°	50	0.099	1.10	81
161.2°	50	0.198	1.10	75
161.2°	400	0.099	1.09	79
161.2°	1000	0.0495	1.07	99
161.2°	1000	0.099	1.07	102
161.2°	2000	0.0495	1.03	113
161.2°	2000	0.099	1.03	112
161.2°	2000	0.198	1.03	102
161.2°	3000	0.0495	1.01	131
161.2°	3000	0.099	1.01	132
161.2°	50	0.060†	1.10	82

*$\rho_{20°,\ 1\ atm}$ and $\rho_{t,p}$ are the densities of the solvent at 20° C and 1 atm and temperature t and pressure p respectively.
†Hydrochloric acid was used as catalyst.

TABLE II

The first-order rate constants of the hydrolysis of diethyl ether in concentrated aqueous acids at 120.1° C and 50 atm

Acid	c_{acid}/mole l.$^{-1}$	$10^6 k$/sec^{-1}
$HClO_4$	0.198	0.30
	1.12	1.85
	2.26	5.7
	3.05	10.7
	4.14	21.8
	5.65	73
H_2SO_4	3.57	10.7
HCl	3.20	17.5

An Arrhenius plot of the second-order constants is given in Fig. 1, in which the vertical lines at each point show a 10% error. The best straight line through the points is shown; it yields for the Arrhenius energy E_A and the entropy of activation $\Delta S^{\ddagger}(= R \ln\{(A/\text{l. mole}^{-1})(h/ekT)\}$ where A is the Arrhenius frequency factor, R is the gas-constant, h is Planck's constant, k is Boltzmann's constant, and T is the temperature)

$$E_A = 31.0 \pm \sim 1 \text{ kcal mole}^{-1},$$

$$\Delta S^{\ddagger} = -9.0 \pm \sim 2.5 \text{ cal deg}^{-1} \text{ mole}^{-1}.$$

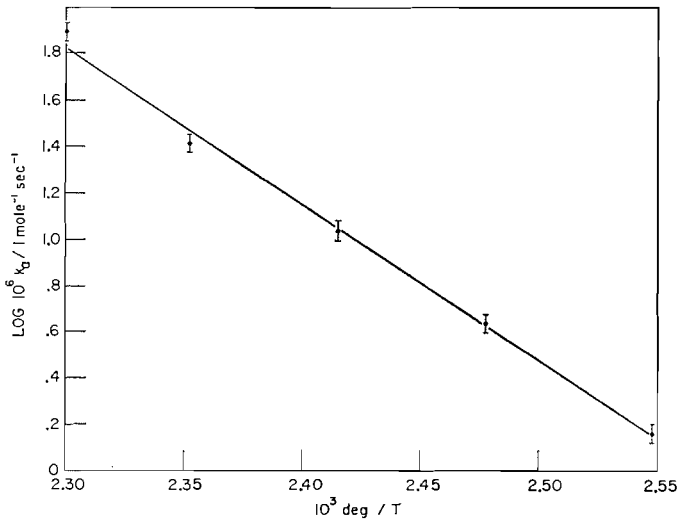

FIG. 1. Log k_a vs. $1/T$ for the acid-catalyzed hydrolysis of diethyl ether between 119 and 161° C.

The points at the highest two temperatures do not fit well with this line, though a good line of slightly smaller slope can be drawn through all but the highest-temperature point, which is about 30% higher than the extrapolated line. It is possible that the Arrhenius energy and the entropy of activation are increasing at the higher temperatures, but the accuracy of the rate constants is not high enough to be sure of it.

The second-order rate constants at 161° C are plotted against pressure in Fig. 2. They

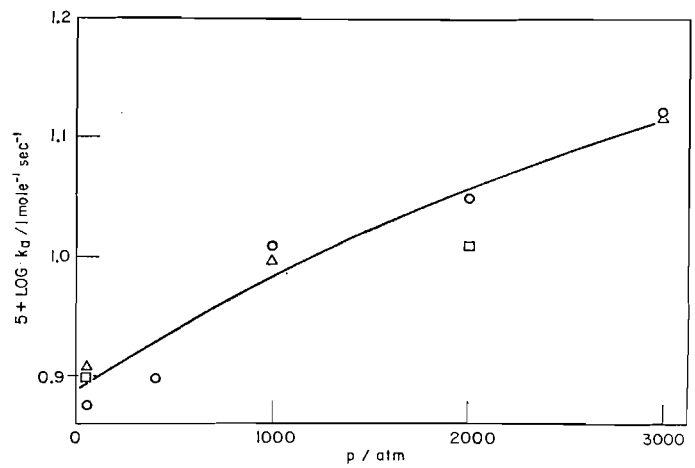

FIG. 2. Log k_a vs. p for the hydrolysis of diethyl ether catalyzed by perchloric acid at 161.2° C. The concentration of catalyst was: triangles, 0.0495 M; circles, 0.099 M; squares 0.198 M.

were fitted by the method of least squares to the equation

$$\log k_a = a+bp+cp^2,$$

and the activation volume $\Delta V^{\ddagger}$ at 1 atm obtained from

$$d \ln k/dp = -\Delta V^{\ddagger}/RT = 2.303b.$$

Can. J. Chem. Downloaded from www.nrcresearchpress.com by 190.90.36.8 on 09/04/12
For personal use only.

We found

$$\Delta V^{\ddagger} = -8.5 \pm \sim 2 \text{ cm}^3 \text{ mole}^{-1} \text{ at } 161^\circ \text{ C, 1 atm.}$$

Our rate constants are in very poor agreement with those of Skrabal and Zahorka (3). Our measurements extrapolated to 95° C give $10^6 k_a = 0.34$ l. mole^{-1} sec^{-1} at 50 atm; Skrabal and Zahorka give for 95° C and 1 atm $10^6 k_a = 0.044$ l. mole^{-1} sec^{-1}, nearly $\frac{1}{8}$ of our value. Skrabal and Zahorka give the rate constant at 125° C, obtained by extrapolation, as 0.0785×10^{-6} l. mole^{-1} sec^{-1}; our interpolated value is 2.57×10^{-6} l. mole^{-1} sec^{-1}, 33 times Skrabal and Zahorka's value. Reduction of our rate constants from 50 atm to 1 atm would make little difference to this disagreement. They also found that in the range 65–95° C the Arrhenius law was not obeyed, the apparent Arrhenius energy decreasing with temperature, whereas we find that it is obeyed in the range 120–150° C, though there may be an *increase* in E_A above this temperature. A partial explanation of this disagreement may be as follows. Skrabal and Zahorka attempted to render small and constant the effect of the vapor-space on the rate constant by keeping the volume of the vapor-space 2 cm^3 and of reaction mixture 12 cm^3. However, the amount of ether in the vapor-space relative to that in the solution will increase as the temperature increases and this will cause the apparent rate constant to be lower than the true rate constant by an amount that increases with increasing temperature. This is at least in the right direction to account for Skrabal and Zahorka's variation of Arrhenius energy with temperature.

In a few cases the reaction mixtures were analyzed for ethylene using the method of Christensen *et al.* (8). Within the experimental error of about 0.3% of the ether initially present no ethylene was found under the following conditions: (i) 14 hours at 120° C and 50 atm in 3.57-*M* sulphuric acid with 49% of the ether hydrolyzed, and (ii) 4 hours at 120° C and 50 atm in 5.65-*M* sulphuric acid with 67% of the ether hydrolyzed. Also, the fact that ether hydrolyzed completely at 120° C, within the experimental error of 2%, to ethanol shows that ethylene is not an important product at 120° C.

DISCUSSION

The second-order constants are independent of acid concentration in dilute acids within experimental error, confirming the much less extensive measurements of Skrabal and Airoldi (9).

As pointed out in the introduction there are two likely mechanisms for the hydrolysis of ether, the A-1 mechanism which is steps [1], [2*a*], and [3*a*], and the A-2 mechanism which is steps [1], [2*b*], and [3*b*], below.

$$(C_2H_5)_2O + H_3O^+ \rightleftharpoons (C_2H_5)_2O^+H + H_2O, \qquad [1]$$

$$(C_2H_5)_2O^+H \xrightarrow{\text{slow}} C_2H_5OH + C_2H_5^+, \qquad [2a]$$

$$C_2H_5^+ + 2H_2O \xrightarrow{\text{fast}} C_2H_5OH + H_3O^+, \qquad [3a]$$

$$(C_2H_5)_2O^+H + H_2O \xrightarrow{\text{slow}} C_2H_5OH + C_2H_5O^+H_2, \qquad [2b]$$

$$C_2H_5O^+H_2 + H_2O \xrightarrow{\text{fast}} C_2H_5OH + H_3O^+. \qquad [3b]$$

The measured volume or entropy of activation is the sum of the volume or entropy change of step [1] and the volume or entropy of activation of the slow step [2*a*] or [2*b*]. It was shown in Part I of this series of papers (4) that the volume change of step [1] is probably small, so that the experimental volume of activation is determined mainly

Can. J. Chem. Downloaded from www.nrcresearchpress.com by 190.90.36.8 on 09/04/12
For personal use only.

by the volume of activation of step [2]. If [2*a*] is the slow step then the transition state is bigger than the reactants and the volume of activation is positive or close to zero; this occurs in the acid-catalyzed hydrolysis of sucrose (4), dimethoxymethane, diethoxymethane, dimethoxyethane, and triethoxymethane (5). If [2*b*] is the mechanism then the conversion of a van der Waals' bond between water and the conjugate acid of the ether to a partial valence bond in the transition state results in a decrease of volume, and the volume of activation is expected to be negative by about 5–10 cm^3 $mole^{-1}$; this occurs in the acid-catalyzed hydrolysis of methyl acetate (4), ethylene oxide, propylene oxide, and isobutylene oxide (6). Similar arguments, which were developed in Part I, apply to the entropy of activation, except that the standard entropy change of the proton-transfer step (1) may be quite high. Consequently, we concluded that an A-1 reaction should have a positive entropy of activation and an A-2 reaction can have either a positive or a negative entropy of activation.

The volume of activation is $-8.5\pm\sim2$ cm^3 $mole^{-1}$, showing that the mechanism is A-2. The entropy of activation is $-9.0\pm\sim2.5$ cm^3 $mole^{-1}$, and this confirms the A-2 mechanism.

It is possible that if increases in E_A and $\Delta S^{\ddagger}$ are beginning to occur at the higher temperatures, as is indicated but not proved by our measurements, an A-1 mechanism is beginning to occur. More work is needed on this point. However, it seems certain that the A-2 mechanism, which is detected by the volumes of activation at 161° C and by the entropy of activation over the range 119°–160°, holds at 120° C.

If the Zucker–Hammett hypothesis (10, 2), that when rates in concentrated acids are proportional to Hammett's acidity function h_0 the mechanism is A-1 and when rates are proportional to concentration of hydrogen ion the mechanism is A-2, is correct then the rate of hydrolysis of diethyl ether should be proportional to concentration of strong acid. Values of H_0 ($= -\log h_0$) are not known for perchloric acid in water at the

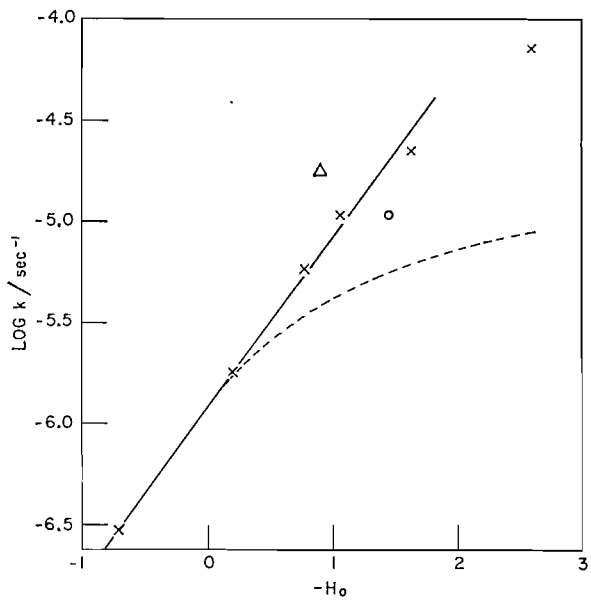

FIG. 3. Log k at 120.1° C and 50 atm vs. $-H_0$ at 25° C and 1 atm for the hydrolysis of diethyl ether catalyzed by acids. The acid was: crosses, perchloric acid; circle, sulphuric acid; triangle, hydrochloric acid. If log $k \propto \log c_{H^+}$ the points would fall near the dashed line.

Can. J. Chem. Downloaded from www.nrcresearchpress.com by 190.90.36.8 on 09/04/12
For personal use only.

temperature and pressure of the measurements, 120.1° C and 50 atm. We have used, therefore, the values appropriate to 25° C and 1 atm (11). These will certainly not be accurate for 120.1° C and 50 atm, but the difference will probably not be enough to invalidate the following discussion. In Fig. 3, log k/sec^{-1} is plotted against $-H_0$, and for comparison the curve that would be obtained if the rate were proportional to concentration of acid is shown. It is quite evident that log k is much more nearly proportional to H_0 than to log c_{H^+}, though the rate at high acidities is somewhat less than strict proportionality would give. The rate in 5.65-M perchloric acid is 8.5 times faster than if it were proportional to c_{HClO_4} and 0.4 times faster than if it were proportional to h_0.

Though there is some uncertainty in the values of H_0 for 120° C and 50 atm, it seems very likely that the Zucker–Hammett hypothesis is not valid for the hydrolysis of diethyl ether. It failed also for the hydrolysis of ethylene oxide (6). The method is inherently empirical, and, since two reactions are now known for which it fails, we must conclude that the relation between rates and h_0 and hydrogen-ion concentration does not distinguish between A-1 and A-2 mechanisms.

Taft, Deno, and Skell, in a recent review (12), refer to work (13) that is not yet fully published that also refutes the Zucker–Hammett hypothesis.

REFERENCES

1. Burwell, R. L. Chem. Revs. **54**, 615 (1954).
2. Long, F. A. and Paul, M. A. Chem. Revs. **57**, 935 (1957).
3. Skrabal, A. and Zahorka, A. Monatsh. Chem. **63**, 1 (1933).
4. Whalley, E. Trans. Faraday Soc. (In press).
5. Koskikallio, J. and Whalley, E. Trans. Faraday Soc. (In press).
6. Koskikallio, J. and Whalley, E. Trans. Faraday Soc. (In press).
7. Bridgman, P. W. Proc. Am. Acad. Arts Sci. **66**, 185 (1931).
8. Christensen, D. E., Hansen, E., and Cheldelin, V. H. Ind. Eng. Chem. Anal. Ed. **11**, 114 (1939).
9. Skrabal, A. and Airoldi, H. Monatsh. Chem. **45**, 13 (1924).
10. Zucker, L. M. and Hammett, L. P. J. Am. Chem. Soc. **61**, 2791 (1939).
11. Paul, M. A. and Long, F. A. Chem. Revs. **57**, 1 (1957).
12. Taft, R. W., Deno, N. C., and Skell, P. S. Ann. Rev. Phys. Chem. **9**, 287 (1958).
13. Boyd, R. H. and Taft, R. W. Abstr. Am. Chem. Soc. 132nd Meeting. 1957. p. P76.

Can. J. Chem. Downloaded from www.nrcresearchpress.com by 190.90.36.8 on 09/04/12
For personal use only.

Can. J. Chem. Downloaded from www.nrcresearchpress.com by 186.233.112.2 on 09/04/12
For personal use only.

REACTION OF TRICHLOROACETONITRILE WITH PRIMARY AND SECONDARY AMINES

PART II. INFRARED SPECTRA OF N-SUBSTITUTED TRICHLOROACETAMIDINES[1, 2]

JOHN C. GRIVAS[3] AND ALFRED TAURINS

ABSTRACT

A correlation between the infrared absorption spectra and the structure of 13 N-mono- and N-di-substituted trichloroacetamidines is presented. N-Alkyl- and N-aryl-trichloroacetamidines associate strongly in the liquid and solid phases, and exist only in the imino form in non-polar solvents. They can be characterized by a strong band (amidine II band) at 1510–1525 cm^{-1} and 1570–1580 cm^{-1} respectively which is attributed to the deformation vibration $\delta(\diagdown\!\diagup N—H)$ of the secondary amino group. The degree of association of N-substituted trichloroacetamidines changes in the following order of substitution:

N-alkyl- > N-aryl- > N-dialkyl.

INTRODUCTION

The free secondary amino group shows only one NH stretching absorption band between 3500 and 3300 cm^{-1}, but hydrogen bonding of this group sometimes gives rise to a second band at lower frequencies. A somewhat narrower frequency range (3400–3200 cm^{-1}) has been established for the stretching vibration, ν(N—H), of the unassociated imino group =NH as is expected from the fact that the environment around the NH group is almost always the same. The deformation vibration, δ(NH), of both secondary amino and imino groups occur between 1650 and 1550 cm^{-1}, but they are usually too weak to be used for identification purposes (1). In the aromatic amines this absorption is complicated by the fact that it occurs in the same region as the aromatic ring vibrations and often causes a modification of these. Certain combinations of structural features are likely to enhance the intensity of the deformation vibration, δ(NH), just as the NH deformation is believed by some authors to be enhanced by the presence of the carbonyl group, with a result of appearance of the amide II band. That has been recently substantiated by Barr and Haszeldine (2), who assigned the deformation vibration, δ(NH), to a strong band near 1500 cm^{-1} showed by secondary perfluoroalkylamines. The same mode has also been reported to be responsible for the absorption near 1510 cm^{-1}, which was observed in the spectra of the secondary aromatic amines (3).

Amidines of the general formula (I)

$$\begin{array}{l} R—C—NHR'' \\ \quad\| \\ \quad NR' \end{array}$$

I

show also the free stretching vibrations ν(NH), between 3440 and 3470 cm^{-1}, but a considerable amount of chemical evidence indicates that monosubstituted and symmetrically disubstituted amidines having different groups at the nitrogen atom exhibit tautomerism (4). Further support for this evidence has been provided by the infrared

[1]*Manuscript received January 7, 1959.*
Contribution from the Department of Chemistry, McGill University, Montreal, Que., with financial assistance from the National Research Council, Ottawa.
[2]*Part I: Grivas, J. C. and Taurins, A. Can. J. Chem.* **36**, *771 (1958).*
[3]*Holder of the National Research Council Studentship, 1957–59.*

studies of the amidines (I), which showed a second weaker absorption, not vanishing upon dilution, near 3400 cm^{-1} (5, 6).

Fabian, Delaroff, and Legrand (5) observed a rather strong band near 1515 cm^{-1} with solutions of the N-alkyl-N′-phenylbenzamidines. This absorption was displaced by 30–40 cm^{-1} toward the higher frequencies in solid state. This led to the conclusion that it was owing to the NH deformation vibration. However, in some cases, the band was confused with the aromatic ring modes which also occur near 1500 cm^{-1}.

Acetamidines (I) with R′,R″ = aryl groups have been reported to exhibit four bands in the region 1550–1200 cm^{-1}, which were effected by the breaking of the hydrogen bonding and deuteration (6). Two of them, near 1540 and 1330 cm^{-1}, were assumed to originate from the coupling of the deformation vibrations, δ(NH), with the antisymmetric mode of the group —C(=N)N, and the other two at 1440 and 1220 cm^{-1} from the coupling mode of the δ(NH) with the ν(N—R).

The C=N stretching vibration has been firmly established as a very strong band between 1690 and 1640 cm^{-1} for open chain compounds. Pickard and Polly (7) quote this absorption at 1655–1615 cm^{-1} for ketimines of the structure $\begin{matrix} R \\ \diagdown \\ \\ \diagup \\ R' \end{matrix}$C=NH. The range of the ν(C=N) is somewhat larger for the substituted amidines (1685–1590 cm^{-1}) and the position or intensity of this band seems to depend on the degree of substitution and the presence of electron-attracting groups attached to the amidine system (5).

The C—N stretching vibrations occur in a wide range together with the C—C skeletal vibrations. This makes the assignments uncertain in many cases. However, Colthup (8) gives a range 1100–1200 cm^{-1} for C_{alk}—N deformation frequency for the secondary aliphatic amines. This was confirmed by Hadži and Škrbljak (3), who mentioned a strong band between 1170 and 1140 cm^{-1} to be associated with skeletal vibrations, in which the C_{alk}—N bonds participate strongly. Colthup's table shows also that the $\nu(C_{ar}—N)$ of amines of the type $_{ar}$—NH—$_{alk}$ occurs at 1350–1280 cm^{-1}, and that the second band of medium intensity at 1240–1290 cm^{-1} should correspond to the $\nu(C_{alk}—N)$ of the same type of secondary amines. Finally, the $\nu(C_{ar}—N)$ was recently located at 1240–1260 cm^{-1} for a series of secondary aromatic amines (3).

EXPERIMENTAL

The trichloroacetamidines subjected to infrared analysis are represented by the formulae II and III:

$$Cl_3C—\underset{\underset{NH}{\|}}{C}—NHR$$

II R = alkyl, phenyl, or substituted phenyl,

$$Cl_3C—\underset{\underset{NH}{\|}}{C}—N\begin{matrix} R' \\ \diagdown \\ \\ \diagup \\ R' \end{matrix}$$

III R′ = alkyl.

The methods of preparation of trichloroacetamidines have been described previously (9). The solid substances were investigated in potassium bromide pellets. Liquid substances were examined by spraying a thin layer between sodium chloride plates. Solutions of the amidines were prepared by dissolving 10 mg of the substance in 1 ml of tetra-

Can. J. Chem. Downloaded from www.nrcresearchpress.com by 186.233.112.2 on 09/04/12
For personal use only.

Can. J. Chem. Downloaded from www.nrcresearchpress.com by 186.233.112.2 on 09/04/12
For personal use only.

TABLE I

Positions of absorption maxima (cm^{-1}) in the infrared spectra of N-substituted trichloroacetamidines

No.	Trichloro-acetamidine	State*	(N—H)	(N=H)	Hydrogen-bonded NH	(CH_3) and $(CH_2)_2$	(C=N)	(C=C) aromatic	(N—H) amidine II	(C=C) aromatic	(C_{ar}—N)	(C—N) HN=C—N	(C_{alk}—N)
1	N-Methyl	L	3490s	3300vs†	3200(sh)–3045s	2950s, 2905s	1635vs		1522vs			1313vs	1152vs
2	N-Ethyl	L	3465s	3340vs‡	3280(sh)–3050s	2970m, 2940s, 2875s	1637vs		1515vs			1314vs	1168vs
		Sol	3465m	3350w	None	2970m, 2930m, 2870w	1642vs		1510vs			1308m	
3	N-*n*-Butyl	L	3445s	3325vs	3200(sh)–3040m	2920vs, 2850s	1633vs		1515vs			1313s	1155vs
4	N-*n*-Amyl	L	3440m	3320s‡	3180(sh)–3030m	2915vs, 2845s	1632vs		1513vs			1312s	1155s
		Sol	3455m	3350w	None	2950(sh), 2925vs, 2855s	1642vs		1512vs				
5	N-Benzyl	S	3330m	3205s‡		2915vw, 2890vw	1635vs	1602m	1545vs	1495s		1338s	1168vs
		Sol	3475m	3370w			1642vs	1602m	1510s	1500sh			
6	N-Phenyl	S	3485s	3370s	3270(sh)–3150vw		1657vs	1594vs	1584vs	1483s	1337s	1237m	
		Sol	3520m	3415m	None		1672vs	1594vs	1580vs	1484s	1327s	1240m	
7	N-*o*-Tolyl	Sol	3500s	3400s		2915vw, 2860(sh)	1670vs	1596s	1577s	1483vs	1327s	1239m	
8	N-*m*-Tolyl	S	3470m	3365m	3320m–3160(sh)	2915vw, 2860(sh)	1652vs	1595vs	1585vs	1486s	1337s	1265m	
		Sol	3500m	3400m	None	2915vw, 2860(sh)	1670vs	1595vs	1580vs	1484s			
9	N-*p*-Tolyl	S	3480m	3370m	3150w	2915w–2850w	1660vs	1610s(sh)	1580vs	1504vs	13375	1237s	
		Sol	3505m	3400m	None	2918w–2860vw	1667vs	1611m	1580vs	1505vs			
10	N-*p*-Ethoxyphenyl	S	3450m	3360m	3330m–3110m	2990m, 2930m, 2890vw	1660vs	1606vs	1627vs	1507vs	1332	1232vs	
		Sol	3500m	3400m	None	2980m, 2920(sh), 2895w	1667vs	1604m	1577vs	1503vs	1322s	1236vs	
11	N,N-Dimethyl	L		3340m		2895s	1603vs					1267vs	1090vs
		Sol		3360m		2895s, 2820(sh)	1607vs					1267vs	
12	N,N-Diethyl	L		3380s		2985vs, 2945vs, 2885s	1593vs						
		Sol		3380m		2985vs, 2945vs, 2880m	1600vs						
13	N-Morpholyl	L		3360m								1275vs	1117vs
		Sol		3365m		2975m–2920m, 2900m–2858s	1601vs					1277vs	

*L, liquid; S, solid; Sol, solution.
†A wide band between 3250 and 3350 cm^{-1}.
‡Wide bands.

chloroethylene. Sodium chloride cells of 1 mm thickness were used. The infrared spectra were recorded with a Perkin–Elmer Model 21 double beam spectrophotometer equipped with a sodium chloride prism. The settings at the instrument were as follows: resolution 927, gain 5, speed 4.5, response 1, suppression 0. The results have been summarized in Tables I and II.

TABLE II

Positions of absorption maxima (cm^{-1}) in the infrared spectra of N-substituted trichloroacetamidines

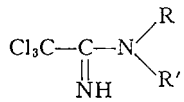

Assignments	R = H R′ = Alkyl	R = H R′ = Aryl	R,R′ = Alkyl
Free $\nu(\rangle N—H)$	3440–3480	3490–3520	
Free $\nu(=N—H)$	3300–3370	3390–3420	3360–3380
Bonded (N—H) (*trans*)	3180–3300	3270–3330	
Bonded (N—H) (*cis*)		3100–3160	
ν(C=N)	1630–1650	1650–1670	1590–1610
Free $\delta(\rangle NH)$ (amidine II band)	1510–1525	1570–1580	
$\nu(C_{ar}—N)$		1320–1340	
ν(C—N) in HN=C—N	1300–1340	1230–1270	1260–1280
$\nu(C_{alk}—N)$	1150–1170		1090–1120(?)
ν(C—C) in $Cl_3C—C$	1025–1070		

RESULTS AND DISCUSSION

I. Region 4000–1800 cm⁻¹

If trichloroacetamidines existed in two tautomeric forms IV*a* and IV*b*

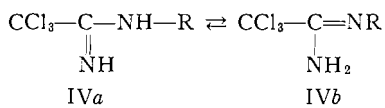

IV*a* IV*b*

present in dilute solutions then more than two absorption bands should appear between 3500 and 3200 cm^{-1}. Or, if the tautomeric equilibrium had been displaced to the right completely (IV*b*), two absorption bands characteristic of the stretching vibrations of the primary amino group should appear, although modified by the double bond at the α-carbon atom. However, the infrared spectra of the N-monosubstituted trichloroacetamidines revealed only two, very sharp, absorptions at 3450–3520 cm^{-1} and at 3350–3415 cm^{-1} in dilute solutions. The intensity of the two bands showed a general increase on passing from N-alkyl- to N-phenyl-derivatives, where both were almost of the same intensity. The second absorption band was of a much lower intensity in the spectra of the N-alkyl-trichloroacetamidines. No inflections were recorded. The results indicate that amidines do not exhibit any tautomerism at least not in dilute tetrachloroethylene solutions.

Furthermore, a comparison of the infrared spectra of N-dialkyl substituted trichloroacetamidines with those of the N-alkyl homologues revealed that the first and the second stretching band of the imino group =NH appear in the same regions and are very close to each other. Thus, in dilute solution N-ethyl- and N-amyl-trichloroacetamidines showed the second band at 3350 and 3347 cm^{-1} respectively, whilst the

Can. J. Chem. Downloaded from www.nrcresearchpress.com by 186.233.112.2 on 09/04/12
For personal use only.

N-dimethyl-, N-diethyl, and N-morpholyl-derivatives exhibited only one band of the free =NH group in this region at 3362, 3382, and 3365 cm^{-1} respectively.

The NH stretching vibration of the secondary amino group was thus assigned to the 3450–3520 cm^{-1} band and the ν(NH) of the imino group to 3350–3415 cm^{-1} absorption. Further evidence in favor of the above assignments was obtained from the position of the ν(C=N) in different types of substitution, which will be discussed later in this paper.

The infrared spectra of all the compounds show that hydrogen bonding is involved to a considerable extent in liquid and solid phases, except the liquid N-dialkyl substituted amidines. The general trend of the displacement of the $\nu(\rangle NH)$ and ν(=NH) to the higher frequencies is shown when the substances are diluted, in accordance with what is expected from a breaking of hydrogen bonding. This displacement is very slight for the change from the liquid to the solution and it is more pronounced in the case of the solid derivatives.

More than two bands appear in the spectra of solid or liquid compounds in addition to the two NH vibrations; their behavior resembles that of the secondary amides, since they disappear upon dilution. Many of the liquids examined possess a weak absorption near 3040 cm^{-1} and it is expected that other bands exist because of the fact that the ν(=NH) band is very broad and exhibits one or two inflections. Its intensity is also higher than the $\nu(\rangle NH)$ while the opposite is true with the spectra obtained by solutions of these substances.

The existence of these absorption bands in addition to the $\nu(\rangle NH)$ and ν(=NH) was established in four of the six solid amidines examined; i.e. N-(*p*-ethoxyphenyl)-trichloroacetamidine absorbed rather strongly at 3450, 3360, 3330, and 3110 cm^{-1}. The last two bands vanished upon dilution, while the first two were displaced to 3498 and 3398 cm^{-1} respectively. Solid N-(*m*-tolyl)trichloroacetamidine showed absorption maxima at 3470, 3365, 3320, and 3160 cm^{-1}; these four bands were replaced by only two strong absorptions at 3500 and 3400 cm^{-1} in dilute solution. The 3050 cm^{-1} weak absorption observed with the N-alkyl-trichloroacetamidines may be confused with the stretching motion of the aromatic C—H group with the N-phenyl derivatives.

Of the two hydrogen atoms of the imino and secondary amino groups, the first one seems to be involved in hydrogen bonding to a greater extent since it is the band near 3350 cm^{-1} which undergoes greater transformation on changing from the condensed phase to the solution. Although more work is necessary in this field, it can be assumed that the absorption near 3300 and 3150 cm^{-1} are due to hydrogen bonding and originate from a *trans* and *cis* arrangement respectively. These absorption bands correspond to the dimer and polymer structures (V and VI), from which the dimer may be stabilized by resonance occurring in a fashion similar to that observed with the carboxylic acids.

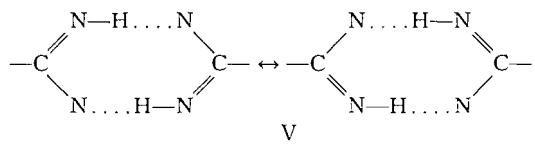

V

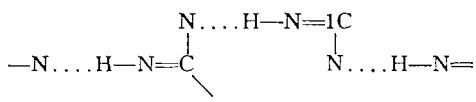

VI

Can. J. Chem. Downloaded from www.nrcresearchpress.com by 186.233.112.2 on 09/04/12
For personal use only.

In conclusion, secondary amidines possess hydrogen bonding to a smaller extent than secondary amides and the N-alkyl-trichloroacetamidines are more strongly associated than the N-aryl derivatives.

II. Region 1800–1200 cm^{-1}

(*a*) *The Stretching,* ν(C=N), *Absorption*

These vibrations were easily recognizable in all the spectra taken, since they appeared as a very strong band between 1590 and 1670 cm^{-1} and did not show any appreciable change in intensity and position, whether the sample was a solid, a liquid, or a solution. The small displacement (5–25 cm^{-1}) to the lower wave lengths upon dilution is quite characteristic in all cases and excludes the possibility of being any NH bending vibration. The position of the ν(C=N) seems to be a function of substitution on the amino nitrogen atom. Thus N-alkyl-trichloroacetamidines absorbed between 1630 and 1645 cm^{-1}, whereas the N-dialkyl compounds at 1590–1610 cm^{-1}. The opposite shift to higher frequencies (1650–1670 cm^{-1}) was recorded with the N-phenyl-trichloroacetamidines.

This behavior can be easily explained and it comes as additional evidence for the non-existence of tautomerism in the amidines examined. Amidines are the resonance hybrid of the following structures (VII).

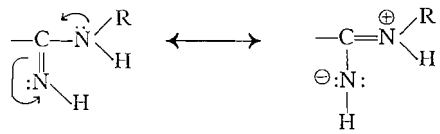

VII

Substitution of the amino hydrogen atom by another alkyl group increases the electron density around the amino nitrogen atom owing to the greater +Is effect. As a consequence the contribution of the polar structure increases, the double bond character of the C=NH double bond decreases, and hence causes a displacement of the ν(C=N) to the lower frequencies which is in fact observed. When R is an electron-attracting group (phenyl) its −Is effect should oppose such an electron movement and depress the resonance within the amidino group. As a result N-phenyl derivatives should absorb at higher frequencies than the corresponding N-alkyl derivatives in agreement with our findings. If tautomerism exists, one of the two tautomers (IX) should be present.

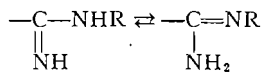

VIII IX

In this case the resonance hybrid can be represented as (X)

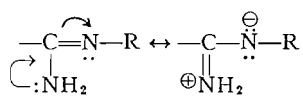

X

and the pattern of the displacement going from the N-alkyl- to the N-dialkyl- and N-phenyl-trichloroacetamidines is expected to be the opposite of that observed.

Can. J. Chem. Downloaded from www.nrcresearchpress.com by 186.233.112.2 on 09/04/12
For personal use only.

Can. J. Chem. Downloaded from www.nrcresearchpress.com by 186.233.112.2 on 09/04/12
For personal use only.

(*b*) *The Amidine II Band*, δ(N—H)

The second very strong absorption in this region appeared near 1515 cm^{-1} for all N-alkyltrichloroacetamidines, and was absent from all the infrared spectra of N-dialkyl derivatives. This immediately suggested that it could be related to the δ(NH) of the secondary amino group. The displacement of this band (1–5 cm^{-1}) to the lower frequencies upon dilution was negligible, since association is weak in the liquid phase, but was indicative of an NH deformation frequency. A rather pronounced shift to lower frequencies was recorded for the N-benzyl derivative, the only aliphatic solid which showed a strong displacement. This compound had a very strong band at 1545 cm^{-1}, in addition to the aromatic absorptions at 1602 and 1495 cm^{-1}. The 1545 cm^{-1} band was displaced to 1510 cm^{-1} upon dilution and the 1495 cm^{-1} absorption peak appeared as a distinct inflection of this band.

In the case of the N-aryl derivatives, the δ(NH) seems to be located near 1580 cm^{-1}, in addition to the two aromatic vibrations. A normal aromatic stretching mode, nevertheless, has been identified between 1600 and 1560 cm^{-1}; although it is always weak, external conjugation increases its intensity, when it becomes a readily recognizable medium band (1).

This possibility was excluded on the following grounds:

(1) The band is very strong in all the spectra.

(2) In the case of the solid N-(*p*-ethoxyphenyl)-trichloroacetamidine, which associates strongly it appeared at 1627 cm^{-1} as a strong absorption, whereas it was found at 1578 cm^{-1} upon dilution.

(3) Richards and Thompson (10) reported only two bands for the aromatic modes near 1600 and 1500 cm^{-1} with the N-aryl acetamides, for which a similar increase in intensity of the 1560–1600 cm^{-1} frequency could be expected.

(4) Since the resonance within the amidine system C(=NH)—NH is opposed to that arising from the aromatic ring, such a conjugation should be reduced greatly, if it existed at all. The assignment of the δ(NH) to the 1515 cm^{-1} absorption for the N-alkyl-trichloroacetamidines and to the 1580 cm^{-1} for the N-aryl analogues might be supported by the findings of Barr and Haszeldine and Hadži and Škrbljak, who located the δ(NH) of the secondary aromatic amines and the secondary perfluoroalkylamines in the same region. It is obvious that the otherwise weak δ(NH) is enhanced through resonance which imposes a partial positive charge on the nitrogen atom.

(*c*) *The Stretching*, ν(C—N), *Frequencies*

Amidines should give rise at least to two absorption bands related mainly to the C—N stretching vibrations. It was clearly understood that only two absorptions of strong and very strong intensity were suitable for the ν(C—N) vibrations in the 1400–1100 region for the N-aryl-substituted trichloroacetamidines, i.e. the 1330 cm^{-1} band for the $\nu(C_{ar}—N)$ and the 1240 cm^{-1} for the ν(C—N) of the amidino grouping. Both values agree with those given by Cothup's table and permit the assumption that the phenyl group "localizes" the C=N double bond to some extent; in agreement with our observation the C=N groups in the phenyl derivative absorb at higher frequencies than the N-alkyl- and N-dialkyl-derivatives.

The ν(C—N) of N-alkyl-trichloroacetamidines occur at higher frequencies; alkyl groups facilitate the resonance within the amidine system, thus imposing a partial double bond character to its (C—N) bond, which therefore should absorb at higher frequencies than the $C_{alk}—N$ bond. This was revealed from a comparison of the infrared spectra recorded for the different classes of substituted amidines on the one hand and from

their absorption in the ultraviolet region on the other. Indeed the amidine ν(C—N) was found to be located near 1310 cm^{-1}, very close to the $\nu(C_{ar}—N)$ in the aromatic compounds, whereas the 1150–1170 cm^{-1} strong absorption should involve mainly $\nu(C_{alk}—N)$ modes, with the N-alkyl-trichloroacetamidines.

No general conclusion could be drawn, for the N-disubstituted derivatives. Nevertheless, a strong band near 1270 cm^{-1} was attributed to the amidine ν(C—N) absorption and the $\nu(C_{alk}—N)$ could be related also to a strong band occurring near 1100 cm^{-1}. It should be pointed out that the ν(C—C) of the $Cl_3C—C$ group was definitely found near 1050 cm^{-1}, in agreement with the spectrum obtained for the trichloroacetonitrile which was used in the preparation of the amidines mentioned above and with the data found in the literature (11).

REFERENCES

1. Bellamy, L. J. The infrared spectra of complex molecules. 2nd ed. Methuen & Co. Ltd., London. 1958.
2. Barr, D. A. and Haszeldine, R. N. J. Chem. Soc. 4169 (1955).
3. Hadzi, D. and Skrbljak, M. J. Chem. Soc. 843 (1957).
4. Shriner, L. R. and Newman, W. F. Chem. Revs. **35**, 378 (1944).
5. Fabian, J., Delaroff, V., and Legrand, M. Bull. soc. chim. France, **287**, 287 (1956).
6. Prevorsek, D. Compt. rend. **244**, 2599 (1957).
7. Pickard, P. L. and Polly, G. W. J. Am. Chem. Soc. **76**, 5169 (1954).
8. Colthup, B. N. J. Opt. Soc. Am. **40**, 397 (1950).
9. Grivas, J. C. and Taurins, A. Can. J. Chem. **36**, 771 (1958).
10. Richards, E. R. and Thompson, W. H. J. Chem. Soc. 1248 (1947).
11. Wait, C. S., Jr. and Janz, J. Cr. J. Chem. Phys. **26**, 1554 (1957).

Can. J. Chem. Downloaded from www.nrcresearchpress.com by 186.233.112.2 on 09/04/12
For personal use only.

Can. J. Chem. Downloaded from www.nrcresearchpress.com by 190.90.36.8 on 09/04/12
For personal use only.

A SURVEY OF THERMODYNAMIC PARAMETERS FOR SOLVOLYSIS IN WATER[1]

R. E. ROBERTSON, R. L. HEPPOLETTE,[2] AND J. M. W. SCOTT[2]

ABSTRACT

A method is suggested for determining the standard state entropies ($S^0_{\neq}$) of the transition state for the neutral hydrolysis of esters in water. This has required the development of methods for approximating initial state parameters where experimental data are lacking.

Characteristic linear correlations between the entropy and enthalpy of activation are observed for hydrolysis in water, as well as for the bimolecular halide exchange reaction in acetone and for acid–base equilibria. Explanations are advanced to explain the observed trends.

From the derived standard state entropies, a method for estimating the charge development in the transition state for the methyl and isopropyl halides is proposed. With this further detailed knowledge of the transition state in the methyl halide series, reasonable values of the activation enthalpy can be calculated from available thermochemical data.

Correlations of kinetic data for reactions in solution have normally been attempted in terms of relative rates and some function of the reactant (1, 2), the solvent (3, 4, 5), or both (6, 7). There is no doubt that the effect of structural changes on the reactivity can be estimated quite fairly by relative rates, provided neither a detailed understanding of the activation process (8, 9) nor a quantitative description of the transition state is required. The next stage of refinement, however, will require a consideration of the derived thermodynamic parameters which characterize the activation process and the transition state. In principle this will require not only that rate data be determined over a wider range of temperature and with greater accuracy (10, 11) than has frequently been judged necessary but also that the corresponding parameters for the solvated initial state of the ester as well as those characterizing the gaseous state be available (8). Differences in the absolute values of the parameters so derived may then be properly analyzed and so provide a quantitative measure of the effect of structure on reactivity. The procedure may be outlined as follows. Consider the reaction:

[1] $$RX_{gas} \xrightarrow{\delta_s F} RX_{solution} \xrightarrow{\Delta F^{\neq}} RX_{transition\ state}.$$

For each ester in the gaseous state there will be an equation of the form

[2] $$F^0_g = E^0 + H^0_g - T\,S^0_g$$

where

$$H^0_g = \int_0^T C_p\,dT$$

and

$$S^0_g = \int_0^T C_p/T\,dT;$$

$S^0_0 = 0$ (third law) but E^0 is indeterminate. Similarly for the solution of the gaseous ester, there will be a corresponding equation with appropriate subscripts incorporating parameters derived from the temperature dependence of the Henry's Law constant

[1]*Manuscript received November 21, 1958.*
Contribution from the Division of Pure Chemistry, National Research Council, Ottawa, Canada.
Issued as N.R.C. No. 5103.
[2]*National Research Council of Canada Postdoctorate Fellow.*

(omitting the zero point energy) and similarly for the transition state. Thus the entropy of the transition state will be a summation of the terms

[3] $$S^0_{\ddagger} = S^0_g + \delta_a S^0 + \Delta S^{\ddagger}$$

and an analysis of changes in $S^0_{\ddagger}$ as a consequence of structural changes will obviously require a consideration of the sum of the changes in each of the contributing terms. Such an analysis has been previously indicated by Moelwyn-Hughes for methyl bromide (12).

The general plan of this paper then follows eq. [3].

1. We propose a simple empirical method for estimating S^0_g values for certain series of esters where these are lacking.

2. Similarly an empirical method is given which provides parameters for the solution processes where the temperature dependences for the corresponding Henry's Law constants are unknown.

3. The entropy and enthalpy values ($\Delta S^{\ddagger}, \Delta H^{\ddagger}$) for the solvolytic process are correlated and related to changes in structure and to the role of the solvent.

4. The problem of charge development which is of such importance in connection with 3 is dealt with in a separate section.

5. Finally the parameters are combined as indicated in eq. [3] to give a limited characterization of the transition state for some alkyl halides and the activation energies for the methyl halides are calculated.

Values for S^0_g

The values of S^0_g (p = 1 atmosphere) have been listed for the methyl halides (13) but not for the other alkyl halides with which we are concerned in this paper. An isolated value has been given for tertiary butyl bromide by Howlett (14). Hence we have used a simple method for the estimation of gas phase entropies based on the S^0_g values of the corresponding hydrocarbons (15) for the isopropyl and tertiary butyl halides.

A term $\delta_x = S^0_g(\text{Me-X}) - S^0_g(\text{Me-H})$ is defined which gives the contribution to the standard state gaseous entropy obtained by replacing a hydrogen atom in the hydrocarbon by a halogen atom. Values for δ_x so calculated based on known values of the methyl halide (13) are given in Table I.

TABLE I

The $\delta_x S^0_g$ contribution of halogen atoms to the standard state entropy of the methyl halides (p = 1 atm)*

Halogen	$\delta_x S^0_g$ e.u.
F	8.8
Cl	11.47
Br	14.24
I	16.35

*It is only for the methyl halides that all the terms on the R.H.S. of eq. [3] have been determined experimentally. As a consequence values for S^0_g and $\delta_a S^0$ for other compounds must be regarded as tentative, especially those for S^0_g, since these have been obtained, by an approach which is undoubtedly oversimplified. Since this paper was written, a much more detailed treatment of the calculation of standard state entropies in cases where experimental values are lacking has been given by Benson and Buss (64) as well as in a recent monograph by Janz (65). It must be emphasized that this lack of precise data in no way alters the broad conclusions which we wish to establish, nor do we suggest that this is the only possible mode of treating these quantities.

To calculate S^0_g(R-X), S^0_g was combined with δ_x in the following manner:

[4] $$S^0_g(\text{RX}) = S^0_g(\text{R-H}) + \delta_x.$$

As a check on the method, the values for ethyl chloride and for *t*-BuBr were calculated, since these were both known.

Can. J. Chem. Downloaded from www.nrcresearchpress.com by 190.90.36.8 on 09/04/12
For personal use only.

Calc.	Lit.
S^0_g(EtCl) = 66.32	65.9 (ref. 13)
S^0_g(*t*-BuBr) = 84.66	80.52 (ref. 14)

Clearly the errors involved for these simple molecules are not too serious. The required values for other compounds determined by this method are recorded in Table VI and compared where possible with the corresponding values calculated by Franklin (16). There is a constant difference of *ca.* 2.6 e.u. between Franklin's values for the isopropyl halides and the values calculated by the above simplified method, but the values for the *t*-BuCl and *t*-BuBr are essentially identical.

Certain special cases arise in which a relative characterization of $F^0_{\ddagger}$ can be obtained without reference to F^0_g. Consider a reaction of a single substrate solvolyzing in a series of solvents or solvent mixtures such as the recent study of the solvolysis of *t*-butyl chloride by Winstein and Fainberg (4):

$$F^0_{\ddagger} = F^0_g + \delta_s F + \Delta F^{\ddagger}. \qquad [5]$$

Since only one compound is involved, for a change of solvent,

$$\delta_M F^0_{\ddagger} = \delta_M \delta_s F + \delta_M \Delta F^{\ddagger}, \qquad [6]$$

i.e. the changes in $F^0_{\ddagger}$ derive only from changes in the solution and activation processes. The use of this relation can be illustrated by reference to the recent data of Winstein and Fainberg (4) for the solvolysis of *t*-butyl chloride in methanol–water mixtures.

By means of the cycle

$$\begin{array}{ccccc} F^0_g & (RX)_g & \xrightarrow{\Delta F^0_g} & (R\oplus.....X^{\ominus})_g & F^0_i \\ & \uparrow \delta_e F & & \downarrow \delta_s F_i & \\ F^0_s & (RX)_s & \xrightarrow[\Delta F^0_{\ddagger}]{} & (R\oplus.....X^{\ominus})_s & F^0_{\ddagger} \end{array}$$

Winstein and Fainberg attempt a separation of the various changes in F^0_g and $F^0_{\ddagger}$ which are due to changes in the solvent. For example it is obvious that by combining the two relations from the above cycle

$$\delta_s F_i = F^0_{\ddagger} - F^0_i \qquad [7]$$

$$F^0_i = F^0_g + \Delta F^0_g \qquad [8]$$

the following relation is obtained for each solvent

$$\delta_s F_i = F^0_{\ddagger} - F^0_g - \Delta F^0_g \qquad [9]$$

and the effect of a change of solvent will be measured by difference

$$\delta_M \delta_s F_i = \delta_M F^0_{\ddagger} - \delta_M \Delta F^0_g, \qquad \delta_M F^0_g = 0. \qquad [10]$$

Clearly changes in $\delta_s F_i$ can only be compared with changes in $\delta_M F^0_{\ddagger}$ if the corresponding $\delta_M \Delta F^0_g$ values are known to $\rightarrow 0$. There is some reason to conclude that the extent of ionization along the MeOH–H_2O mixtures may vary and consequently further discussion of Winstein and Fainberg's dissected values must be postponed until further data are available. While such an approach may be useful in studying the effect of changes in

Can. J. Chem. Downloaded from www.nrcresearchpress.com by 190.90.36.8 on 09/04/12
For personal use only.

solvent, it cannot be extended to a study of the effect of structural differences on reactivity in the absence of a knowledge of the corresponding changes in F_g^0.

TABLE II

Free energy changes for the solvolysis of *t*-butyl chloride in methanol–water mixtures $T = 298.16°$ K

Solvent	$\Delta F^{\ddagger}$	$\delta_s F^*$	$F_{\ddagger}^0$	δ_M
MeOH	25.80	+3.15	$28.95+F_g^0$	10.40
90.17 MeOH/H_2O	24.72	+2.76	$27.48+F_g^0$	8.93
80.09 MeOH/H_2O	23.80	+2.35	$26.15+F_g^0$	7.60
70.45 MeOH/H_2O	23.15	+1.94	$25.09+F_g^0$	6.54
H_2O	19.49	−0.94 (−1.05)†	$18.55+F_g^0$	0

*Winstein and Fainberg values are corrected to the hypothetical standard state used in this paper. This involves a correction of $298.16\times19.53 = 5.823$ kcal. In this and succeeding work we shall use a standard state of 1 mole per liter in both liquid and gaseous state implying $p = 24.466$ atm at 298.16° K. This will involve a correction when comparing our data with those based on other standard states as follows:

Standard states summary

Source	c_g	c_s	p	Conversion factor
1. This paper	1 mole liter^{-1}	1 mole liter^{-1}	22.446 atm	—
2. Glew and Moelwyn-Hughes (17)	1 mole/1.8594×10^4 liter	1 mole liter^{-1}	1 mm Hg	$19.53 = R \ln (760\times22.415)\times(298.16/273.16)$
3. NBS Circular 500 (13)	1 mole/24.466 liter	—	1 atm	$6.35 = R \ln (24.466)$
4. NBS Circular C 461 (15)	1 mole/24.466 liter	—	1 atm	$6.35 = R \ln (24.466)$

†This value was calculated from an extension of the Barclay–Butler Rule (see below).

Initial State Solvation Differences

The solution process for non-electrolytes in water is dominated by the large water–water (*b–b*) interaction in contrast to similar solutions in non-associated solvents where (18) the solute–solute (*a–a*) interactions appear to govern the observed $\delta_s H$ and $\delta_s S$ values. Detailed discussions of aqueous solutions of non-electrolytes have been given by Bernal and Fowler (19), Eley (20), Frank and Evans (21), Glew and Moelwyn-Hughes (17), Feats and Ives (22). The outstanding features of such solution processes may be summarized as follows: (1) large positive ΔC_p values, (2) comparatively large negative $\delta_s H$ and $\delta_s S$ values which are found to be related for any series of alkyl groups attached to a common polar group X by a linear relation of the form

$$\delta_s H = \beta\delta_s S+\gamma, \qquad [11]$$

(3) changes in $\delta_s H$ and $\delta_s S$ appear to follow changes in the size of the solvation shell. The constant (γ) for any given series will include those specific differences in $\delta_s F$ arising as a consequence of differences in the interaction of the anionic portion of the ester with the solvent. The above regularities may be rationalized as follows. A hole must be created in the water for the solute. This will obviously vary with the size of the solute and will be related to the latent heat of evaporation as follows:

$$\delta_\epsilon H = (V_{\text{solute}}/V_{H_2O})\ 10.4 \text{ kcal} \qquad [12]$$

with corresponding values for $\delta_\epsilon S$, while through any series $\delta_R\delta_\epsilon F \simeq 0$. But this cannot be the controlling step in the solution process, since the observed values of $\delta_s H$ and $\delta_s S$ are negative, suggesting a freezing process. This conclusion is supported by the sign of the $\delta_s C_p$ for the solution process of non-electrolytes which is positive and increases with the size of the solute. These facts were noted by Eley (20) and subsequently formed

Can. J. Chem. Downloaded from www.nrcresearchpress.com by 190.90.36.8 on 09/04/12
For personal use only.

Can. J. Chem. Downloaded from www.nrcresearchpress.com by 190.90.36.8 on 09/04/12
For personal use only.

the basis of the "iceberg hypothesis" suggested by Frank and Evans (21) and developed even more specifically by Glew and Moelwyn-Hughes (17). In effect, the mere presence of a cavity removes a measure of librational freedom (20) over an area proportional to the surface area of the solute and thus leads to increased interaction between those water molecules in the solvation shell. This increased interaction as a consequence of loss of librational freedom results in the changes in $\delta_s H$ and $\delta_s S$ and $\delta_s C_p$ which are opposite in sign, and being greater in magnitude than the corresponding values for cavity formation determine the observed sign of these parameters. Finally, solute–solvent interaction must be considered. Since the alkyl groups have low polarizability (with the exception of those containing unsaturated groups) this interaction will largely depend on the polarizability (23) of the anionic portion of the ester leading to the following increasing order of interaction:

$$F < Cl < Br < I < NO_3 < \text{sulphonates} \backsim \text{phosphates}.$$

This solvent–solute interaction will make a specific negative contribution to $\delta_s F$, which is constant throughout any given series. Since it will be less than $(b–b)$ interaction this $(a–b)$ interaction will alter the solvation parameters in the sense

$$[13] \qquad -\delta_x\delta_s F_{ab} = -\delta_x\delta_s H_{ab}; \quad T\,\delta_x\delta_s S_{ab} \approx 0\,.$$

That this is but a first approximation is evident from a consideration of $\delta_s H$ and $\delta_s S$ for ethane–ethylene; MeF, MeCl, and MeBr. These regularities as well as certain deviations are illustrated in Fig. 1, which shows the correlation of $\delta_s H$ vs. $\delta_s S$ values characterizing the solution of a series of hydrocarbons, alcohols, and a series of esters. The values for the latter and some of the former have been approximated by a method to be described below.

Estimation of $\delta_s H$ and $\delta_s S$

The determination of the temperature dependence of the Henry's Law constants for the esters reported here is a long arduous task, where it is at all possible (17). While an attempt will be made to determine values for key compounds, an approximate method was needed as an interim guide for the interpretation of the kinetic data available. The proposed method is based on the interpretation of the solvation process discussed above and on the further assumption that those regularities which formed the basis of the Barclay–Butler rule (24), and hold for the alkane and alcohol series, will also be true for intermediate series. It must be emphasized that the values so determined (Tables III, IV, and VI—excluding the methyl halides) are no better than these assumptions. Frank and Evans (21) comment on the difference in slope between the alcohols and the less polar compounds while Adon, Cox, and Herrington (25) and Glew and Robertson (26) showed a definite separation between the $\delta_s H$ vs. $\delta_s S$ plots for various series of solutes. ΔF in the eq. [14]

$$[14] \qquad \delta_s S = \frac{\delta_s H}{T} - \left(\frac{\delta_s F}{T}\right)$$

depends on polarity but $\delta_s F/T$ is found to remain remarkably constant for a given series. The regularities already noted support the assumption that through each point in the $\delta_s H$–$\delta_s S$ plot corresponding to RX where R = methyl we may draw a line such that

$$[15] \qquad \delta_s S = \beta\delta_s H$$

where $\beta = f(1/T)$ and T will have a value intermediate between that for alcohols, T

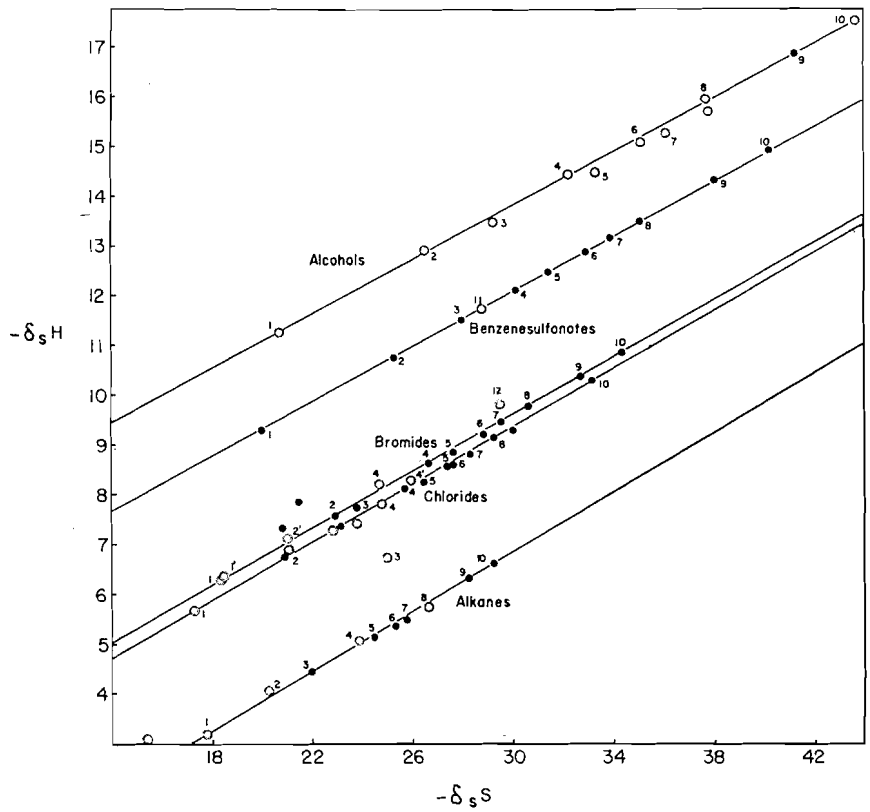

FIG. 1. Estimation of solvation parameters for compounds in water. The numbers refer to Table IV. ○Experimental. ●Estimated.

= 273, and that for the alkanes, T = 300, the variation being assumed proportional to separation along the $\delta_s H$ axis. If the Henry's Law parameters are known for a single member of a series, the $\delta_s H$ vs. $\delta_s S$ plot may be assumed to pass through this point with a slope as given above. Since the solution parameters for the methyl halides were known (17), the corresponding plots were drawn and a line joining methane and methanol was found to approximate to the MeBr and MeI points. The intersection on the chloride and fluoride line did not coincide with the experimental methyl point and the values were accordingly adjusted on the assumption that the deviation was due to some constant $\delta_s H$–$\delta_s S$ contribution associated with X. Lines joining ethane–ethanol, propane–propanol, butane–butanol gave the corresponding EtX, PrX, and BuX points. Since Butler gave $\delta_s H$ vs. $\delta_s S$ values for many alcohols, the above assumptions were used to extend the hydrocarbon plot and so to the corresponding RX values (Table III). The values $\delta_s H$ vs. $\delta_s S$ for ethylamine (27) similarly provide a basis for obtaining the corresponding values for the amines. The only experimental points for comparison are those calculated by Glew (28) from data for EtCl by Nicloux and Scotti-Foglieni (29) and for the *n*-Pr, *i*-Pr bromides and iodides from 1906 data by Rex (30). With the exception of isopropyl chloride the values fall in the predicted range. However, since the experimental values are not consistent among themselves, e.g. $\delta_s S$ (EtCl) < $\delta_s S$ (EtBr), $\delta_s S$ (EtI), $\delta_s S$ (*n*-PrCl) < $\delta_s S$ (EtBr) contrary to what would be expected from relative sizes and polarizabilities (23), we do not regard the deviations between predicted and experimental

Can. J. Chem. Downloaded from www.nrcresearchpress.com by 190.90.36.8 on 09/04/12
For personal use only.

values as significant, and anticipate that more precise data will yield parameters which lie closer to the predicted points. It will be noted that any error in $\delta_s H$ will lead to a compensating error in $\delta_s S$ and displacement along the given plot.

TABLE III

Estimated thermodynamic parameters† for gas solution equilibria of RX

	X					
	-H		-Cl		-Br and -I	
R	$-\delta_s H$	$-\delta_s S$	$-\delta_s H$	$-\delta_s S$	$-\delta_s H$	$-\delta_s S$
1. Methyl	3.2	17.7	5.7	17.1	6.4	18.3
2. Ethyl	4.1	20.0	6.7	21.0	7.0	23.0
4. *n*-Propyl	5.1	23.7	8.1	25.7	8.6	26.5
3. Isopropyl	4.5	22.0*	7.4	23.1	7.8	24.3
8. *n*-Butyl	5.7	26.5	9.1	29.2	9.7	30.5
7. Isobutyl	5.5	25.8	8.9	28.2	9.5	29.5
6. *sec*-Butyl	5.4	25.2*	8.2	27.6	9.2	28.7
5. *t*-Butyl	5.1	24.5	8.2	26.3	8.8	27.5
9. Neopentyl	6.3	28.2	9.9	32.0	10.3	32.5
10. *n*-Pentyl	6.6	29.2	10.3	33.1	10.8	34.3
11. Ethyl acetate						
12. Chloroform						

*Hypothetical.
†See footnote Table I.

Some idea of the influence of the considerable differences in $\delta_s H$ and $\delta_s S$ through a series on the corresponding parameters for the activation process ($\Delta H^{\ddagger}$, $\Delta S^{\ddagger}$) can be judged for the normal series by comparison of the corresponding terms from weak acid–base equilibria studies. In these cases there can be no doubt of the degree of charge development in the ionic form, while in the solvolytic process the transition state has been variously estimated by some to have a charge of $\frac{1}{2}\epsilon$ and others $\rightarrow 1\epsilon$ (see below) (9, 31, 32).

Acid–Base Equilibria Entropy and Enthalpies

The initial state data for the amines can be determined as described above. Those for the acids may be determined if we assume that acetic acid is colinear with ethane and ethanol and determine the $\delta_s H$–$\delta_s S$ point along this line corresponding to $\delta_s F = 1.50$ kcal. The slope of the acid ionization plot was determined as before and, from the predicted values for propionic and butyric acids, $\delta_s F$ values were calculated which agreed (Table IV) within experimental error with the values given by Butler (27). Entropy and enthalpy values for the process of acids and amines and for the corresponding equilibria are recorded in Table IV. A comparison of $\delta_s H/\delta_s S$ with the corresponding $\Delta H/\Delta S$ shows that while the former becomes increasingly negative as the chain lengthens the corresponding ΔS values rapidly converge to a value -24 e.u. The obvious conclusion is that on ionization, reorganization of a solvent will only occur over a limited volume. In any comparison, solvation differences to be significant must occur within this volume (33, 34, 35).

This same consideration will enter into discussions of kinetic parameters where we wish to take account of initial state solvation differences, e.g. the Franklin cycle (see below). Here, too, the development of charge in the activation process results in reorganization of solvent about the "seat of reaction" only, a volume difficult of definition but obviously influenced by the degree of charge development and the structure con-

Can. J. Chem. Downloaded from www.nrcresearchpress.com by 190.90.36.8 on 09/04/12
For personal use only.

TABLE IV

Parameters for hydration and equilibria* for a series of acids and amines

Compound	$\delta_s H$	$\delta_s S$	$\Delta H_{\text{ionization}}$	$\Delta S_{\text{ionization}}$
Formic			− 40	−17.3
Acetic	−14.9	−27.9	−100	−22.1
Propionic	−16.6	−33.9	−170	−22.9
Butyric	−15.91	−40.1	−700	−24.4
Isobutyric	−17.85	−38.80	−799	−24.9
NH_3			1.094	−18.1
$MeNH_2$	−11.45	−22.30	431	−14.0
$EtNH_2$	−12.91	−27.9	− 41	−15.5
n-$PrNH_2$	−14.5	−33.51	−229	−16.5
n-$BuNH_2$	−15.96	−38.9	−453	−17.0
Me_2NH	−13.75	−30.75	1660	− 9.2

*Ref. 36.

tiguous to the bond being broken. Only in the case of such simple compounds as the methyl halides can we assume that this volume includes the entire primary solvation shell characteristic of the initial state. A recognition of the above limitation becomes extremely important when thermodynamic parameters such as the entropy of hydration of ions are being correlated with parameters derived from rate data (10). For the halides it will be noted that the correlation between the $\Delta S^{\ddagger}$ and $\delta_s S$ ion (Fig. 2) is permitted because the complete solvent shell about the forming halide ion in the activation process is influenced just as it is about the corresponding ion. However, the same correlation need not necessarily hold for the nitrate, methanesulphonate, or the benzenesulphonate groups for, although the initial state solvation involves the complete group, the entire solvation shell need not be affected in the transition state (66).

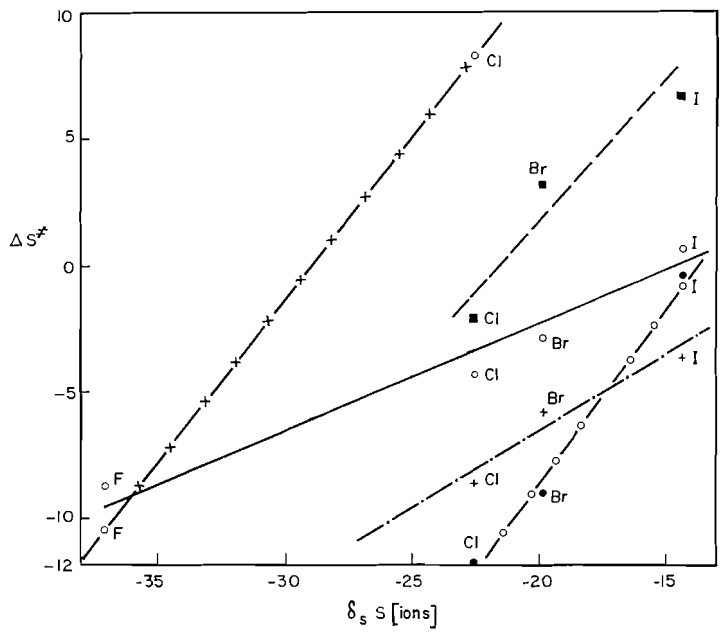

FIG. 2. Correlation between $\Delta S^{\ddagger}$ and $\delta_s S$[ions] for a series of alkyl halides.
—×—×—× *t*-Butyl (50° C) ———— Methyl (25° C)
— — — Isopropyl (25° C) —o—o—o Allyl (50° C)
—·—·—· Ethyl (50° C)

Can. J. Chem. Downloaded from www.nrcresearchpress.com by 190.90.36.8 on 09/04/12
For personal use only.

A distinction must clearly be made between such comparisons as suggested in the previous paragraph and the problem of determining the thermodynamic parameters characterizing the transition state. In such calculations the experimental parameters for the solvation process will enter quite naturally as indicated by eq. [3].

Kinetic Parameters

In Table V are collected a series of parameters characterizing the uncatalyzed solvolysis of esters which have been studied in pure water with sufficient accuracy to warrant comparison. For these compounds, where an accurate determination of $\Delta C_p^{\ddagger}$ had been made, the evaluation of $\Delta H^{\ddagger}$ and $\Delta S^{\ddagger}$ for any temperature between 0 and 100° is convenient. For compounds where $\Delta C_p^{\ddagger}$ can only be estimated the following technique was used.

TABLE V*a*

Summary of activation parameters (at 323.16° K) for the solvolysis of a series of methanesulphonates, benzenesulphonates, and alkyl halides hydrolyzing in water

	Benzene sulphonates		Methane sulphonates		Fluorides		Chlorides		Bromides		Iodides	
	$\Delta H^{\ddagger}$	$\Delta S^{\ddagger}$	$\Delta H^{\ddagger}$	$\Delta S^{\ddagger}$	$\Delta H^{\ddagger}$	$\Delta S^{\ddagger}$	$\Delta H^{\ddagger}$	$\Delta S^{\ddagger}$	$\Delta H^{\ddagger}$	$\Delta S^{\ddagger}$	$\Delta H^{\ddagger}$	$\Delta S^{\ddagger}$
Methyl	20.597	−11.58(1)	20.441	−14.08(3)	25.591	−12.21(5)	25.263	−8.89(6)	24.142	−6.65(6)	25.950	−3.94(6)
Ethyl	21.161	−10.30(1)	21.120	−12.31(3)			24.960	−5.24(6)	24.26	−7.10(6)	25.606	−3.61(6)
Isopropyl	20.791	−3.86(1)	21.424	−3.55(4)			24.960	−5.25(6)	24.36	−1.43(6)	25.527	+1.86(6)
t-Butyl					22.61	−11.36(4)	21.94	+8.32(7,8)				
n-Propyl	20.606	−12.33(1)	20.600	−11.7(3)					23.282	−10.12(10)		
n-Butyl	19.900	−14.7(2)	20.400	−15.00(3)								
n-Amyl	20.100	−13.9(2)										
Isobutyl	23.700	−6.6(2)	24.200	−6.1(3)					26.59	−2.64		
Neopentyl	26.000	−2.8(2)	25.700	−3.5(3)					32.201	−1.37(4)		
Allyl			17.750	−12.21(3)			20.009	−11.68(9)	21.166	−8.91(9)	22.91	−5.34(9)
Benzyl							20.388	−12.35(9)				

1. Ref. (54) 6. Ref. (45)
2. Ref. (55) 7. Ref. (60)
3. Ref. (56) 8. Ref. (62)
4. Ref. (57) 9. Ref. (58)
5. Ref. (59) 10. Ref. (61)

TABLE V*b*

Heat capacity data for the calculation of $\Delta H^{\ddagger}$ and $\Delta S^{\ddagger}$ in V*a*

The following values have been obtained in three different ways:
1. by means of the three-parameter equation (ref. 54),
2. by a plot of E_A vs. T,
3. estimated on the basis of known values by methods 1 or 2 for similar compounds.

Heat capacity of activation ($\Delta C_p^{\ddagger}$ = cal/mole/deg)

	Benzene sulphonate	Methane sulphonate	Fluoride	Chloride	Bromide	Iodide
Methyl	−33.4 (1)	−37.6 (1)	−69 (1)	−52.0 (1)	−46.5 (1)	−56.6 (1)
Ethyl	−34.5 (1)	−36.7 (1)		−50 (3)	−50 (3)	−50 (3)
Isopropyl	−41.2 (1)	−27.4 (1)		−38.5 (1)	−56.4 (1)	−59 (1)
t-Butyl			−50 (3)	−45 (3)		
n-Propyl	−31.3 (1)	−28.8 (2)			−50 (3)	
n-Butyl	−30 (3)	−26.5 (2)				
n-Amyl	−30 (3)					
Isobutyl	−30 (3)				−50 (3)	
Neopentyl	−30 (3)	−23.7 (2)			−50 (3)	
Allyl		−35 (3)		−50.1 (1)	−59 (1)	−46.7 (2)
Benzyl				−40.4 (1)		

*The references for the above parameters are the same as for the corresponding compounds in Table V*a*.

Can. J. Chem. Downloaded from www.nrcresearchpress.com by 190.90.36.8 on 09/04/12
For personal use only.

The rates were determined over a small temperature range, e.g. 40°–50°–60°. The Arrhenius E_A was determined by the method of least squares and this will correspond in the case quoted to E_{50} (mid-point in the experimental range). Since

$$\Delta H^{\ddagger}_{50} = E_{A50} - R \times 323.16 \quad [16]$$

then from k_{50} and $\Delta H^{\ddagger}_{50}$, the $\Delta S^{\ddagger}_{50}$ follows from the absolute rate equation (37). It should be noted that this method does not require any knowledge of $\Delta C_p^{\ddagger}$ and will give results at 50° C of accuracy comparable to those for which $\Delta C_p^{\ddagger}$ has been determined.

Where reactivities made 50° inconvenient or impossible as a mid-point for a series (cf. technique 1 above) e.g. neopentyl bromides or *t*-butyl chloride, $\Delta H^{\ddagger}_T$ and $\Delta S^{\ddagger}_T$ were determined for the mid-point (T) of the experimental range. To evaluate $\Delta H^{\ddagger}_{50}$ and $\Delta S^{\ddagger}_{50}$ we used the formula

$$\Delta H^{\ddagger}_{T+\Delta T} = \Delta H^{\ddagger}_T + \Delta C_p^{\ddagger} \Delta T \quad [17]$$

$$\Delta S^{\ddagger}_{T_1} - \Delta S^{\ddagger}_{T_2} = \Delta C_p^{\ddagger} 2.3026 \ (\log T_1/T_2). \quad [18]$$

This requires a knowledge of $\Delta C_p^{\ddagger}$ for the respective compounds. Here we are guided by experience, the estimated values being shown in Table V*b*. When $\Delta H^{\ddagger}$ and $\Delta S^{\ddagger}$ values are plotted (Fig. 3) a series of linear relations are apparent, revealing definite

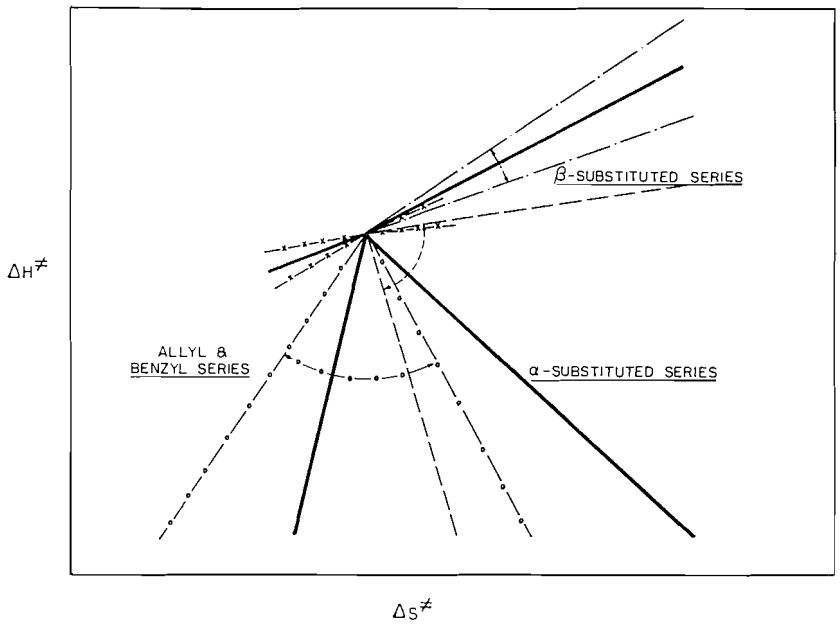

FIG. 3. General profile illustrating the effect of structure on the entropy and enthalpy of activation, for solvolysis reactions in water. The heavy lines indicate average trends; dotted lines indicate specific variations with changing anions.

correlations between the relative values of these parameters and the structure of the alkyl group. Specifically, the values of these coefficients for the α-methyl, β-methyl, straight chain, and unsaturated esters lie on distinct lines which radiate approximately from the methyl group. Functional relationships between $\Delta H^{\ddagger}$ and $\Delta S^{\ddagger}$ for other systems have been noted frequently and an extensive review on this subject has been published by Leffler (38). Hinshelwood (39) has suggested that such correlations are a consequence

Can. J. Chem. Downloaded from www.nrcresearchpress.com by 190.90.36.8 on 09/04/12
For personal use only.

of differences in the lifetime of the transition state but such a suggestion would set kinetic processes apart from the very similar correlations observed in acid–base equilibria (see above and Fig. 4) and those for parameters derived from solution processes. Leffler

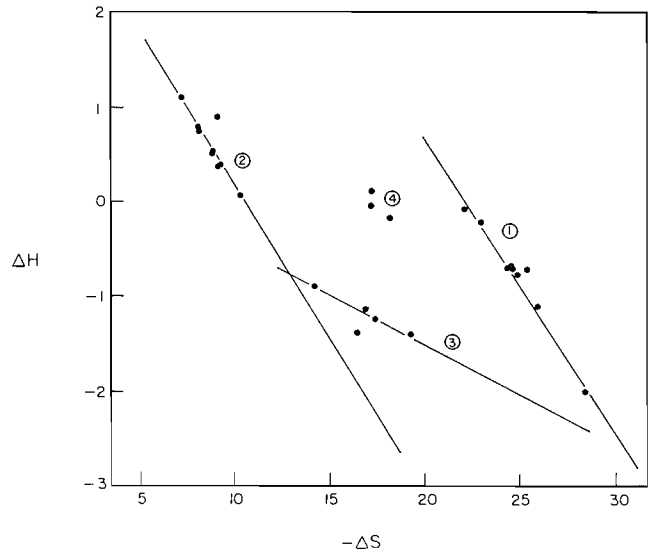

FIG. 4. Linear correlation for the thermodynamic parameters characterizing the dissociation of weak acids: 1, aliphatic acids; 2, amino acids; 3, halogeno-substituted acetic acids; 4, hydroxy acids.

noted that as a consequence of the reorganization of the solvent, on the basis of the Born equation one would expect a linear relation between $\Delta H^{\ddagger}$ and $\Delta S^{\ddagger}$. It would appear that the same argument can be used to include the corresponding changes in enthalpy and entropy arising from solute–solvent interaction as a consequence of other types of force fields involved in the activation process. However, the implication that the linear $\Delta H^{\ddagger}$ and $\Delta S^{\ddagger}$ correlations may be rationalized in terms of differences in solvation is probably an oversimplification. These parameters derived from kinetic studies must include internal as well as solvation differences and a linear correlation in the former implies a similar correlation in the latter or the assumption that the internal contributions to $\Delta H^{\ddagger}$ and $\Delta S^{\ddagger}$ are constant throughout any particular series. In order to rationalize the differences in the slopes of the $\Delta H^{\ddagger}$ and of $\Delta S^{\ddagger}$ correlation (Fig. 3) from our solvolytic data in water, it is convenient to examine, first, the corresponding plot derived from the results published by Ingold and co-workers for the halide exchange reaction in acetone (41). In these latter reactions we may assume that nucleophilic interaction is the dominant factor in the activation process, and the correlation between $\Delta H^{\ddagger}$ and $\Delta S^{\ddagger}$ from these data (Fig. 5) can be rationalized in terms of steric hindrance to nucleophilic attack (41) or a combination of polar and steric effects with the latter predominating (42). Solvation differences must be present, but are probably less specific in organic solvents than in water.

In contrast to the halide exchange reaction, solvation effects are undoubtedly the controlling factor for hydrolysis of esters in water, and the differences evident between the correlation of reaction parameters in Fig. 5 for the halide exchange and in Figs. 3, 6, and 7 for the solvolytic reaction must be rationalized in terms of this change in the controlling factors. From the standpoint of solvation there is also the difference in charge

Can. J. Chem. Downloaded from www.nrcresearchpress.com by 190.90.36.8 on 09/04/12
For personal use only.

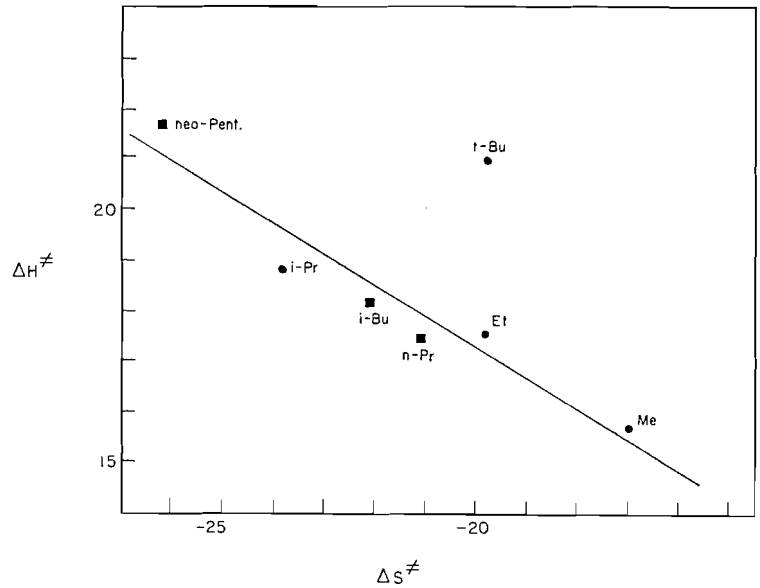

FIG. 5. Effect of structure on the entropy and enthalpy of activation for a bimolecular reaction.

type of the activation process but this is not considered responsible for the trends in the halide exchange parameters. Changes in initial state solvation, as a consequence of β-methylation for any series of esters, will result in successively moving the solvent farther from the carbon at the seat of reaction. The net result will be that, on thermal activation, interaction between the solvent and this carbon will be reduced. Consequently there will be less reorganization of the solvent about the developing carbonium ion in comparison to the reorganization of solvent about the less substituted alkyl group and hence a more positive entropy ($\Delta S^{\neq}$) for the former than for the latter.

Bond making between a particular solvent molecule and the alkyl group will likewise reduce $\Delta H^{\neq}$. Loss of such interaction will have to be compensated for by increased thermal activation and increased solvent interaction with the forming anion, but from the results we must conclude that the effect of this increased interaction on the entropy is not sufficient to compensate for the gain in entropy as a consequence of the decrease in quantum mechanical interaction with the carbonium carbon.

In the halide exchange reaction considered above the dominant driving force came from one direction only—the attack of the nucleophile. In solvolysis, by contrast, as one type of interaction is rendered less effective by structural changes in the alkyl group, alternative paths with higher activation energies become available. The effect of β-methylation in both cases was to raise the enthalpy ($\Delta H^{\neq}$) thus reducing the rate of reaction. The striking difference between the two series is evident in the accompanying entropy changes. Where bond making is dominant, the effect of β-methylation is to impose more stringent requirements on the transition state, leading to more negative entropies and further reducing the rate. In solvolysis, by contrast, as quantum mechanical interaction is reduced through structural change, alternative paths of reaction become available at higher temperatures which are characterized by less reorganization of the solvent and more positive entropy, which to a considerable degree compensates for the higher enthalpy. This difference between the two series can be illustrated by a com-

Can. J. Chem. Downloaded from www.nrcresearchpress.com by 190.90.36.8 on 09/04/12
For personal use only.

Can. J. Chem. Downloaded from www.nrcresearchpress.com by 190.90.36.8 on 09/04/12
For personal use only.

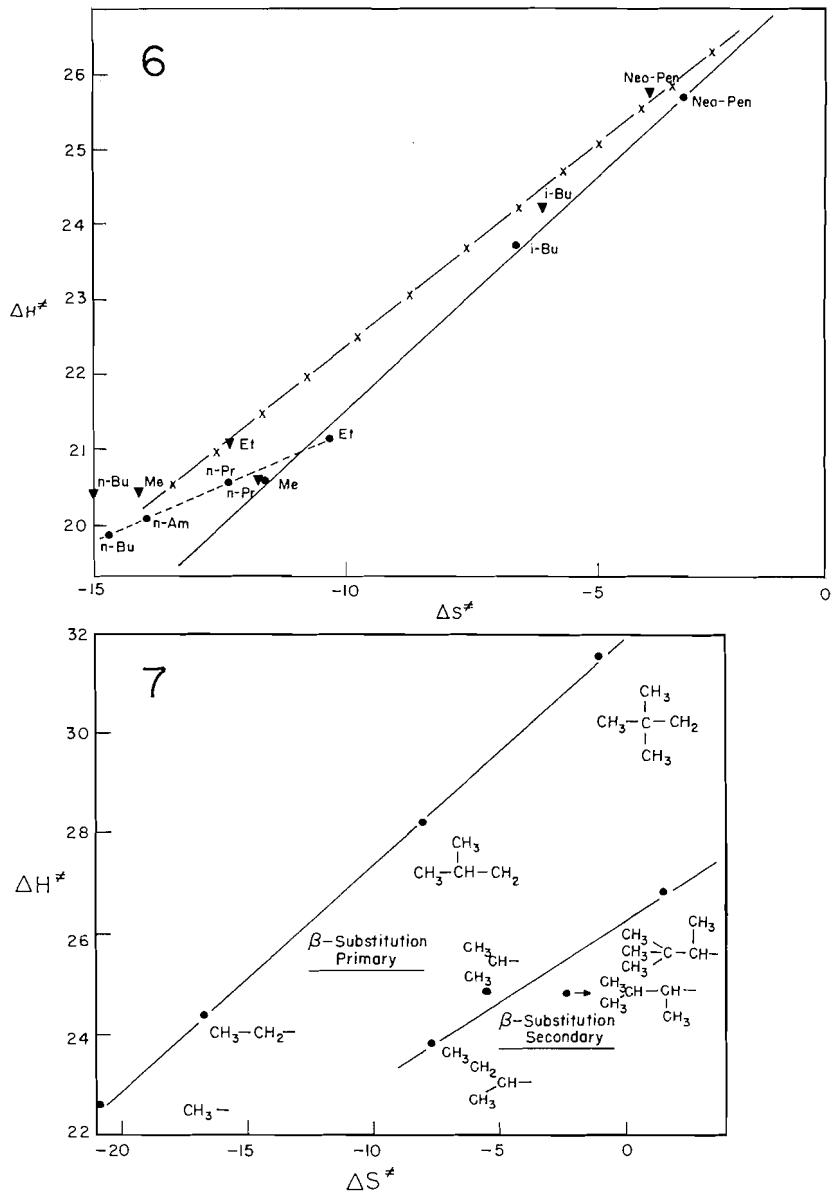

FIG. 6. Correlation of $\Delta H^{\ddagger}$ and $\Delta S^{\ddagger}$ for hydrolysis in water.
—X—X—X Methanesulphonates β-series
——————— Benzenesulphonates β-series
— — — Benzenesulphonates n-series

FIG. 7. Effect of structure on the entropy and enthalpy of activation for solvolysis in acetic acid (ref. 63).

parison of the relative rates $k_{\text{methyl}}/k_{\text{neopentyl}} = 7.7\times10^{6}$ for halide exchange between Cl^- and the alkyl bromides, while the corresponding ratio from solvolysis at 80° C is 16.4. It is noted that the above argument neglects the positive shift in entropy resulting from increased charge development as well as initial state solvation differences.

Such an analysis would lead to the prediction that the values of $\Delta H^{\ddagger}$ and $\Delta S^{\ddagger}$ for the hydrolysis of the normal series of esters would lie close to those corresponding to the

ethyl ester. Since this is not found for the benzenesulphonates (Fig. 6) we must conclude that where steric factors are approximately constant, the effect of other factors such as initial state differences becomes apparent.

Changes in the entropy and enthalpy of activation through the β-substituted primary series of toluenesulphonates solvolyzing in acetic acid (63) show the same general trends both in magnitude and sign (Fig. 7) as was found for the benzenesulphonates hydrolyzing in water. The somewhat reduced slope for the linear $\Delta H^{\ddagger}$ vs. $\Delta S^{\ddagger}$ relation for the former may arise from the reduced importance of quantum mechanical interaction as a consequence of the shift from water to acetic acid as a solvolyzing medium. The difference between the alpha and the beta series arises first from the possibility in the former of a driving force for the reaction arising from an increased tendency toward a change in hybridization from sp^3 to sp^2, which in itself would account for a lowering of the enthalpy and a positive shift in entropy. Secondly, because there is branching close to the seat of reaction, the effect of added α-methyls will exclude solvent more effectively, resulting in an even larger proportional effect by comparison with the β-esters. In addition, in so far as the initial state of the isopropyl or *t*-butyl ester is in some degree more ionic in the initial state than is the corresponding beta compound, then this will further emphasize the difference in entropy between the two series. The combined effect of the above factors will lead to a larger positive shift in the entropy of activation through the alpha series than the corresponding beta series. The difference in the complexity of the contributing factors in the two series is further reflected in the range of values for the parameters through the various series for which data are available to us; contrast the wider range for the alpha than for the beta groups (Figs. 3, 8). In the allyl and benzyl series, where varying charge development in the initial state can alter with the nature of the anionic portion of the molecules, a wider range is also found. Here, however, because the steric factors about the seat of the reaction are relatively constant, the observed changes occur largely in the enthalpy, and solvation differences probably arise from differences in charge development characteristic of the transition state.

Charge Development in the Transition State

In the preceding sections we have shown how to estimate the values of S_g^0 and $\delta_s S$ where they are not known and are now in a position to combine these values with the experimentally determined $\Delta S^{\ddagger}$ according to eq. [3] to get the standard state entropies which characterize the transition state. These values are recorded in Table VI. With the above data available it is now possible to estimate the degree of charge development present in the transition state as follows.

TABLE VI

Summary of thermodynamic parameters for the alkyl halides at 298.16° K

Compound	S_g^0	$\delta_s S$	$\Delta S^0_{\ddagger}$	$S^0_{\ddagger}$
MeF	46.95	−14.11	−8.70	24.14
MeCl	49.62	−17.13	−4.31	28.18
MeBr	52.39	−18.30	−2.91	31.18
MeI	54.50	−18.32	+0.61	36.79
i-PrCl	69.63	−23.08	−2.15	44.40
i-PrBr	72.40	−24.25	+3.11	51.26
i-PrI	74.51	−24.27	+6.67	56.91
t-BuCl	75.54	−26.33	+11.94	61.15

NOTE: We may assume that $\Delta S^{\neq} = \Delta S^0_{\ddagger}$, since the $K^{\ddagger}$ from which $\Delta S^{\ddagger}$ is derived is independent of concentration units (37)—in general this will not be true (see Appendix).

Can. J. Chem. Downloaded from www.nrcresearchpress.com by 190.90.36.8 on 09/04/12
For personal use only.

If the transition state is quasi-ionic it is reasonable to assume

[19] $$S^0_{\ddagger} \propto S^0_R{}^{\oplus} + S^0_X{}^{\ominus} .$$

Making this equation more explicit we may write

[20] $$S^0_{\ddagger} = \mu S^0_R{}^{\oplus} + \alpha S^0_X{}^{\ominus} + c$$

where μ and α and c are constants.

The existence of similar relationships has been noted previously by Hudson and Saville (44) and by Evans and Hamman (10) but has not been set down explicitly as above. The latter, for example, showed a trend between the entropy of solvation for bromide and iodide and the corresponding entropy of activation for two alkyl halides, but such a comparison cannot be strictly true because it fails to take account of initial state differences. It will be noted that these initial state differences are included in the $S^0_{\ddagger}$ and this must be regarded as the main justification for stressing the importance of this term in comparison with the more easily available $\Delta S^{\ddagger}$ value from kinetic measurements.

TABLE VII

Estimation of standard state entropies of alkyl cations

	S^0 ($R^{\oplus}$)*	S^0 ($R^{\oplus}$)†
Me	28.32	—
i-Pr	33.34	57.9 (16)
t-Bu	47.98	63.9 (16)

*Calculated from experimental data.
†Semitheoretical values computed by Franklin (ref. 16).

If a plot of the $S^0_{\ddagger}$ values is made against the standard state entropy of the corresponding halogen ions (Fig. 9), two linear relationships are apparent, the methyl and isopropyl series forming two distinct lines. In the methyl halide series the three halides recently measured in this laboratory (45) gave a linear relationship which loses its precision with the methyl fluoride. This, however, might have been anticipated from the large extrapolation of the rate data required to calculate $S^0_{\ddagger}$ (298.16) for the latter compound. The parameters for these linear plots were determined by the method of least squares (neglecting the fluoride in the methyl series) leading to eqs. [21] and [22].

[21] Methyl $$S^0_{\ddagger} = 0.671\ S^0(X^{\ominus}) + 19.00$$

[22] Isopropyl $$S^0_{\ddagger} = 0.962\ S^0(X^{\ominus}) + 32.07$$

Observed and calculated entropies from these equations are compared in Table VIII, where the standard state entropies of the corresponding halogen ions are also given (13).

TABLE VIII

Comparison of observed and calculated standard state entropies by equations [21] and [22]

		Methyl halides		Isopropyl halides	
	$S^0(X^{\ominus})$	$S^0_{\ddagger obs}$	$S^0_{\ddagger calc}$	$S^0_{\ddagger obs}$	$S^0_{\ddagger calc}$
F	−2.3	24.14	—		
Cl	13.17	28.18	27.83	44.4	44.73
Br	19.29	31.18	31.94	51.26	50.62
I	26.14	36.97	36.54	57.91	57.22

Can. J. Chem. Downloaded from www.nrcresearchpress.com by 190.90.36.8 on 09/04/12
For personal use only.

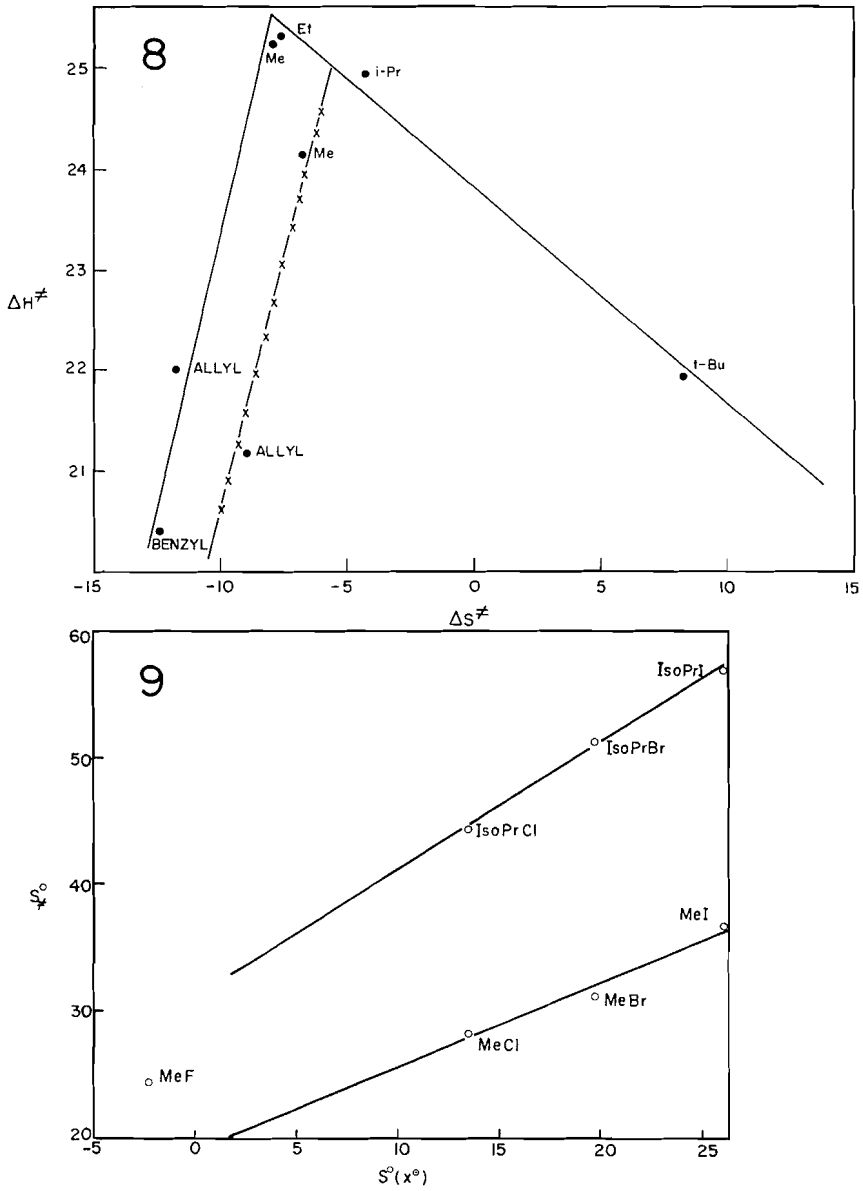

FIG. 8. Correlation of enthalpy and entropy of activation for α-substituted and unsaturated alkyl halides
———— Chlorides —×—×—×— Bromides

FIG. 9. Correlation of $S^0_{\ddagger}$ and $S^0(X^{\ominus})$ for methyl and isopropyl halides.

If we make the assumption that $\mu = \alpha$ and $c = 0$ we can calculate the standard state entropies of the methyl, isopropyl, and *t*-butyl cations ($\alpha = 1$ for the *t*-Bu series).

The coefficients of $S^0(X^{\ominus})$ in the above equations are consistent with the view that the anions are not completely formed in the transition state. Since $\alpha(\text{Me}) < \alpha(i\text{-Pr})$ it would seem that the tendency toward complete ionization increases with α substitution, as is normally assumed. We may safely assume $\alpha = 1$ for the *t*-butyl halides and from this we may calculate $S^0(t\text{-Bu}^{\oplus})$ for the single reasonably accurate value we have in the

Can. J. Chem. Downloaded from www.nrcresearchpress.com by 190.90.36.8 on 09/04/12
For personal use only.

t-butyl series (*t*-BuCl). To give α any further significance must be largely speculative, since it requires a knowledge of how $S^0(X^{\ominus})$ will vary with partial charge development.[3] Currently two views are adopted. Laidler considers (46) $S^0(X^{\ominus}) \propto Z^2$ (Z = charge) and Powell and Latimer (47) consider $S^0(X^{\ominus}) \propto Z$. In this paper we shall adopt Laidler's conclusion because of the successful application by Mason (48) of the Z^2 relationship in discussing the entropy factors in the solvolysis of arylmethyl chlorides.

Thus from eqs. [21] and [22] the charge development for the methyl halides in the transition state is $(0.671)^{\frac{1}{2}}\epsilon = 0.82\epsilon$ and for the isopropyl halides is $(0.962)^{\frac{1}{2}}\epsilon = 0.98\epsilon$.

The Activation Energy for the Methyl Halides

With a guide to the charge development in the methyl halide series it becomes worth while to attempt to calculate again the activation energy for this series. (See for previous work Ogg and Polanyi (49), Evans (32), and Franklin (16).)

Following Franklin we use the cycle:

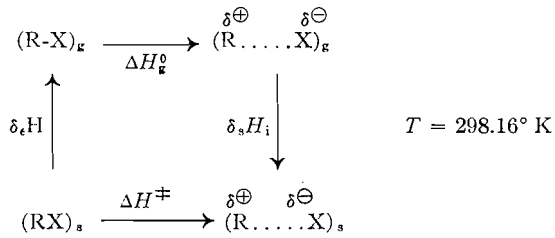

For this calculation we shall require:

(*a*) $\delta_\epsilon H$, the heat of escape of the gaseous methyl halides from solution. This has been measured by Glew and Moelwyn-Hughes (17).

(*b*) ΔH_g^0, the heat of partial ionization of R-X in the gas phase. Calculations for complete ionization are well known (42) (Table IX).

(*c*) $\delta_s H_I$, the combined heats of solution of $R^{\oplus}$ and $X^{\ominus}$ from the gas phase to solution.

The heats of solution for the halide ions have been listed by Latimer, Pitzer, and Slansky (50). These values, it must be noted, are somewhat arbitrary in that they require the total heat of solution of a *pair* of ions to be split up. How this should best be accomplished has not yet been made clear (cf. Moelwyn-Hughes (51)).

TABLE IX

Energies for the ionization of the methyl halides in the gas phase at 298.16° K

Compound	ΔH_g^{0*}		$\Delta H_g^{0\dagger}$
MeF	247.2	—	—
MeCl	223.3	220	223
MeBr	215.2	215	214
MeI	207	208	204

*This paper.
†Streitwieser (ref. 42).

The heat of solvation of the methyl cation represents a much more difficult problem. On a purely electrostatic basis Franklin (16) has estimated the heat of solution as −61 kcal/mole. This value treats the methyl cation as a thermodynamically stable entity

[3]*We are fully aware that other interpretations of the constant α are possible but these will be dealt with in a later communication.*

Can. J. Chem. Downloaded from www.nrcresearchpress.com by 190.90.36.8 on 09/04/12
For personal use only.

when it is in water. This is certainly erroneous, i.e. the methyl cation does not correspond to an ion of given radius and complete octet. We have arrived at an estimate of the heat of solution of the methyl cation which combines both the heat of solvation and the heat of reaction. We consider that both these energy terms are available as driving forces in kinetics. The heat of solvation represents the purely electrostatic portion whilst the heat of reaction is derived from backside attack of the water molecule.

Following Mason (48) we shall apply an equation of the form

$$\Delta H^{\ddagger} = \delta_e H + \alpha^{\frac{1}{2}} \Delta H_g^0 + \alpha \delta_s H_1 \qquad [23]$$

$\alpha^{\frac{1}{2}}$ being equal to the charge development in the transition state.

Values for ΔH_g^0

These have been calculated by Stevenson and quoted by Streitwieser (42). We have recalculated these values from available data (13) using the ionization potential for the methyl radical as 230 kcal/mole and the heat of formation of methyl fluoride as 64 kcal/mole, kindly provided by Dr. Bernstein of these laboratories.

Heat of Solution of the Methyl Cation

Consider the combined processes

$$\begin{array}{ccc} CH_3^{\oplus}(g) + H_2O(g) & \xrightarrow{\Delta H_b} & CH_3OH(g) + H^{\oplus}(g) \\ \downarrow \delta_s H_a & \searrow \Delta H & \downarrow \delta_s H_c \\ CH_3^{\oplus}(s) + H_2O(s) & \xrightarrow{\Delta H_d} & CH_3OH(s) + H^{\oplus}(s) \end{array}$$

We may assume

$$\delta_s H_a + \Delta H_d = \Delta H_b + \delta_s H_c = \Delta H . \qquad [24]$$

Now $\delta_s H_a = \delta_s H(CH_3^{\oplus}) + \delta_l H$ (latent heat of condensation of water),

ΔH_d = heat of reaction of 'solvated' methyl cation to give alcohol + solvated proton. Both processes may be considered to be exothermic, since the 'solvated' methyl cation would not be expected to be thermodynamically stable.

Since $\Delta H_b + \delta_s H_c$ are easily computed we can determine $\Delta H_d + \delta_s H(CH_3^{\oplus})$.

$$\begin{aligned} \Delta H_b &= \Delta H_f^0(H_g^+) + \Delta H_f^0(CH_3OH_g) - \Delta H_f^0(CH_{3g}^+) - \Delta H_f^0(H_2O)_g \\ &= 367.1 - 48.1 - 262.0 + 57.8 \text{ kcals} \\ &= 114.8 \text{ kcals.} \end{aligned}$$

The heat attending the dissolution of 1 gram molecule of hydrohalic acids *as ions* is given by Moelwyn-Hughes (51). The heats of solution of the separate halogen ions have been given by Latimer, Pitzer, and Slansky (50), therefore

$$\delta_s H\ (H^{\oplus}) = \delta_s H\ (H^{\oplus} X^{\ominus}) - \delta_s H\ (X^{\ominus}) . \qquad [25]$$

Combining the above data according to eq. [25] we obtain a mean value for the enthalpy of hydration for the proton of 254.6 kcal/mole.

Latent heat of condensation of water = -10.4 kcal.
Heat of solution of MeOH = -10.7 kcal.
$\Delta H_d + \delta_s H\ (CH_3^{\oplus}) - (-10.4) = 114.8 - 10.7 - 254.6.$
$\Delta H_d + \delta_s H\ (CH_3^{\oplus}) = -140.1$ kcal.

Can. J. Chem. Downloaded from www.nrcresearchpress.com by 190.90.36.8 on 09/04/12
For personal use only.

We can now approximate to $\delta_s H_1$ in the Franklin cycle (previous section) by combining the above figure with the heat of solvation for the appropriate anion (Latimer).

In Table X we have recorded the various quantities which are required to calculate the enthalpy of activation according to eq. [23]. Values for $\delta_s H_1$ are given by the equation

$$\delta_s H_1 = \Delta H_d + \delta_s H\ (CH_3^{\oplus}) + \delta_s H\ (X^{\ominus}).$$

Two values of α have been used: $\alpha = 0.67$ as determined by the relationship (21) for the methyl halides and a slightly higher value $\alpha = 0.74$. The value of $\Delta H^{\pm}$ calculated is extremely sensitive to the value of α adopted. It will be seen from Table X that the value of $\Delta H^{\pm}$ so calculated is in reasonable agreement with experiment, from which we may conclude that in the transition state the water molecule is strongly bonded (both covalently and electrostatically) to the carbon atom undergoing substitution.

TABLE X

Theoretically computed values for $\Delta H^{\pm}$ and associated data at 298.16° K

Compound (RX)	$\delta_s H_i(X^{\ominus})$	$\delta_\epsilon H$	ΔH_g^0 (1)	ΔH_g^0 (2)	$\delta_s H_i$ (1)	$\delta_s H_i$ (2)	Calc. $\Delta H^{\pm}$ (1)	Calc. $\Delta H^{\pm}$ (2)	Obs. $\Delta H^{\pm}$
MeF	−122.6	4.4	202.7	212.6	−176.0	−194.4	31.1	32.6	27.3
MeCl	−88.7	5.7	183.1	192	−153.3	−169.3	35.5	28.4	26.5
MeBr	−81.4	6.3	176.5	185.1	−148.4	−163.9	34.4	27.5	25.3
MeI	−72.1	6.4	169.7	178	−142.2	−157.0	33.9	27.4	27.4

$\delta_s H_i$ (1) is equal to $\alpha[\Delta H_d + \delta_s H_i\ (CH_3^{\oplus}) + \delta_s H_i\ (X^{\ominus})]$ where $\alpha = 0.67$.
$\delta_s H_i$ (2) is equal to $\alpha[\Delta H_d + \delta_s H_i\ (CH_3^{\oplus}) + \delta_s H_i\ (X^{\ominus})]$ where $\alpha = 0.74$.

ΔH_g^0 (1) is equal to $\alpha^{\frac{1}{2}}\Delta H_g^0$ where $(\alpha)^{\frac{1}{2}} = 0.82$: ΔH_i^0 given in Table IX.

ΔH_g^0 (2) is equal to $\alpha^{\frac{1}{2}}\Delta H_g^0$ where $(\alpha)^{\frac{1}{2}} = 0.86$: ΔH_i^0 given in Table IX.

The extension of the above calculations to the isopropyl and *t*-butyl and allyl and benzyl halides has not been carried out for a variety of reasons which are both practical and theoretical. On the practical side the approximate evaluation of the charge development in the *t*-butyl halides from the standard state entropies of activation ($S_{\pm}^0$) is impossible because of their high reactivity. Theoretical objections to any such calculation are equally great.

It will be noted that the ΔH_g^0 values for the isopropyl, *t*-butyl, allyl, and benzyl are considerably less than those for the corresponding methyl halides. This drop in ΔH_g^0 is mainly due to a decrease in the ionization potential of the corresponding radical accompanied by a relatively small bond energy decrease (52). The lowering of the ionization potential is attributed to resonance in the alkyl radical. This is a perfectly reasonable explanation for the gas phase reaction.

In solution, however, the charge stabilization of the forming cation can occur in two distinct ways. First, the localized charge can be solvated, or second, the delocalized charge can be stabilized by solvation. It has been shown in a most elegant paper by Mason (48) that the effect of charge delocalization is to lower the free energy of solvation to a considerable degree. A rough calculation for the benzyl cation indicates that the solvation of the delocalized charge plus the resonance energy is less than the solvation energy of the localized charge by as much as 20 kcal.

The tropylium ion, however, provides a striking example where resonance stabilization, implying delocalized charge, is more favorable than the solvation of the localized charge.

Can. J. Chem. Downloaded from www.nrcresearchpress.com by 190.90.36.8 on 09/04/12
For personal use only.

Even in this case, where resonance stabilization is large (53), there is a definite tendency to revert to the alcohol

$$C_7H_7^{\oplus} + 2H_2O \rightleftharpoons C_7H_7OH + H_3O^{\oplus} \qquad K_{25} = 1.8\times10^{-5}$$

a reaction analogous to the specific localized solvation of a resonating carbonium ion. From the above it would appear that great care must be exercised in rationalizing changes in reactivity as arising from resonance contributions to the transition state, since the solvation of the localized charge may represent a more favorable reaction path. The reasons why we hesitate to use Stevenson's ΔH_g^0 for the gas phase reaction

$$(RX)_g \rightarrow R_g^{\oplus} + X_g^{\ominus}$$

can now be stated for the cases where R = *i*-Pr, *t*-Bu, allyl, and benzyl.

Stevenson's values contain the whole of the resonance energy, since there can be no other mode of stabilization of the positive charge in the gas phase. The only case where ΔH_g^0 can be related to solution kinetics is in the methyl halide series where resonance is negligible in the forming alkyl cation.

The above discussion of the effect of charge delocalization on the free energy of solvation suggests some important criticisms of the calculations by Franklin (16). The errors in calculating the heats and entropies of solvation of the alkyl cations in terms of their relative dimensions only has already been noted. Franklin has also used the values for ΔH_g^0 which contain the resonance energy of the forming cation, although no account has been taken of the effect of this charge distribution on the solvation parameters which as a consequence would be considerably reduced. Thus Franklin's calculations give reasonable results due to a fortuitous cancellation of several errors (4). There is good reason from the $S_{\pm}^0$ vs. $S^0(X^{\ominus})$ relationship (see above) to believe that in water only reactive compounds have reached complete ionization in the transition state ($\alpha = 1$) which Franklin assumes for all compounds. However, Franklin's calculations appear to be correct in principle and should be capable of giving good results with the proviso that the appropriate values for the thermochemical quantities required are available and the transition state is carefully defined.

It will be obvious that the argument presented here rests on the correctness of the assumption (common to all such applications of thermodynamics to kinetic data) that the transition state may be treated as though in equilibrium with the average initial state. We are unaware of any evidence to suggest that such an assumption is unjustified. It will be equally obvious that the work presented here is made possible by the happy combination of accurate kinetic data and reasonable values for the initial state parameters. While it should be possible in principle to extend this treatment to all systems, in practice almost none of the necessary data are available. In this respect we hope that this paper may point the way as well as emphasize the tremendous challenge in this field for both the experimentalist and the theoretician. Yet even if all the necessary thermodynamic parameters were determined for the reactions of interest, a detailed understanding of the activation process would still require that a satisfactory model be constructed, which would satisfy the energetic requirements so determined. In this connection it would appear that the variations in the entropy and enthalpy factors discussed above, in the particular case of hydrolysis, throw far more light on the nature of the transition state than could possibly be derived from a comparison of free energies. While hardly surprising, this needs to be emphasized as a justification for the greatly increased experimental requirements. The above treatment is presented, therefore, not as a panacea,

Can. J. Chem. Downloaded from www.nrcresearchpress.com by 190.90.36.8 on 09/04/12
For personal use only.

but rather as an illustration of what can be done under very favorable experimental conditions and as an example of an essential link in the development of a quantitative treatment of the relation between structure and reactivity for reactions in solution.

ACKNOWLEDGMENT

We wish to acknowledge the criticism and suggestions which we received from Professors K. J. Laidler and P. M. Laughton.

REFERENCES

1. HAMMETT, L. P. Physical organic chemistry. McGraw-Hill Book Company, Inc., New York. 1940. Chap. 7.
2. BRONSTED, J. M. Chem. Revs. **5**, 322 (1928).
3. GRUNWALD, E. and WINSTEIN, S. J. J. Am. Chem. Soc. **70**, 846 (1948).
4. WINSTEIN, S. and FAINBERG, A. J. Am. Chem. Soc. **79**, 5937 (1957).
5. HUDSON, R. F. and BROWN, D. A. J. Chem. Soc. 3352 (1953).
6. SWAIN, C. G. and SCOTT, C. B. J. Am. Chem. Soc. **75**, 141 (1953).
7. MILLER, S. I. (In press).
8. EVANS, M. G. and POLANYI, M. Trans. Faraday Soc. **32**, 1333 (1936).
9. INGOLD, C. K. Structure and mechanism in organic chemistry. Cornell University Press, Ithaca, N.Y. 1953. Chap. 6.
10. EVANS, A. G. and HAMMAN, S. D. Trans. Faraday Soc. **47**, 25 (1951).
11. BENSLEY, B. and KOHNSTAM, G. J. Chem. Soc. 287 (1956).
12. MOELWYN-HUGHES, E. A. Proc. Roy. Soc. (London), A, **220**, 386 (1953).
13. NATIONAL BUREAU OF STANDARDS. Selected values of thermodynamic properties, Circ. 500 (1952).
14. HOWLETT, K. J. Chem. Soc. 2834 (1957).
15. NATIONAL BUREAU OF STANDARDS. Selected values of properties of hydrocarbons, Circ. 461 (1947).
16. FRANKLIN, J. L. Trans. Faraday Soc. **48**, 443 (1952).
17. GLEW, D. N. and MOELWYN-HUGHES, E. A. Discussion Faraday Soc. 15, 1953.
18. EVANS, M. G. Discussions Faraday Soc. 166 (1936).
19. BERNAL, J. D. and FOWLER, E. J. Chem. Phys. **1**, 515 (1933).
20. ELEY, D. D. Trans. Faraday Soc. **40**, 184 (1944).
21. FRANK, H. S. and EVANS, M. W. J. Chem. Phys. **13**, 507 (1945).
22. FEATS, F. S. and IVES, D. J. G. J. Chem. Soc. 2798 (1956).
23. MORRISON, T. S. and JOHNSTONE, N. B. J. Chem. Soc. 3441 (1954).
24. BARCLAY, I. M. and BUTLER, J. A. V. Trans. Faraday Soc. **34**, 1445 (1938).
25. ADON, R. J. L., COX, J. D., and HERRINGTON, E. F. G. J. Chem. Soc. 3188 (1954).
26. GLEW, D. N. and ROBERTSON, R. E. J. Phys. Chem. **60**, 332 (1956).
27. BUTLER, J. A. V. Discussions Faraday Soc. 229 (1936).
28. GLEW, D. N. Private communication.
29. NICLOUX, M. and SCOTTI-FOGLIENI, L. Ann. physiol. physicochim. biol. **5**, 434 (1929).
30. REX, A. Z. physik. Chem. **55**, 355 (1906).
31. EYRING, H. and STEARNS, A. E. J. Chem. Phys. **3**, 778 (1935).
32. EVANS, A. G. Reactions of organic halides in solution. Manchester University Press, Manchester. 1945.
33. HAMMOND, G. S. and HOGLE, D. S. J. Am. Chem. Soc. **77**, 3384 (1955).
34. ROBERTSON, R. E. Can. J. Chem. **33**, 1536 (1955).
35. GODDARD, E. D., HOEVE, C. A. J., and BENSON, G. C. J. Phys. Chem. **61**, 593 (1957).
36. LANDSMAN, D. A. Thesis, St. Andrews, 1955.
37. GLASSTONE, S., LAIDLER, K. J., and EYRING, H. The theory of rate processes. McGraw-Hill Book Company, Inc., New York. 1941. Chap. 1.
38. LEFFLER, J. J. Org. Chem. **20**, 1202 (1955).
39. HINSHELWOOD, C. N. Kinetics of chemical change. Oxford University Press. 1940. Chap. 9.
40. BLACKADDER, D. A. and HINSHELWOOD, C. N. J. Chem. Soc. 2728 (1958).
41. INGOLD, C. K. Quart. Revs. (London), **11**, 1 (1957).
42. STREITWIESER, A. Chem. Revs. **56**, 571 (1956).
43. WYNNE-JONES, W. F. K. and EYRING, H. J. Chem. Phys. **3**, 492 (1935).
44. HUDSON, R. F. and SAVILLE, B. J. Chem. Soc. 4114 (1956).
45. HEPPOLETTE, R. L. and ROBERTSON, R. E. (In press).
46. LAIDLER, K. J. Can. J. Chem. **34**, 1107 (1956).
47. POWELL, R. E. and LATIMER, W. M. J. Chem. Phys. **19**, 1139 (1951).
48. MASON, S. F. J. Chem. Soc. 808 (1958).
49. OGG, R. A. and POLANYI, M. Trans. Faraday Soc. **31**, 604 (1935).
50. LATIMER, W. M., PITZER, K. S., and SLANSKY, C. M. J. Chem. Phys. **7**, 108 (1939).
51. MOELWYN-HUGHES, E. A. Physical chemistry. Pergamon Press, London. 1957. Chap. 18.
52. LANE, M. R., LINNETT, J. W., and OSWIN, H. G. Proc. Roy. Soc. (London), A, **216**, 361 (1953).
53. DOERING, W. VON E. and KNOX, L. H. J. Am. Chem. Soc. **76**, 3203 (1954).
54. ROBERTSON, R. E. Can. J. Chem. **35**, 613 (1957).
55. LAUGHTON, P. M. and ROBERTSON, R. E. Can. J. Chem. **33**, 1207 (1955).

Can. J. Chem. Downloaded from www.nrcresearchpress.com by 190.90.36.8 on 09/04/12
For personal use only.

56. BARNARD, P. W. C. and ROBERTSON, R. E. Unpublished work.
57. ROBERTSON, R. E. Unpublished work.
58. SCOTT, J. M. W. and ROBERTSON, R. E. Unpublished work.
59. GLEW, D. N. and MOELWYN-HUGHES, E. A. Proc. Roy. Soc. (London), A, **211**, 254 (1952).
60. TOMMILA, E., MATTI TIILIKAINEN, and VOIPIO, A. Ann. Acad. Sci. Fennicae, A, **11**, 65 (1955).
61. FIERENS, P. J. C. and KRUYS, P. Bull. soc. chim. Belges, **64**, 542 (1955).
62. LAUGHTON, P. M. and ROBERTSON, R. E. Can. J. Chem. **34**, 1714 (1956).
63. WINSTEIN, S., MORSE, B. K., GRUNWALD, E., SCHREIBER, K. C., and CORSE, J. J. Am. Chem. Soc. **74**, 1113 (1952).
64. BENSON, S. W. and BUSS, J. H. J. Chem. Phys. **29**, 546 (1958).
65. JANZ, G. J. Estimation of thermodynamic properties of organic compounds. Academic Press, Inc., New York. 1958.
66. EVERETT, D. H. Discussions Faraday Soc. **24**, 220 (1957).

APPENDIX

The following scheme for the thermodynamic operators has been adopted. For all chemical reactions (i.e. for parameters derived from rates and equilibria) the symbol Δ carries its usual meaning. For changes in thermodynamic quantities arising from physical or structural changes the following operators have been used:

δ_M = change in medium,
δ_ϵ = change from liquid to gas,
δ_R = change in structure of alkyl group,
δ_X = change in structure of anionic portion of solute,
δ_s = change from gas to solution.

The subscript i, e.g. $\delta_s H_i$, refers to the change in enthalpy in passing ions from gaseous phase to solution. For ionogenic reactions occurring in the gas phase, terms such as ΔF^0_g and ΔH^0_g have been used.

Terms such as $\Delta F^0_{\pm}$ have been used to designate the free energy of activation with respect to a defined standard state. The thermodynamic parameters derived from rate studies and collected in this paper will be independent of the standard state and hence $\Delta F^0_{\pm} = \Delta F^{\pm}$.

Can. J. Chem. Downloaded from www.nrcresearchpress.com by 190.90.36.8 on 09/04/12
For personal use only.

Can. J. Chem. Downloaded from www.nrcresearchpress.com by 196.1.178.254 on 09/04/12
For personal use only.

STERIC INHIBITION OF RESONANCE
II. BOND LENGTHS IN MESO-SUBSTITUTED ANTHRACENES*

JAMES TROTTER†

The crystal structures of several meso-substituted anthracenes have recently been determined by X-ray diffraction methods (1) and reasonably accurate values of the molecular dimensions have been obtained. These detailed investigations have shown that the molecules of 9,10-dibromo- and 9,10-dichloro-anthracene are completely planar (2, 3). In the 9-nitro and 9,10-dinitro derivatives, however, the bulkier nitro groups are markedly tilted out of the aromatic planes about the C–N bonds (4), and correlation with the characteristic nitro group infrared frequencies suggests resultant decreases in resonance interaction between the nitro groups and the aromatic π-electrons (5). The angles of tilt alone do not give directly quantitative measures of the decreases in the conjugation compared with planar models, but resonance involving ionic structures, of type I for 9-nitroanthracene for example, would impart a considerable amount of double bond character to the C–N bond, and in addition cause variations in the N–O bond lengths when compared with those in aliphatic nitro compounds, and in the bond lengths in the anthracene nucleus compared with those in the unsubstituted molecule. It has been shown that in picryl iodide the C–N distances ortho to the iodine atom correspond to single bonds, indicating resonance inhibition, while the conjugated para C–N bond is very much shorter, suggesting a considerable amount of resonance interaction (6). Examination of the bond length variations in meso-substituted anthracenes therefore may give a quantitative account of the resonance interaction, and also indicate the amount of resonance inhibition due to steric effects in those molecules with bulky substituents, such as nitro groups, in the 9 and 10 positions.

The bond lengths, together with the standard deviations, in the molecules studied are compared in Table I with the bond lengths in anthracene (7, 8), the labelling of the carbon–carbon bonds being shown in the diagram. The values in the substituted anthracenes are quoted to 0.001 Å for comparison, although as the standard deviations indicate, the accuracy is much lower than this. The C–Br, C–Cl, C–N, and N–O distances in non-conjugated molecules are included under anthracene.

TABLE I

Bond lengths and standard deviations in meso-substituted anthracenes (Å)

Bond	Anthracene	9,10-Dibromo	9,10-Dichloro	9,10-Dinitro	9-Nitro
a	1.366±0.004	1.409±0.027	1.382±0.015	1.350±0.011	1.399±0.008
b	1.433±0.003	1.417±0.027	1.411±0.015	1.413±0.011	1.434±0.008
c	1.399±0.003	1.374±0.027	1.397±0.015	1.399±0.011	1.400±0.008
d	1.419±0.006	1.463±0.038	1.401±0.021	1.400±0.016	1.413±0.011
e	1.436±0.004	1.471±0.038	1.460±0.021	1.452±0.016	1.437±0.011
C–Br	(1.91)	1.928±0.027	—	—	—
C–Cl	(1.76)	—	1.739±0.016	—	—
C–N	(1.47)	—	—	1.450±0.015	1.482±0.015
N–O	(1.22)	—	—	1.241±0.009	1.216±0.009

*Issued as N.R.C. No. 5068.
†*National Research Council Postdoctorate Fellow.*

Exocyclic Bonds

Since there is no resonance inhibition in the completely planar halogen derivatives, ionic structures (II) ought to make a contribution to the ground state of the molecule. However, the weight of structures of this type, with a positive charge on the halogen atom, is quite small, and only a small contraction of the carbon–halogen bond lengths below the single bond distances would be expected. The C–Cl bond distances in 9,10-dichloroanthracene are slightly less than the normal single bond length, but the difference is scarcely significant. The ionic structures, however, are highly polar and, although their weights are small, they reduce the dipole moment in 9-bromoanthracene, for example, in comparison with a non-conjugated molecule (methyl bromide = 1.78 D, bromobenzene = 1.52 D, 9-bromoanthracene = 1.50 D).

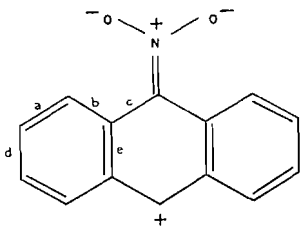

I

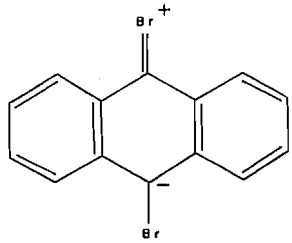

II

In 9-nitroanthracene the nitro group is tilted 85° out of the plane of the aromatic rings, and the C–N bond length (1.48 Å) corresponds to a single bond, indicating that there is little or no resonance between the anthracene nucleus and the nitro group. The C–N bond lengths in 9,10-dinitroanthracene, where the tilt of the nitro groups is 64°, are 1.45 Å, so that in this molecule there is a measurable amount of resonance interaction in spite of the large deviations from planarity. A quantitative measure of the resonance, however, requires a knowledge of the C–N bond length in a fully conjugated molecule such as nitrobenzene, and this length has not been accurately measured. (The conjugated C–N bond lengths in picryl iodide (6) and *p*-nitraniline (9) have been given as 1.35 Å and 1.41 Å respectively.) The C–N bond distances in 9,10-dinitroanthracene are much closer to the single bond length than to the distances in these fully conjugated molecules, so that while there is resonance interaction between the anthracene nucleus and the nitro group, it is much less than in completely planar aromatic nitro compounds. The N–O bond lengths in these nitroanthracenes also suggest that there is little or no resonance between the aromatic rings and the nitro group in 9-nitroanthracene, and a small but measurable interaction in 9,10-dinitroanthracene.

C–C Bonds

Examination of Table I shows that there are no really significant differences between the carbon–carbon bond lengths in the meso-substituted anthracenes studied and those in the unsubstituted molecule, indicating that contributions of ionic structures are too small to effect any measurable changes in the dimensions of the anthracene skeleton.

1. TROTTER, J. Acta Cryst. **11**, 564 (1958).
2. TROTTER, J. Acta Cryst. **11**, 803 (1958).
3. TROTTER, J. Acta Cryst. **12**, 54 (1959).
4. TROTTER, J. Acta Cryst. (In press).
5. TROTTER, J. Can. J. Chem. **37**, 351 (1959).

Can. J. Chem. Downloaded from www.nrcresearchpress.com by 196.1.178.254 on 09/04/12
For personal use only.

6. HUSE, G. and POWELL, H. M. J. Chem. Soc. 1398 (1940).
7. SINCLAIR, V. C., ROBERTSON, J. M., and MATHIESON, A. McL. Acta Cryst. **3**, 251 (1950).
8. CRUICKSHANK, D. W. J. Acta Cryst. **9**, 915 (1956).
9. DONOHUE, J. and TRUEBLOOD, K. N. Acta Cryst. **9**, 960 (1956).

RECEIVED OCTOBER 24, 1958.
DIVISION OF PURE PHYSICS,
NATIONAL RESEARCH COUNCIL,
OTTAWA, CANADA.

Can. J. Chem. Downloaded from www.nrcresearchpress.com by 196.1.178.254 on 09/04/12
For personal use only.

A CRYSTALLINE DERIVATIVE OF 2-*O*-(4-*O*-METHYL-α-D-GLUCOPYRANOSYLURONIC ACID)-D-XYLOPYRANOSE

T. E. TIMELL

2-*O*-(4-*O*-Methyl-α-D-glucopyranosyluronic acid)-D-xylopyranose, the structure of which was first established by Jones and Wise (1), has so far been isolated from some thirty natural plant products. Since no crystalline derivative of this amorphous compound has hitherto been known, it has been characterized by identification of the products obtained on hydrolysis of the original and of the methylated acid. A crystalline *p*-nitrobenzoate of the derived 2-*O*-(4-*O*-methyl-α-D-glucopyranosyl)-glycerol has been prepared (2) but the acetate of the 2-*O*-(4-*O*-methyl-α-D-glucopyranosyl)-D-xylitol is reported to be amorphous (3). A crystalline tetraacetate of the methyl ester methyl glycoside of the aldobiouronic acid has now been prepared and characterized.

Partial hydrolysis of a 4-*O*-methyl glucuronoxylan from white birch wood yielded 2-*O*-(4-*O*-methyl-α-D-glucopyranosyluronic acid)-D-xylopyranose, the structure of which had previously (4) been unequivocally established. Treatment of the derived methyl ester methyl glycoside with acetic anhydride in pyridine gave a sirup, a portion of which crystallized immediately from an ethyl ether solution. After recrystallization, white, small crystals were obtained, easily soluble in acetone, chloroform, ethyl acetate, and tetrahydrofuran, but only sparingly so in ethyl ether and ethanol. The methyl 2-*O*-[methyl-(2,3-di-*O*-acetyl-4-*O*-methyl-α-D-glucopyranosyl) uronate]-3,4-di-*O*-acetyl-D-xylopyranoside had m.p. 200–201° C, $[\alpha]_D^{20}$ +100° in chloroform, and was further characterized through its infrared spectrum and its X-ray diffraction pattern. The residual sirup had a specific rotation slightly lower than that of the crystalline portion (+85°). The data reported by Smith and co-workers (5) for the methyl ester methyl glycoside pentaacetate of two related, anomeric aldobiouronic acids would otherwise suggest that the xylopyranoside moiety was present in the β-configuration. Preparation of methyl ester methyl glycoside tetraacetates of specimens of the same aldobiouronic acid obtained from various natural products gave crystalline compounds with properties identical with those of the present derivative. The corresponding benzoate and *p*-nitrobenzoate esters were amorphous and could not be induced to crystallize.

EXPERIMENTAL

2-O-(4-O-Methyl-α-D-glucopyranosyluronic acid)-D-xylopyranose

A 4-*O*-methyl glucuronoxylan (200 g) from white birch wood (6) was dissolved in 72% sulphuric acid (100 ml). After 24 hours at room temperature, the solution was diluted to 4000 ml and boiled under reflux for 9 hours. Neutralization with barium

6. HUSE, G. and POWELL, H. M. J. Chem. Soc. 1398 (1940).
7. SINCLAIR, V. C., ROBERTSON, J. M., and MATHIESON, A. McL. Acta Cryst. **3**, 251 (1950).
8. CRUICKSHANK, D. W. J. Acta Cryst. **9**, 915 (1956).
9. DONOHUE, J. and TRUEBLOOD, K. N. Acta Cryst. **9**, 960 (1956).

RECEIVED OCTOBER 24, 1958.
DIVISION OF PURE PHYSICS,
NATIONAL RESEARCH COUNCIL,
OTTAWA, CANADA.

Can. J. Chem. Downloaded from www.nrcresearchpress.com by 196.1.178.254 on 09/04/12
For personal use only.

A CRYSTALLINE DERIVATIVE OF 2-*O*-(4-*O*-METHYL-α-D-GLUCOPYRANOSYLURONIC ACID)-D-XYLOPYRANOSE

T. E. TIMELL

2-*O*-(4-*O*-Methyl-α-D-glucopyranosyluronic acid)-D-xylopyranose, the structure of which was first established by Jones and Wise (1), has so far been isolated from some thirty natural plant products. Since no crystalline derivative of this amorphous compound has hitherto been known, it has been characterized by identification of the products obtained on hydrolysis of the original and of the methylated acid. A crystalline *p*-nitrobenzoate of the derived 2-*O*-(4-*O*-methyl-α-D-glucopyranosyl)-glycerol has been prepared (2) but the acetate of the 2-*O*-(4-*O*-methyl-α-D-glucopyranosyl)-D-xylitol is reported to be amorphous (3). A crystalline tetraacetate of the methyl ester methyl glycoside of the aldobiouronic acid has now been prepared and characterized.

Partial hydrolysis of a 4-*O*-methyl glucuronoxylan from white birch wood yielded 2-*O*-(4-*O*-methyl-α-D-glucopyranosyluronic acid)-D-xylopyranose, the structure of which had previously (4) been unequivocally established. Treatment of the derived methyl ester methyl glycoside with acetic anhydride in pyridine gave a sirup, a portion of which crystallized immediately from an ethyl ether solution. After recrystallization, white, small crystals were obtained, easily soluble in acetone, chloroform, ethyl acetate, and tetrahydrofuran, but only sparingly so in ethyl ether and ethanol. The methyl 2-*O*-[methyl-(2,3-di-*O*-acetyl-4-*O*-methyl-α-D-glucopyranosyl) uronate]-3,4-di-*O*-acetyl-D-xylopyranoside had m.p. 200–201° C, $[\alpha]_D^{20}$ +100° in chloroform, and was further characterized through its infrared spectrum and its X-ray diffraction pattern. The residual sirup had a specific rotation slightly lower than that of the crystalline portion (+85°). The data reported by Smith and co-workers (5) for the methyl ester methyl glycoside pentaacetate of two related, anomeric aldobiouronic acids would otherwise suggest that the xylopyranoside moiety was present in the β-configuration. Preparation of methyl ester methyl glycoside tetraacetates of specimens of the same aldobiouronic acid obtained from various natural products gave crystalline compounds with properties identical with those of the present derivative. The corresponding benzoate and *p*-nitrobenzoate esters were amorphous and could not be induced to crystallize.

EXPERIMENTAL

2-O-(4-O-Methyl-α-D-glucopyranosyluronic acid)-D-xylopyranose

A 4-*O*-methyl glucuronoxylan (200 g) from white birch wood (6) was dissolved in 72% sulphuric acid (100 ml). After 24 hours at room temperature, the solution was diluted to 4000 ml and boiled under reflux for 9 hours. Neutralization with barium

hydroxide, filtration through Celite, and evaporation and treatment with Darco G-60 charcoal and Amberlite IR-120 exchange resin yielded a pale yellow solution which was added to a column of Dowex 1-X4 anion exchange resin (acetate form). Neutral sugars were eluted with water (16 liters) after which sugar acids were removed with 30% aqueous acetic acid (16 liters). Evaporation of the acidic eluate yielded a sirup (25 g) which was resolved on 60 sheets of Whatman No. 3 MM filter paper with a solvent system consisting of ethyl acetate – acetic acid – water (9:2:2 v/v). The three main components, namely galacturonic acid, an aldobiouronic acid, and 4-*O*-methyl glucuronic acid (4), were eluted with water from the appropriate strips. Evaporation, treatment with Darco G-60 and Amberlite IR-120, and evaporation to dryness from methanol of the aldobiouronic acid gave a chromatographically pure, white, amorphous powder (10 g), $[\alpha]_D^{20}$ +108° (*c*, 1.0 in water). Anal. Calc. for $C_{12}H_{20}O_{11}$: OCH_3, 9.1%; equiv. wt., 340. Found: OCH_3, 9.2%; equiv. wt., 368.

*Methyl 2-O-[Methyl(4-O-methyl-α-*D*-glucopyranosyl)uronate]-*D*-xylopyranoside*

A portion of the above aldobiouronic acid (1.2 g) was boiled under reflux with 2.5% methanolic hydrogen chloride for 10 hours. After neutralization with silver carbonate, filtration through Celite, and evaporation, a white, fluffy powder was obtained (1.3 g, 100%), $[\alpha]_D^{20}$ +77° (*c*, 1.5 in water). Anal. Calc. for $C_{14}H_{24}O_{11}$: OCH_3, 25.3%. Found: OCH_3, 25.6%.

*Methyl 2-O-[Methyl(2,3-di-O-acetyl-4-O-methyl-α-*D*-glucopyranosyl)uronate]-3,4-di-O-acetyl-*D*-xylopyranoside*

The methyl ester methyl glycoside of the aldobiouronic acid (1.2 g) was dissolved in dry pyridine (75 ml), and redistilled acetic anhydride (25 ml) was added. After 24 hours at room temperature, the solution was poured into ice water (800 ml) and the aqueous solution was extracted with chloroform. The chloroform was extracted three times with ice-cold, 10% hydrochloric acid and subsequently three times with saturated sodium bicarbonate solution. After drying over anhydrous sodium sulphate, the chloroform solution was evaporated to yield a pale yellow sirup (1.70 g, 97%), which was dissolved in boiling ethyl ether (50 ml). On cooling of the solution, crystals immediately formed. The volume was adjusted to 25 ml and crystallization was allowed to proceed at −4° C for 24 hours. The white crystals obtained (0.32 g, 18.3%), m.p. 193–197° C (corrected), $[\alpha]_D^{20}$ +100° (*c*, 1.4 in chloroform), were dissolved in 20 ml of hot, anhydrous ethanol, followed by cooling and addition of the same volume of ethyl ether. The crystals formed (0.20 g) had m.p. 200–201° C, $[\alpha]_D^{20}$ +100° (*c*, 1.5 in chloroform). Anal. Calc. for $C_{22}H_{32}O_{15}$: C, 49.2%; H, 6.02%; OCH_3, 17.3%; $OCCH_3$, 40.1%; mol. wt., 536.3. Found: C, 49.7%; H, 5.93%; OCH_3, 17.0%; $OCCH_3$, 39.8%; mol. wt., 532.

The infrared spectrum of the compound exhibited absorption maxima at the following frequencies (cm^{-1}): 2940, 1745, 1440, 1370, 1225, 1050, 965, 920, 885, 790, 745, and 655. The X-ray powder diagram had the following interplanar lattice spacings in Å:* 8.92 (vs), 6.69 (s), 6.02 (s), 5.29 (s), 4.69 (vs), 4.07 (vs), 3.36 (s), 3.01 (s), 2.62 (m), 2.34 (m), 2.23 (m), 2.10 (m), 1.98 (m), 1.85 (m), 1.75 (w).

The residual sirup had $[\alpha]_D^{20}$ +85° (*c*, 1.5 in chloroform). It could not be induced to crystallize further. Its infrared spectrum was similar, albeit not identical with that of the crystalline portion.

1. Jones, J. K. N. and Wise, L. E. J. Chem. Soc. 2750, 3389 (1952).
2. Gorin, P. A. J. and Perlin, A. S. Can. J. Chem. **36**, 999 (1958).

**The author is grateful to Dr. R. St. J. Manley for providing the X-ray data.*

Can. J. Chem. Downloaded from www.nrcresearchpress.com by 196.1.178.254 on 09/04/12
For personal use only.

3. WHISTLER, R. L. and RICHARDS, G. N. J. Am. Chem. Soc. **80**, 4888 (1958).
4. GLAUDEMANS, C. P. J. and TIMELL, T. E. J. Am. Chem. Soc. **80**, 941, 1209 (1958).
5. MONTGOMERY, R., SMITH, F., and SRIVASTAVA, H. C. J. Am. Chem. Soc. **78**, 2837, 6169 (1956).
6. GLAUDEMANS, C. P. J. and TIMELL, T. E. Svensk Papperstidn. **60**, 869 (1957); **61**, 1 (1958).

RECEIVED DECEMBER 24, 1958.
MCGILL UNIVERSITY AND
PULP AND PAPER RESEARCH INSTITUTE OF CANADA,
MONTREAL, QUEBEC.

Can. J. Chem. Downloaded from www.nrcresearchpress.com by 196.1.178.254 on 09/04/12
For personal use only.

ABSOLUTE CONFIGURATION OF (−)-HOMOSTACHYDRINE*

A. V. ROBERTSON† AND LÉO MARION

Wiehler and Marion (1) isolated and identified a new alkaloid from alfalfa. The laevorotatory compound, which they called (−)-homostachydrine, was shown to be one of the enantiomers of the methyl betaine of pipecolic acid (piperidine-2-carboxylic acid). The proof of structure followed from the identity of the infrared spectra, X-ray powder diagrams, and chromatographic behavior of (−)-homostachydrine hydrochloride and the synthetic hydrochloride of racemic pipecolic acid methyl betaine.

We have now determined the configuration‡ of (−)-homostachydrine by methylating L-(−)-pipecolic acid. The methyl betaine hydrochloride had $[\alpha]_D$ −13°, identical with the value for the natural product (1). Thus (−)-homostachydrine belongs to the L-series of amino acids, and since (−)-pipecolic acid has been correlated with L-aspartic acid (2), the absolute configuration of the betaine is as shown in the formula.

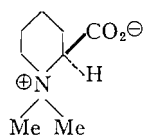

EXPERIMENTAL

Melting points are corrected. The infrared absorption spectra were measured in nujol mulls on a Perkin–Elmer double beam spectrometer model 21B.

L-(−)-*Pipecolic Acid*

Pure synthetic (±)-pipecolic acid hydrochloride was available in this laboratory (1). The acid was resolved with (−)-tartaric acid, $[\alpha]_D^{25}$ −14.2° (7% in water), according to the method of Schweet, Holden, and Lowy (3) (cf. Leithe, ref. 4). (−)-Pipecolic acid-(−)-bitartrate had constant optical activity after three crystallizations, $[\alpha]_D^{25}$ −20.0° (8% in water). After decomposing the diastereoisomer on Amberlite IR-4B ion exchange resin (3), the (−)-pipecolic acid had m.p. 271–272° (copper block) and $[\alpha]_D^{25}$ −25.8° (5% in water). These constants are in good agreement with reported values for natural and synthetic (−)-pipecolic acid (5).

L-(−)-*Homostachydrine Hydrochloride*

(−)-Pipecolic acid was methylated using the procedure of Wiehler and Marion for

*Issued as N.R.C. No. 5081.
†National Research Council of Canada Postdoctorate Fellow.
‡Dr. H. C. Beyerman, Technische Hogeschool, Delft, has also independently established the configuration of homostachydrine, and is publishing his results in Rec. trav. chim. Pays-Bas.

3. WHISTLER, R. L. and RICHARDS, G. N. J. Am. Chem. Soc. **80**, 4888 (1958).
4. GLAUDEMANS, C. P. J. and TIMELL, T. E. J. Am. Chem. Soc. **80**, 941, 1209 (1958).
5. MONTGOMERY, R., SMITH, F., and SRIVASTAVA, H. C. J. Am. Chem. Soc. **78**, 2837, 6169 (1956).
6. GLAUDEMANS, C. P. J. and TIMELL, T. E. Svensk Papperstidn. **60**, 869 (1957); **61**, 1 (1958).

RECEIVED DECEMBER 24, 1958.
MCGILL UNIVERSITY AND
PULP AND PAPER RESEARCH INSTITUTE OF CANADA,
MONTREAL, QUEBEC.

Can. J. Chem. Downloaded from www.nrcresearchpress.com by 190.90.36.8 on 09/04/12
For personal use only.

ABSOLUTE CONFIGURATION OF (−)-HOMOSTACHYDRINE*

A. V. ROBERTSON† AND LÉO MARION

Wiehler and Marion (1) isolated and identified a new alkaloid from alfalfa. The laevorotatory compound, which they called (−)-homostachydrine, was shown to be one of the enantiomers of the methyl betaine of pipecolic acid (piperidine-2-carboxylic acid). The proof of structure followed from the identity of the infrared spectra, X-ray powder diagrams, and chromatographic behavior of (−)-homostachydrine hydrochloride and the synthetic hydrochloride of racemic pipecolic acid methyl betaine.

We have now determined the configuration‡ of (−)-homostachydrine by methylating L-(−)-pipecolic acid. The methyl betaine hydrochloride had $[\alpha]_D$ −13°, identical with the value for the natural product (1). Thus (−)-homostachydrine belongs to the L-series of amino acids, and since (−)-pipecolic acid has been correlated with L-aspartic acid (2), the absolute configuration of the betaine is as shown in the formula.

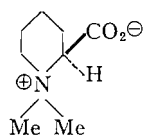

EXPERIMENTAL

Melting points are corrected. The infrared absorption spectra were measured in nujol mulls on a Perkin–Elmer double beam spectrometer model 21B.

L-(−)-Pipecolic Acid

Pure synthetic (±)-pipecolic acid hydrochloride was available in this laboratory (1). The acid was resolved with (−)-tartaric acid, $[\alpha]_D^{25}$ −14.2° (7% in water), according to the method of Schweet, Holden, and Lowy (3) (cf. Leithe, ref. 4). (−)-Pipecolic acid-(−)-bitartrate had constant optical activity after three crystallizations, $[\alpha]_D^{25}$ −20.0° (8% in water). After decomposing the diastereoisomer on Amberlite IR-4B ion exchange resin (3), the (−)-pipecolic acid had m.p. 271–272° (copper block) and $[\alpha]_D^{25}$ −25.8° (5% in water). These constants are in good agreement with reported values for natural and synthetic (−)-pipecolic acid (5).

L-(−)-Homostachydrine Hydrochloride

(−)-Pipecolic acid was methylated using the procedure of Wiehler and Marion for

*Issued as N.R.C. No. 5081.
†National Research Council of Canada Postdoctorate Fellow.
‡Dr. H. C. Beyerman, Technische Hogeschool, Delft, has also independently established the configuration of homostachydrine, and is publishing his results in Rec. trav. chim. Pays-Bas.

the racemic acid (1). The hydrochloride of the methyl betaine which was recrystallized by adding hot ethyl acetate to a boiling solution of the compound in absolute ethanol had m.p. 217–218° (gas evolution) and $[\alpha]_D^{25}$ −13.0° (2% in ethanol). The infrared spectrum and the X-ray powder diagram of the synthetic (−)-homostachydrine hydrochloride were identical in all respects with those of the hydrochloride of the natural material. Similarly, the synthetic and natural samples were chromatographically pure, and indistinguishable from each other, having R_F 0.58 in *n*-butanol – concentrated hydrochloric acid – water (100:20:39) and R_F 0.56 in 95% ethanol – concentrated aqueous ammonia (95:5).

We thank Dr. Maria Przybylska and Mr. R. Lauzon of these laboratories for the X-ray powder diagrams and for the infrared absorption spectra, respectively.

1. Wiehler, G. and Marion, L. Can. J. Chem. **36**, 339 (1958).
2. King, F. E., King, T. J., and Warwick, A. I. J. Chem. Soc. 3590 (1950).
3. Schweet, R. S., Holden, J. T., and Lowy, P. H. J. Biol. Chem. **211**, 517 (1954).
4. Leithe, W. Ber. **65**, 927 (1932).
5. Harris, G. and Pollock, J. R. A. Chem. & Ind. 462 (1953).

Received December 30, 1958.
Division of Pure Chemistry,
National Research Council,
Ottawa, Canada.

SEPARATION OF NICKEL AND COBALT BY PAPER CHROMATOGRAPHY*

Gerhard R. Weidmann

The R_F values of Ni and Co have been determined for *n*-tributyl phosphate (TBP) adjusted with concentrated hydrochloric acid of various concentrations. TBP is as suitable for the separation of Ni and Co by paper chromatography as other solvents mentioned in the literature (1, 2, 3). Before use the reagent was shaken with nitric acid to remove mono- and di-butyl phosphate (4), then distilled and adjusted with HCl of different molarities. Afterwards the organic phase was separated and mixed with methanol in the ratio 2:1 and 1:1.

PROCEDURE

The chromatograms were developed by ascending chromatography. The paper used was Schleicher and Schüll No. 4023*b* (Whatman No. 1). Solutions of Ni- and Co-chlorides each in quantities of 20γ were put on the paper. The process ran 4 hours at a temperature of 22° C. The flow of Co was easily identified by its blue color. On the following pictures Co was marked with α-nitroso-β-naphthol. Ni was identified with an alcoholic solution of dimethyl glyoxime.

RESULTS

The R_F values of Co recorded in Table I show a close dependence on increasing concentration of HCl used to equilibrate the TBP. Ascending concentration of HCl reduces the distance of Co from the liquid front, i.e. the R_F values increase. When working with

**Private contribution.*

Can. J. Chem. Downloaded from www.nrcresearchpress.com by 190.90.36.8 on 09/04/12
For personal use only.

the racemic acid (1). The hydrochloride of the methyl betaine which was recrystallized by adding hot ethyl acetate to a boiling solution of the compound in absolute ethanol had m.p. 217–218° (gas evolution) and $[\alpha]_D^{25}$ −13.0° (2% in ethanol). The infrared spectrum and the X-ray powder diagram of the synthetic (−)-homostachydrine hydrochloride were identical in all respects with those of the hydrochloride of the natural material. Similarly, the synthetic and natural samples were chromatographically pure, and indistinguishable from each other, having R_F 0.58 in *n*-butanol – concentrated hydrochloric acid – water (100:20:39) and R_F 0.56 in 95% ethanol – concentrated aqueous ammonia (95:5).

We thank Dr. Maria Przybylska and Mr. R. Lauzon of these laboratories for the X-ray powder diagrams and for the infrared absorption spectra, respectively.

1. Wiehler, G. and Marion, L. Can. J. Chem. **36**, 339 (1958).
2. King, F. E., King, T. J., and Warwick, A. I. J. Chem. Soc. 3590 (1950).
3. Schweet, R. S., Holden, J. T., and Lowy, P. H. J. Biol. Chem. **211**, 517 (1954).
4. Leithe, W. Ber. **65**, 927 (1932).
5. Harris, G. and Pollock, J. R. A. Chem. & Ind. 462 (1953).

Received December 30, 1958.
Division of Pure Chemistry,
National Research Council,
Ottawa, Canada.

SEPARATION OF NICKEL AND COBALT BY PAPER CHROMATOGRAPHY*

Gerhard R. Weidmann

The R_F values of Ni and Co have been determined for *n*-tributyl phosphate (TBP) adjusted with concentrated hydrochloric acid of various concentrations. TBP is as suitable for the separation of Ni and Co by paper chromatography as other solvents mentioned in the literature (1, 2, 3). Before use the reagent was shaken with nitric acid to remove mono- and di-butyl phosphate (4), then distilled and adjusted with HCl of different molarities. Afterwards the organic phase was separated and mixed with methanol in the ratio 2:1 and 1:1.

PROCEDURE

The chromatograms were developed by ascending chromatography. The paper used was Schleicher and Schüll No. 4023*b* (Whatman No. 1). Solutions of Ni- and Co-chlorides each in quantities of 20γ were put on the paper. The process ran 4 hours at a temperature of 22° C. The flow of Co was easily identified by its blue color. On the following pictures Co was marked with α-nitroso-β-naphthol. Ni was identified with an alcoholic solution of dimethyl glyoxime.

RESULTS

The R_F values of Co recorded in Table I show a close dependence on increasing concentration of HCl used to equilibrate the TBP. Ascending concentration of HCl reduces the distance of Co from the liquid front, i.e. the R_F values increase. When working with

**Private contribution.*

Can. J. Chem. Downloaded from www.nrcresearchpress.com by 190.90.36.8 on 09/04/12
For personal use only.

Can. J. Chem. Downloaded from www.nrcresearchpress.com by 190.90.36.8 on 09/04/12
For personal use only.

PLATE I

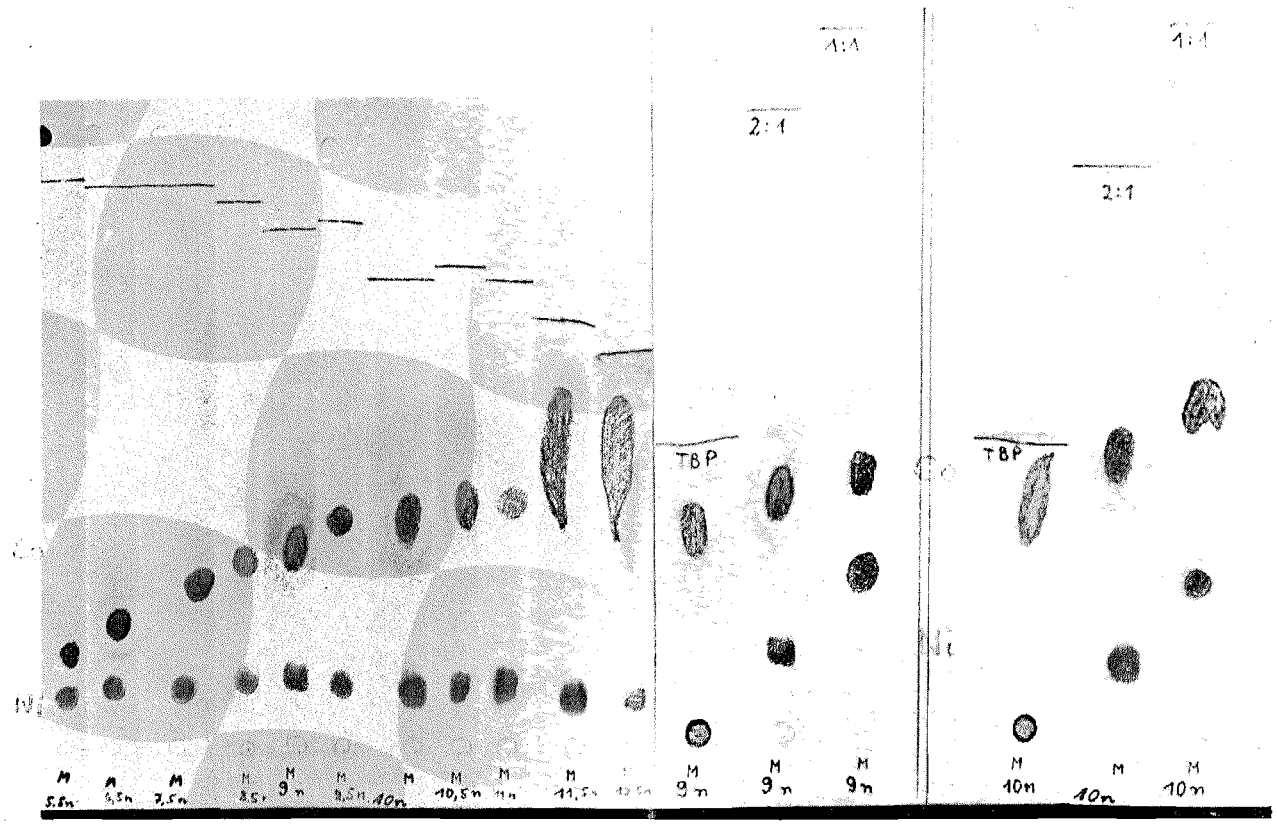

FIG. 1. Flow of Co using TBP/methanol mixture in the ratio 2:1 as a solvent.

FIG. 2. Different flow rates of Co and Ni depending on use of either pure HCl equilibrated TBP or with an admixture of methanol as a solvent.

Can. J. Chem. Downloaded from www.nrcresearchpress.com by 190.90.36.8 on 09/04/12
For personal use only.

highly concentrated HCl, Co will almost reach the liquid front. In this case Co does not flow as a spot any more, but has a long diffuse tail (see Fig. 1). Similar results are obtained when chromatographing Co using TBP as a solvent without admixture of methanol (see Fig. 2).

TABLE I

R_F of Co using a TBP/methanol mixture in the ratio 2:1

TBP adjusted with N HCl	5.5	6.5	7.5	8.5	9.0	9.5	10	10.5	11	11.5	12	12.5
R_F of Co	0.16	0.23	0.28	0.34	0.38	0.43	0.46	0.48	0.52	0.59	0.66	0.74

As Table II shows, the R_F values resulting thereof are considerably higher than those obtained using TBP/methanol mixtures.

TABLE II

R_F values of Co

TBP adjusted with N HCl	Ratio TBP/methanol		
	1:1	2:1	TBP pure
9 N	0.36	0.37	0.7
10 N	0.46	0.46	0.85
12.5 N	—	0.74	—

Previous tests have shown that Ni is not extracted by TBP from an aqueous solution. This effect is apparent in the chromatogram. Figure 2 shows that, when using pure HCl equilibrated TBP, Ni is immobile; and in TBP/methanol mixtures the flow rate is roughly proportional to the quantity of methanol present.

SUMMARY

Sharp chromatographing separations of Ni and Co can be obtained using HCl – equilibrated TBP. It is recommended that the TBP be treated with 9 to 10 molar HCl, and mixed with methanol in the proportion 2:1.

1. BURSTALL, F. H., DAVIES, G. R., LINSTEAD, R. P., and WELLS, R. A. J. Chem. Soc. 516 (1950).
2. BURSTALL, F. H. *et al.* J. Chem. Soc. 1497 (1952).
3. LEDERER, E. Chromatography. Elsevier Publishing Company, New York. 1954.
4. BURGER, L. L. and MCCLANAHAN, E. D. I/EC 50, 153 (1958).

RECEIVED DECEMBER 8, 1958.
COBURG/BAVARIA,
KANONENWEG 33,
WEST GERMANY.

QUENCHING AND VIBRATIONAL-ENERGY TRANSFER OF EXCITED IODINE MOLECULES

B. STEVENS

From their investigation of the effect of foreign gases on the emission spectrum of I_2 $^3\Pi$ ($v' = 26$), Arnot and McDowell (1) obtain collisional transfer coefficients which are

Can. J. Chem. Downloaded from www.nrcresearchpress.com by 190.90.36.8 on 09/04/12
For personal use only.

highly concentrated HCl, Co will almost reach the liquid front. In this case Co does not flow as a spot any more, but has a long diffuse tail (see Fig. 1). Similar results are obtained when chromatographing Co using TBP as a solvent without admixture of methanol (see Fig. 2).

TABLE I

R_F of Co using a TBP/methanol mixture in the ratio 2:1

TBP adjusted with N HCl	5.5	6.5	7.5	8.5	9.0	9.5	10	10.5	11	11.5	12	12.5
R_F of Co	0.16	0.23	0.28	0.34	0.38	0.43	0.46	0.48	0.52	0.59	0.66	0.74

As Table II shows, the R_F values resulting thereof are considerably higher than those obtained using TBP/methanol mixtures.

TABLE II

R_F values of Co

TBP adjusted with N HCl	Ratio TBP/methanol		
	1:1	2:1	TBP pure
9 N	0.36	0.37	0.7
10 N	0.46	0.46	0.85
12.5 N	—	0.74	—

Previous tests have shown that Ni is not extracted by TBP from an aqueous solution. This effect is apparent in the chromatogram. Figure 2 shows that, when using pure HCl equilibrated TBP, Ni is immobile; and in TBP/methanol mixtures the flow rate is roughly proportional to the quantity of methanol present.

SUMMARY

Sharp chromatographing separations of Ni and Co can be obtained using HCl – equilibrated TBP. It is recommended that the TBP be treated with 9 to 10 molar HCl, and mixed with methanol in the proportion 2:1.

1. BURSTALL, F. H., DAVIES, G. R., LINSTEAD, R. P., and WELLS, R. A. J. Chem. Soc. 516 (1950).
2. BURSTALL, F. H. *et al.* J. Chem. Soc. 1497 (1952).
3. LEDERER, E. Chromatography. Elsevier Publishing Company, New York. 1954.
4. BURGER, L. L. and MCCLANAHAN, E. D. I/EC 50, 153 (1958).

RECEIVED DECEMBER 8, 1958.
COBURG/BAVARIA,
KANONENWEG 33,
WEST GERMANY.

QUENCHING AND VIBRATIONAL-ENERGY TRANSFER OF EXCITED IODINE MOLECULES

B. STEVENS

From their investigation of the effect of foreign gases on the emission spectrum of I_2 $^3\Pi$ ($v' = 26$), Arnot and McDowell (1) obtain collisional transfer coefficients which are

Can. J. Chem. Downloaded from www.nrcresearchpress.com by 196.1.178.254 on 09/04/12
For personal use only.

some 10–15 times greater than expected from simple collision theory if a value of 10^{-8} second is assumed for τ_0, the radiative lifetime of the excited I_2 molecule.

In the same way, Polanyi (2) concludes that the collisional transfer efficiencies of H_2 and D_2 are 1 in 55 and 1 in 11 respectively if τ_0 is taken as 3×10^{-7} second. Recently, Arnot and McDowell (3) have corrected Polanyi's results for self-quenching and show that these are consistent with collisional transfer coefficients of 3.9 (H_2) and 7.7 (D_2) times greater than the theoretical values on the assumption that $\tau_0 = 10^{-8}$ second.

Neither Polanyi nor Arnot and McDowell observed self-transfer bands in the absence of foreign gases. In view of the high efficiency of I_2 as third body in I atom recombination (4) a non-quenching collision would be expected to lead to vibrational-energy transfer, and the absence of self-transfer bands may be taken as strong evidence that the collisional efficiency, p, of self-quenching is unity. A similar argument was put forward by Vartanyan (5) in connection with the O_2 quenching of aniline vapor fluorescence.

In their recent note, Arnot and McDowell (3) quote a value of 2.0×10^5 liter mole^{-1} for the I_2 self-quenching constant k_S/k_F measured presumably at 20° C, the temperature of their transfer experiments. Thus from

$$\frac{k_S}{k_F} = p\tau_0 \frac{N}{1000}(r_1+r_2)^2\left\{8\pi RT\left(\frac{1}{M_1}+\frac{1}{M_2}\right)\right\}^{\frac{1}{2}} = 2.0\times10^5 \text{ liter mole}^{-1}$$

with $p = 1$; $r_1 = r_2 = 2.7$ Å; $T = 293°$ K; N = Avogadro number; k_S = self-quenching rate constant; and $k_F = 1/\tau_0$ = radiative decay constant, we have

$$\tau_0 = 1.6\times10^{-6} \text{ second.}$$

This value of τ_0 is some 100 times longer than that usually associated with fluorescence emission but in view of Mulliken's assignment of $^3\Pi$ to this excited state of I_2, (6), the emission is by current definition (7) a phosphorescence of short lifetime due to the heavy atom effect (8). The Z dependence of radiative intersystem transition probabilities would lead us to expect a value closer to $\sim2\times10^{-6}$ second for Cd $^3P_1$ than to $\sim1\times10^{-7}$ second for Hg $^3P_1$.

Experimental transfer coefficients k_T/k_F obtained by Arnot and McDowell both from their own and from Polanyi's results are compared with the theoretical values computed on the basis $\tau_0 = 1.6\times10^{-6}$ second in Table I. k_T is the rate constant for collisional transfer from the 26th vibrational level of I_2*. The collisional transfer efficiency p_T is now intermediate between the values $\ll 1$ obtained from sound dispersion data in the region $v \sim 0$, and unity associated with third body effects on atom recombination in the region $v \sim \infty$. Eliaschevich (9) also adopted the value $\tau_0 = 10^{-8}$ second for the excited I_2

TABLE I

Coefficients for the transfer of vibrational energy from excited I_2 molecules at 20° C

Gas	k_T/k_F liter mole^{-1} Experimental	Theoretical	p_T	Ref.
H_2*	1.9×10^4	7.8×10^5	0.02	2, 3
D_2*	2.7×10^4	5.6×10^5	0.05	2, 3
He	5.31×10^4	5.17×10^5	0.10	1
Ne	2.69×10^4	2.66×10^5	0.10	1
A	1.64×10^4	2.28×10^5	0.07	1
O_2	1.5×10^4	2.2×10^5	0.07	1

*T = 27° C.

Can. J. Chem. Downloaded from www.nrcresearchpress.com by 196.1.178.254 on 09/04/12
For personal use only.

molecule, which is reduced by self-quenching under his experimental conditions to 3.3×10^{-9} second, and obtained collisional transfer coefficients up to 100 times greater than the theoretical values. If $\tau_0 = 1.6 \times 10^{-6}$ second, the reduced lifetime due to self-quenching under the conditions he used is 9.0×10^{-7} second and his transfer coefficients should be reduced by a factor of 270, which brings them into line with the results in Table I.

It is of interest to compare the transfer efficiencies p_T with quenching efficiencies p_Q which may be obtained from the quenching constants k_Q/k_F in the same way; (k_Q is the collisional quenching rate constant). Unfortunately Arnot and McDowell do not give their numerical values for the quenching constants but for He and A these may be calculated from Figs. 3 and 4 (1), in which the slope is given by

$$(k_Q/k_F)/\{1+(k_S/k_F)[I_2]\}.$$

The relevant data are given in Table II along with values obtained for H_2 and D_2 by Arnot and McDowell (3) from Polanyi's results (2). The lower transfer efficiency p_T

TABLE II

Coefficients for quenching of excited I_2 molecules at 20° C

Gas	k_Q/k_F liter mole^{-1}		p_Q
	Experimental	Theoretical	
H_2*	8.4×10^3	7.84×10^5	0.01
D_2*	1.46×10^4	5.60×10^5	0.03
He	3.12×10^4	5.17×10^5	0.06
A	1.01×10^5	2.28×10^5	0.44

*T = 27° C.

for A compared with He may be explained if the higher quenching efficiency p_Q of A is taken into account. Comparable values $p_T{}^0$ obtained on the basis of non-quenching collisions are

$$p_T{}^0 = p_T/(1-p_Q),$$
$$= 0.10 \text{ for He, } 0.13 \text{ for A.}$$

The low transfer efficiency of O_2 can probably be explained in the same way.

It should be noted that the above calculations involve two assumptions. In the first place the collision diameters of the excited and unexcited iodine molecules are assumed to be equal, which is almost certainly not the case. The collision radius calculated from the self-quenching constant taking $\tau_0 = 10^{-8}$ second is 65.6 Å compared with 2.7 Å for the unexcited molecule. This value is unrealistic if quenching is due to a collision-induced predissociation of the excited molecule but could presumably be approached if quenching involves a sensitized predissociation of the quenching molecule as Polanyi has suggested (2). In the absence of direct measurements of τ_0 there is more justification for assigning a value of 2.7 Å to the excited molecule than for assuming a value of 10^{-8} second for its radiative lifetime in view of the electronic transition involved. Use of the larger collision diameter and shorter lifetime would not significantly affect the values of p_T and p_Q given, since in the expression from which they are obtained, the quantity $\tau_0(r_1+r_2)^2$ remains virtually unaltered.

A more serious objection may be made to the second assumption that the collision diameter of the excited I_2* molecule is the same both for quenching and for vibrational-

Can. J. Chem. Downloaded from www.nrcresearchpress.com by 196.1.178.254 on 09/04/12
For personal use only.

energy transfer, particularly if quenching is due to sensitized predissociation at super-kinetic distances. If, however, the quenched molecule predissociates following the collisional removal of 3 or 4 vibrational quanta then quenching and vibrational-energy transfer have similar requirements and the error introduced by this second assumption may not be serious.

1. ARNOT, C. and MCDOWELL, C. A. Can. J. Chem. **36**, 114 (1958).
2. POLANYI, J. C. Can. J. Chem. **36**, 121 (1958).
3. ARNOT, C. and MCDOWELL, C. A. Can. J. Chem. **36**, 1322 (1958).
4. CHRISTIE, M. I., HARRISON, A. J., NORRISH, R. G. W., and PORTER, G. Proc. Roy. Soc. A, **231**, 446 (1955).
5. VARTANYAN, A. T. Izvest. Akad. Nauk S.S.S.R. Ser. Fiz. **3**, 341 (1938).
6. MULLIKEN, R. S. Revs. Modern Phys. **4**, 1 (1932).
7. LEWIS, G. N. and KASHA, M. J. Am. Chem. Soc. **66**, 2100 (1944).
8. MCCLURE, D. S. J. Chem. Phys. **17**, 905 (1949).
9. ELIASCHEVICH, M. Physik. Z. Sowjetunion, **1**, 510 (1932).

RECEIVED DECEMBER 8, 1958.
DEPARTMENT OF CHEMISTRY,
THE UNIVERSITY,
SHEFFIELD 10,
ENGLAND.

Can. J. Chem. Downloaded from www.nrcresearchpress.com by 196.1.178.254 on 09/04/12
For personal use only.

Can. J. Chem. Downloaded from www.nrcresearchpress.com by 196.1.178.254 on 09/04/12
For personal use only.

Canadian Journal of Chemistry

Issued by THE NATIONAL RESEARCH COUNCIL OF CANADA

VOLUME 37 MAY 1959 NUMBER 5

PYRIDINIUM BETAINES OF 1,3-INDANDIONE SERIES[1]

GERASSIMOS FRANGATOS AND ALFRED TAURINS

ABSTRACT

2-Bromo- (II) and 2,2-dibromo-1,3-indandione (III) react with pyridine, 3- and 4-methylpyridine, and 2-, 3-, and 4-pyridinecarboxylic acids to give 1-(3-hydroxy-1-oxo-2-indenyl)-pyridinium hydroxide betaines. In the betaines derived from pyridinecarboxylic acids the negative charge is located not in the carboxylic group but on the carbonyl oxygen atoms.

INTRODUCTION

Stafford (1) has obtained 1-(3-hydroxy-1-oxo-2-indenyl)pyridinium hydroxide, betaine (I), by brominating 1,3-indandione in the presence of pyridine and subsequently treating the intermediate salt with alkali. He assumed that the addition of bromine to pyridine resulted in the formation of pyridine bromide perbromide which formed 2-bromo-1,3-indandione with 1,3-indandione; the latter compound reacted further with pyridine to form a pyridinium salt. These steps appear plausible, but no experimental proof was given to support these assumptions.

It is known, however, that 1,3-indandione produces with bromine only 2,2-dibromo-1,3-indandione (2) and that 2-bromo-1,3-indandione (3) has never been isolated as an intermediate in this bromination. However, this does not exclude the presence of 2-bromo-1,3-indandione in some intermediate steps in the formation of 1-(3-hydroxy-1-oxo-2-indenyl)pyridinium bromide.

A similar reaction of pyridine with 5,5-dibromobarbituric acid produced the betaine of 1-(4-hydroxy-2,6-dioxo-5-tetrahydropyrimidyl)pyridinium hydroxide and 4-pyridylpyridinium bromide hydrobromide. 5-Bromo-5-nitrobarbituric acid and pyridine gave the same products, but 5-bromobarbituric acid did not react (4).

It has been found by Metro and Taurins (5) that 2-bromo-2-nitro-1,3-indandione reacted with pyridine by a different mechanism yielding the pyridinium salt of 2-nitro-1,3-indandione, pyridine hydrobromide, and a black tar containing nitrogen, bromine, and oxygen.

The objective of the present work was to investigate the formation of (I) and similar betaines by the direct interaction of 2-bromo- (II) and 2,2-dibromo-1,3-indandione with pyridine, methylpyridines, and pyridinecarboxylic acids.

DISCUSSION

When 2-bromo-1,3-indandione (II) was added to pyridine, a yellow solution was obtained, the color of which deepened gradually as the reaction proceeded. Upon standing at 20° for several hours, or short heating at 100°, the solution turned very dark. It was

[1]*Manuscript received January 14, 1959.*
Contribution from the Department of Chemistry, McGill University, Montreal, Quebec, with the financial assistance of the National Research Council of Canada, Ottawa, Canada.

felt that 1-(1,3-dioxo-2-indanyl)pyridinium bromide should be formed from (II) in the first step of the reaction as the result of a simple nucleophilic attack by pyridine. Therefore, attempts were made to isolate the bromide by sublimation of the residue obtained after removal of excess pyridine. On sublimation a white pyridinium hydrobromide appeared first and at a higher temperature the betaine (I) sublimed in the form of lustrous yellow crystals. The isolation of these products led to the conclusion that the intermediate 1-(1,3-dioxo-2-indanyl)pyridinium bromide is very reactive and is dehydrobrominated by pyridine in the first stages of the reaction. Furthermore, the isolation of these two products indicates that the bromine atom in (II) can be released also in the form of anion (Formulae sheet I, steps (*c*) and (*d*)).

2,2-Dibromo-1,3-indandione reacted slowly with pyridine at water bath temperature and the color of the mixture deepened gradually. From the reaction mixture two products were isolated, 1-(3-hydroxy-1-oxo-2-indenyl)pyridinium hydroxide, betaine (I), and pyridinium hydrobromide. The latter compound was isolated by removing the excess pyridine *in vacuo* and crystallizing the semisolid residue from alcohol. Both compounds could also be isolated by fractional sublimation. The residue after sublimation was a black tar which contained nitrogen and bromine.

The formation of the betaine may be considered as an elimination of two bromine atoms from each molecule of 2,2-dibromo-1,3-indandione by the action of pyridine. Steps (*c*) and (*d*) are also valid for the reaction of 2-bromo-1,3-indandione with pyridine.

The essential point in this mechanism is that the first bromine atom is removed as Br^+ leaving two electrons at the carbon atom. The second bromine is removed as Br^- in a displacement reaction with pyridine. The formation of two products (betaine I and pyridine hydrobromide) indicates that the mechanism is a two-step elimination. Protons which are necessary for step (*b*) are formed in the bromination reaction of pyridine by Br^+. There is always a black tar formation in the reaction of bromine Br_2 with pyridine (6).

We found that it was impossible to synthesize betaines of the 1,3-indandione series from three isomer methylpyridines using the Stafford procedure. In all cases, even at 0°, there was a rapid tar formation. From the black semisolid products only methylpyridine hydrobromides were isolated by sublimation. Contrary to that, the interaction of 2-bromo- and 2,2-dibromo-1,3-indandione with 3- and 4-methylpyridines gave the corresponding betaines. 2-Methylpyridine produced a black resin with both the reagents, although reactions were attempted under varying conditions of temperature, solvent, and time. 4-Methylpyridine reacted easily with 2,2-dibromo-1,3-indandione in boiling ethanol. On cooling of the red solution, a crystalline compound precipitated which was crystallized and obtained as pure yellow crystals. The reaction occurred also in toluene, but the yield was only about 40%, compared with 67% in ethanol.

3-Methylpyridine was less reactive with 2,2-dibromo-1,3-indandione than its 4-isomer and therefore a longer time and a higher temperature was necessary. Therefore the reaction was carried out in isoamyl alcohol at reflux temperature for 7 hours. The yield of the betaine under such conditions was 77%. The reaction did not occur in methyl or ethyl alcohol resulting in almost quantitative recovery of the starting materials.

The reactions of 3- and 4-methylpyridines with 2-bromo-1,3-indandione were carried out without any solvent at room temperature for 24 hours. Under such conditions 4-methylpyridine reacted with greater ease than pyridine.

The formation of betaines of 2-, 3-, and 4-pyridinecarboxylic acids with 2,2-dibromo-1,3-indandione were of interest because carboxylic groups could be considered as a potential negative center in the betaine. Since pyridinecarboxylic acids have an inner

Can. J. Chem. Downloaded from www.nrcresearchpress.com by 196.1.178.254 on 09/04/12
For personal use only.

Can. J. Chem. Downloaded from www.nrcresearchpress.com by 196.1.178.254 on 09/04/12
For personal use only.

FORMULAE SHEET I

REACTION OF 2-BROMO-1,3-INDANDIONE AND 2,2-DIBROMO-1,3-INDANDIONE WITH PYRIDINE

(*a*)

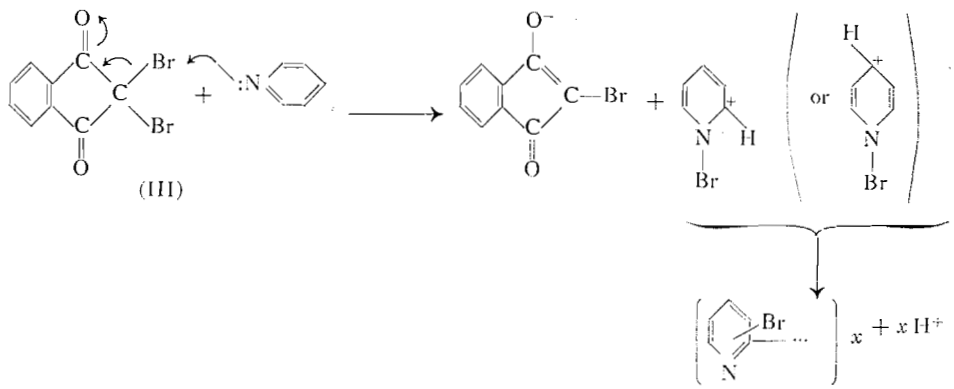

(III)

(*b*)

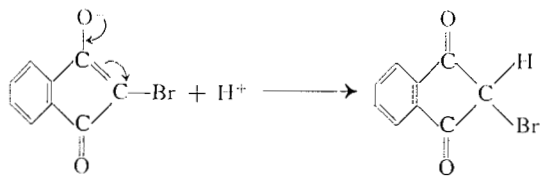

(II)

(*c*)

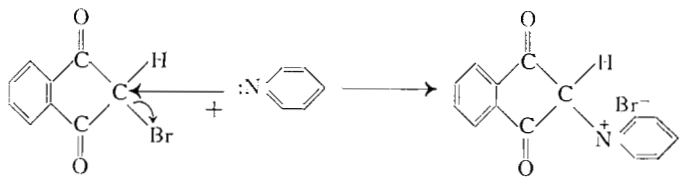

(*d*)

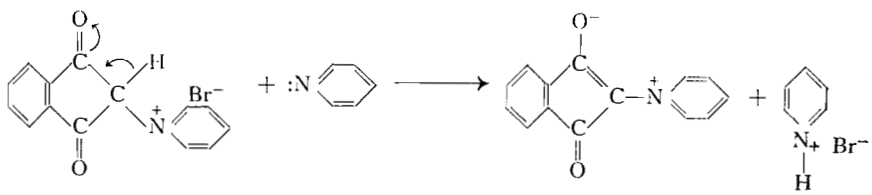

(I)

Can. J. Chem. Downloaded from www.nrcresearchpress.com by 196.1.178.254 on 09/04/12
For personal use only.

salt structure it was expected that the reaction of 2,2-dibromo-1,3-indandione with these acids would proceed with difficulty. This was confirmed experimentally. Higher temperatures and longer reaction time in refluxing isoamyl or *n*-butyl alcohol were necessary for the reaction to be completed. When the reaction mixture had been cooled, the golden-colored product precipitated together with the unreacted excess of pyridinecarboxylic acid. The latter was removed from the mixture by extracting with boiling water or more effectively by treatment with strong mineral acids. Any unreacted 2,2-dibromo-1,3-indandione was removed by extracting with chloroform. 2-Pyridinecarboxylic acid gave a poor yield of the betaine and the reaction was accompanied by fairly strong tar formation.

The presence of the carboxylic group in these betaines was detected by infrared spectroscopy. The betaine of 2-carboxy-1-(3-hydroxy-1-oxo-2-indenyl)pyridinium hydroxide showed weak bands at 2840, 2580, 2470, 2380, and 2300 cm^{-1} given by the stretching vibrations of the hydroxyl of the carboxyl group; 3- and 4-carboxy-isomers gave similar bands at slightly different positions. Also, there was a strong band present at 1725–1732 cm^{-1} in each one of the three betaines derived from pyridinecarboxylic acids. This band was given by the carbonyl of the carboxyl group. The carbonyl absorption of the unsubstituted betaine (Stafford compound) and 4-methyl derivative was very weak at 1725 and 1733 cm^{-1} respectively.

The electronic absorption spectra of the betaines obtained from methylpyridines or pyridinecarboxylic acids were determined and a great similarity in the patterns of these spectra was revealed. In each spectrum the absorption maxima occurred in the regions of 237–243, 311–316, and 386–418 mμ, and the molecular extinction coefficients were of the same order of magnitude. 1-(3-Hydroxy-1-oxo-2-indenyl)4-methylpyridinium hydroxide, betaine, showed a fourth absorption maximum in the region of 300 mμ (Table I and Figs. 1 and 2).

TABLE I

Electronic spectra of betaines of 1-(3-hydroxy-1-oxo-2-indenyl)pyridinium hydroxides (in absolute ethanol solution)

Substituent in the pyridine ring	λ_{max}, mμ	$\log_{10} \epsilon_{max}$
4-CH_3	273, 300, 316, 386	4.53; 3.34; 3.45; 4.13
3-CH_3	241, 313, 400	4.85; 3.36; 3.95
4-COOH	243, 315, 418	4.49; 3.28; 4.09
3-COOH	241, 312, 398	4.81; 3.44; 4.05
2-COOH	240, 311, 396	4.79; 3.33; 4.04

The similarity in spectra of betaines derived from methylpyridines and those obtained from pyridinecarboxylic acids serves to confirm the structures assigned to the latter group of betaines, and leaves no doubt that the carboxylic group does not participate in the formation of the inner salt by becoming the negative center of the dipole.

The absorption spectra of the betaines were determined in absolute alcohol. When attempts were made to measure the absorption spectra in chloroform, it was found that the wavelengths at which the absorption maxima appeared were reproducible but the molecular extinction coefficients were not.

EXPERIMENTAL

For the synthesis of the pyridine betaines of the 1,3-indandione series, three procedures, A, B, and C, were used.

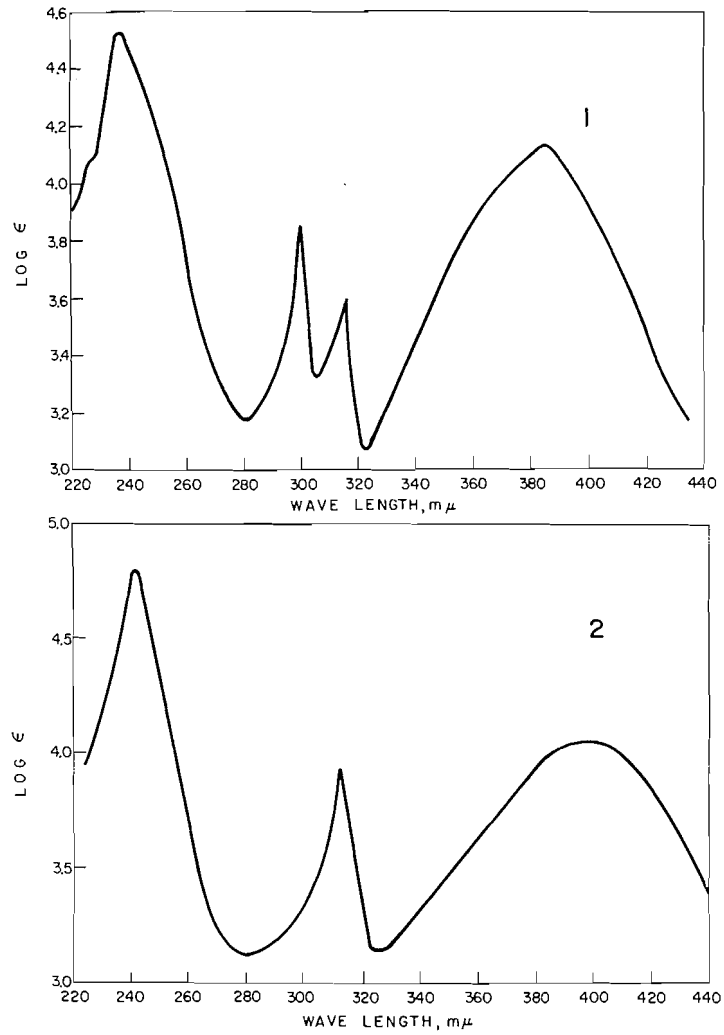

FIG. 1. Electronic absorption spectrum of 1-(3-hydroxy-1-oxo-2-indenyl)4-methylpyridinium hydroxide, betaine.

FIG. 2. Electronic absorption spectrum of 3-carboxy-1-(3-hydroxy-1-oxo-2-indenyl)pyridinium hydroxide, betaine.

Procedure A.—This procedure was applied to the reaction of 2-bromo-1,3-indandione with pyridine and methylpyridines. The method consisted of direct interaction of compounds in the absence of solvents, followed by the removal of excess unreacted materials by extraction, and isolation of the corresponding betaines. The reaction temperature was either 20° for 24 hours, or 100° for 4–6 minutes.

Procedure B.—This method consisted of the direct interaction of 2,2-dibromo-1,3-indandione with excess of pyridine and methylpyridines at 100° for several hours. The excess pyridine compound was removed by distillation in vacuum and the betaine was isolated by sublimation of the residue in vacuum.

Procedure C.—According to this method, 2,2-dibromo-1,3-indandione and pyridine derivatives were dissolved in a solvent (ethyl, *n*-butyl, or isoamyl alcohol, or toluene) and refluxed for 3 to 8 hours. The solvent was removed by distillation at reduced pressure.

Can. J. Chem. Downloaded from www.nrcresearchpress.com by 196.1.178.254 on 09/04/12
For personal use only.

The results are summarized in Table II.

TABLE II

Betaines of 1-(3-hydroxy-1-oxo-2-indenyl)pyridinium hydroxides

Substituent in the pyridine ring	Procedure					Yield, %	M.p., °C (decomp.)	Empirical formula	Elementary analysis					
									C, %		H, %		N, %	
No.	No.	Solvent	Temp., °C	Time					Calc.	Found	Calc.	Found	Calc.	Found
1 3-CH_3	A	No solvent	100	4 min.	82									
	B	No solvent	100	4 hr.	65.8	218	$C_{15}H_{11}NO_2$	75.95	76.20	4.67	4.62	5.90	6.15
	C	Isoamyl alcohol		7 hr.										
	A	No solvent	20	24 hr.	71.7									
2 4-CH_3	C	Ethyl alcohol	78	2 min.		258	$C_{15}H_{11}NO_2$	75.95	76.22	4.67	4.74	5.90	6.19
3 2-COOH	C	*n*-Butyl alcohol	117	3 hr.	27	312	$C_{16}H_9NO_4$	67.41	67.15	4.34	4.17	5.24	4.92
4 3-COOH	C	Isoamyl alcohol	132	6 hr.		317	$C_{16}H_9NO_4$	67.41	67.46	4.34	4.21	5.24	5.02
5 4-COOH	C	Isoamyl alcohol	132	6 hr.	58	351	$C_{16}H_9NO_4$	67.41	67.18	4.34	4.18	5.24	5.04

1-(3-Hydroxy-1-oxo-2-indenyl)pyridinium Hydroxide, Betaine (I)

1. Reaction of 2-Bromo-1,3-indandione with Pyridine (Procedure A)

2-Bromo-1,3-indandione (1.139 g, 0.005 moles) and 3 ml of pyridine were heated on a steam bath for 6 minutes. The dark red solution was poured into 50 ml of water and refluxed for 10 minutes. After being allowed to cool to room temperature, the solution was extracted with three 10-ml portions of ether. The aqueous layer was separated and made alkaline (pH 11) with sodium hydroxide solution. On cooling for 10 hours, the solution deposited 0.75 g of the betaine in 67% yield. The melting point of the substance after crystallizing from ethanol was 257° (decomp.), in agreement with the literature (1). The betaine (I) can be also obtained if the reaction is carried out at room temperature for 24 hours.

2. Reaction of 2,2-Dibromo-1,3-indandione with Pyridine (Procedure B)

(*a*) A sample of 2,2-dibromo-1,3-indandione (1 g, 3.3 millimoles) was added to 3 ml of pyridine and the solution was heated on a steam bath for 3 hours. The excess pyridine was removed under reduced pressure. The solid dark residue was dried in a vacuum desiccator over concentrated sulphuric acid. The material was crystallized from 12 ml of ethyl alcohol and the betaine (I) was obtained in pure form, melting point 257° (decomp.). The yield of (I) was 0.34 g (46.5% of the theoretical).

(*b*) The other product of the reaction, pyridine hydrobromide, was isolated by sublimation (at 120–125° and 1 mm pressure) of the dried reaction mixture in all-glass apparatus. The yield of the substance was 0.475 g. It was purified by repeated sublimations or by recrystallization from a hot mixture of chloroform and styrene. The second fraction, betaine I (0.5 g), sublimed at 185–190° under 1 mm pressure. A black resinous material remained (0.5 g) in the sublimation apparatus. It did not crystallize from various solvents and the analysis showed the presence of nitrogen and anionic bromine.

Can. J. Chem. Downloaded from www.nrcresearchpress.com by 196.1.178.254 on 09/04/12
For personal use only.

1-(3-Hydroxy-1-oxo-2-indenyl)3-methylpyridinium Hydroxide, Betaine

1. Reaction of 2-Bromo-1,3-indandione with 3-Methylpyridine (Procedure A)

The betaine weighed 0.97 g (82% yield) and melted at 218° (decomp.).

2. Reaction of 2,2-Dibromo-1,3-indandione with 3-Methylpyridine

(*a*) *Procedure B.*—The first fraction obtained by the sublimation of the residue from the reaction mixture was 3-methylpyridine hydrobromide (yield 0.23 g). The second fraction was the betaine of 1-(3-hydroxy-1-oxo-2-indenyl)3-methylpyridinium hydroxide, melting point 218° (decomp.). The yield was 0.78 g (65.8%). The black resinous residue which did not crystallize weighed 0.64 g.

(*b*) *Procedure C.*—Five milliliters of 3-methylpyridine was added to a solution of 1.53 g (0.005 moles) of 2,2-dibromo-1,3-indandione in 40 ml of warm isoamyl alcohol. The orange reaction mixture was refluxed for 7 hours, then most of the isoamyl alcohol was distilled at reduced pressure and the viscous orange solution was cooled in an ice bath. The solid material which separated was filtered by suction and washed with two 10-ml portions of ether. On recrystallization from ethyl alcohol it melted at 218° (decomp.). The yield was 0.91 g (0.77%).

1-(3-Hydroxy-1-oxo-2-indenyl)4-methylpyridinium Hydroxide, Betaine

1. By Procedure A

The betaine crystallized from ethyl alcohol in yellow elongated prisms, melting point 258° (decomp.). The yield was 71.7%.

2. By Procedure C

(*a*) 2,2-Dibromo-1,3-indandione (1.53 g, 0.005 moles) was dissolved in 20 ml of ethyl alcohol by refluxing. To this solution 4 ml of 4-methylpyridine was added over a period of 10 minutes. The betaine was isolated in the usual way and melted at 258° with decomposition. The yield was 0.82 g (67% of the theoretical). Molecular weight determination: Calc. for $C_{15}H_{11}NO_2$: 237. Found by the Rast method: 234.

(*b*) In toluene, at reflux temperature of 110.6°, the reaction of the substances mentioned above gave the betaine in a 39% yield.

(*c*) The fractional sublimation of the reaction product gave 0.37 g of 4-methylpyridinium hydrobromide.

2-Carboxy-1-(3-hydroxy-1-oxo-2-indenyl)pyridinium Hydroxide, Betaine

Procedure C.—A sample of 2,2-dibromo-1,3-indandione (0.76 g, 2.5 millimoles) was allowed to react with an excess (2 g) of 2-pyridinecarboxylic acid in 30 ml of boiling *n*-butyl alcohol (b.p. 117°) for 3 hours. The alcohol was removed by distillation under reduced pressure. A solid residue consisting of betaine and excess 2-pyridinecarboxylic acid was left. It was extracted with 8 ml of boiling water to remove the acid. The betaine was dried in vacuum and crystallized several times from *n*-butyl alcohol. A yield of 0.18 g (27% of the theoretical) of the betaine, m.p. 312° (decomp.), was obtained.

3-Carboxy-1-(3-hydroxy-1-oxo-2-indenyl)pyridinium Hydroxide, Betaine

Procedure C.—This compound was prepared in isoamyl alcohol from 3-pyridinecarboxylic acid and 2,2-dibromo-1,3-indandione. It melted at 317° (decomp.) after crystallization from isoamyl alcohol.

4-Carboxy-1-(3-hydroxy-1-oxo-2-indenyl)pyridinium Hydroxide, Betaine

Procedure C.—The betaine was synthesized from 4-pyridinecarboxylic acid and 2,2-dibromo-1,3-indandione in isoamyl alcohol, m.p. 351°.

Can. J. Chem. Downloaded from www.nrcresearchpress.com by 196.1.178.254 on 09/04/12
For personal use only.

REFERENCES

1. STAFFORD, W. H. J. Chem. Soc. 580 (1952).
2. WISLICENUS, W. Ann. **246**, 354 (1888).
3. ROSER, W. and HASELDORF, E. Ann. **247**, 140 (1888).
4. TAYLOR, E. C., JR., PAUDLER, W. W., and CAIN, C. K. J. Org. Chem. **20**, 264 (1955).
5. METRO, S. J. and TAURINS, A. Can. J. Chem. **30**, 466 (1952).
6. MCELVAIN, M. S. and GOESE, M. A. J. Am. Chem. Soc. **65**, 2227 (1943).

Can. J. Chem. Downloaded from www.nrcresearchpress.com by 196.1.178.254 on 09/04/12
For personal use only.

Can. J. Chem. Downloaded from www.nrcresearchpress.com by 196.1.178.254 on 09/04/12
For personal use only.

A GAS CHROMATOGRAPHIC STUDY OF THE ADSORPTIVE PROPERTIES OF A SERIES OF ACTIVATED CHARCOALS[1]

HENRY W. HABGOOD[2] AND JAMES F. HANLAN[3]

ABSTRACT

From measurements of the gas chromatographic retention volumes, the initial slopes of the adsorption isotherms of nitrogen and the simpler hydrocarbons on a series of steam-activated coconut charcoals were determined. The initial heats of adsorption were obtained in the usual way from the temperature dependence. It was found for all gases that both the initial slope of the isotherm and the initial heat of adsorption decreased with increasing degree of activation of the charcoal (i.e. with increasing surface area per g). This suggests that the higher affinity for the very small pores in less activated material more than counterbalances the lower total surface.

Measurements at several different carrier gas flow rates of the relative band width for the charcoals of least and of greatest activation demonstrated, as might be expected, a greater resistance to mass transfer for the former. However, the apparent diffusion coefficients calculated on the assumption that all transport is by gas phase in the pores were nearly the same for each charcoal and showed relatively little variation among the different gases.

INTRODUCTION

The technique of gas chromatography which, in recent years, has been so useful in analytical chemistry may also be applied to some problems in physical chemistry. We have used gas–solid (gas adsorption) elution chromatography to study the adsorptive properties of a series of varyingly activated coconut charcoals. A systematic investigation has been made of the elution peaks obtained for a number of simple hydrocarbon gases from columns of each of the charcoals at a series of temperatures. Each peak is characterized by two quantities, its retention volume and its relative width. The former may be readily identified with the gas–solid distribution coefficient while the latter depends in part on the rate of adsorption.

The retention volume for any given eluate is related to its distribution coefficient between the moving and stationary phases. Cremer and Prior (1) have examined this relationship for gas–solid chromatography, but the best-known development is that for gas–liquid chromatography of Martin and Synge (2). Their simple relationship may be written in the following form to apply to gas–solid chromatography:

$$[1] \qquad \alpha = (V^0_R - V^0_d)/W \cdot 273/T$$

where α is the initial slope of the adsorption isotherm in cc (S.T.P.) adsorbed per g, atm; V^0_R is the limiting value of the retention volume for small samples at column temperature, T, and pressure corrected to zero pressure drop through the column (3); V^0_d is similarly the retention volume for a non-adsorbed component; and W is the weight of adsorbent. Thus α is the net retention volume corrected to standard temperature per g of column material. Porter, Deal, and Stross (4) and others (5, 6, 7) have demonstrated the validity of the equivalent relationship for gas–liquid chromatography provided the sample volume is small compared with the total column volume.

Gas–solid chromatography has the complication of a curved isotherm—i.e. a variable distribution coefficient—and hence equation [1] will only apply to the limiting retention

[1]*Manuscript received October 20, 1958.*
Contribution No. 92 from the Research Council of Alberta, Edmonton, Alberta. Based on a paper presented at the 41st Annual Conference and Exhibition of the Chemical Institute of Canada, Toronto, May 26–28, 1958.
[2]*Associate Research Officer, Research Council of Alberta, and Special Lecturer, Department of Chemical and Petroleum Engineering, University of Alberta.*
[3]*Summer Research Assistant, Summer 1957. Present Address: University of California, Berkeley, California.*

Can. J. Chem. Downloaded from www.nrcresearchpress.com by 196.1.178.254 on 09/04/12
For personal use only.

volume at small sample pressure. The shape of the tail, which is characteristic of the asymmetric peaks usually found with gas–solid chromatography, may give some information about the complete isotherm (8, 9).

While the theory of gas–solid chromatography follows from that for gas–liquid chromatography, it may also be developed directly in terms of the apparent volume of the adsorbate in the presence of the adsorbent (10) by applying the Steele and Halsey equation of state approach to high temperature physical adsorption (11, 12).

The heat of adsorption is obtained from the slope of the log α–$1/RT$ plot. From the definition of α this is seen to be the limiting value at zero coverage of the isosteric heat of adsorption.[4,5]

Generally speaking, the initial slope of the adsorption isotherm is proportional to the product of two quantities, the total surface area and the affinity of the sorbate for the surface. Since the latter is directly related to the heat of adsorption, it is possible, in principle, given a particular model for the adsorption process, to determine the surface area from measurements of α at various temperatures. Steele and Halsey (11, 12), assuming an inverse third power attraction between hard spheres and a smooth surface, fitted the initial slopes of isotherms of the noble gases over a range of temperatures to surface areas fairly close to standard Brunauer–Emmett–Teller areas. Hanlan and Freeman in a paper to be published (10) have applied this method with some additional refinements to the present chromatographic data.

The use of gas–solid chromatography to study the rates of adsorption is based on an interpretation of the relative band widths which follows from the analysis of van Deemter, Zuiderweg, and Klinkenberg (14). These authors, from a development of the "plate" theory of chromatography, related the height equivalent to a theoretical plate, H, to the relative band width, $\Delta S^0/V^0_R$ where ΔS^0 is the volume of carrier gas corresponding to the base of the chromatographic elution peak and V^0_R is the volume to the maximum of the peak. For very small sample volumes giving symmetrical Gaussian peaks the relationship assumes the simple form:

$$[2] \qquad H = L(\Delta S^0/V^0_R)^2/16$$

where L is the length of the column.

The authors showed, from a comparison of the "plate" and "rate" theories, that H is expected to be a function of carrier gas velocity, u, as follows:

$$[3] \qquad H = A + B/u + Cu$$

where A, B, and C are constants for any particular system and may be interpreted respectively in terms of "eddy diffusion", molecular diffusion, and resistance to mass transfer. The last of these determines the rate of adsorption in gas–solid chromatography. A variation of H with u of the form of equation [3] has been obtained by several workers for gas–liquid chromatography (14, 15, 16, 17).

In the present work a tentative interpretation of C in terms of an apparent gas phase diffusion coefficient in the charcoal pores is attempted.

Figure 1 shows a typical chromatogram replotted from the chart record to illustrate the quantities α and H. This chromatogram also illustrates the small but distinct asym-

[4]*Cremer and Prior (1) and more recently Greene and Pust (13) have plotted what is equivalent to log αT against $1/T$ and accordingly obtained a ΔH which is smaller by an amount RT. This difference was not sufficient to influence the linearity of the plots obtained nor the comparison of the ΔH's with literature values.*

[5]*In gas–liquid chromatography an equivalent procedure, i.e. a plot of the logarithm of the retention volume corrected to standard temperature against reciprocal temperature, gives the heat of solution of the solute in the stationary liquid (4).*

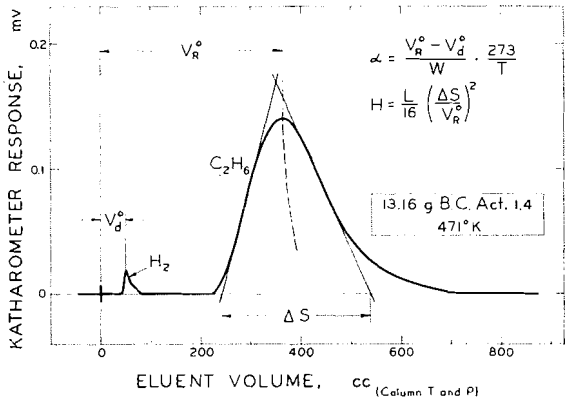

FIG. 1. A typical chromatogram obtained for a mixture of ethane and hydrogen. The usual time–base record is replotted in terms of carrier gas volume. The shoulder on the hydrogen peak results from a trace of air.

metry similar to that generally found with gas–solid chromatograms. Although the treatment referred to above was developed only for symmetrical elution chromatograms we were encouraged to apply it in the present case by the fact that H was found to be independent of sample size over a considerable range.

A major experimental advantage of gas chromatography is its relative speed and simplicity. It is best suited to conditions of fairly mild interaction in order that excessive band broadening and asymmetry do not obscure the center of the peak. This also corresponds to adsorption at temperatures well above the critical where the initial curvature of the isotherm is slight. However, by proper choice of the amount of adsorbent and of the gas flow rate a considerable range of temperatures may be covered.

The activated charcoals used in this study were taken from a series of coconut charcoals which had been steam-activated to varying degrees.[6] Lemieux and Morrison (18), Nay and Morrison (19), and Morrison and Miller (20) had previously studied the adsorptive properties of similar series of charcoals.[7] Their results suggested molecular sieve effects with the charcoals of lower activation; for example, the apparent surface areas for small molecules such as methane and nitrogen were found to be larger than for propane and butane.

By way of confirming the method, measurements were made on a sample of Columbia L-activated coconut charcoal[8] for comparison with the published isotherms of Ray and Box (21).

EXPERIMENTAL

The chromatography column was a copper tube 26 cm long by 1.015 cm inside diameter. It was preceded by a 15-in. length of coiled $\frac{1}{8}$-in. copper tubing and the whole was contained inside a 30-in. furnace made from a copper tube wound uniformly with resistance wire and insulated. There were thermocouples at each end of the column and a thermocouple well ran the length of the heater. The maximum temperature variation over the column was less than 1.0° and usually less than 0.5°.

[6]*These charcoals were kindly provided by Dr. J. L. Morrison of the Department of Chemistry, University of Alberta (now with Connaught Medical Research Laboratories, Toronto), who had obtained them from the Barnebey-Cheney Company, Cassady at Eighth, Columbus 19, Ohio.*

[7]*Unlike the earlier series these new charcoals were not prepared entirely from a single batch of nut shells. There is, therefore, some possibility of non-systematic variation through the series although the results of our work show no indication of this.*

[8]*From Union Carbide and Chemicals Co., Division of Union Carbide Corporation.*

Can. J. Chem. Downloaded from www.nrcresearchpress.com by 196.1.178.254 on 09/04/12
For personal use only.

Can. J. Chem. Downloaded from www.nrcresearchpress.com by 196.1.178.254 on 09/04/12
For personal use only.

Helium was used as a carrier gas, and flows were measured with a soap-bubble manometer corrected for the vapor pressure of the soap solution. The usual flow rate was around 100 cc per minute and retention volumes were found to be independent of flow rate over a considerable range around this value. A Gow-Mac katharometer was used as detector in conjunction with a 1-mv recorder.

The sample volume, 0.185 cc, was the volume of the bore of a two-way stopcock plug which was fitted into the shell of a three-way T-stopcock, the midtube of which led to the gas inlet and a manometer. A constant volume of sample at a known pressure could thus be introduced into the helium stream by turning the plug through 90° while simultaneously closing the helium bypass.

The Barnebey-Cheney charcoals were received as $-6+14$ mesh. This is much coarser than usually used for chromatography. Some preliminary investigations were made to determine the effect of grinding on the chromatographic properties of the charcoal. The finer fractions behaved generally like charcoals of higher activity in the series. Presumably the more highly activated portions of the granules are more fragile and easily broken up. All tests were subsequently carried out with the original material screened to exclude particles larger than 8 mesh. It was hoped that the slight degree of fractionation involved here would not invalidate comparison with conventional measurements made on the whole sample. The relatively large diameter column permitted a fairly uniform packing of this rather coarse material. Furthermore, the use of large particles magnified the effects of diffusional resistances in the charcoal pores.

Each charcoal was dried at 300° and chromatograms were determined at approximately 50° intervals down to as low a temperature as would yield measurable peaks for each gas.

Each solute was introduced as a mixture with hydrogen. While one might introduce a mixture of several non-overlapping gases at once, it is possible that the resultant volumes would be low due to competition for the available surface. Some brief studies of this point, although rather inconclusive, suggested that such effects were slight.

In many cases, particularly with the less active charcoals, several samples of each gas were run at various pressures down to the lowest pressure which would give a detectable peak (from 3–4 mm to 10 cm, depending on the retention volume and subsequent band broadening). It was thus possible to extrapolate the retention volumes to zero concentration. The variation in retention volume was usually less than 1 or 2% but in a few cases with the less active charcoals variations of up to 10% were noted and the limiting values were consequently more uncertain.

EXPERIMENTAL RESULTS

Retention volumes of nitrogen, methane, ethane, propane, the butanes, acetylene, ethylene, and propylene were measured for a sample of Columbia L-activated coconut charcoal, 35–50 mesh. The corresponding values of α from equation [1] are plotted on a logarithmic scale against reciprocal temperature in Fig. 2. Measurements made with a small glass column holding approximately one quarter as much charcoal yielded α's coincident with those from the copper column. For comparison, several values of the estimated initial slopes of the isotherms of Ray and Box (19) are included. The measurements of these authors did not always extend to low adsorbate concentrations, so that except at the higher temperatures there is some uncertainty in drawing the initial slopes. Nevertheless, the general agreement is satisfactory.

The results of Ray and Box for propane and propylene were rather surprising. At 38° and 66° C the adsorption of propylene was greater than that of propane at all pressures

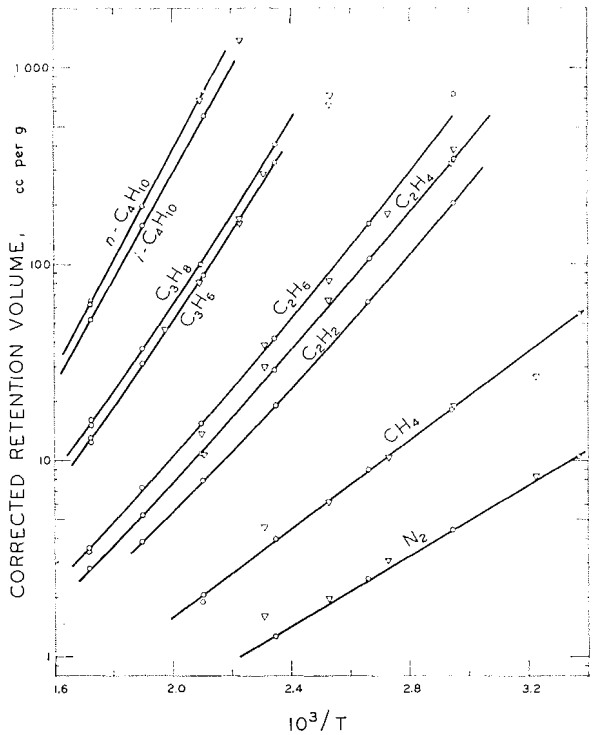

FIG. 2. Corrected retention volume per g (= α from equation [1]) vs. reciprocal temperature for Columbia L charcoal. Also shown (▽) are initial slopes of the isotherms of Ray and Box (21) for all gases except i-C_4H_{10} and C_2H_2. (Only two points are given for C_3H_6 and these lie just below the corresponding C_3H_8 points.)

investigated. At 93° the two were almost identical and at higher temperatures the propane isotherm lay above that of propylene. Lewis, Gilliland, Chertow, and Cadogan (22) found propylene to be more strongly adsorbed at 25°. They suggested that this indicated a special affinity of the carbon surface for double bonds such as that shown by silica gel. However, it may possibly reflect only a greater monolayer capacity resulting from a smaller molecular adsorption area for propylene—the methyl group perhaps projecting free of the surface. The chromatographic measurements are in the region where propane lies above propylene but the slopes of the plot do not give any suggestion of a crossing over at lower temperatures.

The limiting values of the isosteric heats of adsorption at zero coverage follow from the slopes in Fig. 2. The slight curvature in some of the plots is in the direction of decreasing ΔH with temperature. The average heat of adsorption over the interval 200–300° C is plotted in Fig. 3 against the number of carbons in the adsorbate. For comparison the figure includes the calorimetric differential heats of adsorption at 5% coverage for the normal paraffins from ethane to pentane on channel black (Spheron 6) as determined by Schaeffer, Polley, and Smith (23) at 0° C. There does not seem to be any comparable set of measurements reported for activated coconut charcoal. As noted below, the initial isosteric heats of adsorption determined for the Barnebey-Cheney charcoals vary with degree of activation over a range of around twenty-five per cent. Consequently precise agreement with the measurements on carbon black is not to be expected for any particular charcoal.

Can. J. Chem. Downloaded from www.nrcresearchpress.com by 196.1.178.254 on 09/04/12
For personal use only.

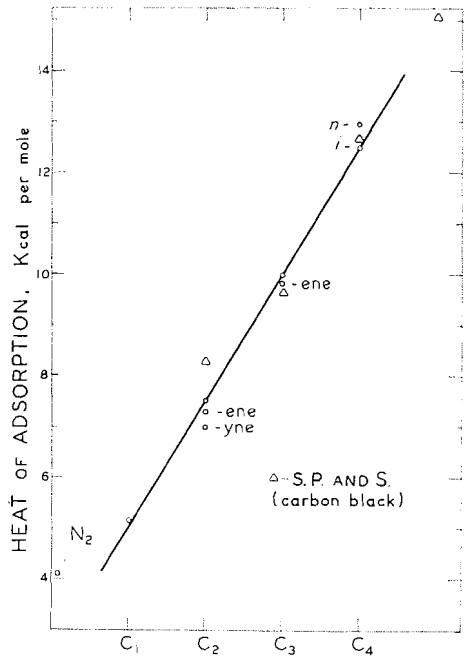

FIG. 3. The initial heats of adsorption on Columbia L charcoal compared with calorimetric values for carbon black at 5% coverage.

The charcoals in the Barnebey-Cheney series on which measurements were made had chloropicrin activities of 0, 1.4, 4.5, 9.5, 51.7, and 89.6. These numbers are times in minutes to break-through for the accelerated chloropicrin test in a standard procedure (air containing 0.286 moles per liter chloropicrin, flowing at 1 liter per minute per cm^2 through a 10-cm column). Since this test is based on a unit volume of packed charcoal the activities were converted to a weight basis using the densities reported by the manufacturer. For comparison with the α values the activities were then expressed as average concentrations at break-through in cc (S.T.P. assuming ideal gas behavior) per g of charcoal and the respective values are then 0, 1.4, 4.7, 10.1, 59.4, 149.0.[9]

For each charcoal a plot similar to Fig. 2 was obtained, and nearly all plots were straight lines. The results with acetylene were erratic. Frequently no peak appeared above 100° and measurements were not continued due to fear of possible polymerization affecting the charcoal surface. The difficulty may have been reaction with the copper tubing. The measurements with the Columbia charcoal which were made near the beginning of the work gave peaks up to 250° C.

The results are summarized in Figs. 4 and 5. Figure 4 shows the values of α for two selected temperatures plotted as functions of the revised chloropicrin activity. Figure 5 shows the heat of adsorption also against activity. Measurements with nitrogen were not always made to low enough temperatures to permit accurate slopes to be drawn.

Morrison and Myshok (24), using conventional methods, studied the adsorption at room temperature and lower of nitrogen and the C_2 hydrocarbons by some charcoals of this series and observed similar trends in initial isotherm slopes and in isosteric heats of adsorption. Their work is being prepared for publication but they have, in the mean-

[9]*The chloropicrin activity of Columbia L charcoal is given by the manufacturers as between 40 and 60 minutes, which corresponds to an average concentration at break-through of 61 to 76 cc/g.*

Can. J. Chem. Downloaded from www.nrcresearchpress.com by 196.1.178.254 on 09/04/12
For personal use only.

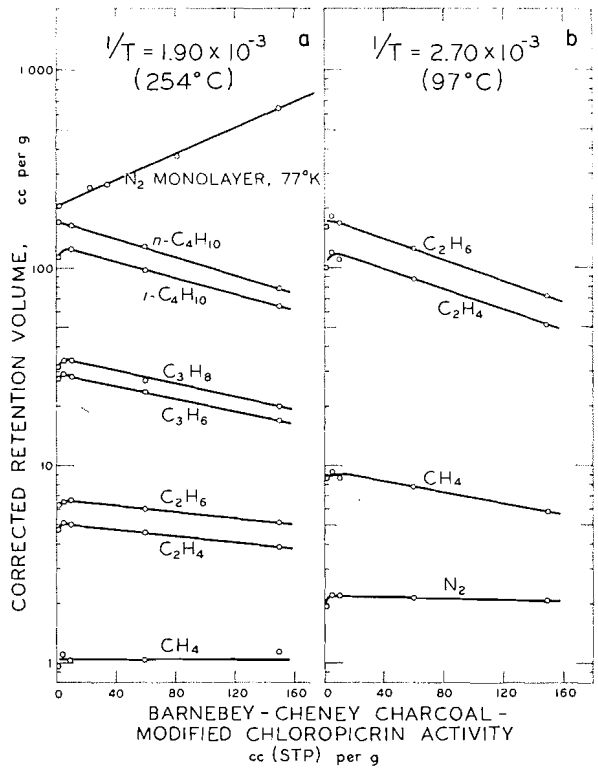

FIG. 4. Corrected retention volumes per g for the Barnebey-Cheney charcoals at 254° C (*a*) and 97° C (*b*). Nitrogen monolayers at 77° K (24) are also shown.

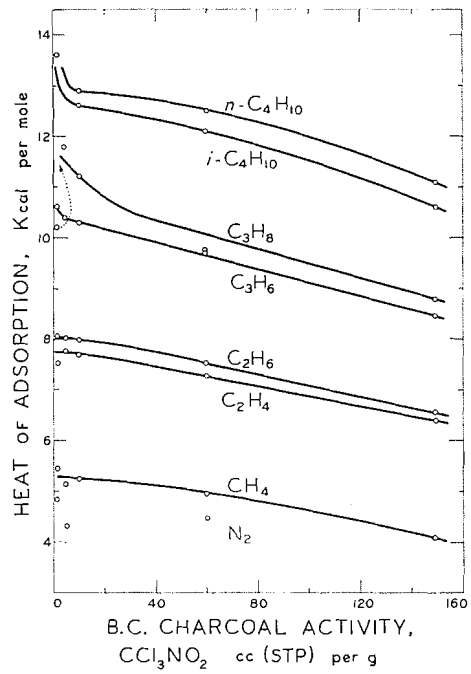

FIG. 5. Initial heats of adsorption for the Barnebey-Cheney charcoals as determined from the slopes of the log α–$1/T$.

Can. J. Chem. Downloaded from www.nrcresearchpress.com by 196.1.178.254 on 09/04/12
For personal use only.

time, provided us with values for the nitrogen monolayer capacities at 77° K for several of the charcoals and these are shown in Fig. 4*a*.

The zero activity charcoal which presumably had been only carbonized but not steam-activated showed some traces of slow adsorption. The retention volumes were within a few cubic centimeters of that of hydrogen in all cases but the peaks showed marked tailing. Conventional adsorption measurements (24) showed that adsorption was very slow but apparently quite considerable.

The variation in relative band width with flow rate was investigated for the charcoals of activities 1.4 and 149 cc/g. Some of the properties of these charcoals are summarized in Table I. The height equivalent to a theoretical plate, H as given by equation [2], was

TABLE I

Characteristics of charcoals of least and greatest activation

Chloropicrin activity, cc/g	1.4	149
Bed density (8–14 mesh granules) cc/g	0.660	0.373
Granule density cc/g (with mercury)	1.110	0.611
Charcoal density cc/g (with helium)	1.87 (100°) 1.969 (25°)	2.075 (100°)
(With CCl_4)	1.299 (25°)	2.095 (25°)

found to be independent of sample pressure over at least a 20-fold range. H is plotted against flow rate for several gases at three temperatures in Fig. 6. Because of the skew-

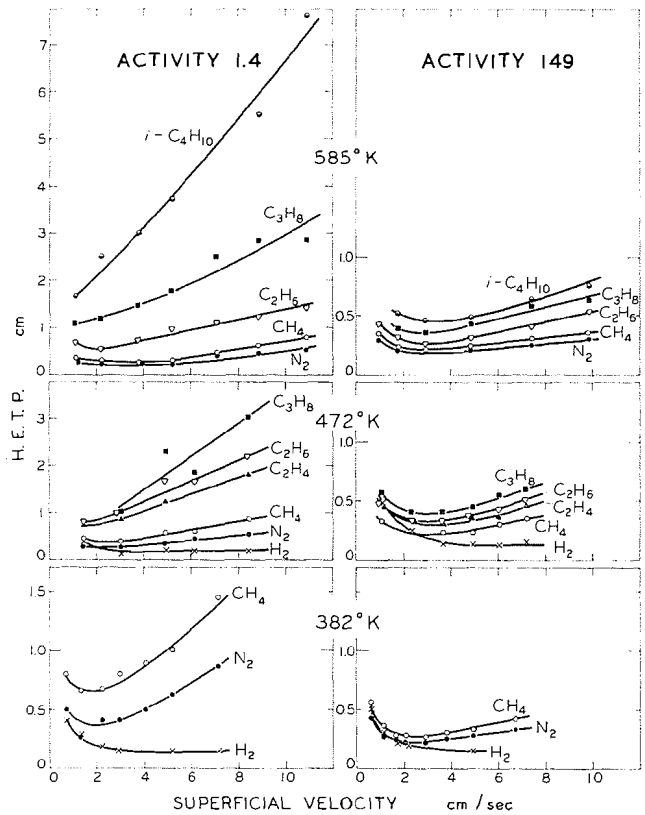

FIG. 6. Variation of H.E.T.P. with flow rate for several gases at 312°, 199°, and 109° C using columns of Barnebey-Cheney charcoals of 1.4 and 149 cc/g activities.

Can. J. Chem. Downloaded from www.nrcresearchpress.com by 196.1.178.254 on 09/04/12
For personal use only.

ness of the peaks (cf. Fig. 1) the retention volume is not identical with the volume corresponding to the intersection of the inflection point tangents and we have for convenience used the retention volume in calculating H. The band-spreading in the connecting tubing has also been neglected but the effect on H of these two factors is likely to be small. It was difficult to get enough measurements at low velocities to determine B in equation [3] so that the values of A and C which are summarized in Table II were obtained from the limiting tangent at high velocities. With few exceptions the A values are close to the limiting H for a non-sorbing gas, 0.10 to 0.15 cm.

TABLE II

Resistance to mass transfer

H.E.T.P. = $A + B/u + Cu$ (fitted only at the high-velocity end)

	Charcoal activity 1.4 cc/g					Charcoal activity 149 cc/g			
Solute	α cc g^{-1} atm^{-1}	A cm^{-1}	C sec	D_p cm^2 sec$^{-1}\times10^2$ (a)	(b)	α cc g^{-1} atm^{-1}	A cm^{-1}	C sec	D_p cm^2 sec$^{-1}\times10^2$
				585° K					
N_2	0.16	0.05	0.045	1.21	3.36		0.13	0.018	—
CH_4	0.56	−0.15	0.085	2.19	6.09	0.74	0.13	0.023	3.62
C_2H_6	2.9	0.25	0.112	3.13	8.70	2.79	0.13	0.038	4.36
C_3H_8	12.0	0.30	0.268	1.50	4.17	8.8	0.13	0.056	3.64
i-C_4H_{10}	30.6	0.32	0.630	0.66	1.83	23.8	0.13	0.066	3.34
				472° K					
N_2	0.44	0.12	0.050	2.59	7.20	—	—	—	—
CH_4	1.74	0.10	0.090	3.23	8.96	1.70	0.02	0.047	2.65
C_2H_4	11.0	0.60 (0.15)	0.158 (.195)	2.50 (2.03)	6.95 (5.64)	7.90	0.05	0.058	3.40
C_2H_6	15.3	0.60 (0.15)	0.195 (0.245)	2.08 (1.65)	5.77 (4.58)	10.6	0.05	0.065	3.14
C_3H_8	98	0.05	0.355	1.19	3.30	54.0	0.10	0.071	3.16
				382° K					
N_2	1.51	0.02	0.118	2.16	6.01	1.75	0.13	0.028	4.03
CH_4	6.9	0.13	0.175	2.14	5.96	5.00	0.13	0.041	4.24

(a) Based on pore volume from helium density.
(b) Based on pore volume from carbon tetrachloride density.

To further interpret the coefficient C we have assumed the total resistance to mass transfer to lie in diffusion along the charcoal pores and have calculated apparent gas phase diffusion coefficients to describe such movement. Use was made of the following equation developed by van Deemter *et al.* (14, equation [49]) for ion-exchange chromatography which describes the resistance due to diffusion in a spherical particle of ion exchange resin:

$$C = \frac{d^2}{2\pi^2} \frac{F_I}{(1-F_I)} \frac{K}{D_{II}} \frac{1}{(1+KF_I/F_{II})^2}$$

where d = particle diameter,
F_I = volume fraction of moving phase,
F_{II} = volume fraction of stationary phase,
K = distribution coefficient, concentration in moving phase/concentration in stationary phase,
and D_{II} = diffusion coefficient in the stationary phase.

To modify this equation to fit the present case the ratio D_{II}/K which describes diffusion

Can. J. Chem. Downloaded from www.nrcresearchpress.com by 196.1.178.254 on 09/04/12
For personal use only.

in the stationary phase in terms of equivalent concentrations in the moving phase was replaced by D_p which accordingly refers directly to gas phase diffusion in the pores. At the same time a factor ϵ was introduced to represent the fraction of external particle surface represented by pore mouths together with a tortuosity factor $\sqrt{2}$ to allow for the greater diffusion path along a system of random pores and the quantity KF_I/F_{II} was replaced by the equivalent expression for gas–solid chromatography. Thus the following expression was obtained:

$$[4] \qquad C = \frac{d^2}{\sqrt{2}\pi^2} \frac{F_I}{(1-F_I)} \frac{1}{\epsilon D_p} \frac{1}{(1+273F_I/\alpha T\rho_b)^2}$$

where ϵ = void fraction in a single granule determined from the densities in mercury and helium or carbon tetrachloride,

D_p = apparent gas phase diffusion coefficient in the charcoal pores, (i.e. all movement along a pore is assumed to occur via the gas phase),

ρ_b = density of the packed bed,

and α = distribution coefficient as given by equation [1].

Values of D_p calculated according to equation [4] are included in Table II. For the 1.4-activity charcoal two sets of values are calculated corresponding to ϵ's determined from the helium and carbon tetrachloride densities.

DISCUSSION

Equilibrium Properties

The somewhat unexpected finding from this work is that the initial slopes of the isotherms all decrease with increasing surface areas of the charcoals. Qualitatively this means that the specific affinity decreases more rapidly than the surface area increases in order that the product of the two should decrease. This decrease in affinity is, of course, reflected in the decreasing heat of adsorption with increasing activation.

As pointed out earlier, α, ΔH, and the surface area are related quantities. It may be shown in the following way that the chromatographically determined α's and ΔH's are consistent with the conventionally measured nitrogen monolayer capacities at 77° K. Consider a simplified form of the initial part of the Langmuir isotherm (25):

$$\alpha = v_m A(T) e^{\Delta H/RT}$$

where v_m is the adsorbate monolayer capacity in cc (S.T.P.) per g. For any given adsorbate at a particular temperature v_m may reasonably be assumed to be a constant fraction of the nitrogen monolayer capacity at 77° K (apart from molecular sieve exclusion effects which may operate with the finer charcoals), and $A(T)$ should be reasonably constant for all charcoals. Consequently the following relationship should hold:

$$\log \alpha - \log v_{m,N_2\,77°} = \text{constant} + \Delta H/RT.$$

Figure 7 shows plots of the left-hand side for the α's and nitrogen monolayer values shown in Fig. 4 against the corresponding ΔH's. The straight lines are arbitrarily drawn in at the correct slopes and, at least for the higher activity charcoals, they fit the points reasonably well. It is doubtful whether any significance should be attached to the actual values of the intercepts, although they seem to be of approximately the correct order of magnitude required by the relationship of Fowler and Guggenheim referred to above (25). The success of this rather crude correlation encourages one to hope that surface areas could in some cases be determined from chromatographic measurements alone.

Can. J. Chem. Downloaded from www.nrcresearchpress.com by 196.1.178.254 on 09/04/12
For personal use only.

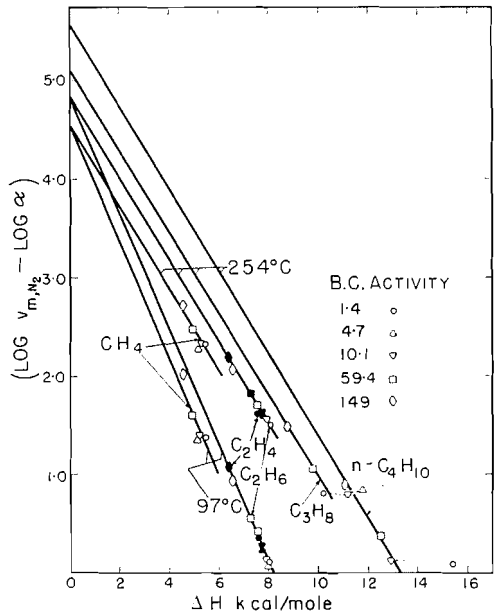

FIG. 7. A test of consistency of the α, ΔH, and nitrogen monolayer capacities (at 77° K) for $1/T = 1.90$ and 2.70×10^{-3}.

This possibility is examined in more detail from a somewhat different point of view in a paper to be published (10).

There is no reason to assume any difference in the chemical nature of the surface as the result of further activation. Therefore, the higher heat of adsorption for the lower activity charcoals is probably due to stronger adsorption in the narrower pores. The initial heat of adsorption with graphitic adsorbents is frequently almost twice the limiting value at higher concentrations, suggesting that the first adsorbate molecules are held by both sides of a narrow crevice. Similar sites will be present, although in smaller proportion, even on the most fully activated charcoals and consequently the range of initial heats is relatively small.

As can be seen from Fig. 4, the variation in surface area (to nitrogen) is much less than the variation in chloropicrin activity. For the most active charcoal the average chloropicrin adsorption at break-through is 149 cc/g. The chloropicrin monolayer capacity was estimated from rough measurements to be around 180 cc/g, which is consistent with the nitrogen monolayer capacity of 630 cc/g. However, when the average chloropicrin concentration at break-through is only 5 cc/g the nitrogen monolayer value is still over 200 cc/g. This discrepancy probably reflects both the slower rates of diffusion in the less active charcoals as well as a relatively lower surface area for chloropicrin due to its exclusion from the smallest pores. By comparing the nitrogen surface areas with those for the previous charcoal series (19), it would appear that significant exclusion of butane would be found only in charcoals of activity less than 5. Exclusion of chloropicrin which is not much larger would hardly extend to much higher activities so that the main reason for the increasing disparity between chloropicrin activities and nitrogen monolayer values must be slower diffusion.

It is perhaps worth considering a little further to what extent a dynamic chromatographic measurement can reflect the true equilibrium adsorption relationship. The

Can. J. Chem. Downloaded from www.nrcresearchpress.com by 196.1.178.254 on 09/04/12
For personal use only.

usual argument is that equilibrium exists at the center of a peak because here the overall rate of transfer is zero (26). This is probably true for a uniform stationary phase. However, each charcoal contains a range of pore sizes. Diffusion in and out of the smaller pores is very slow and consequently broadens the peak but, since this diffusion also opens up a larger surface for adsorption, the broadening is asymmetric in the direction of larger retention volume. In an extreme case, as with the inactivated charcoal, the broadening may be so great as to become indistinguishable from the base line. Thus the asymmetry of a gas–solid chromatogram is at least partly due to the nature of the solid as well as to the curvature of the adsorption isotherm.

This suggests that our method of extrapolation of the peak retention volume to zero sample pressure may be inadequate fully to take account of the retention in the narrowest pores. An alternative procedure considered was to draw in the center line of the peak and take as the retention volume its intersection with the base line. This point was found to be very uncertain, particularly with the less active charcoals, due to the curvature of the center line near the base. We feel, in any case, that the use of such a refinement would change the results relatively little. The direction of any change would be to increase the α's, more so for the less active charcoals and at lower temperatures. Consequently the trend in α and the trend in ΔH may be somewhat stronger than shown in Figs. 4 and 5.

Diffusion Coefficients

The apparent gas phase diffusion coefficients in Table II have been calculated on the assumption of pores of a single size extending through the charcoal granule. For this simplified picture the diffusion coefficients for the 1.4-activity charcoal are slightly larger than those for the 149-activity (taking the values based on the carbon tetrachloride void volumes since transport through channels inaccessible to carbon tetrachloride is likely to be negligible). This is in contrast to the much larger transfer resistance, as shown by the H values, for the 1.4-activity charcoal. However, this resistance, as expressed by C, depends on the total transfer load per unit volume of bed as well as on the specific resistance. The lower α's and lower density of the high-activity charcoal make this load smaller while the greater pore volume increases the cross section for transfer.

The extreme simplifications involved in this picture (e.g. the neglect of the macropore system in the charcoal structure) cast considerable uncertainty on the absolute values of D_p. However, the approximate equality of the values for the two charcoals is consistent with the rather limited range in micropore diameters which appears to be characteristic of steam-activated coconut charcoals. Measurements on an earlier series showed for each charcoal a very narrow spread in micropore sizes around a median diameter which increased only from 18 Å to 25 Å over the series (20).

The mechanism of transient gas flow in small capillaries is usually assumed to be a process of Knudsen diffusion modified by adsorption on the pore walls and by diffusion of the adsorbed phase (27). The apparent gas phase diffusion coefficients corresponding to Knudsen diffusion are decreased by adsorption on the pore walls and increased by diffusion in the adsorbed film. The experimental coefficients vary only a little for the various gases which cover more than a 100-fold range in α values. This suggests that the two factors must nearly balance each other and that diffusion in the adsorbed film is probably quite considerable for strongly adsorbed gases. At these relatively high temperatures this is not unreasonable.

Can. J. Chem. Downloaded from www.nrcresearchpress.com by 196.1.178.254 on 09/04/12
For personal use only.

A more detailed analysis of transport properties in these charcoals is not warranted by the present measurements. We believe, however, that this work has demonstrated the usefulness of gas chromatography in the study of kinetic as well as equilibrium aspects of adsorption.

ACKNOWLEDGMENTS

We wish to thank Dr. J. L. Morrison for his co-operation during this work as well as for giving us samples of the charcoals and, together with Mr. N. W. Myshok, making available some experimental measurements prior to publication. We are grateful to Dr. M. P. Freeman for several helpful suggestions. The co-operation of the Barnebey-Cheney Company in preparing this series of charcoals is also appreciated.

REFERENCES

1. CREMER, E. and PRIOR, F. Z. Elektrochem. **55**, 66 (1951).
2. MARTIN, A. J. P. and SYNGE, R. L. M. Biochem. J. **35**, 1358 (1941).
3. JAMES, A. T. and MARTIN, A. J. P. Biochem. J. **50**, 679 (1952).
4. PORTER, P. E., DEAL, C. H., and STROSS, F. H. J. Am. Chem. Soc. **78**, 2999 (1956).
5. BRADFORD, B. W., HARVEY, D., and CHALKLEY, D. E. J. Inst. Petrol. **41**, 80 (1955).
6. LITTLEWOOD, A. B., PHILLIPS, C. S. G., and PRICE, D. T. J. Chem. Soc. 1480 (1955).
7. ANDERSON, J. R. A. and NAPIER, K. H. Australian J. Chem. **10**, 250 (1957).
8. GLUECKAUF, E. Nature, **156**, 748 (1945).
9. SANGSTER, D. F. Atomic Energy Research Establ. (Gt. Britain), C/M 280 (1956).
10. HANLAN, J. F. and FREEMAN, M. P. Can. J. Chem.
11. STEELE, W. A. and HALSEY, G. D., JR. J. Chem. Phys. **22**, 979 (1954).
12. STEELE, W. A. and HALSEY, G. D., JR. J. Phys. Chem. **59**, 57 (1955).
13. GREENE, S. A. and PUST, H. J. Phys. Chem. **62**, 55 (1958).
14. VAN DEEMTER, J. J., ZUIDERWEG, F. J., and KLINKENBERG, A. Chem. Eng. Sci. **5**, 271 (1956).
15. KEULEMANS, A. I. M. and KWANTES, A. *In* Vapour phase chromatography. *Edited by* D. H. Desty. Butterworth Scientific Publications, London. 1957. p. 150.
16. BRENNAN, D. and KIMBALL, C. J. Inst. Petrol. **44**, 14 (1958).
17. DE WET, W. J. and PRETORIUS, V. Anal. Chem. **30**, 325 (1958).
18. LEMIEUX, R. U. and MORRISON, J. L. Can. J. Research, B, **25**, 440 (1947).
19. NAY, M. A. and MORRISON, J. L. Can. J. Research, B, **27**, 205 (1949).
20. MORRISON, J. L. and MILLER, D. M. Can. J. Chem. **33**, 330 (1955).
21. RAY, G. C. and BOX, E. O., JR. Ind. Eng. Chem. **42**, 1315 (1950).
22. LEWIS, W. K., GILLILAND, E. R., CHERTOW, B., and CADOGAN, W. P. Ind. Eng. Chem. **42**, 1326 (1950).
23. SCHAEFFER, M. D., POLLEY, W. H., and SMITH, W. R. J. Phys. Chem. **54**, 227 (1950).
24. MYSHOK, N. W. M.Sc. Thesis, University of Alberta, Edmonton. September 1958.
25. FOWLER, R. and GUGGENHEIM, E. A. Statistical thermodynamics. Cambridge: The University Press, London. 1949. p. 427.
26. TURKEL'TAUB, N. M., SHWARTSMAN, V. P., NAUMOVA, V. V., and ZHUKOVITSKII, A. A. Zhur. Fiz. Khim. **30**, 417 (1956).
27. BARRER, R. M. and GROVE, D. M. Trans. Faraday Soc. **47**, 826 (1951).

Can. J. Chem. Downloaded from www.nrcresearchpress.com by 196.1.178.254 on 09/04/12
For personal use only.

Can. J. Chem. Downloaded from www.nrcresearchpress.com by 196.1.178.254 on 09/04/12
For personal use only.

THE PARTIAL STRUCTURES OF ACONITINE AND ACONITOLINE[1]

HANS MAYER[2] AND LÉO MARION

ABSTRACT

In aconitoline ($C_{33}H_{41}O_{10}N$), the product of the oxidation of aconitine with chromic acid, the presence of an $\alpha\beta$-unsaturated carbonyl group has been confirmed. The determination of the basic strengths of aconitoline and its various hydrolytic and reduction products revealed a very strong influence of the carbonyl on the basicity of the alkaloid. It was concluded that the secondary hydroxyl that becomes oxidized must be located in close proximity to the nitrogen. Partial structures are suggested to represent both aconitine and aconitoline.

The alkaloid aconitine ($C_{34}H_{47}O_{11}N$) is known to contain three free hydroxyls, four methoxyl groups, an acetate, and a benzoate group. It has further been shown to contain an N-ethyl group so that its empirical formula can be expanded to $C_{19}H_{19}N.C_2H_5$-$(OH)_3(OCH_3)_4(O.COCH_3)(O.COC_6H_5)$ (cf. ref. 1). If in this formula all the oxygenated substituents be replaced by hydrogen the resulting compound would be expressed by $C_{21}H_{33}N$. Similarly, the alkaloid lycoctonine ($C_{25}H_{41}O_7N$) is also expressed by $C_{21}H_{33}N$ when its oxygenated substituents are replaced by hydrogen. It therefore seems legitimate to assume that there is a great deal of similarity between the carbon–nitrogen skeletons of both alkaloids.

Indeed, Schneider (2) has assumed that aconitine possesses the same carbon–nitrogen skeleton as that derived for lycoctonine by X-ray crystallography (3). Of the nine oxygenated substituents of aconitine he has assumed that seven occupied the same positions as the seven oxygenated substituents in lycoctonine, and has assigned to the remaining two positions on the heterocyclic ring I (2, 4). Further, because of the inertness of aconitine towards lead tetraacetate and periodic acid (5), he arranged the substituents in such a way as to avoid the presence of a vicinal glycol in the alkaloid.

It has long been known that aconitine is oxidized by chromic acid to the ketone aconitinone (6), which very readily loses the elements of methanol and gives rise to aconitoline (6, 7, 8). Since β-methoxy ketones were known to eliminate methanol readily and thus gave rise to $\alpha\beta$-unsaturated ketones, Majima and Tamura (6) concluded that aconitoline was an $\alpha\beta$-unsaturated ketone, and that aconitine contained a β-methoxy secondary alcohol system. Schneider (4), who also prepared aconitoline, claimed that the characteristic absorption of the carbonyl group in the infrared and ultraviolet spectra confirmed the presence of an $\alpha\beta$-unsaturated ketone, and he proposed to represent aconitoline by structure II.

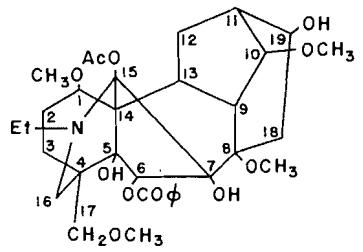

I

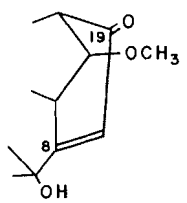

II

[1]*Manuscript received January 20, 1959.*
Contribution from the Division of Pure Chemistry, National Research Council, Ottawa, Canada.
Issued as N.R.C. No. 5118.
[2]*National Research Council of Canada Postdoctorate Fellow.*

Can. J. Chem. Downloaded from www.nrcresearchpress.com by 196.1.178.254 on 09/04/12
For personal use only.

In order to find further evidence regarding the location of the two substituents which by oxidation and loss of methanol give rise to an unsaturated ketone, a fresh study of the oxidation of aconitine with chromic acid has been undertaken.

In our hands the oxidation of aconitine with chromic acid always gave aconitoline directly. The analytical figures confirmed the empirical formula ($C_{33}H_{41}O_{10}N$) already reported (6, 8) and the melting point agreed with that given in the literature. The infrared spectrum of aconitoline contained, besides the ester carbonyl absorption at 1720 and 1730 cm^{-1}, bands at 1677 cm^{-1} (carbonyl) and 720 cm^{-1} (double bond). The ultraviolet spectrum contained four maxima including λ_{max} 232 mμ, log ϵ 4.35 and λ_{max} 305 mμ, log ϵ 2.35. Saponification of aconitoline removed the acetyl and benzoyl groups and gave rise to demethanolaconinone, $C_{24}H_{35}O_8N$, which in the infrared showed a single strong band at 1680 cm^{-1} (carbonyl). Its ultraviolet spectrum showed two maxima (λ_{max} 236 mμ, log ϵ 3.99; λ_{max} 310 mμ, log ϵ 2.34). It has been established that $\alpha\beta$-unsaturation caused a shift of *ca.* 30–40 wave-numbers in the carbonyl absorption in the infrared of six-membered cyclic ketones (9) and the ultraviolet spectrum of demethanolaconinone is characteristic of that of an $\alpha\beta$-unsaturated ketone. Indeed, dihydrodemethanolaconinone ($C_{24}H_{37}O_8N$), the product of the catalytic hydrogenation of demethanolaconinone, in which the double bond is no longer present, shows in the infrared a carbonyl absorption band at 1710 cm^{-1}. This is displaced by 30 wave-numbers from the carbonyl band in the infrared spectrum of demethanolaconinone. β-Methoxy-ketones are known to eliminate the elements of methanol readily and give rise to $\alpha\beta$-unsaturated ketones. Hence aconitine must contain a secondary hydroxyl located in β-position to a methoxyl, as other workers had previously concluded (4, 6, 8).

We have now observed that whereas the pK_a of aconitine is 7.72, that of aconitoline is 3.85. This very marked influence on the basic strength is due to the formation of the carbonyl group, since dihydrodemethanolaconitinone, $C_{33}H_{43}O_{10}N$, prepared by the catalytic hydrogenation of aconitoline, in which the double bond is no longer present has a pK_a 3.85. Furthermore, the action of sodium borohydride either on aconitoline or on dihydrodemethanolaconitinone gave rise to dihydrodemethanolaconitine, $C_{33}H_{45}O_{10}N$, which contained no double bond and in which the carbonyl group had been converted back to a secondary alcohol, and the pK_a of this compound was 6.0. Its ultraviolet absorption spectrum was essentially the same as that of aconitine, and its saponification product, dihydrodemethanolaconine, $C_{24}H_{39}O_8N$, isolated as its hydrochloride, showed no carbonyl absorption in the infrared.

The alkaloid delcosine, which is very closely related to lycoctonine (10, 11), has a pK_a 6.49. It contains a secondary hydroxyl in position 10 (formula I) which[3] is remote from the nitrogen, and when this is oxidized to a carbonyl group (dehydrodelcosine) the pK_a drops to 5.75. The drop in pK_a is only 0.75 unit, whereas a drop of 3.87 units accompanies the formation of aconitoline. Such a dramatic effect on the basic strength indicates that the secondary hydroxyl that becomes oxidized to a carbonyl must be located close to the nitrogen. Hence the location by Schneider of the β-methoxy secondary alcohol system involved in the formation of aconitoline in positions as remote to the nitrogen as carbons 8 and 19 (structure II) is not compatible with these observations.

A β-aminoketone has a much lower basic strength than the hydroxylic base from which it arises, as illustrated by tropine (pK_a 9.80) and tropinone (pK_a 6.98).[4] If then,

[3]*The numbering of the lycoctonine carbon–nitrogen skeleton has been arrived at in consultation with Professor R. C. Cookson and Dr. O. E. Edwards.*

[4]*The basic strengths of tropine and tropinone were determined in 50% ethanol by titration with .055 N p-toluenesulphonic acid in 50% ethanol.*

Can. J. Chem. Downloaded from www.nrcresearchpress.com by 196.1.178.254 on 09/04/12
For personal use only.

like Schneider (2) we assume as a working hypothesis that the carbon–nitrogen structure of aconitine be the same as that of lycoctonine, it appears highly probable that the β-methoxy alcohol system involved in the oxidation to aconitoline is located in ring A, and that that ring is substituted as in partial structure III. That the methoxyl and hydroxyl groups should be as shown in III, and not in the reversed positions, is apparent from the fact that the presence of a hydroxyl in position 1, provided it has the right orientation, should on oxidation lead to the formation of an internal ether as in delcosine (10) and in delsoline (12) and such an internal ether has not been obtained from aconitine. Consequently, aconitoline is represented as IV which is a β-aminoketone.

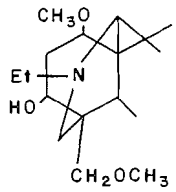

III

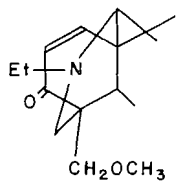

IV

The wave-length at which the maximum (λ_{max} 236 mμ, log ϵ 3.99) occurred in the ultraviolet spectrum of demethanolaconinone, however, indicated a possible further substituent in the α or β position of the $\alpha\beta$-unsaturated ketone system of aconitoline. Since in aconitine the β-position is already substituted with a methoxyl, a second substituent would be more likely to be found in the α-position. Furthermore, such a substituent should be a methoxyl, since were it a hydroxyl it would have been oxidized in the course of the formation of aconitoline. It is well known that α-methoxy-$\alpha\beta$-unsaturated ketones are readily hydrolyzed by acids to α-diketones but aconitoline was recovered quantitatively from such a treatment. Also, the Wolff–Kishner reaction on α-methoxyketones is accompanied by elimination of the methoxyl and formation of a double bond (13). Dihydrodemethanolaconinone was, therefore, reduced by the Wolff–Kishner reaction but the product, $C_{24}H_{39}O_7N$, which showed no carbonyl absorption in the infrared, had the same number of methoxyl groups as the starting material. Hence, there is no substituent between the hydroxyl and methoxyl of ring A in aconitine, and aconitoline is IV.

The location of the acetoxy group in Schneider's proposed structure on the α-position to the nitrogen in the heterocylic ring is also unacceptable. Were the acetoxy group to occupy that position, the hydrochloride of benzoylaconine should be an anhydronium salt and the spectroscopic and other evidence, to be discussed in a later communication, clearly indicate that it is not.

EXPERIMENTAL

All infrared absorption spectra were determined on nujol mulls, unless otherwise mentioned, with a Perkin–Elmer Model 21B spectrometer. For the measurement of the ultraviolet spectra the substances were dissolved in methanol. Basic strengths were determined by titration with .05 *N* *p*-toluenesulphonic acid of solutions of the compounds in 95% ethanol (except when otherwise mentioned).

The aconitine used in the following experiments was recrystallized from methanol–water from which it separated as colorless prisms, m.p. 198–199°[5] (decomp.), when

[5]*Melting points are uncorrected.*

immersed in the bath at 180°. Its pK_a was 7.7, $[\alpha]_D^{24}$ +18.2° (*c*, 1.5 in chloroform). Infrared absorption: 3470 cm^{-1} (OH), 1718 cm^{-1} (ester carbonyls), 1610, 710 cm^{-1} (benzene ring). The homogeneity of the base was tested with a paper chromatogram developed with the organic phase of the mixture isoamyl alcohol, glacial acetic acid, and water (40:15:45). The chromatogram gave only one spot (R_F 0.84).

Aconitoline (Demethanolaconitinone)

Aconitine (4.493 g) was dissolved in acetone (100 ml) and cooled in ice and salt. To the cold solution chromium trioxide (4.50 g) dissolved in cooled acetone (50 ml) was added. The reaction mixture was allowed to stand at room temperature for 3 days, after which the solvent was evaporated under reduced pressure. The dark brown residue was triturated with sulphurous acid (100 ml), sulphur dioxide was bubbled into the mixture, and the resulting dark green solution was extracted with ether (500 ml).

The aqueous liquor was then alkalized with finely powdered sodium carbonate and the precipitate filtered and dried. The dried precipitate was extracted with chloroform (100 ml) in a Soxhlet apparatus. The filtrate was extracted with chloroform (250 ml) and the two chloroform extracts combined and evaporated to dryness. There was left a light yellow froth (3.64 g, 85.5%) that crystallized in contact with ether and *n*-hexane. The product melted at 105–110°, resolidified, and melted again at 205–210° (decomp.). After two recrystallizations from methanol–water, it consisted of colorless prisms (wt., 2.506 g), m.p. 218–220°, $[\alpha]_D^{25}$ +69.0° (*c*, 1.85 in chloroform), pK_a 3.85. Found: C, 64.96; H, 6.75; N, 2.33. Calc. for $C_{33}H_{41}O_{10}N$: C, 64.80; H, 6.76; N, 2.29%. Infrared absorption: 3470 cm^{-1} (OH), 1730, 1720 cm^{-1} (ester carbonyls), 1677 cm^{-1} (six-membered $\alpha\beta$-unsaturated ketone), 1605 and 720 cm^{-1} (benzene).

Ultraviolet spectrum: λ_{max} 232 mμ, log ϵ 4.35; λ_{max} 273 mμ, log ϵ 3.09; λ_{max} 281 mμ, log ϵ 3.0; λ_{max} 305 mμ, log ϵ 2.35.

Aconitoline formed a hydriodide which crystallized in long needles from acetone–ether, m.p. 225–226° (decomp.) when immersed at 200°.

Demethanolaconinone

To a solution of aconitoline (155 mg) in ethanol (10 ml), heated to boiling in a slow stream of nitrogen, was added dropwise an alcoholic *N*-potassium hydroxide solution (0.56 ml), and the reaction mixture was refluxed for 2 hours. The light yellow solution was evaporated to dryness *in vacuo*, water (10 ml) was added, and the solution brought to pH 6 by the dropwise addition of 2 *N* hydrochloric acid. The solution was extracted five times with 25 ml of ether, saturated with sodium carbonate, and extracted five times with 25 ml of chloroform. After drying with sodium sulphate, the chloroform solution was evaporated to dryness *in vacuo*. It left a crystalline froth (115.5 mg, 98% yield) that could not be induced to crystallize.

The froth was dissolved in water (10 ml), the solution was filtered and brought to pH 6 with 2 *N* hydrochloric acid. After evaporation *in vacuo* there remained 126 mg (99% yield) of demethanolaconinone hydrochloride, which crystallized on contact with absolute ethanol, m.p. 220–221° (decomp.). After two recrystallizations from absolute ethanol – ether the colorless needles (95 mg) melted at 220–221° (decomp.), $[\alpha]_D^{24}$ +66.5° (*c*, 1.97 in water). Found: C, 57.37; H, 7.15. Calc. for $C_{24}H_{35}O_8N.HCl$: C, 57.42; H, 7.23%. Infrared absorption: 3320, 3160 cm^{-1} (OH), and a sharp band at 1680 cm^{-1} (six-membered $\alpha\beta$-unsaturated ketone), 720 cm^{-1} (double bond). Ultraviolet spectrum: λ_{max} 229 mμ, log ϵ 3.94; λ_{max} 301 mμ, log ϵ 2.62.

Some of the hydrochloride (38 mg) was dissolved in water (5 ml), the solution was

Can. J. Chem. Downloaded from www.nrcresearchpress.com by 196.1.178.254 on 09/04/12
For personal use only.

saturated with sodium carbonate and extracted five times with 20 ml of chloroform. Evaporation of the chloroform left a residue of 34.5 mg (98% yield) of pure demethanolaconinone, which could not be induced to crystallize. Its ultraviolet spectrum showed λ_{max} 236 mμ, log ϵ 3.99; λ_{max} 310 mμ, log ϵ 2.34.

A quantity of demethanolaconinone was converted to the hydriodide, which crystallized from methanol–ether as colorless prismatic needles, m.p. 240–241° (decomp.) when immersed at 220°. The salt crystallized as a hydrate from which it was not possible to remove all the water. The hydrate dried in air only was used for analysis, $[\alpha]_D^{25}$ +59.2° ±1.5° (*c*, 1.04 in water). Found: C, 44.91; H, 6.53. Calc. for $C_{24}H_{35}O_8N.HI.3H_2O$: C, 44.53; H, 6.54%. Infrared absorption: 3320, 3420 cm^{-1} (OH, H_2O), 1650 cm^{-1} (H_2O), 1680 cm^{-1} (six-membered $\alpha\beta$-unsaturated ketone).

Dihydrodemethanolaconitinone

Aconitoline (113 mg) dissolved in 95% ethanol (5 ml) was hydrogenated at room temperature in the presence of 30% palladium–charcoal (28 mg). After 3.5 hours the reaction was completed (hydrogen uptake 4.28 ml; calc. for 1 mole, 4.55 ml). The catalyst was removed by filtration and the filtrate evaporated to dryness. There was left a colorless froth, 114 mg, which crystallized in contact with ether. After three recrystallizations from aqueous methanol, the product consisted of colorless needles (73 mg), m.p. 220–221° (decomp.) when immersed at 180°, $[\alpha]_D^{25}$ −50° (*c*, 1.1 in chloroform), pK_a 3.85. Found: C, 64.97; H, 7.40. Calc. for $C_{33}H_{43}O_{10}N$: C, 64.58; H, 7.06%. Infrared absorption (fluorolube mull): 3470 cm^{-1} (OH), 1720, 1733 cm^{-1} (ester carbonyl), shoulder at 1705 cm^{-1} (six-membered ketone).

Dihydrodemethanolaconinone

To a solution of dihydrodemethanolaconitinone (363 mg) in ethanol (20 ml) under reflux in a stream of nitrogen, 1.3 ml (2.2 equiv.) of *N*-alcoholic potassium hydroxide was added dropwise and the refluxing continued for 2 hours. The solution was evaporated to dryness *in vacuo* and the residue dissolved in water (10 ml). The aqueous solution was acidified with 10% hydrochloric acid, extracted five times with 20 ml of ether, saturated with sodium carbonate, and extracted five times with 20 ml of chloroform. On evaporation the chloroform solution left a colorless gum (271 mg, 98% yield) which crystallized from acetone – *n*-hexane. After recrystallization from the same mixture, the product consisted of colorless rhombohedral leaflets (255 mg), m.p. 131–133° (decomp.), $[\alpha]_D^{25}$ −52.2° (*c*, 1.11 in chloroform). Found: C, 60.31; H, 7.80. Calc. for $C_{24}H_{37}O_8N.\frac{1}{2}H_2O$: C, 60.48; H, 8.03%. It was not possible to remove all the water by drying *in vacuo* without causing some decomposition. Infrared absorption (in chloroform): 3420 cm^{-1} (OH) and 1710 cm^{-1} (six-membered cyclic ketone).

Dihydrodemethanolaconitine

(*a*) *Reduction of Aconitoline with Sodium Borohydride*

Sodium borohydride (200 mg) was added to a solution of aconitoline (498 mg) in 80% aqueous methanol (40 ml). After the reaction mixture had been left for 1 hour at room temperature the solution was evaporated to dryness *in vacuo* and the residue dissolved in 2 *N* sulphuric acid (20 ml). The solution was extracted five times with 25 ml of ether, saturated with sodium carbonate, and extracted five times with 25 ml of chloroform. Evaporation of the chloroform extract gave a colorless froth (500 mg) which crystallized in contact with ether. The product was recrystallized twice from methanol–water, from which it separated as colorless prisms (321 mg), m.p. 173–174 (decomp.), $[\alpha]_D^{27}$

Can. J. Chem. Downloaded from www.nrcresearchpress.com by 196.1.178.254 on 09/04/12
For personal use only.

+23° (*c*, 1.31 in chloroform), pK_a 6.0±0.1. Found: C, 64.53; H, 7.51. Calc. for $C_{33}H_{45}O_{10}N$: C, 64.38; H, 7.37%. Infrared absorption: 3460 cm^{-1} (OH), 1715, 1730 cm^{-1} (ester carbonyls), 1608 and 702 cm^{-1} (benzene ring). Ultraviolet spectrum: λ_{max} 230 mμ, log ε 4.24; λ_{max} 274 mμ, log ε 3.09; λ_{max} 281 mμ, log ε 3.02.

(*b*) *Reduction of Dihydrodemethanolaconitinone with Sodium Borohydride*

To a solution of dihydrodemethanolaconitinone (101 mg) in 80% aqueous methanol (10 ml), sodium borohydride (50 mg) was added. After the solution had been left for 1 hour at room temperature, it was evaporated to dryness and the residue dissolved in 2 *N* sulphuric acid (10 ml). The solution was washed five times with 20 ml of ether, saturated with sodium carbonate, and extracted five times with 20 ml of chloroform. On evaporation the dried chloroform solution yielded a colorless froth (101 mg) which crystallized when triturated with ether – *n*-hexane. After two recrystallizations from methanol–water the product (47 mg) consisted of colorless prismatic needles, m.p. 171–173° (decomp.), $[\alpha]_D^{27}$ +23.7° (*c*, 1.42 in chloroform). Found: C, 64.48; H, 7.18. Calc. for $C_{33}H_{45}O_{10}N$: C, 64.38; H, 7.37%. The melting point was unchanged by mixture with the dihydrodemethanolaconitine obtained above (*a*) and the infrared absorption spectra were superimposable.

Dihydrodemethanolaconine Hydrochloride

Pure dihydrodemethanolaconitine (148 mg) was hydrolyzed in alkaline solution, as described under demethanolaconinone. The product (106 mg, 95% yield) was a colorless froth. It was dissolved in water (5 ml) and the solution made just acid by the dropwise addition of 10% hydrochloric acid. Evaporation of the acid solution left a colorless froth which crystallized after addition of a few drops of methanol. The crystalline product (108 mg) was recrystallized three times from methanol–ether from which it separated as colorless needles, m.p. 212–213° (decomp.), $[\alpha]_D^{25}$ −19.0±0.6° (*c*, 1.72 in water). Found: C, 56.91; H, 7.87. Calc. for $C_{24}H_{39}O_8N.HCl$: C, 56.96; H, 7.97%. The infrared spectrum contained no absorption attributable to carbonyl or unsaturation.

Attempted Saponification of Demethanolaconinone Hydrochloride

Pure demethanolaconinone hydrochloride (69 mg) was dissolved in 2 *N* hydrochloric acid (10 ml), and the solution refluxed for 2 hours. The solution was then evaporated and the residual colorless froth crystallized from ethanol, from which it separated as colorless needles, m.p. 220–221° when immersed at 200° (decomp.) either alone or in admixture with the starting material. The infrared spectrum of the product was identical with that of the starting material and so was its optical rotation, $[\alpha]_D^{24}$ +66.8° (*c*, 1.53 in water).

Wolff–Kishner Reduction of Dihydrodemethanolaconinone

A mixture of dihydrodemethanolaconinone (101 mg), triethylene glycol (3 ml), and 95% hydrazine (1.2 ml) was immersed in a metal bath preheated to 145°, the temperature raised to 150° and maintained for 1 hour. Potassium hydroxide (520 mg) was then added, the temperature raised gradually to 190°, and maintained between 190–195° for a further 3 hours while a slow stream of nitrogen was passed into the reaction flask. After cooling, the light yellow solution was diluted with water (20 ml), acidified with 2 *N* sulphuric acid, and extracted 10 times with 20 ml of chloroform. The aqueous solution was then alkalized and saturated with solid sodium carbonate and extracted five times with 20 ml of ether. The ether extract when evaporated left a colorless oil which crystallized on addition of some drops of acetone and water (54 mg, yield 55%), colorless

Can. J. Chem. Downloaded from www.nrcresearchpress.com by 196.1.178.254 on 09/04/12
For personal use only.

needles, m.p. 104° (decomp., after beginning to shrink at 80°). Recrystallization from a very concentrated acetone solution gave dihydrodemethanoldehydroxyaconine as rhombohedral leaflets, m.p. 104–106° (decomp.), $[\alpha]_D^{22}$ +21.4° (*c*, 1.04 in chloroform). Found: C, 62.97; H, 8.41; OCH_3, 20.65. Calc. for $C_{24}H_{39}O_7N$: C, 63.55; H, 8.67; 3 OCH_3, 20.53%. The infrared spectrum contained no carbonyl absorption.

ACKNOWLEDGMENTS

We are indebted to Mr. R. Lauzon and Mr. H. Seguin of these laboratories for preparing the infrared spectra and for the microanalyses, respectively. We wish to express our gratitude to Dr. Raymond Paul, Rhône-Poulenc, Paris, who kindly helped us in securing our first supply of aconitine.

REFERENCES

1. STERN, E. S. *In* The alkaloids. Vol. IV. *Edited by* R. H. F. Manske and H. L. Holmes. Academic Press, Inc., New York. 1954.
2. SCHNEIDER, W. Archiv. Pharm. **289**, 703 (1956).
3. PRZYBYLSKA, M. and MARION, L. Can. J. Chem. **34**, 185 (1956).
4. SCHNEIDER, W. and TAUSEND, H. Naturwiss. **44**, 512 (1957).
5. SCHNEIDER, W. Naturwiss. **44**, 492 (1957).
6. MAJIMA, R. and TAMURA, K. Ann. **545**, 1 (1940).
7. LAWSON, A. J. Chem. Soc. 80 (1936).
8. JACOBS, W. A. and CRAIG, L. C. J. Biol. Chem. **136**, 323 (1940).
9. JONES, R. N., WILLIAMS, V. Z., WHALEN, M. J., and DOBRINER, K. J. Am. Chem. Soc. **70**, 2024 (1948).
10. ANET, R., CLAYTON, D. W., and MARION, L. Can. J. Chem. **35**, 397 (1957).
11. SKARIC, V. and MARION, L. J. Am. Chem. Soc. **80**, 4434 (1958).
12. SPARATORE, F., GREENHALGH, R., and MARION, L. Tetrahedron, **4**, 157 (1958).
13. WARNHOFF, E. W. and WILDMAN, W. C. Chem. & Ind. 1293 (1958).

Can. J. Chem. Downloaded from www.nrcresearchpress.com by 196.1.178.254 on 09/04/12
For personal use only.

Can. J. Chem. Downloaded from www.nrcresearchpress.com by 196.1.178.254 on 09/04/12
For personal use only.

CARBONYL AND THIOCARBONYL COMPOUNDS

I *a*. REACTION OF 9-DIAZOXANTHENE WITH *o*-QUINONES

b. THE DIRECT PREPARATION OF HALOGENATED CYCLIC ETHERS FROM CERTAIN THIONES AND THEIR MOLLUSCICIDAL ACTIVITY[1]

NAZIH LATIF AND IBRAHIM FATHY

ABSTRACT

The preparation and properties of 9-diazoxanthene are described. It reacts with tetrachloro- and tetrabromo-*o*-benzoquinone, 4-triphenylmethyl-1,2-benzoquinone, and phenanthraquinone to give the cyclic ethers III*a*, III*b*, IV, and V respectively. The action of hydrochloric acid – dioxane solution on the products is stressed.

Tetrachloro- and tetrabromo-*o*-benzoquinone react with xanthione forming the halogenated cyclic ethers III*a* and III*b* respectively. A 1,2-benzopyran derivative IX is obtained by the action of tetrachloro-*o*-quinone on coumarin-2-thione. IX is toxic to *Biomphalaria boissi* snails in high dilution.

Reaction of 9-Diazoxanthene with o-Quinones

The reactions of diazomethane and diphenyldiazomethane with *o*-quinones have been described by various authors (1). Schönberg and Latif (2) investigated the action of 9-diazofluorene on *o*-quinones and found that it reacts readily with *o*-benzoquinone and *β*-naphthoquinone derivatives to give methylenedioxy derivatives in good yield, but it fails to react with phenanthraquinone under the same conditions.

9-Diazoxanthene has not been described before. It could be prepared by the oxidation of xanthone hydrazone with mercuric oxide in the presence of alkali at room temperature. However, microanalysis could not be carried out, since the substance decomposes at room temperature with the formation of the ketazine. In contrast to diazofluorene, it reacts readily with phenanthraquinone to give the cyclic ether V. It also reacts, but more vigorously, with tetrachloro- I*a*, and tetrabromo-*o*-benzoquinone I*b*, and 4-tri-

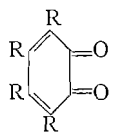

I*a*; R = Cl
I*b*; R = Br

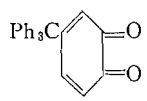

II

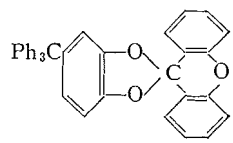

IV

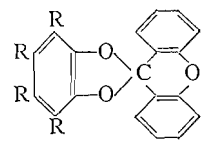

III*a*; R = Cl
III*b*; R = Br

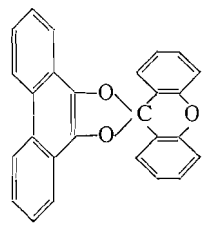

V

phenylmethyl-1,2-benzoquinone II, to give, in excellent yield, the analogous products III*a*, III*b*, and IV, respectively, according to scheme A (2).

[1]*Manuscript received December 9, 1958.*
Contribution from the Organic Chemistry Department, National Research Centre, Dokki, Cairo, Egypt, U.A.R.

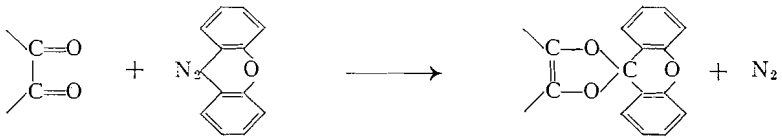

A

The constitution of the products formed is based on the following facts:

(*a*) they are colorless or nearly so,

(*b*) they are readily hydrolyzed by acids, and

(*c*) III*a* and III*b* can be obtained by the reaction between 9,9-dichloroxanthene and the corresponding tetrahalogenocatechol according to scheme B.

The identity of the products obtained from reactions A and B is established by analysis, melting point and mixed melting point, and by their identical infrared spectra.

R = Cl or Br

B

It is observed that all the cyclic ethers obtained in this reaction are readily and quantitatively cleaved by hydrochloric acid in dioxane; for example, when III*a* or III*b* are boiled for 30 minutes with a mixture of concentrated hydrochloric acid and dioxane (1:5), xanthone and the corresponding catechol are obtained in quantitative yield. In the case of V, xanthone and phenanthraquinone are obtained after air oxidation. This is rather remarkable as the analogous products VI and VII obtained by the action of diphenyl- (3) and diphenylene-diazomethane (2) on tetrachloro-*o*-quinone are not similarly attacked. This may be explained by assuming that the proton attacks first the ethereal

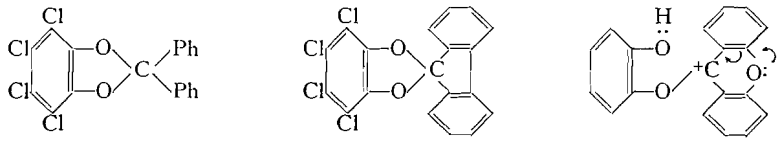

VI VII VIII

oxygen atom and this is followed by the heterolytic fission of the C–O bond, to give a carbonium ion which is stabilized by resonance with the unshared electron pair of the oxygen of the xanthyl residue (4) (cf. VIII for III*a*). However, it is observed that these products are not appreciably cleaved by concentrated sulphuric acid at room temperature, as usually happens with the other methylenedioxy derivatives obtained by the action of diazomethanes on *o*-quinones. This may be attributed to the formation of an oxonium salt which is rather stable under the conditions of the experiment, a property generally shown by xanthenes.

The Direct Preparation of Halogenated Cyclic Ethers from Certain Thiones

Several reactions of thioketones have been described (5), but it is believed that nothing is mentioned about the action of *o*-quinones on cyclic thiones. It is found that the high potential quinones, tetrachloro- and tetrabromo-*o*-benzoquinone, react with xanthione

Can. J. Chem. Downloaded from www.nrcresearchpress.com by 196.1.178.254 on 09/04/12
For personal use only.

in dry benzene at room temperature with the formation of III*a* and III*b*, respectively, according to scheme C.

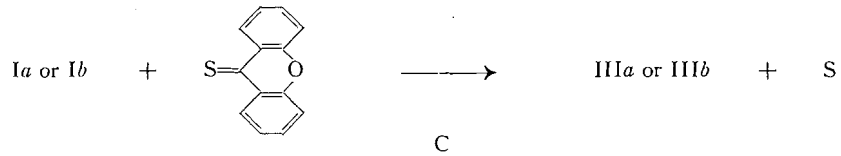

C

However, the reaction is slow at room temperature, but is remarkably accelerated by heat. Thus when I*a* and xanthione are boiled in dry benzene for 1 hour, an 80% yield of III*a* is obtained, whereas, at room temperature, a 75% yield is reached only after 5 days. The reaction of I*b* with xanthione is affected by temperature in almost a similar way. III*a* can also be obtained by heating I*a* and xanthione without a solvent in a carbon dioxide atmosphere.

The identity of the compounds obtained in this reaction with those obtained by either reaction A or B is established by analysis, melting point and mixed melting point, and by similar infrared spectra.

It is found also that tetrachloro-*o*-quinone reacts similarly with coumarin-2-thione in boiling benzene with the formation of a 1,2-benzopyran derivative IX in good yield. The constitution of the product obtained is based on analogy, as well as on the fact that it is colorless and easily hydrolyzed by hydrochloric acid in dioxane to coumarin and tetrachlorocatechol. The absence of sulphur and of the characteristic frequency band of a *d*-lactone (1755 cm^{-1} nujol) (6) shown by coumarin excludes structure X of a 1,4-dioxane, which may result by the addition of the quinone to the double bond of the lactone ring. Addition of *o*-quinones to the double bond in ethylenes, benzofurans, isocoumarins, etc. is well known. However, it is reported that coumarin fails to react with phenathraquinone (7).

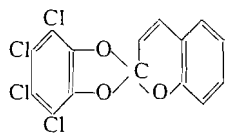

IX

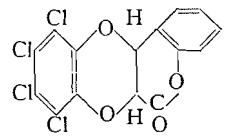

X

The Molluscicidal Activity of Halogenated Cyclic Ethers

Halawani and Latif (8) found that halogenated *o*-benzoquinone and benzodioxole derivatives are toxic to *Biomphalaria boissi* snails—the intermediate host of *Schistosoma mansoni* in Egypt—in high dilutions. The toxicity of the above-mentioned halogenated cyclic ethers has been investigated. It is found that IX kills the snails in concentrations as low as 20 p.p.m. in water during a 24-hour-exposure period to the drug followed by a 72-hour-observation period in fresh water. III*a*, III*b*, IV, and V could not be tested, since they are almost insoluble in the solvents usually used for the test. Details of these experiments will be published separately.

EXPERIMENTAL

Melting points are not corrected. Microanalyses were carried out by A. Bernhardt, Germany.

Preparation of 9-diazoxanthene.—Xanthone hydrazone (4 g), mercuric oxide (7 g), and anhydrous sodium sulphate (1 g) were ground together in a dry mortar, and transferred

Can. J. Chem. Downloaded from www.nrcresearchpress.com by 196.1.178.254 on 09/04/12
For personal use only.

to a dry 100-ml R.B.F. guarded with a calcium chloride tube and containing 50 ml dry ether. One milliliter of a freshly prepared saturated solution of potassium hydroxide in absolute alcohol was added while shaking the mixture for 2 minutes at room temperature (20° C), then stirring for 30 minutes at 10°. The green ethereal solution was filtered off and the residue washed with dry ether. The combined ethereal solutions were concentrated under reduced pressure in the cold, when green crystals of 9-diazoxanthene separated, and filtered. The compound is soluble in most organic solvents in the cold, melts with decomposition at about 60° C (red melt), and turns orange-red when left at room temperature for a few hours.

Xanthone ketazine.—9-Diazoxanthene (0.1 g) was left in a watch glass exposed to air for 24 hours. The orange-red crystals formed were washed with ether and recrystallized from benzene when xanthone ketazine was obtained (m.p. 285° not depressed when admixed with an authentic sample prepared according to Schönberg and Stolpp (9)).

Reaction of tetrachloro-o-quinone with 9-diazoxanthene.—Tetrachloro-*o*-quinone (10) (0.8 g) was added slowly to a dry ethereal solution of diazoxanthene (1.1 g). A vigorous reaction with evolution of gas took place and after a few seconds a yellowish crystalline solid separated. On recrystallization from xylene 9,9-(tetrachloro-*o*-phenylenedioxy) xanthene III*a* separated in colorless crystals,* m.p. 286° (yield almost quantitative). It is difficultly soluble in cold alcohol, acetone, or benzene. Calc. for $C_{19}H_8O_3Cl_4$: C, 53.52; H, 1.87; Cl, 33.3. Found: C, 53.43; H, 2.17; Cl, 32.87%. It dissolves in concentrated sulphuric acid with a deep yellow color and when the solution was kept overnight at room temperature (20° C) and then poured into ice, above 75% of the substance was recovered unchanged.

Hydrolysis of IIIa.—To a solution of concentrated hydrochloric acid (sp. gr. 1.19) (1 ml) in dioxane (5 ml) was added III*a* (0.15 g), the mixture boiled for 30 minutes, and then left to cool. It was then poured into ice and the colorless precipitate formed was filtered, dried, and dissolved in the least amount of boiling methyl alcohol and left to cool. The colorless crystals separated proved to be xanthone (m.p. and mixed m.p. 174°). On addition of dilute hydrochloric acid to the mother liquor a white precipitate was formed. After filtering, drying, and refluxing with acetic anhydride for 30 minutes, the mixture was left to cool, and then poured into ice. The solid formed was recrystallized from methyl alcohol and proved to be the diacetyl derivative of tetrachlorocatechol (melting point and mixed melting point). Using methyl alcohol instead of dioxane, hydrolysis was partial and about 50% of the substance was recovered unchanged.

Reaction between tetrachlorocatechol and 9,9-dichloroxanthene.—Tetrachlorocatechol (0.1 mole) and 9,9-dichloroxanthene (0.1 mole from thionyl chloride and xanthone) were heated together in a test tube protected from moisture at 150° (oil bath) for 1 hour. The reaction mixture was left to cool, washed several times with acetone, and recrystallized from xylene when III*a* was obtained (m.p. 286° undepressed when admixed with an authentic sample prepared by the action of diazoxanthene on tetrachloro-*o*-quinone) (yield about 80%). The product and the authentic sample have identical infrared spectra. Calc. for $C_{19}H_8O_3Cl_4$: C, 53.52; H, 1.87; Cl, 33.3. Found: C, 54.32; H, 2.08; Cl, 32.6%.

Reaction of tetrabromo-o-quinone with 9-diazoxanthene.—Tetrabromo-*o*-quinone (11) (1 g) was added to a crude ethereal solution of diazoxanthene (from 2 g of xanthone hydrazone). A vigorous reaction took place with evolution of gas and the immediate separation of a yellowish deposit. This was filtered off, washed with boiling acetone,

**In a parallel experiment carried out using the crude ethereal solution obtained from the oxidation of xanthone hydrazone as described above, instead of diazoxanthene crystals, the same yield of IIIa was obtained. In the coming experiments this crude ethereal solution will be generally used.*

Can. J. Chem. Downloaded from www.nrcresearchpress.com by 196.1.178.254 on 09/04/12
For personal use only.

Can. J. Chem. Downloaded from www.nrcresearchpress.com by 196.1.178.254 on 09/04/12
For personal use only.

and recrystallized from xylene (using charcoal) when 9,9-(tetrabromo-*o*-phenylenedioxy) xanthene III*b* separated in almost colorless crystals, m.p. 280° (decomp.). Yield almost quantitative. The compound dissolves in concentrated sulphuric acid with a yellow color and most of it was recovered unchanged when poured into ice as in the case of the chloro-analogue. Calc. for $C_{19}H_8O_3Br_4$: C, 37.74; H, 1.32; Br, 52.98. Found: C, 37.68; H, 1.75; Br, 53.24%. When III*b* was boiled with concentrated hydrochloric acid – dioxane as in the case of the chloro-analogue, xanthone and tetrabromocatechol (identified as its diacetyl derivative) were obtained.

Reaction of tetrabromocatechol with 9,9-dichloroxanthene.—Tetrabromocatechol (4 g) and dichloroxanthene (from 2 g of xanthone and thionyl chloride) were dissolved in dry benzene (20 ml), and a few drops of piperidine added. The mixture was refluxed for 3 hours, concentrated, and left to cool. The solid separated was washed with boiling acetone and recrystallized from xylene (using charcoal) when III*b* was obtained in colorless crystals, m.p. 280° (decomp.). Its infrared spectrum is identical with that of the product obtained from diazoxanthene.

Reaction of 4-triphenylmethyl-1,2-benzoquinone with 9-diazoxanthene.—The quinone (12) (1.2 g) was added in very small portions to a crude ethereal solution of diazoxanthene (from 2 g of xanthone hydrazone). A new portion was only added when the reaction from a previous addition had subsided. After all the quinone was added, the reaction mixture was left for 2 hours at room temperature with occasional shaking. The color of the quinone disappeared and a colorless solid was formed. This was recrystallized from xylene when 9,9-(4-triphenylmethyl-*o*-phenylenedioxy) xanthene IV was obtained in colorless crystals, m.p. 264° (yield about 60%). Calc. for $C_{38}H_{26}O_3$: C, 86.01; H, 4.94. Found: C, 86.45; H, 5.28%.

Reaction of phenanthraquinone with 9-diazoxanthene.—The quinone (0.5 g) was added in very small portions to a crude ethereal solution of diazoxanthene (from 2 g xanthone hydrazone) with mild stirring at 37°. When all the quinone had been added, stirring of the reaction mixture was continued for 2 hours. The yellowish solid formed was washed several times with boiling acetone and recrystallized from xylene when (V) was obtained in almost colorless crystals, m.p. 298°. It is insoluble in most organic solvents and gives a deep yellow color with concentrated sulphuric acid. Calc. for $C_{27}H_{16}O_3$: C, 83.5; H, 4.15. Found: C, 84.1; H, 4.35%. V (0.2 g) was refluxed with hydrochloric acid – dioxane solution as above, the reaction mixture was left to cool and then poured into ice. The yellowish solid formed was filtered off using the pump and suction was allowed to continue for 1 hour to facilitate air oxidation. The product was then pressed on a porous plate and recrystallized from benzene. The resulting orange crystals proved to be phenanthraquinone (melting point and mixed melting point). It gives olive green color with concentrated sulphuric acid.

Reaction of tetrachloro-o-quinone with xanthione.—Method "a". The quinone (2.4 g) and xanthione (2.2 g) in dry benzene (15 ml) were refluxed together for 1 hour on the water bath. The red color of the quinone disappeared and the solution became dark brown; it was left to cool. The crystalline solid formed was filtered off and the mother liquor concentrated to obtain another crop of crystalline solid.* The whole crude reaction product was washed with acetone several times and recrystallized from xylene in colorless crystals which proved to be III*a* (m.p. 286° undepressed when admixed with an authentic sample prepared in the above experiments. The product and the authentic sample have

**When the mother liquor was evaporated to dryness under reduced pressure and the residue heated in a carbon dioxide atmosphere at 150° (oil bath) for 1 hour, sulphur collected on the cooler parts of the reaction vessel. Xanthione is stable when heated alone under the same conditions.*

identical infrared spectra.). Yield above 80%. Calc. for $C_{19}H_8O_3Cl_4$: C, 53.52; H, 1.87; Cl, 33.3. Found: C, 53.51; H, 2.07; Cl, 33.04%. *Method "b"*. Tetrachloro-*o*-quinone (0.61 g) and xanthione (0.5 g) were mixed together in a dry test tube protected from moisture. The mixture was heated for 2 hours at 200° (oil bath) while passing carbon dioxide, and then left to cool. The solid mass obtained was ground well, washed with acetone, and recrystallized from xylene (using charcoal) when III*a* was obtained in colorless crystals, m.p. 286° (yield about 50%).

Reaction of tetrabromo-o-quinone with xanthione.—The quinone (1 g) and xanthione (0.5 g) in dry benzene (20 ml) were refluxed together for 1 hour on the water bath. The reaction mixture became dark brown, and yellowish crystals separated. These were filtered off, and the filtrate concentrated and left to cool when another crop of crystals was obtained. The combined crude product was washed with boiling acetone and recrystallized from xylene (using charcoal) when III*b* was obtained in almost colorless crystals, m.p. 280° (decomp.). Its infrared spectrum is identical with that of the products obtained by reactions A and B.

When the quinone and the thione in dry benzene were kept at room temperature in a carbon dioxide atmosphere for 3 days about 75% yield of III*b* separated.

Reaction of tetrachloro-o-quinone with coumarin-2-thione.—The quinone (1.2 g) and the thione (0.8 g) in dry benzene (10 ml) were refluxed for 3 hours. The reaction mixture was filtered while hot, concentrated, and left to cool. The crystals that separated were washed with acetone and recrystallized from benzene when 2,2-(tetrachloro-*o*-phenylenedioxy) benzopyran IX was obtained in colorless crystals, m.p. 214° C. It is soluble in hot acetone, benzene, and chloroform, difficultly soluble in alcohol. Calc. for $C_{15}H_6O_3Cl_4$: C, 47.87; H, 1.59; Cl, 37.7. Found: C, 47.88; H, 1.64; Cl, 37.38%.

Hydrolysis of IX.—IX (0.2 g) was refluxed with a solution of hydrochloric acid in dioxane as usual. The reaction mixture was then poured into ice and filtered and the filtrate left to concentrate slowly at room temperature. The separated colorless crystals were recrystallized from petroleum ether (30–50°) and proved to be coumarin (melting point and mixed melting point). Diluted hydrochloric acid was added to the mother liquor and the white solid obtained was filtered off, dried, and refluxed with acetic anhydride when the diacetyl derivative of tetrachlorocatechol was obtained.

ACKNOWLEDGMENTS

The authors wish to express their appreciation to Dr. E. Bickert, Max-Planck Institut fur Biochemie, München, and to Professor F. G. Baddar, Faculty of Science, A'in Schams University, Cairo, for the determination of infrared spectra.

REFERENCES

1. Adams, R. Organic reactions. Vol. VIII. John Wiley & Sons, Inc., New York. p. 364.
2. Schönberg, A. and Latif, N. J. Chem. Soc. 446 (1952). Horner, L. and Lingnau, E. Ann. **573**, 30 (1951).
3. Schönberg, A., Awad, W. I., and Latif, N. J. Chem. Soc. 1368 (1951).
4. Alexander, E. R. Principles of ionic organic reactions. John Wiley & Sons, Inc., New York. 1950. p. 214.
5. Campaign, E. Chem. Revs. **39**, 1 (1946). Schönberg, A. *In* Houben-Weyl. Methoden Der Organishen Chemie. IX. George Thieme Verlag, Stuttgart. 1955. p. 704.
6. Bellamy, L. J. The infrared spectra of complex molecules. John Wiley & Sons, Inc., New York. 1954. p. 153.
7. Schönberg, A. and Mustafa, A. Chem. Revs. **40**, 181 (1947). Schönberg, A. *et al.* J. Chem. Soc. 1364 (1951).
8. Halawani, A. and Latif, N. J. Egypt. Med. Assoc. **37**, 957 (1954).
9. Schönberg, A. and Stolpp, Th. Ber. **63**, 3102 (1930).
10. Jackson, C. L. and MacLaurin, R. D. Am. Chem. J. **37**, 7 (1907).
11. Zincke, Th. Ber. **20**, 1777 (1887).
12. Zincke, Th. and Wugk, E. Ann. **363**, 284 (1908).

Can. J. Chem. Downloaded from www.nrcresearchpress.com by 196.1.178.254 on 09/04/12
For personal use only.

INFRARED SPECTRA OF ORGANO-PHOSPHORUS COMPOUNDS

III. PHOSPHORAMIDATES, PHOSPHORAMIDOTHIONATES, AND RELATED COMPOUNDS[1, 2]

R. A. McIvor and C. E. Hubley

ABSTRACT

Examination of a number of new phosphorus compounds has provided additional confirmation for many of the group frequencies reported previously. In certain cases additional information has been obtained on the effect of environment on the band positions, and some previously unassigned bands have been attributed to specific structures. In particular, bands previously assigned to P(S), P(S)X, C—H deformation, P—O—(C), P—C, P—S—H, P—S(P), P—N, C—S(P), and C—N(P) are discussed.

Can. J. Chem. Downloaded from www.nrcresearchpress.com by 196.1.178.254 on 09/04/12
For personal use only.

INTRODUCTION

In Parts I and II of this series, characteristic bands were given for various functional groups of organo-phosphorus compounds, in particular P—O—P, P→S, P—O—(C), and P—Cl. A number of new compounds containing P—N bonds has been examined, in addition to those previously discussed, which makes further and revised group frequency assignments possible.

These assignments are simply empirical, based on observations of compounds containing particular atomic groupings. No fundamental studies have been carried out by us to test which particular parts, if any, of the large groupings are responsible for the bands. Thus, for example, while it is always possible to say that compounds containing an isopropoxy group attached to phosphorus will exhibit a triplet of bands between 1100 and 1200 cm^{-1}, the assignment of these bands to specific vibrations has not been attempted and for convenience they have been grouped under R—O—(P), since many other authors in this field have considered at least one band in this region as being a C—O—(P) absorption. Where groups of bands occur in a specific region for many closely related compounds, it is often convenient to discuss all such bands together. More recently, however (1, 2), the strong 1000–1100 cm^{-1} band has been postulated as the C—O—(P) band, while bands near 830 cm^{-1} are considered to be P—O—(C) stretching bands. This C—O assignment seems more in line with the absorption of this grouping in non-phosphorus compounds, but not consistent with the assignment of a 940 cm^{-1} band to P—O(P) and P—O—(H). It should also be noted that the 1000–1100 cm^{-1} band occurs at progressively lower frequencies in the series MeOP, EtOP, *i*-PrOP, whereas the band attributed to C—O stretching in alcohols shifts to higher frequencies with increasing substitution (3).

EXPERIMENTAL

The preparation of some of these compounds is described elsewhere (4, 5). A Baird double-beam recording spectrophotometer was used for all spectra. Band positions are cited to the nearest 0.01 μ for sharp bands and to the nearest 0.05 μ for broad bands. All but three samples, which are marked in the tables, were run as thin films. The solid samples were run as KBr pellets. These were prepared by mixing one part of the sample with 100 parts of KBr in an agate mortar for approximately 1 minute, and then pressing at 75,000–90,000 lb/in.^{2} in a Hilger & Watts evacuated die.

[1]*Manuscript received December 17, 1958.*
Contribution from the Defence Research Chemical Laboratories, Ottawa, Canada.
Issued as D.R.C.L. Report No. 258A.
[2]*Part II, Can. J. Chem.* **36**, *820 (1958).*

Can. J. Chem. Downloaded from www.nrcresearchpress.com by 196.1.178.254 on 09/04/12
For personal use only.

RESULTS AND DISCUSSION

(*a*) P→S

An additional 43 compounds containing P→S have been examined. These compounds have bands in the 740–830 cm^{-1} region with various intensities. However, since the corresponding P→O compounds frequently have similar bands in this region, our earlier assignment of this band to P→S seems less certain. The spectra of most P→S compounds containing *n*-PrO do not have bands in the 770–830 cm^{-1} region, but have one in the 715–770 cm^{-1} region.

A number of compounds of types I and II have been examined both here and in other laboratories (5, 6, 7). I can be converted to II by heating, and the progress of the isomerization can be followed in the infrared. During the isomerization of these compounds there

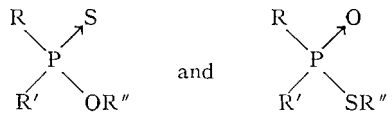

I II

is usually a disappearance of one or more bands in the 740–830 cm^{-1} region with concomitant appearance of P—O and C—S—P bands (see section (*k*) below). Thus compound I (R = Me_2N; R′ = *n*-PrO; R″ = CH_2—CH_2NEt_2) has a very weak band at 790 cm^{-1} which disappears on conversion to the corresponding II isomer.

Since this work was completed a paper by Hooge and Christen (8) has assigned the band discussed in section (*b*) to the P→S link, and related its frequency to the mass of the remaining substituents. This seems to be an excellent suggestion, and consistent with all our observations. The nature of the 740–830 cm^{-1} band remains in doubt.

The 740–830 cm^{-1} band is particularly intense in compounds containing MeO and EtO groups, which usually have an additional strong band in this region, attributed recently to P—O—(C) stretching (1, 2). Such intensification has been frequently noted when two bands associated with the same small group of atoms have closely related frequencies. In this case, however, the effect may be one of simple summation of two superimposed bands. *n*-Propyl and *n*-butyl phosphorus esters have no strong band in this region.

Several additional observations have been made concerning this absorption. As a general rule acids absorb below 770 cm^{-1}. Dichlorides absorb at lower frequencies than the corresponding full esters for any one ester group. For the ester groups absorption usually occurs in this region in the following order of increasing frequency: *n*-propyl > isopropyl > ethyl > methyl. Compounds containing alkyl groups attached to P absorb at lower frequencies than the corresponding phosphates, but since many methylphosphonates have a sharp band near 794 cm^{-1} and a broad one near 758 cm^{-1} the association of either of these with the P→S grouping is dubious. Bands believed to be characteristic are listed in Table I.

(*b*) (O)—P—Cl, (O)—P—S—
↓ ↓
S S

Many new compounds have been examined containing these groupings which are particularly useful for analytical purposes. Further to the information previously reported (7), more examples of phosphonate half-esters are available, all of which absorb

Can. J. Chem. Downloaded from www.nrcresearchpress.com by 196.1.178.254 on 09/04/12
For personal use only.

strongly in the 630 to 641 cm^{-1} region, and two dimethylphosphoramidochloridothionates which absorb near 633 cm^{-1} in contrast with simple phosphorothionates and thionyl dichlorides which absorb near 666 cm^{-1}. Phosphonothionic acids and phosphorothionic acids also absorb in this region but with somewhat lesser intensity. As these compounds probably have the P(S)OH structure primarily, this band (which occurs near 606 cm^{-1} in the phosphonothioic acids) is probably of this type rather than a P—S—(H) stretching as suggested previously (7). Two compounds which possibly contain P—S—P groupings have a doublet at 658 cm^{-1} and 630 cm^{-1}, the components of which retain the same relative intensities during purification procedures. Compounds containing the structure $P(S)CF_3$ also exhibit this band. This band has recently been assigned by Hooge and Christen (8) to the P→S stretching vibration.

Observed bands are listed in Table I.

TABLE I

S
↑
P→S and P—X Bands

Compounds	Band positions in cm^{-1}		Compounds	Band positions in cm^{-1}	
Methyl phosphorodichloridothionate	830	725 704	β-Fluoroethyl methylphosphonochloridothionate	797	634
Ethyl phosphorodichloridothionate	799	728 699	Ethyl dimethylphosphoramidothioic acid	758	662?
n-Propyl phosphorodichloridothionate	758?*	730 694	Ethyl methylphosphonothioic acid	790	602
i-Propyl phosphorodichloridothionate	775	722 685	Dimethyl phosphorothioic acid	810	Not examined
n-Butyl phosphorodichloridothionate	800? 746?	714 694	Ethyl trifluoromethylphosphonothioic acid	794	Not examined
O,O-Dimethyl phosphorodithioic acid	780?	658	β-Fluoropropyl methylphosphonothioic acid	793	606
O,O-Diethyl phosphorodithioic acid	767	658	γ-Fluoropropyl methylphosphonothioic acid	790	606
O,O-Di-*n*-propyl phosphorodithioic acid	741	658	Diethyl dimethylphosphoramidothionate	813	
O,O-Di-*i*-propyl phosphorodithioic acid	757	649	Diethyl diethylphosphoramidothionate	806	
O,O-Di-*n*-butyl phosphorodithioic acid	730	658	Diethyl diisopropylphosphoramidothionate	763	
Sodium O,O-diethyl phosphorodithioate (P)†	775? 769? 746?	730? 694?	Di-*n*-propyl diethylphosphoramidothionate	790	
Triethylammonium diethyl phosphorothioate	766	649	Di-*n*-propyl diisopropylphosphoramidothionate	787 wk 735?	
Triethylammonium di-*n*-propyl phosphorothioate	746	656	Diisopropyl diethylphosphoramidothionate	787	
Triethylammonium di-*n*-butyl phosphorothioate	735?	658	Diisopropyl diisopropylphosphoramidothionate	755	
Triethylammonium ethyl methylphosphonothioate	758?		Di-*n*-butyl diethylphosphoramidothionate	806	
Sodium ethyl trifluoromethylphosphonothioate (P)	754	<625	Di-*n*-butyl diisopropylphosphoramidothionate	787	
Ethylphosphonothionyl dichloride	779	645	Diethyl ethylphosphonothionate	794	
Dimethylphosphoramidothionyl dichloride	766	671	Diethyl methylphosphonothionate	800	
Diethylphosphoramidothionyl dichloride	790? 741	662	OOOO-Tetraethyl trithiopyrophosphate	830 797?	660 631
Diethyl dimethylphosphoramidochloridothionate	806 752?	633	OOOO-Tetraisopropyl trithiopyrophosphate	778 800?	658 629
n-Propyl dimethylphosphoramidochloridothionate	769	633	O-Ethyl-O-β-diethylaminoethyl dimethylphosphoramidothionate	806	
Ethyl methylphosphonochloridothionate	794	629	O-Propyl-O-β-diethylaminoethyl dimethylphosphoramidothionate	794	
γ-Fluoropropyl methylphosphonochloridothionate	794	637	Diethyl trifluoromethylphosphonate	830	649
Cyclohexyl methylphosphonochloridothionate	797	641			

*In this and subsequent tables the symbol ? indicates that the cited band is beyond the normal range for this grouping, or is one of several possible choices. wk = Weak, sh = shoulder, br = broad.

†(P) indicates the spectrum was run as KBr pellet.

(*c*) C—H *Deformation*

Some additional observations have been made in this region, and the characteristic band positions are listed in Table II.

TABLE II
C—H Deformations

Group	Observed bands in cm^{-1}	
Et—P(O)	1460 1399	
Et—P(S)	1453 1389 sh	1381
Me_2N—P	1481 sh 1453	1412 v wk
Et_2N—P(S)	1453 1389 sh	1381
i-Pr_2N—P(S)	1462 1406	1389 sh or wk 1366

Me_2N—P(O) and Me_2N—P(S) absorb at the same positions but in P(S) compounds the 1481 cm^{-1} shoulder is only about one-half the intensity of the neighboring band, whereas in P(O) compounds it is of approximately equal intensity.

(*d*) P—O—(H) *and* P—O—(C) (*900 to 1100 cm*$^{-1}$)

1. EtO *Bands.*—In an earlier paper (7) the occurrence of two bands was mentioned, one between 1100 and 1000 cm^{-1} and another between 1000 and 900 cm^{-1}. Since most Et-containing compounds without EtO—P groupings have weak bands between 1000 and 900 cm^{-1} thought to be associated with a C—C vibration, it is postulated that in P—O—Et compounds this second band is intensified by interaction with the vibration giving rise to the strong absorption between 1000 and 1100 cm^{-1}. P—OEt groups and possibly P—N—C—C groups are the only ones examined that invariably give a band or shoulder in the 962–980 cm^{-1} region for pentavalent compounds and near 917 cm^{-1} for trivalent P compounds. β-Fluoroethoxy phosphorus compounds (two examples) have bands in this region.

2. Acidic compounds.—POOH and PSOH acids and salts generally have a band near 943 cm^{-1} which may be a symmetric P—O stretching for the ions and a P—O(H) stretching in the acids.

(*e*) P—C (*Alkyl*) *and* C—C (*Alkyl*) *Bands*

Examination of more than a dozen new compounds has confirmed the earlier assignments for P—methyl and P—ethyl bands (7). In addition, all compounds containing isopropyl groups (either P—O—*i*-Pr or P—N—*i*-Pr) also have a medium intensity band near 893 cm^{-1} for O—*i*-Pr and near 877 cm^{-1} for P—N—*i*-Pr compounds. P—N—*i*-Pr compounds also have two medium intensity bands in the 625–666 cm^{-1} region. These bands are listed in Table III.

(*f*) P—S—(H)

A number of new examples have been obtained and are listed with other dithioic acids in Table IV.

(*g*) P—S—(P)

Two compounds, although not analytically pure, obtained by reacting dicyclohexylcarbodiimide with diethyl and diisopropyl phosphorodithioic acids had spectra which were different from those of the starting material and the corresponding OOS-trialkyl

Can. J. Chem. Downloaded from www.nrcresearchpress.com by 196.1.178.254 on 09/04/12
For personal use only.

TABLE III
P—C and C—C Bands

Compound	Band positions in cm^{-1}	
Tetraisopropyl monothionopyrophosphate	889	
Diisopropyl dimethylmonothionopyrophosphate	893 (P—Me?)	
Di(isopropyl methylphosphonothionyl) methylphosphonothioate	870	
Isopropyl methylphosphonochloridothionate	897	
Diisopropyl methylphosphonothionate	909?	
	893 sh	
Diisopropyl phosphorochloridothionate	893	
O,O-Diisopropyl phosphorodithioic acid	893	
Sodium diisopropyl phosphate (P)	885	
Isopropyl phosphorodichloridothionate	894	
Diisopropyl diethylphosphoramidothionate	889	
Diisopropyl phosphorofluoridate	901	
Diisopropyl diisopropylphosphoramidothionate	890	664 wk
	877	652 wk
Diethyl diisopropylphosphoramidothionate	881	662
		654 sh
Di-*n*-butyl diisopropylphosphoramidothionate	893?	664
	881	654
Di-*n*-propyl diisopropylphosphoramidothionate	885	664
		654 sh

TABLE IV
P—S—(H) Bands

Compound	Band positions in cm^{-1}
O,O–Dimethyl phosphorodithioic acid	526
	493
O,O-Diethyl phosphorodithioic acid	541
	508
O,O-Di-*n*-propyl phosphorodithioic acid	543
	518
O,O-Di-*i*-propyl phosphorodithioic acid	548
	518
O,O-Di-*n*-butyl phosphorodithioic acid	546
	526

TABLE V
P—Cl Bands

Compound	Band positions in cm^{-1}	
Methylphosphonous dichloride	562 br	
	472 br	
n-Propyl phosphorothionyl dichloride	552?	500 sh
	529?	485
n-Butyl phosphorothionyl dichloride	552	488 wk
	529	
i-Propyl phosphorothionyl dichloride	549	500 sh
	526	488 sh
Ethyl dimethylphosphoramidochloridothionate		515
		465
Dimethylphosphoramidothionyl dichloride		513 br
		461
β-Fluoroethyl methylphosphonochloridothionate		505
		465
Ethyl methylphosphonochloridothionate		510
		469
γ-Fluoropropyl methylphosphonochloridothionate		510
		467

Can. J. Chem. Downloaded from www.nrcresearchpress.com by 196.1.178.254 on 09/04/12
For personal use only.

phosphorodithioate (which cannot be completely excluded as a by-product however) and contained weak diffuse bands near 488 cm^{-1}.

(*h*) P—Cl

New observations recorded in Table V confirm previous assignments.

(*i*) P—N—(C)

Holmstedt and Larsson (9) and Mayhood and Harvey (10) note two bands in P—N-containing compounds, one between 1006 and 989 cm^{-1} and the other between 730 and 704 cm^{-1}. They attribute the latter to P—N stretching, and Larsson (11) has shown that on hydrolysis of the P—N bond the intensity of this band is inversely proportional to the extent of hydrolysis. Mayhood and Harvey noted additional characteristic bands in the 2849–2747 cm^{-1} region for Me_2N and in the 2905–2890 cm^{-1} region for Et_2N compounds.

From electronegativity and mass considerations it is estimated that the P—N—(C) stretching vibration should be very close to the P—O(C) stretching bands. If the 1050 cm^{-1} bands can be attributed to the latter, the band near 1000 cm^{-1} would be the more likely candidate for the P—N stretching vibration. The "absence" of this band in Et_2N compounds noted by Mayhood and Harvey may be due to a perturbation by the 962 cm^{-1} C—C band mentioned earlier, and the P—N stretching is possibly contained in the 1030 cm^{-1} P—O or the 962 cm^{-1} C—C band. Et_2N—P compounds generally have three bands in this region near 1025, 952, and 926 cm^{-1}. In the P—N isopropyl compounds the band near 1000 cm^{-1} is again present.

Since the question of assignments of P—O—(C) and C—O—(P) stretching bands is still controversial, analogies based on these bands are not too useful for assigning P—N—(C) and C—N—(P) bands. The strong band near 943 cm^{-1} in all compounds containing a P—O—P link is consistent with the assignment of P—O—(C) to the 1000–1100 cm^{-1} band. This band is usually not symmetrical, and it is conceivable that the C—O—(P) band should also absorb in this region, particularly since the P—O—(C) band possesses a certain amount of "double bond character".

The 714–770 cm^{-1} band in our experience is mainly associated with N-dimethylamino groups, where it appears in the range 704–725 cm^{-1} for $Me_2NP(O)$ compounds and near 740–769 cm^{-1} for $Me_2NP(S)$ compounds. In $Et_2NP(S)$ compounds a band appears at 714–719 cm^{-1} and in *i*-Pr_2N—P(S) compounds the doublet mentioned previously in section (*e*) is found. From Mayhood and Harvey's work, it appears that the low frequency band is shifted bathochromically when C—P or additional Me_2NP links are present. Band positions are listed in Table VI.

(*j*) C—N—(P)

Bands attributed to groups containing this structure are very strong and tend to hide neighboring bands arising from similar R—O—alkyl structures. The position of these bands suggests that they arise from similar vibration modes as those for P—O—C compounds, previously discussed under R—O—(C) stretching.

1. Me_2N.—Mayhood and Harvey (10) mention bands at 1282–1316, 1190, and 1064 cm^{-1} as characteristic for C—N in Me_2N. All of these bands occur in regions where other absorptions take place so have to be interpreted with caution. Our examples are in agreement with these assignments.

2. Et_2N *and* *i*-Pr_2N.—Et_2N—P compounds all have intense bands near 1210 and 1175 cm^{-1} which are characteristic for this grouping. *i*-Pr_2N—P Compounds have a set

Can. J. Chem. Downloaded from www.nrcresearchpress.com by 196.1.178.254 on 09/04/12
For personal use only.

of five medium intensity bands near 1200, 1183, 1160, 1139 sh, and 1129 cm^{-1}, in addition to those mentioned for other regions of the spectrum. All compounds examined with these two groups contained P(S) as well, so there is a possibility of shifts in the spectra of the corresponding P(O) compounds.

TABLE VI
P—N and C—S—(P) Bands

Compound	Band positions in cm^{-1}	
Diethyl phosphoroamidate	1020?	
	962?	
Diethyl dimethylphosphoroamidate	990	700
Diethyl dimethylphosphoramidothionate	990	748
Ethyl dimethylphosphoramidochloridate	995	725
Ethyl dimethylphosphoramidochloridothionate	990	752
Propyl dimethylphosphoramidochloridothionate	985	766?
Dimethylphosphoramidothionyl dichloride	980	766?
Dimethylphosphoramidyl dichloride	990	725
O-Ethyl S-β-diethylaminoethyl dimethylphosphoramidothioate	985	714
		694
O-Ethyl O-β-diethylaminoethyl dimethylphosphoramidothioate	990	749
O-*n*-Propyl S-β-diethylaminoethyl dimethylphosphoramidothioate	985	714
		697
O-*n*-Propyl O-β-diethylaminoethyl dimethylphosphoramidothioate	990	752
Diethylphosphoramidothionyl dichloride	1026	917
	952	741?
O,O-Diethyl diethylphosphoramidothioate	1026	917 wk
	948	741
O,O-Di-*n*-propyl diethylphosphoramidothioate	1026	924
	948	719?
O,O-Diisopropyl diethylphosphoramidothioate	975?	924
	948 sh	714
O,O-Di-*n*-butyl diethylphosphoramidothioate	975?	924
	952	719
O,O-Diethyl diisopropylphosphoramidothioate	1000	
O,O-Di-*n*-propyl diisopropylphosphoramidothioate	995?	
O,O-Diisopropyl diisopropylphosphoramidothioate	971	
O,O-Di-*n*-butyl diisopropylphosphoramidothioate	995	

(*k*) C—S—(P)

In an earlier paper (7) we attributed a weak band near 641 cm^{-1} to the C—S(P) vibration. Further studies with compounds of type III have indicated that the intensity of a weak band between 667 and 714 cm^{-1} decreases with rupture of the P—S link. This band is tentatively assigned to the P—S—C grouping. It is weak or absent in compounds

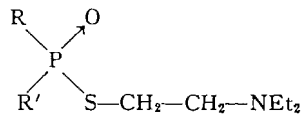

III

where R = R′ = alkoxy, but stronger where R = alkyl and R′ = alkoxy (6), and very prominent where R = Me_2N and R′ = alkoxy (5). Of the phosphonates, Et—P compounds give the strongest band. This may result from either addition to the Et—P and $Me_2NP(O)$ bands or an interaction as described in section (*a*) with concomitant increase in intensity. The formation of a very strong doublet at 714 and 694 cm^{-1} [P—S(C) and $Me_2NP(O)$] (Table VI) with disappearance of bands near 820 and 746 cm^{-1} [P(S) and Me_2N—P(S)] is the most characteristic spectral change during the isomerism IV→V.

Can. J. Chem. Downloaded from www.nrcresearchpress.com by 196.1.178.254 on 09/04/12
For personal use only.

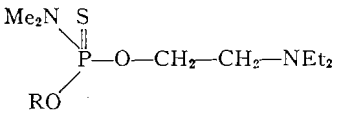

IV

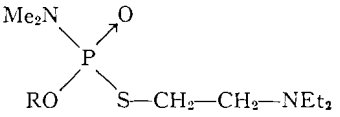

V

The principal group frequencies derived from the tables are summarized in Table VII.

TABLE VII

Group	Frequency range	Intensity
P→S	740–830	Variable
O—P(S)Cl_2	485–488	Weak
	526–529	Strong
	549–552	Strong
	715–730	Strong
	685–705	Strong
$O_2P(S)S$	650–660	Strong
$NP(S)Cl_2$	660–670	Strong
	460–470	Strong
NP(S)Cl and OCP(S)Cl	505–515	Wk to medium
	630–640	Strong
OCP(S)OH	600–610	Strong
PO *i*-Pr	885–900	Wk to medium
PN *i*-Pr	652–654	Medium
	662–664	Medium
	875–885	Wk to medium
	980–990	Strong
	1129	Medium
	1139 sh	
	1160	
	1183	
	1200	
P(O)NMe_2	700–725	Strong
	980–990	Strong
P(S)NMe_2	745–755	Strong
	980–990	Strong
$PNEt_2$	715–740	Medium to strong
	915–925	Medium to strong
	948–950	Medium to strong
	1025	Strong
	1210	Medium
	1175	Medium
P(S)SH	525–550	Medium
	495–525	Medium

ACKNOWLEDGMENTS

The technical assistance of Mr. A. A. Grey of these laboratories in recording the infrared spectra is gratefully acknowledged. The authors are also indebted to Dr. H. J. Bernstein and Mr. L. C. Thomas for helpful comments, and to Dr. K. F. Jennings for samples of the fluorine-containing compounds.

REFERENCES

1. Maarsen, J. W., Smit, M. C., and Matze, J. Rec. trav. chim. **76**, 713 (1957).
2. Mortimer, F. S. Spectrochim. Acta, **9**, 270 (1957).
3. Bellamy, L. J. The infra-red spectra of complex molecules. John Wiley & Sons, Inc., New York. 1954. p. 94.
4. McIvor, R. A., McCarthy, G. D., and Grant, G. A. Can. J. Chem. **34**, 1819 (1956).
5. McIvor, R. A., Miller, R. K., and Grant, G. A. Report in preparation.
6. Tammelin, L. E. Acta Chem. Scand. **11**, 1738 (1957).
7. McIvor, R. A., Grant, G. A., and Hubley, C. E. Can. J. Chem. **34**, 1611 (1956).
8. Hooge, F. N. and Christen, P. J. Rec. trav. chim. **77**, 911 (1958).
9. Holmstedt, B. and Larsson, L. Acta Chem. Scand. **5**, 1179 (1951).
10. Mayhood, J. E. and Harvey, R. B. Can. J. Chem. **33**, 1552 (1955).
11. Larsson, L. Acta Chem. Scand. **6**, 1470 (1952).

Can. J. Chem. Downloaded from www.nrcresearchpress.com by 196.1.178.254 on 09/04/12
For personal use only.

Can. J. Chem. Downloaded from www.nrcresearchpress.com by 196.1.178.254 on 09/04/12
For personal use only.

THE SYNTHESIS OF 2-KETOCYCLOHEXYLSUCCINIC ACID AND RELATED SUBSTANCES

IV. STUDIES ON SOME *CIS*- AND *TRANS*-FUSED γ-LACTONES[1]

E. H. Charlesworth, H. J. Campbell, and D. L. Stachiw

ABSTRACT

The *cis* and *trans* lactones of cyclohexanol-2-acetic acid and cyclohexanol-2-α-propionic acid have been subjected to alkaline hydrolysis to determine the relative ease of ring opening. In addition, a new synthesis by way of a Reformatsky reaction followed by dehydration and cyclization has been shown to yield the *cis* lactone. Finally, the first overtone band of the fundamental carbonyl stretching frequency has been identified.

INTRODUCTION

The reaction of sodiomalonic ester with cyclohexene oxide, followed by hydrolysis and decarboxylation, affords the *trans* lactone (I*a*) (1). An isomeric *cis* lactone (I*b*) is obtained by catalytic reduction of cyclohexanone-2-acetic acid (2).

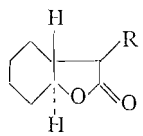

I*a*, R = H
II*a*, R = CH_3

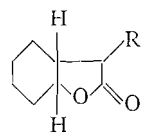

I*b*, R = H
II*b*, R = CH_3

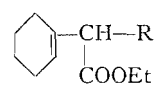

III*a*, R = H
III*b*, R = CH_3

This investigation has shown the latter compound to be identical with the lactone obtained by the acid-catalyzed cyclization of ethyl cyclohexene-1-acetate (III*a*). This substance was produced by a Reformatsky reaction between cyclohexanone and ethyl bromoacetate, followed by dehydration of the β-hydroxy ester with phosphorus pentoxide.

The *cis* and *trans* configurations shown for the lactones follow from (*a*) the known stereochemistry of the reaction of nucleophiles with epoxides (3); (*b*) the known stereochemistry of the catalytic reduction of substituted cyclohexanones (4); and (*c*) the greater ease with which (I*b*) is formed from the corresponding hydroxy acid (2, cf. 5). Similar arguments apply to the lactones (II*a*) (6) and (II*b*), available by essentially the same reactions.

Further support for these configurational assignments is given by studies on the rates of ring opening by alkali. In both cases the isomer assigned the *trans* configuration hydrolyzed more rapidly, as shown in Fig. 1. This was to be expected in view of the less stable *trans* configuration. The greater stability of the methyl-substituted ring is in accordance with the many analogous cases in the literature (7).

All lactones showed peak absorption at about 2.8 μ in the infrared region accessible to the Beckmann D.K. recording spectrophotometer. This is undoubtedly the first overtone (8) of the powerful carbonyl adsorption band observed for (I*a*) and (I*b*) at 5.62 μ and 5.70 μ respectively, by Brewster and Kucera (9). As in the case of the fundamental frequencies, a wavelength shift was observed for these 2.8 μ bands indicating the more strained condition of the *trans* form. Rasmussen and Brattain (10) noticed absorption in this 2.8 μ region by several lactones, but suggested that it might be due to traces of

[1]*Manuscript received January 9, 1959.*
Contribution from the Department of Chemistry, University of Manitoba, Winnipeg, Manitoba.

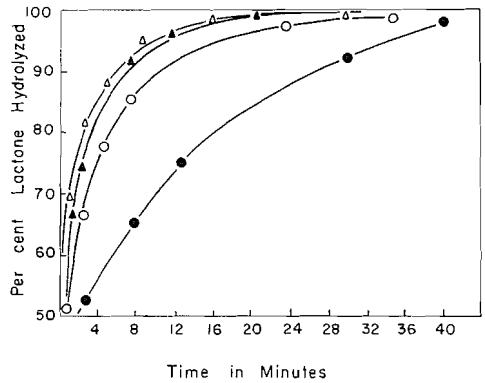

FIG. 1. Rates of hydrolysis of *cis–trans* γ-lactones by .0765 *N* NaOH at 20° C (△—I*a*, ○—I*b*, ▲—II*a*, ●—II*b*).

water. However, in a re-examination of the spectrum of γ-valerolactone in carbon tetrachloride, we find the peak at 2.8 μ to be unaffected by drying the solvent, while a less prominent band at 2.71 μ diminishes (but could not be eliminated altogether). The latter band is undoubtedly due to water, which in carbon tetrachloride alone causes absorption at 2.696 μ; the shift to longer wavelength in the presence of lactones is evidence of hydrogen-bonding between the two molecules.

TABLE I

Some physical constants and derivatives of the lactones

	γ-Lactone of cyclohexanol-2-acetic acid			γ-Lactone of cyclohexanol-2-α-propionic acid		
		cis I*b*			*cis* II*b*	
	trans (I*a*) Method (1)	Method (2)	Reformatsky method	*trans* (II*a*) Method (6)	Reformatsky method	Method (2)
B.p.(per mm)	131–132°/12	129–130°/13	128–128.5°/10	125–128°/10	131–134°/11	132–135°/13
D_4^{20}	1.0859	1.0921	1.0923	1.0519	1.0589	—
n_D^{20}	1.4752	1.4784	1.4773	1.4719	1.4756	1.4751
Position of C=O overtone in millimicrons	2802	2808	2808	2812	2819	2819
M.p. of hydroxy acid	105–106°	—	—	110–111°	—	—
M.p. of hydrazide	167–167.5°	140–141°	140–141°	191–192°	136–137°	—
M.p. of N-benzylamide	141–142°*	97–98°	97–98°*	—	—	—

*Brewster and Kucera (9).

EXPERIMENTAL

Reformatsky Reactions and Subsequent Procedure

Ethyl 1-Cyclohexanolacetate

Cyclohexanone (49 g), zinc filings (33 g), and dry benzene (200 ml) were placed in a 1-l. three-necked flask equipped with a stirrer and condenser. The mixture was heated to boiling and the addition of ethyl bromoacetate (167 g) containing a trace of iodine was begun. At the first sign of reaction, heating was discontinued, the stirrer started, and the addition continued at such a rate that moderate refluxing was maintained. Following addition of the ester, refluxing was continued for a further half hour. No attempt should

Can. J. Chem. Downloaded from www.nrcresearchpress.com by 196.1.178.254 on 09/04/12
For personal use only.

be made to dissolve the unreacted zinc by prolonged heating, as this decreases the yield and quality of the product. A little ice was added to the cooled solution and with the stirrer running, cold sulphuric acid (250 ml, 6 *N*) was added slowly. After half an hour the benzene layer was separated, washed with water and sodium carbonate solution, and dried over calcium chloride. The benzene was removed and the ethyl 1-cyclohexanolacetate (66.5 g, 72% yield) distilled *in vacuo* at 108–118° C (11 mm). Auwers and Ellinger (11) report 141° C (33 mm) and Charlesworth *et al.* (12) 143–146° C (37 mm).

Ethyl Cyclohexene-1-acetate (III*a*)

Ethyl 1-cyclohexanolacetate (50 g) was dissolved in dry benzene (150 ml), and phosphorus pentoxide (40 g) was added to the solution. It was refluxed on the water bath for 3 hours and allowed to cool. The benzene solution was decanted, the porous residue rinsed twice with benzene (25-ml portions), and the washings combined with the main solution. The benzene was removed and the unsaturated ester (30.5 g, 68%) was distilled at 93–95° C (10 mm). Wallach (13) reports 100° C (12 mm).

Lactone of cis-Cyclohexanol-2-acetic Acid (I*b*)

Ethyl cyclohexene-1-acetate (10 g) and sulphuric acid (60 ml, 50% by volume) were heated on the water bath under reflux with stirring for 1 hour. By this time the oily layer had disappeared and the solution was yellow-orange in color. Only a small amount of polymeric material clinging to the walls of the flask was observed. The solution was allowed to cool, water (150 ml) was added, and the solution heated to boiling. It was cooled and extracted four times with ether (50-ml portions). The ethereal extract was washed with saturated salt solution, sodium carbonate solution, and thoroughly dried with anhydrous potassium carbonate. The ether was removed and distillation gave a colorless liquid (5.0 g, 60% yield) with a characteristic smell, which boiled at 129–130° C (13 mm); $n_D^{20} = 1.4784$. It was neutral to litmus and solidified at −20° C into long white needles. The original ethyl cyclohexene-1-acetate does not solidify at −80° C. Found: C, 69.1; H, 8.72%. Calc. for the lactone $C_8H_{12}O_2$: C, 68.6; H, 8.57%.

When crude cyclohexene-1-acetic acid (m.p. 34–36° C) prepared by the hydrolysis of the ester according to the directions of Wallach (13) was treated with 50% sulphuric acid according to the above directions, there was considerably more darkening than with the ester. Acidification of the sodium carbonate washings showed that very little unlactonized acid was left. Distillation gave the lactone in slightly smaller yield (43%), but with the same properties and constants as before. Found: C, 68.8; H, 8.97%. There was more dark viscous distillation residue than in the previous case.

When ethyl 1-cyclohexanolacetate was lactonized according to the above conditions there was considerably more dark polymeric material produced than in the previous cases. The lactone was isolable as before, but only in about 26% yield.

Ethyl α-(1-Cyclohexanol) Propionate

This ester was obtained in 76% yield in a Reformatsky reaction with ethyl α-bromopropionate. It distilled at 115–119° C (11 mm). Wallach reported 125–127° C (12 mm).

Ethyl Cyclohexene-1-α-propionate (III*b*)

This was obtained in 70% yield by dehydration of the previous ester. It boiled at 97–99° C (11 mm) or 68–70° C (1 mm).

Lactone of cis-Cyclohexanol-2-α-propionic Acid (II*b*)

This was obtained in 66% yield by cyclization of the previous unsaturated ester with

Can. J. Chem. Downloaded from www.nrcresearchpress.com by 196.1.178.254 on 09/04/12
For personal use only.

50% sulphuric acid. It boiled at 131–134° C (11 mm); $n_D^{20} = 1.4756$. It did not solidify at −20° C. Found: C, 69.5; H, 9.24%. Calc. for $C_9H_{14}O_2$: C, 70.0; H, 9.15%.

γ-Lactones (Other than by Reformatsky Method)

The preparation of the *cis* lactones by the Reformatsky method (D. L. Stachiw) is described above. These samples were compared with *cis* lactones prepared from the corresponding keto acids by the catalytic hydrogenation method of Newman and Van der Werf (2) and found to be identical in all respects (Table I).

The *trans* lactones (I*a* and II*a*) were prepared by the method of Coffey (1) and of McRae, Charlesworth, and Alexander (6) from cyclohexene oxide.

γ-Lactone of trans-Cyclohexanol-2-methylmalonic Acid

This product was isolated prior to the decarboxylation step in the cyclohexene oxide synthesis of the *trans* lactone (II*a*). After recrystallization from benzene–ligroin, white crystals were obtained melting at 151–152° C. Found: C, 60.98; H, 7.22%; neut. equiv., 198.0. Calc. for $C_{10}H_{14}O_4$: C, 60.6; H, 7.12%; neut. equiv., 198.2.

trans-Cyclohexanol-2-acetic Acid

Upon alkaline hydrolysis and acidification of the *trans* lactone (I*a*) Newman and Van der Werf (2) obtained an acid of m.p. 105–106° C. They claimed that their product was not identical with the 97–102° melting acid obtained by Coffey (1) by hydrogen chloride treatment of the potassium salt of (I*a*) because the latter had a tendency to relactonize in solution. The two methods were repeated and, although several recrystallizations failed to raise the melting point of Coffey's product, a mixed melting point revealed little or no depression. It seems more reasonable, therefore, to view the instability of this low-melting acid as resulting merely from its impurity.

trans-Cyclohexanol-2-α-propionic Acid

The method previously outlined (2) was used to obtain an acid which, after recrystallization from water, melted at 110° C. Found: C, 63.0; H, 9.16%; neut. equiv., 173.5. Calc. for $C_9H_{16}O_3$: C, 62.8; H, 9.31%; neut. equiv., 172.2.

Hydrazide Derivatives

The method described by Coffey (1) was used. A 10% solution of the lactone in alcohol was boiled with hydrazine (95%) for a few minutes. When the solution was cooled, the hydrazide separated.

The Reformatsky-produced lactone (III*a* → I*b*) and the Newman *cis* lactone (I*b*) both gave a hydrazide which, when recrystallized from benzene–ligroin, melted at 140–141° C. Found: N, 16.12%. Calc. for $C_8H_{16}O_2N_2$: N, 16.26%. This derivative was far more soluble in polar and non-polar solvents than the corresponding *trans* hydrazide, which melted at 167.5°, as reported by Coffey (1).

The *trans* lactone of cyclohexanol-2-α-propionic acid (II*a*) gave a derivative which, upon recrystallization from water, melted at 191–192° C. Found: N, 14.76%. Calc. for $C_9H_{18}O_2N_2$: N, 15.04%.

The Reformatsky-produced *cis* lactone (III*b* → II*b*) yielded a hydrazide which, after two recrystallizations from benzene–ligroin, melted at 136–137° C. Found: N, 15.15%. Calc. for $C_9H_{18}O_2N_2$: N, 15.04%.

N-Benzylamide Derivatives

The method used was that of Dermer and King (14). The Reformatsky-produced lactone (1 g) was refluxed with benzylamine (3 ml) in the presence of ammonium chloride

Can. J. Chem. Downloaded from www.nrcresearchpress.com by 196.1.178.254 on 09/04/12
For personal use only.

(1 g). The amide, when recrystallized from benzene–ligroin, melted at 97–98° C. Brewster and Kucera (9) reported an identical melting point for the N-benzylamide prepared from Newman's *cis* lactone.

Hydrolyses of γ-Lactones

The technique used was adapted from that described by Kendall, Osterberg, and MacKenzie (15) for the determination of the rate of ring opening of a γ-lactone. The lactone (1/200 mole) was dissolved in ethanol (25 ml) and introduced into a flask containing .0860 *N* sodium hydroxide (200 ml), stirred gently, and thermostated at 20° C. At periodic intervals, 20-ml portions were withdrawn and run into hydrochloric acid (20 ml, .0896 *N*). The excess acid was then titrated with standard alkali and the hydrolysis rate plotted (Fig. 1).

Infrared Spectra

A Beckmann D.K. recording spectrophotometer was used to investigate the small portion of the infrared region up to 2.85 μ. A pair of quartz cells were used whose 100% line did not deviate more than 3% on either side. The lactone samples were weighed directly into the cell and a measured amount of solvent carbon tetrachloride added.

REFERENCES

1. COFFEY, S. Rec. trav. chim. **42**, 387 (1923).
2. NEWMAN, M. S. and VAN DER WERF, C. A. J. Am. Chem. Soc. **67**, 233 (1945).
3. GRIGSBY, W. E., HIND, J., CHANLEY, J., and WESTHEIMER, F. H. J. Am. Chem. Soc. **64**, 2606 (1942).
4. SIEGEL, S. J. Am. Chem. Soc. **75**, 1317 (1953).
5. ANGYAL, S. J. and MACDONALD, C. G. J. Chem. Soc. 686 (1952).
6. MCRAE, J. A., CHARLESWORTH, E. H., and ALEXANDER, D. S. Can. J. Research, B, **21**, 1 (1943).
7. ELIEL, E. L. Steric effects in organic chemistry. *Edited by* M. S. Newman. John Wiley & Sons, Inc., New York. 1956. p. 119.
8. MARION, L., RAMSAY, D. A., and JONES, R. N. J. Am. Chem. Soc. **73**, 305 (1951).
9. BREWSTER, J. H. and KUCERA, C. H. J. Am. Chem. Soc. **77**, 4564 (1955).
10. RASMUSSEN, R. S. and BRATTAIN, R. R. J. Am. Chem. Soc. **71**, 1073 (1949).
11. AUWERS, K. and ELLINGER, P. Ann. **387**, 200 (1911).
12. CHARLESWORTH, E. H., MCRAE, J. A., and MACFARLANE, H. M. Can. J. Research, B, **21**, 55 (1943).
13. WALLACH, O. Ann. **343**, 51 (1905).
14. DERMER, O. C. and KING, J. J. Org. Chem. **8**, 168 (1943).
15. KENDALL, E. C., OSTERBERG, A. E., and MACKENZIE, B. F. J. Am. Chem. Soc. **48**, 1384 (1926).

Can. J. Chem. Downloaded from www.nrcresearchpress.com by 196.1.178.254 on 09/04/12
For personal use only.

Can. J. Chem. Downloaded from www.nrcresearchpress.com by 196.1.178.254 on 09/04/12
For personal use only.

ON THE COUPLING BETWEEN F^{19} AND H^1 NUCLEI IN *p*-FLUOROTOLUENE[1]

T. SCHAEFER

ABSTRACT

The proton and fluorine high resolution nuclear magnetic resonance spectra of *p*-fluorotoluene are discussed in terms of the case $A_2A_2'X$. The 4×4 submatrices are diagonalized in analytical form and therefore explicit values for all energy levels can be obtained. The spectra are consistent with $J_m^{HF} = J_o^{HF}$, which may be of theoretical interest.

INTRODUCTION

The analysis of high resolution nuclear magnetic resonance spectra normally yields values of the spin–spin coupling constants and of the relative chemical shifts of the resonating nuclei. However, in some special cases the distribution of lines in the spectrum depends only on the sum of the coupling constants. The simplest example of this occurs in the case ABB' (terminology of Bernstein, Pople, and Schneider (1)), in which two nuclei seeing a field H_B may be unequally coupled to a third nucleus seeing a field H_A. Richards and Schaefer (2) analyzed the proton spectrum of 2,5-dichloronitrobenzene and showed that the protons at position 3 and 4 have the same shift and that the line splittings are equal to the average of the coupling constant between protons 3 and 6 and between 4 and 6: $(1/2)(J_m^{HH}+J_p^{HH})$. It does not follow that $J_m^{HH} = J_p^{HH}$.

The proton and fluorine spectra of fluorobenzene indicate a negligible shift between the protons. From the shape of the spectra Baker (3) suggested that the H–F coupling constants are equal. In general the coupling decreases as the number of bonds between the nuclei increases. In view of the work of Gutowsky *et al.* (4) a more likely explanation appears to be that of Roux (5), who interprets the splittings as the average of the H–F coupling constants $(1/5)(2J_o^{HF}+2J_m^{HF}+J_p^{HF})$ without analyzing the spectrum. This interpretation contains the implicit assumption that the signs of the coupling constants are equal. This need not be so (4).

A glance at the proton and fluorine spectra of *p*-fluorotoluene (Fig. 1) would suggest that here also the splittings are given by the average of the H–F coupling constants $(1/2)(J_o^{HF}+J_m^{HF})$. It is the purpose of the present work to show from an explicit analysis that, in fact, $J_o^{HF} = J_m^{HF}$ for this compound. Such a result may be of theoretical interest.

EXPERIMENTAL

p-Fluorotoluene of known purity was kindly loaned by Dr. H. W. Thompson. The proton and fluorine spectra of the pure compound were taken on the high resolution spectrometer in Dr. R. E. Richards' laboratory at Oxford (6). The proton resonance occurs at 29.92000 Mc.p.s. The measurement of line separations is accurate to 1%, while the intensity measurements are good to about 10%.

RESULTS

The proton and fluorine spectra are shown in Fig. 1. The line separations are given in c.p.s. and the number of the lines is such as is convenient for the discussion below.

[1]*Manuscript received January 22, 1959.*
Contribution from the Department of Chemistry, University of Manitoba, Winnipeg, Manitoba.

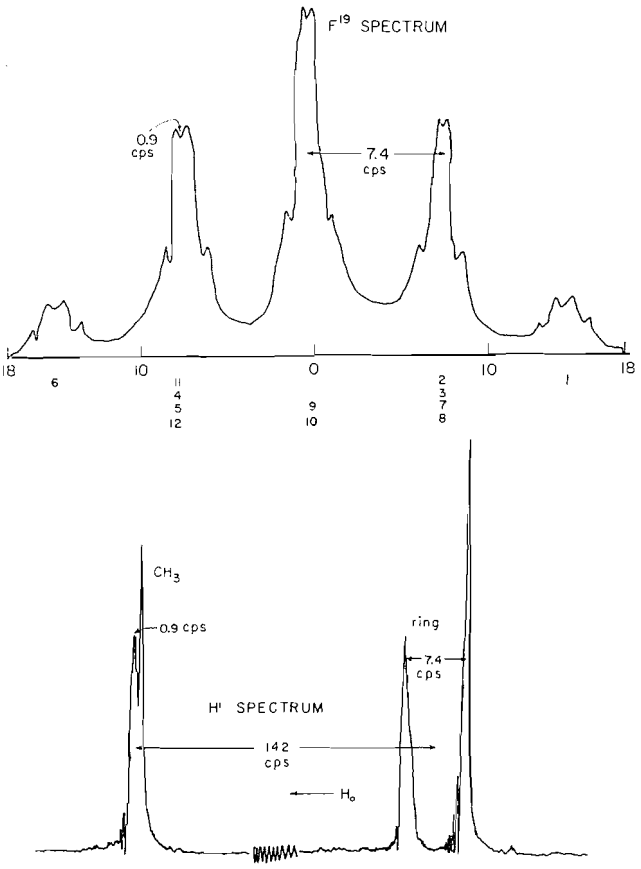

FIG. 1. Fluorine and proton resonance spectra of *p*-fluorotoluene.

DISCUSSION

The ring proton spectrum indicates a negligibly small chemical shift between the protons ortho and meta to the fluorine atom. The intensities of the two lines are the same within experimental error but one is slightly broader and this indicates a very small shift which can be neglected for our purposes. Protons in a methyl group situated ortho or para to a fluorine atom in the benzene ring are normally weakly coupled only to the fluorine nucleus but not to the ring protons (7). In the present instance this coupling is 0.9 c.p.s. Each line in the fluorine spectrum will therefore actually be a quadruplet, while the methyl resonance is a doublet. The splittings due to this coupling are the same in c.p.s., although, of course, not in gauss.

We are interested, however, primarily in the coupling between ring protons and the F^{19} nucleus. Information of a definite nature on this point requires the analysis of the case $A_2A_2'X$.

1. *Analysis of the Case* $A_2A_2'X$

We shall label the protons of the aromatic ring A and A' as shown in Fig. 2 and we shall call the fluorine atom X. The positions in the ring are numbered 1 to 5. Let the field experienced by nuclei A and A' be H_A such that in an applied field H_0, $H_A = H_0(1-\sigma_A)$, and similarly $H_x = H_0(1-\sigma_x)$. There are 10 coupling constants between these

Can. J. Chem. Downloaded from www.nrcresearchpress.com by 196.1.178.254 on 09/04/12
For personal use only.

nuclei and from symmetry we can write:

$$J_{14} = J_{23}, \quad J_{45} = J_{35};$$
$$J_{25} = J_{15}, \quad J_{24} = J_{13};$$
$$J_{12} = J_{34}.$$

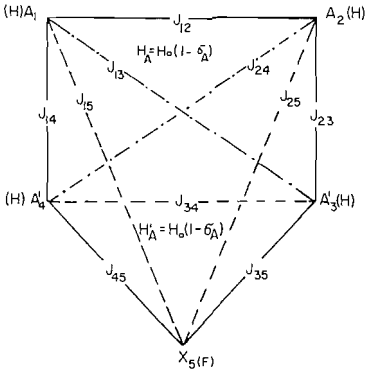

FIG. 2. Model for $A_2A_2'X$.

In the magnetic field H_0, a nucleus of magnetogyric ratio γ will have a nuclear resonance frequency ν_0, such that $\nu_0 = (\gamma/2\pi)H_0$. We shall use ν_0 for the resonance frequency for protons in the applied field and ν_0' for the frequency of the X nucleus resonance.

The initial wave functions are given in Table I together with the diagonal matrix elements. The off-diagonal elements are given in Table II. The matrix is similar to that given by Richards and Schaefer for the case A_2B_2X (8). It is given in full because reference will be made to specific matrix elements later on.

The initial choice of wave functions factorizes the secular determinant considerably. Further simplification arises from the condition that $\nu_0'\sigma_x$ is much larger than any of the spin coupling constants. This condition is of course amply fulfilled when X is fluorine. The determinant resolves itself into four 1×1, ten 2×2, and two 4×4 determinants.

Define positive quantities A, B, C, D, and angles θ, ϕ, ψ, γ, by:

$$\begin{aligned}
A\cos 2\theta &= (1/4)(J_{35}-J_{15}),\\
A\sin 2\theta &= (1/2)(J_{23}+J_{13});\\
B\cos 2\phi &= (1/4)(J_{15}-J_{35}),\\
B\sin 2\phi &= (1/2)(J_{23}+J_{13});\\
C\cos 2\psi &= (1/2)(J_{35}-J_{15}),\\
C\sin 2\psi &= (1/2)(J_{23}-J_{13});\\
D\cos 2\gamma &= (1/4)(J_{15}-J_{35}),\\
D\sin 2\gamma &= (1/2)(J_{13}-J_{23}).
\end{aligned} \qquad [1]$$

When the indicated orthogonal transformations are carried out, we obtain the stationary wave functions and energies given in Tables III and IV. Selection rules allow a maximum number of 110 transitions for the five nuclei. Of these, 46 are combination lines which, because of their weak intensity, will not be further considered. This leaves 16 transitions originating with the X nuclei, 12 of which can now be written down explicitly, whatever the value of the coupling constants. Similarly the A and A' nuclei give rise to 48 lines and 24 of these may now be explicitly tabulated. The 36 transitions are given in Tables V and VI. Later on we shall find explicit values for the other transitions for *p*-fluorotoluene in terms of the experimental parameters.

Can. J. Chem. Downloaded from www.nrcresearchpress.com by 196.1.178.254 on 09/04/12
For personal use only.

TABLE I

No.	Wave function (ψ)	Symmetry	Diagonal elements
1	$\alpha\alpha\alpha\alpha\alpha$	$(A_1)_{5/2}$	$(1/2)\nu_0\,(4-4\sigma_A)+(1/2)\nu_0'(1-\sigma_x)+(1/2)(J_{12}+J_{13}+J_{23}+J_{15}+J_{35})$
2	$\alpha\alpha\alpha\alpha\beta$	$(A_1)_{3/2}$	$(1/2)\nu_0\,(4-4\sigma_A)-(1/2)\nu_0'(1-\sigma_x)+(1/2)(J_{12}+J_{13}+J_{23}-J_{15}-J_{35})$
3	$\sqrt{(1/2)}(\alpha\alpha\alpha\beta\alpha+\alpha\alpha\beta\alpha\alpha)$		$(1/2)\nu_0\,(2-2\sigma_A)+(1/2)\nu_0'(1-\sigma_x)+(1/2)(J_{15}+J_{12})$
4	$\sqrt{(1/2)}(\beta\alpha\alpha\alpha\alpha+\alpha\beta\alpha\alpha\alpha)$		$(1/2)\nu_0\,(2-2\sigma_A)+(1/2)\nu_0'(1-\sigma_x)+(1/2)(J_{35}+J_{12})$
5	$\sqrt{(1/2)}(\alpha\alpha\alpha\beta\beta+\alpha\alpha\beta\alpha\beta)$	$(A_1)_{1/2}$	$(1/2)\nu_0\,(2-2\sigma_A)-(1/2)\nu_0'(1-\sigma_x)+(1/2)(-J_{15}+J_{12})$
6	$\sqrt{(1/2)}(\alpha\beta\alpha\alpha\beta+\beta\alpha\alpha\alpha\beta)$		$(1/2)\nu_0\,(2-2\sigma_A)-(1/2)\nu_0'(1-\sigma_x)+(1/2)(-J_{35}+J_{12})$
7	$\sqrt{(1/2)}(\alpha\beta\alpha\beta\alpha+\beta\alpha\beta\alpha\alpha)$		$(1/2)\nu_0'(1-\sigma_x)+(1/2)(J_{13}-J_{12}-J_{23})$
8	$\sqrt{(1/2)}(\beta\alpha\alpha\beta\alpha+\alpha\beta\beta\alpha\alpha)$		$(1/2)\nu_0'(1-\sigma_x)+(1/2)(-J_{13}-J_{12}+J_{23})$
9	$\alpha\alpha\beta\alpha\alpha$		$(1/2)\nu_0'(1-\sigma_x)+(1/2)(-J_{13}-J_{23}+J_{15}-J_{35}+J_{12})$
10	$\beta\beta\alpha\alpha\alpha$		$(1/2)\nu_0'(1-\sigma_x)+(1/2)(-J_{13}-J_{23}-J_{15}+J_{35}+J_{12})$
11	$\sqrt{(1/2)}(\alpha\beta\alpha\beta\beta+\beta\alpha\beta\alpha\beta)$	$(A_1)_{-1/2}$	$(1/2)\nu_0'(-1+\sigma_x)+(1/2)(J_{13}-J_{12}-J_{23})$
12	$\sqrt{(1/2)}(\beta\alpha\alpha\beta\beta+\alpha\beta\beta\alpha\beta)$		$(1/2)\nu_0'(-1+\sigma_x)+(1/2)(-J_{13}-J_{12}+J_{23})$
13	$\beta\beta\alpha\alpha\beta$		$(1/2)\nu_0'(1-\sigma_x)+(1/2)(J_{12}-J_{13}-J_{23}+J_{15}-J_{35})$
14	$\alpha\alpha\beta\beta\beta$		$(1/2)\nu_0'(1-\sigma_x)+(1/2)(J_{12}-J_{13}-J_{23}-J_{15}+J_{35})$
15	$\sqrt{(1/2)}(\beta\beta\beta\alpha\alpha+\beta\beta\alpha\beta\alpha)$		$(1/2)\nu_0\,(-2+2\sigma_A)+(1/2)\nu_0'(1-\sigma_x)+(1/2)(-J_{15}+J_{12})$
16	$\sqrt{(1/2)}(\alpha\beta\beta\beta\alpha+\beta\alpha\beta\beta\alpha)$		$(1/2)\nu_0\,(-2+2\sigma_A)+(1/2)\nu_0'(1-\sigma_x)+(1/2)(-J_{35}+J_{12})$
17	$\beta\beta\beta\beta\alpha$		$(1/2)\nu_0\,(-4+4\sigma_A)+(1/2)\nu_0'(1-\sigma_x)+(1/2)(J_{12}+J_{13}+J_{23}-J_{15}-J_{35})$
18	$\sqrt{(1/2)}(\beta\beta\beta\alpha\beta+\beta\beta\alpha\beta\beta)$	$(A_1)_{-3/2}$	$(1/2)\nu_0\,(-2+2\sigma_A)-(1/2)\nu_0'(1-\sigma_x)+(1/2)(J_{15}+J_{12})$
19	$(1/\sqrt{2})(\beta\alpha\beta\beta\beta+\alpha\beta\beta\beta\beta)$		$(1/2)\nu_0\,(-2+2\sigma_A)-(1/2)\nu_0'(1-\sigma_x)+(1/2)(J_{35}+J_{12})$
20	$\beta\beta\beta\beta\beta$	$(A_1)_{-5/2}$	$(1/2)\nu_0\,(-4+4\sigma_A)-(1/2)\nu_0'(1-\sigma_x)+(1/2)(J_{12}+J_{13}+J_{23}+J_{15}+J_{35})$
21	$(1/\sqrt{2})(\alpha\alpha\alpha\beta\alpha-\alpha\alpha\beta\alpha\alpha)$	$(B_2)_{3/2}$	$(1/2)\nu_0\,(2-2\sigma_A)+(1/2)\nu_0'(1-\sigma_x)+(1/2)(J_{15}-J_{12})$
22	$(1/\sqrt{2})(\beta\alpha\alpha\alpha\alpha-\alpha\beta\alpha\alpha\alpha)$		$(1/2)\nu_0\,(2-2\sigma_A)+(1/2)\nu_0'(1-\sigma_x)+(1/2)(J_{35}-J_{12})$
23	$(1/\sqrt{2})(\alpha\alpha\alpha\beta\beta-\alpha\alpha\beta\alpha\beta)$	$(B_2)_{1/2}$	$(1/2)\nu_0\,(2-2\sigma_A)-(1/2)\nu_0'(1-\sigma_x)+(1/2)(-J_{15}-J_{12})$
24	$(1/\sqrt{2})(\alpha\beta\alpha\alpha\beta-\beta\alpha\alpha\alpha\beta)$		$(1/2)\nu_0\,(2-2\sigma_A)-(1/2)\nu_0'(1-\sigma_x)+(1/2)(-J_{35}-J_{12})$
25	$(1/\sqrt{2})(\alpha\beta\alpha\beta\alpha-\beta\alpha\beta\alpha\alpha)$		$(1/2)\nu_0'(1-\sigma_x)+(1/2)(-J_{12}+J_{13}-J_{23})$
26	$(1/\sqrt{2})(\beta\alpha\alpha\beta\alpha-\alpha\beta\beta\alpha\alpha)$		$(1/2)\nu_0'(1-\sigma_x)+(1/2)(-J_{12}-J_{13}+J_{23})$
27	$(1/\sqrt{2})(\alpha\beta\alpha\beta\beta-\beta\alpha\beta\alpha\beta)$	$(B_2)_{-1/2}$	$(1/2)\nu_0'(-1+\sigma_x)+(1/2)(J_{13}-J_{12}-J_{23})$
28	$(1/\sqrt{2})(\beta\alpha\alpha\beta\beta-\alpha\beta\beta\alpha\beta)$		$(1/2)\nu_0'(-1+\sigma_x)+(1/2)(-J_{13}-J_{12}+J_{23})$
29	$(1/\sqrt{2})(\beta\beta\beta\alpha\alpha-\beta\beta\alpha\beta\alpha)$		$(1/2)\nu_0\,(-2+2\sigma_A)+(1/2)\nu_0'(1-\sigma_x)+(1/2)(-J_{12}-J_{15})$
30	$(1/\sqrt{2})(\alpha\beta\beta\beta\alpha-\beta\alpha\beta\beta\alpha)$		$(1/2)\nu_0\,(-2+2\sigma_A)+(1/2)\nu_0'(1-\sigma_x)+(1/2)(-J_{12}-J_{35})$
31	$(1/\sqrt{2})(\beta\beta\beta\alpha\beta-\beta\beta\alpha\beta\beta)$	$(B_2)_{-3/2}$	$(1/2)\nu_0\,(-2+2\sigma_A)-(1/2)\nu_0'(1-\sigma_x)+(1/2)(J_{15}-J_{12})$
32	$(1/\sqrt{2})(\beta\alpha\beta\beta\beta-\alpha\beta\beta\beta\beta)$		$(1/2)\nu_0\,(-2+2\sigma_A)-(1/2)\nu_0'(1-\sigma_x)+(1/2)(J_{35}-J_{12})$

TABLE II

Off-diagonal elements

$\mathfrak{H}_{23} = (1/\sqrt{2})J_{35}$, $\mathfrak{H}_{24} = (1/\sqrt{2})J_{15}$, $\mathfrak{H}_{34} = (1/2)(J_{23}+J_{13})$,
$\mathfrak{H}_{56} = (1/2)(J_{23}+J_{13})$, $\mathfrak{H}_{57} = \mathfrak{H}_{58} = (1/2)J_{15}$, $\mathfrak{H}_{59} = (1/\sqrt{2})J_{35}$,
$\mathfrak{H}_{5,10} = \mathfrak{H}_{69} = \mathfrak{H}_{9,10} = 0$, $\mathfrak{H}_{67} = \mathfrak{H}_{68} = (1/2)J_{35}$, $\mathfrak{H}_{6,10} = (1/\sqrt{2})J_{15}$,
$\mathfrak{H}_{7,8} = J_{12}$, $\mathfrak{H}_{7,9} = \mathfrak{H}_{7,10} = (1/\sqrt{2})J_{23}$, $\mathfrak{H}_{89} = \mathfrak{H}_{8,10} = (1/\sqrt{2})J_{13}$,
$\mathfrak{H}_{11,12} = J_{12}$, $\mathfrak{H}_{11,13} = \mathfrak{H}_{11,14} = (1/\sqrt{2})J_{23}$, $\mathfrak{H}_{11,15} = \mathfrak{H}_{12,15} = (1/2)J_{15}$,
$\mathfrak{H}_{11,16} = \mathfrak{H}_{12,16} = (1/2)J_{35}$, $\mathfrak{H}_{12,13} = \mathfrak{H}_{12,14} = (1/\sqrt{2})J_{13}$, $\mathfrak{H}_{13,14} = \mathfrak{H}_{13,16} = \mathfrak{H}_{14,15} = 0$,
$\mathfrak{H}_{13,15} = (1/\sqrt{2})J_{35}$, $\mathfrak{H}_{14,16} = (1/\sqrt{2})J_{15}$, $\mathfrak{H}_{15,16} = (1/2)(J_{23}+J_{13})$,
$\mathfrak{H}_{17,18} = (1/\sqrt{2})J_{35}$, $\mathfrak{H}_{17,19} = (1/\sqrt{2})J_{15}$, $\mathfrak{H}_{18,19} = (1/2)(J_{23}+J_{13})$,
$\mathfrak{H}_{21,22} = (1/2)(J_{23}-J_{13})$,
$\mathfrak{H}_{23,24} = (1/2)(J_{13}-J_{23})$, $\mathfrak{H}_{23,25} = \mathfrak{H}_{23,26} = (1/2)J_{15}$,
$\mathfrak{H}_{24,26} = -\mathfrak{H}_{24,25} = -(1/2)J_{35}$, $\mathfrak{H}_{25,26} = 0$,
$\mathfrak{H}_{27,28} = 0$, $\mathfrak{H}_{27,29} = \mathfrak{H}_{28,29} = -(1/2)J_{15}$,
$\mathfrak{H}_{27,30} = -\mathfrak{H}_{28,30} = -(1/2)J_{35}$, $\mathfrak{H}_{29,30} = (1/2)(J_{23}-J_{13})$,
$\mathfrak{H}_{31,32} = (1/2)(J_{13}-J_{23})$.

2. *The Spectrum of p-Fluorotoluene*

(a) *Fluorine Resonance Spectrum*

The fluorine spectrum has a 7.4-c.p.s. interval between the lines with an intensity distribution of 1:4:6:4:1 within experimental error. From the energies and intensities

Can. J. Chem. Downloaded from www.nrcresearchpress.com by 196.1.178.254 on 09/04/12
For personal use only.

Can. J. Chem. Downloaded from www.nrcresearchpress.com by 196.1.178.254 on 09/04/12
For personal use only.

TABLE III

Stationary wave functions and symmetry

3′	$(1/\sqrt{2})\{-\sin\theta(\beta\alpha\alpha\alpha+\alpha\beta\alpha\alpha)+\cos\theta(\alpha\alpha\alpha\beta+\alpha\alpha\beta\alpha)\}$	$(A_1)_{3/2}$
4′	$(1/\sqrt{2})\{\cos\theta(\beta\alpha\alpha\alpha+\alpha\beta\alpha\alpha)+\sin\theta(\alpha\alpha\alpha\beta+\alpha\alpha\beta\alpha)\}$	
5′	$(1/\sqrt{2})\{-\sin\phi(\alpha\beta\alpha\beta+\beta\alpha\alpha\beta)+\cos\phi(\alpha\alpha\beta\beta+\alpha\alpha\beta\alpha)\}$	$(A_1)_{1/2}$
6′	$(1/\sqrt{2})\{\cos\phi(\alpha\beta\alpha\beta+\beta\alpha\alpha\beta)+\sin\phi(\alpha\alpha\beta\beta+\alpha\alpha\beta\alpha)\}$	
15′	$(1/\sqrt{2})\{\cos\theta(\beta\beta\beta\alpha\alpha+\beta\beta\alpha\beta\alpha)+\sin\theta(\alpha\beta\beta\beta\alpha+\beta\alpha\beta\beta\alpha)\}$	$(A_1)_{-1/2}$
16′	$(1/\sqrt{2})\{-\sin\theta(\beta\beta\beta\alpha\alpha+\beta\beta\alpha\beta\alpha)+\cos\theta(\alpha\beta\beta\beta\alpha+\beta\alpha\beta\beta\alpha)\}$	
18′	$(1/\sqrt{2})\{\cos\phi(\beta\beta\beta\alpha\beta+\beta\beta\alpha\beta\beta)+\sin\phi(\beta\alpha\beta\beta\beta+\alpha\beta\beta\beta\beta)\}$	$(A_1)_{-3/2}$
19′	$(1/\sqrt{2})\{-\sin\phi(\beta\beta\beta\alpha\beta+\beta\beta\alpha\beta\beta)+\cos\phi(\beta\alpha\beta\beta\beta+\alpha\beta\beta\beta\beta)\}$	
21′	$(1/\sqrt{2})\{-\sin\psi(\beta\alpha\alpha\alpha-\alpha\beta\alpha\alpha)+\cos\psi(\alpha\alpha\alpha\beta-\alpha\alpha\beta\alpha)\}$	$(B_2)_{3/2}$
22′	$(1/\sqrt{2})\{\cos\psi(\beta\alpha\alpha\alpha-\alpha\beta\alpha\alpha)+\sin\psi(\alpha\alpha\alpha\beta-\alpha\alpha\beta\alpha)\}$	
23′	$(1/\sqrt{2})\{-\sin\gamma(\alpha\beta\alpha\beta-\beta\alpha\alpha\beta)+\cos\gamma(\alpha\alpha\beta\beta-\alpha\alpha\beta\alpha)\}$	$(B_2)_{1/2}$
24′	$(1/\sqrt{2})\{\cos\gamma(\alpha\beta\alpha\beta-\beta\alpha\alpha\beta)+\sin\gamma(\alpha\alpha\beta\beta-\alpha\alpha\beta\alpha)\}$	
29′	$(1/\sqrt{2})\{\cos\psi(\beta\beta\beta\alpha\alpha-\beta\beta\alpha\beta\alpha)+\sin\psi(\alpha\beta\beta\beta\alpha-\beta\alpha\beta\beta\alpha)\}$	$(B_2)_{-1/2}$
30′	$(1/\sqrt{2})\{-\sin\psi(\beta\beta\beta\alpha\alpha-\beta\beta\alpha\beta\alpha)+\cos\psi(\alpha\beta\beta\beta\alpha-\beta\alpha\beta\beta\alpha)\}$	
31′	$(1/\sqrt{2})\{\cos\gamma(\beta\beta\beta\alpha\beta-\beta\beta\alpha\beta\beta)+\sin\gamma(\beta\alpha\beta\beta\beta-\alpha\beta\beta\beta\beta)\}$	$(B_2)_{-3/2}$
32′	$(1/\sqrt{2})\{-\sin\gamma(\beta\beta\beta\alpha\beta-\beta\beta\alpha\beta\beta)+\cos\gamma(\beta\alpha\beta\beta\beta-\alpha\beta\beta\beta\beta)\}$	

TABLE IV

State	Energy
$3'$, $4'$ $(A_1)_{3/2}$	$\nu_0(1-\sigma_A)+(1/2)\nu_0'(1-\sigma_x)+(1/4)(2J_{12}+J_{15}+J_{35})-A$
	$\nu_0(1-\sigma_A)+(1/2)\nu_0'(1-\sigma_x)+(1/4)(2J_{12}+J_{15}+J_{35})+A$
$5'$, $6'$ $(A_1)_{1/2}$	$\nu_0(1-\sigma_A)-(1/2)\nu_0'(1-\sigma_x)+(1/4)(2J_{12}-J_{15}-J_{35})-B$
	$\nu_0(1-\sigma_A)-(1/2)\nu_0'(1-\sigma_x)+(1/4)(2J_{12}-J_{15}-J_{35})+B$
$15'$, $16'$ $(A_1)_{-1/2}$	$\nu_0(-1+\sigma_A)+(1/2)\nu_0'(1-\sigma_x)+(1/4)(2J_{12}-J_{15}-J_{35})+A$
	$\nu_0(-1+\sigma_A)+(1/2)\nu_0'(1-\sigma_x)+(1/4)(2J_{12}-J_{15}-J_{35})-A$
$18'$, $19'$ $(A_1)_{-3/2}$	$\nu_0(-1+\sigma_A)-(1/2)\nu_0'(1-\sigma_x)+(1/4)(2J_{12}+J_{15}+J_{35})+B$
	$\nu_0(-1+\sigma_A)-(1/2)\nu_0'(1-\sigma_x)+(1/4)(2J_{12}+J_{15}+J_{35})-B$
$21'$, $22'$ $(B_2)_{3/2}$	$\nu_0(1-\sigma_A)+(1/2)\nu_0'(1-\sigma_x)+(1/4)(-2J_{12}+J_{15}+J_{35})-C$
	$\nu_0(1-\sigma_A)+(1/2)\nu_0'(1-\sigma_x)+(1/4)(-2J_{12}+J_{15}+J_{35})+C$
$23'$, $24'$ $(B_2)_{1/2}$	$\nu_0(1-\sigma_A)-(1/2)\nu_0'(1-\sigma_x)+(1/4)(-2J_{12}-J_{15}-J_{35})-D$
	$\nu_0(1-\sigma_A)-(1/2)\nu_0'(1-\sigma_x)+(1/4)(-2J_{12}-J_{15}-J_{35})+D$
$29'$, $30'$ $(B_2)_{-1/2}$	$\nu_0(-1+\sigma_A)+(1/2)\nu_0'(1-\sigma_x)+(1/4)(-2J_{12}-J_{15}-J_{35})+C$
	$\nu_0(-1+\sigma_A)+(1/2)\nu_0'(1-\sigma_x)+(1/4)(-2J_{12}-J_{15}-J_{35})-C$
$31'$, $32'$ $(B_2)_{-3/2}$	$\nu_0(-1+\sigma_A)-(1/2)\nu_0'(1-\sigma_x)+(1/4)(-2J_{12}+J_{15}+J_{35})+D$
	$\nu_0(-1+\sigma_A)-(1/2)\nu_0'(1-\sigma_x)+(1/4)(-2J_{12}+J_{15}+J_{35})-D$

TABLE V

Transitions and intensities of nucleus X

Transition		Energy relative to $\nu_0'(1-\sigma_x)$	Relative intensity
1	$2\rightarrow 1$	$+J_{15}+J_{35}$	1
2	$5'\rightarrow 3'$	$+(1/2)(J_{15}+J_{35})-A+B$	$(\cos\theta\cos\phi+\sin\phi\sin\theta)^2$
3	$6'\rightarrow 4'$	$+(1/2)(J_{15}+J_{35})+A-B$	$(\cos\theta\cos\phi+\sin\phi\sin\theta)^2$
4	$18'\rightarrow 15'$	$-(1/2)(J_{15}+J_{35})+A-B$	$(\cos\theta\cos\phi+\sin\phi\sin\theta)^2$
5	$19'\rightarrow 16'$	$-(1/2)(J_{15}+J_{35})-A+B$	$(\cos\theta\cos\phi+\sin\phi\sin\theta)^2$
6	$20\rightarrow 17$	$-(J_{15}+J_{35})$	1
7	$23'\rightarrow 21'$	$+(1/2)(J_{15}+J_{35})-C+D$	$(\cos\gamma\cos\psi-\sin\gamma\sin\psi)^2$
8	$24'\rightarrow 22'$	$+(1/2)(J_{15}+J_{35})+C-D$	$(\cos\gamma\cos\psi-\sin\gamma\sin\psi)^2$
9	$27\rightarrow 15$	0	1
10	$28\rightarrow 26$	0	1
11	$31'\rightarrow 29'$	$-(1/2)(J_{15}+J_{35})+C-D$	$(\cos\gamma\cos\psi-\sin\gamma\sin\psi)^2$
12	$32'\rightarrow 30'$	$-(1/2)(J_{15}+J_{35})-C+D$	$(\cos\gamma\cos\psi-\sin\gamma\sin\psi)^2$

calculation in Table V and the definitions of A, B, C, D, and angles θ, ϕ, ψ, γ, it is clear

that the only conditions on them consistent with experiment are:

$$\begin{aligned} &A = B = (1/2)(J_{23}+J_{13}),\\ &C = D = (1/2)(J_{23}-J_{13}),\\ &\theta = \phi = \psi = -\gamma = 45°,\\ &J_{15} = J_{35} = \pm 7.4 \text{ c.p.s.} \end{aligned} \qquad [2]$$

TABLE VI

Transitions and intensities of A and A' nuclei

Transitions		Energy relative to $\nu_0(1-\sigma_A)$	Relative intensity
17	$4' \rightarrow 1$	$+(1/4)(2J_{13}+2J_{23}+J_{15}+J_{35})-A$	$2(1+\sin 2\theta)$
18	$17' \rightarrow 16'$	$+(1/4)(-2J_{13}-2J_{23}+J_{15}+J_{35})-A$	$2(1-\sin 2\theta)$
19	$20 \rightarrow 19'$	$+(1/4)(-2J_{13}-2J_{23}-J_{15}-J_{35})-B$	$2(1-\sin 2\phi)$
20	$6' \rightarrow 2$	$+(1/4)(2J_{13}+2J_{23}-J_{15}-J_{35})-B$	$2(1+\sin 2\phi)$
21	$25 \rightarrow 21'$	$+(1/4)(-2J_{13}+2J_{23}+J_{15}+J_{35})-C$	$1+\sin 2\psi$
22	$26 \rightarrow 21'$	$+(1/4)(+2J_{13}-2J_{23}+J_{15}+J_{35})-C$	$1-\sin 2\psi$
23	$27 \rightarrow 23'$	$+(1/4)(-2J_{13}+2J_{23}-J_{15}-J_{35})-D$	$1-\sin 2\gamma$
24	$28 \rightarrow 23'$	$+(1/4)(2J_{13}-2J_{23}-J_{15}-J_{35})-D$	$1+\sin 2\gamma$
25	$29' \rightarrow 26$	$+(1/4)(-2J_{13}+2J_{23}+J_{15}+J_{35})-C$	$1+\sin 2\psi$
26	$29' \rightarrow 25$	$+(1/4)(2J_{13}-2J_{23}+J_{15}+J_{35})-C$	$1-\sin 2\psi$
27	$31' \rightarrow 27$	$+(1/4)(2J_{13}-2J_{23}-J_{15}-J_{35})-D$	$1+\sin 2\gamma$
28	$31' \rightarrow 28$	$+(1/4)(-2J_{13}+2J_{23}-J_{15}-J_{35})-D$	$1-\sin 2\gamma$
29	$3' \rightarrow 1$	$+(1/4)(2J_{13}+2J_{23}+J_{15}+J_{35})+A$	$2(1-\sin 2\theta)$
30	$5' \rightarrow 2$	$+(1/4)(2J_{13}+2J_{23}-J_{15}-J_{35})+B$	$2(1-\sin 2\phi)$
31	$17' \rightarrow 15'$	$+(1/4)(-2J_{13}-2J_{23}+J_{15}+J_{35})+A$	$2(1+\sin 2\theta)$
32	$20 \rightarrow 18'$	$+(1/4)(-2J_{13}-2J_{23}-J_{15}-J_{35})+B$	$2(1+\sin 2\phi)$
33	$25 \rightarrow 22'$	$+(1/4)(-2J_{13}+2J_{23}+J_{15}+J_{35})+C$	$1-\sin 2\psi$
34	$26 \rightarrow 22'$	$+(1/4)(+2J_{13}-2J_{23}+J_{15}+J_{35})+C$	$1+\sin 2\psi$
35	$27 \rightarrow 24'$	$+(1/4)(-2J_{13}+2J_{23}-J_{15}-J_{35})+D$	$1+\sin 2\gamma$
36	$28 \rightarrow 24'$	$+(1/4)(2J_{13}-2J_{23}-J_{15}-J_{35})+D$	$1-\sin 2\gamma$
37	$30' \rightarrow 25$	$+(1/4)(2J_{13}-2J_{23}+J_{15}+J_{35})+C$	$1+\sin 2\psi$
38	$30' \rightarrow 26$	$+(1/4)(-2J_{13}+2J_{23}+J_{15}+J_{35})+C$	$1-\sin 2\psi$
39	$32' \rightarrow 28$	$+(1/4)(-2J_{13}+2J_{32}-J_{15}-J_{35})+D$	$1+\sin 2\gamma$
40	$32' \rightarrow 27$	$+(1/4)(2J_{13}-2J_{23}-J_{15}-J_{35})+D$	$1-\sin 2\gamma$

A possible assignment is shown in Fig. 1. The four transitions involving the F^{19} nucleus which have not yet been calculated will have relative intensities of one and zero energies relative to $\nu_0'(1-\sigma_x)$ for consistency. This remains to be shown.

(*b*) *Proton Resonance Spectrum*

Of the 24 transitions in Table VI, 12 are of nonzero intensity under the conditions [2]. It is to be noted that these have energies $\pm(1/4)(J_{15}+J_{35})$ relative to $\nu_0(1-\sigma_A)$.

In order to calculate energies and intensities for the other 24 proton lines and the 4 flourine lines, the two 4×4 determinants must be solved. This is usually done numerically and would involve an assumption as to the values of J_{23}, J_{13}, and J_{12}. However, a solution in analytical form can be achieved in this case on the assumption that $J_{13} \leqslant 0.5$ c.p.s. and that J_{13} can therefore be neglected. This assumption is in accord with the same result obtained in a variety of other aromatic compounds. Orthogonal matrices can then be found which will diagonalize the two 4×4 matrices. The energies and corresponding eigenfunctions found in this way are given in Table VII. In Table VII quantities a, b, c, d, are related to experimental parameters by:

$$\begin{aligned} a &= J_{12}(-J_{23}+K)^{-1}, & b &= J_{23}(-J_{12}+K)^{-1};\\ c &= J_{12}(J_{23}+K)^{-1}, & d &= J_{23}(J_{12}+K)^{-1}; \end{aligned}$$

with

$$K = (J_{12}^2+J_{23}^2-J_{12}J_{23})^{\frac{1}{2}}.$$

Can. J. Chem. Downloaded from www.nrcresearchpress.com by 196.1.178.254 on 09/04/12
For personal use only.

Remembering that $\sin 2\phi = \sin 2\theta = 1$ and noting that $(1-c-d) = (1-ac-bd) = 0$, the only transitions with nonzero intensity involving these eight states are given in Table VIII. None of these depend on J_{12}. Counting of intensities in Tables V–VIII shows that the distribution and intensity of the predicted lines tallies with experiment. The predicted spectrum depends explicitly on the assumption that $J_o^{HF} = J_m^{HF}$.

TABLE VII

Energies and eigenfunctions for states 7′–14′

	Eigenfunction	Energy
7′	$(1+c^2+d^2)^{-1/2}[\psi_7 - c\psi_8 - (d/\sqrt{2})\psi_9 - (d/\sqrt{2})\psi_{10}]$	$(1/2)\nu_0'(1-\sigma_x)+(1/2)(-J_{12}-J_{23})-K$
8′	$(1+a^2+b^2)^{-1/2}[\psi_7 + a\psi_8 + (b/\sqrt{2})\psi_9 + (b/\sqrt{2})\psi_{10}]$	$(1/2)\nu_0'(1-\sigma_x)+(1/2)(-J_{12}-J_{23})+K$
9′	$(1/\sqrt{3})(\psi_7+\psi_8)+(1/\sqrt{6})(\psi_9+\psi_{10})$	$(1/2)\nu_0'(1-\sigma_x)+(1/2)(J_{12}+J_{23})$
10′	$(1/\sqrt{2})(\psi_9-\psi_{10})$	$(1/2)\nu_0'(1-\sigma_x)+(1/2)(J_{12}-J_{23})$
11′	$(1+c^2+d^2)^{-1/2}[\psi_{11} - c\psi_{12} - (d/\sqrt{2})\psi_{13} - (d/\sqrt{2})\psi_{14}]$	$(1/2)\nu_0'(-1+\sigma_x)+(1/2)(-J_{12}-J_{23})-K$
12′	$(1+a^2+b^2)^{-1/2}[\psi_{11} + a\psi_{12} + (b/\sqrt{2})\psi_{13} + (b/\sqrt{2})\psi_{14}]$	$(1/2)\nu_0'(-1+\sigma_x)+(1/2)(-J_{12}-J_{23})+K$
13′	$(1/\sqrt{3})(\psi_{11}+\psi_{12})+(1/\sqrt{6})(\psi_{13}+\psi_{14})$	$(1/2)\nu_0'(-1+\sigma_x)+(1/2)(J_{12}+J_{23})$
14′	$(1/\sqrt{2})(\psi_{13}-\psi_{14})$	$(1/2)\nu_0'(-1+\sigma_x)+(1/2)(J_{12}-J_{23})$

TABLE VIII

Transitions involving states 7′–14′

Transition	Energy	Relative intensity
10′→ 3′	$\nu_0(1-\sigma_A)+(1/4)(2J_{23}+J_{15}+J_{35})-A$	$1+\sin 2\theta$
9′→ 4′	$\nu_0(1-\sigma_A)+(1/4)(-2J_{23}+J_{15}+J_{35})+A$	$3(1+\sin 2\theta)$
14′→ 5′	$\nu_0(1-\sigma_A)+(1/4)(2J_{23}-J_{15}-J_{35})-B$	$1+\sin 2\phi$
13′→ 6′	$\nu_0(1-\sigma_A)+(1/4)(-2J_{23}-J_{15}-J_{35})+B$	$3(1+\sin 2\phi)$
15′→ 9′	$\nu_0(1-\sigma_A)+(1/4)(2J_{23}+J_{15}+J_{35})-A$	$3(1+\sin 2\theta)$
16′→ 10′	$\nu_0(1-\sigma_A)+(1/4)(-2J_{23}+J_{15}+J_{35})+A$	$1+\sin 2\theta$
18′→ 13′	$\nu_0(1-\sigma_A)+(1/4)(2J_{23}-J_{15}-J_{35})-B$	$3(1+\sin 2\phi)$
19′→ 14′	$\nu_0(1-\sigma_A)+(1/4)(-2J_{23}-J_{15}-J_{35})+B$	$1+\sin 2\phi$
14′→ 10′	$\nu_0'(1-\sigma_x)$	1
13′→ 10′	$\nu_0'(1-\sigma_x)$	1
12′→ 8′	$\nu_0'(1-\sigma_x)$	1
11′→ 7′	$\nu_0'(1-\sigma_x)$	1

ACKNOWLEDGMENTS

I should like to thank Dr. R. E. Richards for the use of his spectrometer and Dr. J. Leane for the measurement of the spectra shown in Fig. 1.

REFERENCES

1. Bernstein, H. J., Pople, J. A., and Schneider, W. G. Can. J. Chem. **35**, 65 (1957).
2. Richards, R. E. and Schaefer, T. J. Molecular Phys. **1**, 331 (1958).
3. Baker, E. B. J. Chem. Phys. **23**, 984 (1955).
4. Gutowsky, H. S., Holm, C. H., Saika, A., and Williams, G. A. J. Am. Chem. Soc. **79**, 4596 (1957).
5. Roux, D. Helv. Phys. Acta, **31**, 511 (1958).
6. Leane, J., Richards, R. E., and Schaefer, T. J. Sci. Instr. (In press).
7. Richards, R. E. and Schaefer, T. Trans. Faraday Soc. **54**, 1447 (1958).
8. Richards, R. E. and Schaefer, T. Proc. Roy. Soc. A, **246**, 429 (1958).

Note Added In Proof: Under highest resolution the high field line of the CH_3 doublet can be resolved further, with splittings of about 0.2 c.p.s. The CH_3 protons appear to be coupled to the ring protons ortho to the CH_3 group. This effect is under investigation and the interpretation is not obvious. The conclusions arrived at above still hold.

Can. J. Chem. Downloaded from www.nrcresearchpress.com by 196.1.178.254 on 09/04/12
For personal use only.

Can. J. Chem. Downloaded from www.nrcresearchpress.com by 196.1.178.254 on 09/04/12
For personal use only.

THE LIMITING CONDUCTANCE OF AQUEOUS SOLUTIONS OF POTASSIUM IODATE, POTASSIUM CHLORATE, AND SILVER NITRATE AT 35.00° C[1]

E. Bock and A. N. Campbell

ABSTRACT

Measurements have been made of the equivalent conductances of aqueous solutions of potassium iodate, potassium chlorate, and silver nitrate at 35.00° C at concentrations ranging from 0.8×10^{-4} to 16×10^{-4} N. From these, the limiting equivalent conductances and association constants A as obtained by the use of the Fuoss–Shedlovsky extrapolation procedure were found to be at 35.0° C:

$\Lambda_0KIO_3 = 138.62$ mhos, $A = 0.8$ l.,
$\Lambda_0KClO_3 = 165.70$ mhos, $A = 0.5$ l.,
$\Lambda_0AgNO_3 = 161.53$ mhos, $A = 0.9$ l.

INTRODUCTION

The fact that aqueous solutions of some salts, especially salts of the oxyacids, behave as moderately strong electrolytes has long been recognized. Several attempts have been made to calculate the association constants of these electrolytes, from conductance data. The various suggested treatments of the experimental data differ from one another in the way in which the effect of ionic attraction on the equivalent conductance is calculated. Thus, in the method proposed by Davis (1), K, the dissociation constant, is obtained through the use of a modified Ostwald dilution law, viz.,

$$K = \frac{\Lambda^2 f_\pm^2}{\Lambda'(\Lambda' - \Lambda)}. \qquad [1]$$

Here Λ is the experimentally determined equivalent conductance at concentration c, Λ' the conductance of one equivalent of free ions, calculated by means of an empirical equation, and f the mean activity coefficient of the electrolyte, usually obtained by means of the Debye-Hückel relationship or modification thereof.

Another treatment, that adopted in the present paper, was suggested by Fuoss and Shedlovsky (2). These authors use a slightly modified Onsager equation in which resistance instead of conductance is considered in its derivation, in combination with the law of mass action. The association constant as well as the limiting equivalent conductance is obtained from a plot of ΛS vs. $c(\Lambda^2 S^2 f_\pm^2)$ where

$$\Lambda S = \Lambda_0 - [c(\Lambda^2 S^2 f_\pm^2)/K\Lambda_0]. \qquad [2]$$

Here Λ, Λ_0, c, and $f_\pm$ have their usual meaning. S is the Shedlovsky (2) function and K is the dissociation constant.

In the present paper Λ_0 and A for the three electrolytes were determined through the use of eq. [2]; the activity coefficient in each case was calculated from the Debye–Hückel approximation

$$\log_{10} f_\pm = -0.5190\sqrt{(\theta c)} \qquad [3]$$

where $\theta = S(\Lambda/\Lambda_0)$ is the degree of dissociation.

[1]*Manuscript received January 26, 1959.*
Contribution from the Chemistry Department of the University of Manitoba, Winnipeg, Manitoba.

Can. J. Chem. Downloaded from www.nrcresearchpress.com by 196.1.178.254 on 09/04/12
For personal use only.

EXPERIMENTAL

The experimental technique has been described elsewhere (3). Potassium iodate and potassium chlorate, both Fisher certified reagents of the highest purity, whose total impurities—mostly ionic in nature—were less than 0.01%, were dried carefully at 150° C and stored over phosphorus pentoxide. The silver nitrate, also a high quality Fisher certified reagent, was fused in darkness and also stored over phosphorus pentoxide.

EXPERIMENTAL RESULTS

Our results are contained in Tables I, II, and III given below.

DISCUSSION

Potassium Iodate

When the results for potassium iodate given in Table I are plotted in the form Λ versus $\sqrt{c}$ the usual straight line plot is obtained. When the best straight line (derived by the method of least squares) is drawn and extrapolated to zero concentration Λ_0 results as 138.62_2 mhos and the slope of the line has a value of -108.03. The Onsager tangent on the other hand has the value -107.43. Thus, to use the language of Fuoss (4), the phoreogram is catabatic to the latter, indicating ion association. When the conductance results are plotted, using eq. [2], a straight line plot again results which on extrapolation yields $\Lambda_0 = 138.61_7$ mhos. The mean deviation from the line, again obtained by the method of least squares as were all subsequent lines, is less than 0.01 of a ΛS unit. The difference between the two Λ_0's is within the experimental error, which is estimated to be 0.01% to 0.02%. This agreement is not surprising since as $c \rightarrow 0$, $S \rightarrow \mathbf{1}$ and $\Lambda \rightarrow \Lambda_0$, so that the intercepts should be identical. Taking the value for the limiting conductance for the potassium ion to be 88.21 mhos (5) the limiting conductance of the iodate ion follows as 50.41 mhos. The association constant as obtained from the slope of the graph of eq. [2] is equal to 0.8 l. It should be pointed out, however, that this association constant is forced to carry all the inadequacy or approximations of eq. [2]. A more realistic association constant and perhaps a slightly better value for Λ_0 would have been obtained

TABLE I

Equivalent conductance of potassium iodate at 35.00° C

Concentration in moles/liter $\times 10^4$	Equivalent conductance in mhos
1.3035	137.397
2.1329	137.040
2.4340	136.948
3.6615	136.584
4.0939	136.431*
5.1986	136.194*
5.6073	136.061
6.6614	135.838
7.1539	135.717
8.3134	135.519
8.7871	135.398
9.9599	135.212
10.425	135.121
11.605	134.944
12.169	134.858
13.342	134.680
16.235	134.282

*These points were not included in the least square calculation since their deviation from the mean is greater than three times the mean deviation.

if the recently proposed treatment of conductance data, derived by Fuoss (6) and based on the latest extension of the conductance equation by Fuoss and Onsager (7), had been employed, but this treatment requires, especially for moderately strong electrolytes whose association constant approaches unity, conductance data in low dielectric constant media, and these are at present lacking. The value of Λ_0 may be taken with confidence to be within 0.02% of its "true" value, but the association constant gives only the order of magnitude.

We greatly regret that in our recent paper (3) on the conductance of potassium iodate at 25° C we overlooked the work of Krieger and Kilpatrick (8), Monk (9), and Spiro (10) on the same subject. We did not encounter the difficulties in the dilute region of concentration experienced by Krieger and Kilpatrick and by Monk. Neither did we observe a scatter as noticed by the former workers nor did we find a change in slope of the curve ΛS vs. $c(\Lambda^2 S^2 f_\pm^2)$ with increase in dilution as reported by Monk, either at 25° C or at 35° C. The mean deviation of ΛS when plotted versus $c(\Lambda^2 S^2 f_\pm^2)$ from a straight line was found to be less than 0.01 of a ΛS unit. The dissociation constant for potassium iodate at 25° C calculated from our data results as 2.0 l.$^{-1}$, a value intermediate between those obtained by the above workers.

Potassium Chlorate and Silver Nitrate

The behavior of these electrolytes was found to be, in general, similar to that of potassium iodate. In both cases the limiting conductances, as obtained by the two

TABLE II

Equivalent conductance of potassium chlorate at 35.00° C

Concentration in moles/liter $\times 10^4$	Equivalent conductance in mhos
0.82043	164.497*
2.3006	163.840*
3.6084	163.355*
5.2357	162.882
6.3990	162.592
7.9999	162.242
9.5265	161.963
10.772	161.734
12.402	161.467
13.814	161.236
15.088	161.067
16.021	160.930

*See footnote of Table I.

extrapolation methods, agree to within the experimental error. Thus for potassium chlorate, Λ_0 derived from the Λ vs. $\sqrt{c}$ plot is 165.45_3 mhos whereas Λ_0 obtained by extrapolation of eq. [2] is 165.47 mhos. Similarly for silver nitrate, Λ_0 obtained by the former procedure, 161.55_3 mhos, is identical within the experimental error, with Λ_0 derived by employing the latter procedure, viz. 161.53_1 mhos. The association constants for potassium chlorate and silver nitrate were found to be 0.5 l. and 0.9 l. respectively. The phoreogram for potassium chlorate was found to be anabatic to the Onsager tangent. Yet the fact that A is equal to 0.5 would seem to indicate that potassium chlorate is associated. A similar behavior was noticed by Fuoss and Kraus (11) for sodium bromate. Moreover, if conductance values for potassium chloride (12), a salt usually taken to be completely dissociated in dilute aqueous solutions, are plotted using eq. [2] a very small A, in fact, one approaching zero, is obtained. Thus it seems that whenever

Can. J. Chem. Downloaded from www.nrcresearchpress.com by 196.1.178.254 on 09/04/12
For personal use only.

TABLE III

Equivalent conductance of silver nitrate at 35.00° C

Concentration in moles/liter $\times 10^4$	Equivalent conductance in mhos
0.84902	160.544*
1.1126	160.346
1.6349	160.148*
2.1291	159.856
2.6514	159.652*
3.1565	159.524
4.8132	159.029
4.8641	159.026
6.1714	158.708
6.4389	158.633
7.4173	158.419
9.1949	158.064
11.075	157.728
12.636	157.479
14.638	157.150

*See footnote of Table I.

eq. [2] yields a slope of reasonable magnitude one is justified in suspecting ion association. For silver nitrate the phoreogram was found to be catabatic to the Onsager tangent, indicating ion association unequivocally.

CONCLUSION

Since the graph obtained by plotting eq. [2] is much more sensitive to errors, especially in the ordinates, than is the graph obtained by plotting Λ vs. $\sqrt{c}$ it is suggested that the limiting equivalent conductance derived from the former be taken as being closer to its "true" value than that derived from the latter. Subtracting from the limiting conductance of potassium iodate and of potassium chlorate the limiting conductance of the potassium ion (viz. 88.2_1 mhos) and from that of silver nitrate the known value of the nitrate ion (13) (viz. 85.48 mhos) there result the following individual limiting ionic conductances at 35.00° C:

$$\lambda_0 IO_3^- = 50.41 \text{ mhos}$$
$$\lambda_0 ClO_3^- = 77.50 \text{ mhos}$$
$$\lambda_0 Ag^+ = 76.05 \text{ mhos}.$$

ACKNOWLEDGMENT

One of us (E.B.) is indebted to the National Research Council of Canada for the award of a student summer research grant.

REFERENCES

1. Davis, C. W. Trans. Faraday Soc. **23**, 351 (1927). Robinson, R. A. and Davis, C. W. J. Chem. Soc. 574 (1937).
2. Fuoss, R. M. and Shedlovsky, T. J. Am. Chem. Soc. **71**, 1496 (1949).
3. Campbell, A. N. and Bock, E. Can. J. Chem. **36**, 1277 (1958).
4. Fuoss, R. M. J. Chem. Educ. **32**, 527 (1955).
5. Gordon, A. R. and Benson, G. C. J. Chem. Phys. **13**, 473 (1945).
6. Fuoss, R. M. J. Am. Chem. Soc. **79**, 3301 (1957).
7. Fuoss, R. M. and Onsager, L. J. Phys. Chem. **61**, 668 (1957).
8. Krieger, K. A. and Kilpatrick, M. J. Am. Chem. Soc. **64**, 7 (1942).
9. Monk, C. B. J. Am. Chem. Soc. **70**, 3281 (1948).
10. Spiro, M. J. Phys. Chem. **60**, 976, 1673 (1956).
11. Fuoss, R. M. and Kraus, C. A. J. Am. Chem. Soc. **79**, 3304 (1957).
12. Shedlovsky, T. J. Am. Chem. Soc. **54**, 1411 (1932).
13. Campbell, A. N. and Bock, E. Can. J. Chem. **36**, 330 (1958).

Can. J. Chem. Downloaded from www.nrcresearchpress.com by 196.1.178.254 on 09/04/12
For personal use only.

Can. J. Chem. Downloaded from www.nrcresearchpress.com by 196.1.178.254 on 09/04/12
For personal use only.

THE CONSTITUTION OF A HEMICELLULOSE FROM SUGAR MAPLE (ACER SACCHARUM)[1]

T. E. TIMELL

ABSTRACT

Partial hydrolysis of the main hemicellulose constituent of sugar maple (*Acer saccharum*) has yielded D-xylose, D-galacturonic acid, 4-*O*-methyl-D-glucuronic acid, and 2-*O*-(4-*O*-methyl-α-D-glucosyluronic acid)-D-xylose. Hydrolysis of the fully methylated polysaccharide gave a mixture of 2-*O*- and 3-*O*-methyl-D-xylose, 2,3-di-*O*-methyl-D-xylose, 2,3,4-tri-*O*-methyl-D-xylose, and 2-*O*-(2,3,4-tri-*O*-methyl-α-D-glucosyluronic acid)-3-*O*-methyl-D-xylose in a mole ratio of 3:111:1:12. The number-average degrees of polymerization of the native and the methylated polysaccharide were 205 and 149, respectively. These data indicate that the hemicellulose is composed of a linear chain of 1,4-linked β-D-xylose residues and that on the average every tenth residue of the chain carries a terminal 4-*O*-methyl-D-glucuronic acid residue attached through its C_2. The structure of the polysaccharide is similar to that of the main hemicellulose component of European beech, white birch, and yellow birch.

Sugar maple is an important hardwood species in the northeastern part of this continent. Ritter and co-workers (1, 2) have studied the general composition of various hemicellulose fractions from this wood and chromatographic evidence for the presence of 4-*O*-methyl glucuronic acid has been reported by Nelson and Schuerch (3). The structure of the same hemicellulose has been studied by Neubauer and Purves (4), who concluded that the polysaccharide was composed of a branched backbone of 1,4-linked xylose residues, some of which carried terminal *O*-methyl glucuronic acid residues. In a previous investigation (5) the molecular properties of a native cellulose from sugar maple were studied. The present paper is concerned with the constitution and properties of the main hemicellulose component of this species.

RESULTS AND DISCUSSION

The high pentosan content of the wood (18.5%) indicated that the preponderant hemicellulose was a xylan. When the wood was extracted with alkali, a hemicellulose was obtained in a yield of 12.4%, giving D-xylose and three uronic acid compounds on partial hydrolysis. The sugar acids were separated from the xylose on an anion exchange resin and the mixture obtained was resolved on a charcoal column to yield galacturonic acid, 4-*O*-methyl glucuronic acid, and an aldobiouronic acid. The hexuronic acids were identified chromatographically whereas the structure of the aldobiouronic acid was proved by the following experiments.

Reduction of the methyl glycoside methyl ester of the aldobiouronic acid followed by hydrolysis gave D-xylose and 4-*O*-methyl-D-glucose. When the neutral disaccharide was methylated to completion and hydrolyzed, 3,4-di-*O*-methyl-D-xylose and 2,3,4,6-tetra-*O*-methyl-D-glucose were obtained. This evidence, together with the specific rotation of the compound (+100°) (6), showed that the acid was 2-*O*-(4-*O*-methyl-α-D-glucosyluronic acid)-D-xylose.

Methanolysis of the fully methylated hemicellulose gave a mixture of glycosides which was saponified and resolved into an acidic and a neutral fraction on an exchange resin. The acid fraction contained only one compound, the ester glycoside of which was reduced with lithium aluminum hydride to yield a crystalline disaccharide, identified as methyl

[1]*Manuscript received January 20, 1959.*
Contribution from the Division of Industrial and Cellulose Chemistry, McGill University, and the Wood Chemistry Division, Pulp and Paper Research Institute of Canada, Montreal, Quebec.

2-*O*-(2,3,4-tri-*O*-methyl-α-D-glucosyl)-3-*O*-methyl-D-xylopyranoside. Hydrolysis of this compound gave the expected 3-*O*-methyl-D-xylose and 2,3,4-tri-*O*-methyl-D-glucose.

The mixture of neutral glycosides was hydrolyzed and resolved by paper chromatography to yield a mixture of 2-*O*- and 3-*O*-methyl-D-xylose, which could be resolved by paper ionophoresis, 2,3-di-*O*-methyl-D-xylose and 2,3,4-tri-*O*-methyl-D-xylose. A quantitative estimation (7), together with the weight of the acidic fraction, indicated a molar ratio of 3:111:1:12 between the mono-, di-, and tri-*O*-methylated xyloses and the latter.

The large quantity of 2,3-di-*O*-methyl-D-xylose, together with the high negative rotation (−80°) of the hemicellulose as well as its consumption of periodate, indicated the presence of 1,4-linked β-D-xylose residues, while the 2,3,4-tri-*O*-methyl-D-xylose undoubtedly originated from the non-reducing end groups. Since no monouronic acids were formed during the methanolysis, the presence of the mono-*O*-methyl xyloses could be accounted for only by incomplete methylation, demethylation, or branching. The fact that their number exceeded that of the tri-*O*-methyl xylose made it certain that branching was not the only factor involved. When the molecular weight of the methylated hemicellulose was determined by osmometry, a value of 27,300 was obtained, corresponding to a number-average degree of polymerization of 149. This was a value somewhat higher than that indicated by the number of non-reducing end groups present (127) and showed that no branching was involved. The mono-*O*-methyl xyloses were therefore artifacts, probably caused by demethylation (8, 9).

The structure of the aldobiouronic acid indicated that the hemicellulose contained residues of 4-*O*-methyl-α-D-glucuronic acid linked by 1,2-glycosidic bonds to the anhydroxylose units. The fact that the 4-hydroxyl was unsubstituted in the xylose moiety of the partly methylated aldobiouronic acid obtained from the methylated hemicellulose, while a methoxyl group was present in this position in the corresponding, fully methylated acid, showed that the acid groups were linked *directly* to the xylan framework. The methoxyl and uronic anhydride content, the yield of aldobiouronic acid from the methylated polysaccharide, and the amount of periodate consumed on oxidation of the hemicellulose all indicated the presence of an average number of 10 xylose residues per acid side chain.

The number-average molecular weight of the acetate derivative of the hemicellulose was 49,300, corresponding to a degree of polymerization of 205. Values of 205 and 217 were obtained from viscosity measurements in cupriethylenediamine and dimethyl sulphoxide, respectively.

Summarizing the above evidence, a tentative structure can now be assigned to the 4-*O*-methyl glucuronoxylan present in sugar maple wood. This polysaccharide consists of a linear framework of approximately 200 1,4-linked β-D-xylose residues. Every tenth residue on the average is linked through its 2-position to a single side chain of 4-*O*-methyl-α-D-glucuronic acid. From recent evidence (10, 11) it appears probable that the polysaccharide contains acetyl groups in its native state and the possibility that at least a portion of it is linked to lignin cannot be excluded (12, 13).

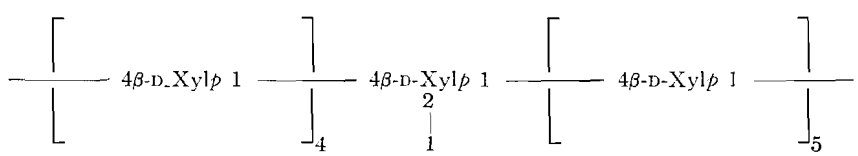

4-*O*-Me-α-D-G*p*A

Can. J. Chem. Downloaded from www.nrcresearchpress.com by 196.1.178.254 on 09/04/12
For personal use only.

Can. J. Chem. Downloaded from www.nrcresearchpress.com by 196.1.178.254 on 09/04/12
For personal use only.

The present polysaccharide is very similar to the 4-*O*-methyl glucuronoxylans previously isolated from the woods of European beech (14), white birch (15), and yellow birch (16) and it is also similar to the main hemicellulose components of Finnish birch (17) and white elm (18). The corresponding polysaccharide of American beech (19), on the other hand, has been claimed to possess a branched xylan backbone and that of trembling aspen (20) evidently contains terminal L-arabofuranose residues. The number-average molecular weight of the hemicellulose is approximately the same as that of other hardwood glucuronoxylans so far studied (21). It is not known, however, whether the alkali used in the extraction of the hemicellulose from the wood has any noticeable depolymerizing effect (22, 23), nor has the weight-average degree of polymerization been determined for any native, undegraded xylan.

EXPERIMENTAL

General experimental conditions were the same as described previously (24). Solvents (v/v) used for separating sugars on the paper chromatogram were (A) ethyl acetate – acetic acid – water (9:2:2), (B) butan-1-ol – pyridine – water (10:3:3), (C) butan-1-ol – ethanol – water (40:11:19), and (D) butan-2-one – water (89:11).

Composition of the Wood

Analyses according to standard methods (9, 15) indicated the following composition of the wood: pentosan (18.5), lignin (22.7), acetyl (2.9), ash (0.3), uronic anhydride (4.4), galactan (trace), glucan (51.7), mannan (2.3), araban (0.8), and xylan (14.8%).

Isolation of the Hemicellulose

Extractive-free wood meal from a sound, 25-year-old specimen of sugar maple* (500 g, 40–60 mesh) was exhaustively extracted by shaking with 24% (w/w) aqueous potassium hydroxide (3.5 liters) as described previously (15, 16, 24). The recovered product was dried from petroleum ether *in vacuo* to give 57 g (12.3%) of a white powder. Anal.: uronic anhydride, 12.05%; methoxyl, 2.09%; $[\alpha]_D^{20}$ −80° (*c*, 1.0 in 2.5% sodium hydroxide). Examination by paper chromatography (solvents A and B) of the hydrolyzate of the hemicellulose suggested the presence of xylose and three uronic acids, two of which corresponded chromatographically to galacturonic acid and 4-*O*-methyl glucuronic acid.

Isolation of the Aldobiouronic Acid

Wood meal (500 g) was treated with 72% sulphuric acid (100 ml) for 24 hours after which the solution was diluted to 2 liters and boiled under reflux for 10 hours. After neutralization with barium hydroxide, filtration through Celite, and evaporation, the solution was added to the top of a cocoanut charcoal column (7.5×25 cm) (25). Most of the neutral sugars were removed with water. Elution with 2% aqueous ethanol removed galacturonic acid and a portion of the 4-*O*-methyl glucuronic acid. Further elution with 4% and 10% ethanol yielded a chromatographically pure aldobiouronic acid (5 g). Anal. Calc. for $C_{12}H_{20}O_{11}$: OCH_3, 9.1; equiv. wt., 340. Found: OCH_3, 9.1; equiv. wt., 326; $[\alpha]_D^{20}$ +100° (*c*, 1.0 in water).

Identification of Hydrolysis Products from the Reduced Aldobiouronic Acid

The aldobiouronic acid (4 g) was boiled under reflux with 2.5% methanolic hydrogen chloride (150 ml) for 7 hours. After neutralization with silver carbonate and filtration through Celite and evaporation, the sirupy ester glycoside was reduced with lithium

**Kindly donated by Mr. Ken Murray, Fitch Bay, Quebec.*

aluminum hydride (4 g) (26) in dry tetrahydrofuran (100 ml) to yield a sirup (3.6 g). A portion of the reduced glycoside (1.2 g) was hydrolyzed with *N* sulphuric acid to give a sugar mixture (1.1 g) which was resolved on sheets of filter paper (solvent A) to yield D-xylose $[\alpha]_D^{20}$ +18° (*c*, 1.0 in water), and 4-*O*-methyl-D-glucose, $[\alpha]_D^{20}$ +58° (*c*, 1.0 in water). The xylose dibenzylidene dimethyl acetal (27) had m.p. and mixed m.p. 210° C and the 4-*O*-methyl-D-glucosazone had m.p. and mixed m.p. 157° C. The infrared spectrum of the latter was identical with that of an authentic specimen.

Methylation and Hydrolysis of the Ester Glycoside of the Aldobiouronic Acid

The ester glycoside of the aldobiouronic acid (2.0 g) was dissolved in dry dimethyl formamide (100 ml) and shaken in the dark with methyl iodide (10 ml) and silver oxide (10 g) (28). The product was recovered as described by Kuhn (28). After addition of chloroform to the reaction mixture, silver salts were removed by filtration. Extraction with aqueous potassium cyanide followed by three extractions with water gave a chloroform solution which was dried with anhydrous sodium sulphate and evaporated to dryness to yield a yellow sirup. Anal. Calc. for $C_{18}H_{34}O_{10}$: OCH_3, 52.8%. Found: OCH_3, 51.0%. The ester glycoside was reduced with lithium aluminum hydride to yield a sugar mixture which was resolved by paper chromatography (solvent C) to give two compounds, chromatographically indistinguishable from a di-*O*-methyl xylose (110 mg) and a tetra-*O*-methyl glucose (130 mg).

*Identification of 3,4-Di-O-methyl-*D*-xylose and 2,3,4,6-Tetra-O-methyl-*D*-glucose*

The di-*O*-methyl xylose, $[\alpha]_D^{20}$ +15° (*c*, 1.0 in water), gave a crystalline 3,4-di-*O*-methyl-*N*-phenyl-D-xylosylamine, m.p. 115° C (29). The tetra-*O*-methyl glucose, $[\alpha]_D^{20}$ +83° (*c*, 3.1 in water), crystallized, melting point and mixed melting point after three recrystallizations from petroleum ether 88–90° C. Anal. Calc. for $C_{10}H_{20}O_6$: OCH_3, 52.7%. Found: OCH_3, 50.0%. The 2,3,4,6-tetra-*O*-methyl-*N*-phenyl-D-glucosylamine had m.p. and mixed m.p. 135–136° C.

Methylation of the Hemicellulose

The hemicellulose (20 g) was dissolved in 40% (w/w) aqueous sodium hydroxide (300 ml) in an atmosphere of nitrogen, after which dimethyl sulphate (200 ml) was added dropwise at 0° C over a period of 8 hours. This treatment was repeated six times at room temperature. The recovered product was dissolved in tetrahydrofuran (2 liters) and powdered sodium hydroxide (200 g) and dimethyl sulphate (300 ml) were added (30). This treatment was repeated twice. The solvent was removed by distillation, and the remainder was washed with water and dissolved in chloroform. The solution was dried and poured into petroleum ether to yield a white, fluffy product (22 g). Anal. Calc. for the fully methylated sodium salt of the hemicellulose: OCH_3, 37.3%. Found: OCH_3, 37.8%. The infrared spectrum indicated the absence of hydroxyl groups.

Hydrolysis and Separation of Acidic and Neutral Sugars

Methylated hemicellulose (10 g) was treated with methanolic hydrogen chloride and the mixture of glycosides (10.8 g) was de-esterified with barium hydroxide (31). The mixture obtained was resolved on a column of Dowex 1-X4 anion exchange resin (acetate form) to yield a mixture of neutral sugars (7.8 g) and an acidic compound (1.7 g).

*Identification of Methyl 2-O-(2,3,4-Tri-O-methyl-α-*D*-glucosyl)-3-O-methyl-α,β-*D*-xylopyranoside*

The above acid compound was converted to its methyl ester methyl glycoside which was reduced with lithium aluminum hydride. The colorless sirup obtained crystallized

Can. J. Chem. Downloaded from www.nrcresearchpress.com by 196.1.178.254 on 09/04/12
For personal use only.

immediately, m.p. and mixed m.p. 167–168° C after recrystallization from ethyl acetate. Anal. Calc. for $C_{16}H_{30}O_{10}$: OCH_3, 40.6%. Found: OCH_3, 40.4%; $[\alpha]_D^{20}$ +93° (*c*, 1.0 in water). The infrared spectrum and the X-ray powder diagram were identical with those of an authentic (31) specimen of methyl 2-*O*-(2,3,4-tri-*O*-methyl-α-D-glucopyranosyl)-3-*O*-methyl-α,β-D-xylopyranoside.

A portion of the disaccharide (600 mg) was hydrolyzed to yield a mixture of methylated sugars which was resolved on the paper chromatogram (solvent D), giving two compounds chromatographically identical with a mono-*O*-methyl xylose and a tri-*O*-methyl glucose. 3-*O*-Methyl-D-xylose, $[\alpha]_D^{20}$ +15° (*c*, 1.0 in water) gave a crystalline aniline derivative, m.p. 134°. The 2,3,4-tri-*O*-methyl-D-glucose had $[\alpha]_D^{20}$ +78° (*c*, 1.0 in water) and aniline derivative with m.p. and mixed m.p. 143°.

Separation and Identification of the Neutral Components

The mixture of neutral glycosides was hydrolyzed and resolved by paper chromatography (solvent D) to yield three fractions. One was a mixture of 2-*O*- and 3-*O*-methyl-D-xylose, resolvable by paper ionophoresis in a borate buffer (32). The main fraction consisted of 2,3-di-*O*-methyl-D-xylose, $[\alpha]_D^{20}$ +25° (*c*, 3.0 in water). Anal. Calc. for $C_7H_{14}O_5$: OCH_3, 34.9%. Found: OCH_3, 35.0%. The 2,3-di-*O*-methyl-*N*-phenyl-D-xylopyranosylamine had m.p. 126–127° C. The last fraction, 2,3,4-tri-*O*-methyl-D-xylose could not be induced to crystallize. Anal. Calc. for $C_8H_{16}O_5$: OCH_3, 48.4%. Found: OCH_3, 47.2%. The infrared spectrum of the sirupy aniline derivative was indistinguishable from that of an authentic specimen.

Quantitative Analysis of the Neutral Components

A small portion of the mixture of neutral sugars was resolved on the paper chromatogram with solvent mixture C. Each paper strip was eluted with water and the concentration of the sugar was determined by the *o*-aminodiphenyl method (7). The average value of three determinations was used. With solvent system D high paper blanks were obtained.

Periodate Oxidation of the Hemicellulose

Periodate oxidations were carried out in the dark with 0.05 *M* solutions of both trisodium paraperiodate and sodium metaperiodate. The amount of periodate consumed, as determined by the arsenite method, was extrapolated to zero time, giving in both cases a consumption of 10.5 mole of oxidant per repeating unit.

Acetylation of the Hemicellulose

Acetylation of the hemicellulose was carried out as described previously (24) essentially according to the method of Carson and Maclay (33). Two acetylations gave a product soluble in chloroform–ethanol (9:1 v/v). Anal. Calc. for the fully acetylated hemicellulose: acetyl, 37.8%. Found: acetyl, 38.3%.

Determination of Molecular Weights

The molecular weights of the original hemicellulose and of its methyl derivative were carried out by osmotic pressure measurements as described elsewhere (24, 34). The results obtained are presented in Table I. Degrees of polymerization were calculated as shown earlier (15).

Estimation of the Intrinsic Viscosity of the Hemicellulose

Intrinsic viscosities were determined with a Craig–Henderson (35) viscometer in *M* cupriethylenediamine and in anhydrous dimethyl sulphoxide as described elsewhere

Can. J. Chem. Downloaded from www.nrcresearchpress.com by 196.1.178.254 on 09/04/12
For personal use only.

(34). The relationship $\bar{P}_n = K[\eta]$, where $[\eta]$ was the intrinsic viscosity and K was 212 and 346, respectively, was used for estimating the degree of polymerization ($\bar{P}_n$).

TABLE I

Osmometry data

Hemicellulose			Methylated hemicellulose		
w*	h†	h/w	w	h	h/w
3.469	1.905	0.549	3.500	3.996	1.142
2.948	1.586	0.538	3.108	3.423	1.102
2.568	1.394	0.543	2.695	2.854	1.059
2.304	1.282	0.556	2.077	2.127	1.024
1.612	0.892	0.553	1.768	1.810	1.024
1.522	0.784	0.515	1.324	1.323	0.999
0	—	0.52	0	—	0.94

*Concentration in g/kg solution (chloroform–ethanol 9:1).
†Osmotic height in cm solvent.

ACKNOWLEDGMENTS

The author wishes to express his gratitude to Mr. W. Steyn and Mr. D. Stoltzenburg for technical assistance.

REFERENCES

1. MITCHELL, R. L. and RITTER, G. J. J. Am. Chem. Soc. **62**, 1958 (1940).
2. MITCHELL, R. L., ROGERS, S. C., and RITTER, G. J. Ind. Eng. Chem. **40**, 1528 (1948).
3. NELSON, R. and SCHUERCH, C. Tappi, **40**, 419 (1957).
4. NEUBAUER, L. G. and PURVES, C. B. Can. J. Chem. **35**, 388 (1957).
5. TIMELL, T. E. Pulp Paper Mag. Can. **59** (No. 8), 139 (1958).
6. GORIN, P. A. J. and PERLIN, A. S. Can. J. Chem. **36**, 999 (1958).
7. TIMELL, T. E., GLAUDEMANS, C. P. J., and CURRIE, A. L. Anal. Chem. **28**, 1916 (1956).
8. LINDBERG, B. Private communication.
9. BARTH, F. W. and TIMELL, T. E. J. Am. Chem. Soc. **80**, 6320 (1958).
10. HÄGGLUND, E., LINDBERG, B., and MACPHERSON, J. Acta Chem. Scand. **10**, 1160 (1956).
11. BOUVENG, H. and LINDBERG, B. Acta Chem. Scand. **10**, 1283 (1956).
12. LINDGREN, B. O. Acta Chem. Scand. **12**, 447 (1958).
13. HAYASHI, A. and TACHI, I. Tappi, **41** (No. 9), 173 A (1958).
14. ASPINALL, G. O., HIRST, E. L., and MAHOMED, R. S. J. Chem. Soc. 1734 (1954).
15. GLAUDEMANS, C. P. J. and TIMELL, T. E. J. Am. Chem. Soc. **80**, 941, 1209 (1958).
16. TIMELL, T. E. To be published.
17. SAARNIO, J., WATHEN, K., and GUSTAFSSON, CH. Acta Chem. Scand. **8**, 825 (1954).
18. GILLHAM, J. K. and TIMELL, T. E. Can. J. Chem. **36**, 1467 (1958).
19. ADAMS, G. A. Can. J. Chem. **35**, 556 (1957).
20. JONES, J. K. N., MERLER, E., and WISE, L. E. Can. J. Chem. **35**, 634 (1957).
21. TIMELL, T. E., GLAUDEMANS, C. P. J., and GILLHAM, J. K. Pulp Paper Mag. Can. **59** (No. 10), 242 (1958).
22. WHISTLER, R. L. and CORBETT, W. M. J. Am. Chem. Soc. **78**, 1003 (1956).
23. ASPINALL, G. O., CARTER, M. E., and LOS, M. J. Chem. Soc. 4807 (1956).
24. CURRIE, A. L. and TIMELL, T. E. Can. J. Chem. **37**, 922 (1959).
25. BARTH, F. W. and TIMELL, T. E. Can. J. Chem. **36**, 1321 (1958).
26. SMITH, F. J. Chem. Soc. 2646 (1951).
27. BREDDY, L. J. and JONES, J. K. N. J. Chem. Soc. 738 (1945).
28. KUHN, R., TRISCHMANN, H., and LÖW, I. Angew. Chem. **67**, 32 (1955).
29. JONES, J. K. N. and WISE, L. E. J. Chem. Soc. 3389 (1952).
30. FALCONER, E. L. and ADAMS, G. A. Can. J. Chem. **34**, 338 (1956).
31. DUTTON, G. G. S. and SMITH, F. J. Am. Chem. Soc. **78**, 3744 (1956).
32. FOSTER, A. B. Advances in Carbohydrate Chem. **12**, 81 (1957).
33. CARSON, J. F. and MACLAY, W. D. J. Am. Chem. Soc. **68**, 1015 (1946).
34. GLAUDEMANS, C. P. J. and TIMELL, T. E. Svensk Papperstidn. **61**, 1 (1958).
35. CRAIG, A. W. and HENDERSON, D. A. J. Polymer Sci. **19**, 215 (1956).

Can. J. Chem. Downloaded from www.nrcresearchpress.com by 196.1.178.254 on 09/04/12
For personal use only.

Can. J. Chem. Downloaded from www.nrcresearchpress.com by 196.1.178.254 on 09/04/12
For personal use only.

ISOTHERMS OF BROMINE ON GRAPHITE[1]

J. G. HOOLEY

ABSTRACT

The isotherms of bromine on eight carbon blacks and on natural graphite have been related to the known structures of these materials. The surface areas can be calculated from the adsorption isotherms and the size of the graphite crystals can be estimated from the extent of hysteresis on desorption. The isosteric heats of adsorption on the surface and between the layers are each 11 kcal mole^{-1}. The formation of residue compounds displaces the isotherms equally at all pressures.

INTRODUCTION

The isotherm of bromine on a natural graphite at 28.8° C has been determined by Reyerson (6) along with the changes in magnetic susceptibility that occur during the process. The purpose of the present work was to study the isotherm at various temperatures and to include carbon blacks of various areas and crystal sizes. A recording vacuum thermobalance (3) and spoon gauge (4) were specially designed for such measurements with bromine and other corrosive vapors.

MATERIALS

1. Carbon black.—G. Cabot Inc., of Boston, donated samples from three sources, each heat-treated to two or three different temperatures. The data supplied with them included an estimate from X-ray data of the average thickness L_c and width L_a of the volumes in which the carbon atoms had the graphite structure. The area of the aggregates of these crystals per gram as calculated from electron microscope data and from B.E.T. adsorption data for N_2 was also given. The effect of heat-treatment on these properties is described elsewhere (7).

2. Graphite.—Natural crystals about 2 mm across were obtained through G. Cabot Inc. from a deposit near Willsboro, N.Y.

3. Bromine.—Analytical material was doubly distilled.

PROCEDURE

A 0.5- to 1-gram sample was weighed, suspended in the balance, evacuated to 0.001 cm, and thermostated to the desired temperature. The positions of the weight- and pressure-measuring transformers were then adjusted and the primary voltage to be applied to each was selected to give suitable sensitivities—all as described in refs. 3 and 4. When the recorded weight had settled down to a constant value, bromine was admitted at any desired pressure up to the saturation value. The pressure and the sample weight were then followed as a function of time by application of the known conversion factors to the millivolt records. At any time the bromine pressure could be increased by opening the tap to the reservoir or decreased by opening the tap to a liquid nitrogen trap at 0.001 cm. Leaving this latter tap open is referred to as reducing the pressure to zero.

For all runs a weight sensitivity of 3.4 mv mg^{-1} and a pressure sensitivity of 3.6 mv mm^{-1} was used. With no sample on the balance pan, any variation in the weight record was less than 0.2 mv over a period of several days. With a sample at 0.001 cm the record was equally constant after any initial loss of volatile material. The buoyancy correction

[1]*Manuscript received January 26, 1959.*
Contribution from the Department of Chemistry, University of British Columbia, with financial assistance from the National Research Council of Canada.

for the spring-pan system was found to be 0.33 mg per cm of mercury of bromine vapor with the reactor tube at 80° C or 25° C. No buoyancy correction was applied to the sample itself because its maximum value would be equivalent to only 0.1 atoms of bromine per 1000 carbon atoms. Adsorption and desorption isotherms were determined at temperatures from 0° C to 80° C. The uptake was plotted as gram atoms of bromine per 1000 g-atoms of carbon and will be referred to as the number of bromine atoms.

RESULTS

The following aspects of the isotherms are related where possible to other known properties of the adsorbent.

1. Hysteresis

(a) Natural Graphite, Untreated

This material showed rapid, reversible but only relatively slight bromine adsorption below a critical pressure dependent on temperature. Thus at 25° C less than 0.5 atoms of bromine (per 1000 carbon atoms) were adsorbed below 1 cm pressure. The critical pressures at 50°, 60°, and 80° C were 6 cm, 12 cm, and above 18 cm, respectively. Above these critical pressures bromine was very slowly adsorbed to a maximum value which increased with the pressure and with the reciprocal of temperature. Then on reducing the pressure, bromine slowly left the material until at zero pressure an amount remained that was independent of time and of temperatures up to 120° C. This is the residue compound studied by Hennig (2). When the cycles were repeated with a single sample of the residue compound obtained by debromination from 15 cm at 25° C the points in Fig. 1 were obtained. Below the critical pressure at a given temperature, less than 0.5 additional bromine atoms were adsorbed and above this pressure a slow adsorption occurred, followed by a hysteresis loop on desorption. The residue composition after each cycle was the same value of 30 bromine atoms. The two loops at 50° and 60° are reproducible in any order if sufficient time is allowed to establish equilibrium. This was as high as 24 hours for large amounts of bromine. For points that are critical in establishing the general shape of a loop, it was shown that no further change occurred in an additional 12 hours. The desorption side of the loop does not close at the critical pressure where adsorption started but continues on down to 2 cm or less before reaching the residue composition. There are five points in this region at 50° and 60° and their compositions were shown to be constant for 24 hours. The curves for 25° were not completed because of the great time required for the larger amounts of bromine adsorbed at this temperature.

(b) Carbon Blacks

These materials showed a rapid adsorption even at the lowest pressure used—0.03 cm. The subsequent isotherm showed hysteresis only if the pressure exceeded the critical value noted for natural graphite. Thus there was no hysteresis at 80° below at least 18 cm and none at 25° below 1 cm. Isotherms at three temperatures for Sterling M.T. 3100 are shown in Fig. 2. The equilibrium values involving hysteresis were reached in an hour or less, which is very rapid compared with the time required for natural graphite. Similar curves were obtained for other carbon blacks, although the amount of hysteresis varied. If the maximum vertical distance between adsorption and desorption curves at 25° C is taken as a measure of hysteresis then its value, listed in Table I, increases with crystal size. Unfortunately the data are insufficient to evaluate the relationship. All that can be said is that the defined hysteresis is proportional to a power of L_a between one and two.

Can. J. Chem. Downloaded from www.nrcresearchpress.com by 196.1.178.254 on 09/04/12
For personal use only.

Hysteresis was also observed when the temperature was changed at constant pressure. The compositions were simply those found on the adsorption and desorption curves for the particular pressure used. With natural graphite the change from one curve to another at constant pressure was extremely slow. Even after 24 hours the change from a 50° curve in Fig. 1 to a 60° curve had progressed only half way and was not followed any further because its rate had dropped to such a low value.

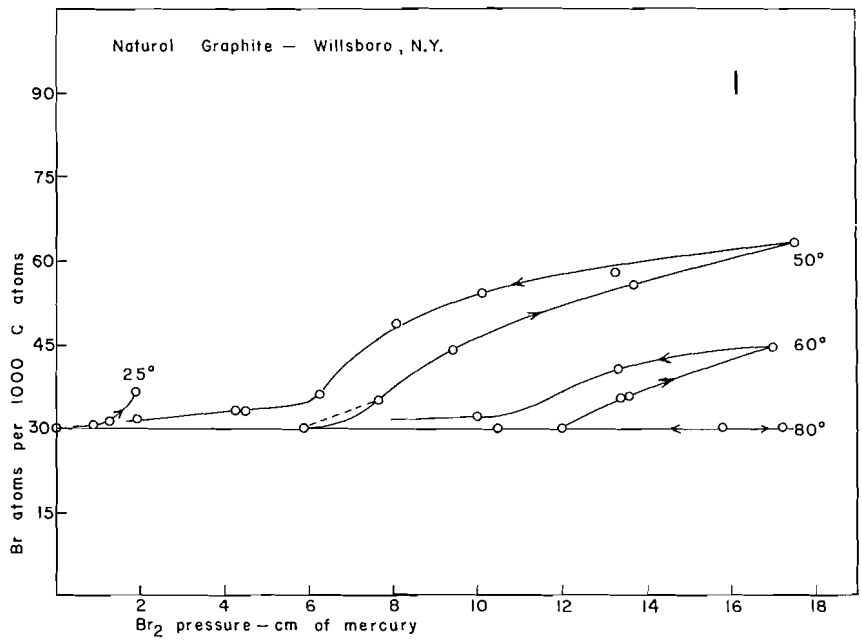

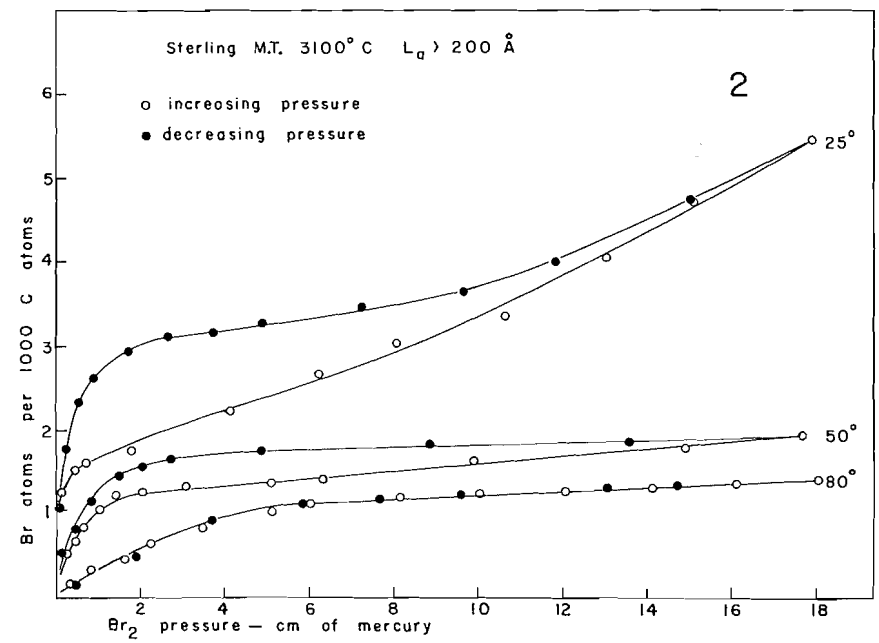

FIG. 1. Isotherms for a residue compound of natural graphite.
FIG. 2. Isotherms for Sterling M.T. 3100° C.

Can. J. Chem. Downloaded from www.nrcresearchpress.com by 196.1.178.254 on 09/04/12
For personal use only.

Can. J. Chem. Downloaded from www.nrcresearchpress.com by 196.1.178.254 on 09/04/12
For personal use only.

2. Residue Compounds

This refers to the bromine that is not removed to a liquid nitrogen trap in a system at 0.001 cm pressure. The time required to reach equilibrium varied up to 24 hours and the final composition was a function of the following conditions. For a given material it increased with the amount of bromine adsorbed before reducing the pressure to zero and with the time of exposure to bromine as reported by Hennig (2). The uptake after 24 hours was zero or very small. The source of carbon black and the temperature of heat-treatment before bromination are also factors. This is shown in Table I where the residue compositions are those obtained after 24 hours' exposure to bromine at 17 cm and 25° C. The values show that for a given source of carbon black the residual bromine content decreases as the temperature of heat-treatment increases.

The effect of the formation of these residue compounds on the isotherms was simply to displace them vertically by an amount equal to the residual bromine content. Any additional effect was not detected. As a result adsorption isotherms were only reproduced in case nothing was done to change the residue composition. In the subsequent use of the isotherms to determine area and isosteric heats only the amount of bromine adsorbed in excess of the residual amount was used in the calculations.

TABLE I

	L_a (Å)	L_c (Å)	Area, meter^2 g^{-1} N_2	Area, meter^2 g^{-1} Electron microscope	Area, meter^2 g^{-1} Br_2	Hysteresis*	Isosteric heat (kcal mole^{-1}) Adsorption	Isosteric heat (kcal mole^{-1}) Desorption	Residual bromine*
Spheron 6 Original	23	13	114	105	124	<0.5	9.5±0.7		15
Spheron 6 1000° C	36	15	91		85	<0.5	10.1±0.9		7
Spheron 6 2700° C	79	48	84		75	0.5	11.2±0.2		0.4
Sterling F.T. Original	28	17	14.5	15.4	25	<0.2	11.2±0.7		8
Sterling F.T. 1500° C	62	39	12.9	16.2	13	0.2	11.2±0.4		0.3
Sterling F.T. 2700° C	132	88	12.5	16.6	12	0.7	8.7±1.4	10.8±0.9† 18.7±3.3‡	0.1
Sterling M.T. Original	34	15	6.6	5.7	6.5	<0.2	11.4±0.7		0.8
Sterling M.T. 3100° C	>200	>200	6.3		7.5	1.2	11.1±1.1	14.6±0.9† 18.8±3.2‡	0.5
Natural graphite							11.7±0.3	16±2‡	30

*Bromine atoms per 1000 carbon atoms.
†Below monolayer value.
‡Above monolayer value.

3. Area Calculations

The B.E.T. equation was applied to the carbon black isotherms at 80° by plotting $p\{\mathrm{Br}/\mathrm{C}(p_0-p)\}^{-1}$ against p/p_0 between partial pressures of 0.03 and 0.12. From the slope of this straight line the areas in Table I were calculated using 12.2 Å^2 as the average area covered per atom of bromine. Except for Sterling F.T. Original the values average (5±10)% higher than the areas from N_2 adsorption data and (10±20)% lower than the electron microscope areas. When similar calculations were made for adsorption isotherms below 80°, larger areas were obtained whenever the plot included pressures above the critical value. Thus the area of Sterling M.T. 3100° calculated from the 0° isotherm was 12.4 and from the 25° isotherm 7.9 meter^2 g^{-1}. The higher values are caused by lamellar adsorption, which will be shown later to occur only above the critical pressure.

4. Isosteric Heats

These were calculated from the adsorption isotherms at 25°, 50°, and 80°. The results are summarized in Table I, where each recorded value is the average for a range of Br/C values from 0.2 to 1.5 monolayers. For Spheron 6 2700° the linearity of the Arrhenius plot is excellent and the standard deviation of the calculated heats at various Br/C values is only 2%. This good behavior is a result of the relatively large surface area, negligible hysteresis, and low residue composition associated with the sample. These combine to make lamellar adsorption and errors in the weighing and in the residue composition less significant. The situation is somewhat less satisfactory for the other carbon blacks. There is, however, no detectable trend of the heat with Br/C content or with temperature. Only on desorption from the two largest crystals and natural graphite is a trend with Br/C content noticeable and that toward lower values as bromine is removed. In Table I the average slopes above and below the monolayer value are used to calculate the two recorded heats of desorption for each of these three samples. All that can be said is that the value is the same as for adsorption below the monolayer value and higher by about 6 kcal per mole above it.

CONCLUSIONS

Because the critical pressure above which hysteresis occurs is the same for natural graphite and for all the carbon blacks it is concluded that the common lamellar structure of these materials is responsible for this behavior. Specifically, intercalation of bromine between the layers occurs only above the critical pressure and because the reverse process is hindered there is hysteresis. As one would expect, the hysteresis increases with the area of the carbon lamella and indeed the extent of hysteresis can be used to estimate the crystal dimension normal to the C axis. Furthermore the transport of bromine in and out of the layers should be and is much slower than the surface adsorption that is the main process below the critical pressure.

The isotherm for this surface adsorption can be used to calculate the surface area from the B.E.T. equation. The values for eight carbon blacks are, with one unexplained exception, within experimental error of the areas calculated from nitrogen adsorption data at low temperature or from electron microscope measurements of the size of the aggregates of graphite crystals. The average area occupied per bromine atom is of course critical in this calculation. The value of 12.2 $Å^2$ used is calculated from the density of the liquid assuming six co-ordination. However, one could equally well use the 11.8 $Å^2$ area per bromine atom in the halogen complexes of violanthrene studied by Professor H. Akamatu (1). He found evidence for a complex with two molecules of bromine to one molecule of the above hydrocarbon with its nine benzene rings. It is also interesting to note that placing bromine molecules over alternate pairs of graphite hexagons gives an average area per bromine atom of 10.5 Å. The atoms would be 0.09 Å from the center of each hexagon.

The isosteric heats in Table I show that the value for adsorption on the surface is within 10% of the value for adsorption between the layers. The best value for the carbon blacks of 11.2 ± 0.2 kcal $mole^{-1}$ agrees well with the 11.4 kcal $mole^{-1}$ reported by Reyerson (5) for adsorption on steam-activated charcoal. These values are only about 4 kcal higher than the heat of vaporization of bromine.

The bromine content of the residue compound increases with the pressure of bromine to which the sample had been exposed. However, the various isotherms for these different contents can be brought to coincidence by subtracting the residue composition at all pressures. This means that the total area available to bromine on the outer surfaces of

Can. J. Chem. Downloaded from www.nrcresearchpress.com by 196.1.178.254 on 09/04/12
For personal use only.

the crystal aggregates and the intercalating properties of the carbon layers are not changed noticeably by formation of the residue compound.

REFERENCES

1. AKAMATU, H., INOKUCHI, H., and MATSUNAGA, Y. Bull. Chem. Soc. Japan, **29**, 2, 213 (1956).
2. HENNIG, G. J. Chem. Phys. **20**, 1438 (1952).
3. HOOLEY, J. G. Can. J. Chem. **35**, 374 (1957).
4. HOOLEY, J. G. Can. J. Chem. **35**, 1414 (1957).
5. REYERSON, L. H. and CAMERON, A. E. J. Phys. Chem. **39**, 181 (1935).
6. REYERSON, L. H., WERTZ, J. E., WELTNER, W., and WHITEHURST, H. J. Phys. Chem. **61**, 1334 (1957).
7. SCHAEFFER, W. D., SMITH, W. R., and POLLEY, M. H. Ind. Eng. Chem. **45**, 1721 (1953).

Can. J. Chem. Downloaded from www.nrcresearchpress.com by 196.1.178.254 on 09/04/12
For personal use only.

Can. J. Chem. Downloaded from www.nrcresearchpress.com by 196.1.178.254 on 09/04/12
For personal use only.

STERIC INHIBITION OF RESONANCE

III. CALCULATION OF RESONANCE ENERGIES AND BOND LENGTHS[1]

JAMES TROTTER[2]

ABSTRACT

In many aromatic nitro compounds steric effects prevent the attainment of complete coplanarity and inhibit resonance interaction between the nitro group and the aromatic π-electrons. The variations with nitro group tilt of resonance energy, electron distribution, and π-bond order in this type of molecule have been calculated by molecular orbital methods, and the corresponding bond length variations have been deduced. The calculated bond lengths for 9,10-dinitroanthracene and 9-nitroanthracene are compared with those measured by X-ray analyses.

INTRODUCTION

Investigations of the crystal and molecular structures of 9-nitroanthracene and 9,10-dinitroanthracene have shown that the nitro groups are tilted markedly out of the planes of the aromatic rings due to the steric effects of neighboring carbon and hydrogen atoms (1, 2), and the resultant decreases in resonance interaction between the nitro groups and the aromatic π-electrons have been correlated with the variations in the characteristic vibration frequencies of the nitro groups (3). Further detailed examination of the bond lengths in these molecules, especially the C–N distances, suggests that the resonance is almost completely inhibited in 9-nitroanthracene, where the nitro group is tilted about the C–N bond 85° from the coplanar position, but that in the 9,10-dinitro derivative, where the tilts are 64°, there is a small but measurable resonance interaction (4).

The changes in the resonance energy and in the bond lengths in aromatic nitro compounds when the nitro group is tilted out of the plane of the aromatic ring may be calculated by molecular orbital methods, and the first section of the present paper describes the calculation of the variation of resonance energy and bond lengths with nitro group tilt (θ) in aromatic nitro compounds in general, nitrobenzene being used as a simple example. Subsequent sections describe the application of these methods to 9-nitroanthracene and 9,10-dinitroanthracene.

NITROBENZENE

In nitrobenzene (Fig. 1) each carbon and oxygen atom contributes one p_z electron to the π-molecular-orbital system, while the nitrogen atom contributes two, so that nine molecular orbitals accommodate 10 electrons. The secular equations

$$\sum c_r^i(H_{rs}-ES_{rs}) = 0$$

were set up in the usual way, using the parameters given in Table I, overlap integrals being taken as zero, and inductive effects neglected (this point will be discussed later). Since the nitrogen atom contributes two electrons its coulomb integral has been taken as $\alpha + \beta$ instead of the usual $\alpha + \frac{1}{2}\beta$ (8). The resonance integral H_{17} varies of course with the angle of tilt, being a maximum when $\theta = 0°$ and a minimum when $\theta = 90°$. By resolving the p_z atomic orbitals along axes at right angles, it can be shown that the value of this resonance integral for any value of θ is given approximately by

$$\beta^\theta = \beta^0 . \cos\theta.$$

[1]*Manuscript received October 31, 1958.*
Contribution from the Division of Pure Physics, National Research Council, Ottawa, Canada.
Issued as N.R.C. No. 5133.
[2]*National Research Council Postdoctorate Fellow.*

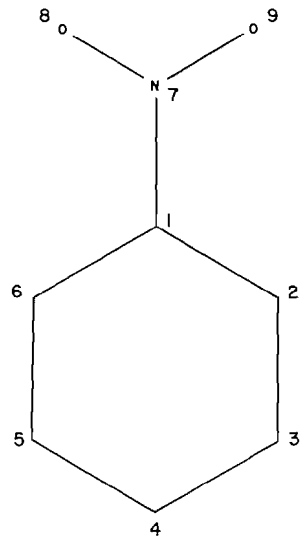

FIG. 1. Numbering used in the computations for nitrobenzene.

TABLE I

Parameters for nitrobenzene

	Coulomb integrals		Resonance integrals
H_{11}	α	H_{12}	β
H_{22}	α	H_{23}	β
H_{33}	α	H_{34}	β
H_{44}	α	H_{45}	β
H_{55}	α	H_{56}	β
H_{66}	α	H_{61}	β
H_{77}	$\alpha+\beta$	H_{17}	$\beta.\cos\theta$
H_{88}	$\alpha+\beta$	H_{78}	$\sqrt{2}\beta$
H_{99}	$\alpha+\beta$	H_{79}	$\sqrt{2}\beta$

The determinant Δ formed by the coefficients of the c_r^i is of the ninth order, and by writing $x = (\alpha - E_i)/\beta$ the molecular energy levels were obtained in terms of β by solving the equation $\Delta = 0$. Using determinants of the variety known as continuants, as described by Goodwin and Vand (5), the secular determinant for nitrobenzene was readily expanded to

$$\Delta_{\text{nitrobenzene}} = \Delta_{\text{benzene}} \cdot \Delta_{\text{nitro group}} - \cos^2\theta(x+1)^2 \cdot P_5$$
$$= (x+1)^3(x-1)[P_5+P_4-5P_3+2P_2+7P_1-11P_0-\cos^2\theta(P_3-P_1)].$$

The energy levels E_i for $\cos\theta = 0, 0.25, 0.50, 0.75, 1.00$ were evaluated, and are listed in Table II. The total π-electron energies and the resonance energies (E_R) due to interaction between the nitro group and the aromatic π-electrons were calculated and are included in the table. The final values of E_R in kcal were obtained by taking $\beta = -20$ kcal/mole.

The variation of E_R with θ is shown in Fig. 2, which indicates that E_R is approximately proportional to $\cos^2\theta$. The curve shows that at a nitro-group tilt of about 60° the energy of resonance interaction between a nitro group and the aromatic π-electrons is about $1\frac{1}{2}$ kcal/mole, compared with about $6\frac{1}{2}$ kcal/mole in a completely planar aromatic nitro compound, so that it is small but not negligible. Guy (6) has calculated for diphenyl

Can. J. Chem. Downloaded from www.nrcresearchpress.com by 196.1.178.254 on 09/04/12
For personal use only.

TABLE II

π-Electron molecular-orbital energy levels (E_i) in order of increasing energy, for various θ

$\theta°$	0	41.4	60	75.5	90
$\cos\theta$	1.000	0.750	0.500	0.250	0.000
$i = 1$	$\alpha+3.2098\beta$	$\alpha+3.1214\beta$	$\alpha+3.0552\beta$	$\alpha+3.0140\beta$	$\alpha+3\beta$
2	$\alpha+1.9554\beta$	$\alpha+1.9726\beta$	$\alpha+1.9869\beta$	$\alpha+1.9966\beta$	$\alpha+2\beta$
3	$\alpha+\beta$	$\alpha+\beta$	$\alpha+\beta$	$\alpha+\beta$	$\alpha+\beta$
4	$\alpha+\beta$	$\alpha+\beta$	$\alpha+\beta$	$\alpha+\beta$	$\alpha+\beta$
5	$\alpha+\beta$	$\alpha+\beta$	$\alpha+\beta$	$\alpha+\beta$	$\alpha+\beta$
6	$\alpha-0.6432\beta$	—	—	—	$\alpha-\beta$
7	$\alpha-\beta$	—	—	—	$\alpha-\beta$
8	$\alpha-1.4024\beta$	—	—	—	$\alpha-\beta$
9	$\alpha-2.1197\beta$	—	—	—	$\alpha-2\beta$
$2\sum_{i=1}^{5} E_i$	$10\alpha+16.3305\beta$	$10\alpha+16.1879\beta$	$10\alpha+16.0842\beta$	$10\alpha+16.0211\beta$	$10\alpha+16\beta$
E_R	0.3305β	0.1879β	0.0842β	0.0211β	0
E_R (kcal/mole)	−6.61	−3.76	−1.68	−0.42	0

derivatives a much more rapid decrease in resonance interaction with increasing θ, and in fact his resonance energy is proportional to $\cos^4\theta$, so that it is quite small at $\theta = 60°$ (about 0.4 kcal/mole). However, he makes the initial assumption that the resonance integral $w(\theta)$ is given by $w(\theta) = w(0)[1+\cos 2\theta]/2$, that is β^θ is proportional to $\cos^2\theta$, and hence his resonance energy is inevitably proportional to $\cos^4\theta$. Dewar (7) on the other hand takes β^θ proportional to $\cos\theta$, and shows that the resonance energy is proportional to $\cos^2\theta$.

In nitrobenzene the most stable configuration has $\theta = 0°$, but in a molecule in which the steric effects of neighboring atoms or groups prevent the attainment of a completely coplanar arrangement, the most stable configuration is determined not only by the resonance energy E_R, but also by the repulsive forces between the oxygen atoms and neighboring groups. The energies of van der Waals attraction and electronic repulsion can be represented by a curve of the form

$$E_v = -\frac{a}{r^6} + \frac{b}{r^n} \qquad (n > 6).$$

The variation of this energy with θ in nitro derivatives of mesitylene and durene is shown in Fig. 3; the energy passes through a slight minimum at the angle corresponding to van der Waals separation, and increases very markedly at smaller θ due to rapidly increasing repulsive forces. The variation of the combined energies, E_R and E_v, with θ is also shown in Fig. 3; there is a minimum in the curve in the region of $\theta = 65°$, so that this is the most stable configuration of the isolated molecules.

Inductive Effects

In heterocyclic molecules uncertainty about the exact values of the various coulomb and resonance integrals generally makes the reliability of the calculated energies rather uncertain. In the present calculations, however, while variation of the parameters changes the values of the energy levels E_i, the resonance energies are changed only slightly. The inductive effect of the nitro group on the carbon parameters, for example, can be allowed for by writing the coulomb integrals of the carbon atoms as $\alpha + m\beta$, where m decreases with increase in the number of bonds between the carbon atom and nitro group. The calculations of the energy levels were repeated taking $m = 0.6$ for carbon atom 1, and zero for the other carbon atoms, the results (for $\theta = 0°$ and 90°) being listed in Table III. Comparison with the values of Table II shows that while the energy levels have

Can. J. Chem. Downloaded from www.nrcresearchpress.com by 196.1.178.254 on 09/04/12
For personal use only.

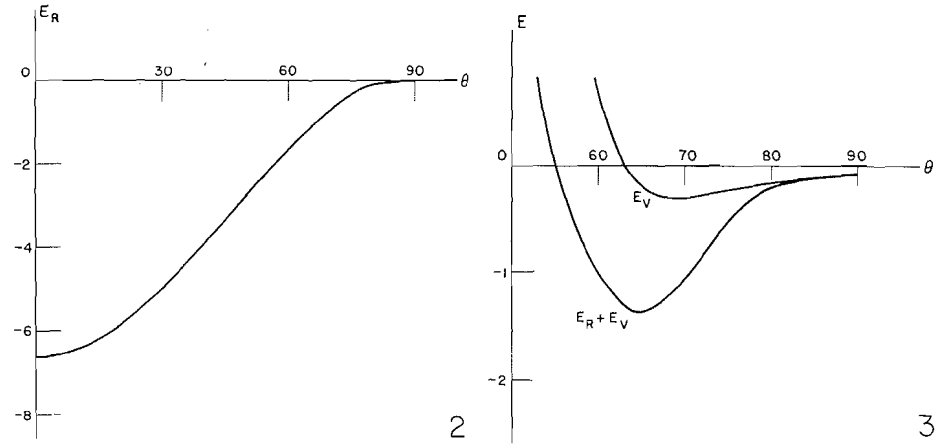

FIG. 2. Energy of resonance interaction (E_R in kcal/mole) between nitro group and aromatic π-electrons as a function of nitro-group tilt (θ).
FIG. 3. Variation of van der Waals energy (E_v) and total energy (E_R+E_v).

TABLE III

Molecular-orbital energy levels, E_i, with allowance for inductive effect

θ	0°	90°
cos θ	1.000	0.000
$i=1$	$\alpha+3.2688\beta$	$\alpha+3\beta$
2	$\alpha+2.0452\beta$	$\alpha+2.1359\beta$
3	$\alpha+1.1845\beta$	$\alpha+1.1995\beta$
4	$\alpha+\beta$	$\alpha+\beta$
5	$\alpha+\beta$	$\alpha+\beta$
6	—	$\alpha-0.8116\beta$
7	—	$\alpha-\beta$
8	—	$\alpha-\beta$
9	—	$\alpha-1.9237\beta$
$2\sum_{i=1}^{5} E_i$	$10\alpha+16.9971\beta$	$10\alpha+16.6707\beta$
E_R	0.3264β	0
E_R (kcal)	−6.53	0

changed, the energy of resonance interaction between a nitro group and aromatic π-electrons differs little from the value calculated neglecting the inductive effect.

Electron Distributions and Mobile Bond Orders

The coefficients c_r^i for each energy level were then evaluated by means of continuants and the π-electron distributions (q_r) and mobile bond orders (p_{rs}) evaluated from the expressions

$$q_r = \sum_i n(c_r^i)^2 \qquad \text{and} \qquad p_{rs} = \sum_i nc_r^i c_s^i \qquad (n = 2).$$

The values for $\theta = 0°$, 60°, 90° are listed in Tables IV and V. The values at $\theta = 0°$ and 90° for $m_1 = 0.6$ are included, and these show that while allowance for the inductive effect of the nitro group changes the charges on the carbon atoms, it produces only quite small differences in the bond orders.

To derive the bond lengths from the calculated bond orders, correlation curves were drawn as described below.

Can. J. Chem. Downloaded from www.nrcresearchpress.com by 196.1.178.254 on 09/04/12
For personal use only.

TABLE IV

π-Electron distribution (q_r)

	r	1	2	3	4	5	6	7	8	9
$m_1 = 0$	$\theta = 0°$	1.006	0.973	1.007	0.976	1.007	0.973	1.009	1.530	1.530
	60°	1.002	0.993	1.000	0.994	1.000	0.993	1.003	1.508	1.508
	90°	1.000	1.000	1.000	1.000	1.000	1.000	1.000	1.500	1.500
$m_1 = 0.6$	$\theta = 0°$	1.213	0.893	1.005	0.923	1.005	0.893	1.000	1.534	1.534
	90°	1.232	0.908	1.005	0.940	1.005	0.908	1.000	1.500	1.500

TABLE V

Mobile bond orders (p_{rs})

	$m_1 = 0$			$m_1 = 0.6$	
Bond	$\theta = 0°$	$\theta = 60°$	$\theta = 90°$	$\theta = 0°$	$\theta = 90°$
1–2	0.628	0.656	0.667	0.610	0.648
2–3	0.675	0.669	0.667	0.679	0.670
3–4	0.661	0.665	0.667	0.659	0.664
1–7	0.322	0.167	0	0.318	0
7–8	0.665	0.696	0.707	0.668	0.707

Carbon–Carbon Bonds

Since the carbon–carbon bond orders in nitrobenzene differ only slightly from those in benzene, only the region of the bond order – bond length curve near the benzene point is of importance, and a linear correlation (Fig. 4*a*) between the single-bond distance for sp^2 hybridization (1.50 Å) and the double-bond distance (1.34 Å) was used, this line passing close to the benzene point (0.667, 1.397).

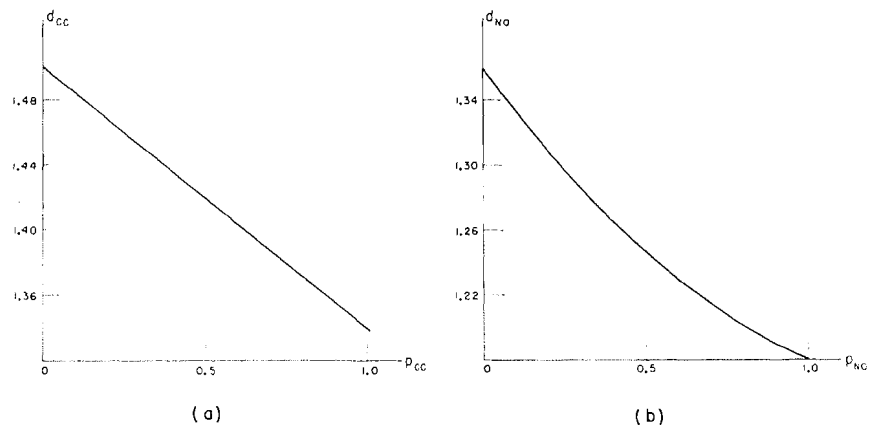

(a) (b)

FIG. 4. Bond order – bond length correlation curves for (*a*) C–C bonds and (*b*) N–O bonds.

Nitrogen–Oxygen Bonds

A curve was drawn (Fig. 4*b*) from the point (0, 1.36) representing the single-bond length to (1.0, 1.18) representing the double-bond distance, and passing close to the point for a non-conjugated nitro compound (0.707, 1.21). Only the range of bond orders around 0.7 is of importance in the present computations.

Carbon–Nitrogen Bonds

Since the mobile bond order of the C–N bonds in aromatic nitro compounds changes

Can. J. Chem. Downloaded from www.nrcresearchpress.com by 196.1.178.254 on 09/04/12
For personal use only.

considerably with the angle of tilt of the nitro group (Table V), the exact form of this correlation curve is of more importance. The curve shown as a full line in Fig. 5 was

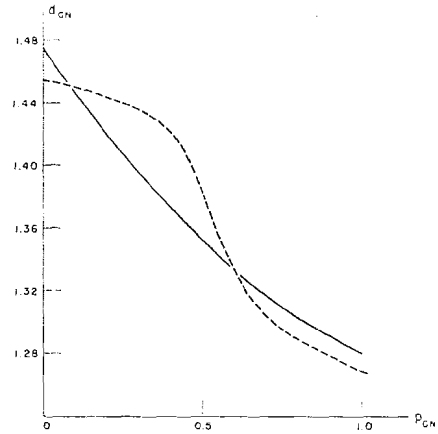

FIG. 5. Correlation curves for C–N bonds.

drawn through (0, 1.475), (0.600, 1.336), and (1.000, 1.280), since Goodwin and Porte (8) have deduced from a consideration of bond orders and lengths in a number of molecules that any reasonable curve must pass close to the point (0.600, 1.336). These authors also suggest that the length of a pure single bond be taken as 1.435 Å to allow for the sp^2 hybridization. However, in aliphatic nitro compounds the C–N distance is about 1.475 Å and since the nitrogen atom is already in a state of sp^2 hybridization, application of a correction for change of hybridization of the carbon atom would give 1.455 Å for the single-bond length to be used in aromatic nitro compounds. An alternative curve using this single-bond distance and of the form suggested by Goodwin and Porte is shown as a broken line in Fig. 5. The two curves differ significantly in the range of bond orders encountered in nitro compounds ($0 \rightarrow 0.3$), and it would be possible to decide between them if some accurate bond length measurements in the bond order range $0 \rightarrow 0.3$ were available. The C–N distance in 9-nitroanthracene (1.482 Å) would suggest that the full curve is more acceptable for nitro compounds, although this length is not known with great accuracy (standard deviation 0.015 Å). An accurate value of the C–N bond length in nitrobenzene would distinguish between the curves, since the lengths corresponding to $p_{CN} = 0.322$ are significantly different (1.391 Å and 1.433 Å) and work is being undertaken to measure this value (and incidentally investigate any possible deviations from exact planarity in this molecule). Meanwhile the full curve will be used in deriving bond lengths, with the bond lengths derived from the broken curve generally being noted for comparison.

The values of the bond lengths for all the bond orders in Table V were read off from the correlation curves, and these are listed in Table VI. The variations of the lengths of the C–C bonds with nitro group tilt are very small, the maximum difference being 0.006 Å (0.009 Å with allowance for the inductive effect, taking $m_1 = 0.6$); similarly the maximum variation for the N–O bonds is 0.007 Å. These variations are generally too small to be measured accurately by X-ray crystal analyses. For the C–N bonds, however, the lengths are 1.475 Å for $\theta = 90°$ and 1.391 Å for $\theta = 0°$ (using the full curve of Fig. 5) and it should be possible to detect this type of variation quite readily. (If the broken correlation curve is used the range is only 1.455 Å to 1.433 Å, but even this variation could be detected by accurate X-ray analysis.)

Can. J. Chem. Downloaded from www.nrcresearchpress.com by 196.1.178.254 on 09/04/12
For personal use only.

TABLE VI
Calculated bond lengths (Å)

	$m_1 = 0$			$m_1 = 0.6$	
Bond	$\theta = 0°$	$\theta = 60°$	$\theta = 90°$	$\theta = 0°$	$\theta = 90°$
1–2	1.399	1.395	1.393	1.402	1.396
2–3	1.392	1.393	1.393	1.392	1.393
3–4	1.394	1.393	1.393	1.394	1.394
1–7	1.391	1.428	1.475	1.391	1.475
7–8	1.220	1.215	1.213	1.219	1.213
Alternative					
1–7	1.433	1.446	1.455	1.434	1.455

MESONITROANTHRACENES

The application of the methods described above to aromatic nitro compounds in which resonance between nitro group and aromatic π-electrons is inhibited due to steric effects requires that some estimation of the C–N resonance integral be made, and this integral is approximately proportional to $\cos\theta$. The angle θ has been accurately measured for 9,10-dinitroanthracene and 9-nitroanthracene in the solid state using X-ray diffraction methods (1, 2), and these values may now be used in computing bond orders, and hence in deriving bond lengths for comparison with those measured by the X-ray methods.

9,10-Dinitroanthracene

In 9,10-dinitroanthracene (Fig. 6) each carbon and oxygen atom contributes one p_z

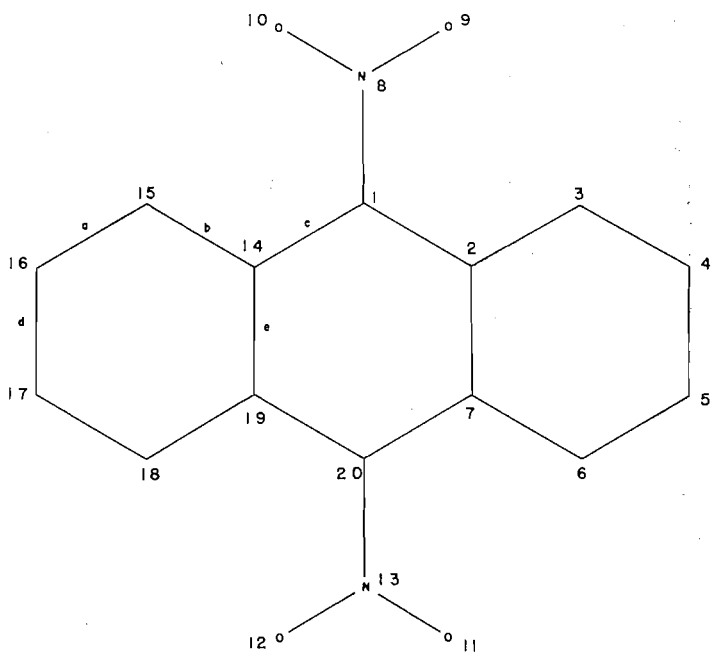

FIG. 6. Numbering used in the computations for 9,10-dinitroanthracene.

electron to the π-molecular-orbital system, while the nitrogen atoms each contribute two, so that 20 molecular orbitals accommodate 22 electrons. The secular equations were set up in the usual way. X-ray analysis has shown that $\theta = 63.7°$, so that the C–N resonance integrals are 0.44β. Overlap integrals were taken as zero, and the inductive

Can. J. Chem. Downloaded from www.nrcresearchpress.com by 196.1.178.254 on 09/04/12
For personal use only.

effects of the nitro groups were neglected since, as shown above, their inclusion causes only small variations in the bond orders and bond lengths.

The secular determinant is of the 20th order, but since the molecule has a center of symmetry, the 20th-order determinant was at once factorized into two 10th-order determinants according as $c_r = \pm c_{21-r}$. Using continuants these determinants were readily expanded to

$$\Delta_{\text{symmetrical}} = (x+1)^2(x-1)^2(x-2)[(P_5+5P_4+7P_3+2P_2+P_1+3P_0) - 0.20(P_3+4P_2+7P_1+6P_0)]$$

$$\Delta_{\text{antisymmetrical}} = (x+1)^2(x-1)^2(x+2)[(P_5+P_4-5P_3-2P_2+P_1+3P_0) - 0.20(P_3-P_1-2P_0)].$$

The π-electron molecular-orbital energy levels, E_i, were evaluated for 9,10-dinitroanthracene, and also, for comparison, for anthracene and the nitro groups separately, corresponding to no resonance interaction ($\theta = 90°$). The energy levels are listed in Table VII, together with the total π-electron energy and resonance energy due to resonance interaction between the nitro groups and the anthracene nucleus. Taking $\beta = -20$ kcal/mole this resonance energy is 2.92 kcal/mole (1.46 kcal/nitro group).

TABLE VII

π-Electron molecular-orbital energy levels, E_i, for 9,10-dinitroanthracene, in order of increasing energy

i	Anthracene + 2 nitro groups	9,10-Dinitroanthracene	Symmetry
1	$\alpha+3\beta$	$\alpha+3.0537\beta$	S
2	$\alpha+3\beta$	$\alpha+3.0397\beta$	A
3	$\alpha+2.4142\beta$	$\alpha+2.3908\beta$	S
4	$\alpha+2\beta$	$\alpha+2\beta$	A
5	$\alpha+1.4142\beta$	$\alpha+1.4118\beta$	S
6	$\alpha+1.4142\beta$	$\alpha+1.4077\beta$	A
7	$\alpha+\beta$	$\alpha+\beta$	S
8	$\alpha+\beta$	$\alpha+\beta$	A
9	$\alpha+\beta$	$\alpha+\beta$	S
10	$\alpha+\beta$	$\alpha+\beta$	A
11	$\alpha+0.4142\beta$	$\alpha+0.4260\beta$	A
12	$\alpha-0.4142\beta$	—	S
13	$\alpha-\beta$	—	S
14	$\alpha-\beta$	—	A
15	$\alpha-\beta$	—	S
16	$\alpha-\beta$	—	A
17	$\alpha-1.4142\beta$	—	S
18	$\alpha-1.4142\beta$	—	A
19	$\alpha-2\beta$	—	S
20	$\alpha-2.4142\beta$	—	A
$2\sum_{i=1}^{11} E_i$	$22\alpha+35.3137\beta$	$22\alpha+35.4596\beta$	
E_R	0	0.1459β	
E_R (kcal/mole)	0	−2.92	

The c_r^i were then evaluated for each energy level and the π-electron distribution and mobile bond orders are listed in Tables VIII and IX. The calculated bond lengths were then derived, using the C–N and N–O correlation curves of the previous section; for C–C bonds however, a best linear correlation was drawn through the points representing the calculated bond orders and observed bond lengths for anthracene (Fig. 7).

9-Nitroanthracene

In 9-nitroanthracene 17 molecular orbitals accommodate 18 electrons, and the secular equations were set up using similar parameters to those for the dinitro derivative. X-ray

Can. J. Chem. Downloaded from www.nrcresearchpress.com by 196.1.178.254 on 09/04/12
For personal use only.

TABLE VIII

π-Electron distributions (q_r) in 9,10-dinitroanthracene

r	Anthracene + 2 nitro groups	9,10-Dinitroanthracene
1	1.000	0.994
2	1.000	0.996
3	1.000	0.999
4	1.000	0.998
8	1.000	1.004
9	1.500	1.508

TABLE IX

Mobile bond orders (p_{rs}) in 9,10-dinitroanthracene

Bond	Anthracene + 2 nitro groups	9,10-Dinitroanthracene
a	0.737	0.736
b	0.535	0.538
c	0.606	0.596
d	0.586	0.587
e	0.485	0.487
C–N	0	0.163
N–O	0.707	0.695

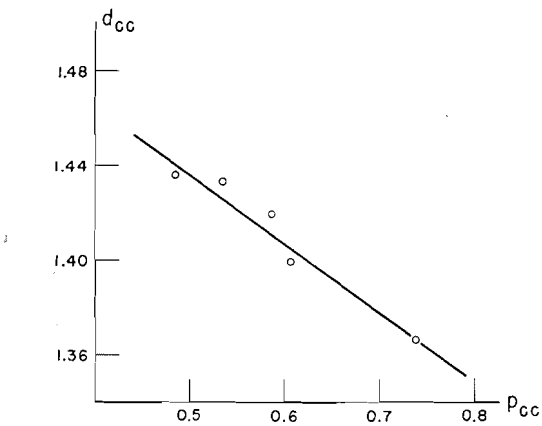

FIG. 7. Correlation curve for C–C bonds, based on the points for anthracene.

analysis has shown that the nitro group is tilted 84.7° out of the aromatic plane so that the C–N resonance integral is 0.09β. The secular determinant is of the 17th order, but since $\cos^2\theta$ is quite small, the energy levels differ little from those in anthracene and a non-conjugated nitro group, and the complete calculations were not carried out. The energy of resonance interaction between the nitro group and the aromatic π-electrons is 0.06 kcal/mole, the C–C and N–O bond orders do not differ significantly from those in the separate, non-conjugated anthracene molecule and nitro group, and the C–N bond order (approximately proportional to $\cos\theta$) is about 0.034. The calculated bond lengths were derived from the same curves as those for 9,10-dinitroanthracene.

DISCUSSION

The energy of resonance interaction between the nitro groups and the anthracene nucleus in 9,10-dinitroanthracene is 2.92 kcal/mole. When the variation of resonance

Can. J. Chem. Downloaded from www.nrcresearchpress.com by 196.1.178.254 on 09/04/12
For personal use only.

energy with nitro-group tilt is combined with the energies of van der Waals attraction and electronic repulsion between the oxygen atoms and neighboring carbon and hydrogen atoms, a curve of the type shown in Fig. 3 is obtained, with a minimum in the region of $\theta = 65°$, in good agreement with the measured tilt (64°). This structure is about 3 kcal/mole more stable than that with $\theta = 90°$. The most stable configuration for 9-nitroanthracene should have the nitro group tilted 64° out of the anthracene plane, but in the solid state crystal forces apparently give minimum energy when $\theta = 85°$.

The calculated bond lengths for anthracene, 9,10-dinitroanthracene, and 9-nitroanthracene are compared in Table X with the distances measured by X-ray crystal

TABLE X

Measured and calculated bond lengths in anthracene, 9,10-dinitroanthracene, and 9-nitroanthracene (Å)

	Anthracene			9,10-Dinitroanthracene			9-Nitroanthracene		
Bond	Meas.	Calc.	Δ	Meas.	Calc.	Δ	Meas.	Calc.	Δ
a	1.366	1.366	0	1.356	1.366	−0.010	1.399	1.366	+0.033
b	1.433	1.426	+0.007	1.414	1.425	−0.011	1.434	1.426	+0.008
c	1.399	1.405	−0.006	1.389	1.408	−0.019	1.400	1.405	−0.005
d	1.419	1.411	+0.008	1.400	1.410	−0.010	1.413	1.411	+0.002
e	1.436	1.440	−0.004	1.452	1.440	+0.012	1.437	1.440	−0.003
C–N	—	—	—	1.450	1.430	+0.020	1.482	1.465	+0.017
Alternative C–N	—	—	—		1.446	+0.004		1.453	+0.029
N–O	—	—	—	1.241	1.215	+0.026	1.216	1.213	+0.003
R.M.S. Δ			0.006			0.016 (0.015)			0.015 (0.017)

analyses, the differences (Δ) and root mean square Δ being included in the table. For anthracene the measured and calculated distances for the various bonds are of course very similar, since the calculated bond orders and observed bond lengths in anthracene have been used in deriving the carbon–carbon correlation curve. The agreement for the C–C bonds in the nitro derivatives is quite satisfactory; only for the *a* bond in 9-nitroanthracene is the difference apparently greater than the estimated experimental error (4), and this latter has probably been slightly underestimated (2). The calculated N–O bond length in 9-nitroanthracene is in very good agreement with the measured value. For 9,10-dinitroanthracene the agreement is not quite so good, although the difference is just within the limits of experimental error.

For the C–N bonds, while the agreement is reasonable, it is still not possible to decide between the two correlation curves shown in Fig. 5. In 9-nitroanthracene the agreement is significantly better when the full curve is used for bond order – bond length correlation, but the broken curve gives better agreement for the dinitro derivative. Further accurate measures of C–N bond lengths in the bond order range $0 \rightarrow 0.3$ are required to establish better correlation for the C–N bonds in nitro compounds, and present investigations by X-ray diffraction methods of the crystal structures of nitro derivatives of mesitylene and durene, and of nitrobenzene, may supply some useful data.

REFERENCES

1. TROTTER, J. Acta Cryst. **11**, 564 (1958).
2. TROTTER, J. Acta Cryst. (In press).
3. TROTTER, J. Can. J. Chem. **37**, 351 (1959).
4. TROTTER, J. Can. J. Chem. **37**, 825 (1959).
5. GOODWIN, T. H. and VAND, V. J. Chem. Soc. 1683 (1955).
6. GUY, J. J. chim. phys. **46**, 469 (1949).
7. DEWAR, M. J. S. J. Am. Chem. Soc. **74**, 3345 (1952).
8. GOODWIN, T. H. and PORTE, A. L. J. Chem. Soc. 3595 (1956)

Can. J. Chem. Downloaded from www.nrcresearchpress.com by 196.1.178.254 on 09/04/12
For personal use only.

Can. J. Chem. Downloaded from www.nrcresearchpress.com by 196.1.178.254 on 09/04/12
For personal use only.

THE KINETICS OF HYDROGEN CHEMISORPTION ON AN IRIDIUM CATALYST[1]

MANFRED J. D. LOW AND H. AUSTIN TAYLOR

ABSTRACT

The kinetics of the chemisorption of hydrogen on an iridium catalyst have been studied at various temperatures and pressures. The rate of adsorption is well defined by the Elovich equation. Isothermal anomalies have been observed and were found to be a function of temperature and initial gas pressure.

Recently it has been shown (1) that the Elovich equation,

$$dq/dt = a\, e^{-\alpha q},$$

will accurately reflect the variation of the amount adsorbed, q, with time, t, in many chemisorption processes. The constants (a) and α were found to vary with temperature, but there was no indication of a pressure dependence. More recently (2, 3) such a pressure dependence has been found in several systems and, in order to investigate further the influence of initial gas pressure on the Elovich parameters, the present investigation was undertaken.

EXPERIMENTAL

The measurements of rates of adsorption were carried out by admitting a known amount of hydrogen to a sample of the catalyst which had been suitably evacuated, and measuring the change of pressure in the constant-volume system. A commercial hydrogenation catalyst, purchased from Baker and Co., Inc., was used as adsorbent. The catalyst consisted of 0.5% iridium supported on the surface of 3×5-mm γ-alumina extrudates.

The catalyst (20.10 g) was placed in a Vycor tube and sealed to the all-Pyrex system. A copious evolution of water and of gas took place on heating the catalyst to 500° C. After an overnight pumping period at that temperature the pressure within the system had fallen to 10^{-6} mm Hg. The catalyst was then treated with palladium-filtered hydrogen at 500° C at a pressure of 60 cm dibutyl phthalate (DBP). After 2 hours the gas was removed, and the adsorbent was pumped on overnight at 500°. This hydrogen treatment was repeated six times. It was found that on pumping at 500°, a vacuum of 10^{-6} mm Hg, or less, could be obtained and maintained after a period of about 6 hours. A minimum pump-off period of 10 hours at 500° was therefore chosen.

It was noticed that the color of the untreated catalyst was black. After pumping, but before the hydrogen treatment, the color was still black. After the first contact with hydrogen, however, the catalyst had turned gray, and remained that color until the end of the series of experiments.

Dead spaces were measured by expansion of helium purified by passage through a charcoal trap cooled with liquid nitrogen. The catalyst was thermostatted at a desired temperature by surrounding the chamber with a Dewar flask filled with solid CO_2, ice, or with the vapors of a boiling liquid. The experiments reported here were made at different initial pressures, P_0, at any one temperature, T, and were numbered consecutively in order of their execution.

[1]*Manuscript received January 28, 1959.*
Contribution from The Nichols Laboratory, New York University, New York 53, New York.

RESULTS AND DISCUSSION

A total of 38 experiments at seven different temperatures were made. It was found that the data of each experiment could be precisely described by use of the Elovich equation. Isothermal anomalies (1) were found. The $q - \log t$ plots of the data appeared as straight lines which, after a certain time, t_b, abruptly changed in slope. These discontinuities, or "breaks", are illustrated by Fig. 1. The data of three sample runs are

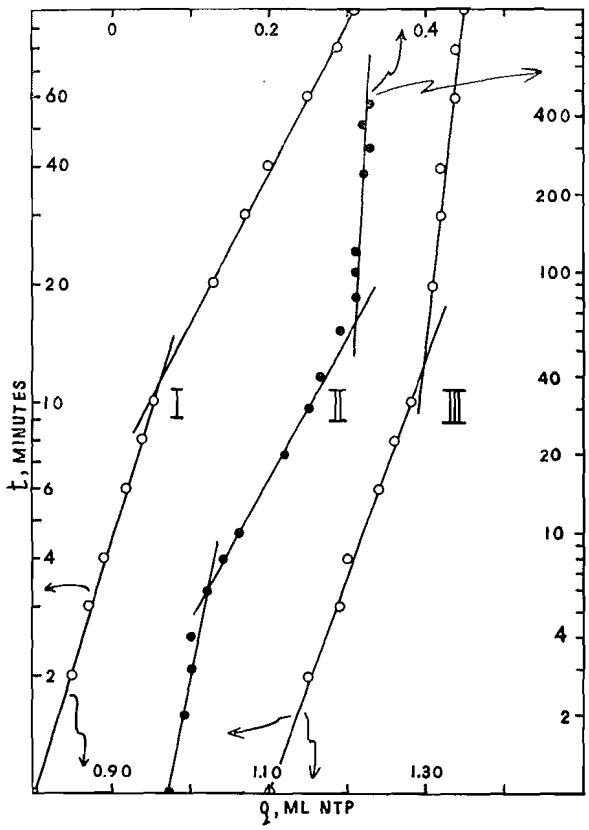

FIG. 1. Adsorption of H_2 on $Ir.Al_2O_3$. Typical runs: I. Run 2, 147°, 34.5 cm DBP; II. Run 28, 257°, 10.4 cm DBP; III. Run 38, −78.5°, 8.8 cm DBP.

shown to be internally consistent. Circles represent experimental points, and the lines were calculated using the equation,

$$q = (2.3/\alpha) \log_{10} (1+a\alpha t).$$

Constants were calculated by a previously described method (4), and are summarized in Table I. The subscripts 1, 2, and 3 identify the parameters corresponding to the 1st, 2nd, or 3rd branches of the curve. The co-ordinates of the break, q_b and t_b, result from the intersection of the 1st and 2nd branches.

It is to be noted that, with the exception of run 38, the slopes of the $q - \log t$ plots increased after t_b. In a few cases, notably with experiments at low pressures, this region of increased slope was followed by one of decreased slope (plot II, Fig. 1). This is not unexpected, since the slope must eventually become zero. The fact that these 3rd branches

Can. J. Chem. Downloaded from www.nrcresearchpress.com by 196.1.178.254 on 09/04/12
For personal use only.

TABLE I

Run No.	P_0 cm DBP	$T°$ C	α_1	α_2	α_3	ln $a_1\alpha_1$	ln $a_2\alpha_2$	ln $a_3\alpha_3$	q_b	t_b
1	68.9		11.5	5.1	—	5.50	1.65	—	1.39	27
2	34.5		15.2	8.7	—	5.30	3.58	—	0.96	11
3	25.8		17.4	11.1	—	5.13	2.96	—	0.79	7
4	59.8	147	12.8	5.1	—	5.34	1.33	—	1.20	21
5	43.2		14.3	7.6	—	4.87	2.07	—	0.96	13
6	9.8		20.0	13.5	19.7	3.83	2.46	4.25	0.50	3
7	18.3		18.1	12.9	—	4.33	2.91	—	0.63	4
8	51.9		15.9	7.4	—	5.94	2.26	—	1.03	11
15	5.9		23.0	9.5	25.6	2.50	0.85	3.56	0.28	2
9	26.0		16.4	8.9	13.5	4.63	2.06	3.87	0.76	6
10	10.0		20.0	10.0	17.7	3.13	1.30	3.08	0.43	3.5
11	4.9	100	35.0	31.0	128.0	1.67	0.40	10.96	0.15	3
12	72.5		10.9	4.8	—	5.27	1.61	—	1.38	18
13	42.5		15.3	8.9	—	5.19	2.52	—	0.93	12
14	26.5		15.2	7.7	—	4.61	1.84	—	0.85	10
16	74.8		14.9	4.1	—	5.51	0.54	—	1.05	19
17	43.7		18.7	9.3	—	4.72	1.81	—	0.71	11
18	26.7		19.5	—	—	3.73	—	—	—	—
19	10.2	200	23.0	11.2	20.4	2.11	0.84	2.60	0.25	2
20	18.4		20.5	10.3	—	3.92	1.73	—	0.51	3
21	5.0		23.0	13.9	37.7	1.30	0.66	3.62	0.16	2
22	60.8		14.8	3.8	—	5.08	0.34	—	0.98	17
23	35.3		20.0	10.3	—	4.22	1.78	—	0.57	6
24	5.0		23.0	14.1	40.0	1.30	0.63	3.73	0.17	2.5
25	61.0		11.5	2.8	—	3.60	−0.19	—	0.99	25
26	35.4		23.0	8.4	—	3.90	0.96	—	0.50	7
27	18.9		33.0	10.4	13.8	3.15	0.67	1.28	0.25	3
28	10.4	257	35.0	12.6	115.0	1.07	−0.12	13.60	0.12	6
29	75.2		12.9	5.2	—	4.00	0.96	—	0.90	12
30	44.4		23.0	9.6	—	4.60	1.47	—	0.54	6
31	31.5		30.2	20.2	—	3.60	2.20	—	0.33	5
32	5.5		27.4	18.0	72.0	0.83	0.41	5.57	0.11	3
33	71.8	56	12.8	5.2	—	7.12	2.12	—	1.52	21
34	9.6		21.0	10.4	17.7	3.93	1.71	3.77	0.49	4
35	68.4	0	15.3	7.0	—	10.81	4.23	—	1.82	20
36	9.2		35.0	13.5	26.4	11.26	3.96	8.97	0.78	4
37	64.2	−78.5	7.7	2.9	—	12.89	4.22	—	4.15	10
38	8.8		12.8	38.0	—	6.12	20.31	—	1.30	13

are linear on a $q - \log t$ plot may be of significance, and suggests that rate measurements be continued to zero rate. Most of the present experiments were terminated after about 100 minutes because the rate of adsorption became quite slow. Thus in run 28, 0.309 ml was adsorbed at 100 minutes, and only 0.325 ml was adsorbed after 420 minutes.

Breaks of a similar nature are to be found in the plots of P_0 versus q_t, the amount adsorbed at time t at 100° C. The plots of Fig. 2 show breaks in the region of $P_0 \sim 10$ cm. This phenomenon was previously observed in the case of the systems H_2 – Ni. kieselguhr (2) and H_2 – Ru. Al_2O_3 (3).

Effect of Initial Pressure

From the data in Table I it can be seen that both α_1 and α_2 are dependent on the initial pressure at each temperature. These dependencies are representable by the equations

$$\alpha_1 = B_1 + C_1 P_0$$

$$\alpha_2 = B_2 + C_2 P_0$$

and Table II lists the values of the constants B and C at the four principal tempera-

Can. J. Chem. Downloaded from www.nrcresearchpress.com by 196.1.178.254 on 09/04/12
For personal use only.

TABLE II

	100° C	147° C	200° C	257° C
B_1	18.871	20.690	23.590	38.126
$-C_1$	0.106	0.129	0.125	0.354
B_2	10.719	14.979	14.030	15.573
$-C_2$	0.075	0.155	0.139	0.167
D	0.460	0.320	0.141	0.00682
E	0.0124	0.0153	0.9129	0.0133
F	1.807	1.740	−0.329	0.932
G	0.228	0.361	0.257	0.211
K	4.330	4.007	3.159	3.367
L	0.0142	0.0261	0.0317	0.0099
M	3.038	3.583	1.566	2.984
N	0.0175	0.0139	0.0381	−0.00651
$-m$	1.504	1.778	1.112	1.842
n	0.331	0.496	0.197	0.175

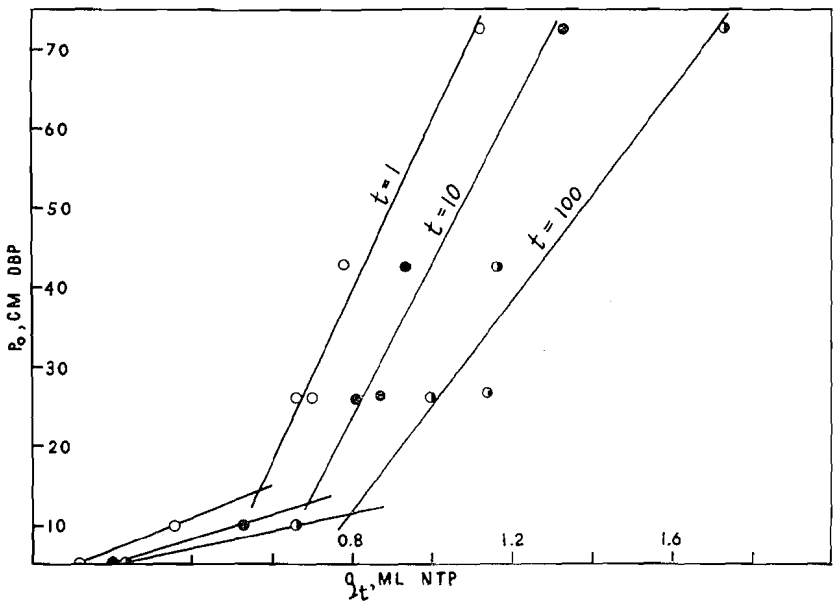

FIG. 2. The variation of q_t with P_0 at 100° C.

tures. In previous studies (2, 3) discontinuities were usually observed in such $\alpha - P_0$ plots, the slope changing abruptly at lower pressures. In the present study a discontinuity was found only at 100° C. Figure 3 shows a plot of both α_1 and α_2 as a function of P_0 at 100°. The data in Table II for 100° refer to the data above 10 cm. Below 10 cm at 100°, $\alpha_1 = 49.41 - 2.94P_0$ and $\alpha_2 = 51.18 - 4.12P_0$. At the other temperatures the constants in Table II cover the whole pressure range studied.

The variation of $\log a_1$ and $\log a_1\alpha_1$ with P_0 followed a pattern similar to that of α, and may be represented by the equations;

$$\log_{10} a_1\alpha_1 = K + LP_0$$

$$\log_{10} a_1 = M + NP_0,$$

the values of the constants at four temperatures being given in Table II. Breaks occurred in the low-pressure region. At 100°, $\log_{10} a_1\alpha_1 = 0.269 + 0.286P_0$; at 200°, $\log_{10} a_1\alpha_1 = 0.522$

Can. J. Chem. Downloaded from www.nrcresearchpress.com by 196.1.178.254 on 09/04/12
For personal use only.

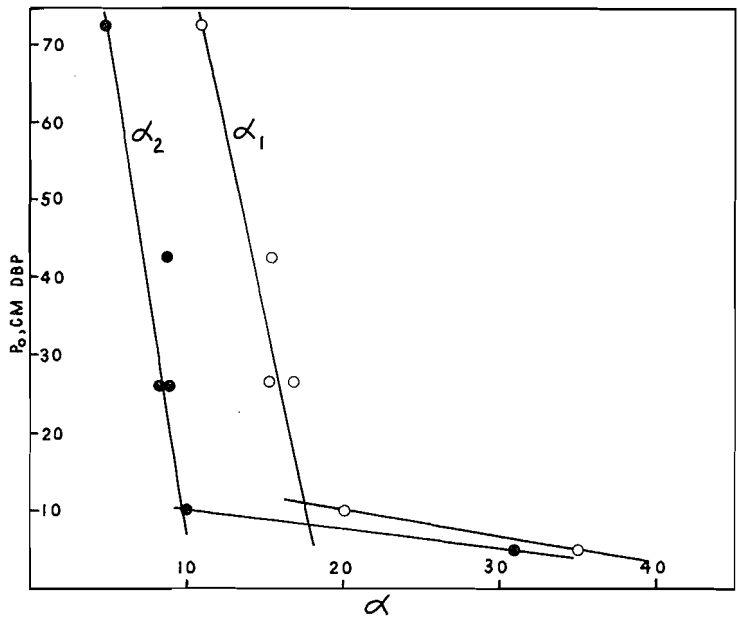

FIG. 3. The variation of α with P_0 at 100° C.

$+0.156P_0$. Since α showed breaks only at 100° but $\log a_1\alpha_1$ has breaks at all temperatures, plots of $\log a_1$ vs. P_0, as expected, showed breaks at all temperatures. The constants of the equation,

$$\log_{10} a_1 = m+nP_0,$$

describing the low-pressure region, are given in Table II. The variation of $\log a_2$ and $\log a_2\alpha_2$ with P_0 is not clearly defined.

It has been noted that breaks occurred in all isotherms. It is interesting that the time of occurrence of the break, t_b, as well as the amount adsorbed at the time of occurrence, q_t, increase linearly with increasing P_0 according to the equations,

$$t_b = F+GP_0,$$
$$q_b = D+EP_0.$$

The values of the constants of these equations at four temperatures are given in Table II. The data at 100° show a break at a P_0 of about 10 cm in a fashion similar to that of α_1 and α_2. Below 10 cm, $q_b = -0.122+0.0554P_0$.

The Influence of Temperature on Parameter Values

In the previous studies it was found that α and $\log a\alpha$ were linear in the reciprocal of the temperature. Since the pressure dependencies of both parameters are more marked in the present study, values of α_1 and $\log a_1\alpha_1$ have been calculated from the previous equations for P_0 values of 60 and 40 cm DBP at each of the four highest temperatures. Since only two runs were made at each of the three lowest temperatures, the pressure dependence is too uncertain to justify a similar treatment. The least square straight line through the four points at each initial pressure expresses the relations, $\alpha_1 = U+V/T$, and $\log_{10} a_1\alpha_1 = X+Y/T$. The values of U, V, X, and Y at each of the initial pressures 60 and 40 cm DBP are given in Table III. The energy of activation of adsorption as

Can. J. Chem. Downloaded from www.nrcresearchpress.com by 196.1.178.254 on 09/04/12
For personal use only.

TABLE III

	P_0 = 60 cm	P_0 = 40 cm
U	28.68	44.13
$-V$	6194	11461
X	1.58	1489
Y	0.564	1741

usually calculated has previously been shown to be expressible as: $E = R(Vq - Y)$, where R is the gas constant. From the values of V and Y it is found that at $P_0 = 60$ cm, $E = -12.36q - 2.97$, and at $P_0 = 40$ cm, $E = 22.88q - 3.48$. Over the whole range of adsorption values of q, E is negative.

Comparison with previous studies on Ni and Ru shows that the values of V and Y may be either positive or negative. The magnitude and the direction of variation of E with coverage, q, present four possibilities which are illustrated in Fig. 4. Case I with

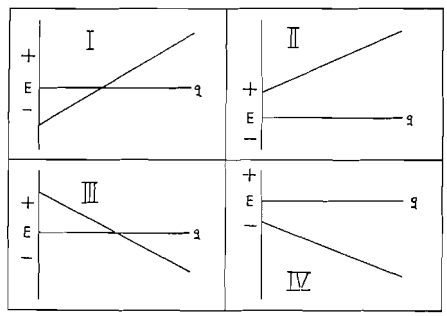

FIG. 4. Linear variation of activation energy with coverage.

V and Y both positive was found in the Ni.kieselguhr system. Case III, with V and Y both negative, was found with Ru.Al_2O_3. Case IV, with V negative and Y positive, is the present study. Case II is approximated by the data of Burwell and Taylor (5) for the adsorption of H_2 on Cr_2O_3. Taking their data, treated by the Elovich equation, given in Table IV of Taylor and Thon (1), for 0.5 atm it is found that $\alpha = (23700/T) - 45.5$, and $\log_{10} a\alpha = (1000/T) - 6$, whence $E = 47q - 2$ kcal. Although V and Y are both positive, the low value of Y leaves E positive except for very small values of q, thus approximating Case II. It is obvious that the interpretation of E as a simple energy of activation is not necessarily an argument for multiplicity of adsorption sites. On the other hand, it would appear inescapable that the changes in adsorption rate, here accentuated as "breaks," as well as the pressure dependencies found, cannot be attributed to a single type of adsorption site. Two or possibly three such types, rather than a spectrum of types, would appear sufficient to account for the observations.

The change in magnitude of a parameter with temperature may be connected with the region of the isobar under consideration. Figure 5 shows estimates of amounts adsorbed at 100 minutes, suggesting that the present experiments were made on the decreasing portion of the isobar. In view of the complexity of the relations it seems too early to comment on the possible physical significance of parameters such as a_2, the mathematical initial rate of the 2nd kinetic stage, or to attempt a general interpretation, much less to attempt to identify the sites concerned. Additional work on other gas–solid systems seems to be required.

Can. J. Chem. Downloaded from www.nrcresearchpress.com by 196.1.178.254 on 09/04/12
For personal use only.

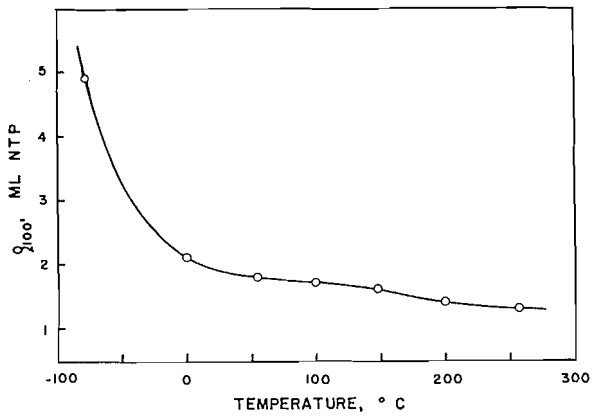

FIG. 5. The "100-minute isobar" of H_2 adsorption on Ir.Al_2O_3 at P_0 = 75 cm DBP.

REFERENCES

1. TAYLOR, H. A. and THON, N. J. Am. Chem. Soc. **74**, 4169 (1952).
2. LEIBOWITZ, L., LOW, M. J. D., and TAYLOR, H. A. J. Phys. Chem. **62**, 471 (1958).
3. LOW, M. J. D. and TAYLOR, H. A. Can. J. Chem. **37**, 544 (1959).
4. SARMOUSAKIS, N. J. and LOW, M. J. D. J. Chem. Phys. **25**, 178 (1956).
5. BURWELL, R. L. and TAYLOR, H. S. J. Am. Chem. Soc. **58**, 697 (1936).

Can. J. Chem. Downloaded from www.nrcresearchpress.com by 196.1.178.254 on 09/04/12
For personal use only.

Can. J. Chem. Downloaded from www.nrcresearchpress.com by 196.1.178.254 on 09/04/12
For personal use only.

THE CONSTITUTION OF A METHYL GLUCURONOXYLAN FROM KAPOK (CEIBA PENTANDRA)[1]

A. L. Currie and T. E. Timell

ABSTRACT

The seed hairs of kapok (*Ceiba pentandra*) on alkaline extraction have yielded a hemicellulose composed of xylose and uronic acid residues. Partial hydrolysis of the polysaccharide gave 2-*O*-(4-*O*-methyl-α-D-glucopyranosyluronic acid)-D-xylopyranose, 4-*O*-methyl-D-glucuronic acid, and, probably, galacturonic acid. Hydrolysis of the fully methylated hemicellulose yielded a mixture of 2-*O*- and 3-*O*-methyl-D-xylose, 2,3-di-*O*-methyl-D-xylose, 2,3,4-tri-*O*-methyl-D-xylose, and 2-*O*-(2,3,4-tri-*O*-methyl-α-D-glucopyranosyluronic acid)-3-*O*-methyl-D-xylopyranose in a molar ratio of 1.1:38:1:6. The number-average D.P. of the native and the methylated polysaccharides was 177 and 124, respectively. On the basis of this and other evidence it is suggested that the average hemicellulose molecule contains approximately 180 1,4-linked β-D-xylopyranose residues, one eighth of which carry a single terminal side chain of 4-*O*-methyl-D-glucuronic acid, attached through an α-glycosidic bond to C_2 of the xylose. The xylan framework contains, on the average, slightly less than two branching points per macromolecule, most of them probably originating from C_3. The number of acid side chains and branches is twice as large as that of the otherwise similar 4-*O*-methyl glucuronoxylan present in the seed hairs of milkweed floss.

In previous investigations the general chemical composition of the seed hairs of kapok was studied (1) as well as the molecular characteristics of their cellulose component (2, 3). The present paper is concerned with the structure and properties of the main hemicellulose constituent.

RESULTS AND DISCUSSION

The high pentosan content (24.4%) of the extractive-free seed hairs indicated that the predominant hemicellulose was based on xylose residues. The considerable amounts of acetyl (8.0%) and uronic anhydride (6.6%) groups present as well as the formation of a methylated glucuronic acid on hydrolysis of the fibers suggested that the polysaccharide in its native state was a partially acetylated methyl glucuronoxylan. When kapok fibers were extracted with aqueous alkali a deacetylated product was obtained in a yield of 18.8%, containing 83.3% pentosan and with $[\alpha]_D^{20}$ −68° in water. Its content of ash, methoxyl, and uronic anhydride indicated the presence of an average of 7.8 anhydroxylose units per methylated uronic acid.

Partial acid hydrolysis of the hemicellulose gave a mixture of sugars which was resolved into a neutral and an acidic portion on a column of anion exchange resin. The neutral part contained mostly D-xylose which crystallized but also traces of glucose, mannose, arabinose, and rhamnose. Elution of the column with dilute acetic acid yielded three sugar acids, namely a monouronic acid, chromatographically identical with galacturonic acid, an aldobiouronic acid, and a mono-*O*-methyl monouronic acid.

The methoxyl content and equivalent weight of the aldobiouronic acid suggested that it consisted of a methoxyuronic acid linked to a pentose residue. A portion of the acid was converted to the corresponding methyl ester methyl glycoside, which was reduced with lithium aluminum hydride and hydrolyzed to yield D-xylose, which crystallized, and 4-*O*-methyl-D-glucose, which was identified through its crystalline osazone (4, 5). The methyl ester methyl glycoside of the aldobiouronic acid was completely methylated, reduced, and hydrolyzed. The mixture of methylated sugars obtained was resolved on a cocoanut charcoal column to yield 3,4-di-*O*-methyl-D-xylose and 2,3,4-tri-

[1]*Manuscript received January 6, 1959.*
Contribution from McGill University and Pulp and Paper Research Institute of Canada, Montreal, Quebec.

O-methyl-D-glucose, both of which were identified through their crystalline aniline derivatives (6, 7). The methylated and reduced glycoside of the aldobiouronic acid was therefore methyl 2-*O*-(2,3,4-tri-*O*-methyl-α-D-glucopyranosyl)-3,4-di-*O*-methyl-D-xylopyranoside. This evidence shows that the aldobiouronic acid was 2-*O*-(4-*O*-methyl-α-D-glucopyranosyluronic acid)-D-xylopyranose. Its high positive rotation (+100° in water) in conjunction with other evidence (8, 9) indicated that the biose linkage was present in the α-configuration.

Reduction and subsequent hydrolysis of the methyl ester methyl glycoside of the mono-*O*-methyl uronic acid gave 4-*O*-methyl-D-glucose, thus showing that the compound was 4-*O*-methyl-D-glucuronic acid.

The hemicellulose was methylated to completion and hydrolyzed with dilute acetic acid. The acidic and neutral sugars formed were separated on an anion exchange resin. The acid fraction contained only one component, namely a partially methylated aldobiouronic acid. Reduction of its methyl ester methyl glycoside yielded a crystalline compound, which was identified through its melting point, specific rotation, infrared spectrum, and X-ray powder diagram as methyl 2-*O*-(2,3,4-tri-*O*-methyl-α-D-glucopyranosyl)-3-*O*-methyl-α,β-D-xylopyranoside, previously isolated from western hemlock (10), sugar maple, and yellow birch (11) wood. Methanolysis of the disaccharide followed by hydrolysis gave a mixture of methylated sugars which was resolved by fractional extraction with chloroform of its aqueous solution. The two sugars obtained were 2,3,4-tri-*O*-methyl-D-glucose and 3-*O*-methyl-D-xylose, both of which were characterized through their aniline derivatives.

The aqueous solution of the neutral sugars was fractionally extracted with chloroform. The first compound removed was chromatographically identical with 2,3,4-tri-*O*-methyl-D-xylose and was tentatively characterized through its infrared spectrum. The second and main portion was 2,3-di-*O*-methyl-D-xylose, identified as its crystalline aniline derivative. The residual aqueous solution contained a mixture of sugars which was resolved by paper ionophoresis to give 2-*O*-methyl-D-xylose together with a smaller quantity of 3-*O*-methyl-D-xylose. A portion of the mixture of neutral sugars was resolved by paper chromatography and subjected to quantitative analysis (12). The molar ratio of mono-, di-, and tri-*O*-substituted xyloses was 1.1: 38:1. The yield of the partially methylated aldobiouronic acid indicated the presence of 6 moles of aldobiouronic acid per mole of tri-*O*-methyl xylose, corresponding to 8 moles of xylose residues per acid group, in accordance with the above evidence.

The large quantity of 2,3-di-*O*-methyl-D-xylose isolated showed that the backbone of the polysaccharide was composed of D-xylopyranose residues linked through positions 1 and 4 and this conclusion was corroborated by results obtained on periodate oxidation of the hemicellulose. The high negative rotation of the original and of the methylated (−57° in chloroform) polysaccharide strongly suggested that the xylose residues were present in the β-configuration. The 2,3,4-tri-*O*-methyl-D-xylose apparently originated from the non-reducing end groups. The fact that the 4-position was unsubstituted in the crystalline, partly methylated aldobiouronic acid, obtained on partial hydrolysis of the methylated hemicellulose, whereas the methylated aldobiouronic acid itself was substituted in this position, indicated that the 4-*O*-methyl-D-glucuronic acid residues were attached *directly* to the framework of the 1,4-linked xylose residues. The structure of the aldobiouronic acid showed that the side chains were present in the α-configuration and were linked to C_2.

None of the acid side groups were evidently removed during the hydrolysis of the

Can. J. Chem. Downloaded from www.nrcresearchpress.com by 196.1.178.254 on 09/04/12
For personal use only.

methylated hemicellulose. The presence of the two mono-*O*-methyl xyloses was therefore due to either incomplete methylation, demethylation, or branching. While some demethylation probably occurred (13, 14), the possibility of branching could not be excluded, especially in view of the fact that one of the mono-*O*-methyl xyloses predominated.

When the number-average molecular weight of the methylated hemicellulose was determined by osmometry (13, 15), a value of 23,400 was obtained. With one 4-*O*-methyl-D-glucuronic acid residue present for every eighth anhydroxylose unit, this corresponded to a degree of polymerization (number of xylose residues in the main chain) of 124. Each methylated macromolecule thus contained on the average 3.0 mono-*O*-methylated, 118 di-*O*-methylated, and 2.7 tri-*O*-methylated xylose residues. This corresponded to the presence of 1.7 branch points per molecule, most of them probably originating from the 3-position of the xylose residues.

A portion of the hemicellulose was converted to the fully substituted acetate derivative which was soluble in chloroform–ethanol. Osmotic pressure measurements gave a number-average molecular weight of 43,700, corresponding to a $\bar{P}_n$ of 177 for the native polymer.

From the above evidence a simplified structure can now be suggested for the main hemicellulose component of the seed hairs of kapok. The xylan framework of this polysaccharide contains an average number of approximately 180 β-D-xylopyranose residues, connected by 1,4-glycosidic bonds and with, on the average, slightly less than two branching points per molecule, most of them probably located at C_3. Every eighth xylose residue has a single, terminal side chain of 4-*O*-methyl-D-glucuronic acid, linked by an α-glycosidic bond to C_2. The exact nature of the branching is unknown.

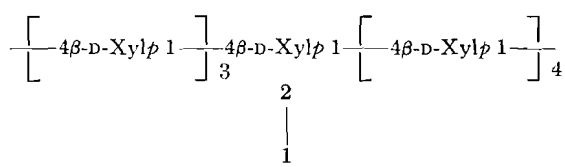

4-*O*-Me-α-D-GpA

The only other seed hair hemicellulose hitherto investigated appears to be that present in the floss of the common milkweed (16). This 4-*O*-methyl glucuronoxylan is similar to, albeit not identical with, that found in kapok, the latter polysaccharide having almost twice as many side chains and branching points as the former. Hemicelluloses containing a branched framework of 1,4-β-linked anhydroxylose units have been isolated also from corncob (17), esparto grass (18), and wheat straw (19, 20). In the dicotyledons, however, the 4-*O*-methyl glucuronoxylans are almost invariably linear (21). Whether the same applies to the related gymnosperm xylans is still uncertain (22). Many xylans have been found to contain single side chains of L-arabofuranose residues, for example those present in cereal straws and in coniferous woods. The absence of such groups in the seed hair xylans so far studied is notable. The molecular weight of the native kapok xylan is approximately the same as that of the corresponding polysaccharides present in milkweed floss (16) and in deciduous woods (21).

EXPERIMENTAL

All specific rotations are equilibrium values and melting points are corrected. Evaporations were carried out *in vacuo* at 40–50° C.

Can. J. Chem. Downloaded from www.nrcresearchpress.com by 196.1.178.254 on 09/04/12
For personal use only.

Can. J. Chem. Downloaded from www.nrcresearchpress.com by 196.1.178.254 on 09/04/12
For personal use only.

Paper Chromatography

Solvents (v/v) used for separating the sugars were (*a*) ethyl acetate – acetic acid – water (9:2:2), (*b*) butan-1-ol–pyridine–water (10:3:3), (*c*) butan-2-one–ethanol–water (20:5:2), (*d*) butan-1-ol–ethanol–water (40:11:19), and (*e*) butan-1-ol–benzene–ethanol–water (6:3:2:1). Whatman No. 1 and No. 3MM filter papers were used and *o*-aminodiphenyl was the preferred spray reagent (12).

Isolation of the Hemicellulose

Kapok seed hairs (1) were exhaustively extracted with ethanol–benzene (1:2, v/v) and subsequently with cold water. The fibers (400 g) were cut into small pieces and shaken with 24% (w/w) aqueous potassium hydroxide (7.6 liters) in an atmosphere of nitrogen for 2 hours. After filtration through sintered glass, the filtrate and the washings were added to a mixture of ethanol (30 liters) and acetic acid (2.6 liters). The precipitate was washed successively on the centrifuge with 80% aqueous methanol, anhydrous methanol, and petroleum ether (b.p. 30–60° C). The product was dried over calcium chloride *in vacuo* for 1 week to yield 75 g of a white, fluffy material, corresponding to 18.8% of the original extractive-free fibers.

Hydrolysis, followed by examination by paper chromatography indicated the presence of mostly xylose and uronic acids. Anal. Pentosan, 83.3%; uronic anhydride, 14.0%; methoxyl, 2.45%; sulphate ash (as potassium), 3.15%; $[\alpha]_D^{20}$ −68° (*c*, 1.0 in 5% sodium hydroxide).

Isolation of Neutral Sugars

The hemicellulose (51 g) was treated with 72% sulphuric acid (120 ml) at room temperature for 2 hours, after which the solution was diluted to 3 liters and boiled under reflux for 6 hours. The solution was neutralized with barium hydroxide, filtered through Celite, and treated with Amberlite IR-120 cation exchange resin for removal of barium ions. Half of the hydrolyzate was slowly passed through a column (5.5×110 cm) of Dowex 1-X4 anion exchange resin. Washing with water removed neutral sugars. On evaporation of the eluate, crystals were obtained which, after recrystallization from 80% ethanol, yielded D-xylose, m.p. and mixed m.p. 144–145° C, $[\alpha]_D^{20}$ +19 (*c*, 1.1 in water). The remaining sirup was resolved on the paper chromatogram (solvent A) to give xylose together with minor quantities of glucose, mannose, arabinose, and rhamnose.

Separation of Sugar Acids

The mixture of sugar acids remaining on the column of exchange resin was resolved by elution with *N* acetic acid to yield two compounds, one being an aldobiouronic acid and the other corresponding in rate of movement on the paper chromatogram (solvent A) and in color produced with the spray reagent to galacturonic acid. Evaporation of the former fraction gave a white, amorphous powder (2.00 g), the infrared spectrum of which was indistinguishable from that of an authentic specimen of 2-*O*-(4-*O*-methyl-α-D-glucopyranosyluronic acid)-D-xylopyranose. Anal. Calc. for $C_{12}H_{20}O_{11}$: OCH_3, 9.1%; equiv. wt., 340. Found: OCH_3, 8.9%; equiv. wt., 351; $[\alpha]_D^{20}$ +100° (*c*, 2.4 in water).

Further elution of the column with 3 *N* acetic acid gave a third sugar acid, chromatographically identical with 4-*O*-methyl glucuronic acid. Anal. Calc. for $C_7H_{12}O_7$: OCH_3, 14.9%; equiv. wt., 208. Found: OCH_3, 13.9%; equiv. wt., 209; $[\alpha]_D^{20}$ +48° (*c*, 1.4 in water).

Reduction and Hydrolysis of the Aldobiouronic Acid

The aldobiouronic acid (0.80 g) was boiled under reflux with 2% methanolic hydrogen

chloride (50 ml) for 11 hours. After neutralization with silver carbonate and treatment with hydrogen sulphide, filtration through Celite and evaporation yielded a clear sirup which was dissolved in dry tetrahydrofuran (100 ml) and reduced with lithium aluminum hydride (2.4 g) in 100 ml of the same solvent. The reduced glycoside was recovered in the usual way and hydrolyzed with *N* sulphuric acid.

Identification of Hydrolysis Products

The mixture of reducing sugars obtained after the hydrolysis was added to a cocoanut charcoal (23) column (3.5×23 cm). Elution with 3% and 10% aqueous ethanol yielded two compounds, corresponding in rate of movement on the paper chromatogram (solvent C) to xylose and 4-*O*-methyl glucose. The xylose (210 mg) crystallized, m.p. 143–144° C, $[\alpha]_D^{20}$ +19° (*c*, 0.8 in water). The 4-*O*-methyl-D-glucose (300 mg), $[\alpha]_D^{20}$ +68° (*c*, 3.0 in water) was converted to the phenylosazone derivative, m.p. and mixed m.p. 156–157° C.

Methylation, Reduction, and Hydrolysis of the Aldobiouronic Acid

A portion of the aldobiouronic acid (1.13 g) was converted to the methyl ester methyl glycoside. The dry sirup obtained was dissolved in dry dimethyl formamide (20 ml) according to Kuhn (24) and methyl iodide (5 ml) and silver oxide (5 g) were added. After shaking for 24 hours, the product was recovered in the usual way and the methylation procedure was repeated twice. The final product had an infrared spectrum which indicated the absence of hydroxyl groups. The sirup (1.02 g) was reduced in ethyl ether (65 ml) with lithium aluminum hydride (2.5 g) to yield a sirup (1.00 g) which was boiled under reflux for 12 hours with 5% methanolic hydrogen chloride followed by refluxing for 10 hours with 0.5 *N* hydrochloric acid.

Identification of 3,4-Di-O-methyl-D-xylose and 2,3,4-Tri-O-methyl-D-glucose

The acid hydrolyzate was added directly to a cocoanut charcoal column (2×13 cm) which was washed with water until the eluate was neutral. Elution with 6% and 10% ethanol gave two compounds, chromatographically (solvent B and D) indistinguishable from 3,4-di-*O*-methyl xylose and 2,3,4-tri-*O*-methyl glucose, respectively. The di-*O*-methyl xylose, electrophoretically (25, 26) identical with the 3,4-di-*O*-methyl derivative, $[\alpha]_D^{20}$ +15° (*c*, 1.1 in chloroform), was converted to the aniline derivative by treatment with aniline dissolved in absolute ethanol at room temperature. After recrystallization from petroleum ether, the 3,4-di-*O*-methyl-*N*-phenyl-D-xylosylamine had m.p. 122.5–123.5° C. The tri-*O*-methyl glucose, $[\alpha]_D^{20}$ +78° (*c*, 2.0 in water), gave crystalline 2,3,4-tri-*O*-methyl-*N*-phenyl-D-glucosylamine, m.p. and mixed m.p. 144–145° C.

Identification of 4-O-Methyl-D-glucuronic Acid

The mono-*O*-methyl hexuronic acid obtained from the column of anion exchange resin was converted to the ester glycoside, reduced with lithium aluminum hydride in tetrahydrofuran, and hydrolyzed with *N* sulphuric acid. Evaporation yielded a sirup, chromatographically (solvent B) identical with 4-*O*-methyl-D-glucose, $[\alpha]_D^{20}$ +56° (*c*, 1.7 in water). The 4-*O*-methyl-D-glucosazone had m.p. and mixed m.p. 156–157° C.

Methylation of the Hemicellulose

The hemicellulose (20 g) was stirred overnight with water (75 ml) and 40% (w/w) sodium hydroxide (100 ml) in an atmosphere of nitrogen, after which dimethyl sulphate (90 ml) was added dropwise over a period of 12 hours. The treatment with alkali and dimethyl sulphate was repeated nine times. The recovered, partially methylated hemicellulose was suspended in tetrahydrofuran (500 ml) and dried over anhydrous sodium sulphate. After removal of the drying agent by filtration, dry dimethyl formamide (500 ml), methyl iodide (5 ml), and silver oxide (5 g) were added (24) and the mixture was

Can. J. Chem. Downloaded from www.nrcresearchpress.com by 196.1.178.254 on 09/04/12
For personal use only.

shaken for 12 hours, after which the same quantities of methylating agents were added and methylation was allowed to proceed for another 12 hours. Tetrahydrofuran was removed by evaporation, chloroform (1000 ml) was added, and dimethyl formamide was removed by continuous extraction with water for 3 days. The dry chloroform extract was concentrated, centrifuged, and poured into petroleum ether (4 liters) to yield a methylated hemicellulose, OCH_3, 37.3% (17.7 g, 80%). Another methylation according to Kuhn (24) failed to raise the methoxyl content of the product. Anal. OCH_3, 37.3%; ash, 0.33%; $[\alpha]_D^{20}$ −57° (*c*, 1.0 in chloroform). The infrared spectrum indicated the absence of hydroxyl groups.

Hydrolysis and Separation of Acidic and Neutral Sugars

A portion of the methylated hemicellulose (7.0 g) was dissolved in glacial acetic acid (75 ml). After addition of water (75 ml), the solution was boiled under reflux for 33 hours, when its rotation was constant. Acetic acid was removed by evaporation and an aqueous solution (500 ml) of the hydrolyzate was added to a column of Dowex 1-X4 exchange resin (acetate form). Neutral sugars were eluted with water after which an acidic compound was removed with 3 *N* acetic acid (1.62 g). Anal. Calc. for $C_{15}H_{26}O_{11}$: OCH_3, 32.5; equiv. wt., 382. Found: OCH_3, 32.3; equiv. wt., 382.

Preparation and Identification of Methyl 2-O-(2,3,4-Tri-O-methyl-α-D-glucopyranosyl)-3-O-methyl-α,β-D-xylopyranoside

The partially methylated aldobiouronic acid (1.38 g) was converted to its methyl ester methyl glycoside, which was reduced with lithium aluminum hydride (1.5 g) in diethyl ether (50 ml). After addition of ethyl acetate and water, the reduced disaccharide was recovered by extraction with chloroform to yield a sirup (1.18 g, 86%) which crystallized on standing. After recrystallization from ethyl acetate, it had a m.p. of 166.5–167.5° C, undepressed on admixture with an authentic specimen of methyl 2-*O*-(2,3,4-tri-*O*-methyl-α-D-glucopyranosyl)-3-*O*-methyl-D-xylopyranoside.* The melting point, infrared spectrum, and X-ray diagram of the material were also identical with those of another authentic specimen, isolated from yellow birch wood (27). Anal. Calc. for $C_{16}H_{30}O_{10}$: OCH_3, 40.6%. Found: OCH_3, 39.0%; $[\alpha]_D^{20}$ +95° (*c*, 0.7 in water). The compound was probably a mixture of the α- and β-xylopyranosides.

A portion (160 mg) of the disaccharide was subjected to methanolysis and subsequent hydrolysis to give an aqueous solution, which, on chromatographic resolution (solvent B), appeared to contain equal amounts of a mono-*O*-methyl xylose and a tri-*O*-methyl glucose. Extraction with chloroform gave a sirup, chromatographically identical with 2,3,4-tri-*O*-methyl-D-glucose (solvent E). The 2,3,4-tri-*O*-methyl-*N*-phenyl-D-glucosylamine had m.p. and mixed m.p. 146–147° C. Evaporation of the remaining aqueous solution gave a compound which was chromatographically identical with 3-*O*-methyl-D-xylose (solvent E). The aniline derivative had an infrared spectrum indistinguishable from that of an authentic specimen. Anal. Calc. for $C_6H_{12}O_5$: OCH_3, 18.9%. Found: OCH_3, 18.8%; $[\alpha]_D^{20}$ +18° (*c*, 1.6 in water).

Separation of the Neutral Components of the Methylated Hemicellulose

The aqueous solution of the neutral sugars from the column of exchange resin was reduced to 500 ml and shaken with chloroform (50 ml) for 3 hours. After having been shaken with water for another 3 hours, the chloroform layer contained only a tri-*O*-methyl xylose (166 mg). The original aqueous solution was extracted continuously with chloroform for 18 hours, the extract was discarded and extraction was continued for another

*The authors are thankful to Professor Fred Smith, University of Minnesota, for providing this sample.

Can. J. Chem. Downloaded from www.nrcresearchpress.com by 196.1.178.254 on 09/04/12
For personal use only.

3 days, yielding a chromatographically pure di-*O*-methyl xylose (1.86 g). The remaining aqueous solution was extracted three times with 20-ml portions of hot ethanol to yield a mixture of mono-*O*-methylated xyloses (154 mg).

Preliminary Characterization of Mono-O-methyl Xyloses

This fraction, $[\alpha]_D^{20}$ +23° (*c*, 2.8 in water), had a methoxyl content (16.3%) somewhat lower than that required for a mono-*O*-methyl xylose. Results obtained on ionophoresis in a borate buffer solution suggested the presence of 2-*O*- and 3-*O*-methyl-D-xylose in an approximate ratio of 2:1.

Identification of 2,3-Di-O-methyl-D-xylose

When seeded with authentic crystals of 2,3-di-*O*-methyl-D-xylose (28), this fraction appeared to crystallize, but the m.p. was 20° higher than expected (96–99° C). Anal. Calc. for $C_7H_{14}O_5$: OCH_3, 34.8%. Found: OCH_3, 33.1%; $[\alpha]_D^{20}$ +26° (*c*, 1.0 in water). The 2,3-di-*O*-methyl-*N*-phenyl-D-xylosylamine, when recrystallized once from ethyl acetate, had m.p. 126–127° C. Slow evaporation of an ethyl acetate – petroleum ether solution gave needles, m.p. 130–131° C. The material is known to be dimorphic (29).

Partial Identification of 2,3,4-Tri-O-methyl-D-xylose

Neither the original compound nor its aniline derivative could be induced to crystallize. The infrared spectra of both were indistinguishable from those of authentic samples.

Quantitative Analysis of the Neutral Components

A small portion of the mixture of neutral sugars was resolved on the paper chromatogram with solvent mixture D. The appropriate paper strips were eluted with water and the concentration of each sugar solution was determined by the *o*-aminodiphenyl method (12). The average value of six determinations was used.

Periodate Oxidation of the Hemicellulose

Periodate oxidations were carried out in the dark with 0.05 *M* sodium metaperiodate containing 2 mg of hemicellulose per ml of solution. Aliquots were taken every day for 6 days and the amount of periodate consumed was determined by the arsenite method. The average consumption after 3–4 days was 8.2 moles per repeating unit, corresponding to a calculated value of 7.8.

Preparation of the Acetylated Hemicellulose

Dry hemicellulose (2 g) was swollen or partially dissolved in dry formamide (40 ml) by shaking for 5 hours. Dry pyridine (80 ml) was added, followed by redistilled acetic anhydride (60 ml). The reaction mixture was cooled with tap water for the first half hour and then shaken mechanically at room temperature for 5 hours, after which it was kept at +4° C for 3 days, the reaction flask being opened occasionally during this time. The mixture was poured into ice water (3 liters) with vigorous stirring and washed on a large Buechner funnel, first with ice-cold 2% hydrochloric acid (30) and subsequently with cold distilled water until neutrality. After the water had been replaced by ethanol and the alcohol by petroleum ether (b.p. 30–60° C), the white product was dried *in vacuo* over calcium chloride for 1 week. A second esterification was carried out in the same way although without the addition of formamide. Anal. Calc. for the fully acetylated hemicellulose: acetyl, 37.3%. Found: acetyl, 37.0% (31).

Determination of the Molecular Weight of the Methyl and Acetyl Derivatives of the Hemicellulose

The osmometer used was of the Zimm–Myerson (15) type as modified by Stabin and

Can. J. Chem. Downloaded from www.nrcresearchpress.com by 196.1.178.254 on 09/04/12
For personal use only.

Immergut (32). Gel cellophane membranes were used, the solvent was a mixture of chloroform and ethanol (9:1, v/v), and the temperature was 30±0.01° C. The osmotic height was measured at five different concentrations by the static method and the values of h/w, the reduced osmotic pressure, were linearly extrapolated to zero concentrations. The results are presented in Table I. The number-average molecular weight and degree of polymerization were calculated as described elsewhere (28).

TABLE I

Osmometry data for the methylated and acetylated hemicelluloses

Methyl derivative			Acetyl derivative		
w*	h†	h/w	w	h	h/w
3.484	4.625	1.328	3.707	2.188	0.590
2.850	3.630	1.274	3.546	2.098	0.592
2.043	2.430	1.189	2.998	1.747	0.583
1.774	2.138	1.205	2.257	1.341	0.594
1.483	—	1.253	1.872	1.136	0.607
0	—	1.10	0	—	0.588

*Concentration in g/kg solution.
†Osmotic height in cm solvent.

ACKNOWLEDGMENTS

The authors are thankful to Dr. R. St. J. Manley for providing the X-ray data. One of them (A.L.C.) also wishes to express his gratitude to the Allied Chemical Corporation for a fellowship and to the Pulp and Paper Research Institute of Canada for a summer stipend.

REFERENCES

1. TIMELL, T. E. Textile Research J. **27**, 854 (1957).
2. TIMELL, T. E. Svensk Papperstidn. **60**, 836 (1957).
3. TIMELL, T. E. Textile Research J. **28**, 270 (1958).
4. SMITH, F. J. Chem. Soc. 2646 (1951).
5. SCHINLE, R. Ber. **65**, 315 (1932).
6. JAMES, S. P. and SMITH, F. J. Chem. Soc. 739 (1945).
7. PEAT, S., SCHLÜCHTERER, E., and STACEY, M. J. Chem. Soc. 581 (1939).
8. BISHOP, C. T. Can. J. Chem. **31**, 154 (1953).
9. GORIN, P. A. J. and PERLIN, A. S. Can. J. Chem. **36**, 999 (1958).
10. DUTTON, G. G. S. and SMITH, F. J. Am. Chem. Soc. **78**, 3744 (1956).
11. TIMELL, T. E. J. Am. Chem. Soc. (In press).
12. TIMELL, T. E., GLAUDEMANS, C. P. J., and CURRIE, A. L. Anal. Chem. **28**, 1916 (1956).
13. GLAUDEMANS, C. P. J. and TIMELL, T. E. J. Am. Chem. Soc. **80**, 941, 1209 (1958).
14. LINDBERG, B. Personal communication.
15. ZIMM, B. H. and MYERSON, I. J. Am. Chem. Soc. **68**, 911 (1946).
16. BARTH, F. W. and TIMELL, T. E. J. Am. Chem. Soc. **80**, 6320 (1958).
17. WHISTLER, R. L. and LAUTERBACH, G. E. J. Am. Chem. Soc. **80**, 1987 (1958).
18. CHANDA, S. K., HIRST, E. L., JONES, J. K. N., and PERCIVAL, E. G. V. J. Chem. Soc. 1289 (1950).
19. EHRENTHAL, I., MONTGOMERY, R., and SMITH, F. J. Am. Chem. Soc. **76**, 5509 (1954).
20. ADAMS, G. A. Can. J. Chem. **30**, 698 (1952).
21. TIMELL, T. E., GLAUDEMANS, C. P. J., and GILLHAM, J. K. Pulp Paper Mag. Can. **59** (No. 10) 242 (1958).
22. PAINTER, T. J. and JONES, J. K. N. (In press).
23. BARTH, F. W. and TIMELL, T. E. Can. J. Chem. **36**, 1321 (1958).
24. KUHN, R., TRISCHMANN, H., and LÖW, I. Angew. Chem. **67**, 32 (1955).
25. FOSTER, A. B. J. Chem. Soc. 982 (1953).
26. BOUVENG, H. and LINDBERG, B. Acta Chem. Scand. **10**, 1283 (1956).
27. TIMELL, T. E. Unpublished results.
28. GILLHAM, J. K. and TIMELL, T. E. Can. J. Chem. **36**, 1467 (1958).
29. EHRENTHAL, I., RAFIQUE, M. C., and SMITH, F. J. Am. Chem. Soc. **74**, 1341 (1952).
30. CARSON, J. F. and MACLAY, W. D. J. Am. Chem. Soc. **68**, 1015 (1946).
31. GENUNG, L. B. and MALLAT, R. C. Ind. Eng. Chem. Anal. Ed. **15**, 319 (1943).
32. STABIN, J. V. and IMMERGUT, E. H. J. Polymer Sci. **14**, 209 (1954).

Can. J. Chem. Downloaded from www.nrcresearchpress.com by 196.1.178.254 on 09/04/12
For personal use only.

Can. J. Chem. Downloaded from www.nrcresearchpress.com by 196.1.178.254 on 09/04/12
For personal use only.

PHOTOCHEMICAL SEPARATION OF MERCURY ISOTOPES

III. THE REACTION OF $Hg^{202}6(^3P_1)$ ATOMS, PHOTOEXCITED IN NATURAL MERCURY VAPOR, WITH HYDROGEN CHLORIDE[1]

C. C. McDonald,[2] J. R. McDowell,[3] and H. E. Gunning[3]

ABSTRACT

An investigation has been made of the reaction of $Hg^{202}6(^3P_1)$ atoms, photoexcited in natural mercury vapor, with flowing hydrogen chloride at 28–30° C. Emphasis has been placed on the effect of reaction parameters on the Hg^{202} content of the calomel product of the reaction.

Under fast-flow conditions it has been found that the calomel product contains 44% Hg^{202}, corresponding to an enrichment of 48% over the normal abundance of 29.8%.

In the presence of unsaturated compounds such as butadiene and benzene the enrichment is markedly increased. With butadiene and benzene as addends, the maximum enrichments were 98% and 85% respectively.

The reaction with pure hydrogen chloride can be explained in terms of the sequence:

$$Hg^{202}6(^3P_1) + HCl \rightarrow Hg^{202}Cl + H \quad [1]$$

$$Hg^{202}6(^3P_1) + HCl \rightarrow Hg^{202} + Cl + H \quad [2]$$

$$Cl + Hg^N + M \rightarrow Hg^NCl + M \quad [3]$$

$$H + HCl \rightarrow H_2 + Cl \quad [4]$$

$$H + Cl + M \rightarrow HCl + M \quad [5]$$

where Hg^N is natural mercury and M is a third body, including the wall.

In the presence of unsaturated compounds (U), additional reactions are postulated to occur:

$$Cl + U \rightarrow \text{products} \quad [6]$$

$$H + U \rightarrow \text{products}. \quad [7]$$

The increased enrichment in the presence of unsaturated addends is explained by the reduced rate of formation of Hg^NCl through cleanup of chlorine and hydrogen atoms by reactions [6] and [7].

Under static conditions, the pure hydrogen chloride reaction formed a calomel product of normal Hg^{202} abundance. This finding is explained as a localized depletion of the unexcited mercury in Hg^{202}, through reaction [1]. With increasing linear flow rate the depletion effect gradually disappears and enrichments maximize at high flow rates.

The Hg^{202} enrichment was found to be very sensitive to the wall temperature of the Hg^{202} source. In a 50:50 v/v mixture of hydrogen chloride and butadiene the enrichment was found to decrease from 68% to 24% as the lamp temperature was raised from 25.5° C to 50° C. The effect is explained by temperature broadening of the emission line leading to overlap of the emission line on absorption contours adjacent to that of Hg^{202}.

Both the rate of deposition of the calomel product and the Hg^{202} enrichment were found to depend upon the concentration of natural mercury in the gas stream for hydrogen chloride – butadiene mixtures. Optimum conditions corresponded to a slight supersaturation of the stream with mercury vapor.

INTRODUCTION

In previous studies in this series (1), conditions have been experimentally defined for the photoexcitation, in natural mercury vapor (Hg^N), of a single isotopic species to the $6(^3P_1)$ state. This technique has been recently applied in a study of the reaction of $Hg^{202}6(^3P_1)$ atoms in Hg^N with water vapor (2, 3). In the water reaction it has been found that the HgO product of the reaction contains 80–90% Hg^{202} when addends are present, such as butadiene-1,3, to suppress the secondary formation of Hg^NO.

The present paper reports the first in a series of studies on the reaction of $Hg^{202}6(^3P_1)$ atoms in Hg^N with hydrogen chloride. Emphasis has been placed on the effects of reaction

[1]*Manuscript received December 29, 1958.*

Joint contribution from the Department of Chemistry, Illinois Institute of Technology, Chicago 16, Illinois, and the Department of Chemistry, University of Alberta, Edmonton, Alberta. This work was supported in part by the U.S. Atomic Energy Commission, under Contract AT(11-1)-43. This support is gratefully acknowledged.

[2]*Present address: Chemical Department, E.I. du Pont de Nemours Company, Wilmington, Delaware.*

[3]*Present address: Department of Chemistry, University of Alberta, Edmonton, Alberta.*

parameters on the Hg^{202} content of the calomel product of the reaction. Enrichment in Hg^{202} in this product would be evidence for primary formation of calomel, presumably by the reaction:

$$Hg^{202}6(^3P_1) + HCl \rightarrow Hg^{202}Cl + H. \quad [1]$$

The details of the investigation follow.

EXPERIMENTAL

The general experimental procedure has been previously described (1, 3). In this study a special rectangular reaction cell was used with faces 2.5×8.0 cm, and an internal path length of 0.10 cm. The cell had two side-arms, terminating in 2/5-spherical joints, for attachment to the flow system. The entire cell was fashioned of Vycor 7910 glass to prevent radiation of wavelength less than 2200 Å from entering the cell.

The source consisted of a quartz electrodeless discharge lamp containing mercury, 98.3 atom per cent in Hg^{202}. The lamp was maintained at 25.5±0.1° C unless otherwise specified. The lamp-cooling assembly has been described (1). The intensity of the radiation at 2537 Å incident upon the cell was monitored by a Westinghouse WL-775 phototube. The photometric unit was identical with that used in the mercury isotope analysis system previously described (4).

The mercury saturator consisted of a 500-cc bulb partially filled with mercury, to which two Liebig condensers were sealed in reflux position. The inner tube of the gas entrance condenser extended into the flask to a point about 1 cm above the mercury surface. In operation the gases entered at the top of the entrance condenser, passed over the refluxing mercury, and left the saturator through the top of the exit condenser. The reaction cell was connected to the exit condenser via a scratched stopcock. The temperatures of the water circulating through exit and entrance condensers were separately controlled from thermostats. The condensers were normally maintained at 30.0±0.1° C.

The gases used in the investigation were the highest-purity grades obtainable from the Matheson Company, East Rutherford, N.J. The benzene used was Fisher A.C.S. grade.

RESULTS

For pure hydrogen chloride a large number of exploratory runs were first performed to determine whether the calomel product of the reaction contained more than the normal abundance of Hg^{202}.

Several runs were first made under static conditions. Analysis showed that the calomel product contained the normal abundance (29.8%) of Hg^{202}, within the experimental error. Under flow conditions, however, the calomel product was found to be consistently enriched in Hg^{202}. The enrichments obtained in these runs varied from 20 to 40%. A systematic study was therefore made of the effect of reaction parameters on the Hg^{202} content of the calomel product.

In Table I the results are given for a series of runs at varying pressures of hydrogen chloride. The linear flow rate was held constant at 600 cm/sec. The light intensity was measured relatively by the photocell response as in the analytical system (4). For this series the incident intensity was 60 units.

Throughout this investigation difficulty was encountered in obtaining good reproducibility for runs done under apparently identical conditions. While the actual absorption measurements were reproducible to ±0.5%, maximum variations of ±5% were encountered, at times, for identical runs.

Can. J. Chem. Downloaded from www.nrcresearchpress.com by 196.1.178.254 on 09/04/12
For personal use only.

TABLE I

The effect of varying substrate pressure on the Hg^{202} enrichment in the solid product of the reaction of $Hg^{202}6(^3P_1)$ atoms, photoexcited in Hg^N, with flowing hydrogen chloride (Linear flow rate = 600 cm/sec. Incident light intensity = 60 units)

Pressure, mm	% Hg^{202}	Fractional enrichment
0.4	37	1.2
1.0	37	1.2
3.0	40	1.3
11.0	38	1.3
17.0	40	1.3
50.0	38	1.3

From Table I, it can be seen that the enrichment is constant within the experimental error over the pressure range, 0.4 to 50 mm. Pressures exceeding 50 mm were avoided to prevent Lorentz-broadening of the hyperfine absorption contours (1).

For the data given in Table I, the mercury saturator was operated under very gentle reflux. With the mercury boiling vigorously, it was found that the enrichments increased by approximately 10%. All ensuing runs were therefore performed under vigorous reflux conditions.

For the data in Table II, the pressure was maintained essentially constant, while

TABLE II

The effect of varying linear flow rate on the Hg^{202} enrichment in the solid product of the reaction of $Hg^{202}6(^3P_1)$ atoms, photoexcited in Hg^N, with flowing hydrogen chloride (Incident light intensity = 60 units)

Pressure, mm	Linear flow rate, cm/sec	% Hg^{202}	Fractional enrichment
4.0	375	41	1.4
1.4	425	43	1.4
1.1	475	43	1.4
1.4	1500	42	1.4
2.3	1500	44	1.5
2.8	1500	44	1.5

the linear flow rate was varied from 375 to 1500 cm/sec. It will be observed that there is a slight increase in enrichment with increasing linear flow rate to a maximum value of 48% at 1500 cm/sec.

Since it was suspected that $Hg^{202}6(^3P_0)$ atoms might be involved in the isotopically specific primary process, the effect of added nitrogen on the enrichment was studied. Representative data are given in Table III. While there appears to be a slight increase in enrichment with increasing nitrogen concentration in the stream, the effect is only slightly larger than the experimental reproducibility.

The failure to obtain pure $Hg^{202}Cl$ in the hydrogen chloride reaction implies that Hg^NCl is also being formed by some mechanism. On the hypothesis that the Hg^NCl arose by the interaction of free chlorine atoms with unexcited Hg^N, various additives were studied to reduce the chlorine-atom concentration.

In Table IV it can be seen that benzene has a marked effect on the Hg^{202} enrichment. With benzene concentrations exceeding approximately 30 mole per cent, the minimum enrichment was 70%. The benzene additive appears maximally effective at concentrations of 70 mole per cent, corresponding to an enrichment of 85%.

Can. J. Chem. Downloaded from www.nrcresearchpress.com by 196.1.178.254 on 09/04/12
For personal use only.

TABLE III

The effect of varying nitrogen concentration on the Hg^{202} enrichment in the solid product of the reaction of $Hg^{202}6(^3P_1)$ atoms, photoexcited in Hg^N, with flowing hydrogen chloride (Linear flow rate = 1500 cm/sec. Incident light intensity = 60 units)

Pressure, mm	Comp. mole %		% Hg^{202}	Fractional enrichment
	HCl	N_2		
2.3	100	0	44	1.5
8.3	80	20	44	1.5
4.8	50	50	47	1.6
6.0	34	66	44	1.5
10.0	20	80	48	1.6

TABLE IV

The effect of varying benzene concentration on the Hg^{202} enrichment in the solid product of the reaction of $Hg^{202}6(^3P_1)$ atoms, photoexcited in Hg^N, with flowing hydrogen chloride (Linear flow rate = 485 cm/sec. Incident light intensity = 60 units)

Pressure, mm	Comp. mole %		% Hg^{202}	Fractional enrichment
	HCl	C_6H_6		
2.3	100	0	44	1.5
3.8	65	35	51	1.7
4.3	37	63	50	1.7
3.6	30	70	55	1.8
8.4	18	82	51	1.7

A number of runs were also done with chlorobenzene as additive. The data are summarized in Table V. The effect of chlorobenzene is quite the reverse of benzene, leading

TABLE V

The effect of varying chlorobenzene concentration on the Hg^{202} enrichment in the solid product of the reaction of $Hg^{202}6(^3P_1)$ atoms, photoexcited in Hg^N, with flowing hydrogen chloride (Linear flow rate = 375 cm/sec. Incident light intensity = 60 units)

Pressure, mm	Comp. mole %		% Hg^{202}	Fractional enrichment
	HCl	C_6H_5Cl		
2.3	100	0	44	1.5
5.0	80	20	44	1.5
6.0	66	34	40	1.3
5.4	50	50	38	1.3
4.0	34	66	38	1.3
6.7	20	80	35	1.2

to a decreased enrichment with increasing mole fraction of chlorobenzene. It is apparent that the photoexcited mercury isotope is being quenched by chlorobenzene with the formation of chlorine atoms. The rate of Hg^NCl formation would therefore be increased over that for pure hydrogen chloride, with a resulting decrease in the Hg^{202} enrichment.

As might be expected, butadiene-1,3 proved to be even more effective than benzene in enhancing the Hg^{202} enrichment. Since butadiene was the most efficient additive encountered in this investigation, it was studied in some detail.

In Table VI, the effect of total pressure on the enrichment is recorded for a mixture containing 50 mole per cent butadiene. The data show clearly that the enrichment reaches a maximum of 98% at a pressure of 5–6 mm. These data were measured at a flow rate of 1500 cm/sec. At lower flow rates the butadiene is less effective. In Table

Can. J. Chem. Downloaded from www.nrcresearchpress.com by 196.1.178.254 on 09/04/12
For personal use only.

TABLE VI

The effect of varying total pressure on the Hg^{202} enrichment in the solid product of the reaction of $Hg^{202}6(^3P_1)$ atoms, photoexcited in Hg^N, with flowing hydrogen chloride containing 50 mole per cent of butadiene (Linear flow rate = 1500 cm/sec. Incident light intensity = 65 units)

Pressure, mm	% Hg^{202}	Fractional enrichment
2.1	53	1.8
4.4	56	1.9
5.6	59	2.0
8.0	54	1.8
16.0	50	1.7
32.0	50	1.7

TABLE VII

The effect of varying total pressure on the Hg^{202} enrichment in the solid product of the reaction of $Hg^{202}6(^3P_1)$ atoms, photoexcited in Hg^N, with flowing hydrogen chloride, containing 50 mole per cent of butadiene (Linear flow rate = 94 cm/sec. Incident light intensity = 65 units)

Pressure, mm	% Hg^{202}	Fractional enrichment
4.0	41	1.4
6.7	52	1.7
10.7	50	1.7
32.0	50	1.7

VII the enrichments are given as a function of total pressure for the same mixture, at a flow rate of 94 cm/sec. The maximum enrichment of 74% occurs at 6–7 mm.

There are many isotopically degradative secondary processes which can be adduced to explain the fact that pure $Hg^{202}Cl$ is not obtained even in the presence of Cl-atom acceptors, such as butadiene. The most obvious of these degradative processes would be the gas phase exchange between $Hg^{202}Cl$ and Hg^N. Some information on the importance of this reaction was obtained by determining the effect upon the enrichment of subliming the calomel deposit a number of times during reaction. This sublimation procedure was carried out for a number of runs, and no difference could be detected, within the experimental error, from those runs in which the calomel product was allowed to accumulate during reaction. An example of the effect of sublimation is given in Table VIII.

The results of a number of runs at various butadiene concentrations and total reaction pressures are given in Table VIII. In none of the runs did the Hg^{202} content of the solid product exceed 59%, corresponding to an enrichment of 98%. From Table VIII it can be seen that higher butadiene concentrations are required at higher total pressures to achieve maximum enrichment.

In order to prevent overlap of the emission line on adjacent hyperfine absorption contours, the temperature of the lamp must be kept below 30° C (1). In this investigation the lamp temperature was maintained constant at 25.5±0.1° C. The uncooled lamp was found to operate at a temperature of approximately 50° C. The decrease in enrichment caused by using an uncooled source is shown in Table VIII. For a mixture containing 50 mole per cent of butadiene, at a total pressure of 4 mm, the enrichment dropped from 68% to 24%, when the cooling water to the lamp was shut off.

Can. J. Chem. Downloaded from www.nrcresearchpress.com by 196.1.178.254 on 09/04/12
For personal use only.

TABLE VIII

The effect of varying butadiene concentration and reaction pressure on the Hg^{202} enrichment in the solid product of the reaction of $Hg^{202}6(^3P_1)$ atoms, photoexcited in Hg^N, with flowing hydrogen chloride (Linear flow rate = 1500 cm/sec. Incident light intensity = 65 units)

Pressure, mm	Comp. mole %		% Hg^{202}	Fractional enrichment
	HCl	C_4H_6		
3.4	90	10	48	1.6
2.0	66	34	47	1.6
4.1	66	34	52	1.7
4.1	66	34	51	1.7*
2.8	50	50	45	1.5
4.0	50	50	37	1.2†
4.1	50	50	50	1.7
4.4	50	50	53	1.8
5.6	50	50	59	2.0
6.3	33	67	48	1.6
8.0	38	62	59	2.0

*Deposit sublimed three times during reaction.
†Lamp uncooled.

Since traces of air are difficult to eliminate completely in fast-flow systems, a study was made of the effect of adding known concentrations of dry air to various mixtures of hydrogen chloride and butadiene. The results are summarized in Table IX. It is

TABLE IX

The effect of varying concentrations of dry air on the Hg^{202} enrichment in the solid product of the reaction of $Hg^{202}6(^3P_1)$ atoms, photoexcited in Hg^N, with flowing hydrogen chloride – butadiene mixtures (Linear flow rate = 1500 cm/sec. Incident light intensity = 65 units)

Pressure, mm	Comp. mole %			% Hg^{202}	Fractional enrichment
	HCl	C_4H_6	Air		
4.2	67	16	17	48	1.6
4.5	59	31	10	52	1.7
4.9	54	29	17	55	1.8
4.9	41	41	18	50	1.7
4.8	28	57	15	44	1.5
7.7	19	71	10	39	1.3

apparent that concentrations of air in the 10–20 mole per cent range decrease slightly the maximum enrichment obtained. However, the effect is only slightly greater than the experimental reproducibility. It is therefore unlikely that traces of air would have any detectable effect on the enrichment values.

In Table X, the effect of varying linear flow rate is shown, for a mixture containing 50 mole per cent of butadiene, at a total reaction pressure of 16.0 mm. In comparing these data with those in previous tables for hydrogen chloride – butadiene mixtures, it should be noted that the light intensity is 60 units for the runs reported in Table X. Previous runs were made at a light intensity of 65 units. It will be noted from Table X that the Hg^{202} enrichment is independent of flow rate up to 750 cm/sec, at a value of $51 \pm 3\%$. However, at 1500 cm/sec, the enrichment has increased to 67%. The enrichment-enhancing effect of increasing linear flow rate is also apparent in comparing the

Can. J. Chem. Downloaded from www.nrcresearchpress.com by 196.1.178.254 on 09/04/12
For personal use only.

TABLE X

The effect of varying linear flow rate on the Hg^{202} enrichment in the solid product of the reaction of $Hg^{202}6(^3P_1)$ atoms, photoexcited in Hg^N, with flowing hydrogen chloride, containing 50 mole per cent of butadiene (Total pressure = 16.0 mm. Incident light intensity = 60 units)

Linear flow rate, cm/sec	% Hg^{202}	Fractional enrichment
188	46	1.5
375	45	1.5
750	44	1.5
1500	50	1.7

data in Tables VI and VII. The effect is most marked for pressures in the 4- to 6-mm range.

The effect of increasing incident light intensity was studied on a hydrogen chloride – butadiene mixture containing 50 mole per cent of butadiene. The total pressure was 4.0 mm and the linear flow rate, 1500 cm/sec. The light intensity was changed by interposing varying thicknesses of Vycor 7910 glass between lamp and cell. The data are given in Table XI. It can be seen that the enrichment increases, with increasing incident

TABLE XI

The effect of increasing incident light intensity on the Hg^{202} enrichment in the solid product of the reaction of $Hg^{202}6(^3P_1)$ atoms, photoexcited in Hg^N, with flowing hydrogen chloride, containing 50 mole per cent of butadiene (Total pressure = 4.0 mm. Linear flow rate = 1500 cm/sec)

Relative incident light intensity	% Hg^{202}	Fractional enrichment
22	48	1.6
30	50	1.7
34	51	1.7
57	53	1.8
68	56	1.9
95	58	1.9

intensity over the entire range of intensities studied.

The final reaction parameter studied was the effect of mercury saturation conditions on the enrichment. In the runs reported to this point in this study the condensers of the mercury saturator were maintained at 30.0±0.1° C. Six feet of pyrex tubing connected the top of the exit condenser to the reaction cell. In order to vary saturation conditions, the 6 ft of connecting tubing were enclosed in a water jacket. To abbreviate the description, the temperature of the exit condenser of the saturator will be referred to as T_c and that of the water-jacketed connecting tubing as T_T.

Normal procedure would correspond closely to $T_c = T_T = 30°$ C, since the uncooled connecting tubing was operated at laboratory temperature, which varied in our case from 28–30° C.

For the mercury saturation studies, a 50:50 v/v mixture of hydrogen chloride and butadiene was used, at a reaction pressure of 4.3 mm, a linear flow rate of 1500 cm/sec, and an incident light intensity of 60 units.

At $T_c = T_T = 30°$ C, sufficient calomel for analysis was obtained in 30 minutes. The average of four runs gave an Hg^{202} abundance of 56±2%. However, as the temperatures

Can. J. Chem. Downloaded from www.nrcresearchpress.com by 196.1.178.254 on 09/04/12
For personal use only.

of the water jackets were reduced the rate of deposition of calomel in the reaction zone was observed to decrease markedly. Thus with $T_c = T_T = 16°$ C, no calomel deposit was observed in four hours of irradiation. With $T_c = T_T = 20°$ C, two hours of irradiation were required before deposition was observed. With $T_c = 20°$ C, and $T_T = 28°$ C, sufficient calomel for analysis was obtained in 80 minutes of irradiation. The Hg^{202} content of the product was 50%. When both T_c and T_T were again raised to 30° C, sufficient calomel for analysis was again obtained in 30 minutes. The Hg^{202} content of the calomel was 58%.

In the final experiment on mercury saturation, the water was drained from the exit condenser of the saturator, and the water-jacketed connecting tubing was replaced by a short piece of uncooled tubing. Under these conditions droplets of mercury formed in the reaction cell, indicating supersaturation of the gas stream with mercury vapor. The average of three runs gave an Hg^{202} abundance of 56±1.5%.

DISCUSSION

In the reaction of $Hg^{202}6(^3P_1)$ atoms, photoexcited in Hg^N, with flowing hydrogen chloride, the fact that a calomel product is formed which is enriched in Hg^{202} can most obviously be explained by a dual primary process mechanism:

$$Hg^{202}6(^3P_1) + HCl \rightarrow Hg^{202}Cl + H \quad [1]$$
$$Hg^{202}6(^3P_1) + HCl \rightarrow Hg^{202} + H + Cl \quad [2]$$
$$Cl + Hg^N + M \rightarrow Hg^NCl + M. \quad [3]$$

Reaction [3] would of course require a third body M to remove heat of recombination.

On the basis of the above sequence, the relative rates of the two primary processes can be estimated from the enrichment data. From the mechanism it follows that the relative rate ratio:

$$R_{Hg^{202}Cl}/R_{Hg^NCl} = \Phi_1/\Phi_2$$

where Φ_1 and Φ_2 are the fractions of the absorbed radiation partitioned to reactions [1] and [2] respectively. The ratio Φ_1/Φ_2 can be calculated from the abundance data, since

$$R_{Hg^{202}Cl}/R_{Hg^NCl} = (A - 29.8)/(100 - A)$$

where A is the percentage abundance of Hg^{202} in the calomel, and 29.8 is the normal Hg^{202} abundance. From our data, the maximum value for $A = 44\%$, whence $\Phi_1/\Phi_2 = 0.25$. In short, reaction [2] is four times more important than reaction [1] at laboratory temperature.

The above calculations are based on the assumption that no isotopic degradation occurs either during reaction or during the recovery of the mercury for analysis. If we allow a maximum uncertainty of ±10% in the A value, the ratio of Φ_2/Φ_1 must be in the range of 3–6. A more detailed investigation of the hydrogen chloride reaction is now in progress in the laboratories of one of us (H.E.G.), as one result of which this ratio should be established more precisely.

The results, given in Table III, indicate that the Hg^{202} enrichment is unaffected by added nitrogen in concentrations up to 80 mole per cent. Although the quenching cross section of hydrogen chloride for $Hg6(^3P_1)$ atoms has not been measured, its value should be at least as large as that for methyl chloride. For methyl chloride and nitrogen, values of 24×10^{-16} cm^2 and 0.274×10^{-16} cm^2 respectively have been obtained (5). Assuming hydrogen chloride to have a quenching cross section of 24×10^{-16} cm^2, hydrogen chloride would be responsible for approximately 96% of the quenching in a mixture containing

Can. J. Chem. Downloaded from www.nrcresearchpress.com by 196.1.178.254 on 09/04/12
For personal use only.

80 mole per cent of nitrogen. Hence it would be necessary to study mixtures very much richer in nitrogen before the role of $Hg^{202}6(^3P_0)$ atoms in the reaction could be assessed.

The three-step sequence proposed for the reaction in pure substrate takes no specific cognizance of the fate of the H atoms produced in reactions [1] and [2]. Rodebush and Speakman (6) have postulated the reaction

$$H + HCl \rightarrow H_2 + Cl \qquad [4]$$

in the mechanism of recombination of H atoms in the presence of hydrogen chloride. If reaction [4] is included in the mechanism, the ratio Φ_1/Φ_2 would be increased from 0.25 to 0.67, since the steady-state calculation leads to the relation:

$$R_{Hg^{202}Cl}/R_{Hg^{N}Cl} = \Phi_1/(1+\Phi_2).$$

If we assume further that a recombination process of the type

$$H + Cl + M \rightarrow HCl + M \qquad [5]$$

occurs, the ratio Φ_1/Φ_2 will lie between 0.25 and 0.67. Studies now in progress should shed light on the importance of steps [4] and [5] to the isotopically specific reaction.

The marked enhancement of the enrichment occurring upon the addition of unsaturated compounds (U), such as butadiene and benzene, to the hydrogen chloride stream could involve reactions of both H atoms and Cl atoms with the unsaturated compounds:

$$Cl + U \rightarrow \text{Products}, \qquad [6]$$
$$H + U \rightarrow \text{Products}. \qquad [7]$$

The rapid reaction of H atoms with unsaturated compounds would be very important if reaction [4] has an appreciable effect on the Cl-atom concentration.

The fact that maximum enrichments of 98% were obtained with butadiene as addend, whereas benzene gave a maximum value of 85%, may indicate that reactions [6] and [7] are faster for butadiene than benzene.

When the lamp–wall temperature was raised from 25 to 50° C, a marked decrease in enrichment occurred. This effect is now being systematically investigated. Since the Doppler-broadening is proportional to the square root of the absolute temperature, it can be shown that an increase of 25° in lamp temperature would result in an increase of emission line width of only 0.1 mÅ. The separation of adjacent hyperfine absorption contours from that of Hg^{202} is about 10 mÅ (1). Hence, at this time, it is apparent that Doppler-broadening alone is insufficient to explain the effect of lamp temperature on the enrichment.

The fact that the addition of chlorobenzene to the hydrogen chloride stream depresses the enrichment indirectly substantiates the proposed mechanism. Quenching of the photoexcited mercury atoms by chlorobenzene apparently leads to the formation of chlorine atoms. The rate of $Hg^{N}Cl$ formation by reaction [3] would therefore be increased, and the over-all enrichment would be reduced.

Since sublimation of the calomel product during reaction did not significantly alter the enrichment, it appears unlikely that exchange reactions of the type:

$$Hg^{202}Cl + Hg^{N} \rightarrow Hg^{N}Cl + Hg^{202} \qquad [8]$$

are important in degrading the isotopic calomel before dimerization on the wall.

The failure to obtain enrichment under static conditions can be explained simply on the basis of the proposed mechanism. Under static conditions the unexcited mercury will become impoverished in Hg^{202} through reaction [1]. Hence the calomel formed in

Can. J. Chem. Downloaded from www.nrcresearchpress.com by 196.1.178.254 on 09/04/12
For personal use only.

reaction [3] will contain less than the normal abundance of Hg^{202}. The enrichment caused by reaction [1] will just correspond to the depletion by reaction [3]. The recovered calomel will therefore contain the normal abundance of Hg^{202}. Now as the linear flow rate is increased the Hg^{202}-depleting effect of reaction [1] on the unexcited mercury will become less and less important. The increase in enrichment with increasing linear flow rate therefore follows from this explanation.

Our findings indicate that, at high flow rates, the enrichment increases with increasing incident light intensity for the hydrogen chloride – butadiene mixtures. The explanation of this effect is not readily forthcoming from the proposed mechanism. It would appear wiser to postpone comment on the light intensity dependence until a more detailed study has been made of the hydrogen chloride – butadiene reaction.

The dependence of both the rate of calomel deposition and the Hg^{202} enrichment on the mercury concentration in the stream for the hydrogen chloride – butadiene reaction again emphasizes the complexity of this system. Since maximum enrichment and efficient calomel deposition are obtained only when the stream is slightly supersaturated with mercury vapor it appears that a layer of natural mercury must be adsorbed on the walls of the reaction vessel before the calomel can deposit. Further studies must be carried out on this system before an adequate explanation can be given for this behavior.

CONCLUSIONS

As a result of this investigation it has been firmly established that a fraction of the quenching collisions between $Hg^{202}6(^3P_1)$ atoms and hydrogen chloride forms a solid mercury compound. From stability considerations it is likely that the primary compound is $Hg^{202}Cl$ rather than $Hg^{202}H$.

From the Hg^{202}-enrichment data, and an assumed mechanism, it can be calculated that the isotopically specific portion of the primary reaction at 28–30° C is in the range 20–40%. It is likely that the two primary processes involve a common intermediate, Hg^{202}–Cl–H*. It would be expected that increasing reaction temperature would favor Cl-atom formation. Studies are now under way at the University of Alberta on the temperature coefficient of the primary reaction.

Further investigations are also in progress on the kinetics of the hydrogen chloride reaction in the presence of unsaturated addends.

ACKNOWLEDGMENTS

The authors would like to express their deep appreciation to Dr. Kenton R. Osborn, Dr. Willard F. Allen, and Mr. John A. Poole for many valuable discussions.

REFERENCES

1. OSBORN, K. R., McDONALD, C. C., and GUNNING, H. E. J. Chem. Phys. **26**, 124 (1957).
2. PERTEL, R. and GUNNING, H. E. J. Chem. Phys. **26**, 219 (1957).
3. PERTEL, R. and GUNNING, H. E. Can. J. Chem. **37**, 35 (1959).
4. OSBORN, K. R. and GUNNING, H. E. J. Opt. Soc. Am. **45**, 552 (1955).
5. DARWENT, B. and PHIBBS, M. J. Chem. Phys. **22**, 110 (1954).
6. RODEBUSH, W. H. and SPEAKMAN, M. L. J. Am. Chem. Soc. **57**, 1040 (1935).

Can. J. Chem. Downloaded from www.nrcresearchpress.com by 196.1.178.254 on 09/04/12
For personal use only.

Can. J. Chem. Downloaded from www.nrcresearchpress.com by 196.1.178.254 on 09/04/12
For personal use only.

REARRANGEMENT STUDIES WITH C^{14}

VII. THE ACETOLYSIS OF METHYL-C^{14}-ISOPROPYLCARBINYL *p*-TOLUENESULPHONATE[1]

A. J. Finlayson and C. C. Lee

ABSTRACT

Acetolysis of methyl-C^{14}-isopropylcarbinyl *p*-toluenesulphonate (I) at reflux temperature gave a mixture of 2-methyl-2-butene (II), 2-methyl-1-butene (III), and 3-methyl-1-butene (IV) with no isolatable quantity of substitution product. The relative amounts of olefins II, III, and IV were measured by gas–liquid chromatography to be 80%, 18%, and 2%, respectively, and these were substantially verified by estimations with the isotope dilution technique. When the acetolysis was carried out at 50° C, besides olefins II, III, and IV, present in relative amounts of 83%, 16%, and 1%, respectively, as determined by gas–liquid chromatography, a small quantity of substitution product, *t*-amyl acetate (V), was obtained. Under the conditions of acetolysis at reflux temperature, however, V was found to decompose to olefins II and III. Degradation of the olefinic products of acetolysis gave, among other compounds, radioactive acetone. Since acetone was derived from the chief product, II, its activity could be attributed to an isotope position rearrangement resulting from a 1,2-methide shift as one of the processes that gave rise to olefin II. This rearrangement amounted to about 2.5% and 0.9%, respectively, in olefin II from acetolysis at reflux temperature and at 50° C. Considering all these results, it may be concluded that both substitution and elimination reactions could take place during acetolysis of I. The substitution reaction proceeded with neighboring hydrogen participation to yield *t*-amyl acetate, which would decompose to olefins II and III at reflux temperature under the acetolysis conditions. In the E_1 reaction during acetolysis of I, processes involving no neighboring group participation to give olefins II and IV, with neighboring hydrogen participation to give olefins II and III, and with neighboring methyl participation to give isotopically rearranged olefins II and IV, all occurred, the process with neighboring hydrogen participation being predominant.

First-order reaction rates for the formolysis of methylisopropylcarbinyl *p*-toluenesulphonate and the acetolysis and formolysis of methylisopropylcarbinyl *p*-bromobenzenesulphonate have been reported by Winstein and Marshall (1) in connection with their studies on neighboring hydrogen and carbon participation. From considerations of relative rates for a series of related secondary sulphonates, it was concluded that there is some assistance to ionization from neighboring group participation during solvolyses of methylisopropylcarbinyl derivatives, though the driving force associated with participation in this system was said to be small (1). No clear-cut differentiation was made on whether participation was from neighboring hydrogen or carbon, nor were any reaction products isolated. In the present work, the acetolysis of methyl-C^{14}-isopropylcarbinyl *p*-toluenesulphonate (I) was carried out, the reaction products identified, and the degrees of isotope position rearrangement determined so as to shed some light on the different routes the reaction may follow during acetolysis.

RESULTS AND DISCUSSIONS

Methyl-C^{14}-isopropylcarbinol was prepared from reaction of isobutyraldehyde with methyl-C^{14}-magnesium iodide. On subjecting this carbinol to the haloform reaction, nonradioactive isobutyric acid was obtained, indicating that all the C^{14} activity was on the methyl carbon. Conversion of the carbinol to sulphonate I was effected by treatment with *p*-toluenesulphonyl chloride in pyridine.

Acetolysis of I at reflux temperature yielded only olefinic products. No acetate fraction could be isolated. The olefins were shown by gas–liquid chromatographic analysis (2), and verified by isotope dilution, to be a mixture of 2-methyl-2-butene (II), 2-methyl-1-

[1]*Manuscript received January 16, 1959.*
Contribution from the Department of Chemistry, University of Saskatchewan, Saskatoon, Saskatchewan.

butene (III), and 3-methyl-1-butene (IV), the relative proportions of these are given in Table I. When the acetolysis was carried out at 50° C, besides olefins II, III, and IV (Table I), a small amount of *t*-amyl acetate (V), but no methylisopropylcarbinyl acetate (VI), was obtained. On subjecting V to treatment under conditions as in the acetolysis at reflux temperature, V decomposed to olefins II and III. There was no decomposition of VI under a similar treatment.

TABLE I

Relative amounts of olefins from acetolyses of methyl-C^{14}-isopropylcarbinyl *p*-toluenesulphonate

		% Composition		
		Analyzed by gas chromato-graphy	Analyzed by radioactivity	
Reaction	Olefin		Run 1	Run 2
Acetolysis at reflux temp.	2-Methyl-2-butene	80	82.8	82.5
	2-Methyl-1-butene	18	14.8	13.8
	3-Methyl-1-butene	2	2.4	3.7
Acetolysis at 50° C	2-Methyl-2-butene	83	79	76
	2-Methyl-1-butene	16		
	3-Methyl-1-butene	1		

Degradations of olefins II, III, and IV are shown by reaction sequences 1–3, the C^{14} labels being indicated on positions as if there were no isotope position rearrangement.

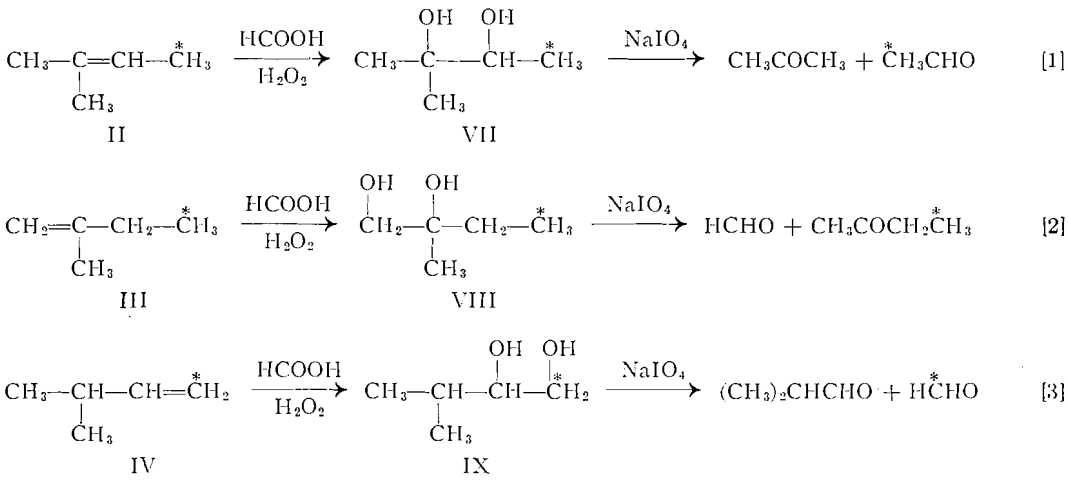

[1] [2] [3]

When a mixture of II, III, and IV was degraded according to these schemes, the products consisted of a mixture of formaldehyde, acetaldehyde, isobutyraldehyde, acetone, and methyl ethyl ketone. Separation of these carbonyl compounds as their 2,4-dinitrophenylhydrazones was effected by adsorption chromatography in a column packed with a 2:1 mixture of silicic acid and celite (3). Desired bands of individual 2,4-dinitrophenylhydrazones were recovered by elution with petroleum ether containing some diethyl ether. Alternatively, the aldehydes in the mixture of carbonyl compounds were first oxidized with potassium permanganate (4) before the chromatographic separation of acetone and methyl ethyl ketone as their 2,4-dinitrophenylhydrazones.

Can. J. Chem. Downloaded from www.nrcresearchpress.com by 196.1.178.254 on 09/04/12
For personal use only.

Can. J. Chem. Downloaded from www.nrcresearchpress.com by 196.1.178.254 on 09/04/12
For personal use only.

For measurements of relative amounts of II, III, and IV by isotope dilution, non-labeled olefin II was obtained by distillation of the commercial material through a long column. Non-labeled olefins III and IV were prepared by the Chugaev reaction with *sec*-butylcarbinol and isobutylcarbinol, respectively (5). From these olefins, inactive glycols VII, VIII, and IX were obtained. The purity of each of these glycols was demonstrated by their cleavage with sodium metaperiodate to give only the expected carbonyl compounds.

The isotope dilution experiments were carried out by adding a known quantity of inactive glycol VII, VIII, or IX to a weighed mixture of VII, VIII, and IX derived from the olefins obtained in an acetolysis. The diluted mixture was cleaved with sodium metaperiodate and the 2,4-dinitrophenylhydrazones of the most abundant products isolated from the chromatographic column. Radioactivity assays of these diluted products of degradation provided data from which the relative amounts of II, III, and IV in the original products of acetolysis can be calculated. For example, in isotope dilution run No. 1, the mixture of olefins II, III, and IV from an acetolysis at reflux temperature was converted to a mixture of glycols VII, VIII, and IX. To 0.0580 g of this glycol mixture, 0.2279 g of inactive VII was added. After degradation and separation by adsorption chromatography, the 2,4-dinitrophenylhydrazones of acetaldehyde and acetone were isolated. Radioactivity assay gave specific activity of 8704 c.p.m. on a molar basis[2] for the 2,4-dinitrophenylhydrazone of acetaldehyde. Since gas–liquid chromatography indicated 80% II in the olefin mixture from acetolysis at reflux temperature, it is reasonable to assume that of the 0.0580 g of undiluted active glycol mixture, 80% was VII. Hence the total activity of the acetaldehyde from 0.0580 g of undiluted glycol mixture is equivalent to $8704\times(0.2279+0.80\times0.0580)$ c.p.m. Correcting to a common basis of 1 g of undiluted active glycol mixture, the corrected activity for the acetaldehyde fraction would be

$$\frac{8704\times(0.2279+0.80\times0.0580)}{0.0580} = 41{,}200 \text{ c.p.m.}$$

Similarly, the corrected activity for the acetone was found to be 1120 c.p.m.

In an analogous way, the active glycol mixture was diluted with inactive VIII or IX. From dilution with VIII, the 2,4-dinitrophenylhydrazones of methyl ethyl ketone and formaldehyde were isolated, while from dilution with IX, only the 2,4-dinitrophenylhydrazone of formaldehyde was eluted for activity assay. Radioactivity data from these experiments as well as from a duplicate run are summarized in Table II.

Since formaldehyde is formed from degradation of both VIII and IX, the activity in the formaldehyde would be derived from both VIII and IX in the undiluted active glycol mixture. The corrected activity for formaldehyde from dilution experiment with either inactive VIII or IX should, therefore, be identical. The actual data (Table II) showed small differences in corrected activities calculated for the two formaldehyde samples from each run. Possibly, in the chromatographic separation of the 2,4-dinitrophenylhydrazones, slight contamination of the formaldehyde derivative by the more highly active derivative of acetaldehyde may contribute to these differences. In any case, the magnitude of the differences between corrected activities of formaldehyde samples, of the order of 300 c.p.m. compared to the total corrected activities for all fractions of around 40,000 to 50,000 c.p.m., should not materially affect the over-all calculation of the relative amounts of olefins II, III, and IV.

[2]*See footnote* †, *Table II.*

TABLE II

Data from isotope dilution of the mixture of glycols derived from the olefins obtained in acetolyses at reflux temperature

Wt. of active glycols (g)		Wt. of inactive diluent (g)		Inactive diluent used	Degradation product assayed	Specific activity (c.p.m. on molar basis†)		Corrected activity per gram of glycol mixture (c.p.m.)		Percentage of total activity‡		Percentage rearrangement in 2-methyl-2-butene	
Run 1	Run 2	Run 1	Run 2			Run 1	Run 2	Run 1	Run 2	Run 1	Run 2	Run 1	Run 2
0.0580	0.0732	0.2279	0.3113	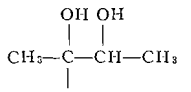	CH_3CHO	8704	6310	41200	31900	80.6	80.5		
					CH_3COCH_3	236	157	1120	800	2.2	2.0	2.6	2.4
0.1078	0.0210	0.1853	0.3105	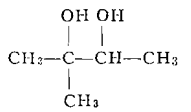	CBr_4*	567	69	1370	1070	2.7	2.7		
0.0845	0.0877	0.1734	0.2177	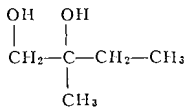	$CH_3COCH_2CH_3$	3400	2052	7580	5470	14.8	13.8		
					HCHO	689	658	1550	1770	3.0	4.5		
0.0975	0.0666	0.1355	0.1079	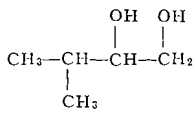	HCHO	781	796	1240	1450	2.4	3.7		

*From reaction of ketonic products with bromine and sodium hydroxide.

†Specific activities in c.p.m. on a molar basis were determined by converting all compounds to barium carbonate and counted as infinitely thick samples of constant geometry in a gas flow Geiger counter. Correction for the presence of non-labeled carbon atoms was made by multiplying the observed activity with the number of carbon atoms per molecule in the compound assayed (6). In the case of CBr_4, the observed activity was multiplied by 2, since acetone has two equivalent methyl groups. All samples were counted for sufficient lengths of time so that statistical errors were within ±2% of the observed activities.

‡The total activity was taken as the sum of the corrected activities of CH_3CHO, CH_3COCH_3, $CH_3COCH_2CH_3$, and HCHO from dilution with inactive 3-methyl-1,2-butanediol. The percentage of total activity in CH_3CHO and CH_3COCH_3 is a measure of the amount of 2-methyl-2-butene in the mixture of olefins from the acetolysis. The percentage of total activity in $CH_3COCH_2CH_3$ and in HCHO from dilution with inactive 3-methyl-1,2-butanediol is taken as measures of 2-methyl-1-butene and 3-methyl-1-butene, respectively.

For the estimation of the relative amounts of olefins II, III, and IV in the original acetolysis products, the total corrected activities of acetaldehyde, acetone, methyl ethyl ketone, and one sample of formaldehyde were taken as representing the total activity of olefins II, III, and IV. The sum of the corrected activities of acetaldehyde and acetone was used as a measure of II, while the corrected activities of methyl ethyl ketone and formaldehyde were used as measures of III and IV, respectively. Since formaldehyde could actually be derived from both III and IV, and since any active formaldehyde from III would have to arise from an isotopically rearranged III, it may be reasonably assumed that any activity of the formaldehyde from III would be small compared to the activity of methyl ethyl ketone. The use of the corrected activity of methyl ethyl ketone alone as a measure of III is, therefore, an acceptable approximation. For these same reasons, the use of the corrected activity of formaldehyde as a measure of IV is also only a good approximation. Furthermore, it should also be pointed out that although the degradation of IV should give rise to formaldehyde and isobutyraldehyde, the activity in the isobutyraldehyde, if any, should be negligibly small, as active isobutyr-

Can. J. Chem. Downloaded from www.nrcresearchpress.com by 196.1.178.254 on 09/04/12
For personal use only.

aldehyde could only result from an isotopically rearranged IV. In Table II, the corrected activities of a number of degradation products are expressed as percentages of total activity. The percentage of total activity for both acetaldehyde and acetone together would be equivalent to the amount of II and the percentages of total activity for methyl ethyl ketone and formaldehyde would be equivalent to the amounts of III and IV, respectively, in the original acetolysis products. These estimated relative amounts of II, III, and IV are also given in Table I for comparison with results from gas–liquid chromatography.

The fact that there was some activity in the acetone fraction from these isotope dilution experiments indicated that there was some isotope position rearrangement in the major acetolysis product, 2-methyl-2-butene (II). For acetolysis at reflux temperature run No. 1, this rearrangement amounted to

$$\frac{1120}{1120+41200}\times 100 = 2.6\%.$$

In the duplicate run, the rearrangement was 2.4% (Table II). This rearrangement very likely arose from a 1,2-methide shift, or neighboring methyl participation, resulting in an acetone with C^{14} on the methyl carbons:

$$CH_3-\underset{\displaystyle CH_3}{\underset{|}{CH}}-\overset{+}{C}H-\overset{*}{C}H_3 \xrightleftharpoons{CH_3\ \text{shift}} CH_3-\overset{+}{C}H-\underset{\displaystyle CH_3}{\underset{|}{CH}}-\overset{*}{C}H_3$$

Collaboration of such a reaction path may be deduced from the following experiment. A sample of the active mixture of glycols VII, VIII, and IX derived from the products of an acetolysis at reflux temperature was diluted with inactive VII and then cleaved with sodium metaperiodate. The resulting mixture of carbonyl compounds was treated with neutral potassium permanganate to destroy the aldehydes (4). An aqueous solution of the remaining acetone and methyl ethyl ketone was recovered by distillation and then treated with bromine and sodium hydroxide to give carbon tetrabromide. The corrected activities of the carbon tetrabromide samples are also included in Table II. If much of the acetone activity were located on the carbonyl carbon, one would expect the corrected activity of the carbon tetrabromide to be less than that of the acetone. Actually, for a given run, carbon tetrabromide showed somewhat greater activity than acetone (Table II). This extra activity in the carbon tetrabromide very likely was derived from the methyl group of methyl ethyl ketone, indicating that there was also a small degree of isotope position rearrangement in 2-methyl-1-butene (III), another product from the acetolysis of I.

When acetolysis of I was carried out at 50° C, as mentioned earlier, a small amount of *t*-amyl acetate was obtained besides a mixture of olefins II, III, and IV. The relative amounts of II, III, and IV, as measured by gas–liquid chromatography, are given in Table I. In addition, the major product, II, was estimated by radioactivity measurements. As before, olefins II, III, and IV from a given run were converted to the glycol mixture, VII, VIII, and IX. This mixture, without dilution, was degraded in the usual manner and the 2,4-dinitrophenylhydrazones of acetaldehyde and acetone isolated from the adsorption chromatographic column. Activity assays on these degradation products as well as on the glycol mixture were carried out. The results from duplicate acetolyses at 50° C are tabulated in Table III. From these results, the isotope position rearrangement in II, as indicated by the activity of the acetone, was calculated (Table III). The sum of

Can. J. Chem. Downloaded from www.nrcresearchpress.com by 196.1.178.254 on 09/04/12
For personal use only.

the activities of acetaldehyde and acetone in a given run is, of course, a measure of the amount of II in the original mixture of olefins II, III, and IV. This estimate of II is also listed in Table I for comparison with gas–liquid chromatographic data.

TABLE III

Radioactivity data from acetolyses at 50° C

Compound assayed	Specific activity (c.p.m. on molar basis)		Percentage of total activity		Percentage rearrangement in 2-methyl-2-butene	
	Run 1	Run 2	Run 1	Run 2	Run 1	Run 2
Glycol mixture from olefinic products	8790	10860	100	100		
CH_3CHO	6900	8125	79	76	0.9	0.9
CH_3COCH_3	62	74				

CONCLUSIONS

From the results presented in the foregoing sections and summarized in Tables I, II, and III, it is clear that a number of reaction routes may be followed in the acetolysis of methyl-C^{14}-isopropylcarbinyl *p*-toluenesulphonate (I). At 50° C, some substitution involving neighboring hydrogen participation took place, giving rise to *t*-amyl acetate (V) as depicted in reaction [4]:

$$\underset{\text{I}}{CH_3{-}CH(CH_3){-}CH(OTs){-}{}^{*}CH_3} + HOAc \longrightarrow \underset{\text{V}}{CH_3{-}C(OAc)(CH_3){-}CH_2{-}{}^{*}CH_3} + TsOH \qquad [4]$$

At reflux temperature, if such a substitution reaction did occur, the product, V, would decompose to olefins II and III. By far the major part of the acetolysis products resulted from elimination reactions. To explain the formation of the various elimination products, processes similar to some of those involved in the E_1 reaction in the acetolysis of the diastereoisomers of 3-phenyl-2-butyl *p*-toluenesulphonate (7) may be postulated. Three processes, depicted by reaction sequences 5, 6, and 7, definitely occurred.

$$I \xrightarrow{-OTs^-} \underset{\text{X}}{CH_3{-}CH(CH_3){-}{}^{+}CH{-}{}^{*}CH_3} \xrightarrow{-H^+} \underset{\text{II}}{CH_3{-}C(CH_3){=}CH{-}{}^{*}CH_3} + \underset{\text{IV}}{CH_3{-}CH(CH_3){-}CH{=}{}^{*}CH_2} \qquad [5]$$

$$I \xrightarrow{-OTs^-} \underset{\text{XI}}{CH_3{-}{}^{+}C(CH_3){-}CH_2{-}{}^{*}CH_3} \xrightarrow{-H^+} \underset{\text{II}}{CH_3{-}C(CH_3){=}CH{-}{}^{*}CH_3} + \underset{\text{III}}{CH_2{=}C(CH_3){-}CH_2{-}{}^{*}CH_3} \qquad [6]$$

$$I \xrightarrow{-OTs^-} \underset{\text{X}_r}{CH_3{-}{}^{+}CH{-}CH(CH_3){-}{}^{*}CH_3} \longrightarrow \underset{\text{II}_r}{CH_3{-}CH{=}C(CH_3){-}{}^{*}CH_3} + \underset{\text{IV}_r}{CH_2{=}CH{-}CH(CH_3){-}{}^{*}CH_3} \qquad [7]$$

(Subscript r is used to denote isotopically rearranged X, II, and IV.)

Can. J. Chem. Downloaded from www.nrcresearchpress.com by 196.1.178.254 on 09/04/12
For personal use only.

Reaction [5] involves ionization of I without anchimeric assistance to secondary carbonium ion X, which gave rise to olefins II and IV. Reaction [6] involves ionization of I with anchimeric assistance from neighboring hydrogen participation resulting in tertiary carbonium ion XI, which gave olefins II and III. Reaction [7] involves ionization of I with anchimeric assistance from neighboring methyl participation to give isotopically rearranged X_r, which resulted in the formation of isotopically rearranged olefins II_r and IV_r. According to Saytzeff's rule (8), one would expect a greater amount of II (or II_r) formed in each of these processes. It is, therefore, not surprising to have found that olefin II was the chief isolatable product from the acetolysis mixture. Of these processes of elimination, reaction [6] may be considered as most important, or as having occurred to the greatest extent, since olefin IV, a measure of reaction [5], and isotopically rearranged II_r, a measure of reaction [7], each amounted to only 2–4% of the over-all reaction products for acetolysis at reflux temperature. Still less IV and II_r, in the order of 1%, were found in the products of acetolysis at 50° C.

On the basis of the present results, it is, of course, not possible to differentiate, that in the neighboring hydrogen and methyl participations, whether the processes involved a series of 1,2-shifts in concrete stages with ion X as the first intermediate (reaction sequences 8 and 9), or whether ions XI and X_r were formed directly from I. Nor can one decide whether non-classical carbonium ions XII and XIII play any role in these reactions, for the present results can be explained with or without postulating the existence of XII and XIII.

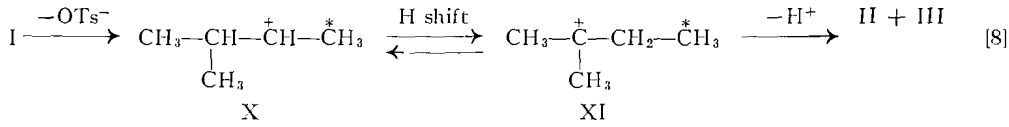

X XI

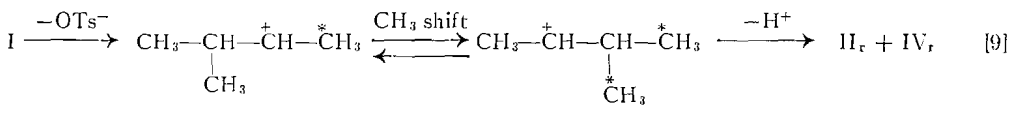

X X_r

XII XIII

It may be recalled that in the degradation of acetone and methyl ethyl ketone to carbon tetrabromide in acetolysis runs 1 and 2 at reflux temperature (Table II), the corrected activity of the carbon tetrabromide was somewhat higher than that of the corresponding acetone. If one were to consider this difference significant and attribute the extra activity in the carbon tetrabromide as arising from the methyl carbon of methyl ethyl ketone, a process involving first a 1,2-methide shift followed by a 1,2-hydride shift would have to be postulated (reaction sequence [10]):

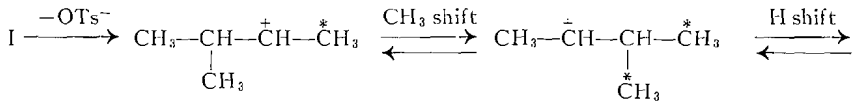

X X_r

Can. J. Chem. Downloaded from www.nrcresearchpress.com by 196.1.178.254 on 09/04/12
For personal use only.

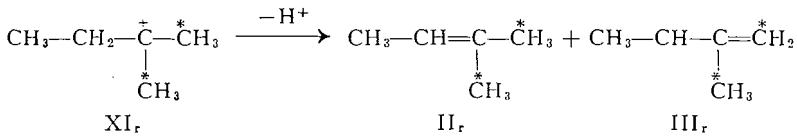

[10]

Methyl ethyl ketone with C^{14} activity on the methyl carbon would thus result from the isotopically rearranged olefin III_r.

In summary, it may be concluded that in the acetolysis of methyl-C^{14}-isopropylcarbinyl *p*-toluenesulphonate (I), both substitution and elimination reactions take place. The substitution proceeds with neighboring hydrogen participation, resulting in the formation of *t*-amyl acetate, which will decompose to olefins at reflux temperature under the acetolysis conditions. In the E_1 reaction during the acetolysis of I, processes involving no neighboring group participation, neighboring hydrogen participation, and neighboring methyl participation all occur, with neighboring hydrogen participation predominant. A process involving first a 1,2-methide shift followed by a 1,2-hydride shift before olefin formation may also take place, though the experimental results only indicate a probability, without an unequivocal proof, of such a reaction route. These conclusions are in excellent agreement with the recent finding of Winstein and Takahashi (9) that the acetolysis of I has a relatively high value of k_Δ/k_s, the ratio of rate constants for anchimerically assisted and unassisted solvolysis processes. These workers attributed k_Δ to neighboring hydrogen participation and accounted for the earlier observation of a low degree of rate acceleration (1) on conformational considerations. Their kinetic studies, however, failed to show the smaller contribution to k_Δ from neighboring methyl participation clearly demonstrated by the present data.

EXPERIMENTAL

Methyl-C^{14}-isopropylcarbinol

Methyl-C^{14}-isopropylcarbinol was prepared by the reaction of isobutyraldehyde with methyl-C^{14}-magnesium iodide. The procedure used was similar to that described for the synthesis of 2-butanol-1-C^{14} (10). A typical preparation is as follows:

Methyl-C^{14}-magnesium iodide, prepared from 13.0 g (0.092 moles) of methyl-C^{14} iodide and 2.9 g (0.12 moles) of magnesium in 180 ml of anhydrous ether, was maintained at −20° C in a dry-ice bath. A solution of 10.8 g (0.15 moles) of freshly distilled isobutyraldehyde in 180 ml of anhydrous ether was added dropwise over a period of 2 hours. The mixture was brought to 0° C and 20 ml of a saturated solution of ammonium chloride was added. The ether layer was separated and the aqueous layer and the precipitated salts were extracted several times with ether. The combined extract was dried over magnesium sulphate, the ether removed, and the residue distilled to give 5.30 g (66%) of the carbinol, b.p. 107–109° C (uncorrected), 3,5-dinitrobenzoate derivative, m.p. 74–75° C (lit. (11*a*), m.p. 76° C).

Isobutyric Acid from Methyl-C^{14}-isopropylcarbinol

A haloform reaction between the carbinol and bromine in sodium hydroxide solution was carried out using a procedure analogous to that employed in the preparation of trimethylacetic acid from pinacolone (12). From 2.80 g (0.032 moles) of methyl-C^{14}-isopropylcarbinol, 1.85 g (65%) of isobutyric acid was obtained. A derivative, the *p*-bromophenacyl ester, showed a m.p. of 77° C (lit. (11*b*), m.p. 77° C). Radioactivity assay showed that this isobutyric acid contained no activity, indicating that all the C^{14} was located on the methyl carbon of methylisopropylcarbinol.

Can. J. Chem. Downloaded from www.nrcresearchpress.com by 196.1.178.254 on 09/04/12
For personal use only.

Methyl-C^{14}-isopropylcarbinyl p-Toluenesulphonate

Methyl-C^{14}-isopropylcarbinyl *p*-toluenesulphonate was prepared from the carbinol by treatment with *p*-toluenesulphonyl chloride in pyridine (13). The product, recrystallized twice from petroleum ether chilled in a dry-ice bath, melted at 20–21° C (lit. (1), m.p. 20.1–20.8° C); the yields obtained were in the order of 60% of theoretical.

Acetolysis of Methyl-C^{14}-isopropylcarbinyl p-Toluenesulphonate

Anhydrous acetic acid containing 0.1 *M* potassium acetate was prepared by refluxing freshly distilled acetic acid, acetic anhydride, and potassium carbonate as described by Cram and Allinger (14). This solution was used for all acetolysis runs. Duplicate acetolyses at reflux temperature and at 50° C were carried out. Typical procedures are given below:

A. Acetolysis at Reflux Temperature

A mixture of 7.15 g (0.030 moles) of methyl-C^{14}-isopropylcarbinyl *p*-toluenesulphonate, 60 ml of anhydrous acetic acid containing 0.1 *M* potassium acetate, and an additional 3.0 g (0.031 moles) of potassium acetate sufficient to neutralize all liberated *p*-toluenesulphonic acid was heated under reflux for 3.5 hours. During the refluxing, the system was flushed with dry nitrogen and any condensable products entrained by the nitrogen were recovered in a dry-ice cooled trap. After the refluxing, the reaction mixture was cooled and extracted with a 3:1 mixture of petroleum ether and ether. The extract was washed with dilute sodium carbonate solution and dried, and the solvent removed. No residue remained, indicating no isolatable quantity of substitution product.

The olefin mixture recovered in the dry-ice cooled trap weighed 1.70 g (82%). It decolorized bromine in carbon tetrachloride very readily. It was distilled once, b.p. 35–38° C, before being used for subsequent analyses by gas chromatography and isotope dilution.

B. Acetolysis at 50° C

A mixture of 13 g (0.054 moles) of methyl-C^{14}-isopropylcarbinyl *p*-toluenesulphonate, 130 ml of anhydrous acetic acid containing 0.1 *M* potassium acetate, and an additional 6.0 g (0.061 moles) of potassium acetate was maintained at 50±1° C and constantly stirred for 14 hours. The olefins formed (1.25 g) were swept out by nitrogen and collected in a dry-ice cooled trap. These olefins were also distilled once, b.p. 35–38° C, before being analyzed.

For the recovery of the product of substitution, the reaction mixture from the acetolysis was poured into 250 g of ice and water and extracted with ether. The extract was washed with water and with dilute sodium carbonate until the washing remained basic. The washed extract was dried and the ether removed. From the colorless residue, a fraction (0.220 g) boiling at 117–118° C was obtained. Its infrared spectrum was identical with that of *t*-amyl acetate and different from that of methylisopropylcarbinyl acetate.

The residue remaining after the distillation of the acetate weighed 4.6 g. On crystallization, 4.0 g of unreacted methyl-C^{14}-isopropylcarbinyl *p*-toluenesulphonate was recovered. Based on the 9.0 g of sulphonate that was not recovered, the yield of olefins was 48% and the yield of *t*-amyl acetate was 4.6%.

Treatment of t-Amyl Acetate in Refluxing Acetolysis Mixture

A mixture of 6.0 g (0.046 moles) of *t*-amyl acetate, prepared from a reaction of *t*-amyl alcohol with acetic anhydride in the presence of zinc chloride (15), 60 ml of anhydrous acetic acid containing 0.1 *M* potassium acetate, and an additional 3.0 g of potassium acetate was gently refluxed for 3.5 hours. The volatile product, which proved to be a

Can. J. Chem. Downloaded from www.nrcresearchpress.com by 196.1.178.254 on 09/04/12
For personal use only.

60:40 mixture of 2-methyl-2-butene (II) and 2-methyl-1-butene (III) according to gas–liquid chromatographic analysis, was swept out by nitrogen and collected in a dry-ice cooled trap as in the acetolysis. The appearance of this olefinic mixture at various time intervals is recorded below:

Time (hours)	Weight of olefins (g)	% Yield
1.5	0.54	17
2.5	0.81	25
3.5	0.97	30

From the reaction mixture, 2.31 g (39%) of unchanged *t*-amyl acetate was recovered.

Treatment of Methylisopropylcarbinyl Acetate in Refluxing Acetolysis Mixture

Methylisopropylcarbinyl acetate was prepared from acetylation of the alcohol with acetyl chloride in pyridine. Treatment of this acetate in the refluxing acetolysis mixture as described for *t*-amyl acetate gave no olefinic product in 3 hours. On working up of the resulting mixture, unchanged acetate was recovered in 80% yield.

Gas–Liquid Chromatography

The olefinic mixture from acetolysis at reflux temperature or at 50° C was analyzed by gas–liquid chromatography. The column was packed with dinonyl phthalate supported on ground firebrick. The olefins passed through the column with helium as carrier gas. The effluent was analyzed by a thermal conductivity cell with the results automatically recorded. Three peaks were obtained corresponding to the three olefins, 2-methyl-2-butene (II), 2-methyl-1-butene (III), and 3-methyl-1-butene (IV). The areas under these peaks were used as measures of the relative amounts of these olefins. The results are tabulated in Table I.

The olefinic product from the treatment of *t*-amyl acetate in the refluxing acetolysis mixture was also analyzed. Only two peaks, corresponding to a 60:40 mixture of II and III, were observed.

Preparations of Non-radioactive Olefins II, III, and IV

2-Methyl-2-butene (II) was obtained from a commercial sample by careful fractionation through an efficient column (16). 2-Methyl-1-butene (III) and 3-methyl-1-butene (IV) were prepared from *sec*-butylcarbinol and isobutylcarbinol, respectively, by the Chugaev reaction according to the modified method described by Whitmore and Simpson (5). These authors (5) reported the details on the reaction with isobutylcarbinol. In the reaction with *sec*-butylcarbinol, from 22.5 g (0.26 moles) of the carbinol treated with equimolar quantities of sodium hydroxide, carbon disulphide, and methyl iodide, the methylxanthate of *sec*-butylcarbinol obtained weighed 32.8 g (73%), b.p. 107–110° C at 15–17 mm, n_D^{25} 1.5225. Anal. Calc. for $C_7H_{14}OS_2$: C, 47.2%; H, 7.92%; S, 36.0%. Found: C, 47.1%; H, 7.72%; S, 35.8%. This xanthate was decomposed at reflux temperature to give a 42% yield of 2-methyl-1-butene (III).

Degradation of Olefins II, III, and IV

Olefin II, III, or IV was degraded by conversion to the corresponding glycol with performic acid (formic acid and hydrogen peroxide) followed by the cleavage of the glycol with sodium metaperiodate to give carbonyl compounds. The procedures used were similar to those described by Roberts, McMahon, and Hine (4) for their degradation

Can. J. Chem. Downloaded from www.nrcresearchpress.com by 196.1.178.254 on 09/04/12
For personal use only.

of isotopically labeled 2-methyl-2-butene (II). The carbonyl compounds, recovered as an aqueous solution by distillation after the reaction with sodium metaperiodate, were converted to the 2,4-dinitrophenylhydrazones which were, in turn, separated by adsorption chromatography. A typical chromatographic separation is as follows:

The chromatographic column, 2.2 cm in diameter and 25 cm in length, was packed with a mixture of silicic acid and celite (2:1 by weight) as described by Gordon and co-workers (3). A 20-mg sample of the 2,4-dinitrophenylhydrazones derived from the degradation of 2-methyl-1-butene (III) was dissolved in 3 ml of chloroform and placed on the top of the column. After the material was adsorbed, 100 ml of low-boiling petroleum ether was added and allowed to percolate into the column under a slight nitrogen pressure. The bands of 2,4-dinitrophenylhydrazones were developed with a 2% solution of diethyl ether in petroleum ether and then eluted by gradually increasing the diethyl ether concentration to 12%. Flow of the solvent was aided by maintaining a nitrogen pressure of about 2 p.s.i.g. on the reservoir of solvent on top of the column. Two bands were eluted. The eluant containing each band was concentrated to about 10 ml whereby the 2,4-dinitrophenylhydrazone crystallized. From the first band, 12.5 mg (90%) of methyl ethyl ketone – 2,4-dinitrophenylhydrazone was recovered. It melted alone and on admixture with an authentic sample at 116–117° C. The second band gave 5.0 mg (80%) of formaldehyde – 2,4-dinitrophenylhydrazone which melted at 161° C. It did not show any melting-point depression when mixed with an authentic sample. No other material was recovered from the column, indicating that the 2-methyl-1-butene (III) degraded was pure.

Similarly, degradation of 2-methyl-2-butene (II) or 3-methyl-1-butene (IV) gave only the 2,4-dinitrophenylhydrazones of the expected carbonyl compounds after the chromatographic separation.

Isotope Dilutions and Degradations of Olefinic Products from Acetolyses at Reflux Temperature

The mixture of radioactive olefins II, III, and IV obtained from each of the duplicate acetolyses at reflux temperature was converted to the corresponding mixture of active glycols, 2-methyl-2,3-butanediol (VII), 2-methyl-1,2-butanediol (VIII), and 3-methyl-1,2-butanediol (IX) by treatment with performic acid (4). Known quantities of this mixture were diluted with weighed amounts of non-radioactive glycol VII, VIII, or IX and then cleaved to give carbonyl compounds. The cleavage was effected by the method of Reeves (17) instead of that of Roberts and co-workers (4) because the former method gave better yields. Details of a typical dilution and degradation are given below:

To 0.0580 g (0.00056 moles) of the mixture of active glycols, derived from acetolysis at reflux temperature run No. 1, was added 0.2279 g (0.0022 moles) of inactive 2-methyl-2,3-butanediol (VII). This diluted glycol mixture was dissolved in 10 ml of water and treated with 10 ml of 0.03 *N* periodic acid and 10 ml of 1 *N* sodium bicarbonate. After it had been left standing at room temperature for 1 hour, the reaction mixture was treated with 10 ml of 1 *N* hydrochloric acid and 10 ml of 1 *N* sodium arsenite solution to destroy the iodine formed. The resulting solution was distilled and the distillate containing the carbonyl compounds was trapped in a dry-ice cooled receiver. This distillate was poured into 250 ml of 2 *N* hydrochloric acid containing 1.20 g (0.006 moles) of 2,4-dinitrophenylhydrazine and allowed to stand for 1 hour at 0° C. The 2,4-dinitrophenylhydrazones formed weighed 1.00 g (79% of the theoretical calculated on the assumption that the diluted glycol mixture was pure 2-methyl-2,3-butanediol). Part of

Can. J. Chem. Downloaded from www.nrcresearchpress.com by 196.1.178.254 on 09/04/12
For personal use only.

these 2,4-dinitrophenylhydrazones was separated, in 50-mg lots, by chromatography in the silicic acid – celite column as previously described. In this particular dilution experiment in which the diluent was inactive VII, the 2,4-dinitrophenylhydrazones of the major degradation products, acetaldehyde and acetone, were isolated from the column and assayed for radioactivity.

Similarly, other portions of the same mixture of active glycols were diluted with inactive glycol VIII or IX and cleaved to give carbonyl compounds which were separated as their 2,4-dinitrophenylhydrazones by chromatography. A fresh silicic acid – celite column was used for each separation. In the dilution with inactive 2-methyl-1,2-butanediol (VIII), the 2,4-dinitrophenylhydrazones of formaldehyde and methyl ethyl ketone were recovered for radioactivity assays. In the dilution with inactive 3-methyl-1,2-butanediol (IX), only the 2,4-dinitrophenylhydrazone of formaldehyde was recovered and its radioactivity measured.

The entire process was repeated using the mixture of active glycols derived from acetolysis at reflux temperature run No. 2.

The radioactivity data are summarized in Table II.

Carbon Tetrabromide from the Ketonic Degradation Products

A portion (0.1078 g) of the mixture of active glycols derived from acetolysis at reflux temperature run No. 1 was diluted with 0.1853 g of inactive 2-methyl-2,3-butanediol (VII) and then cleaved with periodic acid as described above. The solution of carbonyl compound obtained was treated with dilute potassium permanganate solution until the purple color persisted for 1 hour. The excess permanganate was reduced by a few drops of 4% sodium bisulphite and the manganese dioxide removed by filtration. This treatment effectively destroyed all the aldehydes (4). The filtrate was distilled to give a solution containing only the ketonic degradation products, acetone and methyl ethyl ketone. This distillate was added dropwise to a stirred solution of 3.5 g of bromine in 65 ml of 10% sodium hydroxide maintained at 5° C. After the addition, stirring was continued at room temperature for 3 hours. The precipitated carbon tetrabromide was recovered by steam distillation and purified by sublimation. The yield was 0.25 g, m.p. 91–92° C (lit. (11*c*), m.p. 92° C).

A similar reaction using the mixture of active glycols derived from acetolysis at reflux temperature run No. 2 was also carried out.

The radioactivity data are included in Table II.

Degradation of the Olefinic Products from Acetolyses at 50° C

The mixture of active olefins II, III, and IV obtained from each of the duplicate acetolyses at 50° C was converted to the corresponding mixture of active glycols VII, VIII, and IX. Without any dilution with inactive glycol, this mixture was cleaved with periodic acid and the resulting carbonyl compounds subjected to chromatographic separation as their 2,4-dinitrophenylhydrazones. The chief components, the 2,4-dinitrophenylhydrazones of acetaldehyde and acetone, were recovered. Radioactivity assays were carried out on these two 2,4-dinitrophenylhydrazones and on the original mixture of active glycols VII, VIII, and IX. The results are summarized in Table III.

ACKNOWLEDGMENT

The financial assistance given by the National Research Council of Canada is gratefully acknowledged.

Can. J. Chem. Downloaded from www.nrcresearchpress.com by 196.1.178.254 on 09/04/12
For personal use only.

REFERENCES

1. WINSTEIN, S. and MARSHALL, H. J. Am. Chem. Soc. **74**, 1120 (1952).
2. KEULEMANS, A. I. M. Gas chromatography. Reinhold Publishing Corp., New York, N.Y. 1957.
3. GORDON, B. E., WOPAT, F., BURNHAM, H. D., and JONES, L. C. Anal. Chem. **23**, 1754 (1951).
4. ROBERTS, J. D., MCMAHON, R. E., and HINE, J. S. J. Am. Chem. Soc. **72**, 4237 (1950).
5. WHITMORE, F. C. and SIMPSON, C. T. J. Am. Chem. Soc. **55**, 3809 (1933).
6. ROBERTS, J. D., BENNETT, W., HOLROYD, E. W., and FUGITT, C. H. Anal. Chem. **20**, 904 (1948).
7. CRAM, D. J. J. Am. Chem. Soc. **74**, 2137 (1952).
8. INGOLD, C. K. Structures and mechanism in organic chemistry. Cornell University Press, Ithaca, N.Y. 1953. p. 443.
9. WINSTEIN, S. and TAKAHASHI, J. Tetrahedron, **2**, 316 (1958).
10. ROBERTS, J. D., BENNETT, W., MCMAHON, R. E., and HOLROYD, E. W. J. Am. Chem. Soc. **74**, 4283 (1952).
11. SHRINER, R. L., FUSON, R. C., and CURTIN, D. Y. The systematic identification of organic compounds. 4th ed. John Wiley & Sons, Inc., New York, N.Y. 1956. (*a*) p. 280; (*b*) p. 276; (*c*) p. 312.
12. SANDBORN, L. T. and BOUSQUEL, E. W. Organic synthesis, Collective Vol. I. 2nd ed. John Wiley & Sons, Inc., New York, N.Y. 1947. pp. 526–528.
13. MARVEL, C. S. and SEKERA, V. C. Org. Synthesis, **20**, 50 (1940).
14. CRAM, D. J. and ALLINGER, J. J. Am. Chem. Soc. **79**, 2858 (1957).
15. VOGEL, A. I. Practical organic chemistry. Longmans, Green and Company, London. 1948. p. 379.
16. DHAR, M. L., HUGHES, E. D., and INGOLD, C. K. J. Chem. Soc. 2065 (1948).
17. REEVES, R. E. J. Am. Chem. Soc. **63**, 1476 (1941).

Can. J. Chem. Downloaded from www.nrcresearchpress.com by 196.1.178.254 on 09/04/12
For personal use only.

Can. J. Chem. Downloaded from www.nrcresearchpress.com by 196.1.178.254 on 09/04/12
For personal use only.

THE EFFECT OF MOLECULAR OXYGEN ON THE REACTION OF OXYGEN ATOMS WITH *cis*-2-PENTENE[1]

S. SATO[2] AND R. J. CVETANOVIĆ

ABSTRACT

The effect of the presence of nitrogen, oxygen, and nitric oxide on the reaction between *cis*-2-pentene and oxygen atoms has been investigated at room temperature (25±2° C). For production of oxygen atoms use was made of mercury-photosensitized decomposition of nitrous oxide and of the photolysis of nitrogen dioxide at 3660 Å.

In the N_2O work, the presence of molecular oxygen induced the formation of acetaldehyde, propanal, methanol, and ethanol. In the NO_2 work, the amounts of acetaldehyde, propanal, and ethyl nitrate formed increased rapidly with increasing pressure of molecular oxygen. Possible reaction mechanisms for the formation of these compounds are discussed.

Additional information was obtained on the pressure-independent fragmentation in the reaction of oxygen atoms with *cis*-2-pentene.

INTRODUCTION

The reactions of oxygen atoms with various mono-olefins have been extensively investigated in this laboratory and the main features of the reactions have been established (1). As the source of oxygen atoms use was made of mercury-photosensitized decomposition of nitrous oxide (1), photolysis of nitrogen dioxide (2), and activation of oxygen molecules by electrical discharge (3). In the last method, however, excess oxygen molecules present participated in the reaction and led to considerable complexities. Ozone formation was postulated to explain the formation of some of the observed products.

In the photo-oxidation of hydrocarbons by nitrogen dioxide in the air, Haagen-Smit demonstrated the formation of large amounts of ozone (4). Possible mechanisms have been recently reviewed and discussed in some detail by Leighton and Perkins in connection with "smog" formation in the Los Angeles area (5).

The authors have briefly mentioned in a previous paper (2) that photo-oxidation of 1-butene, isobutene, and 2-butene by nitrogen dioxide in the presence of oxygen gives large amounts of propionaldehyde, acetone, and acetaldehyde, respectively, under certain conditions (for example, 3 mm NO_2, 3 mm olefin, and 50 mm oxygen), although the amounts of the main addition products formed remain almost constant in the presence of either nitrogen or oxygen.

A study of the reactions of ozone with a number of olefins in the gas phase is in progress in this laboratory (6). It has been established that ozone produces mainly propanal and formaldehyde from 1-butene, acetone and formaldehyde from isobutene, and propanal and acetaldehyde from 2-pentene. It appears possible then that an intermediate formation of ozone is responsible for some of the major products in the photochemical oxidation of olefins by nitrogen dioxide in the presence of molecular oxygen.

According to Benson and Axworthy (7) and Herron and Schiff (8), the formation of ozone by the third-body reaction

$$O + O_2 + M \rightarrow O_3 + M \qquad [1]$$

is very slow compared with the reactions of oxygen atoms with olefins under conditions stated above. If the aldehydes observed in the photo-oxidation of butenes by nitrogen

[1]*Manuscript received February 3, 1959.*
Contribution from the Division of Applied Chemistry, National Research Council, Ottawa, Canada. Issued as N.R.C. No. 5146.
[2]*National Research Council Postdoctorate Fellow 1956–1958. Present address: Laboratory of Physical Chemistry, Tokyo Institute of Technology, Tokyo, Japan.*

dioxide in the presence of molecular oxygen result from the reactions between ozone and the butenes, there must be another mechanism of formation of ozone. This, perhaps, may involve some radicals (R·) formed in these processes and the following reaction sequence (4, 5):

$$R\cdot + O_2 \rightarrow RO_2\cdot, \quad [2]$$

$$RO_2\cdot + O_2 \rightarrow RO\cdot + O_3. \quad [3]$$

The object of the present work has been to obtain further experimental information on these processes. *cis*-2-Pentene was chosen for the study because the main features of its reaction with oxygen atoms are known and the major products of the reaction with ozone in the gas phase are acetaldehyde and propionaldehyde, both of which are easily measured quantitatively. Photo-oxidation of this olefin by nitrogen dioxide in the presence of nitrogen, nitric oxide, and oxygen was investigated at room temperature and using the wave length of 3660 Å. Also, some additional aspects of the reaction with oxygen atoms produced by mercury-photosensitized decomposition of nitrous oxide were investigated with and without molecular oxygen added with a view of gaining further insight into the mechanism of formation of free radicals by pressure-independent fragmentation in this reaction.

EXPERIMENTAL

The experimental arrangements employed in the two methods of production of oxygen atoms, the mercury-photosensitized decomposition of nitrous oxide (1) and the photolysis of nitrogen dioxide (2), have been reported in the previous papers.

cis-2-Pentene was obtained from the National Bureau of Standards, Washington (impurity 0.07 ± 0.02 mole %). This olefin, nitrogen (Linde Air Products Co.), and nitric oxide (Matheson Co., Inc.) were used without further purification. Oxygen (Dominion Oxygen Co.) was passed through a tube packed with molecular sieve granules to remove traces of water. The method of purification of nitrogen dioxide was the same as reported previously (2).

In the N_2O work, the reaction products were transferred to a LeRoy still (9), and the fraction condensable at $-140°$ C was analyzed by means of gas chromatography (GLC) (10). In the NO_2 work, the products were pumped off at liquid nitrogen temperature and were transferred to a sampling tube containing a drop of mercury. After completion of the reaction of the excess nitrogen dioxide present with mercury, the products were again pumped off at liquid nitrogen temperature and analyzed by GLC. The identity of the reaction products separated by GLC was further confirmed by infrared and mass spectrometric analyses. The amounts of products were measured from the GLC peak areas.

Since a variety of reaction products are formed in these reactions, several GLC columns were used: dimethyl sulpholane (DMS) on glass beads (3 wt. % DMS, 8 ft), dinonyl phthalate (DNP) on glass beads (4 wt. % DNP, 8 ft), and Tricresyl phosphate (TCP) on firebricks (40 wt. % TCP, 40 ft). The last column was used at 90° C and the others at room temperature. The carrier gas was helium.

When the reaction products were passed through the DMS column first, several pairs of compounds remained unresolved: *cis*-2-pentene and acetaldehyde, *trans*-β-pentene oxide and ethyl alcohol, *cis*-β-pentene oxide and methyl nitrate. The first pair was then separated on the TCP column and the last two on the DNP column.

The isolation and identification of *n*-butane formed in the N_2O work was kindly done by Dr. N. F. Foster on a 40-ft GLC column (40 wt. % DMS on firebrick) operated at

Can. J. Chem. Downloaded from www.nrcresearchpress.com by 196.1.178.254 on 09/04/12
For personal use only.

room temperature. Figure 1 shows typical GLC peaks obtained by the DMS column (8 ft).

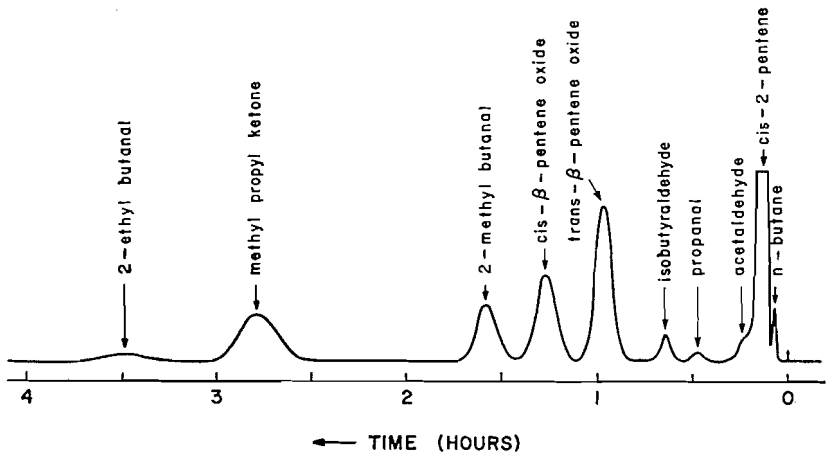

FIG. 1. Typical GL chromatogram obtained using the 8-ft DMS column for the analysis of products of the reaction of oxygen atoms with *cis*-2-pentene.

RESULTS AND DISCUSSION

The Nature of the Pressure-independent Fragmentation in the Reaction of Oxygen Atoms with cis-2-Pentene

As already reported (1), the principal products of the reaction between oxygen atoms and *cis*-2-pentene are *trans*- and *cis*-β-pentene oxide, methyl propyl ketone, and 2-methyl butanal. The first three compounds are produced by internal rearrangements (non-radical mechanisms), while 2-methyl butanal is partly formed by "external" rearrangement (free-radical mechanism). This last process is a consequence of a certain amount of pressure-independent fragmentation which occurs in these reactions (1). (The pressure-dependent fragmentation of the "hot" addition products formed is suppressed already at relatively quite low pressures, except in the case of ethylene and propylene (1, 2).)

In order to obtain further information on the nature of the pressure-independent fragmentation, additional experiments with *cis*-2-pentene and oxygen atoms produced by mercury-photosensitized decomposition of N_2O have been carried out with and without molecular oxygen added. The particular object has been to establish more thoroughly the type of the minor products formed. The results are shown in Table I.

TABLE I

The products of the reaction of oxygen atoms with *cis*-2-pentene
(Oxygen atoms produced by mercury-photosensitized decomposition of N_2O, irradiation time 15 minutes, 25±2° C)

N_2O, mm	*c*-Pe, mm	O_2, mm	GLC peak areas of the products (arbitrary units)											
			t-PO	*c*-PO	2MB	MPK	But	AcA	PrA	*i*-BA	2EB	MeOH	EtOH	H_2O
245	2.7	0	642	462	364	505	53	5	25	87	63	0	0	0
245	2.9	4.4	604	435	100	499	n.d.	535	240	0	0	129	249	ind.
0	6.8	10.2	(10)	8	10	10	n.d.	17	18	0	0	19	(2)	0

c-Pe = *cis*-2-pentene, *t*-PO = *trans*-β-pentene oxide, *c*-PO = *cis*-β-pentene oxide, 2MB = 2-methyl butanal, MPK = methyl propyl ketone, But = *n*-butane, AcA = acetaldehyde, PrA = propanal, *i*-BA = isobutyraldehyde, 2EB = 2-ethyl butanal, MeOH = methyl alcohol, EtOH = ethyl alcohol, n.d. = not determined, ind. = indication. The values in parentheses are of low accuracy.

Can. J. Chem. Downloaded from www.nrcresearchpress.com by 196.1.178.254 on 09/04/12
For personal use only.

In the absence of oxygen, small amounts of butane, propanal, isobutyraldehyde, and 2-ethyl butanal[3] are formed besides the large amounts of the four main addition products. It is significant that these minor products clearly indicate formation not only of free CH_3 but also of free C_2H_5 radicals in the pressure-independent fragmentation. This is also confirmed by the results in the presence of molecular oxygen, which will be discussed further below. In view of this it is suggested that the pressure-independent fragmentation probably results from the decomposition of a very short-lived excited epoxide molecule ($C_2H_5 \cdot CH—CH \cdot CH_3$**), i.e. reactions [8] and [9] in the following scheme:

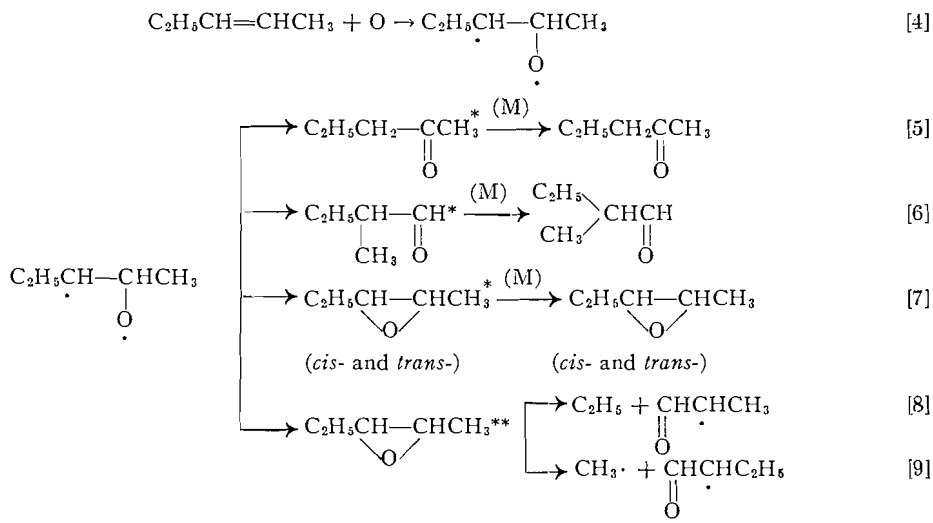

The formation of 2-methyl butanal by "external" rearrangement (1) is then due to the radical combinations

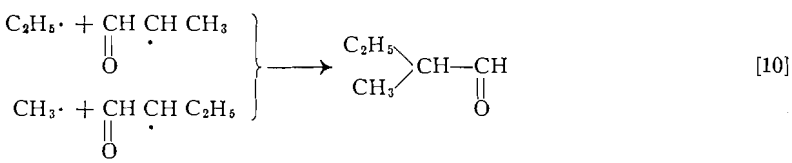

The above mechanism is identical with the general mechanism of addition of oxygen atoms to olefins given previously (1), except that a more detailed course is now postulated for the pressure-independent fragmentation, i.e. reactions [8] and [9]. The presence of both free CH_3 and C_2H_5 radicals is thus accounted for, and the formation of the minor products can then be readily explained by the reactions

$$C_2H_5\cdot + C_2H_5\cdot \rightarrow C_4H_{10} \qquad [11a]$$

$$C_2H_5\cdot + CH_3\cdot \rightarrow C_3H_8 \qquad [11b]$$

$$CH_3\cdot + CH_3\cdot \rightarrow C_2H_6 \qquad [11c]$$

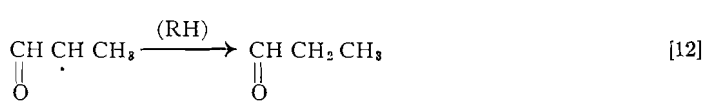

[3]*Mass spectrometer analysis of the fraction isolated by GLC as 2-ethyl butanal indicated also the presence of some unidentified impurities.*

Can. J. Chem. Downloaded from www.nrcresearchpress.com by 196.1.178.254 on 09/04/12
For personal use only.

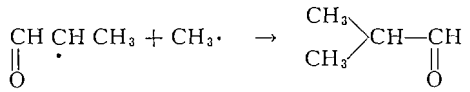

[13]

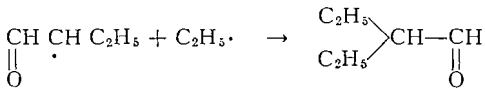

[14]

Since ethane has been observed in the previous work (1) and no analysis for propane could be made in the presence of the huge excess of N_2O, essentially all the observed products are predicted by this scheme.[4]

In the presence of oxygen, large amounts of methyl alcohol, ethyl alcohol, acetaldehyde, and propanal were observed instead of the larger part of 2-methyl butanal (the part formed by "external", free-radical rearrangement), *n*-butane, isobutanal, and 2-ethyl butanal, as shown in Table I. These products did not result from the quenching reaction of oxygen molecules, although the table shows that some quenching reactions involving oxygen molecules in the absence of nitrous oxide occurred, perhaps

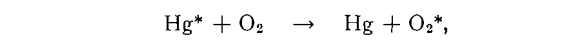

[15]

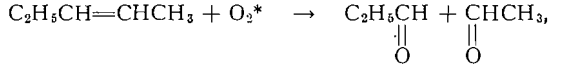

[16]

or

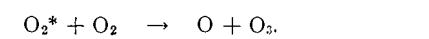

[17]

These reactions (and further reactions of O and O_3) could explain the small amount of products formed in the absence of N_2O.

In the presence of a large amount of nitrous oxide, excited mercury atoms are essentially exclusively quenched by nitrous oxide and the molecular oxygen acts as an efficient scavenger for the free radicals formed in the pressure-independent fragmentation reactions [8] and [9].

The processes which occur in the presence of molecular oxygen are of considerable complexity and are as yet not fully understood. The formation of the alcohols and the aldehydes may be explained tentatively by the following reactions:

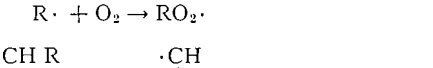

[2]

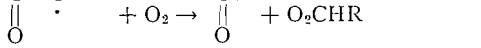

[18]

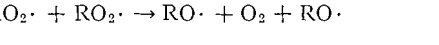

[19]

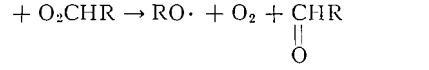

[20]

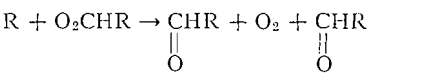

[21]

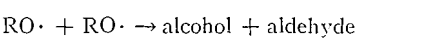

[22]

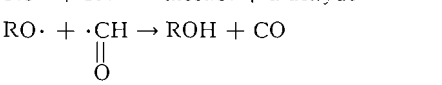

[23]

[4] *Undoubtedly some disproportionation of ethyl radicals occurs as well, but the amount of ethylene thus formed must be relatively quite small and difficult to estimate with certainty by mass spectrometric analysis of the ethane fraction.*

Can. J. Chem. Downloaded from www.nrcresearchpress.com by 196.1.178.254 on 09/04/12
For personal use only.

$$O_2CHR + O_2 \rightarrow \underset{\underset{O}{\|}}{CHR} + O_3 \qquad [24]$$

$$RCH{=}CHR + O_3 \rightarrow \underset{\underset{O}{\|}}{RCH} + O_2CHR \qquad [25]$$

Here R· stands for CH_3· or C_2H_5. Reaction [18] is somewhat similar to the generally assumed initial splitting of an olefin molecule on interaction with ozone (reaction [25]), and O_2CHR is the "zwitter ion" assumed to be formed in this latter process (5). An inspection of the amounts of products in Table I indicates that reactions [2] and [18–23] are capable of explaining the aldehydes and alcohols formed in the presence of oxygen. There is no need then to assume in this case chain processes involving ozone, such as sequences of reactions [2], [3], and [25], or [24] and [25].

Experiments with higher pressures of oxygen have not been attempted in the nitrous oxide work because the quenching reaction [15] is very likely to become important and some additional complications could affect the quantitative aspect of the results.

Photo-oxidation of cis-2-Pentene by Nitrogen Dioxide

Light of wave length of 3660 Å dissociates nitrogen dioxide into nitric oxide and a ground-state oxygen atom (^3P), and the reaction scheme outlined in the previous section should, therefore, be applicable. In this case, however, nitrogen dioxide competes with *cis*-2-pentene for oxygen atoms and also acts as an efficient scavenger for the free radicals formed by the pressure-independent fragmentation, reactions [8] and [9]. As a result a greater complexity of products has to be expected. Figure 2 shows the results of experiments with 3 mm of nitrogen dioxide and 3 mm of *cis*-2-pentene at various irradiation

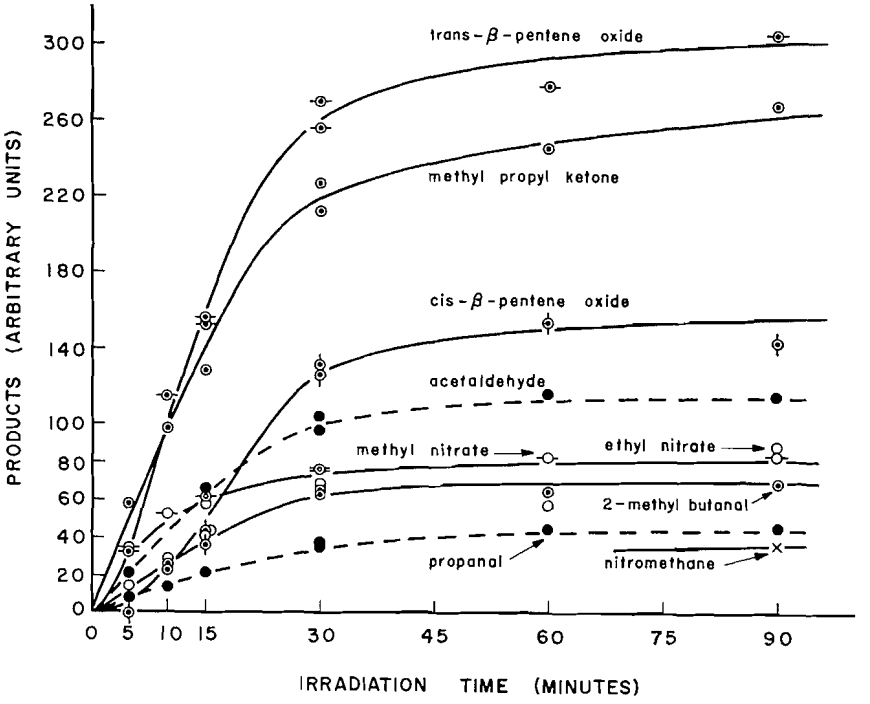

FIG. 2. Yield of the products as a function of irradiation time in the photo-oxidation of *cis*-2-pentene (3 mm) by nitrogen dioxide (3 mm), 25±2° C.

Can. J. Chem. Downloaded from www.nrcresearchpress.com by 196.1.178.254 on 09/04/12
For personal use only.

times. The products formed are *trans*- and *cis*-β-pentene oxide, 2-methyl butanal, methyl propyl ketone, acetaldehyde, propanal, methyl nitrate, ethyl nitrate, nitromethane, and probably nitroethane. The first four compounds are the main products observed in the N_2O work. The curves for *trans*- and *cis*-β-pentene oxide in Fig. 2 show apparent induction periods. These are explainable by a certain amount of thermal reaction between nitrogen dioxide and the pentene oxides formed in the photo-oxidation, as discussed previously (2). The rates of the thermal reactions of butene oxides with nitrogen dioxide are believed to be in the following order: isobutene oxide > *cis*-β-butene oxide > *trans*-β-butene oxide > α-butene oxide. β-Pentene oxides are believed to behave similarly to β-butene oxides.

In order to obtain information on the consumption of nitrogen dioxide under various conditions, a RCA 935 vacuum phototube was placed behind the reaction cell and the intensity of the transmitted light was measured by means of an electronic circuit. Figure 3 shows the fraction of the initially taken 3 mm of nitrogen dioxide consumed at various

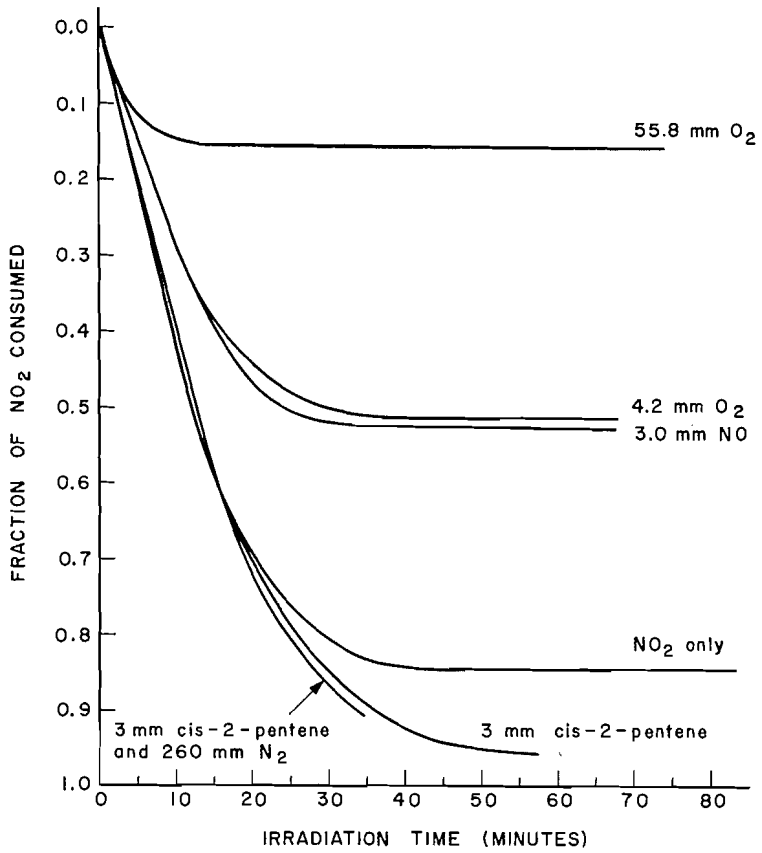

FIG. 3. Consumption of NO_2 as a function of irradiation time. (Initial NO_2 pressure 3 mm, the pressures of added gases are indicated on the curves.)

irradiation times. The greatest part of nitrogen dioxide (in the absence of other compounds) was consumed in about 20 to 30 minutes. In the presence of oxygen or nitric oxide, the consumption was much slower because of more rapid regeneration of nitrogen dioxide when excess of either of these two compounds was added initially.

Can. J. Chem. Downloaded from www.nrcresearchpress.com by 196.1.178.254 on 09/04/12
For personal use only.

Figure 4 shows that pressure effects in the photo-oxidation of *cis*-2-pentene are negligible in the investigated range from 6 to 400 mm, while the photo-oxidations of 1-butene and isobutene showed pressure effects below about 10 mm. Yet, the amounts of acetaldehyde and propanal are seen in Fig. 4 to increase appreciably at pressures below about 10 mm without a noticeable compensating decline in the addition products. This could perhaps be ascribed to a reaction between *cis*-2-pentene and excited oxygen molecules formed in the reaction

$$O + NO_2 \rightarrow NO + O_2^*. \qquad [26]$$

However, nothing definite is known about reactions of this type. There is some scatter of points for the addition products formed, Fig. 4, and some pressure-dependent fragmentation at very low pressures is not ruled out. This view is supported by the observation that the amount of methyl nitrate also increases below about 10 mm.

According to Ford and Endow (11) the three-body reaction

$$O + NO_2 + M \rightarrow NO_3 + M \qquad [27]$$

can successfully compete with reaction [26]. From the values of the rate constants given by these authors for these two reactions, R_{26}/R_{27} is about unity at a pressure of 400 mm when nitrogen is the third body. However, no pressure effect is shown in Fig. 4 at higher pressures, suggesting that reaction [27] is relatively unimportant. These two findings are obviously contradictory except if NO_3 molecules produced in reaction [27] react with *cis*-2-pentene in the same manner as oxygen atoms. This appears somewhat unlikely in view of the following.

Since NO_3 presumably reacts very rapidly with nitric oxide, the effect of additions of nitric oxide was examined as shown in Table II. It is evident from Fig. 3 that with the

TABLE II

Yield of the reaction products as a function of the pressure of nitric oxide
(Oxygen atoms produced by photolysis of NO_2 at 3660 Å, irradiation time 5 minutes, 25±2° C)

NO_2, mm	*c*-Pe, mm	NO, mm	GLC peak areas of the products (arbitrary units)								
			t-PO	*c*-PO	2MB	MPK	AcA	PrA	$MeNO_2$	$MeNO_3$	$EtNO_3$
3.0	3.0	0	394	126	72	341	132	42	(21)	193	131
3.0	3.0	30.4	283	47	99	355	(118)	17	(120)	0	11
3.0	3.0	100	121	20	83	284	(72)	ind.	(130)	0	ind.

c-Pe = *cis*-2-pentene, *t*-PO = *trans*-β-pentene oxide, *c*-PO = *cis*-β-pentene oxide, 2MB = 2-methyl butanal, MPK = methyl propyl ketone, AcA = acetaldehyde, PrA = propanal, $MeNO_2$ = nitromethane, $MeNO_3$ = methyl nitrate, $EtNO_3$ = ethyl nitrate, ind. = indication. The values in parentheses are of low accuracy.

short irradiation times of 5 minutes used in these experiments there could be little variation in the average concentration of nitrogen dioxide as the amount of NO added is varied. The amounts of methyl propyl ketone and 2-methyl butanal remained relatively little affected as the pressure of NO was increased. The observed variations introduce some uncertainty into the quantitative validity of this argument, although they are explainable by the experimental errors and a certain amount of competitive consumption of oxygen atoms in the reaction

$$O + NO + M \rightarrow NO_2 + M.$$

The rapid decline in the two epoxides with increasing amounts of NO added may be ascribed to the considerable reactivity of these compounds. The trends in the amounts of the other products in Table II are of interest for the understanding of the mechanism of their formation and will be discussed further below.

Can. J. Chem. Downloaded from www.nrcresearchpress.com by 196.1.178.254 on 09/04/12
For personal use only.

Can. J. Chem. Downloaded from www.nrcresearchpress.com by 196.1.178.254 on 09/04/12
For personal use only.

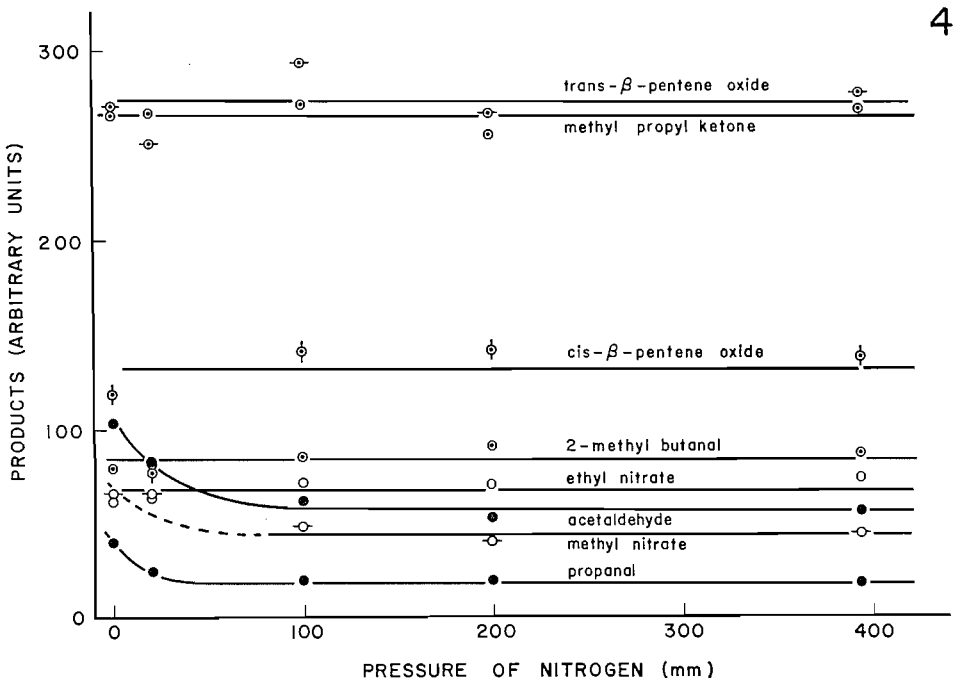

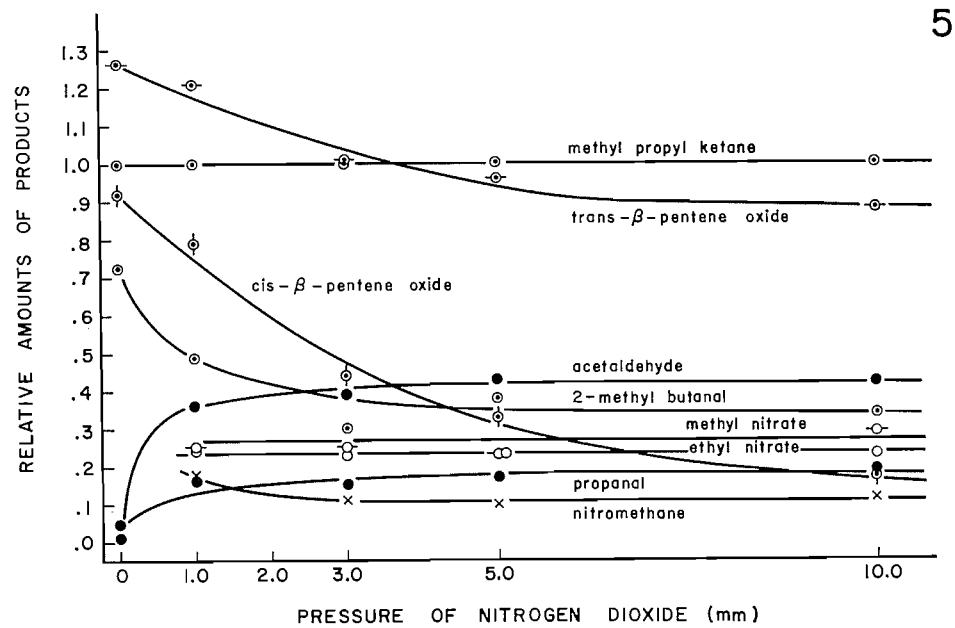

FIG. 4. The effect of pressure on the products formed in the photo-oxidation of *cis*-2-pentene (3 mm initially) by nitrogen dioxide (3 mm initially). Irradiation time 30 minutes, 25±2° C.

FIG. 5. Relative yields of products as a function of initial pressures of nitrogen dioxide in the photo-oxidation of *cis*-2-pentene (3 mm initially). The amounts of methyl propyl ketone formed are taken as unity. Irradiation time 30 minutes, 25±2° C. The points on the ordinate represent the relative amounts of acetaldehyde, propionaldehyde, and the four major addition products observed in the N_2O work, as given in Table I.

The dependence of the relative amounts of products formed (taking methyl propyl ketone as unity) on the pressure of the initially taken nitrogen dioxide is shown in Fig. 5. The decrease in pentene oxides is explained by the thermal reaction of these products with excess nitrogen dioxide. With decreasing NO_2 pressure the relative amounts of these two products tend, within the experimental error, to the relative values found in the N_2O work. The latter are indicated on the ordinate together with the relative values for 2-methyl butanal, acetaldehyde, and propanal (methyl propyl ketone is again taken as unity). The part of 2-methyl butanal formed by external migration (free-radical combination) is completely suppressed already at quite low NO_2 pressure and the part formed by internal migration of methyl radicals remains unaffected by further increasing NO_2 pressure. This is in full agreement with the internal rearrangements described previously (1) and there is no need to discuss here again the mechanism of formation of the four direct addition products. A mechanism for the formation of the products resulting from fragmentation can be proposed with much less certainty and the following scheme is of a tentative character (R· stands for CH_3 and C_2H_5):

$$R\cdot + NO_2 \rightarrow RNO_2, \qquad [28]$$

$$R\cdot + NO_2 \rightarrow RO\cdot + NO, \qquad [29]$$

$$RO\cdot + NO_2 \rightarrow RONO_2, \qquad [30]$$

$$\underset{\cdot}{\mathrm{RCHCH}}\!\!\underset{\mathrm{O}}{\|} + NO_2 \rightarrow \mathrm{RC}\underset{\mathrm{O}}{\overset{\|}{\mathrm{H}}} + CHO\cdot + NO, \qquad [31]$$

$$\underset{\cdot}{\mathrm{RCHCH}}\!\!\underset{\mathrm{O}}{\|} + NO_2 \rightarrow \mathrm{RC}\underset{NO_2\ \mathrm{O}}{\overset{\cdot\ \ \|}{\mathrm{H}}}, \qquad [32]$$

$$CHO\cdot + NO_2 \rightarrow CO + HNO_2. \qquad [33]$$

The radicals are initially formed in the pressure-independent fragmentation reactions [8] and [9]. The products of the last two reactions and nitroethane have not been identified. The observed products are consistent with the reaction scheme. In the presence of added excess NO the following reactions are assumed to occur:

$$R\cdot + NO \rightarrow RNO, \qquad [34]$$

$$RNO + NO_2 \rightarrow RNO_2 + NO, \qquad [35]$$

$$\underset{\cdot}{\mathrm{RCHCH}}\!\!\underset{\mathrm{O}}{\|} + NO \rightarrow \mathrm{RC}\underset{NO\ \mathrm{O}}{\overset{\cdot\ \ \|}{\mathrm{H}}}. \qquad [36]$$

These reactions explain the observed increase in CH_3NO_2 and suppression of the nitrates, propanal, and acetaldehyde (Table II). The product of reaction [36] has not been identified.

The Effect of Molecular Oxygen on the Photo-oxidation of cis-2-Pentene by Nitrogen Dioxide

Photolysis of nitrogen dioxide in the presence of olefins and oxygen in air has been shown to be responsible for "smog" formation in some places on this continent (4, 5). This process is characterized by a remarkable complexity of the recoverable condensable material and is accompanied by appreciable ozone formation. The photolysis of nitrogen dioxide in the presence of *cis*-2-pentene and molecular oxygen studied in the present work is superficially similar to the conditions in polluted atmosphere leading to smog formation. However, the concentrations of NO_2 and the olefin have been very much larger and, as a result, it is difficult to say how much there is in common between the two processes. Nevertheless, it is considered of some interest to report briefly the results of

Can. J. Chem. Downloaded from www.nrcresearchpress.com by 196.1.178.254 on 09/04/12
For personal use only.

the experiments carried out inasmuch as they show the type of products formed under the particular conditions employed.

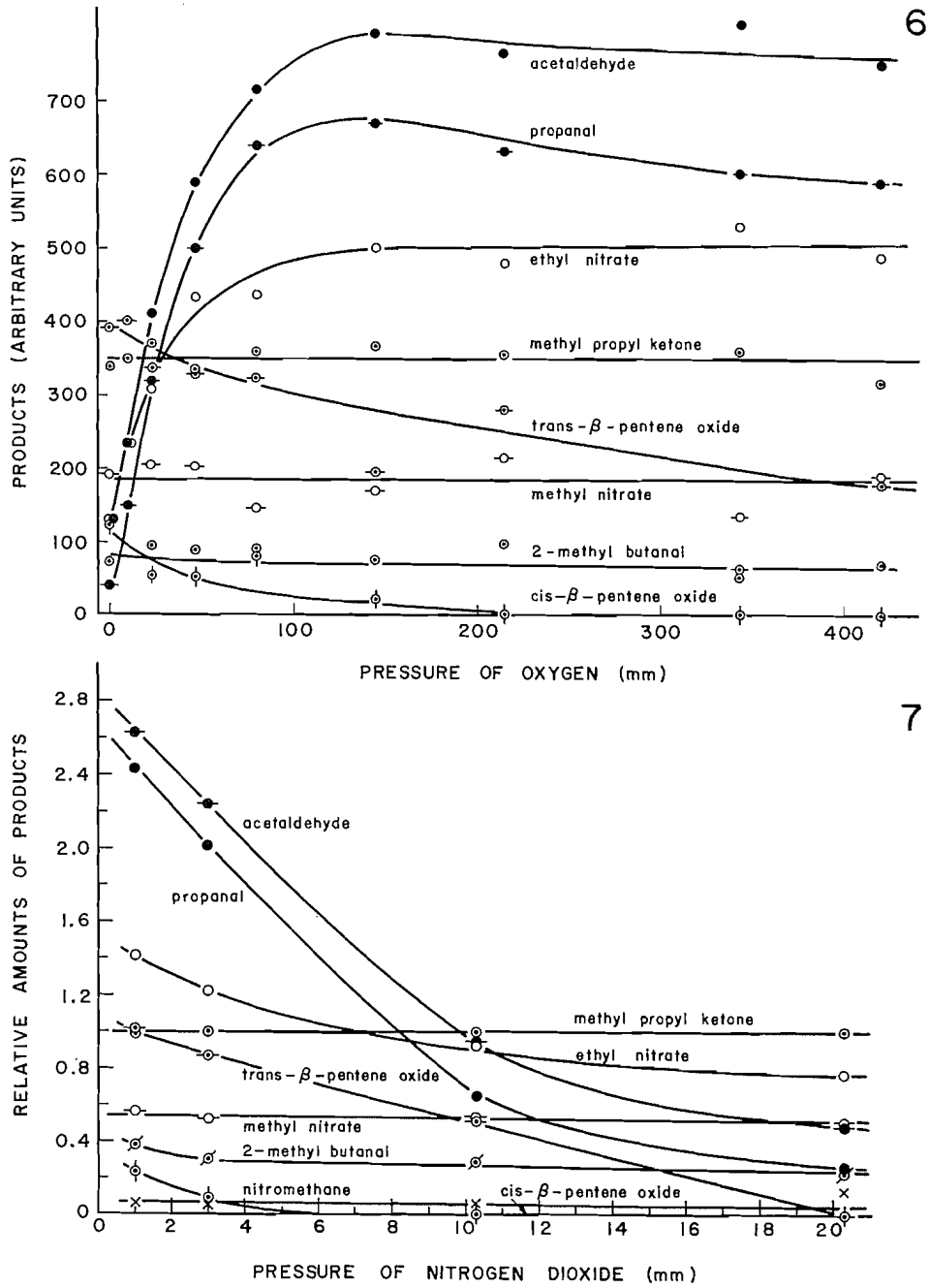

FIG. 6. The amounts of products formed as a function of oxygen pressure (3 mm NO_2, 3 mm *cis*-2-pentene, 25±2° C).

FIG. 7. Relative yields of products in the presence of 100 mm of oxygen as a function of initial pressures of nitrogen dioxide. The amounts of methyl propyl ketone formed are taken as unity (3 mm *cis*-2-pentene, irradiation time 15 minutes, 25±2° C).

Can. J. Chem. Downloaded from www.nrcresearchpress.com by 196.1.178.254 on 09/04/12
For personal use only.

The experimental results are plotted in Figs. 6 and 7, which should be contrasted with Figs. 4 and 5, respectively. It is clear from Fig. 6 that the presence of molecular oxygen induces formation of large amounts of acetaldehyde, propionaldehyde, and ethyl nitrate, although the amounts of the other compounds formed, with the exception of the epoxides, remain constant. The amounts of the two epoxides decrease with increasing oxygen pressure.

The effect of the initial pressure of nitrogen dioxide on the relative yields of products in the presence of 100 mm of oxygen is shown in Fig. 7. It is clear that the formation of acetaldehyde, propionaldehyde, and ethyl nitrate is particularly large at smaller nitrogen dioxide concentrations. The amounts of the two epoxides decline again with increasing NO_2 pressure.

As has already been mentioned, reaction of ozone with 2-pentene in the vapor phase leads to the predominant formation of acetaldehyde and propionaldehyde (6). It is significant that in the photo-oxidation of 1-butene, 2-butene, and isobutene, respectively, in the presence of molecular oxygen large amounts of propionaldehyde, of acetaldehyde, and of acetone are formed and the same compounds are again the predominant products (observed by GLC analysis) in the vapor-phase reaction of ozone with these olefins (6). In view of this, it is probable that in the photo-oxidation experiments carried out in the presence of large amounts of molecular oxygen there was an intermediate formation of ozone, which was, in the case of 2-pentene, responsible for the major part of acetaldehyde and propionaldehyde formed. Here again it is most likely that ozone is not formed to any extent directly from oxygen atoms and molecular oxygen. In the vapor-phase reaction of ozone with *cis*-2-pentene in addition to large amounts of propionaldehyde and acetaldehyde a residue of lower volatility is also formed, the nature of which is being further investigated (6). In one experiment, this residue[5] (after removal of acetaldehyde and propionaldehyde at $-80°$ C) was transferred to the reaction cell containing 3 mm of NO_2. The two were allowed to react thermally for 5 minutes at room temperature and then the product analysis was carried out in the usual manner. The GLC analysis showed peaks in the position of methyl nitrate, ethyl nitrate, *cis*-β-pentene oxide, and methyl propyl ketone and no *trans*-β-pentene oxide nor 2-methyl butanal. This experiment suggests that there are perhaps two potential sources of methyl propyl ketone and gives an example of the complex character of the studied process. In view of the observed complexities it is felt that a detailed discussion of the experimental results will become possible only after considerable additional background knowledge on the reactions of this type is accumulated.

ACKNOWLEDGMENTS

The authors are indebted to Dr. A. W. Tickner for the mass spectrometer analyses and to the Analytical Section of this Division for the infrared analyses.

REFERENCES

1. CVETANOVIĆ, R. J. J. Chem. Phys. **25**, 376 (1956); Can. J. Chem. **36**, 623 (1958); J. Chem. Phys. **30**, 19 (1959).
2. SATO, S. and CVETANOVIĆ, R. J. Can. J. Chem. **36**, 279, 970, 1668 (1958).
3. JARVIE, J. M. S. and CVETANOVIĆ, R. J. Can. J. Chem. **37**, 529 (1959).
4. HAAGEN-SMIT, A. J. and FOX, M. M. Ind. Eng. Chem. **48**, 1484 (1956). HAAGEN-SMIT, A. J., BRADLEY, C. E., and FOX, M. M. Proceedings of the Second National Air Pollution Symposium, Pasadena, Calif. 1952. p. 54.
5. LEIGHTON, P. A. and PERKINS, W. A. Photochemical Secondary Reactions in Urban Air. Report No. 24 of the Air Pollution Foundation, San Marino, Calif. August 1958.

[5]*The authors are thankful to Dr. T. Vrbaški for carrying out the reaction between 2-pentene and ozone.*

Can. J. Chem. Downloaded from www.nrcresearchpress.com by 196.1.178.254 on 09/04/12
For personal use only.

6. VRBAŠKI, T. and CVETANOVIĆ, R. J. To be published.
7. BENSON, S. W. and AXWORTHY, A. E., JR. J. Chem. Phys. **26**, 1718 (1957).
8. HERRON, J. T. and SCHIFF, H. I. Can. J. Chem. **36**, 1159 (1958).
9. LEROY, D. J. Can. J. Research, B, **28**, 492 (1950).
10. CALLEAR, A. B. and CVETANOVIĆ, R. J. Can. J. Chem. **33**, 1256 (1955).
11. FORD, H. W. and ENDOW, H. J. Chem. Phys. **27**, 1156, 1277 (1957).

Can. J. Chem. Downloaded from www.nrcresearchpress.com by 196.1.178.254 on 09/04/12
For personal use only.

Can. J. Chem. Downloaded from www.nrcresearchpress.com by 196.1.178.254 on 09/04/12
For personal use only.

THE TEMPERATURE DEPENDENCE OF THE HYDROLYSIS OF METHYL ESTERS OF CERTAIN ALKYL-SUBSTITUTED BENZENESULPHONATES IN WATER[1]

G. A. HAMILTON[2] AND R. E. ROBERTSON

ABSTRACT

Rate data for the hydrolysis of a series of alkyl-substituted methyl benzenesulphonates are presented and the resulting differences in derived parameters are compared and discussed in an analysis of substituent effects.

Coincident with the hydrolysis studies to be reported on toluenesulphonates (1) a survey was made of the changes in rate and derived parameters for a series of alkyl-substituted benzenesulphonates with the aim of discovering the effect of systematic increase in the size of the anion being produced while the "mechanism" was kept constant through use of the methyl ester. With the realization that the solvent reorganization accompanying the activation process did not necessarily include the total initial solvation shell of the ester (2), the more extensive study of the effect of such groups on solvation was discontinued and the data already determined are published here.

The importance of solvation on the rates of reactions in solution has long been recognized in principle (3) and the general trends analyzed in terms of charge development or distribution. While far from optimum, the benzenesulphonic system provides a means of examining the effect of a substituent on the rate and thermodynamic parameters where there is no steric interference with solvation (para substitution) and where the solvation is altered through the competition of more effective intramolecular interaction (ortho substitution). It is recognized that the latter is not equivalent to the simple screening of a charge by an alkyl group as considered by Everett and Wynne-Jones (4) in discussing the changes in solvation of anions with alkyl substitution but is more closely allied to the effect considered by Evans (5) and Franklin (6) in calculating the heat of solvation of the series $\overset{+}{\text{Me}} \rightarrow t\text{-}\overset{+}{\text{Bu}}$ carbonium ions, where the loss of solvation through solvent exclusion was compensated for by internal resonance effects.

TABLE I

Effect of methyl substituents on relative rates of solvolysis in ethanol and water at 80° C

	Ethanol		Water		Acetic acid	
Ester	$k_1\times10^4$	Rel. rate	$k_1\times10^3$	Rel. rate	$k_1\times10^6$	Rel. rate
Me-*p*-H	1.67_3*	1.0	3.07†, ‡	1.0	1.89	1.0
Me-*p*-Me	1.09_5	0.65	2.19§	0.71	1.27	0.67
Me-*o*-Me	1.41	0.84	2.39	0.78	1.44	0.76
Me-2,4-diMe	0.877	0.52	1.62	0.53	—	—
Me-3,4-diMe	0.905	0.54	1.85	0.60	1.06	0.55
Me-2,4,6-triMe	0.426	0.25	0.309	0.27	—	—

*Ref. 9.
†Ref. 2.
‡Rates calculated from constants Table I, above, and Table V ref. 2.
§Ref. 11.

[1]*Manuscript received November 4, 1958.*
Contribution from the Division of Pure Chemistry, National Research Council, Ottawa, Canada.
Issued as N.R.C. No. 5145.
[2]*Summer Student.*

Whether an alkyl substituent group in a benzenesulphonate will be expected to interfere or in fact increase the solvation of the developing sulphonic anion in the activation process leading to hydrolysis will depend not only on its position and size, but also on the electronic nature of its effect, i.e., whether the effect is simply inductive, or shows evidence of hyperconjugation, or both. To evaluate the possible effect of hyperconjugation one must look for stabilizing influences arising from this cause both in the initial and in the transition states. Formal presentation of typical resonance contributors to the stabilization of these two states are as follows:

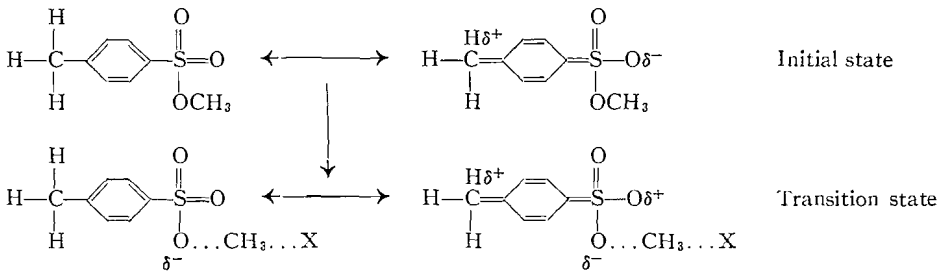

It will be obvious from the above that resonance contributors will be more important in the initial state than in the transition state, since in the latter the developing negative charge will oppose any such electronic shift. Thus we anticipate the initial state for the para-methyl-substituted ester will be stabilized compared to the corresponding state for the unsubstituted ester, and the rate correspondingly reduced. This does not exclude the operation of an inductive effect toward the same end, but evidence that a hyperconjugative effect is present may be gained from a comparison of the relative rates of solvolysis for a series of esters in ethanol and in water (Table I).

If the effect of the methyl group were purely inductive the rate for the meta methyl ester would be the same or slower than that for the para methyl ester. Were the effect purely hyperconjugative, the substituent effect of the meta methyl should be negligible. From Table I it is seen that the relative effect of the para methyl and ortho methyl are about additive to give the value for the 2,4-dimethyl hydrolyzing in ethanol and water of 0.49 (calc.) in both cases and 0.52 and 0.53 (obs.) respectively. If the effect of the para methyl were completely inductive, then the meta methyl should have approximately the same effect and we would anticipate the relative rate values for the 3,4-dimethyl to be 0.30 and 0.42 (calc.) compared with the observed values of 0.53 and 0.60 in ethanol and water, respectively. Hence it may be argued that some considerable fraction of the effect of the para methyl group must be attributed to hyperconjugative stabilization of the initial state.

For the 2,4,6-trimethyl ester, it might be expected the second ortho methyl would not interact with the sulphonic group to the same extent as the first ortho methyl but would have an effect somewhat like an additional para methyl group. Thus the relative rate for the 2,4,6-trimethyl ester might be expected to be intermediate between that calculated assuming the second ortho methyl to duplicate the first (calculated relative rate in ethanol 0.33, in water 0.27) and assuming it is a para methyl (calculated relative rate in ethanol 0.14 and in water 0.20). The observed values of 0.25 and 0.27 in ethanol and water respectively are in fair agreement with this analysis.

The fact that the para methyl substituent may be changed to other para alkyl sub-

Can. J. Chem. Downloaded from www.nrcresearchpress.com by 196.1.178.254 on 09/04/12
For personal use only.

stituents with no change in relative rates (Table II) compared with the unsubstituted ester may be taken as further evidence of compensation between the inductive and hyperconjugative effects. Taft (13) has explained the apparent constancy of the ionization constants of the 4-alkyl-substituted pyridines by a similar balancing of inductive and hyperconjugative effects and our results are in qualitative as well as quantitative agreement with his.

TABLE II

Effect of para alkyl groups on rate of hydrolysis of methyl benzenesulphonates in water at 60° C*

Compound	$k_1 \times 10^4$ sec^{-1}	k_x/k_H
Me-*p*-H†	5.33±1.01	1
Me-*p*-Me‡	3.77±0.01	0.71
Me-*p*-Et	3.80±0.02	0.71
Me-*p*-isoPro	3.77±0.02	0.71
Me-*p*-*t*-Bu	3.80±0.06	0.71
Me-*p*-*n*-Pro	3.68±0.02	0.69

*Actual temperature 60.14° C.
†Ref. 2.
‡Ref. 11.

While comparisons of relative rates such as above give a valuable indication of trends, and largely provide the basis for our knowledge of the relation between structure and reaction rates, the fact that these ratios are temperature dependent encourages a more detailed examination in terms of the parameters derived from the temperature dependence of the rate. In Table III are given the rate data for three methyl esters over a range of

TABLE III

Kinetic data for the hydrolysis of three methyl-substituted benzenesulphonic esters in water

Temp.	Me-3,4-dimethyl benzenesulphonate, $k_1 \times 10^5$ sec^{-1}	Me-2,4-dimethyl benzenesulphonate, $k_1 \times 10^5$ sec^{-1}	Me-2,4,6-trimethyl benzenesulphonate, $k_1 \times 10^5$ sec^{-1}
353.172	$185._8$	$161._7$	83.1_0
348.164	$121._7$	$107._9$	54.2_4
343.166	79.3_1	$70._2$	35.8_3
338.168	50.5_1	45.3_8	22.4_0
333.158	31.3_7	28.5_5	14.1_1
323.159	11.6_4	10.78	5.2_5
313.173	3.97_4	3.79_5	1.80_9
308.170	2.23_3	2.16_4	1.02_5
303.173	1.231	1.21_0	0.57
Standard deviation* $\log k_{obs} - \log k_{calc}$	0.00096	0.0012	0.0010

*The average deviation from the mean of 3 or 4 separate kinetic runs is shown directly after the corresponding rate. The standard deviations between this observed value and the rate calculated from the derived equation [1] are shown here.

temperature. These data fit an empirical equation of the form

$$[1] \qquad \log_{10} k = A/T + B \log_{10} T + C$$

within experimental error and values of the corresponding constants are summarized

Can. J. Chem. Downloaded from www.nrcresearchpress.com by 196.1.178.254 on 09/04/12
For personal use only.

in Table IV. These constants may be interpreted as follows:

$$A = -(\Delta H_0^{\ddagger}/2.303\ R),$$
$$B = (\Delta C_p^{\ddagger}/R)+1,$$
$$C = (\Delta S_0^{\ddagger}-\Delta C_p^{\ddagger})/2.303\ R + \log_{10} k/h,$$

but it is well to recall that this interpretation finally rests on the assumption that an equilibrium exists between the initial and the transition state. Further, in our evaluation of $\Delta S^{\ddagger}$ we assume a frequency factor of $\log kT/h$ which is constant throughout a series and in fact throughout all series. Since we normally are considering $\Delta\Delta S^{\ddagger}$ values within a given series such an assumption is probably acceptable at this preliminary stage of comparison.

TABLE IV

Summary of constants for equation [1]

Benzenesulphonate	*A*	*B*	*C*
Me-3,4-dimethyl	−7408.282	−19.3250	67.48493
Me-2,4-dimethyl	−7067.916	−17.7061	62.33737
Me-2,4,6-trimethyl	−6776.710	−15.1235	54.64063

The thermodynamic parameters calculated from the above data are given in Table V.

TABLE V

Thermodynamic constants at 25° C

Benzenesulphonate	Me-3,4-diMe	Me-2,4-diMe	Me-2,4,6-triMe
k_1 sec$^{-1}\times 10^5$	0.660	0.6596	0.309
$\Delta F^{\ddagger}$ cal/mole	24,514	24,512	24,962
$\Delta H_0^{\ddagger}$ cal/mole	33,898	32,340	31,010
$\Delta H^{\ddagger}_{298.16}$ cal/mole	21,855	21,257	21,455
$-\Delta C_p^{\ddagger}$ cal/mole deg	40.39	37.17	−32.04
$-\Delta S^{\ddagger}$	8.94	10.95	11.64

In Table VI are given the difference functions with unsubstituted methyl benzenesulphonate as the standard. From these a much clearer picture can be gained of the effect of the substituent on the detailed mechanism than was possible from a consideration of relative rates.

TABLE VI

Effect of methyl substitution on thermodynamic constants for the hydrolysis of benzenesulphonic esters in water at 25° C

Ester	k_1 sec$^{-1}\times 10^5$	$\delta_x\Delta H^{\ddagger}_{\text{cal}}$	$\delta_x\Delta C_p^{\ddagger}$	$\delta_x\Delta S^{\ddagger}$
Me-*p*-H	1.166 (1)	0	0	0
Me-*p*-Me	0.799 (0.69)	+197	−2.0	−0.03
Me-*o*-Me	0.998 (0.86)	−540	+6.4	−2.46
Me-3,4-diMe	0.660 (0.57)	+435	−7.0	+0.35
Me-2,4-diMe	0.660 (0.57)	−163	−3.8	+1.66
Me-2,4,6-triMe	0.309 (0.27)	+ 35	+1.4	−2.35

We have noted elsewhere (1) that the *p*-Me raises $\Delta H^{\ddagger}$ by ~200 cal while *o*-Me lowers $\Delta H^{\ddagger}$ by ~−500 cal. If we may assume, on the basis of the above evidence, that the solvation of the para alkyl group is not altered during the activation process, aside from the possibility of a small hyperconjugation effect (and the small $\Delta\Delta S^{\ddagger}$ supports this assumption), then the effect of the *p*-group is to increase the bond energy requiring

Can. J. Chem. Downloaded from www.nrcresearchpress.com by 196.1.178.254 on 09/04/12
For personal use only.

greater thermal activation to achieve the critical charge level characteristic of the transition state. The 3-Me group probably has a somewhat greater inductive effect (7), say $\Delta\Delta H^{\ddagger}$ +225 cal, while if the trend is maintained ortho methyl would be expected to raise $\Delta H^{\ddagger}$ by 275∼300 cal (8). On this basis, the shift to be expected in $\Delta H^{\ddagger}$ for the 2,4-dimethyl will be (+200−500) = −300 compared to the observed value of −175 cal. To rationalize the value of $\Delta H^{\ddagger}$ for the 2,4,6-trimethyl ester we note from an examination of models that if a single ortho methyl interacts with the sulphonic group, the second ortho methyl will not be orientated for interaction. The second ortho methyl will then resemble a more effective (275∼300 cal) para methyl. The interaction of the first ortho methyl will cause a decrease in rotational entropy ($\delta_z\Delta S^{\ddagger}$ ∼2 e.u.) but this will not be duplicated by the second. Thus the predicted $\delta_z\Delta H^{\ddagger}$ will be (+200+275−500) = −25 cal; observed +24 cal, and the $\delta_z\Delta S^{\ddagger}$ is of the same sign and magnitude as for a single ortho methyl. It will be noted that these results are in essential agreement with the additivity relations noted for the relative rates.

Qualitatively, the differences in the heat capacity of activation are in accord with this analysis, but the crude state of our knowledge of the factors influencing this term limits interpretation of small differences. If the $\Delta C_p^{\ddagger}$ observed in hydrolysis arises from the temperature dependence of the $\Delta H^{\ddagger}$ required to break the solvation shell, then it is probable that the observed differences in $\Delta C_p^{\ddagger}$ reflect differences in the degree of involvement of the solvent. As has been noted elsewhere, such large heat capacity differences can hardly be attributed to the solute alone. The changes in $\Delta C_p^{\ddagger}$ are approximately additive. However, even considering the larger experimental error characterizing this parameter, the 2,4-dimethyl value for $\Delta C_p^{\ddagger}$ appears anomalous.

EXPERIMENTAL

Solvents.—Ethanol (absolute) and water were as previously described (9, 2). To acetic acid (reagent) was added sufficient acetic anhydride so that after heating overnight at 100° C approximately 0.05% remained according to analysis of S. Bruckstein (10).

Esters.—The constants characterizing the sulphonyl chloride and the esters are recorded in Table VII. There was no kinetic evidence (non-linear plots) of the presence of any competing impurity in the esters studied.

TABLE VII

Physical constants of methyl esters

Ester	M.p.	M.p. of amide*	Refractive index	Density	Neutral equivalent
Me-*p*-Et		108.5–109.5	1.5148	1.19562	200.9
Me-*p*-*n*-Pro		109.5–111	1.5105	1.16036	—
Me-*p*-isoPro		106–107	1.5116	1.16482	210
Me-*p*-*t*-Bu	68–69	137	—	—	211
Me-2,4-diMe		138.5–139.5	1.5213	1.2055	200.2
Me-3,4-diMe		145.5–146	—	—	200
Me-2,4,6-triMe	43–43.7	143.5–145	—	—	212

*Of corresponding sulphonyl chlorides. These are in essential agreement with values found by previous workers and summarized by Suter (ref. 14).

Kinetic studies.—The rates in water were determined by a conductance method. Details of the method, calculations, and assumptions have been discussed in detail in previous communications (11). The rate data in ethanol and in acetic acid followed the method described by Robertson (9) and Winstein (12) respectively.

Can. J. Chem. Downloaded from www.nrcresearchpress.com by 196.1.178.254 on 09/04/12
For personal use only.

REFERENCES

1. ROBERTSON, R. E. Unpublished work.
2. ROBERTSON, R. E. Can. J. Chem. **35**, 613 (1957).
3. INGOLD, C. K. Structure and mechanism of organic chemistry. Cornell University Press, Ithaca, N.Y. 1951. p. 345 et seq.
4. EVERETT, D. H. and WYNNE-JONES, W. F. K. Trans. Faraday Soc. **35**, 1380 (1939).
5. EVANS, A. G. Reactions of organic halides in solution. Manchester University Press. 1946.
6. FRANKLIN, J. L. Trans. Faraday Soc. 443 (1952).
7. TAFT, R. Steric effects in organic chemistry. John Wiley & Sons, Inc., New York, N.Y. 1956. Chap. 13. Sec. 5.
8. JAFFE, H. Chem. Revs. **53**, 191 (1953).
9. ROBERTSON, R. E. Can. J. Chem. **31**, 589 (1953).
10. BRUCKSTEIN, A. Anal. Chem. **28**, 1920 (1956).
11. ROBERTSON, R. E. Can. J. Chem. **33**, 1536 (1955).
12. WINSTEIN, S., GRUNWALD, E., and INGRAHAM, L. I. J. Am. Chem. Soc. **70**, 821 (1948).
13. TAFT, R. W. Private communication.
14. SUTER, C. M. The organic chemistry of sulphur. John Wiley & Sons, Inc., London. 1944. p. 458 et seq.

Can. J. Chem. Downloaded from www.nrcresearchpress.com by 196.1.178.254 on 09/04/12
For personal use only.

Can. J. Chem. Downloaded from www.nrcresearchpress.com by 196.1.178.254 on 09/04/12
For personal use only.

THE ACETOLYSIS OF SOME HYDROXYTETRAHYDRO-2-PYRANS[1]

THOMAS FRANCIS[2] AND E. VON RUDLOFF

ABSTRACT

The reaction between acetic anhydride and several hydroxytetrahydropyrans in the presence of boron trifluoride has been studied. 2-Methyl-3-hydroxytetrahydropyran, 2-hydroxymethyl-4,5-dihydroxytetrahydropyran, and 3,4-dihydroxytetrahydropyran all underwent normal acetolysis to the expected straight-chain polyol acetates. Optically active forms of *cis*- and *trans*- 3,4-dihydroxytetrahydropyran gave the same, inactive pentanetetrol, showing that racemization of the active centers had accompanied ring cleavage. 2-Hydroxymethyltetrahydropyran gave 1,3,6-hexanetriol besides the expected 1,2,6-isomer. The reagent did not cleave 4-hydroxytetrahydropyran nor dihydro-D-galactal, but the latter underwent hydroxyl inversion to give dihydro-D-altral. 1,5-Anhydro-D-sorbitol (polygalitol) appeared to undergo both ring fission and inversion.

INTRODUCTION

The isolation of several hydroxylated derivatives of tetrahydro-2-pyran from the hydrogenolysis of methyl glycopyranosides (1, 2, 3) stimulated an interest in ring cleavage of this type of cyclic ether as a possible aid in determining their structure and configuration. Relatively few examples of this reaction are cited in the literature (4), in contrast to extensive studies on tetrahydrofurans (4, 5), but it is generally accepted that tetrahydropyrans are much more resistant to cleavage than are their five-membered ring analogues (4, 5). Of the reagents generally used to effect fission of cyclic ethers (4), those involving the use of acetic anhydride and an acid catalyst appeared most attractive, since the cleavage products could be deacetylated readily and the free polyols thus obtained conveniently examined by paper chromatography and periodic acid oxidation.

In preliminary experiments, several different catalysts were used to study the acetolysis of 2-hydroxymethyltetrahydropyran and 3,4-dihydroxytetrahydropyran. The cleavage of 2-hydroxymethyltetrahydropyran using zinc chloride and acetic anhydride for 8 hours at reflux temperature has been reported (6) to yield 1,2,6-hexanetriol triacetate. Re-examination of this reaction now showed that 85% of the starting material was recoverable as its acetate after 4 hours' refluxing and 75% with a reaction period of 28 hours. No trace of cleavage was detected when 3,4-dihydroxytetrahydropyran was subjected to the same conditions for 4 hours. Mixtures of sulphuric acid and acetic anhydride were found to cause some cleavage of 2-hydroxymethyltetrahydropyran but decomposition was extensive and the effect of these reagents on other tetrahydropyrans was not investigated. Trifluoroacetic anhydride promoted acetylation of each of these tetrahydropyrans but there was no evidence of ring opening. However, boron trifluoride was found to catalyze the cleavage without too much general decomposition and its use in the acetolysis of hydroxytetrahydropyrans was, therefore, examined in detail.

DL-*trans*-3,4-Dihydroxytetrahydropyran, treated with excess acetic anhydride saturated with boron trifluoride, split to an extent of 25% with a reaction time of 18 hours at room temperature and to 50% at 100° C for 1 hour, whereas at the higher temperature fission was virtually complete in 4 hours. The cleavage product, after deacetylation and purification, was the expected 1,2,3,5-pentanetetrol. D-*trans*-3,4-Dihydroxytetrahydropyran

[1]*Manuscript received January 23, 1959.*
Contribution from the National Research Council of Canada, Prairie Regional Laboratory, Saskatoon, Saskatchewan.
Issued as N.R.C. No. 5144.
[2]*National Research Council of Canada Postdoctorate Fellow, 1958.*

and L-*cis*-3,4-dihydroxytetrahydropyran were found to yield the same optically inactive pentanetetrol, showing that racemization of the optically active centers had accompanied ring fission. Under similar reaction conditions the triacetate of 2-hydroxymethyl-4,5-dihydroxytetrahydropyran gave a 25% yield of the expected 1,2,3,5,6-hexanepentol, which did not give a solid benzoate or *p*-nitrobenzoate and formed a sirupy pentaacetate.

Cleavage of 2-hydroxymethyltetrahydropyran was complete in 2 hours at room temperature, whilst at 100° C decomposition was extensive. The product from the reaction at room temperature, or lower, was an oil which could not be separated into more than one component by counter-current distribution (210 transfers). The deacetylated product was shown to be a sirupy hexanetriol. However, when oxidized with periodic acid, the material consumed only 0.4 moles of oxidant with the release of 0.4 moles of formaldehyde, indicating that it was a mixture of the expected 1,2,6-hexanetriol and an isomer having no vicinal hydroxyl groups. This mixture of isomers could not be resolved by column chromatography, nor by counter-current distribution (120 transfers), but the isomeric triol was isolated from the mixture by decomposition of the 1,2,6-isomer with periodate. The sirupy product had an infrared spectrum which was similar to that of the 1,2,6-isomer and formed a crystalline tris-*p*-nitrobenzoate having similar spectral properties to those of the 1,2,6-derivative. These data, together with the results from C-methyl determinations, suggested that the compound was most likely 1,3,6-hexanetriol. 1,3,6-Triacetoxyhexane was prepared from tetrahydrofuran-2-acetic acid (7) by lithium aluminum hydride reduction to tetrahydrofuran-2-ethanol and subsequent ring cleavage (8). The triol obtained on deacetylation was shown to be identical with that obtained from 2-hydroxymethyltetrahydropyran. The formation of 1,3,6-hexanetriol besides the 1,2,6-isomer is unexpected, since tetrahydrofuranyl carbinols have given rise to only one triacetate on acetolysis with zinc chloride as catalyst (5). Since the starting material was found to be pure, it could not have been derived from a major impurity, such as tetrahydrofuran-2-ethanol.

Cleavage of a fraction isolated from the hydrogenolysis of α-methyl-D-glucopyranoside and thought to be a hydroxytetrahydropyran derivative (2) was readily effected with the reagent at room temperature in 18 hours. The product, after deacetylation, was 1,4,5-hexanetriol, since it consumed 1.0 mole of periodic acid with the production of 1.0 mole of acetaldehyde, and yielded a tris-*p*-nitrobenzoate. Thus, if no rearrangement had taken place during acetolysis (this assumption is justified, since no isomeric products were isolated) the starting material must have been 2-methyl-3-hydroxytetrahydropyran, a product not unexpected from the hydrogenolysis reaction. The ready cleavage of this 2-alkyl derivative is in accord with the findings on 2-alkyl tetrahydrofurans by Paul (5). The formation of olefinic intermediates presumably was suppressed by the 3-hydroxyl substituent.

4-Hydroxytetrahydropyran was not cleaved to any extent at room temperature, at 65° C, or at 100° C, charring being extensive at the latter temperature. This result was unexpected and cannot be explained by the proposed mechanisms of ether cleavage (4). Similar results were obtained with dihydro-D-galactal and dihydro-D-glucal. When dihydro-D-galactal was first acetylated and then treated with excess reagent at 100° C ring cleavage was also not obtained, showing that the formation of acetic acid in the initial acetylation of the free polyol is not the cause of this failure to cleave the ether. However, after a 10-hour treatment at 100° C dihydro-D-galactal yielded a small amount of dihydro-D-altral. Paper chromatographic analysis of the deacetylated product obtained from dihydro-D-glucal showed the presence of compounds with R_f values corre-

Can. J. Chem. Downloaded from www.nrcresearchpress.com by 196.1.178.254 on 09/04/12
For personal use only.

sponding to dihydrogalactal and dihydroaltral. A similar examination of the reaction product from a small amount of 1,5-anhydro-D-sorbitol (polygalitol) indicated the presence of both fission products (hexitols) and inversion products, besides unreacted starting material.

Burwell (4) proposed as the first step in the catalytic acetolysis of aliphatic ethers the addition of an acetyl cation to the ether oxygen. Presumably this mechanism is also operative in the acetolysis of tetrahydropyrans in the presence of boron trifluoride. The subsequent cleavage of a carbon–oxygen bond of the ether linkage and addition of an acetyl anion to the residual carbonium ion is more difficult to reconcile with the divergent results obtained. An intermediate cation, having the positive charge distributed between the oxygen atom and the carbon atoms in positions 2 and 3, analogous to the cation proposed in the acid-catalyzed cyclization of terpenes (11), would explain, for example, the formation of 1,3,6-hexanetriol in addition to the 1,2,6-isomer from 2-hydroxymethyltetrahydropyran. Such a cation could either cleave directly to such end products, or produce an intermediate olefin, analogous to those isolated by Paul (5) from 2-alkyl tetrahydrofurans. The olefinic diacetate could then be acetylated in the presence of boron trifluoride (12), or might recyclize to tetrahydrofuran-2-ethanol, which would undergo readily ring fission to 1,3,6-hexanetriol. Hydroxyl groups in the 3 position would prevent the formation of such intermediates and lead only to a single, expected product, which is in agreement with the present findings. However, such a mechanism would not explain the resistance to cleavage of the dihydroglycals and 4-hydroxytetrahydropyran. The failure of the former compounds to undergo ring fission may be explained (9) by boron complex formation of the type reported by Angyal and McHugh (10). Aliphatic ethers are known to form stable complexes with boron trifluoride (4) and it is conceivable that complex formation of one type or another prevents the cleavage reaction with some hydroxytetrahydropyrans.

It is concluded that although boron trifluoride is an excellent catalyst for the acetolysis of some tetrahydropyrans, the unexpected results obtained in other cases show that its action is not of a general nature.

EXPERIMENTAL

Paper chromatography was carried out using Whatman No. 1 paper and 1-butanol – ethanol – water (40:11:19, v/v) as solvent. The chromatograms were developed with ammoniacal silver nitrate spray reagent (13) and the distances travelled by compounds relative to rhamnose (R_{Rh}) were measured. Column chromatography was carried out on cellulose using benzene–ethanol–water (500:50:1, v/v) (A), 1-butanol (B), or 1-butanol $\frac{1}{4}$ saturated with water (C) as solvents. In counter-current distribution, a modified 100-tube E.C. Apparatus Co. fractionator was used (14). Deacetylation of polyol acetates was carried out in the manner previously described (2).

3,4-Dihydroxytetrahydropyran

(*a*) DL-*trans-3,4-Dihydroxytetrahydropyran* (*Dihydro*-DL-*xylal*)

A mixture of the diol (1.1 g) and acetic anhydride (10 ml) was saturated with boron trifluoride at such a rate that the internal temperature did not exceed 60° C. The reaction mixture was then heated on a steam bath for 4 hours, cooled, and poured into an ice-cold excess of saturated aqueous sodium carbonate or bicarbonate solution. The mixture was filtered and the residue and filtrate were extracted thoroughly with chloroform which was washed once with water, dried over calcium chloride, and evaporated. After distillation at 170–180° C and 0.5 mm, the cleavage product (2.05 g) was deacetylated.

Can. J. Chem. Downloaded from www.nrcresearchpress.com by 196.1.178.254 on 09/04/12
For personal use only.

Can. J. Chem. Downloaded from www.nrcresearchpress.com by 196.1.178.254 on 09/04/12
For personal use only.

Paper chromatography of the residue indicated a major component, R_{Rh} 1.14, and a minor component, R_{Rh} 1.73, the latter corresponding to unchanged starting material. The mixture was resolved by column chromatography using solvent B, and the cleavage product was thus obtained as a colorless sirup (0.9 g, 72%), b.p. 175–185° C (air bath) at 0.1 mm. Calculated for $C_5H_{12}O_4$: C, 44.11%; H, 8.88%. Found: C, 44.18%; H, 8.83%. The tetrol consumed 2.0 moles of periodic acid with the liberation of 1.0 mole of formaldehyde (15). The tetraacetate of the tetrol, prepared with sodium acetate and acetic anhydride, was a colorless oil, b.p. 175–180° C (air bath) at 0.5 mm; n_D^{20} 1.4442. Calculated for $C_5H_8(OCOCH_3)_4$: C, 51.31%; H, 6.63%; $COCH_3$, 56.6%. Found: C, 51.64%; H, 6.77%; $COCH_3$, 57.1%. The derived tetra-*p*-nitrobenzoate separated as light yellow crystals, m.p. 187° C, from acetone – ethyl acetate. Calculated for $C_{33}H_{24}N_4O_{16}$: C, 54.10%; H, 3.30%; N, 7.65%. Found: C, 54.47%; H, 3.54%; N, 7.68%.

When the cleavage reaction was carried out at 0° C for 18 hours and at room temperature for 24 hours, the product contained about 25% and 50%, respectively, of the tetrol.

(*b*) D-*trans-3,4-Dihydroxytetrahydropyran* (*Dihydro*-D-*xylal*)

Diacetyldihydro-D-xylal (2.0 g) was treated with acetic anhydride (7.5 ml) and boron trifluoride and the resulting tetrol (0.9 g, 67%) was isolated and purified as described above. Periodic acid oxidation of the polyol and analyses of the free polyol and its tetraacetate were consistent with a 1,2,3,5-pentanetetrol structure. The tetrol had no optical rotation in saturated aqueous sodium borate and its derived tetra-*p*-nitrobenzoate was shown by melting point, mixed melting point, and X-ray powder diagram comparison to be identical with that of the tetrol from dihydro-DL-xylal.

(*c*) L-*cis-3,4-Dihydroxytetrahydropyran* (*Dihydro*-L-*arabinal*)

Dihydro-L-arabinal (0.5 g) was cleaved and the derived tetrol (0.3 g, 52%) isolated and purified as described above. The tetrol had no optical rotation in saturated aqueous sodium borate and its tetra-*p*-nitrobenzoate derivative was identical with those of the tetrols from dihydro-D- and dihydro-DL-xylal (melting point, mixed melting point, infrared spectrum, and X-ray powder diagram).

2-Hydroxymethyl-4,5-dihydroxytetrahydropyran

The triacetate of this triol (3.8 g) was treated with acetic anhydride (5 ml) and boron trifluoride at 100° C for 4 hours and the product isolated and purified in the usual way. Paper chromatography of the product indicated that it was a mixture of the starting material and a hexanepentol (R_{Rh} 0.66). The pentol was isolated by column chromatography using solvent C and was a colorless sirup (0.58 g, 25%), n_D^{20} 1.4860. Calculated for $C_6H_{14}O_5$: C, 43.36%; H, 8.49%. Found: C, 43.60%; H, 8.48%. The substance consumed 3.2 moles of periodic acid with the production of 1.8 moles of formaldehyde showing that it was essentially 1,2,3,5,6-hexanepentol. It failed to give a solid benzoate or *p*-nitrobenzoate. The pentaacetate, prepared with sodium acetate and acetic anhydride, was a pale yellow sirup, n_D^{20} 1.4488. Calculated for $C_6H_9(OCOCH_3)_5$: C, 51.06%; H, 6.43%; $COCH_3$, 57.1%. Found: C, 51.08%; H, 6.80%; $COCH_3$, 57.4%.

2-Methyl-3-hydroxytetrahydropyran

One gram of a tetrahydropyran fraction obtained from hydrogenolysis of α-methyl-D-glucopyranoside (2) was treated with acetic anhydride (6 ml) and boron trifluoride at room temperature for 18 hours. The crude product was distilled at 160–170° C (air bath) and 12 mm and was then deacetylated. Paper chromatography of the product indicated that cleavage was complete and that the product was a hexanetriol (R_{Rh} 1.73). The triol was purified by column chromatography in solvent A and by distillation at

130–135° C (air bath) and 0.1 mm giving a colorless sirup (0.64 g, 55%), n_D^{20} 1.4738. Calculated for $C_6H_{14}O_3$: C, 53.71%; H, 10.52%; C-methyl, 20.2%. Found: C, 53.43%; H, 10.50%; C-methyl, 20.2%. The triol consumed 1.0 mole of periodic acid and yielded 1.0 mole of acetaldehyde (16).

The triacetate was a colorless oil, b.p. 105° C (air bath) and 0.1 mm with n_D^{20} 1.4366 (Paul (5) reported n_D^{10} 1.44029; found n_D^{10} 1.4403). Calculated for $C_6H_{11}(OCOCH_3)_3$: C, 55.37%; H, 7.75%; $COCH_3$, 49.6%. Found: C, 54.97%; H, 7.90%; $COCH_3$, 50.7%.

The derived tris-*p*-nitrobenzoate, after several recrystallizations from methanol–acetone, had m.p. 149–150° C. Calculated for $C_{27}H_{23}O_{12}N_3$: C, 55.77%; H, 3.99%; N, 7.23%. Found: C, 55.95%; H, 3.90%; N, 7.24%.

4-Hydroxytetrahydropyran

γ-Pyrone (12.5 g) was hydrogenated in ethanol (75 ml) with Raney nickel (0.6 g) at 100° C and 80 atmospheres pressure for 10 hours. The residual oil, after evaporation of the solvent, was fractionally distilled, yielding 4-hydroxytetrahydropyran (8.5 g), b.p. 90–92° C at 12 mm, n_D^{20} 1.4590. This tetrahydropyran was recovered unchanged from the reaction with boron trifluoride and acetic anhydride at room temperature for 18 hours, at 65° C and at 100° C for 2 hours. At the elevated temperatures charring took place and at 100° C a very small amount of an oil, b.p. 125–130° C (air bath) and 0.1 mm was obtained. The deacetylated product had R_{Rh} 1.62, corresponding to a hexanetriol. The amount obtained was too small for further identification.

Dihydro-D-galactal

Dihydro-D-galactal (0.5 g) was treated with acetic anhydride (5.0 ml) and boron trifluoride at 100° C for 10 hours. The crude product, after deacetylation, showed two major spots, R_{Rh} 1.12 and 1.37, and a weak spot, R_{Rh} 0.74, on paper chromatography. Unchanged dihydrogalactal (0.15 g, R_{Rh} 1.12) was removed from the reaction product by crystallization from methanol – ethyl acetate and the residue was then chromatographed using solvent A. By this means, the material with R_{Rh} 1.37 was isolated and after crystallization from ethyl acetate was identified as dihydro-D-altral by means of mixed m.p. 101–103° C, and by comparison of its X-ray powder diagram with that of an authentic specimen (3). A similar result was obtained using triacetyldihydro-D-galactal and a large excess of acetic anhydride and boron trifluoride.

Dihydro-D-glucal and 1,5-Anhydro-D-sorbitol (Polygalitol)

The product from the reaction of dihydro-D-glucal (R_{Rh} 1.24) with excess acetic anhydride and boron trifluoride at 100° C for 4 hours was deacetylated and paper chromatography of the product showed two major components having R_{Rh} 1.37 and 1.12 and a trace component, R_{Rh} 0.76.

Polygalitol (R_{Rh} 0.74), when similarly treated, yielded a mixture of substances having R_{Rh} values of 0.85, 0.74, 0.45, corresponding to an isomerization product, unchanged starting material, and a hexitol respectively.

2-Hydroxymethyltetrahydropyran

The reaction between 2-hydroxymethyltetrahydropyran (5 g) and acetic anhydride (15 ml) and boron trifluoride was complete in 2 hours at room temperature. The crude acetate mixture was distilled at 117–128° C and 0.5 mm to give a pale yellow oil (6.4 g, 57%) n_D^{20} 1.4472, which failed to separate into more than one component when subjected to counter-current distribution between 70% acetone/petrol (b.p. 60–70° C) when 210 transfers were applied (14). The same oil resulted when the reaction was carried out at

Can. J. Chem. Downloaded from www.nrcresearchpress.com by 196.1.178.254 on 09/04/12
For personal use only.

Can. J. Chem. Downloaded from www.nrcresearchpress.com by 196.1.178.254 on 09/04/12
For personal use only.

room temperature for 24 hours and also when the acetate of the starting material (6.5 g) was similarly reacted with acetic anhydride (9 ml) and boron trifluoride. At 100° C, decomposition was extensive and only a small amount of the oil was isolated. Calculated for $C_6H_{11}(OCOCH_3)_3$: C, 55.37%; H, 7.75%. Found: C, 55.40%; H, 7.85%.

Deacetylation of the above oil yielded a pale yellow sirup, n_D^{20} 1.4720, which did not separate into more than one component on column chromatography using solvent A or on counter-current distribution between water and *n*-butanol with 120 transfers. On paper chromatography it showed a single spot R_{Rh} 1.73, corresponding to a hexanetriol. Calculated for $C_6H_{14}O_3$: C, 53.71%; H, 10.52%. Found: C, 53.89%; H, 10.40%. Oxidation of the sirup with periodic acid resulted in the uptake of 0.4 mole of oxidant and the formation of 0.4 mole of formaldehyde.

The triol mixture (0.5 g) in water (20 ml) and periodic acid (0.5 g) in water (10 ml) was left to stand at room temperature for 2 hours and was then treated with Dowex-1 – bicarbonate until it gave a negative reaction to starch/KI paper. The mixture was filtered and evaporated and formaldehyde removed from the residue by steam distillation. The residue was then dissolved in water, extracted several times with ether, and recovered by evaporation of the aqueous solution. Distillation of the residual material afforded a colorless sirup (0.2 g), b.p. 135° C (air bath) at 0.1 mm, having R_{Rh} 1.73, n_D^{20} 1.4696, and low reducing power to the silver nitrate spray. C alculated for $C_6H_{14}O_3$: C, 53.71%; H, 10.50%. Found: C, 53.40%; H, 10.58%.

The derived tris-*p*-nitrobenzoate, m.p. 130–131° C, crystallized from ethyl acetate. Calculated for $C_{27}H_{23}O_{12}N_3$: C, 55.77%; H, 3.99%; N, 7.23%. Found: C, 56.09%; H, 3.89%; N, 7.23%.

Synthesis of Tetrahydrofuran-2-ethanol

A solution of tetrahydrofuran-2-acetic acid, prepared from tetrahydrofurfuryl bromide (17) by the method of Barger *et al.* (7), (10.5 g) in dry ether (200 ml) was added slowly with stirring to a mixture of lithium aluminum hydride (3.59 g) and dry ether (150 ml). When addition was complete, the mixture was stirred at room temperature for 18 hours and the excess lithium aluminum hydride was then decomposed by careful addition of water. The mixture was then shaken with excess dilute sulphuric acid and the ethereal phase was extracted with aqueous sodium bicarbonate and the aqueous phase again extracted with ether for 18 hours. The ethereal solution of the neutral products was evaporated and the residue distilled at 115–120° C (air bath) and 20 mm giving tetrahydrofuran-2-ethanol (8.0 g, 85%) as a colorless mobile oil n_D^{20} 1.4545. Calculated for $C_6H_{12}O_2$: C, 62.04%; H, 10.41%. Found: C, 61.66%; H, 10.56%.

1,3,6-Hexanetriol from Tetrahydrofuran-2-ethanol

Tetrahydrofuran-2-ethanol (4.06 g) in acetic anhydride (5 ml) was added slowly with stirring to a refluxing mixture of acetic anhydride (15 ml) and zinc chloride (0.3 g) (8). The mixture was refluxed for a further 18 hours and most of the excess anhydride was removed by distillation. The residue was cooled and poured into cold saturated aqueous sodium carbonate. The product was extracted into chloroform, which was washed once with water and dried over calcium chloride and evaporated. The residue was distilled at 120–130° C and 0.5 mm to give 6.5 g (71%) of an oil having n_D^{20} 1.4408. Calculated for $C_6H_{11}(OCOCH_3)_3$: C, 55.37%; H, 7.75%; $COCH_3$, 49.6%. Found: C, 55.58%; H, 7.52%; $COCH_3$, 49.5%.

The oil was deacetylated in the usual way and the triol was purified by column chromatography in solvent A and by distillation at 135° C (air bath) and 0.1 mm. The infrared

spectrum of the sirup, n_D^{20} 1.4753, was indistinguishable from that of the triol of 2-hydroxymethyltetrahydropyran. Confirmation of this identity was obtained by mixed melting point determination and infrared spectra comparison of the derived *p*-nitrobenzoate.

ACKNOWLEDGMENTS

We are grateful to Mr. M. Granat for infrared analyses, to Mr. T. M. Mallard for X-ray powder diagram determinations, to Mr. M. Mazurek and Mr. J. A. Baignée for microanalyses, and also to Dr. A. S. Perlin for his advice and criticism.

REFERENCES

1. BAUER, H. F. and STUETZ, D. E. J. Am. Chem. Soc. **78**, 4097 (1956).
2. RUDLOFF, E. VON, STUETZ, D. E., and BAUER, H. F. Can. J. Chem. **35**, 315 (1957).
3. RUDLOFF, E. VON and TULLOCH, A. P. Can. J. Chem. **35**, 1504 (1957).
4. BURWELL, R. L. Chem. Revs. **54**, 615 (1954).
5. PAUL, R. Bull. soc. chim. France, **8**, 369 (1941).
6. SOCIÉTÉ DES USINES CHIMIQUES RHÔNE-POULENC. Brit. Pat. No. 606,564, Aug. 17, 1943; cf. Chem. Abstr. **43**, 1435f (1949).
7. BARGER, G., ROBINSON, R., and SMITH, H. L. J. Chem. Soc. 718 (1937).
8. GRUMMITT, O., STEARNS, J. A., and ARTERS, A. A. *In* Organic syntheses. Vol. 29. *Edited by* C. S. Hamilton. John Wiley & Sons, Inc., New York. 1949. p. 89.
9. DEAN, F. M. Private communication.
10. ANGYAL, S. J. and MCHUGH, D. J. J. Chem. Soc. 1423 (1957).
11. RE, L. and SCHINZ, H. Helv. Chim. Acta, **41**, 1695 (1958).
12. ZAVGORODNII, S. V. Otdel. Khim. Nauk, 872 (1955); cf. Chem. Abstr. **50**, 9329f (1956); **33**, 5805[9] (1939).
13. PARTRIDGE, S. M. Nature, **158**, 270 (1946).
14. RAYMOND, S. Anal. Chem. **30**, 1214 (1958).
15. LAMBERT, M. and NEISH, A. C. Can. J. Research, B, **28**, 83 (1950).
16. DESNUELLE, P. and NAUDET, M. Bull. soc. chim. France, **12**, 871 (1951).
17. SMITH, L. H. *In* Organic syntheses. Vol. 23. *Edited by* L. I. Smith. John Wiley & Sons, Inc., New York. 1943. p. 88.

Can. J. Chem. Downloaded from www.nrcresearchpress.com by 196.1.178.254 on 09/04/12
For personal use only.

Can. J. Chem. Downloaded from www.nrcresearchpress.com by 196.1.178.254 on 09/04/12
For personal use only.

THE DECOMPOSITION OF SOLID POTASSIUM CHLORATE BY X RAYS[1]

H. G. HEAL[2]

ABSTRACT

Potassium chlorate irradiated with X rays has been found to contain chloride, chlorite, hypochlorite, and occluded oxygen, and probably also substantial amounts of dichlorine hexoxide and a trace of chlorine dioxide. The chlorite and hypochlorite appear to decompose during irradiation to chloride. *G* values are given for 25° and −196°. They vary little with temperature or dose rate.

INTRODUCTION

There has been no previous detailed study of the decomposition of solid potassium chlorate by ionizing radiation. In 1953, however, Hennig, Lees, and Matheson (9) published *G* values for the formation of oxygen when this salt is irradiated in a nuclear reactor, and in the same year the present writer published a brief note mentioning the finding of chlorite, hypochlorite, and chloride in X-irradiated potassium chlorate (6). One of the aims of the investigation reported here was to determine the nature of the decomposition products, which had not been more than tentatively identified. This is not a particularly straightforward matter, since the usual analytical methods only show what is present in a *solution* of the irradiated salt; the substances present in the original crystal are quite likely to be different (7, 8). We have now tried to identify these by examining the absorption spectra of the crystals, in conjunction with ordinary analysis. The other main purpose of this study was to learn what we could about the reaction mechanisms from a rough survey of the kinetics of decomposition.

EXPERIMENTAL

Reagent grade potassium chlorate was recrystallized once by cooling a hot aqueous solution. Rapid cooling gave small platelets, averaging 0.02 mm thick. These were dried for a week at 160°; they then melted quietly when heated, without any trace of decrepitation, showing the absence of water. These crystals were employed in studies of chemical decomposition. Slower cooling gave larger plates from 0.04 mm to 0.15 mm thick, selected specimens of which were used for plotting absorption spectra.

A Machlett OEG-60 X-ray tube, with tungsten target, was the source of radiation employed in the work on chemical decomposition. It was run at 50 kvp, 28 ma, with rectified but not filtered 60-cycle high voltage supply. The sample holder is shown in Fig. 1. Each sample weighed 1.2 to 1.6 mg. It was spread out over the bottom (5 mm in diameter) of a dish pressed from 0.017-mm aluminum foil. Typical samples were seen under the microscope to consist of platelets 0.01 mm to 0.03 mm thick, stacked two or three deep in many places. In order to achieve reasonably uniform rates of energy absorption in such samples, it was necessary to filter out the softer X radiation from the beam. The more filtration is used, the more uniform the rate of energy absorption through the sample, but the lower the dose rate. In the best series of irradiations, only negligible portions of the sample received energy at rates differing by more than 6% from the average for the whole sample. This entailed heavy filtration (294 mg/cm^2 of aluminum) and long irradiations (up to 75 hours). In another series of irradiations with filtration 84 mg/cm^2 of aluminum, the average dose rate was three times as great, but

[1]*Manuscript received January 23, 1959.*
Contribution from the Chemistry Department, University of British Columbia, Vancouver.
[2]*Present address: Chemistry Department, Queen's University, Belfast, Ireland.*

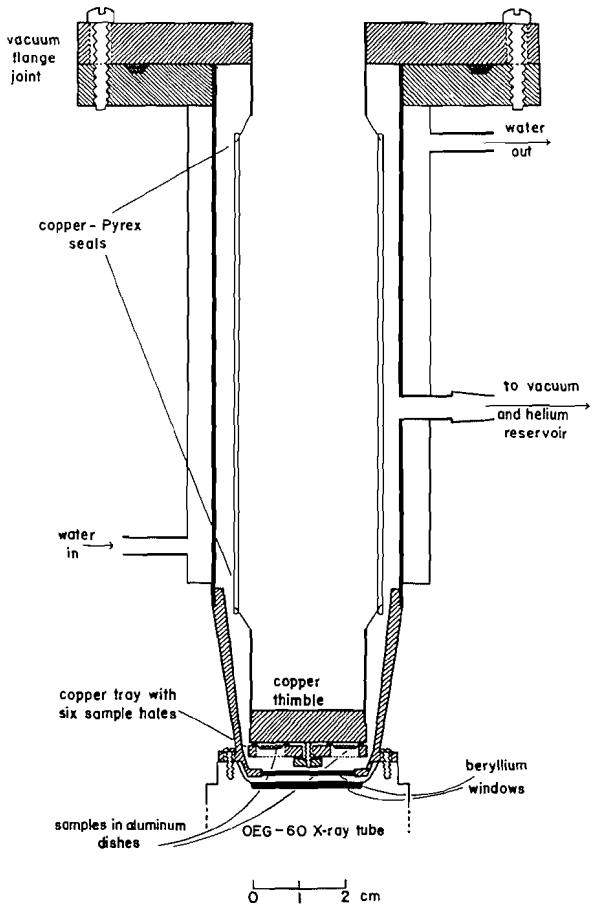

FIG. 1. Irradiation vessel for chemical decomposition studies. The filters are omitted for the sake of clarity. They consisted of aluminum disks which were placed between the two beryllium windows.

some parts of the sample received energy at rates up to 15% different from the average. Most irradiations were performed at 25°±1° under 0.5–1.0 mm of dry helium, which served to conduct away heat generated in the sample by the radiation, and prevented any appreciable rise of temperature. Results quoted for −196° were obtained from single crystals about 0.1 mm thick, which were cemented along one edge to the bottom of the central copper thimble of the irradiation vessel. The vessel was evacuated and the thimble filled with liquid nitrogen.

The absolute energy flux at the position of the samples was measured calorimetrically as described in an earlier publication (6), and the rate of energy absorption in the samples computed using tables of mass absorption coefficients, along with De Waard's formula for the spectral energy distribution of the X rays (1).

The apparatus used for plotting absorption spectra is shown in Fig. 2. The sample, a single crystal plate, was cemented across a hole 3 mm square in a copper block, which was maintained at the desired temperature. This crystal could be made to face either a small beryllium window through which the X-ray beam entered, or, by rotation through 90° on a standard taper joint, a pair of quartz windows through which the light beam of the spectrophotometer passed. The apparatus could be coupled to the

Can. J. Chem. Downloaded from www.nrcresearchpress.com by 196.1.178.254 on 09/04/12
For personal use only.

X-ray tube, a Machlett AEG-50-T, or fitted into the cell compartment of a Cary Model 14 recording spectrophotometer, by arrangements not shown in the diagram. As in the chemical work, the radiation was heavily filtered to ensure a nearly uniform dose rate throughout the crystal.

All sample weighings were done with a Cahn electrobalance sensitive to ± 2 μg.

For the spectrophotometric determination of chlorite and hypochlorite in solutions of irradiated chlorate, the solutions were placed in special quartz optical cells with a light path of 1 cm, but requiring only 0.5 ml of solution. The spectrophotometer was again the Cary Model 14. For the turbidimetric determination of chloride, the transmission of the samples was measured with a Bausch and Lomb Spectronic 20 calorimeter, run from a constant voltage transformer. For convenience, the other details of these procedures are described in the next section.

In order to minimize analytical errors when the degree of decomposition was small, up to six similarly irradiated samples were often combined for one analysis.

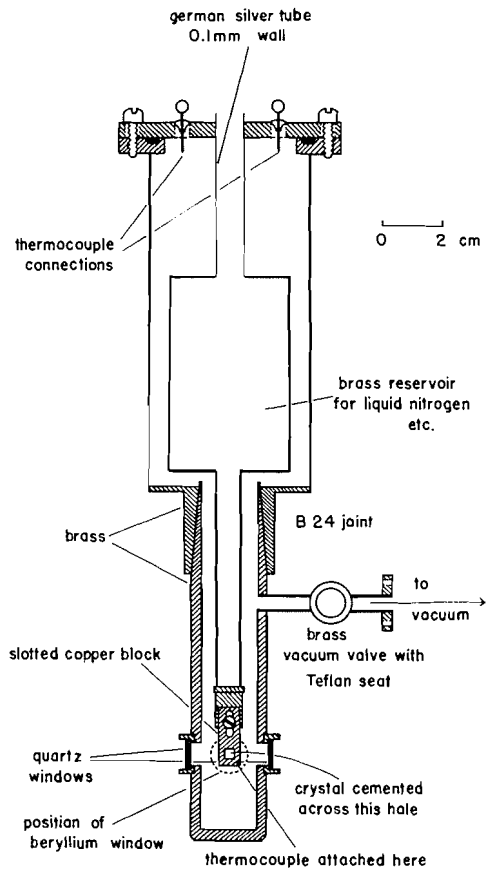

FIG. 2. Irradiation vessel used in the study of absorption spectra.

RESULTS

During irradiation at 25° the crystals darken gradually to a golden-brown tint. Up to about 8% decomposition, practically all the oxygen gas formed remains occluded within the crystals, as shown by the constancy of their weight. Above about 10% decompo-

Can. J. Chem. Downloaded from www.nrcresearchpress.com by 196.1.178.254 on 09/04/12
For personal use only.

sition the crystals "pop" or decrepitate at the slightest touch, presumably because of the oxygen pressure. Hennig, Lees, and Matheson also observed this phenomenon (9). With continued irradiation the crystals disintegrate to a light, fluffy, nearly white powder.

The decomposition products identified with reasonable certainty in irradiated potassium chlorate were oxygen, chloride, chlorite, and hypochlorite ions. Perchlorate ion was probably also present. Other products present in smaller amounts were tentatively identified as dichlorine hexoxide and chlorine dioxide. The methods by which these substances were identified and analyzed for will now be described.

Gas occluded in the irradiated crystals was determined by the microscope slide method described in an earlier publication (5). The crystals were dissolved in 0.025 *M* sodium carbonate which had been saturated with oxygen gas, by bubbling, immediately beforehand, with the object of minimizing errors due to the solubility of oxygen. The gas collected was assumed to be *oxygen*, since chlorine and all its oxides would have dissolved in or reacted with the sodium carbonate solution.

Considering next the *chlorite* and *hypochlorite*, Fig. 3 shows the absorption spectrum of a typical sample of irradiated chlorate, dissolved in 0.025 *M* sodium carbonate (pH

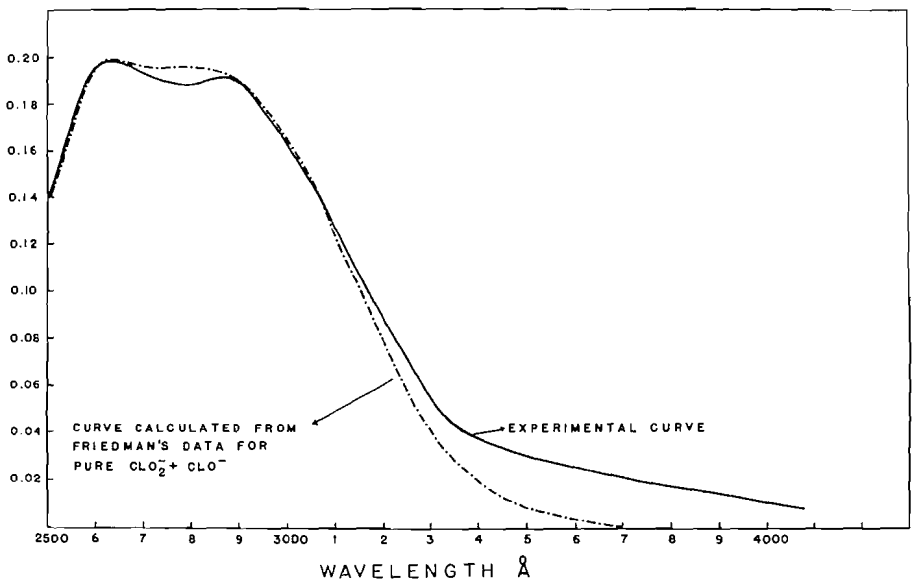

FIG. 3. Spectrum of a solution of irradiated $KClO_3$ in 0.025 *M* Na_2CO_3, compared with the spectrum for an appropriate ClO^-/ClO_2^- mixture from Friedman (ref. 2).

11 approximately). The peak at 2610 Å probably arises from chlorite ion, and the one at 2900 Å from hypochlorite ion. As the figure shows, the experimental spectrum agrees well with that calculated for an appropriate mixture of chlorite and hypochlorite, using Friedman's data for these ions (2). The only serious divergence is in the region 3300 Å to 4000 Å, where the samples always showed a weak absorption not attributable to chlorite or hypochlorite. This disappeared gradually over an hour or so. We attribute it to *chlorine dioxide*, which has an absorption maximum at about 3600 Å and is stated to hydrolyze slowly. The spectra appeared as depicted immediately after the samples were dissolved, suggesting that the chlorite was mostly present as such in the crystals,

Can. J. Chem. Downloaded from www.nrcresearchpress.com by 196.1.178.254 on 09/04/12
For personal use only.

and was not formed by the hydrolysis of chlorine dioxide present in the crystals. The absorption spectra of irradiated crystals themselves support this conclusion. Figure 4 shows a series of spectra for a crystal irradiated at 25°. Peaks developed at 2600 Å and

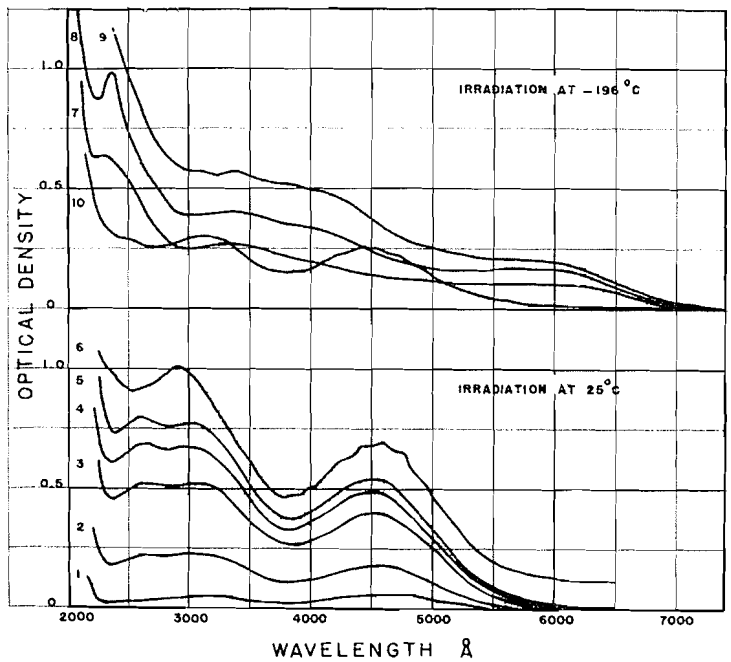

FIG. 4. Absorption spectra of irradiated $KClO_3$ crystals. (All optical densities relative to the unirradiated crystal.)

Below (curves 1 to 6) for crystal irradiated at 25° C. Crystal 0.12 mm thick. (All spectra measured at 25°, except (6).)

(1) After 3.08 hours, irradiation (0.38×10^{23} ev/mole).
(2) After 10.42 hours (1.28×10^{23} ev/mole).
(3) After 25.6 hours (3.15×10^{23} ev/mole).
(4) After 35.7 hours (4.4×10^{23} ev/mole).
(5) After 47.4 hours (5.8×10^{23} ev/mole).
(6) As in (5), but spectrum measured at −196°. The ordinate for this curve has been raised 0.1 unit of optical density for clarity.

Above (curves 7 to 10) for crystal irradiated at −196° C. Crystal 0.04 mm thick. (All spectra measured at −196°.)

(7) After 1 hour and 40 minutes' irradiation (0.86×10^{23} ev/mole).
(8) After 2 hours and 50 minutes' irradiation (1.46×10^{23} ev/mole).
(9) After 4 hours and 50 minutes' irradiation (2.49×10^{23} ev/mole).
(10) After 8 hours' irradiation at −196°, crystal warmed to room temperature for 2 hours, then cooled to −196° again for plotting spectrum (total dose 4.14×10^{23} ev/mole).

3100 Å, which we attribute to chlorite and hypochlorite respectively. The optical densities at the peaks agree within 15% with the values expected from the amounts of chlorite and hypochlorite found by analysis in the crystal, assuming the extinction coefficients in the solid to be the same as in solution. Quantitative analyses for chlorite and hypochlorite were carried out by dissolving the irradiated sample in 0.5 ml of 0.025 *M* sodium carbonate, and measuring optical densities at 2610 Å and 2900 Å. The absorption bands of the two ions overlap, so the amounts of chlorite and hypochlorite were calculated as solutions of a pair of simultaneous equations, using molar extinction coefficients from Friedman's paper.

Chloride could not be tested for by the usual reagent, silver ion in nitric acid solution, since the chlorite already known to be there disproportionates to an uncertain extent to chloride in acid pH's; moreover, silver ion is stated to precipitate silver chloride from

Can. J. Chem. Downloaded from www.nrcresearchpress.com by 196.1.178.254 on 09/04/12
For personal use only.

Can. J. Chem. Downloaded from www.nrcresearchpress.com by 196.1.178.254 on 09/04/12
For personal use only.

hypochlorite solutions (3). Instead, the chloride was allowed to react with silver ion in a weakly alkaline medium (0.01 *M* borax, pH about 9). At this pH, neither silver oxide nor silver borate precipitates, and we established spectrophotometrically that chlorite–hypochlorite mixtures are stable indefinitely. We ascertained by trial that after adding excess silver nitrate, in a very small volume, to a solution of irradiated chlorate in 0.01 *M* borax, and allowing the precipitate of silver chloride to settle, the chlorite and hypochlorite bands appeared in the absorption spectrum of the supernatant liquid exactly as they had been before adding the silver nitrate. This shows that silver nitrate precipitates chloride alone, without interference from chlorite or hypochlorite, in 0.01 *M* borax. For the quantitative estimation of chloride, the sample was dissolved in 1.0 ml 0.01 *M* borax. Water (0.5 ml) was added, followed by 1.5 ml of millimolar silver nitrate, shaking well at each stage. At the same time, a reference solution and two standards were made up. Each contained unirradiated potassium chlorate equal in weight to the sample. The standards contained, in addition, appropriate volumes of millimolar potassium chloride in place of some or all of the water. The quantities of chloride in the standards were chosen to "bracket" that expected for the sample, which had been roughly determined in earlier runs. All solutions were in 10-ml colorimeter test tubes which we had matched. After the solutions were shaken and left to stand for half an hour in the dark, the optical densities of all suspensions were measured at 375 mμ. Control experiments had established that the optical densities in the range we worked with were proportional to the amount of chloride, and (in confirmation of published work (11)) that they reached a maximum steady value in a few minutes less than the half-hour waiting period, at the laboratory temperature (26°).

The amount of gaseous oxygen recovered was less than equivalent to the hypochlorite, chloride, and chlorite, by an amount exceeding any likely experimental error. The most obvious explanation is that some *perchlorate* was formed. This ion could not be directly determined because there appears to be no simple micromethod applicable in the given circumstances. The infrared absorption spectrum of an irradiated sample believed from the material balance to contain 2 mole % of perchlorate was taken by the potassium chloride disk method. It showed a small peak at 1113 cm^{-1} not visible in the spectrum of unirradiated potassium chlorate. This falls close to the main maximum in the spectrum of pure potassium perchlorate (about 1100 cm^{-1}). This observation cannot be considered reliable evidence of perchlorate, since the side of the very strong main chlorate band extends into this region and tends to obscure small structural features. Nevertheless, we consider the formation of perchlorate to be the most likely explanation of the oxygen deficiency, especially in view of Sharman and McCallum's observation that pile-irradiated sodium chlorate contains substantial amounts of perchlorate (14).

The evidence for *dichlorine hexoxide* in irradiated potassium chlorate is derived solely from the absorption spectra of crystals. This substance hydrolyzes to chloric and perchloric acids when dissolved in water, so could not have been detected by any simple chemical method. Figure 4 shows the spectra in question. Besides the bands attributed to chlorite and hypochlorite already mentioned, irradiation at 25° produced a strong band with maximum at 4500 Å, which was responsible for the brown color of the crystals. When the crystal was cooled to −196°, this band developed a structure, as shown. Since this structure only appeared on cooling, it cannot have been an optical effect arising from polarization as described by Pringsheim (13), but must have been a true vibrational structure. The spacing of the subsidiary maxima was irregular and ranged from 570 to 680 cm^{-1}. The structure shows that this band came from a molecular

species, and not a color center. According to published information, no band anywhere near this position is to be found in the spectrum of chlorine or of any of the chlorine oxyanions or oxides, with the exception of Cl_2O_6 (12). The spectrum of this oxide has not been fully investigated, but the long wavelength edge of its absorption band, as described by Goodeve and Richardson (4) corresponds with the long wavelength side of our 4500 Å band.

The spectrum of crystals irradiated at −196°, and then allowed to warm up to 25°, was quite different (Fig. 4). The 4500 Å band was missing, and there was absorption over a considerable range of wavelengths, with one well-defined maximum at 2400 Å and several other ill-defined maxima. When the crystals were warmed to room temperature, the 2400 Å maximum and most of the remaining absorption disappeared, being replaced by a spectrum very similar to that obtained by irradiation at room temperature, including a strong band at 4500 Å. This developed structure on cooling of the crystal, and was obviously due to the same substance as the 4500 Å band produced by irradiation at 25°.

Our data on the *kinetics* of the decomposition are summarized in Fig. 5 and Table I. The figure shows the results of the best series of runs at 25°, viz. those done with the most heavily filtered radiation, and consequently the most nearly uniform dose rate. The main facts about Fig. 5 are as follows. Chlorite and hypochlorite were generated

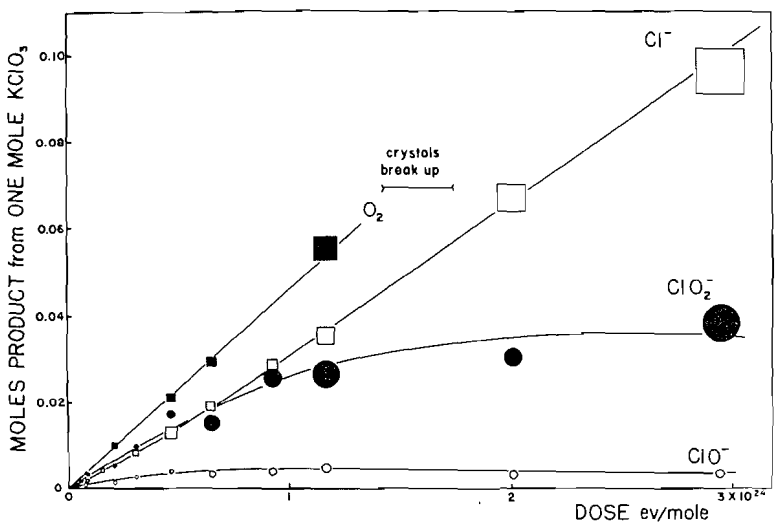

FIG. 5. Yields of chloride, hypochlorite, chlorite, and oxygen on dissolving $KClO_3$ irradiated for various times at 25° (dose rate 0.39×10^{23} ev/mole per hour). Sizes of experimental points represent possible analytical errors.

at rates which decreased with time until their concentrations became roughly steady. Chloride was formed at a rate increasing somewhat with time at first, and then (after a dose of about 10^{24} ev/mole) roughly constant. The final slope of the chloride line is about 25% greater than the initial slope. The rate of formation of oxygen was approximately constant up to the point where it began to escape from the crystals, and could no longer be determined. Some of the points of the chlorite curve are scattered more widely than would be expected from analytical errors alone; the reason is unknown. The general picture for the higher dose rate at 25°, and for the runs at −196° (not plotted, but data given in Table I), was very similar in all respects.

Can. J. Chem. Downloaded from www.nrcresearchpress.com by 196.1.178.254 on 09/04/12
For personal use only.

TABLE I

Initial G values (molecules per 100 ev absorbed) for the formation of products in the X irradiation of potassium chlorate

Temp., ° C	Dose rate, ev/mole per hour	G_{Cl^-}	G_{ClO^-}	$G_{ClO_2^-}$	G_{O_2}	$G_{Cl_2O_6}$	G_{ClO_2}
25	1.24×10^{23}	1.9	0.7	2.6	2.9	—	≈0.2
	0.39×10^{23}	1.3	0.5	2.0	2.5	—	
−196	0.12×10^{23}	—	—	—	—	1.4*	
	0.38×10^{23}	1.1	0.5	1.5	2.0	Not formed	

*Value estimated from optical density of crystal at 5460 Å, using $\epsilon = 80$ (Goodeve and Richardson, ref. 4) (see also ref. 10).

DISCUSSION

Chloride, hypochlorite, and chlorite all appear to be formed at the earliest stages of decomposition accessible to our measurements, viz. a few tenths of one per cent. Probably they all arise directly from chlorate by alternative processes of excitation and subsequent breakdown. The bodies decomposing cannot be positively identified, but are probably not ClO_3 molecules or radicals in their ground state, which are stable. The reactions occurring are likely to be:

$$ClO_3^{-*} \rightarrow Cl^- + O_2 + O \quad [1]$$
$$ClO_3^{-*} \rightarrow ClO^- + O_2 \quad [2]$$
$$ClO_3^{-*} \rightarrow ClO_2^- + O. \quad [3]$$

The perchlorate thought from the material balance to be present might be formed by a reaction between unexcited chlorate ions and O atoms from [1] and [3]:

$$ClO_3^- + O \rightarrow ClO_4^-. \quad [4]$$

The maximum possible yield of perchlorate (taking for discussion the figures for the lower dose rate at 25°) which could be associated with the observed oxygen deficiency is $G_{ClO_4^-} = 1.9$. The yield of O atoms from [1] and [3] is given by $G_O = 3.3$, considerably more than adequate to account for any perchlorate present.

The other main reaction product, thought to be Cl_2O_6, might arise as follows. Irradiation gives rise to positive holes (equivalent to ClO_3 radicals) and electrons in the conduction band. We suggest that at −196° these positive holes do not migrate rapidly, and that the strong ultraviolet absorption observed at this temperature is partly due to ClO_3, which is known to absorb with a maximum just below 3000 Å (12). The spectrum, however, gives no indication of the usual types of trapped electron centers, which would absorb in the region upwards of 5000 Å, and there is a question as to the fate of the electrons. We suggest that these are trapped by some of the O atoms from [1] and [3], which are not accounted for by [4], giving O^- or $O^=$ ions. The oxygen atom has an electron affinity of about 2.2 v, so that it should trap electrons efficiently. The wavelength at which the resulting O ion begins to absorb light would depend on its environment, but is not outside the range of the optical absorption observed in crystals irradiated at −196°. When the crystals are warmed up, some of the positive holes would be annihilated by electrons, while others may migrate together in pairs, forming Cl_2O_6 molecules, which are known to be very stable.

The drop in the net rates of formation of chlorite and hypochlorite as irradiation continues (Fig. 5) can best be explained by the secondary decomposition of these ions to chloride by the radiation:

$$\left.\begin{aligned} ClO_2^{-*} &\rightarrow Cl^- + O_2 \\ ClO^{-*} &\rightarrow Cl^- + O. \end{aligned}\right\} \quad [5]$$

Can. J. Chem. Downloaded from www.nrcresearchpress.com by 196.1.178.254 on 09/04/12
For personal use only.

This might be expected to lead to an increase in the total rate of formation of chloride as irradiation continues. Such an increase is observed, but cannot be given any simple quantitative interpretation. Examination of the data of Fig. 5, for example, discloses that when the concentrations of ClO_2^- and ClO^- are steady, the rates of destruction, and hence also the rates of formation, of these ions must be considerably less than their initial rates of formation; for in this region, the total G_{Cl^-} is only 1.6. If the initial rates of formation of ClO_2^- and ClO^- persisted into the steady state, the rate of formation of chloride from reactions [5] alone would equal $(G_{ClO_2^-}+G_{ClO^-})_{initial} = 2.5$. It seems that the excitons produced by the radiation are used at first mainly in reactions [1] to [3]. Soon, however, the ClO^- and ClO_2^- ions formed in [2] and [3] begin to trap a considerable proportion of the excitons, and use them in reactions [5], causing the yields from [1], [2], and [3] to diminish. ClO^- and ClO_2^- should trap excitons efficiently, since their excitation energies (as shown by their optical absorption) are lower than the minimum excitation energies of ClO_3^- and ClO_4^-. The experimental data do not suffice to give a more detailed picture of exciton utilization. It is interesting to note that the variation of chlorite and hypochlorite concentration with dose in potassium perchlorate (reported in an earlier paper (6)) is very much like that found in potassium chlorate, probably for similar reasons.

The assumption made in the preceding discussion, that all the primary chemical steps are initiated by single excitons, is justified by the small effect of dose rate on the G values (Table I). Reactions involving pairs of excitons would usually proceed at rates proportional to intensity squared, or, what is equivalent, their G values would be proportional to dose rate. Experimentally, all the G values do seem to increase somewhat with dose rate, but not nearly in proportion to it. Since the dose rate was regulated by varying the filtration, this small apparent variation of G values may well be due to systematic errors in the calculations of energy absorption, due among other causes to insufficiently accurate knowledge of the spectral energy distribution of the X rays. The variation of G with temperature over the enormous range from 25° to −196° is so small that none of the reactions can require thermal activation in the ordinary sense.

Our G values for the generation of oxygen (2.5 and 2.9 at 25°) agree well with the values 2.5 and 2.6 reported for pile-irradiated potassium chlorate by Hennig, Lees, and Matheson (9).

ACKNOWLEDGMENT

It is a pleasure to acknowledge the generous support for this investigation received from the Defence Research Board of Canada.

REFERENCES

1. De Waard, R. H. Proc. Acad. Sci. Amsterdam, **49**, 944, 1011 (1946).
2. Friedman, H. L. J. Chem. Phys. **21**, 319 (1953).
3. Gmelin's Handbuch der anorganischen Chemie. System-nummer 6(Chlor). Verlag Chemie G.M.B.H., Berlin. 1927. p. 290.
4. Goodeve, C. F. and Richardson, F. S. Trans. Faraday Soc. **33**, 453 (1937).
5. Heal, H. G. Nature, **172**, 30 (1953).
6. Heal, H. G. Can. J. Chem. **31**, 91 (1953).
7. Heal, H. G. Can. J. Chem. **31**, 1153 (1953).
8. Heal, H. G. Trans. Faraday Soc. **53**, 210 (1957).
9. Hennig, G., Lees, R., and Matheson, M. S. J. Chem. Phys. **21**, 664 (1953).
10. Kalina, M. H. and Spinks, J. W. T. Can. J. Research, B, **16**, 381 (1938).
11. Lamb, A. B., Carleton, P. W., and Meldrum, W. B. J. Am. Chem. Soc. **42**, 253 (1920).
12. Supplement to Mellor's comprehensive treatise of inorganic and theoretical chemistry. The halogens. Vol. I (18). Longmans, Green, & Co., Ltd., London. 1956.
13. Pringsheim, P. J. Chem. Phys. **23**, 369 (1955).
14. Sharman, L. J. and McCallum, K. J. J. Chem. Phys. **23**, 597 (1955).

Can. J. Chem. Downloaded from www.nrcresearchpress.com by 196.1.178.254 on 09/04/12
For personal use only.

Can. J. Chem. Downloaded from www.nrcresearchpress.com by 196.1.178.254 on 09/04/12
For personal use only.

PREPARATION OF SOME FLUORINE-CONTAINING TRISUBSTITUTED AROMATIC HYDROXYLAMINES[1]

B. A. GINGRAS AND C. H. BAYLEY

ABSTRACT

The preparation and properties of aryl dialkyl hydroxylamines in which the aryl group is a fluorobenzene derivative, and the two alkyl substituents are 2-cyano-2-propyl groups, are described.

Fluorine and its inorganic derivatives have been known for some time to be toxic to many live species (1) and, more recently, the high toxicity of fluoroacetic acid and many of its derivatives has been demonstrated (2). Although aromatic fluorine compounds have been prepared in good yields since 1927 (3), it was not until 1949 that the first systematic investigation of their fungistatic properties was undertaken (4). It was found that a number of monofluorinated quinones and nitrophenols showed good activity against the organisms *A. niger*, *A. terreus*, *M. verrucaria*, and *C. globosum*, the last two being cellulolytic. Addition of a second fluorine atom resulted in a decrease in potency and, for the fluoronitrophenols, a loss of activity was obtained by addition of another nitro group. However, in the aromatic hydrocarbon series, addition of a second nitro group markedly increased the potency, the most powerful compound being 2,4-dinitro-5-fluorotoluene (5). There are some indications that with multiple halogen dissimilar halogens give higher potencies, the most effective of all the compounds studied being 1-fluoro-3-bromo-4,6-dinitrobenzene, which, in concentration of 0.8 p.p.m., prevented growth of *A. niger* (6).

Most aromatic fluorinated nitro compounds have a yellow color and impart this to materials to which they are applied. This may be an objectionable feature, especially in the treatment of textile fibers for the suppression of microbiological attack. In the search for new antifungal compounds for this latter type of application, a series of colorless derivatives of fluoronitrobenzene have been prepared. These are O,N,N-trisubstituted hydroxylamines (I), similar to those reported by Gingras and Waters (7).

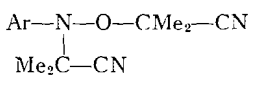

I

They are prepared through a free radical reaction from aromatic *C*-nitroso compounds and 2-cyano-2-propyl free radicals as follows. An aromatic amine (II) is first diazotized and then transformed into the fluorine derivative (IV) through a Schiemann reaction (3, 8). Nitration, followed by mild reduction gives the nitroso compound (VI), which is in turn reduced to the tertiary hydroxylamine (VIII) with two 2-cyano-2-propyl radicals (VII), the latter being produced by thermal dissociation of 2,2′-azo-bis-isobutyronitrile (IX) in solution (9).

In some instances, especially when the resulting mixture from nitration was difficult to separate into pure products, a nitroamine was used as starting material. In these

[1]*Manuscript received February 5, 1959.*
Contribution from the Division of Applied Chemistry, National Research Council, Ottawa, Canada.
Issued as N.R.C. No. 5148.

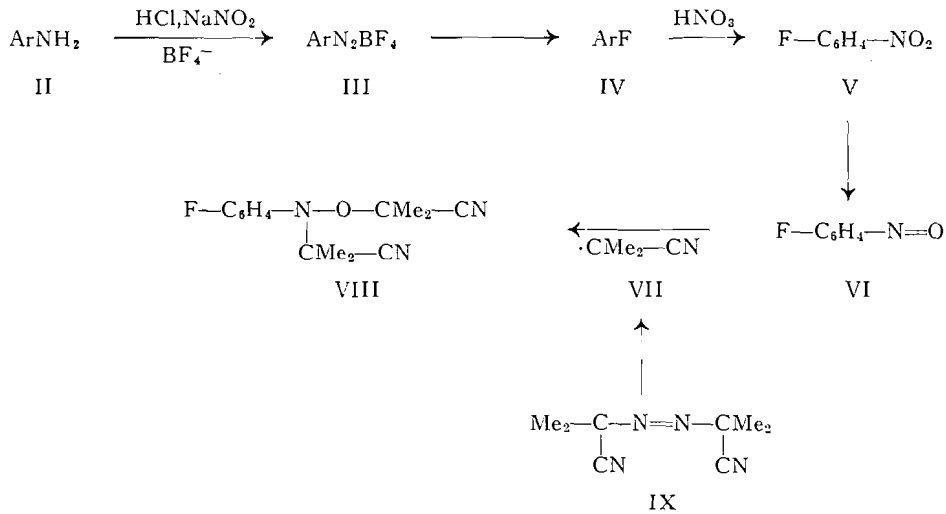

cases, special precautions had to be taken as thermal decomposition of benzene diazonium fluoborates (III) containing a nitro group is difficult to control with resultant possibility of poor yields (8).

The tertiary hydroxylamines together with the intermediate nitro compounds are listed in the table. Except for 2,4-dimethyl-6-nitrofluorobenzene, all the nitro compounds had been previously described.

TABLE

	Fluoronitro compounds: Ar—NO_2			Fluoro tertiary hydroxylamines: Ar—N(CMe_2CN)—O—CMe_2CN		
Starting material	Ar- groups	M.p. or b.p., °C at mm Hg	Lit. m.p. or b.p., °C at mm Hg	M.p., °C	Found, %	Required, %
p-Nitroaniline	4-FC_6H_4—	95/22	95–97.5/22 (11)	121	C, 64.3 H, 6.4 N, 16.0	64.4 6.1 16.0
o-Nitroaniline	2-FC_6H_4—	110/21	110–112/22 (11)	117.5	C, 64.7 H, 6.3 N, 16.2	64.4 6.1 16.0
2-Methyl-5-nitroaniline	3,4-F(Me)C_6H_3—	m.p. 34	m.p. 34 (12)	79	C, 65.2 H, 6.5 N, 15.0	65.5 6.5 15.3
2,4-Dimethyl-6-nitroaniline	2,3,5-F(Me_2)C_6H_2—	m.p. 70	—	88	N, 14.4	14.5
o-Fluorotoluene*	3,4-Me(F)C_6H_3—	m.p. 42 120/25	m.p. 41.5 99.4/13 (13)	86.5	C, 65.9 H, 7.0 N, 15.4	65.5 6.5 15.3
m-Toluidine	2,4-Me(F)C_6H_3—	111/21 †	78.5/3 216/775 (14)	100	C, 65.2 H, 6.5 N, 15.3	65.5 6.5 15.3
p-Fluoroanisole*	2,5-OMe(F)C_6H_3—	m.p. 62	m.p. 61.5 (15)	97.5	C, 61.9 H, 6.3 N, 14.8	61.8 6.2 14.4

*Eastman organic chemical used without further purification.
†Boiling point arrived at by extrapolation.

Can. J. Chem. Downloaded from www.nrcresearchpress.com by 196.1.178.254 on 09/04/12
For personal use only.

The fluorohydroxylamines are white solids, easily purified by chromatography and crystallization. They are practically insoluble in water, but dissolve in most organic solvents. Infrared spectra are of requisite character and, as expected, they are very similar to those obtained for the corresponding chlorine analogs (7). They all show the typical nitrile band at 4.5 μ, a band at 6.25 μ due to vibrations of the aromatic ring, and among others, a medium or strong band in the 9 μ region. Although the latter is indicative of $\diagdown\!\!\diagup$C—F grouping (10), no conclusion can be drawn here, as this region is also characteristic of the C—O and N—O stretching frequencies. Furthermore, the chlorine analogs also show a strong band in this region (7) and hence, it is probable that this is due to some covalencies of the system $\begin{matrix}\text{C}\diagdown\\ \text{C}\diagup\end{matrix}$N—O—C of the hydroxylamines.

Preliminary examination shows that reduction of the nitro compounds to the substituted hydroxylamines resulted in a decrease of potency. Other types of fluorine compounds are being examined simultaneously and it is hoped that a full discussion of the biological results will be published elsewhere.

EXPERIMENTAL

2,2′-Azo-bis-isobutyronitrile was the commercial product Porophor N, (Westville laboratories) and was recrystallized before use, from ethyl acetate, to m.p. 104° C; lit. m.p. 103–104° (16). Diazonium fluoborates were prepared and decomposed by the method of Balz and Schiemann (3, 8). Nitro compounds were reduced to the corresponding nitroso compounds by the method of Lutz and Lytton (17). All melting points were taken on a Fisher–Johns apparatus and are corrected.

p-Fluoronitro- and p-Fluoronitroso-benzene

p-Nitroaniline (34.6 g, 0.25 mole) was converted into *p*-fluoronitrobenzene (15.2 g, 45%) by the Schiemann reaction (8). The preparation of *p*-fluoronitrosobenzene is typical and is described in detail. *p*-Fluoronitrobenzene (14.1 g, 0.1 mole) was dissolved in a mixture of alcohol (42 ml) and water (24 ml) and powdered calcium chloride (1.5 g) was added. The mixture was heated to boiling and zinc dust (20 g) was added in small portions. At the end, the solid residue was removed by filtration and the filtrate was poured into an ice-cold solution of ferric chloride (37 g) in water (600 ml). The dark green precipitate of nitroso compound that formed was separated by filtration, and washed with ice-cold water. The product was purified by steam distillation; yield: 6.5 g (52%).

Reaction between p-Nitrosofluorobenzene and 2,2′-Azo-bis-isobutyronitrile

p-Nitrosofluorobenzene (6.5 g, 0.05 mole) and 2,2′-azo-bis-isobutyronitrile (16.4 g, 0.1 mole) were dissolved in toluene (150 ml) and the solution was heated to 80° C. The azo compound was decomposed and the green color of the nitroso compound soon disappeared. Heating was continued under reflux for 2 hours to assure complete decomposition of the azobutyronitrile. The toluene and radical dimer (tetramethylsuccinonitrile formed by combination of two free radicals VII) (9) were distilled with steam and the residue taken up in ether and dried. After evaporation of the ether, the residue was chromatographed through a column of silica gel. A mixture of benzene and ethyl ether 9:1 eluted ON-di-(2-cyano-2-propyl)-N-(*p*-fluorophenyl) hydroxylamine (5.31 g, 40% from the nitroso compound; 8% over-all yield from original amine; m.p. 121°). The product was recrystallized from aqueous alcohol 80%.

Can. J. Chem. Downloaded from www.nrcresearchpress.com by 196.1.178.254 on 09/04/12
For personal use only.

o-Fluoronitro- and o-Fluoronitroso-benzene

o-Nitroaniline (34.6 g, 0.25 mole) gave 4.4 g (14%) of *o*-fluoronitrobenzene. This gave, by the method previously described, 1.8 g (46%) *o*-fluoronitrosobenzene.

Reaction between o-Fluoronitrosobenzene and 2,2′-Azo-bis-isobutyronitrile

This reaction was carried out as above using 1.8 g (0.15 mole) *o*-fluoronitrosobenzene, 5 g (0.03 mole) azobutyronitrile, and 50 ml toluene. The solution was heated during $2\frac{1}{2}$ hours under reflux and then steam-distilled. The residue from the steam distillation weighed 1.2 g. Chromatographic separation of this residue yielded ON-di-(2-cyano-2-propyl)-N-(*o*-fluorophenyl) hydroxylamine (0.75 g, 20% from the nitroso compound). After recrystallization from aqueous alcohol it had m.p. 117.5°.

3-Fluoro-4-methylnitro- and 3-Fluoro-4-methylnitroso-benzene

2-Methyl-5-nitroaniline (38 g, 0.25 mole) gave 2-methyl-5-nitrobenzenediazonium fluoborate (58 g, 93%) which when decomposed yielded 2-methyl-5-nitrofluorobenzene (25.5 g, 70%). The corresponding 2-methyl-5-nitrosofluorobenzene was obtained in 50% yield (*ca.* 7 g) from 15.5 g (0.1 mole) of nitro compound.

Reaction between 2-Methyl-5-nitrosofluorobenzene and 2,2′-Azo-bis-isobutyronitrile

The nitroso compound (7 g, 0.05 mole) and the azonitrile (16.4 g, 0.1 mole) were dissolved in toluene (100 ml). After the usual $2\frac{1}{2}$ hours' reflux and steam distillation, the residue (4.8 g) was chromatographed. There was obtained from mixtures of benzene: ethyl ether, 4:1 and 2:1, ON-di-(2-cyano-2-propyl)-N-(3-fluoro-4-methylphenyl) hydroxylamine (3.8 g, 28%) which was recrystallized from *n*-hexane to constant m.p. 79°.

2-Fluoro-3,5-dimethylnitro- and 2-Fluoro-3,5-dimethylnitroso-benzene

2,4-Dimethyl-6-nitroaniline (41.5 g, 0.25 mole) gave the corresponding diazonium fluoborate (36.5 g, 55%). The latter decomposed at 220° C to give 2-fluoro-3,5-dimethylnitrobenzene (7.8 g, 25%; m.p. 70°). Calc. for $C_8H_8FNO_2$, mol. wt. 169: C, 56.8; H, 4.8; N, 8.3. Found: C, 57.8; H, 5.2; N, 8.3. Reduction of 5.6 g (0.03 mole) of the nitro compound gave 2-fluoro-3,5-dimethylnitrosobenzene (*ca.* 5 g).

ON-*Di-(2-cyano-2-propyl)*-N-*(2-fluoro-3,5-dimethylphenyl) Hydroxylamine*

Reaction of 2-fluoro-3,5-dimethylnitrosobenzene (*ca.* 5 g, 0.03 mole) and 2,2′-azo-bis-isobutyronitrile (11.5 g, 0.07 mole) in toluene (125 ml) gave 1 g (12%) of the tertiary hydroxylamine. The product was recrystallized from aqueous alcohol; m.p. 88°.

3-Methyl-4-fluoronitro- and 3-Methyl-4-fluoronitroso-benzene

Nitration of *o*-fluorotoluene (60 g, 0.54 mole) with fuming nitric acid (66 ml, sp. gr. 1.5) by the method of Schiemann (11) afforded 3-methyl-4-fluoronitrobenzene (57 g, 67%, b.p. 120° at 25 mm Hg). Reduction of the nitro compound (15.5 g, 0.1 mole) gave the corresponding nitroso compound (*ca.* 7 g, 50%).

ON-*Di-(2-cyano-2-propyl)*-N-*(3-methyl-4-fluorophenyl) Hydroxylamine*

This reaction was carried out as above using 3-methyl-4-fluoronitrosobenzene (*ca.* 7 g, 0.05 mole) and 2,2′-azo-bis-isobutyronitrile (16.4 g, 0.1 mole) in toluene (150 ml). After usual heating, steam distillation, and chromatography, there was obtained the tertiary hydroxylamine (4.8 g, 35%) which was recrystallized from absolute ethyl alcohol to constant m.p. 86.5°.

2-Methyl-4-fluoronitro- and 2-Methyl-4-fluoronitroso-benzene

m-Fluorotoluene (13.4 g) was nitrated with nitric acid (15 g, sp. gr. 1.42) and concen-

Can. J. Chem. Downloaded from www.nrcresearchpress.com by 196.1.178.254 on 09/04/12
For personal use only.

trated sulphuric acid (45 g) to give 2-methyl-4-fluoronitrobenzene (12 g, 70%, b.p. 111° at 21 mm). This was reduced to the corresponding nitroso compound by the usual method.

Reaction between 2-Methyl-4-fluoronitrosobenzene and 2,2'-Azo-bis-isobutyronitrile

This reaction was carried out as before and gave the expected ON-di-(2-cyano-2-propyl)-N-(2-methyl-4-fluorophenyl) hydroxylamine (2.9 g, 25%) which was best recrystallized from ethyl alcohol; m.p. 100°.

2-Methoxy-5-fluoronitro- and 2-Methoxy-5-fluoronitroso-benzene

p-Fluoroanisole (20 g, 0.15 mole) was nitrated by the method of Swarts (15) to give 2-methoxy-5-fluoronitrobenzene (15.7 g, 60%, m.p. 62°). Reduction of the latter (15.7 g, 0.09 mole) gave 2-methoxy-5-fluoronitrosobenzene (7.7 g, 54%).

ON-*Di-(2-cyano-2-propyl)*-N-*(2-methoxy-5-fluorophenyl) Hydroxylamine*

Reaction of 2-methoxy-5-fluoronitrosobenzene (7.7 g, 0.05 mole) with 2,2'-azo-bis-isobutyronitrile (16.4 g, 0.1 mole) gave the expected tertiary hydroxylamine (5 g, 33%), which was recrystallized from *n*-hexane; m.p. 97.5°.

REFERENCES

1. FREAR, D. E. H. Chemistry of the pesticides. 3rd ed. D. Van Nostrand Company Inc., New York. 1955. p. 271.
2. PATTISON, F. L. M. Nature, **172**, 1139 (1953). PATTISON, F. L. M. and MILLINGTON, J. E. Can. J. Chem. **34**, 757 (1956).
3. BALZ, G. and SCHIEMANN, G. Chem. Ber. **60**, 1186 (1927).
4. FINGER, G. C., FINNERTY, J. L., and SCHNEIDER, H. G. Am. Chem. Soc. Abstr. of Papers, 116th Meeting (Atlantic City). p. 17K (1949).
5. FINGER, G. C. and REED, F. H. Wright Air Development Center, Tech. Rept. 54–148, Wright-Patterson A.F.B., Ohio. (1954).
6. FINGER, G. C., REED, F. H., and DUNBAR, J. E. Wright Air Development Center, Tech. Rept. 52–214 (1952).
7. GINGRAS, B. A. and WATERS, W. A. Chem. & Ind. 615 (1953); J. Chem. Soc. 1920 (1954).
8. ROE, A. Organic reactions. Vol. V. John Wiley & Sons, Inc., New York. 1949. p. 193.
9. BICKEL, F. A. and WATERS, W. A. Rec. trav. chim. **69**, 312 (1950).
10. MILLER, F. A. Organic chemistry. Vol. III. *Edited by* Henry Gilman. John Wiley & Sons, Inc., New York. 1953. p. 148.
11. SCHIEMANN, G., PILLARSKY, R., and SCHÜTH, W. Chem. Ber. **62**, 3040 (1929).
12. SCHMELKES, F. C. and RUBIN, M. J. Am. Chem. Soc. **66**, 1631 (1944).
13. SCHIEMANN, G. Chem. Ber. **62**, 1804 (1929).
14. OSTASZYNSKI, A. Bull. soc. sci. lettres Lódź, Classe III, **3**, No. 15, 10 (1952); Chem. Abstr. **49**, 203*i* (1955).
15. SWARTS, F. Bull. acad. roy. Belg. 241 (1913); Chem. Abstr. **8**, 681 (1914).
16. OVERBERGER, C. G., O'SHAUGHNESSY, M. T., and SHALIT, H. J. Am. Chem. Soc. **71**, 2661 (1949).
17. LUTZ, R. E. and LYTTON, M. R. J. Org. Chem. **2**, 68 (1937).

Can. J. Chem. Downloaded from www.nrcresearchpress.com by 196.1.178.254 on 09/04/12
For personal use only.

Can. J. Chem. Downloaded from www.nrcresearchpress.com by 196.1.178.254 on 09/04/12
For personal use only.

NOTES

SZILARD CHALMERS REACTION IN POTASSIUM MANGANATE

R. A. MACKENZIE AND K. J. MCCALLUM

Several investigators have studied the chemical effects following neutron capture by the manganese nucleus in potassium permanganate. Libby (1) showed that when the irradiated solid was dissolved in water, most of the radioactive manganese could be separated with manganese dioxide, but a certain percentage, termed the retention, remained in the form of permanganate ion. The retention was observed to increase when the pH of the solution in which the solid was dissolved was high. Libby postulated that, while some of the radioactive manganese was present in the solid as permanganate ion, some existed as species formed by the loss of one or more oxygen ions from the permanganate ion, such as MnO_3^+ or MnO_2^{+++}. He assumed that these would be reduced to manganese dioxide by water, but would react with hydroxyl ions to form permanganate, thus leading to the observed increase in retention in basic solutions. Later investigations (2, 3) have verified the nature of the observed changes in retention, and have given results which are consistent with the reactions postulated by Libby.

If similar changes occur following neutron capture in potassium manganate, the species trapped in the solid would be of the type MnO_3 or MnO_2^{++}. Libby (1) made preliminary measurements of retention, following the neutron activation of sodium manganate dissolved in basic solution. The retention was less than that observed for permanganates under the same conditions, indicating that the recoil species differed in their behavior under these conditions.

The present note reports the results of a study on the effect of the normality of sodium hydroxide in the solvent on the retention for solid potassium manganate.

Potassium manganate was prepared by boiling a solution of potassium permanganate and potassium hydroxide. The compound was recrystallized from potassium hydroxide solution, the crystals being washed with absolute methanol containing a small amount of dissolved potassium hydroxide, and then with anhydrous ether. The oxidation equivalent of the product corresponded to 95–98% K_2MnO_4 in different preparations.

The solid was exposed to neutrons from a Ra–Be neutron source in a paraffin block. It was then dissolved in sodium hydroxide solutions of known normality, the retention then being determined by methods previously used for studies on potassium permanganate (2).

The results are given in Table I.

TABLE I

Retention in potassium manganate

Solution	% Retention	Solution	% Retention
1 *N* NaOH	46	7.5 *N* NaOH	87
3 *N* NaOH	55	8.5 *N* NaOH	92
5 *N* NaOH	66	10 *N* NaOH	97

The results indicate that the retention increases with increase in concentration of the hydroxyl ion, as was found for potassium permanganate. The recoil species then show

the same general chemical behavior for both salts. Measurements of retention in acid solutions might serve to reveal differences between the species. The disproportionation of manganate ion that occurs in such solutions makes necessary a different method of determining retentions. Attempts to establish a satisfactory method are in progress.

The financial assistance of the National Research Council of Canada is gratefully acknowledged.

1. LIBBY, W. F. J. Am. Chem. Soc. **62**, 1930 (1940).
2. MCCALLUM, K. J. and MADDOCK, A. G. Trans. Faraday Soc. **49**, 1150 (1953).
3. RIEDER, W., BRODA, E., and ERBER, J. Monatsh. **81**, 657 (1950).

RECEIVED FEBRUARY 2, 1959.
DEPARTMENT OF CHEMISTRY,
UNIVERSITY OF SASKATCHEWAN,
SASKATOON, SASKATCHEWAN.

Can. J. Chem. Downloaded from www.nrcresearchpress.com by 196.1.178.254 on 09/04/12
For personal use only.

ELECTRON SPIN RESONANCE ABSORPTION OF ULTRAMARINE: EFFECT OF CATIONS

YOSHIO MATSUNAGA*

Although the origin of the intense blue color of ultramarine is still unexplained, it has been generally accepted that the color is associated with the presence of regulated amounts of alkali and sulphur and the latter seems to be in the form of polysulphide sulphur (1). Gardner and Fraenkel (2) found that ultramarines show E.S.R. absorption and suggested that the paramagnetism arises from some type of sulphur radical. On the other hand, it is well known that the alkali in ultramarine is exchangeable for other bases and the color depends on the kind and the amount of bases. Here we wish to present the results of a study of the effect of cations on E.S.R. absorption of ultramarine.

The synthetic ultramarine supplied by Fisher Scientific Co. (Catalog No. U-1) was used as starting material and treated with large excess of silver nitrate and small amount of water in a sealed tube at 120–140° C for 15 hours. By this method we can replace sodium nearly completely with silver (3, 4). The other ultramarines were prepared by the treatment of the silver derivative with the halide of the desired metal as described by Jaeger (4). E.S.R. absorption was measured at room temperature at a frequency of 9 k Mc/s. The results are given in Table I. The line width is given by the distance in gauss between the points of maximum slope.

TABLE I

E.S.R. absorption of substituted ultramarines

Cation	Color	Line width	*g*-Value	Intensity
Na (original)	Blue	22	2.030	Very strong
Li	Dark violet grey	*ca.*30	2.030	Strong
Na	Dark blue	*ca.*30	2.030	Strong
K	Dark blue	*ca.*30	2.030	Strong
Ag	Brownish yellow	*ca.*35	2.026	Weak
Ca	Green	*ca.*30	2.024	Medium
Sr	Greenish brown	*ca.*30	2.026	Weak
Ba	Brown	*ca.*35	2.027	Weak
Zn	Brown	*ca.*30	2.026	Weak
Cd	Greenish brown	*ca.*30	2.024	Medium

**N.R.C. Postdoctoral Fellow 1957–.*

the same general chemical behavior for both salts. Measurements of retention in acid solutions might serve to reveal differences between the species. The disproportionation of manganate ion that occurs in such solutions makes necessary a different method of determining retentions. Attempts to establish a satisfactory method are in progress.

The financial assistance of the National Research Council of Canada is gratefully acknowledged.

1. LIBBY, W. F. J. Am. Chem. Soc. **62**, 1930 (1940).
2. MCCALLUM, K. J. and MADDOCK, A. G. Trans. Faraday Soc. **49**, 1150 (1953).
3. RIEDER, W., BRODA, E., and ERBER, J. Monatsh. **81**, 657 (1950).

RECEIVED FEBRUARY 2, 1959.
DEPARTMENT OF CHEMISTRY,
UNIVERSITY OF SASKATCHEWAN,
SASKATOON, SASKATCHEWAN.

Can. J. Chem. Downloaded from www.nrcresearchpress.com by 196.1.178.254 on 09/04/12
For personal use only.

ELECTRON SPIN RESONANCE ABSORPTION OF ULTRAMARINE: EFFECT OF CATIONS

YOSHIO MATSUNAGA*

Although the origin of the intense blue color of ultramarine is still unexplained, it has been generally accepted that the color is associated with the presence of regulated amounts of alkali and sulphur and the latter seems to be in the form of polysulphide sulphur (1). Gardner and Fraenkel (2) found that ultramarines show E.S.R. absorption and suggested that the paramagnetism arises from some type of sulphur radical. On the other hand, it is well known that the alkali in ultramarine is exchangeable for other bases and the color depends on the kind and the amount of bases. Here we wish to present the results of a study of the effect of cations on E.S.R. absorption of ultramarine.

The synthetic ultramarine supplied by Fisher Scientific Co. (Catalog No. U-1) was used as starting material and treated with large excess of silver nitrate and small amount of water in a sealed tube at 120–140° C for 15 hours. By this method we can replace sodium nearly completely with silver (3, 4). The other ultramarines were prepared by the treatment of the silver derivative with the halide of the desired metal as described by Jaeger (4). E.S.R. absorption was measured at room temperature at a frequency of 9 k Mc/s. The results are given in Table I. The line width is given by the distance in gauss between the points of maximum slope.

TABLE I

E.S.R. absorption of substituted ultramarines

Cation	Color	Line width	*g*-Value	Intensity
Na (original)	Blue	22	2.030	Very strong
Li	Dark violet grey	*ca.*30	2.030	Strong
Na	Dark blue	*ca.*30	2.030	Strong
K	Dark blue	*ca.*30	2.030	Strong
Ag	Brownish yellow	*ca.*35	2.026	Weak
Ca	Green	*ca.*30	2.024	Medium
Sr	Greenish brown	*ca.*30	2.026	Weak
Ba	Brown	*ca.*35	2.027	Weak
Zn	Brown	*ca.*30	2.026	Weak
Cd	Greenish brown	*ca.*30	2.024	Medium

**N.R.C. Postdoctoral Fellow 1957–.*

Contrary to the replacement of sodium with silver, the exchange of cation in the reverse direction is incomplete. In addition, the loss of a part of the sulphur and the change of oxidation state by the prolonged treatments must be taken into consideration. Although the quantitative explanation of the results is thus complicated by these facts, we can conclude that the concentration of unpaired electrons and the *g*-value depend on the kind of cation. The intensity of E.S.R. absorption is decreased by a factor of 20 to 30 accompanying the replacement of sodium by silver, but the paramagnetism of silver ultramarine can be increased about ten times by treatment with alkali halide. The color of ultramarine also changes nearly reversibly by these replacements. As to the ultramarines containing divalent cations, the replacement of silver seems to be more incomplete (4). However, generally the color of these ultramarines is far from blue and the concentration of unpaired electrons in these samples is less than alkali ultramarines.

It appears that not only the color of ultramarine but also the concentration of unpaired electrons depends on the kind of cation. Besides, the shift of *g*-value by cation exchange suggests that the spin–orbit interaction can be modified by the cation. Therefore, the paramagnetic species is not an isolated sulphur radical but is a complex containing cations. In accordance with the view which regards the color as being due to incompletely oxidized sulphur, it is very likely that unpaired electrons arise from polysulphide ions, however, they can apparently interact with each other through cations. The ability of the cation to couple unpaired electrons seems to be related to its polarizability and its valency. Alkali ions are not so effective for such an interaction.

The author wishes to thank Professor C. A. McDowell and Dr. J. B. Farmer for their interest and encouragement.

1. Emeleus, H. J. and Anderson, J. S. Modern aspects of inorganic chemistry. D. Van Nostrand Company, Inc., New York. 1954. pp. 251–257.
2. Gardner, D. M. and Fraenkel, G. K. J. Am. Chem. Soc. **77**, 6399 (1955).
3. Heumann, K. Ann. **199**, 253 (1879).
4. Jaeger, F. M. and Van Melle, F. A. Proc. Acad. Sci. Amsterdam, **30**, 479, 885 (1927); **32**, 156 (1929).

Received December 15, 1958.
Department of Chemistry,
The University of British Columbia,
Vancouver 8, B.C.

THE ADDITION OF ETHYL RADICALS TO ETHYLENE

F. W. Lampe and F. H. Field

In a recent study (1) of the reaction of ethyl free radicals generated by the photolysis of diethyl ketone, James and Steacie reported the activation energy (assuming zero activation energy for radical coupling) for addition to 1-alkene-type olefins to be 7.0 ± 0.2 kcal/mole. This value is consistent with the value of 7 kcal/mole found by Mandelcorn and Steacie (2) for the addition of methyl radicals to ethylene but is somewhat higher than the value found by Pinder and LeRoy (3) for ethyl radical addition to ethylene. These latter authors generated ethyl radicals by utilizing the mercury-photosensitized decomposition of hydrogen in the presence of ethylene and found an activation energy of 5.5 kcal/mole and a steric factor ratio of 5.0×10^{-5}. A "low" value of 4.6 kcal/mole for the addition of methyl radicals to ethylene can be derived (2) from the data of Raal and Danby (4).

Can. J. Chem. Downloaded from www.nrcresearchpress.com by 196.1.178.254 on 09/04/12
For personal use only.

Contrary to the replacement of sodium with silver, the exchange of cation in the reverse direction is incomplete. In addition, the loss of a part of the sulphur and the change of oxidation state by the prolonged treatments must be taken into consideration. Although the quantitative explanation of the results is thus complicated by these facts, we can conclude that the concentration of unpaired electrons and the *g*-value depend on the kind of cation. The intensity of E.S.R. absorption is decreased by a factor of 20 to 30 accompanying the replacement of sodium by silver, but the paramagnetism of silver ultramarine can be increased about ten times by treatment with alkali halide. The color of ultramarine also changes nearly reversibly by these replacements. As to the ultramarines containing divalent cations, the replacement of silver seems to be more incomplete (4). However, generally the color of these ultramarines is far from blue and the concentration of unpaired electrons in these samples is less than alkali ultramarines.

It appears that not only the color of ultramarine but also the concentration of unpaired electrons depends on the kind of cation. Besides, the shift of *g*-value by cation exchange suggests that the spin–orbit interaction can be modified by the cation. Therefore, the paramagnetic species is not an isolated sulphur radical but is a complex containing cations. In accordance with the view which regards the color as being due to incompletely oxidized sulphur, it is very likely that unpaired electrons arise from polysulphide ions, however, they can apparently interact with each other through cations. The ability of the cation to couple unpaired electrons seems to be related to its polarizability and its valency. Alkali ions are not so effective for such an interaction.

The author wishes to thank Professor C. A. McDowell and Dr. J. B. Farmer for their interest and encouragement.

1. Emeleus, H. J. and Anderson, J. S. Modern aspects of inorganic chemistry. D. Van Nostrand Company, Inc., New York. 1954. pp. 251–257.
2. Gardner, D. M. and Fraenkel, G. K. J. Am. Chem. Soc. **77**, 6399 (1955).
3. Heumann, K. Ann. **199**, 253 (1879).
4. Jaeger, F. M. and Van Melle, F. A. Proc. Acad. Sci. Amsterdam, **30**, 479, 885 (1927); **32**, 156 (1929).

Received December 15, 1958.
Department of Chemistry,
The University of British Columbia,
Vancouver 8, B.C.

THE ADDITION OF ETHYL RADICALS TO ETHYLENE

F. W. Lampe and F. H. Field

In a recent study (1) of the reaction of ethyl free radicals generated by the photolysis of diethyl ketone, James and Steacie reported the activation energy (assuming zero activation energy for radical coupling) for addition to 1-alkene-type olefins to be 7.0 ± 0.2 kcal/mole. This value is consistent with the value of 7 kcal/mole found by Mandelcorn and Steacie (2) for the addition of methyl radicals to ethylene but is somewhat higher than the value found by Pinder and LeRoy (3) for ethyl radical addition to ethylene. These latter authors generated ethyl radicals by utilizing the mercury-photosensitized decomposition of hydrogen in the presence of ethylene and found an activation energy of 5.5 kcal/mole and a steric factor ratio of 5.0×10^{-5}. A "low" value of 4.6 kcal/mole for the addition of methyl radicals to ethylene can be derived (2) from the data of Raal and Danby (4).

Can. J. Chem. Downloaded from www.nrcresearchpress.com by 196.1.178.254 on 09/04/12
For personal use only.

We wish to report here the results of some studies, on the photolysis of azoethane in the presence of ethylene, that support the lower values for the activation energy of the addition reactions.

EXPERIMENTAL

Azoethane was prepared by the method of Leitch (5). Ethylene was Phillips Research Grade, had a stated purity of 99.9+ mole %, and was used without further purification.

The photolyses were carried out in an annular reaction vessel constructed entirely of quartz. The annular space which contained the reacting gases had a thickness (light-path distance) of about 1.5 cm and a length of about 25 cm. The light source, positioned in the center of the vessel, consisted of two 8-watt G.E. "Black-lights" connected in series. The emitted radiation of the "Black-light" peaks at 3660 Å and emits negligible intensity below 3000 Å, thus eliminating the possibility of mercury-sensitized reactions. The gases were circulated by a two-stage Toepler pump, with the dead-space volume being about 20% of the total volume of reaction system.

In all experiments the azoethane pressure was held constant at 40 mm of Hg while the ethylene pressure was varied from 5 to 25 mm of Hg. Nitrogen was measured by assuming it to be the only noncondensible gas at −195° C. After its measurement the nitrogen was removed and the gases condensible at −195° C were analyzed by vapor–liquid partition chromatography.

RESULTS AND DISCUSSION

In all photolyses the only major reaction products observed were nitrogen, ethane, *n*-butane, and *n*-hexane. At the highest conversions in the runs at 175° C, small amounts of butylene were detected. No appreciable amounts of octane or higher hydrocarbons were found.

The main features of the mechanism involved in the photolysis of azoethane have been established (6, 7). The reactions of most importance to this discussion are:

$$C_2H_5N{=}NC_2H_5 + h\nu \rightarrow 2C_2H_5 + N_2 \qquad [R1]$$

$$C_2H_5 + C_2H_5N{=}NC_2H_5 \rightarrow C_2H_6 + C_2H_5N{=}NCH_2CH_2\cdot \qquad [R2]$$

$$C_2H_5 + C_2H_5 \rightarrow C_4H_{10} \qquad [R3]$$

$$C_2H_5 + C_2H_5 \rightarrow C_2H_4 + C_2H_6. \qquad [R3']$$

If ethylene is added to the system, some of the ethyl radicals formed in [R1] will add to it to form butyl radicals, i.e.,

$$C_2H_5 + C_2H_4 \rightarrow C_4H_9. \qquad [R4]$$

The absence of significant amounts of octane indicates, under our experimental conditions, that there is no appreciable addition of butyl radicals to ethylene nor coupling of butyl radicals. Since there is no appreciable addition of butyl radicals to ethylene, it seems reasonable to assume that butyl radicals will not abstract hydrogen from azoethane under these conditions. Also, since there is no appreciable coupling of butyl radicals, it is reasonable to assume that butyl radicals do not couple appreciably with the azoethyl radicals produced in [R2]. Thus, as an approximation, we assume that butyl radicals react only with ethyl radicals, i.e.,

$$C_2H_5 + C_4H_9 \rightarrow C_6H_{14} \qquad [R5]$$

$$C_2H_5 + C_4H_9 \rightarrow C_2H_6 + C_4H_8 \qquad [R6]$$

$$C_2H_5 + C_4H_9 \rightarrow C_2H_4 + C_4H_{10}. \qquad [R7]$$

The usual steady state approximation leads to

$$(1/[C_2H_4])(R_{C_6H_{14}}/R^{\frac{1}{2}}_{C_4H_{10}}) = P_C(k_4/k_3^{\frac{1}{2}}) \qquad [E1]$$

Can. J. Chem. Downloaded from www.nrcresearchpress.com by 196.1.178.254 on 09/04/12
For personal use only.

when the R's denote rates of formation, k's specific reaction rates, and P_C is the probability that in [R5]–[R7] coupling occurs, i.e.,

[E2] $$P_C = k_5/(k_5+k_6+k_7).$$

In Table I we show the results of the photolyses. Each value of $P_C(k_4/k_3^{\frac{1}{2}})$ is the average obtained from at least five experiments with irradiation times varying from 15 to 70 minutes. In the calculation of $P_C(k_4/k_3^{\frac{1}{2}})$, initial ethylene concentrations were used.

TABLE I

Addition of ethyl radicals to ethylene

Temp. (° K)	$[C_2H_4]_0$ (mm at T° K)	$P_C(k_4/k_3^{\frac{1}{2}})\times10^{12}$ (cc/molecule-sec)$^{\frac{1}{2}}$
398	10.2	2.54
398	15.5	2.67
398	20.0	2.64
398	25.0	2.47
423	5.0	3.79
423	10.1	3.71
423	15.0	3.81
423	20.0	3.88
448	5.0	5.62

This does not introduce any error greater than that involved in the analyses, because in all runs the ethylene conversion was below 10% and generally of the order of 2–6%.

The absence of significant amounts of butylene and the fact that [R6] is thermodynamically favored over [R7] suggests that P_C is very close to unity. Assigning P_C a value of unity (an approximation that is not in error by more than 5 or 10%) enables us to make the usual type Arrhenius plot of the rate constant ratios in Table I. Such a plot is shown in Fig. 1 and leads to a value for the activation energy difference, $E_4-\frac{1}{2}E_3$, of 5.5 kcal/mole. The ratio of the pre-exponential factors, $A_4/A_3^{\frac{1}{2}}$, is 2.6×10^{-9} which, upon assumption of a mean collision diameter of 4.0 Å, leads to a steric factor ratio, $P_4/P_3^{\frac{1}{2}}$, of 1.3×10^{-4}.

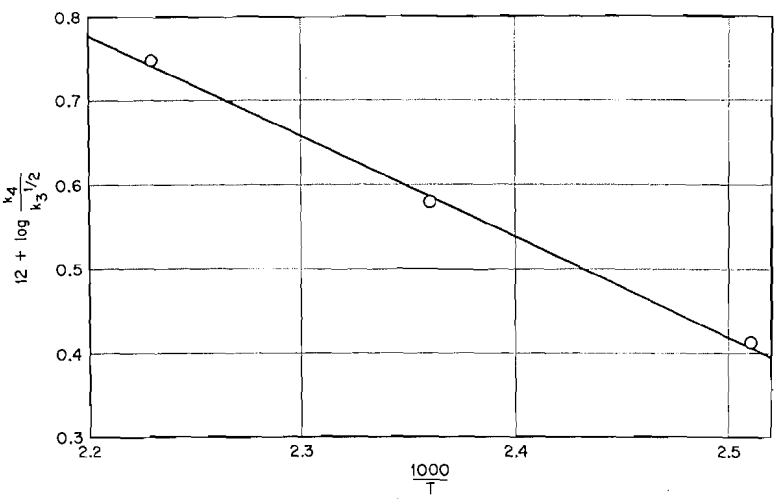

FIG. 1. Arrhenius plot for the addition of ethyl radicals to ethylene.

Can. J. Chem. Downloaded from www.nrcresearchpress.com by 196.1.178.254 on 09/04/12
For personal use only.

The activation energy difference of 5.5 kcal/mole is in excellent agreement with the results of Pinder and LeRoy (3), and consistent with the low value of 4.6 kcal/mole found by Raal and Danby (4) for the addition of methyl radicals to ethylene. Our value of the steric factor ratio is larger than that found by Pinder and LeRoy (3) by a factor greater than two. We can advance no explanation for this difference.

ACKNOWLEDGMENTS

We are indebted to Dr. D. E. Bown for the synthesis of the azoethane and to Mr. J. C. Leutwyler for assistance in the measurements.

1. James, D. G. L. and Steacie, E. W. R. Proc. Roy. Soc. A, **244**, 297 (1958).
2. Mandelcorn, L. and Steacie, E. W. R. Can. J. Chem. **32**, 474 (1954).
3. Pinder, J. A. and LeRoy, D. J. Can. J. Chem. **35**, 588 (1957).
4. Raal, F. A. and Danby, J. C. J. Chem. Soc. 2219 (1949).
5. Renaud, R. and Leitch, L. C. Can. J. Chem. **32**, 545 (1954).
6. Ausloos, P. and Steacie, E. W. R. Bull. soc. chim. Belges, **63**, 87 (1954).
7. Weininger, J. L. and Rice, O. K. J. Am. Chem. Soc. **74**, 6216 (1952).

Received December 29, 1958.
Research and Development Division,
Humble Oil and Refining Company,
Baytown, Texas.

NOTE ON THE DETERMINATION OF CRYSTALLINITY INDEX OF CELLULOSE

M. Kouris, H. Ruck, and S. G. Mason

In a recent communication (1) it was shown that the maximum intensity of air scattering can be used as a reference intensity in determining the X-ray crystallinity index of cellulose. The successful application of the method requires that the following conditions are met:

1. The sample mass must be kept constant to within $\pm 3\%$.
2. I_{as} must be comparable with I_{002}, the intensity of the A_4 cellulose interference.

It now appears that in the earlier work the correct experimental conditions for satisfying the second requirement were fortuitously established.

The purpose of the present note is to draw attention to the recently discovered fact that the second requirement above is satisfied when the thickness of the irradiated sample is about one-third of the optimum thickness as defined by the relation (2)

$$t_m = 1/\mu$$

where μ is the linear absorption coefficient of the sample.

If the optimum sample thickness is used, the absorption of the primary beam will be at a maximum, and the intensity of the air scattering will therefore be disproportionately weak with respect to I_{002} to be used as a reference interference. By reducing the sample thickness to $t_m/3$ the relative intensity of air scattering with respect to I_{002} is increased threefold and I_{as} becomes comparable with I_{002}.

It may also be of interest to point out that preliminary experiments were unable to detect any change in I_{as} with normal variations in atmospheric pressure.

1. Kouris, M., Ruck, H., and Mason, S. G. Can. J. Chem. **36**, 931 (1958).
2. Klug, H. P. and Alexander, L. E. X-Ray diffraction procedures for polycrystalline and amorphous materials. John Wiley & Sons, Inc., New York. 1954. pp. 204–206.

Can. J. Chem. Downloaded from www.nrcresearchpress.com by 196.1.178.254 on 09/04/12
For personal use only.

The activation energy difference of 5.5 kcal/mole is in excellent agreement with the results of Pinder and LeRoy (3), and consistent with the low value of 4.6 kcal/mole found by Raal and Danby (4) for the addition of methyl radicals to ethylene. Our value of the steric factor ratio is larger than that found by Pinder and LeRoy (3) by a factor greater than two. We can advance no explanation for this difference.

ACKNOWLEDGMENTS

We are indebted to Dr. D. E. Bown for the synthesis of the azoethane and to Mr. J. C. Leutwyler for assistance in the measurements.

1. James, D. G. L. and Steacie, E. W. R. Proc. Roy. Soc. A, **244**, 297 (1958).
2. Mandelcorn, L. and Steacie, E. W. R. Can. J. Chem. **32**, 474 (1954).
3. Pinder, J. A. and LeRoy, D. J. Can. J. Chem. **35**, 588 (1957).
4. Raal, F. A. and Danby, J. C. J. Chem. Soc. 2219 (1949).
5. Renaud, R. and Leitch, L. C. Can. J. Chem. **32**, 545 (1954).
6. Ausloos, P. and Steacie, E. W. R. Bull. soc. chim. Belges, **63**, 87 (1954).
7. Weininger, J. L. and Rice, O. K. J. Am. Chem. Soc. **74**, 6216 (1952).

Received December 29, 1958.
Research and Development Division,
Humble Oil and Refining Company,
Baytown, Texas.

NOTE ON THE DETERMINATION OF CRYSTALLINITY INDEX OF CELLULOSE

M. Kouris, H. Ruck, and S. G. Mason

In a recent communication (1) it was shown that the maximum intensity of air scattering can be used as a reference intensity in determining the X-ray crystallinity index of cellulose. The successful application of the method requires that the following conditions are met:

1. The sample mass must be kept constant to within $\pm 3\%$.
2. I_{as} must be comparable with I_{002}, the intensity of the A_4 cellulose interference.

It now appears that in the earlier work the correct experimental conditions for satisfying the second requirement were fortuitously established.

The purpose of the present note is to draw attention to the recently discovered fact that the second requirement above is satisfied when the thickness of the irradiated sample is about one-third of the optimum thickness as defined by the relation (2)

$$t_m = 1/\mu$$

where μ is the linear absorption coefficient of the sample.

If the optimum sample thickness is used, the absorption of the primary beam will be at a maximum, and the intensity of the air scattering will therefore be disproportionately weak with respect to I_{002} to be used as a reference interference. By reducing the sample thickness to $t_m/3$ the relative intensity of air scattering with respect to I_{002} is increased threefold and I_{as} becomes comparable with I_{002}.

It may also be of interest to point out that preliminary experiments were unable to detect any change in I_{as} with normal variations in atmospheric pressure.

1. Kouris, M., Ruck, H., and Mason, S. G. Can. J. Chem. **36**, 931 (1958).
2. Klug, H. P. and Alexander, L. E. X-Ray diffraction procedures for polycrystalline and amorphous materials. John Wiley & Sons, Inc., New York. 1954. pp. 204–206.

Can. J. Chem. Downloaded from www.nrcresearchpress.com by 196.1.178.254 on 09/04/12
For personal use only.

RECEIVED JANUARY 21, 1959.
PHYSICAL CHEMISTRY DIVISION,
PULP AND PAPER RESEARCH INSTITUTE OF CANADA,
MONTREAL, QUEBEC.

STRUCTURE AND REACTIVITY OF C_3H_3 RADICAL*

G. GIACOMETTI†

Recent mass spectroscopic work by Collin and Lossing (1) on the mercury photosensitized decomposition of allene led to the production of the C_3H_3 radical. The latter was then allowed to react with CH_3 radicals, produced thermally from $Hg(CH_3)_2$, and the analysis of the products showed that all the radicals react to form 1-butyne (CH_3—CH_2—CC≡H) and none of the allenic isomer CH_2=C=CH—CH_3.

This fact is to be considered evidence for the structure of the C_3H_3 radical being of the resonant type

$$\dot{\underset{1}{C}}H_2—\underset{2}{C}\equiv\underset{3}{CH} \longleftrightarrow \underset{1}{CH_2}=\underset{2}{C}=\dot{\underset{3}{C}}H \qquad [I]$$

rather than of the pure allenic type

$$CH_2=C=\dot{C}H. \qquad [II]$$

The structure of the radical is actually going to be different in the two cases because if [I] is correct, the two bonds have certainly different lengths, while if [II] is valid, the two bond distances must be approximately the same.

Though one might feel intuitively that resonance is making structure [I] more stable, it is of interest to show that structure [I] is indeed predicted by a very crude molecular orbital approach.

We shall assume that the simple LCAO, MO theory (2) is applicable, neglecting overlap and also π_x–π_y electron interaction. We shall consider equal all the coulomb integrals and take the exchange integrals as a decreasing function of the bond distance (in absolute value).

Indicating by a the C—C bond in [II] and by b and c those in [I], we have:

$$|\beta_b| < |\beta_a| \leqslant |\beta_c|.$$

The total π electron energy for [II] is simply:

$$E_{II} = 4\beta_a$$

while for [I] we have:‡

$$E_I = 2\beta_c + 2\beta_c \left|\sqrt{\left(1 + \frac{\beta_b^2}{\beta_c^2}\right)}\right| \approx 4\beta_c + \beta.$$

Structure [I] is lower in energy than [II] by an amount at least of the order of β, which corresponds to approximately 20–30 kcal/mole. It is then quite clear that the C_3H_3 radical formed from an excited allene molecule is best represented by formulation [I] and has two different bond lengths.

*Issued as N.R.C. No. 5139.
†*National Research Council Postdoctorate Fellow 1957–58. Present address: Instituto di Chimica Fisica, Università di Padova, Padova, Italy.*
‡*The β's are negative quantities. The coulomb integral is taken as zero of the energy scale.*

Can. J. Chem. Downloaded from www.nrcresearchpress.com by 196.1.178.254 on 09/04/12
For personal use only.

RECEIVED JANUARY 21, 1959.
PHYSICAL CHEMISTRY DIVISION,
PULP AND PAPER RESEARCH INSTITUTE OF CANADA,
MONTREAL, QUEBEC.

STRUCTURE AND REACTIVITY OF C_3H_3 RADICAL*

G. GIACOMETTI†

Recent mass spectroscopic work by Collin and Lossing (1) on the mercury photosensitized decomposition of allene led to the production of the C_3H_3 radical. The latter was then allowed to react with CH_3 radicals, produced thermally from $Hg(CH_3)_2$, and the analysis of the products showed that all the radicals react to form 1-butyne (CH_3—CH_2—CC≡H) and none of the allenic isomer CH_2=C=CH—CH_3.

This fact is to be considered evidence for the structure of the C_3H_3 radical being of the resonant type

$$\dot{\underset{1}{C}}H_2—\underset{2}{C}\equiv\underset{3}{CH} \longleftrightarrow \underset{1}{CH_2}=\underset{2}{C}=\dot{\underset{3}{C}}H \qquad [I]$$

rather than of the pure allenic type

$$CH_2=C=\dot{C}H. \qquad [II]$$

The structure of the radical is actually going to be different in the two cases because if [I] is correct, the two bonds have certainly different lengths, while if [II] is valid, the two bond distances must be approximately the same.

Though one might feel intuitively that resonance is making structure [I] more stable, it is of interest to show that structure [I] is indeed predicted by a very crude molecular orbital approach.

We shall assume that the simple LCAO, MO theory (2) is applicable, neglecting overlap and also π_x–π_y electron interaction. We shall consider equal all the coulomb integrals and take the exchange integrals as a decreasing function of the bond distance (in absolute value).

Indicating by a the C—C bond in [II] and by b and c those in [I], we have:

$$|\beta_b| < |\beta_a| \leqslant |\beta_c|.$$

The total π electron energy for [II] is simply:

$$E_{II} = 4\beta_a$$

while for [I] we have:‡

$$E_I = 2\beta_c + 2\beta_c \left|\sqrt{\left(1 + \frac{\beta_b^2}{\beta_c^2}\right)}\right| \approx 4\beta_c + \beta.$$

Structure [I] is lower in energy than [II] by an amount at least of the order of β, which corresponds to approximately 20–30 kcal/mole. It is then quite clear that the C_3H_3 radical formed from an excited allene molecule is best represented by formulation [I] and has two different bond lengths.

*Issued as N.R.C. No. 5139.
†*National Research Council Postdoctorate Fellow 1957–58. Present address: Instituto di Chimica Fisica, Università di Padova, Padova, Italy.*
‡*The β's are negative quantities. The coulomb integral is taken as zero of the energy scale.*

Can. J. Chem. Downloaded from www.nrcresearchpress.com by 196.1.178.254 on 09/04/12
For personal use only.

The experimentally found reactivity at carbon 1 follows in a straightforward way. Both the free valence index and the localization energy criteria, as used for radical addition to unsaturated molecules (3), agree with addition to carbon 1.

Indicating by k the ratio $\frac{\beta_c}{\beta_b} > 1$ we have the free valence indices:

$$f_1 = N_{max} - \frac{1}{\sqrt{(1+k^2)}}, \qquad f_3 = N_{max} - \frac{k}{\sqrt{(1+k^2)}}, \qquad \text{hence } f_1 > f_3$$

and the localization energies (in units of β):

$$E_1 = \sqrt{(1+k^2)} - k, \qquad E_3 = \sqrt{(1+k^2)} - 1, \qquad \text{hence } E_1 < E_3.$$

Of course, this simple theory does not exclude completely addition to carbon 3, the extent of the latter reaction depending mainly on the value to be attributed to k.

Addition to position "three" actually occurs in the case of the cyanoisopropyl radicals:

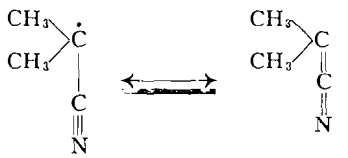

whose π electron system is similar to the one for C_3H_3 radical. They have been found to recombine mainly carbon to carbon but some of the products correspond also to recombination carbon to nitrogen, the ratio being approximately 2:1 (4). In this case, however, the different electronegativities of nitrogen and of the methyl-substituted carbon atom may also play an important role.

1. COLLIN, J. E. L. and LOSSING, F. P. Can. J. Chem. **35**, 778 (1957).
2. (*a*) HÜCKEL, E. Z. Physik, **70**, 204 (1931).
(*b*) COULSON, C. A. and LONGUET-HIGGINS, H. C. Proc. Roy. Soc. A, **191**, 39 (1947).
3. (*a*) COULSON, C. A. J. Chem. Soc. 1435 (1955).
(*b*) GIACOMETTI, G. Nuovo cimento, (10) **3**, 1488 (1956).
4. TALÂT-ERBEN, M. and BYWATER, S. J. Am. Chem. Soc. **77**, 3710 (1955).

RECEIVED NOVEMBER 7, 1958.
DIVISION OF PURE CHEMISTRY,
NATIONAL RESEARCH COUNCIL,
OTTAWA, CANADA.

THE HALF-LIFE OF Pb^{210} (RaD)

B. D. PATE,* D. C. SANTRY,† AND L. YAFFE

Pb^{210} (RaD), a member of the $4n+2$ series, emits soft β^- radiation (0.020 Mev) to form Bi^{210} (RaE), which has a half-life of 5.0 days and emits energetic β^- rays (1.15 Mev). The half-life of RaD has been measured many times. Values ranged from 16.5

**Present address: Department of Chemistry, Brookhaven National Laboratory, Upton, Long Island, N.Y.*
†*Present address: Department of Chemistry, Cambridge University, Cambridge, England.*

Can. J. Chem. Downloaded from www.nrcresearchpress.com by 196.1.178.254 on 09/04/12
For personal use only.

The experimentally found reactivity at carbon 1 follows in a straightforward way. Both the free valence index and the localization energy criteria, as used for radical addition to unsaturated molecules (3), agree with addition to carbon 1.

Indicating by k the ratio $\frac{\beta_c}{\beta_b} > 1$ we have the free valence indices:

$$f_1 = N_{max} - \frac{1}{\sqrt{(1+k^2)}}, \qquad f_3 = N_{max} - \frac{k}{\sqrt{(1+k^2)}}, \qquad \text{hence } f_1 > f_3$$

and the localization energies (in units of β):

$$E_1 = \sqrt{(1+k^2)} - k, \qquad E_3 = \sqrt{(1+k^2)} - 1, \qquad \text{hence } E_1 < E_3.$$

Of course, this simple theory does not exclude completely addition to carbon 3, the extent of the latter reaction depending mainly on the value to be attributed to k.

Addition to position "three" actually occurs in the case of the cyanoisopropyl radicals:

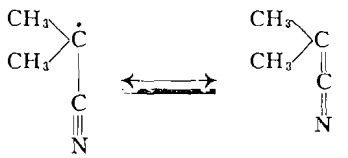

whose π electron system is similar to the one for C_3H_3 radical. They have been found to recombine mainly carbon to carbon but some of the products correspond also to recombination carbon to nitrogen, the ratio being approximately 2:1 (4). In this case, however, the different electronegativities of nitrogen and of the methyl-substituted carbon atom may also play an important role.

1. COLLIN, J. E. L. and LOSSING, F. P. Can. J. Chem. **35**, 778 (1957).
2. (*a*) HÜCKEL, E. Z. Physik, **70**, 204 (1931).
(*b*) COULSON, C. A. and LONGUET-HIGGINS, H. C. Proc. Roy. Soc. A, **191**, 39 (1947).
3. (*a*) COULSON, C. A. J. Chem. Soc. 1435 (1955).
(*b*) GIACOMETTI, G. Nuovo cimento, (10) **3**, 1488 (1956).
4. TALÂT-ERBEN, M. and BYWATER, S. J. Am. Chem. Soc. **77**, 3710 (1955).

RECEIVED NOVEMBER 7, 1958.
DIVISION OF PURE CHEMISTRY,
NATIONAL RESEARCH COUNCIL,
OTTAWA, CANADA.

THE HALF-LIFE OF Pb^{210} (RaD)

B. D. PATE,* D. C. SANTRY,† AND L. YAFFE

Pb^{210} (RaD), a member of the $4n+2$ series, emits soft β^- radiation (0.020 Mev) to form Bi^{210} (RaE), which has a half-life of 5.0 days and emits energetic β^- rays (1.15 Mev). The half-life of RaD has been measured many times. Values ranged from 16.5

**Present address: Department of Chemistry, Brookhaven National Laboratory, Upton, Long Island, N.Y.*
†*Present address: Department of Chemistry, Cambridge University, Cambridge, England.*

Can. J. Chem. Downloaded from www.nrcresearchpress.com by 196.1.178.254 on 09/04/12
For personal use only.

to 23 years and in 1931 the International Radium Standards Commission (1) adopted a value of 22 years.

Since the β^- rays from RaD are so soft, the measurements were not made directly on the RaD, but usually on the Bi^{210} (RaE) daughter in equilibrium with it or on the latter's Po^{210} (RaF) granddaughter, which emits α radiation. A very painstaking measurement of the last type was made by Joliot-Curie (2), who obtained a value of 23 years.

Wagner (3), using an ion chamber, obtained a value of 25 years from a measurement which was carried out for a period of 250 days. In 1955 Tobaillem (4), using a differential ionization chamber, compensated against radium, followed the decay of RaD source for 121 days, and obtained a half-life of 19.4±0.35 years. Merritt, Campion, and Hawkings (5), using a $4\pi\beta$ proportional counter, obtained a value of 22.4±0.4 years for measurements observed over a period of $5\frac{1}{2}$ years. Unfortunately this measurement is not quoted in either the title or the abstract of their paper, and this value became known to us after our series of measurements was completed.

We, in our laboratory, initially used RaD as a standard to monitor the performance of a $4\pi\beta$ proportional counter described previously (6). It soon became apparent that this instrument was sufficiently stable to be used to measure, with good accuracy, the half-lives of long-lived radionuclides.

The Pb^{210} source was chemically purified using standard methods and then sandwiched between aluminum sufficiently thick to absorb all the radiation emitted, other than the β radiation from Bi^{210}. Adequate sealing ensured the exclusion of moisture. This was further checked by intersource comparisons from time to time to ensure source constancy on a short-time basis. The aluminum was thick enough so that no change in geometrical shape could occur which would remove the source from the position of 100% efficiency in the counter (6).

The dead time of the counter was determined from time to time by the well-known 'paired-source' technique, and the correction due to this was of the order of 0.5%. The count rate was great enough so that background and statistical variations in counting rate could be adequately treated.

Activity measurements were carried on for a period of 5 years. Frequency of measurements varied from daily to weekly, so that a large amount of data was accumulated.

The data were analyzed by the method of least squares and yielded a half-life of 23.30 years. The results were broken down into a yearly basis to see whether any consistent variation was occurring which would attest to source impurity. The deviations were random and were of the order of 0.1 year. It is difficult to assess a systematic error to this series of measurements and a value five times this deviation has been used. This yields a value of 23.3±0.5 years in good agreement with Joliot-Curie (2) and Merritt *et al.* (5) but not with Tobaillem (4).

1. International Radium Standards Commission. Revs. Modern Phys. **3**, 427 (1931).
2. Joliot-Curie, I. J. phys. **10**, 388 (1929).
3. Wagner, F. U.S. Atomic Energy Comm. Rept. ANL **4490**, 5 (1950).
4. Tobaillem, J. J. phys. radium, **16**, 235 (1955).
5. Merritt, W. F., Campion, P. J., and Hawkings, R. C. Can. J. Phys. **35**, 16 (1957).
6. Pate, B. D. and Yaffe, L. Can. J. Chem. **33**, 610 (1955).

Received July 7, 1958.
Radiochemistry Laboratory,
Department of Chemistry,
McGill University,
Montreal, Quebec.

Can. J. Chem. Downloaded from www.nrcresearchpress.com by 196.1.178.254 on 09/04/12
For personal use only.

LOW TEMPERATURE IRRADIATION OF MIXTURES OF HBr AND C_2H_4

D. A. ARMSTRONG* AND J. W. T. SPINKS

A 90-c Co^{60} source was used to irradiate solid equimolar mixtures of HBr and C_2H_4 in a 0.5-cm diameter Pyrex cell at liquid nitrogen and liquid oxygen temperature. A few irradiations of liquid equimolar mixtures just above their freezing point (−165° C) (1) were also performed.

An addition reaction was observed at all three temperatures. The product was identified from its vapor pressure and refractive index to be virtually pure ethyl bromide. The addition was followed by evaporating the mixture at given time intervals and measuring its total pressure. For successive irradiations of the same sample, the pressure decreased until it had fallen to 50% of the initial value, i.e., until the addition was complete.

The pressure decrease (as a percentage of the initial pressure of the HBr–C_2H_4 mixture) versus time of irradiation curves for samples which were irradiated continuously are given in Fig. 1. From the dose rate, estimated by ferrous sulphate dosimetry,† an initial G value of about 10^5 was calculated for addition in the liquid samples. For the frozen samples the G values were lower and fell off rapidly with increasing time of irradiation, especially for those irradiated at liquid nitrogen temperature.

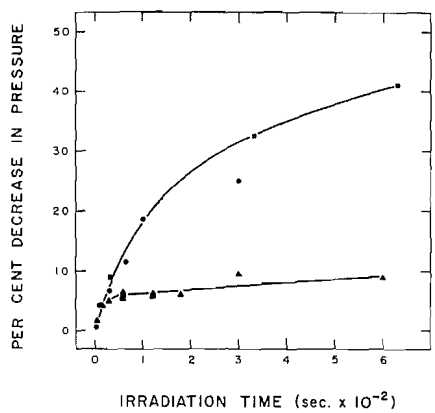

FIG. 1. Percentage decrease in pressure as a function of irradiation time; ■ liquid phase; ● solid phase at liquid oxygen temperature; ▲ solid phase at liquid nitrogen temperature. Dose rate, 450 r per minute.

Unirradiated samples of mixtures of ethylene and hydrogen bromide were stable (cf. (1)), and no addition was observed when an HBr–C_2H_4 mixture was condensed in an empty Pyrex cell which had been previously irradiated.

The high G values are indicative of a chain reaction and it would appear that the radiation produced reactive entities (possibly free radicals, cf. 2, 3, 4, 5) in the liquid and frozen mixtures which subsequently initiated the chain addition. It would seem that for frozen samples the chain reaction must have occurred during melting. In support of this, it was found that the reaction could be initiated in an unirradiated mixture by condensing it onto an irradiated mixture at liquid nitrogen temperature and then melting the combined samples, e.g., when equal amounts of unirradiated and irradiated mixtures

Holder of a Postdoctoral Fellowship.

†*We are indebted to Mr. A. L. Riegert for these measurements.*

Can. J. Chem. Downloaded from www.nrcresearchpress.com by 196.1.178.254 on 09/04/12
For personal use only.

were used, the amount of product formed in the combined sample, on melting, was 60% greater than that formed in the irradiated mixture alone.

We are grateful to the National Research Council and the Atomic Energy of Canada Limited for continued financial support.

1. MAASS, O. and WRIGHT, C. H. J. Am. Chem. Soc. **46**, 2664 (1924).
2. VAUGHAN, W. E., RUST, F. F., and EVANS, T. W. J. Org. Chem. **7**, 477, 491 (1942).
3. NORMAN, L. and PORTER, G. Proc. Roy. Soc. A, **230**, 399 (1955).
4. JONES, T. O., LUEBBE, R. H., WILSON, J. R., and WILLARD, J. E. J. Phys. Chem. **62**, 9 (1958).
5. WILLARD, J. Radiation Research (Abstr.), **9**, 146 (1958).

RECEIVED JANUARY 9, 1959.
CHEMISTRY DEPARTMENT,
UNIVERSITY OF SASKATCHEWAN,
SASKATOON, SASKATCHEWAN.

ELECTRON SPIN RESONANCE ABSORPTION OF BINAPHTHOQUINONES

YOSHIO MATSUNAGA*

Previously we examined the diamagnetic susceptibilities of a number of condensed polycyclic aromatic hydrocarbons and quinones and found that some of them have anomalously small values of susceptibility (1). It was pointed out that this anomaly is characteristic of perylene and its analogues. The localization of π-electrons due to the characteristic molecular structure† and the appearance of a paramagnetic state were suggested as the causes. Although the former suggestion seemed to be in accordance with the predicted tendency for diamagnetic anisotropy given by London's method‡ and no E.S.R. absorption was detected in perylene (2), the existence of unpaired electrons in violanthrone (3, 4) and mesonaphthodianthrene (5) was confirmed by the E.S.R. method. The above-mentioned paramagnetic quinone is dark violet and the hydrocarbon is bluish green; therefore it seemed interesting to know whether the deeply colored polycyclic compounds of a different type can be paramagnetic or not.

Three binaphthoquinones were examined by an E.S.R. spectrometer at a frequency of 9 k Mc/s. Dimethoxybinaphthoquinone (X=OCH_3) was prepared by the oxidation of 1,4-naphthohydroquinone monomethylether with ferricyanide ion as described by Russig (6) and recrystallized from toluene. The sample shows E.S.R. absorption with a line width of 5.6 gauss at a half power. The g-value, estimated by comparison with DPPH, is 2.0036 ± 0.0003. There is one unpaired electron for about 400 molecules of quinone. If this compound is analogous to Chichibabin's hydrocarbon type of carbon biradical, as suggested by Leffler (7), the molecule should be more paramagnetic in the dissolved state. However we could not find E.S.R. absorption from a benzene solution of this compound. The appearance of paramagnetism seems to be limited to the solid state. Unlike Chichibabin's hydrocarbon and Bourdon and Calvin's hindered biphenoquinone (8), the present compound is stable towards oxygen in the solid and in the dissolved states. Binaphthoquinone may belong to the same group of paramagnetic organic compounds as violanthrone (3, 4), mesonaphthodianthrene (5), and metal-free phthalocyanine (9, 10).

*N.R.C. Postdoctoral Fellow, 1957–.

†*In the sense of VB theory the central two or more single bonds can be double only in the excited states.*

‡*Among the compounds of this type, only the anisotropy of perylene was examined by London's method. The predicted value is 1.88 times that of naphthalene. The value given in ref. 1 is in arithmetical error.*

Can. J. Chem. Downloaded from www.nrcresearchpress.com by 196.1.178.254 on 09/04/12
For personal use only.

were used, the amount of product formed in the combined sample, on melting, was 60% greater than that formed in the irradiated mixture alone.

We are grateful to the National Research Council and the Atomic Energy of Canada Limited for continued financial support.

1. MAASS, O. and WRIGHT, C. H. J. Am. Chem. Soc. **46**, 2664 (1924).
2. VAUGHAN, W. E., RUST, F. F., and EVANS, T. W. J. Org. Chem. **7**, 477, 491 (1942).
3. NORMAN, L. and PORTER, G. Proc. Roy. Soc. A, **230**, 399 (1955).
4. JONES, T. O., LUEBBE, R. H., WILSON, J. R., and WILLARD, J. E. J. Phys. Chem. **62**, 9 (1958).
5. WILLARD, J. Radiation Research (Abstr.), **9**, 146 (1958).

RECEIVED JANUARY 9, 1959.
CHEMISTRY DEPARTMENT,
UNIVERSITY OF SASKATCHEWAN,
SASKATOON, SASKATCHEWAN.

ELECTRON SPIN RESONANCE ABSORPTION OF BINAPHTHOQUINONES

YOSHIO MATSUNAGA*

Previously we examined the diamagnetic susceptibilities of a number of condensed polycyclic aromatic hydrocarbons and quinones and found that some of them have anomalously small values of susceptibility (1). It was pointed out that this anomaly is characteristic of perylene and its analogues. The localization of π-electrons due to the characteristic molecular structure† and the appearance of a paramagnetic state were suggested as the causes. Although the former suggestion seemed to be in accordance with the predicted tendency for diamagnetic anisotropy given by London's method‡ and no E.S.R. absorption was detected in perylene (2), the existence of unpaired electrons in violanthrone (3, 4) and mesonaphthodianthrene (5) was confirmed by the E.S.R. method. The above-mentioned paramagnetic quinone is dark violet and the hydrocarbon is bluish green; therefore it seemed interesting to know whether the deeply colored polycyclic compounds of a different type can be paramagnetic or not.

Three binaphthoquinones were examined by an E.S.R. spectrometer at a frequency of 9 k Mc/s. Dimethoxybinaphthoquinone (X=OCH_3) was prepared by the oxidation of 1,4-naphthohydroquinone monomethylether with ferricyanide ion as described by Russig (6) and recrystallized from toluene. The sample shows E.S.R. absorption with a line width of 5.6 gauss at a half power. The g-value, estimated by comparison with DPPH, is 2.0036 ± 0.0003. There is one unpaired electron for about 400 molecules of quinone. If this compound is analogous to Chichibabin's hydrocarbon type of carbon biradical, as suggested by Leffler (7), the molecule should be more paramagnetic in the dissolved state. However we could not find E.S.R. absorption from a benzene solution of this compound. The appearance of paramagnetism seems to be limited to the solid state. Unlike Chichibabin's hydrocarbon and Bourdon and Calvin's hindered biphenoquinone (8), the present compound is stable towards oxygen in the solid and in the dissolved states. Binaphthoquinone may belong to the same group of paramagnetic organic compounds as violanthrone (3, 4), mesonaphthodianthrene (5), and metal-free phthalocyanine (9, 10).

*N.R.C. Postdoctoral Fellow, 1957–.

†*In the sense of VB theory the central two or more single bonds can be double only in the excited states.*

‡*Among the compounds of this type, only the anisotropy of perylene was examined by London's method. The predicted value is 1.88 times that of naphthalene. The value given in ref. 1 is in arithmetical error.*

Can. J. Chem. Downloaded from www.nrcresearchpress.com by 196.1.178.254 on 09/04/12
For personal use only.

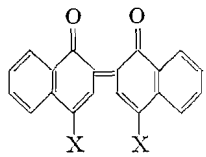

Winslow *et al.* (10) suggested that enough thermal energy can be absorbed at room temperature to produce unpaired electrons in crystals of highly conjugated molecules. However, Akamatu *et al.* (4) found that the spin concentration in violanthrone does not decrease by cooling to liquid nitrogen temperature and considered that the molecules with unpaired electrons are not in excited states. It is well known that polycyclic aromatic compounds are semiconductive and the positive charge carriers in these compounds have high mobility. Therefore, the appearance of unpaired electrons in these cases may have some correlation with the presence of a strong intermolecular charge-transfer force* (11), and unpaired electrons may be trapped at some kind of imperfection in the crystal lattice.

Dichloro- and dibromo-binaphthoquinones (12) were also examined and both of them were found to be paramagnetic to about the same extent as the dimethoxy-derivative. These two compounds are too unstable to be recrystallized, therefore we cannot exclude the possibility that E.S.R. absorption is due to paramagnetic impurities. However, it is very likely that these two quinones have similar magnetic behavior to the well-defined dimethoxy-derivative.

I wish to thank Professor C. A. McDowell for his interest in this work. This research was supported by grants from the National Research Council of Canada.

1. AKAMATU, H. and MATSUNAGA, Y. Bull. Chem. Soc. Japan, **26**, 364 (1953).
2. YOKOZAWA, Y. and MIYASHITA, I. J. Chem. Phys. **25**, 796 (1956).
3. YOKOZAWA, Y. and TATSUZAKI, I. J. Chem. Phys. **22**, 2087 (1954).
4. AKAMATU, H., MROZOWSKI, S., and WOBSCHALL, D. Paper presented at Carbon Conference, Buffalo, N.Y. 1957.
5. MATSUNAGA, Y. Unpublished.
6. RUSSIG, F. J. prakt. Chem. (2) **62**, 30 (1900). GOLDSCHMIDT, S. and WESSBECHER, H. Ber. **61**, 372 (1928).
7. LEFFLER, J. E. The reactive intermediates of organic chemistry. Interscience Publishers, Inc., New York. 1956. p. 54.
8. BOURDON, J. and CALVIN, M. J. Org. Chem. **22**, 101 (1957).
9. INGRAM, D. J. E. and BENNETT, J. E. J. Chem. Phys. **22**, 1136 (1954).
10. WINSLOW, F. H., BAKER, W. O., and YAGER, W. A. J. Am. Chem. Soc. **77**, 4751 (1955).
11. AKAMATU, H., INOKUCHI, H., and MATSUNAGA, Y. Bull. Chem. Soc. Japan, **29**, 213 (1956). MATSUNAGA, Y. Bull. Chem. Soc. Japan, **28**, 475 (1955); J. Chem. Phys. To be published.
12. WILLSTÄTTER, R. and SCHULER, L. Ber. **61**, 362 (1928).

RECEIVED FEBRUARY 2, 1959.
DEPARTMENT OF CHEMISTRY,
UNIVERSITY OF BRITISH COLUMBIA,
VANCOUVER 8, B.C.

**Aromatic hydrocarbon – iodine, typical charge-transfer complex, was found to be highly conductive and rather strongly paramagnetic.*

SUBSTITUTION AND ELIMINATION REACTIONS DURING ACETOLYSIS OF DERIVATIVES OF 3β,6β-DIHYDROXYALLOCHOLANIC ACID

P. ZIEGLER

Tosylation of the 3β,6β-dihydroxy grouping in allosteroids has been reported (1, 2) to yield the corresponding 3β-monotosylates. Replacement of this tosyloxy function by

Can. J. Chem. Downloaded from www.nrcresearchpress.com by 196.1.178.254 on 09/04/12
For personal use only.

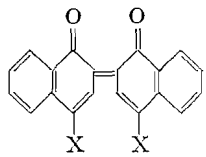

Winslow *et al.* (10) suggested that enough thermal energy can be absorbed at room temperature to produce unpaired electrons in crystals of highly conjugated molecules. However, Akamatu *et al.* (4) found that the spin concentration in violanthrone does not decrease by cooling to liquid nitrogen temperature and considered that the molecules with unpaired electrons are not in excited states. It is well known that polycyclic aromatic compounds are semiconductive and the positive charge carriers in these compounds have high mobility. Therefore, the appearance of unpaired electrons in these cases may have some correlation with the presence of a strong intermolecular charge-transfer force* (11), and unpaired electrons may be trapped at some kind of imperfection in the crystal lattice.

Dichloro- and dibromo-binaphthoquinones (12) were also examined and both of them were found to be paramagnetic to about the same extent as the dimethoxy-derivative. These two compounds are too unstable to be recrystallized, therefore we cannot exclude the possibility that E.S.R. absorption is due to paramagnetic impurities. However, it is very likely that these two quinones have similar magnetic behavior to the well-defined dimethoxy-derivative.

I wish to thank Professor C. A. McDowell for his interest in this work. This research was supported by grants from the National Research Council of Canada.

1. AKAMATU, H. and MATSUNAGA, Y. Bull. Chem. Soc. Japan, **26**, 364 (1953).
2. YOKOZAWA, Y. and MIYASHITA, I. J. Chem. Phys. **25**, 796 (1956).
3. YOKOZAWA, Y. and TATSUZAKI, I. J. Chem. Phys. **22**, 2087 (1954).
4. AKAMATU, H., MROZOWSKI, S., and WOBSCHALL, D. Paper presented at Carbon Conference, Buffalo, N.Y. 1957.
5. MATSUNAGA, Y. Unpublished.
6. RUSSIG, F. J. prakt. Chem. (2) **62**, 30 (1900). GOLDSCHMIDT, S. and WESSBECHER, H. Ber. **61**, 372 (1928).
7. LEFFLER, J. E. The reactive intermediates of organic chemistry. Interscience Publishers, Inc., New York. 1956. p. 54.
8. BOURDON, J. and CALVIN, M. J. Org. Chem. **22**, 101 (1957).
9. INGRAM, D. J. E. and BENNETT, J. E. J. Chem. Phys. **22**, 1136 (1954).
10. WINSLOW, F. H., BAKER, W. O., and YAGER, W. A. J. Am. Chem. Soc. **77**, 4751 (1955).
11. AKAMATU, H., INOKUCHI, H., and MATSUNAGA, Y. Bull. Chem. Soc. Japan, **29**, 213 (1956). MATSUNAGA, Y. Bull. Chem. Soc. Japan, **28**, 475 (1955); J. Chem. Phys. To be published.
12. WILLSTÄTTER, R. and SCHULER, L. Ber. **61**, 362 (1928).

RECEIVED FEBRUARY 2, 1959.
DEPARTMENT OF CHEMISTRY,
UNIVERSITY OF BRITISH COLUMBIA,
VANCOUVER 8, B.C.

**Aromatic hydrocarbon – iodine, typical charge-transfer complex, was found to be highly conductive and rather strongly paramagnetic.*

SUBSTITUTION AND ELIMINATION REACTIONS DURING ACETOLYSIS OF DERIVATIVES OF 3β,6β-DIHYDROXYALLOCHOLANIC ACID

P. ZIEGLER

Tosylation of the 3β,6β-dihydroxy grouping in allosteroids has been reported (1, 2) to yield the corresponding 3β-monotosylates. Replacement of this tosyloxy function by

Can. J. Chem. Downloaded from www.nrcresearchpress.com by 196.1.178.254 on 09/04/12
For personal use only.

means of a variety of nucleophylic reagents such as ammonia and amines (3), thiophenoxide ion (4), and diethyl malonate ion (2) invariably is accompanied by inversion of configuration at C-3. When 3β,6β-dihydroxyallosteroids were treated (1, 5) with mesyl chloride, the corresponding dimesylates were obtained; acetolysis of the latter compounds with acetate ion in acetic acid proceeded with retention of configuration at C-3, giving rise to 3β-acetoxy-Δ^5-steroids. These results can readily be understood by postulating that the 3β-monotosylates undergo a bimolecular substitution reaction which is accompanied by inversion at C-3. On the other hand, with a 3β,6β-dimesylate, dehydromesylation is the initial event leading to the intermediary 3β-mesyloxy-Δ^5-steroid; this unsaturated derivative, under the influence of the π-electrons, is believed (6) to undergo unimolecular heterolysis to provide the stabilized 3β-cation. The latter finally reacts with the weakly nucleophylic acetate ion to yield, with retention of configuration, the 3β-acetoxy-Δ^5-steroid.

The present study describes an analogous case involving methyl 3β,6β-dihydroxyallocholanate (I*a*). Mesylation of I*a* provided the dimesylate I*c*, which, with potassium acetate in aqueous dimethylformamide and subsequent saponification, was converted to 3β-hydroxy-Δ^5-cholenic acid (II). For further characterization, compound II was transformed to the methyl ester. Tosylation of I*a* provided the monotosylate I*b* as well as smaller amounts of the corresponding 3β,6β-ditosylate; acetolysis of I*b* under the same conditions as were used with I*c* and subsequent saponification of the products afforded 3α,6β-dihydroxyallocholanic acid (III). This acid, derived from 3α-hydroxy-6-oxo-allocholanic acid or its acetate methyl ester by catalytic hydrogenation, was previously reported (7, 8, 9) to have melting points in the range 246–251°. Our product, m.p. 248–252°, did not give a depression on mixed melting point with an authentic specimen of III;* elemental analyses of III, even when the sample was dried at 200° in a high vacuum, indicated that the compound retained half a mole of water.* Chromic acid oxidation of this acid provided 3,6-dioxo-allocholanic acid, identified by mixed melting point and conversion to the corresponding methyl ester.

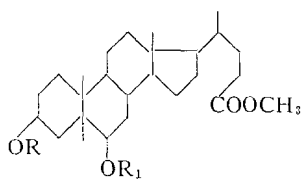

I

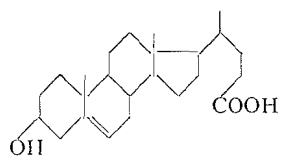

II

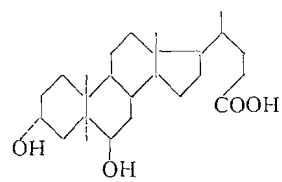

III

a, R = R₁ = H

b, R = H₃C—⟨⟩—SO₂—, R₁ = H

c, R = R₁ = H₃C—SO₂—

EXPERIMENTAL

Methyl 3β,6β-Dimesyloxyallocholanate (I*c*)

Compound I*a* (3 g) dissolved in pyridine (20 ml) was treated at 3° with methanesulphonyl chloride (3.4 g). The mixture was kept at that temperature for 20 hours, the excess reagent was decomposed by addition of a small amount of ice, and the solution was then poured into ice-cold dilute hydrochloric acid. The resulting precipitate was

**Kindly supplied by Dr. A. Schubert of VEB Jenapharm, Jena, East Germany, who also informed us that elemental analyses of his acid III indicated the retention of half a mole of water.*

Can. J. Chem. Downloaded from www.nrcresearchpress.com by 196.1.178.254 on 09/04/12
For personal use only.

filtered off, washed with water, dried, and finally recrystallized from ethyl acetate – ether to afford 3.05 g of I*c*, m.p. 125° (decomp.). Two further recrystallizations from the same solvent system gave the analytical specimen, m.p. 125–127° (decomp.). Anal. Calc. for $C_{27}H_{46}O_8S_2$: C, 57.62; H, 8.24; S, 11.39; OCH_3, 5.51. Found: C, 57.54, 57.57; H, 8.32, 8.26; S, 11.50; OCH_3, 5.69, 5.77.

3β-Hydroxy-Δ⁵-cholenic Acid (II)

A solution of I*c* (3 g) and potassium acetate (7.3 g) in water (4 ml) and dimethylformamide (40 ml) was kept at 120–125° for 5 hours. The mixture was then poured into dilute hydrochloric acid, the resulting precipitate was filtered off, and washed with water. Saponification of the wet solid by refluxing with 4% methanolic potassium hydroxide (40 ml) for 2 hours, followed by addition of dilute mineral acid, provided a solid which was separated by filtration. Crystallization from ethyl acetate afforded 680 mg of substance, m.p. 226–228°, giving an insoluble digitonide and a yellow color with tetranitromethane. Two more recrystallizations from the same solvent gave m.p. 231–233°. Methylation of II with diazomethane and crystallization of the product from hexane gave the methyl ester of II, m.p. 142–143° and $[\alpha]_D^{24}$ −36.2° (*c*, 1.02, dioxane).

Tosylation of Methyl 3β,6β-Dihydroxyallocholanate (I*a*)

To I*a* (2.15 g) dissolved in pyridine (10 ml) was added tosyl chloride (3 g). After 22 hours at 25°, the excess reagent was decomposed by a small amount of ice, the mixture was poured into dilute hydrochloric acid, and the products were extracted with ether–chloroform. The solvent extract was washed with water, dried over sodium sulphate, and evaporated. Crystallization of the residue (3.04 g) from ether (20 ml) yielded 690 mg of material, m.p. 135–140° (decomp.); this was recrystallized from ethyl acetate – ether to give the analytical sample of methyl 3β,6β-ditosyloxyallocholanate, m.p. 133–136° (decomp.). Anal. Calc. for $C_{39}H_{54}O_8S_2$: C, 65.51; H, 7.61; S, 8.97; OCH_3, 4.34. Found: C, 65.45, 65.64; H, 7.60, 7.47; S, 9.11; OCH_3, 4.62, 4.60.

The filtrate from the first crop of ditosylate yielded, on refrigeration, 1.85 g of material, m.p. 140–148°. Three recrystallizations from ethyl acetate – hexane gave pure I*b*, m.p. 150–152° (decomp.) and $[\alpha]_D^{24}$ −13.6° (*c*, 1.75, dioxane). Anal. Calc. for $C_{32}H_{48}O_6S$: C, 68.53; H, 8.63; S, 5.72; OCH_3, 5.53. Found: C, 68.66, 68.70; H, 8.57, 8.65; S, 6.02; OCH_3, 5.75, 5.80.

3α,6β-Dihydroxyallocholanic Acid (III)

Potassium acetate (2.6 g), water (1.3 ml), and dimethylformamide (14 ml) were heated to 110°. After addition of I*b* (1.12 g), the solution was kept at that temperature for 4 hours, whereupon the reaction products were treated with dilute mineral acid and extracted with ether. The residue, obtained from the solvent extract after washing, drying, and evaporating, was refluxed for 2 hours with 4% methanolic potassium hydroxide (50 ml). The saponified mixture was then poured into dilute hydrochloric acid, the precipitate was filtered off, washed with water, and dried. Crystallization of the solid from ethyl acetate afforded 596 mg of material, m.p. 243–245°. Successive recrystallization from methanol, acetone, and ethyl acetate yielded the analytical specimen of III, m.p. 248–252° and $[\alpha]_D^{23}$ +10.7° (*c*, 0.991, dioxane). This compound failed to give an insoluble digitonide and did not react with tetranitromethane. Anal. Calc. for $C_{24}H_{40}O_4 . \frac{1}{2}H_2O$: C, 71.78; H, 10.29. Found: C, 71.86, 72.06, 71.70, 71.74; H, 10.30, 10.17, 10.05, 10.38. These analytical data remained unchanged after a sample had been boiled with sodium hydroxide solution and, after neutralization, had been dried at

Can. J. Chem. Downloaded from www.nrcresearchpress.com by 196.1.178.254 on 09/04/12
For personal use only.

200° in a high vacuum. The methyl ester of III could not be obtained in crystalline form.

Oxidation of III (235 mg) in acetic acid (5 ml) with a solution of chromic acid (150 mg) in water (0.12 ml) and acetic acid (2.5 ml) was carried out at 10° for 1.5 hours. The mixture was then diluted by gradual addition of ice water, whereupon a granular precipitate appeared; this was filtered off, washed with water, dried, and then crystallized twice from ethanol to yield 178 mg of 3,6-dioxo-allocholanic acid, m.p. 206–208°. Methylation of this compound with diazomethane and crystallization of the ester from methanol showed m.p. 149–151.5°. Mixed melting points, both of the acid and the ester, with authentic specimens showed no depressions.

1. Reich, H. and Lardon, A. Helv. Chim. Acta, **29**, 671 (1946).
2. Shoppee, C. W. and Stephenson, R. J. J. Chem. Soc. 2230 (1954).
3. Pierce, J. H., Richards, H. C., Shoppee, C. W., Stephenson, R. J., and Summers, G. H. R. J. Chem. Soc. 694 (1955).
4. Shoppee, C. W., Richards, H. C., and Summers, G. H. R. J. Chem. Soc. 4817 (1956).
5. Reichstein, T. U.S. Patent No. 2,520,656 (1950).
6. Davies, R. H., Meecham, S., and Shoppee, C. W. J. Chem. Soc. 679 (1955).
7. Sugiyama, G. J. Biochem. (Japan), **25**, 157 (1937).
8. Justoni, R. and Pessina, R. Il Farmaco, **11**, 72 (1956).
9. Schubert, A. and Damker, Chr. J. prakt. Chem. **4**, 260 (1957).

Received December 12, 1958.
Research and Development Laboratories,
Canada Packers Ltd.,
Toronto, Ontario.

Can. J. Chem. Downloaded from www.nrcresearchpress.com by 196.1.178.254 on 09/04/12
For personal use only.

Can. J. Chem. Downloaded from www.nrcresearchpress.com by 196.1.178.254 on 09/04/12
For personal use only.

Canadian Journal of Chemistry

Issued by THE NATIONAL RESEARCH COUNCIL OF CANADA

VOLUME 37 JUNE 1959 NUMBER 6

STERIC INHIBITION OF RESONANCE

IV. FURTHER SPECTROSCOPIC STUDIES OF 9-NITROANTHRACENE AND 9,10-DINITROANTHRACENE[1]

JAMES TROTTER[2]

ABSTRACT

The frequencies of the NO_2 symmetrical stretching vibrations, and the ultraviolet absorption spectra, of solutions of 9-nitroanthracene and 9,10-dinitroanthracene have been measured and correlated with the deviations from coplanarity and resultant resonance inhibition.

INTRODUCTION

Detailed X-ray analyses of the crystal and molecular structures of 9-nitroanthracene and 9,10-dinitroanthracene have shown that the nitro groups are twisted* out of the planes of the aromatic rings due to the steric effects of neighboring carbon and hydrogen atoms (1, 2, 3). The variations of the characteristic vibration frequencies of the nitro group indicate resultant decreases in the resonance interactions between the groups and the aromatic π-electrons (4), and further detailed examination of the bond lengths in these molecules suggests that this resonance is almost completely inhibited in 9-nitroanthracene in the solid state, where the nitro group is rotated about the C–N bond 85° from the coplanar position, but that in crystals of the 9,10-dinitro derivative, where the twists are 64°, there is a small but measurable resonance interaction (5).

Calculations by molecular orbital methods (6) have shown that the energy of resonance interaction (E_R) between the nitro group and the aromatic rings in this type of molecule varies as $\cos^2\theta$, where θ is the angle between the planes of the rings and the nitro group. The most stable state of the molecules is determined not only by this resonance energy, but also by the van der Waals attractive and electronic repulsive forces (energy E_v) between the oxygen atoms and neighboring carbon and hydrogen atoms. There is a minimum in the E_v curve at about $\theta = 70°$, the angle corresponding to oxygen–carbon and oxygen–hydrogen separations equal to the sums of the corresponding van der Waals radii (1.7 Å for carbon, 1.4 Å for oxygen, 1.0–1.2 Å for hydrogen). Combination of resonance and van der Waals energies gives a curve with a minimum at about $\theta = 65°$, and the measured deviation from coplanarity in crystals of 9,10-dinitroanthracene (64°) is in excellent agreement with this calculated value. The most stable configuration for an isolated molecule of 9-nitroanthracene should have the nitro group twisted 64° out

[1]*Manuscript received February 3, 1959.*
Contribution from the Division of Pure Physics, National Research Council, Ottawa, Canada.
Issued as N.R.C. No. 5150.
[2]*National Research Council Postdoctorate Fellow.*
**The deviation from coplanarity has been called "twist", rather than "tilt" as in previous communications, since a referee has pointed out that "tilt" tends to suggest a deviation which involves an inclination of the* C–NO_2 *axis from the plane of the aromatic ring system, while the displacement in the molecules studied involves of course a torsional motion of the nitro group about the* C–NO_2 *axis.*

of the anthracene plane, but in the solid state crystal forces apparently result in minimum energy when $\theta = 85°$.

In solution the nitro group twists should be the same in both molecules, 64°, but probably with some oscillation of the groups through $\theta = 90°$, since the potential barrier is only about $1\frac{1}{2}$ kcal/mole (for each nitro group). The angles measured by X-ray diffraction of the crystals have been correlated very nicely with the frequencies of the NO_2 symmetrical stretching vibrations in the solid state, and these frequencies have now been measured in solution to investigate the postulation of equal twists in both molecules. The ultraviolet spectra have also been measured for correlation with the resonance inhibition.

EXPERIMENTAL

The frequencies of the NO_2 symmetrical stretching vibrations of 9-nitroanthracene and 9,10-dinitroanthracene in carbon tetrachloride solution were measured with a Perkin–Elmer model 21 infrared spectrophotometer with a rock salt prism.

The ultraviolet spectrum of 9-nitroanthracene in ethanol solution was measured with a Beckmann D.U. spectrophotometer. Since 9,10-dinitroanthracene is only very sparingly soluble in ethanol, a chloroform–ethanol mixture was used as solvent in measuring its spectrum.

DISCUSSION

The frequencies of the NO_2 symmetrical stretching vibrations in crystals of 9-nitroanthracene and 9,10-dinitroanthracene are 1374 cm^{-1} and 1367 cm^{-1} respectively (4), corresponding to nitro group twists of 85° and 64° (Table I). The corresponding frequencies in carbon tetrachloride solution are 1372 cm^{-1} for both molecules, so that the

TABLE I

NO_2 symmetrical stretching frequencies and nitro group twists

		9-Nitroanthracene	9,10-Dinitroanthracene
Crystals	NO_2 frequency	1374 cm^{-1}	1367 cm^{-1}
	Measured twist	85°	64°
Solutions	NO_2 frequency	1372 cm^{-1}	1372 cm^{-1}
	Deduced twist	64° → 90°	64° → 90°

twists are the same in both molecules in solution. The frequencies in solution cannot however be compared quantitatively with those in the solid state due to the effect of crystal forces, which generally make vibration frequencies a few wave numbers lower than the corresponding frequencies in solution. All that can be deduced is that the twists in both molecules in solution are between 64° and 90°, the value in the most stable configuration possibly depending not only on resonance and van der Waals energies (which would suggest $\theta = 64°$) but also on the effects of solvent–solute interactions.

The positions and intensities of the ultraviolet absorption bands of anthracene (7), 9-nitroanthracene, and 9,10-dinitroanthracene in ethanol solution are listed in Table II. In Table III the frequency shifts of the anthracene absorption maxima resulting from substitution are compared for the 9-cyano- (7), 9-nitro-, and 9,10-dinitro-derivatives. In 9-cyanoanthracene there is no possibility of resonance inhibition due to steric effects, and the cyano group causes a considerable displacement to longer wavelengths of the

Can. J. Chem. Downloaded from www.nrcresearchpress.com by 196.1.178.254 on 09/04/12
For personal use only.

TABLE II

Ultraviolet absorption spectra (wavelengths in mμ)

Anthracene		9-Nitroanthracene		9,10-Dinitroanthracene	
λ_{max}	log ϵ	λ_{max}	log ϵ	λ_{max}	log ϵ
324	3.43	331	3.42	335	3.34
339	3.72	347	3.61	352	3.50
356	3.90	363	3.66	367	3.62
375	3.88	382	3.58	387	3.58

TABLE III

Frequency shifts of anthracene absorption maxima

	Maximum	Frequency, cm^{-1}	Shift from anthracene, cm^{-1}
9-Cyanoanthracene	*E*	28,900	1990
	F	27,510	1960
	G	26,180	1880
	H	24,180	1830
9-Nitroanthracene	*E*	30,210	680
	F	28,820	650
	G	27,550	510
	H	26,180	460
9,10-Dinitroanthracene	*E*	29,850	1040
	F	28,410	1060
	G	27,250	810
	H	25,840	800

E-, *F*-, *G*-, *H*-bands. The corresponding shifts in the 9-nitro derivative are only[1] of about one quarter the magnitude, and those in the 9,10-dinitro about half, of the shifts in the cyano derivative. Although the cyano and nitro derivatives cannot be directly compared, these figures suggest that resonance interaction between a nitro group and the anthracene rings in 9-nitroanthracene and 9,10-dinitroanthracene is about one quarter of the interaction which would be expected in completely planar models. The resonance interaction estimated from the $\cos^2\theta$ relationship is about one fifth ($\cos^2 64°$) that in completely planar molecules, in reasonable agreement with the value deduced from the ultraviolet spectra. The intensities of the bands in the nitro derivatives are significantly lower than in anthracene, again supporting resonance inhibition.

REFERENCES

1. TROTTER, J. Acta Cryst. **11**, 564 (1958).
2. TROTTER, J. Acta Cryst. **12**, 232 (1959).
3. TROTTER, J. Acta Cryst. **12**, 237 (1959).
4. TROTTER, J. Can. J. Chem. **37**, 351 (1959).
5. TROTTER, J. Can. J. Chem. **37**, 825 (1959).
6. TROTTER, J. Can. J. Chem. **37**, 905 (1959).
7. JONES, R. N. Chem. Revs. **41**, 353 (1947).

Can. J. Chem. Downloaded from www.nrcresearchpress.com by 196.1.178.254 on 09/04/12
For personal use only.

Can. J. Chem. Downloaded from www.nrcresearchpress.com by 196.1.178.254 on 09/04/12
For personal use only.

A MANNAN PRODUCED BY BACILLUS POLYMYXA[1]

D. H. BALL[2] AND G. A. ADAMS

ABSTRACT

During the fermentation of glucose, sucrose, or lactose by *Bacillus polymyxa*, a mixture of polysaccharides is formed, one of which has been isolated by mild procedures and shown to contain mannose as the only sugar together with approximately 13% protein. Acid hydrolysis of the methylated mannan gave 2,3,4,6-tetra-*O*-methyl-D-mannose, 2,4,6-tri-*O*-methyl-D-mannose, 3,4,6-tri-*O*-methyl-D-mannose, and 3,4-di-*O*-methyl-D-mannose in the approximate ratio 2:1:1:2. Periodate oxidation results are in agreement with the methylation data and indicate a molecular weight of approximately 3000.

Bacillus polymyxa C3-2* has been studied previously in connection with its ability to ferment carbohydrates to butane-2,3-diol and this organism is of especial interest because it can utilize starch directly (1). The "polymyxins", a series of closely related antibiotics with polypeptide structures, are also produced by various strains of *B. polymyxa* (2). Polysaccharides are formed by these organisms under certain growth conditions and Misaki and co-workers have made a detailed study of the production of polysaccharides by *B. polymyxa* var. *lactoviscosus* (3). This strain, grown on lactose, produced a polysaccharide containing L-rhamnose and D-galactose in the approximate ratio of 2:1. When *B. polymyxa* C3-2 is grown with sucrose as the carbon source, a fructan is formed, presumably by a transfructosidation because this polysaccharide does not occur if glucose or lactose is used. The structure of the fructan was established by Murphy (4) and a preliminary communication reported the isolation of a mannan (5) produced by the same organism. The present paper describes the isolation of this mannan by a mild procedure and investigation of its structure.

B. polymyxa C3-2 was grown on a buffered yeast extract – salts medium with glucose, sucrose, or lactose as the carbon source. A mannan was isolated by the following procedure which was considered unlikely to cause depolymerization or to affect the reducing end group. A mannose-containing polysaccharide fraction was obtained from the cell-free medium by precipitation with ethanol and this material was dissolved in water to give a highly viscous solution. Addition of aqueous Cetavlon (cetyltrimethylammonium bromide) (6, 7) to this solution precipitated the cetyltrimethylammonium salt of an acidic polysaccharide and greatly decreased the viscosity of the residual solution. Addition of sodium borate solution to the latter gave an insoluble cetyltrimethylammonium salt of a polysaccharide–borate complex (8, 9). This precipitate was dissolved in cold 0.1 *N* hydrochloric acid and the free polysaccharide was precipitated by ethanol. It was then redissolved in water and the solution was deionized on columns of ion-exchange resins and lyophilized. This material was very hygroscopic, had $[\alpha]_D$ +82°, and migrated as a single sharp peak on electrophoresis in borate buffer. Mannose was the only sugar present in an acid hydrolyzate. Several amino acids were observed chromatographically after hydrolysis with 6 *N* hydrochloric acid, and nitrogen analysis and a mannose estimation indicated that the preparation contained approximately 13% protein. Methylation of the mannan with methyl sulphate and sodium hydroxide and with silver oxide and methyl iodide in dimethylformamide (10) gave a product which could not be fractionated with

[1]*Manuscript received January 19, 1959.*
Contribution from the Division of Applied Biology, National Research Council, Ottawa, Canada.
Issued as N.R.C. No. 5159.
[2]*National Research Council of Canada Postdoctorate Fellow 1956–1958.*
**From the culture collection of the Division of Applied Biology, National Research Council of Canada, Ottawa.*

Can. J. Chem. Downloaded from www.nrcresearchpress.com by 196.1.178.254 on 09/04/12
For personal use only.

chloroform – light petroleum. The methylated mannan, which showed no hydroxyl absorption in the infrared, was hydrolyzed with formic acid and the neutralized hydrolyzate was fractionated on thick filter paper into di-, tri-, and tetra-*O*-methyl-D-mannose fractions which were present in approximately equal proportions. The syrupy tetra-*O*-methyl-D-mannose was oxidized with bromine water and converted to the crystalline phenylhydrazide of 2,3,4,6-tetra-*O*-methyl-D-mannonic acid. The trimethyl fraction was separated by filter paper electrophoresis into crystalline 3,4,6-tri-*O*-methyl-D-mannose and crystalline 2,4,6-tri-*O*-methyl-D-mannose, present in approximately equal proportions. The dimethyl fraction crystallized and was identified as 3,4-di-*O*-methyl-D-mannose.

On periodate oxidation, the mannan consumed 1.31 mole periodate and liberated 0.46 mole acid per anhydro hexose unit (assuming the presence of 13% protein not attacked by periodate). The oxidized polysaccharide was reduced with potassium borohydride and hydrolyzed. Mannose and glycerol, but not erythritol, were detected in the hydrolyzate indicating the absence in the original polysaccharide of mannose units linked through positions 1 and 4 only (11). The formaldehyde liberated during periodate oxidation at pH 8 was measured by the chromotropic acid method (12) and the results are shown in Fig. 1. The occurrence of overoxidation indicated that the predominant linkage was not 1,6 (13). After reduction of the polysaccharide with potassium borohydride, overoxidation was not observed (Fig. 2), indicating that the reducing end group was linked through position 2 (14). Calculation of the molecular weight from these results (14, 15) gave a value of 2850 and, allowing for 13% protein, this gives an average of 15 mannose units per molecule. The value of 2850 would be minimal because some terminal $1 \rightarrow 2$ linked units may be joined through C_6 position and would not give rise to formaldehyde on periodate oxidation.

These results indicate that the mannan is very similar in structure to that obtained by autolysis of yeast which gives identical methylation results (16, 17, 18). The slime polysaccharide produced by *Saccharomyces rouxii* appears to differ in containing a small proportion only of 1,3 linkages (19). On the basis of methylation data and periodate oxidation, the linkages found to be present in the *B. polymyxa* mannan are shown in the following structure.

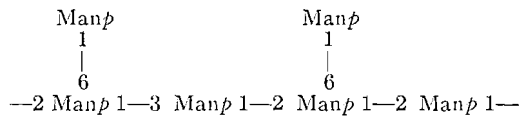

Haworth *et al.* (17) have proposed three possible repeating units for yeast mannan, one of which is the same as shown above.

EXPERIMENTAL

Solutions were concentrated under reduced pressure at 40° C. Optical rotations were determined in water at 23°±3° C unless otherwise stated. Paper chromatography was carried out by the descending method (20) on Whatman No. 1 filter paper using the following solvent systems: (*a*) butan-1-ol–ethanol–water (3:1:1), (*b*) butan-1-ol–pyridine–water (19:3:3), and (*c*) methyl ethyl ketone saturated with water. Sugars were located on chromatograms either by the *p*-anisidine hydrochloride spray (21) or by the silver nitrate and alkali sprays of Trevelyan *et al.* (22).

Preparation of a Mannose-containing Polysaccharide Fraction

The organism, *B. polymyxa* C3-2, was grown on the following medium: Difco yeast extract (5 g), K_2HPO_4 (0.5 g), KH_2PO_4 (0.5 g), $MgSO_4.7H_2O$ (0.2 g), sucrose (70 g) (or

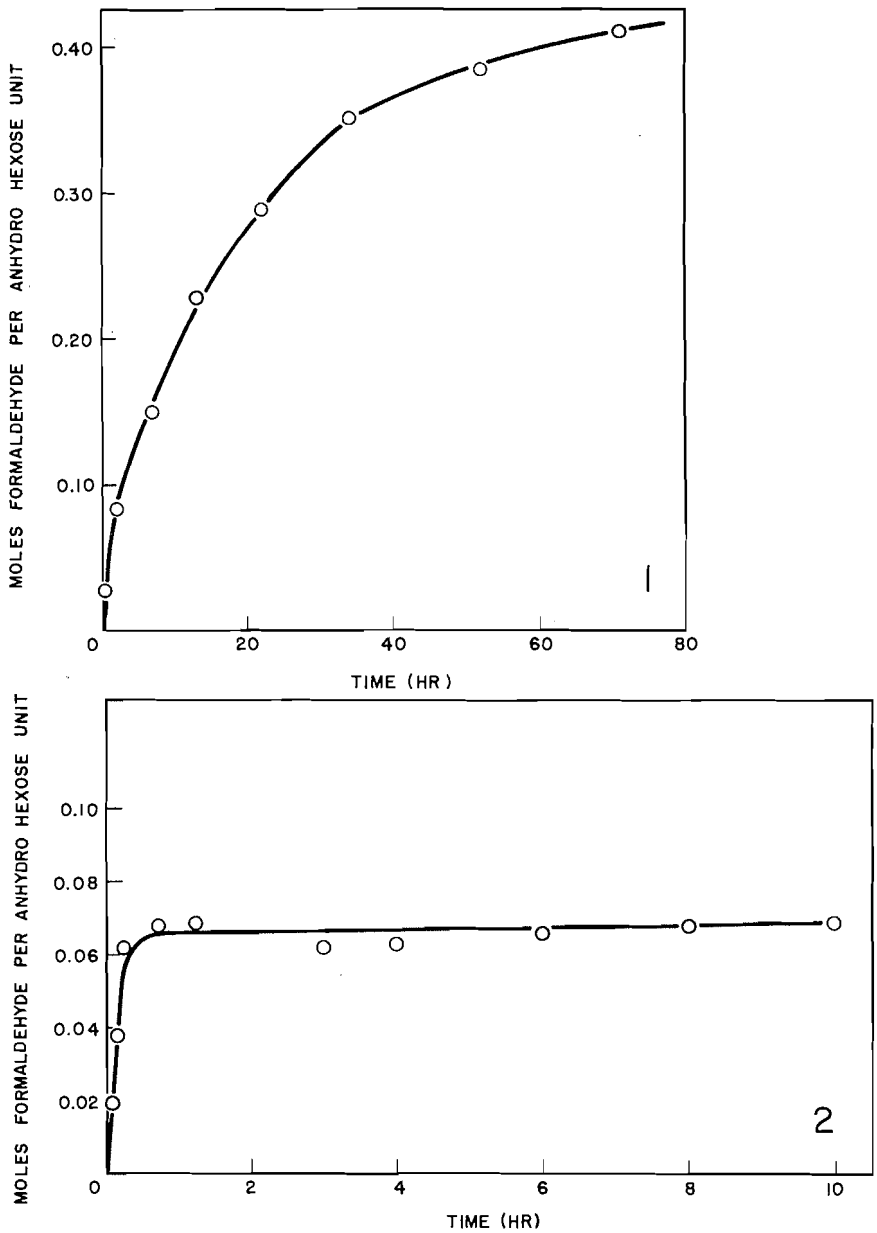

FIG. 1. Liberation of formaldehyde during periodate oxidation of the mannan at 26° C in $M/15$ phosphate buffer, pH 8.

FIG. 2. Liberation of formaldehyde during periodate oxidation of the reduced mannan at 21° C in $M/15$ phosphate buffer, pH 8.

glucose (50 g) or lactose (70 g)), water (1 l.). The medium was sterilized for 15 minutes at 15 p.s.i. in a 3-l. Fernbach flask. Sterile calcium carbonate (16 g) was added to the cooled solution. The inoculum was grown for 24 hours on the same medium (without calcium carbonate), the flask being shaken at 30° C. The inoculum (5 ml) was added to each Fernbach flask and the culture was kept at 30° C and shaken twice daily. The disappearance of sugar was followed on paper chromatograms and, in the case of glucose or

Can. J. Chem. Downloaded from www.nrcresearchpress.com by 196.1.178.254 on 09/04/12
For personal use only.

lactose, by determination of reducing sugar. Fermentations were judged to be complete after 9–10 days (sucrose), 5 days (glucose), 11 days (lactose). The media were then sterilized by heating to 90° C, filtered through cloth, and clarified on a Sharples centrifuge. The clear solution was then concentrated to 1/3 volume and the mannose-containing polysaccharide fraction was precipitated with ethanol (2/3 volume) and collected by centrifugation. Hydrolysis of a portion followed by paper-chromatographic examination indicated the presence of mannose, glucose, and galactose.

Fractionation of the Polysaccharides

To a stirred, viscous solution of the mannose-containing fraction (2.50 g) in water (500 ml) was slowly added a solution of Cetavlon (cetyltrimethylammonium bromide, 10% w/v). Precipitation occurred immediately and was complete after the addition of 10 ml. There was also a marked decrease in viscosity of the solution. The precipitate (fraction A) was collected by centrifugation, washed with water, and the washings were added to the centrifugate. Cetavlon solution (90 ml) was then added and 0.05 *M* sodium borate solution (100 ml) was run in slowly with stirring with precipitation commencing after the addition of 50 ml. The precipitate (fraction B) was collected by centrifugation and washed with water. The supernatant solution was dialyzed and poured into ethanol (4 volume). No further polysaccharide material was precipitated.

Fraction A.—The cetyltrimethylammonium salt of an acidic polysaccharide (fraction A) was not further examined.

Fraction B.—The cetyltrimethylammonium salt of a polysaccharide–borate complex (fraction B) was dissolved in cold 0.1 *N* hydrochloric acid (50 ml) and the free polysaccharide was recovered by precipitation with ethanol (300 ml). The precipitate was recovered by centrifugation, redissolved in water, and the solution was deionized by passage down columns of Amberlite resins IR 120 (H) and IR 45 (OH). The neutral effluent was lyophilized. The product (1.48 g) was hygroscopic and had $[\alpha]_D$ +82°. Found: N, 1.50%. It gave one sharp peak on electrophoresis in 0.05 *M* sodium borate with a mean mobility $\mu = 8.56 \times 10^{-8}$ cm^2 sec^{-1} v^{-1}. After hydrolysis of a portion with dilute acid, mannose was the only sugar detected on paper chromatograms. After hydrolysis with 6 *N* hydrochloric acid at 100° C for 25 hours, paper chromatograms sprayed with ninhydrin indicated the presence of several amino acids. The mannose content of the mannan as determined gravimetrically via the phenylhydrazone (23) was 87.4%.

Methylation of the Mannan

The mannan (1.9 g) was dissolved in water (15 ml) and to the vigorously stirred solution, contained in a three-necked flask under an atmosphere of nitrogen, methyl sulphate (5 ml) and 30% w/v sodium hydroxide solution (15 ml) were added simultaneously and dropwise. After 3 hours, these additions were repeated and the mixture was stirred for a further 12 hours. The solution was then heated on a hot water-bath to destroy residual methyl sulphate and remove methanol. This methylation cycle was repeated twice, water was then added to dissolve sodium sulphate and the mixture was extracted continuously with chloroform. The extracts were dried (Na_2SO_4) and concentrated to a syrup (2.6 g). This was dissolved in dry dimethylformamide (50 ml) and to the solution was added methyl iodide (20 ml) and silver oxide (20 g) (10). The mixture was shaken mechanically at room temperature in the dark for 65 hours. It was then filtered, the grey residue was washed with dimethylformamide, and to the combined filtrate and washings was added the above amounts of methyl iodide and silver oxide and the mixture was shaken for a further 24 hours. The brown-silver residues were removed by filtration, and water (100 ml) was added to the pale yellow solution. Precipitated silver salts were redissolved by

Can. J. Chem. Downloaded from www.nrcresearchpress.com by 196.1.178.254 on 09/04/12
For personal use only.

addition of potassium cyanide solution and the turbid solution was extracted eight times with chloroform, to recover the methylated product. The methylation procedure using methyl iodide and silver oxide was repeated four times. The methylated mannan was recovered as a syrup (2.0 g) which showed no hydroxyl absorption in the infrared and which could not be fractionated with chloroform – light petroleum (b.p. 65–110° C). The syrup had $[\alpha]_D$ +92° (*c*, 2.5 in $CHCl_3$); N, 1.97% and OCH_3, 38.2%.

Hydrolysis of the Methylated Mannan and Separation of the Methyl Ethers

The methylated mannan (1.5 g) was dissolved in 88% formic acid (50 ml) and the solution was heated at 90° C for 18 hours. Formic acid was then removed by evaporation, the residual syrup was taken up in 0.1 *N* hydrochloric acid, and the solution was heated at 90° C for a further 20 hours. The solution was cooled, neutralized by passage down a column of Amberlite resin IR 45 (OH), and concentrated to a syrup which was fractionated on Whatman No. 3MM filter paper, first in solvent *a* and then in solvent *c*. Three fractions were obtained: (*a*) tetra-*O*-methyl-D-mannose (0.41 g), (*b*) tri-*O*-methyl-D-mannose (0.37 g), and (*c*) di-*O*-methyl-D-mannose (0.33 g). These fractions are in a molar ratio of 1.03:1.00:0.95.

2,3,4,6-Tetra-O-methyl-D-mannose

The syrup (100 mg) which had $[\alpha]_D$ +5.6° was oxidized with bromine water. The product was isolated in the usual way and lactonized and the syrupy lactone was converted to the crystalline phenylhydrazide of 2,3,4,6-tetra-*O*-methyl-D-mannonic acid. After recrystallization from benzene, the product had m.p. 183–184° C, not depressed by admixture with an authentic sample, and $[\alpha]_D$ −25° C (*c*, 1.0 in $CHCl_3$) which were in good agreement with the reported values (24).

Tri-O-methyl-D-mannose Fraction

This fraction was separated into two components by electrophoresis on Whatman No. 3MM filter paper in 0.1 *M* sodium borate solution. The components were located by means of guide strips and eluted from the paper with cold water. The aqueous solutions were passed down short columns of Amberlite resin IR 120 (H) and evaporated to syrups which were evaporated three times from methanol to remove borate ions as methyl borate.

Fraction 1.—Fraction 1 gave a brown color with the *p*-anisidine spray and had M_G 0.12 (movement relative to glucose on a paper electrophorogram). It crystallized readily and after recrystallization from ether–*n*-hexane had m.p. 100–102° C not depressed by admixture with authentic 3,4,6-tri-*O*-methyl-D-mannose; $[\alpha]_D$ +21° → +8° (const., 20 hours). These values are in agreement with those reported for this sugar (25).

Fraction 2.—Fraction 2 gave a red color with the *p*-anisidine spray and had M_G 0.0. The syrup crystallized when seeded with authentic 2,4,6-tri-*O*-methyl-D-mannose monohydrate (26) and after recrystallization from ether–*n*-hexane had m.p. and mixed m.p. 63–65° C and $[\alpha]_D$ +17° (no mutarotation).

3,4-Di-O-methyl-D-mannose

The dimethyl mannose crystallized as the monohydrate and after two recrystallizations from ethyl acetate had m.p. 70–73° C not depressed by admixture with an authentic sample (19). $[\alpha]_D$ +17.6° (10 minutes) → +10° (const., 2 hours). Anal.: Calc. for $C_8H_{16}O_6.H_2O$: C, 42.48%; H, 8.02%. Found: C, 42.47%; H, 7.76%.

Periodate Oxidation of the Mannan

Oxidation of the mannan with 0.03 *M* sodium metaperiodate solution at room temperature was complete after 60 hours with the consumption of 1.31 mole of periodate

Can. J. Chem. Downloaded from www.nrcresearchpress.com by 196.1.178.254 on 09/04/12
For personal use only.

and the liberation of 0.46 mole of acid per anhydro hexose unit (all values given are corrected to allow for the 13% protein present). The oxidized polysaccharide was reduced with excess potassium borohydride without prior isolation. After 24 hours at room temperature, the solution was acidified with sulphuric acid and heated at 100° C for 6 hours to hydrolyze the polyol. Chromatographic examination of the deionized hydrolyzate indicated mannose and glycerol only. Erythritol was absent.

The mannan was also oxidized at 27° C with 0.03 *M* sodium metaperiodate in *M*/15 phosphate buffer, pH 8.0, and the formaldehyde liberated was determined by the chromotropic acid method (12). The results, shown in Fig. 1, indicate that extensive overoxidation occurred. After borohydride reduction of the polysaccharide, overoxidation was not observed (Fig. 2). Because only 1 mole of formaldehyde is liberated per mole of polymer, these results give an average molecular weight of 2850 and, allowing for 13% protein, this gives an average of 15 mannose units per molecule.

ACKNOWLEDGMENTS

The authors are grateful to Miss M. T. Clement for assistance with the fermentations, to Professor J. K. N. Jones for samples of 2,4,6- and 3,4,6-tri-*O*-methyl-D-mannose, and to Dr. P. A. J. Gorin for a sample of 3,4-di-*O*-methyl-D-mannose.

REFERENCES

1. LEDINGHAM, G. A. and NEISH, A. C. *In* Industrial fermentations. Vol. II. *Edited by* L. A. Underkofler and R. J. Hickey. Chemical Pub. Co., Inc., N.Y. 1954. p. 27.
2. LONG, P. H. *et al.* Ann. N. Y. Acad. Sci. **51**, 853–1000 (1949).
3. MISAKI, A. *et al.* J. Fermentation Technol. (Japan), **32**, 147, 191, 311, 315, 341 (1954); **36**, 25, 30, 44, 176, 181, 266, 271 (1958).
4. MURPHY, D. Can. J. Chem. **30**, 872 (1952).
5. MURPHY, D., BISHOP, C. T., and ADAMS, G. A. Can. J. Biochem. and Physiol. **34**, 1271 (1956).
6. JONES, A. S. Biochim. et Biophys. Acta, **10**, 607 (1953).
7. BERA, B. C., FOSTER, A. B., and STACEY, M. J. Chem. Soc. 3788 (1955).
8. BARKER, S. A., STACEY, M., and ZWEIFEL, G. Chem. & Ind. 330 (1957).
9. PALMSTIERNA, H., SCOTT, J. E., and GARDELL, S. Acta Chem. Scand. **11**, 1792 (1957).
10. KUHN, R., TRISCHMANN, H., and LOW, I. Angew. Chem. **67**, 32 (1955).
11. HAMILTON, J. K. and SMITH, F. J. Am. Chem. Soc. **78**, 5907 (1956).
12. O'DEA, J. F. and GIBBONS, R. A. Biochem. J. **55**, 580 (1953).
13. HOUGH, L. and PERRY, M. B. Chem. & Ind. 768 (1956).
14. HOUGH, L., WOODS, B. M., and PERRY, M. B. Chem. & Ind. 1100 (1957).
15. UNRAU, A. M. and SMITH, F. Chem. & Ind. 330 (1957).
16. HAWORTH, W. N., HIRST, E. L., and ISHERWOOD, F. A. J. Chem. Soc. 784 (1937).
17. HAWORTH, W. N., HEATH, R. L., and PEAT, S. J. Chem. Soc. 833 (1941).
18. CIFONELLI, J. A. and SMITH, F. J. Am. Chem. Soc. **77**, 5682 (1955).
19. GORIN, P. A. J. and PERLIN, A. S. Can. J. Chem. **34**, 1796 (1956).
20. PARTRIDGE, S. M. Biochem. J. **42**, 238 (1948).
21. HOUGH, L., JONES, J. K. N., and WADMAN, W. H. J. Chem. Soc. 1702 (1950).
22. TREVELYAN, W. E., PROCTOR, D. P., and HARRISON, J. S. Nature, **166**, 444 (1950).
23. HIRST, E. L., JONES, J. K. N., and WOODS, E. A. J. Chem. Soc. 1048 (1947).
24. DREW, H. D. K., GOODYEAR, E. H., and HAWORTH, W. N. J. Chem. Soc. **130**, 1237 (1927).
25. BATT, H. G., HAWORTH, W. N., and HIRST, E. W. J. Chem. Soc. 1395 (1930).
26. PRENTICE, N., CUENDET, L. S., and SMITH, F. J. Am. Chem. Soc. **78**, 4439 (1956).

Can. J. Chem. Downloaded from www.nrcresearchpress.com by 196.1.178.254 on 09/04/12
For personal use only.

Can. J. Chem. Downloaded from www.nrcresearchpress.com by 196.1.178.254 on 09/04/12
For personal use only.

5,6-DIDEOXY-L-ARABINO-HEXOSE (5-DEOXY-5-*C*-METHYL-L-ARABINOSE)[1]

D. J. Ball, A. E. Flood, and J. K. N. Jones

ABSTRACT

A synthesis of 5,6-dideoxy-L-*arabino*-hexose (II) from methyl β-D-galactofuranoside is described.

INTRODUCTION

The isolation of 6-deoxy-5-keto-D-*arabino*-hexose (6-deoxy-D-*arabino*-hexos-5-ulose) (I) from hygromycin has recently been described (1). This substance was converted by reduction to 5,6-dideoxy-D-*arabino*-hexose, which was then characterized as its dithioacetal (1). The purpose of this communication is to describe the synthesis of its optical isomer, 5,6-dideoxy-L-*arabino*-hexose (II). The elimination of tosyloxy (tolyl-*p*-sulphonyloxy) groups situated on vicinal primary and secondary alcoholic groups by heating the esters with sodium iodide is a general reaction (2) which has been observed in the hexitol (3), hexose (4), and inositol series (5).

Crystalline derivatives of ethyl α- and β-D-galactofuranosides are known, but their preparation is tedious. It was observed that an impure syrupy preparation of methyl β-D-galactofuranoside (6) which had been converted to the 2,3,5,6-tetra-toluene-*p*-sulphonate gave, when heated with a solution of sodium iodide in acetone, a crystalline methyl 5,6-didehydroxy-2,3-di-*O*-tosyl-α-L-*arabino*-hexoside (III; R = tosyl = tolyl-*p*-sulphonyl).

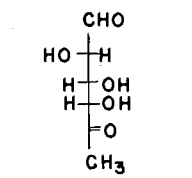

(I)

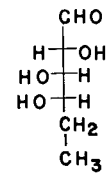

(II)

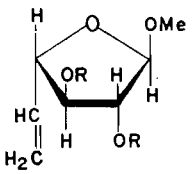

(III)

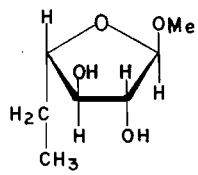

(IV)

Removal of the tosyl groups by reductive saponification yielded crystalline methyl 5,6-didehydroxy-α-L-*arabino*-hexoside (III; R = H) which, when it was reduced (Raney nickel catalyst), furnished 5,6-dideoxy-α-L-*arabino*-hexoside (IV). This substance (IV) was also produced when the unsaturated tosyl derivative of III was reduced by boiling its solution in ethanol in the presence of Raney nickel, followed by reductive saponification of the tosyl groups.

[1]*Manuscript received September 30, 1958.*
Contribution from the Department of Organic Chemistry, Queen's University, Kingston, Ontario.

Tosylation of IV yielded a product indistinguishable from the substance III (R = H) produced by reduction of III (R = tosyl). This experiment proved that inversion of hydroxyl groups had not occurred during removal of the tolyl-*p*-sulphonyl groups in the preparation of III (R = H) and IV.

Both III (R = H) and IV were oxidized by aqueous sodium metaperiodate and yielded significant quantities of iodoform when the oxidized products were allowed to stand in iodine solution. When IV was shaken with ethanethiol and concentrated hydrochloric acid it yielded the diethyl dithioacetal of II. The D-isomer of this derivative was isolated from hygromycin.

When III (R = tosyl) was shaken with silver nitrate and iodine in acetonitrile solution (7), a crystalline deoxy-iodonitrate of III (R = tosyl) was produced. The location of the iodine group in this new product is undecided, as is the decision as to whether the substance is a derivative of L-altrose or of D-galactose.

EXPERIMENTAL

Solutions were evaporated under reduced pressure; optical rotations were determined at 20°±2° C (unless otherwise stated).

*Synthesis of Methyl 5,6-Didehydroxy-2,3-di-O-tolyl-p-sulphonyl-α-*L*-arabino-hexoside* (III; R = Tosyl)

Crude methyl β-D-galactofuranoside (from 50 g of D-galactose (6)) was dissolved in pyridine (500 ml), and toluene-*p*-sulphonyl chloride (250 g) was added to the solution. After 20 hours, the solution was poured (with stirring) onto crushed ice. The syrupy tosyl derivatives were isolated in the usual way. The syrup, without further purification, was heated in acetone solution (500 ml) with sodium iodide (70 g) under reflux. The solution rapidly became brown because of the separation of iodine, and sodium toluene-*p*-sulphonate precipitated. The mixture was filtered at intervals to minimize uneven boiling. (Yield of the sodium salt of toluene-*p*-sulphonic acid, 36.5 g.)

The acetone was removed and the residue was extracted with chloroform. The extracts were washed successively with a solution of sodium thiosulphate and then with water. The chloroform extract was dried ($MgSO_4$) and evaporated to a syrup which rapidly crystallized. The crystals (32 g) were recrystallized from methanol, m.p. 109–110° C, $[\alpha]_D$ −62°±2° (*c*, 0.5 in chloroform). Anal. Calc. for $C_{21}H_{24}O_8S_2$: C, 53.8; H, 5.1; S, 13.7; OMe, 6.5. Found: C, 53.7; H, 5.5; S, 14.7; OMe, 6.5.

*Methyl 5,6-Didehydroxy-α-*L*-arabino-hexoside* (III; R = H)

The di-*O*-tosyl derivative (above) (1 g) was dissolved in ethanol (100 ml), and sodium amalgam (100 g of 3%) was added portionwise with stirring. During the addition, water (150 ml) was added at such a rate that precipitation of the tosyl derivative was avoided. After 12 hours, the solution was made neutral with sulphuric acid and evaporated to dryness. The solid residue was extracted exhaustively with acetone and the extracts were evaporated. The crude crystalline residue (0.21 g) was volatile at 100° C and accordingly it was purified by sublimation at 12 mm/100° C. The product, after sublimation, had m.p. 60° C, $[\alpha]_D^{23}$ −110°±2° (*c*, 0.67), and was analytically pure. The substance moved at 2.4 times the speed of rhamnose in *n*-butyl alcohol – ethanol – water (9:2:2) solvent, and gave a yellow coloration when it was heated with *p*-anisidine hydrochloride. Anal. Calc. for $C_7H_{12}O_4$: C, 52.5; H, 7.6; OMe, 19.4. Found: C, 52.4; H, 7.8; OMe, 22.3.

Can. J. Chem. Downloaded from www.nrcresearchpress.com by 196.1.178.254 on 09/04/12
For personal use only.

Methyl 5,6-Dideoxy-α-L-arabino-hexoside (IV) (*Methyl 5-Deoxy-5-C-methyl-α-L-arabinoside*)

The unsaturated arabinoside derivative (above, 89 mg) was dissolved in methanol and hydrogenated at 20° in the presence of a Raney nickel catalyst (0.5 g). After 20 minutes, the hydrogen uptake (53.4 ml at S.T.P.) was constant. The solution was filtered and the filtrate evaporated. The product was purified by sublimation at 16 mm/100° C. The product had m.p. 63° C and $[\alpha]_D$ 126°±6° (*c*, 0.18). Anal. Calc. for $C_7H_{14}O_4$: C, 51.8; H, 8.7; OMe, 19.1. Found: C, 51.9; H, 8.7; OMe, 19.8.

Both this compound and the unsaturated glycoside were oxidized by sodium metaperiodate solution, with the consumption of more than one mole of reagent, per mole, and with the formation of iodine and iodoform. No formic acid was detected.

Methyl 5,6-Dideoxy-2,3-di-O-tosyl-α-L-arabino-hexoside

The unsaturated tosyl derivative (III; R = tosyl) (116 mg) was dissolved in ethanol (20 ml) and boiled under reflux in the presence of Raney nickel catalyst (0.5 g) for 4 hours. The odor of acetaldehyde was detectable during the reaction. The solution was cooled and filtered, and the filtrate evaporated to a crystalline solid which was purified by recrystallization from ethanol. The product had m.p. 93–94° C, $[\alpha]_D$ −61° (*c*, 2.23 in chloroform). A product which had the same properties was produced when methyl 5,6-dideoxy-α-L-*arabino*-hexoside (IV; 0.1 g) was allowed to react with toluene-*p*-sulphonyl chloride (0.3 g) in pyridine (5 ml) solution overnight. The substance, which was isolated after the pyridine solution had been poured onto ice, weighed 0.21 g and had m.p. 93–94° C, not depressed on admixture with an authentic specimen. Anal. Calc. for $C_{21}H_{26}O_8S_2$: C, 53.6; H, 5.6; S, 13.6; OMe, 6.6. Found: C, 53.8; H, 6.0; S, 12.9; OMe, 6.6.

5,6-Didehydroxy-L-arabino-hexose Diethyl Dithioacetal

Methyl 5,6-dideoxy-α-L-*arabino*-hexoside (0.1 g) was shaken with ethanethiol (0.5 ml) and 6 *N* hydrochloric acid (0.5 ml) for 5 hours. The mixture was twice extracted with chloroform (2-ml portions) and the extracts were washed with sodium bicarbonate solution and then dried ($MgSO_4$). Removal of the chloroform left a syrupy diethyl dithioacetal which crystallized. It was recrystallized from water and had m.p. 110°. Anal. Calc. for $C_{10}H_{22}O_3S_2$: C, 47.3; H, 8.7; S, 25.2. Found: C, 47.4; H, 8.8; S, 24.8.

Iodonitration of Methyl 5,6-Didehydroxy-2,3-di-O-tolyl-p-sulphonyl-α-L-arabino-hexoside

Methyl 5,6-didehydroxy-2,3-di-*O*-tolyl-*p*-sulphonyl-α-L-*arabino*-hexoside (2.34 g; 5 millimole) was dissolved in acetonitrile (50 ml), and to the solution was added silver nitrate (1.70 g; 10 millimole) and iodine (1.27 g; 5 millimole). An immediate precipitate of silver iodide was observed. The mixture was shaken at room temperature for 7 days in a stoppered flask from which light was excluded. The mixture was then filtered and the silver iodide was washed with acetonitrile and air-dried; yield 1.22 g. (The reaction of silver nitrate with iodine to give silver iodide and iodonium nitrate would give 1.17 g of silver iodide from the above amounts of reactants.)

The filtrate was boiled under reflux for 24 hours and a light precipitate was removed by filtration. Concentration of the filtrate afforded a yellow syrup which yielded a further precipitate (probably silver nitrate) when diluted with chloroform. The mixture was again filtered and the filtrate was evaporated to a syrup which crystallized from chloroform – light petroleum (b.p. 60–80° C). Total yield 0.36 g after recrystallization from the same solvents; i.e. 11.0% calculated as the iodonitrate. The compound had

Can. J. Chem. Downloaded from www.nrcresearchpress.com by 196.1.178.254 on 09/04/12
For personal use only.

m.p. 125–126° C and $[\alpha]_D$ −49° (*c*, 5.0 in chloroform). Anal. Calc. for $C_{21}H_{24}INO_{11}S_2$: C, 38.4; H, 3.7; I, 19.3; N, 2.1; S, 9.8. Found: C, 38.4; H, 3.8; I, 18.6; N, 2.6; S, 9.5.

The infrared absorption spectrum showed a strong band at 1642 cm^{-1} which was absent from the spectrum of the parent olefinic compound and is presumably due to the nitrate group. The residual syrup (1.85 g) gave an infrared absorption spectrum with bands of the same relative intensity and therefore probably contains one or more of the other three possible iodonitrates.

A portion of the crystalline iodonitrate (0.10 g) was dissolved in hot ethanol and the solution was refluxed for 90 minutes with hydrazine hydrate (0.03 ml) (8). Excess hydrazine was destroyed by boiling the solution for a further 15 minutes with Raney nickel. The mixture was then filtered and the filtrate was concentrated to an oil which was soluble in water but not soluble in chloroform. The properties of this product indicate that nitrate and tolyl-*p*-sulphonyl groups had both been removed. It was not further examined.

The authors thank the National Research Council for a grant which made this work possible.

REFERENCES

1. MANN, R. L. and WOOLF, D. O. J. J. Am. Chem. Soc. **79**, 120 (1957).
2. TIPSON, R. S. Advances in Carbohydrate Chem. **8**, 201, 205 (1953).
3. BLADON, P. and OWEN, L. N. J. Chem. Soc. 598 (1950).
4. JONES, J. K. N. and THOMPSON, J. L. Can. J. Chem. **35**, 955 (1957).
5. ANGYAL, S. J. and GILHAM, P. T. J. Chem. Soc. 375 (1958).
6. MOWERY, D. F. and FERRANTI, G. R. J. Am. Chem. Soc. **76**, 4103 (1954).
7. MORRIS, L. J. Chem. & Ind. (London), 1291 (1958).
8. ENNOR, K. S. and HONEYMAN, J. J. Chem. Soc. 2586 (1958).

Can. J. Chem. Downloaded from www.nrcresearchpress.com by 196.1.178.254 on 09/04/12
For personal use only.

Can. J. Chem. Downloaded from www.nrcresearchpress.com by 196.1.178.254 on 09/04/12
For personal use only.

IRRADIATION OF AQUEOUS CHLORAL HYDRATE WITH Sr^{90}–Y^{90} BETA RAYS[1]

R. F. Platford and J. W. T. Spinks

ABSTRACT

Air-saturated aqueous chloral hydrate has been irradiated with beta rays and the acid yield as determined by titration has been studied as a function of dose rate, temperature, and initial concentration of the chloral hydrate.

The average lifetime of the intermediates has been found, by means of the rotating sector technique, to be about 0.5 second. Propagation and termination rate constants for the reaction have been calculated and an effort has been made to explain the results observed in terms of a free radical chain reaction.

INTRODUCTION

In 1950 Andrews and Shore (1) reported that aqueous chloral hydrate was decomposed by X rays to yield HCl and other products. The acid yield, measured conductometrically, was found to be linear with radiation dose, and to increase with increasing temperature and initial chloral hydrate concentration, but was reported to be independent of dose rate. Because of the large acid yield, these workers used the system as a sensitive radiation dosimeter.

Freeman *et al.* in 1953 (2) irradiated the same system with Co^{60} γ-rays and found essentially the same results as Andrews and Shore except that they found the acid yield to be dependent on $(\text{dose rate})^{-1/2}$. Freeman also found the radiation yield in air-free solutions to be about one fifth of that in aerated solutions.

Andrews *et al.* (3) have used an agar gel containing chloral hydrate and methyl red as a dosimeter for Van de Graaff electrons.

In the present work the decomposition of chloral hydrate by beta rays is compared with that resulting from gamma rays.

EXPERIMENTAL

Apparatus

Irradiations were carried out with a 40-mc Sr^{90}–Y^{90} medical applicator. The activity was confined to an area of 1 cm^2 and was plated on one face of an aluminum disk to the back of which was attached a rod serving as a handle. Solutions were irradiated in 10-ml pyrex beakers immersed in a thermostat, above which the source was suspended. The dose rate received by the solution was controlled by varying the separation between source and solution.

A rotating sector with a light:dark ratio of 1:2 was constructed from brass of thickness 1335 mg/cm^2. The sector was driven through a reduction drive by a 240-r.p.m. synchronous motor.

Materials

All chemicals were reagent grade or better; the chloral hydrate was Fisher U.S.P. grade. All water was distilled once from alkaline permanganate and once from acidic dichromate solution.

Procedure

The reaction was followed by titration of the acid produced on irradiation. Samples

[1]*Manuscript received February 9, 1959.*
Contribution from the Department of Chemistry, University of Saskatchewan, Saskatoon, Saskatchewan.

were titrated with *ca.* 10^{-2} *N* NaOH from a microburette which could be read to 5×10^{-4} ml. Irradiated solutions were titrated to the same color as unirradiated blanks using bromocresol purple as an indicator.

The energy absorbed on irradiation was estimated by means of the ferrous sulphate dosimeter (0.8 *N* H_2SO_4, 10^{-2} *M* NaCl, 10^{-3} *M* $(NH_4)_2SO_4.FeSO_4.6H_2O$ in air-saturated water). The *G* value (molecules of Fe^{++} oxidized per 100 ev of energy absorbed) was assumed to be 15.5 (4, 5, 6). The Fe^{+++} produced on irradiation was measured by means of its absorption peak at 304 mμ. Dose rates are expressed in rad/min, where 1 rad ≡ 100 erg/g.

Because the densities of irradiated solutions differed from that of the ferrous sulphate solution, a small correction was applied to compensate for differences in stopping power between the two solutions. The stopping power for electrons was assumed proportional to the solution density.

RESULTS

Effect of Dose Rate

The *G* value (molecules of acid produced per 100 ev of energy absorbed) was found to be dependent on dose rate. Also, because of the strong attenuation of beta rays by the solution, the dose rate varied with depth of solution and hence the *G* value was dependent on solution depth (or volume, since the cross sectional area of the solutions was constant). The acid yield vs. dose is shown as a function of dose rate for two different volumes of solution in Figs. 1 and 2. The *G* value, which is equal to 965×(acid yield)/(dose in rad), is shown in Table I as a function of dose rate, and *G* vs. (dose rate)$^{-1/2}$ is plotted in Fig. 3. For comparison, a plot of *G* vs. (dose rate)$^{-1/2}$ is shown for chloral hydrate irradiated with Co^{60} γ-rays for which attenuation of radiation by the solution was very small.

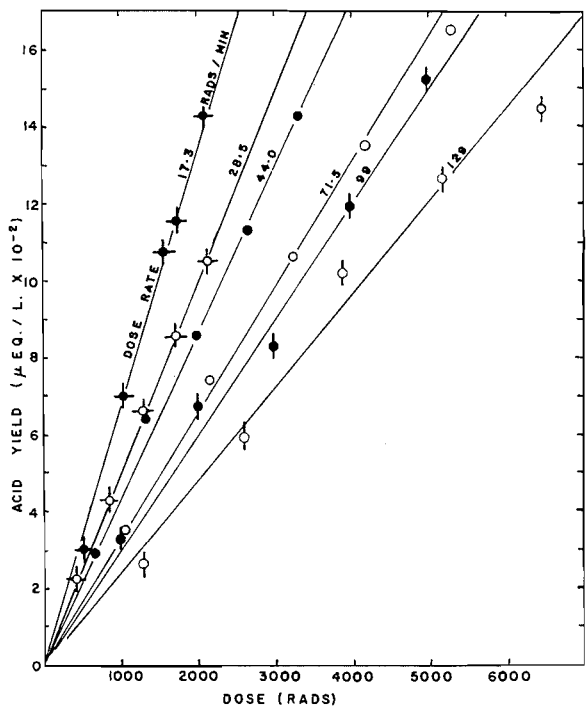

FIG. 1. Effect of dose rate on acid yield in 1 ml of a 1 *M* chloral hydrate solution at 25° C.

Can. J. Chem. Downloaded from www.nrcresearchpress.com by 196.1.178.254 on 09/04/12
For personal use only.

Can. J. Chem. Downloaded from www.nrcresearchpress.com by 196.1.178.254 on 09/04/12
For personal use only.

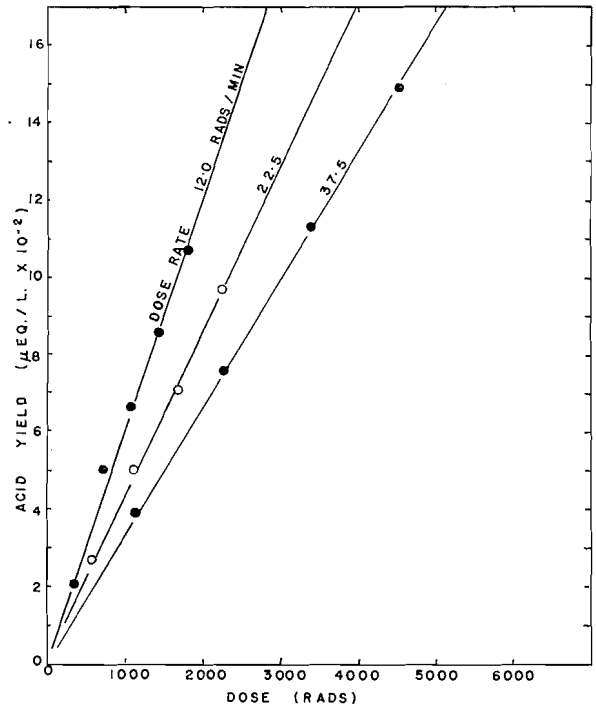

FIG. 2. Effect of dose rate on acid yield in 5 ml of a 1 *M* chloral hydrate solution at 25° C.

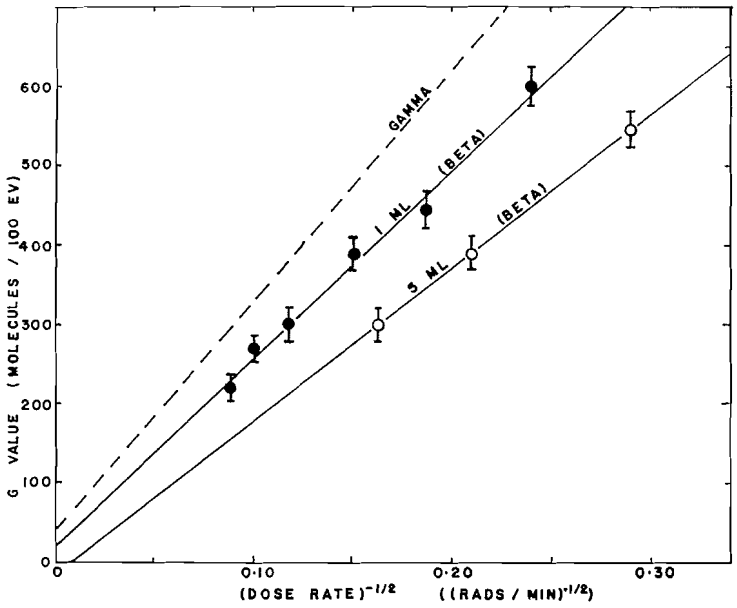

FIG. 3. Effect of dose rate on *G* value for 1 *M* chloral hydrate at 25° C.
– – – – Co^{60} gamma radiation. ——— Sr^{90}–Y^{90} beta radiation.

TABLE I

G value as a function of dose rate for 1 *M* chloral hydrate irradiated at 25° C

Dose rate (rad/min)	*G* value (molecules/100 ev)
1-ml solution (thickness = 2.7 mm)	
129 ±6	220±15
99 ±4	270±15
71.5±2.5	300±20
44.0±1	390±20
28.5±0.7	445±25
17.3±0.4	600±25
5-ml solution (thickness = 13.5 mm)	
37.5±0.8	300±15
22.5±0.4	390±20
12.0±0.4	545±20

Temperature Coefficient

The *G* value was determined at three temperatures and the results are shown in Table II. The temperature coefficient for the reaction was 3.3% per ° C at 25° C, which corresponded to an activation energy of 5.5±1 kcal/mole.

TABLE II

Effect of temperature on *G* value for 1 *M* aqueous chloral hydrate irradiated at 44.0 rad/min (1-ml solution)

Temperature (° C)	*G* value
15.5±0.2	285±20
25 ±0.2	390±20
35 ±0.2	540±20

Effect of Concentration

The results showing the dependence of *G* value on concentration are shown in Table III and in Fig. 4. Since the densities of the more concentrated solutions were so much

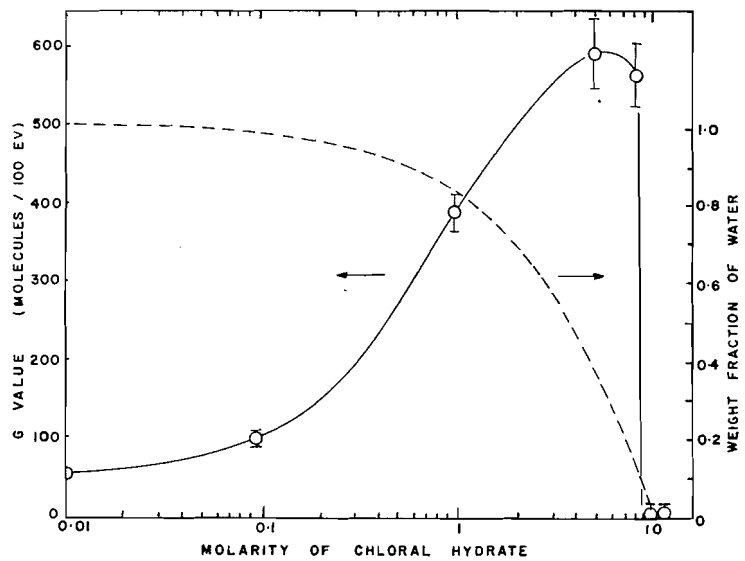

FIG. 4. Effect of initial concentration of chloral hydrate on *G* value for dose rates of 45 rad/min.

Can. J. Chem. Downloaded from www.nrcresearchpress.com by 196.1.178.254 on 09/04/12
For personal use only.

different from that of the dosimeter solution, different dose rates resulted in the two solutions, due to differences in stopping powers per unit *volume*. It was assumed that the stopping power per unit *weight* was the same in both the chloral hydrate and dosimeter solution and that the dose rate in the concentrated chloral hydrate solution was the same as that in an equal weight of dosimeter solution.

The 10 *M* solution was saturated at about 35° C and when cooled to 25° C formed a solid solution which was irradiated in this state.

TABLE III

Effect of concentration on *G* value for chloral hydrate irradiated at 25° C (1-ml solution)

Concentration	*G* value
Dose rate = 45.0 rad/min	
0.01 *M*	53±5
0.1 *M*	100±10
Dose rate = 44.0 rad/min	
1.0 *M*	390±20
5 *M*	600±40
8 *M* (satd.)	570±40
10 *M* (solid soln.)	<25
Solid chloral hydrate	<25

It will be observed that the standard deviations are larger in more concentrated solutions; this was due to a less certain titration end point in the more highly concentrated solutions.

Effect of Intermittent Irradiation

Solutions of 1 *M* chloral hydrate at 25° C were irradiated with pulsed radiation, produced by interposing a rotating sector between source and solution. The effect of pulse time on *G* value is shown in Fig. 5. The reduction in *G* value occurs when the pulse time is about equal to the mean lifetime of the reaction intermediates (7).

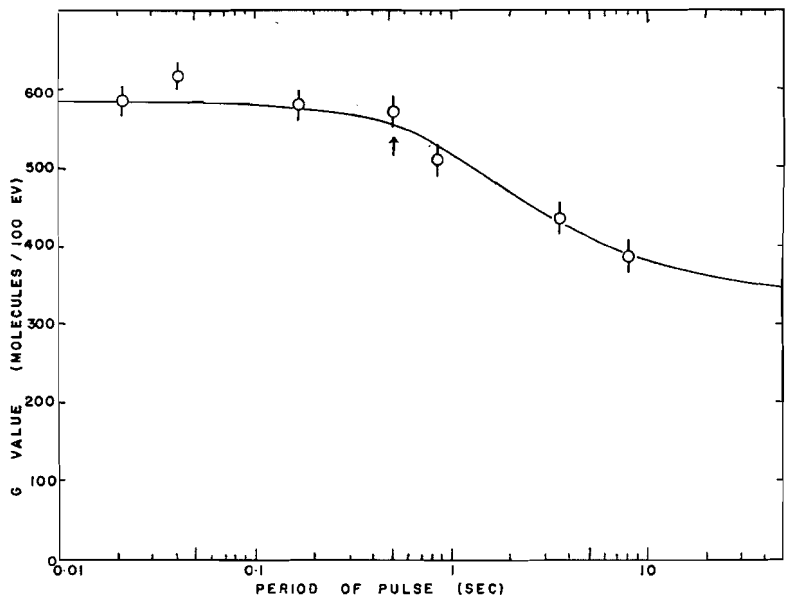

FIG. 5. Effect of intermittent radiation on *G* value. The dose rate with the sector rotating was 18 rad/min The average lifetime of the intermediates corresponds to the period of pulse shown by the arrow.

Can. J. Chem. Downloaded from www.nrcresearchpress.com by 196.1.178.254 on 09/04/12
For personal use only.

Can. J. Chem. Downloaded from www.nrcresearchpress.com by 196.1.178.254 on 09/04/12
For personal use only.

DISCUSSION

The large dose rate dependent G values indicate a chain reaction as the mechanism by which the beta radiolysis proceeds. The dependence of G value on (dose rate)$^{-1/2}$ means that a second-order recombination is responsible for removal of the chain-propagating intermediates. Lack of knowledge of reaction products, however, precluded setting up a reaction mechanism.

The dependence of G on thickness of solution irradiated was explained by assuming that the dose rate varied exponentially with solution depth and that the reaction velocity V varied with the (dose rate)$^{1/2}$ (this is tantamount to saying $G \propto$ (dose rate)$^{-1/2}$).

These conditions give:

$$V_x = KI_x^{\frac{1}{2}}$$

where V_x = reaction rate at depth x in solution,
K = a constant,
I_x = dose rate at depth x in solution,

where x is expressed in g/cm^2.

Also:

$$I_x = I_0\, e^{-\mu x},$$

where I_0 = surface dose rate,
μ = mass absorption coefficient in cm^2/g.

Now we have:

$$V_x = KI_0^{\frac{1}{2}}\, e^{-\mu x/2}.$$

The average reaction rate $\bar{V}$ in a solution of thickness t is given by:

$$\bar{V} = \frac{1}{t}\int_0^t V_x dx = \frac{1}{t}\,(2KI_0^{\frac{1}{2}}/\mu)\,(1-e^{-\mu t/2}).$$

The average dose rate $\bar{I}$ is given by:

$$\bar{I} = I_0(1-e^{-\mu t})/\mu t.$$

Therefore the G value in such a solution is given by:

$$G = \bar{V}/\bar{I} = \frac{2KI_0^{\frac{1}{2}}(1-e^{-\mu t/2})/\mu t}{I_0\,(1-e^{-\mu t})/\mu t},$$

$$G = 2K/[I_0^{\frac{1}{2}}(1+e^{-\mu t/2})].$$

Now $\mu = 6.1$ cm^2/g for solutions used here and $e^{-\mu t/2} = 0.43$ for the 1-ml solution (thickness = 0.27 g/cm^2).

Because absorption of the beta rays was complete in this thickness of solution (1.40 g/cm^2), $\mu t \rightarrow \infty$ for 5-ml solutions.

The *surface* dose rates for 1-ml and 5-ml solutions irradiated at the same *average* dose rates were found by extrapolation of a plot of dose rate vs. solution thickness to zero solution thickness. These dose rates were found to be in the ratio:

$$\frac{I_0\,(1\text{ ml})}{I_0\,(5\text{ ml})} = \frac{1}{3.1}.$$

Substitution into the expression for G value gave:

$$\frac{G\,(1\text{ ml})}{G\,(5\text{ ml})} = \frac{I_0^{\frac{1}{2}}(5\text{ ml})\,(1+e^{-\mu t/2})\,(5\text{ ml})}{I_0^{\frac{1}{2}}(1\text{ ml})\,(1+e^{-\mu t/2})\,(1\text{ ml})} = \frac{\sqrt{3.1}}{1}\,\frac{1}{1.43} = 1.23.$$

The experimental value of the above ratio was found by taking the ratios of the slopes of the 1-ml and 5-ml lines in Fig. 3. This ratio was found to be 1.20. The above explanation accounts for the observed dependence of G value on thickness of solution. The difference between G values for γ-radiation and beta radiation seen in Fig. 3 may also be due to such an effect since the gamma radiation is attenuated even less than beta radiation in a 1-ml solution of the thickness used here.

The dependence of G value on concentration shown in Fig. 4 may be explained by saying that at lower concentrations the probability of reaction of chain-initiating radicals with chloral molecules increased with chloral hydrate concentration; at high chloral hydrate concentrations the water concentration falls off rapidly and very few radicals are produced from the water per unit volume of solution.

The mean lifetime of the reaction intermediates was found to be about 0.5 second and from this figure approximate propagation and termination rate constants were calculated. It can be shown (8) that the termination rate constant k_t is given by:

$$k_t = 1/\tau^2\phi I,$$

where τ = mean lifetime of the free radical intermediates (here = 0.5 second),
ϕ = G value for radical initiation (taken to be 5 radicals/100 ev),
I = dose rate,
k_t = 2.5×10^9 l./mole-sec.

Also, it was assumed that V, the reaction velocity, was given by:

$$V = k_p\,[C](\phi I/k_t)^{\frac{1}{2}},$$

where k_p = propagation rate constant,
$[C]$ = chloral hydrate concentration.

The reaction rate $V = 2.0\times10^{-7}$ mole/l.-sec, $k_p = 2.5\times10^2$ l./mole-sec at a dose rate of 18.0 rad/min.

It would appear that no great difference exists between the beta and gamma radiolysis of aqueous chloral hydrate except for effects due to attenuation of the radiation. This is to be expected since the processes by which chain-initiating radicals are produced are the same in each case.

REFERENCES

1. Andrews, H. L. and Shore, P. A. J. Chem. Phys. **18**, 1165 (1950).
2. Freeman, G. R., Van Cleave, A. B., and Spinks, J. W. T. Can. J. Chem. **32**, 322 (1954).
3. Andrews, H. L., Murphy, R. E., and Lebrun, E. J. Rev. Sci. Instr. **28** (5), 329 (1957).
4. Hochanadel, C. J. and Ghormley, J. A. J. Chem. Phys. **21**, 880 (1953).
5. Saldick, J. and Allen, A. O. J. Chem. Phys. **22**, 438 (1954).
6. Schuler, R. H. and Allen, A. O. J. Chem. Phys. **24**, 56 (1956).
7. Dickinson, R. G. *In* The photochemistry of gases. Reinhold Publishing Corp., New York. 1941. pp. 202–209.
8. Dainton, F. S. and Tordoff, M. Trans. Faraday Soc. **53**, 599 (1958).

Can. J. Chem. Downloaded from www.nrcresearchpress.com by 196.1.178.254 on 09/04/12
For personal use only.

Can. J. Chem. Downloaded from www.nrcresearchpress.com by 196.1.178.254 on 09/04/12
For personal use only.

SOME SPECIFIC FEATURES IN AUTOXIDATION OF METHYL LINOLEATE[1]

N. A. KHAN

ABSTRACT

A scheme of manual counter-current extraction, ingeniously devised, has facilitated quantitative isolation of initial products from autoxidized methyl linoleate under controlled conditions. A sole product of monomeric monohydroperoxide with one spatial configuration has been shown to be the outcome of interactions of oxygen molecule with methyl linoleate. The physical and chemical analyses prove this product as conjugated *cis,trans* methyl linoleate hydroperoxide. The fractionations of its derivative, hydroxystearic acid, and its scission products go to establish the formation of two positional isomers (9- and 13-) exclusively for this *cis,trans* product. Such positional isomers leave no doubt about two possibilities of attack by oxygen on the two 3-C segments in the 5-C system of methyl linoleate containing mobile π electrons. A mechanism has been proposed relevant to the experimental findings. Such initiation processes offer the missing link between neutral methyl linoleate and formation of its hydroperoxide without decomposition. These investigations, thus, emphasize the fact that the initiation processes must be distinguished from the main autoxidation reactions.

In continuation of the previous studies (9) it is necessary to describe the carefully outlined procedures for the isolation of methyl linoleate hydroperoxides. The quantitative isolation of pure hydroperoxides, formed exclusively during the initial stages of autoxidation reactions of methyl linoleate, has been successfully carried out. The purity of such products has also been established through preparation of several derivatives and relevant scission products. Infrared studies on the fatty acid esters and their hydroperoxides have revealed many clues to the mechanism of autoxidation reactions. On the basis of these data and the other experimental facts, the mechanism of the initial attack by oxygen molecule on methylene-interrupted double bonds (5-C system of methyl linoleate) has been presented.

Methyl linoleate (545 g) was freshly prepared from sesame oil acids by bromination and debromination procedures. The *trans* isomers (isolated *trans* absorbing at 10.32 μ) formed during debromination were practically removed through multiple urea complex formation under different conditions. One per cent solution of linoleate sample in methanol was each time saturated at 30° C and crops of crystals were obtained at 4° C, yielding 4.6, 5.9, 7.3, 4.2, and 2.6% of the substance taken. The solution concentration at 1% was restored by evaporation under vacuum at room temperatures 26–31° C. The last filtrate was then passed through a powdered urea column (5 in. × 1/2 in.). After proper elution, 64.7% of methyl linoleate was recovered. Methyl linoleate, thus obtained, was analyzed: I.N. (iodine number), 172.4; isolated *trans*, nil (absorption at 10.32 μ); hydrogen absorption, 1.98 mole/mole. All samples were kept under (dry and oxygen-free) nitrogen and vacuum, below 0° C.

Since we are concerned with the initiation processes only, the extent of oxidation was scrupulously controlled and was not allowed to exceed certain limits. From the previous experiments (10), this limit was set at about 10% oxidation (absorption of 0.1 mole of oxygen per mole which is equivalent to 10% hydroperoxide formation). Consequently, autoxidation of methyl linoleate (50 g) to 10.0% hydroperoxides content was carried out at 0.0° C in 500-ml Erlenmeyer flasks open with loose lids. The quantitative isolation of these hydroperoxides formed at such initial stages and their characterization have been

[1]*Manuscript received January 14, 1959.*
Contribution from the Division of Foods and Nutrition, East Regional Laboratories, Pakistan Council of Scientific and Industrial Research, Tejgaon, Dacca, Pakistan.

considered essential to establish the nature of interactions between oxygen and methyl linoleate containing methylene-interrupted double bonds in a 5-C system. This paper thus deals with the peroxide-forming periods, A and B, and not the final main autoxidation periods, C and D, involving intricate mechanisms with free radicals (10).

Among the methods attempted for isolation of peroxides, the counter-current extraction was found to be the most suitable for keeping the peroxides intact during the isolation procedures. The counter-current extraction between two immiscible solvents was found to be effective in concentrating the oxygenated products. Unluckily, the standard procedures for the counter-current extraction (6) distribute the peroxides over several fractions, and under no conditions is the recovery quantitative. Hence, a scheme of manual counter-current extraction, as represented in Fig. 1, was improvised to separate the

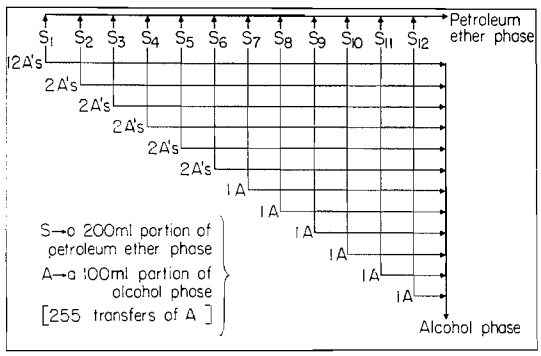

FIG. 1. A scheme of manual counter-current extraction.

oxidized from the unoxidized fraction quantitatively. Two immiscible solvents were first obtained by mixing absolute alcohol (distilled over KOH and zinc dust), petroleum ether (b.p. 30–60° C and free from unsaturable materials (13)), and water in the proportions 5:6:1. The resulting petroleum ether and alcohol phases were allowed to separate and were used as stock solvents. Both the phases were then cooled to 0° C. In Fig. 1, the S rows are 12 separatory funnels, each containing 200 ml of the cold petroleum ether phase. The partially oxidized fatty acid ester was dissolved in the 200 ml of petroleum ether in S_1. Twelve extractions, each with a 100-ml portion (A) of the cold alcohol phase, removed all peroxides from S_1. The subsequent extractions, carried out successively in S_2 through S_{12} by each of these alcohol portions (12 A's, Fig. 1), recovered the majority of peroxides and distributed all unoxidized fatty acid ester together with some peroxides in the petroleum ether phase. These remaining peroxides, in S_2 to S_{12}, inclusive, were extracted by the number of alcohol portions (2 A's and 1 A) indicated at the end of the vertical lines extending from the corresponding petroleum ether phase. This additional extraction of peroxides by fresh solvent is not feasible with the standard counter-current procedures (6). Determination of peroxide values at different steps indicated the efficiency of separation. The peroxide-containing phase of alcohol was kept cooled below 0° C. The precooled oxygen-free nitrogen was bubbled through the above alcohol phase as an added protection. The alcohol phase yielded, in general, 99.0–99.9% of the oxygenated products formed during the autoxidation of fatty acid esters. The unoxidized fraction obtained from the petroleum ether phase contained only 0.0–0.7% of oxygenated products entirely from the unoxidized fatty acid esters, so that the oxygenated products may represent the initial autoxidation process involved. For the convenience of analysis, an aliquot portion

Can. J. Chem. Downloaded from www.nrcresearchpress.com by 196.1.178.254 on 09/04/12
For personal use only.

of the oxygenated products was reduced in a 1% alcohol solution by stannous chloride (5 moles/mole of peroxide), agitating with oxygen-free nitrogen.

Methyl linoleate autoxidized at 0° without agitation gave a peroxide concentrate representing 99.9% of the oxygenated products formed during the autoxidation reactions. The corresponding unoxidized fraction isolated was found to be pure methyl linoleate by the following analysis: hydrogen absorption, 1.98 mole/mole; hydroxyl, 0.0; acid value, 0.0; carbonyl value, 0.0; and polymer, 0.0. Elementary analysis: C, 77.47 and H, 11.52. Calculated for methyl linoleate: C, 77.55 and H, 11.56. The polymer contents were measured by the special microtechnique in distillation (15). The peroxide concentrate having the peroxide value of 6115 meq/kg (theory for methyl linoleate monohydroperoxide, 6125 meq/kg was hydrogenated with 2.92 moles H_2 to yield monohydroxystearic acids (m.p. 75.0–77.5° C (3); hydroxyl, 1.04 moles/mole). The preliminary polarographic studies indicated that peroxide concentrate consists of 100.5% of hydroperoxide. The reduced peroxide concentrate gave the following analysis: hydrogen absorption, 1.99 mole/mole; hydroxyl, 1.02 mole/mole; acid value, 0.0; carbonyl value, 0.0 (17); and polymer, 0.0. Elementary analysis: C, 73.41 and H, 10.89. Calculated for monohydroxy methyl linoleate: C, 73.51 and H, 10.97. The infrared analysis of the above samples also indicated production of almost 100% *cis,trans*-conjugated isomers. Two other samples of peroxide concentrates obtained from methyl linoleate autoxidized under identical conditions gave peroxide values of 6100 and 6135 meq/kg respectively. From these data, the initial autoxidation of methyl linoleate (up to extent of 10% used) gives rise to only monomeric hydroperoxides and no other products. The unoxidized fraction has also been isolated as pure methyl linoleate as shown above and by spectrophotometric analyses. Further confirmation of methyl linoleate monomeric hydroperoxides and its specific isomers has been made through the following experiments.

The infrared absorption of the isolated hydroperoxides at 10.55 μ and 10.15 μ for *cis,trans* isomers was compared with that of pure *cis,trans* isomer of methyl linoleate (under the courtesy of the General Mills' Research Laboratory of Minnesota, U.S.A.). Methyl linoleate hydroperoxides were thus proved to consist of only *cis,trans* isomer. Our attempts to separate other isomers, *trans,trans* in particular, from these methyl linoleate hydroperoxides under suitable conditions, ended in failure. About 90 ml of methanol was saturated with urea at 32° C and mixed with cold 10-ml solution of methyl hydroxy linoleates obtained by reduction of linoleate hydroperoxides (2.54 g). It was left to crystallize at 0° C. The crystals were also washed with cold (−10° C) methanol. The washings and mother liquors were combined and reduced in volume to saturation at about 15–20° C under vacuum. The second crop of crystals was collected under the same conditions. The extractions through cold heptane solvent (80–90° C) from cold aqueous solutions gave three fractions, each of which was found to contain *cis,trans* isomers absorbing at 10.15 μ and 10.55 μ. These experiments from the isolation of peroxides were completed in the course of 14 hours on the same day with a well-planned program. The isolated samples sealed under vacuum were kept in dry ice, wherever possible. (N.B. Such hurried activities in these analyses of *cis,trans* isomers were made possible during the tenure of stay by the author in Minneapolis, Minnesota, U.S.A.) A change was definitely found to occur in the *cis,trans* to *trans,trans* ratios of purified autoxidation products (cf. linoleate hydroperoxides and reduced products) after storage for a certain period of time. During the period of experiments, the samples kept under vacuum below 0° C and used occasionally for analyses showed appreciable conversion to *trans,trans* isomers which rose to almost 10% in amounts within the span

Can. J. Chem. Downloaded from www.nrcresearchpress.com by 196.1.178.254 on 09/04/12
For personal use only.

of a week. Even storage below −50° under vacuum did not stop such conversion. The *trans,trans* isomer (more than 25%) was obtained in all samples in a period of 6–9 months. Hence, it is quite apparent that the experimental conditions, unless scrupulously controlled, may change the true picture of autoxidation products consisting of only *cis,trans* isomer at the initial stages. The survey of literature (3, 5) indicates that all workers who studied kinetics or proposed theories did not consider these initial stages of autoxidation as important and never maintained conditions for keeping the peroxides intact in structure. Consequently, they dealt with only main autoxidation reactions involving decomposition of these peroxides and the resultant free radicals. Our point is related to only where and how autoxidation begins and, hence, much importance is attributed to the initial products unchanged and their energy of formation (10).

Characterization of Methyl Hydroxy Linoleates

Methyl hydroxy linoleates obtained by reduction of hydroperoxides from initial autoxidation of methyl linoleate have been previously shown to be *cis,trans*-conjugated isomers only through infrared analyses. Such products (250 mg) were quantitatively hydrogenated by Adam's platinum catalyst (1) to absorb 1.97 moles H_2 per mole. Methyl hydroxy stearates were subjected to resolution by column chromatography. Alumina was washed with 2 *N* HCl, then with water until neutral, and finally with ethanol. On activation at 150° C for 6 hours, the alumina was poured into a tube (1.0 cm × 110.0 cm) filled with petroleum ether (freed of the unsaturable materials and b.p. 80–90° C). Elution was carried on through petroleum ether containing 0–14% chloroform. Suitable fractions were collected and, through selections, the representative samples were made up. Methyl hydroxy stearates were thus resolved into two fractions (yield, 98.1% of that used) of almost equal weight. These had melting points: first 52.8–51.1° C (found: C, 72.4; H, 12.8; $C_{19}H_{33}O_3$ requires: C, 72.6; H, 12.1) and second 50.8–51.2° C (found: C, 73.2; H, 12.4). They were identified as methyl-, 13-, and 9-hydroxy stearates as done by Bergstrom (4).

Monohydroxystearic acids (40–50 mg) from methyl esters were added to 25% sulphuric acid (3.5 ml) containing 8% chromic acid. Steam was passed through the mixture for about 55 minutes with volume kept constant by additional controlled heating. The distillate was neutralized with alkali. After some concentration under vacuum, the acids were regenerated by sodium bisulphate and extracted with *n*-butanol. The scheme of partition paper chromatography (12) was utilized to analyze these acids; three well-defined intense spots were obtained, two of which had R_f values identical with those of *n*-pentanoic and *n*-hexanoic acids, and the third spot was in a some doubtful position of acids greater than C_8 in chain length. The other faint spots were neglected. For further confirmation, the method of Michael and Schweppe (14) was employed for detecting acids of chain length C_5–C_{18}. The butanol extracts were esterified by means of diazomethane (2) and the corresponding hydroxamic acids were prepared, and the acids *n*-pentanoic, *n*-hexanoic, *n*-nonanoic, and *n*-decanoic were identified. These four acids: C_5, C_6, C_9, and C_{10} can only result from the 9- and 13-hydroxystearic acids, confirming our results in the foregoing section.

Some Concepts on Mechanisms of Autoxidation of Methyl Linoleate

From the above findings, it can be asserted that only two *cis,trans*-conjugated isomers of 9- and 13-linoleate hydroperoxides are formed during autoxidation reactions. No 11-hydroperoxide has been detected in the products. Hence, the formation of 11-peroxide radical ($R^{11}O_2$) and transfer of O_2 to 9- and 13-position seems to be absurd from the modern concepts (cf. transfer of atoms) of electronic interpretation (8, 16). Furthermore,

Can. J. Chem. Downloaded from www.nrcresearchpress.com by 196.1.178.254 on 09/04/12
For personal use only.

the initiation of reaction through free radicals on the 5-C systems of linoleate does not eliminate the formation of 11-isomer. This has been confirmed by the excellent work on free radicals attacking such 5-C systems by Harrison and Wheeler (7). The question of energy to start off the first radical during the interactions of oxygen and linoleate can not be easily thrown off (10, 11).

It is, thus, quite apparent that complex formation already proposed for simple systems (10) may be applied to 5-C systems of methyl linoleate with some modifications. The concepts of non-localization and spread of π electrons (8) have made it possible to present the processes of activation and polarization of 5-C systems and oxygen molecules in the steps I–III of Fig. 2. The first stages of activated complex formation (IV) may involve

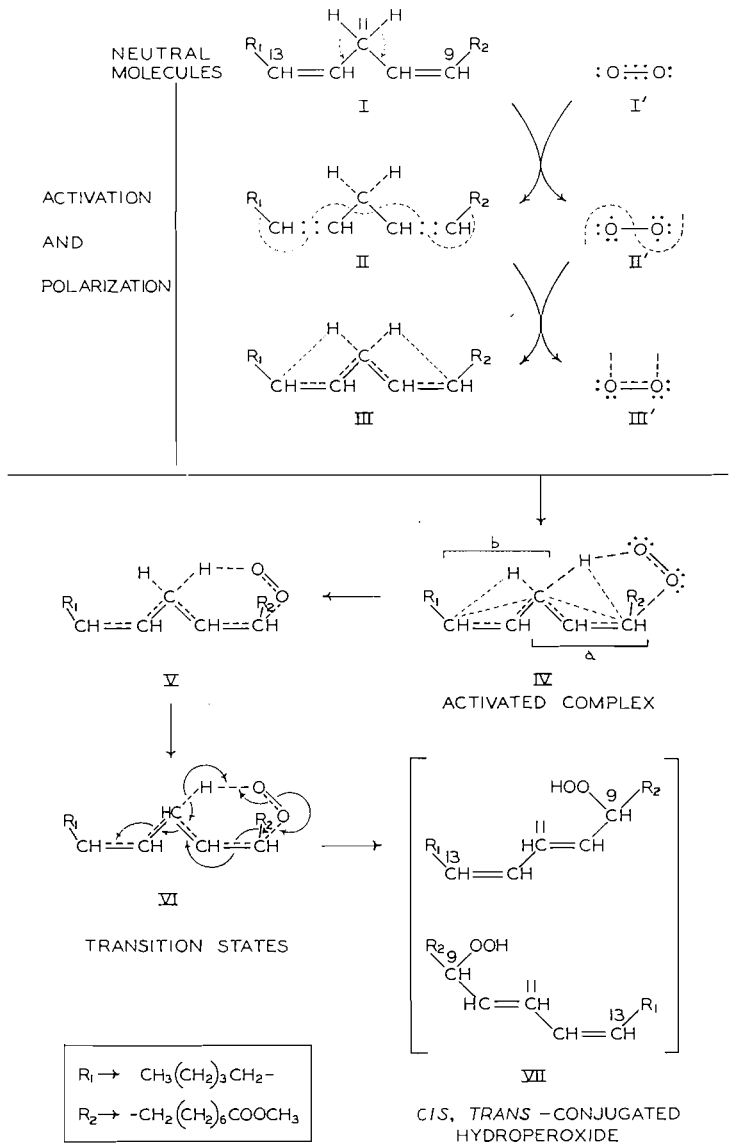

FIG. 2. Mechanism of autoxidation of methyl linoleate.

Can. J. Chem. Downloaded from www.nrcresearchpress.com by 196.1.178.254 on 09/04/12
For personal use only.

either *a* or *b* segment of the 5-C system. The activated complex through *a* (IV) gets its π electrons spread over the whole sphere of reactions including oxygen molecule (V) and then initiates shift of electrons as in VI, Fig. 2, only to give rise to the isomer, 9-hydroperoxide. Similarly, the activated complex through segment *b* (IV) will form 13-isomer of hydroperoxide. That the *cis* to *trans* conversion occurs only in one affected double bond next to hydroperoxide group, is evident from VI–VII, Fig. 2, showing spatial possibilities for 9-isomer. The foregoing mechanisms proposed for methylene-interrupted double bonds (5-C system) of methyl linoleate may account for the clear-cut formation of two conjugated isomers: 9- and 13-*cis*,*trans*-hydroperoxides that have been found as the reaction products of oxygen and methyl linoleate at the initial stages of autoxidation.

It may be noted here that it is of particular interest to consider the above mechanisms as the missing link between neutral methyl linoleate and the formation of its hydroperoxides without decomposition. After peroxide formation, many complicated processes including free radicals may be involved for the main autoxidation reactions which have been studied by various workers, kinetically or otherwise (3, 5). Hence, the proposed mechanisms for the initial reactions do not replace the ideas of free radicals, but these processes only supplement free radical mechanisms that play roles quite later and, consequently, demand careful kinetic studies from a different angle of approach under the conditions prescribed in this paper. Our future plans include such kinetic investigations. Moreover, the mode of complex formation, ahead of free radical reactions, is not new and has been found in many other reaction processes (18). Further details will be published later.

REFERENCES

1. ADAMS, R., VOORHEES, V., and SHRINER, R. L. Org. Syntheses, Coll. Vol. **I**, 463 (1948).
2. ARNDT, F. Org. Syntheses, Coll. Vol. **II**, 165, 461 (1943).
3. BATEMAN, L. Quart. Revs. **8**, 147 (1954).
4. BERGSTROM, S. Arkiv. Kemi, Mineral. Geol. A, **21**, 14 (1945); Nature, **156**, 717 (1945).
5. BOLLAND, J. L. and GEE, G. Trans. Faraday Soc. **42**, 239 (1946).
6. CRAIG, L. C. and CRAIG, D. *In* Technique of organic chemistry. Vol. III. *Edited by* A. Weissberger. Interscience Publishers, Inc., New York. 1950. p. 259.
7. HARRISON, S. and WHEELER, D. H. J. Am. Chem. Soc. **76**, 2379 (1954).
8. HERMANS, P. H. Introduction to theoretical organic chemistry. *Edited and translated by* R. E. Reeves. Elsevier Press Inc., New York. 1954. pp. 71–75.
9. KHAN, N. A. Biochim. et Biophys. Acta, **16**, 159 (1955).
10. KHAN, N. A. Can. J. Chem. **32**, 1149 (1954).
11. KHAN, N. A. J. Am. Oil Chemists' Soc. **30**, 273 (1953).
12. LINDQUIST, B. and STORGÄRDS, T. Acta Chem. Scand. **7**, 87 (1953).
13. MELVILLE, H. W. and COOPER, H. R. J. Chem. Soc. 1988 (1951).
14. MICHAEL, F. and SCHWEPPE, H. Mikrochim. Acta, 53 (1954).
15. PASCHKE, R. F., KERNS, J. R., and WHEELER, D. H. J. Am. Oil Chemists' Soc. **31**, 5 (1954).
16. REMICK, A. E. Electronic interpretations of organic chemistry. 2nd ed. John Wiley & Sons, Inc., New York. 1949. p. 112.
17. SIGGIA, S. Quantitative organic analysis via functional groups. John Wiley & Sons, Inc., New York. 1949.
18. URI, N. J. Am. Chem. Soc. **74**, 5808 (1952). BOOZER, C. E. and HAMMOND, G. S. J. Am. Chem. Soc. **76**, 3861 (1954). MAYO, F. R. J. Am. Chem. Soc. **75**, 6133 (1953).

Can. J. Chem. Downloaded from www.nrcresearchpress.com by 196.1.178.254 on 09/04/12
For personal use only.

Can. J. Chem. Downloaded from www.nrcresearchpress.com by 196.1.178.254 on 09/04/12
For personal use only.

A COMPARISON OF SLATER'S THEORY OF UNIMOLECULAR REACTIONS WITH EXPERIMENTAL DATA[1]

EVERETT THIELE AND DAVID J. WILSON

ABSTRACT

Slater's theory of unimolecular reactions is tested by comparing theoretical and experimental values of the pressure at which the rate constant has fallen off from the high-pressure limit by 5%. A simplified method is used for calculating lower bounds to the theoretical value of this pressure. Agreement with experimental data on cyclobutane, cyclobutene, and nitrogen pentoxide is rather poor; experimental values are lower than the calculated lower bounds.

Slater has set forth a detailed theory of unimolecular gas reactions which is based on a model of a vibrating molecule with a quadratic potential function (1, 2, 3). The molecule reacts when one particular internal co-ordinate (the reaction co-ordinate) attains a critical value. Slater derives an expression for the value of the rate constant at any pressure (k) divided by the value of the rate constant at infinite pressure (k_∞). His expression is $k/k_\infty = I_n(\theta)$, where the right-hand side is an integral depending on n, the number of normal co-ordinates contributing to the reaction co-ordinate, and on θ, which is proportional to pressure. Slater has evaluated this integral for $n = 3, 5, \ldots 13$ at increments of one of $\log_{10}\theta$. For our purposes it is sufficient to determine the value of θ for which $k/k_\infty = 0.95$, from which we shall determine the pressure (P_5) at which the reaction rate has dropped off 5% from its value at the high-pressure limit. Slater has also tabulated these values (3).

The exact application of Slater's theory to a reaction requires a detailed vibrational analysis, a knowledge of the experimental activation energy and of the reaction co-ordinate, and values for the collision diameters of the reactant and any added inert gases. In general, the larger the value of n, the lower is the predicted value of P_5. One upper bound for n is obviously the total number of normal modes of vibration possessed by the reactant molecule. In a molecule possessing symmetry, however, n may be considerably smaller than this if the reaction co-ordinate belongs to one of the symmetry species of the molecule. Even when this is not the case, an upper bound for n can often be determined by considering the symmetry of the less symmetrical molecule resulting when the molecule is distorted by giving the reaction co-ordinate a large value.

For Slater's quantity ν (for definitions of Slater's parameters the reader is referred to ref. 3) one can substitute the high-pressure limit of the pre-exponential factor. This leaves undetermined only the value of Slater's $\Pi_i\mu_i$. A maximum value of this quantity makes P/θ, and also P_5, a minimum. This maximum value is given by Slater (3) as $n^{-\frac{1}{2}n}$, and is obtained by assigning to all the μ_i an equal value. Physically this means that all pertinent normal modes contribute equally to the reaction co-ordinate. Slater has also defined a "representative spread" of the μ_i in such a way that they form a geometric progression with $\mu_1 = 5\mu_n$. P_5 has been calculated for both cases (and is defined as $P_{5\,\mathrm{min}}$ and $P_{5\,\mathrm{rep}}$, respectively) for three unimolecular reactions: the isomerization of cyclobutene, the decomposition of cyclobutane, and the decomposition of nitrogen pentoxide.

Cooper and Walters (4) concluded that the isomerization of cyclobutene to 1,3-butadiene proceeds unimolecularly without the formation of free radicals. If one assumes

[1]*Manuscript received January 29, 1959.*
Contribution from Department of Chemistry, University of Rochester, Rochester 20, New York.

C_{2v} symmetry for the molecule, the reaction co-ordinate is probably of symmetry species A_1. (One expects the reaction co-ordinate to be a simultaneous lengthening of the CH_2—CH_2 and CH=CH bonds and shortening of the CH_2—CH bonds; hydrogen migration seems unlikely and would lead to a too-large pre-exponential factor.) There are eight normal co-ordinates belonging to this species; therefore no more than eight normal vibrations can contribute to the reaction co-ordinate.

The decomposition of cyclobutane has been investigated by several authors (5, 6 *a*) and is thought to be elementary unimolecular. A possible reaction co-ordinate is the simultaneous expansion of two opposite C—C bonds. Although Slater's theory does not apply directly to such a case, we can hypothesize that the sum of these two bond lengths must reach a critical value in order for the reaction to take place. If one considers cyclobutane in such a stretched position prior to reaction, and assumes D_{2h} symmetry, the reaction co-ordinate is a member of the A_g symmetry species, which contains five normal modes.

Alternatively, the stretching of only one C—C bond may be necessary for reaction, in which case the distorted molecule prior to reaction has C_{2v} symmetry. The reaction co-ordinate is of symmetry species A_1, and thus no more than nine normal modes can contribute to it.

An argument against the participation of hydrogen migration to the reaction co-ordinate of cyclobutane is the result of recent unpublished work by Srinivasan and Kellner (both at the University of Rochester), who found that the thermal decomposition of 1,1,2,2-tetradeuterocyclobutane produced essentially no ethylene species of odd molecular weight. We are grateful to these workers for permission to quote their results. (It might be remarked in passing that the work of Rabinovitch and co-workers on dideuterocyclopropane (6 *b*) casts some doubt on the use of a hydrogen migration reaction co-ordinate in the analysis of data on the isomerization of cyclopropane.)

The rate-controlling step in the decomposition of nitrogen pentoxide in the presence of nitric oxide has been found to be unimolecular (7, 8, 9, 10). The reaction co-ordinate might be taken to be the antisymmetric migration of the central oxygen atom away from one nitrogen and toward the other. If, for purposes of computation, the molecule is fixed in a planar configuration, it possesses C_{2v} symmetry. The reaction co-ordinate belongs to symmetry species B_1, and so can be a combination of no more than five normal modes.

Alternatively, the reaction co-ordinate might be the stretching of one N—O bond. For a planar configuration, the distorted molecule possesses C_s symmetry, and 11 normal modes can contribute to the reaction co-ordinate.

Values of $P_{5\ \mathrm{min}}$ and $P_{5\ \mathrm{max}}$ can then be computed for these reactions by means of Slater's tables. (θ_5 for $n = 8$ was calculated by interpolation in Slater's table.) A collision diameter of five Angstroms was used in all calculations.

In two cases there exists a duplication of equivalent reaction co-ordinates within the molecule. Slater has shown that the effect of such a duplication is approximately equal to a multiplication of the over-all rate constant by the degree of duplication (11). Hence no change in the pressure at which $k/k_\infty = 0.95$ should be expected because of this duplication. The results of these calculations and the parameters used are listed in Table I.

It might be noted that, assuming C—C bond stretching is the reaction co-ordinate, Slater's theory is unable to account for the high pre-exponential factor found for cyclobutane. Other examples of "high" pre-exponential factors are known. It has also been

Can. J. Chem. Downloaded from www.nrcresearchpress.com by 196.1.178.254 on 09/04/12
For personal use only.

TABLE I

Experimental data					Theoretical results					
	ν ($\times 10^{13}$ sec^{-1})	E_0 (kcal/mol)	T (° K)	P_5 (mm)		n	$f_{n\,max}$	$P_{5\,min}$ (mm)	$f_{n\,rep}$	$P_{5\,rep}$ (mm)
Cyclobutene	1.2	32.5	422	10		8	20	1100	2.7	8500
Cyclobutane	400	62.5	722	50	Case 1	5	5.65	1.0×10^{7}	1.3	4.4×10^{7}
					Case 2	9	30	1.2×10^{5}	3.3	1.1×10^{6}
Nitrogen pentoxide	50	21	300	1×10^{4}	Case 1	5	5.65	1.7×10^{6}	1.3	7.5×10^{6}
					Case 2	11	70	6.3×10^{3}	5.3	8.3×10^{4}
					Interpolation was used for $n = 8$					

found experimentally that deactivation does not necessarily occur on every collision of an activated molecule with a foreign gas molecule (12, 13); hence the estimate of five Angstroms for the effective collision diameter may well be too high. This would introduce even larger discrepancies between the results of theory and experiment given in Table I.

One concludes that Slater's theory, although certainly the most detailed of the available theories of unimolecular reactions, may require some modifications—perhaps the inclusion of fairly substantial anharmonic interactions between the normal modes, and perhaps the use of a different type of collisional activation mechanism.

REFERENCES

1. SLATER, N. B. Proc. Cambridge Phil. Soc. **35**, 56 (1939).
2. SLATER, N. B. Proc. Roy. Soc. A, **194**, 112 (1948).
3. SLATER, N. B. Phil. Trans. Roy. Soc. London, A, **246**, 57 (1953).
4. COOPER, W. and WALTERS, W. D. J. Am. Chem. Soc. **80**, 4220 (1958).
5. GENAUX, C. T., KERN, F., and WALTERS, W. D. J. Am. Chem. Soc. **75**, 6196 (1953).
6. (*a*) PRITCHARD, H. O., SOWDEN, R. C., and TROTMAN-TICKENSON, A. F. Proc. Roy. Soc. A, **218**, 416 (1953).
   (*b*) RABINOVITCH, B. S., SCHLAG, E. W., and WIBERG, K. B. J. Chem. Phys. **28**, 504 (1958).
7. SMITH, J. H. and DANIELS, F. J. Am. Chem. Soc. **69**, 1735 (1947).
8. MILLS, R. L. and JOHNSTON, H. S. J. Am. Chem. Soc. **73**, 938 (1951).
9. JOHNSTON, H. S. and PERRINE, R. L. J. Am. Chem. Soc. **73**, 4782 (1951).
10. HISATSUNE, I. C., CRAWFORD, B., and OGG, R. A., JR. J. Am. Chem. Soc. **79**, 4648 (1957).
11. SLATER, N. B. Proc. Roy. Soc. A, **218**, 224 (1953).
12. CORDES, H. F. and JOHNSTON, H. S. J. Am. Chem. Soc. **76**, 4264 (1954).
13. WILSON, D. J. and JOHNSTON, H. S. J. Am. Chem. Soc. **75**, 5763 (1953).

Can. J. Chem. Downloaded from www.nrcresearchpress.com by 196.1.178.254 on 09/04/12
For personal use only.

Can. J. Chem. Downloaded from www.nrcresearchpress.com by 196.1.178.254 on 09/04/12
For personal use only.

THE WAX OF THE LEAVES OF PICEA PUNGENS (COLORADO SPRUCE)[1]

E. VON RUDLOFF

ABSTRACT

A chloroform-soluble, neutral wax was isolated from the leaves of Colorado spruce, collected during fall and winter months. The wax was found to consist of sabinic, 14-hydroxytetradecanoic, and juniperic acids, with only minor amounts of non-saponifiables and *n*-fatty acids. 14-Hydroxytetradecanoic acid has not been found before in naturally occurring waxes. A cyclic structure rather than the linear etholides proposed for other conifer waxes is in accord with the analytical data. In the spring and summer months the wax was accompanied by an acidic fraction.

A wax isolated from the leaves of Colorado spruce (*Picea pungens* Engelm.) has been found to differ from the waxes of other conifer leaves (1–7). Leaves harvested in the fall or winter yielded a virtually neutral wax which contained only minor amounts of non-saponifiable material. One of its main constituents is 14-hydroxytetradecanoic acid, which has apparently not been found in natural waxes before. Samples obtained during the spring or summer months, however, had much higher acid values, indicating that seasonal changes occur. Yields of the wax and analytical data are shown in Table I.

TABLE I

Yield and analytical data of waxes

Date of harvest		% Yield (based on dry weight)	Melting point, ° C	Acid value*	Saponification value*	%C	%H	Molecular weight	% Non-saponifiables
Sept./Oct.	1957	0.2–0.25	71–74	0–2	248†	72.92	11.09	860–900	3–4
Dec.	1957	0.25	70–74	0–2	252	—	—	—	—
March/April	1958	0.35	70–73.5	56	184	72.47	11.47	770–800	2–3
May	1958	0.35	69–74	54	—	—	—	—	—
July	1958	0.25	69–74	35	—	—	—	—	—
November	1958	0.25	70–73	5–6	225	74.43	11.77	900–920	1–2
Neutral portion									
March/April	1958	—	70–75	3–5	210	74.36	11.81	920–960	1–2

*Expressed in mg KOH per g wax.
†Saponification value after acetylation: 246.

The neutral wax, after purification, was saponified and the mixture of acids obtained on acidification was fractionated by countercurrent distribution (8). Three distinct fractions, comprising about 90% of the mixture, were obtained after applying 300 or more transfers, and were found to contain sabinic, 14-hydroxytetradecanoic, and juniperic acids, respectively (see Table II). The remaining 10% of the acid mixture was distributed broadly without forming a distinct peak. This was due in part to emulsion formation in tubes containing the less polar material (i.e. normal fatty acids). When the methyl esters were similarly fractionated no emulsification was encountered and the partition of the hydroxy compounds was more favorable, but again no distinct peak was obtained for the less polar compounds. Analysis by vapor-phase chromatography showed that normal fatty acids from lauric to stearic acids were present (see Table II). A substantial seasonal variation was found in the composition of the ω-hydroxy and normal fatty acid

[1]*Manuscript received February 16, 1959.*
Contribution from the National Research Council of Canada, Prairie Regional Laboratory, Saskatoon, Saskatchewan.
Issued as N.R.C. No. 5168 and as Paper No. 259 on the Uses of Plant Products.

mixtures. When the acidic wax isolated in the spring was chromatographed on a silicic acid – celite column a high proportion was recovered as a neutral wax having a composition similar to that isolated in the fall. The small amount (1–4%) of non-saponifiable material isolated had an infrared spectrum which resembled that of *n*-octadecanol; however vapor-phase chromatography showed it to be a mixture of at least four compounds.

TABLE II

Composition of the acidic portion of waxes

Date of harvest		ω-Hydroxy acids			*n*-Fatty acids			
		C_{12}	C_{14}	C_{16}	C_{12}	C_{14}	C_{16}	C_{18}
Sept./Oct.	1957*	22	40	28	(together about 10%)			
Sept./Oct.	1957†	18	45	26	Trace	2	4	5
March/April crude	1958†	13.5	36.5	12.5	7.5	5	10	14.5
March/April neutral	1958†	22.5	44	20.5	2.5	1.5	3	6
November	1958†	17	41	20	Trace	2	5	3

*Countercurrent distribution.
†Vapor-phase chromatography.

The neutrality of the wax, the small percentage of non-saponifiable material present, and the molecular weight of 850 to 950 suggest that the pure wax is composed of about four molecules of the three ω-hydroxy acids, esterified with each other in form of a cyclic polymer. Bougault and Bourdier (1) concluded that the waxes which they isolated consisted of similar esters but in the form of linear polymers, which they named etholides. Such an etholide (m.p. 87.5–88° C) has been prepared from juniperic acid by heat condensation (9). Kariyone *et al.* (5) deduced from their data that such etholides are composed of three to five molecules of juniperic and sabinic acids. A linear polymer would require one free hydroxyl and one free carboxyl group for each molecule. Assuming an average composition corresponding to a linear tetramer of 14-hydroxytetradecanoic acid, the calculated acid value, neutral equivalent, saponification value, and saponification equivalent after acetylation would be 60.7, 923.4, 230.8, and 965.4 respectively. These data do not correspond with those found for either the neutral or acidic wax from Colorado spruce (Table I). Infrared spectra of the neutral wax showed no free hydroxyl groups, and only a small peak for the acidic wax. It is suggested, therefore, that the neutral wax is composed mainly of a cyclic polymer of the ω-hydroxy acids and that the seasonal changes in acidity are caused, in part at least, by ring opening or closure.

Bougault and Cattelain (10) and Tong (7) have suggested that juniperic acid could be used for the production of compounds having musk odor, but the former authors thought the yields too small to be of practical value. Since 14-hydroxytetradecanoic acid forms a 1,14-tetradecanolide having musk odor (11), the same suggestion would apply to the wax from Colorado spruce leaves.

EXPERIMENTAL

Melting points were measured with a Leitz hot stage microscope. Vapor-phase chromatography was carried out with a Beckman GC-2 gas chromatograph using a 2-foot long, $\frac{1}{4}$-inch diameter column of washed silicone on C-22 firebrick (12) and helium as carrier gas. A modified E-C Apparatus Co. Fractionator, Model EC 510, was used in the

Can. J. Chem. Downloaded from www.nrcresearchpress.com by 196.1.178.254 on 09/04/12
For personal use only.

countercurrent distribution experiments (13). Molecular weights were determined by the Rast and isothermal distillation methods (14). Acid values (neutralization equivalents) and saponification equivalents were determined in the usual way, using 90% ethanol as solvent. Because of the low solubility of the waxes, a small amount of chloroform was added and titrations were carried out at 50–60° C. Acetylations were carried out with acetyl chloride and pyridine or dimethylaniline.

Isolation of the Wax

Leaves harvested in the fall of 1957 and spring of 1958 were treated as follows: fresh leaves, 200 g (dry weight approx. 90 g), were macerated in hot 40–60% aqueous alcohol, 1500 ml, with the aid of a 1-gal Waring blendor. The mixture was filtered and the residual pulp extracted similarly with hot benzene – ethanol (2:1 v/v). Both solutions, on reduction to a small volume and cooling, precipitated waxy material which was filtered off. The crude wax was found to be soluble in cold chloroform, hot ethanol, hot acetone, hot benzene, and hot carbon tetrachloride, and was insoluble in water, ether, and petrol.

In later work, the cuticle wax was isolated directly by steeping the fresh needles, 100 g, in chloroform, 500 ml. After it had been left standing for 2 to 3 hours the mixture was filtered and evaporated *in vacuo* (water pump) in a 1-liter flask. The residual material, 1.5 g, formed a thin film along the walls of the flask and was triturated with ether to remove ether-soluble impurities, 0.9 g.

The yields of crude wax at different times of the year are shown in Table I.

Purification of the Wax

The crude wax, 1 g, was dissolved in hot 75% aqueous alcohol (100 ml), and to the solution at 50–60° C was added an equal volume of petrol (b.p. 60–70° C). The mixture was stirred carefully and allowed to cool to room temperature, and the precipitated wax was filtered off. If the wax still had a light green color, the procedure was repeated. The wax was then recrystallized from acetone two or three times to give a constant melting product. If the wax was then further recrystallized from ethanol, ethanol–acetone, or petrol, the melting-point range did not decrease. The constants and analytical data for waxes isolated at various times are shown in Table I.

Separation into Components

The neutral wax (isolated in the fall of 1957, neutral equivalent 267), 1.000 g, was saponified by heating under reflux in 80% aqueous ethanol, 50 ml, containing potassium hydroxide, 1.0 g, for 6 to 8 hours. The non-saponifiable portion was recovered quantitatively by extracting the cold, diluted ethanolic solution three times with an equal volume of petrol (b.p. 60–70° C). The petrol extract was dried over anhydrous sodium sulphate, filtered, and evaporated to dryness. The residue, 0.010 g, had m.p. 51–70° C and an infrared spectrum resembling that of *n*-octadecanol, though not as well defined. Vapor-phase chromatography showed the presence of at least four compounds.

The ethanolic soap solution was evaporated to a small volume, acidified with 10% sulphuric acid solution, and quantitatively extracted with ether. The dried, filtered ethereal solution was evaporated to dryness to yield the free acids, 1.037 g (97.2% of theory, assuming the wax to be composed of etholides only). In another experiment the yield of non-saponifiables was 0.032 g and that of acids 1.040 g (97.6%).

The mixture of acids, 2.0 g, was fractionated by countercurrent distribution, using 60% aqueous ethanol – petrol (b.p. 60–70° C) as solvent system. When 200 transfers were applied three major peaks were obtained (weight analysis) which were not well

Can. J. Chem. Downloaded from www.nrcresearchpress.com by 196.1.178.254 on 09/04/12
For personal use only.

Can. J. Chem. Downloaded from www.nrcresearchpress.com by 196.1.178.254 on 09/04/12
For personal use only.

separated. Applying 400 transfers (withdrawal technique) a better than 90% separation of each component was obtained. Emulsification was troublesome in the most advanced tubes, and a better fractionation was obtained when the methyl esters were used (see below). The amount of each component was calculated and the material at and adjacent to the maxima was combined, evaporated, and recrystallized from acetone. Fraction I (tubes 0–18), 0.42 g (21%), m.p. 82–83.5° C, corresponding to sabinic acid, m.p. 84° C, 84–85° C (1, 9). Calculated for $C_{12}H_{24}O_3$: C, 66.63%; H, 11.18%; neutral equivalent, 216.31. Found: C, 66.91%; H, 11.18%; neutral equivalent, 218.2. The methyl ester was prepared with diazomethane, giving a compound m.p. 31–34° C after three crystallizations from petrol and methanol–water; reported m.p. 34–34.5° C (9). Calculated for $C_{13}H_{26}O_3$: C, 67.78%; H, 11.38%; saponification equivalent, 230.34. Found: C, 68.01%; H, 11.45%; saponification equivalent, 238.3. Acetyl derivative m.p. 42–43.5° C after three crystallizations from petrol (b.p. 60–70° C); reported m.p. 45° C (9).

Fraction II (tubes 19–40), 0.80 g (40%), m.p. 89.5–91.0° C; reported for 14-hydroxytetradecanoic acid, m.p. 91.0–91.5° C (9). Calculated for $C_{14}H_{28}O_3$: C, 68.81%; H, 11.55%; neutral equivalent, 244.36. Found: C, 68.54%; H, 11.35%; neutral equivalent, 246.36. Methyl ester: m.p. 45.5–46.0° C; reported m.p. 47° C (9). Calculated for $C_{15}H_{30}O_3$: C, 69.72%; H, 11.70%; saponification equivalent, 258.39. Found: C, 69.93%; H, 11.79%; saponification equivalent, 259.2. Acetyl derivative: m.p. 53.5–54.5° C; reported m.p. 54–54.5° C (9).

Fraction III (tubes 41–66), 0.56 g (28%), m.p. 94.5–95.5° C; reported for juniperic acid m.p. 95° C (1, 9). Calculated for $C_{16}H_{32}O_3$: C, 70.54%; H, 11.84%; neutral equivalent, 272.42. Found: C, 70.26%; H, 11.60%; neutral equivalent, 274.5. Methyl ester: m.p. 54.5–55.0° C; reported m.p. 55–55.5° C (1, 9). Calculated for $C_{17}H_{34}O_3$: C, 71.28%; H, 11.96%; saponification equivalent, 286.44. Found: C, 71.17%; H, 11.62%; saponification equivalent, 283.5. Acetyl derivative: m.p. 62–64° C; reported m.p. 63° C (9).

The material in tubes 67 and higher, 0.15 g (7.5%), formed no distinct peak. It was combined, esterified, and analyzed by vapor-phase chromatography. Peaks corresponding to lauric (approximately 5%), myristic (20%), palmitic (35%), and stearic (40%) acids were obtained.

The mixture of acids was also fractionated by countercurrent distribution in form of their methyl esters. A satisfactory separation into three hydroxy esters was obtained with 200 transfers using 75% aqueous ethanol – petrol (b.p. 60–70° C) as solvent system. The partition ratios for the C_{12}, C_{14}, and C_{16} ω-hydroxy esters were 0.18, 0.33, and 0.48, respectively, and the relative amounts of each component were practically the same as those found for the free acids.

Chromatography of Acidic Wax

The acidic wax (isolated in the spring of 1958, acid value 56), 1.000 g, was chromatographed on a column, 2.0 cm diameter, of silicic acid – celite (2:1), 50 g, using chloroform as eluent. Fractions of 25 ml were collected. Fractions 5 to 11 yielded 0.93 g of practically neutral wax, m.p. 70–75° C. Found: C, 74.36%; H, 11.81%; acid value 3–5; saponification equivalent, 267; molecular weight, 940–970. Saponification equivalent after acetylation, 272. A small aliquot was saponified and the free acids converted to their methyl esters with diazomethane. The percentage composition of the mixture of methyl esters is shown in Table II.

Vapor-phase Chromatography

All material investigated was injected as concentrated ethereal solutions of the methyl

esters, or, in the case of the non-saponifiables, as dilute ethanolic solutions of the free alcohols. The methyl esters were analyzed at 220° C and 30 p.s.i. pressure (flowrate = 82.55 cc per minute, soap bubble counter). The time of emergence, measured on the chart paper as the distance from the start (solvent peak) to the maximum of each peak, was 1.8, 3.5, 7.0, and 13.9 (±0.2) cm for methyl laurate, myristate, palmitate, and stearate and 5.4, 9.7, and 20.1 (±0.2) cm for the methyl esters of the C_{12}, C_{14}, and C_{16} ω-hydroxy acids, respectively. The areas under the curves were obtained by the triangulation method and the percentage of each component was calculated from its area as compared with the sum of the peak areas. The error on runs with mixture of known amounts of normal fatty acid esters was ±1%. When the non-saponifiable material was analyzed on the same column and at the same temperature, four peaks were recorded.

ACKNOWLEDGMENTS

The author is grateful to Mr. M. Mazurek for carrying out the microanalyses and to Mr. M. Granat for technical assistance and recording the infrared spectra.

REFERENCES

1. BOUGAULT, J. and BOURDIER, L. Compt. rend. **147**, 1311 (1908); J. pharm. chim. **29** (6), 561 (1909); **30**, 10 (1909); **3** (7), 101 (1911).
2. KAUFMANN, H. P. and FRIEDEBACH, M. Chem. Ber. **55**, 1508 (1922).
3. SAKURAI, J. J. Pharm. Soc. Japan, **51**, 34 (1931); **53**, 579 (1933).
4. FUJITA, A. and YOSHIKAWA, T. J. Pharm. Soc. Japan, **71**, 913 (1951).
5. KARIYONE, T., WATANABE, H., and KADOWAKI, H. J. Pharm. Soc. Japan, **72**, 5, 7, 10, 11 (1952).
6. KARIYONE, T. and ISOI, K. J. Pharm. Soc. Japan, **74**, 1312 (1954); **75**, 316 (1955); **76**, 473 (1956).
7. TONG, S. T. Soap, Perfumery & Cosmetics, **27**, 58 (1954).
8. HORN, D. N. S., HOUGEN, F. W., RUDLOFF, E. VON, and SUTTON, D. A. J. Chem. Soc. 177 (1954).
9. CHUIT, P. and HAUSSER, J. Helv. Chim. Acta, **12**, 463 (1929).
10. BOUGAULT, J. and CATTELAIN, E. Compt. rend. **186**, 1746 (1928).
11. CRABALONA, L. L. Brit. Pat. No. 655,428 of July 18, 1951. cf. Chem. Abstr. **46**, 8148ᵉ (1952).
12. CRAIG, B. M. and MURTY, N. L. Can. J. Chem. **36**, 1297 (1958).
13. RAYMOND, S. Anal. Chem. **30**, 1214 (1958).
14. CHILDS, C. E. Anal. Chem. **26**, 1963 (1954).

Can. J. Chem. Downloaded from www.nrcresearchpress.com by 196.1.178.254 on 09/04/12
For personal use only.

Can. J. Chem. Downloaded from www.nrcresearchpress.com by 196.1.178.254 on 09/04/12
For personal use only.

THE BIOGENESIS OF ALKALOIDS

XXI. THE BIOGENESIS OF (−)-HOMOSTACHYDRINE AND THE OCCURRENCE OF TRIGONELLINE IN ALFALFA[1]

A. V. ROBERTSON[2] AND LÉO MARION

ABSTRACT

In an attempt to find the precursor of the piperidine ring in homostachydrine, young alfalfa shoots were fed (*a*) lysine-2-^{14}C, (*b*) lysine-2-^{14}C with pyridoxine, (*c*) lysine-2-^{14}C with pyridoxine and folic acid, and finally (*d*) lysine-2-^{14}C with pyridoxine, folic acid, and methionine. In all cases the homostachydrine isolated from the harvested plants showed no radioactivity. It is shown that homostachydrine is not synthesized at the stage of growth at which the experiments were carried out. Alfalfa has been found to contain a hitherto unreported alkaloid shown to be trigonelline by comparison with an authentic sample. Both homostachydrine and trigonelline are found in the seeds, and are not actively synthesized in the plant until seed formation. Asparagine has also been isolated in relatively high yield.

In the course of experiments on the biosynthesis of stachydrine in alfalfa (*Medicago sativa* L. Grimm) Wiehler and Marion isolated a new alkaloid which they called (−)-homostachydrine (1). The compound was identified as the laevorotatory methyl betaine of pipecolic acid, and it has since been shown to belong to the L-series of amino acids by correlation with L-(−)-pipecolic acid (2, 3).

It has been suggested (1) that homostachydrine is formed in the plant by ring closure of lysine to pipecolic acid followed by the methylation to the betaine. Lysine is known to be a precursor of pipecolic acid in *Phaseolus vulgaris* (4, 5), *Neurospora* (6), and the intact rat (7), and the intermediates of the process have been studied with the aid of enzyme preparations from rat tissue, *Neurospora*, *Pisum sativum*, and *Phaseolus radiatus* (8, 9). The presence of pipecolic acid in alfalfa has yet to be demonstrated but in view of its occurrence in other legumes (10, 11, 12) it would not be surprising if it were found as a nonprotein nitrogen constituent of alfalfa.

We have attempted to provide evidence for the biosynthetic pathway proposed for homostachydrine by feeding lysine-2-^{14}C to 2-week-old alfalfa. A week later the plants were harvested and extracted, but the homostachydrine isolated was radioinactive. In previous experiments on the biosynthesis of stachydrine it was found that ornithine-2-^{14}C was not converted to proline in alfalfa unless pyridoxine was also administered, but even then the stachydrine did not become radioactive (13). In case similar conditions prevailed for the ring closure of lysine, an experiment was performed in which lysine-2-^{14}C and pyridoxine were fed to 2-week-old alfalfa, but again the crystalline alkaloid fraction isolated from the plants a week later was not radioactive. Following the ideas of Wiehler and Marion (14) on stachydrine biosynthesis, folic acid was fed together with lysine-2-^{14}C and pyridoxine in an attempt to stimulate the biological methylation of pipecolic acid, but no radioactivity was incorporated in the homostachydrine subsequently isolated. In a final experiment to influence the biosynthesis of homostachydrine along the proposed route by enhancing the probability of methylation, lysine-2-^{14}C was fed in conjunction with pyridoxine, folic acid, and methionine, but again the alkaloid remained inactive.

These negative results might be interpreted to mean either that lysine is not a pre-

[1]*Manuscript received March 3, 1959.*
Contribution from the Division of Pure Chemistry, National Research Council, Ottawa, Canada.
Issued as N.R.C. No. 5179.
[2]*National Research Council of Canada Postdoctorate Fellow (1957–59).*

cursor of homostachydrine, or that the synthesis of the alkaloid takes place at a later stage of development of the plant, in which case the homostachydrine isolated would have been material stored in the seeds. The second of these interpretations is supported by a result described by Wiehler and Marion (14), who found that after feeding methionine-Me-^{14}C, pyridoxine, and folic acid to alfalfa seedlings, stachydrine became radioactive whereas homostachydrine did not. Assuming that the enzymes controlling methylation of the nitrogen heterocycles are similar, this clearly indicates that only the stachydrine is being synthesized at a plant age of 2 to 3 weeks.

In the last of the experiments with radioactive lysine, the crude betaine hydrochlorides from the reineckate separation were recrystallized without the usual purification through a mercuric chloride complex. The first crop was expected to be homostachydrine hydrochloride (m.p. 217°), but it melted at 240–246°, and after several recrystallizations at 247–250° (decomp.). Elemental analysis of this hydrochloride indicated the formula $C_7H_7O_2N.HCl$, and the ultraviolet spectrum showed aromatic absorption. Since the substance was isolated from the stachydrine fraction from which the stronger bases had already been removed, it was assumed to be a betaine. Thus the choice of structure was reduced to one of the betaines of the three isomeric pyridinecarboxylic acids. Homarine, the α-isomer, was eliminated because its hydrochloride melts at 170° (15). Since the γ-isomer has not been found naturally, trigonelline, the β-isomer, seemed the more likely of the two remaining possibilities. The complete identity of the ultraviolet and infrared spectra, X-ray powder pattern and paper chromatographic properties for the natural sample, and synthetic trigonelline hydrochloride confirmed the structure. Synthetic trigonelline hydrochloride had m.p. 259–260° (decomp.) after softening at 257°, but the melting point of the natural material could not be raised above 250°. Other low-melting samples of trigonelline hydrochloride isolated from natural sources have been reported (16, 17, 18).

In the mercuric chloride precipitation normally used as a final purification step for stachydrine and homostachydrine, trigonelline does not precipitate with the reagent (20% hydrochloric acid saturated with mercuric chloride). Thus in previous work on alfalfa in this laboratory (1, 13, 14, 19) had trigonelline been present it would have remained unnoticed in the filtrate. To see if trigonelline is a normal constituent of the plant, alfalfa seedlings 16 days old and grown with the usual 30 g of seeds per tray (14, 19) were extracted, but trigonelline could not be detected. In the experiment described above in which trigonelline was isolated, 40 g of seeds per tray were used, and experience gained since suggests that this quantity overloads the trays so that although good germination occurred, some seeds did not grow because those already sprouting formed a light shield. This observation suggested that trigonelline may occur in alfalfa seeds and a direct extraction confirmed the idea. Indeed it is present in the betaine fraction of the seeds in a larger amount (38%) than stachydrine (33%) or homostachydrine (29%). It was not discovered in the extraction of seeds by Wiehler and Marion (1) because they used a final mercuric chloride purification. Furthermore, in the butanol – dilute hydrochloric acid system which they used for separating stachydrine (R_F 0.50) and homostachydrine (R_F 0.58) by paper chromatography, trigonelline has the same R_F as choline (0.41). Trigonelline (R_F 0.37) is readily separated from choline (R_F 0.57) in ethanol–ammonia (20). In this system homostachydrine has R_F 0.56 and stachydrine R_F 0.50.

Trigonelline and homostachydrine seem to be formed in alfalfa at the time of seed formation. The trigonelline stored in the seed is used up in the first few days of growth and the homostachydrine disappears between 1 and 5 months, since an extraction of

Can. J. Chem. Downloaded from www.nrcresearchpress.com by 196.1.178.254 on 09/04/12
For personal use only.

plants 5 months old showed stachydrine as the only betaine. Hence the biosynthesis of homostachydrine must take place during the flowering and seed-setting period. The proposed biosynthetic scheme remains as a working hypothesis, but no greater credence can be attached to it in view of recent findings that proline is not involved in the biosynthesis of stachydrine (21).

After removing the proteins in the alfalfa extractions the betaines were separated from the water-soluble residue by leaching with alcohol. The fraction insoluble in alcohol partly crystallized and the recrystallized compound was identified by its elemental analysis, infrared spectrum, and X-ray powder pattern as asparagine. The yield was 2.5% of the weight of the dry plant. Asparagine had been isolated from alfalfa previously (22) but the ease of isolation and the high yield in the present experiments are noteworthy.

EXPERIMENTAL

Melting points are corrected. The infrared absorption spectra were measured in nujol mulls on a Perkin–Elmer double beam spectrometer model 21B.

Feeding Experiments with Lysine-2-^{14}C

Alfalfa seeds were germinated on glass wool as previously described (14, 19) using 300 g in 10 trays (20×30 cm) for the first three experiments and 400 g for the fourth. It was found that discarding the nutrient solution and washing with distilled water each week (14, 19) made the plants too wet and was unnecessary for good growth to an age of 3 weeks.

Experiment 1.—On the 14th day 8.0 mg DL-lysine-2-^{14}C-monohydrochloride (purchased from Tracerlab Inc.) with a total activity of 3.2×10^7 d.p.m. in 500 ml nutrient solution was administered. Plants were harvested on the 20th day.

Experiment 2.—On the 14th day a mixture of 8.5 mg radioactive lysine, total activity 3.5×10^7 d.p.m., and 1 mg pyridoxine hydrochloride in 500 ml nutrient solution was administered. Plants were harvested on the 19th day.

Experiment 3.—On the 10th day a mixture of 7.6 mg radioactive lysine, total activity 3.0×10^7 d.p.m., 1 mg pyridoxine hydrochloride in nutrient solution, and 1 mg folic acid in sodium bicarbonate solution (23) was administered. Plants were harvested on the 20th day.

Experiment 4.—Nutrient solutions containing a total of 22 mg radioactive lysine, total activity 1.8×10^8 d.p.m., 3 mg pyridoxine, 5 mg folic acid in aqueous sodium bicarbonate, and 250 mg (±)-methionine were administered in three portions on the 7th, 11th, and 16th day. Plants were harvested on the 20th day.

Extraction Procedure (cf. 1, 13, 14, 19)

Preliminary defatting of the dried plant material by refluxing (4 hours) with petroleum ether (b.p. 75–90°) was advantageous in avoiding emulsions and giving sharper fractions in subsequent stages. This was particularly important during an extraction of alfalfa seeds. The plant material was boiled with three lots of 70% alcohol, but the extracts were not diluted with water (1) before precipitation of the proteins with lead acetate. After removing the excess of lead as sulphide, the filtrate was evaporated to dryness using octyl alcohol as required to prevent frothing. The alcohol-soluble substances in the resulting dark brown gum could not be obtained by direct extraction on account of the impermeable nature of the material. Of the several methods tried, the best was to dissolve the gum in an equal volume of hot water and slowly add 10 volumes of hot alcohol with vigorous swirling. Most of the material precipitated and after being cooled to 0° the

Can. J. Chem. Downloaded from www.nrcresearchpress.com by 196.1.178.254 on 09/04/12
For personal use only.

supernatant liquid was decanted. This process was repeated twice more. Frequently the gum which was precipitated on adding alcohol crystallized spontaneously, and after recrystallization of the solid from water, large white rhombs having m.p. 234° (decomp.) were obtained in yields from 2–3% of the dry plant weight. The compound was identified as (−)-asparagine hydrate by comparison of its infrared spectrum and X-ray powder pattern with those of an authentic specimen. Found for the anhydrous compound: C, 36.1; H, 6.0; N, 20.8. Calc. for $C_4H_8N_2O_3$: C, 36.4; H, 6.1; N, 21.2%; $[\alpha]_D^{25}$ −5.2° (*c*, 2.0 in water).

The choline and betaine reineckates were separated from the decanted alcoholic extract in the usual way (20, 24, 25, 26). A quicker method of obtaining the hydrochlorides from the reineckates than the precipitation technique (27) was ion exchange chromatography. Amberlite IRA 401 ion exchange resin was rinsed through two cycles with aqueous sodium hydroxide and hydrochloric acid. The chloride form was washed with methanol and a 50-ml tube was filled with the resin. The reineckate (0.50 g) was dissolved in boiling acetone (20 ml) and diluted with methanol (40 ml). The cooled solution was percolated rapidly through the column and eluted with methanol (100 ml), the operation being completed in 10 minutes. If slower flow rates were used, the absorbed reineckate ion began to decompose on the column, discharging an orange impurity. Removal of solvent from the eluate left a quantitative yield of the mixed betaine hydrochlorides, which were best separated by fractional crystallization. Trigonelline hydrochloride is far less soluble than the other two betaines so when present it was separated by using the minimum volume of boiling absolute ethanol for solution. The filtrate after removal of trigonelline was boiled, and successive additions of hot ethyl acetate gave fractions consisting of almost pure homostachydrine hydrochloride. The stachydrine remaining in the filtrate was very difficult to crystallize because contamination due to the homostachydrine still present rendered the mixture much more soluble than pure stachydrine hydrochloride. In the absence of trigonelline the usual mercuric chloride precipitation was very useful in purifying the betaine fraction.

Extraction Results

In the first three experiments with radioactive lysine, the average yield of betaine hydrochlorides was 0.35 g and the mixture was shown by paper chromatography to consist of stachydrine and homostachydrine in a ratio of *ca.* 1:1. In the fourth experiment, using 400 g of seeds, the yield of betaine hydrochlorides was 0.56 g. The first crystalline fraction (0.14 g) after further recrystallization from alcohol had m.p. 247–250° (decomp.). Found: C, 48.9; H, 4.8; N, 7.7; Cl, 20.3. Calc. for $C_7H_7NO_2.HCl$: C, 48.5; H, 4.65; N, 8.1; Cl, 20.4%. Ultraviolet spectrum in ethanol 0.2 *M* with respect to hydrochloric acid, λ_{max} 266 mμ, log ε 3.67. The ultraviolet and infrared spectra, X-ray powder pattern, and paper chromatograms of the natural sample were completely superimposable on those of a synthetic specimen of trigonelline hydrochloride, prepared by methylation of nicotinic acid according to the procedure of Cornforth and Henry (28). The synthetic material had m.p. 259–260° after softening at 257°. None of the above betaine fractions was radioactive.

R_F values of these compounds in butanol – concentrated hydrochloric acid – water (100:20:39) were: homostachydrine, 0.58; stachydrine, 0.50; trigonelline, 0.41; choline, 0.41; and in 95% ethanol – concentrated aqueous ammonia (95:5) were: homostachydrine, 0.56; stachydrine, 0.50; trigonelline, 0.37; choline, 0.57. Descending chromatography was used and the solvent front travelled *ca.* 18 inches, taking 40 hours in the acid system and 18 hours in the alkaline system. The spots were developed with a modi-

Can. J. Chem. Downloaded from www.nrcresearchpress.com by 196.1.178.254 on 09/04/12
For personal use only.

fied Dragendorff's reagent (29) in which the shade of color produced with fresh reagent was characteristic for these compounds. The reagent was made by dissolving potassium iodide (10 g) in water (10 ml) and glacial acetic acid (20 ml). Bismuth subnitrate (3.4 g) was dissolved in small portions with stirring. If necessary, the solution was filtered and then made up to 60 ml with water. For spraying, this stock solution (1 vol) was diluted with 30% acid (9 vol).

In the extraction of trigonelline from 300 g of alfalfa seeds, 0.52 g of betaine hydrochlorides was obtained (0.17% yield). By fractional crystallization 206 mg of trigonelline and 85 mg of homostachydrine hydrochlorides were separated. The remaining stachydrine fraction (0.23 g) was estimated by the intensity of spots on paper chromatograms to be one third homostachydrine, giving the following analysis of the betaine fraction: trigonelline, 38%; stachydrine, 33%; homostachydrine, 29%.

In the extraction of alfalfa 5 months old, 50 plants grown in soil were used, and the roots and aerial portions were treated separately. The former (dry weight 10 g) yielded 15 mg of stachydrine hydrochloride and the latter (dry weight 43 g) yielded 140 mg. No homostachydrine or trigonelline was detected by paper chromatography.

REFERENCES

1. WIEHLER, G. and MARION, L. Can. J. Chem. **36**, 339 (1958).
2. ROBERTSON, A. V. and MARION, L. Can. J. Chem. **37**, 829 (1959).
3. BEYERMAN, H. C. Rec. trav. chim. (In press).
4. GROBBELAAR, N. and STEWARD, F. C. J. Am. Chem. Soc. **75**, 4341 (1953).
5. LOWY, P. H. Arch. Biochem. Biophys. **47**, 228 (1953).
6. SCHWEET, R. S., HOLDEN, J. T., and LOWY, P. H. J. Biol. Chem. **211**, 517 (1954).
7. ROTHSTEIN, M. and MILLER, L. L. J. Am. Chem. Soc. **75**, 4371 (1953); J. Biol. Chem. **211**, 851 (1954).
8. MEISTER, A. and BUCKLEY, S. D. Biochim. et Biophys. Acta, **23**, 202 (1957).
9. MEISTER, A., RADHAKRISHNAN, A. N., and BUCKLEY, S. D. J. Biol. Chem. **229**, 789 (1957).
10. ZACHARIUS, R. M., THOMPSON, J. F., and STEWARD, F. C. J. Am. Chem. Soc. **76**, 2912 (1954).
11. MORRISON, R. M. Biochem. J. **50**, XIV (1952); **53**, 474 (1953).
12. ZACHARIUS, R. M., THOMPSON, J. F., and STEWARD, F. C. J. Am. Chem. Soc. **74**, 2949 (1952); **76**, 2908 (1954).
13. MORGAN, A. and MARION, L. Can. J. Chem. **34**, 1704 (1956).
14. WIEHLER, G. and MARION, L. J. Biol. Chem. **231**, 799 (1958).
15. HOPPE-SEYLER, F. A. Z. physiol. Chem. **222**, 105 (1933).
16. KNOWLES, W. S. and ELDERFIELD, R. C. J. Org. Chem. **7**, 389 (1942).
17. SCHOICHI YANAGITA. J. Pharm. Soc. Japan, **64**, 38 (1944).
18. OGATA, A. and KOMODA, T. J. Pharm. Soc. Japan, **63**, 653 (1943).
19. LEETE, E., MARION, L., and SPENSER, I. D. J. Biol. Chem. **214**, 71 (1955).
20. BREGOFF, H. M., ROBERTS, E., and DELWICHE, C. C. J. Biol. Chem. **205**, 565 (1953).
21. ROBERTSON, A. V. and MARION, L. Can. J. Chem. (In press).
22. VICKERY, H. B. J. Biol. Chem. **60**, 647 (1924); **61**, 117 (1924).
23. LASCELLES, J., CROSS, M. J., and WOODS, D. D. J. Gen. Microbiol. **10**, 267 (1954).
24. STRACK, E. and SCHWANEBERG, H. Z. physiol. Chem. **245**, 11 (1936).
25. GLICK, D. J. Biol. Chem. **156**, 643 (1944).
26. LEE KUM-TATT. Nature, **182**, 655 (1958).
27. KAPFHAMMER, J. and BISCHOFF, C. Z. physiol. Chem. **191**, 179 (1930).
28. CORNFORTH, J. W. and HENRY, A. J. J. Chem. Soc. 601 (1952).
29. PALMER, K. H. (Private communication).

Can. J. Chem. Downloaded from www.nrcresearchpress.com by 196.1.178.254 on 09/04/12
For personal use only.

Can. J. Chem. Downloaded from www.nrcresearchpress.com by 196.1.178.254 on 09/04/12
For personal use only.

THE ACTION OF SODIUM IODIDE ON *O*-*p*-TOLUENE-SULPHONYL-1,4;3,6-DIANHYDRIDES OF D-MANNITOL, D-GLUCITOL, AND L-IDITOL[1]

M. JACKSON AND L. D. HAYWARD

ABSTRACT

In the displacement reaction with sodium iodide in acetic anhydride solution the rates of reaction of four isohexide tosyl esters were compared to that of an *O*-acetyl-*O*-tosylisosorbide recently described. The tosyloxy group in the latter compound was replaced rapidly and was therefore in the 5-*endo*-position, the compound being correctly named 2-*O*-acetyl-5-*O*-*p*-toluenesulphonyl-1,4;3,6-dianhydro-D-glucitol. The product of the reaction was isolated as a crystalline material, and was identified as 2-*O*-acetyl-5-deoxy-5-iodo-1,4;3,6-dianhydro-L-iditol.

INTRODUCTION

The 1,4;3,6-dianhydrides of D-mannitol, D-glucitol, and L-iditol (isomannide (I), isosorbide (II), and isoidide (III)) represent a useful series of compounds for the study of reaction mechanisms from a steric point of view. These compounds possess two fused five-membered rings having a *cis*-arrangement of the ring junction. The rings, being nearly planar, are inclined to one another at an angle of about 120°. Substituents on carbon atoms 2 and 5 can either be on the outside of the V formed by the rings when they are called *exo* (R_2, R_3) or on the inside and named *endo* (R_1, R_4). The conformation of the ring system is rigid in as much as it cannot undergo inversion of the type occurring in cyclohexane conformations and the shape and dimensions of the molecules are therefore fairly well known (2).

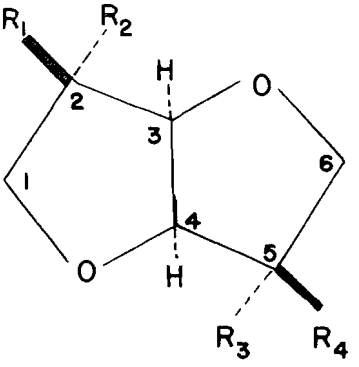

I	R_1 = OH	R_2 = H	R_3 = H	R_4 = OH
II	H	OH	H	OH
III	H	OH	OH	H
IV	OTs	H	H	OTs
V	H	OTs	H	OTs
VI	H	OTs	OTs	H
VII	H	OTs	I	H
VIII	H	O.CO.CH_3	H	OTs
IX	H	O.CO.CH_3	I	H
X	H	I	I	H

[1]*Manuscript received March 2, 1959.*
Contribution from the Department of Chemistry, University of British Columbia, Vancouver, B.C.

Can. J. Chem. Downloaded from www.nrcresearchpress.com by 196.1.178.254 on 09/04/12
For personal use only.

The reaction of sodium iodide with the isohexide di-*O*-*p*-toluenesulphonates (di-*O*-tosylates) has been studied on a qualitative basis by several workers. Hockett *et al.* (3, 4) prepared the 2,5-dideoxy-2,5-diiodo derivative from isomannide di-*O*-tosylate (IV) and a monodeoxy-monoiodo derivative from the isosorbide isomer (V). Matheson and Angyal (5) compared the reaction of these compounds with that of other secondary tosylates by isolating the sodium *p*-toluenesulphonate formed but not the other organic products. These authors found that, in the D-mannitol derivative (IV), both tosyloxy groups are readily replaceable by iodine, but in the D-glucitol derivative (V) only one, and in the L-iditol derivative (VI) neither, tosyloxy group was replaceable. Wiggins and Wood (6), by isolating the dianhydro products, obtained a parallel series of results from reactions of the di-*O*-tosyl and di-*O*-mesyl derivatives with sodium iodide and with lithium chloride respectively. These results confirm that both sulphonoxy groups of the isomannide derivatives and one in the isosorbide derivatives are readily replaced by halide ion, whereas the second group of the isosorbide derivatives and both groups of the isoidide derivatives failed to react under the same conditions.

This behavior was explained (5) by an S_N2 mechanism with attack by the halide ion at the face of the carbon atom opposite the sulphonoxyl group. It may be seen from models that this mode of attack is hindered by the ring system when the group to be displaced is in the *exo* position, as in isoidide derivatives and the 2-position of isosorbide. When the group is *endo*, however, the attack is relatively easy and this situation is found in isomannide derivatives and the 5-position of isosorbide. Other reactions in the isohexide series having an S_N2 mechanism show a similar selectivity (7).

Cope and Shen (1) recently described the preparation of a crystalline *O*-acetyl-*O*-tosyl isosorbide by partial tosylation of the parent compound (II) followed by acetylation. The 2-position was assigned to the *O*-tosyl group since it was considered probable that the *exo*-C_2-hydroxy group was preferentially tosylated.

In the present work the rates of the reaction with sodium iodide of the di-*O*-tosyl isohexides (IV, V, and VI) and of the 2-*O*-tosyl-5-deoxy-5-iodoisoidide (VII) obtained from V were compared to that of the *O*-acetyl-*O*-tosylisosorbide of Cope and Shen in order to show the position of the *O*-tosyl group in the latter compound. Both the sodium *p*-toluenesulphonate and the isohexide products were isolated.

RESULTS AND DISCUSSION

The tosyl esters were treated in acetic anhydride solution at reflux temperature with sodium iodide in the ratio of 1.2 moles of iodide to 1 of *O*-tosyl group. The reaction was stopped at 2, 4, and 8 hours and, after cooling, the precipitated sodium *p*-toluenesulphonate was filtered off and weighed. The yields of the salt obtained are shown in Fig. 1.

The rate curve for the replacement of the tosyloxy group in the *O*-acetyl-*O*-tosylisosorbide closely followed those for the reaction of an *endo* group (IV and one tosyloxy group in V) whereas it was distinctly different from those of the *exo*-tosyl groups (VI and VII). Thus the tosyloxy group in this compound must occupy an *endo* position. In isosorbide this is found at the 5-position and the compound prepared by Cope and Shen (1) was therefore 2-*O*-acetyl-5-*O*-*p*-toluenesulphonyl-1,4;3,6-dianhydro-D-glucitol (VIII).

Confirmation of the rate study came from the isolation in high yield (87%) of a crystalline iodo-compound from the reaction products. This compound melted at 44.0–44.5° C and analyzed correctly for a deoxyiodo-*O*-acetylisohexide. The infrared spectrum con-

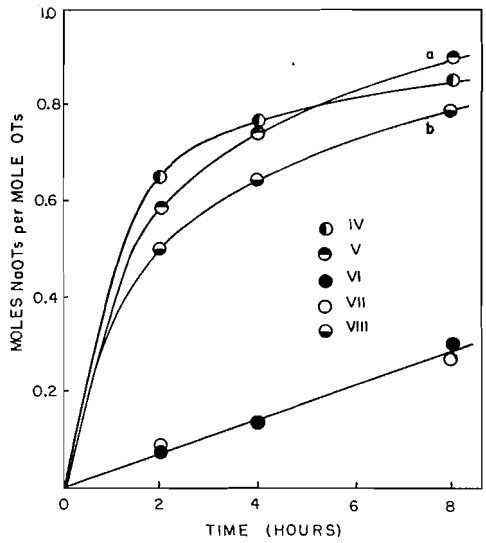

FIG. 1. Rates of replacement of tosyloxy groups by iodine in *O*-tosylisohexides. In acetic anhydride at reflux temperature with 1.2 moles sodium iodide per mole *O*-tosyl group.
(*a*) Sodium iodide, 1.2 moles per mole V; yields calculated for one *O*-tosyl group. With 2.5 moles sodium iodide per mole V the curve was displaced upwards due to the slow reaction of the second tosyloxy group.
(*b*) Acetyldeoxyiodoisoidide isolated in 74% yield.

firmed the presence of the *O*-acetyl group and of the tetrahydrofuran rings. The isoidide configuration was assigned to this compound from comparison with other reactions in this series and the compound was therefore 2-*O*-acetyl-5-deoxy-5-iodo-1,4;3,6-dianhydro-L-iditol (IX).

Cope and Shen (1) found that treatment of the *O*-acetyl-*O*-tosylisosorbide with sodium *t*-butoxide gave a good yield of 1,4;2,5;3,6-trianhydro-D-mannitol and it was proposed that this reaction took place via a normal anhydro-ring-formation reaction, i.e. by an internal displacement of the tosyloxy group by the alkoxide ion formed from the hydrolysis of the *O*-acetyl group. This mechanism is not possible with the *O*-tosyl group in the *endo* position and the *O*-acetyl in the *exo* position. The reaction must therefore proceed via the initial hydrolysis of the *O*-tosyl group followed by the displacement of the *O*-acetyl group or by some transesterification mechanism of the type proposed by Cope and Shen (1).

EXPERIMENTAL

Reaction of the p-Toluenesulphonate Esters of the Isohexides with Sodium Iodide

The sulphur contents, melting points, and specific rotations of the esters together with the reported constants are shown in Table I.

The *O*-tosyl compound (0.005 mole) was dissolved in acetic anhydride (dried and redistilled, 25 ml) and sodium iodide (A.R. grade, 0.0062 or 0.0124 mole) added. The mixture was refluxed for 2 hours, cooled, and left to stand for 30 minutes. The crystalline precipitate was collected by filtration into a weighed sintered glass funnel. The precipitate was washed with acetic anhydride (10 ml) and dried at 100° C to constant weight. The filtrate and washings were combined, refluxed for a further 2 hours, and the precipitate collected as before. The solution from this stage was refluxed for 4 hours before isolation of the final precipitate and the isohexide products.

Can. J. Chem. Downloaded from www.nrcresearchpress.com by 196.1.178.254 on 09/04/12
For personal use only.

TABLE I

p-Toluenesulphonate esters of the 1,4;3,6-dianhydrohexitols (isohexides)

Isohexide	Substituents		Formula	% S		Found		Reported		
	C_2	C_5		Calc.	Found[a]	m.p. (° C)[b]	$[\alpha]_D^{22c}$	m.p. (° C)	$[\alpha]_D$	Reference
Isomannide	OTs	OTs	IV	14.1	13.8	90–91	+95.5	93–94	+98.5	(8)
								89–90	+98.5	(5)
Isosorbide	OTs	OTs	V	14.1	13.6	100–101	+57.4	101–102	+57.8	(5)
								98.3–99.6	+57.4	(3)
Isoidide	OTs	OTs	VI	14.1	13.9	105–105.5	+33.5	90	+38.2	(9)
								105.5–106	+33.2	(6)
								106	+33	(5)
Isoidide	OTs	I	VII[d]	7.52	7.6	82–83	+56.5	90.8–91.3	+52.7	(3)
Isosorbide	OAc	OTs	VIII[e]	9.35	9.2	64–65	+77.9	64–65	+50.5	(1)

[a]Determined by "oxygen flask" method of Lysyj and Zarembo (10).
[b]Compounds were recrystallized from methanol to constant melting points, which are uncorrected.
[c]In chloroform, *c*, 1.1 to 2.0.
[d]Prepared from the reaction of 2.4 moles of sodium iodide on V.
[e]Prepared by partial tosylation of isosorbide following the method of Cope and Shen (1).

After excess acetic anhydride was removed by distillation under reduced pressure, the reaction mixture was shaken with water and chloroform and the aqueous layer was washed with further amounts of chloroform. The combined chloroform extracts were washed with saturated sodium bicarbonate solution, sodium thiosulphate solution (10%), and water, then dried, and evaporated. The resulting syrups crystallized after rubbing at 0° C.

2-O-Acetyl-5-deoxy-5-iodo-1,4;3,6-dianhydro-L-*iditol* (IX)

Treatment of 2-*O*-acetyl-5-*O*-*p*-toluenesulphonyl-1,4;3,6-dianhydro-D-glucitol (2-*O*-acetyl-5-*O*-tosylisosorbide) (VIII) with 1.5 mole excess of sodium iodide as described above gave an 87% yield of crystalline compound. With a 0.24 mole excess of sodium iodide the yield was 74%. Recrystallization several times from methanol gave a product melting at 44.0–44.5° C (uncorr.), $[\alpha]_D^{22}$ +100.5° (*c*, 0.83 in chloroform). Anal. Calc. for a mono-*O*-acetyl-monodeoxy-monoiodoisohexide, $C_8H_{11}IO_4$: C, 32.23; H, 3.72; I, 42.59%. Found: C, 32.46; H, 3.57; I, 42.38%.

The infrared spectrum of the compound (KBr window) showed absorption at 1240, 1370, and 1746 cm^{-1} corresponding to the acetyl group and at 845, 874, and 930 cm^{-1} corresponding to the tetrahydrofuran rings (11).

2,5-Dideoxy-2,5-diiodo-1,4;3,6-dianhydro-L-*iditol* (X)

This compound was isolated from the reaction of 2,5-di-*O*-tosylisomannide (IV) with 0.24 mole excess of sodium iodide. After several recrystallizations from methanol it melted at 65–66° C (uncorr.) and had $[\alpha]_D^{22}$ +110° (*c*, 0.645 in chloroform). Hockett and co-workers (4) had reported m.p. 61–62° C; Wiggins and Wood (6) m.p. 61–63° C, $[\alpha]_D^{19}$ +107.9° (*c*, 1.97 in chloroform).

ACKNOWLEDGMENT

One of us (M.J.) is grateful to the Powell River Company Limited, Powell River, B.C., for the award of a scholarship.

REFERENCES

1. COPE, A. C. and SHEN, T. Y. J. Am. Chem. Soc. **78**, 5912 (1956).
2. MILLS, J. A. Advances in carbohydrate chemistry. Vol. 10. Academic Press, Inc., New York. 1955. p. 46.

Can. J. Chem. Downloaded from www.nrcresearchpress.com by 196.1.178.254 on 09/04/12
For personal use only.

3. HOCKETT, R. C., FLETCHER, H. G., SHEFFIELD, E. L., and GOEPP, R. M. J. Am. Chem. Soc. **68**, 927 (1946).
4. HOCKETT, R. C., FLETCHER, H. G., SHEFFIELD, E. L., GOEPP, R. M., and SOLTZBERG, S. J. Am. Chem. Soc. **68**, 930 (1946).
5. MATHESON, N. K. and ANGYAL, S. J. J. Chem. Soc. 1133 (1952).
6. WIGGINS, L. F. and WOOD, D. J. C. J. Chem. Soc. 1180 (1951).
7. COPE, A. C. and SHEN, T. Y. J. Am. Chem. Soc. **78**, 3177 (1956).
8. MONTGOMERY, R. and WIGGINS, L. F. J. Chem. Soc. 393 (1946).
9. BASHFORD, V. G. and WIGGINS, L. F. J. Chem. Soc. 371 (1950).
10. LYSYJ, I. and ZAREMBO, J. E. Anal. Chem. **30**, 428 (1958).
11. BARKER, S. A. and STEPHENS, R. J. Chem. Soc. 4550 (1954).

Can. J. Chem. Downloaded from www.nrcresearchpress.com by 196.1.178.254 on 09/04/12
For personal use only.

Can. J. Chem. Downloaded from www.nrcresearchpress.com by 196.1.178.254 on 09/04/12
For personal use only.

IONIZATION POTENTIALS OF METHYLAMINES AND ETHYLAMINES BY ELECTRON IMPACT[1]

JACQUES COLLIN

ABSTRACT

Recent determinations of the ionization potentials of methylamines and ethylamines obtained by electron impact have been compared with photoionization results and discussed in relation to the Franck–Condon principle. It seems that the observed discrepancies are mainly due to differences in the sensitivities of the detecting devices.

Six different sets of data on the ionization potentials of aliphatic amines have been published, showing a surprising spread of values going from 0.68 v for methylamine, to 1.60 v for triethylamine, which is much higher than the expected errors of such determinations.

We have therefore remeasured these ionization potentials with a Nier-type mass spectrometer[2] using the semilog method of interpreting the results (1).

TABLE

Ionization potentials of methylamines and ethylamines (in ev)

	Photon impact		Electron impact				
Molecule	(*a*)	(*b*)	(*c*)	(*d*)	(*e*)	(*f*)	This work
Ammonia	10.15	—	—	10.52	—	—	10.34±0.07*
Methylamine	8.97	—	9.8	9.41	9.41	9.65	9.41±0.08
Dimethylamine	8.24	—	9.6	—	9.21	9.5	8.93±0.03
Trimethylamine	7.82	—	9.4	—	9.02	9.2	8.32±0.02
Ethylamine	8.86	<8.8†	—	9.32	—	9.6	9.19±0.05
Diethylamine	8.01	—	—	—	—	9.5	8.44±0.01
Triethylamine	7.50	—	—	—	—	9.1	7.85±0.07

*The errors indicated are precision errors; they only give an idea of the reproducibility of the measurements. The absolute errors can not, of course, be given since no definite interpretation can be given as yet.

†Estimated adlabatic ionization potential; the estimated vertical ionization potential given by the authors is 9.5 v.

(*a*) Watanabe, K. J. Chem. Phys. **26**, 542, 1773 (1957).
(*b*) Hurzeler, H., Inghram, M. G., and Morrison, J. D. J. Chem. Phys. **28**, 76 (1958).
(*c*) Sugden, T. M., Walsh, A. D., and Price, W. C. Nature, **148**, 373 (1941).
(*d*) Morrison, J. D. and Nicholson, A. J. C. J. Chem. Phys. **20**, 1021 (1952).
(*e*) Omura, Higasi, and Baba. Bull. Chem. Soc. Japan, **29**, 504 (1956).
(*f*) Collin, J. Bull. soc. chim. Belges, **62**, 411 (1953).

Our values as well as all previously existing data are given in the table, and the following may be said about them:

1. Our new electron impact results are markedly lower than previous data obtained by the same technique, with the exception of methylamine. All ionization curves were very steep and their initial curvature was practically the same as that of the reference rare gases. This is shown by the fact that the results obtained by taking the 0.1% of 50-v abundance value or the 1% of 50-v abundance value are the same within 0.03 v with the exception of methylamine using krypton as a reference gas, where the difference was 0.08 v.

2. Our results are considerably higher than the photon impact values and the explana-

[1]*Manuscript received November 28, 1958.*
Contribution from Institut de Chimie Générale, Université de Liège, 1b, Quai Fr. Roosevelt, Liège, Belgium.
[2]*These measurements were performed in the laboratories of the National Research Council, Ottawa, Canada.*

tion of the important differences observed is not straightforward. The significance of the values depends mainly on the relative position and shape of the potential energy surfaces for the ion and the molecule. If the internuclear distances are the same for both species no such discrepancies should be observed, both photon and electron impact processes being of the Franck–Condon type. This is, however, no more the case if the equilibrium distances are not the same, the discrepancies arising then from the differences in the sensitivities of the detecting devices. The problem is to find the reasons why such modification of internuclear distances occur in the ion.

It is theoretically thought (2) that the ionization of amines proceeds by removal of a non-bonding electron of the nitrogen lone pair. Another possibility is, however, that the ionization is due to the removal of a σ-bonding electron, as has recently been suggested by Hurzeler, Inghram, and Morrison (3) on the basis of their differential interpretation of photon impact data. These authors have also shown that no adiabatic ionization potential could be obtained from the direct experimental ionization curves, for ethylamine and *n*-propylamine. This would explain the literature discrepancies. Since the C–N, C–C, and C–H bond energies are very much the same in amines and hydrocarbons, however, it does not seem that the removal of a bonding electron from the C–N bond would be so much easier in amines than in hydrocarbons (where for instance $I(C_2H_6)$ = 11.76 v and $I(C_3H_8)$ = 11.21 v (4)). The same argument may be applied to the removal of a bonding electron from a C–H or N–H bond, which must have rather higher ionization potentials since $I(CH_4)$ = 13.12 v (4) on one hand, and since in ammonia the corresponding ionization potential is 15.31 v (5) on the other hand. Moreover the small variation of the ionization potential with the length of the hydrocarbon chain in aliphatic amines (6) compared to a considerable one in hydrocarbons (4) is rather in favor of an ionization process on the nitrogen atom.*

In any case, however, the ionization must bring about a change in the state of hybridization of the nitrogen atom which might be responsible for the modification of internuclear distances, and thus of the potential energy surfaces.

The great variation of ionization potentials with substitution on the nitrogen remains to be explained. It should be remembered that the hybridized valence state of the nitrogen atom in these molecules may be represented by the formulas

$$\text{I} \qquad [\mathrm{N}(1s)^2(2s + \delta 2p)^2(2p + \delta' 2s)^3]$$

and

$$\text{II} \qquad [\mathrm{N}(1s)^2(2s + \delta 2p)^2(2p + \delta' 2s)^2(2p + \delta'' 2s)].$$

State I applies to NH_3 and NR_3 types, with different values of the δ parameter according to the nature of the substituent radical R, and state II applies to NRR_2' types, such as encountered in primary and secondary amines, the values of the δ parameters depending again on the nature of R and R′. Therefore, according to the nature of the radicals R, the non-bonding N atomic orbital $(2s+\delta 2p)$ will have different p character and its energy will not be the same. This is the case for the series NH_3, RNH_2, R_2NH, R_3N and the ionization potentials are expected to vary.

It does not seem probable that electrostatic factors arising from the existence of important dipole moments in those molecules may play a significant role in the ionization processes.

**The cause of the considerable differences between mass spectrometric results, although not evident, should probably mainly be attributed to differences in sensitivity of the mass spectrometers used, as indicated above, and, to a certain extent, to the interpretation of the results by different methods. However, the general trend of variation of ionization potentials with hydrocarbon chain length, as indicated in the work of Morrison and Nicholson, is still of application, notwithstanding the correctness of the absolute values.*

Can. J. Chem. Downloaded from www.nrcresearchpress.com by 196.1.178.254 on 09/04/12
For personal use only.

3. Except for ethylamine and *n*-propylamine where the photon impact evidence seems conclusive (3) and brings information on the relative positions of the potential surfaces for the ground molecular and ionic states, no definite conclusions as to the real meaning of the available data can be given. It seems, however, that electron impact values, being considerably higher than photoionization ones, refer to vertical transition to a vibrationally excited ion; the true reason for the modification of internuclear distances in the ion is not evident.

REFERENCES

1. LOSSING, F. P., TICKNER, A. W., and BRYCE, W. A. J. Chem. Phys. **19**, 1254 (1951).
2. MULLIKEN, R. S. J. Chem. Phys. **3**, 584 (1935).
3. HURZELER, H., INGHRAM, M. G., and MORRISON, J. D. J. Chem. Phys. **28**, 76 (1958).
4. HONIG, R. E. J. Chem. Phys. **16**, 105 (1948).
5. MCDOWELL, C. A. J. Chem. Phys. **24**, 618 (1956).
6. MORRISON, J. D. and NICHOLSON, A. J. C. J. Chem. Phys. **20**, 1021 (1952).

Can. J. Chem. Downloaded from www.nrcresearchpress.com by 196.1.178.254 on 09/04/12
For personal use only.

Can. J. Chem. Downloaded from www.nrcresearchpress.com by 196.1.178.254 on 09/04/12
For personal use only.

THE PROTON RESONANCE SPECTRA OF FURAN AND PYRROLE[1]

R. J. Abraham and H. J. Bernstein

ABSTRACT

Interpretation of the fine structure of the NMR spectra of some five-membered "aromatic" heterocyclic ring compounds indicates that spin coupling constants between adjacent protons on the ring and those across the ring are approximately equal. This is in contrast to the situation in six-membered rings where coupling constants between protons ortho to one another are much larger than those in the meta position.

Quadrupole effects of the N^{14} nucleus in pyrrole broaden the NH signal but do not interfere with the spin coupling of the NH proton with other protons. The surprising result is obtained that the spin couplings of the NH proton with α and β protons in the ring are very nearly equal in magnitude.

The analysis and interpretation of the high resolution proton magnetic resonance spectra of non-benzenoid aromatics have been largely neglected. Corey *et al.* (1) have shown that the magnetic resonance spectra of natural compounds containing furan rings are of considerable help in determining the structure of these compounds, as the position of substitution in the furan ring can be found by inspection of the chemical shift data. Anderson (2) has measured the coupling constants and chemical shifts for 2-bromo-5-chlorothiophen, but no systematic high resolution studies have so far been reported for 5-membered ring compounds.

It is the purpose of this work to present the complete analysis of the spectra of the heterocyclic molecules furan and pyrrole and also to investigate the effect of substitution on the magnitude of the spin–spin coupling constants in these molecules. We shall show that the coupling constants obtained by the analysis of these spectra are very different from those found for benzene systems.

For the analysis of these complex spectra we have employed two simplifying techniques. Firstly, that of substitution to reduce the number of interacting protons: deuterium substitution is preferable as the magnetic constants remain unchanged, but methyl substitution can also be used in many cases since it only changes the coupling constants by a small amount. Secondly, by observing the spectrum of the molecule dissolved in a suitable solvent: very often one group of protons may be more affected by medium effects than the others and this may increase the chemical shift difference between the groups and simplify the fine structure considerably. In particular, the intensity distribution becomes more amenable to simple analytical treatment. This process does not appear to affect the size of the spin coupling constants appreciably, only the chemical shifts. Also, these solution spectra help in an understanding of the nature of the molecular complexes formed in solution and some preliminary investigations of these effects have been made here.

EXPERIMENTAL

The spectra were measured with a Varian V-4300 high resolution spectrometer, incorporating a field stabilizer and operating at 40 Mc/s. A spinning sample tube of 5 mm outside diameter was used. The standard side-band technique was employed to measure the signal separations.

[1]*Manuscript received December 1, 1958.*
Contribution from the Division of Pure Chemistry, National Research Council, Ottawa, Canada. This paper was presented at the Symposium on Molecular Structure, Columbus, Ohio, June 1958.
Issued as N.R.C. No. 5178.

The chemical shifts, expressed here in c.p.s. relative to water as an external reference, were measured with a dioxane or cyclohexane reference capillary, adding 58 c.p.s. to the values measured relative to dioxane, and 142 c.p.s. to those measured relative to cyclohexane.

The accuracy of the chemical shift measurements was estimated to be ± 1 c.p.s. and of the coupling constants, ± 0.1 c.p.s.

The furan compounds used are the commercially available samples. The methylated pyrroles were kindly supplied by Dr. E. Bullock and the deuterated pyrrole by Dr. L. Leitch.

RESULTS AND DISCUSSION

(*a*) *Furans*

We shall consider first the spectra of furan and its derivatives. These spectra are simplified by the large chemical shift difference between the 2,5 and 3,4 protons of the ring due to the strongly electronegative oxygen atom. (This numbering procedure is much more convenient than using α and β when discussing derivatives.)

The spectra of furan and 2-furfurol together establish completely the assignments and coupling constants in these compounds. The spectrum of furan (Fig. 1) consists of two

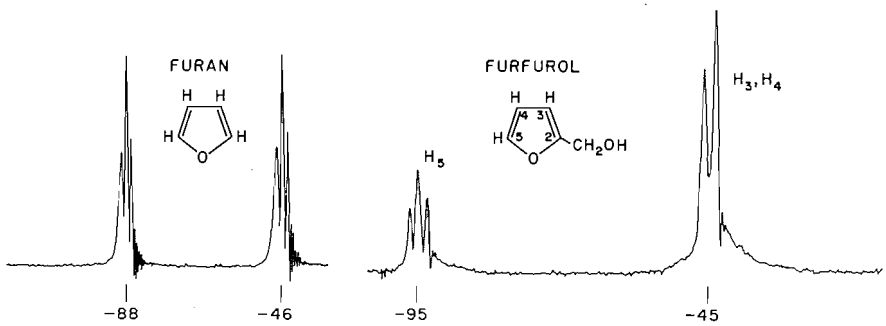

FIG. 1. The proton magnetic resonance spectra of liquid furan and furfurol. The spectrum of the CH_2OH group is not shown. In all figures the direction of increasing applied field is to the right.

widely separated triplets of equal intensity in agreement with earlier observations (1), due obviously to the 2,5 and 3,4 protons of the ring. The spectrum of the ring protons of 2-furfurol (Fig. 1), in which the 2 proton has been replaced by the —CH_2OH group, consists of a low field triplet and a high field doublet of twice the intensity. The intensity distribution immediately shows that the 5 proton is to low field.

The spectrum of furan is of the type A_2X_2 (the nomenclature and full treatment of such systems follows that of Pople, Bernstein, and Schneider (3)). From this analysis, the triplet structure of the component groups in furan can arise when $J_{23} = J_{24}$. The spin coupling constant is then given by the triplet separation and is equal to 1.3 c.p.s. This is confirmed by the spectrum of 2-furfurol. The doublet pattern of the 3 and 4 protons and the triplet structure of the 5 proton are to be expected if $J_{23} = J_{24}$, and from the spectrum the coupling constant is found to be equal to that in furan (1.3 c.p.s.).

Thus in these compounds the adjacent or ortho coupling constant (J_{23}) is almost the same as the cross ring or meta coupling constant (J_{24}), in contrast to the situation in benzene derivatives, where the ortho, meta, and para proton coupling constants are about 8, 2, and 0.5 c.p.s. respectively (4).

Can. J. Chem. Downloaded from www.nrcresearchpress.com by 196.1.178.254 on 09/04/12
For personal use only.

The methylene and hydroxyl peaks of 2-furfurol are not shown in Fig. 1. They are to high field and are single peaks. Presumably any coupling between the methylene and hydroxyl proton is quenched by the rapid exchange of the hydroxyl proton. There is also no coupling between the methylene and the ring protons. This is in contrast to the behavior of other groups in this position (see below). Also the $-CH_2OH$ group does not alter the chemical shift of the 3 proton with respect to the 4 proton of the ring. This is again in contrast to the behavior of other groups in this position. For example, in the case of 2-methyl furan and 2-furfural, the 3 and 4 protons have different chemical shifts, giving rise to an ABX-type spectrum (5), and also the 3 proton spin couples with the protons of the substituent group to further complicate the spectrum.

The spectrum of 2-methyl furan is shown in Fig. 2. On the basis of the chemical shift data obtained for furan and 2-furfurol, we assign the low field peak to the 5 proton. This

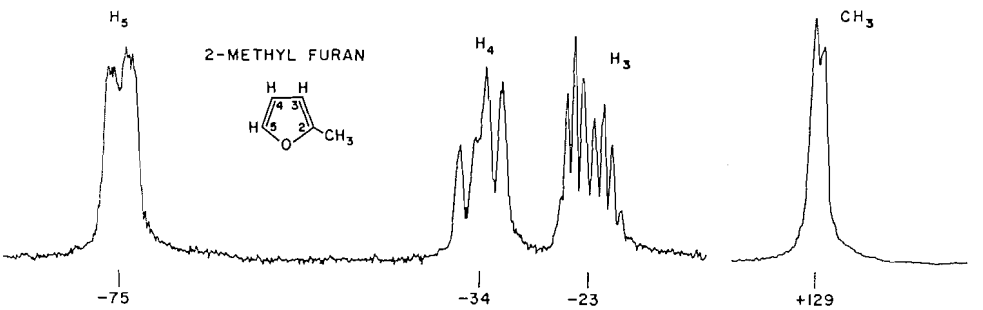

FIG. 2. The proton magnetic resonance spectrum of liquid 2-methyl furan.

is reasonable as the methyl group would not be expected to have any great effect on the electron distribution in the ring. Of the remaining peaks, one of the normal quartet patterns typical of each proton in an ABX-type spectrum (5) is split into more lines by interaction with the methyl group. This group of signals is assigned to the 3 proton since it is reasonable to expect strongest coupling with the proton nearest to the methyl group. The methyl group interaction splits each of the four original lines of this signal into quartets (intensity ratio 1:3:3:1) but the weaker lines will not be observed except on the extreme edges of the signal, so that the main part can be regarded as a quartet split into doublets. However, the splitting due to the methyl is equal to that between the outside pairs of the original quartet so that some overlapping occurs, and thus the complete signal consists of two main triplets with two weak outer lines. The value of the spin coupling constant between CH_3 and H_3 is given directly by the doublet splitting of the methyl group of 0.9 c.p.s. The calculated energies and intensities (i.e. peak heights) for this spectrum are shown along with the observed ones in Table I. Protons 4, 3, and 5 correspond to A, B, and X respectively. Transitions occurring with less than 0.3 c.p.s. separation have been grouped together, as this represents the limit of resolution of the instrument. The intensities for the B group have been normalized separately. The agreement is well within the experimental limits of accuracy. The chemical shifts and spin coupling constants derived from this analysis are given in Table II. The low field signal of proton 5 is not resolved completely into the expected four components, but is more complex and unresolved. This is probably due to a very small interaction of the methyl group with this proton via the oxygen atom. This interaction would be expected to be less than 0.2 c.p.s. and therefore below the limits of resolution of the instrument.

Can. J. Chem. Downloaded from www.nrcresearchpress.com by 196.1.178.254 on 09/04/12
For personal use only.

Can. J. Chem. Downloaded from www.nrcresearchpress.com by 196.1.178.254 on 09/04/12
For personal use only.

TABLE I

Observed and calculated spectra for α-methyl furan

Transition	Origin	Energy (c.p.s.) Calc.	Energy (c.p.s.) Obs.	Relative intensity Calc.	Relative intensity Obs.
1	*B*	0	0	.09	.17
2	*B*	.9	.9	.37	.41
3	*B*	1.1			
4	*B*	1.8	1.8	.56	.56
5	*B*	2.0			
6	*B*	2.7	2.8	.53	.50
7	*B*	2.9			
9	*B*	3.1			
8	*B*	3.8	4.1	.72	.67
10	*B*	4.2			
11	*B*	4.0			
12	*B*	5.1	5.2	.94	.82
13	*B*	4.9			
14	*B*	6.0	6.0	.63	.61
15	*B*	5.8			
16	*B*	6.9	6.7	.16	.22
17	*A*	13.0	13.2	1.26	1.11
18	*A*	14.7	14.7	1.26	1.21
19	*A*	16.1	16.1	.74	.75
20	*A*	17.4	17.6	.74	.71
21	*X*	53.2	53.7	1	1.29
22	*X*	54.8		1	
23	*X*	54.2	55.7	1	1.21
24	*X*	55.8		1	

TABLE II

Chemical shifts and coupling constants for furans (shift relative to water (c.p.s.))

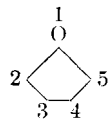

	J_{45}	J_{35}	J_{34}	α	β			
Furan	1.3	1.3		−88	−46			
Furfurol	1.3	1.3		−91	−45	OH +4		CH_2 +38
2-Methyl furan	1.7	1.1	3.5	−75	−34, −23		CH_3 +129	
Furfural	1.5	0.9	3.4	−94	−76, −48		CHO −169	
5-Chlormethyl furfural*			3.8		−76, −50		CHO −166	CH_2 +30

*A bulk susceptibility correction of +15 c.p.s. has been added to the chemical shifts. This value was obtained by a comparison of the chemical shifts in furfural and 5-chlormethyl furfural referred to an internal standard.

The spectrum of furfural is shown in Fig. 3. In this spectrum both the individual groups and their component lines are well separated and thus the formal analysis is quite straightforward. However, the complete assignment cannot be made. The spectrum is an *ABX*-type spectrum modified by the coupling of the aldehyde proton to one of the ring protons. This gives rise to the extra fine structure of the low field signal. The coupling constant

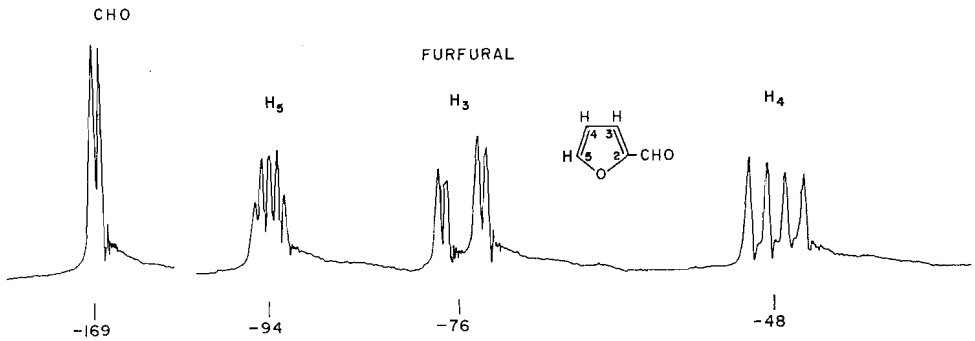

FIG. 3. The proton magnetic resonance spectrum of liquid furfural.

with the aldehyde proton is approximately equal to the spacing in the unperturbed quartet. This results in a quintet of intensity ratio 1:2:2:2:1. The coupling constant is given directly by the size of the aldehyde doublet splitting of 0.7 c.p.s. The remaining chemical shifts and coupling constants for this spectrum are now easily calculated.

However, the assignment of the groups in this spectrum is not clear. On the basis of the chemical shift data, the low field signal would be expected to be that of proton 5 and Corey *et al.* have given this assignment. Further, spin–spin coupling constants are known to be very insensitive to substitution. For example, Richards *et al.* have shown that the coupling constants in a series of para-substituted benzenes vary by less than 10% over a whole range of substituent groups (6). This again supports the assignment of the low field signal in furfural to proton 5 as this would make the coupling constant J_{34} equal to 3.4 c.p.s., in excellent agreement with the value of 3.5 c.p.s. for α-methyl furan.

However, the spin–spin coupling of 0.7 c.p.s. between the aldehyde proton and the proton giving the low field signal would normally be expected to be between the aldehyde proton and the nearest neighbor proton in the ring. On this basis the low field signal would be assigned to proton 3.

This question of the assignment of the low field signal was finally resolved experimentally with the aid of the magnetic resonance spectrum of liquid 5-chlormethyl furfural. In this spectrum the signals of the H_3 and H_4 protons appeared as a quartet (AB group, $J = 3.8$ c.p.s.) and the low field signal of the ring proton spectrum of furfural was absent. This identifies the low field signal with H_5 and further, neither the H_3 proton nor the aldehyde proton showed any signs of fine structure. Thus the surprising result is obtained that fine structure of the aldehyde signal in furfural arises from spin–spin interaction of the aldehyde proton with H_5. The assignments and coupling constants for furfural and 5-chlormethyl furfural are given in Table II. Protons 3 and 4 in furfural are assigned on the basis of the similarity of the coupling constants in furfural to those in α-methyl furan, i.e. the smallest coupling constant is taken as J_{35}. This agrees with the chemical shift data as hydrogen 3 in furfural would be expected to be at lower field than hydrogen 4 due to the influence of the electronegative aldehyde group.

One of the most significant results emerging from this study is the low value of the coupling constants between adjacent protons in these compounds. There are two of these coupling constants, J_{23} and J_{34}, with values of approximately 2 and 3 c.p.s. respectively, in contrast to the value of 8 c.p.s. found in benzene derivatives. These low values we shall show are found also in the pyrrole ring and although thiophen gives a complex and as yet not analyzed spectrum, in 2-bromo-5-chlorothiophen, J_{34} equals 3.9 c.p.s. which is of the

Can. J. Chem. Downloaded from www.nrcresearchpress.com by 196.1.178.254 on 09/04/12
For personal use only.

same magnitude as the above values. Thus the magnitude of the ortho coupling appears to be a function of ring size. This is similar to the behavior in the aromatic hydrocarbon rings (7).

(*b*) *Pyrroles*

The spectrum of pyrrole (Fig. 4) consists of a very broad line at low field (not shown in the figure) due to the hydrogen in the NH group (8), and a complex eight line portion

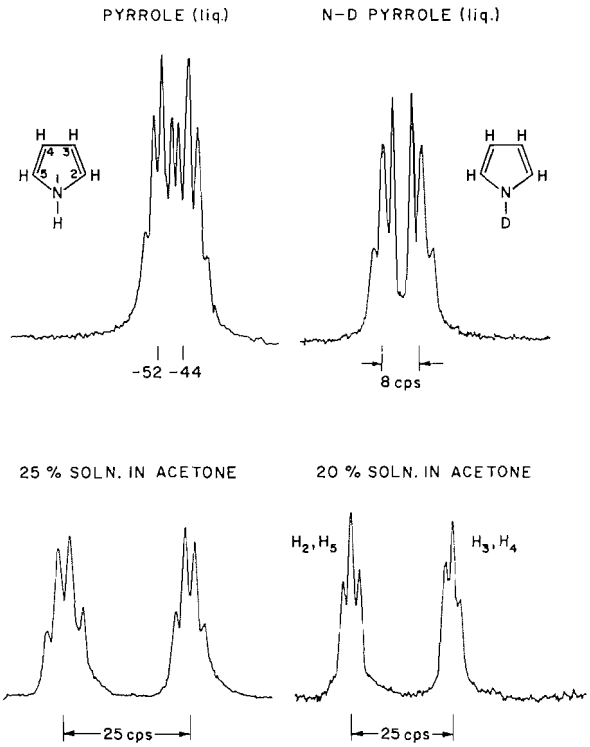

FIG. 4. The proton magnetic resonance spectra of pyrrole and N–D pyrrole. The N–H peak is at low field and not shown.

due to the ring hydrogens. The complete analysis of this A_2B_2X-type spectrum cannot be undertaken without some further experimental results. These were obtained by considering the spectra of pyrrole solutions and also pyrrole derivatives.

The chemical shift difference between the 2,5 and 3,4 protons of pyrrole increases when pyrrole is dissolved in acetone or carbon tetrachloride and the spectrum now splits into two quartets with the 1 proton line shifting to much lower fields and broadening so as to be almost undetectable, but the spacing between the lines in each quartet does not change. Although dilution has effected a considerable simplification in the spectrum, this spectrum can still be interpreted in many ways and the final solution was arrived at by considering the spectra of some methyl- and deuterium-substituted pyrroles. It is apparent that the spectrum of N-deuteropyrrole dissolved in acetone (Fig. 4) is exactly the same as that of furan. This means that in the pyrrole ring as in the furan ring, the ortho coupling constant (J_{23}) equals the meta or cross ring coupling constant (J_{24}) and is equal to the observed separation in the triplets of 1.9 c.p.s. The correct intensity

Can. J. Chem. Downloaded from www.nrcresearchpress.com by 196.1.178.254 on 09/04/12
For personal use only.

pattern for this type of spectrum (triplet ratios 1:2:1) is observed only in the solution case, where the chemical shift is large compared with the spin coupling constant. In the spectrum of the pure liquid these intensities are altered appreciably due to the decrease in the chemical shift, although the separations between the lines remain constant. The spin coupling constants in N-deuteropyrrole must be equal to those in pyrrole and the separation between the lines of the quartets in the solution spectrum of pyrrole is indeed almost equal to this coupling. However, the quartet character in pyrrole must arise from another interaction, namely, the coupling of proton 1 with the other ring protons. In order to obtain the observed spectrum, proton 1 must couple equally to both protons 2 and 3 of the ring and this coupling must be equal to the quadruplet spacing of 2.1 c.p.s. This unexpected result was verified by considering the spectra of 2,3- and 2,5-dimethyl pyrrole (Fig. 5). In the former, protons 4 and 5 will each have a triplet fine structure due

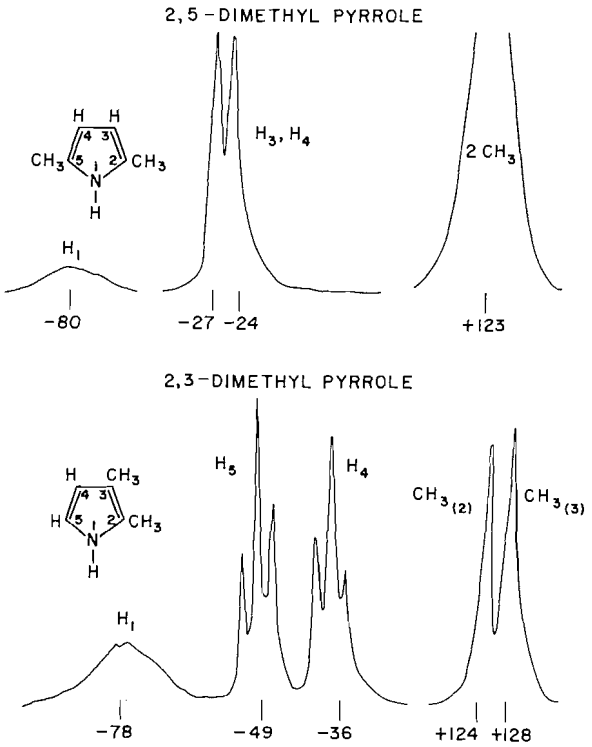

FIG. 5. The proton magnetic resonance spectra of liquid 2,3- and 2,5-dimethyl pyrrole.

to the equal coupling between themselves and proton 1, and in the latter, protons 3 and 4 will be a doublet whose splitting will give directly the coupling constant J_{13} ($=J_{14}$). The coupling constants obtained from these spectra are close to those in pyrrole (see Table III). Note that the splitting due to the spin coupling with the methyl groups is too small to be detected in these compounds. The chemical shift values for these compounds also show that in the pyrroles, as in the furans, the α protons lie to low field (Table III).

The spectrum of 2-methyl pyrrole (Fig. 6) is complicated, as is that of 2-methyl furan, by the different chemical shifts of protons 3 and 4 and the interaction of the methyl

Can. J. Chem. Downloaded from www.nrcresearchpress.com by 196.1.178.254 on 09/04/12
For personal use only.

TABLE III

Chemical shifts and coupling constants for pyrroles (shift relative to water (c.p.s.))

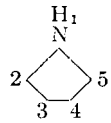

Compound*	J_{45}	J_{35}	J_{34}	J_{15}	J_{14}	N–H	α	β	$(CH_3)_\alpha$	$(CH_3)_\beta$
Pyrrole	2.1	2.1		2.1	2.1	−80	−52	−44		
N–D Pyrrole	2.0	2.0								
α-Methyl pyrrole	2.6	1.5	2.8	2.4	2.8	−80	−52	−43, −34	+124	
50% Acetone soln.	2.6	1.5	2.8	2.4	2.8		−49	−33, −24	+125	
2,3-Dimethyl pyrrole	2.6			2.6	2.6	−78	−49	−36	+124	+128
50% Acetone soln.	2.6			2.6	2.6	−123	−47	−25	+130	+132
2,4-Dimethyl pyrrole						−66	−42	−25	+121	+126
2,5-Dimethyl pyrrole					2.7	−80		−25	+123	
Krypto pyrrole						−62	−42		+121	+125

*The spectrum of the pure liquid is given unless otherwise stated.

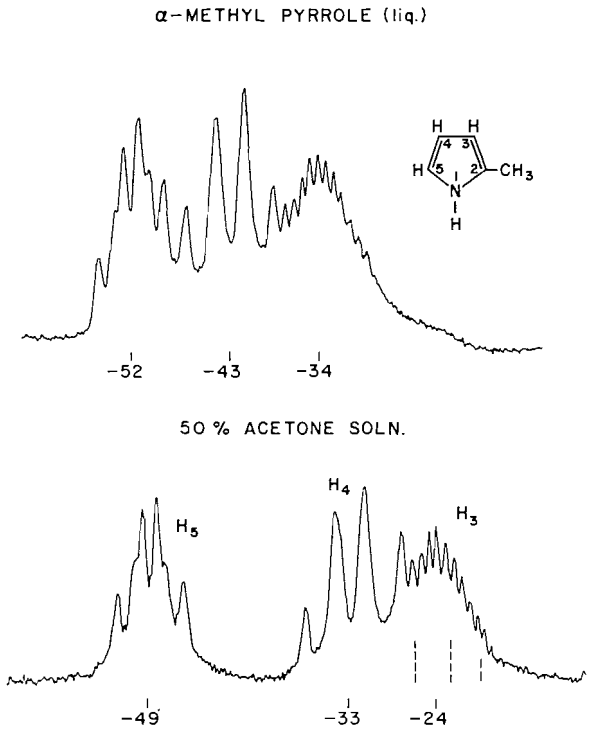

FIG. 6. The proton magnetic resonance spectrum of α-methyl pyrrole. The spectrum of the methyl group is to high field and not shown.

group with proton 3. Although there are several possible assignments for this spectrum, the information obtained from the other pyrrole spectra provides the following means of interpreting this spectrum completely. The low field peak is assigned to proton 5 since the influence of the methyl group on the electron distribution in the ring is small and therefore the order of the chemical shifts would be expected to be the same as in pyrrole.

Can. J. Chem. Downloaded from www.nrcresearchpress.com by 196.1.178.254 on 09/04/12
For personal use only.

The sextet fine structure of this peak results if two of the three coupling constants involved (J_{15}, J_{35}, and J_{45}) are equal. In pyrrole all these constants are equal but in this case we assume that the cross ring coupling J_{35} has decreased whilst the others remain constant. This identifies all the three coupling constants immediately. The assignment for the other two protons is now straightforward, the high field peak is identified unambiguously as that of proton 3 by its complex structure, and the separation of the component lines gives the coupling constant $J_{H_3.CH_3}$, which is equal to 0.6 c.p.s. The quartet structure of proton 4 shows immediately that the three coupling constants (J_{14}, J_{34}, and J_{45}) are all equal. The average values for the coupling constants are given in Table III.

Two other substituted pyrroles were examined, 2,4-dimethyl pyrrole and krypto (3-ethyl-2,4-dimethyl) pyrrole. The ring proton peaks of these substances would be expected to be two triplets and a doublet respectively. In fact, they are spread out into broad humps in each case. This may well be due to some extra splitting due to interaction with the methyl groups, which would be expected to be small and therefore unresolvable.

The results of these investigations in the pyrroles are given in Table III. The coupling constants obtained show again the same characteristics as in the furan ring. The adjacent or ortho coupling (J_{23}) is about the same as the cross ring or meta coupling (J_{24}) although slightly larger than in furan. Also there is some change in the coupling constants even with methyl substitution. There are further effects to be noted here, in particular, the size of the interaction between proton 1 and the ring protons and the almost equal values of J_{12} and J_{13}. The peak for proton 1 is broadened by the quadrupole coupling of the N_{14} nucleus into a very broad single line, though it has been reported that the triplet structure characteristic of the N_{14} interaction does appear at higher temperatures (8). However, the quadrupole coupling has no effect upon the coupling of the NH hydrogen to the ring protons. This is a similar situation to that found in formamide (9).

The invariance of these coupling constants when the compound is dissolved in various solvents is well demonstrated in pyrrole. The spacing between the individual lines in the pyrrole quartets does not change when pyrrole is dissolved in carbon tetrachloride, acetone, methanol, or even glacial acetic acid, although the chemical shift separation between the quartets does change appreciably. Pyrrole is known to form weak hydrogen bonds with itself (10) (although there is still some doubt as to the exact nature of these bonds), and also with solvents like acetone, and thus the observed chemical shift changes in this solvent are very probably due to this effect. However, this hydrogen bonding does not appear to affect the value of the coupling constant between the bonded proton and the other ring protons. Also it can be shown that this hydrogen bonding is not accompanied by any rapid exchange process. The spectrum of pyrrole in methanol at 50° C has still the same pattern as at room temperature although that of the methanol consists only of two sharp peaks, since the rapid exchange of the hydroxyl proton removes any fine structure associated with it. To remove a coupling of about 2 c.p.s., proton 1 would have to have a lifetime shorter than about 0.1 second. Thus the lifetime of proton 1 is certainly longer than 0.1 second, which means the exchange rate is slow under these conditions. This proton, however, can be exchanged, since pyrrole was deuterated in this position using heavy water, although this required many processes before the exchange was complete.

NOTE ADDED IN PROOF

The spectra of furan, furfurol, and pyrrole have been interpreted on the basis that $J_{35} = J_{45}$. This is not the only interpretation of these spectra and a more detailed

Can. J. Chem. Downloaded from www.nrcresearchpress.com by 196.1.178.254 on 09/04/12
For personal use only.

analysis (to be presented in a subsequent publication) shows that the correct coupling constants differ slightly from the values quoted above and in particular the two coupling constants are not equal. The observed splitting in these spectra instead of being equal to J_{35} or J_{45} is equal to $(J_{35}+J_{45})/2$.

REFERENCES

1. COREY, E. J., SLOMP, G., DEV, S., TOBINAGA, S., and GLAZIER, E. R. J. Am. Chem. Soc. **80** (No. 5), 1204 (1958).
2. ANDERSON, W. A. Phys. Rev. **102**, 151 (1956).
3. POPLE, J. A., BERNSTEIN, H. J., and SCHNEIDER, W. G. Can. J. Chem. **35**, 1487 (1957).
4. GUTOWSKY, H. S., HOLM, C. H., SAIKA, A., and WILLIAMS, G. A. J. Am. Chem. Soc. **79**, 4596 (1957).
5. BERNSTEIN, H. J., POPLE, J. A., and SCHNEIDER, W. G. Can. J. Chem. **35**, 65 (1957).
6. RICHARDS, R. E. and SCHAEFFER, T. P. Trans. Faraday Soc. **54**, 1280 (1958).
7. SCHNEIDER, W. G., BERNSTEIN, H. J., and POPLE, J. A. J. Am. Chem. Soc. **80**, 3497 (1958).
8. ROBERTS, J. D. J. Am. Chem. Soc. **78**, 4495 (1956).
9. PIETTE, L. H., RAY, J. D., and OGG, R. A., JR. J. Mol. Spectroscopy, **2**, 66 (1958).
10. JOSIEN, M. L., PINEAU, P., PATY, M., and FUSON, N. J. Chem. Phys. **24**, 1261 (1956).

Can. J. Chem. Downloaded from www.nrcresearchpress.com by 196.1.178.254 on 09/04/12
For personal use only.

Can. J. Chem. Downloaded from www.nrcresearchpress.com by 196.1.178.254 on 09/04/12
For personal use only.

THE BIOGENESIS OF ALKALOIDS

XXII. SOME INTERMEDIATE STEPS IN THE TRANSFORMATION OF TRYPTOPHAN TO GRAMINE[1]

ALBERTO BRECCIA[2] AND LÉO MARION

ABSTRACT

In germinating barley it is known that tryptophan is converted into gramine. In an attempt to find the intermediate steps in this conversion, it has been established that neither 3-indolylacetic acid, 3-indolylglyoxylic acid, 3-indolylaldehyde, nor 3-indolylacetamide (all labelled with ^{14}C in the side chain) was a precursor of gramine. It has been shown, however, that both 3-indolylpyruvic acid and 3-indolylacrylic acid gave rise to radioactive gramine when fed to germinating barley. It is likely that these two acids constitute two intermediates in the pathway tryptophan–gramine.

It has been established earlier (1) that the precursor of the alkaloid gramine is tryptophan, and that the biogenesis involves scission of the side chain of the amino acid not at the indole nucleus as might have been expected, but between the α- and β-carbons (i.e., $R—CH_2—CH(NH_2)CO_2H$). We have now attempted to establish some of the intermediate steps involved in the transformation.

The metabolism of tryptophan, not involving destruction of the indole system, can take place according to Gordon (2) via two potential pathways:

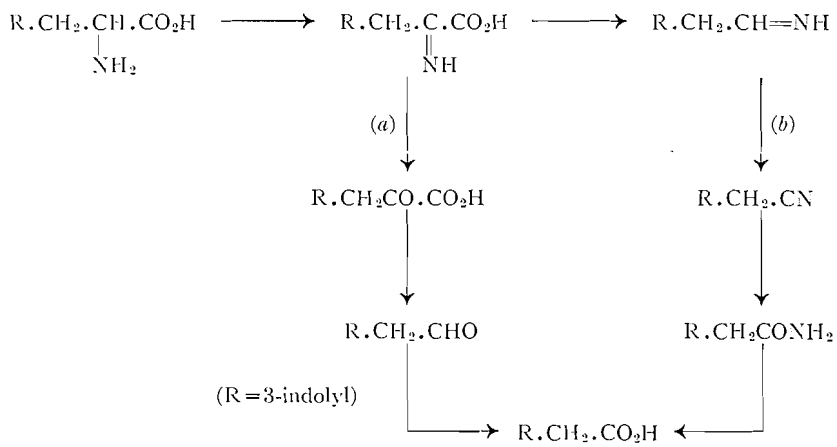

In support of pathway (*a*) Wildman, Ferri, and Bonner (3) had presented evidence that 3-indolylpyruvic acid might be an intermediate in the formation of indolylacetic acid. As a result of paper chromatographic studies, the presence of indolylpyruvic acid has been reported in immature maize kernels (4) and in maize endosperms (5). It has been shown since, however, that indolylpyruvic acid is destroyed on the paper chromatogram under the conditions employed (6) whereas the substance described by Stowe and Thimann (5) is stable, and consequently could not have been indolylpyruvic acid (6).

Furthermore, according to the work of Spenser, Crawhall, and Smyth (7), who have

[1]*Manuscript received February 27, 1959.*
Contribution from the Division of Pure Chemistry, National Research Council, Ottawa, Canada.
Issued as N.R.C. No. 5186.
[2]*National Research Council of Canada Postdoctorate Fellow, 1957–58.*

studied the oxidative decarboxylation of amino acids, it is improbable that indolylpyruvic acid can be an intermediate in the conversion of tryptophan to indolylacetaldehyde.

That indolylacetaldehyde is an immediate precursor of indolylacetic acid in one pathway is indicated by the fact that when homogenates of *Phaseolus mungo* are exposed to X rays the oxidase is blocked, and the aldehyde accumulates in the homogenate while the production of indolylacetic acid decreases (2).

Concerning the second pathway (*b*), indolylacetonitrile has been reported to occur in nature (8, 9, 10), and Stowe and Thimann (11) have shown that *Avena* coleoptiles convert indolylacetonitrile into the corresponding acid.

The metabolism proceeds further, and it has been considered that 3-indolylacetic acid is converted to 3-indolylaldehyde (12) presumably via indolylglyoxylic acid. Manning and Galston (13) have shown, however, that in the presence of indolylacetic acid oxidase from pea seedlings, indolylacetic acid undergoes oxidative conversion into products which do not include 3-indolylaldehyde. They also showed that the aldehyde does not participate as an intermediate in the formation of the final products. On the other hand, their work did not preclude the possibility that in certain plants the metabolism of indolylacetic acid could be via indolylglyoxylic acid to indolylaldehyde, and it was conceivable that the acid and its metabolic products might be intermediates in the conversion of tryptophan to gramine.

When, however, 3-indolylacetic-α-^{14}C acid was fed to germinating barley under conditions identical with those previously described (14), the gramine isolated from the plants showed no radioactivity whatsoever. It was found that most of the radioactivity remained in the nutrient solution (pH 7). The small quantity of radioactivity that became incorporated into the barley was mostly found in the fraction of the extract that contained the acidic and neutral compounds. It thus appeared that the administered indolylacetic acid must have been destroyed very early in the experiment by the action of light or possibly by an oxidase that could be present in the nutrient solution. Indeed, it has been found that 3-indolylacetic acid (100 mg) added to the nutrient solution (100 ml) left after the plants had been harvested was completely destroyed in 3 hours.

In further experiments, 3-indolylglyoxylic-α,β-^{14}C acid was fed to germinating barley, both with and without ascorbic acid, which is known to act as an antagonist of oxidases. The gramine isolated failed to show any radioactivity. 3-Indolylaldehyde (labelled on the aldehydic carbon) was also fed to germinating barley, alone and also in the presence of ascorbic acid. In each case, however, the gramine isolated from the harvested plants was inactive.

In order to test the other possible pathway, 3-indolylacetamide-α-^{14}C was also fed to germinating barley, but with the same negative result.

Unless the negative results described be attributable to the failure of the labelled substances to penetrate into the plant, these results indicate that the conversion of tryptophan to gramine must proceed via a pathway that does not involve 3-indolylacetic acid. It was therefore supposed that the amination necessary for the formation of gramine took place before the rupture of the side chain, i.e., on an indolyl compound still containing a 3-carbon side chain. Such a supposition is supported by the fact that β-(3-indolyl)-acrylic acid and β-(3-indolyl)-lactic acid are known to occur in barley and other plants (9). Although the occurrence of 3-indolylpyruvic acid in plants has not been satisfactorily demonstrated (6), it has been assumed that this acid could be one of the precursors of gramine.

In subsequent experiments 3-indolylpyruvic-β-^{14}C acid was administered to germinating

Can. J. Chem. Downloaded from www.nrcresearchpress.com by 196.1.178.254 on 09/04/12
For personal use only.

barley and the gramine was isolated from the plant after a few days as usual. The gramine thus obtained was radioactive (1.18×10^5 counts per minute per mmole); it was fused with potassium hydroxide and the resulting indolylcarboxylic acid was decarboxylated. The carbon dioxide evolved (isolated as barium carbonate) contained all the radioactivity originally present in the gramine. Hence there has been no randomization and it can be concluded that, as observed previously with tryptophan (1, 14) the β-carbon of the indolylpyruvic acid is still present in the gramine, and that the scission of the side chain of the acid occurred between the α- and β-carbons.

Experiments in which 3-indolylacrylic-β-^{14}C acid was fed to germinating barley were also performed. The results were similar to those obtained with indolylpyruvic acid, and the gramine isolated from the plants was radioactive. The radioactivity again was located on the CH_2 of the gramine, as shown by the results of the degradation of the alkaloid.

EXPERIMENTAL

Preparation of the Labelled Compounds

The indolyl derivatives were prepared by slight modifications of known methods. A sample of each compound was chromatographed on paper to make sure of its purity.

Radioactive gramine was synthesized from polyoxymethylene-^{14}C first hydrolyzed to formaldehyde and then condensed with indole and dimethylamine as described by Kuhn and Stein (15). The yield of radioactive gramine based on polyoxymethylene was 80%. Sp. act. 5.26×10^7 c.p.m. per mmole.

Indolyl-3-aldehyde was prepared via the methosulphate of gramine labelled with ^{14}C in the CH_2 of the side chain by the method of Thesing (16). Using smaller quantities of tetrahydrofuran and glacial acetic acid than those specified resulted in an increased yield of aldehyde, m.p. 196°. Yield 55%. Sp. act. 4.12×10^7 c.p.m. per mmole.

3-Indolylglyoxylic acid was prepared by the condensation of indole with diethyloxalate-1,2-^{14}C (17) obtained by esterification of silver oxalate-1,2-^{14}C with ethyliodide. Sp. act. 3.89×10^7 c.p.m. per mmole.

3-Indolylacrylic-β-^{14}C acid was prepared by condensation of radioactive indolylaldehyde with ethyl malonate in pyridine containing a small quantity of piperidine according to the well-known method. The acid, m.p. 198–200 (decomp.), was obtained in 48.2% yield and 20% of the aldehyde used was recovered. The specific activity of the 3-indolylacrylic acid was 4.32×10^7 c.p.m. per mmole. A paper chromatogram of the acid with the solvent benzene – propionic acid – water (100:70:5) was developed during 12 hours and brought out with a 1% solution of *p*-dimethylaminobenzaldehyde in *N* hydrochloric acid. It showed two spots, one with the R_f of the acid, the other with the same R_f as 3-indolylaldehyde. The radioactivity of the aldehyde spot was 100 counts per minute, and that of the acid spot was 1.0×10^4 counts per minute. Hence the radioactivity of the product is 99% due to the acid and 1% due to the aldehyde still present.

3-Indolylpyruvic-β-^{14}C acid was prepared from radioactive indolylaldehyde as described by Ellinger and Matsuoka (18). Yield 50.3%, m.p. 205–210° (decomp.). Sp. act. 5.04×10^7 c.p.m. per mmole.

3-Indolylacetamide-α-^{14}C was obtained from the action of potassium cyanide on radioactive gramine as described by Snyder and Pilgrim (19). Yield 50.4% based on the gramine, m.p. 149–150°. Sp. act. 4.30×10^7 c.p.m. per mmole.

Administration of the Radioactive Compound to the Barley

A 700-g sample of Charlottetown No. 80 barley was evenly divided among twelve 20×25 cm Pyrex glass trays. Distilled water (50 ml) was added to each of the trays,

Can. J. Chem. Downloaded from www.nrcresearchpress.com by 196.1.178.254 on 09/04/12
For personal use only.

which were placed in a closed germination cabinet. The barley was watered daily. On the sixth day of sprouting, a solution of the labelled substance was added to each of the trays, and the barley allowed to grow for a further 5 days, all as previously described (20).

The barley was harvested on the 11th day of sprouting, the shoots worked up as described before (14), and the gramine isolated.

Because of the low solubility of 2-indolylaldehyde in water, this substance (32 mg, total activity 4.48×10^6 c.p.m.) was dissolved in 65% ethanol (10 ml) and the solution added to the trays of growing barley. After a lapse of 8 hours, distilled water (600 ml) was gradually added to the trays over a period of 6 hours.

The 3-indolylpyruvic acid (50 mg) used in the feeding experiments had a specific activity of 5.04×10^7 c.p.m. per mmole, and the gramine (121 mg) isolated had an activity of 1.18×10^5 c.p.m. per mmole.

The 3-indolylacrylic acid (71 mg) fed to the barley had an activity of 4.32×10^7 c.p.m. per mmole, and the gramine obtained from the plants treated with this acid had a specific activity of 1.86×10^5 c.p.m. per mmole.

Degradation of Gramine

(*a*) Some of the radioactive gramine obtained from the plants was converted to the methiodide and treated with sodium methoxide as described by Madinaveitia (21). The reaction was carried out as in previous cases (14) and the liberated dimethylamine isolated as ethyldimethylamine picrate showed no radioactivity.

(*b*) A quantity of gramine (13 mg) of specific activity 1.38×10^4 c.p.m. per mmole was mixed with inert gramine (150 mg) and fused with potassium hydroxide (3 g) as described previously (14) and the resulting 3-indolylcarboxylic acid was heated at 190–230° in a stream of nitrogen. The stream of nitrogen and evolved gas was bubbled through a barium hydroxide solution, and the precipitated barium carbonate was filtered and dried. It had a specific activity of 1.36×10^4 c.p.m. per mmole.

DISCUSSION

Since neither 3-indolylglyoxylic acid, 3-indolylaldehyde, nor 3-indolylacetamide are precursors of gramine in barley, it is not surprising that as now shown, and as Henry and Leete (22) have recently reported, 3-indolylacetic acid should also fail to act as a precursor of gramine. Unless it be assumed that each of these four labelled substances was destroyed in the nutrient solution instead of penetrating into the plant, as indeed indolylacetic acid was, then it must be concluded that the pathway in the transformation of tryptophan to gramine is not via indolylacetic acid.

On the other hand, both 3-indolylpyruvic acid and 3-indolylacrylic acid are precursors of gramine. Since the alkaloid, obtained from barley fed with indolylacrylic acid, was more strongly radioactive than that isolated from barley fed with indolylpyruvic acid, it is probable that indolylpyruvic acid is the precursor of indolylacrylic acid. It is assumed, therefore, that in the first step of the biogenesis tryptophan is converted by transamination to 3-indolylpyruvic acid from which at a further stage in the same pathway 3-indolylacrylic acid is formed. Experiments are underway to attempt to determine at which stage amination occurs.

REFERENCES

1. LEETE, E. and MARION, L. Can. J. Chem. **31**, 1195 (1953).
2. GORDON, S. A. *In* Wain, R. L. and Wightman, F. The chemistry and mode of action of plant growth substances. Butterworth Scientific Publications, London. 1956. p. 66.

Can. J. Chem. Downloaded from www.nrcresearchpress.com by 196.1.178.254 on 09/04/12
For personal use only.

3. WILDMAN, S. G., FERRI, M. G., and BONNER, J. Arch. Biochem. **13**, 131 (1947).
4. KEFFORD, N. P. J. Exptl. Botany (London), **6**, 129 (1955).
5. STOWE, B. B. and THIMANN, K. V. Nature, **172**, 764 (1953).
6. BENTLEY, J. A., FARRAR, K. R., HOUSLEY, S., SMITH, G. F., and TAYLOR, W. C. Biochem. J. **64**, 44 (1956).
7. SPENSER, I. D., CRAWHALL, J. C., and SMYTH, D. G. Chem. & Ind. 796 (1956).
8. VON DENFFER, D., BEHRENS, M., and FISCHER, A. Naturwiss. **39**, 550 (1952).
9. VLITOS, J. and MEUDT, W. Contribs. Boyce Thompson Inst. **17**, 197 (1953).
10. BLOMMAERT, K. L. J. Nature, **174**, 970 (1954).
11. STOWE, B. B. and THIMANN, K. V. Arch. Biochem. Biophys. **51**, 449 (1954).
12. VON DENFFER, D. and FISCHER, A. Naturwiss. **39**, 549 (1952).
13. MANNING, D. T. and GALSTON, A. W. Plant Physiol. **30**, 225 (1955).
14. BOWDEN, K. and MARION, L. Can. J. Chem. **29**, 1037 (1951).
15. KÜHN, H. and STEIN, O. Ber. **70**, 567 (1937).
16. THESING, T. Chem. Ber. **87**, 507 (1954).
17. ELKS, J., ELLIOTT, D. F., and HEMS, B. A. J. Chem. Soc. 629 (1944).
18. ELLINGER, A. and MATSUOKA, Z. Z. physiol. Chem. **109**, 259 (1920).
19. SNYDER, H. R. and PILGRIM, F. J. J. Am. Chem. Soc. **70**, 3770 (1948).
20. KIRKWOOD, S. and MARION, L. Can. J. Chem. **29**, 30 (1951).
21. MADINAVEITIA, J. J. Chem. Soc. 1927 (1937).
22. HENRY, D. W. and LEETE, E. Abstracts, 134th Am. Chem. Soc. Meeting. Chicago. 1958. p. 43c.

Can. J. Chem. Downloaded from www.nrcresearchpress.com by 196.1.178.254 on 09/04/12
For personal use only.

THE NATURE OF PYRACONITINE[1]

D. J. McCaldin[2] and Léo Marion

ABSTRACT

A new investigation of pyraconitine and pyraconine has confirmed the presence of a skeletal carbonyl in these compounds. Reduction of pyraconitine with sodium borohydride produces a hydrolytic base which no longer contains a carbonyl group. The Wolff–Kishner reaction reduces the carbonyl in pyraconitine, eliminates the elements of methanol, and hydrogenates the resulting double bond as well as hydrolyzing off the benzoyl ester. These observations indicate the presence in aconitine of the sequence $R_2C(OAc).CHOH.CH(OCH_3)$-. On the basis of the structure of aconine previously derived from the X-ray structure of demethanolaconinone the foregoing results determine the skeletal position occupied by the labile acetoxy group in aconitine.

Can. J. Chem. Downloaded from www.nrcresearchpress.com by 196.1.178.254 on 09/04/12
For personal use only.

It has long been known (1) that aconitine ($C_{34}H_{47}O_{11}N$) when pyrolyzed eliminates acetic acid and gives rise to pyraconitine ($C_{32}H_{43}O_9N$). The loss of acetic acid has been variously interpreted as producing an epoxide (1, 2), an ethylenic linkage (3), or a carbonyl group (4). The last interpretation was based on the presence of a broad absorption band in the infrared spectrum of pyraconitine and a weak band in the spectrum of pyraconine hydrochloride. The ethylenic linkage suggested by Schneider (3) would, on the basis of his proposed structure for aconitine, require that the salts of pyraconitine be anhydronium salts, and neither the hydrochloride of pyraconitine nor that of its hydrolytic product pyraconine show the characteristic absorption of anhydronium salts in the infrared, so that this suggestion can be discarded. A new investigation of pyraconitine has therefore been undertaken, and the results obtained confirm the presence of a carbonyl in the pyrolytic products and permit the location of the acetoxy group in the carbon–nitrogen skeleton of the alkaloid.

Crystalline pyraconitine was prepared by heating aconitine to 185–190°. Its saponification product, pyraconine ($C_{25}H_{39}O_8N$), was isolated as the crystalline hydrochloride. The infrared spectrum of pyraconitine contained a split absorption band at 1696–1717 cm^{-1} due to the benzoyl ester carbonyl and a second carbonyl in a six-membered ring. The latter was confirmed by the presence of a weak band at 1709 cm^{-1} in the infrared spectrum of pyraconine, which no longer contains the benzoyl group. In order to ascertain whether this weak carbonyl band was significant a solution of pyraconine in chloroform, of known concentration, was used for the infrared spectrum. The carbonyl band had an extinction coefficient $\epsilon^{(a)}_{max}$ 300, thus showing it to be a true carbonyl absorption band, since the absorption is significant when $\epsilon^{(a)}_{max} > 200$ (5). Furthermore, this absorption peak no longer showed in the infrared spectrum of the Wolff–Kishner reduction product of pyraconitine. On treatment with sodium borohydride, pyraconitine underwent hydrolysis as well as reduction of the carbonyl group to a hydroxyl and gave rise to a compound, $C_{25}H_{41}O_8N$, which in the infrared showed no absorption in the region 1600–1850 cm^{-1}. Had the reaction not involved the reduction of a skeletal carbonyl the product should have been identical with pyraconine, but it proved to be quite different. These results, therefore, confirm the conclusion of Shima and Amiya (4) that the elimination of acetic acid in the pyrolysis of aconitine is accompanied by the formation of a carbonyl group.

[1]*Manuscript received March 18, 1959.*
Contribution from the Division of Pure Chemistry, National Research Council, Ottawa, Canada.
Issued as N.R.C. No. 5190.
[2]*National Research Council of Canada Postdoctorate Fellow.*

The Wolff–Kishner product of pyraconitine had the empirical formula $C_{24}H_{39}O_6N$, and contained only three methoxyl groups. Hence the reaction involved not only the reduction of the carbonyl to a methylene and saponification of the benzoyl group as expected; it also involved the loss of methanol and the hydrogenation of the resulting double bond. The absence of a double bond was evidenced by the infrared spectrum, which contained no absorption bands characteristic of such a function, and also by the attempted catalytic hydrogenation, which yielded the unchanged material. The Wolff–Kishner reaction is known to follow such a course when the carbonyl is α to a methoxyl, although in some cases the product is unsaturated (6).

In order that the elimination of acetic acid might give rise to a ketone it is necessary that the acetoxy group in aconitine be vicinal to a secondary hydroxyl, and to account for the behavior of pyraconine in the Wolff–Kishner reduction it is also necessary that this hydroxyl be vicinal to a methoxy group. It must be concluded, therefore, that aconitine contains the sequence of substituents $R_2C(OAc).CH(OH).CH(OCH_3)$- and that pyraconine contains the sequence $R_2CH.CO.CH(OCH_3)$-, which in the Wolff–Kishner reduction product becomes $R_2CH.CH_2.CH_2$-.

From the X-ray crystallographic study of demethanolaconinone hydriodide trihydrate (7) it follows that the structure of aconine is that represented by formula I. If we assume that no ring enlargement accompanies the pyrolytic reaction, then structure I presents

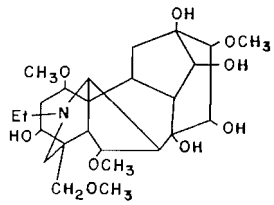

I

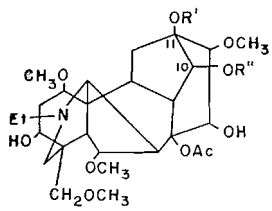

II

only one choice for the location of the acetoxy group in aconitine whose structure is shown by formula II where either R′ or R″ = C_6H_5CO and the other is H. It has previously been shown that the secondary hydroxyl in ring A is unsubstituted (8) and hence the benzoyl ester group can only be in either position 10 or 11 (cf. for numbering see ref. 8). It is hoped from current work to determine which of these two positions is occupied by the benzoyl ester group.

Aconitine possesses many points of similarity with delphinine. Like it, it possesses a bicyclo(1,2,3)octane system (9) which, however, contains one more hydroxyl group due to which the pyrolytic derivatives obtained from the two alkaloids are of a different nature. Jacobs and Pelletier (10) have shown that in delphinine it is a secondary hydroxyl on a five-membered ring that is esterified with benzoic acid. On the assumption that a similar situation exists in aconitine, the structure II (R′ = H, R″ = COC_6H_5) is preferred.

EXPERIMENTAL

All infrared absorption spectra were measured on nujol mulls, unless otherwise mentioned, with a Perkin–Elmer double beam spectrometer Model 21B. The melting points were determined on a Kofler hot stage and were not corrected.

Can. J. Chem. Downloaded from www.nrcresearchpress.com by 196.1.178.254 on 09/04/12
For personal use only.

Pyraconitine

Aconitine (1 g) was heated at 185–190° (metal bath) in a slow stream of nitrogen until effervescence ceased. The pale yellow liquid was cooled and dissolved in the minimum quantity of hot acetone. Hexane was added dropwise until a slight turbidity was observed. After some time pyraconitine crystallized as colorless needles (510 mg), m.p. 167–168° (literature gives 167.5° (1)). It had $[\alpha]_D^{24}$ −103° (*c*, 1.21 in ethanol) and pK_a 7.72 (determined in 50% ethanol). Found: C, 65.26; H, 7.21. Calc. for $C_{32}H_{43}O_9N$: C, 65.62; H, 7.46%. Infrared spectrum: 1696 cm^{-1} (skeletal carbonyl), 1717 cm^{-1} (ester carbonyl), the hydriodide crystallized as pale yellow rosettes from acetone–ether, m.p. 218–220°. Infrared spectrum: 1720 cm^{-1} (broad) due to ester and skeletal carbonyl groups.

Pyraconine

Pyraconitine was saponified with alcoholic sodium hydroxide and the product isolated as the hydrated hydrochloride, which separated from water as colorless prisms, m.p. 135° (literature (2) gives m.p. 135°), $[\alpha]_D^{22}$ −126.7° (*c*, 1.20 in water). Infrared spectrum: 1709 cm^{-1} (six-membered ring carbonyl).

Wolff–Kishner Reduction of Pyraconitine

Pyraconitine (230 mg) was dissolved in triethylene glycol (3 ml) and 95% hydrazine (2.5 ml) added to the solution. The reaction mixture was maintained at 150° for 1 hour under an atmosphere of nitrogen. Solid potassium hydroxide (1 g) was then added to the mixture and the temperature raised and maintained at 185° for a further hour. The dark reaction mixture was cooled and water (10 ml) was added. The aqueous solution was then extracted with six 20-ml portions of ether and the combined extract dried over magnesium sulphate. Evaporation of the ether extract yielded a gum (105 mg) that failed to crystallize, but formed a perchlorate that crystallized from a mixture of acetone and ether as colorless prisms, m.p. 258–259° (decomp.), $[\alpha]_D^{22}$ +61.9 (*c*, 1.25 in ethanol). Found: C, 53.70; H, 7.05; OMe, 17.03. Calc. for $C_{24}H_{39}O_6N.HClO_4$: C, 53.55; H, 7.26; $3OCH_3$, 17.36%.

Sodium Borohydride Reduction of Pyraconitine

Pyraconitine (370 mg) was dissolved in 80% methanol (10 ml) and sodium borohydride (150 mg) was added to the solution. After 1 hour, the solution was evaporated *in vacuo* and the residue dissolved in water (5 ml). The solution was extracted with five 10-ml portions of chloroform and the dried extract evaporated. There was left a gummy residue (280 mg) which formed a hydrochloride that crystallized from aqueous acetone as colorless prisms. The melting point was variable but fusion started at 155–156°, $[\alpha]_D^{21.5}$ −23.4 (*c*, 2.70 in water). Found (sample dried at 50° for 2 hours): C, 54.57; H, 8.27. Calc. for $C_{25}H_{41}O_8N.HCl.2H_2O$: C, 54.10; H, 8.27%. Found (sample dried at 100° at 0.1 mm for 3 days): C, 55.95; H, 8.45. Calc. for $C_{25}H_{41}O_8N.HCl.H_2O$: C, 55.84; H, 8.10%.

ACKNOWLEDGMENTS

We acknowledge our indebtedness to Mr. R. Lauzon and Dr. R. Norman Jones of these laboratories for the preparation of the infrared absorption spectra, and for discussions as to their interpretation.

REFERENCES

1. Dunstan, W. R. and Carr, F. H. J. Chem. Soc. **65**, 178 (1894).
2. Schulze, H. and Liebner, A. Arch. Pharm. **251**, 453 (1913); **254**, 567 (1916).

Can. J. Chem. Downloaded from www.nrcresearchpress.com by 196.1.178.254 on 09/04/12
For personal use only.

3. SCHNEIDER, W. Ber. **89**, 768 (1956).
4. SHIMA, T. and AMIYA, T. Bull. Chem. Soc. Japan, **31**, 657 (1958).
5. ROBERTS, G., GALLAGHER, B. S., and JONES, R. N. Infrared absorption spectra of steroids. Vol. 2. Interscience Publishers, Inc., New York. 1958. p. 4.
6. WARNHOFF, E. W. and WILDMAN, W. C. Chem. & Ind. 1293 (1958).
7. PRZYBYLSKA, M. and MARION, L. Can. J. Chem. **37**, 1116 (1959).
8. MAYER, H. and MARION, L. Can. J. Chem. **37**, 856 (1959).
9. WIESNER, K., BICKELHAUPT, F., and VALENTA, Z. Tetrahedron, **4**, 418 (1958).
10. JACOBS, W. A. and PELLETIER, S. W. J. Am. Chem. Soc. **78**, 3542 (1956).

Can. J. Chem. Downloaded from www.nrcresearchpress.com by 196.1.178.254 on 09/04/12
For personal use only.

Can. J. Chem. Downloaded from www.nrcresearchpress.com by 196.1.178.254 on 09/04/12
For personal use only.

ISOTOPIC AND HOT RADICAL EFFECTS IN THE REACTION OF HYDROGEN ATOMS WITH ETHYLENE[1]

A. H. TURNER[2] AND R. J. CVETANOVIĆ

ABSTRACT

Reactions of D atoms with C_2H_4, H atoms with C_2D_4, and H atoms with C_2H_4 at room temperature are compared. Pronounced differences in the extent of isotopic exchange have been found. The observed isotopic and pressure effects provide evidence for the importance of "hot" ethyl radicals in these reactions and their responsibility for isotopic exchange. The atoms are generated by the mercury-photosensitized decomposition of hydrogen and deuterium and their concentration is sufficiently small so that "atomic cracking" does not occur.

INTRODUCTION

Addition of a hydrogen atom to a molecule of ethylene leads to the formation of an energy-rich ethyl radical. The need to take into account the formation and subsequent reactions of such "hot" ethyl radicals in order to explain and reconcile seemingly divergent experimental information from various sources has been recently stressed by Bradley, Melville, and Robb (1).

In the present work additions of H and D atoms, respectively, to ethylene have been compared at various pressures. Similar systems have been recently studied by Toby and Schiff (2) but at very low pressures and at high atom-to-ethylene ratios so that "atomic cracking" was favored and methane was the main product, with only smaller amounts of ethane and ethylene and traces of butane and propane. In contrast to this in the present work the ratio of concentrations of the atoms and ethylene has been sufficiently small so that atom–radical reactions have been negligible and the only observed products are butane, ethane, and ethylene, resulting from combination and disproportionation of ethyl radicals.

From the observed effect of pressure on the amounts and isotopic structure of products, direct evidence has been obtained for the important role of "hot" ethyl radicals in these reactions as well as for their responsibility for the occurrence of isotopic exchange. The reactions have been carried out at room temperature where attack of thermalized free radicals on H_2 or D_2 is too slow to be of importance. In view of the difference in the strengths of CD and CH bonds an isotopic effect has been anticipated, and it has been found that isotopic exchange occurs when D atoms add to C_2H_4 but not when H atoms add to C_2D_4. As a result the *course* of the reaction in the two cases is quite different. Some information on the mechanism of disproportionation of ethyl radicals has also been obtained.

EXPERIMENTAL

A conventional high vacuum apparatus was used with a cylindrical quartz reaction cell 5 cm in diameter and 10 cm long. Mercury resonance radiation was obtained from a low pressure mercury arc situated some 20 cm from the reaction cell and was roughly collimated with a highly polished aluminum cylinder.

Research grade ethylene was employed and hydrogen was purified by passage through a heated palladium thimble. Tetradeuteroethylene, at least 99 atom % pure, was kindly supplied by Dr. L. C. Leitch of these laboratories.

[1]*Manuscript received February 27, 1959.*
Contribution from the Division of Applied Chemistry, National Research Council, Ottawa, Canada.
Issued as N.R.C. No. 5187.
[2]*National Research Council Postdoctorate Fellow 1955–57. Present address: Carrington Research Laboratory, Petro-Chemicals Limited, Urmston, Manchester, England.*

Can. J. Chem. Downloaded from www.nrcresearchpress.com by 196.1.178.254 on 09/04/12
For personal use only.

RESULTS

All experiments were performed at room temperature and the results for H + C_2D_4, D + C_2H_4, and H + C_2H_4 are given in Tables I, II, and III, respectively. Large excess of hydrogen (or deuterium) and very small amounts of ethylene were used. This ensured essentially quantitative quenching of the Hg $6(^3P_1)$ atoms by hydrogen and also made feasible mass spectrometric analyses of the recovered C_2 hydrocarbons without necessitating excessively long exposures.

Butanes and C_2 hydrocarbons were condensed in liquid nitrogen and, after the unreacted excess hydrogen was pumped off, were separated by a LeRoy still (3), measured with a constant volume gas burette, and then analyzed by mass spectrometry. No products other than those shown in the tables were detected. The observed mass balance was usually slightly below 100%, in all probability due to the difficulty of quantitatively recovering C_2 hydrocarbons from the large excess of hydrogen employed. For this reason, besides the values actually observed for ethylene and ethane, the "corrected" values are also given in the Tables I–III. The latter were calculated by assuming complete recovery of butane and scaling up the C_2 fraction to obtain 100% carbon atom balance. The amount of the C_2 fraction was, therefore, assumed to be equal to the original ethylene less twice the amount of the recovered butane. The relative proportions of ethylenes and ethanes were then calculated from the mass spectrometric analyses of the recovered C_2 fraction. In general, these corrections were not particularly large.

The mass spectrometric analyses were subject to the usual uncertainties in the values of the lighter constituents, especially when they were formed in very small amounts, because of cumulative errors in the corrections for the fragment peaks of the heavier constituents present.[3] Thus in Table I, in addition to the two ethanes, C_2D_5H and $C_2D_4H_2$,

TABLE I

Products of the reaction H + C_2D_4 (25±1° C; exposure 60 minutes; "corrected" values are in italics)

Run	P_{H_2}, mm	C_2D_4 Taken, μmoles	Products (micromoles)					$\frac{(C_2D_5H + C_2D_4H_2)}{(C_4D_8H_2)}$	C_2D_4 Consumed, μmoles
			C_2D_4	C_2D_3H	C_2D_5H	$C_2D_4H_2$	$C_4D_8H_2$		
Q3	51.3	87.0	56.92	0.69	0.40	1.40	12.0	0.150	
			60.3	*0.73*	*0.42*	*1.48*		*0.158*	*26.7*
Q2	99.5	87.0	55.68	0.68	0.41	1.23	13.0	0.126	
			58.1	*0.71*	*0.43*	*1.28*		*0.132*	*28.9*
Q1	299.7	87.3	56.99	0.63	0.44	0.88	13.6	0.097	
			57.7	*0.64*	*0.45*	*0.89*		*0.099*	*29.6*

some $C_2D_3H_3$ is also indicated. However, the analytical uncertainty for this compound is so high that it is not certain whether it is formed at all and it has, therefore, been omitted from the table. Similarly, the figures for C_2D_3H are only approximate. The ratio of C_2D_5H and $C_2D_4H_2$, on the other hand, should be reliable. The C_4 fraction consists in this case of essentially pure $C_4D_8H_2$ (with less than 0.3% of d_9 and d_{10} butanes) and the indications are that the two H atoms are on the terminal carbon atoms. In Table II the figures for C_2H_4, C_2H_3D, C_2H_6, and C_2H_5D are probably not too accurate and, similarly, in the C_4 fraction the figures for C_4H_{10} are not too reliable.

[3]*The mass spectra of the deutero compounds from the American Petroleum Institute catalog of mass spectral data were used where available. In other cases estimates of probable fragment intensities were made by analogy with the known spectra.*

TABLE II

Products of the reaction D + C_2H_4 (25±1° C; exposure 60 minutes in $M_{8,9,10}$, 120 minutes in $M_{6,7}$; initial C_2H_4 88.5 micromoles in all experiments; "corrected" values are in italics)

Run	P_{D_2}, mm	Products (micromoles)											C_2H_4 Consumed, μmoles
		C_2H_4	C_2H_3D	C_2H_6	C_2H_5D	$C_2H_4D_2$	$C_2H_3D_3$	C_4H_{10}	C_4H_9D	$C_4H_8D_2$	$C_4H_7D_3$	Total butane	
M_{10}	49.3	51.7	4.61	4.23	1.81	—	—	0.82	3.28	4.55	0.52	9.17	
		58.3	*5.20*	*4.78*	*2.04*	—	—						*30.2*
M_9	99	36.9	5.83	4.37	1.46	—	—	0.67	3.17	5.29	0.43	9.56	
		52.7	*8.35*	*6.25*	*2.09*	—	—						*35.8*
M_8	300	55.4	3.07	4.10	1.71	—	—	0.33	1.78	8.07	0.33	10.51	
		58.3	*3.23*	*4.31*	*1.80*	—	—						*30.2*
M_6	300	23.9	2.36	4.55	2.98	1.0	0.06	0.82	4.30	17.1	1.73	23.95	
		27.7	*2.73*	*5.25*	*3.43*	*1.4*	*0.07*						*60.8*
M_7	606	21.7	1.76	2.52	2.23	1.12	—	0.95	3.33	20.25	1.05	25.58	
		27.4	*2.23*	*3.19*	*2.82*	*1.42*	—						*61.1*

The analytical uncertainties preclude a detailed quantitative analysis of the pressure dependence of the investigated reactions and for this reason no attempt has been made at present to accumulate more extensive experimental data. Fortunately, the values for the major products formed are in general reasonably reliable. There can, as well, be little doubt of the reality of the general trends observed and in particular of the pronounced difference in the complexity of the products shown in Tables I and II, respectively. As a result a number of conclusions can be safely drawn.

DISCUSSION

A significant result of the present work is the finding that isotopic exchange takes place readily when D atoms add to C_2H_4, even at relatively high pressures of D_2, while there is no exchange when H atoms add to C_2D_4. In the former case the formation of different isotopic butanes indicates, besides C_2H_4D radicals, the presence of C_2H_5 and $C_2H_3D_2$ radicals as well. In the latter case, on the other hand, only C_2D_4H radicals are present.

The amount of isotopic exchange in the reaction of D atoms with C_2H_4 (Table II) increases at lower pressures of D_2 and the following reactions have, therefore, to be considered:

$$C_2H_4 + D \rightarrow C_2H_4D^* \quad [1]$$

$$C_2H_4D^* \rightarrow C_2H_3D + H \quad [2]$$

$$\left[\text{or} \quad C_2H_4D^* + C_2H_4 \rightarrow C_2H_3D + C_2H_5^* \quad [2a]\right]$$

and

$$C_2H_4D^* + M \rightarrow C_2H_4D + M \quad [3]$$

with subsequent reactions of the H atoms produced in reaction [2] and recombination and disproportionation of the ethyl radicals formed. Addition of H atoms to the original ethylene, C_2H_4, produces C_2H_5 and as the conversion increases, D atoms will add to C_2H_3D formed in reaction [2] to give increasing amounts of $C_2H_3D_2$. The observed trends with pressure and over-all conversion in the amounts of various butanes formed in the reaction of D atoms with C_2H_4, as shown in Table II, are in qualitative agreement with the indicated reactions.

In the reaction of H atoms with C_2D_4 (Table I) the only equivalent of reaction [2]

Can. J. Chem. Downloaded from www.nrcresearchpress.com by 196.1.178.254 on 09/04/12
For personal use only.

which occurs is

$$C_2D_4H^* \rightarrow C_2D_4 + H \qquad [4]$$

$$\left[\text{or} \quad C_2D_4H^* + C_2D_4 \rightarrow C_2D_4 + C_2D_4H^* \qquad [4a]\right]$$

but not

$$C_2D_4H^* \rightarrow C_2D_3H + D \qquad [5]$$

$$\left[\text{nor} \quad C_2D_4H^* + C_2D_4 \rightarrow C_2D_3H + C_2D_5^*. \qquad [5a]\right]$$

No isotopic exchange is therefore observed.

The difference between the two cases is readily understandable in view of the difference in the bond dissociation energies between a C–D and a C–H bond as a result of the difference in the zero point energies. When a H atom adds to C_2D_4, the hot $C_2D_4H^*$ radical possesses enough excess energy to undergo reaction [4] but not reaction [5]. When a D atom adds to C_2H_4, on the other hand, the hot $C_2H_4D^*$ radical formed possesses enough excess energy to split off a D or a H atom, and both the statistical and the energetic conditions favor the latter (reaction [2]).

The isotopic structure of the ethanes formed and the pressure effects observed in these experiments are of interest from the point of view of "disproportionation" of ethyl radicals. Under conditions of the present work, ethane could not have been formed by combination of methyl radicals because if this were so appreciable quantities of propane would have been formed as well and this was not the case. Reaction of H atoms with C_2D_4 is relatively simple and the analytical results in Table I for the two ethanes formed, C_2D_5H and $C_2D_4H_2$, are reasonably reliable. (Some $C_2H_3D_3$ might have been produced as well but this is highly uncertain.) C_2D_6 is not formed. These results are not inconsistent with the "head-to-tail" disproportionation mechanism of Wijnen and Steacie (4). The ratio $C_2D_4H_2/C_4D_8H_2$ increases at lower pressures while the ratio of $C_2D_5H/C_4D_8H_2$ is pressure-independent. The following reactions ought then to be considered:

$$C_2D_4H + C_2D_4H \rightarrow C_2D_5H + C_2D_3H \qquad [6]$$

$$C_2D_4H + C_2D_4H \rightarrow C_2D_4H_2 + C_2D_4 \qquad [7]$$

$$C_2D_4H^* + C_2D_4H \rightarrow C_2D_4 + C_2D_4H_2^* \qquad [8]$$

$$C_2D_4H_2^* + M \rightarrow C_2D_4H_2^* + M. \qquad [9]$$

Reactions [6] and [7] involve thermalized radicals and lead, therefore, to a pressure-independent ratio of $C_2D_5H/C_4D_8H_2$. Reaction [8] explains the increase in $C_2D_4H_2$ as the pressure is lowered. It appears therefore necessary to assume that under the conditions employed in these experiments an H atom is abstracted much more readily than a D atom from a hot C_2D_4H radical in spite of the more favorable statistical ratio of D atoms. It is unlikely that $C_2D_4H_2$ was formed by addition of H atoms to C_2D_4H since, if anything, the pressure dependence would then be opposite to that observed.

In contrast to the results obtained in the present work, Dills and Rabinovitch (5) obtained a more complex isotopic structure of the products in an experiment with C_2D_4 and H atoms at a total pressure of about 4 mm, using a simulated point source (nozzle) of H atoms, and maintaining a spherical diffusion reaction zone. The butanes consisted of $C_4D_8H_2$ (83%), C_4D_9H (15%), and C_4D_{10} (2%) and the ethanes of C_2D_6 (63%), C_2D_5H (18%), and $C_2D_4H_2$ (19%). This was interpreted to show that the mechanism of disproportionation is not "head-to-tail" but rather that the disproportionation takes place with more than one atom migrating. This conclusion cannot be of general validity since C_2D_6, C_4D_9H, and C_4D_{10} are not formed in the same reaction under conditions employed in the present work in which the products formed are consistent with a "head-

Can. J. Chem. Downloaded from www.nrcresearchpress.com by 196.1.178.254 on 09/04/12
For personal use only.

to-tail" disproportionation. The more complex isotopic structure of the butane and ethane obtained by Dills and Rabinovitch appears to be due to the particular conditions employed by these authors and the reason for the greater complexity is not quite clear. Perhaps at very low pressures some exchange involving transfer of D atoms does occur. Since reaction [5] is slightly endothermic while [5*a*] is exothermic, the latter would perhaps provide the more readily acceptable mechanism of such an exchange. However, further experimental information is necessary before any firm conclusions can be drawn.

In the reaction of D atoms with C_2H_4 (Table II) no $C_2H_4D_2$ is formed at low conversions, and the disproportionation of C_2H_4D radicals (including also the reactions involving $C_2H_4D^*$) is, therefore, entirely by abstraction of a hydrogen atom.

$$C_2H_4D + C_2H_4D \rightarrow C_2H_5D + C_2H_3D \quad [10]$$

$$C_2H_4D + C_2H_4D^* \rightarrow C_2H_5D^* + C_2H_3D \quad [11]$$

$$C_2H_5D^* + M \rightarrow C_2H_5D + M \quad [12]$$

Abstraction of hydrogen atoms is here favored both statistically and energetically. Only at higher conversions $C_2H_4D_2$ is formed as a result of the eventual addition of D atoms to C_2H_3D produced in the course of the reaction. Formation of C_2H_6 is a consequence of the readily occurring isotopic exchange (reaction [2] or [2*a*]).[4]

A striking feature of the results of the performed experiments is the fact that the isotopic exchange (reactions such as [2] or [2*a*]) and the "hot radical" effects in the disproportionation (reactions such as [8] and [11]) persist to quite high H_2 or D_2 pressures. The occurrence of reactions such as [2] at high pressures could be explained by assuming very short natural lifetimes of the energy-rich radicals and perhaps, as is frequently done, a very readily occurring deactivation by collision for this particular process. The occurrence of reactions such as [8] and [11], on the other hand, must mean that the energy-rich ethyl radicals are deactivated in collisions only extremely slowly and are capable of undergoing preferential disproportionation (and exhibiting as well a strong isotopic effect in disproportionation), even after undergoing numerous collisions in the gas phase with H_2 or D_2 and with ethylene. Thus, for example, although in the reaction of H atoms and C_2D_4 the ratio of the concentrations of hydrogen at a pressure of 100 mm and C_2D_4H (calculated approximately from the rate of formation of $C_4D_8H_2$) is of the order of 10^5 to 10^6, there are still pronounced isotopic and pressure effects in the formation of ethane. Similarly, the pressure dependence of the ratio of disproportionation to combination in the reaction of H atoms with C_2H_4 (Table III) persists to quite high hydrogen pressures.

TABLE III

Products of the reaction H + C_2H_4 (25±1° C; exposure 60 minutes; "corrected" values are in italics)

Run	P_{H_2}, mm	C_2H_4 Taken, μmoles	Products (micromoles)			C_2H_4 Consumed, μmoles	C_2H_6/C_4H_{10}
			C_2H_4	C_2H_6	C_4H_{10}		
M_5	101	88.0	53.4	3.44	12.6		
			59.5	*3.77*		*28.5*	*0.30*
M_1	300	88.9	46.6	2.28	15.0		
			56.7	*2.79*		*32.2*	*0.19*
M_4	616	87.8	51.3	2.36	16.6		
			52.9	*2.40*		*34.9*	*0.14*

[4]*Since all ethane results from disproportionation of ethyl radicals, the relative abundance of* C_2H_6 *and* C_2H_5D *depends on the relative importance of reactions* [2] (*or* [2*a*]) *and* [3], *respectively. In the limiting case when reaction* [3] *is negligible, i.e. as pressure tends to zero, all the ethane would consist of* C_2H_6 (*as long as the conversion is small, i.e. until appreciable quantities of* C_2H_3D *are accumulated*).

Can. J. Chem. Downloaded from www.nrcresearchpress.com by 196.1.178.254 on 09/04/12
For personal use only.

In principle, it might appear to be possible to obtain quantitative information on the lifetimes of the "hot" radicals from a study of the pressure dependence of the yields of the products. The somewhat limited experimental information on pressure effects obtained in the present work and the limitations in analytical accuracy preclude a detailed analysis of this kind. However, the data in Tables I–III appear not to be consistent with the postulates of single hot radical species the rate of deactivation of which depends linearly on pressure.

The finding that abstraction of a hydrogen atom from a hot ethyl radical takes place very readily and that when the hot radical contains both H and D atoms it is the former which are abstracted, makes it necessary, by analogy, to consider the reactions of the type [2*a*] and [4*a*] as the ones which may perhaps be responsible for the isotopic exchange. However, on the basis of the available information the two types of processes (reactions [2] and [4] as contrasted with [2*a*] and [4*a*]) cannot be differentiated. Whether reactions of the latter type occur or not should perhaps be possible to establish by producing hot C_2H_5 radicals from photolysis of mercury diethyl in the presence of C_2D_4.

The ambiguity between these two types of processes may be rather general for exchange reactions of similar kind. Thus, the isotopic exchange and deuterium atom enrichment in the methane formed in the reaction of ethylene (2) or ethane (6), under conditions where atomic cracking takes place, may be due to the reactions of the type

$$CH_3 + D \rightarrow CH_3D^* \qquad [13]$$

$$CH_3D^* \rightarrow CH_2D + H \qquad [14]$$

$$CH_3D^* + M \rightarrow CH_3D + M \qquad [15]$$

as is generally assumed (6), or instead of [14]

$$CH_3D^* + R \rightarrow CH_2D + RH^*, \qquad [14a]$$

where R is D, an ethyl or a methyl radical and RH* may still be to some extent "hot", since the excess energy would be expected to be predominantly transferred into the product (RH*) in which a bond is formed. (Energetically the process simulates to a large extent the sequence of reaction [14] followed by combination of H and R to give RH*.)

Recently Lavrovskaia *et al.* (7) have proposed the following reaction as the one responsible for isotopic exchange in free radical reactions of hydrocarbons:

$$RCH_2\cdot + D_2 \rightarrow RCHD\cdot + HD. \qquad [16]$$

However, we find[5] no isotopic exchange at room temperature between thermalized ethyl radicals (from photolysis of diethyl ketone) and D_2 or C_2D_4. Reactions of this type, therefore, do not occur under conditions of the present experiments and are in general not likely to be important when thermalized radicals are involved.[6] Whether such reactions may occur when the free radicals are "hot" cannot be said at present. In such a case reaction [16] would become analogous to reaction [2*a*], tentatively suggested as a possibility in the present work.

ACKNOWLEDGMENT

The authors are grateful to Dr. A. W. Tickner for mass spectrometer analyses and their interpretation.

[5]*The authors are grateful to Mr. S. Sato for performing these experiments.*
[6]*Reaction [16] is also discussed in reference (6).*

Can. J. Chem. Downloaded from www.nrcresearchpress.com by 196.1.178.254 on 09/04/12
For personal use only.

REFERENCES

1. BRADLEY, J. N., MELVILLE, H. W., and ROBB, J. C. Proc. Roy. Soc. A, **236**, 318 (1956).
2. TOBY, S. and SCHIFF, H. I. Can. J. Chem. **34**, 1061 (1956).
3. LEROY, D. J. Can. J. Research, B, **28**, 492 (1950).
4. WIJNEN, M. H. J. and STEACIE, E. W. R. Can. J. Chem. **29**, 1092 (1951).
5. DILLS, D. H. Lifetimes for decomposition of vibrationally excited dideuteroethyl radicals. Ph.D. Thesis, University of Washington. 1956.
6. BERISFORD, R. and LEROY, D. J. Can. J. Chem. **36**, 983 (1958).
7. LAVROVSKAIA, G. K., MARDALEISHVILI, R. E., and VOEVODSKII, V. V. Voprosy Khim. Kinetiki, Kataliza, i Reakstsionnoi Sposobnosti, Akad. Nauk S.S.S.R., Otdel. Khim. Nauk, 40 (TT-701) (1955).

Can. J. Chem. Downloaded from www.nrcresearchpress.com by 196.1.178.254 on 09/04/12
For personal use only.

Can. J. Chem. Downloaded from www.nrcresearchpress.com by 196.1.178.254 on 09/04/12
For personal use only.

THE REACTION OF POTASSIUM PERSULPHATE WITH THIOGLYCOLIC ACID IN AQUEOUS SOLUTION[1]

J. F. HENDERSON[2] AND C. A. WINKLER

ABSTRACT

The oxidation of thioglycolic acid to dithiodiglycolic acid by potassium persulphate in aqueous solution in the absence of iron did not yield reproducible results, but satisfactory data were obtained when ferrous or ferric ions were added to the system. The catalyst cycle appears to be that ferrous ion is oxidized by persulphate to ferric ion, and the ferric ion is reduced back to ferrous ion by thioglycolic acid. In the absence of persulphate, the reaction of ferric ion with thioglycolic acid in acid solution (pH <3) was second order in both ferric ion and thioglycolic acid concentrations and was markedly inhibited by hydrogen ion.

INTRODUCTION

The rate-controlling step in the thermal decomposition of persulphate ion in aqueous solution has been postulated to be the first-order homolytic dissociation of persulphate to yield sulphate ion radicals (1, 2, 3).

$$S_2O_8^{=} \rightarrow 2SO_4^{\cdot -}$$

The addition of organic compounds to solutions of persulphate in general increases the rate of decomposition of the persulphate ion, but the mechanisms of many of these reactions are not well understood (2, 4, 5, 6, 7).

The reactions of potassium persulphate with alkyl mercaptans in glacial acetic acid – water solution have been discussed in a previous paper from this laboratory (4). Secondary salt effects were observed which tended to make interpretation of the results difficult, but it seemed that persulphate decomposed unimolecularly to yield two sulphate ion radicals which either reacted with the mercaptan or recombined in a solvent "cage".

For the decomposition of persulphate ion in the presence of certain other organic compounds, e.g. methanol and hydrazobenzene, no evidence for the existence of a solvent cage has been found (2, 5, 6). Furthermore, it has been postulated that the sulphate ion radicals in these reaction mixtures were produced by direct reaction between persulphate ion and the organic compound rather than by unimolecular decomposition of persulphate ion (2, 5), though for the persulphate–methanol reaction there is now doubt that this view is correct (6).

The present investigation was planned originally with the intention of obtaining more information about the reactions of persulphate ion with organic compounds, particularly those containing the sulphydryl group. Thioglycolic acid was chosen to permit experiments in aqueous solution, hence avoiding the difficulties encountered in the earlier investigation (4).

Preliminary experiments (8), which will not be described, indicated that 2 moles of thioglycolic acid were oxidized by 1 mole of persulphate to yield 1 mole of dithiodiglycolic acid, but measurements of the reaction rate were quite erratic. Reproducible data were obtained, however, in the presence of soluble iron salts as catalyst, and it was decided to investigate this catalyzed reaction.

[1]*Manuscript received February 5, 1959.*
Contribution from the Physical Chemistry Laboratory, McGill University, with financial assistance from the Canadian Kodak Co., Ltd., and the National Research Council.
[2]*Holder of a Canadian Kodak Company, Ltd., Fellowship.*

Can. J. Chem. Downloaded from www.nrcresearchpress.com by 196.1.178.254 on 09/04/12
For personal use only.

EXPERIMENTAL

Fisher "purified" thioglycolic acid was distilled rapidly at 8 mm Hg and 95° C, and the distillate was stored at 0° C under an atmosphere of nitrogen (9). Its purity was estimated to be 99.5% by diluting weighed quantities with water and titrating these with standard iodine solution, using starch as the indicator.

The other materials employed in this investigation, which were supplied by Brickman and Company, Montreal, were of reagent grade and were used as received.

Either ferrous or ferric ammonium sulphate was used to catalyze the reaction. The ionic strength of the reaction mixture was adjusted by adding potassium sulphate, sulphuric acid, or mixtures of the two. In calculating the ionic strength, allowance was made for the incomplete dissociation of KSO_4^- and HSO_4^- ions (10, 11).

Both the standardized solutions of the reactants and the reaction mixtures were prepared with laboratory distilled water. Prior to mixing, the reactant solutions were swept with nitrogen (99.9%) which was saturated with water vapor and used without further purification. The reaction mixtures were swept with moist nitrogen while experiments were in progress at 24.8±0.02° C.

The progress of the reaction was determined by transferring aliquots from the reaction mixture to 25 ml of approximately 20% phosphoric acid and estimating the thioglycolic acid content by titration with a standard solution of iodine in a solution of potassium iodide. The phosphoric acid, by complexing the ferric ion, served to slow the reaction and to prevent possible complications in the subsequent titration with iodine. Reaction of persulphate with iodide ion during the iodimetric titration was found to be negligible.

For experiments in 0.15 *M* sulphuric acid, both the progress of reaction and the concentration of ferric ion were determined by periodically removing aliquots from the reaction mixture and recording their ultraviolet spectra for wavelengths up to 400 mμ. From the data in Table I it may be inferred that appreciable complex formation did not occur between any of the components present in the reaction mixtures. The concentration of ferric ion in reaction mixtures was estimated from the optical density measured at 325 mμ. The optical densities at lower wavelengths were then corrected for the contri-

TABLE I

Optical density of aqueous solutions of the components and of various mixtures of the components present in the iron-catalyzed persulphate - thioglycolic acid reaction mixtures (sulphuric acid 0.15 M/l. (mole/liter))

Composition of solution	Optical density						
	D330	D310	D290	D270	D250	D230	D210
A. Pure components							
8.02×10^{-4} *M* $S_2O_8^=$				0.005	0.026	0.089	0.367
0.955×10^{-3} *M* TSH				0.005	0.088	0.250	0.722
1.00×10^{-3} *M* TSH				0.005	0.075	0.240	0.783
1.91×10^{-3} *M* TSH				0.012	0.162	0.479	
1.00×10^{-4} *M* TSST				0.024	0.098	0.189	0.331
4.00×10^{-4} *M* Fe^{++}					0.010	0.018	0.020
4.45×10^{-5} *M* Fe^{+++}	0.069	0.110	0.102	0.087	0.157	0.235	0.230
8.00×10^{-5} *M* Fe^{+++}	0.134	0.199	0.185	0.160	0.276	0.408	0.415
B. Mixtures of components							
8.02×10^{-4} *M* $S_2O_8^=$ and 1.91×10^{-3} *M* TSH				0.022	0.190	0.572	
8.02×10^{-4} *M* $S_2O_8^=$ and 4.45×10^{-5} *M* Fe^{+++}	0.069	0.113	0.109	0.098	0.185	0.330	0.630
4.00×10^{-4} *M* Fe^{+++} and 0.955×10^{-3} *M* TSH				0.005	0.103	0.272	0.754
1.00×10^{-4} *M* TSST and 1.00×10^{-3} *M* TSH				0.035	0.184	0.450	
1.00×10^{-4} *M* TSST and 4.00×10^{-4} *M* Fe^{++}				0.028	0.118	0.219	0.364
1.00×10^{-4} *M* TSST and 8.00×10^{-5} *M* Fe^{+++}	0.134	0.199	0.209	0.185	0.386	0.830	0.827

bution by ferric ion and, by using this corrected value, the concentrations of the remaining components in the reaction mixture at any time were calculated using the following equation,

$$[\mathrm{TSST}] = \frac{D - \epsilon_{\mathrm{TSH}}[\mathrm{TSH}]_0 - \epsilon_{S_2O_8^=}[S_2O_8^=]_0}{\epsilon_{\mathrm{TSST}} - 2\epsilon_{\mathrm{TSH}} - \epsilon_{S_2O_8^=}}$$

where D represents the corrected optical density, ϵ the respective extinction coefficients, and $[\mathrm{TSH}]_0$ and $[S_2O_8]_0$ the initial concentrations of thioglycolic acid and persulphate respectively. The results obtained using the spectrophotometric method were in excellent agreement with those obtained using the volumetric method (Fig. 4).

RESULTS

Experiments at a pH of approximately 2 showed the reaction to be first order in the persulphate concentration and zero order in the thioglycolic acid concentration. The first-order rate constant for persulphate disappearance, k_1' in Table II, was directly proportional to the concentration of iron in the system, which indicates that, in the presence of added iron, direct reaction between persulphate and thioglycolic acid was negligible. The effect of ionic strength on the calculated second-order rate constant, $k_1 = k_1'/[\mathrm{Fe}]$, is shown in Fig. 1, and it is apparent that the rate-controlling step of the reaction consists of interaction between doubly charged ions of the opposite sign.

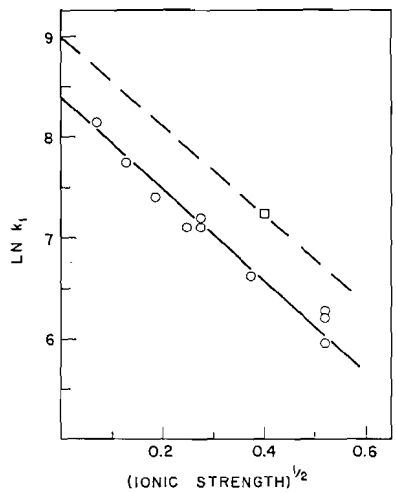

FIG. 1. Variation of the second-order rate constant, k_1, with the ionic strength: —□— see ref. (16, 17).

For reaction mixtures in which the concentration of sulphuric acid was 0.15 M and in which the iron was initially in the ferrous state, the initial rates of reaction and the first-order rate constants at zero time were functions of the initial concentrations of both the persulphate and the thioglycolic acid (Table III). Furthermore, the concentration of ferric ion reached a stationary value which increased with increasing persulphate concentration and decreased with increasing thioglycolic acid concentration (Figs. 2 and 3). Division of the rate of disappearance of persulphate in these reaction mixtures by the product of the persulphate and ferrous ion concentrations at a given instant of time yielded a second-order rate constant corresponding to k_1 which was independent of the reaction mixtures, and for which the average value (651 l. mole^{-1} min^{-1}) was in reasonable agreement with that shown in Fig. 1 at the same ionic strength. As observed

Can. J. Chem. Downloaded from www.nrcresearchpress.com by 196.1.178.254 on 09/04/12
For personal use only.

TABLE II

The effect of different initial concentrations of ferric ion, persulphate, and thioglycolic acid on the rate of disappearance of persulphate at pH $\simeq$ 2

Initial $[Fe^{+++}]$ ($\times 10^5$)	Initial $[S_2O_8^{=}]$ ($\times 10^3$)	Initial [TSH] ($\times 10^3$)	$[K_2SO_4]$	$[H_2SO_4]$	Ionic strength (μ)	k_1' (min^{-1})	$k_1 = k_1'/[Fe]$ (l. M^{-1} min^{-1})
10.0	1.60	4.50	0.00	0.10	0.269	0.0492	492
10.0	3.20	9.00	0.00	0.10	0.269	0.0492	497
10.0	6.40	13.50	0.00	0.10	0.269	0.0492	460
10.0	6.40	4.50	0.00	0.10	0.269	0.0380	380
4.0	3.19	9.72	0.0057	0.010	0.038	0.066	1650
4.0	3.19	4.86	0.0057	0.010	0.038	0.066	1650
4.0	3.19	14.94	0.0057	0.010	0.038	0.066	1650
2.0	8.00	9.40	0.0095	0.10	0.272	0.00782	391
2.0	4.00	9.40	0.0095	0.10	0.272	0.00794	397
2.0	2.40	9.40	0.0095	0.10	0.272	0.00782	391
2.0	1.60	9.40	0.0095	0.10	0.272	0.00794	397
0.8	4.00	9.35	0.0095	0.10	0.272	0.00329	410
4.0	4.00	9.35	0.0095	0.10	0.272	0.01640	410
10.0	4.00	9.35	0.0095	0.10	0.272	0.0398	398

TABLE III

The effect of different initial concentrations of ferrous ion, persulphate, and thioglycolic acid on the rate of disappearance of persulphate in 0.15 M sulphuric acid (ionic strength = 0.224)

Initial $[Fe^{++}]$ ($\times 10^5$)	Initial $[S_2O_8^{=}]$ ($\times 10^3$)	Initial [TSH] ($\times 10^3$)	Initial $\frac{d[S_2O_8^{=}]}{dt}$ (M $l.^{-1}$ min^{-1} $\times 10^5$)	Initial k_1' (min^{-1})
10.0	2.00	10.95	7.1	0.0368
10.0	4.00	10.95	15.5	0.0359
10.0	6.00	10.95	20.0	0.0320
10.0	8.00	10.95	24.0	0.0299
10.0	2.00	4.38	7.0	0.0347
10.0	4.00	4.38	12.7	0.0304
10.0	8.00	4.38	20.0	0.0253
10.0	4.00	2.18	12.1	0.0285
10.0	4.00	7.63	13.0	0.0331
10.0	4.00	15.30	13.0	0.0370
5.0	4.00	10.95	7.5	0.0161
15.0	4.00	10.95	22.0	0.0630

previously for pH$\sim$2, the initial rate of reaction extrapolated to zero when the initial concentration of ferrous ion was decreased to zero indicating that direct reaction between persulphate ion and thioglycolic acid was negligible.

When the added iron was initially in the ferric state, the reaction was preceded by an induction period, but following this induction the rate of reaction was the same as for experiments in which the iron was initially in the ferrous state (Fig. 4). The stationary-state concentration of ferric ion was independent of the valence state of the iron at zero time, although it was not attained for several minutes when the iron was initially in the ferric state. The rate of disappearance of ferric ion during the greater part of the induction period, i.e. before its concentration reached a stationary value, was not influenced by the presence of persulphate (Fig. 5).

To study the reaction between ferric ion and thioglycolic acid in sulphuric acid solutions, the disappearance of ferric ion was followed by the change in optical density at 305 mμ. The thioglycolic acid concentration was in sufficient excess over that of ferric ion to be considered independent of time. The slopes of the straight lines in Fig. 6, which show the second-order dependence of the reaction rate on the ferric ion concentration, are

Can. J. Chem. Downloaded from www.nrcresearchpress.com by 196.1.178.254 on 09/04/12
For personal use only.

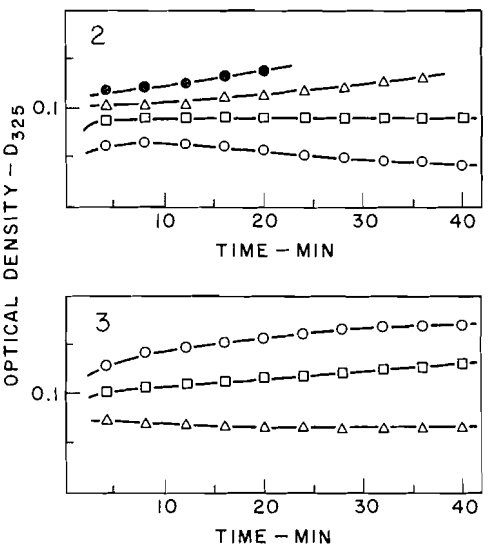

FIGS. 2 AND 3. Effect of different initial concentrations of persulphate and of thioglycolic acid on the optical density at 325 mμ. Initial concn. Fe^{++} 10.0×10^{-5} M/l. Concn. H_2SO_4 0.15 M/l.

FIG. 2. Initial concn. TSH
Initial concn. $S_2O_8^=$
○ 0.00200 M/l.
□ 0.00400 M/l.
△ 0.00600 M/l.
● 0.00800 M/l.

FIG. 3. Initial concn. $S_2O_8^=$ 0.00400 M/l.
Initial concn. TSH
○ 0.00218 M/l.
□ 0.00763 M/l.
△ 0.01530 M/l.

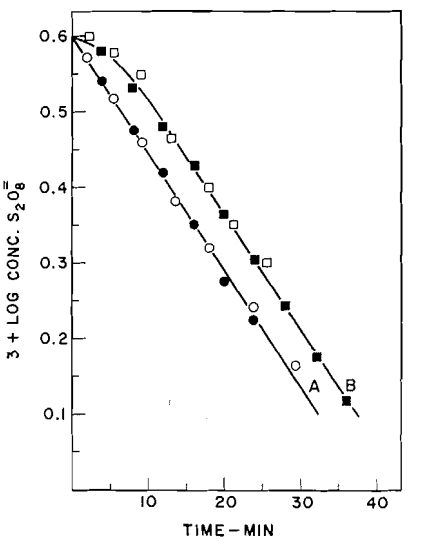

FIG. 4. Effect of the initial oxidation state of the dissolved iron on the rate of disappearance of persulphate.

A Iron initially ferrous
B Iron initially ferric
○, □ Iodimetric analysis
●, ■ Spectrophotometric analysis

Can. J. Chem. Downloaded from www.nrcresearchpress.com by 196.1.178.254 on 09/04/12
For personal use only.

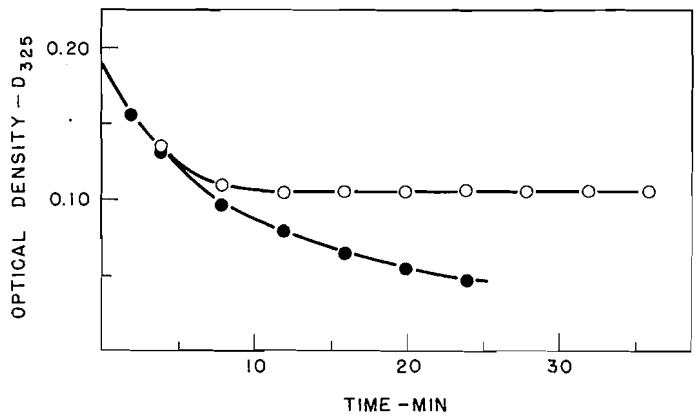

FIG. 5. The variation of optical density at 325 mμ with time when the iron was initially in the ferric state.

Initial concn. TSH 0.01085 M/l. Initial concn. $S_2O_8^=$ ○ 0.00400 M/l. ● 0.00000 M/l.

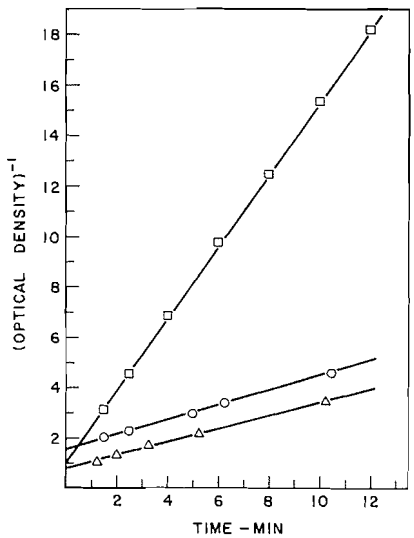

FIG. 6. Effect of different initial concentrations of thioglycolic acid on the rate of reaction between ferric ion and thioglycolic acid.

Initial concn. TSH ○ 0.00488 M/l. □ 0.01220 M/l. △ 0.00488 M/l.

proportional to the square of the thioglycolic acid concentration, indicating the over-all reaction to be of the fourth order. The effect of sulphuric acid concentration on the calculated fourth-order rate constant, k_4''', is shown in Table IV.

When the ferric ion and thioglycolic acid were mixed initially in these experiments, a blue complex was formed which faded rapidly as observed in earlier investigations (13, 14). However, extrapolation of the measured optical densities at 305 mμ to zero time indicated that the optical density of ferric ion was not influenced by thioglycolic acid, and hence that ferric ion – thioglycolic acid complexes were highly dissociated.

The dependence of the fourth-order rate constant on hydrogen ion concentration was

Can. J. Chem. Downloaded from www.nrcresearchpress.com by 196.1.178.254 on 09/04/12
For personal use only.

TABLE IV

Variation of k_4''', the calculated fourth-order rate constant for the ferric ion – thioglycolic acid reaction, with the concentration of sulphuric acid

$[H_2SO_4]$	k_4''' ($l.^2\ M^{-2}\ min^{-1} \times 10^{-6}$)
0.050	242
0.100	27.6
0.150	10.3

determined more exactly by making experiments at various levels of perchloric acid when the ionic strength of the reaction mixtures was adjusted to 1.00 with sodium perchlorate. The reaction was followed by periodically removing aliquots of the reaction mixture and estimating the ferric ion content colorimetrically as the thiocyanate complex (12). Again the thioglycolic acid concentration was in sufficient excess over that of ferric ion to be effectively independent of time. The fourth-order rate constant, k_4', was found to be inversely proportional to approximately the fourth power of the hydrogen ion concentration (Fig. 7). Low concentrations of sulphate ion in these reaction mixtures also caused inhibition (Table V).

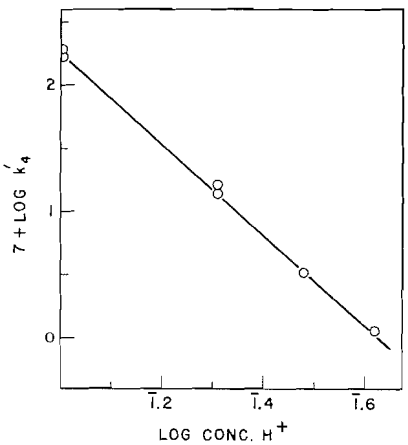

FIG. 7. Effect of perchloric acid concentration on k_4'.

TABLE V

Effect of sulphuric acid concentration on the fourth-order rate constant, k_4'' (ionic strength = 1.00)

$[HClO_4]$	$[H_2SO_4]$	$[SO_4^{=}]$	$[H^+]$	k_4'' ($l.^2\ M^{-2}\ min^{-1} \times 10^{-7}$)	k_4' ($l.^2\ M^{-2}\ min^{-1} \times 10^{-7}$)
0.101	0.0098	0.0070	0.118	63.8	110
0.101	0.0098	0.0070	0.118	71.4	110
0.101	0.0245	0.0170	0.143	22.1	52.5

NOTE: Values of k_4', which were interpolated from Fig. 7, were determined under identical experimental conditions except that sulphate ion was absent.

The fourth-order rate constant, k_4''', for the ferric ion – thioglycolic acid reaction was also determined by dividing the rate of formation of dithiodiglycolic acid in persulphate –

Can. J. Chem. Downloaded from www.nrcresearchpress.com by 196.1.178.254 on 09/04/12
For personal use only.

thioglycolic acid reaction mixtures by the product of the square of the ferric ion concentration and the square of the thioglycolic acid concentration. Its value in these reaction mixtures was approximately 100 times greater than that determined in systems which were identical in every way except that persulphate was absent.

A brief investigation of the reaction between persulphate ion and ferrous ion in the absence of thioglycolic acid showed (Table VI) that the reaction was second order, and

TABLE VI

Comparison of second-order rate constants, k_1, for the ferrous ion – persulphate reaction with those interpolated from Fig. 1

Initial $[S_2O_8^{=}]$	Initial $[Fe^{++}]$	$[K_2SO_4]$	$[H_2SO_4]$	Ionic strength (μ)	k_1 (l. M^{-1} min^{-1})	k_1* (l. M^{-1} min^{-1})
7.88	10.0	0.10	0.0098	0.272	452	448
7.88	10.0	0.00	0.098	0.159	782	730
4.00	10.0	0.00	0.15	0.224	575	513
4.00	20.0	0.00	0.15	0.224	535	513
8.00	20.0	0.00	0.15	0.224	571	513

*See Fig. 1.

that the second-order rate constants, k_1, were in good agreement with those interpolated from Fig. 1. The rate of appearance of ferric ion in these reaction mixtures was estimated from the change in optical density at 305 mμ.

DISCUSSION

Thioglycolic acid in no way influenced the rate of the persulphate ion – ferrous ion reaction, whereas the presence of persulphate caused the reaction between ferric ion and thioglycolic acid to occur more rapidly. It is apparent that the catalyst cycle for the reaction between persulphate ion and thioglycolic acid, in the presence of iron, involves persulphate oxidation of ferrous ion to ferric ion, which is then reduced by thioglycolic acid to ferrous ion.

The mechanism for the reaction between persulphate ion and ferrous ion appears to be well established (15, 16, 17).

$$S_2O_8 + Fe^{++} \rightarrow Fe^{+++} + SO_4^{-} + SO_4^{=} \quad [1]$$

$$SO_4^{-} + Fe^{++} \rightarrow Fe^{+++} + SO_4^{=} \quad [2]$$

The calculated second-order rate constant, k_1, obtained in this investigation was approximately one-half that obtained by Williams *et al.* (16, 17). The difference might result from the much larger hydrogen ion concentrations (100- to 1000-fold) in the present experiments.

For the reaction between ferric ion and thioglycolic acid the results may be explained by postulating the existence of a complex containing two ferric ions and two thioglycolic acid molecules, the reaction rate being governed by the first-order decomposition of this complex. That complexes in the ferric ion – thioglycolic acid system do exist is indicated by the blue color that was produced when the two reactants were mixed initially. Lamfrom and Nielsen (14) have shown that the blue complex disappeared by a first-order process at $-35°$ C in a solvent consisting of 6 parts by volume of ethanol to 10 parts by volume of water. It would appear, therefore, that the blue complex might well consist of two ferric ions and two thioglycolic acid molecules.

Can. J. Chem. Downloaded from www.nrcresearchpress.com by 196.1.178.254 on 09/04/12
For personal use only.

The inhibition by hydrogen and by sulphate ions suggests that mercaptide and hydrated ferric ions were the reactive species and the proposed mechanism is as follows:

$$Fe^{+++} + SO_4^{=} \rightleftarrows FeSO_4^{+}, \quad [4]$$

$$FeSO_4^{+} + SO_4^{=} \rightleftarrows Fe(SO_4)_2^{-}, \quad [5]$$

$$Fe^{+++} + ClO_4^{-} \rightleftarrows FeClO_4^{++}, \quad [6]$$

$$Fe^{+++} + H_2O \rightleftarrows FeOH^{++} + H^{+}, \quad [7]$$

$$TSH \rightleftarrows TS^{-} + H^{+}, \quad [8]$$

$$FeOH^{++} + TS^{-} \rightleftarrows FeOHTS^{+}, \quad [9]$$

$$2FeOHTS^{+} \rightleftarrows Fe_2(OH)_2(TS)_2^{++}, \quad [10]$$

$$Fe_2(OH)_2(TS)_2^{++} \rightarrow 2Fe^{++} + {}^{-}TSST^{-} + 2H_2O. \quad [11]$$

For the experiments made in the absence of sulphate ion, the following relation is obtained,

$$k_4'\,[\text{ferric}]^2\,[\text{thioglycolic acid}]^2 = \frac{k_{11}K_{10}K_9^{\,2}K_8^{\,2}K_7^{\,2}}{[H^+]^4}\,[Fe^{+++}]^2\,[TSH]^2 \quad (i)$$

where [ferric] and [thioglycolic acid] represent the total concentrations of ferric ion and thioglycolic acid respectively in the reaction mixture. Owing to the relatively large concentrations of hydrogen ion used in these experiments, the concentrations of $FeOH^{++}$ and TS^{-} ions should be small (18, 19), and since complex formation between ferric and perchlorate ions occurs only to a very limited extent (20), it follows that

$$[\text{ferric}] \simeq [Fe^{+++}]$$

and

$$[\text{thioglycolic acid}] \simeq [TSH].$$

Therefore

$$k_4' = \frac{k_{11}K_{10}K_9^{\,2}K_8^{\,2}K_7^{\,2}}{[H^+]^4}. \quad (ii)$$

In the presence of low concentrations of sulphate ion

$$[\text{ferric}] = [Fe^{+++}][1+K_4(SO_4^{=})]$$

and

$$k_4'' = \frac{k_{11}K_{10}K_9^{\,2}K_8^{\,2}K_7^{\,2}}{[H^+]^4\,[1+K_4(SO_4^{=})]^2}. \quad (iii)$$

By combining equations (ii) and (iii),

$$K_4 = \frac{\sqrt{(k_4/k_4'')}-1}{[SO_4^{=}]}. \quad (iv)$$

The value of K_4, the association constant of the ferric ion – sulphate complex, calculated in this manner was approximately one-half that determined by Whitekar and Davidson (21).

In the reaction mixtures which were 0.05 to 0.15 M in sulphuric acid, the concentration of free ferric ion may be taken as negligible (21), i.e.

$$[\text{ferric}] = [Fe^{+++}][K_4(SO_4^{=})+K_4K_5(SO_4^{=})^2]$$

and

$$k_4''' = \frac{k_{11}K_{10}K_9^{\,2}K_8^{\,2}K_7^{\,2}}{[H^+]^4\,[K_4(SO_4^{=})+K_4K_5(SO_4^{=})^2]^2}. \quad (v)$$

Can. J. Chem. Downloaded from www.nrcresearchpress.com by 196.1.178.254 on 09/04/12
For personal use only.

Can. J. Chem. Downloaded from www.nrcresearchpress.com by 196.1.178.254 on 09/04/12
For personal use only.

It is interesting to note that the mechanism for the reaction between ferric ion and thioglycolic acid in weakly acidic and in alkaline solution differs markedly from that suggested here for the reaction in more strongly acidic solution (14, 22, 23).

If no account is taken of the relatively rapid ferric ion – thioglycolic acid reaction which occurred in the presence of persulphate, the following sequence of reactions may be suggested for the iron-catalyzed reaction between persulphate and thioglycolic acid:

$$S_2O_8 + Fe^{++} \rightarrow Fe^{+++} + SO_4 + SO_4 \quad [1]$$

$$SO_4 + Fe^{++} \rightarrow Fe^{+++} + SO_4 \quad [2]$$

$$SO_4 + TSH \rightarrow TS\cdot + HSO_4 \quad [3]$$

$$Fe^{+++} + SO_4^{=} \rightleftarrows FeSO_4^{+} \quad [4]$$

$$FeSO_4^{+} + SO_4^{=} \rightleftarrows Fe(SO_4)_2^{-} \quad [5]$$

$$Fe^{+++} + H_2O \rightleftarrows FeOH^{++} + H^{+} \quad [6]$$

$$TSH \rightleftarrows TS^{-} + H^{+} \quad [7]$$

$$FeOH^{++} + TS^{-} \rightleftarrows FeOHTS^{+} \quad [8]$$

$$2FeOHTS^{+} \rightleftarrows Fe_2(OH)_2(TS)_2^{++} \quad [9]$$

$$Fe_2(OH)_2(TS)_2^{++} \rightarrow 2Fe^{++} + {}^{-}TSST^{-} + H_2O \quad [10]$$

$$2TS\cdot \rightarrow TSST \quad [11]$$

Step [1] was rate controlling in reaction mixtures when the pH was approximately 2, but the reduction of ferric ion by thioglycolic was not rapid relative to step [1] in reaction mixtures 0.15 M in sulphuric acid. If step [2] is assumed negligible relative to [3] because of the large excess of thioglycolic acid over ferrous ion, the steady-state assumption may be applied to the concentrations of ferric and ferrous ions to yield the following relation,

$$\frac{D_m - D}{D^2} = \frac{k_4'''}{\epsilon k_1} \frac{[TSH]^2}{[S_2O_8^{=}]} \quad \text{(vi)}$$

where D represents the optical density of the reaction mixture at 325 mμ, D_m the optical density if all the iron had been in the ferric state, and ϵ the extinction coefficient of ferric ion. In actual fact the results from the experiments made in 0.15 M sulphuric acid were found to fit the empirical equation,

$$\frac{D_m - D}{D^2} = \frac{k}{\epsilon k_1 [Fe]^x [TSH]_0} \frac{[TSH]^2}{[S_2O_8^{=}]} \quad \text{(vii)}$$

where $[Fe]^x$ represents the concentration of iron in the system raised to some power x and $[TSH]_0$, the initial concentration of thioglycolic acid.

Furthermore, the values of

$$\frac{k}{k_1 [Fe]^x [TSH]_0}$$

were of the order of 100 times greater than the value of k_4'''/k_1 (Table VII), owing to the influence of persulphate ion on the ferric ion – thioglycolic reaction.

Additional steps in the reaction sequence already shown are necessary to explain, not only the marked influence of persulphate ion on the over-all rate, but also the induction period when iron was initially in the ferric state, and the lack of influence by persulphate on the rate at which ferric ion concentration is decreased to its stationary value during the induction period. A tentative proposal is that either a sulphate ion radical or a

thiyl radical reacts rapidly with a ferric ion – thioglycolic acid complex,

$$SO_4^{\cdot-} + \text{Fe (III) TSH-complex} \rightarrow Fe^{++} + H^+ + TSST + HSO_4^- \quad [12]$$

$$TS\cdot + \text{Fe (III) TSH-complex} \rightarrow Fe^{++} + TSST + H^+. \quad [13]$$

TABLE VII

Comparison of the calculated value of k_4'''/k_1 with the value $\frac{k}{k_1[Fe]^x[TSH]_0}$

Initial $[TSH]_0$ ($\times 10^3$)	$\frac{k}{k_1[Fe]^x[TSH]_0}$ ($\times 10^{-4}$)	k_4'''/k_1 ($\times 10^{-4}$)
10.95	92.3	1.85
4.36	333	1.85

In solutions in which the iron is present initially as ferric ion, free radicals will not be produced at zero time, and reactions [12] and/or [13] will not be important. Due to the production of ferrous ion, however, the persulphate – ferrous ion reaction will begin to occur, giving rise to free radicals and hence to the rapid reactions [12] and/or [13]. Therefore, during the early stages of the reaction before ferric ion and in all probability the free-radical concentrations become stationary, the rate of reduction of ferric ion by thioglycolic acid will increase with time causing a corresponding increase in the over-all reaction rate, and an induction period will result. However, when the iron is initially in the ferrous state, the sulphate ion radicals and ferric ion will be produced at zero time, and reactions [12] and/or [13] will assume an important role at the beginning.

A similar mechanism has been suggested for the uptake of oxygen by mixtures of ferric ion and thioglycolic acid in mildly acidic solution (14).

With existing information, it is extremely difficult to determine either the structure of the complex which entered into this reaction or the nature of the radical, whether sulphate ion or thiyl, which reacted with the complex. Because sulphate ion radicals may react with both ferrous ion and thioglycolic acid, the situation is even more complex, since the relative rates of these two reactions are unknown.

In conclusion, it is apparent that to investigate the uncatalyzed persulphate – thioglycolic acid reaction, as was intended originally, the concentration of dissolved iron in the reaction mixtures, and in all probability the concentration of other metallic ions, would have to be very low.

REFERENCES

1. Green, L. and Masson, D. J. Chem. Soc. **97**, 2083 (1910).
2. Bartlett, P. D. and Cotman, D. J. J. Am. Chem. Soc. **71**, 1419 (1949).
3. Kolthoff, I. M. and Miller, I. K. J. Am. Chem. Soc. **73**, 3055 (1951).
4. Eager, R. S. and Winkler, C. A. Can. J. Research, B, **26**, 527 (1948).
5. Whalley, B. J. P., Evans, H. G. V., and Winkler, C. A. Can. J. Chem. **34**, 1154 (1956).
6. Kolthoff, I. M., Meehan, E. J., and Carr, E. M. J. Am. Chem. Soc. **75**, 1439 (1953).
7. Malinoski, E. R. and Levitt, L. S. Abstracts of Papers, 132nd Meeting, American Chemical Society, New York. 1957. p. 77P.
8. Henderson, J. F. Ph.D. Thesis, McGill University, Montreal. 1958.
9. Leussing, D. L. and Kolthoff, I. M. J. Electrochem. Soc. **100**, 334 (1953).
10. Jenkins, I. L. and Monk, C. B. J. Am. Chem. Soc. **72**, 2695 (1950).
11. Kerker, M. J. Am. Chem. Soc. **79**, 3664 (1957).
12. Kolthoff, I. M. and Sandel, E. B. Textbook of quantitative analysis. 3rd ed. The Macmillan Co., New York. 1952. p. 635.
13. Cannon, B. H. and Richardson, G. W. Biochem. J. **23**, 1242 (1929).
14. Lamfrom, H. and Nielsen, S. O. J. Am. Chem. Soc. **79**, 1966 (1957).

Can. J. Chem. Downloaded from www.nrcresearchpress.com by 196.1.178.254 on 09/04/12
For personal use only.

15. KOLTHOFF, I. M., MEDALIA, A. I., and BAAEN, H. P. J. Am. Chem. Soc. **73**, 1733 (1951).
16. FORDHAM, J. W. L. and WILLIAMS, H. L. J. Am. Chem. Soc. **73**, 4855 (1951).
17. ORR, R. J. and WILLIAMS, H. L. J. Am. Chem. Soc. **77**, 3715 (1955).
18. TURNER, R. C. and MILES, K. E. Can. J. Chem. **35**, 1002 (1957).
19. LARSSON, E. Z. anorg. u. allgem. Chem. **172**, 375 (1928).
20. SYKES, K. W. The kinetics and mechanism of inorganic reactions in solution. Chem. Soc. (London), Spec. Publ. No. 1, p. 64 (1954).
21. WHITEKAR, R. A. and DAVIDSON, N. J. Am. Chem. Soc. **75**, 3081 (1953).
22. LEUSSING, D. L. and KOLTHOFF, I. M. J. Am. Chem. Soc. **75**, 3904 (1953).
23. LEUSSING, D. L. and NEWMAN, L. J. Am. Chem. Soc. **78**, 562 (1956).

Can. J. Chem. Downloaded from www.nrcresearchpress.com by 196.1.178.254 on 09/04/12
For personal use only.

Can. J. Chem. Downloaded from www.nrcresearchpress.com by 196.1.178.254 on 09/04/12
For personal use only.

THE PURIFICATION, DETERMINATION, AND NEUTRON CAPTURE CROSS SECTION OF ACTINIUM-227[1]

M. J. CABELL[2]

ABSTRACT

Procedures are described for (*a*) the separation by ion exchange chromatography of submicrogram quantities of Ac^{227} from its daughters and (*b*) the absolute determination of Ac^{227} by measurement of the rate of growth of α-particle emission from an initially pure source. These procedures are utilized in the determination of the reactor and thermal neutron capture cross sections and the resonance capture integral of Ac^{227} by an activation method.

Assuming 36.5 barns for the thermal neutron capture cross section of Co^{59}, a value of $\sigma_{2200} = 814 \pm 13$ barns has been obtained for Ac^{227}. The resonance capture integral (from 0.5 ev to ∞) was found to be 1177 ± 19 barns relative to 48.6 barns for the resonance capture integral of Co^{59}.

INTRODUCTION

Hughes and Schwartz (1) quote 510 ± 40 barns for the thermal neutron capture cross section of Ac^{227} as determined by a pile oscillator method and 520 ± 50 barns as determined by an activation method; no experimental data are available for either of these measurements. Timma and Russell (2), also using a pile oscillator method, obtained 493 ± 53 barns for the thermal neutron capture cross section. No measurements of differential cross sections or of the resonance capture integral of this isotope have so far been reported in the literature. This paper describes determinations of the reactor and thermal neutron capture cross sections and the resonance capture integral of Ac^{227} by an activation method.

The following nuclear reactions are involved:

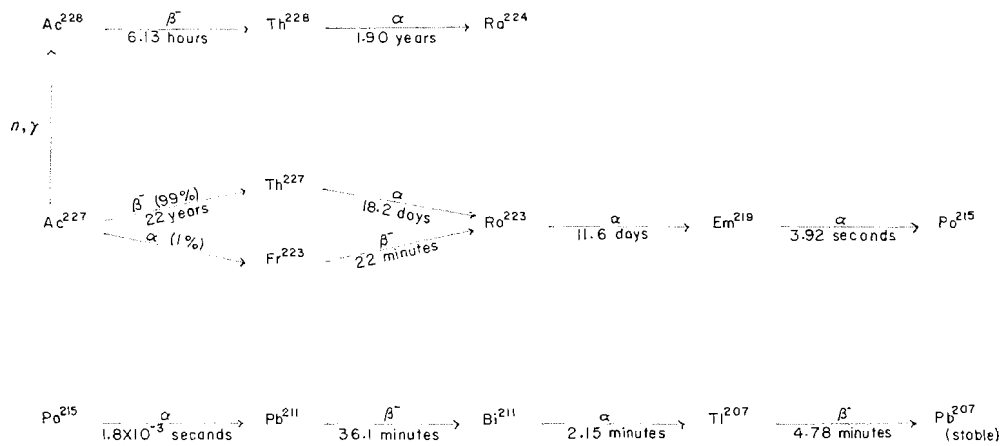

The method used is similar to that described by Cabell (3) and by Cabell, Eastwood, and Campion (4) and involved the irradiation in a high flux position of the NRX reactor of submicrogram amounts of Ac^{227} (*a*) unshielded and (*b*) shielded by 0.0635 cm cadmium. Cobalt monitors were attached to measure both the thermal and the epicadmium fluxes.

[1]*Manuscript received January 23, 1959.*
Contribution from the Research Chemistry Branch, Atomic Energy of Canada Limited, Chalk River, Ontario. Issued as A.E.C.L. No. 745.
[2]*Present address: Atomic Energy Research Establishment, Harwell, Berkshire, England.*

After irradiation the actinium was purified by ion exchange and mounted on thin films for counting. The Ac^{228} content of each source was then determined from measurements of the change in its absolute β-disintegration rate with time. The rise in absolute α-disintegration rate of the same source with time gave a measure of its Ac^{227} content. From these data and the known fluxes the effective cross section for Ac^{227} for pile neutrons, its thermal capture cross section, and its resonance capture integral were calculated.

EXPERIMENTAL METHODS

(*a*) *Preparation of Pure Actinium-227*

A sample of Ac^{227} which had been only partially separated from neutron-irradiated Ra^{226} and contained large quantities of water-soluble salts as additional impurities was received from the Commercial Products Division (Ottawa) of Atomic Energy of Canada Ltd. The actinium was freed from salts by repeated coprecipitation with ferric hydroxide, the iron was removed by anion exchange, and the actinium was separated from the products of its decay and from Ra^{226} by cation exchange (see section on chemical purification). The actinium was finally obtained in 2 ml of 6 *M* nitric acid and this solution was used as a stock for all irradiations.

Aliquots taken from the stock solution were evaporated to dryness on platinum disks and the spectra of the α- and β-particles they emitted were examined. An α-pulse analysis carried out 4 hours after the final separation showed that α-particles from Ac^{227} accounted for about half the total α-particle activity. Separate and growing peaks were identified due to the α-particles from Th^{227}, Ra^{223}, Em^{219}, Po^{215}, and Bi^{211} and accounted for the remainder of the α-particle activity. No evidence of the presence of α-particles from Ra^{226} could be found.

Another source was counted in an internal proportional counter whose anode potential was adjusted for β-particle counting, and the counting rate of the source was determined both uncovered and covered with thin aluminum foils of different thicknesses. The resulting absorption curve showed that most of the uncovered activity was due to the β-particles from Ac^{227} (stopped by 4 mg/cm^2 aluminum corresponding to a maximum energy of 46 kev) and the remainder was almost entirely due to α-particles. All these facts are consistent with the sources being initially radiochemically pure Ac^{227}.

(*b*) *Irradiations*

Fifty-microliter aliquots (approximately 3×10^{-9} g Ac^{227}) of the stock solutions were pipetted into small silica ampoules. Some of these were sealed directly, but those to be irradiated under cadmium and one other were taken to dryness and were then sealed except for a capillary vent. Cobalt monitors were attached and the samples were irradiated for between 5400 ± 2 seconds and 5417 ± 2 seconds as described by Cabell (3).

(*c*) *Chemical Purification of Irradiated Actinium*

Cation and anion exchange chromatography were used to purify the irradiated actinium.

Each cation column consisted of 1.00 g (dry weight) of 200–400 mesh Dowex 50 (hydrogen form) contained in a glass tube 10 cm long and 6 mm in diameter sealed onto a reservoir 10 cm long and 3 cm in diameter. Both column and reservoir were jacketed at 60°. Before they were loaded, the columns were prepared by washing with water.

Each anion column contained 0.25 g of 200–400 mesh Dowex 1 (chloride form) in a tube 6 cm long and 6 mm in diameter sealed onto a reservoir 5 cm long and 1.5 cm in diameter. The anion columns, which were operated at room temperature, were washed with 5 ml of 10 *M* hydrochloric acid before loading.

Can. J. Chem. Downloaded from www.nrcresearchpress.com by 196.1.178.254 on 09/04/12
For personal use only.

The irradiated actinium sample was dissolved in 5 ml of 2 *M* hydrochloric acid and the solution was warmed to 80° before it was fed to a cation exchange column without application of pressure. When the feed had passed, the column was eluted successively with 5 ml of hot 2 *M* hydrochloric acid (to remove bismuth, lead, and francium) and 20 ml of hot 3 *M* nitric acid (to remove radium). Finally the column was eluted with 25 ml of hot 6 *M* nitric acid; the first 5 ml of eluate was rejected and the remainder, which contained the purified actinium, was collected in a centrifuge tube. The Th^{227} daughter of the actinium was left on the column.

The progress of this separation is illustrated in Fig. 1 (each peak was identified by separate experiments using only one of the five components each time).

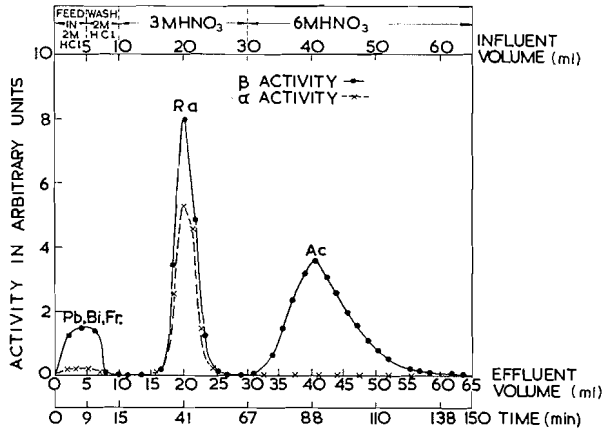

FIG. 1. The separation of Ac^{227} from its daughters by cation exchange chromatography.

Three drops of a ferric nitrate solution (10 mg iron per ml) were added to the eluate obtained from the cation column; the solution was neutralized with ammonia, cooled to room temperature, and the ferric hydroxide precipitate, which carries the actinium, was collected by centrifuging. The precipitate was dissolved in 2 drops of concentrated hydrochloric acid, diluted to 20 ml, and the iron was precipitated again with ammonia. This solution–precipitation cycle was then repeated.

The precipitate was next dissolved in 1 ml of concentrated hydrochloric acid and fed to an anion exchange column at the rate of 0.2 ml/min to remove the iron carrier. After the feed had passed, the column was eluted with 1 ml of 10 *M* hydrochloric acid and the total eluate was collected in a small platinum crucible and evaporated to dryness under an infrared lamp. The crucible was then heated in a furnace at 700° for 5 minutes, cooled, and 2 ml concentrated nitric acid was added and the solution was again evaporated to dryness under an infrared lamp. Finally the residue, which was invisible to the naked eye, was dissolved in 1 ml concentrated nitric acid and the resulting solution was used for making sources on thin films for counting.

(d) Absolute Disintegration-rate Determinations

(1) Determination of Ac^{227}

Ac^{227} decays largely by the emission of β-particles of maximum energy 46 kev (α-particle emission is $1.25 \pm 0.02\%$, Peterson and Ghiorso (5)) and initially attempts were made to determine this isotope by absolute β-disintegration-rate determinations. A series of gold-coated VYNS films of known thickness were prepared and a source of freshly purified

Can. J. Chem. Downloaded from www.nrcresearchpress.com by 196.1.178.254 on 09/04/12
For personal use only.

Ac^{227} was mounted on a film 36 $\mu g/cm^2$ thick. This was β-counted in a 4π counter and then another film was made to adhere to the back of the source before counting again. Additional films were then added, with counting after each addition, until a final total thickness of 260 $\mu g/cm^2$ had been built up. Over this range, 36 to 260 $\mu g/cm^2$, there was a loss of 12% in the measured β-disintegration rate. Since this method of determination is so sensitive to the thickness of the source mount and extrapolation from 36 $\mu g/cm^2$ to zero thickness is uncertain, it was not investigated further.

The measurement of the α-disintegration rates of sources of the α-active daughters of Ac^{227} is not subject to the same difficulties as a second and similar experiment showed. A source of initially pure Ac^{227} which had been prepared 22 days previously was investigated by the same procedure. It was found that over a source mount thickness varied from 37 to 252 $\mu g/cm^2$ there was no change in α-disintegration rate outside the statistical error of each count, i.e. $\pm 0.3\%$.

Since the half-lives of Th^{227} and Ra^{223} are very much greater than those of the other α-particle-emitting daughters of Ac^{227}, for some purposes the sequence of decay by α-particle emission only may be simplified to:

$$Ac^{227} \xrightarrow[\lambda_1]{\beta} Th^{227} \xrightarrow[\lambda_2]{\alpha} Ra^{223} \xrightarrow[\lambda_3]{4\alpha} Pb^{207}\ \text{(stable)}$$

where λ_1, λ_2, and λ_3 are the decay constants of Ac^{227}, Th^{227}, and Ra^{223} respectively. It can be shown that, with this simplification, the α-activity of an initially pure source containing N_0 atoms of Ac^{227} at time t hours after its preparation is given by the expression:

$$[1] \qquad \frac{-d\alpha}{dt} = \frac{N_0\lambda_1\lambda_2}{(\lambda_2-\lambda_1)}\left(e^{-\lambda_1 t}-e^{-\lambda_2 t}+\frac{4\lambda_3(e^{-\lambda_1 t}-e^{-\lambda_3 t})}{(\lambda_3-\lambda_1)}+\frac{4\lambda_3(e^{-\lambda_3 t}-e^{-\lambda_2 t})}{(\lambda_3-\lambda_2)}\right).$$

Since

$$\lambda_1 = (3.66\pm 0.07)\times 10^{-6}\ \text{hours}^{-1}\ \text{(Tobailem (6))},$$
$$\lambda_2 = (1.590\pm 0.007)\times 10^{-3}\ \text{hours}^{-1},$$

and

$$\lambda_3 = (2.472\pm 0.011)\times 10^{-3}\ \text{hours}^{-1}\ \text{(Hagee, Curtis, and Grove (7))},$$

substitution in expression [1] gives:

$$[2] \quad (-d\alpha/dt)\,.\,1/N_0 = 3.670\times 10^{-6}[e^{-\lambda_1 t}-e^{-\lambda_2 t}+4.006(e^{-\lambda_1 t}-e^{-\lambda_3 t})+11.21(e^{-\lambda_3 t}-e^{-\lambda_2 t})]$$

where $-d\alpha/dt$ is expressed in disintegrations per hour.

Expression [2] may be used to calculate N_0 provided there is no loss of Em^{219} ($t_{\frac{1}{2}} = 3.92$ seconds) from the source. The possibility of this was studied in separate experiments using "weightless" sources in a 4π proportional counter. One source was sealed in the counter for several days after which it was α-counted, then removed, and the α-background of the counter was followed for the next 8 hours. The background decayed with a half-life of 35 minutes, showing the presence of Bi^{211} (daughter of Pb^{211}). In a second experiment a high gas flow was passed through the counter into a second and larger counter whose rise in α-counting rate was measured. From these and similar experiments it was concluded that up to 2% of the Em^{219} content of a thin source could diffuse into the counting gas. It was found that any error introduced into the determination of total α-disintegration rate by this effect could be reduced to negligible proportions ($< 0.5\%$) by sealing the source in the counter for at least three hours before measurement and by using a minimum gas flow during the measurement.

Can. J. Chem. Downloaded from www.nrcresearchpress.com by 196.1.178.254 on 09/04/12
For personal use only.

Can. J. Chem. Downloaded from www.nrcresearchpress.com by 196.1.178.254 on 09/04/12
For personal use only.

The possibility of loss of Ra^{223} (and consequently of subsequent decay products) by recoil from the source on emission of an α-particle by Th^{227} must also be considered. Since the recoil energy is 108 kev, the range of Ra^{223} in gold will be of the order 5 $\mu g/cm^2$ and recoils in the direction of the source mount will be successfully trapped, but for a source only 1 atom thick losses of 50% may be expected due to recoil in the opposite direction. In fact it is not possible to make truly "weightless" sources by the method employed in this work, since even the purest reagents inevitably contain traces of non-volatile impurities. The true thickness of the source is seldom known in 4π counting and, in fact, is the largest factor contributing to uncertainty in the technique (see later). In the present work it was known that the recoil effect had no influence on the results. Counting for experiments 3 and 4 of Table II was carried out using sources completely enclosed by gold-coated VYNS films and the results obtained agree with those using uncovered sources. The technique of covering the sources with another thin film was not used except in this one case, since it is clearly unnecessary and additional absorbers should be avoided wherever possible.

Observing these precautions it was found that α-activity measurements made for four or five consecutive days commencing 6 days after preparation of a source gave values for N_0 which agreed with a coefficient of variation of 0.4% to 1.0%. Table I shows the results obtained with one such source.

TABLE I

Determination of Ac^{227} by measurement of its α-particle-emitting daughters

Hours from initial count	α-Count per hour corrected for initial count	$N_0 \times 10^{-10}$
137.1	105920	9.079
159.5	128390	9.098
182.3	151970	9.095
205.8	175800	9.025
231.9	205110	9.050
		Average 9.069 ± 0.032

It is interesting to compare the results obtained by these two possible methods of determining Ac^{227}, i.e. by 4π counting the β-particles emitted and by measurement of the rise in α-particle activity. The former method has been found to give results 23% to 45% lower than the latter for samples prepared from different purifications. These figures emphasize the very large errors which may be expected due to self-absorption when attempts are made to 4π count very weak β-particles even though apparently "weightless" sources are employed.

(*2*) *Determination of* Ac^{228}

The curved line ABC of Fig. 2 shows a decay curve obtained from a purified sample of neutron-irradiated Ac^{227} measured in a 4π proportional counter with its anode potential adjusted for β-particle counting. The shape of the falling portion of the curve, AB, is largely determined by the decay of the β-active Ac^{228} component of the source. By point B most of the Ac^{228} has decayed and the recorded count is largely due to the β-active Ac^{227} component (it has been shown in the previous section that this count cannot be used for the quantitative determination of Ac^{227}).

In addition to the β-particles from Ac^{227} the counter also records pulses arising from α- and β-particles emitted by Th^{227} and its radioactive daughters, and it is the growth of

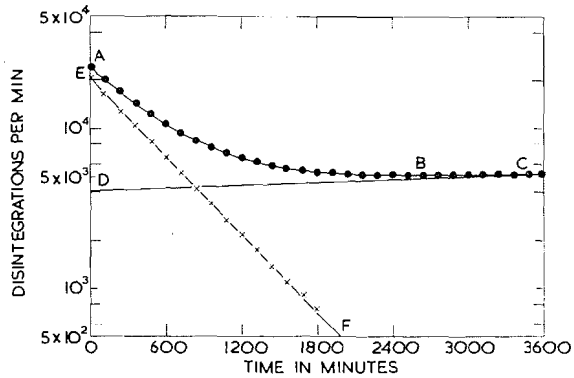

FIG. 2. Decay of neutron-irradiated Ac^{227}.

these which accounts for the upward inclination of the portion of the curve BC. This increase in counting rate follows a form similar to that given in brackets in expression [2], and information obtained by counting after 3 or 4 days (by which time the Ac^{228} will have decayed to about 10^{-5} of its initial amount) was used to correct the portion of the curve AB for these components (line CD). In this way the Ac^{228} contribution alone was obtained and is plotted as points which lie about the line EF which is drawn with a half-life of 6.13 hours, the published value for Ac^{228} (Hahn and Erbacher (8)).

The β-particles emitted by Ac^{228} are mostly highly energetic but 13% have energies below 450 kev (Strominger, Hollander, and Seaborg (9)); sources were therefore examined for possible source mount losses by the technique described above for Ac^{227} particles. It was found that over a source mount thickness varied from 36 to 266 $\mu g/cm^2$ counting rate losses of mixtures of Ac^{227} and Ac^{228} could be ascribed entirely to losses in counting the Ac^{227} component. Using mounts approximately 50 $\mu g/cm^2$ thick losses in counting Ac^{228} would not exceed 0.2% due to this source of error.

A more serious source of error in the absolute disintegration-rate determination of Ac^{228} lies in the possibility of self-absorption in the source itself. Cobble (10) has reported that in certain cases up to 10% losses may occur from apparently "weightless" sources due to this cause and we have shown that for Ac^{227} the losses are even greater. With 450-kev β-particles errors of this magnitude are most unlikely. Since the abundance of the β-particles under consideration is only 13% of the total, we have concluded that the self-absorption losses in determining Ac^{228} in "weightless" sources is much less than one per cent.

(3) Counting Procedure

An important feature of the counting procedure used lay in the fact that after irradiation and purification of the actinium, a single aliquot could be used to determine both the amount of Ac^{227} in that aliquot and also the amount of Ac^{228} which it had yielded on irradiation. Consequently, provided sufficient actinium was purified that adequate counting rates could be obtained, the chemical yield of the purification process was unimportant.

When a batch of irradiated Ac^{227} had been purified, three or four aliquots (sufficient to give between 100 and 1000 β-particle counts/second but whose volume did not need to be known) were mounted on films of approximately 50 $\mu g/cm^2$ thickness and as soon as possible each was counted for α-particles and then, at a higher applied potential, for β-particles in a 4π counter. The progress of β-decay was then followed for 6 or 7 days and

Can. J. Chem. Downloaded from www.nrcresearchpress.com by 196.1.178.254 on 09/04/12
For personal use only.

the absolute β-disintegration rate of the Ac^{228} component during each initial count was determined as described above. The decay of this component was also determined to confirm its identity and purity. From the corrected initial count the absolute β-disintegration rate which the Ac^{228} in each source would have had at the end of the irradiation was calculated using 0.1131 ± 0.0005 hours^{-1} (Hahn and Erbacher (8)) for its decay constant.

The α-particle activities of the same sources were measured again 6 days after their preparation and also on each of the 5 succeeding days after this. Increases in α-particle activity over the initial counts made when the sources were first prepared were used to calculate values of N_0 from the expression:

$$[3] \quad [(d\alpha_0/dt)-(d\alpha/dt)]\cdot 1/N_0 = 3.670\times 10^{-6}[1.013(e^{-\lambda_1 t}-e^{-\lambda_2 t})+4.006(e^{-\lambda_1 t}-e^{-\lambda_3 t}) +11.21(e^{-\lambda_3 t}-e^{-\lambda_2 t})]$$

where $-d\alpha_0/dt$ is the initial counting rate.

Expression [3] differs from expression [2] by a small factor on the right-hand side which arises as follows. The initial α-counts are due to the α-particles emitted in the decay of Ac^{227} to Fr^{223} (plus small activities due to α-active daughters produced during the short time between actinium purification and source counting) and thence to Ra^{223}. Subsequent corrected α-particle counts do not take into account the fact that although all Ac^{227} atoms which disintegrate decay eventually to Ra^{223}, only $98.75 \pm 0.02\%$ (Peterson and Ghiorso (5)) of them decay via Th^{227}. The factor $(e^{-\lambda_1 t}-e^{-\lambda_2 t})$, which expresses the Th^{227} contribution to the total α-particle activity, must therefore be corrected accordingly.

Use of expression [3] rather than [2] for calculations has the merit that a short time may be allowed to elapse between actinium purification and counting without prejudicing the result. This is an advantage when several sources from the same purification have to be counted and, moreover, when it is not possible to determine exactly when the actinium was free from daughters.

For each source the values for N_0 determined on 5 successive days by using expression [3] were averaged and the ratio $(R_{\beta,\,N_0})$ was determined for each film where

$$[4] \quad R_{\beta,\,N_0} = \frac{\text{absolute disintegration rate of the } Ac^{228} \text{ in the source at the end of the irradiation}}{\text{number of atoms of } Ac^{227} \text{ in the source}}.$$

Standard deviations for the three or four separate determinations of $R_{\beta,\,N_0}$ for any one irradiation were calculated and additional uncertainties of 1% and 1.9% were allowed for possible errors in β-disintegration-rate determinations and for errors in the half-lives used in calculating N_0. Distinguishing the results for unshielded and shielded samples by the subscripts 1 and 2 respectively, errors in $(R_{\beta,\,N_0})_1$ varied between 2.6% and 4.2% and errors in $(R_{\beta,\,N_0})_2$ between 5% and 16%.

(4) Measurements with Cobalt Monitors

These have been described by Cabell (3) and by Cabell, Eastwood, and Campion (4).

RESULTS

The results were calculated in terms of the convention advocated by Westcott, Walker, and Alexander (11); application of this convention to the type of experiment described in this paper has been described by Eastwood *et al.* (12).

The measured rate of reaction of a detector, R, is expressed as

$$[5] \quad R = \hat{\sigma}.(nv_0)$$

Can. J. Chem. Downloaded from www.nrcresearchpress.com by 196.1.178.254 on 09/04/12
For personal use only.

where (nv_0) is the conventional flux, i.e. n is the total neutron density in neutrons/cm^3 and v_0 is 2200 m/sec, and $\hat{\sigma}$, the effective cross section, is defined by expression [5]. It is assumed that the neutron spectrum is the sum of two components; an epithermal dE/E flux distribution cut off at a suitable lower limit of energy and a Maxwellian distribution of thermal neutrons at a temperature $T°$ K. The two components overlap in energy since no upper limit is imposed on the Maxwellian component.

It is possible to express $\hat{\sigma}$ as

$$\hat{\sigma} = \sigma_0(g+rs) \quad [6]$$

where r is a measure of the relative density of the epithermal component of the neutron spectrum and g and s are functions of the temperature T which describe the departure of the detector from the $1/v$ law; for true $1/v$ behavior $g = 1$ and $s = 0$.

Values of s and g for a number of elements and isotopes for which differential and resonance integral data are well known have been tabulated by Westcott (13) for a number of temperatures. Amongst these is cobalt.

Since the neutron temperatures are not known in the experiments described here, s is replaced by a temperature-independent term, s_0, such that $s_0 = s\sqrt{(T_0/T)}$. Substitution in equation [6] then gives

$$\hat{\sigma} = \sigma_0\{g+r\sqrt{(T/T_0)}s_0\}. \quad [7]$$

For the cobalt monitors $\sigma_0 = 36.5$ barns, $g = 1$, $r\sqrt{(T/T_0)}$ can be obtained from $(R_{Cd})_{Co}$, the cadmium ratio for Co^{59}, and $s_0 = 0.953$ (Westcott (13)). Therefore, $\hat{\sigma}$ for cobalt can be calculated and substituted in equation [5] to obtain the total flux (nv_0).

Given (nv_0) equation [5] is used to obtain $\hat{\sigma}$ for Ac^{227} and, *if the assumption is made that $g = 1$ for actinium, i.e. that actinium is a $1/v$ absorber in the thermal region*, σ_0 for actinium may then be obtained from equation [7].

The resonance integral for actinium, $(R.I.)_{Ac}$, is given by:

$$(R.I.)_{Ac} = (R.I.)_{Co}\frac{(R_{Cd}-1)_{Co}}{(R_{Cd}-1)_{Ac}}\cdot\frac{(\sigma_0)_{Ac}}{(\sigma_0)_{Co}}. \quad [8]$$

We have used 48.6 barns for the resonance integral of Co^{59}.

The results obtained are recorded in Table II. It is not to be expected that $\hat{\sigma}(Ac^{227})$ will be constant since the experiments extended over a period of months during which the neutron spectrum in the irradiation position (and hence R_{Cd}) changed. An average value of 839 barns was obtained for $\hat{\sigma}(Ac^{227})$.

The four values of $\sigma_0(Ac^{227})$ recorded in Table II were each weighted in proportion to the reciprocal of the square of its error and gave an average value of 814 ± 13 barns. Similar treatment of the four results for $(R.I.)_{Ac}$ gave an average value of 1177 ± 19 barns.

CONCLUSIONS

The thermal capture cross section of Ac^{227} obtained in this work (814 ± 13 barns) is considerably larger than any figure previously obtained. It is not possible to explain why this figure differs from those quoted by Hughes and Schwartz (1) (510 ± 40 barns by a pile oscillator method and 520 ± 50 barns by an activation method) since these authors refer to unpublished work. Timma and Russell (2) give details of their work which led to 493 ± 53 barns, using an oscillator method, and, although no obvious flaw is apparent in their procedure, the possibility of neutron attenuation within the sample does not

Can. J. Chem. Downloaded from www.nrcresearchpress.com by 196.1.178.254 on 09/04/12
For personal use only.

Can. J. Chem. Downloaded from www.nrcresearchpress.com by 196.1.178.254 on 09/04/12
For personal use only.

TABLE II

Results of integral cross section determinations

	Experiments 1 and 2		Experiments 3 and 4		Experiments 5 and 6		Experiments 5 and 7	
	With cadmium cover	Without cadmium cover	With cadmium cover	Without cadmium cover	With cadmium cover	Without cadmium cover	With cadmium cover	Without cadmium cover
$(R_{\beta,N_0})/(1-e^{-\lambda t})$ = Equilibrium rate of production of Ac^{228} from Ac^{227} (sec^{-1})	$(2.12\pm0.17)\times10^{-9}$	$(5.44\pm0.14)\times10^{-8}$	$(2.22\pm0.11)\times10^{-9}$	$(6.26\pm0.27)\times10^{-8}$	$(2.14\pm0.35)\times10^{-9}$	$(6.39\pm0.19)\times10^{-8}$	$(2.14\pm0.35)\times10^{-8}$	$(6.20\pm0.17)\times10^{-8}$
Duration of irradiation (sec) = t	5400 ± 2	5400 ± 2	5417 ± 2	5400 ± 2	5400 ± 2	5400 ± 2	5400 ± 2	5400 ± 2
Co^{60} Activity of monitor (disintegration per sec per mg Co^{59} per sec of irradiation)	3.70 ± 0.04	107.0 ± 0.4	3.84 ± 0.04	118.0 ± 0.5	4.02 ± 0.04	117.0 ± 0.5	4.02 ± 0.04	119.1 ± 0.5
Cd Ratio for Co^{59}	28.93 ± 0.31		30.75 ± 0.33		29.08 ± 0.31		29.60 ± 0.32	
$r\sqrt{(T/T_0)}$	0.0248		0.0233		0.0246		0.0242	
$\hat{\sigma}(Co^{59})$ In barns	37.36 ± 0.01		37.31 ± 0.01		37.36 ± 0.01		37.34 ± 0.01	
nv_0(Neutrons/cm^2 sec)	$(6.71\pm0.08)\times10^{13}$		$(7.41\pm0.09)\times10^{13}$		$(7.34\pm0.08)\times10^{13}$		$(7.47\pm0.09)\times10^{13}$	
$\hat{\sigma}(Ac^{227})$ In barns	811 ± 23		844 ± 37		870 ± 28		829 ± 24	
Cd Ratio for Ac^{227}	25.7 ± 1.5		28.2 ± 1.9		29.8 ± 4.9		28.9 ± 4.7	
$s_0(Ac^{227})$	1.138		1.084		0.916		0.987	
$\sigma_0(Ac^{227})$ In barns	788 ± 23		824 ± 37		851 ± 28		810 ± 25	
Resonance integral of Ac^{227} (from 0.5 ev to ∞) in barns	1185 ± 74		1198 ± 85		1104 ± 189		1104 ± 183	

appear to have been considered. A major uncertainty in using a macro quantity of a rare and highly radioactive material as the sample under investigation might be expected to lie in the chemical purity of the sample, but although Timma and Russell quote no spectrographic or other analyses for the sample they used, they determined its Ac^{227} content by two independent methods (gravimetrically and calorimetrically) with good agreement.

The procedure described here relies entirely on 4π counting methods for the determination of numbers of atoms. The half-lives involved are known with good precision and agreement between published data and those realized during the experiments was excellent. With the present state of our knowledge of 4π counting the major uncertainty lies in the possibility of self-absorption in the source itself. In the experiments described the sources used were invisible to the naked eye and adequate allowance was made for the possibility of self-absorption, taking into account the fact that only relatively energetic particles were of interest. Should these allowances, in fact, be inadequate it is much more likely that the β-counting rather than the α-counting would be in error and consequently the resulting cross section would be higher rather than lower than that quoted here and would make the discrepancy with previous values even greater.

REFERENCES

1. HUGHES, D. J. and SCHWARTZ, R. B. Neutron cross sections. Brookhaven National Laboratory Report BNL 325. 2nd ed. U.S. Govt. Printing Office, Washington, D.C. 1958.
2. TIMMA, D. L. and RUSSELL, L. N. Absorption cross section of actinium-227. Mound Laboratory Report MLM 744. Office of Technical Services, Dept. of Commerce, Washington, D.C. 1952.
3. CABELL, M. J. Can. J. Phys. **36**, 989 (1958).
4. CABELL, M. J., EASTWOOD, T. A., and CAMPION, P. J. J. Nuclear Energy, **7**, 81 (1958).
5. PETERSON, S. and GHIORSO, A. The transuranic elements. Part II. McGraw-Hill Book Co., Inc., New York. 1949. p. 135.
6. TOBAILEM, J. J. phys. radium, **16**, 48 (1955).
7. HAGEE, G. R., CURTIS, M. L., and GROVE, G. R. Phys. Rev. **96**, 817A (1954).
8. HAHN, O. and ERBACHER, O. Physik Z. **27**, 531 (1926).
9. STROMINGER, D., HOLLANDER, J. M., and SEABORG, G. T. Rev. Modern Phys. **30** (No. 2), Part II, 585 (1958).
10. COBBLE, J. W. Determination of absolute disintegration rate using $4\pi\beta$-proportional γ-scintillation coincidence counting. Paper given at the American Chemical Society, 133rd meeting. San Francisco, Calif. April 13–18, 1958.
11. WESTCOTT, C. H., WALKER, W. H., and ALEXANDER, T. K. Second United Nations International Conference on the Peaceful Uses of Atomic Energy, Geneva. September 1–13, 1958. Paper 202.
12. EASTWOOD, T. A. Second United Nations International Conference on the Peaceful Uses of Atomic Energy, Geneva. September 1–13, 1958. Paper 203.
13. WESTCOTT, C. H. Effective cross section values for well-moderated thermal reactor spectra. Atomic Energy of Canada Ltd. Report CRRP 787, August, 1958.

Can. J. Chem. Downloaded from www.nrcresearchpress.com by 196.1.178.254 on 09/04/12
For personal use only.

Can. J. Chem. Downloaded from www.nrcresearchpress.com by 196.1.178.254 on 09/04/12
For personal use only.

PREPARATION AND INFRARED SPECTRA OF DIVINYL SULPHIDE, 2-METHYL-1,3-THIOXOLANE, AND 1,4-THIOXANE[1]

K. K. Georgieff and A. Dupré

ABSTRACT

Dehydration of thiodiglycol at 195°–230° with potassium hydroxide produced a 36% yield of divinyl sulphide, 9–10% of 2-methyl-1,3-thioxolane, 7–8% of 1,4-thioxane, and 3.5% of vinyl 2-hydroxyethyl sulphide. Physical properties and infrared spectra are reported. Divinyl sulphide of high purity for polymer work was obtained by distillation in a Podbielniak column. Precautions that must be observed in the preparation, distillation, and storage are given.

INTRODUCTION

To prepare some divinyl sulphide of high purity for polymer and spectroscopic studies, an examination of the possible methods was made. Dehydrochlorination of mustard gas (2,2′-dichlorodiethyl sulphide) gives reasonable yields (1, 2, 3, 4, 5), but this material is very hazardous to handle, and is not readily available commercially. Dehydrobromination of 2,2′-dibromodiethyl sulphide is less dangerous (6) but this material also is unavailable. Dehydration of thiodiglycol with anhydrous potassium sulphate (7) gives some divinyl sulphide, but also a large proportion of by-products.

$$(CH_2OH.CH_2)_2S \rightarrow (CH_2{=}CH)_2S + 2H_2O$$

Dehydration of thiodiglycol with potassium hydroxide, which has been described more recently by Doumani (8), appeared more promising since no mention of by-products other than 2-hydroxyethyl vinyl sulphide was made. Furthermore, since thiodiglycol is commercially available, investigation of this latter method appeared justified.

Doumani added thiodiglycol slowly to potassium hydroxide and continuously distilled off the divinyl sulphide and water. In this investigation, all of both reagents were added at the beginning and were stirred, but whether this difference in procedure materially affected the yield of divinyl sulphide is not known, since Doumani failed to publish such data. No systematic investigation to determine optimum yield conditions was made, but some precautions which are necessary due to excessive foaming of the thiodiglycol and the ease of polymerization of divinyl sulphide are described in the experimental section.

EXPERIMENTAL

Samples of thiodiglycol were kindly supplied by the Defence Research Laboratories, Shirley Bay, Ontario, and Carbide and Carbon Chemicals Corp., and were used without prior purification. Foaming during the reaction is a problem but may be largely overcome if the following precautions are observed: an oversize reaction flask fitted with a stirrer should be used and the temperature of reaction should be raised very slowly. Also, if it is desired to prepare a second batch, the flask must be thoroughly cleaned before a new charge is added, since even small amounts of residue cause uncontrollable foaming.

The reaction was carried out as follows: into a 500-ml round-bottom flask fitted with an Ace "Tru-bore" stirrer and a distillation column head with a water-cooled condenser were placed 75 ml of thiodiglycol and 75 g of potassium hydroxide pellets (85%). To minimize polymerization, the entire apparatus was evacuated and filled with nitrogen.

[1]*Manuscript received February 17, 1959.*
Contribution from the Research Laboratories, Shawinigan Chemicals Ltd., Shawinigan, Quebec.

Can. J. Chem. Downloaded from www.nrcresearchpress.com by 196.1.178.254 on 09/04/12
For personal use only.

The stirrer was started after adjusting the blade so as to just clear the pellets, and the flask was immersed in a bath of Arochlor 1252. The bath temperature was raised slowly and reaction started at 195°. The organic vapors and water were condensed and drawn off as soon as they formed. Reaction was complete at 230°. The product, which was kept at −50° during the course of the reaction, was allowed to warm up to room temperature and the organic layer separated from the water. The aqueous layer was not further worked up even though it contained several per cent of product. The organic layer was dried with Linde Molecular Sieves No. 4A, stabilized with 1% para-tertiary butylcatechol and 2% copper resinate, and fractionated at a pressure of 105–156 mm Hg (abs.) in a Podbielniak column which had previously been flushed with nitrogen. The distillate receivers were kept at −50° during the distillation.

Since divinyl sulphide polymerizes rapidly at room temperature in the presence of air, the contents of each Podbielniak receiver was redistilled as soon as possible into a closed tube fitted with a stopcock and semiball joint using the high vacuum, low temperature technique (9, 10). By storing the samples in the above tubes at −78° in the complete absence of permanent gases, especially oxygen, it was possible to keep over 90% of the material in a monomeric state for over a year without the use of any stabilizer. Traces of certain impurities markedly decrease the rate of polymerization. For example, purified divinyl sulphide recovered from raw acetylene produced from calcium carbide, which probably still contained minute traces of divinylacetylene, did not polymerize at all under the above conditions in over a year.

Preparation of 2-Methyl-1,3-thioxolane from 2-Mercaptoethanol and Acetaldehyde (11)

Redistilled 2-mercaptoethanol (31.2 g) (obtained from Fisher Scientific Co.) and 17.7 g of freshly distilled acetaldehyde dissolved in 100 ml of cold benzene were charged into a 250-ml, stirred, round-bottom flask, fitted with a distillation column head with a brine-cooled condenser. Some heat was generated on mixing the reagents. Then 8 ml of 0.7 *N* anhydrous hydrogen chloride in ether was added from a dropping funnel over a period of 5 minutes. Slight cooling was required to maintain a temperature of 35–38°. The charge was then heated slowly to the reflux point and maintained there for 4 to 5 hours until the theoretical amount of water formed and was drawn off. The crude product was cooled and extracted with several 10-ml portions of aqueous 10% potassium carbonate solution. The benzene was separated by distillation through a short column at atmospheric pressure and the 2-methyl-1,3-thioxolane was fractionated in a Podbielniak column at 53 mm Hg (abs.). Yields were 77–80% on acetaldehyde and somewhat higher on mercaptoethanol.

Infrared spectra were obtained with a Perkin–Elmer, Model 12-C, single beam spectrometer with a rock salt prism.

RESULTS

The dehydration of thiodiglycol with potassium hydroxide produced a much more complex reaction product than previously indicated (8). After the mixture was separated into several main fractions by distillation in a Podbielniak column, the fractions were further resolved by gas chromatography. The various components so obtained were then identified by their mass, infrared, and ultraviolet spectra. The yield of divinyl sulphide was about 36%. Its spectra and rate of polymerization indicated that the mid-distillation cut was of high purity. Its infrared spectra in the gas and liquid phases are given in Fig. 1.

All three major by-products showed parent peaks of 104 in the mass spectrometer.

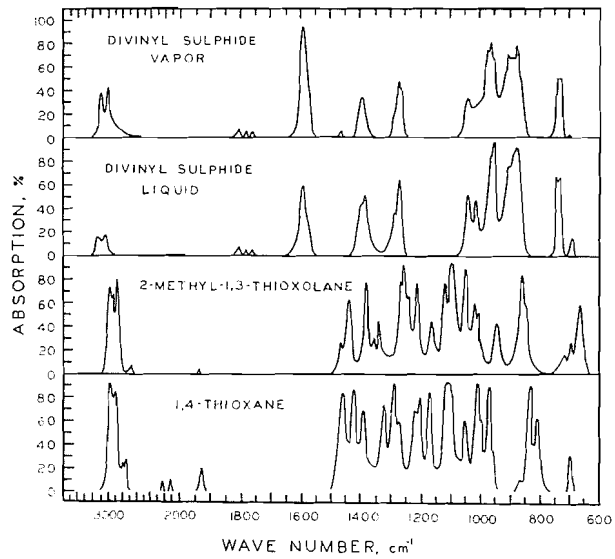

FIG. 1. Infrared spectra. Divinyl sulphide vapor, 34.4 mm pressure in 10-cm cell. Peaks: 3080, 3010, 1806, 1781, 1755, 1592, 1465, 1388, 1286sh, 1272, 1261sh, 1039, 969, 958, 953sh, 914sh, 908, 888, 876, 858sh, 746sh, 738, 733, 696 cm^{-1}.

Divinyl sulphide liquid, 10% by volume in CCl_4 or CS_2 in 0.14-mm cell. Peaks: 3110, 3040, 2970sh, 1588, 1391sh, 1383, 1279, 1265, 1041, 1016, 960sh, 951, 901, 883sh, 874, 736, 729, 685 cm^{-1}.

2-Methyl-1,3-thioxolane, 10% by volume in CCl_4 or CS_2 in 0.128-mm cell. Peaks: 2980, 2940, 2890, 2680, 1934, 1468, 1439, 1380, 1356, 1340, 1267, 1256, 1240, 1212, 1162, 1121, 1095, 1049, 1017, 1007, 996sh, 941, 872sh, 857, 846sh, 712, 691, 661 cm^{-1}.

1,4-Thioxane, 100% in 0.029-mm cell. Peaks: 2960, 2900, 2800, 2750, 2220, 2110, 1925, 1459, 1420, 1388, 1323, 1286, 1272, 1216, 1203, 1172, 1105, 1050, 1006, 993sh, 969, 956sh, 865, 828, 809, 693 cm^{-1}.

The highest boiling one appeared to be vinyl 2-hydroxyethyl sulphide in accordance with the findings of Doumani (8), but in point of quantity it was the smallest. The yield was about 3.5%.

$$(CH_2OH.CH_2)_2S \rightarrow CH_2OH.CH_2.S.CH{=}CH_2 + H_2O$$

Infrared bands at 3500 cm^{-1} and at about 1100 indicated the presence of hydroxyl and ones at 1634 and 945 indicated unsaturation.

The second highest boiling by-product was identified as 1,4-thioxane (*p*-oxathiane). Physical properties, infrared and mass spectra, were identical with those of an authentic sample (purchased from Robinson Brothers Ltd., Great Britain). It also formed by splitting of 1 mole of water from thiodiglycol but in this case, elements were removed from both hydroxyl groups, followed by cyclization.

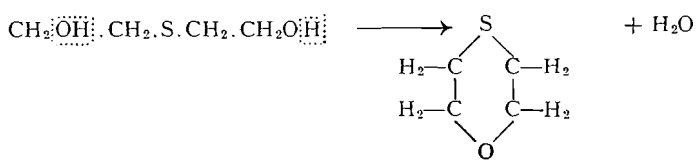

Its formation was not surprising since it was previously obtained from thiodiglycol using potassium sulphate (7) or sulphuric acid (12) as dehydrating agents. The yield was 7–8%. Its infrared spectrum is given in Fig. 1.

The major and third highest boiling by-product was unexpected since its formation

Can. J. Chem. Downloaded from www.nrcresearchpress.com by 196.1.178.254 on 09/04/12
For personal use only.

from thiodiglycol does not appear to have been previously reported. It too formed by splitting of 1 mole of water. Its mass spectrum showed a parent peak of 104 and large peaks at 15 and 89 which suggested a methyl group. Its infrared spectrum (cf. Fig. 1) failed to give any indication of unsaturation or a hydroxyl group. Since a straight chain compound would require one element of unsaturation, a cyclic compound seemed probable. Since it boiled about 27° below 1,4-thioxane, a five-membered ring instead of a six appeared possible. From the above data and since its boiling point was identical with that reported by Copenhaver (13, 14), it appeared that our compound might be 2-methyl-1,3-thioxolane (2-methyl-1,3-oxathiolane).

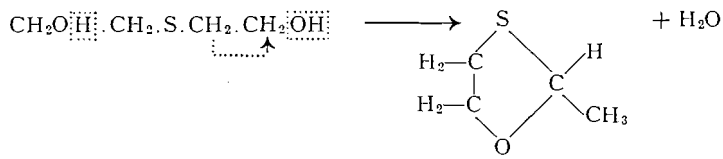

This was confirmed by preparing an authentic sample by the reaction of 2-mercaptoethanol with acetaldehyde in the same manner as Kipnis and Ornfelt (11) prepared 2-isopropyl-1,3-thioxolane from 2-mercaptoethanol and isobutyraldehyde. Physical properties, mass and infrared spectra were identical with those of the compound obtained from the dehydration of thiodiglycol. Its yield from thiodiglycol was 9–10%. The compound appeared to be quite stable at 0° for a period of at least one year.

The lowest boiling by-product obtained was methyl vinyl sulphide. It composed 7–8% of the total volatile product. Identification was made by its boiling point, infrared spectrum (15, 16), and mass spectrum. It is probable that it was formed, in part or in whole, by the dehydration of 2-hydroxyethyl methyl sulphide, which appeared to be a likely impurity in the thiodiglycol. Good mass spectra could not be obtained due to their high boiling points, but on distillation of a few drops from a small charge of the original thiodiglycol in a Podbielniak column, very much larger mass peaks of 74, 61, 47, and 15 were obtained with the distillate than with the residue. This is an indication that some 2-hydroxyethyl methyl sulphide was originally present. Two other by-products were obtained in trace quantities. They had mass parent peaks of 100 and 118 but could not be identified.

Some of the physical properties of the compounds obtained are given below.

TABLE I

Compound	B.p.*	n_D^{20}	d_4^{20}
1,4-Thioxane	67° at 44 mm (abs.)	1.5080	1.105
2-Methyl-1,3-thioxolane	58° at 53 mm (abs.) 130.55° (corr.) at 752 mm	1.4867	1.069
Divinyl sulphide	42.5° at 150 mm	1.5076	
Methyl vinyl sulphide	28° at 155 mm		

*All boiling points are uncorrected except when otherwise stated.

ACKNOWLEDGMENTS

The authors wish to express their thanks to Shawinigan Chemicals Ltd. for permission to publish this paper and to Y. Richard, E. Blais, and E. Beaulieu for their assistance.

Can. J. Chem. Downloaded from www.nrcresearchpress.com by 196.1.178.254 on 09/04/12
For personal use only.

REFERENCES

1. HELFRICH, O. B. and REID, E. E. J. Am. Chem. Soc. **42**, 1208 (1920).
2. BALES, S. H. and NICKELSON, S. A. J. Chem. Soc. **121**, 2137 (1922).
3. BALES, S. H. and NICKELSON, S. A. J. Chem. Soc. **123**, 2486 (1923).
4. LAWSON, W. E. and REID, E. E. J. Am. Chem. Soc. **47**, 2821 (1925).
5. DAVIES, J. S. H. and OXFORD, A. E. J. Chem. Soc. **133**, 224 (1931).
6. RUIGH, W. L. and ERICKSON, A. E. J. Am. Chem. Soc. **61**, 915 (1939).
7. FROMM, E. and UNGAR, B. Ber. B, **56**, 2286 (1923).
8. DOUMANI, T. F. *To* Union Oil Co. of California. U.S. Pat. No. 2,532,612 (1950).
9. SANDERSON, R. T. Vacuum manipulation of volatile compounds. John Wiley & Sons, Inc., New York. 1948. p. 86.
10. GEORGIEFF, K. K., CAVE, W. T., and BLAIKIE, K. G. J. Am. Chem. Soc. **76**, 5494 (1954).
11. KIPNIS, F. and ORNFELT, J. J. Am. Chem. Soc. **71**, 3555 (1949).
12. HEPWORTH, H. J. Chem. Soc. **119**, 1249 (1921).
13. COPENHAVER, J. W. *To* General Aniline and Film Corporation. Brit. Pat. No. 642,253 (1950).
14. COPENHAVER, J. W. *To* General Aniline and Film Corporation. U.S. Pat. No. 2,551,421 (1951).
15. SCHREIBER, K. C. Anal. Chem. **21**, 1168 (1949).
16. PRICE, C. C. and GILLIS, R. G. J. Am. Chem. Soc. **75**, 4750 (1953).

Can. J. Chem. Downloaded from www.nrcresearchpress.com by 196.1.178.254 on 09/04/12
For personal use only.

Can. J. Chem. Downloaded from www.nrcresearchpress.com by 196.1.178.254 on 09/04/12
For personal use only.

SELF-ABSORPTION IN SOURCES PREPARED FOR 4π BETA COUNTING[1]

JANET S. MERRITT, J. G. V. TAYLOR, AND P. J. CAMPION

ABSTRACT

Using the $4\pi\beta$-γ coincidence method the self-absorption of $4\pi\beta$ counting sources prepared by a number of source preparation techniques has been measured for the negatron emitters Cs^{134} (86-kev branch only), Nb^{95}, Hg^{203}, Co^{60}, Sc^{46}, Rb^{86}, Au^{198}, Na^{24}, and the positron branch of Cu^{64}. The self-absorption varied from a few tenths of one per cent to about ten per cent for sources with a mean superficial density of 2 $\mu g/cm^2$ for most of the nuclides studied. Subsidiary experiments were carried out to indicate the variation of self-absorption with source superficial density.

INTRODUCTION

The comparative simplicity of $4\pi\beta$ counting has led to its general use for absolute disintegration rate measurements. It is well known that the chief corrections are those required for absorption in the source and mount. The latter has been extensively discussed (1, 2, 3) and is small for all but the softest beta emitters if thin source mounts are used. Self-absorption cannot be so readily determined, and this is the principal uncertainty in $4\pi\beta$ counting. Hawkings *et al.* (4) progressively diluted a stock solution, and observed the activity (expressed in terms of the original solution) as a function of the dilution factor. At sufficiently high dilutions a constant activity was observed, which was taken to indicate that self-absorption had been eliminated. This procedure has been criticized (5) on the grounds that diluting a stock solution may not decrease the size of the crystals forming an active deposit but merely increase the distance between them. Pate and Yaffe (5) have described a distillation technique for preparing uniformly thin sources and have used this method to set up self-absorption curves for several isotopes (6). Seliger and Schwebel (7) have estimated the self-absorption of a number of isotopes from electron microscope measurements of the crystal sizes. The $4\pi\beta$-γ coincidence method has been used by Gunnink *et al.* (8) to study self-absorption in thin sources prepared by conventional techniques. Assuming that the observed inefficiencies are entirely due to self-absorption they have obtained a curve of per cent loss in 4π counting against maximum beta particle energy. These authors are careful to point out that these losses are "best" averages, and that the value for any one source may deviate considerably from the mean.

In this laboratory a $4\pi\beta$-γ coincidence counting system consisting of a $4\pi\beta$ proportional counter sandwiched between two 3 in. $\times$ 3 in. sodium iodide crystals (9) has been used to investigate the relative merits of various source preparation techniques. The results of six such techniques applied to several isotopes of widely differing maximum beta particle energy are reported here.

EXPERIMENTAL

In their simplest form the equations relating the observed counting rates in a coincidence determination to the absolute disintegration rate, N_0, are:

$$N_\beta = N_0\epsilon_\beta$$
$$N_\gamma = N_0\epsilon_\gamma$$
$$N_c = N_0\epsilon_\beta\epsilon_\gamma$$

[1]*Manuscript received March 11, 1959.*
Contribution from the Physics Division, Atomic Energy of Canada Limited, Chalk River, Ontario. Issued as A.E.C.L. No. 796.

where N_β, N_γ, and N_c are the observed rates in the beta, gamma, and coincidence scalers respectively, and ϵ_β and ϵ_γ are the efficiencies for the beta and gamma detectors. Hence it follows that

$$\epsilon_\beta = N_c/N_\gamma.$$

In practice these equations require several small corrections, the largest of which are due to dead time, accidental coincidences, and backgrounds (9). Since the counter has been shown to have 100% of 4π geometry (9), the inefficiency in the beta detector is due to self-absorption, source mount absorption, and the possibility that the counter–amplifier system may not detect one ion pair.

The following negatron emitters Cs^{134} (86-kev branch only), Nb^{95}, Hg^{203}, Co^{60}, Sc^{46}, Rb^{86}, Au^{198}, Na^{24}, and the positron branch of Cu^{64} were used in this study. Aliquots were deposited on VYNS plastic films (superficial density 5 $\mu g/cm^2$) stretched across aluminum rings 1.5 in. outside diameter, 1.0 in. inside diameter, and 0.022 in. thick. The underside of the plastic film was coated with 15 $\mu g/cm^2$ of gold. After a sample was deposited, a similar gold-coated film was placed over the source so that both gold surfaces were outermost. Provided that the source is not exceptionally thick this second film adheres well to the source material and the first film without forming cavities. The resistance between the center of a film and the mount ring on the coated and uncoated side is about 0.2 and 1.5 meg respectively, while the resistance of a film having no gold on either side is greater than 600 meg. This sandwich technique ensures that no active material can flake off the source, and also provides a more durable source mount for very little increase in total mount thickness compared with a single film coated on both sides.

The correction for absorption in the source mount was determined by observing the efficiency as a function of the number of pairs of gold-coated films added to the sandwich, and extrapolating the resultant "absorption curve" to zero film thickness. The corrections are listed in Table I, those for Cs^{134}, Nb^{95}, Co^{60}, and Na^{24} were measured as described above, while the remainder were found by interpolation.

A small correction required for the threshold detection energy of the counter–amplifier system was estimated as follows. Pulses due to K X rays from Ca^{41}, Cr^{51}, and Fe^{55} observed at the output of the first stage of the amplifier showed that the system was linear in the range 3.3 to 5.9 kev. Comparison of these pulses with the amplitudes of suitably shaped signals fed to the amplifier input from a pulse generator which just failed to register in the beta scaler gave a threshold detection energy of 0.35 ± 0.1 kev when the counter was operated near the center of the plateau. Assuming that self-absorption does not appreciably distort the spectrum, corrections for undetected particles below this threshold energy were calculated using theoretical beta spectral shapes. The corrections for this effect are shown in Table I.

The determination of the efficiency for the 86-kev beta branch in Cs^{134} presented some difficulty owing to the complex nature of the Cs^{134} disintegration scheme. The results for this branch were determined by accepting pulses in the γ-channel corresponding to the sum peak at 1.97 Mev only. In order to increase the efficiency for detecting this peak the outputs of both crystals were added linearly before discrimination, giving a gamma efficiency of 0.03% (as compared with 10 to 15% for the other nuclides). The statistical uncertainty of the efficiency measurement of any one source is estimated to be $\pm 2\%$ for Cs^{134}, while for all the remaining nuclides the corresponding value is $\pm 0.2\%$. The values obtained for the positron branch in Cu^{64} were determined by accepting pulses corresponding to the 0.511-Mev photo peak in the gamma detectors. A correction

Can. J. Chem. Downloaded from www.nrcresearchpress.com by 196.1.178.254 on 09/04/12
For personal use only.

of about 0.3% was necessary for the contribution of the 1.34-Mev gamma ray lying under this peak.

To obtain an indication of the variation of self-absorption with source thickness the beta counting efficiency was measured as a function of the carrier concentration for Au^{198}, Rb^{86}, and Nb^{95}. The results are given in Fig. 1 where the crosshatched area represents the spread in self-absorption which was found.

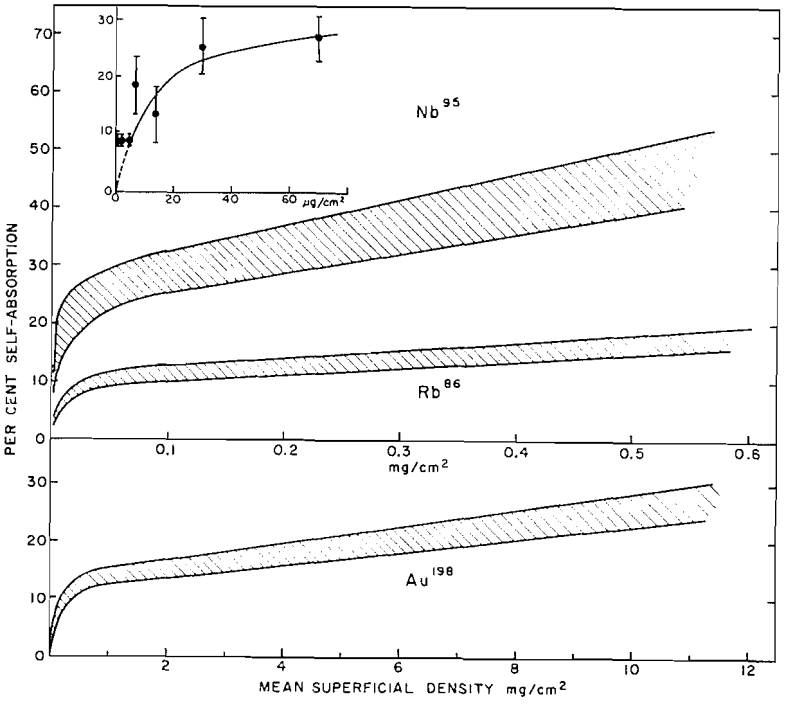

FIG. 1. Per cent self-absorption as a function of the mean superficial density for Au^{198}, Rb^{86}, and Nb^{95}. The Au^{198} and Rb^{86} sources were prepared using the colloidal silica and insulin treatments respectively, while both methods were used in obtaining the curve for Nb^{95}. The inset shows the variation of self-absorption at low mean superficial densities for Nb^{95}.

In order to compare the self-absorption of sources prepared by different methods and with different isotopes, an attempt was made to maintain a mean superficial density of 2 $\mu g/cm^2$, but variations in the area of the deposits may have caused deviations of 50% in this value. In Table I we list the self-absorption, corrected for source mount absorption and threshold detection energy, for a number of isotopes and source preparation techniques. The quoted errors are standard deviations for about five sources. Brief descriptions of, and comments on, the techniques follow according to the column headings of Table I.

(*a*) *Simple evaporation method.*—Aliquots are dried under an infrared lamp and yield a roughly circular deposit of about 1 cm^2. Microscopic inspection shows that this method often results in clumping of the source material, usually around the edge of the deposit, cf. Pate and Yaffe (5). The large errors in this column show the poor reproducibility of the method, especially for the lower energy beta emitters.

(*b*) *Precipitation method.*—A drop of distilled water is added to a source which has been dried as in (*a*). The source is then redried in an atmosphere of ammonia provided by rinsing a beaker with concentrated ammonium hydroxide solution and inverting it

Can. J. Chem. Downloaded from www.nrcresearchpress.com by 196.1.178.254 on 09/04/12
For personal use only.

TABLE I

Per cent self-absorption

Nuclide	Maximum beta energy, Mev	Source mount absorption correction, %	Threshold detection energy correction, %	Self-absorption, %					
				Evaporated (*a*)	Precipitated (*b*)	Insulin-treated (*c*)	"Ludox"-treated (*d*)	Sprayed (*e*)	Distilled (*f*)
Cs^{134}	0.086	5	1.1	39±6		21.4±3.2	18.7±1.3	6.7±0.9	
Nb^{95}	0.16	2	0.5	20.3±2.1		9.3±3.5	8.5±1.0		
Hg^{203}	0.21	2	0.5		5.6±0.6		4.0±0.5		
Co^{60}	0.31	1	0.2	8.7±1.5	3.7±0.5	5.2±1.2	3.6±0.7	1.1±0.6	1.3±0.5
Sc^{46}	0.36	0.7	0.2	5.3±1.7	2.8±0.3	5.1±1.4	2.8±0.4		
Cu^{64}	0.66	0.0	0.00	0.2±0.2			0.1±0.2		
Rb^{86}	0.68	0.3	0.08	2.7±1.1			2.3±0.6	1.0±0.2	
Au^{198}	0.96	0.2	0.06	1.6±0.6		1.4±0.6	0.6±0.4		
Na^{24}	1.39	0.04	0.01	1.0±0.5			0.8±0.3	0.2±0.2	

over the source. These sources appear more uniform and exhibit higher counting efficiencies than similar sources prepared by method (*a*). The ammonia treatment is limited to elements which form insoluble hydroxides, but the technique has been extended by the use of hydrogen sulphide in the preparation of precipitated Hg^{203} sources.

(*c*) *Insulin treatment.*—Insulin solution used as a wetting agent improves the uniformity of evaporated sources and hence their efficiencies, particularly when the solids content is high. Although the usual practice is to remove (prior to depositing the activity) most of the insulin solution from the source mount the solids in the remainder are often considerably more than those contained in many high specific activity solutions, and hence the presence of these solids partially offsets the beneficial properties of the insulin. The sources employed in these studies contained about 2 μg of such residual solids from the insulin. Hence the mean superficial density of sources listed in column (*c*) of Table I is about 4 $\mu g/cm^2$.

(*d*) *Colloidal silica treatment.**—Aliquots are delivered into a small amount of silica sol on a source mount and dried as in (*a*). A freshly prepared $1:10^4$ aqueous dilution of "Ludox" SM (du Pont) has been found convenient. A study of beta efficiencies as a function of the amount of "Ludox" showed that about 10 to 20 μl of the diluted sol (about 0.2 to 0.4 μg residual silica) is optimum for most isotopes. Although high ionic concentrations should be avoided to prevent gelation of the silica, "Ludox" has been successfully used with solutions as acidic as 0.5 *N*.

(*e*) *Spray method.*—The source preparation technique of Carswell and Milsted (11) has been used to prepare almost invisible sources on gold-coated VYNS mounts.† The activity is dissolved in acetone, which is then introduced into a fine glass capillary ($\sim$ 0.005 in. at the tip). When about 3 kv d-c. potential is applied between the source mount and the tip of the capillary a fine spray is ejected. Conditions are adjusted so that the droplets forming the spray evaporate before they reach the source mount. Although the method is presently not quantitative, the yields can be made better than 90% and the convenience of the method together with the low self-absorption obtained suggests its use for the technique proposed by Seliger (12) for the standardization of beta emitters having no γ-ray in their decay scheme. A thin source is prepared from high specific activity material, and counted. The deposit is then completely dissolved,

**This method was developed by W. F. Merritt, who used it to prepare* S^{35} *sources (10).*

†*We are indebted to Drs. Fraser and Milton of this laboratory for the use of their equipment, which is a modification of that described by Carswell and Milsted.*

Can. J. Chem. Downloaded from www.nrcresearchpress.com by 196.1.178.254 on 09/04/12
For personal use only.

carrier added, and the solution made up to volume to form a standardized stock solution. This can then be used to calibrate other similar solutions by direct comparison.

(*f*) *Distillation method.*—Some sources of Co^{60} have been prepared by the distillation method of Pate and Yaffe (5).* These are very uniform deposits which exhibit about the same self-absorption as sprayed sources. For the sources studied the yields were low, but according to (5) the method may be made very nearly 100% quantitative.

DISCUSSION

The self-absorption values obtained by the simple evaporation method and by the use of colloidal silica (columns (*a*) and (*d*), Table I) are shown graphically in Fig. 2,

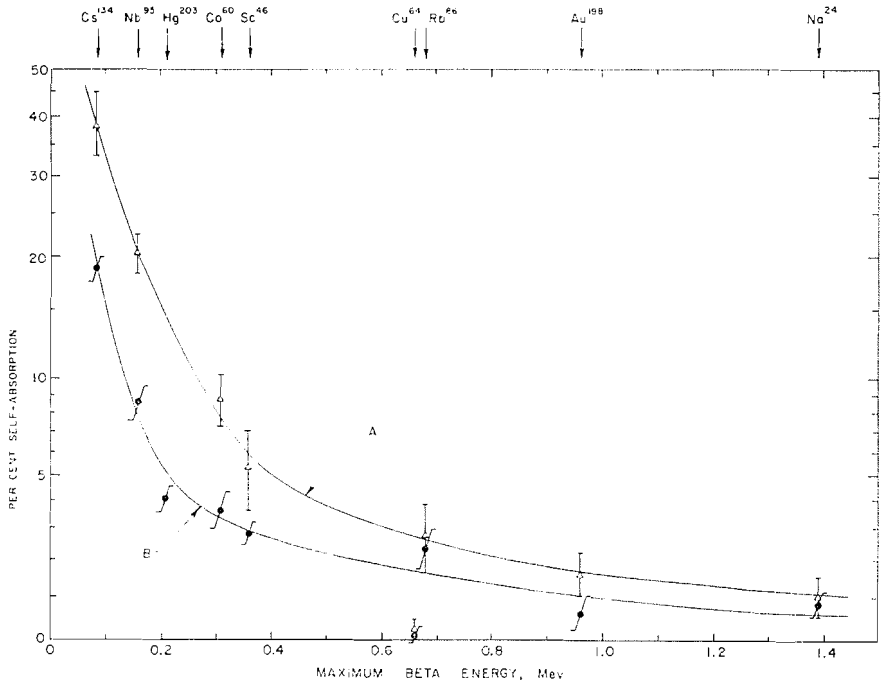

FIG. 2. Per cent self-absorption as a function of beta end point energy for sources of mean superficial density of 2 $\mu g/cm^2$. Curves A and B represent sources prepared by the simple evaporation and colloidal silica methods respectively.

curves A and B respectively. For clarity the results for insulin-treated sources have not been plotted; inspection of Table I shows that they are very similar to those for colloidal silica-treated sources. The results show a comparatively small variation of self-absorption with beta end point energy above about 400 kev, but below this value the absorption rapidly increases. We also note, in agreement with others (8), that the reproducibility in general tends to decrease as the self-absorption increases. On the whole there is good agreement between the self-absorption values obtained by method (*a*) and the experimental results of Gunnink *et al.* (8). Our values are slightly larger than those estimated by Seliger and Schwebel (7), while those obtained for the distilled Co^{60} sources are in agreement with the curve given by Yaffe (6). The use of colloidal silica is seen to be particularly advantageous at low beta end point energies, although no

*We are indebted to Dr. Yaffe and Mr. J. B. Fishman for the preparation of these sources.

Can. J. Chem. Downloaded from www.nrcresearchpress.com by 196.1.178.254 on 09/04/12
For personal use only.

technique that we have investigated to date is capable of reducing self-absorption to negligible proportions. There is one notable deviation from the curves of Fig. 2, viz. the positron branch of Cu^{64}. This may be explained by the fact that owing to the coulomb repulsion effect there are fewer low energy particles in a positron spectrum than in a negatron spectrum having the same end point energy and hence self-absorption effects are smaller.

It should be emphasized that the rapid variation of self-absorption with source thickness (Fig. 1) demands that the source preparation techniques and mean superficial densities be closely similar to those used here if the curves of Fig. 2 are to be used to estimate even approximate self-absorption corrections for $4\pi\beta$ counting. Further, Fig. 1 (inset) and Fig. 8 of (5) show that for sources of smaller mean superficial density it does not necessarily follow that the self-absorption will be significantly less.

REFERENCES

1. SMITH, D. B. A.E.R.E. Rept. I/R 1527 (1954).
2. MANN, W. B. and SELIGER, H. H. J. Research Natl. Bur. Standards, **50**, 197 (1953).
3. PATE, B. D. and YAFFE, L. Can. J. Chem. **33**, 929 (1955).
4. HAWKINGS, R. C., MERRITT, W. F., and CRAVEN, J. H. Proceedings of symposium. Maintenance of Standards, National Physical Laboratory. H.M. Stationery Office, London. 1952.
5. PATE, B. D. and YAFFE, L. Can. J. Chem. **34**, 265 (1956).
6. YAFFE, L. Unpublished results.
7. SELIGER, H. H. and SCHWEBEL, A. Nucleonics, **12** (No. 7), 54 (1954).
8. GUNNINK, R., COLBY, L. J., and COBBLE, J. W. Anal. Chem. To be published.
9. CAMPION, P. J. Intern. J. Appl. Radiation and Isotopes, **4**, 232 (1959).
10. MERRITT, W. F. Unpublished results.
11. CARSWELL, D. J. and MILSTED, J. Nuclear Energy, **4**, 51 (1957).
12. MEASUREMENTS AND STANDARDS OF RADIOACTIVITY. Publication No. 573. National Academy of Sciences, National Research Council, Washington, D.C. p. 47 (1958).

Can. J. Chem. Downloaded from www.nrcresearchpress.com by 196.1.178.254 on 09/04/12
For personal use only.

Can. J. Chem. Downloaded from www.nrcresearchpress.com by 196.1.178.254 on 09/04/12
For personal use only.

NOTES

INDEPENDENCE IN HYDROLYSIS OF CONDENSED PHOSPHATES

M. Joyce Smith

In a series of papers (1) from these laboratories, it was concluded that the hydrolysis of sodium tetrameta-, tetrapoly-, tripoly-, and pyro-phosphate at constant pH and 65.5° C followed first-order kinetics and that hydrolysis of different species in the same dilute solution proceeded independently. A convenient method for making numerical calculations of consecutive reactions was also developed.

When this method was applied to the complete hydrolysis of tetrapolyphosphate near pH 5 using the available rate constants a poor fit was obtained for the curve showing the appearance and disappearance of tripolyphosphate. Either the rate constant for tripolyphosphate at pH 5 or the assumption of independence, or both, might be in error.

Recently an opportunity occurred to investigate the hydrolysis of tetrapolyphosphate using improved chromatographic techniques (2) and carrying out the whole experiment in a reasonably short time without change of personnel.

The results were:

(1) a closer quantitative confirmation of first-order kinetics;
(2) a higher value for the rate constant for tripolyphosphate at pH 5 (6.70×10^{-4} vs. 2.89×10^{-4});
(3) much improved agreement with the theory of consecutive reactions (see Fig. 1); and
(4) confirmation of first-order kinetics by the addition of pyrophosphate and orthophosphate during hydrolysis of tripolyphosphate without effect on the rate constant.

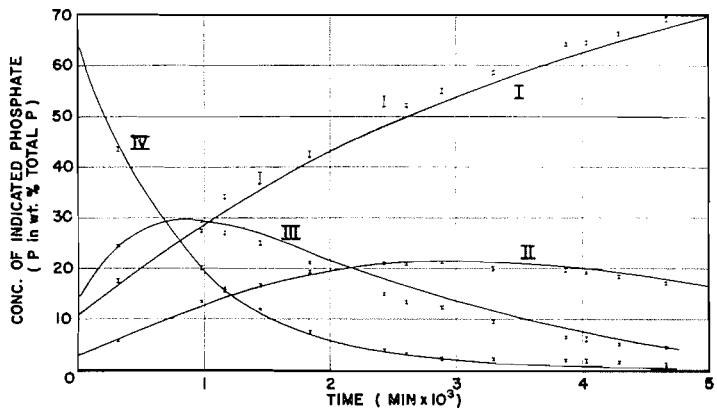

Fig. 1. The course of the reaction degrading tetrapolyphosphate to orthophosphate at 65.5° C and pH = 5.0. Full lines show the proportions of the constituents of the reaction mixture as calculated from the theory of consecutive reactions (1 *d*), individual points show the chromatographically determined values, in duplicate. I, orthophosphate; II, pyrophosphate; III, tripolyphosphate; IV, tetrapolyphosphate.

Since one experiment in the earlier work had given a rate constant of 6.2×10^{-4} at pH 5 for tripolyphosphate, the possibility that it might change drastically in the neigh-

borhood of pH 5 was considered. However, several experiments in the neighborhood of pH 5 showed this not to be the case.

The revised rate constants are given in Table I.

TABLE I

Rate constants for hydrolysis of condensed phosphates (Temp., 65.5° C; Concn., 0.05 at. wt. of P/liter)

Tetrapolyphosphate							
pH				5.0			
$k \times 10^4$				11.7			
Tripolyphosphate							
pH	1.4	3.0		5.0	4.7	4.4	5.3
$k \times 10^4$	86.4	16.2		6.70	7.55	8.40	6.28
Pyrophosphate							
pH	2.8		4.9	5.0			
$k \times 10^4$	4.04		2.99	2.90			

1. (*a*) CROWTHER, J. P. and WESTMAN, A. E. R. Can. J. Chem. **32**, 42 (1954); (*b*) **34**, 969 (1956). (*c*) MCGILVERY, J. D. and CROWTHER, J. P. Can. J. Chem. **32**, 174 (1954). (*d*) WESTMAN, A. E. R. and DELURY, D. B. Can. J. Chem. **34**, 1134 (1956).
2. SMITH, M. J. Anal. Chem. (In press).

RECEIVED FEBRUARY 2, 1959.
ONTARIO RESEARCH FOUNDATION,
43 QUEEN'S PARK,
TORONTO 5, ONTARIO.

THE X-RAY STRUCTURE ANALYSIS OF DEMETHANOL ACONINONE HYDRIODIDE TRIHYDRATE*

MARIA PRZYBYLSKA AND LÉO MARION

The space group of demethanol aconinone hydriodide trihydrate, $C_{24}H_{35}O_8N.HI.3H_2O$, is $P2_12_12_1$ and unit cell dimensions are $a = 14.69$, $b = 22.08$, and $c = 8.33$ Å, with $Z = 4$.

The co-ordinates of the iodine atom, derived from interatomic vector projections, are $x = 0.167$, $y = 0.209$, and $z = 0.169$ (referred to the origin given by the International Tables).

A total of 2773 structure factors has been evaluated out of a possible 3477 which lie within the range of Cu K_α radiation. The $|F|^2_{hkl}$ values were sharpened and modified as described by Donohue and Trueblood (1) and a three-dimensional Patterson synthesis was computed for 30,000 points. Using the results of this function 'Vector Convergence Density' maps (2) were plotted and a thorough examination of vectors of fourfold coincidence and of Fourier projections gave positions of 32 light atoms, excluding the hydrogen atoms.

The scattering curves only for carbon and iodine atoms were used for calculations of the first ($hk0$) and ($0kl$) structure factors. Two cycles of refinement for these two zones established the locations of the remaining four atoms of the molecule and indicated which atoms should be taken as oxygen atoms.

The ring skeleton of the molecule was found to be identical with that of des-(oxymethyl-

**Issued as N.R.C. No. 5158.*

Can. J. Chem. Downloaded from www.nrcresearchpress.com by 196.1.178.254 on 09/04/12
For personal use only.

borhood of pH 5 was considered. However, several experiments in the neighborhood of pH 5 showed this not to be the case.

The revised rate constants are given in Table I.

TABLE I

Rate constants for hydrolysis of condensed phosphates (Temp., 65.5° C; Concn., 0.05 at. wt. of P/liter)

Tetrapolyphosphate							
pH				5.0			
$k \times 10^4$				11.7			
Tripolyphosphate							
pH	1.4	3.0		5.0	4.7	4.4	5.3
$k \times 10^4$	86.4	16.2		6.70	7.55	8.40	6.28
Pyrophosphate							
pH	2.8		4.9	5.0			
$k \times 10^4$	4.04		2.99	2.90			

1. (*a*) CROWTHER, J. P. and WESTMAN, A. E. R. Can. J. Chem. **32**, 42 (1954); (*b*) **34**, 969 (1956). (*c*) MCGILVERY, J. D. and CROWTHER, J. P. Can. J. Chem. **32**, 174 (1954). (*d*) WESTMAN, A. E. R. and DELURY, D. B. Can. J. Chem. **34**, 1134 (1956).
2. SMITH, M. J. Anal. Chem. (In press).

RECEIVED FEBRUARY 2, 1959.
ONTARIO RESEARCH FOUNDATION,
43 QUEEN'S PARK,
TORONTO 5, ONTARIO.

THE X-RAY STRUCTURE ANALYSIS OF DEMETHANOL ACONINONE HYDRIODIDE TRIHYDRATE*

MARIA PRZYBYLSKA AND LÉO MARION

The space group of demethanol aconinone hydriodide trihydrate, $C_{24}H_{35}O_8N.HI.3H_2O$, is $P2_12_12_1$ and unit cell dimensions are $a = 14.69$, $b = 22.08$, and $c = 8.33$ Å, with $Z = 4$.

The co-ordinates of the iodine atom, derived from interatomic vector projections, are $x = 0.167$, $y = 0.209$, and $z = 0.169$ (referred to the origin given by the International Tables).

A total of 2773 structure factors has been evaluated out of a possible 3477 which lie within the range of Cu K_α radiation. The $|F|^2_{hkl}$ values were sharpened and modified as described by Donohue and Trueblood (1) and a three-dimensional Patterson synthesis was computed for 30,000 points. Using the results of this function 'Vector Convergence Density' maps (2) were plotted and a thorough examination of vectors of fourfold coincidence and of Fourier projections gave positions of 32 light atoms, excluding the hydrogen atoms.

The scattering curves only for carbon and iodine atoms were used for calculations of the first ($hk0$) and ($0kl$) structure factors. Two cycles of refinement for these two zones established the locations of the remaining four atoms of the molecule and indicated which atoms should be taken as oxygen atoms.

The ring skeleton of the molecule was found to be identical with that of des-(oxymethyl-

**Issued as N.R.C. No. 5158.*

Can. J. Chem. Downloaded from www.nrcresearchpress.com by 196.1.178.254 on 09/04/12
For personal use only.

ene)-lycoctonine (3). The only chemical evidence used in this investigation was that the ethyl group, which was readily identified, is attached to the nitrogen atom (4, 5). This information allowed us to distinguish the nitrogen atom from the other light atoms of the molecule.

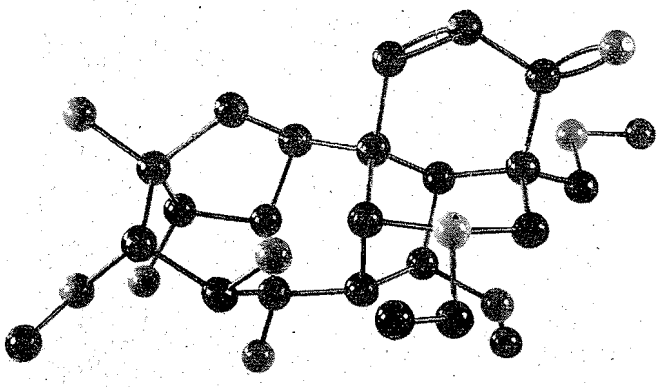

FIG. 1. The molecule of demethanol aconinone.

The calculation of interatomic distances showed the positions of the C=C bond and of the C=O group, which are found to be in agreement with the chemical evidence (6).

The photograph of the molecular model of demethanol aconinone is given in Fig. 1. The structural formula I and the diterpenoid representation of the structure II is also given.

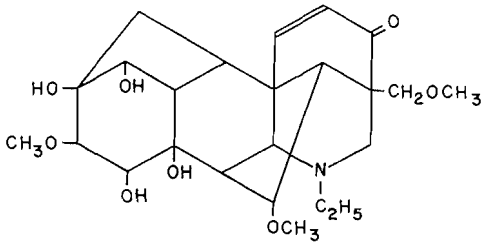

I

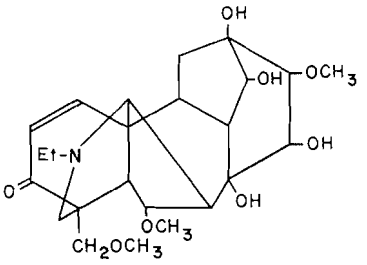

II

Refinement of atomic parameters is proceeding. The present values of the reliability index, $R = \Sigma\big||F_o|-|F_c|\big| \div \Sigma|F_o|$, are: R [001] = 0.16, R [100] = 0.20, and R [010] = 0.22.

Full details of this work will be published elsewhere.

We wish to thank Dr. F. R. Ahmed for computational assistance and for evaluating the Patterson function. We are also indebted to Dr. W. H. Barnes for his continued interest in this investigation, to Miss C. Saunderson for her help with the preparation of X-ray data, and to Dr. H. Mayer for supplying authenticated crystals.

1. DONOHUE, J. and TRUEBLOOD, K. N. Acta Cryst. **5**, 414 (1952).
2. BEEVERS, C. A. and ROBERTSON, J. H. Acta Cryst. **3**, 164 (1950).
3. PRZYBYLSKA, M. and MARION, L. Can. J. Chem. **34**, 185 (1956).
4. JACOBS, W. A. and ELDERFIELD, R. C. J. Am. Chem. Soc. **58**, 1059 (1936).

Can. J. Chem. Downloaded from www.nrcresearchpress.com by 196.1.178.254 on 09/04/12
For personal use only.

5. MAJIMA, R. and TAMURA, K. Ann. **526**, 116 (1936).
6. MAYER, H. and MARION, L. Can. J. Chem. **37**, 856 (1959).

RECEIVED FEBRUARY 4, 1959.
DIVISION OF PURE CHEMISTRY,
NATIONAL RESEARCH COUNCIL,
OTTAWA, CANADA.

Can. J. Chem. Downloaded from www.nrcresearchpress.com by 196.1.178.254 on 09/04/12
For personal use only.

2,4-DIAMINO-2-METHYLPENTANE DIISOCYANATE AND ITS METHYL URETHANE

K. H. KOSSMANN

2,4-Diamino-2-methylpentane is easily prepared from acetone and ammonia via 2,2,4,4-pentamethyl-2,3,4,5-tetrahydropyrimidine ("Acetonine") (1, 2).

While investigating methods of preparation of the diamine it was found desirable to prepare the diisocyanate of diamino-methylpentane and its methylurethane. The procedure used was similar to one given for hexamethylenediamine (3) with the exception that the dihydrochloride was not isolated.

EXPERIMENTAL

A. 2,4-Diamino-2-methylpentane diisocyanate 58 g ($\frac{1}{2}$ mole) of 2,4-diamino-2-methyl-

pentane was dissolved in 500 cc of *sec*-amylbenzene in a 1-liter, 3-necked flask fitted with stirrer, gas inlet, and gas outlet.

Dry HCl gas was bubbled through at 20–25° C, with stirring, until precipitation of the dihydrochloride was complete. The charge was heated with constant stirring to 180–185° C. Phosgene was then introduced, as a gas, for about 16 hours, after which time all the dihydrochloride had disappeared. After filtering, the reaction product was distilled at 10 mm Hg. Diisocyanate (30 g) was obtained, which represented a 35.7% yield. Methylpentanediamine diisocyanate boiled at 90–92° C at 10 mm Hg. Its refractive index at 20° C was 1.4445 (1.4449), its density at 20.5° C was 1.019.

B. The methylurethane of methylpentanediamine diisocyanate was prepared by dissolving 2 g of the diamine in 10 cc of methanol. The mixture warmed up. When it had been cooled the urethane crystallized and was recrystallized from methanol. Its melting point was 81° C.

ACKNOWLEDGMENT

The author wishes to thank Shawinigan Chemicals Limited, Shawinigan Falls, for their permission to publish this note.

1. MATTER, I. E. Helv. Chim. Acta, **31**, 612 (1948).
2. BRADBURY, R. B., HANCOX, N. C., and HATT, H. H. J. Chem. Soc. 1394 (1947).
3. FARLOW, M. W. Org. Syntheses, **31**, 62 (1951).

RECEIVED FEBRUARY 3, 1959.
SHAWINIGAN CHEMICALS LIMITED,
P.O. BOX 330,
SHAWINIGAN FALLS, QUEBEC.

5. MAJIMA, R. and TAMURA, K. Ann. **526**, 116 (1936).
6. MAYER, H. and MARION, L. Can. J. Chem. **37**, 856 (1959).

RECEIVED FEBRUARY 4, 1959.
DIVISION OF PURE CHEMISTRY,
NATIONAL RESEARCH COUNCIL,
OTTAWA, CANADA.

Can. J. Chem. Downloaded from www.nrcresearchpress.com by 196.1.178.254 on 09/04/12
For personal use only.

2,4-DIAMINO-2-METHYLPENTANE DIISOCYANATE AND ITS METHYL URETHANE

K. H. KOSSMANN

2,4-Diamino-2-methylpentane is easily prepared from acetone and ammonia via 2,2,4,4-pentamethyl-2,3,4,5-tetrahydropyrimidine ("Acetonine") (1, 2).

While investigating methods of preparation of the diamine it was found desirable to prepare the diisocyanate of diamino-methylpentane and its methylurethane. The procedure used was similar to one given for hexamethylenediamine (3) with the exception that the dihydrochloride was not isolated.

EXPERIMENTAL

A. 2,4-Diamino-2-methylpentane diisocyanate 58 g ($\frac{1}{2}$ mole) of 2,4-diamino-2-methyl-

pentane was dissolved in 500 cc of *sec*-amylbenzene in a 1-liter, 3-necked flask fitted with stirrer, gas inlet, and gas outlet.

Dry HCl gas was bubbled through at 20–25° C, with stirring, until precipitation of the dihydrochloride was complete. The charge was heated with constant stirring to 180–185° C. Phosgene was then introduced, as a gas, for about 16 hours, after which time all the dihydrochloride had disappeared. After filtering, the reaction product was distilled at 10 mm Hg. Diisocyanate (30 g) was obtained, which represented a 35.7% yield. Methylpentanediamine diisocyanate boiled at 90–92° C at 10 mm Hg. Its refractive index at 20° C was 1.4445 (1.4449), its density at 20.5° C was 1.019.

B. The methylurethane of methylpentanediamine diisocyanate was prepared by dissolving 2 g of the diamine in 10 cc of methanol. The mixture warmed up. When it had been cooled the urethane crystallized and was recrystallized from methanol. Its melting point was 81° C.

ACKNOWLEDGMENT

The author wishes to thank Shawinigan Chemicals Limited, Shawinigan Falls, for their permission to publish this note.

1. MATTER, I. E. Helv. Chim. Acta, **31**, 612 (1948).
2. BRADBURY, R. B., HANCOX, N. C., and HATT, H. H. J. Chem. Soc. 1394 (1947).
3. FARLOW, M. W. Org. Syntheses, **31**, 62 (1951).

RECEIVED FEBRUARY 3, 1959.
SHAWINIGAN CHEMICALS LIMITED,
P.O. BOX 330,
SHAWINIGAN FALLS, QUEBEC.

A SIMPLE THERMOSTATED PROBE ASSEMBLY FOR HIGH RESOLUTION NUCLEAR MAGNETIC RESONANCE SPECTRA

S. BROWNSTEIN

The observation of high resolution nuclear magnetic resonance spectra at a variety of temperatures is desirable to determine rates and activation energies for intramolecular motions (2, 3). The problem of constructing a thermostated probe assembly is complicated by the necessity of spinning the sample rapidly, not using magnetic materials, and having only a small space available. Nevertheless two such probes have been described in the literature (1, 4). Both of these assemblies have the disadvantage of requiring highly skilled glass-blowing techniques, and one of these (4) requires winding of a special receiver coil. In the assembly described here only a simple modification of the commercially available receiver coil unit is required. The apparatus may be easily dismantled and therefore can be used at a variety of frequencies by merely exchanging the receiver coil unit.

A plastic sleeve, tapered at the upper end, is cemented to the base of the probe insert. This mechanically strengthens it and serves as a seal to the thermostated compartment. A slot is cut below the receiving coil, and the insert is lengthened by sealing on an additional length of glass tubing. The resultant probe insert is shown in Fig. 1.

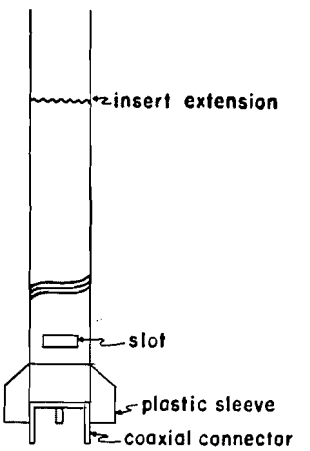

FIG. 1. Modified probe insert.

A cylindrical vacuum jacket, through which a side arm leads, is placed around the insert, fitting against the plastic sleeve at the lower end and supported by a tapered Teflon plug at the upper end. This fits tightly into the probe assembly, with the aid of a Teflon gasket, and is tuned in the usual manner. An aluminum housing, sitting on a cork gasket, with a slot for the glass side arm is screwed to the housing of the probe assembly. An extension of the housing fits snugly against the Teflon plug so that the thermostating air may leave only through the side arm in the aluminum housing. A commercially available sample spinner screws onto the top of the aluminum housing (5). Figure 2 shows the completed assembly with arrows indicating the path of the thermostated air.

The thermostated air was carried to the glass side arm by a Teflon tube wrapped in glass wool and aluminum foil. The temperature was measured by a copper constantan

Can. J. Chem. Downloaded from www.nrcresearchpress.com by 196.1.178.254 on 09/04/12
For personal use only.

Can. J. Chem. Downloaded from www.nrcresearchpress.com by 196.1.178.254 on 09/04/12
For personal use only.

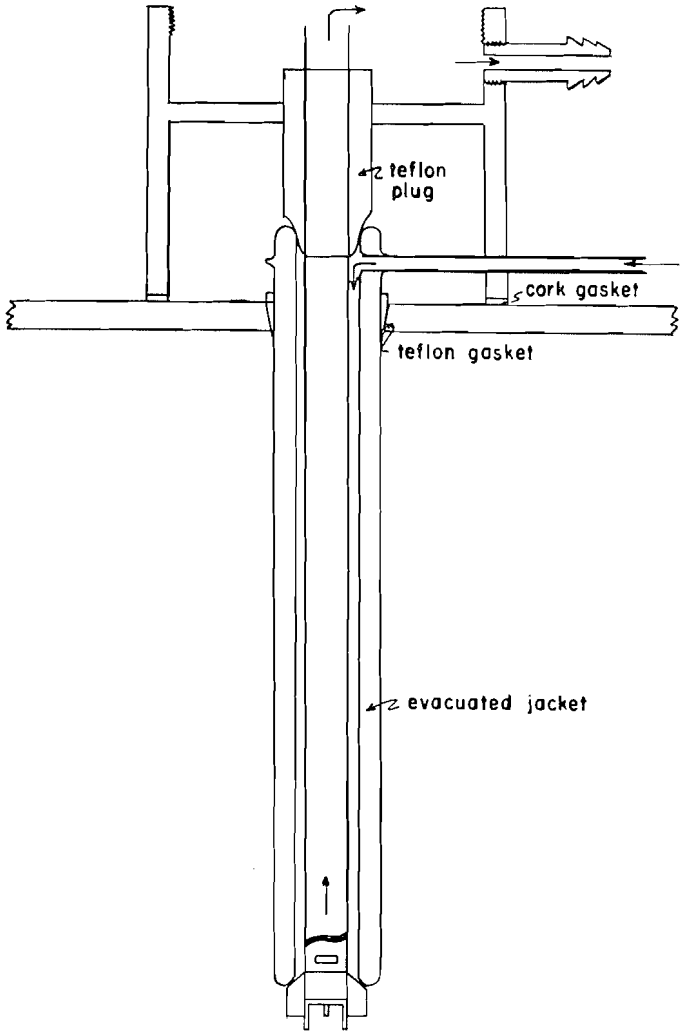

F.G. 2. Thermostating assembly.

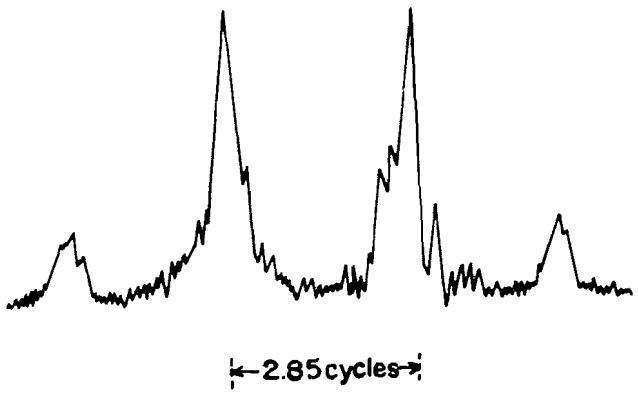

FIG. 3. Resonance of aldehydic proton of acetaldehyde.

thermocouple, B and S gauge 20, inserted through the side arm to 1/4 in. from the receiving coil. This assembly has been operated from −60° to 120° C with resolution equal to that obtained in instruments without a thermostated assembly. Figure 3 shows a trace obtained for the aldehydic proton of acetaldehyde. The resolution is at least one part in 10^8. Since the receiver coil may be tuned without disassembling the apparatus, it is used for routine investigations as well as variable temperature studies.

1. Bernstein, H. J., Schneider, W. G., and Pople, J. A. Proc. Roy. Soc. (London), A, **236**, 515 (1956).
2. Bottini, A. T. and Roberts, J. D. J. Am. Chem. Soc. **78**, 5126 (1956).
3. Gutowsky, H. S. and Holm, C. H. J. Chem. Phys. **25**, 1128 (1956).
4. Shoolery, J. N. and Roberts, J. D. Rev. Sci. Instr. **28**, 61 (1957).
5. Varian Associates, Palo Alto, California. Model V-4331A.

Received January 30, 1959.
Chemistry Department,
Cornell University,
Ithaca, New York.

Can. J. Chem. Downloaded from www.nrcresearchpress.com by 196.1.178.254 on 09/04/12
For personal use only.

SOME HYPOGLYCEMIC THIADIAZOLES

Francis L. Chubb and Jacqueline Nissenbaum

In 1942 Janbon (1) first noticed that 2-sulphanilamido-5-isopropyl-1,3,4-thiadiazole caused hypoglycemia. Bovet and Dubost (2) as well as Loubatières (3) studied the relationship between structure and activity in this series. The present work was undertaken in an effort to prepare some new hypoglycemic thiadiazoles.

A series of 2-arylsulphonamido-5-alkyl-1,3,4-thiadiazoles (Table II) was synthesized according to the following reaction scheme.

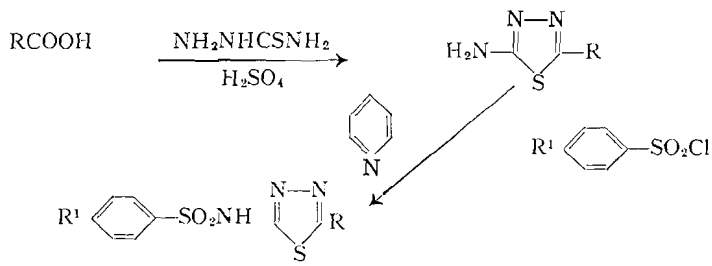

The pharmacology of these compounds will be reported elsewhere.

EXPERIMENTAL

2-Amino-5-alkyl-1,3,4-thiadiazoles (Table I)

A well-stirred mixture of 0.3 mole of fatty acid, 31.5 ml of concentrated sulphuric acid, and 0.25 mole of thiosemicarbazide was slowly heated to 80–90° and maintained at that temperature for 7 hours. After the reaction mixture was cooled, it was poured into ice water and made basic with concentrated ammonia. The crude product, which precipitated upon addition of the ammonia, was filtered and washed with water. It was recrystallized from alcohol–water.

thermocouple, B and S gauge 20, inserted through the side arm to 1/4 in. from the receiving coil. This assembly has been operated from −60° to 120° C with resolution equal to that obtained in instruments without a thermostated assembly. Figure 3 shows a trace obtained for the aldehydic proton of acetaldehyde. The resolution is at least one part in 10^8. Since the receiver coil may be tuned without disassembling the apparatus, it is used for routine investigations as well as variable temperature studies.

1. Bernstein, H. J., Schneider, W. G., and Pople, J. A. Proc. Roy. Soc. (London), A, **236**, 515 (1956).
2. Bottini, A. T. and Roberts, J. D. J. Am. Chem. Soc. **78**, 5126 (1956).
3. Gutowsky, H. S. and Holm, C. H. J. Chem. Phys. **25**, 1128 (1956).
4. Shoolery, J. N. and Roberts, J. D. Rev. Sci. Instr. **28**, 61 (1957).
5. Varian Associates, Palo Alto, California. Model V-4331A.

Received January 30, 1959.
Chemistry Department,
Cornell University,
Ithaca, New York.

Can. J. Chem. Downloaded from www.nrcresearchpress.com by 196.1.178.254 on 09/04/12
For personal use only.

SOME HYPOGLYCEMIC THIADIAZOLES

Francis L. Chubb and Jacqueline Nissenbaum

In 1942 Janbon (1) first noticed that 2-sulphanilamido-5-isopropyl-1,3,4-thiadiazole caused hypoglycemia. Bovet and Dubost (2) as well as Loubatières (3) studied the relationship between structure and activity in this series. The present work was undertaken in an effort to prepare some new hypoglycemic thiadiazoles.

A series of 2-arylsulphonamido-5-alkyl-1,3,4-thiadiazoles (Table II) was synthesized according to the following reaction scheme.

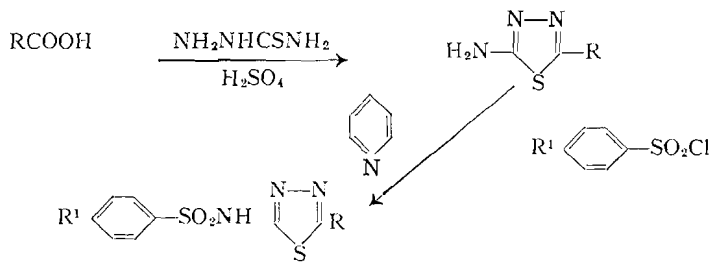

The pharmacology of these compounds will be reported elsewhere.

EXPERIMENTAL

2-Amino-5-alkyl-1,3,4-thiadiazoles (Table I)

A well-stirred mixture of 0.3 mole of fatty acid, 31.5 ml of concentrated sulphuric acid, and 0.25 mole of thiosemicarbazide was slowly heated to 80–90° and maintained at that temperature for 7 hours. After the reaction mixture was cooled, it was poured into ice water and made basic with concentrated ammonia. The crude product, which precipitated upon addition of the ammonia, was filtered and washed with water. It was recrystallized from alcohol–water.

TABLE I

2-Amino-5-alkyl-1,3,4-thiadiazoles

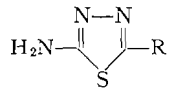

R	M.p., ° C	Yield, %	Formula	Analysis, % Calculated C	Calculated H	Found C	Found H
n-C_3H_7	203–206	80	$C_5H_9N_3S$	*a*			
iso-C_3H_7	182–185	70	$C_5H_9N_3S$	*b*			
n-C_4H_9	194–196	35	$C_6H_{11}N_3S$	*b*			
iso-C_4H_9	228–230	49	$C_6H_{11}N_3S$	*b*			
t-C_4H_9	181–184	54	$C_6H_{11}N_3S$	45.80	7.03	45.84	7.04
sec-C_4H_9	178–180	55	$C_6H_{11}N_3S$	45.80	7.03	45.71	6.82
n-C_5H_{11}	194–196	52	$C_7H_{13}N_3S$	*c*			
iso-C_5H_{11}	214–215	52	$C_7H_{13}N_3S$	49.09	7.59	48.71	7.63

[a]Ohta, M. and Higashijima, T. J. Pharm. Soc. Japan, **72**, 376 (1952).
[b]Wojan, H. and Wuckel, H. Arch. Pharm. **284**, 53 (1951).
[c]Brooks, J. D., Charlton, P. T., Macey, P. E., Peak. D. A., and Short, W. F. J. Chem. Soc. 452 (1950).

TABLE II

2-Arylsulphonamido-5-alkyl-1,3,4-thiadiazoles

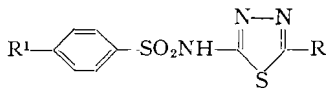

R	R^1	M.p., ° C	Yield, %	Formula	Analysis, % Calculated C	Calculated H	Found C	Found H
n-C_3H_7	CH_3	134–136	59	$C_{12}H_{15}O_2N_3S_2$	48.45	5.08	48.62	5.08
n-C_3H_7	OCH_3	125–127	65	$C_{12}H_{15}O_3N_3S_2$	45.98	4.82	46.01	4.81
n-C_3H_7	OC_2H_5	122–124	62	$C_{13}H_{17}O_3N_3S_2$	47.69	5.24	47.69	5.84
iso-C_3H_7	CH_3	119–121[a]	60	$C_{12}H_{15}O_2N_3S_2$	48.45	5.08	48.36	5.12
iso-C_3H_7	OCH_3	141–142[a]	57	$C_{12}H_{15}O_3N_3S_2$	45.98	4.82	45.96	4.64
iso-C_3H_7	OC_2H_5	128–130	65	$C_{13}H_{17}O_3N_3S_2$	47.69	5.24	47.88	5.53
n-C_4H_9	CH_3	115–116	69	$C_{13}H_{17}O_2N_3S_2$	50.13	5.50	49.89	5.75
n-C_4H_9	OCH_3	121–123	74	$C_{13}H_{17}O_3N_3S_2$	47.69	5.24	47.89	4.98
n-C_4H_9	OC_2H_5	112–113	54	$C_{14}H_{19}O_3N_3S_2$	49.25	5.61	49.49	5.74
iso-C_4H_9	CH_3	174–175	50	$C_{13}H_{17}O_2N_3S_2$	50.13	5.50	49.97	5.61
iso-C_4H_9	OCH_3	148–149	68	$C_{13}H_{17}O_3N_3S_2$	47.69	5.24	47.53	4.75
iso-C_4H_9	OC_2H_5	151–152	67	$C_{14}H_{19}O_3N_3S_2$	49.25	5.61	48.81	5.78
iso-C_4H_9	Cl	154–155	44	$C_{12}H_{14}O_2N_3S_2Cl$	43.40	4.25	43.85	4.45
t-C_4H_9	CH_3	148–150	64	$C_{13}H_{17}O_2N_3S_2$	50.13	5.50	49.95	5.68
t-C_4H_9	OCH_3	140–141	74	$C_{13}H_{17}O_3N_3S_2$	47.69	5.24	47.70	5.09
t-C_4H_9	OC_2H_5	161–162	52	$C_{14}H_{19}O_3N_3S_2$	49.25	5.61	49.22	5.52
t-C_4H_9	Cl	163–165	45	$C_{12}H_{14}O_2N_3S_2Cl$	43.40	4.25	43.30	4.48
sec-C_4H_9	CH_3	111–112	40	$C_{13}H_{17}O_2N_3S_2$	50.13	5.50	49.64	5.67
sec-C_4H_9	OCH_3	97–98	40	$C_{13}H_{17}O_3N_3S_2$	47.69	5.24	47.45	4.74
sec-C_4H_9	OC_2H_9	106–107	50	$C_{14}H_{19}O_3N_3S_2$	49.25	5.61	48.80	5.89
n-C_5H_{11}	CH_3	131–132	73	$C_{14}H_{19}O_2N_3S_2$	51.64	5.89	51.64	5.68
n-C_5H_{11}	OCH_3	133–134	65	$C_{14}H_{19}O_3N_3S_2$	49.25	5.61	48.83	5.64
n-C_5H_{11}	OC_2H_5	116–117	57	$C_{15}H_{21}O_3N_3S_2$	50.69	5.96	50.77	5.77
iso-C_5H_{11}	CH_3	140–141	73	$C_{14}H_{19}O_2N_3S_2$	51.64	5.89	51.86	5.72
iso-C_5H_{11}	OCH_3	141–142	65	$C_{14}H_{19}O_3N_3S_2$	49.25	5.61	48.91	5.78
iso-C_5H_{11}	OC_2H_5	99–100	57	$C_{15}H_{21}O_3N_3S_2$	50.69	5.96	50.62	5.89

[a]Ruschig, H., Korger, G., Aumuller, W., Wagner, H., and Weyer, R. Arzneimittel-Forsch. **8**, 448 (1958), have reported melting points for these compounds.

Can. J. Chem. Downloaded from www.nrcresearchpress.com by 196.1.178.254 on 09/04/12
For personal use only.

2-Arylsulphonamido-5-alkyl-1,3,4-thiadiazoles (*4*) (*Table II*)

A solution of 0.06 mole of the arylsulphonyl chloride in 25 ml pyridine was slowly added with stirring to a solution of 0.06 mole of 2-amino-5-alkyl-1,3,4-thiadiazole in 25 ml pyridine. The resulting solution, after being allowed to stand overnight at room temperature, was slowly added to an excess of 6 *N* hydrochloric acid. The crude product separated, usually as a solid but sometimes as a yellow gum which crystallized on standing. It was dissolved in dilute sodium hydroxide, treated with charcoal, and reprecipitated with hydrochloric acid. The 2-arylsulphonamido-5-alkyl-1,3,4-thiadiazole was recrystallized from alcohol–water.

Microanalyses were performed by Dr. Carl Tiedcke, Teaneck, N.J., U.S.A.

1. JANBON, M., CHAPTAL, J., VEDEL, A., and SCHAAP, J. Montpellier med. **21–22**, 441 (1942).
2. BOVET, D. and DUBOST, P. Compt. rend soc. biol. **138**, 764 (1944).
3. LOUBATIÈRES, A. Compt. rend. soc. biol. **138**, 830 (1944).
4. DAHLBOM, R. and EKSTRAND, T. Svensk Kem. Tidskr. **55**, 122 (1943).

RECEIVED FEBRUARY 20, 1959.
RESEARCH LABORATORIES,
FRANK W. HORNER LIMITED,
MONTREAL, QUEBEC.

NOTE ON THE PHOTOOXIDATION OF TETRAMETHYLRUBRENE*

ROBIN M. HOCHSTRASSER

Badger's group (1) first noticed that tetramethylrubrene (5,6,11,12-tetra-*p*-tolylnaphthacene) crystals change from their normal deep red to a colorless form on exposure to sunlight. This is not a widely observable phenomenon in as much as substances which are photochemically active when dissolved in a suitable solvent do not normally undergo the same reaction in the pure crystalline form. Rubrene (5,6,11,12-tetraphenylnaphthacene) was found to exhibit the same type of decoloration on exposure to ultraviolet irradiation (3), but in this case specially prepared thin films on a large area substrate were necessary. In each case the product is a transannular peroxide.

It is the purpose of this note to report the results of some experiments on the photooxidation of tetramethylrubrene crystals. The experiments were done at 25° C in cells with plane quartz windows. The light source was a 1-kw AH6 water-cooled mercury arc. The apparatus was as previously described by Hochstrasser and Ritchie (3), and differential pressure measurements could be made to within 0.002 mm Hg at total pressures below 25 mm Hg. The oxidation was followed by noting the changes of oxygen pressure in a constant volume system as the crystals were illuminated with near monochromatic light. The small crystals were scratched on to the surface of a quartz disk (in the absence of absorbable light) and the disk was then carefully sealed on to one end of a cylindrical cell. The cell was then evacuated, oxygen allowed in to a known pressure in the dark, and when stability was maintained the crystals were illuminated and the decrease in pressure determined as a function of time. Experiments involving intermittent illumination and irradiation with light at two wavelengths were performed.

**This research was part of a program supported by a grant from the National Research Council of Canada.*

Can. J. Chem. Downloaded from www.nrcresearchpress.com by 196.1.178.254 on 09/04/12
For personal use only.

2-Arylsulphonamido-5-alkyl-1,3,4-thiadiazoles (*4*) (*Table II*)

A solution of 0.06 mole of the arylsulphonyl chloride in 25 ml pyridine was slowly added with stirring to a solution of 0.06 mole of 2-amino-5-alkyl-1,3,4-thiadiazole in 25 ml pyridine. The resulting solution, after being allowed to stand overnight at room temperature, was slowly added to an excess of 6 *N* hydrochloric acid. The crude product separated, usually as a solid but sometimes as a yellow gum which crystallized on standing. It was dissolved in dilute sodium hydroxide, treated with charcoal, and reprecipitated with hydrochloric acid. The 2-arylsulphonamido-5-alkyl-1,3,4-thiadiazole was recrystallized from alcohol–water.

Microanalyses were performed by Dr. Carl Tiedcke, Teaneck, N.J., U.S.A.

1. JANBON, M., CHAPTAL, J., VEDEL, A., and SCHAAP, J. Montpellier med. **21–22**, 441 (1942).
2. BOVET, D. and DUBOST, P. Compt. rend soc. biol. **138**, 764 (1944).
3. LOUBATIÈRES, A. Compt. rend. soc. biol. **138**, 830 (1944).
4. DAHLBOM, R. and EKSTRAND, T. Svensk Kem. Tidskr. **55**, 122 (1943).

RECEIVED FEBRUARY 20, 1959.
RESEARCH LABORATORIES,
FRANK W. HORNER LIMITED,
MONTREAL, QUEBEC.

NOTE ON THE PHOTOOXIDATION OF TETRAMETHYLRUBRENE*

ROBIN M. HOCHSTRASSER

Badger's group (1) first noticed that tetramethylrubrene (5,6,11,12-tetra-*p*-tolylnaphthacene) crystals change from their normal deep red to a colorless form on exposure to sunlight. This is not a widely observable phenomenon in as much as substances which are photochemically active when dissolved in a suitable solvent do not normally undergo the same reaction in the pure crystalline form. Rubrene (5,6,11,12-tetraphenylnaphthacene) was found to exhibit the same type of decoloration on exposure to ultraviolet irradiation (3), but in this case specially prepared thin films on a large area substrate were necessary. In each case the product is a transannular peroxide.

It is the purpose of this note to report the results of some experiments on the photooxidation of tetramethylrubrene crystals. The experiments were done at 25° C in cells with plane quartz windows. The light source was a 1-kw AH6 water-cooled mercury arc. The apparatus was as previously described by Hochstrasser and Ritchie (3), and differential pressure measurements could be made to within 0.002 mm Hg at total pressures below 25 mm Hg. The oxidation was followed by noting the changes of oxygen pressure in a constant volume system as the crystals were illuminated with near monochromatic light. The small crystals were scratched on to the surface of a quartz disk (in the absence of absorbable light) and the disk was then carefully sealed on to one end of a cylindrical cell. The cell was then evacuated, oxygen allowed in to a known pressure in the dark, and when stability was maintained the crystals were illuminated and the decrease in pressure determined as a function of time. Experiments involving intermittent illumination and irradiation with light at two wavelengths were performed.

**This research was part of a program supported by a grant from the National Research Council of Canada.*

Can. J. Chem. Downloaded from www.nrcresearchpress.com by 196.1.178.254 on 09/04/12
For personal use only.

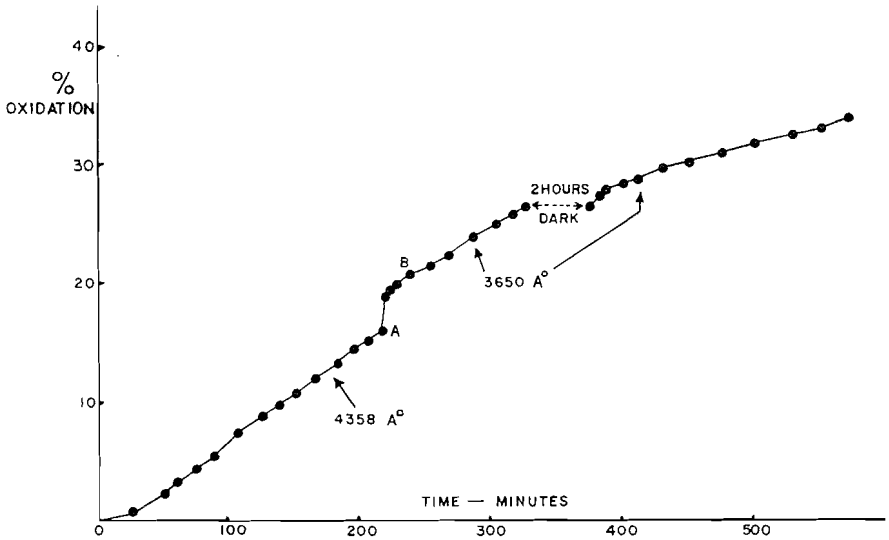

FIG. 1. Photooxidation of tetramethylrubrene crystals (10^{-6} mole of crystal; quanta at 3650 Å approximately double 4358 Å; O_2 pressure 25 mm).

A typical result is shown on Fig. 1 where the extent of the oxidation is plotted against time of irradiation. At A the illumination was discontinued and the crystals left in contact with oxygen for 30 minutes, then reirradiated. The magnitude of the increased rate from A to B was a function of the time of dark contact with oxygen. These results indicate that the photooxidation of tetramethylrubrene is diffusion-controlled. The effects observed when the intensity or the wavelength of the exciting light was changed were again indicative of a diffusional rate-determining step. The absolute rates of oxidation were not reproducible with different crystalline deposits, but the initial rate constants were all of the order of 10^{-10} mole second^{-1} and the quantum yields were approximately 10^{-4} depending on the oxygen pressure. The peroxide is in thermal equilibrium with oxygen but the dissociation is occurring at a negligible rate at this temperature.

Such a system is interesting in as much as not many similar cases are known and certainly not in relation to the combination of molecular oxygen with an aromatic hydrocarbon. As has already been pointed out, crystals of rubrene do not oxidize at a measurable rate even in an atmosphere of oxygen. During the formation of the transannular peroxide a drastic structural change must occur as shown in Fig. 2. Microscopic examination of partly oxidized crystals shows that the oxidation is occurring at the crystal surface.

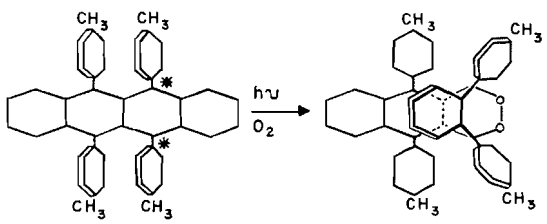

FIG. 2. Schematic representation of the photooxidation of tetramethylrubrene.

Can. J. Chem. Downloaded from www.nrcresearchpress.com by 196.1.178.254 on 09/04/12
For personal use only.

It is reasonably well established that oxidations of this type occur via the triplet state of the molecule attained after intersystem-crossing from the first excited singlet state (4). In a molecular crystal intersystem-crossing will manifest itself as localization of excitation energy within the crystal. This arises from the theory of molecular crystals (2) which shows that the singlet levels of the isolated molecule will be split in the crystal into a broad band ($\sim 3000\ cm^{-1}$), while the triplet splitting will be very small by virtue of the fact that the transition moment integral between the ground singlet and first triplet is negligibly small. In order that the reaction with oxygen can occur, this energy must be transported to the surface of the crystal, where there is an oxygen molecule available. It is the availability of oxygen which is the limiting factor in this case. To accomplish photooxidation, the oxygen must first traverse the peroxide layer. Here the rate of diffusion is measurable, and the observation of a diffusion-controlling step suggests that one reason why other aromatic hydrocarbons containing the basic anthracenic structure do not apparently react with oxygen to any great extent is the imperviousness of the peroxide layer to oxygen. With a bulky molecule such as tetramethylrubrene or even rubrene under special conditions this layer becomes permeable. The discovery of an effect such as this opens up a wide field which should yield much information regarding the transport of electronic excitation energy in molecular crystals. In the near future it is proposed to commence a detailed rotating sector and intensity study of the photooxidation of tetramethylrubrene single crystals.

The author expresses his thanks to Professor G. M. Badger for a sample of tetramethylrubrene.

1. Badger, G. M., Pierce, R. S., Rhodda, H. J., and Walker, I. S. J. Chem. Soc. 3151 (1954).
2. Davydov, A. S. J. Exptl. Theoret. Phys. (U.S.S.R.), **18**, 210 (1948).
3. Hochstrasser, R. M. and Ritchie, M. Trans. Faraday Soc. **52**, 1363 (1956).
4. Reid, C. Quart. Rev. **12**, 224 (1958).

Received March 16, 1959.
Department of Chemistry,
The University of British Columbia,
Vancouver, B.C.

Can. J. Chem. Downloaded from www.nrcresearchpress.com by 196.1.178.254 on 09/04/12
For personal use only.

Can. J. Chem. Downloaded from www.nrcresearchpress.com by 196.1.178.254 on 09/04/12
For personal use only.

Canadian Journal of Chemistry

Issued by THE NATIONAL RESEARCH COUNCIL OF CANADA

VOLUME 37 JULY 1959 NUMBER 7

STUDY OF THE RADIOLYSIS OF BROMAL HYDRATE SOLUTIONS USING C^{14}-LABELLED BROMAL[1]

H. HEUSINGER, R. J. WOODS, AND J. W. T. SPINKS

ABSTRACT

Bromal labelled with C^{14} in the carbonyl group has been used to show that small amounts of carbon dioxide and carboxylic acids are produced in the radiolysis of aqueous bromal solutions. *G* values for the production of CO_2 and carboxylic acid are about 7.5% and 15% of those for HBr production, respectively. The observed yield of carboxylic acid is in agreement with that found by titration.

INTRODUCTION

The decomposition of aqueous bromal hydrate solutions by cobalt-60 gamma rays has already been studied with special reference to the formation of hydrogen bromide (1). Some of the major products of the radiolysis were determined, but it proved difficult to separate those products which were formed in smaller amounts and the quantitative determination of these was not attempted. This suggested the use of labelled bromal, which would facilitate the separation of products using carrier techniques. The determination of the relative activities would give directly the ratio of the products formed.

EXPERIMENTAL

Preparation of C^{14}-Labelled Bromal Hydrate

1-C^{14}-Ethanol[2] (0.1 mc) diluted with 4 g inactive ethanol was oxidized with hot, aqueous dichromate solution (2) and the acetaldehyde produced collected in a bulb cooled in a solid carbon dioxide – methanol bath. The bulb was removed from the cooling bath and equipped with an efficient reflux condenser, through which a drop of dilute sulphuric acid was added. The acetaldehyde became hot and polymerized. The polymer was brominated (3), and the products separated by fractional distillation under reduced pressure. The bromal fraction, b.p. 85–87° C/38 mm, was dissolved in 10 ml acetone, and 3 ml water added. Bromal hydrate (5.5 g, 9×10^3 disintegrations/min mg), m.p. 53.5° C, crystallized as the acetone evaporated. An additional small quantity of bromal was obtained by brominating the low boiling fractions further.

Irradiation of Bromal Hydrate Solutions

Solutions (2 or 3 ml) were irradiated in glass test tubes equipped with gas inlet and outlet tubes and supported in lucite blocks arranged concentrically about a 90-curie Co^{60} source, permitting dose rates of up to 1510 roentgens per minute. Dose rates were measured by determining the ferric ion formed when solutions of ferrous ammonium sulphate were irradiated (4), assuming a *G* value of 15.5 for the formation of ferric ions and a conversion factor of 1 r = 0.975 rad (5).

[1]*Manuscript received January 19, 1959.*
Contribution from the Department of Chemistry, University of Saskatchewan, Saskatoon, Saskatchewan.
[2]*Merck and Co., Montreal, Quebec.*

Gaseous and volatile products were removed by passing a stream of oxygen or hydrogen through the solution either during the irradiation or afterwards. Carbon dioxide was subsequently absorbed from the gas stream by sodium hydroxide solution. In one experiment the oxygen leaving the irradiation tube was passed through a heated platinum catalyst, to oxidize volatile organic compounds to carbon dioxide, before being passed through the sodium hydroxide solution.

Hydrobromic acid and the "total acid" were determined in irradiated solutions of inactive bromal hydrate by titration with silver nitrate solution (eosin) and sodium hydroxide solution (bromophenol blue), respectively.

Counting

In order to get directly comparable values for the radioactivity present in the starting material and the products, all were counted as barium carbonate. The carbonate was counted in a gas-flow proportional counter as infinitely thick samples.

Bromal hydrate, and products other than carbon dioxide, were oxidized to carbon dioxide by warming with an aqueous solution of potassium persulphate containing silver nitrate as a catalyst (6). The carbon dioxide was absorbed in sodium hydroxide solution, carrier sodium carbonate added, and a solution containing ammonium and barium chlorides added to precipitate barium carbonate.

Determination of Carboxylic Acids Formed by Irradiation

To 2 ml of irradiated bromal hydrate solution were added 50 mg inactive bromal hydrate and 40 mg glacial acetic acid, and the solution stirred with 2 g barium carbonate. The neutral solution was filtered, extracted with ether, acidified, and again extracted with ether. Acidic materials were extracted from the ethereal solution with dilute sodium hydroxide solution, a stream of air passed through the alkaline extract to remove dissolved ether, and the organic acids oxidized with persulphate as described above.

RESULTS

The amount of carbon dioxide formed was plotted against the dose of radiation received, as shown in Fig. 1, and the slope of the line measured. Results obtained in this manner,

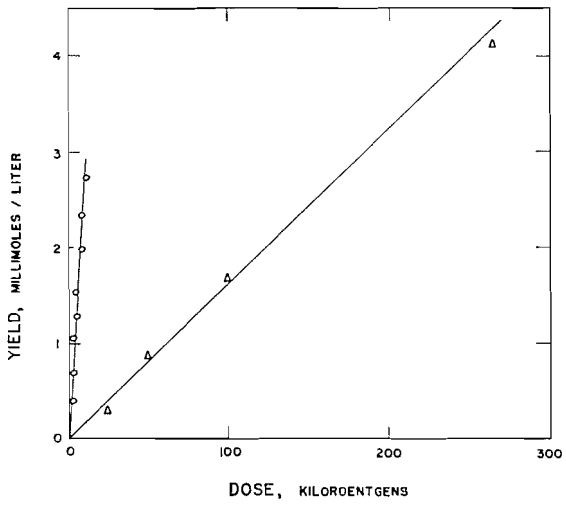

FIG. 1. Production of hydrobromic acid and carbon dioxide on irradiation of 0.2 molar bromal hydrate solution. Dose rate, 216 r/min; ○, HBr; △, CO_2.

3007617

Can. J. Chem. Downloaded from www.nrcresearchpress.com by 196.1.178.254 on 09/04/12
For personal use only.

expressed as G values (1), are given in Table I. Yields of hydrobromic acid, determined by titration are given for comparison. In one experiment the gases from the irradiated solution were passed over a catalyst with oxygen; since this did not increase the yield of carbon dioxide it was assumed that carbon monoxide and other volatile compounds containing the aldehyde–carbon from bromal were absent.

Table II gives yields of hydrobromic acid and the total acid which were determined by titration of irradiated solutions of inactive bromal hydrate. The ratio $G_{\text{total acid}}/G_{\text{HBr}}$ appears to be constant with a value of about 1.16, and to be independent of concentration of bromal hydrate, dose rate, and the presence or absence of oxygen (the "oxygen-depleted" solutions in Table II contained only the oxygen diffusing into the solution from the air above it, oxygen originally present having been used up), although all of these factors have a considerable effect upon the yield of acid. The ratio of $G_{\text{HBr+carboxylic acid}}/G_{\text{HBr}}$ found using labelled bromal (1.15 cf. Table I) agrees well.

TABLE I

Radiolysis products from 0.2 molar aqueous bromal solutions

Gas-saturating soln. during irradiation	Dose rate (r/min)	G_{HBr}	G_{CO_2}	$G_{\text{carboxylic acid}}$	$(G_{\text{CO}_2}/G_{\text{HBr}})\times 100$
Oxygen	216	245	16.2	—	6.6
Oxygen	460	160	12.6	—	7.9
Oxygen	1510	96	7.2	—	7.5
Hydrogen	1510	17.5	0.44	—	2.5
Air (depleted in O_2 during latter stages of irradiation)	460	33.5*	3.5*, †	5.0*	10.4

* Values determined after a single dose of about 100 kr.

† Not changed by oxidation of exit gases.

TABLE II

Hydrobromic acid and total acid produced by radiolysis of aqueous bromal hydrate solutions

Gas-saturating soln. during irradiation	Dose rate (r/min)	Molarity	G_{HBr}	$G_{\text{total acid}}$	$G_{\text{total acid}}/G_{\text{HBr}}$
Oxygen	20	2.0	985	1070	1.09
Oxygen	23.5	2.0	915	1070	1.17
Air (excess O_2 present)	10	0.15	565	625	1.11
Air (excess O_2 present)	19	0.1	375	455	1.21
Air (excess O_2 present)	1100	0.1	69.5	82	1.18
Air (O_2-depleted)	10	0.15	94	100	1.06
Air (O_2-depleted)	19	0.1	121	138	1.14
Air (O_2-depleted)	1100	0.1	14	18	1.29

DISCUSSION

It has already been shown (1) that the radiolysis of aerated, aqueous solutions of bromal hydrate gives hydrobromic acid in such amounts that a chain reaction, initiated by the primary radicals produced by the radiation–water interaction, must be postulated to account for it. Dibromoacetaldehyde, together with a smaller quantity of dibromoacetic acid, was also found among the products of the reaction, although the yields of each could only be estimated approximately. Oxygen was found to be necessary for the highest yields of hydrobromic acid, and was used up during the reaction. The yield fell markedly if the oxygen present in solution was used up or was displaced with nitrogen. About one mole of oxygen was used up for every 3 or 4 moles of hydrobromic acid produced.

Can. J. Chem. Downloaded from www.nrcresearchpress.com by 196.1.178.254 on 09/04/12
For personal use only.

Both the mechanism of the chain reaction and the fate of the oxygen which is consumed are uncertain. The present study was initiated to examine the possibility that carbon–carbon bond fission was a step in the chain reaction that would account for the uptake of oxygen.

Probable chain-initiating reactions between the primary radicals and bromal hydrate are:

$$R\cdot + Br_3C.CH(OH)_2 \rightarrow RBr + Br_2\dot{C}.CH(OH)_2, \quad [1]$$

$$\rightarrow RH + Br_3C.\dot{C}(OH)_2, \quad [2]$$

$$\rightarrow ROH + Br_3C.\dot{C}H(OH), \quad [3]$$

where R· is a hydrogen atom or a hydroxyl radical. Oxygen, if present, could react with the organic radicals to give peroxy radicals which, since stable peroxides have not been detected after irradiation, must subsequently break down. The peroxy radical from reaction [1] would probably break down, the over-all reaction being represented by,

$$Br_2C.CH(OH)_2 + O_2 \rightarrow 2HBr + 2CO_2 + HO_2\cdot. \quad [4]$$
$$\dot{O}_2$$

In this case both carbon atoms appear as carbon dioxide. Peroxy radicals from reactions [2] and [3] would be liable to break down to give the relatively stable tribromomethyl radical, $Br_3C\cdot$, carbon dioxide from the carbonyl carbon atom, and either hydrogen peroxide or water.

Since the amount of carbon dioxide found is only about 7% of the amount of hydrobromic acid it is evident that the fission reactions suggested above, although they may account for the carbon dioxide produced and for part of the oxygen consumed, are not steps in the chain reaction. Furthermore, the carbon dioxide/hydrobromic acid ratio does not vary with dose rate as would be expected if the carbon dioxide were formed in a chain-stopping step; the yield of hydrobromic acid is inversely proportional to the square root of the dose rate (1). Thus, carbon dioxide must be formed by a side reaction which is not part of the chain reaction producing hydrobromic acid. The lower yield of carbon dioxide in the absence of oxygen is in line with the reactions suggested above.

The yield of carboxylic acid also bears a constant ratio to the amount of hydrobromic acid formed and is independent of dose rate, but the yield of acid is too small for it to be formed directly during the chain reaction. The ratio is the same in the presence or absence of oxygen and the acid may result from rearrangement of a proportion of the radicals concerned in the chain reaction. The only carboxylic acid isolated was dibromoacetic acid, suggesting that the rearrangement might be,

$$Br_3C.\dot{C}(OH)_2 \rightarrow Br_2\dot{C}.CBr(OH)_2, \quad [5]$$

followed by removal of hydrogen from a solvent or solute molecule and hydrolysis of the acid bromide. The rearrangement of a number of radicals with the migration of a hydrogen atom has been discussed by Semenov (7), and instances in which a chlorine atom migrates have been given by Wiley (8) and Nesmeyanov (9), the examples given by the latter author involving migration of a chlorine atom from a trichloromethyl group to the adjacent carbon atom. Rearrangement to more stable structures of the organic radicals concerned in the radiolysis of bromal should be favored by the relatively long mean lifetime of the radical chains, about 0.1 to 1 second (10).

Can. J. Chem. Downloaded from www.nrcresearchpress.com by 196.1.178.254 on 09/04/12
For personal use only.

ACKNOWLEDGMENTS

We are grateful to the National Research Council and to the Atomic Energy Control Board for financial support. One of us (H.H.) held a W.U.S.C. Fellowship.

REFERENCES

1. WOODS, R. J. and SPINKS, J. W. T. Can. J. Chem. **35**, 1475 (1957).
2. WERTHEIM, E. J. Am. Chem. Soc. **44**, 2658 (1922).
3. LONG, F. A. and HOWARD, J. W. Org. Syntheses, **17**, 18 (1937).
4. WEISS, J., ALLEN, A. O., and SCHWARZ, H. A. Intern. Conf. on Peaceful Uses of Atomic Energy, **14**, 179 (1956).
5. GRAY, L. H. Brit. J. Radiol. **29**, 355 (1956).
6. CALVIN, M. Isotopic carbon. John Wiley & Sons, Inc., New York. 1949. p. 94.
7. SEMENOV, N. N. Some problems in chemical kinetics and reactivity. Princeton Univ. Press, Princeton, N.J. 1958. p. 68.
8. WILEY, R. H., JARBOE, C. H., HARRELL, J. R., and PARISH, D. J. Proc. Chem. Soc. 347 (1957).
9. NESMEYANOV, A. N., FREIDLINA, R. KH., and KOST, V. N. Doklady Akad. Nauk S.S.S.R. **113**, 828 (1957). NESMEYANOV, A. N., FREIDLINA, R. KH., and ZAKHARKIN, L. I. Doklady Akad. Nauk S.S.S.R. **81**, 199 (1955); Quart. Revs. **10**, 343 (1956).
10. PLATFORD, R. and SPINKS, J. W. T. Can. J. Chem. **37**, 1022 (1959).

Can. J. Chem. Downloaded from www.nrcresearchpress.com by 196.1.178.254 on 09/04/12
For personal use only.

Can. J. Chem. Downloaded from www.nrcresearchpress.com by 196.1.178.254 on 09/04/12
For personal use only.

THE CONFORMATIONS OF THE DIASTEREOMERIC 2,5-DIMETHYL-2,5-DIMETHOXY-3,4-DIPHENYLHEXANES[1]

HENRY SAWATZKY, GEORGE K. WHITE, AND GEORGE F WRIGHT

ABSTRACT

The electric dipole moments of six possible rotamers comprising the two diastereomeric forms of 2,5-dimethyl-2,5-dimethoxy-3,4-diphenylhexane have been calculated vectorially. Comparison of these values with the experimental determination of polarization in benzene and carbon tetrachloride shows that only two of the rotamers of the *dd,ll* form and only one of the *meso* form are present in significant amount. The moment of the *dd,ll* diastereomer decreases with increasing temperature but that of the *meso* form is almost invariant. It is probable that all six central linkages in these diastereomers are hindered from free rotation.

The two diastereomers (I*a* and I*b*) of 2,5-dimethyl-2,5-dimethoxy-3,4-diphenylhexane may be obtained by homopolar reduction of 1-chloromercuri-1-phenyl-2-methoxy-2-methylpropane (1). One of these diastereomers (I*a*) was reported (1) as a non-crystallizable oil, but we have now succeeded, after chromatographic removal of impurities, in the isolation of I*a*, as a low-melting solid.

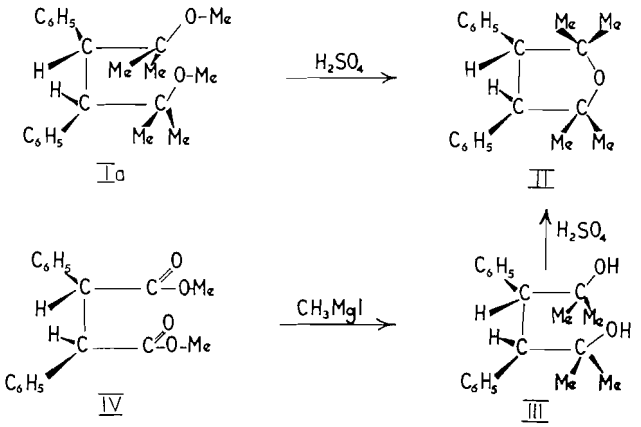

Ia II IV III

The configuration of I*a* has been established (2) by its conversion in concentrated sulphuric acid to the related diastereomer of 2,2,5,5-tetramethyl-3,4-diphenyltetrahydrofuran, II. The configuration of this cyclic ether was established as *dd,ll* because it could be prepared from the diol III, which was obtained from methyl Grignard reagent and *dd,ll*-dimethyl-2,3-diphenylsuccinate, IV (3).

As might be expected in view of the steric convenience in conversion of I*a* or III to II, the other diastereomeric (*meso*) 2,5-dimethyl-2,5-dimethoxy-3,4-diphenylhexane, I*b*, does not form a cyclic ether, V, with ease. It does undergo condensations of the Friedel–Crafts type so that the methoxyisopropyl group on one of the central ("pivot") carbon atoms reacts with the ortho position of a phenyl group on the other "pivot" atom to form 5,5,10,10-tetramethyl-4*b*,5,9*b*,10-tetrahydroindeno[2,1-*a*]indene, VI.

The difference in types of reaction and products formed from I*a* and I*b* would suggest a strong steric influence. Moreover, the specific reactivity with respect to condensing agents (1, 2) shows that the geometry of the diastereomers must be important. For

[1]*Manuscript received January 20, 1959.*
Contribution from the Department of Chemistry, University of Toronto, Toronto, Ontario, Canada.

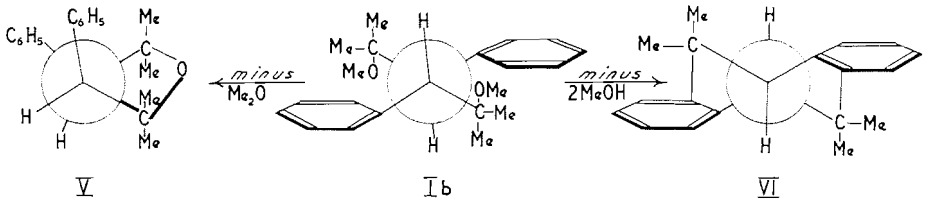

V Ib VI

these reasons we have determined the electric moments of I*a* and I*b* in two solvents and at various temperatures.

The geometry of these diastereomers may be expressed roughly by the rotameric forms (4) in which each would exist if there were restriction toward rotation at the pivot bond. Each diastereomer may be shown as three rotamers which for I*a* are A, B, and C. The three rotamers of the *meso* diastereomer, I*b*, are shown as E, F, and G,

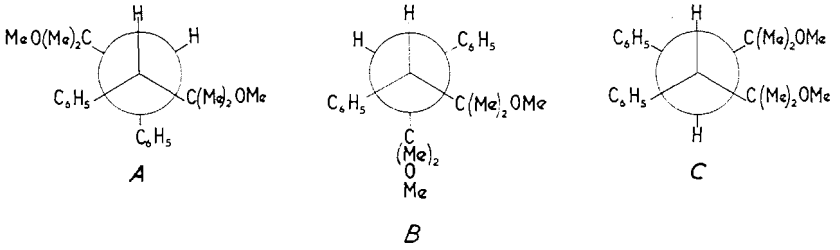

A B C

although it should be noted that F and G are enantiomerically different but geometrically identical. Thus F and G represent one *meso* rotamer while E represents the other.

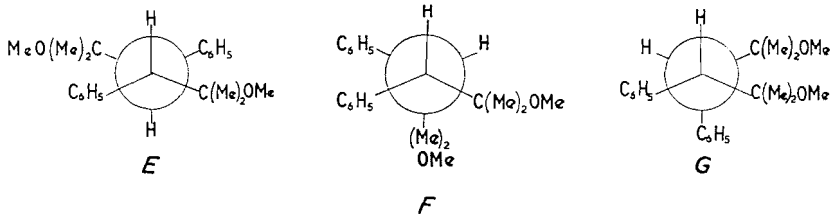

E F G

One realizes that none of these rotamers would have an electric moment equal to zero (even E) because of rotational motion at the isopropylidene and the oxygen linkages. Therefore it is necessary to know the expected moments for different extents of fixity at these linkages before a comparison can be made with experiment. For this purpose we have symbolized the structure of I*a*–I*b* in Fig. 1. In this diagram the carbons are

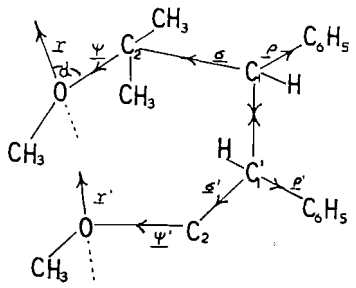

FIG. 1.

Can. J. Chem. Downloaded from www.nrcresearchpress.com by 196.1.178.254 on 09/04/12
For personal use only.

taken as tetrahedral (109°28′) while the oxygen angles are assumed to be 108°. The moment (b) of the phenyl group is chosen as 0.37 Debye while that (a) of the methoxy group is 1.31 D (the observed moment of dimethyl ether). If the unit vectors are defined as shown, σ, ϱ, ψ, τ, σ', ϱ', ψ', and τ', the resultant moments of these vectors (assuming hydrogen compensation) for each rotamer are $a\tau+a\tau'+b\varrho+b\varrho'$.

FREE ROTATION ONLY ABOUT THE ETHER LINKAGE

We shall first consider certain fixed positions for σ, ϱ, ψ, σ', ϱ', ψ' while τ and τ' are rotating freely. In this circumstance (5)

$$[1] \quad \mu^2 = a^2[1+1+2\cos^2 54°\,(\psi.\psi')]+ b^2[1+1+2\varrho.\varrho']+2ab[+\cos 54°\,(\psi\varrho+\psi\varrho')+\cos 54°\,(\psi\varrho'+\psi'\varrho)]$$
$$= 3.706+1.186\psi.\psi'+0.274\varrho.\varrho'+0.570\,(\psi+\psi').(\varrho+\varrho').$$

It is convenient to align Fig. 1 so that "the ethane pivot bond" is parallel (001) to the Z-axis. Now, since the cosine of the angle between Z and ϱ is $+1/3$, ϱ may be written:

$$[2] \quad \varrho = \sqrt{8/9}\cos\phi, \sqrt{8/9}\sin\phi, 1/3 \text{ (as shown in Fig. 2),}$$

similarly

$$\sigma = \sqrt{8/9}\cos\theta, \sqrt{8/9}\sin\theta, 1/3$$

where θ and ϕ represent the polar angles in the plane of projection.

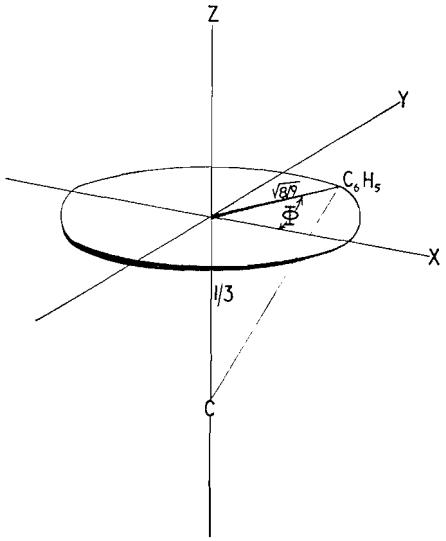

FIG. 2.

Also since $\varrho.\sigma = -1/3$, then $\theta-\phi = \pm 120°$.

We thus need specify only the X-axis in order to get ϱ and σ. This X-axis is best chosen for each isomer according to the symmetry of that particular isomer.

In order to co-ordinatize ψ, it is easiest to take ψ relative to σ in the same manner in which we took σ and ϱ relative to Z.

Since the cosine of the angle between σ and ψ is $-1/3$, ψ may be written as

$$\psi = \sqrt{8/9}\cos\beta\mathbf{k}+\sqrt{8/9}\sin\beta\mathbf{l}+1/3\sigma \text{ (see Fig. 3)}$$

Can. J. Chem. Downloaded from www.nrcresearchpress.com by 196.1.178.254 on 09/04/12
For personal use only.

where $\mathbf{kl}\mathfrak{d}$ form a right-handed triad of unit vectors. Thus $\sqrt{8/9}\cos\beta$ is the projection of ψ on the $\mathbf{k}$-vector of Fig. 3.

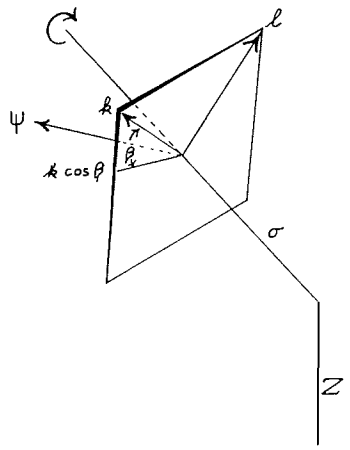

FIG. 3.

Once a particular $\mathbf{l}$ is chosen perpendicular to $\mathfrak{d}$, $\mathbf{k}$ is then fixed and ψ depends only on β. The variation in β corresponds to the rotation of ψ about $\mathfrak{d}$.

Any $\mathbf{l}$ perpendicular to $\mathfrak{d}$ may be chosen, but the following choice simplifies the calculation:

$$\mathbf{l} = (\sin\theta,\ -\cos\theta,\ 0),$$

whence

$$\mathbf{k} = (1/3\cos\theta,\ 1/3\sin\theta,\ -\sqrt{8/9}),$$

i.e. $\mathbf{k}$ is in the (Z, σ) plane, $\mathbf{l}$ is in the (X, Y) plane. Then, as above, if

$$\psi = 1/3\mathfrak{d}+c_2\mathbf{k}+c_3\mathbf{l},$$

substituting,

[3] $$\psi = 1/3\sqrt{8/9}\cos\theta\,(1+\cos\beta)+\sqrt{8/9}\sin\theta\sin\beta,\ 1/3\sqrt{8/9}\sin\theta\,(1+\cos\beta) -\sqrt{8/9}\cos\theta\sin\beta,\ 1/9-8/9\cos\beta.$$

A similar derivation can be made for ψ', or it may be determined intuitively from the symmetry of the molecule about its central bond.

Now the moment of each of the rotamers A–G inclusive may be calculated from ψ and ϱ obtained from equations [2] and [3] after the values for $\psi\cdot\psi'$, $\varrho\cdot\varrho'$, and $(\psi+\psi')\cdot(\varrho+\varrho')$ are determined from the geometry of each rotamer; the moment $(\sqrt{\mu^2})$ may then be determined by substitution into equation [1].

Rotamer A

Reference to the graphic formulation of the A rotamer of the *dd,ll* diastereomer shows the relationship where θ refers to the bonding of the methoxyisopropyl group and ϕ refers to the bonding of the phenyl group. Now for the two central carbon atoms, $A'(x, y, z) = A(-x, y, -z)$, i.e. symmetry about the Y-axis.

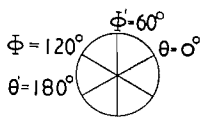

Can. J. Chem. Downloaded from www.nrcresearchpress.com by 196.1.178.254 on 09/04/12
For personal use only.

Then

$$\varrho \cdot \varrho' = -\rho_x^2+\rho_y^2-\rho_z^2(+\rho_y^2-\rho_y^2) = 2\rho_y^2-1,$$

and A,A' refers to all corresponding fixed linkages, in particular ϱ and δ. Similarly

$$\psi \cdot \psi' = 2\psi_y^2-1.$$

So

$$(\varrho+\varrho') \cdot (\psi+\psi') = 4\rho_y\psi_y = -16/9\sqrt{3} \sin \beta$$

since

$$\varrho_y = \sqrt{8/9} \sin \phi = \sqrt{8/9}\sqrt{3/2}$$

and

$$\psi_y = 1/3\sqrt{8/9} \sin \theta (1+\cos \beta)-\sqrt{8/9} \sin \beta \cos \theta = -\sqrt{8/9} \sin \beta,$$

whence

$$\mu^2 = 3.706+1.186(16/9 \sin^2 \beta-1)+(0.274/3)+0.570(-)(16\sqrt{3} \sin \beta/9).$$

Then

$$d\mu^2/d\beta = 0 = \cos \beta (4.216 \sin \beta-1.755).$$

The maximum for μ is then determined as 2.54 D ($\mu^2 = 6.474$) when $\sin \beta = -1$ ($\beta = 270°$, $\cos \beta = 0$), of course with a smaller maximum when $\beta = 90°$ ($\sin \beta = 1$, $\mu^2 = 2.964$). The minimum for μ at $\sin \beta = 1.755/4.216$ ($\beta = 24°36'$ or $155°24'$) is then 1.50 D since $\mu^2 = 2.246$.

Rotamer B

In like manner rotamer B may be evaluated since it differs from rotamer A only in the sense that

$$\varrho_y = \sqrt{8/9} \sin \phi = 0.$$

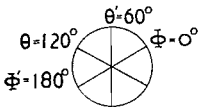

Rotamer C

Symmetrical about X-axis, i.e. $A'(x', y', z') = A(x, -y, -z)$.

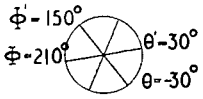

$$\varrho_x = -\sqrt{8/9}.\sqrt{3}/2$$
$$\psi_x = 1/3\sqrt{8/9}.\sqrt{3}/2(1+\cos \beta-\sqrt{3} \sin \beta)$$

Rotamer E

This rotamer, one conformation of the *meso* diastereomer, will be shown to have a moment that is independent of the angle β. Inspection shows that the z co-ordinate of A' = minus the z co-ordinate of A, that is $A'(x', y', z') = A(-x, -y, -z)$.

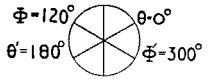

Can. J. Chem. Downloaded from www.nrcresearchpress.com by 196.1.178.254 on 09/04/12
For personal use only.

Can. J. Chem. Downloaded from www.nrcresearchpress.com by 196.1.178.254 on 09/04/12
For personal use only.

So

$$\psi' = -\psi,$$
$$\varrho.\varrho' = -1,$$
$$\psi.\psi' = -1,$$

and

$$(\psi+\psi')(\varrho+\varrho') = 0.$$

Then

$$\mu^2 = 3.706+1.186(-)+0.274(-) = 2.246.$$

Rotamers F and G

The other rotamers of the *meso* isomer are the enantiomorphous F and G in which $A'(\theta', z) = A(\theta+60, -z)$.

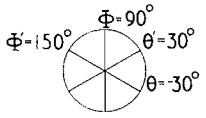

Then

$$\varrho = (\sqrt{8/9}\cos\phi,\ \sqrt{8/9}\sin\phi,\ 1/3)$$
$$\varrho' = \sqrt{8/9}\cos\phi',\ \sqrt{8/9}\sin\phi',\ -1/3$$

and

$$\psi = 1/3\sqrt{8/9}\cos\theta\,(1+\cos\beta)+\sqrt{8/9}\sin\theta\sin\beta,$$
$$1/3\sqrt{8/9}\sin\theta\,(1+\cos\beta)-\sqrt{8/9}\cos\theta\sin\beta, 1/9-8/9\cos\beta.$$

Since

$$\psi = \psi(-30, z) \text{ and } \psi' = \psi(30, -z),$$
$$\psi' = [\sqrt{3}/6\sqrt{8/9}(1+\cos\beta)+1/2\sqrt{8/9}\sin\beta,\ 1/6\sqrt{8/9}(1+\cos\beta)-\sqrt{3}/2\sin\beta,$$
$$-1/9+8/9\cos\beta]$$

so

$$\varrho+\varrho' = -\sqrt{3}/2\sqrt{8/9},\ 3/2\sqrt{8/9},\ 0$$

and

$$\psi+\psi' = \sqrt{3}\sqrt{8/9}\,[1/3(1+\cos\beta),\ -\sin\beta,\ 0]$$
$$\psi.\psi' = 1/27(13+8\cos\beta-32\cos^2\beta)$$
$$\varrho.\varrho' = 1/3.$$

Then

$$d\mu^2/d\beta = 0.098\sin\beta+2.812\cos\beta\sin\beta-1.316\cos\beta = 0$$
$$\sin\beta = 0.468+0.035\tan\beta,$$

whence $\beta = 29°12'$ or $86°18'$ as well as $153°12'$ or $271°24'$ and the maxima and minima may be chosen from these values.

TABLE I

Rotamer moments where all bonds are fixed except the ether linkages

	dd,ll			*meso*	
Rotamer	A	B	C	E	F, G
Angle β for min., μ	24°36′ or 155°24′	180° or 300°	14°14′ or 222°46′	Independent	153°12′
μ, min., Debye	1.50	1.50	1.50	1.50	1.52
Angle β for max., μ	270° or 90°	60°	120°	Independent	271°24′
μ, max., Debye	2.54	1.96	1.81	1.50	2.33

Can. J. Chem. Downloaded from www.nrcresearchpress.com by 196.1.178.254 on 09/04/12
For personal use only.

FREE ROTATION ABOUT ALL BONDS EXCEPT THE PIVOT BOND

In this condition ψ and ψ' (Fig. 1) are presumed to rotate as freely as τ and τ'. Then,

$$\mu^2 = a^2(1+1+2\cos^2(180-\alpha)\cos^2(180-C)(\mathfrak{o}.\mathfrak{o}')+b^2(1+1+2\varrho.\varrho') +2ab[\cos(180-\alpha)\cos(180-C)(\mathfrak{o}.\varrho+\mathfrak{o}.\varrho'+\mathfrak{o}'.\varrho+\mathfrak{o}'.\varrho')]$$

where $\cos C = \mathfrak{o}.\varrho = \mathfrak{o}'\varrho' = -1/3$, i.e. cos of the tetrahedral angle and $\alpha = 180° - 1/2$. The ether angle $= 126°$, whence

$$\mu^2 = 2a^2+2b^2+2ab\cos 54°(+1/3)(-2/3)+a^2.2/9(\mathfrak{o}.\mathfrak{o}')\cos^2 54° +b^2\,2\varrho.\varrho'+2ab\cos 54°.1/3(\mathfrak{o}.\varrho'+\mathfrak{o}'.\varrho).$$

Assuming as before that $a = 1.31$ and $b = 0.37$

$$[4] \qquad \mu^2 = 3.579+0.132(\mathfrak{o}.\mathfrak{o}')+0.274\varrho.\varrho'+0.190(\mathfrak{o}.\varrho'+\mathfrak{o}'.\varrho).$$

This condition of free rotation may be diagrammed as follows:

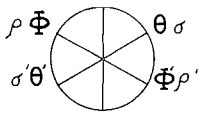

Earlier we specified:

$$\varrho = \sqrt{8/9}\cos\phi,\ \sqrt{8/9}\sin\phi,\ +1/3$$
$$\mathfrak{o} = \sqrt{8/9}\cos\theta,\ \sqrt{8/9}\sin\theta,\ +1/3$$

so ϱ' and $\mathfrak{o}'$ will differ only by the co-ordinate $-1/3$. Then

$$\varrho.\varrho' = 8/9\cos(\phi'-\phi)-1/9$$
$$\mathfrak{o}.\mathfrak{o}' = \{8\cos(\theta'-\theta)-1\}/9$$
$$\mathfrak{o}.\varrho'+\mathfrak{o}'.\varrho = 8/9\,(\cos\theta'-\phi)+\cos(\phi-\theta)-2/9.$$

When the values of θ and ϕ for the five rotamers comprising the two diastereomers are substituted in these equations, the $\sigma.\rho$ values thus obtained may be used in equation [4].

TABLE II

Moments of the rotamers when all but the pivot bonds are freely rotating

	dd,ll			*meso*	
Rotamer	A	B	C	E	F, G
$\varrho.\varrho'$	1/3	−1	1/3	−1	1/3
$\mathfrak{o}.\mathfrak{o}'$	−1	1/3	1/3	−1	1/3
$\mathfrak{o}.\varrho'+\mathfrak{o}'.\varrho$	2/3	2/3	−2	2/3	−2/3
μ^2	3.665	3.476	3.334	3.300	3.588
μ, Debye	1.91	1.86	1.83	1.82	1.89

For a comparison with these calculated moments benzene and carbon tetrachloride solutions of the diastereomers I*a* and I*b* were examined according to techniques described previously (6). Because of the low melting point (45–46°) of the *dd,ll* diastereomer we were unable to measure its distortion polarization by the pelleted solid tech-

nique (7, 8), but the density (1.121) and the dielectric constant (2.460) of the *meso* isomer (pelleted solid) at 23° afforded a P_{e+a} value of 95.5 cc. This experimental value is lower than the electronic polarization (99.9 cc) calculated from additive bond refractions. Since the discrepancy does not alter the moment values appreciably the latter value (99.9 cc) has been subtracted from the total polarization in calculation of the moments recorded in Table III.

TABLE III

Electrical polarizations of the *dd,ll* (I*a*) and *meso* (I*b*) diastereomers of 2,5-dimethyl-2,5-dimethoxy-3,4-diphenylhexane in benzene (C_6H_6) and in carbon tetrachloride (CCl_4)

Diastereomer	Solvent	Temp., °C	$d\epsilon/d\omega$	$d\bar{V}/d\omega$	P_{total}, cc	Moment, Debyes
dd,ll	C_6H_6	20	1.62	0.160	194	2.11
	Same	27	1.35	0.169	178	1.95
	Same	40	0.97	0.176	156	1.69
	CCl_4	20	2.70	0.328	184	1.99
	Same	27	2.36	0.332	173	1.89
	Same	40	2.14	0.333	168	1.83
meso	C_6H_6	20	0.69	0.147	139	1.36
	Same	30	0.67	0.175	136	1.33
	Same	40	0.63	0.177	135	1.33
	CCl_4	20	1.52	0.324	143	1.44
	Same	30	1.40	0.334	140	1.40

According to the data of Table III the diastereomers I*a* and I*b* behave differently from the simple 1,2-disubstituted ethanes and their homologues (Ref. 5, page 355) except for the similarity that moments are apparently higher in benzene than in carbon tetrachloride. But, by contrast, the polarization increases as with rising temperature of 1,2-dichloroethane, its analogues and homologues, whereas the polarizations of I*a* and I*b* decrease with increasing temperature. Moreover, this latter behavior is in contrast with the temperature invariance observed for simple tetrasubstituted ethanes.

The contrast may be attributed to potential energy barriers in I*a* and I*b* which are so complex that they may be described as "group entanglement". In consideration first of the *dd,ll* diastereomer I*a* it may be seen by comparison of Tables II and III that free rotation is excluded by the fact that in this circumstance the moments of rotamers A, B, and C would be almost identical. This expected invariance with respect to temperature does not correspond with the 0.42-D decrease in benzene or the 0.16-D decrease in carbon tetrachloride solution over a 20° temperature rise.

Thus some hindrance to free rotation in the *dd,ll* diastereomer must exist, but the data of Table I are not definitive for an exact assignment. It is probable that rotamer A makes some contribution; indeed it is required to account between its maximum and minimum in respect of isopropylidene conformation for the observed moment (2.11 D) in benzene at 20°. Likewise the maxima and minima of rotamer B at the specified β-angles can account for the entire range of I*a* moment from 20 to 40°. On the other hand the maximum of rotamer C is less than the minimum observed moment in carbon tetrachloride. Therefore one may say that the amount of rotamer C is minimal but no decision can be made in respect of the relative amounts of A and B.

The situation is clearer when one considers the *meso* diastereomer. Certainly the calculated moments of Table II preclude any possibility of free rotation. When rotation restriction at the isopropylidene linkage is considered it may be seen from Table I that

Can. J. Chem. Downloaded from www.nrcresearchpress.com by 196.1.178.254 on 09/04/12
For personal use only.

the presence of rotamer F, G in appreciable amount is unlikely. Because of the maxima and minima the effect of this enantiomeric rotamer ought to be observed as change in moment with respect to temperature. In fact the moment is almost invariant either in benzene or carbon tetrachloride. This situation fits rotamer E, in which the moment is independent of isopropylidene conformation.

While rotamer E seems to describe the *meso* diastereomer I*b* entirely it will be seen that the observed moments (1.33–1.44 D) are lower than have been calculated (Table I) for restriction at the isopropylidene linkage. The only explanation apparent for this discrepancy is that of rotational restriction at the methoxy linkage. Thus it would seem that free rotation is absent in any part of this diastereomer and this circumstance probably applies to the other diastereomer as well. It is in this sense that the term "group entanglement" has been used above.

Of course these arguments may be considered to be trivial; certainly one may draw the conclusions intuitively by inspection of the rotameric formulae A–G. Moreover, these conclusions might have been predicted from the chemical reactions of the diastereomers. However, the present data may be useful in discernment of the intimate mechanisms of the chemical reactions. Certainly it is apparent that the presently popular mechanisms in terms of ionic species appear to be shallow representations of the geometric complexity of diastereomers such as the 2,5-dimethyl-2,5-dimethoxy-3,4-diphenylhexanes. Of course, the symmetrically staggered conformations of formulae A–G also fail to represent entirely the deformations caused by steric effects.

We are grateful to Mr. C. C. Meredith for suggestions which were adopted in improvement of the measuring equipment.

EXPERIMENTAL

dd,ll-2,5-Dimethyl-2,5-dimethoxy-3,4-diphenylhexane (I*b*)

The oil (b.p. 203–205° at 13 mm) previously designated as this diastereomer was purified by passage in hexane solution through a column containing neutral alumina activated at 200° C. The eluate was separated so as to segregate the least ultraviolet fluorescent part. Solvent evaporation left an oil which was dissolved (10 ml per g) in 95% ethanol at 25° and slowly chilled to −78°. Although oil usually separated, eventually crystals, m.p. 41–41.5°, were obtained. Subsequent crystallizations by seeding ethanol, or ethanol–water mixtures at room temperature or below, gave a material melting at 45.6° to 46.3°.

Dielectric Constants of Solutions

The measurements were made by use of an apparatus which has previously been described (9). However, the precision of temperature control has been improved to ±0.04° by alterations in the thermostatting system. Water is circulated through the test cell (Fig. 4) by means of a 1/3-hp centrifugal pump from and to a "slave" bath equipped for controlled heating and cooling by means of a Wheelco Model 7431 recording regulator. Into the test cell at B is fitted a removable 200K thermistor (Western Electric 14A, bottom wet with ethylene glycol), which is held in a connector plug C that may be transferred to a "master" thermostat at entry point F (Fig. 5), which is threaded to accommodate D (Fig. 4). When this thermistor is plugged into G (Fig. 5), which is connected parallel with H (Fig. 4), it is connected with T1 (Fig. 6). The permanent

Can. J. Chem. Downloaded from www.nrcresearchpress.com by 196.1.178.254 on 09/04/12
For personal use only.

Can. J. Chem. Downloaded from www.nrcresearchpress.com by 196.1.178.254 on 09/04/12
For personal use only.

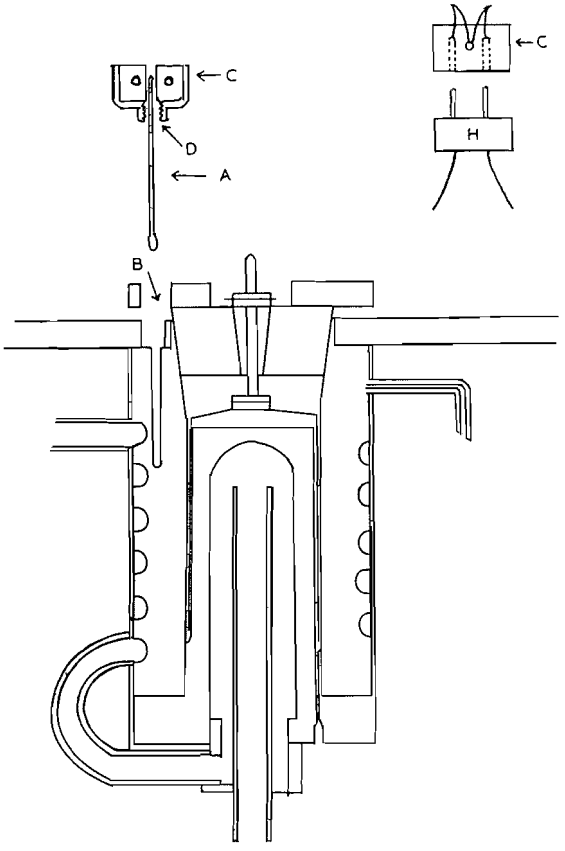

FIG. 4.

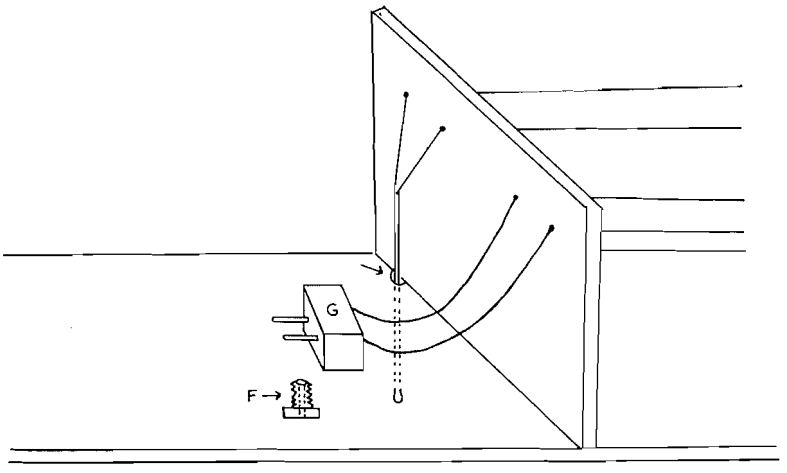

FIG. 5.

thermistor (Fig. 5) in the "master" bath is connected at T2 (Fig. 6) so that the Wheatstone bridge, across which is a 6-v dry cell pack connected via S2, may be balanced by R4 and R5 at the temperature of the master bath.

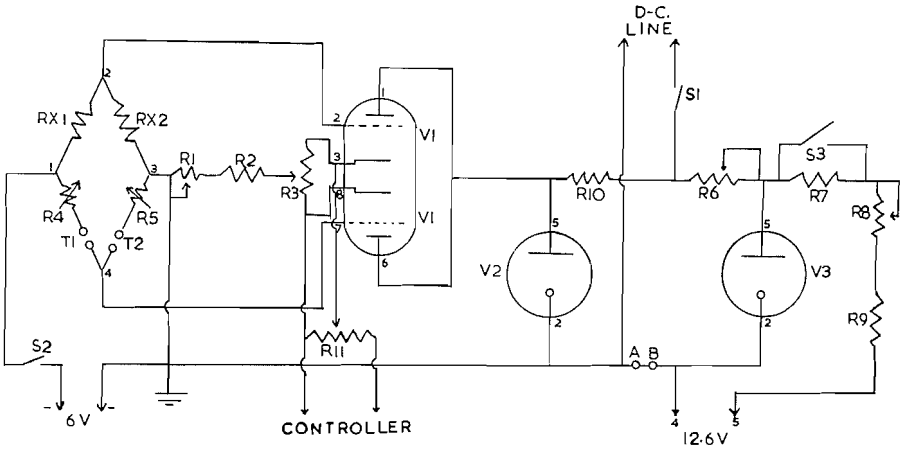

FIG. 6.

When the movable thermistor is returned to B any imbalance in the bridge causes a potential difference at the grids of the twin triode V1–V1 to which a common gas tube regulated d-c. plate supply is available as well as a regulated filament voltage (points 4 and 5, Fig. 6). The amplified imbalance signal, adjusted for scale by R1 and R3 and for sensitivity by R11, is transferred to the "slave" bath regulator (recorder) circuit.

The components of the bridge circuit (Fig. 6) with its voltage-regulated supply are as follows:

R1	0.5 kΩ	R7	1 kΩ	V1–V1	12AT7
R2	0.75 kΩ	R8	0.25 kΩ 10w	V2	VR75
R3	2 kΩ	R9	0.25 kΩ 10w	V3	VR75
R4	25 kΩ	R10	1.5 kΩ 10w	d-c. Line	110 v
R5	25 kΩ	R11	3 kΩ	S3	Push button starter
R6	0.25 kΩ 10w	RX1	100 kΩ		
		RX2	100 kΩ		

The voltage supply regulation is adjusted to 12.6 v by means of R8, and then R6 is adjusted until the current across the otherwise bridged terminals A and B (Fig. 6) is 167–168 ma. The bridge amplifier is adjusted, after a jumper is placed between terminals 2 and 4 of the bridge, by setting R1 to maximum, R11 to minimum resistance; then adjust R3 and R11 until the regulator recorder is in its operating range at sufficient sensitivity. When R11 is returned to minimum resistance R1 is now adjusted so that the potential at either of the 12AT7 grids is 6 v. Again sensitivity is increased via R11, R3 is readjusted to the regulator scale, and the jumper between 2 and 4 is removed.

The specific volumes of solutions between 0.002 and 0.008 weight fraction were determined in the master bath and the dielectric constants were determined at 0.5 mc in

Can. J. Chem. Downloaded from www.nrcresearchpress.com by 196.1.178.254 on 09/04/12
For personal use only.

Can. J. Chem. Downloaded from www.nrcresearchpress.com by 196.1.178.254 on 09/04/12
For personal use only.

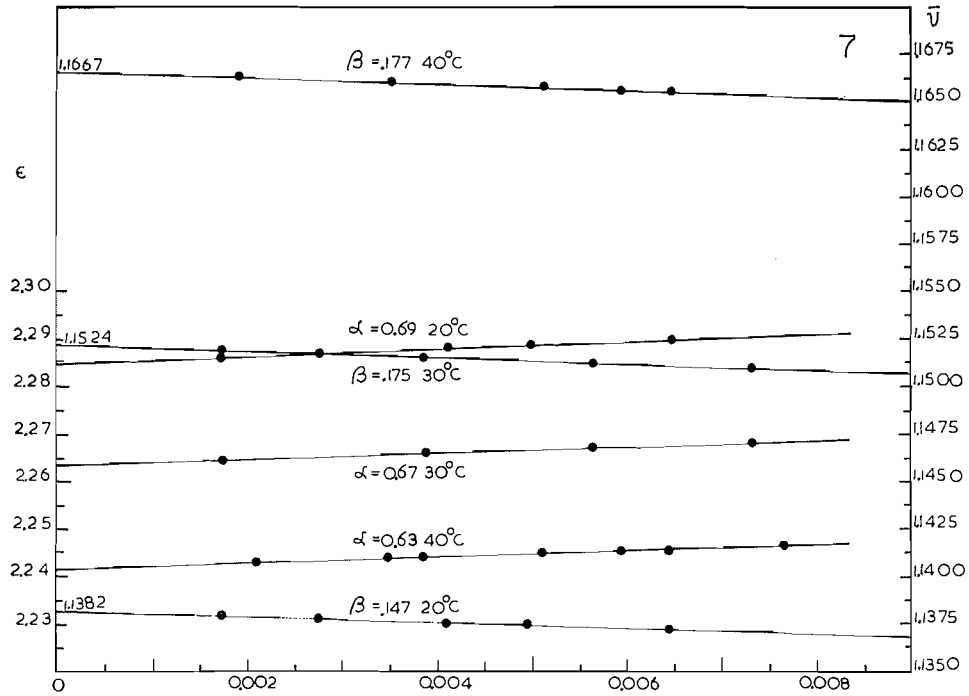

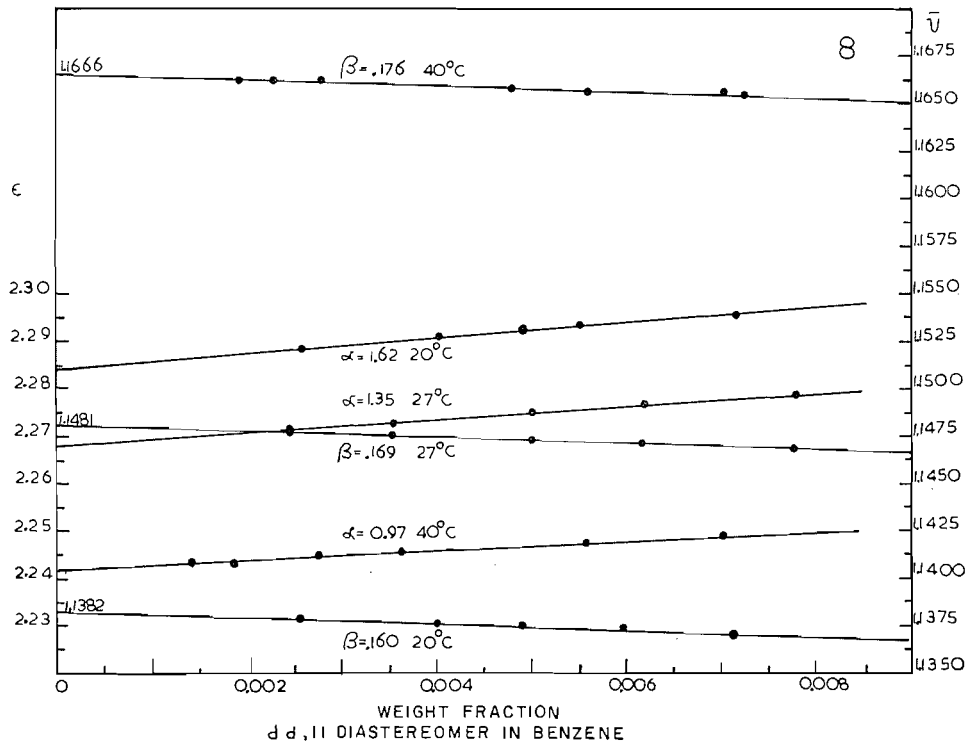

FIGS. 7 AND 8.

benzene and in carbon tetrachloride, the constants of which have been reported recently (6). Typical plots from which $d\bar{V}/d\omega(\beta)$ and $d\epsilon/d\omega(\alpha)$ were obtained are shown in Fig. 7 and Fig. 8. The determinations in carbon tetrachloride were carried out on weight fractions between .001 and .005 and are of comparable precision.

Infrared Spectra

Solutions were examined by the double beam technique (IR4) and frequencies of the absorption peaks are reported as wave numbers, cm^{-1}, for which the molecular extinction coefficients "ϵ" are listed. Benzene solutions were used for the 300–900 cm^{-1} spectral range, while for the 900 and up range carbon disulphide and carbon tetrachloride solutions were used.

The spectra for the benzene solutions are as follows:

meso Diastereomer		*dd,ll* Diastereomer	
cm^{-1}	ϵ	cm^{-1}	ϵ
441	3.6	570	2.5
553	5.9	597	7.1
603	6.3	711	13.1
611	7.5	785	7.5
707	26.3		
717	14.1		
776	16.7		

The spectra for the carbon disulphide solutions are as follows:

meso Diastereomer		*dd,ll* Diastereomer	
cm^{-1}	ϵ	cm^{-1}	ϵ
703	52.8	703	60.3
716	15.9	724	10.2
771	23.5	746	4.3
865	4.5	771	6.3
931	2.8	781	15.5
1028	5.8	823	4.7
1070	50.5	843	2.4
1128	31.0	888	2.4
1159	13.4	928	2.4
1176	20.7	935	2.7
1215	11.6	959	3.0
1233	9.1	998	2.4
1269	5.1	1012	3.3
1363	14.4	1032	5.6
1381	7.7	1069	60.5
1710	7.6	1134	29.0
2180	3.5	1138	30.1
2820	7.6	1177	29.0
2920	19.7	1229	16.9
2940	21.5	1270	2.0
		1343	4.6
		1362	14.1
		1374	18.6
		2820	8.6
		2910	21.5
		2950	25.4
		3020	7.0

Can. J. Chem. Downloaded from www.nrcresearchpress.com by 196.1.178.254 on 09/04/12
For personal use only.

The spectra for carbon tetrachloride solutions are as follows:

meso Diastereomer		*dd,ll* Diastereomer	
cm^{-1}	ϵ	cm^{-1}	ϵ
703	65.2	703	47.2
718	17.4	725	9.1
826	3.6	824	4.7
866	2.9	1032	5.0
1030	5.7	1070	60.6
1083	46.8	1130	25.9
1132	27.8	1141	30.8
1156	12.8	1154	12.1
1161	13.5	1178	29.0
1178	19.8	1226	15.6
1215	9.7	1362	15.1
1233	8.5	1380	19.5
1274	4.9	1455	15.6
1365	17.3	1475	12.1
1388	19.0	1490	9.1
1460	17.1	1600	2.0
1497	107.0	2800	10.8
1605	4.3	2930	23.5
1710	11.9	2950	26.3
2180	2.9	3000	10.7
2820	4.9	3030	7.5
2848	9.2		
2960	19.0		
3010	15.7		
3040	11.9		

REFERENCES

1. BERMAN, L., HALL, R. H., PYKE, R. G., and WRIGHT, G. F. Can. J. Chem. **30**, 541 (1952).
2. SMITH, J. G. and WRIGHT, G. F. Can. J. Chem. **32**, 729 (1954).
3. BROOK, A. G., COHEN, H. L., and WRIGHT, G. F. J. Org. Chem. **18**, 447 (1953).
4. NEWMAN, M. S. Record Chem. Progr. Kresge-Hooker Sci. Lib. **13**, 111 (1952).
5. SMYTH, C. P. Dielectric behavior and structure. McGraw-Hill Book Co., Inc., New York. 1955. p. 234.
6. SAWATZKY, H. and WRIGHT, G. F. Can. J. Chem. **36**, 1555 (1958).
7. MEREDITH, C. C., WESTLAND, L., and WRIGHT, G. F. J. Am. Chem. Soc. **79**, 2385 (1957).
8. PODLESCHKA, P., WESTLAND, L., and WRIGHT, G. F. Can. J. Chem. **36**, 574 (1958).
9. MEREDITH, C. C. and WRIGHT, G. F. Can. J. Technol. **33**, 182 (1955).

Can. J. Chem. Downloaded from www.nrcresearchpress.com by 196.1.178.254 on 09/04/12
For personal use only.

Can. J. Chem. Downloaded from www.nrcresearchpress.com by 196.1.178.254 on 09/04/12
For personal use only.

THE INFRARED SPECTRA OF MALONATES AND OXALATES: TEMPERATURE EFFECT[1]

R. A. ABRAMOVITCH

ABSTRACT

The infrared spectra of a number of malonates and oxalates (as liquid films) were examined at various temperatures and narrower slit widths than had previously been used. The absorption in the 5.8 μ region is very complex, at least four bands being observed in each case. Small but definite temperature effects were recorded for both types of esters. At somewhat wider slit widths only two bands were observed, these occasionally having indistinct shoulders. The spectra of some of the compounds were also measured in both carbon tetrachloride and acetonitrile solutions (two bands observed in each case) and the ratios of the intensities of the two bands compared. A possible explanation of the effects observed is that at least two rotational isomers can exist for each compound and that vibrational coupling of the carbonyl stretching frequencies can occur in each of the rotational isomers.

The infrared spectra of a number of malonic ester derivatives were shown to exhibit two carbonyl stretching bands both in the pure liquid state and in solution (1) (these measurements were carried out on a Grubb–Parsons double-beam spectrometer, type S4, with a sodium chloride prism and at a slit schedule of 1.5 mm). The splitting of the carbonyl band was shown not to be due to either enolization and conjugate chelation or to association. Two further possibilities were considered at that time, these being vibrational coupling and rotational isomerism, but no decision could be reached on the basis of the evidence available. To determine whether, in the absence of rotational isomerism, vibrational coupling was possible the spectra of some cyclic malonates were studied (2). Two carbonyl stretching bands were again observed and since there was no evidence of enolization in these compounds the two bands were attributed to vibrational coupling of the two β-carbonyl groups. This did not, however, eliminate the possibility that in the open chain compounds the two bands could be due to rotational isomerism.

It therefore became necessary to examine the temperature dependence (if any) of the two carbonyl peaks in the case of the open chain compounds. If rotational isomerism did in fact occur, the ratio of the intensities of the two bands should change on raising the temperature, as one of the rotational isomers became favored with respect to the other (3, 4). While this work was in progress Simon and Seyferth (5) reported the spectra of a number of oxalate esters in which two strong carbonyl stretching peaks were observed in every compound examined. It was decided, therefore, to extend our study to the oxalates as well to try and distinguish between rotational isomerism and vibrational coupling. Bellamy and Williams (6) observed a change in the ratios of the intensities of the carbonyl bands due to both rotational isomers of chloroacetone, ω-chloroacetophenone, and related compounds on passing from a solution in acetonitrile to one in carbon tetrachloride, the solvent of high dielectric constant favoring the more polar rotational isomers. The spectra of a few malonates and of diethyl oxalate were measured in both acetonitrile and in carbon tetrachloride to determine whether any such change in the ratio of the intensities did occur.

EXPERIMENTAL

Most of the malonates were commercially available and were purified just before use by repeated fractional distillations. Diethyl methylmalonate was obtained by heating

[1]*Manuscript received February 27, 1959.*
Contribution from the Chemistry Department, University of Saskatchewan, Saskatoon, Saskatchewan.

diethyl methyloxaloacetate (7). Diethyl and dimethyl oxalate were purified by standard methods. Carbon tetrachloride and acetonitrile were AnalaR grade and were redistilled twice just before use.

A Perkin–Elmer model 21 double-beam spectrophotometer with sodium chloride optics was used for the infrared measurements. For the studies of the temperature effect the spectral range from 1800 to 1700 cm^{-1} only was studied. For this purpose a Perkin–Elmer heated cell holder and horizontal cell attachment were used. The compounds were studied as liquid films. Because of evaporation each compound had to be studied at a different "high" temperature at which evaporation was not appreciable. This was checked by running spectra over the same range until a temperature was reached at which no changes in the intensities of the bands occurred in two or more consecutive runs at that temperature. The spectra of the liquids were again recorded after the liquids were cooled to room temperature and the compounds allowed to reach equilibrium for about 15 minutes. The spectra were the same as before heating. Best resolution was observed when only a very thin film of liquid was used (maximum absorption 35–40%) and all spectra were run at speed 4. At higher speeds the resolution was much poorer. Somewhat narrower slit widths ($S' = 6.8\ cm^{-1}$) were used than those usually used for ordinary qualitative runs ($S' = 7.9\ cm^{-1}$), and increased resolution was thus obtained resulting in more bands being observed. A comparison of the number of bands observed at the two slit schedules is given in the discussion. The computed spectral slit width S' was obtained from the mechanical slit width at 1697 cm^{-1} using Williams' equation (8 *a*). The values of the refractive indexes of rock salt used in the calculation of the prism dispersion were those given in Landolt-Börnstein.

The solution spectra were run in compensated 0.028-mm cells, with $S' = 7.9\ cm^{-1}$ at 1697 cm^{-1}.

The standard abbreviations are used: (s) = strong, (m) = medium, (w) = weak, (vw) = very weak, (sh) = shoulder, (br) = broad.

RESULTS AND DISCUSSION

Malonate Esters

The following diethyl malonate derivatives were studied: the dihydrogen-, methyl-, ethyl-, diethyl-, *n*-butyl-, ethylphenyl-, bromo-, and dibromo-malonic esters. All except diethyl methylmalonate had been studied by us before (1) using the Grubb–Parsons S4 spectrophotometer with a slit schedule of 1.5 mm. In nearly all cases two bands had been observed though it was noted that in many examples a weak shoulder was present at 1700–1712 cm^{-1}. In the present study the spectra were first measured over the whole range (2.5–15 μ) with a computed spectral slit width $S' = 7.9\ cm^{-1}$: no bands were observed, overtones or combinations of which would give rise to peaks in the 1770–1700 cm^{-1} region. Two strong bands were observed in all cases in the carbonyl region as reported previously (1), though the position of these differed slightly from those given in the first paper. In some cases, indistinct shoulders were also observed. The shifts in the band maxima are attributed to different resolutions of the two instruments since it is now shown that the two bands observed are really compounded of at least four overlapping strong bands. The spectra were then examined using the heated cell and horizontal attachment at a computed spectral slit width $S' = 6.8\ cm^{-1}$. The results obtained are summarized in Table I.

In all examples the intensity increases or decreases are only small. In the spectrum of diethyl ethylmalonate, raising the temperature to 85° caused the 1753 cm^{-1} shoulder

Can. J. Chem. Downloaded from www.nrcresearchpress.com by 196.1.178.254 on 09/04/12
For personal use only.

TABLE I

Compound	$\nu_{C=O}$ cm^{-1}		
	$S' = 6.8$ cm^{-1}		$S' = 7.9$ cm^{-1} at 30°
	Low temp. (° C)	High temp. (° C)	
Diethyl malonate	(33°)	(82°)	
	1770 (sh) (mw)	1770 (c)	1758 (br)
	1748 (s)	1748 (c)	1740 (br)
	1733 (s)	1733 (c)	
	1722 (s)	1722 (d)	
	1710 (sh) (m)	1710 (c)	
Diethyl ethylmalonate	(33°)	(85°)	
	1775 (sh) (vw)	1775 (sh) (i)	1750 (br)
	1753 (sh) (s)	1753 (i) } br flat	1726 (br)
	1740 (sh) (s)	1740 (d) } maximum	
	1726 (s)	1726 (d)	
	1714 (sh) (m)	1714 (c)	
Diethyl *n*-butylmalonate	(33°)	(75°)	
	—	1772 (w)	1750 (br)
	1750 (sh) (s)	1750 (sh) (i)	1735
	1732 (sh) (s)	1732 (c) } br flat	
	1725 (s)	1725 (d) } maximum	
	1712 (sh) (m)	1712 (sh) (i)	
Diethyl ethylphenylmalonate	(31°)	(85°)	
	1775 (sh) (vw)	1775 (sh) (i)	1750 (indistinct sh)
	1750 (sh) (m)	1750 (sh) (i)	1735
	1735 (sh) (s)	1735 (sh) (d)	1712 (indistinct sh)
	1722 (s)	1722 (d)	
	1713 (sh) (s)	1713 (sh) (i)	
Diethyl bromomalonate	(31°)	(82°)	
	1775 (sh) (m)	1775 (sh) (i)	1776 (indistinct sh)
	1761 (br sh) (s)	1761 (s) (i)	1761 (br sh) (s)
	1742 (s)	1742 (sh) (d)	1744 (br) (s)
	1727 (s)	1727 (d)	1730 (indistinct sh)
	1715 (sh) (w)	1715 (sh) (c)	
Diethyl dibromomalonate	(33°)	(84°)	
	1772 (sh) (w)	1772 (sh) (i)	
	1753 (s)	1753 (i)	
	1742 (sh) (s)	1742 (sh) (d)	
	1727 (sh) (m)	1727 (sh) (d)	
	1712 (sh) (w)	1712 (sh) (c)	

(i) = Slight increase in intensity at the higher temperature.
(d) = Slight decrease in intensity at the higher temperature.
(c) = Approximately constant intensity.

to increase in intensity somewhat and the 1740 cm^{-1} shoulder to decrease slightly in intensity resulting in both these bands becoming merged into one very broad flat maximum. In the case of diethyl *n*-butylmalonate, raising the temperature to 75° resulted in an increase in the intensity of the 1750 cm^{-1} shoulder with respect to the 1732 cm^{-1} shoulder. The latter did not change in intensity but was merged in with the 1725 cm^{-1} band, resulting in a broad flat maximum. Barely discernible shoulders at 1750 and 1712 cm^{-1} were observed in the spectrum of diethyl ethylphenylmalonate at 30° and $S' = 7.9$ cm^{-1}. In the case of diethyl bromomalonate, raising the temperature to 82° caused the 1761 cm^{-1} shoulder to become a resolved maximum while the 1742 cm^{-1} band became a shoulder on the low frequency side of the 1761 cm^{-1} band.

It is clear that open chain malonate esters exhibit four or more bands in the carbonyl stretching region but that due to considerable overlap only two broad maxima can be observed at the slit schedules used in routine qualitative runs (1). This very complex

Can. J. Chem. Downloaded from www.nrcresearchpress.com by 196.1.178.254 on 09/04/12
For personal use only.

system of bands cannot arise through overlap with overtone or combination bands since there are no strong absorptions up to 15 μ which could give rise to them. The slight temperature dependence indicates that rotational isomerism does, in fact, occur. Here, unlike in the case of the α-halogenoketones (4, 6) where the more polar *cis*-configuration is stabilized both by steric repulsion and by some form of dipolar interaction between the halogen and the carbonyl group, the two polar groups are β- to each other and

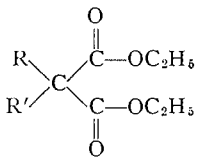

(I)

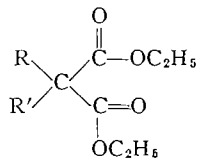

(II)

dipolar effects of the above type would be small. The stabilities of the two rotational isomers would then be governed mainly by steric considerations and, in the case of solutions, by solvent–solute interactions. A consideration of models indicates that steric interactions are similar in both forms I and II so that these should be of comparable stability. Rotational isomers other than the two represented here could, in theory, also exist. It was shown (2) that, in the absence of rotational isomerism, vibrational coupling can occur between two carbonyl groups β- to each other; vibrational coupling could occur then also in the case of the open chain malonates *in each of the rotational isomers*, thus giving rise to at least four bands which would be close together and would overlap considerably. This is actually observed. A study of the temperature effect data indicates that with increasing temperature two of the bands rise somewhat whereas two of them fall, the 1712 cm^{-1} band remaining almost constant. This suggests the possibility that two of the bands are due to one rotational isomer and two to the other (the splitting in each case being due to vibrational coupling) and one of these is slightly more stable at the higher temperature than the other one is, as would be expected if the energy difference between the two forms were small. Due to the complexity of the spectra it doesn't seem possible to attribute any specific bands to any one of the possible rotational isomers at this time.

The spectra of diethyl *n*-butylmalonate and diethyl bromomalonate were also measured in carbon tetrachloride and in acetonitrile. Only two sharp bands were observed. Shifts in the positions of these bands in the two solvents were recorded:

TABLE II

	CCl_4	CH_3CN
Diethyl *n*-butylmalonate	1760, 1743	1754, 1737
Diethyl bromomalonate	1778, 1755	1765, 1749

When taking into account the slight variations in $\Delta\nu_{\frac{1}{2}}$ in the different solvents, the relative intensities of the two bands were very close to each other in both solvents. Though the data are inconclusive the two bands could presumably correspond to two rotational isomers if it is assumed that in the case of the malonates the polarity of the solvent has no effect on the stability of the rotational isomers. It is difficult to see, however, why no vibrational coupling would be observed. Such frequency shifts as are observed

Can. J. Chem. Downloaded from www.nrcresearchpress.com by 196.1.178.254 on 09/04/12
For personal use only.

here on passing from a less to a more polar solvent are well known (8 *b*). An alternative explanation, which involves vibrational coupling, is that each compound is present as a single rotational isomer in each solvent, e.g. form (I) in acetonitrile and form (II) in carbon tetrachloride. This would explain the appearance of only two bands. On the other hand (and this seems more likely), if both rotational isomers are present in solution then the higher of the two bands arising from coupling in one rotational form overlaps with the corresponding one from the other form, as also do the two lower bands.

The dipole moments of some malonate derivatives were measured by Phalnikar (9), who also calculated the expected dipole moments assuming the absence of rotation of the carbethoxyl group about the C—C axis (as for formula I). The calculated values were somewhat high (e.g. diethyl malonate: μ_{calc} 2.72, μ_{obs} 2.54) but that author suggested that this could perhaps be due to induced moments. The moment of diethyl malonate was later measured by Jatkar and Phansalkar (10), who obtained a lower value (2.10 D in benzene solution) by using a new equation instead of the Onsager one. The moment of diethyl malonate as a pure liquid increased from 2.17 D at 31° to 2.29 D at 120° (10), which is consistent with our suggestion that rotational isomers exist but that the energy difference between them is probably small. Further, it is interesting to note that the moment decreased somewhat on going from the pure liquid to a benzene solution. Jatkar and Phansalkar explained the observed moment by assuming free rotation of the two esterified carboxyl groups. Rough calculations indicate that approximately equal amounts of forms (I) and (II) would give rise to a value for the dipole moment of diethyl malonate close to that reported by the above authors. Complete free rotation of the carbethoxyl groups is unlikely in view of the results of dipole moment measurements on monocarboxylic esters (11).

Oxalate Esters

The infrared spectra of dimethyl and diethyl oxalate were examined for temperature dependence in the same way as for the malonates and with similar results. At 30° and $S' = 6.8$ cm^{-1}, diethyl oxalate exhibited the following bands: 1775 (sh), 1760 (sh), 1742, 1733 cm^{-1} (sh), all strong broad bands. At 71°, the 1775 cm^{-1} shoulder increased in intensity, the 1760 cm^{-1} shoulder became a broad rounded maximum at 1756 cm^{-1}, the 1742 cm^{-1} maximum decreased slightly in intensity becoming a shoulder, and the 1733 cm^{-1} shoulder also decreased in intensity. The band observed at 1760 cm^{-1} at 30° is the same as that observed at 1756 cm^{-1} at the higher temperature, but due to considerable overlap with the 1742 cm^{-1} band is not resolved from it. As the latter decreases in intensity the 1756 cm^{-1} band becomes more distinct. Similar observations apply to dimethyl oxalate. These results contrast sharply with those of Miyazawa and Kurantani (12), who only reported a single C=O stretching frequency at 1730 cm^{-1} for dimethyl oxalate, and with those of Simon and Seyferth (5), who reported two bands at 1740 and 1765 cm^{-1} (liquid film) for diethyl oxalate. At 30° and with $S' = 7.9$ cm^{-1} three bands were observed at 1767, 1752 (sh on 1744 band), and 1744 cm^{-1}.

In solution, two bands only were observed: in CCl_4 at 1780 and 1755 cm^{-1}; in acetonitrile at 1774 at 1753 cm^{-1}. In this case, whereas the intensity of the 1755–1753 cm^{-1} band remains approximately the same in both solvents ($\Delta\nu_{\frac{1}{2}}$ practically unchanged), the intensity of the 1780–1774 cm^{-1} band increases considerably on passing from the carbon tetrachloride to the acetonitrile solution, which is in contrast to the results obtained with the malonate esters.

Though the temperature dependence results may be explained on the same basis as were the ones for the malonate esters, i.e. rotational isomerism between (III) and (IV)

Can. J. Chem. Downloaded from www.nrcresearchpress.com by 196.1.178.254 on 09/04/12
For personal use only.

and vibrational coupling of the two α-carbonyl groups in each rotational isomer, it is difficult to explain the solvent effect along those lines. That coupling is possible between two carbonyl groups alpha to each other is seen from the examples of cyclic α-diketones

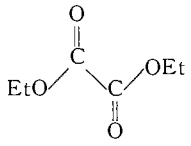

(III)

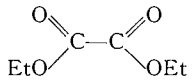

(IV)

(in which no enolization is possible) studied by Leonard and Little (13). The situation in the case of the oxalates is akin to that in the α-chloroketones and α-chloroesters studied by Bellamy and co-workers (4, 6) as far as dipole–dipole interaction goes without, however, the steric repulsion in the *trans*-form (III) which makes the *cis*-form in the α-chloroketones the more stable of the two isomers. One would, therefore, expect (III) to be the predominant molecular species under normal conditions. Both the temperature dependence and the solvent effect indicate that it is not the only species present by any means and that its rotational isomer may be of comparable stability. Some weak intramolecular associative-type interaction in the pure liquid state may also be operative. This might explain the large shift in frequency on passing from the pure liquid state to the solution in the non-polar carbon tetrachloride, and would imply the existence of rotational isomers but no vibrational coupling. (The concentration independence and lack of solvent effect of the infrared spectra of the malonates does not necessarily eliminate such a type of interaction in the pure liquid state.) Again, from the dipole moment of diethyl oxalate (2.06 D in benzene solution), Jatkar and Phansalkar (10) concluded that free rotation of the two ester groups occurs. The moment of the pure liquid was appreciably higher than that of the ester in benzene solution and increased, though less markedly than in the case of diethyl malonate, on raising the temperature, from 2.23 D at 24.8° to 2.27 D at 99°. No definite conclusions about the oxalates may be drawn from the present results, except that contrary to Bellamy's suggestion (14) interaction between adjacent carbonyl groups may be appreciable.

ACKNOWLEDGMENTS

The author wishes to thank the National Research Council for a grant in aid of this research. Thanks are also due to Mr. E. C. Bailey for assistance with the adjustment of the horizontal cell attachment and to Mr. M. J. Kinnear for the purification of the samples used in this study.

REFERENCES

1. ABRAMOVITCH, R. A. Can. J. Chem. **36**, 151 (1958).
2. ABRAMOVITCH, R. A. Can. J. Chem. **37**, 361 (1959).
3. JONES, R. N., FORBES, W. F., and MUELLER, W. A. Can. J. Chem. **35**, 504 (1957).
4. BELLAMY, L. J., THOMAS, L. C., and WILLIAMS, R. L. J. Chem. Soc. 3704 (1956).
5. SIMON, M. S. and SEYFERTH, H. M. J. Org. Chem. **23**, 1078 (1958).
6. BELLAMY, L. J. and WILLIAMS, R. L. J. Chem. Soc. 4294 (1957).
7. COX, R. F. B. and MCELVAIN, S. M. Org. Syntheses, Coll. Vol. **2**, p. 279 (1943).
8. JONES, R. N. and SANDORFY, C. The application of infrared and Raman spectrometry to the elucidation of molecular structure. *In* Technique of organic chemistry. *Edited by* A. Weissberger. Interscience Publishers, Inc., New York. 1956. (*a*) p. 274, (*b*) p. 471.
9. PHALNIKAR, N. L. J. Univ. Bombay, **11** (Pt. 3), 87 (1942); Chem. Abstr. **37**, 3310^2 (1943).
10. JATKAR, S. K. K. and PHANSALKAR, V. K. J. Univ. Poona, Sci. Technol. No. 4, 45 (1953); Chem. Abstr. **48**, 11859^d (1954).

Can. J. Chem. Downloaded from www.nrcresearchpress.com by 196.1.178.254 on 09/04/12
For personal use only.

11. SMITH, J. W. Electric dipole moments. Butterworth Scientific Publications, London. 1955. p. 239.
12. MIYAZAWA, T. and KURANTANI, K. J. Chem. Soc. Japan, **72**, 804 (1951); Chem. Abstr. **47**, 43^d (1953).
13. LEONARD, N. J. and LITTLE, J. C. J. Am. Chem. Soc. **80**, 4111 (1958).
14. BELLAMY, L. J. The infrared spectra of complex molecules. J. Wiley & Sons, Inc., New York. 1954. p. 157.

Can. J. Chem. Downloaded from www.nrcresearchpress.com by 196.1.178.254 on 09/04/12
For personal use only.

Can. J. Chem. Downloaded from www.nrcresearchpress.com by 196.1.178.254 on 09/04/12
For personal use only.

SURFACE ELECTRICAL CONDUCTANCE AND ELECTROKINETIC POTENTIALS IN NETWORKS OF FIBROUS MATERIALS[1]

C. E. MOSSMAN[2] AND S. G. MASON

ABSTRACT

Stream-current, permeability, and conductance measurements were made on cylindrical pads of randomly oriented Dacron, glass, Nylon, and Orlon fibers over a range of electrolyte and solid concentrations. Values of the specific surface conductivity were computed from the conductance data, using equations which were derived from a capillary network theory.

The measured conductance values were independent of pad concentration, increased with increasing electrolyte concentration, and were higher than values calculated from electrical double-layer theory using the measured values of ζ-potential. A number of plausible reasons for the discrepancies are advanced.

INTRODUCTION

When a non-conducting solid is brought into contact with a dilute electrolyte, there is generally an increase in electrical conductivity. This increase, which is most marked with solids of high surface area, is usually associated with the electrical double layer at the solid/liquid interface and is referred to as surface conductance. It is usually considered to be closely related to the conventional electrokinetic effects such as electro-osmosis and electrophoresis.

The present investigation was undertaken to obtain surface conductance data for pads of randomly oriented fibers, as an extension of previous studies (1, 2, 3) of the electrokinetic properties of fibrous materials. To avoid complications, non-swelling fibers (Dacron, glass, Nylon, and Orlon) were used. Values of the ζ-potential were obtained simultaneously by the stream-current method (1, 3).

Previous experimental work on surface conductance has been carried out using glass capillaries (4, 5, 6, 7), glass and other particles (8, 9, 10, 11), and cellulose fibers (12, 13). Wide discrepancies are apparent among the results of different workers and in only a few cases were ζ-potentials measured for the same system. Most of the investigations have yielded surface conductivity values considerably higher than those predicted by the theory outlined below.

THEORETICAL PART

Classical Theory

The surface conductivity is most conveniently defined by considering a non-conducting cylindrical capillary tube filled with an electrolyte. The bulk liquid and the interface are assumed to act as conductors in parallel with a total conductance given by

$$[1] \qquad \frac{1}{R'} = \frac{\pi r^2 \kappa}{L'} + \frac{2\pi r \kappa_s}{L'} = \frac{1}{L'}[a\kappa + f\kappa_s],$$

where R' is the total resistance, and r, f, a, L' are the radius, perimeter, cross-sectional area, and length of the capillary, κ is the specific (volume) conductivity (mho/cm) of the liquid, and κ_s the surface conductivity (mho) of the solid/liquid interface.

[1]*Manuscript received March 3, 1959.*
Contribution from Physical Chemistry Division, Pulp and Paper Research Institute of Canada, and Department of Chemistry, McGill University, Montreal, Que.
[2]*Holder of a Scholarship from the Canadian Federation of University Women, and a Studentship from the National Research Council of Canada.*

A theoretical expression, based on classical diffuse double-layer theory for a plane interface, for κ_s in a capillary has been obtained by several workers (14, 15). In the derivation, it is assumed that the double-layer thickness is much smaller than the capillary radius, and that the potential $\psi(x)$ varies in the double layer from ζ at the surface, where shear motion starts, to zero in the interior of the capillary. It is also assumed that the electrolytes behave as ideal solutions, implying that the results will be strictly valid only at infinite dilution.

The surface conductance is considered to be made up of two parts: (1) an electroosmotic contribution, a result of the mass displacement of the free charge in the double layer; and (2) a term proportional to the mobility of the ions, arising from the fact that the double layer contains more counter ions than the bulk liquid.

The complete theoretical expression for a 1–1 electrolyte may be written

$$\kappa_s = \left(\frac{DnkT}{2\pi}\right)^{\frac{1}{2}}[O+I'] \qquad [2a]$$

where the electroosmotic term

$$O = \frac{kTD}{\pi\eta e}\left[\cosh\left(\frac{e\zeta}{2kT}\right)-1\right] \qquad [2b]$$

and the excess ion mobility term

$$I' = v_+\left[\exp\left(-\frac{e\zeta}{2kT}\right)-1\right]+v_-\left[\exp\left(\frac{e\zeta}{2kT}\right)-1\right] \qquad [2c]$$

where the symbols have the meanings assigned in the List of Symbols (see p. 1163).

It should be noted that, for a given solvent, O is a function of ζ, and I' a function of ζ and the ion mobilities. It is also seen from eq. [2c] that the mobility of the counter ion, i.e. the ion of charge opposite to that of the surface, is the more important in determining I'. Thus when $\zeta > 0$, the right-hand side of eq. [2c] is determined largely by the term containing v_-, and when $\zeta < 0$ by that containing v_+. Similar but more complicated equations can be derived for Z_+-Z_- electrolytes. It follows from eqs. [2] that κ_s depends both on the bulk ion concentration (n) and on the ζ-potential.

Equation [2a] is equivalent to an expression for surface conductivity derived by Bikerman (14). Bikerman assumed that when measurements are made with alternating current there should be no electroosmosis, so that the ion-mobility term is sufficient to describe the surface conductance. However, none of the measurements of the effect of frequency upon κ_s support this assumption (6, 8), and a subsequent theoretical analysis by Rosenhead and Miller (16) has shown that the electroosmotic contribution would become negligible only at frequencies higher than 10 Mc per second.

It is often assumed (12, 17) that at high ionic strengths (κ_s/κ) $\rightarrow$ 0, i.e. that the surface conductance contribution to the total becomes negligible. The validity of this assumption can be demonstrated from the theory by assuming that when ionic strength is varied, the surface charge density, q, remains constant. Under these conditions, the following relation holds (18):

$$\sinh\left(\frac{e\zeta}{2kT}\right) = q\sqrt{\left(\frac{\pi}{2DnkT}\right)} = \frac{1}{\sqrt{n}} \times \text{(constant)}. \qquad [3]$$

Assuming further that the electrolyte is ideal and that

$$\kappa = \lambda n \qquad [4]$$

Can. J. Chem. Downloaded from www.nrcresearchpress.com by 196.1.178.254 on 09/04/12
For personal use only.

and combining eqs. [2*a*] and [4] and reducing, it follows that

$$\frac{\kappa_s}{\kappa} = \frac{1}{\lambda n}\left[\beta\sqrt{n}(O+I')\right]$$

where β is a constant. It follows from eq. [3] that as $n \rightarrow \infty$, $\sinh(e\zeta/2kT) \rightarrow 0$, as a result of which it readily follows that $(O+I') \rightarrow 0$, and hence $(\kappa_s/\kappa) \rightarrow 0$.

κ_s in Porous Media

To obtain κ_s values from the experimental conductance data for pads of fibers, it is necessary to obtain an equation allowing for the complex internal pore structure of the pad. The development given here is similar to that used by Sullivan and Hertel (19) and Goring and Mason (1) for describing viscous and electrokinetic flow in uniformly packed pads of solid particles, starting with the analogues of eq. [1] for straight cylindrical capillaries.

For a single channel inclined at an angle θ to the axis of a pad of thickness L, $L = L' \cos\theta$. Since the total conductance is given by the sum of the individual conductances, it follows from eq. [1] that:

$$\frac{1}{R} = \sum\left[\frac{a\kappa}{L'} + \frac{f\kappa_s}{L'}\right] \qquad [5]$$

where the summation is carried out over all the pores.

The term $\sum \frac{a}{L'}$ may be written as $\sum \frac{a\cos\theta}{L}$ where $\sum a\cos\theta = \xi$, the geometrical "pore factor" (1). Assuming that the distribution functions of pore size and pore orientations are independent of one another, it follows (1) that $\xi = A\epsilon\,\overline{\cos^2\theta}$, where A is the pad cross-sectional area and ϵ is the void fraction. Since $\epsilon = 1-\alpha c$, where c is the solid mass per volume concentration of the pad and α is the specific volume of the fiber, then:

$$\sum \frac{a}{L'} = \frac{A(1-\alpha c)\,\overline{\cos^2\theta}}{L}. \qquad [6]$$

By similar reasoning,

$$\sum \frac{f}{L'} = \frac{1}{L^2}\cdot\overline{\cos^2\theta}\cdot\sum(fL') \qquad [7]$$

where $\sum(fL')$ represents the total surface area of the pad. Also, since $\sum(fL') = \sigma.c.A.L$, where σ is the specific surface per unit mass of material in the pad, the total pad conductance can be written:

$$\frac{1}{R} = \frac{A}{L}\,\overline{\cos^2\theta}\,[(1-\alpha c)\kappa + \sigma c\kappa_s]. \qquad [8]$$

In this equation A, L, and c are obtainable from the dimensions and weight of the pad, κ and R by direct electrical measurement, and σ and α from a liquid permeability measurement on the pad *in situ*.

Thus to calculate κ_s directly from eq. [8], the pore orientation factor $\overline{\cos^2\theta} = \Omega$ must be known. It has been shown empirically (3) that for ionic conductance in fibrous pads

$$\Omega_c = 0.955\,\epsilon. \qquad [9]$$

Eq. [8] can thus be written

$$\kappa_s = \frac{1-\alpha c}{\sigma c R}\left[\frac{1.048\,L}{A(1-\alpha c)^2} - \kappa R\right]. \qquad [10]$$

Can. J. Chem. Downloaded from www.nrcresearchpress.com by 196.1.178.254 on 09/04/12
For personal use only.

Alternately, eq. [8] may be written in terms of the pad cell constant, C ($= \kappa R$):

$$\frac{1}{C} = \frac{A}{L}\,\Omega_c\left[(1-\alpha c)+\sigma c\,\frac{\kappa_s}{\kappa}\right]. \qquad [11]$$

Let C_0 be the pad cell constant at high ionic strengths when $(\kappa_s/\kappa) = 0$; it follows from eq. [11] that

$$\frac{1}{C_0} = \frac{A}{L}\,\Omega_c(1-\alpha c). \qquad [12]$$

By combining eqs. [11] and [12], Ω_c can be eliminated and κ_s computed directly without knowledge of Ω_c:

$$\kappa_s = \kappa\left(\frac{1-\alpha c}{\sigma c}\right)\left(\frac{C_0-C}{C}\right), \qquad [13a]$$

$$= \frac{(1-\alpha c)}{\sigma c R}\,(C_0-\kappa R). \qquad [13b]$$

If the two methods are to give identical values of κ_s, it follows from a comparison of the eqs. [10] and [13*b*] that

$$\left(\frac{L}{C_0}\right)^{\frac{1}{3}} = (0.955\,A)^{\frac{1}{3}}\,(1-\alpha c). \qquad [14]$$

By definition κ_s should be independent of the pad concentration c.

EXPERIMENTAL PART

Materials

The following fibrous materials were used:

1. Nylon: 3 denier delustered.
2. Orlon: continuous filament.
3. Dacron: 1.5 denier staple.
4. Glass fiber: 0.5 μ diam. staple from Glass Fibers Inc., Toledo, Ohio.

All fibers were first chopped into short lengths in a Wiley mill and were then run through a Bauer–McNett classifier, the fractions between the 65- and 150-mesh screens being retained for use.

The solutions used in the experiments were prepared by dilution of stock solutions of HCl, KCl, $CaCl_2$, and $ThCl_4$, their exact normality being determined conductimetrically. Distilled water having a specific conductivity of 1.4×10^{-6} mho/cm was used.

In one series of measurements solutions of KCl in 20% (by volume) ethanol/water were used as electrolytes.

Apparatus

The high-compression cell described previously (2) was used for the permeability, stream-current, and conductance measurements. This arrangement permitted comparison of κ_s values computed from the experimental data (using either eq. [10] or [13]) with those predicted by eq. [2] using ζ-values measured on the same system by the stream-current method.

Reversible Ag–AgCl electrodes were used in the electrical measurements. These were chloridized less heavily than before to reduce the electrical resistance of the chloride layer. Electrodes prepared by anodizing silver electrodes at 1 ma/cm^2 for 15 minutes in 0.1 N HCl were quite stable, showing a slight residual potential and a small polarization effect only at high electrolyte concentrations.

Can. J. Chem. Downloaded from www.nrcresearchpress.com by 196.1.178.254 on 09/04/12
For personal use only.

Pad Formation

Approximately 9 g of fiber was used to form each pad. The fibers were first washed repeatedly in distilled water and then soaked overnight in 4 l. of a 10-l. batch of the electrolyte to be used.

Pad formation and deaeration procedures were identical with those previously described (1, 3). The oven-dry weight of each pad was determined at the end of each experiment, and, together with the measured pad length L and the cross-sectional area A (5.00 cm^2), was used to calculate the pad concentration c.

Surface Conductance Measurements

A complete measurement consisted of measuring R, the resistance of the pad, over a series of pad lengths L at each electrolyte concentration. The specific bulk conductivity κ of each solution was determined using a calibrated conductivity cell placed in the system in series with the high-compression cell. The correction for the specific conductivity of the distilled water was negligible except in very dilute solutions. L was measured to 0.001 cm with a travelling microscope. After compressing the pad in a series of steps, it was possible to expand it to almost its original length for measurements at the next electrolyte concentration by releasing the pressure in the electrodes and streaming some of the electrolyte solution through the cell.

No solution was streamed through the pad during the resistance measurements, although separate experiments revealed no perceptible difference caused by slow streaming of the solution under constant pressure. However, if the solution were streamed rapidly through the system, there was a risk of the equilibrium being disturbed by changes in temperature.

Resistances were measured with a Jones Conductivity Bridge using a Hewlitt–Packard audio-oscillator as a source of 1000 c.p.s. alternating current and a cathode-ray oscilloscope as null-point detector. It was established that the resistances measured at this frequency were the same as the d-c. values, so that there was no low-frequency dispersion effect which was previously observed (20, 21) with fibers swollen by the liquid medium.

Stream-current and Permeability Measurements

By measuring the stream-current function ($I\eta L/pD$) over a range of pad concentrations, ζ was calculated at each electrolyte concentration from the semiempirical equation (ref. 3) expressing the variation of stream current with c:

$$[15] \qquad \left[\frac{I\eta L}{pD}\right]^{2/5} = \left[\frac{Ab\zeta}{4\pi}\right]^{2/5}(1-\alpha c),$$

using the intercept method, and assuming $b = 1$. Typical rectilinear plots of stream-current data are shown in Fig. 1.

Permeability measurements were made on several pads of each material to obtain values of α and the specific surface σ. The rectilinear form of the Kozeny–Carman equation (ref. 3)

$$[16] \qquad (Kc^2)^{1/3} = \frac{(1-\alpha c)}{(5.55\,\sigma^2)^{1/3}},$$

where K is the measured permeability coefficient, was used for this purpose.

RESULTS

Measurement of κ_s

Representative plots of the variation of the pad cell constant C with electrolyte

Can. J. Chem. Downloaded from www.nrcresearchpress.com by 196.1.178.254 on 09/04/12
For personal use only.

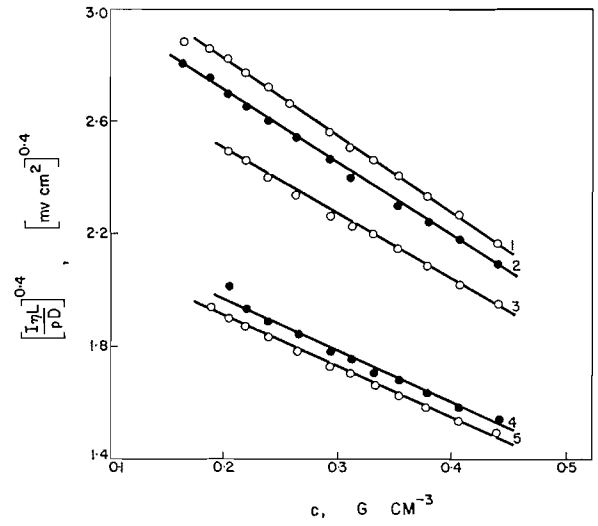

FIG. 1. Rectilinear stream-current – pad concentration plots for Dacron in 7.08×10^{-5}, 1.32×10^{-4}, 3.63×10^{-4}, 2.44×10^{-3}, 3.50×10^{-3} M $CaCl_2$ (lines 1 to 5 respectively).

concentration are shown in Fig. 2 for three concentrations of the same pad; in each case C increased with increasing ionic strength until the plateau value C_0 was reached. For the data illustrated in Fig. 2, the surface conductance represented a maximum of about 30% of the total conductance.

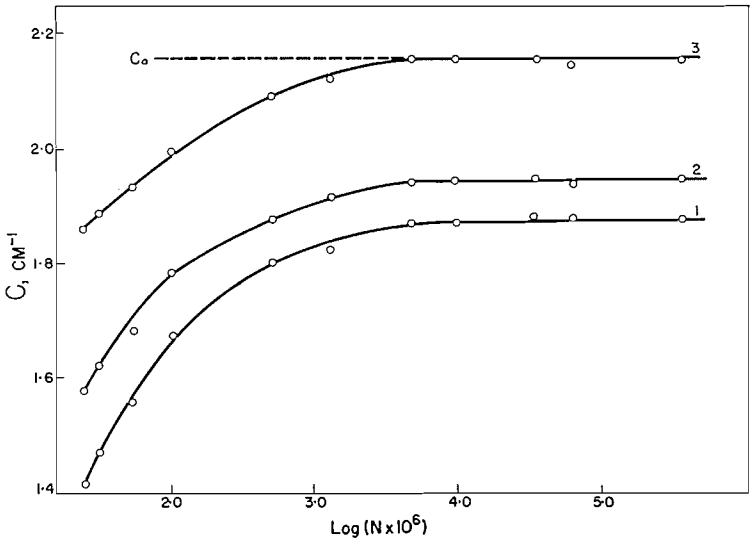

FIG. 2. Pad cell constant versus electrolyte concentration for a pad of Dacron–KCl, at pad concentrations of 0.453, 0.362, and 0.279 g/cc (curves 1 to 3 respectively). As expected from earlier considerations (3), C_0 decreased with increasing pad concentration over this range of void fractions.

Values of κ_s could be calculated from the experimental data using either eq. [10] or [13]. As already pointed out, however, the equations will yield identical results if eq. [14] is satisfied, as was established previously (3). Further confirmation of eq. [14] has been provided by the present data, as is illustrated by the typical linear plots of

Can. J. Chem. Downloaded from www.nrcresearchpress.com by 196.1.178.254 on 09/04/12
For personal use only.

$(L/C_0)^{1/2}$ vs. c shown in Fig. 3. Extrapolation of the lines yields c-intercepts which give α values in excellent agreement with those provided by the rectilinear plots of stream-current and permeability data using eqs. [15] and [16]. An exception was glass, which could not be compressed to values of ϵ sufficiently low (< 0.8) for eqs. [15] and [16] to

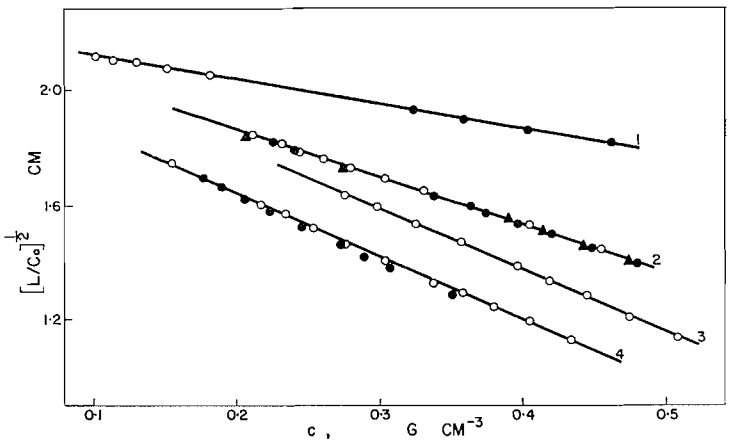

FIG. 3. Rectilinear plots of $(L/C_0)^{1/2}$ versus c for glass, Dacron, Nylon, and Orlon at high concentrations of KCl when $(\kappa_s/\kappa) = 0$ (curves 1 to 4 respectively).

be completely valid. Nevertheless, the conductance plot (Fig. 2) remained linear to void fractions as high as 0.96; the value of α for the glass fiber obtained from Fig. 3 by the intercept method was 0.39 cc/g, which is in good agreement with the specific volume of 0.40 cc/g. Thus eqs. [9] and [14] apply over a much wider range of void fractions than eqs. [15] and [16] (3). The values of σ and α used to compute κ_s are summarized in Table I.

TABLE I

Constants for various fibers

Material	α, cc/g	σ, cm^2/g
Orlon	1.05	3,500
Dacron	0.75	2,860
Nylon	0.96	2,030
Glass	0.39*	32,000†

*From conductivity plot only. Other α's from permeability, stream current, and conductivity.
†Estimated.

Equation [13] was generally used to calculate κ_s, since it was found to yield less scatter, and because it involved no assumptions as to the variation of Ω with ϵ.

At a given electrolyte concentration, κ_s should be independent of the pad concentration c. This condition was generally fulfilled and is illustrated by the typical plots shown in Fig. 4. However, because of the decreased sensitivity of the method at high electrolyte concentrations when C approached C_0, the scatter in κ_s tended to increase. In reporting κ_s, the mean value over a range of pad concentrations was calculated.

Variation of κ_s with Electrolyte Concentration

The increase in κ_s with increasing electrolyte concentration for Dacron–KCl is shown in Fig. 5 for four different pads; it is seen that the results were reproducible. Similar

Can. J. Chem. Downloaded from www.nrcresearchpress.com by 196.1.178.254 on 09/04/12
For personal use only.

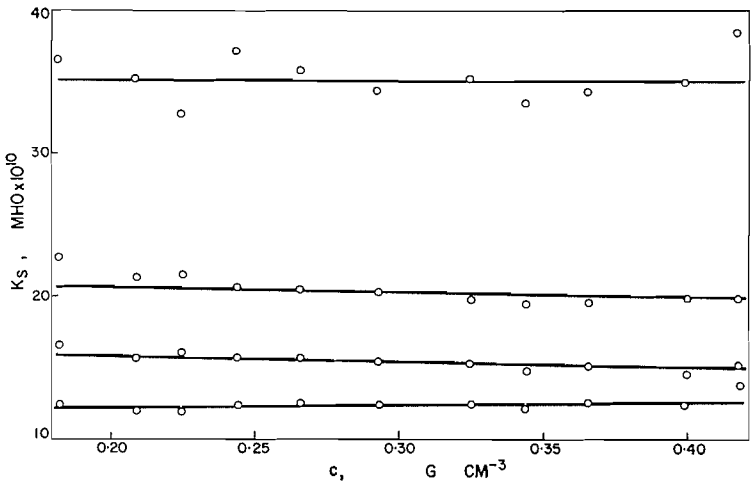

FIG. 4. Experimental values of κ_s at various pad concentrations for Orlon and 5.1×10^{-5}, 8.5×10^{-5}, 1.3×10^{-4}, and 9.6×10^{-4} N KCl (lowest to uppermost curves respectively). Note increasing scatter at higher electrolyte concentrations.

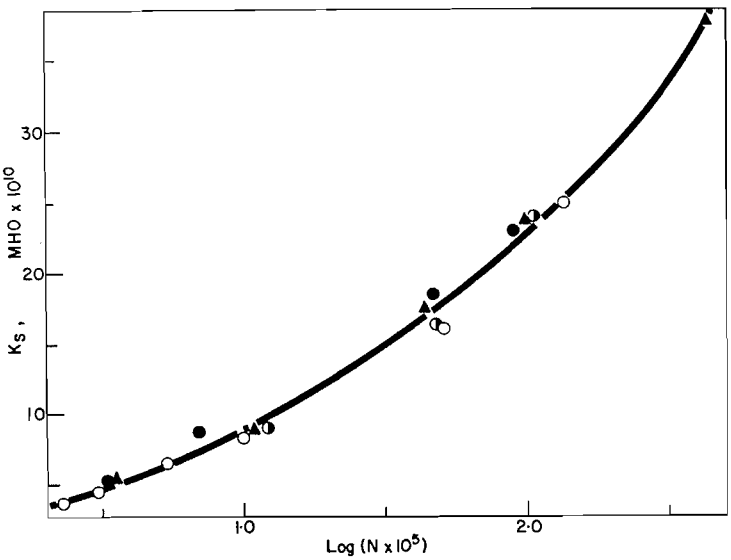

FIG. 5. Reproducibility of κ_s for five different pads of Dacron at various concentrations of KCl.

results were obtained for Dacron–HCl, Dacron–$ThCl_4$, Dacron–KCl (in 20% ethanol), Orlon–KCl, Nylon–KCl, and glass–KCl. In the system Dacron–$CaCl_2$, κ_s increased to a plateau value.

A summary of the data, including measured values of ζ and values of κ_s calculated from eq. [2] using the measured values of ζ and the literature values of the other parameters, is given in Table II. It is interesting to note that at low concentrations of KCl, ζ passed through a maximum and then decreased with increasing electrolyte concentration; this effect was almost negligible in measurements with HCl, while no maximum was observed with $CaCl_2$. This type of behavior has been observed before with various solid systems (23, 24, 25).

Can. J. Chem. Downloaded from www.nrcresearchpress.com by 196.1.178.254 on 09/04/12
For personal use only.

TABLE II

Summary of κ_s and ζ measurements

System	Electrolyte molarity	Experimental ζ eq. [15], mv	Experimental κ_s, mho $\times 10^{10}$	Theoretical κ_s eq. [2], mho $\times 10^{10}$	ψ_0 eq. [17], mv	$10^7 \cdot \delta$, cm	$10^7 \cdot x(\zeta)$, cm
Dacron–KCl	3.3×10^{-5}	−74.0	5.35	0.95			
	4.4×10^{-4}	76.4	17.5	3.65	−156	14.5	5.3
	4.7×10^{-4}	77.2	18.5	3.95	156	14.0	5.0
	8.9×10^{-4}	71.2	23.0	4.35	151	10.2	4.1
	1.0×10^{-3}	58.5	23.8	3.05	150	9.6	5.4
	4.3×10^{-3}	45.5	38.0	3.65	140	4.6	3.5
Dacron–KCl in 20% ethanol/water	4.2×10^{-5}	−108	2.10	1.00	−140	44.4	5.1
	4.5×10^{-5}	101	2.40	0.90	146	42.8	7.1
	8.9×10^{-5}	101	3.60	1.30	148	30.4	5.1
	3.2×10^{-4}	100	4.80	2.40	—	—	
Dacron–HCl	1.6×10^{-5}	−58.5	2.40	1.80	−69	76.1	10.0
	6.9×10^{-5}	46.6	5.30	2.60	72	36.5	13.1
	2.3×10^{-4}	31.0	15.5	2.55	91	19.8	17.6
	1.0×10^{-3}	15.5	30.2	2.05	89	9.6	14.7
Dacron–$CaCl_2$	7.1×10^{-5}	−53.0	7.5	3.9	−70	14.7	1.9
	1.3×10^{-4}	47.0	11.1	3.8	73	10.8	2.3
	1.6×10^{-4}	45.6	11.5	3.8	72	9.7	2.2
	3.6×10^{-4}	38.2	12.6	3.8	66	6.5	2.0
Dacron–$ThCl_4$	1.4×10^{-6}	+10	0.38	0.15			
	5.8×10^{-6}	35	1.65	0.20			
	8.8×10^{-6}	53	2.62	0.38			
	1.4×10^{-5}	65	4.3	0.7			
	2.5×10^{-5}	68	10.5	1.0			
	4.4×10^{-5}	68	17.1	1.4			
	1.8×10^{-4}	55	48.7	2.0			
	3.7×10^{-4}	47	81.2	2.5			
Orlon–KCl	5.1×10^{-5}	−51	12.3	0.50			
	8.5×10^{-5}	58	15.3	0.90			
	1.3×10^{-4}	63	20.0	1.3			
	4.9×10^{-4}	65	35.0	2.7	−187	13.7	7.2
	9.6×10^{-4}	56	35.1	2.7	171	9.8	6.2
	4.6×10^{-3}	37	49.0	2.5	151	4.5	4.3
Nylon–KCl	3.4×10^{-5}	−52	4.4	0.44			
	8.5×10^{-5}	52	3.0	0.68			
	2.3×10^{-4}	48	3.8	0.95			
	4.4×10^{-4}	43	4.8	1.03			
Nylon–HCl	1.9×10^{-5}	−33	6.7	0.80	−109	69.5	63.4
	4.1×10^{-5}		10.4				
	1.0×10^{-4}	20	17.1	0.93	−114	30.0	42.5
	1.4×10^{-4}	16	18.4	1.06	109	25.2	41.2
	3.6×10^{-4}	8.9	21.5	0.70			
Glass–KCl	5.1×10^{-5}	−81	14.5	1.5			
	4.2×10^{-3}	60	45	6.7			

In the KCl systems, for which $v_{K^+} = v_{Cl^-}$ *approximately*, calculations show that the excess ion contribution I' is about twice O. With HCl, I' is approximately $10\times O$ as the result of the high mobility of H^+.

When comparisons can be made, the κ_s values are in fair agreement with results reported by other workers. For example, Hirschler (9) obtained a value of 3.49×10^{-8} mho for glass spheres in 10^{-3} N KCl, while McBain *et al.* (4) reported a value of 4.3×10^{-8} mho for a glass surface in contact with the same concentration of KCl.

According to eq. [2], $\kappa_s = 0$ when $\zeta = 0$. Experiments were undertaken using multivalent cations such as Ce^{3+}, Al^{3+}, and Th^{4+} (as chlorides) in an attempt to pass

Can. J. Chem. Downloaded from www.nrcresearchpress.com by 196.1.178.254 on 09/04/12
For personal use only.

continuously from the normally negative ζ-potential to the positive value. Unfortunately, in each case charge reversal occurred at too low an electrolyte concentration to permit satisfactory conductance measurements near $\zeta = 0$. Previous workers (13, 26) showed that κ_s of cellulose and glass passed through a minimum at the point of charge reversal by Th^{4+}. In the present experiments Dacron became positively charged at 3×10^{-7} M $ThCl_4$; as with the negatively charged systems, κ_s increased with increasing electrolyte concentration.

Without exception the κ_s values from the experimental data were higher than the corresponding theoretical values, the discrepancy becoming more marked as the electrolyte concentration was increased. This is in accord with the experience of other workers, although they are somewhat greater than those recently found by Street (11) using kaolinite suspensions.

DISCUSSION

There are a number of plausible reasons for the discrepancies between measured and theoretical values of κ_s. Without going into the reasons in detail, we may summarize them as follows:

1. The value of σ may be too low, thus yielding incorrectly high "experimental" values of κ_s. The specific surface measured by the liquid permeability method is more properly designated the "hydrodynamic surface" (27), since it measures the area of the envelope of the "hydrodynamic volume". Because of surface roughness and other irregularities in which liquid may be immobilized the correct surface area to be used in eqs. [10] and [13] may be considerably higher than given by eq. [16]. It may be significant that Street used B.E.T. surface areas (based on nitrogen adsorption) in his measurements on kaolinite and which yielded somewhat better agreement of κ_s with theory than reported here (11).

2. In calculating κ_s from the experimental data it is assumed that the appropriate pore orientation factor is Ω_c, the factor for bulk conductance. The correct factor may instead be $\Omega_\zeta = (1-\alpha c)^{3/2}$, the factor for electrokinetic flow (3). Analysis shows that if this is so, the κ_s values of eqs. [10] and [13] would be increased by the factor $0.955/b\sqrt{\epsilon}$, which varies with c. Since $b < 1$ but is otherwise unknown (see below) it is not possible to estimate the magnitude of the effect except that the true κ_s would be increased. Thus there is some doubt of the validity of the capillary network equations, e.g. eq. [5], as has been discussed elsewhere (3).

3. The values of ζ used to calculate κ_s from eq. [2] are those calculated from the stream-current measurements using eq. [15] and assuming that $b = 1$. It has been pointed out, however, that probably $b < 1$ (3), so that the ζ-values used are probably too low. If the experimental values of κ_s listed in Table II are inserted into eq. [2] to calculate values of ζ necessary for the theory to hold, it is found that they are 2 to 10 times the values of ζ given in the same table, corresponding to values of b varying from 1/10 to 1/2. Since b must be constant, this cannot be the whole explanation.

4. In addition to invalidating eq. [16] for calculating σ as mentioned above, surface roughness may require modification of eq. [2]. If electrokinetic flow in the inner portion of the diffuse layer is hindered by irregularities in the surface, it is evident that $\zeta < \psi_0$, where ψ_0 is the potential at the surface. While the electroosmotic flow may be hindered, the excess ion contribution may be unaffected by surface roughness. Equation [2] should then become

$$\kappa_s = \left(\frac{DnkT}{2\pi}\right)^{\frac{1}{2}} [O(\zeta)+I'(\psi_0)] \qquad [17]$$

Can. J. Chem. Downloaded from www.nrcresearchpress.com by 196.1.178.254 on 09/04/12
For personal use only.

thus yielding greater values of κ_s. Table II shows a number of values of ψ_0 calculated by means of eq. [17] using values of ζ and κ_s from the same table. The values do not show any marked variation with electrolyte concentration. On this basis it is possible to estimate the magnitude of the surface roughness.

In classical double-layer theory the potential at any point in the double layer of a 1–1 electrolyte is expressed as a function of distance x from the solid surface as follows:

$$[18] \qquad \frac{x}{\delta} = \log_e \frac{[\exp(e\psi/2kT)+1][\exp(e\psi_0/2kT)-1]}{[\exp(e\psi/2kT)-1][\exp(e\psi_0/2kT)+1]}.$$

Here δ is the effective thickness of the double layer ($= (3.03\times10^{-8}$ cm$)/\sqrt{}$(ionic strength) for aqueous solutions at 25° C). By substituting $\zeta = \psi$ in eq. [18] it is possible to calculate $x(\zeta)$ the distance from the solid surface where $\psi = \psi_0$ to the electrokinetic slipping plane where $\psi = \zeta$. Thus $x(\zeta)$ is the thickness of the hydrodynamically immobilized layer. Values are included in Table II where they may be compared with δ. Bikerman (28) and Eversole and Lahr (29) estimate values of 10^{-6} to 10^{-7} cm as the magnitude of surface irregularities for "smooth" surfaces, which is the same order as $x(\zeta)$. The fact that $x(\zeta)$ is not constant for a given solid (e.g. Dacron) in the presence of various electrolytes indicates that this explanation, although reasonable, cannot account completely for the discrepancies.

Other possible reasons are (i) deviations from the ideal ion conductance eq. [4] at the high counter ion concentrations in the inner part of the double layer, (ii) the effect of adsorbed (i.e. Stern layer (30)) ions, and (iii) immobilization of the water by dielectric saturation in that part of the double layer where the electrical field strength is high (in excess of 10^5 volts/cm (31)); the effect of this on ψ_0 and κ_s is strictly analogous to that of immobilization by surface asperities as considered above.

It must be concluded that the theory of surface conductance has not been established. Evidently more precise and less equivocal measurements on better defined and smooth solids are required for clarification of the phenomena. In the light of the tentative explanations which have been advanced above, however, it is possible that additional studies of surface conductance may throw valuable light on the structure of the electrical double layer.

LIST OF SYMBOLS

a, A = cross-sectional area of capillary and pad (cm^2),
b = proportionality constant in stream-current equation,
c = pad concentration (g cm^{-3}),
C, C_0 = pad cell constant (cm^{-1}) with and without surface conductance contribution,
D = dielectric constant of solvent,
e = electronic charge,
f = perimeter of pore,
I = stream current (μa),
I' = ion-mobility term in surface conductance equation (cm$^{3/2}$ g$^{-1/2}$),
K = permeability coefficient (cm^2),
k = Boltzmann constant (ergs deg^{-1}),
L', L = length of capillary, pad (cm),
n = electrolyte concentration (ions cm^{-3}),
O = electroosmotic term in surface conductance equation (cm$^{3/2}$ g$^{-1/2}$),
p = applied pressure (dynes cm^{-2}),
q = surface charge density (e.s.u. cm^{-2}),

Can. J. Chem. Downloaded from www.nrcresearchpress.com by 196.1.178.254 on 09/04/12
For personal use only.

r = radius of capillary (cm),
R', R = electrical resistance of capillary and pad (ohms),
T = absolute temperature (deg),
v_+, v_- = ion mobilities (g^{-1} $cm^{3/2}$),
x = distance from solid surface (cm),
α = specific volume of fiber (cm^3 g^{-1}),
δ = equivalent thickness of double layer (cm),
$\epsilon = 1-\alpha c$ = void fraction of pad,
σ = specific surface of fiber (cm^2 g^{-1}),
η = viscosity of liquid (poises),
θ = pore orientation with respect to axis of pad,
ψ = electrical potential in double layer (mv),
ζ = zeta-potential,
κ = specific bulk conductivity of electrolyte (mho cm^{-1}),
κ_s = specific surface conductivity (mho),
λ = equivalent conductance (mho cm^2 per ion),
Ω_c, Ω_ζ = pore orientation factors for ion conductance and electrokinetic flow.

REFERENCES

1. GORING, D. A. I. and MASON, S. G. Can. J. Research, B, **28**, 307, 323 (1950).
2. BIEFER, G. J. and MASON, S. G. J. Colloid. Sci. **9**, 20 (1954).
3. BIEFER, G. J. and MASON, S. G. Trans. Faraday Soc. (In press).
4. MCBAIN, J. W., PEAKER, C. R., and KING, A. M. J. Am. Chem. Soc. **51**, 3294 (1929).
5. MCBAIN, J. W. and FOSTER, J. F. J. Phys. Chem. **39**, 331 (1935).
6. URBAN, F., FELDMAN, S., and WHITE, H. L. J. Phys. Chem. **39**, 605 (1935).
7. WHITE, H. L., URBAN, F., and VAN ATTA, E. A. J. Phys. Chem. **36**, 1371 (1932).
8. FRICKE, H. and CURTIS, H. J. J. Phys. Chem. **40**, 715 (1936); **41**, 729 (1937).
9. HIRSCHLER, F. G. Ph.D. Thesis, London University. May 1951.
10. MOONEY, M. J. Phys. Chem. **35**, 331 (1931).
11. STREET, N. Australian J. Chem. **9**, 333 (1956).
12. BRIGGS, D. R. J. Phys. Chem. **32**, 641 (1928).
13. BULL, H. and GORTNER, R. A. J. Phys. Chem. **35**, 309 (1931).
14. BIKERMAN, J. J. Z. physik. Chem., Abt. A, **163**, 378 (1933).
15. URBAN, F., WHITE, H. L., and STRASSNER, E. A. J. Phys. Chem. **39**, 311 (1935).
16. ROSENHEAD, L. and MILLER, J. C. P. Proc. Roy. Soc. (London), A, **163**, 298 (1937).
17. SMOLUCHOWSKI, M. V. VON. Physik. Z. **6**, 529 (1905).
18. NEALE, S. M. and STANDRING, P. T. Proc. Roy. Soc. (London), A, **213**, 530 (1952).
19. SULLIVAN, R. R. and HERTEL, K. L. Advances in colloid science. Vol. I. *Edited by* E. O. Kraemer. Interscience Publishers, Inc., New York. 1942. p. 37.
20. GORING, D. A. I., BIEFER, G. J., and MASON, S. G. Can. J. Research, B, **28**, 339 (1950).
21. MOSSMAN, C. E. Ph.D. Thesis, McGill University, Montreal. 1955.
22. STACKELBERG, M., KLING, W., BENZEL, W., and WILKE, F. Kolloid-Z. **135**, 67 (1954).
23. RUTGERS, A. J., VERLENDE, E., and MOORKENS, M. Proc. Koninkl. Akad. Amsterdam, **41**, 763 (1938).
24. RUTGERS, A. J. Trans. Faraday Soc. **36**, 69 (1940).
25. VERLENDE, E. Proc. Koninkl. Akad. Amsterdam, **42**, 764 (1939).
26. RUTGERS, A. J. and DESMET, M. Natl. Bur. of Standards (U.S.), Circ. No. **524**, 263 (1953).
27. ROBERTSON, A. A. and MASON, S. G. Pulp Paper Mag. Can. **50**, 103 (1949).
28. BIKERMAN, J. J. J. Chem. Phys. **9**, 880 (1941).
29. EVERSOLE, W. and LAHR, P. H. J. Chem. Phys. **9**, 530 (1941).
30. STERN, O. Z. Elektrochem. **30**, 508 (1924).
31. KITCHENER, J. A. and HAYDON, D. A. Nature, **183**, 78 (1959).

Can. J. Chem. Downloaded from www.nrcresearchpress.com by 196.1.178.254 on 09/04/12
For personal use only.

Can. J. Chem. Downloaded from www.nrcresearchpress.com by 196.1.178.254 on 09/04/12
For personal use only.

DISPROPORTIONATION AND RECOMBINATION OF CYANISOPROPYL RADICALS

REARRANGEMENT OF DIMETHYLKETENECYANISOPROPYLIMINE TO TETRAMETHYLSUCCINODINITRILE[1]

M. TALÂT-ERBEN AND A. N. ISFENDIYAROĞLU

ABSTRACT

Evidence is presented that the ketenimine intermediate formed in the thermal decomposition of azo-bis-isobutyronitrile (AIBN) rearranges quantitatively to tetramethylsuccinodinitrile (TMSDN), mainly by a molecular mechanism. Interpretation of experimental data on the basis of a reaction scheme consistent with the nature of the main products and the features of the kinetics of the decomposition permits estimation, by means of a simple diagram, of the extent of disproportionation, as well as that of the normal and abnormal recombination of cyanisopropyl radicals. The result obtained for the latter is in good agreement with that determined previously by an alternative method. The analysis does not exclude absolutely the possibility of side reactions in which the azo-compound partly decomposes by a molecular process, and the intermediate decomposes into free radicals. However, it is concluded that these side reactions, if any, must be of minor importance.

INTRODUCTION

A recent work by the present authors (7) has shown that as much as 55% of the initial recombination of cyanisopropyl radicals is to dimethylketenecyanisopropylimine, an unstable intermediate detected by Talât-Erben and Bywater (6). On the other hand, Bickel and Waters (3) have isolated amounts of the normal dimer, TMSDN, which correspond to an 84% radical recombination. These two results would be compatible only if part of the dinitrile is a transformation product of the intermediate. There are other observations which support this conclusion: The oily fraction, isolated by Talât-Erben and Bywater (6), which contained the ketenimine in a high concentration, slowly deposited TMSDN crystals when left standing, and in an attempt to purify the oil by chromatography, using aluminum oxide as absorbent, these authors obtained a high yield of dinitrile, and none of ketenimine. Moreover, the slope of the experimental curve reported by Bevington (1) for the formation of TMSDN as a function of conversion is not constant during decomposition as would be expected for a product forming solely at the expense of the free radicals; instead, the curve presents a marked convexity towards the conversion axis, which must indicate that a noticeable fraction of the dinitrile is produced from a precursor other than the free radicals.* Therefore, it would be of interest to reconsider the reaction scheme proposed in reference (6), in which the stable products of decomposition of the intermediate would now have to be specified as TMSDN. The reaction scheme under consideration is the following:

[1]
$$\begin{aligned} &R{-}N{=}N{-}R \rightarrow 2R\cdot + N_2 && (k_1)\\ &R\cdot + R\cdot \rightarrow \text{TMSDN} && (k_2)\\ &R\cdot + R\cdot \rightarrow \text{Intermediate} && (k_3)\\ &\text{Intermediate} \rightarrow \text{TMSDN} && (k_4)\\ &R\cdot + R\cdot \rightarrow \text{ISBN} + \text{MAN}. && (k_4) \end{aligned}$$

[1]*Manuscript received March 4, 1959.*
Contribution from the Faculty of Mining Engineering, Technical University of Istanbul, Istanbul, Turkey.
**It is interesting to note that Bevington (1), who ignored the intermediate, considering the shape of this curve, came to the conclusion that the percentage of free radical disproportionation decreases as the decomposition proceeds. However, it will be seen that disproportionation, and recombination as well, remain constant in the whole course of the reaction; the apparent decrease of the former (or the apparent increase of the latter) can be accounted for by the intermediate rearranging to the dinitrile, as suggested quite properly by Walling (8).*

The rate constant for the decay of intermediate has been taken equal to the rate constant of decomposition of the azo-compound in accordance with the features of the kinetics (6). The radical disproportionation products, isobutyronitrile and methacrylonitrile, are denoted as ISBN and MAN respectively.

Integration of the rate equations using the steady-state hypothesis and proper boundary conditions gives for the intermediate the same relations as those of reference (6). In addition, the following relation is obtained between the concentration D of the dinitrile and the time:

$$[2] \qquad 1-\frac{D}{A_0-A} = \frac{k_4}{k_2+k_3+k_4}+\frac{k_3}{k_2+k_3+k_4}\cdot\frac{k_1t}{e^{k_1t}-1}$$

where A_0 and A are the initial concentration and the concentration at any time of azo-compound, respectively. It is seen that if the expressions $k_1t/(\exp k_1t-1)$ and $1-D/(A_0-A)$ are taken as the abscissa and ordinates, respectively, the experimental points will define a straight line, whose slope and ordinate at the origin will be numerically equal to the extent of the abnormal recombination and that of disproportionation, respectively.

Bevington (1) has measured the amounts of TMSDN formed at various stages of the decomposition of 1 mg of AIBN at 60° C, using C^{14}-labelled azo-compound. Bevington's results may be used to check [2] for this particular temperature. Inspection of [2] shows that the slope and the ordinate at the origin of the straight line are exclusive functions of rate constants of free radical recombination reactions; it follows that these geometrical elements must be temperature-independent, owing to the very low activation energies associated with reactions of this kind. To check this, measurements have been carried out at a different temperature, namely 80° C, under the experimental conditions described below.

EXPERIMENTAL

The azo-compound* (Westville Laboratories, Monroe, Connecticut) was recrystallized from benzene; m.p. 102° C decomp. The thermal decomposition was carried out at 80° in toluene (C.P.), in a thermostat controlled to about 0.1°, under a stream of purified nitrogen, with continual shaking. Azo-compound (1.6 to 1.8 g) was decomposed in 50 cc of toluene. At the end of a definite reaction time the solution was cooled quickly to stop the reaction, and transferred quantitatively into a separatory funnel. Fifty cubic centimeters of 1 N HCl were added, and the two phases were stirred vigorously for at least 20 minutes in order to hydrolyze the ketenimine present in, and remove its hydrolytic products from, the toluene solution. This operation of removal of the ketenimine was repeated at least three times with fresh portions of HCl. Then, the toluene layer was taken quantitatively in a weighed crystallization dish, and the solvent evaporated to constant weight under an air current provided by the fan of a fume hood, the window of which was kept low enough to maintain an efficient air flow. Under these conditions the residue must consist of a mixture of the undecomposed AIBN and TMSDN formed, ignoring minor amounts of 2,3,5-trimethyl-2,3,5-tricyanohexane identified by Bickel and Waters (3). ISBN and MAN (both low boiling point liquids) escape along with toluene. The sublimation of TMSDN was studied by using an authentic sample of this compound. It was found that a 4-hour prolongation of the drying period, under the same conditions, caused only about 1% loss of weight. The undecomposed amount of AIBN was calculated,

Kindly supplied by Dr. S. Bywater of the National Research Council of Canada.

Can. J. Chem. Downloaded from www.nrcresearchpress.com by 196.1.178.254 on 09/04/12
For personal use only.

using the value 1.55×10^{-4} sec^{-1} for the rate constant of decomposition at 80° (6). This was subtracted from the weight of the residue to obtain that of TMSDN formed at the particular reaction time.

RESULTS AND DISCUSSION

Experiments were performed at 80° with reaction times of 60, 90, 120, 150, 240, and 900 minutes. The amounts of TMSDN found are given in Fig. 1 (circles), where Bevington's (1) data (squares) at 60° are also quoted. Both sets of points fall nearly on the same curve, as the equation

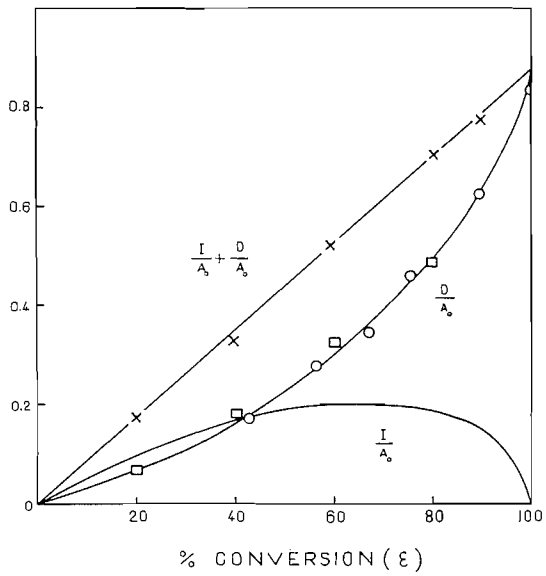

FIG. 1. Moles of TMSDN (upper curve) and ketenimine intermediate (lower curve), present at various stages of the decomposition of 1 mole of AIBN. Circles: Data at 80°; squares: Bevington's (1) results at 60°. The fact that the ordinates of the two curves add up to give a straight line signifies that the intermediate decays quantitatively to TMSDN, and that this decay is almost exclusively a molecular process.

$$[3] \qquad \frac{D}{A_0} = \frac{k_2+k_3}{k_2+k_3+k_4}\epsilon + \frac{k_3}{k_2+k_3+k_4}(1-\epsilon)\ln(1-\epsilon)$$

requires (ϵ is the extent of decomposition). In Fig. 1 the curve for the intermediate, reported in reference (7), whose equation in terms of ϵ is:

$$[4] \qquad \frac{I}{A_0} = -\frac{k_3}{k_2+k_3+k_4}(1-\epsilon)\ln(1-\epsilon),$$

has also been given.

It is seen that the curve $(D/A_0)+(I/A_0)$ versus ϵ must be a straight line if scheme [1] applies. The sums of the ordinates of the two experimental curves at $\epsilon = 0.20$, 0.40, 0.60, 0.80, and 0.90 are also indicated on the same diagram (points marked ×); it is seen that they lie along a straight line, quite satisfactorily. This would be the case only *if* the intermediate decays quantitatively to TMSDN. In fact, it is only in this case that the absolute value of I/A_0 and that of the second term on the right-hand side of [3] are equal, and eliminate each other leaving only the linear term in ϵ. This is simply a requirement of the material conservation. The ordinate of the straight line at $\epsilon = 1$, which

Can. J. Chem. Downloaded from www.nrcresearchpress.com by 196.1.178.254 on 09/04/12
For personal use only.

must measure the total fraction of recombination, is found to be 0.84, in excellent agreement with Bickel and Waters (3). Furthermore, the intersection of the two curves, which occurs at $\epsilon = 0.42$, gives for the ratio k_2/k_3 the value 0.50, which means that the extent of the abnormal recombination of the radicals is twice their normal recombination; this unexpected result can also be seen on Fig. 2. The sum and the ratio of the extent of the two recombinations being now known, their individual values can be calculated as 0.28 and 0.56; the former is in good agreement with the value obtained by an alternative method without making use of the curve for the intermediate (Fig. 2).

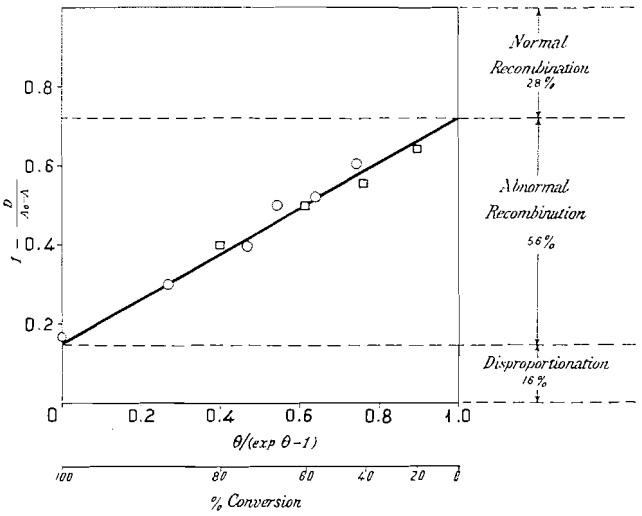

FIG. 2. Graphical estimation of the extent of the normal and abnormal recombination, and dispro portionation. The quantity $1-D/(A_0-A)$ may be called the "apparent" extent of disproportionation; it decreases during decomposition, the true one, $k_4/(k_2+k_3+k_4)$, remaining constant.

As it has already been pointed out, another implication of our reaction scheme is that a plot of $1-D/(A_0-A)$ versus $k_1t/(\exp k_1t-1)$ has to be a straight line, irrespective of the constant temperature at which the amounts D and A are measured. This is shown to be the case in Fig. 2, using again both Bevington's (1) data at 60° and the results of the present work at 80°. It is seen that the slope of the best line gives for the extent of the abnormal recombination the value 0.56, which is in good agreement with that of reference (7).

We have worked out a number of reaction schemes resulting from suitable modifications applied to the one under consideration, in such a way as to make it possible to check some conclusions reached by various authors. For example, Roy *et al.* (5) suggest that the path through the ketenimine intermediate does not involve free radicals. A simple calculation shows that in this case the slope of the straight line of Fig. 2 will be equal to the fraction of AIBN which decomposes molecularly; but, the existing data on the catalyst efficiency of AIBN in styrene and methyl methacrylate polymerization, namely 60% between 30° and 80° (see Tobolsky, A. V. Ann. Rev. Phys. Chem. **7**, 175 (1956), and references given therein), set a limit of 0.40 for the highest possible value of the slope, which would be clearly distinguishable from the observed value of 0.56. This excludes a reaction scheme in which the intermediate is assumed to have a non-radical precursor, although such a scheme would exhibit kinetic features similar to those of the mechanism under consideration. On the other hand, Bevington's (2) conclusion that part of the azo-

Can. J. Chem. Downloaded from www.nrcresearchpress.com by 196.1.178.254 on 09/04/12
For personal use only.

compound decomposes by a molecular mechanism would be inconsistent with the properties of the diagrams presented herein, unless the extent of such a decomposition is negligible. In the same way, it can be shown that a reaction scheme in which it is postulated that at least a fraction of the ketenimine intermediate regenerates cyanisopropyl free radicals, as claimed by Hammond (4), cannot be maintained, unless this fraction is negligibly small. In fact, let P denote disproportionation products, I intermediate, D dimer, ϵ extent of decomposition. The equation $A_0\epsilon = I+D+P$ is true for any mechanism involving an intermediate by any path of formation and decomposition. Now, if the intermediate, which is formed in large quantities, decays to form free radicals, P/A_0 and hence $(I/A_0)+(D/A_0)$ cannot be linear in ϵ. Thus, a free radical successor for the intermediate should also be excluded.

NOTE ADDED IN PROOF

Dr. S. Bywater has kindly drawn our attention to a recent work by Keys, R. T. and Hammond, G. S. Dissertation Abstr. February, 1934 (1959), in which the authors use the ketenimine as initiator in the polymerization of styrene. This may at first sight seem contradictory to the conclusion reached in the present paper that the ketenimine decays molecularly. However, their results indicate that the catalyst efficiency of this compound changes with monomer concentration, and they advance the explanation that "the monomer may complex with the radicals from the decomposition of the initiator thereby to decrease the importance of cage effects". This means that the smaller the monomer concentration the larger the cage effects. Then, in the limiting case of the complete *absence* of monomer, which is the case in our experiments, the "cage effect" (one could rather say "the intramolecular recombination of the two radicals" instead) is predominant. Thus, in the decay of intermediate in a non-reactive solvent there is no noticeable formation of "free" radicals, so that the process exhibits the characteristics of an almost exclusively molecular decomposition.

REFERENCES

1. BEVINGTON, J. C. J. Chem. Soc. 3707 (1954).
2. BEVINGTON, J. C. J. Chem. Soc. 1127 (1956).
3. BICKEL, A. F. and WATERS, W. A. Rec. trav. chim. **69**, 1490 (1950).
4. HAMMOND, G. S. Ann. Rev. Phys. Chem. **8**, 323 (1957).
5. ROY, J.-C., NASH, J. R., WILLIAMS, R. R., JR., and HAMILL, W. H. J. Am. Chem. Soc. **78**, 519 (1956).
6. TALÂT-ERBEN, M. and BYWATER, S. J. Am. Chem. Soc. **77**, 3710 (1955); **77**, 3712 (1955).
7. TALÂT-ERBEN, M. and ISFENDIYAROĞLU, A. N. Can. J. Chem. **36**, 1156 (1958).
8. WALLING, C. Free radicals in solution. John Wiley and Sons, Inc., New York. 1957. p. 514.

Can. J. Chem. Downloaded from www.nrcresearchpress.com by 196.1.178.254 on 09/04/12
For personal use only.

Can. J. Chem. Downloaded from www.nrcresearchpress.com by 196.1.178.254 on 09/04/12
For personal use only.

THE PHASE DIAGRAM OF THE SYSTEM Na_3AlF_6–Na_2SO_4 AND THE DISSOCIATION OF THE CRYOLITE ANION IN MOLTEN SODIUM SULPHATE[1, 2]

KAI GRJOTHEIM, TOR HALVORSEN, AND SIGMUND URNES[3]

ABSTRACT

The binary system Na_3AlF_6–Na_2SO_4 has been investigated. A eutectic point was found at 91 mole % Na_2SO_4. On the Na_3AlF_6 side of the diagram extensive solid solution was found. No solid solution was observed on the Na_2SO_4 side, either by thermal analysis or by Debye–Scherrer diagrams. The freezing point depression of Na_2SO_4 caused by additions of Na_3AlF_6 has been used to evaluate the dissociation scheme of the cryolite anion in a sodium sulphate melt. The calculations favor the following scheme:

$$AlF_6^{3-} = AlF_4^- + 2F^-.$$

INTRODUCTION

Current interest (1, 2) in the structure of molten cryolite has led to the examination of some binary systems containing cryolite. Assuming ideal ionic mixtures, the phase diagrams of these systems may be used for calculations of the dissociation of the cryolite anion. For this purpose, systems without solid solutions but with ions sufficiently similar to justify the assumption of ideal ionic mixtures (3) were chosen.

The first system to be studied was Na_2SO_4–Na_3AlF_6.

EXPERIMENTAL

The experimental techniques involved in the present study have been described in previous papers from this Institute (1, 4, 5, 6, 7).

The investigation was mainly undertaken by careful recording of cooling curves. However, for the determination of the solidus curve the method of Flood and Seltveit (4) was used. By this method, a very small amount is added of a third, radioactive component which is soluble in the liquid, but insoluble in the solid phase. For these experiments Cs^{134} in the form of the chloride was used as a tracer.

The reagents used were sodium sulphate from Merck (Darmstadt, Germany) chemically pure quality, and hand-picked crystals of cryolite from Ivigtut, Greenland.

Some of the experimental data are given in Table I, and the phase diagram is shown in Fig. 1. The eutectic mixture contains 91 mole % Na_2SO_4. The maximum amount of Na_2SO_4 that can be taken in solid solution by Na_3AlF_6 is 80 mole %.

No solution of Na_3AlF_6 in solid Na_2SO_4 was detected, either by thermal analysis or by Debye–Scherrer diagrams made on the samples.

ON THE DISSOCIATION OF CRYOLITE

Structural Models for the Melt and Method of Calculation

Structural interpretations of the liquidus line in systems without solid solubility seem in many cases to give information of considerable value (2).

[1]*Manuscript received in original form November 25, 1958, and, as revised, March 23, 1959.*
[2]*This work is based on a thesis by Tor Halvorsen submitted to The Technical University of Norway in 1956 in partial fulfillment of requirements for the degree Sivilingeniör.*
[3]*Present address: The Royal Norwegian Council for Scientific and Industrial Research, Institute of Silicate Science, The Technical University of Norway, Trondheim, Norway.*

TABLE I

Experimental data on the Na_2SO_4 side of the system Na_3AlF_6–Na_2SO_4

No.	Mole fractions, $N_{Na_2SO_4}$	Observed, ° C: First crystallization	Observed, ° C: Eutectic temperature
1	1.0000	884.1	
2	0.9882	867.6	
3	0.9755	852.8	796.6
4	0.9561	834.7	798.1
5	0.9453	825.5	798.1
6	0.9244	807.2	796.8
7	0.9087	798.6	798.6

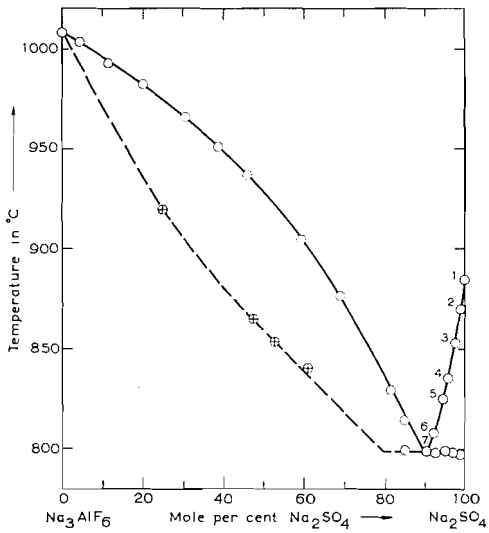

FIG. 1. The system Na_3AlF_6–Na_2SO_4. ○ Liquidus line and eutectic line determined by thermal analysis. ⊕ Solidus line determined with Cs^{134}-tracer by high-temperature filtration.

Investigations by different methods of several binary salt systems with sodium sulphate have by now fairly well established that pure molten sodium sulphate is composed of sodium cations and anions of the sulphate group (6). A review of structural models with corresponding dissociation schemes for pure molten cryolite is given in a previous paper (2).

In the following, the correctness of the most probable of these models will be tested by comparing the calorimetrically determined heat of fusion of sodium sulphate with the heats of fusion that can be evaluated according to the different models from the freezing point depression data of sodium sulphate caused by cryolite additions.

The following two dissociation schemes for the cryolite anion will be considered:

$$AlF_6^{3-} = AlF_4^- + 2F^-$$

$$AlF_6^{3-} = Al^{3+} + 6F^-.$$

The first one will be quantitatively treated here both for complete and part dissociation. The last one has only been considered for the complete dissociation.

Can. J. Chem. Downloaded from www.nrcresearchpress.com by 196.1.178.254 on 09/04/12
For personal use only.

Can. J. Chem. Downloaded from www.nrcresearchpress.com by 196.1.178.254 on 09/04/12
For personal use only.

The equations used in the calculations are well known in classical physical chemistry, but they will be briefly reviewed.

The liquidus line on the sulphate side of the phase diagram gives the composition of the liquid phase which is in equilibrium with pure solid sodium sulphate at the temperature T. The partial free energy of sodium sulphate in the liquid, referred to pure liquid sodium sulphate at the same temperature as the standard state, is given by the following equation:

$$[1] \qquad \overline{\Delta F}_{Na_2SO_4} = \overline{\Delta H}_{Na_2SO_4} - T\overline{\Delta S}_{Na_2SO_4} = -\Delta H_f[1-(T/T_0)]$$

where T_0 is the melting point of pure sodium sulphate and ΔH_f is the heat of fusion. (In obtaining these equations the difference in the specific heat between the solid and liquid sodium sulphate is as usual (8) neglected, because of its small influence.)

In this case we are dealing with mixtures high in sodium sulphate, so we will neglect the energy term in the free energy equation. Equation [1] is thus reduced to

$$[2] \qquad T\overline{\Delta S}_{Na_2SO_4} = \Delta H_f[1-(T/T_0)].$$

In the following we will use Temkin's model (3) of fused salts to evaluate the expression for $\overline{\Delta S}_{Na_2SO_4}$.

The Temkin model can be summarized as follows:

1. The entropy of mixing is entirely configurational.
2. There are two sets of positions in the salt melts, one for the cations and one for the anions.
3. The cations and the anions are randomly distributed over all the cation and anion positions regardless of the magnitude of the charges.

According to this, the partial entropy of sodium sulphate is given by:

$$[3] \qquad \overline{\Delta S}_{Na_2SO_4} = -R \ln (N^2_{Na^+} \cdot N_{SO_4^{2-}})$$

where N_{Na^+} and $N_{SO_4^{2-}}$ are the cation and anion fractions. These ionic fractions will depend on what structural models are chosen for the cryolite anion in the molten mixture.

Plotting $\ln (N^2_{Na^+} \cdot N_{SO_4^{2-}})$ as a function of $1/T$ should give a straight line in the region where $\overline{\Delta H}_{Na_2SO_4}$ can be neglected. The slope of this line should correspond to the calorimetrically determined heat of fusion of sodium sulphate (9). In this way a means is provided to distinguish between different structural models.

RESULTS

If the cryolite anion does not dissociate in the sulphate melt, the ionic fractions of sodium sulphate will be:

$$N_{Na^+} = 1$$

$$N_{SO_4^{2-}} = n_{Na_2SO_4}/(n_{Na_2SO_4}+n_{Na_3AlF_6})$$

where $n_{Na_2SO_4}$ and $n_{Na_3AlF_6}$ are the molar amounts of sodium sulphate and cryolite in the melt.

Plotting for this model $\ln (N^2_{Na^+} \cdot N_{SO_4^{2-}}) = \ln N_{SO_4^{2-}}$ against $1/T$ gives a heat of fusion around 1900 cal/mole as shown by the dashed line in Fig. 2.

Assuming that the cryolite anion dissociates completely into AlF_4^- ions and fluoride ions, we get these expressions for the ionic fractions:

$$N_{Na^+} = 1$$

$$N_{SO_4^{2-}} = n_{Na_2SO_4}/(n_{Na_2SO_4}+3n_{Na_3AlF_6}).$$

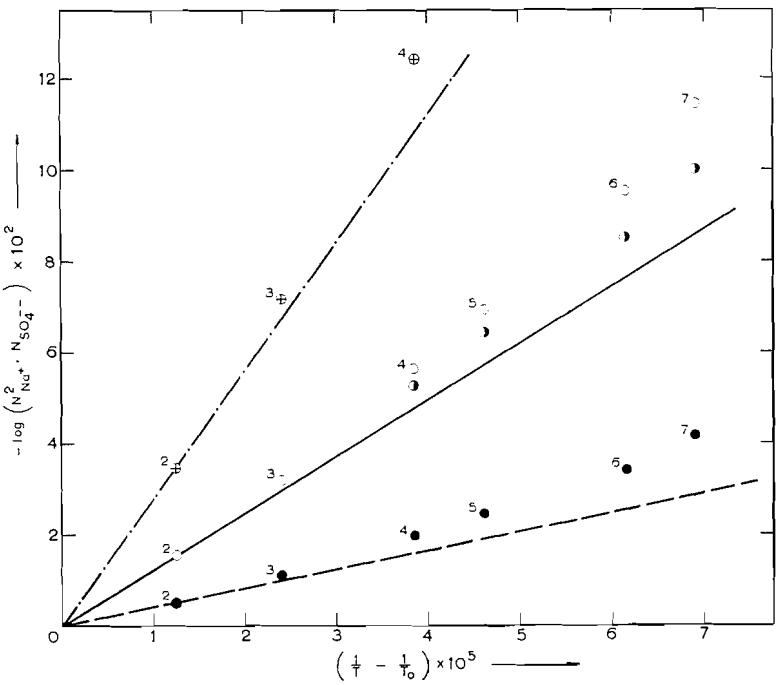

FIG. 2. $-\text{Log}\ (N^2_{Na^+} \cdot N_{SO_4^{2-}})$ versus $1/T$ on the sodium sulphate side of the system Na_3AlF_6–Na_2SO_4, $(N^2_{Na^+} \cdot N_{SO_4^{2-}})$ is calculated according to four different models of the melt. ● Temkin ionic mixture of the ions Na^+, SO_4^{2-}, and AlF_6^{3-}. ○ Temkin ionic mixture of the ions Na^+, SO_4^{2-}, AlF_4^-, and F^-. ◑ Same as above, except AlF_6^{3-} is only partly dissociated into $AlF_4^- + 2F^-$ (with the dissociation constant $K = 0.06$). ⊕ Temkin ionic mixture of the ions Na^+, Al^{3+}, SO_4^{2-}, and F^-. Full line corresponds to the calorimetrical determined heat of melting for sodium sulphate of 5670 cal/mole, dashed line corresponds to 1900 cal/mole, and dashed-dotted line to about 13,000 cal/mole.

A plot (full line in Fig. 2) of $\ln N_{SO_4^{2-}}$ against $1/T$ gives in this case a curve with a limiting slope corresponding to the calorimetrically determined heat of fusion 5670 cal/mole (9).

For comparison, the ionic fractions of Na^+ and SO_4^{2-} are also calculated for an assumed complete dissociation of the cryolite anion into Al^{3+} and $6F^-$ ions. In this case we have:

$$N_{Na^+} = (2n_{Na_2SO_4} + 3n_{Na_3AlF_6})/(2n_{Na_2SO_4} + 4n_{Na_3AlF_6})$$

$$N_{SO_4^{2-}} = n_{Na_2SO_4}/(n_{Na_2SO_4} + 6n_{Na_3AlF_6}).$$

A plot of $\ln (N^2_{Na^+} \cdot N_{SO_4^{2-}})$ against $1/T$ gives in this case a curve (dashed-dotted line in Fig. 2) with a limiting slope corresponding to a heat of fusion around 13,000 cal/mole. (The ionic fractions calculated according to the different models are listed in Table II.)

The results are clearly in favor of the dissociation scheme:

$$AlF_6^{3-} = AlF_4^- + 2F^-.$$

Therefore, a calculation was undertaken using the dissociation constant $K = 0.06$ previously found for this scheme (1, 2). As seen from Fig. 2 this assumption brings the experimental points at higher concentrations closer to the straight line. When a dissociation constant equal to 0.02 is used the points will fall close around the line which corresponds to the heat of fusion of sodium sulphate.

Can. J. Chem. Downloaded from www.nrcresearchpress.com by 196.1.178.254 on 09/04/12
For personal use only.

Can. J. Chem. Downloaded from www.nrcresearchpress.com by 196.1.178.254 on 09/04/12
For personal use only.

TABLE II

Some calculated values for different dissociation schemes of the cryolite anion on the Na_2SO_4 side of the system Na_3AlF_6–Na_2SO_4. The experimental data are taken from Table I

		Calculated as an ideal Temkin mixture of the ions							
		Na^+, SO_4^{2-}, and AlF_6^{3-}		Na^+, SO_4^{2-}, AlF_4^-, and F^-		Na^+, SO_4^{2-}, AlF_6^{3-}, AlF_4^-, and F^- ($K = 0.06$)		Na^+, Al^{3+}, SO_4^{2-}, and F^-	
No.	$\left(\frac{1}{T} - \frac{1}{T_0}\right)10^3$	$N_{SO_4^{2-}}$	$-\log N_{SO_4^{2-}}$	$N_{SO_4^{2-}}$	$-\log N_{SO_4^{2-}}$	$N_{SO_4^{2-}}$	$-\log N_{SO_4^{2-}}$	$N^2_{Na^+} \cdot N_{SO_4^{2-}}$	$-\log(N^2_{Na^+} \cdot N_{SO_4^{2-}})$
1	0	1.0000	0	1.0000	0	1.0000	0	1.0000	0
2	0.0125	0.9882	0.0052	0.9654	0.0153	0.9656	0.0152	0.9222	0.0352
3	0.0240	0.9755	0.0108	0.9299	0.0316	0.9314	0.0309	0.8483	0.0715
4	0.0385	0.9561	0.0195	0.8789	0.0561	0.8849	0.0531	0.7514	0.1241
5	0.0461	0.9453	0.0244	0.8521	0.0695	0.8618	0.0646	0.7043	0.1522
6	0.0615	0.9244	0.0341	0.8030	0.0953	0.8214	0.0855	0.6245	0.2045
7	0.0689	0.9087	0.0416	0.7684	0.1144	0.7940	0.1002	0.5728	0.2420

Discussion of Other Experimental Data for this System

A few freezing point depression measurements were undertaken in sodium sulphate by a simultaneous addition of small amounts of both cryolite and sodium fluoride. To get the points on the straight line corresponding to the calorimetric heat of fusion of sodium sulphate it was necessary, for this mixture, to use a dissociation constant $K = 0.04$, to be compared with 0.06 above.

The complete dissociation of AlF_6^{3-} into $6F^-$ ions and one Al^{3+} ion in sulphate melt can be also ruled out from some other experimental evidence. This reaction scheme leads to free Al^{3+} ion. However, at the actual temperatures Al^{3+} will be a stronger acid than SO_3. The following reaction will therefore take place:

$$2Al^{3+} + 3SO_4^{2-} = Al_2O_3 + 3SO_3(g).$$

Thus addition of $Al_2(SO_4)_3$ or $KAl(SO_4)_2$ to sodium sulphate melts leads to SO_3 evolution corresponding to the reaction just mentioned.

If aluminum fluoride is added to a sodium sulphate melt, there will not be sufficient fluoride to form any stable AlF_4^- complex and we should thus expect a reaction between Al^{3+} and the sulphate ion. To test this the following experiments were carried out. In a platinum crucible, Na_2SO_4, with small additions of AlF_3, was heated to melting. The whole system was kept just above the melting point of sodium sulphate in an inactive atmosphere for about half an hour. The heating resulted in a loss of weight corresponding to about one mole of SO_3 given off for each two moles of AlF_3. However, if NaF is added to the charge before the run, a little in excess of the composition $NaAlF_4$, no loss in weight is observed, neither does any addition of cryolite to sodium sulphate give any loss of weight by melting.

CONCLUSIONS

Cryoscopic data for the liquid mixtures of $NaCl$–Na_2SO_4 and $NaBr$–Na_2SO_4 (4) indicate that these systems are essentially ideal over a wide concentration range. Careful measurements of e.m.f. between oxygen electrodes in the system Na_2SO_4–Na_2CO_3 (10) have shown the ideality of that system. It is, thus, fair to assume that a liquid mixture containing the ionic species Na^+, F^-, AlF_4^-, AlF_6^{3-}, and SO_4^{2-} should also show ideal behavior. In that case it may be concluded from this study of the system Na_2SO_4–Na_3AlF_6 that cryolite anion dissociates in sodium sulphate melt according to the scheme

$$AlF_6^{3-} = AlF_4^- + 2F^-,$$

with a dissociation constant of the same order as previously found by similar calculations for the cryolite anion in the system NaF–AlF_3. The surprisingly good agreement may indicate that the AlF_4^- ion is fairly stable at these temperatures.

REFERENCES

1. GRJOTHEIM, K. Contribution to the theory of the aluminium electrolysis. Kgl. Norske Videnskab. Selskabs, Skrifter, No. 5 (1956).
2. BRYNESTAD, J., GRJOTHEIM, K., and URNES, S. Z. Elektrochem. (In press).
3. TEMKIN, M. Acta Physicochim. U.R.S.S. **20**, 411 (1945).
4. SELTVEIT, A. and FLOOD, H. Acta Chem. Scand. **12**, 1030 (1958).
5. FLOOD, H., FÖRLAND, T., and NESLAND, A. Acta Chem. Scand. **5**, 1193 (1951).
6. FLOOD, H., FÖRLAND, T., and GRJOTHEIM, K. The physical chemistry of melts. A symposium on the nature of molten slags and salts held by the Nuffield Research Group in Extraction Metallurgy, London. February 20, 1952. Printed by Institution of Mining and Metallurgy, London. 1953. p. 49.
7. GRJOTHEIM, K., GRÖNVOLD, F., and KROGH-MOE, J. J. Am. Chem. Soc. **77**, 5824 (1955).
8. GUGGENHEIM, E. A. Mixtures. The Clarendon Press, Oxford. 1952. p. 11.
9. COUGHLIN, J. P. J. Am. Chem. Soc. **77**, 868 (1955).
10. FLOOD, H., FÖRLAND, T., and MOTZFELDT, K. Acta Chem. Scand. **6**, 257 (1952).

Can. J. Chem. Downloaded from www.nrcresearchpress.com by 196.1.178.254 on 09/04/12
For personal use only.

Can. J. Chem. Downloaded from www.nrcresearchpress.com by 196.1.178.254 on 09/04/12
For personal use only.

REACTIONS OF TITANIUM HALIDES WITH ORGANOMETALLIC COMPOUNDS

I. STOICHIOMETRY OF THE REACTIONS BETWEEN TITANIUM TETRACHLORIDE AND SOME ORGANOMETALLIC COMPOUNDS[1]

ALBERTO MALATESTA[2]

ABSTRACT

The over-all stoichiometry of the reactions involving titanium tetrachloride and various organometallic compounds has been determined. While titanium tetrachloride reacts with aluminum ethyldichloride and lead tetraethyl according to a 1:1 stoichiometry for any ratio investigated, the reaction between aluminum triethyl and titanium tetrachloride proceeds according to different paths when the ratio of the reagents is changed. Equations describing the reactions between aluminum triethyl and titanium tetrachloride, where the stoichiometries are respectively 1:1, 1:2, 1:3, are derived. Although a certain amount of hydrogen has been isolated after hydrolysis of the products of these reactions, no definite evidence is found for the presence of Ti(II).

In all the experiments (except those in which an Al/Ti ratio greater than unity was used) substantial amounts of ethyl chloride and ethylene have been found, together with the main gaseous components, ethane and butane. A higher alkane was also isolated from the solid products of the reaction and is equal to the quantity of ethane liberated.

INTRODUCTION

The reaction of organometallic compounds with titanium derivatives has been under investigation for a long time (1) in an attempt to prepare compounds containing titanium–carbon bonds. Gilman and Jones (2), reacting phenylmagnesium bromide with tetrabutyl titanate in ether at about 8° C, succeeded in demonstrating the formation of a Ti–C bond by a test with Michler's ketone which developed slowly but ultimately became strong in color. The colors appearing in the reaction mixture, attributable to titanous compounds, led to the conclusion that the phenyl–titanium bond decomposes spontaneously giving phenyl radicals and Ti(III). In the case of a reaction mixture of methylmagnesium bromide and tetrabutyl titanate, the formation of Ti(III) and methane was observed to proceed at the same rate. Herman and Nelson (3), using phenyl lithium and isopropyltitanate in ether at 8–15° C, succeeded in preparing a compound whose analysis led to the formulation $C_6H_5Ti(OC_3H_7)_3 \cdot LiOC_3H_7 \cdot LiBr \cdot (C_2H_5)_2O$. This compound was reacted further with an excess of titanium tetrachloride, and phenyltitanium triisopropoxide was isolated with a yield of 53%. This compound is very stable, it melts at 88–90° C and shows no darkening after 1 year of storage at 10° C. On being heated at 100–120° C it decomposes giving a violet compound. In a second paper the same authors (4) report some information on the stability of titanium–carbon bonds as a function of the alkyl or aryl groups involved in the organometallic bond, of the number of these groups attached to the titanium atom, and of the nature of the other groups bonded to the metal atom. Using phenylmagnesium bromide and titanium tetrabutylate in different ratios, they found that a different organotitanium compound is formed for each ratio used. They based their conclusions on the rate of spontaneous decomposition of solutions of the organometallic compounds. Although no clear-cut evidence is given, the formation of highly unstable polyphenyltitanium compounds is favored when higher ratios are used, while more stable mono-substituted phenyltitanium compounds are formed at lower ratios. Ti(II) was found at higher ratios (from hydrogen evolved upon

[1]*Manuscript received March 19, 1959.*
[2]*Present address: Dunlop Research Centre, Toronto 8, Ontario.*

hydrolysis of the products of the reaction) suggesting that diphenyltitanium may be present as a relatively stable organometallic compound. Summers and Uloth (5), reacting bis-(cyclopentadienyl)-titanium halides with several lithium aryls, succeeded in preparing relatively stable compounds containing two titanium–carbon bonds.

The present series of experiments was carried out in order to determine the over-all stoichiometry involved in the alkylation reaction of titanium tetrachloride with various organometallic compounds.

EXPERIMENTAL

Materials

$AlEt_3$ (Ethyl Corp.) was vacuum-distilled through a short Vigreux column and stored at room temperature. The purity of the product was checked by gravimetric analysis with 8-hydroxyquinoline (6 *b*) and potentiometrically (7) in order to determine the amount of aluminum triethyl, aluminum diethyl monohydride, and aluminum alkoxide derivatives. The aluminum triethyl used in this investigation was 99.8% pure. No aluminum hydride derivatives were found and the only impurities present were aluminum alkoxide compounds.

$AlEtCl_2$ was prepared according to the procedure of Grosse and Mavity (8), distilled through a Vigreux column, and stored at room temperature. Gravimetric analysis gave a purity of 99.9%.

$TiCl_4$ (Fisher) was purified according to the procedure of Gilchrist (9).

$PbEt_4$ (Ethyl Corp.) was dehydrated with anhydrous magnesium sulphate, filtered, and stored in a dark bottle under nitrogen. The purity of the product was determined iodometrically (6 *a*) and was 99.2%.

Prepurified nitrogen (Mathieson) was used as an inert gas to prevent contamination of the reaction materials. Before use the gas was passed through alumina activated at 250° C and calcium hydride.

Procedure

The organometallic compounds and titanium tetrachloride react together with gas evolution. A specially designed reaction vessel of known volume connected to a mercury manometer (made with a calibrated capillary tubing) and by a high-vacuum stopcock to a vacuum system was used to study the reaction (Fig. 1).

The apparatus was heated for at least 12 hours at 100° C in vacuum and then assembled in nitrogen atmosphere. Before assembling the apparatus, two glass ampoules, each containing a weighed amount of reactants, were introduced through the female joint. This was then closed with a male ground-glass joint fitted with a long glass rod. By small vertical movements of the rod it was possible to break the two ampoules. Before breaking the ampoules the system was evacuated to 10^{-3} mm of Hg and then cooled at $-35°$ C. After the ampoules were broken the temperature of the vessel was slowly raised to 0° C and maintained there in order to insure a smooth reaction. After a few minutes the vessel was introduced into a thermostat and kept at $35\pm0.1°$ C until the reaction was complete. The end of the reaction was indicated by stabilization of the level in the mercury manometer. From a knowledge of the final pressure (obtained from the difference between the reading of the mercury manometer and the barometric pressure, less the vapor pressure of the reagent present in excess),[3] the number of moles of gas liberated during

[3]*The vapor pressure values of the reagents were determined at 35±0.1° C in the apparatus used for the investigation here reported. In this way it was also possible to ascertain that while lead tetraethyl and aluminum ethyldichloride are stable under vacuum, aluminum triethyl split off ethylene. At 35±0.1° C, the moles of ethylene liberated per mole of aluminum triethyl are* 5.61×10^{-4}.

Can. J. Chem. Downloaded from www.nrcresearchpress.com by 196.1.178.254 on 09/04/12
For personal use only.

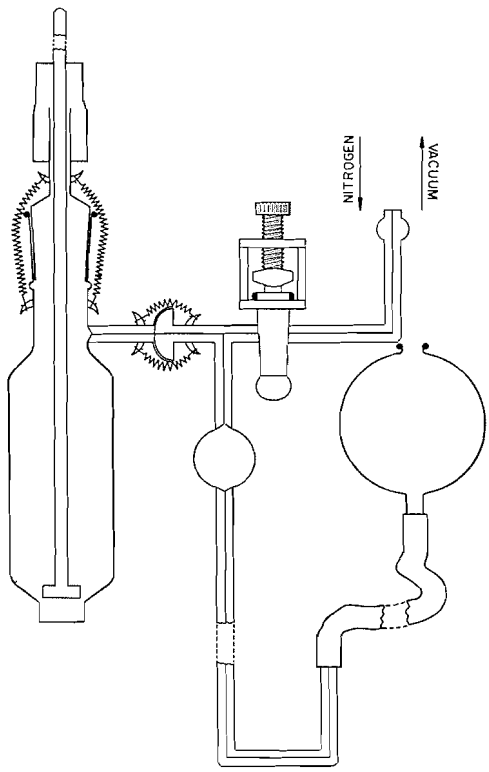

FIG. 1. Reaction vessel.

the reaction was calculated. Since the amount of gas formed is dependent on the amount of the organotitanium derivative produced in the alkylation reaction of titanium tetrachloride,[4] the moles of the organometallic compound reacted with titanium tetrachloride were then calculated from the moles of gas liberated after the determination of its composition by mass spectrometry. After the removal of the gas sample for the analysis, the vessel was frozen at $-35°$ C and the gas was pumped off. When the original pressure (10^{-3} mm of Hg) was restored, carefully degassed water was introduced.

The temperature of the system was raised to 0° C, and, after the hydrolysis was complete, the gas was again analyzed by mass spectrometry. Atmospheric pressure was then restored with nitrogen and the Ti(III) was determined with Fe(III) in the presence of ammonium thiocyanate as an indicator (4). At the end of each experiment a waxy substance was found in the vessel. This substance, soluble in organic solvents, had a molecular weight (determined by the cryoscopic method in benzene) which varied between 750 and 1000 and was characterized by I.R. spectroscopy as a high alkane (4).

A few reactions were duplicated in the apparatus described using a pressure of 545 mm of Hg, or the atmospheric pressure instead of the pressure of 10^{-3} mm of Hg. Since no appreciable differences have been found in quantity and composition of the gas liberated in these experiments and in comparable experiments conducted at 10^{-3} mm of Hg, it is

[4]*C. F. Feldman, L. C. Arnold, and D. W. McDonald, in a paper presented at the 131st National Meeting of the American Chemical Society, Miami, Florida, April 1957, reported that with the aluminum triisobutyl – titanium tetrachloride system at a ratio* Al/Ti *1.2:1, the reduction of* Ti(IV) *to* Ti(III) *according to the reactions* $AlR_3 + TiCl_4 \rightarrow AlR_2Cl + TiCl_3R$ *and* $TiCl_3R \rightarrow TiCl_3 + R\cdot$ *was more than 90% complete in 20 minutes. See also reference 2.*

Can. J. Chem. Downloaded from www.nrcresearchpress.com by 196.1.178.254 on 09/04/12
For personal use only.

concluded that the evolution of the gas observed in the reactions between organometallic compounds and titanium tetrachloride is not influenced by the pressure at which the experiments were conducted.

The ampoules were made with capillary tips at one end, and had a predetermined volume. They were filled according to the following procedure: the organometallic compounds and the titanium tetrachloride were stored in separate specially designed glass containers (Fig. 2) each with a side arm through which prepurified nitrogen could

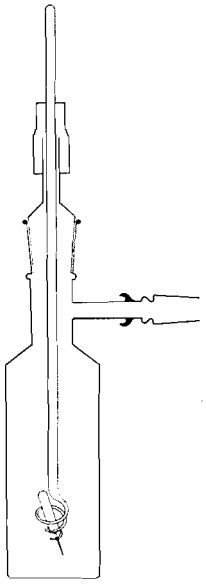

FIG. 2. Container for the sampling of the reagents.

be introduced when necessary. The container was closed with a male joint fitted with a glass rod. The end of the rod introduced into the container was formed as a thin spiral on which the glass ampoules could be conveniently placed with the tip down. All the ampoules were previously heated in vacuum for at least 24 hours and filled with nitrogen. The apparatus, containing the substance and the ampoule, was evacuated, and upon complete evacuation the tip of the ampoule was inserted below the liquid level, by pushing down the glass rod. Nitrogen was admitted slowly thus filling the ampoule with liquid. On exposure to air the ampoules containing both the organometallic compounds and the titanium tetrachloride became sealed by reaction of the air with the compound present in the capillary tip. The ampoules containing lead tetraethyl were sealed with a microflame. All the ampoules used in this investigation were filled at the same time. The analysis for the purity of each compound was actually performed using the product sampled at the start, in the middle, and at the end of the operation, in order to verify that the sampling procedure did not change the purity of the reagents. Analyses were also made at the end of the investigation in order to check that the purity of the material had not changed during that time.

EXPERIMENTAL RESULTS

Reaction of $AlEtCl_2$ *and* $TiCl_4$

Aluminum ethyldichloride and titanium tetrachloride react quite smoothly with the formation of a reddish-brownish precipitate. A qualitative evaluation of the rate of gas

Can. J. Chem. Downloaded from www.nrcresearchpress.com by 196.1.178.254 on 09/04/12
For personal use only.

evolution shows that, whatever the ratio between the organometallic compound and titanium tetrachloride there is no considerable difference in the rate. The gases evolved during the reaction are mainly ethane and butane. Substantial amounts of ethylene and ethyl chloride are also liberated and traces of higher alkanes. The absolute molar amount of each gas liberated per mole of aluminum ethyldichloride used is plotted against the molar ratio of aluminum ethyldichloride and titanium tetrachloride in Fig. 3.

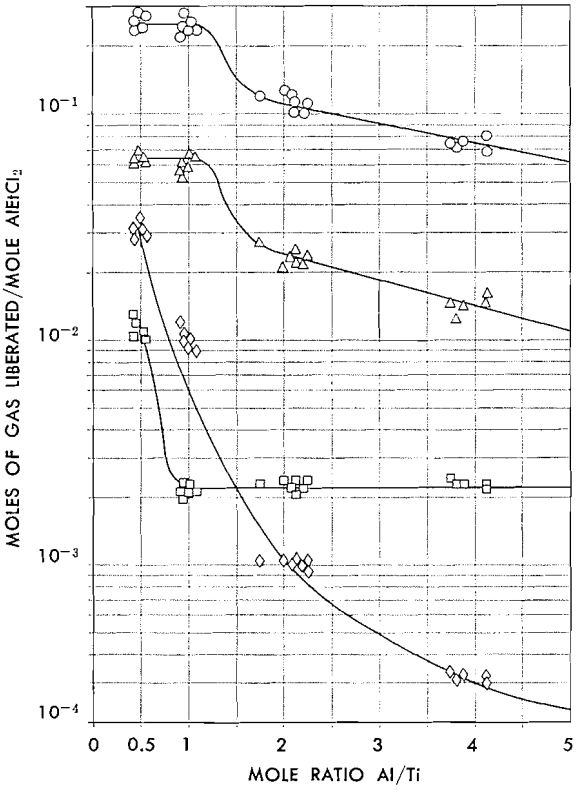

FIG. 3. Reaction of $AlEtCl_2$ with $TiCl_4$. Molar amounts of ethane, butane, ethylene, and ethyl chloride liberated per mole of $AlEtCl_2$ used vs. the molar ratio of $AlEtCl_2$ and $TiCl_4$.
○ Ethane □ Ethylene
△ Butane ◇ Ethyl chloride

An interesting result is the presence of ethyl chloride in the gas evolved during the reaction. The amount of this component is very close to the amount of butane evolved, especially at ratios Al/Ti below 1. The presence of ethyl chloride demonstrates that part of the alkylated form of titanium is decomposed according to the equation [1] proposed by Friedlander and Oita (10).

$$TiCl_3R \rightarrow TiCl_2 + RCl \qquad [1]$$

Titanium dichloride obtained from this reaction reacts with the excess of titanium tetrachloride present for every ratio, according to the reaction [2] which is completely

$$TiCl_2 + TiCl_4 \rightleftharpoons 2TiCl_3 \qquad [2]$$

shifted to the right at room temperature (11). The presence of ethylene, already ascertained by Gilman (12) in similar reactions, and of the waxy polymer, already mentioned,

Can. J. Chem. Downloaded from www.nrcresearchpress.com by 196.1.178.254 on 09/04/12
For personal use only.

throws light on the fate of the ethyl radicals split from the alkylated product. The sum of the moles of ethylene found in the gas and of the polymer found in the reaction vessel is equal, within experimental error, to the amount of ethane liberated.[5] After decomposition with water, the analysis of the gas reveals no hydrogen for any ratio of Al/Ti, thus ruling out the possibility of having Ti(II) as a product of the reaction. The gases produced during the hydrolysis are mainly ethane and a small amount of butane. The acid solution containing the titanium was analyzed for Ti(III) content.

TABLE I

Molar amounts of $AlEtCl_2$ and $TiCl_4$ used and reacted; average valence of titanium in the product of the reaction

$AlEtCl_2$ (mole)	$TiCl_4$ (mole)	$\frac{AlEtCl_2}{TiCl_4}$	$TiCl_4$ reacted (mole)	$AlEtCl_2$ reacted (mole)	$\frac{AlEtCl_2 \text{ reacted}}{TiCl_4 \text{ reacted}}$	$TiCl_4$ mole reduced (%)	Ti, av. valence
1.97×10^{-2}	4.25×10^{-3}	4.17	3.68×10^{-3}	4.57×10^{-3}	1.24	86.5	3.14
1.67	4.04	4.15	3.17	3.75	1.18	76.5	3.24
2.21	5.70	3.88	4.28	4.57	1.07	75.0	3.25
2.35	6.20	3.76	4.40	4.99	1.13	72.0	3.28
1.96	5.26	3.74	3.85	4.52	1.17	73.2	3.27
1.39	6.24	2.23	4.71	6.57	1.39	75.5	3.25
1.56	7.07	2.21	5.02	7.28	1.45	71.0	3.29
1.06	4.95	2.14	3.90	5.20	1.33	79.0	3.21
1.64	7.77	2.11	5.66	7.65	1.35	72.9	3.27
1.77	8.39	2.10	6.23	8.46	1.35	74.2	3.26
1.67	8.27	2.01	6.57	9.38	1.42	79.5	3.22
2.00	1.34×10^{-2}	1.76	0.93×10^{-2}	1.05×10^{-2}	1.13	69.5	3.33
1.69	1.69	1.00	1.09	1.22	1.12	64.5	3.36
0.81	0.82	0.98	0.50	0.62	1.24	60.5	3.40
1.10	1.12	0.98	0.72	0.78	1.08	64.5	3.32
0.74	0.77	0.95	0.40	0.47	1.17	60.1	3.40
1.94	2.06	0.94	1.24	1.40	1.13	60.1	3.40
1.34	1.46	0.92	0.84	0.85	1.01	57.7	3.42
1.25	1.36	0.91	0.80	0.92	1.15	58.5	3.42
1.17	1.30	0.90	0.75	0.79	1.05	57.5	3.43
0.92	1.69	0.54	0.58	0.64	1.10	34.3	3.66
1.24	2.45	0.51	0.83	0.83	1.00	34.0	3.66
0.99	1.95	0.50	0.64	0.68	1.06	32.9	3.66
0.82	1.67	0.49	0.82	0.85	1.04	32.2	3.68
0.68	1.39	0.49	0.44	0.50	1.14	31.6	3.69
0.97	2.04	0.47	0.62	0.72	1.16	30.2	3.70
1.09	2.39	0.45	0.72	0.74	1.03	30.0	3.70

In Table I are reported the amounts of the reagents used, the amount of the reagents reacted, the per cent of Ti(IV) reduced, and the average valence of the metal in the product of the reaction.

Reaction of $PbEt_4$ *and* $TiCl_4$

These two compounds react as smoothly as aluminum ethyldichloride and titanium tetrachloride, with the formation of a brownish-blackish precipitate. In this case an approximate evaluation of the rate of gas evolution shows that no large difference exists in the rate of the reaction between the two reagents for any ratio studied and that the gases evolved during the reaction are mainly ethane and butane with substantial amounts of ethylene and ethyl chloride and traces of higher alkanes. In Fig. 4 the absolute amount of each gas liberated per mole of lead tetraethyl used is plotted against the ratio

[5]*An exhaustive discussion on the relationship between the mechanism of the decomposition of the organometallic compounds of the transition metals and their stability is reported by Cotton, F. A. Chem. Revs.* **55**, *551 (1955).*

Can. J. Chem. Downloaded from www.nrcresearchpress.com by 196.1.178.254 on 09/04/12
For personal use only.

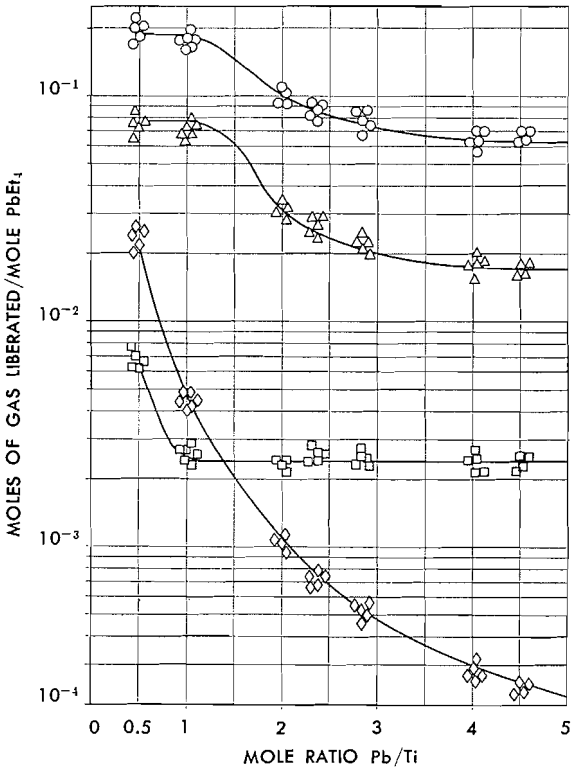

FIG. 4. Reaction of $PbEt_4$ with $TiCl_4$. Molar amounts of ethane, butane, ethylene, and ethyl chloride liberated per mole of $PbEt_4$ used vs. the molar ratio of $PbEt_4$ and $TiCl_4$.
○ Ethane □ Ethylene
△ Butane ◇ Ethyl chloride

$PbEt_4/TiCl_4$. It is possible to conclude that ethyl chloride also results in this case from a reaction of the same type as in equation [1]. After hydrolysis, the analysis of the gas shows no hydrogen for any ratio of Pb/Ti. The gases present after decomposition are mainly ethane and a trace of butane. The solution containing the titanium was titrated with Fe(III) and the amount of Ti(III) was determined. After the titration the solution was filtered and the solid collected was dissolved in hot *n*-heptane. From the solution a white powder was recovered. This substance was purified by crystallization from *n*-heptane and analyzed for chlorine. The compound was identified as $PbEt_3Cl$. (Anal. Calc. for $PbEt_3Cl$: Cl, 10.71. Found: Cl, 10.69.)

In Table II are reported the quantities of reagents used, the amount of the reagents reacted, the per cent of titanium tetrachloride reduced, and the average valence of the metal in the product of the reaction.

Reaction of $AlEt_3$ *and* $TiCl_4$

Aluminum triethyl and titanium tetrachloride react very fast even at low temperature with the formation of blackish-brown precipitate depending on the ratio of Al/Ti used. An approximate evaluation of the rate in this case was quite difficult because the reaction is completed in a few minutes. It is also doubtful at what temperature the alkylation reaction was actually conducted although the standard technique already described was used. In spite of these difficulties the results were reproducible enough to be interpreted.

Can. J. Chem. Downloaded from www.nrcresearchpress.com by 196.1.178.254 on 09/04/12
For personal use only.

TABLE II

Molar amounts of $PbEt_4$ and $TiCl_4$ used and reacted; average valence of titanium in the product of the reaction

$PbEt_4$ (mole)	$TiCl_4$ (mole)	$\frac{PbEt_4}{TiCl_4}$	$TiCl_4$ reacted (mole)	$PbEt_4$ reacted (mole)	$\frac{PbEt_4 \text{ reacted}}{TiCl_4 \text{ reacted}}$	$TiCl_4$ mole reduced (%)	Ti, av. valence
1.89×10^{-2}	4.16×10^{-2}	4.54	3.82×10^{-3}	3.71×10^{-3}	0.97	91.8	3.08
1.91	4.21	4.53	3.95	3.99	1.01	93.8	3.06
1.73	4.08	4.24	3.86	4.01	1.04	94.5	3.06
2.37	6.21	3.82	5.72	5.72	1.00	92.1	3.08
1.95	7.99	2.44	6.54	6.61	1.01	81.9	3.18
1.10	5.01	2.17	4.03	4.03	1.00	80.4	3.19
1.58	7.71	2.08	6.51	6.71	1.03	84.5	3.16
1.68	8.26	2.03	6.86	6.72	0.98	83.1	3.17
0.94	0.92×10^{-2}	1.02	0.68×10^{-2}	0.68×10^{-2}	1.00	74.1	3.25
1.37	1.37	1.00	1.03	1.05	1.02	75.4	3.24
0.98	0.97	1.01	0.70	0.69	0.98	72.3	3.28
1.10	1.13	0.97	0.83	0.81	0.98	73.8	3.26
0.98	1.94	0.51	1.13	0.95	0.84	58.1	3.42
0.65	1.34	0.48	0.77	0.63	0.82	57.1	3.43
0.97	2.01	0.48	1.15	0.95	0.83	57.3	3.43
1.10	2.41	0.56	1.34	1.05	0.78	55.4	3.44

In this case also the gases formed during the alkylation reaction were mainly ethane and butane and traces of higher alkanes, but if the ratio Al/Ti was kept above the value 1, ethylene and ethyl chloride were not found. These two components appear in substantial amount when ratios of Al/Ti less than unity are used.

In Fig. 5 the absolute amount of each gas liberated per mole of aluminum triethyl used is plotted against the ratio $AlEt_3/TiCl_4$.

After hydrolysis, analysis of the gas showed that ethane was the principal component, and that a small amount of butane was also present. Hydrogen was also found in small amounts only for ratios of Al/Ti greater than unity. In Table III are reported the quantity of reagents used, the amount of the reagents reacted, and the per cent of titanium tetrachloride reduced. The amount of $TiCl_2$, which can be calculated from the hydrogen evolved on hydrolysis, is not reported here because no other direct evidence of its presence in the alkylated material is available. While it is possible to have compounds of Ti(II) as direct products of the alkylation reaction, it is also possible that such products could be formed by thermal effects from higher valence compounds during the hydrolysis itself. This possibility is discussed later. Nevertheless, the moles of titanium dichloride calculated from the hydrogen evolved represented only a small per cent (about 5%) of the initial amount of $TiCl_4$ used for all the ratios of Al/Ti above 1.81.

DISCUSSION

The alkylation of titanium tetrachloride with various organometallic compounds reported is a well-defined reaction, at least with organometallic compounds of low activity such as aluminum ethyldichloride and lead tetraethyl. With these compounds the stoichiometry of the reaction follows reaction [3] for any ratio investigated. The

$$MR_x + TiCl_4 \rightarrow MR_{x-1}Cl + TiCl_3R \qquad [3]$$

formation of a specific compound as a product of the alkylation is demonstrated by a constant rate of gas evolution during the reaction and by the almost constant composition of the gas obtained for any ratio of the reagents used. For the reaction between

Can. J. Chem. Downloaded from www.nrcresearchpress.com by 196.1.178.254 on 09/04/12
For personal use only.

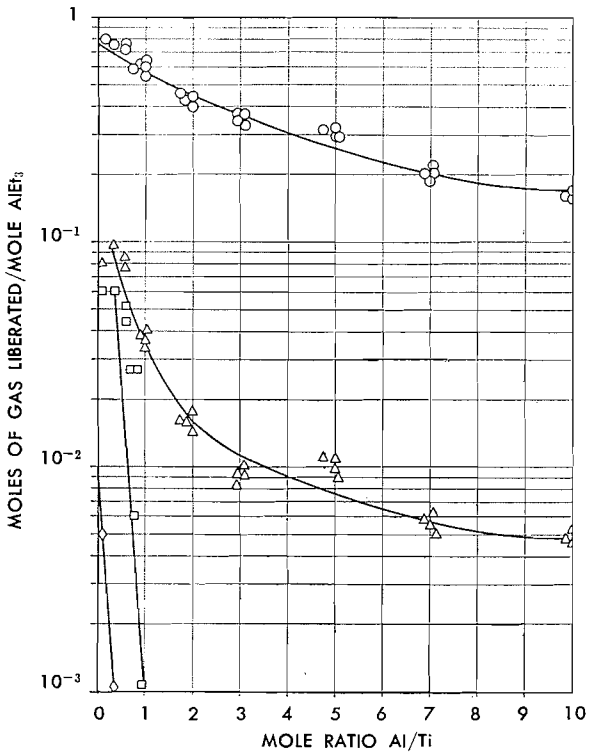

FIG. 5. Reaction of $AlEt_3$ with $TiCl_4$. Molar amounts of ethane, butane, ethylene, and ethyl chloride liberated per mole of $AlEt_3$ used vs. the molar ratio of $AlEt_3$ and $TiCl_4$.
○ Ethane □ Ethylene
△ Butane ◇ Ethyl chloride

TABLE III

Molar amounts of $AlEt_3$ and $TiCl_4$ used and reacted

$AlEt_3$ (mole)	$TiCl_4$ (mole)	$\frac{AlEt_3}{TiCl_4}$	$TiCl_4$ reacted (mole)	$AlEt_3$ reacted (mole)	$\frac{AlEt_3 \text{ reacted}}{TiCl_4 \text{ reacted}}$	$TiCl_4$ mole reduced (%)
3.99×10^{-2}	3.99×10^{-3}	10.00	3.99×10^{-3}	4.44×10^{-3}	1.11	100.0
3.99	5.58	7.15	5.57	5.77	1.03	99.9
0.62	1.31	4.76	1.31	1.53	1.15	99.9
1.21	4.32	2.94	4.32	3.10	0.72	100.0
0.77	4.23	1.81	4.21	2.47	0.59	99.7
0.75	4.51	1.66	4.42	2.59	0.59	99.8
0.61	5.65	1.07	5.64	2.67	0.47	99.9
0.63	7.36	0.86	6.43	3.05	0.47	87.4
0.67	1.01×10^{-2}	0.67	6.75	3.66	0.54	67.2
0.73	1.32	0.55	7.35	4.32	0.59	55.8
0.59	1.41	0.42	7.57	3.86	0.51	53.5
0.39	1.71	0.23	7.57	2.80	0.37	44.2
0.55	2.51	0.22	1.17×10^{-2}	3.99	0.34	46.8
0.60	3.72	0.16	1.12	4.04	0.36	30.2
0.36	2.75	0.13	0.69	2.40	0.35	25.0
0.57	4.80	0.12	0.91	3.53	0.39	18.9

aluminum triethyl and titanium tetrachloride, it is not possible to derive a constant stoichiometric relationship for the various ratios used. However, it appears that for

Can. J. Chem. Downloaded from www.nrcresearchpress.com by 196.1.178.254 on 09/04/12
For personal use only.

an Al/Ti ratio greater than 3 the reaction goes according to reaction [4], while for Al/Ti ratios below 0.5 reaction [5] is followed. Since it is possible to observe a continuous

$$AlEt_3 + TiCl_4 \rightarrow AlEt_2Cl + TiCl_3R \quad [4]$$

$$AlEt_3 + 3TiCl_4 \rightarrow AlCl_3 + 3TiCl_3R \quad [5]$$

variation in the ratios of reacted aluminum triethyl and titanium tetrachloride from 1 to 0.35, it is difficult to determine boundary lines dividing the regions where the reactions [4], [5], and [6] occur.

$$AlEt_3 + 2TiCl_4 \rightarrow AlEtCl_2 + 2TiCl_3R \quad [6]$$

The reactions [4] and [6] do not account for the further reduction of titanium to the bivalent state.

The formation of Ti(II), which probably becomes apparent only upon hydrolysis, can occur according to the reactions [7] and [7′]

$$TiCl_3 + AlEt_3 \rightarrow TiCl_2R + AlEt_2Cl \quad [7]$$

$$TiCl_2R \rightarrow TiCl_2 + R\cdot \quad [7']$$

or according to the reactions [8] and [8′].

$$TiCl_4 + 2AlEt_3 \rightarrow TiCl_2R_2 + 2AlEt_2Cl \quad [8]$$

$$TiCl_2R_2 \rightarrow TiCl_2 + 2R\cdot \quad [8']$$

While both reactions may be responsible for the formation of Ti(II), it is probably true that the course of reaction [7] is hindered by its heterogeneity. Reaction [8], with the production of Ti(IV) alkyl derivatives (which are the only stable organometallic compounds of titanium isolated (4, 5)), is more likely responsible for the formation of Ti(II). Since no titanium metal has been found after hydrolysis of the alkylated material, and since titanium can form di-, tri-, and tetra-substituted derivatives as well as complex anions (using its empty *d*-orbitals), all the alkylation reactions which produce those organotitanium compounds which give titanium metal directly or by disproportionation on hydrolysis can be eliminated. It is reasonable to assume, at this point, that the alkylation of titanium tetrachloride proceeds only through the reaction schemes from [3] to [8]. Among all the possible organotitanium compounds only TiR_2Cl_2 and $TiRCl_3$ are likely to be present as tetra-substituted derivatives, while the only one likely to be present as a tri-substituted derivative is $TiRCl_2$.

Saltman and co-workers (13) found that with a Al/Ti ratio of 0.33 (in the case of a reaction of aluminum triisobutyl and titanium tetrachloride) the amount of solid obtained from the reaction per mole of $TiCl_4$ consumed is very similar in weight and composition to a mixture of 1 mole of $AlCl_3$ and 3 moles of $TiCl_3$. This result calls for a stoichiometry as in equation [5], which was derived using a completely different experimental procedure.

The possibility of having titanium as a complex anion has been suggested by Summers and Uloth (5) in order to explain the solubility of bis-(cyclopentadienyl)-titaniumdiphenyl in ether when an excess of phenyl lithium is added, according to the equilibrium equation [9], with the formation of dark orange-brown or nearly black solutions.

$$Ph_2[(C_5H_5)_2Ti] + PhLi \rightleftharpoons Ph_3[(C_5H_5)_2Ti]^- Li^+ \quad [9]$$

This possibility is reported here in order to discuss the observations of Friedlander and Oita (10) that the product of the reaction of aluminum triethyl with titanium tetrachloride for ratio values equal or less than unity gave negative tests with Michler's

Can. J. Chem. Downloaded from www.nrcresearchpress.com by 196.1.178.254 on 09/04/12
For personal use only.

ketone, indicating that all the alkyl compound either reacted with titanium tetrachloride or was held in an inactive complex. For a ratio Al/Ti greater than 2.5, strong positive Michler's ketone tests were observed thus indicating the presence of an excess of aluminum alkyl while between ratios 2.5 and 1, weakly positive test results were obtained, indicating the formation of new carbon–metal bonds or the formation of a complex which modified the properties of the aluminum alkyls. The mechanism of the reaction of Michler's ketone with a carbon–metal bond (14) consists of co-ordination of the oxygen of the carbonyl group with the metal, followed by migration of the group R with its electrons according to equation [10].

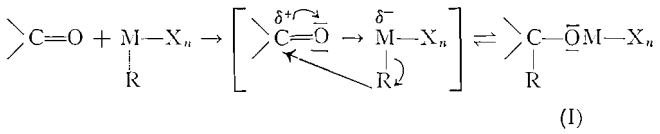

[10]

(I)

It is possible that if the color test (based on the hydrolysis of (I) and a chromatic reaction of the tertiary alcohol (15)) is negative, the co-ordination of the carbonyl does not occur. In presence of titanium derivatives this could only be explained by the fact that the empty *d*-orbitals of the metal are already occupied. The presence in the system of anions of the type suggested by Summers and Uloth (5) can explain why the Michler's ketone test failed to give positive results.

REFERENCES

1. CAHOURS, A. Ann. **122**, 48 (1862). CHALLENGER, F. and PRITCHARD, F. J. Chem. Soc. **125**, 864 (1924). BROWNE, H. O. and REID, E. E. J. Am. Chem. Soc. **49**, 830 (1927). KOEHLER, H. Ber. **13**, 1626 (1880). LEVY, L. Ann. chim. et phys. **25** (6), 433 (1892). PATERNO, E. and PERATONER, A. Ber. **22**, 467 (1889). SCHUMANN, A. Ber. **21**, 1079 (1888).
2. GILMAN, H. and JONES, R. G. J. Org. Chem. **10**, 505 (1945).
3. HERMAN, D. F. and NELSON, W. K. J. Am. Chem. Soc. **75**, 3877 (1953).
4. HERMAN, D. F. and NELSON, W. K. J. Am. Chem. Soc. **75**, 3882 (1953).
5. SUMMERS, R. and ULOTH, R. H. J. Am. Chem. Soc. **76**, 2278 (1954).
6. KOLTHOFF, I. M. and SANDELL, E. B. Textbook of quantitative inorganic analysis. The Macmillan Co., New York. 1948. (*a*) p. 624, (*b*) p. 638.
7. BONITZ, E. Ber. **88**, 742 (1955).
8. GROSSE, A. V. and MAVITY, J. M. J. Org. Chem. **5**, 106 (1940).
9. CLABAUGH, W. S., LESLIE, R. T., and GILCHRIST, R. J. Research Natl. Bur. Standards, **55**, 261 (1955).
10. FRIEDLANDER, H. N. and OITA, K. Ind. Eng. Chem. **49**, 1885 (1957).
11. FARBER, M. and DARNELL, A. J. J. Phys. Chem. **59**, 156 (1955).
12. GILMAN, H., JONES, R. G., and WOODS, L. A. J. Am. Chem. Soc. **76**, 3615 (1954).
13. SALTMAN, W. M., GIBBS, W. E., and LAL, J. J. Am. Chem. Soc. **80**, 5615 (1958).
14. ROBINSON, R. Chem. Age, **74**, 997 (1956).
15. GILMAN, H. and SCHULTZE, F. J. Am. Chem. Soc. **47**, 2002 (1925).

Can. J. Chem. Downloaded from www.nrcresearchpress.com by 196.1.178.254 on 09/04/12
For personal use only.

Can. J. Chem. Downloaded from www.nrcresearchpress.com by 196.1.178.254 on 09/04/12
For personal use only.

THE ALKALOIDS OF INULA ROYLEANA[1]

O. E. Edwards and M. N. Rodger[2]

ABSTRACT

Royline and inuline, previously isolated from *Inula royleana*, have again been isolated from this source, and shown to be lycoctonine and anthranoyl-lycoctonine respectively. The presence of a third known alkaloid, methyl-lycaconitine has also been established. This is the first recorded occurrence of lycoctonine and its derivatives outside the family Ranunculaceae.

Inula royleana DC. Prod., a perennial plant of the family Compositae, with reputed medicinal value, is found in the lower reaches of the Himalayas. Its extractives had been previously examined by two groups of workers. In 1944 Chopra, Kohli, and Handa (1) isolated an alkaloid, m.p. 120–121° $[\alpha]_D$ −42.5° to which they gave the name royline, and assigned the empirical formula $C_{21}H_{33}O_6N$. These workers were unable to isolate any crystalline derivatives of this base other than an aurichloride, m.p. 142° (decomp.) for which no analysis was given. Chatterjee and Talapatra (2) later examined this plant and isolated the same alkaloid. They changed its name to royline and altered the empirical formula to $C_{21}H_{35-37}O_6N$. In addition, these workers found another alkaloid, m.p. 165° (decomp.) $[\alpha]_D$ +44.3°, which they called inuline. This analyzed correctly for $C_{16}H_{23}O_4N$, and gave a crystalline chloroplatinate which analyzed for $C_{32}H_{46}O_8N_2 . H_2PtCl_6$.

We have re-examined the roots of *Inula royleana*, and have isolated and characterized three alkaloids, two of which correspond to those encountered by the Indian workers.

The dried root gave a phenomenal yield of alkaloid (*ca.* 5%), most of which was extracted by methylene chloride when a solution of its salt was adjusted to pH 8. This material was a complex mixture which was not readily separated by chromatography on alumina. After solvent precipitation of the darker colored components, the bases were separated by countercurrent distribution between benzene and buffer of pH 5. Royline remained in the early tubes, while inuline moved rapidly with the benzene phase, and both alkaloids were obtained pure after 180 transfers.

Inuline, when submitted to paper chromatography and paper electrophoresis proved to be homogeneous. The base formed a highly crystalline perchlorate, m.p. 206° (decomp.) which analyzed for $C_{32}H_{46}O_8N_2 . HClO_4$. On alkaline hydrolysis of the alkaloid two fragments were isolated—a base, $C_{25}H_{43}O_8N$, and a fluorescent amino acid $C_7H_7O_2N$. The latter fragment was identified as anthranilic acid by direct comparison with an authentic specimen. The basic fragment was similarly identified as the monohydrate of the known alkaloid lycoctonine. Inuline is therefore anthranoyl-lycoctonine. In accord with this, inuline and anthranoyl-lycoctonine[3] showed no depression of melting point on admixture, and their infrared spectra were identical. The corresponding perchlorates also proved to be identical. We were able to confirm that our material corresponded to that obtained by the earlier workers (I.R., melting point, mixed melting point, and rotation) using a sample kindly supplied by Mrs. A. Chatterjee whom we cordially thank.

[1]*Manuscript received April 10, 1959.*
Contribution from the Division of Pure Chemistry, National Research Council, Ottawa, Canada.
Issued as N.R.C. No. 5228.
[2]*National Research Council of Canada Postdoctoral fellow.*
[3]*The anthranoyl-lycoctonine isolated from D. consolida (Marion, L. and Edwards, O. E. J. Am. Chem. Soc.* **69**, *2010 (1947)) crystallized when seeded with a sample from Goodson's collection, kindly provided by Dr. T. M. Sharp. The two materials proved identical, with m.p. 155–164°. The m.p. of 172° recorded by Goodson (3) could not be duplicated.*

Can. J. Chem. Downloaded from www.nrcresearchpress.com by 196.1.178.254 on 09/04/12
For personal use only.

Royline was also shown to be homogeneous by paper chromatography. Comparison of the base and its perchlorate with lycoctonine and its perchlorate proved the identity of the two alkaloids. We were again able to confirm that the material in our hands was the same as that examined by the earlier workers using a sample supplied by Mrs. A. Chatterjee. This sample had a rotation identical with that of lycoctonine, hence the reported negative rotation (1) for royline is in error.

The bulk of the alkaloids from the roots was separated manually in large funnels (12 transfers) using the above solvent system, but moving the lower phases.

The contents of the first three funnels were rich in inuline. The contents of the later funnels would not crystallize. The material from funnels 7–9 was redistributed (100 transfers) between benzene and buffer of pH 5. The major peak (tubes 34 to 79) was still non-crystalline, hence was redistributed between benzene and buffer of pH 4 (100 transfers). The material corresponding to the main peak (tubes 11 to 45) proved to be homogeneous. It could not be obtained crystalline, but it gave a crystalline hydriodide, m.p. 201° (decomp.). The base on hydrolysis gave lycoctonine and 1-methylsuccinyl-anthranilic acid. This suggested that it was methyl-lycaconitine, and comparison of the hydriodide with a sample kindly supplied by Professor R. C. Cookson, whom we cordially thank, established the identity (I.R., melting point, mixed melting point). Methyl-lycaconitine had previously been isolated by Goodson (3) and by Cookson, Page, and Trevett (4). These workers were also unable to induce the base to crystallize.

In addition to the major component found in the distribution at pH 4 there were four minor components, one moving more slowly than methyl-lycaconitine, and the remaining three moving more rapidly. These bases have not as yet been crystallized but each has a distinctive infrared spectrum, especially over the carbonyl and aromatic absorption regions.

The aqueous mother liquor from which the main basic fraction had been extracted was made strongly alkaline, and extracted with chloroform. The base obtained was largely lycoctonine (royline).

Alkaline hydrolysis of the material precipitated by the initial benzene–hexane separation of the weak bases (see experimental) gave a further yield of lycoctonine, and this fraction may well consist largely of oxidation and decomposition products formed from methyl-lycaconitine during drying of the root and subsequent operations.

Inula royleana now becomes the richest known source of lycoctonine. Now that the alkaloids isolated by the previous workers have proved to be lycoctonine and anthranoyl-lycoctonine we suggest that the names "royline" and "inuline" be deleted from the chemical literature.

Lycoctonine and its derivatives have been found in *Aconitum lycoctonum* and all the *Delphinium* species which have been carefully examined; but their presence in *Inula royleana* is the first recorded occurrence of these alkaloids outside the family Ranunculaceae. It seems remarkable to us that not only should an alkaloid as complex as lycoctonine be synthesized by a plant belonging to an entirely different family from the previously known sources, but that it should be esterified with the same complex acid.

EXPERIMENTAL

Melting points were taken in an open tube unless marked (K), in which case they were taken on the Kofler block. Infrared spectra were taken as "Nujol" mulls on a Perkin–Elmer model 21 spectrophotometer.

Can. J. Chem. Downloaded from www.nrcresearchpress.com by 196.1.178.254 on 09/04/12
For personal use only.

Isolation and Separation of the Alkaloids

Inula royleana was obtained from an Indian source by the S. B. Penick Co. through the good offices of Dr. H. R. Schmidt. The finely ground dry roots (25 lb) were extracted exhaustively with methanol at room temperature, and the methanolic extract taken to dryness under reduced pressure. The material so obtained was dissolved in dilute sulphuric acid and the neutral and acidic material removed by extraction with methylene chloride.

The methylene chloride solution was back-washed with dilute sulphuric acid. The combined aqueous layers were taken to pH 8 using sodium carbonate and again extracted with methylene chloride. This extract was evaporated under reduced pressure to give a dark brown gum (498 g) ("weak bases").

The pH of the aqueous layer was raised to 11 and the solution extracted with chloroform. The chloroform was removed under reduced pressure to yield a dark brown gum (70 g) ("strong bases").

A portion of the crude weak base (25 g) was dissolved in the minimum quantity of benzene and an equal volume of hexane added. The dark gum which precipitated was laid aside. The mother liquors were evaporated under reduced pressure, and the material obtained (15 g) separated into its components in a Craig apparatus for countercurrent distribution. Four tubes were loaded with a benzene solution of the alkaloids (40 ml; 10 ml per tube) and the material was moved through 180 tubes against citric acid – phosphate buffer of pH 5. The contents of the last 29 tubes yielded 4.4 g of pure inuline, while the material identified as royline (2.2 g) was left in the early benzene layers. Both alkaloids crystallized from aqueous methanol as needles, and were shown to be homogeneous by paper chromatography. The homogeneity of inuline was also checked by paper electrophoresis.

A preliminary examination of the "strong base" fraction indicated that this consisted largely of royline. The weak bases insoluble in benzene–hexane, on alkaline hydrolysis gave a 45% yield of lycoctonine.

Inuline

The base had m.p. 145–154° (decomp.) undepressed on admixture with anthranoyl-lycoctonine, and $[\alpha]_D$ +51° ($CHCl_3$). Comparison (melting point, mixed melting point, I.R., rotation) of the base with a sample of inuline supplied by Mrs. A. Chatterjee confirmed their identity. The infrared spectrum of inuline was identical with that of anthranoyl-lycoctonine. The perchlorate of the base crystallized from ethanol as needles m.p. 206° (decomp.) undepressed on admixture with the perchlorate from anthranoyl-lycoctonine. Found: C, 55.91; H, 7.01. Calc. for $C_{32}H_{46}O_8N_2.HClO_4$: C, 55.94; H, 6.85.

Hydrolysis of Inuline

Inuline (220 mg) was refluxed for 45 minutes with 1% ethanolic potassium hydroxide. The solution was cooled and extracted with chloroform, and the chloroform solution on evaporation under reduced pressure afforded lycoctonine, crystallizing from aqueous methanol as needles, m.p. 115–123° (decomp.), undepressed on admixture with an authentic sample of lycoctonine. The infrared spectra of the two samples were also identical. Found: C, 61.77; H, 8.74; N, 2.93. Calc. for $C_{25}H_{43}O_8N$: C, 61.83; H, 8.93; N, 2.88.

On neutralization of the hydrolysis mother liquors and extraction with chloroform, anthranilic acid was obtained, identical with an authentic specimen (melting point, mixed melting point, I.R., and U.V.). Found: C, 61.62; H, 4.98; N, 9.97. Calc. for $C_7H_7O_2N$: C, 61.31; H, 5.15; N, 10.21.

Royline

The base had m.p. 115–123° (decomp.) undepressed on admixture with lycoctonine hydrate, and $[\alpha]_D$ +47 (EtOH). Comparison of the base with a sample of royline supplied by Mrs. A. Chatterjee (melting point, mixed melting point, I.R., rotation) confirmed their identity. The infrared spectrum of royline was identical with that of lycoctonine hydrate.

The perchlorate of the base crystallized from ethanol as needles, m.p. 215° (decomp.) undepressed on admixture with the perchlorate from lycoctonine.

Methyl-lycaconitine

The main bulk of the "weak bases" (*ca.* 400 g) was dissolved in benzene and the less soluble components precipitated by hexane. The remaining solution was evaporated to dryness, leaving 155 g of pale yellow alkaloid. This was taken up in benzene and separated manually in large funnels (12 transfers), the moving phase being in this case the buffer solution of pH 5. The contents of funnels 1–3 (55 g) proved to be largely inuline and yielded 37 g of crystalline base. Funnels 7–9 contained 21 g of alkaloid which was separated by a further 100 transfers on the Craig countercurrent apparatus using the same solvent system. Fractions 85–98 from this separation afforded 3.6 g of inuline, and fractions 1–12 gave 0.5 g of royline. Funnels 4–6 from the manual separation contained 41 g of alkaloid which could not be crystallized, hence this was distributed between benzene and buffer pH 5 in the countercurrent apparatus (100 transfers). The bulk of the alkaloid was found in fractions 34–79, and this material (14 g) was redistributed between benzene and buffer pH 4 in the Craig countercurrent apparatus (100 transfers). Five components were thus separated. The major component (tubes 11–45, 6.6 g) could not be crystallized, but gave a crystalline hydriodide, m.p. 199–201° (K), undepressed on admixture with an authentic specimen of methyl-lycaconitine hydriodide. The infrared spectra of the hydriodide of the base and of methyl-lycaconitine hydriodide were identical.

Hydrolysis of Methyl-lycaconitine

The base (404 mg) was refluxed for 45 minutes with 1% ethanolic potassium hydroxide. On cooling of the reaction mixture and extraction with chloroform, lycoctonine was obtained, and was recrystallized from aqueous ethanol as needles (256 mg) m.p. 115–123° (decomp.) undepressed on admixture with an authentic sample of lycoctonine. The infrared spectrum of the material obtained was identical with that of lycoctonine.

On acidification and further extraction of the hydrolysis mother liquors with chloroform, 1-methylsuccinyl-anthranilic acid was obtained (81 mg) which recrystallized from acetone–hexane as needles, m.p. 150–154° (K) with sintering at 146°, $[\alpha]_D$ −6° (EtOH). Found: C, 56.89; H, 5.02. Calc. for $C_{12}H_{13}O_5N$: C, 57.37; H, 5.22. (Goodson (3) reports a melting point of 155° with sintering at 147° $[\alpha]_D$ −7° (EtOH).)

ACKNOWLEDGMENTS

The authors wish to thank Mr. A. Knoll for technical assistance, Mr. H. Seguin for the microanalyses, and Mr. R. Lauzon for the infrared spectral determinations. We gratefully acknowledge the co-operation of Dr. A. Chatterjee, University of Calcutta, in informing us of their observations, and providing us with reference samples.

REFERENCES

1. CHOPRA, I. C., KOHLI, J. D., and HANDA, K. L. Indian J. Med. Research, **33**, 139 (1945).
2. CHATTERJEE, A. and TALAPATRA, S. Proc. 44th Indian Sc. Congr. Part III, p. 124 (1957).
3. GOODSON, J. A. J. Chem. Soc. 139 (1943).
4. COOKSON, R. C., PAGE, J. E., and TREVETT, M. E. J. Chem. Soc. 4028 (1954).

Can. J. Chem. Downloaded from www.nrcresearchpress.com by 196.1.178.254 on 09/04/12
For personal use only.

Can. J. Chem. Downloaded from www.nrcresearchpress.com by 196.1.178.254 on 09/04/12
For personal use only.

ACTIVATION ENERGIES OF SEMICONDUCTORS WITH THE ZINC BLENDE STRUCTURE[1]

W. B. PEARSON

ABSTRACT

Difficulties of determining the binding energies and effective charges on the atoms are the main reason why no systematic explanation of the variation of the size of the energy gap among members of the simplest family of semiconductors—those with the zinc blende structure—has ever been given. It is shown that by the choice of suitable atomic parameters for discussing the activation energies of these compounds these difficulties may be avoided, and the variation of the size of the energy gap between one compound and another can be systematically accounted for. In the treatment which develops no particular distinction need be made between the III–V, II–VI, and I–VII compounds, and it is concluded that the anomalously high or low activation energies, which certain compounds appear to have, are just the result of the relative sizes of the cations and anions in influencing the polarization of the bonds.

INTRODUCTION

Energy band calculations of semiconductors involve so much labor and difficulties that they do not provide a ready means of determining activation energies from the properties of the component atoms of the semiconductor. More intuitive chemical approaches have also made singularly little progress and it has not so far been possible, for instance, even to give a self-consistent discussion of the variation of activation energy among the compounds of the simplest family of semiconductors—those with the zinc blende type of structure. Welker (11) has shown essentially that the activation energy of a semiconductor depends on the binding energy and on the effective charges on the atoms. However, Folberth (3) has pointed out that consideration of Welker's rules alone is insufficient to explain the relative variation of activation energy among the III–V compounds with the zinc blende structure. The size of the energy gap depends both on the binding energy and on the extent of the modulation of the crystalline field in the compound semiconductor. Folberth postulates a linear relationship between the degree of modulation and the polarization of the chemical bonds, and establishes the relative size of the modulation of the crystalline field in a number of III–V compounds from calculated values of the polarization. Nevertheless, this work does not lead to an understanding of the variation of the activation energies of *all* compounds with the zinc blende structure since he deals only with the III–V compounds and then ignores some of these without comment.

Another method of approach has been developed by Goodman (4) in discussing the relative variation of electron mobilities in some semiconductors with the zinc blende structure. He determined the "ionic contribution" to the activation energy for the compounds from a linear relationship between the square root of the size of the energy gap and the reciprocal of the square of the interatomic distance, which he established for the truly homopolar Group IV semiconductors with the diamond structure. However, it does not seem possible to develop this approach further to describe the variation of the activation energies of these compounds, and the reason appears to be that no account is taken of the relative atomic sizes of the component atoms which are also significant.

[1]*Manuscript received March 16, 1959.*
Contribution from the Division of Pure Physics, National Research Council, Ottawa, Canada.
Issued as N.R.C. No. 5225.

Can. J. Chem. Downloaded from www.nrcresearchpress.com by 196.1.178.254 on 09/04/12
For personal use only.

DISCUSSION

The two main difficulties in developing a chemical discussion of the activation energies of compounds with the zinc blende structure along lines suggested by the work of Welker and Folberth are the determination of the binding energy and the effective charges on the atoms. Although some information of the latter may be gained by calculation from experimental data (cf. Wolff (2), Picus *et al.* (10), and Ehrenreich (1)) or perhaps by the arguments used by Pauling (cf. 8), there is no comprehensive knowledge of these charges which can be drawn on at present. Faced with these difficulties it seems that some progress may be made by indirect means, by comparing for these compounds atomic parameters to which the binding energy and effective charges are related, without ever considering the quantities explicitly.[2] For instance, Mooser and Pearson (6) have recently given a classification of normal valence compounds with simple atomic ratios in terms of two parameters: $\bar{n}$, the average principal quantum number of the valence electrons of the component atoms, and Δx, the difference of the electronegativities of the component atoms. These two parameters, which respectively describe the loss of directional character of covalent bonds in the compounds as the metallic character and as the ionic character increase, give a sharp separation of the compounds into groups with different structures and co-ordinations. Together or severally they bear a loose relationship to the binding energy and to the atomic size which is important in the modulation of the crystalline field in compounds of the zinc blende type. However, Δx alone is not sufficient to take account of the effective charges on the atoms of such compounds which depend on the polarization of the bonds, and this in turn depends on the relative sizes of the cation and anion. For reasons which are discussed more fully below we take the ratio of the cationic and anionic radii r_c/r_a as a measure of the polarization.

Several interesting facts appear when we examine the observed activation energy, ΔE_{obs}, of compounds with the zinc blende structure and of the Group IV elements with the diamond structure as a function of $\bar{n}$, Δx, and r_c/r_a. In each of the three isoelectronic series of substances shown in Table I we can investigate the variation of ΔE_{obs} as a

TABLE I

Substances in isoelectronic series considered

Substance	$\bar{n}$	ΔE_{obs} at 0° K	Δx*	Lattice spacing a in Å	r_c/r_a†
Si	3	1.21	—	5.4308	1
AlP‡	3	3.0	0.6	5.43	1.145
Ge	4	0.75	—	5.6575	1
GaAs	4	1.53	0.5	5.64	1.068
ZnSe	4	2.58	0.9	5.664	1.149
CuBr	4	2.94	1	5.69	1.216
Sn	5	0.08	—	6.4892	1
InSb	5	0.25	0.3	6.476	1.059
CdTe	5	1.45	0.6	6.477	1.121
AgI	5	2.8	0.75	6.50	1.195

*Values taken from Gordy and Thomas' (5) recently reviewed values of electronegativity.

†Based on Pauling and Huggins' tetrahedral radii (see e.g. Wells (12)).

‡A value of ΔE_{obs} = 5.0 ev for a hypothetical compound MgS with the zinc blende structure is consistent with the activation energies of the other members of the series with $\bar{n}$ = 3. MgS actually has the rock salt type of structure.

[2]*Since there are only bonds of one type in the zinc blende structure, it is reasonable not to have to consider the binding energy explicitly. This would not, however, be the case in, say, the chalcopyrites where bonds of two types occur and the energy gap would essentially depend on the weaker of the two bonds.*

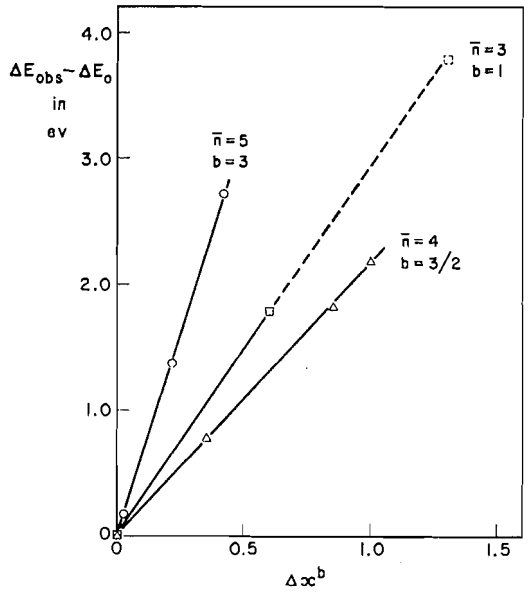

FIG. 1. Plots of $\Delta E_{obs} - \Delta E_0$ against Δx^b for three isoelectronic series of compounds. See text and Tables I and II.

function of Δx at a constant $\bar{n}$ value and at an r_c/r_a value which is approximately constant (taking Pauling's (7) single bond radii), or regularly increasing (taking tetrahedral radii, Pauling and Huggins (9)). We find (Fig. 1) that relationships of the type

$$\Delta E_{obs} = \Delta E_0 + c.\Delta x^b$$

hold in each of these series when ΔE_0 is the activation energy of the isoelectronic Group IV element and c and b are constants having the values depending on $\bar{n}$ given in Table II.

TABLE II

$\bar{n}$	ΔE_0 in ev	c	b
3	1.21	2.97	1
4	0.75	2.19	1.5
5	0.082	6.4	3

An approximately linear function of the average interatomic distance (lattice spacing) of substances in each of the three isoelectronic series is represented by b.

The form of these relationships for the isoelectronic series of substances indicates that no distinction need be made between the III–V, II–VI, and I–VII compounds if suitable parameters are chosen to discuss their activation energies, so that questions of whether a formal transference of one, two, or three valence electrons from anion to cation takes place in these compounds are avoided. As far as we are aware it has only previously been possible to obtain relationships between activation energies and atomic or bulk properties of compounds with the zinc blende structure which are of one type, e.g. the III–V or the II–VI compounds.

Using the above relationship for $\bar{n}$ values of 3, 4, and 5, we can derive the activation energy contours on an $\bar{n}$ vs. Δx plot shown in Fig. 2 so that the observed activation

Can. J. Chem. Downloaded from www.nrcresearchpress.com by 196.1.178.254 on 09/04/12
For personal use only.

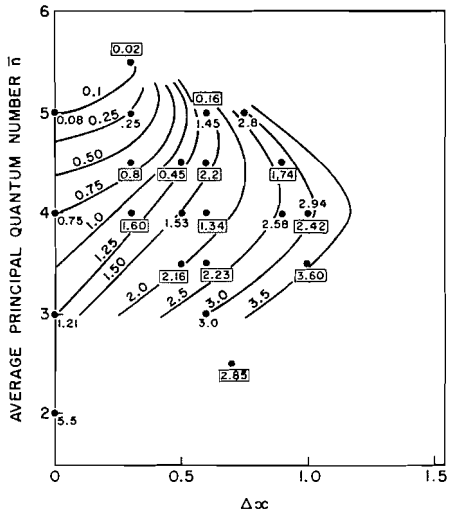

FIG. 2. Isoactivation energy contours on a $\bar{n}$ vs. Δx plot. These have been derived for the three isoelectronic series of compounds using the data in Fig. 1 and the unenclosed numbers are the observed activation energies for these compounds. The numbers enclosed in rectangles are the observed activation energies of the remaining compounds with the zinc blende structure.

energies of the remaining compounds with the zinc blende structure can be compared with the predicted values, ΔE_{pred}. As such a diagram only allows us to take account of $\bar{n}$ and Δx values, we would expect the observed and predicted activation energies of compounds to agree only if their r_c/r_a values were the same as those of the appropriate compounds of the isoelectronic series for which the contours were derived.[3] As Table III shows, this is indeed the case. The activation energies of AlAs, GaP, and ZnS with $\bar{n} = 3.5$ (and HgTe) are correctly predicted to within an average of 3% as their r_c/r_a values differ little from those interpolated from the isoelectronic series of compounds (i.e. $\Delta(r_c/r_a)$ in Table III). On the other hand the predicted and observed activation energies of compounds with $\bar{n} = 4.5$ and the remaining compounds with $\bar{n} = 4$ and $\bar{n} = 5$ differ widely, and this divergence systematically accompanies the difference between their r_c/r_a values and those of the isoelectronic series of compounds ($\Delta(r_c/r_a)$ in Table III). These compounds all contain one component atom from the fifth or sixth periods, the other coming from a lower period. The value of ΔE_{pred} is always *too small* when the *anion* comes from the fifth period and *too large* when the cation comes from the fifth or sixth periods. Now there is a much larger difference in atomic size between elements in the fourth and fifth periods, than between elements in the third and fourth,

[3]*In order to make this comparison with substances having fractional values of $\bar{n}$, we interpolate values as follows, say for $\bar{n} = 4.5$:*

$$(r_c/r_a)_{\bar{n}=4.5} = \{(r_c/r_a)_{\bar{n}=4} + (r_c/r_a)_{\bar{n}=5}\}/2.$$

In order to compare the r_c/r_a values of compounds in the isoelectronic series with r_c/r_a values of the remaining compounds we define

$$\Delta(r_c/r_a) = (r_c/r_a)_{\text{isoelectronic compound}} - (r_c/r_a)_{\text{other compound}}$$

comparing together III–V or II–VI compounds with the same $\bar{n}$, or interpolated $\bar{n}$, values. Thus for example

$$\Delta(r_c/r_a)_{CdS} = (r_c/r_a)_{ZnSe} - (r_c/r_a)_{CdS}.$$

The reason for this is that r_c/r_a for tetrahedral radii is an approximately linear function of the atomic number of the anion or cation in a series of isoelectronic compounds going from the Group IV element to the I–VII compound.

Can. J. Chem. Downloaded from www.nrcresearchpress.com by 196.1.178.254 on 09/04/12
For personal use only.

TABLE III

Compounds having $\bar{n}$ values from 3 to 5 which are not in the isoelectronic series considered

Compound	$\bar{n}$	ΔE_{obs} (ev)	Δx*	ΔE_{pred} (ev)	$(\Delta E_{pred} - \Delta E_{obs})$ (ev)	r_c/r_a*	$\Delta(r_c/r_a)$†
BAs	3	—	0	1.2	Large and negative(?)	0.746	0.399
AlAs	3.5	2.16	0.5	1.99	−0.17	1.068	0.04
GaP	3.5	2.23	0.6	2.23	0	1.146	−0.04
ZnS	3.5	3.60	1.0	3.48	−0.12	1.260	−0.014
AlSb	4	1.60	0.3	1.12	−0.48	0.927	0.141
InP	4	1.34	0.6	1.76	0.42	1.309	−0.241
CdS	4	2.42	1.0	2.94	0.52	1.423	−0.274
GaSb	4.5	0.8	0.3	0.66	−0.14	0.927	0.136
InAs	4.5	0.45	0.5	1.16	0.71	1.220	−0.156
ZnTe	4.5	2.2	0.6	1.41	−0.79	0.992	0.143
CdSe	4.5	1.74	0.9	2.74	1.0	1.298	−0.164
HgSe	5	0.16 ?	0.6	1.45	1.29	1.298	−0.177

*See footnotes to Table I.
†See footnote on page 1194.

or fifth and sixth, periods. In all of these compounds, therefore, with $\bar{n}$ having values of 4, 4.5, or 5, the values of r_c/r_a are appreciably larger or smaller, depending on whether the cation or the anion comes from the fifth period, than the values estimated from compounds of the three isoelectronic series upon which the $\bar{n}$ vs. Δx relationship for ΔE_{obs} was based. We would therefore expect that the polarization of the bonds and hence the effective atomic charges in these compounds would differ considerably from those in corresponding compounds of the isoelectronic series.

Let us consider the polarization of, say, a III–V compound with the zinc blende structure; the basic assumption in considering the chemical bonding is that an electron is transferred from the five-valent atom to the three-valent atom so that each atom has four valence electrons and forms four shared electron pair bonds. The formal charges on the atoms are then $:\dot{\underset{\cdot\cdot}{\text{III}}}^{-}\ :\dot{\underset{\cdot\cdot}{\text{V}}}^{+}:$. Polarization of the bonds in this structure involves the movement of the electron pairs from the center of the bonds towards the five-valent atom, thus reducing the formal charges on the atoms. Therefore the greater the polarization, the smaller the effective charges on the atoms (provided of course that the polarization is not so strong as to reverse the charges on the atoms), and hence the smaller is the activation energy of the compound. The polarization depends on the relative sizes of the anions and cations and also on the principal quantum number of their valence electrons and on the electronegativity difference. The larger the cation and the smaller the anion, the greater is the polarization of the bonds in these compounds and we therefore take the ratio of the cationic to anionic radii, r_c/r_a, as a measure of the polarization.

As shown in Table III, HgSe, InAs, CdSe, InP, and CdS, with r_c/r_a values considerably greater than those of compounds in the corresponding isoelectronic series, all have activation energies lower than those predicted, because a negative $\Delta r_c/r_a$ value means a greater polarization of the bonds, smaller effective charges on the atoms, and hence lower activation energies. The converse is true for GaSb, ZnTe, AlSb, and BAs, which have positive $\Delta r_c/r_a$ values and hence higher activation energies.

Can. J. Chem. Downloaded from www.nrcresearchpress.com by 196.1.178.254 on 09/04/12
For personal use only.

Can. J. Chem. Downloaded from www.nrcresearchpress.com by 196.1.178.254 on 09/04/12
For personal use only.

CONCLUSION

We are thus led to the conclusion that the variation of the activation energy in compounds of the zinc blende type (with $\bar{n}$ values from 3 to 5.5) is perfectly systematic and it can be accounted for by the use of three atomic properties, $\bar{n}$, Δx, and r_c/r_a. The treatment does not require that any particular distinction be made between the III–V, II–VI, and I–VII families of compounds. The apparently anomalously large or small activation energies of some compounds such as ZnTe and InAs, which have previously led to difficulties of interpretation, are shown to be the result of excessively small or excessively large polarization of the bonds when either the anion or the cation alone comes from the fifth or sixth periods. The discussion, however, fails to reach a satisfying quantitative conclusion since we have been unable to calculate the activation energies of all compounds with the zinc blende structure from the values of $\bar{n}$, Δx, and r_c/r_a alone. Relationships giving the sign and magnitude of $(\Delta E_{pred} - \Delta E_{obs})$ in terms of $\Delta(r_c/r_a)$ do exist, but they depend on the $\bar{n}$ value of the compounds.

Our investigation suggests that the observed activation energy of SiC is lower than expected and this could be accounted for by polarization of the bonds, but there is little value in entering into a discussion of SiC, or in attempting to predict the activation energy of the compound BP, until the activation energy of cubic BN with $\bar{n} = 2$ is known, since this would only involve uncertain extrapolations.

ACKNOWLEDGMENTS

I am very grateful to Drs. D. K. C. MacDonald and E. Mooser for many stimulating discussions about theories, interpretations, and activation energies.

NOTE ADDED IN PROOF

This correlation of the activation energies of compounds with the zinc blende structure is based on examination of compounds lying along a non-planar section in $\bar{n}$–Δx–r_c/r_a space for which activation energy contours can be constructed. All compounds lying above this section, that is having greater r_c/r_a values, have activation energies smaller than those expected for a compound with the same $\bar{n}$ and Δx values which lies in the section, and the converse is true for compounds with smaller r_c/r_a values which lie below the section. Compounds with r_c/r_a values lying in the section have their activation energies correctly predicted. This is in complete accord with the expected polarization of the bonds in these substances, provided that it is assumed that the cations still possess small effective negative charges and the anions positive charges (i.e. that the polarization is not so strong as to reverse the formal charges on the covalently bonded atoms). On the other hand the percentage ionic character of the bonds in these compounds determined from infrared measurements (Picus *et al.* (10)) and microcleavage studies (Wolff (2)) suggests that the cations are positively charged and the anions are negatively charged.

REFERENCES

1. Ehrenreich, H. Phys. and Chem. Solids, **2**, 131 (1957).
2. Wolff, G. A. Private communication.
3. Folberth, O. G. Z. Naturforsch. **13a**, 856 (1958).
4. Goodman, C. H. L. J. Electronics, **1**, 115 (1955).
5. Gordy, W. and Thomas, W. J. O. J. Chem. Phys. **24**, 439 (1956).
6. Mooser, E. and Pearson, W. B. Acta Cryst. (In press).
7. Pauling, L. J. Am. Chem. Soc. **69**, 542 (1947).
8. Pauling, L. Proc. Natl. Acad. Sci. **36**, 433 (1950).
9. Pauling, L. and Huggins, M. L. Z. Krist. **87**, 205 (1934).
10. Picus, G., Burstein, E., Henvis, B. W., and Hass, M. Phys. and Chem. Solids, **8**, 282 (1959)
11. Welker, H. Z. Naturforsch. **7a**, 744 (1952)
12. Wells, A. F. Structural inorganic chemistry. 2nd ed. Clarendon Press, Oxford. 1954. p. 50.

Can. J. Chem. Downloaded from www.nrcresearchpress.com by 196.1.178.254 on 09/04/12
For personal use only.

THE BIOGENESIS OF ALKALOIDS

XXIII. THE ROLE OF PROLINE AND ORNITHINE IN THE BIOGENESIS OF STACHYDRINE[1]

A. V. Robertson[2] and Léo Marion

ABSTRACT

When methionine-Me-^{14}C, pyridoxine, and folic acid were fed to growing alfalfa, the stachydrine isolated from the plant was radioactive. This observation supports the assumption that stachydrine arises from proline by methylation since pyridoxine has been shown to induce the formation of proline from ornithine in the plant. However, the administration of labelled ornithine, pyridoxine, folic acid, and methionine to alfalfa failed to produce the radioactive alkaloid. Similar experiments were performed in which methionine-Me-^{14}C and folic acid, methionine-Me-^{14}C and pyridoxine, and finally methionine-Me-^{14}C alone were fed to alfalfa, and in each case the stachydrine isolated from the plant was radioactive, while the homostachydrine remained inactive. Feeding proline-carboxyl-^{14}C to alfalfa failed to produce radioactive stachydrine. It must be concluded that in alfalfa which is 2 to 3 weeks old, stachydrine is actively synthesized although homostachydrine is not. The implications of these observations are discussed.

The biogenesis of stachydrine in alfalfa (*Medicago sativa* L. Grimm) has been studied in this laboratory for some time (1, 2, 3). In these studies the assumption has always been made that stachydrine was formed in the plant by methylation of proline, and that the latter has for its precursor ornithine. Indeed, in higher plants, it has been shown that ornithine is the precursor of the disubstituted N-methylpyrrolidine ring of hyoscyamine (4) and of the monosubstituted N-methylpyrrolidine ring of nicotine (5, 6). Leete, Marion, and Spenser (1) administered ornithine-2-^{14}C to 2-week-old alfalfa seedlings, but found that the stachydrine isolated from the plants a week later was not radioactive. In further experiments this result was confirmed, and it was established that the proline in the plant was not active either although glutamic acid, aspartic acid, and glycine were (2). Even in 12-week-old alfalfa, stachydrine and proline were not actively synthesized from ornithine (2). When, however, ornithine-2-^{14}C together with pyridoxine was administered to 7-day-old seedlings, the proline isolated from the plants 12 days later was radioactive although the stachydrine was not (2). Feeding glutamic acid-2-^{14}C and pyridoxine to 2-week-old alfalfa seedlings also produced radioactive proline, but again the stachydrine was inactive (3). The effect of feeding radioactive glutamic acid without pyridoxine has not been examined. To test the possibility that stachydrine formation might not occur until a later stage of growth, ornithine-2-^{14}C was fed to flowering alfalfa plants, 9 months old, but the stachydrine subsequently isolated was not radioactive (7).

From the foregoing results it was concluded that although the conversion of glutamic acid and ornithine to proline occurs in the presence of pyridoxine the methylation of proline to stachydrine does not take place in alfalfa at an age of 2–3 weeks. In an attempt to stimulate the plant methylation processes, alfalfa seedlings were treated with ornithine-2-^{14}C, pyridoxine, and methionine, but the stachydrine obtained showed no radioactivity (7). In a further effort to enhance the probability of methylation, Wiehler and Marion (3) found that after feeding methionine-Me-^{14}C, pyridoxine, and folic acid, the stachydrine was radioactive. On the assumption that proline was the precursor of stachydrine, they concluded that the young plants were deficient in folic acid and that the artificial appli-

[1]*Manuscript received March 16, 1959.*
Contribution from the Division of Pure Chemistry, National Research Council, Ottawa, Canada.
Issued as N.R.C. No. 5226.
[2]*National Research Council of Canada Postdoctorate Fellow.*

cation of this compound had induced the biosynthesis of stachydrine. However, if the substance being methylated to produce stachydrine is not proline, other interpretations are possible, and the purpose of the present work was to examine this possibility. Nevertheless it is definitely established that although proline is a normal constituent of alfalfa, no interconversion with ornithine takes place in plants 2–3 weeks old unless pyridoxine is added; interconversion between glutamic acid and proline also occurs in the presence of pyridoxine.

If folic acid is really a necessary co-factor for the biological methylation of proline then administration of ornithine-2-^{14}C with pyridoxine and folic acid should produce radioactive stachydrine. This experiment was performed on plants 2 weeks old, and inactive methionine and ornithine were added as well to boost the concentration of these amino acids. The purified mixture of stachydrine and homostachydrine hydrochlorides (8) isolated after a week was not radioactive. The result was surprising and it suggested that the presence of folic acid was incidental to the formation of radioactive stachydrine from Me-labelled methionine. A small scale repetition of the experiment of Wiehler and Marion using radioactive methionine, pyridoxine, and folic acid confirmed their result. Similar experiments were then performed on 2-week-old alfalfa by feeding methionine-Me-^{14}C and folic acid, methionine-Me-^{14}C and pyridoxine, and finally methionine-Me-^{14}C alone. In all of these experiments the betaine fraction was radioactive, and paper chromatographic assay showed the whole of the activity was present in the stachydrine and that the homostachydrine was inactive. These results lend further support to the suggestion made in Part XXI of this series of studies (9) that homostachydrine is not formed until a later stage of development and that translocation of this alkaloid stored in the seeds is the reason for its isolation from alfalfa seedlings. From the facts described it seems that at least a partial synthesis of stachydrine is actively going on in the plant during the first 3 weeks of growth in the absence of pyridoxine and folic acid, and also that proline might not be involved in the chain of precursors. As a check on the role of proline in stachydrine biogenesis, proline-carboxyl-^{14}C was fed to alfalfa on the 17th day of growth and after 2 days the plants were harvested. The crystalline mixture of stachydrine and homostachydrine hydrochlorides was not radioactive.

To sum up, and assuming that ornithine-2-^{14}C in conjunction with pyridoxine is equivalent to proline-2-^{14}C, the radioactivity of ring-labelled or carboxyl-labelled proline is not incorporated in stachydrine at a plant age when experiments with methionine-Me-^{14}C indicate that the synthesis of the alkaloid is taking place. At first glance these results indicate that proline is not a precursor of stachydrine, but this conclusion is difficult to accept on general chemical and biogenetic grounds. Assuming, however, that the alkaloid is in fact derived from the expected amino acids, there are three hypotheses which are not eliminated on the basis of the present evidence. Firstly stachydrine may be ultimately derived from the expected amino acid precursors, but the stages of the synthesis occur at different times so that the final step is a methylation of an intermediate which is so far undetected in alfalfa, and which is preformed from proline and stored in some suitable form. Secondly there may be a specific reversible equilibrium between preformed stachydrine (the alkaloid having been formed from the amino acid at a different period of growth) and administered methionine or some intermediate to which methionine-methyl may be transferred, leading to methyl exchange, such as

2-S-adenosylmethionine-Me* + stachydrine-Me $\rightleftharpoons$ 2-S-adenosylmethionine-Me + stachydrine-Me*.

Thirdly[3] the site of stachydrine synthesis may be highly localized and possibly not

[3]*We are grateful to Dr. I. D. Spenser, McMaster University, for suggesting this third possibility.*

Can. J. Chem. Downloaded from www.nrcresearchpress.com by 196.1.178.254 on 09/04/12
For personal use only.

all amino acids can enter this site preformed. For instance, yeast cells readily assimilate methionine, but do not apparently take up proline (10). Methionine (or at least its methyl group) can obviously penetrate the site of stachydrine synthesis, and it could be assumed that proline, glutamate, and ornithine cannot, and must be formed *in situ* to be utilized. This would explain the finding that radio-proline, when fed, did not give rise to stachydrine, and that proline, isolated after administration in the presence of pyridoxine of radio-ornithine or radio-glutamate, was labelled, whereas stachydrine was not.

The second of these assumptions involving a methylation equilibrium is not too probable, because processes involving only the betaine methyl groups are unlikely since homostachydrine is not affected. In the first hypothesis N-methyl proline (hygric acid) should be involved, and the results of feeding carboxyl-labelled hygric acid are being examined. It seems that either the first or third hypothesis is more probable than the assumption that proline might not be a precursor of stachydrine.

EXPERIMENTAL

The alfalfa seedlings were grown and the alkaloids were isolated as described previously (9).

Radioactive Ornithine Experiment

Alfalfa seeds (300 g) were germinated on glass wool in 10 trays (20×30 cm). On the 16th day, DL-ornithine-2-^{14}C-monohydrochloride (208.5 mg, total activity 5×10^7 d.p.m., purchased from Tracerlab Inc.), DL-methionine (100 mg), folic acid (2 mg), and pyridoxine hydrochloride (2 mg) were administered in nutrient solution. These materials were fed again in the same quantities on the 21st day and the plants were harvested the next day. The alcoholic extract of the dried plants contained 3% of the radioactivity administered, and 0.465 g of betaine hydrochlorides was obtained. After purification via the mercuric chloride complex and recrystallization, the mixture of stachydrine and homostachydrine hydrochlorides was radioinactive.

Radioactive Methionine Experiments

For each of these four experiments, 30 g of seeds were germinated in one tray. On the 16th day, the plants were fed the following compounds in aqueous solution:

Experiment 1.—Methionine-Me-^{14}C (25 mg, total activity 3.05×10^7 d.p.m.), pyridoxine hydrochloride (1 mg), folic acid (0.5 mg).

Experiment 2.—Methionine-Me-^{14}C as for 1, folic acid (0.5 mg).

Experiment 3.—Methionine-Me-^{14}C as for 1, pyridoxine hydrochloride (0.5 mg).

Experiment 4.—Methionine-Me-^{14}C as for 1.

After 1 day only 1–2% of the radioactivity remained in the nutrient solutions and only 0.1–0.3% after 2 days, so the plants were harvested on the 18th day. The alcoholic extract contained 11–13% of the activity administered. The alkaloid fractions were purified by means of a mercuric chloride precipitation but the mixture of betaines was very difficult to crystallize because of inorganic and other impurities which could not be removed on this small scale. The alkaloid mixtures had activities of about 400 d.p.m./mg, and paper chromatographic assay (3) in butanol – hydrochloric acid and ethanol–ammonia (9) showed that the stachydrine contained all the radioactivity in each case. The crude choline reineckate from each experiment was radioactive and averaged about 500 d.p.m./mg.

Radioactive Proline Experiment

Alfalfa seeds (250 g) were grown in 10 trays. On the 17th day, proline-carboxyl-^{14}C

Can. J. Chem. Downloaded from www.nrcresearchpress.com by 196.1.178.254 on 09/04/12
For personal use only.

(9.2 mg, total activity 6.4×10^7 d.p.m., purchased from Volk Radiochemical Co.) was fed, as usual. A small part of this activity (3.5%) remained in the nutrient solution after 1 day, and less than 2% after 2 days. The plants were harvested on the 19th day. The alcoholic extract contained 1.8% of the radioactivity administered. Sixty-eight per cent of the activity in the extract was present in the protein fraction, and the remaining activity stayed in the filtrate after precipitating the betaine reineckates. The pure crystalline mixture of stachydrine and homostachydrine hydrochlorides (0.283 g) was not radioactive, nor was the crystalline asparagine (2.53 g) or choline chloride (0.46 g).

REFERENCES

1. LEETE, E., MARION, L., and SPENSER, I. D. J. Biol. Chem. **214**, 71 (1955).
2. MORGAN, A. and MARION, L. Can. J. Chem. **34**, 1704 (1956).
3. WIEHLER, G. and MARION, L. J. Biol. Chem. **231**, 799 (1958).
4. LEETE, E., MARION, L., and SPENSER, I. D. Nature, **174**, 650 (1954).
5. LEETE, E. Chem. & Ind. 537 (1955).
6. DEWEY, L. J., BYERRUM, R. U., and BELL, C. D. Biochim. et Biophys. Acta, **18**, 141 (1955).
7. MASSICOT, J. and MARION, L. Unpublished work.
8. WIEHLER, G. and MARION, L. Can. J. Chem. **36**, 339 (1958).
9. ROBERTSON, A. V. and MARION, L. Can. J. Chem. **37**, 1043 (1959).
10. BARTON-WRIGHT, E. C. Wallerstein Labs. Communs. **15**, 115 (1952).

Can. J. Chem. Downloaded from www.nrcresearchpress.com by 196.1.178.254 on 09/04/12
For personal use only.

Can. J. Chem. Downloaded from www.nrcresearchpress.com by 196.1.178.254 on 09/04/12
For personal use only.

DEGRADATIVE STUDIES ON λ-CARRAGEENIN[1]

K. MORGAN[2] AND A. N. O'NEILL[3]

ABSTRACT

λ-Carrageenin was subjected to partial acetolysis. Chromatography of the deacetylated products on charcoal led to the isolation of D-galactose, 3-*O*-α-D-galactopyranosyl-D-galactose (A), and a crystalline trisaccharide (B) tentatively identified as *O*-α-D-galactopyranosyl-(1 → 3)-*O*-α-D-galactopyranosyl-(1 → 3)-D-galactose. Periodate oxidation of the polysaccharide indicated the presence of more than one type of linkage in the polymer.

The name carrageenin (1, 2) was first applied to the polysaccharide which can be extracted with hot water from certain red seaweeds, where it occurs as an intercellular constituent. The main source of carrageenin is the alga *Chondrus crispus*, but similar material has been isolated from *C. ocellatus* (3) and *Gigartina stellata* (4).

In 1953, Smith and Cook (5) reported the separation of two major discrete polysaccharide components from carrageenin. This was achieved by fractionation with potassium chloride which, when added to a dilute solution of carrageenin, causes one component to gel. This gel fraction, which constitutes approximately forty per cent of unfractionated carrageenin, has been designated κ-carrageenin. It has been shown (6) to be composed of residues of 3,6-anhydro-D-galactose and sulphated D-galactose in approximately equimolar amounts. The other major polysaccharide component is insensitive to potassium ion, and can be recovered from the mother liquor by ethanol precipitation (5, 7, 8); this fraction has been termed λ-carrageenin. In addition to κ- and λ-carrageenin, minor amounts of other polysaccharides occur in carrageenin preparations as indicated by the detection of small amounts of L-galactose, glucose, and xylose in hydrolyzates (8).

Although the structure of λ-carrageenin has not been extensively investigated, results from X-ray analysis (9) and periodate oxidation (8) of the polysaccharide, together with data from methylation of unfractionated carrageenin (4, 10, 11, 12), suggest that it consists essentially of a sulphated galactan in which D-galactose residues are linked glycosidically through positions 1 and 3, and bear sulphate half-ester groups on position 4. The purpose of the present work was to obtain definitive evidence for the fundamental structural linkage in λ-carrageenin.

The polysaccharide was isolated from commercial carrageenin by fractionation with potassium chloride (5, 7, 8). Analytical figures for three separate preparations are shown in Table I. Acid hydrolyzates of the preparations were shown chromatographically to contain galactose and a trace of xylose only.

Since sulphated polysaccharides do not lend themselves easily to examination by exhaustive methylation, a method involving partial degradation was indicated. This was accomplished most satisfactorily by acetolysis, in which degradation of the polymer was accompanied by rapid desulphation to give a good yield of neutral oligosaccharide acetates.

λ-Carrageenin was treated with a mixture of acetic anhydride and acetic acid containing sulphuric acid (6%) at 25° C for 71 hours, and the sulphate-free product was deacetylated

[1]*Manuscript received March 23, 1959.*
Contribution from the National Research Council, Atlantic Regional Laboratory, Halifax, Nova Scotia. Issued as N.R.C. No. 5217.
[2]*National Research Council of Canada Postdoctorate Fellow 1957–1959. Present address: Department of Microbiology, Yale University, New Haven, Conn., U.S.A.*
[3]*Deceased May 7, 1958.*

TABLE I

Analytical results for λ-carrageenin preparations

Preparation	$[\alpha]_D^{25}$†	Galactose, %	3,6-Anhydro-D-galactose, %‡	SO_3K, %	Total recovery, %	Molar ratio, $\frac{\text{galactose}}{SO_3K}$
λ–1	+69.8°	46.2	2.1	46.8	93.0	0.74
λ–2	+71.2°	48.3	1.4	47.6	95.9	0.75
λ–IP*	+71.2°	48.2	1.0	47.8	96.0	0.75

*Refractionated material from sample λ-1.
†*c*, 0.33 in water.
‡Determined colorimetrically (28).

with methanolic sodium methoxide. The reducing power of the solution corresponded to an apparent degree of conversion into galactose of 45%. The deacetylated acetolyzate was adsorbed on a column of charcoal–Celite. Elution with water yielded D-galactose, characterized as its β-penta-acetate, and a small amount of xylose, detected chromatographically. The oligo- and higher saccharides were recovered by elution of the column with aqueous ethanol (50% v/v). Hydrolysis of a small portion, followed by chromatographic examination, indicated that the oligosaccharides present were composed of galactose residues only.

The oligosaccharides were separated on a charcoal–Celite column by stepwise elution with aqueous ethanol (13) (see Fig. 1). One disaccharide (A), one trisaccharide (B), and

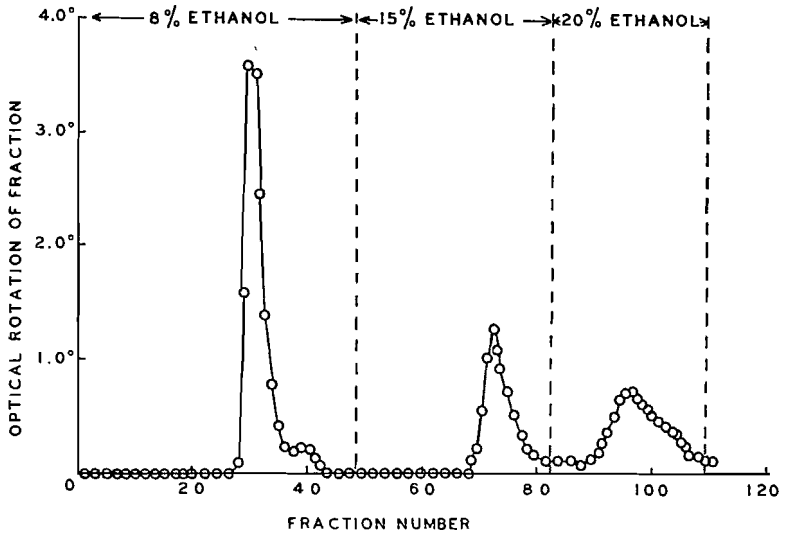

FIG. 1. Charcoal fractionation of oligosaccharide mixture from a deacetylated acetolyzate of λ-carrageenin.

an impure tetrasaccharide fraction (C) were isolated. These travelled on chromatograms at the relative rates expected for a polymer-homologous series (14). A fraction (D) containing the higher saccharides was also recovered from the column. The physical properties of the di- and tri-saccharides and their derivatives are recorded in Table II.

The disaccharide (A) was not obtained crystalline but afforded crystalline β-octa-*O*-acetyl and phenylosazone derivatives. On paper chromatograms and ionophoretograms

Can. J. Chem. Downloaded from www.nrcresearchpress.com by 196.1.178.254 on 09/04/12
For personal use only.

TABLE II

Properties of the products from a deacetylated acetolyzate of λ-carrageenin (45.0 g)

Sugars	Yield (g)	M.p.	$[\alpha]_D^{25}$†	β-Acetate derivative‡ M.p.	β-Acetate derivative‡ $[\alpha]_D^{25}$
Monosaccharide	3.8	—	+80.0°	142°	+23.7°
Disaccharide	3.75	—	+155.0°	157.5–158.5°	+109.1°
Trisaccharide	2.15	237–239° (decomp.)	+146.0°	275–277°	+105.5°
Tetrasaccharide*	2.15	—	—	—	—
Higher molecular weight sugars	6.0	—	—	—	—

*Contains trace of contaminating trisaccharide.
†In water.
‡In chloroform.

it was located as a single discrete spot and moved at markedly different rates from those of 4-*O*- and 6-*O*-α-D-galactopyranosyl-D-galactose. Its high specific optical rotation (+155°, water) indicated that it was α-linked, and distinguished it from 3-*O*-β-D-galactopyranosyl-D-galactose, which has $[\alpha]_D$ +63° (15). Hydrolysis of the methylated disaccharide yielded 2,3,4,6-tetra-*O*-methyl-D-galactose and 2,4,6-tri-*O*-methyl-D-galactose, characterized as their crystalline aniline derivatives. Periodate oxidation (25) of the disaccharide (1 mole) under unbuffered conditions led to an initial rapid uptake of 4.2 moles of oxidant and the production of 2.2 moles of formic acid (see Fig. 2). The disaccharide is thus identified as 3-*O*-α-D-galactopyranosyl-D-galactose.

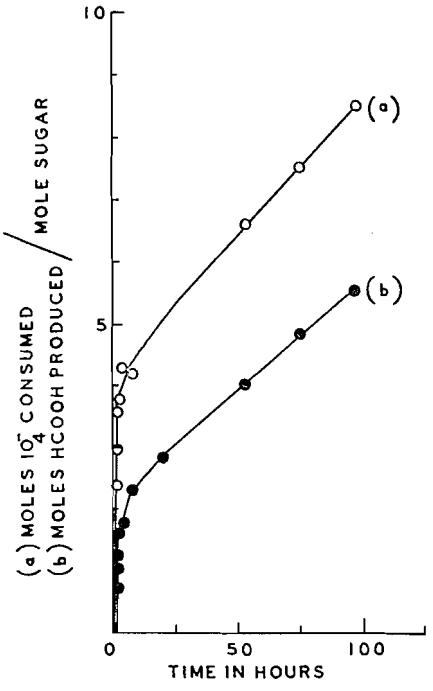

FIG. 2. Oxidation of disaccharide in 0.004 *M* solution with 0.125 *M* sodium metaperiodate at 25° C.

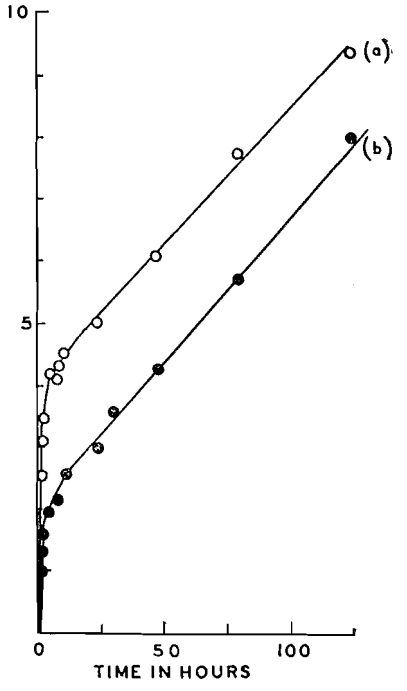

FIG. 3. Oxidation of trisaccharide in 0.003 *M* solution with 0.125 *M* sodium metaperiodate at 25° C.

Can. J. Chem. Downloaded from www.nrcresearchpress.com by 196.1.178.254 on 09/04/12
For personal use only.

The trisaccharide (B) crystallized, and gave a crystalline β-hendeca-*O*-acetyl derivative. Partial hydrolysis of the trisaccharide yielded galactose and one disaccharide only. The latter was chromatographically and ionophoretically indistinguishable from (A). Its specific optical rotation (+146°, water) suggested that both galactosidic linkages were in the α-configuration. Periodate oxidation (25) of the trisaccharide gave results similar to those obtained for the disaccharide as shown in Fig. 3, thereby indicating that both glycosidic linkages are (1 → 3). The trisaccharide is therefore suggested to be *O*-α-D-galactopyranosyl-(1 → 3)-*O*-α-D-galactopyranosyl-(1 → 3)-D-galactose.

Portions of fractions (C) and (D) were partially hydrolyzed. Chromatographic and ionophoretic examinations of the hydrolyzates indicated the presence of one disaccharide and one trisaccharide, the mobilities of which were identical with those of (A) and (B), respectively.

Oxidation of the three separate preparations of λ-carrageenin in 0.05 *M* sodium metaperiodate resulted in each case in the uptake of 0.15 mole of periodate and the production of 0.05 mole of formic acid per anhydrogalactose residue.

DISCUSSION

The foregoing results corroborate the evidence of Smith *et al.* (8) that the λ-carrageenin molecule is composed mainly, if not exclusively, of D-galactopyranose residues. Also, their conclusion that the xylose found in carrageenin hydrolyzates arises from a contaminating xylan is supported by the fact that the total oligo- and higher saccharide fraction isolated in the present work was free from xylose residues. The analyses of λ-carrageenin preparations for galactose and sulphate (Table I) show that a large proportion of the galactose residues are disulphated.

The structural evidence presented here shows that the λ-carrageenin molecule is composed mainly of α-1:3 galactosidic linkages, and also suggests that the di-, tri-, and tetra-saccharides, (A), (B), and (C), are members of a homologous series composed uniformly of α-(1 → 3)-linked-D-galactopyranose residues. The substantial yield of these sugars, and the failure to detect the presence of other di- and tri-saccharides in the deacetylated acetolyzate, indicate a paucity in the polymer of other types of linkages. That other linkages are present, however, is clear from the fact that λ-carrageenin is susceptible to periodate ion. The periodate uptake and the yield of formic acid observed in the present work correspond to the presence, for every 20 D-galactose residues, of one residue bearing three contiguous, unsubstituted hydroxyl groups, and of a second residue bearing two such hydroxyl groups. Methylation data for unfractionated carrageenin (4, 10, 11, 12) indicate the presence of some 1 → 6 linkages in the polysaccharide mixture. In the λ-carrageenin molecule, therefore, two such linkages may be present for every 20 residues. Whether these linkages occur in linear chains of galactose residues, or constitute branch points, remains quite obscure, as also does the distribution of the half-ester sulphate groups.

EXPERIMENTAL

Chromatograms were developed on Whatman No. 1 filter paper with the following solvent systems: (*a*) 1-butanol–ethanol–water (4:1:1); (*b*) 1-butanol–pyridine–water (6:4:3); (*c*) 1-propanol – ethyl acetate – water (6:1:3); and (*d*) 1-butanol – acetic acid – water (4:1:5; upper phase). Sugars were located by spraying with benzidine (16), silver nitrate (17), or aniline hydrogen phthalate (18) reagents, and their mobilities are quoted relative to galactose (R_{Gal}).

Can. J. Chem. Downloaded from www.nrcresearchpress.com by 196.1.178.254 on 09/04/12
For personal use only.

Can. J. Chem. Downloaded from www.nrcresearchpress.com by 196.1.178.254 on 09/04/12
For personal use only.

Electrophoresis was carried out using Whatman No. 1 paper, supported horizontally, and a borate buffer (pH 10) (19). A potential difference of 500–600 v was applied, corresponding to a current of *ca.* 20–25 ma. Sugar spots were detected with the benzidine spray reagent (16).

Melting points were determined with a Kofler micro melting point apparatus. Solutions were concentrated under reduced pressure at 40–45° C. Polysaccharide samples were analyzed for galactose by complete hydrolysis and then determination of the reducing sugar by the Somogyi method (20). Sulphate determinations were made on completely hydrolyzed polysaccharide samples by precipitation with barium chloride.

Preparation of λ-Carrageenin

An aqueous solution of commercial carrageenin[4] was treated with potassium chloride, and the resulting gel removed as previously described (7, 8). The λ-carrageenin was precipitated from the mother liquor by addition of ethanol to a final concentration of 38–40% (v/v), and was collected in a Sharples centrifuge. After the precipitate was washed with aqueous ethanol (50% v/v), followed by ethanol, and then ether, a white fibrous polysaccharide (λ-1) was obtained. The yield from 65 g of commercial carrageenin was 20 g. A further quantity (λ-2; 30 g) was prepared in the same way.

A portion (3 g) of λ-1 was dissolved in aqueous potassium chloride (0.25 *M*; 1.75 l.) at 65° C. The solution was cooled to 20° C and centrifuged at 15,000 r.p.m. for 30 minutes, when a small amount of gel separated. Addition of aqueous "Cetavlon" (20% w/v; 25 ml) to the centrifugate yielded a precipitate (21) which was separated by centrifugation, washed with water, and dissolved in aqueous potassium chloride (2 *M*; 1 l.). Ethanol (1 l.) was added, and the precipitated material was collected (centrifuge) and washed with aqueous ethanol (60% v/v). The precipitate was then dissolved in water (750 ml) and the solution dialyzed against aqueous potassium acetate (0.0025 *M*) until free from chloride ion. From the impermeate a purified sample of λ-carrageenin (λ-IP; 2.25 g) was recovered in the usual way.

Analytical figures for preparations λ-1, λ-2, and λ-IP are given in Table I. In each case, samples hydrolyzed with 0.1 *N* hydrochloric acid at 100° C for 24 hours yielded galactose and a trace of xylose only, detected chromatographically.

Partial Acetolysis of λ-Carrageenin

A sample of λ-carrageenin (λ-1 + λ-2; 45 g), dried *in vacuo* at 60° C for 24 hours, was added slowly during 30 minutes to a rapidly stirred mixture of acetic anhydride (250 ml), glacial acetic acid (180 ml), and concentrated sulphuric acid (25 ml) at 0–5° C. After the mixture was shaken at 25° C for 71 hours the small amount of insoluble material which remained was removed by filtration. The filtrate was poured into ice-cold water (2.5 l.), which was then made neutral to Congo red with solid sodium bicarbonate. The precipitated material was separated by filtration, washed with water, and dried to a white, amorphous powder (29.5 g). The filtrate was extracted by shaking with chloroform (3×500 ml), and the combined chloroform extracts dried and concentrated to a yellow syrup (10.2 g). The two products contained no detectable sulphate, and were combined. The total product (39.5 g) was dissolved in methanol (410 ml), and a solution of sodium methoxide (0.5% sodium in methanol) (135 ml) was added. The mixture was kept at 5° C for 20 hours, and water was then added until the precipitated sugars just redissolved. The solution was neutralized with Amberlite resin IR-120, filtered, and concentrated to a syrup (22.0 g). The reducing power of the product corresponded to an apparent degree

[4]*Product of the Seaplant Chemical Corporation, New Bedford, Mass., U.S.A.*

of conversion into galactose of 45%. Chromatographic examination indicated the presence of galactose and a trace of xylose, together with three oligosaccharide components (A, B, and C) which had R_{Gal} values in solvent *d* of 0.56, 0.33, and 0.20, respectively. Some higher saccharides were also present.

Fractionation of the Deacetylated Acetolyzate

The above product (22 g) was adsorbed on a column of charcoal–Celite (1:1 w/w; adsorbent, 90×4.8 cm), and the monosaccharide components removed by elution with water (1 l.). The oligo- and higher saccharides were recovered by elution of the column with aqueous ethanol (50% v/v; 5 l.); the eluate was concentrated to a syrup (18.3 g), a portion of which, when hydrolyzed in 0.1 *N* hydrochloric acid at 100° C for 24 hours and examined chromatographically, revealed the presence of galactose only.

The oligo- and higher saccharide mixture was readsorbed on a column of charcoal–Celite (1:1 w/w; adsorbent, 68×8.0 cm), which was then eluted stepwise with increasing concentrations of ethanol in water (13). Fractions (150 ml) were collected under reduced pressure as described by Whelan *et al.* (22). The course of the elution was followed polarimetrically (see Fig. 1). Appropriate fractions were combined, concentrated to dryness, and examined chromatographically.

Elution of the column with 8% (v/v) aqueous ethanol displaced component A (3.75 g in 2.5 l.). Aqueous ethanol (15% v/v; 2.5 l.) then displaced component B (2.15 g), and fraction C (2.15 g) was eluted with 20% (v/v) aqueous ethanol (2.5 l.). The higher saccharides, D (6.0 g), were then eluted with 50% (v/v) aqueous ethanol (5 l.).

Examination of the Fractions

(*i*) *Monosaccharide Components*

Concentration of the aqueous eluate from the first charcoal–Celite column afforded a syrup (3.8 g) which was shown chromatographically to contain galactose and a trace of xylose. A portion (1 g) was acetylated with acetic anhydride and sodium acetate (23), and yielded β-D-galactopyranose penta-acetate, m.p. 142° C, $[\alpha]_D^{25}$ +23.7° (*c*, 0.6, chloroform).

(*ii*) *Component A*

The amorphous powder, $[\alpha]_D^{25}$ +155° (*c*, 0.3, water), had R_{Gal} 0.56 (solvent *b*). Authentic specimens of 4-*O*- and 6-*O*-α-D-galactopyranosyl-D-galactose had R_{Gal} 0.50 and 0.35, respectively, in the same solvent, and had ionophoretic mobilities different from that of A. The molecular weight of the sugar, determined iodometrically (24), was 330.

Oxidation of the disaccharide (71.6 mg) in sodium metaperiodate (0.125 *M*; 50 ml) is illustrated in Fig. 2. Both periodate uptake and formic acid liberation were followed iodometrically (25). Extrapolation of the overoxidation curves indicated that in the initial rapid oxidation, the disaccharide (1 mole) consumed 4.2 moles of periodate and yielded 2.2 moles of formic acid.

Acetylation of the disaccharide (23) (800 mg) yielded a crystalline β-octa-acetate (800 mg) which, after recrystallization from ethanol, had m.p. 157.5–158.5° C and $[\alpha]_D^{25}$ +110.2° (*c*, 0.5, chloroform). Calculated for $C_{28}H_{38}O_{19}$: C, 49.3%; H, 5.6%. Found: C, 49.53%; H, 5.76%.

A solution of the disaccharide (200 mg) in water (2 ml) was heated at 100° C with phenylhydrazine (1.5 ml) and 2 *N* acetic acid (7.5 ml) to yield a crystalline phenylosazone which, after recrystallization from ethanol, had m.p. 227–229° (decomp.) and $[\alpha]_D^{25}$ +114.6° (*c*, 0.2, pyridine).

Can. J. Chem. Downloaded from www.nrcresearchpress.com by 196.1.178.254 on 09/04/12
For personal use only.

Can. J. Chem. Downloaded from www.nrcresearchpress.com by 196.1.178.254 on 09/04/12
For personal use only.

A solution of the disaccharide (430 mg) in water (3 ml) was stirred at 0° C in an atmosphere of nitrogen; dimethyl sulphate (2 ml) and aqueous sodium hydroxide (30% w/w; 3 ml) were added. After 2 hours the solution was warmed to 25° C, treated with dimethyl sulphate (9 ml) and aqueous sodium hydroxide (30% w/w; 5 ml), added over a period of 45 minutes, and then warmed to 40° C for 1 hour. Methylation in this way was repeated three times. The solution was then heated at 100° C for 2 hours, neutralized with acetic acid, and extracted with chloroform. Evaporation of the extract afforded a syrup, which was further methylated three times with methyl iodide (20 ml) and silver oxide (4 g). The product crystallized, and after two recrystallizations from *n*-hexane (yield 143 mg) it had m.p. 110–115° C, $[\alpha]_D^{25}$ +95.5° (*c*, 0.7, chloroform). Found: OMe, 53.9%. Calculated for $C_{20}H_{38}O_{11}$: OMe, 54.6%.

The methylated disaccharide (60 mg) was hydrolyzed in 0.25 *N* sulphuric acid (5 ml) at 100° C for 20 hours. The solution was then neutralized with barium carbonate, filtered, and concentrated to a syrup (55 mg). Chromatography of the hydrolyzate indicated the presence of two components, *X* and *Y*, which travelled at rates identical with those of 2,3,4,6-tetra-*O*-methyl-D-galactose and 2,4,6-tri-*O*-methyl-D-galactose, respectively. They were separated on a sheet of Whatman No. 3 MM paper with benzene–ethanol–water (200:47:15 v/v; upper phase) (26) as the developing solvent.

Component *X* afforded a crystalline aniline derivative which, after recrystallization from ethanol and ethyl acetate, had m.p. 198–199° C, undepressed on admixture with *N*-phenyl-2,3,4,6-tetra-*O*-methyl-D-galactosylamine, and $[\alpha]_D^{25}$ −79.6° → −36.4° (24 hours) (*c*, 0.5, acetone).

Component *Y* crystallized, and was recrystallized from ethyl acetate – petroleum ether. It had m.p. 103–105° C. The derived *N*-phenyl-glycosylamine had m.p. 173–174° C, undepressed on admixture with *N*-phenyl-2,4,6-tri-*O*-methyl-D-galactosylamine, and $[\alpha]_D^{25}$ −91° → −41° (24 hours) (*c*, 0.4, acetone). For purposes of comparison, authentic 2,4,6-tri-*O*-methyl-D-galactose was prepared by the method of Bell (27).

(*iii*) *Component B*

The amorphous material had R_{Gal} 0.26 (solvent *b*). It was crystallized from 95% (v/v) aqueous methanol and the product had m.p. 237–239° C (decomp.) and $[\alpha]_D^{25}$ +146° (*c*, 0.5, water). Upon partial hydrolysis in 0.1 *N* hydrochloric acid the trisaccharide yielded galactose and one disaccharide only, detected chromatographically. The latter was chromatographically and ionophoretically indistinguishable from 3-*O*-α-D-galactopyranosyl-D-galactose.

The molecular weight of the sugar was found (24) to be 490. Calculated for $C_{18}H_{32}O_{16}$: C, 42.87%; H, 6.35%. Found: C, 42.38%; H, 6.44%.

Oxidation of the trisaccharide (81 mg) with sodium metaperiodate (0.125 *M*; 50 ml) (25) gave results, illustrated in Fig. 3, similar to those obtained for the disaccharide (see Fig. 2). The trisaccharide (1 mole) consumed 4.02 moles of periodate and yielded 1.93 moles of formic acid.

Acetylation of the trisaccharide (500 mg) (23) afforded a crystalline β-hendeca-acetate (100 mg). After recrystallization from ethanol the product had m.p. 275–277° C and $[\alpha]_D^{25}$ +106.0° (*c*, 0.05, chloroform). Calculated for $C_{40}H_{54}O_{16}$: C, 49.70%; H, 5.60%. Found: C, 49.48%; H, 5.69%.

(*iv*) *Fraction C*

Paper chromatography of this fraction revealed the presence of a small amount of contaminating trisaccharide. Partial hydrolysis of a small portion in 0.1 *N* hydrochloric acid for 1 hour, followed by paper chromatography, showed that galactose, one disac-

charide, and one trisaccharide were present in the hydrolyzate. The chromatographic mobilities of the di- and tri-saccharides corresponded to those of components (A) and (B), respectively.

(*v*) *Fraction D*

This fraction contained the penta- and higher saccharides from the deacetylated acetolyzate. Partial hydrolysis of small portions in 0.1 *N* hydrochloric acid for periods of 1, 2, 3, and 5 hours yielded in each case only one di-, one tri-, and one tetra-saccharide, detected chromatographically. These had R_{Gal} values identical with those of the components (A), (B), and (C), respectively.

Periodate Oxidation of λ-Carrageenin

A sample of λ-carrageenin (637 mg) was oxidized with sodium metaperiodate (0.05 *M*; 250 ml). The reaction solution was stored in the dark at 25° C, and at intervals aliquots were removed for the determination of the periodate uptake and formic acid production. Determinations were made at each time in duplicate.

(*a*) *Periodate Uptake*

An aliquot (10 ml) was transferred to a flask containing 0.05 *N* sodium arsenite (25 ml) and after 15 minutes the excess sodium arsenite was titrated against 0.02 *N* iodine.

Time (hours)	2	4.5	7.5	29	55	103	127	175	217	290	318
Periodate uptake (moles $\times 10^2$)	7.8	9.4	9.4	11.2	11.9	12.7	12.7	14.7	15.0	14.7	15.2

(*b*) *Formic Acid Production*

An aliquot (5 ml) was added to ethylene glycol (0.5 ml) and the solution stored in the dark at 25° C for 30 minutes. Neutral potassium iodide (10% w/v; 2 ml) was then added and the liberated iodine titrated rapidly against 0.005 *N* sodium thiosulphate.

Time (hours)	1.5	5	19	43	74	118	165	193	212
Formic acid produced (moles $\times 10^2$)	1.3	2.0	2.7	2.9	3.4	3.8	5.1	5.1	5.0

ACKNOWLEDGMENTS

Samples of 4-*O*-α-D-galactopyranosyl-D-galactose and 6-*O*-α-D-galactopyranosyl-D-galactose were very kindly provided by Professor E. Pacsu and Professor J. K. N. Jones.

The assistance of Dr. T. J. Painter in the preparation of this paper is gratefully acknowledged.

REFERENCES

1. SCHMIDT, C. Ann. **51**, 29 (1844).
2. STANFORD, E. C. C. J. Soc. Arts. **10**, 185 (1862).
3. MORI, T. and TSUCHIYA, Y. J. Agr. Chem. Soc. Japan, **15**, 1065 (1939).
4. DEWAR, E. T. and PERCIVAL, E. G. V. J. Chem. Soc. 1622 (1947).
5. SMITH, D. B. and COOK, W. H. Biochim. et Biophys. Acta, **45**, 232 (1953).
6. O'NEILL, A. N. J. Am. Chem. Soc. **77**, 6324 (1955).
7. SMITH, D. B., COOK, W. H., and NEAL, J. L. Arch. Biochem. Biophys. **53**, 192 (1954).
8. SMITH, D. B., O'NEILL, A. N., and PERLIN, A. S. Can. J. Chem. **33**, 1352 (1955).
9. BAYLEY, S. T. Biochim. et Biophys. Acta, **17**, 194 (1955).
10. BUCHANAN, J., PERCIVAL, E. E., and PERCIVAL, E. G. V. J. Chem. Soc. 51 (1943).
11. JOHNSTON, R. and PERCIVAL, E. G. V. J. Chem. Soc. 1994 (1950).

Can. J. Chem. Downloaded from www.nrcresearchpress.com by 196.1.178.254 on 09/04/12
For personal use only.

12. DILLON, T. and O'COLLA, P. Proc. Roy. Irish Acad. **54**, 51 (1951).
13. WHISTLER, R. L. and DURSO, D. F. J. Am. Chem. Soc. **72**, 677 (1950).
14. FRENCH, D. and WILD, G. M. J. Am. Chem. Soc. **75**, 2612 (1953).
15. HIRST, E. L. and PERLIN, A. S. J. Chem. Soc. 2622 (1954).
16. BACON, J. S. D. and EDELMAN, J. Biochem. J. **48**, 114 (1951).
17. PARTRIDGE, S. M. Biochem. J. **42**, 238 (1948).
18. PARTRIDGE, S. M. Nature, **164**, 443 (1949).
19. FOSTER, A. B. Chem. & Ind. 1050 (1952).
20. SOMOGYI, M. J. Biol. Chem. **160**, 69 (1945).
21. BERA, B. C., FOSTER, A. B., and STACEY, M. J. Chem. Soc. 3788 (1955).
22. WHELAN, W. J., BAILEY, J. M., and ROBERTS, P. J. P. J. Chem. Soc. 1293 (1953).
23. ERWIG, E. and KOENIGS, W. Ber. **22**, 2207 (1889).
24. MCLEOD, M. and ROBINSON, R. Biochem. J. **23**, 517 (1929).
25. BOBBIT, J. M. Advances in Carbohydrate Chem. **11**, 1 (1956).
26. ADAMS, G. A. Can. J. Chem. **33**, 56 (1955).
27. BELL, D. J. and WILLIAMSON, S. J. Chem. Soc. 1196 (1938).
28. YAPHE, W. Nature, **183**, 44 (1959).

Can. J. Chem. Downloaded from www.nrcresearchpress.com by 196.1.178.254 on 09/04/12
For personal use only.

Can. J. Chem. Downloaded from www.nrcresearchpress.com by 196.1.178.254 on 09/04/12
For personal use only.

RADIATION-INDUCED ADDITION OF HBr TO C_2H_4 IN THE GASEOUS STATE[1]

D. A. ARMSTRONG[2] AND J. W. T. SPINKS

ABSTRACT

The gas phase addition of hydrogen bromide to ethylene in a pyrex irradiation cell was induced by the action of Co^{60} γ-rays. Dose rates were calculated by means of the Bragg–Gray cavity principle from saturation ionization currents measured in air in a similar cell. The only product detected was ethyl bromide and the ion pair yield was of the order of 10^5. The rate of addition was followed with an electrically adjusted "spoon gauge" and was studied (*a*) with HBr in great excess, (*b*) with HBr and C_2H_4 in equal concentration, (*c*) with C_2H_4 in great excess. For condition (*a*) the rate showed a first-order dependence on $[C_2H_4]$, an approximate second-order dependence on [HBr], a negative temperature coefficient, and a dose rate exponent of unity. It was concluded that the reaction rate was determined by the same step as for the photobromination reaction and that wall termination predominated. For conditions (*b*) and (*c*) the dose rate exponent was found to be approximately 0.5 indicating a predominance of mutual termination. Definite conclusions with regard to the termination reaction were not possible but the data suggested that certain ion–molecule reactions may precede ion combinations.

Investigations of the fast electron or γ-radiolysis of gaseous systems are usually hindered by the low product yields obtained. However, in systems where there is a free radical chain reaction of appreciable chain length this difficulty should be considerably reduced. Such chain reactions are to be found in the addition of halogens and hydrogen halides to the olefins. Quantum yields of 10^4 or greater have been observed (1, 2) in the photosensitized bromination of ethylene, and although the gas phase addition of hydrogen halides to the olefins has not been investigated in very great detail, the work of Vaughan, Rust, and Evans (3) indicated that an analogous type of chain reaction was probably responsible for the rapid photoaddition of hydrogen bromide to ethylene and propylene. These considerations, together with the relative ease with which hydrogen bromide can be handled, and the fact that its X-radiolysis in the gaseous state has recently been investigated (4), led to the choice of the hydrogen bromide – ethylene reaction as the subject for the present study.

The work of Vaughan, Rust, and Evans was largely confined to the addition of hydrogen bromide to propylene. They found that the photochemical reaction was extremely rapid, provided the wave length of the light used was sufficiently short for dissociation of the hydrogen bromide into a hydrogen and a bromine atom (< 2900 Å). Photosensitization at longer wave lengths could be achieved by the addition of acetone, bromine, and lead tetraethyl (or other substances which gave rise to free radicals on photolysis). In all cases the "abnormal" type addition was observed, the product being almost entirely *n*-propyl bromide. Methyl iodide and iodine inhibited the reaction. Large quantities of oxygen somewhat reduced the rate of addition and gave rise to significant yields of an oxidation product, but, in contrast to the bromination reaction (cf. 1, 2), complete inhibition by oxygen was never observed.

The ethylene reaction proceeded at about the same rate as the propylene reaction, and "the data of certain individual experiments" indicated an approximate proportionality between the rate of ethyl bromide formation and the product of the hydrogen bromide and ethylene concentrations. The effect of oxygen on the ethylene reaction was

[1]*Manuscript received February 25, 1959.*
Contribution from the Department of Chemistry, University of Saskatchewan, Saskatoon, Saskatchewan.
[2]*Present address: University of Alberta, Calgary, Alberta.*

similar to its effect on the propylene reaction. A mechanism for the addition, which involved bromine atoms and bromo-ethyl free radicals, was proposed.

In this study the main characteristics of the radiation-induced addition were examined, and where possible the results have been discussed in the light of data obtained from the photochemical studies already mentioned.

EXPERIMENTAL

The 90-c Co^{60} unit, which was used as the source of radiation in all experiments, has been described (5).

A diagram of the jacketed pyrex irradiation cell is given in Fig. 1. One end of the cell, A, was attached through capillary tubing to a 2-mm-bore vacuum-seated stopcock, C, and a ground joint. The opposite end was similarly connected to a "spoon gauge",

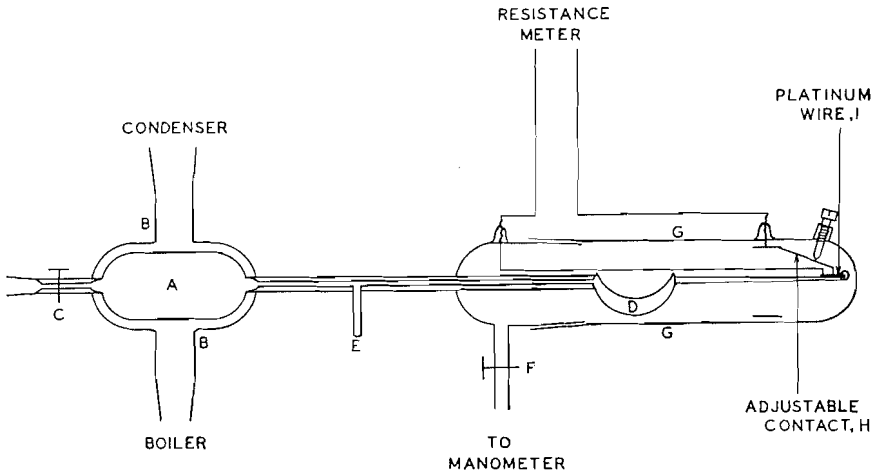

FIG. 1. The apparatus.

D, and a cold trap, E. The volumes of the cell and associated "dead space" were 35.2 and 6.6 ml, respectively. The envelope, G, of the gauge was connected through stopcock, F, and several feet of copper tubing to a mercury manometer located on the exterior wall of the irradiation cave. A resistance meter, also located outside the cave, was wired in series with the electrical contacts, H and I, on the gauge. This device was used as a "null instrument" for equating the envelope pressure and the internal gauge-cell pressure. (In practice it was usually necessary to apply a small correction to the pressure indicated by the external manometer.) Pressure measurements were reproducible to within 0.1 mm and could be made continuously during an irradiation.

The cell was maintained at a constant temperature by surrounding it with a suitable vapor generated in a boiling-flask beneath it. The condensed vapor ran down the outer wall of the jacket, B, thus returning to the boiling-flask without dropping on the walls of the cell. Most experiments were performed at the boiling point of ether. The vapor temperature, indicated by a thermometer located just above the cell, showed minor day-to-day fluctuations of about $\pm 0.1°$ C from the mean value, but was constant over the duration of any one experiment. The thermometer showed the same reading when placed directly in the neck of the boiling-flask.

The cell jacket, stopcock, and gauge envelope were firmly fastened to a metal frame which could be placed in any one of three fixed irradiation positions, approximately

Can. J. Chem. Downloaded from www.nrcresearchpress.com by 196.1.178.254 on 09/04/12
For personal use only.

3, 9, and 18 cm from the source. As shown in Fig. 2, the stopcock and gauge were shielded from the direct Co^{60} radiation by the source assembly. The dose rate at each irradiation position was measured with a pyrex-walled ionization chamber, of the same dimensions as the irradiation cell, supported in a pyrex jacket on a similar frame. The inner surface of the chamber was silvered to render it conducting, and a polythene cap, which carried the aluminum collecting-electrode, was inserted at the open end. Electrical contact between the grounded portion of the cap and the silvered chamber wall was achieved by the use of "Aquadag" paste. Ion currents were measured with a Townsend balance.

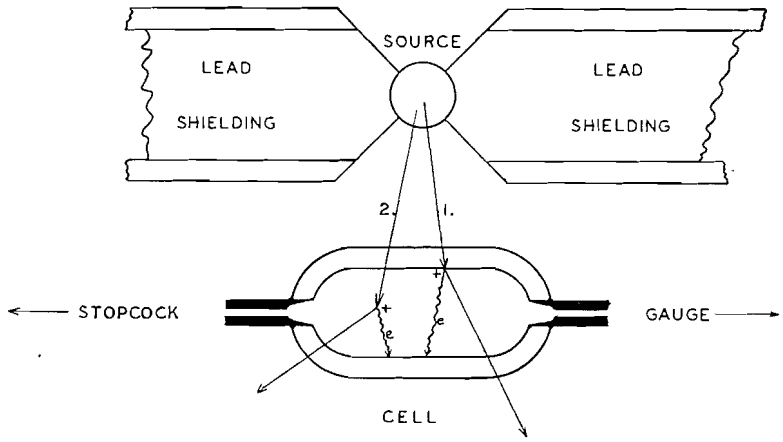

FIG. 2. Schematic diagram of reaction cell and Co^{60} source.

A vacuum line fitted with storage bulbs and a gas-measuring apparatus, to which the irradiation cell could be attached, was used for storing the reactants and preparing the desired mixtures for irradiation. The pumping system consisted of a Cenco Hyvac oil pump and a Todd single stage mercury diffusion pump. Ultimate vacua of about 10^{-5} mm of mercury were obtained with this combination.

Ethylene of 99.5% purity was obtained from a cylinder supplied by the Ohio Chemical and Surgical Equipment Co. of Cleveland. This material was subjected to two or three bulb-to-bulb distillations and then stored. Hydrogen bromide from a cylinder supplied by the Matheson Co. of Ohio was freed from traces of water by passing it over fused calcium bromide. A further purification by bulb-to-bulb distillation was carried out before the gas was stored. A sample of this gas was absorbed in water and titrated with silver nitrate. The bromide analysis showed 100.3% of the theoretical.

Hydrogen bromide was also prepared by warming a mixture of potassium bromide, phosphorus pentoxide, and syrupy phosphoric acid. This gas was purified in the same way. Similar rates of addition were obtained with hydrogen bromide from both sources.

The cell and associated apparatus were evacuated to a pressure of 10^{-4} mm or less before use. A gas mixture of the required composition was synthesized and the cold trap, E, of the irradiation cell was immersed in liquid nitrogen. The gases were then slowly admitted to the cell through stopcock, C. After they had been condensed, the stopcock was closed and the liquid nitrogen removed from E. As the condensed gases evaporated, the pressure in the gauge envelope was increased at a corresponding rate by admitting air through F. After the cell had been set up in the irradiation cave and the vapor bath had attained thermal equilibrium, the initial pressure in the cell was measured on the

Can. J. Chem. Downloaded from www.nrcresearchpress.com by 196.1.178.254 on 09/04/12
For personal use only.

external manometer by "zeroing" the spoon gauge. The envelope pressure was then reduced by about 1 mm and the irradiation was started. The time at which the envelope and cell pressures became equal was noted and the envelope pressure was subsequently reduced by a further 1 mm. In this way, successive pressure readings could be taken every 30–40 seconds during an irradiation.

On completion of an experiment, the gas mixture was carefully removed from the cell and gauge, the envelope pressure being reduced at the same rate as the internal cell pressure. As a standard procedure, the cell was filled with an atmosphere of ethylene when it was not in use, and whenever it was necessary to regrease stopcock, C. Air was not admitted to the cell unless it was unavoidable, as it seemed to produce fluctuations in the rate of reaction. Dow-Corning High Vacuum Silicone grease was used wherever possible on the apparatus, as it was more resistant to hydrogen bromide and ethyl bromide than Apiezon grease.

In calculating the reaction rate or concentration of either component in the reaction cell, corrections were made for the gas drawn into the cell from the gauge as the pressure fell. It was assumed that the initial concentrations of ethylene and hydrogen bromide in the gauge and cell were identical and that their relative concentrations in the gauge remained unaltered as the pressure fell. The results were, in general, consistent with this assumption.

Dosimetry

The number of ion pairs formed in the ionization chamber per unit volume per second in air was calculated from the saturation ionization currents for each of the three irradiation positions. These values, corrected to N.T.P. were 18.9_2, 4.7_2, and $1.3_8 \times 10^9$ ion pairs per milliliter per second, respectively.

There are two processes which may contribute to the ionization of the gas in the chamber: (1) ionization by fast electrons ejected from the chamber wall, and (2) ionization by fast electrons formed by the interaction of γ-rays with the electrons of the gas molecules in the chamber. Both processes have been illustrated in Fig. 2. Theoretical estimates, based on γ-ray interaction cross sections, show that with Co^{60} γ-radiation process (2) can only account for about 0.5% of the total ionization in the chamber in air at N.T.P. For dosimetry purposes the ionization can therefore be treated as being exclusively of type (1) and the Bragg–Gray cavity principle (6) can be used to estimate the dose rate in gas mixtures in the irradiation cell, which was similar to the ionization chamber in dimensions and wall thickness (2 mm). The electrons ejected from the wall of the cell will possess energies varying from about 1 Mev down. Their number per unit dose, and energy distribution, will be determined by the wall material* and will be independent of the gas in the cell, provided the conditions of the Bragg–Gray cavity theory hold. In traversing the cell these electrons will lose energy by interactions with the electrons of the gas molecules, giving rise to excitations as well as ionizations. The rate of loss of energy per unit length of fast electron track in the gas (or "stopping power" of the gas) can be calculated from the Bethe or the Block formula (6). For an electron of given energy traversing a medium containing only one element of atomic number Z, the latter formula may be written in the form:

$$-\left(\frac{dE}{dx}\right) = S_A \times [C] = \frac{2\pi r_0^2 m_0 c^2 Z}{\beta^2} \{\Phi - 2 \log_e I\} [C]$$

**It is necessary to assume that the layer of silver on the wall of the ionization chamber does not appreciably alter the electron flux or energy distribution.*

Can. J. Chem. Downloaded from www.nrcresearchpress.com by 196.1.178.254 on 09/04/12
For personal use only.

where the quantities r_0, m_0, c, and β have their usual significance, and Φ is the value of the Block function calculated for the particular fast electron energy. $[C]$ is the number of atoms per unit volume of the medium, and I is their mean ionization–excitation potential. S_A is the stopping power per atom of the element.

Assuming that the Bragg law of additivity of stopping powers holds, values of (dE/dx) can be calculated for hydrogen bromide and ethylene from the individual atomic stopping powers of hydrogen, bromine, and carbon. The following values were obtained for fast electrons of 0.3-Mev energy:

$$-(dE/dx)_{HBr} = 2.1_2\times10^{-22}\times[HBr] \text{ Mev/cm}$$

$$-(dE/dx)_{C_2H_4} = 1.20_7\times10^{-22}\times[C_2H_4] \text{ Mev/cm}$$

$$-(dE/dx)_{air} = 2.7_4\times10^{-3} \text{ Mev/cm at N.T.P.}$$

where the concentrations of ethylene and hydrogen bromide must be expressed in molecules/ml. The values of I used were: $I_H = 13$ ev, $I_C = 67$ ev, and $I_{Br} = 328$ ev (7). For consistency, $-(dE/dx)_{air}$ was also calculated.

According to the Bragg–Gray principle, the number of ion pairs formed in ethylene ($J_{C_2H_4}$) can be calculated from the number found in air (J_{air}) with the aid of the formula:

$$J_{C_2H_4} = J_{air}\times\frac{W_{air}}{W_{C_2H_4}}\times\frac{(dE/dx)_{C_2H_4}}{(dE/dx)_{air}} \text{ ion pairs/ml second}$$

where W is the energy required to create a single ion pair in the particular gas.

The value of the quantity $(dE/dx)_{C_2H_4}/(dE/dx)_{air}$ varies with the electron energy and should be averaged over the entire electron energy spectrum. However, it is unlikely that the ratio of the stopping powers of ethylene and air for 0.3-Mev electrons will be very different from the weighed mean ratio for the electron distribution from Co^{60} radiation in the glass cells used (cf. ref. 9). Hence:

$$J_{C_2H_4} = J_{air}\times5.6_6\times[C_2H_4]\times10^{-20} \text{ ion pairs/ml second.}$$

The values of W were chosen from recent results reported in the literature (8). No experimental value of W_{HBr} has been reported, but a theoretical estimate of 26.5 ev by Platzman has been cited (2). Using this value, one obtains a similar formula for ionization in hydrogen bromide:

$$J_{HBr} = J_{air}\times9.8_5\times[HBr]\times10^{-20} \text{ ion pairs/ml second.}$$

This is probably somewhat less accurate than that for ethylene. A combination of these formulae with the values of J_{air} for radiation positions I, II, and III yields:

position I: $J_{total} = \{[HBr]+0.57_5[C_2H_4]\}\times1.8_6\times10^{-9}$ ion pairs/ml second
position II: $= \{[HBr]+0.57_5[C_2H_4]\}\times4.6_5\times10^{-10}$ ion pairs/ml second
position III: $= \{[HBr]+0.57_5[C_2H_4]\}\times1.3_6\times10^{-10}$ ion pairs/ml second.

It may be noted that a correction should be applied to these formulae to make allowance for energy which is lost from the radiation cell (10) due to the escape of the higher energy δ-rays (or secondary electrons) from the radiation cell. This depends on the gross stopping power of the gas in the cell, and hence on the gas pressure and composition. At the lowest pressures used in these experiments J_{total} might be about 10% lower than calculated by the above formulae. Under conditions where the gross stopping power was equivalent to air at N.T.P., J_{HBr} would be only about 3% less than estimated,

Can. J. Chem. Downloaded from www.nrcresearchpress.com by 196.1.178.254 on 09/04/12
For personal use only.

and $J_{C_2H_4}$ should be almost unaffected. In view of the uncertainty involved in estimating this correction and the approximations already made, the formulae have been used without correction.* They are probably correct to within $\pm 10\%$ when ethylene is the main component.

RESULTS

Two methods were employed in identifying the product of the reaction:

(1) A gas chromatogram of the material produced, from which ethylene and hydrogen bromide had been separated by virtue of their higher vapor pressures, showed only one peak after it was scanned for 33 minutes. The time of appearance (13.5 minutes) and "skewness" of this peak were identical with those of the peak from a commercial sample of ethyl bromide.

(2) A number of experiments were performed in which the hydrogen bromide remaining after irradiation was determined by absorption. It was found that the hydrogen bromide consumed in the irradiation corresponded closely to the over-all pressure decrease. This indicated a mole-for-mole addition of HBr to ethylene, and this conclusion received further support from the observation that the over-all pressure decrease in experiments where the reaction was taken to virtual completion corresponded to complete consumption of the component present in lower concentration.

These results are in accordance with the photochemical work, and because of the long chain length (see below) the species formed in the initiation and termination processes would be present in relatively small amounts and could only be detected by the use of special techniques.

The rate of addition of hydrogen bromide to ethylene was investigated under three distinct sets of conditions: (1) the hydrogen bromide concentration greatly exceeded the ethylene concentration, (2) the hydrogen bromide and ethylene concentrations were approximately equal, (3) the ethylene concentration greatly exceeded the hydrogen bromide concentration.

I. HBr *in Excess*

Over a period of several months the rates of addition were reproducible to within $\pm 10\%$ under any given set of conditions. However, duplicate experiments in the same series usually agreed to within $\pm 5\%$. The pressure decrease versus time curves for two identical experiments have been given in Fig. 3. These were carried out at 33.9° C with hydrogen bromide and ethylene concentrations of 10.5 and 1.5×10^{18} molecules per ml, respectively, at the highest of the three possible dose rates. From the estimated dose rate ($2.1_4 \times 10^{10}$ ion pairs per ml per second) an ion pair yield of about 2×10^5 was calculated.

All experiments showed an induction period of about 60 seconds and there was no obvious relation between its magnitude and the concentration of either component. Experiments in which the irradiation was interrupted usually showed a second induction period (see Fig. 3). The initial induction periods could be attributed to "clean-up" of an inhibiting impurity in the cell at a concentration of the order of 10^{12} molecules/ml (3×10^{-5} mm of Hg pressure). However, the second induction periods cannot be explained in this way.

In some experiments there appeared to be a small postirradiation reaction (of the order of 1 mm), which was complete in a few minutes. It seems likely that this post-

**In any case the majority of experiments were carried out at a gross stopping power in the range 0.8–1.2 times that of air.*

Can. J. Chem. Downloaded from www.nrcresearchpress.com by 196.1.178.254 on 09/04/12
For personal use only.

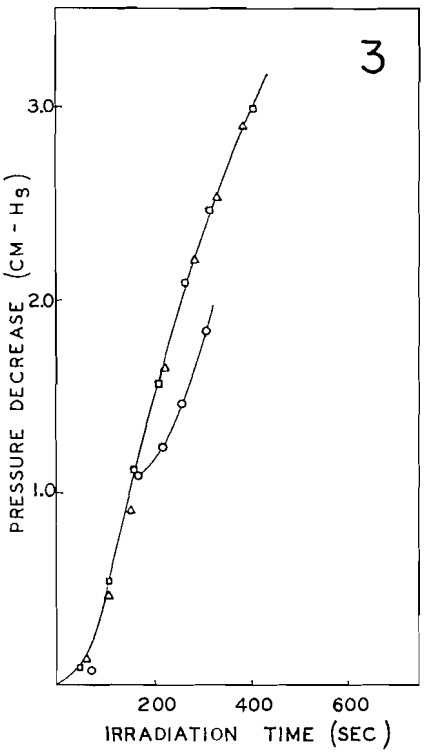

FIG. 3. Pressure decrease versus time curves for three similar experiments at 33.9° C.

$[C_2H_4]_0 = 1.5\times10^{18}$ (molecules/ml)
$[HBr]_0 = 10\times10^{18}$ (molecules/ml).

A second induction period in an interrupted experiment is also shown.

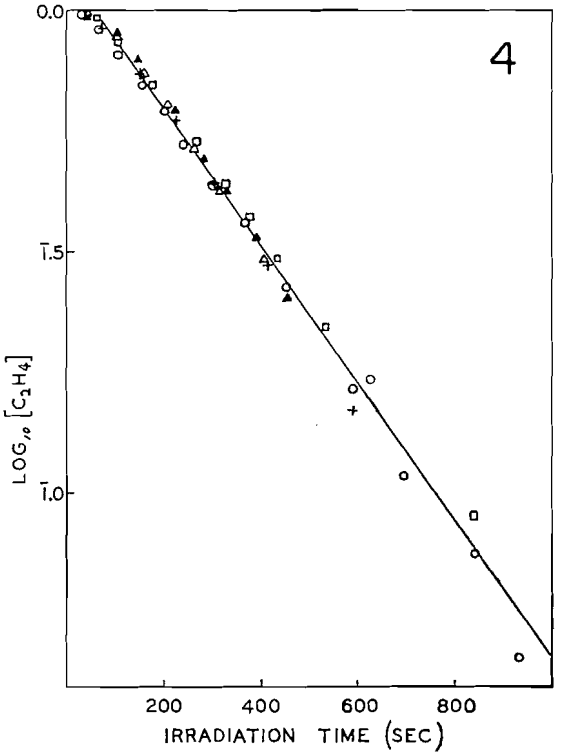

FIG. 4. First-order plots for ethylene consumption at 33.9° C and $[HBr]_0 = 10^{19}$ molecules/ml.

$[C_2H_4]_0$ (molecules/ml)	
2.92×10^{18}	○
2.08	□
1.60	▲
1.57	△
0.68	+

irradiation effect is an inverse Budde–Draper effect and that the induction periods may be partly, but not wholly, due to Budde–Draper effect (cf. (11)). Other effects such as interaction of the radiation with the walls of the radiation cell may also contribute.

The dependence of the rate on ethylene concentration was studied over the range $0.6–2.9\times10^{18}$ molecules/ml of ethylene. In these experiments the initial hydrogen bromide concentration was 10.6×10^{18} molecules/ml and the cell temperature, 33.9° C. Plots of $\log_{10}[C_2H_4]$ versus time have been given in Fig. 4. It would appear that there is a first-order dependence of the rate on ethylene concentration, and values of the first-order rate constant (i.e., rate/$[C_2H_4]$) taken over the first 50% of the reaction, have been summarized in Table I. They showed a tendency to fall off as the ethylene concentration was increased.

The dependence on hydrogen bromide concentration over the range $4–21\times10^{18}$ molecules/ml was investigated at the same temperature. The ethylene concentration was kept within the range $1.4–1.6\times10^{18}$ molecules/ml. Rates of addition, determined from first-order plots for ethylene consumption, have been given in Table I. A log–log plot of the rate versus hydrogen bromide concentration indicated an exponent slightly greater than 2 for [HBr] at this temperature.

Experiments at 54° and 25° C were also performed, using the same ethylene con-

Can. J. Chem. Downloaded from www.nrcresearchpress.com by 196.1.178.254 on 09/04/12
For personal use only.

TABLE I

Rate of addition of hydrogen bromide to ethylene: HBr in excess

[HBr], molecules/ml	$[C_2H_4]$, molecules/ml	k_I = Rate/$[C_2H_4]$, sec^{-1}	[HBr]+0.575 $[C_2H_4]$, molecules/ml	$\bar{D}$, cm^2/sec	Average [HBr], molecules/ml	$F^* = \frac{1}{6} \times \frac{[HBr]\,JRd^2}{\bar{D} \times 16(Rate/[C_2H_4])}$
			(*a*) Dependence on $[C_2H_4]$			
33.9° C						
10.5×10^{18}	2.92×10^{18}	3.24×10^{-3}	12.2×10^{18}	0.184	9.0×10^{18}	8.16×10^{31}
10.8	2.08	3.24	12.0	0.192	9.8	8.47
10.6	1.60	3.54	11.5	0.198	9.7	7.04
10.4	1.57	3.71	11.3	0.199	9.5	6.40
10.7	0.68	3.71	11.1	0.210	10.4	6.68
			(*b*) Dependence on [HBr]			
33.9° C						
20.6×10^{18}	1.48×10^{18}	14.8×10^{-3}	21.5×10^{18}	0.108	19.7×10^{18}	11.9×10^{31}
11.6	1.45	4.20	12.5	0.183	10.7	7.80
10.6	1.60	3.54	11.5	0.200	9.7	7.04
10.6	1.54	3.03	11.5	0.200	9.7	8.24
10.4	1.57	3.71	11.3	0.203	9.5	6.40
5.97	1.46	1.09	6.81	0.329	5.46	4.67
5.69	1.50	0.756	6.58	0.344	4.82	5.44
4.08	1.50	0.396	4.95	0.440	3.21	4.00
53.9° C						
10.5×10^{18}	1.55×10^{18}	1.76×10^{-3}	11.4	0.208	10.25	14.3
5.86	1.46	0.423	6.7	0.340	5.68	11.8
24.8° C						
11.0×10^{18}	1.55×10^{18}	4.61×10^{-3}	11.9	0.192	9.83	5.92
10.7	1.57	4.73	11.6	0.196	9.86	5.53
6.05	1.46	1.39	6.89	0.324	5.06	3.47
			(*c*) Dependence on *J*			
33.9° C				*J* (ion pairs/ml sec)	Log_{10} (*J*)	Log_{10} (Rate/$[C_2H_4]$)
10.6×10^{18}	1.60×10^{18}	3.54×10^{-3}	11.5	2.14×10^{10}	10.331	$\bar{3}.549$
10.4	1.57	3.71	11.3	2.10×10^{10}	10.323	$\bar{3}.569$
10.46	1.40	0.960	11.3	5.25×10^{9}	9.720	$\bar{4}.983$
10.5	1.45	0.208	11.3	1.54×10^{9}	9.187	$\bar{4}.318$

*For convenience these values have all been reduced by a factor of 1/6.

centration as above and two hydrogen bromide concentrations. As shown in Table I, the reaction rate decreased with increasing temperature.

A dose rate exponent of approximately unity was observed for hydrogen bromide and ethylene concentrations of 10.5 and 1.5×10^{18} molecules/ml, respectively, at 33.9° C. A logarithmic plot of rate versus dose rate has been presented in Fig. 5.

II. HBr *and* C_2H_4 *Present in Approximately Equal Concentrations*

Three experiments performed under these conditions were followed to almost 100% addition. The results have been summarized in Table II*a*, where the reaction rates at various stages have been included. The initial concentrations of hydrogen bromide were approximately the same in each experiment (10^{19} molecules/ml), while the concentrations of ethylene were slightly less than, equal to, and slightly greater than the hydrogen bromide concentrations in experiments 1, 2, and 3, respectively. In a fourth experiment, a gas mixture similar in composition to that of experiment 2 was irradiated in position II until a steady rate had been attained and measured. It was then irradiated in position I, and the steady rate again measured. A log–log plot of the two rates against dose rate has been included in Fig. 5. It is apparent that the dose rate exponent has fallen at the higher ethylene concentration and is approaching a value of 0.5.

Can. J. Chem. Downloaded from www.nrcresearchpress.com by 196.1.178.254 on 09/04/12
For personal use only.

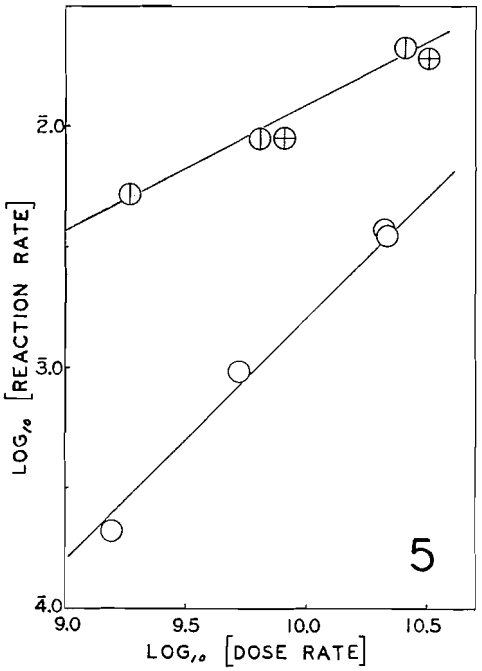

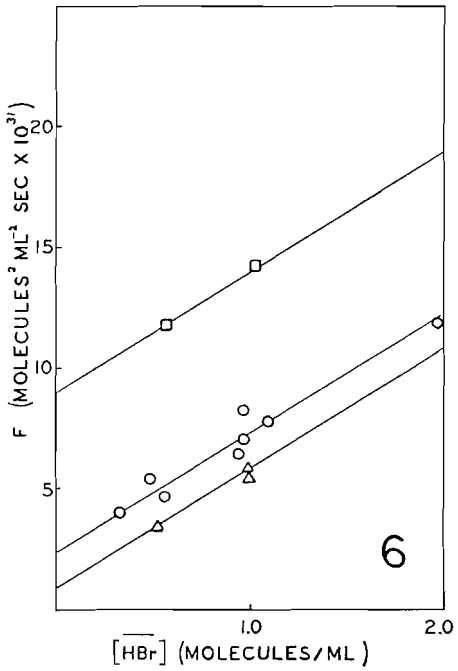

FIG. 5. Logarithmic plots of rate versus dose rate for experiments at 33.9° C.

[HBr] (molecules/ml)
⊖ 10^{18}
⊕ 10^{19}
○ 10^{19}

[C_2H_4] (molecules/ml)
2×10^{19}, 10^{19} } ordinates displaced by +1.00
10^{18}

FIG. 6. The function, $F = \frac{1}{6}\times\frac{[HBr][C_2H_4]\ JRd^2}{\bar{D}\times Rate\times 16}$, plotted against [$\overline{HBr}$].

Temperature, ° C 54.0 □
33.9 ○
25.0 △

III. C_2H_4 *Present in Excess*

The data for these experiments have been given in Table II*b*. The dose rate exponent was again determined from a fourth experiment, in which the concentrations were similar to those of experiment 5. This time the gas mixture was irradiated first in position II and then in position III. The rates obtained in these two irradiations, together with the rate from experiment 2, have been plotted in Fig. 5. The gradient of this logarithmic plot indicated a dose rate exponent of about 0.5 under the conditions existing.

DISCUSSION

The Initiation Process

The following reactions, originally suggested by Eyring, Hirschfelder, and Taylor, were found by Zubler, Hamil, and Williams (4) to be consistent with their experimental results on the X-radiolysis of hydrogen bromide:

$$HBr \rightsquigarrow HBr^+ + e \qquad [1]$$

$$e + HBr \rightarrow H + Br^- \qquad [2]$$

$$Br^- + HBr^+ \rightarrow H + 2Br \qquad [3]$$

$$H + HBr \rightarrow H_2 + Br. \qquad [3a]$$

Can. J. Chem. Downloaded from www.nrcresearchpress.com by 196.1.178.254 on 09/04/12
For personal use only.

TABLE II

Rate of addition of hydrogen bromide to ethylene

	$[C_2H_4]$, molecules/ml $\times 10^{18}$	[HBr], molecules/ml $\times 10^{18}$	Rate, molecules/ml sec $\times 10^{15}$	[A′]	[B′]
	(*a*) Reactants present in approximately equal concentrations				
1.	5.68	9.26	13.5	5.88×10	1.34×10^{-8}
	4.26	7.87	9.71	5.95	
	2.84	6.48	6.12	6.09	
	1.42	5.12	2.79	6.16	
2.	8.53	8.84	16.2	5.34×10	1.35×10^{-8}
	7.10	7.42	12.4	5.26	1.28
	5.68	6.02	9.05	5.22	1.21
	4.27	4.57	5.28	4.65	
	2.84	3.16	2.61	3.80	
	1.42	1.74	0.78	3.76	
3.	12.2	8.62	22.1	5.72×10	1.45×10^{-8}
	10.9	7.27	18.9	5.83	1.48
	9.61	5.94	14.6	5.52	1.40
	8.36	4.66	9.70	4.87	1.22
	7.05	3.30	6.15	4.34	1.08
	5.72	1.96	2.80	3.44	0.84
	4.90	1.32	1.60	3.06	0.82
	(*b*) C_2H_4 present in excess				
4.	20.1	2.84	7.10	2.59×10	1.00×10^{-8}
	20.0	2.56	6.82	2.78	1.00
	19.8	2.27	6.44	2.76	1.01
	19.6	1.99	5.35	2.54	0.945
	18.6	1.42	3.61	2.45	0.915
	18.5	1.14	3.06	2.32	0.900
5.	21.2	1.14	2.58	1.97×10	0.75×10^{-8}
	21.0	0.853	1.84	1.70	0.70
	20.8	0.568	1.18	1.55	0.65
	20.6	0.284	0.520	1.31	0.57
	20.4	0.142	0.218	1.06	0.46
6.	10.0	1.42	1.41	1.68×10	0.65×10^{-8}
	9.9	1.28	1.13	1.45	0.69
	9.7	0.994	1.00	1.69	0.69
	9.6	0.710	0.71	1.44	0.64
	9.5	0.570	0.57	1.53	0.63

NOTE: In calculating the values of [A′] it was assumed that the contribution of HBr to M could be neglected (cf. ref. (1), results of Section I). $k' = k_{16}/k_{11a}$ at 33.9° from Section I; all experiments at 33.9° C.

These reactions explained the destruction of four molecules of HBr per ion pair formed and indicate that in the present system four initiating radicals (H and Br) would be produced from each HBr^+ ion.

More recent work (12) has shown that ion–molecule reactions are generally rapid. In fact it seems that they will compete with ion combinations under certain conditions. The reaction (cf. ref. 12*a*):

$$HBr^+ + HBr \rightarrow H_2Br^+ + Br \qquad [4]$$

should therefore be considered in addition to those given above especially when HBr is present in high concentrations as in the experiments reported in Section I of this paper. Neutralization of the H_2Br^+ ion by bromide ions might give rise to two or four initiating radicals:

$$Br^- + H_2Br^+ \rightarrow H_2 + 2Br \qquad [5a]$$

$$HBr + H + Br \qquad [5b]$$

$$2H + 2Br. \qquad [5c]$$

Can. J. Chem. Downloaded from www.nrcresearchpress.com by 196.1.178.254 on 09/04/12
For personal use only.

Since the positive ions are probably surrounded by a cluster of HBr molecules, which would act in essentially the same way as a solvent cage does in liquid phase photolyses, it seems unlikely that these dissociative ion combinations will be 100% efficient in forming radicals unless a considerable amount of energy is released as kinetic energy. While undoubtedly a large amount of energy would be released in reactions [5*a*] and [5*b*], this is not likely to be the case for reaction [5*c*]. Consequently, reaction [4] would probably be followed by reactions [5*a*] or [5*b*], but not by reaction [5*c*]. The number of initiating radicals formed per initial HBr^+ ion would then still be four.

Excited hydrogen bromide molecules formed in the reaction mixture could dissociate to radicals, thus enhancing the number of initiations. However, excited species did not seem to play a major role in the X-ray-induced decomposition of HBr. In this study the results of Section I (HBr in excess) were therefore interpreted on the assumption that four initiating radicals were formed per ion pair and that the number formed through excitations was negligible.

In the experiments of Sections II and III, where the ethylene concentration was high, positive ions would have been formed by the direct ionization of ethylene molecules:

$$C_2H_4 \rightsquigarrow C_2H_4^+ + e \qquad [6]$$

or possibly by ion–molecule reactions (cf. ref. 12*a*) such as:

$$HBr^+ + C_2H_4 \rightarrow HBr + C_2H_4^+ \qquad [7]$$

$$HBr^+ + C_2H_4 \rightarrow C_2H_5^+ + Br \qquad [8a]$$

$$C_2H_4^+ + C_2H_4 \rightarrow C_3H_5^+ + CH_3 \qquad [8b]$$

and:

$$C_2H_4^+ + HBr(+M) \rightarrow C_2H_5Br^+(+M). \qquad [9]$$

As the reaction proceeded and the concentration of ethyl bromide increased, it too would have suffered ionization (see ref. 13):

$$C_2H_5Br \rightsquigarrow C_2H_5Br^+ + e. \qquad [10]$$

The electron capture process:

$$e + C_2H_5Br \rightarrow C_2H_5 + Br^- \qquad [11]$$

is a likely one (13*a*, 14) and might have competed with reaction [2] as the hydrogen bromide was consumed.

Neutralization of the positive ions $C_2H_4^+$, $C_2H_5^+$, $C_3H_5^+$, and $C_2H_5Br^+$ by negative bromide ions would undoubtedly furnish a large number of radicals, and although there is no specific information about ion combinations of this type, it is clear that the number of initiating radicals formed might vary from one positive ion to another. The number of initiations per ion pair would therefore be sensitive to the competition between the various ion–molecule reactions cited above, and thus also to the relative concentrations of HBr and C_2H_4. Under the conditions existing in Sections II and III the initiation process is therefore likely to be much more complex than for those of Section I.

Section I

The results in Table I indicated a first-order dependence of the reaction rate on ethylene concentration. However, the value of the rate constant fell as the ethylene concentration increased. This may have been due to the occurrence of reactions [18] and [19] (see below), but since the value of k_I decreased by only 20% for a fourfold change in ethylene concentration, these processes could not have been very significant under the conditions existing in Section I. The linearity of the first-order plots for ethylene

Can. J. Chem. Downloaded from www.nrcresearchpress.com by 196.1.178.254 on 09/04/12
For personal use only.

consumption over 90% of the reaction supports this conclusion and also shows that there was no appreciable change in the number of initiating radicals formed per ion pair* as the ethylene was replaced by ethyl bromide.

The following mechanism (in accordance with the bromine atom theory of abnormal addition) was proposed by Vaughan and co-workers for the photoaddition of hydrogen bromide to ethylene:

$$h\nu + HBr \rightarrow H + Br \quad [12]$$

$$Br + C_2H_4 \rightarrow C_2H_4Br \quad [13]$$

$$C_2H_4Br + HBr \rightarrow C_2H_5Br + Br. \quad [14a]$$

It may be observed that reaction [14*a*] is probably some 10 kcal exothermic, while the alternative propagating mechanism would involve the endothermic reaction:

$$C_2H_5 + HBr \rightarrow C_2H_5Br + H$$

and could not therefore account for the rapid addition observed.

This mechanism may be compared with that of Schumacher and co-workers (1) for the bromination of ethylene:

$$h\nu + Br_2 \rightarrow 2Br \quad [15]$$

$$Br + C_2H_4 \rightarrow C_2H_4Br \quad [13]$$

$$C_2H_4Br \rightarrow C_2H_4 + Br \quad [16]$$

$$C_2H_4Br + Br_2 \rightarrow C_2H_4Br_2 + Br. \quad [14b]$$

The same propagating radicals, Br and C_2H_4Br, are involved in both mechanisms, and reaction [16] should obviously be included in the mechanism for the hydrobromination.

In either system, termination may occur by any one of the following processes, or possibly by a combination of them (cf. 15 and 16):

$$Br + \text{wall} \rightarrow \tfrac{1}{2}Br_2 \quad [17]$$

$$Br + Br + M \rightarrow Br_2 + M \quad [18]$$

$$Br + C_2H_4Br \rightarrow C_2H_4Br_2 \quad [19a]$$

or

$$\rightarrow C_2H_4 + Br_2 \quad [19b]$$

$$2C_2H_4Br \rightarrow C_2H_4 + C_2H_4Br_2 \quad [20a]$$

or

$$\rightarrow C_4H_8Br_2. \quad [20b]$$

The process involved will depend largely on the relative concentrations of Br and C_2H_4Br, and application of the principle of stationary states leads to the following relation between the concentrations of these species:

[i] $$[Br]/[C_2H_4Br] = (k_{14a}[HBr]+k_{16})/k_{13}[C_2H_4] \text{ for hydrobromination}$$

[ii] $$= (k_{14b}[Br_2]+k_{16})/k_{13}[C_2H_4] \quad \text{for bromination.}$$

Since only the ratio k_{16}/k_{14b} is known, estimates of the above concentration ratio cannot be made with certainty in either system. However, reactions [17] and [18] were apparently the main modes of termination in the photobromination reaction at 60° C for ethylene pressures less than 8 cm. It may thus be concluded that at least under these conditions (which approach those of Section I in the present study) the bromine atom concentration is appreciably greater than the concentration of bromo-ethyl radicals.

**It is improbable that the value of W for C_2H_5Br will be very different from those of HBr and C_2H_4. Assuming that the Bragg law of additivity of stopping powers holds, there should therefore be no marked change in the number of ion pairs formed in the cell as the reaction proceeds.*

Can. J. Chem. Downloaded from www.nrcresearchpress.com by 196.1.178.254 on 09/04/12
For personal use only.

The dose rate exponent of unity in Section I indicated linear termination. Assuming that this was due to reaction [17] the following rate expression may be derived (cf. ref. 2).

$$\text{Rate} = \frac{k(R.J)k_{13}[C_2H_4][HBr]}{\bar{D}\{[HBr]+k_{16}/k_{14a}\}}$$

where k is a constant, $\bar{D}$ the mean diffusion coefficient for bromine atoms in the reaction mixture, J the dose rate in ion pairs per milliliter per second, and R the number of initiations per ion pair (taken as 4). Since both J and $1/\bar{D}$ are directly proportional to the hydrogen bromide pressure, this expression accounts for the observed dependence of the rate on hydrogen bromide concentration, as well as for the first-order dependence on ethylene concentration and the dose rate exponent of unity.

In theory the reaction rate for wall-terminated chain reactions in cylindrical vessels should be proportional to the square of the cell diameter (cf. ref. 17). The above rate expression may therefore be rearranged to:

$$\frac{k'\times d^2\times(J\times R)\times[C_2H_4][HBr]}{\bar{D}\times\text{Rate}} = \frac{[HBr]}{k_{13}}+\frac{k_{16}}{k_{13}k_{14a}}$$

where k' is a second constant having a value of 1/16 in this case and d is the cell diameter. Values of the left-hand side of this expression, denoted as the function F, have been given in Table I and are plotted against the hydrogen bromide concentration in Fig. 6 for the three temperatures studied. The mean diffusion coefficient, $\bar{D}$, was calculated for each individual experiment. The results are consistent with the above rate expression, and the following values of k_{16}/k_{14a} were calculated from the ratio of the intercepts to the slopes of the lines obtained in Fig. 6: 2.0, 4.8, 18.4×10^{18} molecules/ml at 25, 34, and 54° C, respectively. These values of k_{16}/k_{14a} would require an activation energy difference of 14 ± 2 kcal for $E_{16}-E_{14a}$. This seems rather high since Schmitz *et al.* (1) obtained a value of only 6 kcal for $E_{16}-E_{14b}$, and Anderson *et al.* (18) found that $E_{14a}-E_{14b}$ for ethyl radicals was very small. More detailed studies of both systems would be required to establish the reason for this discrepancy, but in view of certain criticisms made by Kistiakowski and Sternberg (2) it seems that the low value for $E_{16}-E_{14b}$ may be in error. With this exception the results of Section I are consistent with the wall termination mechanism and with the work on the photobromination of ethylene. The value of k_{16}/k_{14a} at 34° C has been used in Sections II and III.

A point of interest is the fact that in the bromination reaction at 60° C the reaction rate rose as the pressure of inert gas (CF_2Cl_2) in the reaction cell was increased, and passed through a maximum at 200 mm. Above this pressure the intensity exponent fell from 1.0 to 0.5, and wall termination ceased to predominate. In contrast, no evidence of a maximum was observed in this study up to hydrogen bromide pressures of 600 mm. This difference in behavior of the two systems may be attributed to a poor third-body efficiency of hydrogen bromide and to the larger diameter of the reaction cell used in the previous study (5.9 cm as opposed to 2.6 cm). (By substituting these values of d in the rate equations for the two systems, estimates of the values of k_{13} in the two systems may be made. These agreed within a factor of 2, and were of the order of 4×10^{10} mole ml^{-1} sec^{-1}. Such a value would seem to be reasonable for a radical addition reaction of this type.)

Sections II and III

The results of Sections II and III may be discussed together since the mechanism of termination in each was apparently almost exclusively by mutual interaction of the

Can. J. Chem. Downloaded from www.nrcresearchpress.com by 196.1.178.254 on 09/04/12
For personal use only.

chain centers. Relation [i] shows that the chances of mutual termination by reactions [19] or [20] increase with the ethylene concentration. However, according to Schumacher and co-workers ethylene is about five times as efficient a third body for bromine atom combination as Freon, and in view of the results of Section I it seems likely that ethylene will also be more efficient when compared to hydrogen bromide. The probability of reaction [18] occurring would therefore also increase with ethylene concentration.

Termination by reactions [18], [19], and [20] leads to the following three rate expressions, respectively.

$$[A] \qquad \text{Rate} = \frac{k_{13}}{k_{18}^{\frac{1}{2}}}(RJ)^{\frac{1}{2}}\frac{[HBr][C_2H_4]}{[M]^{\frac{1}{2}}\{[HBr]+k_{16}/k_{14a}\}}$$

$$[B] \qquad = \sqrt{\frac{k_{13}k_{14a}}{2k_{19}}}(RJ)^{\frac{1}{2}}\frac{[HBr][C_2H_4]^{\frac{1}{2}}}{\{[HBr]+k_{16}/k_{14a}\}^{\frac{1}{2}}}$$

$$[C] \qquad = (k_{14a}/k_{20}^{\frac{1}{2}})(RJ)^{\frac{1}{2}}[HBr].$$

These expressions may be rearranged to the forms:

$$[A'] \qquad \frac{k_{13}R^{\frac{1}{2}}}{k_{18}^{\frac{1}{2}}} = \frac{\text{Rate}[M]^{\frac{1}{2}}\{[HBr]+k_{16}/k_{14a}\}}{J^{\frac{1}{2}}[HBr]\times[C_2H_4]}$$

$$[B'] \qquad \sqrt{\frac{k_{13}\cdot k_{14a}R}{2k_{19}}} = \frac{\text{Rate}\,\{[HBr]+k_{16}/k_{14a}\}^{\frac{1}{2}}}{J^{\frac{1}{2}}[HBr][C_2H_4]^{\frac{1}{2}}}$$

and

$$[C'] \qquad \frac{k_{14a}R^{\frac{1}{2}}}{k_{20}^{\frac{1}{2}}} = \frac{\text{Rate}}{J^{\frac{1}{2}}[HBr]}.$$

The right-hand sides of expressions [A'] and [B'] have been calculated for various points on the reaction–time curves of each individual experiment and are given in Tables II*a* and *b*.

The initial rates of experiments 1, 2, and 3 gave fairly consistent values of either [A'] or [B'], but over the course of each experiment both the [A'] (experiment 1 excepted) and [B'] values fell by almost 50%. Fluctuations of a similar nature were observed in the values of [C'] which have not been given. It is not possible, therefore, to draw definite conclusions from the present experiments as to which mode of termination predominates at high ethylene pressures, but, whichever this may be, it seems that the variations in [A'], [B'], or [C'] could be explained by a dependence of R on hydrogen bromide pressure. This would account for the similar results of Section III and might be attributed to a competition between ion–molecule reactions as already discussed. More definite conclusions could be drawn if the mechanism of termination at high ethylene pressures were established by independent photochemical experiments.

In conclusion, the similarities between the photoinitiated bromination and the radiation-induced hydrobromination may be summarized: (1) similar chain lengths (10^5), (2) same rate-controlling step at low ethylene pressures ($Br + C_2H_4 \rightleftharpoons C_2H_4Br$), (3) negative temperature coefficient, and (4) similar modes of termination dependent on the third-body efficiency of the gases present and the cell diameter.

ACKNOWLEDGMENTS

We are grateful to the National Research Council and to the Atomic Energy of Canada Limited for continued financial assistance. One of us (D.A.A.) held a National Research Council Postdoctoral Fellowship. We are grateful to Doctors Cormack and Bardwell for helpful assistance.

Can. J. Chem. Downloaded from www.nrcresearchpress.com by 196.1.178.254 on 09/04/12
For personal use only.

REFERENCES

1. SCHMITZ, H., SCHUMACHER, H. J., and JAGER, A. Z. physik. Chem. B, **51**, 281 (1942).
2. KISTIAKOWSKI, G. B. and STERNBERG, J. C. J. Chem. Phys. **21**, 2218 (1953).
3. VAUGHAN, W. F., RUST, F. F., and EVANS, T. W. J. Org. Chem. **7**, 477, 491 (1942).
4. ZUBLER, E. G., HAMIL, W. H., and WILLIAMS, R. R. J. Chem. Phys. **23**, 1263 (1955).
5. RIEGERT, A. L. and SPINKS, J. W. T. Proc. 7th Hot Labs. Conf., Cleveland. 315 (1959).
6. HINE, G. H. and BROWNELL, G. L. Radiation chemistry. Academic Press, Inc., New York. 1956.
7. (*a*) BAKKER, C. J. and SEGRE, E. Phys. Rev. **81**, 489 (1951). (*b*) BRAND, W. Phys. Rev. **104**, 691 (1956).
8. (*a*) JESSE, P. W. and SADAUKIS, J. Phys. Rev. **107**, 766 (1957). (*b*) WEISS, J. and BERNSTEIN, W. Radiation Research, **6**, 603 (1957).
9. CORMACK, D. V., HUMMEL, R. W., JOHNS, H. E., and SPINKS, J. W. T. J. Chem. Phys. **22**, 6 (1954).
10. (*a*) BURCH, P. R. Radiation Research, **3** (4), 361 (1955). (*b*) SPENCER, L. V. and ATTIXE, F. H. Radiation Research, **3**, 239 (1955).
11. FONTIJN, A. and SPINKS, J. W. T. Can. J. Chem. **35**, 1397 (1957).
12. (*a*) SCHISSLER, D. O. and STEVENSON, D. P. J. Chem. Phys. **24**, 926 (1956). (*b*) LAMPE, F. W., FIELD, F. H., and FRANKLIN, J. L. A. J. Am. Chem. Soc. **79**, 6132 (1957).
13. (*a*) MORRISON, J. D. and NICHOLSON, A. J. C. J. Chem. Phys. **20**, 1021 (1952). (*b*) ISRA, A. P. J. Chem. Phys. **26**, 18 (1957).
14. MAGEE, J. L. and BURTON, M. J. Am. Chem. Soc. **73**, 523 (1951).
15. TROTMAN-DICKENSON, A. F. Gas kinetics. Butterworth Scientific Publications, London. 1955.
16. BENSON, S. W. and BIRSS, J. H. J. Chem. Phys. **28**, 301 (1958).
17. DAINTON, F. S. Chain reactions. Methuen & Co. Ltd., London. 1955.
18. ANDERSON, H. C. and VAN ARTSDALEN, E. R. J. Chem. Phys. **12**, 479 (1944).

Can. J. Chem. Downloaded from www.nrcresearchpress.com by 196.1.178.254 on 09/04/12
For personal use only.

Can. J. Chem. Downloaded from www.nrcresearchpress.com by 196.1.178.254 on 09/04/12
For personal use only.

NOTES

AMENDMENT TO A PAPER BY W. MEHL AND J. O'M. BOCKRIS

J. O'M. Bockris

In the paper entitled "On the mechanism of electrolytic deposition and dissolution of silver" (Can. J. Chem. **37**, 190 (1959)) the following Acknowledgment should appear before the References.

Thanks are due to the American Electroplaters' Society for the financial support of the work. It is wished to express appreciation for helpful comments made on the experimental work by members of the Supervising Committee of this Society.

Received March 31, 1959.
John Harrison Laboratory of Chemistry,
University of Pennsylvania,
Philadelphia, Pa., U.S.A.

NOTE ON THE INTRINSIC VISCOSITY OF POLYSTYRENE IN MIXED SOLVENTS*

J. F. Henderson† and C. A. Winkler

The ability of solvents to dissolve high polymers, especially polystyrene, and the properties of the resulting solutions is a subject that has received much attention (1, 2, 3, 4, 5, 6). The following is a brief account of results obtained from a few experiments which were made in this laboratory.

The intrinsic viscosity of polystyrene dissolved in binary mixtures of methanol with benzene, bromobenzene, and chloroform was determined, and the results are shown in Fig. 1. Although benzene is a better solvent than bromobenzene for polystyrene, more methanol is required to precipitate polystyrene from bromobenzene than from benzene. Both this result and those of earlier investigations (1, 2) indicate that knowledge of the intrinsic viscosity of a polymer in a given solvent does not permit prediction of either the variation of intrinsic viscosity with addition of non-solvent or the amount of non-solvent required to produce precipitation.

The expansion of a polymer molecule from its unperturbed dimensions, and consequently the intrinsic viscosity of the polymer solution, depends upon the relative magnitudes of the heat of dilution and of the entropy of dilution parameters (7). It was decided to investigate solutions of polystyrene in binary mixtures of three different types of solvents, the solvents being characterized by their heat of dilution and entropy of dilution parameters.

Measurements of the intrinsic viscosity of a polystyrene sample dissolved in several mixtures of methyl ethyl ketone and benzene were made, for which solvents the values of κ_1, the heat of dilution parameters, are approximately equal (7). The intrinsic viscosity

*Financial assistance was received from the Canadian Kodak Co., Ltd. and the National Research Council.
†Holder of a Canadian Kodak Company Ltd. Fellowship.

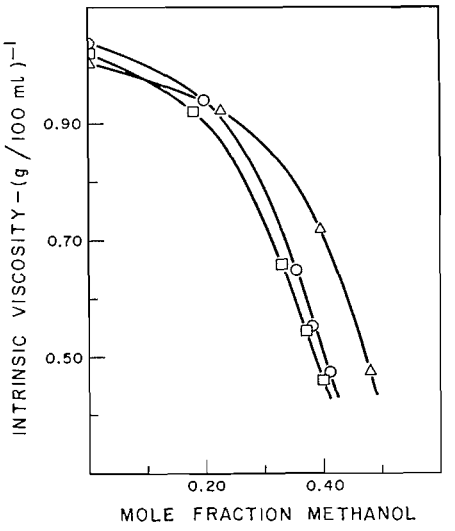

FIG. 1. The intrinsic viscosity of polystyrene ($[\eta]_\theta = 0.43$) in solvent mixtures containing methanol at 24.2° C.

○ Benzene
□ Chloroform
△ Bromobenzene

was very nearly linear in solvent composition and was independent of temperature for all solvent compositions (Fig. 2). On the other hand, the intrinsic viscosity of polystyrene in mixtures of benzene and cyclohexane, for which the entropy parameters, ψ_1, were approximately equal (7), was not linear in solvent composition and in the solvents rich in cyclohexane the intrinsic viscosity was temperature-dependent (Fig. 2) (3). It seems evident, therefore, that the relations between the composition of a mixture of two solvents and the two parameters κ_1 and ψ_1 are different.

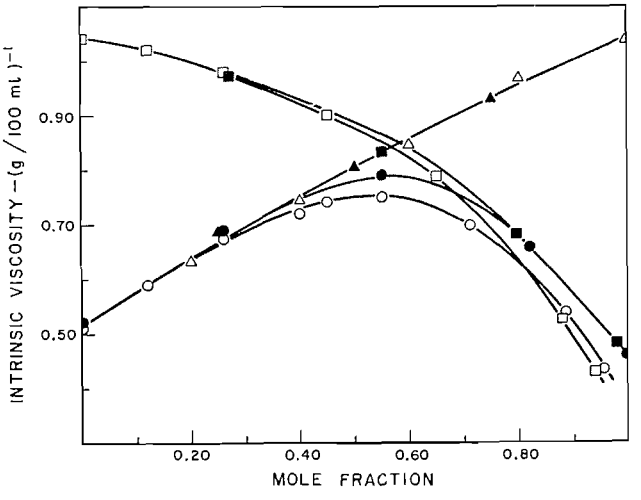

FIG. 2. The intrinsic viscosity of polystyrene ($[\eta]_\theta = 0.43$) in binary mixtures of benzene, cyclohexane, and methyl ethyl ketone.

○ Cyclohexane and methyl ethyl ketone at 24.2° C
△ Benzene and methyl ethyl ketone at 24.2° C
□ Benzene and cyclohexane at 24.2° C
● Cyclohexane and methyl ethyl ketone at 40.5° C
▲ Benzene and methyl ethyl ketone at 40.5° C
■ Benzene and cyclohexane at 40.5° C

Can. J. Chem. Downloaded from www.nrcresearchpress.com by 196.1.178.254 on 09/04/12
For personal use only.

The intrinsic viscosity of polystyrene dissolved in mixtures of methyl ethyl ketone and cyclohexane increased to a maximum and then decreased with increasing cyclohexane concentration. In the solvent mixtures rich in cyclohexane the intrinsic viscosity increased with increasing temperature (Fig. 2). These results bear a striking resemblance to those for polystyrene dissolved in mixtures of acetone and methylcyclohexane (5).

The addition of cyclohexane to polystyrene dissolved in methyl ethyl ketone will cause the values of both κ_1 and ψ_1 to increase. To account for the curves in Fig. 2, it is suggested that, in solvent mixtures rich in methyl ethyl ketone, ψ_1 will increase at a greater rate than κ_1 with increasing cyclohexane concentration. However, when the cyclohexane concentration is in excess of a given value, κ_1 will increase at the greater rate with increasing cyclohexane concentration. Hence, the difference $\psi_1 - \kappa_1$, and therefore the intrinsic viscosity, will first increase and then decrease with addition of cyclohexane to the solvent mixture. This suggestion is in accord with the observed behaviors of solutions of polystyrene in benzene – methyl ethyl ketone and in benzene–cyclohexane mixtures.

If different relations exist between the composition of a mixture of two solvents and the two parameters κ_1 and ψ_1, it becomes immediately possible to account at least qualitatively for cosolvency and for the observation, for example, that more methanol is required to precipitate polystyrene from bromobenzene than from benzene. Unfortunately, there is little information about the dimensions of polymer molecules in mixtures of specific types of solvents.

It should be noted that a truly adequate theoretical explanation of these observations would require that solvent mixtures be considered, not as single components as done above, but as two components, and this would require knowledge of the thermodynamic interactions between the polymer and each solvent and between the solvents themselves. This has been done for solutions of polystyrene in benzene–cyclohexane mixtures (8) but not for solutions of polystyrene in benzene – methyl ethyl ketone and cyclohexane – methyl ethyl ketone mixtures since information about solvent–solvent interactions in the latter systems is not available.

1. ADELSTEIN, P. Z. and WINKLER, C. A. Can. J. Research, B, **28**, 194 (1950).
2. ALFREY, T., JR., GOLDBERG, A. I., and PRICE, J. A. J. Colloid Sci. **5**, 251 (1950).
3. FOX, T. G., JR. and FLORY, P. J. J. Am. Chem. Soc. **73**, 1909 (1951).
4. OUTER, P., CARR, C. I., and ZIMM, B. H. J. Chem. Phys. **18**, 830 (1950).
5. PATIT, S. R., COLOMBO, G., and MARK, H. J. Polymer Sci. **6**, 295 (1951).
6. SHULTZ, A. R. and FLORY, P. J. J. Am. Chem. Soc. **75**, 5681 (1953).
7. FLORY, P. J. Principles of polymer chemistry. Cornell Univ. Press, Ithaca, New York. 1953. p. 622.
8. SHULTZ, A. R. and FLORY, P. J. J. Polymer Sci. **15**, 231 (1955).

RECEIVED MARCH 24, 1959.
THE PHYSICAL CHEMISTRY LABORATORY,
MCGILL UNIVERSITY,
MONTREAL, QUEBEC.

Can. J. Chem. Downloaded from www.nrcresearchpress.com by 196.1.178.254 on 09/04/12
For personal use only.

Can. J. Chem. Downloaded from www.nrcresearchpress.com by 196.1.178.254 on 09/04/12
For personal use only.

NOTES

AMENDMENT TO A PAPER BY W. MEHL AND J. O'M. BOCKRIS

J. O'M. Bockris

In the paper entitled "On the mechanism of electrolytic deposition and dissolution of silver" (Can. J. Chem. **37**, 190 (1959)) the following Acknowledgment should appear before the References.

Thanks are due to the American Electroplaters' Society for the financial support of the work. It is wished to express appreciation for helpful comments made on the experimental work by members of the Supervising Committee of this Society.

Received March 31, 1959.
John Harrison Laboratory of Chemistry,
University of Pennsylvania,
Philadelphia, Pa., U.S.A.

NOTE ON THE INTRINSIC VISCOSITY OF POLYSTYRENE IN MIXED SOLVENTS*

J. F. Henderson† and C. A. Winkler

The ability of solvents to dissolve high polymers, especially polystyrene, and the properties of the resulting solutions is a subject that has received much attention (1, 2, 3, 4, 5, 6). The following is a brief account of results obtained from a few experiments which were made in this laboratory.

The intrinsic viscosity of polystyrene dissolved in binary mixtures of methanol with benzene, bromobenzene, and chloroform was determined, and the results are shown in Fig. 1. Although benzene is a better solvent than bromobenzene for polystyrene, more methanol is required to precipitate polystyrene from bromobenzene than from benzene. Both this result and those of earlier investigations (1, 2) indicate that knowledge of the intrinsic viscosity of a polymer in a given solvent does not permit prediction of either the variation of intrinsic viscosity with addition of non-solvent or the amount of non-solvent required to produce precipitation.

The expansion of a polymer molecule from its unperturbed dimensions, and consequently the intrinsic viscosity of the polymer solution, depends upon the relative magnitudes of the heat of dilution and of the entropy of dilution parameters (7). It was decided to investigate solutions of polystyrene in binary mixtures of three different types of solvents, the solvents being characterized by their heat of dilution and entropy of dilution parameters.

Measurements of the intrinsic viscosity of a polystyrene sample dissolved in several mixtures of methyl ethyl ketone and benzene were made, for which solvents the values of κ_1, the heat of dilution parameters, are approximately equal (7). The intrinsic viscosity

*Financial assistance was received from the Canadian Kodak Co., Ltd. and the National Research Council.
†Holder of a Canadian Kodak Company Ltd. Fellowship.

Can. J. Chem. Downloaded from www.nrcresearchpress.com by 196.1.178.254 on 09/04/12
For personal use only.

Canadian Journal of Chemistry

Issued by THE NATIONAL RESEARCH COUNCIL OF CANADA

VOLUME 37 AUGUST 1959 NUMBER 8

HYDROGENOLYSIS OF CARBOHYDRATES

VII. METHYL β-L-ARABOPYRANOSIDE-1-C^{14} [1]

THOMAS FRANCIS[2] AND A. S. PERLIN

ABSTRACT

Methyl β-L-arabopyranoside-1-C^{14} was hydrogenolyzed in the presence of copper chrome oxide catalyst at 250° C, yielding an approximately equimolar mixture of optically inactive *cis*- and *trans*-3,4-dihydroxytetrahydropyran-C^{14}, together with 2,3-dihydroxypentane-C^{14}. The latter was formed by reductive ring-opening of the tetrahydropyrandiols. Ether cleavage of each of the cyclic diols afforded 1,2,3,5-tetrahydroxypentane-C^{14} in which the tracer was distributed about equally between carbons 1 and 5. Carbon-14 in the pentanediol was distributed in a similar manner. The results show that both the 2- and 4-hydroxyl groups of the original pentoside are prone to reductive cleavage, and that *cis*- and *trans*-glycol groups in the cyclic diols are formed by isomerization. They suggest that hydrogenolysis of the methoxyl group takes place initially, accompanied by isomerization, to give a mixture of tetrahydropyrantriols in which the 2- and 4-hydroxyl groups have equivalent reactivity.

In Part V of this series (1) methyl β-L-arabopyranoside (I) was shown to isomerize readily at 180° C in the presence of hydrogen and copper chromium oxide catalyst to a mixture of methyl D- and L-pentosides. This finding offered an explanation of the earlier report (2) that the arabinoside is hydrogenolyzed at 250° to form optically inactive *cis*- and *trans*-3,4-dihydroxytetrahydropyran (dihydro-DL-arabinal and -DL-xylal), rather than the expected L-isomers (II and III, respectively). Clearly, the glycosidic methoxyl group is easily hydrogenolyzed and the 3-hydroxyl group, though isomerized (1), is stable, but it was not possible to decide from these data whether the 2- or 4-hydroxyl group (or both) is cleaved reductively. In the present study this problem has been examined by tracer techniques using methyl β-L-arabopyranoside-1-C^{14}.

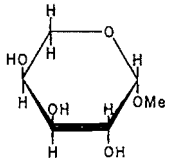

I

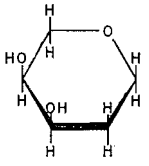

II

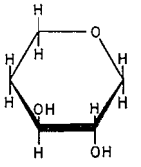

III

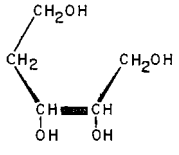

IV

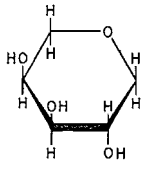

V

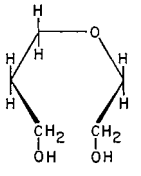

VI

[1]*Manuscript received April 13, 1959.*
Contribution from the National Research Council of Canada, Prairie Regional Laboratory, Saskatoon, Saskatchewan.
Issued as N.R.C. No. 5234 and as Paper No. 260 on the Uses of Plant Products.
[2]*National Research Council of Canada Postdoctorate Fellow, 1957–58.*

Can. J. Chem. Downloaded from www.nrcresearchpress.com by 196.1.178.254 on 09/04/12
For personal use only.

The dihydroglycal-C^{14} fraction, isolated as the major product from hydrogenolysis of the labelled L-arabinoside at 250°, comprised an approximately equimolar mixture of *cis*- and *trans*-isomers, in agreement with the earlier finding (2). Acetonation of the mixture afforded the *O*-isopropylidene derivative of the *cis*-diol, and the *trans*-isomer remaining was freed from a small proportion of unacetonated *cis*-diol by selective lead tetraacetate oxidation of the latter. The purified isomers were optically inactive.

Acetolysis of the diols-C^{14} in the presence of boron trifluoride (3) yielded from each the tetraacetate of 1,2,3,5-tetrahydroxypentane (IV). Following deacetylation the tetritols were oxidized with periodate, and the formaldehyde produced was isolated as the dimedon derivative or the 2,4-dinitrophenylhydrazone. Since the formaldehyde was derived either from carbon 1 or carbon 5 of the original methyl L-arabinoside, or from both, its specific activity provided a measure of the percentage survival of the 2- and 4-hydroxyl groups of the glycoside. Thus, if only the 4-hydroxyl group had been hydrogenolyzed all of the carbon-14 should have been located in the formaldehyde, but inactive formaldehyde should have been obtained if the 2-position was attacked exclusively. In fact, the formaldehyde from the *cis*- and *trans*-isomers contained 40–45% of the total activity (Table I), showing clearly that the 2- and 4-hydroxyl groups were cleaved

TABLE I

Specific activity of products from methyl β-L-arabopyranoside-1-C^{14}

Compound	Specific activity (mμc/mmole)	Per cent reduction at C_2	Per cent reduction at C_4
Methyl β-L-arabopyranoside-1-C^{14}	47.2		
cis,trans-3,4-Dihydroxytetrahydropyran-C^{14}	47.4		
Formaldehyde from *cis*-3,4-dihydroxytetrahydropyran-C^{14} *			
As dimedon (sp. activity 1.25 mμc/mM CO_2)	21.2		44.8
As 2,4-dinitrophenylhydrazone (sp. activity 2.73 mμc/mM CO_2)	19.1	58.1†	39.0
Formaldehyde from *trans*-3,4-dihydroxytetrahydropyran-C^{14}*			
As dimedon (sp. activity 1.25 mμc/mM CO_2)	21.2		45.1
As 2,4-dinitrophenylhydrazone (sp. activity 2.63 mμc/mM CO_2)	18.4	57.2†	40.5
Acetaldehyde from 2,3-dihydroxypentane-C^{14}			
As 2,4-dinitrophenylhydrazone (sp. activity) 2.10 mμc/mM CO_2)	16.8		35.5
Propionaldehyde from 2,3-dihydroxypentane-C^{14}			
As 2,4-dinitrophenylhydrazone (sp. activity) 3.07 mμc/mM CO_2)	27.6	58.5	

*By periodate oxidation of derived 1,2,3,5-tetrahydroxypentane.
†Calculated by difference from average of the C_4 values.

reductively almost to the same extent. The results show also, contrary to the original interpretation (2), that the presence of *cis*- and *trans*-1,2-diol groups in the products is not related necessarily to the occurrence of such groups in the methyl L-arabinoside, but to isomerization. Thus, *cis*- and *trans*-glycol groups are located in the tetrahydropyrandiols at positions corresponding to both the 2,3- and 3,4-positions of the glycoside.

The approximately equivalent reactivity of the 2- and 4-hydroxyl groups in methyl L-arabinoside contrasts with hydrogenolysis mainly of the 4-position in methyl α-D-glucopyranoside (4, 5). Possibly hydrogenolysis of the pentoside is initiated at carbon 1 giving rise, also as a result of isomerization (1), to a mixture of 1,5-anhydropentitols (e.g., V). In the latter mixture the 2- and 4-hydroxyl groups would be more nearly equivalent than in the parent glycosides and hence reduced at about the same rate. The survival in each molecule of one of these groups together with the 3-hydroxyl group may be attributed to the resistance of 1,2-diols and the instability of 1,3-diols to hydro-

Can. J. Chem. Downloaded from www.nrcresearchpress.com by 196.1.178.254 on 09/04/12
For personal use only.

genolysis (6). Relatively greater reactivity of the 4-position in methyl D-glucoside possibly is associated with the influence of the primary carbinol group.

About one-third of the hydrogenolysis product consisted of a low-boiling oil which yielded a *p*-nitrobenzoate corresponding to that of a pentanediol. This product was found to be mainly 2,3-dihydroxypentane, for it consumed about one mole of periodate with production of acetaldehyde and propionaldehyde. Previously, methoxypentanediols were reported present in the reaction mixture (2), but, since polyols may give spurious methoxyl values (7), it is likely that the product actually encountered was the pentane-2,3-diol. The diol was produced also by hydrogenolysis of the isolated tetrahydropyrandiols, and hence was a secondary reaction product resulting from reductive cleavage of the cyclic ether group. When the C^{14}-labelled glycoside was used as starting material the propionaldehyde obtained from the pentanediol by periodate cleavage accounted for 58%, and the acetaldehyde 36%, of the tracer (Table I). These data show again that the 2- and 4-positions of the methyl pentoside are both subject to reduction, and correspond closely to the data obtained with the tetrahydropyrandiols.*

Another possible procedure was examined for evaluating the distribution of tracer in the tetrahydropyrandiols. The diols were oxidized with periodate and the resulting dialdehydes reduced to give the corresponding dihydroxy ether (VI). Cleavage of VI was expected to afford ethylene glycol and 1,3-dihydroxypropane, the specific activities of which would indicate the relative proportion of carbon 1 from the L-arabinoside-C^{14} in each fragment. However, the ether linkage of VI proved to be particularly resistant, and the low yield of products obtained made the procedure unattractive for use with the small quantity of radioactive diols available.

EXPERIMENTAL

Methyl β-L-arabopyranoside-1-C^{14}, m.p. 171–173°, was prepared by methanolysis (8) of L-arabinose-1-C^{14}.

Paper chromatography was carried out with Whatman No. 1 paper using *n*-butanol: ethanol:water (40:11:19) as solvent and ammoniacal silver nitrate as the spray reagent (9).

Melting points are corrected.

Radioactive samples were combusted and the specific activity of the carbon dioxide liberated was measured by the procedure of Buchanan and Nakao (10). Reproducibility of the measurements was about ±3%.

Hydrogenolysis of Methyl β-L-Arabopyranoside-1-C^{14}

Methyl β-L-arabopyranoside-1-C^{14} (47.6 mμc/mmole) (6.0 g) in dioxan (100 ml) was shaken for 5 hours at 250° with copper chromium oxide catalyst (1.25 g) in an atmosphere of hydrogen at 2000 p.s.i. The syrupy product (3.2 g) obtained after removing the catalyst and evaporating the solvent was found by paper chromatography to consist of two main components (R_F 0.52 and 0.82). Distillation at 0.3 mm afforded the faster-travelling of these components as an oil (1.0 g), b.p. 51–65° (bath temp.), n_D^{20} 1.4404, and the second as an oil (1.5 g), b.p. 81–90°, n_D 1.4630. The latter product was identified by paper chromatography as 3,4-dihydroxytetrahydropyran and, by plotting its rate of uptake of lead tetraacetate, was found to consist of a 45:55 mixture of *cis*- and *trans*-isomers (cf.

**Cleavage of the ether ring in tetrahydropyran derivatives with boron trifluoride – acetic anhydride has been found in at least one instance to produce positional isomers (3). Formation of* IV *from* II *or* III, *however, did not appear to involve such a side reaction (3). The distribution of tracer in 2,3-dihydroxypentane affords an independent check on the latter acetolysis reaction, by showing that labelling in the tetrahydroxypentane is that expected for normal ring-opening of the cyclic ether.*

ref. 2). Separation of the isomers on chromatograms could not be effected by adding boric acid to the solvent, nor by column chromatography on cellulose using benzene: ethanol:water (500:50:1).

cis-3,4-Dihydroxytetrahydropyran-C^{14}

The higher-boiling oil (1.0 g) was dissolved in acetone (50 ml) containing 1% concentrated sulphuric acid. After 24 hours at room temperature the solution was neutralized with anhydrous potassium carbonate, filtered, and evaporated. The residual syrup was dissolved in water and the solution extracted 3 times with ether. Acetic acid (10 ml, 30%) was added to the extract, the ether evaporated, and the solution heated on the steam bath for 1 hour. Removal of the solvent gave a syrup (R_F 0.51) which was purified by distillation. Weight 0.27 g, $[\alpha]_D^{24}$ 0°±0.1° (*c*, 2, satd. borax). Treatment of the product with *p*-toluenesulphonyl chloride in pyridine gave *cis*-di-*O*-*p*-toluenesulphonyl-3,4-dihydroxytetrahydropyran, m.p. 131–132°; the infrared absorption spectrum was indistinguishable from that of an authentic specimen.

trans-3,4-Dihydroxytetrahydropyran-C^{14}

The water-soluble fraction from the acetonation procedure (0.56 g) appeared, from its rate of lead tetraacetate uptake, to contain about 15% of *cis*-isomer. The latter was preferentially removed by lead tetraacetate oxidation and the product worked up as described earlier (2), affording an oil (0.31 g), R_F 0.57, $[\alpha]_D^{24}$ 0°±0.1° (*c*, 2, satd. borax). The derived tosyl ester had m.p. 159–162°, and gave an infrared absorption spectrum indistinguishable from that of *trans*-di-*O*-*p*-toluenesulphonyl-3,4-dihydroxytetrahydropyran.

1,2,3,5-Tetrahydroxypentane-C^{14}

The tetritol was prepared from the *cis*- and *trans*-diols by acetolysis in the presence of boron trifluoride as described earlier (3), and separated from a small proportion of starting material by column chromatography on cellulose using *n*-butanol. The *trans*-isomer (0.31 g) and the *cis*-isomer (0.27 g) each yielded 0.19 g of tetritol.

Periodate Oxidation of 1,2,3,5-Tetrahydroxypentane-C^{14} *and Isolation of Formaldehyde*

(*a*) Oxidation of the tetritol with periodate and recovery of liberated formaldehyde as the dimedon derivative was carried out according to the procedure of Bell (11). In a typical experiment, the tetritol (0.10 g) derived from *cis*-3,4-dihydroxypyran-C^{14} yielded 0.20 g of formaldehyde dimedon, m.p. and mixed m.p. 192–193°.

(*b*) In a typical experiment, the tetritol (0.09 g) in water (20 ml) was oxidized with periodic acid (0.40 g) for 4 hours. Dowex-1 resin (bicarbonate form) was added until a negative starch–iodide test was obtained, the solution was concentrated, the distillate being trapped in a solution of 2,4-dinitrophenylhydrazine in dilute hydrochloric acid. After it was dried, the recovered hydrazone was purified by chromatography on silicic acid:Supercel (2:1) using Skelly B containing 5% ether (12). Weight 0.09 g, m.p. 166–167°, undepressed by admixture with formaldehyde 2,4-dinitrophenylhydrazone.

2,3-Dihydroxypentane-C^{14}

The low-boiling oil consumed 0.96 mole of periodic acid per mole, producing 0.86 mole of acetaldehyde (estimated colorimetrically (13)), and 0.13 mole of formaldehyde (estimated colorimetrically (14)). On treatment with excess *p*-nitrobenzoyl chloride in hot pyridine it afforded a di-*O*-*p*-nitrobenzoate, m.p. 168–169° after recrystallization

Can. J. Chem. Downloaded from www.nrcresearchpress.com by 196.1.178.254 on 09/04/12
For personal use only.

Can. J. Chem. Downloaded from www.nrcresearchpress.com by 196.1.178.254 on 09/04/12
For personal use only.

from ethyl acetate. Calc. for $C_{19}H_{18}O_8N_2$: C, 56.71%; H, 4.51%; N, 6.96%. Found: C, 56.80%; H, 4.50%; N, 6.73%.

The oil (0.10 g) in water (25 ml) was treated with periodic acid (0.20 g) for 1.5 hours, the solution was neutralized with Dowex-1 resin, and a solution of 2,4-dinitrophenylhydrazine in dilute hydrochloric acid was added. A precipitate which formed was collected, dried, and chromatographed on silicic acid:Supercel as described above. Two fractions were isolated, the first having m.p. 157°, after recrystallization from ethanol, undepressed by admixture with propionaldehyde 2,4-dinitrophenylhydrazone. Calc. for $C_9H_{10}O_4N_4$: C, 45.38%; H, 4.23%. Found: C, 45.85%; H, 4.01%. The second fraction, recrystallized from ethanol, had m.p. 159–164°. Calc. for $C_8H_8O_4N_4$: C, 42.90%; H, 3.60%. Found: C, 43.30%; H, 3.72%.

2,3-Dihydroxypentane from Hydrogenolysis of 3,4-Dihydroxytetrahydropyran

A mixture of *cis*- and *trans*-3,4-dihydroxytetrahydropyran (4.4 g) was treated for 24 hours under the hydrogenolysis conditions described above. The product (1.5 g), which on chromatographic examination appeared to consist mainly of 2,3-dihydroxypentane, distilled at 45–55°/0.05 mm (bath temp.) to give an oil, having an infrared absorption spectrum indistinguishable from that of 2,3-dihydroxypentane, n_D^{25} 1.4412. The derived *p*-nitrobenzoate had m.p. 165–167°, undepressed by admixture with 2,3-dihydroxypentane di-*p*-nitrobenzoate; the X-ray diffraction patterns of the two diesters were indistinguishable.

Hydroxyethyl-(3-hydroxy)n-propyl Ether (VI)

A mixture of *cis*- and *trans*-3,4-dihydroxytetrahydropyran (2.4 g) in water (40 ml) was treated with periodic acid (4.8 g) for 5 hours. Excess periodate and iodate were removed with Dowex-1 resin (bicarbonate form), the solution was evaporated to half volume and added dropwise to a solution (30 ml) of sodium borohydride (1.5 g). After 18 hours excess Amberlite IR-120 was added, the filtrate was concentrated to dryness, and boric acid removed by repeated (4 times) addition and evaporation of methanol. The product (1.65 g), b.p. 115–125°/0.8 mm (bath temp.), was a viscous oil, n_D^{24} 1.4515, R_F 0.66. It yielded a *p*-nitrobenzoate which solidified when taken up in ether and, after four recrystallizations from methyl ethyl ketone – ether, had m.p. 98–100°. Calc. for $C_{19}H_{18}O_9N_2$: C, 54.55%; H, 4.34%; N, 6.70%. Found: C, 54.73%; H, 4.26%; N, 6.54%.

Cleavage of the Dihydroxy Ether (VI)

(*a*) Treatment of the dihydroxy ether with acetic anhydride – boron trifluoride as described above for 3,4-dihydroxytetrahydropyran yielded only trace amounts of cleavage products.

(*b*) The syrupy ether (0.15 g), in acetic anhydride (2 ml) containing freshly fused zinc chloride (0.15 g), was heated on the steam bath for 12 hours. Cold saturated potassium carbonate was added and the neutral solution extracted three times with chloroform. Evaporation of the chloroform solution yielded a residue which was treated with 0.1 *M* sodium methoxide for 18 hours. The solution was neutralized with Amberlite IR-120 and concentrated, giving a dark syrup (0.074 g). Chromatographic examination indicated that the product consisted of ethylene glycol and 1,3-dihydroxypropane, and a minor, slower-moving component which was not starting material. The spot corresponding to ethylene glycol was absent from the chromatogram when the mixture was treated beforehand with periodic acid, and formaldehyde was produced in the oxidation as shown by isolation of formaldehyde dimedon (6 mg from 30 mg of cleavage product), m.p. and mixed m.p. 186–189°.

ACKNOWLEDGMENTS

The authors express their gratitude to Dr. A. C. Neish for a generous sample of L-arabinose-1-C^{14}. Dr. P. A. J. Gorin contributed valuable suggestions. Carbon-14 assays were carried out by J. Dyck, and microanalyses by T. Mazurek; infrared spectra and X-ray diffraction patterns were prepared by Inez Gaffney and M. Granat.

REFERENCES

1. PERLIN, A. S., RUDLOFF, E. VON, and TULLOCH, A. P. Can. J. Chem. **36**, 921 (1958).
2. BAUER, H. F. and STUETZ, D. E. J. Am. Chem. Soc. **78**, 4097 (1956).
3. FRANCIS, T. and RUDLOFF, E. VON. Can. J. Chem. **37**, 972 (1959).
4. RUDLOFF, E. VON, BAUER, H. F., and STUETZ, D. E. Can. J. Chem. **35**, 315 (1957).
5. RUDLOFF, E. VON and TULLOCH, A. P. Can. J. Chem. **35**, 1504 (1957).
6. ADKINS, H. Reactions of hydrogen. 4th Printing. Univ. of Wis. Press, Madison, Wis. (1946).
7. RUDLOFF, E. VON. Anal. Chim. Acta, **16**, 294 (1957).
8. FISCHER, E. Ber. **26**, 2400 (1893).
9. PARTRIDGE, S. M. Nature, **158**, 270 (1946).
10. BUCHANAN, D. L. and NAKAO, A. J. Am. Chem. Soc. **74**, 2389 (1952).
11. BELL, D. J. J. Chem. Soc. 992 (1948).
12. ROBERTS, J. D. and GREEN, C. Ind. Eng. Chem. Anal. Ed. **18**, 335 (1946).
13. DESNEULLE, P. and NAUDET, M. Bull. soc. chim. France, **12**, 871 (1945).
14. LAMBERT, M. and NEISH, A. C. Can. J. Research, B, **28**, 83 (1950).

Can. J. Chem. Downloaded from www.nrcresearchpress.com by 196.1.178.254 on 09/04/12
For personal use only.

Can. J. Chem. Downloaded from www.nrcresearchpress.com by 196.1.178.254 on 09/04/12
For personal use only.

ADSORPTION OF STERICALLY HINDERED PHENOLS ON CARBON[1]

OWEN H. WHEELER[2] AND ERIC M. LEVY

ABSTRACT

The Freundlich isotherms for the adsorption of some ortho-alkylated phenols on carbon from cyclohexane solution have been determined. The minimum surface area covered by the adsorbed phenols is compared with the area of the molecules themselves. Large alkyl groups ortho to the hydroxyl group greatly reduce the adsorption.

INTRODUCTION

The importance of steric effects in reactions occurring in a homogeneous phase is now well understood (1), but few data are available concerning the effect of steric hindrance in heterogeneous reactions. The kinetic rate-controlling step in such reactions is often the adsorption of the reactants on the surface of an adsorbent, and such a process will be considerably influenced by steric effects.

The adsorption of a series of ortho-alkylated phenols on carbon from cyclohexane solution has been studied. Phenols were chosen since they should be strongly adsorbed and can be easily analyzed. Carbon is a suitable adsorbent since it contains neither strongly acidic nor basic groups, and cyclohexane is a convenient inert solvent which is available in a state of high purity.

The effective surface area of the carbon used was first determined by the standard method (2) of adsorption of nitrogen at liquid air temperature.

The results of the adsorption of the phenols were expressed in the form of the Freundlich isotherm equation ($x/m = k.c^n$, where x is the amount adsorbed by m grams of adsorbent, and c is the equilibrium concentration of the adsorbate) as plots of x/m against c (Fig. 1). In all cases the graphs show limiting values of the amounts of phenol adsorbed, which must correspond to the formation of unimolecular layers.

EXPERIMENTAL

Reagents

Carbon

This was a sample of Darco G-60 adsorbent carbon supplied by the Atlas Powder Company of Canada, Ltd. The manufacturer's analysis was: ash content 2–5%, water solubles 0.1–0.2%, acid solubles 0.5%, pH of water extract 5–6, moisture 5–10%. The loss of weight of a sample dried to constant weight at 145° C corresponded to a moisture content of 5.2%. The sample used was dried under these conditions and stored over phosphorus pentoxide.

Gases

Nitrogen and helium were Canadian Liquid Air Company's pure samples and were dried prior to use.

Phenols

Phenol (Allied Chemical and Dye Corporation, absolute), *p-tert*-butylphenol (Dow Chemical Company), and 2,6-dimethylphenol (Aldrich Chemical Company) were used without further purification. 2,6-Diisopropylphenol (Aldrich) was vacuum-distilled twice.

[1]*Manuscript received February 19, 1959.*
Contribution from Department of Chemistry, Dalhousie University, Halifax, N.S.
[2]*Present address: Department of Chemistry, College of Agriculture and Mechanic Arts, Mayaguez, Puerto Rico.*

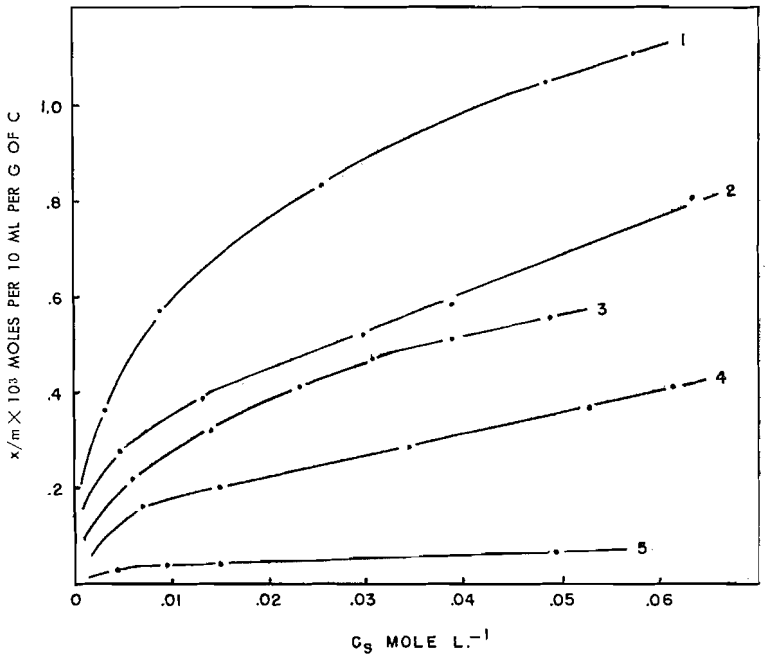

FIG. 1. Adsorption of phenols. 1. Phenol. 2. 2,6-Dimethylphenol. 3. *p-tert*-Butylphenol. 4. 2,6-Diisopropylphenol. 5. 2,6-Di-*tert*-butylphenol.

A yellow-colored impurity persisted in the product. 2,6-Di-*tert*-butylphenol (Aldrich) was recrystallized twice from ethanol.

The physical constants of the phenols are given in Table I.

TABLE I

Physical constants of phenols

	M.p./b.p.[a]	λ_{max}[b]
Phenol	43.0° (41°)	271 (1520), 276 (1450)[c]
p-tert-Butylphenol	97° (100°)	277 (1810)
2,6-Dimethylphenol	49.0° (49.0°)	273 (1450), 276 (1400)[c]
2,6-Diisopropylphenol	107.5°/110 mm, n_D^{20} 1.5124	273 (1700), 276 (1650)[c]
2,6-Di-*tert*-butylphenol	37.0° (39°)	272 (1410), 275 (1340)[c]

[a]Literature values in parentheses, ref. 16. [b]Wavelength of maximal absorption in mμ. Molar extinction coefficients (ε) in parentheses. [c]Inflection.

Aromatic Hydrocarbons

Benzene, *o*- and *p*-xylene, isopropyl- and *tert*-butyl-benzene, and mesitylene were Eastman-Kodak white label grade and were distilled before use (see Table II for physical constants).

Solvents

Cyclohexane was Fisher or Eastman-Kodak spectro-grade and was used as received. The 95% alcohol was a commercial grade which was free from aromatics as judged from its ultraviolet adsorption.

Can. J. Chem. Downloaded from www.nrcresearchpress.com by 196.1.178.254 on 09/04/12
For personal use only.

TABLE II
Physical constants of hydrocarbons

	B.p.[a]	n_D^{25}	λ_{max}[b]
Benzene	80.2° (80.1°)	1.5000	254.5 (186)
o-Xylene	143.5° (144.9°)	1.5030	263 (245)
p-Xylene	138.5° (138.3°)	1.4924	268.5 (243) 274.5 (269)
Isopropylbenzene	152.5° (152.4°)	1.4875	260 (180)
tert-Butylbenzene	170.0° (169.1°)	1.4894	278 (178)
Mesitylene	165.0° (164.7°)	1.4922	255 (193)

[a]Literature values in parentheses. [b]Wavelength of principal maxima in mμ. Molar extinction coefficients in parentheses.

Specific Surface Area of Carbon

The apparatus used was similar to that of Emmett and Brunauer (2) and consisted of an adsorption bulb connected by narrow bore glass tubing to a calibrated gas burette and a mercury manometer, attached to a conventional high vacuum line. The dead space in the adsorption bulb containing the carbon specimen was determined from pressure–volume measurements using helium. A series of pressure–volume experiments were then carried out with pure nitrogen while the adsorption vessel was immersed in liquid air. An adsorption isotherm of residual pressure against volume of nitrogen adsorbed was constructed and gave a limiting value of nitrogen required to form a unimolecular layer at 78° K of 42.0 cm^3 for 0.5424 g of carbon. Using the value of the effective area of nitrogen molecule at −195.8° C of 16.2 $Å^2$ (3), the corresponding specific surface area of the carbon is 1.15×10^3 $meter^2$ per g. This is in agreement with the findings of other workers (3) and Kipling states that "there has recently been a downward trend in surface area values of Darco G from 2123 $meter^2/g$ to 1295 $meter^2/g$" (3).

Adsorption of Phenols on Carbon

Samples of 10 ml of solutions of varying concentrations (0.01 to 0.1 *M*) of the phenols in cyclohexane were shaken with 0.200 g of carbon in 12-ml centrifuge tubes fitted with ground glass stoppers. The shaking was carried out by tumbling the tubes end-over-end at *ca.* 75 r.p.m. with a constant speed motor for ½ hour. It was found that in the case of phenol itself adsorption on the carbon was very rapid for the first 10 minutes and essentially complete after ½ hour. A very slow increase in adsorption took place with a longer time of contact. The suspensions were centrifuged for 5 minutes, and 5-ml portions of the clear solutions were removed with a pipette, care being taken not to disturb the carbon. All these operations were carried out in a constant-temperature room maintained at 20.5±0.5°. The 5-ml aliquots were diluted with 95% ethanol to give solutions of about 4×10^{-4} *M*, and the concentration of unadsorbed phenol was determined by measuring the intensity of ultraviolet absorption at the wavelength of maximal absorption of the phenol (270 to 275 mμ, see Table I). Graphs of the amount of phenol in moles adsorbed per gram of carbon against unadsorbed phenol are given in Fig. 1.

The adsorption of the aromatic hydrocarbons was determined in like manner and the results are expressed graphically in Fig. 2.

Surface Area Occupied by Phenol Molecules

The experimental area of the surface of the adsorbent occupied by one molecule of phenol was calculated (Table III, column 3) from the limiting amount of phenol adsorbed

Can. J. Chem. Downloaded from www.nrcresearchpress.com by 196.1.178.254 on 09/04/12
For personal use only.

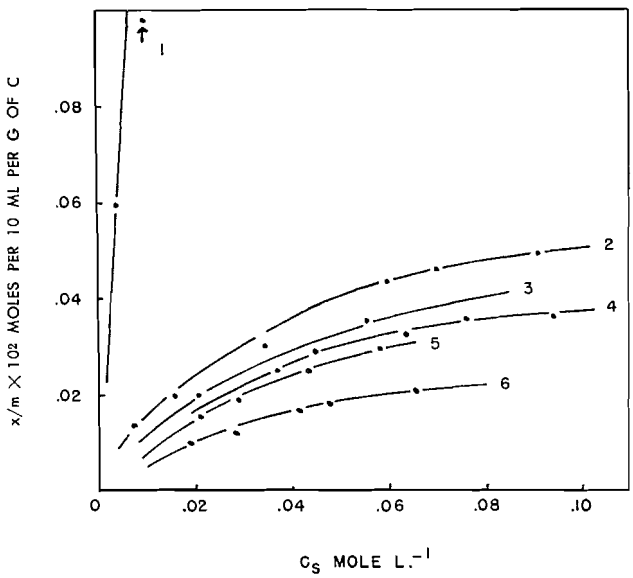

FIG. 2. Adsorption of hydrocarbons. 1. Benzene. 2. Mesitylene. 3. *o*-Xylene. 4. *p*-Xylene. 5. *tert*-Butylbenzene. 6. Isopropylbenzene.

(in moles per 10 ml of solution per gram of carbon) and the known active surface area of the carbon sample.

TABLE III

Surface area occupied by phenol molecules

Phenol	Moles/g 10 ml $\times 10^3$	Exptl. area (A_E)	Calc. area (A_c)	(A_E/A_c)
Phenol	0.97	200	33	6.0
p-tert-Butyl	.52	368	45	8.2
2,6-Dimethyl	.35	550	49	11.2
2,6-Diisopropyl	.175	1090	64	17.0
2,6-Di-*tert*-butyl	.048	3980	64	62.0

The surface area of each phenol molecule in the plane of the benzene ring was calculated (Table III, column 4) using the value of bond distances and the radius of the hydrogen atom given by Pauling (4) and the ring carbon–methyl and carbon–hydroxyl distances of Badger (5). The ratio of the experimental surface area covered by a phenol molecule to the plane surface area of the molecule (assuming "square packing") is given in the last column of Table III.

DISCUSSION

If it is assumed that the phenols are adsorbed with the benzene ring parallel to the surface of the adsorbent, then the fraction of the available surface covered in the case of phenol and *p-tert*-butylphenol is only 1/6 and 1/8, respectively. For the ortho dialkyl-substituted phenols the fraction is 1/11, 1/17, and 1/62 for methyl, isopropyl, and *tert*-butyl groups, respectively. The small fraction of the surface covered even in the case of phenol itself suggests that adsorption of the phenols takes place only at certain "active centers" on the adsorbent. The decreasing adsorption of 2,6-dimethyl and 2,6-

Can. J. Chem. Downloaded from www.nrcresearchpress.com by 196.1.178.254 on 09/04/12
For personal use only.

diisopropylphenol is consistent with the increasing steric shielding of the hydroxyl group and suggests that this group is largely responsible for the adsorption. The greatly decreased adsorption of 2,6-di-*tert*-butylphenol must be due to the large steric size of the *tert*-butyl groups, and the effect of their steric hindrance is also manifest in the physical properties (6) and chemical reactions (7, 8, 9) of this phenol. Carlton and Bradbury (10) have studied the paper chromatographic behavior of these phenols and they found that while alkyl groups in the meta- and para-positions have little effect on the adsorption, in the case of ortho-alkylated phenols the adsorption decreases with increasing size of the substituent. Under their conditions 2,6-di-*tert*-butylphenol was not adsorbed at all. The decreased adsorption of *o*-toluic acid as compared with benzoic acid on carbon (11), and of *o*-cresol and *o*-anisidine as compared to their *p*-analogues on silicic acid (12), has also been observed.

Recently Hallum and Drushel (13) have advanced infrared and polarographic evidence that the surface of carbon black contains free hydroquinone and quinone groups. These could constitute the "active centers" for adsorption of the phenols by hydrogen bonding, and since the hydroquinone and quinone groups do not cover the entire free surface it is understandable that the phenols can cover only part of the available surface area.

Though the principal adsorption force will be hydrogen bonding a further possibility is interaction between the π-electrons of the phenol rings and those of the "aromatic structure" of the graphite surfaces on the carbon particles. Experiments with aromatic hydrocarbons (see Fig. 2) show that although benzene itself is easily adsorbed the effect of alkyl substituents is to greatly reduce adsorption. This is true whether there is one, or more than one, group in ortho- or para-positions or whether the groups are methyl, isopropyl, or *tert*-butyl. Thus, since phenol and *p-tert*-butylphenol are adsorbed to similar extents, π-electron interaction cannot contribute to the forces of adsorption to any large extent. However, there is a small difference between these two phenols, which suggests that adsorption is with the plane of the benzene ring parallel to the surface of the carbon, since if the molecule were perpendicular to the surface no difference would be observed. (The electronic effect of the *p-tert*-butyl groups (donating electronic charge to the ring) (14) will increase the acid strength of the phenol and increase the strength of hydrogen bonding, producing an effect which would be opposite to that observed.)

The steric effect of the ortho alkyl groups in the phenols will decrease their acid strengths by inhibiting resonance with the benzene ring (14), and this in turn will decrease the strength of hydrogen bonding. Thus it appears that the ortho-alkylated phenols are adsorbed weakly, due both to the direct steric effect of the alkyl groups preventing hydrogen bonding and to their indirect effect of weakening this hydrogen bonding.

Spectra of the Phenols

The ultraviolet absorption spectra of the phenols shows some interesting effects. Thus *p-tert*-butylphenol absorbs at a higher wavelength and with a higher intensity than phenol itself. This is attributable to the inductive effect of the *tert*-butyl group increasing the electron density in the ring. The displacement to higher wavelength also results in submergence of the inflection at *ca.* 275 mμ which is present in all the other phenols measured.

In the case of 2,6-dimethyl-, 2,6-diisopropyl-, and 2,6-di-*tert*-butyl-phenol, though the wavelengths of the maxima do not change, the intensities of absorption increase and then decrease with increasing size of the group. This must be due to the opposing effect of

Can. J. Chem. Downloaded from www.nrcresearchpress.com by 196.1.178.254 on 09/04/12
For personal use only.

increasing inductive effect (which will increase the intensity) and increasing steric effect (which will decrease the intensity) (15) on passing from methyl, through isopropyl, to *tert*-butyl.

ACKNOWLEDGMENTS

The authors are indebted to the Atlas Powder Company, Canada, Ltd., Brantford, Ont., and Dow Chemicals, Midland, Mich., for gifts of Darco carbon and *p-tert*-butylphenol, respectively.

REFERENCES

1. BROWN, H. C. J. Chem. Soc. 1248 (1956).
2. EMMETT, P. R. and BRUNAUER, S. J. Am. Chem. Soc. **59**, 310 (1957).
3. KIPLING, J. J. Quart. Revs. (London), **10**, 1 (1956).
4. PAULING, L. The nature of the chemical bond. Cornell Univ. Press, Ithaca, N.Y. 1944.
5. BADGER, G. M. Structures and reactions of aromatic compounds. Cambridge University Press, London. 1954.
6. DAVIES, M. and MEAKINS, R. J. J. Chem. Phys. **26**, 1584 (1957).
7. STILLSON, G. H., SAWYER, D. W., and HUNT, C. K. J. Am. Chem. Soc. **67**, 303 (1945).
8. COFFIELD, T. H., FILBEY, A. H., ECKE, G. G., and KOLKA, A. J. J. Am. Chem. Soc. **59**, 310 (1937).
9. COFFIELD, T. H., FILBEY, A. H., ECKE, G. G., and KOLKA, A. J. J. Am. Chem. Soc. **79**, 5019 (1957).
10. CARLTON, J. K. and BRADBURY, W. C. J. Am. Chem. Soc. **78**, 1069 (1956).
11. HARTMAN, R. J., KERN, R. A., and BOBALEK, E. G. J. Coll. Sci. **1**, 271 (1946).
12. LE ROSEN, A. L., CARLTON, J. K., and MOSELEY, P. B. Anal. Chem. **25**, 666 (1953).
13. HALLUM, J. V. and DRUSHEL, H. V. J. Phys. Chem. **62**, 110 (1958).
14. BROWN, H. C., MCDANIEL, D. H., and HAFLIGER, O. Determination of organic structure by physical methods. *Edited by* E. A. Braude and F. C. Nachod. Academic Press, Inc., New York. 1955. Chap. 14.
15. BRAUDE, E. A. and SONDHEIMER, F. J. Chem. Soc. 3754 (1955).
16. PARDEE, W. A. and WEINRICH, W. Ind. Eng. Chem. **36**, 595 (1944).

Can. J. Chem. Downloaded from www.nrcresearchpress.com by 196.1.178.254 on 09/04/12
For personal use only.

Can. J. Chem. Downloaded from www.nrcresearchpress.com by 196.1.178.254 on 09/04/12
For personal use only.

THE ISOLATION AND PROPERTIES OF LIGNINS OBTAINED BY THE ACIDOLYSIS OF SPRUCE AND ASPEN WOODS IN DIOXANE–WATER MEDIUM[1]

J. M. Pepper, P. E. T. Baylis,[2] and E. Adler

ABSTRACT

A study has been made of the isolation of a lignin fraction from spruce and aspen wood meals using a low temperature (90–95° C) acidolysis involving a dioxane–water (9:1) solvent medium containing the equivalent of 0.2 *N* hydrochloric acid. The effect of extraction time on the yield of precipitated lignin and ether-soluble material, and on the methoxyl content of these products, was investigated. For both species prolonged extraction times led to greater yields of lignin with lower methoxyl content.

Further acidolysis of isolated spruce lignin led to no significant loss of methoxyl indicating the stability of this group to these reaction conditions. With increasing times of acidolysis of the aspen wood, a slow rise in the carbon–methyl/methoxyl ratio was observed for the isolated lignins. This is in agreement with earlier findings for the spruce lignin. The yields of vanillin and syringaldehyde from aspen lignin on alkaline nitrobenzene oxidation were much less than those from wood meal, and the relative yield of syringaldehyde was higher.

It is suggested that this type of lignin may be only mildly modified during extraction and hence suitable for subsequent chemical investigation. The significance of the findings is discussed.

An attempt has been made to isolate the lignin fraction from both spruce and aspen woods, in yields sufficiently high that the product may be considered representative of the lignin in the wood and yet remain in a form suitable for subsequent extensive chemical investigation. It is well established that rearrangements, which occur during the ethanolysis of wood meal, give rise in both the soluble Hibbert monomers (1) and in the ethanol lignin (2) to an increased percentage of carbon–methyl groupings over that of the original, acetoxy-free, wood meal. This suggested the need for a readily available lignin in which these acid-catalyzed rearrangements could be studied more systematically. The importance of the nature of the extracting solvent in typical alcoholysis reactions has been emphasized by Schuerch (2, 4), who stated, "The low reported yields of lignin alcoholysis products are mainly the result of the slight solubility of the products in the solvent rather than solely the result of polymerization reactions". Other workers (5, 6) have also emphasized the importance of using an aqueous organic solvent system for increased lignin solubility. The well-known alcoholysis procedure for the isolation of lignin suffers primarily from the disadvantage of solvent–lignin interaction. Thus the use of methanol or ethanol was excluded since the ready etherification of various lignin alcoholic groups would yield a product whose analysis for either methoxyl or carbon–methyl respectively would be difficult to interpret.

The use of dioxane in a typical solvolysis reaction has been studied (1), but has led to conflicting reports as to its usefulness. However, dioxane–water appeared to offer many advantages as a solvolysis medium: it has been shown to be a good solvent (5); dioxane is not known to react with lignin to any appreciable extent, and such a system, at reflux, would provide a moderately elevated extraction temperature. The presence of small amounts of a mineral acid (usually hydrochloric acid) are necessary in the lignin solvolysis

[1]*Manuscript received March 13, 1959.*
Contribution from the Institut för Organisk Kemi, Chalmers Tekniska Högskola, Goteborg, Sweden; and from the Department of Chemistry, University of Saskatchewan, Saskatoon, Saskatchewan. Presented, in parts, at the 40th and 41st Annual Conferences, Chemical Institute of Canada, at Vancouver, June 3–5, 1957, and at Toronto, May 26–28, 1958. Abstracted, in part, from a M.Sc. thesis submitted by P.E.T.B., October, 1957.
[2]*Present address: Ontario Research Foundation, Toronto, Ontario.*

reaction. Concentrations of such acid ranging from 0.01 to 3.8% have been reported (1) but no detailed study appears to have been reported on the effect of this variable on yields of isolated lignins. Schuerch (4) reported that in a series of experiments involving the solvolysis of spruce lignin in a chloroform–ethanol system, the decrease in hydrogen chloride concentration from 1.75 to 0.7% substantially lowered the rate of delignification. Konkin and Rogovin (7), in a study of the delignification of wood using ethylene glycol for ½ hour at 180° C, showed that a slight decrease in the amount of lignin dissolved occurred if the hydrogen chloride concentrations were varied from 0.1 to 0.02%. The most commonly used acid concentration is 0.2 *N* (0.7%) and this is used throughout this research.

A. ISOLATION OF LIGNIN FROM SPRUCE WOOD

In a series of preliminary experiments to compare the suitability of various solvent systems, pre-extracted spruce wood meal was suspended in the solvent medium containing 0.2 *N* (by weight) dry hydrogen chloride and refluxed for 4 hours in a nitrogen atmosphere. The solvents chosen were chloroform–methanol (4:1), dioxane–methanol (9:1) as recommended by Schuerch (3), dioxane, and dioxane–water (9:1). The reaction mixture was filtered, and the filtrate, after neutralization with sodium bicarbonate, was concentrated to a small volume. The lignin was precipitated by forcing this concentrate, as a fine stream, under the surface of 1% sodium sulphate solution. The lignin was removed by centrifugation and decantation and the mother liquors were exhaustively extracted with ether. The residual wood meal, the lignin, and the ether-soluble extract* were dried to constant weight and analyzed for methoxyl content. The results are given in Table I.

TABLE I

Preliminary lignin extraction experiments[a]

Solvent	Temp., °C	Residual pulp		Lignin		Ether extract		Total methoxyl recovery, %
		Recovery, %	Methoxyl, %	Weight, g(% K.L.)[b]	Methoxyl, %	Weight, g(% K.L.)[b]	Methoxyl, %	
$CHCl_3$–CH_3OH (4:1) H_2O[c]	55	79.9	6.58	1.35 (19.6)	16.5	—	—	—
$CHCl_3$–CH_3OH (4:1)	55	77.6	6.55	1.0 (14.5)	20.9	0.073 (1.06)	25.2	123
Dioxane–CH_3OH (9:1)	80	54.2	3.48	4.3 (64)	21.4	0.88 (12.8)	27.2	134
Dioxane	96	65.5	4.23	3.52 (51)	12.2	1.41 (20.5)	15.0	110
Dioxane–water (9:1)	94	50.5	2.20	5.13 (74.5)	14.4	1.46 (21.2)	10.9	97.5

[a]Pre-extracted spruce wood (25 g); solvent (200 ml); 0.2 *N* HCl; reflux time, 4 hours, under nitrogen.
[b]Expressed as percentage of the Klason lignin.
[c]The wood meal was first refluxed for 4 hours with 0.2 *N* HCl, then filtered and treated as indicated.

The significant alkylation as indicated by the marked increased total methoxyl content in those experiments using methanol supports this well known reaction of lignin. This alkylation reaction has been studied (8) and explained as being due to the etherification of benzyl alcohol groups or the re-etherification of benzyl ether groups. The effect of an acid treatment of the wood meal prior to the chloroform–methanol extraction was limited. There is an indication that some added methylatable hydroxyl groups were liberated but that some condensation occurred to decrease the solubility of the lignin. The advantage of using aqueous dioxane over dioxane alone is indicated by the significantly increased yield and methoxyl content of the isolated lignin. It would appear that,

**It must be pointed out that the small amounts of dioxane introduced during the precipitation process modify the solubility of the extracted substances.*

Can. J. Chem. Downloaded from www.nrcresearchpress.com by 196.1.178.254 on 09/04/12
For personal use only.

in the aqueous system, some carbohydrate or other non-methoxyl-containing fragments that appear with the lignin in the pure dioxane extraction have been separated and appear instead in the ether extract giving rise to the relatively lower methoxyl content of this fraction.

Since it had been shown that the dioxane–water (9:1) solvent system was effective for lignin extraction, the effect of the time of reflux was studied. Similar experiments were conducted with the reflux times of 1, 2.5, 4.0, and 8.0 hours. The components of the reaction mixture were obtained and analyzed as before. The results are given in Table II.

TABLE II

Effect of reflux time on isolation of spruce lignin[a]

Time, hours	Residual pulp		Lignin		Ether extract		Total methoxyl recovery, %
	Recovery, %	Methoxyl, %	Weight, g(% K.L.)[b]	Methoxyl, %	Weight, g(% K.L.)[b]	Methoxyl, %	
1.0	73	3.62	2.25 (32.5)	16.1	0.74 (10.8)	15.9	94.3
2.5	62	2.44	3.77 (55)	15.0	1.23 (17.8)	11.7	90.0
4.0	52	1.73	4.95 (72)	14.3	1.66 (24.1)	10.4	91.5
4.0[c]	50.5	2.2	5.13 (74.5)	14.4	1.46 (21.2)	10.9	97.5
8.0	42.5	1.16	6.56 (95)	12.7	1.95 (28.3)	6.74	89.5

[a]Pre-extracted spruce wood (25 g); dioxane–water (9:1) (200 ml); 0.2 *N* HCl; reflux temperature, 90–94° C, under nitrogen.
[b]Expressed as percentage of Klason lignin.
[c]Included from Table I to indicate order of reproducibility.

There is no evident variation in methoxyl recovery with time of reflux, but the average value of 92.5% appears sufficiently significant to suggest a small but rapid acid-catalyzed loss of methoxyl. This could arise by the hydrolysis of methyl acetal linkages or by the solubilization of methoxyl-bearing components which are not extracted by ether. The lignin extracted by the 1-hour treatment was of a light tan color and its methoxyl content of 16.1% agrees with that reported by Björkman (6) for a sample of spruce milled wood lignin whose methoxyl content of 15.8%, after correction for 1.9% hydrolyzable carbohydrates, becomes 16.1%. A similar 1-hour preparation analyzed for carbon, 64.6; hydrogen, 5.55%; results, which again agree closely with the elemental analysis of other extracted lignins.

The steady decrease, with time of extraction, of the methoxyl content of both the isolated lignin and the corresponding ether extracts may be explained as follows. Either the protolignin is non-homogeneous, at least with respect to its ease of extraction, and the higher percentage methoxyl components are most readily liberated and solubilized (e.g., terminal units), or the isolated "lignin" fraction contains increasingly larger relative amounts of carbohydrate fragments. This latter situation could arise as the result of the direct isolation of such lignin–carbohydrate portions pre-existing in the wood, or as a result of secondary condensations between solubilized lignin and carbohydrate fragments.

It was felt that some information might be obtained regarding the homogeneity of the protolignin if a stepwise isolation were conducted and the lignin products examined at each stage. To this end the residual pulp from the 1-hour extraction procedure (25 g wood meal) was treated under the same experimental conditions for a further $1\frac{1}{2}$ hours and the solubilized lignin and ether extracts obtained. This was repeated again on the second pulp residue. The lignin yields with methoxyl content given in brackets, obtained by the successive extraction periods of 1, 1.5, and 1.5 hours, were 2.25 g (16.1%), 0.684 g

Can. J. Chem. Downloaded from www.nrcresearchpress.com by 196.1.178.254 on 09/04/12
For personal use only.

(14.85%), and 0.514 g (14.5%). The corresponding ether extracts were 0.774 g (14.9%), 0.338 g (8.45%), and 0.21 g (4.62%). There is a considerable decrease in the total available lignin products as compared to those obtained by either the one-step 2.5 hours or the one-step 4.0 hours extraction. The chemical nature of these products isolated by the successive stepwise method varied considerably, indicating a non-homogeneity of the lignin substance. It must be pointed out that each wood residue was dried first in the air then in a vacuum desiccator over phosphorus pentoxide, and it is conceivable that during this time oxidation or condensation occurs which decreases the ease of subsequent isolation.

The ready availability, light tan color, high methoxyl content, and solubility in dioxane–water (9:1) of the lignin isolated by the 1-hour treatment was considered as sufficient indication that this material would prove suitable for extended chemical studies. Thus, studies could be made on the effect of increasing times of acidolysis on the establishment of carbon–methyl groups by rearrangement, and on the liberation of free phenolic hydroxyl groupings. For this purpose solvent-extracted wood meal (300 g) was extracted, as before, for a 1-hour period. The resulting lignin weighed 31.2 g (37.8% of the Klason lignin) and analyzed for 15.53% methoxyl. The ether extract yielded a dark colored oil fraction, 7.92 g (9.6% of the Klason lignin) which was not studied further.

Samples of this dioxane–water lignin were subsequently refluxed further under similar conditions for periods of 3, 11, 23, and 47 hours. The resulting reaction products were studied as before, the lignin recovered by precipitation into 1% sodium sulphate, and the ether-soluble oils extracted from the aqueous filtrate. The results of these treatments are given in Table III.

TABLE III

Acidolysis of isolated dioxane–water lignins[a]

Run	Sample (g)	Reflux (hours)	Lignin recovered		Ether extract		Methoxyl recovery (%)
			Weight (g)	OCH_3 (%)	Weight (g)	OCH_3 (%)	
A	4.0017	3	3.1432	16.2	0.394	17.52	93.0
B	4.0255	11	3.0178	16.4	0.473	16.75	91.5
C	4.0024	23	3.1103	16.19	0.457	18.4	94.5
D	4.003	47	3.0599	16.06	0.426	16.7	90.5

[a]Reaction medium: dioxane–water (9:1) (100 ml); 0.2 *N* HCl.

The consistently high methoxyl content of the recovered lignins indicates the stability of this grouping to these reaction conditions. This fact, together with the close similarity in the amounts of the ether extracts, suggests a rapid release of these lower molecular weight fragments from this lignin. Support is thereby also given to the belief that the decrease in methoxyl content of both the isolated lignin and the ether-soluble extracts, with increasing time of acidolysis of the original wood (see Table II), is a result of the simultaneous isolation of lower methoxyl content portions. A progressive darkening in color of the isolated lignins from run A through D indicates a distinct chemical change which, however, did not result in a change of the methoxyl content. The analytical results showing the increasing content of both carbon–methyl and of free phenolic hydroxyl groups with increased time of acidolysis have been reported and their significance to the chemistry of spruce lignin discussed (9). It is obvious that extensive rearrangements or other structural changes were occurring as a result of the prolonged treatment.

Can. J. Chem. Downloaded from www.nrcresearchpress.com by 196.1.178.254 on 09/04/12
For personal use only.

Can. J. Chem. Downloaded from www.nrcresearchpress.com by 196.1.178.254 on 09/04/12
For personal use only.

B. ISOLATION OF LIGNIN FROM ASPEN WOOD

The method of lignin isolation described above offered a simple but rapid means of obtaining, in good yields, a light, tan-colored material suitable for further extensive chemical studies. The method was then applied to a typical angiosperm, *Populus tremuloides*. The effects of time of extraction on the yields of the precipitated lignin and the ether-soluble oils along with their respective methoxyl contents are given in Table IV.

TABLE IV

Effect of reflux time on isolation of aspen lignin[a]

Reflux time (hours)	Residual pulp		Lignin recovered[b]					Ether extract			Total OCH_3 recovery (%)
			Weight			Methoxyl		Weight		OCH_3 (%)	
	Recovery (%)	OCH_3 (%)	A (g)	B (g)	Total (% K.L.)	A (%)	B (%)	(g)	(% K.L.)		
0.5	80.5	2.63	1.75	0.17	42.2	21.0	15.9	0.34	7.5	19.1	77.8
1.0	73.0	1.87	2.36	0.11	54.3	21.5	12.8	0.54	11.9	18.7	75.0
2.5	64.0	0.77	2.71	0.42	68.8	20.8	15.6	0.39[c]	8.6	11.5	62.4[c]
4.0	61.2	0.30	3.22	0.01	71.0	20.3	12.9	0.99	21.8	15.8	66.8
8.0	56.9	0.32	3.34	0.13	76.3	19.5	15.6	1.41	31.0	14.4	71.5
48.0	46.5	0.69	4.85	0.02	107.	16.3	—	1.26	27.7	12.4	80.0

[a]Reaction conditions: extracted wood meal (25 g); dioxane–water (9:1) (200 ml); 0.2 *N* HCl; reflux temperature, 90–94° C, under nitrogen.
[b]Lignin A refers to that fraction obtained from the neutralized filtrate; lignin B to that fraction obtained from $NaHCO_3$ layer.
[c]Unknown mechanical loss during evaporation.

One of the striking features of this extraction of aspen wood meal is the consistently low recovery of methoxyl as compared to that obtained from spruce wood by a similar treatment. Two possible reasons for this poor recovery may be suggested; either a significant proportion of the original methoxyl is present in an acid labile form, e.g., acetal linkage, or it is associated with readily hydrolyzable carbohydrate fractions which remain unrecovered in the aqueous residue. As high as 15% of the methoxyl of aspen wood has been reported (10) to be associated with the holocellulose.

The steady decrease in the methoxyl content of the isolated lignins and of the ether extracts with times of extraction from 0.5 to 48 hours follows a pattern similar to that found for spruce and may be likewise explained. The high (21%) methoxyl content of the lignin isolated after ½-hour or 1-hour treatments is in general agreement with the several values reported by Brauns (1) ranging from 20.4 to 20.9% and slightly higher than the 19.4% reported for native aspen lignin (11). The results presented in Table IV suggest that as a result of extended acidic treatment secondary reactions occur involving the isolated lignin and residual carbohydrate components. The significantly increasing methoxyl content of the pulps after longer than 4 hours' extraction time indicates a recombination of methoxyl-bearing components and pulp residues.

The characteristic reaction of hardwood lignin whereby it may be oxidized by hot alkaline nitrobenzene solution to produce vanillin and syringaldehyde was applied to the isolated lignins recorded in Table IV. These results are given in Table V.

It is very significant that even after only a ½-hour acidolysis treatment, the yields of vanillin and syringaldehyde have been markedly decreased over those obtainable using wood meal alone. No results were obtained respecting the aldehyde yields of the ether extract, but since it represented only 7.5% of the total lignin, the possible aldehyde yields would be less than this value. The combined yields of vanillin and syringaldehyde from the isolated lignin and from the residual pulp of the ½-hour extraction procedure

TABLE V

The alkaline nitrobenzene oxidation of isolated aspen lignins

	Yields of aldehydes[a]								
Reflux time (hours)	0[b,c]	0.5	1.0	2.5	4.0	8.0	48	0.5[c]	(Wood residue)
Vanillin	17.0	8.2	8.4	6.2	5.7	5.0	4.6	1.39	
	14.1	8.4	10.5	6.3	4.1	4.8	3.6	1.46	
	14.9	7.8	7.3	6.6	4.4	4.1	3.3	1.31	
	19.5								
Mean	16.6	8.1	8.7	6.4	4.7	4.6	3.8	1.39	
Syringaldehyde	33.7	24.0	24.8	18.3	15.3	11.2	6.4	1.89	
	32.6	22.0	25.5	16.9	13.4	10.5	5.8	2.20	
	33.0	23.7	21.4	18.1	12.6	9.9	5.1	2.11	
	36.1								
Mean	33.9	23.2	23.9	17.8	13.8	10.5	5.8	2.07	
Total vanillin and syringaldehyde	50.5	31.3	32.6	24.2	18.5	15.1	9.6	3.46	
Ratio S/V	2.0	2.9	3.0	2.8	2.9	2.3	1.5	1.5	

[a]Reported as percentage by weight of the isolated lignin.
[b]Solvent-extracted wood meal.
[c]Reported as percentage by weight of the original Klason lignin.

amounted to only 9.49 and 25.3%, as compared to yields of 16.6 and 33.9% respectively obtained from the wood meal itself and calculated as percentage of the Klason lignin. This marked difference suggests a very rapid change in chemical structure, under the conditions of the acidolysis, into a form which no longer is oxidized to the phenolic aldehydes. A strikingly similar result was observed previously by Kavanagh and Pepper (12), who showed that if similar wood meals were subjected to a 2.5-hour pretreatment with 8% sodium hydroxide, then on subsequent oxidation with nitrobenzene yields of vanillin and syringaldehyde were only 9.65 and 22.6% respectively. It seems clear that as a result of either an acid- or base-catalyzed reaction, structural changes in the lignin occur rapidly either prior to, during, or after solution of the lignin fraction.

The methoxyl content of aspen lignin may be considered to arise from the methoxyl groups associated with the guaiacyl and syringyl nuclei of the lignin substance. If a typical guaiacyl-containing unit be represented by $C_{10}H_{12}O_4$ and a typical syringyl-containing unit by $C_{11}H_{14}O_5$, a ratio of these two units of close to 2:1 respectively would be equivalent to a combined methoxyl content of 21% as found for the least modified isolated lignin (see Table IV). As may be seen from Table V the actual ratios of vanillin to syringaldehyde as obtained by the alkaline nitrobenzene oxidations are all (except in the 48-hour experiment) close to 1:3. Since neither vanillin nor syringaldehyde is lost to any appreciable extent by this treatment (12), the inverse ratio and high relative yields of syringaldehyde may be explained as follows. Under the conditions of the reaction a secondary condensation occurs involving the reactive 5-position of the 1-substituted guaiacyl nuclei giving rise to products that no longer can be oxidized to vanillin. No such secondary reaction is possible for the fractions composed of syringyl nuclei.

The increasing carbon–methyl content of the isolated spruce wood lignin with increasing time of subsequent further acidolysis treatment has already been reported (9). The carbon–methyl/methoxyl ratio increased from 0.04 to 0.20 as a result of a 48-hour

Can. J. Chem. Downloaded from www.nrcresearchpress.com by 196.1.178.254 on 09/04/12
For personal use only.

acidolysis treatment. Similarly, for the lignin isolated from aspen wood the carbon–methyl/methoxyl ratio was shown to increase with increasing times of acidolysis during isolation. After 0.5, 1.0, 2.5, 4.0, 8.0, and 48.0 hours of acidolysis, the average carbon–methyl/methoxyl ratio was 0.13, 0.10, 0.11, 0.15, 0.22, and 0.29 respectively.

These results again indicate the rearrangements that readily occur intramolecularly in isolated lignins. They emphasize too the requirement of short times of extraction in order to obtain a representative lignin fraction. Earlier workers (2) had shown that for maple negligible amounts of carbon–methyl groups existed in the whole wood other than those derivable from the readily hydrolyzable acetate groupings.

The application of this procedure of lignin isolation to both spruce and aspen woods gives rise in good yields to a readily obtained product, which, on preliminary examination, appears to be only moderately changed from protolignin. In comparison it appears that aspen wood lignin is isolated rather more easily than that from spruce wood. It appears too, that there is evidence in the former case for an initial rapid extraction of about two-thirds of the lignin followed by a slower rate of extraction of the remainder. There is no similar inflection in the rate of lignin isolated from spruce. This effect may be associated with the proved dinuclear character of the hard wood lignins as compared to the greater homogeneity of the softwood lignins. This suggested greater ease of cleavage, and subsequent dissolution of fragments with syringyl-type nuclei is supported by the evidence presented regarding the relative yields of aldehydes obtained by oxidation.

EXPERIMENTAL

Preparation and Analysis of Wood Meal

Spruce wood.—Swedish spruce wood meal was extracted continuously with a mixture of ethanol–benzene (1:1) for 53 hours, air-dried, and finally dried to constant weight in a vacuum desiccator over phosphorus pentoxide. Anal: Klason lignin, 27.55%; methoxyl, 4.85%.

Aspen wood.—Native Saskatchewan aspen (*Populus Tremuloides*) sapwood, 20 mesh, was extracted with ethanol–benzene (1:1) for 45 hours, air-dried, and finally dried to constant weight over phosphorus pentoxide. Anal.: Klason lignin, 18.2%; methoxyl, 5.13%.

Solvent.—The dioxane was purified according to the procedure of Fieser (13).

General Procedure for Lignin Isolation

A procedure typical of that used for all acidolysis treatments is as follows. Pre-extracted wood meal (25 g) was placed in a 2-liter, 3-necked flask fitted with a reflux condenser, a nitrogen bubbler, and a dropping funnel. The flask was evacuated at the water aspirator (10–15 minutes), the connection to the pump closed, and the solvent system (200 ml of dioxane–water (9:1) containing 1.46 g dry HCl gas) added slowly from the dropping funnel. The reaction mixture was heated using a heating mantle and refluxed gently for varying periods of time of 0.5, 1.0, 2.5, 4.0, 8.0, and 48 hours under a nitrogen atmosphere. For the experiments using aspen wood the reaction mixture was stirred using a magnetic stirrer. The reaction mixture was allowed to cool, filtered whilst blanketed with nitrogen, and the residue washed on the filter with a further 50 ml of the same solvent. The residual pulp was dried to constant weight and analyzed for methoxyl content.

The filtrate was neutralized with excess sodium bicarbonate and allowed to stand overnight. The liquid layer was concentrated under reduced pressure, using a nitrogen leak, to a thick syrupy consistency, dissolved in ca. 30 ml of the solvent, and forced

Can. J. Chem. Downloaded from www.nrcresearchpress.com by 196.1.178.254 on 09/04/12
For personal use only.

under pressure (syringe bulb) in a fine stream under the surface of 250 ml of a 1% Na_2SO_4 solution. The precipitated lignin was separated by centrifugation and decantation, washed thoroughly with water, and centrifuged three times more, and finally dried to constant weight in a vacuum desiccator over P_2O_5. In the case of the aspen wood experiments, the sodium bicarbonate sludge layer was dissolved in a large excess of water (60 ml) and acidified with hydrochloric acid. The lignin thus precipitated is referred to as lignin B in Table IV.

Those lignins isolated by the short periods of reflux (0.5–1.0 hours) were light tan-colored powders, but the color darkened as the time of reflux increased. These lignins were all slightly hygroscopic, highly susceptible to static electricity when dry, soluble in pure dioxane or dioxane containing a few per cent water, and soluble in glacial acetic acid and sodium hydroxide but only slightly soluble in ether and carbon tetrachloride.

The alkaline nitrobenzene oxidations were conducted according to the procedure of Stone and Blundell (14).

The carbon–methyl analyses were determined according to the procedure outlined by Smith and Shriner (15).

ACKNOWLEDGMENTS

One of the authors (J.M.P.) wishes to acknowledge the granting to him by the University of Saskatchewan of a year's study leave in Sweden, where the research on spruce was performed. Acknowledgment is also made of the financial assistance provided by the Saskatchewan Research Council for the work on the aspen wood. Thanks are expressed to Miss R. Sins for assistance with the methoxyl and carbon–methyl analyses.

REFERENCES

1. Brauns, F. E. The chemistry of lignin. Academic Press Inc., New York. 1952. Chap. XV.
2. McGregor, W. S., Evans, T. H., and Hibbert, H. J. Am. Chem. Soc. **66**, 41 (1944).
3. Schuerch, C. J. Am. Chem. Soc. **73**, 2385 (1951).
4. Schuerch, C. J. Am. Chem. Soc. **74**, 5061 (1952).
5. Pepper, J. M. and Hagerman, D. C. Can. J. Chem. **32**, 614 (1954).
6. Björkman, A. Ind. Eng. Chem. **49**, 1395 (1957).
7. Konkin, A. A. and Rogovin, Z. A. Chem. Abstr. **48**, 360 (1954).
8. Adler, E. and Gierer, J. Acta Chem. Scand. **9**, 84 (1955).
9. Adler, E., Pepper, J. M., and Eriksoo, E. Ind. Eng. Chem. **49**, 1391 (1957).
10. Freeman, R. D. and Peterson, F. C. Ind. Eng. Chem. Anal. Ed. **13**, 803 (1941).
11. Buchanan, M. A., Brauns, F. E., and Leaf, R. L. J. Am. Chem. Soc. **71**, 1297 (1949).
12. Kavanagh, K. R. and Pepper, J. M. Can. J. Chem. **33**, 24 (1955).
13. Fieser, L. F. Experiments in organic chemistry. 3rd ed. D. C. Heath and Co., Boston. 1955.
14. Stone, J. E. and Blundell, N. J. Anal. Chem. **23**, 771 (1951).
15. Smith, W. T. and Shriner, R. L. The systematic identification of new organic compounds. John Wiley & Sons, Inc., New York. 1956.

Can. J. Chem. Downloaded from www.nrcresearchpress.com by 196.1.178.254 on 09/04/12
For personal use only.

Can. J. Chem. Downloaded from www.nrcresearchpress.com by 196.1.178.254 on 09/04/12
For personal use only.

HYDRONIUM ION ABSORPTION IN THE REGION 1.7 μ[1]

W. J. Biermann and J. B. Gilmour

ABSTRACT

Optical absorption of the hydronium ion in the region 1.7 μ was measured in solutions of nitric acid and perchloric acid in the concentration range 0.01 to 4.0 moles per liter. Above 0.1 molar the absorption did not follow Beer's Law, being smaller than predicted from the low concentration behavior. This enhanced transparency is attributed to a "negative absorption" band, associated with the change in solvent structure, found in this spectral region.

INTRODUCTION

In an attempt to establish relationships between the thermochemical properties of aqueous solutions of strong acids and the structures of these solutions, the degree of dissociation of the acid is an indispensable quantity. The limited information presently available has been based, for the most part, on observations of the optical absorption or Raman spectra of undissociated molecules and the anions produced in dissociation (1, 6, 7, 9, 10, 12). The degree of dissociation of a few oxyacids, notably nitric and perchloric acids, seems to be reliably established over a wide concentration range, but these methods are not applicable to binary strong acids.

While casting about for alternate methods of studying the dissociation of strong acids in aqueous solutions, we observed the near infrared absorption spectra of a number of aqueous solutions of strong acids (2). In all cases, these spectra showed a strong absorption band centered in the region of 1.7 μ (5800 cm^{-1}). It appeared reasonable to classify this as an harmonic of a fundamental vibrational frequency of the hydronium ion. Very shortly thereafter, Giguère and Falk (5) reported broad absorption peaks for the hydronium ion at 2900 cm^{-1} and 3300 cm^{-1}.

A study of this absorption band over a range of concentrations was undertaken, primarily to determine the applicability of Beer's Law. If Beer's Law were obeyed, a useful method would be available for the determination of the degree of dissociation of acids in water. Nitric acid and perchloric acid solutions were chosen because the hydronium ion concentrations of these can be calculated with some degree of confidence from existing data.

EXPERIMENTAL

Nitric and perchloric acid solutions were prepared by diluting concentrated reagent grade chemicals with conductivity water. The diluted solutions were analyzed by titration with carbonate-free sodium hydroxide solutions, using bromcresol purple as indicator. The percentages of light transmitted by the diluted solutions were measured on a Beckmann DK-II spectrophotometer, using 1.0-cm Corex cells at room temperature. Conventional procedures were used to insure temperature similarity between the solution and the water-filled reference cell, to correct for inequalities of cell length, and to minimize the chance of gross error by a suitable schedule of repetition of observations.

The experimental results are summarized in Tables I and II, which give the average absorbancy ($\log_{10} I_0/I$) and the wavelength of the maximum of the absorption peak for a range of concentrations of nitric acid and perchloric acid from 0.01 to 4.0 molar. All the absorbancy values were measured at the wavelength of maximum absorption. Figure 1

[1]*Manuscript received March 16, 1959.*
Contribution from the Department of Chemistry, University of Manitoba, Winnipeg, Manitoba.

TABLE I

Absorbancy data for aqueous perchloric acid solutions

Concentration, moles $HClO_4$/liter	Absorbancy, $\log_{10} I_0/I$	Wavelength (μ) of max. absorption
0.009706	0.0067	
0.01948	0.0156	
0.02925	0.0252	
0.03912	0.0313	1.730
0.04836	0.0383	1.738
0.05795	0.0453	1.738
0.06937	0.0550	1.741
0.07754	0.0696	1.736
0.09733	0.0775	1.736
0.1957	0.152	1.738
0.2936	0.225	1.738
0.6303	0.458	1.738
0.7305	0.526	1.735
0.9358	0.650	1.732
1.233	0.823	1.727
1.562	0.983	1.723
1.967	1.153	1.715
2.423	1.286	1.712
2.933	1.385	1.708
3.859	1.477	1.700

TABLE II

Absorbancy data for nitric acid solutions

Concentration, moles HNO_3/liter	Absorbancy, $\log_{10} I_0/I$	Wavelength (μ) of max. absorption
0.00928	0.0073	1.735
0.01878	0.0161	1.735
0.04762	0.0417	1.735
0.09413	0.0834	1.734
0.1998	0.173	1.732
0.3839	0.323	1.734
0.5645	0.460	1.731
0.7433	0.587	1.730
0.9534	0.730	1.726
1.171	0.863	1.721
1.581	1.093	1.714
2.005	1.264	1.710
2.492	1.407	1.705
3.044	1.507	1.697
3.909	1.576	1.696

is a graphical presentation of the absorbancy, plotted against concentration. The solid lines are extensions of the limiting slopes and, since both of these acids are substantially completely dissociated in the concentration range studied, are approximately the loci which would be anticipated if the absorption followed Beer's Law. Figure 2 shows the low concentration absorbancy versus concentration plot, in which Beer's Law is obeyed within the accuracy of observation.

DISCUSSION

That the phenomenon being observed is more complex than a simple absorption of light by H_3O^+ is shown by four types of behavior inconsistent with the simple picture:

1. Absorbancy falls off too rapidly with concentration. If the experimental results are used to compute degrees of dissociation on the assumption that Beer's Law is applicable, these are much lower than the values consistently obtained by other methods.

Can. J. Chem. Downloaded from www.nrcresearchpress.com by 196.1.178.254 on 09/04/12
For personal use only.

2. The wavelength of the peak maximum shifts to a lower value as the concentration increases.

3. Nitric acid appears to be "stronger" than perchloric acid, whereas all other investigations have shown perchloric acid to be the stronger.

4. The limiting value of the extinction coefficient differs between nitric and perchloric acids.

The shift in the peak maximum is a particularly strong indication that the entity being observed does not retain its physical structure throughout the concentration range.

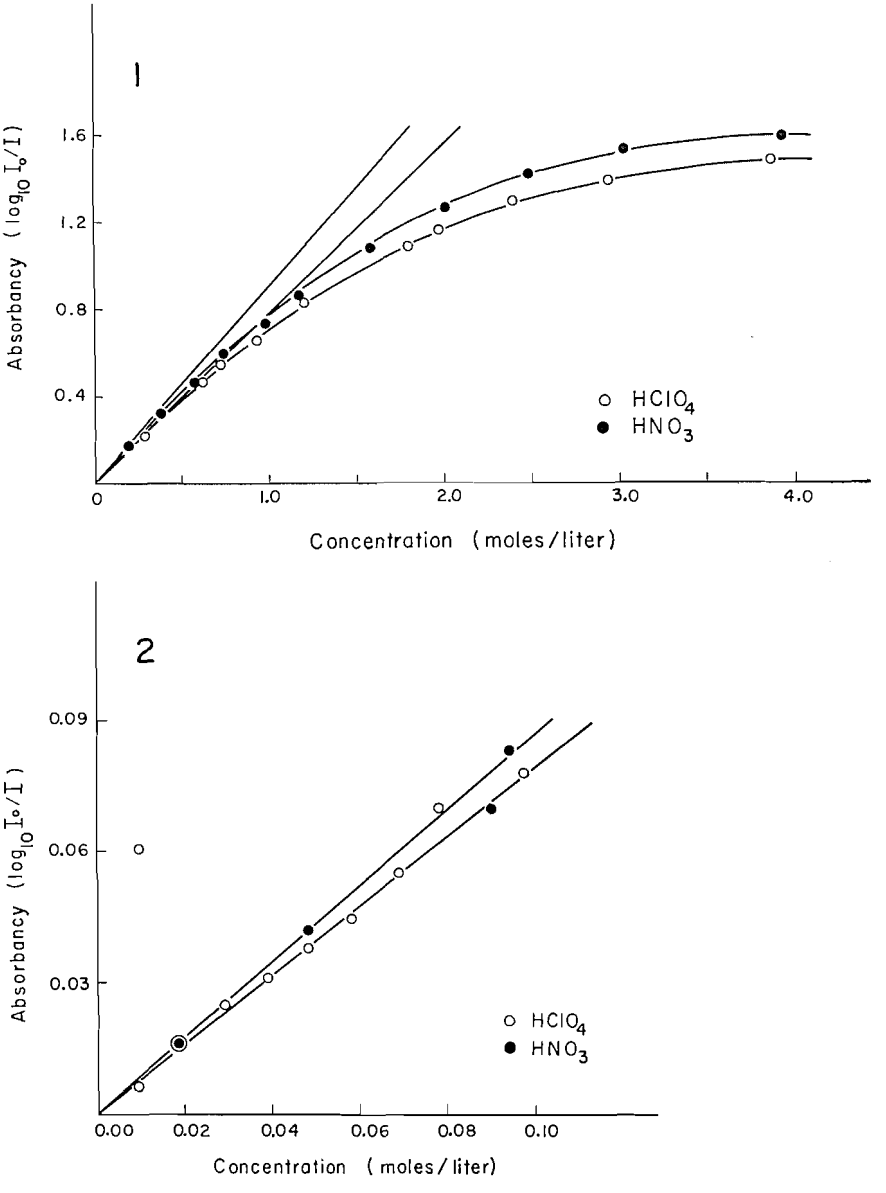

FIG. 1. Absorbancy of aqueous solutions of nitric and perchloric acids in the region 1.7 μ.
FIG. 2. Absorbancy of nitric and perchloric acid solutions at low concentrations.

Can. J. Chem. Downloaded from www.nrcresearchpress.com by 196.1.178.254 on 09/04/12
For personal use only.

It is quite certain that the H_3O^+ ion, which has three hydrogen atoms available for bonding to oxygen atoms and a positive charge, is connected by hydrogen bonding to the surrounding water molecules. Raman studies by Cross, Burnham, and Leighton (4) have shown that at low temperature water has a fourfold co-ordination structure, but above 26° C the twofold co-ordination structure predominates. The structure of course is a dynamic one; over a long range there would appear to be repetition of units, but nevertheless there is a short range order. Hence, the co-ordination or hydration sphere of the H_3O^+ ion would include not free water molecules but a structure at least similar to that of water itself, and would therefore be subject to any change in the solvent, which would be reflected by a change in the co-ordination sphere of the hydronium ion.

If this picture is close to the true model of a dissociated acid in water, one can expect a change in the nature of the $H_3O^+.nH_2O$ hydrate with concentration. At higher concentrations, hydronium ions would compete for available water units in order to form co-ordination spheres. Once these co-ordination spheres are formed, they would be subject to any change in the structure of the solvent.

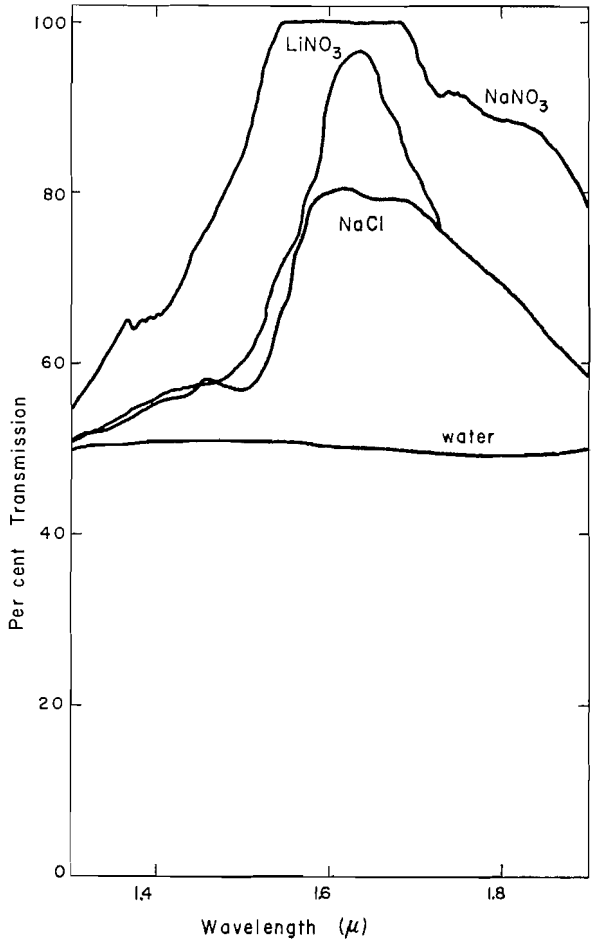

FIG. 3. Optical transmission of some salt solutions relative to the transmission of water in the region 1.7 μ.

Can. J. Chem. Downloaded from www.nrcresearchpress.com by 196.1.178.254 on 09/04/12
For personal use only.

It is well known that the association of water is disturbed by an electrolyte. Bernal and Fowler (3) first suggested that electrolyte ions cause a rearrangement of the structure of liquid water. Leighton and Burnham (8) showed that zinc chloride, when dissolved in water, causes a shift in the short frequency component of a main Raman band. Using the X-ray diffraction curves of lithium chloride, sodium chloride, and potassium chloride in aqueous solution at 15° C, Stewart (11) demonstrated that with increasing ionic concentration, the amount of fourfold co-ordination of water is lessened.

The absorbancy values observed above 1 molar are lower than would be anticipated from available dissociation data. Introduction of ions would undoubtedly cause some measure of distortion of the structure of water, probably through orientation of water dipoles, especially in the case of a small ion. The water in an ionic solution might then absorb less light than pure water at the same wavelength. (One can conveniently call this "negative absorption".) The existence of some such negative absorbance mechanism, superimposed on the position absorbance of the hydronium ion, offers a facile explanation for the low absorbancies found for nitric and perchloric acids.

If such a negative absorption is caused by the introduction of hydronium ions, it should also be caused by introduction of any small positively charged ions which are hydrated, such as sodium or lithium ions. Since they will have no positive absorption in this region, solutions containing sodium or lithium ions should be more transparent than water in the spectral region 1.7 μ. Figure 3 shows shapes of curves which resulted when the absorbancies of lithium nitrate, sodium nitrate, and sodium chloride solutions were compared to water. As predicted, all of the solutions gave negative absorption in the region of the absorbance peak of the acids. These solutions were all approximately 1 molar.

It is planned to examine the applicability of Beer's Law to the other two absorption bands reported for the hydronium ion and to examine the "negative absorption" of a series of solutions containing small cations.

ACKNOWLEDGMENTS

Financial assistance given by the National Research Council is gratefully acknowledged. We are also indebted to the Canadian Government Rust Research Laboratory for the use of their facilities.

REFERENCES

1. BETHELL, D. E. and SHEPPARD, N. J. Chem. Phys. **21**, 1421 (1953).
2. BIDINOSTI, D. R. Private communication.
3. BURNAL, J. D. and FOWLER, R. H. J. Chem. Phys. **1**, 515 (1933).
4. CROSS, R. C., BURNHAM, J., and LEIGHTON, P. A. J. Am. Chem. Soc. **59**, 1134 (1937).
5. GIGUÈRE, P. A. and FALK, M. Can. J. Chem. **35**, 1195 (1957).
6. GUTOWSKY, H. and SAIKA, A. J. Chem. Phys. **21**, 1688 (1953).
7. HOOD, G. C., REDLICH, O., and REILLY, C. A. J. Chem. Phys. **22**, 207 (1954).
8. LEIGHTON, P. A. and BURNHAM, J. J. Am. Chem. Soc. **59**, 424 (1937).
9. REDLICH, O. Chem. Revs. **39**, 333 (1946).
10. REDLICH, O. Monatsh. **86**, 329 (1955).
11. STEWART, G. W. J. Chem. Phys. **7**, 869 (1939).
12. YOUNG, T. F. and BLATZ, L. A. Chem. Revs. 44, 93 (1949).

Can. J. Chem. Downloaded from www.nrcresearchpress.com by 196.1.178.254 on 09/04/12
For personal use only.

Can. J. Chem. Downloaded from www.nrcresearchpress.com by 196.1.178.254 on 09/04/12
For personal use only.

THE ARRANGEMENT OF BRANCHING IN AN ARABINO-XYLAN FROM WHEAT FLOUR[1]

CONSTANCE M. EWALD[2] AND A. S. PERLIN

ABSTRACT

The manner in which L-arabinofuranose branches are arranged along the xylan chain of the pentosans has been examined. The approach used was based on the fact that D-xylose units engaged in branching are resistant to periodate oxidation whereas other sugar residues are readily attacked. Selective degradation of oxidized portions of the polymer with phenylhydrazine or sulphurous acid enabled the isolation of fragments which corresponded to branch points in the original pentosans. D-Xylose and xylobiose were the major products obtained, and xylotriose a minor product. The results indicate that L-arabinose branches of the polysaccharide occur sometimes on isolated D-xylose residues, sometimes on two adjacent D-xylose units, less frequently on three, but not on four, five, etc., consecutive D-xylose residues along the chain.

A water-soluble polysaccharide fraction isolated from wheat flour has been shown to contain a group of closely related pentosans composed of D-xylose and L-arabinose (1, 2). Structure I (A_F = L-arabinofuranosyl; X_P = D-xylopyranosyl) was suggested as an average representation of these pentosans (2), a formulation which has received support in more recent studies (3). Pentosans from a variety of plant sources appear to have a similar type of structure, differing mainly in the relative proportion of the two pentoses or in containing D-glucuronic acid (or a methyl ether of it) as a third component sugar

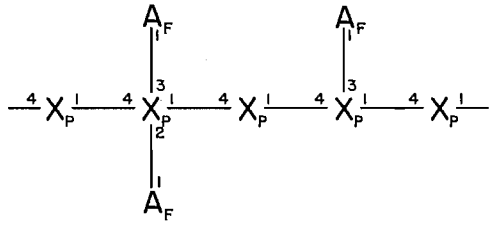

I

(e.g., 4, 5, 6, 7, 8 and references therein). Major structural features are a linear chain of β-D-xylopyranose units joined by (1 → 4)-linkages, and L-arabinofuranose (or uronic acid) end groups, which, in at least some of the polysaccharides (2, 4, 7), are attached directly by (1 → 2)- or (1 → 3)-linkages to the xylan chain. The available data do not define how the branches in these polysaccharides are arranged, and are consistent with a variety of sequences. Thus, branching may be uniform throughout (II white circles = D-xylopyranosyl; dark circles = L-arabinofuranosyl), in some molecules the incidence of side chains very high (III), or a mixture of arrangements (IV), may be found. The current paper deals with attempts to obtain more definitive information about the mode of branching in the wheat flour pentosans.*

[1]*Manuscript received April 20, 1959.*
Contribution from the National Research Council of Canada, Prairie Regional Laboratory, Saskatoon, Saskatchewan. Presented at the 41st Annual Conference, The Chemical Institute of Canada, Toronto, May 26–28, 1958.
Issued as N.R.C. No. 5262 and as Paper No. 261 on the Uses of Plant Products.
[2]*Research assistant, 1953.*
**Detailed information about the arrangement of branching in complex polysaccharides is generally lacking. The chain length of branches in polymers such as glycogen or amylopectin, for example, must be regarded at present as an average value rather than an accurate representation of the size of each branch.*

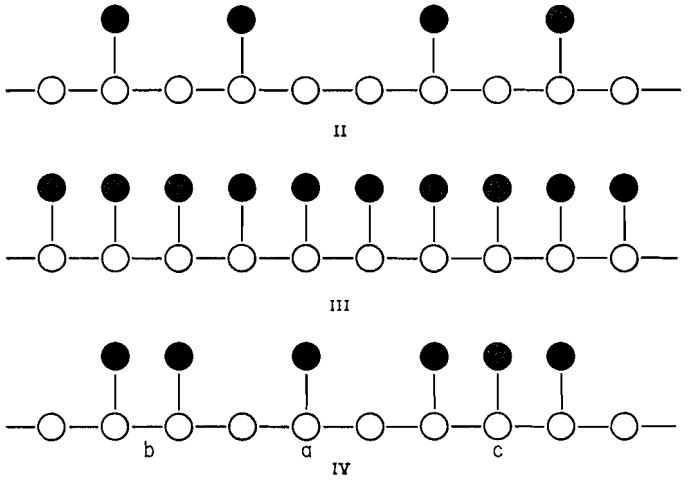

In devising an approach to this problem the following considerations were made. Treatment of the pentosans with periodate promotes oxidation of the L-arabinose units and D-xylose units which do not constitute branch points. Selective removal of oxidized residues and isolation of unoxidized portions of the molecule as intact fragments should then permit a distinction between II, III, IV, etc. According to this scheme, for example, structure II would afford D-xylose, III a polymeric xylan, and structure IV mono-, di-, and tri-saccharides.

A means for degrading dialdehydes* from periodate oxidation through reaction with phenylhydrazine acetate was developed by Barry (9). The method has been used effectively in examining the fine structure of several polysaccharides which are oxidized partially by periodate (9, 10, 11, 12, 13, 14) facilitating the removal of oxidized portions of the polymers. With a dialdehyde such as V the reagent cleaves the oxygen-bridge and forms glyoxal bis(phenylhydrazone) and triose phenylosazone. It was to be expected, therefore, that the Barry reaction would remove oxidized L-arabinofuranose units (the L-isomer of V) from the oxidized pentosans. Similarly, a dialdehyde (VI) adjacent to a second dialdehyde residue (R) yields osazones of glyoxal and glycerose. However, when R is an unoxidized unit the dialdehyde may yield a hydrazone of VII (R = glycosyl) in addition to glyoxal bis(phenylhydrazone), or the glycosidic bond may be cleaved giving triose phenylosazone and a sugar, the latter being converted in turn to an osazone. These reactions were expected to occur with disruption of the partially oxidized xylan chain.

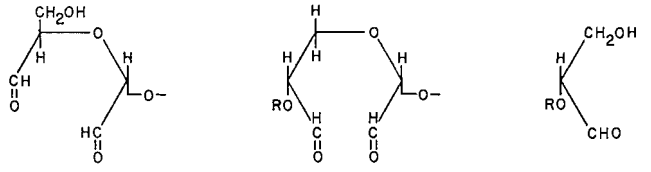

V VI VII

*The dialdehydes may exist in equilibrium with several cyclic modifications (Michell, J. H. and Purves, C. B. J. Am. Chem. Soc. **64**, 589 (1942)). For a recent discussion of these structural types see Goldstein, I. J., Lewis, B. A., and Smith, F. J. Am. Chem. Soc. **80**, 939 (1958).

Can. J. Chem. Downloaded from www.nrcresearchpress.com by 196.1.178.254 on 09/04/12
For personal use only.

Can. J. Chem. Downloaded from www.nrcresearchpress.com by 196.1.178.254 on 09/04/12
For personal use only.

Depending on the arrangement of branches in the polymer, it was evident that the Barry degradation could yield a complex mixture of products. As osazones, the unoxidized fragments might be especially difficult to separate and characterize, particularly since they would represent as a maximum only about 30% of the original polysaccharide (2). Alternatively, by avoiding use of excess phenylhydrazine, it was found that only a portion of the liberated sugars are converted into osazones and hence could be examined by conventional sugar techniques. In this modification of Barry's procedure, low molecular weight osazones were readily separated from other components of the reaction mixture, and the water-soluble fraction was treated with benzaldehyde to decompose hydrazones (15) which might have been formed. The aqueous solution then afforded in low yield approximately equal amounts of D-xylose and 4-*O*-β-D-xylopyranosyl-D-xylose (xylobiose) as the major products. Xylotriose (16), characterized tentatively, was a minor product, but oligosaccharides of higher molecular weight were not found.*

With excess phenylhydrazine acetate, the oxidized polysaccharide was degraded extensively to low molecular weight fragments and no product corresponding to a xylan was isolated. This finding made it unlikely, therefore, that a substantial proportion of the L-arabinose units are to be found in a densely packed arrangement as in III. Chromatographic examination of the reaction mixture indicated the presence of xylosazone, xylobiosazone, and only traces of higher molecular weight products, in addition to a very large proportion of glyoxal and glyceraldehyde osazones. A partial separation of these products was achieved by column chromatography on silicic acid – Celite (17).

Another procedure examined briefly as a possible means for selectively degrading the periodate-oxidized pentosans employed graded hydrolysis with sulphurous acid. Periodate dialdehydes are remarkably resistant to hydrolysis with mineral acids (18, 19), but are smoothly hydrolyzed by sulphurous acid (20). Progressive gentle hydrolysis of the oxidized pentosans with a saturated solution of sulphur dioxide produced xylose, xylobiose, and a trace of xylotriose (followed chromatographically in small-scale experiments). A small proportion of arabinose which had escaped, or was resistant to, oxidation by periodate (2) was also found on the chromatograms. The two oligosaccharides were hydrolyzed in turn by continued treatment, but no other oligosaccharides were detected.

The data obtained by use of these different procedures are consistent, and indicate that L-arabinose residues in the wheat flour pentosans are linked to isolated D-xylose units (IV*a*), or to two consecutive D-xylose units (IV*b*); occasionally, branching appears to involve three consecutive D-xylose units (IV*c*). It is possible, however, that the pentosans contain branches arranged in yet other ways which have not been detected by the methods used.

EXPERIMENTAL

Water-soluble wheat flour pentosans were prepared from commercial unbleached flours by the acetylation procedure described earlier (1) or by the method of Simpson (21).

Paper chromatography was carried out on Whatman No. 1 paper. Circular chromatograms (22) were used for osazones, the solvent being toluene–ethanol–water (270:30:1) (12) and variations of this mixture to speed up or slow development.

Pentosan was determined by the orcinol method (23).

Preparation of Periodate-oxidized Pentosans

The pentosans (10 g) were moistened with ethanol, pasted in water, and the solution was adjusted to a volume of 700 ml with water. Sodium periodate (17 g) in water (300 ml)

In a preliminary report of this work (Ewald, C. M. and Perlin A. S. Chem. in Can. **10 (No. 4), 62 (1958)) only D-xylose and xylobiose were listed as relevant degradation products.*

Can. J. Chem. Downloaded from www.nrcresearchpress.com by 196.1.178.254 on 09/04/12
For personal use only.

was added and the solution stored at 16° in the dark for 100 hours. Excess periodate was reduced with ethylene glycol, the solution was concentrated *in vacuo* at 40–45° to about one-third volume, and acetic acid added with stirring until a copious precipitate formed. The precipitate, which was insoluble in water, was filtered off and washed with water until it gave a negative starch iodide test, then washed with methanol, and dried. Weight 9.5 g. The dialdehyde content of the product, measured potentiometrically by the hydroxylamine method (24) was 0.67 mole per mole, in good agreement with the measured periodate uptake of 0.65–0.70 mole per mole (2). Pentosan content, 33%.

Partial Degradation of Oxidized Pentosans with Phenylhydrazine Acetate

Oxidized pentosans (7 g) in 45% ethanol (650 ml) were heated on the steam bath together with phenylhydrazine (20 ml) and acetic acid (20 ml) for 1.5 hours. The clear solution obtained was concentrated *in vacuo* at 45–50° to a thick slurry which was taken up in water and extracted exhaustively with ether. Paper chromatographic examination indicated that the ether extract contained osazones mainly of glyoxal and glyceraldehyde and of xylose in low proportion, and that the water extract contained mainly xylose, xylobiose in about equal proportion, and a trace of xylotriose together with dark material which streaked heavily on the paper. Two other trace products detected in the water extract (R_{xylose} 0.7 and 0.4) were eluted from paper chromatograms in one run and found by acid hydrolysis to contain xylose and arabinose.

Benzaldehyde (6 ml) and benzoic acid (0.5 g) in ethanol (150 ml) were added to the water extract (200 ml), the solution was heated on a steam bath for 8 hours and then evaporated at 45° almost to dryness. Water was added, the solution was extracted with chloroform (three times), then exhaustively with ether, and concentrated to dryness. Weight 1.73 g. Extraction of the residue with hot ethanol and evaporation of the ethanol afforded a yellow powder (0.83 g) a portion of which (0.65 g) was transferred to a column (2×20 cm) of coconut charcoal (25). Water (200 ml) eluted a dark brown solution which contained some xylose and xylobiose. Gradient elution (26) of the column with aqueous ethanol up to a concentration of 35% afforded a series of fractions.

The first fraction (0.10 g), $[\alpha]_D^{23}$ +13° (*c*, 2, water), contained mainly D-xylose, which crystallized from methanol–ethanol m.p. 141–143°, undepressed; the X-ray diffraction pattern was indistinguishable from that of D-xylose. The derived (2,5-dichlorophenyl)-hydrazone had m.p. 133–136°, undepressed by admixture with D-xylose(2,5-dichlorophenyl)hydrazone (27).

A second fraction (0.08 g), $[\alpha]_D^{23}$ −21° (*c*, 2.7, water), yielded, on acetylation with hot acetic anhydride – sodium acetate, a product having m.p. 154–156°; a mixed melt and comparison of X-ray diffraction diagrams showed that the product was 4-*O*-β-D-xylopyranosyl-β-D-xylose hexaacetate (16). Calc. for $C_{22}H_{30}O_{15}$: C, 49.44%; H, 5.66%. Found: C, 49.62%; H, 5.91%.

At higher alcohol concentrations, a third product was obtained (0.02 g), $[\alpha]_D^{23}$ −44° (*c*, 2, water). On a paper chromatogram it corresponded to xylotriose but appeared to be admixed with a small proportion of another oligosaccharide(s), for, in addition to xylose, it yielded arabinose as a minor hydrolytic product. Its infrared absorption spectrum was closely similar to that of xylotriose; that of the syrupy derived acetate was indistinguishable from the infrared spectrum of hexa-*O*-acetyl-β-xylotriose. Oligosaccharides of higher molecular weight were not obtained, even by washing the column with 60% ethanol.

The water-soluble material not extracted into hot ethanol was a yellow powder (0.65 g) which contained 57% of pentosan, and hence appeared to be an incompletely degraded

polymeric residue. This material was examined further by partial hydrolysis with sulphurous acid (below).

Treatment of Oxidized Pentosans with Excess Phenylhydrazine Acetate

The procedure of Barry and Mitchell (12) was used. Oxidized pentosans (2.7 g) were taken up in 65% ethanol (115 ml), phenylhydrazine (10 ml) and acetic acid (12 ml) were added, and the mixture heated under reflux for 3.5 hours. Material which deposited on cooling (wt. 1.6 g) was readily soluble in ethanol and, after recrystallization from aqueous ethanol had m.p. 165–167°, undepressed by admixture with glyoxal bis(phenylhydrazone). Calc. for $C_{14}H_{14}N_4$: C, 70.56%; H, 5.92%. Found: C, 70.87%; H, 6.03%.

The filtrate was concentrated giving a syrup, part of which was soluble in hot water. The aqueous solution was extracted exhaustively with ether, phenylhydrazine (3 ml) and acetic acid (3.5 ml) were added, it was then heated on the steam bath for 2.5 hours, and again extracted exhaustively with ether. Evaporation of the water afforded a dark syrup (0.91 g), part of which (0.40 g) was insoluble in 80% ethanol. The insoluble portion contained 43% of pentosan and the soluble material 24% of pentosan, and appeared to be incompletely degraded products.

Paper chromatographic examination of the fraction insoluble in hot water (1.5 g) indicated that it contained osazones of glyoxal and glycerose mainly, xylose, xylobiose, and slower moving components in trace amounts. Attempts to resolve this mixture by countercurrent distribution or chromatography on alumina were unsuccessful. (Two batches of alumina tested were much more retentive than the adsorbent used by Barry and Mitchell (12).) On a column of silicic acid – Celite (2:1) (17),* the compounds corresponding on a chromatogram to glyoxal and triose phenylosazones were eluted with ether, and the addition of ether containing 5% of ethanol then eluted material corresponding on a chromatogram mainly to xylosazone. Removal of the solvent afforded a solid product (0.07 g) which, after two recrystallizations from benzene, had m.p. 164–166° (decomp.), and gave an X-ray diagram indistinguishable from that of D-xylose phenylosazone. Elution with ether containing 15% of ethanol yielded a second fraction (0.09 g) which did not crystallize, but which appeared from its chromatographic mobility and infrared absorption spectrum to be mainly xylobiose phenylosazone. Higher concentrations of alcohol promoted elution of only trace quantities of other materials.

The ether extracts appeared (paper chromatograms) to contain osazones of glyoxal, triose, and xylose, and on concentration, afforded a large proportion of *N*-acetylphenylhydrazine (combined wt. 4.2 g), colorless plates, m.p. 125–127°.

Graded Hydrolysis of Periodate-oxidized Pentosans with Sulphurous Acid

An amount (0.05 g) of oxidized pentosans was suspended in water (2.5 ml) in a pressure flask (200 ml capacity), sulphur dioxide gas introduced to saturation (20), and the flask sealed. Several samples prepared in this way were heated on the steam bath for varying periods; within a few minutes the polysaccharide swelled and then dissolved. After the chosen heating interval the flasks were unsealed, most of the excess sulphur dioxide was removed with a stream of nitrogen, and the solutions were neutralized with Dowex-1 (bicarbonate form). Paper chromatographic examination indicated that most of the arabinose was liberated within 0.5 hour together with small proportions of xylose and xylobiose; at 1.5 hours xylose and xylobiose were the major products, and a trace of xylotriose was present; on further hydrolysis the spots corresponding to xylobiose and xylotriose diminished in intensity.

**The use of this adsorbent was kindly suggested by Dr. Thomas Francis.*

Can. J. Chem. Downloaded from www.nrcresearchpress.com by 196.1.178.254 on 09/04/12
For personal use only.

The partially degraded water-soluble polymer remaining from the reaction with phenylhydrazine (above), treated with sulphurous acid under the same conditions, also yielded (chromatographic evidence) xylose and xylobiose as the major products together with minor proportions of xylotriose and arabinose; oligosaccharides of higher molecular weight were not detected on the chromatograms.

ACKNOWLEDGMENTS

The technical assistance of J. Giroux and J. W. L. C. Christ is gratefully acknowledged. Microanalyses were carried out by J. A. Baignee and M. Mazurek; X-ray diagrams and infrared spectra were prepared by T. M. Mallard and Inez Gaffney. The authors express their thanks to Dr. F. J. Simpson for a sample of wheat flour pentosans, to Almonte Flour Mills, Almonte, Ont., for a sample of wheat flour, and to Dr. C. T. Bishop for a specimen of xylotriose.

REFERENCES

1. PERLIN, A. S. Cereal Chem. **28**, 370 (1951).
2. PERLIN, A. S. Cereal Chem. **28**, 382 (1951).
3. MONTGOMERY, R. and SMITH, F. J. Am. Chem. Soc. **77**, 3325 (1955).
4. ADAMS, G. A. Can. J. Chem. **30**, 698 (1952).
5. HIRST, E. L. J. Chem. Soc. 2974 (1955).
6. JONES, J. K. N., MERLER, E., and WISE, L. E. Can. J. Chem. **35**, 634 (1957).
7. ASPINALL, G. O. and FERRIER, R. J. J. Chem. Soc. 638 (1958).
8. ASPINALL, G. O. and MCKAY, J. E. J. Chem. Soc. 1059 (1958).
9. BARRY, V. C. Nature, **152**, 537 (1943).
10. DILLON, T., O'CEALLACHAIN, D. F., and O'COLLA, P. Proc. Roy. Irish Acad. B, **55**, 165, 331 (1953).
11. BARKER, S. A., BOURNE, E. J., and STACEY, M. J. Chem. Soc. 3084 (1953).
12. BARRY, V. C. and MITCHELL, P. W. D. J. Chem. Soc. 4020 (1954).
13. FINAN, P. A. and O'COLLA, P. Chem. & Ind. (London), 493 (1958).
14. HIRST, E. L., O'DONNELL, J. J., and PERCIVAL, E. Chem. & Ind. (London), 834 (1958).
15. HERZFELD, A. Ber. **28**, 440 (1895).
16. WHISTLER, R. L. and TU, C. C. J. Am. Chem. Soc. **73**, 1389 (1951).
17. ROBERTS, J. D. and GREEN, C. Ind. Eng. Chem. Anal. Ed. **18**, 335 (1946).
18. JACKSON, E. L. and HUDSON, C. S. J. Am. Chem. Soc. **60**, 989 (1938).
19. MICHELL, J. H. and PURVES, C. B. J. Am. Chem. Soc. **64**, 589 (1942).
20. MOYER, J. D. and ISBELL, H. S. Anal. Chem. **29**, 1862 (1957).
21. SIMPSON, F. J. Can. J. Microbiol. **1**, 131 (1954).
22. RUTTER, L. Nature, **161**, 435 (1948).
23. MEIJBAUM, W. Z. physiol. Chem. Hoppe-Seyler's, **258**, 117 (1939).
24. GLADDING, E. K. and PURVES, C. B. Paper Trade J. **116** (No. 14), 26 (1943).
25. BARTH, F. W. and TIMELL, T. E. Can. J. Chem. **36**, 1321 (1958).
26. ALM, R. S., WILLIAMS, R. J. P., and TISELIUS, A. Acta Chem. Scand. **6**, 826 (1952).
27. MANDL, I. and NEUBERG, C. Arch. Biochem. Biophys. **35**, 326 (1952).

Can. J. Chem. Downloaded from www.nrcresearchpress.com by 196.1.178.254 on 09/04/12
For personal use only.

Can. J. Chem. Downloaded from www.nrcresearchpress.com by 196.1.178.254 on 09/04/12
For personal use only.

REACTION OF TRICHLOROACETONITRILE WITH PRIMARY AND SECONDARY AMINES

PART III. STRUCTURE OF AMIDINIUM CATION IN THE LIGHT OF INFRARED STUDY[1, 2]

JOHN C. GRIVAS[3] AND ALFRED TAURINS

ABSTRACT

The infrared spectra of 14 trichloro- and trifluoro-acetamidine hydrochlorides were studied. It was concluded that protonation occurs at the imino nitrogen atom of the N-substituted amidines. Both nitrogens of the amidine grouping, C(=N)N, become electron-deficient due to resonance leading to the single structure (III), regardless of which of the tautomers is present in the equilibrium mixture, and of the number and type of substituents on the amidine nitrogen atoms. These findings predestine to *failure* any attempts to isolate the two amidine tautomers, whenever amidinium salts are involved as intermediates.

INTRODUCTION

The assignment of the $-NH_3^+$, $\rangle NH_2^+$, and $\rangle NH^+$ frequencies presents a difficult problem, which has not yet been solved successfully. The infrared spectra of amine hydrohalides show many bands in the stretching region, which cannot be fully assigned. This complexity is undoubtedly due to the strong hydrogen bonding occurring in the solid phase, whereas the free vibrations are not well known since considerable difficulty is encountered in dissolving these salts in non-polar solvents.

The topic has been reviewed by Bellamy (1), by Witkop (2), and by Heacock and Marion (3). The last investigators identified the NH_2^+ deformation mode between 1620 and 1560 cm^{-1} in a series of secondary amine hydrochlorides.

Stone, Craig, and Thompson (4) were able to arrive at more definite conclusions, comparing the spectra of amine salts with those of their deuterated compounds. Thus, the $\rangle NH_2^+$ asymmetrical stretching frequency was found close to 2920 cm^{-1} and the corresponding symmetrical mode at 2780 to 2825 cm^{-1} for some secondary amine hydrochlorides. They also located the deformation frequency, $\delta(NH_2^+)$, between 1560 and 1600 cm^{-1}, in agreement with the findings of Heacock and Marion. The same authors assigned the stretching vibrations, $\nu(\rangle NH^+)$, to the band between 2330 and 2680 cm^{-1}, shown by tertiary amine hydrochlorides.

More recently Chenon and Sandorfy (5) discussed the complexity of the stretching NH^+ modes and reported the $\delta(NH_3^+)$ frequencies at 1510–1600 cm^{-1}. The strong band which appears in many cases near 2000 cm^{-1} was attributed to a combination mode between the scissoring vibration and a very anharmonic band near 400 cm^{-1}.

To our knowledge, the infrared absorption of the NH^+ vibrations of the amidinium cation has not yet been studied. However, Prevoršek (6) suggested the following structure for some N,N′-disubstituted amidine hydrochlorides, on the basis of their infrared spectra.

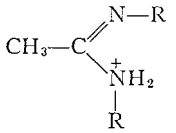

[1]*Manuscript received April 9, 1959.*
Contribution from the Department of Chemistry, McGill University, Montreal, Quebec, with financial assistance from the National Research Council, Ottawa, Canada.
[2]*Part II: Grivas, J. C. and Taurins, A. Can. J. Chem.* **37**, *795 (1959).*
[3]*Holder of the National Research Council Studentships, 1957–58 and 1958–59.*

Can. J. Chem. Downloaded from www.nrcresearchpress.com by 196.1.178.254 on 09/04/12
For personal use only.

EXPERIMENTAL

The infrared spectra were recorded on a Perkin–Elmer model 21 double-beam spectrophotometer equipped with a sodium chloride prism. Fluorolube T-45 mulls were used, since Nujol absorbs strongly at 2800–3000 cm^{-1}. A similar cell unit provided excellent compensation between 4000 and 1350 cm^{-1}. The results are summarized in Tables I, II, and III.

Preparation of Hydrochloride Salts

About 100 mg of freshly purified and dry amidine was dissolved in 20 ml of absolute ether and cooled to 0° C in an ice–salt bath. A stream of dry hydrogen chloride gas was passed through this solution, with continuous stirring by means of a magnetic stirrer, until no precipitation was observed. The white crystalline hydrochlorides were filtered off and dried under vacuum. Although they could not be recrystallized, since they decomposed easily, they were pure and suitable for infrared investigation.

Preparation of Deuterium Chloride Salts of N-*Methyltrifluoroacetamidine-d_2 and* N-*Methyltrichloroacetamidine-d_2*

The same procedure as above was followed and gaseous deuterium chloride was used. All the operations were conducted in a dry nitrogen atmosphere.

Deuterated amidines and the free bases were prepared by known methods (7), or by procedures which will be presented in another paper. All unknown parent compounds were analyzed.

RESULTS AND DISCUSSION

Amidines are monobasic compounds, since they form monosalts with a variety of acids. A literature search revealed that very little is known with respect to the structure of the amidinium cation, which must have an important bearing on the understanding of the chemical behavior of the amidine grouping. Some authors do not draw any distinction between the two nitrogen atoms of amidines.

Theoretical considerations, however, combined with the results of this investigation by the infrared spectroscopy method, may definitely elucidate the course of protonation. Irrespective of the type and number of substituents on the nitrogen atoms, the amidine system is represented by formula (I):

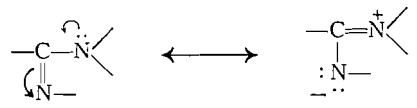

(I*a*) (I*b*)

Such a structure as shown allows for only one charged resonance form having a negative charge on the imino nitrogen and a positive charge on the other. Consequently, the imino group would be expected to accept the proton during the salt formation. Such protonation should yield a resonance hybrid receiving contributions from the two structures shown in formula (II). As a result,

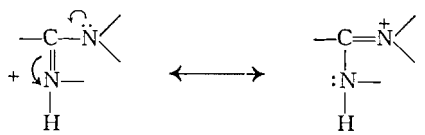

(II)

both nitrogen atoms would become electron-deficient to a degree (III), which should depend on the substituents to some extent. The decreased electron density on nitrogen atoms should prevent any further protonation.

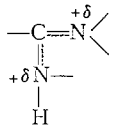

(III)

The protonation of both the plausible tautomeric forms of amidines must give one and the same compound (IV) stabilized by resonance, as outlined in the following scheme:

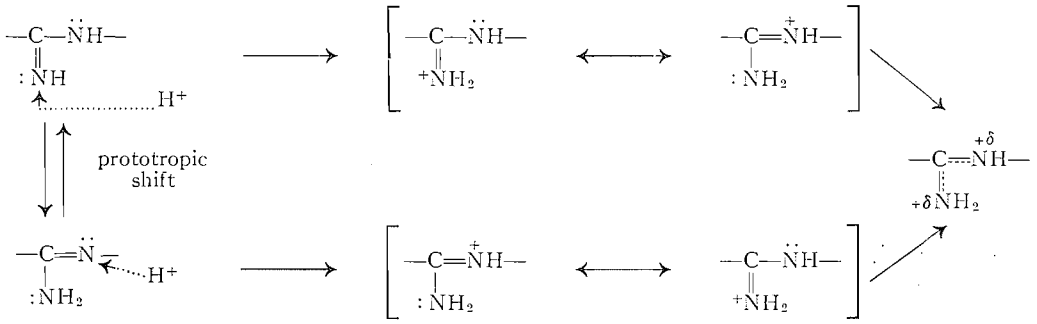

(IV)

This course must be valid in any case, independently of the kind of substitution, and predestines to failure any attempts to isolate the two tautomers, whenever intermediate salt formation occurs. It should be mentioned here that many such unsuccessful attempts have been made, even recently, and in all cases methods leading to salt intermediates were used.

An alternative course of protonation can be written as follows:

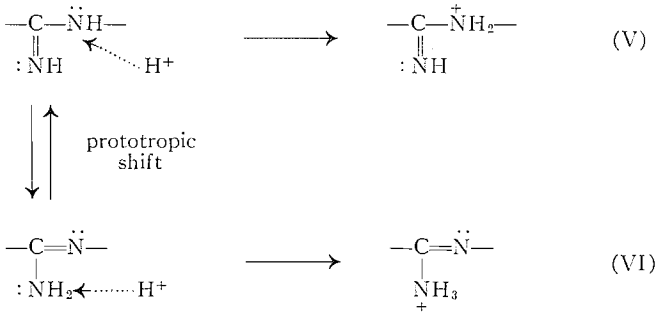

(V) (VI)

It is obvious that formulae (V) and (VI) represent two relatively unstable isomers, since resonance stabilization is prevented.

The infrared spectra of the amidine hydrochlorides examined showed characteristically only the stretching vibrations of the $\overset{+}{N}H$ group and the complete absence of any absorption bands of free or bonded NH group (Tables I and II).

Can. J. Chem. Downloaded from www.nrcresearchpress.com by 196.1.178.254 on 09/04/12
For personal use only.

TABLE I

Positions of absorption maxima (cm^{-1}) in the infrared spectra of N-substituted trichloroacetamidine hydrochlorides

No.	Trichloro-acetamidine hydrochloride	M.p. (decomp.)	$\nu(\rangle\overset{+}{N}H)$		and $\nu(=\overset{+}{N}H_2)$†		$\nu(C=\overset{+}{N})$	$\delta(=\overset{+}{N}H_2)$	$\delta(\overset{+}{N}H)$
1	N-Methyl-	229°	3100sh,	*2930vs*,*	2800sh,	2300w	1680vs	1620m	1500m
2	N-Ethyl-	224–225°	3060sh,	*2950vs*,*	2800sh,	2340w	1687vs	1640m	1520s
3	N,N-Dimethyl-	175–176°	2970sh,	2910sh,	*2860vs*,*	2340w	1617vs	1530s	None
4	N,N-Diethyl-	202°	3040sh,	2990sh,	*2860vs*,*	2340sh	1607vs	1540s	None
5	N-Phenyl-	182–183°	2820sh,	*2710vs*,*	2600sh,	2360m	1630vs	?	1550s
6	N-*o*-Tolyl-	214–216°	2800sh,	*2680vs*,*	2600sh,	2360m	1625vs	1555m	1575m
7	N-*m*-Tolyl-	193–195°	*2830vs*,*	*2740vs*,*	2600sh,	2360w	1635s	1550m	1585m

*Very broad strong bands.

†Bands have no sharp peaks; positions of absorption maxima represent only approximate values.

TABLE II

Positions of absorption maxima (cm^{-1}) in the infrared spectra of N-substituted trifluoroacetamidine hydrochlorides

No.	Trifluoro-acetamidine hydrochlorides	M.p. (decomp.)	$\nu(\rangle\overset{+}{N}H)$		and $\nu(=\overset{+}{N}H_2)$†		$\nu(C=\overset{+}{N})$	$\delta(=\overset{+}{N}H_2)$	$\delta(\rangle\overset{+}{N}H)$
1	N-Methyl-	219–221°	3150m,	2970vs,	*2910vs*,*	2780m	1717vs	1655vw	1560vw
2	N-Ethyl-	189–191°	3130m,	*2900vs*,*	2760sh,	2360w	1707vs	1650m	1560m
3	N,N-Dimethyl-	169–171°	3000sh,	*2850vs*,*	2780sh,	2330w	1655vs	1585s	—
4	N,N-Diethyl-	133–135°	2960sh,	*2780vs*,*	2360w		1645vs	1580s	—
5	N-Phenyl-	179–180°	*2840vs*,*	2770sh,	2630sh,	2360m	1685vs	1537s	1525s

*Very broad strong bands.

†Bands have no sharp peaks; positions of absorption maxima represent only approximate values.

A broad and very strong band was shown instead, between 2600 and 3000 cm^{-1}, which possessed two to three well-defined inflections. This absorption includes, of course, the CH stretching vibrations; their separation being impossible with the low dispersion prism used. In addition a broad weak absorption band appeared near 2350 cm^{-1} in all cases.

The striking feature of all the spectra was the complete absence of the strong bands near 2000 cm^{-1} (5) and between 2600 and 2000 cm^{-1}. Furthermore the strongest absorptions occurred at higher frequencies in the corresponding amine hydrochlorides, as was firmly established from a comparison of two amidine hydrochlorides with their deuterated analogues (Table III). Since the greater the positive charge on a nitrogen atom the greater is the displacement of its NH^+ stretching vibrations towards the lower frequencies (1), this observation may definitely demonstrate that only partial positive charges are present in the amidinium cation, which does not agree with structures (V) and (VI).

The stretching $\nu(C=\overset{+}{N})$ vibrations were easily detected since they showed the strongest band between 1600 and 1700 cm^{-1}. Moreover, deuterium chloride salts of two deuterated N-alkylamidines established this assignment, since they displaced all $\delta(\overset{+}{N}H)$ absorptions. This frequency seems to be quite sensitive to small changes, because substitution of the two amino and imino hydrogens by deuterium in N-methyltrifluoro- and N-methyltrichloro-acetamidine salts reduced the absorption frequency by about 20 cm^{-1}, and formula (III) indicates that some distortion of the almost planar configuration of the molecule is likely to occur.

Can. J. Chem. Downloaded from www.nrcresearchpress.com by 196.1.178.254 on 09/04/12
For personal use only.

TABLE III*a*

Absorption maxima (cm^{-1}) in the infrared spectra of N-methyltrichloro- and N-methyltrifluoro-acetamidines and their salts

No.	Compound	ν(NH)	ν(=NH)	ν(ND)	ν(=ND)	$\nu(NH^+)$	$\nu(ND^+)$
1	$F_3C-C(=NH)-NHCH_3$	3515	3380				
2	$F_3C-C(=ND)-NDCH_3$			2585	2470		
3	$F_3C-C(=NH\leftrightarrow HN^+)-CH_3$					2910	
4	$F_3C-C(=ND\leftrightarrow DN^+)-NDCH_3$						2200vs*
5	$Cl_3C-C(=NH)-NHCH_3$	3480	3355				
6	$Cl_3C-C(=ND)-NDCH_3$			2570	2465		
7	$Cl_3C-C(=NH\leftrightarrow HN^+)-NHCH_3$					2930	
8	$Cl_3C-C(=ND\leftrightarrow DN^+)-NDCH_3$						2260vs

*Also 2420 (s), 2190 (s), and 2110 (s) peaks.

TABLE III*b*

Comparison of ν(NH)/ν(ND) ratios of absorption maxima (cm^{-1}) in the infrared spectra of N-methyltrichloro- and N-methyltrifluoro-acetamidines and their salts

Compound No.	$\frac{\nu(NH)}{\nu(ND)}$	$\frac{\nu(=NH)}{\nu(=ND)}$	$\frac{\nu(NH^+)}{\nu(ND^+)}$
1/2	1.36	1.37	
3/4			1.32
5/6	1.31	1.31	
7/8			1.30

There was no difficulty in the identification of the $\delta(=NH_2^+)$ modes with the N-dialkyl compounds, since only one band was present and suitable for this assignment between 1530 and 1590 cm^{-1}.

Two peaks of medium to strong intensity appeared in the spectra of the N-substituted compounds. Although no decisive conclusions could be drawn, the one existing very close to the amidine II band in the corresponding free bases was attributed to the $\delta(>NH^+)$ of the secondary amino group, and the other to the $\delta(=NH_2^+)$ frequency.

The present study suggests quite clearly that protonation is always initiated at the imino group, and the distribution of the positive charge over the two nitrogens takes place in agreement with this theory.

Can. J. Chem. Downloaded from www.nrcresearchpress.com by 196.1.178.254 on 09/04/12
For personal use only.

REFERENCES

1. BELLAMY, L. J. The infrared spectra of complex molecules. 2nd ed. Methuen and Co. Ltd., London. 1958.
2. WITKOP, B. Experientia, **10**, 420 (1954).
3. HEACOCK, R. A. and MARION, L. Can. J. Chem. **34**, 1782 (1956).
4. STONE, P. J., CRAIG, J. C., and THOMPSON, H. W. J. Chem. Soc. 52 (1958).
5. CHENON, B. and SANDORFY, C. Can. J. Chem. **36**, 1181 (1958).
6. PREVORŠEK, D. Compt. rend. **244**, 2599 (1957); Bull. soc. chim, France, 788 (1958).
7. GRIVAS, J. C. and TAURINS, A. Can. J. Chem. **36**, 771 (1958).

Can. J. Chem. Downloaded from www.nrcresearchpress.com by 196.1.178.254 on 09/04/12
For personal use only.

Can. J. Chem. Downloaded from www.nrcresearchpress.com by 196.1.178.254 on 09/04/12
For personal use only.

THE REACTION OF NITROACETONITRILE WITH AROMATIC AMINES[1]

JOHN C. GRIVAS[2] AND ALFRED TAURINS

ABSTRACT

It has been shown by infrared spectroscopic study that the alleged N-aryl-nitroacetamidines are in fact the salts of nitroacetonitrile with aromatic amines.

RESULTS AND DISCUSSION

Studies have been made of the reactions of nitroacetonitrile with various amines in an attempt to examine the influence of electronegative groups attached to the α-carbon atom of acetonitrile on the formation of the amidines. The reaction forming alleged N-phenyl-, N-*o*-tolyl-, and N-(2,4-dimethylphenyl)-nitroacetamidine has been reported (1) to occur almost instantaneously in ether at about 0° C.

Early observations were made, showing that ammonia gas decomposed the alleged N-phenylnitroacetamidine in ether solution, to give a precipitate of ammonium salt of nitroacetonitrile while aniline remained in solution. Passing hydrogen chloride gas through a similar solution caused the amidine to decompose into aniline hydrochloride and nitroacetonitrile.

The hydrolysis of these alleged amidines to their starting materials was attributed recently (2) to the formation of a resonance-stabilized carbonium ion, although no other amidines are known to hydrolyze in this way.

It seemed doubtful to us that the amidines of nitroacetonitrile and aromatic amines could be formed so readily, since the reaction between the more electropositive carbon atom of the carbon–nitrogen triple bond of trichloroacetonitrile, with primary aromatic amines, takes place only very slowly at room temperature, even in polar solvents (3). Furthermore, the reported behavior of the reaction products towards ammonia and hydrogen chloride, and their solubilities, could be explained better if they were salts rather than amidines. Since nitroacetonitrile is about as acidic as acetic acid, the reaction of the salts with ammonia and hydrogen chloride could then be represented by the following scheme:

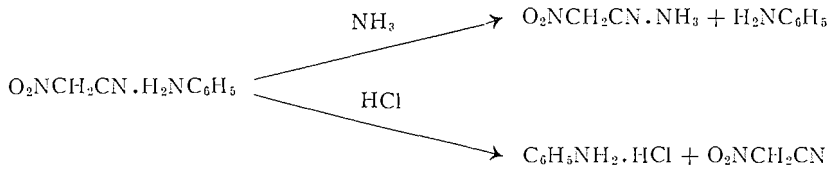

In view of these contradictory facts, we have prepared the three addition compounds in question, and investigated their infrared spectra, together with that of ammonium salt of nitroacetonitrile, $NH_4^+[O_2NCHCN]^-$. The results are summarized in Table I.

The presence of very sharp strong absorption bands in the infrared spectra of the four compounds, due to the (C≡N) vibrations being very close to 2200 cm^{-1}, suggested immediately that no addition occurred across the carbon–nitrogen triple bond. The four

[1]*Manuscript received April 9, 1959.*
Contribution from the Department of Chemistry, McGill University, Montreal, Que., with financial assistance from the National Research Council, Ottawa, Canada.
[2]*Holder of the National Research Council Studentship 1957–58 and 1958–59.*

TABLE I

Positions of absorption maxima (cm^{-1}) in the infrared spectra of nitroacetonitrile salts $[O_2NCHC{\equiv}N]^-\ H_3\overset{+}{N}R$

Assignment	R = H	R = C_6H_5—	R = CH_3—OC_6H_4—	R = 2,4$(CH_3)_2C_6H_3$
$\nu(NH_3^+)$		3060m†	3100sh	3100m
		2540m	3010m‡	3000s‡
			2710m	2730s
			2560s	2580vs
			2360sh	2100m
$\nu(NH_4^+)$	3060vs*			
	2780s			
$\nu(C{\equiv}N)$	2210s	2200s	2200s	2205s
$\delta(NH_3^+)$		1578m	1535m	1623m
		1525m		
$\nu_{asym}(NO_2)$	1500vs	1480vs	1500vs	1505vs
$\delta(NH_4^+)$	1430vs			
$\nu_{sym}(NO_2)$	1345vs	1320vs	1330vs	1328vs
ν(C—N)	1185vs	1260s	1235vs	1222vs
			1222vs	1207vs
ν(C—C)	977vs	945s	955s	948vs

*Broad band at 3200–2900 cm^{-1} including Nujol absorptions.
†Broad band at 2600–3100 with inflections at 3130 and 2740 cm^{-1} including Nujol and CH absorptions.
‡Broad bands.

salts absorbed at a frequency even lower than the conjugated aliphatic nitriles (2235–2215 cm^{-1}), as one might expect for a strongly resonating carbanion structure.

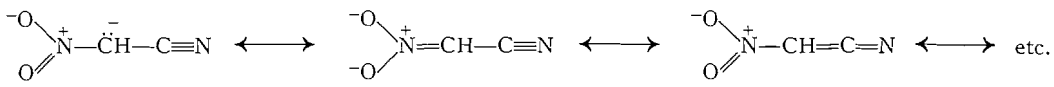

On the other hand, the two NH stretching vibrations, characteristic of the N-substituted amidines, which occur between 3300 and 3500 cm^{-1} (4) were completely absent. New wide strong bands appeared in the region 2500–3100 cm^{-1}, corresponding to the (NH_3^+) modes and indicating that the aromatic amines were present in the form of salts.

Finally, resonance within the carbanion ion caused a remarkable frequency shift in the asymmetric stretching vibration of the $-NO_2$ group to the lower part of the absorption range (1500 cm^{-1}), whereas the similar symmetric mode showed absorption at 1320–1345 cm^{-1}.

EXPERIMENTAL

The infrared spectra of the nitroacetonitrile salts were recorded on a Perkin–Elmer Model 21 double beam spectrophotometer. Nujol mulls of the solid compounds were prepared and spread between NaCl plates. A similar cell containing Nujol was used for compensation.

The substances were prepared according to described procedures (1, 2). They were purified in small quantities by careful sublimation at low pressure and, since they were slightly explosive, at a temperature not exceeding 50°.

REFERENCES

1. STEINKOPF, W. J. prakt. Chem. **81** [2], 97, 103 (1910).
2. RIED, W. and KÖHLER, E. Ann. **598**, 145 (1956).
3. GRIVAS, J. C. and TAURINS, A. Can. J. Chem. **36**, 771 (1958).
4. GRIVAS, J. C. and TAURINS, A. Can. J. Chem. **37**, 1260 (1959).

Can. J. Chem. Downloaded from www.nrcresearchpress.com by 196.1.178.254 on 09/04/12
For personal use only.

Can. J. Chem. Downloaded from www.nrcresearchpress.com by 196.1.178.254 on 09/04/12
For personal use only.

KINETIC EQUATIONS FOR ENZYME REACTIONS IN THE PRESENCE OF POWERFUL INHIBITORS[1]

RICHARD M. KRUPKA AND KEITH J. LAIDLER

ABSTRACT

Steady-state equations are worked out for the case of a competitive inhibitor that is present in concentrations comparable with that of the enzyme; allowance is made for the inhibitor attached to the enzyme. Two cases are considered: in case 1 the enzyme and inhibitor form a simple addition complex, while in case 2 a molecule is split off. Methods of graphical analysis of rate data are described.

INTRODUCTION

In the development of steady-state equations for enzyme systems (1) the assumption is generally made that the enzyme concentration is much less than the concentrations of substrates, inhibitors, and activators; allowance is therefore not made for the fact that the amounts of these substances that are present in the free state are, owing to complexing with the enzyme, less than the total amounts. This assumption is justified for most systems. However, when very powerful inhibitors such as diisopropyl phosphorofluoridate (DFP) are present their molar concentrations are frequently comparable with those of the enzyme. There is, therefore, need for steady-state equations appropriate to this situation.

Such equations are developed in the present paper, and they are applied to some data obtained in the following paper. Two cases are considered: in the first, the enzyme forms a simple addition compound with the inhibitor, while in the second the complexing is accompanied by the splitting-off of a molecule. In both cases the inhibition is regarded as competitive, since this appears always to be the situation for inhibitors of this type.

STEADY-STATE EQUATIONS

Case 1: The Enzyme and Inhibitor Form a Simple Addition Complex

This case is represented by the equations

$$E+S \underset{k_{-1}}{\overset{k_1}{\rightleftarrows}} ES \overset{k_2}{\rightarrow} E+\mathrm{P}$$

$$E+I \overset{K_1}{\rightleftarrows} EI.$$

K_1 is the equilibrium constant for the formation of the enzyme–inhibitor complex, and is defined by

$$[1] \qquad K_1 = [\mathrm{EI}]/([\mathrm{E}][\mathrm{I}]).$$

A constant $\bar{K}$, equal to the reciprocal of the conventional Michaelis–Menten constant, is defined by

$$[2] \qquad \bar{K} = [\mathrm{ES}]/([\mathrm{E}][\mathrm{S}]) = k_1/(k_{-1}+k_2).$$

[1]*Manuscript received February 27, 1959.*
Contribution from the Department of Chemistry, the University of Ottawa, Ottawa, Canada.

Can. J. Chem. Downloaded from www.nrcresearchpress.com by 196.1.178.254 on 09/04/12
For personal use only.

The total concentrations of enzyme and inhibitor are given by

[3] $$[E]_0 = [E]+[ES]+[EI]$$

[4] $$[I]_0 = [I]+[EI].$$

The rate in the absence of inhibitor is given by

[5] $$v_0 = (k_2\bar{K}[E]_0[S])/(1+\bar{K}[S])$$

while the general rate is given by

[6] $$v = k_2[ES] = k_2\bar{K}[E][S].$$

From [5] and [6] it follows that

[7] $$[E] = \frac{v}{v_0}\frac{[E]_0}{1+\bar{K}[S]}$$

and

[8] $$[ES] = \frac{v}{v_0}\frac{[E]_0\bar{K}[S]}{1+\bar{K}[S]}.$$

From [3] and [4] it follows that

[9] $$[EI] = (K_I[E][I]_0)/(1+K_I[E])$$

and using [7],

[10] $$[EI] = \frac{vK_I[E]_0[I]_0}{v_0(1+\bar{K}[S])+vK_I[E]_0}.$$

Introduction of the expressions [7], [8], and [10] into eq. [3] gives rise to

[11] $$[E]_0 = \frac{v}{v_0}[E]_0+\frac{vK_I[E]_0[I]_0}{v_0(1+\bar{K}[S])+vK_I[E]_0}.$$

This rearranges to

[12] $$[I]_0+\left(\frac{v}{v_0}-1\right)[E]_0 = \left(\frac{v_0}{v}-1\right)\frac{1+\bar{K}[S]}{K_I}.$$

Experimental results for this type of system may therefore be analyzed by plotting

$$[I]_0+\left(\frac{v}{v_0}-1\right)[E]_0$$

against $(v_0/v-1)$ for a given substrate concentration; from the slope of the line K_I can then be calculated provided that $\bar{K}$ is known from separate studies in the absence of inhibitor. An example of this type of plot is shown below.

Case 2: Complexing Associated with the Splitting-off of a Molecule

This case is represented by

$$E+S \underset{k_{-1}}{\overset{k_1}{\rightleftarrows}} ES \xrightarrow{k_2} E+P$$

$$E+I \overset{K_I}{\rightleftarrows} X+Y$$

where X is the complex and Y the molecule split off. The concentrations of X and Y must always be identical, and will be written as [X].

Equations [1] to [4] are now replaced by

$$[13] \qquad K_1 = [X]^2/([E][I])$$

$$[14] \qquad \bar{K} = [ES]/([E][S])$$

$$[15] \qquad [E]_0 = [E]+[ES]+[X]$$

$$[16] \qquad [I]_0 = [I]+[X].$$

From [13] and [16] it follows that

$$[17] \qquad [X]^2+K_1[E][X]-K_1[E][I]_0 = 0.$$

From [7] and [8]

$$[18] \qquad [E]+[ES] = (v/v_0)[E]_0$$

so that using [15]

$$[19] \qquad [X] = [E]_0\left(1-\frac{v}{v_0}\right).$$

Introduction of [7] and [19] into [17] gives

$$[20] \qquad [E]_0^2\left(1-\frac{v}{v_0}\right)^2+K_1\frac{v}{v_0}\frac{[E]_0^2}{1+\bar{K}[S]}\left(1-\frac{v}{v_0}\right)-K_1\frac{v}{v_0}\frac{[E]_0[I]_0}{1+\bar{K}[S]} = 0,$$

which reduces to

$$[21] \qquad 1-\frac{v}{v_0} = \frac{K_1}{1+\bar{K}[S]}\left[\frac{[I]_0}{[E]_0\{(v_0/v)-1\}}-\frac{v}{v_0}\right].$$

The value of K_1 could now be determined from a plot of $1-v/v_0$ against

$$\frac{[I]_0}{[E]_0\{(v_0/v)-1\}}-\frac{v}{v_0}.$$

APPLICATION TO EXPERIMENTAL DATA

In the work described in the following paper rates have been measured for the α-chymotrypsin-catalyzed hydrolysis of hydrocinnamic ester, over a range of pH values and of concentrations of DFP. Figure 1 shows a case 1 plot for the rates obtained at pH 8.1; the experimental details are given in the following paper. The plot is seen to be satisfactorily linear when the degree of inhibition ($v_0/v-1$) is small. At high inhibitor concentrations, however, there are very significant deviations from linearity, in the sense that the inhibition is much greater than would be predicted from the behavior at low inhibitor concentrations. This effect is attributed tentatively to the formation of a second complex of the type EI_2, as found with other enzyme–substrate systems (for example, urease (2), carboxypeptidase (3), acetylcholinesterase (4); cf. also ref. 1, pp. 71–77, 260–263).

The slope of the linear portion of the curve is 1.93×10^{-6}, and from this, since [S] = 1.17×10^{-3} and $\bar{K}$ = 2500, a value of 2.04×10^{6} is calculated for K_1. It is of interest that use of the simple conventional inhibition equation

$$[22] \qquad v/v_0 = (1+\bar{K}[S])/(1+\bar{K}[S]+K_1[I])$$

Can. J. Chem. Downloaded from www.nrcresearchpress.com by 196.1.178.254 on 09/04/12
For personal use only.

leads to a K_i value of 1.2×10^6, which is much less than the true value. The equations developed in the present paper will always give higher K_i values than the simple formula, which overestimates the concentrations of inhibitor present free in the solution.

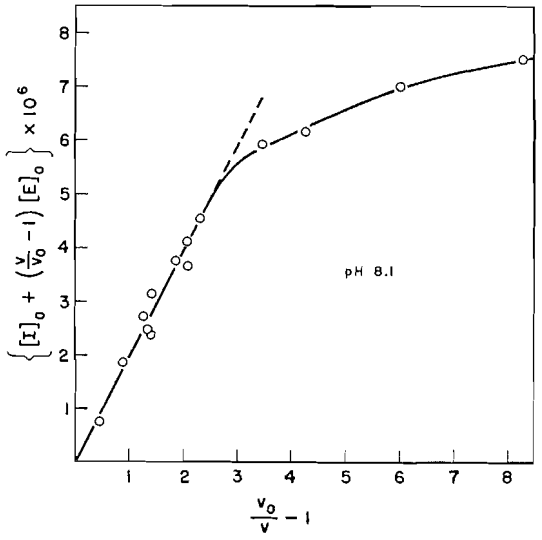

FIG. 1. A plot showing that the mechanism of case 1 is applicable at low inhibitor concentrations.

A plot of the data according to the case 2 mechanism did not give a straight line even at low inhibitor concentrations, and it is concluded that this situation is not applicable. Although the reaction of DFP with the enzyme is accompanied by the liberation of HF (5), it may be that the fluoride ions remain attached to the protein so that equation [1] applies rather than equation [13].

ACKNOWLEDGMENT

The authors are grateful to the Defence Research Board for their support of this work under Grant DRB-9510-06.

REFERENCES

1. LAIDLER, K. J. The chemical kinetics of enzyme action. The Clarendon Press, Oxford. 1958. Chap. 3.
2. LAIDLER, K. J. and HOARE, J. P. J. Am. Chem. Soc. **71**, 2699 (1949).
3. LUMRY, R., SMITH, E. L., and GLANTZ, R. R. J. Am. Chem. Soc. **73**, 4330 (1951).
4. WILSON, I. B. and BERGMANN, F. J. Biol. Chem. **186**, 683 (1950).
5. JANSEN, E. F., NUTTING, M. D. F., JANG, R., and BALLS, A. K. J. Biol. Chem. **185**, 209 (1950).

Can. J. Chem. Downloaded from www.nrcresearchpress.com by 196.1.178.254 on 09/04/12
For personal use only.

Can. J. Chem. Downloaded from www.nrcresearchpress.com by 196.1.178.254 on 09/04/12
For personal use only.

KINETICS OF THE INHIBITION OF α-CHYMOTRYPSIN BY METHANOL AND DFP[1]

BERNARD R. STEIN[2] AND KEITH J. LAIDLER

ABSTRACT

A study has been made of the kinetics of the α-chymotrypsin-catalyzed hydrolysis of methyl hydrocinnamate in the presence of various concentrations of methanol, of eserine, and of diisopropyl phosphorofluoridate (DFP). In 20% methanol the pH optimum, using a substrate concentration of 1.20×10^{-3} *M*, is 7.8; in pure water it is 8.3; and at intermediate pH's the optimum varies between these values. No inhibition was observed with eserine. In aqueous solution the character of the inhibition by DFP differs from that in alcohol solutions; the inhibition is of the competitive type, and the inhibition constant varies with pH in essentially the same manner as does the rate of the reaction. This result suggests that DFP interacts with the same active groups on the enzyme as are responsible for the hydrolysis of the substrate. A specific mechanism for inhibition is suggested.

INTRODUCTION

Studies of the influence of inhibitors on the rates of enzyme reactions have contributed considerably to an understanding of the mechanisms of enzyme action. In a recent paper (1) the kinetics of the α-chymotrypsin-catalyzed hydrolysis of methyl hydrocinnamate have been studied in the presence of hydrocinnamic acid, and it has been concluded that this inhibitor interacts with the enzyme at its active center, and that this active center contains a negatively charged group in addition to the acidic and basic groups actually responsible for the hydrolysis of the substrate.

In the present investigation this general line of attack on the chymotrypsin system has been extended to a study of the inhibition of the enzyme by methanol and by diisopropyl phosphorofluoridate (DFP). The main purpose of the work with methanol was to relate previous kinetic studies in 20% methanol–water mixtures with those that we are at present carrying out in pure aqueous solutions. Since 20% methanol solutions are far from physiological, and since (as shown below in the case of inhibition by DFP) the behavior is sometimes quite different in the two media, it seemed to be of interest to carry out kinetic studies in pure water and to relate the results to those obtained in the presence of alcohol.

The inhibition of α-chymotrypsin by DFP has been very thoroughly investigated (2, 3, 4, 5, 6, 7, 8, 9) but always, it would appear, using solvents containing propanol or other alcohols. Under the conditions previously employed the DFP reacts stoichiometrically with the enzyme, with the release of hydrogen fluoride, in accordance with the following equation:

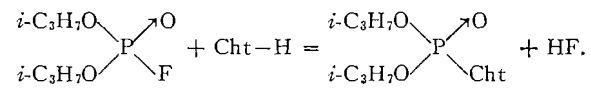

In previous studies this reaction has appeared to proceed essentially to completion, although the inhibitor can be displaced from the enzyme by the action of electrophilic reagents such as hydroxylamine (10, 11, 12, 13, 14, 15, 16).

In our experiments in pure aqueous solutions we have found definite evidence for reversibility; the DFP indeed acts as a competitive inhibitor. The behavior has been

[1]*Manuscript received February 27, 1959.*
Contribution from the Department of Chemistry, the University of Ottawa, Ottawa, Canada.
[2]*Present address: Army Research Office, Arlington, Virginia, U.S.A.*

investigated over a range of inhibitor concentrations and pH values, and conclusions drawn about the nature of the interaction between the DFP molecule and the active center of the enzyme.

EXPERIMENTAL

Materials

The enzyme and ester were as described in the previous paper (1), and the methanol was purified by distillation. The DFP was a pure sample supplied by the Defence Research Chemical Laboratories, Shirley Bay, Ontario.

Kinetic Procedure

The rate measurements were carried out using a pH-stat, manufactured by the Ole Dich Company of Copenhagen, together with a radiometer automatic titrator. Calomel and glass electrodes in the reaction mixture together with the titrator allowed the pH to be recorded, and when the pH fell below the designated value the pH-stat injected 0.02 *M* sodium hydroxide from a syringe micropipette into the reaction system. The pH-stat contains a rotating drum on which a record is made of alkali added vs. time; since the alkali is added in increments of about 10^{-4} cc, the record is extremely smooth and allows rates to be measured with great accuracy. All rates quoted are initial rates.

The reaction vessel was a small glass cell maintained at constant temperature (20.0° C) by circulation of thermostatically controlled water through an outer jacket. Fifteen milliliters of reaction mixture was employed in each case, and stirring was done magnetically. Various enzyme concentrations were employed, mostly in the region of 3×10^{-6} *M*. Owing to the limited solubility of the substrate in pure water, runs could not be done at concentrations higher than about 3×10^{-3} *M*; most were done at about 1.2×10^{-3} *M*. To avoid changes in ionic strength all runs were carried out at a sodium chloride concentration of 0.1 *M*. The total volume of sodium hydroxide solution added during a run never exceeded 3% of the total volume, and was usually less than this; the correction required is therefore very small.

RESULTS

Inhibition by Methanol

The work of Laidler and Barnard (17) showed that in 20% methanol there is a well-defined pH optimum at 7.8. In the present study runs were made at methanol concentrations varying from zero to 12%, and at pH values ranging from 7.5 to 8.5. The results are shown in Table I and Fig. 1, in which are included the rates measured by Laidler and Barnard (17) in 20% methanol–water mixtures.

TABLE I

Rate of hydrolysis of hydrocinnamic ester in the presence of methanol
Rates in $mole^{-1}\ sec^{-1}\times10^{9}$ Temperature = 20.0° C
$[E]_0 = 3.33\times10^{-6}$ *M* [S] = 1.2×10^{-3} *M* [NaCl] = 0.1 *M*

% Methanol (by volume)	Rate at pH				
	7.5	7.8	8.1	8.3	8.5
0	138.7	160.3	185.5	190.7	165.2
0.66	100.8	136.1	150.0	151.7	133.2
2.0	70.8	91.2	100.0	96.5	82.7
4.0	39.4	59.1	68.0	63.0	56.7
8.0	18.5	29.0	31.4	28.0	23.4
12.0	12.5	21.0	21.9	18.0	11.2
20.0	5.0	8.5	7.5	5.5	3.0

Can. J. Chem. Downloaded from www.nrcresearchpress.com by 196.1.178.254 on 09/04/12
For personal use only.

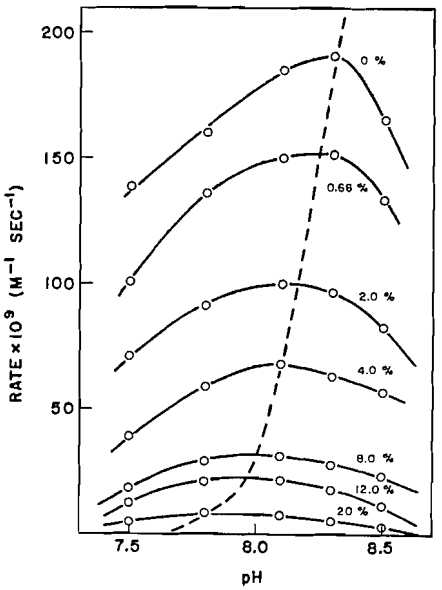

FIG. 1. Plots of rate against pH for various concentrations of methanol. The dotted line shows the variation of the pH optimum.

Lack of Inhibition by Eserine

Since eserine (physostygmine), which has the structure

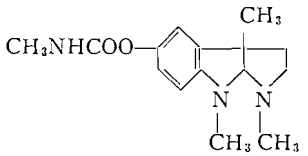

is a very powerful inhibitor for cholinesterase, a study has been made of its action on chymotrypsin. Rate measurements have been made, using the same conditions as above, at pH values varying from 7.5 to 8.7 and at eserine:enzyme molar ratios of up to 40. There was no inhibition under any of the conditions employed.

Inhibition by DFP

In the majority of our experiments with DFP the procedure was to add the aqueous solution of the inhibitor to the enzyme solution which had previously been brought to the required pH by addition of sodium hydroxide; this addition was carried out slowly with the vessel connected to the pH-stat, so that no change in pH occurred, and the mixture was then allowed to stand, with stirring, for 10 minutes. The substrate was then added slowly and the reaction followed with the recorder.

Table II shows some typical results using this procedure. It is to be noted that even when the inhibitor was considerably in excess of the enzyme the inhibition is not complete; this was the case even when the inhibitor–enzyme ratio was as high as 4:1. This result is in marked contrast to that obtained by Jansen and co-workers (2), who used a propanol–water mixture as solvent and acetyl tyrosine ethyl ester as substrate. They found that when the molar ratio of DFP to enzyme was greater than unity there was

Can. J. Chem. Downloaded from www.nrcresearchpress.com by 196.1.178.254 on 09/04/12
For personal use only.

TABLE II

Typical results showing that the DFP inhibition is reversible
Temperature = 20.0° C
[NaCl] = 0.1 M [S] = 1.17×10^{-3} M $[E]_0 = 3.03\times10^{-6}$ M

[DFP] $\times10^6$	$[DFP]/[E]_0$	% inhibition
1.18	.39	17.0
2.36	.78	28.6
3.54	1.17	45.1
4.72	1.56	48.0
5.36	1.77	61.8
8.04	2.65	83.2
10.72	3.54	87.8

practically 100% inhibition. This observation was confirmed by us using their experimental conditions, but using pure water as solvent the inhibition was much less strong, as shown in Table II. We tentatively attribute this difference to the fact that the alcohol interacts with the HF formed and in this way displaces the equilibrium.

The interaction between DFP and chymotrypsin is thus reversible under our conditions. Experiments were also carried out to determine whether the behavior was competitive or non-competitive with respect to the substrate. This was done by determining the degree of inhibition at various substrate concentrations; the degree of inhibition was found to be reduced by increasing the substrate concentration, so that it is concluded that the behavior is competitive.

The above work was done by measuring initial rates. Further evidence that the inhibition is reversible and competitive under our reaction conditions was provided by studies of the time course of the reactions. Experiments were carried out in which the DFP and substrate were mixed first, after which the enzyme was added. It was found that the greater the substrate:inhibitor ratio the less was the falling-off of the rate as the reaction proceeded. It follows that the substrate competes with the inhibitor and can displace it from the enzyme surface.

Measurements were then carried out with a view to determining the association constant K_I between the enzyme and the inhibitor. In this series of experiments the enzyme and inhibitor were mixed first, after which substrate was added and initial rates measured using the pH-stat.

As discussed in the preceding paper, the inhibition by DFP can, at low inhibitor concentrations, be interpreted in terms of the mechanism

$$E+S \underset{k_{-1}}{\overset{k_1}{\rightleftarrows}} ES \xrightarrow{k_2} E+P$$

$$E+I \overset{K_I}{\rightleftarrows} EI.$$

Allowance must be made for the inhibitor that becomes bound to the enzyme, and the resulting kinetic equation is [12] of the preceding paper.

The data have been analyzed in terms of this equation, and plots similar to that of the preceding paper were obtained at all pH values. The resulting K_I values are shown in Table III. The variation of K_I with pH is shown in Fig. 2, which also shows the variation of rate with pH at a substrate concentration of 1.20×10^{-3} M.

Can. J. Chem. Downloaded from www.nrcresearchpress.com by 196.1.178.254 on 09/04/12
For personal use only.

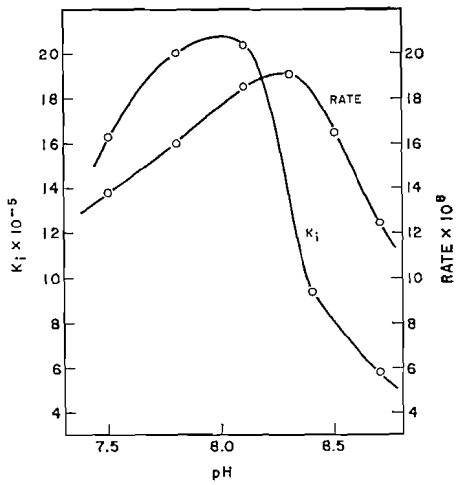

FIG. 2. Plots of K_i against pH and of rate against pH at a substrate concentration of 1.20×10^{-3} M.

TABLE III

Results for the inhibition of α-chymotrypsin by DFP

Temperature = 20.0° C

[NaCl] = 0.10 M [S] = 1.17×10^{-3} M $[E]_0 = 3.03\times10^{-6}$ M

pH	$\bar{K}$	$(1+\bar{K}[S]) \times10^6/K_i$	$K_i \times10^{-5}$
7.5	2730	29.6	14.2
7.8	2600	2.03	19.9
8.1	2500	1.93	20.4
8.4	2010	3.58	9.35
8.7	1570	4.96	5.72

DISCUSSION

The influence of methanol on the kinetics of the α-chymotrypsin – hydrocinnamic ester system was treated by Barnard and Laidler (18) as a dielectric constant effect. This may well be the case under the conditions of the previous experiments, in which the methanol concentration varied from 15 to 25%. However, the very marked inhibition brought about by small amounts of methanol, as found in the present work, is too great to be explained as a solvent effect, and is probably due to a specific interaction between the enzyme and the methanol. The methanol may well interfere with hydrogen bonding at the active center and in this way affect markedly the interaction between the enzyme and the substrate. The small shift in pH optimum is understandable on the same basis.

The complete lack of inhibition by eserine indicates that the negatively charged group on the chymotrypsin molecule (indicated by the work with hydrocinnamic acid (1)) is not able to interact with a positively charged group on the eserine molecule. This anionic site on chymotrypsin therefore differs in character from that on the cholinesterase molecule, which is markedly inhibited by eserine.

The most significant result of the present investigation is that the inhibitor constant K_i varies with pH in approximately the same manner as does the reaction rate itself. It follows from this that the reaction between the enzyme and DFP is of a similar nature to that between the enzyme and the substrate.

Previous work, including studies of the pH dependence of the rate (17, 19, 20, 21),

Can. J. Chem. Downloaded from www.nrcresearchpress.com by 196.1.178.254 on 09/04/12
For personal use only.

has suggested that the hydrolytic action of the enzyme involves a simultaneous nucleophilic attack by an imidazole nitrogen atom and an electrophilic attack by a protonated ω-amino ion. It is postulated that a similar process occurs when the enzyme forms a complex with the DFP molecule, and the reaction may be represented as

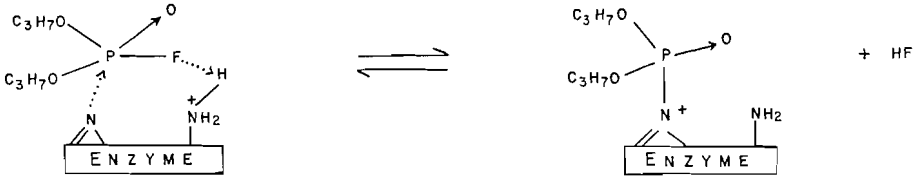

This proposal relates to the reversible binding of the inhibitor. The irreversible inhibition may be due to the transfer of the $(C_3H_7O)_2PO$- group from the imidazole ring to a neighboring serine residue.

ACKNOWLEDGMENTS

The authors are indebted to Mr. E. K. Gill for help with the experimental work and to Dr. R. M. Krupka for help with the analysis of the experimental data. They are also grateful to the Defence Research Board for their support of this work under Grant DRB 9510-06.

REFERENCES

1. Canady, W. J. and Laidler, K. J. Can. J. Chem. **36**, 1289 (1958).
2. Jansen, E. F., Nutting, M. D. F., Jang, R., and Balls, A. K. J. Biol. Chem. **179**, 189 (1949).
3. Jansen, E. F., Nutting, M. D. F., and Balls, A. K. J. Biol. Chem. **179**, 201 (1949).
4. Jansen, E. F., Nutting, M. D. F., Jang, R., and Balls, A. K. J. Biol. Chem. **185**, 209 (1950).
5. Schaffer, N. K., May, S. C., and Summerson, W. H. J. Biol. Chem. **202**, 67 (1953).
6. Schaffer, N. K., Harshman, S., and Engle, R. R. J. Biol. Chem. **214**, 799 (1955).
7. Jandorf, B. J., Michel, H. O., Schaffer, N. K., Egan, R., and Summerson, W. H. Discussions Faraday Soc. **20**, 134 (1955).
8. Wagner-Jauregg, T. and Hackley, B. E. J. Am. Chem. Soc. **75**, 2125 (1953).
9. Weil, L., James, S., and Buchert, A. R. Arch. Biochem. Biophys. **46**, 266 (1953).
10. Wilson, I. B. J. Biol. Chem. **190**, 111 (1951).
11. Wilson, I. B. J. Biol. Chem. **199**, 113 (1952).
12. Wilson, I. B. and Meislich, E. K. J. Am. Chem. Soc. **75**, 4628 (1953).
13. Wilson, I. B. and Ginsberg, S. Biochim. et Biophys. Acta, **18**, 168 (1955).
14. Wilson, I. B. Discussions Faraday Soc. **20**, 119 (1955).
15. Davies, D. R. and Green, A. L. Discussions Faraday Soc. **20**, 269 (1955).
16. Davies, D. R. and Green, A. L. Biochem. J. **63**, 529 (1956).
17. Laidler, K. J. and Barnard, M. L. Trans. Faraday Soc. **52**, 497 (1956).
18. Barnard, M. L. and Laidler, K. J. J. Am. Chem. Soc. **74**, 6099 (1952).
19. Laidler, K. J. Trans. Faraday Soc. **51**, 550 (1955).
20. Laidler, K. J. Discussions Faraday Soc. **20**, 302 (1955).
21. Laidler, K. J. The chemical kinetics of enzyme action. The Clarendon Press, Oxford. 1958. pp. 147–149.

Can. J. Chem. Downloaded from www.nrcresearchpress.com by 196.1.178.254 on 09/04/12
For personal use only.

Can. J. Chem. Downloaded from www.nrcresearchpress.com by 196.1.178.254 on 09/04/12
For personal use only.

NOTE ON THE DETECTION OF AN APPARENT PHASE TRANSITION OF ADSORBED WATER ON POROUS VYCOR GLASS BY MEASUREMENTS OF DIMENSIONAL CHANGES[1]

C. HODGSON[2] AND R. MCINTOSH

ABSTRACT

A new technique is described for detecting possible phase transitions of adsorbates. The method involves the measurement of length changes of the solid, but only solids for which the surface-to-volume ratio is large could be used with the present form of instrument because of its moderate sensitivity. Using this measurement an apparent phase transition for water adsorbed on porous Vycor glass has been detected at approximately −22° C.

The detection of phase changes occurring in adsorbates on solids has been attempted in a variety of ways. Among these are the dependence of equilibrium pressure on temperature, the anomalies of carefully determined cooling curves, and dilatometric techniques (1, 2, 3). The experimental evidence is not always readily acceptable because of the methods employed.

Recently Puri, Singh, and Myer (4) reported the experimental detection of the formation of the "solid" phase for a variety of adsorbate–adsorbent systems by means of measurements of equilibrium pressures. These authors compared their data with predicted freezing point depressions based upon the Kelvin theory of capillary condensation and the assumption that the adsorbed "solid" would have the same equilibrium vapor pressure as that of bulk solid. This implies that the adsorbed "solid" is not under any negative pressure due to concave menisci, which could well be valid, and also that the adsorbed "solid" has the properties of bulk solid, which is unlikely. The validity of the latter assumption could be directly established by a measurement of equilibrium pressure over the adsorbate.

In view of the earlier work from this laboratory (5, 6), the contraction of the adsorbent system due to concave menisci seems reasonably well established. If the effects of menisci could be appreciably changed by forming the solid phase a marked expansion of the system might be expected. It should be noted that the change of molar volume of the adsorbate could also produce an effect. Discrimination between these two causes should be possible using an adsorbate for which the solid molar volume is less than that for liquid, e.g. benzene. A further reason to employ such an adsorbate is given below.

An expansion on lowering temperature, and a contraction through the same range of temperature when the system is rewarmed, have now been established for water adsorbed on porous Vycor glass (see Fig. 1). The phenomenon may exist for water contents below the beginning of the hysteresis loop, but experimental precision in determining length changes makes this speculation. However, because the extent of the anomaly increases markedly for water contents above the inception of the hysteresis loop the effect is probably associated with water condensed in the pores.

The Kelvin theory as applied by Puri, Singh, and Myer (4) does not rationalize our experimental observations since (*a*) the transition should be sharp as all the liquid menisci have the same radius of curvature for a given relative pressure, and (*b*) the transition temperature should depend upon the relative pressure corresponding to the adsorbate content.

[1]*Manuscript received April 3, 1959.*
Contribution from the Department of Chemistry, University of Toronto, Toronto, Ontario.
[2]*Graduate Student and holder of N.R.C. Studentship (1958–59), Union Carbide Fellowship (1957–58).*

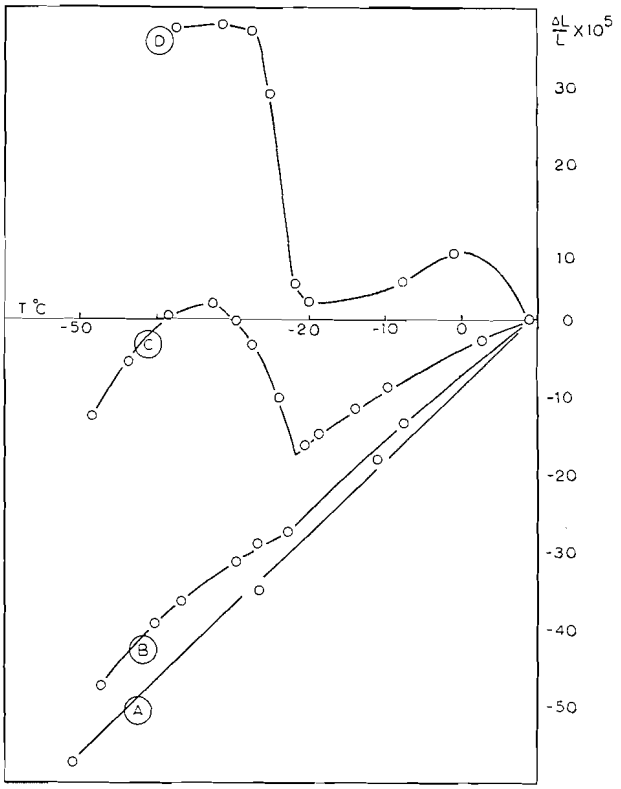

FIG. 1. Plot of fractional length change against decreasing temperature for water contents of:
A, 0.0221 g per g. C, 0.175 g per g.
B, 0.138 g per g. D, 0.195 g per g (desorption branch).

Curve "A" in Fig. 1 for a water content of 0.0221 g water per g glass, i.e. well below the beginning of the hysteresis loop, is approximately linear; curve "B" for a water content on the lower part of the adsorption branch of the hysteresis loop begins to show a slight anomaly at −22° C; while curves "C" and "D" show large anomalies. In the cases "C" and "D" the water contents are high on the adsorption and desorption branches respectively, but the evidence of transition again appears at −22° C in both cases. An unexplained hysteresis on reversing the direction of temperature change has been observed, but has been omitted from the figure.

For a given quantity adsorbed, the transition temperature of the adsorbed matter, relative to that of bulk material, depends upon the relative displacements of the molar free energy versus temperature curves of the adsorbed phases from those of the bulk. The assumption of concave menisci for the adsorbed "liquid" predicts a lowering of its curve relative to that for bulk liquid. The same assumption might be made in dealing with the "solid" phase except for the difficulty of obtaining the value of the surface free energy of the "solid". As pointed out above, the molar free energy of the adsorbed "solid" would be expected to be lower than that of the bulk solid but we have been unable to determine the low pressures with sufficient accuracy to establish the relative values. However, the known compressibility of Vycor-adsorbate systems (7), the negative pressure generated by the liquid menisci, and the measured expansion of about 20 μ in

Can. J. Chem. Downloaded from www.nrcresearchpress.com by 196.1.178.254 on 09/04/12
For personal use only.

the transition range (see system "C") combine to suggest that the effect of concave menisci has not been completely eliminated after the transition to "solid".

Whether or not effects due to menisci must be assumed for the "solid" adsorbate can be demonstrated. Hysteresis is caused, in the general view, by the shapes of the voids and the radius of curvature of menisci appropriate to the adsorption or desorption conditions. Thus hysteresis should vanish from an isotherm determined at a temperature where "solid" adsorbate is the stable form, provided that effects due to menisci do not exist for the "solid" phase. The equilibrium pressures for water are too low to make this test conveniently, but it might be possible using benzene. The necessary experiments are now being begun.

Full details of the experiments with water and an expanded discussion of the thermodynamic theory will be published at a later date.

The authors would like to express their thanks to Dr. M. H. Panckhurst for many helpful discussions. Grateful acknowledgment is also made to the National Research Council and to the Advisory Committee on Research, University of Toronto, for financial support of this work.

REFERENCES

1. BATCHELOR, R. W. and FOSTER, A. G. Trans. Faraday Soc. **40**, 300 (1944).
2. IWAKAMI, Y. J. Chem. Soc. Japan, **72**, 259 (1951).
3. PURI, B. R., SHARMA, L. R., and LAKHANPAL, M. L. J. Phys. Chem. **58**, 289 (1954).
4. PURI, B. R., SINGH, D. D., and MYER, Y. P. Trans. Faraday Soc. **53**, 530 (1957).
5. AMBERG, C. H. and MCINTOSH, R. Can. J. Chem. **30**, 1012 (1952).
6. QUINN, H. W. and MCINTOSH, R. Proc. 2nd International Congress of Surface Activity. Butterworth Scientific Publications, London. 1957.
7. QUINN, H. W. and MCINTOSH, R. Can. J. Chem. **35**, 745 (1957).

Can. J. Chem. Downloaded from www.nrcresearchpress.com by 196.1.178.254 on 09/04/12
For personal use only.

Can. J. Chem. Downloaded from www.nrcresearchpress.com by 196.1.178.254 on 09/04/12
For personal use only.

ULTRAVIOLET IRRADIATION OF PYRIMIDINE DERIVATIVES

III. INFLUENCE OF HYDROGEN CYANIDE ON THE PHOTOLYSIS[1]

A. M. Moore

ABSTRACT

The presence of HCN in concentrations up to 0.05 *M* in aqueous, buffered solutions of uracil, uridine, and 1,3-dimethyluracil has been shown to divert the normal course of the photochemical hydration reactions of these compounds as a result of photochemically induced combination between HCN and the pyrimidine derivative. A simple calculation indicates that HCN is more efficient than water in reacting with activated uracil molecules by a factor of about 10^3. The possible general significance of such nucleophilic addition reactions in the photochemistry of nucleic acids is discussed.

INTRODUCTION

Evidence has been accumulating during the past 5 years (reviewed in 11) to indicate that the principal initial photochemical reaction of aqueous solutions of uracil and cytosine, their nucleosides, and nucleotides consists of the addition of a molecule of water to the 5,6 double bond of the pyrimidine ring. The studies that have been reported in this connection have been made with dilute solutions of the pyrimidine compounds in water or in buffer. Although it is interesting to speculate from such evidence about the possible biological significance of the photochemical hydration reaction, it is important to remember that our knowledge of such reactions is very limited and that, in any case, the analogy between the simple aqueous systems that have been studied and the situation involved in the irradiation of complex nucleic acid molecules in vivo leaves something to be desired.

The present paper reports the results of a study of the influence of hydrogen cyanide, in low concentration, upon the course of the photochemical hydration of uracil and certain of its derivatives. The rather large effect observed makes it clear that the course of the hydration reaction may be greatly modified by the presence of other components of the solution.

The choice of hydrogen cyanide for these experiments was, of course, made not on physiological but on chemical grounds. The addition of hydrogen cyanide and other weak acids to conjugated mono-olefinic carbonyl compounds—in which class we may include uracil and its derivatives—has been extensively studied (cf. for example, ref. 3). Furthermore, the ready availability of carbon-14-labelled cyanide makes it a convenient tool for such study.

METHODS

General

Irradiations were carried out with the apparatus previously described (8) using low-pressure mercury arcs (wavelength mainly 2537 Å) as light source. The spectroscopic changes were determined on samples withdrawn after various irradiation times with either a Beckman DU or DK2 spectrophotometer.

The solutions which were irradiated contained the pyrimidine compounds (10^{-4} *M*), phosphate buffer (0.5 *M*, pH 7.0), various concentrations of HCN added from a stock solution of KCN (0.5 *M*) which was titrated to pH 7.0 with HCl just before use, and KCl,

[1]*Manuscript received April 16, 1959.*
Contribution from the Biology Branch, Atomic Energy of Canada Limited, Chalk River, Ontario.
Issued as A.E.C.L. No. 831.

added as required, so that all solutions had the same total chloride concentration (0.05 *N*).

The uracil and uridine used in these experiments were obtained commercially. The former was recrystallized twice from water and dried at room temperature *in vacuo*. The 1,3-dimethyluracil was prepared from this purified uracil by the method of Davidson and Baudisch (2) and was purified by recrystallization from 95% ethanol, (m.p. 122° C; $\epsilon = 8600$ at 2660 Å). The KCN and KCl were reagent grade.

C^{14}-Labelled Compounds

The $HC^{14}N$ was prepared by the method of McCarter (4) starting with $BaC^{14}O_3$ provided by Atomic Energy of Canada Ltd. As the final stage of purification it was distilled into 0.1 *N* KOH in which form it was stored until required.

The uracil-2-C^{14} was the same preparation as that previously reported (6).

EXPERIMENTAL AND RESULTS

Effect of HCN *on the Irradiation of Uracil*

Solutions of uracil were irradiated in the presence of HCN in concentrations ranging from zero to 0.05 *M*. The results (Fig. 1) show that the presence of HCN accelerated the photochemical destruction of uracil in a striking manner. Unirradiated controls showed no change in spectrum on standing in the presence of 0.05 *M* HCN for periods up to 30 minutes.

It has been reported (13) that, without HCN, about 50% of the uracil destroyed by irradiation with filtered 2537 Å light may be regenerated by heating or by acid treatment. In our own experiments, using the unfiltered light from low-pressure mercury arcs, 42–43% of the loss in optical density (2600 Å) produced by irradiation was restored by heating (100° C; 5 minutes; pH 1), and this proportion was independent of the extent of decomposition for optical density decreases of 51 to 86%. On the other hand, after irradiation (6 minutes) in the presence of 0.05 *M* HCN until the optical density had decreased by 67%, the restoration on heating amounted to only 6.5%.

Effect of HCN *on the Irradiation of 1,3-Dimethyluracil*

The quantum yield for the photodecomposition of 1,3-dimethyluracil in simple aqueous solution is about twice as large as that for uracil (see 11), and the photodecomposition curves are correspondingly steeper. No effect of HCN on the rate of reaction was observed. However, after irradiation until the optical density had fallen to 8–9% of its initial value, it was found that the extent of recovery that ensued upon heating decreased as the concentration of HCN was increased. Thus, for HCN concentrations of 0, 0.005, 0.01, and 0.05 *M* the recoveries were 100, 93, 91, and 70% respectively. Without irradiation no effect of HCN (0.05 *M*) on the spectrum of 1,3-dimethyluracil was detectable.

Effect of HCN *on the Irradiation of Uridine*

Uridine, like uracil, was decomposed more rapidly in the presence of HCN (0.05 *M*) than in simple aqueous solution (Fig. 2). A sample which had been irradiated for 5 minutes in the presence of 0.05 *M* HCN was subsequently heated to promote regeneration of the uridine. The spectrum, after this treatment, indicated that partial recovery had occurred. The final optical density at 2610 Å was only about 38.9% of the density before irradiation. By contrast, uridine irradiated in the absence of cyanide gave 97.5% recovery on heating. This latter finding agrees with the observation of Rapport and Canzanelli (10) of virtually 100% regeneration of uridine after irradiation in water for short times.

Can. J. Chem. Downloaded from www.nrcresearchpress.com by 196.1.178.254 on 09/04/12
For personal use only.

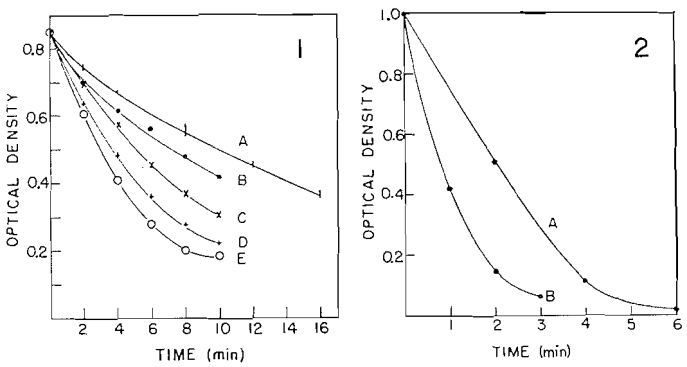

FIG. 1. Irradiation of uracil (10^{-4} M) in presence of various concentrations of HCN. All solutions, pH 7.0.

Curve	A	B	C	D	E
Concentration of HCN	0	0.01 M	0.02 M	0.03 M	0.05 M

FIG. 2. Irradiation of uridine (10^{-4} M) without HCN (curve A) and with 0.05 M HCN (curve B).

Test for Spontaneous Reaction of Uridine with HCN

A solution 10^{-2} M with respect to uridine and 0.05 M with respect to HCN (pH 7) was allowed to stand at room temperature in a glass-stoppered flask. Samples were withdrawn at 0, 6, and 24 hours, diluted 1:100 with water, and their spectra determined. After 24 hours at room temperature a final sample was heated at 70° C for 20 minutes before dilution and examination. The absorption spectrum showed no significant change in any of these samples.

Irradiation of Uracil and Uridine in Presence of $HC^{14}N$

Although an effect of HCN on the course of irradiation was evident in the foregoing experiments, it was not certain that it involved actual combination between cyanide and pyrimidine. In order to settle this point three experiments were performed with labelled reagents. In one, uracil-2-C^{14} was irradiated along with ordinary cyanide; in the second, ordinary uracil was irradiated along with $HC^{14}N$; in the third, ordinary uridine was irradiated with $HC^{14}N$. The products of all three experiments were chromatographed together on paper using *n*-propanol:water, 70:30 by volume, as solvent, and the materials on the chromatogram were located both by autoradiography and by contact printing with ultraviolet (2537 Å) light (5) (Fig. 3).

In the experiments with labelled uracil and ordinary cyanide, three radioactive spots (R_f, 0.24, 0.50, and 0.62) were found in addition to uracil itself (R_f 0.58). Ordinary uracil and labelled cyanide gave four prominent radioactive spots. Three of these (R_f 0.24, 0.50, and 0.62) evidently corresponded to the same products as were obtained with labelled uracil. The other spot (R_f 0.36) was presumably due to a substance derived only from the $HC^{14}N$ since it was absent when the labelling was reversed.

The result of the experiments with uridine tends to support this conclusion. Here again there were four main radioactive spots. One spot corresponded in position to the R_f 0.36 component of the uracil–$HC^{14}N$ lane; the other three spots (R_f 0.19, 0.49, and 0.59) appear to be the analogues of the spots at R_f 0.24, 0.50, and 0.62 observed with uracil, the slightly lower R_f values corresponding to the fact that uridine itself has a slightly lower R_f than uracil, 0.51 compared with 0.58 in this experiment.

The individual lanes of these chromatograms were also counted in a gas flow proportional counter designed for counting chromatograms. Typical results are given in Fig. 4. The two components with R_f 0.24 and 0.62, respectively, in the uracil–HCN lanes were

Can. J. Chem. Downloaded from www.nrcresearchpress.com by 196.1.178.254 on 09/04/12
For personal use only.

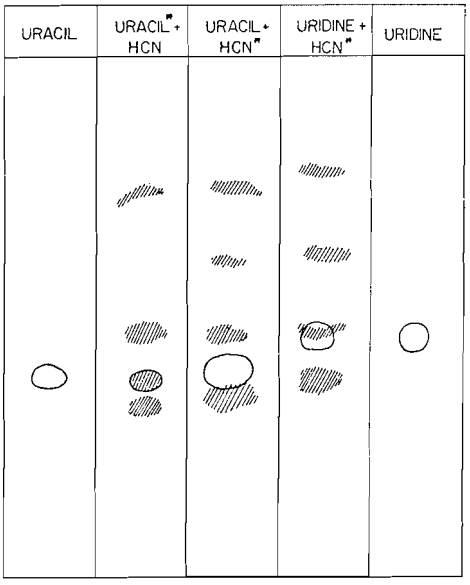

FIG. 3. Paper chromatogram of products of irradiation of pyrimidines in presence of HCN. C^{14}-Labelled reagents are indicated by asterisks in the column headings. Ultraviolet-(2537 Å)-absorbing spots are outlined; radioactive spots, located by autoradiography, are indicated by diagonal shading.

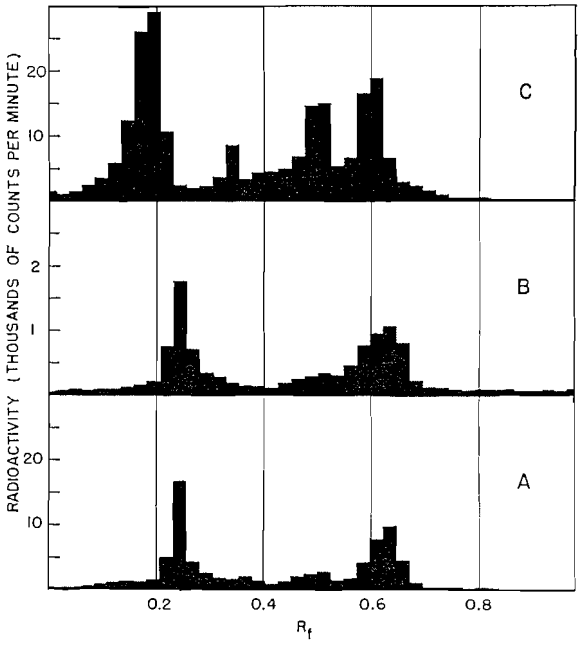

FIG. 4. Reaction products formed on irradiating pyrimidines (0.01 *M*) with HCN (0.05 *M*). 50-μl samples were chromatographed on paper(*n*-propanol:water 70:30 v/v)and the lanes were counted separately with a gas flow proportional counter. (A) Ordinary uracil and labelled HCN irradiated 6 hours. (B) Labelled uracil and ordinary HCN irradiated 4 hours. (C) Uridine and labelled HCN irradiated 3 hours.

Can. J. Chem. Downloaded from www.nrcresearchpress.com by 196.1.178.254 on 09/04/12
For personal use only.

approximately equal in amount and together accounted for 80 to 90% of the activity on the lanes in different runs, while the component with R_f 0.50 accounted for about 10% of the activity. In the uridine–HCN experiments the component of R_f 0.19 amounted to about 42% of the total activity and those with R_f 0.49 and 0.59 each contributed about 25% of the total activity.

The products of the uracil–HCN experiments were also chromatographed using *n*-butanol saturated with water as developing solvent. Irrespective of which component carried the C^{14} initially, the chromatograms exhibited three prominent radioactive components of R_f 0, 0.27, and 0.37. An additional minor component of R_f 0.11 was present in the experiments in which the HCN was labelled.

DISCUSSION

The experiments described in the foregoing pages show that when HCN is present during the irradiation of uracil, 1,3-dimethyluracil, or uridine, the activated pyrimidine reacts preferentially with it. This is made clearly evident by the extent to which the presence of the HCN reduces the yield of "reversible" product in all three cases, by the net increase in the rate of photochemical destruction of uracil and uridine, and by the chromatographic analysis of the products of irradiation using C^{14}-labelled reagents. It was also shown that the reactions with HCN were photochemical, not spontaneous.

The fact that 0.05 *M* HCN largely suppresses the formation of the "reversible" product in the case of uracil suggests that HCN is particularly efficient in competing with water for the excited uracil molecules. This matter is considered in detail in the appendix to this paper in which it is estimated that the specific reaction rate of excited uracil molecules with HCN is greater than that with water by a factor of about 10^3.

The chromatographic experiments using C^{14} demonstrated that there were multiple products. Uracil and uridine each yielded three principal products of reaction with HCN, which account for about 90% of the total reaction in each case. The most likely product in the reaction with uridine would be the nitrile of 5,6-dihydroorotidine. Other possibilities include the isonitrile and its hydrolysis products. At present the evidence does not permit a decision regarding the identity of the observed products but it may be noted that the disappearance of the ultraviolet absorption maximum (ca. 2600 Å) suggests reactions that eliminate the 5,6 double bond of the pyrimidine ring.

These results with cyanide fit into a general scheme according to which nucleophilic addition may be considered the primary photochemical reaction of the uracil derivatives. Mulliken (9) and Braude (1) have developed the concept that the first electronic excited state of compounds such as the aromatic ketones may be represented as a zwitterion with the negative charge on the oxygen and the positive charge on a carbon at the opposite end of the conjugated chain. Wang (14) has applied this concept to the pyrimidines, suggesting that the absorption of an ultraviolet quantum by a molecule of 1,3-dimethyluracil, in water solution, converts it to the structure I, which then undergoes a typical nucleophilic addition reaction with water.

The original state of polarization of the pyrimidine ring would be expected to have a considerable effect on the probability of attaining such a structure. For example, comparing uracil (II) with thymine (III) the hyperconjugating effect of the methyl group at position 5 would be expected to oppose the development of a positive charge on the carbon at position 6 thereby making thymine less susceptible than uracil to nucleophilic addition at the 5,6 double bond. In fact, thymine is much more resistant than uracil to photodecomposition and does not appear to undergo the 5,6 hydration reaction (12).

Can. J. Chem. Downloaded from www.nrcresearchpress.com by 196.1.178.254 on 09/04/12
For personal use only.

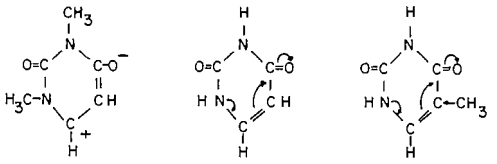

I II III

Extending the concept one would predict that other nucleophilic agents might be induced to participate in the photochemical reactions of the pyrimidines. The results of the present experiments support this prediction. Observations have also been reported (7, 11) to indicate that ethanol, like water, undergoes reversible addition to the 5,6 double bond of 1,3-dimethyluracil and uracil under the influence of ultraviolet light.

There is thus a growing body of evidence supporting the view that photoinduced nucleophilic addition may be a general reaction of the substituted uracils. Not all additions of this sort will be as easily reversed as in the case of water; indeed the addition of cyanide appears to be irreversible. In considering the fate of pyrimidines irradiated in vivo we may expect to encounter other examples of a similar nature. Such reactions might be significant when pyrimidines are irradiated as constituents of nucleic acid molecules, where they are ideally situated to undergo reactions with neighboring pyrimidines or purines especially in structures like the Watson–Crick model of deoxyribonucleic acid (15).

ACKNOWLEDGMENTS

The assistance of Miss Shena M. Anderson and of Mr. C. H. Thomson in the work described in this report is gratefully acknowledged.

REFERENCES

1. Braude, E. A., Sondheimer, F., and Forbes, W. F. Nature, **173**, 117 (1954).
2. Davidson, D. and Baudisch, O. J. Am. Chem. Soc. **48**, 2397 (1926).
3. Ingold, C. K. Structure and mechanism in organic chemistry. Cornell University Press, Ithaca. 1953. p. 676 ff.
4. McCarter, J. A. J. Am. Chem. Soc. **73**, 483 (1951).
5. Markham, R. and Smith, J. D. Biochem. J. **45**, 294 (1949).
6. Moore, A. M. and Boylen, J. B. Arch. Biochem. Biophys. **54**, 312 (1954).
7. Moore, A. M. and Thomson, C. H. *In* Progress in radiobiology. Oliver and Boyd, Ltd. Edinburgh. 1956.
8. Moore, A. M. and Thomson, C. H. Can. J. Chem. **35**, 163 (1957).
9. Mulliken, R. S. J. Chem. Phys. **7**, 14, 20, 121 (1953).
10. Rapport, D. and Canzanelli, A. Science, **112**, 469 (1950).
11. Shugar, D. and Wierzchowski, K. L. Polska Akad. Nauk, Quarterly Biochem. Suppl. 4, 243 (1958).
12. Shugar, D. and Wierzchowski, K. L. Biochim. et Biophys. Acta, **23**, 657 (1957).
13. Sinsheimer, R. L. Radiation Research, **1**, 505 (1954).
14. Wang, S. Y. J. Am. Chem. Soc. **80**, 6196 (1958).
15. Watson, J. D. and Crick, F. H. C. Nature, **171**, 737 (1953).

APPENDIX

The absorption of ultraviolet light by a uracil molecule raises it into an excited state. Its excitation energy may then be dissipated by both physical and chemical processes. The principal physical process is likely to be the transfer of vibrational energy to the solvent water molecules during collisions. Fluorescence has not been observed and is, in any case, unlikely because the lifetime of excited molecules with respect to radiation is generally long compared with the interval between collisions with the solvent molecules. The chemical processes, on the other hand, are known to be of two kinds: one

Can. J. Chem. Downloaded from www.nrcresearchpress.com by 196.1.178.254 on 09/04/12
For personal use only.

leading to a labile product that is capable of regenerating uracil, and another (or possibly more than one) leading to irreversible destruction of uracil. These two processes have roughly equal quantum yields (13).

The net effect of the physical and chemical processes of energy dissipation together with a fixed rate of energy input will be the establishment of an equilibrium concentration of excited molecules $[u^*]$ which will vary with time during irradiation. It will be convenient to refer to its initial value as $[u^*]_0$.

We may thus summarize the processes of energy dissipation:

[1] $$u^* + H_2O \xrightarrow{k_1} u.HOH \text{ (reversible chemical reaction)},$$

[2] $$u^* \xrightarrow{k_2} X \text{ (irreversible chemical reaction)},$$

[3] $$u^* + H_2O \rightarrow u + H_2O^* \text{ (physical deactivation by collision)}.$$

Equation [2] may represent several reactions, in which case k_2 will be the weighted mean rate constant for all the irreversible chemical processes. Reactions [1] and [2] are the only processes leading to a decrease in the concentration of uracil. Thus the total initial rate of disappearance of uracil will be $k_1.[u^*]_0[H_2O] + k_2[u^*]_0$ or, since the rates of reactions [1] and [2] are known to be roughly equal, we may represent the total initial rate approximately as $2k_1.[u^*]_0[H_2O]$.

In the presence of HCN we will have additional chemical reactions which may be lumped together as:

[4] $$u^* + HCN \xrightarrow{k_4} u.HCN \text{ (irreversible chemical reaction)}$$

where k_4 represents the weighted mean rate constant for the various reactions of u^* and HCN. We may neglect any effect of HCN on the purely physical processes of energy transfer for the concentrations of HCN employed in these experiments and, since this is still the principal mode of deactivation, the chemical quantum yields being of the order 0.01 mole per einstein, we may assume that $[u^*]_0$ will be essentially unchanged by the addition of the HCN. The initial rate of disappearance of uracil in the presence of HCN will therefore be $k_4[u^*]_0[HCN] + 2k_1.[u^*]_0[H_2O]$.

The ratio of the initial rates with and without HCN is:

$$\frac{k_4[u^*]_0[HCN]+2[k_1][u^*]_0[H_2O]}{2k_1[u^*]_0[H_2O]} = 1 + \frac{k_4[HCN]}{2k_1[H_2O]}.$$

In the experimental section the initial rate of disappearance of uracil during irradiation in the presence of 0.05 M HCN was found to be about 2.4 times the rate without HCN (Fig. 1), i.e.,

$$(k_4[0.05])/(2k_1[55.5]) = 1.4,$$

whence

$$k_4/k_1 = \text{ca. } 3100.$$

Even making allowance for the approximations involved in this derivation it appears that k_4 is larger than k_1 by a factor of the order of 10^3. This could explain the fact that the formation of the "reversible" product, 6-hydroxyhydrouracil, is almost completely suppressed in the presence of 0.05 M HCN.

Can. J. Chem. Downloaded from www.nrcresearchpress.com by 196.1.178.254 on 09/04/12
For personal use only.

Can. J. Chem. Downloaded from www.nrcresearchpress.com by 196.1.178.254 on 09/04/12
For personal use only.

CONDUCTANCE IN THE RANGE OF MEDIUM CONCENTRATION[1]

A. N. Campbell and R. J. Friesen

ABSTRACT

Equivalent conductances, densities, and viscosities of aqueous solutions of ammonium nitrate, of silver nitrate, and of lithium nitrate were determined at 25° C and at 35° C at concentrations ranging from 0.01 *N* to 1.0 *N*.

Experimental equivalent conductances have been compared with those calculated by the Wishaw–Stokes and Falkenhagen–Leist equations. Suitable choice of one parameter, the distance of closest approach, permits reproduction of the experimental data with an error of less than 0.5%. A study of the deviations of the calculated from the experimental conductances reveals that the distance of closest approach (so-called) varies appreciably with concentration and temperature.

In previous papers from this laboratory, we have reported our experimental results on conductances, densities, and viscosities of concentrated solutions (1). More recently, we have ventured into the field of extreme dilution (2). In the concentrated region, we have always compared our experimental results for equivalent conductance with the values calculated by means of the equations of Wishaw and Stokes (3) and of Falkenhagen and Leist (4); it is therefore not necessary to reproduce here these often-quoted equations. In the region of high concentration, the agreement between observed and calculated results is far from exact, and this is to be expected since neither of the above equations makes any assumptions other than those of the Debye–Hückel–Onsager treatment, and it is hardly to be expected that this relatively simple treatment would account for the behavior of the (presumably) complicated concentrated solutions.

We therefore decided to determine, with a high degree of accuracy, the conductances, densities, and viscosities, in a range of concentration varying from 0.01 *N* to 1.0 *N*, of those electrolytes with which much of our previous work has been done, viz. ammonium nitrate, silver nitrate, and lithium nitrate. The presumption was that agreement between calculated and observed conductances would be much better if the above equations have even approximate validity. We worked at the two temperatures, 25° C and 35° C. Our technique has been described frequently and need not be repeated here. The conductances of ammonium nitrate were corrected for hydrolysis by the method of Campbell and Bock (2); in the most dilute solution the correction amounts to 0.11 mho.

EXPERIMENTAL RESULTS

The experimental results are given in Tables I to VI. Three fundamental properties (density, specific conductance, and relative viscosity) and two derived properties (equivalent normality or molarity and equivalent conductance) are given for each solution.

DISCUSSION OF RESULTS

The densities are accurate to 0.002%, weight per cent concentration to 0.01%, and hence equivalent concentration to 0.015%. The accuracy of specific conductance measurements depends principally on the knowledge of the cell constant and this is known within 0.02%. Hence, equivalent conductances are within ±0.05% of their true values.

[1]*Manuscript received May 1, 1959.*
Contribution from the Department of Chemistry, University of Manitoba, Winnipeg, Manitoba.

Can. J. Chem. Downloaded from www.nrcresearchpress.com by 196.1.178.254 on 09/04/12
For personal use only.

TABLE I

Data for ammonium nitrate solutions

At 25.00° C					At 35.00° C				
Concn. (mole/l.)	Density (g/ml)	Specific conductance (mho/cm $\times 10^6$)	Equiv. conductance (mho)	Rel. viscosity	Concn. (mole/l.)	Density (g/ml)	Specific conductance (mho/cm $\times 10^6$)	Equiv. conductance (mho)	Rel. viscosity
0.009893	0.99740	1350.9	136.47	0.999	0.009864	0.99439	1616.0	163.73	0.999
0.020033	0.99776	2671.8	133.32	0.998	0.019972	0.99472	3192.9	159.78	0.999
0.029175	0.99801	3830.7	131.26	0.998	0.029087	0.99498	4577.8	157.31	0.999
0.039970	0.99839	5170.5	129.33	0.997	0.039851	0.99540	6177.1	154.94	0.998
0.047956	0.99866	6146.3	128.13	0.996	0.047808	0.99559	7341.2	153.49	0.997
0.050005	0.99872	6395.0	127.86	0.998	0.049851	0.99566	7637.5	153.14	0.998
0.059997	0.99901	7601.0	126.66	0.996	0.059813	0.99594	9073.9	151.65	0.998
0.070046	0.99938	8792.6	125.50	0.997	0.069828	0.99628	10495.5	150.28	0.998
0.079920	0.99967	9955.0	124.54	0.996	0.079673	0.99658	11880.9	149.08	0.997
0.089968	1.00003	11130.3	123.70	0.996	0.089684	0.99687	13280.7	148.04	0.997
0.10001	1.00036	12285.5	122.83	0.995	0.099691	0.99720	14661.3	147.03	0.998
0.15363	1.00208	18344	119.39	0.993	0.15315	0.99894	21863	142.73	0.996
0.20090	1.00360	23529	117.10	0.990	0.20026	1.00041	28020	139.89	0.995
0.30230	1.00684	34302	113.46	0.986	0.30130	1.00353	40792	135.37	0.992
0.39993	1.00990	44327	110.83	0.982	0.39859	1.00650	52637	132.04	0.992
0.49647	1.01296	53993	108.74	0.977	0.49478	1.00951	64031	129.40	0.988
0.59710	1.01613	63832	106.90	0.975	0.59498	1.01251	75588	127.03	0.987
0.69976	1.01937	73640	105.23	0.973	0.69727	1.01575	87124	124.94	0.987
0.79943	1.02246	82966	103.77	0.968	0.79655	1.01877	98031	123.06	0.984
0.90237	1.02566	92510	102.51	0.967	0.89905	1.02189	109146	121.39	0.984
0.99976	1.02868	101306	101.32	0.963	0.99578	1.02458	119441	119.94	0.982

TABLE II

Data for silver nitrate solutions

At 25.00° C					At 35.00° C				
Concn. (mole/l.)	Density (g/ml)	Specific conductance (mho/cm $\times 10^6$)	Equiv. conductance (mho)	Rel. viscosity	Concn. (mole/l.)	Density (g/ml)	Specific conductance (mho/cm $\times 10^6$)	Equiv. conductance (mho)	Rel. viscosity
0.010156	0.99842	1267.0	124.75	1.001	0.010127	0.99549	1519.5	150.04	1.002
0.019394	0.99981	2354.2	121.39	1.003	0.019335	0.99678	2824.9	146.10	1.003
0.029459	1.00125	3503.3	118.92	1.004	0.029369	0.99820	4199.9	143.00	1.004
0.039998	1.00278	4675.2	116.89	1.004	0.039873	0.99966	5604.3	140.55	1.004
0.049659	1.00411	5720.5	115.20	1.003	0.049507	1.00104	6854.4	138.45	1.005
0.058313	1.00530	6643.7	113.93	1.003	0.058136	1.00224	7958.2	136.89	1.005
0.068343	1.00675	7691.4	112.54	1.004	0.068130	1.00362	9212.8	135.22	1.007
0.080014	1.00842	8895.5	111.18	1.005	0.079763	1.00526	10652.4	133.55	1.007
0.089961	1.00978	9902.2	110.07	1.005	0.089681	1.00663	11858	132.23	1.008
0.10063	1.01127	10968.2	109.00	1.005	0.10032	1.00811	13143	131.01	1.008
0.14915	1.01809	15655	104.96	1.008	0.14867	1.01485	18738	126.04	1.011
0.19797	1.02494	20148	101.77	1.011	0.19734	1.02167	24108	122.16	1.016
0.29997	1.03920	28982	96.62	1.016	0.29899	1.03580	34657	115.91	1.022
0.39976	1.05316	37051	92.68	1.022	0.39842	1.04961	44288	111.16	1.029
0.55271	1.07455	48674	88.06	1.027	0.55080	1.07082	58120	105.52	1.037
0.59523	1.08033	51646	86.77	1.030	0.59314	1.07654	61665	103.96	1.038
0.69928	1.09476	58860	84.17	1.038	0.69679	1.09087	70246	100.81	1.050
0.79154	1.10758	64962	82.07	1.046	0.78873	1.10364	77488	98.24	1.058
0.89509	1.12196	71594	79.99	1.053	0.89180	1.11783	85278	95.63	1.066
1.00088	1.13649	77977	77.91	1.062	0.99713	1.13225	92985	93.25	1.076

If $\mathring{a}$, the distance of closest approach in angstroms, is treated as the unknown in the equations of Falkenhagen–Leist and Wishaw–Stokes, it is possible to solve for this quantity, and to plot it as a function of concentration. This has been done in Figs. 1, 2, and 3, which are typical of many similar diagrams. In Fig. 1, $\mathring{a}$ of the Falkenhagen–Leist

TABLE III

Data for lithium nitrate solutions

At 25.00° C					At 35.00° C				
Concn. (mole/l.)	Density (g/ml)	Specific conductance (mho/cm $\times 10^6$)	Equiv. conductance (mho)	Rel. viscosity	Concn. (mole/l.)	Density (g/ml)	Specific conductance (mho/cm $\times 10^6$)	Equiv. conductance (mho)	Rel. viscosity
0.010572	0.99751	1083.0	102.44	1.000	0.010540	0.99446	1306.2	123.93	1.000
0.021061	0.99793	2105.4	99.97	0.999	0.020996	0.99485	2534.9	120.73	1.002
0.029775	0.99830	2920.0	98.07	1.004	0.029683	0.99523	3525.9	118.79	1.003
0.038848	0.99866	3770.3	97.05	1.005	0.038729	0.99559	4540.1	117.23	1.006
0.050821	0.99897	4861.3	95.66	—	0.050664	0.99589	5848.5	115.44	—
0.059158	0.99949	5604.1	94.73	1.007	0.058975	0.99640	6745.2	114.37	1.008
0.069872	0.99991	6533.8	93.51	1.009	0.069654	0.99679	7861.2	112.86	1.010
0.076234	1.00010	7095.4	93.07	1.008	0.075999	0.99700	8531.6	112.26	1.008
0.091701	1.00079	8448.0	92.13	1.011	0.091418	0.99770	10157.2	111.11	1.012
0.10111	1.00112	9247.6	91.46	1.011	0.10079	0.99798	11114.3	110.27	1.014
0.14980	1.00332	13290	88.72	1.017	0.14929	0.99997	15960	106.91	1.020
0.19937	1.00506	17267	86.61	1.022	0.19874	1.00186	20724	104.28	1.024
0.29918	1.00902	24887	83.19	1.043	0.29821	1.00576	29822	100.00	1.044
0.39900	1.01293	32130	80.53	1.042	0.39769	1.00960	38460	96.71	1.045
0.45941	1.01532	36341	79.10	1.050	0.45787	1.01192	43479	94.96	1.055
0.58142	1.02009	44546	76.62	1.060	0.57945	1.01662	53234	91.87	1.066
0.71135	1.02509	52771	74.18	1.075	0.70889	1.02154	62994	88.86	1.081
0.81640	1.02930	59193	72.51	1.087	0.81351	1.02566	70605	86.79	1.094
0.91101	1.03301	64745	71.00	1.098	0.90862	1.02929	77198	84.96	1.106
1.00464	1.03667	69959	69.64	1.114	1.0010	1.03287	83338	83.26	1.117

TABLE IV

Ammonium nitrate solutions at 25° C

I	II	III	IV	V	VI
0.01	136.47	136.4	136.61	136.59	136.5
0.02	133.32	133.0	133.54	133.51	133.4
0.03	131.26	131.0	131.56	131.50	—
0.04	129.33	128.9	129.69	129.62	129.4
0.048	128.13	127.7	128.52	128.44	128.2
0.05	127.86	127.6	128.24	128.15	—
0.06	126.66	126.1	126.99	126.89	126.6
0.07	125.50	125.1	125.89	125.78	125.4
0.08	124.54	124.0	124.90	124.78	—
0.09	123.70	123.2	123.99	123.85	123.4
0.10	122.83	122.3	123.15	123.01	—
0.15	119.39	118.6	119.59	119.38	—
0.2	117.10	116.0	117.19	116.95	115.9
0.3	113.46	111.8	113.46	113.14	—
0.4	110.83	108.9	110.83	110.45	—
0.5	108.74	106.2	108.78	108.35	106.1
0.6	106.90	104.3	107.08	106.56	—
0.7	105.23	102.4	105.56	105.04	—
0.8	103.77	100.5	104.34	103.77	100.4
0.9	102.51	99.1	103.23	102.63	—
1.0	101.32	97.6	102.30	101.68	97.7

NOTE: Column

I Gives the rounded concentration, moles per liter.

II Experimental equivalent conductance.

III Experimental equivalent conductance multiplied by relative viscosity.

IV Equivalent conductance calculated by Falkenhagen equation, $\mathring{a}$ = 2.625 Å.

V As for IV, except $\mathring{a}$ = 2.560 Å.

VI Equivalent conductance, calculated by Robinson–Stokes equation, with $\mathring{a}$ = 2.75 Å.

Can. J. Chem. Downloaded from www.nrcresearchpress.com by 196.1.178.254 on 09/04/12
For personal use only.

Can. J. Chem. Downloaded from www.nrcresearchpress.com by 196.1.178.254 on 09/04/12
For personal use only.

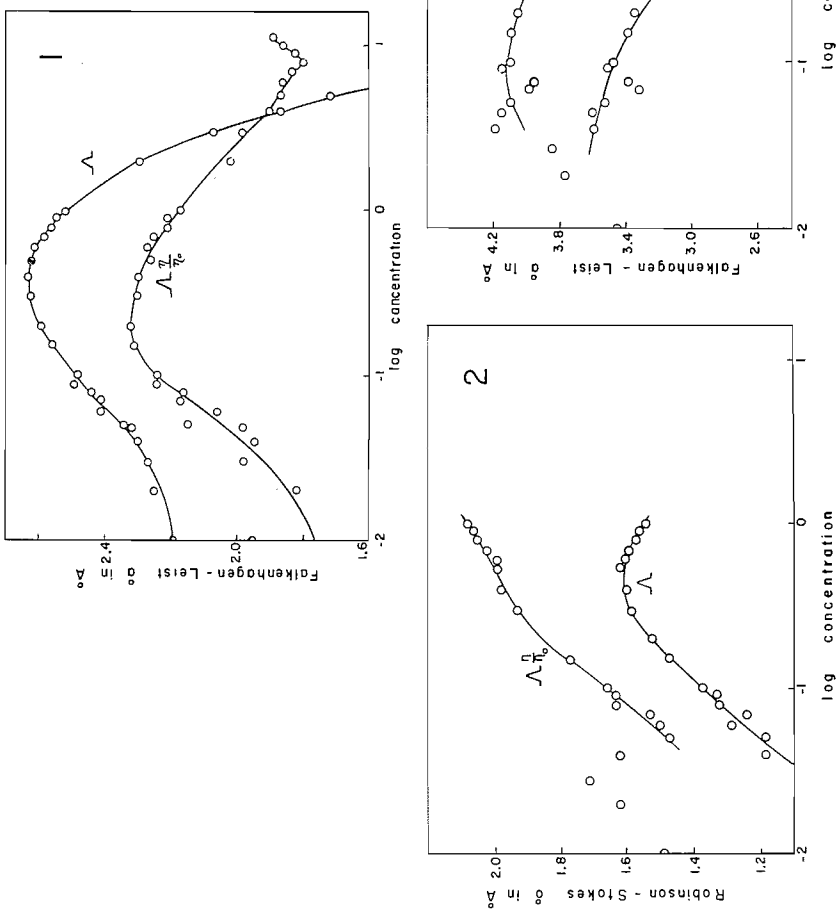

FIG. 1. $\mathring{a}$(F–L) vs. log c, NH_4NO_3 at 25° C.

FIG. 2. $\mathring{a}$(R–S) vs. log c, $AgNO_3$ at 25° C.

FIG. 3. $\mathring{a}$(F–L) vs. log c, $LiNO_3$ at 25° C.

Can. J. Chem. Downloaded from www.nrcresearchpress.com by 196.1.178.254 on 09/04/12
For personal use only.

TABLE V

Silver nitrate solutions at 25° C

I	II	III	IV	V	VI	VII
0.01	124.75	124.7	124.70	124.8	124.68	124.8
0.02	121.39	121.7	121.65	121.9	—	121.9
0.03	118.92	119.4	119.22	119.7	119.28	119.6
0.04	116.89	117.3	117.14	117.6	117.20	117.6
0.05	115.20	115.5	115.53	116.0	115.60	116.1
0.06	113.93	114.3	114.23	114.8	114.32	115.1
0.07	112.54	113.0	112.90	113.5	112.97	113.6
0.08	111.18	111.7	111.49	112.2	111.54	112.3
0.09	110.07	110.6	110.37	111.1	110.42	111.3
0.10	109.00	109.6	109.26	110.1	109.33	110.3
0.15	104.96	105.8	105.08	106.2	105.17	106.4
0.2	101.77	102.9	101.75	103.0	101.82	103.3
0.3	96.62	98.1	96.39	98.2	96.43	98.4
0.4	92.68	94.7	92.40	94.6	92.37	94.9
0.55	88.06	90.4	87.58	90.4	87.53	90.5
0.6	86.77	89.4	86.47	89.5	86.37	89.6
0.7	84.17	87.4	83.99	87.3	83.81	87.2
0.8	82.07	85.8	82.02	85.5	81.81	85.4
0.9	79.99	84.2	80.07	83.9	79.79	83.7
1.0	77.91	82.7	78.27	82.4	77.91	82.0

NOTE: Column

I Rounded concentration, moles per liter.
II Experimental equivalent conductance.
III Experimental equivalent conductance multiplied by relative viscosity.
IV Calculated equivalent conductance, Falkenhagen equation, $\mathring{a}$ = 1.51 Å.
V Same as IV, except $\mathring{a}$ = 1.80 Å.
VI Calculated equivalent conductance, Robinson–Stokes, $\mathring{a}$ = 1.54 Å.
VII Same as VI, except $\mathring{a}$ = 2.00 Å.

TABLE VI

Lithium nitrate solutions at 25° C

I	II	III	IV	V
0.01	102.44	102.4	102.31	102.6
0.02	99.97	99.9	99.57	100.1
0.03	98.07	98.5	97.94	98.6
0.04	97.05	97.5	96.57	97.3
0.05	95.66	96.2	95.05	96.1
0.06	94.73	95.4	94.11	95.3
0.07	93.51	94.4	93.07	94.4
0.08	93.07	93.9	92.51	94.0
0.09	92.13	93.1	91.30	92.9
0.10	91.46	92.5	90.57	92.3
0.15	88.72	90.3	87.80	90.1
0.2	86.61	88.5	85.76	88.3
0.3	83.19	86.7	82.43	85.9
0.4	80.53	83.9	80.11	84.2
0.5	79.10	83.1	78.98	83.4
0.6	76.62	81.2	77.11	82.0
0.7	74.18	79.7	75.48	81.2
0.8	72.51	78.9	75.17	—
0.9	71.00	78.0	—	—
1.0	69.64	77.6	—	—

NOTE: Column

I Rounded concentration, moles per liter.
II Experimental equivalent conductance.
III Experimental equivalent conductance multiplied by relative viscosity.
IV Calculated equivalent conductance, Falkenhagen equation, $\mathring{a}$ = 3.00 Å.
V Same as IV, except $\mathring{a}$ = 4.00 Å.

equation, for ammonium nitrate at 25° C, is plotted against log c; one curve refers to equivalent conductance without viscosity correction, the other to conductance multiplied by relative viscosity. In Fig. 2, the $\mathring{a}$ of the Wishaw–Stokes equation, for silver nitrate at 25° C, is plotted against log c. In Fig. 3, the Falkenhagen–Leist $\mathring{a}$, for lithium nitrate, is plotted against log c. It is apparent that $\mathring{a}$ is far from constant; often it appears to pass through a maximum. Theoretically, $\mathring{a}$ should be independent of concentration and even, perhaps, of temperature. In fairness, however, it should be pointed out that this method of treatment forces $\mathring{a}$ to absorb not only all the imperfections in the conductance equations but any experimental error as well.

Considering the Falkenhagen–Leist equation only, it appears that $\mathring{a}$ determinations in dilute solutions show greater scatter than in concentrated solutions. The reason for this is that $\mathring{a}$ appears only in the linear and quadratic divisors $(1+Ka)$ and $(1+1/2\sqrt{2}Ka+1/6K^2a^2)$, both of which approach unity with dilution. The more dilute the solution, the greater the uncertainty in the determination of $\mathring{a}$ from conductance.

Curves similar to Figs. 1, 2, and 3, for the higher temperature (35° C), show that above 0.1 N there is no doubt that two different $\mathring{a}$ values are necessary to reproduce the experimental results at the two temperatures.

Despite the apparent variations in $\mathring{a}$, however, if a suitable "best" value of $\mathring{a}$ is chosen, it is possible to reproduce the values of equivalent conductance, between 0.01 N and 1.0 N, within 0.5 mho, using either the Falkenhagen–Leist or the Wishaw–Stokes equation. This is shown in Tables IV, V, and VI, which are self-explanatory. Although it might seem that, on theoretical grounds, the Wishaw–Stokes equation is less acceptable than that of Falkenhagen–Leist, the agreement between calculation and experiment is better with the former equation: this we have observed before.

REFERENCES

1. CAMPBELL, A. N. and KARTZMARK, E. M. Can. J. Research, B, **28**, 43 (1950). CAMPBELL, A. N., GRAY, A. P., and KARTZMARK, E. M. Can. J. Chem. **31**, 617 (1953). CAMPBELL, A. N., DEBUS, G. H., and KARTZMARK, E. M. Can. J. Chem. **33**, 1508 (1955).
2. CAMPBELL, A. N. and BOCK, E. Can. J. Chem. **36**, 330 (1958).
3. WISHAW, B. F. and STOKES, R. H. J. Am. Chem. Soc. **76**, 2065 (1940).
4. FALKENHAGEN, H., LEIST, M., and KELBG, G. Ann. Phys. **11**, 51 (1952).

Can. J. Chem. Downloaded from www.nrcresearchpress.com by 196.1.178.254 on 09/04/12
For personal use only.

Can. J. Chem. Downloaded from www.nrcresearchpress.com by 196.1.178.254 on 09/04/12
For personal use only.

LIGHT ABSORPTION STUDIES

PART XIV. THE ULTRAVIOLET ABSORPTION SPECTRA OF PHENOLS[1]

J. C. Dearden and W. F. Forbes

ABSTRACT

A spectral analysis of benzene derivatives is extended to substituted phenols. The discussion emphasizes hydrogen bonding and steric effects which occur in phenols. Some of the phenolic absorption bands are ascribed to locally excited states.

INTRODUCTION

The effect of the hydroxy group on the electronic spectra of benzene derivatives is of interest for a number of reasons. First, phenols are known to give rise to various forms of hydrogen bonding, and hence the investigation of spectral effects which may be ascribed to hydrogen bonding affords further information concerning the nature of the hydrogen bond. Next, compounds which may be regarded as substituted phenols, for example flavones, frequently occur as natural products, and hence an understanding of phenolic spectra assists in the identification and quantitative estimation of such naturally occurring compounds. Lastly, previous papers in this series have attempted to analyze the spectra of benzene derivatives in terms of mesomeric and steric interactions, and it is therefore of interest to test these hypotheses on the observed spectra of phenols.

The ultraviolet spectra of a number of phenols have previously been investigated by other workers (1, 2, 3, 4, 5), but whenever convenient we have redetermined the spectra in order to ensure near-identical conditions.

THE SPECTRUM OF PHENOL

Phenols generally exhibit two absorption bands in the spectral region under investigation, that is, between 200 and 360 mμ. The band at longer wavelength is referred to as the *C*-band, and the band at shorter wavelength as the *B*-band. This assignment corresponds to the assignment for anilines and is based on similar reasoning (cf. ref. 6). The data for phenol are listed in Table I.

The bands are somewhat altered with change of solvent, and it has been shown by Coggeshall and Lang (3) that some of these spectral changes do not depend on *stable* hydrogen-bonded complexes, although there is evidence that some of the observed spectral changes are caused by some type of hydrogen bonding (5). Various forms of intermolecular hydrogen bonding are certainly possible, involving both the hydrogen atom of the hydroxy group and the oxygen atom. The wavelength displacement between the spectra in the vapor phase and in cyclohexane solution must also result from some solute–solvent interaction; but the latter interaction is unlikely to be associated with hydrogen bonding because similar displacements are observed for phenols and anilines (cf. ref. 6). In more concentrated solutions of phenol in cyclohexane, yet other spectral effects occur, presumably caused by intermolecular hydrogen bonding between phenol molecules (see ref. 4).

The fine structure of the *C*-band for phenol or anisole in cyclohexane or similar inert media is fairly characteristic of these chromophores, and can often be recognized in substituted, including sterically hindered, phenols (see also later section). The fine structure disappears if the phenolic species no longer contributes appreciably to the

[1]*Manuscript received November 10, 1958.*
Contribution from the Memorial University of Newfoundland, St. John's, Newfoundland.

TABLE I

Absorption maxima of phenol in various solvents

(Values in italics represent inflections in this and subsequent tables)

Solvent	*B*-Band		*C*-Band		Source
	λ_{max}(mμ)	ϵ_{max}	λ_{max}(mμ)	ϵ_{max}	
Vapor phase	205	†	261 264 266.5 *ca. 270* 273	†	*
Cyclohexane (*B*-band concn. = 2.3×10^{-4} moles/l.)	210	6000	263 269 276	1400 2200 2100	*
Ether	218	6400	266 271 277.5	1600 2200 1800	*
Ethanol	218.5	6000	*ca. 266* 271 *276*	*1500* 1900 *1450*	*
Water	210	6000	268 *273*	1500 *1250*	*
0.1 *N* HCl	210	6000	268 *273*	1600 *1300*	*
N NaOH	234	10500	285	2700	*
Conc. H_2SO_4	231.5	9500	261 *ca. 271* 278–279	830 *980* 1150	*

*This series of papers. †Intensities not determined.

observed spectrum; as for example in the *C*-band of *m*-nitro- or *m*-amino-phenol, where the compound absorbs preferentially as nitrobenzene or aniline (see Table II). The fine structure of the *C*-band also disappears for intramolecularly hydrogen-bonded molecules such as salicylaldehyde (see Table II), but the fine structure *is* noticeable for a number of orthosubstituted phenols even in ethanolic solution (see Table III). The most probable explanation seems to be that this fine structure is caused by vibrational sublevels and that a hydrogen bond may obscure this fine structure. Hence, the fine structure is frequently reduced if the phenol is associated with a solvent molecule by means of an intermolecular hydrogen bond (see Table I) or if the phenol molecule is intramolecularly hydrogen-bonded, but the fine structure does become evident if steric interactions hinder the formation of a hydrogen bond (see section on orthosubstituted phenols).

In sodium hydroxide solution the phenolic spectrum is radically altered, and the spectrum is assumed to correspond to the phenolate ion. For phenol in basic medium, compared with cyclohexane solution, a wavelength displacement of 24 mμ is observed for the *B*-band and a displacement of 16 mμ is observed for the *C*-band (see Table I). As expected, similar wavelength displacements are not observed for the spectrum of anisole (see ref. 7).

THE SPECTRA OF PARASUBSTITUTED PHENOLS

The spectra of substituted phenols are listed in Table II.

Table II lends support to the naming of the *B*-bands, that is, as bands corresponding to the so-called *B*-bands in benzene, acetophenone, nitrobenzene, benzoic acid, and

Can. J. Chem. Downloaded from www.nrcresearchpress.com by 196.1.178.254 on 09/04/12
For personal use only.

Can. J. Chem. Downloaded from www.nrcresearchpress.com by 196.1.178.254 on 09/04/12
For personal use only.

TABLE II

Absorption maxima of substituted phenols

		Para isomer				Meta isomer						Ortho isomer					
		B-Band		*C*-Band		Phenolic *B*-band		2nd *B*-band		*C*-Band		Phenolic *B*-band		2nd *B*-band		*C*-Band	
Substituent	Solvent	$\lambda_{max}(m\mu)$	ϵ_{max}	$\lambda_{max}(m\mu)$	ϵ_{max}	$\lambda_{max}(m\mu)$	ϵ_{max}	$\lambda_{max}(m\mu)$	ϵ_{max}	$\lambda_{max}(m\mu)$	ϵ_{max}	$\lambda_{max}(m\mu)$	ϵ_{max}	$\lambda_{max}(m\mu)$	ϵ_{max}	$\lambda_{max}(m\mu)$	ϵ_{max}
-OH	Cyclohexane	223	4400*	*ca. 285*	*2500**	*ca.217*	*6800**	—	—	*ca. 268*	*1650**	214	6800	—	—	*ca. 270*	*2200*
				289	2800					273.5	2150					274	2500
				292	2900					279.5	1800					280	2250
				ca. 299	*2200*												
$-OCH_3$	Cyclohexane	224	7000	*ca. 285*	*2900*			220	5400†	*ca. 267*	*1300*			216	6200†	*ca. 270*	*2250*
				288	3150					271.5	1650					273.5	2550
				291	3100					278	1550					279.5	2150
				298	2350												
$-NH_2$	Cyclohexane*	235	7150‡	304	2550‡			234	6800	284	2300			235	7000	288	3300
	Water	229	6100‡	294	2000‡			229	6400	278	1900			229	6150	281	2700
	pH 3 or 0.1 *N* HCl	218.5	6240§	262.5	1450§	217	6300	*ca. 212*	*6150†*	269	1900	210	6500†			268	2100
										ca. 273	*1700*					*ca. 273*	*1800*
$-CH_3$	Cyclohexane	220	5900	268	1400	214	6100			271	1600	213	7000			270	1850
				271.5	1600					277	1850					276	1750
				274	1850												
				277	2150												
				283.5	1950												
$-C_2H_5$	Cyclohexane	221	7250	*ca. 267*	*1400*							212	7450			*ca. 268*	*1400*
				270	1600											270	2000
				273	1800											276	1900
				276	2200												
				282	2000												
$-CH(CH_3)_2$	Cyclohexane	220	6850	*ca. 267*	*1350*							211	7500			*ca. 264*	*1500*
				ca. 270	*1500*											270	2100
				ca. 272	*1700*											276	2000
				275	2100												
				281	1900												
$-C(CH_3)_3$	Cyclohexane	219	6800	*ca. 268*	*1500*							213	5900			*ca. 263*	*1400*
				274	2100											268.5	2050
				280	2050											275	2100

Can. J. Chem. Downloaded from www.nrcresearchpress.com by 196.1.178.254 on 09/04/12
For personal use only.

TABLE II (*Concluded*)

Absorption maxima of substituted phenols

		Para isomer				Meta isomer						Ortho isomer					
		B-Band		*C*-Band		Phenolic *B*-band		2nd *B*-band		*C*-Band		Phenolic *B*-band		2nd *B*-band		*C*-Band	
Substituent	Solvent	$\lambda_{max}(m\mu)$	ϵ_{max}	$\lambda_{max}(m\mu)$	ϵ_{max}	$\lambda_{max}(m\mu)$	ϵ_{max}	$\lambda_{max}(m\mu)$	ϵ_{max}	$\lambda_{max}(m\mu)$	ϵ_{max}	$\lambda_{max}(m\mu)$	ϵ_{max}	$\lambda_{max}(m\mu)$	ϵ_{max}	$\lambda_{max}(m\mu)$	ϵ_{max}
-F	Cyclohexane	210–211	4200	267	1700	211.5	5200			*ca. 262*	*1150*	212	5800			262	1250
				269.5	2200					266.5	1450					266	1600
				272.5	2500					272	1300					272	1400
				275.5	2750												
				278.5	3100												
				ca. 282	*2000*												
				285	2600												
-Cl	Cyclohexane	224	8800	*ca. 273*	*1400*	216	6500			266	1300	212	6450			*ca. 265*	*1550*
				279	1850					272	2050					271	2350
				287	1700					279	2000					278	2450
-Br	Cyclohexane	224	10250	*ca. 273*	*1300*	210	7500†			266	1450	212	8700			*ca. 266*	*1750*
				279.5	1750	*215*	*7000*			272	2300					272	2700
				287	1500					279	2250					279	2650
-I	Cyclohexane	230.5	15000	273.5	1300									218	9250†	268	2200
		ca. 235	*12400*	279.5	1450									224	8300	274	3000
				288	1100									229	6500	281.5	2800
-CHO	*n*-Hexane	265–266	19000	—	—	213	19000†	244	10000	302	2900	215	17000†	250	11000	324–325	3600
		ca. 274	*15500*					250	9500	*ca. 307*	*2800*			257	11700		
		281	12000†														
		288	6000†														
	0.1 *N* NaOH	330	27900§	—	—§	237	23900‖	267	6200‖	357	2600‖	226.5	18200‖	264.5	7500‖	377	6700‖
$-NO_2$	Cyclohexane	295	11300*	—	—*	225	11000*	262	5750*	319	2150*	*ca. 230*	*4000*	269	7350	342	3700
	Water	313–314	9300	—	—	228	7650	272	5950	328	1950	*ca. 230*	*3700*	276	6350	346	3050
	0.1 *N* or *N* NaOH	402.5	19200§	—	—§	251.5	11000‖	291	4500‖	392	1500‖	*250*	*5000‖*	282	4300‖	416	4800‖
-COOH	Cyclohexane	251	15000	—	—			235–236	6500	296	2900			237–238	8000	307	4400
	Ethanol	253–254	15000	—	—			234–235	6000	301	2300			236	7500	307	3700

*In cyclohexane containing *ca.* 2% ether. †*B*-Band assignment doubtful. ‡Aniline absorption. §Ref. 8. ‖Ref. 9.

benzaldehyde, although the excited state of phenol may represent a locally excited state (see below). This follows because the gradual displacement of the band for a series of compounds such as phenols indicates that the main absorption band in phenol (and incidentally aniline) is of similar nature for the compounds listed in Table II. Further, as shown in Parts XI and XII (10, 11), this same band, for example in *p*-hydroxyacetophenone, can likewise be related to the *B*-band in acetophenone. This confirms the suggestion that *all* the above-mentioned absorption bands may be described as *B*-bands.*

The *B*-band in phenol is shown to be displaced to longer wavelength on parasubstitution. If the parasubstituent is electron-withdrawing, this displacement is greater, *qualitatively* related to the electron-withdrawing effect of the substituent, and the usual high-intensity band corresponding to an extended conjugated system is obtained. The wavelength displacements with respect to phenol in cyclohexane are parallel to the displacements in the aniline series (6). The *quantitative* relation observed between spectra of parasubstituted nitrobenzenes, acetophenones, and benzaldehydes (10, 11) is, however, absent for the displacements observed between parasubstituted anisoles and phenols, since in the latter example the straight line plot of the wavelength displacements does not pass through the origin (see following paper).

As will also be shown in the following paper and elsewhere, this difference can be rationalized by assuming that the *B*-band in phenol involves transitions which should be associated to an appreciable extent with locally excited states of type I. In support of this hypothesis the following may be cited: (i) the *B*-band of phenol at 210 mμ in

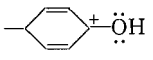

I

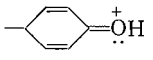

II

cyclohexane is displaced by about 7 mμ from the corresponding band in benzene, a wavelength displacement similar to that associated with the short-range interaction of the hydroxy group (see section on metasubstituted phenols); (ii) if phenol is assumed to absorb at longer wavelength, because hypothetical structures of type II contribute more appreciably to the electronic excited state, the above-mentioned relationship between wavelength displacements in parasubstituted anisoles and phenols becomes more nearly quantitative (see following paper); (iii) steric effects in the *B*-band of phenol are different from those which would be anticipated for a band associated with transitions to excited states of type II (see section on orthosubstituted phenols); (iv) the anomalous nature of the wavelength displacements for phenols has previously been noted by Doub and Vandenbelt (8); and (v) the bathochromic wavelength displacement obtained for the spectra of metasubstituted phenols compared with the spectrum of phenol when the metasubstituent is electron-withdrawing can be explained since an electron-withdrawing substituent has been assumed to facilitate resonance forms of type II (see ref. 6) and this therefore can account for the anomalous *bathochromic* wavelength displacement (see the discussion of the spectra of metasubstituted phenols).

**Alternatively, it has been proposed that the B-band of compounds like, for example, nitrobenzene should be related to the C-band of benzene, that is to the band occurring in benzene at ca. 250 mμ. Wepster (12), in the course of a discussion on steric effects, suggests that this latter argument is supported because for sterically hindered nitrobenzenes the absorption band in hexane remains near 250 mμ, that is, near the C-band absorption of benzene. Our interpretation is to regard this band in substituted nitrobenzenes as a nitrobenzene B-band, since the latter band also occurs near 250 mμ. We believe that our argument receives support from the absorption maxima of sterically hindered p-nitroanilines in ethanol. These maxima are all reported to occur near 380 mμ (12), that is, near the maximal absorption of p-nitroaniline, and the maxima for these examples do not therefore revert to a maximum near 250 mμ.*

Can. J. Chem. Downloaded from www.nrcresearchpress.com by 196.1.178.254 on 09/04/12
For personal use only.

It may be noted that this hypothesis assumes that the absorption of parasubstituted phenols such as *p*-cresol, hydroquinone, or *p*-bromophenol may still involve locally excited states of type I with both substituents exerting only a secondary effect. However, in compounds of this type, structures involving appreciable resonance interaction with at least one substituent seem more probable because the second substituent facilitates additional electronic interaction. The relevant structures may be represented by resonance forms of types III and IV, and consideration of structure IV also suggests that structure

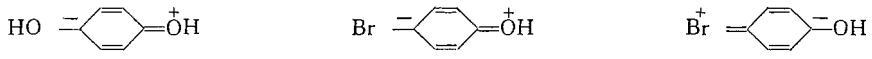

III IV V

V cannot be ruled out. The actual contributing structures will depend on the relative over-all electronegativities of the two substituents in the ground and excited states. For phenols in basic media, a different type of resonance interaction presumably occurs in the excited state because of the replacement of the phenol group by the phenolate ion. Since this resonance interaction will be reflected in the maximal wavelengths it follows that the mesomeric interaction between the hydroxy group and the benzene ring is less than the mesomeric interaction between the amino group and the benzene ring. Extending the argument one step further, the maximal absorptions suggest an order of mesomeric interaction $PhO^- > PhNH_2 > PhOH > PhNH_3^+$.

The *C*-band shows the expected changes if the parasubstituent is electron-withdrawing, namely, with increase of mesomeric interaction the *C*-band usually becomes progressively less pronounced (see Table II and Ref. 13). If the parasubstituent is electron-donating, the fine structure of the *C*-band is frequently enhanced, the effect being most pronounced for the spectra of *p*-methyl- and *p*-fluoro-phenol in cyclohexane. It is worth noting that the fine structure of the *C*-band in these latter compounds is considerably more pronounced than for the corresponding meta isomers (see Table II). This is surprising since increased molecular symmetry is generally assumed to simplify the absorption spectra, and one would therefore have expected the fine structure of the *C*-band to be less pronounced in the para isomer than in the meta isomer.

THE SPECTRA OF METASUBSTITUTED PHENOLS

In metadisubstituted benzene derivatives direct resonance interaction is ruled out by definition, and hence we would expect two *B*-bands corresponding to the two monosubstituted benzene derivatives (cf. refs. 6, 10, 11). Both these bands may be modified because of the other substituent, either by means of secondary short-range electronic interactions (cf. ref. 7), or possibly because of the buttressing effect (cf. refs. 14, 15). It is, of course, possible that one of the two *B*-bands may be obscured, either because of overlap by the other *B*-band or because of *A*-band absorption (cf. ref. 13), and these factors may also prevent a reliable band assignment for some examples. On the other hand, characteristic properties like the fine structure of the phenolic *C*-band assist in the band assignments.

These generalizations are illustrated for phenols in Table II. If the non-phenolic substituent is electron-withdrawing, it is found that the non-phenolic *B*-bands are normally displaced to longer wavelength on account of the secondary interaction of the hydroxy group, and this displacement is of the order of 7 mμ for a number of compounds (cf. ref. 7). This wavelength displacement of *ca.* 7 mμ suggests that the hydroxy group tends

Can. J. Chem. Downloaded from www.nrcresearchpress.com by 196.1.178.254 on 09/04/12
For personal use only.

to facilitate the absorption of the non-phenolic chromophore. The hypothesis may be illustrated by structures of type VI, by analogy with similar structures used in previous arguments (cf. ref. 10). In basic media the secondary interaction is considerably increased, because of the replacement of the hydroxy group by the O^--entity, and bathochromic wavelength displacements of up to 25 mμ (for *m*-nitrophenol compared with nitrobenzene) are observed.

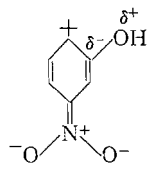

VI

As has previously been noted by Lemon (2, cf. also ref. 7),* the effect of alkali on the spectra of hydroxybenzaldehydes and hydroxyacetophenones is greatest in the para isomers.

Our data also show that for the *B*-bands the displacement in the para isomers in basic media is much more pronounced. For example, the phenolic *B*-band of *m*-nitrophenol on passing from neutral to alkaline solution shows a wavelength displacement of 23.5 mμ (see Table II), comparable with the displacement of 24 mμ for phenol (see Table I). In the para isomer, presumably because appreciable primary resonance interaction occurs, the displacement of the *B*-band, caused by the addition of alkali, is *ca.* 90 mμ (see Table II). These observations may be of some practical importance. For example, if the *B*-band of an acetyl-substituted phenol on changing the solvent from neutral to basic medium does not show a bathochromic wavelength displacement greater than *ca.* 25 mμ, it may be assumed that no uninhibited, direct mesomeric interaction occurs between the hydroxy and acetyl groups.

The effect of the second substituent on the *phenolic B*-band is also illustrated for some of the compounds listed in Table II. Unfortunately, the relevant absorption band frequently occurs at too short a wavelength to be identified with certainty. However, for a few compounds the band assignment presents little difficulty, as for example, in *m*-nitrophenol where the phenolic absorption is appreciably displaced to longer wavelength (see Table II). This latter displacement has previously been ascribed to the nitrosubstituent facilitating the phenolic absorption (10). This bathochromic displacement for the phenolic *B*-band in compounds like *m*-nitrophenol may be related to the changes in the integrated absorption intensities for the infrared hydroxyl absorption in phenols, since the integrated absorption intensity for compounds like *m*-nitrophenol is greater than for phenol (17, 18), and since increased integrated absorption intensities, like bathochromic wavelength displacements in the *B*-band, may be related to increased mesomeric interactions.

It should be noted that when the metasubstituent is electron-withdrawing, the phenolic *B*-band appears sometimes to be moved to longer wavelength (see Table II), whereas the anilinic *B*-band under these conditions is moved to shorter wavelength (see ref. 6). More-

**Lemon arrives at this conclusion, although for the ortho and meta isomers he considers what we believe to be the C-band, whereas for the para isomers he considers the B-band. Another example of what we believe is an incorrect assignment is provided by the reported data for the intense o-hydroxyacetophenone band near 315–330 mμ, which has been described as a B-band (K-band, see ref. 16), whereas we would regard it as a displaced C-band.*

Can. J. Chem. Downloaded from www.nrcresearchpress.com by 196.1.178.254 on 09/04/12
For personal use only.

Can. J. Chem. Downloaded from www.nrcresearchpress.com by 196.1.178.254 on 09/04/12
For personal use only.

over, these wavelength displacements are parallel in the corresponding infrared bands. For example, in *m*-nitroaniline compared with aniline (19), the NH_2 stretching vibration is moved to higher frequency, that is to shorter wavelength, whereas the OH stretching vibration in *m*-nitrophenol compared with phenol is moved to lower frequency. These anomalous wavelength displacements for phenols can be explained by assuming that the *B*-band of phenol occurs at unusually *short* wavelength because of the contribution of locally excited states of type I (see section on parasubstituted phenols). In this way, the above-mentioned comparisons involving phenol are rendered invalid, in the sense that metasubstituted phenols compared with hypothetical phenol molecules containing more similar contributions of locally excited states than aniline may still afford the anticipated hypsochromic wavelength displacement.

If the above assignments are accepted, examination of the relative intensities of the two *B*-bands suggests that the phenolic *B*-band absorption usually occurs preferentially. For example, in *m*-nitrophenol, compared with the two monosubstituted parent compounds, the nitrobenzene *B*-band absorption decreases, whereas the phenolic absorption increases in intensity. A similar relative intensity increase is observed for the aniline *B*-band in *m*-nitroaniline (6), although the relative increase in the intensity of the phenolic *B*-band is less than for the anilinic *B*-band. These observations may be rationalized by a converse of the mechanism postulated to account for the increased extinction coefficient in associated benzoic acid molecules (see ref. 20). There it was shown that an electron-withdrawing substituent, in the absence of direct resonance interaction, gives rise to an increased maximal extinction coefficient. Likewise, in metasubstituted anilines or phenols the nitro group may be assumed to increase the probability of the phenolic or anilinic transition, and conversely, the *m*-hydroxy and the *m*-amino substituents may be assumed to have the effect of relatively *weakening* the nitrobenzene absorption, the effects being more pronounced for the meta-amino substituent, which donates electrons more effectively.

Some of the *C*-bands in metasubstituted phenols show the expected changes. For example, if the metasubstituent is electron-withdrawing the *C*-bands are enhanced compared with the *C*-bands in para isomers (cf. ref. 13).

THE SPECTRA OF ORTHOSUBSTITUTED PHENOLS

The *B*-bands of the ortho isomers frequently resemble the *B*-bands of the meta isomers. For example, for *o*-nitrophenol in 0.1 *N* NaOH where intramolecular hydrogen bonding is ruled out, the nitrobenzene band at 282 mμ, $\epsilon = 4300$, is similar to the nitrobenzene *B*-band in the meta isomer which occurs at 291 mμ, $\epsilon = 4500$ (9). The phenolic *B*-band is considerably reduced in intensity and occurs in the ortho isomer as an inflection at 250 mμ, $\epsilon = 5000$, whereas in the meta isomer it occurs at 251.5 mμ, $\epsilon = 11{,}000$ (9, and see Table II). For *o*-nitrophenol in basic solution there is therefore no evidence for appreciable resonance interaction. Similar spectral effects are observed in other examples listed in Table II, and the examples of 2,4- or 2,4,6-substituted nitrobenzenes when an ortho-alkyl substituent does not contribute to the direct resonance interaction, have previously been mentioned in this paper in the discussion of parasubstituted phenols. Effects of this type may also be noted in the *B*-bands of a number of parasubstituted phenols in neutral solution when, on introduction of two *t*-butyl groups in the ortho-positions, no appreciable wavelength displacement is observed, but a decreased extinction coefficient indicative of steric interactions is obtained (21).

This absence of resonance interaction may be ascribed to steric interactions, and steric interactions are also indicated by a number of other physical properties, such as the decreased intermolecular hydrogen bond formation in sterically hindered phenols (3, 15, 22, cf. also 23), and more generally by the failure of sterically hindered phenols to exhibit normal phenolic properties (cf. for example, ref. 21). These observed steric effects may be associated, at least partly, with the two unshared electron pairs on the oxygen atom, since a steric effect caused entirely by the more distant hydrogen atom of the hydroxy group would not account satisfactorily for the observed steric effects (cf. ref. 24, p. 360). The *B*-band in orthosubstituted phenols does not normally undergo a pronounced wavelength displacement even if the orthosubstituents are bulky as in diortho-*t*-butylphenol (see Table III). The absence of this spectral effect, characteristic of steric inhibition of resonance in many other conjugated systems, has already received an explanation (see section on parasubstituted phenols, which tentatively ascribes the

TABLE III

Absorption maxima of orthosubstituted phenols in cyclohexane and ethanol

	Cyclohexane		Ethanol	
Orthosubstituents	λ_{max}(mμ)	ϵ_{max}	λ_{max}(mμ)	ϵ_{max}
H,H (*B*-Band)	210	6000	218.5	6000
H,H (*C*-Band)	263	1400	*ca. 266*	*1500*
	269	2200	271	1900
	276	2100	*276*	*1450*
H,CH_3 (*B*-Band)	213	7000	213	7100
H,CH_3 (*C*-Band)	270	1850	272	2050
	276	1750	*ca. 276*	*1800*
H,$CH(CH_3)_2$ (*B*-Band)	211	7500	215	6200
H,$CH(CH_3)_2$ (*C*-Band)	*ca. 264*	*1500*	271	2250
	270	2100	*ca. 276*	*2000*
	276	2000		
H,$C(CH_3)_3$ (*B*-Band)	213	5900	216	5100
H,$C(CH_3)_3$ (*C*-Band)	*ca. 263*	*1400*	271	2300
	268.5	2050	277	2050
	275	2100		
CH_3,CH_3 (*B*-Band)	211–212	7900	*ca. 214*	*8500*
CH_3,CH_3 (*C*-Band)	269	1500	271	1550
	275	1600	*ca. 275*	*1450*
$CH(CH_3)_2$,$CH(CH_3)_2$ (*B*-Band)	211	9200	*ca. 214*	*8000*
$CH(CH_3)_2$,$CH(CH_3)_2$ (*C*-Band)	269	1900	270.5	1850
	275.5	1950	*ca. 275*	*1700*
$C(CH_3)_3$,$C(CH_3)_3$ (*B*-Band)	211	7500	*ca. 212*	*7600*
$C(CH_3)_3$,$C(CH_3)_3$ (*C*-Band)	268	1800	268	1550
	275	1800	274	1500
H,Cl (*B*-Band)	212	6450	216	6400
H,Cl (*C*-Band)	*ca. 265*	*1550*	274.5	2350
	271	2350	*ca. 280*	*2000*
	278	2450		
H,Br (*B*-Band)	212	8700	*ca. 214*	*8450*
H,Br (*C*-Band)	*ca. 266*	*1750*	275.5	2750
	272	2700	*ca. 281*	*2350*
	279	2650		

Can. J. Chem. Downloaded from www.nrcresearchpress.com by 196.1.178.254 on 09/04/12
For personal use only.

phenolic absorption to transitions involving locally excited states). Steric interactions are, however, indicated in the ultraviolet spectra by the *absence* of the usual wavelength displacements between solutions in cyclohexane and ethanol. That is, whereas between solutions of phenol in cyclohexane and ethanol a wavelength displacement of 8 mμ is observed in the *B*-band (see Table I), no such displacement is observed for solutions of strongly sterically hindered phenols (see Table III for the spectra of various orthosubstituted phenols in cyclohexane and ethanol). Our explanation, following the suggestion of Coggeshall and Lang (3), is to ascribe a reduced wavelength displacement to steric interactions inhibiting solvent–solute interactions between phenol and solvent molecules.

Yet another spectral effect which may be associated with steric interactions is the progressive *increase* in extinction coefficient of the *C*-band for the spectra of orthosubstituted phenols in alkaline solution with increased size of the orthosubstituent (cf. ref. 13). The relevant *C*-band data are listed in Table IV, and Table IV also shows that the *B*-bands are not appreciably affected under these conditions.

TABLE IV

Absorption maxima of orthosubstituted phenols in alkaline solution (*N* aqueous NaOH)

	B-Band		*C*-Band	
Orthosubstituents	λ_{max}(mμ)	ϵ_{max}	λ_{max}(mμ)	ϵ_{max}
H,H	234	10500	285	2700
H,CH_3	235	9000	286	3200
H,C_2H_5	236	8400	287	3400
H,$CH(CH_3)_2$	236	8900	287	3700
CH_3,CH_3	238	8000	285	3400
$CH(CH_3)_2$,$CH(CH_3)_2$	238–239	8100	289	4550
$C(CH_3)_3$,$C(CH_3)_3$*	247–248	8300	292–293	4800

*Solution contains *ca.* 1% ethanol.

Next, in neutral solution, there is evidence for intramolecular hydrogen bonding, and the spectral effects ascribed to hydrogen bonding are more pronounced for orthosubstituted phenols than for the corresponding anilines (cf. ref. 6). The evidence is obtained by comparing the *B*-bands of a number of orthosubstituted phenols with the *B*-bands of the meta isomers, where the former *B*-bands show a bathochromic wavelength displacement accompanied by an increased absorption intensity.

Since these spectral changes are much more pronounced in orthosubstituted phenols than in the corresponding anisoles (see following paper) it is assumed that the spectral changes must be caused, at least partly, by intramolecular hydrogen bonding. Evidence for an intramolecular hydrogen bond in, for example, *o*-nitrophenol is also provided by the appreciably displaced hydroxyl band in the infrared region at 3240 cm^{-1} for *o*-nitrophenol compared with the band at 3590 cm^{-1} for the meta and para isomers (25, 26, cf. also refs. 27, 28, 29). Further evidence is provided by the C–H bending frequency at 748 cm^{-1} for *o*-nitrophenol (30).

EXPERIMENTAL

The ultraviolet absorption spectra were determined by standard methods using a Unicam SP500 spectrophotometer. For each compound at least two independent sets of observations were made. Some of the spectra have previously been described in this series.

Can. J. Chem. Downloaded from www.nrcresearchpress.com by 196.1.178.254 on 09/04/12
For personal use only.

The phenols were mostly commercial materials, purified by distillation or recrystallization until their boiling points or melting points showed them to be sufficiently pure. The solvents used were spectroanalyzed cyclohexane (Fisher) or commercially available absolute ethanol. The spectra of the aminophenols and dihydroxybenzenes were determined as quickly as possible to prevent oxidation. With this end in mind, the air in the flasks containing these solutions was also replaced by nitrogen.

ACKNOWLEDGMENTS

The authors are greatly indebted to Miss Florence Jackman for very competent technical assistance in the determination of some of the spectral data. They also wish to thank the Fisheries Research Board of Canada for financial support, since the major part of this work was carried out under a contract between the Fisheries Research Board of Canada and Memorial University of Newfoundland. The authors further acknowledge the general assistance of the National Research Council in support of these studies.

REFERENCES

1. BURAWOY, A. and CHAMBERLAIN, J. T. J. Chem. Soc. 2310 (1952).
2. LEMON, H. W. J. Am. Chem. Soc. **69**, 2998 (1947).
3. COGGESHALL, N. D. and LANG, E. M. J. Am. Chem. Soc. **70**, 3283 (1948).
4. KEUSSLER, V. VON. Z. Elektrochem. **58**, 136 (1954).
5. NAGAKURA, S. and BABA, H. J. Am. Chem. Soc. **74**, 5693 (1952).
6. FORBES, W. F. and LECKIE, I. R. Can. J. Chem. **36**, 1371 (1958).
7. FORBES, W. F. and RALPH, A. S. Can. J. Chem. **36**, 869 (1958).
8. DOUB, L. and VANDENBELT, J. M. J. Am. Chem. Soc. **69**, 2714 (1947).
9. DOUB, L. and VANDENBELT, J. M. J. Am. Chem. Soc. **71**, 2414 (1949).
10. FORBES, W. F. Can. J. Chem. **36**, 1350 (1958).
11. DEARDEN, J. C. and FORBES, W. F. Can. J. Chem. **36**, 1362 (1958).
12. WEPSTER, B. M. Progress in stereochemistry. Vol. 2. *Edited by* W. Klyne and P. B. D. de la Mare. Butterworth Scientific Publications, London. 1958. pp. 112 and 110.
13. FORBES, W. F., MUELLER, W. A., RALPH, A. S., and TEMPLETON, J. F. Can. J. Chem. **35**, 1049 (1957).
14. FORBES, W. F. and MUELLER, W. A. J. Am. Chem. Soc. **79**, 6495 (1957).
15. SEARS, W. C. and KITCHEN, L. J. J. Am. Chem. Soc. **71**, 4110 (1949).
16. KANENIWA, N. J. Pharm. Soc. Japan, **76**, 253 (1956).
17. BROWN, T. L. J. Phys. Chem. **61**, 820 (1957).
18. STONE, P. J. and THOMPSON, H. W. Spectrochim. Acta, **10**, 17 (1957).
19. KRUEGER, P. J. and THOMPSON, H. W. Proc. Roy. Soc. A, **243**, 143 (1957).
20. FORBES, W. F. and TEMPLETON, J. F. Can. J. Chem. **36**, 180 (1958).
21. COHEN, L. A. J. Org. Chem. **22**, 1333 (1957).
22. BOWMAN, R. S., STEVENS, D. R., and BALDWIN, W. E. J. Am. Chem. Soc. **79**, 87 (1957).
23. CARLTON, J. K. and BRADBURY, W. C. J. Am. Chem. Soc. **78**, 1069 (1956).
24. WEPSTER, B. M. Rec. trav. chim. **76**, 357 (1957).
25. HOYER, H. Ber. **89**, 146 (1956).
26. GINETTI, Y. Naturwiss. **41**, 333 (1954).
27. FRANCK, B., HÖRMANN, H., and SCHEIBE, S. Ber. **90**, 330 (1957).
28. FLEET, M. ST. C. Spectrochim. Acta, **10**, 21 (1957).
29. FRANCEL, R. J. J. Am. Chem. Soc. **74**, 1265 (1952).
30. KROSS, R. D., FASSEL, V. A., and MARGOSHES, M. J. Am. Chem. Soc. **78**, 1332 (1956).

Can. J. Chem. Downloaded from www.nrcresearchpress.com by 196.1.178.254 on 09/04/12
For personal use only.

Can. J. Chem. Downloaded from www.nrcresearchpress.com by 196.1.178.254 on 09/04/12
For personal use only.

LIGHT ABSORPTION STUDIES

PART XV. THE ULTRAVIOLET ABSORPTION SPECTRA OF ANISOLES[1]

J. C. Dearden and W. F. Forbes

ABSTRACT

Anisoles, compared with phenols, possess similar spectral properties, except that properties determined mainly by the hydrogen atom of the hydroxy group are modified. In this way, comparison of the ultraviolet absorption spectra of phenols and anisoles permits, for example, the study of the spectral effects of hydrogen bonding and the study of steric interactions involving the hydroxy and methoxy groups.

INTRODUCTION

In previous parts of this series (1) it was found that ultraviolet *B*-band spectra can often be interpreted by assuming that the *B*-bands of ultraviolet spectra are determined predominantly by mesomeric and steric interactions. Phenolic spectra, which were examined in the previous paper (1*a*), were found to be of interest since they provide good examples of secondary interactions such as intramolecular hydrogen bonding. The phenolic *B*-band is also of interest, since it is believed to be determined by so-called locally excited states; that is, in the absence of appreciable direct mesomeric interaction between the hydroxy group and the benzene ring, the benzene ring is assumed to determine the observed absorption band with the hydroxy group exerting only a secondary influence. The anisole spectra provide an evident extension of this investigation, and we have therefore determined, or redetermined, a number of the relevant anisole spectra.

THE SPECTRUM OF ANISOLE

Table I lists the main absorption maxima of anisole in the region 210–330 mμ.

Anisole in cyclohexane absorbs maximally at 220 mμ, that is, at longer wavelength than the corresponding absorption of phenol at 210 mμ (1*a*). We deduce from this that the methoxy group does not merely exert a "secondary" interaction on the benzene ring, as has been postulated for the spectrum of phenol, since such a secondary interaction would cause a wavelength displacement of only *ca.* 7 mμ relative to benzene (see ref. 1*a* and section on metasubstituted anisoles). This in turn suggests that some additional mesomeric interaction occurs between the methoxy group and the benzene ring or, in other words, that the transitions leading to the *B*-band in anisole involve a smaller proportion of locally excited states compared with the transitions leading to the *B*-band in phenol.

The important question arises why locally excited states should preferentially contribute to this absorption in phenol. One possible explanation is that in phenol the O—H bond is aligned approximately parallel to the plane of the benzene ring (I*a*), whereas in anisole, partly for steric reasons, the O—CH_3 bond is directed out of the plane of the benzene ring as in I*b*. To satisfy this explanation, it must further be assumed that this direction of the O—CH_3 bond as in I*b* favors the overlap of the unshared electrons of the oxygen atom with the π-electrons of the benzene ring, and that in this way additional resonance interaction is possible. This explanation is consistent with the observation that the spectrum of phenol in ether or ethanol solution, which presumably involves the attachment of a solvent molecule to the phenolic hydrogen atom and hence causes an

[1]*Manuscript received February 12, 1959.*
Contribution from the Memorial University of Newfoundland, St. John's, Newfoundland.

TABLE I

Absorption maxima of anisole in various solvents*

Solvent	*B*-Band		*C*-Band	
	λ_{max} (mμ)	ϵ_{max}	λ_{max} (mμ)	ϵ_{max}
Vapor	214	†	*ca. 254* *ca. 259* 261 266 267 272.5	†
Cyclohexane‡	220 *ca. 223*	7500 *6000*	263 269 275	1400 2100 2100
Ether	219	7400	263.5 269 275.5	1300 1900 1700
Ethanol	219	7000	264 269 275	1350 1800 1600
Water	217	4300	*ca. 261* 267 273	*1200* 1600 1300
0.1 *N* HCl	217	4900	267 272	1700 1400
N NaOH	221	3600	267 273	1700 1400
Conc. H_2SO_4	235–236	11300	281	1350

*Values in italics represent inflections in this and subsequent tables.
†Intensities not determined.
‡Solute concentration = 2.3×10^{-4} moles/l.

increase in the effective size of the hydroxy group, shows maximal absorption at or near 218 mμ (1*a*), namely much like that of anisole in most solvents (see Table I). This therefore may imply that under these conditions structures such as I*a*, partly for steric reasons, tend to change into structures of type I*b* which facilitate orbital overlap and which tend to give rise to a maximal absorption near 218 mμ.*

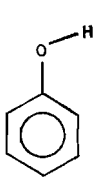

I*a*

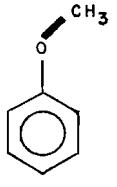

I*b*

The *C*-band fine structure, which is observed in cyclohexane solution for the spectra of both anisole and phenol, is evident, though to a lesser extent, for anisole in aqueous and alcoholic solution. It almost disappears for phenol in the latter solvents (1*a*). This reduced fine structure in the *C*-bands of both anisoles and phenols is ascribed to solute–solvent interactions (cf. ref. 1*a*). A striking difference between the spectra of phenol and anisole is the different behavior of both *B*- and *C*-band maxima on changing the

**For a full discussion concerning the conformation of the methoxy group, with particular emphasis on the tendency of the methoxy group to be coplanar with the benzene ring, see Wheland, G. W. Resonance in organic chemistry. John Wiley & Sons, Inc., New York. 1955. pp. 238–243.*

Can. J. Chem. Downloaded from www.nrcresearchpress.com by 196.1.178.254 on 09/04/12
For personal use only.

solvent from neutral to basic; the phenolic bands are appreciably displaced to longer wavelength (1*a*), while addition of alkali to an aqueous solution of anisole only slightly displaces the *B*-band (by 4 mμ), and does not displace the *C*-band (see Table I).

THE SPECTRA OF PARASUBSTITUTED ANISOLES

As in previous parts (1), the spectra of paradisubstituted benzene derivatives may be classified into spectra of compounds when both substituents are electron-donating, or electron-withdrawing, and into spectra of compounds when one substituent is electron-donating and the other electron-withdrawing. For the former group, the spectrum of the disubstituted benzene compound usually resembles the spectrum of the monosubstituted parent compound, that is, the transition involves locally excited states with the second substituent exerting only a secondary influence on the spectrum. If in the former group, in addition, the two substituents are dissimilar, the spectrum of the monosubstituted compound will involve the substituent which interacts preferentially with the benzene ring. These generalizations are illustrated by the data in Table II.

The earlier *B*-band spectra of parasubstituted anisoles listed in Table II usually show the anisole-type spectrum. Exceptions are provided when the methoxy substituent does not preferentially interact with the benzene ring. For example, for *p*-aminoanisole, and incidentally for the meta and ortho isomers also, in non-acidic media an aniline-type *B*-band is obtained, and for *p*-iodoanisole an iodobenzene-type spectrum is obtained. This may be illustrated by assuming structures of type II or III to be involved preferentially in the transitions leading to the spectra of *p*-fluoro- and *p*-iodo-anisole.*

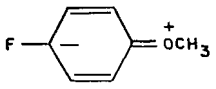

II

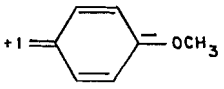

III

If the parasubstituent is electron-withdrawing (see lower part of Table II) the anticipated appreciable wavelength displacements, accompanied by intensity increases, are observed in the *B*-band. These wavelength displacements are shown in Fig. 1 to be parallel to the wavelength displacements obtained for phenols. The electron-withdrawing substituent may be visualized as facilitating the formation of resonance forms of type IV.

**The second substituent will in this way exert only a secondary effect on the B-band. Thus the location of the B-band remains essentially unaltered between p-fluoroanisole and anisole. Fluorobenzene, by contrast, shows the following, quite different, B-band absorption in cyclohexane solution, that is, λ_{max} 204 mμ, ε = 6600. Iodobenzene, on the other hand, shows a B-band reasonably similar to that of p-iodoanisole, that is: λ_{infl} 223 mμ, ε = 9400; λ_{max} 227 mμ, ε = 12,700; and λ_{max} 232 mμ, ε = 12,000 (see also Table II). Moreover, the bathochromic B-band wavelength displacements reported by Schubert et al. (3) on determining the B-bands in the vapor phase and in cyclohexane solution are 2.8 and 4.6 mμ for p-fluoroanisole and anisole respectively, while there is a hypsochromic wavelength displacement of 2 mμ for fluorobenzene. Therefore in only one of the two examples will the "second" substituent be a halogen atom, and it follows from this that care must be taken in deducing the order of electron release for the halogen atoms from the spectra of para-halogen-substituted anisoles (cf. refs. 3, 4).*

It may also be noted that the C-band spectral changes do not entirely bear out this analysis, since the C-band changes suggest a different pattern for p-fluoroanisole and the other three para-halogen-substituted anisoles. However, although we are not strictly concerned with C-band changes at this time, it may be observed that the location of the C-band maxima are closer to the location of the C-band maxima in anisole than to the location of these maxima in fluorobenzene (λ_{max} 246.5 mμ, ε = 350; λ_{max} 252 mμ, ε = 750; λ_{max} 258 mμ, ε = 1100; and λ_{max} 264 mμ, ε = 1050), and the C-band fine structure in p-fluoroanisole is also obtained for para-alkyl-substituted anisoles and cannot therefore be associated specifically with the fluoro substituent. In addition, the iodobenzene C-band fine structure (λ_{infl} 246 mμ, ε = 590; λ_{max} 251 mμ, ε = 670; λ_{max} 255.5 mμ, ε = 710; and λ_{max} 261 mμ, ε = 620) is similar to that in p-iodoanisole (see Table II).

Can. J. Chem. Downloaded from www.nrcresearchpress.com by 196.1.178.254 on 09/04/12
For personal use only.

Can. J. Chem. Downloaded from www.nrcresearchpress.com by 196.1.178.254 on 09/04/12
For personal use only.

TABLE II

Absorption maxima of substituted anisoles in cyclohexane solution

	Para isomer				Meta isomer						Ortho isomer					
	B-Band		*C*-Band		Anisole *B*-band		2nd *B*-band		*C*-Band		Anisole *B*-band		2nd *B*-band		*C*-Band	
Substituent	λ_{max} (mμ)	ϵ_{max}	λ_{max} (mμ)	ϵ_{max}	λ_{max} (mμ)	ϵ_{max}	λ_{max} (mμ)	ϵ_{max}	λ_{max} (mμ)	ϵ_{max}	λ_{max} (mμ)	ϵ_{max}	λ_{max} (mμ)	ϵ_{max}	λ_{max} (mμ)	ϵ_{max}
-OCH_3	210–211	5700*	*ca. 280*	*2500*	220	7300	—	—	*ca. 267*	*1700*	225	7150	—	—	271	2450
	226	9700	286.5	3200					271.5	2200					275	2550
			290	3200					277.5	2150					280	1900
			297	2550												
-OH	223–224	7000	*ca. 285*	2900	220	5400			*ca. 267*	*1300*	216	6200			*ca. 270*	*2250*
			288	3150					271.5	1700					273.5	2550
			291	3100					278	1550					279.5	2150
			298	2350												
-NH_2	236	9100	300	2600			233–234	6400	283	2250			237	8500	286	3450
			303	2650					*ca. 289*	*1800*						
-NH_2†	230	7900	293	2000			229	6400	279	2000			231	6900	278	2650
															280	2700
-NH_2‡	219.5	8250	269.5	1450	218.5	7700			267.5	1800	215.5	6800			267	1950
			ca. 275	*1200*					*ca. 273*	*1550*					273	1700
-CH_3	222.5	8600	268	1450	217	7000			*ca. 266*	*1300*	215.5	7500			270	2000
			271	1600	*ca. 220*	*6800*			270.5	1800	*ca. 220*	*7100*			276	1900
			274	1900					277.2	1900						
			276.5	2200												
			283	2050												
-F	*ca. 211*	*5000**	*ca. 267*	*1650*	218	7500			*ca. 263*	*1250*	217.5	7100			264.5	1450
	216–217	5400	269.5	2150					266.5	1550					268	1700
			272.5	2500					272.5	1450					273	1450
			275	2750												
			278.5	3200												
			284.5	2750												

Can. J. Chem. Downloaded from www.nrcresearchpress.com by 196.1.178.254 on 09/04/12
For personal use only.

TABLE II (*Concluded*)

Absorption maxima of substituted anisoles in cyclohexane solution

	Para isomer				Meta isomer						Ortho isomer					
	B-Band		*C*-Band		Anisole *B*-band		2nd *B*-band		*C*-Band		Anisole *B*-band		2nd *B*-band		*C*-Band	
Substituent	λ_{max} (mμ)	ϵ_{max}	λ_{max} (mμ)	ϵ_{max}	λ_{max} (mμ)	ϵ_{max}	λ_{max} (mμ)	ϵ_{max}	λ_{max} (mμ)	ϵ_{max}	λ_{max} (mμ)	ϵ_{max}	λ_{max} (mμ)	ϵ_{max}	λ_{max} (mμ)	ϵ_{max}
-Cl	227	11700	*ca. 273*	*1400*	219	7300			*ca. 266*	*1350*	218	7500			*ca. 267*	*1600*
			279	1900					272	2150	222	7400			272.5	2400
			287	1850					279	2150					280	2450
-Br	226	12500	*ca. 274*	*1350*	*ca. 218*	*8500*			*ca. 267*	*1450*	*ca. 218*	*8300*			*ca. 268*	*1800*
			279	1750					272.5	2350	*ca. 223*	*7400*			273.5	2750
			287	1550					279.5	2300					280.5	2800
-I	233	19000	273.5	1450	213	25500*	*ca. 224*	*9200**	268	1950			*ca. 227*	*8700**	269	2400
	ca. 237	*15800*	279	1600			228.5	9500	274.5	2700			231	10200*	275.5	3400
			288	1200					282	2550			235.5	10000*	283	3250
$-COCH_3$	261.5	18000	—	—	214	25000*	244	8500	298	2800	211	20300*	*ca. 237*	*8100*	294.5	3550
	ca. 268	*14500*					*ca. 250*	*6100*	*ca. 308*	*2100*			241	8350	*ca. 304*	*2500*
	ca. 278	*11200*														
-CHO§	265	18500	—	—	216	23500	246	9200‖	304	3000	211	20000*	246	10500	306	4600
	ca. 272	*16000*			220	22500	*ca. 251*	*8900*‖	*ca. 313*	*2700*			*ca. 253*	*8500*	*ca. 314*	*4200*
	278	12500														
	286	5500														
$-NO_2$	291	12100	—	—	223	13000	260	6100	313	2400	—	—	248–249	3400	304	2500
$-NO_2$†	313	10500	—	—	228	8900	273.5	6000	330	2050¶	*ca. 232*	*4300*	264	4300	333	2900
-COOH	255	17300	—	—	211	26000*	238	8500	295	3200			229	8000	282	2950
	ca. 268	*13500*							*ca. 301*	*2900*			*ca. 236*	*5000*	*ca. 286*	*2750*
	ca. 269	*9000*													289	2750

*B-Band assignment doubtful. †In aqueous solution. ‡In 0.1 N HCl. §In n-hexane solution. ‖These values should replace those previously reported (see ref. 1*c*). ¶Ref. 2.

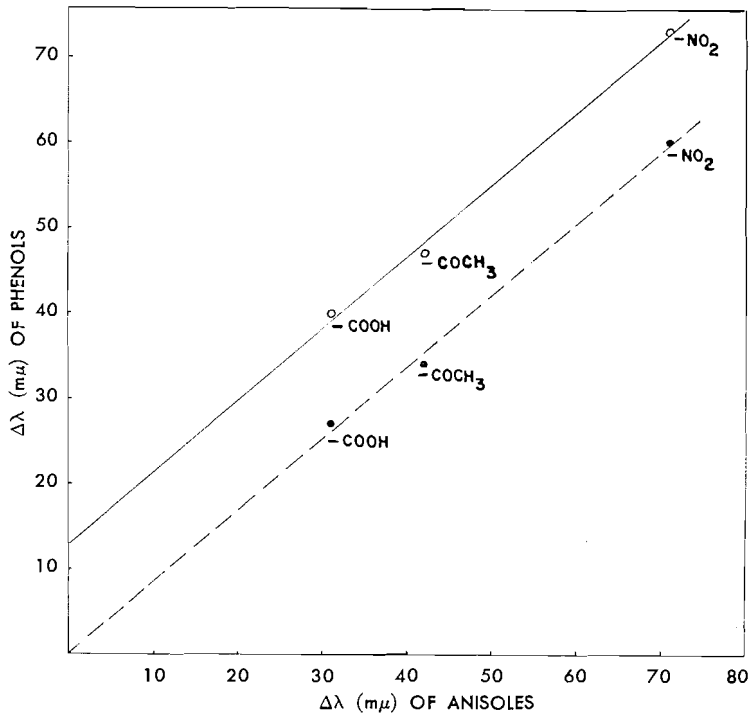

FIG. 1. Wavelength displacements ($\Delta\lambda$) of the *B*-band obtained in neutral inert solution on introducing an electron-withdrawing parasubstituent in anisole and phenol. (Values from this study, and ref. 1*a*.) The dotted line shows the plot if the phenolic absorption at 223 mμ is used as the reference compound (see text). ○ $\Delta\lambda$ for phenols taken as (λ_{max} −210). ● $\Delta\lambda$ for phenols taken as (λ_{max} −223).

The appreciable wavelength displacements for parasubstituted phenols are calculated with reference to a hypothetical absorbing species absorbing maximally at 223 mμ, and

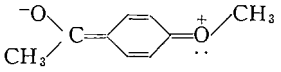

IV

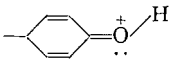

V

involving in its transitions structures of type V to an appreciable extent. If, on the other hand, the phenolic absorption in cyclohexane at 210 mμ is assumed to involve preferentially electronic excited states of type V and is taken as the reference point, then the straight line, as shown in Fig. 1, does not pass through the origin. The data thus lend support to the suggestion made in the previous paper concerning the supposed absence of appreciable mesomeric interaction for phenol in cyclohexane solution (see section on the spectrum of anisole and ref. 1*a*).

The *C*-bands of para- and meta-substituted anisoles undergo the previously noted general changes (1*e*). Moreover, the *C*-band spectral changes are similar for para- and meta-substituted phenols and anisoles (see previous paper).

THE SPECTRA OF METASUBSTITUTED ANISOLES

The *B*-bands of meta- and ortho-substituted anisoles are again classified into *B*-bands associated with the anisole chromophore, and into *B*-bands associated with the other

Can. J. Chem. Downloaded from www.nrcresearchpress.com by 196.1.178.254 on 09/04/12
For personal use only.

monosubstituted benzene chromophore (cf. refs. 1*a*, *b*, *c*, *d*). The two types of *B*-bands are in this way observed in a number of meta- and ortho-substituted anisoles.*

Using this classification, it may first be noted that the "secondary effect" of the methoxy group on the *B*-band associated with the non-anisole, monosubstituted benzene chromophoric system is as anticipated. That is, the non-anisole *B*-bands are generally bathochromically displaced by *ca.* 7 mμ for compounds where the second substituent is electron-withdrawing (see Table II and cf. ref. 6), and it is thus assumed that the overall effect of the methoxy group facilitates the formation of electronic excited states.

The effect of the second substituent on the anisole *B*-band is very similar to the effect of the same substituent on the phenolic *B*-band. Both the phenol and anisole *B*-bands are frequently displaced to longer wavelength if the second substituent is electron-withdrawing, and the displaced *B*-bands are sometimes more intense than for the parent compounds, namely phenol or anisole. For compounds of this type the observed intensities of the *B*-bands also suggest that the anisole *B*-band absorption occurs preferentially (see Table II). This again supports the previously noted generalization that, in the absence of direct primary resonance interaction, an electron-withdrawing substituent tends to cause an intensity increase (see refs. 1*a*, 1*d*, 7).

THE SPECTRA OF ORTHOSUBSTITUTED ANISOLES

Comparing the *B*-bands of orthosubstituted phenols and anisoles it is found that frequently only the *B*-band of the phenol is appreciably intensified and displaced to longer wavelength. Other secondary interactions may evidently contribute to these observed spectral changes but the data certainly provide qualitative evidence for intramolecular hydrogen bonding, since the above-mentioned spectral changes are most pronounced if a strong intramolecular hydrogen bond is expected. Qualitative evidence for intramolecular hydrogen bonding may also be obtained by comparing the spectra of ortho isomers with those of the meta isomers; for intramolecularly hydrogen-bonded phenols the bathochromic wavelength displacement and intensity increase in both *B*- and *C*-bands are greater between the ortho- and meta-substituted phenols than between the corresponding anisoles. A fuller discussion of semiquantitative methods, which may be used to estimate the strength of the intramolecular hydrogen bond in orthosubstituted phenols and related compounds, will be presented in a separate communication.

Steric effects have, by implication, been noted in the section on the spectrum of anisole since it has been tentatively assumed that, partly for steric reasons, the methoxy group in anisole is directed out of the plane of the benzene ring. It follows that an orthosubstituent would not be expected readily to cause an appreciable wavelength displacement or intensity decrease, since the methoxy group is already dislodged from the plane of the benzene ring. In fact, even for bulky orthosubstituents, the maximal *B*-band absorption still occurs close to 220 mμ (see Table III). It should be noted, however, that for compounds such as 2,6-dimethylanisole or *tert*-butoxybenzene appreciable spectral changes can be discerned in the *C*-band (see Table III and ref. 8). For example, the *C*-band of 2,6-dimethylanisole as shown in Table III is considerably less intense than the *C*-band

**Only one B-band is usually observed for the para isomer, although a band that may, incorrectly, be assumed to be a second B-band occurs in compounds like p-nitroanisole at λ_{max} 227 mμ, ε = 7000 (in water). However, this absorption band, which also occurs in p-nitrophenol at λ_{max} 227 mμ, ε = 7000 (in water), is not a B-band, since in basic solution this band of p-nitrophenol still occurs at λ_{max} 226 mμ, ε = 6500 (in N NaOH) (5). If the absorption band were a B-band, addition of alkali would appreciably displace the band to longer wavelength (1a) and because this is not so, the absorption bands near 227 mμ in p-nitrophenol and p-nitroanisole are both assumed to be A-bands.*

Can. J. Chem. Downloaded from www.nrcresearchpress.com by 196.1.178.254 on 09/04/12
For personal use only.

in 3,5-dimethylanisole. The latter compound in cyclohexane solution absorbs as follows: λ_{max} 219–220 mμ, ϵ = 7250 (*B*-band); λ_{infl} *ca.* 264 mμ, ϵ = 900; λ_{infl} *ca.* 268 mμ, ϵ = 1250; λ_{max} 271 mμ, ϵ = 1450; λ_{infl} *ca.* 274 mμ, ϵ = 1250; and λ_{max} 278 mμ, ϵ = 1700. 2,5-Dimethylanisole also absorbs similarly, thus: λ_{max} 219 mμ, ϵ = 7200 (*B*-band); λ_{infl} *ca.* 266 mμ, ϵ = 1400; λ_{infl} *ca.* 270 mμ, ϵ = 1900; λ_{max} 273 mμ, ϵ = 2100; and λ_{max} 278.5 mμ, ϵ = 2150.

TABLE III

Absorption maxima of orthosubstituted anisoles in cyclohexane and ethanol

	Cyclohexane				Ethanol			
	B-Band		*C*-Band		*B*-Band		*C*-Band	
Orthosubstituents	λ_{max} (mμ)	ϵ_{max}	λ_{max} (mμ)	ϵ_{max}	λ_{max} (mμ)	ϵ_{max}	λ_{max} (mμ)	ϵ_{max}
H,H	220	7500	263	1400	219	7000	264	1350
	ca. 223	*6000*	269	2100			269	1800
			275	2100			275	1600
H,CH_3	215.5	7500	270	2000	215.5	6800	269	1850
	ca. 220	*7100*	276	1900	*ca. 219*	*6700*	275	1750
$H,CH(CH_3)_2$	216	7200	*ca. 263*	*1450*	216.5	7100	*ca. 263*	*1450*
	220	7100	269	2100	*ca. 220*	*7000*	269	2050
			275.5	2000			275	1900
$H,C(CH_3)_3$	216.5	7200	*ca. 262*	*1350*	*ca. 217*	*7000*	*ca. 262*	*1400*
	221	7300	268	2000	221	7200	268	2000
			274.5	2000			274.5	1900
CH_3,CH_3	212	8350	262.5	345	*ca. 211*	*8350*	262	315
			266	340			266	310
			270.5	300			270	260
$CH(CH_3)_2,CH(CH_3)_2$	212	9400	263	400	*ca. 211*	*9200*	263	380
			ca. 265	*385*			*ca. 265*	*365*
			270	360			269.5	335

Table III lists the spectra of some orthosubstituted anisoles. The data show that changing the solvent from cyclohexane to ethanol has practically no effect on the observed *B*- and *C*-bands of many of these compounds. This absence of solvent effect has previously been noted for orthosubstituted phenols. Both phenol and anisole data are therefore consistent with the explanation put forward in the previous paper, that a large orthosubstituent prevents solvent–solute interaction between the unshared electron pair of the oxygen atom and the ethanol molecules.

The frequent similarity of the spectra of the ortho and meta isomers, which has been observed for phenols (1*a*), is also observed for the anisole analogues. However, there are some significant differences. Thus, the intensity decreases which may be caused partly by steric interactions are frequently more pronounced for anisoles. For example, comparing the nitrobenzene *B*-bands of the meta and ortho isomers of nitrophenol and nitroanisole, it is found that the decrease of the ϵ_{max} values in the ortho isomers is more pronounced for *o*-nitroanisole. Unfortunately, this example does not lend itself to unambiguous analysis since in neutral solution intramolecular hydrogen bonding affects the *B*-band of *o*-nitrophenol, while in basic solution the effective size of the methoxy group is compared with that of the O^- group rather than with the effective size of the hydroxy group. However, it seems certain that a steric factor contributes to the relatively low ϵ_{max} value of *o*-nitroanisole in various solvents (see Table II). Supporting evidence for the

Can. J. Chem. Downloaded from www.nrcresearchpress.com by 196.1.178.254 on 09/04/12
For personal use only.

ability of the methoxy group to cause steric inhibition of resonance is further provided by the spectrum of 2,6-dimethoxynitrobenzene in cyclohexane solution (λ_{max} 276 mμ, ϵ = 1700) which shows a yet more pronounced decrease in intensity for the nitrobenzene *B*-band. Further, for ortho-halogen-substituted phenols and anisoles, the ϵ_{max} values of the ortho-fluoro and ortho-chloro compounds are *smaller* for the phenols than for the anisoles, but for the ortho-bromo compound, that is, for a larger orthosubstituent, the ϵ_{max} value of the orthosubstituted phenol is *greater* than that of the anisole (see Table II and ref. 1*a* for the relevant *B*-bands; for evidence of steric interactions because of the methoxy group, see also refs. 9, 10).

In orthosubstituted anisoles there is also evidence that large steric interactions contribute to more pronounced spectral changes. For example, in 2,6-dimethylanisole a hypsochromic wavelength displacement, indicative of steric interaction, is obtained in the *B*-band, and the *C*-band is very considerably reduced in intensity (see Table III). It may finally be noted that in many hindered phenols and anisoles, that is, in compounds where *C*-band fine structure is evident in both cyclohexane and ethanol solutions, a relative decrease in intensity occurs for the long wavelength peak of the *C*-band in ethanol solution (see, for example, in Table III the *C*-bands of *o-tert*-butylanisole in cyclohexane and ethanol solution).

EXPERIMENTAL

The ultraviolet absorption spectra were determined by standard methods using Unicam SP 500 spectrophotometers. For each compound at least two independent sets of observations were made. Some of the spectra have previously been described in this series and elsewhere. Whenever possible, the anisole spectra were determined under conditions identical with those under which the phenolic spectra had been determined. Frequently, but not always, our data were in good agreement with recent values reported by other workers (cf. refs. 4, 5, 11, 12, 13).

The anisoles were mostly commercial materials, purified by distillation or recrystallization until their boiling points or melting points showed them to be sufficiently pure. The solvents used were spectroanalyzed cyclohexane (Fisher) or commercially available absolute ethanol.

ACKNOWLEDGMENTS

The authors are greatly indebted to Mr. D. L. Coffen for very competent technical assistance in the preparation of some of the compounds.

They also wish to thank the Fisheries Research Board of Canada for financial support, since the major part of this work was carried out under a contract between the Fisheries Research Board of Canada and the Memorial University of Newfoundland. The authors further acknowledge the general assistance of the National Research Council in support of these studies.

REFERENCES

1. (*a*) DEARDEN, J. C. and FORBES, W. F. Can. J. Chem. **37**, 1294 (1959).
(*b*) FORBES, W. F. and LECKIE, I. R. Can. J. Chem. **36**, 1371 (1958).
(*c*) DEARDEN, J. C. and FORBES, W. F. Can. J. Chem. **36**, 1362 (1958).
(*d*) FORBES, W. F. Can. J. Chem. **36**, 1350 (1958).
(*e*) FORBES, W. F., MUELLER, W. A., RALPH, A. S., and TEMPLETON, J. F. Can. J. Chem. **35**, 1049 (1957).
2. DOUB, L. and VANDENBELT, J. M. J. Am. Chem. Soc. **71**, 2414 (1949).

Can. J. Chem. Downloaded from www.nrcresearchpress.com by 196.1.178.254 on 09/04/12
For personal use only.

3. SCHUBERT, W. M., CRAVEN, J. M., and STEADLY, H. Unpublished information.
4. BURAWOY, A. and THOMPSON, A. R. J. Chem. Soc. 4314 (1956).
5. DOUB, L. and VANDENBELT, J. M. J. Am. Chem. Soc. **69**, 2714 (1947).
6. FORBES, W. F. and RALPH, A. S. Can. J. Chem. **36**, 869 (1958).
7. FORBES, W. F. and TEMPLETON, J. F. Can. J. Chem. **36**, 180 (1958).
8. BADDELEY, G., SMITH, N. H. P., and VICKARS, M. A. J. Chem. Soc. 2455 (1956).
9. ENEBÄCK, C. Acta Chem. Scand. **11**, 895 (1957).
10. LITVINENKO, L. M. and GREKOV, A. P. Zhur. Obscheĭ Khim. **27**, 3332 (1957); Chem. Abstr. **52**, 9041 (1958).
11. BURAWOY, A. and CHAMBERLAIN, J. T. J. Chem. Soc. 2310 (1952).
12. DOUB, L. and VANDENBELT, J. M. J. Am. Chem. Soc. **77**, 4535 (1955).
13. COMMINS, B. T. and LINDSEY, A. J. Anal. Chim. Acta, **15**, 446 (1956).

Can. J. Chem. Downloaded from www.nrcresearchpress.com by 196.1.178.254 on 09/04/12
For personal use only.

Can. J. Chem. Downloaded from www.nrcresearchpress.com by 196.1.178.254 on 09/04/12
For personal use only.

PHOTOCHEMICAL SEPARATION OF MERCURY ISOTOPES

IV. THE REACTION OF $Hg^{202}6(^3P_1)$ ATOMS, PHOTOEXCITED IN NATURAL MERCURY VAPOR, WITH METHYL CHLORIDE AND ISOPROPYL CHLORIDE[1, 2]

K. R. OSBORN[3] AND H. E. GUNNING[4]

ABSTRACT

A detailed investigation has been made of the reaction of $Hg^{202}6(^3P_1)$ atoms, photoexcited in natural mercury vapor (Hg^N), with methyl chloride, at room temperature. Data are also reported on the reaction with isopropyl chloride as substrate. Hg^{202} enrichment in the calomel product is taken as evidence of its formation in the primary quenching reaction.

Under static conditions the methyl chloride reaction was found to form calomel with the natural Hg^{202} abundance (29.8%). With increasing flow rate a progressive increase in Hg^{202} abundance was observed. Maximum enrichments were found at fast flow rates, low substrate pressures, and high values for the absorbed light intensity (I_A). The most highly enriched calomel obtained in this study contained 50.4% Hg^{202}. With increasing I_A, a corresponding increase in flow rate was required to achieve maximum Hg^{202} enrichment. The addition of propylene or butene-1 to the methyl chloride stream was found to result in a slight decrease in Hg^{202} abundance over that for the pure substrate.

The isotopically specific aspects of the reaction are explained in terms of the sequence:

$$RCl + Hg^{202}6(^3P_1) \rightarrow Hg^{202}Cl + R \quad [1]$$

$$RCl + Hg^{202}6(^3P_1) \rightarrow R + Cl + Hg^{202}6(^1S_0) \quad [2]$$

$$Cl + Hg^N + M \rightarrow Hg^NCl + M \quad [3]$$

where M represents a third body, including the wall. The decrease in enrichment observed at high substrate pressures is shown to be due to Lorentz-broadening effects on the hyperfine absorption contours of Hg^N. The failure to obtain enrichment under static conditions is explained by the depletion in Hg^{202} of the Hg^N in the cell through reaction [1].

The investigation shows that there are two primary processes operative in the mercury-$6(^3P_1)$-photosensitized decomposition of alkyl chlorides, in one of which calomel is formed. These processes presumably involve a common short-lived intermediate R—Cl—Hg.

INTRODUCTION

In the investigation reported in this paper, the technique of mono-isotopic mercury-$6(^3P_1)$-photosensitization, in natural mercury vapor (Hg^N), developed in a previous study in this series (1), has been used to study the reaction of $Hg^{202}6(^3P_1)$ atoms, in Hg^N, with two alkyl chlorides. The effect of reaction parameters on the Hg^{202} content of the calomel product of the methyl chloride reaction has been investigated in some detail. Preliminary experiments with isopropyl chloride as substrate are also given for comparative purposes. As in the earlier investigation with hydrogen chloride (2), Hg^{202} enrichment in the calomel product is taken as evidence of formation of the product in the primary quenching process.

In an investigation of the reaction of flowing hydrogen chloride with $Hg^{202}6(^3P_1)$ atoms in Hg^N, McDonald, McDowell, and Gunning (2) found that the calomel product contained a maximum of 44% Hg^{202}, under conditions of fast flow and low substrate pressure. This Hg^{202} abundance corresponds to an enrichment of 48% over the natural Hg^{202} abundance of 29.8%. In the presence of unsaturated addends, such as butadiene-1,3, the Hg^{202} enrichment was found to increase to a maximum of 98%.

[1]*Manuscript received March 31, 1959.*
Joint contribution from Department of Chemistry, Illinois Institute of Technology, Chicago 16, Illinois and Department of Chemistry, University of Alberta, Edmonton, Alberta.
[2]*This work was supported in part by the U.S. Atomic Energy Commission under contract AT(11-1)-43. This support is gratefully acknowledged.*
[3]*Present address: E. I. du Pont de Nemours Company, Wilmington, Delaware.*
[4]*Present address: Department of Chemistry, University of Alberta, Edmonton, Alberta.*

The $Hg^N6(^3P_1)$-photosensitized decomposition of methyl chloride has been investigated by Masson and Steacie (3) over the pressure range 10–640 mm at temperatures from 72 to 328° C. These authors concluded that the calomel product, under the afore-mentioned conditions, arises from the secondary reaction of unexcited Hg^N with CH_2Cl radicals. By photosensitization of a single isotopic species, as in the present study, fairly unequivocal evidence can be obtained on the importance of primary formation of mercury compounds in alkyl chloride reactions. The present investigation was undertaken, therefore, to gain further insight into the nature of the primary process in the mercury-$6(^3P_1)$-photosensitized decomposition of calomel-forming substrates.

EXPERIMENTAL

The high-vacuum flow system was so arranged that reproducible gas flow rates could be achieved for compounds which were either gases (CH_3Cl) or liquids ($(CH_3)_2CHCl$) at room temperature. The pressure of the flowing gas was measured with a manometer upstream from the reaction cell. Flow rates were determined by calibrated capillary flow meters situated on the entrance and exit sides of the reaction cell.

The methyl chloride was taken directly from a cylinder. To obtain a fixed pressure of isopropyl chloride vapor, the temperature of the liquid was held constant in a modified Ward still (4). The flow rate was controlled with a Warrick–Fugassi valve (5). Efficient saturation of the gases with Hg^N was accomplished by allowing the gases to pass through an operating "umbrella-type" mercury diffusion pump. The exit condenser of the pump was temperature-regulated to ± 0.5° C by circulating water from a thermostat through its jacket.

The reaction cells used were rectangular in shape, with faces 2.5 cm × 8.0 cm and an internal path length of 0.1 cm. They were made of Vycor 7910 glass, and attached to the system by offset arms, terminating in 12/5 spherical joints.

The Hg^{202} source and photometric apparatus have been previously described (2). The reaction cell was located 5 cm from the source. A rectangular slit was used to confine the beam within the cell faces. A portion of the transmitted radiation was focussed on a Westinghouse WL-775 photocell by means of a quartz lens.

A special procedure was employed in the determination of the relative mean absorbed light intensity during a run. The relative intensity of the source could be obtained at any time by rotating the cell through 90° out of the light path. Before attaching the cell to the system, the transmission of the cleaned, Hg^N-free, cell was first measured in the absorbiometric analysis apparatus (6). With the cell in position, and the Hg^N-saturated gas flowing through the system, the transmission was again measured. From these data, together with the calibration curve obtained on the analysis system (6), the fraction of light absorbed by the Hg^N in the cell, and the Hg^N concentration, could be calculated. During the reaction, the determination of absorbed intensity was complicated by the accumulation of the calomel product on the faces of the reaction cell. Preliminary experiments showed that the transmitted intensity was reduced by calomel deposition to approximately one-half of the initial value in the first 5–10 minutes of irradiation. At this half-time point, the cell was rotated out of the light beam, and the faces were heated with a Bunsen burner until the calomel had sublimed away. After it was cooled, the cell was again moved into the light beam. It was consistently observed in this procedure that subsequent calomel deposition occurred largely in the area to which the original calomel product had been sublimed. Thus the transmitted intensity did not decrease as rapidly in the latter part of the run, as in the initial period. Usually

Can. J. Chem. Downloaded from www.nrcresearchpress.com by 196.1.178.254 on 09/04/12
For personal use only.

the transmitted intensity was again reduced to one-half after 30 to 60 minutes of further irradiation. The run was terminated at this point by rotating the cell out of the light path. The method of recovering the isotopic mercury from the calomel, and the procedure for isotopic analysis, have been previously described (1, 6). Before the reaction cell was used again, it was cleaned with hot aqua regia, rinsed, and dried at 120° C. In order to obtain reproducible enrichment data, it was found necessary, also, to heat the cell to a dull red heat prior to each run.

The methyl chloride, propylene, and butene-1 used were Matheson C.P. grade, with minimum purity of 99%. The isopropyl chloride used had a boiling range of 34–36° C. It was purified by several trap-to-trap distillations before use.

RESULTS

A preliminary series of runs was first made on the methyl chloride reaction. The Hg^{202} abundance in the calomel product was studied as a function of flow rate, at a fixed pressure of 7 mm. The incident intensity, I_0, was maintained essentially constant in this series. It should be noted that throughout this paper intensity will be expressed in terms of scale divisions on the 5×10^{-10} ampere scale of the Beckmann Ultrohmeter, used for monitoring the photocell output (6). Since the relative positions of all optical components were held constant in this investigation, the intensity values given are directly proportional to the absolute intensities.

The data are presented in Table I, and shown graphically in Fig. 1. It will be noted that two "saturation temperatures" were used. By this term is meant the temperature of the water circulating through the exit arm of the mercury saturator. From Fig. 1, it can be seen that the Hg^{202} abundance increases directly with the flow rate. With the saturator temperature at 9° C the abundance appears to maximize at 42.7% Hg^{202}. Considerably higher abundances were found with the saturator temperature at 20° C. At a flow rate of 22.5 liter $minute^{-1}$, an abundance of 50.4% Hg^{202} was obtained at the higher saturator temperature. It should also be pointed out, at this time, that no enrichment was found under static conditions. In Fig. 1, it can be seen that the Hg^{202} abundance approaches the natural value of 29.8% as the flow rate goes to zero.

Under the conditions of constant I_0, saturator temperature, and substrate pressure obtaining in the first series, variations were observed in the intensity absorbed by the

TABLE I

The effect of flow rate on the Hg^{202} content of the solid product of the reaction of $Hg^{202}6(^3P_1)$ atoms, photoexcited in Hg^N, with methyl chloride

Pressure, mm	Saturation temperature, ° C	Flow rate, liter min^{-1}	Incident intensity, I_0	Hg^{202} abundance, atom %
7.00	20.5	0.18	0.67	31.0
7.00	20.5	0.26	0.68	34.3
6.73	20.5	0.41	0.64	38.4
7.06	20.0	0.90	0.68	38.7
6.60	18.5	3.88	0.69	41.8
7.62	20.5	11.0	0.65	46.0
6.64	20.5	22.5	0.65	50.4
7.06	9.5	0.46	0.65	33.8
6.62	8.2	5.34	0.64	42.8
6.45	9.0	9.70	0.63	42.6

Can. J. Chem. Downloaded from www.nrcresearchpress.com by 196.1.178.254 on 09/04/12
For personal use only.

mercury vapor. In subsequent runs, therefore, the effect of this parameter was studied in some detail.

To evaluate the intensity, I_A, absorbed by the mercury in the reaction cell, the ratio of transmitted to incident intensity was determined for the evacuated cell ($\bar{T}_C$) and also for the cell under reaction conditions ($\bar{T}_R$). The two faces of the cell were assumed to be identical, and the fraction of light transmitted by the incident face, by the filter-product rule, was taken as the square root of $\bar{T}_C$. With I_0 as the mean incident intensity of the lamp during the reaction, I_A was calculated from the equation

$$I_A = \bar{T}_C^{\frac{1}{2}}(1-\bar{T}_R/\bar{T}_C)I_0 = \bar{T}_C^{\frac{1}{2}}.A.I_0.$$

Values of A were determined at the beginning of the run, and also following sublimation of the calomel at the half-time point, in most of the runs.

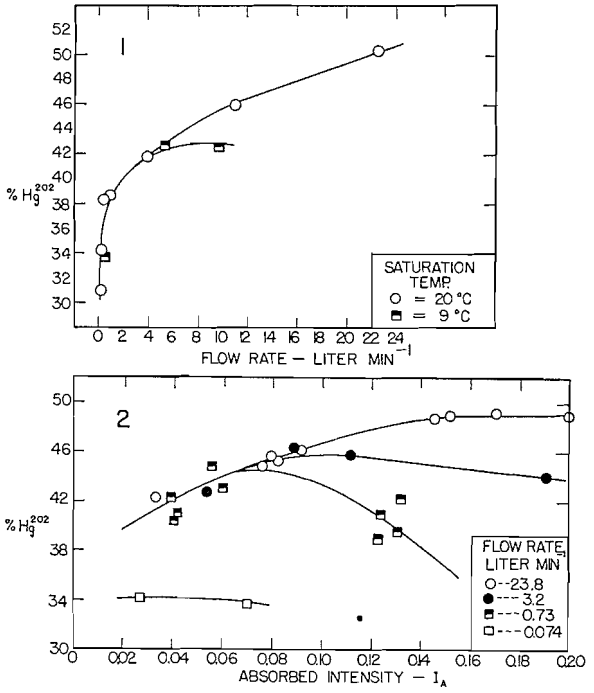

FIG. 1. The effect of flow rate on the abundance of Hg^{202} in the calomel product of the methyl chloride reaction, at two saturation temperatures.

FIG. 2. The effect of I_A on the abundance of Hg^{202} in the calomel product of the methyl chloride reaction, at four flow rates.

In Table II, the Hg^{202} abundance is shown as a function of I_A, for mean flow rates of 0.074, 0.73, 3.2, and 23.8 liter minute^{-1}. In the graphical representation of the data in Fig. 2 it would appear that the Hg^{202} abundance passes through a maximum then decreases with increasing absorbed intensity, except at the highest flow rate used, i.e. 23.8 liter minute^{-1}. In other words, for each absorbed intensity there is a minimum value of the flow rate which must be achieved in order to obtain maximum isotopic enrichment. These minimal flow rate values increase with increasing absorbed intensity. With the flow rate sufficiently high to eliminate any enrichment-depressing effect of this parameter, the Hg^{202} abundance clearly increases with increasing absorbed intensity.

Can. J. Chem. Downloaded from www.nrcresearchpress.com by 196.1.178.254 on 09/04/12
For personal use only.

TABLE II

The effect of flow rate and absorbed intensity on the Hg^{202} content of the solid product of the reaction of $Hg^{202}6(^3P_1)$ atoms, photoexcited in Hg^N, with methyl chloride

	Pressure, mm	Flow rate, liter min^{-1}	Saturation temperature, °C	Absorption (A) Initial	Absorption (A) Half-time	I_0	I_A	Hg^{202} abundance, atom %
	7.86	25	20.0	0.320		0.146	0.033	42.3
	7.14	25.4	20.5	0.346		0.305	0.076	44.9
	7.00	18.2	29.6	0.385		0.655	0.080	45.8
	6.76	21.0	30.5	0.364	0.377	0.710	0.083	45.4
	6.94	23.1	21.0	0.264		0.496	0.092	46.2
	6.59	25.7	20.5	0.389	0.410	0.527	0.146	48.8
	7.21	25.8	20.5	0.333		0.645	0.152	49.0
	6.45	25.2	19.5	0.338	0.408	0.580	0.171	49.2
	6.80	23.5	21.0	0.402	0.394	0.700	0.200	48.9
	6.86	27.2	30.6	0.436	0.410	0.655	0.204	50.2
	6.58	21.2	30.7	0.428	0.444	0.590	0.206	49.8
Average values	6.9	23.8						
	7.13	3.94	20.5	0.484	0.468	0.360	0.054	42.8
	6.96	3.13	21	0.489	0.500	0.570	0.089	46.4
	7.69	2.77	20.5	0.425	0.378	0.885	0.112	45.9
	6.87	3.22	20.5	0.402	0.522	0.560	0.191	44.0
Average values	7.2	3.2						
	6.80	0.73	21.2	0.291	0.328	0.178	0.039	42.2
	6.8	0.7	31.5	0.303	0.312	0.192	0.041	40.4
	6.46	0.78	20.5	0.180	0.276	0.270	0.042	41.1
	6.80	0.76	21.0	0.164	0.225	0.418	0.056	44.8
	6.80	0.76	21.2	0.232	0.292	0.325	0.060	43.1
	6.52	0.74	31	0.328	0.287	0.574	0.123	39.0
	6.59	0.73	21.5	0.277	0.328	0.565	0.124	41.0
	6.8	0.7	31.1	0.258	0.260	0.737	0.131	39.6
	6.66	0.72	21.9	0.244	0.244	0.750	0.132	42.2
Average values	6.7	0.73						
	6.60	0.076	21.5	0.095	0.163	0.775	0.027	34.2
	6.65	0.072	22.5	0.162		0.630	0.070	33.8
Average values	6.6	0.074						

It should be emphasized that the I_A values are initial absorbed intensities averaged from the readings taken at the beginning of the run and after sublimation of the calomel at the half-time point. The average intensity of radiation absorbed during the run would be about three-fourths of the reported I_A values.

The variation-in-intensity technique, described above, was used to study the effect of varying I_A on the Hg^{202} abundance, for several substrate pressures, at a constant flow rate of 2.7 ± 0.7 liter $minute^{-1}$. The data for substrate pressures of 0.27, 136, and 314 mm are shown in Table III. From Table II, data are available for the same flow rate at a substrate pressure of 7.2 mm. At the lowest pressures of 0.27 and 7.2 mm, the I_A values had to be corrected for incomplete quenching. Since the absorption path was only 0.1 cm, and the pressure of Hg^{202} was small, imprisonment of the hyperfine component was assumed to be negligible. The Stern–Volmer relation (7) should therefore be valid under these conditions. To make the correction the values of I_A, derived from the absorption data, were multiplied by $Z\tau/(1+Z\tau)$, where Z is the number of collisions per second of one Hg^{202} atom with the methyl chloride, and τ is the lifetime in seconds of the $Hg^{202}6(^3P_1)$ state. The Z values were calculated from Maxwell's collision frequency equation, with the collision cross section taken as the quenching cross section of methyl chloride for $Hg^N6(^3P_1)$ atoms. This value has been found by Darwent and Phibbs (8) to be 24×10^{-16} cm^2. The question of the magnitude of the lifetime, τ, of the $Hg^{202}6(^3P_1)$

Can. J. Chem. Downloaded from www.nrcresearchpress.com by 196.1.178.254 on 09/04/12
For personal use only.

TABLE III

The effect of pressure and absorbed intensity, at constant flow rate, on the Hg^{202} content of the solid product of the reaction of $Hg^{202}6(^3P_1)$ atoms, photoexcited in Hg^N, with methyl chloride

	Pressure, mm	Flow rate, liter min^{-1}	Saturation temperature, ° C	Absorption		I_0	I_A	Hg^{202} abundance, atom %
				Initial	Half-time			
	0.27	1.99	19.5	0.436	0.526	0.072	0.012	37.4
	0.27	2.05	20.6	0.496	0.398	0.170	0.024	38.6
	0.27	2.15	20.0	0.375	0.412	0.545	0.038	41.1
	0.27	2.27	21.2	0.395	0.482	0.520	0.040	40.4
Average values	0.27	2.1						
	132	3.20	20.5	0.308	0.322	0.144	0.036	41.8
	135	3.18	20.0	0.328	0.311	0.194	0.049	42.8
	134	3.39	20.2	0.344	0.354	0.316	0.088	42.8
	142	3.29	20.2	0.350	0.338	0.555	0.148	45.4
Average values	136	3.3						
	312	1.60	21.3	0.252	0.320	0.070	0.032	37.9
	316	1.59	21.2	0.252	0.315	0.138	0.062	39.5
	313	1.53	20.0	0.256	0.292	0.545	0.117	40.7
Average values	314	1.6						

state has been discussed in an earlier paper in this series (1). For the lifetime of the $6(^3P_1)$ state of the even-mass mercury isotopes, Lennuier and Cojan (9) obtained 1.12×10^{-7} seconds. This value was used in the present calculations. The correction factors for incomplete quenching applied at the pressures of 0.27 and 7.2 mm were 0.19 and 0.88 respectively. It should be noted that the I_A values given in Table II are uncorrected for incomplete quenching.

The Hg^{202} abundance vs. I_A curves, corrected for incomplete quenching, are shown for the four pressures, 0.27, 7.2, 136, and 314 mm in Fig. 3. The enrichment-depressing effect of high substrate pressure is clearly shown at 314 mm. The values obtained in the 0.27–136 mm range all appear to fall on the same curve within the experimental error.

At low methyl chloride pressures, collisional transfer of energy between $Hg^{202}6(^3P_1)$ and Hg^N atoms could conceivably become important. From resonance radiation imprisonment measurements, Holstein, Alpert, and McCoubrey (10) have estimated that the mean quenching cross section of Hg^N is 10^{-13} cm^2. Knowing the quenching cross sections

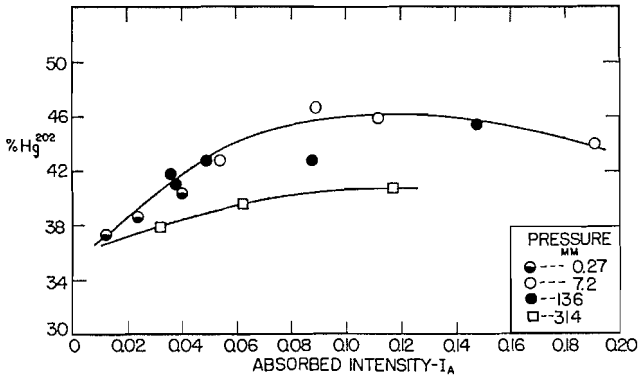

FIG. 3. The effect of I_A at constant flow rate on the abundance of Hg^{202} in the calomel product of the methyl chloride reaction at four substrate pressures.

Can. J. Chem. Downloaded from www.nrcresearchpress.com by 196.1.178.254 on 09/04/12
For personal use only.

of Hg^N and methyl chloride, it is possible to obtain the relative quenching of $Hg^{202}6(^3P_1)$ by Hg^N and methyl chloride from the collision frequency equation. At the lowest substrate pressure used, i.e. 0.27 mm, and with a mercury vapor pressure corresponding to equilibrium at 21° C, it was calculated that 99% of the $Hg^{202}6(^3P_1)$ atoms were quenched by methyl chloride. Quenching by Hg^N atoms was therefore considered negligible in the present investigation.

In all of the experiments reported in this paper on the effect of various reaction parameters on the Hg^{202} abundance, a consistent procedure was used in treating the reaction cell between experiments. Following the removal of the calomel product by solution in boiling concentrated hydrochloric acid, the cell was cleaned in aqua regia, to remove any traces of calomel or mercury, rinsed in distilled water, dried at 120° C, and heated to a dull red with a gas–oxygen flame. The flaming served to burn off any polymeric material formed on the cell during reaction. With repeated use it was observed that the transmission of the cleaned, Hg^N-free, cell slowly decreased. To improve the transmission, the cell was immersed in concentrated hydrofluoric acid for 30 minutes, rinsed, dried, and flamed. The transmission, following this treatment, was considerably higher. However, the Hg^{202} content of the calomels formed in succeeding experiments was found to be lower than before the treatment.

In order to determine whether surface factors influenced the Hg^{202} abundance, a series of 10 consecutive runs were performed, on the same cell, and under essentially the same reaction conditions. The runs differed only in the method of cell treatment between successive experiments. The data are summarized in Table IV.

It is apparent from the data that the aqua regia treatment, followed by flaming, is necessary to obtain maximum enrichments reproducibly. Furthermore, it appears that

TABLE IV

The effect of cell-cleaning methods in consecutive runs under constant reaction conditions on the Hg^{202} content of the solid product of the reaction of $Hg^{202}6(^3P_1)$ atoms, photoexcited in Hg^N, with methyl chloride

Cell treatment	Pressure, mm	Flow rate, liter min^{-1}	Saturation temperature, ° C	Absorption		I_0	I_A	Hg^{202} abundance, atom %
				Initial	Half-time			
30 minutes in conc. HF, rinsed, dried, flamed	6.77	25.4	20.5	0.316	0.380	0.580	0.163	46.6
Cell flamed only	6.87	26.5	20.5	0.315	0.340	0.290	0.076	40.8
Cell flamed only	6.45	25.8	20.1	0.408	0.418	0.617	0.203	46.6
Cell cleaned in aqua regia, rinsed, dried, flamed	6.80	23.5	21.2	0.402	0.394	0.630	0.200	48.9
No treatment	6.42	24.9	21.0	0.414	0.428	0.650	0.213	40.5
No treatment	7.20	19.8	20.7	0.377	0.418	0.604	0.190	43.4
Cell cleaned in aqua regia, rinsed, dried, flamed	6.74	20.6	20.5	0.363	0.370	0.618	0.181	43.6
Cell cleaned in aqua regia, rinsed, dried, flamed	6.45	25.2	19.5	0.338	0.408	0.582	0.171	49.1
Cell cleaned in aqua regia, rinsed, dried, flamed	6.32	21.8	20.7	0.285	0.305	0.291	0.068	47.3
Cell cleaned in aqua regia, rinsed, dried, flamed	6.58	21.2	30.6	0.428	0.444	0.590	0.206	49.8

Can. J. Chem. Downloaded from www.nrcresearchpress.com by 196.1.178.254 on 09/04/12
For personal use only.

the "recovery" of the cell surface from other treatments is not immediate. In the last five runs in Table IV it can be seen that the untreated cell does not yield high values for the enrichment until two runs have been performed using the aqua regia method.

The possibility of isotopic degradation in the calomel product by gas-phase exchange reactions between $Hg^{202}Cl$ and Hg^{N} has been considered in an earlier study in this series (2) on the reaction of $Hg^{202}6(^3P_1)$ atoms with hydrogen chloride – butadiene mixtures. It was found that repeated sublimation of the calomel product did not alter the Hg^{202} abundance, compared to that for unsublimed calomel.

In this investigation, exchange between Hg^{N} vapor and isotopically enriched solid calomel was examined. A deposit of enriched calomel was first laid down in the cell under the following reaction conditions: 6.87 mm pressure of methyl chloride, at a flow rate of 0.7 liter minute^{-1}, a saturation temperature of 20° C, and an absorbed intensity of 0.159. The lamp was then turned off, and the Hg^{N}-saturated methyl chloride was allowed to flow through the cell for an additional 30 minutes. The Hg^{202} abundance was found to be 40.8%, the value to be expected under the conditions of the experiment. This experiment would suggest that exchange between gaseous Hg^{N} and isotopically enriched solid calomel is not significant under the conditions of this investigation.

The reaction between photoexcited Hg^{202} atoms and solid calomel is another exchange reaction which could be influential in determining the Hg^{202} abundance. This possibility was investigated by depositing a layer of $Hg^{N}{}_2Cl_2$ by irradiating the Hg^{N}-saturated stream of methyl chloride with an electrodeless discharge source containing Hg^{N}. The deposit was sublimed from the cell face and the system was evacuated. A stream of nitrogen, presaturated with Hg^{N}, was then allowed to flow through the system, under irradiation with the Hg^{202} source. After 30 minutes the run was stopped and the mercury from the calomel was analyzed. An Hg^{202} content of 29.7% was found, corresponding to the natural abundance. This experiment would suggest that neither $Hg^{202}6(^3P_1)$ atoms nor $Hg^{202}6(^3P_0)$ atoms can displace the mercury atoms in solid calomel.

The effect on the Hg^{202} enrichment of adding unsaturated hydrocarbons to the methyl chloride stream was studied using propylene and butene-1 as addends. The data are summarized in Table V. In this table the I_A values given were determined as described above. The numbers are proportional to the absorbed intensity for the Hg^{N}-saturated gas mixture. The fraction of I_A partitioned in competitive quenching to methyl chloride is designated in Table V as $I_A(CH_3Cl)$. To obtain $I_A(CH_3Cl)$, the I_A values were multiplied by the relative quenching factor $[Z(CH_3Cl)/Z(G)]/[1+Z(CH_3Cl)/Z(G)]$: where $Z(CH_3Cl)$ and $Z(G)$ represent respectively the number of collisions between Hg^{202} and methyl chloride and between Hg^{202} and the added gas. For calculating the collision frequency ratio, quenching cross sections of 31 and 33.5×10^{-16} cm^2 were used respectively for propylene and butene-1 (11). In addition to the correction of I_A for competitive quenching, the fraction of light escaping by resonance fluorescence was also considered.

From Table V, it can be seen that the addition of propylene and butene-1 has a slightly depressing effect on the Hg^{202} content in comparison with the value for the pure substrate, under comparable conditions. From the four runs with varying concentrations of butene-1, it would appear that the enrichment-depressing effect of this addend decreases with increasing concentration.

As a preliminary study on the effect of the alkyl side chain on the isotopically specific reaction, a series of 19 runs was done with isopropyl chloride as substrate. Reaction pressure was varied from 0.16 to 308 mm, and the flow rate from 0.0007 to 11.20 liter minute^{-1}.

Can. J. Chem. Downloaded from www.nrcresearchpress.com by 196.1.178.254 on 09/04/12
For personal use only.

TABLE V

The effect of added gases on the Hg^{202} content of the solid product of the reaction of $Hg^{202}6(^3P_1)$ atoms, photoexcited in Hg^N, with methyl chloride at a flow rate of 20.5 ± 1.5 liter $minute^{-1}$

Added gas	P (Total), mm	P (CH_3Cl), mm	P, mm	% added gas	I_A	I_A (CH_3Cl)	Hg^{202} abundance, atom %
Propylene	4.89	3.46	1.43	28.3	0.175	0.093	42.2
Propylene	4.90	3.53	1.37	28.0	0.175	0.095	44.2
Butene-1	5.51	3.47	2.04	37.0	0.202	0.110	42.0
Butene-1	4.63	3.06	1.57	33.8	0.233	0.113	41.4
Butene-1	4.69	4.28	0.41	8.7	0.222	0.149	40.4
Butene-1	4.76	4.35	0.41	8.6	0.133	0.099	38.5
None	4.63	4.63	0	0	0.130	0.130	44.0

As with methyl chloride, maximum enrichments were obtained at low pressures and high flow rates. The highest Hg^{202} abundance was 44.1%, for a pressure of 6.42 mm and a flow rate of 8.0 liter $minute^{-1}$. This point fits on the curve for methyl chloride, shown in Fig. 1, for the same saturation temperature of 20° C.

DISCUSSION

In a previous paper (2) in this series, on the reaction of $Hg^{202}6(^3P_1)$ atoms, in Hg^N, with hydrogen chloride, it was pointed out that there are two factors which must be considered before the significance of reaction parameters in the kinetics can be properly assessed. These factors are (*a*) the Lorentz-broadening effects of substrate pressure on the hyperfine absorption contours, and (*b*) the depletion in Hg^{202} of the Hg^N present in the reaction zone through isotopically specific processes. These factors will first be discussed.

By analogy with the hydrogen chloride reaction (2), the formation of a calomel product, enriched in Hg^{202}, in the reaction of methyl chloride with $Hg6(^3P_1)$ atoms, in Hg^N, could be ascribed to the sequence:

$$CH_3Cl + Hg^{202}6(^3P_1) \rightarrow CH_3 + Hg^{202}Cl \quad [1]$$

$$CH_3Cl + Hg^{202}6(^3P_1) \rightarrow CH_3 + Cl + Hg^{202}6(^1S_0) \quad [2]$$

$$Hg^N + Cl + M \rightarrow Hg^NCl + M \quad [3]$$

where M represents a third body in the gas phase, or the wall.

The Lorentz-broadening effects of methyl chloride on the five absorption contours of the 2537 Å line of Hg^N have been discussed in some detail in a previous paper (1). Quantitative estimates were there made of the fraction of Hg^{202} resonance radiation absorbed by Hg^N with increasing methyl chloride pressure. From these data, and the Hg^{202} abundances in the present investigation, an approximate calculation can be made of the magnitude of the Lorentz effect in the methyl chloride reaction. On the basis of the three-step mechanism above, the ratio, R, of the rates of $Hg^{202}Cl$ to Hg^NCl formation is related to the fractional Hg^{202} abundance, α, in the calomel product by the equation:

$$R = (\alpha - 0.298)/(1-\alpha),$$

where 0.298 is the α value for natural mercury. The calculation can only be made for low I_A values, under which conditions Hg^{202} depletion of the Hg^N in the irradiated zone should be negligible, as required by reaction [3]. From Fig. 3 it can be seen that at substrate pressures less than 136 mm, there is no appreciable pressure effect on the Hg^{202} enrichments, since the abundance values all lie on the same curve within the

Can. J. Chem. Downloaded from www.nrcresearchpress.com by 196.1.178.254 on 09/04/12
For personal use only.

Can. J. Chem. Downloaded from www.nrcresearchpress.com by 196.1.178.254 on 09/04/12
For personal use only.

experimental error. From this curve the value of $\alpha = 0.44$, for $I_A = 0.06$; whence, from the above equation, $R = 0.25_4$. From reference 1 the fraction of incident Hg^{202} radiation absorbed by Hg^{202} atoms, at a methyl chloride pressure of 314 mm, is 0.70. The apparent R value at this substrate pressure will therefore be $(0.70)(0.25_4) = 0.17_8$. Substituting this value in the above equation an α value of 0.40 is obtained. From Fig. 3, the experimental value is 0.395, for $I_A = 0.06$ and $P = 314$ mm.

From the above calculation, the Lorentz effect would appear sufficient to account for the decrease in Hg^{202} abundance at high substrate pressures. This subject will be dealt with in greater detail in forthcoming papers from this program.

From Fig. 2, it would appear that the Hg^{202} abundances, at a fixed flow rate, increase with increasing I_A to a maximum value and then fall off. The maximum value becomes progressively greater with increasing flow rate. This behavior can be adequately explained in terms of a localized depletion of the Hg^{202} content of the Hg^N in the reaction zone through reaction [1]. Under such conditions reaction [3] takes place with mercury containing less than the normal abundance (29.8%) of Hg^{202}. The net Hg^{202} enrichment found in the recovered calomel will thereby be reduced. This depletion effect would be minimized at high flow rates and low I_A values. The extreme case of Hg^{202} depletion would of course occur under static conditions. Here a calomel containing the normal Hg^{202} abundance was recovered. The static behavior points up the fact that the photochemical reaction is very much faster than the rate of evaporation of the liquid Hg^N present in the reaction cell. All of the Hg^N present must be consumed in primary and secondary calomel-forming reactions in order for Hg^NCl to be recovered.

Since the relative mean absorbed intensities (I_A) were determined under reaction conditions, the net decrease in the Hg^{202} content of the Hg^N with decreasing flow rate can be calculated. In Table II, the three sets of runs at flow rates of 23.8, 0.73, and 0.074 liter minute^{-1} were performed consecutively with the same reaction cell. For each set the A values were averaged and the corresponding mean concentrations of Hg^{202} were obtained from the calibration curve of the absorbiometric analysis unit (6). The results of the calculations are shown in Table VI, with the mean Hg^{202} concentrations

TABLE VI

The effect of flow rate on the concentration of Hg^{202} atoms in the reaction zone, in the reaction of $Hg^{202}6(^3P_1)$ atoms in Hg^N with methyl chloride

Flow rate, liter minute^{-1}	Average absorption	N^{202}, atoms cm$^{-3}\times10^{-13}$	Equilibrium temp., ° C
23.8	0.335	1.45	21.2
0.73	0.231	0.93	16.1
0.074	0.128	0.52	9.8

(N^{202}) given as the number of Hg^{202} atoms per cc. The progressive decline in the N^{202} values with decreasing flow rate is clearly evident. In the last column of Table VI the equilibrium temperatures of liquid Hg^N are given corresponding to the vapor concentrations of Hg^N indicated by the N^{202} values. At the highest flow rate (23.8 liter minute^{-1}), the equilibrium temperature corresponds, within the experimental error, to the temperature of the exit condenser of the mercury saturator. However, at the lowest flow rate (0.074 liter minute^{-1}) the equilibrium temperature is 11.4° C below the saturator temperature. These calculations show up clearly the Hg^{202}-depleting effect of reaction [1] on the Hg^N in the light zone. It should further be noted that these results prove the efficiency

of the method used for saturating the gas stream with Hg^N. This is evident from the fact that the equilibrium temperature is the same as the saturation temperature at the highest flow rate employed.

From the preceding considerations, it seems reasonable to conclude that the Hg^{202} abundances in the methyl chloride reaction are invariant in both substrate pressure and volume flow rate when the actual data are corrected for Lorentz-broadening of the hyperfine absorption contours and depletion of Hg^{202} in the Hg^N present during reaction.

The specific nature of the primary processes occurring in the reaction of methyl chloride with $Hg^{202}6(^3P_1)$ atoms was the focus of interest in this study. Pertinent to this, the quenching cross section of methane for $Hg^N6(^3P_1)$ atoms is only 0.08×10^{-16} cm^2 (7), whereas that of methyl chloride is 24×10^{-16} cm^2 (8). The substitution of chlorine in the methane molecule results therefore in well over a 300-fold increase in quenching cross section. From these data alone one would expect that chemical quenching would occur almost exclusively at the C—Cl bond in methyl chloride. In their study of the methyl chloride reaction with $Hg^N6(^3P_1)$ atoms, at elevated temperatures, Masson and Steacie (3) came to this conclusion on the basis of the nature and quantum yields of the products formed. The results of the present work substantiate this conclusion and show further that at least part of the calomel product recovered originates in the primary quenching reaction. It should be emphasized that this study indicates primary calomel formation in the room temperature reaction. It would be expected that increasing reaction temperature would favor reaction [2] over reaction [1]. Hence our results are not necessarily in disagreement with the conclusions of Masson and Steacie (3) that the primary process is exclusively reaction [2] at elevated temperatures.

From the fact that the calomel recovered is not pure $Hg^{202}Cl$, it would appear necessary to postulate the two primary processes, [1] and [2], to allow for secondary Hg^NCl as well as primary $Hg^{202}Cl$ formation. That calomel is forming by secondary reactions is clearly indicated by the effect of flow rate and intensity, discussed above, on the Hg^{202} abundance. Further evidence for reaction [2] has recently been obtained in further studies on the methyl chloride reaction (12). It has been found that hydrogen chloride is an important product of the reaction at room temperature. The presence of this product can be most readily explained by the reaction:

$$Cl + CH_3Cl \rightarrow HCl + CH_2Cl. \qquad [4]$$

This step has been previously postulated by Masson and Steacie (3) to explain HCl formation in the reaction at higher temperatures. It is likely that the two primary processes involve a common intermediate, since reaction parameters do not appear to influence the ratio of the rates of the two processes.

To this point it has been implied that secondary Hg^NCl formation arises by direct reaction of Cl atoms with Hg^N in the presence of a third body, as shown in reaction [3]. For their higher temperature conditions, Masson and Steacie (3) concluded that calomel formed by the reaction:

$$CH_2Cl + Hg^N \rightarrow Hg^NCl + CH_2. \qquad [5]$$

In the present investigation, CH_2Cl radicals will be available not only through reaction [4] but also from abstraction reactions of methyl radicals, formed in [1] and [2], with the substrate (13):

$$CH_3 + CH_3Cl \rightarrow CH_4 + CH_2Cl. \qquad [6]$$

Can. J. Chem. Downloaded from www.nrcresearchpress.com by 196.1.178.254 on 09/04/12
For personal use only.

It would be expected that these radicals would be consumed mainly through recombination (3):

$$2CH_2Cl \rightarrow C_2H_4Cl_2. \qquad [7]$$

With increasing I_A, there would be a localized build-up in Cl atom concentration, favoring reactions [3] and [4]. This should result in no net change in the Hg^{202} abundances, since $Hg^{202}Cl$ is simultaneously being formed in reaction [1]. However, if $Hg^{N}Cl$ is also being formed by [5], and since any increase in I_A will enhance the steady-state concentration of CH_2Cl radicals, the rate of $Hg^{N}Cl$ formation will increase more rapidly than that for $Hg^{202}Cl$ formation, with a resulting decrease in the Hg^{202} content of the recovered calomel. This is contrary to our findings, since actually an increase in Hg^{202} content was observed with increasing I_A. It appears therefore unlikely that reaction [5] is significant under our reaction conditions. It should further be noted that a similar intensity effect was found in the reaction of $Hg^{202}6(^3P_1)$ atoms in Hg^{N} with hydrogen chloride – butadiene mixtures (2).

It is possible that the reason for the positive intensity effect should be sought in the nature of reaction [3]. With increasing I_A, the localized enhancement of Cl atom concentration may result in a decreased efficiency in reaction [3] through its third-body restriction. Any reduction in the efficiency of [3] would result in a net increase in the Hg^{202} content of the recovered calomel.

From Table V it can be seen that the addition of propylene or butene-1 to the methyl chloride stream results either in no change or a slight decrease in the Hg^{202} content of the recovered calomel. While it is likely that these addends are slightly more efficient than methyl chloride in removing Cl atoms, any beneficial effect of this type in suppressing $Hg^{N}Cl$ formation will be compensated by a decreased I_A partitioned to the methyl chloride through competitive quenching effects from the added olefins.

The influence of cell-cleaning techniques on the Hg^{202} abundance is summarized in Table IV. The behavior suggests that isotope exchange reactions in product recovery may be playing a role in determining the Hg^{202} abundance found in the mercury recovered from the calomel product. Thus the physical condition of the cell surface may determine the extent to which Hg^{N} adsorbs upon it. In the recovery of Hg^{202}-enriched mercury from the calomel the importance of isotopic degradation through exchange reactions between Hg^{202} ions and Hg^{N} will be determined by the quantity of Hg^{N} adsorbed on the calomel product. This problem has been discussed in an earlier publication (14). The importance of exchange reactions in investigations of this type is currently being studied in the laboratories of one of us (HEG).

From the preliminary study of the isopropyl chloride reaction there is no evidence that an increase in the carbon chain length has any influence on the enrichment process.

CONCLUSIONS

As a result of this investigation it can be concluded that $Hg6(^3P_1)$ atoms react with alkyl chlorides through two primary modes:

$$RCl + Hg6(^3P_1) \rightarrow HgCl + R$$

$$RCl + Hg6(^3P_1) \rightarrow R + Cl + Hg6(^1S_0).$$

Through the technique of initiating the photosensitized decomposition with $Hg^{202}6(^3P_1)$ atoms in Hg^{N}, it has been possible to show that the calomel product is formed partially in the primary quenching reaction, and partially by secondary reactions of the type:

$$Cl + Hg + M \rightarrow HgCl + M.$$

Can. J. Chem. Downloaded from www.nrcresearchpress.com by 196.1.178.254 on 09/04/12
For personal use only.

The two primary modes of decomposition presumably involve the same short-lived intermediate in which the mercury atom is associated with the chlorine of the alkyl chloride. For alkyl halides in general the scission of the intermediate R—X—Hg into HgX and R would presumably be favored with increasing bond strength of the HgX. For this reason studies are now in progress in the laboratories of one of us (HEG) on the reaction of $Hg^{202}6(^3P_1)$ atoms in Hg^N with alkyl fluorides. Here it is conceivable that higher Hg^{202} enrichments would be obtained because of the greater stability of HgF compared to HgCl.

ACKNOWLEDGMENTS

The authors would like to express their deep appreciation to Dr. C. C. McDonald, Dr. Willard F. Allen, Mr. John A. Poole, Mr. Richard Pertel, and Mr. J. K. S. Wan for many helpful discussions.

REFERENCES

1. Osborn, K. R., McDonald, C. C., and Gunning, H. E. J. Chem. Phys. **26**, 124 (1957).
2. McDonald, C. C., McDowell, J. R., and Gunning, H. E. Can. J. Chem. **37**, 930 (1959).
3. Masson, C. R. and Steacie, E. W. R. J. Chem. Phys. **19**, 183 (1951).
4. LeRoy, D. J. Can. J. Research, B, **28**, 492 (1950).
5. Warrick, E. and Fugassi, P. Ind. Eng. Chem. Anal. Ed. **15**, 13 (1943).
6. Osborn, K. R. and Gunning, H. E. J. Opt. Soc. Am. **45**, 552 (1955).
7. Mitchell, A. and Zemansky, M. Resonance radiation and excited atoms. Cambridge University Press, London. 1934.
8. Darwent, B. and Phibbs, M. J. Chem. Phys. **22**, 110 (1954).
9. Lennuier, R. and Cojan, J. Compt. rend. **231**, 1450 (1950).
10. Holstein, T., Alpert, D., and McCoubrey, A. Phys. Rev. **85**, 985 (1952).
11. Darwent, B., Phibbs, M., and Hurtubise, F. J. Chem. Phys. **22**, 859 (1954).
12. Wan, K. J. S. and Gunning, H. E. To be published.
13. Ridge, M. S. and Steacie, E. W. R. Can. J. Chem. **33**, 396 (1955).
14. Gunning, H. E. Can. J. Chem. **36**, 89 (1958).

Can. J. Chem. Downloaded from www.nrcresearchpress.com by 196.1.178.254 on 09/04/12
For personal use only.

Can. J. Chem. Downloaded from www.nrcresearchpress.com by 196.1.178.254 on 09/04/12
For personal use only.

THE MECHANISMS OF OXYMERCURATION[1]

M. J. Abercrombie, Alan Rodgman, K. R. Bharucha, and George F Wright

ABSTRACT

The oxymercuration of norbornenes has been found to be acid-catalyzed, and to give oxymercurials which have a higher dipole moment and greater stability toward deoxymercuration than do their diastereomers in which the configuration of the mercuri linkage has been inverted. Since these properties can be correlated with those of the oxymercurials from norbornenedicarboxylic acids (partly published heretofore and elaborated in the present report) the configurations of which are known, it follows that the configurations of the oxymercurials from norbornene are ↑↓ (*trans*). But these configurations must be opposite to those of the oxymercurials from cyclohexene, cyclopentene, α-terpineol, and the geoisomeric stilbenes, the formations of which are not acid-catalyzed and the dipole moments of which are lower than those of the diastereomers inverted with respect to the mercuri linkage. The configuration of these oxymercurials must be ↓↓ (*cis*) and the mechanism of their formation must be different from the acid-catalyzed oxymercuration of norbornene. The mechanism for *cis* (↓↓) addition has previously been suggested as non-ionic. Calculation of the electric moments of these ↓↓ diastereomers shows that hindrance to group rotation must prevail. It is reasonable to attribute the relative ease with which they may be deoxymercurated to this hindrance.

For some years there has been a difference of opinion in respect of the mechanism whereby the elements of hydroxy- or alkoxy-mercuric salts add to alkenes. This controversy is of interest beyond that of the oxymercurials because oxymercuration may provide an insight of alkene reactions not provided by less definitive reactions of these hydrocarbons. Thus it has been observed that oxymercuration is generally entirely stereospecific, with simple second-order kinetics in which a *cis*-geometric isomer is oxymercurated at a faster rate than is its *trans*-modification. However, none of these characteristics define the mechanism of reaction.

In 1935 the reaction was specified as an addition of molecular hydroxy- or alkoxymercuric acetate to the carbon–carbon double bond (1), and this belief that the added groups were in contiguous (so-called *cis*) configuration was reiterated in 1947 (2). Meanwhile, the alternative postulation has been made (3) that an ionized alkane–mercurinium salt is first formed from an ionizable mercuric salt and an alkene. The cation of this salt is subsequently attacked by a nucleophilic hydroxide or alkoxide ion, with inversion, to produce the oxymercurial in which the added groups are in the non-contiguous (so-called *trans*) relationship to one another. This mechanism is portrayed here for the oxymercuration of 1,4-methylene-Δ^2-cyclohexene (norbornene, I).

It might be predicted from this mechanism that the reaction would be favored by a system in which the ionization of mercuric salts would be enhanced. Moreover, the prevalence of the two possible products, 3-↓-methoxy-1,4-↑↑-methylenecyclohexyl-2-↑-mercuric salt (IV) versus 3-↓-acetoxy-1,4-↑↑-methylenecyclohexyl-2-↑-mercuric salt (III), ought to depend upon the relative activities of the anions $X^{\ominus}$ (usually acetate) and $OCH_3^{\ominus}$ in the system.

The oxymercuration of norbornene, I, has been found to conform with these predictions. A quantitative yield of III is formed rapidly when I is treated with mercuric acetate (X = OAc) in acetic acid. More specifically, a 0.34 molar solution of mercuric acetate in 2,5-dioxahexane converts 1 equivalent of norbornene into nearly pure 3-↓-acetoxy-1,4-↑↑-methylenecyclohexyl-2-↑-mercuric salt (III, X = Cl after treatment with aqueous sodium chloride, m.p. 126–128°) in 98% yield during 30 minutes. Neither rate

[1]*Manuscript received March 31, 1959.*
Contribution from the Department of Chemistry, University of Toronto, Toronto, Ontario, Canada.

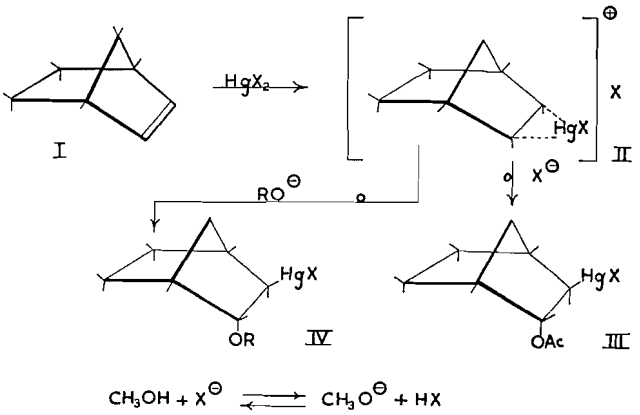

nor yield is diminished by inclusion of either 1 or 0.1 equivalent of boron fluoride etherate, although 0.1 equivalent of pyridine decreases the yield to 62% and 1 equivalent to 24% during 30 minutes. The effect of pyridine may be expected because of its tendency to coordinate with mercuric salts.

The configuration of this oxymercurial has been studied. The position of the acetoxy group in III (X = Cl) has been proved by saponification to be 3-↓-hydroxy-1,4-↑↑-methylene-2-↑-cyclohexylmercuric chloride (IV, R = H). This substance may be reduced by use of hydrazine hydrate in large excess to 3-↓-hydroxy-1,4-↑↑-methylenecyclohexane, identical with that obtained by Alder, Stein, and Rickert (4, 5) and configurationally established by Alder and Windemuth (6). The position of the chloromercuri group seems to be *trans* (↑) with respect to the acetoxy substituent according to the comparatively high dipole moment (3.6 Debye) which III (X = Cl) displays in dioxane. Therefore, the oxymercuration seems to have occurred via the alkane–mercurinium salt, II.

The same mode of reaction seems to occur when an equivalent of methanol is included with the mercuric acetate and norbornene in 2,5-dioxahexane but the product is IV (R = CH_3), as might be expected if methoxide ion were strongly nucleophilic in this medium. The configuration of 3-↓-methoxy-1,4-↑↑-methylene-2-↑-cyclohexylmercuric chloride (IV) corresponds with that of III because the 3-↓-hydroxy analogue to which III has been converted may be methylated in good yield (7) to the methoxy analogue, IV.

In protonic media the oxymercuration of norbornene is less simple. In water a mixture of III and IV (R = H, X = Cl after sodium chloride treatment) is obtained from which pure IV may be obtained by saponification. In methanolic solution, 0.00025 molar in I, and mercuric acetate a 97% yield of a mixture comprising 65% of IV (R = CH_3) and 35% of III is obtained. This behavior, not usual in the preparation of oxymercurials, would seem to be due to competition in nucleophilic attack of an intermediate like II by alkoxide and acetate ions. The following experiments substantiate this belief.

In Table I, items 1 to 4, is shown a series of experiments in which the molarity of norbornene and mercuric acetate in methanol has been lowered by dilution with this solvent. The products from these 90-minute experiments have been analyzed by melting point – composition diagram and by acetyl determinations.

It may be seen that upon increased dilution the yield is first increased and then essentially is constant. Of greater significance is the increasing amount of methoxymercurial (IV) instead of acetate (III) in the product. Item 11 shows that this tendency is independent of the absolute quantity of mercuric acetate in the system, although item 12, like

Can. J. Chem. Downloaded from www.nrcresearchpress.com by 196.1.178.254 on 09/04/12
For personal use only.

TABLE I

Oxymercuration of norbornene by mercuric acetate in methanol during 90 minutes followed by dilution into aqueous sodium chloride (X = Cl)

Item	Molarity of I and $Hg(OAc)_2$ in MeOH $\times 10^3$	Excess equiv. $Hg(OAc)_2$	Equiv. NaOAc	Equiv. HOAc	Total yield, %	% IV in total
1	0.5				86	61
2	0.25				97	66
3	0.1				93	73
4	0.07				95	86
5	0.25			1	85	80
6	0.25			5	69	73
7	0.25			20	69	67
8	0.25		1		73	21
9	0.25		2		60	15
10	0.25		10		81	10
11	0.04	9			99	90
12	0.12	3			90	60

item 1, shows that a high ratio of mercuric acetate to norbornene tends to decrease the formation of IV in favor of III. These behaviors might be expected if formation of methoxide ion were a consequence of equation [i] to which the reaction of equation [i] furnished little acetate because of limited dissociation.

Consideration of equations [i]–[vii] permits explanation of the results shown in Table I.

$$Hg(OAc)_2 \rightleftharpoons HgOAc^{\oplus} + OAc^{\ominus} \qquad [i]$$

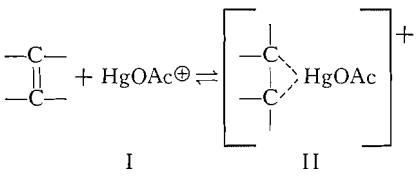

I II [ii]

$$HOAc \rightleftharpoons H^{\oplus} + OAc^{\ominus} \qquad [iii]$$

$$ROH + OAc^{\ominus} \rightleftharpoons RO^{\ominus} + HOAc \qquad [iv]$$

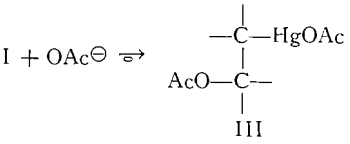

III [v]

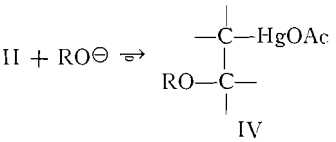

IV [vi]

$$Hg(OAc)_2 + ROH \rightleftharpoons RO-HgOAc + HOAc \qquad [vii]$$

$$HgO + 2HOAc \rightarrow Hg(OAc)_2 + H_2O \qquad [viii]$$

The reaction involving norbornene (I), mercuric acetate, and methanol may be adequately described by these equations. Dilution of the solution of reactants with methanol as indicated in items 1–4, Table I, would result in increased formation of methoxide ion and reduction of acetate ion by equation [iv]; thus favoring the formation of IV as described by equation [vi] at the expense of formation of III by equation [v]. Reduction of acetate ion would result in increased formation of the acetoxymercurinium ion (equa-

Can. J. Chem. Downloaded from www.nrcresearchpress.com by 196.1.178.254 on 09/04/12
For personal use only.

tion [i]). Thus increased dilution of the reactants with methanol would favor increased ionization of the mercuric acetate and would result in an increased yield of III plus IV in 90 minutes.

An equilibrium shift of the reaction described by equation [i] ought to be enhanced more by the ionization of acetic acid than by mercuric acetate. This expectation is realized in item 5 and to a certain extent in item 6, by comparison with item 2, but item 7 shows when addition of acetic acid reaches the 20-equivalent level the presence of acetate ion starts to favor the formation of III to the detriment of IV.

Inclusion of varying amounts of acetic acid (items 5–7, Table I) should reduce the over-all per cent yield in 90 minutes. The reason for this reduction is readily found by interpretation of equations [i]–[vii]. The increase in the ratio of III:IV produced by addition of acetic acid (and thus increased acetate ion) is explicable by consideration of the ratio, acetate:methoxide ion.

Inclusion of sodium acetate, a salt highly ionized in methanol compared with acetic acid, should further enhance the effect observed with added acetic acid. Addition of 10 equivalents of sodium acetate (item 10) increases the amount of the acetoxymercurial III to 90% of the total product.

According to these evidences of ionic participation it would follow that conditions in which basic mercuric salts would be prevalent ought to decrease the rate of reaction. This condition has been devised by inclusion of mercuric oxide into the methanolic system 0.25 molar in norbornene and mercuric acetate. In this experiment, the reaction shown in equation [viii] would be operative together with the reactions described by equations [i]–[vii]. After 4 hours the total yield is only 70% but the acetic acid liberated from this amount of oxymercuration has by this time dissolved the suspended mercuric oxide. Subsequently the yield rises to 90%. Of interest is the observation that the 90% yield contains at least 10% more of the methoxymercurial than is obtained from the reaction system in which no mercuric oxide is present.

This evidence that methoxymercuration of norbornene is retarded in a basic or neutral environment would indicate that this reaction would be favored in acidic media. The data of Table II substantiate this prediction.

The addition of only 0.02 equivalent of sulphuric acid increases the amount of methoxymercurial, IV, relative to the acetate, III, from 67 to 85%. While the addition of larger amounts of sulphuric acid tends slightly to decrease the total yield (deoxymercuration), the percentage of IV in this total actually is increased. It would appear that the bisulphate ion, itself not sufficiently nucleophilic to undergo neutralizing addition to an alkane–mercurinium salt, removes acetate ion from the system according to equation [ix]. The behavior of methoxyfluoboric acid

$$Hg(OAc)_2 + H^{\oplus} + HSO_4^{\ominus} \leftrightarrows HgOAc^{\oplus} + HSO_4^{\ominus} + HOAc \qquad [ix]$$

and *p*-toluenesulphonic acid probably are similar. In this connection it may be observed that hydrochloric acid does not increase the yield of IV, undoubtedly because it is converted to mercuric chloride which is largely unionized.

It may be seen from the table that odd electron donors such as benzoquinone, hydroquinone, and *tert*-butylhydroperoxide are entirely ineffective. To be sure stannous chloride and ferrous sulphate are both effective for augmentation of IV over the acetate, III, but they may be functioning in formation of complex anions. The augmentation by the ferrous salt is of especial interest if the present findings are contrasted to an earlier report of the preparation of 3-methoxymethylenecyclohexylmercuric chloride (8) in which

Can. J. Chem. Downloaded from www.nrcresearchpress.com by 196.1.178.254 on 09/04/12
For personal use only.

TABLE II

The effect of catalysts on oxymercuration with norbornene and mercuric acetate 0.25 molar in methanol during 90 minutes

Catalyst	Equiv. of catalyst	Total yield, %	% of IV in product: From acetyl content	% of IV in product: By thermal analysis
Sulphuric acid	0.02	92		85
	0.10	85	90	89
	0.50	85		93
	1.00	85		93
p-Toluenesulphonic acid hydrate	0.10	90	86	83
	2.5	95		95
Ferrous sulphate	0.05	75	80	79
Boron fluoride etherate	0.10	95	90	89
Stannous chloride	0.10	65	79	81
Hydroquinone	0.10	93		69
Benzoquinone	0.10	95		68
Hydrochloric acid	0.10	83		68
tert-Butylhydroperoxide	0.10	93		67
None		97		67
Pyridine	0.10	95	58	55
	1.00	89	37	30
Trimethylamine	0.10	90	24	21

a good yield in high purity seemingly was obtained with a system comprised only of norbornene, mercuric acetate, and methanol. In view of our findings with this system, we presume that a contaminant such as ferrous salt must have been present in Rowland's system since otherwise he could not have obtained the high yield of methoxymercurial which he reported. Rather he should have obtained a mixture of III and IV.

In addition to the substances which accelerate the methoxymercuration over the formation of 3-↓-acetoxy-1,4-↑↑-methylenecyclohexyl-2-↑-mercuric salt (III), it may be seen from Table II that tertiary amines like pyridine and trimethylamine strongly retard methoxymercuration in favor of the formation of III. This must be due to the augmentation of acetate ion from the acetic acid formed in the system. Of course these nitrogen-containing electron-donors have been known previously to retard methoxymercuration, and earlier in this report it was shown that pyridine retarded the formation of III in 2,5-dioxahexane. Probably these latter effects are inconsequential to the argument of Table II. It may be seen that the presence of the amines did not appreciably diminish the total yield in methanol. Actually, the effect of either acids or bases on the rate of norbornene oxymercuration has not been evaluated in the present study because the reaction, even without addends, is very fast. Although 90 minutes has been allowed in these studies in order that all reactions would be standardized with respect to time, it is known that the 0.25 molar reaction in methanol at 20° C is complete within 45 seconds.

One may ask how this evidence for an ionic mechanism of oxymercuration may be correlated with previous experience of the general reaction. For example, it has been shown (9) that acetic acid retards one oxymercuration while the removal of acetic acid by evaporation from another, typical, reaction increases the rate (10). Moreover the evidence for ↑↑ (*cis*) addition is strong in respect of general oxymercuration (11), except for an X-ray diffraction study (12) which may be questioned in view of recent opinions about the flexibility of the cyclohexane ring. In view of these experiences the present results might seem to be anomalous.

Can. J. Chem. Downloaded from www.nrcresearchpress.com by 196.1.178.254 on 09/04/12
For personal use only.

Can. J. Chem. Downloaded from www.nrcresearchpress.com by 196.1.178.254 on 09/04/12
For personal use only.

An explanation has been sought, and found, in the chemical and physical properties of the norbornene methoxymercurials. First, the stability of the product designated as 3-↓-methoxy-1,4-↑↑-methylenecyclohexyl-2-↑-mercuric chloride (IV, R = Me, X = Cl) is unusually high. This stability is apparent also in the products obtained when IV is treated with excess hydrazine hydrate. For the first time this reaction has yielded methoxyalkyl bis-mercurials; both diastereomers have been obtained as solids which were separable by fractional crystallization. Either diastereomer can be reconverted to the original chloromercurial, IV, so that the reconversion of the bis-mercurial is stereospecific. We consider the higher melting (108°) bis-mercurial to be the meso isomer, V; also it has the higher dipole moment (2.17 D in benzene).

A second evidence of the stability of IV has been observed by the diastereomeric equilibration of IV (↓↑) with its isomer (↓↓, VI) with a small amount of hydrazine hydrate. This reaction has been shown (13) to give diastereomeric mixtures of 2-oxycyclohexyl and 2-oxycyclopentyl mercurials. The more stable diastereomer in the mixture may be isolated by treatment with methanolic hydrogen chloride which deoxymercurates the other diastereomer. The recovered diastereomer, which has been designated as β, has always heretofore been that one *not* obtained by oxymercuration of the alkene.

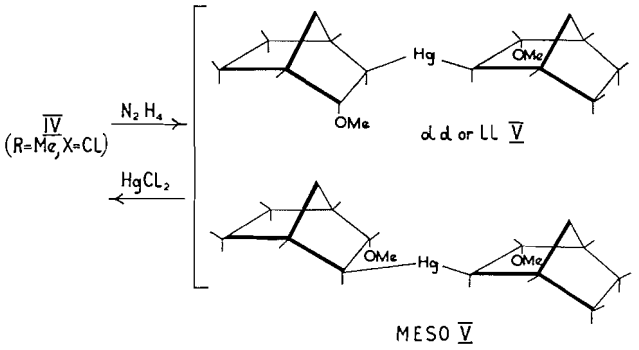

In contrast, the diastereomer recovered by partial deoxymercuration of the mixture of IV and VI is IV, the product of oxymercuration, in good yield. In order to isolate VI (at best, in small amount) an arduous fractional crystallization of the IV–VI mixture is required. This separation may be facilitated slightly by first converting the IV–VI mixture into a bis-mercurial mixture containing all four diastereomers, of which V represents a pair. This is accomplished by treatment of the IV–VI mixture with excess of hydrazine hydrate. When the four-diastereomer mixture is treated cautiously with less than the stoichiometric amount of methanolic hydrogen chloride for the reaction, the amount of VI in the mixture of IV and VI has been enhanced. Probably steric effects have altered the relative rates of diastereomeric scission.

The properties of VI do not resemble those of the previously known cyclic β-chloromercurials. It has been pointed out above that VI is more easily deoxymercurated than is IV, and this contrast to other cyclic α=β pairs is confirmed by the observation that the dipole moment of VI is found to be lower than that of IV. It would seem from these properties that the configurations of the norbornene oxymercurials are opposite to those of other oxymercurials such as are prepared from terpineol (14), cyclopentene (13), and cyclohexene (13, 15).

According to this definition of the configurations those assigned by Winstein, Traylor, and Garner (15) must be incorrect.

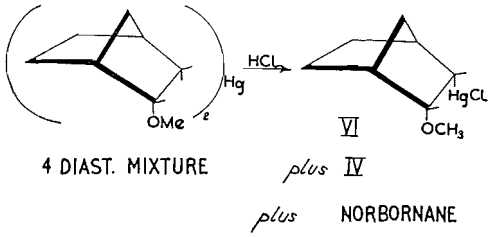

In contrast to the oxymercurations of cyclopentene and cyclohexene it may be said that the oxymercuration of norbornene is abnormal. This unusual behavior may not be unexpected in view of the dipole moments observed (Table III) for norbornane and norbornene, which would indicate a displacement of the electronic fields in these substances. Moreover, it has been shown previously (16, 17) that bromination of the norbornene-2,3-dicarboxylic acids does not follow the common ↑↓ addition of bromine to the double bond. During the remainder of this report it will be shown that some of these dicarboxylic acids also are abnormal in respect of oxymercuration.

During our previous work (11) with 1,4-↑↑-methylene-Δ^5-cyclohexene-2,3-↓↓-dicarboxylic acid (endo-norbornene-2,3-dicarboxylic acid, VII) we did not discern any abnormality when we established the *cis* (↓↓) configuration for the product (VIII) obtained by treatment of VII with aqueous mercuric acetate. Although the compound shown graphically as VIII could, alternatively, be 5-↓-hydroxy-anhydro-[6-↓-hydroxymercuri-2-↓-carboxy]-1,4-↑↑-methylenecyclohexane-3-↓-carboxylic acid, the choice of which transannular bridge is open is configurationally unimportant. Either form would be expected to undergo dehydration upon treatment with acetic anhydride to give 5-↓-hydroxy-anhydro-[6-hydroxymercuri-2-↓-carboxy]-1,4-↑↑-methylenecyclohexane-3-↓-carboxylic acid, γ-lactone (IX). The configuration of IX (and therefore of VIII) must be ↓↓ in respect of the oxy- and mercuri-linkages because its molecular weight has been determined cryoscopically as 381. The calculated molecular weight of IX is 382, so a polyester structure is not involved. The configuration of VIII and IX must therefore be ↓↓ as well.

It may be expected that the chloromercurial XI derived from VIII by acidification with hydrochloric acid also will have the ↓↓ configuration. But XI may be obtained directly by treatment of the unsaturated acid, VII, with mercuric chloride in water. This observation by Mr. J. H. Robson marks the first instance of oxymercuration in which participation of a basic mercuric salt cannot be postulated. Indeed, the near-quantitative yield is only lowered by 15% when 2 equivalents of hydrogen chloride are included with the mercuric chloride, although the otherwise very rapid reaction is retarded by this extra acid. The behavior is strongly suggestive of an ionic reaction which will be discussed later in this report.

When either VIII or IX is treated with aqueous sodium stannite the expected precipitation of metallic mercury occurs, and this presumably homopolar reaction (18) yields a diastereomeric mixture. Careful acidification with acetic acid precipitates VIII, perhaps in the anhydromercurial form mentioned above. After removal of VIII the filtrate may be acidified further by use of hydrochloric acid to yield the diastereomeric 5-↓-hydroxy-6-↑-chloromercuri-1,4-↑↑-methylenecyclohexane-2,3-↓↓-dicarboxylic acid, γ-lactone (X). This compound may be deoxymercurated (by treatment with concentrated hydrochloric acid) to the same 5-↓-hydroxy-1,4-↑↑-methylenecyclohexane-2,3-↓↓-di-

Can. J. Chem. Downloaded from www.nrcresearchpress.com by 196.1.178.254 on 09/04/12
For personal use only.

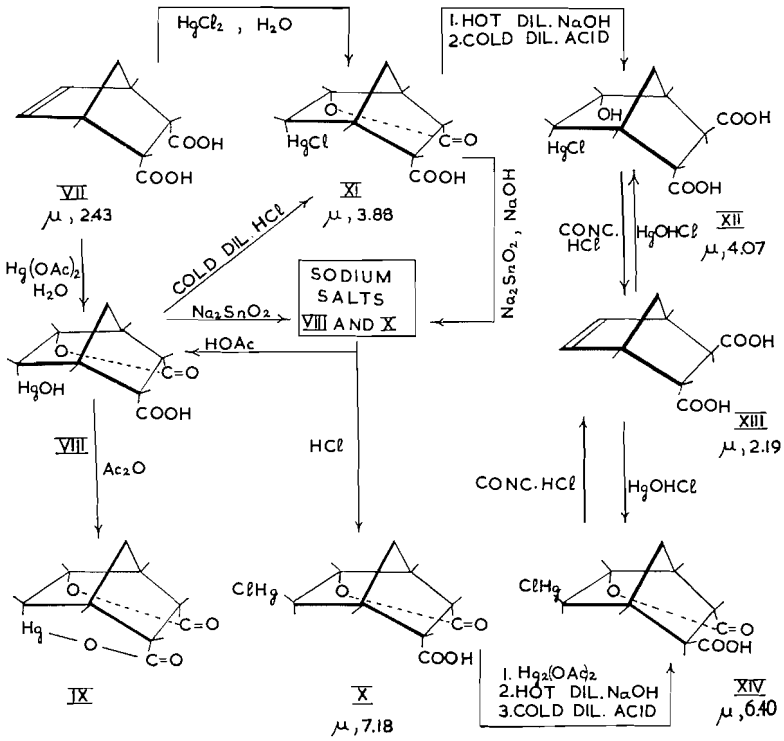

carboxylic acid, γ-lactone, obtained (more easily) by similar deoxymercuration of XI. The latter also yields, with sodium stannite, a mixture from which X may be isolated but the yield is lower, probably because of the presence of chloride ion.

When XI is boiled with aqueous sodium hydroxide it is converted (evidently via lactone hydrolysis) by prototropic rearrangement into 5-↓-hydroxy-6-↓-chloromercuri-1,4-↑↑-methylenecyclohexane-2-↓-3-↑-dicarboxylic acid (XII). The alteration in the rearranged substance is proved by deoxymercuration to 1,4-↑↑-methylene-Δ^5-cyclohexene-2-↓-3-↑-dicarboxylic acid by means of hydrochloric acid. Further proof is obtained when XII is treated with sodium amalgam, which effects replacement of chloromercuri by hydrogen. The product (which shows no tendency toward spontaneous lactonization) evidently is 5-↓-hydroxy-1,4-↑↑-methylenecyclohexane-2-↓-3-↑-dicarboxylic acid.

The prototropic rearrangement of XI→ XII is replicated by the conversion X → XIV, although the absence of chloride ion is essential to the latter conversion. The chloride was precipitated as calomel. The 2-carboxyl group seems to be rearranged, since XIV is the lactone of what must be 5-↓-hydroxy-6-↑-chloromercuri-1,4-↑↑-methylenecyclohexane-2-↑-3-↓-dicarboxylic acid. Confirmation of this structure assignment follows deoxymercuration of XIV with concentrated hydrochloric acid, which yields 1,4-↑↑-methylene-Δ^5-cyclohexene-2,3-↓↑-dicarboxylic acid (XIII). Moreover, replacement of the chloromercuri group (with sodium amalgam) by hydrogen leads to the known 5-↓-hydroxy-1,4-↑↑-methylenecyclohexane-2-↑-3-↓-dicarboxylic acid, γ-lactone (19).

The oxymercurial from norbornene has been assigned the ↑↓ configuration and that from 1,4-↑↑-methylene-Δ^5-cyclohexene-2,3-↓↓-dicarboxylic acid (VII) the ↓↓ configuration (XI), yet both reactions seem to proceed by the same (ionic) mechanism. It might then be expected that a reaction would exist in which both ↓↓ and ↑↓ configurations would

Can. J. Chem. Downloaded from www.nrcresearchpress.com by 196.1.178.254 on 09/04/12
For personal use only.

appear in the product. This expectation is realized in the treatment of 1,4-↑↑-methylene-Δ^5-cyclohexene-2,3-↑↓-dicarboxylic acid (XIII) with basic mercuric chloride in water, since both XII and XIV are obtained as products with the former predominating.

From these examples, it seems reasonable to assume that the norbornenes are oxymercurated uniquely via a π complex with mercuric salts which once was specified for alkenes in terms of an alkene–mercurinium ion (3). The favored neutralization of such an intermediate seems to occur from that region of the norbornane cage farthest from the methylene bridge. The mercuri group will then be situated in that region of the cage where the methylene bridge is predominant, unless it is attracted by an anionic group such as carboxyl in an available (↓) position. The simplest instance where both neutralizing anion and mercuri-attracting anion are two ↓↓ carboxyl groups is exemplified by the π-co-ordinated mercuric salt, XV, which is transformed to IX.

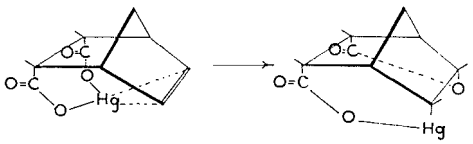

XV IX

When only one ↓ carboxyl group is available, as in 1,4-↑↑-methylene-Δ^5-cyclohexene-2-↓-3-↑-dicarboxylic acid (XIII), it seems to play either of the two roles alternatively. Thus it may neutralize the cation XVII formed via the intermediate XVI to yield XIV, or it may attract the mercuri group while hydroxyl ion is the neutralizing species, in which case XII is formed. One might expect in these circumstances that some of the 5-↑-OH diastereomer would be formed despite a preferential anionic approach to the cage. We have not found this diastereomer, but we cannot affirm its absence in view of the difficulties of separation. We shall now present evidence that such anionic neutralization does occur.

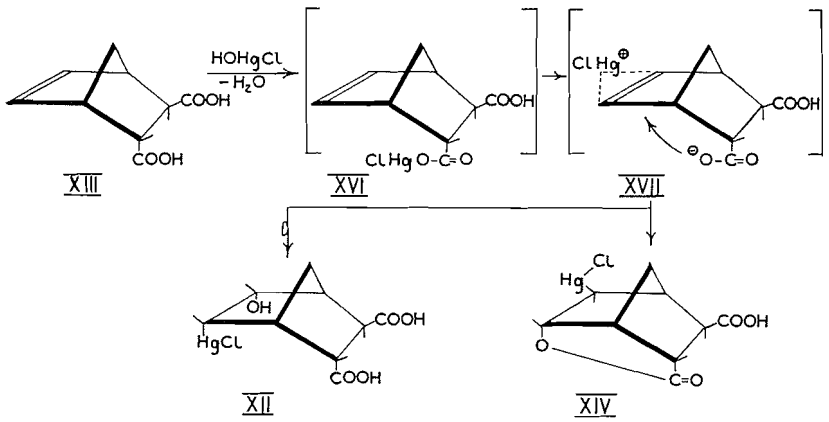

XIII XVI XVII XII XIV

This evidence is afforded by oxymercuration of dimethyl 1,4-↑↑-methylene-Δ^5-cyclohexene-2,3-↓↓-dicarboxylate (XVIII). Previously, the hydroxymercuration of this substance was reported (11) and the product was specified as 5-↓-hydroxy-6-↓-chloromercuri-2-↓-carbomethoxy-1,4-↑↑-methylenecyclohexane-3-↓-carboxylic acid, γ-lactone (XXII). It is now known that XXII from this reaction is contaminated with 5-↑-hydroxy-6-↓-

Can. J. Chem. Downloaded from www.nrcresearchpress.com by 196.1.178.254 on 09/04/12
For personal use only.

chloromercuri-2-↓-carbomethoxy-1,4-↑↑-methylenecyclohexane-3-↓-carboxylic acid, perhaps as its methyl ester, XXIII, though neither has been isolated. However, the presence of this mono- or di-ester impurity is shown by saponification of the entire product. The main product of this saponification is 5-↓-hydroxy-6-↓-chloromercuri-1,4-↑↑-methylenecyclohexane-2,3-↓↓-dicarboxylic acid, γ-lactone (XI), as well as some of the 2-↓-3-↑-dicarboxylic acid (XII) arising by prototropic rearrangement of XI. The remainder is isolated as 5-↑-hydroxy-6-↓-chloromercuri-1,4-↑↑-methylenecyclohexane-2-↓-3-↑-dicarboxylic acid (XXIV), the chemistry of which is discussed below. Thus the dimethyl ester of VII is shown to oxymercurate both ↓↓ and ↓↑, the former being predominant.

When dimethyl 1,4-↑↑-methylene-Δ^5-cyclohexene-2,3-↓↓-dicarboxylate (XVIII) is treated with mercuric acetate in acetic acid, the reaction is very rapid. The main product, almost pure, is dimethyl 5-↑-acetoxy-6-↓-chloromercuri-1,4-↑↑-methylenecyclohexane-2,3-↓↓-dicarboxylate (XXIII, Z = CH_3CO) plus a small quantity of 5-↓-hydroxy-6-↓-chloromercuri-2-↓-carbomethoxy-1,4-↑↑-methylenecyclohexane-3-↓-carboxylic acid, γ-lactone (XXII, X = Cl). When XXIII (Z = CH_3CO) is hydrolyzed, a prototropic rearrangement of one carboxyl group occurs to yield XXIV. This shift is indicated because

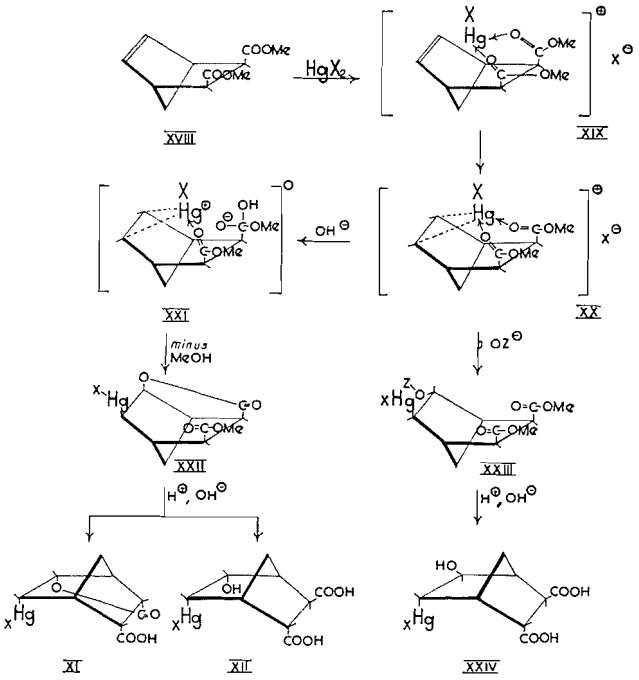

deoxymercuration of XXIV with hydrochloric acid yields 1,4-↑↑-methylene-Δ^5-cyclohexene-2-↓-3-↑-dicarboxylic acid (XIII). However, XXII (X = Cl), which may be prepared in excellent yield by mercuration of XVIII with an aqueous solution of mercuric acetate, and XXIII (Z = Me, X = Cl) prepared by methoxymercuration of XVIII, both deoxymercurate with hydrochloric acid to yield 5-↓-hydroxy-1,4-↑↑-methylenecyclohexane-2,3-↓↓-dicarboxylic acid, γ-lactone. Of course, this does not indicate which carboxyl group in XXIII has diastereomerically shifted. Indeed, XXIV could be either 5-↑-hydroxy-6-↓-chloromercuri-1,4-↑↑-methylenecyclohexane-2-↓-3-↑- or 2-↑-3-↓-dicarboxylic acid, but a pyrolytic reaction seems to supply this information.

Can. J. Chem. Downloaded from www.nrcresearchpress.com by 196.1.178.254 on 09/04/12
For personal use only.

The 5-↑-hydroxy-6-↓-chloromercuri-1,4-↑↑-methylenecyclohexane-2-↓-3-↑-dicarboxylic acid (XXIV) exists in two forms which evidently are polymorphs since the distortion polarizations and the infrared spectra (900–300 cm^{-1}) are practically identical although the melting points and X-ray diffraction patterns are different. The lower melting of these polymorphs tends slowly to resolidify slightly above its melting point of 194°. If it is maintained at 194–200° for 15 minutes the recognizable product is 5-↓-hydroxy-6-↑-chloromercuri-1,4-↑↑-methylenecyclohexane-2-↑-3-↓-dicarboxylic acid, γ-lactone (XIV). This inversion of the methylene bridge seems to be characteristic of the configuration of XXIV (since XII did not rearrange in this manner) and probably is a consequence of the 5-↑-hydroxy configuration. The rearrangement may be described in terms of the intermediates XXV and XXVI, and is typical of dehydration which otherwise would establish a bridgehead unsaturation.

In order to eliminate the possibility that the oxymercuration position assignments were incorrect, and that XXIV and XII differed only in the configuration of the chloromercuri group, the acid XXIV has been treated with sodium amalgam. The product has been designated as 5-↑-hydroxy-1,4-↑↑-methylenecyclohexane-2-↓-3-↑-dicarboxylic acid; certainly it is not identical with the acid of like composition which has been obtained by reduction of XII. It would seem that XXIV and XII differ in the configuration of the hydroxyl group.

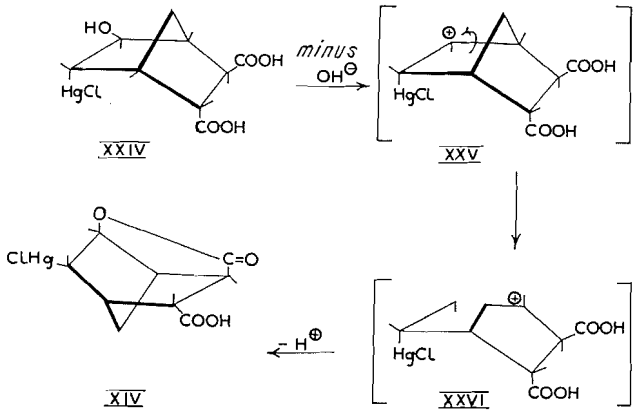

The configurations of the oxymercurials derived from dimethyl 1,4-↑↑-methylene-Δ^5-cyclohexene-2,3-↓↓-dicarboxylate seem to be established and the mode of their formations may be suggested. The mechanism may be described essentially as was that of the corresponding acid. If the ester (XVIII) co-ordinates with mercuric acetate (X = OAc) a near-ionic form, XIX, may occur. Within the electropositive portion further co-ordination with the π bond (XX) will be a prelude to further reaction. If the reaction occurs in water, hydroxyl ion may be expected to perform the first step of an ester hydrolysis, i.e. to add to the carbomethoxyl group and form the externally neutral dipole, XXI. This internal mercurinium salt, by loss of methanol, would then culminate in the principal product, XXII. If some hydroxyl ion (or the ever-present acetate ion X) were to attack rearward of the mercurinium linkage (OH or OAc = OZ) then the product of inversion (XXIII) is expected and, in small amount, is obtained. In absence of the hydrolytic reaction, that is, when the reaction medium is acetic acid, XXIII, the product

Can. J. Chem. Downloaded from www.nrcresearchpress.com by 196.1.178.254 on 09/04/12
For personal use only.

of inversion, is obtained in 93% yield, and XXII in small amount (0.5%). This attack by acetate from the region of the cage where the methylene bridge predominates is contrary to that observed with norbornene. This opposite behavior is attributed in the present mechanism to the complexity of the ion, XX.

In connection with the ionic mechanism which has been postulated for the norbornenedicarboxylic acids and their derivatives it may be recalled that inclusion of boron fluoride etherate during the oxymercuration of norbornene largely excluded the acetoxy derivative, III, in favor of the methoxy derivative, IV (R = Me). This behavior is expected when acetate and methoxide ions are competing in an ionic process because of the preferential stabilization of methoxide ion by the Lewis acid, BF_3. It is of interest that the oxymercuration of the ester, XVIII, in methanol leads to XXIII in which Z is almost entirely aceto. However, a mixture is formed in which Z is partly methyl when boron fluoride is included with the methanol. Since the measured dipole moment of this methoxy derivative is of the same magnitude as that of XXIII (Z = CH_3CO), we presume that the configuration is identical. The mechanism of reaction thus seems to be the same as that postulated for oxymercuration of norbornene.

It will be noted in the preceding paragraph that configurational identity has been claimed on the basis of dipole moments. Also configurational relationships must be established between the mercurials from norbornenedicarboxylic acids (the configuration of which has been established by definitive physical and chemical criteria) and the mercurials from norbornene. Therefore the basis for the relationship according to the moment values of Table III must be established.

It must be understood that the moment values per se do not establish configurations but only relate known to unknown configurations. Moreover the moment values must only be considered of qualitative significance. Of course the actual values, all determined at 20° in dioxane (the only non-polar solvent in which all the mercurials are soluble), are reliable within 0.1 D. However, the vectorial assignments and the group moments must be chosen somewhat arbitrarily; indeed another set might have been chosen which would designate configurations opposite to those specified in this report. Nevertheless, like much physical interpretation based on factual logic and non-factual assumptions, the moment calculations are at least self-consistent. As such they suffice to relate the configurations assigned in this report.

Among the group moment assignments which must be made for the calculation is that of the chloromercuri group. A linear (20) and later an angular (21, 22) (+)C—Hg—Cl(−) has been proposed. The angularity must be revised anew in view of evidence (23) that the C—Hg moment is not negligible. Indeed, the measured polarizations of mercuracyclohexane and mercuracycloheptane (0.86 and 0.90 D respectively) show that the bond moment of C—Hg is 1.31 D, negative with respect to carbon, if the C—Hg—C angle is 140°. Then despite uncertainty of mercurial bond angles (23) one may assign to a typical mercurial, *n*-propylmercuric chloride (3.70 D), a C—Hg—Cl bond angle of about 80° if the Hg—Cl moment is 3.2 D. The latter value has been chosen in consideration of the increasing dipole moment of alkylmercuric halides with ascent of the homologous series (23). Essentially these assignments designate mercury as the positive end of the angular alkanemercuric chloride dipole.

A structural assignment must also be made for the gamma–lactone linkage. This assignment has not been made previously, perhaps because the reported values, 3.8 (24) to 4.1 D (25), for γ-butyrolactone are abnormally high by contrast with non-cyclic

Can. J. Chem. Downloaded from www.nrcresearchpress.com by 196.1.178.254 on 09/04/12
For personal use only.

TABLE III

Electrical polarizations (cc) in dioxane at 20° C, moment in Debye units

	$\Delta\epsilon/\Delta\omega$	$\Delta\bar{V}/\Delta\omega$	P_T	P_{e+a} pellet	R_D calc.	μ
5-↓-Hydroxy-2-carbomethoxy-1,4-↑↑-methylene-cyclohexane-3-↓-carboxylic acid, γ-lactone	15.53	0.165	542.9		45.1	4.86
1,4-↑↑-Methylene-Δ⁵-cyclohexene-2,3-↓↑-dicarboxylic acid (XIII)	3.50	0.220	143.4		42.0	2.19
Same, except-2,3-↓↓-dicarboxylic acid (VII)	4.35	0.295	164.3		42.0	2.42
1,4-↑↑-Methylenecyclohexane-2,3-↓↓-dicarboxylic acid	5.50	0.230	204.8		42.4	2.78
1,4-↑↑-Methylenecyclohexane-2,3-↓↑-dicarboxylic acid	4.40	0.210	172.7		42.4	2.49
5-↓-Hydroxy-1,4-↑↑-methylenecyclohexane-2,3-↓↓-dicarboxylic acid, γ-lactone	16.70	0.265	535.1		40.4	4.85
5-↓-Hydroxy-1,4-↑↑-methylenecyclohexane-2-↑-3-↓-dicarboxylic acid, γ-lactone	18.30	0.275	578.8		40.4	5.06
Dimethyl 5-↑-acetoxy-6-↓-chloromercuri-1,4-↑↑-methylenecyclohexane-2,3-↓↓-dicarboxylate (XXIII, Z = CH_3CO, X = Cl)	6.30	0.545	579.5		78.9	4.87
Norcamphane (norbornane)	0.09	0.210	34.11		30.1	0.43
Norbornene (I)	0.28	0.185	35.6		29.7	0.53
5-↑-Methoxy-1,4-↑↑-methylenecyclohexane-2,3-↑↑-dicarboxylic acid	6.00	0.295	249.9		47.6	3.10
5-↑-Hydroxy-1,4-↑↑-methylenecyclohexane-2,3-↓↓-dicarboxylic acid	7.25	0.612	557.5	88.9	60.2	4.73
dd,ll-2,2′-↑↑-Mercuri-bis-3-↓-methoxy-1,4-↑↑-methylenecyclohexane, m.p. 68° (V, *dd,ll*)	1.0417	−0.36364	156.8	81.1	81.8	1.93
dl,ld of same, m.p. 108° (V, *dl,ld*)	1.250	−0.3333	176.2	81.4	81.8	2.17
3-↓-Methoxy-1,4-↑↑-methylenecyclohexyl-2-↑-mercuric chloride (IV, R = Me, X = Cl)	6.250	−0.4500	427.5		52.4	4.22
3-↓-Methoxy-1,4-↑↑-methylenecyclohexyl-2-↓-mercuric chloride (VI)	2.857	−0.555	214.2		52.4	2.77
3-↓-Acetoxy-1,4-↑↑-methylenecyclohexyl-2-↑-mercuric chloride (III)	4.40	0.505	329.8		57.1	3.60
5-↓-Hydroxy-6-↓-chloromercuri-1,4-↑↑-methylene-cyclohexane-2-↓-3-↑-dicarboxylic acid (XII)	5.33	0.605	405.6		56.4	4.07
5-↓-Hydroxy-6-↑-chloromercuri-1,4-↑↑-methylene-cyclohexane-2-↑-3-↓-dicarboxylic acid, γ-lactone (XIV)	9.90	0.610	716.1		56.4	6.40
5-↓-Hydroxy-6-↑-chloromercuri-1,4-↑↑-methylene-cyclohexane-2,3-↓↓-dicarboxylic acid, γ-lactone (X)	16.10	0.585	1143.4		56.4	7.18
Same, except -6-↓-chloromercuri- (XI)	4.85	0.600	373.0		56.4	3.88
5-↓-Hydroxy-6-↓-chloromercuri-2-↓-carbomethoxy-1,4-↑↑-cyclohexane-3-↓-carboxylic acid, γ-lactone (XXII)	4.50	0.545	366.6		61.1	3.81
Dimethyl 5-↑-methoxy-6-↓-chloromercuri-1,4-↑↑-methylenecyclohexane-2,3-↓↓-dicarboxylate (XXIII, Z = Me, X = Cl)	5.80	0.537	508.2		74.2	4.54

little-constrained esters. It seems reasonable to explain this high value as an alteration of bond moments in the —C—O—(C=O)—C linkage from [0.7, 0.7, 2.3, 0.4] to [0.8, 0.5, 2.8, 0.4], after which the moment for γ-butyrolactone is calculated as 4.0 D.

However, the moments of the 5-↓-hydroxy-1,4-↑↑-methylenecyclohexane-2,3-↓↓-dicarboxylic acid, γ-lactone (μ = 4.85 D), and the 2,3-↑↓-diastereomer (μ = 5.06 D) markedly exceed that of γ-butyrolactone. Part of this abnormality may be ascribed to the norbornane ring since a moment of 0.43 D has been observed (Table III) for this hydro-

Can. J. Chem. Downloaded from www.nrcresearchpress.com by 196.1.178.254 on 09/04/12
For personal use only.

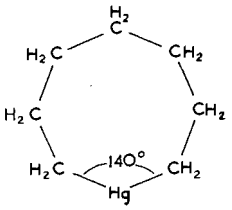

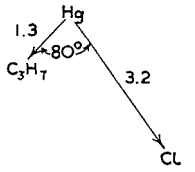

carbon. The carboxyl group will also contribute, but neither contribution suffices to explain the high moment which has been observed, especially for the 2,3-↑↓-diastereomer. However, it is probable that the additional constraint imposed by the norbornane cage accentuates the alteration in bond moment which has been suggested for γ-butyrolactone.

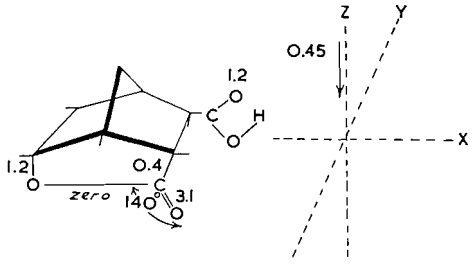

XXVII

These considerations have suggested the model XXVII in which the alcohol bond is extended to 1.2 D and the carbonyl bond is extended to 3.1 D, while the ester bond is decreased to zero. This condition represents a resonance hybridization of the O—C=O linkage. Moreover the constraint imposed by non-planarity of the γ-lactone ring has distorted the cyclohexane ring so that the ↓ linkages are inclined 18° toward the center of the cage, thus forcing the equatorial ↑ linkage into a plane containing atom 2, 3, 5, and 6. These linkages are assumed to be spread 30° outward from the *X*-axis.

The moment of the free carboxyl group has been estimated as 1.2 D by calculation from the observed moments of 1,4-↑↑-methylenecyclohexane-2,3-↓↓-dicarboxylic acid (μ = 2.78 D) and 1,4-↑↑-methylenecyclohexane-2,3-↑↓-dicarboxylic acid (μ = 2.49 D) after subtraction of the norbornane cage moment (0.45 D). In order to simplify subsequent calculations the moment of the carboxyl groups (either ↑ or ↓) has been assumed to be symmetrical about the C—COOH bond. That is to say that the hydroxyl group in the carboxyl is in *cis* relationship to the carbonyl group.

In these circumstances the moment summation with respect to the co-ordinate axes is found to be 4.86 D for 5-↓-hydroxy-1,4-↑↑-methylenecyclohexane-2,3-↓↓-dicarboxylic acid, γ-lactone, and 5.04 D for the 2,3-↑↓-diastereomer. If the C—Hg group moment assigned previously (1.31 D, C ← Hg) is added to each of these γ-lactones in the appropriate sense the following R—Hg moments arise from the calculation.

Calculation of the moment of 5-↓-hydroxy-6-↓-chloromercuri-1,4-↑↑-methylenecyclohexane-2,3-↓↓-dicarboxylic acid, γ-lactone, from XXVIII may be made as follows:

$$\mu = [(3.79)^2+(3.22)^2-2(3.79)(3.22)\cos 41°\cos 13°\sin 10°]^{\frac{1}{2}} = 4.6 \text{ D}.$$

It is not surprising that this value, based on harmonic rotation at a rate exceeding 500 kc/second, is appreciably higher than the observed moment (3.88 D) since free rotation

Can. J. Chem. Downloaded from www.nrcresearchpress.com by 196.1.178.254 on 09/04/12
For personal use only.

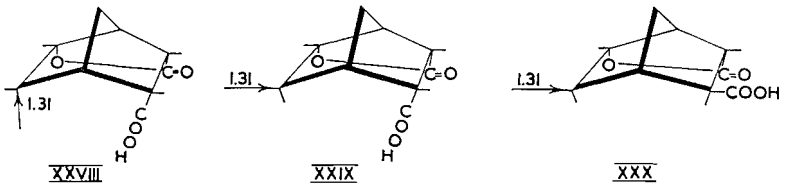

$\mu_{R\text{-}Hg}$ = 3.79 D where $\tan\mu_Y/\mu_Z = \tan 11°$ and $\tan\mu_X/\mu_Z = \tan 43°$

$\mu_{R\text{-}Hg}$ = 5.87 D where $\tan\mu_Y/\mu_X = \tan 23°$ and $\tan\mu_Z/\mu_X = \tan 43°$

$\mu_{R\text{-}Hg}$ = 6.31 D where $\tan\mu_Y/\mu_X = \tan 18°$ and $\tan\mu_Z/\mu_X = \tan 27°$

would be most improbable. Calculation at position 6 for the quadrant directions of Hg → Cl shows that when this vector points toward the 2-position the moment would be 6.2 D; away from position 2, 2.3 D; toward position 5, 5.0 D; and away from position 5, 4.3 D. Therefore the observed moment is about what would be expected if rotation were hindered within the realm of the norbornane cage, thus minimizing the 6.2 D and the 5.0 D conformations.

The moment calculation from XXIX for 5-↓-hydroxy-6-↑-chloromercuri-1,4-↑↑-methylenecyclohexane-2,3-↓↓-dicarboxylic acid, γ-lactone (X), assuming free rotation, is 7.0 D. While this is lower than the observed moment (7.18 D) the slight discrepancy is not unexpected in view of possible hindrance when Hg → Cl is directed toward C_5. This conformation detracts slightly from the total because of the angle of 120° which the Hg—C bond makes with the C_5—C_6 bond. Consequently, the observed moment may be expected to be slightly higher than that calculated for harmonic free rotation.

However, a greater discrepancy exists between observed moment (6.4 D) and that calculated (7.50 D) from the partial structure, XXX, for 5-↓-hydroxy-6-↑-chloromercuri-1,4-↑↑-methylenecyclohexane-2-↑-3-↓-dicarboxylic acid, γ-lactone (XIV). Several explanations are possible to account for this discrepancy. First, the assumption that the carboxyl group is bound so that its group moment is linear may apply to the ↓ position where it is "bound" by the lactone resonance but not to the ↑ (actually equatorial) position. Thus it may contribute, together with the chloromercuri group, three rotators in the structure. The equation for a single rotator would then not apply. More likely is the possibility that this heavy molecule exists as a carboxylic acid dimer which is stable even in very dilute solution because of the non-hindered equatorial carboxyl group. This hydrogen-bridging would effectively lower the moment. Some evidence for this bridging is found in the fact that the moment in dioxane increases from 6.40 D at 25° to about 6.6 D at 70°.

However, it is advisable to consider only qualitatively any moment value in which more than two rotators are involved. For this reason there are numerous entries in Table III for which no calculations are attempted. However, a typical example may be chosen in the observed moment of 3-↓-acetoxy-1,4-↑↑-methylenecyclohexyl-2-↑-mercuric chloride (3.6 D, III). When the accepted value (1.80 D) for the acetoxy group (26) in its *cis* conformation is used with a calculated moment angle of 121° the over-all molecular moment where two rotators are inclined at 120° is 4.0 D. However, the discrepancy may be made to disappear and then to reappear in a moment value lower than that observed by alteration in the rotations at the ether linkage and the carbonyl linkage in the acetoxy

Can. J. Chem. Downloaded from www.nrcresearchpress.com by 196.1.178.254 on 09/04/12
For personal use only.

group. Since the anharmonicity of these rotators is unknown, the calculation is of little significance.

The moment calculation for 3-↓-methoxy-1,4-↑↑-methylenecyclohexyl-2-↑-mercuric chloride (IV) is more propitious because only two rotators are involved. The rotation is assumed to be harmonic. One rotator is C—Hg—Cl with a group moment of 3.67 D and moment angle 79° from C—Hg. The other rotator is a combined norbornane plus methoxyl moment (μ_0 = 1.30+0.43 cos 55° = 1.59 D). The rotator axes are separated by 65°. The resultant is 4.12 D, slightly low by comparison with the observed moment of 4.22 D. This discrepancy may be attributed to anharmonicity such as was postulated for the 2,3-↓↓-dicarboxy analogue (X) because of slight steric hindrance.

When μ for 3-↓-methoxy-1,4-↑↑-methylenecyclohexyl-2-↓-mercuric chloride (VI) is calculated on the same free-rotatory basis as is the diastereomer, IV, the value, 3.4 D, is considerably higher than has been measured (2.88 D). However, a consideration of the quadrant conformations shows that XXXIV surely is excluded on the basis of hindrance between chloromercuri and methoxy. Probably XXXII is excluded for the same reason. The average calculated moment due to XXXI and XXXIII is 2.86 D, in agreement with the observed value.

The reasonable adjustments which have been made in calculation are required to bring the norbornane oxymercurials of unknown configuration into correlation with the known configuration of the norbornane dicarboxylic acid mercurials. However, these adjustments have a further significance because those diastereomers (↓↓) in which hindrance is assumed to exist are also the ones which are most easily deoxymercurated.

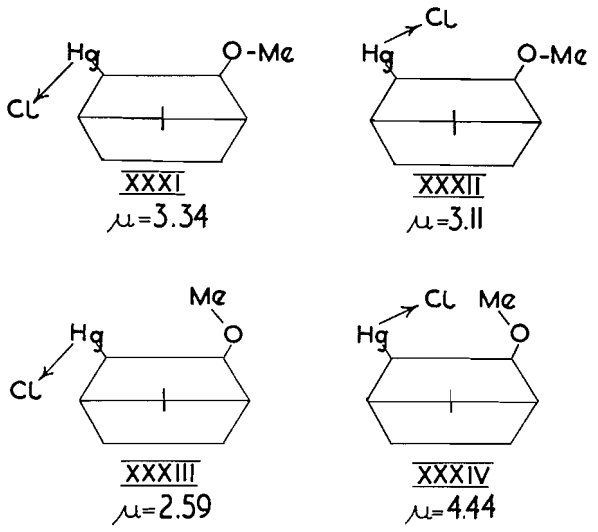

The mechanism of deoxymercuration has been suggested variously as due to polar (27) and steric effects (28), and both probably are operative. Certainly the extreme resistance of alkylmercuric halides and the moderate resistance of arylmercuric halides toward demercuration, in contrast to comparatively easy deoxymercuration, shows that polarity of substituents is significant. The static aspects of steric effect have been shown by experiment to be profound. Additionally, and related both to polarity and geometry, are the internal degrees of freedom. The acceptance of the deoxymercurating agent either

Can. J. Chem. Downloaded from www.nrcresearchpress.com by 196.1.178.254 on 09/04/12
For personal use only.

by co-ordination with the oxy group (polar mechanism) or in concerted cyclic transition states (steric (28)) must be related to molecular flexibility. The rigidity imparted by the norbornane cage makes it possible to correlate the moment values with the ease of deoxymercuration and thus to justify the behavior of 5-↓-hydroxy-6-↓-chloromercuri-1,4-↑↑-methylenecyclohexane-2,3-↓↓-dicarboxylic acid, γ-lactone (XI), and the simpler mercurial, VI, which is configurationally related to it.

In summary, the calculations show that since the dipole moment of 5-↓-hydroxy-6-↓-chloromercuri-1,4-↑↑-methylenecyclohexane-2,3-↓↓-dicarboxylic acid, γ-lactone (XI, the configuration of which is known), is lower than that of 5-↓-hydroxy-6-↑-chloromercuri-1,4-↑↑-methylenecyclohexane-2,3-↓↓-dicarboxylic acid, γ-lactone (X), the moment of the norbornene methoxymercurial (which is higher than that of the diastereomer to which it may be rearranged) designates it as 3-↓-methoxy-1,4-↑↑-methylenecyclohexyl-2-↑-mercuric chloride. The addition of the elements of methoxymercuric salts to norbornene thus occurs in the ↓↑ (so-called *trans*) manner. In part, this is true for oxymercuration of all norbornenes except 1,4-↑↑-methylene-Δ^5-cyclohexene-2,3-↓↓-dicarboxylic acid (VII). The oxymercuration of all norbornenes seems to be acid-catalyzed. This catalysis as well as the ultimate configuration indicates that oxymercuration of norbornenes occurs by an ionic mechanism which may be expressed in terms of a cationic intermediate such as the alkene–mercurinium ion postulated by Lucas, Hepner, and Winstein (3).

But the oxymercuration of cyclohexene, for which this postulate was made, is neither acid-catalyzed nor does the product resemble the oxymercurial from norbornene in respect of moment magnitude and resistance toward deoxymercuration. The same dissimilarity applies to the oxymercurials of cyclopentene, α-terpineol, and also of the stilbenes if conformational aspects are taken into consideration. Although the postulation of Lucas, Hepner, and Winstein seems to apply to a bicyclic alkene in which electron field distortion is probable, this postulation is unrealistic in respect of the conformationally restricted type of alkene for which it was promulgated. The latter type seems to be oxymercurated by a molecular mechanism which causes ↓↓ (so-called *cis*) addition. However, ↑↓ oxymercuration might be found to occur among α,β-unsaturated carbonyl compounds.

The authors wish to thank the National Research Council for funds in support of this research, and also Dr. Henry Richmond for aid in some of the moment calculations.

EXPERIMENTAL

Physical Constants

Melting points have been corrected against reliable standards (29). X-Ray diffraction patterns have been made with Cu K_α (Ni-filtered) radiation and are expressed as relative intensities $[I/I_1]$ for d spacings in Å. Temperature composition diagrams have been determined (1° per minute) by the method of Rheinboldt and Kirscheim (30). Electrical polarizations in dioxane solutions were made with the apparatus and method described previously (31), and no value of $\Delta\epsilon/\omega_2$ or $\Delta\bar{V}/\omega_2$ was accepted unless the extrapolation matched the ϵ and $\bar{V}$ for pure dioxane. Distortion polarizations were determined from compressed pellets and/or additive group refractions.

Purification of Reagents

The norbornene (1,4-↑↑-methylene-Δ^2-cyclohexene, 100 g) was shaken twice at 50° with 200 ml of 5% aqueous ferrous sulphate in a separatory funnel under nitrogen, then twice with 50-ml portions of water. After it was dried under nitrogen with magnesium sulphate the norbornene was distilled under nitrogen at 95–97°, then fractionated under

Can. J. Chem. Downloaded from www.nrcresearchpress.com by 196.1.178.254 on 09/04/12
For personal use only.

nitrogen in a 100-plate column, reflux ratio 1:35, b.p. 97–98°, m.p. 45–47°. The mercuric acetate was crystallized from acetic acid (2.5 ml per g) and was washed with anhydrous ether until the odor of acetic acid no longer could be detected.

3-↓-Hydroxy-1,4-↑↑-methylenecyclohexyl-2-↑-mercuric Chloride (IV, R = H, X = Cl)

A system consisting of 0.94 g (0.01 mole) of norbornene with 3.18 g (0.01 mole) of mercuric acetate and 0.2 ml of concentrated nitric acid in 35 ml of water was allowed to react 1 day and then was treated with aqueous sodium chloride. The product (88%) melted at 124–128° and was purified for analysis (see Table IV) by crystallization from 1:1 ethanol–water. When the nitric acid was not included the crude melting point was 119–125° and treatment with alkali was required to saponify the acetate which was present as an impurity. The other derivatives of Table IV were prepared by treatment with the appropriate sodium halide.

3-↓-Acetoxy-1,4-↑↑-methylenecyclohexyl-2-↑-mercuric Acetate (III, X = OAc)

To 6.36 g (0.02 mole) of mercuric acetate suspended in 30 ml of 2,5-dioxahexane was added 1.88 g (0.02 mole) of norbornene. After 5.5 hours the insoluble substance was filtered off and washed with 30 ml of dioxahexane, 6.55 g (79%), m.p. 98–100°. The substance was obtained in 84% yield by use of acetic anhydride as the reaction medium (32). Calc. for $C_{11}H_{16}HgO_4$: Hg, 48.7. Found: Hg, 49.3.

4-↓-Acetoxy-1,4-↑↑-methylenecyclohexyl-2-↑-mercuric Chloride (III, X = Cl)

(*a*) *By Acetylation*

To 2 ml of anhydrous pyridine was added 0.5 g (0.0014 mole) of 3-↓-hydroxy-1,4-↑↑-methylenecyclohexyl-2-↑-mercuric chloride. To this solution was added 1 ml (0.0065 mole) of acetic anhydride. After 2 days at room temperature the system was poured into 20 ml of cold 5% aqueous sodium chloride. The slowly solidifying product (0.56 g, 98%) melted at 122–124°. After two crystallizations from acetone the melting point (130°) of the product was not depressed by a sample prepared according to procedure (*b*). The substance was found by flotation in thallium formate – malonate at 5° to have a density of 2.37.

(*b*) *By Salt Exchange*

The compound may be obtained in 8% yield by dilution of the mother liquors from the acetate (see above) with aqueous sodium chloride. Alternatively, 1.04 g (0.0025 mole) of 3-↓-acetoxy-1,4-↑↑-methylenecyclohexyl-2-↑-mercuric acetate was shaken with 25 ml of 5% aqueous sodium chloride for 2 hours, converting it to 0.87 g (88%) of the chloromercurial, m.p. 124–128°. Crystallization from acetone (7 ml per g) raised this melting point to 130.8–131.8° (0.63 g).

The X-ray diffraction pattern was determined: [10] 14.40; [7] 4.77, 4.27, 3.86, 3.53, 2.79; [6] 5.71, 2.41; [5] 5.27, 3.12, 2.47; [4] 8.58, 5.90, 4.00, 3.62, 3.06, 2.98, 2.90, 2.51, 2.25; [3] 3.41, 3.25, 2.66, 2.62, 2.35, 2.31, 2.14; [2] 4.13, 2.19, 2.10, 1.96, 1.93, 1.86, 1.81, 1.77; [1] 7.02, 3.34, 2.27, 2.06, 2.00, 1.72, 1.64, 1.36, 1.24, 1.34; [0.5] 4.95, 2.85. Calc. for $C_9H_{13}ClHgO_2$: C, 27.8; H, 3.34; Hg, 51.6. Found: C, 28.0; H, 3.47; Hg, 52.0.

(*c*) *From Norbornene*

To 5 ml of anhydrous peroxide-free 2,5-dioxahexane was added 0.4 g (0.0017 mole) of mercuric acetate with or without a catalyst. To this suspension was added 0.11 g (0.0017 mole) of norbornene and the system was agitated for 4.5 hours, then filtered into 15 ml of 5% aqueous sodium chloride. After 1.5 hours, filtration with water-washing gave 0.65 g (98%), m.p. 126–128°, when no catalyst was added. Addition of boron fluoride

Can. J. Chem. Downloaded from www.nrcresearchpress.com by 196.1.178.254 on 09/04/12
For personal use only.

etherate depressed the melting point but not the yield. Addition of 0.00017 mole of pyridine depressed both (62%, m.p. 122–155°) while 0.0017 mole of this retarder depressed both to 24%, m.p. 121–125°. Under the latter conditions a prolonged reaction time (11 hours) increased this low yield to 41%, m.p. 122–124°. The catalytic effect of an equivalent of methanol was found to be negative since a yield of 70%, m.p. 120–125°, was obtained. None of these products gave a melting point depression upon admixture with the purified product of procedures (*a*) and (*b*). Reaction in glacial acetic acid (15 ml) was more rapid than in dioxahexane. The clear solution, after 30 minutes, was drowned in 30 ml of 5% aqueous sodium chloride giving a quantitative yield, m.p. 127–129°. Two crystallizations from acetone (6 ml per g) raised this melting point to 130°.

3-↓-Methoxy-1,4-↑↑-methylenecyclohexyl-2-↑-mercuric Chloride (IV, R = Me, X = Cl)

(*a*) *By Methylation*

From a 250-ml claisen flask containing 80 ml of sulphur-free toluene was distilled 15 ml to remove water. Then 0.59 g (0.015 atom) of potassium and 10 ml of sodium-dried *tert*-butyl alcohol was added. When solution was complete the excess of *tert*-butyl alcohol was distilled off. Then 1.8 g (0.005 mole) of 3-↓-hydroxy-1,4-↑↑-methylenecyclohexyl-2-↑-mercuric chloride was dissolved in the stirred system. After 90 minutes the whole was partially vacuum-distilled to remove *tert*-butyl alcohol. To the remainder was added 1.89 g (0.015 mole) of pure dimethyl sulphate. After the solution was stirred for 90 minutes 40 ml of 10% aqueous sodium hydroxide was added. The remaining toluene was vacuum-distilled off after 15 minutes. The residue, diluted with 90 ml of 1.5% aqueous sodium chloride, was treated exhaustively with gaseous carbon dioxide. The precipitate, 1.4 g (77%), m.p. 119–122°, was crystallized from absolute ethanol, m.p. 121–123°. A mixture melting point with the methoxymercurial prepared according to procedure (*b*) or by Rowland's procedure (8) was not lowered. The density, determined by flotation at 5° in an aqueous thallium formate – malonate solution, was 2.41. Oxidation with alkaline permanganate was difficult and much unchanged mercurial was recovered. However, a 10% yield of 1,3-↓↓-cyclopentanedicarboxylic acid, m.p. 119°, was obtained.

(*b*) *By Standard Oxymercuration*

To 10 ml of absolute methanol containing the catalyst (see Table II) was added 0.23 g (0.0025 mole) of norbornene. To the homogeneous solution was added with shaking 0.80 g (0.0025 mole) of mercuric acetate. The homogeneous reaction continued for 90 minutes; then the system was chilled to 5° and this temperature was maintained while 20 ml of 5% aqueous sodium chloride was added. The system kept at 5° during 2 hours was filtered, washed with water, and vacuum-dried. The typical yield with 0.5 equivalent of boron fluoride was 0.85 g (95%), m.p. 115–118°, or with 0.2 equivalent of ferrous sulphate was 95%, m.p. 108–114°. The product was analyzed as described below or was crystallized from hot carbon tetrachloride (1 ml per g), m.p. 120–121°. Melting point ranges were determined in the Rheinboldt apparatus, the temperature–composition diagram having been determined from known mixtures of methoxy- and acetoxy-mercurials which were together dissolved in chloroform and evaporated. The acetyl content of the known mixtures and the products were determined by the method of Friedrich (33).

(*c*) *From Mercuric Chloride*

A mixture of 0.94 g (0.01 mole) of norbornene and 2.71 g (0.01 mole) of mercuric chloride in 25 ml of methanol was maintained for 10 hours and then chilled to −60° and filtered to remove 0.67 g, m.p. 89.5–91.5°, which contained 0.30 g of benzene-insoluble mercuric chloride. The filtrate was diluted to a volume of 45 ml and was filtered quickly, 0.49 g,

Can. J. Chem. Downloaded from www.nrcresearchpress.com by 196.1.178.254 on 09/04/12
For personal use only.

m.p. 121–122°. The total yield (0.86 g, 24%) was crystallized from 2:1 hexane–benzene, m.p. 122–123°. A mixture melting point with the pure products of procedures (*a*) and (*b*) was not lowered.

(*d*) *By Mercuric Acetate plus Mercuric Oxide*

Suspensions of 10 ml of absolute methanol, 0.80 g (0.0025 mole) of mercuric acetate, and 0.10 g (0.0005 mole) of alkali-free yellow mercuric oxide were stirred under reflux in nitrogen for 8 hours. Each was then stirred for various periods of time after 0.23 g (0.0025 mole) of norbornene was added, then was chilled and treated with 20 ml of 5% aqueous sodium chloride and chilled to 5° overnight. The yield after 15 minutes and also after 4 hours was 70%, m.p. 92–101°, but after 12 hours it was 90%, m.p. 92–106°, indicating a retarded formation of methoxymercurial. The marked acceleration after 4 hours undoubtedly is related to the disappearance of suspended material after this time interval.

TABLE IV

Preparation and properties of 2-↓-alkoxy-1,4-↑↑-methylenecyclohexyl-2-↑-mercuric halides (IV) from equimolar amounts of norbornene (1) and mercuric acetate in the protonic medium (ROH), then treated with alkali halides (MX)

Properties	R = H X = Cl	R = H X = Br	R = H X = I	R = Me X = Cl	R = Me X = Br	R = Et X = Cl	R = Et X = Br
Yield	88	90	93	91	97	78	93
M.p., ° C	128.6–129.3	130.7–131.2	146.6–147.2	123.0–123.7	89.3–89.8	64–65	80.4–81.2
% C:							
calc.	24.2	21.4	19.2	26.6	23.7	28.8	25.8
found	24.5	21.3	19.1	26.7	23.5	28.6	25.2
% H:							
calc.	3.20	2.81	2.52	3.63	3.20	4.01	3.58
found	3.62	2.99	2.57	3.77	3.40	4.17	3.44
% Hg:							
calc.	57.8			55.6		53.6	
found	57.6			56.2		53.5	
X-ray diagram							
[10]	8.63			9.50		13.80	
[9]	4.78			6.06		3.65	
[8]	5.12			5.12		5.57	
	3.31			4.95		4.55	
	3.51			3.56		3.42	
[7]	2.92			2.93		8.50	
	2.58			3.70		5.61	
	3.08			3.93		5.34	
[6]	2.80			3.35		4.30	
	2.54			3.06		4.20	
[5]	2.45			3.48		6.94	
	2.15			2.62		6.53	
	2.03			2.51		5.05	
	1.98			2.24		4.10	

2,2′-↑↑-Mercuri-bis-3-↓-methoxy-1,4-↑↑-methylenecyclohexane (V, *dd,ll and* V, *dl,ld*)

To 100 ml of 85% hydrazine hydrate chilled to −70° was added 27 g (0.0075 mole) of 3-↓-methoxy-1,4-↑↑-methylenecyclohexyl-2-↑-mercuric chloride. The temperature was allowed to rise slowly to that of the ice bath into which the system was transferred. After 20 minutes a pink color was observed which changed to blue-black. After 12 hours at 25° the whole was heated on the steam bath for 3 hours, then chilled for 12 hours.

Can. J. Chem. Downloaded from www.nrcresearchpress.com by 196.1.178.254 on 09/04/12
For personal use only.

Can. J. Chem. Downloaded from www.nrcresearchpress.com by 196.1.178.254 on 09/04/12
For personal use only.

The aqueous layer and the metallic mercury were decanted from the white solid (12 g, 70%, m.p. 70–110°) which was heated with 100 ml more of hydrazine hydrate on the steam bath for 11 hours. Chilling yielded 4.3 g (25%) of crude product, m.p. 62–66°, softening at 55°. The same color change and the same yield, but with lower melting point (56.2–57.5°), may be obtained if 1 mole of mercurial in 5 moles of 2.5% aqueous alkali is treated with 0.5 mole of stannous chloride dihydrate during 24 hours.

This mixture of two diastereomers may be separated by 'triangular' crystallization utilizing methanol in which the higher melting isomer is relatively insoluble and methanol–water from which the lower melting isomer may be crystallized. Finally the higher melting isomer was crystallized from acetone, m.p. 107.5–108°. The lower melting isomer finally was crystallized from methanol, m.p. 66–66.5°. The ratio of high to low was found to be 6 to 1. Calc. for $C_{16}H_{26}O_2Hg$: C, 42.7; H, 5.76. Found (high): C, 42.8; H, 5.73. Found (low): C, 42.7; H, 5.67. The X-ray pattern for the high melting diastereomer was [10] 10.64, 10.00, 5.82, 5.60; [6] 4.21, 3.87, 3.77, 3.47, 3.26; [4] 2.74, 2.65, 2.22, while that of the low melting isomer was [10] 11.33, 5.34, 4.79; [9] 7.76, 7.53, 3.90; [8] 3.61, 3.46; [6] 3.09, 3.02, 2.68, 2.59, 2.36, 2.40; [3] 2.15, 2.10.

When either the high or low melting isomer was refluxed for 3 hours with 2 equivalents of mercuric acetate in methanol, and then was treated with sodium chloride, the crude chloromercurials melted at 120–122°. A mixture melting point with 3-↓-methoxy-1,4-↑↑-methylenecyclohexyl-2-↑-mercuric chloride was not lowered. In each instance about 10% of bis-mercurial was recovered unchanged. The same chloromercurial, m.p. 121–122°, was obtained when either isomer was treated with methanolic hydrochloric acid for 5 minutes. Either isomer could be heated to 115° for 40 minutes without change.

An unsuccessful attempt was made to synthesize the bis-mercuri diastereomers by converting 0.9 g (0.0025 mole) of 3-↓-methoxy-1,4-↑↑-methylenecyclohexyl-2-↑-mercuric chloride either to the organomercuric acetate by 0.41 g of silver acetate or to the organomercuric hydroxide by treatment with silver oxide, both in methanol, followed by treatment with norbornene (0.47 g, 0.005 mole) and 12 mg of boron fluoride etherate. After 1 day the original mercurials were recovered unchanged.

1,4-↑↑-Methylenecyclohexan-↓-yl Phenylurethane

To 1.40 g (0.004 mole) of 3-↓-hydroxy-1,4-↑↑-methylenecyclohexyl-2-↑-mercuric chloride in 18 ml of methanol was added a solution of 0.32 g (0.008 mole) of sodium hydroxide in 1 ml of distilled water. This solution was refluxed 6 hours with 0.47 ml (0.008 mole) of 85% hydrazine hydrate; 0.70 g (87%) of the mercury was filtered off as the metal.

The filtrate, diluted with 75 ml of water, was ethyl ether-extracted (75 ml) and the extract was evaporated to 5 ml. The solid which crystallized, m.p. 151–152°, 0.28 g (62%), was 2-hydroxy-1,4-↑↑-methylenecyclohexane (no mercury). A mixture melting point with an authentic sample of 2-↓-hydroxy-1,4-↑↑-methylenecyclohexane (34) gave no depression. A 0.01-g (0.0009 mole) portion of the alcohol was treated with 1 equivalent of phenyl isocyanate in 3 ml of hexane for 1 day. The urethane, 0.15 g (60%), melted at 158–159° before and 160–161° after crystallization from benzene, mixture melting point not lowered.

3-↓-Methoxy-1,4-↑↑-methylenecyclohexyl-2-↓-mercuric Chloride (VI)

To 25.2 g (0.07 mole) of 3-↓-methoxy-1,4-↑↑-methylenecyclohexyl-2-↑-mercuric chloride (IV, R = Me, X = Cl) in 750 ml of water plus 5.60 g (0.14 mole) of sodium hydroxide was added 0.3 g of 100% hydrazine hydrate. After 6 hours the cooled system was ether-

extracted (30 ml) and the aqueous, metallic, and non-aqueous phases were separated. The aqueous phase was acidified with acetic acid to yield a variable amount of original mercurial admixed with bis-mercurial and product, m.p. 78–95°, mixture melting point with original mercurial 80–110°, maximum amount 12.1 g (48%).

The non-aqueous phase was evaporated leaving an oil, 4.80 g, which was dissolved in 35 ml of hot methanol. Then 2 ml of concentrated hydrochloric acid was added to the slightly warm solution. After 30 minutes at room temperature water was added to turbidity. The system was extracted by chloroform and this extract was vacuum-evaporated leaving 1.80 g of semisolid which was crystallized from carbon tetrachloride (11 ml per g), 1.5 g, m.p. 113–114°, 6% yield. Crystallization from absolute ethanol (30 ml per g) raised this melting point to 117.7–118.5°, recovery 45%. A mixture melting point with the original mercurial was lowered to 80–85°. Diffraction pattern: [10] 11.62; [8] 5.14, 4.14, 3.37, 3.14; [6] 6.91, 6.28, 5.21; [5] 3.09; [4] 3.87, 3.46, 2.15, 2.10. Calc. for $C_6H_{13}ClHgO$: C, 26.6; H, 3.63; Hg, 55.6. Found: C, 26.7; H, 3.74; Hg, 55.0.

In a variation the concentrate from the non-aqueous extract of the reaction system was shaken for 15 minutes with 150 ml of 10% hydrochloric acid. The gummy solid was dissolved in 125 ml of absolute ethanol, and 2 ml of 5% aqueous sodium chloride was added. After 30 minutes a precipitate appeared (m.p. 110–112°, yield 12%), which was purified to m.p. 117.5–118.5° as described above.

A mixture of this ↓↓-diastereomer and the ↑↓-diastereomer from which it was formed (0.1 g of each in 10 ml of methanol) was treated with 0.2 ml of hydrochloric acid for 40 minutes. Addition of sodium hydroxide precipitated mercuric oxide which was filtered off. The filtrate, upon acidification with acetic acid, precipitated 0.06 g (30%), m.p. 112–117°. Crystallization from absolute ethanol raised this melting point to 120–122°. A mixture melting point with the ↓↓-diastereomer was lowered to 95° while no depression was observed upon admixture with the ↑↓-diastereomer.

2-↓-Methoxy-1,4-↑↑-methylenecyclohexane

A suspension of 11 g (0.03 mole) of 3-↓-methoxy-1,4-↑↑-methylenecyclohexyl-2-↑-mercuric chloride in 50 ml of water was shaken slowly and 100 g (0.1 atom) of 2% sodium amalgam was added. After 12 hours the system was steam-distilled and the non-aqueous phase of the distillate was dried with magnesium sulphate and distilled, b.p. 59–62°, at 30 mm, 1.90 g (50%), n_D^{20} 1.4574. It was redistilled, b.p. 154–155°, at 750 mm, n_D^{20} 1.4572. This product could not be frozen at −80° C. The same product was obtained by reduction of 3-↓-methoxy-1,4-↑↑-methylenecyclohexyl-2-↑-mercuric chloride with an excess of hydrazine hydrate and by methylation of 2-↓-hydroxy-1,4-↑↑-methylenecyclohexane in diethyl ether by use of sodamide and methyl iodide. Calc. for $C_8H_{14}O$: C, 76.1; H, 11.25; OCH_3, 24.6. Found: C, 76.1; H, 11.17; OCH_3, 25.1.

5-↓-Hydroxy-6-↓-chloromercuri-1,4-↑↑-methylenecyclohexane-2,3-↓↓-dicarboxylic Acid, γ-Lactone, μ = 3.88 D (XI)

A solution of 1.82 g (0.01 mole) of 1,4-↑↑-methylene-Δ^5-cyclohexene-2,3-↓↓-dicarboxylic acid in 50 ml of water at 80° was agitated while 2.70 g (0.01 mole) of mercuric chloride dissolved rapidly. The product appeared within 6 seconds and was filtered off when the system was cool, m.p. 202°, 3.97 g (95%). By crystallization via solution in dimethylformamide and gradual precipitation with chloroform (the first slight precipitate being discarded) it melted at 225–226° when inserted about 10° below this melting point. The X-ray diffraction pattern was [10] 4.55; [9] 4.74; [8] 4.00; [7] 6.13, 6.57, 7.25; [5] 2.78; [4] 3.50; [3] 2.57; [2] 2.88, 2.98; [1] 5.51, 3.06; [0.5] 4.16, 3.43.

Can. J. Chem. Downloaded from www.nrcresearchpress.com by 196.1.178.254 on 09/04/12
For personal use only.

A repetition of this experiment in which 2 ml (0.02 mole) of concentrated hydrochloric acid was included showed that the reaction was retarded both with respect to time of appearance of product and disappearance of inorganic mercury. However, the ultimate yield was 2.68 g (89%). The delay was still longer (20 minutes) before the first precipitate appeared when 4 ml (0.04 mole) of hydrochloric acid was included and the final yield after 1 day was 75%. Conversely the inclusion of 4 ml (0.01 mole) of 10% aqueous sodium hydroxide in the system reduced the time for appearance of product to 3 seconds; the ultimate yield was 93%.

5-↓-Hydroxy-6-↓-chloromercuri-1,4-↑↑-methylenecyclohexane-2-↓-3-↑-dicarboxylic Acid, $\mu = 4.07$ (XII)

(*a*) *By Isomerization of* XI ($\mu = 3.88$ *D*)

A solution of 41.7 g (0.10 mole) of 5-↓-hydroxy-6-↓-chloromercuri-1,4-↑↑-methylene-2,3-↓↓-dicarboxylic acid ($\mu = 3.88$) in 400 ml (1.0 mole) of 10% aqueous sodium hydroxide was refluxed for 2 hours, then cooled slowly, finally chilled and acidified by acetic acid to pH 5. The precipitate, 12.65 g of impure diastereomer, $\mu = 3.88$, melted at about 200°. The filtrate was made basic to pH 7.5, then was vacuum-evaporated to a 100-ml volume, and then was acidified cold to pH 2 with hydrochloric acid. The 15-g crop, m.p. about 190°, was dissolved in 50 ml of dimethylformamide, filtered, and treated with 80 ml of chloroform. After a precipitate (10 g, m.p. 206°) was filtered off, the filtrate was vacuum-evaporated. The residue was crystallized from 250 ml of boiling water to give 5 g (12%), m.p. 219–219.5°, strongly depressed by admixture with the diastereomer: μ, 3.88. Recrystallization from dimethylformamide–chloroform or from boiling water raised this melting point to 223–223.5° (sample inserted at 215°). Calc. for $C_9H_{11}O_5HgCl$: C, 24.8; H, 2.54. Found: C, 25.0; H, 2.75. The X-ray diffraction pattern was found to be [10] 12.10; [9] 5.12; [8] 3.56; [7] 3.07; [6] 4.67; [5] 6.23; [4] 6.65, 3.97; [3] 10.9, 5.94. The substance largely survived treatment with concentrated hydrochloric acid for 5 minutes but during 50 minutes it was converted to 1,4-↑↑-methylene-Δ^5-cyclohexene-2,3-↑↓-dicarboxylic acid (XIII), m.p. 184–185°, not depressed by mixture melting point with an authentic sample.

When the mercurial, $\mu = 4.07$, was dissolved in cold alkali and potentiometrically titrated with standard hydrochloric acid it showed by three inflections (corresponding with 3 equivalents) that the substance was not a lactone. Treatment with acetic anhydride failed to convert this hydroxydicarboxylic acid to a γ-lactone.

(*b*) *By Oxymercuration of* XIII

A solution of 76.7 g (0.38 mole) of 1,4-↑↑-methylene-Δ^5-cyclohexene-2-↓-3-↑-dicarboxylic acid (XIII) in 3 liters of boiling water was treated with 103 g (0.38 mole) of mercuric chloride. The precipitating system was cooled to 25°, and then 300 ml (0.75 mole) of 10% aqueous sodium hydroxide was added (pH 5). After 8 hours the system was acidified to pH 2. The precipitate was filtered off, washed with methanol and ether, and then vacuum-dried, 145 g, m.p. 211–212°. This crude product was extracted with 1300 ml of boiling water leaving 132 g, m.p. 222–223°. A hot solution in dioxane (10 ml per g) precipitated about 70%, m.p. 217°. The remaining 30% was obtained from the filtrate by addition of an equal volume of diethyl ether and was nearly pure XII, m.p. 218–219°. The process should be repeated with the 70%, m.p. 217°, which yields less pure XII, m.p. 213–214°. All of the crops of XII (estimated total yield, 25%) may be purified by crystallization from boiling water (10 ml per g), m.p. 220–221°.

Can. J. Chem. Downloaded from www.nrcresearchpress.com by 196.1.178.254 on 09/04/12
For personal use only.

Can. J. Chem. Downloaded from www.nrcresearchpress.com by 196.1.178.254 on 09/04/12
For personal use only.

The aqueous filtrates and the initial precipitates from dioxane crystallizations are rich in XIV. After the latter had been removed as is described below the final aqueous filtrates yielded about 20 g of unchanged norbornenedicarboxylic acid, XIII.

5-↓-Hydroxy-6-↓-hydroxymercuri-1,4-↑↑-methylenecyclohexane-2-↓-3-↑-dicarboxylic Acid

A solution of 2.15 g (0.005 mole) of 5-↓-hydroxy-6-↓-chloromercuri-1,4-↑↑-methylenecyclohexane-2-↓-3-↑-dicarboxylic acid (XII) in 4 ml (0.01 mole) of 10% aqueous sodium hydroxide was shaken with 0.8 g (0.055 mole) of silver oxide for 2 hours, then filtered by suction to remove a mixture of silver oxide and chloride from which 0.70 g (98%) of the chloride was isolated by washing the mixture with nitric acid.

The filtrate from the mixture was acidified to pH 5.6 with acetic acid; the precipitate which appeared momentarily redissolved. When no precipitate appeared after 12 hours the system was further acidified to pH 5 with 10% aqueous acetic acid. The precipitate was filtered off and dissolved in 30 ml of 1% aqueous sodium hydroxide. The solution was clarified by means of Norite, then was filtered, and the filtrate was acidified with acetic acid. After 36 hours at 4° the precipitate was filtered off, 0.70 g (34%), m.p. 198°. Resolution in alkali with Norite treatment gave a solution from which no precipitate appeared upon saturation with carbon dioxide gas. Acidification by acetic acid to pH 5.2 gave a gelatinous precipitate (0.55 g), which was dissolved in alkali, treated with Norite, filtered, and acidified by use of acetic acid, m.p. 200.5–201°. Calc. for $C_9H_{12}O_6Hg$: C, 25.9; H, 2.90. Found: C, 25.8; H, 3.13.

When this substance was dissolved in dilute alkali, and then dilute hydrochloric acid was added, the melting point (221°) of the precipitate was not depressed by admixture with 5-↓-hydroxy-6-↓-chloromercuri-1,4-↑↑-methylenecyclohexane-2-↓-3-↑-dicarboxylic acid (XII).

5-↓-Hydroxy-1,4-↑↑-methylenecyclohexane-2-↓-3-↑-dicarboxylic Acid

A solution of 1.08 g (0.0025 mole) of 5-↓-hydroxy-6-↓-chloromercuri-1,4-↑↑-methylenecyclohexane-2-↓-3-↑-dicarboxylic acid (XII) in 4 ml (0.005 mole) of 5% aqueous sodium hydroxide was chilled to 4°, and 6.5 g (0.01 atom Na) of sodium amalgam was added at once. Next day the system was filtered and the chilled filtrate was acidified with concentrated hydrochloric acid. The crystalline precipitate (0.24 g) melted at 210–211°, decomp. The chilled filtrate after 5 days yielded 0.12 g, m.p. 209–210° (total 72%). The whole was crystallized from 1.5 ml of hot water and also from hot ethyl acetate, m.p. 210–211°, decomp. A mixture melting point with 5-↑-hydroxy-1,4-↑↑-methylenecyclohexane-2-↓-3-↑-dicarboxylic acid was lowered to 192°. Calc. for $C_9H_{12}O_5$: C, 54.1; H, 6.04. Found: C, 54.1; H, 6.14. The X-ray diffraction pattern is [10] 5.30; [9] 4.38, 4.79; [8] 3.38; [6] 5.68, 3.65; [5] 4.23; [4] 5.98; [3] 3.79, 2.70, 3.22; [2] 2.79, 2.97; [1] 2.16, 2.00, 2.50.

5-↓-Hydroxy-6-↑-chloromercuri-1,4-↑↑-cyclohexane-2-↑-3-↓-dicarboxylic Acid, γ-Lactone, μ = 6.40 (XIV)

(*a*) *By Oxymercuration*

After the product obtained by treatment of 0.38 mole of 1,4-↑↑-methylene-Δ^5-cyclohexene-2-↓-3-↑-dicarboxylic acid was extracted to remove XII there remained impure crops (m.p. 208–213°) from dioxane crystallizations, and also filtrates from aqueous extractions and crystallizations. The latter were vacuum-evaporated and the whole was dissolved in hot water (10 ml per g), cooled, and filtered. Evaporation of the filtrates to 1/2–1/3 volume gave precipitates of XIV melting at 228–236°. These crops represent a

total isolable yield of about 40% of theoretical. The final purification was effected by crystallization from hot dioxane (23 ml per g), m.p. 237–238°. Calc. for $C_9H_9ClHgO_4$: C, 25.7; H, 2.18. Found: C, 25.3; H, 2.43. The X-ray diffraction pattern was [10] 13.5; [9] 8.97; [8] 7.29; [7] 10.45; [4] 3.66; [3] 4.27; [2] 6.19, 5.04; [1] 3.01. Treatment for 1 hour with twice its weight of concentrated hydrochloric acid converted the mercurial into 1,4-↑↑-methylene-Δ^5-cyclohexene-2-↓-3-↑-dicarboxylic acid, m.p. 186–187°, authenticated by mixture melting point.

When a solution of 150 mg of this mercurial (μ = 6.40 D) and 150 mg of 5-↓-hydroxy-6-↓-chloromercuri-1,4-↑↑-methylenecyclohexane-2-↓-3-↑-dicarboxylic acid (μ = 4.07 D) in 80 ml of dioxane was treated with 0.5 ml of concentrated hydrochloric acid for 3 hours the vacuum-evaporated system could be extracted with chloroform to yield only one mercurial, which, crystallized from water, melted at 230°, 60 mg, with powder diagram identical with that shown above for the compound, μ = 6.40 D. The chloroform-insoluble portion yielded 1,4-↑↑-methylene-Δ^5-cyclohexene-2-↓-3-↑-dicarboxylic acid, m.p. 186–187°, with X-ray powder diagram [10] 4.99; [5] 4.34; [4] 3.92; [2] 4.61, 4.51, 3.44, 3.19; [1] 6.43, 5.62, 3.01, 2.95, 2.68. This pattern is in contrast to that determined for 1,4-↑↑-methylene-Δ^5-cyclohexene-2,3-↓↓-dicarboxylic acid, m.p. 179–180°, which is [10] 6.10; [9] 4.44; [8] 4.23; [5] 4.95; [3] 3.86, 3.25; [2] 2.79, 2.73; [1] 5.47, 5.18, 5.06, 3.49, 2.39. The reader is cautioned about the subtle difference between this latter pattern and that of the product of platinum-catalyzed reduction, 1,4-↑↑-methylenecyclohexane-2,3-↓↓-dicarboxylic acid, m.p. 161–161.5°: [10] 6.25; [9] 4.45; [8] 4.32; [5] 5.05; [3] 3.91, 3.35, 3.27, 2.79, 2.48; [2] 5.23; [1] 5.62, 5.45, 3.82, 2.93, 2.72.

A solution of 0.86 g (0.002 mole) of 5-↓-hydroxy-6-↑-chloromercuri-1,4-↑↑-methylenecyclohexane-2-↑-3-↓-dicarboxylic acid, γ-lactone, in 4 ml (0.005 mole) of 5% aqueous sodium hydroxide was chilled and treated at once with 5.2 g (0.008 atom Na) of 3.5% sodium amalgam. After 7 hours the system was filtered and the chilled filtrate was acidified strongly with concentrated hydrochloric acid. The crystals, 0.25 g, m.p. 127–128° (70%), were recrystallized from benzene (50 ml per g), m.p. 132–133.5°. A mixture melting point with 5-↓-hydroxy-1,4-↑↑-methylenecyclohexane-2-↑-3-↓-dicarboxylic acid, γ-lactone, was not depressed.

(*b*) *By Isomerization*

A mixture of 1.82 g (0.0032 mole) of 5-↓-hydroxy-6-↑-chloromercuri-1,4-↑↑-methylenecyclohexane-2,3-↓↓-dicarboxylic acid, γ-lactone (X, μ = 7.18), and 0.82 g (0.0032 mole) of mercurous acetate in 25 ml of methanol was refluxed for 8 hours. Then it was diluted with water and made slightly alkaline. Darco was added and the dirty yellow precipitate was filtered off. The filtrate was acidified by addition of acetic acid to yield 1.00 g of chloride-free precipitate of indistinct melting point.

This precipitate was refluxed 3 hours in 20 ml of 4% aqueous sodium hydroxide, then chilled and acidified to pH 5.0 by addition of acetic acid. After 12 hours 0.48 g of infusible precipitate was filtered off. The filtrate upon acidification to pH 2 with dilute hydrochloric acid yielded 0.22 g, m.p. 233–235°, not depressed by admixture with the mercurial, μ = 6.40, prepared by oxymercuration, but was depressed by the mercurials X (μ = 7.18) and XII (μ = 4.07).

The infusible precipitate, 0.48 g, was dissolved in 10% aqueous sodium chloride and then was acidified with 12% hydrochloric acid. The precipitate, m.p. 211–213°, was crystallized from water, m.p. 223–224°, not depressed by admixture with the reagent mercurial, X.

Can. J. Chem. Downloaded from www.nrcresearchpress.com by 196.1.178.254 on 09/04/12
For personal use only.

5-↓-Hydroxy-6-↑-chloromercuri-1,4-↑↑-methylenecyclohexane-2,3-↓↓-dicarboxylic Acid, γ-Lactone, μ = 7.18 D (X)

To a solution of 1.13 g (0.005 mole) of stannous chloride dihydrate in 50 ml (0.02 mole) of 1.6% aqueous sodium hydroxide was added 4.00 g (0.01 mole) of 5-↓-hydroxy-anhydro-[6-↓-hydroxymercuri-2-↓-carboxy]-1,4-↑↑-methylenecyclohexane-3-↓-carboxylic acid (11) and then 2.7 cc (0.0068 mole) more of aqueous 10% sodium hydroxide; final pH was 8. After 1 hour the black precipitate was filtered off. The cold filtrate was strongly and quickly acidified with 12% hydrochloric acid in order to redissolve the precipitated tin salts; then a granular precipitate appeared. After 12 hours the precipitate was filtered off and washed with water, 1.95 g (47%), m.p. 204–205°. Crystallization from methanol (0.6 g per ml, Darco) raised this melting point to 225.5–226°. Mixture melting points with the mercurials of moments of 3.88, 4.07, and 6.40 D all were depressed. X-Ray diffraction pattern is [10] 6.70; [7] 12.10; [5] 6.15, 5.02, 4.88, 4.00, 3.62, 3.14; [4] 3.32, 2.74, 5.32, 4.38; [1] 4.58, 4.22, 3.07. Calc. for $C_9H_9ClHgO_4$: C, 25.7; H, 2.17. Found: C, 26.2; H, 2.31.

When 0.10 g of this product and of the diastereomeric mercurial, μ = 3.88 D, were mixed and treated with 0.5 ml of concentrated hydrochloric acid for 5 minutes the diluate with an equal volume of water yielded 6 mg with X-ray diffraction pattern corresponding with the product, μ = 7.18 D. When the latter was treated alone with 1.4 times its weight of concentrated hydrochloric acid for 45 minutes at least 30% of it survived, m.p. 216–217°, not depressed by admixture with the pure reagent, μ = 7.18 D. However, a reaction period of 12 hours yielded only 5-↓-hydroxy-1,4-↑↑-methylenecyclohexane-2,3-↓↓-dicarboxylic acid, γ-lactone, m.p. 202°, not depressed by admixture with the authentic lactone (35). The lactone was characterized further by methylation as described below.

5-↓-Hydroxy-2-↓-carbomethoxy-1,4-↑↑-methylenecyclohexane-3-↓-carboxylic Acid, γ-Lactone

A solution of 7.28 g (0.04 mole) of 5-↓-hydroxy-1,4-↑↑-methylenecyclohexane-2,3-↓↓-dicarboxylic acid, γ-lactone, m.p. 201–202°, in 32 ml (0.08 mole) of 10% aqueous sodium hydroxide was heated to boiling for several minutes, then cooled to 25°, and 6.72 g (0.08 mole) of sodium bicarbonate was added in 50 ml of water. Then 15.2 ml (0.16 mole) of dimethyl sulphate was added and the system was stirred for 2 days. The whole was then exhaustively extracted with chloroform. The evaporated extracts were crystallized from water, 4.79 g, 61%, m.p. 76–77°. This product was crystallized from benzene – commercial hexane (1:1, 40 ml per g), m.p. 81–82°. X-Ray diagram was [10] 5.38; [8] 4.73; [6] 6.53; [5] 3.99, 3.50, 3.39; [3] 3.81, 2.85; [2] 5.94, 4.38, 3.27; [1] 7.59, 4.94, 2.27. Calc. for $C_{10}H_{12}O_4$: C, 61.3; H, 6.17. Found: C, 61.3; H, 6.23.

5-↓-Hydroxy-2-↑-carbomethoxy-1,4-↑↑-methylenecyclohexane-3-↓-carboxylic Acid, γ-Lactone

When 1.96 g (0.01 mole) of 5-↓-hydroxy-2-↓-carbomethoxy-1,4-↑↑-methylenecyclohexane-3-↓-carboxylic acid, γ-lactone, m.p. 81–82°, was treated for 45 minutes with a solution of 0.23 g (0.01 atom) of sodium in 15 ml of methanol and then with 0.95 ml (0.01 mole) of dimethyl sulphate a rise in temperature was observed at the last step. After 1 hour the solvent was removed under vacuum and replaced with water. The product (1.46 g, 70%, m.p. 67–68°) was crystallized from boiling ethyl ether (1.2 ml per g), m.p. 68.3–68.8°. X-Ray diagram: [10] 5.15; [9] 4.59; [5] 5.64; [3] 6.60, 4.23; [2] 3.83, 3.46, 2.87; [1] 3.68, 2.58, 2.11. This substance was recovered unchanged after 6 hours with 1 equivalent of 10% aqueous mercuric acetate. When the substance was saponified during 1 hour with 10% aqueous alkali at 80° or was hydrolyzed by concentrated hydro-

Can. J. Chem. Downloaded from www.nrcresearchpress.com by 196.1.178.254 on 09/04/12
For personal use only.

chloric acid during 1 minute it yielded 5-↓-hydroxy-1,4-↑↑-methylenecyclohexane-2-↑-3-↓-dicarboxylic acid, γ-lactone, m.p. 132.8–133°, authentic according to mixture melting point and elemental analysis. Calc. for $C_{10}H_{12}O_4$: C, 61.3; H, 6.17. Found: C, 61.8; H, 6.32.

1,4-↑↑-Methylene-Δ⁵-cyclohexene-2,3-↑↓-dicarboxylic Acid (XIII)

When prepared by sodium methoxide saponification of dimethyl 1,4-↑↑-methylene-Δ⁵-cyclohexene-2,3-↓↓-dicarboxylate (35) the compound melted at 186.5° after crystallization from hot acetonitrile (25 ml per g). The powder diagram is reported above.

Dimethyl 5-↑-Acetoxy-6-↓-chloromercuri-1,4-↑↑-methylenecyclohexane-2,3-↓↓-dicarboxylate (XXIII, Z = CH_3CO, X = Cl)

(*a*) *In 2,5-Dioxahexane*

To a solution of dimethyl 1,4-↑↑-methylene-Δ⁵-cyclohexene-2,3-↓↓-dicarboxylate (m.p. 37°, 1.05 g, 0.0047 mole) in 10 ml of anhydrous 2,5-dioxahexane was added 1.45 g (0.0046 mole) of mercuric acetate. After 74 hours of agitation the system (in which all of the solid had dissolved) was poured into 40 ml of 2.5% aqueous sodium chloride. The oil soon crystallized, 1.925 g (83%), m.p. 153–158°. Four crystallizations from methanol raised the melting point to 177°. Diffraction pattern was [10] 5.64; [9] 6.41; [8] 11.47, 6.96; [7] 4.80, 3.88; [6] 3.23; [4] 4.50, 3.66; [3] 4.17, 3.48. Calc. for $C_{13}H_{17}ClHgO_6$: C, 30.9; H, 3.38; OCH_3, 12.3. Found: C, 30.6; H, 3.54; OCH_3, 12.1.

(*b*) *In Methanol*

To 2.10 g (0.01 mole) of the dimethyl ester in 35 ml of anhydrous methanol was added 3.18 g (0.01 mole) of mercuric acetate. The salt dissolved during 25 minutes. After 8 hours the system was filtered into 100 ml of 5% aqueous sodium chloride. The precipitate (4.57 g, 95%, m.p. 163–165°) was crystallized from absolute methanol (25 ml per g), m.p. 171–172°.

(*c*) *In Acetic Acid*

A solution of 10.5 g (0.047 mole) of the ester used in procedure (*a*) and 14.5 g (0.046 mole) of mercuric acetate in 50 ml of glacial acetic acid was let stand for 12 hours, then was poured into 350 ml of 3% aqueous sodium chloride. The precipitate was filtered off after 1 hour, washed with water and with methanol, and vacuum-dried, 22.1 g (93%), m.p. 173–174°. Crystallization from methanol (55 ml per g) raised this melting point to 177–177.2° (11.4 g). Subsequent crops, m.p. 175–168°, obtained by chilling and by concentration of the mother liquor finally left a filtrate which was vacuum-evaporated. The residue was twice purified by solution in warm dimethylformamide (12 ml per g), filtration of the slight precipitate appearing at 25°, and then dilution with an equal volume of chloroform. The product (0.13 g, 0.5%), m.p. 229–229.5°, was found to be 5-↓-hydroxy-6-↓-chloromercuri-2-↓-carbomethoxy-1,4-↑↑-methylenecyclohexane-3-↓-carboxylic acid, γ-lactone (XXII, X = Cl) (11). Identification was made by mixture melting point after it was found that the substance prepared from the ester and mercuric acetate in water also melted at 229° (rather than 223.5°) after sufficient purification. The two products gave the same X-ray powder pattern.

When 3 g of the dimethyl 5-↑-acetoxy-6-↓-chloromercuri-1,4-↑↑-methylenecyclohexane-2-↓-3-↑-dicarboxylate was reduced by 2 g of lithium aluminum hydride in tetrahydrofuran (slow addition followed by reflux) with hydrolysis by aqueous ammonium chloride, the product, m.p. 78-84°, weight 0.85 g, upon crystallization from commercial pentane

Can. J. Chem. Downloaded from www.nrcresearchpress.com by 196.1.178.254 on 09/04/12
For personal use only.

melted at 81.5–83°. It reacts rapidly with alkaline permanganate to yield a product which may be 2,3-dimethylol-1,4-↑↑-methylene-Δ^5-cyclohexene.

5-↑-Hydroxy-6-↓-chloromercuri-1,4-↑↑-methylenecyclohexane-2-↓-3-↑-dicarboxylic Acid (XXIV)

A solution of 5.15 g (0.01 mole) of dimethyl 5-↑-acetoxy-6-↓-chloromercuri-1,4-↑↑-methylenecyclohexane-2,3-↓↓-dicarboxylate in 36 ml (0.09 mole) of 10% aqueous sodium hydroxide was maintained at room temperature for 15 hours, then chilled and acidified cautiously to pH 2 with concentrated hydrochloric acid. The precipitation which commenced after 15 minutes was complete after 1 day at 4°. Filtration gave 2.59 g (60%), m.p. 183–184° (inserted at 160°). Quick crystallization from boiling water (10 ml per g) raised this melting point to 184–184.5°. The X-ray diffraction pattern was [10] 4.21, 5.05; [9] 5.79; [8] 5.60; [7] 3.44; [6] 3.26, 3.14; [5] 3.03; [3] 2.39; [2] 2.74; [1] 2.66, 3.91. The infrared band spectrum of polyethylene wax pellets (6000 p.s.i. at 23°) containing 5% is reported in wave numbers [cm^{-1}] at specified per cent transmissions: [316] 46; [352] 82; [388] 85; [410–17] 88; [428] 76; [451] 83; [553] 73; [648] 50; [678] 68; [794] 68; [884] 53. The density of the solid at 23° was 2.420 and the extrapolated dielectric constant of pellets was 3.917, so P_{e+a} is 88.5 cc. Calc. for $C_9H_{11}ClHgO_5$: C, 24.9; H, 2.56. Found: C, 25.0; H, 2.70.

When this substance was dissolved and boiled in water (7–8 ml per g) for 15 minutes the crystals which separated upon cooling melted first at 216–217° and then after an identical crystallization at 221–222°. The X-ray diffraction pattern was [10] 9.65; [9] 5.80; [8] 3.64; [7] 7.22; [6] 4.21, 4.25; [5] 4.56, 4.83, 5.26; [4] 3.22, 3.07; [3] 3.35, 3.50; [2] 2.94; [1] 2.82. The infrared band spectrum (5% in polyethylene wax compressed at 6000 p.s.i.) was recorded in [cm^{-1}] at indicated per cent transmissions: [316.8] 42; [351] 75; [390] 76; [414] 76; [429] 66; [453] 71; [550] 58; [649] 42; [675] 54; [696–702] 55; [791] 42; [841] 40; [881] 35. The density of the solid substance at 23° was 2.453 and the dielectric constants of pellets of various thicknesses were extrapolated to zero thickness for $\epsilon = 4.019$, whence P_{e+a} is 88.9 cc. Calc. for $C_9H_{11}ClHgO_5$: C, 24.9; H, 2.56. Found: C, 24.7; H, 2.53.

The melting point was not depressed when the substance was quickly crystallized from water or other solvents, but when it was dissolved in alkali and then reprecipitated by addition of hydrochloric acid the modification, m.p. 184–185°, reappeared. The latter could again be converted to the 221–222° variety by 15-minute reflux in boiling water. The high melting variety decomposed completely when heated under vacuum at its melting point and did not yield any of compound XIV. The filtrate from the original acidified reaction system was found to yield at least 0.59 g of 1,4-↑↑-methylene-Δ^5-cyclohexene-2,3-↓↑-dicarboxylic acid, m.p. 187°. Treatment of the mercurial with concentrated hydrochloric acid also gave this product, authenticated by mixture melting point.

It was observed that the low melting 5-↑-hydroxy-6-↓-chloromercuri-1,4-↑↑-methylenecyclohexane-2-↓-3-↑-dicarboxylic acid at its melting point tended oftentimes to resolidify after melting. This property was utilized by heating 0.2 g, m.p. 184–185°, in a test tube under continuous water aspirator vacuum by immersion into a paraffin bath heated from 185° to 193° during 15 minutes. After cooling to 25° the residue was extracted with 10 ml of hot acetone. This extract was treated with commercial hexane to incipient turbidity. After several hours the system was filtered to remove a slight precipitate. Then the filtrate was vacuum-evaporated to leave a syrup which solidified when moistened with methanol. The solid product, 0.08 g (24%), melted at 232–232.5°, and was found

Can. J. Chem. Downloaded from www.nrcresearchpress.com by 196.1.178.254 on 09/04/12
For personal use only.

by mixture melting point to be identical with 5-↓-hydroxy-6-↑-chloromercuri-1,4-↑↑-methylenecyclohexane-2-↑-3-↓-dicarboxylic acid, γ-lactone (m.p. 234°). The X-ray diffraction pattern also was identical with that of XIV.

5-↑-Hydroxy-1,4-↑↑-methylenecyclohexane-2-↓-3-↑-dicarboxylic Acid

A solution comprised of 129.6 g (0.3 mole) of 5-↑-hydroxy-6-↓-chloromercuri-1,4-↑↑-methylenecyclohexane-2-↓-3-↑-dicarboxylic acid in 480 ml (0.6 mole) of 5% aqueous sodium hydroxide was prepared during 2 hours of stirring. Then 442 g (0.66 atom Na) of 3.5% sodium amalgam was added with stirring during 2 hours, the temperature being maintained at 33°. Five hours later the system was filtered, chilled, strongly acidified by addition of 75 ml of concentrated hydrochloric acid, and continuously extracted with diethyl ether. The first 14-hour extract contained 7.9 g of unchanged mercurial as ether-insoluble material. Subsequently the extraction was continued for 40 hours longer.

The total extract (except for unchanged mercurial) was evaporated, dissolved in 200 ml of ethyl acetate, and then placed on a chromatographic column, 70 mm O.D. by 150 cm long of 100–170-mesh silica gel which had been deactivated by washing with U.S.P. chloroform. The column was first eluted with 4 liters of chloroform and the eluate was discarded. Likewise the first 2 liters of eluate were discarded after 2 liters of 1:1 chloroform – ethyl acetate (purified) and then pure ethyl acetate was used for elution. The next 1.5 liters yielded about 10 g of 1,4-↑↑-methylene-Δ^5-cyclohexene-2-↓-3-↑-dicarboxylic acid, m.p. 182–183°. The subsequent eluant (5 liters) yielded a semisolid upon evaporation which was crystallized from hot ethyl acetate to yield 55 g, m.p. 155–160° (90%). Recrystallization from ethyl acetate raised this melting point to 184.5°. The crystallization is accomplished by solution in 10–20 ml of solvent per gram after which 40% of the solvent is distilled off. The rate of crystal growth usually requires 4 to 5 days. Calc. for $C_9H_{12}O_5$: C, 54.1; H, 6.08. Found: C, 53.9; H, 6.04. The X-ray diffraction pattern was [10] 4.21, 5.05; [9] 5.79; [8] 5.60; [7] 3.44; [6] 3.26, 3.14; [5] 3.03; 3] 2.39; [2] 2.74; [1] 2.66, 3.91.

5-↓-Hydroxy-6-↓-chloromercuri-2-↓-carbomethoxy-1,4-↑↑-methylenecyclohexane-3-↓-carboxylic Acid, γ-Lactone (XXII, X = Cl)

A solution of 7.95 g (0.025 mole) of mercuric acetate in 80 ml of water was shaken with 5.25 g (0.025 mole) of molten dimethyl 1,4-↑↑-methylene-Δ^5-cyclohexene-2,3-↓↓-dicarboxylate (m.p. 37.5–38°) until the oil dissolved (8 minutes). Thirty minutes later the system was shaken vigorously while a solution of 1.5 g of sodium chloride in 5 ml of water was added slowly. The crude precipitate, methanol-washed and vacuum-dried, weighed 10.2 g, m.p. 201–203° (95%). This product was dissolved in 35 ml of dimethylformamide at 100°. The precipitate formed upon cooling weighed 6.45 g, m.p. 229–229.5° (60%). A methoxyl analysis showed 7.31% OCH_3, calc. 7.19%. The strongest lines of the X-ray diffraction pattern are [10] 9.30; [9] 4.61; [8] 3.61; [7] 2.92; [6] 5.81; [5] 6.55, 2.43; [4] 2.04. Recrystallization from dimethylformamide raised the melting point to 230.5–231°.

When this ester lactone (0.5 g) was dissolved in 1 ml of concentrated hydrochloric acid and the solution, after 12 hours, was diluted with water and let stand 1 week, crystals were obtained. The product, 0.115 g, m.p. 195–196°, was crystallized from hot water, m.p. 201°. A mixture melting point with 5-↓-hydroxy-1,4-↑↑-methylenecyclohexane-2,3-↓↓-dicarboxylic acid, γ-lactone, was not lowered.

Saponification of the pure ester lactone was effected by maintaining a solution of 2.57 g (0.005 mole) in 18 ml (0.045 mole) of 10% aqueous sodium hydroxide for about 12 hours after which the system was boiled for ½ hour. Acidification with 12% hydrochloric

Can. J. Chem. Downloaded from www.nrcresearchpress.com by 196.1.178.254 on 09/04/12
For personal use only.

Can. J. Chem. Downloaded from www.nrcresearchpress.com by 196.1.178.254 on 09/04/12
For personal use only.

acid gave 1.96 g, m.p. 181°. Extraction with 40 ml of boiling water left 0.70 g, m.p. 219–220°, which was not lowered by admixture with XI. The cooled filtrate gave 0.68 g, m.p. 196–197°, from which successive crops of XI could be obtained. The final crop, 0.33 g, melted at 209–210° and was impure 5-↓-hydroxy-6-↓-chloromercuri-1,4-↑↑-methylenecyclohexane-2-↓-3-↑-dicarboxylic acid (XII) of X-ray diffraction pattern [10] 5.14; [8] 12.02; [7] 3.55, 3.94; [5] 3.07; [4] 4.30; [3] 4.47, 6.25; [2] 5.92, 6.73; [1] 10.84, 3.74.

A by-product was also found to be formed in the oxymercuration. When the dimethylformamide contained in the mother liquors from crystallization of the 10.2 g portion (above) was evaporated the residue upon quick crystallization from boiling water melted at 181°. After another quick crystallization it melted at 187–188° and resolidified to melt again at 214°. These properties identify it as 5-↑-hydroxy-6-↓-chloromercuri-1,4-methylenecyclohexane-2-↓-3-↑-dicarboxylic acid (XXIV). Further proof was obtained by heating 0.2 g under vacuum from 195 to 204° during 20 minutes. An acetone extract of the cooled residue, evaporated and treated with methanol, gave 0.05 g of 5-↓-hydroxy-6-↑-chloromercuri-1,4-methylenecyclohexane-2-↑-3-↓-dicarboxylic acid, γ-lactone (XIV), m.p. 232–233°, with partial X-ray diagram [10] 7.13; [9] 5.65; [7] 2.35; [6] 3.50; [5] 2.84; [4] 4.05.

Dimethyl 5-↑-Methoxy-6-↓-chloromercuri-1,4-↑↑-methylenecyclohexane-2,3-↓↓-dicarboxylate (XXIII, Z = Me, X = Cl)

To a solution of dimethyl 1,4-↑↑-methylene-Δ^5-cyclohexene-2,3-↓↓-dicarboxylate (1.05 g, 0.0047 mole) in anhydrous methanol containing 0.5 g (0.0035 mole) of boron fluoride etherate was added 1.58 g (0.005 mole) of mercuric acetate. After 4 minutes the salt dissolved, and after 10 minutes the whole was poured into 50 ml of 5% aqueous sodium chloride. After 2 days at 4° the precipitate was filtered, water-washed, and dried, 1.78 g, m.p. 97–121°. This mixture of acetoxy- and methoxy-mercurials was fractionally crystallized from ethyl acetate – isooctane solutions to give impure acetoxymercurial (X-ray diffraction pattern) and pure dimethyl chloromercurimethoxymethylenecyclohexanedicarboxylate, 0.5 g (10%), m.p. 130–131°. X-Ray diffraction pattern is [10] 6.96; [9] 3.97; [8] 5.34; [7] 3.42, 3.08; [6] 4.62; [5] 5.94, 4.27; [4] 2.91. A longer reaction time (36 hours) gave a lower weight yield (1.55 g) of higher (107–114°) melting point. Calc. for $C_{12}H_{17}ClHgO_5$: C, 30.2; H, 3.56; OCH_3, 19.5. Found: C, 30.4; H, 3.64; OCH_3, 19.1.

When XXIII was treated with concentrated hydrochloric acid, and after 1 hour, the system was evaporated to 20% of the original volume crystals of 5-↓-hydroxy-1,4-↑↑-methylenecyclohexane-2,3-↓↓-dicarboxylic acid, γ-lactone, appeared, m.p. 198°. Crystallization from water raised this melting point to 201–202° and a mixture melting point with an authentic sample was not lowered.

5-↑-Methoxy-1,4-↑↑-methylene-2,3-↑↑-[1′-↑-hydroxy-Δ^2-propene-1′,3′-ylene]-cyclohexane

A solution of 5-↑-methoxy-1,4-↑↑-methylene-2,3-↑↑-propenylenecyclohexane (prepared in 92% yield by use of sodamide rather than sodium (36)) in 200 ml of pure acetic anhydride was added dropwise to a stirred ice-cooled suspension of selenium dioxide (67.2 g, 0.6 mole) in 25 ml of water. Following then a comparable procedure (37), an acetate, b.p. 147° (12 mm), was obtained, n_D^{20} 1.4974, 87 g, 65%, % C, 71.0, % H, 8.40. Hydrolysis by the prescribed method gave an 83% yield of the methoxy alcohol, b.p. 148° (11 mm), n_D^{20} 1.5145. Calc. for $C_{11}H_{16}O_2$: C, 73.3; H, 8.88; Found: C, 73.8; H, 8.78.

5-↑-Methoxy-1,4-↑↑-methylene-2,3-↑↑-propenonylenecyclohexane

Following the recommended procedure (37) upon the methoxy alcohol described above an 83% yield was obtained, b.p. 147° (11 mm), n_D^{20} 1.5188, λ_{max} 225 mμ, E_{max} 8,650. Calc. for $C_{11}H_{14}O_2$: C, 74.1; H, 7.85. Found: C, 73.7; H, 7.70.

5-↑-Methoxy-1,4-↑↑-methylenecyclohexane-2,3-↑↑-dicarboxylic Acid

To a stirred solution of the unsaturated ketone (1.5 g) in 30 ml of acetone plus 1 ml of water was added 8 g of potassium permanganate during 10 minutes (37); the system boiled. After 2 hours of stirring 10 ml of water was added, followed by 20 ml of methanol. After 30 minutes the permanganate was reduced so the manganese dioxide was filtered off and washed with acetone and water. The residue from the vacuum-evaporated filtrate was dissolved in 10 ml of water and the solution acidified to pH 4 was saturated with sodium chloride and thoroughly extracted by ethyl ether. The extracts, evaporated, left 1.1 g of sticky solid which was crystallized from benzene–methanol and from water to give 0.68 g, m.p. 149–152°. Crystallization from methanol – ethyl acetate gave 0.37 g, m.p. 166–167°. Calc. for $C_{10}H_{14}O_5$: C, 56.0; H, 6.58. Found: C, 56.4; H, 6.73. X-Ray diffraction pattern is [10] 4.99; [9] 5.73; [8] 3.91; [7] 4.26; [6] 5.45.

Stability of Mercurials Toward Concentrated Hydrochloric Acid

After 1 year a suspension of 0.2 g of butylmercuric chloride in 2 ml of concentrated hydrochloric acid at room temperature was filtered to recover 0.19 g of the mercurial. The filtrate was evaporated to a volume of 1 ml and then was made basic with aqueous sodium hydroxide. No mercuric oxide was precipitated. The result was unaltered by inclusion of 0.01 g of mercurous chloride into the system.

A suspension of 0.1 g of cyclopentylmercuric chloride in 2 ml of concentrated hydrochloric acid and 1 ml of dioxane was refluxed for 1 day. The mercurial was all recovered unchanged, m.p. 112°. The inclusion of 0.01 g of mercuric chloride did not alter this result.

A mixture of 0.200 g each of β-2-chloromercuricineole and of phenylmercuric chloride in 2 ml of methanol was treated with 2 ml of concentrated hydrochloric acid. The system, which became warm, was cooled to room temperature and was stirred for 30 minutes. After dilution with water the solid phase was filtered off, 0.175 g, m.p. 255–256°, which was proved by mixture melting point to be phenylmercuric chloride. Addition of alkali to the filtrate gave 0.258 mmole of mercuric oxide.

REFERENCES

1. WRIGHT, G. F. J. Am. Chem. Soc. **57**, 1993 (1935).
2. ROMEYN, J. and WRIGHT, G. F. J. Am. Chem. Soc. **69**, 697 (1947).
3. LUCAS, H. J., HEPNER, F. R., and WINSTEIN, S. J. Am. Chem. Soc. **61**, 3102 (1939).
4. ALDER, K. and STEIN, G. Ann. **525**, 183 (1936).
5. ALDER, K. and RICKERT, H. F. Ann. **543**, 1 (1940).
6. ALDER, K. and WINDEMUTH, E. Ber. **71**, 1939 (1938).
7. PARK, W. R. R. and WRIGHT, G. F. Can. J. Chem. **35**, 1088 (1957).
8. ROWLAND, R. L. J. Am. Chem. Soc. **73**, 2381 (1951).
9. BROOK, A. G., RODGMAN, A., and WRIGHT, G. F. J. Org. Chem. **17**, 988 (1952).
10. RODGMAN, A. and WRIGHT, G. F. J. Org. Chem. **18**, 1617 (1953).
11. MCNEELY, K. H., RODGMAN, A., and WRIGHT, G. F. J. Org. Chem. **20**, 714 (1955).
12. BROOK, A. G. and WRIGHT, G. F. Acta Cryst. **4**, 50 (1951).
13. BROOK, A. G., DONOVAN, R., and WRIGHT, G. F. Can. J. Chem. **31**, 536 (1953).
14. BROOK, A. G. and WRIGHT, G. F. J. Org. Chem. **22**, 1314 (1957).
15. WINSTEIN, S., TRAYLOR, T. G., and GARNER, C. S. J. Am. Chem. Soc. **77**, 3741 (1955); **77**, 3747 (1955).
16. BERSON, J. A. J. Am. Chem. Soc. **76**, 4069 (1954).
17. KWART, H. and KAPLAN, L. J. Am. Chem. Soc. **76**, 4078 (1954).
18. WRIGHT, G. F. Can. J. Chem. **30**, 268 (1952).
19. ALDER, K. and STEIN, G. Ann. **514**, 1 (1934).
20. SMYTH, C. P. J. Org. Chem. **6**, 421 (1941).
21. CURRAN, B. C. J. Am. Chem. Soc. **64**, 830 (1942).
22. SIPOS, J. C., SAWATZKY, H., and WRIGHT, G. F. J. Am. Chem. Soc. **77**, 2759 (1955).
23. SAWATZKY, H. and WRIGHT, G. F. Can. J. Chem. **36**, 1555 (1958).
24. LONGSTER, G. F. and WALKER, E. E. Trans. Faraday Soc. **49**, 228 (1953).
25. MARSDEN, R. J. B. and SUTTON, L. E. J. Chem. Soc. 1383 (1936).

Can. J. Chem. Downloaded from www.nrcresearchpress.com by 196.1.178.254 on 09/04/12
For personal use only.

26. SMYTH, C. P. Dielectric behavior and structure. McGraw-Hill Book Co., Inc., New York. 1955. p. 308.
27. WHITMORE, F. C. Chem. Eng. News, **26**, 672 (1948).
28. BERG, O. W., LAY, W. P., RODGMAN, A., and WRIGHT, G. F. Can. J. Chem. **36**, 358 (1958).
29. WRIGHT, G. F. Can. J. Technol. **34**, 89 (1956).
30. RHEINBOLDT, H. and KIRSCHEIM, M. J. prakt. Chem. **113**, 348 (1926).
31. MEREDITH, C. C., WESTLAND, L., and WRIGHT, G. F. J. Am. Chem. Soc. **79**, 2385 (1957).
32. BROOK, A. G. and WRIGHT, G. F. Can. J. Chem. **28**, 623 (1950).
33. FRIEDRICH, A. Die Praxis der quantitativen organischen Mikroanalyse. F. Deiticke Co., Leipzig. 1934.
34. KOMPA, G. and BECKMANN, S. Ann. **512**, 172 (1934).
35. DIELS, O. and STEIN, G. Ann. **514**, 1 (1934).
36. BRUSON, H. A. and REINER, T. W. J. Am. Chem. Soc. **68**, 8 (1946).
37. BARTLETT, P. D. and SCHNEIDER, A. J. Am. Chem. Soc. **68**, 6 (1946).

Can. J. Chem. Downloaded from www.nrcresearchpress.com by 196.1.178.254 on 09/04/12
For personal use only.

Can. J. Chem. Downloaded from www.nrcresearchpress.com by 196.1.178.254 on 09/04/12
For personal use only.

PRESSURE EFFECT AND MECHANISM IN ACID CATALYSIS

V. THE HYDROLYSIS OF ACETIC ANHYDRIDE[1]

J. KOSKIKALLIO,[2] D. POULI,[3] AND E. WHALLEY

ABSTRACT

The spontaneous and the acid-catalyzed hydrolyses of acetic anhydride have been measured as a function of temperature over the range 0 to 40° C, as a function of pressure over the range 0 to 3 kb at 0° C, and as a function of solvent over the range 0 to 70.3% w/w acetone–water at 0° C. The results are discussed with reference to the mechanisms of the hydrolyses. The volume and entropy of activation of the acid-catalyzed hydrolysis are $-17.1 \pm \sim 1.3$ cm^3 mole^{-1} and ~ -20 cal deg^{-1} mole^{-1}, showing that the mechanism

$$Ac_2\overset{+}{O}H \rightarrow AcOH + Ac^+,$$

suggested because the rate was proportional to Hammett's h_0, is not correct. It follows that the Zucker–Hammett hypothesis is invalid for this reaction, as we have shown previously for other reactions, and hence that it does not provide a valid method of distinguishing between the A-1 and A-2 mechanisms.

1. INTRODUCTION

The acid-catalyzed hydrolysis of acetic anhydride has been studied by Kilpatrick (1) and by Gold and Hilton (2, 3). It is usually accepted that the first step in the hydrolysis is the equilibrium transfer of a proton to the anhydride. The second step is most likely either a unimolecular decomposition of the conjugate acid (A-1 mechanism) or a bimolecular addition of or substitution by a water molecule (A-2 mechanism). Gold and Hilton (2) measured the rate constants in concentrated acids and found that the first-order constants were much more nearly proportional to Hammett's acidity function h_0 than to hydrogen-ion concentration. They deduced from this that the mechanism is most likely A-1. However, we have shown in previous papers (4, 5) that some reactions that follow h_0 rather than hydrogen-ion concentration are actually A-2, and so the conclusion of Gold and Hilton is doubtful. We have also shown (4, 5, 6, 7) that the pressure coefficient of an acid-catalyzed reaction can help to elucidate mechanism, and in this paper we report a study of the effect of pressure on the acid-catalyzed hydrolysis of acetic anhydride. There are many possible mechanisms. First, there are two possible locations of the proton in the conjugate acid, the carbonyl oxygen and the ether oxygen. Both forms can react by an A-1 decomposition, an A-2 substitution by water, or an A-2 addition of water, which may be either slow, or fast and followed by a slow step. Consequently, unique conclusions are not to be expected. In order to accumulate useful information the effects of temperature and solvent composition have also been studied.

In order to follow the acid-catalyzed reaction it is necessary to study the spontaneous reaction, and similar measurements have been made for this reaction.

2. EXPERIMENTAL METHODS

Reagent-grade acetic anhydride and acetone, and technical-grade aniline distilled in the presence of zinc and solid sodium hydroxide, were used. The acetone–water solvent mixtures were made up by volume at 25° C.

[1]*Manuscript received April 16, 1959.*
Contribution from the Division of Applied Chemistry, National Research Council, Ottawa, Canada. Issued as N.R.C. No. 5265.
[2]*N.R.C. Postdoctorate Fellow, 1957–58. Present address: Department of Chemistry, University of Helsinki, Helsinki, Finland.*
[3]*Summer student, 1958.*

Can. J. Chem. Downloaded from www.nrcresearchpress.com by 196.1.178.254 on 09/04/12
For personal use only.

The high-pressure technique was essentially that described in Part II (7). The apparatus has been somewhat improved by using heavier-walled capillary tube to connect the syringe to the valve, so reducing the number of breakages of the tube, and by measuring the pressures at 1000 b and higher by means of a 3-kb Heise Bourdon gauge of accuracy about 0.1%. Runs at 1 b were done in stoppered flasks.

Initial concentrations of acetic anhydride were 0.1–0.2 *M*. For reactions that were acid-catalyzed the acetic anhydride was dissolved in standard acid. Both reactant and solvent were heated or cooled to the temperature of the experiment before mixing. Analysis was done by pipetting 1 to 5 ml of solution (chosen to give a final titer of about 50 ml of barium hydroxide) into 0.3 *M* aqueous aniline. Acetic anhydride reacts quantitatively and rapidly with aniline to give acetanilide and acetic acid; the acetic acid was titrated, together with the acid catalyst and the acetic acid already produced by hydrolysis, with standard barium hydroxide. The difference between the titer and that of a fully hydrolyzed sample is proportional to the anhydride concentration. The half-lives were, at the higher temperatures, rather short, and the pipettes used for taking samples were cooled or heated to the temperature of the experiment; the sample was blown in about 2 seconds from the pipette to the aniline solution, and the time at which this occurred was the time corresponding to the sample. The smallest half-life for the high-pressure experiments was about $1\frac{1}{2}$ hours, so the sampling introduced only a very small error.

The reactions were kinetically of first order up to 75% of complete reaction. The first-order rate constant k is the sum of spontaneous and acid-catalyzed terms, thus

$$k = k_0 + k_a c_{H^+},$$

where k_0 is the first-order constant for the spontaneous reaction, k_a the second-order constant for the acid-catalyzed reaction, and c_{H^+} is the concentration of hydrogen ion. The spontaneous and acid-catalyzed rate constants were calculated from measurements in pure solvent and in acidified solvent respectively. It was calculated from the final values of k_0 and k_a and the dissociation constants of acetic acid in the solvents used, assuming these to be the same as in water–dioxane mixtures (8) of the same dielectric constant as the water–acetone mixtures, that catalysis by hydrogen ions derived from the acetic acid produced in the hydrolysis is negligible. This is verified by the linear first-order plots.

The 0° C bath was maintained by ice; in order to reduce corrosion of the high-pressure equipment small amounts of sodium dihydrogen phosphate were added to the bath, so its temperature was not exactly 0° C. Small corrections ($< 2\%$) were made to convert the rate constants to 0° exactly using the Arrhenius equation.

The reproducibility of the rate constants was about $1\frac{1}{2}\%$, and the accuracy is probably about 2%.

3. RESULTS

Spontaneous Hydrolysis

The rate constants for the spontaneous hydrolysis are given as a function of temperature, pressure, and composition, in Table I. The only direct comparison with other measurements that can be made is for pure water at 0° C and 1 atm. Under these conditions Kilpatrick (1) found $k_0 = 432 \times 10^{-6}$ sec^{-1}, and Gold (9) found 460×10^{-6} sec^{-1}, in satisfactory agreement with the mean of our values, 468×10^{-6} sec^{-1}. Other results of Gold cannot be compared directly with ours because they were not measured at common

TABLE I

Rate constants for the spontaneous hydrolysis of acetic anhydride

Temp., °C	% w/w of acetone in solvent	p/b	$10^6 k_0$/sec^{-1}
0	0	1	464
			451
			484
	20.8	1	149
			150
	44.1	1	28.2
			28.0
		506	45.3
			44.6
		1025	63.3
			69.2
		2008	144
			150
		2900	257
	70.3	1	2.65
			2.72
19.37	44.1	1	120
			121
29.61	44.1	1	225
			220
			225
39.86	44.1	1	383
			372

conditions. Consequently, we have interpolated graphically Gold's rate constants at constant temperature to 44.1% w/w acetone by plotting log k_0 vs. concentration of acetone. The interpolated values are compared with ours on an Arrhenius plot in Fig. 1. The agreement is satisfactory, though Gold's values are somewhat lower than ours.

The Arrhenius energy E_A of the equation

$$\ln k_0 = A\, e^{-E_A/RT},$$

where A is a constant, R is the gas constant, and T is the temperature, decreases with increasing temperature, as found by Gold (9). Our values of E_A calculated from rate constants at adjacent temperatures are given in Table I; they agree well with those of Gold for other acetone concentrations. The entropy of activation $\Delta S^{\ddagger}$ calculated from the equation

$$A = (ekT/h)\, e^{\Delta S^{\ddagger}/R}$$

where k is Boltzmann's constant and h is Planck's constant, is also given; it also decreases as the temperature increases.

The rate constants at constant pressure are plotted on a van't Hoff plot in Fig. 2. The volume of activation at 0° C and 1 b was obtained from the graphically measured slope of the curve at 1 b. It is

$$\Delta V^{\ddagger} = -22.0 \pm \sim 1.5 \text{ cm}^3 \text{ mole}^{-1} \text{ at } 0°\text{ C, 1 b.}$$

Can. J. Chem. Downloaded from www.nrcresearchpress.com by 196.1.178.254 on 09/04/12
For personal use only.

Can. J. Chem. Downloaded from www.nrcresearchpress.com by 196.1.178.254 on 09/04/12
For personal use only.

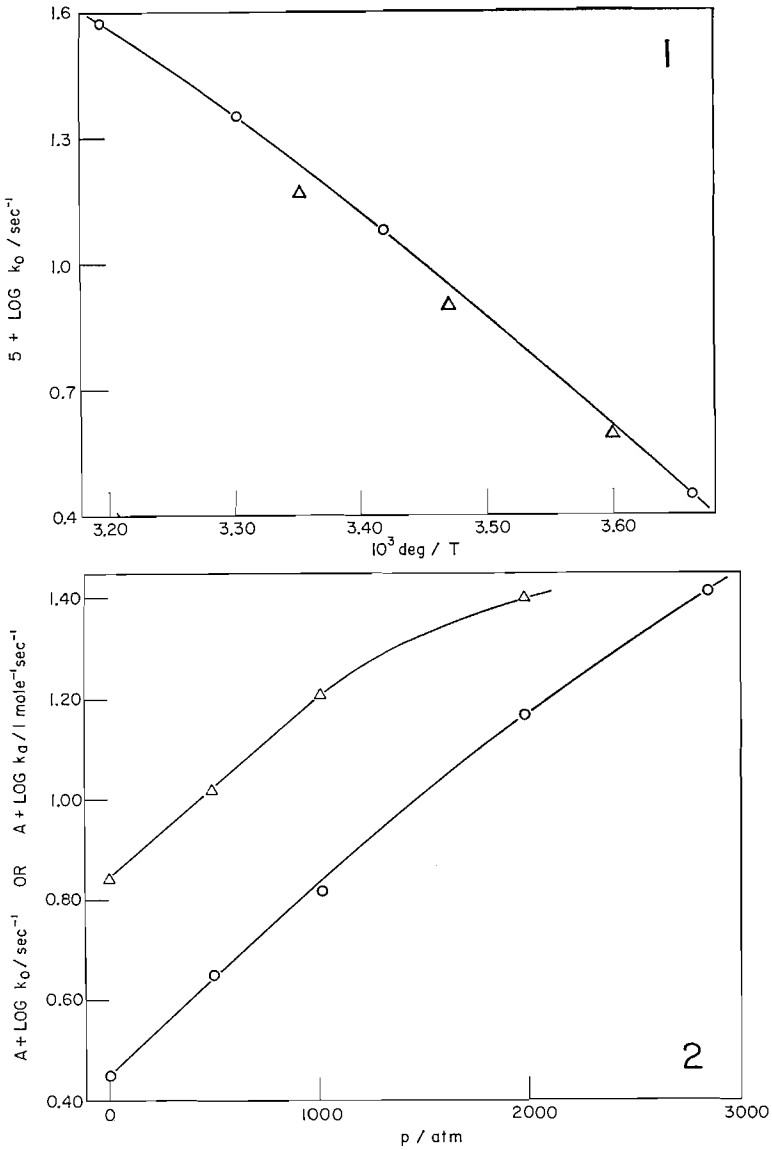

FIG. 1. Plot of log k_0 vs. $1/T$. Crosses: this paper. Circles: interpolated to 44.1% w/w acetone in water from Gold's results.

FIG. 2. Plot of log k_0 and log k_A vs. p. Circles: k_0. Triangles: k_A.

Acid-catalyzed Hydrolysis

The rate constants for the acid-catalyzed hydrolysis are given as a function of temperature, pressure, and solvent composition, in Table II. The acid concentrations are those at the temperature of the experiment and the pressure of 1 atm calculated from concentrations at room temperature using the data of Thomas and McAllister (10) on the volumes of acetone–water mixtures at various temperatures; because the compression of acetone–water mixtures is not known it is not possible to give rate constants under pressure, but only values of $k/c_{H^+}{}^0 = k_A\rho_p/\rho_{1\,b}$, where ρ_p and $\rho_{1\,b}$ are the densities of the solution at the temperature of the experiment and at pressures p and 1 b respectively.

TABLE II

Rate constants for the acid-catalyzed hydrolysis of acetic anhydride

Temp., ° C	% w/w of acetone	p/b	c_{HClO_4}/mole l.$^{-1}$*	$(10^3k/c_{H^+}{}^0)$/l. mole^{-1} sec^{-1}
0	20.8	1	0.1197	0.472
			0.2436	0.498
	44.1	1	0.0980	0.229
			0.1959	0.224
			0.4834	0.228
			0.1718	0.219
			0.2457	0.203
			0.2851	0.229
		506	0.2031	0.328
			0.1011	0.334
		1025	0.1011	0.533
			0.1011	0.525
			0.2390	0.481
			0.2400	0.520
			0.2572	0.506
		2008	0.1011	0.808
			0.2585	0.753
	70.3	1	0.1109	0.0717
				0.0733
19.37		1	0.0954	1.37
			0.0954	1.56
			0.1908	1.39
29.61		1	0.1187	3.70
			0.2319	3.68
39.86		1	0.0945	8.90
			0.1890	9.03

*c_{HClO_4} is that at the temperature of the experiment and 1 atm.

TABLE III

Arrhenius energies and entropies of activation for the spontaneous and acid-catalyzed hydrolyses of acetic anhydride

Temp. range, ° C	Spontaneous hydrolysis		Acid-catalyzed hydrolysis	
	E_A / kcal mole^{-1}	$\Delta S^{\ddagger}$ / cal deg^{-1} mole^{-1}	E_A / kcal mole^{-1}	$\Delta S^{\ddagger}$ / cal deg^{-1} mole^{-1}
0–19.37	11.95	−37.6	15.34	−21.1
19.37–29.61	10.56	−42.3	16.19	−18.2
29.61–39.86	9.68	−45.2	16.31	−17.8

The Arrhenius energy and the entropy of activation both increase with temperature as shown by the data in Table III, in which E_A and $\Delta S^{\ddagger}$ [$= R \ln (A/\text{l. mole}^{-1})(h/ekT)$] calculated from adjacent temperatures are given. The changes are less marked than those for the spontaneous hydrolysis, but seem reasonably certain.

The values of log $k/c_{H^+}{}^0$ as a function of pressure at 0° C are shown in a van't Hoff plot in Fig. 2. The slope of the curve at 0° C and 1 b as measured graphically is

$$RTd \ln (k/c_{H^+}{}^0)/dp = -\Delta V^{\ddagger} + \chi RT = +18.5 \pm \sim 1 \text{ cm}^3 \text{ mole}^{-1}$$

where χ is the compressibility of the pure solvent.

The compression of acetone–water mixtures has been measured only at 1000 atm and 25° C (11) and 30° C (12). The compressibility of acetone has not been measured at

Can. J. Chem. Downloaded from www.nrcresearchpress.com by 196.1.178.254 on 09/04/12
For personal use only.

0° C, but it appears from the compilation of McGowan (13) that it will be close to 120×10^{-6} atm^{-1} at 0° C and 1 atm. Newitt and Weale (11) point out that the compression of acetone–water mixtures at 25° C and 1000 atm is roughly linear in the mole fraction. Using this assumption and the compressibility of water at 0° C given by McGowan we find $\chi RT = 1.4$ cm^3 mole^{-1} at 0° C and 1 b. Consequently, for the acid-catalyzed hydrolysis

$$\Delta V^{\ddagger} = -17.1\pm\sim1.3 \text{ cm}^3 \text{ mole}^{-1} \text{ at } 0° \text{ C, 1 b}$$

the uncertainty having been increased to allow for the uncertainty in the compressibility.

4. DISCUSSION

Spontaneous Hydrolysis

The volume of activation, $-22.0\pm\sim1$ cm^3 mole^{-1} at 0° C and 1 b, is very similar to that for the spontaneous hydrolysis of ethylene oxide (14). The mechanism is likely (9) to be the attack of a water molecule on a molecule of acetic anhydride, and a considerable separation of charges occurs. The low volume of activation confirms this; the volume lost due to the formation of a partial valence bond between water and acetic anhydride is expected to contribute only about -5 to -10 cm^3 mole^{-1} to the volume of activation (14), and the remaining part of $\Delta V^{\ddagger}$, -16 to -11 cm^3 mole^{-1}, is presumably due mainly to electrostriction of the solvent.

Acid-catalyzed Hydrolysis

There are many possible mechanisms for the acid-catalyzed hydrolysis of acetic anhydride. The proton can be on either the carbonyl oxygen or the ether oxygen. Either form can react by the A-1 or the A-2 mechanism. The A-2 mechanism can take on several forms according as the incoming water molecule substitutes or adds, and, if it adds, according as the slow step is the formation or decomposition of the adduct.

Gold and Hilton (3) have shown that the rate of hydrolysis in concentrated aqueous acids is nearly proportional to Hammett's acidity function h_0, and is not proportional to c_{H^+}. They assumed that the Zucker–Hammett hypothesis, that rates of A-1 reactions are proportional to h_0 and those of A-2 reactions are proportional to c_{H^+}, holds, and deduced that the slow step is

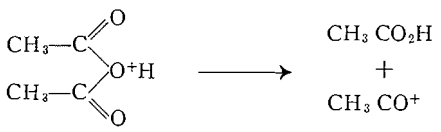

[4.1]

in which the proton is on the ether oxygen in the reactive conjugate acid. If the slow step were reaction [4.1], then according to arguments developed in Part I of this series (6) and confirmed experimentally for the A-1 hydrolyses of formals, acetals, and ethyl orthoformate in Part II (7), both the volume and entropy of activation would be positive. In fact, both are negative, $\Delta S^{\ddagger}$ being ~-20 cal deg^{-1} mole^{-1} and $\Delta V^{\ddagger}$ being -17.1 cm^3 mole^{-1}. The slow step is not, therefore, reaction [4.1]. The A-1 reaction

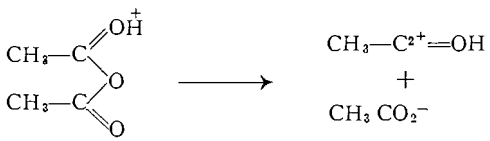

[4.2]

Can. J. Chem. Downloaded from www.nrcresearchpress.com by 196.1.178.254 on 09/04/12
For personal use only.

is consistent with the experimental $\Delta V^{\ddagger}$ and $\Delta S^{\ddagger}$ because, due to electrostriction of the solvent, the greatly increased polarity in the transition state would make both the volume and the entropy less than that of the conjugate acid. Thus an A-1 mechanism is possible, but only if a separation of charges occurs in the transition state. The justification of the Zucker–Hammett hypothesis requires that this does not occur, and so it ought not to apply to reaction [4.2]. Consequently, we conclude that the hydrolysis of acetic anhydride is another reaction for which the Zucker–Hammett hypothesis is invalid. We have shown previously that the hydrolyses of ethylene oxide (4) and of diethyl ether (5) do not follow the Zucker–Hammett hypothesis, and Taft, Deno, and Skell (15) refer to other evidence that refutes it. There can be no doubt that the Zucker–Hammett hypothesis does not reliably distinguish between A-1 and A-2 reactions.

The acid-catalyzed hydrolysis of acetic anhydride is formally similar to the acid-catalyzed hydrolysis of aliphatic esters, acetic anhydride being considered as acetyl acetate. It is instructive, therefore, to compare the various quantities of activation of the two hydrolyses. The volume of activation for the hydrolysis of methyl acetate in 44.1% w/w acetone–water is -13.3 cm^3 mole^{-1} at 35° C (16), similar to that for acetic anhydride. The entropy of activation for the hydrolysis of ethyl acetate in 56% w/w acetone–water is, from the data in ref. (17), -26.1 cal deg^{-1} mole^{-1}, again very similar to that for the hydrolysis of acetic anhydride. Unfortunately for a simple explanation of these similarities, the solvent effects are quite different. The logarithm of the ratio of rate constants in 20.8% w/w and 70.3% w/w acetone–water is -0.825 at 0° C for acetic anhydride, while for ethyl acetate it is, from the data in ref. (17), -0.330 at 35° C and for methyl propionate it is, from the data in ref. (18), -0.354 at 25° C. For comparison, the logarithm of the ratio of the *second-order* rate constants for the spontaneous hydrolysis of acetic anhydride is, from our results, -1.284. As we discussed above, the transition state for the spontaneous hydrolysis is probably very polar. The simple conclusion from the volumes and entropies of activation is that the transition state for the hydrolysis of acetic anhydride is similar to that for the hydrolysis of aliphatic esters; the simple conclusion from the solvent effects is that the transition state for the hydrolysis of acetic anhydride is considerably more polar. The resolution of these apparently contradictory conclusions will await more experimental data.

REFERENCES

1. Kilpatrick, M. J. Am. Chem. Soc. **50**, 2891 (1928).
2. Gold, V. and Hilton, J. J. Chem. Soc. 838 (1955).
3. Gold, V. and Hilton, J. J. Chem. Soc. 843 (1955).
4. Koskikallio, J. and Whalley, E. Trans. Faraday Soc. **55**, 815 (1959).
5. Koskikallio, J. and Whalley, E. Can. J. Chem. **37**, 788 (1959).
6. Whalley, E. Trans. Faraday Soc. **55**, 798 (1959).
7. Koskikallio, J. and Whalley, E. Trans. Faraday Soc. **55**, 809 (1959).
8. Conway, B. E. Electrochemical data. Elsevier Pub. Co., Inc., Amsterdam. 1952. p. 196.
9. Gold, V. Trans. Faraday Soc. **44**, 506 (1948).
10. Thomas, K. T. and McAllister, R. A. A.I.Ch.E. Journal, **3**, 161 (1957).
11. Newitt, D. M. and Weale, K. E. J. Chem. Soc. 3092 (1951).
12. Stutchbury, J. E. Austral. J. Chem. **9**, 536 (1956).
13. McGowan, J. C. *In* Handbook of chemistry and physics. *Edited by* C. E. Hodgman. 39th ed. Chemical Rubber Publishing Co., Cleveland, Ohio. 1957–58. p. 2008.
14. Koskikallio, J. and Whalley, E. Can. J. Chem. **37**, 783 (1959).
15. Taft, R. W., Deno, N. C., and Skell, P. S. Ann. Rev. Phys. Chem. **9**, 287 (1958).
16. Osborn, A. R. and Whalley, E. Unpublished work.
17. Nair, P. M. and Ananthakrishnan, S. V. Proc. Indian Acad. Sci. A, **32**, 85 (1950).
18. Hockersmith, J. L. and Amis, E. S. Anal. Chim. Acta, **9**, 101 (1953).

Can. J. Chem. Downloaded from www.nrcresearchpress.com by 196.1.178.254 on 09/04/12
For personal use only.

Can. J. Chem. Downloaded from www.nrcresearchpress.com by 196.1.178.254 on 09/04/12
For personal use only.

THE LUMINESCENCE OF COMPLEX MOLECULES IN RELATION TO THE INTERNAL CONVERSION OF EXCITATION ENERGY. PART I[1]

ROBIN M. HOCHSTRASSER

ABSTRACT

The relative fluorescence yields of a variety of double molecules have been measured as a function of the wavelength of exciting light. In some cases the yield from the second excited state is lower than from the first. This effect is attributed to either photodecomposition or to the enhancement of intramolecular energy transfer processes which can compete with the internal conversion between the excited singlet states. The experiments on bianthrone have suggested a method of elucidating the mechanism of the photochromic isomerization of this compound.

INTRODUCTION

The fluorescence of the vast majority of aromatic compounds arises from the radiative transition – first excited singlet to ground (singlet) state. On excitation to higher electronic states this same luminescence is observed and usually with unchanged yield. This implies that the rate of internal conversion to the radiating level is fast compared to the rate of intersystem crossing between upper excited states of different multiplicity. It has been suggested (3) that the fall-off in fluorescence yield of dibromoanthracene excited with light below 3000 Å is due to heavy atom-induced intersystem crossing to the second triplet level. This indicates comparable rates for these competing processes. Preliminary studies have indicated that a variety of molecules which are apparently quite stable photochemically have luminescence efficiencies which are anomolous in terms of the above rule.

In this work the relative luminescence yields of a series of double molecules have been measured as a function of the exciting wavelength. A double molecule is one consisting of two identical parts coupled through a conjugating linkage.

EXPERIMENTAL

The fluorescence measurements were made by illuminating the samples contained in a Vycor tube or silica cell with the beam from a hydrogen lamp and Beckman D.U. monochromater. The luminescence was detected over a 20° region centering at 70° to the main beam by means of an end-on-type photomultiplier with S11 response. The incident radiation was filtered out by 1.5 cm of a saturated solution of sodium nitrite in water. By using suitable Corning filters, the cutoff could be extended to longer wavelengths. This combination provided good cutoff at 3950 Å. The relative quantal output of the hydrogen lamp was known at each wavelength from 2500–3800 Å in terms of the luminescence of pure anthracene, which is known to be constant over this region (3, 4). The range was extended to 4100 Å by calibrating the lamp output against the luminescence intensity from a totally (99%) absorbing solution of tetracene. The fluorescence yield of tetracene is independent of the exciting light wavelength in this region of its absorption. The hydrogen lamp becomes less continuous above 3700 Å but good reproducibility could be obtained by opening up the monochromater slit for this range of excitation. All the solutions which were studied absorbed at least 99% of the incident light throughout the exposed pathlength. The solvents were ethyl alcohol or petroleum ether. The low temperature experiments were performed in a quartz Dewar with an optically clear

[1]*Manuscript received March 16, 1959.*
Contribution from the Department of Chemistry, University of British Columbia, Vancouver, B.C.

base. Rigid glasses were either alcohol, ether–alcohol, or E.P.A., depending on solubility of the compound. The same results were obtained from cracked and optically clear rigid glasses. Luminescence measurements may be radically affected by small amounts of impurities. The criterion for purity in this work was taken to be reproducibility after two further purifications by different methods. These methods involved recrystallization, sublimation, and chromotography. III, VI, VII, VIII, IX, and X were synthesized by Dr. Y. Matsunaga. IV and V were synthesized according to the method of A. Willemart (12). They were purified on alumina. I and II were Delta chemicals samples with fluorescent impurities. The fluorescence spectrum of each substance was examined on a Cary Recording Spectrometer. In no case did the spectrum of the purified material change when the wavelength of the exciting light was altered.

RESULTS AND DISCUSSION

Plots of the relative luminescence yields against exciting wavelength are shown on Figs. 1–3. Some of the curves show slight variations of the order of 3% which cannot be taken as real under the present experimental conditions.

(*A*) *1,1-Binaphthyl* (I); *2,2-Binaphthyl* (II); *α,α-Di-β-naphthol* (III)

These substances have long absorption tails and there is an unusually large separation of absorption and fluorescence, indicating substantial distortion in the excited state. The fluorescence yields of (I), (II), and (III) crystals at 25° C and −183° C were independent of exciting light. Alcoholic solutions and rigid glasses of (I) and (III) also retained constant yields of emission over the range 2500 Å–3500 Å.

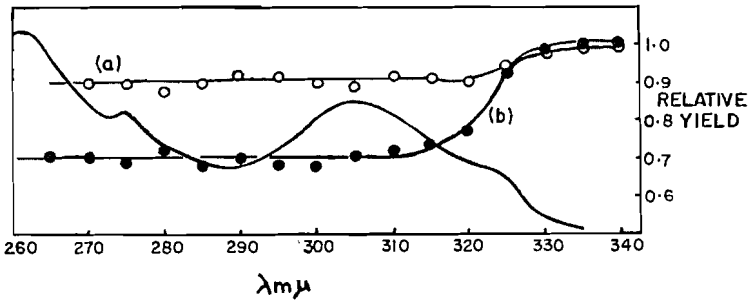

FIG. 1. The variation of the fluorescence yield of 2,2-binaphthyl with wavelength of exciting light. (*a*) crystal (*b*) alcohol solution or rigid alcohol glass. Smooth curve is the approximate absorption spectrum of 2,2-binaphthyl with log (extinction) as abscissa.

The results for (II) are given in Fig. 1. The fluorescence yield is constant to about 3275 Å, and below this exciting wavelength the luminescence falls off by about 30%. This is the type of effect that would be observed if an impurity was emitting above 3200 Å. Commercial (II) is green and even after many recrystallizations the color is greenish, although no impurities can be detected by absorption in a 10-cm path. After purification on alumina, one can obtain with difficulty colorless crystals with a bluish tinge. Such phenomena are reminiscent of the effects of very small quantities of tetracene in anthracene where energy transfer is highly efficient (1). The appearance of the blue fluorescence was accepted as a criterion of purity in this case. The absorption spectrum of (II) differs from (I) in the same manner as that of biphenyl differs from benzene. Free rotation of one ring relative to the other is sterically allowed and conjugative

Can. J. Chem. Downloaded from www.nrcresearchpress.com by 196.1.178.254 on 09/04/12
For personal use only.

interaction may occur, resulting in a red shift of the spectrum (5). It is feasible that the double molecule (II) has two closely lying electronic states at low energies. Such a splitting could arise through a weak interaction between the ring systems and if this is the case electric dipole transitions to one of these states may be more or less forbidden than transitions to the other state, depending on the degree of interaction (7, 9). The results indicate that there is an enhancement of the fluorescence when the excitation is in the long wavelength tail, that is, in the region of the 0–0 transition. It is possible that population of the upper state vibrational levels which are always below the crossing line of the singlet and triplet energy surfaces can occur in this case. In any case this system deserves detailed individual study and will be discussed in a future part of this series.

(*B*) *9,10-Di-α-naphthylanthracene* (IV); *9,10-Di-β-naphthylanthracene* (V); *9,9'-Dianthryl* (VI); *9,9'-Dianthran-10,10-diol* (VII)

The quantum yields of these compounds are independent of the wavelength of exciting light from 2600 to 3900 Å. This conclusion applies to crystals at 25° C and −183° C, alcoholic solutions at 25° C, and to rigid alcohol glasses. The actual quantum yields of luminescence from all but VII were higher than that of anthracene.

(*C*) *trans-Stilbene* (VIII); *p-Dimethoxystilbene* (IX); *Di-α-ethoxynaphthostilbene* (X); *α,β-Bis (9,9'-anthronylidene)-ethane* (XI)

No fluorescence could be detected from XI crystals below 6000 Å.

The luminescence yields in Fig. 2 relate to alcoholic solutions of X and XI and crystals of IX at −183°. There is little difference between rigid glass and viscous solution except in relation to the absolute fluorescence yield which is always greater in the glass. It

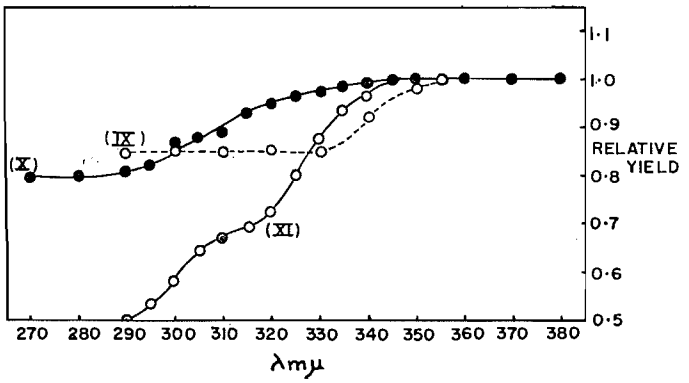

FIG. 2. Fluorescence yields as functions of the wavelength of exciting light for IX, X, and XI.

can be seen that double molecules of this type exhibit a marked wavelength dependence, which may be due either to photochemical reaction in upper excited states or to an intramolecular energy transfer process which is much more efficient in the upper excited state than in the fluorescent state. With the exception of XI, which is in any case too complex a molecule to permit a detailed study, it is felt that the fall-off in fluorescence yield may be caused by a lowering of the potential energy barrier to rotation about the ethylenic double bond in the upper excited states. The different results obtained with VIII on the one hand and with IX and X on the other would be attributed to the double bond character of the ethylenic link in each of these types. The naphthalenic groups will certainly be out of plane even in the trans form and consequently there will be less

Can. J. Chem. Downloaded from www.nrcresearchpress.com by 196.1.178.254 on 09/04/12
For personal use only.

conjugative interaction through the central double bond. If the time spent in an upper excited state is of the order of 10^{-12} seconds then the frequency of twist must be of the same order as a few hundred vibration frequencies if the fall-off in yield is due to this process. This corresponds to a considerable lowering of the barrier. The phosphorescence contribution to the total luminescence curve in Fig. 2 must be negligible under these experimental conditions as the same curve was obtained in solution at room temperature and in rigid glasses at liquid nitrogen temperature. In all cases no permanent changes in the absorption spectrum could be detected which would have indicated a photoprocess occurring with a significant quantum yield. Some experiments were done using completely oxygen-free solutions and no differences were obvious. In the case of *trans*-stilbene the fluorescence yield was constant throughout the absorbing region. The fluorescence yield was also measured as a function of temperature for crystalline VIII and no discontinuities were observed.

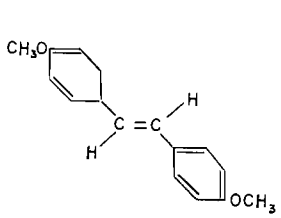

IX

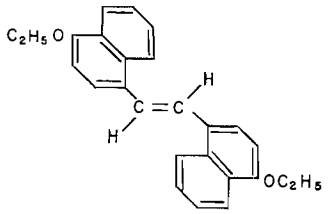

X

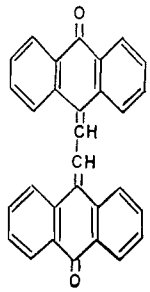

XI

(*D*) *Bianthrone* (XII)

This substance is photochromic (6), thermochromic (11), and photochemically reactive (12). The bianthrone used in this work was recrystallized twice from dichloroethane, sublimed *in vacuo*, then chromatographed twice on alumina. Even under these conditions a fluorescent impurity was shown to be present. (XII) did not fluoresce in solution at 25°, i.e. the apparatus would detect very low light levels corresponding to fluorescence yields of the order of 10^{-3}. In ether–isopentane glass at −183° C the fluorescence yield varied with exciting energy in the manner shown in Fig. 3 along with the absorption spectrum of bianthrone.

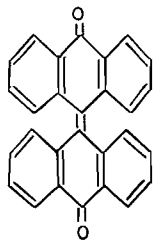

XII

The fluorescence yield is constant throughout the first absorption band but falls off to about 50% of this value below 3400 Å. During irradiation in the low energy band the so-called colored form of bianthrone is being produced, and the constancy of the luminescence yield indicates that the process of photochromism is also independent of

Can. J. Chem. Downloaded from www.nrcresearchpress.com by 196.1.178.254 on 09/04/12
For personal use only.

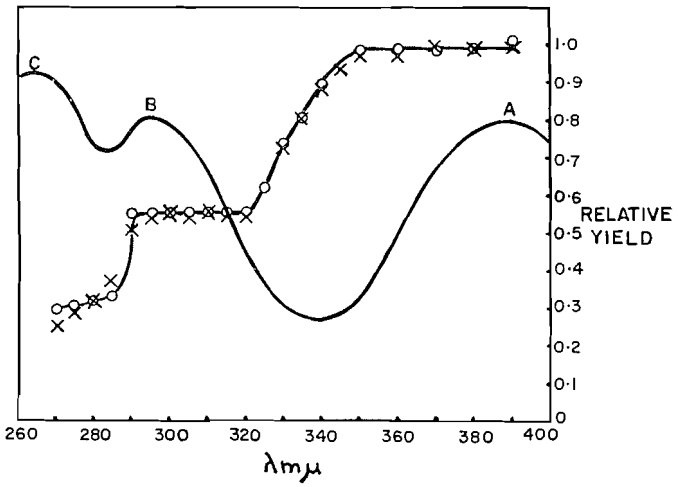

FIG. 3. The fluorescence of bianthrone as a function of the wavelength of exciting light.
○ In ether–isopentane glass.
× After U.V. irradiation in non-rigid medium.
— Absorption spectrum of bianthrone. The absorption at A corresponds to a $n \rightarrow \pi^*$ transition while B and C are probably $\pi \rightarrow \pi^*$.

the excitation energy over this region; such considerations will apply if only the formation of the photochromic isomer is in competition with fluorescence. The similarity of the fluorescence curves for bianthrone in ether–isopentane and the pre-irradiated sample—which is green due to reversion to photochromic isomer—indicates that the same fluorescence is being observed in each case. The actual yield was diminished slightly owing to reabsorption by the long wavelength band of the colored form. The absorption band at 2950 Å is due to a higher electronic transition, and either an internal conversion process, *other* than the rearrangement of the electronic excitation of this state into the vibrational modes of the fluorescent state, is occurring *or* the probability of photodecomposition is enhanced by exciting the molecule to this state. Here again the barrier to isomerism may be very slight in the higher levels of excitation. This is tantamount to an increased probability of intersystem crossing in the upper state as it is likely that the photochromic isomer is the molecule in its lowest triplet state. Hirshberg and Fischer (6) point out that no photochemical reactions other than photochromism occur at low temperatures.

CONCLUSIONS

As a rule the fluorescence yield is independent of the wavelength of the exciting light. Some double molecules have provided striking exceptions to this rule. The exceptions have arisen in the first place when there is slight conjugative interaction between two aromatic ring systems; e.g., 1,1′-binaphthyl exhibits normal behavior while 2,2′-binaphthyl is exceptional. Secondly, exceptions also arise when the molecule can be photochemically isomerized, e.g., naphthostilbene and bianthrone respectively.

It is likely that the configurations of the latter type of molecule in the excited states will differ markedly from those in the ground state. In particular the relative orientation of the ring systems may change considerably. This consideration is supported by the large separation of emission and absorption for the compounds studied here.

Can. J. Chem. Downloaded from www.nrcresearchpress.com by 196.1.178.254 on 09/04/12
For personal use only.

That some of the phenomena reported here may be due in part to an enhancement of the rate of intercombination between states of different multiplicity may only be considered as an interesting conjecture at this stage. It is likely that deformation of a π-molecular orbital, such as in the case of the trinitrobenzene complexes of aromatic hydrocarbons (10), could result in a considerable increase in the rate of intersystem crossing. With molecules such as naphthostilbene and bianthrone this rate may be unusually great in the upper excited states if there is a reasonable distortion. Such a distortion would necessarily increase the $\pi-\sigma$ interactions in the molecule and it is known that the main contribution to the spin orbital coupling in these molecules arises from interactions of this type (8).

It has been the purpose of the first part of this paper to present the results of fluorescence studies on a variety of double molecules. It is apparent that a detailed study of the photochemistry of some of these systems will be necessary before more certain conclusions can be reached. Subsequent parts of this series will describe such studies as well as results on the phosphorescence of these and similar molecules and new results on the phosphorescence and fluorescence of N-heteroaromatics and their derivatives.

ACKNOWLEDGMENTS

This research was supported by a grant from the National Research Council of Canada. Thanks are due to Dr. Y. Matsunaga for gifts of the compounds as indicated in the text, and to Dr. C. Reid for many helpful discussions.

REFERENCES

1. Bowen, E. J., Mikiewicz, E., and Smith, F. W. Nature, **159**, 706 (1947).
2. Brockmann, H. and Mühlmann, R. Ber. **82**, 348 (1949).
3. Ferguson, J. To be published.
4. Förster, T. Fluoresenz organischer Verbindungen. Vandenhoek und Ruprecht, Gottingen. 1951.
5. Friedel, R. A., Orchin, M., and Reggel, L. J. Am. Chem. Soc. **70**, 199 (1948).
6. Hirshberg, Y. and Fischer, E. J. Chem. Soc. 629 (1953).
7. Levinson, G. S., Simpson, W. T., and Curtis, W. J. Am. Chem. Soc. **79**, 4314 (1957).
8. McLure, D. S. J. Chem. Phys. **20**, 682 (1952).
9. McRae, E. G. and Kasha, M. J. Chem. Phys. **28**, 721 (1958).
10. Moodie, M. M. and Reid, C. J. Chem. Phys. **22**, 252 (1954).
11. Theilacker, W., Kortum, G., and Friedheim, G. Ber. **83**, 508 (1950). Grubb, W. J. and Kistiakowsky, G. B. J. Am. Chem. Soc. **72**, 419 (1950).
12. Willemart, A. Compt. rend. **201**, 1201 (1935).

Can. J. Chem. Downloaded from www.nrcresearchpress.com by 196.1.178.254 on 09/04/12
For personal use only.

Can. J. Chem. Downloaded from www.nrcresearchpress.com by 196.1.178.254 on 09/04/12
For personal use only.

THE LOW TEMPERATURE PREPARATION OF ANHYDROUS TITANIUM IV BROMIDE AND ANHYDROUS TITANIUM IV IODIDE FROM BENZENE SOLUTIONS

KARL H. GAYER AND GERALD TENNENHOUSE

A recent series of experiments required supplies of anhydrous titanium IV bromide and anhydrous titanium IV iodide. The usual methods for preparing titanium IV bromide by passing either bromine vapor or hydrogen bromide gas over a heated mixture of titanium dioxide and carbon or titanium metal were found to be too time-consuming for frequent use. Consequently the following method was devised.

EXPERIMENTAL

Preparation of Titanium Tetrabromide

The following experimental procedures, which required an inert atmosphere, were carried out in a dry box in which the air had been dried over P_2O_5. Hydrogen bromide gas, flowing at approximately 350 cubic centimeters per minute, was dried by being passed through a porous tower of phosphorus pentoxide. This dry gas was directed into the reaction vessel.

A solution of titanium IV chloride was made by adding 35 g of redistilled titanium IV chloride to 71 g of reagent grade benzene in a 250-ml two-necked flask. The flask was maintained at 0° C by means of a salt–ice bath. Hydrogen bromide gas was bubbled into this solution. After 20 minutes of gassing the solution had turned from colorless to yellow to red. After 1 hour, the gassing was stopped and the solution permitted to rise in temperature to 25° over a period of 3 hours. The benzene was distilled off. This was followed by the titanium IV bromide. The portion boiling between 229° and 232° was collected. The product obtained in 80% yield based on $TiCl_4$ was found to melt at 39° C and boil at 231° C. The literature (1, 2) lists the melting point and boiling point as 39° C and 230° C respectively. The compound was analyzed gravimetrically for both titanium and bromide. The following are mean values of three determinations:

Calculated values for	Ti = 13.03%	Br = 86.97%
Experimental values for	Ti = 13.17%	Br = 86.81%

The anhydrous product is an orange-red solid at room temperature, which sublimes readily and is extremely hygroscopic, fuming strongly in air. It is soluble in acetone and ether. It could not, however, be crystallized from these solvents. Furthermore, the product is soluble without reaction in benzene and carbon tetrachloride.

Preparation of Anhydrous Hydrogen Iodide

Anhydrous hydrogen iodide free of elementary iodine was prepared by distilling a mixture of 80 g of reagent potassium iodide in 400 ml 85% phosphoric acid. The resulting product, slightly contaminated with water and iodine, was purified by passing it over an intimate mixture of red phosphorus and iodine, then through a condenser maintained at 0° C to remove iodine, and finally over phosphorus pentoxide.

Preparation of Titanium Tetraiodide

The hydrogen iodide prepared above was bubbled (at approximately 400 cc per minute) into a round-bottom flask containing 35 g of redistilled titanium IV chloride and 88 g

of reagent grade benzene. The flask was kept at 0° C by means of an ice–salt bath. After 5 minutes, the solution had turned dark. The addition of hydrogen iodide was continued for 1 hour. After the mixture had been left to stand for 30 minutes at 0° C, it was freed of excess hydrogen iodide by vigorous gassing with dry nitrogen. The mixture was kept overnight at 0° C after which the titanium iodide was filtered off. The product was recrystallized, then dried under reduced pressure of 25 mm Hg, and sealed in a bent glass tube about 30 cm in length. Finally, the product was sublimed by immersing one end of the tube in an ice–salt bath while gently heating the other end. The purple solid collected in the cold part of the tube. A 70% yield, based on $TiCl_4$ was obtained. Analysis: The titanium was precipitated as the oxide, ignited, and weighed. The iodide was determined by preliminary oxidation with KIO_3, followed by titration with standard $Na_2S_2O_3$ solution. The following are mean values of three determinations:

Calculated values for	Ti = 8.62%	I = 91.38%
Experimental values for	Ti = 8.49%	I = 91.46%

The product is extremely hygroscopic, fuming strongly in air. It is readily soluble in water, forming a brown-colored solution. On standing for several weeks out of contact with the air, the brown solution becomes colorless. The product is soluble without reaction in benzene and carbon tetrachloride.

1. INORGANIC SYNTHESES. *Edited by* W. C. Fernelius. Vol. II. McGraw-Hill Book Co., Inc., New York. 1946. (*a*) p. 114, (*b*) p. 115.
2. SCOTT, W. W. Standard methods of chemical analysis. Vol. I. 5th ed. D. Van Nostrand Company, Inc., 1939. (*a*) p. 191, (*b*) p. 454, (*c*) p. 981.

RECEIVED MARCH 5, 1959.
DEPARTMENT OF CHEMISTRY,
WAYNE STATE UNIVERSITY,
DETROIT 2, MICHIGAN.

Can. J. Chem. Downloaded from www.nrcresearchpress.com by 196.1.178.254 on 09/04/12
For personal use only.

A NEW SYNTHESIS OF 5-HYDROXYTRYPTOPHAN*

GERASSIMOS FRANGATOS AND FRANCIS L. CHUBB

The biological significance of 5-hydroxytryptophan has been established. It is an important metabolite of tryptophan and is a precursor of serotonin (5-hydroxytryptamine) (1). In recent years serotonin has been the subject of an extensive study by many workers due to its potential importance in the function of the autonomic and central nervous system (2).

The first synthesis of 5-hydroxytryptophan was reported by Ek and Witkop (3), and is an application of the gramine synthesis developed by Snyder and Smith (4). A second synthesis of 5-hydroxytryptophan, which is also an application of the gramine synthesis, has recently been reported by Koo, Avakian, and Martin (5). The synthesis herein reported is an application of the convenient tryptophan synthesis of Warner and Moe (6). This method eliminates the difficult and tedious preparation of 5-benzyloxyindole.

The *p*-benzyloxyphenylhydrazone of γ,γ-dicarbethoxy-γ-acetamido-butyraldehyde (I) was prepared, and cyclized, without isolation, to form ethyl β-(5-benzyloxyindolyl-3)-α-carbethoxy-α-acetamidopropionate (II). This was identical with material prepared

**Based on a paper presented at the 41st Annual Conference of the Chemical Institute of Canada, Toronto, May 26–28, 1958.*

of reagent grade benzene. The flask was kept at 0° C by means of an ice–salt bath. After 5 minutes, the solution had turned dark. The addition of hydrogen iodide was continued for 1 hour. After the mixture had been left to stand for 30 minutes at 0° C, it was freed of excess hydrogen iodide by vigorous gassing with dry nitrogen. The mixture was kept overnight at 0° C after which the titanium iodide was filtered off. The product was recrystallized, then dried under reduced pressure of 25 mm Hg, and sealed in a bent glass tube about 30 cm in length. Finally, the product was sublimed by immersing one end of the tube in an ice–salt bath while gently heating the other end. The purple solid collected in the cold part of the tube. A 70% yield, based on $TiCl_4$ was obtained. Analysis: The titanium was precipitated as the oxide, ignited, and weighed. The iodide was determined by preliminary oxidation with KIO_3, followed by titration with standard $Na_2S_2O_3$ solution. The following are mean values of three determinations:

Calculated values for	Ti = 8.62%	I = 91.38%
Experimental values for	Ti = 8.49%	I = 91.46%

The product is extremely hygroscopic, fuming strongly in air. It is readily soluble in water, forming a brown-colored solution. On standing for several weeks out of contact with the air, the brown solution becomes colorless. The product is soluble without reaction in benzene and carbon tetrachloride.

1. INORGANIC SYNTHESES. *Edited by* W. C. Fernelius. Vol. II. McGraw-Hill Book Co., Inc., New York. 1946. (*a*) p. 114, (*b*) p. 115.
2. SCOTT, W. W. Standard methods of chemical analysis. Vol. I. 5th ed. D. Van Nostrand Company, Inc., 1939. (*a*) p. 191, (*b*) p. 454, (*c*) p. 981.

RECEIVED MARCH 5, 1959.
DEPARTMENT OF CHEMISTRY,
WAYNE STATE UNIVERSITY,
DETROIT 2, MICHIGAN.

Can. J. Chem. Downloaded from www.nrcresearchpress.com by 196.1.178.254 on 09/04/12
For personal use only.

A NEW SYNTHESIS OF 5-HYDROXYTRYPTOPHAN*

GERASSIMOS FRANGATOS AND FRANCIS L. CHUBB

The biological significance of 5-hydroxytryptophan has been established. It is an important metabolite of tryptophan and is a precursor of serotonin (5-hydroxytryptamine) (1). In recent years serotonin has been the subject of an extensive study by many workers due to its potential importance in the function of the autonomic and central nervous system (2).

The first synthesis of 5-hydroxytryptophan was reported by Ek and Witkop (3), and is an application of the gramine synthesis developed by Snyder and Smith (4). A second synthesis of 5-hydroxytryptophan, which is also an application of the gramine synthesis, has recently been reported by Koo, Avakian, and Martin (5). The synthesis herein reported is an application of the convenient tryptophan synthesis of Warner and Moe (6). This method eliminates the difficult and tedious preparation of 5-benzyloxyindole.

The *p*-benzyloxyphenylhydrazone of γ,γ-dicarbethoxy-γ-acetamido-butyraldehyde (I) was prepared, and cyclized, without isolation, to form ethyl β-(5-benzyloxyindolyl-3)-α-carbethoxy-α-acetamidopropionate (II). This was identical with material prepared

**Based on a paper presented at the 41st Annual Conference of the Chemical Institute of Canada, Toronto, May 26–28, 1958.*

from the reaction of ethyl acetamidomalonate with 5-benzyloxygramine. Saponification and partial decarboxylation of II, followed by hydrolysis of the acetamido group, gave 5-benzyloxytryptophan (III). 5-Hydroxytryptophan (IV) was obtained by hydrogenolysis of III.

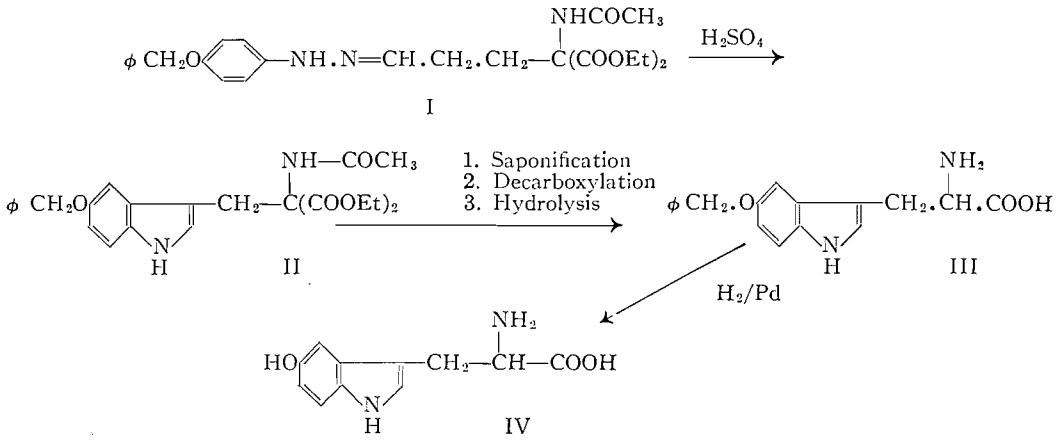

EXPERIMENTAL

Ethyl β-(5-Benzyloxyindolyl-3)-α-carbethoxy-α-acetamidopropionate (II)

A mixture of 85 g of ethyl acetamidomalonate (4), 0.4 g of sodium methoxide, and 200 ml of absolute ethanol was cooled to 0° with stirring. A thin slurry formed and then 31 ml of acrolein was added during 1.5 hours, keeping the temperature at 0–3°. The stirring was continued for 2 hours at 0–3°. Then 85 g of *p*-benzyloxyphenylhydrazine (7) and 10 ml of glacial acetic acid were added with vigorous stirring. The reaction mixture was heated to 50°, with stirring, and maintained at that temperature until the hydrazine went into solution. The resulting dark solution of II was kept at room temperature overnight. It was then transferred to a three-necked flask and water was added to bring the total volume to 1.5 liters. After 70 ml of concentrated sulphuric acid was added, the mixture was stirred vigorously and refluxed for 3 hours. The ethyl β-(5-benzyloxyindolyl-3)-α-carbethoxy-α-acetamidopropionate soon crystallized. The reaction mixture was cooled and filtered to yield 160 g of crude product. Three recrystallizations from toluene followed by one from aqueous ethanol gave 135 g (75.5%) of pure II, m.p. 169°, undepressed on admixture with an authentic sample prepared according to ref. 5. Anal. Calculated for $C_{25}H_{28}N_2O_6$: C, 66.36; H, 6.24; N, 6.19. Found: C, 66.60; H, 6.28; N, 6.08.

5-Benzyloxytryptophan (III)

The ester II (50 g) was saponified, decarboxylated, and deacetylated according to the procedure of Koo, Avakian, and Martin (5). The intermediate dicarboxylic acid was not purified before decarboxylation and deacetylation to form 5-benzyloxytryptophan (III).

The crude III was purified according to the following procedure. 5-Benzyloxytryptophan (20 g) was warmed with 100 ml of water and 1 liter of ethanol. If solution was not complete then 1% sodium hydroxide was added dropwise until the material all dissolved. After treatment with charcoal and filtration, the solution was cooled and adjusted to pH 6.6 with acetic acid. The 5-benzyloxytryptophan began to crystallize

Can. J. Chem. Downloaded from www.nrcresearchpress.com by 196.1.178.254 on 09/04/12
For personal use only.

immediately. In case it separated as a gel, warming and stirring converted it to the crystalline form. A total of 29 g (88.5%) of III, m.p. 276–280° was obtained.

5-Hydroxytryptophan (IV)

5-Hydroxytryptophan was prepared by catalytic hydrogenolysis of III according to the procedure of Koo, Avakian, and Martin (5).

1. UDENFRIEND, S., TITUS, E., WEISSBACH, H., and PETERSON, R. E. J. Biol. Chem. **219**, 335 (1956).
2. PAGE, I. H. Physiol. Rev. **38**, 277 (1958).
3. EK, A. and WITKOP, B. J. Am. Chem. Soc. **76**, 5579 (1954).
4. SNYDER, H. R. and SMITH, C. W. J. Am. Chem. Soc. **66**, 350 (1944).
5. KOO, J., AVAKIAN, S., and MARTIN, G. J. J. Org. Chem. **24**, 179 (1959).
6. WARNER, D. T. and MOE, O. A. J. Am. Chem. Soc. **70**, 2763 (1948).
7. MENTZER, C., BEAUDET, C., and BORY, M. Bull. soc. chim. France, 421 (1953).

RECEIVED APRIL 24, 1959.
RESEARCH LABORATORIES,
FRANK W. HORNER LIMITED,
MONTREAL, QUEBEC.

THE EFFECT OF AMINES AND PHENOLS ON THE GAS-PHASE OXIDATION OF *n*-BUTANE AND ISOBUTANE*

K. U. INGOLD AND I. E. PUDDINGTON

In recent years the antiknock efficiency of a large number of fuel additives has been measured. Among the more powerful fuel additives are amines both aliphatic and aromatic (1, 2, 3, 4), and aromatic compounds in general (2, 5).

From an examination of the high and low temperature oxidation of diisopropyl ether, Chamberlain and Walsh (6, 7) concluded that inhibition of this reaction by aromatic compounds and, therefore, the antiknock ability of aromatic compounds, was due primarily to the electronic properties of the ring, nitrogen, and other side groups merely modifying the properties of the ring. However, it has since been shown by using deuterated amine antiknocks that, in the internal combustion engine, aromatic amines owe their antiknock efficiency to their ability to destroy chain-propagating radicals ($X^{\cdot}$) by the reaction (3)

$$X^{\cdot} + ArNHR \rightarrow XH + Ar\dot{N}R \qquad [1]$$

where $Ar\dot{N}R$ is a less reactive radical than $X^{\cdot}$. The effect of deuterated antiknocks on the low temperature oxidation of hydrocarbons has, however, not been previously studied.

The present work involved a brief investigation of the effect of aniline and aniline N—D_2 on the low temperature oxidation of two simple paraffins, viz. *n*-butane and isobutane. The effect of a few other amines and phenols was also examined with a view to comparing inhibitor efficiencies in gas- and liquid-phase (8) hydrocarbon oxidations.

The oxidation was studied in a conventional apparatus, except that the progress of the reaction was measured by means of a diaphragm manometer to avoid contamination of the reaction vessel with mercury. The butane (70 mm) and oxygen (280 mm) were premixed before being admitted to the cylindrical Pyrex reaction vessel (15 cm long, 4 cm diameter). The oxidation of *n*-butane was studied at 275° C and isobutane in the range 275°–310° C. The pressure–time curves for both butanes are S-shaped, and although the

*Issued as N.R.C. No. 5266.

Can. J. Chem. Downloaded from www.nrcresearchpress.com by 196.1.178.254 on 09/04/12
For personal use only.

immediately. In case it separated as a gel, warming and stirring converted it to the crystalline form. A total of 29 g (88.5%) of III, m.p. 276–280° was obtained.

5-Hydroxytryptophan (IV)

5-Hydroxytryptophan was prepared by catalytic hydrogenolysis of III according to the procedure of Koo, Avakian, and Martin (5).

1. UDENFRIEND, S., TITUS, E., WEISSBACH, H., and PETERSON, R. E. J. Biol. Chem. **219**, 335 (1956).
2. PAGE, I. H. Physiol. Rev. **38**, 277 (1958).
3. EK, A. and WITKOP, B. J. Am. Chem. Soc. **76**, 5579 (1954).
4. SNYDER, H. R. and SMITH, C. W. J. Am. Chem. Soc. **66**, 350 (1944).
5. KOO, J., AVAKIAN, S., and MARTIN, G. J. J. Org. Chem. **24**, 179 (1959).
6. WARNER, D. T. and MOE, O. A. J. Am. Chem. Soc. **70**, 2763 (1948).
7. MENTZER, C., BEAUDET, C., and BORY, M. Bull. soc. chim. France, 421 (1953).

RECEIVED APRIL 24, 1959.
RESEARCH LABORATORIES,
FRANK W. HORNER LIMITED,
MONTREAL, QUEBEC.

THE EFFECT OF AMINES AND PHENOLS ON THE GAS-PHASE OXIDATION OF *n*-BUTANE AND ISOBUTANE*

K. U. INGOLD AND I. E. PUDDINGTON

In recent years the antiknock efficiency of a large number of fuel additives has been measured. Among the more powerful fuel additives are amines both aliphatic and aromatic (1, 2, 3, 4), and aromatic compounds in general (2, 5).

From an examination of the high and low temperature oxidation of diisopropyl ether, Chamberlain and Walsh (6, 7) concluded that inhibition of this reaction by aromatic compounds and, therefore, the antiknock ability of aromatic compounds, was due primarily to the electronic properties of the ring, nitrogen, and other side groups merely modifying the properties of the ring. However, it has since been shown by using deuterated amine antiknocks that, in the internal combustion engine, aromatic amines owe their antiknock efficiency to their ability to destroy chain-propagating radicals ($X^{\cdot}$) by the reaction (3)

$$X^{\cdot} + ArNHR \rightarrow XH + Ar\dot{N}R \qquad [1]$$

where $Ar\dot{N}R$ is a less reactive radical than $X^{\cdot}$. The effect of deuterated antiknocks on the low temperature oxidation of hydrocarbons has, however, not been previously studied.

The present work involved a brief investigation of the effect of aniline and aniline N—D_2 on the low temperature oxidation of two simple paraffins, viz. *n*-butane and isobutane. The effect of a few other amines and phenols was also examined with a view to comparing inhibitor efficiencies in gas- and liquid-phase (8) hydrocarbon oxidations.

The oxidation was studied in a conventional apparatus, except that the progress of the reaction was measured by means of a diaphragm manometer to avoid contamination of the reaction vessel with mercury. The butane (70 mm) and oxygen (280 mm) were premixed before being admitted to the cylindrical Pyrex reaction vessel (15 cm long, 4 cm diameter). The oxidation of *n*-butane was studied at 275° C and isobutane in the range 275°–310° C. The pressure–time curves for both butanes are S-shaped, and although the

*Issued as N.R.C. No. 5266.

Can. J. Chem. Downloaded from www.nrcresearchpress.com by 196.1.178.254 on 09/04/12
For personal use only.

rate of pressure increase is at first very small, there is no initial decrease in pressure at these temperatures. The onset of a pressure increase has been shown (9) to mark a transition from a surface-inhibited reaction to an autocatalytic reaction in which effects resulting from chain-branching predominate and surface effects are much less important. For this reason, the amines and phenols were added not only at the start of the reaction ($\Delta p = 0$) where their effect might be due to their action on the surface, but were also added during the course of the reaction after a definite pressure increase had occurred and the induction period was over.

Since most of the additives had rather low vapor pressures at room temperature, they were stored in traps separated from the reaction vessel by metal valves; both traps and valves could be heated to 100° C. Helium at 1 atmosphere pressure was admitted to the traps and after residence for at least half an hour was used to carry the additive into the reaction vessel. Induction periods (defined as the time required for a pressure increase of 1.0 mm) are summarized in the table, all values being averages of at least two experiments.

TABLE

Effect of amines and phenols on the induction period of *n*-butane and isobutane
(Butane 70 mm, oxygen 280 mm, helium 180 mm)

Additive	Additive pressure (mm)	Added at Δp (mm)	*n*-Butane (275° C) induction period (seconds)	Isobutane (310° C) induction period (seconds)
None	—	—	140	400
He	—	0	125	140
He + aniline	9.0	0	1620	3900
He + aniline N—D_2	9.0	0	1090	2350
He + phenol	9.0	0	210	270
He + *o*-toluidine	4.5	0	750	1100
He + N-methylaniline	4.5	0	700	1200
He + *p*-cresol	3.5	0	160	185
He + piperidine	9.0	0	440	30
He + pyrrole	9.0	0	650	150
He + ammonia	9.0	0	165	110
He	—	2.7	20	10
He + aniline	9.0	2.7	110	250
He + aniline N—D_2	9.0	2.7	100	200
He	—	4.5	16	5
He + aniline	9.0	4.5	64	160
He + phenol	9.0	4.5	36	9
He + *o*-toluidine	4.5	4.5	55	40
He + N-methylaniline	4.5	4.5	60	40
He + *p*-cresol	3.5	4.5	22	7
He + piperidine	9.0	4.5	90	5
He + pyrrole	9.0	4.5	84	15
He + ammonia	9.0	4.5	30	5

Analysis of the reactants at the end of the induction period showed that the addition of aniline at the start of the reaction decreases the rate of butane consumption during the induction period. Aniline is, therefore, a true inhibitor for the oxidation of both butanes.

The reduced inhibiting effect of aniline N—D_2 compared with aniline shows that the rate-controlling step of at least a part of the inhibition must involve rupture of the N—D or N—H bond. This result is in agreement with the results of Brown *et al.* (3) on the antiknock efficiency of N-methylaniline and N-deutero-methylaniline. Although the conclusions of Walsh (7) that aromatic compounds inhibit by virtue of the electronic properties of the ring are not invalidated, this factor would seem to be of little importance with aromatic amines.

Can. J. Chem. Downloaded from www.nrcresearchpress.com by 196.1.178.254 on 09/04/12
For personal use only.

Since the isotope effect exists when aniline is added, both at the start of the reaction and during its course when surface effects are at a minimum, inhibition probably occurs to a fairly large extent in the gas phase. The reduction in the isotope effect when aniline is added during the reaction suggests that some exchange may occur, probably on the walls between the deuterated aniline and the various oxygenated products. The isotope effect is somewhat less than when aniline is used to inhibit liquid phase oxidations (8).

The results obtained with aniline, phenol, N-methylaniline, and *p*-cresol, all of which have also been studied in the liquid phase (8), show that the range of inhibitor efficiencies is smaller in the gas than in the liquid phase. By analogy with the results obtained with aniline these additives also probably inhibit by way of reaction [1].

Pyrrole and piperidine were studied to see if there was any correlation between the base strength of amines and their inhibiting efficiency. These two compounds have similar inhibiting power on the oxidation of diethyl ether (10) yet pyrrole is an extremely weak base while piperidine is a strong base. Both amines inhibit the *n*-butane oxidation. At 310° C pyrrole has only a small inhibiting effect on isobutane, while piperidine behaves as a strong catalyst. The catalytic action of piperidine occurs at temperatures as low as 275° C where, judging by the results with *n*-butane, the piperidine itself is probably not decomposed or oxidized appreciably. At low temperatures pyrrole also becomes a catalyst, although a rather weak one. For example, at 297° C the induction period for isobutane with helium alone is 1400 seconds, for pyrrole 1000 seconds, and for piperidine 100 seconds. The catalysis by both amines is not likely to be due to their decomposition, since such catalysis would be expected to increase with temperature. Ammonia, also, acts as an inhibitor with *n*-butane and as a catalyst with isobutane. The difference in behavior of these three compounds with the two butanes suggests that different intermediates are involved in the oxidation of the butanes. Inhibition of the *n*-butane oxidation may be due to reaction [1]. The catalysis observed with isobutane suggests that a catalyzed decomposition of the chain-branching intermediate is of considerable importance.

1. Boyd, T. A. Ind. Eng. Chem. **16**, 893 (1924).
2. Callendar, H. L. Aeronaut. Research Comm. Rept. No. 1018 (1925).
3. Brown, J. E., Markley, F. X., and Shapiro, H. Ind. Eng. Chem. **47**, 2141 (1955).
4. Brennan, J. A., Giammaria, J. J., and Oberright, E. A. Ind. Eng. Chem. **51**, 77 (1959).
5. Spiers, H. M. Technical data on fuel. British Natl. Comm. World Power Conf. (London). 1935.
6. Chamberlain, G. H. N. and Walsh, A. D. Trans. Faraday Soc. **45**, 1032 (1949).
7. Walsh, A. D. Trans. Faraday Soc. **45**, 1043 (1949).
8. Ingold, K. U. and Puddington, I. E. Ind. Eng. Chem. (In press).
9. Batten, J. J. and Ridge, M. J. Australian J. Chem. **8**, 370 (1955).
10. Waddington, D. J. 7th Symposium on Combustion. Preprints, 13, 1958.

Received April 13, 1959.
Division of Applied Chemistry,
National Research Council of Canada,
Ottawa, Canada.

Can. J. Chem. Downloaded from www.nrcresearchpress.com by 196.1.178.254 on 09/04/12
For personal use only.

Can. J. Chem. Downloaded from www.nrcresearchpress.com by 176.9.209.113 on 09/04/12
For personal use only.

Canadian Journal of Chemistry

Issued by THE NATIONAL RESEARCH COUNCIL OF CANADA

VOLUME 37 SEPTEMBER 1959 NUMBER 9

THE THERMODYNAMIC PROPERTIES OF THE SYSTEM CELLULOSE – WATER VAPOR[1]

JOHN L. MORRISON[2] AND MATTHEW A. DZIECIUCH[3]

ABSTRACT

The heats of wetting by water of cotton cellulose containing various amounts of adsorbed and desorbed water were measured. These measurements together with those of the water vapor sorption isotherm were used to calculate the integral and differential enthalpies, free energies, and entropies of adsorption. Irreversible effects were avoided by vacuum-drying all samples at room temperature. The differential enthalpy values suggest hydrogen bonding. The differential entropies are explained in terms of changes in both the adsorbate and adsorbent.

The surface area of the cellulose is calculated by applying the Brunauer–Emmett–Teller and Harkins–Jura equations to the adsorption isotherm. The changes in the differential enthalpies and entropies of adsorption follow the same sequence as the changes in film formation given by the surface area calculations.

No hysteresis was observed in the heats of wetting of adsorbed and desorbed samples. It is concluded that the hysteresis of the sorption isotherm is an entropy phenomenon. This supports Barkas' explanation of hysteresis in terms of plastic deformation of a gel.

INTRODUCTION

Measurement of the amounts, the vapor pressures, and the energies involved when water vapor is added to and removed from fibrous natural polymers have made it possible to calculate in detail the thermodynamic properties of the systems silk fibroin – water vapor and wool keratin – water vapor (1, 2, 3). The present report includes the same kind of measurements on the system cellulose – water vapor.

Wahba also made similar measurements on the cellulose – water vapor system (4). However, we believe that Wahba's drying procedures introduce an irreversible effect. A similar but larger effect is shown in the work of Argue and Maass (5), who made the first detailed measurements of the heats of wetting of cellulose by water.

Babbitt (6) made a comprehensive analysis of the adsorption isotherm of the cellulose – water vapor system and was the first to apply the Brunauer, Emmett, and Teller adsorption isotherm equation (7) to this system. In the present work, surface area measurements have assisted us in interpreting the thermodynamic properties.

EXPERIMENTAL

Calorimetric measurement of the heats of wetting by liquid water of cellulose equilibrated with various amounts of adsorbed and desorbed water vapor is the basis of the

[1]*Manuscript received April 13, 1959.*

Contribution from the Department of Chemistry, University of Alberta, Edmonton, Alberta. Based on a thesis submitted to the Faculty of Graduate Studies, University of Alberta, in partial fulfillment of the requirements for the M.Sc. degree, June, 1958. Presented in part to the 133rd Meeting of the American Chemical Society, San Francisco, California, U.S.A., April 13–18, 1958.

[2]*Formerly Professor of Chemistry, University of Alberta, Edmonton, Alberta. Present address: Connaught Medical Research Laboratories, University of Toronto, Toronto, Ontario.*

[3]*Graduate student, University of Alberta, 1956–58.*

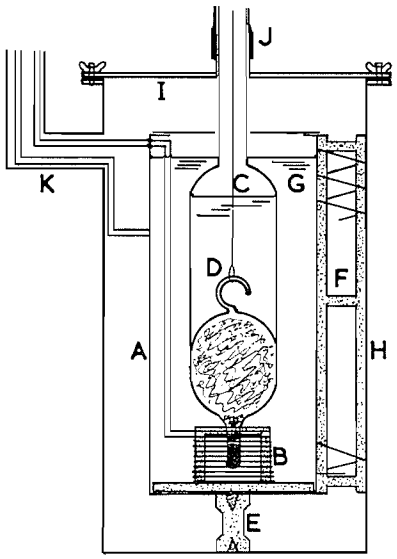

FIG. 1. The adiabatic calorimeter.

enthalpy calculations. Measurement of the adsorption and desorption isotherms is the basis of the corresponding free energy calculations. The entropies of sorption then follow from the well-known equation connecting the three thermodynamic functions.

Calorimeter

The adiabatic calorimeter (Fig. 1) was a simplified version of one by Howard and Culbertson (8). An inner cylindrical copper can, A, 2 inches in diameter by 5.5 inches long, was secured on a small lucite pedestal E inside an outer concentric copper jacket H with an air gap of 0.75 inch. A thermel F of 21 pairs of copper–constantan junctions supported on a light lucite frame was placed between the concentric walls. A 100-ohm manganin wire, non-inductively wound on a lucite frame, served as a calibration heater coil B and was placed in the bottom of the inner can.

The flanged lid I of the outer can had a central brass tube to act as a bearing for the glass reaction cell D. A side tube K from the outer can carried the wiring of the thermels and heater. The complete assembly rested in a well-stirred crock containing water. A rubber tube J was clamped to the lid-bearing to prevent leakage of water from the crock into the calorimeter.

Adiabatic control, sensed by the thermel and a sensitive galvanometer, was obtained manually by hot and cold water streams. Temperature changes were measured by a pair of thermistors (Stantel Type F, Standard Telephone and Cables, Ltd., England, total resistance about 3500 Ω at 25° C) immersed in the outer water bath and connected to a wheatstone bridge reading to 0.1 Ω. (Simultaneously, for some experiments, the resistance was measured by a Sargent Recorder, Model S-72150.) Electrical duplication of the heat changes was obtained with a circuit (9) which included an electronic voltage stabilizer to give a constant voltage (5 to 10 v). Between particular heat of wetting experiments, the outer crock was maintained at constant temperature by a thermoregulator and heater assembly, and at least 20 hours was allowed for the calorimeter and reaction cell to come to thermal equilibrium. All experiments were started at about 24.5° C.

Can. J. Chem. Downloaded from www.nrcresearchpress.com by 176.9.209.113 on 09/04/12
For personal use only.

A double compartment glass reaction cell D was used for contacting the cellulose and liquid water (Fig. 1). The cellulose in the lower compartment was sealed under vacuum. This ensured complete wetting when the breaking of the glass septum by pulling on a looped wire C allowed the water in the upper compartment to enter the lower one. The glass tube of the reaction cell passes through the calorimeter lid and is suspended by a coupling to a reciprocating stirring device. The main parts of the reaction cell are suspended in a heat transfer fluid G (light grade vacuum pump oil) in the inner can. After a sample has been prepared, the vacuum seal which is finally made at the lower end of the reaction cell is pinched into a paddle shape to act as a stirrer. This stirrer is suspended just inside the electrical heater B, thus securing dissipation of the heat evolved by the heater and by the wetting process. A new glass cell is required for each experiment.

Adsorption Apparatus

The sorption isotherm of cellulose and water vapor was determined with a vacuum apparatus similar to that used by Wiig and Juhola (10) for charcoal. About 8 g cellulose were placed in a detachable cylindrical glass bulb fitted with a vacuum stopcock and ground glass joint. The bulb had a central glass tube with several perforations to hasten equilibration. The vapor pressure was measured with an oil (Apiezon B) manometer and cathetometer, and the amount of water in the sample was obtained by detaching and weighing the assembly. Special precautions were taken in experiments near saturation vapor pressure because the top surface of the water bath thermostat had a slightly lower temperature than the bulk of the thermostat. A small heating coil was clasped around the tubes of the adsorption cell and the water reservoir to prevent condensation. The manometer was maintained at a temperature slightly above that of the thermostat. The isotherm was measured at 24.6° C.

Preparation of Cellulose

Standard cellulose was prepared from absorbent cotton (Johnson and Johnson Red Chain) by the same method as that of Argue and Maass (5), with the exception that *the cellulose was never allowed to dry above room temperature.*

All of the samples of cellulose, both for the calorimetry and for the sorption isotherm, were evacuated at room temperature for a minimum of 24 hours by means of a system including a mercury diffusion pump, magnesium perchlorate drying tube, a glass trap in dry ice – acetone mixture, and a rotary oil vacuum pump. "Stick" vacuums were consistently obtained as shown by the McLeod gauge. It was found that evacuation for 2 or 3 days neither reduced the moisture content nor produced a higher heat of wetting than for samples evacuated for 24 hours.

Samples for heat of wetting experiments (about 1 g) were placed in the lower compartment of the reaction cell; a small plug of Pyrex glass wool was inserted to prevent singeing of the cellulose. A vacuum stopcock and a male ground glass joint were sealed to the lower compartment, and the assembly was evacuated to constant weight. The dry weight of the cellulose was obtained by weighing the assembly after removing the grease (Apiezon L) from the ground glass joint with ether. All other joints and all stopcocks were greased with Dow Corning High Vacuum Silicone Grease, but Apiezon L is more easily removed because of its yellow color and hydrocarbon nature.

Samples were prepared with various adsorbed and desorbed water contents by contacting water vapor in an otherwise evacuated line. In each case at least 24 hours (11) were allowed for the final equilibration *after* the addition or removal of water. Also, at

Can. J. Chem. Downloaded from www.nrcresearchpress.com by 176.9.209.113 on 09/04/12
For personal use only.

least 24 hours were allowed for saturation with water vapor *before* the water was partially removed for the desorption experiments. Thus, at least 48 hours were required to prepare adsorption samples and 72 hours to prepare desorption samples for the calorimeter.

The correction for the heat of bulb-breaking (12) when water entered the evacuated bulb containing cellulose was calculated to be about 0.2 cal for each cell. A blank run on an empty cell gave a value of about 0.15 cal, so that this was subtracted from the heat of wetting of each sample. It happens that this correction does not affect any of the thermodynamic functions except the net enthalpy ΔH at saturation.

RESULTS AND CALCULATIONS

Drying Temperatures and the Heats of Wetting

The heats of wetting of standard cellulose with varying water contents, both adsorbed and desorbed, are given in Table I and Fig. 2. It would appear that within the experimental error, there is no hysteresis between the "adsorbed" and "desorbed" heats of wetting.

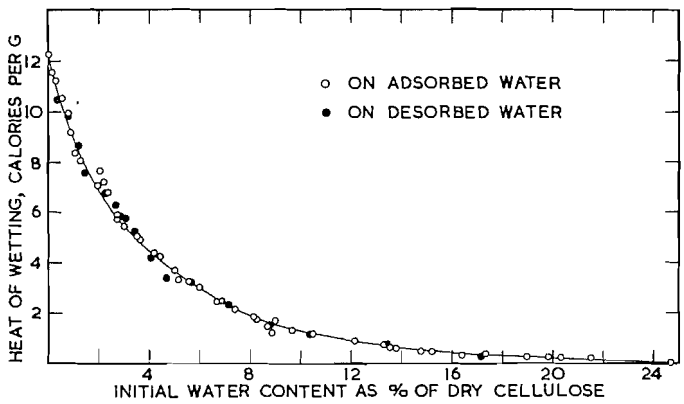

FIG. 2. The heats of wetting by water of cotton cellulose containing various amounts of adsorbed and desorbed water.

TABLE I

Heats of wetting of cotton cellulose by water

Adsorption		Adsorption		Adsorption		Desorption	
Water content, %	Heat of wetting, cal/g	Water content, %	Heat of wetting, cal/g	Water content, %	Heat of wetting, cal/g	Water content, %	Heat of wetting, cal/g
0	12.28	3.46	5.08	12.13	0.92	0.35	10.50
0	12.36	3.60	4.90	13.31	0.74	0.74	9.89
0	12.34	4.12	4.41	13.48	0.66	1.17	8.69
0.17	11.61	4.40	4.25	13.75	0.61	1.38	7.62
0.29	11.30	4.98	3.70	14.78	0.48	1.62	7.13
0.55	10.56	5.13	3.34	15.20	0.45	2.20	6.78
0.77	9.97	5.59	3.24	16.36	0.33	2.61	6.33
0.88	9.21	5.97	3.02	17.28	0.42	2.81	5.90
1.05	8.40	6.66	2.47	18.94	0.25	3.00	5.80
1.28	8.06	6.89	2.49	19.79	0.25	3.38	5.25
1.45	8.05	7.36	2.18	20.28	0.21	4.01	4.18
1.95	7.08	8.14	1.88	21.51	0.23	4.67	3.40
2.06	7.67	8.15	1.80	24.67	0.03	5.67	3.23
2.20	7.22	8.70	1.53	28.43	0	7.11	2.39
2.35	6.80	8.88	1.21	33.31	0	8.76	1.56
2.72	5.93	9.00	1.73	35.59	0	10.37	1.19
2.73	5.74	9.67	1.31			13.40	0.73
2.97	5.46	10.44	1.17			17.20	0.34

Can. J. Chem. Downloaded from www.nrcresearchpress.com by 176.9.209.113 on 09/04/12
For personal use only.

There is more scatter in the heats of wetting of samples below 3% water content than above. We believe that this is due to difficulty in removing the last traces of water from the cellulose rather than to errors in the calorimetry.

The heats of wetting obtained here are significantly higher than those obtained by Argue and Maass (5) and Wahba (4). For example, our value for dry cellulose was 12.33 cal/g whereas theirs were 10.16 and 10.72 respectively.

Argue and Maass heated their samples in air at 100° C, while Wahba heated his cellulose *in vacuo* at 65° C. In contrast, our samples were never permitted to go above room temperature. Kouris, Ruck, and Mason (13) also found that drying cellulosic material (a purified sulphite pulp) at elevated temperatures lowers the heat of wetting significantly compared with drying at room temperature.

There is some evidence that the cellulose–water system undergoes a change around 40° to 50° C. For example, Collins (14) found a parallel break in the curves of the cross-sectional area changes *and* the regain when plotted against temperature, with a complete change in direction occurring in the range 40° to 50° C.

Wahba and Nashed (15), on the basis of the experimental determination of adsorption isotherms at different temperatures, found that the isosteric heats of adsorption decreased markedly above an optimum temperature of from 40° to 50° C for "unstabilized" cellulose. They attribute this change to the development of new adsorbing centers above the optimum temperature.

The absence of hysteresis in the heats of wetting probably was found because the samples were dried at room temperature. Wahba and Nashed (16) found some hysteresis when they dried cellulose at 65° C and Argue and Maass (5) found even more when they dried it at 100° C.

The scatter in the heat of wetting values at very low moisture contents may arise from a high energy of activation for the transfer of water out of and into the cellulose fibers. Thus, room temperature drying increases the difficulty of obtaining reproducible drying. If we had used smaller samples, and evacuated them for longer times, the scatter probably would be reduced. Above the moisture content of the monolayer value (later), the scatter is much smaller in spite of the smaller amount of heat to be measured. It follows quite reasonably that the energy of activation for the removal of the upper layers is much less than for the first layer of sorbed water.

Thermodynamic Calculations

The heat of wetting data are used to calculate the integral and differential net enthalpies of sorption ΔH and $\overline{\Delta H}$ in calories per 100 g cellulose (above the heat of condensation of water vapor to liquid).

The adsorption isotherm (Table II and Fig. 3) is used to calculate the integral and differential free energies of adsorption, following the method of Dole and McLaren (17), see also (1, 2), which is similar to that of Wahba (4).

Finally, the integral and differential net entropies of adsorption are calculated from the enthalpies and free energies by the equations

$$\Delta S = (\Delta H - \Delta F)/T \quad \text{and} \quad \overline{\Delta S} = (\overline{\Delta H} - \overline{\Delta F})/T.$$

The various thermodynamic data are given in Table III and the differential properties are plotted in Fig. 4.

Adsorption Areas

Babbitt (6) applied the Brunauer, Emmett, and Teller (B.E.T.) equation (7) to Urquhart and Williams' cellulose – water vapor isotherm (18). Bull applied the same

Can. J. Chem. Downloaded from www.nrcresearchpress.com by 176.9.209.113 on 09/04/12
For personal use only.

TABLE II

Sorption isotherms of water vapor on cellulose at 24.6° C

Relative pressure	Adsorption, %	Desorption, %	Relative pressure	Adsorption, %	Desorption, %
0.025	1.00	1.18	0.55	5.97	7.03
0.05	1.49	1.71	0.60	6.52	7.66
0.075	1.86	2.10	0.65	7.13	8.31
0.10	2.13	2.45	0.70	7.81	9.02
0.15	2.65	3.02	0.75	8.58	9.84
0.20	3.09	3.52	0.80	9.53	10.88
0.25	3.48	3.94	0.85	10.72	12.21
0.30	3.87	4.37	0.90	12.55	14.0
0.35	4.22	4.84	0.95	15.25	16.7
0.40	4.61	5.37	0.975	17.0	19.2
0.45	5.02	5.92	0.99	19.1	21.3
0.50	5.47	6.47	1.00	~25	~25

TABLE III

Calculated thermodynamic properties of the cellulose–water system

n	P/P_0	$-\Delta H$	$-\Delta F$	$-\Delta S$	$-\overline{\Delta H}$	$-\overline{\Delta F}$	$-\overline{\Delta S}$
0	0	0	0	0	7600	—	—
.025	.008	165	83	0.28	5730	3100	8.83
.05	.021	297	148	0.50	4640	2300	7.86
.075	.042	405	202	0.68	4050	1900	7.22
.10	.071	498	247	0.84	3350	1570	5.98
.15	.156	640	313	1.10	2230	1095	3.81
.175	.207	695	337	1.20	1935	930	3.37
.20	.265	740	358	1.28	1720	785	3.14
.25	.387	820	391	1.47	1480	565	3.07
.30	.492	888	416	1.58	1360	420	3.15
.35	.582	952	434	1.74	1130	320	2.72
.40	.656	1005	448	1.87	860	250	2.05
.45	.720	1047	459	1.97	690	197	1.65
.50	.773	1080	468	2.05	525	152	1.25
.55	.817	1105	475	2.11	380	118	0.88
.60	.853	1122	481	2.16	330	94	0.79
.65	.881	1140	485	2.20	315	76	0.80
.70	.901	1154	488	2.24	250	62	0.63
.75	.919	1165	491	2.26	210	48	0.54
.80	.932	1176	493	2.29	180	38	0.48
.90	.965	1195	496	2.35	95	23	0.24
1.0	.984	1204	497	2.37	75	13	0.21
1.1	.990	1208	497.5	2.39	50	6	0.15
1.2	.995	1218	497.5	2.42	30	—	—
1.3	.998	1225	—	—	20	—	—
1.4	.9995	1230	—	—	—	—	—

NOTE: n, moles per 100 g cellulose; ΔH and ΔF, calories per 100 g cellulose; $\overline{\Delta H}$ and $\overline{\Delta F}$, calories per mole of water; ΔS, entropy units per 100 g cellulose; $\overline{\Delta S}$, entropy units per mole of water.

equation to a large number of protein – water vapor adsorption isotherms (19). In both cases the B.E.T. equation fitted the lower part of the adsorption isotherm.

Dunford and Morrison (20) have shown that the Harkins–Jura (H.J.) equation (21) applied to the upper part of Bull's isotherms and, by using Liang's correlation (22), they found the *same* monolayer content for both the B.E.T. and H.J. equations.

Applying these equations to the present isotherm, we obtain monolayer contents of 3.19 and 3.29 g water per 100 g cellulose for the B.E.T. and H.J. equations, respectively. The relative pressures over which these equations apply are 0.075 to 0.30 *and* 0.68 to

Can. J. Chem. Downloaded from www.nrcresearchpress.com by 176.9.209.113 on 09/04/12
For personal use only.

Can. J. Chem. Downloaded from www.nrcresearchpress.com by 176.9.209.113 on 09/04/12
For personal use only.

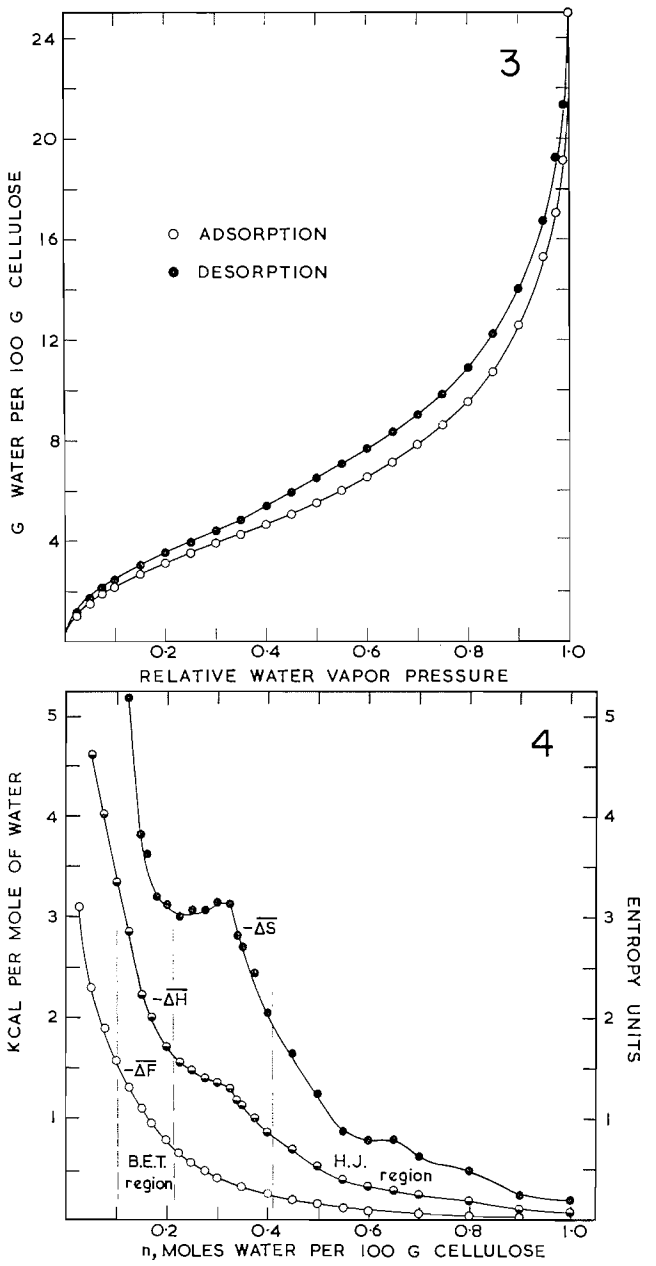

FIG. 3. The adsorption and desorption isotherms of water vapor on cotton cellulose. The points here are from smoothed curves obtained from measurements that extended over 3 months and included a total of 83 points; a minimum of 24 hours was allowed between each point.

FIG. 4. The net differential enthalpy, free energy, and entropy of adsorption of water by cotton cellulose.

1.0, respectively. For comparison, Wahba's data (4) yielded monolayer contents of 3.080 *and* 3.085 g, for the relative pressure range of 0.075 to 0.37 *and* 0.60 to 1.0, respectively. Urquhart and Williams' data (18) gave monolayer values of 3.38 and 3.60 g respectively.

Can. J. Chem. Downloaded from www.nrcresearchpress.com by 176.9.209.113 on 09/04/12
For personal use only.

DISCUSSION

Isotherm Equations and Areas

The application of theoretical adsorption equations to water vapor – natural polymer systems such as the present one helps us to interpret the thermodynamic data. The finding that at least two different equations, the B.E.T. and the H.J. equations, are required to account for the major part of the adsorption isotherm suggests either or both of two interpretations, (*a*) that a phase change occurs in the state of the adsorbed film (21) or (*b*) that a new phase appears as the relative pressure increases.

We note here that the B.E.T. equation is based on an immobile film with adsorption on definite sites, while the H.J. equation is based on a mobile condensed film.

Following the suggestion of Dunford and Morrison (20) with respect to the adsorption of water vapor by proteins, we consider that the adsorption of water vapor by cellulose from the dry state to saturation takes place as follows: a monolayer of immobilized water molecules is completed well before a relative pressure of 0.5 is reached, while further adsorption occurs *above* this monolayer; no surface is developed beyond that occupied by the monolayer; some multilayers, also immobile, are built up until the onset of a condensed film occurs at a relative pressure of about 0.6. Since the H.J. equation is based on *monolayer* film formation, it is suggested that the condensed film may appear as a new phase above an underlying "iceberg" phase of immobilized water (23).

The interpretation given here is in part confirmed by the observations of Hermans and co-workers (24). When the density of cotton cellulose is plotted against water content, a very well-defined maximum occurs at about 3.1% water content. This corresponds in their terms to the "formation of the first hydrate", and in our terms to the completion of a monolayer of immobilized water. Subsequently, there is evidence from their data of additional hydration up to 10 to 12% water content, succeeded by a density of sorbed water indistinguishable from that of liquid water.

A Comparison of Cellulose and the Fibrous Proteins

When the differential entropy and enthalpy curves (Fig. 4) of the cellulose – water vapor system are compared with those for silk fibroin and wool keratin (1, 2, 3), it is seen that the curves of the cellulose system are not as *definite* in their features. Whereas the breaks in the $\overline{\Delta H}$ and $\overline{\Delta S}$ curves of the two protein systems are very definite, and these breaks coincide very well with the B.E.T. and H.J. equation ranges, the same features in the corresponding cellulose curves are much less definite. For example, the beginning and end of the B.E.T. ranges of the two proteins coincide with the minimum and maximum respectively of the breaks in the $\overline{\Delta S}$ curves. In contrast, the B.E.T. range for cellulose begins earlier and it ends before the second break in the $\overline{\Delta S}$ curve.

It is possible that in the case of the proteins, the first monolayer is largely completed before the second and higher layers begin to form. In contrast, Babbitt has suggested for cellulose "that condensation begins in the second layer long before the first is completed" (6).

There is much evidence to suggest that cellulose is a much less reproducible material than the fibrous proteins. In our experience with the three fibers, the proteins are much less sensitive to high temperature drying than cellulose. Wool keratin can be dried in vacuum up to 80° C without affecting its heat of wetting (25), and it shows no hysteresis in its heat of wetting curve (2). Probably silk fibroin could also be heated nearly to this temperature without changing its adsorption properties, because on drying at 100° C it shows only a small hysteresis in its heat of wetting curve (1). Moreover, this

hysteresis is in the opposite direction to that observed for cellulose (5). Hutton and Gartside (26) have shown after very careful experiments that silk fibroins of Japanese, Chinese, and Italian origin gave exactly the same sorption isotherms.

In contrast, as already noted, cellulose is very sensitive to its mode of drying (see also Brown and co-workers (27)) and other features of its past history.

Perhaps the most important evidence for the contrast between protein fibers and cellulose is given by Mellon, Korn, and Hoover (28). They found that complete solution and reprecipitation of fibroin and keratin did not essentially alter their sorption isotherms. On the other hand, it is well known that solution and reprecipitation of cellulose always result in very large increases in the amount of water adsorbed.

Differential Enthalpy and Hydrogen Bonding

Although less definite than the fibrous proteins, nevertheless cellulose reveals the same kinds of breaks in its differential enthalpy and entropy curves. The enthalpy $\overline{\Delta H}$ decreases rapidly and levels off somewhat at -1.4 kcal per mole water adsorbed. This is comparable to the first layer heat value, -1.44, which Babbitt obtained for cellulose from one of the constants in the B.E.T. equation (6). It is also similar to the value obtained in this laboratory for mercerized cotton cellulose (29).

The value, -1.4, is significantly lower than the corresponding one, -2.4, which was obtained for both fibroin and keratin (1, 2, 3). As in the latter cases, we consider that the value -1.4 corresponds to a single hydrogen bond between water molecules and cellulose. Since the $\overline{\Delta H}$ values are net ones above the heat of condensation to liquid water, the hydrogen bond values would be $-4.5+(-1.4) = -5.9$ kcal per mole water, which is reasonable (30).

The high initial values of $\overline{\Delta H}$ may be due in part to the formation of two or more hydrogen bonds (15) per adsorbed water molecule; also, there may be a contribution from the release of tensions within the excessively dried cellulose. After the break in the region of monolayer formation, $\overline{\Delta H}$ decreases continuously up to saturation vapor pressure when it is indistinguishable from that of condensation on liquid water.

Entropy Changes

The differential entropy of adsorption for the cellulose – water vapor system is given in Fig. 4. The entropy curve exhibits a minimum similar to that of the fibrous proteins (3). Kelsey and Clarke (31) have a break in their $\overline{\Delta S}$ curve for a wood – water vapor system at about 8% to 9% water content. Since their wood adsorbed about 1.65 times as much water as pure cellulose, their observation is consistent with our maximum at a moisture content of 5.4%.

The explanation of the entropy curve is based on the assumption that both the adsorbate and adsorbent are contributing to $\overline{\Delta S}$ and $\overline{\Delta H}$. It is considered that after the *minimum* in $\overline{\Delta S}$ ($n = 0.25$) the contribution of the adsorbent is negligible on the *adsorption* side.

Pure adsorption, being an ordering process, contributes negative entropy ($-\overline{\Delta S}$ = +value). On the other hand, the disorganization of a highly dried gel (cellulose, fibroin, etc.) by water, contributes positive entropy ($-\overline{\Delta S}$ = −value). The high initial values of $-\overline{\Delta S}$ are probably due to adsorption of water, while the very rapid decrease to a minimum may be due in part to the disordering of the dried gel and in part to the replacement of two or more hydrogen bonds per water molecule by one per molecule. Then $-\overline{\Delta S}$ recovers up to a maximum. Here it is suggested that the disordering of the gel is

Can. J. Chem. Downloaded from www.nrcresearchpress.com by 176.9.209.113 on 09/04/12
For personal use only.

largely completed and the ordering due to adsorption asserts itself sufficiently to give a net recovery in $-\overline{\Delta S}$.

Adsorption into the second layer is less ordering than into the first so that $-\overline{\Delta S}$ continues to fall off after the maximum.

There is only a suggestion of a second break in the $-\overline{\Delta S}$ curve at $n = 0.70$, which corresponds to the pronounced break in the fibroin and keratin curves (1, 2, 3). A revision of a former explanation (3) is given here for the second and final break. It has already been suggested that well before the final break is reached, the contribution of the adsorbent to $-\overline{\Delta S}$ is negligible. The final break is considered to be a recovery in $-\overline{\Delta S}$ *after* the onset of a mobile film.

The transition from an immobile to a mobile film, *or* the appearance of a new mobile film above the immobile one, probably is marked by the beginning of the H.J. range, and is a disordering effect ($-\overline{\Delta S} = -$value). Thus, the net $-\overline{\Delta S}$ decreases more rapidly than if such a transition did not occur. But, after it has occurred, further adsorption (an ordering effect) continues and there is some recovery in $-\overline{\Delta S}$. Finally, the entropy changes become indistinguishable from condensation on liquid water.

Hysteresis

The adsorption–desorption isotherm for the cellulose – water vapor system exhibits a well-known hysteresis. Everett and Whitton (32) have discussed the validity of calculating thermodynamic properties of systems which exhibit such a permanent hysteresis. They have shown that these systems are thermodynamically stable, and differ from more familiar thermodynamic systems in having at least one other (an internal) variable.

It has been found that there is no hysteresis in the enthalpies of adsorption and desorption of water vapor on cellulose (also wool keratin and probably silk fibroin). Since the sorption curves determine the free energy functions, it follows that hysteresis in these systems is an entropy phenomenon.

The absence of hysteresis in the enthalpy seems to rule out the suggestion that hysteresis in the sorption isotherm involves the uncovering of new, more active sites on the desorption branch. Thus, Wahba and Nashed (15) suggest that the water molecules are more tightly held on the desorption side so that the vapor pressure is lower than on the adsorption side for the same amount of water sorbed.

If the hysteresis in the sorption isotherm is an entropy phenomenon, we would look for a difference in the arrangements (ordering) of the system on the two sides of the hysteresis loop rather than a difference in the bonding energies (enthalpies). It is difficult to conceive of the water alone having a different arrangement on the two sides of the loop, without the cellulose also being different. In fact, it is more usual that the adsorbent determines the arrangement of the adsorbate than the opposite. The general observation that the hysteresis of the water sorption isotherms of these fibrous systems is an entropy phenomenon supports Barkas' explanation of these hystereses (33).

Barkas explains hysteresis in terms of plastic deformation of a gel on the desorption of water vapor. This sets up internal stresses which affect the vapor pressure in a way analogous to the effect of an external hydrostatic pressure on the vapor pressure of a liquid. Thus, the vapor pressure on the desorption side is decreased by increased stresses on that side of the hysteresis loop.

We are suggesting that on the adsorption side of the hysteresis, the stresses of a completely dried gel have been largely removed in the low vapor pressure region of water uptake and that beyond about a monolayer, the isotherm is essentially stress-free up to saturation. Otherwise, it is difficult to understand the fit of the B.E.T. and H.J. equations

Can. J. Chem. Downloaded from www.nrcresearchpress.com by 176.9.209.113 on 09/04/12
For personal use only.

to the lower and upper parts of the adsorption isotherms with the same area being found for both equations. Attempts to fit these equations to the desorption side have been unsatisfactory. In the case of cellulose, the points do not lie on a 'good' straight line; and when the 'best' one is drawn, the H.J. monolayer area is at least 10% higher than the B.E.T. area.

Barkas predicted that there should be a hysteresis in the volume of the gel on the two sides of the loop. He found such to be the case for the wood – water vapor system (34). However, he calculated that in the case of *solid* filaments the volume hysteresis would be too small to observe experimentally. Hermans and his co-workers (24) confirmed this in the case of solid filaments of regenerated cellulose.

However, Collins (14), in some work apparently overlooked by Barkas, observed a definite hysteresis in the diameter of cotton cellulose fibers which have been treated with 15% NaOH to smooth them. Here, the same result as Barkas found for wood was observed in that the volume on the desorption side was greater than on the adsorption side.

Correspondingly, the differential entropy curve of desorption lies below that of adsorption. Since these are negative entropies, the desorption side has a higher positive entropy and is, therefore, more disordered than the adsorption side. This observation is consistent with the volume hysteresis.

A calculation based on Collins' measurements and on Urquhart and Williams' sorption isotherm for cellulose treated with 15% NaOH (35) shows, for example, that at 8% water content, the cross-sectional area changes are 9.7% on the adsorption side and 11% on the desorption. At 13% water content, the cross-section changes are 15.3% and 17.3% respectively.

Recently, Chakravarty (36) observed a similar hysteresis in the cross-sectional areas of single jute fibers at different relative humidities. However, Chakravarty found that there was no measurable hysteresis below a relative humidity of 25%, which corresponds to about one monolayer content for cellulose. This observation when taken together with Hermans and his co-workers' observations on isotropic solid filaments suggests that hysteresis may be largely an interfibrillar phenomenon rather than one within any single microfibril.

In conclusion, our work emphasizes the importance of measuring and reporting both the adsorption and desorption isotherms of systems which exhibit hysteresis. Unfortunately, this has not been done in many cases reported in the literature. For example, Bull in his classical work (19) measured the adsorption isotherms of about 18 protein materials. In the case of five of these (silk, wool, collagen, gelatin, and lyophilized egg albumin) he stated that "equilibrium was approached from both the wet and dry side of the equilibrium point". He found that "there is some hysteresis between a relative pressure of 0.15 and 0.65 while above and below these humidities the agreement is very good. In reporting the adsorption curves for the above five proteins, an average of the adsorption and desorption curves has been given." Here, Bull has assumed that hysteresis is a transient phenomenon; moreover, in calculating the "average of the adsorption and desorption curves", he does not indicate which of the two averages he used, the average at equal relative vapor pressure or at equal water content.

ACKNOWLEDGMENT

The authors are pleased to acknowledge grants in aid of this work made by the National Research Council of Canada.

Can. J. Chem. Downloaded from www.nrcresearchpress.com by 176.9.209.113 on 09/04/12
For personal use only.

Can. J. Chem. Downloaded from www.nrcresearchpress.com by 176.9.209.113 on 09/04/12
For personal use only.

REFERENCES

1. DUNFORD, H. B. and MORRISON, J. L. Can. J. Chem. **33**, 904 (1955).
2. MORRISON, J. L. and HANLAN, J. F. Proc. Second Intern. Congr. Surface Activity (London), **2**, 322 (1957).
3. MORRISON, J. L. and HANLAN, J. F. Nature, **179**, 528 (1957).
4. WAHBA, M. J. Phys. & Colloid Chem. **54**, 1148 (1950).
5. ARGUE, G. H. and MAASS, O. Can. J. Research, **12**, 564 (1935).
6. BABBITT, J. D. Can. J. Research, A, **20**, 143 (1942).
7. BRUNAUER, S., EMMETT, P. H., and TELLER, E. J. Am. Chem. Soc. **60**, 309 (1938).
8. HOWARD, F. L. and CULBERTSON, J. L. J. Am. Chem. Soc. **72**, 1185 (1950).
9. STURTEVANT, J. M. *In* Physical methods of organic chemistry. Vol. I. *Edited by* A. Weissberger. Interscience Publishers Inc., New York. 1945. p. 331.
10. WIIG, E. O. and JUHOLA, A. J. J. Am. Chem. Soc. **71**, 561 (1949).
11. ASHPOLE, D. K. Proc. Roy. Soc. (London), A, **212**, 112 (1952).
12. GUDERJAHN, C. A., PAYNTER, D. A., BERGHAUSEN, P. E., and GOOD, R. J. J. Chem. Phys. **28**, 520 (1958).
13. KOURIS, M., RUCK, H., and MASON, S. G. Can. J. Chem. **36**, 931 (1958).
14. COLLINS, G. E. J. Textile Inst. **21**, T311 (1930).
15. WAHBA, M. and NASHED, S. J. Textile Inst. **48**, T1 (1957).
16. WAHBA, M. and NASHED, S. Proc. Egyptian Acad. Sci. **8**, 128 (1952).
17. DOLE, M. and MCLAREN, A. D. J. Am. Chem. Soc. **69**, 651 (1947).
18. URQUHART, A. R. and WILLIAMS, A. M. J. Textile Inst. **15**, T559 (1924).
19. BULL, H. B. J. Am. Chem. Soc. **66**, 1499 (1944).
20. DUNFORD, H. B. and MORRISON, J. L. Can. J. Chem. **32**, 558 (1954).
21. JURA, G. and HARKINS, W. D. J. Am. Chem. Soc. **68**, 1941 (1946).
22. LIANG, S. C. J. Phys. & Colloid Chem. **55**, 1410 (1951).
23. KLOTZ, I. M. Science, **128**, 815 (1958).
24. HERMANS, P. H. Physics and chemistry of cellulose fibers. Elsevier Pub. Co., Inc., N.Y. 1949.
25. BRIGHT, N., CARSON, T., and DUFF, G. M. J. Textile Inst. 44, T587 (1953).
26. HUTTON, E. A. and GARTSIDE, J. J. Textile Inst. **40**, T161 (1949).
27. BRICKMAN, W. J., DUNFORD, H. B., TORY, E. M., MORRISON, J. L., and BROWN, R. K. Can. J. Chem. **31**, 550 (1953).
28. MELLON, E. F., KORN, A. H., and HOOVER, S. R. J. Am. Chem. Soc. **71**, 2761 (1949).
29. CHAPMAN, R. and MORRISON, J. L. Unpublished results.
30. COULSON, C. A. Research, **10**, 149 (1957).
31. KELSEY, K. E. and CLARKE, L. N. Australian J. Appl. Sci. **7**, 160 (1956).
32. EVERETT, D. H. and WHITTON, W. I. Trans. Faraday Soc. **48**, 749 (1952).
33. BARKAS, W. W. Trans. Faraday Soc. **38**, 194 (1942).
34. BARKAS, W. W. Nature, **162**, 32 (1948).
35. URQUHART, A. R. and WILLIAMS, A. M. J. Textile Inst. **16**, T155 (1925).
36. CHAKRAVARTY, A. C. Textile Research J. **28**, 878 (1958).

Can. J. Chem. Downloaded from www.nrcresearchpress.com by 176.9.209.113 on 09/04/12
For personal use only.

ADDITION OF PHENYL ISOTHIOCYANATE TO PYRROLES[1]

E. BULLOCK[2] AND R. J. ABRAHAM[2]

ABSTRACT

Pyrrole and alkyl pyrroles react spontaneously with phenyl isothiocyanate to produce C-substituted derivatives. The structures of the products are confirmed by physical methods. The reaction is catalyzed by organic bases.

Alkyl pyrroles react with phenyl isocyanate; the speed of reaction varies widely, depending on the substituents on the pyrrole ring. Where the pyrrole has a free α-position, the product is considered to be the α-anilide, e.g., I*a*. Reaction with α, α'-disubstituted pyrroles is slow and is thought to yield β-anilides, e.g. II*a* (1).

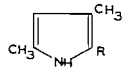

I

(*a*) R = CO.NH.Ph
(*b*) R = CS.NH.Ph

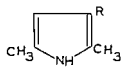

II

(*a*) R = CO.NH.Ph
(*b*) R = CS.NH.Ph

Generally, phenyl isocyanate reacts only sluggishly with "active" carbon atoms (e.g. with acetoacetic ester (2)) though the formation of IV from Fischer's Base (III) is rapid (3).

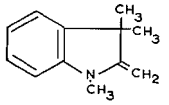

III

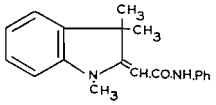

IV

Phenyl isothiocyanate is less reactive than the oxygen analogue towards water (4), amines (5), and acetoacetic ester, though it reacts readily with sodioethyl acetoacetate (11). The reaction with pyrroles is often rapid and the products are easily isolated (no competing side reaction with water). The thioanilides are converted to the corresponding anilides by alkaline peroxide.

In the ultraviolet, I*b* has a single absorption band of high intensity, while II*b* has two weaker bands at shorter wavelengths. This corresponds well with the difference in absorption of the α-(VII*a*) and β-(VII*b*) carboxylic acids (7).

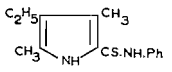

V

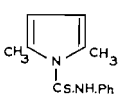

VI

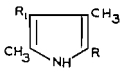

VII

(*a*) R = COOEt, R_1 = H
(*b*) R = H, R_1 = COOEt

[1]*Manuscript received April 16, 1959.*
Contribution from the Division of Pure Chemistry, National Research Council, Ottawa, Canada. Issued as N.R.C. No. 5272.
[2]*National Research Council Postdoctorate Fellow.*

N.M.R. spectra were recorded on several of these derivatives. The cryptopyrrole adduct shows no signal due to pyrrole C—H protons (8) and is therefore the α-thioanilide V (Fig. 1*a*). This compound is very similar (e.g. in infrared and ultraviolet spectra) to I*b*, which must therefore belong to the α-series, a fact confirmed by the proton resonance (Fig. 1*b*).

The nuclear magnetic resonance spectrum of II*b* confirms the structure since, apart from the single β-proton signal (Fig. 1*c*) the presence of two different sets of $-CH_3$ protons (Fig. 1*d*) rules out the symmetrical N-substituted compound (VI).

There is a qualitative relationship between the degree of alkyl substitution on the pyrrole nucleus and the rate of reaction with isothiocyanate in the α-series (Table I). The work on the anilides (1) shows a similar trend.

TABLE I

Reaction rates of substituted pyrroles

	Reaction (heating time)	Derivative	Yield (%)
Pyrrole	7 hours	α	3
α-Methyl	40 minutes	α	88
2,4-Dimethyl	10 minutes	α	90
2,4-Dimethyl-3-ethyl	2 minutes	α	100 (approx.)
2,3,4-Trimethyl	1 minute	α	100
2,3-Dimethyl	15 minutes	α	95
3,4-Dimethyl	5 minutes	α	73
2,5-Dimethyl	12 hours	β	7
2,3,5-Trimethyl	$1\frac{1}{2}$ hours	β	45

The reaction is base-catalyzed and solvent-sensitive. In several cases dissolution of the reactants (10%) in NN-dimethyl formamide (cf. 9) gives almost quantitative yields of thioanilides after 12 hours at room temperature and is the most convenient method of preparation; similar solutions in heptane yield no isolable product after 7 days.

Addition of triethylamine to mixtures of phenyl isothiocyanate with pyrrole, 2,4-, and 2,5-dimethyl pyrrole causes a marked increase in reaction rate and in the yield of the anilide.

The reaction with 2,3,5-trimethylpyrrole is interesting since it is faster than that of pyrrole and is comparable with α-methyl pyrrole. Thus, despite the steric effect of two adjacent methyl groups this β-position approaches the α-position of the simpler compound in reactivity.

Unlike the oxygen analogue, phenyl isothiocyanate failed to react with tetramethyl pyrrole (cf. 13) under vigorous conditions.

The variation of reaction rate with substitution may be due to two effects: (*a*) a general increase in the reactivity of the pyrrole ring with alkyl substitution and (*b*) the similarly increasing basicity of the pyrroles.

The close similarity of the reactions of isothiocyanates and isocyanates suggests that the mechanisms are analogous. The base catalysis observed for the pyrrole reaction indicates that as in the "normal" reaction with amines formation of a reactive complex (10) probably involving the pyrrole nitrogen atom is an intermediate step.

EXPERIMENTAL

Melting points are uncorrected.

Pyrryl carbanilides were prepared for comparison purposes according to Treibs and Ott (1).

Can. J. Chem. Downloaded from www.nrcresearchpress.com by 176.9.209.113 on 09/04/12
For personal use only.

Can. J. Chem. Downloaded from www.nrcresearchpress.com by 176.9.209.113 on 09/04/12
For personal use only.

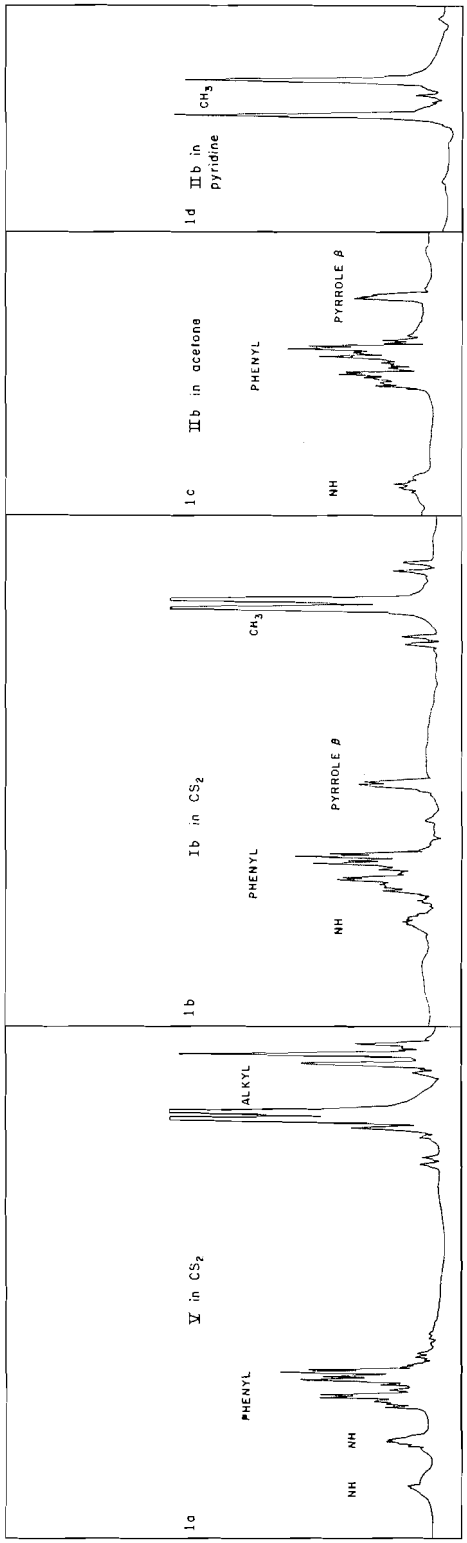

FIG. 1. N.M.R. spectra of pyrryl thiocarbanilides.

General Procedure for Isothiocyanate Reactions

The pyrrole was treated with approximately 10% excess of phenyl isothiocyanate and the mixture heated on the steam bath, the conditions being given for individual compounds in Table I. When the reaction mixture became very viscous, cold heptane was added; the product usually solidified when scratched with a glass rod. The solid was filtered and washed with heptane, then crystallized from a small volume of ether to which heptane was carefully added.

Pyrrole-2-thiocarbanilide

The reaction was far from complete after 7 hours and isolation of the product was made difficult by the presence of the reactants. The product was soluble in many organic solvents but was finally crystallized from heptane to yellow plates, m.p. 96–97° (3%). Calc. for $C_{11}H_{10}N_2S$: C, 65.31; H, 4.98; N, 13.85. Found: C, 64.96; H, 4.86; N, 13.92.

2-Methylpyrrole-5-thiocarbanilide

The thioanilide crystallized to thick yellow needles (88%), m.p. 109.5–111°. Calc. for $C_{12}H_{12}N_2S$: C, 66.62; H, 5.59; N, 12.95. Found: C, 66.46; H, 5.41; N, 12.65.

2,4-Dimethylpyrrole-5-thiocarbanilide

The product (90%) was crystallized to long yellow needles, m.p. 112–115°. Calc. for $C_{13}N_{14}N_2S$: C, 67.79; H, 6.13; N, 12.17. Found: C, 67.73; H, 5.76; N, 11.95. Ultraviolet spectrum: λ_{max} 344, λ_{infl} 218 mμ; log ϵ_{max} 4.38, log ϵ_{infl} 4.12 (95% ethanol). Infrared spectrum (nujol mull): 3380, 3340, 1603, 1500, 1482, 1448, 1427, 1375, 1355, 1315, 1288, 1235, 1207, 1155, 1027, 1008, 986, 945, 892, 820, 802, 744, 695, 680, 642 cm^{-1}.

2,5-Dimethylpyrrole-3-thiocarbanilide

The reactants were heated on the steam bath for 12 hours after which time the reaction mixture was black. The product was isolated by sublimation (0.5 mm, 150°) from the black solid obtained on addition of heptane to the reaction mixture, as small white needles, m.p. 194° (7%). Calc. for $C_{13}H_{14}N_2S$: C, 67.79; H, 6.13; N, 12.17. Found: C, 67.96; H, 5.77; N, 12.13. Ultraviolet spectrum: λ_{max} 319–325, 263, 217 mμ; log ϵ_{max} 4.09, 4.09, 4.32 (95% ethanol). Infrared spectrum (nujol mull): 3170, 1595, 1527, 1493, 1372, 1337, 1315, 1304, 1285, 1219, 1199, 1127, 1067, 1025, 1002, 966, 910, 790, 755, 712, 700, 682, 653 cm^{-1}.

In $CHCl_3$ solution, the NH band resolves to two peaks at 3380, 3440 cm^{-1}.

2,3-Dimethylpyrrole-5-thiocarbanilide.—2,3-Dimethylpyrrole-5-thiocarbanilide was isolated as thick yellow needles (95%), m.p. 144–145°. Calc. for $C_{13}H_{14}N_2S$: C, 67.79; H, 6.13; N, 12.17. Found: C, 68.13; H, 6.00; H, 12.15.

3,4-Dimethylpyrrole-2-thiocarbanilide.—3,4-Dimethylpyrrole-2-thiocarbanilide was obtained as yellow needles (73%), m.p. 118–119.5. Calc. for $C_{13}H_{14}N_2S$: C, 67.79; H, 6.13; N, 12.17. Found: C, 67.75; H, 6.06; N, 12.01.

2,4-Dimethyl-3-ethylpyrrole-5-thiocarbanilide

An almost quantitative yield of the product was isolated as thick yellow needles, m.p. 98–99°. Calc. for $C_{15}H_{18}N_2S$: C, 69.72; H, 7.02; N, 10.84. Found: C, 69.93; H, 6.87; N, 10.91.

2,3,4-Trimethylpyrrole-5-thiocarbanilide.—2,3,4-Trimethylpyrrole-5-thiocarbanilide was obtained in quantitative yield, m.p. 123–124°. Calc. for $C_{14}H_{16}N_2S$: C, 68.34; H, 6.60; N, 11.21. Found: C, 68.74; H, 6.49; N, 11.11.

Can. J. Chem. Downloaded from www.nrcresearchpress.com by 176.9.209.113 on 09/04/12
For personal use only.

2,3,5-Trimethylpyrrole-4-thiocarbanilide.—2,3,5-Trimethylpyrrole-4-thiocarbanilide was formed in good yield when the reactants were heated alone (or with triethylamine) for 1½ hours on the steam bath. Shorter reaction times yielded a product which was difficult to purify owing to the presence of starting material. Addition of heptane gave a dark gummy solid which when washed with ether yielded a yellow powder which was crystallized from chloroform–heptane as yellow prisms, m.p. 195–196° (45%). Calc. for $C_{14}H_{16}N_2S$: C, 68.34; H, 6.60; N, 11.21. Found: C, 68.12; H, 6.47; N, 11.37. Ultraviolet spectrum: λ_{max} 313 (broad), λ_{infl} 292 mμ; log ϵ_{max} 4.16, log ϵ_{infl} 4.10 (95% ethanol).

2,3,4,5-Tetramethylpyrrole.—2,3,4,5-Tetramethylpyrrole yielded no derivative under the following conditions: heating for 1 minute, 1 hour, 3 hours, heating for 3 hours then 24 hours at room temperature, standing for 48 hours at room temperature.

Oxidation of Thioanilides to Anilides (6)

Thioanilide (0.2 g) was dissolved in ethanol–water (10:1) in which 1 pellet of sodium hydroxide was dissolved. Hydrogen peroxide solution (100 vol., 1 ml) was added to the cold solution dropwise with shaking, and crystalline material appeared in the mixture soon after the addition of all the peroxide. After 30 minutes the product was isolated by pouring the reaction mixture into water (100 ml) and crystallized from chloroform–heptane.

(*i*) 2-Methylpyrrole-5-thiocarbanilide yielded 0.11 g of the corresponding anilide, m.p. 174–176° alone or mixed with authentic material (lit. 173° (1)).

(*ii*) 2,4-Dimethylpyrrole-5-carbanilide (0.15 g), m.p. 161° (lit. (1) 163°), was isolated.

(*iii*) Cryptopyrrole-5-thiocarbanilide yielded the corresponding anilide (0.06 g), m.p. 128–129° alone or mixed with authentic material (lit. (1) 137° for sublimed material or 131° (12)).

Comparison of Catalyzed and Uncatalyzed Reactions

The pyrrole (1 ml) was mixed with phenyl isothiocyanate (1 ml, 1.13 g) in each of two vessels to one of which triethylamine (3 drops) was added. The reactions were stopped by the addition of heptane (50 ml) and the product filtered off.

In the pyrrole case a black solid was produced in the catalyzed reaction from which two products, one white unidentified, the other the yellow thioanilide, were isolated and separated by fractional crystallization. In the other cases the crude solid was dried and weighed for comparison (a single recrystallization of these materials yielded products of good melting point).

Compound	Heating time	Uncatalyzed	Catalyzed
Pyrrole	6 hours	0.025 g 1.5%	0.17 g 10%
2,4-Dimethylpyrrole	2 minutes	1.40 g 73%	1.66 g 86%
2,5-Dimethylpyrrole	2½ hours	0 0	0.21 g 11%

ACKNOWLEDGMENTS

Analyses are by Mr. H. Seguin and the infrared spectra were recorded by Mr. R. Lauzon.

REFERENCES

1. TREIBS, A. and OTT, W. Ann. **577**, 19 (1952).
2. DIECKMANN, W. Ber. **33**, 2002 (1900).
3. COENEN, M. Chem. Ber. **80**, 546 (1947).

Can. J. Chem. Downloaded from www.nrcresearchpress.com by 176.9.209.113 on 09/04/12
For personal use only.

4. CAIN, J. C. and COHEN, J. B. J. Chem. Soc. 328 (1891).
5. BUU HOI, N. P., XUONG, N. G., and SUU, V. T. J. Chem. Soc. 2815 (1958).
6. MCKAY, A. F., SKULSKI, M., and GARMAISE, D. L. Can. J. Chem. **36**, 150 (1958).
7. COOKSON, G. H. J. Chem. Soc. 2789 (1953).
8. ABRAHAM, R. J. and BERNSTEIN, H. J. Can. J. Chem. **37**, 1056 (1959).
9. LIEBER, E. and RAMACHANDRAN, J. Chem. & Ind. 1406 (1958).
10. BAKER, J. W. and BAILEY, D. N. J. Chem. Soc. 4649 (1957).
11. WORRALL, D. E. J. Am. Chem. Soc. **40**, 418 (1918).
12. FISCHER, H., SÜS, O., and WEILGUNY, F. G. Ann. **481**, 159 (1930).
13. TREIBS, A. and DERRA-SCHERER, H. Ann. **589**, 196 (1954).

Can. J. Chem. Downloaded from www.nrcresearchpress.com by 176.9.209.113 on 09/04/12
For personal use only.

Can. J. Chem. Downloaded from www.nrcresearchpress.com by 176.9.209.113 on 09/04/12
For personal use only.

MOLTEN SALTS

THE DENSITY AND ELECTRICAL CONDUCTIVITY OF THE SYSTEMS: $AgNO_3$–$Ba(NO_3)_2$, –$Ca(NO_3)_2$, AND –$Mg(NO_3)_2$ [1]

J. W. Murphy and F. E. W. Wetmore

ABSTRACT

The density and electrical conductivity of the systems $AgNO_3$–$Ba(NO_3)_2$, –$Ca(NO_3)_2$, and –$Mg(NO_3)_2$ have been determined from 210 to 320° and from 0 to 20 equiv. %. The addition of magnesium nitrate causes the greatest shrinkage of the equivalent volume and reduction of the conductivity, barium nitrate the least.

The low conductivity of the binary melts is explained in terms of a mechanism involving restricted jumps and variation of the energy barrier with temperature and kind of ion added.

To date there have been few systematic studies of the density and electrical conductivity of binary salt melts comprising other than uni-univalent salts. This report concerns melts of silver nitrate with additions of barium, calcium, and magnesium nitrates.

EXPERIMENTAL

Materials

The silver nitrate was of reagent grade with a limit of 0.02% impurity, dried by oven-heating and finally by fusion. Barium nitrate of reagent grade was dried in an oven in which the temperature was slowly raised to a point just short of fusion. Calcium nitrate was prepared from reagent tetrahydrate by holding it at 300° for more than a day and heating it to 450° for an hour before use. Magnesium nitrate was prepared from reagent hexahydrate by vacuum-exsiccation from 50° slowly up to 150° (1); the weight of the charge was determined periodically. The salts were stored under dry air. Dryness of the melts was assured by the fact that their properties (density, conductivity, and freezing point) were not altered by longer periods of drying or by being held at high temperatures for several days during the runs; it is also significant that on heating the melts through more than 100° and returning them to the original temperature, the properties were not changed.

Apparatus

The apparatus used for the determination of density and conductivity differed from that used by Spooner (2) in only a few respects. The furnace was fitted with top and bottom plate heaters, which improved the homogeneity of the temperature of the melt. The silica conductivity cell was similar to that used by Lorenz and Kalmus (3), open at the bottom and having the lower electrode in the main body of the melt; the position of this electrode was found to be not critical.

Calibration with potassium chloride solution (4) showed the cell constant to be 801.93 cm^{-1} at 25°; appropriate correction was made for the expansion of the silica at higher temperatures. The bridge circuit was similar to that recommended by Jones and Josephs (5); both ratio arms were 1000 ohms. The signal leaving the bridge could be sent through a wide-band (400 to 10,000 c.p.s.) filter or through one sharply peaked. The amplitude and phase angle of the signal were observed on a cathode ray tube.

[1]*Manuscript received April 20, 1959.*
Contribution from the Department of Chemistry, University of Toronto, Toronto, Ontario.

Procedure

Preliminary determinations of the apparent resistance of the melts with frequencies from 400 to 10,000 c.p.s. showed that it varied inversely as the square root of the frequency. The small polarization, not exceeding 0.05%, was thereafter conveniently determined by measuring the apparent resistance at two frequencies, 1000 and 4000 c.p.s.

Both conductivity and density measurements were made at intervals of about 12°, first with rising temperature and then with falling. The results fell on one smooth curve. Melts containing 1, 2, 3, 4, 5, 10, and 20 equiv. % of calcium and magnesium nitrate were studied; the dictate of solubility limited the addition of barium nitrate to 5 equiv. %.

RESULTS

From the measured buoyancies and resistances were derived equations of density and specific conductivity as functions of temperature. From these equations the equivalent volume and equivalent conductivity were calculated for intervals of 10°. The deviations of the original data from the equations indicated that the equivalent volumes of Table I are precise within 0.04%, the conductivities of Table II within 0.1%.

The equivalent volume of a melt, whether unary or binary, is the volume of 1 equivalent of nitrate ion with its associated equivalent of cation. Calculation of the shrinkage to be expected from simple replacement of silver ion by an equivalent amount of divalent ion (one-half as many) can be based on the reported (6) radii of the ions. The absolute values must depend on the assumption of the volume to be ascribed to an ion, varying, for example, from an extreme of $4.2\,r^3$ (spherical) to the other extreme of $8\,r^3$ (cubic). The relative shrinkages do not depend on this assumption; they are 1.0:2.0:2.5 for Ba:Ca:Mg. The actual shrinkages shown in Table I are $2.5N_2$, $5.5N_2$, and $7.3N_2$, corresponding to 1.0:2.2:2.9. In the melt, compared with the condition for which the radii were determined, the magnesium ion is most closely bound to the nitrate ions, the barium ion least.

TABLE I

Equivalent volume (cm^3 g-equiv.$^{-1}$) of the systems $AgNO_3$–$M(NO_3)_2$

Temp., °C	Equiv. %, divalent nitrate					
	0	3	5	10	20	M
210	42.82	42.74				Ba
		42.66	42.56	42.27	41.70	Ca
		42.60	42.46	42.07	41.47	Mg
230	43.07	42.99				Ba
		42.90	42.80	42.52	41.94	Ca
		42.85	42.71	42.32	41.72	Mg
260	43.44	43.36	43.32			Ba
		43.28	43.18	42.89	42.30	Ca
		43.22	43.08	42.69	42.10	Mg
290	43.83	43.75	43.70			Ba
		43.66	43.56	43.26	42.67	Ca
		43.60	43.47	43.07	42.48	Mg
320	44.22	44.14	44.10			Ba
		44.05	43.94	43.65	43.05	Ca
		43.99	43.86	43.46	42.87	Mg

Can. J. Chem. Downloaded from www.nrcresearchpress.com by 176.9.209.113 on 09/04/12
For personal use only.

Can. J. Chem. Downloaded from www.nrcresearchpress.com by 176.9.209.113 on 09/04/12
For personal use only.

Flood, Forland, and Grjotheim (7) suggested that the addition of divalent salt to univalent salt with a common ion could create vacancies in the melt. The shrinkages found here are of a magnitude which indicates the possibility of only small formation of vacancies, if any.

If ideality in conductivity is defined as the absence of effect of the presence of one ion on the mobility of another, then $\Lambda = N_1\Lambda_1^0 + N_2\Lambda_2^0$, in which N_i is the equivalent fraction of component i and Λ_i^0 is the equivalent conductivity of pure component i, is the condition of ideality. Since the melting points of the divalent nitrates lie well above the decomposition temperature of silver nitrate, comparison of real with ideal behavior is restricted to melts containing a high proportion of silver nitrate.

TABLE II

Equivalent conductivity (ohms cm^{-2} g-equiv.$^{-1}$) of the systems $AgNO_3$–$M(NO_3)_2$

Temp., °C	Equiv. %, divalent nitrate					
	0	3	5	10	20	M
210	27.76	26.31				Ba
		26.05	24.86	22.11	16.91	Ca
		25.76	24.59	21.63	16.30	Mg
230	31.99	30.48				Ba
		30.19	28.94	25.99	20.33	Ca
		29.85	28.58	25.34	19.53	Mg
260	38.18	36.56	35.46			Ba
		36.23	34.88	31.70	25.46	Ca
		35.84	34.43	30.84	24.35	Mg
290	44.15	42.44	41.32			Ba
		42.06	40.63	37.27	30.61	Ca
		41.61	40.10	36.25	29.15	Mg
320	49.92	48.10	46.97			Ba
		47.68	46.16	42.71	35.78	Ca
		47.17	45.61	41.56	33.92	Mg

Table II and the solid curves of Fig. 1 show the real behavior; the broken line indicates the ideal contribution of silver nitrate alone, $N_1\Lambda_1^0$. The conductivity of the melt is much less than that of silver nitrate diluted by a non-conducting substance; assumption of lack of conductivity on the part of the divalent nitrate will therefore not alone explain the low conductivity.

Van Artsdalen and Yaffe (8) pointed out that shrinkage of the equivalent volume (quasi-lattice) would increase the electrostatic energy barrier for the conducting species. At 260° a melt containing 20 equiv. % magnesium nitrate, for example, shows a conductivity 20% less than $N_1\Lambda_1^0$. The volume is only 3% less than that of silver nitrate, corresponding to 1% reduction in interionic spacing and 2% increase in coulomb force. This increase in the energy barrier can account for about one-third of the observed decrease.

The suggestion of Van Artsdalen and Yaffe can be extended by supposing that silver ion is the important carrier of charge and that it moves by jumping from one cation site to another, but not to a site occupied by a cation closely bound to its anion neighbors. In comparison with pure silver nitrate there would be in the binary melt only N_1 as many silver ions and only some N_1 as many sites to which jumps are possible. The contribution of silver nitrate, without allowance for an increase in the energy barrier,

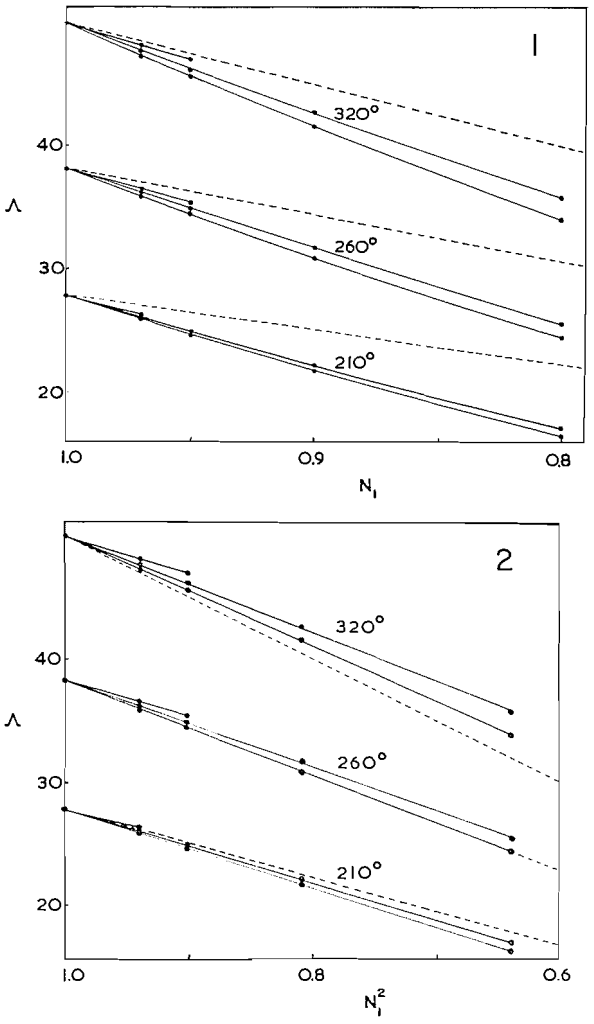

FIG. 1. The equivalent conductivity of silver nitrate with addition of divalent nitrate. The broken line shows the value of $N_1\Lambda_1^0$. In descending order the three solid curves in each group refer to barium, calcium, and magnesium nitrate, respectively.

FIG. 2. The equivalent conductivity of silver nitrate with addition of divalent nitrate. The broken line shows the value of $N_1^2\Lambda_1^0$. In descending order the three solid lines in each group refer to barium, calcium, and magnesium nitrate, respectively.

would be approximately $N_1^2\Lambda_1^0$. The solid lines of Fig. 2 show that Λ is essentially linear in N_1^2, but not exactly equal to $N_1^2\Lambda_1^0$. The deviations with change of temperature and divalent ion are in qualitative agreement with the views expressed above. The energy of activation of the conduction process decreases with rising temperature (2), and it can be seen from the expression $\Lambda = A.\exp(-E/RT)$ that the increase in the energy barrier with shrinkage of the quasi-lattice will be most pronounced at low temperature. The fall of conductivity should be greatest for addition of magnesium ion, least for barium ion. Both of these expectations are borne out.

Can. J. Chem. Downloaded from www.nrcresearchpress.com by 176.9.209.113 on 09/04/12
For personal use only.

ACKNOWLEDGMENTS

The authors gratefully acknowledge the financial support received from the National Research Council of Canada and the Advisory Committee on Scientific Research of this University.

REFERENCES

1. SHOMATE, C. and KELLEY, K. K. J. Am. Chem. Soc. **66**, 1490 (1944).
2. SPOONER, R. C. and WETMORE, F. E. W. Can. J. Chem. **29**, 777 (1951).
3. LORENZ, R. and KALMUS, H. T. Z. physik. Chem. **59**, 17 (1907).
4. JONES, G. and PRENDERGAST, M. J. Am. Chem. Soc. **59**, 731 (1937).
5. JONES, G. and JOSEPHS, R. C. J. Am. Chem. Soc. **50**, 1049 (1928).
6. PAULING, L. The nature of the chemical bond. Cornell Univ. Press, Ithaca, N.Y. 1939. p. 326.
7. FLOOD, H., FORLAND, T., and GRJOTHEIM, K. The physical chemistry of melts. Inst. of Mining and Metallurgy. London. 1953. p. 46.
8. VAN ARTSDALEN, E. R. and YAFFE, I. S. J. Phys. Chem. **59**, 118 (1955).

Can. J. Chem. Downloaded from www.nrcresearchpress.com by 176.9.209.113 on 09/04/12
For personal use only.

Can. J. Chem. Downloaded from www.nrcresearchpress.com by 176.9.209.113 on 09/04/12
For personal use only.

THE NUCLEAR MAGNETIC RESONANCE SPECTRA OF TRIARYL CARBONIUM IONS[1]

R. B. MOODIE,[2] T. M. CONNOR,[3] AND ROSS STEWART

ABSTRACT

The N.M.R. spectra of the triphenylmethyl cation and several of its derivatives substituted with methyl, methoxyl, and *tert*-butyl groups in the meta or para position have been obtained in trifluoroacetic acid – trifluoroacetic anhydride solution. The ring protons and substituent protons are all shifted to lower fields, i.e. are less shielded in the carbonium ions than in the neutral compounds of similar structure. The chemical shifts for the substituent protons are greater for para than for meta substituents and for mono- rather than tri-substituted ions. With each ion only a single peak was observed for the substituent protons but the ring protons were, in some cases, well resolved. The theoretical implications of these results are discussed.

INTRODUCTION

Triaryl carbinols are known to ionize in strongly acid solution to give carbonium ions.

$$Ar_3COH + 2H^+ \rightleftharpoons Ar_3C^+ + H_3O^+$$

The stability of these ions depends mainly on the extent of resonance interaction between the central electron-deficient carbon atom and the aromatic rings. Substituents which can aid this charge dispersal are known to have very large stabilizing effects on the carbonium ion. Thus the equilibrium constant for the ionization of tri-*p*-anisylcarbinol is larger by a factor of 3×10^7 than that of unsubstituted triphenylcarbinol (1). The effect of substituents in the meta position is much smaller since direct resonance interaction is not possible.

There are in addition two steric factors which are known to influence this electronic interaction. They are, first, the effect of bulky ring substituents such as *tert*-butyl in inhibiting solvation of the rings (2), and second, the steric interaction at the ortho positions. This latter effect precludes the formation of the electronically favored planar structure. The actual structure is open to question and it has been suggested that only one or two of the rings are conjugated with the central carbon atom (3). There is evidence, however, that favors, at least for the symmetrically substituted ions, a symmetrical "propeller" structure in which the π orbitals of each ring overlap to the same extent with the central carbon atom's p orbital (4, 5).

This paper reports a study of the nuclear magnetic resonance spectra of some substituted triarylmethyl cations in which the frequency of the aromatic and substituent proton resonances gives information about the distribution of the positive charge. The only previously reported N.M.R. spectra of carbonium ions are those of some protonated aromatic hydrocarbons (6) and the tropylium cation (7).

In order to compare the chemical shifts with those of neutral compounds containing similar groups, we sought a solvent which was sufficiently acidic to cause complete ionization of the triarylcarbinols, which would dissolve such compounds as toluene and anisole, and which was free from proton resonances in the region to be studied. A solution of trifluoroacetic acid in trifluoroacetic anhydride was found to be a suitable solvent system.

[1]*Manuscript received May 11, 1959.*
Contribution from the Chemistry Department, University of British Columbia, Vancouver, B.C., Canada.
[2]*National Research Council Postdoctoral Fellow, 1958–59.*
[3]*Holder of a National Research Council Studentship 1957–59.*

Can. J. Chem. Downloaded from www.nrcresearchpress.com by 176.9.209.113 on 09/04/12
For personal use only.

EXPERIMENTAL

The nuclear magnetic resonance spectra were recorded on a Varian 4300 spectrometer at 40 Mc, using an external water marker. In some cases the aromatic proton resonances were also examined at 60 Mc. Shifts were measured using conventional side band and interpolation techniques. Since all the solutions were dilute and the volume susceptibilities of the triarylmethyl cations are expected to be similar, the bulk susceptibility corrections are negligible so that the measured shifts can be compared directly. In each case the sample consisted of a 10% solution of the carbinol in a solvent of 1.5 *M* trifluoroacetic acid in trifluoroacetic anhydride sealed off *in vacuo*. The diamagnetic properties of the solvent were not appreciably changed over the range 1.5 to 3 *M* acid since the position of the proton resonances of toluene did not change.

The visible spectra of 3×10^{-4} *M* triphenylcarbinol (λ_{max} 410 mμ, ϵ 43,500, λ_{max} 425 mμ, ϵ 42,200) and of 1.5×10^{-4} *M* tri-*p*-anisyl carbinol (λ_{max} 478 mμ, ϵ 87,000) in the trifluoroacetic acid – trifluoroacetic anhydride solvent were measured with a Cary Model 14 recording spectrophotometer using cells of 0.1-cm path length. The spectrum appeared to be unchanged in more concentrated solutions (ca. 4×10^{-2} *M*) using cells of 10^{-3}-cm path length, but the volatility of the solvent precluded any precise determination with these cells.

The absorption maxima and extinction coefficients are very similar to those of the carbonium ions in sulphuric acid solution (triphenylmethyl cation: λ_{max} 404 mμ, ϵ 40,000, λ_{max} 431 mμ, ϵ 40,000 (2), tri-*p*-anisylmethyl cation: λ_{max} 483 mμ, ϵ 91,000 (8)). It was assumed that complete ionization also occurred in the slightly more concentrated solutions used for the N.M.R. spectral measurements. The N.M.R. spectra would, however, not necessarily reveal the presence of a small amount of the unionized triarylmethyl trifluoroacetate since in the equilibrium below,

$$CF_3CO_2CAr_3 \rightleftharpoons Ar_3C^+ + CF_3CO_2^-,$$

the rate of interconversion of the ionized and unionized forms may be too fast for separate substituent proton resonances to be observed.

The N.M.R. and visible spectra of *m*-methoxyphenyl diphenylcarbinol and tri-*m*-methoxyphenylcarbinol in this solvent were found to be quite different from the other carbinols studied. There seems to us to be some doubt as to the nature of the colored species formed in this solvent and their spectra are not further discussed here.

Preparation of Carbinols

The carbinols in Table I were prepared from the indicated starting materials by conventional Grignard syntheses.

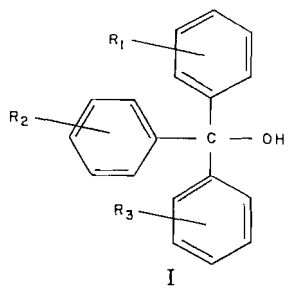

I

TABLE I

Preparation of carbinols

	R_1	R_2	R_3	Starting materials	M.p., ° C (found)	M.p., ° C (literature)
I	*p*-Me	—	—	*p*-MeC_6H_4Br, $(C_6H_5)_2CO$	76–9	78–9 (9)
II	*p*-Me	*p*-Me	—	C_6H_5Br, $(p\text{-}MeC_6H_4)_2CO$	73	75 (10)
III	*p*-Me	*p*-Me	*p*-Me	*p*-MeC_6H_4Br, $(p\text{-}MeC_6H_4)_2CO$	94–5	94 (11)
IV	*m*-Me	—	—	*m*-MeC_6H_4Br, $(C_6H_5)_2CO$	62–5	67 (12)
V	*m*-Me	*m*-Me	*m*-Me	*m*-MeC_6H_4Br, *m*-MeC_6H_4COOMe	70–2	69–71 (13)
VI	*p*-MeO	—	—	*p*-$MeOC_6H_4Br$, $(C_6H_5)_2CO$	60	60 (14) 82 (15)
VII	*p*-MeO	*p*-MeO	*p*-MeO	*p*-$MeOC_6H_4Br$, *p*-$MeOC_6H_4COOMe$	82–3	81–2 (2)
VIII	*m*-MeO	—	—	*m*-$MeOC_6H_4Br$, $(C_6H_5)_2CO$	87–9	88 (14)
IX	*m*-MeO	*m*-MeO	*m*-MeO	*m*-$MeOC_6H_4Br$, *m*-$MeOC_6H_4COOMe$	117–9	119.4 (14)
X	*p*-^{t}Bu	—	—	*p*-$^t BuC_6H_4Br$, $(C_6H_5)_2CO$, HCl	134–6[a]	133–4[a] (16)

[a]These melting points refer to *p-tert*-butylphenyl diphenylchloromethane which was prepared and used directly for the N.M.R. measurements.

Compounds IV and V gave poor yields and were purified by alumina chromatography. Compounds III and VI were purified by conversion to the triarylchloromethane and after several recrystallizations reconversion to the carbinol, as described by Gomberg (15). We are indebted to Mr. L. J. Muenster for the preparation of compound III.

RESULTS AND DISCUSSION

Table II records the chemical shifts of the aromatic and substituent protons measured from an external water marker at 40 Mc. In the case of the aromatic protons, these measurements were made to the largest peak except in the case of the tri-*p*-anisylmethyl cation where the measurement is to the center of the symmetrical quartet.

TABLE II

Chemical shifts of aromatic and substituent protons in cycles per second

Compound from which cation was derived	Aromatic shift (to main peak)	Substituent shift
Triphenylcarbinol	−101.0	—
p-Tolyl diphenylcarbinol (I)	− 98.0	+102.5
Di-*p*-tolyl phenylcarbinol (II)	− 94.75	+104.5
Tri-*p*-tolylcarbinol (III)	− 93.5	+105.5
m-Tolyl diphenylcarbinol (IV)	− 95.5	+112.5
Tri-*m*-tolylcarbinol (V)	− 89.0	+112.5
p-Anisyl diphenylcarbinol (VI)	− 96.0	+ 42.0
Tri-*p*-anisylcarbinol (VII)	− 87.5	+ 47.0
p-tert-Butylphenyl diphenylchloromethane (X)	−101.0	+151.0
Compound		
tert-Butylbenzene	− 76.0	+161.5
Anisole	− 68.0	+ 59.5
Toluene	− 69.0	+124.0

The Substituent Protons

In no cases were multiple substituent proton peaks observed. This is expected for the symmetrical propeller form but is also consistent with the one-ring-conjugated form if one assumes that the interconversion of isomers is too rapid to be detected by N.M.R. No splitting of the substituent proton resonances of the tri-*p*-anisylmethyl and tri-*p*-tolylmethyl cations was observed when the solutions were cooled to −80°.

Greater shielding of the substituent protons is observed in the carbonium ions sub-

Can. J. Chem. Downloaded from www.nrcresearchpress.com by 176.9.209.113 on 09/04/12
For personal use only.

stituted in all three para positions compared with those with only one para substituent. In the latter case greater stability would be expected for a structure in which the substituted ring occupies a position of greater conjugation with the central carbon than the other two rings. This effect should be less marked with metasubstituted compounds, where the direct resonance interaction with the substituent is not possible, and in fact no difference was observed in the shielding of the substituent protons for the *m*-tolyl diphenylmethyl and tri-*m*-tolylmethyl cations.

The greater shift between toluene and the tri-*p*-tolylmethyl cation (18.5 c/s) than between anisole and the tri-*p*-anisylmethyl cation (12.5 c/s), in spite of the greater contribution to stability that a methoxy substituent makes, shows the importance of hyperconjugative structures in the former case.

A considerable loss of shielding is also observed going from *tert*-butylbenzene to the *p-tert*-butylphenyl diphenylmethyl cation (10.5 c/s). However, it is not possible to say whether this is purely an inductive effect or involves carbon–carbon hyperconjugation.

The Ring Protons

The effect of the substituents is to increase the shielding of the ring protons as can be seen by comparison with the triphenylmethyl cation (Table II). In the monosubstituted compounds this effect in the substituted ring is partly offset by the presumed greater conjugation it has with the central carbon atom. The result is that the signals from substituted and unsubstituted rings overlap.

The fine structure of the aromatic peaks is shown in Figs. 1–6. Figures 1 and 2 show the spectra of the triphenylmethyl cation at 40 Mc and at 60 Mc respectively and give us some information regarding the distribution of positive charge within the rings.

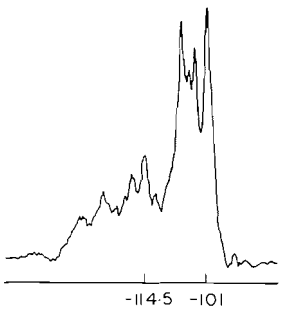

FIG. 1. Spectrum of aromatic protons of the triphenylmethyl cation at 40 Mc.

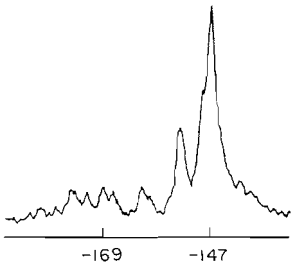

FIG. 2. Spectrum of aromatic protons of the triphenylmethyl cation at 60 Mc.

Resonance theory predicts that the meta protons should be more shielded than either the ortho or para protons in a carbonium ion. (This argument does not apply to molecules like nitrobenzene, for which it has been shown by Corio and Dailey (17) that the ortho hydrogens are least shielded with the meta and para proton peaks superimposed at higher field. The proximity of the latter is reasonable since the Hammett substituent constants (18) for meta and para nitro groups are close, i.e. resonance is of minor importance in nitrobenzene.) The complexity of the triphenylmethyl cation spectrum is due to coupling between aromatic protons and prevents complete identification of the proton signals. The group of peaks at low field however (below 157 c/s), can be assigned to the para protons since they occupy the theoretical value of one fifth of the area of the curve. The meta and ortho proton peaks overlap at higher field. (This agrees with

Can. J. Chem. Downloaded from www.nrcresearchpress.com by 176.9.209.113 on 09/04/12
For personal use only.

S.C.M.O. calculations of π electron densities (19).) This is similar to the N.M.R. spectrum of protonated pentamethylbenzene in which the para substituent is the least shielded (6).

A factor which we will call ortho electrostatic interaction may be important in determining the charge distribution in triarylmethyl cations. The propeller form of the ion will be of lowest energy when the three rings are folded close to one another to enable maximum overlap to occur with the central p orbital. The ortho carbons are very close in this form, however, and electrostatic repulsion between these partially positively charged atoms may be expected to render the para positions relatively more positive.

FIG. 3. Spectrum of aromatic protons of p-tolyl diphenylmethyl cation at 60 Mc.

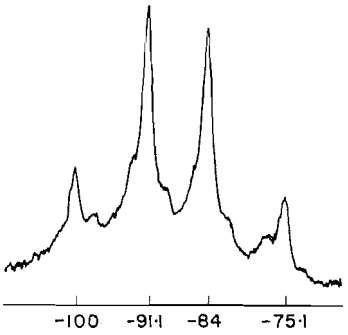

FIG. 4. Spectrum of aromatic protons of tri-p-anisylmethyl cation at 40 Mc.

The spectrum of the mono-para methyl ion (Fig. 3) resembles that of the unsubstituted triphenylmethyl cation with the single peak due to the substituted ring superimposed on the main peak. The peaks at low field are probably due to the para protons in the unsubstituted rings since the area under the peaks below -154 c/s is approximately one seventh of the area under the whole aromatic proton spectrum.

The spectrum of the tri-p-anisylmethyl cation at 40 Mc shows a well-resolved quartet (Fig. 4) due to coupling between ortho and meta positions. Assuming negligible cross ring coupling this quartet may be considered as a superposition of two AB cases in the notation of Bernstein, Pople, and Schneider (20). Using their theory one may calculate the absolute values of the spin-coupling constant, J, and chemical shift, δ, between the ortho and meta protons. J is given directly by the separation of the right- or left-hand pair of lines, which is 8.9 c/s, and the separation of the inner pair of lines (7.1 c/s) is given by $2C-J$ where $C = \frac{1}{2}[\delta^2+J^2]^{\frac{1}{2}}$. This gives a value of $\delta = 13.3$ c/s. Values of J, the ortho coupling constant, found by other authors range from 8.2 c/s to 8.6 c/s (20, 21). This value may also be compared with the value of 8.0 ± 0.5 c/s found for

Can. J. Chem. Downloaded from www.nrcresearchpress.com by 176.9.209.113 on 09/04/12
For personal use only.

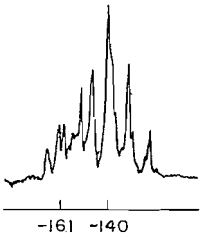

FIG. 5. Spectrum of aromatic protons of *p*-anisyl diphenylmethyl cation at 60 Mc.

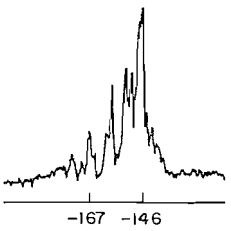

FIG. 6. Spectrum of aromatic protons of *p-tert*-butylphenyl diphenylmethyl cation at 60 Mc.

protonated dianisylethylene in sulphuric acid. In the case of the tri-*p*-tolyl ion, this quartet is not resolved even at 60 Mc, and the aromatic protons give rise to only a single sharp peak.

The spectra of the aromatic protons of the *p*-anisyl diphenylmethyl and *p-tert*-butylphenyl diphenylmethyl cations were recorded at 60 Mc as shown in Figs. 5 and 6. A well-resolved fine structure was observed but no definite assignments could be made.

The meta-methyl-substituted ions illustrate an interesting point. Table II shows that a meta methyl substituent shields the ring protons to a greater extent than does a para methyl substituent. This is because the electron-donating properties of the methyl group function to donate negative charge to the electron-deficient ring but, because of its meta location, it is unable to interact directly by resonance with the central electron-deficient carbon atom.

Di-p-anisylethylene in Sulphuric Acid

The N.M.R. spectrum of 1,1-di-*p*-anisylethylene in sulphuric acid was recorded in connection with other work and its similarity to that of the triarylmethyl cations warrants its being discussed briefly here. The spectrum of the resulting carbonium ion is shown in Fig. 7. Thanks are due to Mr. A. L. Gatzke for the preparation of this compound.

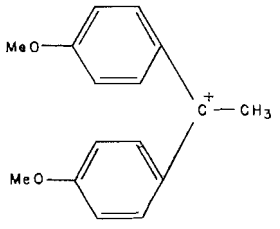

II

Like the tri-*p*-anisylmethyl cation there is a well-resolved quartet due to the coupled ortho and meta protons, the chemical shift between the two halves of the quartet being 32 c/s. The methoxy protons and the methyl protons are at higher field but the high degree of positive charge in the latter, which are in a hyperconjugating position, is reflected in the large shift to low field (−85 c/s) from the cyclohexane marker.

It is of interest to note that the N.M.R. and visible spectra of this compound in trifluoroacetic acid – anhydride solvent is quite different to that in sulphuric acid. Anomalous visible spectra in carboxylic acid solvents for this compound have previously been observed by other workers (8, 22, 23).

Can. J. Chem. Downloaded from www.nrcresearchpress.com by 176.9.209.113 on 09/04/12
For personal use only.

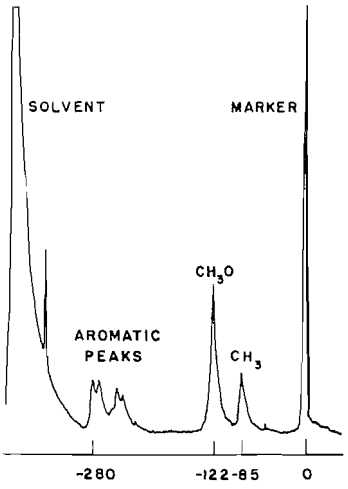

FIG. 7. Spectrum of 1,1-di-*p*-anisylethylene in sulphuric acid at 40 Mc.

ACKNOWLEDGMENTS

The authors wish to thank Dr. K. B. Wiberg and Mr. B. Nist of the University of Washington for allowing us to use their 60-Mc Varian spectrometer. Helpful discussions with Dr. C. Reid are also acknowledged.

Two of us (R.B.M. and T.M.C.) wish to thank the National Research Council for the fellowship and studentship.

REFERENCES

1. DENO, N. C., JARUZELSKI, J. J., and SCHRIESHEIM, A. J. Am. Chem. Soc. **77**, 3044 (1955).
2. SCHUBERT, W. M., ROBINS, J., and HAUN, J. L. J. Am. Chem. Soc. **79**, 910 (1957).
3. DENO, N. C., JARUZELSKI, J. J., and SCHRIESHEIM, A. J. Org. Chem. **19**, 155 (1954).
4. SHARP, D. W. A. and SHEPPARD, N. J. Chem. Soc. 674 (1957).
5. MASON, S. F. *In* Gray, G. W. Steric effects in conjugated systems. Butterworth Scientific Publications, London. 1958. p. 52.
6. MACLEAN, C., VAN DER WAALS, J. H., and MACKOR, E. L. Mol. Phys. **1**, 274 (1958).
7. LETO, J. R., COTTON, F. A., and WAUGH, J. S. Nature, **180**, 978 (1957).
8. GATZKE, A. L. M.Sc. Thesis, University of British Columbia, Vancouver, British Columbia. 1959.
9. WITTIG, G. and CLAUSNIZER, R. Ann. **588**, 145 (1954).
10. MUSTAFA, A., ASKER, W., and HISHMAT, O. H. J. Am. Chem. Soc. **77**, 5127 (1955).
11. BARTLETT, P. D. and JONES, J. E. J. Am. Chem. Soc. **65**, 1837 (1942).
12. BRAND, K., GABEL, W., and ROSENKRANZ, E. Ber. B, **70**, 296 (1937).
13. FABER, A. C. and NAUTA, W. T. Rec. trav. chim. **61**, 469 (1942).
14. MARVEL, C. S., WHITSON, J., and JOHNSTON, H. W. J. Am. Chem. Soc. **66**, 415 (1944).
15. GOMBERG, M. Chem. Revs. **1**, 91 (1924).
16. MARVEL, C. S., MEULLER, M. B., HIMEL, C. M., and KAPLAN, J. F. J. Am. Chem. Soc. **61**, 2771 (1939).
17. CORIO, P. L. and DAILEY, B. P. J. Am. Chem. Soc. **78**, 3043 (1956).
18. HAMMETT, L. P. Physical organic chemistry. McGraw-Hill Book Co., Inc., New York. 1940. p. 184. TAFT, R. W. J. Am. Chem. Soc. **79**, 1045 (1957).
19. POPLE, J. A. J. Phys. Chem. **61**, 6 (1957).
20. BERNSTEIN, H. J., SCHNEIDER, W. G., and POPLE, J. A. Can. J. Chem. **35**, 65 (1957).
21. POPLE, J. A., SCHNEIDER, W. G., and BERNSTEIN, H. J. Can. J. Chem. **35**, 1060 (1957).
22. EVANS, A. G., JONES, N., JONES, P. M. S., and THOMAS, J. H. J. Chem. Soc. 2757 (1956).
23. EVANS, A. G., JONES, P. M. S., and THOMAS, J. H. J. Chem. Soc. 104 (1957).

Can. J. Chem. Downloaded from www.nrcresearchpress.com by 176.9.209.113 on 09/04/12
For personal use only.

Can. J. Chem. Downloaded from www.nrcresearchpress.com by 176.9.209.113 on 09/04/12
For personal use only.

THE SYSTEM Li^+–Na^+–K^+–SO_4^{--} AND WATER, AT 25.0° C[1]

A. N. Campbell and E. M. Kartzmark

ABSTRACT

The above system is a further stage in the study of the five-component system, containing the radicals Li_2, Na_2, K_2, Cl_2, SO_4, and water. The double salts occurring are $Li_2SO_4 \cdot K_2SO_4$ and $3K_2SO_4 \cdot Na_2SO_4$: no ternary salt is formed.

This paper is the fourth instalment of our study of the five-component system containing the radicals Li_2, Na_2, K_2, Cl_2, SO_4, and water, at 25.0° C. So far as we are aware, this is the first complete study which has been made of a five-component system of this type. The work has now been in progress for 4 years: a bibliography is given in references 1 and 2.

According to the Jänecke method of graphic representation the finished study will be represented by a solid model within an equilateral triangular pyramid. All the surfaces of this model have now been studied, the present study being the final one, that of one of the triangular surfaces. It remains only to study the interior of the solid model.

Turning to the present study, the component ternary systems are: (*a*) Li_2SO_4–Na_2SO_4–H_2O; (*b*) Na_2SO_4–K_2SO_4–H_2O; (*c*) Li_2SO_4–K_2SO_4–H_2O. Systems (*a*) and (*c*) have been studied by us and system (*b*) is well known. We have shown (2) that in system (*c*) the double salt $Li_2SO_4 \cdot K_2SO_4$ exists in contact with solution at 25° C, though the solution is not congruently saturating. In system (*a*) no double salt forms (at 25° C) but there is an extensive series of solid solutions of lithium sulphate in sodium sulphate. In system (*b*), the well-known glaserite or Penny's salt ($3K_2SO_4 \cdot Na_2SO_4$) occurs as the end member of a series of solid solutions of potassium sulphate in sodium sulphate.

In the present quaternary system, there is the possibility that ternary salts, containing all three metallic ions, may occur, in addition to the above named double salts, but no such ternary salt has been found.

EXPERIMENTAL

The technique is simple and has been described frequently (1, 2). In previous papers we have referred to the extreme difficulty of determining sulphate radical in the presence of alkalis and we have been forced to such expedients as determining density and viscosity, in order to analyze the systems, procedures which call for extreme experimental accuracy (because of the slight differences in physical property for the different ions), notably in the determination of density. For the present study we turned with relief to the flame photometer as a means of analysis for alkali metals. We used a Beckmann DU instrument with flame photometer attachment. Since this instrument is dependent on constancy of flame intensity, it must be calibrated afresh for each analysis. Standard solutions, containing from 10 to 100 parts per million of lithium sulphate, sodium sulphate, or potassium sulphate, respectively, were made up and preserved in plastic containers. Before each analysis, a curve of instrument reading versus content of given salt was determined experimentally for each salt. The reading for the unknown, in the appropriate region of the spectrum, then gives the salt content in parts per million. Since the unknown always contained the three salts simultaneously present, the possibility existed that

[1]*Manuscript received May 7, 1959.*
Contribution from the Chemistry Department, University of Manitoba, Winnipeg, Manitoba.

TABLE I

Solubilities in the quaternary system at 25° C

Liquid phase in mole %			Nature of solid phase	Moles water/ mole salt
Li_2SO_4	Na_2SO_4	K_2SO_4		
100	—	—	$Li_2SO_4 \cdot H_2O$	17.8
74.6	25.4	—	$Li_2SO_4 \cdot H_2O$ + s.s. of Li_2SO_4 in Na_2SO_4†	13.7
29.0	71.0	—	Na_2SO_4 anhyd. + $Na_2SO_4 \cdot 10H_2O$	18.0
—	100	—	$Na_2SO_4 \cdot 10H_2O$	28.4
95.0	—	5.0	$Li_2SO_4 \cdot H_2O$ + $Li_2SO_4 \cdot K_2SO_4$	15.4
63.0	—	37.0	$Li_2SO_4 \cdot K_2SO_4$ + K_2SO_4	27.5
—*	—	100	K_2SO_4	80.8
—*	77.3	22.7	$Na_2SO_4 \cdot 10H_2O$ + $Na_2SO_4 \cdot 3K_2SO_4$	22.4
—*	37.5	62.5	K_2SO_4 + $Na_2SO_4 \cdot 3K_2SO_4$	44.4
77.0	21.0	2.0	$Li_2SO_4 \cdot H_2O$ + s.s. of Li_2SO_4 in Na_2SO_4	15.8
88.5	4.5	7.0	$Li_2SO_4 \cdot H_2O$ + $Li_2SO_4 \cdot K_2SO_4$	16.1
85.0	10.0	5.0	$Li_2SO_4 \cdot H_2O$ + $Li_2SO_4 \cdot K_2SO_4$ + s.s. of Li_2SO_4 in Na_2SO_4	15.7
83.0	12.0	5.0	$Li_2SO_4 \cdot H_2O$ + s.s. of Li_2SO_4 in Na_2SO_4	16.5
84.9	9.1	6.0	$Li_2SO_4 \cdot H_2O$ + $Li_2SO_4 \cdot K_2SO_4$	16.0
17.2	71.9	10.9	Na_2SO_4 anhyd. + $Na_2SO_4 \cdot 10H_2O$	17.1
13.0	72.5	14.5	Na_2SO_4 anhyd. + $Na_2SO_4 \cdot 10H_2O$ + $Na_2SO_4 \cdot 3K_2SO_4$	18.9
11.7	73.5	14.8	$Na_2SO_4 \cdot 10H_2O$ + $Na_2SO_4 \cdot 3K_2SO_4$	17.7
27.8	58.7	13.5	Na_2SO_4 anhyd. + $Na_2SO_4 \cdot 3K_2SO_4$	15.6
49.5	20.1	30.4	$Li_2SO_4 \cdot K_2SO_4$ + K_2SO_4	23.0
47.3	22.1	30.7	$Na_2SO_4 \cdot 3K_2SO_4$ + $Li_2SO_4 \cdot K_2SO_4$ + K_2SO_4	22.5
27.0	26.0	47.0	$Na_2SO_4 \cdot 3K_2SO_4$ + K_2SO_4	34.2
44.0	21.0	35.0	$Na_2SO_4 \cdot 3K_2SO_4$ + K_2SO_4	25.7
46.0	26.0	28.0	$Na_2SO_4 \cdot 3K_2SO_4$ + $Li_2SO_4 \cdot K_2SO_4$	22.2
29.8	56.8	13.4	Na_2SO_4 anhyd. + $Na_2SO_4 \cdot 3K_2SO_4$	15.1
48.0	46.0	6.0	s.s. of Li_2SO_4 in Na_2SO_4 + $Li_2SO_4 \cdot K_2SO_4$	16.0
53.0	42.0	5.0	s.s. of Li_2SO_4 in Na_2SO_4 + $Li_2SO_4 \cdot K_2SO_4$	16.5
67.0	27.0	6.0	s.s. of Li_2SO_4 in Na_2SO_4 + $Li_2SO_4 \cdot K_2SO_4$	16.7
45.0	32.0	23.0	$Li_2SO_4 \cdot K_2SO_4$ + $Na_2SO_4 \cdot 3K_2SO_4$	19.2
44.0	37.0	19.0	$Li_2SO_4 \cdot K_2SO_4$ + $Na_2SO_4 \cdot 3K_2SO_4$	17.6
42.0	43.0	15.0	$Li_2SO_4 \cdot K_2SO_4$ + $Na_2SO_4 \cdot 3K_2SO_4$	17.2
38.0	53.0	9.0	Na_2SO_4 anhyd. + $Li_2SO_4 \cdot K_2SO_4$ + $Na_2SO_4 \cdot 3K_2SO_4$	16.9

*Reference 3.
†s.s. = solid solution.

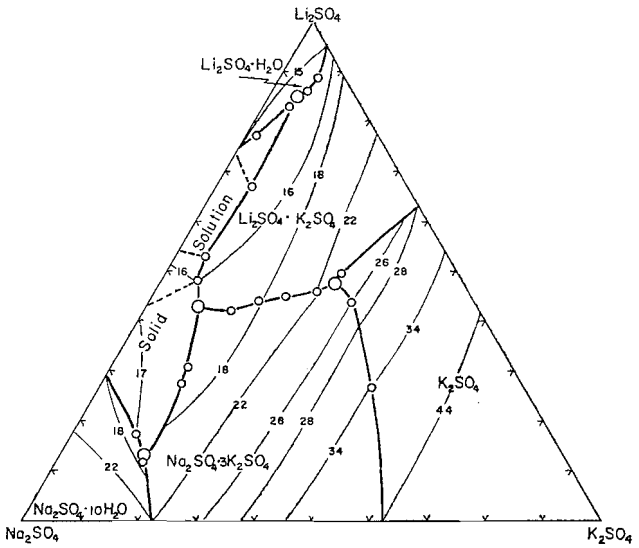

FIG. 1.

Can. J. Chem. Downloaded from www.nrcresearchpress.com by 176.9.209.113 on 09/04/12
For personal use only.

one salt might interfere with another, but we convinced ourselves by the analysis of numerous mixtures of known composition that this was not so here. The accuracy is not high, $\pm 1\%$ at best, but, within these limits, the results are completely dependable. In a study which involved the Schreinemakers' method of the "wet rest", this accuracy would scarcely be good enough but it was sufficient for the present study.

RESULTS

The numerical results are given in Table I and represented graphically in Fig. 1. The isohydrores (lines of equal water content) are of necessity, as in all such studies, to some extent hypothetical, at least in their curvature, but such curves are most instructive in evaporation studies.

DISCUSSION

The dotted lines in the area marked "solid solution" (which would normally be the area of anhydrous sodium sulphate) give a rough indication of the composition of the solid phase (solid solution of sodium sulphate in lithium sulphate). Figure 1 also shows the absence of any ternary salt; all the solid phases are to be found already in the component ternary systems. The main areas of the equilibrium diagram are those of K_2SO_4, $K_2SO_4 \cdot Li_2SO_4$, and $3K_2SO_4 \cdot Na_2SO_4$.

REFERENCES

1. CAMPBELL, A. N. and KARTZMARK, E. M. Can. J. Chem. **34**, 672 (1956). CAMPBELL, A. N. KARTZMARK, E. M., and LOVERING, E. G. Can. J. Chem. **36**, 1511 (1958).
2. CAMPBELL, A. N. and KARTZMARK, E. M. Can. J. Chem. **36**, 171 (1958).
3. HAMID M. A. J. Chem. Soc. 199 (1926).

Can. J. Chem. Downloaded from www.nrcresearchpress.com by 176.9.209.113 on 09/04/12
For personal use only.

Can. J. Chem. Downloaded from www.nrcresearchpress.com by 176.9.209.113 on 09/04/12
For personal use only.

THE REACTION OF SULPHURYL CHLORIDE WITH GLYCOSIDES AND SUGAR ALCOHOLS. PART I[1]

P. D. Bragg, J. K. N. Jones, and J. C. Turner

ABSTRACT

The reaction of sulphuryl chloride with methyl α-D-glucopyranoside, methyl 4,6-*O*-benzylidene-α-D-glucoside, methyl β-D-arabinopyranoside, D-mannitol, 2,5-*O*-methylene-D-mannitol, dulcitol, and sucrose is described.

INTRODUCTION

Helferich and his co-workers in a series of papers (1, 2, 3) described the action of sulphuryl chloride on methyl α- and methyl β-D-glucopyranoside, mannitol, and trehalose. They isolated crystalline products in which the hydroxyl groups had either been replaced by chlorine atoms or bridged by cyclic sulphate groups. The compound derived from methyl α-D-glucopyranoside was shown to contain 2 chlorine atoms and a cyclic sulphate group (1). The cyclic sulphate ring could be opened by treatment with base, and the sulphate group so formed hydrolyzed with hydrochloric or sulphuric acid to yield a dichloro-dideoxy hexose (2).

In the present work, this reaction was applied to glycosides and hexitols, and an attempt was made to determine the structure of the desulphated chloro-sugars.

The dichloro-dideoxy hexose from methyl α-D-glucopyranoside was prepared by Helferich's method (1). On periodate oxidation this compound (I) in 24 hours consumed 2 moles periodate and liberated 2 moles of formic acid.

Although all the periodate was consumed rapidly the second molecule of acid was liberated more slowly suggesting that hydrolysis of the formyl ester (II) was occurring. These results are only consistent with I being 4,6-dichloro-4,6-dideoxy hexose. Periodate oxidation of the methyl glycoside of I (0.87 mole periodate; 26 hours) substantiated this conclusion. Helferich had previously suggested that 1 chlorine atom was at $C_{(6)}$ because of the ease with which it could be removed by alkali (3).

The dichloro-dideoxy hexose was reduced with potassium borohydride. The dichloro-dideoxy hexitol was obtained as an impure syrup which rapidly consumed 1.56 moles periodate liberating 0.73 mole formic acid and formaldehyde (not estimated), which is only consistent with the assignment of chlorine atoms to $C_{(4)}$ and $C_{(6)}$.

The structure of the original compound is therefore probably methyl 4,6-dichloro-4,6-dideoxy-α-D-hexoside 2,3-sulphate. The elimination of the hydroxyl group at $C_{(4)}$ by the chlorine atom might occur with inversion of configuration to give the D-galactose configuration. This problem is now under investigation. The presence of a 2,3-sulphate

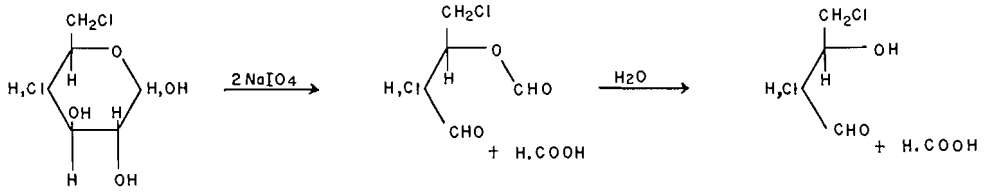

I II

[1]*Manuscript received October 27, 1958.*
Contribution from the Department of Chemistry, Queen's University, Kingston, Ontario.

group was also suggested by the isolation of an analogous methyl 4,6-*O*-benzylidene-α-D-glucoside 2,3-sulphate by the action of sulphuryl chloride on methyl 4,6-*O*-benzylidene-α-D-glucoside.

Hydrolysis of the cyclic sulphate derivative eliminated the methyl glycoside and benzylidene groups and gave glucose only, showing that removal of the sulphate group occurred without inversion of the hydroxyl groups on $C_{(2)}$ and $C_{(3)}$ unless the initial formation of the cyclic ester had also resulted in inversion.

Methyl β-D-arabinopyranoside was converted by sulphuryl chloride to a methyl monochloro-monodeoxy pentoside cyclic sulphate which could be desulphated to yield a monochloro-monodeoxy pentose. The results of periodate oxidation (2 moles periodate consumed with the liberation of 2 moles acid) indicated that the chlorine atom was located on $C_{(4)}$. Periodate oxidation (1.1 moles; 26 hours) of the methyl α-glycoside confirmed this. The monochloro-monodeoxy pentose gave a *p*-nitrophenylosazone without loss of chlorine showing that the chlorine atom was not on $C_{(1)}$ or $C_{(2)}$ of the pentose. The very probable structure of the original compound would therefore be methyl 4-chloro-4-deoxy-β-pentoside 2,3-sulphate.

Both dulcitol and D-mannitol readily give crystalline compounds with sulphuryl chloride and in both cases 4 chlorine atoms and a cyclic sulphate group are introduced. 2,5-*O*-Methylene-D-mannitol gave a trichloro-trideoxy-mono-*O*-methylene hexitol.

The cyclic sulphate ester of the mannitol derivative is very resistant to acid hydrolysis. Very little acetolysis of this compound occurred at 25° C, but appreciable hydrolysis of the sulphate group followed by acetylation occurred at 100° C. Deacetylation of the product then yielded a substance (contaminated with starting material) with a chromatographic mobility consistent with that of a tetrachloro-tetradeoxy hexitol. The impure product consumed 0.77 mole periodate (46 hours) suggesting that the sulphate group in the original compound bridged adjacent hydroxyl groups (presumably on $C_{(3)}$–$C_{(4)}$).

Sucrose yielded a product which appeared to be a mixture of di- and tri-chlorodeoxy sucrose disulphates. The structure of the glucose moiety is similar to that from methyl α-D-glucopyranoside since the same 4,6-dichloro-4,6-dideoxy hexose can be obtained from both. The remaining cyclic sulphate group and chlorine atom are located on the fructose portion of the molecule. The position of these groups was not determined since the vigorous conditions of hydrolysis necessary to cleave the interglycosidic linkage destroyed the fructose moiety, but it is probable by comparison with the anhydrides of sucrose (4), that the sulphate group spans $C_{(3')}$–$C_{(6')}$ or $C_{(1')}$–$C_{(4')}$ with the chlorine atom on $C_{(1')}$ or $C_{(6')}$ respectively.

EXPERIMENTAL

Melting points are uncorrected and were determined on a Kofler microheating stage. Optical rotations were measured at 24° C. All evaporations were carried out under reduced pressure.

General Method

Redistilled sulphuryl chloride (7 ml) was added to a mixture of pyridine (30 ml) and chloroform (100 ml), which had been dried over potassium hydroxide pellets and anhydrous sodium sulphate respectively. The temperature of the solution was maintained at 5° C while the glycoside or hexitol (4 g; dried over phosphoric oxide) was added with vigorous stirring. After 2 hours the reaction mixture was poured into ice water and the chloroform layer separated, well washed with water, and dried (sodium hydrogen carbonate). Concentration afforded a syrup which was decolorized with charcoal if

Can. J. Chem. Downloaded from www.nrcresearchpress.com by 176.9.209.113 on 09/04/12
For personal use only.

necessary. Crystallization was spontaneous, but purification by extracting the product into ether was sometimes imperative.

Methyl α-D-Glucopyranoside

With sulphuryl chloride, methyl α-D-glucopyranoside gave long colorless needles (1.8 g) which, recrystallized from ether – light petroleum (40–60° C), had m.p. 104–105° C, $[\alpha]_D$ +140° (*c*, 1.99 in methanol). Analysis: Calc. for $C_7H_{10}O_6Cl_2S$: C, 28.7%, H, 3.4%; Cl, 24.2%; S, 10.9%. Found: C, 28.9%; H, 3.4%; Cl, 24.1%; S, 11.1%.

Methyl Dichloro-dideoxy Hexoside and Dichloro-dideoxy Hexose

The above compound (1.8 g) dissolved in methanol saturated with ammonia at 0° C (50 ml) was kept at room temperature for 24 hours. Concentration gave a partially crystalline syrup which was heated at 100° C for 14 hours with *N* sulphuric acid (50 ml). The acid was neutralized with barium carbonate and the solution deionized by passage through Amberlite IR-120 and Duolite A4 resin columns. The eluate was concentrated to a syrup (0.74 g) which slowly crystallized. An aqueous solution of the syrup was continuously extracted with chloroform. The chloroform extract on evaporation yielded crystals, m.p. 158° C, $[\alpha]_D$ +184° (*c*, 2.1 in water). Analysis: Calc. for $C_7H_{12}O_4Cl_2$: C, 36.3%; H, 5.2%; Cl, 30.7%. Found: C, 36.2%; H, 5.3%; Cl, 31.0%. On concentration of the aqueous solution white needle-shaped crystals were obtained. Recrystallized from ethanol–water, the dichloro-dideoxy hexose had m.p. 183–186° C (decomp.), $[\alpha]_D$ +132° (5 minutes) → 98° (equilibrium; 24 hours) (*c*, 0.69 in methanol). Analysis: Calc. for $C_6H_{10}O_4Cl_2$: C, 33.2%; H, 4.6%. Found: C, 33.6%; H, 4.7%.

The dichloro-dideoxy hexose (115 mg) was reduced for 1 hour with potassium borohydride (365 mg) in water (50 ml). Excess borohydride was destroyed with acetic acid, and after deionization with resin, the major component (R_f 0.56) *n*-butanol:ethanol:water = 3:1:1 was separated as a syrup (47 mg) on paper chromatograms, $[\alpha]_D$ 0° (*c*, 1.0 in water).

Methyl β-D-Arabinoside

Methyl β-D-arabinoside and sulphuryl chloride yielded colorless needles (1.6 g) which, recrystallized from ether – light petroleum (80–100° C), had m.p. 108.5° C, $[\alpha]_D$ −89° (*c*, 0.97 in methanol). Analysis: Calc. for $C_6H_9O_6SCl$: S, 13.1%; Cl, 14.5%. Found: S, 13.3%; Cl, 14.1%.

Methyl Monochloro-monodeoxy Pentoside and Monochloro-monodeoxy Pentose

Both were prepared from the compound derived from methyl β-D-arabinoside by treatment with methanolic ammonia followed by sulphuric acid as described above. The methyl pentoside crystallized as white needles which after recrystallization from ether – light petroleum (b.p. 60–80° C) had m.p. 102–104° C, $[\alpha]_D$ +119° (*c*, 2.25 in water). Analysis: Calc. for $C_6H_{11}O_4Cl$: C, 39.5%; H, 6.0%; Cl, 19.5%. Found: C, 39.6%; H, 6.2%; Cl, 19.8%. Monochloro-monodeoxy pentose had m.p. 128–131° C, $[\alpha]_D$ +57° (10 minutes) → 0° (equilibrium, 6 hours) (*c*, 0.98 in methanol). Analysis: Calc. for $C_5H_9O_4Cl$: C, 35.6%; H, 5.3%. Found: C, 35.8%; H, 5.8%.

The product (95 mg) in 50% acetic acid (2 ml) was added to *p*-nitrophenylhydrazine (0.3 g) in glacial acetic acid (2 ml) and heated at 100° C for 1 hour. Crystals of the *p*-nitrophenylosazone were precipitated. After they were washed with water and ether, they had m.p. 224° C. Analysis: Calc. for $C_{17}H_{17}O_6N_6Cl$: N, 13.7%; Cl, 8.7%. Found: N, 11.7%; Cl, 7.1%.

Methyl 4,6-O-Benzylidene-α-D-glucopyranoside

This reacted with sulphuryl chloride to give long colorless needles (2 g) which slowly darkened over a period of days with liberation of benzaldehyde. When recrystallized

Can. J. Chem. Downloaded from www.nrcresearchpress.com by 176.9.209.113 on 09/04/12
For personal use only.

Can. J. Chem. Downloaded from www.nrcresearchpress.com by 176.9.209.113 on 09/04/12
For personal use only.

from chloroform – light petroleum it had m.p. 107° C (decomp.). A sodium fusion showed chlorine to be absent from the molecule. Analysis: Calc. for $C_{14}H_{16}O_8S$: S, 9.3%. Found: S, 9.0%. Treatment first with methanolic ammonia and then with sulphuric acid gave chromatographically homogeneous glucose which was characterized as its *p*-nitroanilide derivative, m.p. 186° C, $[\alpha]_D$ +192° (*c*, 0.85 in water).

D-*Mannitol*

With sulphuryl chloride, D-mannitol afforded needle-shaped crystals (1.5 g) which when recrystallized from chloroform – light petroleum had m.p. 105° C, $[\alpha]_D$ +88° (*c*, 2.84 in methanol). Analysis: Calc. for $C_6H_8O_4Cl_4S$: C, 22.6%; H, 2.5%; Cl, 44.7%; S, 10.0%. Found: C, 22.8%; H, 2.8%; Cl, 44.3%; S, 10.4%.

The compound (4.2 g) was heated at 95–100° C for $2\frac{1}{2}$ hours in acetic anhydride (30 ml) and sulphuric acid (1.5 ml). The dark brown solution was poured into ice water, which was then extracted with chloroform. The chloroform extract was washed with an aqueous sodium hydrogen carbonate solution, dried (anhydrous magnesium sulphate), and was concentrated to a syrup. Following decolorization with charcoal, the syrup was deacetylated with sodium methoxide at 5° C. Excess sodium methoxide was removed with carbon dioxide, and after dilution with water, the solution was continuously extracted with ether. Concentration of the ether extract afforded a syrup (0.9 g) which gave a single spot (R_f 0.79) with the periodate–anisidine spray (5) on chromatography in butan-1-ol:ethanol:water (3:1:1) solvent.

Mono-anhydro-trichloro-trideoxy Hexitol

The compound (2.7 g) obtained from mannitol was treated with methanolic ammonia and with sulphuric acid, as previously described, to yield colorless needles (0.6 g) m.p. 102° C, $[\alpha]_D$ 0° (*c*, 0.86 in methanol). Analysis: Calc. for $C_6H_9O_2Cl_3$: C, 32.8%; H, 4.1%; Cl, 48.5%. Found: C, 33.0%; H, 4.1%; Cl, 46.2%.

*2,5-O-Methylene-*D*-mannitol*

2,5-*O*-Methylene-D-mannitol and sulphuryl chloride yielded a crystalline product (1.1 g); when recrystallized from ethanol–water it had m.p. 116° C and $[\alpha]_D$ −42° (*c*, 1.73 in methanol). Analysis: Calc. for $C_7H_{11}O_3Cl_3$: C, 33.6%; H, 4.4%; Cl, 42.7%. Found: C, 33.7%; H, 4.3%; Cl, 42.9%. In the infrared a hydroxyl peak was obtained. The methylene group was not removed by treatment with *N*-sulphuric acid at 100° C for 5 hours.

Dulcitol

Dulcitol and sulphuryl chloride gave a crystalline product (1.4 g) m.p. 116° C. Analysis: Calc. for $C_6H_8O_4Cl_4S$: C, 22.6%; H, 2.5%; Cl, 44.7%; S, 10.0%. Found: C, 22.6%; H, 2.7%; Cl, 44.3%; S, 10.4%.

Sucrose

Sucrose (4 g) was dissolved in pyridine (80 ml) at the boiling point and the solution then cooled to 5° C. Chloroform (90 ml) was added and the slight precipitate produced was redissolved by the further addition of pyridine (10 ml). Sulphuryl chloride (7 ml) was added dropwise with stirring to the cooled solution (5° C). After 2 hours the liquid was poured into ice water, the chloroform layer washed with water and dried (magnesium sulphate). Concentration gave a syrup (2.9 g), and from a chloroform solution of this the product was precipitated by ether as a pale yellow solid, m.p. 94–99° C. Analysis: Calc. for $C_{12}H_{16}O_{13}S_2Cl_2$: S, 12.7%; Cl, 14.1%. Calc. for $C_{12}H_{15}O_{12}S_2Cl_3$: S, 12.3%; Cl, 20.4%. Found: S, 12.4%; Cl, 16.8%.

Hydrolysis (*N* sulphuric acid, 24 hours) gave a complex mixture of substances but mainly 4,6-dichloro-4,6-dideoxy hexose identical with that derived from methyl α-D-

glucoside. After separation on a cellulose column using *n*-butanol:water (19:1) it had m.p. and mixed m.p. 186° C (decomp.). Calc. for $C_6H_{10}O_4Cl_2$: C, 33.2%; H, 4.6%; Cl, 32.7%. Found: C, 33.4%; H, 4.7%; Cl, 32.6%.

Compounds reacting with the resorcinol spray (ketoses) (6) were largely absent from the hydrolysis mixture.

TABLE I

Substance	Time of oxidation (hours)	Consumption of periodate (mole/molecule)	Acid production (mole/molecule)
Methyl dichloro-dideoxy hexoside	1.08	0.16	
	20	0.79	0.00
	26	0.87	
	43	1.13	0.00
Dichloro-dideoxy hexose	1	1.40	1.14
	4	2.05	1.89
	7	2.05	2.01
	24	2.09	1.96
Dichloro-dideoxy hexitol	1	1.49	
	5	1.56	0.73
	24	1.56	0.73
Methyl monochloro-monodeoxy pentoside	1.08	0.15	
	20	1.01	0.00
	26	1.10	
	43	1.22	0.00
Monochloro-monodeoxy pentose	1	1.62	1.09
	4	1.87	1.42
	7	1.87	1.42
	24	1.93	1.72
Tetrachloro-tetradeoxy hexitol	1	0.46	
	4	0.52	
	23	0.67	0.00
	46	0.77	0.00

Periodate Oxidation of Chloro-sugars

About 25 mg of the substance, accurately weighed, was dissolved in water (50 ml) and 0.3 *M* sodium metaperiodate (2 ml) added. Aliquots were removed at intervals and the consumption of periodate and the production of formic acid measured (7, 8). Dichloro-dideoxy hexitol gave formaldehyde (characterized as the dimedone complex, m.p. 188° C) (9) on periodate oxidation.

Mono-anhydro-trichloro-trideoxy hexitol was not attacked by periodate.

ACKNOWLEDGMENT

Part of this work was supported by the Sugar Research Foundation, Inc., to whom the authors wish to express their thanks.

REFERENCES

1. HELFERICH, B. Ber. **54**, 1082 (1921).
2. HELFERICH, B., LÖWA, A., NIPPE, W., and RIEDEL, H. Ber. **56**, 1083 (1923).
3. HELFERICH, B., SPROEK, G., and BESLER, E. Ber. **58**, 886 (1925).
4. LEMIEUX, R. U. and BARRETTE, J. P. J. Am. Chem. Soc. **80**, 2243 (1958).
5. BRAGG, P. D. and HOUGH, L. J. Chem. Soc. 4050 (1958).
6. HOUGH, L., JONES, J. K. N., and WADMAN, W. H. J. Chem. Soc. 796 (1952).
7. NEUMÜLLER, G. and VASSEUR, E. Arkiv Kemi, **5**, 235 (1953).
8. ANDERSON, D. M. W., GREENWOOD, C. T., and HIRST, E. L. J. Chem. Soc. 225 (1955).
9. BELL, D. J. J. Chem. Soc. 994 (1948).

Can. J. Chem. Downloaded from www.nrcresearchpress.com by 176.9.209.113 on 09/04/12
For personal use only.

Can. J. Chem. Downloaded from www.nrcresearchpress.com by 176.9.209.113 on 09/04/12
For personal use only.

REACTIONS OF BUTENES AND METHYL BUTENES ON A ZINC OXIDE CATALYST[1]

M. G. HAMPTON[2] AND R. J. CVETANOVIĆ

ABSTRACT

Reactions of butene-1, isobutene, 3-methyl butene-1, and 2-methyl butene-2 on ZnO catalysts have been investigated at 615°. The formation of the observed products is discussed in terms of a sequence of surface processes incorporating dissociation of the bonds in β position to the double bond, with formation of chemisorbed allyl and substituted allyl radicals.

INTRODUCTION

A study of dehydrogenation of butene-1 on semiconducting oxide catalysts between 500 and 650° has been conducted recently in this laboratory (1). The activity and selectivity to butadiene formation of "valency-controlled" ZnO and NiO catalysts were discussed in terms of their electrical properties. Thus, after it was doped with lithia, zinc oxide became inactive, while the catalysts with small additions of gallia, although showing the same activity as pure zinc oxide, were distinctly more selective. An explanation was suggested by assuming an important role in these reactions of "excess" electrons in the *n*-type semiconductors.

The present work has been carried out in an attempt to obtain further information on the mechanism of dehydrogenation on zinc oxide catalysts from a comparative study of the reactions of several structurally related olefins. Zinc oxide containing 1 atom % Ga^{+++} in the lattice was used because of its somewhat greater selectivity (1). The reactions were carried out at 615°.

EXPERIMENTAL

The apparatus used is illustrated in Fig. 1. It consisted of a reactor, circulating pump, boiler, and storage lines. The reactor consisted of a silica tube connected to the rest of the apparatus by pyrex–silica graded seals. The catalyst pellets were placed in a silica spoon as shown. Two leads through tungsten–glass seals were provided for conductivity measurements. Larger flat pellets containing Pt-foil leads were used for conductivity determinations by means of an a-c. bridge. In most of the work small cylindrical pellets of the catalyst ($\frac{1}{8}$ in. × $\frac{1}{8}$ in. × $\frac{1}{8}$ in.) were used. A 14/30 standard joint facilitated catalyst removal and changing. The temperature of the furnace round the reactor was controlled by a chromel–alumel thermocouple placed in a well in the silica tube.

The olefins were introduced to the evacuated 2-liter flask, then mixed with nitrogen to give a total pressure of about 760 mm Hg. The ratio of the olefin to nitrogen was about 1:12 in all experiments. Nitrogen was also let into the reactor system, so that with the water in the boiler boiling vigorously, the total pressure in the reactor section was also about 760 mm. The stopcocks isolating the 2-liter volume from the reaction system could then be opened, and the gases circulated continuously using a reciprocating plunger pump as described by Watson (2). The pumping rate and the volume of the reaction system were such that the gas phase was circulated once in just over 2 minutes. Average run duration was about 30 to 40 minutes, with occasional runs up to 90 minutes. During a run samples of the gas phase were withdrawn at intervals into 50-ml receiving bulbs, and the condensable content frozen out with liquid nitrogen. The permanent

[1]*Manuscript received May 14, 1959.*
Contribution from the Division of Applied Chemistry, National Research Council, Ottawa, Canada. Issued as N.R.C. No. 5281.
[2]*National Research Council Postdoctorate Fellow 1956–57.*

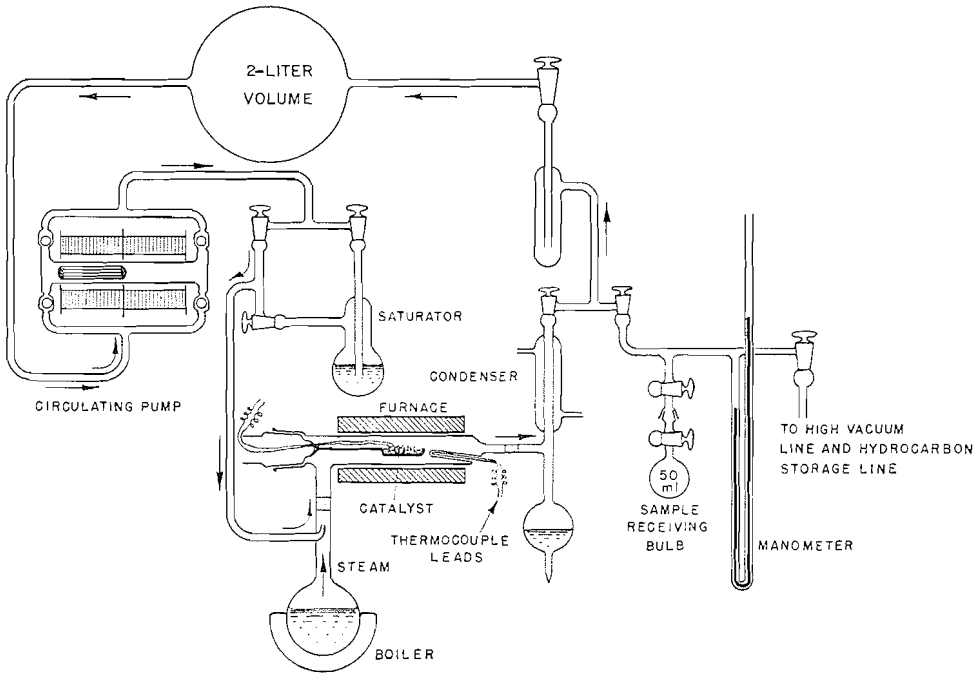

FIG. 1. Diagram of the apparatus.

gases were then pumped away, and the residual samples analyzed by means of a mass spectrometer. Analyses for H_2 and CH_4 in the large excess of non-condensable gas were as a rule not made. To distinguish between certain isomers in the products, gas chromatographic analysis was sometimes used.

Research grade olefins were employed.

RESULTS

Reactions of the following olefins were investigated: butene-1, isobutene, 3-methyl butene-1, and 2-methyl butene-2.

Butene-1

Butene-1 undergoes extensive dehydrogenation, the main products being C_4H_6, C_3H_6, and C_2H_4 in the approximate ratio 2:2:1. The production of butadiene is favored by the presence of moisture, which suppresses side reactions rather than aiding dehydrogenation directly. The results are summarized in Table I. The average dehydrogenation selectivity is about 40% for about 40% decomposition of butene-1.

Isobutene

Isobutene undergoes practically no decomposition and no butadiene is formed. This indicates that no isomerization of the carbon skeleton of the molecule occurs.

3-Methyl Butene-1

3-Methyl butene-1 is very reactive, the main products being C_4H_8 and C_4H_6 in the presence of moisture, that is, the loss of a methyl group is the main reaction. In the presence of oxygen, added to the gas stream, C_5H_8 was the main product, much less C_4H_6 being produced. The presence of oxygen however slowed down the over-all decomposition rate. The results are summarized in Table II.

Can. J. Chem. Downloaded from www.nrcresearchpress.com by 176.9.209.113 on 09/04/12
For personal use only.

TABLE I

Dehydrogenation and decomposition of butene-1

Diluting gas	% Reaction* (after 22 min)	Dehydrogenation selectivity, %	Main products†			Catalyst
			Butadiene	Propylene	Ethylene	
Moist N_2	43.4	44.5	14.5	16.0	7.8	ZnO + 1% Ga
Steam + N_2	41.0	41.4	14.8	16.7	7.6	ZnO + 1% Ga
Moist N_2 + 27 mm O_2	40.0	39.0	12.2	12.2	7.9	ZnO + 1% Ga
Dry N_2	62.9	29.6	13.0	21.7	20.0	ZnO + 1% Ga
Steam + N_2	26.0	23.5	5.5	12.3	4.3	Zn metal
Dry N_2	54.1	22.0	11.0	19.6	15.4	Zn metal

*Isomerization is not taken into account in evaluating % reaction.
†Expressed as percentages of the total carbon in the products.

2-Methyl Butene-2

2-Methyl butene-2 produces mainly C_5H_8 and C_4H_8 with only very small amounts of C_4H_6. The results are summarized in Table II. The results show that double-bond isomerization to give 3-methyl butene-1 does not occur, otherwise the products of decomposition of the latter hydrocarbon would also be found. This was confirmed by gas chromatographic analysis.

TABLE II

Dehydrogenation and decomposition of 3-methyl butene-1 and 2-methyl butene-2 on ZnO + 1% Ga

Olefin	Diluting gas	% Reaction* (after 22 min)	Dehydrogenation selectivity, %	Main products†				
				C_5H_8	C_4H_8	C_4H_6	C_3H_6	C_2H_4
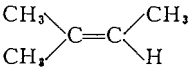	Steam + N_2	30.0	48.0	13.1	9.4	1.1	3.0	3.0
(2-Methyl butene-2)	Steam + N_2 + 44 mm O_2	42.5	41.2	12.6	8.4	—	9.4	—
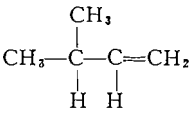	Steam + N_2	82.8	9.7	5.0	9.0	21.0	11.5	21.5
(3-Methyl butene-1)	Steam + N_2 + 29 mm O_2	56.0	22.1	12.4	10.0	10.2	8.4	8.4

*Isomerization is not taken into account in evaluating % reaction.
†Expressed as percentages of the total carbon in the products.

As the amount of butadiene produced by the decomposition of 2-methyl butene-2 was very small even after about 20 recycles, it appeared that the butene produced in this reaction was mainly the unreactive isobutene. Gas chromatographic analysis of the C_4H_8 fraction showed that the butene consisted of 75% isobutene, 25% *trans*-butene-2, and no *cis*-butene-2 or butene-1.

DISCUSSION

The processes studied in the present work involve dissociation of C—H and C—C bonds at the surface of the catalyst. In general C—C bonds in hydrocarbons are considerably weaker than C—H bonds and this factor alone would favor cracking over dehydrogenation. Selectivity to dehydrogenation is in general determined by the ability of a particular catalyst to dissociate preferentially the C—H bonds. This in general

Can. J. Chem. Downloaded from www.nrcresearchpress.com by 176.9.209.113 on 09/04/12
For personal use only.

depends not only on the properties of the catalyst but also on the reaction conditions, such as temperature, contact time, etc. The present experiments were carried out at a single temperature and under conditions which might have favored the cracking processes and somewhat exaggerated their importance. Thus, over a period of time there was some accumulation of metallic zinc on the colder parts of the reaction vessel. For these reasons some of the results were independently checked (3) under similar conditions but with certain additional precautions. The ratio of the dead volume to the catalyst volume in the reaction zone was also reduced. Some differences were observed, particularly a tendency for reduction of cracking relative to dehydrogenation. In the case of 2-methyl butene-2, for example, only isoprene and 2-methyl butene-1 were formed. The main features of the reactions, however, remained very similar. The present results will, therefore, be discussed as obtained under the particular experimental conditions employed. Further study of these processes on the same and some other catalysts at various temperatures is in progress.

The reactions of the individual olefins studied show some characteristic differences. It is known from infrared studies of chemisorbed olefinic hydrocarbons (4) that there are under certain conditions and on some metals at least three and perhaps more than three points of contact (with the necessary corresponding dissociative chemisorption of hydrogen atoms). On hydrogenation–dehydrogenation catalysts the processes of dissociative and associative chemisorption, dehydrogenation and hydrogenation, and of desorption with isomerization or polymerization, are closely related. The predominance of one or the other of these processes depends on the surface concentrations of adsorbed species (in particular that of hydrogen) and on the rates of their formation by adsorption and of their mutual interactions and desorption, both of which are functions of temperature and the nature of the catalyst. The extent of dissociative "stripping" of hydrogen atoms and of the number of contacts with the surface may, therefore, vary widely with the conditions. The kinetic differences observed in the present work should be contrasted with the identical infrared spectra of chemisorbed isomeric *n*-hexenes (4). The adsorbed complexes in the case of 3-methyl butene-1 and 3-methyl butene-2, for example, cannot be identical under conditions of the present work.

In order to explain in a consistent manner the products of dehydrogenation and isomerization observed in the present work a sequence of dissociative processes, following energetically favorable paths, is postulated. This incorporates dissociative chemisorption of the weak C—C and C—H bonds in β position to the double bonds. On the present catalyst at 615° C the weaker β C—C bonds appear to be broken more readily than the stronger β C—H bonds, although this may vary with the type of catalyst used and the temperature. Thus, in the case of butene-1 the breakage of β C—H and β C—C bonds may lead to the formation of butadiene and propylene, respectively. These two compounds are formed in approximately equal amounts in spite of the fact that there are two β C—H bonds and only one β C—C bond indicating that the latter break more readily. In 3-methyl butene-1 there are two β C—C bonds and only one β C—H bond and the reaction involves predominantly cracking to lower hydrocarbons, with butadiene as the main product. The presence of two weak β C—C bonds also explains the high reactivity of this compound. On the other hand, 2-methyl butene-2 possesses no β C—C bonds but only the stronger β C—H bonds, and is consequently much less reactive and direct dehydrogenation is the main reaction. The very low reactivity of isobutene can be partly explained in the same manner, but the main factor appears to be that a conjugated system of double bonds to form C_4H_6 is impossible without rearrangement to a straight chain carbon skeleton. As a result any dissociative chemisorption is eventually

Can. J. Chem. Downloaded from www.nrcresearchpress.com by 176.9.209.113 on 09/04/12
For personal use only.

followed by recombination with the initially dissociated H atoms to regenerate isobutene. The dependence of the over-all reactivity under comparable conditions and of the selectivity to dehydrogenation of these olefins on the number of β C—C and β C—H bonds is shown in Table III.

TABLE III

Comparison of the reactivity and selectivity to dehydrogenation with the number of β C—C and β C—H bonds in the olefins

Olefin	% Reaction* (after 22 min)	Dehydrogenation selectivity,* %	Number of β C—C bonds	Number of β C—H bonds
$(CH_3)_2C{=}CH_2$	Small	—	None	6
$(CH_3)_2C{=}C(CH_3)H$	30.0	48.0	None	9
$CH_3{\cdot}CH_2{\cdot}CH{=}CH_2$	41.0	41.4	1	2
$(CH_3)_2CH{\cdot}CH{=}CH_2$	82.8	9.7	2	1

*Isomerization is not taken into account in evaluating % reaction.

The dissociation of the bonds in β position to the double bond may constitute the initial step in the catalytic process (a purely dissociative mechanism), or the dissociation may be preceded by an initial interaction of the catalyst with the double bond (a combined associative–dissociative mechanism). The two possibilities are in many respects very similar and are difficult to distinguish experimentally. Both lead to the formation of chemisorbed allyl or substituted allyl radicals. In the purely dissociative mechanism the double-bond shift can be visualized as occurring through a 1,3 switch in the position of attachment of the allylic radical to the surface, and the dissociative process can then be further propagated through the breakage of bonds β to the shifted double bond, with formation of dienes. Some energetic restrictions have to be imposed to accommodate, for example, the lack of isomerization of 3-methyl butene-2 to 3-methyl butene-1.

In the combined associative–dissociative mechanism the energetic restrictions can be introduced by assuming an "orientation" in the initial interaction of the catalyst with the olefin. It can be assumed that (*a*) the initial attachment to the surface takes place at the "less-substituted" of the two carbon atoms of the olefinic double bond, (*b*) a C—H or a C—C bond in β position to the original double bond is broken and a new double bond is formed, (*c*) if there are C—H (or C—C) bonds in β position to the new double bond, these may be broken in turn and dienes formed, (*d*) alternatively and simultaneously recombination may take place with chemisorbed H atoms to regenerate the olefin but with the double bond shifted one position. This is represented for the olefins of interest in connection with the present work in the following scheme.

Isobutene

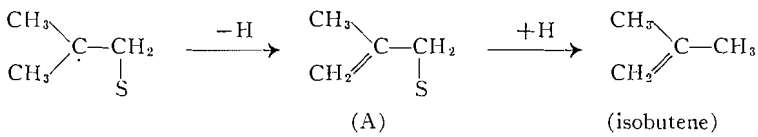

Can. J. Chem. Downloaded from www.nrcresearchpress.com by 176.9.209.113 on 09/04/12
For personal use only.

Butene-1

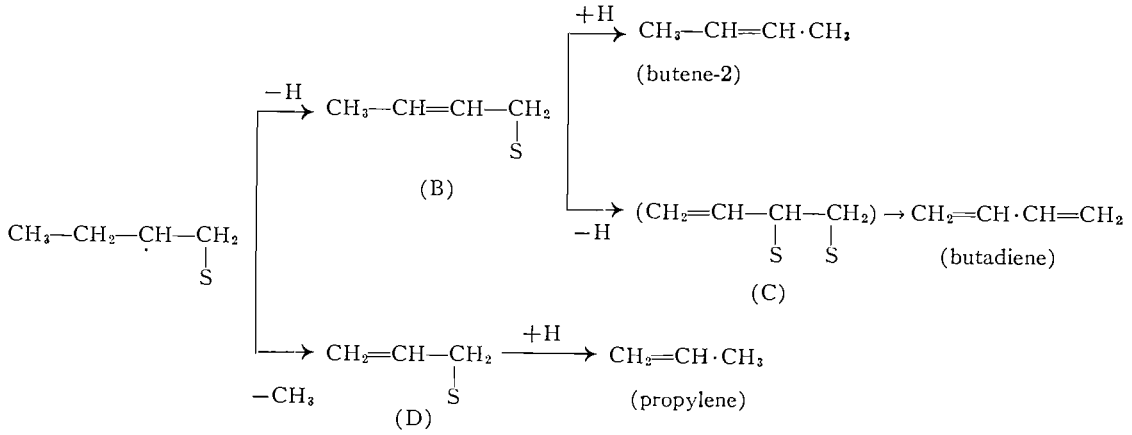

2-Methyl Butene-2

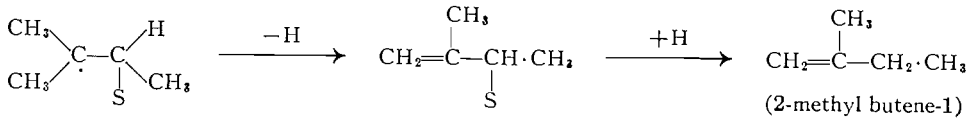

(E)

2-Methyl Butene-1

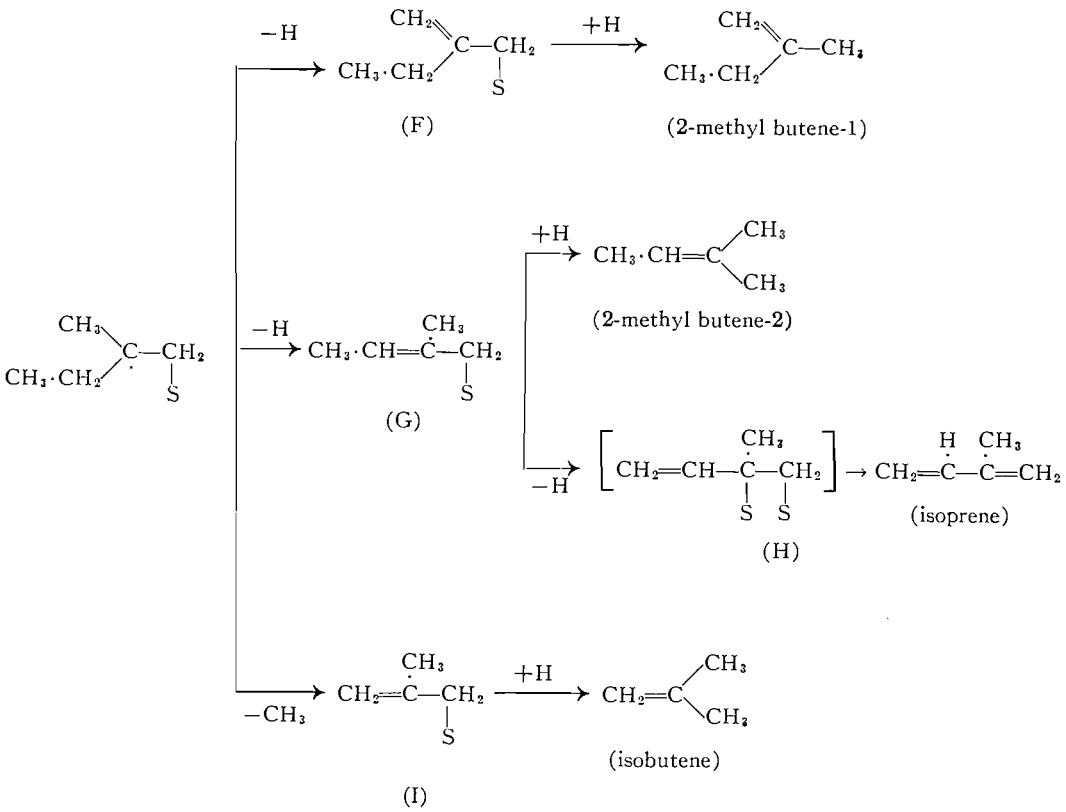

Can. J. Chem. Downloaded from www.nrcresearchpress.com by 176.9.209.113 on 09/04/12
For personal use only.

3-Methyl Butene-1

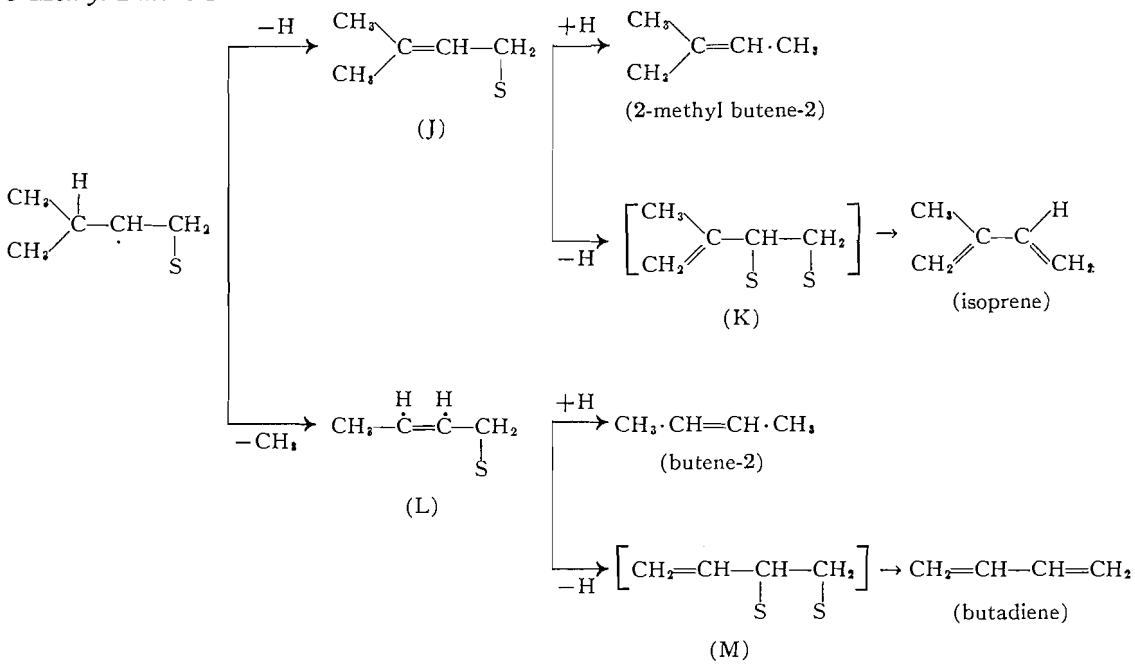

The products predicted in this scheme for various olefins by consistent application of the mechanism summarized in the four points given above agree well with the observed products if, for the moment, the formation of the cracking products ethylene and propylene is disregarded in most cases. Thus, no isomerization of 2-methyl butene-2 to 3-methyl butene-1 is predicted, although the double bond should shift in the opposite direction to form 2-methyl butene-1. This last compound should then produce isoprene and isobutene, which are the main products formed. No butadiene is predicted nor is it formed to any extent. On the other hand, in the case of 3-methyl butene-1, isoprene, butadiene, and butene-2 (but only a trace of butene-1 or isobutene (3)) are all formed in substantial amounts. Furthermore, the primary isomerization product is 2-methyl butene-2, as predicted, rather than 2-methyl butene-1 (3).

In the proposed scheme of reactions no cracking into ethylene and propylene (with one exception) is considered. This type of cracking can be formally explained in a consistent manner by assuming that in the intermediates (B), (G), (J), and (L) the incipient new double bond may break. In the case of the intermediates such as (A), (D), etc. where an analogous split would liberate CH_2, this cracking probably does not occur to any extent. Thus, isobutene is stable, 3-methyl butene-1 forms large amounts of propylene and ethylene, while 2-methyl butene-2 forms very little of these compounds.

The dissociative and associative mechanisms of olefin chemisorption have been the subject of numerous studies and discussions. The difficulty of unambiguous differentiation between the two (and the "hydrogen-switch" mechanism) is well recognized (5) .The number of points of contact indicated for the complexes (A), (B), etc. and their positions in the olefin molecules are necessarily arbitrary. In the case of the complexes (C, H, K, M) preceding dienes the formal application of the associative mechanism leads to 1,2-diadsorbed species with a double bond in 3 position, as shown in the above scheme. The

Can. J. Chem. Downloaded from www.nrcresearchpress.com by 176.9.209.113 on 09/04/12
For personal use only.

purely dissociative mechanism discussed earlier, on the other hand, leads to 1,4-diadsorbed molecules with a double bond in 3 position. Formation of transitory double bonds in chemisorbed hydrocarbons, somewhat similar though not identical with those depicted here, was recently postulated by Burwell *et al.* (6) in order to explain racemization of (+)3-methylhexane occurring concurrently with H—D exchange on some metal surfaces.

The condition of the catalytic surface appears to play an important role in determining the relative extents of cracking, dehydrogenation, and isomerization. Thus in the reaction of butene-1 over-all reaction increased but the amount of butadiene formed remained unaltered in the absence of moisture, as shown in Table I. The presence of moisture seems to be essential in suppressing the cracking. The role of moisture may be to prevent the exposure of the Zn atoms by covering the surface with hydroxyl groups. The promotion of cracking by Zn is perhaps due to the relatively strong bond between this metal and CH_3 (7), which is stronger than the corresponding bond with hydrogen.

The sensitivity of the catalytic surface to the ambient atmosphere reflected itself in a strong increase in conductivity, almost to that of metallic zinc as soon as any hydrocarbon was admitted to the system. This held true even when oxygen was present in the gas phase, in spite of the normally observed decrease in conductivity of *n*-type semiconductors as the partial pressure of oxygen is increased.

Under dry conditions appreciable quantities of benzene (up to 14% after 35 to 40 recycles) were formed from butene-1. While the mechanism of formation of benzene is not understood, it is likely that it results from recombination of acetylenic residues. A mixture of butadiene and ethylene failed to yield any benzene under similar reaction conditions.

ACKNOWLEDGMENTS

The authors are thankful to Dr. A. W. Tickner for mass spectrometer analyses and to the Analytical Section of this Division for several gas chromatographic analyses.

REFERENCES

1. Rowlinson, H. C. and Cvetanović, R. J. Advances in Catalysis, **9**, 243 (1957).
2. Watson, J. S. Can. J. Technol. **34**, 373 (1956).
3. Foster, N. F., Barker, G. R., and Cvetanović, R. J. Unpublished results.
4. Eischens, R. P. and Pliskin, W. A. Advances in Catalysis, **10**, 1 (1958).
5. Condon, F. E. Catalysis. *Edited by* P. H. Emmett. Vol. 6. Reinhold Publishing Corp., New York. 1958. Chap. 2.
6. Burwell, R. L., Jr., Shim, B. K. C., and Rowlinson, H. C. J. Am. Chem. Soc. **79**, 5142 (1957).
7. Price, S. J. W. and Trotman-Dickenson, A. F. Trans. Faraday Soc. **53**, 1208 (1957).

Can. J. Chem. Downloaded from www.nrcresearchpress.com by 176.9.209.113 on 09/04/12
For personal use only.

Can. J. Chem. Downloaded from www.nrcresearchpress.com by 176.9.209.113 on 09/04/12
For personal use only.

OXYMERCURATION OF Δ^5-[2,2,2]-BICYCLOÖCTENE[1]

D. D. K. Chiu and George F Wright

ABSTRACT

It has now been shown that an earlier assignment of configuration in which 1,4-↑↑-ethylene-Δ^5-cyclohexenedicarboxylic acids and their derivatives were presumed to form with mercuric salts 5-↓-hydroxy-6-↓-anionomercuri-1,4-↑↑-ethylenecyclohexanedicarboxylic acid derivatives is incorrect. Instead 5-↓-hydroxy-6-↑-anionomercuri-1,4-↑↑-ethylenecyclohexanedicarboxylic acid derivatives are formed, similarly with the homologous 5-↓-hydroxy-6-↑-anionomercuri-1,4-methylenecyclohexane-2,3-dicarboxylic acid derivatives. This similarity is exemplified by comparable dipole moments. The exception is 5-↓-hydroxy-6-↓-chloromercuri-1,4-↑↑-methylenecyclohexane-2,3-↓↓-dicarboxylic acid, γ-lactone, which has a configuration opposite to all of the others of these series having boat-type cyclohexane ring conformations. The exception is attributed to steric effects.

The oxymercuration of Δ^5-[2,2,2]-bicycloöctene has been reported and the stereochemistry has been specified (1). It has now been proved that this configurational assignment is incorrect. The error may be summarized in terms of two formulae reproduced here, together with their identifying numbers, from page 719 of the previous report (1).

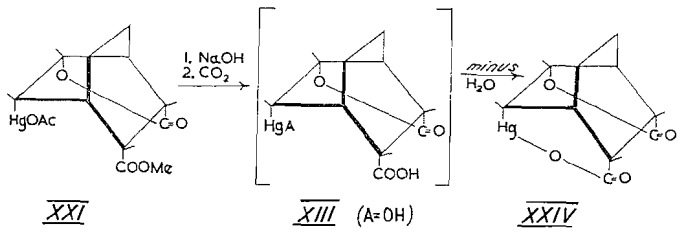

XXI XIII (A=OH) XXIV

According to the statement of McNeely *et al.* (1), the structure of 2-↓-carbomethoxy-5-↓-hydroxy-6-↓-acetoxymercuri-1,4-↑↑-ethylenecyclohexane-3-↓-carboxylic acid, γ-lactone (XXI), was proved by its careful saponification to 5-↓-hydroxy-*anhydro*-[6-↓-hydroxymercuri-2-↓-carboxy]-1,4-↑↑-ethylenecyclohexane-3-↓-carboxylic acid, γ-lactone (XXIV), the molecular weight of which was demonstrated cryoscopically in diphenylmercury. It will be shown that McNeely *et al.* did not have XXIV at all, but, instead, an hydroxymercurial diastereomeric with XIII (A = OH) which was contaminated with its chloromercurial. The content of this mixture has now been shown by a critical study of the X-ray diffraction pattern (1) of what McNeely *et al.* thought to be XXIV.

During the present investigation it has been found that the same dicarboxylic acid, γ-lactone, may be obtained by oxymercuration of 1,4-ethylene-Δ^5-cyclohexene-2,3-↓↓-dicarboxylic anhydride (I) as was formerly obtained from dimethyl 1,4-↑↑-ethylene-Δ^5-cyclohexene-2,3-↓↓-dicarboxylate. The anhydride seems to survive as such in aqueous media. However, a mercuric salt is formed by addition of mercuric chloride to the aqueous solution of the anhydride. Oxymercuration occurs very rapidly in this acidic system, and neutralization is required only to avoid an equilibrium due to the reverse reaction, deoxymercuration. By analogy with the oxymercuration reactions of the 1,4-↑↑-methylene-

[1]*Manuscript received April 8, 1959.*
Contribution from the Department of Chemistry, University of Toronto, Toronto, Ontario, Canada.

Δ^5-cyclohexene system (2) the reaction with the homologue, I, should be acid-catalyzed and should lead to a ↑↓ (*trans*) configuration of the oxy and mercuri addends. Then the product is 5-↓-hydroxy-6-↑-chloromercuri-1,4-↑↑-methylenecyclohexane-2,3-↓↓-dicarboxylic acid, γ-lactone (II), unless lactonization has occurred with inversion.

A re-examination of the oxymercuration of dimethyl 1,4-ethylene-Δ^5-cyclohexene-2,3-↓↓-dicarboxylate (III) shows that inversion during lactonization is very unlikely. The product is clearly dimethyl 5-↓-hydroxy-6-↑-acetoxymercuri-1,4-↑↑-ethylenecyclohexane-2,3-↓↓-dicarboxylate (IV). However, this substance (m.p. 136–137°) is quite unstable. Methanol is eliminated during crystallization and especially at the melting point, whereupon resolidification occurs. The remainder after loss of methanol melts at 188–189°, and is 2-↓-carbomethoxy-5-↓-hydroxy-6-↑-acetoxymercuri-1,4-↑↑-ethylenecyclohexane-3-↓-carboxylic acid, γ-lactone (V). This substance (reported previously (1) as having acetoxymercuri in the ↓ configuration) is thus formed under conditions where inversion is unlikely.

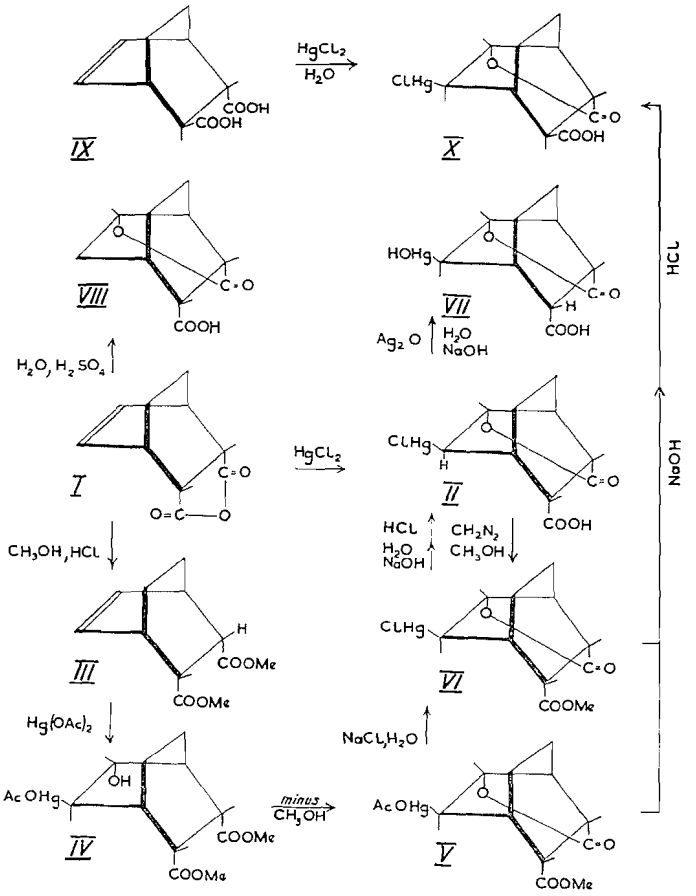

Treatment of V with aqueous sodium chloride converts it to 2-↓-carbomethoxy-5-↓-hydroxy-6-↑-chloromercuri-1,4-↑↑-ethylenecyclohexane-3-↓-carboxylic acid, γ-lactone (VI). This ester may be saponified by use of the stoichiometric quantity of 10% alkali to the acid identical with II. Therefore, it would seem that the anhydride (I) and the ester (III) were oxymercurated to the same product unless some rearrangement occurred during the saponification.

Can. J. Chem. Downloaded from www.nrcresearchpress.com by 176.9.209.113 on 09/04/12
For personal use only.

Can. J. Chem. Downloaded from www.nrcresearchpress.com by 176.9.209.113 on 09/04/12
For personal use only.

In order to eliminate this possibility we have converted the acid (II) to the ester (VI) by treatment with diazomethane in diethyl ether – methanol. Although this reagent attacks oxymercurials vigorously, forming chloromethylmercuric chloride (3), the esterification may be accomplished in fair yield at a reaction temperature of −80°. The product is identical with the ester (VI), thus precluding rearrangement during the saponification of VI.

When a chloromercurial such as II is treated with alkali the hydroxymercurial, 5-↓-hydroxy-6-↑-hydroxymercuri-1,4-↑↑-ethylenecyclohexane-2,3-dicarboxylic acid, γ-lactone (VII), is expected. In order to ensure absence of chloromercurial, silver oxide should be included, and acidification should be effected with carbonic acid. In these circumstances the product seems to be VII. Although the elemental analyses show percentage errors of 2% for carbon and 13% for hydrogen they are still much closer to theoretical values than was reported by McNeely *et al.* (1) for their substance, which at any rate contained the chloromercurial II according to its X-ray diffraction pattern.

Indeed the poor analysis is more to be expected of the free hydroxymercurial than of the 5-↓-hydroxy-*anhydro*-[6-↑-hydroxymercuri-2-↓-carboxy]-1,4-↑↑-ethylenecyclohexane-3-↓-carboxylic acid, γ-lactone, which McNeely *et al.* thought the product to be. Hydroxymercuri compounds are difficult to purify, partly because they react with carbon dioxide. Of course, the analysis does not differentiate, at best, between the structure VII and that of the diastereomeric 5-↓-hydroxy-*anhydro*-[6-↓-hydroxymercuri-2-↓-carboxy]-1,4-↑↑-ethylenecyclohexane-3-↓-carboxylic acid predicated on the configurational assignment by McNeely *et al.* However, a potentiometric titration in which only 1 equivalent of alkali is consumed vitiates the possibility of this alternative non-lactonic isomer. In any circumstance there is no evidence for the *anhydro* structure and hence no evidence for the ↓↓ addition reported previously.

Proof for structure II is afforded by its high dipole moment (7.30, Table I) which compares with 7.19 Debye for 5-↓-hydroxy-6-↑-chloromercuri-1,4-methylenecyclohexane-2,3-↓↓-dicarboxylic acid, γ-lactone, of proved structure (2). Since the moments of 1,4-↑↑-methylenecyclohexane-2,3-↓↓-dicarboxylic anhydride (4.8 D) (4), 1,4-↑↑-methylenecyclohexane-2-↓-3-↑-dicarboxylic acid (2.19 D), and 5-↓-hydroxy-1,4-↑↑-methylenecyclohexane-2,3-↓↓-dicarboxylic acid, γ-lactone (4.85 D), also are closely comparable with those of the higher homologues (Table I) the structural analogy seems to be reasonable.

A similar comparison can be made between 5-↓-hydroxy-6-↑-chloromercuri-1,4-ethylenecyclohexane-2-↑-3-↓-dicarboxylic acid, γ-lactone (X, 6.91 D), and the methylene homologue (μ = 6.40) (2). The synthesis of X has been effected by prolonged treatment of VI with alkali (1), and also by treatment of 1,4-↑↑-ethylene-Δ^5-cyclohexene-2-↓-3-↑-dicarboxylic acid (IX) (5) with aqueous mercuric chloride. The postulated prototropic configurational shift of 2-carboxyl in II by action of alkali is thus confirmed.

Unfortunately, for a complete demonstration of configurational differences by comparison of dipole moments we have been unable to convert II to the diastereomeric 5-↓-hydroxy-6-↓-anionomercuri-1,4-↑↑-ethylenecyclohexane-2,3-↓↓-dicarboxylic acid, γ-lactone (XIII, A = Cl). When II is treated with hydrazine hydrate a mixture of products is obtained, one of which is the original substance, II. The other seems to be either a hydrolyzate or a polymorph of II since it may be converted to II when it is maintained for a few minutes at a temperature below the melting point. Probably some of XIII is actually formed but we have been unable to isolate it.

In summary the [2,2,2]-bicyclo-2-octenes seem to oxymercurate like the homologous

TABLE I

Dipole moments of 1,4-↑↑-ethylenecyclohexanes in dioxane at 20°

Substance	$d\epsilon/d\omega$	$dV/d\omega$	P_T	R_D calc.	μ, D
1,4-↑↑-Ethylenecyclohexane-2,3-↓↓-dicarboxylic anhydride	15.70	0.180	499	44	4.65
5-↓-Hydroxy-1,4-ethylenecyclohexane-2,3-↓↓-dicarboxylic acid, γ-lactone (VIII)	14.60	0.286	505	45	4.68
5-↓-Hydroxy-6-↑-chloromercuri-1,4-↑↑-ethylenecyclohexane-2,3-↓↓-dicarboxylic acid, γ-lactone (II)	16.15	0.597	1182	61	7.30
5-↓-Hydroxy-6-↑-chloromercuri-1,4-ethylenecyclohexane-2-↑-3-↓-dicarboxylic acid, γ-lactone (X)	14.50	0.581	1065	61	6.91
1,4-↑↑-Ethylenecyclohexane-2-↓-3-↑-dicarboxylic acid (IX)	3.30	0.203	150	47	2.21
Dimethyl 1,4-↑↑-ethylene-Δ^5-cyclohexene-2,3-↓↓-dicarboxylate (III)	3.90	0.120	197	42	2.59
2-↓-Carbomethoxy-5-↓-hydroxy-6-↑-chloromercuri-1,4-↑↑-ethylenecyclohexane-3-↓-carboxylic acid, γ-lactone (VI)	17.03	0.594	1283	66	7.60

[2,2,1]-bicyclo-2-heptenes in a manner which is different from that occurring with cyclohexenes, cyclopentenes, α-terpineol, and the stilbenes. Reaction with the bicyclic compounds seems to be acid-catalyzed. An over-all ↑↓ (*trans*) addition occurs in contradistinction to that observed with the other alkenes. The fixed boat conformation of the bicyclic alkenes may be involved in this abnormality.

One difference in oxymercuration between the bicycloheptene and bicycloöctene series is apparent. Although 1,4-methylene-Δ^5-cyclohexene-2,3-↓↓-dicarboxylic acid seems to oxymercurate by an ionic mechanism, it nevertheless yields a 2,3,5,6-↓↓↓↓-diastereomer. By contrast 1,4-↑↑-ethylene-Δ^5-cyclohexene yields the 2,3,5-↓↓↓-6-↑-diastereomer. It would seem that in one instance (XI) the mercuric ion is endo-co-ordinated, while in XII exo-co-ordination maintains. The difference is thus defined as a steric one.

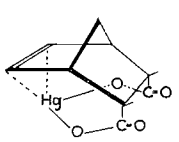

XI

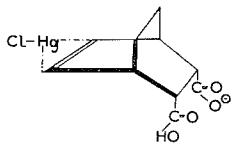

XII

The authors are grateful to the National Research Council for financial aid.

EXPERIMENTAL*

1,4-↑↑-Ethylenecyclohexane-2,3-↓↓-dicarboxylic Anhydride

A solution of 0.20 g (0.00112 mole) of 1,4-↑↑-ethylene-Δ^5-cyclohexene-2,3-↓↓-carboxylic anhydride (6) (I) in 20 ml of absolute ethanol was reduced within 25 minutes by hydrogen in presence of 0.018 g of platinum oxide containing 0.002 g of Darco. The product (0.20 g, 79%, m.p. 176–177°) was crystallized from 1:2 commercial hexane – acetone (30 ml/g), m.p. 186–186.8°. X-Ray diffraction pattern was [10] 5.38; [6] 5.15, 5.02; [5] 3.61; [4] 7.02; [3] 4.60, 3.96, 2.66; [2] 2.96, 3.30, 3.17; [1] 3.04, 3.11, 6.29, 4.15, 3.43, 2.50, 2.19, 2.38, 1.99, 1.93.

Melting points have been corrected against reliable standards (Can. J. Technol. **34, 89 (1956)). The X-ray diffraction patterns are recorded for* Cu K_α (Ni-*filtered*) *radiation in* Å *at relative intensities* $[I/I_1]$.

Can. J. Chem. Downloaded from www.nrcresearchpress.com by 176.9.209.113 on 09/04/12
For personal use only.

5-↓-Hydroxy-6-↑-chloromercuri-1,4-↑↑-ethylenecyclohexane-2,3-↓↓-dicarboxylic Acid, γ-Lactone (II)

To a solution of 34.0 g (0.191 mole) of I in 2840 ml of water at 80° was added 51.8 g (0.191 mole) of mercuric chloride with vigorous agitation. A precipitate appeared immediately and a test for mercuric ion was almost negative. After 10 hours alkali was added to a pH of 4.5. The system tested negatively (20% alkali) for mercuric or mercurous ion. The precipitate was filtered, thrice washed with distilled water, and vacuum-dried, 73 g (85%), m.p. 197–199° (decomp.). Crystallization from acetone (4 ml/g) raised this melting point to 208–208.5° (decomp.); % C, 27.7; % H, 2.67. The X-ray diffraction pattern was obtained as follows: [10] 8.19; [9] 6.15; [8] 4.16; [6] 3.28; [4] 4.84; [3] 3.81, 5.19, 6.77; [2] 3.94, 5.57, 2.92, 4.10; [1] 3.19, 3.14, 3.01, 2.86, 2.74, 2.64. When the substance was treated for 1 hour with concentrated hydrochloric acid the anhydride (I) was regenerated and identified by mixture melting point (147–148°). When II was dissolved in 4 equivalents of alkali and back-titrated with hydrochloric acid it neutralized 2 equivalents.

Dimethyl 5-↓-Hydroxy-6-↑-chloromercuri-1,4-↓↓-ethylenecyclohexane-2,3-↓↓-dicarboxylate (IV)

A suspension of 12 g (0.0535 mole) of dimethyl 1,4-↑↑-ethylenecyclohexane-2,3-↓↓-dicarboxylate (III) (7, 8) (m.p. 70–70.8°) in a solution of 17 g (0.0535 mole) of mercuric acetate in 120 ml of water was stirred for 8 hours. The filtered precipitate weighed 13.7 g (51%) and melted at 135–137°, with evolution of methanol, demonstrated as the dinitrobenzoate. The melt then resolidified and remelted at 183–185° (decomp.). The diffraction pattern of the filtered precipitate was [10] 6.91; [9] 8.42; [8] 4.09; [7] 5.34, 5.12; [6] 3.53; [5] 3.80; [4] 3.29; [3] 4.84, 2.75. Crystallization of this substance from any medium that we tried, but specifically from methanol (4 ml/g), converted it to 2-↓-carbomethoxy-5-↓-hydroxy-6-↑-acetoxymercuri-1,4-↑↑-ethylenecyclohexane-3-↓-carboxylic acid, γ-lactone (V), m.p. 188.5–189°, X-ray pattern [10] 10.84; [9] 4.56; [8] 6.44, 6.68; [5] 4.27; [4] 3.57; [3] 2.80, 3.75, 8.54. When this product was treated with aqueous sodium chloride it yielded VI.

2-↓-Carbomethoxy-5-↓-hydroxy-6-↑-chloromercuri-1,4-↑↑-ethylenecyclohexane-3-↓-carboxylic Acid, γ-Lactone (VI)

Methanol (800 ml) at 0° was freed from acidic substances by treatment with a solution containing 0.0064 mole of diazomethane in diethyl ether which had previously been dried over potassium hydroxide. Into this colorless methanol–ether mixture was dissolved 0.93 g (0.00216 mole) of 5-↓-hydroxy-6-↑-chloromercuri-2-↓-carboxy-1,4-↑↑-ethylenecyclohexane-3-↓-carboxylic acid, γ-lactone (II), at 0°. This solution at −80° was then mixed with a solution at −80° of ethereal diazomethane (0.0174 mole). The system was allowed to warm to 20° during several hours. Then a gray precipitate was filtered off. The vacuum-evaporated filtrate left 0.65 g, m.p. 182–184° (decomp.). Crystallization from acetone (4 ml/g) gave 0.12 g of unchanged II (mixture melting point). Partial evaporation of the mother liquor gave 0.16 g (17%), m.p. 199–201°. This melting point was raised to 204–205° by crystallization from acetone; a mixture melting point with VI prepared by treatment of V with aqueous sodium chloride was not lowered although admixture with II lowered the melting point 20°.

5-↓-Hydroxy-6-↑-chloromercuri-1,4-↑↑-ethylenecyclohexane-2-↑-3-↓-dicarboxylic Acid, γ-Lactone (X)

To a solution of 0.64 g (0.00327 mole) of 1,4-↑↑-ethylene-Δ^5-cyclohexene-2-↑-3-↓-dicarboxylic acid (IX) (9) in 52 ml of water at 70° was added 0.88 g (0.00327 mole) of mercuric

Can. J. Chem. Downloaded from www.nrcresearchpress.com by 176.9.209.113 on 09/04/12
For personal use only.

chloride. After it was cooled to room temperature the system was neutralized to pH 5.6–6.0 (2 ml 10% aqueous sodium hydroxide). A precipitate appeared which redissolved upon addition of 3.5 ml more of the alkali (pH 7.6, no mercuric oxide). After 20 hours the solution was acidified at 0° by addition of 2.2 ml of 10% hydrochloric acid (pH 3.0). The precipitate, 0.81 g (58%), melted at 194–200° (decomp.). Crystallization from acetone (10 ml/g) raised this melting point to 208.5–209°, mixture melting point with II lowered to 194°. No depression was observed upon admixture with the substance obtained by McNeely *et al.* by 1-day saponification (3 equivalents alkali) of 2-↓-carbomethoxy-5-↓-hydroxy-6-↑-acetoxymercuri-1,4-↑↑-ethylenecyclohexane-3-↓-carboxylic acid, γ-lactone, and subsequent acidification with hydrochloric acid. The X-ray diffraction pattern was [10] 4.79; [8] 8.79, 3.24; [7] 1.95; [6] 5.45; [5] 5.98; [4] 6.91; [3] 2.81; [2] 3.00, 2.30; [1] 3.08, 2.70, 2.61. Calc. for $C_{10}H_{11}ClHgO_4$: C, 27.8; H, 2.60. Found: C, 28.0; H, 2.67. Treatment of this product with concentrated hydrochloric acid yielded 1,4-↑↑-ethylene-Δ^5-cyclohexene-2,3-↑↓-dicarboxylic acid, m.p. 210–211°.

5-↓-Hydroxy-6-↑-hydroxymercuri-1,4-ethylenecyclohexane-2,3-↓↓-dicarboxylic Acid, γ-Lactone (VII)

A solution of 3.40 g (0.0073 mole) of 2-↓-carbomethoxy-5-↓-hydroxy-6-↑-acetoxymercuri-1,4-↑↑-ethylenecyclohexane-3-↓-carboxylic acid, γ-lactone (V), in 29 ml of 1% aqueous sodium hydroxide was let stand for 34 hours. The precipitate weighed 1.5 g (53%), m.p. 222–226° (decomp.). This melting point was raised to 239–241° by washing with chloroform, methanol, and diethyl ether. Further purification was effected by solution in 1% aqueous alkali (pH 10) followed by acidification by means of gaseous carbon dioxide. The precipitate, washed with acetone, melted at 244–244.5°. Calc. for $C_{10}H_{12}O_5Hg$: C, 29.1; H, 2.93. Found: C, 28.5; H, 3.17. The X-ray diffraction pattern was found to be [10] 8.72; [9] 6.25; [8] 3.33; [6] 4.27; [5] 2.67; [4] 3.05; [3] 3.65, 4.50, 1.97; [2] 3.92, 3.44, 3.25; [1] 2.03, 7.85, 6.93, 5.55. The same diffraction pattern was obtained for the product obtained when II (0.65 g, 0.0015 mole) in 2.45 ml of 5% aqueous alkali containing 0.46 g (0.002 mole) of silver oxide was filtered and then acidified by means of carbon dioxide gas. A comparison of the diffraction pattern with that reported by McNeely *et al.* shows that their compound must have been a mixture of VII and II.

Treatment of 5-↓-Hydroxy-6-↑-chloromercuri-1,4-↑↑-ethylenecyclohexane-2,3-↓↓-dicarboxylic Acid, γ-Lactone (II), *with Hydrazine Hydrate*

To an alkaline solution of 5.0 g (0.0116 mole) of II in 46.5 ml (0.058 mole) of 5% aqueous sodium hydroxide was added 0.6 ml (0.012 mole) of hydrazine hydrate. After 1 day the filtered system was acidified (pH 3) by use of hydrochloric acid at 0°. Slow precipitation yielded 3.0 g, m.p. 181–183°, which upon crystallization from methanol (10 ml/g) melted at 208–208.5°, mixture melting point with II not lowered (10%). The filtrate upon evaporation left a residue which was crystallized from methanol (1 ml/g), m.p. 207.5–208° (4%). Although this substance seemed to be different from II in respect of its solubility in methanol and also in respect of its X-ray diffraction pattern: [10] 6.41; [8] 8.84; [5] 5.12, 4.19; [4] 3.17; [3] 3.77, 3.46, 4.31; [2] 3.90, 3.26; [1] 4.56, 4.49, 3.39 (and despite the fact that a mixture melting point with II was not depressed), it was evidently configurationally the same as II. Thus when it was heated to 195° for 5 minutes its X-ray diffraction pattern became identical with II. Moreover, it would not form an anhydromercurial when it was converted to the hydroxymercurial by treatment with silver oxide and alkali. It may be a polymorph or, alternatively, the non-lactonic hydroxy acid.

Can. J. Chem. Downloaded from www.nrcresearchpress.com by 176.9.209.113 on 09/04/12
For personal use only.

5-↓-Hydroxy-1,4-↑↑-ethylenecyclohexane-2,3-↓↓-dicarboxylic Acid, γ-Lactone (VIII)

The substance was prepared by the recorded method (5) by heating 2.0 g (0.0112 mole) of 1,4-↑↑-ethylenecyclohexane-2,3-↓↓-dicarboxylic anhydride (I) in 22 g of 50% (w/w) sulphuric acid for 5 hours at 90°. After neutralization with sodium bicarbonate (pH 3) the precipitate was dissolved by extraction with chloroform. Evaporation of this solvent left 1.15 g (52%), m.p. 168–178°. Two crystallizations from acetone raised this melting point to 198–198.5°. The X-ray diffraction pattern was [10] 5.82; [9] 5.60; [6] 6.72; [5] 4.29; [4] 3.85, 2.90; [3] 4.94, 4.60; [2] 5.15, 2.98, 4.07; [1] 2.76, 3.18, 3.33. Potentiometric titration showed that 1 equivalent of alkali neutralized this substance. Calc. for $C_{10}H_4O_{12}$: C, 61.2; H, 6.16. Found: C, 61.3; H, 6.11.

1,4-↑↑-Ethylene-Δ⁵-cyclohexene-2,3-↓↑-dicarboxylic Acid (IX)

To a solution of 9.56 g (0.0625 mole) of fumaryl chloride in 55 ml of dry diethyl ether at −10° was gradually added a solution of 10 g (0.125 mole) of 1,3-cyclohexadiene in 55 ml of dry ether at −10°. After 1 hour at this temperature the system was maintained at 25° for 12 hours and then was shaken with 20 ml of 10% aqueous sodium hydroxide for 4 hours. Acidification of the aqueous layer yielded 8.40 g (68%), m.p. 199–204°. Crystallization from commercial hexane – acetone (1:5, 5 ml/g) raised the melting point to 210–211°. Calc. for $C_{10}H_{12}O_4$: C, 61.3; H, 6.16. Found: C, 61.0; H, 6.05.

1,4-Ethylenecyclohexane-2,3-↓↑-dicarboxylic Acid

A solution of 0.20 g (0.002 mole) of 1,4-↑↑-ethylene-Δ⁵-cyclohexene-2,3-↓↑-dicarboxylic acid in 20 ml of absolute ethanol plus 0.02 g of platinum oxide with 0.002 g of Darco was reduced within 35 minutes by 26.7 ml of hydrogen. After filtration of the catalyst the solution was evaporated, leaving 0.20 g (99%), m.p. 234–235°. After crystallization from commercial hexane – acetone (1:5, 60 ml/g) it melted at 235.0–235.5°.

REFERENCES

1. McNeely, K. H., Rodgman, A., and Wright, G. F. J. Org. Chem. **20**, 714 (1955).
2. Abercrombie, M. J., Bharucha, K. R., Rodgman, A., and Wright, G. F. Can. J. Chem. **37**, 1328 (1959).
3. Sawatzky, H. and Wright, G. F. Can. J. Chem. **36**, 1555 (1958).
4. Kwart, H. and Kaplan, L. J. Am. Chem. Soc. **75**, 3356 (1953).
5. Alder, K. and Stein, G. Ann. **514**, 1 (1934).
6. Diels, O. and Alder, K. Ann. **460**, 98 (1928).
7. Bode, H. Ber. **70**, 1167 (1937).
8. West, T. F. J. Chem. Soc. 140 (1941).
9. Alder, K. and Stein, G. Ann. **514**, 197 (1934).

Can. J. Chem. Downloaded from www.nrcresearchpress.com by 176.9.209.113 on 09/04/12
For personal use only.

Can. J. Chem. Downloaded from www.nrcresearchpress.com by 176.9.209.113 on 09/04/12
For personal use only.

PHOTOCHEMICAL SEPARATION OF MERCURY ISOTOPES

V. FURTHER STUDIES ON THE REACTION OF $Hg^{202}6(^3P_1)$ ATOMS, PHOTOEXCITED IN NATURAL MERCURY VAPOR, WITH HYDROGEN CHLORIDE[1]

J. R. McDowell, C. C. McDonald,[2] and H. E. Gunning

ABSTRACT

A further study has been made of the reaction of $Hg^{202}6(^3P_1)$ atoms, in natural mercury vapor (Hg^N), with hydrogen chloride under flow conditions at room temperature. Emphasis has been placed in this study on the effect of reaction parameters and mercury-recovery techniques on the Hg^{202} content of the solid calomel formed in the reaction.

For pure hydrogen chloride the Hg^{202} content of the calomel was found to be $39.9\pm0.3\%$, compared to the natural abundance of 29.8%. With 20–40 mole % of butadiene-1,3 in the hydrogen chloride, calomels containing 83–84% of Hg^{202} were consistently obtained.

The isotopically specific aspects of the reaction in pure hydrogen chloride can be adequately explained by the sequence:

$$Hg^{202}6(^3P_1) + HCl \rightarrow Hg^{202}Cl + H \quad [1]$$

$$Hg^{202}6(^3P_1) + HCl \rightarrow Hg^{202} + H + Cl \quad [2]$$

$$Cl + Hg^N + M \rightarrow Hg^NCl + M \quad [3]$$

$$H + HCl \rightarrow H_2 + Cl \quad [4]$$

where M in reaction [3] is a third body or the wall. From the Hg^{202}-abundance data and steady-state considerations, it has been shown that the ratio of partitioning of the absorbed radiation to [1] and [2], respectively, $= \Phi_1/\Phi_2 = 0.40\pm0.02$. In short, 29% of the primary reaction proceeds by the isotopically specific step [1].

The Hg^{202} content of the calomel product was found to increase markedly when unsaturated hydrocarbons were added to the hydrogen chloride stream. The addends studied included butadiene-1,3, benzene, isoprene, acetylene, propylene, and ethylene in order of decreasing effectiveness. In the presence of the unsaturated addend (U) two additional reactions were postulated to occur:

$$Cl + U \rightarrow \text{product} \quad [7]$$

$$H + U \rightarrow \text{product}. \quad [8]$$

From steady-state calculations the effectiveness of the addend can be shown to be determined by the rate ratio, k_8/k_4.

For the maximally enriching mixture of hydrogen chloride and butadiene, the effect of variations in lamp temperature and reaction pressure was studied. At lamp temperatures exceeding approximately 35° C, reduced enrichments were obtained owing to emission-line broadening. A progressive reduction in enrichment was also observed with substrate pressures greater than 25 mm, owing presumably to Lorentz-broadening of the hyperfine absorption contours of the Hg^N in the reaction cell.

The Hg^{202} content of the calomel product was determined by resonance radiation absorbiometry. The apparent Hg^{202} abundances of the mercury recovered from the calomel product were found to depend strongly on the method used for isolating the enriched mercury from the calomel. Evidence was obtained for the occurrence of isotopically degradative exchange reactions during the recovery process. A recovery technique was developed which appeared to eliminate this exchange degradation.

INTRODUCTION

In an earlier paper in this series (1), experimental techniques were described for the photoexcitation, in natural mercury vapor (Hg^N), of a specific mercury isotopic species (Hg^i) to the $6(^3P_1)$ state. For mercury-$6(^3P_1)$-photosensitized reactions wherein mercury-containing products are formed, the aforementioned technique of monoisotopic photosensitization may be used to determine the extent to which mercury compounds are formed in the primary process. Primary formation of mercury compounds would be

[1]*Manuscript received April 16, 1959.*
Contribution from the Department of Chemistry, University of Alberta, Edmonton, Alberta.
[2]*Present address: Chemical Department, E. I. du Pont de Nemours Co., Wilmington, Delaware.*

indicated when the mercury product is enriched in the isotope undergoing photoexcitation. For a substrate, XY, the general mechanism may be represented by the sequence:

$$Hg^{i}6(^3P_1) + XY \rightarrow Hg^{i}X + Y \quad [1]$$

$$Hg^{i}6(^3P_1) + XY \rightarrow Hg^{i} + X + Y \quad [2]$$

$$X + Hg^{N} + M \rightarrow Hg^{N}X + M \quad [3]$$

where M represents a third body, including the wall. The two primary processes, [1] and [2], presumably involve the same intermediate. Reaction [3], the isotope-diluting step, may be reduced in importance by the addition of compounds which will react rapidly with the free radicals, X and Y. Under these conditions, products highly enriched in the isotope under photoexcitation can be obtained.

Pertel and Gunning (2, 3) studied the reactions of $Hg^{202}6(^3P_1)$ atoms, in Hg^{N}, with N_2O, O_2, and H_2O under flow conditions. For N_2O and O_2 the HgO product was found to contain the normal abundance (29.8%) of Hg^{202}. However, the HgO product of the water vapor reaction contained 33–35% Hg^{202}. Reaction [1] appears therefore to be significant in the H_2O reaction and unimportant for N_2O and O_2. Evidence in favor of the above-cited general mechanism was obtained by studying the Hg^{202} enrichment when unsaturated addends, such as butadiene-1,3, were added to the water vapor stream. Under these conditions the HgO product was found to contain a maximum of 85% Hg^{202}.

The principles of monoisotopic mercury photosensitization and their application to the study of the mechanisms of reactions involving collisions of the second kind have been reviewed by Gunning (4).

A study has recently been made of the reactions of $Hg^{202}6(^3P_1)$ atoms, in Hg^{N}, with flowing hydrogen chloride (5). Under fast-flow conditions it was found that the pure substrate yielded a calomel product containing 44% Hg^{202}. With butadiene-1,3 and benzene as addends, calomels containing respectively 59% and 55% Hg^{202} were obtained under optimum conditions. In the investigation (5) difficulty was encountered in obtaining good reproducibility in the Hg^{202}-enrichment data. It was suspected that exchange reactions were occurring between Hg^{202} ions and adsorbed Hg^{N} during the recovery for analysis of the isotopic mercury from the calomel product.

The present investigation represents a further study of the reaction of $Hg^{202}6(^3P_1)$ atoms, in Hg^{N}, with flowing hydrogen chloride. The various experimental factors which influence the Hg^{202}-enrichment values have been sought out in order to obtain maximum precision in the kinetic data. Emphasis has been placed on the reaction in the presence of various unsaturated addends, in order to find conditions of maximum isotopic enrichment.

The details of the investigation follow.

EXPERIMENTAL

For detailed descriptions of the experimental techniques employed in this study, reference should be made to earlier papers in this series (5, 3, 1). The particular experimental assembly used was essentially identical with that described in reference 3. The quartz-electrodeless discharge source used in this study contained mercury, 98.3 atom % in Hg^{202}. The lamp-wall temperature was maintained constant to $\pm 0.05°$ C.

In the earlier study (5) of the hydrogen chloride reaction the calomel reaction product was removed from the cell by filling the cell with hot, concentrated, hydrochloric acid. The acid-filled cell was immersed in boiling water until the product had dissolved. After the acid solution had been neutralized with base to a pH of 5–6, the isotopic mercury was recovered by immersing a coil of pure copper wire in the solution.

Can. J. Chem. Downloaded from www.nrcresearchpress.com by 176.9.209.113 on 09/04/12
For personal use only.

Can. J. Chem. Downloaded from www.nrcresearchpress.com by 176.9.209.113 on 09/04/12
For personal use only.

For this investigation two, totally different, methods were studied for recovering the isotopic mercury for absorbiometric analysis (6). The two recovery procedures will be referred to as the NH_3 method and the HCl method.

In the NH_3 method, 3 ml of concentrated ammonium hydroxide were poured into the reaction cell, and the cell was shaken so that the liquid completely contacted the calomel product, as evidenced by blackening of the product associated with the formation of $HgNH_2Cl + Hg$. After it was drained, the cell was rinsed thoroughly with distilled water, attached via ground joints to a high-vacuum system, and evacuated for 6 hours. While still under evacuation, the cell was heated strongly with a gas–oxygen flame until the product in the cell was completely white in color, indicating that any free mercury had been driven off. The cell was then removed from the evacuation system, and the product was dissolved in a mixture consisting of 2 ml concentrated nitric acid, 3 ml concentrated hydrochloric acid, and 5 ml of water. The aqua regia was allowed to remain in the cell for 10 minutes. After neutralization to pH 4–5 with sodium hydroxide solution, mercury was recovered from the solution with a copper coil.

In the HCl method, 3 ml of concentrated hydrochloric acid, at 100° C, were poured into the cell and allowed to remain there for a specified time. The solution was then drained from the cell, and neutralized as in the NH_3 method. The isotopic mercury was recovered from the solution by plating on copper as before.

The gases used in this investigation were the highest-purity grades available from the Matheson Company, East Rutherford, N.J. The benzene and isoprene used were A.C.S. grade.

RESULTS

In the runs with pure hydrogen chloride the solid product of reaction was observed to form as a white deposit, mainly in the reaction zone. However, some deposit could be observed in the connecting tubing downstream from the reaction cell. The combined product from several runs was examined by X-ray diffraction. The patterns showed that the material was Hg_2Cl_2, with some weak lines indicating, perhaps, a trace of $HgCl_2$. The product was found to be (*a*) insoluble in cold water, (*b*) slightly soluble in cold, concentrated hydrochloric acid, and (*c*) very soluble in hot hydrochloric acid. In the presence of ammonium hydroxide the product turned black. There is therefore little doubt that the white product is finely divided calomel.

When butadiene was added to the hydrogen chloride stream, the white deposit was observed to form as in the runs with pure substrate. However, during the reaction the white deposit became gradually coated with a thin film of transparent polymer. It was further observed that the quantity of white product formed, in a fixed duration of exposure, decreased with increasing mole fraction of butadiene in the stream. The decreasing yield of product with increasing butadiene concentration can obviously be ascribed to competitive quenching of the photoexcited atoms by the butadiene.

In the first series of runs the Hg^{202} abundance in the calomel product was studied as a function of the butadiene concentration in the stream. A fast flow rate was used, which was maintained essentially constant at 304–383 ml/sec at 25° C and reaction pressure. The total pressure was kept at 9.4 ± 2 mm, while the concentration of butadiene was varied from 0–55 mole %. The lamp-wall temperature was held constant at 23.00 ± 0.05° C. For recovery of mercury from the calomel product, the NH_3 method was used. The results are represented graphically in Fig. 1. It will be noted that as the concentration of butadiene is increased, the Hg^{202} abundance rises rapidly to a maximum

value of 75% at 20 mole % of butadiene. At higher butadiene concentrations, the isotopic abundance slowly decreases toward the natural abundance value.

In order to compare directly the effect of recovery methods on the Hg^{202} abundances, a second series of runs was done on the hydrogen chloride–butadiene system. This series differed from the preceding one only in that the isotopic mercury was recovered from the product by the HCl method. The hot acid was left in the cell for 10 minutes before draining.

The results of this series are shown graphically as the upper curve in Fig. 1. The cell pressure was held within the range, 7.4–12.3 mm. The flow rate was maintained at 360 ± 10 ml/sec. For any given run, the lamp-wall temperature was kept constant to $\pm0.05°$ C. The total range of lamp-wall temperature over the series was 23.0–24.0° C.

A comparison of the two curves in Fig. 1 points up clearly the marked effect of recovery methods on the Hg^{202} abundances in the mercury from the solid reaction product. In the second series an average maximum abundance value of 83% was obtained, and this maximum was invariant in butadiene concentration from 20 to at least 40 mole % of butadiene. Even at 70 mole % butadiene the abundance has only decreased to 72%.

It is also pertinent to note that the two recovery methods did not appreciably influence the Hg^{202} abundance for pure hydrogen chloride. The two methods gave an average value of $39.9\pm0.3\%$.

In the HCl method of mercury recovery, it was found that isotopic degradation occurred if the hot acid was left in contact with the product in the reaction cell for more than 10 minutes. The following example is representative of this degradative effect: In one run the acid was left in contact with the product for 5 minutes, after which time the acid was drained and the cell washed thoroughly with distilled water. The mercury recovered from the acid contained 66.2% Hg^{202}. The undissolved deposit in the cell was then treated with another aliquot of hot acid. The acid was left in the cell for 2 hours. The analysis of the recovered mercury gave 52.8% Hg^{202}. Since the normal abundance of Hg^{202} is 29.8%, the fractional enrichment has decreased from 1.22 to 0.77 in the prolonged acid treatment. This represents a degradation of 37%.

In all subsequent runs reported in this paper, the HCl method was used, with the hot acid left in contact with the product for 10 minutes.

In order to assess the importance of lamp-wall temperatures on the hydrogen chloride–butadiene system, the lamp-wall temperature was varied from 4 to 48.5° C. A maximally enriching mixture of hydrogen chloride and butadiene was used, containing 22 mole % of butadiene. Flow rates were kept within the range 350–370 ml/sec at a cell pressure of 10.9 ± 0.6 mm. It should be noted that difficulty was encountered in maintaining constant lamp intensity at 4° C. At this temperature flickering was observed in the blue emission from the lamp. As the lamp-wall temperature was raised, the brilliance of the lamp steadily increased. The rate of production of product was also observed to increase with increasing lamp-wall temperature.

The data on Hg^{202} abundance vs. lamp-wall temperature are shown in Fig. 2. There is some change in the Hg^{202} abundance when the lamp-wall temperature is lowered from 23° C to 4° C. However, in view of the instability of the lamp at 4° C, it is doubtful whether the small decrease is significant. At temperatures beyond 35° C, the Hg^{202} abundance drops sharply. This effect will be discussed later in this paper.

The variation in Hg^{202} content with increasing cell pressure was studied over the range 10–100 mm. The reaction mixture contained 22 mole % of butadiene as in the lamp-wall temperature studies. The flow rate was held constant at 360 ± 10 ml/sec. The lamp temperature was 23.0° C.

Can. J. Chem. Downloaded from www.nrcresearchpress.com by 176.9.209.113 on 09/04/12
For personal use only.

The data are graphically represented in Fig. 3. It is quite apparent from the graph that pressure-broadening of the absorption contours is an extremely important factor in studies of this type. Maximum enrichments are only obtained for the hydrogen chloride – butadiene mixture at pressures less than about 25 mm.

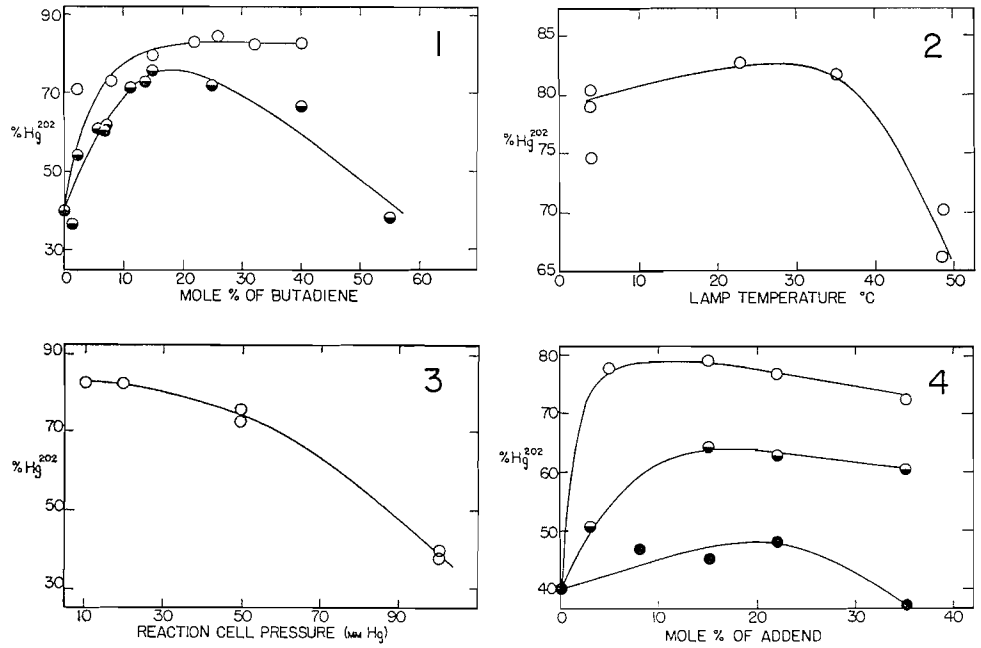

FIG. 1. Hg^{202} abundance vs. mole % of butadiene. ○ HCl method. ◒ NH_3 method.
FIG. 2. Hg^{202} abundance vs. lamp-wall temperature for hydrogen chloride containing 22 mole % of butadiene.
FIG. 3. Hg^{202} abundance vs. reaction cell pressure for hydrogen chloride containing 22 mole % of butadiene.
FIG. 4. Hg^{202} abundance vs. mole % of addend. ○ Benzene. ◒ Isoprene. ● Ethylene.

The efficiency of an unsaturated addend in increasing the Hg^{202} abundance will be related directly to its ability to remove radicals associated with the formation of $Hg^{N}Cl$, if the mechanism proposed in this paper is accepted. A number of addends, in addition to butadiene, were therefore studied in order to obtain a measure of relative efficiencies. In Table I, ethylene, propylene, acetylene, isoprene, benzene, and butadiene are compared with respect to their influence on the Hg^{202} abundance. The concentrations of all addends in the hydrogen chloride stream was 35 mole %. The lamp temperature was 20.0° C. The flow rate was held at 350–375 ml/sec at a total reaction pressure of 10 mm. From Table I, it is apparent that at the chosen concentration of 35 mole %, butadiene is the most efficient addend. In order of decreasing effectiveness follow benzene, isoprene, acetylene, propylene, and ethylene. Surprisingly enough, ethylene is quite ineffective as an addend at the chosen concentration.

Since the effectiveness of an addend could depend upon its concentration, three of the above unsaturated compounds, benzene, isoprene, and ethylene were selected for more detailed study. The results are represented graphically in Fig. 4. While the results at varying concentrations do not change the order of effectiveness of the three addends, they do establish the concentrations at which each addend is maximally effective. The maximum abundances obtained for the three addends were 78.7, 64.0, and 48.1 for benzene, isoprene, and ethylene respectively.

Can. J. Chem. Downloaded from www.nrcresearchpress.com by 176.9.209.113 on 09/04/12
For personal use only.

TABLE I

The effect of various unsaturated addends on the Hg^{202} content of the solid product of the reaction of $Hg^{202}6(^3P_1)$ atoms in Hg^N with flowing hydrogen chloride*

Addend	Concentration, mole %	Hg^{202} abundance, atom %
Ethylene	35	37·1
Propylene	35	40·6
Acetylene	35	51·5
Isoprene	35	60·6
Benzene	35	72·3
Butadiene	35	82·0

*Lamp temperature = 20.0° C; flow rate = 350–375 ml/sec; cell pressure = 10 mm.

DISCUSSION

For pure hydrogen chloride the general mechanism proposed in the Introduction becomes:

$$Hg^{202}6(^3P_1) + HCl \rightarrow Hg^{202}Cl + H \quad [1]$$

$$Hg^{202}6(^3P_1) + HCl \rightarrow Hg^{202} + H + Cl \quad [2]$$

$$Cl + Hg^N + M \rightarrow Hg^NCl + M. \quad [3]$$

In the earlier study (5) it was pointed out that Cl atoms are also likely formed by abstraction reactions of the H atoms, generated in [1] and [2], with the substrate

$$H + HCl \rightarrow H_2 + Cl. \quad [4]$$

It would be expected that [4] would be at least as fast as the corresponding abstraction reaction with methyl radicals:

$$CH_3 + HCl \rightarrow CH_4 + Cl. \quad [5]$$

For this reaction Cvetanović and Steacie [7] found a collision yield of 2×10^{-4} at 28° C, corresponding to a maximum activation energy of 5.1 kcal per mole. Reaction [4] could therefore be of considerable importance in the present investigation. On the other hand, the recombination of H and Cl atoms, discussed in the earlier paper (5),

$$H + Cl + M \rightarrow HCl + M, \quad [6]$$

should be unimportant under our conditions owing to the high concentration of Hg^N, which is being constantly replenished in the fast-flow system. Reaction [3], therefore, should account almost exclusively for Cl atom consumption.

For the four-step mechanism, [1]–[4], the relative rate ratio, from steady-state considerations,

$$R_{Hg^NCl}/R_{Hg^{202}Cl} = (1 + \Phi_2)/\Phi_1 = (100-A)/(A-29.8),$$

where Φ_1 and Φ_2 are the relative fractions of the chemically quenched radiation partitioned to [1] and [2] respectively, and A is the percentage Hg^{202} abundance in the recovered calomel. In the present study the A value for pure substrate was found to be 39.9 ± 0.3, whence $(1+\Phi_2)\,(\Phi_1) = 6.0\pm0.2$, and $\Phi_1/\Phi_2 = 0.40\pm0.02$. In the first paper on this reaction (5), an A value of 44% was obtained, corresponding to $\Phi_1/\Phi_2 = 0.68$. In view of the higher analytical reproducibility obtained in this study, together with the fact that the A values were obtained for two totally different methods of mercury recovery, the Φ_1/Φ_2 value of 0.40 ± 0.02 should be more reliable than the earlier one.

Can. J. Chem. Downloaded from www.nrcresearchpress.com by 176.9.209.113 on 09/04/12
For personal use only.

It is interesting to compare the value of the ratio, Φ_1/Φ_2, for hydrogen chloride to that obtained in the reaction of $Hg^{202}6(^3P_1)$ atoms, in Hg^N, with water vapor. Pertel and Gunning (2, 3) obtained a value for A of $33.4\pm1.0\%$ for pure substrate. For water vapor the corresponding four-step sequence would be:

$$Hg^{202}6(^3P_1) + HOH \rightarrow Hg^{202}OH + H \quad [1']$$
$$Hg^{202}6(^3P_1) + HOH \rightarrow Hg^{202} + H + OH \quad [2']$$
$$OH + Hg^N + M \rightarrow Hg^NOH + H \quad [3']$$
$$H + HOH \rightarrow H_2 + OH. \quad [4']$$

From the A value $\Phi_1/\Phi_2 = 0.10\pm0.03$. In short, the isotopically specific primary process is some four times more important in hydrogen chloride than in water vapor. It would be expected that the importance of [1] would be related to the stability of the mercury compound formed in the reaction. Since HgCl is considerably more stable than HgOH, compound formation should be favored for hydrogen chloride. The stability consideration would be partially offset, however, by the larger number of vibrational degrees of freedom, available in HgOH, to take up excess energy associated with the quenching process.

It should be emphasized that the Φ_1/Φ_2 values for hydrogen chloride and water vapor are minimum values since any isotopically degradative exchange processes operative either in the reaction, or during recovery of the mercury for analysis, would lower the apparent value of the abundance, and yield a spuriously low value for Φ_1/Φ_2.

As stated earlier in this paper, the major emphasis in the present investigation was placed on the effect of unsaturated addends on the Hg^{202}-abundance values. Here considerable progress was made over the previous investigation (5). Average maximum abundances of 83% were consistently obtained at butadiene concentrations of 20–40 mole %, whereas the highest abundance obtained hitherto was 59% for hydrogen chloride–butadiene mixtures. In this connection the question naturally arises whether degradative reactions have now been completely eliminated in product recovery. In the previous study the calomel was dissolved from the cell in concentrated hydrochloric acid at 100° C. No attempt was made to control the time of contact of the reaction products with the hot acid. From the present study this contact time would appear to be very critical if exchange degradation is to be minimized. Optimum conditions involve a contact time not exceeding 10 minutes, followed by rapid neutralization of the acid extract.

It is instructive to compare the maximum enrichments obtained in the hydrogen chloride and water vapor reactions, for butadiene as the addend. Pertel and Gunning (3) found that the maximally enriched HgO product of the water reaction contained 85% Hg^{202}, at a butadiene concentration of 21 mole %. From Fig. 1, it can be seen that the most highly enriched $Hg^{202}Cl$ contained 84.2% Hg^{202}, and the corresponding butadiene concentration was 26 mole %. Hence the maximum Hg^{202} abundances and the butadiene concentrations are almost identical in the two reactions. Since the HgO product was removed with cold, dilute hydrochloric acid, whereas hot concentrated acid was required to dissolve the HgCl product, and since it has been shown (3) that high acid concentrations favor exchange degradation, it appears probable that exchange reactions are unimportant for the HCl method of calomel recovery. In Fig. 1 the effect of exchange degradation is clearly shown. The consistently lower values obtained by the NH_3 method must be ascribed to this type of isotopic degradation. The fact, apparent from Fig. 1, that exchange degradation becomes more extensive at higher butadiene concentrations, suggests that the controlling factor is the ratio of the quantities of enriched calomel to adsorbed mercury present in the cell. With increasing butadiene concentrations, the

Can. J. Chem. Downloaded from www.nrcresearchpress.com by 176.9.209.113 on 09/04/12
For personal use only.

competitive quenching progressively reduces the product yield for a fixed duration of exposure. The quantity of adsorbed mercury on the other hand should be relatively independent of quenching partitioning. The fact that the HCl method, as shown in Fig. 1, leads to maximum Hg^{202} abundances which are invariant in butadiene concentration is further evidence that exchange has been eliminated by using this technique for product recovery.

For the hydrogen chloride reaction the unsaturated addend (U) would serve to remove both Cl and H atoms:

$$Cl + U \rightarrow \text{products} \quad [7]$$
$$H + U \rightarrow \text{products}. \quad [8]$$

If, for the mechanism of the reaction with addend, we consider steps [1]–[4], together with [7] and [8], it can be readily shown by steady-state calculations that the effectiveness of the addend at fixed mole fraction is determined by the ratio of k_8/k_4 only. The corresponding steps for the water reaction would be:

$$OH + U \rightarrow \text{products} \quad [7']$$
$$H + U \rightarrow \text{products}. \quad [8]$$

The fact that almost identical maximum enrichments are obtained in the hydrogen chloride and water vapor reactions, with butadiene as addend, suggests that reaction [8], which is common to both mechanisms, is the dominant factor in determining the effectiveness of the addend. Maximum enrichment would occur when the H atoms are disappearing almost exclusively by reaction [8]. On this basis other reasons must be sought for the failure to obtain maximum abundances identical with the Hg^{202} content of the lamp isotope (98.3% Hg^{202}).

In order to obtain maximum abundances identical with that of the lamp isotope, the emission line must not overlap hyperfine absorption contours adjacent to that of Hg^{202}. If some overlap is occurring at lamp-wall temperatures of 23° C, it would be expected that a decrease in source temperature would reduce the extent of this overlap. Figure 2 shows clearly that reduced lamp-wall temperature does not improve enrichment. On the other hand, increasing lamp temperature does result in a decreased enrichment, showing thereby that the absorption-line width does indeed increase significantly over the range of lamp temperatures studied. No appreciable overlap occurs until lamp-wall temperatures exceeding 35° C are reached. The problem of lamp-wall temperature is, however, complicated by the fact that the enrichment apparently increases with increasing absorbed intensity (5). This effect may obscure any increase in enrichment associated with a decrease in lamp temperature. The slight maximum in enrichment shown in Fig. 2, at approximately 20° C, may arise from the net effect of the intensity and broadening factors. The problem can only be answered unequivocably by a total isotopic analysis of the maximally enriched products in the hydrogen chloride and water reactions. Mass spectrometric studies are now underway in the laboratories of one of us (H.E.G.) as one result of which considerable light should be shed on the importance of overlap in these reactions.

The results shown in Figs. 2 and 3 on the effects of increasing lamp-wall temperature and substrate pressure on the enrichment point up clearly the importance of broadening factors in emission and absorption of the Hg^{202} enrichment. These data offer further confirmation for the proposed mechanism in that these broadening influences would operate only in the primary act of absorption.

Can. J. Chem. Downloaded from www.nrcresearchpress.com by 176.9.209.113 on 09/04/12
For personal use only.

Can. J. Chem. Downloaded from www.nrcresearchpress.com by 176.9.209.113 on 09/04/12
For personal use only.

The variation of enrichment with substrate pressure for the maximally enriching hydrogen chloride – butadiene system as shown in Fig. 3 serves to define clearly the pressure beyond which Lorentz-broadening becomes significant. At total pressures below 25 mm the Lorentz effect does not appear detectably to broaden the hyperfine absorption contours.

The broadening influences on the emission line apparently cause appreciable overlap when the lamp-wall temperature is increased from 23° C to 48° C. The Doppler effect is quite inadequate to account for this broadening. An increase of 25° C would result in an increase of emission-line half-width by the Doppler effect of only 0.1 mÅ, whereas the hyperfine contours are separated by approximately 10 mÅ (1). However, with increasing lamp temperature, the vapor pressure of mercury will rise rapidly leading to increased self-reversal (1) of the resonance line. Furthermore, there will be a marked increase in the lamp current. Pressure- and current-broadening will therefore be simultaneously operative at higher lamp temperatures.

In Table I,e % effectiveness of six unsaturated addends are compared, at a concentration of 35 mol the. From the foregoing discussion on the mechanism of the reaction in the presence of addends, it would appear that these relative efficiencies are primarily determined by the rate of addition of H atoms to the double bond, as shown in reaction [8]. In Figs. 1 and 4, the curves for the variation in Hg^{202} abundance with concentration for the four addends show that the order of decreasing effectiveness is butadiene, benzene, isoprene, and ethylene. It should be emphasized that the effectiveness of an addend will be very sensitive to small differences in the activation energy of reaction [8], since absolute rate constant ratios are the determining factor.

From the proposed mechanism, it would be expected that the Hg^{202} abundance should increase with increasing addend concentration, and approach asymptotically the Hg^{202} abundance in the lamp. However, even with butadiene, the most effective addend studied, the abundance maximizes at an average value of 83%, some 15% lower than the Hg^{202} abundance in the mercury present in the lamp. From this investigation, it seems unlikely that the discrepancy can be attributed to broadening either in emission or absorption, since the range of influence of these parameters has been examined in the present investigation. There is apparently some other process operative in these reactions, which leads to degradation of the $Hg^{202}Cl$ formed in [1]. The same situation exists in the water reaction. In the laboratories of one of us (H.E.G.) further investigations are in progress on the detailed kinetics of these reactions. It is hoped that these studies will lead to a more complete understanding of the mechanism involved in reactions of this type.

CONCLUSIONS

By minimizing exchange reactions in product recovery, and determining quantitatively the influence of broadening factors in emission and absorption, the kinetics of the reaction of $Hg^{202}6(^3P_1)$ atoms, in Hg^N, with hydrogen chloride has been placed on a more quantitative basis than proved possible in the earlier study (5). It has now been established that the ratio Φ_1/Φ_2 has the value of 0.40 ± 0.02 at room temperature.

Under the conditions defined in this paper, the hydrogen chloride reaction could be used to advantage in the preparation of Hg^{202} from natural mercury. It has now been shown that enrichments equal to those obtainable in the water reaction can be conveniently produced in the hydrogen chloride system.

In both the hydrogen chloride and water vapor reactions, the effectiveness of an unsaturated addend, in increasing the Hg^{202} abundance in the recovered mercury product, is

apparently determined primarily by the rate of addition of H atoms to the double bond in the addend.

In both the hydrogen chloride and water reactions, the maximum abundances obtained are still some 15 atom % lower than that of the lamp isotope. Mass spectrometric studies now in progress on the total isotopic analysis of the enriched mercury in the solid reaction products and related investigations should be of considerable value in determining the reason for the discrepancy.

ACKNOWLEDGMENTS

This work was supported in part by the National Research Council of Canada through Block Term Grant No. NRC-BT-74. This assistance is most gratefully acknowledged.

One of us (J.R.M.) would like to express his deep appreciation to the International Nickel Company for generous Fellowship support.

REFERENCES

1. OSBORN, K. R., McDONALD, C. C., and GUNNING, H. E. J. Chem. Phys. **26**, 124 (1957).
2. PERTEL, R. and GUNNING, H. E. J. Chem. Phys. **26**, 219 (1957).
3. PERTEL, R. and GUNNING, H. E. Can. J. Chem. **37**, 35 (1959).
4. GUNNING, H. E. Can. J. Chem. **36**, 89 (1958).
5. McDONALD, C. C., McDOWELL, J. R., and GUNNING, H. E. Can. J. Chem. **37**, 930 (1959).
6. OSBORN, K. R. and GUNNING, H. E. J. Opt. Soc. Am. **45**, 552 (1955).
7. CVETANOVIĆ, R. J. and STEACIE, E. W. R. Can. J. Chem. **31**, 158 (1953).

Can. J. Chem. Downloaded from www.nrcresearchpress.com by 176.9.209.113 on 09/04/12
For personal use only.

Can. J. Chem. Downloaded from www.nrcresearchpress.com by 176.9.209.113 on 09/04/12
For personal use only.

THELEPHORIC ACID[1]

G. READ[2] AND L. C. VINING

ABSTRACT

The electronic and infrared absorption spectra of thelephoric acid and its leucoacetate indicate that the structure at present accepted for the pigment is incorrect. It is suggested from an interpretation of these spectra, together with a re-evaluation of the reported properties of thelephoric acid and its derivatives, that the substance may be a hydroxylated terphenyl containing internal quinhydrone and benzofuran systems (e.g. (V)).

Structure (I), proposed by Kögl, Erxleben, and Jänecke (8), is widely quoted for thelephoric acid, which occurs in several lichens and many of the higher fungi (6, 14). The sparing solubility of a compound of this structure in sodium bicarbonate and sodium carbonate solutions is surprising. Furthermore, (I) does not fall into any of the broad groups of naturally occurring compounds and is difficult to reconcile with accepted theories of biogenesis. Recently Millward and Whiting (10) have shown that synthetic 1,2′-phenanthryl-1,3-butadiene differs in melting point from the hydrocarbon of that structure reported to be formed by zinc dust distillation of acetylthelephoric acid (8). They concede that polymorphism or the unlikely survival of a *cis*-form could account for

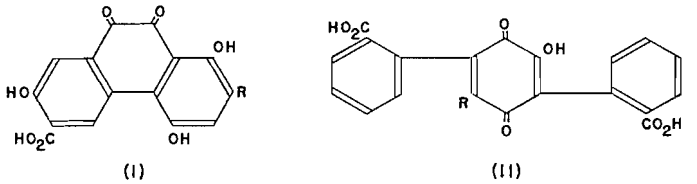

(I) (II)

(I) and (II) R = $[CH:CH]_2CO_2H$

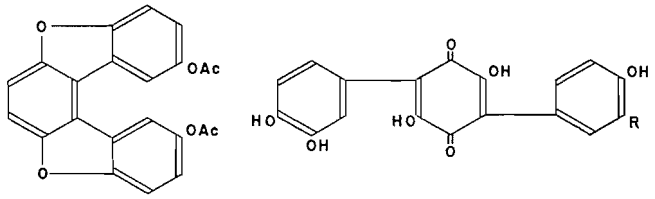

(III) (IV)

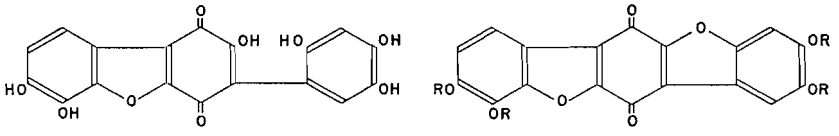

(V) (VI)

[1]*Manuscript received April 24, 1959.*
Contribution from the National Research Council of Canada, Prairie Regional Laboratory, Saskatoon, Saskatchewan.
Issued as N.R.C. No. 5287.
[2]*National Research Council of Canada Postdoctorate Fellow, 1957–59. Present address: The Dyson Perrins Laboratory, Oxford University, Oxford, England.*

the difference, but their doubt concerning the nature of this product seems especially pertinent in view of Kögl and Erxleben's claim that a dienoic acid side chain is lost from muscarufin (II) in a comparable reaction (7). Only limited amounts of material were available for the classical degradations of the pigment (8), and it seemed desirable to confirm the structure by modern physical methods.

Small samples of thelephoric acid and its "leucopentaacetate" were obtained through the generosity of Professor S. Shibata. The infrared spectrum of the pigment was not well defined suggesting heterogeneity. It showed a single peak (1629 cm^{-1}; (s)) in the carbonyl stretching region. The leucoacetate gave peaks in this region at 1760 cm^{-1} (s) (acetate) and 1630 cm^{-1} (w). In view of the absence of any bands attributable to carboxyl groups, the accepted structure for thelephoric acid is clearly untenable. Moreover, the ultraviolet absorption of the leucoacetate (Fig. 1) is inconsistent with that of an acetoxylated phenanthryldienoic acid.

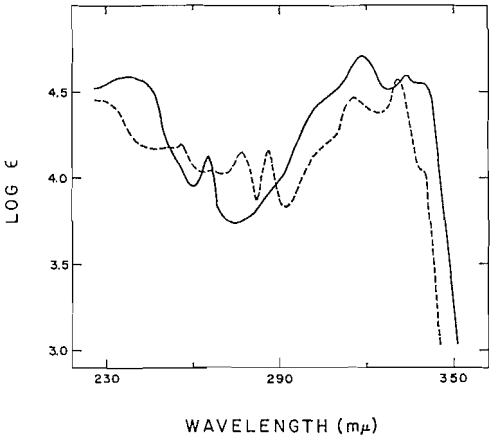

FIG. 1. Absorption spectra of thelephoric acid leucoacetate (———), and 2,11-diacetoxybenzobis-[1,2-*b*,4,3-*b*']-benzofuran (– – –) (III).

A striking property of thelephoric acid is its intense blue-black color in the solid state, whereas a solution in pyridine is wine-red in color and shows an absorption maximum at only 493 mμ. This suggests a quinhydrone, and the color, insolubility, stability to recrystallization, and color reactions of this material are reminiscent of the internal diphenyl quinhydrone systems examined by Erdtman (3). Thomson has also noted (14) that, like thelephoric acid, 5,6-dihydroxy-1,4-naphthoquinone gives a cornflower-blue solution in aqueous pyridine, and the terphenyl quinone, polyporic acid, behaves similarly (11). A quinhydrone structure would account for the single carbonyl band at 1629 cm^{-1} in the infrared spectrum of thelephoric acid. Other possible assignments for this band are a quinomethine, an extended quinone, or a perihydroxylated quinone, but the last can be excluded by the ultraviolet spectrum of the leucoacetate which, if representing a single chromophore, is incompatible with any fused-ring aromatic system. This spectrum is basically similar to that of dibenzofuran, but bathochromic and hyperchromic displacement of the 280-mμ band suggests a more extended system. It, in fact, closely resembles that of 3-aminodibenzofuran (13), but its absorption in the region of 320 mμ is higher (log ε 4.70 vs. 4.22). The absorption from 290 to 360 mμ shows a marked similarity to that of the terphenyl (III) (Fig. 1), but there are differences between 240 and 290 mμ. The infrared spectra of the leucoacetate and (III) are basically similar and show, in common

Can. J. Chem. Downloaded from www.nrcresearchpress.com by 176.9.209.113 on 09/04/12
For personal use only.

with the pigment, weak aromatic absorption bands between 1550 and 1635 cm^{-1}, and strong bands at ca. 1025 (aromatic ether) and 800 cm^{-1} (two adjacent aromatic hydrogens). The pigment and leucoacetate also show a band at ca. 870 cm^{-1} (isolated aromatic hydrogen). The properties of the materials examined are therefore compatible with highly oxygenated terphenyl derivatives, the occurrence of which in higher fungi and lichens has frequently been reported (6, 14).

In attempting to rationalize the published evidence for structure (I) with the current spectral data, the possibility cannot be ruled out that the two samples of thelephoric acid are different. Unfortunately, the material examined by Kögl *et al.* was not obtainable, but in view of the close agreement in properties reported for the two compounds (2), this possibility seems remote. Moreover, a specimen kindly supplied by Dr. J. Gripenberg had an infrared spectrum virtually identical with that of the Japanese sample.

The initial analytical figures obtained by Asahina and Shibata for the pigment (2) agree with $C_{18}H_{10}O_9$, e.g. (V), in addition to the $C_{20}H_{12}O_9.H_2O$ formula adopted. Carbon and hydrogen analyses obtained by both the Japanese and European workers for the acetate fit a $C_{26}H_{16}O_{12}$ molecule, e.g. (VI; R = Ac), while the analyses obtained by Asahina and Shibata for the leucoacetate agree with the required figures for the leucoacetate of (VI; R = Ac). In reported analyses for thelephoric acid, the hydrogen values are all low for $C_{20}H_{12}O_9$, and the carbon values variable (59.89 to 60.99%). Furthermore, Asahina and Shibata could only approach the required analysis for structure (I) by prolonged drying of the sample at elevated temperatures at which (V) might be expected to dehydrate. Analyses obtained would also be given by a 1:1 mixture of (V) and (VI; R = H). Under the conditions used, acetylation and reductive acetylation of such a mixture might be expected to yield a single acetate, e.g. (VI; R = Ac), and leucoacetate. It is therefore suggested that (V) or a closely related isomer represents the structure for thelephoric acid as initially isolated by the Japanese workers. Such a compound might be formally derived from leucomelone (IV; R = H) (1) by hydroxylation to the terphenyl quinone (IV; R = OH), oxidation to a diquinone, rearrangement, and hydroxylation.

The isolation from compounds such as (VI; R = Ac) of the key hydrocarbon from which 2-phenanthroic acid and subsequently phenanthrene were obtained is conceivable if the initial result of zinc dust distillation is a fission of the quinone ring leading to substituted benzofuran and phenyl fragments. A condensation analogous to that in which phenanthrene is formed by pyrolysis of benzofuran and benzene (9) might then yield a phenanthrene derivative such as 2-vinyl phenanthrene (m.p. 116.5–118° C) (12) which is similar in analysis to the reported 1,2-phenanthrylbuta-1,3-diene (m.p. 126° C).

The authors realize that this hypothesis leaves unexplained many aspects of the chemistry of thelephoric acid but hope that it may serve to stimulate further studies by chemists with access to the substance.

EXPERIMENTAL

Infrared spectra of the compounds in pressed potassium bromide disks were measured with a Perkin–Elmer double beam spectrometer, model 21. Because of the poor solubility and the smallness of the samples, solution spectra could not be obtained.

The ultraviolet and visible absorption spectra were measured on a Warren Spectracord double beam recording spectrophotometer, model 3000. Thelephoric acid was examined in pyridine, the remaining samples in freshly purified dioxane. The leucoacetate of thelephoric acid showed λ_{max} 238, 265, 318, and 334 mμ, log ϵ 4.64, 4.18, 4.77, and 4.64 respectively, based on a molecular formula $C_{30}H_{22}O_{14}$.

Can. J. Chem. Downloaded from www.nrcresearchpress.com by 176.9.209.113 on 09/04/12
For personal use only.

2,11-Diacetoxybenzobis-[1,2-*b*,4,3-*b*']-benzofuran (III) was prepared according to the method used by Erdtman (4) and had m.p. 236–238° C. (Erdtman reports m.p. 236–237° C.) Found: C, 70.51%; H, 3.92%. Calculated for $C_{22}H_{14}O_6$: C, 70.58%, H, 3.77%. Ultraviolet absorption maxima at 257, 265.5, 277, 286, 315, 331 mμ, log ϵ 4.19; 4.04, 4.16, 4.17, 4.46, 4.55 respectively; inflexion at 233 mμ, log ϵ 4.50. The *p*-terphenyl structure assigned to this compound at the time it was first prepared has since been corrected (5).

ACKNOWLEDGMENTS

The authors wish to express their appreciation to Professor S. Shibata, Tokyo University, Japan, and to Dr. J. Gripenberg, Finland Institute of Technology, Helsingfors, for gifts of samples, and to Miss I. M. Gaffney for measurement of the infrared spectra.

REFERENCES

1. Akagi, M. J. Pharm. Soc. Japan, **62**, 129 (1942).
2. Asahina, Y. and Shibata, S. Chem. Ber. **72**, 1531 (1939).
3. Erdtman, H. Proc. Roy. Soc. A, **143**, 191 (1934).
4. Erdtman, H. Proc. Roy. Soc. A, **143**, 228 (1934).
5. Erdtman, H. and Wachtmeister, C. A. *In* Festschrift Arthur Stoll. Birkhäuser, Basel. 1957. p. 153.
6. Gripenberg, J. Acta Chem. Scand. **12**, 1411 (1958).
7. Kögl, F. and Erxleben, H. Ann. **479**, 11 (1930).
8. Kögl, F., Erxleben, H., and Jänecke, L. Ann. **482**, 105 (1930).
9. Kraemer, G. and Spilker, A. Chem. Ber. **23**, 84 (1890).
10. Millward, B. B. and Whiting, M. C. J. Chem. Soc. 903 (1958).
11. Murray, J. J. Chem. Soc. 1345 (1952).
12. Price, C. C. and Halpern, B. D. J. Am. Chem. Soc. **73**, 818 (1951).
13. Sawicki, E. and Ray, F. E. J. Am. Chem. Soc. **75**, 2519 (1953).
14. Thomson, R. H. Naturally occurring quinones. Butterworth Scientific Publications, London. 1957.

Can. J. Chem. Downloaded from www.nrcresearchpress.com by 176.9.209.113 on 09/04/12
For personal use only.

Can. J. Chem. Downloaded from www.nrcresearchpress.com by 176.9.209.113 on 09/04/12
For personal use only.

CATALYTIC ACTIVATION OF HYDROGEN IN AQUEOUS SOLUTION BY THE CHLOROPALLADATE(II) ION[1]

J. HALPERN, J. F. HARROD, AND P. E. POTTER[2]

ABSTRACT

The kinetics of the reduction of ferric chloride by molecular hydrogen in aqueous solution, in the presence of chloropalladate(II), were examined. The latter acts as a homogeneous catalyst for the reaction. The rate-law was found to be,

$$-d[H_2]/dt = k[H_2][PdCl_4^{=}]$$

where

$$k = 6.6\times10^{11} \exp[-20{,}000/RT] \text{ liter mole}^{-1} \text{ sec}^{-1}.$$

The mechanism of the reaction is discussed.

INTRODUCTION

Metallic palladium is readily precipitated from aqueous solutions of palladous chloride by reduction with hydrogen. Ipatieff and Tronev (1) found this reaction to be autocatalytic, in line with the well-known heterogeneous catalytic activity of palladium for hydrogenation reactions in general. However, when oxidizing substrates such as ferric chloride were present in the solution, precipitation of the palladium was preceded by an induction period during which the substrate underwent reduction. Since metallic palladium apparently was absent during this stage, this observation suggests that the dissolved palladium salt may be acting as a homogeneous catalyst for the hydrogenation of the substrate. This paper describes a kinetic study of the reaction, the results of which confirm this view.

Previously, the ability to activate hydrogen homogeneously and catalyze its reactions in solution has been demonstrated for ions and complexes of only a few other metals notably copper, silver, mercury, and cobalt (2, 3). Importance has been attached to the study of these systems, not only for their intrinsic interest, but also because of the insight they provide into the mechanism of action of related heterogeneous and enzymic catalysts, which often cannot be elucidated directly because of their greater chemical and kinetic complexity (4).

EXPERIMENTAL

Hydrated palladous oxide, precipitated with NaOH from a solution of reagent grade palladous chloride and washed thoroughly, was dissolved in 3 *M* HCl to give a stock solution of H_2PdCl_4. The concentration of palladium was determined by precipitation with dimethylglyoxime. Hydrogen was obtained from Canadian Liquid Air Co., passed through a "deoxo" catalytic purifier to remove oxygen, and dried over P_2O_5. Other chemicals were of reagent grade.

Several procedures for making the desired kinetic measurements were examined. The most satisfactory of these proved to be the determination of the rate of catalytic reduction

[1]*Manuscript received May 19, 1959.*
Contribution from the Department of Chemistry, University of British Columbia, Vancouver, B.C. Support of this work through grants from the National Research Council of Canada and Imperial Oil Limited is gratefully acknowledged.
[2]*Present address: Inorganic Chemistry Department, Imperial College of Science and Technology, London S.W.7, England.*

Can. J. Chem. Downloaded from www.nrcresearchpress.com by 176.9.209.113 on 09/04/12
For personal use only.

of ferric chloride by measuring the volume of hydrogen taken up at constant pressure. The results reported in this paper were obtained by this method, the details of which have been previously described (5). An attempt was also made to examine the kinetics of the catalyzed reduction of dichromate by the procedure used earlier to study the activation of hydrogen by silver salts (6), that is, bubbling hydrogen through the solution and following the decrease in dichromate concentration spectrophotometrically. The overlap of the palladium and dichromate absorption bands and the tendency of metallic palladium (a powerful heterogeneous catalyst) to form prior to complete reduction of the dichromate, limited the accuracy of this procedure but, on the whole, the results obtained by the two methods were in satisfactory accord.

RESULTS AND DISCUSSION

The kinetics of the reduction of ferric chloride, in the presence of palladium chloride, were found to be,

$$[1] \qquad -d[H_2]/dt = k[H_2][PdCl_4^{=}].$$

Typical rate plots showing the uptake of H_2 are given in Fig. 1. Since the concentrations of $PdCl_4^{=}$ and of H_2 remain constant while ferric chloride is being reduced the kinetics are of pseudo zero-order. Reduction of palladous chloride itself commenced only when reduction of $FeCl_3$ to $FeCl_2$ was nearly complete and was marked by an increase in the rate of H_2 uptake due to autocatalysis by metallic Pd; prior to this point the reaction is apparently homogeneous.

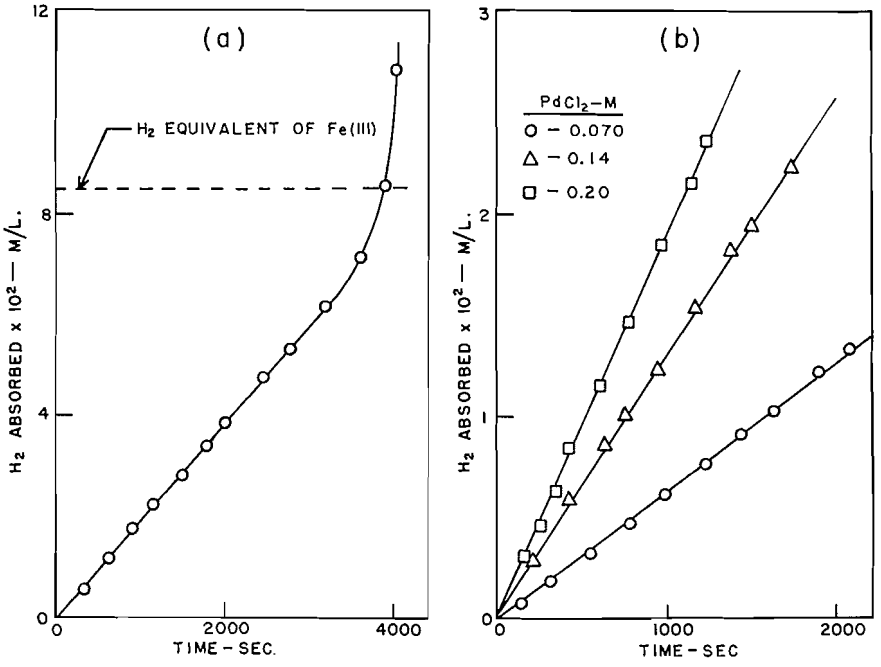

FIG. 1. Typical rate plots at 80°, 450 mm H_2. (*a*) 0.20 *M* $PdCl_2$, 0.17 *M* $FeCl_3$; reduction of $FeCl_3$ carried to completion; (*b*) 0.2 *M* $FeCl_3$, various $PdCl_2$ concentrations.

The kinetic results in Table I are in accord with equation [1]. Values of k, determined from the slopes of the zero-order rate plots using equation [1], are seen to be substantially independent of the initial concentrations of $FeCl_3$, $PdCl_2$, and H_2 over a considerable

range of each. The concentration of H_2 was calculated using the solubility data of Wiebe and Gaddy (7), correcting for the effect of HCl. The latter correction (−18% for 3 *M* HCl) was based on room temperature data (8) but it is unlikely that the error due to this is appreciable.

TABLE I

Summary of kinetic data at 80° C

$[PdCl_2]$ (molar)	H_2 (mm)	$[H_2]\times10^4$ (molar)[a]	Initial $[FeCl_3]$ (molar)	Medium	Rate of H_2 uptake $\times10^6$ (mole liter^{-1} sec^{-1})	k (liter mole^{-1} sec^{-1})
0.070	450	3.6	0.20	3 *M* HCl	7.0	0.28
0.113	450	3.6	0.20	3 *M* HCl	11.5	0.28
0.141	450	3.6	0.20	3 *M* HCl	12.5	0.25
0.141	450	3.6	0.10	3 *M* HCl	12.9	0.25
0.188	450	3.6	0.20	3 *M* HCl	17.3	0.26
0.226	450	3.6	0.20	3 *M* HCl	21.5	0.26
0.203	436	3.5	0.15	3 *M* HCl	20.0	0.28
0.203	340	2.7	0.15	3 *M* HCl	14.7	0.27
0.203	275	2.2	0.15	3 *M* HCl	12.8	0.29
0.203	190	1.5	0.15	3 *M* HCl	8.1	0.26
0.203	70	0.5	0.15	3 *M* HCl	3.0	0.27
0.203	450	3.6	0.15	5 *M* HCl	20.7	0.28
0.203	450	3.6	0.15	3 *M* HCl; 2 *M* NaCl	14.9	0.20
0.203	450	3.6	0.15	3 *M* HCl; 2 *M* $NaClO_4$	20.1	0.28
0.203	450	3.6	0.15	3 *M* HCl; 2 *M* $HClO_4$	25.7	0.35

[a]Based on estimated solubility of H_2 in 3 *M* HCl, 6.1×10^{-4} mole atm^{-1}. Data for other media not corrected for variation in solubility.

Varying the HCl concentration from 3 *M* to 5 *M* had no effect on k. Since the predominant palladium species in this region is the chloropalladate(II) ion, $PdCl_4^=$ (9), it appears probable that this is the catalytic species. Addition of 2 *M* $NaClO_4$ was also without effect on the rate while 2 *M* NaCl decreased, and 2 *M* $HClO_4$ increased, the rate slightly. These effects are small and attributable to changes in the solubility of hydrogen since they follow the same pattern as do the activity coefficients of non-electrolytes in general (10, 11).

At HCl concentrations below 3 *M* erratic results were obtained because of the tendency of metallic palladium to form (resulting in complications due to heterogeneous catalysis) prior to complete reduction of the substrate. Similar complications were encountered in experiments using $Pd(ClO_4)_2$ in perchloric acid solution. While these experiments failed to yield quantitative information, it was possible to conclude qualitatively that the catalytic activities of the uncomplexed Pd^{++} ion and the lower chloride complexes are lower than that of $PdCl_4^=$; this was also the case for the ethylenediamine complex.

Kinetic measurements at temperatures ranging from 66 to 87.5° yielded the Arrhenius plot in Fig. 2, fitted by the equation,

$$k = 6.6\times10^{11}\exp[-20{,}000/RT] \text{ liter mole}^{-1}\text{ sec}^{-1}.$$

The frequency factor corresponds to an entropy of activation of −6.8 e.u.; this value is in the normal range for a simple bimolecular reaction in solution, and suggests that there is little charge redistribution during formation of the activated complex.

The kinetics described above resemble those found previously for the activation of hydrogen by Cu^{++}, Ag^+, Hg^{++}, and their complexes (2, 12). In a number of these systems it has been shown that the rate-determining step involves heterolytic splitting of H_2

Can. J. Chem. Downloaded from www.nrcresearchpress.com by 176.9.209.113 on 09/04/12
For personal use only.

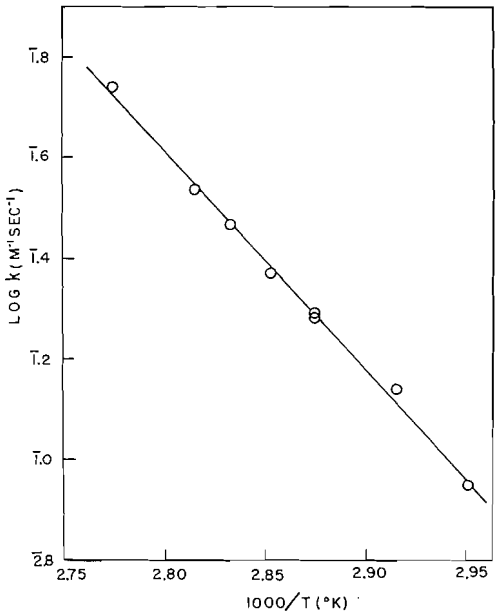

FIG. 2. Arrhenius plot for k.

by the catalytic species* with the formation of a catalyst–hydride complex which is reoxidized in a subsequent rapid reaction with the substrate. It seems likely that the present reaction also proceeds through this type of mechanism, that is,

$$PdCl_4^{=} + H_2 \xrightarrow{k} HPdCl_3^{=} + HCl \qquad [2]$$

$$HPdCl_3^{=} + 2FeCl_3 \xrightarrow{\text{fast}} PdCl_4^{=} + HCl + 2FeCl_2. \qquad [3]$$

Attempts have been made to correlate the catalytic activities of metal ions and complexes with their electron configurations (13, 4). Thus, most of the metal ions which have been found to activate hydrogen in solution have nearly filled or just filled d-shells, and it has been suggested that their catalytic activity is related to their high electron affinities. Attention has also been directed (13, 4) to a link between catalytic activity in homogeneous and heterogeneous systems, suggested by the observation that most of the ions which are catalytically active in solution are "isoelectronic" with metals (Ni, Co, Pd, Pt, etc.) which are good heterogeneous hydrogenation catalysts. The appearance of catalytic activity for a complex of Pd^{++} ($4d^8$; isoelectronic with Ru) is consistent with this pattern. Attention should also be directed to the striking parallel between the postulated hydride intermediate, $HPdCl_3^{=}$, and the electronically analogous complexes of the type $HPtCl(PR_3)_2$, described by Chatt (14).

REFERENCES

1. IPATIEFF, V. V., JR. and TRONEV, V. G. Compt. rend. acad. sci. U.R.S.S. **1**, 624 (1935).
2. HALPERN, J. Quart. Revs. (London), **10**, 463 (1956).
3. WELLER, S. and MILLS, G. A. Advances in Catalysis, **8**, 163 (1956).
4. HALPERN, J. Advances in Catalysis. (In press).

**In the case of Ag^+, there is also an alternative path of activation, second-order in Ag^+, probably involving homolytic-splitting of H_2 in the rate-determining step (12).*

Can. J. Chem. Downloaded from www.nrcresearchpress.com by 176.9.209.113 on 09/04/12
For personal use only.

5. CHALK, A. J. and HALPERN, J. J. Am. Chem. Soc. (In press).
6. WEBSTER, A. H. and HALPERN, J. J. Phys. Chem. **60**, 280 (1956).
7. WIEBE, R. and GADDY, V. L. J. Am. Chem. Soc. **56**, 76 (1934).
8. SEIDELL, A. Solubilities of inorganic and metal organic compounds. Vol. 1. 3rd ed. D. Van Nostrand Co., Inc., New York. 1940. p. 557.
9. DROLL, H. A., BLOCK, B. P., and FERNELIUS, W. C. J. Phys. Chem. **61**, 1000 (1957).
10. RANDALL, M. and FAILEY, C. F. Chem. Revs. 4, 271 (1927).
11. AKERLOF, G. J. Am. Chem. Soc. **57**, 1196 (1935).
12. WEBSTER, A. H. and HALPERN, J. J. Phys. Chem. **61**, 1239, 1245 (1957).
13. HALPERN, J. J. Phys. Chem. **63**, 398 (1959).
14. CHATT, J., DUNCANSON, L.A., and SHAW, B.L. Proc. Chem. Soc. 343 (1957); Chem. & Ind. 859 (1958).

Can. J. Chem. Downloaded from www.nrcresearchpress.com by 176.9.209.113 on 09/04/12
For personal use only.

Can. J. Chem. Downloaded from www.nrcresearchpress.com by 176.9.209.113 on 09/04/12
For personal use only.

RELATIONS BETWEEN HEATS OF FORMATION FOR INORGANIC SYSTEMS[1]

A. D. WESTLAND

ABSTRACT

Some empirical relationships dealing with the heats of formation of crystalline compounds are interrelated. A more general relation based upon functions derived from heats of formation and applicable to dissolved species as well as crystals is described. The relation may be used as a criterion for thermal data and for estimation of heats of formation. Deviations of literature values from those predicted by the relation are discussed in the light of structural features.

In recent years a number of empirical relations have been found to exist concerning heats of formation or lattice energies of crystalline ionic compounds (1–5). While presenting one of these (4), Hoppe showed it to be a more general case of the relation discovered by Fomin (3). It is the purpose of this paper to show that both of these relations and that of Karapet'yants (5) are special cases of a more general one.

Hoppe derived his method from certain theoretical considerations which were, however, in error. He supposed that the quantity

$$[1] \qquad \nabla^*(\mathrm{F,O})_{\mathrm{Me}} = -\frac{\Delta H^*(\mathrm{MeF}_{2x})}{\text{equivalents}} - \frac{\Delta H^*(\mathrm{MeO}_x)}{\text{equivalents}}$$

in which ΔH^* is the heat of formation of the compound from gaseous atoms in their ground states, would be invariant for the fluorides and oxides of various metals, Me, providing non-coulombic contributions to the lattice bonding are not involved. The conclusion drawn from this was that ∇^*-functions for various series of compounds of a given set of cations would yield a straight line if plotted one against the other. For example, one might plot ∇^*-functions for the nitrates of group I and II metals against the ∇^*-functions for the chlorides of the same metals. The second term in the expression for ∇^* may be taken as the thermal datum for the oxide in each case. Linearity was indeed observed.

The linearity is more correctly rationalized as follows: If we express ΔH^* by means of the Born–Haber cycle using the fundamental electrostatic expressions of Born, we have

$$[2] \qquad -\Delta H^* = \frac{NAe^2}{r^+ + r^-} + \frac{B}{(r^+ + r^-)^n} + \frac{C}{(r^+ + r^-)^6} - I + E - D$$

in which N is Avogadro's number, e is the charge on the ions in electrostatic units, A is the Madelung factor, B is a constant, C is a function of the ionic polarizabilities and zero-point frequencies, I is the sum of the ionization potentials of the metal, E is the electron affinity of the non-metal, D is the dissociation energy of the non-metal, r^+ is the cation radius, r^- is the anion radius, and n is the so-called Born exponent. Upon substitution of this in equation [1], the I terms disappear by subtraction and in plotting one ∇^*-function against another, the $E-D$ terms make up the constant of linearity. Otherwise the ∇^*-functions consist of a linear combination of terms of the form: $(r^+ + a)^{-p}$ where r^+ is a variable taking the values of the radii of the various cations and a is the constant anion radius. The exponent p may have the values 0, n, or 6. The corresponding terms of ΔH^* have decreasing significance in this order.

[1]*Manuscript received March 9, 1959.*
Contribution from the Department of Chemistry, University of Ottawa, Ottawa, Ontario.

Two functions $(r^+ + a_1)^{-p}$ and $(r^+ + a_2)^{-p}$ will be in approximately linear relation one to another, that is the slope at various points of a plot of one function against the other for corresponding values of r^+ will be approximately constant, if

$$[3] \qquad \frac{d(r^+ + a_1)^{-p}}{d(r^+ + a_2)^{-p}} = \left(\frac{r^+ + a_2}{r^+ + a_1}\right)^{p+1}$$

is essentially constant. It follows that the same condition leads to linearity between ∇^*-functions. For $p = 1$ the change in the derivative is never large over the range of values of r^+, a_1, and a_2 encountered in practice. One can easily see upon inserting the ionic radii of alkali halides, oxides, etc., that the maximum change in passing from lithium to caesium amounts to 18%. In terms of the slope of a curve this is not a large change. Thus if a line is being drawn through experimental points governed by this function a departure from linearity is hardly noticed. However, the terms containing higher values of p result in expressions giving plots which are slightly less satisfactory approximations to straight lines.

Since $\nabla^*(F,O)_{Me}$ is not invariant for various metals, Hoppe concluded that there is a certain amount of non-coulombic bonding present. He maintained further that the ∇^*-function is a measure of such non-coulombic bonding. The above development shows that the ∇^*-function indicates not so much departure from purely ionic bonding; rather it simply reflects the change in ionic size.

It is evident that Hoppe's relation is unnecessarily complicated. It is sufficient to plot the quantities ΔH^{**} defined by

$$[4] \qquad -\Delta H^{**} = (-\Delta H_f + S + I)/\text{equivalents}$$

in which ΔH_f is the heat of formation of the compound from the elements in their standard states and S is the sublimation energy of the metal component. This has the advantage that only one thermochemical quantity is required in addition to S and I. The last two quantities are known for most metals to a sufficient degree of accuracy, for good plots are obtained in general. An error of a few per cent in S or I has a negligible effect on the plots in practice.

We are now in a position to compare Hoppe's device with that of Karapet'yants. The latter plotted lattice energies in the same manner that Hoppe plotted ∇^*-functions and obtained straight line plots for compounds of elements in the same valence state. That is, he obtained a straight line for compounds of univalent elements, a different one for bivalent elements, and so on.

By plotting ΔH^{**}-values one combines the two methods to give a more general one. Moreover, since $(r^+ + r^-)^{-p}$ is symmetrical in r^+ and r^-, it follows that series of compounds each containing a common cation instead of a common anion could be employed for setting up a linearity relation. This may be done by defining

$$[5] \qquad -\Delta H^{**} = (-\Delta H_f + D - E)/\text{equivalents.}$$

A better approximation to a straight line plot is possible. If one plots the logarithm of the lattice energies per equivalent, the slope is still more nearly constant in a given case because the exponent p in $(r^+ + a)^{-p}$ is no longer significant, for the expression analogous to [3] is

$$[6] \qquad \frac{d \log (r^+ + a_1)^{-p}}{d \log (r^+ + a_2)^{-p}} = \frac{r^+ + a_2}{r^+ + a_1} .$$

Plots of this sort are shown in Figs. 1 and 2.[2] In the first figure the lines were drawn so as

[2]*These and other heats of formation were taken from the National Bureau of Standards Circular 500.*

Can. J. Chem. Downloaded from www.nrcresearchpress.com by 176.9.209.113 on 09/04/12
For personal use only.

to fit the points of the group II metals best. Departure from the line may be expected when there is considerable covalent contribution to the bonding.

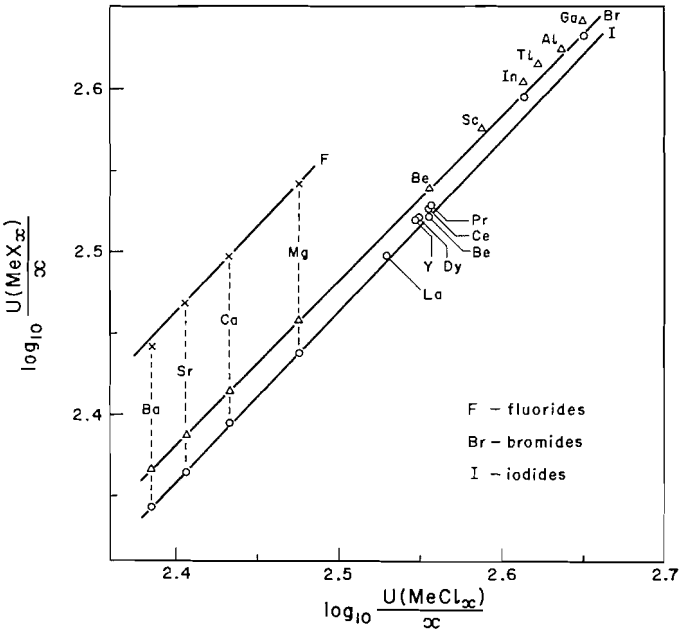

FIG. 1. Logarithmic plots of the lattice energies of fluorides, bromides, and iodides of bi- and ter-valent ions against the lattice energies of the chlorides.

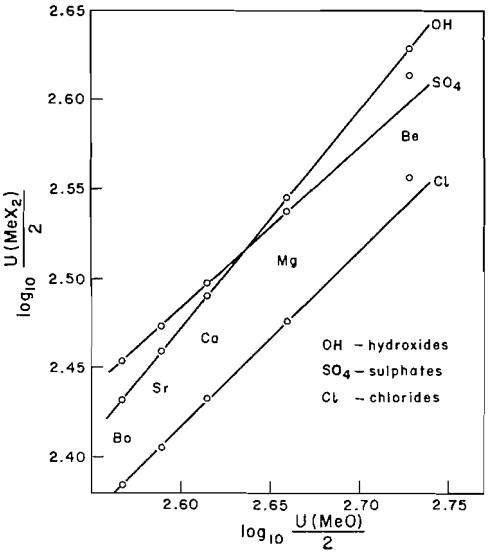

FIG. 2. Logarithmic plots of lattice energies: hydroxides, sulphates, and chlorides of group II*a* elements against the corresponding oxides.

It might be expected that the relation is only as good as the Born equation for lattice energy. It appears to be very much better, however. Thus the form of the Born equation would lead one to expect that the crystal structure, i.e. the value of the Madelung con-

Can. J. Chem. Downloaded from www.nrcresearchpress.com by 176.9.209.113 on 09/04/12
For personal use only.

stant, would have to be the same along a series of compounds. Such is not necessarily the case. This is demonstrated in Fig. 2. Thus even though all the group II*a* metal oxides with the exception of BeO have the same crystal structure, this is not true of the sulphates and chlorides for example. Here the magnesium and calcium compounds differ in structure but there is no irregularity in the plots due to this.

It is evident that the difference in the energy due to change in the Madelung factors of the chlorides from magnesium to barium is compensated by some other effect(s). The difference in the Madelung factors of $CaCl_2$ and $MgCl_2$ is not great, so that it would appear that the alteration in ionic radius with change in co-ordination (6) could account for the compensation. The change in co-ordination in this instance is from the asymmetric environment of the chloride ions in $MgCl_2$ to the symmetric environment in $CaCl_2$ and $SrCl_2$. In passing from $SrCl_2$ to $BaCl_2$ there is an increase in co-ordination number; this would be accompanied by an increase in Madelung factor but also an increase of a few per cent in ionic radius. It is remarkable how small is the over-all effect of minor changes in structure. By "minor" is meant such changes as those involving only structures of high co-ordination ($\geqslant 6$). The alkali nitrates provide another example of a series involving several structure changes, but which may yet be related very satisfactorily to the corresponding halides.

If, on the other hand, a structure of 4:4 or 4:2 co-ordination appears in a series otherwise composed of structures of higher co-ordination, a major change in Madelung factor is involved. Such is the case in the series of group II oxides at beryllium. Thus the singularity at this element may be accounted for, provided that the (as yet unknown) chloride structure could be shown to have a Madelung factor close to that of the other group II chlorides. It is significant that there is no discrepancy in a plot of hydroxide and sulphide values against oxide values. In the sulphate–oxide plot there is again a discrepancy at beryllium of exactly the same magnitude as in the chloride–oxide case.

Molecular volume provides an analogous linearity relation. This may, therefore, be used in many cases such as the above-mentioned to decide whether a discrepancy is due to an experimental error or a structural singularity. If the cause is structural, this will in general be reflected in the additivity of atomic increments (7).

APPLICATIONS TO DISSOLVED SPECIES

The coulombic energy of ion–dipole attraction is proportional to $(r^+ + r^-)^{-2}$ in which r is the "thermochemical radius" (8) of the dipole molecule. The polarization energy is proportional to $(r^+ + r^-)^{-4}$. We should therefore expect the linearity relationships to be applicable to heats of solvation (or heats of solution), and this is indeed so.

Figure 3 illustrates the relation between $-\Delta H^{**}$ for solvation of a number of ions and the $-\Delta H^{**}$-values for the corresponding crystalline chlorides. The $-\Delta H^{**}$-values for solvation were obtained by adding $S + I$ to the standard heats of formation of the aqueous ions. It should be noted that the linear relationship demands that either the number of solvent molecules co-ordinated per equivalent of charge on the ion is the same in all cases, or there is a gradual change in effective co-ordination number such that the linearity is preserved. The former condition seems improbable but the latter is quite plausible, representing one more instance of the uniformity of behavior along a series of ions.

A singularity appears in the case of lithium. The point may lie off the curve because of a large covalent contribution to the Li—O bond. This has been suggested previously in explanation of the bond length. It may be seen that the periodic groups are better con-

Can. J. Chem. Downloaded from www.nrcresearchpress.com by 176.9.209.113 on 09/04/12
For personal use only.

sidered individually, for a slightly better line could be drawn through the points of the group II*a* metals than that shown and the subgroups of the tervalent metals appear to fall on separate lines.

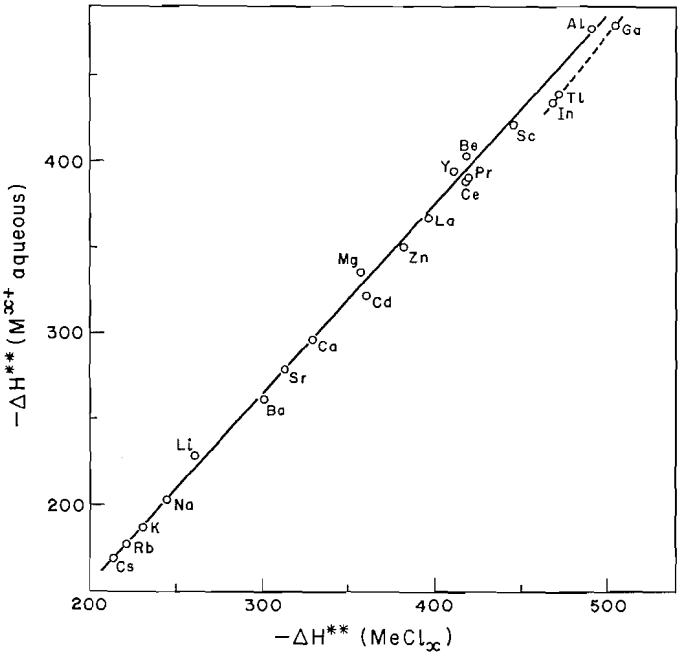

FIG. 3. Plot of $-\Delta H^{**}$-values for uni-, bi-, and ter-valent ions in the aqueous standard state against the corresponding function for anhydrous chlorides.

The heat of formation of a complex compound in aqueous solution may be combined with the solvation energy to obtain the heat of formation of the compound from gaseous ligands and ions (9). The series of group II*a*–EDTA or –citrate complexes serves to demonstrate that the linear relationship extends to these compounds as well. This is hardly a useful fact, however, as the energy of the complex is not much different than the energy of the solvated ion in all cases in which the stability constant is measurable.

REFERENCES

1. LONG, L. H. Quart. Revs. **7**, 134 (1953).
2. KAPUSTINSKII, A. F. Izvest. Akad. Nauk S.S.S.R. Otdel. Khim. Nauk, 568, 581 (1948).
3. FOMIN, V. V. Zhur. Fiz. Khim. **27**, 1689 (1953).
4. HOPPE, R. Z. anorg. u. allgem. Chem. **296**, 104 (1958).
5. KARAPET'YANTS, M. KH. Zhur. Fiz. Khim. **28**, 1136 (1954).
6. GOLDSCHMIDT, V. M. Ber. **60**, 1263 (1927).
7. BLITZ, W. Raumchemie der festen Stoffe. Verlag L. Voss, Leipzig. 1934.
8. KAPUSTINSKII, A. F. Compt. rend. acad. sci. U.R.S.S. **32**, 59 (1941).
9. GEORGE, P. Rec. trav. chim. **75**, 671 (1956).

Can. J. Chem. Downloaded from www.nrcresearchpress.com by 176.9.209.113 on 09/04/12
For personal use only.

Can. J. Chem. Downloaded from www.nrcresearchpress.com by 176.9.209.113 on 09/04/12
For personal use only.

THE PHOTOOXIDATION OF AZOMETHANE. II[1,2]

R. L. STRONG[3] AND K. O. KUTSCHKE

ABSTRACT

In a further investigation of the photooxidation of azomethane it was found that the yields of all products depend on the fractional conversion in a manner which suggests that some inhibitor is produced. Products from experiments at lower pressures of azomethane are obtained in yields appropriate to the higher conversions. Only very small changes in yields are observed for relatively large variations in light intensity. The implications of these facts to the mechanism of the photooxidation are discussed.

In an earlier investigation of the photooxidation of azomethane (1) it was postulated that formaldehyde should be a major product of the reaction. It proved impossible to detect this product, however, presumably because of the well-known tendency of the material to polymerize at temperatures below 100° C (2).

Preliminary work, indicating that formaldehyde was indeed an important product, was done as follows. The mixture of reaction products, unreacted azomethane, and oxygen was condensed at −196° C in a small side arm attached to a grease-free reaction system. After the side arm was allowed to warm to room temperature, the vapor phase was removed by pumping for several minutes and the side arm sealed off. The invisible residue in the side arm was dissolved in dilute H_2SO_4 and the chromotropic acid test (3) applied to the resulting solution. Positive identification was achieved, which was not due to hydrolysis of residual azomethane as shown by the absence of a test on the unphotolyzed mixture.

A reaction system was constructed based on this technique for the analysis of formaldehyde.

EXPERIMENTAL

The reaction system consisted of a fused quartz reaction cell (4.8 cm i.d., 10 cm long, ~180 cm^3 volume), a glass-enclosed, magnetically driven stirrer, a U-tube through which the cell contents were circulated, and connecting tubing. Reactants were introduced from storage and manometers through a stainless steel diaphragm valve (Hoke, No. 413) and led to the analytical system through a similar valve. The entire system, including the valves but excluding the U-tube, was housed in a thermostatted air oven. Gradients and fluctuations in the region of the cell were less than 1° C. Other parts of the oven had larger gradients so that temperature differences of as much as 5° C existed between the cell and other units in the oven. The U-tube, which extended through the walls of the oven, could be kept at oven temperature with heating tape or cooled to any temperature desired.

Gases were led from the reaction system through heated tubing to a removable U-tube (Dow Corning Silicone greased joints), and thence to a Hg cutoff leading to LeRoy stills (4) and a grease-free gas burette.

[1]*Manuscript received May 8, 1959.*
Contribution from the Division of Pure Chemistry, National Research Council, Ottawa, Canada.
Issued as N.R.C. No. 5290.
[2]*For Part I see ref. 1.*
[3]*National Research Council Postdoctorate Fellow 1954–55. Present address: Department of Chemistry, Rensselaer Polytechnic Institute, Troy, N.Y.*

After an exposure the products were condensed at −196° C in the U-tube of the reaction system and non-condensables (CO, O_2, N_2, and any CH_4) transferred to the gas burette, measured, and analyzed as before (1). Condensables were transferred to the removable U-tube (with the reaction system U-tube above 100° C to ensure depolymerization of formaldehyde) and the outlet valve closed. Three cycles of warming to room temperature and recondensation at −196° C in the removable U-tube followed to polymerize the formaldehyde. The cutoff to the LeRoy still (held at −196° C) was opened and the removable U-tube warmed quickly to room temperature; after 3 minutes the cutoff was closed. Blank experiments showed that this procedure resulted in complete transfer of azomethane in that no formaldehyde could be detected in unoxidized azomethane subjected to the same analysis. Had any azomethane remained, a positive test would have resulted owing to subsequent hydrolysis of the azo compound.

Carbon dioxide and nitrous oxide were removed from the LeRoy still at −155° C and submitted for mass spectrometric analysis. Usually a small amount of formaldehyde escaped polymerization and contaminated the CO_2–N_2O mixture. Formaldehyde contributes to the peak at m/e 30, which was used as the basis for the N_2O–CO_2 analysis. Since a reproducible sensitivity could not be obtained for formaldehyde in the mass spectrometer, so that a correction could not be made using the formaldehyde peak at m/e 29, it is felt that the N_2O results are slightly high. For similar reasons the subsequent formaldehyde determination may be 10–15% low.

In some experiments azomethane was removed from the LeRoy still at −100° C; the residue of liquid products were identified mass spectrometrically and gas chromatographically. The major constituents were water and methanol with the latter in much greater yield; Φ_{CH_3OH} was of the order of unity.

After separation of all other products, air was admitted to the U-tube, the tube removed, and the polymerized formaldehyde dissolved in 1 *N* H_2SO_4 (three washings, 1 cm^3 each). One cm^3 of this solution was pipetted into a 15×150-mm glass-stoppered tube, 10 drops of chromatropic acid (Eastman Kodak P230, 2.5 g dry powder in 25 cm^3 water) added, and the solution acidified with 7 cm^3 of concentrated H_2SO_4. The tube was stoppered, heated for 30 minutes in boiling water, cooled, and diluted to 50 ml in a volumetric flask. Transmission readings were taken at 570 mμ (using a reagent blank in the Beckman DU) and converted to absolute quantities with the aid of the measured extinction coefficient, 1.7×10^4, obtained with standard formaldehyde solutions.

Azomethane was obtained from Dr. L. C. Leitch of these laboratories. Traces of low-boiling impurities were removed at −119° C, while heavier material was retained at −80° C by low temperature distillation *in vacuo*; large head and tail fractions were rejected. The material retained had a vapor pressure of 6.6 mm at −80° C. Oxygen was generated by heating $KMnO_4$ and dried by passage through traps at −196° C.

The optical system—a S-500 Hanovia Hg arc, lenses, stops, and a Corning 5860 filter—produced a nearly parallel beam which filled the cell. More than 95% of the light absorbed was of wavelength 3660 Å (5). The intensity of the light could be varied by the use of neutral density filters of chromel on quartz, whose transmission was calibrated with a Beckman DU spectrophotometer at the wavelength used.

RESULTS

An attempt was made to do experiments under conditions similar to those described in the second experimental section of the earlier work (1). It became apparent, however, that the stirring was not as effective at low pressures in the present system as it had been in the earlier apparatus. This was shown by the lack of reproducibility of nitrogen yields

Can. J. Chem. Downloaded from www.nrcresearchpress.com by 176.9.209.113 on 09/04/12
For personal use only.

Can. J. Chem. Downloaded from www.nrcresearchpress.com by 176.9.209.113 on 09/04/12
For personal use only.

and the lack of effect when the stirrer was not operated. It was possible to show definitely that formaldehyde was present in large yields, although not as large as had been predicted (1). Moreover, the yield of carbon monoxide was much higher than had been found in Part I. In those experiments in which the liquid product was separated, methanol was found gas chromatographically in approximately the same yield as had been found in the earlier work. It is concluded that formaldehyde is, in fact, a major product under these conditions, but the postulated equality between formaldehyde and methanol was not found. Possibly the necessity of making the experiments at room temperature followed by heating the reaction mixture to ~100° C before analysis contributed to the lack of reproducibility.

A parameter which has received scant attention in photooxidation systems, but which is of major importance in many thermal oxidations, is that of exposure time. Hentz (6) has observed an induction period for the production of carbon monoxide in the photooxidation of acetone. An investigation was made of the effect of the time of exposure on the product ratios in the present system. The general form of the product–time curves is shown by the data of Fig. 1. It is difficult to state unequivocally from these data whether

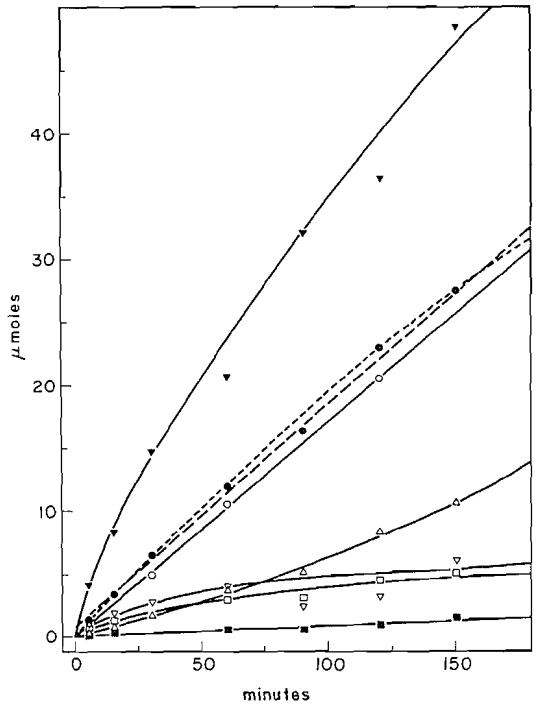

FIG. 1. Variation of products with time at 124° C. Conditions: $p_A \sim 82$ mm, $p_{O_2} \sim 11$ mm, $I_a \sim 1 \times 10^{13}$ quanta/cm³ sec. ○ N_2, $p_{O_2} = 0$; ● N_2, the dotted lines show two possible interpretations; △ CO; ▽ CH_2O; □ N_2O; ■ CO_2; ▼ O_2 consumption.

the nitrogen–time relationship is linear with a small positive intercept or whether it should be extrapolated to the origin as a curve. A careful search was made of possible nitrogen impurities in the reactants and for nitrogen formed in a thermal dark reaction. The total nitrogen expected from such sources was less than about ten per cent of the value of the apparent intercept. This is evidence for curvature in the nitrogen–time plot in the presence of oxygen.

In the absence of oxygen, but with otherwise identical initial conditions, it was observed that the yield of nitrogen was a linear function of time up to rather large fractional decompositions of the order of a few per cent. Thus the ratio of the amount of a product formed in a photooxidation to the amount of nitrogen which would have been formed had oxygen been absent is a measure of the quantum yield of that product since it has been shown that $\Phi_{N_2} = 1$ in the photolysis of azomethane (5). The quantum yields shown in Fig. 2

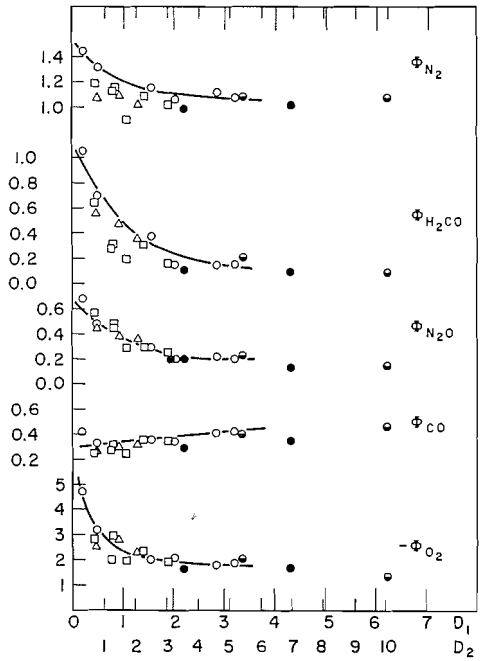

FIG. 2. Variation of product ratios with conversion at 124° C.
○ p_A 82 mm, p_{O_2} 11 mm, I_a 1×10^{13} quanta/cm³ sec.
□ p_A 82 mm, p_{O_2} 11 mm, I_a 3×10^{12} quanta/cm³ sec.
△ p_A 82 mm, p_{O_2} 11 mm, I_a 3×10^{11} quanta/cm³ sec.
● p_A 22 mm, p_{O_2} 11 mm, I_a 0.9×10^{13} quanta/cm³ sec.
◒ p_A 39 mm, p_{O_2} 11 mm, I_a 1.1×10^{13} quanta/cm³ sec.
D_1 and D_2 are approximate measures of the conversion in per cent. The smooth curves were drawn through the open circles and other points plotted later.

were obtained in this manner. The abscissae of Fig. 2 are measures, perhaps arbitrary, of the fractional decomposition of azomethane. D_1 is the ratio of the amount of molecular nitrogen plus that of nitrous oxide found to the amount of azomethane initially introduced in the reaction system (~290 cm³), while D_2 is the similar ratio based on azomethane in the cell alone (~180 cm³). The use of D_1 implies complete and instantaneous efficiency of the stirring mechanism, while D_2 assumes that the stirring is completely ineffective. With the pressures used here it is probable that D_1 is nearer to the true decomposition. Both measures are arbitrary in that it is assumed that each molecule of azomethane which is removed from the system leads either to nitrous oxide or molecular nitrogen. Later work (7) suggests that other nitrogen-containing compounds cannot account for more than 10–15% of the total azomethane disappearance. Thus it would appear that the D_1 abscissae in Fig. 2 are probably accurate to within 10–15%; the relative values are somewhat more precise, of course. Data are shown for N_2, CO, CH_2O, N_2O, and O_2

Can. J. Chem. Downloaded from www.nrcresearchpress.com by 176.9.209.113 on 09/04/12
For personal use only.

consumption. The yields of carbon dioxide were always small ($\Phi_{CO_2} \sim 0.1$) and rather badly scattered, owing more to the low value of the yield than to any other factor. For this reason the carbon dioxide data is not included in Fig. 2. No attempt was made to determine methanol in most of the experiments.

DISCUSSION

Two experimental conditions have been investigated in this work, viz., fractional decomposition and light intensity. It is apparent from an examination of Fig. 2 that a variation in light intensity by a factor of about thirty is without large effect, while an increase in the extent of conversion from $\sim 1/2$ to 1% is responsible for a pronounced decrease in the yields of all products except that of carbon monoxide. The first observation is rather surprising, although the second is, perhaps, less so.

In general terms it would seem that as the reaction progresses, some compound is formed which acts as an inhibitor to the main reaction. It is difficult to identify this inhibitor specifically. Because of the low value which has been quoted (8) for the activation energy of the reaction of methyl radicals with formaldehyde, it was thought possible that radicals in the system could react with formaldehyde thus consuming formaldehyde and possibly acting as a source of the carbon monoxide found, as has been suggested before (6, 9). Such a suggestion would, indeed, explain the results, in a qualitative way at least. Assuming that nitrous oxide arises as suggested earlier (1), a competition for radicals will be set up such as reactions [1] and [2]

$$R + CH_2O \rightarrow RH + CHO \qquad [1]$$

$$R + CH_3N_2CH_3 \rightarrow RH + CH_2N_2CH_3 \qquad [2]$$

$$CH_2N_2CH_3 + O_2 \rightarrow CH_2O + N_2O + CH_3. \qquad [3]$$

Step [3] may occur in stages involving $CH_3N_2CH_2O_2$ radicals;* R is some radical in the system. If CHO reacts with oxygen as in [4],

$$CHO + O_2 \rightarrow HO_2 + CO, \qquad [4]$$

it is expected that an induction period should be observed in the production of carbon monoxide, and that the apparent rate of production of formaldehyde should decrease so that the concentration observed approaches a stationary value in time. Moreover, as more radicals are consumed by [1], fewer are available to react in [2] so that the rate of nitrous oxide production and the chain length should decrease with fractional decomposition. If the quantum yield of oxygen consumption is taken as approximately proportional to the probability of chain propagation (reactions [2] and [3]), then both these expectations are realized qualitatively. Further work (7) to be reported later suggests that this concept, while qualitatively correct, cannot withstand quantitative examination in the light of the more extensive data available. Whatever may be the identity of the specific inhibitor produced, it seems obvious that considerable care should be exercised in the interpretation of photooxidation data in which this effect is not studied in detail.

The lack of variation of the quantum yields with intensity also presents considerable difficulties for interpretation. Jolley (10) has observed that the yields of most products from the photooxidation of diethyl ketone vary with intensity according to the equation $\Phi = a + bI_a^{-\frac{1}{2}}$. If the same type of mechanism is applicable here, the numerical value of

*The referee has pointed out that the radical $CH_3N{=}\dot{N}CH_2{-}OO\cdot$ might also exist in the form $CH_3N{-}\dot{N}CH_2OO$, a formulation which enhances the plausibility of [3] as the over-all reaction.

Can. J. Chem. Downloaded from www.nrcresearchpress.com by 176.9.209.113 on 09/04/12
For personal use only.

b must be such that the second term makes a negligible contribution to the yield. The second term involves the formation of a product in a propagation reaction, such as the combination [2] and [3], along with some other reactions which oxidize methyl radicals, presumably to methoxy radicals. The first term, on the other hand, represents the same product formed in an initiation or termination reaction; because of the inverse square root dependence on intensity it would appear that termination was mutual. It is difficult to conceive of a source of nitrous oxide other than [2] and [3]. If this is in fact the sole source of nitrous oxide, then the yields of this product should be the most sensitive to changes in intensity since the first term is missing. The opposite is observed.

A possible explanation is that termination is linear in radicals, e.g., a two-step adduct formation with azomethane, with the first stage rate determining. In this case radical concentration becomes proportional to the first power of light intensity, and the yield of nitrous oxide by the mechanism suggested becomes independent of the light intensity.

A few experiments were done with lower azomethane pressures as indicated in Fig. 1. The yields at lower azomethane pressures are those appropriate to the larger conversions, as determined by extrapolation of the lower conversion data, although a trend to lower yields is just discernible at the lowest pressure for almost all the products. This would be consistent with the decreasing importance of a chain reaction at lower substrate pressures. It has been suggested (11, 12, 13) that the association of a methyl radical and oxygen requires a third body in the usual experimental conditions. The relatively slight effect of azomethane pressure on product yields, if degree of conversion is also considered, is inconsistent with this hypothesis, but the data are insufficient to permit a thorough test.

ACKNOWLEDGMENTS

The authors wish to thank Dr. E. W. R. Steacie for his advice and encouragement during this investigation. They are indebted to Mrs. Frances Kutschke and Mrs. June Garlick for the mass spectrometric analyses.

They are indebted to Dr. Calvert for a manuscript of his paper (ref. 13) prior to publication.

REFERENCES

1. HOEY, G. R. and KUTSCHKE, K. O. Can. J. Chem. **33**, 496 (1955).
2. WALKER, J. F. Formaldehyde. Reinhold Publishing Corp., New York. 1953.
3. BRICKER, C. E. and JOHNSON, H. R. Ind. Eng. Chem. Anal. Ed. **17**, 400 (1945).
4. LEROY, D. J. Can. J. Research, B, **28**, 492 (1950).
5. JONES, M. H. and STEACIE, E. W. R. J. Chem. Phys. **21**, 1018 (1953).
6. HENTZ, R. R. J. Am. Chem. Soc. **75**, 5810 (1953).
7. WENGER, F. and KUTSCHKE, K. O. Unpublished work.
8. KODAMA, S. and TAKEZAKI, Y. J. Chem. Soc. Japan, **73**, 13 (1952).
9. RALEY, J. H., PORTER, L. M., RUST, F. F., and VAUGHAN, W. E. J. Am. Chem. Soc. **73**, 15 (1951).
10. JOLLEY, J. E. J. Am. Chem. Soc. **79**, 1537 (1957).
11. HOARE, D. E. and WALSH, A. D. Trans. Faraday Soc. **53**, 1102 (1957).
12. CHRISTIE, M. I. Proc. Roy. Soc. A, **244**, 411 (1958).
13. SLEPPY, W. C. and CALVERT, J. G. J. Am. Chem. Soc. **81**, 769 (1959).

Can. J. Chem. Downloaded from www.nrcresearchpress.com by 176.9.209.113 on 09/04/12
For personal use only.

Can. J. Chem. Downloaded from www.nrcresearchpress.com by 176.9.209.113 on 09/04/12
For personal use only.

THE REACTION OF METHYL RADICALS WITH FORMALDEHYDE[1]

A. R. BLAKE[2] AND K. O. KUTSCHKE

ABSTRACT

The pyrolysis of di-*t*-butyl peroxide has been reinvestigated and used as a source of methyl radicals to study the abstraction reaction between methyl radicals and formaldehyde. At low [HCHO]/[peroxide] ratios the system was simple enough for kinetic analysis, and a value of 6.6 kcal/mole was obtained for the activation energy. At higher [HCHO]/[peroxide] ratios the system became very complicated, possibly due to the increased importance of addition reactions.

INTRODUCTION

The reaction between methyl radicals and formaldehyde has been previously studied by Kodama and Takezaki (1) and by Toby and Kutschke (2), who used the photolysis of azomethane as a source of methyl radicals. They obtained values of 5.6 and 6.2 kcal/mole, respectively, for the activation energy of the process. It seemed desirable to re-investigate the reaction using the pyrolysis of di-*t*-butyl peroxide as a source of methyl radicals. This source possesses the advantage that there is little abstraction reaction between methyl radicals and the molecule which produces the radicals.

EXPERIMENTAL

Methyl radicals were produced by the pyrolysis of di-*t*-butyl peroxide in a Pyrex glass reaction vessel (volume = 550 cm^3) the temperature of which was controlled to within 0.1° C. To start the reaction the reactants were expanded into the cell from a preheater maintained at 80° C, at which temperature no measurable decomposition of the peroxide took place in a period of 30 minutes. The reaction was stopped by expansion into a liquid-nitrogen-cooled trap. The products were analyzed by conventional methods. CH_4 and CO were separated from the remaining products at −210° C, and the CO measured as CO_2 after oxidation in a copper oxide furnace at 260° C. Methane was removed directly from the furnace and measured. Ethane was distilled from Ward stills at −180° C. The purity of each fraction was checked mass spectrometrically in some experiments. The remaining mixture of liquid products and unreacted starting materials was removed for further analysis. Liquid product analyses for acetone, *t*-butanol, and acetaldehyde were carried out gas chromatographically on a 10-ft column consisting of 30% nonyl-phthalate on firebrick, with a small proportion of polyethylene glycol added to the phthalate to cut down tailing of the peaks. No substances were detected other than the residual reactants and those products for which analyses are given.

Di-*t*-butyl peroxide, from the Novadel-Agene Corporation, contained traces of acetone and methanol and approximately 1/2% *t*-butanol. The first two were entirely removed by chromatographic purification; the *t*-butanol content was reduced to $< 0.1\%$ by this treatment. Isobutane was Phillips Research Grade. Formaldehyde was prepared by heating α-polyoxymethylene followed by distillation *in vacuo*. All these materials were thoroughly outgassed before use.

[1]*Manuscript received May 14, 1959.*
Contribution from the Division of Pure Chemistry, National Research Council, Ottawa, Canada.
Issued as N.R.C. No. 5289.
[2]*National Research Council Postdoctorate Fellow 1957–59.*

Can. J. Chem. Downloaded from www.nrcresearchpress.com by 176.9.209.113 on 09/04/12
For personal use only.

RESULTS AND DISCUSSION

In preliminary experiments the pyrolysis of di-*t*-butyl peroxide was reinvestigated in the temperature range 101–145° C, alone and in the presence of isobutane. The mechanism for the decomposition is well established (3)

$$\text{peroxide} \rightarrow 2(CH_3)_3CO \quad [1]$$

$$(CH_3)_3CO \rightarrow CH_3 + (CH_3)_2CO \quad [2]$$

$$2CH_3 \rightarrow C_2H_6 \quad [3]$$

$$CH_3 + \text{peroxide} \rightarrow CH_4 + \text{radical} \quad [4]$$

$$CH_3 + \text{radical} \rightarrow \text{stable products} \quad [5]$$

$$CH_3 + CH_3 - CH(CH_3) - CH_3 \rightarrow CH_4 + CH_3 - C(CH_3) - CH_3. \quad [6]$$

Peroxide Alone

The results for the decomposition of peroxide alone are given in Table I. Assuming

TABLE I

Pyrolysis of di-*t*-butyl peroxide

Temp., °C	Peroxide, initial, mm	Time, sec	C_2H_6, μmole	CH_4, μmole	k_1, 10^{-4} sec^{-1}	$k_4/k_3^{\frac{1}{2}}$, (mole cm^{-3})$^{-\frac{1}{2}}$ sec$^{-\frac{1}{2}}$
103.2	18.5	9888	3.30	0.06	0.0056	0.018
111.9	12.0	6467	3.55	0.09	0.0203	0.051
116.4	14.3	3700	4.85	0.12	0.0417	0.070
116.6	13.2	3032	3.55	0.13	0.0410	0.097
120.2	14.3	2704	5.52	0.12	0.0639	0.074
120.5	14.4	2702	4.31	0.12	0.0639	0.090
122.3	13.9	4038	10.2	—	0.084	—
128.9	13.3	1430	6.90	0.33	0.174	0.23
129.5	13.2	1746	9.70	0.17	0.198	0.107
135.2	13.0	700	7.55	0.32	0.392	0.370
138.5	13.8	450	8.00	0.06	0.600	0.080
141.8	16.0	800	20.0	0.30	0.770	0.170
143.2	21.4	488	20.8	0.26	0.970	0.140
145.4	10.1	484	12.3	0.28	1.24	0.189

every molecule of peroxide decomposed gives rise to a molecule of ethane or methane then:

$$k_1 = \frac{1}{t} \ln \frac{a}{a - x}$$

and

$$\frac{R_{CH_4}}{R_{C_2H_6}^{\frac{1}{2}}} = \frac{k_4}{k_3^{\frac{1}{2}}} \cdot \frac{1}{[\text{peroxide}]}$$

where a is the initial peroxide concentration, x the amount of methane and ethane formed, and t the time. A plot of log k_1 against $1/T$ is given in Fig. 1. This leads to a rate constant, $k_1 = 2.5 \times 10^{16} \exp(-38{,}700/RT)$ sec^{-1}, in excellent agreement with those previously determined (3, 4, 5, 6, 7, 8). The amount of methane formed in the reaction was small (usually less than 3% of the ethane) and analysis was difficult. An approximate estimate of $E_4 - \frac{1}{2}E_3$ gave 14.5±2.5 kcal/mole. The correspondence between acetone

formation and total methyl radical recovery was good (Table II).* No *t*-butanol was detected in any experiments

TABLE II

Acetone formation in the pyrolysis of di-*t*-butyl peroxide

Temp., °C	% decomposition of peroxide	Acetone, μmole	$2C_2H_6 + CH_4$, μmole	Divergence, %
119.3	1.52	4.00	4.06	1.5
119.1	1.26	5.64	5.47	3
102.5	0.63	1.35	1.30	3.8
131.5	3.0	3.76	3.76	0

Peroxide in the Presence of Isobutane

These experiments were performed in order to establish that our experimental system produced the same value for E_6 as had been determined by other methods. The results are presented in Table III, and the Arrhenius plot in Fig. 2. The value of $E_6 - \frac{1}{2}E_3 = 7.7$ kcal/mole is in good agreement with the value of 7.6 found by Trotman-Dickenson and

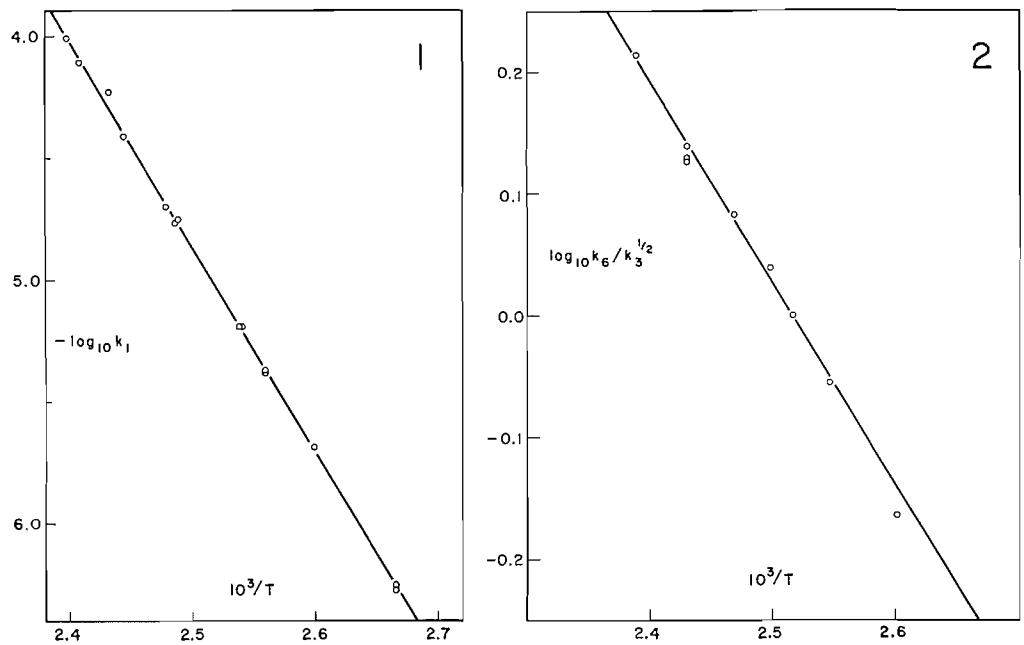

FIG. 1. Arrhenius plot for the pyrolysis of di-*t*-butyl peroxide.
FIG. 2. Arrhenius plot for the reaction of methyl radicals with isobutane.

Steacie (9) from the photolysis of acetone. It is higher than the values of Rebbert and Steacie (10), 7.3 kcal/mole, from the photolysis of $Hg(CH_3)_2$, and Jones and Steacie (11), 6.7 kcal/mole, from the photolysis of azomethane.

Recently Alexandrova, Yu. A., Yui-Li, K., Pravednikov, A. N., and Medvedev, S. S. (Doklady Akad. Nauk, S.S.S.R. **123, 1029 (1958)) have suggested that acetone can be formed in a bimolecular reaction of t-butoxy radicals, the other product being methyl isobutyl ether. The concentration range (> 0.2 mole/l. in isopropyl benzene solution) in which the effect of this reaction was observed, the lack of methyl isobutyl ether among the products in the present work, and the good balance between acetone and hydrocarbon products found here all suggest that the bimolecular reaction is not of importance in our experimental conditions.*

Can. J. Chem. Downloaded from www.nrcresearchpress.com by 176.9.209.113 on 09/04/12
For personal use only.

TABLE III

Pyrolysis of di-*t*-butyl peroxide isobutane mixtures

Temp., ° C	Peroxide, 10^{-6} mole/cc	Isobutane, 10^{-6} mole/cc	R_{CH_4}, 10^{-12} mole/cc sec	$R_{C_2H_6}$, 10^{-12} mole/cc sec	$k_6/k_3^{\frac{1}{2}}$, (mole $cm^{-3})^{-\frac{1}{2}}$ $sec^{-\frac{1}{2}}$
145.5	0.280	1.89	13.2	17.4	1.63
137.5	0.391	0.233	1.97	17.2	1.62
137.4	0.330	0.218	1.45	12.5	1.52
137.5	0.265	0.386	2.02	10.0	1.47
137.4	0.273	0.919	13.2	17.4	1.34
137.8	0.326	1.18	3.92	9.15	1.33
137.4	0.306	2.94	5.05	9.45	1.38
131.3	0.330	1.63	3.73	3.35	1.21
126.4	1.22	0.57	2.89	1.48	1.10
124.0	0.292	1.60	1.92	1.42	1.00
119.5	0.310	1.64	1.04	0.526	0.875
111.3	0.330	1.60	0.462	0.173	0.68

It was found that at low isobutane pressures $k_6/k_3^{\frac{1}{2}}$ decreased with increasing isobutane pressure, but above 20 mm Hg there was no change with increasing pressure. Consequently all rate measurements were made above this pressure.

Peroxide in the Presence of Formaldehyde

At low formaldehyde/peroxide ratios (below 0.2, except at high temperatures), the following simple mechanism is obeyed

$$CH_3 + HCHO \rightarrow CH_4 + CHO \quad [7]$$

$$CHO + CH_3 \rightarrow CH_4 + CO \quad [8]$$

$$CHO + CH_3 \rightarrow CH_3CHO \quad [9]$$

along with reactions [1] to [5]. This leads to the expression

$$[I] \qquad R_{CH_4}/R_{C_2H_6}^{\frac{1}{2}} = (k_7/k_3^{\frac{1}{2}})\,[HCHO]\,(1+k_8/(k_8+k_9)).$$

Acetaldehyde is formed in the reaction at low pressures in very small quantities, the value of R_{CH_3CHO}/R_{CO} being < 0.10. Therefore $k_8/(k_8+k_9)$ can be approximated by unity. This approximation will have little effect on the activation energy as the term will certainly have a small temperature coefficient. Throughout this work we have used the approximate expression

$$[II] \qquad R_{CH_4}/R_{C_2H_6}^{\frac{1}{2}} = 2(k_7/k_3^{\frac{1}{2}})\,[HCHO].$$

We consider that reaction [10] probably does not play an important role in the over-all

$$2CHO \rightarrow HCHO + CO \quad [10]$$

reaction scheme, as the methyl radical concentration, as estimated from the absolute rate of ethane formation, is high throughout. It is difficult to check this point in a satisfactory manner experimentally. Table IV shows the experimental results at low formaldehyde/peroxide ratios, and in Fig. 3 the data are plotted according to equation [II]. The Arrhenius plot is given in Fig. 4. This leads to a rate equation

$$k_7/k_3^{\frac{1}{2}} = 3.8\times10^4 \exp(-6600/RT)\ (\text{mole cm}^{-3})^{-\frac{1}{2}}\ \text{sec}^{-\frac{1}{2}}.$$

The activation energy is in good agreement with the value of 6.2 kcal/mole obtained by Toby and Kutschke (2). It is interesting to compare it with the 6.8 kcal/mole obtained

Can. J. Chem. Downloaded from www.nrcresearchpress.com by 176.9.209.113 on 09/04/12
For personal use only.

TABLE IV

The pyrolysis of di-*t*-butyl peroxide in the presence of formaldehyde

Temp., °C	f/p*	R_{CH_4}	$R_{C_2H_6}$	R_{CO}	R_{CH_2CHO}	R_{H_2}	$R_{CH_4}/R_{C_2H_6}^{\frac{1}{2}}[P]$
		10^{-11} mole/cm³ sec					(mole cm^{-3})$^{-\frac{1}{2}}$ sec$^{-\frac{1}{2}}$
147.3	0.197	1.03	3.64	0.580			5.65
147.3	0.360	1.66	3.05	—			10.2
147.2	0.396	1.86	3.25	—			10.7
147.2	0.630	2.27	2.57	1.60			17.2
142.5	0.097	1.24	2.28	0.680			3.74
142.5	0.275	2.64	3.20	1.42			7.60
142.2	0.430	1.41	1.43	0.740			12.4
142.2	0.702	1.97	1.16	1.09			18.7
142.2	1.15	3.14	1.27	1.76			26.0
134.5	0.089	0.530	1.68	0.272			2.21
134.5	0.360	0.700	1.48	0.360			3.25
134.7	0.510	1.05	1.39	0.510			4.75
128.2	0.045	0.360	1.31	0.195			0.98
128.9	0.042	0.623	1.91	0.312			1.12
129.0	0.088	0.500	1.09	0.276			1.93
129.0	0.114	0.820	1.21	0.425			2.20
128.9	0.189	0.980	1.07	0.540			3.50
122.1	0.0341	0.656	1.57	0.336			0.670
122.7	0.0415	0.740	1.55	—			0.810
122.2	0.0650	1.10	1.33	0.630			1.16
122.0	0.0625	1.20	1.38	0.670			1.17
122.2	0.100	1.50	1.09	0.820			1.71
142.2	0.430	1.41	1.43	0.609	0.31	0.04	12.4
143.5	0.949	2.59	1.36	1.46	0.34	0.08	21.1
142.2	1.153	3.14	1.25	1.76	0.58	0.18	26.1
142.0	2.825	3.22	0.338	2.34	0.47	0.32	54.5
123.7	0.473	0.247	0.867	0.151	0.05	0.01	8.80
123.7	0.788	0.327	0.658	0.224	0.06	0.01	12.2
123.5	1.809	0.445	0.402	0.327	0.06	0.04	21.8

*f/p = [HCHO]/[peroxide] initial.

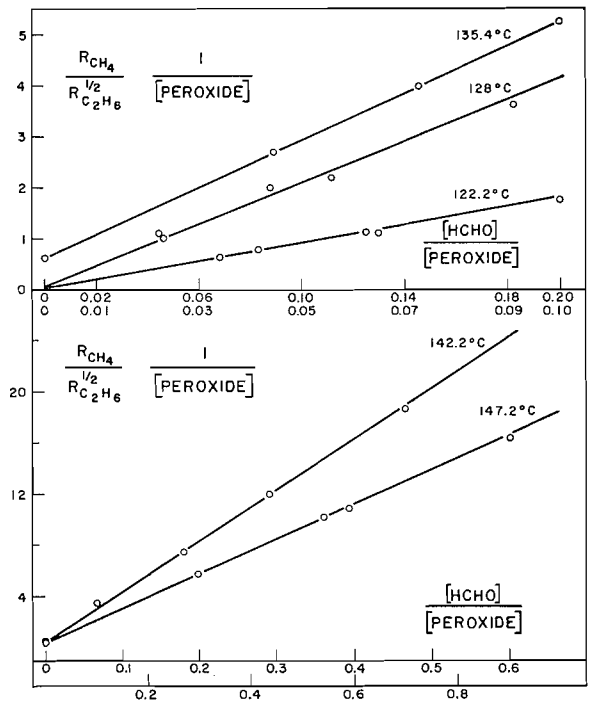

FIG. 3. The pyrolysis of peroxide and formaldehyde at low formaldehyde/peroxide ratios. 147.2° C, lower abscissa scale; 142.2° C, upper abscissa scale; 135.4° C, upper abscissa scale, ordinate origin at 0.5 scale units; 128° C, upper abscissa scale; 122.7° C, lower abscissa scale.

Can. J. Chem. Downloaded from www.nrcresearchpress.com by 176.9.209.113 on 09/04/12
For personal use only.

by Ausloos and Steacie (12) for the corresponding reaction with acetaldehyde. Hoare (13) has also determined $k_7/k_3^{\frac{1}{2}}$ at 120° C. He obtained 10.1 (mole cm^{-3})$^{-\frac{1}{2}}$ sec$^{-\frac{1}{2}}$ compared with our value of 7.9 (mole cm^{-3})$^{-\frac{1}{2}}$ sec$^{-\frac{1}{2}}$ at the same temperature.

At higher HCHO/peroxide ratios the system becomes very complicated. Measurable amounts of hydrogen and acetaldehyde are produced and the plots of $R_{CH_4}/R_{C_2H_6}^{\frac{1}{2}}$[peroxide] against [HCHO]/[peroxide] show a very marked deviation from linearity (see, for example, Fig. 5). Some data are shown in the second part of Table IV. This last observation has been made previously in other systems by Brinton and Volman (5) in the reaction between methyl radicals and ethylene imine and by Brinton (14) in the reaction between methyl radicals and ethylene. It seems clear that the deviations are most marked in systems where there is a possibility of methyl radicals undergoing addition reactions. Fuller and Rust (15) have demonstrated recently that alkyl radicals add quite readily to formaldehyde. It is possible that reaction of a second methyl radical

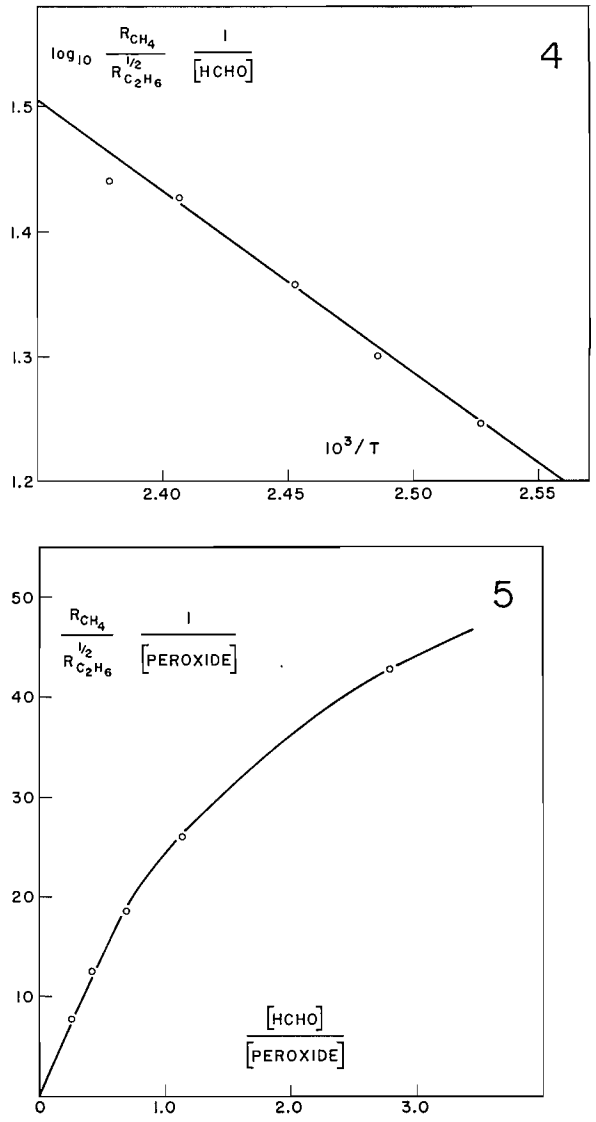

FIG. 4. Arrhenius plot for the reaction of methyl radicals with formaldehyde.
FIG. 5. The pyrolysis of peroxide and formaldehyde at 142.2° C.

Can. J. Chem. Downloaded from www.nrcresearchpress.com by 176.9.209.113 on 09/04/12
For personal use only.

with the methyl radical – formaldehyde complex to produce a molecule of ethane could account for the deviations observed.

The ratio of acetaldehyde/CO in these experiments was approximately 0.25. This is not, however, a reliable measure of the relative rates of reactions [8] and [9], as acetaldehyde might also be produced in the decomposition of methyl radical – formaldehyde addition compounds.

ACKNOWLEDGMENTS

We wish to thank Dr. E. W. R. Steacie for his interest in this work, and Miss Bernice Thornton for mass spectrometric analyses.

REFERENCES

1. KODAMA, S. and TAKEZAKI, Y. J. Chem. Soc. Japan, **73**, 13 (1952).
2. TOBY, S. and KUTSCHKE, K. O. Can. J. Chem. **37**, 672 (1959).
3. RALEY, J. H., RUST, F. F., and VAUGHAN, W. E. J. Am. Chem. Soc. **70**, 88 (1948).
4. JAQUISS, M. T., ROBERTS, J. S., and SZWARC, M. J. Am. Chem. Soc. **74**, 6005 (1952).
5. BRINTON, R. K. and VOLMAN, D. H. J. Chem. Phys. **20**, 25 (1952).
6. LOSSING, F. P. and TICKNER, A. W. J. Chem. Phys. **21**, 907 (1953).
7. PRITCHARD, G. O., PRITCHARD, H. O., and TROTMAN-DICKENSON, A. F. J. Chem. Soc. 1425 (1954).
8. BIRSS, F. W., DANBY, C. J., and HINSHELWOOD, C. Proc. Roy. Soc. (London), A, **239**, 154 (1957).
9. TROTMAN-DICKENSON, A. F. and STEACIE, E. W. R. J. Chem. Phys. **19**, 329 (1951).
10. REBBERT, R. E. and STEACIE, E. W. R. J. Chem. Phys. **21**, 1723 (1953).
11. JONES, M. H. J. and STEACIE, E. W. R. Can. J. Chem. **31**, 505 (1953).
12. AUSLOOS, P. and STEACIE, E. W. R. Can. J. Chem. **32**, 593 (1954).
13. HOARE, D. E. Trans. Faraday Soc. **49**, 1292 (1953).
14. BRINTON, R. K. J. Chem. Phys. **29**, 781 (1958).
15. FULLER, G. and RUST, F. F. J. Am. Chem. Soc. **80**, 6148 (1958).

Can. J. Chem. Downloaded from www.nrcresearchpress.com by 176.9.209.113 on 09/04/12
For personal use only.

Can. J. Chem. Downloaded from www.nrcresearchpress.com by 176.9.209.113 on 09/04/12
For personal use only.

THE INFRARED SPECTRA OF SOME DNP-α-AMINO ACIDS[1, 2]

FELIX FRIEDBERG[3] AND MYLOUS S. O'DELL

ABSTRACT

The infrared spectra of some DNP-α-amino acids were examined using the KBr technique in the region 5000 to 625 cm^{-1}. There is sufficient variation in spectra of closely related DNP-amino acids to allow positive identification even though the spectra on the whole are more strikingly similar than they are different. Differences in varying degrees were also noted between L- and DL-forms.

INTRODUCTION

The DNP[4]-derivatives of amino acids recently have assumed importance in amino acid sequence studies on peptides and proteins (1). While the KBr pellet spectra of a large number of the amino acids (2, 3), and also of their 3-phenyl-2-thiohydantoins (4), are reported in the literature, there is little information with regard to the infrared spectra of DNP-derivatives.[5] This study was undertaken to compare the spectra (*a*) of the DNP-derivatives of amino acids with the spectra of the corresponding free amino acids as given in the literature, (*b*) of the DNP-derivatives of comparable L- and DL-amino acids, and (*c*) of the DNP-derivatives of structurally related acids, to see whether such compounds can be identified by their spectra.

EXPERIMENTAL

The spectra were taken on a Model No. 21 Perkin–Elmer spectrophotometer (equipped with sodium chloride optics). Pellets were made by first mixing the DNP-amino acids with KBr in an agate mortar, and then pressing the material in the Perkin–Elmer die, under evacuation. The DNP-amino acids had been prepared in this laboratory by the method of Levy and Chung (5), and each was crystallized several times and found pure by paper chromatography. Melting points for all derivatives were determined and are essentially in agreement with the values given in literature (6).

DISCUSSION

Table I lists and characterizes the spectral absorption bands in the 5000 to 625 cm^{-1} region. As a result of dipolar ion structure many amino acids possess a characteristic absorption frequency at about 1587 cm^{-1} which is related to the COO^- group, as well as a relatively weak absorption at about 2128 cm^{-1} which may be attributed to NH frequencies in the $—NH_3$ ion. The absence of this absorption peak at 2128 cm^{-1} in the case of DNP-derivatives of amino acids, where the amino group is attached to the dinitrophenyl ring, was therefore expected.

[1]*Manuscript received April 16, 1959.*
Contribution from the Department of Biochemistry, Howard University Medical School, Washington, D.C. This work was supported in part by a grant from the American Cancer Society.
[2]*Spectra deposited with Documentation of Molecular Spectroscopy, Butterworth Scientific Publications, London, England.*
[3]*Work done during tenure of Lederle Medical Faculty Award.*
[4]*DNP is used as an abbreviation for 2,4d-initrophenyl.*
[5]*The first systematic study of the vibrational spectra of α-amino acids was made by Edsall and his co-workers (J. Phys. Chem.* ***41****, 133 (1937); J. Chem. Phys.* ***4****, 1 (1936);* ***5****, 225, 508 (1937); J. Am. Chem. Soc.* ***65****, 1767 (1943);* ***71****, 474 (1950); and more recently J. Am. Chem. Soc.* ***80****, 3807, 3813, 3818, 3823, 3827 (1958). This work is concerned primarily with Raman spectra in aqueous solutions. The first infrared studies were published by Freyman and his co-workers (J. phys. radium,* ***7****, 30 (1936)).*

Can. J. Chem. Downloaded from www.nrcresearchpress.com by 176.9.209.113 on 09/04/12
For personal use only.

TABLE I

Absorption spectra in the infrared in the 5000–625 cm^{-1} region[a]

DNP-L-arginine 245–250 (*d*)[b]	3311sh 3236SB		2882MB			1658SB 1618SB	1580SB 1570sh	1520SB	1484SS 1464sh 1451sh	1408SB	1387SS	1335SB
DNP-L-alanine 182	3311MS	3058MB			1718SS	1675MB 1623SS	1590SS	1522SS 1502MS	1464WB	1414SB	1359SB	1333sh
DNP-DL-alanine 180.5	3279MS	3058MB			1709SS	1618SS	1587SS	1522SS 1499MS	1464WB	1414SB	1364sh	1333SB
DNP-L-aspartic 186–187	3279MS	3058MB	2857MB		1712SB	1618SS	1590SS	1546MS 1522SS 1499SS		1425SB 1395SS	1361SB	1333SB
Bis-DNP-L-cysteine 155–158	3279MS	3058MB	2907WB		1748SS	1613SB	1590SB	1515SB 1511sh		1427MB	1385MB	1333SB
Di-DNP-L-cystine 118–121	3311sh 3289MS				1745MB	1616SS	1590SS	1520SB		1422MB		1333SB
DNP-glycine 209	3311MS				1712SS	1608SS	1595sh	1517SB 1497SS	1447MS 1441sh	1422sh 1412SB	1362SS	1335SB
Di-DNP-L-histidine 219	3268MS	3058MB			1715MB	1618sh 1613SB	1582SS	1511SB		1416SB 1412sh	1362MS 1359sh	1333sh 1326SB 1321sh
DNP-hydroxy-L-proline 174–178	3425SB 3319sh	3095WB	2950WB		1744SB	1610SB	1588SB	1533SB 1512SB	1464vw 1439MB 1450sh		1384sh	1345SB
DNP-L-isoleucine 109–110	3289MS	3058MB	2924MB	2538vwB	1712SS	1618SS	1587SS	1515SB	1456MB	1412SS	1364MS	1333SB
DNP-DL-isoleucine 174.5	3289WS	3030MB	2915MB 2833sh		1712SS	1621SS	1582SS	1517MS 1502MS	1453WB	1412SS	1377WS 1361MS	1332SB
DNP-L-leucine 102	3289SS	3030SB	2899SB		1712SB	1618SB	1587SB	1513SB 1495SB	1464SB	1422SB	1385SS 1364SS	1325SB

Can. J. Chem. Downloaded from www.nrcresearchpress.com by 176.9.209.113 on 09/04/12
For personal use only.

TABLE I (*Continued*)

Absorption spectra in the infrared in the 5000–625 cm^{-1} region[a]

DNP-L-arginine 245–250 (*d*)[b]	1277SB	1250SB		1176sh	1139SB	1094MB		1054MB				948vw	919MB	
DNP-L-alanine 182	1302MS	1261SB 1230SB	1217MB	1157SS	1140MB	1124MB	1072WB	1057MS				940WB	919WB	
DNP-DL-alanine 180.5	1292SB 1284sh	1242SB 1232sh		1172MB 1156MS		1119SS		1053MB					916MB	
DNP-L-aspartic 186–187	1282SB	1229SB	1220sh	1151SS	1136SS	1109SB		1056SS	1040MB 1037sh			928SB	915MB	905SB
Bis-DNP-L-cysteine 155–158	1290SB	1244SB 1239sh		1171MB	1143SB 1135sh	1107SB 1100sh		1050MB					918MB 916sh	902WB
Di-DNP-L-cystine 118–121	1299sh 1292SB				1140sh 1135MB	1105MB		1058MB					926MB	
DNP-glycine 209	1307SB 1290SB	1250sh 1232SB		1155SS	1131SS	1105SS		1056MB		996MS	978WB	945MB	922SS	
Di-DNP-L-histidine 219	1285sh	1230SB	1222sh		1144SB 1133SB	1103SB		1054MB	1026MB	996SB	971MB	952MB 936MB	918MB	
DNP-hydroxy-L-proline 174–178	1285sh	1245WB	1210vw	1183MB	1152MS	1125MS	1074MS			997MS	980MS		927WS	903vWB
DNP-L-isoleucine 109–110	1285SB	1244SB	1222SB	1163sh	1147SS 1134SB	1121MB 1101MB		1056MB			966WB		921MB 919sh	
DNP-DL-isoleucine 174.5	1290SS	1261sh 1247SB 1232sh 1229sh			1149SS	1124MS 1098MB		1054WS		1008vw	965WB		918MB	
DNP-L-leucine 102	1302MB 1276SB	1261SB 1232SB	1206SB	1151SS	1139WB 1125SB	1094SB	1076SB	1054SB			958MB	939SB	917SB	

DNP-L-arginine 245–250 (*d*)[b]			831MS	811MB		763MB	743SB	722MB					645MB	
DNP-L-alanine 182			833WB 828WS			765WB	743MB	720WB			667WB			
DNP-DL-alanine 180.5			832WB	817WS		763WB	743MB	724WB 720sh						
DNP-L-aspartic 186–187		858WB	832MS	807MS	785WB	762WB	744SS[1]	716SB	687WB	680WB	678WB	658WB	644WB	
Bis-DNP-L-cysteine 155–158	877WB		833MS	819MB		762WB	745MB 732MS	718MB				660WB		
Di-DNP-L-cystine 118–121			832MB				743MB							
DNP-glycine 209	889WB 886sh		835MS	818SS		762WS	745SS	714WB	695WB	684WB		657MB		
Di-DNP-L-histidine 219	885WB 879vw	870WB	832MB	822MB 818sh		759WB	743MS	719MB						
DNP-hydroxy-L-proline 174–178	882vwB		832vwS	810SS		758WS	743SS	724vwB		689MB		653MB		
DNP-L-isoleucine 109–110			831MS 826MB	821MB		765WB	743MS 733MB	719WB						
DNP-DL-isoleucine 174.5			830WS	818MS	791vw	760vw	743MB	717WB	690vw		667vw		644WB	
DNP-L-leucine 102			831SB	817SB	774MB	767MS	741SS	711SB	699WB	685MB	665MB			

Can. J. Chem. Downloaded from www.nrcresearchpress.com by 176.9.209.113 on 09/04/12
For personal use only.

TABLE I (*Continued*)

Absorption spectra in the infrared in the 5000–625 cm^{-1} region[a]

DNP-DL-leucine 132–133	3322WS		3058WB		2899MB					1712SS	1618SS	1592SS
Di-DNP-L-lysine 178–180	3300WS		3058WB		2890WB					1715MS	1618SS	1587SS
E-DNP-L-lysine 197–200	3333MS				2841SB					1724MS	1618SS	1587SS
DNP-DL-methionine 122	3279MS		3058MB		2874MB					1718SB	1618sh	1590SS
											1608SS	
DNP-L-phenylalanine 191	3279SS	3195sh	3077sh		2882sh		1965WB	1821WB	1742SS	1715sh	1618sh	1580SS
	3247sh	3175sh								1701sh	1608SS	
DNP-DL-phenylalanine 219	3279MS	3205sh	3058sh	3003sh			1980WB	1818WB	1742SS	1701sh	1613SS	1580SS
	3247sh	3185sh								1686sh		
		3145sh										
DNP-L-proline 138	3356WB		3049MB		2833MB					1712SS	1603SS	1577SS
DNP-DL-serine 197–201	3344SS		3077sh	3021sh	2899SB				1757SS		1616SS	1592sh
	3300SS			2959sh								1587SS
				2941sh								
DNP-DL-threonine 178–179	3390SB		3086MS		2899SB				1757SS		1618SS	1587SS
	3333SS											
DNP-L-tryptophan 217–221 (*d*)	3401SS		3096MB		2915MB					1715SS	1613SS	1582SS
	3322MS											
Di-DNP-L-tyrosine 184 (*d*)	3390sh		3058WB								1613SS	1582SS
	3279WB											
Di-DNP-DL-tyrosine 207 (*d*)	3378MS		3058WB							1715SS	1616SS	1582SS
	3279MS											
DNP-L-valine 132–133	3311SS	3215SS		2950SS	2915SS				1748SS		1618SS	1587SS
		3145sh									1610sh	
DNP-DL-valine 187–189	3279MS			3003MvB	2924MB	2571WB				1712SS	1623SS	1587SS
					2890sh							

Can. J. Chem. Downloaded from www.nrcresearchpress.com by 176.9.209.113 on 09/04/12
For personal use only.

TABLE I (*Continued*)

Absorption spectra in the infrared in the 5000–625 cm^{-1} region[a]

DNP-DL-leucine 132–133		1517SS	1499MS	1464WS		1422SS	1387vw	1355MS	1332SB	1302MB	1277MB	1261SB	1222MS	
Di-DNP-L-lysine 178–180		1517SS				1416SS			1337SB	1307MB	1269MB		1229MB	
E-DNP-L-lysine 197–200		1522SB				1420SS		1361MS	1330SB	1312SB			1238SB	1195SB
DNP-DL-methionine 122	1541WB	1513SS	1499SB			1420SB		1357MS	1330SS	1307SB	1274SB	1266sh	1244SB	1198MB
						1416sh							1229sh	
DNP-L-phenylalanine 191	1534WB	1515SS	1488SS	1451MS	1437sh	1420sh	1401SB	1362MS	1325SB	1307sh			1236SB	1203sh
							1395sh							
DNP-DL-phenylalanine 219	1538WB	1517SS	1486SS	1451WB	1439sh	1420MB	1393SB	1366MS	1330sh	1314sh	1287sh		1245SS	1205MB
									1321sh	1300sh	1282sh		1235SB	
									1318SS	1294SS				
DNP-L-proline 138		1520SB	1495SS		1447MS	1420MB	1377SS		1326SB	1297sh	1274sh		1221MB	
										1290SB				
DNP-DL-serine 197–201		1513SS	1495SS	1456MS	1431sh	1412SS		1362SS	1335SB	1316SB	1279sh	1266SS	1232SB	1198SB
DNP-DL-threonine 178–179		1520SS	1495SB			1420SB	1395sh	1364SB	1335SS	1316SB	1277SB		1235SB	1206SB
							1389sh	1357sh						
							1381MB							
DNP-L-tryptophan 217–221 (*d*)	1531MS	1515SS	1493MB	1449MS		1418SB		1361sh	1332SB	1290SB	1276SB		1250SB	1198SB
													1227SB	
Di-DNP-L-tryosine 184 (*d*)	1527SB		1502MS			1412MB			1340SB			1266SB		
			1479MS											
Di-DNP-DL-tryosine 207 (*d*)	1531sh	1517SS	1490SS		1439sh	1416SS		1362MB	1330SS	1312sh	1274SB		1248sh	1205SS
													1239SB	
DNP-L-valine 132–133	1541SS	1520SS	1490SS	1466MS	1447sh	1427MS	1406SS	1372SS	1333SB	1299SB			1245SS	
						1425sh	1391sh						1238sh	
													1235sh	
DNP-DL-valine 187–189	1529sh	1520sh	1508SB	1462MS		1412SS		1362MS	1332SB	1309SS	1284SB	1261SB	1242SB	
				1451MS										

Can. J. Chem. Downloaded from www.nrcresearchpress.com by 176.9.209.113 on 09/04/12
For personal use only.

TABLE I (*Continued*)

Absorption spectra in the infrared in the 5000–625 cm^{-1} region[a]

DNP-DL-leucine 132–133	1164MS	1148WB	1122MB 1112MB	1095WB		1058WB				958WB			916WS	
Di-DNP-L-lysine 178–180	1181WS	1140MB	1130MB 1107WB			1054WB							917WB	
E-DNP-L-lysine 197–200			1131SB 1122sh 1117SB	1088sh	1076MB	1053MB						922MB		
DNP-DL-methionine 122	1183MS 1170MS	1144SS	1127MS	1100sh 1093MB		1057MB			987WB	966WB 959sh	939WB	921MS	917sh 907WB	
DNP-L-phenylalanine 191	1188SB 1174sh	1156sh 1147SB 1138sh	1130sh	1094sh 1091SB	1071MB	1054SS	1028WB 1026WB	997WB	987WB 976WB	963WB	926MS		913MS	881WB
DNP-DL-phenylalanine 219	1175sh	1159SB 1144SB	1136sh 1131sh	1094SS	1075MS	1054MS	1027WB		983WB	965WB	928WB	923WB 919sh	916sh 909WS	883WB
DNP-L-proline 138	1178MB	1159MS 1145MB	1119MB	1094MB		1063MB	1040WB		976MB				909MB	878WB
DNP-DL-serine 197–201		1153SB	1131sh 1112SB		1067SB	1062sh					934MB		915SB	887MB
DNP-DL-threonine 178–179		1155SB	1126sh 1124sh 1105SB		1083SB	1057SB	1024MB		986WB	966WB	934MB		911MB	
DNP-L-tryptophan 217–221 (*d*)		1143SS	1120MB 1104MB	1093MB		1058MB						923vw	913WB	882WB
Di-DNP-L-tryosine 184 (*d*)	1190MB	1161WS 1144MB	1133sh 1105WB			1064WB 1057sh	1015WB					923MB		889vw
Di-DNP-DL-tryosine 207 (*d*)		1147MB	1121MS 1107MS	1089MB		1062MB		1006WB			939MB 929WB	921vw	914MB	
DNP-L-valine 132–133	1176SS 1174sh 1170sh	1149SS	1125SS 1100SS			1055MS	1029sh			968WS	945WB 926MS			885vwS
DNP-DL-valine 187–189	1174WB	1151SB	1124MB 1100MB			1055WB				953WB		918MB		

Can. J. Chem. Downloaded from www.nrcresearchpress.com by 176.9.209.113 on 09/04/12
For personal use only.

TABLE I (*Concluded*)

Absorption spectra in the infrared in the 5000–625 cm^{-1} region[a]

DNP-DL-leucine 132–133		831WS 825WS				763vw	743MS	715WB	709vw	685MB		654WB
Di-DNP-L-lysine 178–180		831WB	817WB			761vw	741MS		709vw 703vw			
E-DNP-L-lysine 197–200		831MS	818MB			763WB	741MS		699MB			
DNP-DL-methionine 122		830MB	817MB	797WB	784WB	762WB	743MS	720WB	714WB	676WB		
DNP-L-phenylalanine 191	849WB	831WB	817SS			768sh 762SS	743MS	717MB	711sh 703SS		661SB	648MB
DNP-DL-phenylalanine 219	855WB	833WB		811MS		765MB	744WB	719MS 717sh	707MS		663sh 662MS	648MB
DNP-L-proline 138		829MS		805MS	773WB	755WS	741SS	724MB		690WB		647WB
DNP-DL-serine 197–201		827SS				768sh 763MB	744SS	715MB		690MB	658MB	
DNP-DL-threonine 178–179	867MB	834sh 828MB				764WB	750MB 744MS	715MB			660WB	
DNP-L-tryptophan 217–221 (*d*)		830MS	821MB			768WB 755MB	741MB		707WB		658WB	
Di-DNP-L-tryosine 184 (*d*)	866vw 855vw	833MB	814vw		784vw	765vw	744MB				667WB	
Di-DNP-DL-tryosine 207 (*d*)		831WB	820MB		778MB	760vw	750MB 742SB		711MB			
DNP-L-valine 132–133		834MS	820SS			762MB	749MB	722SB 718SB				
DNP-DL-valine 187–189		830WB	819MS			761WS	749sh 745MS	720WB		692vw	669WB	

[a]W weak intensity, M medium intensity, S strong intensity, B broad band, S sharp band, sh shoulder, vw very weak band.
[b]These numbers represent uncorrected melting points.

Can. J. Chem. Downloaded from www.nrcresearchpress.com by 176.9.209.113 on 09/04/12
For personal use only.

Amino acids have been reported to show marked similarity in their infrared spectra in the region of 1587 to 1333 cm^{-1}. Bands at 1587 and 1408 cm^{-1} have been related, respectively, to the antisymmetrical and symmetrical stretching vibrations of the ionized carboxyl group of the dipolar ions. None of the free amino acids studied lacked the 1408 cm^{-1} band. Among those in which the 1587 cm^{-1} band was not observed were L-threonine and L-proline (3). All of the DNP-derivatives examined by us, however, exhibit the bands at 1587 and 1408 cm^{-1}, and hence the implication is possible that these compounds are dipolar ions. For the free amino acids, a band at 1515 cm^{-1} due to an N–H deformation motion of the α-amino group has been reported, L-leucine, L-serine, and hydroxy-L-proline being among the exceptions (3). Again, there are no such exceptions among the DNP-derivatives studied by us; but we believe that the band here represents antisymmetrical aromatic NO_2 stretch rather than NH-deformation. In the case of free amino acids, bands at 1449 and 1370 cm^{-1} are due to antisymmetrical and symmetrical CH_3 and possibly CH_2 deformation motions, respectively. Among the free amino acids in which the 1449 cm^{-1} band was not apparent were L-valine, L-phenylalanine, hydroxy-L-proline, L-aspartic acid, and L-lysine (3). While the DNP-derivatives of L-aspartic acid and L-lysine (both mono- and di-) and in addition of L-cysteine, L-cystine, L-histidine (di-), L-tyrosine (di-), and DL-threonine do not show the band, those of L- and DL-valine, L- and DL-phenylalanine, and hydroxy-L-proline exhibit it weakly or as a shoulder. In the spectrum of free glycine only, the 1370 cm^{-1} band was lacking (3), and in that of its DNP-derivative it is present. Furthermore, the DNP-derivatives of L-cystine (di-), L-lysine (di-) (unlike the monosubstituted forms), and DNP-L-tyrosine (di-) do not show this band. A 1333 cm^{-1} band has been considered to be related to a CH_2 wagging motion and the only exception among the free amino acids was due to L-alanine (3). None of the DNP-amino acids studied lacks this band. It should be emphasized, however, that bands in the region 1330–1370 will be difficult to interpret, as symmetrical aromatic NO_2 stretch is in this region and is usually intense.

While many free amino acids possessed a band at 2564 cm^{-1}, provisionally assigned to the C–H stretching motion (3), but more likely due to overtone or combinations of the strongly anharmonic $N–H_n$ deformations, it is missing in almost all DNP-derivatives. On the other hand, the spectra of DNP-derivatives with the exception of DNP-L-tyrosine (di-) and DNP-L-arginine possess a band at 1724 cm^{-1}, a band which is not exhibited by the free amino acids.

The spectrum of the racemic form of DNP-alanine differs very little from that of its optically active form. The spectrum of the former does not show the band at 1727 cm^{-1} or that at 1261 cm^{-1}. In the case of DNP-isoleucine, the differences are also not very marked. There is an additional band at 733 cm^{-1} in the spectrum of the active form. The spectrum of the active form of leucine shows additional bands at 1206, 1076, 939, and 775 cm^{-1}. The shoulders at 1420 and at 1203 cm^{-1} of DNP-L-phenylalanine turn into medium broad bands for the DL-form. This L-form has an additional band at 1188, while the DL-form also has an additional band at 1294 cm^{-1}. For tyrosine the shoulder at 3390 cm^{-1} of the L-isomer is a definite dip in the spectrum of the racemic mixture. A striking difference is the absence of the intense and sharp band at 1715 cm^{-1}, the medium band at 1479 cm^{-1}, and the weak one at 1161 cm^{-1} in the DL-form of this amino acid. The DL-form has additional bands at 1362, 1239, 1121, 1089, 939, 750, and 711 cm^{-1}. The shoulder at 1529 cm^{-1} for DNP-DL-valine turns into a definite band for the L-form. The major differences, however, between the spectra for the L- and DL-forms of this amino acid lie between 1429 to 1250 cm^{-1} where the L-form has clearly resolved bands at 1427, 1309, and 1261 cm^{-1}.

The question arises as to whether structurally related DNP-amino acids can be readily differentiated. In the case of DNP-L-proline versus DNP-hydroxy-L-proline, for instance, the former has pronounced additional peaks at 1377, 1290, 1221, 1159, 1094, 1040, and 773 cm^{-1}, the latter at 1245, 997, and 927 cm^{-1}. The 3226-cm^{-1} band, however, reported to be present in the free hydroxy-prolines but not in the spectrum of free proline and assumed to reflect the presence of the —OH group in the former (3), is absent in the spectra of the DNP-derivatives of either L-hydroxyproline or L-proline.

The spectra of DNP-L-valine and DNP-L-isoleucine would be expected to resemble each other. DNP-L-isoleucine has additional bands at 3058, 1222, 1121, and 733 cm^{-1}, DNP-L-valine at 1490, 1427, 1176, and 945 cm^{-1}. In the case of the spectrum of the corresponding free amino acids, L-isoleucine, unlike L-valine, shows a sharp and discrete band at 1462 cm^{-1} (3). Such a distinguishing difference is ruled out for the DNP-derivative of these amino acids.

It would be surprising if the infrared spectra of closely related compounds did not reveal some differences by which pure, individual samples of such compounds could be differentiated from each other. A review of the table suggests that among the DNP-L-amino acids studied the spectra on the whole are more strikingly similar than they are different, and that the use of the spectral tool for purposes of identification is much weaker and less reliable than such procedures as chromatography. There are, however, some DNP-amino acids (e.g., leucine and isoleucine) which are difficult to identify by chromatography and hence spectral analysis after purification would still be of value. Even the spectra of structurally very similar DNP-amino acids show sufficient variation to allow positive identification.[6]

REFERENCES

1. SANGER, F. Biochem. J. **39**, 507 (1945); **45**, 563 (1949).
2. LEIFER, A. and LIPPINCOTT, E. R. J. Am. Chem. Soc. **79**, 5098 (1957).
3. KOEGEL, R. J., GREENSTEIN, J. P., WINITZ, M., BIRNBAUM, S. M., and MCCALLUM, R. A. J. Am. Chem. Soc. **77**, 5708 (1955).
4. RAMACHANDRAN, L. K., EPP, A., and MCCONNELL, W. B. Anal. Chem. **27**, 1734 (1955).
5. LEVY, A. L. and CHUNG, D. J. Am. Chem. Soc. **77**, 2899 (1955).
6. RAO, K. R. and SOBER, H. A. J. Am. Chem. Soc. **76**, 1328 (1954).

[6]*While it is recognized that polymorphism can result in spectral changes due to the alterations in the immediate environments of the vibrating groups, no attempt has been made here to evaluate this factor.*

Can. J. Chem. Downloaded from www.nrcresearchpress.com by 176.9.209.113 on 09/04/12
For personal use only.

Can. J. Chem. Downloaded from www.nrcresearchpress.com by 176.9.209.113 on 09/04/12
For personal use only.

FREE RADICALS BY MASS SPECTROMETRY

XVI. Hg-PHOTOSENSITIZED DECOMPOSITIONS OF BIACETYL, ACETYLACETONE, AND ACETONYLACETONE[1]

A. G. HARRISON[2] AND F. P. LOSSING

ABSTRACT

The Hg($^3P_1$)-photosensitized decomposition of biacetyl proceeds by a central bond fission. Of the resulting acetyl radicals, at least 27% survive the primary act long enough to react with other radicals, or with a second excited Hg atom. Under conditions of high illumination, there is evidence that Hg($^3S_1$) atoms produced by stepwise excitation also play a part in the reaction by forming excited biacetyl molecules with a lifetime of the order of 1 millisecond. The photosensitized decompositions of acetylacetone and acetonylacetone were examined qualitatively. The former dissociates mainly into an acetyl and an acetonyl radical, and the latter mainly if not exclusively to form CH_3CO and $C_2H_4COCH_3$ radicals. Further reactions of these radicals, and a possible structure for the $C_2H_4COCH_3$ radical, are also discussed.

INTRODUCTION

The photochemical behavior of biacetyl has been the subject of many investigations, mainly as a result of its well-known fluorescence and the complicating factors which this introduces into the mechanism of the acetone photolysis. However, no study of the reaction of biacetyl with excited mercury atoms appears to have been published. Earlier work supplies ample evidence that both CH_3 and CH_3CO radicals are produced in the direct photolysis. The addition of NO was found (1) to suppress the formation of methane and ethane. Blacet and Bell (2, 3) found that the addition of iodine was also effective in this respect, and they concluded that the primary decomposition step at 2654 Å could most probably be written as:

$$CH_3COCOCH_3 + h\nu_{2654} \rightarrow 2CH_3CO. \qquad [1]$$

As a result of energy carry-over, one or both acetyl radicals could dissociate immediately into CH_3 and CO. This work, in agreement with that of Anderson and Rollefson (1), indicated that the decomposition reaction is wholly free radical in nature, and that no molecular rearrangement to form C_2H_6 occurs. Some evidence (4) that ethane could be formed directly by dissociation of a long-lived excited biacetyl molecule has not been substantiated by later work.

The flash photolysis of biacetyl was examined by Porter (5) and by Porter and Norrish (6). Their observations were in agreement with reaction [1] as a primary step, but they concluded that the more complete dissociation

$$CH_3COCOCH_3 + h\nu \rightarrow 2CH_3 + 2CO \qquad [2]$$

predominated, even at 4200 Å. Since the energy available at 4200 Å is insufficient for reaction [2], there is reason to believe that thermal energy from the flash must have been involved. Their conclusions as to the relative occurrence of reactions [1] and [2] are consequently open to question (7).

The photolysis of biacetyl at 2700, 3650, and 4358 Å and its relationship to fluorescence has been discussed in some detail by Noyes and his co-workers (8, 9). They concluded

[1]*Manuscript received April 29, 1959.*
Contribution from the Division of Pure Chemistry, National Research Council, Ottawa, Canada.
Issued as N.R.C. No. 5291.
[2]*National Research Council of Canada Postdoctorate Fellow 1957–59.*

that at 2700 and 3650 Å the primary step [1] given by the earlier work was essentially the correct one, but that the reaction might more correctly be written:

$$CH_3COCOCH_3 + h\nu \rightarrow 2\alpha CH_3CO^* + (2-2\alpha)CH_3CO. \quad [3]$$

The evidence suggested that at 2700 Å one of the acetyl radicals dissociated immediately (i.e. $\alpha = 0.5$) and the primary dissociation was therefore kinetically indistinguishable from a primary dissociation step:

$$CH_3COCOCH_3 + h\nu \rightarrow CH_3 + CH_3COCO \quad [4]$$

followed by an immediate dissociation of the radical:

$$CH_3COCO \rightarrow CH_3CO + CO. \quad [5]$$

At 3650 Å the situation is complicated by the existence of two excited species giving rise to the short-lived and long-lived fluorescences. They found the primary quantum yield at 4358 Å to increase with light intensity. From this observation, and on the basis that the 66 kcal/mole available at 4358 Å is probably insufficient to dissociate biacetyl, they came to the tentative conclusion that the observed dissociation at 4358 Å proceeded by a collision of two excited biacetyl molecules having a lifetime of about 1.8×10^{-3} second. This conclusion, together with the fact that the fluorescence of biacetyl is not excited at wavelengths shorter than 3130 Å (9), is of importance in explaining an unusual feature of the mercury-photosensitized decomposition of biacetyl observed in the present work.

The photochemical behavior of acetylacetone (2,4-pentanedione) and of acetonylacetone (2,5-hexanedione) does not appear to have been investigated before.

EXPERIMENTAL

The mercury-photosensitized reactions were carried out at 55° C in a fast-flow reactor using helium as a carrier. At a point just past the end of the illuminated zone, a small fraction of the reaction stream flowed through an orifice directly into the ionization chamber of a mass spectrometer, enabling observation of free radical products, as well as of stable products, to be made. This apparatus and its operating characteristics have been described (10, 11). A new design of ion source having some modifications to permit a higher pumping speed in the ionization chamber was employed (12).

The effect of light intensity on the biacetyl decomposition was studied by the use of metal screens. Screens with different degrees of transmission were prepared from brass screen having an original transmission of about 39%, by reducing the wire diameter in dilute nitric acid. A rough index of the transmission of the etched screens could be had by measuring the hole-to-wire ratios with a low-power microscope fitted with a micrometer traversing screw. Pieces of suitable width cut from these etched screens were then rolled into cylindrical form so that they could be placed in the annular space between the lamp and the reactor tube. The transmission coefficient for each screen was then measured in place by observing the reduction it caused in the amount of ethylene decomposed in the reactor on illumination by the lamp. The transmission coefficients measured in this way agreed quite closely with those obtained by observation of the hole-to-wire ratios.

MATERIALS

The biacetyl, acetylacetone, and acetonylacetone were Eastman Kodak Co. white label grade, further purified by vacuum distillation. The sample of $Hg(CD_3)_2$ was obtained from Merck and Co. (Montreal).

Can. J. Chem. Downloaded from www.nrcresearchpress.com by 176.9.209.113 on 09/04/12
For personal use only.

Can. J. Chem. Downloaded from www.nrcresearchpress.com by 176.9.209.113 on 09/04/12
For personal use only.

RESULTS AND DISCUSSION

Biacetyl

A qualitative examination of the products of the mercury-photosensitized reaction of biacetyl, using low-energy electrons for the detection of the parent peaks of free radicals and stable products, showed the presence of CH_3 radicals in considerable abundance. Other parent peaks showing significant increases were those of acetone, ketene, ethane, carbon monoxide, and methane. However, a definite increase for the acetyl radical (mass 43) could not be obtained, even using higher partial pressures of biacetyl. No increase in the mass 85 ($CH_3COCOCH_2$) or mass 71 (CH_3COCO) peaks was found. The failure to detect these radicals using low-energy electrons was not conclusive evidence for their absence, however, since acetyl radicals were also not detected by this means. A further search was made for radicals by means of the addition of mercury dimethyl to the reaction stream. In earlier work (12, 13) it was found that CH_3 radicals produced by the mercury-photosensitized decomposition of $Hg(CH_3)_2$ provided a means for detecting the presence of a free radical R by observation of the formation of the combination product:

$$CH_3 + R \rightarrow CH_3R. \qquad [6]$$

This technique was found to be a valuable aid in detecting radicals for which the sensitivity of detection using low-energy electrons appeared to be rather low. The addition of a small partial pressure of $Hg(CH_3)_2$ to the reaction stream containing biacetyl resulted in a greatly increased yield of acetone, showing that acetyl radicals were present. The combination product of the $CH_3COCOCH_2$ radical with CH_3, on the other hand, was not found, indicating that this radical, which on thermochemical grounds would be stable at 55° C, was not present in significant amounts. To provide a means of detecting the CH_3COCO radical, $Hg(CD_3)_2$ was added to the reaction stream. The combination product $CH_3COCOCD_3$ was not found, although CH_3COCD_3 was produced in abundance. It may be concluded that the CH_3COCO radical, if formed at all, must have dissociated immediately. The addition of CD_3 radicals was found to reduce greatly the yield of CH_3COCH_3, showing that most, if not all, of the acetone was formed by radical combination and not by a molecular rearrangement of biacetyl.

The composition of the reaction products from the biacetyl decomposition was examined quantitatively as a function of the length of the illuminated zone by means of the movable shutter described previously (10, 11). Using 50-volt electrons, mass spectra were obtained at different shutter positions, and analyses were carried out in the usual way. The amounts of biacetyl decomposed, and of the products CO, acetone, ketene, ethane, methane, and methyl produced at the different shutter positions are given in Table I. The amounts of CH_3 were calculated with the assumption that the CH_3^+ contribution

TABLE I

Length of illuminated zone, mm	Biacetyl decomposed, μ	Products from biacetyl, μ						Balance (%) of:	
		CO	$CO(CH_3)_2$	CH_2CO	C_2H_6	CH_3	CH_4	O	C
5	0.096	0.12_1	0.014	0.021	0.020	0.03_5	0.010	81.3	75.5
10	0.221	0.26_9	0.049	0.053	0.049	0.09_6	0.008	83.9	81.9
15	0.401	0.41_8	0.115	0.064	0.085	0.11_4	0.011	73.9	74.4
20	0.566	0.73_6	0.216	0.086	0.146	0.15_1	0.018	91.7	89.1
25	0.790	1.02_8	0.333	0.107	0.212	0.14_7	0.028	92.9	89.6
30	0.996	1.34_6	0.400	0.131	0.276	0.16_7	0.038	94.2	89.5

from the CH_3CO radical was negligible. The actual yields of CH_3 are therefore rather smaller than those given in Table I. The increasing defect in the C and O balances at the shorter lengths of illuminated zone probably results from the inability to include a quantitative measurement for the CH_3CO radical. Although no increase in the mass 43 peak could be detected using low-energy electrons, a small remainder was left in the 50-volt spectra in all cases after correction for contributions from biacetyl and acetone.

The distribution of products is consistent with a primary dissociation into two acetyl radicals:

$$CH_3COCOCH_3 + Hg(^3P_1) \rightarrow CH_3CO + CH_3CO^* + Hg(^1S_0). \quad [7]$$

The present work provides no clear indication as to what fraction of the acetyl radicals formed in this reaction dissociate immediately by the reaction

$$CH_3CO^* \rightarrow CH_3 + CO. \quad [8]$$

However, a significant fraction does survive for an appreciable time, either as a result of receiving insufficient activation in the primary step, or as a result of deactivation:

$$CH_3CO^* + M \rightarrow CH_3CO + M. \quad [9]$$

The following radical combination reactions also occur:

$$CH_3CO + CH_3 \rightarrow CH_3COCH_3 \quad [10]$$

$$2CH_3 \rightarrow C_2H_6. \quad [11]$$

In agreement with the findings of earlier work on acetone (11), the low yield of methane shows that the disproportionation reaction

$$CH_3 + CH_3CO \rightarrow CH_2{=}CO + CH_4 \quad [12]$$

is quite slow compared with reaction [10]. If all the methane were produced by reaction [12] and all the acetone by reaction [10], the ratio k_{12}/k_{10} would be given by the ratio of methane to acetone. At the longest contact time this ratio was 0.095. This probably represents an upper limit to k_{12}/k_{10}. The large excess of ketene over methane supports the conclusion reached in earlier work (11) that acetyl radicals are decomposed by excited mercury atoms as follows:

$$CH_3CO + Hg^* \rightarrow CH_2{=}CO + H + Hg. \quad [13]$$

The fate of the H atom is not known; possibly it reacts with an acetyl radical to give a second molecule of ketene. Since no acetaldehyde is formed, it is evident that ketene is not produced in a primary molecular rearrangement reaction. The rapid decrease in the yield of acetone at shorter contact times supports the evidence given above that acetone was formed by reaction [10] and not by the possible molecular rearrangement:

$$CH_3COCOCH_3 + Hg^* \rightarrow CH_3COCH_3 + CO + Hg. \quad [14]$$

A similar conclusion can be reached for ethane. Assuming, then, that acetone and ketene are formed only by reactions [10] and [13], it may be concluded that at least 0.27 of the acetyl radicals survive the primary dissociation step for a time sufficiently long to permit them to react with methyl radicals or a second excited mercury atom. Whether they survive as a result of deactivation (reaction [9]), or as a result of not being sufficiently excited in reaction [7], cannot be decided from the present results.

A graphical representation of the data on biacetyl, given in Fig. 1, shows an unexpected feature. The amount of biacetyl decomposed did not increase linearly with the length of the illuminated zone as had been found for all other compounds examined, but curved

Can. J. Chem. Downloaded from www.nrcresearchpress.com by 176.9.209.113 on 09/04/12
For personal use only.

Can. J. Chem. Downloaded from www.nrcresearchpress.com by 176.9.209.113 on 09/04/12
For personal use only.

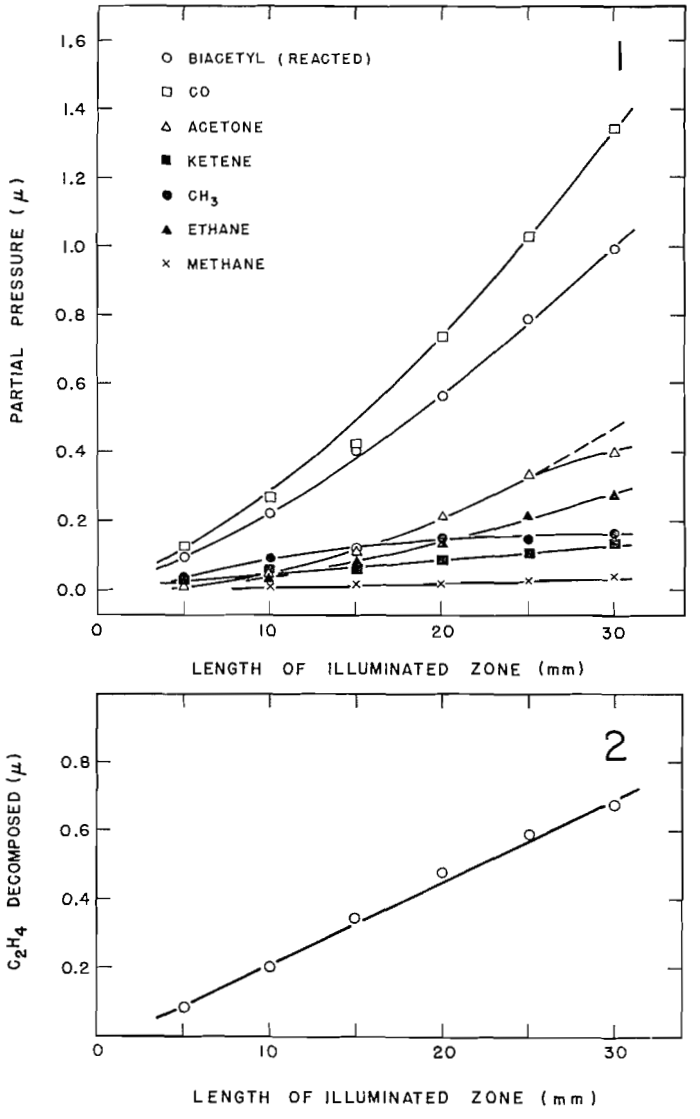

FIG. 1. Decomposition of biacetyl.
FIG. 2. Ethylene decomposed as a function of the length of the illuminated zone.

progressively upward. In order to ensure that this non-linear behavior did not result from inequalities in the amount of 2537-Å radiation entering the reactor at different points along its length (as a result of polymeric deposits, for example), a calibration was carried out using ethylene. As shown in Fig. 2, the relation for ethylene was linear. The curvature evident in Fig. 1 was consequently considered to be a real, and not an instrumental, effect. Such an effect would be produced if an appreciable fraction of the biacetyl decomposed by a process involving an intermediate whose lifetime was not negligible compared to the transit time through the illuminated zone, which was about 1×10^{-3} second. A reasonable assumption would be that this species was the metastable state of biacetyl B**, having a lifetime of 1.8×10^{-3} second. As discussed above, this

species was considered by Noyes and co-workers (8, 9) to account for the dissociation of biacetyl at 4358 Å by a second-order process:

$$2B^{**} \rightarrow B + \text{products.} \qquad [15]$$

If, in the present work, some fraction of the biacetyl were dissociating by this mechanism, the question arises as to how B** could be formed. Since biacetyl shows no fluorescence in the 2380–3130 Å (9) it appears unlikely that B** could be formed by collisions with $^3P_1$ mercury atoms. The radiation from a mercury lamp of the type used in this work does contain an appreciable amount of radiation at longer wavelengths, particularly at 3130, 3650, and 4358 Å. The possibility that B** could be formed by direct absorption of 3650- and 4358-Å radiation was checked by placing a filter, in the form of a split cylinder of Corning 7040 glass, between the lamp and the reactor tube to remove 2537 Å while allowing 3650 Å to pass. With this filter in place, it was found that no measurable decomposition of biacetyl occurred, showing that direct absorption of 3650- or 4358-Å radiation was not responsible for the effect, and that the explanation must be sought in terms of 2537-Å radiation and excited mercury atoms.

The dependence of biacetyl decomposition on the total light intensity was investigated using the metal screens described above, with the result shown in Fig. 3. For purposes of comparison, the dependence for acetone decomposition was also examined. Within the

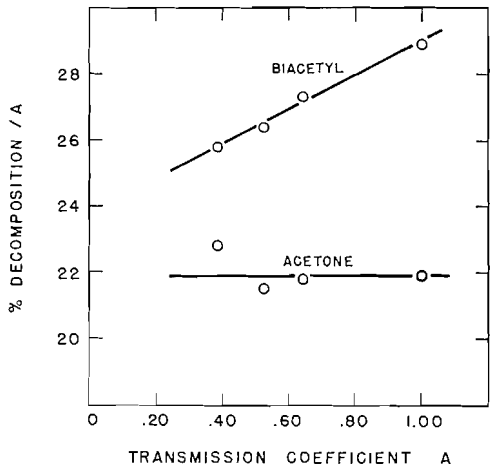

FIG. 3. Dependence of extent of decomposition on the light intensity.

experimental error the amount of acetone decomposed per millisecond was found to be proportional to the amount of light passing through the screen. The amount of biacetyl decomposed, on the other hand, depended on some order of light intensity greater than one. This lends further support to the view that a second-order decomposition process such as reaction [15] must be involved.

A positive identification of this process is not possible from the present work, but it is of interest to speculate as to how the B** state of biacetyl could be activated. Since the incident flux of 2537-Å radiation in the reaction cell is very high (greater than 10^{18} quanta/sec cc (10)) the fraction of the total number of mercury atoms which are at any instant in the $^3P_1$ state is quite appreciable. The probability of absorption of a quantum of 4358 Å by a $^3P_1$ atom to give a mercury atom in the 7^3S_1 state is therefore not negligible. This process of stepwise excitation is well known (14). Since the B**

Can. J. Chem. Downloaded from www.nrcresearchpress.com by 176.9.209.113 on 09/04/12
For personal use only.

state of biacetyl is known to be formed by direct absorption of 4358 Å it is not unreasonable to assume that this state could also be formed by a collision in which a $^3S_1$ mercury atom is quenched to a $^3P_1$ atom. On the assumption that the incident radiation I contains a fraction x of 4358-Å radiation, the remainder being 2537 Å, the following interactions may be considered:

[16] $\quad Hg + h\nu_{2537} \rightarrow Hg^3P_1 \qquad +\frac{d}{dt}[Hg^3P_1] = k_{16}(1-x)I[Hg]$

[17] $\quad Hg^3P_1 + h\nu_{4358} \rightarrow Hg^3S_1 \qquad +\frac{d}{dt}[Hg^3S_1] = k_{17}I[Hg^3P_1]$

[18] $\quad Hg^3P_1 \rightarrow Hg + h\nu_{2537} \qquad -\frac{d}{dt}[Hg^3P_1] = [Hg^3P_1]/\tau_1$

[19] $\quad Hg^3S_1 \rightarrow Hg^3P_1 + h\nu_{4358} \qquad -\frac{d}{dt}[Hg^3S_1] = [Hg^3S_1]/\tau_2$

[20] $\quad Hg^3P_1 + B \rightarrow Hg + B^* \qquad -\frac{d}{dt}[Hg^3P_1] = k_{20}[Hg^3P_1][B]$

[21] $\quad Hg^3S_1 + B \rightarrow Hg^3P_1 + B^{**} \qquad -\frac{d}{dt}[Hg^3S_1] = k_{21}[Hg^3S_1][B]$

Application of the steady-state treatment to these equations gives the relation:

[22] $$\frac{[Hg^3S_1]}{[Hg^3P_1]} = \frac{k_{17}x}{k_{16}(1-x)}\frac{[Hg^3P_1]}{[Hg]}\left(\frac{1/\tau_1 + k_{20}[B]}{1/\tau_2 + k_{21}[B]}\right).$$

The lifetime of Hg^3S_1, $\tau_2 = 5.75\times10^{-8}$ second (15), is not greatly different from that of Hg^3P_1, for which $\tau_1 = 1.0\times10^{-7}$ second (14). Since the absorption coefficients are proportional to the reciprocal of the lifetimes, k_{16} and k_{17} are, to a first approximation, nearly equal. Nothing is known about the quenching efficiency of biacetyl for Hg^3S_1 atoms, but if it is assumed that it is not greatly different from that for Hg^3P_1 atoms, then $k_{20} \approx k_{21}$ and expression [22] reduces to:

[23] $$\frac{[Hg^3S_1]}{[Hg^3P_1]} = \frac{x}{1-x}\frac{[Hg^3P_1]}{[Hg]}f$$

in which the factor f is of the order of unity. On the basis (from Fig. 3) that some 10% of the amount of biacetyl decomposed does so by a second-order process, the right-hand side of equation [23] would have to have a value of about 0.2. Under the existing experimental conditions this may not be beyond the bounds of possibility.

In order to demonstrate conclusively that Hg^3S_1 atoms were the activating agent, it would have been necessary to filter out 4358-Å radiation while allowing 2537 Å to pass. While this might be possible given sufficient space between the lamp and the reactor tube, it could not be accomplished in the 2–3 mm annular space available in the present reaction system.

Acetylacetone and Acetonylacetone

The products of the mercury-photosensitized reactions of acetylacetone and acetonylacetone were very briefly examined, but no quantitative analyses of the products were made. In the decomposition of acetylacetone, the use of low-energy electrons indicated that three free radicals were formed, at mass 15 (methyl), mass 43 (acetyl), and mass 57 (CH_3COCH_2). The stable products were CO, some ethane, ketene, and acetone. Addition

Can. J. Chem. Downloaded from www.nrcresearchpress.com by 176.9.209.113 on 09/04/12
For personal use only.

of CH_3 radicals to the reaction stream resulted in an increased yield of acetone and ethane, and the appearance of a peak at mass 72. The latter was attributed to the formation of methyl ethyl ketone by combination of methyl with acetonyl radicals. There was no indication of the formation of $CH_3COCH_2COCH_2CH_3$, suggesting that the $CH_3COCH_2COCH_2$ radical was not present in significant amounts. These qualitative results suggest that acetylacetone decomposes mainly by a split into two radicals:

$$CH_3COCH_2COCH_3 + Hg^* \rightarrow CH_3COCH_2 + CH_3CO. \quad [24]$$

Since the CH_3CO radical could be detected at low-electron energies, it is possible that a considerably larger fraction of the CH_3CO radicals survives the primary step than in the case of biacetyl.

The mode of reaction with acetylacetone with excited mercury atoms is undoubtedly quite complicated in detail. Acetylacetone vapor is 76.5% in the enol form under equilibrium conditions (16) and at first sight it might be thought that the keto and enol forms could be excited at different higher states and dissociate by different modes. However, it appears from the present experiments that CH_3CHO, a reasonable product from the dissociation of an enol-type excited molecule, is not formed to any extent. It is interesting to note that in the mass spectrum (No. 806 in the API Mass Spectral Catalog) there are no ions such as $CH_3{}^+COH$ which might arise from dissociation of an enol-type parent ion. There is no reason to believe, therefore, that the keto–enol tautomerism also exists among the excited and ionic states of acetylacetone.

A qualitative examination of the products formed by the mercury-photosensitized decomposition of acetonylacetone was also carried out in the same way. Using low-energy electrons, products were found having the following parent peaks: mass 15 (CH_3), mass 42 (ketene), and mass 43 (CH_3CO). No increase in the mass 57 peak, corresponding to the acetonyl radical, was found. Other products formed were ethane, acetone, products having parent masses of 70 and 86, and possibly a little ethylene. The addition of CH_3 radicals (from $Hg(CH_3)_2$) to the reaction stream gave a greatly enhanced yield of the products of mass 58 and 86, indicating the presence of radicals of mass 43 and 71. This shows that the predominating mode of dissociation is into two radicals according to the reaction:

$$CH_3COCH_2CH_2COCH_3 + Hg^* \rightarrow CH_3CO + C_2H_4COCH_3 + Hg. \quad [25]$$

Since no methyl ethyl ketone was formed on the addition of CH_3 radicals it may be concluded that the concentration of acetonyl radicals was negligibly small, and that the alternative mode of dissociation

$$CH_3COCH_2CH_2COCH_3 + Hg^* \rightarrow 2CH_3COCH_2 + Hg \quad [26]$$

occurred to a much smaller extent, if at all.

A third mode of dissociation is possible:

$$CH_3COCH_2CH_2COCH_3 + Hg^* \rightarrow CH_3 + COCH_2CH_2COCH_3 + Hg. \quad [27]$$

However, the addition of CD_3 radicals (from $Hg(CD_3)_2$) to the reaction stream did not result in any formation of the combination product $CD_3COCH_2CH_2COCH_3$ at mass 117. Although this experiment strongly suggests that no $COCH_2CH_2COOH_3$ radicals were present, it is possible that some of the radicals at mass 71 arose from reaction [27] followed immediately by a loss of CO from the large radical. On the other hand, the large yield of CH_3CO radicals shows that a large fraction of the radicals of mass 71 was formed by reaction [25]. In view of earlier observations that free radicals may react

Can. J. Chem. Downloaded from www.nrcresearchpress.com by 176.9.209.113 on 09/04/12
For personal use only.

rapidly with excited Hg atoms (10, 11) the small amount of product of mass 70 may have been formed by the reaction:

$$C_2H_4COCH_3 + Hg^* \rightarrow CH_2 = CHCOCH_3 + H + Hg. \qquad [28]$$

In view of the unexpected stability of the $C_2H_4COCH_3$ radical, further experiments were carried out in an attempt to obtain a more exact identification. A simple bond rupture as in equation [25] would be expected to give a radical having the structure $\dot{C}H_2CH_2COCH_3$. The addition product of this radical with the added CH_3 radicals would therefore be expected to be methyl *n*-propyl ketone. The mass spectrum of this ketone shows major peaks at masses 86, 71, and 57.[3] Although the observed addition product had major peaks at masses 86 and 71, the peak at mass 57 was much too small for this product to be methyl *n*-propyl ketone. The lack of a mass 57 peak would be explained if the addition product were instead methyl isopropyl ketone, which has major peaks at masses 86 and 71, but not at mass 57. This observation suggests that the large radical formed in reaction [25] had the structure $\dot{C}H_3CHCOCH_3$ rather than the structure $\dot{C}H_2CH_2COCH_3$, presumably as a consequence of a hydrogen atom shift in the excited molecule prior to dissociation. If such were the case the stability of the $C_2H_4COCH_3$ radical would be explained, since for the former one can write two resonating structures:

$$CH_3\dot{C}H{-}\underset{\underset{O}{\|}}{C}CH_3 \leftrightarrow CH_3CH{=}\underset{\underset{O\cdot}{|}}{C}CH_3.$$

The $\dot{C}H_2CH_2COCH_3$ radical, on the other hand, would be expected to dissociate easily into C_2H_4 and $COCH_3$. Without a more definite identification of the ketone addition product, this conclusion as to the identity of the $C_2H_4COCH_3$ radical must be regarded as tentative.

REFERENCES

1. ANDERSON, H. W. AND ROLLEFSON, G. K. J. Am. Chem. Soc. **63**, 816 (1941).
2. BLACET, F. E. and BELL, W. E. Discussions Faraday Soc. **14**, 70 (1953).
3. BLACET, F. E. and BELL, W. E. J. Am. Chem. Soc. **77**, 5332 (1954).
4. ASCAH, R. G., BURTON, M., RICCI, J. E., and DAVIS, T. W. J. Chem. Phys. **14**, 487 (1946).
5. PORTER, G. Proc. Roy. Soc. (London), A, **200**, 284 (1950).
6. KHAN, M. A., NORRISH, R. G. W., and PORTER, G. Proc. Roy. Soc. (London), A, **219**, 450 (1953).
7. STEACIE, E. W. R. Atomic and free radical reactions. 2nd ed. Reinhold Publishing Corp., New York. 1954.
8. SHEATS, G. F. and NOYES, W. A., JR. J. Am. Chem. Soc. **77**, 1421 (1955).
9. NOYES, W. A., JR., PORTER, G. B., and JOLLEY, J. E. Chem. Revs. **56**, 49 (1956).
10. LOSSING, F. P., MARSDEN, D. G. H., and FARMER, J. B. Can. J. Chem. **34**, 701 (1956).
11. LOSSING, F. P. Can. J. Chem. **35**, 305 (1957).
12. KEBARLE, P. and LOSSING, F. P. Can. J. Chem. **37**, 389 (1959).
13. COLLIN, J. and LOSSING, F. P. Can. J. Chem. **35**, 778 (1957).
14. MITCHELL, A. C. G. and ZEMANSKY, M. W. Resonance radiation and excited atoms. Cambridge University Press, London. 1934.
15. RANDALL, R. H. Phys. Rev. **35**, 1161 (1930).
16. CONANT, J. B. and THOMPSON, A. F., JR. J. Am. Chem. Soc. **54**, 4039 (1932).

[3]*The data in the Mass Spectral Catalog, API Project 44, are in disagreement as to the spectrum of methyl n-propyl ketone. Spectra Nos. 299 and 378 show a large 57 peak, but No. 651 shows instead a mass 57 peak of only 0.35. A spectrum of methyl n-propyl ketone obtained in the present work agreed with spectra Nos. 299 and 378 in this respect. It is possible that a misprint in No. 651 has given 0.35 instead of 10.35 for the mass 57 peak.*

Can. J. Chem. Downloaded from www.nrcresearchpress.com by 176.9.209.113 on 09/04/12
For personal use only.

Can. J. Chem. Downloaded from www.nrcresearchpress.com by 176.9.209.113 on 09/04/12
For personal use only.

STERIC INHIBITION OF RESONANCE

V. NITROMESITYLENE[1]

JAMES TROTTER[2]

ABSTRACT

A detailed X-ray investigation of the crystal structure of nitromesitylene has shown that the nitro group is twisted 66° out of the plane of the aromatic ring about the C—N bond. The resulting decrease in resonance interaction compared with a completely planar model has been correlated with the characteristic NO_2 vibration frequencies.

INTRODUCTION

The physical properties of the nitro and acetyl derivatives of mesitylene and durene indicate that resonance interaction between the nitro and acetyl groups and the aromatic rings is markedly reduced in comparison with nitrobenzene and acetophenone, suggesting that the steric effect of the methyl groups prevents the attainment of completely coplanar configurations (1).

The dipole moments, for example, of conjugated aromatic nitro compounds, such as nitrobenzene (I), are larger than those of the corresponding aliphatic molecules, the moment of nitrobenzene in benzene solution being 3.95 Debye units compared with about 3.3 D for an aliphatic nitro compound. The increased dipole moments are due to contributions from ionic structures (II and III) which are at a maximum when the nitro

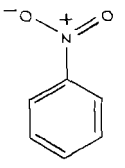

I

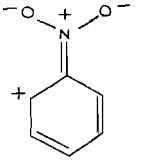

II

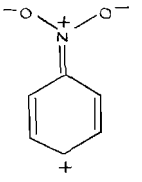

III

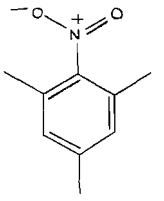

IV

group is coplanar with the aromatic ring. The introduction of methyl groups ortho to the nitro group, as in nitromesitylene (IV), reduces the dipole moment to 3.65 D, suggesting that the nitro group is twisted out of the plane of the benzene nucleus, and the contributions of structures II and III are reduced.

[1]*Manuscript received February 27, 1959.*
Contribution from the Division of Pure Physics, National Research Council, Ottawa, Canada.
Issued as N.R.C. No. 5292.
[2]*National Research Council Postdoctorate Fellow.*

Raman spectra evidence leads to similar conclusions. The Raman shift corresponding to the NO_2 symmetrical stretching vibration is at 1367 cm^{-1} in phenylnitromethane, $Ph.CH_2.NO_2$, where the nitro group is not conjugated with the ring, and at 1341 cm^{-1} in nitrobenzene; the frequency in nitromesitylene is 1363 cm^{-1}, much closer to the value in the non-conjugated molecule, again indicating a significant inhibition of the resonance between the nitro group and the aromatic π-electrons. The ultraviolet absorption spectrum of nitromesitylene also suggests a marked reduction in the resonance interaction.

Similar deviations from coplanarity and consequent resonance inhibition are to be expected in 9-nitroanthracene and 9,10-dinitroanthracene where the nitro group environments are similar to those in nitromesitylene. Detailed investigations of the crystal structures of these anthracene derivatives by X-ray diffraction methods have shown that the nitro groups are twisted markedly out of the planes of the aromatic rings, by 64° in crystals of 9,10-dinitroanthracene, and by 85° in crystals of the 9-nitro derivative. The reductions in resonance interaction resulting from these deviations from coplanarity have been correlated with the infrared spectra and with the bond length variations in the molecules, the energy of resonance interaction between a nitro group and the aromatic π-electrons in 9,10-dinitroanthracene in the solid state being about one-fifth of that in a completely planar model, while for 9-nitroanthracene this resonance energy is negligible. Configurations with 64° twist are the most stable for isolated molecules of both substances, but in crystals of 9-nitroanthracene crystal forces apparently result in minimum energy when the twist is 85°. In solution the angles are the same in both molecules, the exact values possibly depending on solvent–solute interactions.

The present communication describes the extension of these investigations to nitromesitylene; the angle between the plane of the nitro group and the aromatic plane has been determined by an accurate X-ray analysis of the crystals, and the resultant resonance inhibition has been correlated with the characteristic vibration frequencies of the nitro group, both in the solid state and in solution.

EXPERIMENTAL

Infrared Spectra

The spectra measured (Fig. 1) were those of pure nitromesitylene in carbon tetrachloride solution and dispersed in a Nujol mull, as observed with a Perkin–Elmer model 21 infrared spectrophotometer with a rock salt prism.

X-Ray Analysis

Crystals of nitromesitylene are orthorhombic with four molecules in a unit cell of dimensions $a = 15.14$, $b = 8.41$, $c = 7.26$ Å, space group $Pna2_1$. The structure was determined from projections along the three principal crystallographic axes. All the carbon atoms and the nitrogen atom lie on one plane, but the oxygen atoms lie one above and one below this plane at distances of 0.95 Å, so that the nitro group is twisted very markedly out of the plane of the aromatic ring about the C—N bond, the angle between the planes of the benzene ring and the nitro group being 66.4°. Figure 2 shows a projection of the structure along the *b*-axis; the benzene ring is perpendicular to the plane of projection so that the individual atoms are not resolved, but the large deviation of the oxygen atoms from coplanarity is well illustrated. Full details of the crystal structure analysis are published elsewhere (2).

Can. J. Chem. Downloaded from www.nrcresearchpress.com by 176.9.209.113 on 09/04/12
For personal use only.

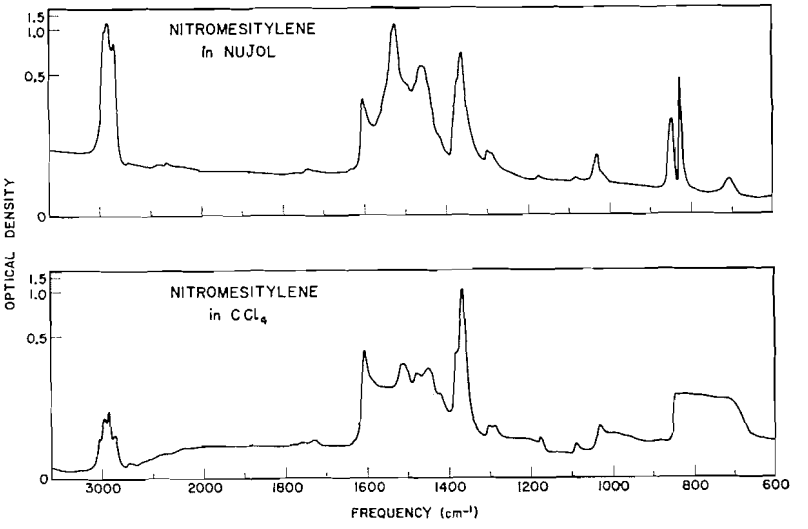

FIG. 1. Infrared spectra.

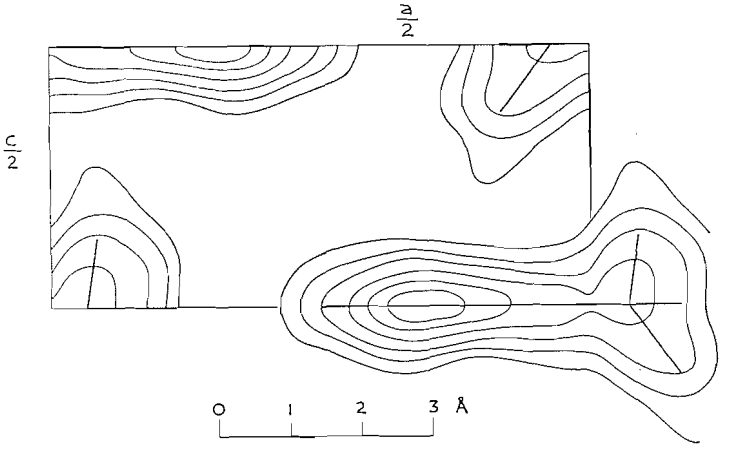

FIG. 2. Projection of the structure of nitromesitylene along the *b*-axis.

DISCUSSION

The spectra of nitromesitylene in the range 3500 cm^{-1} to 600 cm^{-1} in carbon tetrachloride solution and dispersed in a Nujol mull are shown in Fig. 1, and the peak positions and intensities of the absorption bands are listed in Table I, some peaks of course being masked by the carbon tetrachloride or Nujol bands. The strong absorption at 1364 cm^{-1} in solution and 1362 cm^{-1} in the solid state can be assigned to the NO_2 symmetrical stretching vibration. The NO_2 antisymmetrical stretching vibration cannot be assigned quite so unambiguously, as with the nitroanthracenes, but is probably at 1531 cm^{-1}. The absorption maximum at 828 cm^{-1} corresponds to the C—N stretching vibration.

The characteristic NO_2 frequencies in nitromesitylene are compared in Table II with the corresponding frequencies in conjugated (3) and non-conjugated (4) nitro compounds and with those in 9-nitroanthracene and 9,10-dinitroanthracene. The twists of the nitro

Can. J. Chem. Downloaded from www.nrcresearchpress.com by 176.9.209.113 on 09/04/12
For personal use only.

TABLE I

Frequencies and intensities of absorption bands

Solution (CCl_4)		Solid (Nujol mull)		
Frequency, cm^{-1}	Intensity	Frequency, cm^{-1}	Intensity	Vibration
3030	w			Aromatic C—H stretching
2975	m			CH_3 antisymmetrical stretching
2930	m			CH_3 stretching
2875	w			CH_3 symmetrical stretching
1606	m	1604	m	C=C (aromatic) stretching
		1531 (sh)	s	NO_2 antisymmetrical stretching
		1525	s	C=C (aromatic) stretching
1478	m			CH_3 bending
1450	m			CH_3 symmetrical bending
1420 (sh)	w	1419 (sh)		CH_3 bending
1380 (sh)	m	1373 (sh)	m	CH_3 antisymmetrical bending
1364	s	1362	s	NO_2 symmetrical stretching
1303	w	1300	w	
1288	w	1288 (sh)	w	
1178	w	1177	w	
1090	w	1085	w	Characteristic aromatic bands
1031	w	1033	w	
		849	m	Aromatic C—H out-of-plane vibration
		828	s	C—N stretching

TABLE II

Characteristic nitro-group frequencies (cm^{-1}) and deviations from coplanarity in nitromesitylene and related molecules

Molecule	NO_2 stretching		C—N stretching	NO_2 twist, θ in degrees
	Symmetrical	Antisymmetrical		
Non-conjugated	1377	1586	800→900	90.0
9-Nitroanthracene	1374	1540	836	84.7
Nitromesitylene	1362	1531	828	66.4
9,10-Dinitroanthracene	1367	1542	831	63.7
Conjugated	1349	1518	849	0

groups out of the aromatic planes are included in the last column of the table. The NO_2 symmetrical stretching vibration in nitromesitylene at 1364 cm^{-1} in solution and at 1362 cm^{-1} in the solid state indicates, as in 9,10-dinitroanthracene, that resonance interaction between the nitro group and the aromatic π-electrons is markedly reduced in comparison with a completely conjugated nitro compound, but is not negligible. This conclusion is in agreement with the effect which would be predicted from the measured twist of the nitro group out of the aromatic plane, the predicted resonance energy being about one-fifth ($\cos^2 66.4° = 0.16$) of that for a planar model.

As with the nitroanthracenes the frequencies in solution cannot be directly correlated with the values in the crystals and with the twists of the nitro groups out of the aromatic planes, since the possible effects of solvent–solute interactions cannot be estimated; it can only be deduced that the angle in solution is between 66° and 90°.

REFERENCES

1. WHELAND, G. W. Resonance in organic chemistry. John Wiley & Sons, Inc., New York. 1955.
2. TROTTER, J. Acta Cryst. (In press).
3. RANDLE, R. R. and WHIFFEN, D. H. J. Chem. Soc. 4153 (1952).
4. SMITH, D. C., PAN, C., and NIELSEN, J. R. J. Chem. Phys. **18**, 706 (1950).

Can. J. Chem. Downloaded from www.nrcresearchpress.com by 176.9.209.113 on 09/04/12
For personal use only.

Can. J. Chem. Downloaded from www.nrcresearchpress.com by 176.9.209.113 on 09/04/12
For personal use only.

SOLVOLYSIS IN HYDROGEN AND DEUTERIUM OXIDE

III. ALKYL HALIDES[1]

P. M. LAUGHTON[2] AND R. E. ROBERTSON

ABSTRACT

Rate data for the hydrolysis of a series of α- and β-methylated allyl, benzyl, and cycloalkyl halides in light and heavy water are compared. The major factor determining the rate ratio k_{D_2O}/k_{H_2O} appears to be the relative stability of the initial solvation shell. When the relative viscosity of H_2O and D_2O is used as a measure of the relative stability of structure in bulk solvent, the observed kinetic isotope effect and the temperature dependence of the isotope effect can be rationalized in terms of accepted properties of aqueous solutions.

Attention is drawn to the anomalous rate ratio $k_{RBr}/k_{RI} > 1$ which appears to be characteristic of solvolysis of these alkyl halides in pure water in contrast to other media.

In an extension of recent solvolytic studies of strongly solvated substrates, chiefly sulphonates (1), rates were obtained for the solvolysis of a variety of halogen compounds in light and heavy water. This work was done on the premise that the isotope effect derived from the rate ratio k_{D_2O}/k_{H_2O} was insensitive to temperature, a conclusion based on earlier work on the benzenesulphonates and methanesulphonates (2). However, a recent determination of $\Delta C_p^{\ddagger}$ for isopropyl bromide in light and heavy water (3) has cast doubt on the general applicability of this assumption. Since it was not practical to determine the $\Delta C_p^{\ddagger}$ for each of the alkyl halides for which we had a rate ratio at one temperature, we give here the rate ratios at the convenient experimental temperatures, both because we propose to refer to them later and because even subject to the above proviso they provide, for the detailed mechanism of hydrolysis, clues which deserve discussion.

EXPERIMENTAL

The methods of measuring kinetic rates were similar to those used previously (4). Easily volatile solutes were added under vacuum to the reaction flask, containing deaerated water and the potassium salt of the corresponding acid (0.003 *M*) either from a gas burette or from an evacuated side arm. With some solutes of low solubility, especially the benzyl bromides, a saturated solution was formed, and a fritted glass disk in the filling line was required to remove the small undissolved globules of the halide. With these latter solutes, supersaturation difficulties were occasionally encountered, as shown by non-linear rate plots.

Most of the halides were commercial samples (chiefly Eastman Kodak-White Label), distilled before use with a Fenske (low boiling) or Vigreux (high boiling) column, and passed through an alumina column to give refractive indices in agreement with published values. The following compounds were prepared by the methods indicated: cyclopentyl chloride (5), *p*-methylbenzyl bromide (6), neopentyl bromide (7), and *t*-butyl fluoride (8).

DISCUSSION OF RESULTS

The rates of hydrolysis in light and heavy water and rate ratios for a series of saturated alkyl halides are given in Table I. Similar data for a series of unsaturated or cyclic

[1]*Manuscript received May 20, 1959.*
Contribution from the Division of Pure Chemistry, National Research Council, and the Department of Chemistry, Carleton University, Ottawa, Canada. Presented in part at the Toronto Meeting of the Chemical Institute of Canada, May 27, 1958.
Issued as N.R.C. No. 5288.
[2]*Department of Chemistry, Carleton University, Ottawa, Canada.*

Can. J. Chem. Downloaded from www.nrcresearchpress.com by 176.9.209.113 on 09/04/12
For personal use only.

TABLE I

Solvolytic rate constants for the reaction of alkyl halides, RX, in hydrogen and deuterium oxide

X	R	Temp. (° C)	$k_{D_2O}\times10^5$ sec^{-1}	$k_{H_2O}\times10^5$ sec^{-1}	k_{D_2O}/k_{H_2O}
Cl	Me[a]	89.96	4.38	5.64[b]	$.78_0$
	Et	100.00	9.33 ± .06	11.48	.81
	i-Pr	98.64	75.7 ± .03	100.0 ±1.1	$.75_7$
	t-Bu[a]	4.00	95.0	136.7[c]	.70
		14.03	473	636	.74
	n-Pr	100.00	5.58	6.81	.82
Br	Me[a]	70.50	8.55	10.65[b]	$.80_3$
		80.00	22.0	27.1	$.81_0$
		89.95	54.8	67.0	$.81_8$
	Et	98.66	113.8 ± .2	139.5 ± .4[c]	$.81_6$
	i-Pr[a]	50.00	8.84	11.29[d]	$.78_0$
	n-Pr	79.99	13.15 ± .05	16.14[e]	$.81_5$
	i-Bu	80.00	1.652	1.406	.85
		100.00	35.5 ± .1	42.5	$.83_5$
	*neo*Pen	90.00	4.25 ± .004	5.08 ± .04	$.83_8$
		100.17	13.8	16.2 ± .1	.85
I	Me	79.99	6.68 ± .04	8.19 ± .06[b]	$.81_6$
	Et	98.64	71.1 ± .1	87.8 ± .7[f]	$.81_0$
	i-Pr	80.01	211 ±1	275 ± .4	$.76_7$
	n-Pr	100.00	45.1 ± .4	54.9 ± .4	$.82_2$
	i-Bu	99.90	28.6	35.5 ± .4	.81
F	*t*-Bu	90.24	42.5 ± .02	51.8 ± .16	$.82_0$

[a]Values taken from Paper I of this series (2).
[b]Previous data by Moelwyn-Hughes (9).
[c]Data by Tommila (10, 11).
[d]Value of Winstein *et al.* (12), 1.16×10^{-4} sec^{-1}.
[e]Previous data by Fierens, 25–60° C (13).
[f]Higher than the value of Moelwyn-Hughes (9) at 100° C.

TABLE II

Solvolytic rate constants for the reaction of some allylic, benzylic, and cyclic halides in hydrogen and deuterium oxide

Halide	Temp. (° C)	$k_{D_2O}\times10^5$ sec^{-1}	$k_{H_2O}\times10^5$ sec^{-1}	k_{D_2O}/k_{H_2O}
CH_2=$CHCH_2Cl$	74.99	23.3± .05	29.5± .2	$.79_2$
$PhCH_2Cl$	60.00	45.8± .2	58.3± .1[b]	$.78_5$
p-$MeC_6H_4CH_2Cl$	29.98	64.4± .1	86.2± .5	$.74_7$
$PhCHCl_2$	29.98	198 ± .4	297 ±2	$.66_6$
$PhCCl_3$	5.10	307 ±15	387 ±5	.79
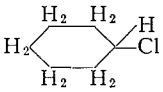	60.01	17.7± .03	23.2± .1	$.76_0$
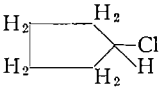	98.64	76.2± .2	93.2± .2	$.81_7$
CH_2=$CHCH_2Br$	60.00	69.0± .3	89.6± .4[c]	$.77_0$
$PhCH_2Br$[a]	29.98	20.2	27.5	$.73_5$
p-$MeC_6H_4CH_2Br$	20.00	104.8± .2	140.6±1.1	$.74_5$
o-$MeC_6H_4CH_2Br$	20.00	41.5± .2	56.0± .3	$.74_2$
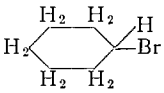	59.98	224 ±2	292 ±1	$.76_6$

[a]Data taken from Paper I of this series (2).
[b]Previous data by Olivier at 30° (15).
[c]Previous data by Fierens, 15–51° (13).

Can. J. Chem. Downloaded from www.nrcresearchpress.com by 176.9.209.113 on 09/04/12
For personal use only.

compounds are given in Table II. The rate ratios for benzal chloride and benzotrichloride were included since Bensley and Kohnstam have recently suggested (16) that these compounds react by an ionizing mechanism.

The model we have used for aqueous solutions in previous papers (4, 17) has approximated to that proposed by Frank and Evans (18). However, the term "iceberg" has a connotation of a greater degree of rigidity than is intended. The problem is to find some graphic word which will take account of the high degree of structure in water and at the same time take cognizance of the dynamic situation demonstrated by self-diffusion (19) and solvation exchange (20, 21). This semantic difficulty is both illustrated and in some degree accommodated by Frank's "fluttering cluster" hypothesis (22). For the sake of simplicity, however, we have chosen to discuss the isotope effect in terms of the static term "structure" in spite of the limitations which this abstraction implies. The opposing effects of non-electrolytes and ions on the associated water in aqueous solutions are conveniently discussed in terms of characteristic changes in structure, and when considered differentially, these changes provide a basis for interpreting the isotope effect observed when D_2O replaces H_2O as a medium for hydrolysis.

Aqueous Solutions of Non-Electrolytes and Ions

When a non-electrolyte is introduced into water, its mere presence removes some degree of librational freedom (23, 18), or in terms of Frank's "fluttering cluster" theory (22) its presence interferes with the shifting centers of organization in such a way as to cause a greater interaction between those molecules immediately contiguous to the non-electrolyte. This has been described as leading to the formation of icebergs about the solute but it is probably a better approximation to specify that a particular water molecule in the primary solvation shell spends more time in each configuration than is characteristic of bulk water (24, 25). The net effect of this loss of freedom will clearly be proportional to the number of water molecules in the surface layer thus leading to such regularities between structures and solvation parameters as are recognized in the Barklay–Butler rule (26).

Evidence that the stability of the solvation shell about non-electrolytes in aqueous solutions decreases with rising temperature is derived from the decrease in the negative enthalpy characterizing the gas–solution equilibria (i.e. $\delta_s C_p$ is positive). In the activation process for hydrolysis the energy required to break down this initial state solvation shell ($\Delta F^{\ddagger}_{str}$) will also be expected to show a similar temperature dependence. This has been invariably found (17) with the obvious difference that since $\Delta H^{\ddagger}$ is positive, $\Delta C^{\ddagger}_p$ is negative for the latter process.

The added energy required to reorganize this initial state solvation shell is given formal recognition in equation [1]

$$[1] \qquad \Delta F^{\ddagger} = \Delta F^{\ddagger}_{I} + \Delta F^{\ddagger}_{str} - \Delta F^{\ddagger}_{R\delta+} - \Delta F^{\ddagger}_{X\delta-}$$

where $\Delta F^{\ddagger}$,* the free energy of activation, is shown to be the difference between (*a*) the energy of bond breaking plus the energy required for the breakdown of the initial state solvation shell and (*b*) the sum of the two terms representing the interaction of the water with the transition state. The intention here is *not* to suggest that complete charge development has necessarily been achieved in the transition state but rather to emphasize interaction with the cationic and anionic functions of the solute.

Ions of intermediate size such as $Cl^{\ominus}$, $Br^{\ominus}$, or $I^{\ominus}$, in contrast to non-electrolytes, appear to have a net structure-breaking effect on water (17), or to use the Bernal–Fowler

*Symbols are the same in this paper as in ref. 17.

description, such ions raise the structural temperature of the water (27). The specific effect will be strongly dependent on the charge density at the surface of the ion, and for singly charged ions this leads to the well-known gradation of solvation properties with size (28, 29). The extension of such considerations to the effect of charge development on adjacent water molecules in the activation process would seem obvious. The majority of salts are known to be more soluble in H_2O than in D_2O (30) presumably because the former already has a less stable structure (see below), and it would seem equally probable that in the hydrolysis of neutral esters, the transition state would be favored by H_2O over D_2O in agreement with the observed isotope effect. It is unlikely, however, that this is the major factor determining the k_{D_2O}/k_{H_2O} ratio.

Kinetic Isotope Effect

In all of those experimental situations where a breakdown of water–water structure is involved, e.g. viscosity (31), mobility of ions (32), self-diffusion (19), dielectric relaxation (33), D_2O invariably gives evidence of a greater degree of structure than H_2O at the same temperature. Since each of the above physical reorganization processes appears to depend on the same elementary step, the similarity found for the isotope effect in each of these processes is to be expected. In terms of the formalism noted above we have adopted this isotope ratio as a measure of the relative structural stability of D_2O versus H_2O toward reorganization. Since the activation process for the hydrolysis of the alkyl halides will involve a reorganization of solvent from a condition characterizing the solvation of non-electrolytes to that characterizing the solvation of the quasi-ionic transition state, it would seem reasonable that the above norm when coupled with recognized differences in the structural stability of water contiguous to non-electrolytes and to ions would provide a convenient basis for discussing the observed isotope effects (k_{D_2O}/k_{H_2O}). To use viscosity as a measure of structural stability in a kinetic equation is by no means novel (34, 35), although this factor is normally considered to have negligible effect on the reaction rate (36).

Formal representation of the kinetic isotope effect follows directly from equation [1]

$$[2] \qquad -RT \ln k_{D_2O}/k_{H_2O} = \delta_M \Delta F^{\ddagger} = \delta_M \Delta F^{\ddagger}_{str} - \delta_M \Delta F^{\ddagger}_{R^{\delta+}} - \delta_M \Delta F^{\ddagger}_{X^{\delta-}}$$

and in the following an attempt will be made to evaluate the relative contribution of the three factors on the right-hand side of equation [2].

If we consider the isotope effect for fluidity (ϕ_{D_2O}/ϕ_{H_2O}) as a normal value for the relative stability of water structure toward reorganization, then it will be apparent that the kinetic isotope effect at any temperature as indicated by the rate ratio (k_{D_2O}/k_{H_2O}) tends toward values either below or above this norm (Fig. 1). This grouping of relative kinetic isotope effects with respect to the assumed "norm" follows, to a remarkable degree, the changes to be expected in the relative stability of the initial state solvation shell.

Just as small ions may be regarded as raising the structural temperature of the water molecules associated with them, so non-electrolytes may be considered to lower the structural temperature of the surrounding water molecules. For solutes such as the alkyl halides, which do not interact strongly with the primary solvation shell, the isotope effect arising from the breakdown of the more stable initial state solvation shell will reflect this added stability, and hence will correspond to a lower temperature, that is, a larger isotope effect than for the corresponding "normal" ϕ_{D_2O}/ϕ_{H_2O} value which reflects the relative stability of the water structures at the experimental temperature. Since on this hypothesis the kinetic isotope effect (k_{D_2O}/k_{H_2O}) will largely arise from water–water

Can. J. Chem. Downloaded from www.nrcresearchpress.com by 176.9.209.113 on 09/04/12
For personal use only.

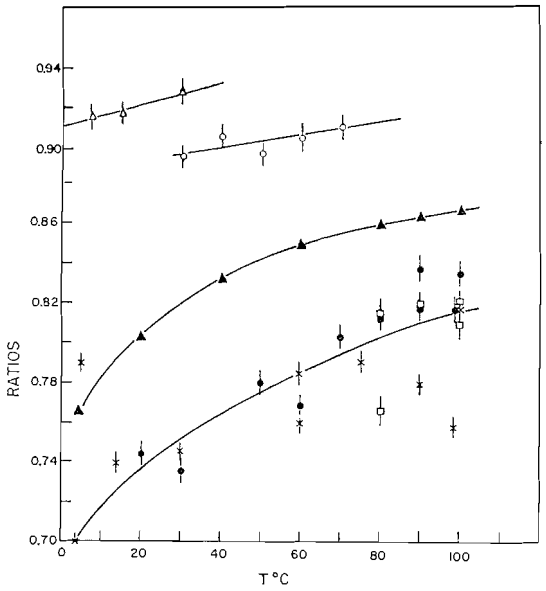

FIG. 1. The kinetic isotope effect caused by a change of medium from H_2O to D_2O over a range of temperatures compared with the corresponding isotope effect expressed by the relative fluidities of the two solvents.

△ Isopropyl benzenesulphonate (ref. 1).
○ Methyl benzenesulphonate (ref. 2).
× Chlorides (Tables I and II).
● Bromides (Tables I and II).
□ Iodides (Tables I and II).
▲ Relative fluidities (ref. 31).

interaction, this ratio will tend to be the same for all esters at a given temperature, a conclusion supported by the results in Tables I and II. That this conclusion is not exactly true is not too surprising, since small effects will be expected to arise as a consequence of characteristic differences in the solvation of the alkyl halides and differentially result in the observed scatter of points (Fig. 1). On the other hand, esters containing the sulphonic group show a much smaller isotope effect and in terms of the present formalism may be regarded as raising the structural temperature of the water solvating the initial state, thus decreasing the relative difference between rates in D_2O and H_2O. The difference between the halides and the sulphonates becomes larger at lower temperatures, the characteristic curve for the halides lying below and roughly paralleling the "normal" viscosity isotope curve while the isotope ratios for the solvolysis of the sulphonates change by but a few per cent through the temperature range 5–80° C.

Apparently *t*-butyldimethylsulphonium ion with a rather weak field also belongs to the class of molecules that interact strongly, like the sulphonates, and hence have a reduced isotope ratio ($k_{D_2O}/k_{H_2O} = 0.94$). On the other hand, methyl nitrate (0.83 at 85° C) and benzenesulphonyl chloride (0.63 at 10° C) and methanesulphonyl chloride (0.63 at 20° C) do not. Indeed the latter compounds, along with benzal chloride (0.66 at 30° C) and benzotrichloride, (0.79 at 5.1° C) show such wide deviations from the norm as to suggest major differences in mechanism.

There appears to be a minor trend toward a decreased isotope effect through the α-methylated series (Table I) and a tendency for some of those molecules which from other considerations would be expected to have a greater degree of charge development in the transition state to give isotopic ratios which lie below the "normal curve". If these molecules were more ionic in the initial state the predicted ratio would lie above

Can. J. Chem. Downloaded from www.nrcresearchpress.com by 176.9.209.113 on 09/04/12
For personal use only.

the normal curve as shown by the sulphonates. An opposite effect would suggest some minor contribution to the isotope effect from $\delta_M \Delta F^{\ddagger}_{R\,\delta+}$ and $\delta_M \Delta F^{\ddagger}_{X\,\delta-}$ as discussed above. Before any particular significance can be attached to such deviations, however, the temperature dependence of the ratios must be examined for the individual solutes.

The Halide Anomaly

While it is not the purpose of this paper to discuss the effect of changes in structure on the rate of alkyl halides hydrolyzing in water, although this would appear to be the first time that such data have been published for many of the substrates in Tables I and II, it is of interest to note that the relative rates of hydrolysis of alkyl halides are in the unusual order $k_{\text{bromide}} > k_{\text{iodide}} > k_{\text{chloride}}$. This order was first noted by Moelwyn-Hughes 20 years ago (9) for the methyl compounds and is now seen to be characteristic of other alkyl halides hydrolyzing in water. The "normal" order of reactivity $k_{\text{iodide}} > k_{\text{bromide}}$ is found for all bimolecular displacement reactions at a saturated carbon atom of which we are aware (see the recent review by Streitwieser for a summary (37)) save for displacement by OH^- in water (9), and is also the order for the solvolysis of tertiary halides in 80/20 ethanol–water where the mechanism has been assumed to approach a limiting (11), i.e. an ionization or S_N1, type.

Since this reversal of order cannot be attributed to a change in the alkyl group from one which requires a large degree of nucleophilic interaction (primary halides) to the tertiaries where this requirement is reduced if not absent, and since the order for the so-called border line compounds (the isopropyl halides hydrolyzing in 60/40 ethanol–water (37)) is also the normal order $k_{\text{iodide}} > k_{\text{bromide}}$, we are led to conclude that the the reverse order found for halides in pure water derives from some peculiarity in ion–dipole interaction which favors the bromide in the above reactions: note for example the order of the mobilities Br > I > Cl.

ACKNOWLEDGMENT

We wish to acknowledge the careful technical assistance of Mr. S. Sugamori throughout the course of this investigation.

REFERENCES

1. Robertson, R. E. and Laughton, P. M. Can. J. Chem. **35**, 1319 (1957).
2. Laughton, P. M. and Robertson, R. E. Can. J. Chem. **34**, 1714 (1956).
3. Heppolette, R. L. and Robertson, R. E. Unpublished work.
4. Robertson, R. E. Can. J. Chem. **33**, 1536 (1955).
5. Yarnall, W. A. and Wallis, E. S. J. Org. Chem. 4, 284 (1939).
6. Atkinson, E. F. J. and Thorpe, J. F. J. Chem. Soc. **91**, 1687 (1907).
7. Sommer, L. H., Blankman, H. D., and Miller, P. C. J. Am. Chem. Soc. **76**, 803 (1954).
8. Cooper, K. A. and Hughes, E. D. J. Chem. Soc. 1183 (1937).
9. Moelwyn-Hughes, E. A. Proc. Roy. Soc. A, **164**, 295 (1938).
10. Tommila, E., Tülikainen, M., and Voipoi, A. Ann. Acad. Sci. Fennicae, A, **II**, 26 (1955).
11. Tommila, E. Suomen Kemistilehti, A, **29**, 205 (1956).
12. Winstein, S., Grunwald, E., and Jones, H. W. J. Am. Chem. Soc. **73**, 2700 (1951).
13. Fierens, P. J. C. and Kruys, P. Bull. soc. chim. Belges, **64**, 542 (1955).
14. Scott, J. M. W. and Robertson, R. E. Unpublished work.
15. Olivier, S. C. J. Rec. trav. chim. **33**, 891 (1934).
16. Bensley, B. and Kohnstam, G. J. Chem. Soc. 287 (1956).
17. Robertson, R. E., Heppolette, R. L., and Scott, J. M. W. Can. J. Chem. **37**, 803 (1959).
18. Frank, H. S. and Evans, M. J. Chem. Phys. **13**, 507 (1945).
19. Wang, J. H. J. Phys. Chem. **58**, 686 (1954).
20. Posey, F. A. and Taube, H. J. Am. Chem. Soc. **79**, 4285 (1957).
21. Connick, R. E. and Poulson, R. E. J. Chem. Phys. **30**, 759 (1959).
22. Frank, H. S. and Wen, Yen-Yang. Discussions Faraday Soc. **24**, 133 (1957).
23. Eley, D. D. Trans. Faraday Soc. **35**, 1421 (1939).
24. Haggis, G. H., Hasted, J. B., and Buchanan, T. J. J. Chem. Phys. **20**, 1452 (1952).

Can. J. Chem. Downloaded from www.nrcresearchpress.com by 176.9.209.113 on 09/04/12
For personal use only.

25. SAMILOV, O. Discussions Faraday Soc. **24**, 141 (1957).
26. BARKLAY, I. M. and BUTLER, J. A. V. Trans. Faraday Soc. **35**, 1445 (1939).
27. BERNAL, J. D. and FOWLER, R. H. J. Chem. Phys. **1**, 1 (1933).
28. LAIDLER, K. J. Can. J. Chem. **34**, 1107 (1956).
29. GURNEY, R. W. Ionic processes in solution. McGraw-Hill Book Co., Inc., New York. 1953. Chap. 10.
30. TAYLOR, H. S., CALEY, E. R., and EYRING, H. J. Am. Chem. Soc. **55**, 4334 (1933).
31. HARDAY, R. C. and COTTINGTON, R. L. J. Research Natl. Bur. Standards, **42**, 573 (1949).
32. CHITTUM, J. P. and LA MER, V. K. J. Am. Chem. Soc. **59**, 2425 (1937).
33. COLLIE, C. H., HASTED, J. B., and RITSON, D. M. Proc. Phys. Soc. **60**, 145 (1948).
34. MOELWYN-HUGHES, E. A. J. Chem. Soc. 95 (1932).
35. MOELWYN-HUGHES, E. A. Trans. Faraday Soc. **33**, 91 (1937).
36. GLASSTONE, S., LAIDLER, K. J., and EYRING, H. The theory of rate processes. McGraw-Hill Book Co., Inc., New York. 1941. p. 401.
37. STREITWIESER, A., JR. Chem. Revs. **56**, 571 (1956).

Can. J. Chem. Downloaded from www.nrcresearchpress.com by 176.9.209.113 on 09/04/12
For personal use only.

Can. J. Chem. Downloaded from www.nrcresearchpress.com by 176.9.209.113 on 09/04/12
For personal use only.

SYNTHESIS OF CYCLIC PHOSPHOROUS ACID ESTERS BY TRANSESTERIFICATION[1]

ALEXIS A. OSWALD

ABSTRACT

Five- and six-membered cyclic phosphorous acid esters were synthesized by transesterification of phosphites with 1,2- and 1,3-glycols: Diethyl hydrogen phosphite was transesterified to give cyclic hydrogen phosphites. Partial transesterification of tris-2-chloroethyl phosphite resulted in cyclic 2-chloroethyl phosphites.

Organic phosphites are potentially important chemicals as antioxidants in the petroleum and plastics industry (1, 2, 3). Their usefulness is limited, however, by their hydrolytic instability. Recently, the extreme resistance of *cis*-1,3-cyclohexylidene phosphate to hydrolysis was reported (4). This report together with earlier knowledge (5) regarding the stability of 2,3-dimethyl-2,3-butylene hydrogen phosphite initiated the present work of synthesizing new cyclic phosphites.

SYNTHESIS OF CYCLIC HYDROGEN PHOSPHITES

One of the earliest methods for synthesizing dialkyl esters of phosphorous acid is the direct esterification (6, 7) by heating phosphorous acid with the appropriate alcohol. The first syntheses of cyclic hydrogen phosphites were probably accomplished by starting from phosphorous acid and various glycols. However, there is little evidence of a single pure product being isolated (8).

Another method for the synthesis of cyclic hydrogen phosphites is the hydrolysis of cyclic chlorophosphites (5, 9, 10, 11) or alkyl phosphites (5). Saunders and his co-workers (12) reported the synthesis of a cyclic secondary diphosphite by reacting phosphorus trichloride with an excess of ethylene glycol.

In the course of this work, the transesterification of diethyl hydrogen phosphite with 1,2- and 1,3-glycols was accomplished. When 3-chloro-1,2-propylene glycol was used for transesterification, the known 3-chloro-1,2-propylene hydrogen phosphite or 2-hydroxy-4-chloromethyl-1,3,2-dioxaphospholane (13) was obtained. Analogously, the formation of other cyclic hydrogen phosphites with five-membered (dioxaphospholane) and six-membered (dioxaphosphorinane) ring structures was presumed according to the following equations:

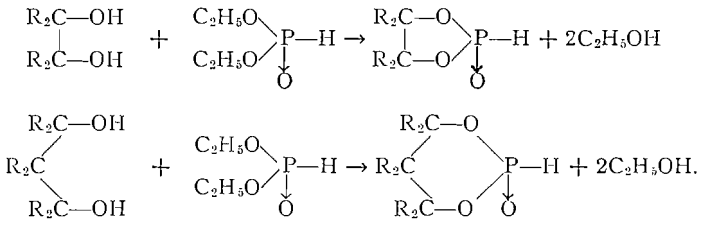

R = H or alkyl

In the transesterification experiments, 1 mole of 1,2- or 1,3-glycol was used per mole of hydrogen phosphite. The reactions were carried out between 130 and 140° C at

[1]*Manuscript received April 23, 1959.*
Contribution from the Research Department, Imperial Oil Limited, Sarnia, Ontario, Canada.

120–150 mm. When the liberation of the by-proudct ethanol ceased, the remaining crude product was fractionated at pressures between 2 and 3 mm. The purified compounds are liquids with the exception of the white crystalline 2-hydroxy-5,5-dimethyl-1,3,2-dioxaphosphorinane. Some of the physical and analytical data and the yields of the compounds obtained are shown in Table I.

TABLE I

Cyclic hydrogen phosphites

Formula	B.p. (° C/mm)	Refractive index (n_D^{20})	Phosphorus (%) Calc.	Phosphorus (%) Found	Yield (%)
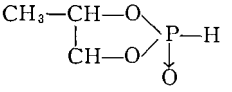	84–86/2.3	1.4580	25.4	23.9	78
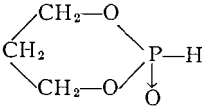	97–98/2.5	1.4522	25.4	24.9	79
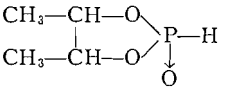	84–85/2.3	1.4616	22.8	23.1	75
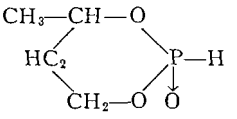	103–104/2.3	1.4547	22.8	22.8	76
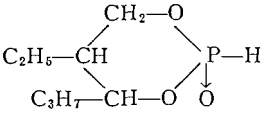	117–118/2.5	1.4600	16.1	16.3	78
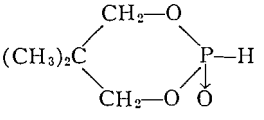	103–104/2.3	m.p. 53–55°	20.6	20.2	85
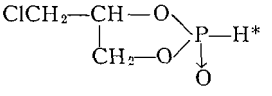	125–126/2.3	1.4910	19.8	19.7	83
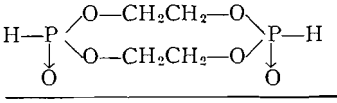	117–118/2.3	1.4751	28.7	28.2	56

*First synthesized by Arbuzov and Zoroastrova (10).

Unequivocal syntheses of the cyclic butylene hydrogen phosphites were also carried out to prove the five- and six-membered ring structures respectively. These syntheses started from the appropriate butanediols and phosphorus trichloride. In this manner, the corresponding cyclic chlorophosphites (11, 12) were prepared. These compounds yielded the cyclic hydrogen phosphites after hydrolysis with the stoichiometric amounts of water.

Can. J. Chem. Downloaded from www.nrcresearchpress.com by 176.9.209.113 on 09/04/12
For personal use only.

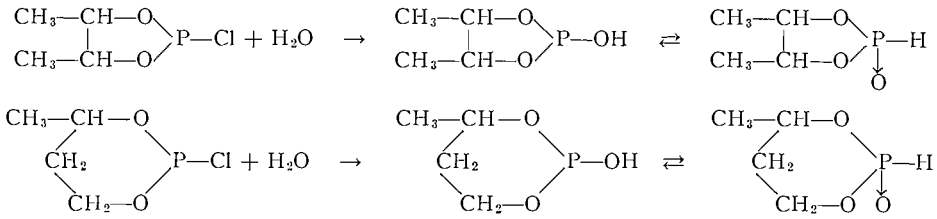

It can be assumed from the high yield of the product of hydrolysis that the water attack results in the selective removal of the chlorine without ring opening. The identity of the infrared spectra of the compounds obtained in this manner with the butanediol transesterification products verifies the assumed five- and six-membered ring structures.

All the liquid cyclic hydrogen phosphites prepared are highly viscous materials with high boiling points. These properties probably indicate intermolecular association as shown by B. A. Arbuzov and Vinogradova (13) in the case of dialkyl phosphites. In the case of the hydrogen phosphite tautomer such an association can be depicted as follows:

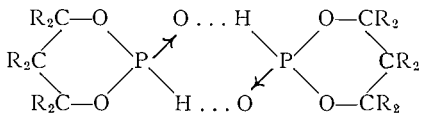

This assumption is supported by the observation that the cyclic hydrogen phosphites prepared from the chlorophosphites became viscous only after several days' standing after distillation.

Transesterification with ethylene glycol resulted in a compound having an identical boiling point with the cyclic diethylene diphosphite mentioned previously.

SYNTHESIS OF CYCLIC PHOSPHITES

Transesterification of phosphite esters was first performed by Milobendzki and Szulgin (14). They prepared propyl- and butyl-diphenyl phosphite from triphenyl phosphite by the action of the corresponding sodium alcoholates according to the following equation:

$$(Ph—O)_3P + NaOR \rightarrow (Ph—O)_2POR + Ph—ONa.$$

Some patents claim transesterification of triarylphosphites with alcohols (1, 2); for example, the synthesis of alkyl diaryl phosphites by the following reaction:

$$(ArO)_3P + HOR \rightarrow (ArO)_2POR + HOAr.$$

A recent German patent (15) claims the transesterification of tris-2-chloroethyl phosphite with several alcohols. However, in this work the transesterification reaction with polyhydric alcohols was mentioned as giving polymeric products.

The reinvestigation of the latter transesterification in these laboratories revealed some new facts suggesting the formation of monomeric cyclic phosphite esters by partial transesterification of tris-2-chloroethyl phosphite with 1,2- and 1,3-glycols.

In previous work, cyclic phosphite esters have also been synthesized from the corresponding cyclic chlorophosphites, which in turn were prepared from phosphorus trichloride and diols; in both cases with the help of an acid-binding agent (pyridine) (10, 11, 16, 17).

Can. J. Chem. Downloaded from www.nrcresearchpress.com by 176.9.209.113 on 09/04/12
For personal use only.

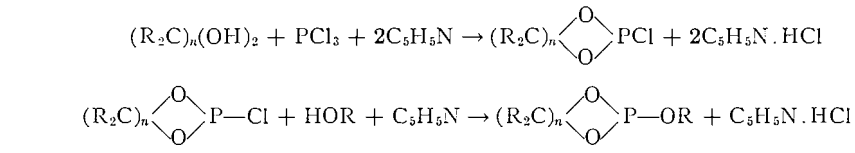

Similar compounds can be synthesized starting with an alkyl dichlorophosphite and a diol.

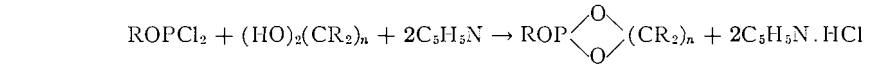

Cyclic catechol phosphites were prepared by an analogous method starting from catechol and phosphorus trichloride (18, 19). Chloroethyl catechol phosphite was synthesized by reacting ethylene oxide with catechol chlorophosphite according to the following reaction equation (20):

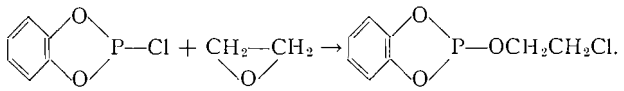

The stability of the cyclic phosphite esters is greatest for six-membered rings (10, 11, 16, 17).

Partial transesterification of 1 mole of tris-2-chloroethyl phosphite with 1 mole of 1,2- or 1,3-glycol was attempted. At elevated temperature and reduced pressure about 2 moles ethylene chlorohydrin per mole of phosphite was removed from the reaction mixture as indicated by the amount of the distillate in the receiver and the weight loss of the reaction mixture. After redistillation, the distillate was identified as ethylene chlorohydrin by boiling point, refractive index, and infrared spectrum. The formation of five- and six-membered cyclic chloroethyl phosphites is suggested according to the following general equations:

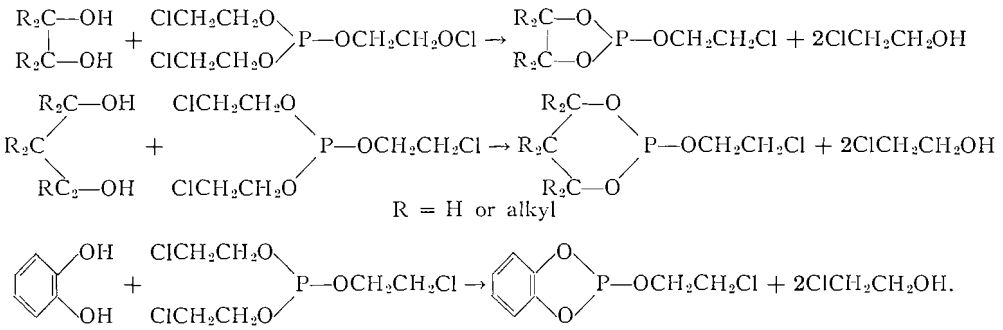

The lower glycols used in these reactions were not miscible with the tris-2-chloroethyl phosphite, but after standing at room temperature homogeneous mixtures were obtained. For preparative purposes, the reaction was performed by heating the ingredients between 60 and 100° C *in vacuo*, and the ethylene chlorohydrin distilled as it was formed. The remaining crude product was fractionated *in vacuo* yielding the purified, colorless cyclic chloroethyl phosphites usually as liquids, immiscible with water. Some of the physical and analytical data and the yields obtained are shown in Table II.

Can. J. Chem. Downloaded from www.nrcresearchpress.com by 176.9.209.113 on 09/04/12
For personal use only.

TABLE II

Cyclic 2-chloroethyl phosphites

Formula	B.p. (° C/mm)	Refractive index (n_D^{20})	Chlorine Calc.	Chlorine Found	Yield (%)
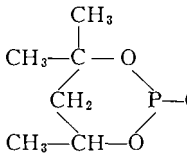	105–107/2	1.4534	15.67	16.05	80
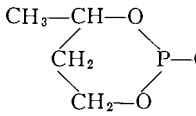	98–100/2.5	1.4680	17.88	18.30	75
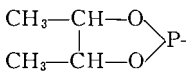	107–109/3	1.4650	17.88	17.90	70
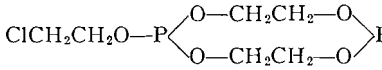	108–110/2	1.4898	20.82	19.85	20‡
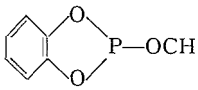	82–84/2	1.5390	16.24	16.50	85

*For data on compound prepared by independent synthesis see Experimental part.

†Highly viscous liquid; tentative formula. For ethylene-2-chloroethyl phosphite Arbuzov (10) gives the following data: b.p. 78.5–79.5° at 65 mm, n_D^{20} 1.4755.

‡The greater part of the raw product is polymeric material, which cannot be distilled.

§Previously prepared by Kabachnik (20), who found b.p. 107–108° at 2.5 mm and n_D^{20} 1.5430. Catechol-2-chloroethane-phosphonic acid has b.p. 167–170° at 4.5 mm and n_D^{20} 1.5502 as reported by Kabachnik and co-workers (21).

Unequivocal syntheses of the cyclic butylene 2-chloroethyl phosphites were also carried out to prove the five-membered 1,3,2-dioxaphospholane and the six-membered 1,3,2-dioxaphosphorinane ring structures respectively. In these syntheses the corresponding cyclic chlorophosphites (10, 11) were reacted with ethylene chlorohydrin to give the cyclic 2-chloroethyl phosphites.

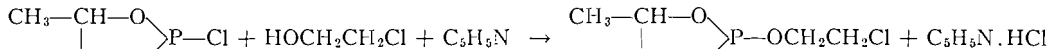

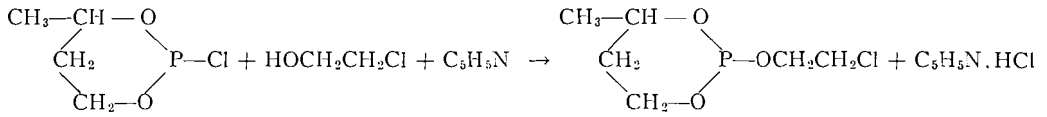

In the course of these reactions, if carried out below room temperature, Arbuzov transformation and ring opening are not likely to occur. Therefore, the identity of the infrared spectra of the compounds with the corresponding transesterification products supports the presence of the cyclic phosphite structures. A further indication of this structure is given by the comparison of the boiling point and refractive index of the catechol transesterification product with catechol 2-chloroethyl phosphite prepared by Kabachnik (20) from catechol chlorophosphite.

Can. J. Chem. Downloaded from www.nrcresearchpress.com by 176.9.209.113 on 09/04/12
For personal use only.

Can. J. Chem. Downloaded from www.nrcresearchpress.com by 176.9.209.113 on 09/04/12
For personal use only.

EXPERIMENTAL

Preparation of Cyclic Hydrogen Phosphites by Transesterification

Diethyl hydrogen phosphite (27.6 g, 0.2 m (mole)) and 1,2- or 1,3-glycol (0.2 m) were placed in a round bottom flask connected to a Claisen head fitted with a downward condenser and a receiver for vacuum distillation. The resulting solution was heated to 130° C at 120–160 mm pressure under nitrogen. The reaction proceeded as shown by the distillation of ethanol. Ethanol evolution ceased after about 3 hours' heating at the above temperature.

The remaining crude product was fractionated at 2 to 3 mm. The cyclic hydrogen phosphites were obtained as very viscous, colorless liquids. The yields and other data are given in Table I. Some high boiling materials remained in the distillation flask and were probably polymeric.

Preparation of Cyclic Chlorophosphites

To a solution of phosphorus trichloride (68.7 g, 0.5 m) in anhydrous ether (200 ml) a mixture of 2,3- or 1,3-butanediol (45 g, 0.5 m), pyridine (79 g, 1 m), and ether (200 ml) was added with vigorous stirring, while the temperature was kept below −5° C. The precipitated pyridinium chloride was removed by filtration and washed with ether. The combined clear filtrate was fractionated. After the removal of the ether, the cyclic chlorophosphites were distilled in vacuum and were obtained as colorless liquids.

Starting from 2,3-butanediol, 67 g (87%) 2-chloro-1,3,2-dioxaphospholane boiling at 54–56° C at 10 mm was obtained. The refractive index was n_D^{20} 1.4700. (Lucas and co-workers (11) obtained apparently the same product without an acid-binding agent. It had a boiling point of 66° C at 15 mm and a refractive index of n_D^{20} 1.4696.)

When 1,3-butanediol was used, the method gave 2-chloro-4-methyl-1,3,2-dioxaphosphorinane (69.5 g, 98%) boiling at 55–57° C at 10 mm. The refractive index of this product was n_D^{20} 1.4670. (Arbuzov and Zoroastrova (10) reported b.p. 65° C at 12 mm and n_D^{20} 1.4700. Lucas and co-workers (11) gave b.p. 66.6–67.5° C at 15 mm and n_D^{20} 1.4884.)

Synthesis of Cyclic Hydrogen Phosphites by the Hydrolysis of Cyclic Chlorophosphites

To a mixture of water (3.6 g, 0.2 m) and benzene (100 ml), the solution of the chlorophosphite (0.2 m) in benzene (250 ml) was added, while it was shaken. The reaction mixture was then stirred for one-half hour. The resultant clear, homogeneous solution was fractionated in vacuum, when the benzene solvent was removed at first under 160 mm pressure. The raw product was then distilled at 2 mm of mercury.

2-Chloro-4,5-dimethyl-1,3,2-phospholane gave on hydrolysis 2-hydroxy-4,5-dimethyl-1,3,2-phospholane (26 g, 95%). The product was obtained between 81° and 83° C at 2 mm and had a refractive index, n_D^{20} 1.4610. Comparison of infrared spectra showed identity with the 2,3-butanediol transesterification product.

Similarly, by the hydrolysis of 2-chloro-4-methyl-1,3,2-phosphorinane, this procedure resulted in the formation of 2-hydroxy-4-methyl-1,3,2-dioxaphosphorinane obtained as a colorless liquid (25 g, 92%) between 101 and 102° C at 2 mm. The refractive index is n_D^{20} 1.4528. Although this product was a mobile liquid after distillation, it became quite viscous after a few days and was similar to the transesterification product with 1,3-butanediol. The identity of the two products was then proved by comparison of their infrared spectra.

Preparation of Cyclic 2-Chloroethyl Phosphites by Transesterification

Tris-2-chloroethyl phosphite (26.9 g, 0.1 m) and 1,2- or 1,3-glycol (0.1 m) were placed in a round bottom flask connected with a Claisen head, downward condenser, and receiver

for vacuum distillation. The contents became homogeneous within 5 minutes when heated in a water bath. Reaction was performed at 18 mm under nitrogen. The heating was continued for about 1 hour, during which time the evolution of ethylene chlorohydrin was complete.

The colorless crude product was fractionated at 2–3 mm pressure to obtain the pure products as clear, colorless liquids, immiscible in water. See Table II for properties and yields.

Preparation of Cyclic 2-Chloroethyl Phosphites from Cyclic Chlorophosphites

To a solution of the cyclic chlorophosphite (30.9 g, 0.2 m) (2-chloro-4,5-dimethyl-1,3,2-dioxaphospholane and 2-chloro-4-methyl-1,3,2-dioxaphosphorinane respectively) in ether (200 ml), ethylene chlorohydrin (16.1 g, 0.2 m) and subsequently pyridine (15.8 g, 0.2 m) were added dropwise with stirring at 0° C or lower. After the addition, the reaction mixture was allowed to come to room temperature with continued stirring. Pyridinium chloride was removed by filtration and the filtrate was fractionated.

In this manner, beginning with 2-chloro-4,5-dimethyl-1,3,2-dioxaphospholane between 56 and 60° C at 1 mm, 31 g (79%) 2-(β-chloroethoxy)-4,5-dimethyl-1,3,2-dioxaphospholane (2,3-butylene-2-chloroethyl phosphite) was obtained, n_D^{20} 1.4659. The spectrum of this compound was identical with the product of transesterification reported in Table II.

When the same method was used, 2-chloro-4-methyl-1,3,2-phosphorinane gave 33 g (86%) 2-(β-chloroethoxy)-4-methyl-1,3,2-dioxaphosphorinane distilled between 54 and 56° C at 1 mm and having a refractive index of n_D^{20} 1.4697. This compound had an identical spectrum with the corresponding transesterification product reported in Table II.

ACKNOWLEDGMENTS

The author is greatly indebted to Mr. A. J. Stephenson for the infrared spectra, to Mr. E. G. Ulbricht and Miss A. F. Fischel for the phosphorus analyses, and to Mr. J. F. Eagen for the chlorine analyses.

REFERENCES

1. Reuter, R. U.S. Pat. No. 2,280,450 (1942).
2. Gzemski, F. C. U.S. Pat. No. 2,353,558 (1944).
3. Hecker, A. C. and Leistner, W. E. U.S. Pat. No. 2,860,115 (1958).
4. Brown, D. M. and Higson, H. M. J. Chem. Soc. 2034 (1957).
5. Arbuzov, A. E. and Azanovskaya, M. M. Izvest. Akad. Nauk S.S.S.R. Otdel. Khim. Nauk, 473 (1949).
6. Arbuzov, A. E. J. Russ. Phys. Chem. Soc. **46**, 291 (1914).
7. Baker, A. A. and Brown, J. H. U.S. Pat. No. 2,670,368 (1954).
8. Kosolapoff, G. M. Organophosphorus compounds. J. Wiley & Sons, Inc., New York. 1950. p. 189.
9. Carré, M. P. Compt. rend. **136**, 756 (1903).
10. Arbuzov, A. E. and Zoroastrova, V. M. Izvest. Akad. Nauk S.S.S.R. Otdel. Khim. Nauk, 208 (1948).
11. Lucas, H. J., Mitchell, F. W., Jr., and Scully, C. N. J. Am. Chem. Soc. **72**, 5491 (1950).
12. Cook, H. G., Ilett, J. D., Saunders, B. C., Stacey, G. J., Watson, H. G., Wilding, J. G. E., and Woodcock, S. J. J. Chem. Soc. 2921 (1949).
13. Arbuzov, B. A. and Vinogradova, V. S. Izvest. Akad. Nauk S.S.S.R. Otdel. Khim. Nauk, 507 (1952).
14. Milobendzki, T. and Szulgin, K. Chemik Polski, 66 (1917); Chem. Abstr. **13**, 2867 (1919).
15. Gumlich, W. and Wriss, F. A. German Pat. No. 1,011,866 (1957).
16. Arbuzov, A. E. and Zoroastrova, V. M. Izvest. Akad. Nauk S.S.S.R. Otdel. Khim. Nauk, 770 (1952).
17. Arbuzov, A. E. and Zoroastrova, V. M. Izvest. Akad. Nauk S.S.S.R. Otdel. Khim. Nauk, 799 (1952).
18. Arbuzov, A. E. and Valitova, F. G. Izvest. Akad. Nauk S.S.S.R. Otdel. Khim. Nauk, 529 (1940).
19. Reich, W. S. Nature, **157**, 133 (1946).
20. Kabachnik, M. J. Izvest. Akad. Nauk S.S.S.R. Otdel. Khim. Nauk, 631 (1947).
21. Kabachnik, M. J., Rossiiskaya, P. A., and Novikova, N. N. Izvest. Akad. Nauk S.S.S.R. Otdel. Khim. Nauk, 97 (1947).

Can. J. Chem. Downloaded from www.nrcresearchpress.com by 176.9.209.113 on 09/04/12
For personal use only.

Can. J. Chem. Downloaded from www.nrcresearchpress.com by 176.9.209.113 on 09/04/12
For personal use only.

L'ARYLATION DES QUINONES PAR LES SELS DE DIAZONIUM

V. SUR LA SYNTHÈSE DE 5-ARYLTOLUQUINONES[1]

P. BRASSARD ET P. L'ÉCUYER

RÉSUMÉ

Tout comme la chloroquinone la toluquinone réagit en milieu tampon avec les sels de diazonium aromatiques pour donner des monoaryltoluquinones. Cependant, par contraste avec les réactions de la première, qui donnent naissance à deux isomères monoarylés, les réactions de cette dernière n'ont permis d'isoler qu'un seul isomère monoarylé. Celui-ci est fort probablement la 2-méthyl-5-aryl-1,4-benzoquinone, car il a été vérifié dans un travail ultérieur que tel est bien le cas pour la 2-méthyl-5-phényl-1,4-benzoquinone.

Diverses 1,4-benzoquinones monosubstituées réagissent en milieu tampon avec les sels de diazonium pour donner des 1,4-benzoquinones bisubstituées. Ainsi, selon ces conditions, une monoaryl-1,4-benzoquinone (I = Ar) donne naissance à une 2,5-bisaryl-1,4-benzoquinone (II, X = Ar) (1, 2), tandis que la chloroquinone (I, X = Cl) fournit un mélange de deux monoaryl-1,4-benzoquinones isomères que nous avons d'abord cru être la 2-chloro-3-aryl-1,4-benzoquinone et la 2-chloro-6-aryl-1,4-benzoquinone (II, X = Cl) (3, 4).

X = Cl, CH_3 ou Ar Ar = groupe aryle

Tout comme la chloroquinone, la toluquinone (I, X = CH_3) en milieu tampon aqueux réagit avec les sels de diazonium aromatiques. La réaction est cependant beaucoup plus lente avec cette dernière, à moins que l'activité du sel de diazonium ne compense partiellement la faible réactivité de la toluquinone. Nous avons réalisé la synthèse de diverses monoaryltoluquinones (Tableau I) et nous n'avons toujours isolé qu'une seule substance, bien qu'il soit possible qu'un autre isomère soit présent dans le produit d'au

TABLEAU I

2-Méthyl-5-aryl-1,4-benzoquinones

1,4-Benzoquinone	P.f., °C	Solvant	Formule	Analyse	
				% calculé	% trouvé
2-Méthyl-5-phényl-	107–109	Méthanol–acétone–eau (2:1:1)	$C_{13}H_{10}O_2$	C, 78.77 H, 5.09	C, 78.9 H, 5.0
2-Méthyl-5-(*o*-bromophényl)-	133–134	Acétone	$C_{13}H_9O_2Br$	C, 56.34 H, 3.27 O, 11.55 Br, 28.84	C, 56.0 H, 3.3 O, 11.4 Br, 28.8
2-Méthyl-5-(*p*-chlorophényl)-	128–130	Méthanol–acétone–eau (2:1:1)	$C_{13}H_9O_2Cl$	C, 67.11 H, 3.90	C, 66.9 H, 3.9
2-Méthyl-5-(*o*-nitrophényl)-	130–131.5	Acétone–méthanol	$C_{13}H_9O_4N$	C, 64.20 H, 3.73 N, 5.76	C, 64.1 H, 3.8 N, 5.7
2-Méthyl-5-(*m*-nitrophényl)-	185–185.5	Acétone	$C_{13}H_9O_4N$	C, 64.20 H, 3.73 N, 5.76	C, 64.2 H, 3.8 N, 5.8
2-Méthyl-5-(*p*-nitrophényl)-	156–158	Éthanol–acétone	$C_{13}H_9O_4N$	C, 64.20 H, 3.73 N, 5.76	C, 64.7 H, 3.9 N, 6.0

[1]*Manuscrit reçu le 1 juin 1959.*
Contribution du Département de Chimie, Faculté des Sciences, Université Laval, Québec, Qué.

moins quelques réactions. L'isomère isolé est fort probablement la 2-méthyl-5-aryl-1,4-benzoquinone (II, X = CH_3). C'est du moins la conclusion qu'il s'impose de tirer d'un travail ultérieur (5) dans lequel nous avons pu vérifier que, dans le cas de la condensation de la toluquinone avec le chlorure de benzène–diazonium, c'est bien la 2-méthyl-5-phényl-1,4-benzoquinone que l'on obtient.

Les monoaryltoluquinones sont des solides cristallins jaunes. Elles s'obtiennent avec des rendements variant de 20 à 85% selon les difficultés qu'on a à surmonter lors de leur purification.

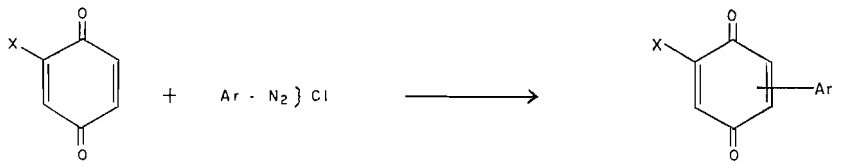

(I) (II)

PARTIE EXPÉRIMENTALE[2]

On diazote, entre 0 et 5°, l'amine (0.05 mole) dissoute dans un mélange de 12.5 ml d'acide chlorhydrique concentré et de 50 ml d'eau, en ajoutant une solution de nitrite de sodium (3.5 g) dans de l'eau (10 ml). La solution limpide du sel de diazonium est ensuite versée dans un mélange de 6.8 g (0.055 mole) de toluquinone, de 20.4 g (0.3 mole) d'acétate de sodium trihydraté et de 500 ml d'eau, qui est agité mécaniquement. Sauf pour les sels de diazonium les moins actifs, le dégagement d'azote se produit lentement même à la température ambiante. Sinon, on porte le mélange à 35–40° en plongeant le récipient dans un bain-marie. On continue d'agiter pendant quelques heures et on abandonne ensuite le mélange réactionnel à la température ambiante jusqu'à ce que le dégagement gazeux soit terminé (12 à 24 heures). On filtre ou décante la solution aqueuse, lave à l'eau le précipité ou le résidu et sèche ce dernier.

Il est quelquefois assez difficile de purifier l'aryltoluquinone, car elle est parfois contaminée par une quantité variable de résines. Celles-ci sont très solubles dans l'acétone, moins dans le méthanol et presque pas dans l'éther de pétrole. Par ailleurs, les aryltoluquinones sont aussi passablement solubles dans l'acétone, moins dans le méthanol et peu dans l'éther de pétrole. En conséquence, on ne réussit quelquefois à se débarasser complètement des résines par cristallisation dans le méthanol qu'en faisant bouillir à plusieurs reprises la solution avec du noir animal. D'autre part, en cristallisant dans l'acétone (noir animal) non dilué, on obtient vite l'aryltoluquinone à l'état pur. Dans les deux cas toutefois, le rendement s'en trouve considérablement diminué.

Les deux meilleures façons de procéder pour la purification des aryltoluquinones semblent les suivantes: (*a*) Comme la 2-méthyl-5-phényl-1,4-benzoquinone est relativement soluble dans l'éther de pétrole (p.é. 65–110°) bouillant, on l'extrait à plusieurs reprises dans ce solvant, on évapore les extraits à siccité sous pression réduite et on cristallise ensuite dans le mélange acétone–méthanol–eau (1:2:1); (*b*) quant aux autres aryltoluquinones qui sont trop peu solubles dans l'éther de pétrole bouillant, on les cristallise directement dans un mélange de méthanol–acétone ou méthanol–acétone–eau et on les décolore au noir animal.

[2]*Les points de fusion (p.f.) ne sont pas corrigés. Ils ont été déterminés dans un appareil de Vanderkamp.*

Can. J. Chem. Downloaded from www.nrcresearchpress.com by 176.9.209.113 on 09/04/12
For personal use only.

REMERCIEMENTS

Nous remercions la Shell Oil Company of Canada et le Conseil National de Recherches du Canada pour des bourses d'études qu'ils ont accordées à l'un d'entre nous (P. B.).

BIBLIOGRAPHIE

1. KVALNES, D. E. J. Am. Chem. Soc. **56**, 2478 (1934).
2. BRASSARD, P. et L'ÉCUYER, P. Can. J. Chem. **36**, 700 (1958).
3. GÜNTHER, F. Brevet allemand 508,395 (1924).
4. BRASSARD, P. et L'ÉCUYER, P. Can. J. Chem. **36**, 814 (1958).
5. HOEGERLE, K. et L'ÉCUYER, P. Can. J. Chem. (Soumis).

Can. J. Chem. Downloaded from www.nrcresearchpress.com by 176.9.209.113 on 09/04/12
For personal use only.

Can. J. Chem. Downloaded from www.nrcresearchpress.com by 176.9.209.113 on 09/04/12
For personal use only.

EBULLIOMETRY AND THE DETERMINATION OF THE MOLECULAR WEIGHTS OF POLYMERS

PART I. THE SMALL EBULLIOMETER[1]

W. R. BLACKMORE

ABSTRACT

An ebulliometer that has been in routine use for the determination of the number average molecular weight of polymers is described. The results obtained with two different series of polythenes (which were also measured elsewhere) are given. These results show this ebulliometer to be subject to experimental difficulties which limit it to number average molecular weights of perhaps 20,000 depending on the precision required.

INTRODUCTION

Ebulliometry is the measurement of the difference in boiling point between a solution and a pure solvent at the same pressure. The technique may be used to measure the number average molecular weight of a polymer.

In the earliest work in ebulliometry, Beckmann (1) submerged one of his thermometers directly in the boiling liquid, first in the solvent and then in the solution, but the temperature difference thus determined was not accurately reproducible. It was found that there was superheat in the liquid and this was subject to large random fluctuations. Molecular weights of only the simplest compounds could be determined in this way. The situation was markedly improved by Cottrell (2), who first suggested the use of a vapor-lift pump. It was found that when pumped liquid was allowed to trickle down over a surface so that a thin film of liquid was in contact with solvent vapor, then temperature equilibrium was rapidly established. Furthermore this temperature was much more constant than in the main body of the boiling liquid itself (3).

Once the Cottrell pump had been introduced and the noise level reduced so greatly, it was not long before two transducers (4, 5) more sensitive than Beckmann thermometers were used in ebulliometry. These are still used in modern times (6, 7). After World War II new temperature-sensitive resistors, called thermistors (8), were developed to the point of being made available commercially. As applied in ebulliometry a steady-state temperature difference is established between two thermistors, each forming one arm of a Wheatstone bridge circuit. The temperature difference causes a resistance difference between the thermistor arms and this, in turn, produces an unbalance voltage which is amplified and recorded. In our apparatus the measured change in this unbalance voltage corresponding to the addition of weighed polymer pellets permits the polymer number average molecular weight $\bar{M}_n$ to be computed.

APPARATUS

Description of Glassware

The ebulliometer is shown in Fig. 1. This modified form of Ray ebulliometer (7) was designed in the Research Department of the Plastics Division of Imperial Chemical Industries Limited. The drawing was provided through the courtesy of Dr. Burnett.

[1]*Manuscript received April 3, 1959.*
Contribution from the Central Research Laboratory, Canadian Industries Limited, McMasterville, Que. A preliminary account of this work was presented to the Chemical Institute of Canada Meeting, Vancouver, June 1957.

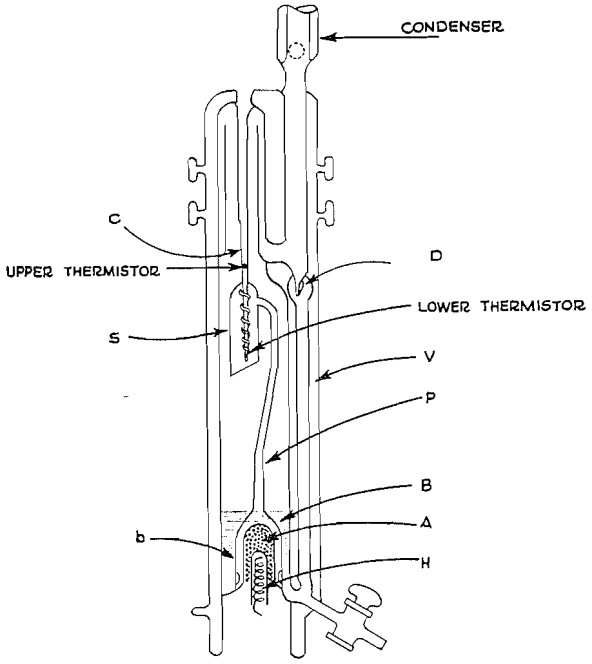

FIG. 1. The small ebulliometer.

The ebulliometer proper is protected from ambient temperature fluctuations by the silvered, vacuum jacket (V). Initially solvent is maintained at its boiling point in the boiler (B) by a bayonet heater (H) which heats by radiation and is not in contact with the boiling liquid. Polymer additions are made through the condenser. The stippled region (A) of the figure indicates crushed glass which has been fused to the inner surface of the boiler to promote boiling. The Cottrell pump (P) consists of a bell (*b*) and the stack up which boiling liquid is lifted by bubbles of vapor. When the liquid is ejected by the pump it is channelled by a spiral down the central core (C) which houses both thermistors. The shield (S) protects the lower tip of the well from any condensate which might roll down from the uppermost regions of the ebulliometer. The positioning of the thermistors is approximately as shown. The drop-counter (D), after Swietoslawski (3), was intended to provide a measure of the boil-up rate. In fact, it is frequently a source of experimental difficulty. Polymer pellets which only dissolve slowly may stick there temporarily and plug the condenser return line. This spreads a film of polymer on the upper reaches of the ebulliometer and spoils the run. The difficulty may be avoided by eliminating the drop-counter entirely. To protect the ebulliometer from atmospheric pressure fluctuations, it is connected by a wide-bore glass tube (2 in. diameter) to a 25-liter surge bottle which vents to the atmosphere through a length of capillary tubing. This does not reduce the pressure fluctuations within the ebulliometer produced by the surging liquid itself but it does remove the effects of draughts. Since improperly matched thermistors in Wheatstone bridge circuits may be very sensitive to atmospheric pressure changes it may be necessary to protect the ebulliometer from relatively long-term pressure drifts during the day. To do this a Cartesian Diver manostat (10) may be employed to control the pressure in the surge bottle.

Another experimental problem is that of thermal e.m.f.'s. Since a direct-current

Can. J. Chem. Downloaded from www.nrcresearchpress.com by 176.9.209.113 on 09/04/12
For personal use only.

thermistor bridge has been used with this ebulliometer, room temperature changes may produce drifts in the thermal e.m.f.'s which are large enough compared to the signals which are to be measured to seriously affect the results. This problem has been brought under control by mounting the ebulliometer and its associated electrical equipment in a thermostatted air bath. The design is not critical, the only requirement being that the box be large enough. The temperature is controlled at $34\pm0.5°$ C with a thermistor controller (11). The thermistor (32A11 V.E. Co.) (12) is situated close to the fan and main heater so that the response time may be fast. It should be pointed out that thermostatting does not remove the problem of thermal e.m.f.'s but merely renders the effects tractable.

Description of Electrical Components

The Wheatstone bridge is made up of two 52A11 V.E. Co. (12) thermistors which have been calibrated and matched in a manner to be described below. The remaining two arms of the Wheatstone bridge are fixed wire-wound resistors of accurately known resistance (nominally 2500 Ω) in series with a decade resistance box. Initially a Leeds–Northrup Model 9835-B, direct-current microvolt amplifier was used as the bridge output detector but this was replaced several years ago by a Liston–Becker (9), Model 14, breaker-type d-c. amplifier. The latter instrument is more sensitive. The amplifier output is fed through a resistance–capacitance network into a Brown "Electronik" potentiometer recorder (10 mv full scale).

It has been found desirable to use shielded cabling throughout. In those places where space was limited, for instance in the thermistor well, the Teflon coated leads were covered by a braided shield which was slipped as close to the extremities as possible. Thermal-free solder (with a low thermal e.m.f. to copper), supplied by the Liston–Becker Company (9), was used on all bridge connections. Originally all connections in the bridge were soldered. But during the course of time it has been found that it is more useful to have the leads from the bridge resistors enter a shielded junction box fitted with four double-pole single-throw heavy copper switches. With this arrangement it is easily possible to change thermistors, or to substitute wire-wound resistors for the thermistors if the electrical circuitry must be tested. All shields are connected directly to one ground point to avoid ground loops.

Thermistor Calibration

The thermistors which are to be calibrated are maintained at whatever temperature is desired in a large copper block. This copper block is heated by radiation and may be maintained (11) at any temperature, at least up to 300° C, with a precision of 0.001° C. The temperature of the copper block is measured with a platinum resistance thermometer and a Mueller bridge. The thermometer was calibrated at the National Physical Laboratory, Teddington, England. The resistances of the thermistors are measured with a Wheatstone bridge (Type 3352) manufactured by the Tinsley Company (13). A microvolt d-c. amplifier has been used to detect unbalance when thermistors are being calibrated, and this has been either a Liston–Becker (9) or the Leeds and Northrup. The unbalance voltage is fed from the amplifier to a Brown Electronik recorder. It is thus possible to follow slight changes in block temperature as well as measure the thermistor resistance simultaneously. The thermistor current normally used in calibrating a thermistor is about 25 μa so that the thermistor is only heated to a small fraction of a degree above its ambient temperature. Generally four or five thermistors are suspended in oil in the central well of the copper block simultaneously. It is thus possible to measure their

Can. J. Chem. Downloaded from www.nrcresearchpress.com by 176.9.209.113 on 09/04/12
For personal use only.

resistances consecutively at any one temperature before shifting the block temperature one or two degrees and taking another series of measurements.

BRIEF DESCRIPTION OF THEORY AND CALCULATION OF RESULTS

Fundamentally the apparatus behaves as follows: the two thermistor arms of the Wheatstone bridge are maintained at slightly different temperatures, because one thermistor is at the boiling point of the solvent while the other thermistor is at the boiling point of the solution. This difference in temperature, between the two thermistors, produces a resistance difference between them, and this, in turn, produces an unbalanced voltage signal from the bridge which is amplified and then displayed on the recorder. The actual value of the unbalance voltage which appears with a solution in the ebulliometer is of no particular significance. The only subject of concern is the *change* in this voltage produced when a pellet of solute of known weight is added to the boiling solution (or solvent).

It can be shown (14) that for any Wheatstone bridge in which all arms are of resistance R, except for one which has a resistance $R+\Delta R$, the unbalance voltage e_5 appearing at the detector is given by an expression of the form

$$[1] \qquad e_5 = k \,.\, i_b \,.\, \Delta R$$

where k is a constant,
i_b is the bridge current,
and ΔR the difference in resistance between the arms of the bridge.

The equation relating the resistance of a thermistor and its temperature (8) is

$$[2] \qquad R = R_0 \, e^{B/T}$$

where R is the thermistor resistance at temperature T °K,
R_0 is the thermistor resistance at some arbitrary reference temperature,
B is a constant related to the material of which the thermistor is made,
and T is the absolute temperature at which the resistance is desired.

Hence, assuming that we have two perfectly matched thermistors with the same R_0 and B, then if these are maintained at two slightly different temperatures T and $T+\Delta T$ their resistances will differ by an amount

$$[3] \qquad \Delta R = \frac{-B}{T^2} \,.\, R \,.\, \Delta T \,.$$

Thus substituting [3] into [1] we obtain an expression for the unbalance voltage obtained from a Wheatstone bridge when the two thermistor arms are maintained at temperatures differing by $\Delta T°$. This expression is

$$[4] \qquad e_5 = \frac{-kB}{T^2} \,.\, i_b \,.\, R \,.\, \Delta T \,.$$

The boiling point elevation (15) for an ideal solution (or any solution at infinite dilution) is given by

$$[5] \qquad \Delta T = \frac{R_g T^2}{L_g} \,.\, N_2$$

where R_g is the gas constant,
L_g the molar heat of vaporization,
T the boiling point in degrees Kelvin,
and N_2 the mole fraction of solute.

Can. J. Chem. Downloaded from www.nrcresearchpress.com by 176.9.209.113 on 09/04/12
For personal use only.

When [5] is substituted in [4] and the constants are combined, an expression of the form

$$e_5 = Ki_b \,.\, R \,.\, N_2 \qquad [6]$$

is obtained. This relates the unbalance voltage to the mole fraction of solute in the solution. But as has been mentioned earlier, the *change* in unbalance voltage with *change* in solute concentration is the only measurement actually used in this work. That is

$$\Delta e_5 = Ki_b \,.\, R\Delta N_2. \qquad [7]$$

Now $N_2 = n_2/(n_1+n_2)$ where n_1 is the number of moles of solvent; and for dilute solutions $n_1+n_2 \simeq n_1$. Therefore $N_2 \simeq n_2/n_1$ and since $n_2 = w_2/M_2$ where w_2 is the weight of solute of molecular weight M_2, equation [7] becomes

$$M_2 = K \,.\, i_b \,.\, R \,.\, \frac{M_1}{w_1}\frac{\Delta w_2}{\Delta e_5} \qquad [8]$$

and the molecular weight M_2 of the desired component is given in terms of quantities which are either measurable or known. When the second component is a polymer then M_2 is identical with $\bar{M}_n$, the number average molecular weight (16). Equation [5] for the boiling point elevation was used for simplicity and is not strictly applicable to polymer solutions. An equation of the type used by Smith (17) would be more precise.

During the course of a run the values of interest are the changes in e_5 brought about by the addition of a series of polymer pellets. The cumulative shift ($\Sigma\Delta s$) of the recorder pen, which is proportional to the boiling point elevation, is plotted versus the cumulative weight Σw (proportional to the concentration) of polymer added. It is found experimentally that for low molecular weight materials the cumulative shift so obtained is frequently a linear function of the total weight of material added, i.e.

$$\Sigma\Delta s = a \,.\, \Sigma w; \qquad [9]$$

but as the molecular weight of the material increases it is sometimes necessary to go to a quadratic equation

$$\Sigma\Delta s = a_0\Sigma w + a_1\Sigma w^2. \qquad [10]$$

This, however, is quite a common finding with polymer solutions (e.g. with osmotic pressures) and it is only in the limit of infinite dilution that one might expect a simple linear relation to hold. In the case where the linear relationship holds, the value of interest is the slope of the plot of $\Sigma\Delta s$ versus Σw. In the quadratic case ($\Sigma\Delta s/\Sigma w$) is plotted versus Σw and the value of the intercept at $\Sigma w = 0$ is used. The values of ($\Sigma\Delta s/\Sigma w$) for the polymer so obtained must then be related to the molecular weight of the polymer. The simplest method of doing this is to use a standard material, the molecular weight of which is known. Then using the relation

$$\bar{M}_n\left(\frac{\Sigma\Delta s}{\Sigma w}\right)_{\text{polymer}} = M_s\left(\frac{\Sigma\Delta s}{\Sigma w}\right)_{\text{standard}} \qquad [11]$$

it is possible to calculate the molecular weight of the unknown. This comparative procedure is recommended by Swietoslawski ((3), pp. 171–173). The technique, as we have used it frequently, consists of adding benzil pellets (the standard material) consecutively to establish the benzil sensitivity, i.e. the ($\Sigma\Delta s/\Sigma w$) for benzil for that day; then polymer pellets are added to this benzil solution and the $\Sigma\Delta s/\Sigma w$ for the polymer determined. The molecular weight of the polymer is then calculated using equation [11].

Can. J. Chem. Downloaded from www.nrcresearchpress.com by 176.9.209.113 on 09/04/12
For personal use only.

It may be objected at this point that the possibility of interaction between polymer and standard when both are added to the same solvent would vitiate this procedure entirely. This problem is discussed in greater detail later (21). Our results to date indicate that the procedure is safe, at least for benzil and polythene.

It may be mentioned as an aside, at this point, that the sensitivity attainable with thermistors and high gain amplifiers is so great that choosing a solvent because of its high ebullioscopic constant is no longer meaningful. Most ebullioscopic constants are within a factor of 10 of each other and any change in this value from solvent to solvent is easily compensated for by increasing the amplifier gain. A similar argument may be applied to the question of using a two-thermistor bridge or a four-thermistor bridge. The latter has twice the sensitivity of the former but the difficulty of matching four thermistors is more than twice that of matching two. Hence a two-thermistor bridge is used and gives more than adequate sensitivity.

EXPERIMENTAL RESULTS

The small ebulliometer has been in routine use for 4 years. During this time a large number of different samples has been determined with molecular weights ranging from the low hundreds to about 30,000. Rather than reproduce all the results, two series only will be discussed. These show, as well as any, the nature of the difficulties encountered. Furthermore each series was independently determined in another laboratory so that a check is provided. Those polymers other than polythene which have been measured gave similar problems.

The first series tested consisted of four polythene fractions (17) which had been prepared at Imperial Chemical Industries Limited, Alkali Division, where they were designated 47A/3/1, 2, 4, and 9. The results obtained at Imperial Chemical Industries Limited and Canadian Industries Limited are listed in Table I.

TABLE I

Comparison of I.C.I. and C-I-L results with some polythene fractions

	I.C.I. ebulliometer		C-I-L ebulliometer		
Sample No.	CCl_4	Toluene	CCl_4	Toluene	No. of runs
47A/3/1	4500	4000	4300	4320±130	2
47A/3/2		7090		6910, 6950, 6870	3
47A/3/4		11700		10000, 10500	2
47A/3/5	17280	13000			
47A/3/9	29400	20300	28200	16000, 17800	2

Sample No. 47A/3/5 has been included in this table even though it was not measured at Canadian Industries Limited because a tentative explanation for the different results obtained with the two solvents will be given in the discussion.

The next series of comparative determinations was performed by Dr. F. Sirianni of the Division of Applied Chemistry, National Research Council, Ottawa. The apparatus employed (18) permits a measurement of the depression of the vapor pressure over a solution compared with that over the solvent. His measurements were made with toluene solutions at 75° C. The results are listed in Table II.

One other sample has been determined both elsewhere and at Central Research Laboratory. This was a polystyrene which had been characterized both by osmometry and the method of radioactive end groups (22). The results were given as 24,000 and 20,000 respectively. Our result was 17,000.

Can. J. Chem. Downloaded from www.nrcresearchpress.com by 176.9.209.113 on 09/04/12
For personal use only.

TABLE II

Comparison of N.R.C. and C-I-L results with whole polythene samples

Alkathene melt index	N.R.C. results	C-I-L	
		CCl_4	Toluene
200000	2550	2400	2500
20000	4800	4680	4660
7000	6850	7100	7300, 6900
700	7750		7200, 6700
2	14150		10400
0.2	24350		18400

DISCUSSION OF RESULTS

It will be seen from Table I that the results obtained with the same samples in both ebulliometers agree quite well. The uncertainty with any one sample in toluene in the Canadian Industries Limited ebulliometer was least for low values of M_n and increased to about 10% at the highest M_n. The individual results are plotted in Fig. 2.

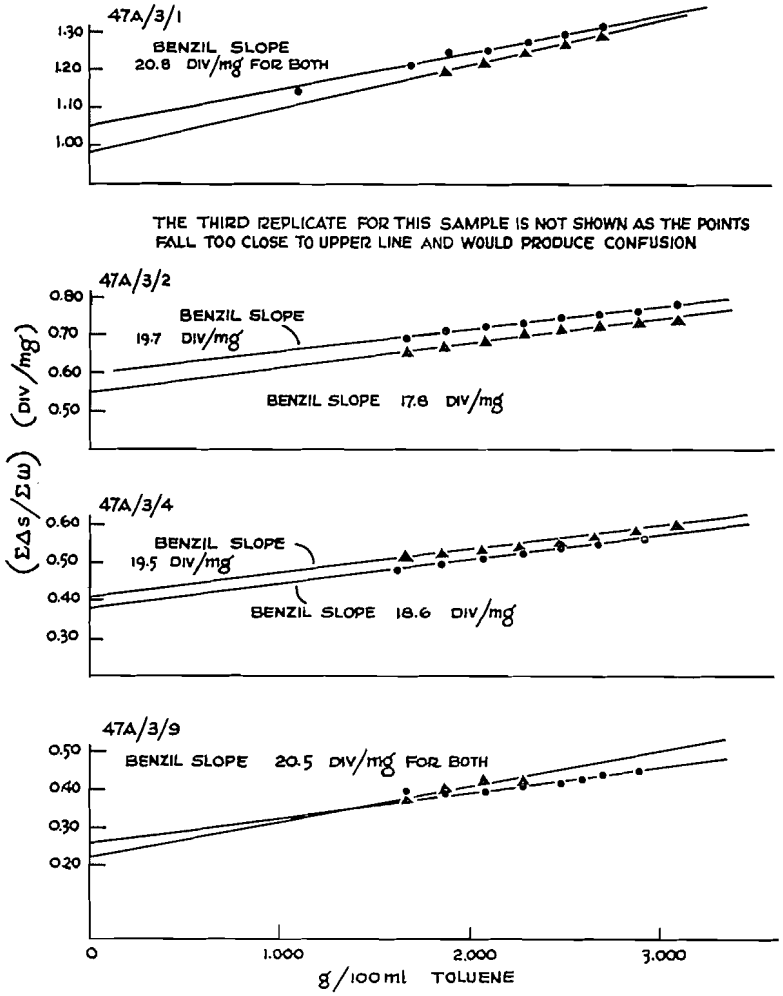

FIG. 2. Replicate runs on polythene fractions.

Can. J. Chem. Downloaded from www.nrcresearchpress.com by 176.9.209.113 on 09/04/12
For personal use only.

Two major points concerning the results in Table II and Fig. 2 should be discussed. The first is the remarkably large discrepancy between the value of M_n for sample 47A/3/9 in toluene compared with CCl_4, both at Imperial Chemical Industries and Canadian Industries Limited. A tentative explanation is that the high molecular weight species present in each added pellet do not dissolve in CCl_4 because of its low boiling point. Richards (19) and Myers (20) have both shown that the solubility of a polythene may be very sensitive to temperature. The percentage deviation between the results in CCl_4 and toluene increases as the value of M_n increases, which is in keeping with this explanation. Experimentally, since polythene floats on CCl_4, undissolved portions of the added pellets would be difficult to see because of the foam and the narrow viewing slit in the small ebulliometer. This explanation is, however, only tentative because Smith (17) also obtained high results in *n*-octane (boiling point 125° C) where the effect should not occur.

The second major point concerns the foam level during these runs. The "constant foam level" zone (see Foam, Part II (21)) was reached by using about 250 mg polythene in 15 ml solvent as the first addition. Subsequent additions were about 30 mg each. This means that the error introduced by the "foam shift" is hidden in the first value of $\Delta s/w$. Since this initial value of $\Delta s/w$ affects all subsequent values when the cumulative sums in $\Sigma\Delta s/\Sigma w$ are formed the error must be transmitted to the whole line. The magnitude of this error is unknown but the fact that it exists probably explains the increasing difference in results obtained between the next series measured at the National Research Council and Canadian Industries Limited.

The results of the second comparative series are shown in Table II. The agreement is good for the low molecular weight materials but there is an increasing disparity as the value of M_n increases. It is believed that the fault lies in the ebulliometer. This series provided a more stringent test of the ebulliometer for two reasons: (1) whole polymer produced more foam at lower polymer concentrations than did a fraction of comparable molecular weight and (2) the initial polymer concentration was low in each run of this series. This meant usually that the foam level changed during the run with consequences which are discussed later (21).

ACKNOWLEDGMENTS

The author wishes to thank Dr. D. C. West for his assistance in the early stages of this study, Mr. E. Lister for the skill and willingness with which this and other ebulliometers were constructed, Messrs. D. Hudson and R. Richard, by whom most of the measurements were made. The author is also indebted to Mr. H. Smith, Imperial Chemical Industries, Alkali Division, for having provided the series of polythene fractions; to Dr. A. F. Sirianni, National Research Council, Ottawa, for having performed the comparative measurements on the whole polythene samples; to Dr. H. T. Hookway for providing the polystyrene sample which had been characterized osmotically at the National Chemical Laboratory, Teddington, England, and which had been prepared and characterized radioactively by D. P. W. Allen of the British Rubber Producers Research Association.

REFERENCES

1. BECKMANN, E. Z. physik. Chem. **4**, 532 (1889).
2. COTTRELL, F. G. J. Am. Chem. Soc. **41**, 721 (1919).
3. SWIETOSLAWSKI, W. Ebulliometric measurements. Reinhold Publishing Corp., New York. 1945.
4. MENZIES, A. W. C. J. Am. Chem. Soc. **43**, 2309, 2314 (1921).
5. SAXTON, B. and SMITH, R. P. J. Am. Chem. Soc. **54**, 2626 (1932).

Can. J. Chem. Downloaded from www.nrcresearchpress.com by 176.9.209.113 on 09/04/12
For personal use only.

6. MORAWETZ, H. J. Polymer Sci. **6**, 117 (1951).
7. RAY, N. H. Trans. Faraday Soc. **48**, 809 (1952).
8. ADEY, A. W. Radio Physics Lab. Defence Research Telecommunications Establishment, Ottawa, Project Report No. 22-1-2 (1957).
9. LISTON-BECKER INSTRUMENT COMPANY, Stamford, Connecticut.
10. MANOSTAT CORPORATION, 20 N. Moore Street, New York 13, N.Y.
11. WOOD, H. H. Canadian Industries Ltd., McMasterville, Que., Report CRL-57-30. 1957.
12. VICTORY ENGINEERING CORPORATION, Springfield Road, Union, N.J.
13. H. TINSLEY & COMPANY, Smiths Falls, Ontario.
14. HARRIS, F. K. Electrical measurements. John Wiley & Sons, Inc., New York. 1952.
15. GLASSTONE, S. Textbook of physical chemistry. 2nd ed. D. Van Nostrand Company, Inc., New York. 1946.
16. HILDEBRAND, J. Solubility of non-electrolytes. 3rd ed. Reinhold Publishing Corp., New York. 1950.
17. SMITH, H. Trans. Faraday Soc. **52**, 402 (1956).
18. TREMBLAY, R., SIRIANNI, A. F., and PUDDINGTON, I. E. Can. J. Chem. **36**, 725 (1958).
19. RICHARDS, R. B. Trans. Faraday Soc. **42**, 10 (1946).
20. MYERS, C. S. J. Polymer Sci. **13**, 549 (1954).
21. BLACKMORE, W. R. Can. J. Chem. **37**, 1517 (1959).
22. ALLEN, P. W. and PLACE, M. A. J. Polymer Sci. **26**, 386 (1957).

Can. J. Chem. Downloaded from www.nrcresearchpress.com by 176.9.209.113 on 09/04/12
For personal use only.

Can. J. Chem. Downloaded from www.nrcresearchpress.com by 176.9.209.113 on 09/04/12
For personal use only.

EBULLIOMETRY AND THE DETERMINATION OF THE MOLECULAR WEIGHTS OF POLYMERS

PART II. BACKGROUND NOISE IN THE SMALL EBULLIOMETER[1]

W. R. Blackmore

ABSTRACT

It is shown that the usual form of ebulliometer is subject to at least three sources of noise. Those discussed here are (1) pressure fluctuations over the boiling liquid surface, (2) the Cottrell pump, and (3) the foam which appears on many polymer solutions when maintained at the boiling point. Background noise in this, and other ebulliometers commonly employed, may be large compared to the size of the signals expected for dilute high polymer solutions. Consequently further progress in ebulliometry is dependent on the development of a new ebulliometer with a much lower background noise.

INTRODUCTION

In any measurement the most important quantity is the signal-to-noise ratio. In ebulliometry, with high polymer solutions, the signal is frequently only a small boiling point elevation of perhaps 1000 microdegrees (μ° C). But the ebulliometer itself, because of the nature of its operation, introduces random temperature fluctuations, called noise. This noise is often an appreciable fraction of the signal to be measured. Thus even with pure solvent boiling and being pumped, the noise may be ± 150 μ° peak to peak, while as the concentration of polymer increases the noise also increases and may rise by a factor of five or six over the pure solvent noise. It is obvious that reducing the noise in an ebulliometer is greatly to be desired. The object of this work was to discover the sources of noise in the small ebulliometer (1).

EXPERIMENTAL SECTION

(1) *To Show the Principal Source of Background Noise*

The thermistor bridge normally used in the small ebulliometer only measures differential temperatures. To discover at which thermistor the noise is greater, the thermistor bridge was opened and the behavior of the thermistors was followed individually. To do this the Tinsley Wheatstone bridge (1), the Leeds and Northrup microvolt d-c. amplifier, and the Brown recorder were used. To facilitate the measurements the conditions were chosen so that the background noise would be much greater than normal. The ebulliometer was connected to a 25-liter surge bottle which was closed off from the atmosphere. The three traces obtained are shown in Fig. 1. It is obvious that most of the temperature fluctuation is produced at the lower thermistor which is exposed to the pumped liquid. The fluctuations recorded for the lower thermistor represent peak-to-peak fluctuations of ± 2.7 m° C. By comparison the upper thermistor trace shows only a slow drift produced by a slight increase in pressure in the surge bottle. The third trace is also most instructive. This was obtained when the tube connecting the ebulliometer to the surge bottle was closed off near the ebulliometer. This meant that pressure waves travelling up inside the ebulliometer from the surging boiling surface were now unable to dissipate themselves in the surge bottle and were reflected back down into the ebulliometer. The disastrous effect on

[1]*Manuscript received April 3, 1959.*
Contribution from the Central Research Laboratory, Canadian Industries Limited, McMasterville, Que.

the temperature stability at the upper thermistor is obvious. This noise represents peak-to-peak temperature fluctuations of ± 4.8 m° C. It must be emphasized that these conditions have been chosen for purely illustrative purposes; in normal operation the noise level is considerably lower.

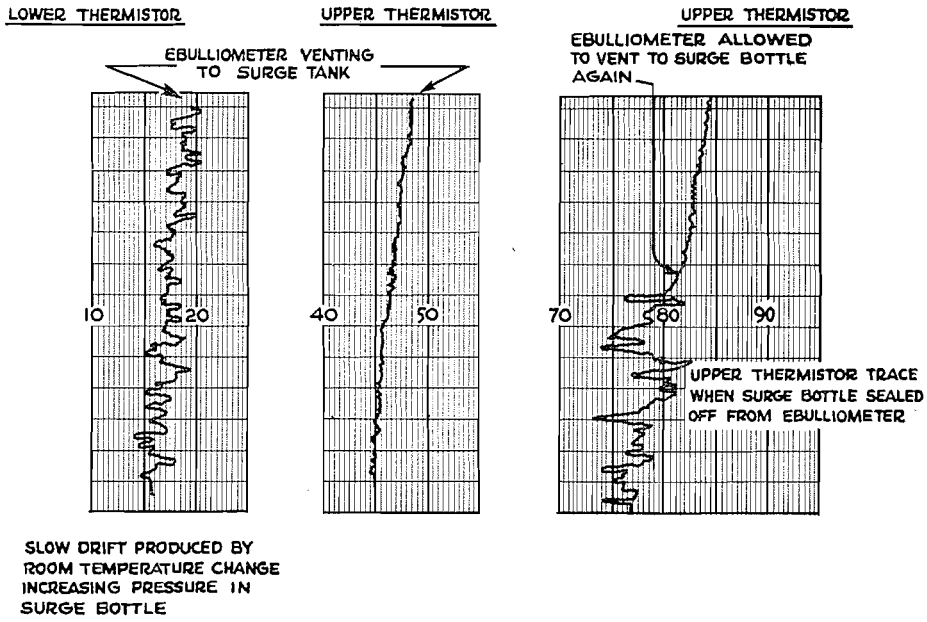

FIG. 1. Temperature fluctuations at individual thermistor wells.

The similarity of the trace obtained from the lower thermistor compared with that from the upper thermistor when the ebulliometer was closed off from the surge bottle raises one of the fundamental questions about background noise in ebulliometry. The question is this. The lower thermistor is subject in this ebulliometer to pressure fluctuations coming from (*a*) the boiling surface in the pot and (*b*) vapor puffs as the liquid is ejected by the the pump. Are these responsible for the noise at the lower thermistor? Under normal operating conditions the trace noise is of the order of $\pm(100 \rightarrow 150)$ μ° C for toluene. Differences of only $\pm(2 \rightarrow 3)$ μ Hg in the pressures of the vapors around each thermistor region would produce temperature fluctuations of the order mentioned.

(*2*) *To Show the Effects of the Boil-up Rate and Radiation from the Pump Heater on the Thermistors*

The first method used to investigate the effect of heater current variations was to follow the unbalance voltage from the differential bridge as a function of heater current, with a constant volume of solvent in the ebulliometer and the amplifier gain set high enough so that the background noise was clearly visible on the recorder. A curve typical of the results obtained is shown in Fig. 2. This curve was calculated from the differential thermistor bridge output by attributing the temperature changes to the lower thermistor and assuming the upper thermistor temperature was constant. The vertical bar at each point on the graph indicates the peak-to-peak noise level. The volume chosen was 15 ml of pure toluene for which the minimum heater current required in order for the pump just to operate is 3.0 amperes. The unbalance voltage from the thermistor bridge at this heater

Can. J. Chem. Downloaded from www.nrcresearchpress.com by 176.9.209.113 on 09/04/12
For personal use only.

current was chosen as the arbitrary zero. For any heater current above or below 3.0 amperes the trace indicated that the lower thermistor came to an equilibrium temperature which was higher than its temperature at the minimum heater current required for pumping. The noise increased with increased current too.

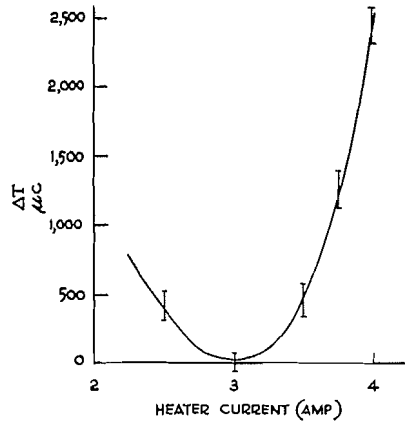

FIG. 2. Temperature difference between thermistors vs. pump heater current.

To understand this it was necessary to open the thermistor bridge and measure the resistances of the thermistors individually with the Tinsley Wheatstone bridge. The results obtained are indicated graphically in Fig. 3. The temperature change experienced by each thermistor was calculated relative to its temperature at the lowest heater current shown; pressure corrections were applied where necessary. No attempt to establish

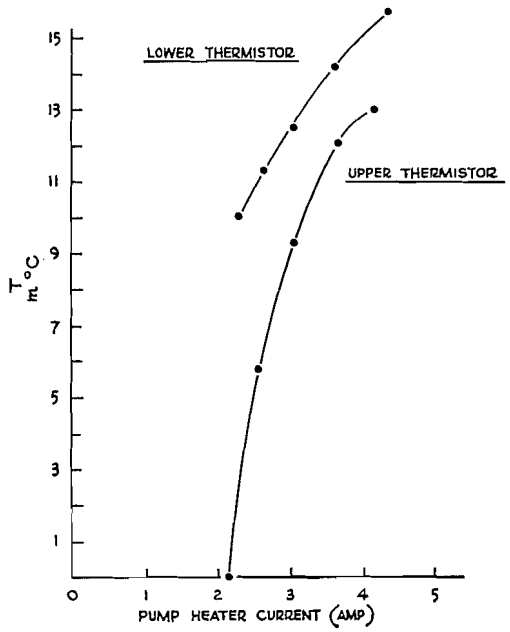

FIG. 3. Individual thermistor equilibrium temperature vs. pump heater current.

Can. J. Chem. Downloaded from www.nrcresearchpress.com by 176.9.209.113 on 09/04/12
For personal use only.

the absolute true minimum temperature difference between the thermistors was made since equipment of greater precision would have been required. For any one heater current each thermistor assumed an equilibrium temperature which was quite stable. Since the same form of curve was obtained with 10 ml in the boiler the relationship was not a function of the pumping rate. The results were attributed to (1) the changed boil-up rate, which established a new pressure head within the ebulliometer, and (2) radiation from the heater, which affected each thermistor, after multiple reflections by the silvered wall of the vacuum jacket.

(3) The Cottrell Pump

It seems reasonable to suppose that the energy required for any Cottrell pump to just operate must be proportional to the height through which the liquid is to be lifted and the mass of liquid to be pumped. Thus the energy required may be written as equal to

$$k.h.V.d.g.,$$

where k is a constant relating to pump efficiency, h is the height from boiling surface to pump exit, V and d are the volume and density of the fluid in the pump stack, and g is the acceleration due to gravity. This expression was tested by comparing CCl_4 and toluene at heater currents such that the pump just worked. From the equation we have $h_2d_2 = h_1d_1$, and since the density of CCl_4 (2) at its boiling point (76.7° C) is 1.483 g/ml while that of toluene at its boiling point (110.6° C) is 0.779 g/ml we would expect that the pump would only operate if the height for CCl_4 were half of that for toluene. An experimental check showed qualitative agreement with this analysis. The height was altered by working with different volumes of solvent. This relation also shows why a Cottrell pump works so much more easily (with less energy input from the heater) when foam, with its low density, is being pumped.

(4) To Show the Effect of Hydrostatic Head on Superheat

The unbalance voltage from the thermistor bridge was measured as a function of different volumes of solvent in the boiler. The heater current was held constant and the ebulliometer surge bottle was closed off from the atmosphere so that the pressure would not change. The experiment was started with 30 ml of toluene in the ebulliometer. After enough of a trace had been taken to allow a measure of the noise and to prove that this value of unbalance voltage was constant at that volume, 5 ml of toluene were allowed to drain out the stopcock without disturbing the heater current or the pressure. The recorder pen shifted to its new position and the whole procedure was repeated until the final volume was 10 ml. Once again the temperature difference between thermistors was least when the pump was just working. And the pump noise was also least at this point. When the volume was so low that the pump no longer worked the upper thermistor temperature was lower compared with that of the lower thermistor than it had been. To make sure that this interpretation was correct once again the thermistor bridge was opened up and the resistances of the individual thermistors followed separately. The curve obtained with the differential bridge is shown in Fig. 4 while the other two are given in Fig. 5. The curve shown in Fig. 4 was calculated from the thermistor bridge output by attributing the temperature changes to the lower thermistor and assuming the upper thermistor temperature was constant. In Fig. 5 the temperature change experienced by each thermistor was calculated relative to its temperature at a volume of 20 ml. A vapor ring was visible in the condenser at all volumes.

Can. J. Chem. Downloaded from www.nrcresearchpress.com by 176.9.209.113 on 09/04/12
For personal use only.

Can. J. Chem. Downloaded from www.nrcresearchpress.com by 176.9.209.113 on 09/04/12
For personal use only.

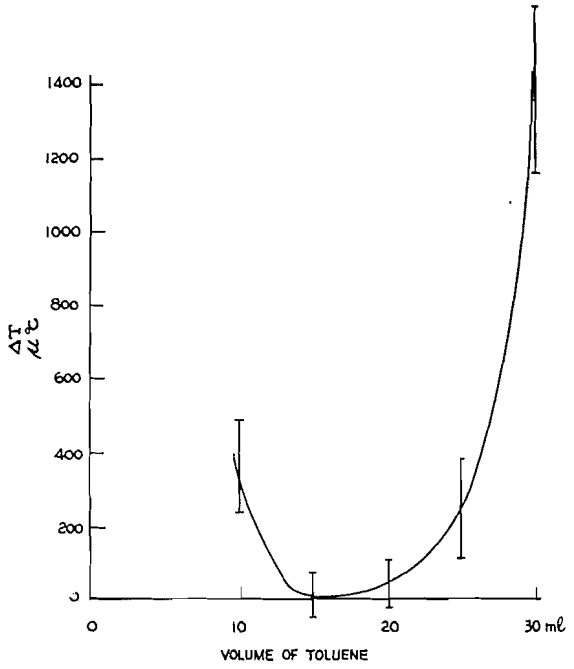

FIG. 4. Temperature difference between thermistors vs. volume of pure toluene in boiler at constant heater current (2.8 amperes).

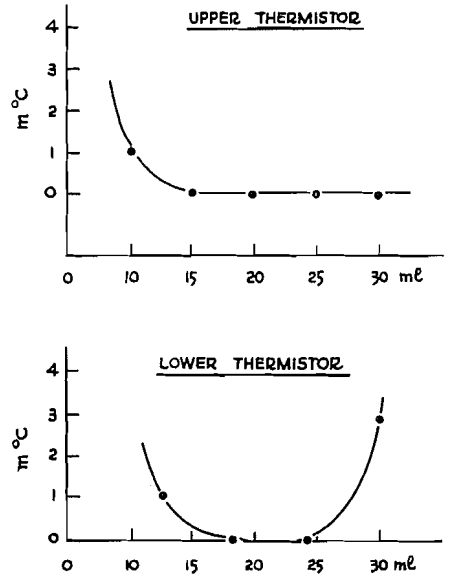

FIG. 5. Individual thermistor equilibrium temperature vs. volume of toluene in the boiler at constant heater current (2.8 amperes).

When these results are interpreted we are almost forced to conclude that the superheat in the liquid leaving the pump does not flash off immediately but rather requires more time to come to equilibrium than is available in the short run down the spiral around the

thermistor well. Since the hydrostatic head acting on the liquid in the pump bell is greatest at 30 ml, and the superheat and the pump rate are also greatest at this point the relatively vast quantity of liquid pouring over the lower thermistor may not have time to come to true equilibrium.

(*5*) *To Demonstrate the Effects of Foam in an Ebulliometer*

Many polymer solutions produce foam in the ebulliometer when maintained in a state of vigorous boiling. We have found, as did Smith (3), that both increasing molecular weight and wider molecular weight distribution in a polymer increase the amount of foam formed in the ebulliometer. Usually all the foam does not appear at once. Thus for a given polymer, in a low concentration region, there may be no foam, then in a slightly higher concentration zone there is increasing foam until finally another concentration zone of constant foam appears. Graphically this may be illustrated as in Fig. 6. When different

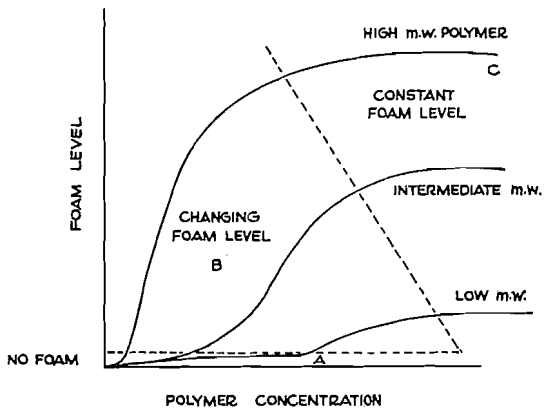

FIG. 6. Schematic representation of the foam level vs. polymer concentration for polymers of increasing molecular weight.

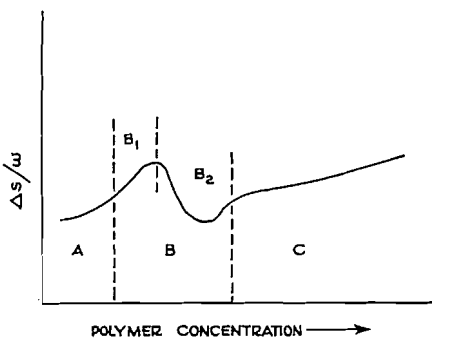

FIG. 7. Schematic representation of effect of foam level on sensitivities of successive polymer additions.

solvents are compared it is found that the behavior is similar but the "changing foam level" zone may have shifted along the concentration axis. For instance a polythene in CCl_4 produces more foam at lower concentrations than the same polythene in toluene.

Experiments to show the "foam shift" are reported below, but meanwhile a schematic representation will be given, which shows the effect most simply. Suppose successive polythene pellets, each of the same weight, are added to an ebulliometer operating with pure solvent in the boiler. Depending on the molecular weight of the material, we might obtain a curve such as that shown in Fig. 7. In region A no foam is present. In region B_1

Can. J. Chem. Downloaded from www.nrcresearchpress.com by 176.9.209.113 on 09/04/12
For personal use only.

foam begins to be established and the measurement indicates a total elevation which is the sum of the true boiling point elevation plus an elevation associated with the change in foam level. In region B_2, although the foam increases slightly, one measures lower values for $\Delta s/w$. Finally in region C the foam level is constant and $\Delta s/w$ increases with Σw as one expects for a polymer. Quite obviously the presence of changing amounts of foam accompanies serious changes in the polymer sensitivity.

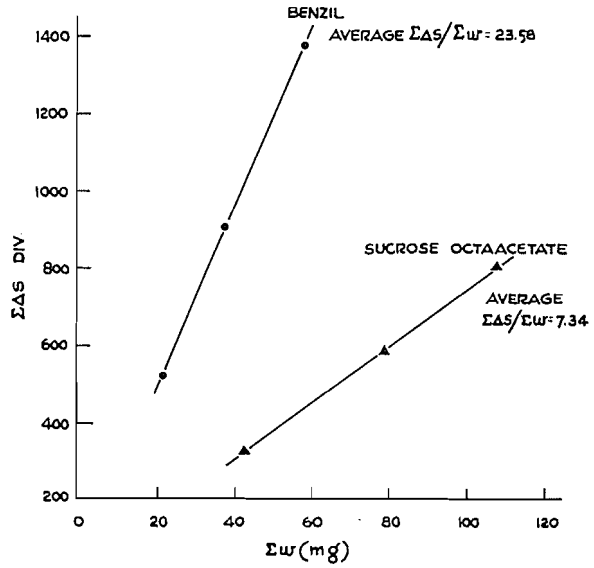

FIG. 8. Typical plots of $\Sigma\Delta s$ vs. Σw for alternate additions of low molecular weight materials.

Some experiments with foam will now be described. The first demonstrates that once the foam level is constant the sensitivity is constant. This fact was established as follows: the small ebulliometer operating with toluene was given a few benzil additions and the sensitivity measured. Then 60 mg of a polythene known to produce a great deal of foam were added, and the benzil sensitivity was measured again. The results are given in Table I.

TABLE I

Effect of foam on benzil sensitivity

Foam level	Trace noise, div peak-to-peak	Benzil		
		Δs, div	w, mg	$(\Delta s/w)$, div/mg
None	±2	54	4.3	12.6
None	±2	39	3.1	12.6
	Polythene foamer added			
Large amount of foam	±3	69	4.7	14.7
	±3	70	4.8	14.6
	±3	139	9.5	14.6
	±4	109	7.5	14.5
	More foamer added			
Extremely heavy foam	±9	161	8.9	18.1
	±9	143	8.8	16.3
This solution boiled all night and another benzil addition was made in the morning				
	±9	126	7.4	17.0

Can. J. Chem. Downloaded from www.nrcresearchpress.com by 176.9.209.113 on 09/04/12
For personal use only.

It is now necessary to establish whether (*a*) the changing foam level, (*b*) the different polymer concentration, or (*c*) the different benzil concentration produces the different benzil sensitivity. First it will be established (Table II) that the benzil sensitivity is independent of the benzil concentration.

TABLE II

Benzil sensitivity as a function of benzil concentration in toluene

Noise, div	Δs, div	w, mg	$(\Delta s/w)$, div/mg	$(\Sigma\Delta s/\Sigma w)$, div/mg
±2	45	3.86	11.7	11.7
±2	87	7.35	11.8	11.8
±2	90	7.64	11.8	11.8
±2	36	3.02	11.9	11.8
±2	94	7.75	12.1	11.9
±2	65	5.50	11.8	11.9

Next, the results in Table III show that the benzil sensitivity increases slowly with polymer concentration but not with the amount of foam present, while the individual polymer sensitivities change with the foam level established by the particular polymer addition. In the final stages of the polymer additions when the amount of foam present is not altered by an addition then the $\Sigma\Delta s/\Sigma w$ increases with Σw along a respectable straight line.

TABLE III

Effect of foam on polythene sensitivity

Substance added	Noise level	Δs, div	w, mg	$(\Delta s/w)$	Σw	$(\Sigma\Delta s/\Sigma w)$	Comments
Benzil	±2	79	6.45	12.2	6.45	12.2	No foam
	±2	51	4.00	12.8	10.45	12.4	
Polythene	±2	34	32.4	1.05	32.4	1.05	
Benzil	±2	42	3.15	13.3	13.60	12.6	
	±2	48	3.80	12.6	17.40	12.6	
Polythene	±2	39	32.0	1.22	64.4	1.13	Slight foam on surface
Benzil	±2	43	3.30	13.0	20.70	12.7	of boiling liquid but
	±2	43	3.34	12.9	24.04	12.7	none around thermistor well
Polythene	±2	87	60.1	1.45	124.5	1.29	Definite small surface
Benzil	±3	65	5.1	12.7	29.14	12.7	foam and slight froth
Polythene	±3	80	62.5	1.28	187.0	1.28	in umbrella at lower
Benzil	±3	48	3.75	12.8	32.89	12.7	thermistor. Remains
Polythene	±3	91	61.9	1.47	248.9	1.33	approximately con-
Benzil	±3	44	3.2	13.8	36.09	12.8	stant hereafter
Polythene	±3	100	63.7	1.57	312.6	1.38	
Benzil	±3	72	5.3	13.6	41.39	12.9	

(6) Solvent Purity and Benzil–Polymer Interaction

In this work the comparative method requiring the addition of a standard substance to the solution of the unknown has been employed for the reasons advanced by Swietoslawski ((4), pp. 171–173). The solvent used has been toluene ("from Sulfonic Acid") produced by Distillation Products Inc. It was assumed that neither the polythenes nor the benzil would associate with any impurity. Given this, the only difficulty which

Can. J. Chem. Downloaded from www.nrcresearchpress.com by 176.9.209.113 on 09/04/12
For personal use only.

might have arisen was a volatile impurity. To measure the effect of a volatile impurity increasing concentrations of water were added to boiling toluene in the small ebulliometer with the results given in Table IV.

TABLE IV

% water, g/100 cc	Ratio of wet toluene noise to noise for pure dry toluene
0	1
1.4	5
4.8	7
12.0	20

The toluene normally used was tested with Karl Fischer reagent and found to be dry (.0016 g/100 cc). No regularly repeating fluctuations were ever observed in a trace which would have indicated a volatile impurity. The reasons for using benzil (diphenyldiketone) as a reference substance are that it is (1) easily purified, (2) stable to heat and light, (3) non-hygroscopic, and (4) easily soluble in common organic solvents.

The next problem is whether the introduction of benzil may produce some interaction with the polythene solutions. To test this several experiments were performed. First a series of benzil additions was made to pure boiling toluene. This gave a completely linear plot of cumulative shift $\Sigma\Delta s$ versus total weight added Σw. The relationship has been proved linear up to concentrations as high as 10% (g/cc). The next experiment was to measure the benzil sensitivity ($\Delta s/w$) for alternate additions both before and after the introduction of a quantity of low molecular weight material, e.g. sucrose octaacetate. No change in sensitivity (Fig. 8) could be detected. If the formula weight for benzil is assumed known the molecular weight calculated for sucrose octaacetate from the data in Fig. 8 is 676.7, which is in error by 0.28%. This proved the feasibility of the method for solutions in which neither sensitivity was a function of the concentration. The next step was to do a run on a pure polythene solution. This was a low molecular weight material ($M_n = 3000$) and a plot of ($\Sigma\Delta s/\Sigma w$) versus Σw for this polymer was a straight line. No attempt was made to calculate a molecular weight from this series of polythene additions; the run was being used simply to determine whether the polymer sensitivity ($\Delta s/w$) increased with Σw. It did, in fact, quite slowly. Then a new run was made; this time the benzil sensitivity was measured after each polythene addition. It was found that the benzil sensitivity increased with increasing polymer concentration with the same slope as had the polymer plot of ($\Sigma\Delta s/\Sigma w$) versus Σw. Consequently it was concluded that the benzil did not affect the polymer, and conversely.

DISCUSSION OF RESULTS

The problems which may arise from (*a*) pressure fluctuations in the ebulliometer, (*b*) changes in the boil-up rate, (*c*) radiation from the heater acting on the thermistors, and (*d*) uneven delivery from the pump each may be corrected by fairly obvious changes in design. This has, in fact, been done with an ebulliometer to be described later in this series.

The real problems are to understand (1) why polymer solutions produce noise which increases as a function of the concentration and (2) how to explain the "foam shift". From the foregoing results it appears that a constant amount of foam in the ebulliometer is not troublesome. The principal difficulty arises when the amount of foam is changed by the addition of polymer for then the shift measured is not necessarily the true boiling point elevation but also has associated with it what is called a "foam shift".

Can. J. Chem. Downloaded from www.nrcresearchpress.com by 176.9.209.113 on 09/04/12
For personal use only.

The first attempt to explain the foam shift was an argument to the effect that the dissipation constant of foam at the lower thermistor was less than that of liquid. Consequently, since thermistors must always float slightly above the ambient temperature, if less heat were taken away from the lower well by foam than by liquid, then the boiling point elevation measured on the addition of a material which changed the foam level would be greater than the true value. Unfortunately, measurements of the dissipation constant proved that this was not the case. The dissipation constant was unchanged whether foam or liquid engulfed the well.

The next approach was to consider the hypothesis advanced by Smith (3) to explain the curves he obtained. It was supposed there that adsorption in the foam at low bulk concentrations gave a polymer "excess" in the foam which consequently produced a greater boiling point elevation than that expected. At higher polymer concentrations this foam adsorption represented a much smaller percentage of the material present and, as well, approached a saturated value so that the measured elevations corresponded much more closely to the true values. This satisfactorily explained the shape of the curves obtained with toluene. But the same shape curve was not obtained with CCl_4 although foam (3) appeared even earlier in this solvent. Hence surely the effect should have been found there too.

CONCLUSIONS

The results quoted have shown three sources of noise in an ebulliometer of a design similar to most now employed throughout the world. These are:

(1) instantaneous pressure differences in the vapors surrounding each detector element,

(2) remnants of superheat in the liquid ejected by the Cottrell pump, and

(3) the foam produced by most polymer solutions when maintained at the boil.

Each of these may be corrected by fairly obvious changes in design. This has been done with the new ebulliometer to be described later in this series.

ACKNOWLEDGMENTS

The author wishes to thank Drs. A. T. Williamson and S. S. Grimley for the many clarifying discussions of the problems mentioned in this paper.

REFERENCES

1. BLACKMORE, W. R. Can. J. Chem. **37**, 1508 (1959).
2. TIMMERMANS, J. (*Editor*). Physical chemical constants of pure organic compounds. Elsevier Press, Inc., N.Y. 1950. pp. 152, 224.
3. SMITH, H. Trans. Faraday Soc. **52**, 402 (1956).
4. SWIETOSLAWSKI, W. Ebulliometric measurements. Reinhold Publishing Corp., New York. 1945.

Can. J. Chem. Downloaded from www.nrcresearchpress.com by 176.9.209.113 on 09/04/12
For personal use only.

Can. J. Chem. Downloaded from www.nrcresearchpress.com by 176.9.209.113 on 09/04/12
For personal use only.

ELECTROMIGRATION OF IONS ABSORBED BY FILTER PAPER[1]

R. A. BAILEY[2] AND L. YAFFE

ABSTRACT

The variation with absorbance of the zone mobilities and obstructive factors for a number of inorganic ions has been investigated in acetic acid and in ammonium hydroxide at several concentrations. The results agree with the form of the semiempirical equation of Crawford and Edward. For a given ion the apparent obstructive factor defined as

$$\rho_{app} = \frac{\text{zone mobility}}{\text{free solution mobility}}$$

remains fairly constant as the concentration of the background electrolyte is changed, except in the very dilute region. However, the apparent obstructive factor varies with the ion and the background electrolyte indicating that specific effects, which are not considered in the equation, are important.

INTRODUCTION

The separation of ions by electromigration in paper has received much attention in recent years, but it is for the most part an empirical technique. Theories have been proposed to account for the behavior of ions under the conditions which prevail in this process and, although they are based on a somewhat naive model, they seem to be at least qualitatively valid. In order to see to just what extent these theories are applicable, there is a great need for accurate and reproducible measurements of zone mobilities under conditions where all of the many variables are fixed. This is especially so in the case of inorganic ions. In this paper we shall show that, while the zone mobilities (defined as the velocity under unit voltage gradient of the zone of ions on the paper) of inorganic ions in paper do follow the existing theories in a general manner, specific effects are present which cannot be accounted for satisfactorily.

Electromigration of ions in paper was first treated fundamentally by Kunkel and Tiselius (1). Their treatment was later modified by Edward (2). In the model used, the zone mobility U_z of an ion migrating in paper is given by the expression

[1] $$U_z = \rho U_F$$

where U_F is the mobility of the ion in free solution, and ρ is a correction factor called the obstructive factor (2) which is the reciprocal of the square of the conventional tortuosity factor (3). This correction factor stems from the fact that the path followed by the ion in paper would be more tortuous than in free solution since the ion must now detour around the inert fibers of the paper.

If L is the length of the paper and L^1 the length of the crooked channel in it, which the ion must follow, it is readily shown that

[2] $$\rho = \left(\frac{L}{L^1}\right)^2 = \frac{K^1}{K}$$

where K^1 is the conductance of the solution when it is in the paper, and K its conductance in the free state. It is possible, then, to estimate the value of the obstructive factor from conductance measurements.

[1]*Manuscript received May 25, 1959.*
Contribution from the Radiochemistry Laboratory, Department of Chemistry, McGill University, Montreal, Que. with financial assistance from the National Research Council of Canada, Ottawa, Canada.
[2]*Holder of National Research Council Studentships, 1957–58 and 1958–59.*

Can. J. Chem. Downloaded from www.nrcresearchpress.com by 176.9.209.113 on 09/04/12
For personal use only.

Crawford and Edward (4) have considered the variation of the obstructive factor ρ with the volume of liquid present per unit weight of paper (the absorbance) and, in certain cases, their results make it possible to calculate this obstructive factor. Their treatment was based on a semiempirical equation devised by Biefer and Mason (5) giving the conductance of pads of randomly oriented, non-conducting, non-swelling fibers, which in turn was obtained from the theoretical equation

$$K^1 = \frac{kf(\theta)A\epsilon}{L}. \qquad [3]$$

Here, k is the specific conductivity of the solution, A is the cross-sectional area of the pad and solution, L is its length, and ϵ is its void fraction:

$$\epsilon = \frac{V_L}{V_L + V_s}$$

where V_L is the volume of the liquid, and V_s the volume of the solid fibers. $f(\theta)$ is an orientation factor which was originally equated to the void fraction on experimental grounds. Subsequent work (5) has shown that better agreement with experiment is obtained if $f(\theta) = \alpha\epsilon$ where α is a constant which is close to unity. Measurements with cellulose acetate, Dacron, nylon, and glass fibers give a mean value of 0.955 (5). Then

$$K^1 = \frac{kA\alpha\epsilon^2}{L}. \qquad [4]$$

Since $A = (V_L + V_s)/L$, then substituting for A and ϵ gives

$$\alpha\epsilon = \frac{K^1L^2}{kV_L},$$

but

$$\rho = \frac{K^1}{K} = \frac{K^1L^2}{kV_L}. \qquad [5]$$

Thus

$$\alpha\epsilon = \rho.$$

The absorbance a is

$$a = \frac{V_L}{\text{weight of solid}}.$$

Applying this we get

$$\rho = \alpha\left(\frac{a}{a + v_s}\right) \qquad [6]$$

where v_s is the specific volume of the fibers.

Cellulose fibers are known to swell in aqueous solution. If X is the fractional increase in fiber volume that is effective in hindering ion migration, then

$$\epsilon = \frac{V_L - XV_s}{V_L + V_s}.$$

Then, from equations [4] and [5]

$$\rho = \alpha\left(\frac{a - 2v_sX}{a + v}\right). \qquad [7]$$

Crawford and Edward, using conductance measurements, found that values of X between 0.1 and 0.2 fitted most of their experimental obstructive factors for inorganic salt solutions; α was taken as unity.

From equation (6) it is possible to calculate the obstructive factor for non-swelling fibers such as glass, if the theory is correct. The only uncertain factor in the equation is α. This can be assumed to be unity with only a small error, or it can be taken as 0.96 from the work of Biefer and Mason. The expression $f(\theta) = \alpha\epsilon$, on which equations [6] and [7] depend, is admittedly empirical, but it does seem to be well founded experimentally.

The above model makes no allowance for specific interactions between the ions and the fiber. It is true that the value of ρ obtained from conductance measurements may include effects of adsorption and may therefore show a dependence on the electrolyte used, but the measurements so far made in this connection have been with solutions of much higher concentrations than is usual for the ions moving in a separation, so that the paper is 'overloaded'. It is possible that adsorption effects at low concentrations are more marked. Furthermore, the background electrolyte itself may well affect the way in which the ion interacts with the paper. This would not be shown from conductance measurements.

By the use of radioactive tracers, we have been able to check any low concentration effects and test the validity of these empirical equations.

EXPERIMENTAL

The paper was placed between two brass plates, 60×25 cm in size, and insulated by polythene film of about 0.01-in. thickness. Water from a constant temperature bath ($25.0 \pm 0.5°$ C) was circulated through copper tubing which was soldered to the backs of these plates. In a few experiments at lower temperature, the control was not as good. Measurements with a thermocouple in contact with the paper showed that at an applied potential of 30 v/cm, a current of 1 milliampere could be carried for each centimeter width of the paper with an increase of less than 0.5° C in the actual temperature of the strip. This is approximately the rise calculated by assuming an equilibrium between the amount of heat generated in the paper and that conducted across the polythene insulation.

Wood and Strain (6) have shown that electroosmotic flow of the background electrolyte is largely eliminated if the electrodes are placed in direct contact with the paper. We used this arrangement and, when necessary, prevented interference from the electrolytic products by moistening the zones at the ends of the paper with a suitable buffer solution which trapped the ions so formed without itself giving an interfering ion. These buffer zones also served to keep the voltage drop across the electrodes nearly constant without manual control. This procedure was chosen in preference to correcting for electroosmotic flow by the motion of zones of uncharged substances. Such corrections are always subject to uncertainty about the relative effects of adsorption on the motion of the ion and the indicator substance. Also, if the flow of electrolyte is not uniform, as when the liquid flows from both ends of the strip toward the center (the 'wick effect') (7), the effect of this flow on the migrating ion is difficult indeed to determine from the motion of the indicator zones. When uncharged materials, particularly H_2O_2, were used as indicators in our technique, these materials showed no measurable motion.

Voltages were measured by means of a vacuum tube voltmeter connected to platinum probes that were at some distance from the ends of the paper strip so that voltage

Can. J. Chem. Downloaded from www.nrcresearchpress.com by 176.9.209.113 on 09/04/12
For personal use only.

drops across the platinum foil electrodes and the buffer zones were not considered. Separate measurements showed that the voltage gradient in that part of the strip where the migration took place was uniform, and remained so for the duration of an experiment.

In order to obtain known reproducible absorbances of the paper, the desired volume of electrolyte was spread as uniformly as possible over the strip from a pipette. The buffer zones were moistened to the same absorbance. The electrolyte was allowed to spread for $\frac{1}{2}$ hour or more and the solution to be investigated was applied at the starting line as a spot or a streak. This method of moistening the strip was quite satisfactory except at very low absorbances.

There are certain advantages in using radioactive materials in this work. The zones of material are very easily detected by their radiations so that no chemical tests are necessary, and exceedingly small amounts of material can be used so that the ionic strength of the moving zone is not appreciably different from that of the background solution. Although the influence of concentration of the moving ion on its zone mobility has not yet been adequately studied, it is known that there is an effect. Our work indicates that, at least in non-complexing media, the zone mobility decreases slowly with increasing concentration, while at the same time the zone becomes broader. The latter was reported also by Maki (8). The solutions used here were sufficiently dilute to render the effects of concentration entirely negligible; indeed, the Na^{22} was effectively 'carrier-free', i.e. ca. 10^{-8} molar.

Na^{22}, Cs^{137}, Tl^{204} (as Tl^{+}), Cl^{36} (as chloride), Co^{60}, and Zn^{65} were the radioactive tracers used. Inactive Cu^{++}, Cd^{++}, and Fe^{+++} were used in the form of 0.001 *M* solutions of the nitrate; some of the experiments with Zn^{++} and Co^{++} were done with similar inactive solutions. The volume applied was in most cases 10 microliters. The volume of Tl^{+} was usually 5 μl, however, and in other cases some experiments were made with 20 or 50 μl of solution.

The active ions were detected by cutting the strip into sections 1 cm (occasionally 0.5 cm) broad, and measuring each with a Geiger counter. The inactive ions were detected with a solution of dithizone in CCl_4 or by exposure to H_2S.

The papers used were Whatman No. 52 chromatography paper, 5.1 cm wide, and Reeve Angel 934AH glass fiber filter paper, 2.9 cm wide. The length of the paper available for migration varied in different experiments from 20 to 50 cm, and actual distances of migration ranged from about 15 to 50 cm.

RESULTS AND DISCUSSIONS

In order to calculate the zone mobility, U_z, it is first necessary to determine U_F, the mobility of the ion in question in the solution used as background electrolyte. This must be estimated from the ionic conductance at infinite dilution by taking into account the effects of ionic strength and viscosity. We must consider the effects of foreign ions and uncharged molecules on the ion studied, and this makes an accurate calculation of U_F very difficult. For instance, the value of the dielectric constant, which enters into all conductance equations, is probably appreciably different in 6 *M* acetic acid from what it is in pure water, but we are unable to make a satisfactory allowance for such changes. Fortunately all solutions used have quite a low ionic strength, and the correction given by the limiting form of the Onsager equation, taking the constants to be those for pure water, probably serves as well as that which could be obtained from more complicated equations which are largely untested under conditions such as we are considering. In addition, the change in mobility due to ionic strength alone is small

Can. J. Chem. Downloaded from www.nrcresearchpress.com by 176.9.209.113 on 09/04/12
For personal use only.

compared with the effect of viscosity. Therefore, we have corrected for ionic strength by the Onsager equation and divided this result by the relative viscosity to get U_F. The result, although perhaps crude, is not likely to involve an error greater than that in the experimentally determined zone mobilities.

Each of the zone mobilities included in these results represents the mean of three or more experiments, usually carried out with different voltage gradients and migration times. Figure 1 shows the variation of the zone mobilities of Fe^{+++}, Co^{++}, Ni^{++}, Cu^{++}, Zn^{++}, and Cd^{++} with absorbance in 2.36 M acetic acid at 5° C. The curves are linear in most cases. The precision of these measurements is not sufficient to show the slight curvature that would be present if equation [7] were valid.

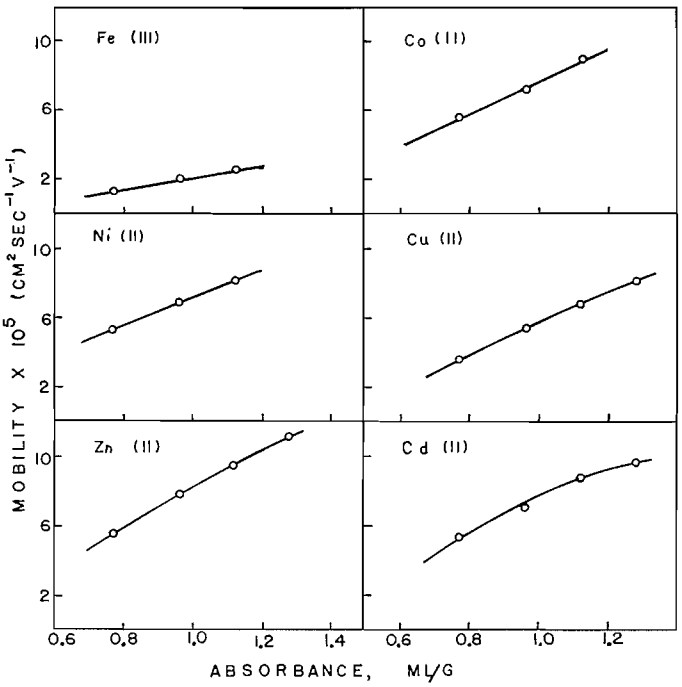

FIG. 1. Zone mobility vs. absorbance for several positive ions in 2.36 M acetic acid. Whatman No. 52 paper; 5±1° C.

Results for Cs^+ at 25° C in a variety of background electrolyte solutions are given in Fig. 2. They show the same nearly linear form as do the previous examples. In Fig. 3 the apparent obstructive factor is compared with the obstructive factor calculated from equation [7] using the values of X that give the best over-all fit for the experimental data. The calculated and experimental curves agree very well in most instances.

It is of interest to consider ρ_{app}, i.e. zone mobility/free solution mobility, as a function of concentration of background electrolyte at fixed absorbance. This is given for a number of ions in acetic acid and ammonium hydroxide in Tables I and II. The zone mobility is plotted as a function of concentration for Cs^+ in acetic acid, in Fig. 4, and is typical of all examples investigated. At acetic acid concentrations above about 0.05 M, the curve of zone mobility concentration decreases. This is the sort of behavior that would be expected from ionic strength and viscosity considerations. In this region, ρ_{app} has a nearly constant value for most ions, although there seems to be a tendency

Can. J. Chem. Downloaded from www.nrcresearchpress.com by 176.9.209.113 on 09/04/12
For personal use only.

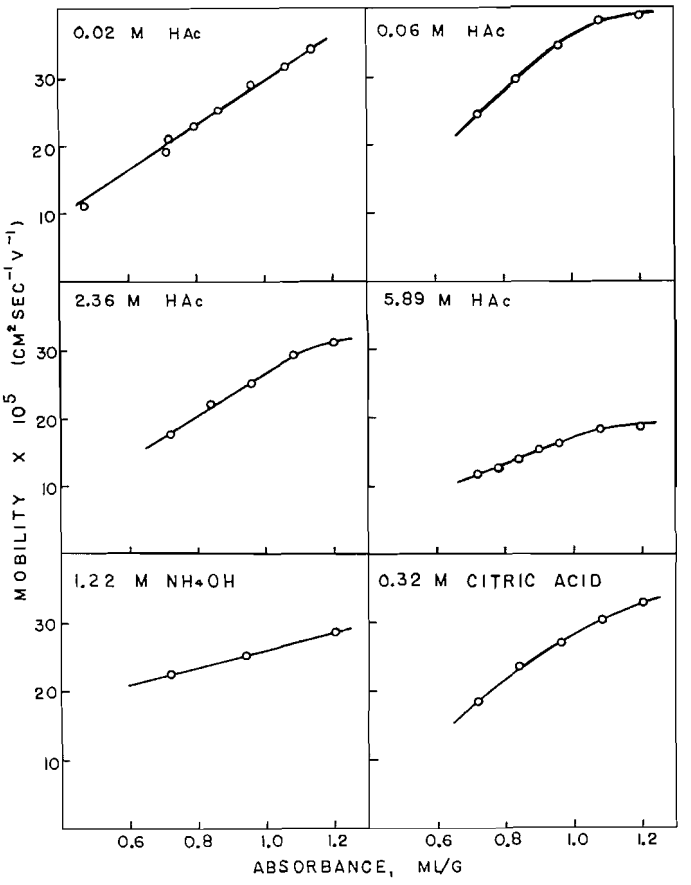

FIG. 2. Zone mobility vs. absorbance for Cs^+ in several background electrolytes. Whatman No. 52 paper; 25.0±0.5° C.

for it to fall off to some extent at higher concentrations. In the more dilute region, the zone mobility decreases quite markedly, and consequently ρ_{app} decreases also. Although this would require a corresponding increase in X if equation [7] were to be obeyed, there is no suggestion that the swelling of the cellulose fibers undergoes any particular change at this point. In fact the reduction of mobility with decreasing concentration seems to set in at a value more characteristic of the valence type of the moving ion than of the nature of the background electrolyte. The maximum zone mobility seems to occur close to 0.06 M for the univalent ions in both acetic acid and ammonium hydroxide, but at 0.5 M for the bivalent ions in acetic acid. Extensive measurements in this dilute region have been made only with Cs^+, however, and for other ions mainly the behavior at the higher concentrations is considered.

The cause of the decrease in zone mobility at low background electrolyte concentrations may be due to adsorption effects, since considerable trailing of the zones occurs, and the spots have the 'comet' shapes typical of adsorption (9). The fact that, in the more highly ionized citric acid, the decrease does not occur until a considerably lower concentration is reached indicates that the ionic strength may be important in this connection, and there are also other factors that cannot be excluded.

Can. J. Chem. Downloaded from www.nrcresearchpress.com by 176.9.209.113 on 09/04/12
For personal use only.

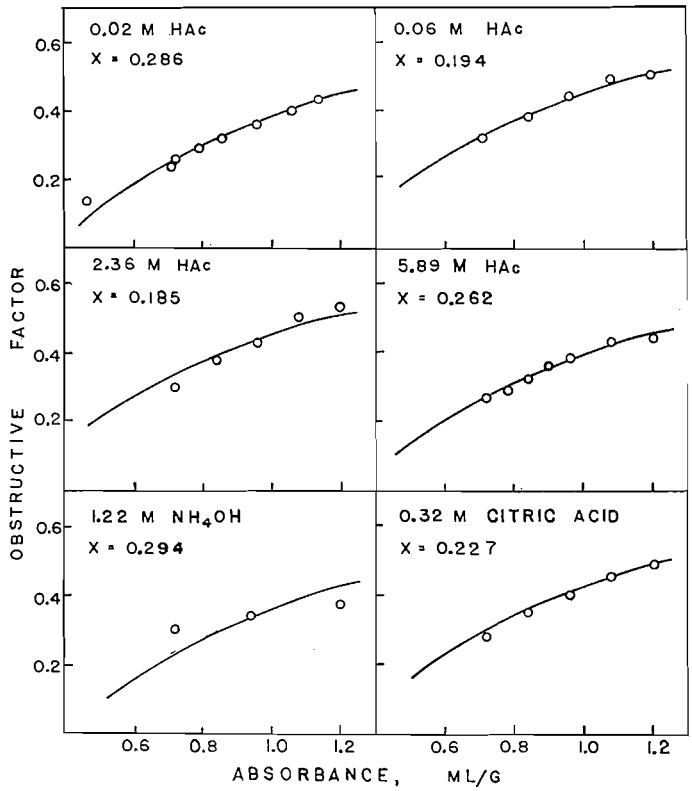

FIG. 3. Comparison of calculated and experimental (or apparent) obstructive factors as a function of absorbance for Cs^+ in several background electrolytes. The curves are calculated from equation [7] using the values of X indicated. The circles represent experimental points. Whatman No. 52 paper; 25.0±0.5° C.

Equation [7] assumes that there is no specific interaction between the migrating ion and the paper, and that consequently the obstructive factor is the same for all ions. That this is not the case is shown by the data in Tables I and II. ρ_{app} differs quite appreciably from ion to ion, and for the same ion in different background electrolytes. Evidently, since Na^+ has the largest ρ_{app}, it is the least obstructed, or hindered, of the ions studied, followed by Cs^+ and then by Tl^+. Zn^{++} and Cd^{++} are hindered somewhat more, while Cu^{++} shows the lowest ρ_{app} and is slowed to the greatest extent. It is obvious that the picture of an ion moving down a crooked channel is too simple to explain this process completely. By postulating absorption, one can explain the variation of ρ_{app} on the basis of different strengths of binding between the cellulose and the various ions. It is known that ions may travel through a portion of the swollen fiber (i.e. that the fractional increase, X, that is effective in hindering ion migration is less than the total fractional increase in volume on swelling (10, 11)). The bivalent ions seem to be more hindered than the univalent, but there are not enough examples to make any generalization between ρ_{app} and size or charge. Greater interaction with the negative acetate ions may be in part responsible for this increased hindrance.

A negative ion such as Cl^- might have different absorptive properties with respect to cellulose, but for the most part there seems to be little difference in its behavior, as shown in Table III. The mobility drops sharply in very dilute solutions, as for positive ions.

Can. J. Chem. Downloaded from www.nrcresearchpress.com by 176.9.209.113 on 09/04/12
For personal use only.

Can. J. Chem. Downloaded from www.nrcresearchpress.com by 176.9.209.113 on 09/04/12
For personal use only.

TABLE I

Zone mobilities of several positive ions in various concentrations of acetic acid

Ion	Concentration of acetic acid, moles/liter	U_z, $cm^2\ v^{-1}\ sec^{-1} \times 10^5$	ρ_{app}
Cs^+	0.01	27.8	0.35
	0.02	28.8	0.36
	0.04	31.2	0.40
	0.06	34.5	0.44
	0.59	30.9	0.43
	1.18	28.8	0.43
	2.36	25.1	0.43
	5.89	16.2	0.38
Na^+	0.06	24.8	0.49
	0.59	22.1	0.47
	1.18	20.7	0.48
	2.36	18.1	0.48
	5.89	13.4	0.49
Tl^+	0.06	27.0	0.36
	0.59	25.4	0.36
	2.36	21.1	0.37
	5.89	13.4	0.32
Cu^{++}	0.06	10.2	0.18
	0.59	10.4	0.20
	1.18	11.0	0.22
	2.36	9.0	0.21
	3.40	7.2	0.19
	5.89	5.1	0.17
Zn^{++}	0.06	15.7	0.30
	0.59	15.8	0.33
	1.18	16.1	0.35
	2.36	12.6	0.32
	3.40	10.7	0.31
	5.89	7.7	0.27
Cd^{++}	0.06	14.9	0.30
	0.59	15.3	0.33
	1.18	15.1	0.36
	2.36	11.6	0.32
	3.40	9.4	0.29
	5.89	6.9	0.26

NOTE: Absorbance, 0.96 ml/g, Whatman No. 52 paper, 25.0±0.5° C.

TABLE II

Zone mobilities of some positive ions in various concentrations of ammonium hydroxide

Ion	Concentration of NH_4OH, moles/liter	U_z, $cm^2\ v^{-1}\ sec^{-1} \times 10^5$	ρ_{app}
Cs^+	0.06	28.9	0.37
	0.61	26.1	0.34
	2.4	23.8	0.33
	6.1	21.5	0.33
Na^+	0.06	21.3	0.42
	0.61	19.9	0.41
	2.4	19.6	0.43
	6.1	17.9	0.43
Tl^+	0.06	15.6	0.21
	0.61	12.4	0.17
	1.22	11.8	0.16
	2.4	10.7	0.15
	6.1	9.5	0.15

NOTE: Absorbance 0.94 ml/g, Whatman No. 52 paper, 25.0±0.5° C.

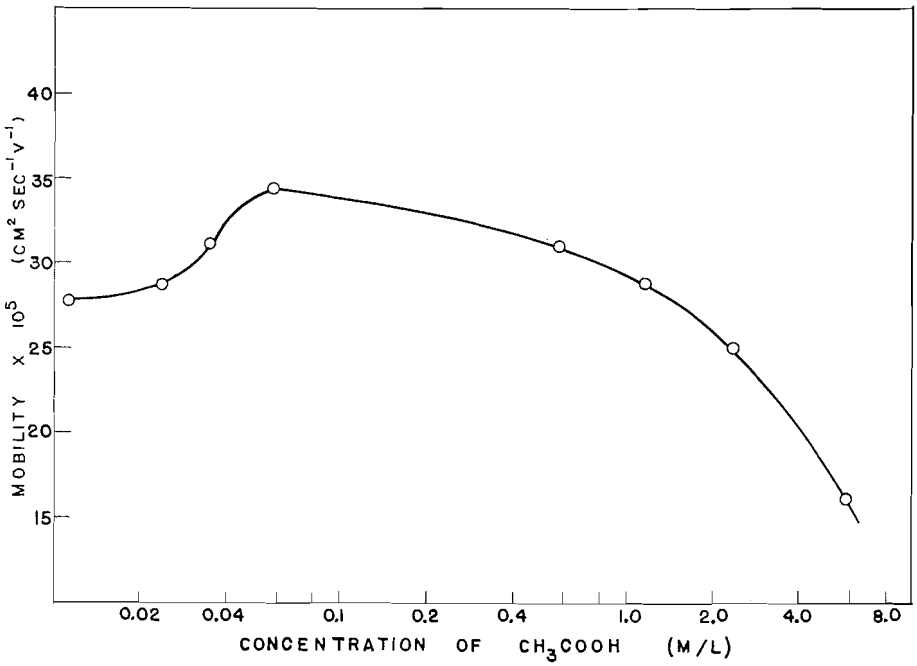

FIG. 4. Zone mobility vs. concentration for Cs^+ in acetic acid. Absorbance 0.96 ml/g; Whatman No. 52 paper; 25.0±0.5° C.

TABLE III

Zone mobility of Cl^- in varying concentrations of acetic acid and ammonium hydroxide

Background electrolyte	Concentration of background electrolyte, moles/liter	U_z, $cm^2\ v^{-1}\ sec^{-1} \times 10^5$	ρ_{app}
Acetic acid	0.02	15.2	0.20
	0.06	30.3	0.39
	0.59	26.3	0.37
	1.18	24.1	0.36
	2.36	20.1	0.35
	5.89	16.0	0.38
NH_4OH	0.6	24.8	0.33
	2.4	24.0	0.34
	6.1	22.2	0.34

NOTE: Absorbance 0.96 ml/g, Whatman No. 52 paper, 25.0±0.5° C.

Fibers such as glass do not swell in aqueous solutions, so it should be possible to apply equation [6] to electromigration in glass fiber filter paper. In Figs. 5 and 6 are shown the mobilities of Na^+ and Cl^- respectively, in such a medium with acetic acid as background electrolyte. Glass paper appears to absorb positive ions to a much greater extent than does cellulose paper. At any rate both Cs^+ and Tl^+ showed very extensive trailing, and Na^+ trailed considerably in acetic acid of less than 1 M concentration. The calculated value of ρ, assuming v_s to be 0.43 and α to be 0.96, is 0.84 for the absorbance used. In the high-concentration regions (above 1 M) U_z, calculated using this value of ρ, agrees fairly well with the experimental value, considering the errors involved in both the experimental and the calculated values.

Can. J. Chem. Downloaded from www.nrcresearchpress.com by 176.9.209.113 on 09/04/12
For personal use only.

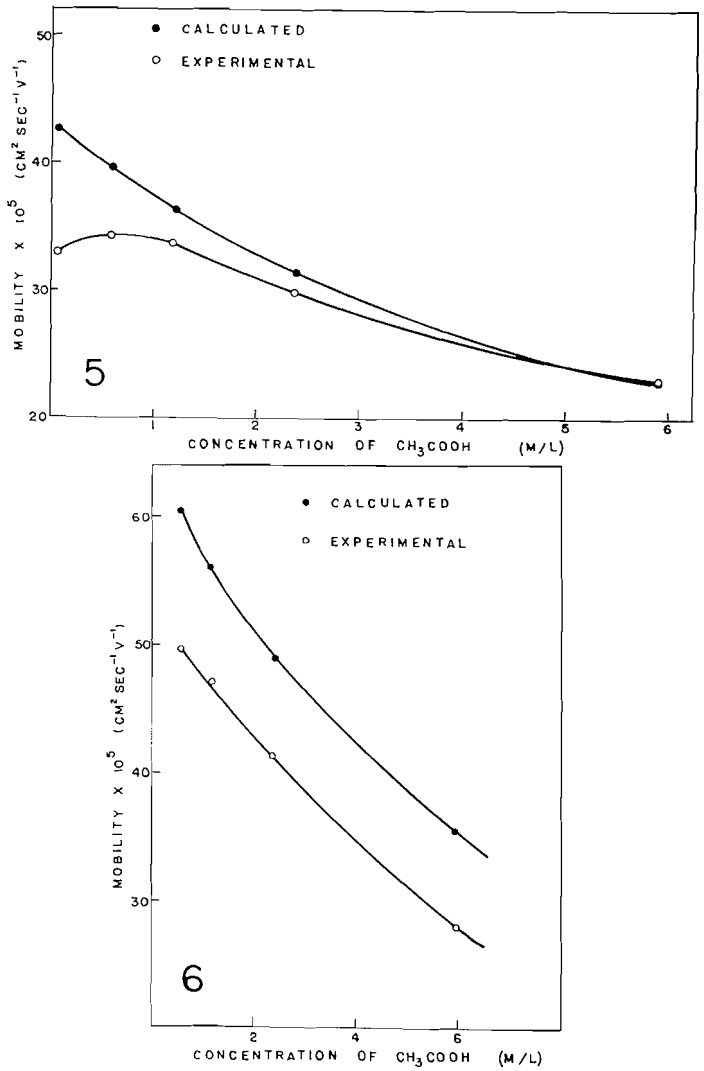

FIG. 5. Comparison of experimental zone mobilities of Na^+ in acetic acid with those calculated from equation [6]. Reeve Angel 934AH glass fiber filter paper; absorbance 3.36 ml/g; 25.0±0.5° C.

FIG. 6. Comparison of experimental zone mobilities of Cl^- in acetic acid with those calculated from equation [6]. Reeve Angel 934AH glass fiber filter paper; absorbance 3.36 ml/g; 25.0±0.5° C.

However, the data for Cl^- under the same conditions show very poor agreement between calculated and experimental results; the hindrance of Cl^- in glass is considerable compared with that for Na^+.

The results shown here indicate that specific interactions of appreciable magnitude can affect the zone mobilities of ions in both cellulose and glass papers. The equation of Crawford and Edward, relating obstructive factor to absorbance for cellulose papers, gives an approximate fit to the experimental results if the value of the swelling factor is properly chosen. In general, this factor varies for each ion and for each background electrolyte, usually falling between 0.13 and 0.45. It is apparent that these changes in X reflect factors other than swelling of the fibers. These may include adsorption of the ions and migration through the swollen volume of the fiber.

Can. J. Chem. Downloaded from www.nrcresearchpress.com by 176.9.209.113 on 09/04/12
For personal use only.

Using glass fiber paper, it is possible to calculate an idealized obstructive factor free from any uncertain swelling factor, and for Na^+ in fairly concentrated acetic acid the calculated zone mobilities agree quite well with the experimental. For Cl^-, on the other hand, they do not. Most of the ions studied so far in glass paper showed a large amount of trailing indicative of adsorption. It is clear that further work in this or in a similar non-swelling material with ions which show no adsorption is required.

REFERENCES

1. KUNKEL, H. G. and TISELIUS, A. J. Gen. Physiol. **35**, 89 (1951).
2. EDWARD, J. T. J. Chromatography, **1**, 446 (1958).
3. SCHEIDEGGER, A. E. The physics of flow in porous media. University of Toronto Press, Toronto. 1957.
4. CRAWFORD, R. and EDWARD, J. T. Anal. Chem. **29**, 1543 (1957).
5. BIEFER, G. J. and MASON, S. G. Trans. Faraday Soc. (In press).
6. WOOD, S. E. and STRAIN, H. H. Anal. Chem. **26**, 1869 (1954).
7. STRAUCH, L. and ANDREC, K. Vestnik. Sloven. kemi. društva, **3**, 127 (1956).
8. MAKI, M. Japan Analyst, **4**, 377 (1955).
9. WEBER, R. Helv. Chim. Acta, **36**, 424 (1953).
10. BIKERMAN, J. J. J. Phys. Chem. **46**, 724 (1942).
11. GORING, D. A. I. and MASON, S. G. Can. J. Research, B, **28**, 307 (1950).

Can. J. Chem. Downloaded from www.nrcresearchpress.com by 176.9.209.113 on 09/04/12
For personal use only.

Can. J. Chem. Downloaded from www.nrcresearchpress.com by 176.9.209.113 on 09/04/12
For personal use only.

THE STRUCTURE OF AN ARABOGALACTAN FROM MONTEREY PINE (PINUS RADIATA)[1]

D. J. BRASCH[2] AND J. K. N. JONES

ABSTRACT

The two major components of the water-soluble polysaccharides from Monterey pine (*Pinus radiata*) are an arabogalactan and a glucomannan. The arabogalactan contained L-arabinose and D-galactose in the ratio 1 to 8. The polysaccharide is highly branched in structure and contains end groups of L-arabofuranose and of D-galactopyranose. Removal of the L-arabinose residues leaves a highly ramified galactan.

INTRODUCTION

When wood meal which has been extracted with organic solvents is exhaustively washed with cold water a mixture of polysaccharides is readily obtained. The quantities and constituents of this mixture vary widely with the species of wood used, but usually the polysaccharides isolated are one or more of four general types: wood starches, pectic materials, arabogalactans, or glucomannans.

Starch is known to occur to the extent of 0.5% to 5% in woods and can be detected by the usual blue coloration with iodine. Care must be taken in the interpretation of this test since certain wood hemicelluloses are also stained blue with iodine (1). When starch is present it usually occurs in the sapwood, and often the starch granules can be detected microscopically. Wood starches on hydrolysis give mainly D-glucose, although a starch-like polysaccharide which apparently contained uronic acid groups has been isolated from oakwood.

The second group of polysaccharides which may occur in the cold water extracts of wood are the pectic materials. The main polysaccharide of the pectic group is a polymer of α-1 $\rightarrow$ 4-linked D-galacturonic acid units which are either fully or partly esterified and which may have attached to them residues of L-arabinose or D-galactose. Araban and galactan are frequently found associated with pectic acid.

The term arabogalactan has been given to the third group of polysaccharides occurring in the cold water extracts, especially of coniferous woods, since these polysaccharides on hydrolysis give mainly L-arabinose and D-galactose. Western larch (*Larix occidentalis*) contains up to 15% of an arabogalactan (2), European larch (*Larix decidua*) yields the so-called ϵ-galactan (3), while many other gymnosperms (4, 5, 6, 7, 8, 9, 10) contain lesser amounts of polysaccharides which are structurally similar to the arabogalactan of western larch. It is not yet clear whether or not the arabogalactans are homogeneous polysaccharides, (but see (2)).

The last of the types of polysaccharides which occurs in the aqueous extract of coniferous woods belongs to the glucomannan group. Several coniferous woods are known to yield polysaccharides of this type (11, 12, 13), but their chemistry has not yet been investigated in such detail as that of the associated arabogalactans.

When wood meal from Monterey pine (*Pinus radiata*) is extracted with water a complex mixture of polysaccharides is obtained. These can be separated, as described by Adams (10) and by Jones and Painter (11) into a polysaccharide fraction which is

[1]*Manuscript received May 4, 1959.*
Contribution from the Department of Chemistry, Queen's University, Kingston, Ontario.
[2]*Present address: Dominion Laboratory, Department of Scientific and Industrial Research, Wellington, New Zealand.*

precipitated by Fehling's solution; the glucomannan fraction; and one which is not precipitated by this reagent, the arabogalactan. This paper discusses the chemistry of the arabogalactan.

The polysaccharide was obtained as a white, water-soluble powder which on hydrolysis gave L-arabinose and D-galactose in a ratio of 1 to 8.2. All attempts to separate this polysaccharide into fractions with different properties were unsuccessful even when the polysaccharide, its acetate, or methyl ether was used.

Oxidation of the polysaccharide with sodium metaperiodate resulted in the consumption of approximately 1 mole of metaperiodate and the formation of 0.35 mole of formic acid per 162 g of polysaccharide. These figures indicate that for every sugar unit which is oxidized with the production of formic acid one other sugar residue is oxidized without the formation of formic acid, and one sugar residue is unattacked. This suggested that the polysaccharide is highly branched or that it consists of a linear polymer which contains a variety of differently linked sugars.

When the polysaccharide was hydrolyzed under mild conditions oligosaccharides were produced and two were tentatively identified as 6-*O*-β-D-galactopyranosyl- and 3-*O*-β-D-galactopyranosyl-D-galactose.

The methylated polysaccharide on hydrolysis gave a complex mixture of sugars. The following major constituents were identified: 2,3,5-tri-*O*-methyl-L-arabinose (I), 2,3,4,6-tetra-*O*-methyl-D-galactose (II), 2,4,6-tri-*O*-methyl-D-galactose (III), 2,3,4-tri-*O*-methyl-D-galactose (IV), and 2,4,-di-*O*-methyl-D-galactose (V).

The molar ratio of sugars I + II:III + IV:V was approximately 1:1:1. This proves that the polysaccharide is of the branched-chain type. When the arabogalactan was heated in dilute oxalic acid solution (14) all the L-arabinose was eliminated together with a small quantity of D-galactose and traces of other sugars. The ease of elimination of the L-arabinose indicated that it was all present in the polysaccharide in the furanoside form and probably as end group since no L-arabinose-containing oligosaccharides were isolated.

The arabinose-free polysaccharide termed "galactan" had a low positive rotation which indicated that the sugars were united by β-galactosidic linkages. The galactan was oxidized by sodium metaperiodate, approximately 1.1 moles of periodate were consumed and 0.5 mole of formic acid produced per 162 g of polysaccharide. The increase in yield of formic acid indicated that removal of the L-arabinose residues (probably from the —OH at C_3 of D-galactose) has resulted in the exposure of D-galactose residues which possess hydroxyl groups on each of three adjacent carbon atoms. These hexose residues thus become end groups or 1,6-linked D-galactose residues.

The methylated "galactan" on hydrolysis gave sugars II, III, IV, and V. The ratio of these sugars was II:III + IV:V of 1.0:1.1:1.0. The amount of 2,4,6-tri-*O*-methyl-D-galactose (III) was 10 times less than that of 2,3,4-tri-*O*-methyl-D-galactose (IV). It is evident that the formic acid produced on oxidation of the galactan by metaperiodate was derived almost equally from the end groups D-galactopyranose residues and from 1,6-linked D-galactopyranose residues.

These results do not allow the advance of a unique structure for the arabogalactan. However, it can be said that the polysaccharide is of the branched-chain type and that it resembles in structure the several other arabogalactans which have been isolated by other workers (4, 5, 6, 7, 8, 9, 10).

The structure of the glucomannan which is associated with arabogalactan will form the subject of a later communication.

Can. J. Chem. Downloaded from www.nrcresearchpress.com by 176.9.209.113 on 09/04/12
For personal use only.

Can. J. Chem. Downloaded from www.nrcresearchpress.com by 176.9.209.113 on 09/04/12
For personal use only.

EXPERIMENTAL

All melting points are uncorrected. Optical rotations were determined at 25° C and in water unless otherwise stated. All solutions were concentrated under reduced pressure and at a temperature not exceeding 40° C.

Sheet paper chromatography was carried out on Whatman No. 1 chromatographic paper by the descending method (15). The following solvent systems were used: A_1, ethyl acetate:acetic acid:formic acid:water (18:3:1:4); A_2, ethyl acetate:acetic acid:water (9:2:2); B, butan-1-ol:pyridine:water (10:3:3), and C, butan-1-ol:ethanol:water (10:3:3, all v/v). After development the sugars and derivatives were located on the chromatograms by spraying them with a 1% solution of *p*-anisidine hydrochloride in butan-1-ol (16) or with a 1% solution of silver nitrate in acetone followed by spraying with 2% ethanolic sodium hydroxide (17). The rates of movements of sugars are quoted relative to a standard sugar, e.g. R_{gal} (relative to galactose), while the movement of methyl sugars is quoted relative to tetramethyl-D-glucose (i.e. the R_g value). Infrared absorption spectra were recorded using a Perkin–Elmer Model 21 instrument in conjunction with potassium bromide pellets or 7% chloroform solution (w/v) in sodium chloride cells.

Description and Preparation of Wood Sample

The sample of Monterey pine wood used in this work was from a 25-year-old tree grown in North Island, New Zealand. The wood was received in log form, each log being about four feet long. The wood showed 2.8 to 4.2 annual growth rings per inch. It was converted into wood meal using a circular wood-working saw and air-dried to a moisture content of 9.8%. The wood (3 kg) was then extracted under reflux with ethanol (95%):benzene (2:1, v/v) for 16 hours. The residue was then extracted with ethanol (95%) under reflux for 8 hours, and dried in air.

Isolation of the Water-soluble Polysaccharide

The air-dried wood meal (500 g) was extracted with stirring, with water (10 liters) at 20° C for 16 hours. During this process toluene was added to the top of the slurry to obviate bacterial action. The wood was filtered through linen, and the process repeated using fresh water. The combined washings from 3 kg of wood were concentrated to 1 liter and centrifuged. The clear solution was then poured into ethanol (12 liters) which contained a little barium chloride and the precipitate collected. The precipitate was redissolved in water (200 ml) and reprecipitated by the addition of ethanol (800 ml). Repetition of this process (twice) gave a white product (4.3 g). Anal. ash, 2.9%; Klason lignin, 3.4%.

A sample of the product (50 mg) was hydrolyzed with 2 *N* sulphuric acid for 6 hours at 98° C. Paper chromatographic examination of the hydrolyzate (solvents A_1, A_2, and C) revealed the presence of arabinose, galactose, glucose, and mannose together with traces of xylose, rhamnose, and uronic acid.

Separation of Polysaccharides by Electrophoresis on Glass Paper

The crude polysaccharide was examined by electrophoresis on glass fiber paper (18) using both borate buffer (0.025 *N*) and sodium hydroxide (2 *N*). In one experiment at 400 v and 40 ma for 2 hours, using buffer at pH 10.7, the crude polysaccharide was separated into two distinct components. It was possible to repeat the separation, though reproducibility was not always satisfactory. In all experiments the endosmosis was considerable. Two components were also indicated by electrophoresis at 120 v, 60 ma, using sodium hydroxide (2 *N*) to dissolve the polysaccharide.

Can. J. Chem. Downloaded from www.nrcresearchpress.com by 176.9.209.113 on 09/04/12
For personal use only.

Fractionation of the Crude Polysaccharide by Copper Complex Formation

The polysaccharide (25 g) was dissolved in water (3 liters) and the solution centrifuged. Fehling's solution (100 ml) was added to the clear solution and, after 4 hours, the precipitated copper salts were collected. The top clear solution was dialyzed and, when the solution was free from copper salts, it was concentrated to 1 liter and Fehling's solution again added. The precipitated copper complex was collected and the top clear solution dialyzed until it was free from salts. The solution was concentrated and poured into alcohol and the precipitated polysaccharide (11.2 g), an *arabogalactan*, was collected. The combined precipitated copper complexes were washed with water and decomposed by maceration for 1 minute with ice-cold ethanol which contained concentrated hydrochloric acid (1% v/v). The residue was washed with ethanol and then redissolved in water. It was purified via its copper complex twice more and finally isolated as a white powder (10.7 g), a *glucomannan*.

Characterization of the Sugars from the Arabogalactan

The polysaccharide (0.30 g) was hydrolyzed for 6 hours with N hydrochloric acid at 100° C. The sugar mixture was isolated and separated chromatographically. L-Arabinose, $[\alpha]_D$ +96° (c, 2.0), was characterized as its diphenylhydrazone, m.p. 201° C, not depressed in admixture with an authentic specimen, and D-galactose, $[\alpha]_D$ +78° (c, 0.5), was characterized as its N-methyl-N-phenyl hydrazone, m.p. and mixed m.p. 190° C. The ratio of sugars, determined chromatographically (19), was found to be 1:8.2 (mean value). (Attempts to separate an araban from the arabogalactan by extracting the solid with 70% ethanol (v/v) were unsuccessful.)

Acetylation of Arabogalactan

The arabogalactan (0.20 g) was dissolved in formamide (10 ml), pyridine (10 ml) was then added followed by acetic anhydride (20 ml), which was added in 10 portions of 2 ml over a 2-hour period. After 16 hours the solution was poured on to ice and the precipitate collected. The dried product was reacetylated as described above and yielded arabogalactan acetate, $[\alpha]_D$ −5° (c, 1.2 in chloroform), which was readily soluble in dioxane, chloroform, and acetone. All attempts to fractionate this material were unsuccessful.

Periodate Oxidation of the Arabogalactan

A sample of arabogalactan was deionized by passing its solution in water through columns of Amberlite Resin IR-120 (H form) and Duolite A-4 Resin (OH form), and the polysaccharide was isolated.

Duplicate samples (approximately 50 mg each) were dissolved in water. Sodium metaperiodate solution (3 ml, 0.3 M) was added and the solution was made up to 100 ml. Oxidations were carried out at 23° C with the exclusion of light. At intervals aliquots (5 ml) were withdrawn and the amounts of metaperiodate consumed and formic acid liberated were determined. Found: moles of metaperiodate consumed and formic acid produced per mole of anhydro hexose: 0.52, 0.20 (3 hours); 0.91, 0.36 (8 hours); 1.04, 0.39 (20 hours); 1.10, 0.43 (44 hours); 1.19, 0.51 (68 hours).

Methylation of the Arabogalactan Acetate

Acetylated arabogalactan (6.9 g) was dissolved in acetone (500 ml) and methylated by the dropwise addition of sodium hydroxide (30% v/v; 150 ml) and dimethyl sulphate (50 ml) in the usual way. The resulting partially methylated polysaccharide (5.5 g) was remethylated as described above. After eight such treatments examination of the product in the infrared indicated that the amount of free hydroxyl groups had become small and constant. The product was therefore methylated by the procedure of Kuhn *et al.*

(20) and a practically completely methylated product was isolated. The pale yellow solid (3.9 g) had $[\alpha]_D$ −57° (*c*, 4.5 in chloroform) and $[\alpha]_D$ −37° (*c*, 3.9 in acetone). The infrared spectrum showed a very low concentration of hydroxyl (band at 3500–3600 cm^{-1}). Attempts to fractionate the methylated product by solution in chloroform – light petroleum (b.p. 60–80° C) were unsuccessful. Practically all the material dissolved when a ratio of chloroform – light petroleum of 3:1 (v/v) was reached.

Hydrolysis of the Methylated Arabogalactan

The methylated galactoaraban (2.5 g) was dissolved in formic acid (50% v/v) and heated at 97° C until no further change in optical rotation occurred (6 hours). The water was distilled off and the residual formic acid was removed by three codistillations with water. The hydrolysis was completed by dissolving the syrup in sulphuric acid (2 *N*) and heating the solution at 90° C for 4 hours. The cooled solution was neutralized ($BaCO_3$), centrifuged, and the clear solution concentrated with the addition of 1 drop of acetic acid. The syrup (2.1 g) had $[\alpha]_D$ +55° (*c*, 3.1 in methanol) and contained at least five components (paper chromatography).

Separation of the Methylated Sugars

A portion (1.7 g) of the mixture of methylated sugars was separated by partition chromatography on a column of powdered cellulose (21) using butan-1-ol and light petroleum (b.p. 100–120° C) (3:7) as eluent. The solvent mixture was later changed to a 1:1 ratio, followed by pure butan-1-ol and then by water. The following seven fractions were collected and their components identified.

Fraction 1. The first fraction (141 mg) was chromatographically identical with 2,3,5-tri-*O*-methyl-L-arabinose in solvents A and B. A portion (0.12 g) of the syrup was oxidized with bromine water and converted to 2,3,5-tri-*O*-methyl-L-arabonic acid which was characterized as its derived amide. The product had m.p. 134–135° C, not depressed on admixture with an authentic specimen, and $[\alpha]_D$ +20° (*c*, 2.0).

Fraction 2. This fraction (155 mg) was a mixture of 2,3,5-tri-*O*-methyl-L-arabinose and 2,3,4,6-tetra-*O*-methyl-D-galactose (which could be separated paper chromatographically) (solvents A_1, B, and C). The ratio of sugars was judged to be approximately 2:1 from chromatographic evidence. It was not further examined.

Fraction 3. Fraction 3 (133 mg) behaved in solvents A and B like 2,3,4,6-tetra-*O*-methyl-D-galactose. It had $[\alpha]_D$ +102° (*c*, 1.5) but did not crystallize. When a portion of the syrup (0.1 g) was heated with ethanolic aniline for 3 hours 2,3,4,6-tetra-*O*-methyl-*N*-phenyl-D-galactosylamine crystallized, it had m.p. and mixed m.p. 196° C and $[\alpha]_D$ −80° (*c*, 2.0 in acetone). No other sugar could be identified in this fraction.

Fraction 4. This fraction (30 mg) crystallized. The crystals possessed properties which were indistinguishable from those of 2,4,6-tri-*O*-methyl-D-galactose, m.p. 99–100° C, $[\alpha]_D$ +85° (*c*, 1.1). On heating its solution in ethanol with aniline, needlelike crystals of 2,4,6-tri-*O*-methyl-*N*-phenyl-D-galactosylamine separated, m.p. and mixed m.p. 178° C.

Fraction 5. This fraction (208 mg) consisted of two components which moved at the same rate as 2,3,4- and 2,4,6-tri-*O*-methyl-D-galactose. The syrup was heated with ethanolic aniline for 8 hours and the solvent then removed. The residue on recrystallization from ethanol yielded a mixture of needle- and plate-like crystals, the latter predominating. The two products were separated by hand picking. The needlelike crystals were identical with 2,4,6-tri-*O*-methyl-*N*-phenyl-D-galactosylamine, m.p. 175° C. The plates were not distinguishable from 2,3,4-tri-*O*-methyl-*N*-phenyl-D-galactosylamine, m.p. 162–164° C not depressed on admixture with an authentic specimen. No other derivative was isolated.

Can. J. Chem. Downloaded from www.nrcresearchpress.com by 176.9.209.113 on 09/04/12
For personal use only.

Fraction 6. Fraction 6 (315 mg) contained one component only. This sugar was indistinguishable from 2,3,4-tri-*O*-methyl-D-galactose on paper chromatograms (solvents A and B). With ethanolic aniline it yielded 2,3,4-tri-*O*-methyl-*N*-phenyl-D-galactosylamine, m.p. and mixed m.p. 166–168° C, $[\alpha]_D$ −60° → +40° (equil.) (*c*, 1.3 in methanol).

Fraction 7. The last fraction (521 mg) crystallized. Recrystallization from acetone – light petroleum yielded 2,4-di-*O*-methyl-D-galactose, monohydrate, m.p. 98–100°, $[\alpha]_D$ 119° → 85° (24 hours) (*c*, 2.0). When the sugar was heated with ethanolic aniline it gave the derived *N*-phenyl-galactosylamine, m.p. 218°–220° C, $[\alpha]_D$ −180° (*c*, 1.0 in pyridine).

The molar ratios of the sugars were determined by the method of Hirst and Jones (19). Found: total end group in molar ratios (0.97), tri-*O*-methyl fraction (1.0), di-*O*-methyl fraction (1.0).

Partial Hydrolysis of the Arabogalactan

The arabogalactan (0.10 g) was hydrolyzed for 1 hour at 95° C with sulphuric acid (0.1 *N*). Chromatographic analysis of the neutralized solution revealed the presence of substantial amounts of galactose and arabinose plus minor amounts of three oligosaccharides with (*a*) R_{gal} 0.34 (solvent A_1) and 0.42 (solvent A_2), (*b*) R_{gal} 0.20 (solvent A_1) and 0.26 (solvent A_2), and (*c*) R_{gal} 0.13 (solvent A_1) and 0.14 (solvent A_2). The oligosaccharide (*a*) and (*b*) moved at rates very similar to those of galactobiose (1,6-β-linked) and galactobiose (1,3-β-linked). In a second experiment arabogalactan (4.98 g) was dissolved in oxalic acid solution (0.026 *N*, 200 ml) and heated at 95° C for 5 hours. The cooled solution was neutralized ($CaCO_3$), centrifuged, the clear solution concentrated, and the concentrate poured into ethanol. The precipitated degraded polysaccharide was collected, washed with ethanol, dissolved in water, and reprecipitated in ethanol, yield 3.49 g. The supernatant solutions were concentrated and the syrupy concentrate (1.19 g) was examined chromatographically (solvents A_1, A_2, and C). The major component of the syrup was arabinose; associated with it were significant quantities of galactose and trace quantities of xylose and rhamnose. The ratio of arabinose to galactose was 2 to 1.

The degraded polysaccharide, henceforth termed *galactan*, on hydrolysis yielded D-galactose only (paper chromatography).

The galactan had $[\alpha]_D$ +13° (*c*, 3.5) and contained 0.9% ash and 0.3% Klason lignin. Attempted fractionation of the galactan by (*a*) ethanol precipitation from neutral or acidic aqueous solution, (*b*) by copper complex formation, and (*c*) by glass paper electrophoresis was unsuccessful.

Periodate Oxidation of the Galactan

The galactan (ash-free) was oxidized with sodium metaperiodate solution as described for the oxidation of the arabogalactan. Found: moles of metaperiodate consumed and moles of formic acid produced per anhydrohexose residue: 1.17, 0.60 (8 hours); 1.35, 0.80 (25 hours); 1.61, 1.12 (48 hours); 1.95, 1.45 (72 hours). Extensive over-oxidation had occurred.

Methylation of the Galactan

Prior to methylation the galactan was reduced with sodium borohydride. The galactan (2.97 g) was dissolved in water (50 ml), and a solution of sodium borohydride (25 mg) in water (10 ml) was added. After 4 hours acetic acid (1 ml) was added and the reduced polysaccharide was methylated by adding dropwise to its solution sodium hydroxide (300 ml, 30%) and dimethyl sulphate (100 ml) during 5 hours. After 16 hours the partially methylated product (2.71 g) was isolated and the methylation procedure was repeated. The product was then methylated (twice) by the Kuhn procedure (20) in dimethyl-

Can. J. Chem. Downloaded from www.nrcresearchpress.com by 176.9.209.113 on 09/04/12
For personal use only.

formamide. The resultant methylated polysaccharide (2.1 g) was a crisp pale yellow solid. Anal. Found: OMe, 45.3%. The product had $[\alpha]_D$ −49° (*c*, 5.3 in chloroform) and −29° (*c*, 4.9 in methanol). Infrared examination of the solid indicated that it contained very little free hydroxyl.

An attempt was made to fractionate the methylated polysaccharide by dissolution in a series of mixtures of boiling *n*-hexane and chloroform in the usual way. Almost all of the material (1.58 g) was soluble in the solvent when the ratio of *n*-hexane to chloroform was 4:1 (v/v).

Fission of the Methylated Galactan

The methylated galactan (1.4 g) was dissolved in formic acid (90% v/v) and the solution was heated at 95° C for 6 hours. The solution was evaporated to dryness and formic acid removed by three codistillations with water. The hydrolysis was then continued by heating the syrup in *N* sulphuric acid for 5 hours at 95° C. The mixture was cooled, neutralized ($BaCO_3$), and centrifuged. The top clear solution was acidified (acetic acid) and evaporated to a syrup, (1.2 g), $[\alpha]_D$ +65° (*c*, 2.0 in methanol).

Isolation of the Methylated Sugars

Paper chromatographic examination of a portion (1 g) of the syrup indicated the presence of at least four methylated sugars. These were separated on a column of cellulose using the procedure described above.

Fraction 1. The first component (0.34 g) eluted from the column behaved chromatographically like 2,3,4,6-tetra-*O*-methyl-D-galactose (solvents A_1 and B) and had $[\alpha]_D$ +112° (*c*, 1.4). A sample when heated with ethanolic aniline yielded 2,3,4,6-tetra-*O*-methyl-*N*-phenyl-D-galactosylamine, m.p. 195–197° C, not depressed on admixture with an authentic specimen.

Fraction 2. The second fraction (0.03 g) was identified chromatographically as 2,4,6-tri-*O*-methyl-D-galactose (solvents A_1 and B) and was characterized as the *N*-phenyl-D-galactosylamine derivative, m.p. and mixed m.p. 179° C.

Fraction 3. This fraction (0.08 g) was a mixture of two methyl sugars. The slower moving and major component moved at the same rate as 2,3,4-tri-*O*-methyl-D-galactose. It gave a characteristic brown color with the *p*-anisidine hydrochloride spray, while the faster moving component gave a pink color and was indistinguishable from the 2,4,6-tri-*O*-methyl isomer. The mixed sugars were converted into the mixed crystalline *N*-phenyl-D-galactosylamines which were separated by hand.

Fraction 4. Fraction 4 (0.15 g) was homogeneous and identical with 2,3,4-*O*-trimethyl-D-galactose. Treatment with ethanolic aniline yielded the corresponding D-galactosylamine derivative, m.p. and mixed m.p. 167–169° C, $[\alpha]_D$ −65° → 45° (5 hours) *c*, 1.1) in methanol.

Fraction 5. This fraction (0.27 g) crystallized and was identified as 2,4-di-*O*-methyl-D-galactose monohydrate, m.p. and mixed m.p. 100° C, $[\alpha]_D$ 116° (5 minutes, *c*, 1.7). When it was heated with ethanolic aniline 2,4-di-*O*-methyl-*N*-phenyl-D-galactosylamine, m.p. and mixed m.p. 216° C was obtained.

Fraction 6. The last fraction (0.005 g) was eluted from the column with water. It represented 0.5% of the original hydrolyzate and was probably a monomethyl galactose.

Estimation of Molar Ratios of the Methylated Sugars

The molar ratios of the methylated sugars in the hydrolyzate were determined by the method of Hirst, Hough, and Jones (19). Anal. Found: ratio of 2,3,4,6-tetra-, to tri-,

Can. J. Chem. Downloaded from www.nrcresearchpress.com by 176.9.209.113 on 09/04/12
For personal use only.

to 2,4-di-*O*-methyl-D-galactose: 1.0:1.1:1.0. The ratio of 2,4,6-tri-*O*-methyl- to 2,3,4-tri-*O*-methyl-D-galactose was 1 to 10 as determined from the weight of fractions isolated from the cellulose column.

ACKNOWLEDGMENTS

The authors thank the National Research Council for a grant. They gratefully acknowledge the award of a scholarship by Canadian Industries Limited to one of them (D.J.B.). They also thank Dr. L. E. Wise and The Institute of Paper Chemistry, Appleton, Wisconsin, U.S.A., for the supply of sawdust.

REFERENCES

1. CAMPBELL, W. G. Biochem. J. **29**, 1068 (1935).
2. BOUVENG, H. O. and LINDBERG, B. Acta Chem. Scand. **12**, 1977 (1958).
3. PETERSON, F. C., MAUGHAN, M., and WISE, L. E. Cellulosechemie, **15**, 109 (1934).
4. WISE, L. E., HAMER, P. L., and PETERSON, F. C. Ind. Eng. Chem. **25**, 184 (1933).
5. NIKITIN, N. I. and SOLOVIEV, I. A. J. Appl. Chem. (U.S.S.R.), **8**, 1016 (1935); Chem. Abstr. **30**, 5563 (1936).
6. ITO, T. Cellulose Ind. **13**, 4 (1937); Chem. Abstr. **31**, 6872 (1937).
7. SCHORGER, A. W. and SMITH, D. F. J. Ind. Eng. Chem. **8**, 494 (1916).
8. BRAUNS, F. E. Science, **102**, 155 (1945).
9. BISHOP, C. T. Can. J. Chem. **35**, 1010 (1957).
10. ADAMS, G. A. Can. J. Chem. **36**, 755 (1958).
11. JONES, J. K. N. and PAINTER, T. J. Chem. Soc. 573 (1959).
12. SMITH, F. Paper presented at 128th Meeting of the American Chemical Society, Minneapolis, Minn. Sept. 1955.
13. DUTTON, G. S. and HUNT, K. J. Am. Chem. Soc. **80**, 5697 (1958).
14. BYWATER, R. A. S., HAWORTH, W. N., HIRST, E. L., and PEAT, S. J. Chem. Soc. 1983 (1937).
15. PARTRIDGE, S. M. Biochem. J. **42**, 238 (1948).
16. HOUGH, L., JONES, J. K. N., and WADMAN, W. H. J. Chem. Soc. 1702 (1950).
17. TREVELYAN, W. E., PROCTOR, D. D., and HARRISON, J. S. Nature, **166**, 444 (1950).
18. SMITH, F. and LEWIS, B. A. J. Am. Chem. Soc. **79**, 3929 (1957).
19. HOUGH, L., HIRST, E. L., and JONES, J. K. N. J. Chem. Soc. 928 (1949).
20. KUHN, R., TRISCHMANN, H., and LÖW, I. Angew. Chem. **67**, 32 (1955).
21. HOUGH, L., JONES, J. K. N., and WADMAN, W. H. J. Chem. Soc. 528 (1949).

Can. J. Chem. Downloaded from www.nrcresearchpress.com by 176.9.209.113 on 09/04/12
For personal use only.

Can. J. Chem. Downloaded from www.nrcresearchpress.com by 176.9.209.113 on 09/04/12
For personal use only.

THE PHOTOOXIDATION OF AZOMETHANE. III[1]

F. WENGER[2] AND K. O. KUTSCHKE

ABSTRACT

It is confirmed that the yields of all products in the photooxidation of azomethane at relatively high oxygen pressure depend on conversion in a manner which would be explained if a reactive hydrogen donor were produced in the early stages of the reaction. Evidence is presented which indicates that formaldehyde cannot be active as an inhibitor in the system at 162° C. It is suggested that methyl radicals react with oxygen in two ways. The third order formation of methyl peroxy radicals leads to methoxy radicals and, eventually, to methanol, while the bimolecular reaction between methyl radicals and oxygen leads to a vibrationally excited state of formaldehyde. The latter is thought to undergo oxidization to performic acid, which acts as the inhibitor in the system. Yields of formaldehyde, of nitrogen in excess of that formed in the primary process, and of nitrous oxide are linearly related regardless of the conversion up to about 4%. Methanol is a major product of the oxidation and, if account is taken of its yield, a carbon balance of the order of 90% is obtained.

INTRODUCTION

In view of the convenience of azomethane as a photochemical source of methyl radicals, this compound has been used in the past for studies of the reaction of methyl radicals with oxygen (1, 2, 3). While it was possible to obtain an approximate value for the rate constant of this association reaction (1), assuming it to be bimolecular (see (3) and (4) for a discussion of this point), many of the features of the over-all photooxidation remained unsettled. This was particularly true with respect to the dependence of the rates of formation of most of the products on the extent of conversion.

Earlier work was hampered by the lack of reliable techniques for formaldehyde detection (1) and measurement (2). The present report describes the techniques for measurement of formaldehyde and methanol yields. Experimental conditions have been limited to the region of high oxygen pressure where methane and ethane are absent (1), an observation which was confirmed in the present study. The absence of methane renders highly improbable the participation of "hot" methyl radicals such as have been postulated from other methyl radical sources (5). Data have been obtained at 121° and 161° C. The lower limit was chosen to ensure that formaldehyde would not polymerize in the system, while the upper limit was dictated by the appreciable rate of a thermal reaction at temperatures slightly above it.

EXPERIMENTAL

Apparatus

The apparatus was basically the same as used in an earlier investigation (2). Improvements in the thermostatted air bath housing the cell lowered local temperature differences from point to point within the oven to 1° C. The volume of the reaction system—U-tube, reaction cell, and circulating pump—was 255 cm^3; that of the cell itself, 180 cm^3. Some changes were made in the analytical system to permit the use of the modified procedures for liquid product analysis described below. Actinic light, mainly of 3660 Å, was obtained from a Hanovia S-500 mercury arc and a Corning 5860 filter (6).

Materials

Azomethane was obtained from Merck of Canada (Montreal). After several bulb-to-bulb distillations a middle fraction was stored at room temperature in a blackened bulb

[1]*Manuscript received May 8, 1959.*
Contribution from the Division of Pure Chemistry, National Research Council, Ottawa, Canada.
Issued as N.R.C. No. 5295.
[2]*National Research Council Postdoctorate Fellow 1955–57. Present address: Mellon Institute, 4400 Fifth Avenue, Pittsburgh 13, Pa., U.S.A.*

behind a mercury cutoff. Oxygen was prepared by heating potassium permanganate and purified by passage through a trap at −196° C. Formaldehyde-O^{18} was obtained as paraformaldehyde from Dr. L. C. Leitch of these laboratories; it had been prepared by exchange of the polymer with enriched water under reflux. Heating of the polymer liberated the monomer, which was freed of residual water by distillation from −78° to −196° C. Mass spectrometric analysis indicated an O^{18} content of 2.4%, although the water used in the exchange was more highly enriched. It is thought that only the surface layers of the polymer had been exchanged by the treatment used.

The trisodium salt of chromotropic acid (4,5-dihydroxy-2,7-naphthalene disulphonic acid, trisodium salt) used in formaldehyde and methanol analyses was prepared by titration of an aqueous solution of Eastman Kodak chromotropic acid, disodium salt. On adding ethanol a white, crystalline material separated, which was filtered and dried. This crude material soon turned violet when left to stand. The substances causing the colored oxidation products—impurities and probably the quarternary salt of the acid—were less soluble in ethanol–water mixtures and were removed by fractional precipitation. Material prepared in this manner was stored for months in the dark with no change in its analytical behavior.

Photooxidation Procedure

Azomethane was outgassed in the storage bulb prior to each run; the required pressure, as measured on a manometer at room temperature, was built up in the hot cell; and the contents of the reaction system were condensed at −196° C in the U-tube. Oxygen was admitted to the reaction system to the required pressure and measured on a McLeod gauge external to the oven. The volume of the cold U-tube was small relative to that of the whole reaction system so that negligible error was introduced by measuring oxygen pressure with the U-tube at −196° C. After the valve leading to the storage and measuring manifold was closed, the U-tube was heated to the cell temperature and the gases mixed by means of the circulating stirrer.

Considerable care was taken in the experiment with added formaldehyde to ensure that the results would not be uncertain due to polymerization of that material. An accurately known amount of formaldehyde was introduced as follows. Two bulbs of known volume ratio and equipped with breakoff points were connected via stopcocks to a manifold containing formaldehyde vapor at approximately the required pressure. After time was allowed for pressure equilibration, the stopcocks were closed, the formaldehyde condensed at −196° C, the bulbs detached from the stopcocks at a sealoff point, and the contents of one bulb analyzed by the chromotropic acid procedure (see below). From the known volume ratio, the quantity in the second bulb could be calculated. This second bulb was sealed to the reaction system in the oven, and azomethane was introduced as usual and stored temporarily outside the oven in a trap on the analytical system. The breakoff was broken, the monomeric formaldehyde condensed in the U-tube at −196° C, and the formaldehyde introduction bulb sealed from the system. Azomethane was returned to the cold U-tube, oxygen introduced as usual, and the gases mixed.

Analysis of Products

(*a*) *Gaseous Products*

After photolysis the contents of the reaction system were condensed in a trap at −196° C and the non-condensable gases (N_2, CO, and O_2) were transferred to a gas burette, measured, and analyzed over copper – copper oxide at 250° C with a contact time of 2 hours as described earlier (1, 2). The contents of the trap were allowed to warm to room

Can. J. Chem. Downloaded from www.nrcresearchpress.com by 176.9.209.113 on 09/04/12
For personal use only.

temperature in a volume of connecting tubing defined by the valve leading to the reaction system and a stopcock near the trap, and were recondensed and warmed three times thus polymerizing the bulk of the formaldehyde (2). Unpolymerized material was transferred to a LeRoy still (7) held at −196° C. Nitrous oxide, carbon dioxide, unpolymerized formaldehyde, and some of the azomethane were transferred at −130° C from this still to a second at −196° C. By heating the second still to −160° C, nitrous oxide and carbon dioxide were transferred to the gas burette, measured, and submitted for mass spectrometric examination. By following this procedure in detail less than 1% formaldehyde impurity was found in the carbon dioxide – nitrous oxide fraction.

(*b*) *Formaldehyde*

A method based on the chromotropic acid procedure (8) was used. Formaldehyde and any azomethane from the second LeRoy still, along with the formaldehyde from the U-tube (depolymerized by heating), were condensed with liquid nitrogen on top of 4 ml of a frozen aqueous solution containing 150 mg of the trisodium salt of chromotropic acid contained in a small pear-shaped reaction flask. The flask was removed from the vacuum system at a ground joint, warmed to room temperature, and mixed well. Azomethane was removed by bubbling a stream of water-saturated nitrogen through the solution. Blank experiments showed that this procedure removed completely the excess azomethane and retained formaldehyde quantitatively. The solution was acidified with 12 ml concentrated H_2SO_4, heated in boiling water for 30 minutes, and cooled. After dilution the extinction at 570 mμ was measured on a Beckmann DU spectrophotometer and the amount of formaldehyde determined from a calibration curve. For samples expected to contain more than 200 γ formaldehyde proportionally larger quantities of reagents were used.

(*c*) *Methanol*

Products remaining in the first LeRoy still (mainly methanol, water, and the bulk of the unreacted azomethane) were distilled to a reaction flask containing 4 ml distilled water. Azomethane was removed on a stream of nitrogen as before; 400 mg chromotropic acid, disodium salt, and 0.5 ml concentrated H_2SO_4 were added and a 3-ml fraction, containing all the methanol (as shown by calibration experiments), was transferred by distillation to a second reaction flask. Methanol was oxidized by potassium permanganate and the resulting formaldehyde determined with chromotropic acid as described above (9). A set of similarly treated methanol standards was used to construct the calibration curve of extinction vs. amount of methanol.

Since the yield in the oxidation step of this procedure is small (~10%) small amounts of formaldehyde, present in this liquid product fraction or produced by hydrolysis of azomethane or other products of the photooxidation, if carried over in the distillation step will yield high values for the amount of methanol. In using the method of Bricker and Vail (10) to separate synthetic methanol – formaldehyde mixtures, formaldehyde was always found in the methanol fraction. This could be prevented by heating the solution to 100° C for a half an hour prior to distillation or by maintaining a low pH during the distillation as was outlined above. This latter method was adopted because the liquid products from the first LeRoy still appeared to contain small amounts of unidentified compounds, presumably products of the addition of radicals to azomethane. These compounds were not removed by the stream of nitrogen. Moreover, they did not react with the chromotropic acid salt (as would free formaldehyde if present) so that they appeared in the methanol distillate where they were hydrolyzed to formaldehyde during subsequent acid treatment causing high methanol yields. The addition of sulphuric acid prior to distillation yielded a distillate free of formaldehyde and hydrolyzable substances.

Can. J. Chem. Downloaded from www.nrcresearchpress.com by 176.9.209.113 on 09/04/12
For personal use only.

In some parallel experiments the methanol determination was verified by gas chromotography or, after removal of the bulk of the azomethane by distillation, by infrared analysis.

RESULTS

Analyses are given for the amounts of nitrogen, carbon monoxide, carbon dioxide, methanol, and formaldehyde formed and for oxygen disappearance. Water was detected mass spectrometrically and the rough estimate of its yield on this basis was in essential agreement with that calculated from a consideration of the hydrogen and oxygen material balances. Formic acid and acetaldehyde were detected mass spectrometrically in very small yields in the liquid product fraction. An otherwise unidentifiable peak at mass number 104 was tentatively assigned to the compound $CH_3OOCH_2N_2CH_3$. It is possible that this compound is an important intermediate in nitrogen production at low oxygen pressure.

In the early series of experiments (Table I and Fig. 1) methanol analyses were not attempted and formaldehyde yields are probably low due to adsorption or polymerization on room temperature connecting tubing; this was corrected in the later experiments by heating the tubing to about 140° C.

TABLE I

Products of azomethane photooxidation

p_{azo} = 57 mm, p_{O_2} = 8.5 mm at 0° C, Temp. = 119° C

Time (minutes)	μmoles of: N_2	CO	CO_2	N_2O	CH_2O	$-O_2$
			$I_a = 1.3\times10^{13}$, quanta/cm³ sec			
10	2.36	0.36	0.27	0.54	0.80	—
20	5.44	1.03	—	—	1.47	—
40	11.28	2.45	0.54	2.10	—	—
60	15.4	4.24	0.80	2.54	4.28	—
90	23.1	7.36	1.52	3.26	5.31	45
150	39.7	14.3	2.27	3.61	6.91	78
210	49.7	22.1	4.19	5.66	8.34	97
90	21.4			Oxygen absent		
			$I_a = 6.3\times10^{13}$, quanta/cm³ sec			
5	6.56	1.47	0.13	0.94	2.10	
11	15.6	3.97	0.54	2.19	2.77	
20	24.1	7.81	0.94	2.10	4.50	
30	35.8	12.6	1.25	2.81	6.78	
40	46.2	17.8	1.56	3.48	8.12	
20	22.5			Oxygen absent		

Table I shows the data for a set of experiments at 120° C using two different light intensities. An examination of these data shows that light intensity changes of a factor of about five have little effect on product ratios for any given degree of conversion as indicated by the amount of nitrogen and nitrous oxide found. The data for the lower intensity are plotted in Fig. 1 showing the general trend of the amounts of the various products formed with illumination time. Both the very small intensity dependence and the trend shown in Fig. 1 confirm results reported previously (2).

The data shown in Table II were taken after the improvements in the analytical system noted above had been achieved. If it is assumed that each molecule of azomethane which is decomposed leads to either a molecule of nitrogen or of nitrous oxide, then the

Can. J. Chem. Downloaded from www.nrcresearchpress.com by 176.9.209.113 on 09/04/12
For personal use only.

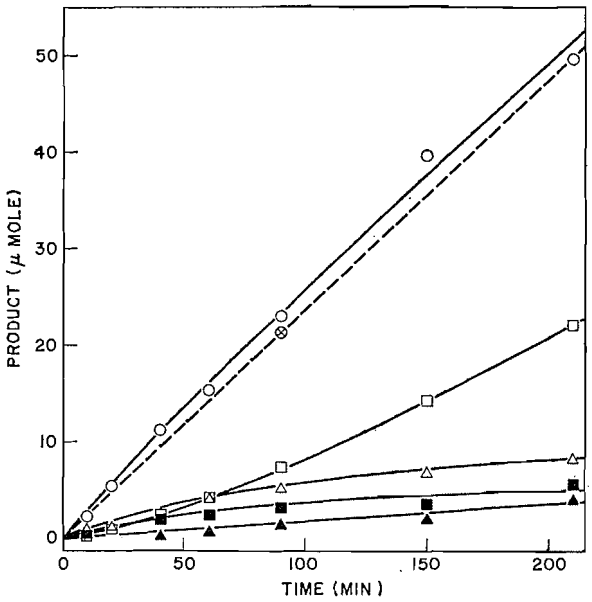

FIG. 1. Time dependence of products, 119° C. ○ N_2; ⊗ N_2, oxygen absent; □ CO; ■ N_2O; △ CH_2O; ▲ CO_2.

ratio $(n_{N_2}+n_{N_2O})/n_A$ is an approximate measure of the fractional conversion of the azomethane. Here $n_{N_2}+n_{N_2O}$ represents the total number of moles of nitrogen and nitrous oxide found and n_A represents the initial number of moles of azomethane in the reaction system (255 cm^3). This corresponds to the conversion D_1 of the earlier work (2); to obtain conversions based on the cell volume (D_2 of (2)) multiply by 1.42. By plotting the data against fractional conversion rather than time of illumination at least some compensation is achieved for the effects of small variations in light intensity from one experiment to another.

TABLE II

Products of azomethane photooxidation
p_{azo} = 57 mm, p_{O_2} = 7 mm at 0° C

Time (minutes)	μmoles of:							% of:			
	N_2	CO	CO_2	N_2O	CH_2O	CH_3OH	$-O_2$	m_C	m_H	m_O	m_I
					Temp. = 121° C; $I_a = 4.5\times10^{13}$ quanta/cm^3 sec						
5	4.24	1.56	0.09	0.71	1.47	4.55	—	77	71	—	103
9	7.58	1.56	0.13	1.12	2.23	8.34	—	70	73	—	66
15	—	—	0.58	1.92	—	—	—	—	—	—	—
20	17.1	5.35	0.80	2.41	5.93	16.7	—	74	67	—	104
30	—	—	—	—	8.16	26.4	—	—	—	—	—
40	30.6	11.19	1.69	3.30	10.39	31.4	—	80	72	—	110
20	16.0	Oxygen absent									
					Temp. = 121° C; $I_a = 3\times10^{11}$ quanta/cm^3 sec						
520	3.17	0.67	0.36	1.65	2.77	6.91	3.84	111	115	166	65
960	5.84	1.56	0.98	2.50	3.39	12.6	14.9	100	103	74	59
1500	9.46	2.54	1.78	3.79	4.37	16.2	24.4	94	93	62	69
					Temp. = 162° C; $I_a = 4.7\times10^{13}$ quanta/cm^3 sec						
5	4.77	1.16	0	2.10	3.43	7.36	7.7	87	88	91	78
10	9.05	2.94	0.71	3.39	5.40	12.3	16.4	86	80	78	98
20	16.8	7.09	1.47	4.82	7.18	22.7	—	89	81	—	101
31	25.0	11.6	2.05	6.29	9.28	34.3	42	91	83	78	101
30	21.1	Oxygen absent									

Can. J. Chem. Downloaded from www.nrcresearchpress.com by 176.9.209.113 on 09/04/12
For personal use only.

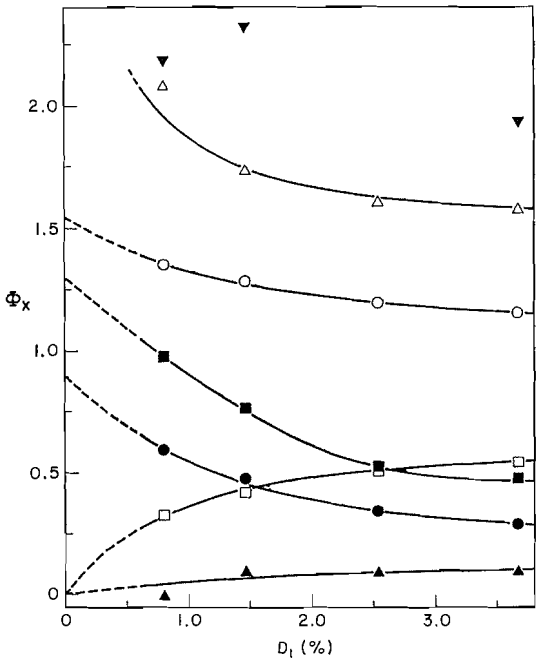

FIG. 2. Dependence of quantum yields on conversions, 162° C. ○ N_2; ● N_2O; □ CO; ■ CH_2O; △ CH_3OH; ▲ CO_2; ▼ O_2.

Figure 2 contains the data taken at 162° C (Table II) plotted as apparent quantum yields Φ_X, calculated as the ratio of the amount of product X actually found to the amount of nitrogen which would have been formed had oxygen been absent in the experiment. Extrapolations to zero conversion are arbitrary except in the case of carbon monoxide where the shape of the amount vs. time curve (similar to that of Fig. 1) strongly suggests that the quantum yield vanishes at zero conversion. The large increase in Φ_{CO} is accompanied by a decrease in Φ_{N_2O} and Φ_{CH_2O}. The actual decrease in Φ_{CH_3OH} might not be as large as indicated because the curve drawn is strongly dependent on the yield at the lowest conversion where small errors in the analytical method would be exaggerated. However, it seems quite certain that Φ_{CH_3OH} does decrease as conversion is increased.

Data for the lower temperature experiments are illustrated in Fig. 3. Instead of Φ_X the quantity ρ_X, defined as $n_X/(n_{N_2}+n_{N_2O})$, is plotted against conversion. ρ_X is a measure of the yield of the product X per molecule of azomethane decomposed. The use of ρ eliminates any assumption regarding the comparison of experiments in the presence and absence of oxygen and the possibility that such a comparison is not valid over a large range of intensity. In general the trends of ρ_X with conversion are similar to those of Φ_X except when X is N_2. ρ_{N_2} decreases at low conversion because of the increase in the relative amount of nitrous oxide, although Φ_{N_2} in fact increases in this region in a manner analogous to that shown in Fig. 2. Values of Φ_X at 120° C, read from a graph similar to that of Fig. 2 at conversions such that the yields had attained their approximately steady values, are, $\Phi_{N_2} \sim 1.0$; $\Phi_{N_2O} \sim 0.1$; $\Phi_{CO} \sim 0.4$; $\Phi_{CO_2} \sim 0.06$; $\Phi_{CH_3OH} \sim 1.0$; $\Phi_{CH_2O} \sim 0.2$. In drawing curves to obtain these values, no account was taken of the very low intensity experiments in Table II; owing to the lack of data at high conversion and low intensity it is not possible to make an estimate of limiting quantum yields for these conditions. However, it would seem definite that all Φ_X increase at low intensity. This fact, together with

Can. J. Chem. Downloaded from www.nrcresearchpress.com by 176.9.209.113 on 09/04/12
For personal use only.

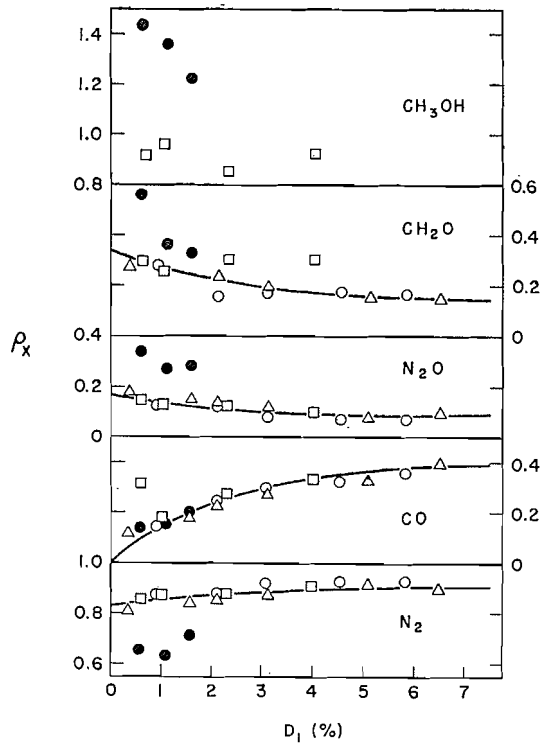

FIG. 3. Change of product ratios (ρ_x) with conversion, ~ 120° C. ○ Table I, $I_a = 6.3\times10^{13}$; □ Table II, $I_a = 4.5\times10^{13}$; △ Table I, $I_a = 1.3\times10^{13}$; ● Table II, $I_a = 2.7\times10^{11}$.

Φ_{CH_3OH} 2.5 at about 1% conversion strongly suggests that a short chain is operating which is inhibited at higher conversions and higher light intensity. Inhibition of a chain by increase in oxygen pressure is suggested by other work, but the present data are taken at an oxygen pressure such that any inhibition from this source should be fully developed.

Earlier work on this problem (1, 2) as well as other photooxidation studies has been hampered by very low product balances. Using the assumption mentioned earlier, to the effect that nitrogen and nitrous oxide found are proportional to azomethane decomposition, it is seen that carbon recovery in per cent is given by $m_C = (100/2)\Sigma\rho_X$ where the summation extends over all products containing carbon. Similarly, the hydrogen recovery is $m_H = (100/6)\,(4\rho_{CH_3OH}+2\rho_{CH_2O})$. Oxygen recovery is given by $m_O = 100(n_{CO}+2n_{CO_2}+n_{N_2O}+n_{CH_2O}+n_{CH_3OH})/2n_{O_2}$ where the n_X is the numbers of moles of products X recovered and n_{O_2} is the oxygen consumption. Values calculated on this basis are reported in Table II; the data of Table I have not been treated in this way since methanol was not determined. Rather surprisingly, methanol yields are sufficiently large to raise the carbon balance to reasonably high values. It would thus appear that no major products of the reaction have been neglected. One possibility cannot be ruled out entirely. If some high molecular weight nitrogenous compound were produced possessing a carbon to nitrogen atomic ratio less than unity, the balances cited would be too large. It is difficult to visualize the formation of such compounds in this system, however. The converse hypothesis, that high molecular weight products are formed, but that they possess a carbon–nitrogen

Can. J. Chem. Downloaded from www.nrcresearchpress.com by 176.9.209.113 on 09/04/12
For personal use only.

ratio greater than unity, is probably true and could account for $m_C < 1$. Such compounds could be formed by radical addition to the nitrogen–nitrogen double bond, a reaction of considerable importance in the absence of oxygen (1, 6).

DISCUSSION

Nitrogen, Formaldehyde, and Nitrous Oxide

Following our earlier work (1) it is considered that the primary process in the photolysis is unaffected by the presence of oxygen.

$$CH_3N_2CH_3 + h\nu \rightarrow 2CH_3 + N_2 \quad [1]$$

The strongest evidence supporting this hypothesis is data taken at low azomethane pressure, high oxygen pressure, and low temperature. It was shown (1) that for these conditions $-\Phi_{azo} = \Phi_{N_2} \sim 1$, which could hardly be true if deactivation of excited molecules were occurring. The low temperature is expected to favor deactivation if it occurred.

For other conditions values of $\Phi_{N_2} > 1$ have been observed here and in earlier work (1, 2). A similar observation has been made in the azoethane photooxidation (11). The data may be correlated empirically as is done in Fig. 4. In this plot, at 162° C, the amount of formaldehyde produced is linearly related to the amount of nitrous oxide, as is the amount of secondary nitrogen. The latter is defined as the nitrogen produced in excess of that which would have been formed had oxygen been absent in the experiment. Although curvature may be present in these plots, a linear relation represents the data adequately within experimental error. Such a correlation strongly suggests a common source for secondary nitrogen, nitrous oxide, and formaldehyde. Nitrous oxide has been considered (1) to arise via the mechanism

$$R + CH_3N_2CH_3 \rightarrow RH + CH_2N_2CH_3 \quad [2]$$

$$CH_3N_2CH_2 + O_2 \rightarrow CH_3 + N_2O + CH_2O. \quad [3]$$

Reaction [3] is written as an over-all reaction and might occur in stages involving the $CH_3N_2CH_2O_2$ radical. R is some radical in the system capable of abstracting hydrogen from azomethane. A parallel reaction yielding the secondary nitrogen might be

$$CH_3N_2CH_2 + O_2 \rightarrow CH_3O + N_2 + CH_2O. \quad [4]$$

If these are the only important reactions producing secondary nitrogen, nitrous oxide, and formaldehyde, the difference between formaldehyde and secondary nitrogen should equal the amount of nitrous oxide found. The broken line in Fig. 4, which is drawn with a slope of unity, is a reasonable representation of the data. At the lower temperature the correlation does not hold. Data at 124° C from an earlier investigation (2) show a similar trend but are rather badly scattered. Thus it is not possible to obtain the activation energy difference between [3] and [4]. From Fig. 4 a value $k_3/k_4 = 1.8$ is obtained at 162° C.

Earlier data show that [3] and [4] are slow compared to the third order (3, 12) reaction [5]

$$CH_3 + O_2 + M \rightarrow CH_3O_2 + M. \quad [5]$$

This may be seen by comparing (at 161° C) the oxygen pressure at which Φ_{N_2O} attains its approximately limiting value (~ 1 mm) with that required for Φ_{CH_4} to decrease to negligible values (~ 0.1 mm) (Figs. 3 and 4 of (1)). Thus there exists a region of oxygen pressure between these limits where CH_3O_2 and $CH_2N_2CH_3$ are present in the system. If these may react as in [6] and the resulting peroxide decomposes, in part, by [7] and [8],

Can. J. Chem. Downloaded from www.nrcresearchpress.com by 176.9.209.113 on 09/04/12
For personal use only.

Φ_{N_2} should increase at oxygen pressures below about 1 mm and decrease again at a very low oxygen pressure where [5] becomes a less predominant fate for methyl radicals.

$$CH_3O_2 + CH_2N_2CH_3 \rightarrow CH_3O_2CH_2N_2CH_3 \quad [6]$$

$$CH_3O_2CH_2N_2CH_3 \rightarrow CH_3O + OCH_2N_2CH_3 \quad [7]$$

$$OCH_2N_2CH_3 \rightarrow CH_2O + N_2 + CH_3 \quad [8]$$

A careful examination of the dependence of Φ_{N_2} on oxygen pressure (Fig. 1 of (1)) shows that such a trend exists. The tentative mass spectrometric identification of $CH_3O_2CH_2N_2CH_3$ among the products in the current work supports this hypothesis as well. An analogous effect has been observed in the photooxidation of azoethane (11), and a similar scheme might be used to explain part of the variation in Φ_{CO} with oxygen pressure in acetone photooxidation (13).

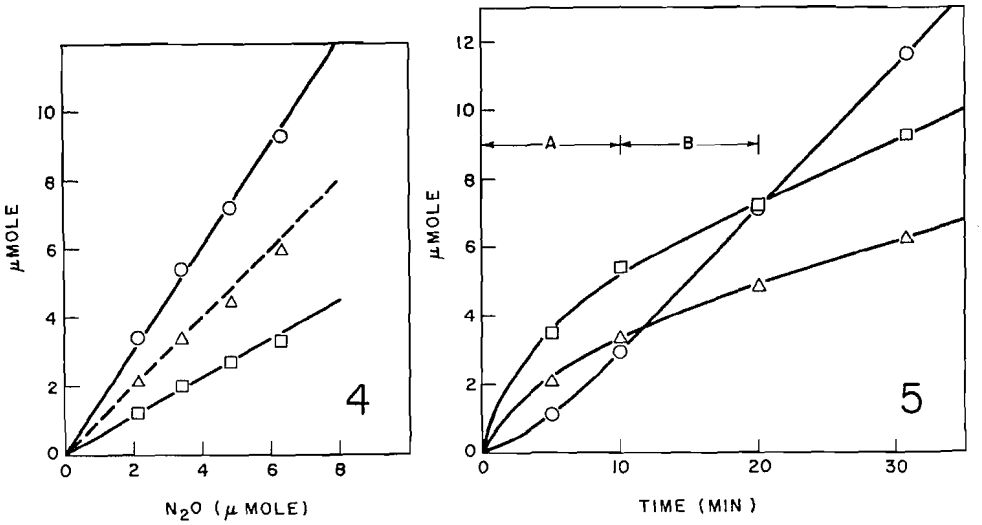

FIG. 4. Correlation of formaldehyde, secondary nitrogen, and nitrous oxide, 162° C. ○ CH_2O; □ $(N_2)_{secondary}$; △ CH_2O–$(N_2)_{secondary}$. The broken line has a slope of unity.
FIG. 5. Possible formaldehyde inhibition, 162° C. ○ CO; □ CH_2O; △ N_2O.

If the reactions analogous to [2], [3], [4], [6], [7], and [8] occur in the acetone photooxidation, the material balance method (4) of determining the third body requirement for [5] is open to some question since more than two methyl radicals are released to the system per quantum absorbed. The determination of k_5 using azomethane photooxidation (1) included the chain steps [2] and [3] but did not consider [6], [7], and [8]. Occurrence of [4] further complicates the situation in either case.

Formation of Methanol

It seems unlikely that the large yields of methanol found here can be explained without the presence of relatively high concentrations of methoxy radicals. If such is indeed the case then methanol could arise in reaction [2], with R the CH_3O radical, and possibly in [9] as well.

$$2CH_3O \rightarrow CH_3OH + CH_2O \quad [9]$$

Empirically it is found that the material balance [I] holds reasonably well over a large range of conversion and temperature.

$$CH_3OH = 2CO + CO_2 + CH_2O \quad [I]$$

Can. J. Chem. Downloaded from www.nrcresearchpress.com by 176.9.209.113 on 09/04/12
For personal use only.

This is shown in the last column of Table II as the ratio $m_I = (2CO + CO_2 + CH_2O)/CH_3OH$. At the very low intensity the relationship is no longer obeyed.

It would appear that, in addition to [2] and [9], which produce equivalent quantities of methanol and formaldehyde if [3] and [4] are the sole fates of $CH_2N_2CH_3$ radicals, there is another source of methanol. This further source involves the production of 2 molecules of methanol and 1 of carbon monoxide or 1 each of carbon dioxide and methanol. A single source need not lead to both oxides of carbon; possibly two such sources are involved. Moreover, the inclusion of carbon dioxide in [I] is somewhat dubious. Because of the relatively small yields of this product, an equally reasonable value of m_I could be obtained if carbon dioxide were not considered. Since methanol production by this means appears to be associated with carbon monoxide formation and the yield of this product depends most strongly on conversion, a discussion of the additional methanol formation is deferred to a later section.

Occurrence of [2] and [9] as sources of methanol requires the presence of methoxy radicals. Reaction [4] is not, of course, a sufficiently copious source of that radical. The product of [5] is almost certainly a methyl peroxy radical, and some scheme must be devised to transform the peroxy methyl radical to a methoxy. Using an earlier suggestion of Bell *et al.* (14) reaction [10] has been postulated for this conversion (1).

$$2CH_3O_2 \rightarrow 2CH_3O + O_2 \qquad [10]$$

Unless other fates are possible for CH_3O_2 radicals, [10] is inevitable regardless of intensity. Such another fate might be abstraction from some hydrogen donor in the system to form methyl hydroperoxide. All attempts to identify this compound have been fruitless (1). While it might be objected that mercury vapor present in the system might catalyze the decomposition of the peroxide, the results of Marcotte and Durbetaki (15) in the acetone photooxidation are inconsistent with this objection. Thus it is concluded that if [10] occurs it will be unaffected by light intensity. Recently McDowell and Sharples (16) have shown that reactions, thought to be analogous to [10], of acetyl and propionyl peroxy radicals proceed with almost unit collision yield. The products in those cases were written as diacetyl or dipropionyl peroxides and molecular oxygen, but the products were not isolated. In view of the higher temperatures used here it might be anticipated that the products would be those of O—O bond fission in the resulting peroxide. Hence [10] is considered an efficient reaction.

Other mechanisms have been suggested for this conversion. The identification of small, stationary concentrations of ozone in some photooxidation systems has led to the suggestion (3, 17) that [11] might be efficient in the transformation.

$$RO_2 + O_2 \rightarrow RO + O_3 \qquad [11]$$

Ozone is thought to be consumed by rapid reaction with alkyl radicals so that its concentration never reaches readily detectable levels.

While the precise mechanism operating in this system remains unknown, it seems necessary to postulate that the methyl radicals produced in [1], [3], and [8] are, for the most part, rapidly and efficiently converted to methoxy radicals probably via the methyl peroxy radical.

Dependence of Products on Conversion

The decrease with conversion of the apparent yields of nitrogen, nitrous oxide, formaldehyde, and methanol, as illustrated in Figs. 1 to 3, accompanied by an increase in the carbon monoxide yield, strongly suggests that an inhibitor is produced in the early stages of the reaction. Radicals, presumably mostly methoxy, react with this inhibitor

Can. J. Chem. Downloaded from www.nrcresearchpress.com by 176.9.209.113 on 09/04/12
For personal use only.

rather than with azomethane, resulting in a decreased chain length for the over-all reaction and production of carbon monoxide from the inhibitor. The time scale of the events—many minutes—precludes the possibility that the phenomenon involves a radical acting as an inhibitor.

Because of the relatively small energy requirements for abstraction of the aldehydic hydrogen, aldehydes have been thought to act in the manner required by the present observations. A scheme involving formaldehyde has been suggested in the azomethane photooxidation (2). This involved the mechanism outlined below in which the radical R is probably methoxy.

$$R + CH_2O \rightarrow RH + CHO \qquad [a]$$

$$R + CHO \rightarrow RH + CO \qquad [b]$$

$$O_2 + CHO \rightarrow CO + HO_2 \qquad [c]$$

$$R + CH_3N_2CH_3 \rightarrow RH + CH_2N_2CH_3 \qquad [d]$$

$$CH_2N_2CH_3 + O_2 \rightarrow CH_2O + N_2O + CH_3 \qquad [e]$$

If, as seems reasonable, [*c*] and [*e*] are considered to follow rapidly after [*a*] and [*d*] respectively, so that the latter reactions are rate determining, it is seen that the instantaneous rate ratio is obtained as [II]

$$[II] \qquad r_{CO}/r_{N_2O} = k_a[F]/k_d[A].$$

Figure 5 is used to test this suggestion. During the period from 10 to 30 minutes r_{N_2O} is essentially constant while the instantaneous concentration of formaldehyde, [F] of equation [II], has increased from about 2.1×10^{-5} mole/l. at 10 minutes to about 3.6×10^{-5} mole/l. at 30 minutes. Thus r_{CO} should have increased by a factor of about 1.7 if [II] is to hold. Obviously r_{CO} is essentially constant in this interval.

Further confirmation of the incorrectness of the hypothesis is obtained from the experiment with added formaldehyde-O^{18}, done at 162° C. Formaldehyde was added in an amount (5.13 μmole) calculated to be equivalent to that found at the end of a 10-minute exposure. If formaldehyde were essentially inert in the system, the amounts of various products expected are those corresponding to the time interval A of Fig. 5. Conversely, if formaldehyde acts as the inhibitor, the amounts expected are those pertaining to time interval B. Products observed and those expected under the two conditions are shown in Table III. It is seen that the observed values are in excellent agreement with those expected if formaldehyde were inert in the system.

TABLE III

Photooxidation of azomethane formaldehyde mixture
p_{azo} = 57 mm, p_{O_2} = 7 mm at 0° C
Formaldehyde added 5.13 μmole

	Products in μmole		
		Expected	
	Observed	Abstraction from H_2CO	No abstraction from H_2CO
N_2	9.19	8.03	9.05
CO	2.90	4.15	2.94
CO_2	0.85	0.76	0.71
N_2O	3.70	1.43	3.39
CH_2O	9.01	6.91	10.5

Can. J. Chem. Downloaded from www.nrcresearchpress.com by 176.9.209.113 on 09/04/12
For personal use only.

A further observation from this experiment involves the isotopic composition of carbon monoxide. This product, along with unreacted oxygen, was compressed into the copper – copper oxide furnace and the resulting carbon dioxide submitted for mass spectrometric examination. Blacet and Taylor (17) have concluded that oxygen required for the conversion of carbon monoxide to the dioxide arises solely from the excess gas phase oxygen, and that no exchange occurred. Hence it was anticipated that exchange of any CO^{18} present was unlikely. However, conditions were not identical in the two cases (especially in regard to contact time and the state of oxidation of the catalyst) so that the results might not be significant. It was observed that the carbon dioxide so formed had precisely the naturally occurring composition (obs. $CO^{16}O^{16}$ 99.59%, $CO^{16}O^{18}$ 0.41%, $CO^{18}O^{18}$ absent; natural composition $CO^{16}O^{16}$ 99.60%, $CO^{16}O^{18}$ 0.399%, $CO^{18}O^{18}$ 0.0004%). Had abstraction occurred from the added formaldehyde somewhat less than 2.4% of the carbon dioxide should have been enriched. By itself the isotopic result is of little value because of low O^{18} concentrations and lack of proved techniques. Agreement between the conclusions reached here and those outlined above, however, suggests that the results are more than fortuitous. It is hoped to continue work along these lines in the future.

On the basis of the evidence outlined, it is difficult to treat formaldehyde differently from any other product in the system. The parallelism between the yields of formaldehyde, secondary nitrogen, and nitrous oxide (Fig. 4) had already suggested this. It is, however, possible to obtain a qualitative explanation of this parallelism even if further oxidation of formaldehyde occurs (2). As shown here this explanation leads to quantitative inconsistencies and must be abandoned.

Various other intermediates have been suggested in thermal oxidation reactions but no direct evidence is available from the present work which would permit a decision in this matter. Another qualitatively correct hypothesis is worthy of examination, however. It has been suggested by Hoare and Walsh (4) and by Christie (12) that the oxidation of a methyl radical proceeds via the third order reaction [5] and a bimolecular reaction [12].

$$CH_3 + O_2 \rightarrow CH_2O + OH \qquad [12]$$

The products of [12] were not discussed in detail but Christie's evidence is strongly in favor of its occurrence; she suggests those shown as probable products. It might be pointed out further that if the products of [12] retain the energy of the exothermic reaction, it is conceivable that a goodly percentage of this energy is held by the formaldehyde. The products of [3], [4], [8], and [9], the latter being especially exothermic, are not thought to be in high vibrational levels. The activated complex for [9], for example, presumably involves a relatively simple H-abstraction type of configuration in which vibrations are not excited (18). High vibrational levels must be involved in the complex of [12], however, and it is thought that these are carried over in the formaldehyde product.

It is suggested that this excited formaldehyde is oxidizable by some mechanism which cannot be specified in detail, but which must not be available to normal formaldehyde. Such a process can be designated by the over-all reaction [13].

$$CH_2O^* + O_2 \rightarrow HCO_3H \qquad [13]$$

It is possible to devise a scheme, on the basis of performic acid as the elusive intermediate, which does in fact satisfy most of the data.

$$CH_3O + HCO_3H \rightarrow CH_3OH + CO_3H \qquad [14]$$

$$CO_3H \rightarrow CO_2 + OH \qquad [15]$$

$$CH_3O + CO_3H \rightarrow CH_3OH + O_2 + CO \qquad [16]$$

Can. J. Chem. Downloaded from www.nrcresearchpress.com by 176.9.209.113 on 09/04/12
For personal use only.

The mechanism is thought to operate in a manner generally similar to the formaldehyde mechanism discussed before. At very low conversions, $\backsim 1/2\%$ in this work, the concentration of performic acid is too low to affect the course of the reaction and a short chain reaction occurs (at 162° C $\Phi_{N_2} + \Phi_{N_2O}$ extrapolates to 2.5 at zero conversion). As conversion increases performic acid is consumed in [14], [15], and [16], leading to new products—the oxides of carbon—so that its concentration is held at a low, stationary level which was not detected analytically. This particular scheme has the advantage that the production of carbon dioxide with an induction period is also accounted for explicitly. Because of the small yields the actual presence of an induction period cannot be demonstrated conclusively (Figs. 2 and 3), but its occurrence would not be inconsistent with data. An alternative suggestion, that excited formaldehyde itself acts as the intermediate, can be eliminated on the basis of the time scale of the phenomenon.

Over-all Mechanism

Hydroxyl radicals, formed in [12] and [15], are thought to react as do methoxy. Thus [17], [18], [19], and [20] are postulated for their disappearance.

$$OH + CH_3N_2CH_3 \rightarrow H_2O + CH_2N_2CH_3 \qquad [17]$$

$$OH + HCO_3H \rightarrow H_2O + CO_3H \qquad [18]$$

$$OH + CO_3H \rightarrow H_2O + CO + O_2 \qquad [19]$$

$$OH + CH_3O \rightarrow H_2O + H_2CO \qquad [20]$$

An over-all mechanism composed of reactions [1] to [20] will explain the time dependence and is consistent with stability of formaldehyde in the system. The weakest point is, of course, the formation of performic acid for the presence of which no direct evidence has been obtained. It is seen that water is the only product not determined aside from presumably small quantities of performic acid. In the range of oxygen pressure used here, reactions [6], and thus [7] and [8], are unimportant. Conversion of methyl peroxy to methoxy is assumed to proceed via [10] only; reaction [11] is not considered here. Formaldehyde is formed in [3], [4], [9], and [20]. The difference

$$(H_2CO)_{total} - ((N_2)_s + N_2O) = (H_2CO)_{9,20} \qquad [III]$$

is shown in Fig. 4 to be negligible so that [9] and [20] cannot be significant at this temperature.

Unfortunately only the series of experiments at 162° C are sufficiently complete to be used as a test of the mechanism. In view of this, only material balances can be used to evaluate the scheme proposed. Moreover, because of the effect of conversion on the rates, comparisons can be made only after the rates have attained limiting values. These have been estimated graphically yielding limiting values at 162° C as follows; N_2 0.77, CO 0.42, CO_2 0.069, N_2O 0.14, CH_2O 0.25, CH_3OH 1.07, O_2 consumption 1.27 (all values are in μmole/minute). Since nitrogen is produced in the primary step at a rate of 0.70 μmole/minute, the limiting rate for secondary nitrogen is 0.07 μmole/minute.

If the amount of performic acid remaining at the end of an experiment can be neglected, the sum of the rate of formation of carbon monoxide and of carbon dioxide is a direct measure of the rate of [12]. Moreover, since [9] and [20] are not important, the difference between the limiting rates of formation of methanol and that of secondary nitrogen is a measure of the rate of [5]. Hence,

$$[IV] \qquad k_{12}/k_5[M] = (R_{CO}+R_{CO_2})/(R_{CH_3OH}-(R_{N_2})_s).$$

Can. J. Chem. Downloaded from www.nrcresearchpress.com by 176.9.209.113 on 09/04/12
For personal use only.

Using the limiting rates given above, $k_{12}/k_5[M] = 0.49$. A number of expressions may be derived relating $k_{12}/k_5[M]$ to the limiting rates of various products; all such expressions lead to similar values for the rate ratio. This value may be compared to that of 0.12 obtained from Christie's data (12) where M was methyl iodide. Differences in the temperature of the two experiments and possibly different efficiencies of methyl iodide and azomethane as third bodies might account for the factor of four difference. The uncertainties in both determinations are large.

It can be shown that oxygen consumption is given by either [V*a*] or [V*b*].

$$[Va] \qquad -R_{O_2} = \frac{4k_{12}+k_5[M]}{k_{12}+k_5[M]}\left((R_{N_2})_{prim}+\tfrac{1}{2}R_{N_2O}\right)+(R_{N_2})_s+R_{N_2O}-R_{CO}$$

$$[Vb] \qquad = \frac{2k_{12}+k_5[M]}{k_{12}+k_5[M]}\left((R_{N_2})_{prim}+\tfrac{1}{2}R_{N_2O}\right)+(R_{N_2})_s+R_{N_2O}+R_{CO_2}$$

[V*a*] yields 1.22 and [V*b*] 1.30 to be compared to an observed rate of 1.27 μmole/minute when limiting rate values are used. Thus the mechanism suggested yields the observed rate with reasonable success once approximately steady rates are reached.

Since water was not determined quantitatively it is not possible to test the predications of the mechanism for this product. It might be pointed out, however, that if each hydroxyl radical formed in [12] and [15] abstracts hydrogen to form water (as suggested by [17], [18], [19], with [20] thought not important) then the rate of water production when steady rates are attained is given by

$$[VI] \qquad R_{H_2O} = R_{CO}+2R_{CO_2}.$$

If [VI] is evaluated using the limiting rates, $R_{H_2O} = 0.56$ μmole/minute corresponding to a limiting value of the quantum yield of 0.8. The mechanism also predicts that

$$[VII] \qquad R_{CH_3OH}+R_{H_2O} = (R_{N_2})_s+R_{N_2O}+2R_{CO}+R_{CO_2}.$$

Comparison of [I] and [III], which are correct empirically as demonstrated earlier, with [VII] suggests that the yield of water should be negligible, which cannot be reconciled to the prediction of [VI]. Until more extensive data are available it seems fruitless to speculate further in regard to the formation of water.

A decrease of intensity yields an increase in the relative yields of products formed in propagation reactions (Fig. 3). However, the fact that the rates depend on conversion as well makes an investigation of the effect of intensity difficult to interpret until more data are available at various conversions and intensities.

It is concluded that the mechanism suggested is not complete, especially in regard to water formation, but that the trends of the product yields are reasonably well accounted for by that mechanism.

ACKNOWLEDGMENTS

The authors wish to thank Dr. E. W. R. Steacie for his continued interest in this work and to acknowledge the assistance of Mrs. Frances Kutschke and Miss Bernice Thornton with the mass spectrometric analysis.

They also wish to thank Dr. J. G. Calvert for manuscript copies of his papers (see ref. 3) prior to publication.

Can. J. Chem. Downloaded from www.nrcresearchpress.com by 176.9.209.113 on 09/04/12
For personal use only.

REFERENCES

1. HOEY, G. R. and KUTSCHKE, K. O. Can. J. Chem. **33**, 496 (1955).
2. STRONG, R. L. and KUTSCHKE, K. O. To be published.
3. HANST, P. L. and CALVERT, J. G. J. Phys. Chem. **63**, 71 (1959). SLEPPY, W. C. and CALVERT, J. G. J. Am. Chem. Soc. **81**, 769 (1959).
4. HOARE, D. E. and WALSH, A. D. Trans. Faraday Soc. **53**, 1102 (1957).
5. MARTIN, R. B. and NOYES, W. A., JR. J. Am. Chem. Soc. **75**, 4183 (1953).
6. JONES, M. H. and STEACIE, E. W. R. J. Chem. Phys. **21**, 1018 (1953).
7. LEROY, D. J. Can. J. Research, B, **28**, 492 (1950).
8. BRICKER, C. E. and JOHNSON, H. R. Ind. Eng. Chem. **17**, 400 (1945).
9. BOOS, R. N. Anal. Chem. **20**, 964 (1948).
10. BRICKER, C. E. and VAIL, W. A. Anal. Chem. **22**, 720 (1950).
11. CERFONTAIN, H. and KUTSCHKE, K. O. To be published.
12. CHRISTIE, M. I. Proc. Roy. Soc. (London), A, **244**, 411 (1958).
13. MARCOTTE, F. B. and NOYES, W. A., JR. Discussions Faraday Soc. **10**, 236 (1951); J. Am. Chem. Soc. **74**, 783 (1952).
14. BELL, E. R., ROLEY, J. H., RUST, F. F., SEUBOLD, F. H., and VAUGHAN, W. E. Discussions Faraday Soc. **10**, 242 (1951).
15. MARCOTTE, F. B. and DURBETAKI, A. *Quoted by* W. A. Noyes, Jr. Discussions Faraday Soc. **10**, 308 (1951).
16. MCDOWELL, C. A. and SHARPLES, L. K. Can. J. Chem. **36**, 251, 258, 268 (1958).
17. BLACET, F. E. and TAYLOR, R. P. Ind. Eng. Chem. **48**, 1505 (1956). SHUBERT, C. C. and PEASE, R. N. J. Chem. Phys. **24**, 919 (1956); J. Am. Chem. Soc. **78**, 2044 (1956).
18. BYWATER, S. and ROBERTS, R. Can. J. Chem. **30**, 773 (1952).

Can. J. Chem. Downloaded from www.nrcresearchpress.com by 176.9.209.113 on 09/04/12
For personal use only.

Can. J. Chem. Downloaded from www.nrcresearchpress.com by 176.9.209.113 on 09/04/12
For personal use only.

THE SYNTHESIS OF 5-DEOXY-5-*S*-ETHYL-D-THREO-PENTULOSE[1]

J. K. N. JONES AND D. L. MITCHELL

ABSTRACT

The microbiological oxidation of 1-deoxy-1-*S*-ethyl-D-arabitol by *Acetobacter suboxydans* has yielded syrupy 5-deoxy-5-*S*-ethyl-D-*threo*-pentulose from which a crystalline phenylosazone identical with the one prepared from 5-deoxy-5-*S*-ethyl-D-*xylo*-pentose was obtained. A syrupy 3,4-*O*-isopropylidene-5-deoxy-5-*S*-ethyl-D-*threo*-pentulose and its crystalline 2,5-dichlorophenylhydrazone were prepared.

INTRODUCTION

The microbiological oxidation of terminal substituted polyhydric alcohols by *Acetobacter suboxydans* has been the subject of investigation in several laboratories (1, 2, 3). Recently, we reported that 1-deoxy-1-*S*-ethyl-D-glucitol was oxidized to 6-deoxy-6-*S*-ethyl-L-sorbose (3), and in this communication we report the microbiological oxidation of a structurally similar polyol, 1-deoxy-1-*S*-ethyl-D-arabitol (I), to 5-deoxy-5-*S*-ethyl-D-*threo*-pentulose (II). The ω-deoxy analogue, 5-deoxy-D-*threo*-pentulose, $[\alpha]_D$ −5° in water, has been prepared by an aldolase-catalyzed condensation between acetaldehyde and dihydroxyacetone monophosphate (4); it was also most likely obtained when 1-deoxy-D-arabitol was oxidized by *A. suboxydans* (1).

When the culture medium contained sorbitol (0.4%), 1-deoxy-1-*S*-ethyl-D-arabitol was completely oxidized after 10 days to a strongly reducing compound. Copper reducing values previously published also support this conclusion (3). However, when sorbitol was not included in the medium, oxidation proceeded at a slower rate and was incomplete after 8 days. The oxidation product (II), $[\alpha]_D$ −41° in ethanol, which was obtained as a chromatographically pure syrup, revealed a strong absorption band in the carbonyl stretching frequency at 1710 cm^{-1}, while the corresponding 5-deoxy-5-*S*-ethyl-(D-*xylo*- and L-*arabino*-pentoses) possessed only a trace of carbonyl absorption and must therefore exist almost entirely as furanoses. Periodate oxidation of (II) at pH 3.7 followed by an estimation of the liberated formaldehyde (0.6 mole) indicated that the reducing compound had a primary alcohol group and that the site of enzymic oxidation was not at carbon 1. It appeared that periodate oxidation took place mainly between carbons 1 and 2. However, cleavage between carbons 2 and 3, or carbons 3 and 4, is possible although it could lead to an intermediate (i.e. glycollic acid) which is very stable to further attack by periodate ion (5). If enzymic oxidation occurred at a site other than the first carbon atom, the formation of a furanol ring system would be prohibited and the molecule would most likely exist in a zigzag conformation. The hydroxyl groups at carbons 3 and 4 would then be favorably situated for scission by periodate ion and also for ketal formation. Reaction of the ketose (II) with acidified acetone led to the formation of a strongly reducing *O*-isopropylidene derivative which possessed strong absorption at the carbonyl and carbon–hydrogen stretching frequencies. Considerable reduction of the absorption peak in the hydroxyl region of this compound was observed when its spectrum was compared with that of the ketose (II). Periodate oxidation of the *O*-isopropylidene derivative at pH 7 liberated formaldehyde (0.6 mole), which indicated

[1]*Manuscript received May 19, 1959.*
Contribution from the Department of Chemistry, Queen's University, Kingston, Ontario.

that carbons 1 and 2 were not involved in ketal formation. Reaction of the *O*-isopropylidene derivative (III) with 2,5-dichlorophenylhydrazine produced a small amount of the crystalline 2,5-dichlorophenylhydrazone (IV) which gave absorptions in the infrared corresponding to hydroxyl, —C=N—, and ketal groups (6). This evidence indicates that the biochemical oxidation product is the acyclic 2-pentulose, 5-deoxy-5-*S*-ethyl-D-*threo*-pentulose (II) and that the derived ketal is 3,4-*O*-isopropylidene-5-deoxy-5-*S*-ethyl-D-*threo*-pentulose (III). These conclusions are also consistent with the well-known enzyme specificity for oxidations at pH 6.

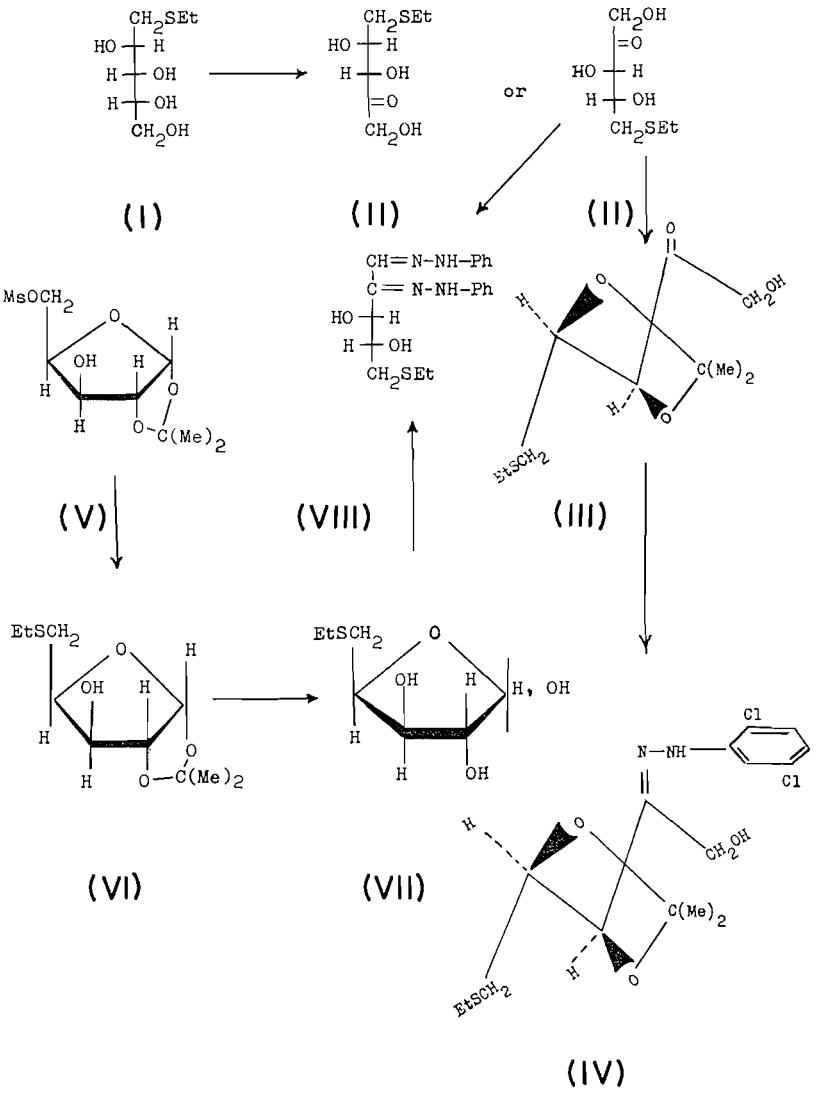

Independent proof of the structure (II) was obtained through the synthesis of 5-deoxy-5-*S*-ethyl-(D-*xylo*- (VII) and L-*arabino*-pentose) via the 1,2-*O*-isopropylidene-5-*O*-toluene-*p*- (or methane-) sulphonyl ester (e.g. (V) → (VI)). The thioethyl aldoses (VII) displayed physical properties different from the thioethyl ketose (II). However, 5-deoxy-5-*S*-ethyl-

Can. J. Chem. Downloaded from www.nrcresearchpress.com by 176.9.209.113 on 09/04/12
For personal use only.

D-*xylo*-pentose gave a phenylosazone (VIII) identical with that which was prepared from (II) but which differed from the phenylosazone of 5-deoxy-5-*S*-ethyl-L-*arabino*-pentose. Therefore, the hydroxyls at carbons 3 and 4 of (II) possess the D-*threo*-configuration.

EXPERIMENTAL

Solutions were concentrated under reduced pressure (ca. 15 mm) and at 40° C or less. Melting points were uncorrected and optical rotations were determined in water unless otherwise stated. Paper chromatography was carried out by the descending method on Whatman No. 1 filter paper using the following solvent systems (v/v): (*a*) ethyl acetate – acetic acid – formic acid – water (18:3:1:4); (*b*) ethyl acetate – acetic acid – water (9:2:2); (*c*) butan-1-ol–ethanol–water (9:3:3); and (*d*) butan-1-ol–pyridine–water (10:3:3). Non-reducing compounds were detected on paper chromatograms with an alkaline silver nitrate spray reagent (7) and reducing compounds were detected with *p*-anisidine hydrochloride reagent (8). The rate of movement of the compound on paper chromatograms is quoted relative to that of rhamnose (R_{Rh} value). Infrared absorptions were measured as solutions in chloroform or as a powder suspended in a potassium bromide pellet on a Perkin–Elmer Model 21 spectrophotometer and wave numbers are given to within ± 10 cm^{-1}.

*5-Deoxy-5-S-ethyl-*D*-threo-pentulose*

A broth consisting of 1-deoxy-1-*S*-ethyl-D-arabitol (3) (0.42 g), sorbitol (0.2 g), yeast extract* (0.1 g), and potassium dihydrogen phosphate (0.01 g) in tap water (50 ml) was autoclaved (15 p.s.i., 30 minutes), cooled, inoculated with *Acetobacter suboxydans* (A.T.C.C. No. 621), and stored at 28° C for 10 days. Paper chromatographic examination of the medium then indicated the formation of a single major reducing constituent, besides sorbose, which gave an orange-red (apricot) color with the *p*-anisidine hydrochloride reagent. Chromatographic comparison with 5-deoxy-5-*S*-ethyl-L-*arabino*-pentose and 5-deoxy-5-*S*-ethyl-D-*xylo*-pentose, which both gave bright pink colors with the same reagent, indicated that it was a different compound because its rate of movement was slower in solvent systems (*c*) and (*d*). The rates of movement were practically identical in solvent systems (*a*) and (*b*). With the orcinol – trichloroacetic acid spray reagent no color reaction was produced but with the silver nitrate reagent a very rapid formation of silver resulted.

The broth was poured with stirring into ethanol (150 ml) and the cell debris was separated by filtration. After concentration of the filtrate, the oxidation product was separated on Whatman 3 MM filter paper and was obtained as a chromatographically pure syrup (0.20 g, 67%). The syrup was soluble in water, ethanol, acetone, and chloroform. A specimen which was dried *in vacuo* for 4 days was dissolved in chloroform (3% w:v) and its absorption measured in the infrared. A strong, sharp peak in the carbonyl stretching frequency at 1710 cm^{-1} was observed; $[\alpha]_D$ $-41° \pm 2°$ (*c*, 0.9, ethanol). After 3 weeks' storage at room temperature, the syrup was re-examined by paper chromatography, and revealed streaking in the vicinity of the constituent, presumably due to the development of isomers via keto $\rightleftarrows$ enol tautomerism. Some time later a second reducing constituent appeared with a rate of movement approximately that of rhamnose (solvent *a*).

In another experiment, *Acetobacter suboxydans* was grown on the same medium described above except that sorbitol was not included. After 8 days' oxidation, the

**Nutritional Biochemicals Corporation, Cleveland, Ohio, U.S.A.*

Can. J. Chem. Downloaded from www.nrcresearchpress.com by 176.9.209.113 on 09/04/12
For personal use only.

substrate and oxidized product appeared to be present on paper chromatograms in a ratio of 1:1.

TABLE I

Paper chromatographic values

Solvent system	(*c*)	(*d*)
R_{Rh} value of:		
5-Deoxy-5-*S*-ethyl-L-*arabino*-pentose	2.11*	1.98*
5-Deoxy-5-*S*-ethyl-D-*threo*-pentulose	2.02	1.86
5-Deoxy-5-*S*-ethyl-D-*xylo*-pentose	2.14	2.00

*Mean of two measurements.

*5-Deoxy-5-S-ethyl-*D*-threo-pentulose Phenylosazone*

A portion of the syrupy 5-deoxy-5-*S*-ethyl-D-*threo*-pentulose (ca. 50 mg) was dissolved in a mixture of phenylhydrazine (0.1 ml), acetic acid (0.2 ml), and water (2 ml) and the solution was heated to 80° C for 2 hours. The derived phenylosazone was collected after the solution had been cooled and diluted with water. It was recrystallized from a small volume of ethanol and the product was washed with cold (−60° C) ethanol. Several recrystallizations gave a product of constant melting point 158–159° C (decomp.) which possessed an infrared absorption spectrum identical with that of the phenylosazone derived from 5-deoxy-5-*S*-ethyl-D-*xylo*-pentose. Mixed melting point 155–156° C, $[\alpha]_D^{20} -29° \pm 4°$ (*c*, 1.2, pyridine). Anal. Calc. for $C_{19}H_{24}N_4O_2S$: C, 60.0; H, 6.7. Found: C, 59.5; H, 6.4.

*3,4-O-Isopropylidene-5-deoxy-5-S-ethyl-*D*-threo-pentulose*

Syrupy 5-deoxy-5-*S*-ethyl-D-*threo*-pentulose (ca. 75 mg) was dissolved in acetone (50 ml) containing concentrated sulphuric acid (1 drop) and the solution was shaken for 18 hours. After neutralization with barium carbonate, filtration, and concentration of the filtrate, the resulting syrup was examined by paper chromatography and infrared spectroscopy. A compound which moved much faster than the original material and which had R_{Rh} 2.7 (solvent (*a*)) was detected on the chromatogram as an orange-colored spot (*p*-anisidine hydrochloride); it also gave an immediate reaction with the silver nitrate – sodium hydroxide reagent. Traces of acetone were removed by repeated codistillation with chloroform, and a chloroform solution of the *O*-isopropylidene derivative was examined in the infrared. It possessed a medium weak absorption band at 3350 cm^{-1} and a medium strong absorption band at 1709 cm^{-1}. When the syrup was examined chromatographically in high concentration, a trace of 5-deoxy-5-*S*-ethyl-D-*threo*-pentulose was detected, $[\alpha]_D$ 21.5° (*c*, 0.6, ethanol).

*3,4-O-Isopropylidene-5-deoxy-5-S-ethyl-*D*-threo-pentulose 2,5-Dichlorophenylhydrazone*

A solution of the syrupy *O*-isopropylidene derivative (30 mg) and 2,5-dichlorophenylhydrazine (30 mg) in methanol (10 ml) were heated under reflux for 3 hours. After removal of the solvent, the light brown syrup was redissolved in *n*-hexane (5 ml), the solution was chilled in a solid carbon dioxide – ethanol mixture, and crystallization was induced by rubbing the walls of the flask with a spatula. The white powder (10 mg), m.p. 89–91° C, absorbed strongly in the infrared at 1595 cm^{-1} and the carbonyl absorption at 1710 cm^{-1} was present as a very weak peak barely detectable over the background fluctuation. Absorptions were also recorded at 1458 (m), 1378 (vs), 1250 (s), 1234 (vs), 1200 (s), 1160 (vs), 1087 (vs), 1033 (vs), and 794 (s) cm^{-1}. Anal. Calc. for $C_{16}H_{22}Cl_2N_2O_3S$: C, 48.8; H, 5.6. Found: C, 48.5; H, 5.4.

Can. J. Chem. Downloaded from www.nrcresearchpress.com by 176.9.209.113 on 09/04/12
For personal use only.

Can. J. Chem. Downloaded from www.nrcresearchpress.com by 176.9.209.113 on 09/04/12
For personal use only.

*1,2-O-Isopropylidene-5-deoxy-5-S-ethyl-*D*-xylo-pentose*

1,2-*O*-Isopropylidene-5-*O*-methanesulphonyl-D-xylose (1.08 g, m.p. 136–137° C (9)) and freshly prepared sodium thioethylate (0.70 g) in acetone (25 ml) were heated to 100° C in a pressure bottle for 2 hours. The solution was cooled and concentrated, and the acetone removed by several codistillations with water. The aqueous solution was extracted thrice with ether and the ethereal extracts were shaken once with ice cold, dilute sulphuric acid, twice with water, and were finally dried (Na_2SO_4). The ethereal extract was concentrated and the residual pale yellow syrup was dissolved in a small volume of *n*-hexane and the solution was cooled in a solid carbon dioxide – ethanol mixture. Crystallization was induced by rubbing the walls of the vessel with a spatula. The product (0.4 g, 42%) was collected and washed thoroughly with cold (−60° C) *n*-hexane. The product had m.p. 64–65° C, and $[\alpha]_D$ −58° (*c*, 0.9, ethanol).

The reported constants were: m.p. 66.5–67.5° C, $[\alpha]_D$ −57.5° (ethanol) (10).

A test portion of the product was hydrolyzed with acetic acid for 3 hours under reflux. Removal of the solvents and acetic acid left a syrup which was soluble in chloroform. Examination of this solution in the infrared revealed only a trace of absorption in the vicinity of 1710 cm^{-1}.

*5-Deoxy-5-S-ethyl-*D*-threo-pentose Phenylosazone*

A solution of 1,2-*O*-isopropylidene-5-deoxy-5-*S*-ethyl-D-*xylo*-pentose (100 mg) in 50% aqueous alcohol (10 ml) and glacial acetic acid (5 drops) was hydrolyzed by heating for 3 hours under reflux. Water was added and the ethanol and acetone were removed by several codistillations with water. Phenylhydrazine (0.2 ml) and acetic acid (0.2 ml) were added and the phenylosazone was prepared according to the method previously described. The bright yellow product after recrystallization from a small volume of ethanol followed by washing with cold (−60° C) ethanol melted at 155–156° C, $[\alpha]_D^{20}$ −28°±4° (*c*, 1.1, pyridine). Anal. Calc. for $C_{19}H_{24}N_4O_2S$: C, 60.0; H, 6.7; S, 8.4. Found: C, 59.9; H, 6.3; S, 8.3.

*1,2-O-Isopropylidene-5-deoxy-5-S-ethyl-*L*-arabino-pentose*

1,2-*O*-Isopropylidene-5-*O*-toluene-*p*-sulphonyl-L-arabinose (1.09 g, m.p. 129–130° C (11)) and freshly prepared sodium thioethylate (0.5 g) in acetone (25 ml) were heated at 100° C in a pressure flask for 2 hours. Water was added and the acetone was removed by several codistillations with water. The aqueous solution was then extracted twice with chloroform and the chloroform extracts were washed successively with cold, dilute sulphuric acid and then with water. The dried (Na_2SO_4) solution was concentrated to a crystalline mass which was readily recrystallized from a small volume of *n*-hexane to yield needles (0.61 g, 82%) melting at 88° C, $[\alpha]_D$ 1.3° (*c*, 0.8, ethanol). Anal. Calc. for $C_{10}H_{18}O_4S$: C, 51.3; H, 7.7; S, 13.7. Found: C, 51.2; H, 7.8; S, 13.8.

*5-Deoxy-5-S-ethyl-*L*-arabino-pentose*

1,2-*O*-Isopropylidene-5-deoxy-5-*S*-ethyl-L-*arabino*-pentose (0.46 g) was hydrolyzed for 3 hours with Amberlite IR-120 (H) resin (20 cc, wet volume) suspended in 50% aqueous ethanol (25 ml). The solution was filtered through a charcoal pad, concentrated, and the resulting syrup was redissolved in ethyl acetate. The solution was clarified by percolation under gravity through a fine porosity sintered glass funnel. Concentration yielded a colorless syrup (0.38 g) which revealed a single reducing constituent by paper chromatography and possessed no carbonyl absorption in the infrared; $[\alpha]_D$ −32°±2° (*c*, 0.9, ethanol).

Further hydrolysis with 0.05 *N* hydrochloric acid for 1.5 hours at 80° C, followed by deionization on Duolite A-4 (OH) resin, yielded a colorless syrup with $[\alpha]_D$ −29.5° (*c*, 3.3, ethanol). Since the optical rotation of the product was not significantly changed by the second acid hydrolysis, hydrolysis by the resin was considered complete.

*5-Deoxy-5-S-ethyl-*L*-erythro-pentose Phenylosazone*

The crystalline phenylosazone was prepared from syrupy 5-deoxy-5-*S*-ethyl-L-*arabino*-pentose (66 mg) in the usual way to yield a product that melted at 157° C after recrystallization from aqueous ethanol. The infrared absorption spectrum differs in minor features from 5-deoxy-5-*S*-ethyl-D-*threo*-pentose phenylosazone; the major difference was the absence of a peak at 817 cm^{-1} in the 5-deoxy-5-*S*-ethyl-L-*erythro*-derivative. The mixed melting point with both specimens of 5-deoxy-5-*S*-ethyl-D-*threo*-pentose phenylosazone was 120–135° C; $[\alpha]_D^{20}$ +19°±4° (*c*, 0.9, pyridine). Anal. Calc. for $C_{19}H_{29}N_4O_2S$: C, 60.0; H, 6.7; S, 8.4. Found: C, 59.5; H, 6.8; S, 8.7.

Determination of the Formaldehyde Liberated

Samples (0.5–1.5 mg; accurately weighed) were dissolved in buffer solution or 40% aqueous pyridine containing 0.3 *M* sodium metaperiodate solution (0.5 ml) and were made up to 10 ml. At intervals, aliquot samples (1 ml) were withdrawn and the formaldehyde was estimated by the chromotropic acid method (12). A trial experiment indicated that pyridine did not interfere in the estimation.

TABLE II

Liberation of formaldehyde during periodate oxidation

Compound	pH	Time (hours) 0.08	0.25	0.50	1.0	20
5-Deoxy-5-*S*-ethyl-D-*threo*-pentulose	3.7[a]	0.60[c]		0.63	0.60	
	40% pyridine		0.64			0.59
3,4-*O*-Isopropylidene-5-deoxy-5-*S*-ethyl-D-*threo*-pentulose	7.6[b]	0.33				0.61
	40% pyridine		0.38			0.43

[a, b] 0.5 *M* acetate buffer.

[c] Moles of formaldehyde liberated per mole of substrate.

ACKNOWLEDGMENTS

The authors wish to thank Dr. N. K. Richtmyer of the National Institute of Arthritis and Metabolic Diseases, National Institute of Health, Bethesda, Maryland, for cultures, and Dr. D. H. Ball for generous specimens of 1,2-*O*-isopropylidene-5-*O*-methane-sulphonyl-D-xylose and 1,2-*O*-isopropylidene-5-*O*-toluene-*p*-sulphonyl-L-arabinose. One of us (D.L.M.) thanks the Ontario Research Foundation for a scholarship.

REFERENCES

1. Bollenback, G. N. and Underkofler, L. A. J. Am. Chem. Soc. **72**, 741 (1950).
2. Richtmyer, N. K., Stewart, L. C., and Hudson, C. S. J. Am. Chem. Soc. **72**, 4934 (1950).
3. Hough, L., Jones, J. K. N., and Mitchell, D. L. Can. J. Chem. **37**, 725 (1959).
4. Gorin, P. A. J., Hough, L., and Jones, J. K. N. J. Chem. Soc. 2140 (1953).
5. Fleury, P., Courtois, J., Perles, R., and Le Dizet, L. Bull. soc. chim. France, 347 (1954).
6. Barker, S. A., Bourne, E. J., Pinkard, R. M., and Whiffen, D. H. J. Chem. Soc. 807 (1959).
7. Trevelyan, W. E., Proctor, D. P., and Harrison, J. S. Nature, **166**, 444 (1950).
8. Hough, L., Jones, J. K. N., and Wadman, W. H. J. Chem. Soc. 1702 (1950).
9. Ball, D. H. Unpublished work. Department of Chemistry, Queen's University, Kingston, Ontario.
10. Raymond, A. L. J. Biol. Chem. **107**, 88 (1934).
11. Levene, P. A. and Compton, J. J. Biol. Chem. **116**, 189 (1936).
12. O'Dea, J. F. and Gibbons, R. A. Biochem. J. **55**, 580 (1953).

Can. J. Chem. Downloaded from www.nrcresearchpress.com by 176.9.209.113 on 09/04/12
For personal use only.

Can. J. Chem. Downloaded from www.nrcresearchpress.com by 176.9.209.113 on 09/04/12
For personal use only.

SODIUM DITHIONITE, DECOMPOSITION IN AQUEOUS SOLUTION AND IN THE SOLID STATE[1]

M. W. Lister and R. C. Garvie

ABSTRACT

The decomposition of sodium dithionite has been investigated in alkaline aqueous solution. Under these conditions it decomposes by a first order reaction with a rate constant of 4.5×10^{-4} min^{-1} at 88.5° C and an activation energy of 26.5 kcal/g-molecule. The ionic strength, and the concentration of the sodium hydroxide also present, affect the rate to some extent. A possible mechanism is suggested. The decomposition of solid sodium dithionite was also examined, and was found to give the best fit to the equations deduced assuming random nucleation, followed by linear growth of nuclei, with possible ingestion and interference of reacting zones. The activation energy of nucleus growth is 32 to 33 kcal/g-molecule, and that for nucleation probably between 40 and 45 kcal/g-molecule.

The decomposition of aqueous solutions of sodium dithionite was examined by K. and E. Jellinek (1). They established that the products were sodium thiosulphate and bisulphite, so that the equation for the reaction is:

$$2Na_2S_2O_4 + H_2O \rightarrow Na_2S_2O_3 + 2NaHSO_3.$$

The quantities of the various products agreed with this equation. They measured the rate of decomposition in solutions containing varying, but usually large, amounts of sodium bisulphite. From the ionization constants of sulphurous acid (2), the pH of these solutions must have been about 4.5. They found a second order reaction, fairly rapid even at room temperature: the rate constant was 0.044 $(g\text{-molecule/l.})^{-1}$ min^{-1} at 32° C. The rate constants at various temperatures give only a moderately straight line in a plot of log (rate constant) against 1/temperature (they did not themselves put their results in this form); the activation energy appears to be close to 8 kcal/g-molecule.

This is a remarkably low activation energy, when it is remembered that the mechanism proposed is one involving the collision of two doubly charged ions, followed by the breaking of at least one chemical bond. The details of the reaction are not entirely clear, but whatever mechanism is suggested must include at least one bond rupture. The most obvious solution of this difficulty would be to suppose that at the pH used, the dithionite is partly present as $HS_2O_4^-$, or even as $H_2S_2O_4$ molecules, and that these react. Accordingly, experiments were made on the decomposition of sodium dithionite in alkaline solution; and, as will be seen below, these show that the rates in alkaline solution are quite different from those reported by K. and E. Jellinek. The reaction was examined over a range of ionic strength and temperature.

The decomposition of solid sodium dithionite has been examined by Deines and Elstner (3), who found the products to be sodium thiosulphate and sulphite and sulphur dioxide. This is sufficiently similar to the reaction in solution that it seemed worth while to obtain some quantitative information on the decomposition of the solid, particularly in order to compare the activation energies of the reaction under the different circumstances.

EXPERIMENTAL

The chief difficulty in these experiments is that sodium dithionite solutions can be

[1]*Manuscript received April 17, 1959.*
Contribution from the Department of Chemistry, University of Toronto, Toronto, Ontario, Canada.

oxidized by atmospheric oxygen, so air must be rigorously excluded, both during the run, and during manipulation of samples. The apparatus used was similar to that of K. and E. Jellinek, modified only in details. The solutions were made up in a flask under a positive pressure of purified nitrogen. During the run this flask was immersed in a water thermostat, and the contents were stirred with a mercury sealed stirrer. At intervals samples were sucked up into a nitrogen-filled burette, and then a measured volume of solution was immediately run into excess oxidizing agent. The details of the analysis are given below.

In the experiments with solid sodium dithionite, the apparatus consisted of a long pyrex tube, with a sintered glass disk fixed across the middle of it. The tube was wound with suitable resistance wire and insulation, and a thermocouple was placed just above the glass disk. During the actual run the thermocouple was embedded in the sodium dithionite. The temperature at the thermocouple was maintained constant by connecting it to a potentiometer, and sending the off-balance current through a light-and-mirror galvanometer, the light being reflected on to a photocell. The photocell activated a relay which introduced a small extra resistance into the heating circuit when the temperature rose. The temperature was thus controlled to 0.1° C. Nitrogen was passed through the tube and disk, and, for a run, sodium dithionite was placed on the disk. As soon as it had come to temperature, a sample was removed by a small glass scoop, weighed, and analyzed; further samples were taken at suitable intervals.

In the solution runs, the solutions were always kept alkaline with sodium hydroxide. This is slowly used up, as the total reaction is:

$$2Na_2S_2O_4 + 2NaOH \rightarrow Na_2S_2O_3 + 2Na_2SO_3 + H_2O,$$

but the runs were never carried beyond the point where the sodium hydroxide was exhausted. The ionic strength was adjusted by addition of sodium fluoride. This salt was chosen because it did not interfere with the analyses, and is of a simple ionic type. As the equation shows, the ionic strength rises during the reaction. In the results given below, the initial ionic strength is recorded. Most of the runs were kept fairly short, so that the change in ionic strength was not above 0.05, as it was expected that the rate would vary considerably with ionic strength. As it turned out, there is some such variation, but it was not very large. For the most part, evidence of the order of the reaction was obtained by starting runs at different dithionite concentrations, but in the run shown in Fig. 1, the analyses were continued long enough to give fairly definite evidence of this from this run alone.

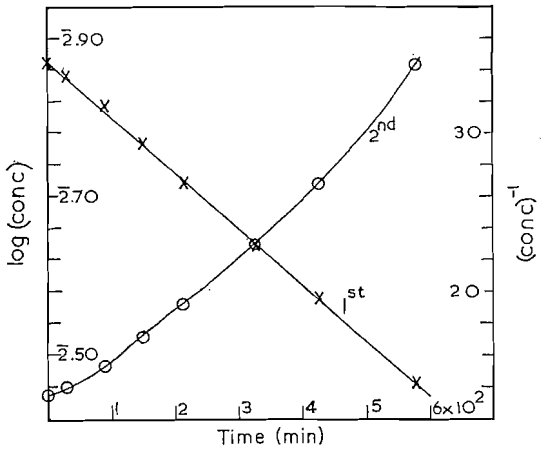

FIG. 1.

Can. J. Chem. Downloaded from www.nrcresearchpress.com by 176.9.209.113 on 09/04/12
For personal use only.

Can. J. Chem. Downloaded from www.nrcresearchpress.com by 176.9.209.113 on 09/04/12
For personal use only.

The analysis for dithionite in alkaline solution presents some difficulties that are not encountered in neutral or weakly acid solution. K. and E. Jellinek used the reduction of ammoniacal copper (II) sulphate for their analyses. In alkaline solution this reagent gives a heavy black precipitate (probably a sulphide) with dithionite, and the method is impracticable. Hahn (4, 5) used titration with ferric chloride, in the presence of a mixed indicator of potassium thiocyanate and ferricyanide, but this was found to give irregular results in alkaline solution. However, it worked well for the analyses of solid sodium dithionite, and was used in runs with the solid. The method finally used in the solution runs was that due to Smith (6). A known volume of dithionite was run into excess ammoniacal silver nitrate; silver is then precipitated. This was filtered off, washed, dissolved in nitric acid, and titrated with chloride by the Volhard method. The chief difficulty was that sometimes the precipitate was so finely divided that filtration was virtually impossible, and samples were occasionally lost because of this.

The reagents used were all of analytical reagent quality, with the exception of the sodium dithionite. The purest available solid was about 90% sodium dithionite, the main impurities being the decomposition products, sodium thiosulphate and sulphite. Recrystallization did not much improve this as some decomposition always occurred. Solutions were made from this, and were then analyzed in order to be able to calculate the ionic strength. This was then adjusted to the desired value by adding sodium fluoride.

RESULTS

The runs were generally not long enough to distinguish unambiguously the order of the reaction solely from one run. Accordingly in Table I the results are given in the form of the best values of the first order rate constants (k_1), and the second order rate constants (k_2), obtained in the usual way from a plot of time against log (concentration) or (concentration)$^{-1}$. This table also gives runs at various ionic strengths, at various temperatures, and at various initial sodium hydroxide concentrations.

TABLE I

Decomposition of sodium dithionite in aqueous solution

Run	Temp., °C	Initial ionic strength	Initial ($Na_2S_2O_4$), molar	Initial (NaOH), molar	k_1, min^{-1}	k_2, (g-molecule/l.)$^{-1}$ min^{-1}
1	88.5	0.70	0.064	0.10	4.3×10^{-4}	7.4×10^{-3}
2	88.5	0.67	0.062	0.10	4.4	8.0
3	88.5	0.70	0.034	0.10	4.6	15.1
4	88.5	0.70	0.123	0.10	4.6	4.0
5	88.5	0.70	0.069	0.20	6.3	10.6
6	88.5	0.70	0.130	0.20	6.4	6.1
7	88.5	0.71	0.142	0.20	6.1	5.6
8	88.5	0.74	0.067	0.05	4.3	7.0
9	88.5	0.70	0.067	0.15	5.5	9.6
10	88.5	0.35	0.068	0.10	2.9	4.5
11	88.5	0.99	0.063	0.10	5.0	7.5
12	88.5	1.53	0.065	0.10	5.8	10.5
13	98.0	0.71	0.065	0.10	11.3	18.9
14	84.1	0.70	0.065	0.10	3.0	5.15
15	79.4	0.69	0.059	0.10	1.65	3.0
16	98.0	0.70	0.074	0.20	16.0	35.8

The first thing that is apparent from this table is that the reaction is first order in dithionite. Runs 1 to 4, or 5 to 7, where all other variables are kept constant show this clearly. Figure 1 shows a plot of log (concentration) and (concentration)$^{-1}$ against time for run 16. This gives a better straight line for a first order reaction. This, as well as the great differences in over-all rate, proves that the reaction in alkaline solution is not the

same as that examined by K. and E. Jellinek. The obvious explanation of this is that under the conditions of their experiments the solution contained $HS_2O_4^-$ or $H_2S_2O_4$, and that these decompose faster than $S_2O_4^{--}$. Similar behavior is, of course, found with other acids and their salts, e.g. thiosulphates and hypochlorites. There seem to be no reliable values of the ionization constants of dithionous acid, so it is impossible to calculate the concentrations of $HS_2O_4^-$ or $H_2S_2O_4$ in K. and E. Jellinek's experiments. With an activation energy as low as 8 kcal, as calculated from their results, it seems quite probable that molecules of dithionous acid are reacting.

The effect of varying concentrations of sodium hydroxide can be seen from runs 8, 1, 9, and 5. The rate increases somewhat at higher sodium hydroxide concentrations, but the change is very small at lower concentrations. Presumably hydroxide ions catalyze the reaction to some extent, but the effect is not proportional to their concentration.

Ionic strength was varied in runs 10 to 12, taken together with earlier runs at an ionic strength of 0.7. The results show a moderate change in rate with ionic strength, higher ionic strengths giving increased rates. Somewhat similar behavior is, of course, found in other ionic reactions.

Variation in temperature in runs 13 to 15 gave rate constants which show a reasonably linear plot of log k against $1/T$ of the usual sort. The activation energy is 26 kcal/g-molecule (or perhaps, $26\frac{1}{2}$ kcal/g-molecule). If $k = A\,e^{-E/RT}$, then, expressing k_1 in (seconds)$^{-1}$, log $A = 10.9$, or ln $A = 25.1$. This is a somewhat low figure, but not exceptionally so. This is for concentrations of hydroxide ion low enough for them apparently not to affect the rate to any great extent.

The mechanism of the reaction cannot be deduced with any certainty from these results. The most plausible suggestion, perhaps, is that the initial, and slowest, stage is a reaction with water:

$$S_2O_4^{--} + H_2O \rightarrow HSO_2^- + HSO_3^-$$

followed by a more rapid further reaction of HSO_2^- with dithionite ions:

$$HSO_2^- + S_2O_4^{--} \rightarrow HSO_3^- + S_2O_3^{--}.$$

This suggestion is very tentative. However, if it is correct, the reaction is really bimolecular, and $d[S_2O_4^{--}]/dt = -k_2[S_2O_4^{--}].[H_2O]$. Allowing for the concentration of water, and if $k_2 = A_2\,e^{-E/RT}$, then log $A_2 = 9.2$ (time in seconds), a fairly typical figure (7).

DECOMPOSITION OF THE SOLID

It seemed of interest to compare rates in the solid with those in solution, although if the above suggestion about the mechanism is correct, the reaction must necessarily go by a different route in the solid. Finely ground solid (between 100 and 200 mesh) was used, and the fraction decomposed at different times is given in Table II.

These results give typical S-shaped curves when the fraction decomposed (represented by α in the equations below) is plotted against time. Various equations have been proposed to explain similar curves for other reactions of solids (e.g. (8)), the different equations being based on different mechanisms. In applying them, there is a difficulty because the sample took a finite time to come to the temperature of the run, and consequently there is some doubt about the true zero of time for the reaction. To avoid this difficulty the method generally adopted was to plot the observed time to reach a given value of α against the calculated time to reach the same value. This was done for the range of α from 0.1 to 0.95, and a suitable equation should give a straight line for the resulting graph. Even so the decision between various equations is not too easy, since all give, if

Can. J. Chem. Downloaded from www.nrcresearchpress.com by 176.9.209.113 on 09/04/12
For personal use only.

TABLE II

Decomposition of solid sodium dithionite

Run 1: 155° C								
Time (min)	30	60	90	120	150	180	210	240
α	0.038	0.065	0.092	0.151	0.230	0.355	0.458	0.610
Time (min)	272	30	333	362				
α	0.772	0.834	0.908	0.953				
Run 2: 160° C								
Time (min)	30	60	93	120	150	165	180	195
α	0.081	0.123	0.225	0.366	0.623	0.712	0.798	0.900
Time (min)	210	225						
α	0.941	0.962						
Run 3: 165° C								
Time (min)	15	30	45	60	75	90	107	120
α	0.062	0.095	0.145	0.257	0.405	0.563	0.737	0.854
Time (min)	135	150	165					
α	0.939	0.983	0.994					
Run 4: 170° C								
Time (min)	15	30	45	60	75	90	105	
α	0.076	0.204	0.507	0.741	0.902	0.978	0.989	

α is plotted against time, roughly linear middle sections, similar to what is found experimentally; and consequently graphs of calculated against experimental times were always linear over a considerable range in the middle. Hence a decision for or against a possible mechanism largely depended on the ends of the curves.

The equations quoted by Garner (8) may be divided into those which take account of overlap and interference between growing reaction zones, and those which do not. The latter are only applicable in the early stages of the reaction, and so cannot be applied here. On the former, the following deductions seem possible.

1. Branching Nuclei, Interfering During Growth

Garner and Hailes (9) suggested that nuclei might initially form very rapidly up to a certain maximum number, and thereafter increase by branching. At the same time nuclei might disappear as centers of reaction by becoming totally surrounded by reacted material. The chance of this happening was taken to be proportional to α. If N is the number of nuclei at time, t, these assumptions mean that

$$dN/dt = k_3N - k_4\alpha N$$

where k_3 and k_4 are constants. If each nucleus grows linearly with time, $d\alpha/dt = k_1N$, the nuclei being supposed to grow out in one dimension and not as spheres. Hence the curve of α against t will have an inflexion at $\alpha = \alpha_1 = k_3/k_4$. If $N = 0$ at $\alpha = 0$, these equations lead to

$$\ln [\alpha/(2\alpha_1 - \alpha)] = k_3t + C$$

where C is an integration constant.

In the present curves α_1 is about 0.5 (as was found in other cases by Garner and Hailes), and a plot of $\ln [\alpha/(1-\alpha)]$ against t was fairly linear. The values of k_3 were calculated to be:

T	155	160	165	170	° C
k_3	1.9	3.3	5.4	8.2×10^{-2}	min^{-1}.

These values make the activation energy for the growth process 36 kcal/g-molecule.

Can. J. Chem. Downloaded from www.nrcresearchpress.com by 176.9.209.113 on 09/04/12
For personal use only.

There is some deviation from this equation if α is small, but in any case the approximations made in deriving it are not valid at low values of α. This is because the assumption that $N = 0$ at $\alpha = 0$ is not really correct. If we assume that $N = N_1$, a small number, when $\alpha = 0$, the equation becomes:

$$\ln \{(\alpha - N_1k_1/k_3)/(2\alpha_1 - N_1k_1/k_3 - \alpha)\} = k_3(1 - N_1k_1/k_3\alpha_1)t + C.$$

As α evidently approaches unity at large values of t, presumably

$$2\alpha_1 - N_1k_1/k_3 = 1.$$

Fairly good lines are obtained if $N_1k_1/k_3 = 0.04$ for all runs; the resulting values of k_3 are:

T	155	160	165	170	°C
k_3	2.35	3.65	5.6	9.05×10^{-2}	min^{-1}.

These give an activation energy of 34.1 kcal/g-molecule.

2. Random Surface Nucleation Followed by Rapid Surface Growth

Here it is proposed that random nucleation occurs, but once it has occurred on a grain of the material either the entire surface, or certain faces of it, is rapidly covered with a reaction zone, which then moves slowly towards the center. If N_0 is the total number of grains, and N of these are nucleated, then $dN/dt = k_1(N_0 - N)$. If the reaction zone moves at a constant speed, α is given by:

$$\alpha = (1/k_1t_0)\ (e^{-k_1t} + k_1t - 1)$$

where t_0 is the time any one grain takes to decompose. This is valid up to $t = t_0$, as it does not allow for some grains having totally decomposed. If $t > t_0$, α is given by:

$$\alpha = 1 - (1/k_1t_0)\ (e^{k_1t_0} - 1)\ e^{-k_1t}.$$

When these equations were compared with the experimental curves, it was not possible to get a good fit. In particular they make α rise much too rapidly at first as compared with experiment, though this improves somewhat if k_1t_0 is very large. However, it seems unlikely that this is the correct mechanism. Other assumptions about the proportion of the surface nucleated led to modified equations, but none were found to give a good agreement with experiment.

3. Random Surface Nucleation, but no Rapid Surface Growth

On this picture nucleation starts at a point on the surface of the grain, and the reacted zone spreads inwards like a growing sphere. If each grain is itself spherical, the fraction of any grain reacting in time, t, is

$$\alpha_1 = 4(t/t_0)^3 - 3(t/t_0)^4$$

where t_0 is the time for any grain to react completely. If nucleation is random the equations for α are:

[i] $t < t_0$; $\alpha = (24A^3 + 72A^4)\ (e^{-U/A} - 1) - 3U^4 + 4U^3 + 12AU^3 - 12AU^2 - 36A^2U^2 + 24A^2U + 72A^3U$

[ii] $t > t_0$; $\alpha = 1 - e^{-U/A}[24A^3 + 72A^4 - (12A^2 - 48A^3 + 72A^4)\ e^{1/A}]$

where $U = t/t_0$ and $A = 1/k_1t_0$, and k_1 is the rate constant for the nucleation process.

Can. J. Chem. Downloaded from www.nrcresearchpress.com by 176.9.209.113 on 09/04/12
For personal use only.

These equations make the rise in α too steep at first unless k_1t_0 is fairly large (about 7 or more), under which conditions the rate of nucleation is rapid compared with the time for a particle to react. However, even if k_1t_0 is large a plot of U against experimental times for the same α does not give a good straight line. Hence this is probably not the correct mechanism.

4. Random Nucleation with Ingestion of Nuclei

Here it is proposed that nuclei are formed at random throughout the material, and the radii of the nuclei grow at a constant rate. Allowance is made for the impingement of the nuclei on each other. This leads to the equation:

$$-\ln (1-\alpha) = B(e^{-U}-1+u-u^2/2+u^3/6)$$

where $u = k_1t$, and k_1 is the rate constant for nucleation. B is a constant equal to $8\pi N_0k_2^3/V_0k_1^3$, where N_0 is the total number of nuclei, k_2 is the rate of nucleus growth, and V_0 is the total volume of material (10).

The form of the curves is little altered by changes in B, so that it is not possible to deduce the best value of B with any precision. Plots of u against the experimental time for the same values of α give good lines if B is fairly large (about 10), though the data for 170° C fit a somewhat smaller value of B (about 2 to 5). If B is 10 at all temperatures, values of k_1 are:

T	155	160	165	170	° C
k_1	2.55	4.3	7.15	10.2×10^{-3}	min^{-1}.

This gives a linear plot of log k_1 against $1/T$ corresponding to an activation energy of 35.7 kcal/g-molecule.

However, B should vary with temperature, and as the activation energy of nucleation is presumably larger than that of growth, B should fall with increasing temperature. Different values of B at 170° C, with $B = 10$ at 155° C, give the following activation energies:

B (170° C)	10	5	2	1
E_1	35.7	39.0	45.4	50.4 kcal/g-molecule
E_2	35.7	33.2	31.9	31.1 kcal/g-molecule.

Here E_1 is the activation energy of nucleation, and E_2 that of growth. If $B = 5$ at 170° C, then $k_1 = 12.0\times10^{-3}$ min^{-1}; if $B = 2$, $k_1 = 15.5\times10^{-3}$ min^{-1}, both at 170° C.

As a general conclusion, this last equation undoubtedly gives the best agreement with the experimental points, and is somewhat superior to the equation for the branching mechanism; so probably the correct mechanism is one of random nucleation and linear growth. Although some other mechanisms have been definitely excluded above, one cannot be certain that some hitherto unsuggested mechanism might not also fit the experimental points. Because of the small change in the curves representing random nucleation and linear growth as B varies, it is not possible to separate all the rate constants, but that for the nucleation rate must be approximately as indicated above. The activation energy for growth is 32 to 33 kcal/g-molecule, while the most that can be said about the activation energy for nucleation is that it is probably 40 to 45 kcal/g-molecule. As is to be expected, these are considerably larger than the solution activation energy of $26\frac{1}{2}$ kcal/g-molecule.

Can. J. Chem. Downloaded from www.nrcresearchpress.com by 176.9.209.113 on 09/04/12
For personal use only.

REFERENCES

1. JELLINEK, K. and JELLINEK, E. Z. physik. Chem. **93**, 325 (1919).
2. LANGE, N. A. Handbook of chemistry. Handbook Pubs., Inc., Sandusky, Ohio. 1956. p. 1202.
3. DEINES, O. and ELSTNER, G. Z. anorg. u. allgem. Chem. **191**, 340 (1930).
4. HAHN, F. L. Anal. Chim. Acta, **3**, 62 (1949).
5. HAHN, F. L. Anal. Chim. Acta, **3**, 65 (1949).
6. SMITH, J. H. J. Am. Chem. Soc. **43**, 1307 (1921).
7. SMITH, J. H. J. Am. Chem. Soc. **43**, 76 (1921).
8. GARNER, W. E. Chemistry of the solid state. Butterworth Scientific Publications, London. 1955. Chap. 7.
9. GARNER, W. E. and HAILES, H. R. Proc. Roy. Soc. A, **139**, 576 (1933).
10. AVRAMI, M. J. Chem. Phys. **7**, 1103 (1939); **8**, 212 (1940).

Can. J. Chem. Downloaded from www.nrcresearchpress.com by 176.9.209.113 on 09/04/12
For personal use only.

Can. J. Chem. Downloaded from www.nrcresearchpress.com by 176.9.209.113 on 09/04/12
For personal use only.

GAS ADSORPTION CHROMATOGRAPHY[1]

JAMES F. HANLAN AND MARK P. FREEMAN[2]

ABSTRACT

It is found that the "retention volume" in gas adsorption chromatography may be identified in a very simple way with the concept of "apparent volume" in the equation of state for high temperature physical adsorption first derived by Halsey *et al.* It is shown that a considerable body of experimental chromatographic data reduces down to the two parameters of the theory in a reasonable way. The single parameter describing temperature dependence is seen to be related simply to the number of carbons in the skeleton for a series of hydrocarbons, while the parameter describing column capacity shows regular, though unanticipated, behavior. This theoretical connection provides a complete link between static measurements and gas adsorption chromatography.

Gas adsorption chromatography or gas solid chromatography is the name applied to the chromatographic process using an adsorbent as the fixed phase and a gas as the mobile phase. It is useful chiefly in the chromatographic separation of mixtures of permanent gases and vapors of low-boiling liquids for which purpose it seems more suitable than the more frequently encountered gas–liquid partition chromatography.

As it is commonly used, gas adsorption chromatography apparatus is very similar to that employed in gas–liquid partition chromatography with the substitution of an adsorbent for the fixed bed. It is characterized by requiring a much more sensitive temperature control for reproducible results. Elution chromatography and frontal analyses may be performed in either case, but the adsorption chromatogram is characterized by asymmetric break-through curves which have thus far defied a simple quantitative interpretation. This latter fact has complicated a theoretical interpretation by the "theoretical plate" analysis so useful in the partition chromatogram (1).

At the same time, the aforementioned sensitivity to temperature change in adsorption chromatography makes it possible to separate virtually any mixture on the same column by judiciously selecting the temperature (barring chemisorption), whereas in partition chromatography it is often necessary to change the liquid employed in the fixed phase.

This work represents an attempt to present a comprehensive theoretical framework for the interpretation of gas adsorption chromatographic results in terms of the rigorously derived equation of state for the interaction of gases and surfaces developed by Halsey *et al.* (2, 3, 4, 5, 6) also (7, 8). Such an interpretation would necessarily link gas chromatographic results to the static measurements employed in these investigations, as well as provide the desired predictive information about temperature dependence for the chromatogram.

The experimental data (9) used in the verification of the theory derived here were obtained by Dr. H. Habgood of the Research Council of Alberta, Edmonton, Alberta, Canada, and one of us (James F. Hanlan) at that laboratory.

The experimental observation made by these investigators indicating the suitability of the gas–surface interaction state equation was that when the logarithm of the retention volume (10) (which is defined as the volume of gas leaving the column while a given

[1]*Manuscript received in original form December 18, 1958, and, as revised, April 7, 1959.*
Contribution from the Department of Chemistry, University of California, Berkeley, California.
[2]*Present address: Research Division, American Cyanamid Company, Stamford, California.*

constituent is passing through the column) of gas A minus that for H_2 is plotted vs. $1/T$, a fairly good straight line relationship holds (Fig. 1). This is reminiscent of the concept of "excess volume" in the theory of Halsey *et al.* which exhibits similar behavior.

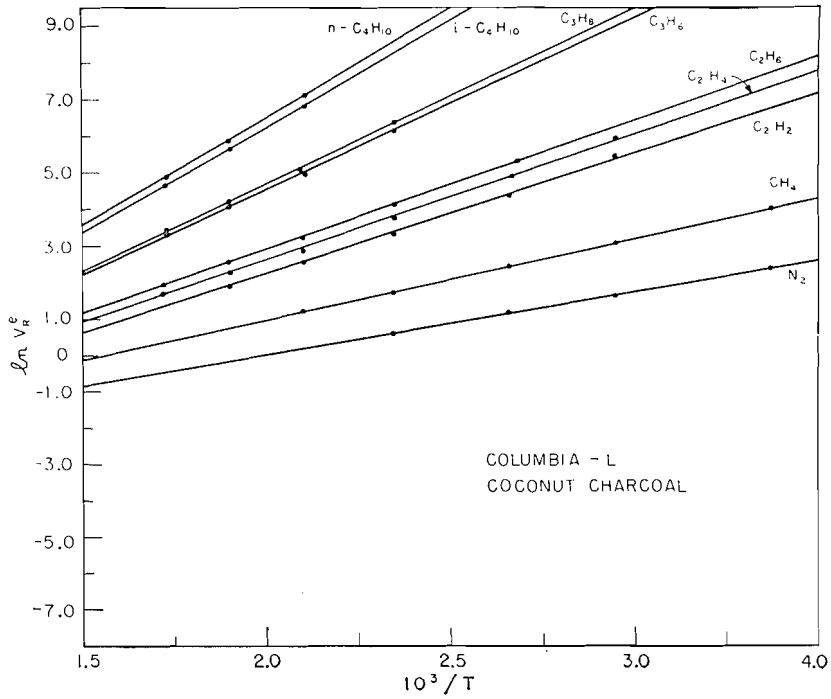

FIG. 1. The natural logarithm of the experimental excess retention volume on Columbia L charcoal plotted vs. reciprocal temperature for several gases. Five points of the original data have been discarded where marked deviations from the trend were observed. These deviations were not systematic and were probably attributable to experimental error.

THEORY

A basic underlying assumption will be implicitly made in the following derivation. Namely, it will be assumed that some sort of equilibrium exists within the gas phase passing through the column so that the gas systems (molecules or atoms) are always at their equilibrium distribution with respect to the gas surface potential well. This assumption is supported by the observation (10) that retention volume is independent of flow rate over a wide range of flow rates.

The retention volume is given as the product of retention time and flow rate through the column:

$$[1] \qquad V_R = F \cdot t_A = (\eta kT/P) \cdot t_A$$

where F is the flow rate in cm³/sec (at column temperature T and pressure P) and η is the flow rate in systems per second; t_A is the time lag between introducing the mixture and detection of constituent A at the other end. Now, the apparent volume of a vessel containing an adsorbent is just given by:

$$[2] \qquad V_a = NkT/P$$

where V_a is just the imaginary volume that would be required to hold N systems of ideal gas at temperature T and pressure P. If these two concepts are linked, a very

Can. J. Chem. Downloaded from www.nrcresearchpress.com by 176.9.209.113 on 09/04/12
For personal use only.

simple picture emerges for the adsorption chromatogram in terms of the time required for constituent A to get through the column. Namely, if all gas systems pass through the column at the same flow rate, the time to get through is going to vary directly as the apparent volume traversed. That is, one could think of equivalent empty columns of the same diameters, but of lengths proportional to the apparent volumes. This would suggest an immediate formal identification of apparent volume and retention volume so that for a pure constituent the equation of state would be immediately applicable. Unfortunately, gas chromatography always involves a mixture of gases and although the gas–surface equation of state gives an apparent volume in this case, it is not immediately obvious what this means in terms of retention volume. This becomes particularly true when considering gas imperfections and lateral interactions on the surface.

The equation of state (5) for the interaction of a binary mixture of gases and a surface is given by:

$$\frac{1}{V_a} = \frac{X_A}{V_A^0} + \frac{X_B}{V_B^0} - N\left(\frac{C_0}{V_a^{0\,3}}\right) \qquad [3]$$

where the mole fraction of G is X_G(G = A, B) and

$$V_G^0 = V_{geo} + B_{GS} \qquad [4]$$

and is the apparent volume for pure constituent G at zero pressure.

Further,

$$\frac{C_0}{V_0^3} = \frac{X_A^2 C_{AAS}}{(V_A^0)^3} + \frac{X_B^2 C_{BBS}}{(V_B^0)^3} + \frac{X_A X_B C_{ABS}}{V_A^0 V_B^0}\left(\frac{1}{V_A^0} + \frac{1}{V_B^0}\right) \qquad [5]$$

V_{geo} is the true or geometric volume enclosed by the vessel in which the gas is interacting with the surface and excluded by a geometric surface running through the gas–solid interface beyond which gas systems are assumed not to penetrate.

$$B_{GS} = \int_{V_{geo}} [\exp\{-\phi_{ls}^G/kT\} - 1]\, d\tau_i^G \qquad [6]$$

where $d\tau_i^G$ is the differential volume element for the ith gas system of species G and ϕ_{ls}^G is the potential energy function for the interaction of a specific system of this type with the surface. This integral has been tabulated for two potential energy models both of which have been quite successful in interpreting experimental results:

(1) the hard sphere–inverse cube model (2):

$$\phi_{ls}^G = -\epsilon_G^* \frac{D^3}{x^3} \qquad [7]$$

where ϵ_G^* is the depth of the potential energy well at the hard sphere repulsion distance, $x = D$, and

(2) the 9-3 model (7):

$$\phi_{ls}^G = \left(\frac{3\sqrt{3}\epsilon^*}{2}\right)\left[\left(\frac{s_0}{s}\right)^9 - \left(\frac{s_0}{s}\right)^3\right] \qquad [8]$$

where ϵ^* is as before and s_0 is the gas–surface separation where the attractive and repulsive energies just cancel. This second potential energy model will be used throughout the paper as it is somewhat easier to use. A reduced form of this integral (B_{GS}/As_0) (where A is the area) for this potential model is in reference (7) with three additional values tabulated in Table I.

Can. J. Chem. Downloaded from www.nrcresearchpress.com by 176.9.209.113 on 09/04/12
For personal use only.

TABLE I
Addition to the Appendix in reference 7

ϵ^*/kT	B_{AS}/As_0
13.087	8.291×10^4
14.627	3.625×10^5
16.166	1.579×10^6

$C_{GG'S}$ can be broken up into a gas imperfection factor and a term involving the simultaneous interaction of two gas systems of type G and G′ and the surface (8):

$$C_{GG'S} = -2(V_G^0 + V_{G'}^0 - V_{geo})B_{GG'} + C' \quad [9]$$

where $B_{GG'}$ is the (mixed) second virial coefficient and

$$C' = \int \{\exp[-\phi_{1s}^{G}/kT]-1\} \int \{\exp[-\phi_{2s}^{G'}/kT]-1\}\{\exp[-\phi_{12}^{GG'}/kT]-1\}\, d\tau_1^G, d\tau_2^{G'}. \quad [10]$$

The most successful model for this integration to date is tabulated in the appendix of reference (8) for a single constituent. This involves the 9-3 potential model for gas–surface attraction and a hard sphere repulsion at distance $^n r_0$ between the interacting gas systems. This integral is given as a function of the reduced gas–surface potential energy and the distance ratio $\delta = s_0/^n r_0$.

Equations [3], [4], and [5] undergo considerable simplification if it is assumed that the carrier gas, B, has no net attraction to the surface or to other gas systems (apparently true for He at room temperature and above). If ideal behavior is likewise assumed for the bulk carrier phase, then

$$B_{BS} = B_{BB} = B_{AB} = C_{BBS} = C_{ABS} = 0 \quad [11]$$

and equation [5] becomes

$$\frac{C_0}{V_0^3} = \frac{X_A^2 C_{AAS}}{V_A^{0\,3}}. \quad [12]$$

Equation [4] for the carrier reduces to:

$$V_B^0 = V_{geo}. \quad [13]$$

Substituting [12] and [13] in [3] yields:

$$\frac{1}{V_a} = \frac{X_A}{V_A^0} + \frac{X_B}{V_{geo}} - \frac{NX_A^2 C_{AAS}}{V_A^{0\,3}}. \quad [14]$$

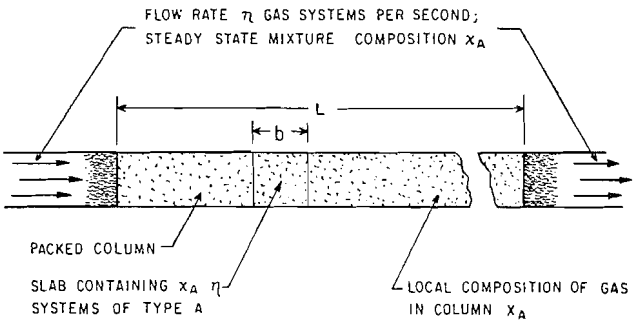

FIG. 2. Schematic representation of the adsorption chromatographic column.

Can. J. Chem. Downloaded from www.nrcresearchpress.com by 176.9.209.113 on 09/04/12
For personal use only.

Can. J. Chem. Downloaded from www.nrcresearchpress.com by 176.9.209.113 on 09/04/12
For personal use only.

To effect the necessary derivation, it is convenient to assume a steady state mixture (composition χ_A) to be flowing in and out of the column (Fig. 2) at a flow rate of η systems per second. The necessary enrichment of A in the column results in a local composition of X_A which is generally different from χ_A. Clearly $\chi_A\eta$ is the number of systems of type A leaving the column each second. The same number of systems of type A must cross every boundary in the column each second so that b, the length of a slab of column containing $\chi_A\eta$ systems of type A, divided into L, the length of the column, will give the time required for a labeled front in gas A to travel the length of the column. (This does not allow for column end effects, but this will be taken care of below.)

[15] $$t_A = L/b$$

If the extensive quantities in the slab are denoted by double primes and use is made of the definition of mole fraction, then [14] may be rewritten:

[16] $$\frac{N''}{V_{a''}} = \frac{N_{A''}}{V^0_{A''}} + \frac{N_{B''}}{V_{geo''}} - \frac{N_{A''}{}^2 C_{AAS''}}{V^{0\,3}_{A''}}.$$

But by definition $N_{A''} = \chi_A\eta$. Using the assumed ideality of the carrier gas

$$N_{B''} = P_B V_{geo''/kT} = (1-\chi_A) P V_{geo''/kT}$$

and relation [2] [16] may be written:

[17] $$\frac{P}{kT} = \frac{\eta}{V^0_{A''}} - \chi_A\eta^2 \frac{C_{AAS''}}{V^{0\,3}_{A''}}.$$

If the extensive quantities per unit length are denoted by single primes, [17] becomes:

[18] $$\frac{P}{kT} = \frac{\eta}{bV^0_{A'}}\left[1 - \chi_A\eta \frac{C_{AAS'}}{bV^{0\,2}_{A'}}\right]$$

or solving for b (assuming the term on the right in the brackets, eq. [18], to be small):

[19] $$b \approx \frac{\eta kT}{PV^0_{A'}}\left[1 + \frac{\chi_A P C_{AAS'}}{kTV^0_{A'}}\right]^{-1}.$$

Using relations [15] and [1] one finally obtains for V_R

[20] $$V_{R_A} = V^0_A + \chi_A P \frac{C_{AAS}}{kT}.$$

The retention volume for the carrier gas by the same analysis is just

[21] $$V_{R_{carrier}} = V_{geo}.$$

To be consistent with the data as they were received and to subtract out the effect of unpacked parts of the column and end effects so far as possible, one must subtract equation [21] from equation [20] to get an excess retention volume:

[22] $$V^e_R = B_{AS}\left(1 + \frac{\chi_A P}{kT}\frac{C_{AAS}}{B_{AS}}\right).$$

One sees that under the conditions of the derivation if χ_A is zero then the excess retention volume is just equal to B_{AS} which is identical with

[22a] $$V_{ex}|_{p=0} = V^0_A - V_{geo} = B_{AS}$$

for the static measurements. C_{AAS} has generally been observed to be negative while

B_{AS} is always positive or negligible so that the usual case will have a higher concentration of gas A going through the column faster (lower retention volume), which means that a narrow rectangular initial distribution will tend to skew forward. This is what is observed and in fact the gas adsorption chromatogram is usually characterized by sharp anterior and sloping posterior edge. At very low partial pressures where chromatograms are usually run, this will produce a negligible error if retention time is measured to the peak which is the easiest part of the chromatogram to identify. At the same time, if frontal analysis is performed at different mole fractions, one may determine C_{AAS} experimentally. This would seem like a good way to obtain this experimentally elusive parameter, which is still of considerable theoretical interest (8).

It was found necessary in the course of the derivation to assume $1 \gg \chi_A P C_{AAS}/kTV_A^0$ or its equivalent. For a specific system all these quantities may be evaluated independently by static measurements. Take as an example argon on carbon black (Black Pearls No. 71) (7) at 273° K,

$$\begin{aligned}
&\text{sample wt.} = 10.63 \text{ g},\\
&C_{AAS} = -240\times10^{-20}(\text{cm})^6,\\
&V_A^0 = 150 \text{ cm}^3,\\
&kT = 3.72\times10^{-20} \text{ cc atm},\\
&V_{geo} = 28.5 \text{ cm}^3,\\
&B_{AS} = 121.5 \text{ cm}^3,
\end{aligned}$$

or

$$\frac{\chi\Delta P C_{AAS}}{kTV_A^0} = -.43\,\chi_A|_{p=1 \text{ atm}}.$$

If the mole fraction of A in the gas phase is kept below, say, 0.1 then the assumption that this product is much less than unity is clearly all right for this particular assembly. It would seem that if it were not small, no peak would be distinguished, which probably sets the lower temperature limit to gas adsorption chromatography.

Enthalpy of Adsorption

Using a model for physical adsorption based on the Gibbs boundary condition, one may consider the interaction to be a phase change from the gas phase to an imaginary two dimensional phase of zero volume. It has been shown (7) that the surface excess partial molar enthalpy at zero coverage is given by the derivative:

$$[23] \qquad \frac{\partial \ln T/V_{ex}^0}{\partial\, 1/RT} = \Delta H = \frac{\partial \ln T/V_R^e}{\partial\, 1/RT}$$

where V_{ex}^0 and V_R^e are those volumes at zero pressure and mole fraction respectively. Finally, using the definition of retention volume and keeping a constant flow rate (systems/second)

$$[24] \qquad \frac{\partial \ln (t_A - t_B)}{\partial\, 1/T} = \frac{-\Delta H}{R}$$

where B is as before a noninteracting constituent. This enthalpy may be related unambiguously to the parameter ϵ^* (7) which provides a way of getting this parameter without curve fitting. The enthalpy derived thus is of questionable predictive value because of a considerable temperature coefficient, especially at high temperatures, but

Can. J. Chem. Downloaded from www.nrcresearchpress.com by 176.9.209.113 on 09/04/12
For personal use only.

it is equal to the initial calorimetric heat of adsorption (L'Hospital's rule) and as such is of interest. Equation [23] is of course easier to apply than equation [24], which has been derived by a different approach (11). These authors did not correct for the interstitial dead space, but they did correct for the time spent in the unpacked region of flow at the ends of the column.

Effect of a Column Pressure Differential

Because of the short loosely packed columns and low rate used in gas adsorption chromatography, one would not expect the relatively large difference between P_i (inlet pressure) and P_o (outlet pressure) encountered in gas–liquid partition chromatography. However, in the framework of this theory any differential that exists can be handled readily.

Recognizing that [1] holds in any differential slab of the column, we obtain

$$\frac{\partial t_A}{\partial \zeta} = \frac{P(\zeta)}{\eta k T} \frac{\partial V_R}{\partial \zeta} \qquad [25]$$

where ζ is the distance from the exit of the column. Making use of d'Arcy's formula for the laminar seepage of a perfect gas through a long capillary* and our boundary conditions,

$$P_{(\zeta)}^2 = P_o^2 + \frac{P_i^2 - P_o^2}{L} \zeta. \qquad [26]$$

From differentiation of [20]

$$\frac{\partial V_R}{\partial \zeta} = V_{A'}^0 + \frac{\chi_A C_{AAS'}}{kT} P_{(\zeta)} \qquad [27]$$

where the primed quantities are again the values per unit length. One may now write an expression for the retention time (using [25], [26], and [27]):

[28]

$$t_A = \int_{\zeta=0}^{\zeta=L} \frac{\partial t_A}{\partial \zeta} d\zeta = \frac{V_{A'}^0}{\eta k T} \int_{\zeta=0}^{\zeta=L} \left(P_o^2 + \frac{P_i^2 - P_o^2}{L} \zeta \right)^{\frac{1}{2}} d\zeta + \frac{\chi_A C_{AAS'}}{\eta (kT)^2} \int_{\zeta=0}^{\zeta=L} \left(P_0^2 + \frac{P_i^2 - P_o^2}{L} \zeta \right) d\zeta.$$

Integrating the right-hand side of equation [28] yields:

$$t_A = \frac{2 V_{A'}^0}{3 \eta k T} \left\{ \frac{P_i^3 - P_o^3}{P_i^2 - P_o^2} \right\} + \frac{\chi_A C_{AAS}}{\eta (kT)^2} \{ (P_i + P_o)^2 - 2 P_i P_o \} \qquad [29]$$

where V_A^0 and C_{AAS} are those quantities for the entire volume. If one makes the approximation that the geometric mean pressure is equal to the arithmetic mean pressure P_m, (a completely justified approximation if $P_i \leqslant 1.30\ P_o$)

$$P_m^2 = \left[\frac{(P_i + P_o)}{2} \right]^2 = P_i P_o. \qquad [30]$$

Equation [29] may be written

$$t_A = \frac{V_A^0}{\eta k T} P_m + \frac{\chi_A C_{AAS}}{\eta (kT)^2} P_m^2. \qquad [31]$$

*Suggested by referee I.

Can. J. Chem. Downloaded from www.nrcresearchpress.com by 176.9.209.113 on 09/04/12
For personal use only.

Leaving P in equation [1] undefined for the moment, one may substitute from [31] for t_A and solve for the measured V_R:

$$[32] \qquad V_R = V_A^0 \frac{P_m}{P} + \frac{\chi_A C_{AAS}}{kT} \frac{P_m^2}{P}.$$

In practice, the flow rate is determined in a measuring device at some other temperature and pressure and is corrected to column conditions assuming ideal gas behavior. If the P used in the correction is the mean column pressure, then clearly

$$[33] \qquad V_R = V_{geo} + B_{AS} + \chi_A \frac{C_{AAS}}{kT} P_m.$$

Comparing [20] and [22*a*] with [33] it is apparent that if the mean pressure is used a column pressure drop introduces no difficulty in the interpretation of the data in terms of the integrals B_{AS} and C_{AAS}.

It may be pointed out that the correction factor for pressure drop along the column (12) proposed by James and Martin:

$$\frac{2}{3} \frac{(P_i/P_o)^3 - 1}{(P_i/P_o)^2 - 1}$$

reduces to

$$P_m/P_o$$

(where P_i, P_o, and P_m have the same significance as above) if the approximation [30] is assumed valid.

Effect of Another Elutant

Helium is moderately hard to obtain and so the question arises whether this theory can be used with a cheaper elutant such as hydrogen or nitrogen. An analysis of the behavior of B_{AS} and the relations leading to the derivation of equation [22] leads to the following conclusions:

(*a*) If the elutant is hydrogen, He may be used as the marker with no other modification.

(*b*) If the elutant is N_2 or a heavier gas, He or H_2 may still be used as the marker. The mixture must be run at a somewhat lower mole fraction for each constituent in order to preserve peaks.

(*c*) Even if the parameter C_{AAS} is quite large the pressure behavior will be dominated (5) (and hence obscured) by $C_{N_2N_2S}$.

Clearly this theory should be no more difficult to use for N_2 than for He but the sensitivity will necessarily be decreased due to the requirement of lower mole fraction for the major components and of course the fact that nitrogen is quite likely to be less different from the gas analyzed for than is He or H_2.

It is interesting that there is nothing in this theory to contradict the notion that a helium marker can move through the column considerably faster than the eluting nitrogen. This is probably easiest to understand in terms of the motion of equivalent empty columns.

Interpretation of Data

The data received by the authors were in the form V_R^e as a function of T. However, the V_R^e had been corrected to 273° K and were converted back to column temperature for application of the theory. The adsorbents used were three coconut charcoals designated Columbia L, BC-4, and BC-90. The last two charcoals were identical except for degree of activation. A hydrogen marker was used to measure the retention time of the

Can. J. Chem. Downloaded from www.nrcresearchpress.com by 176.9.209.113 on 09/04/12
For personal use only.

helium, which introduced some error because of the higher interaction energy of hydrogen and the surface, but an attempt to estimate the effect of this error on the part of the authors showed the error to be negligible within experimental error. The time interval was measured between the peak of the hydrogen marker and the peak of the constituent. As the authors had no way of determining this peak height all data were assumed to be at zero-mole fraction of A. The usual practice does not exceed this by much. The V_R^e's received had been divided by the weight of the adsorbent, but this is by no means necessary for use of the theory.

To fit the data and evaluate the parameters As_0 and ϵ^*/k, it is convenient to use a plot (7) of

$$\ln \frac{B_{AS}}{As_0} \quad \text{vs.} \quad \epsilon^*/kT.$$

One then estimates an ϵ^*/k and plots

$$\ln V_R^e \quad \text{vs.} \quad \left(\frac{\epsilon^*}{k}\right)_{\text{trial}}.$$

Next a

$$\ln As_0$$

is chosen for the data such that the sum of the deviations is zero when

$$\ln \frac{V_R^e}{As_0} \quad \text{vs.} \quad \left(\frac{\epsilon^*}{k}\right)_{\text{trial}}$$

is plotted. The trial value of ϵ^*/k is then systematically varied until the sum of the squares of the deviations of the data from the theoretical plot is a minimum. This procedure may be programed for an electronic computer and the result obtained accurately and rapidly as was done for this work. The final values of ϵ^*/kT and $\ln (B_{AS}/As_0)$ are shown in Table II along with the standard deviation from the curve. A deviation of .03 represents, for example, an average error in V_R^e of 3%. The data are shown thus fitted in Fig. 3. The fit is entirely satisfactory. The values of the parameters required are given in Table III. Since one has two parameters characterizing the chromatogram it would be desirable to make them independent of the amount of column packing used. By its nature ϵ^*/k is already this way, but, of course, the product As_0 is simply extensive in the area (and presumably in the weight) of the packing material. One way to reduce this product to a reproducible parameter would be to divide by the weight of packing material as was done here. Another way would be to subtract the logarithm of As_0 for some calibrating gas such as nitrogen from $\ln As_0$ for each gas and thereby remove the extensive element.

How reproducible any of these parameters would be when determined by different investigators with different columns is of course not known, nor has an attempt been made as yet to directly compare parameters derived from chromatographs with those from static measurements.

Analysis of Trends in the Parameters

Once ϵ^* is known, the complete temperature dependence of V_R^e is known so that it is of interest to see what sorts of predictions one might make about this quantity. The data presented here correlate well with several molecular and bulk properties, but the best correlation for the hydrocarbon series is to the number of carbon atoms in the skeleton (Fig. 4). This is clearly a good linear correlation suggesting the possibility that

Can. J. Chem. Downloaded from www.nrcresearchpress.com by 176.9.209.113 on 09/04/12
For personal use only.

Can. J. Chem. Downloaded from www.nrcresearchpress.com by 176.9.209.113 on 09/04/12
For personal use only.

TABLE II

Gas	Surface BC-4			Surface BC-90		
	ϵ^*/kT	ln (B_{AS}/As_0)	Standard deviation	ϵ^*/kT	ln $B_{AS}/As_0)$	Standard deviation
N_2	6.945	5.586	.0164	5.090	3.940	.0642
	6.251	4.962		4.537	3.457	
	5.532	4.327		4.032	2.016	
	4.962	3.829		3.641	2.672	
CH_4	8.587	7.086	.0363	5.006	3.867	.0231
	7.724	6.293		4.462	3.392	
	6.837	5.488		3.966	2.958	
	6.151	4.873		3.581	2.619	
	5.500	4.299		—	—	
	4.981	3.845		—	—	
C_2H_4	10.045	8.443	.0537	8.010	6.555	.0558
	9.063	7.527		7.140	5.762	
	8.086	6.625		6.345	5.047	
	7.336	5.940		5.730	4.502	
	6.566	5.246		5.220	4.054	
C_2H_6	10.545	8.914	.0535	8.552	7.053	.0836
	9.493	7.927		7.623	6.201	
	8.489	6.995		6.775	5.432	
	6.878	5.525		5.573	4.364	
C_3H_6	10.782	9.136	.0152	8.493	6.998	.0283
	9.786	8.201		7.670	6.243	
	8.760	7.246		6.987	5.624	
	—	—		6.465	5.155	
C_3H_8	11.121	9.457	.0231	10.152	8.544	.0296
	10.109	8.503		9.022	7.488	
	9.049	7.514		8.147	6.681	
	—	—		7.422	6.019	
	—	—		6.868	5.516	
i-C_4H_{10}	—	—	—	9.953	8.356	.0212
	—	—		9.067	7.530	
	—	—		8.390	6.903	
n-C_4H_{10}	—	—		10.415	8.792	
				9.488	7.923	.0475
				8.780	7.264	

Can. J. Chem. Downloaded from www.nrcresearchpress.com by 176.9.209.113 on 09/04/12
For personal use only.

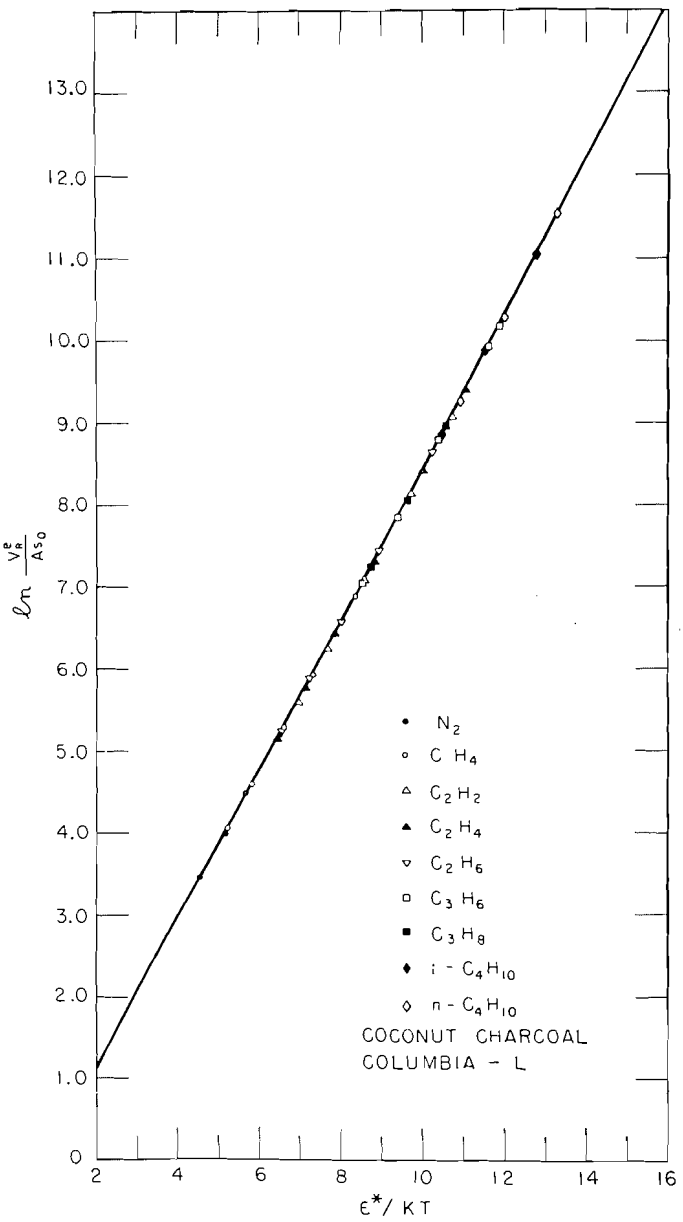

FIG. 3. Fit of the chromatographic results to the reduced curve of the theory for several gases interacting with Columbia L charcoal.

TABLE III

Surface	Gas	ϵ^*/k (° K)	ln As_0 (units of cm³/g)	ln $\frac{As_0\|A}{As_0\|N_2}$
Columbia L	N_2	1938	−2.83	—
	CH_4	2484	−2.83	0.0
	C_2H_2	3656	−3.69	0.86
	C_2H_4	3758	−3.48	0.65
	C_2H_6	3820	−3.30	0.47
	C_3H_6	4945	−3.77	0.94
	C_3H_8	5062	−3.81	0.98
	i-C_4H_{10}	6078	−4.20	1.37
	n-C_4H_{10}	6320	−4.40	1.57
BC-4	N_2	2078	−3.34	—
	CH_4	2570	−3.07	0.27
	C_2H_4	3789	−3.58	−0.24
	C_2H_6	3969	−3.64	−0.30
	C_3H_6	5055	−4.04	−0.70
	C_3H_8	5219	−4.20	−0.86
BC-90	N_2	1906	−2.94	—
	CH_4	1875	−1.87	1.07
	C_2H_4	3000	−2.46	0.48
	C_2H_6	3203	−2.53	0.41
	C_3H_6	4016	−2.75	0.19
	C_3H_8	4266	−3.03	−0.09
	i-C_4H_{10}	5211	−3.51	−0.57
	n-C_4H_{10}	5453	−3.75	−0.81

in a more heterogeneous series one could sum over different types of heavy atoms or functional groups in the molecule to obtain an accurate estimate of ϵ^*/k. This possibility should be thoroughly checked because of the obvious analytical applications of such a correlation.

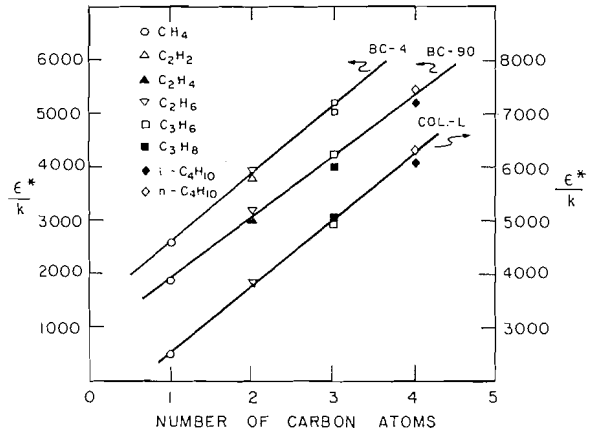

FIG. 4. Observed trends in the value of the parameter ϵ^*/k for all hydrocarbon assemblies analyzed as a function of the number of carbon atoms in the interacting gas.

The parameter As_0 when suitably normalized is as characteristic of a given gas–surface interaction as is ϵ^*/k, and so the two parameters together should serve as positive means to identify a particular molecular species for a precalibrated solid whether or not the column itself has been precalibrated. The detailed behavior of As_0 as an area-depen-

Can. J. Chem. Downloaded from www.nrcresearchpress.com by 176.9.209.113 on 09/04/12
For personal use only.

Can. J. Chem. Downloaded from www.nrcresearchpress.com by 176.9.209.113 on 09/04/12
For personal use only.

dent parameter is somewhat less satisfactory than has been observed for rare-gas atoms on carbon blacks. Even in this case there was the rather remarkable phenomenon that As_0 decreased as atomic size (and interaction energy) increased. For a constant area, this could mean a somewhat closer distance of balanced attractive and repulsive potentials. Likewise, it could mean a considerable area of small crevices or capillaries more accessible to the smaller atom than the larger. Finally, it could indicate the presence of hot-spots (7) (portions of the surface with much higher energy of interaction). This effect is much magnified in these chromatographic data (possibly because of the non-spherical systems?). For example, the parameter As_0 for Columbia L charcoal increases by 400% in going from normal butane to methane, whereas by way of comparison, changing from argon to helium on carbon black with static measurements increased As_0 by only 30%. Finally, note that when the charcoal is activated as in going from BC-4 to BC-90 (presumably by the water gas or some similar reaction) the energy of interaction for all hydrocarbons drops by about 20–30% at the same time the specific values of the parameters As_0 increase by a factor of 3.25. This is in contrast to the behavior of nitrogen which decreases in energy by 2.6% and increases in the value of the product As_0 by 52% in the same activation process.

In Table IV can be seen the increase of the area with activation. This calculation, of course, requires the approximation that s_0 be nearly the same for a given gas on the two

TABLE IV

A	$\ln \frac{As_0\vert_{\text{BC-90}}}{As_0\vert_{\text{BC-4}}}$	$\frac{A\vert_{\text{BC-90}}}{A\vert_{\text{BC-4}}}$
CH_4	1.17	3.22
C_2H_4	1.29	3.63
C_2H_6	1.11	3.04
C_3H_6	1.12	3.06
C_3H_8	1.20	3.32
Mean value	1.178	3.25

different surfaces. The values for the different gases are remarkably uniform with a mean value of 3.25 for the ratio of the area of charcoal BC-90 to that of BC-4. This compares well with the monolayer areas of 630 and 200 m^2/g respectively (9). If s_0 is estimated as one half the interlayer thickness of graphite, 1.7 Å, (13) plus one half the van der Waal's radius of the adsorbate, the area is calculated from the parameter As_0 to be of the order of the monolayer area. The decrease of ϵ^* with activation points to surface heterogeneity, for example, crevices which upon widening with activation would permit fewer adsorbent nearest neighbors per adsorbed molecule. This might be expected to appear under these conditions, i.e., low pressure and high temperature, where such effects would not be "washed out" by large numbers of strong lateral interactions. The similarity of the ratios of the monolayer areas and of our A's may be taken to mean that all portions of a heterogeneous surface increase equally. On the other hand, this may be interpreted as indicating that the surface is, in fact, homogeneous. More work is definitely indicated in this area.

Note that acetylene stands out as being rather exceptional. This gas was used on the BC-4 charcoal where it gave a reasonable value of ϵ^*/k but an apparently anomalous

value of the parameter As_0. At the time the experiments were performed the investigators felt that this gas was somehow interacting chemically with the column and therefore did not use it, throughout their experiments.

DISCUSSION

It has been shown that the concept of excess retention volume in gas adsorption chromatography not only provides a simple physical analog in terms of equivalent empty column lengths but also relates in a simple way to the concept of excess apparent volume. This quantity was introduced by Halsey *et al.* when treating the theory of the van der Waals interaction of gas and surface in the same temperature region where gas adsorption chromatography is carried out.

A considerable number of data were fitted to the curve and were found to fit within experimental error yielding reasonable values of the two parameters. The parameter describing the temperature dependence was seen to be highly predictable from a knowledge of the number of carbons in a hydrocarbon and the parameter describing column capacity showed some interesting though as yet uninterpreted behavior. Even without this interpretation the theoretical framework should be very useful to the practicing chromatographer.

To the theoretical investigator, it is clear that gas adsorption chromatography though possibly less accurate than static measurements makes up for it in much greater speed and ease of manipulation. The use of frontal analyses to get C_{AAS} looks especially promising.

ACKNOWLEDGMENTS

The authors wish to express their appreciation for the co-operation of Dr. Habgood and the Research Council of Alberta. In addition, they would like to thank Professor T. Vermeulen of this university for many helpful discussions.

The calculations reported here were done under the free time allocation for unsupported research on an IBM 701 computer. This computer is supported jointly by the Regents of the University of California, International Business Machines Corporation, and the National Science Foundation.

REFERENCES

1. PHILLIPS, C. Gas chromatography. Butterworth Scientific Publications, London. 1956. p. 11.
2. STEELE, W. A. and HALSEY, G. D., Jr. J. Chem. Phys. **22**, 979 (1954).
3. STEELE, W. A. and HALSEY, G. D., Jr. J. Phys. Chem. **59**, 57 (1955).
4. FREEMAN, M. P. and HALSEY, G. D., Jr. J. Phys. Chem. **59**, 181 (1955).
5. KWAN, T., FREEMAN, M. P., and HALSEY, G. D., Jr. J. Phys. Chem. **59**, 600 (1955).
6. CONSTABARIS, G. and HALSEY, G. D., Jr. J. Chem. Phys. **27**, 1433 (1957).
7. FREEMAN, M. P. J. Phys. Chem. **62**, 723 (1958).
8. FREEMAN, M. P. J. Phys. Chem. **62**, 729 (1958).
9. HABGOOD, H. W. and HANLAN, J. F. Can. J. Chem. **37**, 843 (1959).
10. JANAK, J. J. Chem. Listy, **47**, 464 (1953).
11. GREENE, S. A. and PUST, H. J. Phys. Chem. **62**, 55 (1958).
12. JAMES, A. T. and MARTIN, A. J. P. Biochem. J. **50**, 679 (1952).
13. PAULING, L. Nature of the chemical bond. Cornell Univ. Press, Ithaca, N.Y. 1948. p. 172.

Can. J. Chem. Downloaded from www.nrcresearchpress.com by 176.9.209.113 on 09/04/12
For personal use only.

Can. J. Chem. Downloaded from www.nrcresearchpress.com by 176.9.209.113 on 09/04/12
For personal use only.

ALKALOIDS OF LYCOPODIUM ANNOTINUM

PART II. ISOLATION OF FOUR NEW ALKALOIDS[1, 2]

F. A. L. ANET AND N. H. KHAN

ABSTRACT

Countercurrent distribution of the alkaloids of *Lycopodium annotinum* gave four new bases: annofoline, lycofoline, and α- and β-lofoline. Annofoline, $C_{16}H_{25}O_2N$, contained a keto and a hydroxyl group. Lycofoline, $C_{16}H_{25}O_2N$, possessed at least one hydroxyl group and possibly a double bond. α- and β-Lofoline each had the formula $C_{18}H_{29}O_3N$ and contained a hydroxyl and an O-acetyl group.

Anet and Eves (1) described the separation of the crude alkaloid mixture from *Lycopodium annotinum* by countercurrent distribution into a "chloroform-soluble" and a "buffer- (pH 6.0) soluble" fraction. From the former fraction they isolated a new alkaloid, lycodine. In the present paper we report work on the latter fraction, as a result of which four new alkaloids have been isolated and characterized.

The buffer-soluble fraction mentioned above (1) was subjected to 57-transfer countercurrent distribution with the system chloroform–buffer of pH 7.0, with the buffer solution as the moving phase. Weight analysis of the distribution gave the pattern shown in Fig. 1A. Although the alkaloid concentration used was such that overloading resulted, causing changes in the pH of the buffer, the separation obtained was not far from that expected on the basis of a constant distribution coefficient for each alkaloid. The alkaloids in tubes 10 to 42 are at present under investigation, but it may be noted here that acrifoline (2, 3) could be isolated from tubes 26 to 34.

The peak represented by tubes 46 to 57 (Fig. 1A) was too wide to represent a single alkaloid, a conclusion supported by the results of paper chromatography and infrared analysis. Due to the high partition coefficients, however, the various components making up the peak were badly resolved. All the same, tubes 46 to 52 readily yielded a crystalline alkaloid (α-lofoline described below), but only in small yield. In order to improve the separation, the alkaloid contents of tubes 46 to 57 were mixed and subjected to another countercurrent distribution, but this time with the system chloroform–buffer of pH 8.0. The distribution (Fig. 1B) obtained showed three peaks, two of which overlapped.

The tubes 21 to 32 (Fig. 1B) yielded a crystalline alkaloid, and paper chromatography indicated that this was the main component present. The compound obtained had m.p. 211–212°, and its properties were unchanged after chromatography on alumina or after repeated recrystallizations. Analysis gave the formula $C_{18}H_{29}O_3N$ and further showed the presence of one O-acetyl group and at least two C-methyl groups. The infrared spectrum (Fig. 2A) confirmed the presence of an O-acetyl group (bands at 1720 cm^{-1} and at 1225 cm^{-1}, 1240 cm^{-1}) and also indicated the presence of a hydroxyl group (band at 3200 cm^{-1}), thus accounting for all the oxygen atoms. The general properties and formula of this compound do not correspond with any known alkaloid and we therefore propose the name α-lofoline for it. α-Lofoline gave a methiodide, m.p. 266–267°.

Paper chromatography indicated the presence of two alkaloids in tubes 36 to 51 (Fig. 1B) which were not completely resolved in the distribution. It was found best to

[1]*Manuscript received May 19, 1959.*
Contribution from the Department of Chemistry, University of Ottawa, Ottawa, Canada.
[2]*Part I of this series is considered to be the paper entitled "Lycodine, a new alkaloid of Lycopodium annotinum" by F. A. L. Anet and C. R. Eves (see reference 1).*

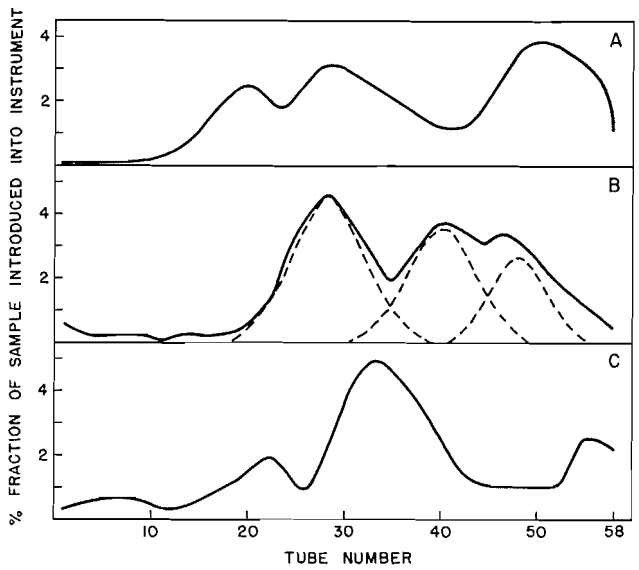

FIG. 1. Countercurrent distribution of various alkaloid fractions mentioned in the text: A, with the system chloroform–buffer of pH 7; B, chloroform–buffer of pH 8.0; C, chloroform–buffer of pH 8.2. In each case the buffer solution is the moving phase. The dotted lines represent theoretical distributions.

mix the contents of all these tubes and to separate the two components by chromatography on alumina. The first alkaloid eluted had, after recrystallization and sublimation, m.p. 156–157°. Analysis gave the formula $C_{16}H_{25}O_2N$ and showed the presence of at least one C-methyl group. The infrared spectrum (Fig. 2B) indicated a hydroxyl group (band at 3400 cm^{-1})and a carbonyl group (band at 1700 cm^{-1}, probably a ketone in a six-membered ring). The properties of this alkaloid showed it to be new, and we propose the name annofoline for it. Annofoline gave a perchlorate, m.p. 234–236°, and a methiodide, m.p. 308–309°.

The second alkaloid eluted from the alumina chromatogram had, after recrystallization, m.p. 144–145°. Analysis indicated the formula $C_{16}H_{25}O_2N$ and the presence of a C-methyl group. The infrared spectrum (Fig. 2C) showed the presence of one or more hydroxyl groups (band at 3300 cm^{-1}), but no carbonyl group. A very faint band at 1670 cm^{-1} may indicate unsaturation. This compound also appeared to be new and we have named it lycofoline. It gave a hydrobromide, m.p. 274–275°, and a methiodide, m.p. 263–264°. In the last few tubes of the distribution (Fig. 1B) there was present a small amount of a compound showing a band at 1740 cm^{-1} (in CCl_4) in the infrared, but no attempt was made to isolate the compound responsible for this absorption.

It was noticed that the distribution shown in Fig. 1A had a pronounced minimum at tube 42. It was already known (1) that alkaloids with a partition coefficient (buffer of pH 5.0 versus chloroform) near unity were not present to any appreciable extent in the crude alkaloid mixture. These facts enabled us to modify our original preliminary separation, which divided the alkaloid into two groups, into one where three groups were obtained. This was done (Fig. 3) without greatly increasing the number of transfers, and without any of the major components of the crude alkaloid mixture occurring in more than one group. The solvent system used was chloroform–buffer of pH 7.0. The buffer-soluble fractions B_1' to B_3' gave after a 60-transfer countercurrent distribution in

Can. J. Chem. Downloaded from www.nrcresearchpress.com by 176.9.209.113 on 09/04/12
For personal use only.

Can. J. Chem. Downloaded from www.nrcresearchpress.com by 176.9.209.113 on 09/04/12
For personal use only.

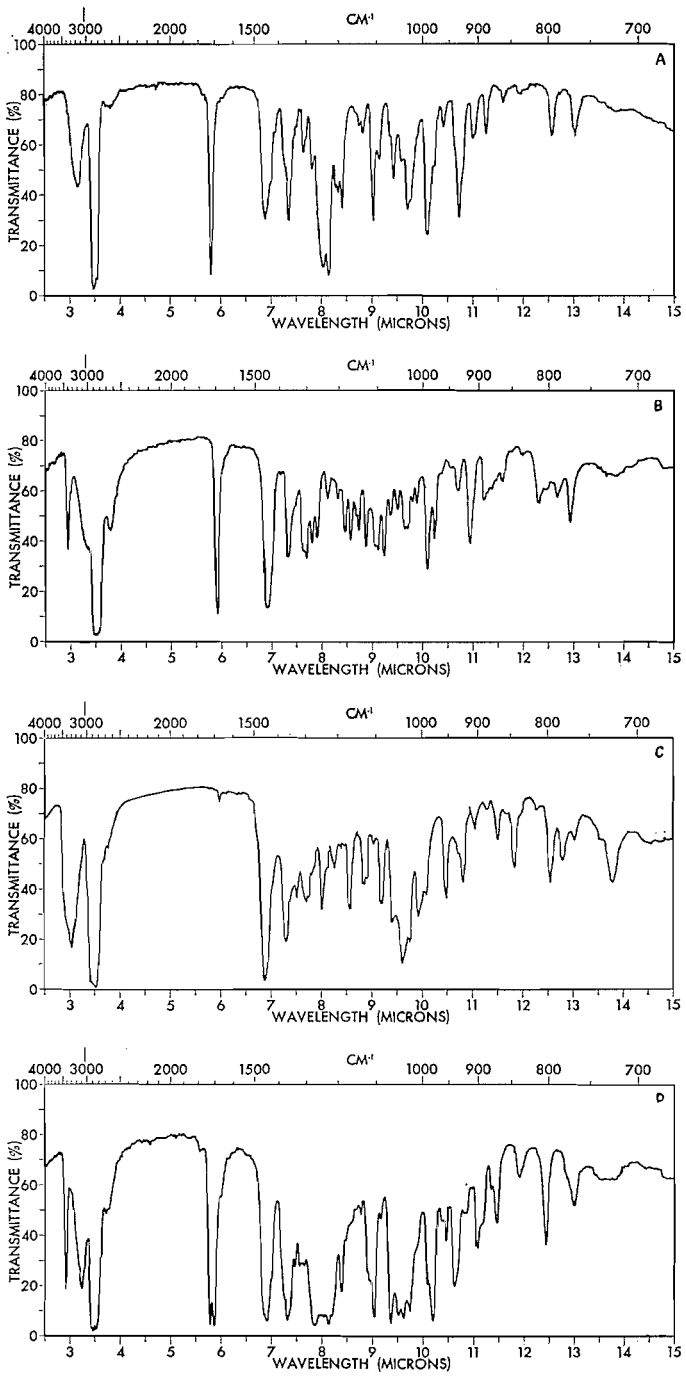

FIG. 2. Infrared absorption spectra in Nujol mull measured on a Perkin–Elmer "Infracord": A, α-lofoline; B, annofoline; C, lycofoline; D, β-lofoline.

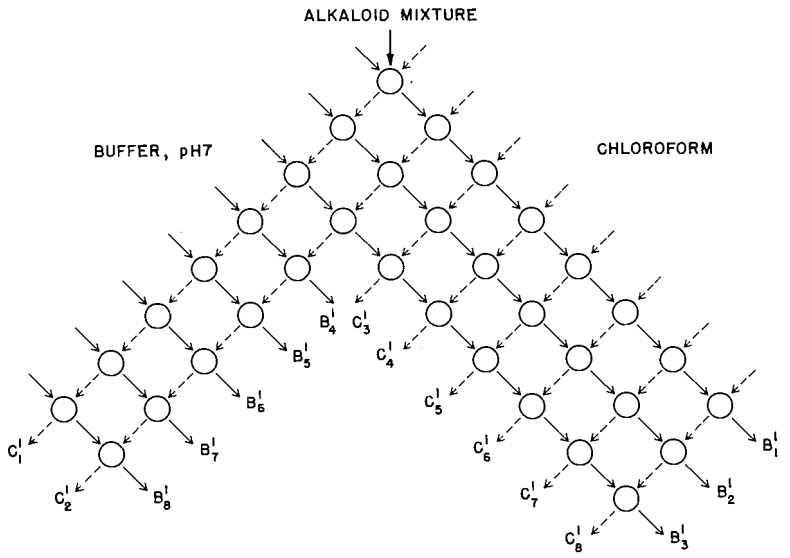

FIG. 3. Modified Bush and Densen extraction pattern. The circles represent phase separation, and the full lines show the advancement of the buffer solutions, and the dotted lines that of the chloroform solutions.

the system chloroform–buffer of pH 8.2 the pattern shown in Fig. 1C. Thus about the same separation was obtained as before but with one 60-transfer countercurrent distribution less.[3]

The distribution pattern of Fig. 1C was somewhat different from that of Fig. 1B. In the first place the peak corresponding to α-lofoline was much less intense in Fig. 1C than in Fig. 1B, and there was a new peak (tubes 52 to 58) in Fig. 1C not present in Fig. 1B. Furthermore, the peak occurring at tubes 16 to 26 contained not only α-lofoline, but also another new alkaloid resembling it closely, and which we have named β-lofoline. The two alkaloids were separated by careful chromatography on alumina. β-Lofoline had m.p. 166–167°, and analysis gave the formula $C_{18}H_{29}O_3N$ and showed the presence of one O-acetyl group and two C-methyl groups. The infrared spectrum (Fig. 2D) indicated a hydroxyl group (free hydroxyl, 3400 cm^{-1}, and bonded hydroxyl, 3100 cm^{-1}) and an O-acetyl group (bands at 1700 cm^{-1}, 1730 cm^{-1} and at 1225 cm^{-1}, 1270 cm^{-}).[1] The splitting of the carbonyl band of the acetyl group is probably related to the fact that there are two hydroxyl frequencies. In carbon tetrachloride solution both α- and β-lofoline showed only one (free) hydroxyl band and one carbonyl band (1720 cm^{-1}); therefore the effect with β-lofoline is not intramolecular. Thus in the crystals of β-lofoline the carbonyl groups of some molecules are not hydrogen-bonded whilst the carbonyl groups of other molecules are intermolecularly hydrogen-bonded. The new peak at tubes 52 to 58 (Fig. 1C) may represent hydrolysis products of α-lofoline and β-lofoline. Preliminary experiments have shown that the hydrolysis products of α- and β-lofoline have the same R_f values and partition coefficients as the alkaloids present in the new peak. This would also explain why the amount of lofolines in the second lot of alkaloid (see Fig. 1C) was less than in the first lot (Fig. 1B).

[3]*The middle fractions (B_4' to B_8' and C_3' to C_8') have been found by Mr. G. Dong in these laboratories to contain the same alkaloids as those present in tubes 10 to 42 of the countercurrent distribution given in Fig. 1A. Also, the chloroform-soluble fractions (C_1' and C_2') have been found by Mr. M. V. Rao to contain all the anno-tinine, lycodine, and lycopodine present in the original mixture.*

Can. J. Chem. Downloaded from www.nrcresearchpress.com by 176.9.209.113 on 09/04/12
For personal use only.

The pK_a's, rotations, and other properties of the alkaloids are summarized in Table I. Degradative work on these alkaloids will be reported in a future paper.

TABLE I

New alkaloids isolated from *L. annotinum*

Alkaloid	Formula	M.p.	pK_a in 50% aqueous methanol	$[\alpha]_D$ in ethanol	R_f*	Methiodide, m.p.
α-Lofoline	$C_{18}H_{29}O_3N$	211–212°	9.7	− 52°	0.58	266–267°
β-Lofoline	$C_{18}H_{29}O_3N$	166–167°	9.55	− 6°	0.51	296–297°
Annofoline	$C_{16}H_{25}O_2N$	156–157°	9.15	−131°	0.31	308–309°
Lycofoline	$C_{16}H_{25}O_2N$	144–145°	9.1	− 75°	0.53	263–264°

*Chromatography on Whatman No. 1 paper buffered to pH 7.0 and developed with *n*-butanol saturated with water (see also Experimental).

In a recent paper (4) Achmatowicz and Rodewald described the isolation of some new alkaloids, in the form of their methiodides, from *L. annotinum* of European origin. However, none of these alkaloids seems to correspond with the alkaloids which we have isolated.

EXPERIMENTAL

The infrared spectra, apart from those given in Fig. 2, were measured in carbon tetrachloride solution (1%) in a 1-mm cell on a Perkin–Elmer single-beam double-pass instrument. The paper chromatograms were obtained on Whatman No. 1 paper buffered with the pH mentioned in the text, and developed with butanol saturated with water. The absolute R_f values of the alkaloids varied appreciably, but the relative values were constant. The alkaloidal spots were revealed by spraying with a modified Dragendorff reagent (5). Equivalent weights (E.W.) and pK_a were determined by microtitrations with 0.1 *N* hydrochloric acid in 50% aqueous methanol.

Preliminary Separation of the Crude Alkaloid

The first lot of alkaloid to be investigated was the same as that described (1) previously. The crude alkaloid left after the removal of most of the annotinine by crystallization was partitioned repeatedly between chloroform and a buffer of pH 6 using the extraction scheme of Bush and Densen (6) so as to obtain six chloroform phases and six buffer phases. The alkaloid in the first four buffer phases (B1 to B4 of reference (1)) were combined for the present study and will be referred to as fraction B.

A second lot of alkaloid mother liquors from a different extraction of plant material was also investigated, but was treated differently from the above in view of the results obtained with fraction B.

Countercurrent Distribution with the System Chloroform–Buffer of pH 7.0

Fraction B (8.6 g) was dissolved in chloroform (120 ml) and the solution was placed in the first three tubes of a 60-tube Craig countercurrent distribution apparatus (7) and partitioned between chloroform and citrate–phosphate buffer of pH 7.0. Fifty-seven transfers were made, after which every third tube was analyzed. Aliquots (usually 2 ml) of each phase of a tube were removed, mixed, and made alkaline and the bases extracted with chloroform. The alkaloid left after removal of the solvent was weighed to give the distribution shown in Fig. 1A. The samples obtained from the weight analysis were submitted to paper chromatography (paper buffered at pH 6.0) and their infrared

Can. J. Chem. Downloaded from www.nrcresearchpress.com by 176.9.209.113 on 09/04/12
For personal use only.

spectra measured. Whilst α-lofoline could be crystallized from the alkaloid in tubes 46 to 52, the yield was small and it was preferable to separate the alkaloids present in tubes 46 to 57 by another countercurrent distribution.

Countercurrent Distribution with the System Chloroform–Buffer of pH 8.0

The alkaloid was recovered from tubes 46 to 57 in the usual way and submitted to 58 transfers in the above system, the alkaloid being placed in the first two tubes of the apparatus. The tubes were analyzed as described before and the distribution pattern of Fig. 1B was obtained.

Isolation of α-Lofoline

The alkaloid in tubes 21 to 32 of the above distribution was isolated and crystallized from methanol to give thick colorless prisms, m.p. 211–212°. To obtain a good yield it was found desirable to chromatograph the mother liquors on alumina, using successively benzene, benzene–chloroform, and chloroform as the eluants. α-Lofoline was very soluble in methanol and chloroform but sparingly soluble in ether or petroleum ether. The alkaloid was best recrystallized from benzene, and was sublimed (120–130° at 0.05 mm) for analysis. Calc. for $C_{18}H_{29}O_3N$: C, 70.32; H, 9.51; N, 4.56; 2C—CH_3, 9.8; O—$COCH_3$, 14.0%; M.W., 307.4. Found: C, 70.56, 70.56; H, 9.54, 9.54; N, 4.63; C—CH_3, 10.60; O—$COCH_3$, 14.21%; M.W. (Rast), 291, 312; E.W., 310, 310; pK_a, 9.7, 9.7; $[\alpha]_D$ −52° (*c*, 2.0 in ethanol).

α-Lofoline Methiodide

α-Lofoline (20 mg) was dissolved in a mixture of methanol (1 ml) and methyl iodide (0.5 ml) and the mixture was refluxed for 10 minutes. The solvent was removed by evaporation and the methiodide was crystallized from methanol–acetone. Yield, 16 mg, m.p. 266–267°. Calc. for $C_{18}H_{29}O_3N.CH_3I$: C, 50.78; H, 7.18; I, 28.24%. Found: C, 51.08; H, 7.04; I, 28.04%.

Isolation of Annofoline

The alkaloid in tubes 36 to 41 of the above distribution (with the buffer of pH 8) was isolated and crystallized from methanol–ether, but the m.p. was 115–130°. Three recrystallizations raised the m.p. to 148–150° and this changed to 156–157° after sublimation (120–130° at 0.05 mm). It was found that a much better yield of pure annofoline could be obtained by chromatography on alumina of the contents of tubes 36 to 51. Elution with benzene–chloroform gave annofoline, whilst elution with chloroform gave lycofoline (see below). Annofoline had similar solubilities to α-lofoline, and when its solution in carbon tetrachloride (but not chloroform) was allowed to evaporate in the presence of air, an intense orange-yellow residue was left. This test was not given by α- or β-lofoline but lycofoline gave a crimson-red color. For analysis a sublimed sample was used. Calc. for $C_{16}H_{25}O_2N$: C, 72.96; H, 9.57; N, 5.32; C—CH_3, 5.96%; M.W., 263.4. Found: C, 72.85, 73.05; H, 9.51, 9.59; N, 4.91; C—CH_3, 6.91%; M.W. (Rast), 270, 283; E.W., 259, 267; pK_a, 9.1, 9.2; $[\alpha]_D$ −131° (*c*, 2.0 in ethanol).

Annofoline Methiodide

The methiodide of annofoline crystallized on addition of methyl iodide (0.8 ml) to a solution of the alkaloid (60 mg) in acetone (2 ml). The mixture was refluxed for 5 minutes, cooled, and the methiodide collected. It was recrystallized from water, m.p. 308–309°. Yield, 40 mg. Calc. for $C_{16}H_{25}O_2N.CH_3I$: C, 50.37; H, 6.94; I, 31.31%. Found: C, 50.30; H, 6.70; I, 31.50%.

Can. J. Chem. Downloaded from www.nrcresearchpress.com by 176.9.209.113 on 09/04/12
For personal use only.

Annofoline Perchlorate

A methanolic solution of perchloric acid was added to a solution of the alkaloid in methanol until a slight excess was present. Ether was added to the solution and the perchlorate crystallized on scratching. After recrystallization from methanol–ether it melted at 234–236°. Calc. for $C_{16}H_{25}O_2N.HClO_4.H_2O$: C, 50.30; H, 7.65%. Found: C, 50.08; H, 7.35%.

Isolation of Lycofoline

The alkaloid in tubes 42 to 51 of the above distribution (with the buffer of pH 8.0) was isolated and converted into the hydrobromide by the addition of concentrated hydrobromic acid to the methanolic solution of the alkaloid. Addition of ether gave a crystalline salt, which after three crystallizations from methanol–ether was converted to the base. The base was sublimed (110–130° at 0.05 mm) and then crystallized from ether. Lycofoline was obtained as prisms, m.p. 144–145°. For analysis it was sublimed *in vacuo*, m.p. unchanged. Calc. for $C_{16}H_{25}O_2N$: C, 72.96; H, 9.57; N, 5.32; C—CH_3, 5.69%; M.W., 263.4. Found: C, 72.77, 72.66; H, 9.51, 9.59; N, 5.11; C—CH_3, 4.96%; M.W. (Rast), 239; E.W., 264, 267; pK_a, 9.05, 9.1; $[\alpha]_D$ −75° (*c*, 2.0 in ethanol). A better yield of lycofoline was obtained by chromatography of the mixture of annofoline and lycofoline as described in the procedure for the isolation of annofoline.

Lycofoline Hydrobromide

For analysis the hydrobromide was recrystallized from methanol–ether and dried at 117° *in vacuo*, m.p. 274–275°. Calc. for $C_{16}H_{25}O_2N.HBr$: C, 56.05; H, 7.61%. Found: C, 55.64, 55.68; H, 7.55, 7.42%.

Lycofoline Methiodide

Lycofoline (34 mg) was dissolved in methanol (1.5 ml) and the solution was refluxed for 10 minutes with methyl iodide (0.5 ml). The solvent was removed and the methiodide was crystallized from methanol. Yield, 15 mg, m.p. 263–264°. Calc. for $C_{16}H_{25}O_2N.CH_3I$: C, 50.37; H, 6.94; I, 31.31%. Found: C, 50.65; H, 6.99; I, 31.58%.

Improved Separation of Crude Alkaloid

A second batch of crude alkaloid (after removal of the annotinine) (60 g) was partitioned between chloroform and a citrate–phosphate buffer of pH 7.0 using the modified Bush and Densen extraction pattern of Fig. 3. The extractions were carried out with 1 liter of each phase. The fractions B_1' to B_3' were combined and the alkaloid extracted in the usual way. The mixture (20 g) so obtained was divided into three equal lots, and each was subjected to a 60-tube countercurrent distribution with the solvent system chloroform and boric acid – sodium hydroxide buffer of pH 8.2. The distribution pattern given in Fig. 1C was obtained.

Isolation of β-Lofoline

Annofoline and lycofoline were isolated from tubes 28 to 43 and were separated as described above by chromatography on alumina. Tubes 16 to 26, however, did not give α-lofoline in pure state easily. Indeed, paper chromatography (paper buffered at pH 7.0) showed two spots of very similar R_f values (0.58, 0.51). The mixture was therefore chromatographed on alumina. Elution with benzene, benzene–chloroform, and chloroform gave first β-lofoline, followed by α-lofoline. The β-lofoline was crystallized from methanol–ether, m.p. 160–166°, raised to 166–167° after two recrystallizations from ether. For analysis a sample was sublimed (120–130° at 0.05 mm). Calc. for $C_{18}H_{29}O_3N$: C, 70.32; H, 9.51; N, 4.56; 2C—CH_3, 9.8; O—$COCH_3$, 14.00%; M.W., 307.4. Found: C, 70.18,

Can. J. Chem. Downloaded from www.nrcresearchpress.com by 176.9.209.113 on 09/04/12
For personal use only.

70.14; H, 9.45, 9.69; N, 4.84; C—CH_3, 8.83; O—$COCH_3$, 15.6%; M.W. (Rast), 322; E.W., 311; pK_a, 9.55; $[\alpha]_D$ −6° (*c*, 2.0 in ethanol).

β-Lofoline Methiodide

To a solution of the alkaloid (20 mg) in methanol (2 ml), methyl iodide (0.5 ml) was added, and the mixture was refluxed for 10 minutes. The solvent was removed and the methiodide was crystallized from methanol. Yield, 10 mg, m.p. 296–297° (decomp.). Calc. for $C_{18}H_{29}O_3N.CH_3I$: C, 50.78; H, 7.18%. Found: C, 50.90; H, 6.80%.

ACKNOWLEDGMENTS

The authors thank Dr. Léo Marion for providing the mother liquors from the crystallization of annotinine. One of us (N. H. K.) wishes to thank the Colombo Plan authorities for the award of a scholarship and the Pakistan Council of Scientific and Industrial Research for financial support.

REFERENCES

1. ANET, F. A. L. and EVES, C. R. Can. J. Chem. **36**, 902 (1958).
2. MANSKE, R. H. F. and MARION, L. J. Am. Chem. Soc. **69**, 2126 (1947).
3. PERRY, G. S. and MACLEAN, D. B. Can. J. Chem. **34**, 1189 (1956).
4. ACHMATOWICZ, O. and RODEWALD, W. Roczniki Chem. **32**, 485 (1958).
5. MUNIER, R. and MACHEBOEUF, M. Bull. soc. chim. biol. **33**, 846 (1951).
6. BUSH, M. T. and DENSEN, P. M. Anal. Chem. **20**, 121 (1948).
7. CRAIG, L. C. and POST, O. Anal. Chem. **21**, 500 (1949).

Can. J. Chem. Downloaded from www.nrcresearchpress.com by 176.9.209.113 on 09/04/12
For personal use only.

Can. J. Chem. Downloaded from www.nrcresearchpress.com by 176.9.209.113 on 09/04/12
For personal use only.

SYNTHESIS OF 2,4-THIAZOLIDINEDIONE-2-AZINES AND 2,4-THIAZOLIDINEDIONE-2-DIMETHYLHYDRAZONES FROM THIOCYANOESTERS AND HYDRAZINES[1]

PAUL E. GAGNON, JEAN-L. BOIVIN,[2] AND GORDON M. BROWN[3]

ABSTRACT

Thiocyanoesters were prepared from 2-bromoesters and potassium thiocyanate, and a series of substituted thiazolidinedione-2-azines was obtained from these thiocyanoesters using hydrazine hydrate. The structure of the thiazolidinedione-2-azines was determined by hydrolysis using hydrochloric acid in ethanol. The reaction of thiocyanoesters with dimethylhydrazine, generally speaking, was analogous to their reaction with hydrazine, but there were many differences. Only 1 mole of alcohol was eliminated rather than 2, and there was no apparent reaction for the ethyl 2-thiocyanononanoate and the methyl phenylthiocyanoacetate. Furthermore, the reaction of methyl 2-thiocyanoisobutyrate with dimethylhydrazine did not give a 2,4-thiazolidinedione-2-dimethylhydrazone but rather an addition product, *N*-dimethylamino-*S*-(1-methyl-1-carbomethoxy) ethylisothiourea. To illustrate the reactivity of the thiocyano group, benzyl thiocyanate was treated with hydrazine and the product was found to be dibenzyldisulphide, and ammonia was evolved. Similarly, trimethylene dithiocyanate gave the dimer of trimethylene disulphide. Finally, benzyl thiocyanate formed an addition product with dimethylhydrazine which was *N*-dimethylamino-*S*-benzylthiourea.

INTRODUCTION

Ethyl thiocyanoacetate, which was prepared for the first time by Heintz (1) from ethyl chloroacetate and potassium thiocyanate, contains an active methylene group and, consequently, is structurally similar to ethyl cyanoacetate which is easily alkylated in the presence of a catalyst. Thus for a time it was considered that a series of thiocyanoesters might be prepared from ethyl thiocyanoacetate itself. However, Claesson (2) discovered that if ethyl thiocyanoacetate was treated with ethyl bromide, the products were ethyl thiocyanate and ethyl bromoacetate.

$$C_2H_5Br + NCSCH_2COOC_2H_5 \rightarrow C_2H_5SCN + BrCH_2COOC_2H_5$$

Therefore, the thiocyanoesters had to be synthesized from the corresponding 2-bromoesters which, in turn, were obtained by esterification of the bromoacids.

$$RCH_2COOH \rightarrow RCHBrCOOH \rightarrow RCHBrCOOR' \rightarrow RCH(SCN)COOR'$$

In 1910, Frerichs and Förster (3) reported that when an aqueous solution of hydrazine hydrate was shaken with ethyl thiocyanoacetate, an exothermic reaction ensued producing a precipitate which was insoluble in all common solvents. The analysis suggested the formula $C_6H_6N_4O_2S_2$. This compound decomposed without melting and was assigned the structure of 3,3-bis-pseudothiohydantoin.

$$2NCSCH_2COOC_2H_5 + H_2NNH_2 \rightarrow \begin{array}{l} CH_2\text{——}CO \quad CO\text{——}CH_2 \\ \quad | \quad\quad | \quad\quad | \quad\quad | \\ S\text{—}C\text{—}N\text{——}N\text{—}C\text{—}S \\ \quad\quad \| \quad\quad\quad \| \\ \quad\quad NH \quad\quad NH \end{array} + 2C_2H_5OH$$

The authors also claimed that the above compound was obtained from hydrazodithiodicarbonamide and chloroacetic acid in aqueous solution.

[1]*Manuscript received May 1, 1959.*
Contribution from the Department of Chemistry, Laval University, Quebec, Que. This paper constitutes part of a thesis submitted to the Graduate School, Laval University, in partial fulfillment of the requirements for the degree of Doctor of Science.
[2]*Canadian Armament Research and Development Establishment, Valcartier, Quebec.*
[3]*Graduate student, holder of National Research Council of Canada Studentships in 1957–59.*

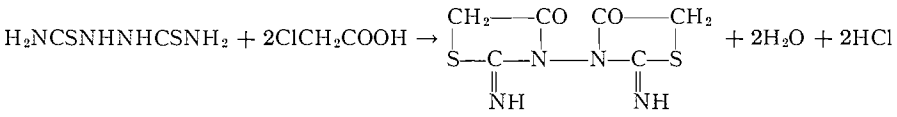

Some years later, Stephen and Wilson (4) investigated the reaction between hydrazodithiodicarbonamide and ethyl chloroacetate. They established the structure of the product by treating it with boiling concentrated hydrochloric acid in which it gradually dissolved. After evaporation, the solid obtained was extracted with hot chloroform, giving 2,4-thiazolidinedione identified by a mixed melting point with an authentic sample. The residue, after the extraction, was proved to be hydrazine hydrochloride. From the two hydrolysis products, then, it is obvious that the original compound obtained from hydrazodithiodicarbonamide and ethyl chloroacetate was 2,4-thiazolidinedione-2-azine.

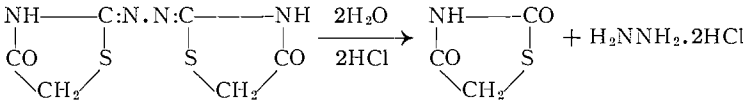

Stephen and Wilson claimed that the compound prepared by Frerichs and Förster gave the same products when boiled with concentrated hydrochloric acid. The compound of which they spoke was prepared from hydrazodithiodicarbonamide and chloroacetic acid; no mention was made of the reaction between ethyl thiocyanoacetate and hydrazine hydrate.

In 1913, Frerichs and Höller (5) studied the reactions of hydrazodithiodicarbonamide with haloacids, specifically 2-bromopropionic and 2-bromobutyric acids. The compounds obtained were regarded as substituted 3,3-bis-pseudothiohydantoins. The melting points reported by Frerichs and Höller were not sharp, which leads one to believe that difficulties in purification were encountered.

Stephen and Wilson (6) also undertook the preparation of the same compounds by the method of Frerichs and obtained from hydrazodithiodicarbonamide and 2-bromopropionic acid a solid melting at 289° C which, on hydrolysis with concentrated hydrochloric acid, gave rise to the known 5-methyl-2,4-thiazolidinedione. Similarly, the compound obtained from hydrazodithiodicarbonamide and 2-bromobutyric acid melting at 233° C gave on acid hydrolysis the known 5-ethyl-2,4-thiazolidinedione. The structure of these two compounds must be, therefore, 5-methyl- and 5-ethyl-2,4-thiazolidinedione-2-azine, respectively.

RESULTS AND DISCUSSION

Thiocyanoesters

The thiocyanoesters were prepared from the corresponding bromoesters using a 50% excess of potassium thiocyanate as recommended by Allen (7). Generally speaking, 80% alcohol was used for the lower members, and as the chain length increased to seven and eight carbons 90% alcohol was employed since the latter were not completely miscible with 80% alcohol.

The methyl phenylthiocyanoacetate was not synthesized using the sequence of reactions followed for alkyl thiocyanoacetates. Direct bromination of phenyl acetic acid puts the bromine in the ring, not in the side chain, even when no catalyst is used (8). To prepare the desired ester, then, mandelic acid was employed as the starting material. Esterification by the method of Clinton and Laskowski (9) gave the corresponding methyl

Can. J. Chem. Downloaded from www.nrcresearchpress.com by 176.9.209.113 on 09/04/12
For personal use only.

ester in good yield. The methyl phenylchloroacetate was then prepared by treatment of the mandelate with thionyl chloride in accordance with the procedure given by McKenzie and Barrow (10), and the phenylthiocyanoacetate was obtained directly from the above compound by the usual method.

It was noted that the inductive effect played a very important part in the time required to form the thiocyanoesters. In the case of ethyl chloroacetate, both the chlorine atom and the carbethoxy group are electron attracting, leaving the alpha carbon atom with a residual positive charge which attracted the attacking thiocyanate ion. The substitution, therefore, took place quite rapidly. The alpha carbon atom, in the case of alkyl-substituted thiocyanoesters, is more negatively charged than in the non-substituted ester, due to the fact that alkyl groups are electron repelling, and so the attacking thiocyanate ion approaches less rapidly as is seen by the reflux time necessary for the completion of the reaction.

The methyl 2-thiocyanoisobutyrate and the methyl 2-thiocyanoisovalerate required a much longer period of heating, due to the electron repulsion of the two methyl groups toward the same carbon atom. The approach of the negatively charged thiocyanate ion is greatly hindered by the strongly negative charges on the second carbon atom. True to the electronic theory that the inductive effect dies out after one methylene group, the preparation of methyl 2-thiocyanoisohexanoate was performed easily. In spite of the repulsion of the methyl groups, the site of the perturbation was too far removed from the second carbon atom to hinder the replacement of the bromine atom, and no extra time was required in the preparation of the above-mentioned ester. The phenylthiocyanoacetate required but a small reflux period due to the fact that the phenyl group is electron attracting, leaving the alpha carbon atom with a net positive charge and facilitating greatly the approach of the attacking thiocyanate ion.

2,4-Thiazolidinedione-2-azines

A method of improving the yields was devised for the azines by finding a suitable solvent. Methanol was finally selected as the medium in spite of the fact that it itself is a by-product of the reaction and thus tends to set up an equilibrium. If the addition of the reagent was not performed with care, the reaction mixture boiled; however, by introducing a dropwise solution of hydrazine hydrate in methanol, the temperature did not become too great and solid products were obtained.

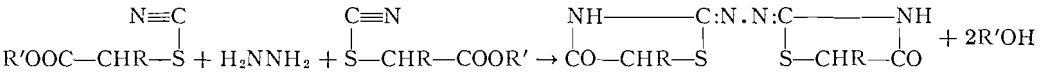

The structure was established by boiling these compounds with concentrated hydrochloric acid in ethanol (11). Substituted 2,4-thiazolidines were obtained and their melting points compared favorably with those reported in the literature. The second product of hydrolysis was identified as hydrazine hydrochloride, thus establishing without a doubt the structure of the compounds being hydrolyzed as 2,4-thiazolidinedione-2-azines.

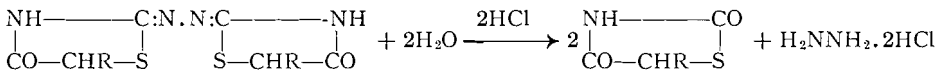

The above results prove conclusively that thiocyanoacetates and hydrazine hydrate give the same azines as hydrazodithiodicarbonamide and 2-haloacetic acids.

Can. J. Chem. Downloaded from www.nrcresearchpress.com by 176.9.209.113 on 09/04/12
For personal use only.

2,4-Thiazolidinedione-2-dimethylhydrazones

If dimethylhydrazine and thiocyanoesters, which were mutually soluble, were mixed without a solvent, the reaction, which was endothermic at the time of the addition, after a few minutes became uncontrollably exothermic with charring of the reaction mixture. It was found that for the preparation of lower molecular weight members of this series, formamide was an excellent solvent as the product was insoluble and precipitated out when the mixture was left to stand overnight.

$$RCH(SCN)COOR' + (CH_3)_2NNH_2 \rightarrow \begin{matrix} NH\text{———}C{:}N.N(CH_3)_2 \\ | \qquad\qquad | \\ CO\text{—}CHR\text{—}S \end{matrix} + R'OH$$

The reaction mixture generally darkened to amber, but the reactions themselves were not exothermic, except in the case of ethyl thiocyanoacetate, which was moderately so.

Unfortunately, the complete series of thiocyanoesters was not soluble in formamide and another solvent had to be found for those of higher molecular weight. If the reaction between dimethylhydrazine and methyl 2-thiocyanohexanoate was performed using nitrobenzene as the solvent, a solid product was obtained which separated out when the mixture was left to stand overnight. No exothermic reaction was observed and the mixture darkened only slightly to yellow. The yield obtained by this method was almost the same as that obtained by using formamide. Another solvent employed was *o*-nitroanisole which gave results similar to those obtained by nitrobenzene. To determine the structure of these compounds, they were hydrolyzed with hydrochloric acid in ethanol and two products were obtained, the known 2,4-thiazolidinediones and dimethylhydrazine hydrochloride.

$$\begin{matrix} NH\text{———}C{:}N.N(CH_3)_2 \\ | \qquad\qquad | \\ CO\text{—}CHR\text{—}S \end{matrix} + H_2O + HCl \rightarrow \begin{matrix} NH\text{———}CO \\ | \qquad\quad | \\ CO\text{—}CHR\text{—}S \end{matrix} + (CH_3)_2NNH_2.HCl$$

There was no apparent reaction when ethyl 2-thiocyanononanoate and methyl phenylthiocyanoacetate were treated with 1,1-dimethylhydrazine. The lack of reaction on the part of the thiocyanononanoate is not easily explained. The fact that it is an ethyl ester rather than a methyl ester might have some effect on the cyclization but could scarcely inhibit the addition of the hydrazine to the thiocyano group. Since no product was obtained, even when the solution was cooled strongly, it must be concluded that the addition did not occur which could possibly be explained by steric hindrance. Perhaps the coiled heptyl chain blocks the thiocyanate group from the attacking hydrazine. The absence of reaction of the phenylthiocyanoacetate can be theoretically explained. The triple bond in methyl phenylthiocyanoacetate is less polar than in the alkyl-substituted thiocyanoacetates, as the phenyl group is electron attracting.

In the reaction between methyl 2-thiocyanoisobutyrate and 1,1-dimethylhydrazine using the same conditions as before, it was found that the product had a much lower melting point than expected. This posed a problem until it was found that the substance was water soluble and all the 2,4-thiazolidinedione-2-dimethylhydrazones were insoluble in water. It was suspected then that the reaction between dimethylhydrazine and methyl 2-thiocyanoisobutyrate consisted of a simple addition which was confirmed by analysis. No coloration was obtained upon treatment with ferric chloride. The fact that no cyclization occurred must be due to the effect of the two methyl groups on the second carbon atom.

Can. J. Chem. Downloaded from www.nrcresearchpress.com by 176.9.209.113 on 09/04/12
For personal use only.

Disulphides

When benzyl thiocyanate was treated with hydrazine hydrate in ethanol at reflux temperature, the product was found to be dibenzyldisulphide.

$$2C_6H_5CH_2SCN + 4H_2NNH_2.H_2O \rightarrow C_6H_5CH_2SSCH_2C_6H_5 + 8NH_3 + N_2 + 2CO_2$$

(HN=CH—N=N—CH=NH) ↓

The same product was formed when the reaction was carried out at room temperature although, due to occlusion of the solvent which had deepened in color to dark red, the product was not as pure. However, the yields obtained at room temperature are greater than at the reflux temperature of ethanol.

The reaction at room temperature was very interesting since certain effects were discovered which had escaped notice at the higher temperature. A strong smell of ammonia was produced, and a small amount of precipitate was obtained which contained no sulphur. This compound was suspected to contain a guanidine function and accordingly benzaldehyde and cinnamaldehyde derivatives were prepared. However, the melting points of the condensation products did not correspond with the melting points of the mono-, di-, or tri-amino/guanidine derivatives reported in the literature (12, 13). It was not possible, then, to establish the identity of this by-product.

Also trimethylene dithiocyanate was treated with hydrazine hydrate in ethanol at room temperature. A solid separated out almost immediately, which on being subjected to qualitative test showed the absence of nitrogen. Its melting point was similar to that of a compound described by Hagelberg (14), who prepared it by the treatment of trimethylene dithiocyanate with potassium hydroxide.

$$NCS(CH_2)_3SCH + 2KOH \rightarrow (CH_2)_3S_2 + KCN + KOCN + H_2O$$

However, he was not certain whether it was the simple trimethylene disulphide that was formed or its dimer. Therefore, a molecular weight determination was made using the method of Rast (15), and calculations proved that indeed the dimer hexamethylene tetrasulphide had been formed.

Isothioureas

Benzyl thiocyanate was also treated with 1,1-dimethylhydrazine. The reaction was performed at room temperature in ether, and the product started to separate almost immediately as a viscous liquid which crystallized upon standing. The suspected *N*-dimethylamino-*S*-benzylisothiourea was soluble in water as expected and the analysis was correct for $C_{10}H_{15}N_3S$.

$$C_6H_5CH_2SCN + (CH_3)_2NNH_2 \rightarrow C_6H_5CH_2SC(=NH)NHN(CH_3)_2$$

However, upon treatment of an aqueous solution of the compound with ferric chloride, a blood-red coloration was obtained, characteristic of thiocyanate ion. In addition, aqueous mercurous nitrate gave a grey precipitate of mercury, also indicative of a thiocyanate.

When the substance was dissolved in ethylene chloride and treated with concentrated sulphuric acid, a solid separated out which, according to analysis results, was the sulphate salt of 1,1-dimethyl-2-benzylhydrazine, $C_6H_5CH_2NHN(CH_3)_2.H_2SO_4$. At the same time, these results definitely eliminated the possibility of the product being a sulphate salt of the isothiourea mentioned above.

It is obvious that a rearrangement has occurred, perhaps due to the acidic medium induced by the sulphuric acid, or else by the basicity of the original mixture of benzyl

Can. J. Chem. Downloaded from www.nrcresearchpress.com by 176.9.209.113 on 09/04/12
For personal use only.

thiocyanate and dimethylhydrazine, in which case the product $C_{10}H_{15}N_3S$ must be the thiocyanic acid salt of 1,1-dimethyl-2-benzylhydrazine. If, however, the rearrangement is brought about by hydrogen ions, then treatment of the isothiourea with ferric chloride and mercurous nitrate, both of which are acidic in aqueous solution, could still conceivably give a positive test for thiocyanate ion.

The addition product obtained from dimethylhydrazine and methyl 2-thiocyanoisobutyrate gave no red coloration when treated with ferric chloride; therefore it must be an isothiourea derivative, and one would suspect the formation of a similar type of compound from the analogous reaction under discussion.

EXPERIMENTAL

2-Bromoacids

The 2-bromoacids were obtained by treatment of aliphatic fatty acids with dry bromine in the presence of phosphorus trichloride, according to the procedures of Clarke and Taylor (16) and of Marvel (17), although the conditions varied slightly from those suggested by the above authors in that, in general, the reactions were performed at lower temperatures for longer periods of time.

Methyl 2-Bromoesters

The esters were synthesized from the bromoacids by the method of Clinton and Laskowski (9). The following preparation is representative.

Methyl 2-bromoheptanoate.—2-Bromoheptanoic acid (150 g, 0.72 mole), methanol (70 g, 2.2 moles), ethylene chloride (250 ml), and concentrated sulphuric acid (3 ml) were heated under reflux for 11 hours and diluted with water. The organic layer was washed with carbonate solution and water and dried over sodium sulphate. After removal of the solvent, the ester was distilled, b.p. 87–88° C/6 mm, n_D^{25} 1.4531. Yield, 117 g (73%). Calc. for $C_8H_{15}BrO_2$: C, 43.06; H, 6.79; Br, 35.82%. Found: C, 43.18; H, 6.70; Br, 35.72%.

Methyl 2-bromoöctanoate.—This ester was obtained in the same manner, b.p. 105° C/7 mm, n_D^{25} 1.4544. Calc. for $C_9H_{17}BrO_2$: C, 45.57; H, 7.24; Br, 33.70%. Found: C, 45.86; H, 7.07; Br, 33.78%.

2-Thiocyanoesters

The bromoesters (or in the case of ethyl thiocyanoacetate and methyl phenylthiocyanoacetate, the chloroesters) were transformed into the corresponding thiocyano-compounds by the action of potassium thiocyanate in aqueous alcohol. The particulars are given in Table I.

2,4-Thiazolidinedione-2-azines

When thiocyanoesters were treated dropwise at room temperature with a solution of hydrazine hydrate in alcohol, a precipitate was produced after the whole had been left to stand overnight. The properties of the azines are recorded in Table II.

Hydrolysis of the azines.—5-Ethyl-2,4-thiazolidinedione-2-azine (1 g) was heated under reflux for 18 hours with concentrated hydrochloric acid (40 ml) and ethanol (80 ml). After the solution was evaporated to dryness, the solid was extracted several times with boiling benzene. When the benzene solution was concentrated to small volume and cooled, crystals were obtained, which upon recrystallization from benzene ligroine (2:1) melted at 64–66° C (6). The residue was dissolved in a small quantity of water and buffered with a slight excess of sodium acetate. Upon the addition of a solution of benzaldehyde in ethanol, a yellow precipitate of benzalazine was obtained, m.p. 91–93° C (18).

Can. J. Chem. Downloaded from www.nrcresearchpress.com by 176.9.209.113 on 09/04/12
For personal use only.

Can. J. Chem. Downloaded from www.nrcresearchpress.com by 176.9.209.113 on 09/04/12
For personal use only.

TABLE I

Thiocyanoesters, $R_1R_2C(SCN)COOR_3$

R_1	R_2	R_3	Time of reflux, hours	Medium	B.p. °C	B.p. mm	Yield, %	Refract. index, 25° C	Formula	Analysis: Calculated C	Calculated H	Calculated N	Found C	Found H	Found N
H	H	C_2H_5	2	80% ethanol	113–115	11.5	67	1.4677	$C_5H_7NO_2S$	*					
CH_3	H	CH_3	5	90% methanol	108–109	19	55	1.4707	$C_5H_7NO_2S$	†					
C_2H_5	H	CH_3	8	80% methanol	114–117	16	76	1.4676	$C_6H_9NO_2S$	†					
CH_3	CH_3	CH_3	10	80% methanol	88–89	9	75	1.4624	$C_6H_9NO_2S$	†					
C_3H_7	H	CH_3	6	80% methanol	114	7	70	1.4666	$C_7H_{11}NO_2S$	48.52	6.41	8.09	48.71	6.42	8.31
i-C_3H_7	H	CH_3	12	80% methanol	109	11	68	1.4674	$C_7H_{11}NO_2S$	†					
C_4H_9	H	CH_3	6	80% methanol	119–120	7	74	1.4663	$C_8H_{13}NO_2S$	51.30	7.01	7.48	51.63	6.72	7.66
i-C_4H_9	H	CH_3	7	80% methanol	115	8	68	1.4660	$C_8H_{13}NO_2S$	51.30	7.01	7.48	51.61	6.81	7.52
C_5H_{11}	H	CH_3	6	90% methanol	133–134	7	61	1.4667	$C_9H_{15}NO_2S$	53.69	7.53	6.96	53.93	7.55	6.90
C_6H_{13}	H	CH_3	6	90% methanol	143	6	67	1.4665	$C_{10}H_{17}NO_2S$	55.77	7.97	6.51	56.08	8.09	6.67
C_7H_{15}	H	C_2H_5	6	80% ethanol	164	6	75	1.4617	$C_{12}H_{21}NO_2S$	59.21	8.71	5.76	58.71	8.65	6.18
C_6H_5	H	CH_3	3	80% methanol	176	8.5	73	1.5514	$C_{10}H_9NO_2S$	57.94	4.39	6.76	57.54	4.39	7.10

*Ruhemann, S. J. Chem. Soc. **95**, 119 (1909).

†Wheeler, H. L. and Barnes, B. J. Am. Chem. Soc. **24**, 60 (1900).

Can. J. Chem. Downloaded from www.nrcresearchpress.com by 176.9.209.113 on 09/04/12
For personal use only.

TABLE II

2,4-Thiazolidinedione-2-azines, 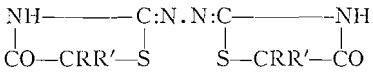

R	R′	Reaction time, days	Solvent	M.p., °C	Yield, %	Formula	Analysis					
							Calculated			Found		
							C	H	N	C	H	N
H	H	4	Dioxane	Dec.	40	$C_6H_6N_4O_2S_2$	*					
CH_3	H	7	Dioxane	285–286	39	$C_8H_{10}N_4O_2S_2$	37.19	3.91	21.69	37.14	4.11	21.90
C_2H_5	H	14	80% dioxane	235–236	38	$C_{10}H_{14}N_4O_2S_2$	41.93	4.94	19.57	42.30	5.26	19.14
CH_3	CH_3	14	80% dioxane	342	41	$C_{10}H_{14}N_4O_2S_2$	41.93	4.94	19.57	42.41	4.96	19.39
C_3H_7	H	7	Methanol	246.5–247.5	45	$C_{12}H_{18}N_4O_2S_2$	45.83	5.78	17.82	45.78	5.82	17.73
i-C_3H_7	H	4	80% dioxane	291	54	$C_{12}H_{18}N_4O_2S_2$	45.83	5.78	17.82	46.08	5.94	17.52
C_4H_9	H	12	Methanol	233–234	38	$C_{14}H_{22}N_4O_2S_2$	49.09	6.49	16.36	49.35	6.31	16.85
i-C_4H_9	H	5	80% dioxane	274–275	39	$C_{14}H_{22}N_4O_2S_2$	49.09	6.49	16.36	49.08	6.47	16.57
C_5H_{11}	H	14	Methanol	217.5–218.5	42	$C_{16}H_{26}N_4O_2S_2$	51.86	7.09	15.12	52.31	7.19	14.81
C_6H_{13}	H	16	Methanol	218–220	28	$C_{18}H_{30}N_4O_2S_2$	54.23	7.60	14.06	54.24	7.46	13.93
C_7H_{15}	H	5	Methanol	223–224	34	$C_{20}H_{34}N_4O_2S_2$	56.29	8.05	13.13	56.00	8.05	13.01
C_6H_5	H	6	80% dioxane	307–307.5	26	$C_{18}H_{14}N_4O_2S_2$	56.52	3.70	14.65	56.07	3.98	14.06

*Frerichs, G. and Förster, P. Ann. **371**, 227 (1910).

Can. J. Chem. Downloaded from www.nrcresearchpress.com by 176.9.209.113 on 09/04/12
For personal use only.

TABLE III

2,4-Thiazolidinedione-2-dimethylhydrazones, 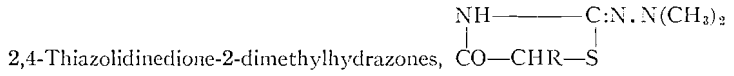

R	Reaction time, days	Medium	Solvent	M.p., ° C	Yield, %	Formula	Analysis					
							Calculated			Found		
							C	H	N	C	H	N
H	5	$HCONH_2$	Ethanol	199–201	21	$C_5H_9N_3OS$	37.71	5.71	26.40	37.74	5.83	26.21
CH_3	3	$HCONH_2$	Ethanol	178–180	34	$C_6H_{11}N_3OS$	41.59	6.41	24.26	41.64	6.39	24.28
C_2H_5	3	$HCONH_2$	60% methanol	158–159	35	$C_7H_{13}N_3OS$	44.89	7.01	22.44	44.93	7.01	22.24
C_3H_7	3	$HCONH_2$	60% methanol	147–148	32	$C_8H_{15}N_3OS$	47.73	7.53	20.88	47.76	7.55	20.68
i-C_3H_7	4	$C_6H_5NO_2$	70% methanol	174–177	45	$C_8H_{15}N_3OS$	47.73	7.53	20.88	47.68	7.53	21.03
C_4H_9	4	$C_6H_5NO_2$	60% methanol	138.5–139.5	39	$C_9H_{17}N_3OS$	50.19	7.97	19.52	50.15	7.93	19.79
i-C_4H_9	7	$C_6H_5NO_2$	60% methanol	166.5–168	39	$C_9H_{17}N_3OS$	50.19	7.97	19.52	50.35	7.84	19.74
C_5H_{11}	7	$C_6H_5NO_2$	70% methanol	116–117	34	$C_{10}H_{19}N_3OS$	52.35	8.36	18.32	52.46	8.33	18.07
C_6H_{13}	7	$C_6H_5NO_2$	70% methanol	118–119	34	$C_{11}H_{21}N_3OS$	54.27	8.71	17.27	54.26	8.60	17.02

2,4-Thiazolidinedione-2-dimethylhydrazones

When thiocyanoesters were treated with 1,1-dimethylhydrazine in a suitable solvent at room temperature, solids separated out after the whole had been left to stand overnight. No special precautions were required in the additions. The dimethylhydrazones prepared in this manner are listed in Table III.

Hydrolysis of the dimethylhydrazones.—5-Ethyl-2,4-thiazolidinedione-2-dimethylhydrazone (2 g) was treated with ethanol (80 ml) and concentrated hydrochloric acid (40 ml) at reflux temperature for 12 hours and the resulting solution was evaporated to dryness. After the benzene solution was extracted thoroughly with boiling benzene and concentrated to small bulk, the residue was left to stand in the refrigerator where crystals of 5-ethyl-2,4-thiazolidinedione were obtained, m.p. 63–64° C. The fraction insoluble in benzene was dissolved in water, a little sodium acetate was added, and this solution was treated with *m*-nitrobenzaldehyde in ethanol. After the solution was heated for a few minutes on a hot plate, a cloudiness developed, and solidification occurred when it was left to stand in the cold. The *m*-nitrobenzaldehyde dimethylhydrazone so formed caused no depression in the melting point of an authentic sample of this material, prepared as follows: *m*-Nitrobenzaldehyde dissolved in a small quantity of warm ethanol was treated with an excess of 1,1-dimethylhydrazine and two drops of glacial acetic acid. The solution was heated on a hot plate until little solvent remained, whereupon it was allowed to cool and the residue crystallized, m.p. 57–58° C. The compound was recrystallized from methanol, leaving the melting point unchanged. Calc. for $C_9H_{11}N_3O_2$: N, 21.75%. Found: N, 21.58%.

N-Dimethylamino-S-(1-methyl-1-carbomethoxy) Ethylisothiourea

Methyl 2-thiocyanoisobutyrate (15.0 g, 0.094 mole), dimethylhydrazine (6.0 g, 0.100 mole), and nitrobenzene (15 ml) were mixed at room temperature and allowed to stand for 4 days. After it was filtered out and washed with ligroine, the solid product was recrystallized from *t*-amyl alcohol, m.p. 136–138° C. Yield, 5.8 g (28%). Further recrystallization using the same solvent gave a sample melting at 140° C. Calc. for $C_8H_{17}N_3O_2S$: C, 43.80; H, 7.83; N, 19.16%. Found: C, 44.19; H, 7.88; N, 19.02%.

Dibenzyl Disulphide

Benzyl thiocyanate was prepared from benzyl chloride in the usual manner, m.p. 42–44° C (19). The thiocyanate (10 g, 0.067 mole) in ethanol (50 ml) was treated with hydrazine (3.4 g, 0.068 mole) at room temperature, and the resulting solution was allowed to stand for 3 days. The color of the reaction mixture deepened to dark red and a small amount of precipitate of the same color was obtained. After the solution was diluted with ether (100 ml), the product was filtered and when the filtrate was concentrated, a solid separated out, m.p. 70.5–72° C, which contained no nitrogen. Recrystallization from ethanol gave 4.2 g (51%) of the dibenzyl disulphide, m.p. 72–73° C (20).

Trimethylene Disulphide

Hydrazine hydrate (6.3 g, 0.126 mole) was added to a solution of trimethylene dithiocyanate (10 g, 0.063 mole) in ethanol (50 ml) at room temperature. The reaction was slightly exothermic, accompanied by darkening of the mixture to deep yellow. After the mixture was left to stand for 20 hours, the precipitate was filtered and washed with alcohol and ether, m.p. 73–75° C. Yield, 6.4 g (95%). Recrystallization from chloroform gave a product containing no nitrogen, m.p. 75–76° C (14). Molecular weight determinations showed that this material was in reality the dimer of trimethylene disulphide. Calc. for $C_6H_{12}S_4$: 212. Found (Rast method): 198.

Can. J. Chem. Downloaded from www.nrcresearchpress.com by 176.9.209.113 on 09/04/12
For personal use only.

N-dimethylamino-S-benzylisothiourea

Dimethylhydrazine (4.3 g, 0.072 mole) was introduced, with shaking, into a solution of benzyl thiocyanate (10 g, 0.067 mole) in ether (25 ml) at room temperature. After 5 minutes had elapsed, an oil started to separate out, and at the end of 65 hours solidification occurred. The white solid was filtered and washed with ether, m.p. 72–74° C. Yield, 12.1 g (86%). Six recrystallizations from *t*-amyl alcohol afforded a pure product, m.p. 76–77° C. Calc. for $C_{10}H_{15}N_3S$: C, 57.37; H, 7.24; N, 20.08%. Found: C, 57.56; H, 7.23; N, 20.17%.

A small quantity of the above compound was dissolved in ethylene chloride and treated with a few drops of concentrated sulphuric acid. The solution was allowed to stand overnight in a refrigerator and a solid product was obtained, m.p. 114–115° C. Recrystallization from butanol gave rise to the pure sulphate salt of 1,1-dimethyl-2-benzylhydrazine, m.p. 116° C. Calc. for $C_9H_{14}N_2.H_2SO_4$: C, 43.53; H, 6.51; N, 11.29%. Found: C, 43.80; H, 6.63; N, 11.31%.

REFERENCES

1. HEINTZ, A. Ann. **136**, 223 (1865).
2. CLAESSON, P. Ber. **10**, 1346 (1877).
3. FRERICHS, G. and FÖRSTER, P. Ann. **371**, 227 (1910).
4. STEPHEN, H. W. and WILSON, F. J. J. Chem. Soc. 1415 (1928).
5. FRERICHS, G. and HÖLLER, H. Ann. **398**, 256 (1913).
6. STEPHEN, H. W. and WILSON, F. J. J. Chem. Soc. 2826 (1928).
7. ALLEN, P., JR. J. Am. Chem. Soc. **57**, 198 (1935).
8. RADZISZEWSKI, B. Ber. **2**, 208 (1869).
9. CLINTON, R. O. and LASKOWSKI, S. C. J. Am. Chem. Soc. **70**, 3135 (1948).
10. MCKENZIE, A. and BARROW, F. J. Chem. Soc. **99**, 1917 (1911).
11. WINTHROP, S. O. and GAVIN, G. Can. J. Chem. **36**, 879 (1958).
12. STALLÉ, R. and KRAUCH, K. J. Prakt. Chem. **83**, 306 (1913).
13. LIEBER, E. and STROJNY, E. J. J. Org. Chem. **17**, 518 (1952).
14. HAGELBERG, L. Ber. **23**, 1083 (1890).
15. RAST, K. Ber. **55**, 1051, 3727 (1922).
16. CLARKE, H. T. and TAYLOR, E. R. Org. Syntheses, **4**, 9 (1925).
17. MARVEL, C. S. Org. Syntheses, **21**, 74 (1941).
18. HATT, H. H. Org. Syntheses, **16**, 51 (1936).
19. WHEELER, H. L. and MERRIAM, H. F. J. Am. Chem. Soc. **23**, 283 (1901).
20. BERGMANN, E. and HERVEY, J. Ber. **62**, 893 (1929).

Can. J. Chem. Downloaded from www.nrcresearchpress.com by 176.9.209.113 on 09/04/12
For personal use only.

Can. J. Chem. Downloaded from www.nrcresearchpress.com by 176.9.209.113 on 09/04/12
For personal use only.

THE CHEMICAL COMPOSITION OF THE HEARTWOOD EXTRACTIVES OF TAMARACK (LARIX LARICINA (DU ROI) K. KOCH)[1]

G. V. NAIR[2] AND E. VON RUDLOFF

ABSTRACT

The acetone-soluble constituents of the heartwood of tamarack have been investigated. The flavanonols taxifolin and aromadendrin were isolated in 0.30 and 0.05% yield and a trace amount of quercetin was obtained. Tropolones could not be detected, nor was there any evidence for resin acids. The major portion of the extract consisted of esters of ferulic, phthalic, and long-chain fatty acids. Eicosanyl ferulate was isolated as such, whereas the other constituents were identified after saponification. Gas liquid chromatography of the fatty acid mixture indicated the presence of palmitic, palmitoleic, oleic, linoleic, and linolenic acids as well as small amounts of C_{14}, stearic, and C_{20} acids. From the non-saponifiable portion β-sitosterol, eicosanol, and nonan-2-ol were isolated. The acetone extract also contained free D-galactose and L-arabinose.

INTRODUCTION

Whereas the heartwood constituents of pine trees (1, 2) and those of the commercially important west coast conifers (1, 2, 3) have been studied extensively, larch heartwood constituents have not been investigated to any great extent. Gripenberg (4) has isolated from *Larix decidua* (*L. europea*) taxifolin ((+)-2,3-dihydroquercetin) and aromadendrin ((+)-2,3-dihydrokaempferol) and has shown that the distylin isolated from *L. leptolepis* (5, 6) is a mixture of these two flavanonols (nomenclature (2)). Brewerton (7) made a thorough investigation of the heartwood constituents of *L. decidua* and *L. leptolepis* grown in New Zealand and found, besides taxifolin and aromadendrin, trace amounts of a flavanone (m.p. 252° C), a phytosterol, and unidentified lignin- and tannin-like material, but no resin acids.

Tamarack is a small- to medium-sized larch tree found across Canada from the Atlantic coast to northern British Columbia and in Alaska. The wood of this species is often quite oily and is resistant to decay. Although it is used for railway ties, telegraph poles, and posts, it has found little commercial use. The present study of the acetone-soluble heartwood constituent was made on mature trees obtained from the Prince Albert and the Winnipeg areas. The freshly milled heartwood contained about 2.5% (on a dry weight basis) of acetone-soluble, non-volatile extractives.

Preliminary investigation on the total extract and a saponified portion thereof, by spot tests and paper chromatography, indicated the presence of a steroid, flavanoid constituents, and free sugars. Tropolones of the thujaplicin type were not detected on a paper chromatogram (8), nor were resin acids encountered. The concentrated acetone extract deposited a mixture of sugars, consisting of D-galactose (0.15% over-all yield, based on the dry weight of heartwood extracted) and L-arabinose (0.04%). The extraction of these acetone-insoluble sugars is explained by the presence of 15% moisture in the wood. The proportion of galactose to arabinose is the same as that found by Campbell *et al.* (9) in the ε-galactan of larch wood (*Larix decidua*), and it is conceivable that the free sugars were derived from polysaccharides by hydrolysis in the plant.

[1]*Manuscript received May 25, 1959.*
Contribution from the National Research Council of Canada, Prairie Regional Laboratory, Saskatoon, Saskatchewan.
Issued as N.R.C. No. 5293.
[2]*National Research Council of Canada Postdoctorate Fellow, 1958–60.*

Conventional fractionation of the extract into petrol- or ether-soluble neutral compounds and acidic and phenolic constituents by treatment with aqueous alkali was unsatisfactory because of emulsion formation and incomplete separations. Therefore, the extract was divided into acetone-, benzene-, and petrol-soluble portions and then further fractionated as indicated (see Fig. 1). The acetone-soluble, benzene-insoluble portion (0.34%) consisted of flavonoid material. Paper chromatography of this material gave two spots corresponding to aromadendrin (R_f 0.8) and taxifolin (R_f 0.6) with the solvent system of Gripenberg (4), containing 1% acetic acid to prevent tailing. The

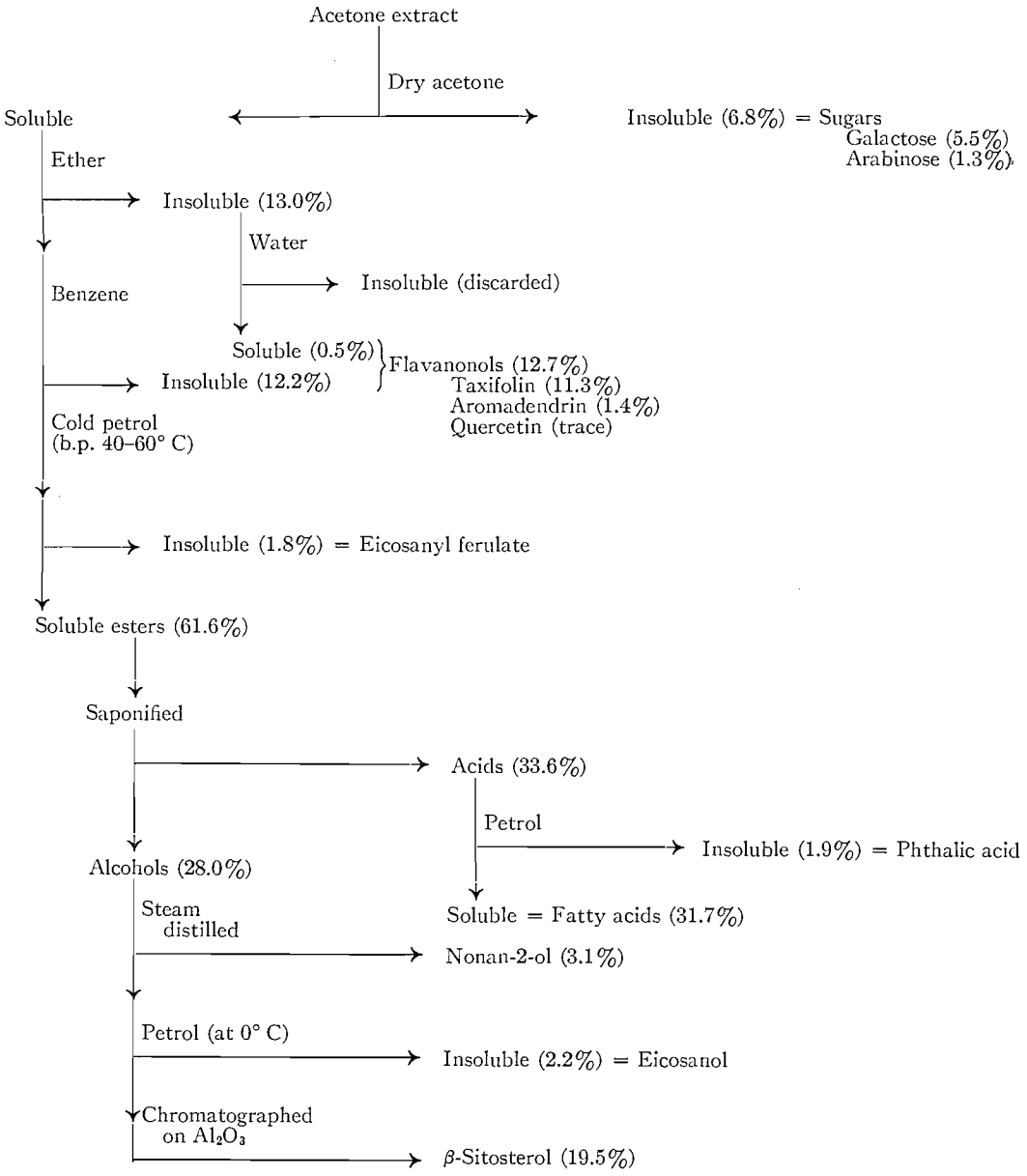

FIG. 1. Fractionation scheme and yields of compounds (based on the weight of acetone extract).

Can. J. Chem. Downloaded from www.nrcresearchpress.com by 176.9.209.113 on 09/04/12
For personal use only.

mixture was resolved almost completely on a cellulose powder column, giving an over-all yield of 0.04% of aromadendrin and 0.30% of taxifolin. When the column was washed with 50% aqueous ethanol a trace amount of quercetin was obtained.

The benzene-soluble, cold petrol-insoluble portion contained an ester, m.p. 61–62° C (0.05%), which was soluble in very dilute alkali, but which precipitated in more concentrated solutions. The infrared spectrum suggested an aromatic ester with a free hydroxyl group and a double bond in conjugation with the aromatic ring. It resembled closely the spectrum of methyl ferulate, except that the C–H absorption was much more intense. Alkaline hydrolysis produced eicosanol and ferulic acid in equimolar proportions, showing the ester to be eicosanyl ferulate.

The petrol-soluble portion formed the major part of the extract and it was comprised mainly of long-chain esters (infrared spectrum). Fractional distillation *in vacuo* did not yield pure components, and gas liquid chromatography was not feasible because of the low volatility of these esters. A portion of the material was saponified and the acidic and neutral fractions were investigated separately. From the non-saponifiable mixture nonan-2-ol, eicosanol, and β-sitosterol were isolated. From the acidic portion phthalic acid was obtained by crystallization. Phthalic acid or its esters are not often found in nature. Haagen-Smit *et al.* (10) report phthalic acid to occur in Zinfandel grapes and recently Kohlbrenner and Schuerch (11) have found *l*-2-octyl-β-sitosteryl phthalate in the extractives of Sitka spruce wood. The major portion of the acidic fraction was composed of long-chain fatty acids, with the unsaturated members predominating. Gas liquid chromatography resolved the methylated mixture and major peaks corresponding to palmitic, palmitoleic, oleic, linoleic, and linolenic acids and minor peaks corresponding to C_{14}, stearic, and C_{20} acids were recorded.

The resistance of heartwood to decay is ascribed to the presence of compounds having phenolic properties, e.g. the pinosylvins in pine heartwood (1, 12) and thujaplicins in thuja species (13). The present findings would indicate, therefore, that tamarack owes its resistance to decay to the presence of the flavanonols and ferulic acid esters.

EXPERIMENTAL

Melting points were measured with a Leitz hot stage microscope. Gas liquid chromatograms were obtained with a Beckman GC-2 chromatograph using washed silicone (14) or polyester (15) on C-22 firebrick columns (18 to 24 in. long, $\frac{1}{4}$ in. diameter). Infrared spectra were recorded by the KBr disk method or the film technique on a Perkin–Elmer Model 21 double beam recording spectrophotometer. All known compounds were identified by mixed melting point and infrared spectra comparison with authentic samples.

Extraction of the Wood

Logs of mature tamarack trees were obtained from the Prince Albert district, Saskatchewan, and from the Winnipeg area, Manitoba. The heartwood was cut out and milled in a hammer mill and then reduced to coarse sawdust in a Wiley mill. The air-dried wood (12.7 kg, 15% moisture content) was extracted with acetone in a Soxhlet extractor for 36 hours. The acetone extract was reduced to dryness by evaporation *in vacuo* in a rotary evaporator, at about 50° C, giving a dark brown, viscous material (302 g).

Preliminary Tests

The magnesium – hydrochloric acid test on an alcoholic solution of the extract was positive for flavanonols. Precipitation tests with digitonin or cyclohexylamine on the extract did not indicate the presence of free sterols or resin acids. When the test was

Can. J. Chem. Downloaded from www.nrcresearchpress.com by 176.9.209.113 on 09/04/12
For personal use only.

Can. J. Chem. Downloaded from www.nrcresearchpress.com by 176.9.209.113 on 09/04/12
For personal use only.

repeated on a saponified portion, positive results were obtained with digitonin. Paper chromatography, using *n*-butanol – acetic acid – water (4:1:1.8 v/v) (16) and *p*-anisidine spray (17) showed that the mixture contained sugars with R_f values corresponding to galactose and arabinose. With impregnated paper, petrol (b.p. 50–60° C), and diazotized benzidine spray (8) the chromatograms showed no spots corresponding to tropolones. When Gripenberg's method (4) was applied, spots corresponding to aromadendrin and taxifolin (see below) were obtained.

Isolation and Identification of Sugars

The concentrated acetone extract when left to stand yielded crystalline material (14.1 g). The total extract was then taken up in dry acetone (0.5 l.) when more solid material was deposited (6.4 g). The solid material was removed by filtration and crystallized from methanol to yield a crude product, m.p. 142–155° C, $[\alpha]_D^{24.6}$ +79.12 (*c*, 0.77, H_2O). Paper chromatography showed the presence of galactose and arabinose only, and the mixture was resolved by treatment with α-methyl-α-phenyl hydrazine (9). D-Galactose-*N*-methyl-*N*-phenyl hydrazone (1.636 g, corresponding to 80.55% galactose), m.p. 185–186° C, $[\alpha]_D^{22.8}$ −18.98 (*c*, 0.66, pyridine), and arabinose, m.p. 158–160° C, $[\alpha]_D^{23.8}$ +121.59 (*c*, 0.52, H_2O), were isolated.

Isolation and Identification of Flavanonols

The acetone-soluble material, after filtration and reduction to a small volume, was taken up in excess ether (1.25 l.). The ether-insoluble material was separated, dried (39 g), and extracted repeatedly with boiling water, the insoluble residue being discarded. The ether-soluble portion was evaporated to dryness and re-extracted with benzene. The benzene-insoluble portion (36.5 g) was combined with the water-soluble portion (1.5 g) and analyzed by paper chromatography (4). When 1% acetic acid was added to the solvent mixture (chloroform–ethanol–water, 8:2:1 v/v, lower phase) tailing of the flavanonols was prevented. With the bis-diazotized benzidine spray reagent (18) brown spots corresponding to aromadendrin (R_f 0.8) and taxifolin (R_f 0.6) were obtained. An aliquot of the mixture of flavanonols (3.75 g) was resolved on a cellulose powder column (50×4.5 cm), using the same solvent system (4.5 l.) as eluent. Fractions of 20 ml were collected and tested individually by paper chromatography. Tubes 1 to 70 contained aromadendrin (0.314 g), m.p. 236–237° C (from $CHCl_3$), $[\alpha]_D^{24.6}$ +44.72 (*c*, 0.5, water–acetone, 1:1). When the compound was recrystallized from water the m.p. was 128–130° C. This dimorphism has apparently not been noted before. Tubes 71 to 89 contained a mixture (0.077 g) of aromadendrin and taxifolin in about equal amounts. Taxifolin (3.307 g) was obtained from tubes 90 to 195, m.p. 238–240° C (from $CHCl_3$ and ethanol), $[\alpha]_D^{24}$ +47.71 (*c*, 0.75, water–acetone). When the column was washed with 50% aqueous ethanol (1:1) a yellow solid (0.006 g) was obtained on evaporation of the solvent. Crystallization from aqueous ethanol gave quercetin, m.p. 310–312° C, $[\alpha]_D^{24}$ +142.2 (*c*, 0.53, water–acetone).

Isolation and Identification of Eicosanyl Ferulate

The benzene-soluble material (191 g) was repeatedly triturated with cold petrol (b.p. 40–60° C). The petrol-insoluble material (5.5 g) on recrystallization from cyclohexane gave a compound, m.p. 61–62° C. Found: C, 75.76%; H, 10.70%; molecular weight (Rast), 533. Calc. for $C_{30}H_{50}O_4$: C, 75.95%; H, 10.54%; molecular weight, 474.52.

The ester (0.5 g) in chloroform (5 ml) was treated with excess bromine in chloroform. Evaporation of the solvent left a solid tribromide, m.p. 98° C (from petrol, b.p. 40–60° C). Found: C, 51.96%; H, 7.21%. Calc. for $C_{30}H_{49}O_3Br_3$: C, 51.65%; H, 7.03%. The ester

(2.1 g) was hydrolyzed by refluxing in a 20% aqueous potassium hydroxide solution (150 ml) containing ethanol (50 ml) for 15 hours. The ethanol was removed by distillation, and the cold aqueous residue was extracted with ether. The ether extract was washed, dried, and evaporated to dryness (1.3 g). The residue was recrystallized (from acetone) to yield *n*-eicosanol, m.p. 71–72° C. Found: C, 80.70%; H, 14.10%. Calculated for $C_{20}H_{42}O$: C, 80.53%; H, 14.06%. The aqueous soap solution was acidified to pH 2–3 with 10% aqueous sulphuric acid and extracted three times with ether. The ether extract was washed with a saturated aqueous solution of sodium chloride, dried, and the solvent was distilled off. The residual solid (0.85 g) was recrystallized from ethyl acetate – cyclohexane to give pure ferulic acid, m.p. 175–176° C. Found: C, 62.05%; H, 5.19%. Calc. for $C_{10}H_{10}O_4$: C, 61.86%; H, 5.19%.

Petrol Extract

The petrol-soluble portion formed the major part of the heartwood extract (185 g). Fractional vacuum distillation did not resolve the mixture into single components. Because of the low volatility of the mixture, gas liquid chromatography was not successful. However, an infrared spectrum of the mixture indicated the presence of a large amount of long-chain esters. An aliquot (40 g) of the material was saponified under reflux with 20% aqueous potassium hydroxide solution (200 ml) and ethanol (100 ml) for 15–20 hours. The reaction mixture was separated into non-saponifiables (18.7 g) and acids (22.25 g) in the usual manner.

The non-saponifiable material was exhaustively steam distilled, the distillate (2 l.) saturated with sodium chloride and thrice extracted with ether (200 ml each). The ethereal solution was washed with saturated sodium chloride solution, dried over anhydrous sodium sulphate, and then distilled, yielding a sweet-smelling liquid (2.3 g), b.p. 75–77° C at 12 mm. Found for a redistilled sample: C, 74.78%; H, 14.00%; n_D^{27} 1.4310. Calc. for $C_9H_{20}O$: C, 74.46%; H, 14.48%. The derived α-naphthyl urethane was crystallized from carbon tetrachloride, m.p. 55–56° C. This corresponds to the melting point of the α-naphthyl urethane of nonan-2-ol (m.p. 55.5° C) (19).

The non-volatile residue was dissolved in petrol (b.p. 40–60° C) and kept at 0–2° C for several days, when eicosanol (1.3 g), m.p. 71–72° C, crystallized. A portion of the residual material (2.4 g) was chromatographed on neutral alumina (Brockmann). Elution with petrol (b.p. 40–60° C) and ether (1:1 v/v) gave 0.3 g of unsaponified esters. With ether-ethanol (1:1 v/v) a solid (1.8 g) was eluted which had m.p. 141° C after crystallization from ethanol. It gave a positive Lievermann–Burchard reaction, and formed an acetate, m.p. 123–124° C, and a benzoate, m.p. 143–144° C, which correspond with those of β-sitosterol (20). Found: C, 83.78%; H, 12.30%. Calc. for $C_{29}H_{50}O$: C, 83.99%; H, 12.15%.

The acid mixture contained petrol-insoluble material (1.25 g) which crystallized from acetone to give phthalic acid, m.p. 201–203° C; anilide, m.p. 165–166° C. The petrol-soluble acids were converted to their methyl esters with diazomethane and analyzed by gas liquid chromatography. When the polyester column was used, peaks corresponding to two C_{14} acids (0.5% and 0.6% respectively), palmitic (7.0%), palmitoleic (7.1%), stearic (1.9%), oleic (20.0%), linoleic (31.8%), linolenic (25.2%), and two C_{20} acids (1.5% and 3.0% respectively) were obtained.

ACKNOWLEDGMENTS

We wish to express our thanks to the Forestry Branch of the Department of Natural Resources for obtaining the wood, to Mr. M. Granat for technical assistance, to Miss

Can. J. Chem. Downloaded from www.nrcresearchpress.com by 176.9.209.113 on 09/04/12
For personal use only.

I. M. Gaffney for the infrared spectra, to Mr. M. Mazurek for the microanalyses, and to Dr. C. G. Youngs for help in gas liquid chromatographic separations. We are also grateful to Professor H. Erdtman, Royal Institute of Technology, Stockholm, who kindly supplied authentic samples of taxifolin and aromadendrin, and for his advice and suggestions.

REFERENCES

1. ERDTMAN, H. *In* Progress in organic chemistry. Vol. 1. *Edited by* J. W. Cook. Butterworth Scientific Publications, London. 1952. pp. 22–63.
2. ERDTMAN, H. *In* Perspectives in organic chemistry. *Edited by* A. Todd. Interscience Publishers, Inc., New York. 1956. p. 453.
3. GARDNER, J. A. F. and BARTON, G. M. Forest Prods. J. **8**, 3 (1958).
4. GRIPENBERG, J. Acta Chem. Scand. **6**, 1153 (1952).
5. HASEGAWA, M. and SHIRATO, T. J. Chem. Soc. Japan, **72**, 223 (1951).
6. MIGITA, N., NAKANO, J., and TOROI, T. J. Japan Tech. Assoc. Pulp Paper Ind. **5**, 399 (1951); Chem. Abstr. **46**, 1254^g (1952).
7. BREWERTON, H. V. New Zealand J. Sci. Technol. B, **37**, 626 (1956).
8. WACHTMEISTER, C. A. and WICKBERG, B. Acta Chem. Scand. **12**, 1335 (1958).
9. CAMPBELL, W. G., HIRST, E. L., and JONES, J. K. N. J. Chem. Soc. 774 (1948).
10. HAAGEN-SMIT, A. J., HIROSAWA, F. N., and WANG, T. H. Food Research, **14**, 472 (1949).
11. KOHLBRENNER, P. J. and SCHUERCH, C. J. Org. Chem. **24**, 166 (1959).
12. ERDTMAN, H. Naturwissenschaften, **27**, 130 (1939).
13. ERDTMAN, H. and GRIPENBERG, J. Nature, **161**, 719 (1948).
14. CRAIG, B. M. and MURTY, N. L. Can. J. Chem. **36**, 1297 (1958).
15. CRAIG, B. M. J. Am. Oil Chemists' Soc. (In press).
16. NEISH, A. C. Can. J. Biochem. and Physiol. **35**, 159 (1957).
17. HOUGH, L., JONES, J. K. N., and WADMAN, W. H. J. Chem. Soc. 1702 (1950).
18. LINDSTEDT, G. Acta Chem. Scand. **4**, 448 (1950).
19. PICKARD, R. H. and KENYON, J. J. Chem. Soc. **99**, 56, 70 (1911).
20. COOK, J. W. and PAIGE, M. F. C. J. Chem. Soc. 336 (1944).

Can. J. Chem. Downloaded from www.nrcresearchpress.com by 176.9.209.113 on 09/04/12
For personal use only.

Can. J. Chem. Downloaded from www.nrcresearchpress.com by 176.9.209.113 on 09/04/12
For personal use only.

NOTES

4-NITROPYRENE*

P. M. G. Bavin†

Nitration of pyrene has afforded only the 1-isomer (1, 8). Since the introduction of the nitro group into polycyclic hydrocarbons through the diazonium compounds does not proceed in high yield (3), other indirect routes to the unknown nitropyrenes seemed to offer advantages.

One such alternative, the dehydrogenation of the nitrohexahydropyrene (I*a*) with chloranil, has been used to prepare 4-nitropyrene (II*a*) for the first time.

The nitrohexahydropyrene (I*a*) and the corresponding amine (I*b*) and its N-acetyl derivative (I*c*) have been described previously (7). These have been prepared again and the fluoro compound (I*d*) has been described for the first time. Other substitution products of *sym*-hexahydropyrene have been described (5, 6, 8).

It is curious that Neresheimer's work (7) was not included in Vollmann's paper (8) although carried out in the same laboratory and at the same period.

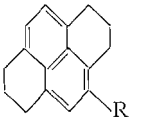

I

I*a*, R = NO_2 I*c*, R = $NH.CO.CH_3$
I*b*, R = NH_2 I*d*, R = F

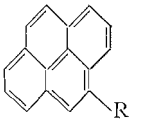

II

II*a* R = NO_2
II*b* R = NH_2

EXPERIMENTAL

Melting points are uncorrected.

4-Nitro-1,2,3,6,7,8-hexahydropyrene (I*a*)

In a typical experiment, *sym*-hexahydropyrene (3 g) was nitrated with nitric acid (0.8 ml, d. 1.42) in acetic anhydride (250 ml). The solution rapidly turned red. After 48 hours at room temperature, acetic anhydride was destroyed with water and the products isolated with chloroform. Purification of the crude nitro compound by chromatography from pentane–benzene (5:1) on acid-washed alumina followed by crystallization from methanol–acetone afforded pure (I*a*) (1.9–2.4 g) as bright yellow needles, m.p. 92–93° (lit. m.p. 92–95° (7)). Calculated for $C_{16}H_{15}NO_2$: C, 75.87; H, 5.97%. Found: C, 75.97; H, 5.74%.

The impure nitro compound rapidly turned brown when exposed to light.

4-Amino-1,2,3,6,7,8-hexahydropyrene (I*b*)

4-Amino-1,2,3,6,7,8-hexahydropyrene was prepared by reducing the nitro compound (I*a*) with hydrazine and palladized charcoal (2). It crystallized from heptane as almost

*Ring index numbering.
†I.C.I. Fellow.

colorless slender needles, m.p. 132–133° (lit. m.p. 134–135° (7)). Calculated for $C_{16}N_{17}N$: C, 86.05; H, 7.67; N, 6.27%. Found: C, 86.15; H, 7.76; N, 6.28%.

N-*Acetyl-4-amino-1,2,3,6,7,8-hexahydropyrene* (I*c*)

N-Acetyl-4-amino-1,2,3,6,7,8-hexahydropyrene crystallized from toluene as colorless slender needles, m.p. 290–292° (lit. m.p. 280–282° (7)). Calculated for $C_{18}H_{19}NO$: C, 81.47; H, 7.22; N, 5.28%. Found: C, 81.28; H, 7.28; N, 5.26%.

4-Fluoro-1,2,3,6,7,8-hexahydropyrene (I*d*)

4-Fluoro-1,2,3,6,7,8-hexahydropyrene, prepared in the usual way (4), crystallized from methanol as slender white needles, m.p. 111–112°. Calculated for $C_{16}H_{15}F$: C, 84.93; H, 6.68%. Found: C, 84.73; H, 6.91%.

4-Nitropyrene (II*a*)

The pure hexahydro compound (I*a*), (1 g), was boiled under reflux for 24 hours with a solution of chloranil (5 g) in xylene (30 ml). After it was cooled the mixture was diluted with hexane (30 ml), decanted from the dark hydroquinone, and passed through a column of alumina. Elution was continued with hexane–benzene (5:1). The eluted material was further purified by rechromatographing from hexane, only the orange-brown band eluting as a yellow solution being retained. (These colors correspond exactly to those shown by 1-nitropyrene (1).)

Crystallization from methanol containing a little acetone afforded slender orange needles, m.p. 196–197.5°. Calculated for $C_{16}H_9NO_2$: C, 77.72; H, 3.67%. Found: C, 77.40; H, 3.51%.

4-Aminopyrene (II*b*)

4-Aminopyrene was prepared from (II*a*) by reduction with hydrazine and palladized charcoal (2). It crystallized from heptane as bright yellow platelets, m.p. 191–193° with decomposition (lit. m.p. 182° (7)).

ACKNOWLEDGMENTS

Most of this work was completed at the University of Ottawa during the tenure of a National Research Council of Canada Postdoctorate Fellowship (1954–56). The author is indebted to Dr. W. L. Mosby (American Cyanamid Co., Bound Brook) for drawing his attention to and supplying a copy of the P.B. Report (7).

1. BAVIN, P. M. G. Thesis, London. 1952.
2. BAVIN, P. M. G. Can. J. Chem. **36**, 238 (1958).
3. BAVIN, P. M. G. and DEWAR, M. J. S. J. Chem. Soc. 4477 (1955).
4. BAVIN, P. M. G. and DEWAR, M. J. S. J. Chem. Soc. 4486 (1955).
5. CLAR, E. J. Chem. Soc. 2168 (1949).
6. COOK, J. W. and HEWETT, C. L. J. Chem. Soc. 401 (1933).
7. NERESHEIMER, H. P. B. Report 70840, frames 12871/6.
8. VOLLMANN, H., BECHER, H., CORELL, M., and STREECK, H. Ann. **531**, 1 (1937).

RECEIVED MARCH 19, 1959.
THE DEPARTMENT OF CHEMISTRY,
THE UNIVERSITY,
KINGSTON-UPON-HULL,
EAST YORKSHIRE, ENGLAND.

Can. J. Chem. Downloaded from www.nrcresearchpress.com by 176.9.209.113 on 09/04/12
For personal use only.

KINETICS OF THE THERMAL REACTION OF HYDROGEN PEROXIDE WITH HYDROGEN*

W. FORST

The thermal reaction of hydrogen peroxide with hydrogen has been studied by McLane (1), who worked around 500° C in a flow system without reaching any definite conclusions. In the present brief study it was found that under suitable conditions the reaction of hydrogen peroxide with hydrogen proceeded with a pressure increase in a closed system. This means that in addition to the over-all process

$$H_2 + H_2O_2 \rightarrow 2H_2O,$$

the reaction

$$H_2O_2 \rightarrow H_2O + \tfrac{1}{2}O_2$$

must also be occurring because it is the only conceivable process capable of increasing the number of molecules. Presence of oxygen in the system was confirmed by following the reaction to completion. The pressure in the system rose to a maximum, and then slowly declined (Fig. 1), indicating a slow hydrogen–oxygen reaction. Sometimes there occurred an explosion shortly before the pressure maximum was reached (i.e. shortly before all the

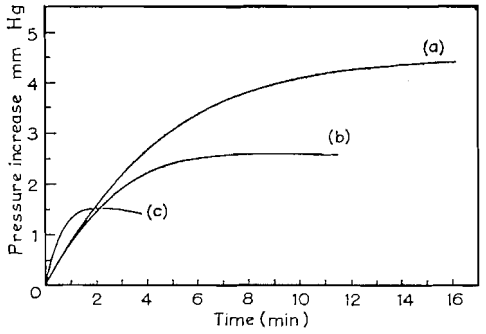

FIG. 1. Rate curves in the presence and absence of hydrogen. (*a*) Peroxide only. (*b*) Peroxide + 19.2 mm H_2 initially. (*c*) Peroxide + 96.2 mm H_2 initially. Initial pressure of peroxide 9.6 mm Hg in all three cases.

hydrogen peroxide had disappeared). This behavior finds a ready explanation in the inhibiting action of hydrogen peroxide in hydrogen–oxygen explosions at the second limit (2). Comparison of rate curves in the presence and absence of hydrogen (Fig. 1) shows that qualitatively the effect of hydrogen is twofold: (1) the rate is faster; (2) the pressure increase is smaller.

Apparatus and technique were described previously (3). All experiments were done at 431.5° C, where the slow hydrogen–oxygen reaction is not important. However, to avoid all complications arising from this reaction, only initial rates were measured and considered significant; these results are summarized in Figs. 2 and 3. Each point is the average of two successive runs on the same H_2–H_2O_2 mixture.

The interpretation of the results is complicated by two factors: (1) the time-dependence of the pressure rise in the H_2O_2–H_2 reaction system represents the rate of formation of oxygen, which, unlike in the case of the pressure rise in the H_2O_2 system, bears no simple

**This work was supported in part by the Office of Scientific Research of the U.S. Air Force under Contract No. AF 18(600)-492.*

Can. J. Chem. Downloaded from www.nrcresearchpress.com by 176.9.209.113 on 09/04/12
For personal use only.

relationship to the rate of disappearance of peroxide; (2) under the experimental conditions (H_2O_2 pressure below 20 mm Hg, hydrogen pressure below 100 mm Hg) the decomposition of hydrogen peroxide is unimolecular and second order (3, 4). If the proposed (3) scheme for this decomposition is accepted, then the initial rate of oxygen formation R_0, in the presence of one inert foreign gas X, is given by (cf. eq. VII′, ref. 3)

$$[1] \qquad R_0 = (d[O_2]/dt)_{t\to 0} = a_1[H_2O_2]_0^2 + a_4[H_2O_2]_0[X]_0,$$

where the subscript zero refers to initial conditions, and

a_1 = second order rate constant for activation with peroxide,
a_4 = second order rate constant for activation with inert gas X.

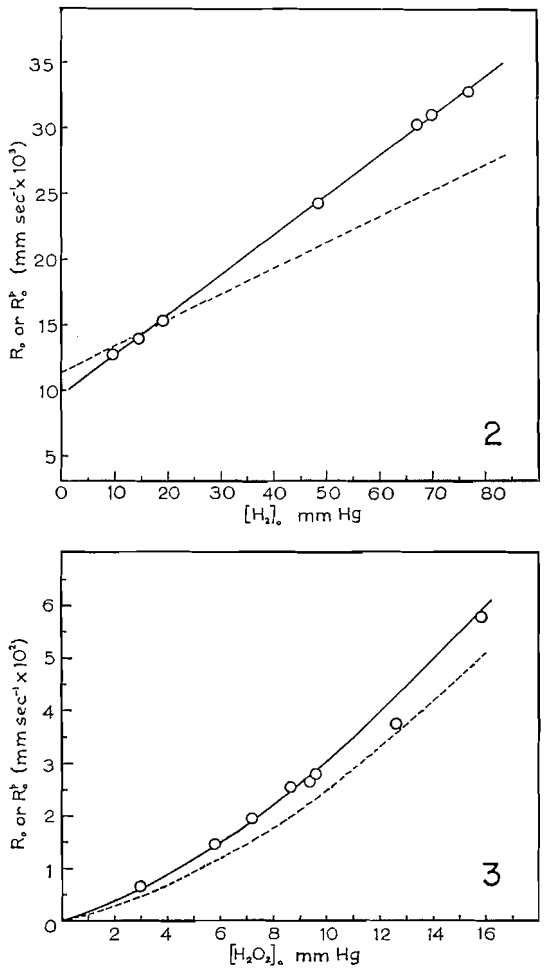

FIG. 2. Solid line: Experimental initial rate R_0 plotted vs. initial hydrogen pressure. Broken line: R_0^p (theoretical physical component of initial rate) plotted vs. initial hydrogen pressure. Initial hydrogen peroxide concentration constant at 9.6 mm Hg in both cases.

FIG. 3. Solid line: Experimental initial rate R_0 plotted vs. initial peroxide pressure. Broken line: R_0^p (theoretical physical component of initial rate) plotted vs. initial peroxide pressure. Initial hydrogen pressure constant at 57.9 mm Hg in both cases.

Can. J. Chem. Downloaded from www.nrcresearchpress.com by 176.9.209.113 on 09/04/12
For personal use only.

Can. J. Chem. Downloaded from www.nrcresearchpress.com by 176.9.209.113 on 09/04/12
For personal use only.

Equation [1] makes it at once apparent that the initial rate of oxygen formation R_0 will depend on initial hydrogen concentration even if hydrogen did not chemically react, that is, the mere presence of hydrogen as a collision medium will increase R_0. This may be referred to as the physical effect of hydrogen, the magnitude of which depends on $a_4^{H_2}$, the second order rate constant for activation with hydrogen. The experimentally determined initial rate R_0 must contain the contribution of both the physical and chemical effects of hydrogen, because it is difficult to account for the results in Fig. 1 by physical activation alone. By working out the necessary algebra it is easy to show that R_0 will be equal to the sum of the two contributions:

$$\begin{aligned} R_0 &= R_0^{p}+R_0^{c} \\ &= a_1[H_2O_2]_0^2+a_4^{H_2}[H_2O_2]_0[H_2]_0+R_0^{c}, \end{aligned}$$

where R_0^{p} is a term representing the physical effect and R_0^{c} a term representing the chemical effect of hydrogen on initial rate. This equation shows that for constant $[H_2O_2]_0$, R_0^{p} is linear in initial hydrogen concentration. From Fig. 2 it is apparent that for $[H_2O_2]_0$ = constant the experimentally determined R_0 is also linear in $[H_2]_0$, and therefore R_0^{c} must be likewise linear in initial hydrogen concentration at constant $[H_2O_2]_0$; hence the reaction is seen to be first order with respect to hydrogen.

The broken line in Fig. 2 represents a plot of R_0^{p} vs. $[H_2]_0$ for $[H_2O_2]_0$ = constant = 9.6 mm Hg taking $a_4^{H_2} = 2.1\times10^{-5}$ mm sec^{-1}, a value obtained by assuming that the collision/collision efficiency of hydrogen relative to H_2O_2 reactant is the same as that of He relative to the same reactant. This is a first approximation based on results of Volpe and Johnston (5), who found experimentally that these efficiencies were equal in the case of nitryl chloride reactant. The value of a_1 was taken from ref. 3. The discrepancy in the intercepts of the two lines is partly due to error in peroxide concentration (which enters the intercept squared), and partly to a slight shift in surface condition.

Figure 3 represents experimental results obtained at fixed initial hydrogen concentration. The broken line is a theoretical plot of R_0^{p} vs. $[H_2O_2]_0$ assuming $a_4^{H_2} = 2.1\times10^{-5}$ mm sec^{-1}, as before. If R_0^{c} is now written

$$R_0^{c} = k[H_2O_2]_0^{x}[H_2]_0,$$

where k = rate constant for the reaction of peroxide with hydrogen, and x = the unknown power of the peroxide concentration in the rate expression, then the plot of $R_0-R_0^{p}$ vs. $[H_2O_2]_0$ will be a curve if $x > 1$, and a straight line if $x = 1$. This is plotted in Fig. 4, again for $a_4^{H_2} = 2.1\times10^{-5}$ mm sec^{-1}, and is seen to result in a straight line. The linearity of

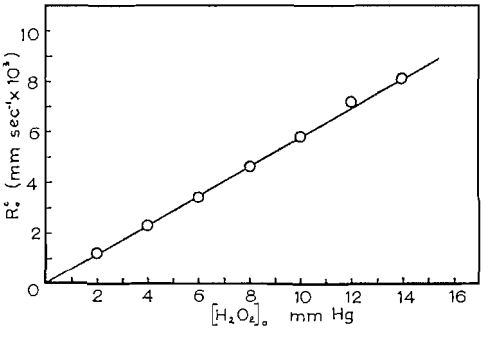

FIG. 4. The difference $R_0 - R_0^{p}$ (from Fig. 3) plotted vs. initial peroxide concentration, with initial hydrogen pressure constant at 57.9 mm Hg.

this plot does not depend on the assumed value for $a_4^{H_2}$, although the slope does. The reaction is thus seen to be first order in peroxide as well, and so the reaction may be described by the equation

$$R_0 = a_1[H_2O_2]_0^2 + (a_4^{H_2} + k)\,[H_2O_2]_0[H_2]_0. \qquad [2]$$

On the basis of this result some speculation may be made concerning the probable mechanism. If reactions involving oxygen are neglected on the ground that they would not affect the initial rate, hydrogen is likely to enter only into reactions

$$OH + H_2 \rightarrow H_2O + H \qquad [a]$$

$$H + H_2O_2 \rightarrow H_2O + OH, \qquad [b]$$

for which there seems to be good evidence from other sources ([*a*], ref. 6; [*b*], refs. 2, 7, 8). It turns out, however, that these two reactions, when combined with reactions postulated (3) in the decompostion of hydrogen peroxide, will not result in an increase of oxygen formation as required by eq. [2]. A closer look at the mechanism shows that there are two types of reactions that will increase the rate of formation of oxygen (but will not necessarily lead to the desired order in peroxide or hydrogen).

(1) Reactions in which one radical disappears and another radical appears, with the simultaneous formation of oxygen, for example,

$$HO_2 + H_2O_2 \rightarrow OH + O_2 + H_2O$$

or

$$HO_2 \rightarrow H + O_2.$$

These reactions do not involve the intervention of hydrogen and therefore presumably should occur also in the decomposition of pure peroxide. However, they lead there to unsatisfactory results (9, 10).

(2) Chain-branching reactions not involving oxygen. This restricts the choice of likely reactions considerably; in fact, the only reaction seems to be

$$H_2 + HO_2 \rightarrow 2OH + H \qquad [c]$$

suggested by Kassel and Storch (11) and used by them to derive a mechanism for the second explosion limit in the hydrogen–oxygen reaction. If reactions [*a*], [*b*], and [*c*] are added to the reactions postulated in the decomposition of pure peroxide (3), a rate expression for the rate of formation of oxygen may be derived which has the form [2]. However, reaction [*c*] has a very high endothermicity, some 67 kcal if $D(H–O_2)$ is taken as 47 kcal (12), so that a more direct evidence for reaction [*c*] would be required before this mechanism can be accepted.

ACKNOWLEDGMENTS

Thanks are due to Professor P. A. Giguère of Laval University for his continued interest, and to Professor O. K. Rice of the University of North Carolina for permission to write this paper during the tenure of a postdoctoral fellowship.

1. McLane, C. K. J. Chem. Phys. **18**, 972 (1950).
2. Forst, W. and Giguère, P. A. J. Phys. Chem. **62**, 340 (1958).
3. Forst, W. Can. J. Chem. **36**, 1308 (1958).
4. Hoare, D. E., Protheroe, J. B., and Walsh, A. D. Nature, **182**, 654 (1958).
5. Volpe, M. and Johnston, H. S. J. Am. Chem. Soc. **78**, 3903 (1956).
6. Lewis, B. and von Elbe, G. Combustion, flames and explosions. Academic Press, Inc., New York. 1951.
7. Geib, K. H. Z. physik. Chem. A, **169**, 161 (1934).
8. Baldwin, R. R. and Mayor, L. Paper presented at the 7th Symposium on Combustion, Oxford. 1958.

Can. J. Chem. Downloaded from www.nrcresearchpress.com by 176.9.209.113 on 09/04/12
For personal use only.

9. GIGUÈRE, P. A. and LIU, I. D. Can. J. Chem. **35**, 283 (1957).
10. CONWAY, D. C. J. Phys. Chem. **61**, 1579 (1957).
11. KASSEL, L. S. and STORCH, H. H. J. Am. Chem. Soc. **57**, 672 (1935).
12. FONER, S. N. and HUDSON, R. L. J. Chem. Phys. **23**, 1364 (1955).

RECEIVED MAY 4, 1959.
DEPARTMENT OF CHEMISTRY,
LAVAL UNIVERSITY,
QUEBEC, QUE.

Can. J. Chem. Downloaded from www.nrcresearchpress.com by 176.9.209.113 on 09/04/12
For personal use only.

TRANSIENTS IN THE FORMATION OF ANODIC OXIDE FILMS

L. YOUNG

With certain metals, in particular, tantalum (1) and niobium (2) when the ionic (film-building) current density through the anodic oxide film is suddenly increased, the field strength in the oxide "overshoots" before settling to the new steady state value corresponding to the new current density. Dewald (1) has shown that the behavior is inconsistent with the model (which he advanced to explain the Tafel slope anomalies) in which the space charge due to the mobile metal ions is uncompensated by other sources of space charge. A more realistic model would have a concentration (say, ϕ cm^{-3}) of mobile metal in the electrically neutral oxide. The net space charge may then be either negative or positive. The steady state equations for this model, with ϕ independent of field strength, have been published (3).

The purpose of the present communication is to show that Dewald's result for his case (which corresponds to $\phi = 0$) may be generalized to $\phi \neq 0$.

We have

$$\partial E/\partial t = (pI_0 - i)/KK_0 \quad \text{(differentiated Gauss' equation)}$$
$$\partial E/\partial x = q(n-\phi)/KK_0 \quad \text{(Poisson's equation)}$$
$$i = q\mu_0 \exp \beta E \quad \text{(conventional equation for the ionic current at high fields)}$$

where E = field strength in the oxide at distance x from the metal, t = time after current is changed, I_0 = current density for $t < 0$, pI_0 = current for $t > 0$, i = current in oxide at distance x from the metal, n = concentration of mobile metal ions,

$$\mu_0 = \nu \exp(-W/kT)$$

where ν = vibration frequency and

$$W = \text{activation energy at zero } E, \text{ and } \beta = qa/kT$$

where a = half ionic jump distance within the oxide. By eliminating n and i, and putting (following Dewald)

$$R = \mu_0 KK_0 \exp(\beta E)/\beta pI_0 t$$
$$T = \beta pI_0 t/KK_0$$
$$z = x/D$$

where D = total oxide thickness; with, in addition,

$$\alpha = \phi\beta Dq/KK_0$$

and

$$\epsilon = (n_0 - \phi)/\phi$$

9. GIGUÈRE, P. A. and LIU, I. D. Can. J. Chem. **35**, 283 (1957).
10. CONWAY, D. C. J. Phys. Chem. **61**, 1579 (1957).
11. KASSEL, L. S. and STORCH, H. H. J. Am. Chem. Soc. **57**, 672 (1935).
12. FONER, S. N. and HUDSON, R. L. J. Chem. Phys. **23**, 1364 (1955).

RECEIVED MAY 4, 1959.
DEPARTMENT OF CHEMISTRY,
LAVAL UNIVERSITY,
QUEBEC, QUE.

Can. J. Chem. Downloaded from www.nrcresearchpress.com by 176.9.209.113 on 09/04/12
For personal use only.

TRANSIENTS IN THE FORMATION OF ANODIC OXIDE FILMS

L. YOUNG

With certain metals, in particular, tantalum (1) and niobium (2) when the ionic (film-building) current density through the anodic oxide film is suddenly increased, the field strength in the oxide "overshoots" before settling to the new steady state value corresponding to the new current density. Dewald (1) has shown that the behavior is inconsistent with the model (which he advanced to explain the Tafel slope anomalies) in which the space charge due to the mobile metal ions is uncompensated by other sources of space charge. A more realistic model would have a concentration (say, ϕ cm^{-3}) of mobile metal in the electrically neutral oxide. The net space charge may then be either negative or positive. The steady state equations for this model, with ϕ independent of field strength, have been published (3).

The purpose of the present communication is to show that Dewald's result for his case (which corresponds to $\phi = 0$) may be generalized to $\phi \neq 0$.

We have

$$\partial E/\partial t = (pI_0 - i)/KK_0 \quad \text{(differentiated Gauss' equation)}$$
$$\partial E/\partial x = q(n-\phi)/KK_0 \quad \text{(Poisson's equation)}$$
$$i = q\mu_0 \exp \beta E \quad \text{(conventional equation for the ionic current at high fields)}$$

where E = field strength in the oxide at distance x from the metal, t = time after current is changed, I_0 = current density for $t < 0$, pI_0 = current for $t > 0$, i = current in oxide at distance x from the metal, n = concentration of mobile metal ions,

$$\mu_0 = \nu \exp(-W/kT)$$

where ν = vibration frequency and

$$W = \text{activation energy at zero } E, \text{ and } \beta = qa/kT$$

where a = half ionic jump distance within the oxide. By eliminating n and i, and putting (following Dewald)

$$R = \mu_0 KK_0 \exp(\beta E)/\beta pI_0 t$$
$$T = \beta pI_0 t/KK_0$$
$$z = x/D$$

where D = total oxide thickness; with, in addition,

$$\alpha = \phi\beta Dq/KK_0$$

and

$$\epsilon = (n_0 - \phi)/\phi$$

where n_0 is the concentration of metal ions just inside the oxide for $t < 0$, we obtain

$$\partial R/\partial z + (1/R)\partial R/\partial T + \alpha R = 1.$$

The general solution is

$$f\{z + (1/\alpha)\log(1-\alpha R),\ T - \log(R/(1-\alpha R))\} = 0.$$

The boundary conditions are

$$R(z, 0) = R(0,0)\{1+\epsilon(1-\exp(-\alpha z))\}$$
$$R(0,T) = R(0,0)p^r/(1+(p-1)e^{-T/r})^r$$

where r = ratio of ionic jump distance at the interface to that within the oxide.

Solutions satisfying these conditions are

$$R = \{(1-\alpha R(0,0)p)e^{-\alpha z}-1\}/\{\alpha(1-p)e^{-T}-\alpha\}$$
$$(p-1)(e^{\alpha z}e^{-T}R)^{1/r} = p(R(0,0))^{1/r} - ((1-e^{\alpha z})/\alpha + R e^{\alpha z})^{1/r}.$$

These solutions join at

$$z = z_s$$

where

$$(e^{\alpha z_s}-1)/\alpha = R(0,0)(e^T-1).$$

For a given z, $\partial R/\partial T$ is always positive for $p > 1$ and always negative for $p < 1$, so that there is no overshoot.

This communication is published by permission of the Defence Research Board.

1. Dewald, J. F. J. Phys. Chem. Solids, **2**, 55 (1957).
2. Young, L. Trans. Faraday Soc. **52**, 502 (1956).
3. Young, L. Can. J. Chem. **37**, 276 (1959).

Received May 19, 1959.
British Columbia Research Council,
University of British Columbia,
Vancouver 8, British Columbia.

Can. J. Chem. Downloaded from www.nrcresearchpress.com by 176.9.209.113 on 09/04/12
For personal use only.

Can. J. Chem. Downloaded from www.nrcresearchpress.com by 176.9.209.113 on 09/04/12
For personal use only.

Canadian Journal of Chemistry

Issued by THE NATIONAL RESEARCH COUNCIL OF CANADA

VOLUME 37 OCTOBER 1959 NUMBER 10

SELF-DIFFUSION IN POLYCRYSTALLINE NICKEL[1]

J. R. MACEWAN,[2] J. U. MACEWAN, AND L. YAFFE

ABSTRACT

The self-diffusion of nickel has been studied in polycrystalline samples by a sectioning technique. There is evidence of grain boundary diffusion below temperatures of 1150° C. The results obtained between 1150° and 1400° C are representative of volume diffusion and are represented by the expression

$$D = 3.36\, e^{-69,800/RT}.$$

A comparison is made with the results of other self-diffusion studies using Zener's hypothesis.

INTRODUCTION

The most precise measurements made on the rate of volume self-diffusion in metals have been carried out with single crystal specimens. Measurements made with polycrystalline specimens have been in good agreement with those made with single crystal specimens only when the diffusion study was confined to temperatures close to the melting point of the metal. None of the reported investigations (1, 2, 3) made of the self-diffusion of nickel in polycrystalline samples have satisfied this criterion. Therefore, it was thought worth while to report some work on the rate of nickel self-diffusion in the temperature range 1050° to 1400° C.

EXPERIMENTAL

Diffusion coefficients were obtained by the standard sectioning method (4) and by a modification of Gruzin's integral residue method (5). In some cases both techniques were employed to analyze the same specimen, which permitted a direct comparison of the results obtained with each.

The nickel tracer employed contained two long-lived isotopes, Ni^{63} decaying with the emission of a 67-kev β-particle and Ni^{59} decaying by K-electron capture with the emission of a Co K_α X-ray (6). A Co^{58}, gamma-emitting impurity present in the tracer solution was completely removed by an ion exchange procedure (7). In the 2π internal source proportional counter employed, the ratio of detected disintegrations of Ni^{63} to Ni^{59} was in excess of 5×10^3 for almost all sources counted. Thus, with one exception which will be discussed later, it was assumed that the tracer consisted of a single active species, Ni^{63}.

The diffusion specimens consisted of polycrystalline nickel cylinders about 0.60 in. in diameter with the active tracer electroplated on one face. The total analyzed impurity

[1]*Manuscript received May 22, 1959.*
Contribution from the Department of Metallurgical Engineering and the Radiochemistry Laboratory, Department of Chemistry, McGill University, Montreal, Que., with financial assistance from the Defence Research Board.
[2]*Present address: Fuel Development Branch, Atomic Energy of Canada Limited, Chalk River, Ontario.*

content in the cylinders was less than 0.08%, with the principal impurities being Fe, 0.04; Co, 0.015; and Cu, 0.01%. Each cylinder was annealed at 1400° C for 24 hours to produce a coarse stable grain size prior to the electrodeposition of the tracer from an ammonia – ammonium sulphate solution. Grain diameters in individual specimens varied from 3 to 10 mm. Thickness of the tracer layer was about one micron. Uniformity of the active plating was checked by measuring the counting rate at nine positions on the active surface through an aluminum diaphragm with a 3/32-in. hole. These counting rates were converted to thicknesses with a self-absorption curve for Ni^{63} (8), and specimens with thickness variations greater than $\pm 3\%$ were rejected.

For the diffusion anneal, duplicate specimens were positioned in recrystallized alumina crucibles with the active faces touching to minimize loss of the tracer by evaporation. This assembly was placed in a preheated tube furnace with a constant temperature zone 5 in. in length where the samples were surrounded by a pure hydrogen atmosphere to prevent oxidation. By charging and discharging the samples to and from a hot furnace, errors in the length of the diffusion anneal were less than 0.2%, even for the shortest times. Temperatures were controlled to within $\pm 0.5°$ C by backing off most of the potential from the Pt/(Pt – 13% Rh) control thermocouple with a standard potential source and feeding the amplified difference to a Speedomax proportional temperature controller. The temperature of the specimens was measured during each run with a certified Pt/(Pt–Rh) thermocouple, corrections being made for thermocouple sheath losses. The diffusion anneal temperatures should be accurate to $\pm 2.0°$ C.

After the diffusion anneal, one of the duplicate specimens was sectioned in the standard manner. The specimen was mounted in a lathe-collet so that the face ran true to ± 0.002 mm, and at least 1.2 mm was removed from the diameter to eliminate edge effects. Then successive facing cuts from 0.025 to 0.040 mm, in thickness were made to provide samples for activity measurements. The turnings were weighed to determine the slice thickness for comparison with direct micrometer measurements made on the specimen. As the nickel cuttings did not represent a suitable source for counting of the low energy Ni^{63} β-particles, the cuttings were dissolved in concentrated hydrochloric acid and the nickel electroplated on to copper planchets to form a 0.70-in. diameter deposit. The method employed has been described elsewhere (8). In all cases, sufficient nickel was deposited to form an infinitely thick source (4.5 mg/cm^2 or greater), so that the observed counting rate was directly proportional to the specific activity of the source. The reproducibility in preparing sources in this manner was better than $\pm 1\%$. Whenever possible, sufficient counts were recorded to give counting statistics of $\pm 1\%$.

The second specimen was treated in an identical fashion except for the following change in procedure. Before taking each facing cut, the activity of the active face was measured by mounting the specimen in the 2π internal source counter using a special baseplate. A diaphragm with a central hole smaller than the specimen diameter prevented β-particles emitted from the specimen sides being detected. The activity measured in this manner represents the specific activity of the Ni^{63} in a layer less than one micron below the surface. Previous work (8) on the self-absorption of Ni^{63} showed that over half the detected activity in an infinitely thick sample of uniform specific activity is emitted from a depth within 0.5 μ of the sample surface. Thus in a diffusion couple where the activity is decreasing in a Gaussian manner with increasing depth below the surface, the counting rate measured on the surface can be assumed to be proportional to the specific activity of the metal forming the surface layer.

Can. J. Chem. Downloaded from www.nrcresearchpress.com by 176.9.209.113 on 09/04/12
For personal use only.

Can. J. Chem. Downloaded from www.nrcresearchpress.com by 176.9.209.113 on 09/04/12
For personal use only.

RESULTS AND DISCUSSION

For volume diffusion, the concentration $C(x, t)$ of the tracer isotope in a layer at distance X below the surface after an annealing time t is given by the equation,

$$C(x, t) = C_0/\sqrt{\pi Dt}\, e^{-X^2/4Dt},$$

where C_0 is the total quantity of tracer deposited on the specimen face and D is the diffusion coefficient. The diffusion coefficient is calculated from the slope of the straight line plot of log $\bar{C}$ versus $\bar{X}^2$. Typical plots obtained at temperatures of 1197° and 1152° C are shown in Fig. 1. The plot at 1197° C is typical of those obtained at all temperatures equal to or above 1200° C. It can be seen that log $\bar{C}$ varies as $\bar{X}^2$ for all values of $\bar{X}$ indicating that the diffusion occurring at these temperatures is typical of volume diffusion. However, in the concentration penetration curve obtained at 1152° C, log $\bar{C}$ varies as $\bar{X}^2$ for shallow penetrations, while at deeper penetrations log $\bar{C}$ varies as $\bar{X}$. This mixed type of penetration curve is obtained when neither grain boundary nor volume diffusion predominate in a diffusion couple. Wajda (9) has shown that with this type of specimen the volume diffusion coefficients obtained from the initial linear portion of the log $\bar{C}$ versus $\bar{X}^2$ are generally higher than those obtained from single crystal specimens at the same temperature.

Excellent agreement, within 1%, was obtained between duplicate diffusion couples treated by the standard sectioning method. However, when the same specimen was treated by both surface-activity-sectioning and sectioning techniques, the D values for the former method were always slightly lower. For the five samples treated by both methods, this difference varied from 1.5 to 9.0%, with an average deviation of 5.6%. This is reflected in Fig. 1 where the penetration curve determined by the surface-sectioning method has a steeper slope than that obtained in the conventional manner for the same specimen. About one per cent of this diffusion is a result of neglecting the enhanced counting rate at the surface for low values of $\bar{X}$ due to detection of the more penetrating Ni^{59} radiation from much deeper portions of the diffusion specimen. This effect would tend to make the diffusion coefficients obtained with the surface-activity-sectioning method too low. The diffusion coefficients obtained by the normal method are about 1.0% too high as a result of using slices of finite thickness. No convincing explanation can be offered for the residual discrepancy of 3.6%.

The activation energy, Q, and frequency factor, D_0, for volume diffusion are related by the Arrhenius equation:

$$D = D_0\, e^{-Q/RT}.$$

To obtain values for Q and D_0, the measured values of D were plotted against $1/T$ as in Fig. 2. The open circles represent the average values found by the normal sectioning method for the duplicate specimens annealed at one time, while the solid points represent the surface-activity-sectioning value for one of these specimens. A correction was made to the diffusion constants for lattice expansion, but no allowance was made for an isotopic mass effect. Johnson's (10) original work, which suggested that Graham's law applied to metallic diffusion as well as to gaseous diffusion, has not been substantiated by more recent work (11).

It can be seen that the values found for the temperature range 1150° to 1400° C lie on a straight line. The coefficients measured below 1150° C lie above the extrapolated line of best fit for the high temperature results indicating that sufficient grain boundary

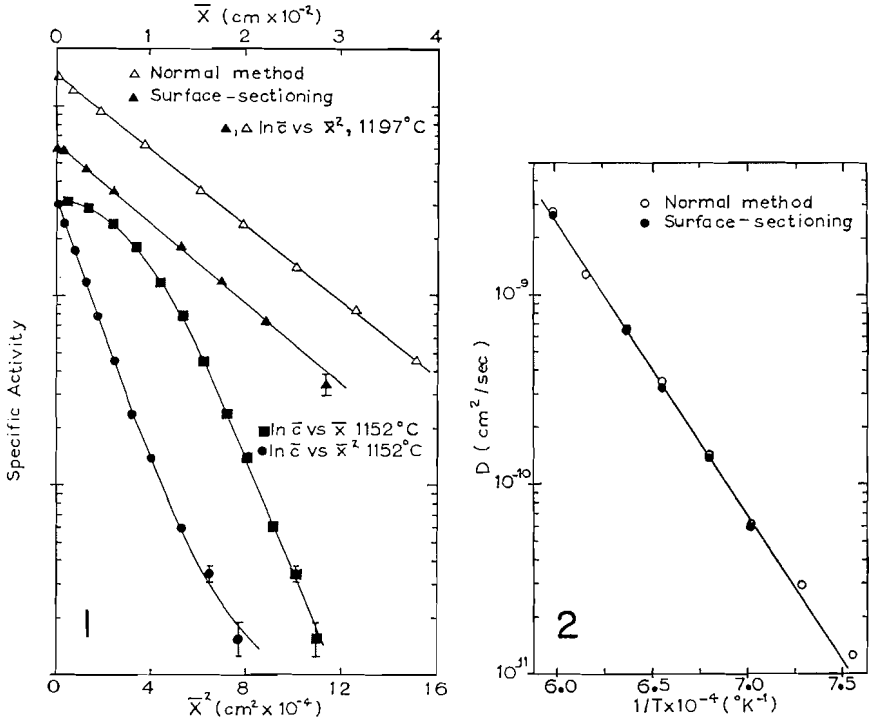

FIG. 1. Concentration penetration curves obtained at 1152° C and at 1197° C. The curves at 1152° C assume the form generally associated with grain boundary diffusion.
FIG. 2. Activation energy plot.

diffusion has occurred in those specimens to invalidate the results. To obtain a comparison between the results obtained by both methods employed, both sets of data were fitted individually by least mean squares. For the standard sectioning method

$$D = 3.66\, e^{-(70{,}000\pm1700)/RT}$$

and for the surface-activity-sectioning method

$$D = 3.04\, e^{-(69{,}000\pm600)/RT}.$$

The results obtained by the two methods of analysis are in good agreement although the surface-activity-sectioning data have a slightly smaller standard deviation. Thus this work gives an average value of 3.36 cm²/sec for the frequency factor, D_0, and 69.8 kcal/mole for the activation energy, Q.

For comparison, the values found in other investigations are tabulated below:

TABLE I
Self-diffusion data for nickel

Reference	Q (kcal/mole)	D_0 (cm²/sec)	Temp. range (° C)	Method
(1)	61–65	—	250–1250	Surface activity
(2)	66.8	1.27	1150–1250 870–1230	Sectioning surface activity
(3)	63.8	0.33	1100–1175	Sectioning
This work	69.8	3.36	1150–1400	Sectioning

Can. J. Chem. Downloaded from www.nrcresearchpress.com by 176.9.209.113 on 09/04/12
For personal use only.

Can. J. Chem. Downloaded from www.nrcresearchpress.com by 176.9.209.113 on 09/04/12
For personal use only.

Burgess and Smoluchowski's work, apparently incomplete, can be regarded only as a preliminary study. Their results were obtained by a surface activity technique, not specified in detail, below a temperature of 1250° C. No value was reported for the frequency factor.

The activation energy obtained by Reynolds *et al.* in a study of nickel self-diffusion throughout the Au–Ni system cannot be given too much weight because of the narrow temperature range investigated. However, their measured diffusion coefficients differ by only 4% from those obtained in this work.

Hoffman, Pikus, and Ward's reported diffusion coefficients in the temperature range 1150–1250° C are also in good agreement with the results obtained in this work. The differences in activation energy are reflected in a small but consistent difference in D values at temperatures outside the range where the two investigations overlap. Hoffman *et al.* employed a decrease in surface activity technique for their measurements below 1150° C. However, inspection of their data shows that all their diffusion coefficients obtained above a temperature of 1147° C, both by surface activity and sectioning techniques are consistent with an activation energy higher than that reported. Therefore, if their low temperature measurements yielded results which were high, their reported activation energy would be low.

There are two factors which could cause high values for the D values obtained by the decrease in surface activity method employed in the investigation by Hoffman *et al.*: grain boundary diffusion or an incorrect choice of k, the absorption coefficient of the β-radiation from Ni^{63}. Direct measurements of k by the present authors (8) and by Schweitzer *et al.* (12) for self-absorption of Ni^{63} in a 2π geometry have shown that at least two absorption coefficients are needed to explain the observed results assuming exponential absorption of radiation. One of these coefficients is much larger than, and the other comparable to, that obtained in an external absorption measurement. The narrow angle counter geometry employed by Hoffman will tend to minimize this effect but certainly not eliminate it. The combined effect of these two absorption coefficients is to make self-absorption more rapid in the source than anticipated and will lead to high values for D in samples where little diffusion has taken place, i.e. at low temperatures.

Zener (13) in a theoretical analysis of the activation process for diffusion in face-centered cubic metals proposed the following correlation between the entropy of activation for diffusion, ΔS, the temperature coefficient of Young's modulus, μ^1/μ_0, and the activation energy

$$(\Delta S/R) = \ln (D_0/a^2\nu) = \lambda(\mu^1/\mu_0)(Q/R)$$

where a is the lattice parameter, R the gas constant, and ν the Debye frequency. The particular choice of the constant, $\lambda = 0.55$, was such as to make the correlation exact for the accurately determined values of D_0 and Q for the self-diffusion of silver (14).

A plot of $\Delta S/R$ versus $(\mu^1/\mu_0)(Q/R)$ is given in Fig. 3 for the commonly accepted self-diffusion data for Ag, Au, Cu, Ni, Pb, and Pt. The straight line shown has a slope of 0.55, corresponding to Zener's suggested value for the constant λ. The dotted lines connecting various points for the same metal are not intended to have any particular significance, but rather to simplify inspection of the graph.

Inspection of the graph shows that there is a rough correlation between values of $\Delta S/R$ and $(\mu^1/\mu_0)(Q/R)$. A point of some interest is that the value from Makin, Rowe, and LeClaire's (15) recent careful study of gold self-diffusion falls just above the curve.

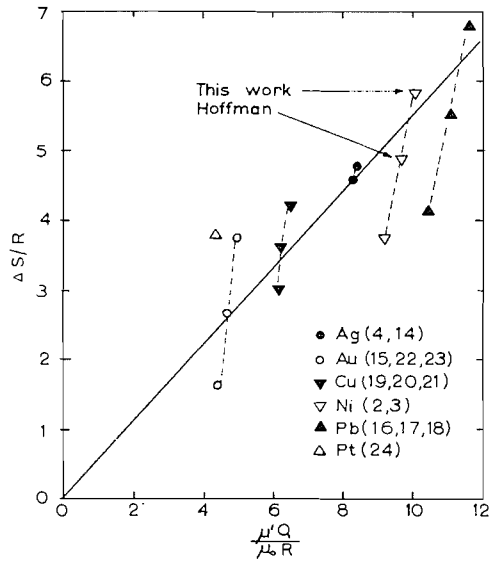

FIG. 3. Correlation between $\Delta S/R$ and $(\mu^1/\mu_0)(Q/R)$ for self-diffusion in various face-centered cubic lattice metals.

Thus, if we accept Zener's correlation with $\lambda = 0.55$ as exact, it is apparent that the activation energy for self-diffusion in nickel falls somewhere between that found in this work and that found by Hoffman *et al.* While there is no real justification for this observation, it is interesting to note that with $\lambda = 0.57$, the correlation line would pass through or close to points representing self-diffusion studies in Au, Ag, Cu, Pb, and the value found for nickel in this research.

ACKNOWLEDGMENT

The authors wish to express their gratitude to the Defence Research Board for grants received.

REFERENCES

1. BURGESS, H. and SMOLUCHOWSKI, R. J. Appl. Phys. **26**, 491 (1955).
2. HOFFMAN, R. E., PIKUS, F. W., and WARD, R. A. Trans. A.I.M.E. **206**, 483 (1956).
3. REYNOLDS, J. E., AVERBACH, B. L., and COHEN, M. Acta Met. **5**, 29 (1957).
4. JOHNSON, W. A. Trans. A.I.M.E. **143**, 107 (1941).
5. GRUZIN, P. L. Doklady Akad. Nauk S.S.S.R. **86**, 289 (1952).
6. BROSI, A. R., BORKOWSKI, C. J., CONN, E. E., and GREISS, J. C., JR. Phys. Rev. **81**, 391 (1951).
7. MOORE, G. E. and KRAUS, K. A. J. Am. Chem. Soc. **73**, 9 (1951); **74**, 843 (1952).
8. MACEWAN, J. R., MACEWAN, J. U., and YAFFE, L. Can. J. Chem. **37**, 649 (1959).
9. WAJDA, E. S. Acta Met. **2**, 184 (1954).
10. JOHNSON, W. A. Trans. A.I.M.E. **166**, 114 (1946).
11. LAZARUS, D. and OKKERSE, B. Phys. Rev. **105**, 1677 (1957).
12. SCHWEITZER, G. K., STEIN, B. R., and NEHLS, J. W. J. Phys. Chem. **56**, 692 (1952).
13. ZENER, C. J. Appl. Phys. **22**, 372 (1951).
14. SLIFKIN, L., LAZARUS, D., and TOMIZUKA, T. J. Appl. Phys. **23**, 1032 (1952).
15. MAKIN, S. M., ROWE, A. H., and LECLAIRE, A. D. Proc. Phys. Soc. B, **70**, 545 (1957).
16. SEITH, W. and KEIL, A. Z. Metallk. **25**, 104 (1933).
17. NACHTREIB, N. H. and HANDLER, G. S. J. Chem. Phys. **23**, 1569 (1955).
18. OKKERSE, B. Acta Met. **2**, 551 (1954).
19. MAIER, M. S. and NELSON, H. R. Trans. A.I.M.E. **147**, 39 (1942).
20. RAYNOR, C. L., THOMASSEN, L., and ROUSE, L. J. Trans. Am. Soc. Metals, **30**, 313 (1942).
21. KUBASCHEWSKI, O. Trans. Faraday Soc. **46**, 713 (1950).
22. OKKERSE, B. Phys. Rev. **103**, 1246 (1956).
23. GATOS, H. C. and KURTZ, A. D. Trans. A.I.M.E. **200**, 616 (1954).
24. KIDSON, G. V. and ROSS, R. Intern. Conf. on Radioisotopes in Scientific Research, Unesco/NS/RIC/216 (1957).

Can. J. Chem. Downloaded from www.nrcresearchpress.com by 176.9.209.113 on 09/04/12
For personal use only.

Can. J. Chem. Downloaded from www.nrcresearchpress.com by 176.9.209.113 on 09/04/12
For personal use only.

DIFFUSION OF Ni^{63} IN IRON, COBALT, NICKEL, AND TWO IRON–NICKEL ALLOYS[1]

J. R. MacEwan,[2] J. U. MacEwan, and L. Yaffe

ABSTRACT

The self-diffusion of nickel and the diffusion of Ni^{63} into iron, cobalt, and two iron–nickel alloys was studied using the technique of decrease in surface activity, The nickel self-diffusion results are compared to previously reported values. Nickel is found to diffuse more slowly than iron in the iron-rich portion of the iron–nickel system. The rate of nickel diffusion increases with increasing nickel content. A comparison is made between the present results for diffusion of Ni^{63} into iron, cobalt, and nickel with reported values for diffusion of Co^{60} and Fe^{59} in the same metals. In each solvent, the magnitudes of the activation energies, Q, are such that $Q_{Ni} > Q_{Co} > Q_{Fe}$.

INTRODUCTION

The transition elements iron, cobalt, and nickel are interesting both theoretically and experimentally because they exhibit marked similarities in properties. All assume a face-centered cubic lattice structure at high temperatures and possess nearly similar atomic radii. Therefore, it was thought worth while to investigate the rate of diffusion of Ni^{63} in pure iron, cobalt, and nickel. The studies were in a temperature range where only face-centered cubic lattice phases exist, and all diffusion data refer to the three metals in this condition. These results should permit some conclusions to be drawn concerning diffusion in these metals as other investigators have already reported data for diffusion of cobalt and iron tracers in iron, cobalt, and nickel.

The rate of self-diffusion of nickel in the iron-rich portion of the iron–nickel system was investigated to complement work reported by other investigators on the rate of self-diffusion of iron in the same region. The results should permit a comparison to be made between rates of diffusion of iron and nickel atoms in this technologically interesting portion of the iron–nickel system.

EXPERIMENTAL

The self-absorption characteristics of Ni^{63} β-radiation are such that, in a thick sheet containing the tracer isotope, over half the activity detected over a face comes from radiation emitted within 0.5 μ of that surface (1). Since the specific activity of the tracer decreases in a Gaussian manner below the diffusion interface, it has been shown (2) that in a specimen where diffusion has taken place the counting rate determined over the surface is directly proportional to the specific activity of the tracer on the surface. This characteristic of Ni^{63} β-radiation suggested the use of the following technique for measuring diffusion coefficients.

The solution to Fick's law corresponding to the diffusion of an infinitely thin layer of tracer into a semi-infinite medium, the diffusion coefficient D assumed constant, is

$$C(x, t) = (C_0/\sqrt{\pi D t})\, e^{-x^2/4Dt} \qquad [1]$$

where C_0 is the quantity of tracer deposited on the surface, $C(x, t)$ is the concentration in a layer at distance x below the surface, and t is the diffusion time. For the limiting

[1]*Manuscript received June 9, 1959.*
Contribution from the Department of Metallurgical Engineering and the Radiochemistry Laboratory, Department of Chemistry, McGill University, Montreal, Que., with financial assistance from the Defence Research Board.
[2]*Present address: Fuel Development Branch, Atomic Energy of Canada Limited, Chalk River, Ontario.*

case where $x = 0$ the above equation becomes

$$C(0,t) = C_0/\sqrt{\pi Dt}. \quad [2]$$

If C_0 is evaluated, the diffusion coefficient can then be determined by measuring the change of surface activity with time. This method overcomes the necessity of knowing accurately the self-absorption coefficients for Ni^{63} β-radiation.

The purified tracer isotope employed contained two long-lived isotopes, Ni^{63} decaying by the emission of a 67-kev β-particle and Ni^{59} decaying by K-electron capture with the emission of a Co K_α X-ray (3). Even in a specimen diffused for a long time, the contribution of the more penetrating Ni^{59} radiation to the counting rate measured at the active surface was less than 0.5%. Therefore, it was assumed that the tracer contains only one active species, Ni^{63}. All samples were measured in a 2π internal source counter (1).

The rate of diffusion of Ni^{63} was studied in five metals, 99.92% purity nickel, 99.91% purity iron, 99.5% purity cobalt, and two iron–nickel alloys prepared from electrolytic iron and nickel containing 5.79 and 14.88% Ni. All these metals were melted and cast *in vacuo*. The three pure metals were obtained from National Research Corporation, Cambridge, Mass., and we are indebted to Mr. H. V. Kinsey, Mines Branch, Department of Mines and Technical Surveys, Ottawa, Ontario, for preparing the two alloys. Disks, 0.650 in. in diameter and 0.15 in. thick, were machined from these metals for diffusion specimens. After each specimen was annealed at 1400° C for 24 hours, it was carefully faced on a lathe followed by grinding on a series of polishing papers, finishing on 4/0 grade. Aliquots containing equal amounts of Ni^{63} tracer then were electrodeposited on the face of each specimen from an ammonia – ammonium sulphate electroplating solution. The active deposit was about one micron in thickness. Satisfactory deposits were obtained only when the specimens were given an anodic pretreatment in a 25% sulphuric acid solution to remove the oxide layer. Specimens where the tracer was non-uniformly plated or where the total quantity deposited differed by more than $\pm 1.5\%$ from the intended amount were discarded.

Ten specimens, a pair for each metal investigated, were placed in a recrystallized alumina crucible and diffusion-annealed simultaneously. Loss of tracer by evaporation was minimized by placing the faces of duplicate specimens in contact. Welding of the specimens was prevented by washing the active faces with a dilute suspension of fine alumina powder in alcohol. The furnace was maintained at the annealing temperature and specimens were introduced and removed at this temperature. Corrections were made when necessary to keep the error in the effective diffusion time within 0.4% by a method suggested by Ham, Parke, and Herzig (4). The furnace had a constant temperature zone 5 in. in length and was controlled to $\pm 0.5°$ C. The specimen temperatures were measured to $\pm 1.5°$ C with a certified Pt/(Pt – 10% Rh) thermocouple. An atmosphere of purified hydrogen was employed to prevent oxidation of the specimens.

At least four successive annealing treatments at the desired annealing temperature were employed to obtain each diffusion coefficient. These times were chosen to give equal intervals on a $1/\sqrt{t}$ axis. The surface activities were measured using a diaphragm with an opening 0.55 in. in diameter over the active surface to minimize edge effects arising from surface diffusion.

In addition to the slope of the plot of $C(0,t)$ versus $1/\sqrt{t}$, it is necessary to know C_0, in order to calculate the diffusion coefficient. The following procedure was selected as giving the most accurate value for C_0. Two nickel specimens, annealed at 1209° C, were sectioned on a lathe. Before each section was removed, the counting rate of the

Can. J. Chem. Downloaded from www.nrcresearchpress.com by 176.9.209.113 on 09/04/12
For personal use only.

exposed face was measured to determine $C(x,t)$ for various values of x. The area under the curve of $C(x,t)$ versus x was integrated to determine a value for C_0. Agreement between the duplicate specimens was within 1%. The diffusion coefficient calculated from equation [2] for the mean value of C_0 was in excellent agreement with that calculated from the sectioning data in the normal manner using equation [1]. This agreement indicates that good results should be obtainable with this surface activity technique. As an identical quantity of tracer was deposited on each specimen, it was sufficient to measure C_0 in this manner for one pair of specimens.

RESULTS AND DISCUSSION

The experimental curves for all specimens at a diffusion temperature of 1209° C are shown in Fig. 1, and are typical of those obtained at all temperatures. For surface activities below 4500 c.p.m., the curves are linear conforming to equation [2] and extrapolate to pass through the origin. However, for the diffusion of nickel into iron, cobalt, and the two iron–nickel alloys the plots are curved in the initial region, the curvature corresponding to a decrease in the diffusion coefficients with time. This curvature represents either a concentration dependence of the diffusion coefficient or a failure to satisfy the boundary conditions of equation [2] by using a tracer layer of finite thickness. This latter supposition was not substantiated, as a check experiment showed that a plot of $C(0,t)$ versus $1/\sqrt{t}$ is linear for nickel self-diffusion even for diffusion times short enough to promote much less diffusion than that obtained in those specimens where curvature was observed. Therefore, while the tracer layer was thin enough to satisfy the boundary

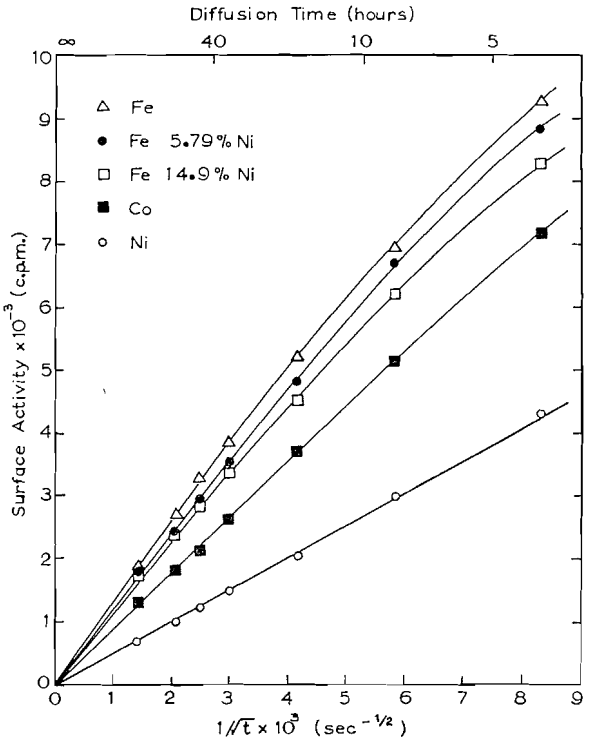

FIG. 1. Variation of surface activity with diffusion time for Ni^{63} diffusing into various metals and alloys at 1209° C.

Can. J. Chem. Downloaded from www.nrcresearchpress.com by 176.9.209.113 on 09/04/12
For personal use only.

conditions of equation [2], it appears to have been thick enough to cause a concentration effect.

A similar time dependence of the diffusion coefficient was observed by Martin, Johnson, and Asaro (5), who studied the rate of diffusion of Au^{198} into copper at low solute concentrations. At 1000° C the diffusion coefficient varied with annealing time, decreasing steadily for the first 30 hours and then assuming a constant value for longer times. No noticeable improvement was obtained when the thickness of the Au^{198} layer was decreased by a factor of 50. Therefore, this time dependence of the diffusion coefficient for short annealing times may not be entirely associated with a dependence of the diffusion coefficient on concentration, but it may be partially associated with an enhanced rate of diffusion caused by lattice strains introduced by the large concentration gradient existing at the start of an experiment.

The diffusion coefficients were calculated in each case from the linear portions of the plots. In this region, the concentration of tracer atoms has decreased sufficiently that each diffusing tracer atom is completely surrounded by host atoms so that there is a negligible concentration effect. Diffusion coefficients were obtained for each system at the following temperatures: 1152°, 1209°, 1271°, 1327°, and 1400° C.

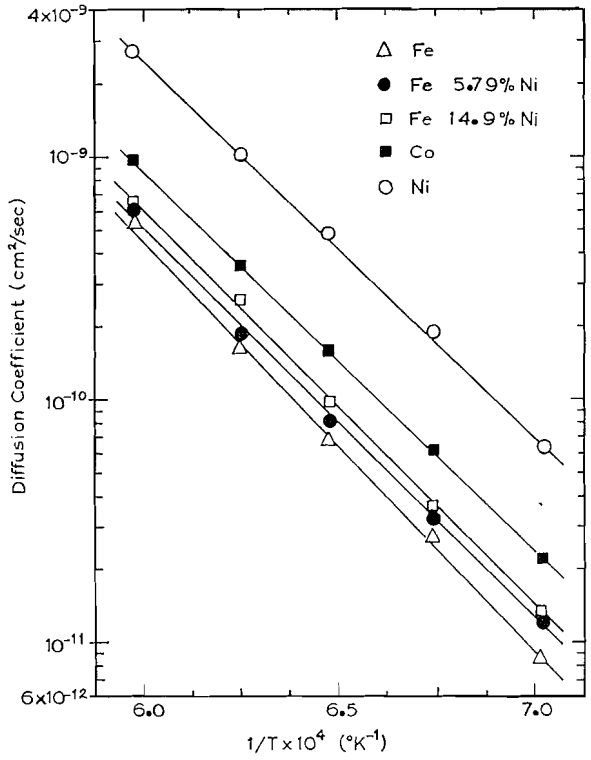

FIG. 2. Activation energy plots for Ni^{63} diffusion.

The activation energy, Q, and frequency factor, D_0, for volume diffusion are related by the Arrhenius equation:

$$D = D_0 e^{-Q/RT}.$$

To obtain values for Q and D_0, the experimental D values were plotted against $1/T$ as

Can. J. Chem. Downloaded from www.nrcresearchpress.com by 176.9.209.113 on 09/04/12
For personal use only.

in Fig. 2. A correction was made to each coefficient to compensate for lattice expansion. The data for each system were fitted by the method of least squares, on the assumption that the temperatures were correct, and gave the values for the activation energy and frequency factor shown in Table I.

TABLE I

Values of Q and D_0 for Ni^{63} diffusion

Solvent	D_0 (cm^2/sec)	Q (kcal/mole)
Ni	5.12	71.0±1.8
Co	1.25	72.1±1.4
Fe	6.92	77.6±2.0
Fe 5.8% Ni	2.11	73.5±2.0
Fe 14.88% Ni	5.00	75.6±1.2

A comparison of the present results for self-diffusion of nickel with those of a previous investigation (2) shows that the two studies are in close agreement as is shown in Table II where the values are tabulated. Both investigations gave higher values for the activation energy than that reported by Hoffman, Pikus, and Ward (6).

TABLE II

Summary of D_0 and Q values for nickel self-diffusion

Reference	D_0 (cm^2/sec)	Q (kcal/mole)	Method
(6)	1.27	66.8	Sectioning and surface activity
(2)	3.36	69.8	Sectioning
This work	5.12	71.0	Surface activity

The slightly higher activation energy found in this investigation compared with that previously reported by the same authors may be a result of slight errors introduced by evaporation of tracer from the active face, as a surface activity method is more sensitive to these losses than a sectioning method. However, any losses must have been negligible as no traces of activity were found on the supporting crucible even after the anneals at 1400° C. The good agreement between this and the previous investigation where a sectioning method was employed can be taken as evidence for the accuracy of the surface activity method employed in this investigation. No comparison of these results for nickel self-diffusion to those for other face-centered metals will be attempted here, as this topic was fully discussed when the previous results were reported (2).

Theoretical attempts to correlate the diffusion rate of various solutes in the same solvent at low solute concentration have been based on two different concepts. Lazarus (7) has deduced expressions for D_0 and Q for solute diffusion in a monovalent solvent taking into account the screened coulombic potential surrounding the impurity atom. These expressions suggest that elements to the left of the solvent atom in the periodic table should diffuse more slowly with higher values of D_0 and Q, while those to the right should diffuse more rapidly with lower values of D_0 and Q. This theory has had partial success in correlating the results for various solute atoms in silver and copper. Swalin (8) has attempted to correlate the results for the diffusion of various solutes in nickel solely on a size effect. He argues that the increased strain induced when solute

Can. J. Chem. Downloaded from www.nrcresearchpress.com by 176.9.209.113 on 09/04/12
For personal use only.

atoms larger than the solvent atoms pass through the saddle point should result in slower rates of diffusion and higher values for D_0 and Q, and the converse for smaller impurities.

The three transition elements iron, cobalt, and nickel are interesting from the theoretical viewpoint because of the similarity in their properties. All assume a face-centered cubic structure at high temperatures and have atomic radii which are nearly equal. Therefore, any differences in diffusion rates should be associated with the valency these atoms assume when dissolved in one another. Thus a comparison of the activation energies for self-diffusion and tracer-impurity diffusion is of interest. The appropriate values of Q and D_0, are tabulated in Table III for diffusion in the solvents iron, cobalt, nickel, and copper.

TABLE III

D_0 and Q values for self-diffusion and tracer-impurity diffusion in some transition elements

Solute	Solvent	D_0 (cm^2/sec)	Q (kcal/mole)	Reference
Fe		1.0	69.0	(9)
Co	Fe	1.2×10^5	104.0	(10)
Ni		6.92	77.6	This work
Fe		0.21	62.7	(11)
Co	Co	0.83	67.7	(11)
Ni		1.25	72.1	This work
Fe		8.4×10^{-3}	51.0	(12)
Co	Ni	1.46	68.3	(13)
Ni		5.12	71.0	This work
Fe		1.4	51.8	(14)
Co	Cu	1.93	54.1	(14)
Ni		2.70	56.5	(14)
Cu		0.32	46.8	(14)

Before discussing the significance of the data in Table III it should be pointed out that the data for the diffusion of iron into nickel and for cobalt into iron seem questionable. The value of D_0 found for diffusion of Fe^{59} into nickel is 8.4×10^{-3} cm^2/sec. This is suspect on the basis of Zener's (16) theory because it corresponds to a negative entropy of activation. The activation energy for the diffusion of Co^{60} into iron seems very high. It will be interesting to see if these values are confirmed in future investigations.

As observed by Mackliet (14) in the case of diffusion in the solvent copper, the tracer impurities iron, cobalt, and nickel all have larger activation energies than was obtained for copper self-diffusion. This is in general agreement with the Lazarus screening theory which predicts that elements which have a negative value of excess valency, Z, should have higher activation energies than for solvent self-diffusion. However, he found that $Q_{Ni} > Q_{Co} > Q_{Fe}$, which is contrary to the predictions expected if we assign to these elements their excess valence on a basis of their position in the periodic table. It is of interest to note that this trend also holds when the solvents are respectively iron, cobalt, and nickel with the single exception for diffusion of cobalt into iron. An explanation of this trend in activation energies for these transition elements will have to await clarification of the concept of valence in these metals.

Darken (17) has deduced expressions relating the interdiffusion coefficients, D_c, in a binary alloy at a given composition to the self-diffusion coefficients D_a^* and D_b^* of the

Can. J. Chem. Downloaded from www.nrcresearchpress.com by 176.9.209.113 on 09/04/12
For personal use only.

individual species in the same alloy. In the case of the iron–nickel system, which is thermodynamically ideal in the gamma region (18), these expressions reduce to

$$[3] \qquad D_c = N_{Fe}D_{Ni}^* + N_{Ni}D_{Fe}^*$$

where N_{Fe} and N_{Ni} are the atomic fractions of iron and nickel in the alloy. The variation of the interdiffusion coefficient, D_c, with composition in the iron–nickel system was investigated by Wells and Mehl (19) at 1300° C. Their data for D_c are plotted along with our data obtained for D_{Ni}^* in Fig. 3. A complete study of the variation of D_{Fe}^* with composition in the iron–nickel system was made by Neiman and Shinyaev (20) in the temperature range 1055 to 1148° C. Unfortunately their data are suspect at the nickel-rich end, because their D_0 values for diffusion in this range are low enough to correspond to negative entropies of activation. Therefore, in Fig. 3, we have only shown Gruzin's data for D_{Fe}^* in pure iron (9), and for D_{Fe}^* in two iron–nickel alloys containing 20% and 25% nickel (21).

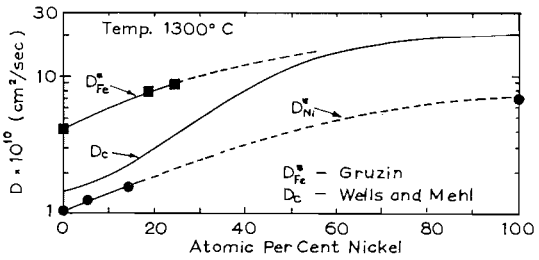

FIG. 3. Variation of the diffusion coefficients with composition in the iron–nickel system.

Considering that the data represent the results of four separate investigations, the correlation is remarkably good. While there is no evidence to justify the extrapolations shown, it is apparent that nickel atoms diffuse at about one-quarter the rate of iron atoms in the iron-rich portion of this system and probably throughout the entire system. This is in agreement with the observations of Seith and Kottman (22), who observed porosity in the iron-rich portion of an iron–nickel couple during a Kirkendall-effect experiment (23). While the data are not in sufficient agreement to test the validity of Darken's equations it is interesting to note that $D_c \rightarrow D_{Ni}^*$ as $N_{Fe} \rightarrow 1$ in agreement with equation [3].

Examination of the data in Table II indicates that there may be a trend towards lower activation energies for nickel self-diffusion in this system with increasing nickel content. There is a definite trend towards faster rates of nickel self-diffusion with increasing nickel content, which also suggests that the activation energy should decrease.

ACKNOWLEDGMENT

The authors wish to express their gratitude to the Defence Research Board for grants received.

REFERENCES

1. MACEWAN, J. R., MACEWAN, J. U., and YAFFE, L. Can. J. Chem. **37**, 649 (1959).
2. MACEWAN, J. R., MACEWAN, J. U., and YAFFE, L. Can. J. Chem. **37**, 1623 (1959).
3. BROSI, A. R., BORKOWSKI, C. L., CONN, E. E., and GREISS, J. C., JR. Phys. Rev. **81**, 391 (1951).
4. HAM, J. L., PARKE, R. M., and HERZIG, A. J. Trans. Am. Soc. Metals, **31**, 877 (1943).
5. MARTIN, A. B., JOHNSON, R. P., and ASARO, F. J. Appl. Phys. **25**, 369 (1954).
6. HOFFMAN, R. E., PIKUS, F. W., and WARD, R. A. Trans. A.I.M.E. **206**, 483 (1956).

Can. J. Chem. Downloaded from www.nrcresearchpress.com by 176.9.209.113 on 09/04/12
For personal use only.

7. LAZARUS, D. Impurities and imperfections. Impurities and imperfections in metallic diffusion. American Society for Metals, Cleveland, Ohio. 1955. Chap. 5.
8. SWALIN, R. A. Acta. Met. **5**, 443 (1957).
9. GRUZIN, P. L., KORNEV, N. Y., and KURDYUMOV, G. V. Reports Acad. Sci. Ukr.S.S.R. **80**, 49 (1951).
10. GRUZIN, P. L. Doklady Akad. Nauk S.S.S.R. **94**, 681 (1954).
11. MEAD, H. W. and BIRCHENALL, C. E. Trans. A.I.M.E. **203**, 994 (1955).
12. NEIMAN, M. B., CHINYAEV, A. YA., and DZANTIEV, B. G. Doklady Akad. Nauk S.S.S.R. **91**, 265 (1953).
13. RUDER, R. C. and BIRCHENALL, C. E. Trans. A.I.M.E. **191**, 142 (1951).
14. MACKLIET, C. A. Phys. Rev. **109**, 1964 (1958).
15. RAYNOR, C. L., THOMASSON, L., and ROUSE, L. S. Trans. Am. Soc. Metals, **30**, 313 (1942).
16. ZENER, C. J. Appl. Phys. **22**, 372 (1951).
17. DARKEN, L. S. Trans. A.I.M.E. **175**, 184 (1948).
18. KUBASCHEWSKI, O. and GOLDBECK, O. Trans. Faraday Soc. **45**, 948 (1949).
19. WELLS, C. and MEHL, R. F. Trans. A.I.M.E. **145**, 329 (1941).
20. NEIMAN, N. B. and SHINYAEV, A. YA. Doklady Akad. Nauk S.S.S.R. **102**, 969 (1955).
21. GRUZIN, P. L. and KUZNETSOV, E. V. Doklady Akad. Nauk S.S.S.R. **93**, 809 (1953).
22. SEITH, W. and KOTTMAN, A. Angew. Chem. **64**, 379 (1952).
23. SMIGELSKAS, A. D. and KIRKDENDALL, E. O. Trans. A.I.M.E. **171**, 130 (1947).

Can. J. Chem. Downloaded from www.nrcresearchpress.com by 176.9.209.113 on 09/04/12
For personal use only.

Can. J. Chem. Downloaded from www.nrcresearchpress.com by 176.9.209.113 on 09/04/12
For personal use only.

THE REACTION BETWEEN DIPHENYLAMINE AND NITRATES IN ULTRAVIOLET LIGHT[1,2]

B. B. Coldwell and S. R. McLean[3]

ABSTRACT

Under the activating influence of short-wave ultraviolet light, diphenylamine and nitrate ions in solution or on filter paper react to yield a yellow-colored product. Between pH 4 and 10 this consists mainly of 2-nitrodiphenylamine and 4-nitrodiphenylamine. Over this range of pH, the absorption maxima at 405 mμ did not shift; however, the intensity of absorption appeared to reach a minimum at or near neutrality and then increase rapidly as the solution was made more alkaline. The reaction rate was not affected by lowering the concentration of diphenylamine from 0.38% to 0.038%. A similar change in nitrate concentration decreased the rate 5.4 times. No evidence of nitroso compounds was found. Possible mechanisms are suggested.

INTRODUCTION

In a previous paper (1), it was noted that diphenylamine and nitrate ions reacted to form a yellow-colored product when irradiated with short-wave ultraviolet light. The reaction appeared specific and was made the basis of a spot test for inorganic nitrates. Subsequently, Hayward (2) found the reaction applicable to nitrate esters and used it for detecting these on paper chromatograms. We have confirmed Hayward's observation and, also, have found the reaction useful in identifying various kinds of explosives (3). The present work is concerned mainly with the identification of the products of the photochemical reaction.

EXPERIMENTAL AND RESULTS

(*A*) *Identification of Products Formed on Paper*

Sixty sheets of Whatman No. 1 filter paper (18×22 in.) were immersed for a few seconds in aqueous 1% sodium nitrate solution, air-dried, then immersed again in an ethanolic solution of diphenylamine (1% in 95% ethanol), air-dried, and exposed to short-wave ultraviolet radiation for 10 minutes on each side. The source and filters used have been described (1). The yellow-colored material was extracted from the paper with 95% ethanol in a modified Soxhlet assembly. The alcoholic extract was evaporated to dryness under vacuum on a constant temperature bath at 80° C. A total of 14.4 g, mostly unreacted diphenylamine, was recovered.

The material was dissolved in warm, redistilled petroleum ether (boiling range 30–50° C), and chromatographed on alumina columns (1×30 cm) which were prewashed with ethyl ether followed by petroleum ether. The columns were developed with petroleum ether. Two yellow bands separated, one (1P) weakly and the other (2P) very strongly absorbed by the alumina. Fraction 1P together with most of the unreacted diphenylamine was eluted from the columns with petroleum ether; the eluates were combined and evaporated to dryness under vacuum on a constant temperature bath at 35° C. Approximately 12.4 g were recovered. Repeated passes through the column eventually gave a fraction (44.8 mg) whose absorption maxima (see Table I) in the visual

[1]*Manuscript received June 5, 1959.*
Contribution from the Crime Detection Laboratories, Royal Canadian Mounted Police, Ottawa, Canada.
[2]*Published with the permission of the Commissioner, R.C.M.P., Ottawa.*
[3]*Present address: Canadian Titanium Pigments Ltd., Montreal, Quebec.*

TABLE I

Spectrophotometric properties of diphenylamine, nitro derivatives, and fractions isolated from the photochemical reaction between diphenylamine and nitrate

Substance	Position of maxima, mμ		Position of minima, mμ	
	Literature (4)	Observed*	Literature (4)	Observed*
Diphenylamine	285	283–285	249	248–249
2-Nitrodiphenylamine	422–423 257–259	415–425 257–259	323–327 238–239	319–324 237–239
Fraction 1P		415–420 256–260		324–328 236–239
Fraction 1S		418–422		
4-Nitrodiphenylamine	390 257	386–388 254–256	305–306	304–306
Fraction 2P		386–390 254–257		308–312 240–242
Fraction 3S		388–394 254–256		290–300 234–237
Fraction 2S		442–450 291–293 256–257 243–245 233–234		374–380 272–274 249–250 240–242
Fraction 4S (acidic solution)		575–580 237–239		465–475 226–228
Fraction 4S (basic solution)		575–580 239–241		450–470 228–229

*Spectra determined with a Spectracord using 1-cm silica and Corex cells and absolute ethanol as solvent.

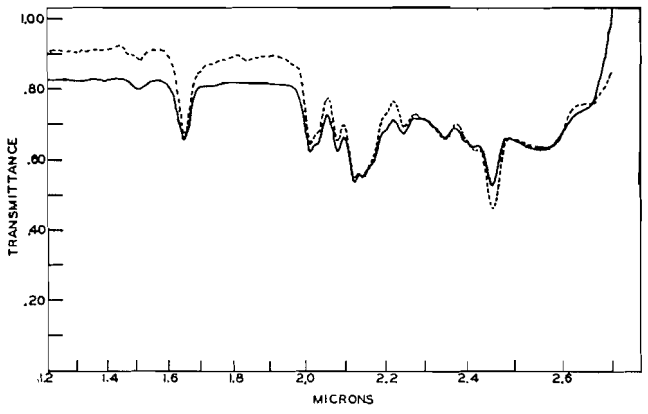

FIG. 1. Near infrared spectra of 2-nitrodiphenylamine (———) and fraction 1P (- - -) in carbon tetrachloride. Obtained with Spectracord using 1-cm silica cells.

and ultraviolet regions were in good agreement with those reported for 2-nitrodiphenylamine (4). The near- and far-infrared spectra of this fraction also were identical with those of 2-nitrodiphenylamine (see Figs. 1 and 2). From the absorptivity of 2-nitrodiphenylamine and the absorbance at 420–425 mμ, it was calculated that fraction 1P contained approximately 80% of 2-nitrodiphenylamine. The spectra, melting point[4] (35–50° C),

[4]*All melting points are uncorrected.*

Can. J. Chem. Downloaded from www.nrcresearchpress.com by 176.9.209.113 on 09/04/12
For personal use only.

and adsorbent characteristics of a 4 to 1 mixture of 2-nitrodiphenylamine and diphenylamine were identical with those of fraction 1P. It was concluded, therefore, that the yellow component of fraction 1P was 2-nitrodiphenylamine.

Fraction 2P was eluted from the adsorbent with acetone and evaporated to dryness under vacuum at 35° C. Approximately 0.24 g was recovered. This was rechromatographed on alumina using benzene – petroleum ether (1:1) as the developing solvent.

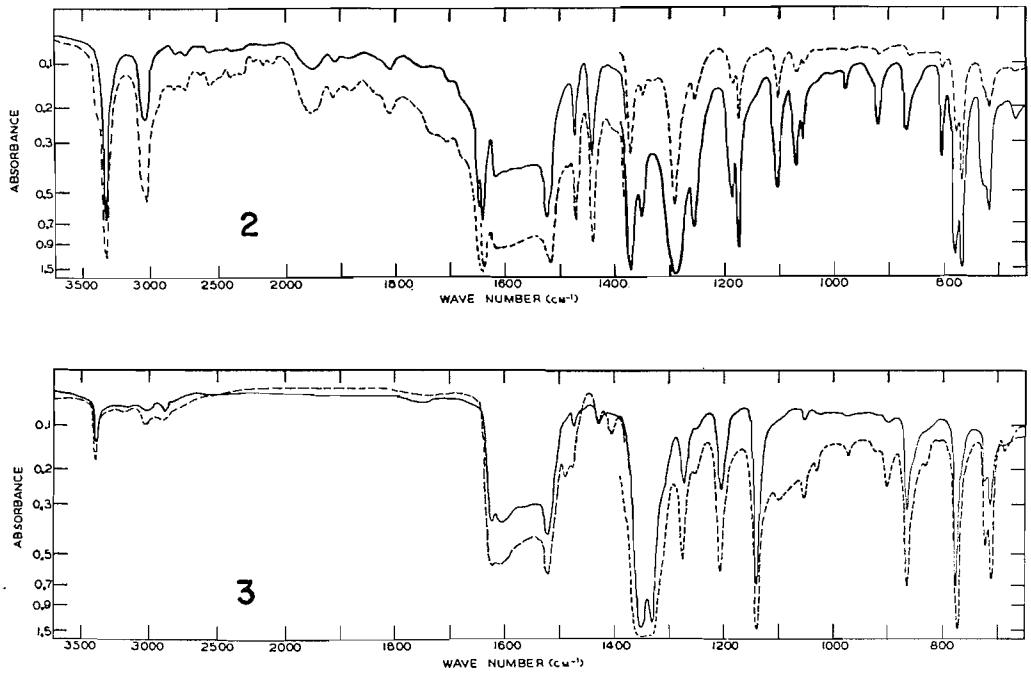

FIG. 2. Infrared spectra of 2-nitrodiphenylamine (———) and fraction 1P (– – –). Instrument: Perkin–Elmer Model 21, double beam, with sodium chloride optics. Solvent: carbon tetrachloride from 3600 to 1385 cm^{-1}, carbon disulphide from 1385 to 650 cm^{-1}.

FIG. 3. Infrared spectra of 4-nitrodiphenylamine (———) and fraction 2P (– – –). Conditions: as given in Fig. 2.

The colored eluate when concentrated gave 187.5 mg of yellow crystals. After recrystallizing twice from carbon tetrachloride the material melted at 133.5–134° C. A mixed melting point determination with a known[5] sample of 4-nitrodiphenylamine (m.p. 136–137° C) gave no depression. Absorption maxima in the ultraviolet and visible spectral regions were in agreement with those reported for 4-nitrodiphenylamine (see Table I). The infrared spectra of 2P and 4-nitrodiphenylamine were also identical (see Fig. 3). It was concluded that fraction 2P was 4-nitrodiphenylamine.

(B) Identification of Products Formed in Solution

A saturated solution of calcium nitrate tetrahydrate in 95% ethanol was made 1% with respect to diphenylamine. Ten 100-ml aliquots of this solution in a 1-l. beaker were exposed to short-wave ultraviolet radiation for 1 hour. The solutions were combined, taken to dryness, and chromatographed on alumina using petroleum ether to develop the chromatogram, as described above. Four bands gradually developed. The first band

[5]*Obtained from Dr. K. N. Trueblood, Department of Chemistry, University of California, Los Angeles, whose assistance is gratefully acknowledged.*

Can. J. Chem. Downloaded from www.nrcresearchpress.com by 176.9.209.113 on 09/04/12
For personal use only.

(1S), yellow in color, was eluted with petroleum ether. To elute the remaining bands off the column, ethyl ether was added to the petroleum ether, the proportions being increased gradually from 4:1 to 1:1. The second (2S) and third (3S) bands were orange and yellow, respectively. The fourth band (4S) was colored blue and remained at the top of the column. It was removed from the adsorbent with 95% ethanol.

Fraction 1S was concentrated and rechromatographed several times until finally crystals were obtained having an absorption maximum in the visible region characteristic of 2-nitrodiphenylamine (see Table I). Because of the difficulty in separating diphenylamine from 2-nitrodiphenylamine, additional purification of this fraction was not attempted.

Fraction 2S was concentrated and rechromatographed with 1:1 petroleum ether – ethyl ether. The absorption maxima exhibited in the ultraviolet and visible regions are given in Table I. There was insufficient material available to characterize this fraction further.

Fraction 3S was concentrated to a small volume and the orange-yellow crystals which separated were recrystallized twice from carbon tetrachloride (m.p. 132–132.5° C) and identified as 4-nitrodiphenylamine by a mixed melting point determination. The absorption maxima in the ultraviolet and visual regions (see Table I) and the infrared spectra of this material corresponded to those of 4-nitrodiphenylamine.

The wavelengths of maximum and minimum absorption of fraction 4S were almost identical in acidic and alkaline solutions (see Table I). The blue-colored material was insoluble in water. It appeared to be different from the blue quinoidal compound formed on the oxidation of diphenylamine with strong oxidizing agents (5). The latter on dilution with alcohol changed from a deep blue to a brownish yellow with the formation of a greenish brown precipitate. Similar changes were not observed with fraction 4S.

(C) Effect of pH on Reaction in Solution

Mixtures of diphenylamine and sodium nitrate, each 0.38% in aqueous ethanol (13 parts ethanol to 8 parts distilled water by volume), were adjusted to a known pH with hydrochloric acid or potassium hydroxide and exposed to short-wave ultraviolet radiation for 30 minutes without stirring. The pH, color, and visual spectra were then recorded. Some of the data are summarized in Table II and in Fig. 4.

TABLE II

Effect of pH on the ultraviolet-light-induced reaction between diphenylamine and nitrate. (Diphenylamine, 0.38%; sodium nitrate, 0.38%; solvent, ethanol 13 parts and water 8 parts; exposure, 30 minutes)

pH				
Initial	After exposure	Position of maxima,* mμ	Absorbance	Color of solution
3.0	3.0	398–401	0.240	Dark blue
		525–550	0.500	
4.0	5.5	402–408	0.595	Red-brown
		525–550	0.220	
5.0	7.2	405	0.490	Dark yellow
6.0	7.3	405	0.480	Yellow
8.0	8.0	405	0.565	Yellow
10.0	9.0	405	0.780	Yellow

*Determined with Spectracord using 1-cm Corex cells.

At pH 3, the main end product of the reaction appears to be the blue-colored substance found in fraction 4S. This is quite evident from curve 1, Fig. 4. As the pH rises,

Can. J. Chem. Downloaded from www.nrcresearchpress.com by 176.9.209.113 on 09/04/12
For personal use only.

the blue substance disappears and the absorption at 405 mμ becomes more pronounced. There is evidence that the absorption at 405 mμ reaches a maximum at pH 4, decreases to a minimum at or near neutrality, and then rises sharply as the solution is made more alkaline. This trend is evident from the data in Table II and was observed in another series of experiments where the concentration of diphenylamine and nitrate was 0.038% for each. The production of 2-nitrodiphenylamine and 4-nitrodiphenylamine would appear to be responsible for the absorption at 405 mμ. A 1 to 1 mixture of these two compounds in 13 to 8 ethanol–water exhibited an absorption maximum at 403–404 mμ, which shifted to 406 mμ when the mixture contained twice as much 2-nitrodiphenylamine as 4-nitrodiphenylamine.

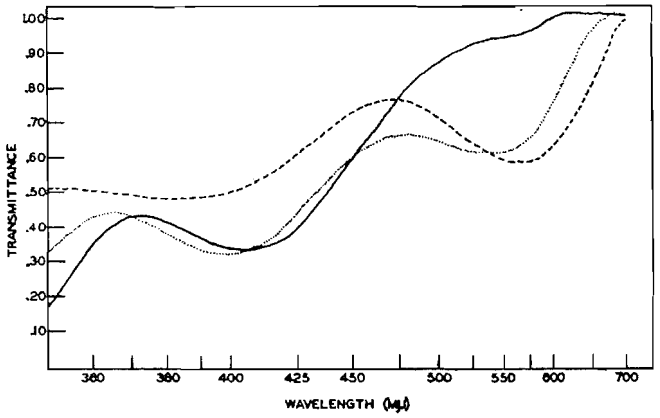

FIG. 4. Effect of pH on the visible spectra of diphenylamine–nitrate solutions irradiated with ultraviolet light. Solvent: 13 parts ethanol to 8 parts distilled water by volume. Concentration: diphenylamine and sodium nitrate each 0.38% (w/v). Exposure time: 30 minutes. Instrument: Spectracord with 1-cm Corex cells. Curve 1: – – –, pH 2.5. Curve 2: . . ., pH 3.0. Curve 3: ———, pH 5.0.

The magnitude of the absorbance at 405 mμ was not affected by lowering the diphenylamine concentration from 0.38% to 0.038% but was decreased 5.4 times by the same change in the nitrate concentration. At these concentrations a linear relationship was observed between absorbance and time of exposure, over a period of 2.5 hours.

(D) Nitrite and Diphenylamine

A solution of sodium nitrite (0.038%) and diphenylamine (0.038%) in aqueous ethanol (13 parts ethanol to 8 parts water by volume) was colorless between pH 11.0 and 6.2 and exhibited no absorption between 360 and 700 mμ. When irradiated for 1 hour the mixture turned a light yellow color and showed weak absorption in the region of 435 to 460 mμ (also given by irradiated diphenylamine solution) and strong absorption below 360 mμ (not shown by irradiated diphenylamine solution).

Increasing the acidity, without exposure to ultraviolet light, caused the solution to turn yellow. At pH 5.1 relatively sharp absorption maxima were observed at 388, 372, and 358 mμ. As the pH was lowered still further, the absorption below 360 mμ became stronger and overshadowed the absorptions at higher wavelengths which appeared as a shoulder between 370 and 390 mμ. Neutralization of the acidic solution did not change its visible spectrum. The spectrum at pH 2 was similar to that at pH 10 and resembled that of N-nitrosodiphenylamine. Similar results were obtained with more concentrated solutions.

Can. J. Chem. Downloaded from www.nrcresearchpress.com by 176.9.209.113 on 09/04/12
For personal use only.

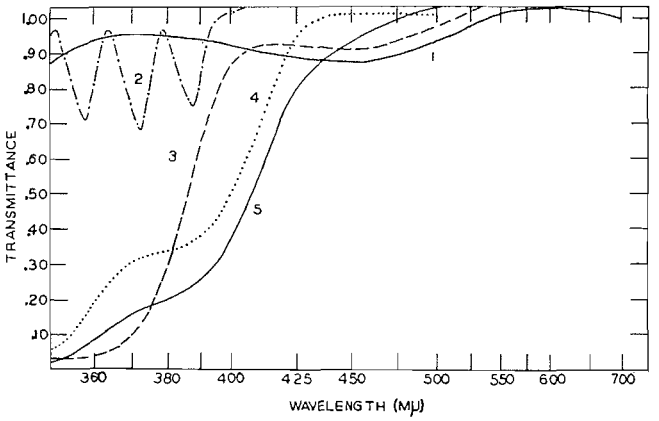

FIG. 5. The effect of ultraviolet radiation and pH on the visible spectra of diphenylamine, diphenylamine–nitrite solutions, and N-nitrosodiphenylamine. Solvent: ethanol 13 parts and distilled water 8 parts by volume. Instrument: Spectracord with 1-cm Corex cells. Curve 1: 0.038% diphenylamine exposed 1 hour to short-wave ultraviolet light. Curve 2: a solution of diphenylamine and sodium nitrite, each 0.038%, pH 5.1. Curve 3: same as curve 2, pH 7.5, irradiated 1 hour. Curve 4: same as curve 2, pH 2 and pH 10. Curve 5: N-nitrosodiphenylamine (0.1%).

The spectra of acidic (pH 5.5) diphenylamine–nitrite solutions could not be duplicated by exposing the corresponding original mixtures (pH 7.5) to short-wave ultraviolet light for varying periods of time. The spectrum of irradiated N-nitrosodiphenylamine (0.1% in 13 to 8 ethanol–water solution) was unchanged from the original. These results are illustrated in Fig. 5.

DISCUSSION

It is evident that between pH 4 and 10 the yellow end products formed during short-wave ultraviolet radiation of diphenylamine–nitrate mixtures, either in solution or on paper, consist largely of 2-nitrodiphenylamine and 4-nitrodiphenylamine. While the actual mechanism whereby these derivatives are formed remains uncertain, two pathways appear possible, (*a*) direct N-nitrosation of diphenylamine followed by rearrangement to the C-nitroso compound and subsequent oxidation (6), and (*b*) direct nitration of the phenyl rings (7).

Nitrate ion is reduced to nitrite ion by ultraviolet light, particularly at wavelengths below 2650 Å and around 3000 Å (8, 9). The reduction proceeds more rapidly in alkaline than in neutral or acidic solutions (10). It is claimed also that solid nitrate salts form nitrite near the surface when irradiated at 2500 Å (11, 12). Under our experimental conditions, the concentration of nitrite, determined with a modified Griess reagent (13), in aqueous alcoholic sodium nitrate solutions increased linearly with time of exposure to short-wave ultraviolet radiation. A 10-fold increase in nitrate concentration increased the rate of nitrite production by a factor of 3.

Further, the concentration of nitrite increased with rising pH, the amount present at pH 10 being more than twice that present at pH 3. These results agree with those of Villars (7) and Warburg (8). Thus, with increasing alkalinity there is an increase in the amount of yellow product and nitrite. Both of these increase linearly with time of exposure and both are affected in a similar manner by a change in concentration of nitrate. Warburg (8) pictures the reduction of nitrate by light as a unimolecular reaction in which the nitrate ion becomes activated by absorption of a quantum of light energy (90 to 100 kcal) and subsequently dissociates into nitrite and oxygen:

$$NO_3^- + h\nu \rightarrow (NO_3^-)^1 \rightarrow NO_2^- + O.$$

Can. J. Chem. Downloaded from www.nrcresearchpress.com by 176.9.209.113 on 09/04/12
For personal use only.

These facts suggest that the nitro derivatives might have resulted from very rapid oxidation of the C-nitroso derivatives of diphenylamine. In the presence of oxygen, oxidation of the labile nitroso compounds would be expected to take place rapidly, particularly in alkaline solution. This may explain why no evidence of nitroso derivatives was found on chromatographing the yellow reaction products or on spectral examination of irradiated diphenylamine–nitrate solutions. Certainly, the differences in the reactions taking place in irradiated diphenylamine–nitrate solutions, irradiated diphenylamine–nitrite solutions, and acidified solutions of the latter, as evidenced from a study of their spectra, suggest atomic oxygen plays a key role.[6]

On the other hand, the absence of nitroso compounds in the reaction products enhances the possibility of derivative formation through direct nitration of the ring. The activated nitrate radical might react with diphenylamine in this manner.

ACKNOWLEDGMENT

The authors are indebted to Mr. R. Ironside, Division of Applied Chemistry, National Research Council, Ottawa, for recording the infrared spectra.

REFERENCES

1. COLDWELL, B. B. and McLEAN, S. R. Can. J. Chem. **36**, 652 (1958).
2. HAYWARD, L. D. Private communication.
3. COLDWELL, B. B. Analyst. In press.
4. SCHROEDER, W. A., WILCOX, P. E., TRUEBLOOD, K. N., and DEKKER, A. O. Anal. Chem. **23**, 1740 (1951).
5. KEHRMANN, F. and MICEWITZ, ST. Ber. **45**, 2641 (1912).
6. DAVIS, T. L. and ASHDOWN, A. A. Ind. Eng. Chem. **17**, 674 (1925).
7. SCHROEDER, W. A., MALMBERG, E. W., FONG, L. L., TRUEBLOOD, K. N., LANDERL, J. D., and HOERGER, E. Ind. Eng. Chem. **41**, 2818 (1949).
8. GILLAM, A. E. and MORTON, R. A. J. Soc. Chem. Ind. (London), **46**, 415 (1927).
9. VILLARS, D. S. J. Am. Chem. Soc. **49**, 326 (1927).
10. WARBURG, E. Z. Elektrochem. **25**, 334 (1919).
11. NARAYANSWAMY, L. K. Trans. Faraday Soc. **31**, 1411 (1935).
12. KRISHNAN, K. S. and GUHA, A. C. Proc. Indian Acad. Sci. A, **1**, 242 (1934).
13. SNELL, F. D. and SNELL, C. T. Colorimetric methods of analysis. Vol. 2. 3rd ed. D. Van Nostrand Co., Inc., New York. 1949. p. 804.

[6]*The Referee has suggested that under these conditions it appears likely atomic oxygen would react first with the solvent, by electron capture or otherwise, to form intermediate products which could function as the oxidizing agent. This is certainly a possibility.*

Can. J. Chem. Downloaded from www.nrcresearchpress.com by 176.9.209.113 on 09/04/12
For personal use only.

Can. J. Chem. Downloaded from www.nrcresearchpress.com by 176.9.209.113 on 09/04/12
For personal use only.

A STUDY ON THE STRUCTURE OF THE CYCLOPENTADIENYL ANION WITH C^{14} AS TRACER[1]

R. TKACHUK[2] AND C. C. LEE

ABSTRACT

Starting with formaldehyde-C^{14}, 1,2-dibromocyclopentane-4-C^{14} (XI) was synthesized in eight steps. Conversion of XI to cyclopentadiene was accomplished in three different ways, namely: the dehydrobromination of XI with quinoline at 195–198° C, the preparation of 1,2-bis-(trimethylammonium)-cyclopentane-4-C^{14} hydroxide from XI followed by thermal decomposition, and the conversion of XI to 3,5-dibromocyclopentene followed by reaction of the latter with magnesium in dry ether. Degradations of the samples of cyclopentadiene obtained by these three synthetic routes showed a completely randomized distribution of the C^{14} activity, with 20% of the total activity on each of the five carbon positions. These results led to the conclusion that these preparations of cyclopentadiene very likely involved ionization to the cyclopentadienyl anion. The randomized distribution of C^{14} in the resulting products thus furnishes a strong indication that all five carbon positions in the cyclopentadienyl anion are equivalent.

INTRODUCTION

The acidity of cyclopentadiene was first recognized in 1900 by Thiele (1), and its potassium salt was prepared in 1901 (2). This salt is stable, though very reactive. The reason for the stability of salts containing the cyclopentadienyl anion has been given as early as 1928, by Goss and Ingold (3), and is that this ion has six (π) electrons, distributed over the entire five-membered ring, thus constituting a stable aromatic system similar to benzene. The resonance energy of this ion has been calculated to be about 42 kcal per mole (4).

Salts of cyclopentadiene with organic cations are also known. Pyridinium cyclopentadienylide has been described by Lloyd and Sneezum (5) and by Kosower and Ramsey (6). Triphenylphosphonium cyclopentadienylide has also been reported (7).

From theoretical considerations and physical chemical measurements, a number of workers (4, 8–12) have predicted that the negative charge on the cyclopentadienyl anion will not be localized on a particular carbon atom but will be distributed over the

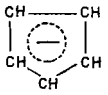

(I)

ion as a whole, as depicted by I. In the present study, attempts were made to obtain, by the tracer technique, some direct experimental evidence in support of these theoretical predictions.

If it were possible to synthesize cyclopentadiene-5-C^{14} (II), conversion of this compound to its potassium salt followed by regeneration should yield a cyclopentadiene in which the C^{14} distribution could provide definitive evidence for the structure of the cyclopentadienyl anion. Should the anion have the symmetrical electronic structure I, on

[1]*Manuscript received June 8, 1959.*
Contribution from the Department of Chemistry, University of Saskatchewan, Saskatoon, Sask.
[2]*Canadian Industries Limited Fellow, 1956–1958.*

regeneration of cyclopentadiene from the anion, the proton would have an equal probability of attaching itself to any one of the five equivalent carbons, resulting in the formation of a mixture of equal amounts of cyclopentadiene with the C^{14} label on the 1-, 2-, 3-, 4-, or 5-position.

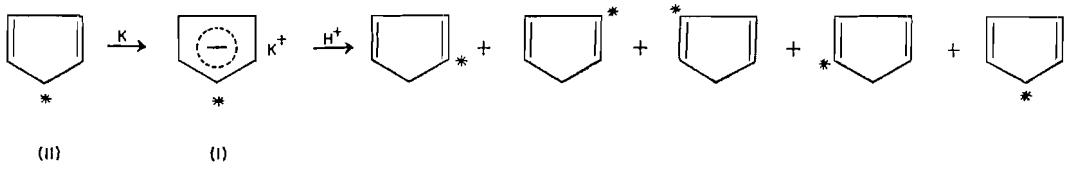

(II) (I)

Effectively, on degradation, one-fifth of the original C^{14} activity in II would be located on each carbon position of the sample of regenerated cyclopentadiene.

RESULTS AND DISCUSSION

As a suitable precursor for the attempted syntheses of cyclopentadiene-5-C^{14} (II), *trans*-1,2-dibromocyclopentane-4-C^{14} (XI) was chosen because it can give rise to cyclopentadiene by a number of different routes. The synthesis of XI was accomplished according to the following sequence of transformations.

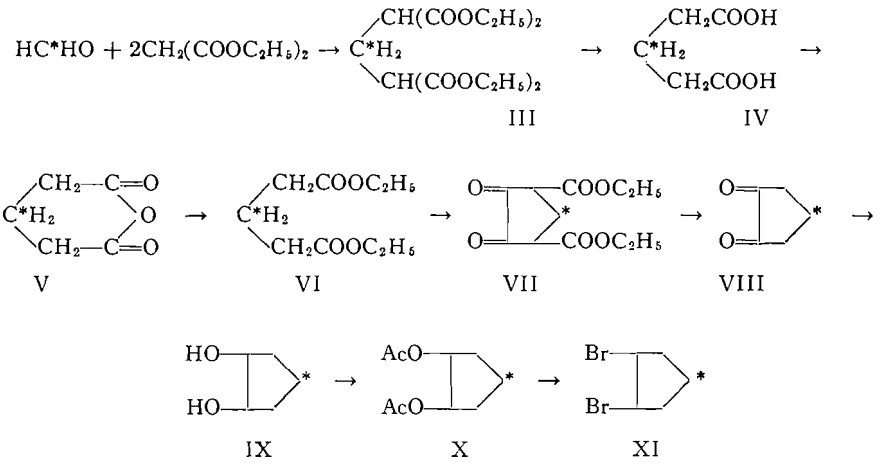

Tetraethyl propane-1,1,3,3-tetracarboxylate-2-C^{14} (III) was prepared by the condensation of formaldehyde-C^{14} and diethyl malonate. It was hydrolyzed to give glutaric acid-3-C^{14} (IV), which was, in turn, converted to glutaric anhydride-3-C^{14} (V) by treatment with acetic anhydride. Esterification of V gave diethyl glutarate-3-C^{14} (VI), which, on a Dieckmann condensation with diethyl oxalate, yielded 3,5-dicarboethoxy-1,2-cyclopentanedione-4-C^{14} (VII). Hydrolysis of VII afforded 1,2-cyclopentanedione-4-C^{14} (VIII). Reduction of VIII with sodium borohydride in water gave *trans*-1,2-cyclopentanediol-4-C^{14} (IX), which in turn was acetylated with acetic anhydride in pyridine to give *trans*-1,2-diacetoxycyclopentane-4-C^{14} (X). Treatment of X with hydrogen bromide in anhydrous acetic acid yielded *trans*-1,2-dibromocyclopentane-4-C^{14} (XI). The over-all yield of XI from formaldehyde-C^{14} was 11.4%.

To ascertain that *trans*-1,2-dibromocyclopentane-4-C^{14} (XI) was labeled as designated, it was degraded by the following scheme.

Can. J. Chem. Downloaded from www.nrcresearchpress.com by 176.9.209.113 on 09/04/12
For personal use only.

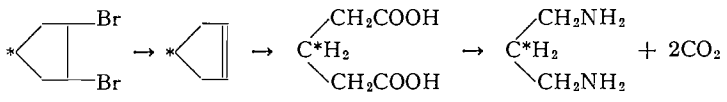

XI XII XIII XIV XV

The debromination of XI with zinc dust in ethanol yielded cyclopentene-4-C^{14} (XII). Ozonolysis of XII gave glutaric acid (XIII), which was degraded by the Schmidt reaction to give trimethylene-1,3-diamine (XIV) and carbon dioxide (XV). Radioactivity assays were carried out on the glutaric acid (XIII), on the diamine (XIV) as its dihydrogen bromide, and on the carbon dioxide (XV) precipitated as barium carbonate. The results, given in Table I, indicated that XIV contained all and XV contained none of the activity originally present in XI, showing that the label was not in positions 1 and 2. Thus, the designation that XI was labeled only in position 4 was likely correct.

TABLE I

C^{14} activities in products from degradation of 1,2-dibromocyclopentane-4-C^{14}

Compound analyzed	C^{14} activity[a] (mμc/mmole)
Glutaric acid (XIII)	415
Trimethylene-1,3-diamine dihydrogen bromide from XIV	421
Barium carbonate from XV	0.18

[a]C^{14} activity in millimicrocuries per millimole of sample was assayed as CO_2 gas with a vibrating reed electrometer supplied by Nuclear-Chicago Corporation.

The synthesis of cyclopentadiene from XI was accomplished by three different routes. The first synthesis was effected by the heating of XI with quinoline at 195–198° C to give cyclopentadiene-*x*-C^{14} (XVI*a*). The procedure was similar to one reported in 1904 for the preparation of 1,3-cyclohexadiene from 1,2-dibromocyclohexane (13). The second synthesis involved the thermal decomposition of 1,2-bis-(trimethylammonium)-cyclopentane-4-C^{14} hydroxide (XVIII) according to the following sequence of conversions.

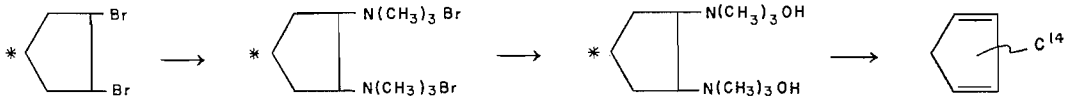

(XI) (XVII) (XVIII) (XVIb)

Treatment of XI with trimethylamine in acetone gave 1,2-bis-(trimethylammonium)-cyclopentane-4-C^{14} bromide (XVII). In turn, XVII was converted to XVIII with silver oxide in water. The decomposition of XVIII at 150° C afforded another sample of cyclopentadiene-*x*-C^{14} (XVI*b*). The third synthesis was carried out according to procedures reported fairly recently in the literature. It involved first the conversion of XI to cyclopentene-4-C^{14} (XII). Treatment of XII with N-bromosuccinimide and benzoyl peroxide in carbon tetrachloride gave 3,5-dibromocyclopentene (XIX)(14). Reaction of XIX with magnesium in dry ether (15) yielded a third sample of cyclopentadiene-*x*-C^{14} (XVI*c*).

The samples of cyclopentadiene-*x*-C^{14} obtained from the various syntheses were degraded by the following series of reactions.

Can. J. Chem. Downloaded from www.nrcresearchpress.com by 176.9.209.113 on 09/04/12
For personal use only.

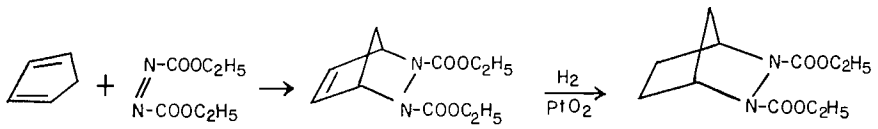

(XX) (XXI)

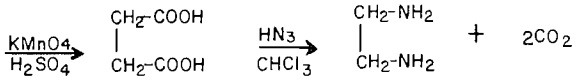

(XXII) (XXIII) (XXIV)

A Diels–Alder type of reaction between cyclopentadiene-x-C^{14} and diethyl azodicarboxylate gave the adduct, the diethyl ester of 2,3-dihydrazabicyclo (2.2.1)-5-heptene-2,3-dicarboxylic acid-x-C^{14} (XX). Hydrogenation of XX gave the diethyl ester of 2,3-dihydrazabicyclo (2.2.1) heptane-2,3-dicarboxylic acid-x-C^{14} (XXI). To yield succinic acid (XXII), XXI was oxidized with potassium permanganate. A Schmidt reaction with XXII resulted in the formation of ethylene-1,2-diamine (XXIII) and carbon dioxide (XXIV); XXIII was isolated as the dihydrogen bromide and XXIV as barium carbonate. C^{14} assays were carried out on XXI, XXII, the dihydrogen bromide from XXIII, and the barium carbonate from XXIV; XXI contained the total activity originally present in the cyclopentadiene-x-C^{14}. The difference in activities between XXI succinic acid (XXII) represented the activity in the 5-position (the methylene position) of cyclopentadiene. The activity in the 1- and 4-positions of cyclopentadiene was represented by the C^{14} in the carbon dioxide (XXIV) as well as by the difference between the activities of succinic acid (XXII) and ethylene-1,2-diamine (XXIII). Finally, the activity in the 2- and 3-positions of cyclopentadiene was given by the C^{14} in XXIII. The results of the C^{14} measurements are summarized in Table II.

TABLE II

C^{14} activities in products of degradation of cyclopentadiene-x-C^{14}

Source of cyclopentadiene	Compound analyzed	C^{14} activity (mμc/mmole)	% activity (XXI = 100)	% activity calc. for randomized distribution
Synthesis No. 1[a]	Hydrogenated Diels–Alder adduct (XXI)	26.73	100	100
	Succinic acid (XXII)	21.76	81.3	80
	Ethylene-1,2-diamine dihydrogen bromide from XXIII	10.78	40.3	40
	Barium carbonate from XXIV	10.92	40.9	40
Synthesis No. 2[b]	Hydrogenated Diels–Alder adduct (XXI)	43.56	100	100
	Succinic acid (XXII)	35.00	80.2	80
	Ethylene-1,2-diamine dihydrogen bromide from XXIII	17.44	40.1	40
	Barium carbonate from XXIV	17.64	40.5	40
Synthesis No. 3[c]	Hydrogenated Diels–Alder adduct (XXI)	2.09; 5.10[d]	100; 100[d]	100
	Succinic acid (XXV)	1.65; 3.97[d]	79; 78[d]	80
	Barium carbonate from XXIV	0.96	46	40

[a]Dehydrobromination of 1,2-dibromocyclopentane-4-C^{14} with quinoline.
[b]Thermal decomposition of 1,2-bis-(trimethylammonium)-cyclopentane-4-C^{14} hydroxide.
[c]Reaction of 3,5-dibromocyclopentene with magnesium in dry ether.
[d]Duplicate run.

Can. J. Chem. Downloaded from www.nrcresearchpress.com by 176.9.209.113 on 09/04/12
For personal use only.

The data in Table II clearly show that the samples of cyclopentadiene-*x*-C^{14} (XVI*a*, XVI*b*, XVI*c*) obtained from *trans*-1,2-dibromocyclopentadiene-4-C^{14} (XI) by the three synthetic routes were not the hoped for cyclopentadiene-5-C^{14}. Instead, they were samples of cyclopentadiene with the C^{14} activity completely randomized over all the five carbon positions. Such a distribution of C^{14} activity may be explained on the assumption that the cyclopentadienyl anion with symmetrical structure I is involved in these preparations. In the dehydrobromination of XI with quinoline (synthesis No. 1), the cyclopentadiene formed may immediately undergo reversible ionization-regeneration with quinoline acting as proton acceptor.

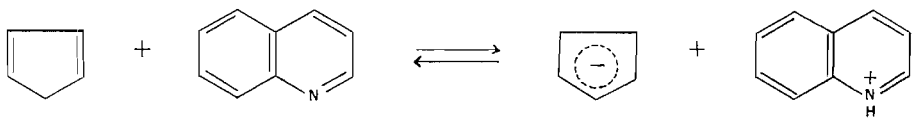

Considering the thermal decomposition of 1,2-bis-(trimethylammonium)-cyclopentane-4-C^{14} hydroxide (XVIII) (synthesis No. 2), first of all, the designation of the C^{14} location in XVIII is most probably correct since the conversion of XI to XVIII involved an S_N2 type of direct displacement and a double decomposition reaction both of which are not likely to cause isotope position rearrangements. Moreover, XVIII was prepared in a manner analogous to the synthesis of *n*-propyl-3-C^{14}-trimethylammonium hydroxide, which has been found to undergo successful thermal decomposition to propene-1-C^{14} (16). The randomized C^{14} distribution in the cyclopentadiene from synthesis No. 2 may, therefore, be again explained on the basis that the cyclopentadiene formed immediately undergoes reversible ionization-regeneration.

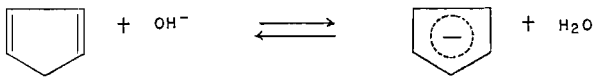

The interpretation of the results from synthesis No. 3 is more difficult. In the conversion of cyclopentene-4-C^{14} (XII) to 3,5-dibromocyclopentene (XIX) by treatment with N-bromosuccinimide and benzoyl peroxide, the possibility of allylic shifts cannot be excluded. Thus, the location of the C^{14} labels in XIX cannot be definitely designated. Furthermore, the mechanism for the transformation of XIX to cyclopentadiene in the presence of magnesium and dry ether is not well understood. Therefore, it is uncertain at what stage of the synthesis randomization of the C^{14} activity occurs. If one were to assume that there is no isotope position rearrangement in the conversions of XII to XIX and XIX to cyclopentadiene, then the randomized C^{14} distribution in the cyclopentadiene obtained from synthesis No. 3 might be explained in the same manner as in syntheses 1 and 2, namely, the cyclopentadiene formed immediately undergoes a reversible ionization-regeneration. Under the conditions employed in this synthesis, a Grignard reagent type of species may be present and serve as a base in promoting the ionization of the cyclopentadiene to its anion.

From the above considerations, it is clear that although the original intention of securing evidence on the structure of the cyclopentadienyl anion via cyclopentadiene-5-C^{14} was not successfully realized, the C^{14} distribution found in the samples of cyclopentadiene synthesized in these experiments does have a bearing on the problem under study. The completely randomized distribution of the C^{14} labels in the synthetic cyclopentadiene, at least in the samples from syntheses No. 1 and 2, likely resulted from an

Can. J. Chem. Downloaded from www.nrcresearchpress.com by 176.9.209.113 on 09/04/12
For personal use only.

involvement of the cyclopentadienyl anion during the synthetic processes. Thus, this randomization of the C^{14} activity in the cyclopentadiene furnishes a strong, though indirect, indication that all five carbon positions in the cyclopentadienyl anion are equivalent, as depicted in structure I.

EXPERIMENTAL

The condensation of formaldehyde-C^{14} with diethyl malonate to give tetraethyl propane-1,1,3,3-tetracarboxylate-2-C^{14} (III), the hydrolysis of III to glutaric acid-3-C^{14} (IV), and the conversion of IV to glutaric anhydride-3-C^{14} (V) were carried out according to procedures given in Cason and Rapaport (17). Starting with 16 g (0.53 mole) of formaldehyde-C^{14} (0.5 mc) as 35% formalin and 160 g (1.0 mole) of diethyl malonate, the yield of III, b.p. 163–166° C at 1.4 mm (lit. (17), b.p. 168–171° C at 4 mm), was 138.5 g (83%). Hydrolysis of the 138.5 g of III in 138 ml of concentrated hydrochloric acid gave a crude glutaric acid (IV), which was heated at 100° C for 1 hour with 85 ml of acetic anhydride to give glutaric anhydride-3-C^{14} (V). After vacuum distillation and crystallization from benzene and dry ether, the yield of product, m.p. 55–56° C (lit. (17), m.p. 55–56° C), was 24.8 g (52% based on the tetraethyl ester III).

Diethyl Glutarate-3-C^{14} (VI)

The conversion of glutaric anhydride-3-C^{14} to the diethyl ester was effected by treatment with absolute ethanol in the presence of toluene and concentrated sulphuric acid. The method used was similar to that given by Micovic for the preparation of diethyl adipate (18). From 24.8 g of V, 40 g (99% of theoretical) of diethyl glutarate-3-C^{14}, b.p. 84–85° C at 1.4 mm (lit. (19*a*), b.p. 103–104° C at 7 mm), was obtained.

3,5-Dicarboethoxy-1,2-cyclopentanedione-4-C^{14} (VII)

The Dieckmann condensation between diethyl glutarate-3-C^{14} (40.0 g, 0.21 mole) and diethyl oxalate (31.5 g, 0.22 mole) was carried out according to a procedure given by Hauser and Hudson (20). The product (VII), crystallized twice from ethanol and water, melted at 116–117° C (lit. (20), m.p. 115° C). The yield was 41.4 g (81%).

1,2-Cyclopentanedione-4-C^{14} (VIII)

Under an atmosphere of carbon dioxide, a mixture of 41.3 g (0.17 mole) of 3,5-dicarboethoxy-1,2-cyclopentanedione-4-C^{14} and 160 g of 20% sulphuric acid was refluxed gently in a wax bath for 2.5 hours. The reaction mixture was cooled, saturated with ammonium sulphate, and then continuously extracted with ether for 10 hours. A carbon dioxide atmosphere was also maintained throughout the extraction period. After removal of the ether from the extract, the residue was distilled under reduced pressure to give 12.7 g (76%) of product, b.p. 67–69° C at 1.4 mm; m.p. 54–55° C (lit. (21), m.p. 56° C).

Air rapidly decomposes this diketone, especially at room temperature. However, when kept under nitrogen or carbon dioxide at approximately −5° C, it is stable for at least two years.

trans-1,2-Cyclopentanediol-4-C^{14} (IX)

To 4.0 g (0.041 mole) of 1,2-cyclopentanedione-4-C^{14} in 50 ml water, 2.31 g (0.61 mole) of sodium borohydride was slowly added with cooling and shaking. The reaction which took place was quite vigorous, and the mixture turned yellowish during the reduction. After standing at room temperature for 3 hours, the solution was heated to boiling to destroy any excess sodium borohydride. The resulting solution, after cooling, was extracted continuously with ether for 72 hours. On removal of the ether from the extract and vacuum distillation of the residue, 2.3 g (65%) of product was obtained with a b.p.

Can. J. Chem. Downloaded from www.nrcresearchpress.com by 176.9.209.113 on 09/04/12
For personal use only.

of 80–82° C at 1.2 mm (lit. (22), b.p. 93° C at 2 mm). The di-*p*-nitrobenzoate derivative melted alone and on admixture with the same derivative from authentic *trans*-1,2-cyclopentanediol at 141–142° C (lit. (22), di-*p*-nitrobenzoate derivative, m.p. 143° C). It is reasonable that only the *trans*-isomer was isolated since the *cis*-isomer is known to form a stable complex with boric acid (23).

trans-1,2-Diacetoxycyclopentane-4-C^{14} (X)

The *trans*-1,2-cyclopentanediol-4-C^{14} was acetylated by treating 2.3 g (0.023 mole) of the diol with a mixture of 20 ml of acetic anhydride and 40 ml of pyridine at 100° C for 4 hours. After cooling, the reaction mixture was neutralized with 10% hydrochloric acid and then extracted three times with 35-ml portions of ether. The extract was dried over potassium carbonate, the ether removed, and the residue vacuum-distilled to give 2.7 g (65%) of product, b.p. 61–65° C at 1.4 mm (lit. (24), b.p. 85.5–86.5° C at 3.5 mm). Analysis: Calc. for $C_9H_{14}O_4$: C, 58.05%; H, 7.58%; acetyl, 46.3%. Found: C, 57.88%; H, 7.54%; acetyl, 46.4%.

In another preparation of the diacetate (X), 0.81 g of the diol (IX), 4.0 g of acetic anhydride, and 12 ml of pyridine were refluxed for 1.5 hours, the reaction mixture being protected from atmospheric moisture by means of a drying tube containing Drierite. The excess acetic anhydride and pyridine were removed under reduced pressure with a water aspirator pump and the residue vacuum-distilled, yielding 1.4 g (95%) of product boiling at 60° C at 1.2 mm.

trans-1,2-Dibromocyclopentane-4-C^{14} (XI)

This preparation was carried out in a manner similar to that used in the synthesis of 2,3-dibromobutane from 2,3-diacetoxybutane (25).

Into a 12-mm (O.D.) Pyrex glass tube with wall thickness of 1 mm was placed 1.38 g of *trans*-1,2-diacetoxycylopentane-4-C^{14} and 7.0 ml of saturated hydrogen bromide in acetic acid, the latter prepared by saturating pure acetic acid with dry hydrogen bromide gas at 35° C. The glass tube was sealed and then heated for 2 hours in boiling water. During this period, the reaction mixture darkened appreciably. After the mixture had cooled, the tube was opened and the solution poured onto crushed ice, neutralized with sodium bicarbonate solution, and extracted three times with 40-ml portions of low boiling petroleum ether. The extract was dried with anhydrous sodium carbonate, the solvent removed, and the residue vacuum-distilled, yielding 1.33 g (78%) of product, b.p. 44–46° C at 1.4 mm (lit. (26), b.p. 76.5–77.5° C at 18.5 mm). Analysis: Calc. for $C_5H_8Br_2$: Br, 70.2%. Found: Br, 70.8%.

Degradation of trans-1,2-Dibromocyclopentane-4-C^{14} (XI)

Cyclopentene-4-C^{14} (XII)

Cyclopentene-4-C^{14} (XII) was prepared from XI by a method similar to that used in the preparation of 2-pentene from 2,3-dibromopentane (27). To 2.0 g of granular, 20-mesh zinc metal in 3 ml of ethanol at 50° C, 1.3 g (0.0057 mole) of *trans*-1,2-dibromocyclopentane-4-C^{14} was added dropwise over a period of 10 minutes. A vigorous reaction took place, the cyclopentene being distilled over as it was formed into a receiver cooled in a dry ice – acetone bath. To insure complete recovery of the cyclopentene, the reaction mixture was heated just to the boiling point of ethanol. The weight of the product was 0.35 g (84%).

Ozonolysis of Cyclopentene-4-C^{14}

Ozonolysis of cyclopentene-4-C^{14} (XII) was effected in the same manner as reported

Can. J. Chem. Downloaded from www.nrcresearchpress.com by 176.9.209.113 on 09/04/12
For personal use only.

Can. J. Chem. Downloaded from www.nrcresearchpress.com by 176.9.209.113 on 09/04/12
For personal use only.

for the ozonolysis of cyclohexene (28). Starting with a solution of XII from 1.3 g of XI in 20 ml of absolute methanol, ozonization followed by decomposition of the ozonide in formic acid and hydrogen peroxide gave 0.62 g (87% based on the dibromide XI) of glutaric acid-3-C^{14} (XIII), m.p. 97° C (lit. (19*a*), m.p. 97–98° C).

The Schmidt Reaction on Glutaric Acid-3-C^{14}

This was carried out according to procedures already described in the literature (29, 30). From 198 mg (1.5 mmoles) of XIII, the yield of barium carbonate from the carbon dioxide absorbed in carbonate-free sodium hydroxide solution was 300 mg (52%), while the yield of trimethylene-1,3-diamine-2-C^{14} dihydrogen bromide was 49.5 mg (14%). Analysis: Calc. for $C_3H_{12}N_2Br_2$: C, 15.27%; H, 5.13%; N, 11.87%; Br, 67.7%. Found: C, 15.32%; H, 5.05%; N, 12.02%; Br, 68.0%.

Cyclopentadiene-x-C^{14} (XVI*a*) *from Dehydrobromination of trans-1,2-Dibromocyclopentane-4-*C^{14} (XI) *with Quinoline* (*Synthesis No. 1*)

In a 25-ml pear-shaped flask with a side arm as gas inlet was placed 2.82 g (0.0124 mole) of XI and 7.98 g (0.0168 mole) of freshly distilled quinoline. The flask was also fitted with a reflux condenser whose jacket temperature was kept at 45–47° C. The whole system was swept with dry nitrogen leading to a receiver cooled in a dry ice – acetone bath. The reaction mixture was heated in a wax bath to 195–198° C, whereupon a reaction set in as evidenced by much charring and bubbling. After the main evolution of volatile material had ceased, the mixture was kept at 198° C for an additional 10 minutes to insure complete reaction. The product in the receiving vessel was distilled into a calibrated centrifuge tube by heating the original receiver to 50–53° C. This distillation separated the cyclopentadiene from higher boiling materials such as quinoline that may have been present. The volume of product was 0.5 ml, corresponding to an approximate yield of 50% if all this product were pure cyclopentadiene.

A solution of the above product in ether was treated with maleic anhydride giving rise to the cyclopentadiene – maleic anhydride adduct which melted at 162–163° C (lit. (15), m.p. 163–164° C).

Another derivative of the above cyclopentadiene was the liquid adduct formed with diethyl azodicarboxylate which, on reaction with bromine, yielded the diethyl ester of 2,3-dihydraza-5,6-dibromobicyclo (2.2.1) heptane-2,3-dicarboxylic acid, m.p. 66–67° C (lit. (31), m.p. 67° C).

There was some indication that some cyclopentene may also have been formed in this reaction. After treatment of the redistilled product with excess diethyl azodicarboxylate, a small amount of liquid boiling at 39–41° C (lit. (19*b*), b.p. for cyclopentene, 44–46° C) was recovered. This liquid was unsaturated and showed an infrared spectrum similar to that of authentic cyclopentene.

Cyclopentadiene-x-C^{14} (XVI*b*) *from Thermal Decomposition of 1,2-Bis-(trimethylammonium)-cyclopentane-4-*C^{14} *Hydroxide* (*Synthesis No. 2*)

1,2-Bis-(trimethylammonium)-cyclopentane-4-C^{14} *Bromide* (XVII)

A mixture of 0.639 g (0.0028 mole) of *trans*-1,2-dibromocyclopentane-4-C^{14} (XI) and 2.0 ml of acetone[3] containing 2.65 g (0.045 mole) of trimethylamine was placed in a Pyrex glass tube, 12 mm O.D., with 1 mm wall thickness. The tube was sealed and heated at 80° C for 66 hours. During this period a mass of white crystals was deposited in the

[3]*A search for a suitable solvent for this reaction showed that acetone gave the best results as compared with nitromethane, nitrobenzene, acetonitrile, benzyl alcohol, and acetophenone* (*cf. discussion of the effects of solvent on the Menschutken reaction given by Streitwieser* (*32*)).

reaction mixture. After the mixture had cooled, the sealed tube was opened and the solvent and excess trimethylamine evaporated off. The product was recrystallized from a mixture of ethanol and ethyl acetate. The yield of the quaternary ammonium salt (XVII) was 1.11 g (76%). Analysis: Calc. for $C_{11}H_{26}N_2Br_2$: C, 38.15%; H, 7.57%; N, 8.10%; Br, 46.2%. Found: C, 38.24%; H, 7.39%; N, 8.07%; Br, 46.2%.

1,2-Bis-(trimethylammonium)-cyclopentane-4-C^{14} *Hydroxide* (XVIII)

To a solution of 1.11 g of 1,2-bis-(trimethylammonium)-cyclopentane-4-C^{14} bromide (XVII) in 20 ml of water, moist, freshly prepared silver oxide was slowly added until the color of silver oxide persisted after the solution had been standing for 1 hour at room temperature. The silver bromide which precipitated was filtered off and washed with 15 ml of water. The filtrate and washings were combined, and the water removed at 45–50° C with the aid of a water aspirator pump. The quaternary ammonium hydroxide, which remained behind as a yellowish oil, was used directly for the next reaction.

Cyclopentadiene-x-C^{14} (XVI*b*)

The above quaternary ammonium hydroxide (XVIII) was transferred to a 15-ml pear-shaped flask equipped with a nitrogen bubbler and a reflux condenser with its jacket temperature maintained at 50° C. The reflux condenser was connected to a receiver immersed in a dry ice – acetone bath. With a slow stream of dry nitrogen flushing through the system, the reaction flask was heated in a wax bath to 150° C whereupon a smooth reaction took place. The reaction temperature was kept at 150° C for 10 minutes and then raised to 160° C for an additional 15 minutes. The product trapped in the receiver was dissolved in 15 ml of low boiling petroleum ether containing 0.4 g of ordinary cyclopentadiene as carrier. This solution of diluted cyclopentadiene-*x*-C^{14} was washed four times with 15-ml portions of cold water, dried with Drierite, and then it was used directly for degradation to determine the C^{14} distribution. In preliminary preparations, the yield of cyclopentadiene, identified by the formation of the maleic anhydride adduct, m.p. 162–163° C, was found to be of the order of 20%.

Cyclopentadiene-x-C^{14} (XVI*c*) *from Reaction of 3,5-Dibromocyclopentene with Magnesium in Dry Ether* (*Synthesis No. 3*)

Cyclopentene-4-C^{14} (XII)

Cyclopentene-4-C^{14} (XII) was prepared from *trans*-1,2-dibromocyclopentane-4-C^{14} (XI) as described under the method of degradation of XI.

3,5-Dibromocyclopentene-x-C^{14} (XIX)

One gram (0.015 mole) of cyclopentene-4-C^{14} was brominated by refluxing for 4 hours with a mixture of 5.4 g (0.030 mole) of N-bromosuccinimide and 50 mg of benzoyl peroxide in 70 ml of carbon tetrachloride. The product, recovered as described by Cope and co-workers (14), weighed 2.12 g (64%), b.p. 50–60° C at 1.2 mm (lit. (14), b.p. 52–73° C at 3 mm).

Cyclopentadiene-x-C^{14} (XVI*c*) (*15*)

In a 15-ml pear-shaped flask fitted with reflux condenser, dropping funnel, and inlet to provide a nitrogen atmosphere was placed 0.432 g (0.018 mole) of magnesium turnings and 5.0 ml of absolute ether. The magnesium was activated by the addition of a few drops of ethyl bromide. Then with frequent shaking, 2.00 g (0.0088 mole) of 3,5-dibromocyclopentene-*x*-C^{14} (XIX) in 5.0 ml of absolute ether was added dropwise over a period of 15 minutes. The reaction was very vigorous. After the addition of XIX was completed, the mixture was allowed to stand at room temperature for 30 minutes with frequent shaking. The product, along with ether, was distilled, the distillate being

Can. J. Chem. Downloaded from www.nrcresearchpress.com by 176.9.209.113 on 09/04/12
For personal use only.

collected in a dry-ice-cooled receiver. This distillate was used directly for the degradation of the cyclopentadiene-*x*-C^{14}. In preliminary preparations, the cyclopentadiene was identified by the formation of the adduct with maleic anhydride, m.p. 162–163° C.

Degradation of Cyclopentadiene-x-C^{14}

Diethyl Ester of 2,3-Dihydrazabicyclo (2.2.1)-5-heptene-2,3-dicarboxylic Acid (XX)

An ether solution containing 0.50 g (0.0076 mole) of cyclopentadiene-*x*-C^{14} and 1.32 g (0.0076 mole) of diethyl azodicarboxylate, the latter prepared from reaction of hydrazine with ethyl chloroformate followed by oxidation with chlorine (33), was heated in a sealed tube at 45° C for 12 hours. After removal of the solvent, the residue was distilled under vacuum, yielding 1.73 g (95%) of a very viscous product, b.p. 110–113° C at 0.12 mm (lit. (31), b.p. 121° C at 0.5 mm). On addition of bromine, the dibromo derivative obtained melted at 66–67° C (lit. (31), m.p. 67° C).

Diethyl Ester of 2,3-Dihydrazabicyclo (2.2.1) heptane-2,3-dicarboxylic Acid (XXI)

In the glass liner of the hydrogenator bomb were placed 2.00 g (0.0083 mole) of the above Diels–Alder adduct (XX) in 20 ml of absolute ethanol and 0.05 g of platinum oxide. Hydrogenation was effected by shaking the system for 4 hours under a hydrogen pressure of about 450 p.s.i. The required drop in pressure for the small quantity of reactant used was negligible so it was not recorded. The product was isolated by filtering off the catalyst, removing the ethanol by means of a water aspirator pump, and vacuum-distilling the residue. The fraction collected weighed 1.77 g (88%), b.p. 112–114° C at 0.2 mm (lit. (31), b.p. 121° C at 5 mm).

Succinic Acid (XXII) *from* XXI

A mixture of 1.00 g (0.0041 mole) of hydrogenated ester XXI, 6.5 g (0.041 mole) of potassium permanganate, and 100 ml of water was heated on a steam bath with occasional shaking for 25 minutes. After the mixture had cooled, the excess permanganate and manganese dioxide were reduced by slow addition of sodium bisulphite. The resulting colorless solution was continuously extracted with ether for 48 hours. The extract was dried with Drierite, the ether removed by distillation, and the residue maintained at 60–70° C under water pump vacuum until a yellowish, crystalline residue remained. This residue, after being washed with chloroform, weighed 0.253 g (52%). It was purified by three successive recrystallizations, suitable solvent for the recrystallization being diethyl ketone, anhydrous tetrahydrofuran, or water acidified with hydrochloric acid. The m.p. of the purified product was 184–185° C (lit. (19*c*), m.p. 184.5–185° C).

Schmidt Reaction with Succinic Acid

Succinic acid (50 mg, 0.42 mmole) was converted to succinic anhydride by treatment with 30 λ (0.34 mmole) of phosphorus oxychloride, and then the anhydride was subjected to reaction in 0.43 ml of 100% sulphuric acid containing 85 mg (1.3 mmoles) of sodium azide. The detailed procedure has been reported by Phares and Long (34). The carbon dioxide liberated was trapped in carbonate-free sodium hydroxide solution and then precipitated as barium carbonate. The yield of barium carbonate was in the order of 80%. The reaction mixture was made basic with sodium hydroxide solution and distilled to give an aqueous solution of ethylene-1,2-diamine as described by Phares and Long (34). Isolation of the ethylene-1,2-diamine as a solid derivative was effected by acidifying the distillate with hydrobromic acid, evaporating almost to dryness, adding ethanol, and collecting the crystalline product formed. The yield of ethylene-1,2-diamine dihydrogen bromide was 52 mg (55%). Analysis: Calc. for $C_2H_{10}N_2Br_2$: N, 12.63%; Br, 72.0%. Found: N, 12.59%; Br, 72.4%.

Can. J. Chem. Downloaded from www.nrcresearchpress.com by 176.9.209.113 on 09/04/12
For personal use only.

ACKNOWLEDGMENTS

The award of the C-I-L Fellowship to one of us (R.T.) and the financial support given by the National Research Council of Canada are gratefully acknowledged.

REFERENCES

1. THIELE, J. Ber. **33**, 666 (1900).
2. THIELE, J. Ber. **34**, 68 (1901).
3. GOSS, F. R. and INGOLD, C. K. J. Chem. Soc. 1268 (1928).
4. ROBERTS, J. D., STREITWIESER, A., JR., and REGAN, C. M. J. Am. Chem. Soc. **74**, 4579 (1952).
5. LLOYD, D. and SNEEZUM, N. S. Chem. & Ind. (London), 1221 (1955); Tetrahedron, **3**, 334 (1958).
6. KOSOWER, E. M. and RAMSEY, B. G. J. Am. Chem. Soc. **81**, 856 (1959).
7. RAMIREZ, F. and LEVY, S. J. Org. Chem. **21**, 488 (1956); J. Am. Chem. Soc. **79**, 67 (1957).
8. HÜCKEL, E. Z. Physik, **70**, 204 (1931); Grundzüge der Theorie ungesättigter und aromatische Verbindungen. Verlag Chemie, G.M.B.H., Berlin. 1938. pp. 71–85.
9. WHELAND, G. W. J. Chem. Phys. **2**, 474 (1934).
10. DOERING, W. VON E. and KNOX, J. H. J. Am. Chem. Soc. **76**, 3203 (1954).
11. WILKINSON, G. W., COTTON, F. A., and BIRMINGHAM, J. M. J. Inorg. & Nuclear Chem. **2**, 95 (1956).
12. FRITZ, H. P. Ber. **92**, 780 (1959).
13. CROSSLEY, A. W. J. Chem. Soc. 1403 (1904).
14. COPE, A. C., ESTER, L. L., JR., EMERY, J. R., and HAVEN, A. C., JR. J. Am. Chem. Soc. **73**, 1199 (1951).
15. REID, E. B. and YOST, J. F. J. Am. Chem. Soc. **72**, 1807 (1950).
16. FRIES, B. A. and CALVIN, M. J. Am. Chem. Soc. **70**, 2235 (1948).
17. CASON, J. and RAPAPORT, H. Laboratory text in organic chemistry. Prentice-Hall Inc., New York. 1950. pp. 289–291.
18. MICOVIC, M. V. Organic synthesis. Collective Vol. II. John Wiley & Sons, Inc., New York. 1943. p. 264.
19. HEILBRON, I. and BUNBURY, H. M. Dictionary of organic compounds. Eyre and Spottiswoode, Ltd., London. 1953. (*a*) Vol. II, p. 606; (*b*) Vol. I, p. 647; (*c*) Vol. IV, p. 383.
20. HAUSER, C. R. and HUDSON, B. E., JR. Organic reactions. Vol. 1. John Wiley & Sons, Inc., New York. 1942. p. 284.
21. HESSE, G. and BÜCKING, E. Ann. **563**, 31 (1949).
22. OWEN, L. N. and SMITH, P. N. J. Chem. Soc. 4026 (1952).
23. HERMANS, P. H. Z. anorg. u. allgem. Chem. **142**, 83 (1925).
24. VERKADE, P. E., COOPS, J., JR., VERKADE-SANDBERGEN, A., and MAAN, C. J. Ann. **477**, 279 (1930).
25. WINSTEIN, S. and LUCAS, H. J. J. Am. Chem. Soc. **61**, 1581 (1939).
26. ZELINSKY, N. D. and LEWINA, R. J. Ber. **66**, 477 (1933).
27. LUCAS, H. J., SCHLATTOR, M. J., and JONES, R. C. J. Am. Chem. Soc. **63**, 22 (1941).
28. BAILY, P. S. J. Org. Chem. **22**, 1548 (1957).
29. LOFTFIELD, R. B. J. Am. Chem. Soc. **73**, 4707 (1951).
30. ROBERTS, J. D., SEMENOV, D. A., SIMMONS, H. E., JR., and CARLSMITH, L. A. J. Am. Chem. Soc. **78**, 601 (1956).
31. DIELS, O., BLOM, J. M., and KOLL, W. Ann. **443**, 242 (1925).
32. STREITWIESER, A., JR. Chem. Revs. **56**, 571 (1956).
33. RABJOHN, N. Org. Syntheses, **28**, 58 (1948).
34. PHARES, E. F. and LONG, M. V. J. Am. Chem. Soc. **77**, 2556 (1955).

Can. J. Chem. Downloaded from www.nrcresearchpress.com by 176.9.209.113 on 09/04/12
For personal use only.

Can. J. Chem. Downloaded from www.nrcresearchpress.com by 176.9.209.113 on 09/04/12
For personal use only.

A PRELIMINARY STUDY OF THE VAPOR PERMEABILITY OF CELLOPHANE[1]

W. L. ARCHER[2] AND S. G. MASON

ABSTRACT

The water vapor permeability of cellophane was measured over adsorption–desorption cycles and was found to parallel the sorption isotherm. When a constant vapor pressure was applied on the low pressure side of the membrane, the mass flow rate was independent of the vapor pressure used and showed hysteresis on desorption. The permeabilities of methanol, ethanol, and benzene were found to increase with increasing vapor pressure.

INTRODUCTION

In this note we describe some rather careful measurements of the diffusion of water and other substances through cellophane when a controlled difference in vapor pressure was maintained across the membrane. The measurements were made originally to determine their usefulness in studying swelling phenomena in cellulose. Because the measurements were time-consuming and the permeation phenomena complicated, the technique was abandoned in favor of liquid permeability methods (1, 2).

Since the transmission of gases and vapors through polymeric films is receiving considerable attention (3, 4), our results may prove to be of some interest. Doty, Aiken, and Mark (5) have shown that the water vapor permeability of cellophane varies non-linearly with the vapor pressure gradient. They proposed a mechanism of vapor transfer comprising an activated diffusion by the sorption and desorption of water molecules at active spots on the internal surface of the cellulose.

Several investigators have pointed out the similarity in shape between the water sorption isotherm and permeability of cellophane (6, 7). This observation has been confirmed and extended in the present study.

EXPERIMENTAL PART

Apparatus

Measurements were made in an evacuated system consisting essentially of a vapor source, a cellophane barrier, and a cold trap to condense the permeating vapor. The sorption of the vapor by a separate piece of cellophane was measured simultaneously on the high pressure side of the membrane.

The same cellophane membrane was used in all the permeability measurements and was held in a stainless steel cell (Fig. 1). The cell consisted of two half-cells bolted together at central flanges by eight symmetrically placed steel bolts. The membrane was clamped between the inner lapped ring surfaces of the flanges. A groove B cut in the flanges provided a mercury well to seal the edges of the membrane. The free area of membrane was 19.68 cm^2.

The cell was connected to the vacuum system by two tapered ends machined to fit female standard ground glass joints. Effective bonding of the steel and glass was obtained with high vacuum cement. The cell was immersed in a constant temperature water bath. A vacuum of 10^{-4} mm Hg was readily obtained.

[1]*Manuscript received June 10, 1959.*
Contribution from the Physical Chemistry Division, Pulp and Paper Research Institute of Canada, and the Department of Chemistry, McGill University, Montreal, Quebec.
[2]*Holder of Studentships (1947–48 and 1948–49) from the National Research Council.*

Can. J. Chem. Downloaded from www.nrcresearchpress.com by 176.9.209.113 on 09/04/12
For personal use only.

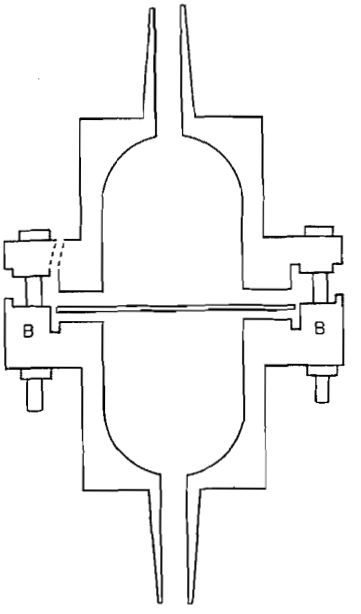

FIG. 1. Vapor permeability cell.

Vapor was supplied from bulbs at C (Fig. 2), thermostatted separately from the permeability cell to provide the required relative vapor pressures next to the membrane. Saturated solutions of potassium acetate and potassium thiocyanate, and distilled water, provided a complete range of relative humidities. A mixture of methanol and glycerol provided low methanol vapor pressures. Due to the low loss rate of vapor by permeation, mechanical agitation of the reservoir was not required. Dissolved air was removed by several cycles of freezing and thawing under vacuum. The temperature of the vapor tube bath was controlled to $\pm 0.02°$ C.

The vapor pressure gradient across the membrane was measured by mercury manometers at D and E (Fig. 2).

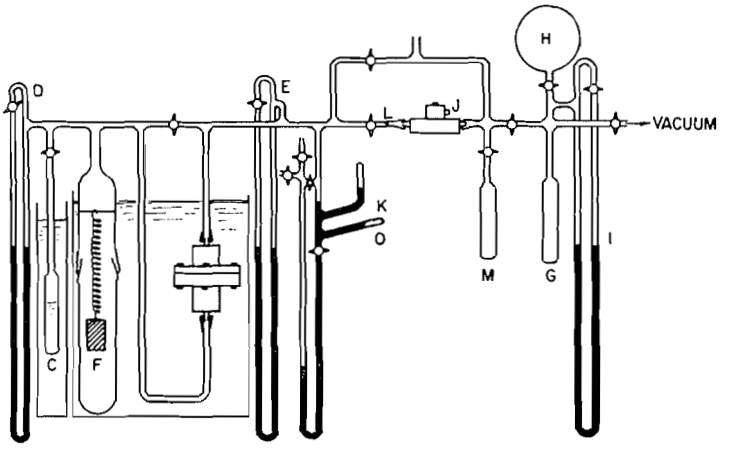

FIG. 2. Vapor permeability apparatus.

Sorption measurements were carried out with a cellophane sample suspended by a quartz spiral spring (sensitivity = 1.08 mg/mm) in a sorption cell at F. Vapor sorption was determined by measuring the extension of the quartz spring with a cathetometer, and was expressed as a percentage of the dry weight.

The vapor passing through the membrane was condensed in a cold trap G using liquid nitrogen, and measured by subsequent expansion into a known volume of the system. A calibrated volume H was used both to determine the volume of this portion of the system and to provide extra space for the expansion of large amounts of condensate. The resulting pressures were measured with a mercury manometer I.

Constant vapor pressures were maintained as required on the "dry" or low pressure side of the membrane by a solenoid-operated needle valve J. Valve action was controlled by a mercury contact switch K operating through a relay. For increased sensitivity, a fine orifice L was inserted in advance of the needle valve. Dry side vapor pressures were maintained constant to ± 0.1 mm Hg.

Materials

Both the permeability membrane and the sorption sample were cut from a single sheet of Canadian Industries Limited PT 600 (non-waterproofed) cellophane. The glycerol plasticizer was removed by extraction in water at 60° C for 2 hours.

Procedure

For several days prior to each sorption–desorption cycle, the system was continuously evacuated to remove sorbed vapors and gases from the glass tubing and the cellophane. During the time required to reach a constant transmission rate, the vapors passing through the membrane were collected in a cold trap M (Fig. 2). For a permeability measurement, this cold trap was closed off and the transmitted vapor collected in cold trap G.

All permeability and sorption measurements were carried out at $30 \pm .01$° C.

The permeabilities were expressed in terms of the mass flow rate q in g sec^{-1}, and a vapor permeability P_v defined by

$$[1] \qquad q = P_v A(\Delta p)$$

where A is the area of membrane (= 19.68 cm^2), and (Δp) is the vapor pressure difference across the membrane in dynes/cm^2. In view of the uncertainty of the thickness of the partially swollen membrane and of other complications, no attempts were made to calculate absolute permeability coefficients.

RESULTS AND DISCUSSION

Permeability to Water Vapor

1. Steady State

To ensure that a constant vapor transmission rate was attained, a series of flow rate measurements was made at each relative humidity until a constant flow rate was reached. A typical curve illustrating the change in flow rate accompanying an increase in relative humidity on the "wet" side is shown in Fig. 3. The time to reach a constant flow rate was found to decrease with increasing relative humidity, and to be shorter during sorption than during desorption. These trends were evident from the times to half-value, i.e. the time for the initial 50% change in flow rate to occur. The corresponding times to half-value for sorption were approximately one-half those of P_v at low R.H.; above 40% R.H. the times were substantially the same.

Can. J. Chem. Downloaded from www.nrcresearchpress.com by 176.9.209.113 on 09/04/12
For personal use only.

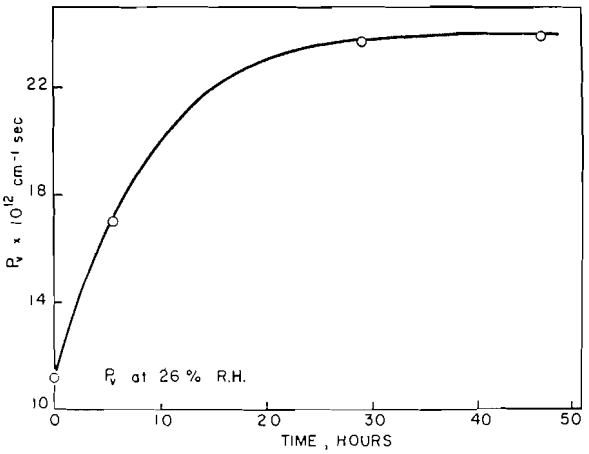

FIG. 3. Approach of permeability to equilibrium value on increasing relative humidity from 26 to 40%. Dry side at 0% R.H. The time to half-value in this experiment was 6.0 hours.

2. Permeability at Zero Back Pressure

Permeabilities for a complete sorption–desorption cycle are given in Table I. These measurements were made with zero vapor pressure on the low pressure side of the membrane.

TABLE I

Water vapor permeability (zero back pressure)

Relative humidity (wet side), %	Δp, mm Hg	$q \times 10^8$, g sec^{-1}	$P_v \times 10^{12}$, cm^{-1} sec	Moisture content, %
Adsorption				
11	3.5	6.12	0.67	4.5
26	8.2	24.2	1.12	6.5
40	12.8	79	2.38	8.3
55	17.5	234	5.03	10.8
80	25.5	1000	14.8	17.9
Desorption				
94	30.0	2000	25.1	30.6
80	25.5	1016	15.0	19.1
60	19.1	294	5.80	12.8
40	12.8	116	3.43	10.0
26	8.2	56.4	2.61	8.1
11	3.5	13.6	1.47	5.8

The permeabilities in Table I are approximately four times those reported by Doty *et al.* (5) for a comparable grade of cellophane. This is not a serious discrepancy in view of the wide variations in permeability reported by these authors for commercial films of different manufacture.

The permeability and sorption data are plotted in Fig. 4 and as others have found (6, 7) roughly parallel one another. During desorption, the curve of Fig. 4 is seen to exhibit a permeability hysteresis at relative humidities below 60%. This behavior was confirmed several times. Both the adsorption and desorption portions of the P_v curve in Fig. 4 extrapolate smoothly to the origin indicating that dry cellophane is impervious to water.

Can. J. Chem. Downloaded from www.nrcresearchpress.com by 176.9.209.113 on 09/04/12
For personal use only.

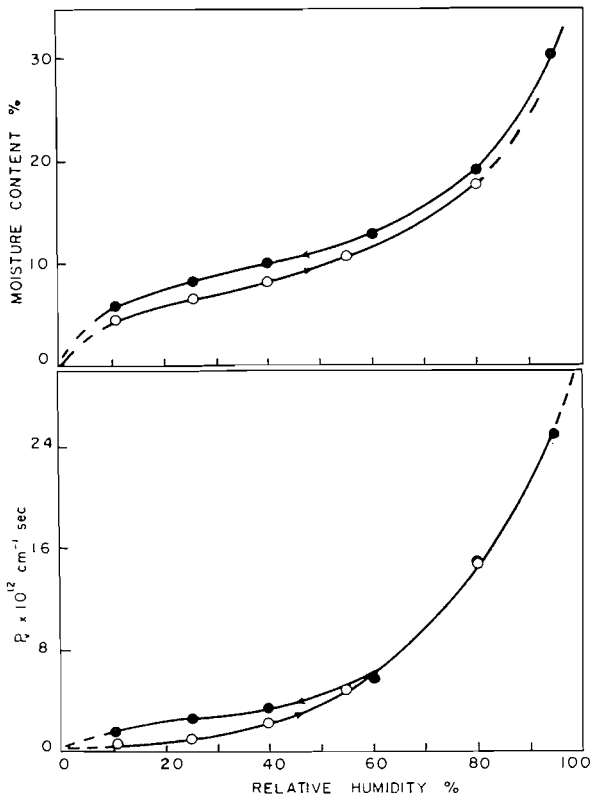

FIG. 4. Water vapor sorption (upper part) and permeability at zero back pressure (lower part) for adsorption (open circles) and desorption (solid circles).

3. Reduced Moisture Gradients

The effect of reducing the moisture gradient across the membrane was studied by introducing constant water vapor pressures on the low pressure side of the membrane. The results obtained with pressures corresponding to 20% R.H. are given in Table II

TABLE II

Water vapor permeability
(20% relative humidity on low pressure side)

Relative humidity (wet side), %	Δp, mm Hg	$q \times 10^8$, g sec^{-1}	$P_v \times 10^{12}$, cm^{-1} sec
Adsorption			
26	1.8	12.9	2.7
55	11.2	360	12.1
65	14.1	730	21.2
75	17.0	1320	29.2
Desorption			
70	15.5	1080	26.2
65	14.1	920	24.8
55	11.2	500	16.8
33	4.2	105	9.5

Can. J. Chem. Downloaded from www.nrcresearchpress.com by 176.9.209.113 on 09/04/12
For personal use only.

for a complete cycle. These data together with values at 0, 10, and 15% R.H. are shown in Fig. 5. In order to show the trends more clearly, values of q have been plotted.

Figure 5 shows that the reduction in moisture gradient across the membrane has caused an increase in the vapor transmission rate at all relative humidities. The q curves during adsorption for the three back pressures used coincide, indicating that the increase in q is independent of the pressure used.

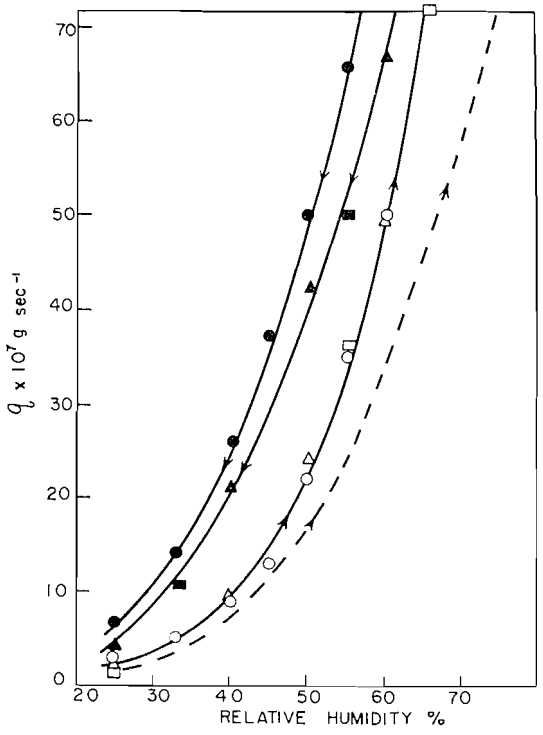

FIG. 5. Water vapor flow rates during adsorption (open points) and desorption (solid points) at 10% (circles), 15% (triangles), and 20% (squares) relative humidity on the low pressure side. The broken line is for adsorption at zero R.H. on the low pressure side.

A second effect of a reduced moisture gradient is seen in the extension of the permeability hysteresis to relative humidities above 60%. There also appears to be a trend toward a reduction in the magnitude of the hysteresis as the low pressure side relative humidity is increased.

TABLE III

Organic vapor permeabilities (zero back pressure)

Permeant	Δp, mm Hg	$q \times 10^8$, g sec^{-1}	$P_v \times 10^{14}$, cm^{-1} sec	% sorption
Methanol	45.5	1.47	1.21	1.4
	81.9	10.5	4.85	1.8
	133	94	26.7	6.9
Ethanol	40.0	0.93	1.08	—
	60.1	2.50	1.57	—
	79.0	7.09	3.39	—
Benzene	67.6	2.32	1.3	0.03
	97.7	7.26	2.8	0.08

Can. J. Chem. Downloaded from www.nrcresearchpress.com by 176.9.209.113 on 09/04/12
For personal use only.

Permeability to Organic Vapors

Various organic vapors are adsorbed less than water and it was thought that P_v might be independent of Δp when the sorption became negligible. The permeabilities of methanol, ethanol, and benzene at zero back pressure are given in Table III. These data show that the permeability to organic vapors is considerably less than to water vapor. The flow rate of methanol vapor, for example, at 45.5 mm Hg pressure is less than 1/600 that of water vapor at 25.5 mm Hg pressure (Table I).

Sorption measurements on methanol and benzene are included in Table III and show that P_v increases with the sorptions.

It is seen from Table III that P_v did not remain constant but in all cases increased with increase in Δp.

REFERENCES

1. CARROLL, M. and MASON, S. G. Can. J. Technol. **30**, 294 (1952).
2. KUZMAK, J., ARCHER, W. L., and MASON, S. G. To be published.
3. WAACK, R., ALEX, N. H., FRISCH, H. L., STANNET, V., and SZWERC, M. Ind. Eng. Chem. **47**, 2524 (1955).
4. BARRER, R. M. Diffusion in and through solids. Cambridge Univ. Press, London. 1941.
5. DOTY, P. M., AIKEN, W. H., and MARK, H. Ind. Eng. Chem. Anal. Ed. **16**, 686 (1944).
6. CHARCH, W. H. and SCROGGIE, A. G. Paper Trade J. **101**, 201 (1935).
7. TAYLOR, R. L., HERRMANN, D. B., and KEMP, A. R. Ind. Eng. Chem. **28**, 1255 (1936).

Can. J. Chem. Downloaded from www.nrcresearchpress.com by 176.9.209.113 on 09/04/12
For personal use only.

Can. J. Chem. Downloaded from www.nrcresearchpress.com by 176.9.209.113 on 09/04/12
For personal use only.

PARTIAL SPECIFIC VOLUME MEASUREMENTS BY DIFFERENTIAL SEDIMENTATION[1]

W. G. MARTIN, C. A. WINKLER,[2] AND W. H. COOK

ABSTRACT

The partial specific volumes of several macromolecules were determined from their sedimentation rates in aqueous and heavy water solutions with results comparable to those obtained by conventional methods. Corrections for the changes in weight due to isotopic exchange were obtained from measurements on small quantities of material with a quartz spiral balance. Measurements of the partial specific volumes of bovine plasma albumin, polyvinyl alcohol, glycine, and triglycylglycine in both aqueous and heavy water media, made with a magnetic float apparatus, indicate that isotopic exchange has no significant effect on the macromolecular volume. The sedimentation method is therefore a micro method that does not require a knowledge of the concentration of macromolecules and which is applicable to mixtures that are resolvable during sedimentation.

INTRODUCTION

In a recent paper (1) it was shown that measurement of the differential rate of sedimentation of macromolecules dissolved in water or deuterium oxide solvents could yield a sufficiently accurate estimate of their partial specific volume ($\bar{v}$) to be useful in estimating molecular size by sedimentation methods. Although the inherent accuracy is less than that of the conventional methods (pycnometry and magnetic float), the procedure has several advantages: it can be used when only small amounts of material (ca. 10 mg) are available; other methods require purified material whereas the sedimentation method should be applicable to mixtures, provided the boundaries can be resolved; finally, this method is applicable to materials (lipoproteins) where density and other properties are altered by contact with immiscible organic liquids used to establish density gradient columns. These advantages are so great in the preparative stages of any new biological macromolecule, or with any scarce material, that further study and development of the method were well justified.

As mentioned in the earlier paper (1), other investigators (2) have used salts and nonelectrolytes to alter the density of the media of sedimentation. Since these substances interacted with the sedimenting solutes and brought about spurious results, Sharp *et al.* (3) sedimented viruses in heavy water media. Recently polystyrene latex spheres were sedimented in aqueous and heavy water mixtures (4, 5), but here hydration and isotopic exchange of labile hydrogen were not involved. Katz and Schachman (6) have obtained an adequate value of $\bar{v}$ from sedimentation of deoxyribonucleic acid at constant concentration in media in which the density was altered by the addition of heavy water. However, with most biological macromolecules it is necessary to consider the extent of exchange of labile hydrogen atoms in heavy water media. True, as in our earlier paper, isotopic exchange may be estimated for well-known materials, but not so for new unknown macromolecules. Therefore a procedure for determining the degree of substitution on micro quantities of material by direct weighing was developed and critically compared with the substitution indicated by density methods. In addition to measurements on

[1]*Manuscript received June 15, 1959.*
Contribution from the Division of Applied Biology, National Research Council, Ottawa, Canada, and the Physical Chemistry Laboratory, McGill University, Montreal, Quebec. This paper constitutes part of a thesis submitted to the Graduate School, McGill University, by W.G.M., in partial fulfillment of the requirements for the degree of Doctor of Philosophy.
Issued as N.R.C. No. 5320.
[2]*Department of Chemistry, McGill University, Montreal, Quebec.*

proteins, some relatively extensive measurements were made on glycine and triglycylglycine where substitution is proportionately higher. Finally, the aqueous – heavy water sedimentation procedure was tested on mixtures of proteins of known and unknown $\bar{v}$ to confirm the applicability and accuracy of the procedure as applied to such systems.

MATERIALS

Crystalline bovine plasma albumin lot No. A1201 (Pentex Inc.), crystalline bovine β-lactoglobulin lot No. 0053B (Armour and Co.), and triglycylglycine lot No. 7484 (Nutritional Biochemicals Corp.) were used without further purification and will be referred to as BPA, βLG, and TGG, respectively. Polyvinyl alcohol (Shawinigan Chemicals Ltd.), termed PVA, was dissolved in distilled water, centrifuged, filtered, and then lyophilized. The PVA had a remnant of 12 acetate groups per 100 mers owing to incomplete alcoholysis. Glycine (Eastman) was dissolved in warm water and filtered from a slurry of charcoal and celite, then precipitated with methanol, washed with methanol–ether, and dried at 45° C *in vacuo*.

Livetin (7), the water-soluble protein of hen egg yolk, was separated into its α–β-components and γ-components by the procedures of Martin *et al.* (8, 9). Lipovitellin of yolk was prepared by the method of Joubert and Cook (10). It was possible to store the α–β-livetin in a lyophilized condition but the lipovitellin and γ-livetin had to be stored at 5° C in solution.

A stock of distilled water was prepared by adding potassium permanganate to alkaline tap water and distilling with a minimum of reflux. The distillate, redistilled with a minimum of reflux, was assumed to have a density of 0.997074 g/ml at 25.000° C.

Deuterium oxide (99% D_2O) and a quartz spiral were purchased from Merck & Co., Inc., and Microchemical Supply Co., respectively.

METHODS

The sedimentation procedures were as described previously (1) with some modifications. Solutes in appropriate solvents were dialyzed at 5° C against solvent. Suitable dilutions were then made using diffusate as diluent. Viscosity and density measurements on diffusates were made with Ostwald–Fenske type viscometers and with a Mohr–Westphal balance, respectively, at 20° C, since sedimentation experiments were controlled at this temperature. Solute concentrations were determined from measurements with a differential refractometer (11) from previously determined values of the specific index increments. Transfer of solutions was effected by use of dry syringes to minimize exchange of heavy water with atmospheric moisture.

In order to interpret the changes in $\bar{v}$ of macromolecules brought about by isotopic exchange, the direct weight increase upon exposure to heavy water was measured on a McBain–Bakr quartz spiral balance (Fig. 1). The balance apparatus consisted of vacuum pump A, oil diffusion pump B, gas inlet control system C and D, trap E, ionization gauge F, pyrex glass balance case containing quartz spiral and sample basket, and movable permanent magnets L. Capillary tube G permitted insertion of syringe needles. Heater M containing thermometer N was removable. Auxiliary apparatus could be connected at H.

Aluminum foil baskets were dipped into silicone grease dispersed in benzene, and then dried at 110° C. Baskets with capacity of 1 or 2 ml weighed about 40 to 60 mg. The spiral was calibrated *in vacuo* by measuring the extension caused by the addition of calibrated platinum weights. Extensions were measured with a Wild cathetometer

Can. J. Chem. Downloaded from www.nrcresearchpress.com by 176.9.209.113 on 09/04/12
For personal use only.

Can. J. Chem. Downloaded from www.nrcresearchpress.com by 176.9.209.113 on 09/04/12
For personal use only.

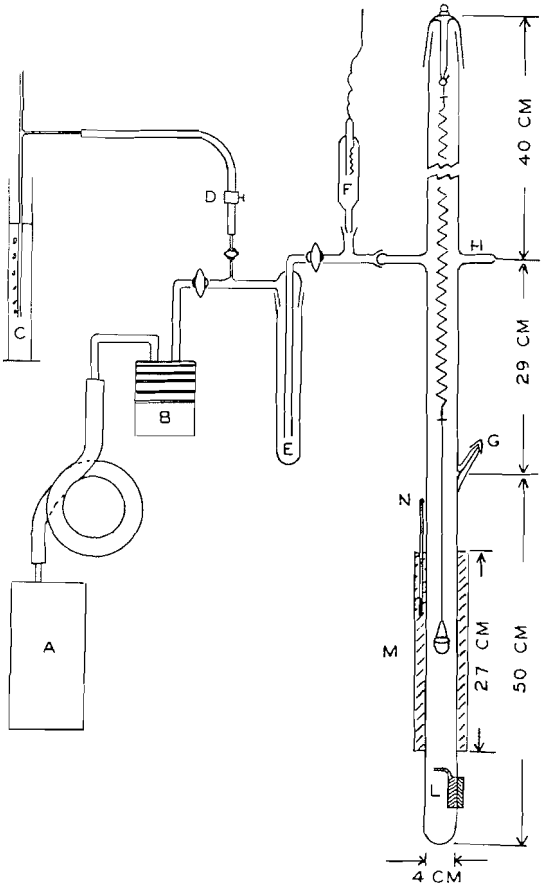

FIG. 1. Quartz spiral balance apparatus.

at 25° C to 0.01 mm with a precision of reading of ±0.02 mm. The sensitivity of the spiral was 1.00±0.02 mg/mm extension with loads ranging from 24 to 198 mg.

Measurements were made of spiral extension *in vacuo* with the empty basket suspended and the trap E immersed in liquid nitrogen. Then nitrogen gas was slowly admitted to the system through the trap until atmospheric pressure was reached. About 150 mg of sample was added to the basket and the system evacuated until constant weight was reached. Nitrogen gas was admitted to the system through the trap and about 1 ml of water was directed into the basket through capillary G while the basket was supported by the magnets. After an equilibrium period of 15 to 20 hours the basket was lowered in the balance case and the sample was frozen *in situ*. Lyophilization was brought about and evacuation continued until constant weight again occurred. Similarly, two to three applications of deuterium oxide were applied to the sample and sometimes followed by two more applications of water. Equilibrium weights were also obtained at selected temperatures (< 105° C) by adjustment of the movable furnace M about the basket. Once a sequence of exchanges had commenced, the trap E was kept immersed in liquid nitrogen. When deuterium oxide was added to samples, a small flow of nitrogen gas passed through the system by way of the trap.

To provide a standard of comparison with $\bar{v}$ obtained by the sedimentation method, $\bar{v}$ was also determined from measurements of density made with a magnetic float apparatus (12, 13). Usually weighed quantities of diffusate were placed in the float chamber and then weighed amounts of concentrated stock solutions were added, with density measurements being made upon each addition. However, owing to the impossibility of dialysis of glycine or TGG solutions, solvents were obtained by cryosublimation from their frozen solutions, and solvents and residual concentrated solutions used in the manner of the diffusates and solutions mentioned above.

Solute concentrations for the float measurements were based on dry weight. Deuterated samples were brought to constant weight, then two additions of water were made with intervening drying to get the dry weight of the protonated sample. At the temperature of 105° C *in vacuo*, employed for the other materials, glycine samples failed to reach constant weight, and therefore the effect of temperature on glycine was examined with the spiral balance. Based on these measurements, glycine was brought to constant weight at 70° C *in vacuo*.

RESULTS

Difficulty in achieving constant dry weight of glycine samples at 105° C *in vacuo* is understandable in view of the results shown in Fig. 2 for the spiral extension when the basket containing glycine was heated to various temperatures. Rapid loss of weight, accompanied by sublimation of the sample, occurred *in vacuo* at temperatures above 74° C. The other materials presented no serious drying difficulties. Even with the lipid-containing lipovitellin, only a slight loss in weight occurred between 25 and 91° C *in vacuo*.

The extent of exchange of deuterium for hydrogen atoms in the materials is shown in Table I, 97.4% deuterium oxide being the exchange medium. In a few instances experiments with the spiral balance had to be repeated owing to dusting or loss of small pieces of the material during drying. Concentrated solutions gave less trouble in this respect.

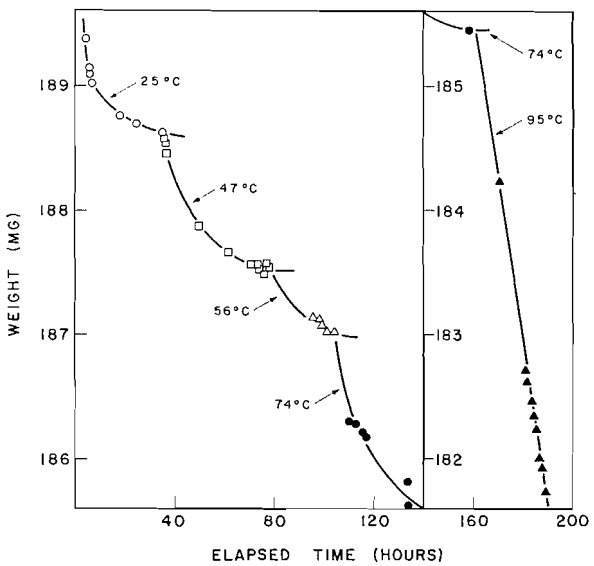

FIG. 2. Weight (extension) of glycine as a function of temperature and heating time *in vacuo*.

Can. J. Chem. Downloaded from www.nrcresearchpress.com by 176.9.209.113 on 09/04/12
For personal use only.

TABLE I

Labile hydrogen exchange*

Sample	Weight increase observed, %	Theoretical weight increase, %
BPA	1.52	1.52
βLG	—	1.5
PVA	1.79	1.75
Glycine	3.84	3.89
TGG	—	2.4
Lipovitellin + X protein	1.33	—
α- + β-Livetin	1.32	—
γ-Livetin	1.36	—

*Based upon 97.4% of D_2O and equilibrium at 25° C.

The isotopic exchange of deuterium with the labile hydrogen atoms of BPA was investigated at intermediate concentrations of heavy water and the results shown in Fig. 3 illustrate the essential linearity of the relation between volume per cent of heavy water and the percentage weight increase of the material.

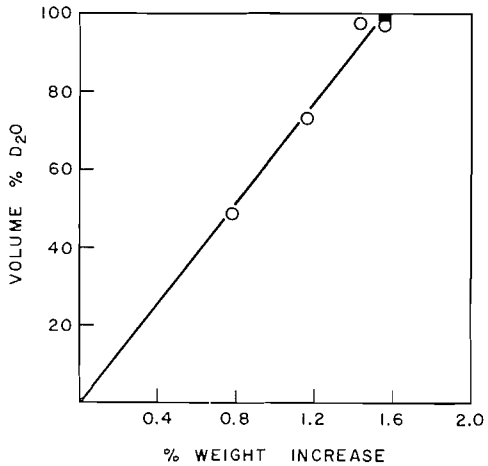

FIG. 3. Relation between D_2O concentration and weight increment of bovine plasma albumin. ○ Experimental. ■ Calculated.

From the exchange measurements or, lacking these, published data, the value of k (1) was calculated from

$$[1] \qquad k = 1+[(\Delta w)(d_1-d_0)/\Delta d]$$

where Δw is the weight increase per gram of sample, (d_1-d_0) is the increment in density of the solvent due to deuterium oxide, and Δd is the increment in density of 100% deuterium oxide over the density of water.

$$[2] \qquad f\eta s = Mk(1-\bar{v}k^{-1}d)$$

was given in the previous paper (1), where f, η, s, M, d are the frictional coefficient, solvent viscosity, sedimentation coefficient, molecular weight of the macromolecule, and solvent density, respectively. As shown in Fig. 4 the relation between $\eta s/k$ and d/k for BPA and PVA (concentration 0.4 g/100 ml) in media of varying concentrations of heavy water

Can. J. Chem. Downloaded from www.nrcresearchpress.com by 176.9.209.113 on 09/04/12
For personal use only.

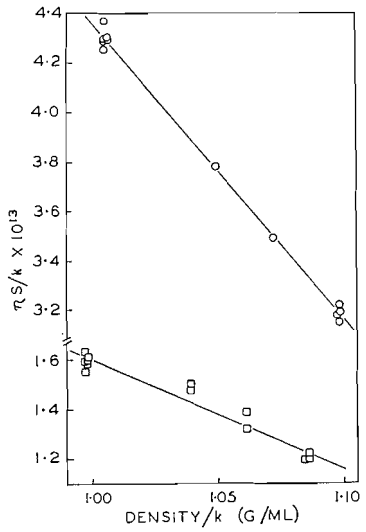

FIG. 4. Relation between $\eta s/k$ (solvent) and d/k (solvent) for bovine plasma albumin and polyvinyl alcohol. ○ BPA. □ PVA.

is essentially linear, as expected from inspection of equation [2]. Moreover, from the intercepts at the values of $\eta s/k$ equal to zero, where $\bar{v}$ equals the reciprocals of the intercepts d/k, $\bar{v}$ was 0.735±0.003, and 0.735±0.013, for BPA and PVA, respectively.

Since the above results and those of others (2, 3, 6) demonstrate the linearity of equation [2] when heavy water is used to alter the density of the solvent, the equation

$$[3] \qquad \bar{v} = (\eta_2/\eta_1 - ks_1/s_2)(d_1\eta_2/\eta_1 - d_2s_1/s_2)^{-1},$$

derived in the earlier paper (1), was used to calculate $\bar{v}$ from sedimentation experiments on macromolecules including single solutes and mixtures. Sedimentation coefficients were extrapolated to zero solute concentration by use of relative values of diluted initial stock solutions and are recorded in Table II, as are also the related solvent viscosities

TABLE II

Summary of sedimentation results and related measurements

Materials	Temp., °C	s^0 uncorr., Svedbergs		η, centipoise		d, g/ml		k
		1	2	1	2	1	2	
Individual macromolecules								
BPA, 0.2 *N* NaCl	25	4.78±0.04	2.97±0.03	0.912	1.117	1.005	1.113	1.015
PVA, 0.2 *N* NaCl	25	2.14±0.03	1.22±0.03	0.912	1.117	1.005	1.113	1.018
α–β-Livetin, 0.2 *N* NaCl	20	3.77±0.05	2.36±0.01	1.030	1.269	1.008	1.112	1.013
γ-Livetin, buffer*	20	7.28±0.06	4.67±0.07	1.033	1.274	1.012	1.116	1.014
In mixtures								
BPA (with βLG), 0.2 *N* NaCl	20	4.36±0.05	2.76±0.06	1.026	1.259	1.006	1.112	1.015
βLG (with BPA), 0.2 *N* NaCl	20	2.74±0.08	1.66±0.05	1.026	1.259	1.006	1.112	1.015
Lipovitellin (with X), buffer†	20	9.71±0.01	5.31±0.01	1.101	1.357	1.019	1.122	1.013
Protein X (with lipovitellin), buffer†	20	6.36±0.16	3.34±0.29	1.101	1.357	1.019	1.122	1.013

*Glycine, pH or pD 9.5, μ 0.2.

†Glycine, pH or pD 9.0, μ 0.3 + 0.05 *M* $MgSO_4$.

s, η, and d values refer to the solvents and temperatures indicated.

1 refers to aqueous solvent.

2 refers to heavy water solvent.

Can. J. Chem. Downloaded from www.nrcresearchpress.com by 176.9.209.113 on 09/04/12
For personal use only.

and densities. The values of k were based upon measured values (Table I) except for βLG, where k was estimated from the amino acid composition (14). Values of $\bar{v}$ obtained by the sedimentation method are shown in Table III. The errors were calculated according to equation

$$[4] \qquad \Delta\bar{v} = \eta_1\eta_2(kd_1-d_2)(s_1+s_2)(d_1s_2\eta_2-d_2s_1\eta_1)^{-2}[(\Delta^2s_1 + \Delta^2s_2)/2]^{\frac{1}{2}}$$

where Δ is to be read "the standard error of" (1).

From measurements of density with the magnetic float apparatus of solutions BPA, PVA, glycine, and TGG in water and heavy water, $\bar{v}$ values were computed for the protonated and deuterated macromolecules, as shown in Tables III and IV. Based upon the measured $\bar{v}$, the fractional changes in $\bar{v}$ upon exchange of labile hydrogen atoms with deuterium atoms were calculated and compared with the values to be expected from the degree of substitution given in Table I.

TABLE III

Partial specific volumes of macromolecules (ml/g)

Material	Calculated	Published or observed by conventional methods	Sedimentation method	
			Alone	In mixtures
BPA	0.734* (15)	0.734_9† (13) 0.7342±0.0002†	0.734±0.001†	0.72±0.02* (with βLG)
PVA	0.75*	0.766±0.001†	0.78±0.01†	
βLG	0.746* (15)	0.751* (17)	—	0.75±0.03* (with BPA)
Lipovitellin	—	0.781† (10)	—	0.779±0.003* (with X)
Protein X	—	—	—	0.79±0.03* (with lipovitellin)
γ-Livetin	—	0.726±0.001† (9)	0.70±0.02*	—
α–β-Livetin	—	—	0.72±0.02*	—

NOTE: Temperatures applicable, *20° C, †25° C.
PVA contains 12 acetate groups per 100 mers.
Values without references are from this work.

In Table III the calculated values of $\bar{v}$ for BPA and βLG were reported by McMeekin and Marshall (15), while that of PVA was obtained by use of the atomic volume increments derived by Traube (16). Of the published values of $\bar{v}$, that of BPA (13), lipovitellin (10), and γ-livetin (9) were obtained by use of a magnetic float, while that of βLG (17) was obtained presumably by use of pycnometers.

DISCUSSION

The weight increases (Table I) that occur upon exchange of labile hydrogen atoms with deuterium atoms are accompanied by changes in $\bar{v}$ as shown by the data in Table IV. The experimentally determined decreases in $\bar{v}$ of PVA, TGG, and glycine were in reasonable agreement with the values calculated on the assumption that the volume occupied by deuterium atoms in a material is similar to that of the displaced hydrogen atoms. The decrease in $\bar{v}$ of BPA was less than the theoretical value, although complete exchange would be expected on the basis of the spiral balance measurements. However, Robertson (18) has reported that an expansion is likely to occur in the direction of the hydrogen bonds upon deuteration, an effect of greater importance in BPA than in PVA, TGG, or glycine. The extent of such an effect on proteins would be unpredictable owing to the several types of hydrogen bonding. Errors in $\bar{v}$ due to measurements with the

Can. J. Chem. Downloaded from www.nrcresearchpress.com by 176.9.209.113 on 09/04/12
For personal use only.

TABLE IV

Partial specific volumes from float apparatus measurements

	Substance			
	BPA	PVA	TGG	Glycine
$\bar{v}_p \times 10^3$, 25° C, ml/g	734.2±0.2	765.9±0.6	590.7±1.2	575.4±1.5
$\bar{v}_D \times 10^3$, 25° C, ml/g	728.2±1.3	754.4±3.5	576.6±1.9	544.9±0.8
$(-\Delta\bar{v}/\bar{v}_p) \times 10^3$ (found)	8.2±1.3	15.0±3.5	24±3	53±3
$(-\Delta\bar{v}/\bar{v}_p) \times 10^3$ (theory)	15.5	17.9	24	40

NOTE: Subscripts p and D refer to protonated and deuterated TGG and glycine values at $c \to 0$.

float apparatus have already been discussed (12, 13) and, even with the added difficulties of dealing with heavy water, are not enough to account for the small $\Delta\bar{v}$ for BPA.

Specific volumes of organic substances with known composition and functional groups can be calculated from atomic volume increments derived by Traube (16) and recently employed by others to evaluate $\bar{v}$ of proteins (19, 15). Calculated and experimental values of $\bar{v}$ for BPA and other proteins agree well if the decrease in volume due to charged groups (electrostriction) is ignored. Electrostriction should occur in proteins as it does in amino acids and peptides. Cohn and Edsall (19) report electrostriction values of 13.5, 16.1, and 16.1 for glycine, glycylglycine, and diglycylglycine, while in this work values of 12.6 and 19.1 ml/mole were obtained for glycine and triglycylglycine, respectively. Thus the effect of electrostriction in proteins must be nullified by a compensating factor. There may be a steric effect due to the folding and packing of the peptide chains whereby a small volume (excluded volume) is rendered inaccessible to solvent (20, 13), although the exchange reactions in heavy water showed a ready accessibility in BPA.

The available and observed $\bar{v}$ values for the macromolecules used in this study are summarized in Table III. Obviously, calculated values can be reported only for materials of known composition and functional groups. Clearly, the sedimentation method with BPA permits evaluation of $\bar{v}$ in complete agreement with calculated and magnetic float values, despite the small $\Delta\bar{v}$ value discussed above. Applied to a mixture of BPA and βLG, the value of $\bar{v}$ for BPA was about 1.5% lower and that for βLG in agreement with the calculated and reported values. The agreement of $\bar{v}$ of lipovitellin by the sedimentation and float methods indicates the applicability of the sedimentation method to lipoproteins. The minor sedimenting component, termed protein X, which always accompanies lipovitellin at pH 9.0, had a $\bar{v}$ value of 0.79±0.03 by the sedimentation method, which serves to distinguish it from γ-livetin, which had a $\bar{v}$ of 0.70±0.02 by sedimentation and 0.726±0.001 by the float method, although these two substances have similar sedimentation and electrophoretic characteristics in aqueous media. It is likely that protein X is a lipoprotein. Although the α–β-livetins could not be resolved sufficiently for accurate measurement of their individual $\bar{v}$ values, the value obtained for the mixture is reasonable for protein material.

It is worth mentioning, perhaps, that values of $\bar{v}$ are obtainable by sedimentation measurements without recourse to knowledge of solute concentration. In fact, the evaluations of $\bar{v}$ from the experiments on mixed macromolecules were made on the basis of relative concentrations only. Also, since the concentrations of the macromolecules in the mixtures were low and extrapolations were made to zero concentration, the Johnston–Ogston effect (21) would be small. In any case, the effect would be similar in aqueous and heavy water solutions.

Can. J. Chem. Downloaded from www.nrcresearchpress.com by 176.9.209.113 on 09/04/12
For personal use only.

Thus it would be possible to obtain $\bar{v}$ of macromolecules even in impure preparations in which resolvable boundaries are evident upon sedimentation in aqueous and heavy water media. A 1-ml sample containing about 10 mg of solute may be dialyzed versus solvent, dilutions made, and sedimentation coefficients determined. Density and viscosity may easily be measured upon the diffusate. The extent of isotopic exchange may be estimated or measured by direct weight increase on a quartz spiral balance of suitable sensitivity. By differentiation of equation [3] it may be estimated that neglect of this factor will introduce an error of about four to six per cent in $\bar{v}$. However, by taking an estimated figure of about 1.015 for k of protein, the error involved would be within the error of the sedimentation method of evaluating the partial specific volumes.

ACKNOWLEDGMENTS

The authors wish to thank Mr. J. Giroux and Mr. D. R. Muirhead for valuable technical assistance.

REFERENCES

1. MARTIN, W. G., COOK, W. H., and WINKLER, C. A. Can. J. Chem. **34**, 809 (1956).
2. LAUFFER, M. A. and BENDET, I. J. The hydration of viruses. *In* Advances in virus research. Vol. II. Academic Press, Inc., New York. 1954. p. 241.
3. SHARP, D. G., BEARD, D., and BEARD, J. W. J. Biol. Chem. **182**, 279 (1950).
4. SHARP, D. G. and BEARD, J. W. J. Biol. Chem. **185**, 247 (1950).
5. CHENG, P. Y. and SCHACHMAN, H. K. J. Polymer Sci. **16**, 19 (1955).
6. KATZ, S. and SCHACHMAN, H. K. Biochim. et Biophys. Acta, **18**, 28 (1955).
7. PLIMMER, R. H. A. J. Chem. Soc. **93**, 1500 (1908).
8. MARTIN, W. G., VANDEGAER, J. E., and COOK, W. H. Can. J. Biochem. and Physiol. **35**, 242 (1957).
9. MARTIN, W. G. and COOK, W. H. Can. J. Biochem. and Physiol. **36**, 153 (1958).
10. JOUBERT, F J. and COOK, W. H. Can. J. Biochem. and Physiol. **36**, 389 (1958).
11. BRICE, B. A. and HALWER, M. J. Opt. Soc. Am. **41**, 1033 (1951).
12. MACINNES, D. A., DAYHOFF, M. O., and RAY, B. R. Rev. Sci. Instr. **22**, 642 (1951).
13. CHARLWOOD, P. A. J. Am. Chem. Soc. **79**, 776 (1957).
14. SPRINGALL, H. D. The structural chemistry of proteins. Butterworth Scientific Publications, London. 1954.
15. MCMEEKIN, T. L. and MARSHALL, K. Science, **116**, 142 (1952).
16. TRAUBE, J. Ann. **290**, 43 (1896).
17. PEDERSEN, K. O. Biochem. J. **30**, 961 (1936).
18. ROBERTSON, J. M. Organic crystals and molecules. Cornell Univ. Press, Ithaca, N.Y. 1953.
19. COHN, E. and EDSALL, J. T. Proteins amino acids and peptides, Reinhold Publishing Corp., New York. 1943.
20. EDSALL, J. T. The proteins. Vol. IB, *Edited by* H. Neurath and K. Bailey. Academic Press, Inc., New York. 1953.
21. JOHNSTON, J. P. and OGSTON, A. G. Trans. Faraday Soc. **42**, 789 (1946).

Can. J. Chem. Downloaded from www.nrcresearchpress.com by 176.9.209.113 on 09/04/12
For personal use only.

Can. J. Chem. Downloaded from www.nrcresearchpress.com by 176.9.209.113 on 09/04/12
For personal use only.

THE MECHANISM OF THE PHOTOOXIDATION OF ACETALDEHYDE AT ROOM TEMPERATURE[1]

JACK G. CALVERT AND PHILIP L. HANST[2]

ABSTRACT

The initial rates of product formation in the photooxidation of acetaldehyde at room temperature have been determined through the use of infrared spectrometry. The rates of formation of the products peroxyacetic acid, carbon monoxide, carbon dioxide, methanol, formic acid, and acetic acid were determined in experiments with various pressures of acetaldehyde, oxygen, and added gases. The amounts of methylhydroperoxide and acetylperoxide formed in all of the experiments were below the detection limit of the analytical methods. The results require that some modification and corrections be made to the mechanism suggested by McDowell and Sharples.

INTRODUCTION

Recently McDowell and Sharples (1) published a series of kinetic studies of the photooxidation of acetaldehyde and propionaldehyde. The reactions were followed by the titration of the peroxyacid formed. Reported here is a study of the photooxidation of acetaldehyde in which a more detailed product analysis has been made through infrared absorption spectroscopy. The results show that the simple mechanism which McDowell and Sharples have inferred from their rate studies is very incomplete, and in some respects, it is incorrect. Some suggested modifications and corrections to their mechanism are presented.

EXPERIMENTAL

Apparatus and Materials

Our experiments were basically similar to those of McDowell and Sharples (1). We used comparable amounts of acetaldehyde in oxygen, and we photolyzed at room temperature with light in the range 3000–3300 Å. In order to accelerate the rates and facilitate the identification of the products of the chain-initiating and chain-terminating reactions, we used intensities about 1000 times those employed by McDowell and Sharples.

The acetaldehyde (Eastman-Kodak, white-label, fractionated at reduced pressure), oxygen (Linde tank gas), and other added gases were mixed in a 10-cm Pyrex-body infrared absorption cell which was mounted in the sample beam of a Perkin–Elmer Model 21 double beam infrared spectrometer. The side of the cell was exposed to the radiation from a Pyrex-jacketed, water-cooled, high pressure mercury arc (AH-6) which was fastened about 10 inches from the cell. The absorption characteristics of the water jacket and the cell body limited the effective radiation to the range 3000–3300 Å. The maximum intensity of the light absorbed by the aldehyde was near 3100 Å.

The other reactant gases and standards for analysis were obtained as follows: tetramethylethylene was the research grade Phillips product; peroxyacetic acid and acetylperoxide were obtained from Becco and purified by distillation at reduced pressure; ozone was prepared as needed by a simple ozonizer apparatus; the oxides of carbon were reagent gases of the Air Reduction Co.; methanol was the Mallinckrodt Analytical

[1]*Manuscript received May 25, 1959.*
Contribution from the McPherson Chemical Laboratory, The Ohio State University, Columbus 10, Ohio.
[2]*Present address: Physics Section, AVCO Research and Advanced Development, Wilmington, Massachusetts, U.S.A.*

Reagent; acetic acid was the DuPont Reagent product; nitrogen was the Linde dry tank gas.

Procedures and Results

The total pressure of the reaction mixture was adjusted to about 740 mm by the addition of nitrogen gas. Infrared absorption spectra of the products of the runs and standard gases were measured under similar conditions of pressure, resolution, and absorption.

The scale expansion feature of the Perkin–Elmer Model 21 infrared spectrometer made possible the determination of initial rates of formation of the products. Since it appears that similar application of this valuable technique has not been made in previous published kinetic studies, we wish to describe the method briefly. The scale expansion enables one to magnify small absorptions by selection of a 5-, 10-, or 20-fold signal amplification. With this amplification "initial" rates are easily measurable on amounts of material which normally would escape detection by infrared analysis. In the study here reported an accurate rate could be determined after only a few tenths of one per cent conversion of the reactants. The concentrations of the products were determined at the characteristic absorption regions: peroxyacetic acid, 8.1 and 3.05 μ; acetic acid, 7.7 μ; carbon dioxide, 4.31 μ; carbon monoxide, 4.63 μ; methanol, 9.68 μ; formic acid, 9.05 μ; methylhydroperoxide, 12.2 μ; acetylperoxide, 8.6 and 11.75 μ; methane, 7.7 μ; ethane, 12.4 μ; acetaldehyde, 3.7, 5.69 μ. There were no unexplained regions of absorption. Illustrative of the rate data obtained by this method is that given in Fig. 1

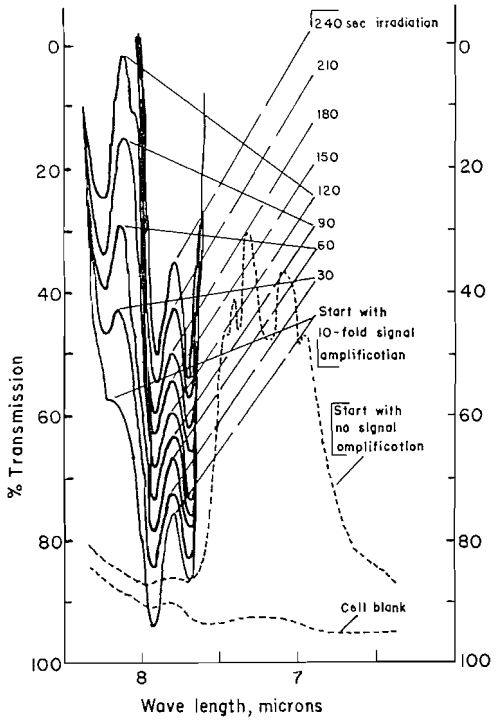

FIG. 1. A typical portion of the infrared absorption spectrum of an irradiated acetaldehyde–oxygen mixture, recorded during run 2 of Table I: the upper dotted curve shows the initial absorption of the mixture without amplification; the multiple peaks at 7.8 (due to CH_3CO_2H) and 8.1 μ (due to CH_3CO_3H) were recorded with a 10-fold signal amplification after successive 30-second exposures.

Can. J. Chem. Downloaded from www.nrcresearchpress.com by 176.9.209.113 on 09/04/12
For personal use only.

Can. J. Chem. Downloaded from www.nrcresearchpress.com by 176.9.209.113 on 09/04/12
For personal use only.

TABLE I

Initial rates of product formation in the photooxidation of acetaldehyde (3000–3300 Å, temperature 20°)

Run No.	Pressure of reactant or added gases, mm			Initial rates of product formed, mm/min					R_{CH_3OH}	$R_{CO_2} + R_{CH_3OH}$
	O_2	CH_3CHO	Added gas	CO_2	CH_3OH	CO	CH_3CO_2H	CH_3CO_3H	R_{CO_2}	$2R_{CH_3CO_3H}$
1	690	42.5	None	0.11	0.13	0.29	—	—	1.2	—
2	650	42.5	N_2, 50	0.12	0.13	0.30	0.020	0.55	1.1	0.23
3	247	42.5	N_2, 471	0.12	0.14	0.32	0.009	0.59	1.2	0.22
4[a]	43	42.5	N_2, 640	0.27	0.32	0.29	0.014	1.15	1.2	0.26
5	25	42.5	N_2, 670	0.29	0.34	0.29	0.015	1.13	1.2	0.28
6	8	42.5	N_2, 680	0.61	0.53	0.29	0.021	1.88	0.9	0.30
7	2	42.5	N_2, 700	—	—	—	0.021	2.29	—	—
8[b]	0	42.5	N_2, 700	0.00	0.00	0.09_4	0.000	0.00	—	—
9	745	5.0	None	0.0059	0.0052	0.026	0.0057	< 0.01	0.9	> 0.56
10	8	5.0	N_2, 730	0.022	0.017	0.025	0.0053	0.026	0.8	0.75
11	650	42.5	CH_3CO_3H, 4	0.14	0.14	—	0.14	loss	1.0	—
12	12	42.5	CH_3CO_3H, 4; N_2, 680	0.31	0.27	0.24	0.063	0.38	0.9	—
13	700	42.5	O_3 < 1	0.87[c]	0.90[c]	0.29	—	—	1.0	—
14[d]	676	42.5	$Me_2C{=}CMe_2$, 20	0.017	0.046	0.18	0.0057	< 0.05	2.7	—
15[d]	11	42.5	$Me_2C{=}CMe_2$, 12	0.0081	0.053	0.12	0.0041	< 0.05	6.5	—

[a]After 10 minutes' exposure there was no detectable amount of CH_3O_2H (on 20-fold amplification) at its absorption band at 12.2 μ or $(CH_3CO_2)_2$ at its 8.6- and 11.8-μ bands; $R_{CH_3O_2H} < 0.003$ mm/minute; $R_{(CH_3CO_2)_2} < 0.0005$ mm/minute.

[b]Other measurable product rates in this O_2-free run were: $R_{C_2H_6} = 0.01_4$; $R_{CH_4} = 0.083$.

[c]These rates have been corrected for a large thermal reaction, so the accuracy of them is not large.

[d]Possible traces of CH_3COCH_3 formed as detected at the characteristic band near 8.2 μ.

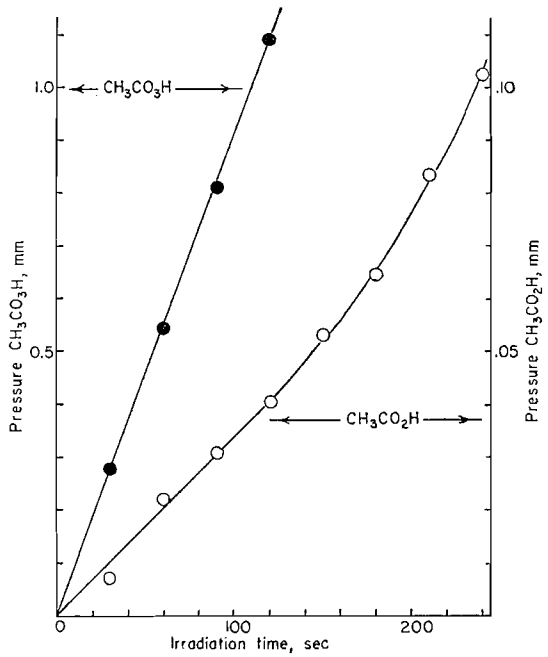

FIG. 2. Pressures of the peracetic acid and acetic acid products as a function of irradiation time (calculated from the data of Fig. 1, and recorded during run 2 of Table I).

(obtained for run 2 of Table I). Shown are the 7.8- (acetic acid) and 8.1-μ (peroxyacetic acid) regions scanned with 10-fold signal amplification after successive exposures each of 30 seconds' duration. These data yielded the product pressure – time plot of Fig. 2. All of the initial product rate data summarized in Table I were obtained from similar absorption measurements.

One of the products of the reaction, formic acid, is not shown in Table I since it was impossible to determine it accurately with small conversions; the major absorption bands

TABLE II

Mass balance of the products of the photooxidation of acetaldehyde at room temperature (experiments with 30 minutes' exposure)

	Run	
	1	2[a]
Pressure O_2, mm	670	670
Pressure CH_3CHO, mm	34	32
Products pressure in mm		
Peroxyacetic acid	2.8	1.4
Acetic acid	0.4	0.2
Methanol	2.6	0.5
Formic acid (as monomer)	2.2	0.5
Carbon dioxide	1.8	0.5
Carbon monoxide	2.0	0.7
Acetylperoxide	None detected	None detected
Methylhydroperoxide	None detected	None detected
Acetaldehyde, unreacted	27.3	29.4
Total acetaldehyde accounted for	34.8	32.4

[a]Intensity of run 2 is about one-third that of run 1; the arc-to-cell distance was increased.

Can. J. Chem. Downloaded from www.nrcresearchpress.com by 176.9.209.113 on 09/04/12
For personal use only.

overlapped those of the reactant, acetaldehyde. A test for the mass balance of the products was made in similar experiments in which a more extensive conversion was allowed (exposure time 30 minutes). These results are shown in Table II. It is seen that an adequate accounting can be made for all of the acetaldehyde which has reacted.

There was no measurable dark reaction between oxygen and acetaldehyde under any of the conditions used. When ozone was added to the oxygen–aldehyde mixture a rapid dark reaction occurred for which correction was made to estimate the "photochemical" rates (run 13, Table I).

DISCUSSION

Limitations of the McDowell and Sharples Mechanism

Our data show that the McDowell and Sharples mechanism (1) of acetaldehyde photooxidation should be revised in several important respects. First, the conventional chain-initiating steps which they suggest involving peroxy radicals seem unimportant for this system:

$$CH_3CHO + h\nu \rightarrow CH_3 + CHO \qquad [I]$$

$$R + O_2 \rightarrow RO_2 \ (R = CH_3 \text{ or } CHO) \qquad [1]$$

$$RO_2 + CH_3CHO \rightarrow RO_2H + CH_3CO. \qquad [2]$$

Methylhydroperoxide, one of the expected products of reaction [2], was below the detection limit of the infrared equipment using the most sensitive 20-fold signal amplification. We estimate that the rate of formation of this product, if formed at all, must be less than 0.003 mm/minute. If this result is coupled with the facts that the chain lengths are relatively short in our experiments,* and methylhydroperoxide is comparatively stable under the conditions used (2), then reaction [2] of the McDowell and Sharples mechanism must be unimportant in the photooxidation of acetaldehyde.

Secondly, the expected product of the termination step of the McDowell and Sharples mechanism, acetylperoxide, was not formed in detectable quantities in our experiments; its rate of formation in run 4 of Table I must have been less than 0.0005 mm/minute, if it was formed at all. Obviously, one should question the McDowell and Sharples assignment of the kinetic rate constant of the termination reaction derived from rotating sector experiments to the reaction [3]:

$$2CH_3CO_3 \rightarrow (CH_3CO)_2O_2 + O_2. \qquad [3]$$

Thirdly, cognizance should be taken of the variety of products other than peroxyacetic acid which are formed in the photooxidation of acetaldehyde, as they are not insignificant, and a proper consideration of them should help in the correct mechanism choice.

Revised Mechanism of Acetaldehyde Photooxidation

In view of our findings in the study of the azomethane photooxidation (2) and data here presented, we favor a mechanism of acetaldehyde photooxidation involving ozone as an intermediate product. Ozone has not been detected by direct spectroscopic observations in the irradiated acetaldehyde–oxygen system. However, it is a reasonable extrapolation

*$\Phi_{CO} \cong 0.2$ *in the oxygen-free acetaldehyde photolysis at 25° and 3130 Å (3). Using the rate data of Table I, run 8 (in the absence of oxygen) and run 7, one estimates the maximum chain length for peroxyacetic acid formation in these experiments to be about 20; this assumes that the primary efficiency of free radical formation in acetaldehyde photolyses at 3130 Å is 0.2 (4, 5). The estimate of chain length represents a maximum since the primary efficiency may be considerably higher (0.8) in experiments at low oxygen pressures. See the discussion in the section on the primary efficiency.*

Can. J. Chem. Downloaded from www.nrcresearchpress.com by 176.9.209.113 on 09/04/12
For personal use only.

to this system from the systems in which it has been observed. If we accept the hypothesis of ozone participation in the mechanism, we expect the steady state concentration of ozone to be very low (10^{-3} to 10^{-5} mm) because of its rapid reaction [4] with free radicals.

$$O_3 + R \rightarrow RO + O_2 \qquad [4]$$

Reaction [4] would not have the three-body restriction which has been observed for the reaction of methyl radicals with O_2 (6, 7, 8), and it would be considerably faster. We consider the mechanism here proposed to be a reasonable postulate which is consistent with the facts at hand and is worthy of further testing.

Chain-initiating Steps

It is probable that the formation of CH_3O_2 (and CHO_3) radicals in the photooxidation of acetaldehyde occurs as the first step in the reaction of CH_3 (and CHO) with O_2. The fact that the expected products, CH_3O_2H and HCO_3H, are not found in the photooxidation of acetaldehyde, but rather CH_3OH and HCO_2H are observed, suggests the rapid removal of these radicals by some other path than H-abstraction. We feel that the removal of CH_3O_2 (and HCO_3) may occur either by the mechanism of Bell and coworkers (9),

$$2CH_3O_2 \rightarrow 2CH_3O + O_2, \qquad [5]$$

or by the alternative reactions which we have favored in the azomethane photooxidation (2);

$$CH_3O_2 + O_2 \rightarrow CH_3O + O_3 \qquad [6]$$

$$HCO_3 + O_2 \rightarrow HCO_2 + O_3. \qquad [7]$$

In either case chain initiation in the photooxidation of acetaldehyde is presumed to involve the CH_3O and HCO_2 radicals; this interpretation is consistent with the observed products. If reaction [5] were the source of CH_3O we would expect some H-abstraction from aldehyde and a detectable yield of CH_3O_2H (the rate of [5] is proportional to $[CH_3O_2]^2$); to expect this reaction to occur to the exclusion of [2], whose rate is proportional to $[CH_3O_2][CH_3CHO]$, seems unrealistic. Thus we favor the alternative mechanism of CH_3O and HCO_2 formation in reactions [6] and [7].

Chain-termination Reactions

Some obvious alternatives to the unobserved acetylperoxide formation for chain termination are reactions [8], [9], and [10]:

$$2CH_3O \rightarrow CH_3OH + CH_2O \qquad [8]$$

$$CH_3O + CH_3CO_3 \rightarrow CH_2O + CH_3CO_3H \qquad [9]$$

$$CH_3O + CH_3CO_2 \rightarrow CH_2O + CH_3CO_2H. \qquad [10]$$

Under our conditions CH_2O would be rapidly converted to CHO_2H, with small amounts of CO, CO_2, and possibly other products (2).

The Efficiency of Radical Formation in Acetaldehyde Photooxidation

Note in Fig. 3 the increase in the rate of formation of the peroxyacetic acid, methanol, and carbon dioxide products as the oxygen pressure is lowered. We interpret this to indicate an increased quantum efficiency of radical formation at the lower oxygen pressures. That is, a certain fraction of the excited acetaldehyde molecules are deactivated by oxygen, and the fraction so deactivated before the possible decomposition into radicals decreases with decrease in oxygen pressure. With this interpretation we estimate from

Can. J. Chem. Downloaded from www.nrcresearchpress.com by 176.9.209.113 on 09/04/12
For personal use only.

the relative rates of CH_3CO_3H formation at the high and the low oxygen pressures that about 76% of the electronically excited ($\lambda \cong 3100$ Å) molecules of acetaldehyde which normally decompose in the absence of oxygen can be deactivated at the high concentrations of oxygen. This value checks well with the observed deactivation of 3130 Å light-activated acetaldehyde by added iodine. In this case it has been estimated that 75% of the electronically excited aldehyde molecules which decompose in the absence of iodine are deactivated when iodine is added (10).

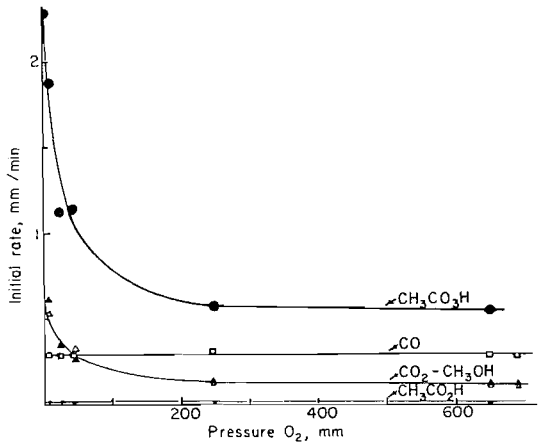

FIG. 3. Initial rates of formation of products of the photooxidation of acetaldehyde as a function of oxygen pressure: $P_{CH_3CHO} = 42.5$ mm; $P_{N_2} + P_{O_2} + P_{CH_3CHO} \cong 740$ mm; wave lengths of absorbed light, 3000–3300 Å; temperature, 20°.

Mechanism of Formation of CO_2 *and* CH_3OH

From the data of Table I the ratio R_{CH_3OH}/R_{CO_2} is seen to be near unity. In Fig. 3 it is seen that the rate of increase of CO_2 and CH_3OH at low oxygen pressures parallels that for CH_3CO_3H. In view of these results we first postulated that the CO_2 and CH_3OH arose from the thermal or photochemical decomposition of a portion of the primary product peroxyacetic acid. However, the initial rates of formation of CO_2 and CH_3OH are not measurably increased when peroxyacetic acid is added at the start of the run (see runs 11 and 12 of Table I), so that these products clearly are not derived from peroxyacetic acid. The only difference in the runs with added peroxyacid is the acceleration of the rate of CH_3CO_2H formation. This effect will be described later.

If we accept the conversion of CH_3 to CH_3O in the acetaldehyde–oxygen system, then there are several alternatives which may be considered in the explanation of the CO_2 and CH_3OH rate data.

$$CH_3CO_3 + M \rightarrow CH_3O + CO_2 + M \quad [11]$$

$$CH_3CO_3 + O_2 \rightarrow CH_3CO_2 + O_3 \quad [12]$$

$$CH_3CO + O_3 \rightarrow CH_3CO_2 + O_2 \quad [13]$$

$$CH_3CO_2 \rightarrow CH_3 + CO_2. \quad [14]$$

The relative constancy of the ratio, $(R_{CO_2} + R_{CH_3OH})/2R_{CH_3CO_3H}$, of Table I, is consistent with the occurrence of reaction [11], provided that the CH_3CO_3 radical decomposition is in the second order region and that [11] is usually followed by CH_3OH formation

Can. J. Chem. Downloaded from www.nrcresearchpress.com by 176.9.209.113 on 09/04/12
For personal use only.

by H-abstraction. It is likely that peroxyacetic acid is formed in the chain-propagating reaction [15], which is commonly proposed.

$$CH_3CO_3 + CH_3CHO \rightarrow CH_3CO_3H + CH_3CO. \qquad [15]$$

If we assume that [11] and [15] are homogeneous reactions and that these reactions are the major sources of the CO_2, CH_3OH, and CH_3CO_3H, then we can explain the small variation of the ratio, $(R_{CO_2} + R_{CH_3OH})/2R_{CH_3CO_3H}$, in terms of the differences in the efficiencies of CH_3CHO, O_2, and N_2 as M in reaction [11]. However, the increase in this ratio at low aldehyde pressures suggests that CH_3CHO is a poorer M than N_2 and O_2, a result which is unexpected.

We favor the alternative reactions for CO_2 and CH_3OH formation, [12], [13], and [14]; these suggest the formation and participation of ozone. In terms of this mechanism choice, the observed simultaneous increase in CH_3OH, CO_2, and CH_3CO_3H can be rationalized as follows: as the oxygen pressure is lowered, the rate of radical formation from the photodecomposition of acetaldehyde is increased; assuming reactions [6] and [7], we expect the ozone concentration to increase, and thus [13] and [14] would become more important. As the ratio of $[O_2]/[CH_3CHO]$ is increased, one expects that the fraction of the CH_3CO_3 radicals which form peroxyacetic acid in [15] would decrease compared to that reacting by [12]. This is the trend observed in the last column of Table I.

Some support for the participation of ozone in the photooxidation of acetaldehyde was obtained in runs 13, 14, and 15 of Table I. In run 13 a small quantity of ozone was added at the start of the run. Ozone initiates the thermal oxidation of acetaldehyde, and dark reaction was observed. However, after correction for the large dark rates, the "photochemical" rates of CO_2 and CH_3OH formation were much in excess of their normal values; compare runs 2 and 13 of Table I. The conclusions from this experiment are not unambiguous, but the results provide indirect support of the reactions [13] and [14]. In experiments 14 and 15 quantities of tetramethylethylene were added to the acetaldehyde–oxygen mixture. The indication of a trace of infrared light absorption near 8.2 μ suggests the formation of CH_3COCH_3 in these experiments. We have interpreted this as evidence for the presence of ozone in these experiments; ozone reacts rapidly with tetramethylethylene to form acetone (2). The amount of acetone formed in these experiments was much less than that found in the azomethane–oxygen–tetramethylethylene experiments reported previously (2), but the thermal reactivity of ozone with acetaldehyde might account for the difference.

Until the spectroscopic tests for ozone in the irradiated acetaldehyde–oxygen mixtures are made, one can consider ozone participation only as an interesting possibility, but we feel that there is strong indirect evidence that favors its consideration.

The Formation of Carbon Monoxide and Acetic Acid

The mechanism of formation of carbon monoxide and acetic acid is by no means clear from this work. It has been demonstrated that peroxyacetic acid is converted to acetic acid in the irradiated aldehyde–oxygen mixtures (see runs 11 and 12 of Table I). The acceleration of rate of formation of acetic acid with time is apparent in Fig. 2, even after only 2 minutes of irradiation. However, initial rates of formation of acetic acid do not parallel those of the peroxyacetic acid, so that the origin of the acetic acid formed initially by the conversion of peroxyacetic acid is ruled out. Perhaps the acetic acid is formed from CH_3CO_2 radicals which do not react entirely by [14] but to a minor extent abstract hydrogen from acetaldehyde or disproportionate with CH_3O reaction [11]. The alternative of acetic acid formation directly from electronically excited acetaldehyde molecules can not be excluded.

Can. J. Chem. Downloaded from www.nrcresearchpress.com by 176.9.209.113 on 09/04/12
For personal use only.

There are several possible sources of CO, for example, CH_2O photodecomposition, or reactions of the radicals, HCO, HCO_3, and CH_3CO. It appears to be formed in non-chain processes at a rate proportional to the absorbed light intensity.

In conclusion it should be stated that the photooxidation of acetaldehyde is a complex process, quite different from the simple oxidation mechanism which seems to be accepted currently. Much additional experimentation will be necessary to establish many of the interesting details of this reaction.

ACKNOWLEDGMENT

The authors gratefully acknowledge the financial support of this work by the United States Public Health Service, National Institutes of Health, Bethesda, Maryland.

REFERENCES

1. McDOWELL, C. A. and SHARPLES, L. K. Can. J. Chem. **36**, 251 (1958).
2. HANST, P. L. and CALVERT, J. G. J. Phys. Chem. **63**, 71 (1959).
3. LEIGHTON, P. A. and BLACET, F. E. J. Am. Chem. Soc. **55**, 1766 (1933).
4. BLACET, F. E. and HELDMAN, J. D. J. Am. Chem. Soc. **64**, 889 (1942).
5. BLACET, F. E. and LOEFFLER, D. E. J. Am. Chem. Soc. **64**, 893 (1942).
6. HOARE, D. E. and WALSH, A. D. Trans. Faraday Soc. **53**, 1102 (1957).
7. CHRISTIE, M. I. Proc. Roy. Soc. (London), A, **224**, 411 (1958).
8. SLEPPY, W. C. and CALVERT, J. G. J. Am. Chem. Soc. **81**, 769 (1959).
9. BELL, E. R., RALEY, J. H., SEUBOLD, F. H., and VAUGHAN, W. E. Discussions Faraday Soc. **10**, 242 (1951).
10. CALVERT, J. G., PITTS, J. N., JR., and THOMPSON, D. D. J. Am. Chem. Soc. **78**, 4239 (1956).

Can. J. Chem. Downloaded from www.nrcresearchpress.com by 176.9.209.113 on 09/04/12
For personal use only.

Can. J. Chem. Downloaded from www.nrcresearchpress.com by 176.9.209.113 on 09/04/12
For personal use only.

THE STUDY OF ELECTRICALLY DISCHARGED O_2 BY MEANS OF AN ISOTHERMAL CALORIMETRIC DETECTOR[1]

L. ELIAS, E. A. OGRYZLO,[2] AND H. I. SCHIFF

ABSTRACT

Molecular oxygen was subjected to an electrodeless discharge in the pressure range 0.1–3 mm Hg. The oxygen atom concentration was measured as a function of time in a flow system by means of a movable atom detector which consisted of a platinum wire coated with a suitable catalyst for atom recombination. The atom concentration was calculated from the heat liberated when the detector was operated under isothermal conditions. The surface recombination was found to be first order in the atom concentration. A value of 7.7×10^{-5} was obtained for the recombination coefficient (γ) on Pyrex. No temperature dependence for γ was observed. The gas phase recombination of oxygen atoms was found to be consistent with the mechanism

$$O + O_2 + M \rightarrow O_3 + M$$
$$O + O_3 \rightarrow 2O_2$$

The rate constant for the third-order reaction was found to have a value of 1.0×10^{14} cc^2 mole^{-2} sec^{-1}, and a small negative temperature dependence.

Evidence was also obtained for the presence of considerable amounts of excited molecular oxygen in electrically activated O_2.

INTRODUCTION

Considerable interest has been shown recently in the reactions of atomic oxygen, particularly those which occur in the upper atmosphere. To study the rates of recombination or reaction of oxygen atoms, it is necessary to know how their concentration changes with time. Such rapid reactions are often best studied in flow systems with movable atom detectors. Of the various methods available for measuring atom concentrations, isothermal calorimetry appears to be the most readily adaptable for use as a movable probe. This method was used successfully by Tollefson and Le Roy (1) to study the kinetics of hydrogen atom reactions. They measured the heat liberated by the recombination of H-atoms on a platinum or tungsten wire mounted on an adjustable column of mercury. The same technique has been used in the present study with minor modifications.

The present work was undertaken to study the kinetics of the recombination of oxygen atoms obtained by subjecting molecular oxygen to an electrical discharge. In the course of the investigation, evidence was obtained which strongly suggests the presence of considerable amounts of excited molecular oxygen.

EXPERIMENTAL

Principle of the Method

Normal oxygen is passed over a spiral of platinum wire coated with a material of high catalytic activity for recombining atoms. A known electric current "i_0" is passed through the wire, and its resistance R is measured. The gas is then activated by electrical discharge. The atoms which reach the wire are recombined on its surface. To compensate for the heat liberated by the atom recombination, the current through the wire is reduced to some new value "i", such that its resistance, and consequently its temperature, is restored

[1]*Manuscript received June 18, 1959.*
Contribution from the Department of Chemistry, McGill University, Montreal, Quebec. This work has been supported in part by the Air Force Cambridge Research Center under Contract No. AF19(604)-1488, and in part by the Defence Research Board of Canada.
[2]*Holder, National Research Council Fellowship 1956–58.*

to the initial value. The difference in electrical energy required to keep the wire isothermal can readily be calculated from the relation:

$$[1] \qquad \Delta W = R(i_0^2 - i^2).$$

Since the temperature of the wire is the same in the presence and in the absence of atoms, loss of heat by radiation or conduction through the leads should be unaltered. Thus, if the wire removes all the atoms from the gas stream, the flow rate of atoms F_0 can be deduced from the equation

$$[2] \qquad F_0 = \Delta W/\Delta H$$

where ΔH is the heat of atom recombination, 58.5 kcal/mole of O-atoms. The validity of this relation will be considered below.

Materials

Reproducible results could be obtained only when the nitrogen content in the oxygen was low. The presence of this impurity could be detected readily from the afterglow produced by the reaction of O-atoms with the NO formed in the discharge. U.S.P. grade tank oxygen supplied by Linde Air Products, rated at less than 0.1% nitrogen, was used. Oxygen was also produced by thermal decomposition of $KMnO_4$ and from liquified tank oxygen from which the first 80% of the distillate had been discarded. The oxygen from all three sources gave identical results for the recombination rates.

Nitric oxide, obtained from the Matheson Company, was purified by repeated trap-to-trap distillations; NO_2 was made by reaction of NO with O_2. All other gases were commercial products of reagent grade purity.

Apparatus

A conventional flow system was used for all experiments. A linear velocity of 20 to 40 cm/sec and a pressure of 0.5 to 5 mm Hg was found to be suitable for atom recombination studies. The flow rates of all gases were adjusted by means of fine-control needle valves and measured by calibrated U-tube flowmeters. All mercury surfaces were covered with "octoil".

The oxygen was activated by a "Raytheon" microwave generator operating at 2450 Mc/sec with a maximum power output of 125 w. The discharge could be excited in a 13 mm O.D. quartz tube over a pressure range from 0.1 to 20 mm Hg. The use of a Pyrex rather than a quartz tube resulted in some foreign material being liberated from the glass which produced erratic results.

The discharge tube was connected at A by a 20-cm length of Pyrex tubing to the reaction tube shown in Fig. 1; the inner diameter was 17.5 mm and its length was 35 cm. It was surrounded by a jacket B through which thermostatted liquid could be circulated and which was, in turn, surrounded by a vacuum jacket C. Inert gases, NO and NO_2 were introduced at G into the gas stream through a multiple jet located a few centimeters below the top of the jackets. The pressure was measured by McLeod gauges connected at M_1 and M_2. The reaction tube was cleaned frequently with dilute solutions of HF.

The detector D_1 was mounted on a rack which could be moved by rotation of a pinion attached to a standard taper joint equipped with an "O"-ring. The platinum ring R was attached to the top of the rack to ensure that the detector maintained a central position in the reaction tube.

The movable detector D_1, and the stationary detector D_2, were made of 60-cm lengths of No. 30 gauge platinum wire coiled into spirals. Since platinum was found to be in-

Can. J. Chem. Downloaded from www.nrcresearchpress.com by 176.9.209.113 on 09/04/12
For personal use only.

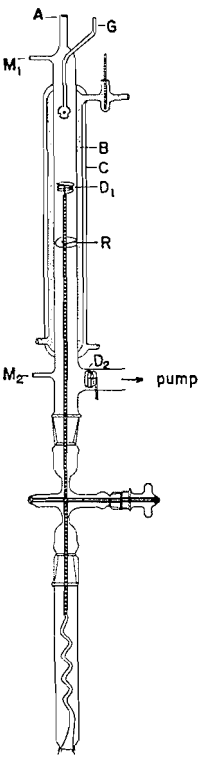

FIG. 1. Reaction tube: A, O_2 and O entry; G, multiple jet for reactant entry; M_1 and M_2, McLeod gauges; B, thermostatting jacket; C, vacuum jacket; D_1, movable detector; D_2, fixed detector.

efficient in recombining O-atoms, a layer of silver was deposited on the wire by electrolysis. A more adherent coating was obtained by heating the electroplated wire until the surface became shiny. When subjected to an atmosphere containing O-atoms, the metal is rapidly converted to the oxide, which forms an excellent catalyst for O-atom recombination.[3]

The oxides of cobalt, nickel, manganese, and copper were also found to be good catalysts. For the length of platinum wire used, zinc and cadmium coatings were only about half as efficient in destroying the atoms.

The detector formed one arm of a Wheatstone bridge. The current through the detector was determined from the potential drop across a standard resistor forming the adjacent arm of the bridge. To keep the bridge in balance when the oxygen was activated, the current through the detector was altered by means of a variable resistor in series with the bridge.

RESULTS AND DISCUSSION

(1) *Test of Detector*

Equation [2] is valid only if the detector removes all the atoms from the gas stream. To test this, measurements were made simultaneously with detectors D_1 and D_2. When the movable detector D_1 was above the pumping lead, D_2 showed no heat effect. When D_1 was lowered below the pumping lead, D_2 showed the same change in wattage previously shown by D_1 when it was just above the pumping lead.

A further test for the catalytic activity of the detector is obtained when a small amount

[3]*A stable detector could not be made from silver metal, since the thickness of the oxide layer would change with time.*

Can. J. Chem. Downloaded from www.nrcresearchpress.com by 176.9.209.113 on 09/04/12
For personal use only.

of NO is added to the gas stream. The green glow resulting from the reaction

$$O + NO \rightarrow NO_2 + h\nu$$

provides a very sensitive test for the presence of O-atoms.[4]

The glow was found to be completely extinguished by the detector. The sharp discontinuity of the glow at the detector also indicated that the rate of removal of atoms from the gas stream was controlled by the linear flow rate of the gas, and not by diffusion resulting from the atom concentration gradient established at the detector.

If the heat measured corresponds to the heat of recombination of all the atoms, it should be independent of the detector temperature. For the silver detector used, this was found to be true up to a detector temperature of 100° C. At higher temperatures the measured atom concentration decreased, and the NO–O glow was seen to extend beyond the detector. The temperature at which this occurs depends on the size of the detector. This indicated that, as the temperature increases, the silver oxide surface becomes less efficient, so that a larger surface area is required to effect complete recombination.

This observation is interesting for another reason. The method can be criticized on the grounds that the temperature distribution along the detector will be different when it is heated electrically only, and when the upper rings of the spiral are also heated by atom recombination, even though the electrical resistance may be the same in both cases. However, the atom concentration measured when the atoms are recombined on the first few rings (at the lower temperatures) was the same as when a number of rings were required (at higher temperatures). This effect must therefore be negligible.

(*2*) *Effect of Thermal Conductivity*

If the detector is to operate under truly isothermal conditions, it is necessary for the rate of heat loss to be identical in the presence and in the absence of atoms. This condition will be satisfied for radiation and conduction along the leads. However, the heat lost by conductivity in the gas could be altered if the gas temperature or composition changes upon activation of the gas.

The temperature of the discharged gas was measured by substituting a 1-mm glass-covered thermistor for the detector. Argon and helium, passed through the discharge at the same pressure, showed no increase in temperature at distances greater than 10 cm beyond the discharge. A maximum temperature rise of 2° C was observed in the center of an activated O_2 stream at the same distance. To determine the effect of such a temperature change on the detector readings, normal oxygen, initially at 25° C, was passed through the reaction tube which was thermostatted at 5° C. The difference in electrical energy required to keep the temperature of the wire constant at the top and in the middle of the reaction tube was found to be less than 0.004 w. This can be compared with a maximum value of 0.03 w calculated from the heat capacity of the oxygen. The heat given to the detector by atom recombination is in the order of 1.0 w. Thus, the effect of a 2° rise in gas temperature will be well within experimental error.

The change in thermal conductivity due to change in composition of the oxygen when it is subjected to electrical discharge will also have a negligible effect on the detector readings. The steady-state ozone concentration is very low, while excited molecular oxygen will not be expected to have a thermal conductivity appreciably different from normal oxygen. The slight change in thermal conductivity due to the presence of O-atoms above the detector would be expected to produce a change in detector reading which is less than the experimental error.

[4]*The glow also provides a good test for the design of the inlet jet, since the mixing pattern can be readily observed. Furthermore, it can be used to determine the upper limit of reactant flow rate in an O-atom reaction which can be used before encountering back diffusion of reactant.*

Can. J. Chem. Downloaded from www.nrcresearchpress.com by 176.9.209.113 on 09/04/12
For personal use only.

Can. J. Chem. Downloaded from www.nrcresearchpress.com by 176.9.209.113 on 09/04/12
For personal use only.

(3) Comparison with other Techniques for Determining Atom Concentrations

Experiments with discharges through mixtures of oxygen and argon or helium at a fixed total pressure showed that the ratio of atomic to molecular oxygen increased as the partial pressure of oxygen in the mixture decreased. An attempt was therefore made to prepare a known atom concentration by complete dissociation. However, the maximum atom concentration measured by the detector never exceeded 85% of that corresponding to complete dissociation. It is possible that complete dissociation could not be achieved in this way.

A comparison was made between the atom concentrations measured by the detector and by a Wrede gauge (2). The gauge was constructed from a fritted disk having a maximum pore diameter of 5 μ; the pressure difference across the disk was measured with a sensitive pressure transducer (Statham Instrument Co.). A small silver coil was placed near the disk, on the transducer side, to ensure complete atom recombination. Comparisons were made over the pressure range 0.7 to 3.3 mm. In this region the atom concentration measured by the detector was proportional to that measured by the Wrede gauge but higher by about 10%.

An attempt was made to measure the atom concentration by chemical titration. This method had previously been found to be very successful in testing the accuracy of a platinum detector in measuring deuterium atom concentrations (3). Since the reaction between D-atoms and ethylene is very rapid, introduction of an excess of C_2H_4 consumed all the D-atoms within a few millimeters of the inlet jet. The amount of deuterium atoms in the products was determined mass spectrometrically and used to calculate the atom concentration. The concentrations determined in this manner were found to agree with those determined by the detector within 0.5%.

Kaufman (4) has recently used an NO_2 titration for estimating O-atom concentrations. The reaction

$$NO_2 + O \rightarrow NO + O_2 \qquad [1]$$

is much faster than the light-emitting reaction

$$NO + O \rightarrow NO_2 + h\nu. \qquad [2]$$

Consequently, if the flow rate of NO_2 is gradually increased, a glow will be observed until the NO_2 concentration equals the O-atom concentration. At this point all the O-atoms will be consumed by reaction [1] and the glow will recede to the jet. This method was found by us to yield the same atom concentration within experimental error as the method of Spealman and Rodebush (5). These workers titrated the O-atoms with a large excess of NO_2, trapped the products at liquid air temperature, and measured the amount of NO formed. The O-atom concentration measured by NO_2 titration was found to be proportional to that measured by the silver oxide detector but lower by approximately 25%.

(4) Evidence for the Existence of Excited Molecules

The discrepancy between the atom concentrations determined by the detector and by the NO_2 titration may be due to the presence of some other species which does not react with NO_2 but which liberates heat on the detector. A cobalt oxide detector was found to show an even greater discrepancy with the titration value, which suggests that it is an even more efficient surface for deactivating the second species. To test this suggestion, a number of additional experiments were performed.

When the movable detector D_1 (Fig. 1) was coated with cobalt oxide while the fixed

detector D_2 was coated with silver oxide, no heat was liberated on D_2. However, when D_1 was silver oxide while D_2 was cobalt oxide, an appreciable amount of heat was measured by D_2.

When a sufficient amount of C_2H_4 was introduced through the inlet jet to consume all the atoms, the cobalt oxide detector still measured an appreciable quantity of heat. When an excess of NO_2 was used to destroy all the atoms, a silver oxide detector at D_1 measured only a very small amount of heat, while a cobalt detector below this at D_2 measured an amount of heat which was even greater than it measured before the NO_2 was introduced. This could be due to the additional excited O_2* formed in the reaction

$$NO_2 + O \rightarrow NO + O_2^*.$$

When a mercury mirror was deposited just beyond the discharge tube, no atoms passed this point, as evidenced from the lack of glow when NO was introduced through the inlet jet. Nevertheless, heat was liberated on the cobalt detector, which corresponded to over 25% of the heat measured by the detector in the absence of the mercury mirror. The magnitude of this heat effect decreased only very slowly down the reaction tube, thus indicating a long lifetime for the excited species.[5]

Addition of NO, NO_2, CO_2, and C_2H_4 after the mercury mirror had no effect on the heat measured by the cobalt detector. The new species therefore does not appear to be ozone, which is known to react rapidly with NO and C_2H_4.

Norrish and co-workers (6) have presented evidence that vibrationally excited O_2 molecules are deactivated in approximately one collision in 5000 by CO_2, and in one collision in 500 by NO_2. However, addition of these gases in large amounts did not decrease the heat measured by the detector. The species therefore does not appear to be vibrationally excited molecules.

The most likely excited species appears to be electronically excited O_2. If these molecules are in the $^1\Delta g$ state as suggested by Foner and Hudson (7), and by Herron and Schiff (8), the observed heat effect would correspond to about 10% of the gas being present in this form, in agreement with estimates made by these authors.

As a result of these studies, it was learnt that a freshly prepared silver oxide coated detector of the dimensions given would recombine all the atoms but deactivate only a negligible amount of the excited molecules. After five or six experiments the detector measured an increasing proportion of excited molecules and was then replated. Freshly prepared detectors were used to measure the recombination of oxygen atoms.

(5) *Recombination of* O-*Atoms*

The oxygen atom concentration was measured along a 20-cm length of the reaction tube over a pressure range from 0.5 to 5 mm Hg. Figure 2 shows typical second-order, and Fig. 3 typical first-order, plots for the atom concentration – time dependence. It is apparent that the atom recombination follows first-order kinetics. The following mechanism is consistent with these observations:

$$O + \text{wall} \rightarrow \tfrac{1}{2}O_2 + \text{wall} \quad [3]$$

$$O + O_2 + M \rightarrow O_3 + M \quad [4]$$

$$O + O_3 \rightarrow 2O_2 \quad [5]$$

where M is any third body.

[5]*The same effect could be obtained if the atoms were destroyed by addition of* NO_2 *rather than by the mercury deposit.*

Can. J. Chem. Downloaded from www.nrcresearchpress.com by 176.9.209.113 on 09/04/12
For personal use only.

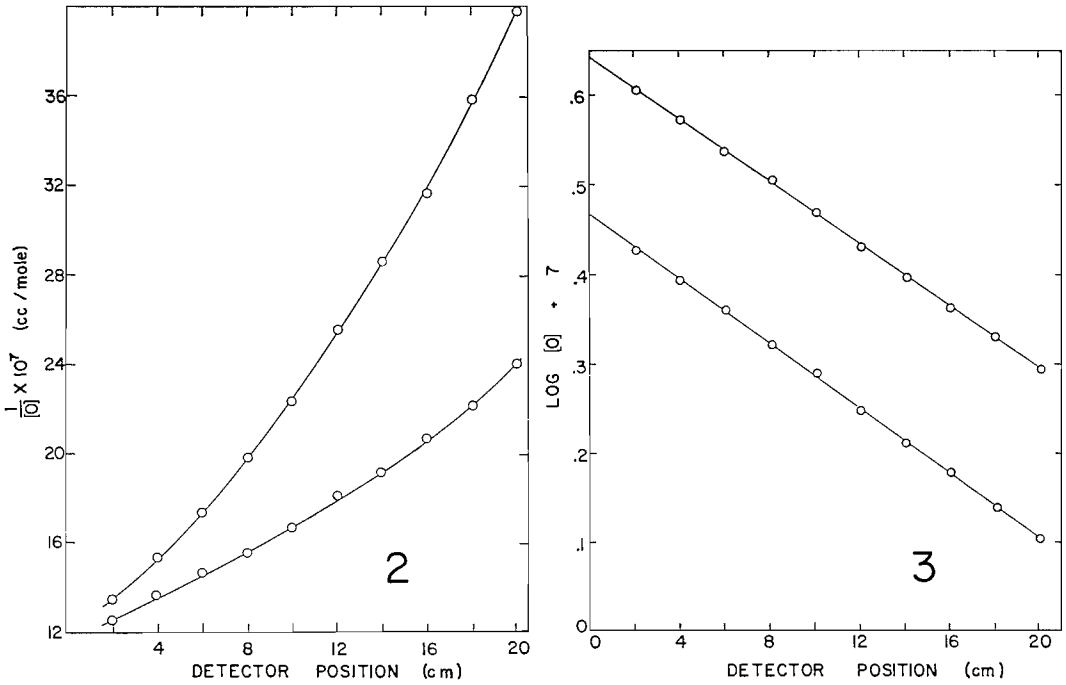

FIG. 2. Typical second-order plots of oxygen atom disappearance.
FIG. 3. Typical first-order plots of oxygen atom disappearance.

A steady-state condition can be assumed for the ozone concentration. Benson and Axworthy (9) give values of 1.3×10^9 cc mole^{-1} sec^{-1} for k_5, and 7.9×10^{13} cc^2 mole^{-2} sec^{-1} for k_4 at 293° K. If O-atoms form 10% of the gas leaving the discharge, calculations show that 70% of the steady-state ozone concentration is attained before the gas enters the reaction vessel at 0.5 mm Hg pressure, and virtually 100% at higher pressures. With this assumption the rate equation for the atom disappearance can be integrated to give:

$$\frac{1}{t}\ln\frac{[O_0]}{[O]} = k_3 + 2k_4[O_2][M]$$

where $[O_0]$ is the atom concentration at the top of the reaction tube, where t is taken as zero.

Figure 4 shows a plot of the left-hand side of this equation against $[O_2][M]$ for M = O_2. The intercept of this curve, k_3, can be used to calculate the surface recombination coefficient γ from the relation:

$$\gamma = 2k_3r/c$$

where r is the radius of the reaction tube and c is the average velocity of the atoms.

The average value of γ obtained from several sets of measurements was 0.77×10^{-4}. This can be compared with the value of 1.2×10^{-4} obtained by Linnett and Marsden (10) and 0.2×10^{-4} by Kaufman (11). Kistiakowsky and Volpi (12) deduced a minimum value of 2×10^{-4} from indirect measurements of N-atom reactions. Herron and Schiff (8) reported a value of 1.1×10^{-4} based on the assumption that all recombinations occur on the wall, and their figure therefore represents an upper limit.

Can. J. Chem. Downloaded from www.nrcresearchpress.com by 176.9.209.113 on 09/04/12
For personal use only.

The slopes of the curves in Fig. 4 yielded an average value for k_4 of 1.0×10^{14} cc^2 mole^{-2} sec^{-1}. This figure is in good agreement with the value of 2×10^{14} cc^2 mole^{-2} sec^{-1} reported by Kaufman (4) and the value of 0.79×10^{14} cc^2 mole^{-2} sec^{-1} obtained by Benson and Axworthy (9) from the thermal decomposition of ozone.

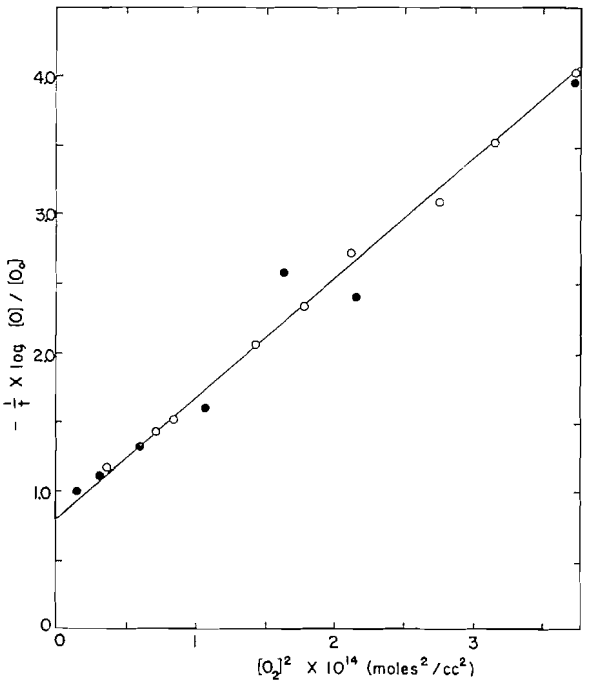

FIG. 4. The dependence of the oxygen atom disappearance on the pressure.

No differences in the rate of recombination were observed when helium or argon molecules were used as third bodies. Addition of CO_2 increased the rate of recombination but in a somewhat erratic way. If CO_2 acts simply as a third body, i.e.

$$O + O_2 + CO_2 \rightarrow O_3 + CO_2, \qquad [6]$$

the integrated rate equation could be written in the form

$$\frac{1}{t}\ln\frac{[O_0]}{[O]} - 2k_4[O_2]^2 = k_3 + 2k_6[O_2][CO_2].$$

A plot of the left-hand side of this equation against $[O_2][CO_2]$ should yield a straight line with slope $2k_6$. However, the data deviated from linear behavior to a larger extent than the estimated experimental error. No unequivocal explanation can be offered for this deviation at the present time. The best straight line through the data gave a value of $k_6 = 2.6\times10^{14}$ cc^2 mole^{-2} sec^{-1}. Thus the relative efficiency of M in reaction [4] was found to be 1.0, 1.0, 1.0, and 2.6 for O_2, He, A, and CO_2 respectively. Kaufman (4) found relative values of 1.0, 1.0, 1.0, and 10 for O_2, A, N_2, and CO_2. Benson and Axworthy (9) found relative values of 1.0, 0.78, 0.93, and 2.4 for O_2, He, N_2, and CO_2.

In order to estimate the effect of temperature on the rate of atom recombination, measurements were made with the reaction tube thermostatted at $-60°$ C. The results are plotted as closed circles in Fig. 4. They suggest that the temperature coefficients for both the gas phase and wall recombinations are zero.

Can. J. Chem. Downloaded from www.nrcresearchpress.com by 176.9.209.113 on 09/04/12
For personal use only.

Can. J. Chem. Downloaded from www.nrcresearchpress.com by 176.9.209.113 on 09/04/12
For personal use only.

However, at this temperature it is doubtful whether the assumption of a steady-state ozone concentration is justified. Benson and Axworthy (9) have reported an activation energy of 6 kcal mole^{-1} for reaction [5], which yields a rate constant for this reaction at $-60°$ C of 2×10^7 cc mole^{-1} sec^{-1}. Assuming that the room temperature steady-state O_3 concentration is achieved before the gas enters the reaction zone, then, at this temperature and at the pressures used in these experiments, the rate of removal of O-atoms by reaction [5] is 400 times slower than by reaction [4], and can therefore be neglected. The integrated rate equation for atom recombination then becomes:

$$\frac{1}{t}\ln\frac{[O_0]}{[O]} = k_3+k_4[O_2][M].$$

On this basis the results obtained indicate no temperature coefficient for k_3 but a small negative Arrhenius activation energy of about 0.7 ± 0.2 kcal mole^{-1} for k_4, which can be compared with a value of 0.6 kcal mole^{-1} reported by Benson and Axworthy (9).

Oxygen atoms recombine much more slowly in the gas phase than do other atoms such as iodine (13, 14, 15), bromine (13, 16), nitrogen (17, 18), or hydrogen (19). Moreover, these atoms recombine by the reaction

$$X + X + M \rightarrow X_2 + M \qquad [7]$$

which is second order in the atom concentration, while the recombination of oxygen atoms was found to be first order in the atom concentration.

The rate of oxygen atom recombination by reactions [4] and [5] relative to recombination by reaction [7] when $M = O_2$ would be

$$\frac{2k_4}{k_7}\frac{[O_2]}{[O]}.$$

Since k_4 was found to be 1.0×10^{14} cc^2 mole^{-2} sec^{-1} and $[O_2]/[O] \simeq 20$ for most of the experiments, the relative rates are $4\times10^{15}/k_7$. If 10% of the recombination had occurred by reaction [7], curvature would have been found in the first-order plots. This leads to the conclusion that $k_7 \leqslant 4\times10^{14}$ cc^2 mole^{-1} sec^{-1}.

Third-order recombination reactions such as [7] can be expressed in terms of elementary reactions by at least three mechanisms:

$$[A]\quad X + X \rightleftharpoons X_2^* \qquad [a]$$
$$X_2^* + M \rightarrow X_2 + M \qquad [b]$$
$$[B]\quad X + M \rightleftharpoons XM^* \qquad [c]$$
$$XM^* + X \rightarrow X_2 + M \qquad [d]$$
$$[C]\quad X + M \rightleftharpoons XM^* \qquad [c]$$
$$XM^* + M' \rightleftharpoons XM + M' \qquad [e]$$
$$XM + X \rightarrow X_2 + M \qquad [f]$$

If reactions [a], [c], and [e] represent equilibria, the rates of atom recombination will be: by mechanism [A]

$$-d[X]/dt = K_a k_b[X]^2[M],$$

by mechanism [B]

$$-d[X]/dt = K_c k_d[X]^2[M],$$

by mechanism [C]

$$-d[X]/dt = K_c K_e k_f[X]^2[M].$$

Mechanism [*A*] predicts the correct order of magnitude for the third-order rate constant for many atom recombinations on the basis of simple collision theory. However, it encounters difficulties in explaining the variation of the rate constant with the nature of the third body, and the negative temperature coefficients observed for these reactions. Keck (20) has recently suggested means of circumventing these difficulties.

Mechanism [*B*] was originally proposed by Rabinowich (21) and is capable of explaining the effects of different third bodies, and the negative temperature coefficients.

Mechanism [*C*] has been strongly supported by Bunker and Davidson (15) to explain their observations of the recombination of iodine atoms. It possesses several inherent advantages over mechanism [*B*]. The negative temperature coefficient is immediately accounted for by the difference in bond strength of XM and the activation energy of reaction [*f*]. The relative efficiencies of third bodies can be explained in terms of the XM bond strength.

The results of the present study can be considered in the light of mechanism [*C*]. In the presence of large amounts of oxygen, $M = O_2$ and $MX = O_3$. Since the bond strength in O_3 is 24 kcal/mole, $k_e \gg k_{-e}$, and a steady-state rather than an equilibrium ozone concentration is established. The mechanism then reduces to that proposed earlier for the disappearance of O-atoms. Under these conditions the over-all third-order reaction becomes first order in [O], in agreement with experiment—a fact which cannot be explained by mechanism [*A*] or [*B*] alone.

Bunker and Davidson (15) have attributed the large differences in the third-body efficiencies for iodine recombination to the differences in the XM bond strengths. In the case of O-atom recombination, added inert gas can only influence reaction [*e*] and only small differences in third-body efficiencies should be observed. Although this is found to be true, Benson and Axworthy (9) report the same order of efficiencies for third bodies in the O-atom system as do Bunker and Davidson (15) in the I-atom system. Further studies of relative third-body efficiencies seem indicated.

REFERENCES

1. Tollefson, E. E. and Le Roy, D. J. J. Chem. Phys. **16**, 1057 (1948).
2. Wrede, E. Instrumentkunde, **48**, 201 (1928).
3. Toby, S. Ph.D. Thesis, McGill University, Montreal. 1955.
4. Kaufman, F. Proc. Roy. Soc. (London), A, **247**, 123 (1958).
5. Spealman, M. L. and Rodebush, W. H. J. Am. Chem. Soc. **57**, 1474 (1935).
6. Libscomb, F. J., Norrish, R. G. W., and Thrush, B. A. Proc. Roy. Soc. A, **233**, 455 (1956).
7. Foner, S. N. and Hudson, R. L. J. Chem. Phys. **25**, 601 (1956).
8. Herron, J. T. and Schiff, H. I. Can. J. Chem. **36**, 1159 (1958).
9. Benson, S. W. and Axworthy, A. E. J. Chem. Phys. **26**, 1718 (1957).
10. Linnett, J. W. and Marsden, D. G. H. Proc. Roy. Soc. (London), A, **234**, 489 (1956).
11. Kaufman, F. J. Chem. Phys. **28**, 352 (1958).
12. Kistiakowski, G. B. and Volpi, G. A. J. Chem. Phys. **27**, 1141 (1957).
13. Strong, R. L., Chien, J. C., Graff, P. E., and Wellard, J. E. J. Chem. Phys. **26**, 1287 (1957).
14. Christie, M. I., Harrison, A. J., Norrish, R. G. W., and Porter, G. Proc. Roy. Soc. (London), A, **231**, 446 (1955).
15. Bunker, D. L. and Davidson, N. J. Am. Chem. Soc. **80**, 5085, 5090 (1958).
16. Britton, D. and Davidson, N. J. Chem. Phys. **25**, 810 (1956).
17. Herron, J. T., Franklin, J. L., Bradt, P., and Dibeler, V. H. J. Chem. Phys. **29**, 230 (1958).
18. Wentinck, T., Sullivan, J. O., and Wray, K. L. J. Chem. Phys. **29**, 231 (1956).
19. Careri, G. J. Chem. Phys. **21**, 749 (1953).
20. Keck, J. C. J. Chem. Phys. **29**, 410 (1958).
21. Rabinowich, E. Trans. Faraday Soc. **33**, 283 (1937).

Can. J. Chem. Downloaded from www.nrcresearchpress.com by 176.9.209.113 on 09/04/12
For personal use only.

Can. J. Chem. Downloaded from www.nrcresearchpress.com by 176.9.209.113 on 09/04/12
For personal use only.

THE REACTION OF OXYGEN ATOMS WITH NO[1, 2]

E. A. Ogryzlo[3] and H. I. Schiff

ABSTRACT

In the reaction between NO and O-atoms, the concentration of NO remains essentially unaltered. The reaction can therefore be considered as a NO-catalyzed recombination of O-atoms. Its rate can be conveniently studied by following the disappearance of O-atoms by an isothermal calorimetric technique. The reaction was found to be third order, first order in the concentrations of O, NO, and M, where M is some third body. The third-order rate constant was found to be 1.85×10^{16} cc^2 mole^{-2} sec^{-1} when M = O_2, A, or He and 2.0×10^{16} cc^2 mole^{-2} sec^{-1} when M = CO_2. The rate constant was found to have a slight negative temperature coefficient which corresponded to a negative Arrhenius activation energy of about 0.2 kcal/mole. A detailed mechanism for the reaction has been proposed.

INTRODUCTION

The preceding paper (1) described an isothermal calorimetric technique for following the rate of disappearance of oxygen atoms. The present section describes the application of this technique to the study of the reaction of O-atoms with nitric oxide. This reaction proceeds by the sequence:

$$O + NO + M \rightarrow NO_2 + M \quad [1]$$

$$O + NO_2 \rightarrow NO + O_2 \quad [2]$$

where M represents some third body. Since reaction [2] is much more rapid than reaction [1] at the pressures used in this study (2, 3), the NO concentration is essentially constant, and the entire reaction may be considered as a NO-catalyzed recombination of O-atoms. It can therefore be studied conveniently by the isothermal calorimetric method.

The purpose of the study was to determine the rate constant for the reaction, and to attempt to learn something of the detailed mechanism.

EXPERIMENTAL

The apparatus, the method of purification of the materials, and the method used to measure the atom concentration have been described in the previous paper (1). The reaction was studied over a total pressure range from 1.21 to 3.05 mm Hg. Helium, argon, and CO_2 were used in addition to O_2 as third bodies; the partial pressures of these gases were varied by a factor of 5. Argon and helium were added with the oxygen through the discharge, while the CO_2 was added through a separate jet in the reaction vessel.

The O-atom concentration was first measured along the reaction tube, in the absence of NO, with a silver oxide detector. NO was then added through the multiple jet inlet and, after steady conditions had been established, the atom concentration was again determined as a function of position in the reaction tube. Finally, the discharge was extinguished and the detector readings again taken to give the "i_0" readings for the conditions obtaining while NO was flowing through the tube.

In the preceding paper (1), evidence was presented to indicate that a freshly prepared silver oxide surface detected O-atoms only and did not detect any excited molecules.

[1]*Manuscript received June 18, 1959.*
Contribution from the Department of Chemistry, McGill University, Montreal, Quebec.
[2]*This work has been supported in part by the Air Force Cambridge Research Center under Contract No. AF19(604)-1488, and in part by the Defence Research Board of Canada.*
[3]*Holder, National Research Council Fellowship 1956–58.*

Since such a detector is imperative for the present work, it was frequently tested by introducing a large excess of NO, sufficient to destroy all the atoms. Under these conditions a satisfactory detector registered no heat effect below the reaction zone (as delineated by the glow). Since studies made with a cobalt oxide detector indicated that NO does not deactivate excited molecules, it can be concluded that the silver oxide detector measures atoms only. Further support for this conclusion will be presented in the following discussion.

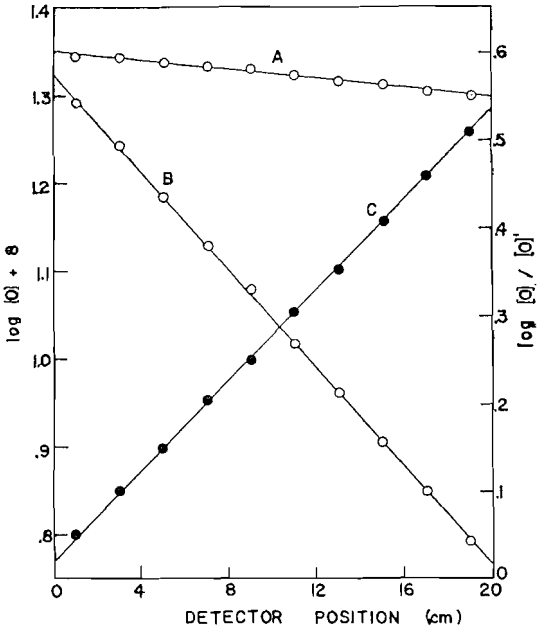

FIG. 1. Oxygen atom decay curves: A, in the absence of NO; B, in the presence of NO; C, the difference between A and B.

RESULTS AND DISCUSSION

Figure 1 shows the O-atom decay curves obtained for a typical experiment. Curve A shows the decrease in O-atom concentration obtained in the absence of NO; curve B shows the more rapid decay of O-atoms in the presence of NO. This decay also appears to be first order in the atom concentration.

It has been shown that, in the absence of NO, the first-order decay of O-atoms is consistent with the mechanism

$$O + W \rightarrow \tfrac{1}{2}O_2 + W \qquad [3]$$

$$O + O_2 + M \rightarrow O_3 + M \qquad [4]$$

$$O + O_3 \rightarrow 2O_2 \qquad [5]$$

where W represents the wall of the reaction vessel.

The integrated rate equation is

$$[i] \qquad \frac{1}{t}\log\frac{[O_0]}{[O]} = k_3[W] + 2k_4[O_2][M]$$

where $[O] = [O_0]$ at $t = 0$.

Can. J. Chem. Downloaded from www.nrcresearchpress.com by 176.9.209.113 on 09/04/12
For personal use only.

When NO is introduced, the following additional reactions may be considered:

$$O + NO + M \rightarrow NO_2 + M \quad [1]$$

$$O + NO_2 \rightarrow NO + O_2 \quad [2]$$

$$O_3 + NO \rightarrow NO_2 + O_2. \quad [6]$$

The reaction of O_3 with NO_2 need not be considered, since it is a relatively slow reaction (4) and the steady-state concentrations of both these species are low.[4]

If steady-state conditions are assumed for both O_3 and NO (or NO_2), the integrated rate equation for O-atom disappearance becomes:

$$[ii] \qquad \frac{1}{t}\log\frac{[O_0]'}{[O]'} = k_3[W]+2k_4[O_2][M]+2k_1[NO][M].$$

Since the flow rate of NO was always kept below 10% of the total flow rate, the values of t and $[O_2]$ in equations $[i]$ and $[ii]$ can be assumed to be identical for the same detector position. The equations can then be subtracted to yield

$$[iii] \qquad \log\frac{[O]}{[O]'} = \log\frac{[O_0]}{[O_0]'}+2tk_1[NO][M].$$

Thus, if the difference of the logarithms of the atom concentrations at a given detector position is plotted against the detector position, a straight line should be obtained with slope equal to $2k_1[NO][M]$. This plot is shown as curve C in Fig. 1. Similar straight line plots were obtained in all cases where the detector measured atoms only. If, however, the detector also measured excited molecules, the plots showed considerable curvature, as

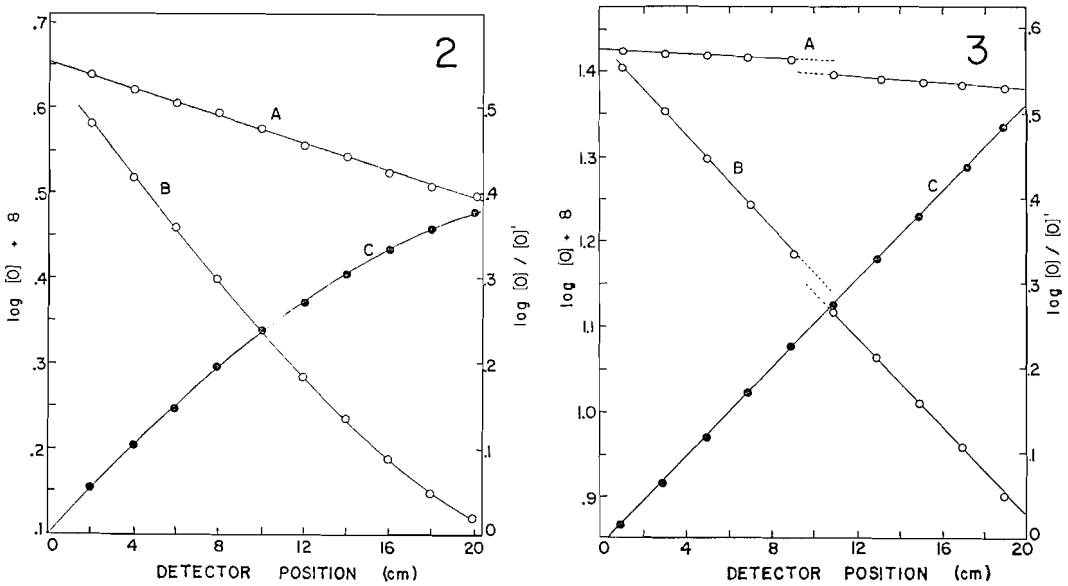

FIG. 2. Oxygen atom decay curves measured with a detector which also measured excited molecules: A, in the absence of NO; B, in the presence of NO; C, the difference between A and B.

FIG. 3. Oxygen atom decay curves showing the effect of a piece of silver placed half way down the reaction tube: A, in the absence of NO; B, in the presence of NO; C, the difference between A and B.

[4]*Similarly, the reactions*

$$NO_2 + O + M \rightarrow NO_3 + M$$

$$NO_3 + O \rightarrow NO + O_2$$

if they occur, can be shown, by using estimates of the rate constants (5), to have a negligible effect on the rate of O-atom disappearance.

Can. J. Chem. Downloaded from www.nrcresearchpress.com by 176.9.209.113 on 09/04/12
For personal use only.

shown in Fig. 2. A detector which gave such a curve always registered a heat effect when sufficient NO was added to consume all the atoms.

There remained the possibility that some reaction might be occurring on the detector. To test this, a piece of silver oxide was placed half way down the reaction tube. The discontinuities in curves A and B of Fig. 3 show that this silver oxide destroys some of the atoms. Nevertheless, the difference curve C shows no discontinuity at this position, which clearly indicates that the NO–O-atom reaction is occurring predominantly in the gas phase.

TABLE I

Expt. No.	Total pressure (mm Hg)	Temp. (° C)	O_2 flow (moles/sec $\times 10^6$)	NO flow (moles/sec $\times 10^6$)	Inert gas flow (moles/sec $\times 10^6$)	Slope (meter^{-1})	$k \times 10^{-16}$ cc^2 mole^{-2} sec^{-1}
A-1	2.14	293	99.0	3.20	—	1.73	1.78
A-2	2.68	293	133.4	3.20	—	1.86	1.73
A-3	2.08	293	95.0	6.87	—	3.44	1.79
A-4	2.08	293	98.0	2.04	—	1.00	1.68
F-3	2.23	293	88.3	3.43	—	2.45	1.97
F-4	2.15	293	88.3	3.43	—	2.72	1.99
E-3	3.27	279	160	3.50	—	2.98	1.75
E-4	1.38	279	55.8	3.50	—	1.91	1.90
					Argon		
D-1	2.87	279	23.4	3.5	107.9	2.61	1.65
D-2	2.36	279	16.3	3.5	92.7	3.25	2.38
D-3	2.12	279	15.0	3.5	82.3	2.06	2.40
D-4	3.05	279	23.4	3.5	122.5	3.72	2.23
D-5	3.16	279	23.4	3.5	131.6	3.34	2.05
D-6	1.84	280	20.0	3.5	61.4	2.56	2.25
D-7	3.34	279	23.4	3.5	146.5	3.43	2.12
F-1	2.72	296	49.1	3.43	67.6	2.70	1.80
F-2	2.23	296	49.1	3.43	43.2	2.52	1.95
F-5	2.71	293	49.1	3.77	67.6	2.45	1.96
					Helium		
E-1	3.21	279	23.4	3.5	131	3.28	1.90
E-2	1.21	279	23.4	3.5	20.0	2.22	2.09
F-6	2.88	293	49.1	3.77	73.6	3.58	1.86
F-7	3.05	279	81.9	1.92	52.7	2.12	1.90
					CO_2		
B-1	2.68	294	46.6	1.30	70.7	0.97	1.75
B-2	2.67	213	46.6	1.30	70.7	2.69	1.90
B-3	2.70	294	44.3	3.40	70.7	2.55	1.70
B-4	2.60	213	46.3	3.40	65.7	8.50	2.26
B-5	2.57	294	24.4	3.50	84.8	3.30	2.40
B-6	2.55	213	25.0	3.50	84.8	10.2	2.70
B-7	2.75	294	51.3	3.50	67.9	3.30	2.15
B-8	2.75	213	51.3	3.50	67.9	9.80	2.40

The results are shown in Table I. The capital letters prefixing the experiment numbers refer to separate series in which the same detector and reaction vessel were employed. Column 7 gives the slope of equation [*iii*].

Inspection of the data indicates that the over-all reaction is third order, first order in the concentrations of atomic oxygen, nitric oxide, and third body. Wall reactions cannot be significant since they would show zero or reciprocal pressure dependence. Helium, argon, and molecular oxygen appear to be equally efficient as third bodies within experimental error. The average value of the rate constant at 20° C is $1.85 \pm 0.10 \times 10^{16}$ cc^2 mole^{-2} sec^{-1} and $2.04 \pm 0.20 \times 10^{16}$ cc^2 mole^{-2} sec^{-1} at 6° C. Although the mean deviations in

Can. J. Chem. Downloaded from www.nrcresearchpress.com by 176.9.209.113 on 09/04/12
For personal use only.

these values would cause them to overlap, there does seem to be an indication of a small negative temperature coefficient. These values can be compared with the value of 1.8×10^{16} cc^2 mole^{-2} sec^{-1} obtained by Ford and Endow (5) at 25° C from a study of the photolysis of NO_2, and the value of 2.5×10^{16} cc^2 mole^{-2} sec^{-1} obtained by Kaufman (6) and the value of 2.7×10^{16} cc^2 mole^{-2} sec^{-1} obtained by Harteck *et al.* (7) from a study of the rate of decrease in the light intensity accompanying this reaction.

Carbon dioxide appears to be more efficient as a third body by about 10%. This is a somewhat smaller effect than found by Kaufman (6), who reported a rate constant for the reaction with CO_2 as third body of $4-5\times10^{16}$ cc^2 mole^{-2} sec^{-1}. An estimate of the temperature coefficient for the reaction can be obtained for the reactions in which CO_2 was introduced. Pairs of experiments in series B were performed in rapid succession with all conditions kept constant with the exception of the reaction tube temperature. The ratios of the rate constants for the pairs B-2 and B-1, B-4 and B-3, B-6 and B-5, B-8 and B-7, are 1.1, 1.3, 1.1, and 1.1 respectively. The average of these ratios corresponds to a negative Arrhenius activation energy of 0.24 kcal/mole.

Mechanism of the Reaction

A third-order association reaction can be analyzed in terms of successive bimolecular collisions. A collision between the two associating partners can be considered to produce a short-lived intermediate which will dissociate again unless it experiences a collision with a third body M, which removes sufficient energy to leave the product in a potential well. Thus, reaction [1] can be considered to be the result of the successive reactions

$$O + NO \rightarrow NO_2^* \quad [7]$$

$$NO_2^* \rightarrow NO + O \quad [8]$$

$$NO_2^* + M \rightarrow NO_2 + M. \quad [9]$$

Reaction [8] must be much faster than reaction [9] if third-order kinetics is to be obtained. The over-all rate will depend mainly on the lifetime of NO_2^*, i.e. on the rate of reaction [8]. Due to its greater number of degrees of freedom, the NO_2^* complex may have a considerably longer lifetime than the complexes formed by collision of two atoms.

An additional fate for the excited NO_2^* must also be considered. The reaction is accompanied by the emission of radiation, in what appears to be a continuum, but might have a closely banded structure. This radiation could be produced in the reaction:

$$NO_2^* \rightarrow NO_2 + h\nu. \quad [10]$$

Kaufman (6) has found that the rate of light emission is much slower than the rate of oxygen atom disappearance in the pressure range used here. This would correspond to the condition that $k_9[M] \gg k_{10}$. This condition, along with the assumption of steady-state concentrations for NO_2^* and NO, can be used to derive an expression for the rate of oxygen atom disappearance in the form:

$$-\frac{d[O]}{dt} = 2\frac{k_7}{k_8}k_9[O][NO][M]$$

in agreement with the empirical rate equation.

Furthermore, it can be readily shown that the rate of light emission is

$$I = \frac{d[h\nu]}{dt} = \frac{k_7}{k_8}k_{10}[NO][O]$$

Can. J. Chem. Downloaded from www.nrcresearchpress.com by 176.9.209.113 on 09/04/12
For personal use only.

in agreement with the second-order dependence found by Kaufman. However, recent studies of the recombination of iodine atoms (8, 9, 10) suggests that an alternate mechanism might be proposed in which M participates in the initial step:

$$O + M \rightarrow OM^* \quad [11]$$

$$OM^* \rightarrow O + M \quad [12]$$

$$OM^* + NO \rightarrow NO_2^{\ddagger} + M \quad [13]$$

$$NO_2^{\ddagger} \rightarrow NO_2 + h\nu \quad [14]$$

$$NO_2^{\ddagger} + M \rightarrow NO_2 + M. \quad [15]$$

This mechanism is also capable of explaining a third-order rate for atom disappearance and a second-order rate for light emission.

The relative importance of the two mechanisms will depend on the relative lifetimes of NO_2^* and OM*. It might be expected that the second mechanism would be much more sensitive to the nature of the third body. For example, one would expect quite different lifetimes for O_3^* and OA*. The observation that O_2 and A seem to be equally efficient as third bodies might therefore be considered to favor the first mechanism. Furthermore, if O_3^* is the excited molecule formed in the first step when O_2 is the third body, one would expect the rate of oxygen atom disappearance to be similar in the presence and in the absence of NO, i.e. the rate of reaction [13] should not change appreciably if O is substituted for NO. However, the presence of NO increased the rate of atom disappearance by at least an order of magnitude.[5]

It might also be argued that the reaction [14] in the second mechanism seems less likely to give rise to a continuum than does reaction [10] since $NO_2^{\ddagger}$ will be more stabilized than NO_2^*. However, Neuberger and Duncan (11) found a "pseudo" continuum emitted when NO_2 was irradiated with light of energies insufficient to cause dissociation, although there may be some doubt as to whether the excited state of NO_2 reached in this way has any connection with the one reached by the NO–O reaction. The data available at present do not permit an unequivocal choice between these two mechanisms. It is hoped that some work currently in progress in these laboratories on the light-emitting step will help in a decision.

REFERENCES

1. ELIAS, L., OGRYZLO, E. A., and SCHIFF, H. I. Can J. Chem. **37**, 1680 (1959).
2. HERRON, J. T. and SCHIFF, H. I. Can. J. Chem. **36**, 1159 (1958).
3. FORD, H. W. and ENDOW, N. J. Chem. Phys. **27**, 1277 (1957).
4. FORD, H. W., DOYLE, G. J., and ENDOW, N. J. Chem. Phys. **26**, 1336 (1957).
5. FORD, H. W. and ENDOW, N. J. Chem. Phys. **27**, 1156 (1957).
6. KAUFMAN, F. Proc. Roy. Soc. (London), A, **247**, 123 (1958).
7. HARTECK, P., REEVES, R. R., and MANNELLA, G. J. Chem. Phys. **29**, 1333 (1958).
8. STRONG, R. L., CHIEN, J. C., GRAFF, P. E., and WELLARD, J. E. J. Chem. Phys. **26**, 1287 (1957).
9. CHRISTIE, M. I., HARRISON, A. J., NORRISH, R. G. W., and PORTER, G. Proc. Roy. Soc. (London), A, **231**, 446 (1955).
10. BUTLER, D. and DAVIDSON, N. J. Chem. Phys. **25**, 810 (1956).
11. NEUBERGER, D. and DUNCAN, A. B. J. Chem. Phys. **22**, 1693 (1954).

[5]*The occurrence of reaction [2] simply doubles the rate of atom consumption.*

Can. J. Chem. Downloaded from www.nrcresearchpress.com by 176.9.209.113 on 09/04/12
For personal use only.

Can. J. Chem. Downloaded from www.nrcresearchpress.com by 176.9.209.113 on 09/04/12
For personal use only.

THE MERCURY-PHOTOSENSITIZED DECOMPOSITION OF BENZALDEHYDE, ACROLEIN, AND CROTONALDEHYDE[1]

A. G. HARRISON[2] AND F. P. LOSSING

ABSTRACT

The Hg^3P_1-photosensitized decomposition of benzaldehyde at low pressure and high radiation intensity forms predominantly a polymeric material. In the fraction of the reaction which forms the identifiable final products benzene and carbon monoxide, both a direct molecular rearrangement and a free radical split to phenyl and formyl radicals occur. The decomposition reactions of acrolein and crotonaldehyde involve the three primary processes:

$$\begin{aligned} RCHO + Hg^* &\rightarrow RH + CO + Hg \\ &\rightarrow R + CHO + Hg \\ &\rightarrow RCO + H + Hg. \end{aligned}$$

INTRODUCTION

In the photolytic and mercury-photosensitized decompositions of aldehydes three possible primary processes can occur:

$$RCHO \rightarrow R + CHO \quad [1]$$

$$RCHO \rightarrow RH + CO \quad [2]$$

$$RCHO \rightarrow RCO + H. \quad [3]$$

Where R is an alkyl group other than methyl, further primary processes involving rearrangements and bond splitting in this group are possible, and the course of the reaction may become quite complicated.

The direct photolysis and the mercury-photosensitized decomposition of acetaldehyde have both been studied in some detail. In the direct photolysis at 2537 to 3130 Å the main primary process is reaction [1], although part of the reaction appears to proceed by reaction [2] (1). In the reaction of acetaldehyde with $Hg(^3P_1)$ atoms (2) the primary decomposition is almost exclusively to form methyl and formyl radicals, although the experimental results could not rule out the possibility that 5% of the reaction proceeded by reaction [2]. There was no evidence for the occurrence of reaction [3].

Very little work has been done on the relative importance of these primary processes when R is an unsaturated group capable of conjugating with the aldehydic function. In this case it might be expected that the proportions of the three possible steps would change. Blacet and Roof (3) studied the photolysis of crotonaldehyde in the 2400–2600 Å region and found no decomposition; however, Volman, Leighton, Blacet, and Brinton (4) found that during the photolysis of crotonaldehyde at 2537 Å tellurium mirrors were removed, indicating the presence of radicals. They postulated the following reaction:

$$CH_3{-}CH{=}CH{-}CHO + h\nu \rightarrow CH_3{-}CH{=}CH + CHO. \quad [4]$$

Blacet, Fielding, and Roof (5) studied the direct photolysis of acrolein and postulated that the primary process was to some extent the following:

$$CH_2{=}CH{-}CHO + h\nu \rightarrow CH_2{=}CH + CHO. \quad [5]$$

[1]*Manuscript received June 18, 1959.*
Contribution from the Division of Pure Chemistry, National Research Council, Ottawa, Canada. Issued as N.R.C. No. 5324.
[2]*National Research Council of Canada Postdoctorate Fellow 1957–59.*

By mirror-removal experiments Volman and co-workers (4) showed that radicals were produced at 2537 and 2810 Å.

No work has been reported on the direct photolysis of benzaldehyde or on the mercury-photosensitized decomposition of any of the three conjugated aldehydes: crotonaldehyde, acrolein, and benzaldehyde. In view of the few results available it was thought that some information on the relative importance of the three primary processes in the mercury-photosensitized decomposition of these aldehydes would be of interest.

EXPERIMENTAL

The reactions were studied by passing the reactant at a few microns pressure, together with mercury vapor, in a stream of helium through a photochemical reactor attached to a mass spectrometer. The apparatus and procedure have been described previously (2, 6, 7).

In recent work (7, 8) the addition of methyl radicals, produced by the photosensitized decomposition of dimethyl mercury, to the reaction products has been found to be a convenient method of detecting free radicals, particularly those which are difficult to detect directly with low energy electrons. This method of detection of a radical R depends on the occurrence of the combination reaction

$$R + CH_3 \rightarrow RCH_3. \qquad [6]$$

It is worth while to consider briefly the conditions upon which the success of this method of radical detection and identification depends. The method will work only if conditions are such that radical recombination reactions predominate over radical attack on stable molecules. Although radical–radical reactions are several orders of magnitude faster than radical–substrate reactions, the concentration of radicals in conventional photochemical work is usually so small that radical–substrate reactions nevertheless predominate. However, as has been pointed out previously (7), conditions in the present reactor are considerably different. In the present system some 10–20% of the parent compound is decomposed in the order of 10^{-3} second with the result that the concentrations of radicals can be relatively high. In the case of acetone (2) the concentration of methyl radicals was approximately 1/10 that of the parent compound for most of the contact time. Under such conditions radical–radical reactions would be expected to predominate.

Of course, as the fraction of the reaction proceeding by a free radical mechanism decreases the occurrence of radical–radical reactions will also decrease. However, when using methyl radicals as a radical detector this effect can be counterbalanced by increasing the amount of methyl radicals added to the system.

The sensitivity of this method for the detection of a radical R is dependent on many variables: among others, the rate of recombination, the ratio of recombination to disproportionation, and the sensitivity of the mass spectrometer to the product RCH_3. It is therefore impossible to put the limits of radical detection by this method on an absolute scale.

Materials

The benzaldehyde, acrolein, and crotonaldehyde were all Eastman-Kodak "White-Label" materials purified by bulb-to-bulb distillation and degassed before use. The benzaldehyde-d_6 was prepared by Dr. L. C. Leitch and was 94.7% pure. The impurity was chiefly benzaldehyde-d_5.

Can. J. Chem. Downloaded from www.nrcresearchpress.com by 176.9.209.113 on 09/04/12
For personal use only.

RESULTS AND DISCUSSION

Benzaldehyde

The only identifiable products found in the mercury-photosensitized decomposition of benzaldehyde were benzene and carbon monoxide. The major part of the reaction ($\sim 80\%$) appeared to proceed to the formation of a yellowish polymer which deposited on the walls of the reactor and rapidly caused a reduction in the amount of light transmitted. As the results in Table I show, the amounts of benzene and carbon monoxide produced were equal, suggesting that the deposit was a polymer of benzaldehyde and not of one of the reaction products.

TABLE I
Benzaldehyde decomposition

Benzaldehyde decomposed		Products		Yield (%)	
(μ)	(%)	C_6H_6	CO	C_6H_6	CO
0.92	11.7	0.166	0.172	18.1	18.8

No radicals could be detected at low electron energies. A search was therefore made for radicals by the addition of methyl radicals as previously discussed. Upon the addition of methyl radicals a peak at mass 92 of approximately 7 mm was produced. A peak was also produced at mass 91, the intensities at mass 92 and 91 being in the correct ratio for toluene. These results demonstrate the presence of the phenyl radical in the system, suggesting as a primary step the reaction:

$$C_6H_5CHO + Hg^* \rightarrow C_6H_5 + CHO + Hg. \quad [7]$$

However, one cannot rule out the possibility that the primary reaction proceeds by the formation of the benzoyl radical, which then rapidly decomposes to form a phenyl radical and carbon monoxide.

$$C_6H_5CHO + Hg^* \rightarrow C_6H_5CO + H + Hg \quad [8]$$

$$C_6H_5CO \rightarrow C_6H_5 + CO \quad [9]$$

No formation of acetophenone, the addition product of C_6H_5CO and CH_3, was observed, indicating that the C_6H_5CO concentration was very small. An estimate of the bond dissociation energy $D(C_6H_5—CO)$ can be made from the heat of formation of CO and recent estimates of the heat of formation of the phenyl radical ($\Delta H_f = 70$ kcal/mole) (9) and the benzoyl radical ($\Delta H_f = 15.6$ kcal/mole) (10). These values lead to $D(C_6H_5—CO) = 28$ kcal/mole. Since the benzoyl radical should therefore be stable at 55° C, the failure to detect it either directly or by CH_3 addition must be taken as evidence that reaction [8] does not occur to a significant extent.

Reaction [7] undoubtedly occurs to some extent, the observed products benzene and carbon monoxide being formed by the subsequent reaction:

$$C_6H_5 + CHO \rightarrow C_6H_6 + CO. \quad [10]$$

To determine the importance of reactions [7] and [10] relative to a possible direct molecular rearrangement to benzene and carbon monoxide:

$$C_6H_5CHO + Hg^* \rightarrow C_6H_6 + CO + Hg \quad [11]$$

experiments were carried out with C_6H_5CHO–C_6D_5CDO mixtures. In the absence of the free radical processes [7] and [10] all the benzene produced in such mixtures should be

Can. J. Chem. Downloaded from www.nrcresearchpress.com by 176.9.209.113 on 09/04/12
For personal use only.

either C_6H_6 or C_6D_6. The amount of isotopically mixed benzenes relative to the C_6H_6 and C_6D_6 benzenes should therefore provide an index of the amount of benzene formed by reaction [11].

TABLE II

Decomposition of C_6D_5CDO–C_6H_5CHO mixtures

Aldehyde decomposed (μ)		Product benzenes (μ)				% free radical reaction
C_6D_5CDO	C_6H_5CHO	C_6D_6	C_6D_5H	C_6H_5D	C_6H_6	
1.46	—	0.257	0.026_6	—	—	—
0.599	1.36	0.078_7	0.031_4	0.016_3	0.190	34.0
0.646	0.569	0.090_7	0.017_9	0.013_6	0.075_4	32.0

In Table II are recorded the results obtained in the decomposition of benzaldehyde-d_6 and of two mixtures of benzaldehyde-d_6 and ordinary benzaldehyde. Because of the formation of polymer it was necessary to keep the period of illumination as short as possible, therefore the yield of carbon monoxide was not measured in these experiments. The small amount of C_6D_5H formed in the decomposition of benzaldehyde-d_6 alone arises from the small percentage of benzaldehyde-d_5 present in the original material. The results given for the two mixtures were corrected by this factor.

Assuming that for the isotopic aldehydes the same fraction of the total reaction proceeds by formation of free radicals, and similarily that the rate of reaction [10] is the same for all isotopic species, it is possible to calculate from the results of the two experiments the fraction proceeding by steps [7] and [10]. If these assumptions are valid the amount of the mixed benzenes, C_6D_5H and C_6H_5D, formed in each experiment should be equal. The observed agreement was not too satisfactory, presumably because the amounts formed were quite small compared to the experimental error. For purposes of calculation the amounts of C_6H_5D and C_6D_5H were averaged. The final column of Table II shows that of that fraction of the total reaction which produced benzene, 33% did so by a free radical mechanism. There was no evidence for the formation of mixed aldehydes suggesting that the recombination reaction

$$C_6H_5 + CHO \rightarrow C_6H_5CHO \qquad [12]$$

must be much slower than the disproportionation reaction [10].

Acrolein

Using low energy electrons no free radicals could be detected in the photosensitized decomposition of acrolein. From a comparison of the 50-v spectra with and without illumination the principal products were found to be ethylene, acetylene, carbon monoxide, and a small amount of hydrogen. At higher partial pressures of aldehyde a substance of mass 54 was formed. This was identified as 1,3-butadiene, presumably formed by the dimerization of vinyl radicals.

On the addition of methyl radicals to the system a compound of parent mass 42 was formed. This compound was identified as propylene and confirms the presence of the vinyl radical. This suggests the primary step:

$$CH_2{=}CH{-}CHO + Hg^* \rightarrow CH_2{=}CH + CHO + Hg. \qquad [13]$$

In addition, a small amount of product of mass 70 was also formed. This compound was probably vinyl methyl ketone, suggesting the occurrence to some extent of the additional

Can. J. Chem. Downloaded from www.nrcresearchpress.com by 176.9.209.113 on 09/04/12
For personal use only.

primary step:

$$CH_2{=}CH{-}CHO + Hg^* \rightarrow CH_2{=}CH{-}CO + H + Hg. \quad [14]$$

The product yields obtained by varying the length of the illuminated zone are given in Table III and shown graphically in Fig. 1. The carbon and oxygen balances were low,

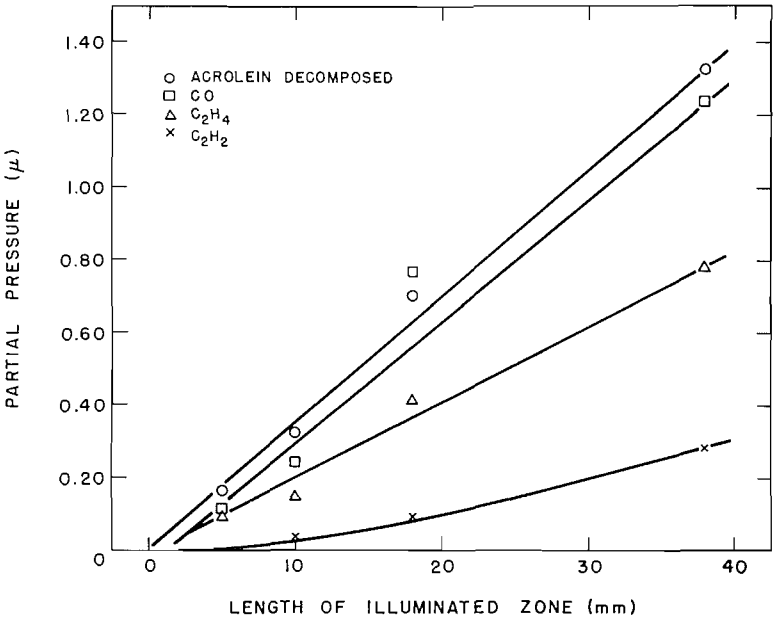

FIG. 1. Mercury-photosensitized decomposition of acrolein.

TABLE III

Acrolein decomposition (partial pressure acrolein 4.85 μ)

Length of illuminated zone (mm)	Acrolein decomposed		Products (μ)			Product balance	
	(μ)	(%)	CO	C_2H_4	C_2H_2	% C	% O
38	1.33	27.4	1.23	0.783	0.282	84.5	92.9
18	0.700	14.4	0.768	0.417	0.095	68.9	(109.7)
10	0.320	6.58	0.244	0.152	0.037	64.8	76.3
5	0.165	3.38	0.114	0.095	0.00	61.4	69.1

probably as a result of the presence of radicals which were not included in the material balances. The curved nature of the plot of the acetylene yield versus the length of illuminated zone suggests that acetylene was not produced in a primary step. The only primary step producing acetylene which would be energetically possible is the reaction:

$$CH_2{=}CH{-}CHO + Hg^* \rightarrow C_2H_2 + CH_2O + Hg. \quad [15]$$

The absence of formaldehyde as a product indicates that this reaction does not occur. Several secondary reactions can be postulated to explain the formation of acetylene

$$C_2H_3 + Hg^* \rightarrow C_2H_2 + H + Hg \quad [16]$$

$$C_2H_3 \rightarrow C_2H_2 + H \quad [17]$$

$$2C_2H_3 \rightarrow C_2H_2 + C_2H_4 \quad [18]$$

$$C_2H_4 + Hg^* \rightarrow C_2H_2 + H_2 + Hg. \quad [19]$$

Can. J. Chem. Downloaded from www.nrcresearchpress.com by 176.9.209.113 on 09/04/12
For personal use only.

From heats of formation, assuming $D(C_2H_3—H) \leqslant 110$ kcal/mole, $D(H—C_2H_2)$ can be calculated to be $\geqslant 36$ kcal/mole; therefore the decomposition reaction [17] should be very slow at the temperature of the reactor (55° C). It is possible that the acetylene could be produced by reaction [18]. However, most of the ethylene must arise by some other mechanism since in all cases more ethylene was produced than acetylene. The relatively large yield of ethylene, the apparent low concentration of vinyl radicals, and the absence of products containing the CHO group all suggest that a large proportion of the reaction proceeds by a molecular rearrangement mechanism:

$$CH_2{=}CH—CHO + Hg^* \rightarrow CH_2{=}CH_2 + CO + Hg. \quad [20]$$

The presence of the vinyl and acrylyl radical, as shown by the methyl addition products propylene and vinyl methyl ketone, strongly suggest the occurrence of two other primary processes:

$$CH_2{=}CH—CHO + Hg^* \rightarrow CH_2{=}CH + CHO + Hg \quad [13]$$

$$CH_2{=}CH—CHO + Hg^* \rightarrow CH_2{=}CH—CO + H + Hg. \quad [14]$$

From the present experiments it is not possible to determine the relative importance of the three primary processes.

Crotonaldehyde

Difficulties were encountered in identifying the products formed in the mercury-photosensitized decomposition of crotonaldehyde. For this reason an identification of all primary reactions and an estimate of their relative importance could not be made. The main products detected were carbon monoxide, propylene, a product of mass 40, a small amount of acetylene, and a very small amount of a product of mass 56. Use of low energy electrons led to detection of a radical mass 41. The addition of methyl radicals caused a small but definite increase at mass 84 indicating the presence of the crotonyl radical in small amounts and thus suggesting the occurrence of the primary reaction:

$$CH_3—CH{=}CH—CHO + Hg^* \rightarrow CH_3—CH{=}CH—CO + H + Hg. \quad [21]$$

The large amount of propylene produced suggested that the main primary step was the molecular rearrangement:

$$CH_3—CH{=}CH—CHO + Hg^* \rightarrow CH_3—CH{=}CH_2 + CO + Hg. \quad [22]$$

It was not possible to determine whether the radical of mass 41 was formed by the primary reaction:

$$CH_3—CH{=}CH—CHO + Hg^* \rightarrow CH_3—CH{=}CH + CHO + Hg \quad [23]$$

or by the reaction of Hg* with propylene produced in reaction [22] as follows:

$$CH_2{=}CH—CH_3 + Hg^* \rightarrow CH_2{=}CH—CH_2 + H + Hg. \quad [24]$$

Since a considerable amount of propylene was present, and since propylene has a large cross section for reaction with excited Hg atoms (6), the latter alternative appears more probable.

CONCLUSIONS

The mercury-photosensitized decomposition of benzaldehyde under the present conditions leads primarily to the formation of a polymeric material. However, that portion of the reaction which results in identifiable products has been shown to involve two primary processes, a molecular rearrangement to form benzene and carbon monoxide

Can. J. Chem. Downloaded from www.nrcresearchpress.com by 176.9.209.113 on 09/04/12
For personal use only.

and a free radical split to form phenyl and presumably formyl radicals, with 33% of the reaction occurring by the free radical mechanism. No evidence was found for the formation of benzoyl radicals and hydrogen atoms. This mode of decomposition is quite different from that of acetaldehyde, in which no molecular rearrangement was found to occur, and free radicals only were formed.

The reactions of both acrolein and crotonaldehyde appear to involve three primary processes

$$RCHO + Hg\ ^3P_1 \rightarrow RH + CO + Hg \quad [25]$$

$$\rightarrow R + HCO + Hg \quad [26]$$

$$\rightarrow RCO + H + Hg. \quad [27]$$

For both these compounds the results suggest that the main reaction is the molecular rearrangement [25], with reaction [26] occurring to a lesser extent and reaction [27] only to a very slight extent. The results for acrolein and crotonaldehyde do not permit quantitative determinations of the relative importance of the three steps.

REFERENCES

1. STEACIE, E. W. R. Atomic and free radical reactions. 2nd ed. Reinhold Publishing Corp., New York. 1954.
2. LOSSING, F. P. Can. J. Chem. **35**, 305 (1957).
3. BLACET, F. E. and ROOF, J. G. J. Am. Chem. Soc. **58**, 73 (1936).
4. VOLMAN, D. H., LEIGHTON, P. A., BLACET, F. E., and BRINTON, R. K. J. Chem. Phys. **18**, 203 (1950).
5. BLACET, F. E., FIELDING, G. H., and ROOF, J. G. J. Am. Chem. Soc. **59**, 2375 (1937).
6. LOSSING, F. P., MARSDEN, D. G. H., and FARMER, J. B. Can. J. Chem. **34**, 701 (1956).
7. KEBARLE, P. and LOSSING, F. P. Can. J. Chem. **37**, 389 (1959).
8. COLLIN, J. and LOSSING, F. P. Can. J. Chem. **35**, 778 (1957).
9. SZWARC, M. and WILLIAMS, D. J. Chem. Phys. **20**, 1171 (1952).
10. SZWARC, M. and TAYLOR, J. W. J. Chem. Phys. **22**, 270 (1954).

Can. J. Chem. Downloaded from www.nrcresearchpress.com by 176.9.209.113 on 09/04/12
For personal use only.

Can. J. Chem. Downloaded from www.nrcresearchpress.com by 176.9.209.113 on 09/04/12
For personal use only.

THE POLYOXYPHENOLS OF WESTERN RED CEDAR (THUJA PLICATA DONN.)

I. ISOLATION AND PRELIMINARY CHARACTERIZATION OF PLICATIC ACID[1]

J. A. F. Gardner, G. M. Barton, and Harold MacLean

ABSTRACT

An amorphous, optically active, heat and light sensitive, polyoxyphenolic acid ($pK_a = 3$) has been isolated from the mixture of polyoxyphenols present in the aqueous extractive of western red cedar. Analyses of crystalline derivatives are consistent with a molecular formula of $C_{20}H_{22}O_{10}$. Color tests, spectra, methylation, and alkaline nitrobenzene oxidation results indicate it to be a propylphenol dimer, a lignan acid, in which one aromatic ring is 3-methoxy-4-hydroxyphenyl and the other is 3,4-dihydroxy-5-methoxyphenyl. Acetylation results and lactone formation require the presence of three alcoholic hydroxyls, one of which is in the γ position to the carboxyl.

In a previous paper (1), the presence in the acetone extractive of western red cedar of several water-soluble polyoxyphenols was reported. This phenolic mixture constituted 4 to 5% of wood samples having acetone solubilities of 10 to 14%. These substances were also extracted with water and accounted for the main portion (85–95%) of the hot-water extractive of butt outer heartwood which was found to have hot-water solubilities ranging from 10 to 23% (2). This indicated high content of natural phenolic substances together with the availability of large volumes of western red cedar wood as mill and forest residue in British Columbia prompted a detailed investigation of the chemistry of the phenolic constituents.

Paper chromatography of the aqueous extractive, a brown resin, showed the presence of at least seven different phenols and arabinose. By steaming the mixture during aqueous extraction of the wood, the steam-volatile tropolones, thujic acid and methyl thujate, were virtually eliminated. The arabinose and other non-phenols in the extractive were removed by treatment with lead acetate solution and regeneration of the phenols from the precipitated lead salts. Attempts to fractionate the regenerated phenols with a variety of solvents were made, and the separation efficiency was checked by means of paper chromatography of the fractions. In this manner it was established that a major component ($R_f = 0.9$, carbon dioxide – water) was very soluble in water and, compared with the others, practically insoluble in ethyl acetate. Thus, thorough extraction of the phenolic mixture with ethyl acetate gave a residue which was paper chromatographically pure in respect to carbohydrates and other phenols. This product was an amorphous brown powder which gave positive tests for pyrocatechol, methoxyl, and carboxyl groups. In view of its acidity and source, this substance was termed plicatic acid.

Additional quantities of plicatic acid were isolated simply by extracting it from the mixture of phenols in methyl ethyl ketone with sodium bicarbonate solution. The yield was 40% of the aqueous extractive, but since the product was brown in color and failed to crystallize or give crystalline methyl ethers with diazomethane, milder methods of isolation not involving the use of acids and alkalis were investigated.

Column chromatography with a variety of packings including cellulose, magnesol–

[1]*Manuscript received June 15, 1959.*
Contribution from the Vancouver Laboratory, Forest Products Laboratories of Canada, a Division of the Forestry Branch, Department of Northern Affairs and National Resources. Paper presented at the 133rd National Meeting, American Chemical Society, San Francisco, California, April 13–18, 1958.

Can. J. Chem. Downloaded from www.nrcresearchpress.com by 176.9.209.113 on 09/04/12
For personal use only.

celite, alumina, and ion-exchange resins was examined. The low solubility of the aqueous extractive in most solvents limited the loading of most columns to very small quantities. Also, although weakly basic ion-exchange resins separated plicatic acid from the other phenols, acid was required to elute the plicatic. The most successful column separation of the phenols was obtained with a weakly acid (carboxylic) cation-exchange resin which is also useful in the separation of flavonoids (3). Elution with water of a column loaded with the aqueous extractive yielded plicatic acid and the phenols, R_f .7 and .5 (carbon dioxide – water), in that order with some overlapping. Subsequent graded elution with water–ethanol gave the phenols of R_f .52 and .03 and finally a mixture of the remainder, R_f .03, .06, and .1. Paper chromatography showed that the first plicatic acid eluted from the column was contaminated with arabinose. Subsequent fractions showing no contamination were combined and lyophilized to provide amorphous plicatic acid in small quantities (1 g or less).

Consideration of the high solubility of plicatic acid in water and very poor solubility in ethyl acetate together with the poor solubility of the other phenols in water and their good solubility in ethyl acetate led to isolations on a larger scale by a six-stage countercurrent distribution of the aqueous extractive between these two solvents. This procedure provided almost equal quantities of chromatographically pure plicatic acid and plicatic acid contaminated with 5–6% of arabinose and traces of other sugars in a combined yield of 40% on the aqueous extractive.

As obtained by the column or countercurrent distribution technique, the plicatic acid was a very light tan-colored, amorphous, optically active powder, very soluble in water, soluble in absolute acetone and ethanol, and very slightly soluble in ethyl acetate and ether.

The color reaction with aqueous ferric chloride was pinkish purple shifting to blue-green at neutrality and thence to deep red in sodium carbonate solution. This indication of the presence of adjacent phenolic hydroxyls was confirmed by positive tests with ferrous sulphate, ammonium molybdate, titanium chloride, and bromine solutions. A test for three vicinal phenolic hydroxyls with ferrous sulphate – potassium tartrate solution was negative, but the chlorine – sodium sulphite test for pyrogallol derivatives was positive. Alkaline nitrobenzene oxidation gave a 4% yield of vanillin. A test for methylenedioxy groups was negative.

Solutions of plicatic acid were unstable to sunlight, rapidly turning dark red-brown in color. Heating the solid or an aqueous solution caused a gradual conversion to another phenol of R_f 0.7 (carbon dioxide – water) having an infrared absorption characteristic of a γ-lactone. This substance, according to paper chromatography, was identical with one of the other phenols occurring with plicatic acid in the cedar extractive. Acidification of an alkaline solution regenerated plicatic acid.

Elementary analyses and molecular weight determinations indicated an empirical formula for plicatic acid of $C_{20}H_{24}O_{10}$. For two methoxyl groups and one carboxyl group per molecule, this requires a methoxyl content of 14.6% and a neutral equivalent of 424. The best values found were 13.7% and 432 respectively. The heating (65–100° C) necessary for moisture removal prior to analyses also caused some decomposition making analytical results on plicatic acid itself subject to question.

Methylation of plicatic acid with dimethyl sulphate and alkali in aqueous acetone solution followed by diazomethane in dioxane gave a crystalline product which could also be obtained in poorer yield directly from plicatic with diazomethane. Analytical values for carbon, hydrogen, and methoxyl content and molecular weight fitted an empirical

formula of $C_{24}H_{30}O_{10}$. This corresponds to the methyl ester of the trimethyl ether of a plicatic acid containing two fewer hydrogens per molecule than the formula above. Since dehydrogenation during diazomethane methylation is unlikely and the analytical values for plicatic are based on amorphous heat-labile material, the $C_{20}H_{22}O_{10}$ formula for plicatic acid is favored.

The methyl ester of the trimethyl ether effervesced when heated above its melting point, evolving methanol and yielding a crystalline product which analyzed as the trimethyl ether lactone, $C_{23}H_{26}O_9$. The lactone character was confirmed by the appearance of a strong band in the infrared absorption spectrum at 1784 cm^{-1}, the region assignable to the carbonyl group of five-membered lactones (4) and disappearance of the band at 1716 cm^{-1} assignable to the carbonyl group in the ester (5). The infrared absorption spectrum of the lactone also indicated additional hydroxyl group content.

Acetylation of plicatic acid in acetic anhydride and pyridine gave an amorphous product analyzing for methoxyl content as a hexaacetate.

The neutralization curve for plicatic acid disclosed it to be a strong acid, $pK_a = 3$, comparable to orthohydroxybenzoic acids. However, in acids of this type having strong intramolecular hydrogen bonding the absorption band in the infrared spectrum assignable to the carbonyl occurs below 1680 cm^{-1} (5), whereas for plicatic acid the band assignable to the carbonyl is at 1713 cm^{-1}, a frequency normal for monobasic aliphatic acids.

The high acidity of plicatic acid indicated it would displace acetic acid from its salts. Treatment of an alcoholic solution with alcoholic potassium acetate precipitated a crystalline monopotassium salt, $C_{20}H_{21}O_{10}K$, in high yield. Therefore the possibility of isolating and purifying plicatic acid directly from the aqueous extractive by precipitation as the potassium salt is now being examined.

The analytical and molecular weight results on plicatic acid and its crystalline derivatives indicate it to be a propylphenol dimer of the lignan type and, pending completion of degradative studies, some deductions may be made as to the nature of the aromatic nuclei. The formation of some vanillin by oxidation indicates one aromatic ring to be 3-methoxy-4-hydroxyphenyl. The presence of two additional phenolic hydroxyls adjacent to one another is shown by the methylation data and the color tests. This together with the positive test for pyrogallol derivatives indicates a vicinal arrangement of these two phenolic hydroxyls with the other methoxyl on the other aromatic ring. In addition to the three phenolic hydroxyls and one carboxylic hydroxyl which, with two methoxyls, account for seven of the 10 oxygens required by the empirical formula, $C_{20}H_{22}O_{10}$, there are three alcoholic hydroxyls as shown by formation of a hexaacetate. One of these is used in γ-lactone formation by the methyl ester of the trimethyl ether, and the other two account for the hydroxyl band remaining in the infrared absorption spectrum of the lactone. Thus the formula for plicatic acid can be provisionally written: $C_6H_3(OH)(OCH_3).C_5H_4(OH)_3(COOH).C_6H_2(OH)_2(OCH_3)$, and it is reasonable to conclude that it is a highly hydroxylated lignan acid. Structural investigations are continuing.

While no lignan acids have been isolated from plant material heretofore, many of the lactones have (6), and it is significant that the infrared absorption spectrum of the lactone of methylated plicatic acid is similar to those published for the podophyllotoxin series (4).

The presence in plicatic acid of unetherified neighboring phenolic hydroxyls as in another lignan, nordihydroguaiaretic acid, a well-known commercial antioxidant, justifies its testing as an antioxidant. Similarly, biological testing of it and its lactone derivatives is in order in view of the fact that many lactones have marked physiological activity and some are valuable medicinals (7).

Can. J. Chem. Downloaded from www.nrcresearchpress.com by 176.9.209.113 on 09/04/12
For personal use only.

Can. J. Chem. Downloaded from www.nrcresearchpress.com by 176.9.209.113 on 09/04/12
For personal use only.

EXPERIMENTAL

Evaporations were conducted under reduced pressure at 40° C. Melting points were determined on a Fisher–Johns apparatus and are uncorrected. Carbon and hydrogen analyses were by Clark Microanalytical Laboratory, Urbana, Illinois. Infrared absorption spectra were determined on a Baird Atomic KM-1 spectrophotometer. Solvent mixtures for paper chromatography were carbon dioxide – water and butanol – acetic acid – water (40–10–50) for phenols and the latter and butanol–pyridine–water (10–3–3) for sugars.

Preparation of the Aqueous Extractive of Western Red Cedar

Straw-colored shingle mill spalts were ground in a Wiley mill to pass a 20-mesh screen. The wood meal (1.49 kg moisture-free basis, TAPPI hot-water solubility, 14.5%) was leached with four batches of hot water in an earthenware crock. The temperature was maintained at 100° C and agitation achieved by passing steam into the mixture. Results were as follows:

Extraction time (hours)	Volume of extract (liters)	Solids content (g)
2	14.3	84.4
1	7.7	27.1
1	7.0	13.4
1/2	9.3	11.8
Totals	38.3	136.7

After the solution was cooled, the combined extract was decanted from settled solids (10 g) and evaporated at reduced pressure to a viscous brown syrup, (168 g, 25% moisture). Yield based on the wood, 8.5% or 59% of the TAPPI hot-water solubility. Paper chromatograms (carbon dioxide – water) showed spots for phenols at R_f 0, .03, .07, .12, .16, .50, .70, .90. Color tests for thujaplicins were negative. Paper chromatograms showed arabinose and traces of other sugars.

Isolation of Plicatic Acid from Aqueous Extractive

(*a*) *By Sodium Bicarbonate Extraction of Lead-precipitated Phenols*

Aqueous extractive (331 g, moisture-free basis) in water solution was treated with lead acetate solution (900 g in 2 l.) and the precipitated white lead salts (427 g) removed by filtration. A portion (273 g) of the lead salt was agitated with 2-butanone (2 l.) containing excess sulphuric acid (6 *N*). After filtration, the 2-butanone solution was extracted with 5% sodium bicarbonate solution (500 ml, 3×250 ml). The bicarbonate solution after back extraction with 2-butanone was saturated with sodium chloride, acidified with dilute sulphuric acid (12 *N*), and extracted with 2-butanone (2×500 ml, 2×100 ml). The 2-butanone solution was dried over sodium sulphate and evaporated to yield brown amorphous plicatic acid (119 g), which in paper chromatography showed no contamination with sugars or other phenols.

(*b*) *By Column Chromatography*

Aqueous extractive (2.6 g, moisture-free basis) in warm water (400 ml) was added to a column bed (5 cm × 30 cm) of Amberlite IRC-50 (H) (Rohm and Haas, Philadelphia, Penn.) at a rate of 1.5 ml/minute. The column was eluted at the same rate, first with water and then with graded ethanol–water using a fraction collector loaded with 15-ml tubes. The contents of each fifth tube were checked by paper chromatography. The water

eluted arabinose and phenols of R_f .9, .7, and .5 in that order with partial overlapping. The ethanol–water eluted phenols of R_f .52, .03, and a mixture of R_f .03, .06, and .1 in that order. Fractions which were pure by paper chromatography were combined and lyophilized. Total yields were estimated from the pure yields and paper chromatographic data on fractions showing overlapping as follows:

Tube No.	Eluant	R_f of phenols	Yield of pure material (mg)	Total yield estimated (mg)
0–40	H_2O	—	—	—
40–80	H_2O	.90	650	1250
65–140	H_2O	.70	—	200
80–200	H_2O	.50	215	525
200–320	5–20% EtOH	.52	110	225
310–330	20–25% EtOH	.03	30	100
330–340	25–30% EtOH	.03		
		.06	200	200
		.10		
	Totals		1105	2500

The plicatic acid (R_f 0.9) obtained was a light tan, amorphous powder.

(*c*) *By Countercurrent Distribution with Ethyl Acetate – Water*

Aqueous extractive solids (12 g) were added to a 1-liter separatory funnel containing water-saturated ethyl acetate (400 ml) and ethyl-acetate-saturated water (400 ml) and the mixture shaken 5 minutes before separation. The water layer was transferred to a second funnel and similarly treated with fresh ethyl acetate while the ethyl acetate layer was treated with fresh water in the first funnel. This procedure was repeated through six stages involving six funnels until the original water was in funnel six in contact with the last added ethyl acetate and the original ethyl acetate was in funnel one in contact with the last added water. The water layer in funnel six on lyophilization yielded plicatic acid (2.5 g) contaminated with 7–9% arabinose (as determined by quantitative paper chromatography). The combined water layers from funnels four and five with the ethyl acetate layers from five and six yielded paper chromatographically pure plicatic acid (2.3 g), R_f in carbon dioxide – water, 0.9; in butanol – acetic acid – water, 0.4, a light tan-colored powder; $[\alpha]_D^{21}$ −9.99 (water). Ultraviolet absorption in water: min. 256 mμ (log ϵ = 3.23); max. 281 mμ (log ϵ = 3.58); shoulder, 307 mμ (log ϵ = 2.42). Infrared absorption, ν_{max}^{KBr} in cm^{-1}: 3340, 1713, 1611, 1518, 1200, 1088. Calc. for $C_{20}H_{24}O_{10}$: C, 56.6; H, 5.71; OCH_3, 14.6; mol. wt. and neutral equivalent, 424.2; for $C_{20}H_{22}O_{10}$: C, 56.9; H, 5.26; OCH_3, 14.67; mol. wt. and neutral equivalent, 422.2. Found: C, 56.24; H, 5.84; OCH_3, 13.7; mol. wt. (Rast), 433; neutral equivalent, 432. Approximate pK_a from pH at half-neutralization, 3.0.

Color tests with aqueous solutions of plicatic acid were as follows: aqueous ferric chloride, pinkish purple shifting to blue and then red on addition of sodium carbonate; ammonium molybdate and acetic acid (8), reddish brown; with Folin–Denis reagent (9) blue; ferrous sulphate – sodium potassium tartrate at pH 5.6 (10), negative; titanium chloride, yellow; chlorine – sodium sulphite (11), red; Gaebel test for methylenedioxy groups (12), negative.

A quantitative alkaline–nitrobenzene oxidation test, using the technique of Stone and Blundell (13) showed 4% vanillin formation.

Repeated attempts to obtain a crystalline acetate or benzoate of plicatic acid were

Can. J. Chem. Downloaded from www.nrcresearchpress.com by 176.9.209.113 on 09/04/12
For personal use only.

unsuccessful. The amorphous product of treatment with acetic anhydride and pyridine in benzene solution was precipitated in fractions by stepwise addition of ligroin. The last most soluble fraction had a methoxyl content of 9.1; calculated for a hexaacetate, $C_{32}H_{34}O_{16}$, 9.17.

Plicatic Acid Trimethyl Ether Methyl Ester

Plicatic acid (5 g) in a mixture of water (5 ml) and acetone (9 ml) was treated with dimethyl sulphate (4 ml) and 5 *N* sodium hydroxide dropwise at reflux for 2 hours while maintaining the pH at 8–9. The methylated plicatic precipitated as the white sodium salt during the latter stages of the reaction. The reaction mixture was acidified to pH 3, the acetone removed, and the mixture extracted with chloroform. The residue from evaporation of the chloroform solution was methylated in dioxane with excess diazomethane to yield a product which crystallized from benzene in 42% yield. Melting point after recrystallization from benzene 204–205° C $[\alpha]_D^{22}$ −29.9 ($CHCl_3$).

A methylation of plicatic acid in methanol directly with diazomethane gave the same product contaminated with large amounts of black ether-soluble tar which complicated the purification and reduced the yield of pure product to 23%.

The product, recrystallized from benzene, contained benzene of crystallization. Recrystallization from ethanol gave colorless crystals m.p. 203–204° C. Calc. for $C_{24}H_{30}O_{10}$: C, 60.24; H, 6.32; OCH_3, 38.9; mol. wt., 478.6. Found: C, 59.91; H, 6.02; OCH_3, 38.7; mol. wt. (Rast), 478. Infrared spectrum, ν_{max}^{KBr} in cm^{-1}: 3460, 1716, 1588, 1522, 1511, 1451, 1422, 1256, 1235, 1215, 1128, 1002, 861.

Plicatic Acid Trimethyl Ether Lactone

The trimethyl ether methyl ester on the melting point stage was observed to evolve a gas after melting and then recrystallize. The material evolved was condensed and found to be methanol and the solid, m.p. 252–255° C had an infrared absorption characteristic of a γ-lactone. Accordingly the ester (0.1 g) was heated under nitrogen at 220° C until evolution of gas had ceased and the material had resolidified. Recrystallization from ethanol gave colorless crystals, m.p. 257° C. Calc. for $C_{23}H_{26}O_9$: C, 61.93; H, 5.88; OCH_3, 34.72. Found: C, 61.82; H, 5.99; OCH_3, 34.66. Infrared spectrum, ν_{max}^{KBr} in cm^{-1}: 3450, 1784, 1593, 1518, 1465, 1425, 1322, 1255, 1220, 1126, 992, 862.

Potassium Plicatate

Plicatic acid (2 g) in anhydrous ethanol (50 ml) was treated with anhydrous potassium acetate (0.6 g) in ethanol (10 ml). The white salt which precipitated immediately was separated on the centrifuge and washed well with ethanol (70 ml) before drying under pressure at 65° C. Yield 1.5 g (68.5% of theory). The product was quite soluble in methanol and could be reprecipitated by addition of ethanol. Calc. for $C_{20}H_{21}O_{10}K$: C, 52.16; H, 4.60; OCH_3, 13.45; K as sulphated ash, 18.82. Found: C, 52.17; H, 5.11; OCH_3, 13.39; K as sulphated ash, 18.7. The infrared absorption spectrum was characteristic of the salt of an organic acid (5), ν_{max}^{KBr} in cm^{-1}: 3340, 1610 and 1600 (broad doublet), 1515, 1350–1320 (broad), 1205, 1090, 872.

ACKNOWLEDGMENT

The authors are indebted to Canadian Forest Products Limited for supplying cedar wood samples.

Can. J. Chem. Downloaded from www.nrcresearchpress.com by 176.9.209.113 on 09/04/12
For personal use only.

REFERENCES

1. BARTON, G. M. and GARDNER, J. A. F. Pulp Paper Mag. Can. **55** (10), 132 (1954).
2. MACLEAN, H. and GARDNER, J. A. F. Forest Prods. J. **6**, 510 (1956).
3. GAGE, T. B., MORRIS, Q. L., DETTY, W. E., and WENDER, S. H. Science, **113**, 522 (1951).
4. SCHRECKER, H. W. and HARTWELL, J. L. J. Am. Chem. Soc. **75**, 5916 (1953).
5. BELLAMY, L. J. The infrared spectra of complex molecules. Methuen & Co. Ltd., London. 1954.
6. HEARON, W. M. and MACGREGOR, W. S. Chem. Revs. **55**, 957 (1955).
7. HAYNES, L. J. Modern methods of plant analysis. Vol. II. Springer-Verlag, Berlin. 1955. p. 584.
8. QUASTEL, J. H. Analyst, **56**, 311 (1931).
9. FOLIN, O. and DENIS, W. J. Biol. Chem. **12**, 239 (1912).
10. KURSANOV, A. L. and ZAPROMETOV, M. N. Biokhimiya, **14**, 467 (1949).
11. CAMPBELL, W. G., MACGOWAN, J. G., and BRYANT, S. A. Biochem. J. **32**, 2138 (1938).
12. GAEBEL, G. O. Arch. Pharm. **248**, 225 (1910).
13. STONE, J. E. and BLUNDELL, M. J. Anal. Chem. **23**, 771 (1951).

Can. J. Chem. Downloaded from www.nrcresearchpress.com by 176.9.209.113 on 09/04/12
For personal use only.

Can. J. Chem. Downloaded from www.nrcresearchpress.com by 176.9.209.113 on 09/04/12
For personal use only.

INFRARED SPECTRA AND STRUCTURE OF POLYALDEHYDES

III. POLYACETALDEHYDE AND POLYPROPIONALDEHYDE[1]

A. NOVAK[2] AND E. WHALLEY

ABSTRACT

Acetaldehyde and propionaldehyde have been polymerized at room temperature and pressures of about 10 kb. The infrared spectra of the polymers have been investigated and it is shown that the polymers have the formula $HO(CHR.O)_nH$. The spectra are too complicated to be understood if there is only one monomer unit in the repeating unit of the chain; there are at least two units.

1. INTRODUCTION

Polyacetaldehyde was first made approximately simultaneously by Letort (1) and by Travers (2) by cooling acetaldehyde in liquid nitrogen. The molecular weight of a sample was about a half-million (3). A note (4) describes briefly its infrared spectrum, which indicates that its structure is $(CHCH_3.O)_n$, confirming Staudinger's suggestion (5). Attempts to polymerize propionaldehyde by this method failed (6). The higher aliphatic aldehydes, butyraldehyde and higher homologues, polymerize under pressures of about 10 kb (7, 8) to give compounds that are presumed to have the structure $(CHR.O)_n$, but an attempt to polymerize acetaldehyde by subjecting it to a pressure of 9 kb and 40° C failed (9). Low-molecular-weight polymers of acetaldehyde have been made (10) by treating mixtures of acetaldehyde and acetaldehyde diethylacetal with a small amount of concentrated sulphuric acid at −40 to +20° C, and the structure $C_2H_5O(CHCH_3.O)_nC_2H_5$ was suggested. Propionaldehyde has apparently not been polymerized previously except by the aldol condensation.

In this paper we describe the preparation of polymers of acetaldehyde and propionaldehyde by subjecting the monomers to pressures of about 9 kb at room temperature. The infrared spectra and X-ray diffraction patterns of these polymers, of low-temperature polyacetaldehyde, and of the polymer from acetaldehyde and acetal have been obtained in order to help elucidate the structures.

2. EXPERIMENTAL METHODS AND RESULTS

Eastman-Kodak White-Label acetaldehyde, acetal, and propionaldehyde were used. They were dried with Drierite and distilled before use in a fractionating column in an atmosphere of dry air. Acetaldehyde-d_1 (CH_3CDO) and propionaldehyde-d_1 (C_2H_5CDO) were prepared from nitroethane and nitropropane respectively by the method described by Leitch (11).

High-pressure Polymerization

The monomers were subjected to pressures of about 9 kb for 1–2 days at room temperature. The reaction vessel was a 1-cm³ stainless-steel test tube closed by a piston that was fitted with an *o*-ring. The vessel was filled with aldehyde, stoppered, and put into the high-pressure end of an intensifier which was then pressurized. When the monomers were almost free of water the polymerization was almost complete in 1–2 days and the

[1]*Manuscript received March 25, 1959.*
Contribution from the Division of Applied Chemistry, National Research Council, Ottawa, Canada.
Issued as N.R.C. No. 5309.
[2]*N.R.C. Postdoctorate Fellow, 1956–58.*

polymers were tacky solids. The proportion polymerized and the viscosity of the product decreased rapidly when small amounts of water were added to the monomer. For example, the azeotropic mixture of propionaldehyde and water, which contains about 1.9% of water in the form of the hydrate (12), polymerized under pressure only to the extent of about 30%, as estimated from the intensity of the C=O stretching band in a solution of the mixture in carbon tetrachloride, and after evaporation of the monomer the polymer remained as a liquid probably of low molecular weight as estimated from the intensity of the OH end group stretching band (see below). If we can anticipate our conclusions about structure, this is probably due to the equilibrium

$$\frac{1}{n}H_2O + RCHO \rightleftharpoons \frac{1}{n}HO(CHR.O)_nH$$

being dependent upon the amount of water present. At 1 atm pressure and room temperature the polymers depolymerized spontaneously to the parent aldehyde. The depolymerization of the solid polymer was rather slow and took several weeks at room temperature if it was exposed to the atmosphere so that the monomer could evaporate. If the monomer was not allowed to evaporate, or if the polymer was liquid, or if it was dissolved in carbon tetrachloride, depolymerization was complete, as determined by the infrared spectrum, in a few days. Presumably depolymerization occurs faster in a less viscous medium.

Low-pressure Polymerization of Acetaldehyde

The low-temperature polymer was made by condensing the vapor at liquid-nitrogen temperatures as described by Bevington and Norrish (13). A polymer of low molecular weight was prepared by treating a mixture of acetaldehyde and acetal in molar ratio 6:1 at −40° C with a drop of concentrated sulphuric acid (10). After 2 hours the acid was neutralized with sodium bicarbonate and the mixture dried with Drierite and filtered. The dimer and trimer were distilled off under reduced pressure; an oily liquid remained.

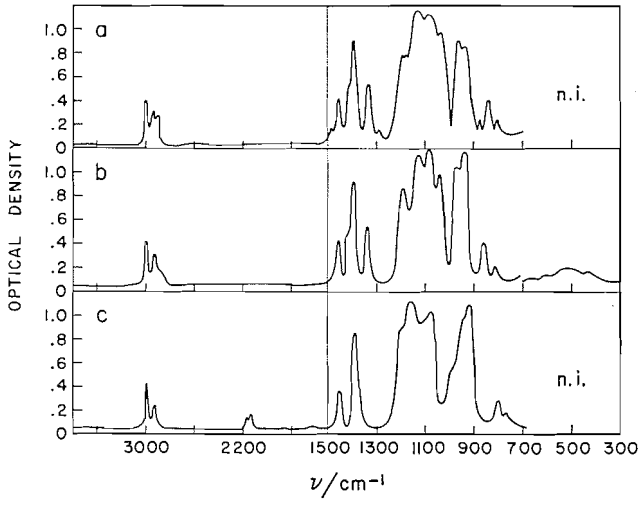

FIG. 1. Infrared spectrum of polyacetaldehyde: (*a*) low-molecular-weight polymer from acetaldehyde and acetal, (*b*) high-pressure polyacetaldehyde, (*c*) high-pressure polyacetaldehyde-d_1.

Can. J. Chem. Downloaded from www.nrcresearchpress.com by 176.9.209.113 on 09/04/12
For personal use only.

The polymers were examined spectroscopically as thin films pressed between sodium chloride or cesium bromide windows and as solutions in carbon tetrachloride. The spectra were recorded between 4000 and 700 cm^{-1} using a Perkin–Elmer Model-21 infrared spectrophotometer equipped with a rock salt prism, and between 700 and 300 cm^{-1} with a Beckmann IR-4 spectrophotometer equipped with a cesium bromide prism. The infrared spectra of polyacetaldehyde and polypropionaldehyde are shown in Figs. 1 and 2, and the wave numbers and relative intensities of the bands are given in Tables I and II.

X-ray diffraction photographs of films were taken with a Debye–Scherrer powder-camera, diameter 114.7 mm, using nickel-filtered copper radiation. Polyacetaldehyde gave two diffuse rings corresponding to interplanar spacings of 3.9 and 7.2 Å; polypropionaldehyde gave three diffuse rings corresponding to interplanar spacings of 2.1, 4.1, and 9.0 Å.

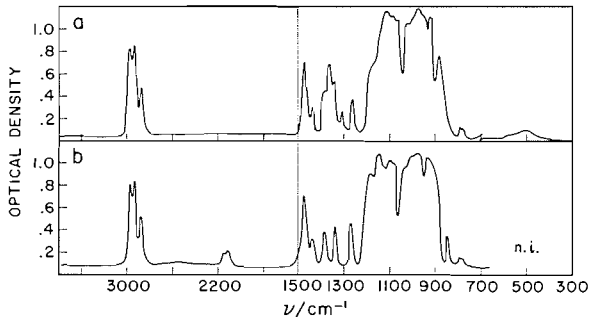

FIG. 2. Infrared spectrum of: (*a*) polypropionaldehyde, and (*b*) polypropionaldehyde-d_1.

TABLE I

Infrared spectra of polyacetaldehyde and polyacetaldehyde-d_1

$(-CHCH_3-O-)_n$			$(-CDCH_3-O-)_n$		
Wave No. cm^{-1}	Intensity	Tentative approximate description	Wave No. cm^{-1}	Intensity	Tentative approximate description
3440	Variable, w	OH stretching	3440	Variable, w	OH stretching
2980	m	CH_3 asym. stretching	2980	m	CH_3 asym. stretching
2920	m	CH_3 sym. stretching	2920	m	CH_3 sym. stretching
2860	sh	CH stretching	2160	w	CD stretching
			2140	w	
1445	m	CH_3 asym. bending	1445	m	CH_3 asym. bending
1400	sh	CH bending			
1380	s	CH_3 sym. bending	1380	s	CH_3 sym. bending
1335	m	CH bending			
1187	s	CH_3 rocking	1195	sh	CH_3 rocking, C—O and C—C stretching, and C—D bending
1130	vs	C—O and C—C stretching	1165	vs	
1085	vs		1100	sh	
1040	vs		1078	vs	
970	vs		990	sh	
			950	vs	
935	vs		925	vs	
845	m	C—H bending	787	m	C—D bending
810	w		760	w	
620	sh	C—O and C—C bending			
490	w				
450	sh				

Can. J. Chem. Downloaded from www.nrcresearchpress.com by 176.9.209.113 on 09/04/12
For personal use only.

TABLE II

Infrared spectra of polypropionaldehyde and polypropionaldehyde-d_1

$(—CHC_2H_5—O—)_n$			$(—CDC_2H_5—O—)_n$		
Wave No. cm^{-1}	Intensity	Tentative approximate description	Wave No. cm^{-1}	Intensity	Tentative approximate description
3460	Variable, w	OH stretching	3460	Variable, w	OH stretching
2960	s	C—H stretching	2960	s	CH_3, CH_2, and C—H stretching
2925	s		2925	s	
2870	m		2870	m	
			2150	w	C—D stretching
			2125	w	
1468	s	CH_2 bending	1468	s	CH_2 bending
1443	m	CH_3 asym. bending	1443	m	CH_3 asym. bending
1380	sh	CH_3 sym. bending	1380	m	CH_3 sym. bending
1360	s	C—H bending			
1345	m	CH_2 wagging	1342	m	CH_2 wagging
1305	m	C—H bending			
1265	m	CH_2 twisting	1270	m	CH_2 twisting
1175	sh	CH_3 rocking	1182	vs	CH_3 rocking, C—O and C—C stretching, and C—D bending
1120	vs	C—O and C—C stretching	1150	vs	
1085	vs		1108	vs	
1050	sh		1092	vs	
1020	vs		1045	sh	
1010	sh		1007	vs	
975	vs		980	vs	
960	sh		940	vs	
925	vs		920	sh	
895	m	C—H bending	855	m	C—D bending
795	w	CH_2 rocking?	790	w	CH_2 rocking
780	w		773	w	
520	sh	C—O and C—C bending	n.i.		
480	w				

3. DISCUSSION

(*i*) *Polyacetaldehyde*

The infrared spectra of low-temperature and high-pressure polyacetaldehyde were identical, except for the intensity of the minor bands in some samples in the region of 3300 cm^{-1} which we ascribe to end groups (see below). Chemical evidence (14) and previous spectroscopic evidence (4) show that the low-temperature polymer has the structure $(CHCH_3.O)_n$. Detailed examination of the spectra, which is described below, fully agrees with this. Hence, the low-temperature and high-pressure polymers are identical, except perhaps for molecular weight. There is a weak band at 3440 cm^{-1} which varies in intensity from sample to sample. It is probably due to OH end groups; the formula is thus $HO(CHCH_3.O)_nH$.

The X-ray diffraction patterns of thin films of both low-temperature and high-pressure polymer show only two diffuse rings which correspond to spacings of about 3.9 and 7.2 Å, in agreement with the spacings reported for the low-temperature polymer (14). Filaments were drawn from the polymers, but X-ray diffraction photographs of them showed no orientation. It has been suggested (14) that the broad rings are due to intrachain spacings. However, the corresponding spacings of other polyaldehydes are greater than those of polyacetaldehyde by an amount that increases as the bulk of the side chain increases (15). It seems more likely, therefore, that these broad bands are due to interchain and not to intrachain distances.

The infrared spectrum of the polymer obtained from acetaldehyde and acetal is similar

Can. J. Chem. Downloaded from www.nrcresearchpress.com by 176.9.209.113 on 09/04/12
For personal use only.

Can. J. Chem. Downloaded from www.nrcresearchpress.com by 176.9.209.113 on 09/04/12
For personal use only.

to that of polyacetaldehyde and confirms the proposed structure (10) $C_2H_5O(CHCH_3.O)_n$-C_2H_5. The bands in the skeletal stretching region (1200–900 cm^{-1}) are slightly displaced from, and their relative intensities are somewhat different from, those of high-molecular-weight polyacetaldehyde. In addition, a few weak bands or shoulders appear near 2880, 1470, 1295, 1170, and 870 cm^{-1}; they are probably due to the ethyl end groups.

The infrared spectra of high-pressure polyacetaldehyde and polyacetaldehyde-d_1 are shown in Fig. 1. The bands in the skeletal stretching and skeletal bending regions are broad, in contrast to those of polychloral (15), probably because there are many rotational isomers present. However, if, as seems likely, the polymer chain is kinked at a small proportion of the C—O bonds and the interaction between the chains is small, the spectrum will resemble that of the isolated regular (i.e. repeating) chain. In particular, the number of strong bands observed should be close to the number expected for an isolated regular chain, and the bands will be broader than for the regular chain because rotational isomers are present. Similar assumptions about other polymers have been made by others (16, 17), and we tentatively assume that they are true for polyacetaldehyde and poly-propionaldehyde. The observation that the infrared spectrum of polyacetaldehyde in solution is similar, except that the bands are broader, to the spectrum of the pure polymer verifies that interaction between chains does not produce major changes in the number of strong bands. Davison (18) has shown that the presence of rotational isomers causes broadening of the bands in polyesters and related compounds. The assumption that the number of strong bands in a moderately kinked chain is close to the number expected for a regular chain allows us to obtain some tentative information about the structure of the polymer chain. Unfortunately, there appears to be no simple way of counting the number of kinks and so of verifying our assumption directly. We were not able to obtain oriented specimens of polyacetaldehyde or polypropionaldehyde and so could not obtain the dichroisms, probably because the melting point is below room temperature.

If there is one monomer unit in the repeat of polyacetaldehyde there are $3\times7-4 = 17$ fundamental frequencies that may be optically active, because only those vibrations that are in phase in all repeat units can be active in a perfect chain. These frequencies may be approximately divided as follows. Between 3000 and 2700 cm^{-1} two asymmetrical (which are probably not resolvable) and one symmetrical CH_3 stretching frequency and one CH stretching frequency are expected. Between 1500 and 1300 cm^{-1} two asymmetrical (which may not be resolvable) and one symmetrical CH_3 bending frequency are expected. Only one CH bending frequency is expected in this region, the other being probably below 1200 cm^{-1}, because deuterated chloral hydrate (19) has only one band in this region, and a band near 1100 cm^{-1} that is present in acetals and absent in ketals has been ascribed (20) to the CH bending mode. Between 1300 and 700 cm^{-1} two CH_3 rocking (which may not be resolved), one CH bending, and three skeletal (CO and CC) stretching bands are expected.

In the spectrum of polyacetaldehyde there are three bands in the 3-μ region, 2980, 2920, and 2860 cm^{-1}. The 2860-cm^{-1} shoulder disappears on deuteration and is replaced by two bands at 2160 and 2140 cm^{-1}. The 2860-cm^{-1} shoulder is thus a CH stretching band and the 2980- and 2920-cm^{-1} bands are the CH_3 asymmetrical and symmetrical stretching bands respectively. The two bands at 2160 and 2140 cm^{-1} may both be CD stretching fundamentals of the regular chain or one may be a band characteristic of the non-crystalline polymer, as occurs in the CH stretching region in polychloral (15), or one may be an overtone whose intensity is increased by Fermi resonance.

Can. J. Chem. Downloaded from www.nrcresearchpress.com by 176.9.209.113 on 09/04/12
For personal use only.

In the range 1500–1300 cm^{-1} there are three medium or strong bands, 1445, 1380, and 1335 cm^{-1}, and a shoulder, 1400 cm^{-1}. The 1400- and 1335-cm^{-1} bands disappear on deuteration and are thus CH bending bands; two CH bending bands are also present in polychloral (15) at 1360 and 1325 cm^{-1}. The bands at 1445 and 1380 cm^{-1} do not shift on deuteration and are straightforwardly assigned to the asymmetrical and symmetrical CH_3 bending modes, respectively.

The bands below 1200 cm^{-1} are not so easily identified. There are very intense and broad bands at 1187, 1130, 1085, 1040, 970, and 935 cm^{-1}. No band similar to the 1187-cm^{-1} band is observed in the spectra of the polyaldehydes which do not contain methyl groups, such as polymers of formaldehyde (21), chloral (15), and mono- and di-chloroacetaldehyde (22), and it might be due to the CH_3 rocking vibrations which are expected in this region (23). This mode involves appreciable skeletal stretching motion (23) and so may absorb strongly. The remaining bands in the 1200–900 cm^{-1} region are likely to be due to C—O and C—C stretching vibrations; they are similar to bands in the spectra of acetals and of other polyaldehydes. The changes in this region on deuteration are difficult to interpret because the bands overlap and are broad. Two CD bending bands, corresponding to the CH bending bands 1400 and 1335 cm^{-1}, should be here.

There is a medium band at 845 cm^{-1} and a weak band at 810 cm^{-1} which are replaced on deuteration by bands at 787 and 760 cm^{-1}. They might be associated with the low-frequency C—H bending mode. The shifts, however, are small and if they are CH bending bands they must be strongly coupled with skeletal motions; presumably other bands in the region 1200–1000 cm^{-1} shift but the shifts are masked by the overlapping of bands.

In the remaining part of the spectrum there occurs only one very broad weak band at 490 cm^{-1} with shoulders at 510 and 450 cm^{-1}. Similar bands occur in the spectra of acetals (20) and other polyaldehydes (15, 21, 22, 25) and are probably due to skeletal bending motions.

It is not easy to interpret the spectrum on the grounds of one monomer unit in the repeat unit. Thus, there are two higher-frequency C—H bending bands where only one is expected; there are eight bands in the region 1250–700 cm^{-1} where there are only six expected if the two CH_3 rocking modes are resolved and only five if, as seems very likely, they are not. If the assumption that we have made, that the kinking of the chain does not greatly effect the number of strong bands, is true then there are at least two monomer units in the repeat unit of the polymer chain.

(ii) Polypropionaldehyde

Polypropionaldehyde is very similar to polyacetaldehyde in chemical properties and in infrared spectrum. It is therefore a substituted polyoxymethylene and has the monomer unit $(CHC_2H_5.O)$, as expected from the ease of polymerization and depolymerization. A broad weak band at 3460 cm^{-1} occurs in some samples; it is probably an OH stretching band due to the end groups. The polymer is therefore $HO(CHC_2H_5.O)_nH$. The X-ray powder diagram has two diffuse rings that correspond to spacings of about 9.0 and 4.1 Å. This and the broadness of the skeletal stretching and bending bands show (see below) that the polymer is amorphous. The broad rings on the X-ray diagram probably relate to interchain rather than to intrachain distances, as argued above for polyacetaldehyde. The infrared spectra can be analyzed, as was that of polyacetaldehyde, to show that there is probably more than one monomer unit in the repeat. The assumptions made are the same as those made for polyacetaldehyde, i.e. that rotational

isomerism and interaction between chains broadens the infrared bands but does not produce much change in the number of strong bands. By analogy with polyacetaldehyde and polychloral it is likely that only the CH bending and skeletal stretching and possibly the CH stretching modes will give information about the structure. If there is one monomer in the repeat unit then one CH stretching, one CH bending, and four skeletal stretching bands are expected.

There are three strong bands in the 3-μ region, at 2960, 2925, and 2870 cm^{-1}. They do not shift on deuteration, and so are due mainly to methyl and methylene groups. Though no shifts are observed on deuteration, two bands, 2150 and 2125 cm^{-1}, appear in the spectrum of polypropionaldehyde-d_1. At least one band is CD bending and, as with polyacetaldehyde, both may be fundamentals of the crystalline polymer, one may be a band characteristic of the disordered regions of the polymer, or one may be an overtone in resonance with the fundamental.

In the region 1500–1200 cm^{-1} there are medium or strong bands at 1468, 1443, 1380, 1345, 1305, and 1265 cm^{-1}. The 1360- and 1305-cm^{-1} bands disappear on deuteration and, as we argued for similar bands in polyacetaldehyde, are probably higher-frequency CH bending bands. The 1443- and 1380-cm^{-1} bands are close to those of polyacetaldehyde and are therefore probably respectively asymmetrical and symmetrical CH_3 bending bands. The remaining three bands, 1468, 1345, and 1265 cm^{-1}, are not present in polyacetaldehyde and shift but slightly on deuteration. They are therefore probably CH_2 bending modes and, on grounds of frequency by comparison with small molecules, are probably the bending, wagging, and twisting modes respectively.

The 1200–900 cm^{-1} region is less straightforward. There are about nine strong or very strong bands. A shoulder at 1175 cm^{-1} might, by analogy with polyacetaldehyde and smaller molecules, be due to the CH_3 rocking modes. The remaining are probably skeletal stretching bands. There are therefore about eight skeletal stretching bands. If there is one monomer unit in the repeating unit only four are expected. This together with the two CH bending bands at 1400–1300 cm^{-1} shows that, if kinking does not cause many new strong bands, then there is probably more than one monomer unit in the repeating unit of the chain. In the spectrum of polypropionaldehyde-d_1 the bands in this region are shifted and their intensities changed. The interpretation of this is uncertain because CD bending bands are expected here.

In the remaining part of the spectrum there are medium or weak bands at 895, 795, 780, and 480 cm^{-1}. The 895-cm^{-1} band is replaced on deuteration by a band at 855 cm^{-1}. It is likely that CH bending is an important contributor to this mode. The bands at 795 and 780 cm^{-1} shift little on deuteration and are not observed in polyacetaldehyde. They may be CH_2 rocking modes, which are expected about here. The very broad weak band at 480 cm^{-1} accompanied by a shoulder at about 590 cm^{-1} is due to skeletal bending vibrations.

We have seen that the spectra of polyacetaldehyde and polypropionaldehyde are considerably more complicated than they would be if there was only one monomer unit in the repeat unit. In particular, there are twice as many high-frequency CH bending and somewhat less than twice as many skeletal stretching bands as are expected for one monomer unit. No further information is obtainable from the infrared spectrum at present. It is interesting to note, however, that polyformaldehyde has a helical configuration (24) which is probably formed from gauche conformations of the C—O bonds (25). The stable conformation of the smallest molecules derived from polyformaldehyde dimethoxymethane, is the double gauche form (26, 27). It seems not unlikely that the

Can. J. Chem. Downloaded from www.nrcresearchpress.com by 176.9.209.113 on 09/04/12
For personal use only.

higher homologues of dimethoxymethane, i.e. 1,1-dimethoxyethane and 1,1-dimethoxypropane, have a stable conformation similar to that of dimethoxymethane. If this is so then a chain of such units, such as are polyacetaldehyde and polypropionaldehyde, would be expected to have at equilibrium at low temperatures a spiral structure similar to that of polyformaldehyde. The infrared spectra are certainly consistent with a spiral structure, but do not prove it. As outlined previously (21), for all cyclic structures but the trivial plane zigzag, each mode of vibration of the monomer splits into two infrared-active modes, of species A and E_1 (E in some of the simpler spirals). Consequently, if the spiral were perfect, then two high-frequency CH bending and six (polyacetaldehyde) and eight (polypropionaldehyde) skeletal stretching modes would be expected to be active. These are approximately the number of strong bands found in the spectra, and so, if rotational isomerism does not cause many new strong bands, the spectra are consistent with the structures' being spirals.

ACKNOWLEDGMENTS

The authors are very grateful to Dr. L. D. Calvert for taking the X-ray diffraction photographs and to Mr. A. Lavergne for help with the high-pressure equipment.

REFERENCES

1. LETORT, M. Compt. rend. **202**, 767 (1936).
2. TRAVERS, M. Trans. Faraday Soc. **32**, 246 (1936).
3. MUTHANA, M. S. and MARK, H. J. Polymer Sci. **4**, 91 (1949).
4. SUTHERLAND, G. B. B. M., PHILPOTTS, A. R., and TWIGG, G. H. Nature, **157**, 267 (1946).
5. STAUDINGER, H. Trans. Faraday Soc. **32**, 246 (1936).
6. LETORT, M. and DUVAL, X. Compt. rend. **216**, 58 (1943).
7. BRIDGMAN, P. W. and CONANT, J. B. Proc. Nat. Acad. Sci. **15**, 680 (1929).
8. CONANT, J. B. and TONGBERG, C. O. J. Am. Chem. Soc. **52**, 1659 (1930).
9. FAWCETT, E. W. and GIBSON, R. O. J. Chem. Soc. 386 (1934).
10. FENNE, D. J. and MUGDAN, M. U.S. Pat. No. 2,607,804 (1952).
11. LEITCH, L. C. Can. J. Chem. **33**, 400 (1955).
12. SMITH, T. E. and BONNER, R. F. Ind. Eng. Chem. **43**, 1169 (1951).
13. BEVINGTON, J. C. and NORRISH, R. G. W. Proc. Roy. Soc. (London), A, **196**, 363 (1949).
14. RIGBY, H. A., DANBY, C. J., and HINSHELWOOD, C. N. J. Chem. Soc. 234 (1948).
15. NOVAK, A. and WHALLEY, E. Trans. Faraday Soc. In press.
16. TOBIN, M. C. J. Chem. Phys. **23**, 891 (1955).
17. LIANG, C. Y., KRIMM, S., and SUTHERLAND, G. B. B. M. J. Chem. Phys. **25**, 543 (1957), and later papers.
18. DAVISON, W. H. T. J. Chem. Soc. 3270 (1955).
19. NOVAK, A. and WHALLEY, E. Unpublished work.
20. BERGMANN, E. D. and PINCHAS, S. Rec. trav. chim. **71**, 161 (1952).
21. NOVAK, A. and WHALLEY, E. Trans. Faraday Soc. In press.
22. NOVAK, A. and WHALLEY, E. Can. J. Chem. **37**, 1722 (1959).
23. JONES, R. N. and SANDORFY, C. In A. WEISSBERGER. *Editor.* Technique of organic chemistry. Vol. IX. Interscience Publishers, Inc., New York. 1956. p. 342.
24. WILMSHURST, J. K. Can. J. Chem. **36**, 285 (1958).
25. NOVAK, A. and WHALLEY, E. Can. J. Chem. **37**, 1718 (1959).
26. SAUTER, E. Z. physik. Chem. B, **21**, 161 (1933).
27. SHIMANOUCHI, T. and MIZUSHIMA, S. J. Chem. Phys. **23**, 707 (1955).
28. MIZUSHIMA, S., MORINO, Y., and KUBO, M. Physik. Z. **38**, 459 (1937).
29. AOKI, K. J. Chem. Soc. Japan, Pure Chem. Sect. **74**, 110 (1953).

Can. J. Chem. Downloaded from www.nrcresearchpress.com by 176.9.209.113 on 09/04/12
For personal use only.

Can. J. Chem. Downloaded from www.nrcresearchpress.com by 176.9.209.113 on 09/04/12
For personal use only.

THE INFRARED SPECTRA AND STRUCTURE OF POLYALDEHYDES

IV. THE HIGHER POLYALDEHYDES[1]

A. NOVAK[2] AND E. WHALLEY

ABSTRACT

The polymers of *n*- and iso-butyraldehyde and *n*-valeraldehyde, which were made by subjecting the aldehydes to pressures of about 8 kb, have been examined by infrared spectroscopy. They are homologues of polyformaldehyde, having the formula $HO(CHR.O)_nH$.

I. INTRODUCTION

The polymerization under pressure of aliphatic aldehydes was first observed by Bridgman and Conant (1) and by Conant and Tongberg (2). The polymers were quite different from those obtained by the aldol condensation, and they readily reverted to the monomers at normal temperature and pressure. Conant and Peterson (3) suggested that they were homologues of polyformaldehyde on the grounds that polymerization and depolymerization was relatively easy and was not catalyzed by bases.

We have investigated the infrared spectra of polymers of *n*- and iso-butyraldehyde, *n*-valeraldehyde, and *n*-heptaldehyde and confirm the structure suggested by Conant and Peterson. This paper reports this work.

2. EXPERIMENTAL METHODS AND RESULTS

The aldehydes were Eastman Kodak White-Label products; they were dried with Drierite several times and were fractionated in an atmosphere of dry air before use. Their infrared spectra were recorded for comparison purposes and to check the substantial absence of water and hydrates. The polymers were prepared by subjecting the monomers to pressures of about 9 kb at room temperature for about one day; this was done by placing them in 1-cm^3 stainless-steel test tubes which were sealed with a plug carrying an *o*-ring and put into the high-pressure end of a pressure intensifier of standard design. Polymerization was usually almost complete; monomer and lower polymers were removed if necessary by extraction with ethanol. Poly-*n*-butyraldehyde was a waxy solid, poly-*n*-valeraldehyde was a viscous liquid, and poly-*n*-heptaldehyde was a solid; all were soluble in ether and carbon tetrachloride and insoluble in ethanol. Poly-isobutyraldehyde was a hard transparent solid that was insoluble in the commoner solvents.

At room temperature all the polymers reverted to monomer. The depolymerization of poly-*n*-butyraldehyde in carbon tetrachloride solution was followed by infrared spectroscopy; depolymerization was complete in about 30 hours at room temperature. Poly-*n*-butyraldehyde was stored for several months in ethanol at about $-10°$ C without apparent depolymerization. No attempt was made to store the other polymers.

The polymers were investigated spectroscopically as films or as suspensions in nujol and hexachlorobutadiene. The spectra were recorded between 4000 and 700 cm^{-1} using a Perkin–Elmer infrared spectrophotometer, Model 21, with a sodium chloride prism, and between 700 and 300 cm^{-1} using a Beckmann IR-4 spectrophotometer with a cesium bromide prism. The spectra are shown in Fig. 1, and the wave numbers and relative intensities of the bands are listed in Table I.

[1]*Manuscript received March 25, 1959.*
Contribution from the Division of Applied Chemistry, National Research Council, Ottawa, Canada. Issued as N.R.C. No. 5308.
[2]*N.R.C. Postdoctorate Fellow, 1956–58.*

TABLE I

Infrared spectra of polyaldehydes, $(CHR—O—)_n$

$R = CH_3(CH_2)_2$		$R = CH_3(CH_2)_3$		$R = CH_3(CH_2)_5$		$R = (CH_3)_2CH$	
Wave No. cm^{-1}	Intensity	Wave No. cm^{-1}	Intensity	Wave No. cm^{-1}	Intensity	Wave No. cm^{-1}	Intensity
		3440	Variable, w	3440	Variable, w		
2940	vs			2940	vs	2940	vs
2920	vs	2920	vs	2920	vs	2920	vs
2860	s	2860	vs	2850	vs	2860	s
1470	s	1470	s	1470	s	1475	s
1460	s	1460	sh	1460	sh	1463	sh
1436	m	1436	m	1436	m		
1372	s	1380	s, b	1374	s	1382	s
1345	s	1355	s	1355	s	1368	s
		1342	sh	1345	sh	1353	s
				1325	m	1335	m
1295	w	1285	w	1300	w	1304	m
1270	w	1250	w	1276	w		
1238	m	1220	m	1255	w		
				1225	m		
				1200	m		
						1190	s
1165	sh	1140	sh	1150	sh	1158	s
1125	vs, b			1130	vs	1130	s
1105	vs, b	1095	vs, vb	1102	vs	1060	vs
1090	vs, b			1050	s	1025	vs
1050	s	1050	sh	1036	vs	1008	vs
1007	vs, b	1005	vs, vb	1025	vs		
982	vs, b			1015	s	990	s
960	sh	960	sh	990	s	968	vs
914	vs	935	vs, vb	948	m	918	sh
				905	m	908	vs
840	w	875	sh	870	w	845	m
825	w			785	w	840	m
755	sh	780	w, b	760	w		
740	w	730	w	722	m	676	w
				610	w	628	vw
				544	m	519	m
530	w, vb	530	w, vb	455	w	495	sh
				390	w	456	m

NOTE: b=broad, vb=very broad.

X-ray diffraction photographs were taken on a Debye–Scherrer powder-camera using Ni-filtered Cu radiation. The lattice spacings are listed in Table II.

3. DISCUSSION

The infrared spectra (Fig. 1 and Table I) confirm Conant and Peterson's suggestion (3) that the polymers are substituted polyoxymethylenes. Thus, there are strong bands in the region 1200–900 cm^{-1}; i.e. in the region of C—O stretching bands, and there are no very strong broad bands near 3400 cm^{-1}, showing that OH groups in quantity are absent. Broad weak bands at about 3440 cm^{-1} occur in the spectra of some samples and are probably due to OH end groups; those samples in which the band is missing are probably of higher molecular weight. The chemical formula of the polyaldehydes is thus $HO(CHR.O)_nH$ and they are analogues of polyformaldehyde (4–6), polychloral (7), polyacetaldehyde (8), and polypropionaldehyde (8). The polymerization can be represented thus,

$$RCHO + \frac{1}{n}H_2O \rightleftharpoons \frac{1}{n}HO(CHR.O)_nH,$$

Can. J. Chem. Downloaded from www.nrcresearchpress.com by 176.9.209.113 on 09/04/12
For personal use only.

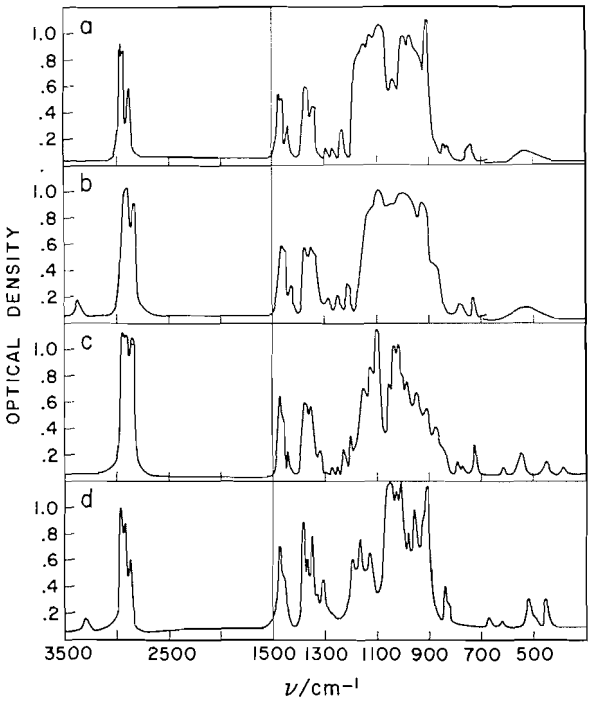

FIG. 1. Infrared spectra of polyaldehydes: (*a*) poly-*n*-butyraldehyde film; (*b*) poly-*n*-valeraldehyde film; (*c*) poly-*n*-heptaldehyde mull in nujol and hexachlorobutadiene; (*d*) poly-isobutyraldehyde mull in nujol and hexachlorobutadiene.

and the position of equilibrium is evidently displaced from almost completely on the left to nearly completely on the right by pressures of about 9 kb.

It is not possible to identify the infrared bands in detail. Undoubtedly C—H stretching modes are in the region 3000–2700 cm^{-1}, C—H bending modes in the region 1500–1200 cm^{-1}, skeletal stretching modes in the region 1200–700 cm^{-1}, with probably some of the lower-frequency C—H bending modes, and skeletal bending modes in the region 700–300 cm^{-1}. The spectra are too complicated to analyze in more detail at the present time.

It should be noted that the bands in the skeletal bending and stretching regions are broad in poly-*n*-butyraldehyde and poly-*n*-valeraldehyde and that the X-ray diagram of poly-*n*-butyraldehyde shows only a few diffuse halos. The X-ray diffraction diagram of poly-*n*-valeraldehyde could not be taken because it decomposed rapidly; since it is a viscous liquid it is likely to be amorphous. On the other hand, the infrared spectra of poly-isobutyraldehyde and poly-*n*-heptaldehyde in the skeletal bending and stretching regions are sharp and the X-ray diagrams for these polymers have relatively sharp rings. We conclude from this evidence that the polymers of *n*-butyraldehyde and *n*-valeraldehyde are amorphous and that the broadness of the infrared bands is caused by the presence of rotational isomers. It is unlikely that the broadness is due to intermolecular effects because the spectrum of poly-*n*-butyraldehyde in carbon tetrachloride solution is similar to that of the film. The polymers of isobutyraldehyde and *n*-heptaldehyde are relatively crystalline, and the sharpness of the infrared bands confirms that they contain relatively few rotational isomers.

Can. J. Chem. Downloaded from www.nrcresearchpress.com by 176.9.209.113 on 09/04/12
For personal use only.

TABLE II

Interplanar spacings of polyaldehydes, $(CHR.O)_n$

$R = CH_3(CH_2)_5$		$R = CH_3CH_2CH_2$		$R = (CH_3)_2CH$	
Spacing Å	Intensity	Spacing Å	Intensity	Spacing Å	Intensity
13.1	100	12.0 }	Halo 100	9.3	100 vb
11.5	100	9.0 }			
7.44	30			7.9	60 vb
6.53	50				
5.87	50			5.5	10
5.00	40	4.8 }	Halo 100		
4.66	50	4.0 }		4.6	60 b
4.18	90 b			3.95	20
3.65	50				
3.46	25			3.5	40 b
3.09	25				
2.87	25			2.65	5
2.67	25				
2.50	25 b			2.40	10 b
2.29	25			2.25	2 b
2.23	25				
2.17	30	2.05	20	2.04	5

The lattice spacings corresponding to the rings of the most intense lines of the X-ray diffraction photographs (Table II) increase with increasing length of the side groups. As we have pointed out before (8), it is likely because of this increase that these spacings are related to interchain rather than to intrachain distances.

REFERENCES

1. BRIDGMAN, P. W. and CONANT, J. B. Proc. Nat. Acad. Sci. **15**, 680 (1929).
2. CONANT, J. B. and TONGBERG, C. O. J. Am. Chem. Soc. **52**, 1659 (1930).
3. CONANT, J. B. and PETERSON, W. R. J. Am. Chem. Soc. **54**, 628 (1932).
4. STAUDINGER, H. Die hochmolekularen organischen Verbindungen. Springer-Verlag, Berlin. 1932.
5. PHILPOTTS, A. R., EVANS, D. O., and SHEPPARD, N. Trans. Faraday Soc. **51**, 1051 (1955).
6. NOVAK, A. and WHALLEY, E. Trans. Faraday Soc. In press.
7. NOVAK, A. and WHALLEY, E. Trans. Faraday Soc. In press.
8. NOVAK, A. and WHALLEY, E. Can. J. Chem. **37**, 1710 (1959).

Can. J. Chem. Downloaded from www.nrcresearchpress.com by 176.9.209.113 on 09/04/12
For personal use only.

Can. J. Chem. Downloaded from www.nrcresearchpress.com by 176.9.209.113 on 09/04/12
For personal use only.

INFRARED SPECTRA AND STRUCTURE OF POLYALDEHYDES

V. POLYMONOCHLOROACETALDEHYDE AND POLYDICHLOROACETALDEHYDE[1]

A. NOVAK[2] AND E. WHALLEY

ABSTRACT

The polymers of monochloroacetaldehyde and dichloroacetaldehyde have been examined by infrared spectroscopy. They are homologues of polyformaldehyde, having the formula $HO(CHR.O)_nH$. X-ray-diffraction powder photographs show that they are fairly crystalline.

1. INTRODUCTION

It has been known for some time that mono- and di-chloroacetaldehyde form trimers and polymers (1–3). Trimers are produced when the aldehydes are treated with concentrated sulphuric acid; they are crystalline substances with well-defined melting points (1–3) and are probably analogous to paraldehyde. Monochloroacetaldehyde polymerizes fast when allowed to stand in sealed tubes to give a substance described as amorphous (1) which has the same empirical formula as the aldehyde. Dichloroacetaldehyde, when purified, rapidly forms a similar substance that has the same empirical formula as the aldehyde. Both polymers are insoluble in water and alcohol, and that derived from monochloroacetaldehyde is insoluble also in ether and chloroform. They have no sharp melting points and they decompose to the parent aldehyde when heated to above 120° C. No work on the nature of these substances has been reported.

As part of our program of investigation of the structures of polyaldehydes (4–7) we have investigated the infrared spectra and X-ray powder diagrams of these polymers in order to elucidate their structure. This paper reports the results of this work.

2. EXPERIMENTAL AND RESULTS

Monochloroacetaldehyde (40% water solution) and dichloroacetaldehyde were commercial samples. Monochloroacetaldehyde solution was treated with concentrated sulphuric acid and distilled. The distillate formed a crystalline substance of melting point about 40–50° C which is probably the hydrate (1); this was treated again with concentrated sulphuric acid, and the vapor of the aldehyde which was obtained was dried by being passed through a tube containing calcium chloride heated at 100° C. The vapors when condensed polymerized rapidly to a solid which had similar properties to the polymer previously described (1). The commercial dichloroacetaldehyde was a rather viscous substance whose infrared spectrum indicates that it is a mixture mainly of a polymer whose structure is described below, aldehyde, and water. A small amount of concentrated sulphuric acid was added to this mixture and it was then distilled, and the vapor was dried in a similar manner to that used for monochloroacetaldehyde. The distillate polymerized into a block of translucent soft solid. The polymer was dissolved in acetone and precipitated with methanol. The precipitate was filtered and dried under reduced pressure.

The samples were examined as mulls in nujol and hexachlorobutadiene; the polymer of dichloroacetaldehyde was examined also in chloroform solution and as a film that was obtained by evaporating a solution of the polymer in acetone. The spectra were recorded

[1]*Manuscript received March 25, 1959.*
Contribution from the Division of Applied Chemistry, National Research Council, Ottawa, Canada. Issued as N.R.C. No. 5307.
[2]*N.R.C. Postdoctorate Fellow 1956–58.*

between 4000 and 700 cm^{-1} using a Perkin–Elmer infrared spectrophotometer, Model 21, with a rock salt prism and a Beckmann IR-4 spectrophotometer with a cesium bromide prism. The infrared spectra of the polymers are shown in Fig. 1 and the wave numbers and relative intensities of the bands are listed in Table I.

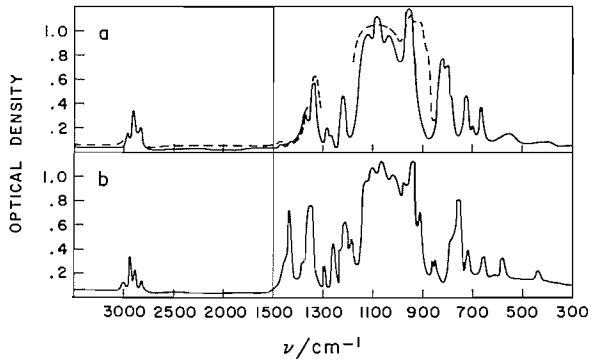

FIG. 1. Infrared spectra. (*a*) Polydichloroacetaldehyde: solid line, film: dotted line, in solution in $CHCl_3$. (*b*) Polymonochloroacetaldehyde: suspensions in nujol and hexachlorobutadiene.

TABLE I

Infrared spectra of polymers of mono- and di-chloroacetaldehyde

$(CHCH_2Cl—O—)_n$			$(CHCHCl_2—O—)_n$		
Wave No. cm^{-1}	Intensity	Approximate description	Wave No. cm^{-1}	Intensity	Approximate description
3460	Variable, w	OH stretching	3420	Variable, w	OH stretching
3000	w	CH stretching	3005	m	CH stretching
2935	m		2940	m	
2890	m		2870	m	
2820	w				
			1460	w	Combinations
1445	sh	CH_2 bending	1430	w	
1434	s				
			1370	m	CH bending
1375	sh		1338	s	
1350	s				
1298	m	CH bending,	1287	m	$CHCl_2$ bending
1265	m	CH_2 wagging, and	1265	m	
1230	sh	CH_2 twisting	1217	s	
1216	s		1132	vs	C—O stretching
1192	m		1087	vs	
			1040	vs	
			955	vs	
1135	vs, b				
1105	vs				
1065	vs		815	vs	C—C and C—Cl stretching
1025	vs		800	vs	
975	vs		775	sh	
942	vs	C—O, C—C, and	725	s	
915	s	C—Cl stretching,	710	w	
862	m	CH_2 rocking, and	675	m	
852	m	CH bending			
790	s		550	m, b	Skeletal bending
762	s				
730	m				
716	w				
660	m				
620	w	Skeletal bending			
580	m				
440	w				

Can. J. Chem. Downloaded from www.nrcresearchpress.com by 176.9.209.113 on 09/04/12
For personal use only.

The X-ray powder photographs were taken with a Debye–Scherrer camera using nickel-filtered copper radiation. The lattice spacings calculated from the X-ray photographs are given in Table II.

TABLE II

X-Ray powder diagrams of polymers of mono- and di-chloroacetaldehyde

$(CHCH_2Cl—O—)_n$		$(CHCHCl_2—O—)_n$	
Spacing Å	Intensity	Spacing Å	Intensity
7.76	100	8.32	100
5.45	50	4.99 to 4.41	30
4.35 to 3.63	75 Halo	4.41 to 3.62	75
3.85	90	3.42	40
3.45	90	3.13	50
3.06	30	2.83	50
2.93	30	2.32	30
2.74	50	2.01	25
2.60	40		
2.44	60		
2.14	40		
2.00	25		

3. DISCUSSION

The infrared spectra have very strong bands in the region 1200–900 cm^{-1} that must involve C—O stretching motions. There are no carbonyl stretching bands and only very weak bands in the region of the OH stretching band. This evidence together with the ease of polymerization and depolymerization shows that the structure of the polymers is $(CHR.O)_n$ where R is either the monochloromethyl or dichloromethyl group. There are weak bands in the spectra of some samples in the region of 3400 cm^{-1} which are probably due to OH stretching vibrations. It is likely that the OH groups are at the ends of the chains, and so the formulas are $HO(CHR.O)_nH$. The polymers are thus substituted polyoxymethylene glycols, entirely analogous to the other polymers discussed in this series of papers.

The X-ray diffraction photographs have relatively sharp rings, indicating that the polymers are fairly crystalline, as we found also for polychloral. The bands in the skeletal stretching region of the spectra are broader than those of polychloral and narrower than those of polyacetaldehyde and polypropionaldehyde. It seems likely that the broadness is due, at least partly, to the presence of rotational isomers in the non-crystalline parts of the spectrum. This is supported by the skeletal stretching bands in the spectrum of polydichloroacetaldehyde in chloroform solution, which probably contains more rotational isomers than the solid, being much broader than those of the solid.

We have seen previously (4–7) that the spectra of the simpler polyaldehydes have more bands than they would have if there were only one monomer unit in the repeating unit, and it is pertinent to inquire if this is so also for polymonochloroacetaldehyde and polydichloroacetaldehyde. We make the same assumption that we have made previously, viz. that the amorphous regions of the polymers cause the infrared bands to broaden but do not cause many new bands.

Can. J. Chem. Downloaded from www.nrcresearchpress.com by 176.9.209.113 on 09/04/12
For personal use only.

Polydichloroacetaldehyde

If there is one monomer unit in the repeating unit then there are $3\times7-4 = 17$ potentially active fundamentals, which can be approximately divided into 6 CH and 11 skeletal vibrations, though there may, of course, be strong interaction between the lower-frequency CH and the skeletal vibrations. There are two kinds of CH group $CC(O—)_2H$ and $CCCl_2H$. The two CH bending frequencies of the $CC(O—)_2H$ group are expected, according to arguments presented in reference 5, to be one above 1300 cm^{-1} and one below 1200 cm^{-1}. The two CH bending frequencies of the $CCCl_2H$ group are expected to be between 1300 and 1200 cm^{-1} by analogy with smaller molecules containing a similar group (8). Thus, the bands expected are summarized as follows: 3000–2700 cm^{-1}, two C—H stretching bands; 1500–1200 cm^{-1}, three C—H bending bands; 1200–600 cm^{-1}, one C—H bending and five skeletal stretching bands.

In the observed spectrum there are three medium bands near 3005, 2950, and 2870 cm^{-1}; they are probably all fundamentals, being strong for ternary combinations, but one may be characteristic of the amorphous polymer, as we found with polychloral.

In the region 1500–1200 cm^{-1}, there are weak bands at 1460 and 1430 cm^{-1} and medium or strong bands at 1370, 1339, 1287, 1265, and 1217 cm^{-1}. The weak 1460- and 1430-cm^{-1} bands are probably combination bands; CCl vibrations frequently give bands about here. The others are likely to be all CH fundamentals.

In the region 1200–600 cm^{-1} there are 10 bands, at 1132, 1087, 1040, 955, 815, 800, 775, 725, 710, and 675 cm^{-1}. Most are very strong and they are probably all fundamentals, mostly skeletal stretching bands. The 1132-, 1087-, 1040-, and 955-cm^{-1} bands are, by analogy with other polyaldehydes, probably due mainly to C—O stretching modes.

There are many more bands than expected for a one-monomer-unit repeat. Thus, there are five C—H bending bands, where only three are expected; there are nine bands in the skeletal stretching region, where only six are expected. We conclude, therefore, that there are at least two monomer units in the repeat.

Polymonochloroacetaldehyde

If there is one monomer unit in the repeating unit the number of bands expected in the different regions are as follows: 3000–2700 cm^{-1}, one CH and two CH_2 stretching bands; 1500–1200 cm^{-1}, one CH bending and CH_2 bending, wagging, and twisting bands; 1200–600 cm^{-1}, one CH bending, one CH_2 rocking, and four skeletal (C—O, C—C, and C—Cl) stretching bands.

In the region 3000–2700 cm^{-1} there are four bands, 3000, 2935, 2890, and 2820 cm^{-1}; as with polychloral, they may not all be fundamentals of the crystalline polymer.

In the region 1500–1200 cm^{-1} there are bands at 1445, 1434, 1375, 1350, 1298, 1265, 1230, 1216, and 1192 cm^{-1}. Allowing for the possibility that some of these are overtone or combination bands, or bands due to non-crystalline regions, there are many more than the four expected for a one-monomer repeat.

In the region 1200–600 cm^{-1} there are bands at 1135, 1105, 1065, 1025, 975, 942, 915, 862, 852, 790, 762, 730, 716, 660, and 610 cm^{-1}. Again, allowing for the possibility of overtones and combination bands, and the possibility that a few may be due to amorphous regions (cf. the 630-cm^{-1} band in polychloral) there are many more than the six bands expected for a one-monomer repeat.

We conclude, therefore, that there is more than one monomer unit in the repeating unit.

ACKNOWLEDGMENT

We are very grateful to Dr. L. D. Calvert for taking the X-ray diffraction photographs.

Can. J. Chem. Downloaded from www.nrcresearchpress.com by 176.9.209.113 on 09/04/12
For personal use only.

REFERENCES

1. NATTERER, K. Monatsh. Chem. **3**, 442 (1882).
2. FRIEDRICH, R. Ann. **206**, 251 (1881).
3. JACOBSEN, O. Ber. **8**, 87 (1875).
4. NOVAK, A. and WHALLEY, E. Trans. Faraday Soc. In press.
5. NOVAK, A. and WHALLEY, E. Trans. Faraday Soc. In press.
6. NOVAK, A. and WHALLEY, E. Can. J. Chem. **37**, 1710 (1959).
7. NOVAK, A. and WHALLEY, E. Can. J. Chem. **37**, 1718 (1959).
8. DAASCH, L. W., LIANG, C. Y., and NIELSEN, J. R. J. Chem. Phys. **22**, 1293 (1954).

Can. J. Chem. Downloaded from www.nrcresearchpress.com by 176.9.209.113 on 09/04/12
For personal use only.

INTERACTION BETWEEN KETONE AND TERTIARY AMINE GROUPS[1]

OWEN H. WHEELER[2] AND ERIC M. LEVY[3]

ABSTRACT

Vapor pressure studies of trimethylamine and ketones in heptane solution have shown that unstable complexes are formed with cyclohexanone at 0° and with cyclohexanone and cyclopentanone at −40°. No complex formation was observed with methylethyl ketone, diethyl ketone, or cyclopentanone at 0°.

Can. J. Chem. Downloaded from www.nrcresearchpress.com by 176.9.209.113 on 09/04/12
For personal use only.

Robinson and co-workers (1, 2) originally suggested that there was some type of interaction between a keto group and a tertiary amine group in certain alkaloids having these groups in a large-membered ring, to explain the masked reactivity of the keto group (1) and the large displacement of its infrared stretching frequency from its normal value (2). Later Leonard and co-workers (3, 4, 5) prepared a series of cyclic aza-acyloins and found evidence for transannular interaction in 8- (3, 5), 9- (4), and 10- (5) membered rings between the ketone and tertiary amine group. This was demonstrated by infrared and ultraviolet absorption (6) studies.

Anet, Bailey, and Robinson (2) found no evidence for interaction between acetone and triethylamine or between cyclopentanone and N-methyl piperidine by infrared measurements in chloroform solution. However, the amine would preferentially interact with the chloroform (7) and hinder association between the amine and ketone, and the evidence of these workers cannot be considered conclusive. Thus, though interaction between keto and amine groups within the same ring has been amply proved, no sound evidence has been published concerning possible interaction between ketone and amine groups in separate molecules.

Infrared and ultraviolet measurements are probably not the best method of observing weak interactions resulting in unstable complex formation, since such measurements must be carried out in dilute solution and cannot readily be made at low temperatures. Moreover these measurements will only detect interactions which result in a change in the electron density of the keto group. Vapor pressure studies, however, are usually made with solutions of moderate concentration, and the lower limit of temperature is only governed by the measurable vapor pressure of one (or more) component, and the method is not limited to specific types of interaction. In this study the vapor pressure of trimethylamine above a *n*-heptane solution and above solutions of the ketones, methylethyl ketone, diethyl ketone, cyclohexanone, and cyclopentanone in *n*-heptane has been measured. Trimethylamine was chosen as a conveniently volatile, non-sterically hindered amine and methylethyl ketone and diethyl ketone as examples of reactive and unreactive acyclic ketones, and cyclohexanone and cyclopentanone as examples of a very reactive and a moderately reactive cyclic ketone. The results are expressed in terms of Henry's law (8) (P solute $= K.N$ solute) and negative deviations are assumed to be due to complex formation (8) caused by interaction between the ketones and the amine.

[1]*Manuscript received March 31, 1959.*
Contribution from the Departments of Chemistry of the College of Agriculture and Mechanic Arts, University of Puerto Rico, Mayaguez, Puerto Rico, and Dalhousie University, Halifax, N.S. Published as Part XII of Structure and Properties of Cyclic Compounds. Part XI, Can. J. Chem. **36**, *656 (1958).*
[2]*Present address: College of Agriculture and Mechanic Arts, Mayaguez, Puerto Rico.*
[3]*Present address: Dalhousie University, Halifax, N.S.*

Can. J. Chem. Downloaded from www.nrcresearchpress.com by 176.9.209.113 on 09/04/12
For personal use only.

EXPERIMENTAL

n-Heptane

This was a sample from Matheson, Coleman, and Bell and was distilled over sodium (see Table I).

TABLE I

Physical constants*

	B.p. (° C)	n_D^{20}
n-Heptane	98.3 (98.43)	1.3884 (1.3879)
Methylethyl ketone	79.5 (79.50)	1.3786 (1.3784)
Diethyl ketone	101.6 (101.70)	1.3929 (1.3929)
Cyclopentanone	129.5 (130.6)	1.4369 (1.4366)
Cyclohexanone	155.7 (155.65)	1.4506 (1.4510)

*Values from International Critical Tables in parenthesis.

Trimethylamine

Eastman-Kodak white-label grade was dried over calcium hydride as described below.

Ketones

Eastman-Kodak white-label samples were dried over anhydrous calcium sulphate and fractionally distilled before use (see Table I).

Apparatus

The apparatus was similar to that used by Brown and Brady (9) and consisted of a flat-bottomed reaction flask of known volume (65.00 ml) joined by narrow-bore glass tubing to a differential mercury barometer, connected by a narrow-bore stopcock to a storage vessel of known capacity (534.0 ml), itself joined to another differential mercury barometer. The whole was attached to a conventional high-vacuum line which incorporated bulbs for the purification and storage of trimethylamine.

Method

A sample of 10 ml of purified *n*-heptane was introduced into the reaction flask together with two small Teflon-covered magnetic stirring bars, and was frozen and pumped out several times to remove dissolved air. Trimethylamine, which had been dried with calcium hydride, and freed from non-condensable gases, was distilled into the storage vessel. Small quantities were introduced into the reaction vessel and the amount admitted obtained from the known volume of the storage vessel and the pressure decrease on its manometer. The reaction vessel was immersed in a constant temperature bath (at 0° of ice; at −39.50° a slush bath of diethyl ketone (10), and at −63.55° of chloroform (11), and stirred by a strong permanent bar magnet mounted externally on a slow-speed motor. The reaction vessel was stirred continuously for about 10 to 15 minutes when the pressure ceased to drop and the residual pressure was noted. This process was repeated a number of times with pressures up to 160 mm of mercury, taking about 15 readings. All pressure readings were taken at constant volume by adjusting the amount of mercury in the barometers to a fixed mark on one limb.

The experiments were repeated with 10-ml samples of 1.0 *M* solutions of the ketones in *n*-heptane.

The amount of trimethylamine in solution is the difference between the amount added from the storage vessel and the amount remaining in the gas phase above the reaction vessel (this was usually $< 3\%$ the total amount; see Table II for typical data).

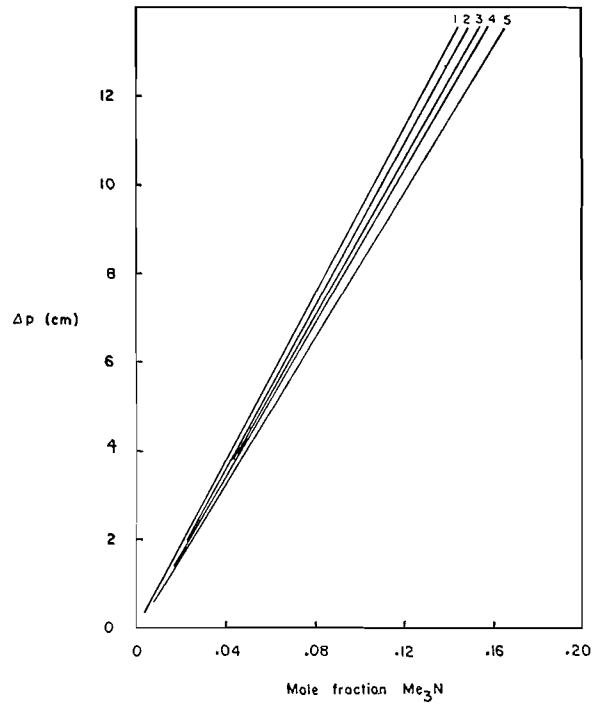

FIG. 1. Henry's law plot at 0° C. 1. Methylethyl ketone. 2. Diethyl ketone. 3. Cyclopentanone. 4. *n*-Heptane (pure). 5. Cyclohexanone.

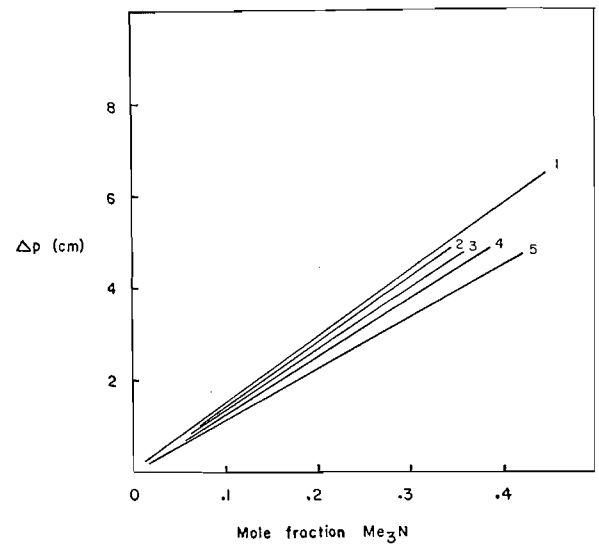

FIG. 2. Henry's law plots at −40° C. 1. Pure *n*-heptane. 2. Methylethyl ketone. 3. Diethyl ketone. 4. Cyclopentanone. 5. Cyclohexanone.

Can. J. Chem. Downloaded from www.nrcresearchpress.com by 176.9.209.113 on 09/04/12
For personal use only.

TABLE II

Typical data for cyclohexanone at 0° C*

Δp† (mm)	n_{Me_3N} added $\times 10^4$	$P_{equil.}$ soln. (mm)	n_{Me_3N} gas phase $\times 10^4$	n_{Me_3N} soln. $\times 10^4$	N_{Me_3N} soln.
5.34	15.5	0.56	0.181	15.3	0.0212
13.43	39.1	4.11	1.33	37.8	.0506
25.24	73.5	7.36	2.38	71.1	.0914
42.18	123	12.03	3.88	119	.144
54.92	160	14.52	4.68	155	.180
66.62	194	17.11	5.53	189	.211

*1 M in n-heptane (10 ml).
†Pressure difference on "storage" manometer.

The amount of trimethylamine was converted to its mole fraction and these values are plotted against the pressure of trimethylamine above the solution (corrected for the small vapor pressure of the solvent) in Figs. 1 and 2. The Henry's law constants (K in $P = K.N$) were determined from the slope of the straight lines and are given in Table III.

DISCUSSION

The slopes of the graphs at both 0° C (Fig. 1) and −40° C (Fig. 2) for solutions containing the ketones are little different from the slopes of the graphs for pure n-heptane, showing that no very stable complex is formed. The vapor pressures at −63.55° were too small to obtain reliable data.

The graphs of methylethyl ketone, diethyl ketone, and cyclopentanone at 0° (Fig. 1 and Table III) all lie above that of n-heptane itself. Such positive deviations from Henry's law can be attributed to a decrease in the association (8) of the solute ketone molecules in the presence of trimethylamine. Cyclohexanone, however, shows a small but definite negative deviation and this must be due to association (8) between the ketone and trimethylamine. Assuming that a 1:1 complex is formed the dissociation constant

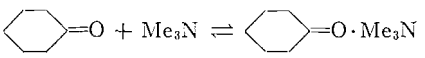

of the complex will be given (9) by $K_D = N$ (ketone) $\times P(Me_3N)/N$ (complex). At any given pressure of trimethylamine above the solution the difference between the mole fraction of trimethylamine in the cyclohexanone solution and in pure n-heptane must be the amount which has reacted with the cyclohexanone. The mean of three values of the dissociation constant so calculated is 1550 mm, which corresponds to a very unstable complex with a dissociation pressure of some 2 atmospheres. This result neglects any possible positive deviation from Henry's law, resulting from decreased association of the ketone itself, which will be masked by the negative deviation produced by association of the ketone and amine. If the graph of cyclohexanone is compared with that of diethyl ketone, for which complex formation is very unlikely, then the value of K_D is 1010 mm, which still corresponds to a very unstable complex.

The results at −40° (Fig. 2 and Table III) show small negative deviations from Henry's law in the cases of methylethyl and diethyl ketone and larger negative deviations for cyclohexanone and cyclopentanone. These larger deviations must be due to complex formation and give values of K_D for cyclohexanone of 95 mm and only 165 mm for cyclopentanone.

Can. J. Chem. Downloaded from www.nrcresearchpress.com by 176.9.209.113 on 09/04/12
For personal use only.

TABLE III

Henry's law constants*

	0° C	−40° C
n-Heptane	86.4	14.8
Cyclohexanone	81.4	11.1
Cyclopentanone	88.4	12.3
Diethyl ketone	90.8	13.3
Methylethyl ketone	94.4	13.8

*In cm of Hg.

The data for cyclohexanone may be treated in another manner. In general the reaction may be expressed by

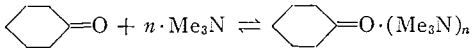

where n is the number of moles of trimethylamine reacting with 1 mole of cyclohexanone. If a is the original concentration of ketone and b and c are the equilibrium concentrations of trimethylamine and the complex, respectively, then

$$K_D = (a-c).b^n/c.$$

The concentration of the complex c is measured by the amount of trimethylamine which has reacted (say d) and $c = d/n$. Since the concentration of complex is very small compared to the initial concentration of the ketone, then

$$a-c = a-d/n = a.$$

The equation thus reduces to

$$K_D = nab^n/d$$

or

$$\log d = n \log b + \log na - \log K_D.$$

In any experimental run b and d are the only variables and thus a graph of log d against log b will be linear with slope of n and an intercept of (log na − log K_D). The results of cyclohexanone at 0° give a straight line through nine points which has a slope of 1.02 (see Fig. 3), corresponding to the formation of a 1:1 complex, and a value of K_D of 14.3 moles $l.^{-1}$. A similar graph for the data at −40° gives $n = 1.04$ and $K_D = 13.1$ moles $l.^{-1}$. These values should be compared to the very high reactivity of cyclohexanone in equilibrium reactions involving addition to the ketone group, such as cyanohydrin formation with $K_D = 0.00059$ in 95% ethanol (12) and $K_D = 0.060$ mole $l.^{-1}$ in 80% dioxane (13) (both at 25° C). The small difference (if real) between the dissociation constants of complex formation at 0° and −40° C corresponds to a heat of formation (ΔH) of only +0.27 kcal mole.

While the non-reactivity of methylethyl and diethyl ketones towards trimethylamine is not surprising, since these ketones are known to be unreactive (14), the low reactivity of cyclohexanone is surprising, and must be contrasted with the ready interaction of ketone and amine groups in the same ring. The interaction in ring compounds, however, occurs more readily in 8- (3, 5), 9- (4, 15), and 10- (5, 16, 17) membered rings, in which the bridged product will have fused 5- or 6-membered rings, and may have a favorable free energy or entropy difference (18) with respect to the monocyclic compound.

Can. J. Chem. Downloaded from www.nrcresearchpress.com by 176.9.209.113 on 09/04/12
For personal use only.

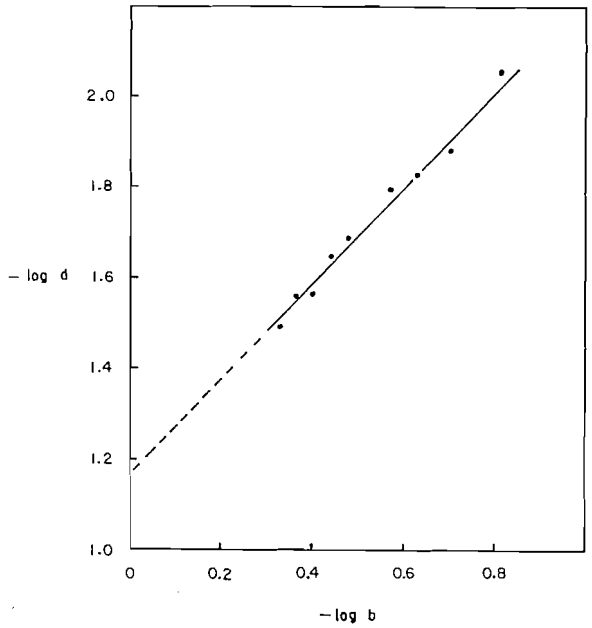

FIG. 3. Data for cyclohexanone at 0° C.

ACKNOWLEDGMENTS

One of the authors (E.M.L.) wishes to acknowledge financial support in the form of a bursary from the National Research Council of Canada. The helpful comments of the referee are also acknowledged.

REFERENCES

1. KERMACK, W. O. and ROBINSON, R. J. Chem. Soc. **121**, 427 (1922).
2. ANET, F. A. L., BAILEY, A. S., and ROBINSON, R. Chem. & Ind. (London), **36**, 944 (1953).
3. LEONARD, N. J., FOX, R. C., ŌKI, M., and CHIAVARELLI, S. J. Am. Chem. Soc. **76**, 630 (1954).
4. LEONARD, N. J., FOX, R. C., and ŌKI, M. J. Am. Chem. Soc. **76**, 5708 (1954).
5. LEONARD, N. J., ŌKI, M., and CHIAVARELLI, S. J. Am. Chem. Soc. **77**, 6234 (1955).
6. LEONARD, N. J. and ŌKI, M. J. Am. Chem. Soc. **77**, 6239 (1955).
7. KORINEK, G. J. and SCHNEIDER, W. G. Can. J. Chem. **35**, 1157 (1957).
8. HILDEBRAND, J. H. and SCOTT, R. L. The solubility of non-electrolytes. Reinhold Publishing Corp., New York. 1950.
9. BROWN, H. C. and BRADY, J. D. J. Am. Chem. Soc. **74**, 3570 (1952).
10. DREISBACH, R. R. and MARTIN, R. A. Ind. Eng. Chem. **41**, 2875 (1949).
11. STULL, D. K. J. Am. Chem. Soc. **59**, 2726 (1937).
12. WHEELER, O. H. and ZABICKY, J. Z. Can. J. Chem. **36**, 656 (1958).
13. WHEELER, O. H. and MATEOS, J. L. Can. J. Chem. **36**, 712 (1958).
14. EVANS, D. P. and YOUNG, J. R. J. Chem. Soc. 1310 (1954).
15. LEONARD, N. J., ŌKI, M., BRADER, J., and BOAZ, H. J. Am. Chem. Soc. **77**, 6237 (1955).
16. MOTTUS, E. H., SCHWARZ, H., and MARION, L. Can. J. Chem. **31**, 1144 (1953).
17. ANET, F. A. L. and MARION, L. Can. J. Chem. **32**, 452 (1954).
18. ALLINGER, N. J. Org. Chem. **21**, 915 (1956).

Can. J. Chem. Downloaded from www.nrcresearchpress.com by 176.9.209.113 on 09/04/12
For personal use only.

Can. J. Chem. Downloaded from www.nrcresearchpress.com by 176.9.209.113 on 09/04/12
For personal use only.

A SHORTER SYNTHESIS OF GLUTATHIONE[1]

CASIMIR BERSE, ROGER BOUCHER, AND LUCIEN PICHÉ

ABSTRACT

A preparation of glutathione is proposed, in which the cystinyl residue is at one stage only partially reduced, to uncover the basic groups necessary for ensuing condensation, but without cleavage of the disulphide linkage. This affords an economy of intermediate steps but it does not provide a substantial increase in over-all yield of the hormone.

Synthesis of glutathione was accomplished with difficulty and in low over-all yields (1–5). The latest preparations (6, 7) report yields of 4 to 6% and the peptide is still prepared from yeast (8, 9). New synthetical methods are of potential value for its production and also to the study of analogues of glutathione.

= NO_2–C$_6$H$_4$–CH_2–O–C(=O)–

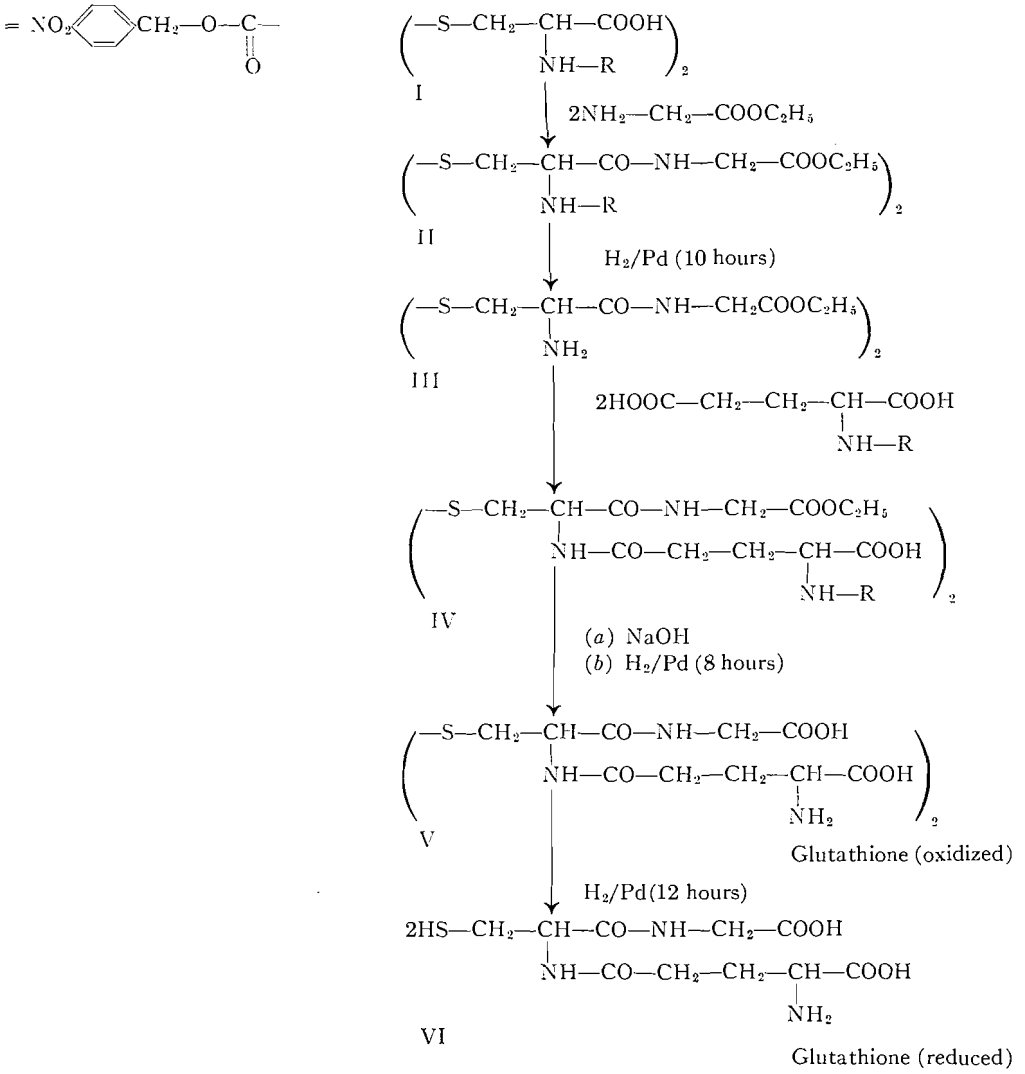

[1]*Manuscript received April 22, 1959.*
Contribution from the Department of Chemistry, Faculty of Science, Université de Montréal, Montreal, Quebec.

Can. J. Chem. Vol. 37 (1959)

In a previous publication (10), we have shown the possibility of reducing peptidic derivatives of di-(N-*p*-nitrocarbobenzoxy)-L-cystine either partially to L-cystinyl peptides or completely to L-cysteinyl derivatives by appropriately controlled hydrogenation on palladium catalyst. This has afforded a favorable short route to glutathione through the following steps: di-(N-*p*-nitrocarbobenzoxy)-L-cystine I was condensed with glycine ethyl ester in the presence of N,N′-dicyclohexylcarbodiimide (11); the intermediate ester II was partially reduced to uncover the amino groups of the L-cystine residue without cleaving its disulphide linkage. The resulting diethyl L-cystinyldiglycinate III was condensed with 2 equivalents of *p*-nitrocarbobenzoxy-L-glutamic acid to provide an ester IV in which the glutathione structure has been assembled. Saponification (*a*) and partial reduction (*b*) of IV lead to oxidized glutathione V. Complete hydrogenation on palladium catalyst leads to glutathione VI.

This procedure, involving fewer steps to oxidized glutathione, affords an over-all yield of 10% on cystine; the reduced form of the hormone is provided in 6.6% yield.

EXPERIMENTAL

Melting points, unless otherwise indicated, have been determined in semicapillary tubes and are uncorrected. In some cases where the materials decomposed, instantaneous melting points have been determined on the Maquenne block.

Diethyl di-(N-*p-nitrocarbobenzoxy*)-L-*cystinyldiglycinate* II

To a solution of glycine ethyl ester hydrochloride (5.6 g, 0.04 mole) in 50 ml of dimethylformamide and 10 ml of acetonitrile, 9.5 ml of tri-*n*-butylamine and di-(N-*p*-nitrocarbobenzoxy)-L-cystine (12 g, 0.02 mole) were added. After cooling of the solution to −5°, dicyclohexylcarbodiimide (9 g) was added and the mixture was kept at this temperature for 30 minutes. The reaction mixture was allowed to come to room temperature and set aside for 1 day. It was acidified with 5 ml of glacial acetic acid (to decompose excess reagent). The insoluble urea was removed; 200 ml of chloroform and 350 ml of water were added. The chloroformic solution was washed with *N* HCl, 5% aqueous sodium bicarbonate, and dried over anhydrous sodium sulphate. The solvent was evaporated *in vacuo* and the residue was recrystallized from nitromethane. Yield: 12.3 g (80%). Identity was ascertained through comparison by melting point, mixed melting point, and optical rotation with the product described in a previous publication (10).

*Diethyl-*L-*cystinyldiglycinate Dihydrochloride* III

Diethyl di-(N-*p*-nitrocarbobenzoxy)-L-cystinyldiglycinate (6 g, 0.08 mole) was dissolved in a mixture of dimethylformamide (25 ml) and ethanol 80% (50 ml). The compound was hydrogenated for 10 hours at room temperature and at atmospheric pressure over 10% palladium on carbon (2 g). The catalyst was removed by filtration and the solvent was evaporated *in vacuo* at 50°. The resulting syrup was triturated with *N* HCl (30 ml) and the filtrate evaporated *in vacuo*. The residue after treatment with water and Norit gave a white amorphous hygroscopic powder. Yield: 2.5 g (70%). Anal. Calc. for $C_{14}H_{26}N_4O_6S_2.2HCl$: C, 34.78; H, 5.84; N, 11.59%. Found: C, 34.79; H, 5.82; N, 11.70%.

*p-Nitrocarbobenzoxy-*L-*glutamic Acid*

L-Glutamic acid (12.3 g) was dissolved in 42 ml of 4 *N* NaOH; 20 ml of purified dioxane were added. The solution was stirred vigorously and cooled to 0°; *p*-nitrocarbobenzoxyl chloride (19 g) dissolved in 50 ml of dioxane was added in 5 portions (30 minutes). During

Can. J. Chem. Downloaded from www.nrcresearchpress.com by 176.9.209.113 on 09/04/12
For personal use only.

reaction, the pH was maintained at 11 with 2 *N* NaOH. Stirring was continued for 0.5 hour after the addition of all reactants. The mixture was allowed to come to room temperature and 300 ml of water were added. The resulting alkaline solution was washed twice with ethyl acetate and acidified to Congo red with 1 *N* HCl. The precipitate was collected and recrystallized from a mixture of ethanol and water. Yield: 21 g (77%); m.p. 157–158°; $[\alpha]_D^{25}$ −8.0 (*c*, 0.9 in ethanol, 95%). Anal. Calc. for $C_{13}H_{14}O_8N_2$: C, 47.85; H, 4.32; N, 8.58%. Found: C, 47.68; H, 4.32; N, 8.55%.

Diethyl di-(N-*p-nitrocarbobenzoxy-γ-*L-*glutamyl*)-L-*cystinyldiglycinate* IV

To a solution of diethyl L-cystinyldiglycinate dihydrochloride (2.2 g, 4.5 mmole) in 30 ml of dimethylformamide and 5 ml of acetonitrile, 2 ml of tri-*n*-butylamine and *p*-nitrocarbobenzoxy-L-glutamic acid (2.7 g, 8 mmole) were added. After the solution had been cooled to −5°, dicyclohexylcarbodiimide (2 g) was added and the mixture was kept at this temperature for 30 minutes. The reaction mixture was allowed to come to room temperature and allowed to stand for 1 day. It was acidified with 1 ml glacial acetic acid. The insoluble urea was removed and 200 ml of ethyl acetate and 300 ml of water were added. The ethyl acetate solution was washed with *N* HCl and water, then dried over anhydrous sodium sulphate. The solvent was evaporated *in vacuo*. Yield: 2.8 g (60%).

Di-(N-*p-nitrocarbobenzoxy-γ-*L-*glutamyl*)-L-*cystinyldiglycine*

The crude product obtained above (2.7 g) was dissolved in methanol (20 ml), and *N* NaOH (2% excess) was added in two portions. The mixture was stirred at 0–5° for a first hour and at room temperature for another. It was acidified with HCl. The crude product, an oil, was dissolved in ethanol. The solvent was evaporated *in vacuo* and the residue was dissolved in dioxane; precipitation with ether yielded 1.9 g of product (74%).

Glutathione (Oxidized) V

Di-(N-*p*-nitrocarbobenzoxy)-γ-L-glutamyl-L-cystinyldiglycine (2 g) was dissolved in 80% ethanol (25 ml). The compound was hydrogenated for 8 hours at room temperature and at atmospheric pressure over 10% palladium on carbon (1 g). After filtration, the catalyst was washed with water and the washings were combined with the first filtrate. The solvent was evaporated *in vacuo* and the residue was triturated with water. The filtrate was concentrated and glutathione (oxidized) was precipitated by addition of absolute ethanol. Yield: 0.7 g (55%); m.p. 175–195°; $[\alpha]_D^{25}$ −92.8 (*c*, 1.2 in water). Literature (12, 13) m.p. 170–195°; $[\alpha]_D^{27}$ −93.9 (*c*, 1.0 in water).

Glutathione VI

Glutathione (oxidized) (0.4 g) was dissolved in 25 ml of water. The compound was hydrogenated for 12 hours at room temperature and at atmospheric pressure over palladium (13) (200 mg). The catalyst was removed by filtration and the filtrate was concentrated *in vacuo*. By addition of ethanol (95%) to the syrupy residue, the glutathione precipitated. Yield: 0.26 g (65%); m.p. 190° decomp., $[\alpha]_D^{25}$ −20.6 (*c* 1.5 in water). (Literature (2) m.p. 190°; $[\alpha]_D^{27}$ −21.3 (*c*, 2% in water).) Anal. Calc. for $C_{10}H_{17}N_3O_6S$: C, 39.08; H, 5.58; N, 13.67. Found: C, 39.00; H, 5.48; N, 13.62%.

ACKNOWLEDGMENTS

This research was supported by a National Research Council grant. One of us (R.B.) is also indebted to the Quebec Bureau of Research for a bursary.

Can. J. Chem. Downloaded from www.nrcresearchpress.com by 176.9.209.113 on 09/04/12
For personal use only.

REFERENCES

1. HARINGTON, C. A. and MEAD, T. H. Biochem. J. **29**, 1602 (1935).
2. DU VIGNEAUD, V. and MILLER, G. L. J. Biol. Chem. **116**, 469 (1936).
3. HEGEDÜS, B. Helv. Chim. Acta, **31**, 737 (1948).
4. RUDINGER, J. and SORM, F. Collection Czechoslovak Chem. Commun. **16**, 214 (1951).
5. GOLDSCHMIDT, S. and JUTZ, C. Chem. Ber. **86**, 1116 (1953).
6. AMIAR, G., HEYMES, R., and VELLUZ, L. Bull. soc. chim. France, 698 (1956).
7. KING, F. E., CLARK-LEWIS, S. W., and WADE, R. J. Chem. Soc. 880 (1957).
8. HOPKINS, F. G. J. Biol. Chem. **84**, 269 (1929).
9. KENDALL, E. C., MCKENZIE, B. F., and MASON, H. L. J. Biol Chem. **84**, 657 (1929).
10. BERSE, C., BOUCHER, R., and PICHÉ, L. J. Org. Chem. **22**, 805 (1957).
11. SHEEHAN, J. C., and HESS, G. P. J. Am. Chem. Soc. **77**, 1067 (1955).
12. HUNTER, G. and EAGLES, B. A. J. Biol. Chem. **72**, 165 (1927).
13. JOHNSON, J. M. and VOEGTLIN, C. J. Biol. Chem. **75**, 710 (1927).

Can. J. Chem. Downloaded from www.nrcresearchpress.com by 176.9.209.113 on 09/04/12
For personal use only.

Can. J. Chem. Downloaded from www.nrcresearchpress.com by 176.9.209.113 on 09/04/12
For personal use only.

THE PHOTOLYSIS OF TRIFLUOROMETHYL CYANIDE[1]

A. BRUCE KING[2] AND E. W. R. STEACIE

ABSTRACT

The photolysis of CF_3CN at 1849 Å has been studied. The major products are hexafluoroethane, cyanogen, and perfluoro-3-methyl-2-aza-2-butene.

The experimental value for $k_3/k_2^{\frac{1}{2}}$ is:

$$10^{-9.08\pm.13}\, e^{-5.00\pm.21 \text{ kcal mole}^{-1}/RT} \text{ molecule}^{-\frac{1}{2}} \text{ cc}^{\frac{1}{2}} \text{ sec}^{-\frac{1}{2}},$$

where:

$$CF_3 + CF_3 \rightarrow C_2F_6, \qquad [2]$$

$$CF_3 + CF_3CN \rightarrow (CF_3)_2CN. \qquad [3]$$

Another product was isolated in smaller amounts and has been tentatively identified as perfluorotrimethyl-aza-2-pentene.

INTRODUCTION

Earlier work on the photolysis of CH_3CN (1) showed the mechanism to be so complex that a unique interpretation was difficult. It was felt that the vulnerability of the C—H bond, both to break in the primary step and to subsequent abstraction, led to the wide variety of reaction paths and products. It was thus hoped that a study of the photolysis of CF_3CN would give information for the interpretation of the CH_3CN studies. In particular the importance of reaction [8]:

$$CN + CF_3CN \rightarrow C_2N_2 + CF_3 \qquad [8]$$

was sought.

EXPERIMENTAL

Photolyses were carried out in a cylindrical quartz reaction vessel 4.8 cm long and 4.7 cm in diameter, which was connected to a mercury-free system with a Hoke No. 413 high-vacuum stainless-steel valve. The windows of the cell were 1.00-mm-thick quartz, each of which transmitted about 75% of the 1849 Å radiation used in this work. The initial pressure in the reaction cell was measured with a quartz spiral Bourdon gauge nulled with a mercury manometer. When a mixture of gases was desired in the reaction cell, the appropriate amounts of the gases were premixed in a 125-cc bulb with a magnetically driven stirrer and then expanded into the reaction cell. The techniques described by McElcheran *et al.* (1) were used; the reaction products were transferred to the analytical system through a silicone oil diffusion pump, a stopcock, and two liquid nitrogen traps to keep the mercury vapor in the analytical system out of the reaction cell.

The cell was placed inside a cylindrical furnace which was mounted on an optical bench. The quartz spiral low-pressure mercury lamp and the platinum photocell were also mounted on the optical bench as part of an airtight system with the furnace tube. This permitted nitrogen to flow through the light path and yet allowed the lamp and photocell to be easily moved for heating the windows of the reaction cell with a torch.

[1]*Manuscript received June 18, 1959.*
Contribution from the Division of Pure Chemistry, National Research Council, Ottawa, Canada.
Issued as N.R.C. No. 5332.

[2]*National Research Council Postdoctorate Fellow 1956–58. Present address: Chemical Physics Department, Stanford Research Institute, Menlo Park, California, U.S.A.*

Can. J. Chem. Downloaded from www.nrcresearchpress.com by 176.9.209.113 on 09/04/12
For personal use only.

The nitrogen was passed through the system at approximately 200 cc min^{-1} by means of a small heater in a Dewar of fresh liquid nitrogen. Provision was also made to introduce glass plates between the lamp and the reaction cell. A Vycor plate (Corning No. 7910) was inserted when only 2537 Å radiation was desired and several 3-mm-thick quartz plates were inserted to reduce the 1849 Å intensity to about 20% of the usual value.

Because of polymer formation during the photolysis it was necessary at the end of each run to fill the cell with an atmosphere of oxygen and flame both windows to red heat. This removed the polymer from the windows and ends of the cylindrical walls, but after a number of runs some polymer was built up on the walls of the central section of the cell. The relative amount of polymer was determined for each run by the drop in transmitted 1849 Å radiation during the photolysis and this intensity decrease was as high as 50% for some of the higher-pressure experiments.

The photocell consisted of a semicylindrical cathode of platinum (2) mounted in a quartz envelope that had been thinned slightly in front of the cathode to decrease the light absorption by the envelope. Before the photocell was sealed off, it was evacuated overnight at 10^{-6} mm of Hg with the envelope heated to 500° C, and then the cathode was heated with an induction heater (two thin strips of platinum had been spot-welded to the top and bottom of the cathode to complete the loop and give more effective coupling) until the cathode was no longer sensitive to 2537 Å light. This was determined by measuring the photocurrent produced by a low-pressure Hg lamp with a Vycor plate in front of the photocell. The effective area of the photocell was about 4 cm^2 and the operating anode potential was 135 v. Photocurrents of the order of 10^{-9} amp were obtained in this work and were measured with a Keithley electrometer and decade resistance attachment. After more than a year of use, the photocell remained completely insensitive to the 2537 Å radiation of the mercury lamp.

The volatile products were condensed at −195° C and then separated by distillation from a Ward–Leroy still (3). The C_2F_6 and the bulk of the CF_3CN were removed at −150° C and condensed in a liquid nitrogen trap until the distillation pressure had dropped to approximately half the value of the equilibrium pressure during the bulk of the distillation. This procedure removed at least 95% of the CF_3CN, but none of the higher-boiling products. The CF_3CN–C_2F_6 mixture was then reacted in a micro-hydrogenation tube with about 500 mm of hydrogen over a nickel–kieselguhr catalyst (4) at 85° C for 1 to 2 hours. This converted about 95% of the CF_3CN, principally to higher-boiling amines. The excess hydrogen was pumped off at liquid nitrogen temperature, and the products of the hydrogenation were distilled from −140° C to a liquid nitrogen trap. The quantity of this fraction (cut No. 4) was measured in a gas burette and sealed off in a sample tube for mass spectrometric analysis. This cut consisted mainly of the unreacted CF_3CN, the C_2F_6 (from the photolysis only; none was found in a blank hydrogenation), and some ammonia. This procedure thus served to concentrate the C_2F_6 from about 1% of the original fraction to an appreciable component that could readily be measured by mass spectrometry.

Other fractions of the photolysis reaction products were taken at −130° C (cut No. 1), −115° C (cut No. 2), and the residual higher boiling compounds that remained condensed at −115° C were collected as cut No. 3. The total quantity of each of the samples was measured on a gas burette and then the sample was sealed in a tube for mass spectrometric analysis. The total volume of the inlet system of the mass spectrometer was calibrated by expanding samples of known quantities of pure nitrogen (similar sample size to the unknown samples) into the spectrometer, measuring the

m/e 28 peak height, and comparing with the nitrogen sensitivity. Calculation of analyses for two component samples where standards were not available is described in the Appendix.

The CF_3CN was obtained from Peninsular Chemresearch Inc., practical grade, and was purified by several fractionations from −80° C to −195° C. The hexafluoroacetone was obtained by reacting the hydrate (Merck Chemical) with phosphorus pentoxide, followed by several vacuum fractionations. This gas was stored in a blackened bulb until used.

RESULTS

Mass spectrometric analyses indicated that cut No. 1 contained the remaining CF_3CN (pattern given in Table I) and some of the C_2N_2, while cut No. 2 contained the remainder of the C_2N_2 and a fluorinated product. The pattern for this product is listed in Table I and is consistent with the pattern to be expected for perfluoro-3-methyl-2-aza-2-butene ($(CF_3)_2C{=}NCF_3$, hereafter called MAB). This type of compound gives mass spectral patterns with a small parent peak (m/e 233), medium-sized peaks corresponding to loss of one or two fluorine atoms (m/e 214 and 195), a large peak for loss of a CF_3 group (m/e 164), and a large m/e 69 peak. All other peaks are also consistent with the structure of MAB. Further evidence of consistency with the proposed structure is indicated by the metastable transitions observed which are also listed in Table I. In every case they correspond to transitions of the important ions in the spectrum by typical reaction paths found in mass spectral fragmentation patterns, e.g. references 5 and 6.

TABLE I

Mass spectral patterns for CF_3CN and MAB

m/e	CF_3CN	MAB	m/e	CF_3CN	MAB	
12	5.3		131		0.2	
24	0.5		145		5.2	
26	11.6		164		(100.)	
27	1.7		165		3.7	
31	25.8	9.8	169		0.3	
38	4.2		171		0.2	
50	50.2	12.8	176		2.1	
51	0.6		195		4.3	
57	2.5		214		35.7	
69	311.	242.	233		0.8	
70	3.5	2.8	Metastable ions observed and suggested transition			
76	(100.)	11.8				
77	2.5		None observed		m/e	Transition
81		0.7				
93		1.1			29.	164 → 69
95	5.1	1.2			32.8	76 → 50
100		1.8			60.9	214 → 114
114		16.7			79.	164 → 114
119		1.3			115.5	233 → 164
126 + $m^{\mp}$		2.6			125.9	214 → 164

Because of lack of mass spectral standards for MAB and because of troubles in obtaining a reproducible cyanogen standard (apparently due to absorption problems), the effective sensitivities of the cyanogen m/e 52 peak and the MAB m/e 164 peak were determined by the method described in the Appendix. A typical plot of equation [A-3] for a set of analyses performed on the same day is shown in Fig. 1 with the sensitivities of C_2N_2 and MAB being determined from the slope and the intercept, respectively, of the straight

Can. J. Chem. Downloaded from www.nrcresearchpress.com by 176.9.209.113 on 09/04/12
For personal use only.

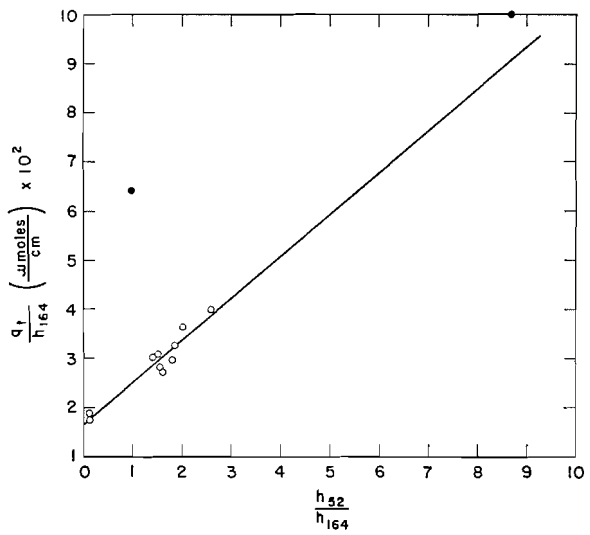

FIG. 1. Plot of equation [*A*-3] for a typical group of cut No. 2 analyses. Open circles used to determine linear plot and closed circles are for points above the line that indicate an additional component present.

line. These sensitivities were used to calculate the absolute amounts of C_2N_2 and MAB in the samples of cut No. 2 as well as samples of cut No. 1 that were analyzed at the same time.

Cut No. 4 was analyzed for C_2F_6 by using the *m/e* 119 peak. Because of absorption of the ammonia and amines in the sample, a complete analysis of the sample was not undertaken. Rather, by expanding the total sample into the calibrated volume on the inlet system of the mass spectrometer, one could relate the partial pressure of C_2F_6 (from the *m/e* 119 peak height) directly to the absolute amount of C_2F_6 in the sample.

The small amount of high-boiling products (cut No. 3) was analyzed on the mass spectrometer and found to contain two major components. One component was distinguished by peaks at *m/e* 96 and 97 (as well as 77, 76, 69, etc.) and is tentatively identified as 2,2,2-trifluoroethylideneimine ($CF_3CH{=}NH$) or a similar partially hydrogenated compound. This compound must arise from reaction of photolytic species or photolysis products with adsorbed water on the walls or with the silicone oil in the diffusion pump, because this compound was not found after a similar fractionation procedure on a sample of CF_3CN that had not been photolysed.

The pattern assigned to the major component of cut No. 3 is shown in Table II. Because of the small quantity of this product in any of the samples, the smaller-sized peaks are subject to considerable scatter and only the major peaks are listed. Many of the lower mass peaks are also omitted because of interference from the other component. The higher mass peaks are consistent with a molecular weight of 383 (loss of one fluorine atom gives *m/e* 364; loss of CF_3 gives *m/e* 314, which is a major peak, etc.). This would indicate a formula of $C_7F_{15}N$ and would probably be either perfluoro-3,4,4-trimethyl-2-aza-2-pentene ($CF_3C(CF_3)_2C(CF_3){=}NCF_3$) or perfluoro-2,4,4-trimethyl-3-aza-2-pentene ($CF_3C(CF_3)_2N{=}C(CF_3)_2$), hereafter called TAP. A plot of equation [*A*-3] for cut No. 3 (Fig. 2) indicates that the amounts of the two major components present are proportional to the *m/e* 314 and 96 peak heights and that there are no other compounds consistently present in significant quantity in these samples (see Appendix).

Can. J. Chem. Downloaded from www.nrcresearchpress.com by 176.9.209.113 on 09/04/12
For personal use only.

TABLE II

Mass spectrum of TAP

m/e	Relative peak height	m/e	Relative peak height
31	5.0	196	2.1
50	4.5	214	9.
69	270.	221	2.3
76	4.7	226	11.7
112	3.5	245 and 246	12.
114	2.	259	11.2
131	4.0	264	22.6
138	1.5	271	2.3
145	2.	295	1.4
146	1.	303	0.8
150	2.1	310	3.9
159	3.	314	(100.)
164	9.	322	1.
169	4.3	328	3.
176	3.6	342	4.6
192	2.6	354	1.
195	1.6	364	5.5

The sensitivities for these two components were determined from the graph and were used to calculate the absolute amount of TAP formed.

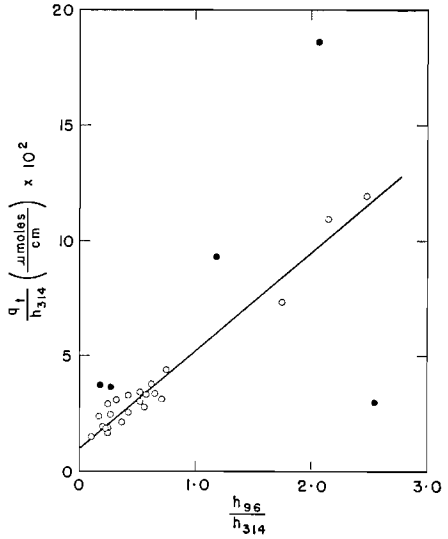

FIG. 2. Plot of equation [*A*-3] for a group of cut No. 3 analyses. Open circles used to determine linear plot and closed circles are for points above the line that indicate an additional component present.

On the basis of the reaction mechanism one might expect perfluorodiisopropylidene hydrazine ($(CF_3)_2C{=}N{-}N{=}C(CF_3)_2$(PDH)), or its isomer perfluoro-3,4-dimethyl-2,5-diaza-2,4-hexadiene ($CF_3N{=}C(CF_3)C(CF_3){=}NCF_3$), as a product. This compound would have a parent peak at *m/e* 328 and significant peaks at *m/e* 309, 290, and 259. Peaks are observed at *m/e* 328, 310, and 259, but the ratio of these peak heights to the *m/e* 314 peak height is reasonably constant (although with more scatter than some of the other peaks in the spectrum of TAP), indicating that traces of PDH may be present, but that the major contribution to these peaks comes from the same compound that gives the *m/e* 314 peak. (A coincidental proportionality between the yields of two different products for all runs under the variety of conditions studied is very unlikely.)

Can. J. Chem. Downloaded from www.nrcresearchpress.com by 176.9.209.113 on 09/04/12
For personal use only.

Can. J. Chem. Downloaded from www.nrcresearchpress.com by 176.9.209.113 on 09/04/12
For personal use only.

The polymer formation (measured as the decrease in the logarithm of the 1849 Å light transmitted) as a function of irradiation time was found to be linear after an initial induction period. The slope of the linear region was found to be proportional to the square root of the CF_3CN pressure at constant light input (uncorrected for the change in optical density of the CF_3CN) and approximately proportional to the incident intensity at constant pressure. One photolysis was carried out on a mixture of CF_3CN and CF_3COCF_3 with 2537 Å light so that only CF_3COCF_3 would undergo photolysis. No polymer formation was detected with 1849 Å light after the run, although a 20–30% decrease in intensity was observed for runs on CF_3CN alone at 1849 Å at the same pressure and temperature. This indicated that the formation of polymer required reactants in addition to the $CF_3\cdot$ radical and CF_3CN. This fact, and the induction period observed, indicate that the polymer must arise from polymerization of the cyanogen formed during the photolysis.

A blank photolysis of CF_3COCF_3 at 2537 Å in the reaction cell that was partially coated with paracyanogen gave a C_2F_6/CO ratio of about 0.6, indicating an appreciable loss of $CF_3\cdot$ radicals by addition to the unsaturated paracyanogen. This is also confirmed by the observation of the evolution of C_2F_6 on heating the polymer formed in the photolysis of CF_3CN. Because of loss of some of the C_2N_2 product by polymerization and some of the $CF_3\cdot$ radicals by reaction with the polymer, attempts at absolute quantum measurements in order to test the existence of reaction [8] are useless.

The absorption coefficient of CF_3CN at 1849 Å was found to vary with temperature and a statistical analysis of the data taken during the course of this work yielded:

$$\epsilon = 10^{1.483\pm.045}\, e^{-1620\pm70 \text{ cal mole}^{-1}/RT} \text{ mole}^{-1} \text{ l. cm}^{-1}.$$

This rather significant dependence on temperature would seem to indicate that the 1849 Å line coincides with the edge of an absorption band. The same situation occurs for CH_3CN (7), and thus it would appear that the substitution of fluorine atoms on the methyl group of CH_3CN does not shift the absorption band edge very much.

DISCUSSION

The experimental data are summarized in Table III. On the basis of these data and the other results discussed above, the following mechanism is proposed:

$$CF_3CN + h\nu \rightarrow CF_3 + CN, \quad [1]$$

$$CF_3 + CF_3 \rightarrow C_2F_6, \quad [2]$$

$$CF_3 + CF_3CN \rightarrow (CF_3)_2C{=}N\cdot, \quad [3]$$

$$CF_3 + (CF_3)_2CN\cdot \rightarrow (CF_3)_2C{=}NCF_3\,(\text{MAB}), \quad [4]$$

$$CF_3 + \text{MAB} \rightarrow \rightarrow \rightarrow \text{TAP}, \quad [5]$$

$$CN + CN + M \rightarrow C_2N_2 + M, \quad [6]$$

$$C_2N_2 + R(CN?) \xrightarrow{\text{wall?}} \text{paracyanogen}. \quad [7]$$

The formation of MAB proceeds through reactions [3] and [4] with reaction [3] the rate-determining step. An Arrhenius plot of $R_{MAB}/R_{C_2F_6}^{\frac{1}{2}}[CF_3CN]$ is shown in Fig. 3 and gives

$$k_3/k_2^{\frac{1}{2}} = 10^{-9.09\pm.11}\, e^{-5.05\pm.17 \text{ kcal mole}^{-1}/RT} \text{ molecule}^{-\frac{1}{2}} \text{ cc}^{\frac{1}{2}} \text{ sec}^{-\frac{1}{2}}.$$

The mechanism for the formation of TAP is subject to some doubt, but the best kinetic agreement has been found for $R_{TAP}/R_{MAB}R_{C_2F_6}^{\frac{1}{2}}t$ (where t is the reaction time),

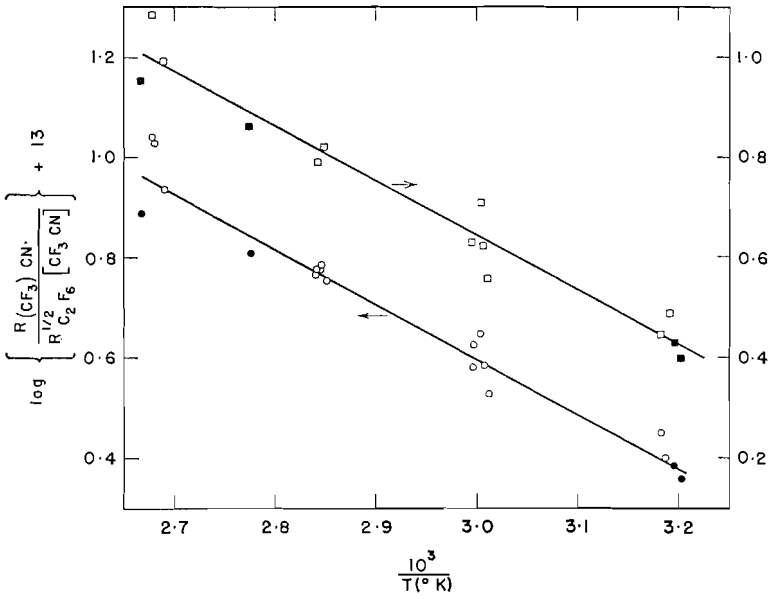

FIG. 3. Arrhenius plot of $k_3/k_2^{\frac{1}{2}}$. Circles (lower plot) represent $R_{(CF_3)_2CN\cdot} = R_{MAB}$. Squares (upper plot) represent $R_{(CF_3)_2CN\cdot} = R_{MAB} + 2R_{TAP}$. Solid circles and squares indicate low-intensity runs.

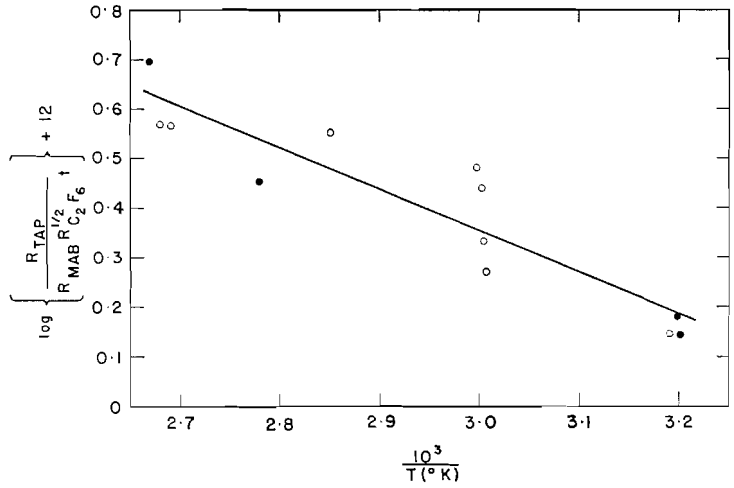

FIG. 4. Arrhenius plot of $k_5/k_2^{\frac{1}{2}}$. Solid circles indicate low-intensity runs.

indicating the rate-determining step for the formation of TAP is the addition of $CF_3\cdot$ to MAB. An Arrhenius plot of this function is shown in Fig. 4 and the lack of effect of intensity on the plot indicates this function represents the rate-determining step for the formation of TAP. From Fig. 4 and assuming the average concentration of MAB is $\frac{1}{2}R_{MAB}t$, one obtains:

$$k_5/k_2^{\frac{1}{2}} = 10^{-8.81\pm.22}\, e^{-3.87\pm.33 \text{ kcal mole}^{-1}/RT} \text{ molecule}^{-\frac{1}{2}} \text{ cc}^{\frac{1}{2}} \text{ sec}^{-\frac{1}{2}}.$$

It is difficult to decide what additional reaction steps following reaction [5] must be involved to explain the formation of TAP. The difficult part is the origin of the perfluoro-

Can. J. Chem. Downloaded from www.nrcresearchpress.com by 176.9.209.113 on 09/04/12
For personal use only.

TABLE III

Summary of experimental results

Run No.	Concn. of CF_3CN (molecule $cc^{-1} \times 10^{-18}$)	Temp. (° K)	Rel. initial incident intensity	Time (sec $\times 10^{-4}$)	Molecule cc^{-1} sec^{-1} $\times 10^{-11}$ of:				R_{MAB} / $R_{C_2F_6}{}^{\frac{1}{2}}[CF_3CN]$ (molecule$^{-\frac{1}{2}}$ $cc^{\frac{1}{2}}$ $sec^{-\frac{1}{2}}$ $\times 10^{13}$)	R_{TAP} / R_{MAB}-$R_{C_2F_6}{}^{\frac{1}{2}}t$ (molecule$^{-\frac{1}{2}}$ $cc^{\frac{1}{2}}$ $sec^{-\frac{1}{2}}$ $\times 10^{12}$)	$R_{MAB}+2R_{TA}$ / $R_{C_2F_6}{}^{\frac{1}{2}}$-$[CF_3CN]$ (molecule$^{-\frac{1}{2}}$ $cc^{\frac{1}{2}}$ $sec^{-\frac{1}{2}}$ $\times 10^{13}$)
					$R_{C_2F_6}$	R_{MAB}	$R_{C_2N_2}$	R_{TAP}			
59	1.826	314.2	2.38	6.06	1.24	0.687	2.01	0.037	2.50	(2.52)†	2.78
61	2.40	313.4	2.40	6.48	2.34	3.29	5.18	0.144	2.83	1.39	3.08
64	1.597	312.8	0.400	30.40	0.113	0.411	0.514	0.0200	2.42	1.51	2.68
65	3.124	312.2	0.418	24.55	0.193	0.987	0.978	0.0480	2.27	1.39	2.49
52	0.599	332.0	1.84	6.13	0.783	0.564	2.23	0.018	3.36	1.86	3.58
54	1.130	333.8	1.88	6.32	0.977	1.33	3.73	0.080	3.78	3.04	4.24
51	1.717	332.4	1.86	6.64	1.188	2.25	5.59	0.112	3.81	2.16	4.19
56	2.36	332.6	2.38	6.42	1.548	4.13	3.75	0.289	4.45	2.76	5.09
55	2.97	333.8	2.44	6.18	1.71	5.16	5.02	n.d.*	4.21	—	—
46	0.482	351.8	1.96	6.20	0.294	0.482	1.95	0.010	5.85	(1.94)†	6.10
50	1.610	351.8	1.87	6.65	0.850	2.80	4.29	n.d.*	5.98	—	—
63	2.15	351.2	2.04	7.60	1.065	4.23	4.07	n.d.*	6.00	—	—
49	2.74	350.8	2.40	6.82	1.170	5.31	9.80	0.443	5.68	3.56	6.60
66	1.045	360.2	0.382	32.76	0.049	0.469	0.049	0.0305	6.41	2.84	7.26
70	1.007	371.6	2.32	7.01	0.737	2.35	3.43	0.165	8.58	3.68	9.79
69	1.566	373.0	2.10	6.26	0.731	4.49	4.47	0.283	10.60	3.71	11.99
68	2.083	373.3	2.20	6.46	0.727	6.09	5.72	n.d.*	10.85	—	—
71	2.103	374.7	0.320	23.8	0.0404	1.030	0.957	0.0800	7.70	4.95	8.90

NOTE: *n.d., not determined.
†Outside 2.5 × standard deviation.

Can. J. Chem. Downloaded from www.nrcresearchpress.com by 176.9.209.113 on 09/04/12
For personal use only.

t-butyl group. This may have required breaking a C—N bond, possibly by addition of two CF_3 radicals to MAB and then breaking of the C—N bond due to steric repulsion. If the *t*-butyl radical is an intermediate, one would expect perfluoroneopentane as a detectable product. From the boiling point of this compound (8), one would expect it to appear in cut No. 2 and to give a large *m/e* 219 peak, but none is observed.

Another possibility is that the C—N bond does not break until after 2 molecules of the original CF_3CN are associated in some intermediate compound that contains a number of additional CF_3 groups. This would not require the *t*-butyl radical as an intermediate, but again the absence of any other obvious intermediate is difficult to explain. Still another possibility is that TAP is not the actual product, but rather none of the higher mass peaks (above *m/e* 364) in the pattern of the actual product is stable. Thus the C—N bond has been broken on electron impact of the compound in the mass spectrometer to give a pattern resembling TAP. (It should be emphasized that the kinetic dependence for the formation of the compound giving the *m/e* 314 peak is much better understood from the data available than the structure of the compound.)

If TAP is formed by the reaction of MAB, then $k_3/k_2^{\frac{1}{2}}$ should be corrected for the number of $(CF_3)_2CN\cdot$ radicals or MAB molecules that are consumed in the formation of TAP. If two $(CF_3)_2CN\cdot$ radicals are assumed to be precursors for each molecule of TAP, $k_3/k_2^{\frac{1}{2}}$ would be determined from $(R_{MAB}+2R_{TAP})/R_{C_2F_6}{}^{\frac{1}{2}}[CF_3CN]$. A plot of this function (also shown in Fig. 3) results in a value for $(k_3/k_2^{\frac{1}{2}})_{corr}$ of:

$$10^{-9.08\pm.13}\, e^{-5.00\pm.21 \text{ kcal mole}^{-1}/RT} \text{ molecule}^{-\frac{1}{2}} \text{ cc}^{\frac{1}{2}} \text{ sec}^{-\frac{1}{2}}.$$

It is seen that the uncertainty in the number of precursor $(CF_3)_2CN\cdot$ radicals in the formation of TAP will have only a small effect on the experimental value of k_3.

Using the latter value of $k_3/k_2^{\frac{1}{2}}$, assuming $E_2 = 0$, collision diameters for CF_3, CF_3CN, and MAB as 4.0, 7.0, and 8.0 Å, respectively, and a temperature of 343° K, one calculates $E_3 = 5.0\pm.2$ kcal mole^{-1}, $E_5 = 3.9\pm.3$ kcal mole^{-1}, $p_3/p_2^{\frac{1}{2}} = 2.2\times10^{-5}$, $p_5/p_2^{\frac{1}{2}} = 3.4\times10^{-5}$. If p_2 is taken to be unity, then p_3 and p_5 are about 2×10^{-5} and 3×10^{-5}, respectively.

Reactions [3] and [5] are similar to the addition of CH_3 radicals to simple olefins where the activation energies are about 5–7 kcal mole^{-1} and the steric factors are about 4×10^{-4} (9). The activation energies observed here are about the same, but the steric factors are lower by about a factor of 20. This decrease from the hydrocarbon case is presumably due to the increased size of the fluorinated groups.

ACKNOWLEDGMENTS

The authors wish to express their appreciation to Drs. K. O. Kutschke and F. P. Lossing for helpful discussions. They also wish to thank Miss B. Thornton for the mass spectrometric analyses and Mr. G. Ensel for making some of the glassware used in this work.

REFERENCES

1. McElcheran, D. E., Wijnen, M. H. J., and Steacie, E. W. R. Can. J. Chem. **36**, 321 (1958).
2. DuBridge, L. A. Phys. Rev. **29**, 451 (1927).
3. Leroy, D. J. Can. J. Research, B, **28**, 492 (1950).
4. Shepp, A. and Kutschke, K. O. Can. J. Chem. **32**, 1112 (1954).
5. Bloom, E. G., Mohler, F. J., Wise, C. E., and Wells, E. J. J. Research Nat. Bur. Standards, **43**, 65 (1949).
6. King, A. B. and Long, F. A. J. Chem. Phys. **29**, 374 (1958).
7. Platt, J. R. and Klevens, H. B. Rev. Modern Phys. **16**, 182 (1941).
8. Dresdner, R. D. J. Am. Chem. Soc. **78**, 876 (1956).
9. Mandelcorn, L. and Steacie, E. W. R. Can. J. Chem. **32**, 414 (1954).

Can. J. Chem. Downloaded from www.nrcresearchpress.com by 176.9.209.113 on 09/04/12
For personal use only.

APPENDIX

Consider the case of a mass spectral analysis on a two-component mixture where each of two peaks in the spectrum can be attributed solely to each component. The total pressure (p_t) is equal to the sum of the partial pressures of the two components and thus:

$$p_t = (h_1/S_1)+(h_2/S_2), \qquad [A\text{-}1]$$

where h refers to the peak height and S the sensitivity of the particular component.

If the total quantity of the sample (q_t) is known and the entire sample is expanded into a volume (V), then:

$$q_t/V = (h_1/S_1)+(h_2/S_2), \qquad [A\text{-}2]$$

and rearranging,

$$q_t/h_2 = (h_1/h_2)(V/S_1)+(V/S_2). \qquad [A\text{-}3]$$

A plot of q_t/h_2 vs. h_1/h_2 for a series of samples of varying relative composition will give the constants V/S_1 and V/S_2 from the slope and intercept, respectively. Since the absolute quantity of each component is:

$$q_1 = h_1(V/S_1), \qquad [A\text{-}4]$$

the absolute quantity can be calculated from the peak height in the individual samples and the constant determined from the plot of equation [A-3] for a set of analyses. No standards are therefore required and the volume (V) need not be known, merely that it is the same for all of the samples. If different volumes have to be used for different sample sizes, only the ratio of volumes needs to be known.

The presence of a third component in all of the samples will cause a scatter of the plot, but an occasional impurity in only a few samples will show up as a few points above the line with the remainder of the analyses giving a good linear plot. Figures 1 and 2 show this latter type of deviation, indicating that there are no significant additional components present in cuts No. 2 and No. 3.

This technique has the added advantage that if one of the components shows preferential absorption on the walls of the inlet system of the mass spectrometer, no effect on the linearity of equation [A-3] will be observed if the fraction of the component absorbed is independent of the total quantity of that component present. The V/S_1 thus obtained is an effective reciprocal sensitivity and the correct absolute quantities will still be obtained when the effective reciprocal sensitivity is used in equation [A-4].

Can. J. Chem. Downloaded from www.nrcresearchpress.com by 176.9.209.113 on 09/04/12
For personal use only.

Can. J. Chem. Downloaded from www.nrcresearchpress.com by 176.9.209.113 on 09/04/12
For personal use only.

AN ASYMMETRIC SYNTHESIS OF D- AND L-MANNOSAMINE[1]

A. N. O'NEILL[2]

ABSTRACT

The addition of ammonia to the ethylenic bond of D-arabo-tetraacetoxy-1-nitrohexene-1 was stereospecific and formed a crystalline product, 1-nitro-1-deoxy-N-acetyl-D-mannosaminol. Application of the Nef reaction to this compound gave 2-amino-2-deoxy-D-mannose, which was isolated as the crystalline pentaacetate and further characterized as the hydrochloride by deacetylation with hydrochloric acid. In the deacetylation of the pentaacetate with barium methoxide, however, an abnormal epimerization occurred to yield N-acetyl-D-glucosamine.

L-Mannosamine pentaacetate was synthesized in a similar manner from L-arabo-tetraacetoxy-1-nitrohexene-1.

The general chemistry of the simple α-nitroölefins has been investigated extensively. It has been found, in agreement with theoretical considerations, that the α-nitro group, by virtue of its powerful inductive and resonance effects, strongly activates the double bond, thereby facilitating attack in the β-position by nucleophilic reagents. Thus the addition of such reagents as ethyl malonate (7, 8), alcohols (10), thiols (5), ammonia and amines (6), nitroparaffins (11), hydrogen cyanide (2), Grignard reagents (9, 1), and arylacetonitriles (3) to α-nitrostyrene, nitroethylene, α-nitropropylene, etc. has been easily accomplished in the presence of basic catalysts.

Some of the more complex acetylated carbohydrate C-nitroölefins with an olefinic bond in conjugation with the nitro group have been prepared (16), but their reactivities have not been studied other than in the synthesis of 2-deoxy aldoses by selective hydrogenation of the double bond (16, 17). These compounds are readily obtained from the aldoses with one less carbon atom by condensation with nitromethane. This is followed by acetylation and elimination of 1 mole of acetic acid by treatment with a mild base under the conditions of the Schmidt and Rutz reaction (15). The resulting acetylated nitroölefins are obtained in good yield and in general are easily crystallized. As the primary C-nitro group can readily be converted into an aldehyde by the Nef reaction, these compounds should provide excellent starting materials for the synthesis of hexosamines by the addition of ammonia, and branched-chain carbohydrates by the addition of nitroparaffins, malonic ester, or other nucleophilic reagents.

The addition of amines and ammonia to the more simple α-nitroölefins has been studied by Heath and Rose (6), who found the reaction a general one. However the yields were variable, due partly to the instability of the resulting 2-nitroalkylamine in which the basic group caused rapid decomposition of the nitro compound, and partly to the tendency of the nitroölefins to polymerize under the influence of the amine.

In the present investigation both D- and L-arabo-tetraacetoxy-1-nitrohexene-1 were synthesized from D- and L-arabinose by the method of Sowden (16). The addition of ammonia to the olefinic bond was readily accomplished by adding the acetylated nitroölefin slowly to a saturated solution of ammonia in anhydrous methanol at 0°. The product, obtained in 82% yield, was a very stable, white, crystalline solid. Its aqueous solution was neutral. Microanalysis and the infrared spectrum indicated the presence of a N-acetyl group. The absorption spectrum showed the typical bands, types I and II,

[1]*Manuscript received June 8, 1959.*
Contribution of the National Research Council of Canada, Atlantic Regional Laboratory, Halifax, Nova Scotia.
Issued as N.R.C. No. 5333.
[2]*Deceased. Manuscript completed by B. A. Bolto.*

of a secondary amide at 1640 and 1550 cm^{-1} respectively. This compound would not undergo the rapid decomposition characteristic of the basic unsubstituted 2-nitroalkylamines because it contains a neutral amide group, which must result from an acyl migration from O to N during the concomitant addition and de-O-acetylation reactions.

From the addition reaction only one of the two possible diastereoisomers was isolated. A search for the second isomer in the mother liquors from the crystallization failed to reveal its presence. The compound isolated was shown to have the *erythro* configuration about carbon atoms two and three by its subsequent conversion into derivatives of mannosamine.

It is reasonable to assume that this addition reaction proceeds through a primary nucleophilic attack by the ammonia or amide ion on the β-carbon atom of the acetylated nitroölefin. If Cram's rule of "steric control of asymmetric induction" (4) can be applied, then the ammonia would enter preferably from the least-hindered side of the double bond when the rotational conformation of the C—C bond is such that the double bond is flanked by H and OAc, the two least bulky groups attached to the adjacent asymmetric center. This should lead to a predominance of the erythroisomer, as was actually obtained (Fig. 1). However, in this case, this simple interpretation is complicated by the possible interaction of the carbonyl carbon atom of the migrating acyl group with the incoming amino group. If the addition of ammonia at the double bond is complete before the

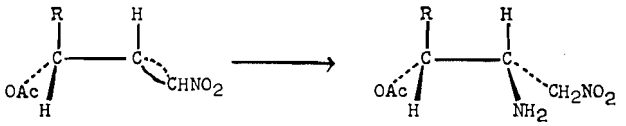

Fig. 1. R = $(CHOAc)_2.CH_2OAc$

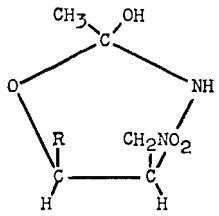

Fig. 2. R = $(CHOAc)_2.CH_2OAc$

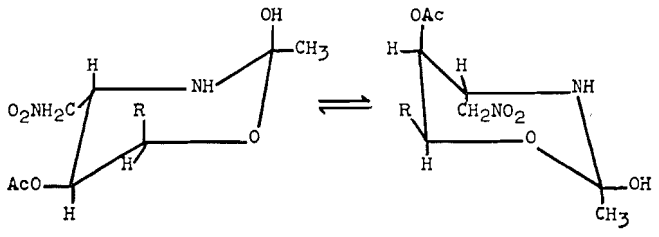

Fig. 3. R = $CHOAc.CH_2OAc$

Can. J. Chem. Downloaded from www.nrcresearchpress.com by 176.9.209.113 on 09/04/12
For personal use only.

acyl migration takes place, then the acyl group concerned could originate from C_3, with a planar five-membered ring as the intermediate (Fig. 2), or from C_4, with a non-planar six-membered ring as the intermediate (Fig. 3). In each case the nitrogen atom of the amino group can attack the carbonyl carbon atom of the migrating acyl group from either side. In Fig. 3, only one of the two possible configurations for the transient asymmetric center is given.

It is difficult to predict the most favored course of the rearrangement. In each of the above two cases, an intermediate is involved in which there is strong non-bonded repulsion

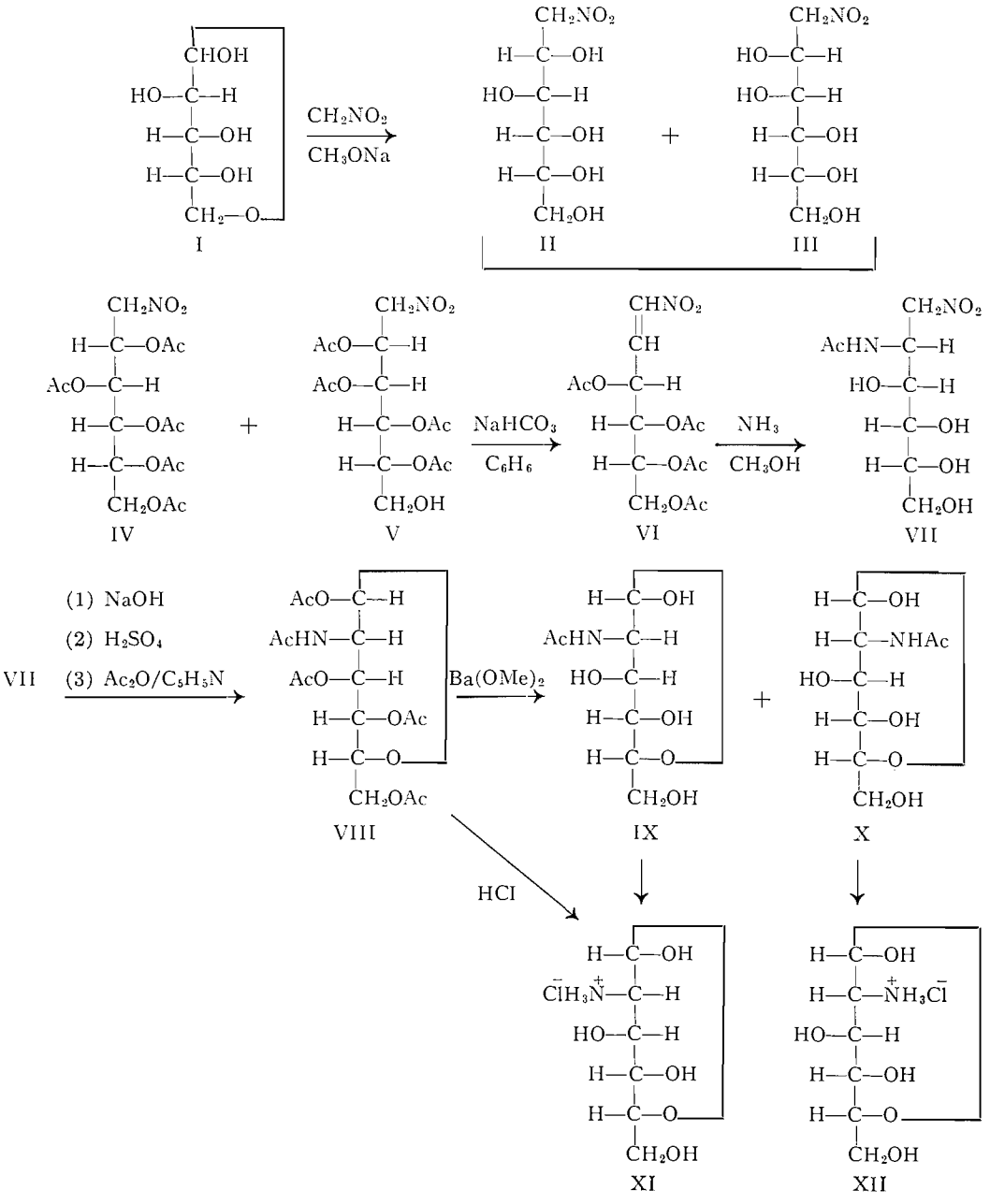

Can. J. Chem. Downloaded from www.nrcresearchpress.com by 176.9.209.113 on 09/04/12
For personal use only.

Can. J. Chem. Downloaded from www.nrcresearchpress.com by 176.9.209.113 on 09/04/12
For personal use only.

between fairly large groups, or in which bulky groups are in axial conformations. The addition product VII was treated with sodium hydroxide and the resulting sodium salt of the *aci*-nitro form treated with sulphuric acid under the conditions of the Nef reaction. Acetylation of the crude syrup so obtained yielded a crystalline pentaacetate of which the melting point and specific rotation agreed with values reported by Levene (13) for the β-pentaacetate of epichitosamine (β-D-mannosamine pentaacetate). The compound was further characterized as the hydrochloride by deacetylation with hydrochloric acid when agreement with the reported specific rotation was again obtained (13). Further evidence that XI was indeed D-mannosamine hydrochloride was obtained by a positive Elson–Morgan reaction, and by a degradation to D-arabinose with ninhydrin in pyridine (18).

However, deacetylation of the pentaacetate with barium methoxide gave 80–90% yields of N-acetyl-D-glucosamine (X) and only traces of N-acetyl-D-mannosamine (IX). These compounds were characterized as the hydrochlorides. This is evidence of an unusual epimerization during deacetylation in which a catalytic amount of barium methoxide was used, and is another example of the abnormal behavior of this compound. Thus, as the hydrochloride, it shows no mutarotation, nor is it oxidized by bromine or mercuric oxide. In fact treatment of D-mannosamine hydrochloride with mercuric oxide yields crystalline 2,5-anhydro-D-glucose (14).

For purposes of confirmation and for comparison of physical properties, derivatives of D-mannosamine were synthesized by a modification of Levene's original method (12). D-Glucosamine was oxidized to D-glucosaminic acid and epimerization accomplished in aqueous pyridine to form D-mannosaminic acid. After conversion to the lactone hydrochloride, reduction with sodium amalgam yielded D-mannosamine hydrochloride. The pentaacetate was formed in the usual manner and deacetylated with barium methoxide, when N-acetyl-D-glucosamine was again obtained with only traces of N-acetyl-D-mannosamine. But deacetylation of the pentaacetate with hydrochloric acid gave a quantitative yield of D-mannosamine hydrochloride.

The corresponding enantiomorphs of compounds II to VIII were synthesized by the same method from L-arabinose.

EXPERIMENTAL

All rotations were measured in a 2-dm tube with a Rudolph polarimeter. Melting points were observed on a Kofler micro-melting-point apparatus and are corrected. The infrared spectra were determined in nujol mulls with a Baird double-beam infrared spectrophotometer, model 4-55.

D-*Arabo-tetraacetoxy-1-nitrohexene-1* (VI)

This compound was synthesized from D-arabinose according to the method of Sowden (16), by condensation with nitromethane, acetylation, and elimination of 1 mole of acetic acid from the resulting mixture of acetylated C-nitroalcohols (IV and V). The yield of D-arabo-tetraacetoxy-1-nitrohexene-1 (VI) from 25 g of D-arabinose was 30 g; m.p. 115–116°, $[\alpha]_D^{24}$ +33° (c = 1.0 in chloroform). Main infrared absorption bands: 2900, 1740, 1667, 1530, 1460, 1379, 1220, 1122, 1078, 1050, 972, 953, and 853 cm^{-1}. Anal. Calc. for $C_{14}H_{19}O_{10}N$: C, 46.54; H, 5.30; N, 3.88. Found: C, 46.31; H, 4.87; N, 3.76%.

The corresponding L-arabo-tetraacetoxy-1-nitrohexene-1 prepared in the same manner from L-arabinose had m.p. 114–116°, $[\alpha]_D^{25}$ −34° (c = 1.0 in chloroform), and gave an identical infrared absorption spectrum.

Can. J. Chem. Downloaded from www.nrcresearchpress.com by 176.9.209.113 on 09/04/12
For personal use only.

1-Nitro-1-deoxy-N-*acetyl*-D-*mannosaminol* (VII)

Finely powdered D-arabo-tetraacetoxy-1-nitrohexene-1 was added slowly, in portions and with continuous shaking, to 500 ml of absolute methanol saturated with anhydrous ammonia at 0°. Each portion was allowed to dissolve before the next was added. When all of the acetylated nitroölefin was added the solution was left at 5° for 18 hours. Methanol and ammonia were removed by distillation under reduced pressure. This left a crystalline residue. It was recrystallized twice from methanol to give long needles; yield 16 g (82%), m.p. 172–173°, $[\alpha]_D^{24}$ −13.2° (c = 1.1 in water). Anal. Calc. for $C_8H_{16}O_7N_2$: C, 38.09; H, 6.40; N, 11.11. Found: C, 37.99; H, 6.14; N, 11.05%. Main infrared absorption bands: 3330, 2930, 1640, 1570, 1550, 1460, 1379, 1300, 1240, 1122, 1080, 1023, 943, 908, and 855 cm^{-1}.

The enantiomorphous 1-nitro-1-deoxy-N-acetyl-L-mannosaminol had m.p. 172–172.5° and $[\alpha]_D^{24}$ +14.9° (c = 1.5 in water). Its infrared absorption spectrum was identical with that of the D-isomer.

2-Acetamido-2-deoxy-1,3,4,6-tetra-O-*acetyl*-β-D-*mannose* (VIII)

An amount of 10 g of the above crystalline addition product was dissolved in 25 ml of 2 *N* sodium hydroxide at 5° and added dropwise with shaking to 12 ml of sulphuric acid in 15 ml of water also at 5°. During the addition the temperature was maintained at 10–15° by external cooling. The solution was neutralized with warm barium hydroxide solution and filtered. Two drops of acetic acid were added and the filtrate concentrated to a syrup under reduced pressure. It was further dried by the distillation of added ethanol, and finally over phosphorus pentoxide in a vacuum desiccator.

This syrupy material was acetylated for 3 days at 0° with acetic anhydride (125 ml) and pyridine (100 ml). The acetylation mixture was poured into 500 ml of ice and water and extracted with chloroform. The chloroform extract was washed twice with dilute sodium bicarbonate, four times with dilute copper sulphate, four times with water, and dried over anhydrous sodium sulphate. Distillation of the solvent under reduced pressure left a yellow syrup which was crystallized from absolute ethanol and recrystallized from ethanol–ether; yield 13 g (84% from VII), m.p. 162–163°, $[\alpha]_D^{24}$ −17.0° (c = 1.8 in chloroform). Anal. Calc. for $C_{16}H_{23}O_{10}N$: C, 49.35; H, 5.95; N, 3.60. Found: C, 49.44; H, 5.73; N, 3.50%. Levene (13) reported m.p. 158–159° and $[\alpha]_D^{20}$ −18° for his preparation of β-D-mannosamine pentaacetate.

The corresponding compound in the L-series had m.p. 162–163°, $[\alpha]_D^{25}$ +18.0° (c = 1.1 in chloroform).

2-Amino-2-deoxy-α-D-*mannose Hydrochloride* (XI)

β-D-Mannosamine pentaacetate was completely deacetylated by dissolving 200 mg in 4 ml of 2 *N* hydrochloric acid and heating on the steam bath for 4½ hours. After concentration under reduced pressure small amounts of residual water, hydrochloric acid, and acetic acid were removed by co-distillation with ethanol. The resulting dark brown crystalline material was dissolved in a small amount of water, decolorized with charcoal, and, after filtration through a cotton and asbestos plug, crystallized by the addition of ethanol; yield 107 mg. The product reduced Fehling's solution, and gave the characteristic Elson–Morgan reaction for hexosamine hydrochlorides. A small amount when degraded in a sealed tube with ninhydrin and pyridine by the method of Jeanloz (18) gave only D-arabinose as determined by paper chromatography. This compound had an indefinite melting point and showed no mutarotation; $[\alpha]_D^{25}$ −4° (c = 1.0 in 3% hydrochloric acid). Anal. Calc. for $C_6H_{14}O_5NCl$: C, 33.26; H, 6.48; N, 6.50; Cl, 16.44.

Found: C, 33.05; H, 6.36; N, 6.70; Cl, 16.40%. Levene (13) reported no mutarotation for his preparation of D-mannosamine hydrochloride, $[\alpha]_D$ −4.7° in 5% hydrochloric acid.

2-Acetamido-2-deoxy-D-glucose (X)

A portion (10 g) of the syrupy β-D-mannosamine pentaacetate was dissolved in 150 ml of absolute methanol, cooled to 0°, and treated at this temperature for 24 hours with 20 ml of 0.4 *N* barium methoxide. The solution was diluted with an equal volume of water, deionized by shaking with exchange resins Amberlite IR-120 and IR-45, filtered, and the filtrate concentrated to a syrup by distillation under reduced pressure. This was crystallized from ethanol–ether to yield 0.75 g of crystalline material and 5.0 g of syrup. The crystalline material, after recrystallization, had m.p. 193–196° with decomposition starting at 185°; $[\alpha]_D^{26}$ +75.0° (5 minutes), +69.0° (15 minutes), +58.2° (30 minutes), and +43.8° at equilibrium (4 hours); (c = 1.2 in water). Anal. Calc. for $C_8H_{15}O_6N$: C, 43.43; H, 6.84; N, 6.33. Found: C, 43.53; H, 6.79; N, 6.48%.

Both the crystalline material and the syrup gave the characteristic Elson–Morgan reaction for N-acetyl hexosamines. The crystalline material was further deacetylated with hydrochloric acid by dissolving 100 mg in 1 ml of 2 *N* hydrochloric, treating on the steam bath for 2 hours, and working up the material as described in the preceding preparation of D-mannosamine hydrochloride. It was recrystallized from aqueous ethanol; yield 93 mg. It reduced Fehling's solution and gave the Elson–Morgan color reaction for hexosamine hydrochlorides. An $[\alpha]_D^{25}$ of +82.4° at 5 minutes and +73° at 18 hours (c = 0.91 in water) established that the material was D-glucosamine hydrochloride, and that the crystalline N-acetyl hexosamine was N-acetyl-D-glucosamine and not N-acetyl-D-mannosamine.

However, when the syrupy material was treated with hydrochloric acid in the same manner, the product had $[\alpha]_D^{24}$ +18.0° changing to +15.5° after 26 hours (c = 2.2 in water). Fractional crystallization of some of this hydrochloride produced D-glucosamine hydrochloride ($[\alpha]_D^{25}$ +98° (5 minutes), +76° (17 hours; c = 1.1 in water)) and a small amount of D-mannosamine hydrochloride ($[\alpha]_D^{26}$ −4°; c = 1.0 in 2.5% hydrochloric acid). Thus the syrupy N-acetyl hexosamine was a mixture of N-acetyl-D-glucosamine and N-acetyl-D-mannosamine, while the crystalline material was pure N-acetyl-D-glucosamine. Of the total yield of N-acetyl derivative, 80–90% was estimated as N-acetyl-D-glucosamine.

Alternate Preparation of D-Mannosamine Hydrochloride

D-Mannosamine was synthesized by a modification of the method of Levene (12). D-Glucosamine hydrochloride (80 g) was first oxidized in aqueous solution with yellow mercuric oxide (200 g) to give D-glucosaminic acid in 50% yield, $[\alpha]_D^{25}$ −14° (c = 1.3 in 2.5% hydrochloric acid). Epimerization was accomplished by refluxing 40 g of D-glucosaminic acid dissolved in 400 ml water containing 40 ml pyridine on a steam bath for 24 hours. The D-mannosaminic acid was obtained by fractional crystallization from the large amount of starting material. The recovered D-glucosaminic acid was treated twice again with aqueous pyridine in the same manner. Each treatment yielded about 4 g of D-mannosaminic acid which was further purified by many recrystallizations from aqueous ethanol, $[\alpha]_D^{24}$ +10° (c = 1.5 in 2.5% hydrochloric acid). The D-mannosaminic acid was converted into its lactone hydrochloride by treatment with ethanolic hydrogen chloride containing a small amount of benzaldehyde; yield 75%, $[\alpha]_D^{24}$ +45° (c = 1.4 in water). Reduction of the lactone with 2.5% sodium amalgam yielded D-mannosamine hydrochloride; yield

Can. J. Chem. Downloaded from www.nrcresearchpress.com by 176.9.209.113 on 09/04/12
For personal use only.

60% from the lactone. Recrystallization from water containing a small amount of methanol gave pure material, $[\alpha]_D^{24}$ −4.0° (c = 2.0 in 2.5% hydrochloric acid).

Acetylation of the hydrochloride with pyridine and acetic anhydride in the usual manner gave β-D-mannosamine pentaacetate, m.p. 161–162°, $[\alpha]_D^{24}$ −18° (c = 1.5 in chloroform). Deacetylation with barium methoxide again yielded predominantly N-acetyl-D-glucosamine. But deacetylation with hydrochloric acid gave a quantitative yield of D-mannosamine hydrochloride.

REFERENCES

1. BUCKLEY, G. D. J. Chem. Soc. 1494 (1947).
2. BUCKLEY, G. D., HEATH, R. L., and ROSE, J. D. J. Chem. Soc. 1500 (1947).
3. BUCKLEY, G. D., HUNT, F. G., and LOWE, A. J. Chem. Soc. 1504 (1947).
4. CRAM, D. J. and ABD ELHAFEZ, F. A. J. Am. Chem. Soc. **74**, 5828 (1952).
5. HEATH, R. L. and LAMBERT, A. J. Chem. Soc. 1477 (1947).
6. HEATH, R. L. and ROSE, J. D. J. Chem. Soc. 1486 (1947).
7. KOHLER, E. P. and ENGELBRECHT, H. J. Am. Chem. Soc. **41**, 764 (1919).
8. KOHLER, E. P. and BARRETT, G. R. J. Am. Chem. Soc. **48**, 1770 (1928).
9. KOHLER, E. P. and STONE, J. F. J. Am. Chem. Soc. **52**, 761 (1930).
10. LAMBERT, A., SCAIFE, C. W., and WILDER-SMITH, A. E. J. Chem. Soc. 1474 (1947).
11. LAMBERT, A. and PIGGOTT, H. A. J. Chem. Soc. 1489 (1947).
12. LEVENE, P. A. J. Biol. Chem. **36**, 73 (1918).
13. LEVENE, P. A. Hexosamines and mucoproteins. Longmans, Green and Co., Ltd., London. 1925. p. 16.
14. LEVENE, P. A. J. Biol. Chem. **39**, 69 (1919).
15. SCHMIDT, E. and RUTZ, G. Ber. **61**, 2142 (1928).
16. SOWDEN, J. C. and FISCHER, H. O. L. J. Am. Chem. Soc. **69**, 1048 (1947).
17. SOWDEN, J. C. J. Am. Chem. Soc. **72**, 808 (1950).
18. STOFFYN, P. J. and JEANLOZ, R. W. Arch. Biochem. Biophys. **52**, 373 (1954).

Can. J. Chem. Downloaded from www.nrcresearchpress.com by 176.9.209.113 on 09/04/12
For personal use only.

Can. J. Chem. Downloaded from www.nrcresearchpress.com by 176.9.209.113 on 09/04/12
For personal use only.

SYNTHESIS OF SUGARS FROM SMALLER FRAGMENTS

PART XI. SYNTHESIS OF L-GALACTOHEPTULOSE[1]

J. K. N. JONES AND N. K. MATHESON[2]

ABSTRACT

1,3-Dihydroxy-2-propanone phosphate condenses with L-threose in the presence of the enzyme aldolase to yield L-galactoheptulose phosphate, from which the heptose was prepared.

Dihydroxyacetone phosphate (1,3-dihydroxy-2-propanone phosphate) which was formed from D-fructose 1,6-diphosphate has been shown to yield new sugar derivatives when its solution is incubated at pH 6.5 with aldehydes in the presence of crude pea aldolase or purified muscle aldolase (1). The reaction takes place between the aldehyde and an enzyme–substrate complex which involves aldolase and dihydroxyacetone phosphate (2). In particular three of the possible aldotetroses, D-erythrose (3), L-erythrose (4), and D-threose (5) have been shown to condense with dihydroxyacetone phosphate in the presence of aldolase and the resultant heptulose derivatives have the D-*threo* configuration on carbon atoms 3 and 4.

It was considered of interest to examine the behavior of the fourth aldotetrose, L-threose. At pH 6.5, L-threose and dihydroxyacetone phosphate (produced by the cleavage of fructose diphosphate with aldolase) in the presence of aldolase gave a low yield of L-galactoheptulose 1-phosphate which was converted to the crystalline sugar. No other heptulose could be detected chromatographically (an orcinol – trichloroacetic acid spray was used for the detection of heptuloses on chromatograms (6)). The ultraviolet absorption of the product formed on heating the heptulose with cysteine and sulphuric acid (7) was measured at 5080 Å, and its intensity indicated that 1 mole of L-threose had yielded 0.021 mole of heptulose. Thus all the aldotetroses condense with dihydroxyacetone phosphate in the presence of aldolase to yield heptulose derivatives which possess the D-*threo* configuration on carbon atoms 3 and 4.

In view of the results of other workers (8, 9) which indicated that these condensations take place without the intervention of enzymes a reaction mixture which was composed of dihydroxyacetone (1,3-dihydroxy-2-propanone), L-threose, and aldolase at pH 6.5 was studied. The presence of heptulose was determined colorimetrically by the method of Dische (7). The reaction products were also separated on paper chromatograms which were sprayed with orcinol–trichloroacetic acid (6). No heptulose was detected by either method. The formation of heptulose was therefore enzymic and involved dihydroxyacetone as its phosphate.

EXPERIMENTAL

Preparation of L-*Threose*

2,4-*O*-benzylidene-L-threose was prepared by the method of Neish (10). The *O*-benzylidene group was removed by heating the derivative in 10% acetic acid solution at 100° C for 1 hour. The solution was extracted three times with ether and the extracts were evaporated under diminished pressure to half their original volume. This concentration of aldotetrose was used in the enzymic experiments.

[1]*Manuscript received June 22, 1959.*
Contribution from the Department of Chemistry, Queen's University, Kingston, Ontario.
[2]*Present address: Tobacco Research Institute, P.O. Box 172, Mareeba, Queensland, Australia.*

Can. J. Chem. Downloaded from www.nrcresearchpress.com by 176.9.209.113 on 09/04/12
For personal use only.

D-*Fructose Sodium Diphosphate*

Commercial barium salt was deionized on a column of Amberlite ion-exchange resin IR-120, the acidity of the eluate was neutralized with sodium hydroxide, after which the solution was evaporated to a small volume and the concentrate was cooled to 0° C.

The efflorescent crystalline hydrate which separated was collected on a filter, washed with the cold water, and quickly transferred to a desiccator. The dried salt was a pale yellow powder.

The chromatographic behavior of this substance corresponded to that of authentic D-fructose 1,6-diphosphate.

Reaction of L-*Threose,* D-*Fructose Diphosphate, and Crystalline Muscle Aldolase*

A solution of L-threose (3.0 g) and the sodium salt of D-fructose diphosphate (3.0 g) was adjusted to pH 6.5 with dilute acetic acid. Twice-recrystallized muscle aldolase (50 mg) was added and the volume was adjusted to 150 ml. The solution was kept at 37° C and 1-ml aliquots were taken at intervals (see Table I). Each sample was mixed with an equal volume of 2 *N* sulphuric acid and heated on a boiling water bath for 15 minutes to stop enzyme action. The heptulose content was then estimated by the method of Dische (7) with cysteine hydrochloride and sulphuric acid as follows. One milliliter of the sample was made up to 10 ml, and 1 ml of this solution was treated with 5 ml of sulphuric acid reagent at 0° C. The color at 5080 Å which developed after the solution had been left to stand for 18 hours was measured on a Unicam SP 600 spectrophotometer.

TABLE I

Yield of heptose as determined by the colorimetric procedure of Dische (7)

Time (hours)	Heptulose synthesis: aldolase, D-fructose 1,6-diphosphate, L-threose (log *E* 5080 Å)	Blank experiment: aldolase, dihydroxyacetone, L-threose (log *E* 5080 Å)
0	0.17	0.18
0.5	0.20	0.17
1.5	0.23	0.17
6.0	0.51	0.18
24	0.66	0.17
72	0.76	0.16

A calibration curve made by using D-galactoheptulose as the heptose sugar gave a linear relationship between concentration and intensity of color.

The pH of the reaction solution showed a drop towards lower values with time and this pH was adjusted to the original value by the addition of a few drops of sodium acetate solution. Sulphuric acid (2 *N*, 150 ml) was added to the solution which was heated at 100° C for 6 hours in order to hydrolyze phosphate esters. The sulphuric acid was partially neutralized with barium hydroxide and neutralization was completed with barium carbonate.

The barium salts were removed by centrifugation and the supernatant liquid was passed through a column of Amberlite IR4B (acetate) and IR 120 ion-exchange (H) resins. The eluate was reduced in volume by evaporation under diminished pressure to give a syrup which was separated into three fractions on a column of powdered cellulose using butane-1-ol and water (9:1) as eluent.

Fraction I.—Fraction I (0.030 g) co-chromatographed with dihydroxyacetone and gave the same color with the *p*-anisidine hydrochloride reagent as did dihydroxyacetone.

Fraction II.—Fraction II (0.082 g) co-chromatographed with D-fructose and gave the same color with the orcinol – trichloroacetic acid reagent.

Fraction III.—Fraction III (0.079 g) co-chromatographed with L-galactoheptulose and on trituration with ethanol gave L-galactoheptulose, m.p. and mixed m.p. 100–101°, $[\alpha]_D^{22°}$ −90° → −80° (*c*, 1.1 water).

Reaction of Dihydroxyacetone with L-*Threose and Aldolase at pH 6.5*

A solution of L-threose (0.30 g) and dihydroxyacetone (0.30 g) in water was adjusted to pH 6.5 with acetic acid, crystalline muscle aldolase (5 mg) was then added, the volume made up to 15.0 ml, and the solution kept at 37° C. One-milliliter aliquots were taken at 0, 0.5, 1.5, 6.0, 24, and 72 hours, and the heptulose estimated (7). The absorption at 5080 Å at the elapse of these times is recorded in the table.

The authors thank the National Research Council for grants and for a Postdoctoral Fellowship (to N. K. Matheson).

REFERENCES

1. MEYERHOF, O. and SCHULZ, W. Biochem. Z. **289**, 87 (1936).
2. TOPPER, Y. J., MEHLER, A. H., and BLOOM, D. Science, **126**, 1287 (1957).
3. HOUGH, L. and JONES, J. K. N. J. Chem. Soc. 4047 (1952).
4. JONES, J. K. N. and KELLY, R. B. Can. J. Chem. **34**, 95 (1956).
5. GORIN, P. A. J. and JONES, J. K. N. J. Chem. Soc. 1537 (1953).
6. KLEVSTRAND, R. and NORDAL, A. Acta Chem. Scand. **4**, 1320 (1950).
7. DISCHE, Z. J. Biol. Chem. **204**, 983 (1953).
8. STACEY, M. Biological synthesis of carbohydrates. Roy. Inst. Chem. (London), Monograph No. 2, 6 (1956).
9. GASCOIGNE, J. A., OVEREND, W. G., and STACEY, M. Chem. & Ind. (London), 402 (1959).
10. NEISH, A. C. Can. J. Chem. **32**, 334 (1954).

Can. J. Chem. Downloaded from www.nrcresearchpress.com by 176.9.209.113 on 09/04/12
For personal use only.

Can. J. Chem. Downloaded from www.nrcresearchpress.com by 176.9.209.113 on 09/04/12
For personal use only.

LYCOPODIUM ALKALOIDS

VIII. LYCOPODINE[1]

D. B. MacLean and W. A. Harrison[2]

ABSTRACT

Information pertaining to the position of the carbonyl group relative to the nitrogen atom and to the size of one of the nitrogen rings in lycopodine has been obtained through a study of the reactions of α- and β-cyanobromolycopodine.

Lycopodine, $C_{16}H_{25}ON$, is the major alkaloid of several species of *Lycopodium*. It is known that it contains a tertiary nitrogen atom, a carbonyl group, and no other functional groups, and it can be inferred that it has a combination of four carbocyclic and/or heterocyclic rings (1).

The first degradative work on lycopodine was carried out by Marion and Manske (2), who dehydrogenated the alkaloid and isolated from the reaction 7-methylquinoline and 5,7-dimethylquinoline along with several other uncharacterized bases. Thus, there may be present in the alkaloid a reduced quinoline ring system. The reaction of lycopodine with cyanogen bromide was studied by MacLean, Manske, and Marion (1) and later by Barclay and MacLean (3). From the cyanogen bromide reaction two isomeric cleavage products, α- and β-cyanobromolycopodine, I and II, respectively, were isolated. The bromo group in I was shown to be primary by its conversion to an acetate, hydrolysis of the acetate to an alcohol, and oxidation of the latter to a carboxylic acid without loss of carbon. An attempt to carry out an analogous series of reactions on II failed in the first step, for, instead of the expected acetate, a different compound III, $C_{17}H_{24}ON_2$, was formed, apparently in a cyclization reaction. The carbonyl group in lycopodine is ketonic and is present in a six-membered or larger ring on the basis of its absorption in the infrared near 1700 cm^{-1} (1). Barclay and MacLean (3) have shown that the carbonyl group is flanked on one side by a methylene group through the formation of a benzylidene derivative from α-cyanolycopodine. In the present study the reactions of α- and β-cyanobromolycopodine have been extended to give information on the size of one of the two nitrogen rings and on the position of the carbonyl group relative to the nitrogen atom.

α-Cyanobromolycopodine I was converted to the carboxylic acid IV reported by MacLean, Manske, and Marion (1). Reduction of the acid IV with sodium borohydride yielded the hydroxy acid V, $C_{17}H_{26}O_3N_2$. This hydroxy acid failed to form a lactone on treatment with catalytic amounts of *p*-toluene sulphonic acid in a boiling benzene solution and a close relationship between the carbonyl and the nitrogen in the direction of the α-cleavage is precluded. Hydrolysis of the acid IV with aqueous alcoholic hydrochloric acid yielded an impure amino acid hydrochloride VI. Treatment of a solution of VI in methanol with a solution of diazomethane in ether yielded a mixture from which the lactam VII, $C_{16}H_{23}O_2N$, was isolated. The lactam had ketonic absorption in its infrared spectrum at 1700 cm^{-1} and lactam absorption at 1635 cm^{-1}. The latter is in the region characteristic of six-membered or larger ring lactams. Reduction of VII with

[1]*Manuscript received June 25, 1959.*
Contribution from the Burke Chemical Laboratories, Hamilton College, McMaster University, Hamilton, Ontario. Part of this work was taken from the thesis of W. A. Harrison presented to the Faculty of Graduate Studies in May, 1957 in partial fulfillment of the requirements for the M.Sc. degree.
[2]*Holder of National Research Council Studentship 1956–57, 1957–58, and 1958–59.*

Can. J. Chem. Downloaded from www.nrcresearchpress.com by 176.9.209.113 on 09/04/12
For personal use only.

lithium aluminum hydride yielded dihydrolycopodine VIII, identified by comparison with an authentic sample prepared by the reduction of lycopodine with lithium aluminum hydride. It can be concluded that no rearrangements in the carbon skeleton occurred in the above reaction sequence.

MacLean, Manske, and Marion (1) reported that β-cyanobromolycopodine II reacted with potassium acetate in an unexpected manner and formed compound III in an elimination reaction rather than undergoing displacement to form an acetate. We have confirmed this result. We have found, however, that treatment of II with silver acetate in boiling benzene yielded a mixture of III and an acetate. The presence of the acetate in the reaction mixture was indicated by an examination of the infrared spectrum of the crude reaction product. To facilitate the separation of compound III from the other product of reaction, the mixture was hydrolyzed and then separated by chromatography into two components. The less strongly adsorbed fraction proved to be compound III formed in 82% yield, while the more strongly adsorbed proved to be the β-alcohol, $C_{17}H_{26}O_2N_2$, IX formed in 18% over-all yield from the β-bromide. The crude product IX had absorption bands in the infrared attributable to a carbonyl group and a hydroxyl group. In an alternate method of separation, the crude reaction mixture from the silver acetate reaction was treated directly with sodium borohydride in ethanol. Chromatographic separation of the product of this reduction yielded III in 72% yield and a new compound, $C_{17}H_{28}O_2N_2$, X in 23% yield. Compound X was also obtained by treatment of IX with sodium borohydride. Compound X showed no carbonyl absorption in its infrared spectrum, but had strong hydroxyl absorption as well as the usual cyanamide absorption. The compound X was oxidized by the Oppenauer method to the keto alcohol IX, and in this manner IX was obtained in crystalline form.

The low yield of alcohol in the silver acetate reaction coupled with the difficulty in isolation of the β-bromide II led us to seek an alternative source of the β-alcohol IX. In the reaction of lycopodine with cyanogen bromide, Barclay and MacLean (3) reported that an alcohol fraction was formed in small yield along with the two isomeric bromides. From this alcohol fraction they isolated, after treatment with acetic anhydride, α-cyanoacetoxylycopodine XI, previously reported by MacLean, Manske, and Marion (1). We have treated this alcohol fraction with sodium borohydride and have obtained a mixture from which we have isolated compounds III and X and a new compound XII. Compound XII proved to be identical with the product obtained when α-cyanohydroxylycopodine was reduced with sodium borohydride. In this manner a sufficient quantity of the β-alcohol was obtained for degradative study.

The chromic acid oxidation of IX yielded a non-crystalline acid XIII which was converted to a crystalline methyl ester XIV, $C_{18}H_{26}O_3N_2$, on treatment with diazomethane. The analysis indicated that no loss in carbon had occurred in the oxidation reaction and one can safely conclude that the alcohol IX is a primary alcohol. Reduction of the crude β-acid XIII with sodium borohydride yielded a neutral product XV, $C_{17}H_{24}O_2N_2$, with the properties of a lactone. It had no hydroxyl absorption in its infrared spectrum, but had a strong peak at 1743 cm^{-1} when the spectrum was determined in nujol mull, and at 1761 cm^{-1} when it was determined in a carbon tetrachloride solution. This is a borderline region between five-membered and six-membered lactones and it can be concluded that the carbonyl group is separated from the nitrogen atom by three or four carbon atoms about the periphery of the molecule in the direction of the β-cleavage.

In proposing a model to account for these reactions it is inviting to use the hexahydrojulolidine ring system which is present in annotinine, the only alkaloid of this group of

known structure (4, 5). In making use of this ring system it is convenient to place the carbonyl group in the position shown in the partial formula below.

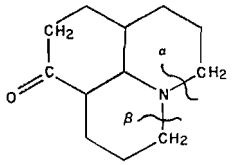

Those carbon atoms which are definitely known are so indicated, and the α- and β-cleavages are designated. This model is in agreement with the data presented here, namely, that the ring broken in the α-cleavage is six-membered and that the carbonyl group is located close to the nitrogen atom about the periphery of the molecule in the direction of the β-cleavage, but not in the direction of the α-cleavage. The model also accounts for the carbonyl frequency in the infrared spectrum of lycopodine. It does not attempt to account for the fourth ring of lycopodine nor for the C-methyl group which is present in the alkaloid.

EXPERIMENTAL

Lycopodine

The alkaloid was isolated from *L. flabelliforme* by the procedure described by Barclay and MacLean (3). It melted at 116° after recrystallization from petroleum ether. Calc. for $C_{16}H_{25}ON$: one C-methyl, 6.1%. Found: 5.0%.

Reaction of Lycopodine with Cyanogen Bromide

The reaction was carried out and the products isolated according to the procedure of Barclay and MacLean (3).

Oxidation of α-Cyanohydroxylycopodine

α-Cyanohydroxylycopodine (1.9 g), prepared by the method of MacLean, Manske, and Marion (1), was dissolved in 40 ml of 90% acetic acid and the solution added slowly to a solution of 4 g of chromium trioxide in 60 ml of 90% acetic acid. The temperature was maintained at -10 to $-15°$ during the addition, and the mixture was stirred at this temperature for a further 4 hours. The excess chromic acid was destroyed with methanol and the mixture was then evaporated to dryness. Water was added to the residue and the mixture was exhaustively extracted with chloroform. The chloroform solution was extracted with sodium carbonate solution and the carbonate extract acidified and extracted with chloroform. Evaporation of the second chloroform solution yielded 1.2 g of non-crystalline acid. The crude acid crystallized on standing, but a suitable solvent system for its recrystallization was not found. It was characterized as its methyl ester reported previously (1).

Preparation of the Lactam VII

The acid IV (1.2 g) was dissolved in 12 ml of *n*-propanol and treated with 60 ml of 2 *M* hydrochloric acid. The mixture was heated on the steam bath for 15 hours and then evaporated to dryness. The residue was washed several times with warm ether to remove unreacted starting material. There remained a residue of 1.1 g of crude amino acid hydrochloride.

The hydrochloride was dissolved in methanol, an excess of diazomethane in ether was added, and the mixture allowed to stand for 1 hour before it was taken to dryness.

Can. J. Chem. Downloaded from www.nrcresearchpress.com by 176.9.209.113 on 09/04/12
For personal use only.

The crude product was dissolved in chloroform and washed with dilute hydrochloric acid. The chloroform solution yielded, on evaporation, 0.5 g of crude product which was purified by chromatography on an alumina column using chloroform as eluant. Practically all the material was eluted in a single band. The chloroform was evaporated and the residue dissolved in low boiling petroleum ether from which it crystallized in needles. Recrystallization from the same solvent gave an analytical sample which melted at 159–161°. Calc. for $C_{16}H_{23}O_2N$: C, 73.6; H, 8.88; N, 5.4%. Found: C, 73.9; H, 9.29; N, 5.2%. The infrared spectrum showed a strong band at 1635 cm^{-1} in the lactam region, as well as the usual carbonyl band at 1700 cm^{-1}. The over-all yield of lactam from α-cyanohydroxylycopodine was about 30%.

The acid washings from the purification of the lactam were worked up and yielded 0.3 g of an amino acid ester. The ester was slowly converted to the lactam by refluxing in xylene. This was shown by the infrared spectrum of the crude product, which exhibited a decrease in the intensity of the ester carbonyl absorption at 1730 cm^{-1} and the appearance of the lactam carbonyl band at 1635 cm^{-1}.

Reduction of the Lactam VII *with Lithium Aluminum Hydride*

A sample of the lactam VII (0.15 g), dissolved in anhydrous tetrahydrofuran, was added with stirring to a solution of lithium aluminum hydride (0.2 g) in tetrahydrofuran. The mixture was heated under reflux for 4 hours and then allowed to stand overnight. The excess hydride was decomposed with wet tetrahydrofuran, the solution filtered, and the precipitated hydroxides extracted thoroughly with chloroform. The combined tetrahydrofuran and chloroform extract was evaporated to dryness and the residue was purified by chromatography on an alumina column using chloroform as eluant. From the chloroform eluant a residue was obtained which crystallized from ether – petroleum ether. This material proved to be identical with a sample of dihydrolycopodine prepared by the reduction of lycopodine with lithium aluminum hydride. The melting point of a mixture of the two samples was not depressed and their infrared spectra were identical.

Reduction of the Acid IV *with Sodium Borohydride*

The acid IV (0.3 g) was dissolved in an aqueous sodium carbonate solution and treated with an excess of sodium borohydride. After the mixture had stood at room temperature for 12 hours, the excess sodium borohydride was destroyed with acetone and the mixture evaporated to dryness. The residue was taken up in water, acidified with hydrochloric acid, and the resulting mixture extracted with chloroform. The chloroform extract was dried and evaporated to yield a crystalline residue in virtually quantitative yield. Recrystallization from ether, in which the compound is only sparingly soluble, gave an analytical sample which melted at 193–194°. The compound analyzed for a monohydrate. Calc. for $C_{17}H_{26}O_3N_2 \cdot H_2O$: C, 62.9; H, 8.70; N, 8.6%. Found: C, 63.0; H, 8.35; N, 8.7%. Loss in weight on drying: Calc., 5.5%; found, 5.8%.

Reduction of α-Cyanohydroxylycopodine with Sodium Borohydride

α-Cyanohydroxylycopodine (0.2 g) was dissolved in ethanol and treated with an excess of sodium borohydride. After a period of 3 hours the excess borohydride was destroyed by the addition of acetone and the mixture evaporated to dryness. Water was added to the residue and the mixture was extracted with chloroform. The chloroform extract was dried and evaporated to dryness to yield a crystalline residue in virtually quantitative yield. Recrystallization from acetone yielded an analytical sample which

Can. J. Chem. Downloaded from www.nrcresearchpress.com by 176.9.209.113 on 09/04/12
For personal use only.

melted at 195–197°. Calc. for $C_{17}H_{28}O_2N_2$: C, 69.8; H, 9.65; N, 9.6%. Found: C, 70.1; H, 9.97; N, 9.2%.

Treatment of β-Cyanobromolycopodine II *with Silver Acetate*

Silver acetate (1.0 g) was added to a solution of 0.82 g of β-cyanobromolycopodine in benzene (80 ml) and the mixture heated under reflux for 5 hours. After the insoluble salts had been removed by filtration, the benzene solution was evaporated to give 0.67 g of non-crystalline material. The infrared spectrum (film) of the crude product showed bands at 1700 and 1735 cm^{-1}, attributed to ketone and acetate carbonyl groups respectively, as well as a strong band at 1675 cm^{-1} characteristic of the cyclized compound III.

To facilitate separation of the cyclized and non-cyclized products, the acetate which had been formed was hydrolyzed to the alcohol by treating the mixture for 2.5 hours with potassium hydroxide (0.8 g) in boiling methanol (20 ml). The methanol was evaporated, water added to the residue, and the mixture extracted with chloroform. The oil obtained on evaporation of the extract was chromatographed on alumina with chloroform as the eluant. The first fractions yielded 0.52 g (82%) of crystalline cyclized compound III, identified by comparison with a sample prepared according to the procedure of MacLean, Manske, and Marion (1). A yellow band which moved more slowly down the column yielded 0.12 g (18%) of an almost colorless oil, the infrared spectrum of which had absorption bands in the hydroxyl, cyanamide, and carbonyl regions. Reduction of this crude keto alcohol IX is described below.

A second silver acetate reaction was carried out using 0.47 g of β-cyanobromolycopodine. In this run the cyclized compound – acetate mixture was reduced with sodium borohydride and the resulting mixture separated by chromatography on alumina with chloroform as the eluant. This procedure yielded 0.26 g (72%) of the cyclized compound III and 0.09 g (23%) of compound X described below.

Reduction of β-Cyanohydroxylycopodine IX *with Sodium Borohydride*

The non-crystalline alcohol IX (0.12 g) obtained by the foregoing procedure was dissolved in 95% ethanol, sodium borohydride (0.1 g) added, and the mixture left overnight at room temperature. When the reaction mixture was worked up in the usual manner a nearly quantitative yield of a crystalline product was obtained which melted at 181–182° after recrystallization from acetone. Calc. for $C_{17}H_{28}O_2N_2$: C, 69.8; H, 9.65; N, 9.6%. Found: C, 69.9; H, 9.43; N, 8.9%.

The infrared spectrum of the compound showed a band at 3360 cm^{-1} in the hydroxyl region, cyanamide absorption at 2195 cm^{-1}, and no absorption in the carbonyl region.

Sodium Borohydride Reduction of the Alcohol Fraction from the Cyanogen Bromide Reaction

An ethanol solution containing the alcohol fractions (3.6 g) from a number of reactions of lycopodine with cyanogen bromide was added to a solution of 1.0 g of sodium borohydride in 95% ethanol. The reaction mixture was allowed to stand overnight at room temperature. The excess hydride was destroyed by the addition of formalin and the solution taken to dryness. Water was added to the residue, the mixture extracted with chloroform, and the chloroform extract washed with dilute hydrochloric acid. The non-crystalline basic material which was recovered from the acid washings weighed 0.22 g. The neutral fraction obtained on evaporation of the chloroform solution was dissolved in acetone. Concentration of the acetone solution yielded 0.31 g of a crystalline com-

Can. J. Chem. Downloaded from www.nrcresearchpress.com by 176.9.209.113 on 09/04/12
For personal use only.

pound, m.p. 193–196°, which was identical with compound XII obtained by borohydride reduction of α-cyanohydroxylycopodine.

The material recovered by evaporation of the mother liquors from the crystallization above was dissolved in chloroform and adsorbed on an alumina column. Elution with 99:1 chloroform–methanol first yielded a fraction containing 0.43 g of cyclized compound III, followed by a brown band (0.43 g) from which no crystalline compounds could be isolated. Evaporation of the next fractions yielded an additional 0.78 g of crystalline compound XII. This diol was closely followed down the column by another compound (0.22 g, m.p. 179–181°) which was found by a mixed melting point determination and comparison of infrared spectra to be identical with that obtained by sodium borohydride reduction of β-cyanohydroxylycopodine. Further elution of the column yielded only non-crystalline material of complex composition. The yields of cyclized compound III, α-cyanohydroxydihydrolycopodine XII, and β-cyanohydroxydihydrolycopodine X were 12%, 30%, and 6%, respectively.

Oppenauer Oxidation of β-Cyanohydroxydihydrolycopodine X

To 0.60 g of β-cyanohydroxydihydrolycopodine X partially dissolved in anhydrous benzene (70 ml) were added 5 ml of acetone and 1.5 g of aluminum isopropoxide. The mixture was heated under reflux for 11 hours and then poured into water. The benzene layer was separated and the aqueous phase extracted with more benzene. The crude product obtained by evaporation of the combined benzene extract was dissolved in chloroform and adsorbed on an alumina column. Evaporation of the fractions collected on elution with chloroform yielded 0.38 g of β-cyanohydroxylycopodine which melted at 123–124° after crystallization from ether – petroleum ether. Calc. for $C_{17}H_{26}O_2N_2$: C, 70.3; H, 9.03; N, 9.7%. Found: C, 69.8; H, 8.82; N, 10.0%.

The infrared spectrum showed absorption bands at 3475 cm^{-1} in the hydroxyl region, 2195 cm^{-1} in the cyanamide region, and 1685 cm^{-1} in the carbonyl region. The spectrum of a non-crystalline film of the compound was found to be identical with that of the non-crystalline alcohol obtained by hydrolysis of the product of the reaction of β-cyanobromolycopodine with silver acetate.

Elution of the column with 95:5 chloroform–methanol gave a fraction containing 0.09 g of unreacted diol.

Oxidation of β-Cyanohydroxylycopodine with Chromic Acid

A solution of 0.15 g of β-cyanohydroxylycopodine (m.p. 123–124°) in 90% acetic acid was added dropwise over 1.5 hours to a stirred solution of chromium trioxide (0.3 g) in 90% acetic acid maintained at −5 to −10°. The reaction mixture was stirred 3 hours longer, during which time the temperature rose to 0°. After the excess chromium trioxide had been destroyed by the addition of methanol, the mixture was evaporated under reduced pressure. Water was added to the residue and the mixture extracted repeatedly with chloroform. The chloroform solution was extracted with aqueous sodium bicarbonate and the bicarbonate solution acidified and extracted with chloroform. Evaporation of the chloroform yielded 0.11 g (70%) of a non-crystalline acid, whose infrared spectrum (film) showed absorption maxima at 1695 (ketone carbonyl), 1710 (acid carbonyl), and 2200 cm^{-1} (cyanamide), and absorption in the hydroxyl region.

A sample of the acid (35 mg) was converted to the methyl ester by dissolving it in methanol and treating it with an excess of an ether solution of diazomethane. After it had stood for 2 hours the solution was evaporated and the residue dissolved in chloro-

Can. J. Chem. Downloaded from www.nrcresearchpress.com by 176.9.209.113 on 09/04/12
For personal use only.

form. The chloroform solution was washed with aqueous sodium bicarbonate and then evaporated. The product crystallized readily and melted at 127–129° after recrystallization from ether – petroleum ether. Calc. for $C_{18}H_{26}O_3N_2$: C, 67.9; H, 8.23; N, 8.8%. Found: C, 67.8; H, 8.41; N, 8.9%.

The infrared spectrum of the ester showed absorption at 1700 (ketone carbonyl), 1725 (ester carbonyl), and 2210 cm^{-1} (cyanamide).

Reduction of the Acid XIII *with Sodium Borohydride*

A solution of the non-crystalline acid XIII (70 mg) in aqueous sodium bicarbonate was added to an ethanolic solution of sodium borohydride. After the reaction mixture had stood at room temperature for 2 hours, the excess hydride was destroyed by adding formalin, and the mixture evaporated. The residue was acidified with dilute hydrochloric acid and extracted with chloroform. The chloroform extract was washed with aqueous sodium bicarbonate and then evaporated to give 45 mg (68%) of a crystalline neutral compound. A small amount of starting material was recovered when the bicarbonate washings were acidified and extracted with chloroform, but no hydroxy acid was detected. Recrystallization of the neutral compound from ether yielded colorless needles, m.p. 201–203°. Calc. for $C_{17}H_{24}O_2N_2$: C, 70.8; H, 8.39; N, 9.7%. Found: C, 70.7; H, 8.52; N, 9.8%.

The infrared spectrum of the neutral compound exhibited cyanamide absorption and a single band in the carbonyl region which appeared at 1761 cm^{-1} when the spectrum was determined in carbon tetrachloride solution, and at 1743 cm^{-1} when determined in nujol mull. There was no absorption in the hydroxyl region.

ACKNOWLEDGMENTS

We wish to express our thanks to the National Research Council and the Ontario Research Foundation for financial assistance.

REFERENCES

1. MacLean, D. B., Manske, R. H. F., and Marion, L. Can. J. Research, B, **28**, 460 (1950).
2. Marion, L. and Manske, R. H. F. Can. J. Research, B, **20**, 153 (1942).
3. Barclay, L. R. C. and MacLean, D. B. Can. J. Chem. **34**, 1519 (1956).
4. Przybylska, M. and Marion, L. Can. J. Chem. **35**, 1075 (1957).
5. Wiesner, K., Valenta, Z., Ayer, W. A., Fowler, L. R., and Francis, J. E. Tetrahedron, **4**, 87 (1958).

Can. J. Chem. Downloaded from www.nrcresearchpress.com by 176.9.209.113 on 09/04/12
For personal use only.

Can. J. Chem. Downloaded from www.nrcresearchpress.com by 176.9.209.113 on 09/04/12
For personal use only.

THE CONSTITUTION OF THE SODIUM – ACID PHOSPHATE GLASSES[1, 2]

A. E. R. Westman, M. Joyce Smith, and P. A. Gartaganis

ABSTRACT

The preparation of phosphate glasses containing sodium and hydrogen is described. The over-all composition was calculated from the Na/P ratio of the starting mixture and the hydrogen content determined by a zinc oxide ignition. The chemical constitution was determined paper-chromatographically employing recent improvements in technique.

Close resemblance between the molecular weight distributions of the sodium–acid glasses and the strong phosphoric acids is shown by the results, but it is also shown that there is no sharp transition to the molecular weight distribution shown by the sodium, potassium, and lithium glasses.

The importance of stoichiometry on the constitution of glass is discussed, together with the statistical models from which several theories are derived to predict the distribution of the polymers in a glass. The theories of Van Wazer and Parks, which show the most satisfactory agreement with the experimental results, receive detailed consideration.

INTRODUCTION

Glasses with compositions in the Na_2O–H_2O–P_2O_5 system between the orthophosphate and the metaphosphate compositions were studied, in particular glasses containing both hydrogen and sodium cations. New methods of preparation involved the progressive dehydration of orthophosphate mixtures to give a series of compositions following the lines on Fig. 1. In the preliminary examination compositions on the line $T = 20$ were also studied.

The development of the separation of phosphate anions by paper chromatography has been described by Hettler (1). The latest techniques used in this laboratory, especially a

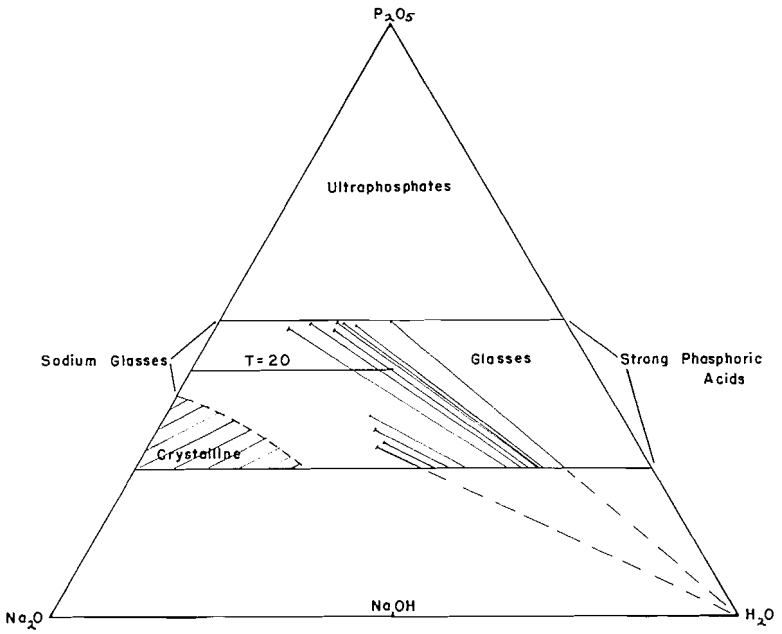

FIG. 1. Glasses in the Na_2O–H_2O–P_2O_5 system.

[1]*Manuscript received June 17, 1959.*
Contribution from the Ontario Research Foundation, 43 Queen's Park, Toronto 5, Ontario. This paper was presented at the American Chemical Society Symposium on Phosporus, Boston, April 5–10, 1959.
[2]*Published with the permission of the American Chemical Society.*

Can. J. Chem. Downloaded from www.nrcresearchpress.com by 176.9.209.113 on 09/04/12
For personal use only.

new method of quantitative estimation of phosphorus, have been described recently (2) and give greater precision and reliability.

The chromatographic separation of the condensed phosphate anions made it possible to determine the constitutions of the soluble glasses, i.e. the proportions of each chain length. The first study of the change in the size distribution with composition was carried out by Westman and Crowther (3) on the Na_2O–P_2O_5 system, the sodium glasses. However, only glasses with a number-average chain length, $\bar{n}$, higher than 3 were obtainable crystal-free. Many attempts to obtain clear sodium glasses of lower $\bar{n}$ have not yet yielded satisfactory results, although experiments are still in progress, notably with the through-flame apparatus originally devised by Haller (4). Secondly, the system H_2O–P_2O_5, the strong phosphoric acids, was studied by Huhti and Gartaganis (5) and also by Thilo and Sauer (6) and Ohashi and Sugatani (7). Some modification of techniques was necessary because these compositions give rise to hygroscopic, syrupy liquids at room temperatures. Certain significant differences were observed between the distributions obtained for the sodium glasses and the acids from these two studies, the principal being the absence of orthophosphate in sodium glasses and the existence of "free-water" in the acids. Two further investigations into the effect of the cation on distribution were begun. The distributions obtained from glasses containing lithium and potassium as cations have already been published (8). They were similar to those of the original sodium glasses, no orthophosphate being detected; however there were differences too large to be ascribed to experimental error alone. The object of the present study was to obtain the distribution patterns of glasses having a sodium–hydrogen ratio of unity, and to determine the effect of the substitution of sodium by hydrogen at one particular cation to phosphorus ratio.

EXPERIMENTAL

Preliminary Works

Attempts to prepare sodium–acid glasses with Na/H = 1 by heating phosphorus pentoxide with sodium hydrogen pyrophosphate in a sealed pyrex flask, as in the case of the strong phosphoric acids, were unsuccessful and dangerous because the pyrex, leached by the phosphate, became brittle and exploded. "Vycor" brand, 96% silica glass was found to be resistant to attack and so small tubes of Vycor were prepared as containers.

Starting materials consisted of $Na_2H_2P_2O_7$ and either P_2O_5 or an equimolecular mixture of Na_2HPO_4 and NaH_2PO_4. (The $Na_2H_2P_2O_7$, Na_2HPO_4, and NaH_2PO_4 were previously dried at 110° C.) The mixtures were homogenized by vigorous shaking, a portion was sealed in a Vycor tube and placed in a furnace at 650° or 800° C. A clear liquid was obtained in 10 minutes. The tube was carefully removed (the worker wearing protective shields) and plunged horizontally into a bath of water. When cool the tube was broken open and a sample of the glass was dissolved in alkaline solution and chromatographed. Tubes were processed singly due to the frequency of explosion, both in the furnace and on quenching.

Despite the difficulties, data were obtained for a range of number-average chain lengths, $\bar{n}$ = 1.1 to 9.0. These were communicated to Van Wazer and Parks to illustrate their distribution theory and were published by them as preliminary values (9). In this laboratory, publication of the detailed results was delayed because an error was detected in the preparation. When the number of molecules per 100 atoms of phosphorus indicated by the chromatographic analysis, "N", was compared with the number derived from the cation to phosphorus ratio of the starting material, the agreement was found to be unsatisfactory at high cation–phosphorus ratios. Appreciable quantities of water had

escaped from the liquid phase and, on quenching, condensed on the upper portion of the tube, leaving the bulk of glass poor in hydrogen and with a correspondingly increased average chain length. This was confirmed by experiment showing that packing the tubes as fully as possible lowered the average chain length again and that the surface layer of the glass with adsorbed water had a very different constitution from the bulk of the glass. The techniques adopted to avoid this error are described later.

The glass prepared by the earlier technique with an average chain length $\bar{n} = 5$ was sufficiently defined to be used in admixture with a sodium glass $\bar{n} = 5$ to examine the effect of a change in cation. The mixtures were melted quickly in a platinum crucible over a burner and quenched between copper blocks. No general increase in average chain length was detected.

Final Preparation of Glasses

Efforts were made to avoid the unknown composition change due to loss of water to the vapor phase. A lowering of the temperature required to give a clear melt was sought in an alternative starting mixture including sodium – acid tetrametaphosphate (10) but no significant improvement in results was observed. Finally, a method was adopted whereby the composition (%) with respect to hydrogen was determined after the glass was made by ignition with zinc oxide. The standard deviation of this determination was 0.12.

Glasses of number-average chain length greater than three were obtained by quenching between copper blocks, at 1-minute intervals, the liquids resulting from melting and partially dehydrating certain mixtures of pure monobasic sodium orthophosphate and standard orthophosphoric acid (85.454%) in a platinum crucible over a Meeker burner. Usually six glasses of decreasing water content resulted from one starting mixture. A second series covering a smaller range of compositions, due to shorter intervals of dehydration, permitted glasses to be obtained with Na/H near unity. Most were clear, brittle, crystal-free glasses, but if insufficient water was removed, very viscous liquids similar to the strong phosphoric acids resulted. The end of a dehydration series was controlled by the formation of fibrous "hypoly" material, as the metaphosphate composition was approached. This appeared crystalline under the petrographic microscope and would not remelt.

The chemical constitution of each glass was determined by dissolving a few fragments in sodium bicarbonate solution maintaining the pH at approximately 8, separating the various molecular species on a filter paper chromatogram, and analyzing by the new technique (2). By adding the other fragments to a weighed, fired crucible containing zinc oxide (approx. 2 g), the water content (in %) was determined from the loss in weight from firing at 550° C for 1 hour.

Glasses having a sodium to phosphorus ratio greater than .83 (i.e. $\bar{n} = 3$ when Na = H) required a starting mixture of mono- and di-basic orthophosphates without orthophosphoric acid. These mixtures lost almost all of their water content before melting. Glasses of these compositions were obtained, however, by returning to a sealed Vycor-tube technique. Mixtures of the correct sodium to phosphorus ratio, but rich in water content (i.e. using $NaH_2PO_4.H_2O$ crystals in part), were sealed into Vycor tubes and heated to 350° C for about one hour. The liquid was homogenized by rolling the tube over the floor of the furnace (with all due precautions) and then removed vertically and allowed to cool to room temperature. The coefficients of expansion of the Vycor and the phosphate glass were sufficiently different to allow the phosphate lump to be lifted cleanly away from the fractured Vycor tube. Carefully avoiding the upper surface layer and possible absorbed water, we chromatographed part of the lump and ignited part to determine the water

Can. J. Chem. Downloaded from www.nrcresearchpress.com by 176.9.209.113 on 09/04/12
For personal use only.

content and thus the composition of the bulk of the phosphate glass. Again, a series of varying composition was obtained by varying the proportion of hydrated and anhydrous NaH_2PO_4; slight variations were also effected by using tubes of various lengths and different temperatures of melting, both of the latter influencing the proportion of the water existing in the vapor phase.

DATA

The constitution of some 150 glasses with compositions located along the solid lines in Fig. 1 were obtained. For these glasses it was found that the Na/H ratio had little effect on the observed constitutions so all of the results, including those for Na = H, could be represented adequately by the curves in Fig. 2 (11). The abscissa "T" is defined by

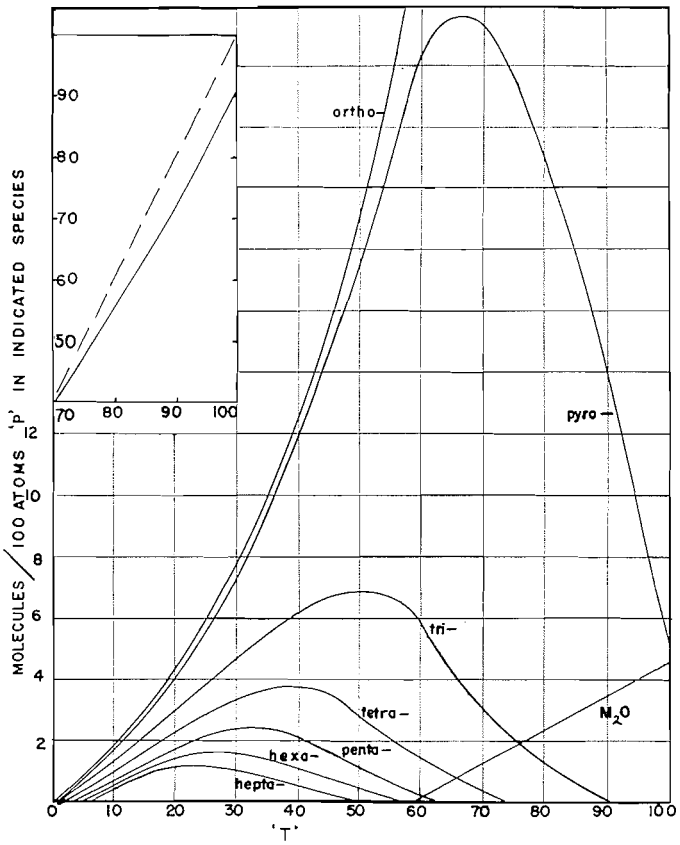

FIG. 2. The variation of distributions with T for the sodium–acid glasses. Inset: solid line, extension of orthophosphate curve; broken line, orthophosphate proportion in a system containing only ortho- and pyro-fractions.

$T = 50(M/P-1)$ where M/P is the cation to phosphorus atomic ratio (see also Stoichiometry later), "T" therefore represents the number of molecules per 100 phosphorus atoms for the particular composition. The ordinate indicates the number of molecules appearing in each fraction for a total of 100 atoms of phosphorus. The value of "T" for each glass was calculated from its water content using the following equation:

[1] $$T = 100/\bar{n} = 50\ (x+w(ax+b)/(1-w)-1)$$

Can. J. Chem. Downloaded from www.nrcresearchpress.com by 176.9.209.113 on 09/04/12
For personal use only.

where w = % water content/100, $a = Na_2O/H_2O = 3.440$, $b = P_2O_5/H_2O = 7.885$, and x = molecular ratio $Na_2O:P_2O_5$. The curve marked "M_2O", i.e. "free water or sodium hydroxide" in Fig. 2 is derived from the difference between "T" and "N", the latter being the total of the molecules observed in the chromatographic analysis per 100 atoms of phosphorus, i.e. those molecules not detected chromatographically, "hypoly" being negligible. At smaller values of "T" the number-average chain length of the hypoly material can be deduced from $T-N$. A check on the methods of preparation and chromatographic analyses is provided when both M_2O and "hypoly" are negligible.

DISCUSSION

Qualitative Comparisons

The distributions observed in Fig. 2 are similar to those of the strong phosphoric acids in that free M_2O and orthophosphate are present; the latter does not occur in the sodium glasses. When only ortho- and pyro-phosphate are present their proportion is fixed as indicated by the broken line in the insert on Fig. 2, but the experimental points for both the sodium–acid glasses and the strong phosphoric acids tend to follow the lower solid line. This was explained by Huhti and Gartaganis (5) in the case of the acids by assuming "free water" to exist in equilibrium with the phosphoric acids. Their auxiliary experiments and those of other workers (6, 7) confirmed this explanation. In the case of the sodium–acid glasses, free M_2O may again explain the points below the theoretical line. However, it was difficult to prepare bubble-free glasses in this region and it was possible for moisture trapped in the bubbles to result in a higher value of T. This was borne out when the deliberate analysis of specimens containing some bubbles showed values for % total phosphorus as orthophosphate, approximately 5% lower than the samples without bubbles indicated by the solid line in the inset on Fig. 2. More experiments, possibly with other techniques, are needed in this region.

A closer comparison of the curves in Fig. 2 with the corresponding curves for the strong acids and the alkali metal glasses revealed the following differences:

(*a*) The orthophosphate content of the acid glasses was greater than that of either the strong acids or the sodium glasses, the latter being zero. The preliminary experiments at $\bar{n} = 5$ described above showed that as hydrogen replaced sodium as cation, the orthophosphate content of the glasses increased *gradually* to a very flat maximum or plateau over the acid glass compositions before dropping very slightly at the strong phosphoric acid composition. Thus, there was no particular arrangement of hydrogen and sodium atoms necessary for the development of orthophosphate.

(*b*) The maximum in the curve for pyrophosphate in Fig. 2 is to the right of that for the strong acids.

(*c*) The sodium–acid glasses and the acids had much higher hypoly contents than the sodium glasses. At low values of T the sodium–acid glasses contained less hypoly than the acids; at high T values, more hypoly; the hypoly contents being the same at about $T = 20$.

(*d*) Free water occurred in much the same mole percentages and over the same range of T in both the acid glasses and acids.

(*e*) The ring phosphates found in the alkali metal glasses were not found in either the acids or the sodium–acid glasses studied. Studies of compositions closer to the left side of Fig. 1 are indicated.

Can. J. Chem. Downloaded from www.nrcresearchpress.com by 176.9.209.113 on 09/04/12
For personal use only.

Some of the above comparisons are seen later in Fig. 4 where the agreement between theoretical and experimental results is shown for three of the fractions.

Phase Relations

Morey (12) investigated phase relations in sealed tubes for systems with compositions along a line in Fig. 1 from H_2O to $NaPO_3$. A comparison with the data of this paper is of interest in connection with the much discussed question of the relation of glass constitution to the constitution of the primary phase. The molecules, or molecule-ions, that form the primary phase may exist as such in the glass or may be formed from smaller units as the crystal grows. There is evidence for the first of these possibilities in this case. The cyclic trimetaphosphate crystals (Morey's $NaPO_3I$) grow in glasses containing trimetaphosphate rings near the $NaPO_3$ composition.

STOICHIOMETRY

For a particular cation or combination of cations M, the chromatographic analysis of a properly fused and quenched glass depends solely on the M/P atomic ratio of that glass. This means that stoichiometry is an important factor in determining the constitution of a glass.

Stoichiometric ideas can be introduced in several ways. The method developed in papers from this laboratory starts from the number-average chain length. Other approaches include that of Stevels (13) and Van Wazer and Parks (9).

Number-average Chain Length

If only polymers of the general formula $M_{n+2}P_nO_{3n+1}$ are involved, then the number-average chain length, $\bar{n}$, is related to the M/P atomic ratio by the equation

$$\bar{n} = 2/(M/P-1) \qquad [2]$$

where M and P stand for corresponding numbers of cation and phosphorus atoms respectively. If for a particular $\bar{n}$, we consider 100 phosphorus atoms, then on stoichiometric grounds alone the constitution might be such that all the polymers had the same formula $MO_{\frac{1}{2}}.(MPO_3)_{\bar{n}}.O_{\frac{1}{2}}M$ and there would be $100/\bar{n}$ such polymers. The MPO_3 units, 100 in all, could then be distributed in other ways among the $100/\bar{n}$ polymers. The number of polymers per 100 phosphorus atoms remains the same, depending only on $\bar{n}$, and being given by [1] above.

When ring compounds are formed, the number of linear polymers per 100 phosphorus atoms is unchanged, but there are fewer MPO_3 groups to distribute among them. A single long linear polymer can also rearrange according to equation [5] (following) to form a branched or cross-linked polymer with the same M/P ratio and without altering the above empirical formula so long as the "length" of the new polymer is defined by the number of phosphorus atoms it contains. However, when branching or cross-linking is accompanied by an increase in molecular weight, as when two polymers go together to form the new polymer, splitting off M_2O, then the M/P ratio of the polymer decreases.

When the M/P atomic ratio = 1 the number-average chain length becomes infinite (equation [2]). For M/P atomic ratios < 1, branching or cross-linking accompanied by higher molecular weights, postulated by Van Wazer, creates "ultraphosphates" (14). As the M/P ratio is reduced through unity a sharp change from finite linear polymers to infinite (wall-to-wall) polymers, or cross-linked structures, is unlikely. In the experimental

Can. J. Chem. Downloaded from www.nrcresearchpress.com by 176.9.209.113 on 09/04/12
For personal use only.

data for glasses just below the metaphosphate line there is some indication of branched or cross-linked material.

Bridging and Non-bridging Oxygens

A number of glass technologists, notably Stevels (13), introduce stoichiometric ideas into the discussion of silicate glasses by distinguishing between bridging and non-bridging oxygens.

Stevels defines the number of non-bridging oxygens per silicon atom, X, and the number of bridging oxygens per silicon atom, Y, as follows:

[3] $$X = 2(O/Si) - 4$$

[4] $$Y = 8 - 2(O/Si)$$

where the symbols O and Si stand for numbers of atoms of oxygen and silicon respectively and $X + Y = 4$.

Criteria for finite chains, infinite chains, and cross-linked structures are then given in terms of Y, as $O < Y < 2$, $Y = 2$, and $Y > 2$ respectively. The silicate glasses of commerce have values of Y from 3 to 3.4. Glasses can be made in the laboratory having Y values between 3 and 2 and, by special means, below 2.

When this approach is applied to phosphate glasses it is found to be algebraically equivalent to the methods just given, except that there is no provision for unreacted M_2O or rings. A phosphorus–oxygen tetrahedron is only capable of bonding to three other tetrahedra and cannot form a three-dimensional network, as do the SiO_4 tetrahedra. In its usual crystalline modification P_4O_{10} consists of isolated cage structures each built of four PO_4 tetrahedra. In other forms sheets of PO_4 tetrahedra occur but no three-dimensional networks. Thus, it is interesting to note: (*a*) that the silicate glasses of commerce on this basis have a more cross-linked structure than even P_2O_5 in the phosphate series; (*b*) that bonding a cation to a SiO_4 tetrahedron renders it equivalent to a PO_4 tetrahedron, i.e. NaSi may substitute for P; and (*c*) that, using Stevels' equations [3] and [4], the phosphate glasses with which this paper is concerned are in the range of $O < Y < 2$ or very much below the commercial silicate glasses. Each of these comments is illustrated in Table I.

TABLE I

Stoichiometric comparison of silicate and phosphate compositions

Composition of silicate	X	Y	O/Si or O/P ratio	Composition of phosphate
SiO_2	0	4	2	
$Na_2Si_2O_5$	1	3	2.5	P_2O_5
Na_2SiO_3	2	2	3	$NaPO_3$
	3	1	3.5	$Na_4P_2O_7$
	4	0	4	Na_3PO_4

Parks–Van Wazer Approach

Parks and Van Wazer (9) define chemical groups to which chemical symbols and names are assigned as follows:

Symbol	Name	Symbol	Name
o = M_3PO_4	Ortho group	**b** = $PO_{2.5}$	Branching group
e = $M_2PO_{3.5}$	End group	**u** = MOM	Unreacted M_2O
m = MPO_3	Middle group	(**2e**) = $M_4P_2O_7$	Pyro group

Can. J. Chem. Downloaded from www.nrcresearchpress.com by 176.9.209.113 on 09/04/12
For personal use only.

They also define R as the M/P ratio.

All polymers and molecules envisaged in a glass may be constructed from these building units and are subject to the chemical equations

[5] $$2\mathbf{m} = \mathbf{b}+\mathbf{e}$$

[6] $$2\mathbf{e} = \mathbf{m}+\mathbf{o}$$

[7] $$2\mathbf{o} = 2\mathbf{e}+\mathbf{u}$$

or

[8] $$2\mathbf{o} = (\mathbf{2e})+\mathbf{u}.$$

The compound $\mathbf{u} = M_2O$ is not considered to break down further.

Equilibrium constants designated K_1, K_2, K_3, and K'_3 are written for equations [5], [6], [7], and [8] respectively in terms of mole fractions represented by the corresponding italicized letters. This approach is proving very useful for classifying a wide variety of polymer systems. The choice of the constants K_1, K_2, K_3, K'_3 to fit the experimental results as closely as possible permits deductions concerning the degree of ionization of the cations. Conversely, if previous assumptions regarding ionization are made, the change in ortho and unreacted units with composition (M/P) is forecast. In general the shapes of the curves obtained by calculation agree well with the experimental results. This is clearly shown in Fig. 3 where the solid lines indicate the experimental data for the acid glasses and the broken lines the curves derived from the selection of the constants as $K_1 = 0$, $K_2 = 0.08$, and $K_3 = 0.02$. However, no choice of K values will bring the maximum for ends anywhere but at $R = 2$, which does not agree with the experimental data. One must assume in this case that the K values change slightly with composition.

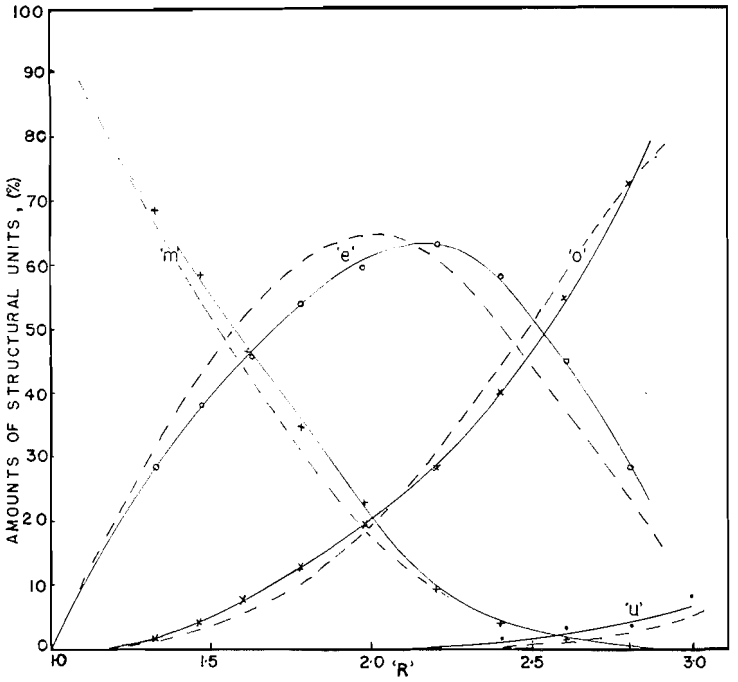

FIG. 3. Comparison of theoretical and experimental amounts of structural units ('*m*', middles; '*e*', ends; '*o*', ortho; '*u*', unreacted M_2O). (Theoretical curves (broken lines) obtained using $K_1 = 0$, $K_2 = 0.08$, and $K_3 = 0.02$.)

Can. J. Chem. Downloaded from www.nrcresearchpress.com by 176.9.209.113 on 09/04/12
For personal use only.

Distribution Theories

Since knowledge of the structural units present and their proportions does not define the distribution of polymers to be expected in a glass, various statistical models have been proposed. Van Wazer has discussed a Poisson model; a random reorganization model, based on a flexible chain theory; and, with Parks, a rigid-rod model (9).

The Poisson model has been shown to fit only a limited range of compositions and does not fit the data given in this paper so it will not be discussed further.

It is also possible to invoke mass law theory, which is essentially statistical in origin. This was applied to the chromatographic data for the strong phosphoric acids (5).

Mass Law Theory

This can be applied in as many ways since one can write chemical equations purporting to govern the dynamic equilibrium occurring in the molten glass, or liquid state, etc. In the paper cited, the equilibrium between water, pyrophosphoric acid, and orthophosphoric acid was considered. Thus, unreacted M_2O, i.e. water, was the common factor. This could have been extended to the higher acids present but two difficulties are encountered: (*a*) the number of equilibrium constants involved becomes very large and (*b*) the data required to confirm their validity would have to be very comprehensive and accurate. This is one reason why Van Wazer and Parks worked with structural units, since five or six such units suffice for all polymers.

An alternative method would be to regard orthophosphate as a common factor in all the equilibria since, whatever the mechanism, the polymers gain or lose PO_4 tetrahedra in maintaining an equilibrium. This method has possibilities in the low molecular weight acid glasses and acids, but suffers the two disadvantages already given for the mass law approach and, in addition, when dealing with the non-acid glasses, the difficulty arises that charge density considerations suppress the formation of orthophosphate, as explained by Van Wazer (9). On the other hand, hydrolysis studies indicate that linear phosphate polymers tend to degrade by splitting orthophosphate groups off the end so this approach would have the benefit of starting from chemical knowledge of the polymer properties. One could only hope for some empirical relation relating the equilibrium or other constants with chain length.

Van Wazer–Parks Distributions

Another approach, followed by Van Wazer–Parks, is to set up a statistical model, being guided more or less by the known properties of phosphates and the nature of the distributions to be fitted. They used the results for the strong acids (5) and the authors' preliminary results for the sodium-acid glasses and showed that with some smoothing of the data, a reasonable fit could be obtained using the flexible chain model but not the rigid-rod model. Since the preliminary data do not differ markedly from the more reliable data reported here, a theoretical distribution based on the flexible chain model in the limiting case where there is no branching was computed from

$$[9] \qquad w_n = \frac{n}{\bar{n}(\bar{n}-1)}\left(\frac{\bar{n}-2}{\bar{n}-1}\right)^{n-2}\left(1-\frac{o}{1-u}\right)$$

where n = the chain length of a polymer; w_n = the weight fraction of the total phosphorus in polymers of length n; and $\bar{n}$ = the number-average chain length of the glass, computed by including only the polymers having $n \geqslant 2$. Allowance is made in the equation [9] for "o" and "u", the mole fractions of orthophosphate and unreacted M_2O,

Can. J. Chem. Downloaded from www.nrcresearchpress.com by 176.9.209.113 on 09/04/12
For personal use only.

which are not considered to be polymers but diluents. Their proportion was predicted by the selection of K_1, K_2, and K_3 as shown in Fig. 3.

The comparisons afforded by Table II show that the Van Wazer–Parks distribution (9) fits the observed values remarkably well, considering that the probabilities are introduced from very general physical ideas. The individual chemical properties of the polymers are most likely to influence the system which contains only a few species, especially when these exhibit the striking differences associated with the first members of a homologous series. Thus the ability of statistical models to fit the high molecular weight contributions but not the low ones is understandable. The slight differences between sodium, potassium, and lithium glasses can similarly be attributed to chemical influences.

If the distribution for $T = 10$ is plotted in terms of molecules, it will be seen that, although the number-average chain length is 10, the maximum is still at $n = 2$. Most statistical models result in distributions in which the mode moves away from the origin quickly as the mean is increased.

It will be noted that the observed values for $T = 20$ and $T = 10$ in Table II are practically constant for $n = 2$ or greater. If this holds for the hypoly fraction, it indicates a very flat and long distribution above $n = 7$ which accentuates the difficulty just mentioned.

In Fig. 4 the agreement between distributions derived from the flexible chain model and the results of both the acid – sodium phosphate glasses and the strong phosphoric acids has been indicated in the case of pyro-, tri-, and hypoly-phosphate. Clearly the distributions in the sodium glass system require a modified theory such as that provided by the rigid-rod model.

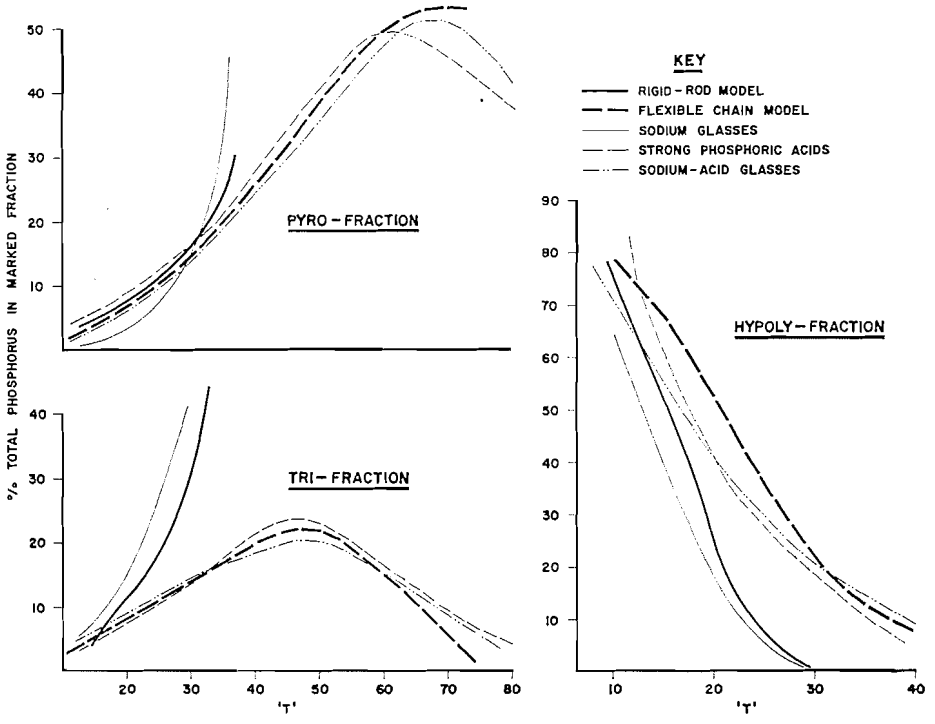

FIG. 4. Comparison of the theoretical and experimental distributions.

Can. J. Chem. Downloaded from www.nrcresearchpress.com by 176.9.209.113 on 09/04/12
For personal use only.

TABLE II

Sodium–acid glasses
(Comparisons of experimental and theoretical distributions)

		Ortho	Pyro		Tri		Tetra		Penta		Hexa		Hepta		Hypoly	
T	u	E*	E	[9]	E	[9]	E	[9]	E	[9]	E	[9]	E	[9]	E	[9]
90	3.5	72.4	28.0		0.3											
80	2.9	54.5	42.3		4.1											
70	1.4	39.8	50.6	52.9	9.5	6.5	1.4	0.7								
60		28.3	48.4	50.3	17.2	15.6	5.4	4.3	1.1	1.1		0.3				
50		19.5	35.2	37.2	20.6	21.8	11.2	11.3	5.9	5.5	3.1	2.6	0.8	1.2	3.8	0.9
40		12.7	24.0	24.8	18.6	20.3	15.2	14.8	10.0	10.0	7.2	6.6	3.8	4.2	9.2	6.6
30		7.8	14.9	14.1	14.1	14.4	13.7	13.1	11.7	11.2	9.6	9.2	7.7	7.3	20.8	22.9
20		3.9	8.9	6.5	9.0	7.8	8.8	8.3	9.0	8.3	9.0	7.9	8.4	7.4	43.0	49.9
10		1.5	3.4	1.6	4.2	2.2	3.8	2.6	4.1	3.0	4.2	3.2	3.5	3.4	73.5	82.5

*E, experimental values; [9], values calculated from eq. [9].

CONCLUSIONS

Change of Cation

From the discussion of the experimental results in the first part of this paper, it will be evident that a distribution theory which fits the strong acids will give a reasonable fit for glass compositions in the Na_2O–P_2O_5–H_2O diagram, Fig. 2, as far as the center line where Na/H atomic ratio = 1. At higher ratios the effect of the smooth reduction of both orthophosphate and hypoly will have to be taken into account. Also, it has been shown that a shift of cation to K or Li makes a significant but small change in the nature of the distributions.

The postulation of statistical models, however, has served a useful purpose. While not always fitting the data within the experimental error, the fit has been good enough to support the general thesis that some sort of reorganization governed largely by chance encounters is taking place in a molten phosphate glass, that the equilibrium can be frozen in by quick quenching, and that it governs the distributions observed by means of filter paper chromatography as well as by the physical methods used by Van Wazer.

Statistical Models

More than one statistical model plus certain stoichiometrical conditions derived from experiment are necessary in general to give a good fit to the observed molecular weight distributions. However, the most general conclusion is that, despite the differences which have been pointed out, the distributions of molecular weight are much the same over a considerable range of cations.

The relations of the constitution of the phosphate glasses to that of the silicate glasses will be better understood when more work has been done on the silicate glasses having a higher M/Si atomic ratio and on the phosphate glasses with a lower M/P ratio.

More work on the physical properties of the phosphate glasses whose constitution has been established appears to be a logical development.

ACKNOWLEDGMENTS

The authors wish to express their gratitude to Anne Mueller for her careful technical assistance and also to the Research Corporation, New York, for their support.

REFERENCES

1. HETTLER, H. J. Chromatog. **1**, 389 (1958).
2. SMITH, M. J. Anal. Chem. **31**, 1023 (1959).

Can. J. Chem. Downloaded from www.nrcresearchpress.com by 176.9.209.113 on 09/04/12
For personal use only.

3. WESTMAN, A. E. R. and CROWTHER, J. J. Am. Ceram. Soc. **37**, 420 (1954).
4. LANDIS, B. M. M.Sc. Thesis presented to the University of Toledo, Toledo, Ohio. 1956. (Work supervised by W. Haller.)
5. HUHTI, A.-L. and GARTAGANIS, P. A. Can. J. Chem. **34**, 785 (1956).
6. THILO, E. and SAUER, R. J. prakt. Chem. **4**, 324 (1957).
7. OHASHI, S. and SUGATANI, H. Bull. Chem. Soc. Japan, **30**, 864 (1957).
8. WESTMAN, A. E. R. and GARTAGANIS, P. A. J. Am. Ceram. Soc. **40**, 293 (1957).
9. (*a*) VAN WAZER, J. R. and PARKS, J. R. J. Am Chem. Soc. **79**, 4890 (1957).
(*b*) VAN WAZER, J. R. Phosphorus and its compounds. Vol. I. Interscience Publishers, Inc., New York. 1958.
10. GRIFFITH, E. J. J. Am. Chem. Soc. **73**, 3867 (1956).
11. SMITH, M. J. M.Sc. Thesis presented to the University of Birmingham, Birmingham, England. 1959. (Now available from University Microfilm Center, Ann Arbor, Michigan.)
12. MOREY, G. W. J. Am. Chem. Soc. **75**, 5794 (1953).
13. STEVELS, J. M. Glass Ind. **35**, 657 (1954).
14. VAN WAZER, J. R. and GRIFFITH, E. J. J. Am. Chem. Soc. **77**, 6140 (1955).

Can. J. Chem. Downloaded from www.nrcresearchpress.com by 176.9.209.113 on 09/04/12
For personal use only.

Can. J. Chem. Downloaded from www.nrcresearchpress.com by 176.9.209.113 on 09/04/12
For personal use only.

THE PREPARATION OF D-RIBOSE-1-C^{14}, D-ARABINOSE-1-C^{14}, AND D-2-DEOXYRIBOSE-1-C^{14} [1]

D. H. MURRAY AND G. C. BUTLER

ABSTRACT

D-Ribose-1-C^{14} and D-arabinose-1-C^{14} have been synthesized by a modified Sowden–Fischer procedure in which the mixed sodium nitropentitols resulting from the condensation of erythrose and $C^{14}H_3NO_2$ have been submitted to a Nef reaction. The epimeric labelled pentoses were isolated by cellulose column chromatography in an over-all radiochemical yield of 19%.

Mixed nitropentitols-1-C^{14} have been acetylated, partially deacetylated with sodium bicarbonate in a non-polar solvent, and hydrogenated to yield triacetoxy-1-nitropentane-1-C^{14}. The mixture of this material and the accompanying undeacetylated nitropentitols gave rise, via a Nef reaction, to D-2-deoxyribose-1-C^{14} (6.3%), D-ribose-1-C^{14} (3.1%), and D-arabinose-1-C^{14} (2.9%).

INTRODUCTION

The Fischer cyanhydrin (1–4) and the Sowden–Fischer (5, 6, 7) methods of lengthening an aldose chain have both been employed in the preparation of labelled aldoses. The cyanhydrin procedure has generally afforded better radiochemical yields of the desired aldoses but is somewhat tedious. Most of the procedures reported to date employing either method have involved separation of epimeric compounds at an early stage, thus necessitating twice the manipulation of labelled compounds. It is more convenient to carry isomeric materials through one series of reactions and to separate them at a terminal stage. Chromatography on cellulose columns (8) constitutes a convenient method for achieving such separation on a preparative scale.

Rappoport and Hassid (6) have employed a Sowden–Fischer procedure and cellulose column chromatography in preparing L-arabinose-1-C^{14}. Although the yield of labelled pentose reported was only 3% based on the starting C^{14}-nitromethane, the simplicity of the method was attractive. The Sowden–Fischer method has also been adapted to the preparation of deoxyaldoses, and it thus appeared possible that it might be employed for the preparation of the two sugars of nucleic acids, D-ribose and D-2-deoxyribose in Cl-labelled form. Figure 1 shows the routes followed.

D-*Ribose-1*-C^{14} *and* D-*Arabinose-1*-C^{14}

D-Erythrose was condensed with an equimolecular amount of C^{14}-nitromethane in sodium methoxide solution. The mixed sodium nitropentitols formed were submitted to a Nef reaction according to the reaction conditions employed by Mahler (5), with two modifications. First, because of the ready decomposition of sodium nitroalditols in aqueous solutions, the alkaline solution of mixed sodium nitropentitols was added to concentrated acid from a jacketed funnel maintained at 0°. Second, it was to be expected that toward the end of the addition the dilution which had occurred would reduce the concentration of acid to a point where the Nef reaction would not take place. To avoid this possibility, the sodium nitropentitols were dissolved in a minimal volume of ice water and added to a larger amount of concentrated acid than that reported by Sowden (9). The pentoses formed were separated using a cellulose column and aqueous acetone as eluting solvent. The yield of pentose-1-C^{14} based on C^{14}-nitromethane was 19%.

[1]*Manuscript received June 26, 1959.*
Contribution from the Department of Biochemistry, University of Toronto, Toronto, Ontario.

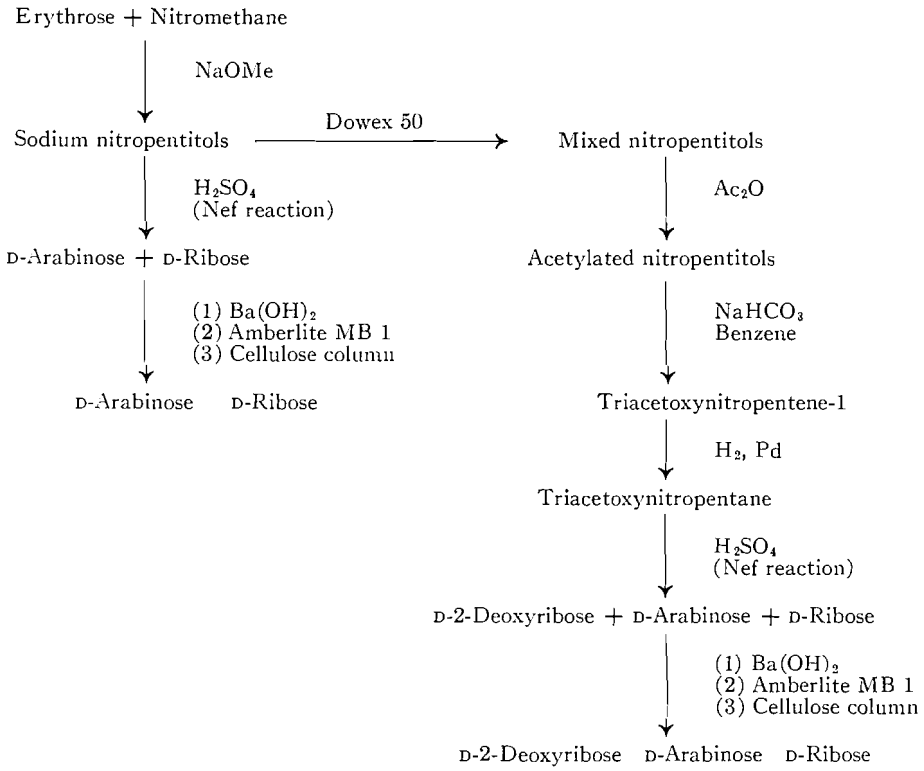

FIG. 1. Scheme of synthesis for labelled pentoses.

A fast-running radioactive fraction containing a small amount of tetrose-1-C^{14} (10) was eluted from the column ahead of the ribose-1-C^{14}. When excess nitromethane was employed in preliminary non-radioactive experiments, a similar small fraction was regularly observed but yields of pentose up to 65% were obtained. With the smaller amounts of C^{14}-nitromethane a reduction in the yield of pentose-1-C^{14} occurred. The reasons for this are discussed in a separate communication (10).

D-*2-Deoxyribose-1*-C^{14}

There seemed to be three potentially feasible routes to deoxyribose-1-C^{14}. Application of a Fischer glycal method (11) starting from D-arabinose-1-C^{14} (1), or a Ruff degradation of the metasaccharinic acids (12) resulting from the alkaline isomerization of D-glucose-2-C^{14} (13) would produce the desired labelled sugar. Both these routes, however, could be anticipated to give low radiochemical yields. On first consideration a Sowden–Fischer procedure starting from erythrose and nitromethane seemed equally unpromising. Although Sowden has prepared D-2-deoxyribose in over-all yield of 21% based on the starting erythrose (14), other workers have obtained less than 1% yields of the deoxy sugar by this route (15). On further examination it appeared that Sowden (9) adequately explained the reasons for this low yield and we therefore undertook the preparation of D-2-deoxyribose-1-C^{14} by his method.

In most cases the erythrose used for the preparation of ribose and arabinose was obtained from 4,6-ethylidene glucose. As discussed elsewhere (10), use of this material in the preparation of the deoxyribose may result in a small but significant contamination

Can. J. Chem. Downloaded from www.nrcresearchpress.com by 176.9.209.113 on 09/04/12
For personal use only.

of the desired deoxy sugar. By employing benzylidene sorbitol as the source of erythrose this contamination could be avoided.

Erythrose was condensed with an equimolecular amount of C^{14}-nitromethane to yield a mixture of epimeric C-nitropentitols which, after acetylation and subsequent treatment with bicarbonate in a non-polar solvent, gave rise to an acetylated nitroölefin. Partial hydrogenation of this material afforded the 1-nitro-1,2-deoxy-3,4,5-triacetoxypentane.

The intermediate compounds in the above procedure are crystallizable with difficulty (15). However, Sowden has shown (7) that acceptable yields of deoxyribose are attainable without separation of intermediates. Moreover, in the interest of best utilization of carbon-14, advantage was taken of the fact that nitropentitols which were not acetylated, as well as acetylated nitropentitols which were not deacetylated (and would not therefore be available for hydrogenation), would both give rise, via the Nef reaction, to ribose-1-C^{14} and arabinose-1-C^{14}, and the whole preparative procedure could be made to yield these two pentoses in addition to deoxyribose-1-C^{14}.

The total product of the hydrogenation step, in alkaline solution, was submitted to a Nef reaction. After deionization the mixture of pentoses was separated on a cellulose column using aqueous acetone. A radiochemical yield of 12% of pentoses based on nitromethane was obtained.

As in the synthesis of ribose-1-C^{14} and arabinose-1-C^{14} a fast-running fraction carrying significant radioactivity was observed. This was concluded to be 2-deoxytetrose-1-C^{14}, for reasons given in a separate communication (10). As for the ribose–arabinose case, the reactions leading to this by-product, when equimolecular amounts of erythrose and C^{14}-nitromethane were used in the initial condensation reaction, led to a considerable reduction in the yield of deoxyribose-1-C^{14}. In pilot experiments employing excess non-radioactive nitromethane, yields of about 30% of deoxyribose based on the starting erythrose were obtained.

EXPERIMENTAL

D-*Ribose and* D-*Arabinose-1*-C^{14}

D-Erythrose was prepared from 4,6-ethylidene-D-glucose (m.p. 181–183°) by the procedure described for L-erythrose (6). C^{14}-Nitromethane was obtained from Merck and Company, Montreal, and had a specific activity of about 4 mc per g.

Sodium Nitropentitols-1-C^{14}

A sodium methoxide solution (2.4 g of sodium in 50 ml of absolute methanol) was added dropwise, with stirring, to a solution of erythrose (8.3 g) and C^{14}-nitromethane (3.7 ml) in 50 ml of methanol. After 2 hours the reaction mixture was cooled to 0–10° in an ice bath. The cooled mixture was stirred for a further 12 hours, 100 ml of cold anhydrous ether added, and the precipitated sodium nitropentitols collected by filtration. They were washed on the filter with cold methanol – ether (1:1) and ether – petroleum ether (1:1). While still moist the sodium salts were transferred rapidly to a vacuum desiccator containing P_2O_5, which was then evacuated until all solvent had been removed. The yield of dry sodium nitropentitols was 8.28 g (60% based on nitromethane).

Nef Reaction

A solution of the sodium nitropentitols (2.5 g in 15 ml of ice water) was added dropwise, over a 2-hour period, from a cold (0–5°) jacketed dropping funnel to a cold (−20 to −18°) stirred solution of 6 ml of concentrated sulphuric acid and 7.5 ml of water. After the addition was complete, the stirred reaction mixture was allowed to approach 0° slowly over a period of 1 hour.

Can. J. Chem. Downloaded from www.nrcresearchpress.com by 176.9.209.113 on 09/04/12
For personal use only.

Can. J. Chem. Downloaded from www.nrcresearchpress.com by 176.9.209.113 on 09/04/12
For personal use only.

Deionization and Separation of Pentoses

The resulting solution was diluted by slow addition of 200 ml of ice water and adjusted to pH 4.0 with cold barium hydroxide solution. A few drops of glacial acetic acid were added; the barium sulphate was removed by centrifugation and washed eight times with water. The combined supernatant and washings were concentrated to a small volume at a temperature below 35°, charcoaled, and passed, under suction, through a column of 40 g of Amberlite-MB 1. The column was washed with 200 ml of water, and 0.1 *M* sodium sulphate was passed through the resin until the first faint positive test of sulphate was obtained in the eluate. A few milligrams of resin were added to the eluate, stirred, and removed by filtration. After concentration at reduced pressure (below 35° C), powdered cellulose was added and concentration continued to dryness. To remove the last traces of water, alcohol, and subsequently acetone, were added and removed under reduced pressure. The dry cellulose powder (on which the C^{14}-pentoses were absorbed) was washed with dry acetone on to a cellulose column (5 cm by 50 cm) through which absolute acetone had been passed for 4–6 hours. A pad of filter paper was placed above the cellulose and pressed down firmly. The column was developed with 98% acetone until the fast-running fractions were eluted. Ribose was eluted with 93% acetone and arabinose with 80% acetone. A 40-minute collection time and a flow rate of about 1 ml per minute were used throughout. Pentose was located in the eluate with orcinol reagent (16).

The ribose-containing fractions were combined and concentrated to a syrup at reduced pressure. Alcohol was added and distilled at reduced pressure, twice, to remove the last traces of acetone. The syrup was dissolved in water, charcoaled, and passed through a bacterial filter. The arabinose-containing fractions were combined and treated similarly. No attempt was made to crystallize the pentoses since it was convenient to use aqueous solutions directly in biological experiments. Aliquots of the solutions were taken for determination of pentose and of radioactivity. The pentoses were identified by orcinol reactions and paper strip chromatography with the appropriate authentic samples as markers.

The yields of labelled pentose were: D-ribose-1-C^{14}, 300 mg, 17,400 counts/min mg; D-arabinose-1-C^{14}, 297 mg, 18,100 counts/min mg. The total yield of C^{14}-pentose was 19.1% based on nitromethane.

D-*2-Deoxyribose-1*-C^{14}

D-*Erythrose*

Twenty grams of β-benzyl-4,6-benzylidene-D-glucoside (17, 18) in methanol solution was hydrogenated with 3 g of Raney nickel catalyst, at 3 atmospheres pressure, for 72 hours. After removal of the catalyst, excess of benzene was added to the methanol filtrate. Concentration under reduced pressure removed methanol. Further benzene was added and concentration continued until precipitation occurred. The crude benzylidene sorbitol was collected by filtration, stirred with 50 ml of ethylacetate–chloroform (1:1), refiltered, washed, and dried. One crystallization from ethanol yielded pure benzylidene sorbitol (m.p. 132–134°). From this material D-erythrose was obtained in 85% yield by periodate oxidation as described by Sowden (14).

Acetylated Nitropentitols-1-C^{14}

A solution of 0.85 g of sodium in 40 ml of absolute methanol was added dropwise over a half-hour period to a stirred, cool (10° C) solution of erythrose (3.04 g) and C^{14}-nitromethane (0.5 ml diluted to 1.3 ml with non-radioactive nitromethane) dissolved in 40 ml of methanol. The cool reaction mixture was stirred for a further 15 hours, stored

Can. J. Chem. Downloaded from www.nrcresearchpress.com by 176.9.209.113 on 09/04/12
For personal use only.

in the cold room overnight, and the sodium nitropentitols collected as described in the procedure for ribose-1-C^{14} and arabinose-1-C^{14}. The sodium nitropentitols were dissolved in 200 ml of ice water and the sodium removed by passage through a cooled column of 40 ml of Dowex 50 (hydrogen form). The eluate and further water washings of the column were charcoaled, filtered, and concentrated to dryness at a temperature below 35°. Alcohol was added to the resulting partly crystalline mass and distilled under reduced pressure. This procedure was repeated three times to remove the last traces of water. After storage over P_2O_5 *in vacuo* the product weighed 2.36 g (51% based on nitromethane). Acetic anhydride (30 ml) and one small drop of concentrated sulphuric acid were added and stirred for 6 hours until the syrupy nitropentitols had dissolved. The reaction mixture was heated at 95° with stirring for 30 minutes, cooled, and 100 ml of ice water added to hydrolyze the excess acetic anhydride. After being stirred for 20 minutes the cold mixture was extracted with three 75-ml portions of chloroform. The combined chloroform extracts were washed twice with ice water, dried over calcium chloride, charcoaled, filtered, and concentrated to a syrup. Benzene was added and removed under reduced pressure. This procedure was repeated eight times to remove the last traces of acetic acid. The product weighed 3.83 g corresponding to an 84% yield of the acetylated nitropentitols.

Deacetylation and Hydrogenation

The acetylated compound, 60 ml of dry benzene and 4.5 g of sodium bicarbonate were refluxed with rapid stirring for $2\frac{1}{2}$ hours, cooled, charcoaled, filtered, and concentrated to a syrup. Alcohol was added and removed under reduced pressure. The syrup was finally completely freed of solvent under high vacuum to yield 2.83 g of presumed triacetoxynitropentene-1. The syrup was dissolved in 50 ml of ethanol, 300 mg of palladium black was added, and hydrogenation carried out at room temperature and atmospheric pressure. After 21 minutes the rate of uptake of hydrogen had become slow and the hydrogenation was terminated. The catalyst was removed by filtration and the ethanol filtrate concentrated to a syrup.

Nef Reaction

The syrup was dissolved in 8 ml of ethanol, cooled to 10°, and 24 ml of 2 *N* NaOH also at 10° was added dropwise with rapid stirring over a 20-minute period. The resulting alkaline solution was employed in a Nef reaction under the same conditions as those for the preparation of ribose-1-C^{14} and arabinose-1-C^{14}. (Eight milliliters of concentrated sulphuric acid and 10 ml of water were used.)

Deionization and Separation of Pentoses

The resulting solution was deionized and the mixture of pentoses transferred to a cellulose column by the same procedure given for the ribose–arabinose case. The column was developed with 99% acetone for 8 hours. (Forty-minute collection time and elution rate of 1 ml per minute.) After 8 hours the eluting solvent was changed to 97% acetone until the deoxyribose-1-C^{14} was eluted; ribose and arabinose were eluted as described previously. The three pentoses were obtained as syrups and, as previously described, dissolved in water for biological experiments. Aliquots were taken for determination of pentose and of radioactivity. The three pentoses were identified by diphenylamine (19) (for the deoxyribose-1-C^{14}) and orcinol (for the ribose-1-C^{14} and arabinose-1-C^{14}) reactions and by paper strip chromatography with the appropriate authentic samples as markers. The yields of labelled pentoses (based on nitromethane) were: D-2-deoxyribose-1-C^{14}, 202 mg (6.3%), 6800 counts/min mg; D-ribose-1-C^{14}, 112 mg (3.1%), 7200 counts/min mg; D-arabinose-1-C^{14}, 106 mg (2.9%), 7100 counts/min mg.

ACKNOWLEDGMENT

The authors are grateful to the National Research Council of Canada for funds which defrayed part of the cost of this study.

REFERENCES

1. FRUSH, H. L. and ISBELL, H. S. J. Research Natl. Bur. Standards, **51**, 307 (1953).
2. ISBELL, H. S., KARABINOS, J. V., FRUSH, H. L., HOLT, N. B., SCHWEBEL, A., and GALKOWSKI, T. T. J. Research Natl. Bur. Standards, **48**, 163 (1952).
3. ISBELL, H. S., FRUSH, H. L., and HOLT, N. B. J. Research Natl. Bur. Standards, **53**, 217 (1954).
4. ISBELL, H. S., FRUSH, H. L., and HOLT, N. B. J. Research Natl. Bur. Standards, **53**, 325 (1954).
5. MAHLER, H. R. U.S. Atomic Energy Comm. Document AECD-2400 (1948).
6. RAPPOPORT, D. A. and HASSID, W. Z. J. Am. Chem. Soc. **73**, 5524 (1951).
7. SOWDEN, J. C. J. Biol. Chem. **180**, 55 (1949).
8. BINKLEY, W. W. Advances in Carbohydrate Chem. **10**, 55 (1955).
9. SOWDEN, J. C. Advances in Carbohydrate Chem. **6**, 291 (1951).
10. MURRAY, D. H. and BUTLER, G. C. To be published.
11. OVEREND, W. G. and STACEY, M. Advances in Carbohydrate Chem. **8**, 68 (1953).
12. SOWDEN, J. C. J. Am. Chem. Soc. **76**, 3541 (1954).
13. ISBELL, H. S., FRUSH, H. L., and SCHAFFER, R. J. Research Natl. Bur. Standards, **54**, 201 (1955).
14. SOWDEN, J. C. J. Am. Chem. Soc. **72**, 808 (1950).
15. OVEREND, W. G., STACEY, M., and WIGGINS, L. F. J. Chem. Soc. 1358 (1949).
16. MCRARY, W. L. and SLATTERY, M. C. Arch. Biochem. **6**, 151 (1945).
17. RAYMOND, A. L., TYSON, R. S., and LEVENE, P. A. J. Biol. Chem. **130**, 47 (1939).
18. RICHTMYER, N. K. J. Am. Chem. Soc. **56**, 1633 (1934).
19. DAVIDSON, J. N. and WEYMOUTH, C. Biochem. J. **38**, 379 (1944).

Can. J. Chem. Downloaded from www.nrcresearchpress.com by 176.9.209.113 on 09/04/12
For personal use only.

Can. J. Chem. Downloaded from www.nrcresearchpress.com by 176.9.209.113 on 09/04/12
For personal use only.

NOTES

A RAPID DETERMINATION OF SOME SURFACE PROPERTIES OF SOLIDS

H. P. Schreiber and M. H. Waldman

INTRODUCTION

Among the important properties of a solid used as an adsorbent, catalytic agent, filler, etc., are its specific surface area ($\bar{A}$) and its maximum adsorption capacity ($\bar{V}_{max}$) for a given adsorbate. Standard techniques are available for accurate determinations of these quantities; for example, surface areas can be measured by the B.E.T. method (1) or by electron microscopy (2), adsorption capacities from suitable adsorption isotherms. When routine determinations of such surface properties are required and demands on accuracy are not too stringent, these techniques become overly time consuming. In such cases a rapid method of determination is wanted. To this end, a simplification of the B.E.T. procedure has recently been reported (3). This note is believed to describe a more widely applicable and rapid method of estimating the desired surface properties.

BASIS OF METHOD

The present method relies on a correlation between the surface area and adsorption capacity of a solid on the one hand, and the heat of adsorption in the given system, on the other. For the coverage of any fraction θ of surface per gram of adsorbent,

$$(\bar{A}) = k(\Delta\bar{H}_\theta) \qquad [1]$$

and

$$(\bar{V}_{max}) = k'(\Delta\bar{H}_\theta) \qquad [2]$$

where $(\Delta\bar{H}_\theta)$ denotes the integral heat of adsorption per gram of adsorbent, and k and k' are unspecified proportionality parameters. Thus, provided k and k' are known, an experimental evaluation of $(\Delta\bar{H}_\theta)$ would give an estimate of the required solid characteristic in any specified system.

In this method, a quantity proportional to the heat of adsorption is measured rapidly using apparatus characteristic of differential thermal analysis (d.t.a.). Since results are always comparative, the proportionality between the true and the measured reaction quantity need not be known explicitly.

EXPERIMENTAL

The quantity proportional to the heat of adsorption is measured in apparatus, the essentials of which are shown in Fig. 1. The d.t.a. cell is connected through a manifold system to the usual high vacuum components. Cup A of the cell holds the experimental sample; cup B is the reference arm, containing sintered glass of small specific surface. Chromel–alumel thermocouples (T_1 and T_2) are immersed into the cups, and connected to a Leeds–Northrup Type 9835B d-c. amplifier, the latter to a single pen recording potentiometer. The reservoir R contains the adsorbate, the vapor pressure of which can be read on the constant-volume mercury manometer. Provision was made to append additional d.t.a. cells as indicated. About one gram of adsorbent is weighed into the

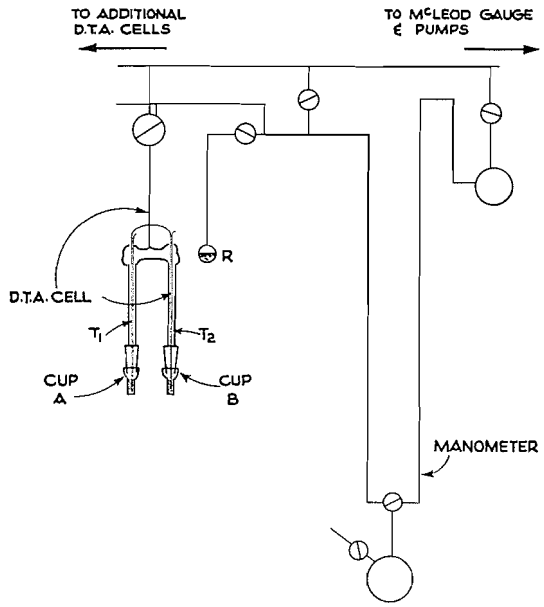

FIG. 1. Sample cell and vacuum system for reaction area determination.

reaction cup. The adsorbent is evacuated for about one hour at room temperature, or sufficiently long to establish a residual pressure of about 10^{-5} mm over the sample. The sample cell is then thermostated at the desired temperature, the dead space volume is exposed to the adsorbate, and the vapor finally admitted to the evacuated sample. The course of the interaction is recorded until no temperature gradient exists between sample and reference arms of the cell. In general, this involves about 10 minutes' operating time. The area under the time–temperature curve is found using a planimeter. This area, divided by the mass of adsorbent involved, is taken to be proportional to the heat of adsorption. Hereafter, the quantity is referred to as the "reaction area".

RESULTS AND DISCUSSION

The procedure for rapid surface area and adsorption capacity measurements was established using commercially available carbon blacks as adsorbents. Water, *n*-butane, and ethyl chloride were chosen as convenient adsorbates. Nine carbon blacks were involved in the water adsorption work, carried out at 25.5° C. Three types of carbon black were used in conjunction with the butane and ethyl chloride, these experiments being done at 0° C. In order to evaluate the parameters k and k', conventional values of $\bar{A}$ and $\bar{V}_{max}$ were needed (equations [1], [2]). Surface areas of the carbon blacks were obtained by the usual nitrogen adsorption technique in a B.E.T. apparatus (1). Maximum adsorption capacities were found only for butane and ethyl chloride adsorption, from the 0° C isotherms.

A description of the carbon black samples, their nitrogen adsorption and various "reaction areas", and the pertinent maximum adsorption capacities, are recorded in Table I. Each "reaction area" is the mean of two separate results. These did not deviate more than 8% about the mean. A correlation seems to exist between the "reaction areas" and the surface areas and maximum adsorption capacities. This is more readily seen by evaluating the proportionality parameters k and k'. In so doing, the pertinent

Can. J. Chem. Downloaded from www.nrcresearchpress.com by 176.9.209.113 on 09/04/12
For personal use only.

"reaction area" was substituted for the heat of adsorption. The values are given in Table II.

TABLE I

Surface areas, adsorption capacities, and reaction areas for adsorption of water, butane, and ethyl chloride on carbon blacks

Sample	Description	N_2 surface areas (m^2/g)	Reaction areas (cm^2/g)			$\bar{V}_{max}$ (cc/g)	
			H_2O (25.5° C)	n-C_4H_{10} (0° C)	EtCl (0° C)	n-C_4H_{10} (0° C)	EtCl (0° C)
1	Fine porous channel	327	88.0	54.2	50.6	470	300
2	Medium porous channel	139	42.0	—	—	—	—
3	Coarse porous channel	106	31.0	—	—	—	—
4	Coarse porous channel	112	35.5	—	—	—	—
5	Medium porous channel	125	36.5	—	—	—	—
6	Medium porous channel	140	38.0	—	—	—	—
7	Fine non-porous furnace	131	15.0	23.2	21.3	205	110
8	Medium non-porous furnace	76	8.8	—	—	—	—
9	Medium non-porous furnace	80	—	13.5	13.0	115	50
10	Coarse non-porous furnace	43	5.5	—	—	—	—

TABLE II

Proportionality parameters for adsorption of water, butane, and ethyl chloride on carbon blacks

Sample	$k \times 10^{-4}$			k' (cm)	
	H_2O	n-C_4H_{10}	EtCl	n-C_4H_{10}	EtCl
1	3.80	6.10	6.50	8.70	5.90
2	3.30	—	—	—	—
3	3.40	—	—	—	—
4	3.20	—	—	—	—
5	3.40	—	—	—	—
6	3.70	—	—	—	—
7	8.70	5.60	6.10	8.80	5.20
8	8.50	—	—	—	—
9	—	5.80	6.10	8.50	4.00
10	7.80	—	—	—	—

The parameter k appears to be constant for each interacting pair. The "reaction area" can therefore serve as a measure of the apparent surface area of the adsorbent in each system. Similarly, the value k' appears to be a constant characteristic of the interacting system, although there is a relatively large spread in the case of ethyl chloride adsorption. Thus, in each specified system an estimate of $\bar{V}_{max}$ is possible from the reaction datum. Provided, therefore, a given adsorbent–adsorbate system has been calibrated by means of a standard determination of surface area or maximum adsorption capacity, the described technique can be used to estimate these characteristics absolutely with an accuracy of some 15%. The total determination time of under two hours constitutes a very pronounced time saving over standard techniques.

A further use of this technique should be in routine control of the surface properties of a given solid. The precision of the "reaction area" determination is about 10–15%, so that changes in the quantity beyond this limit in a selected adsorption process indicate significant changes in the surface characteristics of the adsorbent under consideration. If absolute values are not required, there is no need for prior calibration of the system. If several d.t.a. cells are used, up to 30 or 40 such "surface characterizations" can be

Can. J. Chem. Downloaded from www.nrcresearchpress.com by 176.9.209.113 on 09/04/12
For personal use only.

performed per day by a single operator. Although the method had been utilized only in conjunction with carbon blacks, it should be broadly applicable to any adsorbent.

Some further aspects of the data merit brief discussion. Table II shows that k changes only slightly from the butane to the ethyl chloride system. This is reasonable; the apparent surface area is not likely to vary greatly when the probe molecules are approximately equal in size, as is the case here. In the case of water adsorption, the k value is sensitive to differences between channel and furnace blacks, but seems constant in each group. The absence of pore structure in the furnace blacks doubtless lowers the effective number of sites for water adsorption, thus raising the value of k. The water molecule is, presumably, sufficiently small to gain entry into some of the pores of the channel blacks, resulting in a relatively large heat of adsorption, hence a low k value. The apparent constancy of k for ethyl chloride and butane adsorption suggests that little penetration of the pore structure of the channel blacks occurs with these adsorbates.

The proportionality parameter k' is considerably greater for butane than for ethyl chloride. Since the "reaction areas" in these cases are approximately equal (see Table I), a given surface region of the black seems to accommodate greater amounts of butane than ethyl chloride prior to bulk liquefaction. In view of the polar nature of the ethyl chloride molecule, this result seems reasonable.

1. Brunauer, S., Emmett, P. H., and Teller, E. J. Am. Chem. Soc. **60**, 309 (1938).
2. Anderson, R. B. and Emmett, P. H. J. Appl. Phys. **19**, 367 (1948).
3. Starkweather, F. M. and Palumbo, D. T. J. Electrochem. Soc. **104**, 287 (1957).

Received April 24, 1959.
Canadian Industries Limited,
Central Research Laboratory,
McMasterville, Quebec.

STEROIDS. CXV. THE SYNTHESIS OF HALOGENATED STEROID HORMONES, 4-CHLORO-19-NOR HORMONE ANALOGS*

O. Mancera and H. J. Ringold

In an earlier paper (1) we noted that halogenation of progesterone at C-4 virtually eliminates progestational activity. It was thus of considerable interest to convert the extremely potent progestational agents (2), 19-nor: 17α-methyl- (3), 17α-ethynyl- (3), 17α-vinyl- (4), and 17α-ethyltestosterone (5) as well as 19-norprogesterone (6) into their 4-chloro analogs for evaluation of gestational activity. This transformation was readily accomplished by converting the parent steroids I into their 4,5-oxides (II) by reaction with alkaline hydrogen peroxide followed by hydrochloric acid treatment to yield directly the 4-chloro-Δ^4-3-ketones (III). This sequence is one first described in the cholesterol series by Shaw and Stevenson (7) and later described in the hormones series by ourselves (1) and by Camerino *et al.* (8). An alternate synthesis involving direct halogenation has been described by Petrow and co-workers (9) while a later paper by a Schering group (10) describes the synthesis of 4-halo hormone analogs by the addition of hypohalous acid to Δ^4-3-ketones.

In the case at hand 17α-methyl-19-nortestosterone (I*a*), 17α-ethynyl-19-nortestosterone (I*b*), and 19-norprogesterone (I*e*) were each reacted for periods of 35 minutes to 1 hour

Paper CXIV, Kincl, F. A. and Garcia, M. Ber. **92, 595 (1959).*

Can. J. Chem. Downloaded from www.nrcresearchpress.com by 176.9.209.113 on 09/04/12
For personal use only.

performed per day by a single operator. Although the method had been utilized only in conjunction with carbon blacks, it should be broadly applicable to any adsorbent.

Some further aspects of the data merit brief discussion. Table II shows that k changes only slightly from the butane to the ethyl chloride system. This is reasonable; the apparent surface area is not likely to vary greatly when the probe molecules are approximately equal in size, as is the case here. In the case of water adsorption, the k value is sensitive to differences between channel and furnace blacks, but seems constant in each group. The absence of pore structure in the furnace blacks doubtless lowers the effective number of sites for water adsorption, thus raising the value of k. The water molecule is, presumably, sufficiently small to gain entry into some of the pores of the channel blacks, resulting in a relatively large heat of adsorption, hence a low k value. The apparent constancy of k for ethyl chloride and butane adsorption suggests that little penetration of the pore structure of the channel blacks occurs with these adsorbates.

The proportionality parameter k' is considerably greater for butane than for ethyl chloride. Since the "reaction areas" in these cases are approximately equal (see Table I), a given surface region of the black seems to accommodate greater amounts of butane than ethyl chloride prior to bulk liquefaction. In view of the polar nature of the ethyl chloride molecule, this result seems reasonable.

1. Brunauer, S., Emmett, P. H., and Teller, E. J. Am. Chem. Soc. **60**, 309 (1938).
2. Anderson, R. B. and Emmett, P. H. J. Appl. Phys. **19**, 367 (1948).
3. Starkweather, F. M. and Palumbo, D. T. J. Electrochem. Soc. **104**, 287 (1957).

Received April 24, 1959.
Canadian Industries Limited,
Central Research Laboratory,
McMasterville, Quebec.

STEROIDS. CXV. THE SYNTHESIS OF HALOGENATED STEROID HORMONES, 4-CHLORO-19-NOR HORMONE ANALOGS*

O. Mancera and H. J. Ringold

In an earlier paper (1) we noted that halogenation of progesterone at C-4 virtually eliminates progestational activity. It was thus of considerable interest to convert the extremely potent progestational agents (2), 19-nor: 17α-methyl- (3), 17α-ethynyl- (3), 17α-vinyl- (4), and 17α-ethyltestosterone (5) as well as 19-norprogesterone (6) into their 4-chloro analogs for evaluation of gestational activity. This transformation was readily accomplished by converting the parent steroids I into their 4,5-oxides (II) by reaction with alkaline hydrogen peroxide followed by hydrochloric acid treatment to yield directly the 4-chloro-Δ^4-3-ketones (III). This sequence is one first described in the cholesterol series by Shaw and Stevenson (7) and later described in the hormones series by ourselves (1) and by Camerino *et al.* (8). An alternate synthesis involving direct halogenation has been described by Petrow and co-workers (9) while a later paper by a Schering group (10) describes the synthesis of 4-halo hormone analogs by the addition of hypohalous acid to Δ^4-3-ketones.

In the case at hand 17α-methyl-19-nortestosterone (I*a*), 17α-ethynyl-19-nortestosterone (I*b*), and 19-norprogesterone (I*e*) were each reacted for periods of 35 minutes to 1 hour

Paper CXIV, Kincl, F. A. and Garcia, M. Ber. **92, 595 (1959).*

Can. J. Chem. Downloaded from www.nrcresearchpress.com by 176.9.209.113 on 09/04/12
For personal use only.

with alkaline hydrogen peroxide in cold methanol solution to give a mixture (1) of the corresponding 4β,5β- and 4α,5α-epoxides. Without purification the epoxide mixtures were treated for 1 hour with concentrated hydrochloric acid in acetone solution (1), thus giving a high yield of the 4-chloro-Δ^4-3-keto compounds II*a*, II*b*, and II*e*.

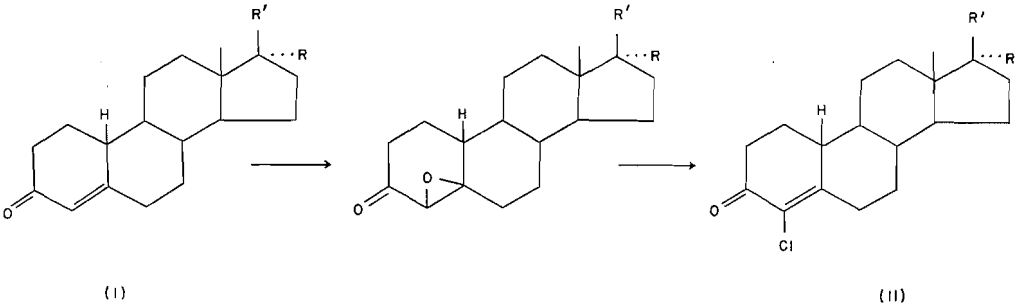

(I) (II)

(*a*) R = CH_3; R′ = OH
(*b*) R = C≡CH; R′ = OH
(*c*) R = $CH{=}CH_2$; R′ = OH
(*d*) R = CH_2CH_3; R′ = OH
(*e*) R = H; R′ = $COCH_3$

Hydrogenation of 4-chloro-17α-ethynyltestosterone (II*b*) in pyridine (11) over a palladium – calcium carbonate catalyst and interrupted at 1.1 equivalents hydrogen uptake gave 4-chloro-17α-vinyltestosterone (II*c*) in 70% yield, while hydrogenation of II*b* in dioxane (12) with palladium – barium sulphate, interrupted at 2.1 moles uptake, gave the 17α-ethyl compound (II*d*) in 60% yield. When tested* in the Clauberg assay by either the oral or subcutaneous route, compounds II exhibited only a relatively low order of progestational activity.

EXPERIMENTAL

Melting points are uncorrected. Rotations were determined in chloroform and ultraviolet absorption spectra in 96% ethanol.

4-Chloro-17α-methyl-19-nortestosterone (II*a*).—A solution of 17α-methyl-19-nortestosterone (I*a*) (10 g) in methanol (250 ml) was cooled to 0° and then treated dropwise and successively with 35% hydrogen peroxide (40 ml) and 10% sodium hydroxide (16 ml). After it had been left to stand for 35 minutes at 0–5° the solution was poured into water and extracted with ethyl acetate. Evaporation of the washed extract gave 11 g of crude epoxide as a semicrystalline product exhibiting no selective absorption in the ultraviolet. The epoxide without further purification was dissolved in acetone (100 ml), and concentrated hydrochloric acid (10 ml) was added. The solution, after being kept for 1 hour at room temperature, was poured into salt water and the product extracted with methylene chloride. The extract was washed successively with water, sodium carbonate solution, water, and then evaporated. The residue in 200 ml of benzene–hexane (1:1) was adsorbed on 300 g of neutral alumina, whereupon acetone–hexane crystallization of the benzene eluate gave 6.32 g of 4-chloro-17α-methyl-19-nortestosterone (II*a*), m.p. 145–148°. The analytical specimen from acetone–ether exhibited m.p. 148–151°, λ_{max} 255 mμ, log ϵ 4.12, $[\alpha]_D$ +42°.† Anal. Calc. for $C_{19}H_{27}ClO_2$: C, 70.67; H, 8.43; Cl, 10.98. Found: C, 70.68; H, 8.39; Cl, 10.61.

**Bio-assays by T. Endocrine Laboratories, Madison, Wisc.*

†After completion of our work this compound was reported by Camerino et al. (ref. 8b) with m.p. 151–152°, λ_{max} 255 mμ, log ϵ 4.14.

Can. J. Chem. Downloaded from www.nrcresearchpress.com by 176.9.209.113 on 09/04/12
For personal use only.

4-Chloro-17α-ethynyl-19-nortestosterone (II*b*).—17α-Ethynyl-19-nortestosterone (I*b*) (10 g) was epoxidized and then treated with acid as described above for the 17-methyl analog. The residue was chromatographed on neutral alumina and the benzene and benzene–ether 4:1 fractions crystallized from acetone–hexane to yield 5.54 g of II*b*, m.p. 186–188°, λ_{max} 225 mμ, log ε 4.11, $[\alpha]_D$ +7°. Anal. Calc. for $C_{20}H_{25}ClO_2$: C, 72.16; H, 7.57; Cl, 10.65. Found: C, 72.49; H, 7.46; Cl, 10.69.

4-Chloro-19-norprogesterone (II*e*).—19-Norprogesterone (0.8 g) in methanol (100 ml) at 0° was treated with 3.5 ml of 35% hydrogen peroxide and 1.4 ml of 10% sodium hydroxide and stirred for 1 hour at 0–5°. A small amount of insoluble material was removed and the filtrate poured into salt water. The crude epoxide mixture (0.83 g) was isolated by ethyl acetate extraction and then dissolved in 40 ml of acetone, and 1 ml of concentrated hydrochloric acid was added. After the solution had stood for 1 hour at room temperature, water, salt, and ice were added, the precipitate was collected, washed, dried, and recrystallized from acetone–hexane, yielding 0.61 g of II*e*, m.p. 169–172°. Recrystallization from the same solvents afforded the analytical sample, m.p. 174–177°, λ_{max} 256 mμ, log ε 4.11, $[\alpha]_D$ +127°. Anal. Calc. for $C_{20}H_{27}O_2Cl.\frac{1}{2}C_3H_6O$: C, 70.96; H, 8.31; Cl, 9.74%. Found: C, 71.01; H, 7.93; Cl, 9.68.

4-Chloro-17α-vinyl-19-nortestosterone (II*c*).—4-Chloro-17α-ethynyl-19-nortestosterone (5 g) in pyridine (100 ml) was hydrogenated at 25° and 580 mm over 2 g of pre-reduced 2% palladium – calcium carbonate catalyst. When hydrogen uptake reached 1.1 equivalents (2 to 3 hours in general) the reduction was interrupted, the catalyst removed, and the solvent concentrated *in vacuo*. The oily residue was taken up in ethyl acetate, the solution washed with dilute acid, carbonate solution, and then water. Evaporation and crystallization of the product from acetone–hexane gave 3.54 g of the vinyl compound (II*c*), m.p. 115–118°. Two recrystallizations from the same solvent pair produced the analytical specimen, m.p. 124–126°, λ_{max} 255 mμ, log ε 4.13, $[\alpha]_D$ +51°. Anal. Calc. for $C_{20}H_{27}ClO_2$: C, 71.69; H, 8.15; Cl, 10.59. Found: C, 71.42; H, 8.05; Cl, 10.71.

4-Chloro-17α-ethyl-19-nortestosterone (II*d*).—The reduction at 25° and 580 mm of 2 g of 4-chloro-17α-ethynyl-19-nortestosterone (II*b*) in 160 ml of dioxane over 0.8 g of pre-hydrogenated 10% palladium – barium sulphate catalyst was stopped after the uptake of 2.1 equivalents of hydrogen (ca. 3 hours). The catalyst was filtered and the solution concentrated to dryness, whereupon acetone–hexane crystallization of the reduced product gave 1.20 g of 17α-ethyl compound (II*d*), m.p. 122–125°. Repeated crystallization yielded the pure substance, m.p. 126–128° (mixture melting point depression with II*c*), λ_{max} 256 mμ, log ε 4.14, $[\alpha]_D$ +47°. Anal. Calc. for $C_{20}H_{29}O_2Cl$: C, 71.34; H, 8.68; O, 9.50. Found: C, 71.30; H, 8.69; O, 9.58.

1. Ringold, H. J., Batres, E., Mancera, O., and Rosenkranz, G. J. Org. Chem. **21**, 1432 (1956).
2. McGinty, D. and Djerassi, C. Ann. N. Y. Acad. Sci. **71**, 500 (1958).
3. Djerassi, C., Miramontes, L., Rosenkranz, G., and Sondheimer, F. J. Am. Chem. Soc. **76**, 4092 (1954).
4. Sandoval, A., Miramontes, L., Rosenkranz, G., and Sondheimer, F. J. Am. Chem. Soc. **75**, 4117 (1953).
5. Colton, F. B., Nysted, L. N., Riegel, B., and Raymond, A. L. J. Am. Chem. Soc. **79**, 1123 (1957).
6. Miramontes, L., Rosenkranz, G., and Djerassi, C. J. Am. Chem. Soc. **73**, 3540 (1951).
7. Shaw, J. I. and Stevenson, R. J. Chem. Soc. 3549 (1955).
8. (*a*) Camerino, B., Patelli, B., and Vercellone, A. J. Am. Chem. Soc. **78**, 3540 (1956). (*b*) Camerino, B., Modelli, R., and Patelli, B. Farmaco, (Pavia), **13**, 52 (1958); Chem. Abstr. **52**, 13768 (1958).
9. Kirk, D. N., Patel, D. K., and Petrow, V. J. Chem. Soc. 1184 (1956).
10. Oliveto, E. P., Gerold, C., and Hershberg, E. B. J. Am. Chem. Soc. **79**, 3596 (1957).

Can. J. Chem. Downloaded from www.nrcresearchpress.com by 176.9.209.113 on 09/04/12
For personal use only.

11. RUZICKA, L. and MÜLLER, P. Helv. Chim. Acta, **22**, 755 (1939).
12. HERSHBERG, E. B., OLIVETO, E. P., GEROLD, C., and JOHNSON, L. J. Am. Chem. Soc. **73**, 5073 (1951).

RECEIVED JUNE 12, 1959.
RESEARCH LABORATORIES,
SYNTEX, S. A.,
APDO. POSTAL 2679,
MEXICO, D. F.

THE STREAMING BIREFRINGENCE OF CELLULOSE MICELLES: A CONFIRMATION OF THE THEORY FOR RIGID RODS

D. F. MACLENNAN* AND S. G. MASON

INTRODUCTION

Theories of streaming birefringence have been reviewed by Edsall (1) and by Cerf and Scheraga (2). Peterlin and Stuart (3, 4) have developed a theory for the orientation of rigid ellipsoids of revolution which permits the calculation of particle lengths from streaming birefringence data. Donnet (5) has made a comparison of the lengths of tobacco mosaic virus particles measured directly from electron micrographs and those calculated from flow birefringence measurements using the theory of Peterlin and Stuart. Good agreement between the two methods was obtained.

This note deals with similar measurements on a cellulose sol.

EXPERIMENTAL

Apparatus

The streaming birefringence apparatus, used in this work, is the concentric cylinder type with rotating outer cylinder. A longitudinal section of the cylinders and optical system is shown in Fig. 1.

The outer cylinder, made of stainless steel, has an internal diameter of 3.40 cm and an inside length of 6.35 cm. Four interchangeable stainless steel inner cylinders, 6.30 cm long and having different diameters, make it possible to vary the annular gap from 1.5 mm to 0.2 mm and the velocity gradient up to 10^4 sec^{-1}.

The light source is a General Electric A-H4 100-watt mercury arc with a filter combination to isolate the 546-mμ mercury line.

Cellulose Sol

The sol was prepared (6) by boiling 10 g bleached sulphite wood pulp in 5 *N* sulphuric acid for 3.5 hours, and the residue, after it was washed, was dispersed in 2 l. of distilled water.

To narrow the distribution of particle sizes the sol was then centrifuged at 3500 *g* for 1 hour in a Spinco preparatory ultracentrifuge and the supernatant sol was used for the measurements.

Electron micrographs of the rod-like cellulose particles were made using palladium-shadowed specimens.

RESULTS AND DISCUSSION

The distribution of particle lengths from the electron micrographs is given in Table I. The experimental values of the extinction angle χ over a range of gradients G and using three different stators are plotted in Fig. 2.

The electron micrographs indicate that the cellulose particles range in length from 1500 Å to 6500 Å. From this information a theoretical extinction angle curve, character-

*Holder of a Studentship (1951–52) and a Fellowship (1952–53) from the National Research Council of Canada.

Can. J. Chem. Downloaded from www.nrcresearchpress.com by 176.9.209.113 on 09/04/12
For personal use only.

11. RUZICKA, L. and MÜLLER, P. Helv. Chim. Acta, **22**, 755 (1939).
12. HERSHBERG, E. B., OLIVETO, E. P., GEROLD, C., and JOHNSON, L. J. Am. Chem. Soc. **73**, 5073 (1951).

RECEIVED JUNE 12, 1959.
RESEARCH LABORATORIES,
SYNTEX, S. A.,
APDO. POSTAL 2679,
MEXICO, D. F.

THE STREAMING BIREFRINGENCE OF CELLULOSE MICELLES: A CONFIRMATION OF THE THEORY FOR RIGID RODS

D. F. MACLENNAN* AND S. G. MASON

INTRODUCTION

Theories of streaming birefringence have been reviewed by Edsall (1) and by Cerf and Scheraga (2). Peterlin and Stuart (3, 4) have developed a theory for the orientation of rigid ellipsoids of revolution which permits the calculation of particle lengths from streaming birefringence data. Donnet (5) has made a comparison of the lengths of tobacco mosaic virus particles measured directly from electron micrographs and those calculated from flow birefringence measurements using the theory of Peterlin and Stuart. Good agreement between the two methods was obtained.

This note deals with similar measurements on a cellulose sol.

EXPERIMENTAL

Apparatus

The streaming birefringence apparatus, used in this work, is the concentric cylinder type with rotating outer cylinder. A longitudinal section of the cylinders and optical system is shown in Fig. 1.

The outer cylinder, made of stainless steel, has an internal diameter of 3.40 cm and an inside length of 6.35 cm. Four interchangeable stainless steel inner cylinders, 6.30 cm long and having different diameters, make it possible to vary the annular gap from 1.5 mm to 0.2 mm and the velocity gradient up to 10^4 sec^{-1}.

The light source is a General Electric A-H4 100-watt mercury arc with a filter combination to isolate the 546-mμ mercury line.

Cellulose Sol

The sol was prepared (6) by boiling 10 g bleached sulphite wood pulp in 5 *N* sulphuric acid for 3.5 hours, and the residue, after it was washed, was dispersed in 2 l. of distilled water.

To narrow the distribution of particle sizes the sol was then centrifuged at 3500 *g* for 1 hour in a Spinco preparatory ultracentrifuge and the supernatant sol was used for the measurements.

Electron micrographs of the rod-like cellulose particles were made using palladium-shadowed specimens.

RESULTS AND DISCUSSION

The distribution of particle lengths from the electron micrographs is given in Table I. The experimental values of the extinction angle χ over a range of gradients G and using three different stators are plotted in Fig. 2.

The electron micrographs indicate that the cellulose particles range in length from 1500 Å to 6500 Å. From this information a theoretical extinction angle curve, character-

*Holder of a Studentship (1951–52) and a Fellowship (1952–53) from the National Research Council of Canada.

Can. J. Chem. Downloaded from www.nrcresearchpress.com by 176.9.209.113 on 09/04/12
For personal use only.

Can. J. Chem. Downloaded from www.nrcresearchpress.com by 176.9.209.113 on 09/04/12
For personal use only.

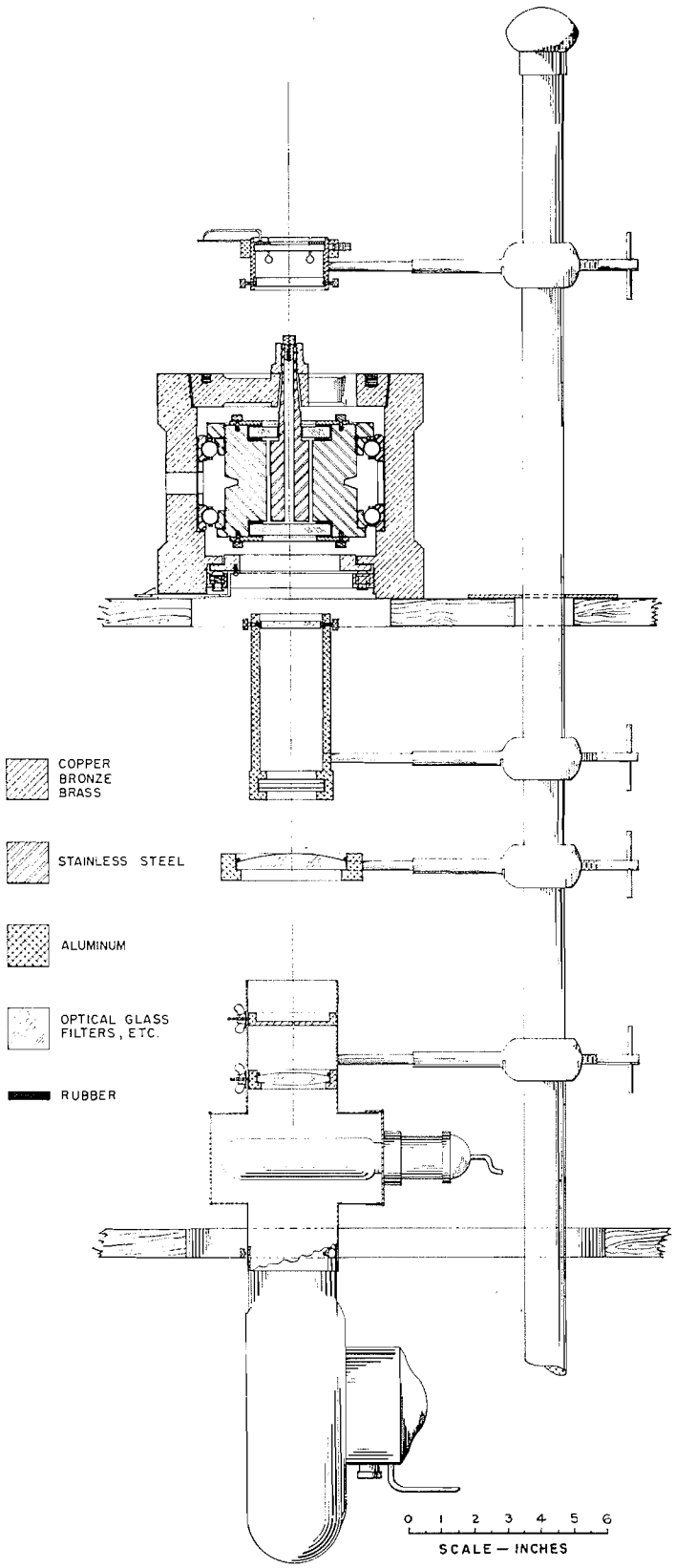

FIG. 1. Sectional view of the streaming birefringence apparatus.

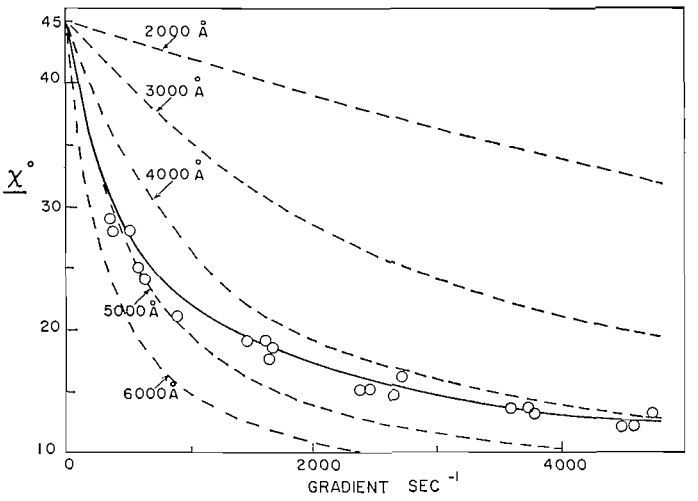

FIG. 2. Extinction angle at various gradients. The points represent experimental values with three different annular gaps in the apparatus. The solid line is calculated from the measured length distribution, and the broken lines are calculated for monodisperse particles of the lengths indicated.

TABLE I
Length distribution from electron micrographs

Range (Å)	Percentage of particles
1500–2500	12
2500–3500	21
3500–4500	27
4500–5500	22
5500–6500	18

istic of a solution of particles having this length distribution, has been calculated.

A rotary diffusion constant, θ, has been calculated for each length range using the Perrin formula (7)

$$[1] \qquad \theta = \frac{3kT}{16\pi\eta a^3}(-1+2\log_e 2p)$$

where k is the Boltzmann constant, T is the absolute temperature, η is the solvent viscosity, a is the length of the semimajor axis, and p is the axis ratio.

Since, as may be seen from eq. [1], θ is much more sensitive to a than to p, the use of an approximate value of p in these calculations is permissible. The latter was taken to be 16, the approximate value estimated from the electron micrographs.

From values of θ and p, theoretical values of χ can be obtained for any velocity gradient from the tables of Scheraga, Edsall, and Gadd (8).

Values for a polydisperse sol, made up of particles of the measured lengths in the proper proportions, have been calculated using the theory of Sadron (9). According to this theory the extinction angle of a polydisperse system is given by

$$[2] \qquad \tan 2\chi = \left(\sum_i \delta_i \sin 2\psi_i\right) \Big/ \left(\sum_i \delta_i \cos 2\psi_i\right)$$

where ψ_i is the extinction angle, and δ_i the birefringence which would be produced by the ith component alone in a given solvent at a given velocity gradient.

Can. J. Chem. Downloaded from www.nrcresearchpress.com by 176.9.209.113 on 09/04/12
For personal use only.

According to Peterlin and Stuart (4) the birefringence Δn of a polydisperse system is given by

$$[3] \qquad \Delta n = \frac{2\pi c}{n_0}(g_1 - g_2) f(\alpha, p)$$

where c is the concentration of the particles expressed as volume fraction, n_0 is the index of refraction of the isotropic solution at rest, $(g_1 - g_2)$ is an optical factor, and $f(\alpha, p)$ is an orientation factor. If $(g_1 - g_2)$ is assumed to be constant, δ_i may be replaced in eq. [2] by $c_i f_i$ where c_i is the concentration and f_i the orientation factor of the ith component of the sol. The relative values of c_i were taken from the distribution (Table I) and f_i and ψ_i were obtained from the tables (8).

The modified equation is

$$[4] \qquad \tan 2\chi = \sum_i c_i f_i \sin 2\psi_i \Big/ \sum_i c_i f_i \cos 2\psi_i.$$

The curve calculated from eq. [4] is shown as the solid line in Fig. 2. Included for comparison as broken lines are the calculated values for monodisperse sols of various lengths. It is seen that the experimental values are in good agreement with the theoretical curve based on the measured length distribution.

1. EDSALL, J. T. Advances in Colloid Sci. **1**, 269 (1942).
2. CERF, R. and SCHERAGA, H. A. Chem. Revs. **51**, 185 (1952).
3. PETERLIN, A. Z. Physik, **111**, 232 (1938).
4. PETERLIN, A. and STUART, H. A. Z. Physik, **112**, 1, 129 (1939).
5. DONNET, J. B. J. Polymer Sci. **12**, 53 (1954).
6. RANBY, B. G. Discussions Faraday Soc. **11**, 158 (1951).
7. PERRIN, F. J. phys. radium, **5** (7), 497 (1934).
8. SCHERAGA, H. A., EDSALL, J. T., and GADD, J. O., JR. J. Chem. Phys. **19**, 1101 (1951).
9. SADRON, C. J. phys. radium, **9** (7), 381 (1938).

RECEIVED JUNE 9, 1959.
PHYSICAL CHEMISTRY DIVISION,
PULP AND PAPER RESEARCH INSTITUTE OF CANADA AND
DEPARTMENT OF CHEMISTRY, MCGILL UNIVERSITY,
MONTREAL, QUEBEC.

NOTE ON THE REACTION OF HYDROGEN ATOMS WITH CYANOGEN*

CATHERINE HAGGART† AND C. A. WINKLER

During a study of the reactions of CN radicals formed in mixtures of cyanogen and active nitrogen, it became of interest to know the extent to which cyanogen was capable of reacting with hydrogen atoms and CN radicals with molecular hydrogen. Using a fast flow system, Geib and Harteck (1) observed that hydrogen atoms react with cyanogen to produce hydrogen cyanide and traces of methylamine and ammonia. Pease and Robertson (2) reported that, in a static system at 550° C, the reaction of cyanogen and molecular hydrogen followed a chain mechanism, initiated by the formation of CN radicals, and they suggested that hydrogen cyanide was formed by the reactions of CN radicals with molecular hydrogen and of hydrogen atoms with cyanogen. The reaction of molecular hydrogen with CN radicals, formed in the sodium flame reaction with cyanogen, was observed by Hartel and Polanyi (3) to produce hydrogen cyanide and to require an activation energy of some 7 kcal.

**Financial assistance received from the Canadian Industries Limited, and the National Research Council.*
†*Holder of a C.I.L. Fellowship, 1958–59.*

Can. J. Chem. Downloaded from www.nrcresearchpress.com by 176.9.209.113 on 09/04/12
For personal use only.

According to Peterlin and Stuart (4) the birefringence Δn of a polydisperse system is given by

$$[3] \qquad \Delta n = \frac{2\pi c}{n_0}(g_1 - g_2) f(\alpha, p)$$

where c is the concentration of the particles expressed as volume fraction, n_0 is the index of refraction of the isotropic solution at rest, $(g_1 - g_2)$ is an optical factor, and $f(\alpha, p)$ is an orientation factor. If $(g_1 - g_2)$ is assumed to be constant, δ_i may be replaced in eq. [2] by $c_i f_i$ where c_i is the concentration and f_i the orientation factor of the ith component of the sol. The relative values of c_i were taken from the distribution (Table I) and f_i and ψ_i were obtained from the tables (8).

The modified equation is

$$[4] \qquad \tan 2\chi = \sum_i c_i f_i \sin 2\psi_i \Big/ \sum_i c_i f_i \cos 2\psi_i.$$

The curve calculated from eq. [4] is shown as the solid line in Fig. 2. Included for comparison as broken lines are the calculated values for monodisperse sols of various lengths. It is seen that the experimental values are in good agreement with the theoretical curve based on the measured length distribution.

1. EDSALL, J. T. Advances in Colloid Sci. **1**, 269 (1942).
2. CERF, R. and SCHERAGA, H. A. Chem. Revs. **51**, 185 (1952).
3. PETERLIN, A. Z. Physik, **111**, 232 (1938).
4. PETERLIN, A. and STUART, H. A. Z. Physik, **112**, 1, 129 (1939).
5. DONNET, J. B. J. Polymer Sci. **12**, 53 (1954).
6. RANBY, B. G. Discussions Faraday Soc. **11**, 158 (1951).
7. PERRIN, F. J. phys. radium, **5** (7), 497 (1934).
8. SCHERAGA, H. A., EDSALL, J. T., and GADD, J. O., JR. J. Chem. Phys. **19**, 1101 (1951).
9. SADRON, C. J. phys. radium, **9** (7), 381 (1938).

RECEIVED JUNE 9, 1959.
PHYSICAL CHEMISTRY DIVISION,
PULP AND PAPER RESEARCH INSTITUTE OF CANADA AND
DEPARTMENT OF CHEMISTRY, MCGILL UNIVERSITY,
MONTREAL, QUEBEC.

NOTE ON THE REACTION OF HYDROGEN ATOMS WITH CYANOGEN*

CATHERINE HAGGART† AND C. A. WINKLER

During a study of the reactions of CN radicals formed in mixtures of cyanogen and active nitrogen, it became of interest to know the extent to which cyanogen was capable of reacting with hydrogen atoms and CN radicals with molecular hydrogen. Using a fast flow system, Geib and Harteck (1) observed that hydrogen atoms react with cyanogen to produce hydrogen cyanide and traces of methylamine and ammonia. Pease and Robertson (2) reported that, in a static system at 550° C, the reaction of cyanogen and molecular hydrogen followed a chain mechanism, initiated by the formation of CN radicals, and they suggested that hydrogen cyanide was formed by the reactions of CN radicals with molecular hydrogen and of hydrogen atoms with cyanogen. The reaction of molecular hydrogen with CN radicals, formed in the sodium flame reaction with cyanogen, was observed by Hartel and Polanyi (3) to produce hydrogen cyanide and to require an activation energy of some 7 kcal.

**Financial assistance received from the Canadian Industries Limited, and the National Research Council.*
†*Holder of a C.I.L. Fellowship, 1958–59.*

Can. J. Chem. Downloaded from www.nrcresearchpress.com by 176.9.209.113 on 09/04/12
For personal use only.

The reaction between hydrogen atoms and cyanogen was studied over a range of temperatures up to 430° C, at various flow rates of cyanogen. Hydrogen atoms were formed in a conventional Wood–Bonhoeffer (4) system. Hydrogen cyanide and unreacted cyanogen were the only substances trapped at liquid air temperature after reaction had occurred and no polymer was formed during the reaction. Analysis for hydrogen cyanide in the presence of cyanogen was made as described by Rhodes (5), by absorbing both products in a known volume of acidified silver nitrate solution, from which cyanogen was quantitatively recovered by slowly drawing nitrogen through the absorber and then into a train of Wallis bubblers (6) containing sodium hydroxide solution. The excess silver nitrate was titrated with potassium thiocyanate using ferrous ammonium sulphate as indicator, and the cyanide content of the bubblers was estimated by titration with silver nitrate with potassium iodide as indicator (7).

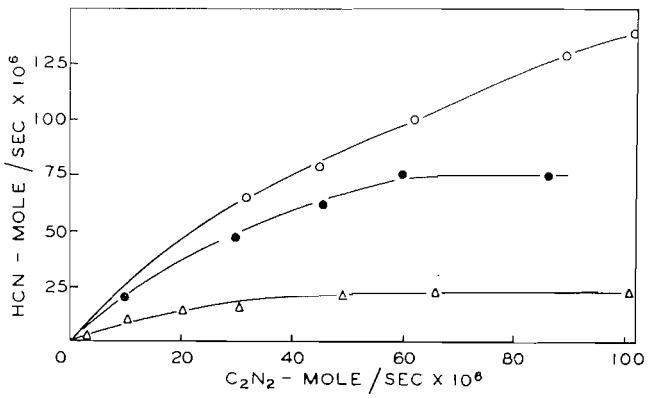

FIG. 1. Production of hydrogen cyanide in the reaction of hydrogen atoms with cyanogen. Temperature in ° C: △, 68; ●, 268; ○, 430.

The relations between the hydrogen cyanide production and cyanogen flow rate at three temperatures are shown in Fig. 1. Even at the lowest temperature used (68° C), the maximum rate of hydrogen cyanide production exceeded by a factor of three the flow rate of hydrogen atoms as determined from the maximum amount of hydrogen bromide that could be decomposed under comparable conditions (8). As the temperature was increased, the maximum production of hydrogen cyanide increased rapidly, until at 430° C it was some twenty times the flow rate of hydrogen atoms from the discharge tube. It seems quite apparent, therefore, that the reaction occurs by a chain mechanism, presumably as follows:

$$(CN)_2 + H \rightarrow HCN + CN \quad [1]$$

$$CN + H_2 \rightarrow HCN + H. \quad [2]$$

Termination of the chain might, of course, occur by recombination of hydrogen atoms or CN radicals, or by the interaction of hydrogen atoms and CN radicals.

1. GEIB, K. H. and HARTECK, P. Ber. B, **66**, 1815 (1933).
2. PEASE, R. N. and ROBERTSON, N. C. J. Am. Chem. Soc. **64**, 1880 (1942).
3. HARTEL, P. and POLANYI, M. Z. physik. Chem. B, **11**, 97 (1930).
4. BONHOEFFER, K. F. Z. physik. Chem. **113**, 199 (1924).
5. RHODES, F. N. Ind. Eng. Chem. **4**, 652 (1912).
6. WALLIS, T. Ann. **345**, 352 (1906).
7. KOLTHOFF, I. M. and SANDELL, E. B. Textbook of quantitative inorganic analysis. Rev. ed. The MacMillan Co., New York. 1948.

Can. J. Chem. Downloaded from www.nrcresearchpress.com by 176.9.209.113 on 09/04/12
For personal use only.

8. WILES, D. M. and WINKLER, C. A. J. Phys. Chem. **61**, 620 (1957).

RECEIVED JUNE 22, 1959.
PHYSICAL CHEMISTRY LABORATORY,
MCGILL UNIVERSITY,
MONTREAL, QUEBEC.

THE MERCURY-DISCHARGE REDUCTION OF PHOSPHORUS TRICHLORIDE

ARTHUR FINCH

Little information is available concerning the preparation or properties of simple halogen compounds containing the P—P bond; P_2Br_4 and P_2F_4 are unknown, and only P_2I_4 is well characterized (1). Early work by Besson (2) on the effect of an electrodeless discharge on mixtures of phosphorus trichloride and hydrogen resulted in the production of (presumably) P_2Cl_4, and similar recent work by Gutmann (3) led to unidentified liquid products. Attempts to make the tetrachloride by chemical reactions using P_2I_4 have been unsuccessful (4). The work reported below involves the reduction of phosphorus trichloride vapor by a high-voltage mercury arc, using conditions successfully adopted by Schlesinger and collaborators (5) for the continuous production of unstable boron subhalides.

EXPERIMENTAL

Apparatus and Materials

A "square-four" design discharge tube, similar to that previously used (5) was employed, with a discharge path of about 6 cm. A 2000-volt, 15-ma output transformer was operated under conditions appropriate to give a satisfactory discharge; the potential actually used varied between 1000 volts and 1300 volts, depending on the pressure in the system.

Phosphorus trichloride was redistilled at 74° C, passed into a high-vacuum line of conventional design, and fractionated through a −45.2° bath into a −78° trap. The vapor pressure of the purified compound was 65 mm at about −10°, in agreement with published results (6). Phosphorus trichloride vapor was circulated through the discharge cell either by a circulating pump or by distillation from a −63° bath to a −196° trap.

Results

Extensive decomposition occurred, with the production of dark red and yellow involatile solids on the walls of the discharge tubes, a dark grey scale on the surface of the mercury electrodes, and small quantities of a volatile liquid.

The volatile fraction was transferred to a fractionating system, and condensed as white crystals at −45° after passing a −23° bath. Using the Stock melting-point technique, and a pentane thermometer calibrated at the National Physical Laboratory to ±1°, the crystals were found to melt sharply between −34° and −35° C. The colorless liquid produced on melting the crystals decomposed at room temperature in vacuum, giving yellow involatile solids, and phosphorus trichloride, identified by measurements in a micro vapor-pressure apparatus. The liquid fumed in air, and reacted vigorously with water. Samples were distilled into weighed tubes under vacuum, hydrolyzed, and analyzed for chlorine and phosphorus, using standard procedures. Typical results calculated for P_2Cl_4 (Cl, 69.5%; P, 30.5%) were as follows. Sample 1: weight, 0.3041 g; Cl, 69.3%; P, 29.8%. Sample 2: weight, 0.2520 g; Cl, 69.6%; P, 30.4%. During the hydrolysis some non-condensable gas, presumably hydrogen, was evolved, suggesting the breaking of a P—P bond, though measurement was not possible in the apparatus available. The nature

Can. J. Chem. Downloaded from www.nrcresearchpress.com by 176.9.209.113 on 09/04/12
For personal use only.

8. WILES, D. M. and WINKLER, C. A. J. Phys. Chem. **61**, 620 (1957).

RECEIVED JUNE 22, 1959.
PHYSICAL CHEMISTRY LABORATORY,
MCGILL UNIVERSITY,
MONTREAL, QUEBEC.

THE MERCURY-DISCHARGE REDUCTION OF PHOSPHORUS TRICHLORIDE

ARTHUR FINCH

Little information is available concerning the preparation or properties of simple halogen compounds containing the P—P bond; P_2Br_4 and P_2F_4 are unknown, and only P_2I_4 is well characterized (1). Early work by Besson (2) on the effect of an electrodeless discharge on mixtures of phosphorus trichloride and hydrogen resulted in the production of (presumably) P_2Cl_4, and similar recent work by Gutmann (3) led to unidentified liquid products. Attempts to make the tetrachloride by chemical reactions using P_2I_4 have been unsuccessful (4). The work reported below involves the reduction of phosphorus trichloride vapor by a high-voltage mercury arc, using conditions successfully adopted by Schlesinger and collaborators (5) for the continuous production of unstable boron subhalides.

EXPERIMENTAL

Apparatus and Materials

A "square-four" design discharge tube, similar to that previously used (5) was employed, with a discharge path of about 6 cm. A 2000-volt, 15-ma output transformer was operated under conditions appropriate to give a satisfactory discharge; the potential actually used varied between 1000 volts and 1300 volts, depending on the pressure in the system.

Phosphorus trichloride was redistilled at 74° C, passed into a high-vacuum line of conventional design, and fractionated through a −45.2° bath into a −78° trap. The vapor pressure of the purified compound was 65 mm at about −10°, in agreement with published results (6). Phosphorus trichloride vapor was circulated through the discharge cell either by a circulating pump or by distillation from a −63° bath to a −196° trap.

Results

Extensive decomposition occurred, with the production of dark red and yellow involatile solids on the walls of the discharge tubes, a dark grey scale on the surface of the mercury electrodes, and small quantities of a volatile liquid.

The volatile fraction was transferred to a fractionating system, and condensed as white crystals at −45° after passing a −23° bath. Using the Stock melting-point technique, and a pentane thermometer calibrated at the National Physical Laboratory to ±1°, the crystals were found to melt sharply between −34° and −35° C. The colorless liquid produced on melting the crystals decomposed at room temperature in vacuum, giving yellow involatile solids, and phosphorus trichloride, identified by measurements in a micro vapor-pressure apparatus. The liquid fumed in air, and reacted vigorously with water. Samples were distilled into weighed tubes under vacuum, hydrolyzed, and analyzed for chlorine and phosphorus, using standard procedures. Typical results calculated for P_2Cl_4 (Cl, 69.5%; P, 30.5%) were as follows. Sample 1: weight, 0.3041 g; Cl, 69.3%; P, 29.8%. Sample 2: weight, 0.2520 g; Cl, 69.6%; P, 30.4%. During the hydrolysis some non-condensable gas, presumably hydrogen, was evolved, suggesting the breaking of a P—P bond, though measurement was not possible in the apparatus available. The nature

Can. J. Chem. Downloaded from www.nrcresearchpress.com by 176.9.209.113 on 09/04/12
For personal use only.

of the hydrolysis products in the analogous compound P_2I_4 has been studied in detail by Kolitowska (9), who has shown that the final products include HI, H_3PO_2, H_3PO_3, PH_3, ($P_{12}H_6$), and it is expected that similar results obtain for the present compound. Molecular weight determinations by depression of vapor tension of carbon tetrachloride gave the values 191 and 194 for different samples (calculated for P_2Cl_4, 204). Thus the liquid was P_2Cl_4, and exhibited the general appearance and properties described by Besson, though the melting point was 6° lower. Using a single cell, some 200 mg per day were formed by a semiautomatic process.

Lack of volatility at low temperatures, and the rate of decomposition at room temperature, precluded vapor-pressure measurements. By analogy with the fluorination of B_2Cl_4 to form a more volatile and stable compound (7), attempts were made to replace the chlorine by fluorine, using similar Swarts-type reactions. No evidence for volatile compounds other than phosphorus trichloride, and very small amounts of a very volatile gas, presumably phosphorus trifluoride, was obtained. Further experiments to synthesize the tetrafluoro compound are in progress.

The electrode scale was completely soluble in warm nitric acid without apparent evolution of phosphine. Complete analysis, using standard gravimetric techniques, gave the following results. Sample 1: Hg, 86.4%; Cl, 10.7%; P, 2.6%. Sample 2: Hg, 86.2%; Cl, 10.9%; P, 2.6%. Thus in distinction to Gutmann's experiments with copper electrodes, a simple metal phosphide was not formed. It is of interest to note, that mercury tetratritaphosphide Hg_3P_4 is produced by the action of P_2I_4 on mercury at elevated temperatures (8), and the electrode scale is presumably a mixture of this with other mercury phosphides and chlorides.

The colored involatile deposits on the walls of the tubes were pyrophoric, and were similar to the mixture of red and yellow phosphorus described by Gutmann.

ACKNOWLEDGMENTS

It is a pleasure to acknowledge helpful discussions from Dr. A. G. Foster, and financial assistance from Imperial Chemical Industries Limited.

1. LEUNG, Y. C. and WASER, J. J. Phys. Chem. **60**, 539 (1956).
2. BESSON, A. and FOURNIER, L. Compt. rend. **150**, 102 (1910).
3. GUTMANN, V. Monatsh. Chem. **86**, 98 (1954).
4. GAUTIER, A. Compt. rend. **78**, 286 (1874).
5. URRY, G., WARTIK, T., MOORE, R. E., and SCHLESINGER, H. I. J. Am. Chem. Soc. **76**, 5293 (1954).
6. INTERNATIONAL CRITICAL TABLES, III, 213 (1933).
7. FINCH, A. and SCHLESINGER, H. I. J. Am. Chem. Soc. **80**, 3573 (1958).
8. VAN HAAREN, A. and PARTHEIL, A. Arch. Pharm. **238**, 35 (1900).
9. KOLITOWSKA, J. H. Roczniki Chem. **15**, 29 (1935).

RECEIVED JUNE 12, 1959.
DEPARTMENT OF CHEMISTRY,
ROYAL HOLLOWAY COLLEGE,
UNIVERSITY OF LONDON,
ENGLEFIELD GREEN, ENGLAND.

INFRARED SPECTRUM OF AMMONIUM HYDROPEROXIDE

OSVALD KNOP* AND PAUL A. GIGUÈRE

Ammonia and hydrogen peroxide form a 1:1 compound which is remarkable in that its melting point, 25° C (1), lies some 100° above that of the ammonia–water analogue (2).

**Present address: Department of Chemical Engineering, Nova Scotia Technical College, Halifax, N.S.*

Can. J. Chem. Downloaded from www.nrcresearchpress.com by 176.9.209.113 on 09/04/12
For personal use only.

of the hydrolysis products in the analogous compound P_2I_4 has been studied in detail by Kolitowska (9), who has shown that the final products include HI, H_3PO_2, H_3PO_3, PH_3, ($P_{12}H_6$), and it is expected that similar results obtain for the present compound. Molecular weight determinations by depression of vapor tension of carbon tetrachloride gave the values 191 and 194 for different samples (calculated for P_2Cl_4, 204). Thus the liquid was P_2Cl_4, and exhibited the general appearance and properties described by Besson, though the melting point was 6° lower. Using a single cell, some 200 mg per day were formed by a semiautomatic process.

Lack of volatility at low temperatures, and the rate of decomposition at room temperature, precluded vapor-pressure measurements. By analogy with the fluorination of B_2Cl_4 to form a more volatile and stable compound (7), attempts were made to replace the chlorine by fluorine, using similar Swarts-type reactions. No evidence for volatile compounds other than phosphorus trichloride, and very small amounts of a very volatile gas, presumably phosphorus trifluoride, was obtained. Further experiments to synthesize the tetrafluoro compound are in progress.

The electrode scale was completely soluble in warm nitric acid without apparent evolution of phosphine. Complete analysis, using standard gravimetric techniques, gave the following results. Sample 1: Hg, 86.4%; Cl, 10.7%; P, 2.6%. Sample 2: Hg, 86.2%; Cl, 10.9%; P, 2.6%. Thus in distinction to Gutmann's experiments with copper electrodes, a simple metal phosphide was not formed. It is of interest to note, that mercury tetratritaphosphide Hg_3P_4 is produced by the action of P_2I_4 on mercury at elevated temperatures (8), and the electrode scale is presumably a mixture of this with other mercury phosphides and chlorides.

The colored involatile deposits on the walls of the tubes were pyrophoric, and were similar to the mixture of red and yellow phosphorus described by Gutmann.

ACKNOWLEDGMENTS

It is a pleasure to acknowledge helpful discussions from Dr. A. G. Foster, and financial assistance from Imperial Chemical Industries Limited.

1. LEUNG, Y. C. and WASER, J. J. Phys. Chem. **60**, 539 (1956).
2. BESSON, A. and FOURNIER, L. Compt. rend. **150**, 102 (1910).
3. GUTMANN, V. Monatsh. Chem. **86**, 98 (1954).
4. GAUTIER, A. Compt. rend. **78**, 286 (1874).
5. URRY, G., WARTIK, T., MOORE, R. E., and SCHLESINGER, H. I. J. Am. Chem. Soc. **76**, 5293 (1954).
6. INTERNATIONAL CRITICAL TABLES, III, 213 (1933).
7. FINCH, A. and SCHLESINGER, H. I. J. Am. Chem. Soc. **80**, 3573 (1958).
8. VAN HAAREN, A. and PARTHEIL, A. Arch. Pharm. **238**, 35 (1900).
9. KOLITOWSKA, J. H. Roczniki Chem. **15**, 29 (1935).

RECEIVED JUNE 12, 1959.
DEPARTMENT OF CHEMISTRY,
ROYAL HOLLOWAY COLLEGE,
UNIVERSITY OF LONDON,
ENGLEFIELD GREEN, ENGLAND.

INFRARED SPECTRUM OF AMMONIUM HYDROPEROXIDE

OSVALD KNOP* AND PAUL A. GIGUÈRE

Ammonia and hydrogen peroxide form a 1:1 compound which is remarkable in that its melting point, 25° C (1), lies some 100° above that of the ammonia–water analogue (2).

**Present address: Department of Chemical Engineering, Nova Scotia Technical College, Halifax, N.S.*

Can. J. Chem. Downloaded from www.nrcresearchpress.com by 176.9.209.113 on 09/04/12
For personal use only.

Solid ammonia hydrates are known from various investigations (3–5) to be of the molecular, or addition type: $NH_3 \cdot H_2O$, etc. On the other hand, the Raman spectra of the ammonia – hydrogen peroxide compound in the molten state as well as in aqueous solutions (6, 7) show no indication whatsoever of the characteristic bands of the NH_4^+ ion, thereby confirming that under such conditions both component molecules essentially preserve their identity. In view of its relatively high melting point it is conceivable that in the solid state the ammonia – hydrogen peroxide compound is ionic, $NH_4^+O_2H^-$, like the alkali metal hydroperoxides. To answer the question we decided to measure its infrared spectrum. In the meantime we came across a short note by Simon and Kriegsman (8) establishing definitely the ionic nature of crystalline ammonium hydroperoxide from the NH_4^+ ion bands at 3041 and 3152 cm^{-1}. The present results lead to the same conclusion and provide further data on the O_2H^- ion.

Preparation of samples suitable for the infrared spectra presented considerable difficulty due to the marked tendency of the solid to decompose and react with atmospheric moisture. The usual methods of (*a*) grinding of the bulk solid to a fine powder, (*b*) mull in Nujol, (*c*) evaporation of a solution in alcohol, and (*d*) pressing in a KBr disk were tried without success. Satisfactory results could be obtained only by the deposition technique (9) using an evacuated glass absorption cell. First, hydrogen peroxide vapor from a liquid sample 99.9% pure was condensed in a thin film on a rock salt plate cooled with liquid nitrogen. Then a suitable amount of ammonia gas was deposited on top of the solid peroxide film. Mixing of the two vapors before condensation turned out to be unsuitable because of the large difference in the volatility of the two components. As long as the temperature remained in the neighborhood of −180° C no reaction took place between the two solids; when the liquid nitrogen was replaced by acetone – dry ice the compound was formed readily, and the excess ammonia was then pumped off. Traces of water, either from leakage of moisture or from decomposition of the peroxide vapor, yielded complex spectra arising presumably from some ternary compounds, identified since by means of thermal analysis (10).

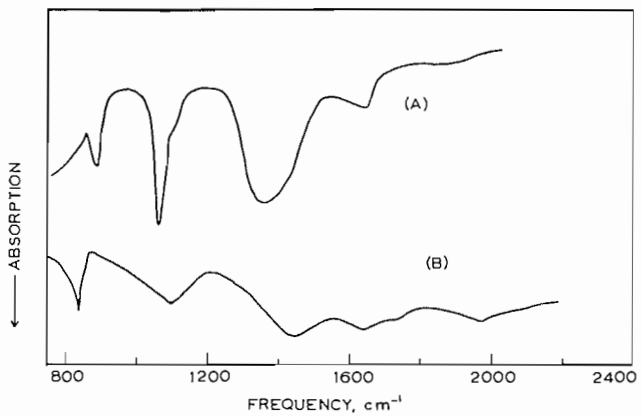

FIG. 1. Infrared spectra of (*a*) unreacted films of anhydrous ammonia and hydrogen peroxide deposited at −180° C, and (*b*) ammonium hydroperoxide.

The infrared spectrum in the rock salt region (Fig. 1) shows the well-known bands of the NH_4^+ ion at 1630 and 1450 cm^{-1} (11), plus a medium-intense band at 1100 cm^{-1} and the sharp O—O stretching band at 836 cm^{-1}. The latter, which coincides exactly with the

Can. J. Chem. Downloaded from www.nrcresearchpress.com by 176.9.209.113 on 09/04/12
For personal use only.

Raman band, represents an appreciable decrease from the corresponding frequency in hydrogen peroxide, 880 cm^{-1} (12). This implies a lowering of some 10% in the force constant and a lengthening of about 0.02 Å of the O—O bond. Undoubtedly the formal negative charge on the O_2H^- ion is responsible for this effect through (*a*) increase in covalent radius of the terminal O atom and (*b*) repulsion between the latter and the bonding electron cloud. Another example of this is the isocyanate ion (13) the fundamental frequencies of which are noticeably lower that those of isocyanic acid (14). Conversely, the formal positive charge on the hydroxylammonium ion increases the NO stretching frequency and shortens the N—O distance, as shown recently by infrared spectroscopy (15).

The 1100 cm^{-1} band reported here for the first time is not found in the spectra of ammonium salts; therefore it must belong to the O_2H^- ion, most likely to the bending mode. The only other possibility is an overtone or combination involving some lattice frequency, but this seems precluded by its relatively high intensity. Although somewhat low for an OH bending mode (ν_6 = 1380 cm^{-1} in crystalline H_2O_2), the present assignment is reasonable since lengthening of the O—O bond must reduce appreciably the OH bending frequency. Lastly the OH stretching band could not be identified positively in infrared because of strong interference from the NH stretching bands of the ammonium ion. In the Raman spectrum (8) a band at 3112 cm^{-1} has been assigned tentatively to the hydrogen-bonded OH in agreement with the above reasoning. As no X-ray data are available on crystalline hydroperoxides one can only surmise that hydrogen bonds of the type O—H . . . O exist between the neighboring perhydroxyl ions.

It seemed desirable to supplement this work by a study of an alkali metal hydroperoxide. To that effect some NaO_2H was prepared by reacting (in a dry box) pure, reagent grade sodium peroxide with absolute ethanol. The dry solid was ground under an inert atmosphere and the finer particles were allowed to settle on a salt window. The spectra showed bands at 718 (w), 814 (s), 873 (s), 1009 (s), 1325 (s), 1361 (w), 1427 (s), 1555 (w), and 1622 (s) cm^{-1}, indicating that, in spite of all precautions, the sample had reacted with atmospheric carbon dioxide and possibly contained traces of a hydroperoxidate, $2NaO_2H \cdot H_2O_2 \cdot 4H_2O$ (12).

In conclusion it appears that the acid strength of hydrogen peroxide, though greater than that of water (pK = 11.65 at 25°), is not sufficient to ionize ammonia in the liquid state. Only when thermal agitation is reduced on cooling do the strong hydrogen bonds O—H . . . N ionize and the resulting field leads to spatial organization of the ions. On the other hand, with a stronger base like tetramethylammonium, hydrogen peroxide ionizes even in solution (6).

The authors are grateful to the National Research Council for financial help.

1. Maass, O. and Hatcher, W. H. J. Am. Chem. Soc. **44**, 2472 (1922).
2. Postma, S. Rec. trav. chim. **39**, 516 (1920).
3. Waldrom, R. L. and Hornig, D. F. J. Am. Chem. Soc. **75**, 6079 (1953).
4. Gutowsky, H. S. and Fujiwara, S. J. Chem. Phys. **22**, 1782 (1954).
5. Siemons, W. J. and Templeton, D. H. Acta Cryst. **7**, 194 (1954).
6. Simon, A. and Marchand, M. Zeit. anorg. Chem. **262**, 191 (1950).
7. Simon, A. and Uhlig, U. Ber. **85**, 977 (1952).
8. Simon, A. and Kriegsman, H. Naturwissenschaften, **42**, 14 (1955).
9. Wagner, E. L. and Hornig, D. F. J. Chem. Phys. **18**, 296 (1950).
10. Chin, D. Unpublished results.
11. Miller, F. A. and Wilkins, C. H. Anal. Chem. **24**, 1253 (1952).
12. Schumb, W. C., Satterfield, C. N., and Wentworth, R. L. Hydrogen peroxide. Reinhold Publishing Corp., New York. 1955.
13. Pal, N. N. and Sen Gupta, P. N. Indian J. Phys. **5**, 13 (1930).

Can. J. Chem. Downloaded from www.nrcresearchpress.com by 176.9.209.113 on 09/04/12
For personal use only.

14. HERZBERG, G. and REID, C. Discussions Faraday Soc. **9**, 92 (1950).
15. FRASCO, D. L. and WAGNER, E. L. J. Chem. Phys. **30**, 1124 (1959).

RECEIVED JUNE 29, 1959.
DEPARTMENT OF CHEMISTRY,
LAVAL UNIVERSITY,
QUÉBEC, QUÉBEC.

Can. J. Chem. Downloaded from www.nrcresearchpress.com by 176.9.209.113 on 09/04/12
For personal use only.

Can. J. Chem. Downloaded from www.nrcresearchpress.com by 176.9.209.113 on 09/04/12
For personal use only.

Canadian Journal of Chemistry

Issued by THE NATIONAL RESEARCH COUNCIL OF CANADA

VOLUME 37 NOVEMBER 1959 NUMBER 11

SYNTHESIS, REACTIONS, AND PROPERTIES OF SOME HIGHLY HINDERED DIPHENYL ETHERS[1, 2]

MARJORIE ALLEN[3] AND R. Y. MOIR

ABSTRACT

In the Hems synthesis of diphenyl ethers, an ortho-carbonyl offered less obstruction when held in a lactone ring than when present as an ester. Side reactions interfered with the Hems synthesis of highly hindered diphenyl ethers, and the highly hindered, highly activated ethers produced in the synthesis were easily cleaved by nucleophilic reagents, often in a few minutes at room temperature. The latter fact added a lively interest to the transformation of the ethers into other derivatives. Three of these were of special interest: (*a*) methyl 2-(6′-amino-4′-carbomethoxy-2′-nitrophenoxy)benzoate (VI*c*) which existed in remarkably stable dimorphic forms, (*b*) the dibenzoxazepine VIII, and (*c*) the quadruply orthosubstituted, asymmetrical 7-(4′-carbomethoxy-6′-laevo-menthoxyacetamino-2′-nitrophenoxy)metameconine (IX). Attempts to isolate diastereoisomeric substances having the diphenyl ether link as an element of asymmetry failed, the classical explanation of the low configurational stability (due to bending and twisting of bonds) being superior to the quantum mechanical explanation of a tunnelling oscillation of oxygen.

This paper describes the synthesis of diphenyl ethers bearing three or four groups ortho to the ethereal linkage, their conversion into asymmetrical derivatives, and our tentative conclusion that the unsymmetrical derivatives cannot be resolved into optical isomers at room temperature. The most interesting part of the paper describes the synthetic methods that must be used in the face of the very great ease of disruption of the ethereal linkage.

Synthesis of Hindered Diphenyl Ethers

Ullmann's reaction (1, 2) is not very useful for the synthesis of hindered diphenyl ethers[4] (3, 4, 5, 6, 7, 8, 9). A more powerful method is the well-known reaction of a phenol, a base, and an activated aryl halide (10, 11, 12). Considerable activation is required in the aryl halide: with low activation, as with *p*-fluoronitrobenzene, the reaction occasionally fails with as few as two ortho substituents (13), but with greater activation successes with three ortho groups are common, and using the great activation of picryl chloride, Dahlgard and Brewster (14) recently succeeded in making two quadruply orthosubstituted diphenyl ethers. In this method, the large number, position, and similarity of the activating groups required are an embarrassment in further synthetic steps. A more promising synthesis discovered by Borrows, Clayton, Hems, and Long (15) has as its essential step the reaction of a phenol with an activated N-phenylpyridinium salt.

One main advantage of the new method is its lower requirements for activation (9, 15). The discoverers of the reaction felt that at least two nitro groups were required, but

[1]*Manuscript received July 6, 1959.*
Contribution from the Department of Chemistry, Queen's University, Kingston, Ontario.
[2]*Most of the material is taken from a thesis written by Mrs. Marjorie Allen at Queen's University in April, 1959, in partial fulfillment of the requirements of the degree of Master of Arts. Some (referred to this footnote) is taken from a paper given by R. Y. Moir at the Symposium in Organic Chemistry of the Chemical Institute of Canada at Montreal, March 9, 1954.*
[3]*Canadian Industries, Limited, Fellow, 1958–59.*
[4]*See footnote 2.*

Can. J. Chem. Downloaded from www.nrcresearchpress.com by 176.9.209.113 on 09/04/12
For personal use only.

McRae, Moir, Ursprung, and Gibbs (9) and at almost the same time Grundon and Perry (16) showed that activation by one nitro and one carbomethoxy group sometimes sufficed. Constantin and L'Écuyer (17) later showed that one nitro and one formyl group were sufficient in several instances. This theoretically small extension of the limits of activation has already been of considerable service to those interested in the synthesis of cularine and the bis-benzylisoquinoline alkaloids (9, 16, 17, 18).

The new synthesis may produce highly hindered diphenyl ethers with fantastic ease from moderately activated reactants. Thus N-(4-carbomethoxy-2,6-dinitrophenyl)-pyridinium chloride (I*a*) with 7-hydroxymetameconine[5] (III) gave the maximally orthosubstituted ether IV*a*, while the slightly activated N-(4-carbomethoxy-2-

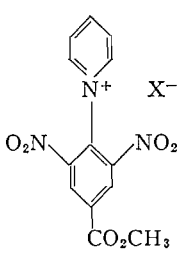

I*a*: $X^- = Cl^-$
I*b*: X^- = Anion of II*a*

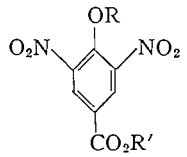

II*a*: R = H; R′ = CH_3
II*b*: R = R′ = H
II*c*: R = R′ = CH_3

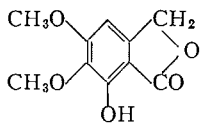

III

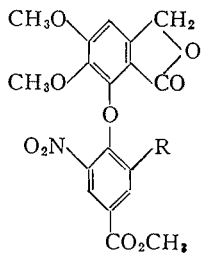

IV*a*: R = NO_2
IV*b*: R = NH_2
IV*c*: R = NHOAc

nitrophenyl)pyridinium tosylate reacted easily with III to give the triply orthosubstituted ether V*a* (9). In this paper it is shown that I*a* reacts with methyl salicylate to give the triply orthosubstituted ether VI*a* with ease. Nevertheless, since 1952 we have accumulated many more failures than successes with the method. For example, methyl salicylate, which smoothly reacts with I*a*, has repeatedly failed to react with the less activated N-(4-carbomethoxy-2-nitrophenyl)pyridinium tosylate, which in turn reacts smoothly with III. These examples must closely illustrate the lower limit of activation for ortho-carbomethoxydiphenyl ethers (compare reference 17).

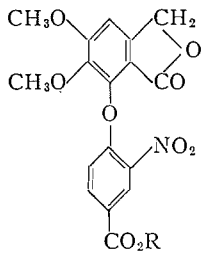

V*a*: R = CH_3
V*b*: R = H

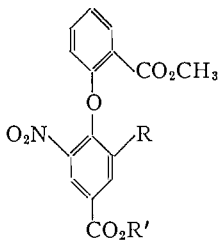

VI*a*: R = NO_2; R′ = CH_3
VI*b*: R = NO_2; R′ = H
VI*c*: R = NH_2; R′ = CH_3
VI*d*: R = NHOAc; R′ = CH_3

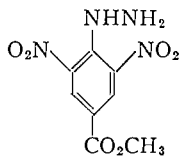

VII

One new side reaction is conveniently described here. In the new preparation of VI*a*, as well as in the repetition of the synthesis of IV*a*, the same quaternary salt, N-(4-carbomethoxy-2,6-dinitrophenyl)pyridinium 4′-carbomethoxy-2′,6′-dinitrophenoxide (I*b*) was

[5]*The numbering scheme for the metameconines is that of Chemical Abstracts. A different scheme was used in our previous papers in this journal.*

isolated in considerable yield. Its proof of structure by synthesis and degradation is described in the experimental part. Quaternary salts have previously been isolated from two sources in the synthesis: (*a*) from a simple double decomposition of the ionic reactants, or (*b*) from a nucleophilic attack of pyridine upon an activated diphenyl ether (the reverse of the synthetic reaction) (19). The salt I*b* must have arisen in still a third way, the simplest explanation being that it arose from the hydrolysis of the very unstable reactant I*a*, probably during the isolation of the products. If this explanation is correct, then water attacks I*a* at the 1-position of the benzene ring, while hydroxide ion attacks it at the 2-position of the pyridine ring (see Experimental section) (20), a conclusion that raises the most interesting questions about the mechanism of the synthesis.

Other side reactions will be reported in a later paper, together with the limitations they set upon the scope of the synthesis.

Reactions of Highly Hindered, Highly Activated Diphenyl Ethers

Nucleophilic scissions of the ethers described in this paper occur with remarkable rapidity; apparently a considerable energy of steric compression aids the well-known effects of activation (11). The experimental methods described below were designed to avoid disruption of the sensitive ethereal linkages while (*a*) introducing asymmetry into the molecules or (*b*) hydrolyzing ester groups to free carboxyl groups with a view to possible resolutions.

The ether V*a* is readily cleaved by alkali (9) but careful control of the conditions of saponification has now been found to give the free acid V*b* in very high yield and purity. With the more highly activated ether VI*a*, good yields on saponification were no longer possible. The best yields of the free acid VI*b* were given by 5 minutes' contact of VI*a* with aqueous potassium hydroxide at room temperature; scission of VI*a* was easily detectable after only 1 minute's contact! The conditions which served to give excellent yields in the saponification of V*a* completely degraded VI*a* to the phenolic acid II*b*.

With more nucleophilic reagents it was not possible to prevent nucleophilic attack upon the ether. Methoxide ion (provided by barium hydroxide in methanol) degraded VI*a* *without* saponification to the ester II*c* in 3 minutes at room temperature. (The reagent was shown to be capable of saponifying II*a* to the barium salt of II*b*.) Hydrazine and Raney nickel gave the phenylhydrazine VII without concurrent reduction of the nitro groups.

Selective reduction of one nitro group was achieved with iron and acetic acid. The ether IV*a* was reduced to IV*b*, and the ether VI*a* to VI*c*. These very fortunate reductions provided the asymmetry needed for possible resolvability. Each of the amino esters was characterized through its acetyl derivative (IV*c* and VI*d*, respectively). The amino ester VI*c* exhibits a dimorphism remarkable in that both forms sometimes crystallize together spontaneously from the same mother liquor. The very reproducible double melting point is shown in Plate I.

When the amino ester VI*c* was heated to 210°, it was converted into its lactam (VIII), which was also produced more directly by the reduction of the dinitro ester VI*a* with stannous chloride in the presence of hydrochloric acid. The interesting ring system of VIII (21) is accompanied by substituents well placed for further synthesis. It might be added that the formation of VIII and of the monoacetyl derivatives IV*c* and VI*d*, the scissions of the ethers, and the methods of synthesis provide unequivocal proofs of the structures suggested in this paper and the previous one (9).

The amino ester IV*b* was converted into its N-laevo-menthoxyacetyl derivative IX, the farthest step in our development of the chemistry of metameconine (8, 9, 22), and the most highly hindered asymmetrical diphenyl ether we have yet been able to produce.

Can. J. Chem. Downloaded from www.nrcresearchpress.com by 176.9.209.113 on 09/04/12
For personal use only.

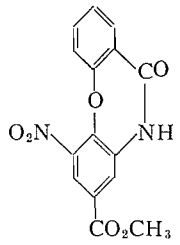

VIII

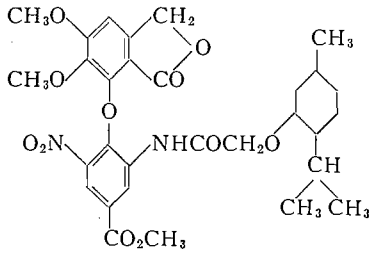

IX

Resolvability of Highly Hindered Diphenyl Ethers

Many years ago it was suggested[6] on the basis of a study of models (9) that suitably hindered diphenyl ethers might be resolvable into optical isomers. During the course of our work, Dahlgard and Brewster (14) reported their failure to resolve an unspecified highly substituted diphenyl ether. They further suggested that such a resolution might be theoretically impossible if there exists a "tunnelling" oscillation of the ethereal oxygen analogous to the oscillation that destroys asymmetry in substituted ammonias. That was not our independent appraisal of the problem, and a study of the models shows that inversion with the allowed rotations converts a diphenyl ether into itself.

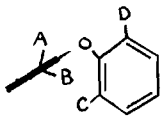

X

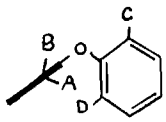

XI

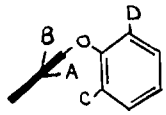

XII

In compound X, A is behind the plane of the paper, and B is in front. Inversion through oxygen converts X into XI, while concerted rotation of the two benzene rings about the oxygen bonds converts XI into X. Neither X nor XI can be made to coincide with XII, the mirror image of X, unless interfering groups are forced past each other.

However, we have failed to separate into diastereoisomers either the brucine salt of V*b*, or the much more highly hindered amide IX. Moreover, neither of these compounds exhibited any mutarotation in solution, so that apparently even the lower order of configurational stability, observed by Adams and his co-workers (23) for slightly hindered diphenyls, is absent. Dahlgard and Brewster (14) showed that increasing orthosubstitution of diphenyl ethers is accompanied by the gradual disappearance of absorption bands near 3000 Å in the ultraviolet spectra. They felt that this was due to the growing lack of coplanarity between the benzene rings with the consequent loss of quininoid resonance, and they concluded that rotational isomers of diphenyl ethers do exist, though they may not be sufficiently stable to be isolated as such. The triply orthosubstituted ether V*a* showed marked absorption near 2900 Å, while the maximally orthosubstituted ethers VI*c* and IX showed only very weak bands near 3550 Å and 3250 Å, respectively. Accepting the interpretation of Dahlgard and Brewster does lead to the reasonable conclusion that

[6]*See footnote 2.*

FIGS. 1–5. Dimorphism of methyl 2-(6′-amino-4′-carbomethoxy-2′-nitrophenoxy)benzoate (VI*c*).
FIG. 1. "Plate" form at room temperature. FIG. 2. "Plate" form melting at 135°, with the "prism" form already beginning to grow in the melt. FIG. 3. Growth of "prism" form, 136–141°. FIG. 4. Complete solidification at 141°. FIG. 5. Melting of "prism" phase at 144–145°. (Photomicrographs by Professor J. R. Allen.)

Can. J. Chem. Downloaded from www.nrcresearchpress.com by 176.9.209.113 on 09/04/12
For personal use only.

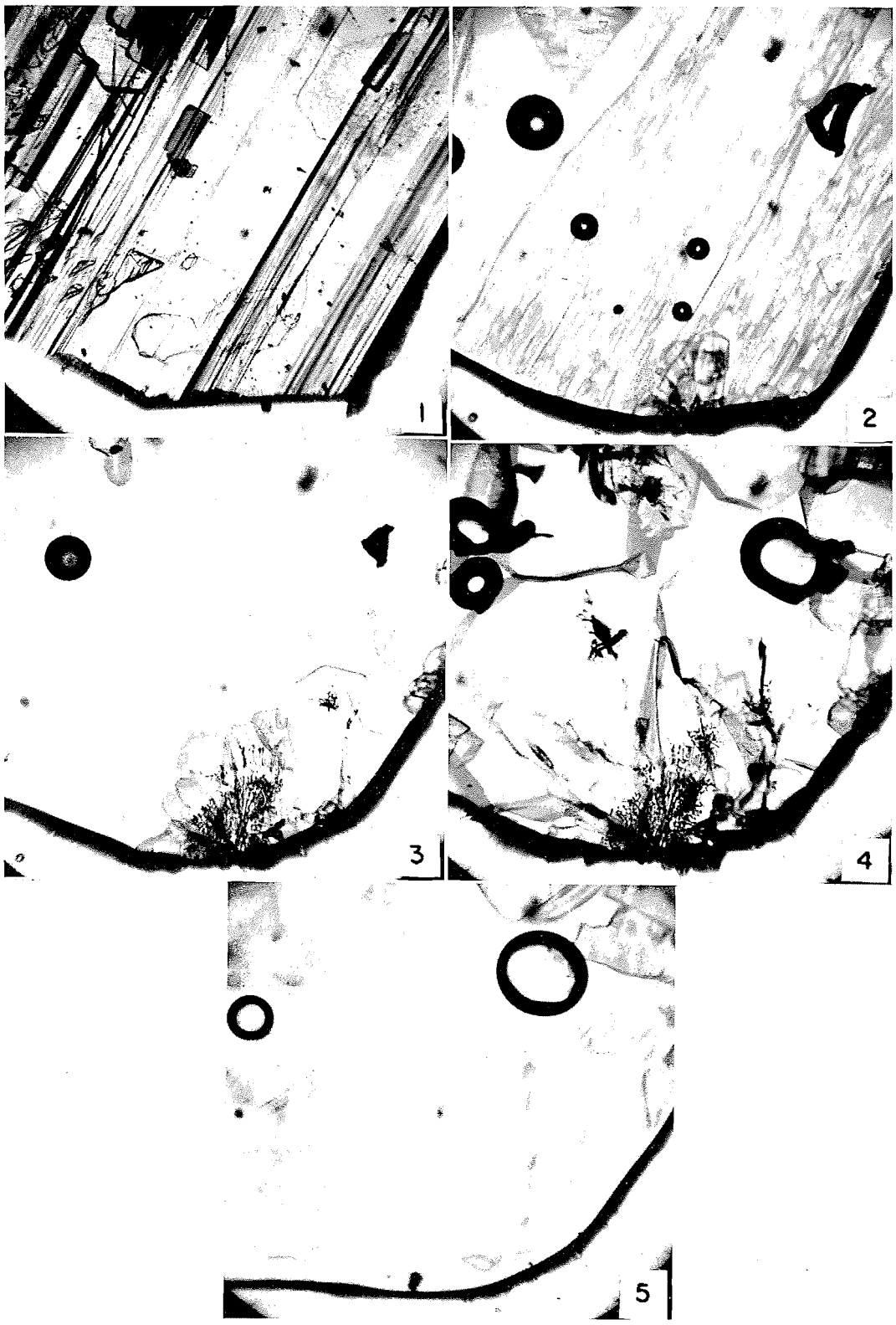

Allen and Moir — Can. J. Chem.

Can. J. Chem. Downloaded from www.nrcresearchpress.com by 176.9.209.113 on 09/04/12
For personal use only.

Can. J. Chem. Downloaded from www.nrcresearchpress.com by 176.9.209.113 on 09/04/12
For personal use only.

there is little steric interference with coplanarity in V*a*, but that there is marked interference in VI*c* and IX.

EXPERIMENTAL

Melting points, unless otherwise stated, were determined in an instrument of high precision (24). Melting points followed by (k) were performed on a Koffler Micro Hot Stage and lowered 3–5° to agree with precision capillary melting points within less than 1° up to 250°. Uncorrected melting points were determined in the Fisher–Johns apparatus; comparison with the precision apparatus at one point near the center of the range used here showed the instrument to read about 3° high. Infrared spectra with one exception were done with potassium bromide disks containing 0.8% to 2% by weight of the sample. Ultraviolet spectra were determined with the Beckman recording spectrophotometer. Pyridine was heated under reflux with barium oxide, distilled from the barium oxide, and stored over fresh barium oxide.

7-(4'-Carbomethoxy-2'-nitrophenoxy)metameconine (V*a*)

A repetition of the previous procedure (9) showed that no by-product of the type described below (see under IV*a*) could be isolated.

7-(4'-Carboxy-2'-nitrophenoxy)metameconine (V*b*)

The methyl ester (V*a*) (5.52 g) was mechanically stirred at 76–81° for 30 minutes with a solution of potassium hydroxide (2.9 g) in water (30 ml) and 95% ethanol (30 ml). The solution was immediately cooled and acidified; the fine needles which slowly deposited were recovered, washed, and dried; yield 88%, m.p. 236.0–237.8°. Two recrystallizations from dilute acetic acid gave the analytical sample of V*b*, m.p. 237.4–238.4°, in agreement with the indirectly characterized material previously obtained (9). Found: C, 54.28; H, 3.52%. Calc. for $C_{17}H_{13}O_9N$: C, 54.40; H, 3.49%.

The *brucine salt* of this acid was subjected to three lengthy fractional crystallizations from acetone and from methanol; the salt fractions all showed similar, wide, melting ranges with unsatisfactory upper limits, and their habits varied. A typical fraction of the salt (3.03 g) had m.p. 174.5–177.5° (uncorr.), and $[\alpha]_D^{21} = -7°$ (in chloroform), with no mutarotation at all in the period of 4 to 71 minutes after formation of the solution. Free acid was liberated from the salt by very cautious acidification in the cold of initial, central, and final fractions, but all the acid fractions had zero rotation. Attempts were also made to induce spontaneous crystallization of one enantiomorph of the free acid, using new apparatus free from scratches, great precautions to destroy random seeds, and seeding from single, well-formed crystals with early interruption of the recrystallization process, but all the attempts gave acids of zero rotation.

7-(4'-Carbomethoxy-2',6'-dinitrophenoxy)metameconine (IV*a*)

A repetition of the previous experiments (9) showed the presence of a by-product. Methyl 4-chloro-3,5-dinitrobenzoate (I*a*) (1.65 g) (15) and dry pyridine (10 ml) were warmed on the steam bath for 5 minutes, the pyridinium salt separating as crystals. 7-Hydroxymetameconine (III) (1.35 g, m.p. 158–159°) (9) was added and the heating continued for 90 minutes. The deep red solution was poured onto ice and the product, which soon solidified, was recovered, dried, and recrystallized from acetone to give a mixture of (*a*) pale yellow prisms, and (*b*) long, deep yellow needles. The products were separated mechanically by swirling away the lighter needles in the acetone mother liquor, a process which greatly simplified the subsequent purifications. After a second recrys-

Can. J. Chem. Downloaded from www.nrcresearchpress.com by 176.9.209.113 on 09/04/12
For personal use only.

tallization from acetone the prisms gave 1.4 g of pure 7-(4′-carbomethoxy-2′,6′-dinitrophenoxy)metameconine (IV*a*), m.p. 210–211° (k). Found: N, 6.55%. Calc. for $C_{18}H_{14}N_2O_{11}$: N, 6.45%. The crystals were stable in air (cf. ref. 9), but they were decomposed by light.

The yellow needles, after another recrystallization from acetone, melted at 240–242° (uncorr.). They are shown below to be N-(4-carbomethoxy-2,6-dinitrophenyl)pyridinium 4′-carbomethoxy-2′,6′-dinitrophenoxide (I*b*).

7-(6′-Amino-4′-carbomethoxy-2′-nitrophenoxy)metameconine (IV*b*)

Iron powder (0.27 g) was heated on the steam bath for 1 hour with a solution of 7-(4′-carbomethoxy-2′,6′-dinitrophenoxy)metameconine (IV*a*) (1.0 g) in glacial acetic acid (60 ml). The mixture was evaporated to dryness and the residue thoroughly extracted with water and then with boiling methanol (100 ml). A yellow powder (0.4 g), m.p. 230–233° (k) was thus obtained; two recrystallizations from acetone gave the analytical sample, m.p. 234–235° (k). Found: C, 53.63; H, 3.99; N, 7.18%. Calc. for $C_{18}H_{16}O_9N_2$: C, 53.47; H, 3.96; N, 6.93%.

7-(6′-Acetamino-4′-carbomethoxy-2′-nitrophenoxy)metameconine (IV*c*)

The above amino compound (IV*b*) (0.1 g) was heated 5 minutes with acetic anhydride (2 ml) and concentrated sulphuric acid (1 drop). The solution was poured into water and boiled to decompose the acetic anhydride. White needles, m.p. 197–199° (k) were deposited from the cooled solution. Two crystallizations from 50% aqueous methanol raised their m.p. to 206–207° (k). Found: C, 54.16, 54.14; H, 4.14, 4.02; N, 6.08, 6.50%. Calc. for $C_{20}H_{18}O_{10}N_2$: C, 53.81; H, 4.04; N, 6.28%.

7-(4′-Carbomethoxy-6′-laevo-menthoxyacetamino-2′-nitrophenoxy)metameconine (IX)

The amino compound IV*b* (0.539 g), laevo-menthoxyacetyl chloride (0.31 g), $[\alpha]_D = -85.75°$ (*c*, 2.13 in chloroform) (25), and chloroform (30 ml) were heated under reflux for 6 hours. The crystals (0.1 g) which separated from the cooled solution had a m.p. of 228–232° (k), undepressed by admixture with authentic IV*b*. Evaporation of the mother liquors and trituration of the oily residue with petroleum ether gave a solid, which was sensitive to light, in a yield of 0.7 g, m.p. 183°. Five successive recrystallizations gave products of the following melting points (k): (from ethanol) 185–190°; (from ethanol) 188–191°; (from methanol) 188–190°; (from benzene – petroleum ether) 188–190°; (from ethanol) 188–189°; thus there was no evidence for the presence of stable diastereoisomers. Stout white needles. Found: C, 60.23; H, 6.08; N, 4.85%. Calc. for $C_{30}H_{36}O_{11}N_2$: C, 60.00; H, 6.00; N, 4.67%.

A solution of the menthoxy-amide (IX) (0.1467 g) in chloroform (solution volume 5 ml) was observed in the polarimeter; nine readings were taken over the period from 5 minutes to 68 hours after the formation of the solution, each reading, as well as the instrument's zero-point, being the mean of 10 observations. The corrected readings varied smoothly from the initial value of −0.85° to the final value of −0.89°; the variation was probably not significant. The initial value gives $[\alpha]_D = -29°$ and a molar rotation of −174°; under approximately the same conditions the molar rotation of purified menthoxyacetic acid was found to be −190°. The lack of mutarotation, and the approximate agreement of the molar rotations, were regarded as significant.

Methyl 2-(4′-Carbomethoxy-2′,6′-dinitrophenoxy)benzoate (VI*a*)

Methyl 4-chloro-3,5-dinitrobenzoate (2.6 g) and dry pyridine (15 ml) were heated

Can. J. Chem. Downloaded from www.nrcresearchpress.com by 176.9.209.113 on 09/04/12
For personal use only.

5 minutes on the steam bath. Methyl salicylate (1.5 ml) was then added and the heating continued for 90 minutes. The dark colored solution deposited a bright yellow gum on being poured onto ice (100 g); when the gum had solidified it was recovered, washed with water, and dried. The crude mixed product was separated into its components in any of three ways.

(*a*) Recrystallization from acetonitrile gave bright yellow needles, m.p. 241–242° (uncorr.) in a yield of 0.4 g, or 11%. Evaporation of the mother liquors followed by recrystallization of the residue from ethanol gave the diphenyl ether VI*a*, m.p. 109.5–110.5°, yield 2.1 g (56%). One more recrystallization from ethanol gave the analytical sample, m.p. 110.6–111.2°. Found: C, 51.12; H, 3.50; N, 7.71%. Calc. for $C_{16}H_{12}O_9N_2$: C, 51.06; H, 3.22; N, 7.45%.

(*b*) Extraction with hot ethanol left the yellow needles undissolved; the ether was recovered by dilution of the ethanol. Further recrystallizations gave the same two products as before.

(*c*) The crude product was washed with dilute hydrochloric acid (which decomposed the yellow needles) and then recrystallized twice from ethanol to give the pure ether, m.p. 110–111°. On a larger scale, 23.3 g (73% of theory) of the twice recrystallized ether VI*a*, m.p. 110–111°, was made in this more convenient way.

The yellow needles are shown below to be N-(4-carbomethoxy-2,6-dinitrophenyl)-pyridinium 4′-carbomethoxy-2′,6′-dinitrophenoxide (I*b*).

Stability of Methyl 2-(4′-Carbomethoxy-2′,6′-dinitrophenoxy)benzoate (VI*a*) *in Pyridine*

The dinitroether VI*a* (0.5 g) and dry pyridine (5 ml) were heated on the steam bath for 30 minutes, poured onto ice, the precipitate recovered and recrystallized from methanol. The product (0.4 g) had m.p. 111°, undepressed by admixture with the original ether. Hence the quaternary salt (I*b*) did not arise from nucleophilic attack upon the diphenyl ether.

Scissions of the Diphenyl Ether Linkage; Preparation of Methyl 2-(4′-Carboxy-2′,6′-dinitrophenoxy)benzoate (VI*b*)

(*a*) *With Hot Potassium Hydroxide*

The dimethyl ester VI*a* (0.3 g) was heated under gentle reflux for 30 minutes with 10% aqueous potassium hydroxide solution. The cooled, acidified solution deposited white crystals, m.p. 254–255° (uncorr.). Analyses were approximately correct for 3,5-dinitro-4-hydroxybenzoic acid (II*b*), and the identification was confirmed by mixture melting point with authentic material (made by saponification of the methyl ester II*a*, and twice recrystallized from ethanol; the melting point of 254–255° (uncorr.) was considerably higher than that (244–246°) observed by Christianson) (26).

(*b*) *With Cold Potassium Hydroxide*

The dimethyl ester VI*a* (3.0 g) was dissolved in hot ethanol and the solution rapidly cooled to give a suspension of very fine crystals. Potassium hydroxide solution (18 ml of 10%) was slowly added and the mixture shaken at room temperature for 5 minutes. Ether (50 ml) was then added, and the mixture acidified, separated, and the aqueous layer extracted with three 50-ml portions of ether. Exhaustive back extraction of the combined ethereal layers with cold sodium bicarbonate solution (each extract being rapidly chilled and acidified after the extraction) followed by re-extraction with ether of the acidified sodium bicarbonate extracts, and evaporation of the final, dried, ethereal extracts, gave a pale yellow oil containing some crystals. Recrystallization of the oily mixture from methanol gave 1.1 g of light-sensitive crystals m.p. 175–185°. Three more

Can. J. Chem. Downloaded from www.nrcresearchpress.com by 176.9.209.113 on 09/04/12
For personal use only.

wasteful recrystallizations from methanol gave the analytical sample of 2-(4′-carboxy-2′,6′-dinitrophenoxy)benzoate, m.p. 214–215° (k). Found: C, 49.81; H, 2.90; N, 7.62%. Calc. for $C_{15}H_{10}O_9N_2$: C, 49.72; H, 2.76; N, 7.74%.

When a similar preparation was acidified after the reaction had proceeded for only 1 minute at room temperature, a strong odor of methyl salicylate could be detected. This observation, together with the isolation of the free dinitro acid (II*b*) in (*a*) part, and the rapid saponification observed in the less activated ether (V*a*) (see above), made it sufficiently clear that it was the less activated ester group which remained in compound VI*b*.

(*c*) *With Acids*

When the dimethyl ester VI*a* was heated under reflux with dilute acetic acid containing a little *p*-toluenesulphonic acid, it was recovered unchanged almost quantitatively. An attempted transesterification with glacial acetic acid and *p*-toluenesulphonic acid gave no detectable methyl acetate in the fractionating column, and again the recovery of unchanged material was almost quantitative. When concentrated sulphuric acid was allowed to react with the ester at room temperature for 14 hours, and the mixture poured into water, recovery of the starting material was lower, and a strong odor of methyl salicylate showed that some rupture of the ethereal linkage had occurred.

(*d*) *With Methoxide Ion*

The dimethyl ester VI*a* (2 g) was dissolved in a methanolic solution of barium hydroxide hydrate (64 ml of a solution containing 18 g of the hydrate per liter) and allowed to react for 3 minutes at room temperature. No precipitate formed. The deep red solution was then acidified, diluted with water, and extracted with ether. The ethereal extracts were dried and evaporated; the yellow oil remaining (1.7 g) had a strong odor of methyl salicylate. Extraction of an ethereal solution of the oil with aqueous sodium bicarbonate, removal of the ether, and recrystallization of the residue from methanol gave white crystals in a yield of 0.6 g, whose m.p. of 54–55° was not depressed by admixture with authentic methyl 3,5-dinitro-4-methoxybenzoate (II*c*) (prepared by the action of diazomethane upon II*a*, and recrystallized from methanol, m.p. 52–53°).

Methyl 3,5-dinitro-4-hydroxybenzoate (II*a*) (1 g) was dissolved in 150 ml of the same solution of barium hydroxide hydrate in methanol, and allowed to stand 3 days at room temperature. The bright orange crystals (1.7 g) of the barium salt were recovered, suspended in water (150 ml), and acidified; the free acid slowly precipitated and on recovery it had a m.p. of 249–250° (uncorr.) undepressed by admixture with authentic II*b*. Thus the scission of the ether had been accomplished by direct nucleophilic attack of methoxide, and not, for example, by hydrolysis followed by methylation of the free phenolic group by the activated methyl ester.

(*e*) *With Hydrazine*

The dimethyl ester VI*a* (1 g) was suspended in absolute alcohol and treated with a solution of hydrazine hydrate (0.4 g) in ethanol (2 ml). A little Raney nickel was added and the mixture heated under reflux for 1 hour, more ethanol being added to keep the product in solution. The hot solution was filtered from the Raney nickel and cooled; the red crystals (0.3 g) which separated were recovered and thrice recrystallized from ethanol to give thick red needles of 4-carbomethoxy-2,6-dinitrophenylhydrazine (VII), m.p. 171° (k). Found: C, 37.58; H, 3.26; N, 22.03%. Calc. for $C_8H_8O_6N_4$: C, 37.51; H, 3.12; N, 21.87%. The phenylhydrazine reacted with benzaldehyde to give a derivative which on purification consisted of orange plates, m.p. 241° (k), not further characterized.

Can. J. Chem. Downloaded from www.nrcresearchpress.com by 176.9.209.113 on 09/04/12
For personal use only.

Can. J. Chem. Downloaded from www.nrcresearchpress.com by 176.9.209.113 on 09/04/12
For personal use only.

Methyl 2-(6'-Amino-4'-carbomethoxy-2'-nitrophenoxy)benzoate (VI*c*)

The dinitro ester VI*a* (1 g) was dissolved in glacial acetic acid (25 ml) and gently warmed to 30° with iron powder (0.45 g). The temperature then rose spontaneously to 55° and was kept at 50–55° for 15 minutes by external cooling. Allowed to cool by itself during 30 minutes more, the mixture was then filtered from a precipitate which was washed with hot glacial acetic acid. The combined filtrates were evaporated to dryness, the residue thoroughly extracted with ether, the ether evaporated, and the residual oil recrystallized from methanol with charcoal to give 0.5 g of yellow crystals, m.p. 134–138°. Five successive recrystallizations from methanol gave crystals of grossly erratic shape and melting point. In a second preparation, the product was recrystallized once from methanol and then five times from benzene, with the same erratic results (which were therefore not due to solvent of crystallization) (see below). The final analytical sample so obtained consisted of needles, m.p. 135° (k). Found: N, 8.16%; and on another sample: C, 55.67, 55.63%; H, 4.08, 3.92%. Calc. for $C_{16}H_{14}O_7N_2$: C, 55.49; H, 4.08; N, 8.09%.

Dimorphism of Methyl 2-(6'-Amino-4'-carbomethoxy-2'-nitrophenoxy)benzoate (VI*c*)

The analytical sample of the amino ester VI*c* (0.2 g, m.p. 139°) was heated at 150° for 45 minutes to give a clear yellow melt without any signs of decomposition. Allowed to cool slowly, the melt produced crystals of m.p. 141–143°; admixture with the starting material gave an intermediate m.p. of 137–139°. Recrystallization of the solidified material from methanol gave a mixture of crystals of two distinct forms: (*a*) pale yellow "prisms" (*b*) slightly darker yellow "plates". The two forms were separated by hand, and careful examination of the prisms (type "*a*") under the microscope showed them to be perfectly free from crystals of type "*b*". Nevertheless, recrystallization of the prisms from methanol gave plates of type "*b*". Careful heating of these plates on the hot stage of the microscope showed melting to begin at 135°; at 137° crystals of the prism type "*a*" appeared in the melt, and at 139° the sample had solidified entirely into the prism form, which then melted at 144–145°. This sequence, remarkable for its reproducibility, has twice been recorded photomicrographically by Professor J. R. Allen, as shown in Plate I.

Infrared spectra of the solid plates and prisms in potassium bromide disks showed differences in the regions of 1300 to 1375 cm^{-1}, and 3280 to 3300 cm^{-1}, but the infrared spectra of chloroform solutions of the two forms were identical.

Methyl 2-(6'-Acetamino-4'-carbomethoxy-2'-nitrophenoxy)benzoate (VI*d*)

The amino ester VI*c* (0.1 g, m.p. 142°), acetic anhydride (1 ml), and concentrated sulphuric acid (1 drop) were heated together to complete solution, then diluted with water (20 ml) and heated to destroy the acetic anhydride. When cool, the solution deposited pale yellow needles which after four recrystallizations from aqueous ethanol gave the colorless analytical sample m.p. 149–150° (k). Found: C, 55.43, 55.29; H, 4.19, 4.29; N, 7.75%; on another sample: N, 7.14, 7.35%. Calc. for $C_{18}H_{16}O_8N_2$: C, 55.68; H, 4.12; N, 7.22%.

8-Carbomethoxy-6-nitro-11-oxo-10,11-dihydro-dibenz[b,f][1,4]oxazepine (Lactam of 2-(6'-Amino-4'-carbomethoxy-2'-nitrophenoxy)benzoic Acid (VIII)

(*a*) The amino ester VI*c* (0.2 g, m.p. 135°) was heated in an oil bath at 210° for 30 minutes. Decomposition was evident, and the cooled melt was a black tar coated with white crystals. Extraction with hot methanol left the white crystals as an insoluble residue, m.p. 315–316° (k).

(*b*) The dinitro ester VI*a* (0.5 g), dissolved in glacial acetic acid (15 ml), was heated for

30 minutes on the steam bath with a solution of stannous chloride dihydrate (1.0 g) in concentrated hydrochloric acid (2 ml). White needles were recovered from the cooled reaction mixture; one recrystallization from glacial acetic acid gave 0.1 g of fluffy needles, m.p. 289–291° (uncorr.), and two more similar recrystallizations gave the analytical sample, m.p. 315–316° (k). Found: C, 57.75; H, 3.59; N, 8.83%. Calc. for $C_{15}H_{10}O_6N_2$: C, 57.32; H, 3.19; N, 8.92%. The melting point was not depressed by admixture with the product from (*a*), and the infrared spectra of the two preparations were identical.

Supposed N-(*4'-Carbomethoxy-2',6'-dinitrophenyl*)*pyridinium Chloride* (I*a*)

Methyl 4-chloro-3,5-dinitrobenzoate (2.6 g) (15) in dry benzene (20 ml) was treated with dry pyridine (1.5 ml). After 1 hour the slightly sticky yellow crystals were recovered, washed with benzene and then with acetone, dissolved in warm ethanol, and reprecipitated with ether to give white prisms (3.0 g, 88%), m.p. 117–120°. Since they decomposed very rapidly indeed they were characterized indirectly as described below.

N-(*4-Carbomethoxy-2,6-dinitrophenyl*)*pyridinium 4'-Carbomethoxy-2',6'-dinitrophenoxide* (I*b*)

(*a*) The pyridinium chloride I*a* (3.4 g) was dissolved in water (10 ml) and shaken with silver oxide (freshly prepared from 3.4 g of silver nitrate). Filtered from the silver compounds, the solution was slowly added to a suspension of methyl 3,5-dinitro-4-hydroxybenzoate (II*a*) (27) (2.5 g) in boiling water (150 ml). The bright yellow precipitate was recovered, washed with water, and then with acetone (100 ml) to remove unchanged phenol. The initial melting point of 236–237° (decomp.) was raised to 242–243° (k) (decomp.) by two recrystallizations from acetone. Found: C, 46.67, 46.52; H, 2.72, 2.77%. Calc. for $C_{21}H_{15}O_{13}N_5$: C, 46.25; H, 2.77; N, 12.84%.

(*b*) The yellow needles, m.p. 240–242° (uncorr.), obtained as a by-product in the preparation of IV*a* as described above were the same substance as that obtained in (*a*) part (mixture melting point, identical infrared spectra). Found: C, 47.90; H, 2.89; N, 12.88%. The presence of the activated N-phenylpyridinium group was shown by the slow solubility of the crystals in cold dilute potassium hydroxide to give a deep red coloration (20)—a test not given by the diphenyl ethers or dinitrohydroxybenzoic acids of this series. When this preparation of the quaternary salt (0.35 g) was heated for 3 hours on the steam bath with dry pyridine (3 ml) and the mixture poured onto ice, the solid recovered and recrystallized from acetone, unchanged quaternary salt was obtained in a yield of 0.2 g, m.p. 240–242° (uncorr.). Thus the salt is resistant to hydrolysis and to transformation into a diphenyl ether (19).

(*c*) The yellow needles, m.p. 241–242°, isolated from the preparation of VI*a* as above were also identical with those from (*a*) and (*b*) (mixture melting point, infrared spectra). Another sample of the yellow needles from the same source was recrystallized four times from acetonitrile and twice from acetone. Found: C, 46.18, 46.18; H, 2.30, 2.25; N, 12.98, 12.85%. Allowed to stand in the cold with dilute potassium hydroxide solution, the crystals slowly gave the deep red color characteristic of activated N-phenylpyridinium compounds.

Further proof of identity and structure is given in the next section.

Decomposition of the Quaternary Salt I*b*

(*a*) A sample of the quaternary salt I*b* (3.0 g, prepared as in "*a*" above) was stirred 5 minutes with dilute hydrochloric acid. The deep yellow color of the phenoxide was slowly replaced by the cream color of the insoluble decomposition product. This precipitate on recovery was shown to be methyl 3,5-dinitro-4-hydroxybenzoate (II*a*) by melting point and mixture melting point—a demonstration of the anion of the quaternary salt.

Can. J. Chem. Downloaded from www.nrcresearchpress.com by 176.9.209.113 on 09/04/12
For personal use only.

The aqueous filtrates after being neutralized with sodium bicarbonate gradually deposited a yellow solid which was recovered next morning, yield 0.88 g. Four recrystallizations from acetone converted it to long pale yellow needles, m.p. 244–245° (uncorr.) (decomp.).

(*b*) A sample of I*b*, recovered from the preparation of IV*a*, and as described in part (*b*) of the previous section, gave the same results. In particular, the precipitate from the neutralized solution had the same infrared spectrum as that described in part (*a*) of this section. Thus the identity of the two specimens of I*b* had been demonstrated.

ACKNOWLEDGMENTS

The research was made possible by a grant from the National Research Council, and by the grant of a Fellowship to one of us (M. A.) by Canadian Industries, Limited. We wish to thank Miss Shelagh Courtenay for determining the infrared spectra reported in the paper.

REFERENCES

1. ULLMANN, F. Ber. **37**, 854 (1904).
2. UNGNADE, H. E. Chem. Rev. **38**, 405 (1946).
3. KING, H. J. Chem. Soc. 1157 (1939).
4. MANSKE, R. H. F. and LEDINGHAM, A. J. Am. Chem. Soc. **72**, 4797 (1950).
5. KULKA, M. and MANSKE, R. H. F. J. Am. Chem. Soc. **75**, 1322 (1953).
6. BRUCKHAUSEN, F. VON, OBEREMT, H., and FELDHAUS, A. Ann. **507**, 144 (1933).
7. FALTIS, F. and ZWERINA, K. Ber. **62**, 1034 (1929).
8. MCRAE, J. A., VAN ORDER, R. B., GRIFFITHS, F. H., and HABGOOD, T. Can J. Chem. **29**, 482 (1951).
9. MCRAE, J. A., MOIR, R. Y., URSPRUNG, J. J., and GIBBS, H. H. J. Org. Chem. **19**, 1500 (1954).
10. BOST, R. W. and NICHOLSON, F. J. Am. Chem. Soc. **57**, 2368 (1935).
11. BUNNETT, J. F. and ZAHLER, R. E. Chem. Revs. **49**, 273 (1951).
12. RARICK, M. J., BREWSTER, R. Q., and DAINS, F. B. J. Am. Chem. Soc. **55**, 1289 (1933).
13. BARNES, J. H., BORROWS, E. T., ELKS, J., HEMS, B. A., and LONG, A. G. J. Chem. Soc. 2824 (1950).
14. DAHLGARD, M. and BREWSTER, R. Q. J. Am. Chem. Soc. **80**, 5861 (1958).
15. BORROWS, E. T., CLAYTON, J. C., HEMS, B. A., and LONG, A. G. J. Chem. Soc. S190 (1949).
16. GRUNDON, H. F. and PERRY, H. J. H. J. Chem. Soc. 3531 (1954).
17. CONSTANTIN, R. and L'ÉCUYER, P. Can. J. Chem. **36**, 1627 (1958).
18. CROWDER, J. R., GRUNDON, M. F., and LEWIS, J. R. J. Chem. Soc. 2142 (1958).
19. BECKWITH, A. L. and MILLER, J. J. Org. Chem. **19**, 1416 (1954).
20. ZINCKE, T. Ann. **330**, 361 (1904).
21. BREWSTER, R. Q. and STRAIN, F. J. Am. Chem. Soc. **56**, 117 (1934).
22. MANSKE, R. H. F., MCRAE, J. A., and MOIR, R. Y. Can. J. Chem. **29**, 526 (1951).
23. YUAN, H. C. and ADAMS, R. J. Am. Chem. Soc. **54**, 4434 (1932).
24. MERRIAM, F. C. Anal. Chem. **20**, 1246 (1948).
25. READ, J. and GRUBB, W. J. J. Soc. Chem. Ind. **51**, 329T (1932).
26. CHRISTIANSON, W. G. J. Am. Chem. Soc. **48**, 465 (1926).
27. CAVILL, G. W. K. J. Soc. Chem. Ind. **64**, 212T (1945).

Can. J. Chem. Downloaded from www.nrcresearchpress.com by 176.9.209.113 on 09/04/12
For personal use only.

Can. J. Chem. Downloaded from www.nrcresearchpress.com by 176.9.209.113 on 09/04/12
For personal use only.

GUANIDINE COMPOUNDS

III. THE PREPARATION OF TRIACETYLGUANIDINE AND ITS TRANSFORMATION WITH ALCOHOL[1, 2]

R. GREENHALGH AND R. A. B. BANNARD

ABSTRACT

Triacetylguanidine has been prepared and shown to undergo stepwise deacetylation in the presence of alcohol to guanidine acetate. Diacetylguanidine has been shown to have a m.p. 176–177° and not 166° as previously reported.

Acetylation of guanidine under mild conditions gave a compound m.p. 110–112°, in 82% yield, which had not previously been reported by Korndorfer (1), Grundmann and Beyer (2), Ryabinin (3), or Cockburn and Bannard (4). The substance could be purified by crystallization from acetone or sublimation *in vacuo*. Its ultraviolet spectrum differed from those of model diacetyl- and monoacetyl-guanidine derivatives. The diacetylguanidines showed two bands in the regions 222–229 mμ and 255–265 mμ, and the monoacetylguanidines only one band at 230–236 mμ (5). Analytical data gave an empirical formula $C_7H_{11}O_3N_3$, which together with acetyl and molecular weight determinations showed the compound to be triacetylguanidine.

The most important property of triacetylguanidine is its instability in the presence of hot alcohol. Treatment with ethanol at 75° for 30 minutes or repeated recrystallization from methanol gave a compound, m.p. 176–177°, which sublimed unchanged *in vacuo*. This compound was shown to be different from monoacetylguanidine acetate (m.p. 178–180°), since admixture with an authentic sample depressed the melting point, also the infrared spectra of the two compounds differed. No free acetic acid was present, as indicated by the fact that no sodium hydroxide was consumed on potentiometric titration. The ultraviolet spectrum indicated a diacetylguanidine and the analytical data agreed with this. Confirmation was obtained by the preparation of a picrate m.p. 162–164°, which analyzed for diacetylguanidine picrate. Previously, Ryabinin (3) had obtained a substance, m.p. 166°, which he designated as diacetylguanidine and which gave a picrate, m.p. 162–164°. Since we could also isolate the compound, m.p. 176–177°, by following Ryabinin's procedure for acetylation of guanidine, we concluded his sample was impure. A possible explanation for the failure of previous workers to isolate the triacetyl derivative could be their use of more vigorous conditions. Treatment of triacetylguanidine with acetic acid led to a number of unstable intermediates, which on drying *in vacuo* gave the diacetyl derivative. The acetic acid formed during acetylation under these vigorous conditions could be expected to yield these intermediates, which on drying as Ryabinin did, would give diacetylguanidine.

When diacetylguanidine was treated with ethanol under conditions similar to those used with triacetylguanidine a compound, m.p. 187–189°, was obtained which was shown to be identical with monoacetylguanidine. Monoacetylguanidine in its turn when treated with ethanol gave guanidine acetate. Thus we were able to deacetylate triacetylguanidine

[1]*Manuscript received June 15, 1959.*
Contribution from Defence Research Chemical Laboratories, Ottawa, Canada.
Issued as D.R.C.L. Report No. 304.
[2]*Part II. Can. J. Chem.* **36**, *1541 (1958).*

to guanidine acetate in a stepwise manner, each step proceeding with a yield greater than 55%. In acidic methanol, deacetylation occurs even more readily, as can be shown by treatment of diacetylguanidine in methanol with 1 equivalent of acetic acid, when monoacetylguanidine acetate is formed almost instantaneously. On substituting N,N-dimethylformamide for methanol as solvent no deacetylation occurs, although monoacetylguanidine is readily converted to the acetate salt in the presence of 1 equivalent of acetic acid.

No attempt was made to study the kinetics of the stepwise deacetylation, but the high yields obtained would suggest that it is not a simple first-order sequential reaction.

EXPERIMENTAL[3]

Triacetylguanidine

Guanidine acetate (500 mg) was heated for 1 hour on the steam bath with acetic anhydride (5 ml). The solution was taken to dryness *in vacuo* yielding a colorless oil which slowly crystallized. Recrystallization from acetone gave 636 mg (82%) of colorless thick needles, m.p. 110–112°. Calc. for $C_7H_{11}O_3N_3$: C, 45.40; H, 5.99; N, 22.69; CH_3CO, 69.7%; mol. wt., 184. Found: C, 45.47; H, 5.86; N, 22.94; CH_3CO, 68.65%; mol. wt., 182. The compound could also be purified by sublimation *in vacuo* (70–80° at 0.005 mm). Ultraviolet spectrum in ethanol, λ_{max} 214 mμ, ϵ_{max} 15,260; λ_{max} 250 mμ, ϵ_{max} 9712: (concn. 0.8 mg/100 ml).

Conversion of Triacetylguanidine to Diacetylguanidine

Triacetylguanidine (503 mg) was dissolved in ethanol (1.0 ml) and heated for 30 minutes at 75°. When the solution was concentrated, colorless prisms separated. They were recrystallized from methanol–ether, yielding 275 mg (71%) of diacetylguanidine, m.p. 176–177°. Calc. for $C_5H_9O_2N_3$: C, 41.95; H, 6.34; N, 29.36; CH_3CO, 60.15%. Found: C, 41.86; H, 6.33; N, 29.51; CH_3CO, 58.7%. On admixture with an authentic sample of monoacetylguanidine acetate, m.p. 178–180°, the melting point was depressed to 164°. Diacetylguanidine sublimed unchanged at 105–110° at 0.005 mm. Ultraviolet spectrum in ethanol λ_{max} 212 mμ, ϵ_{max} 8921; λ_{max} 248 mμ, ϵ_{max} 16,840: (concn. 1.09 mg/100 ml). The picrate was prepared by adding the theoretical amount of picric acid in methanol to diacetylguanidine in methanol, m.p. 162–164°. Calc. for $C_{11}H_{12}O_9N_6$: C, 35.49; H, 3.25; N, 22.58%. Found: C, 35.73; H, 3.19; N, 22.05%.

Conversion of Diacetylguanidine to Monoacetylguanidine

Diacetylguanidine (250 mg) was treated with ethanol as above. The colorless prisms obtained were recrystallized from methanol–ether, m.p. 188–190°, yield, 103 mg (55%). Identified by mixed melting point and infrared spectrum as monoacetylguanidine.

Conversion of Monoacetylguanidine to Guanidine Acetate

Monoacetylguanidine (250 mg) was treated with ethanol as above. Recrystallization of the crude product from methanol–ether gave 187 mg (74%) of colorless prisms, m.p. 227–229°. Identified by infrared spectrum and no depression of melting point on admixture with a sample of guanidine acetate.

ACKNOWLEDGMENTS

The authors wish to thank J. Helie for the analysis and S. Head and A. Grey for ultraviolet and infrared determinations.

[3]*All melting points are corrected.*

Can. J. Chem. Downloaded from www.nrcresearchpress.com by 176.9.209.113 on 09/04/12
For personal use only.

REFERENCES

1. KORNDORFER, G. Arch. Pharm. **241**, 467 (1903).
2. GRUNDMANN, C. and BEYER, E. Ber. **83**, 452 (1950).
3. RYABININ, A. A. J. Gen. Chem. U.S.S.R. **22**, 541 (1952).
4. COCKBURN, W. F. and BANNARD, R. A. B. Can. J. Chem. **35**, 1285 (1957).
5. GREENHALGH, R. and BANNARD, R. A. B. Unpublished work.

Can. J. Chem. Downloaded from www.nrcresearchpress.com by 176.9.209.113 on 09/04/12
For personal use only.

Can. J. Chem. Downloaded from www.nrcresearchpress.com by 176.9.209.113 on 09/04/12
For personal use only.

AN ELECTRON DIFFRACTION STUDY OF ELECTROPOLISHED IRON[1]

P. B. SEWELL,[2] C. D. STOCKBRIDGE,[2] AND M. COHEN

ABSTRACT

Iron has been electropolished over a range of voltage and current in the acetic acid–perchloric acid bath. Under optimum conditions an "atomically smooth" surface has been obtained as evidenced by marked refraction effects in the electron diffraction patterns. There is also evidence for a thin film on the electropolished surface which thickens on further exposure to air to form a preferentially oriented cubic iron oxide. Light etching in nitric acid removed the film and formed a surface which, on diffraction, gave the more normal spot pattern of iron.

INTRODUCTION

The behavior of metals in corrosion and oxidation studies is very dependent on the original method of surface preparation. Mechanical polishing leads to plastic deformation of the structure which may penetrate quite deeply into the metal. Some impurities and original oxide film may be introduced into the metal by the polishing agent. Subsequent etching to remove the deformed layer can lead to surfaces with high and variable surface roughness factors. Hydrogen reduction may introduce hydrogen into the metal and roughen the surface. For these reasons there has been a great deal of interest in the use of electropolishing as a method of surface preparation.

Satisfactory electropolishing gives rise to an undulating surface which may best be described as "atomically smooth" (1). During reflection electron diffraction examination, the incident electron beam enters such a surface at varying angles of grazing incidence. Each resulting diffraction image is thus built up of a series of diffracted beams suffering slightly different refraction displacements towards the shadow edge. The over-all effect is the elongated spot pattern commonly found with electropolished surfaces (2).

Pashley (1) indicates that on a flat substrate uniform films of the order of 2 Å thick (monolayers) may be detected by electron diffraction under favorable conditions. Available information suggests that a layer of material 25–50 Å thick completely obscures the low angle diffraction maxima of a flat substrate (3, 4, 5). It follows that marked refraction streaking of the substrate pattern and low background scatter strongly suggest freedom from such extensive contamination.

There have been a number of attempts to produce "clean" and smooth iron surfaces by electropolishing. Recently Ladage (6) has reported the satisfactory electropolishing of iron in an ortho-phosphoric–chromic acid bath. Boswell (7) has electropolished iron in a chromic–acetic acid bath. Both these baths may contaminate the surface with chromium or phosphorus compounds.

Electropolishing polycrystalline iron in the perchloric–acetic anhydride bath (8), Cohen (9) obtained surface films which obscured the substrate. Iron surfaces polished in a bath of different composition (10) were also contaminated by a film estimated to be about 100 Å thick by electron microscopy. Wilman *et al.* (11, 12, 13) have polished iron single crystals in the perchloric–acetic anhydride bath (8) and claim to have produced clean "atomically smooth" surfaces. The somewhat restricted spot elongation that is

[1]*Manuscript received June 24, 1959.*
Contribution from the Division of Applied Chemistry, National Research Council, Ottawa, Canada.
Issued as N.R.C. No. 5349.
[2]*N.R.C. Postdoctorate Research Fellow. Present address: Bell Telephone Laboratories, Whippany, N.J., U.S.A.*

apparent in their published patterns and the absence of diffuse spots from an air-formed film suggest that much of their surface was etched.

The present paper describes a procedure for preparing an iron surface by electropolishing which, as evidenced by electron diffraction, is a closer approximation to a clean "atomically smooth" condition than has heretofore been achieved.

EXPERIMENTAL

A Ferrovac iron (Al 0.0005%, C 0.007%, Cr 0.002%, Mn 0.0002%, Ni 0.0009%, Si 0.002%, S 0.0015%) sheet, 10 mil in thickness, cut into 1.5×5.0-cm coupons with a 2.5-cm × 2-mm tail was used. As received, this iron contained excessive oxide inclusions, which rendered optical judgment of electropolishing impossible. To remove this oxide, several Ferrovac coupons, mechanically polished down to 4/0's were reduced for 99 hours in wet hydrogen followed by a further 84 hours in dry hydrogen continuously above 1100° C.

Metallographic examination of this iron showed that the oxide inclusions had been largely removed. The slow cooling after the high-temperature treatment led to sufficient grain growth in the polycrystalline sheet to allow diffraction patterns to be obtained from single grains.

The internally clean iron polycrystals were electropolished in a 20/1 glacial acetic acid/70% perchloric acid solution under an optimum bath potential of 105±5 volts d-c. (ripple $\not>$ 300 millivolts). This bath was chosen since the iron surfaces were required for corrosion studies in the absence of avoidable contaminants. Thus complete removal of a perchlorate/acetate anolyte is more likely than a chromium, phosphate, or sulphate anolyte. The "areal average" current density was 0.4–0.5 Å/cm² under proper conditions of stirring in the bath geometry illustrated in Fig. 1. With an initial bath temperature of 17±2° C each coupon was polished for a total period of 3 minutes in 10-second bursts.

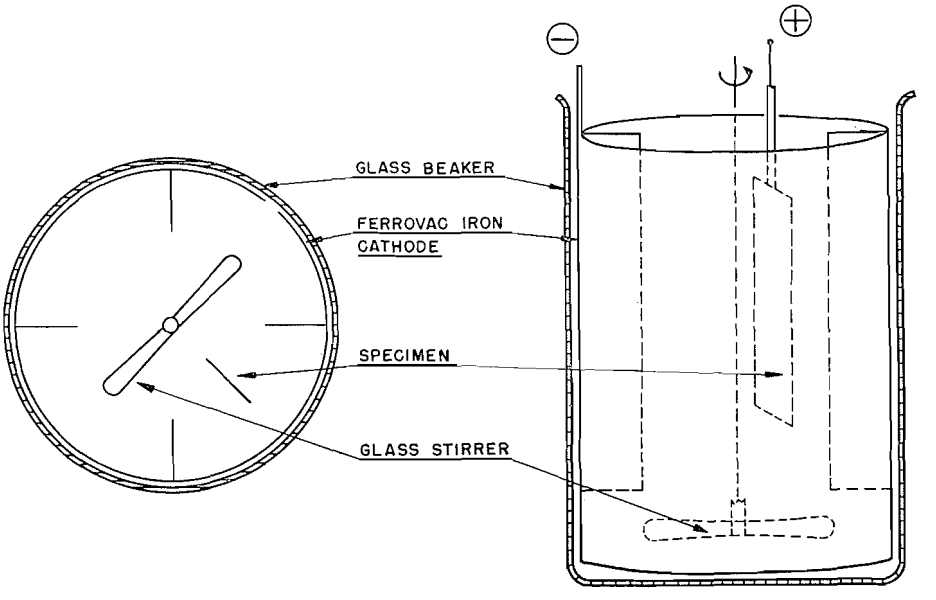

FIG. 1. Schematic diagram of electropolishing cell.

Each 10-second treatment resulted in the removal of iron to a depth of 1.2 μ. While waiting for the bath to cool, we washed the coupon in a jet of anhydrous redistilled

Can. J. Chem. Downloaded from www.nrcresearchpress.com by 176.9.209.113 on 09/04/12
For personal use only.

methyl alcohol and held it inverted. On removal from the final 10- to 15-second electropolish (which was also found to be a sufficient period to eradicate the effects of the subsequent etching employed), the coupon was withdrawn from the bath under potential and washed generously (200 ml) and immediately in a jet of anhydrous methyl alcohol.

At 1000-diameter magnification such coupon surfaces were optically featureless save for sharp steps at the few grain boundaries. These steps, initially present on the iron after reduction, were not removed by prolonged electropolishing.

A number of polishing variables were investigated. The best results were obtained by polishing in fresh solutions. Such coupon surfaces gave the most marked refraction elongation in diffraction patterns and the best optical polish. Coupons polished in solutions which had been used repeatedly gave some degree of refraction elongation until the solution took on a brown coloration. The presence of ferric ion was suspected of having deleterious effects.

Optimum stirring conditions were determined by trial and error. Inadequate agitation of the bath by stirring gave rise to local etching even at optimum polishing conditions, while excessive agitation disrupted the anolyte layer causing irregular polishing.

A cell voltage of less than 100, for example, 80 volts, produced plateaux with flower-like peripheries on an otherwise well-polished surface. Electron diffraction showed relatively weak iron spots with a high background, which indicated a contaminated surface. At cell voltages of greater than 110, for example, 120 volts, a smooth clean surface with microetching just visible at 1000 diameters was obtained and little evidence of refraction elongation of the diffraction spots was observed.

The removal of the coupon with or without disconnecting the applied potential appeared to make no difference provided the anolyte was displaced quickly. Allowing the anolyte to disperse in the polishing solution caused the surface to pick up excess contamination, as evidenced by a higher ratio of background scatter to spot intensity. In contrast, leaving the anolyte on the iron surface after removal from the bath caused sufficient etching within 60 seconds to obliterate refraction elongation of the diffraction spots.

After final rinsing in alcohol the coupons were transferred under methyl alcohol to the specimen chamber of the electron diffraction camera. In subsequent etching experiments the coupon was agitated under 0.05% nitric acid in conductivity grade water, washed generously with an alcohol jet, and returned to the camera while still moist.

All electron diffraction photographs were taken using a camera length of 50 cm and an accelerating voltage of 50 kilovolts.

RESULTS

The results shown are typical of those obtained from large crystals which developed in the coupons during annealing. The crystal chosen for study had a (521) plane almost parallel to the macroscopic surface, and the diffraction pattern observed with the electron beam parallel to the [$\bar{1}$13] zone axis is indexed in Fig. 2. The specimen was bent slightly to allow the electron beam to be incident on the surface of this particular crystal. The resulting lattice distortion prevented the formation of sharp Kikuchi lines. Many orders of reflection were observed at the one setting of angle of incidence.

On electropolishing this specimen under optimum polishing conditions, Fig. 3 was obtained. Figure 3 shows marked refraction elongation of all spots towards the shadow edge, characteristic of an "atomically smooth" surface. A diffuse spot not belonging to the iron pattern is visible below the (220) iron reflection in Fig. 3. This is attributed to an overgrowth film which also contributed to the background scatter. After a 15-second etch

Can. J. Chem. Downloaded from www.nrcresearchpress.com by 176.9.209.113 on 09/04/12
For personal use only.

in 0.05% nitric acid, the diffuse background was reduced and the iron pattern increased in intensity (Fig. 4). A diffuse spot still appearing below the (220) iron reflection indicates that some oriented overgrowth was again present on the surface. Little change in the spot elongation suggests that most of the substrate metal was unaffected. (Double spots appearing in Figs. 4, 5, and 6 occurred as a result of the unintentional location of a second crystal of similar orientation in the incident beam.) Figures 5 to 8 illustrate the effect of further etching. Refraction elongation of the iron reflections was gradually reduced and the intensity of the spot from the overgrowth diminished. The diffraction spots in Fig. 8 are characteristic of an etched surface where diffraction is a result of transmission through etch structures.

Exposure of an electropolished surface to the atmosphere at 20° C for 17 hours resulted in Fig. 9. The intensity of the overgrowth spot below the (220) iron reflection has greatly increased and numerous other diffuse reflections are visible.

DISCUSSION

(*1*) *Diffraction Pattern from Substrate*

The details of refraction phenomena in electron diffraction have been discussed by a number of authors (14, 15). Relationships between the angle of incidence of the electron beam (ϕ), the Bragg angle of reflection within the crystal (θ), and the inner potential of the specimen (Φ) are developed in the above literature. A discussion of refraction effects on electropolished surfaces has recently been published (16). The gradual change of refraction elongation of the iron reflections may be discussed with reference to the idealized models in Fig. 10.

On an atomically flat surface (Fig. 10(*a*)), the electron beam suffers refraction as it enters and leaves the crystal through the same surface plane SS' by the path $ABCDE$. It may be shown to suffer an angular displacement of $2(\theta-\phi)$ from the direction of the electron beam in the absence of refraction $FBCDG$. For metal crystals, the inner potential giving rise to this refraction effect is generally of the order of 10 to 15 volts positive. The resulting angular displacement of the electron beam may be about 0.017 radian for low orders of reflection and grazing angles of incidence. If the distance between the specimen and the photographic plate in the diffraction apparatus is 50 cm, the displacement is recorded as an 8.5-mm shift of the diffraction spot towards the shadow edge of the photograph. Some symmetrical spot broadening may be expected due to lack of penetration of the beam normal to the surface of the specimen, resulting in diffraction spots of the type illustrated in Fig. 10(*a*). Such discrete spot displacements are observed on cleavage faces of many crystals and are clearly demonstrated by cleaved rock-salt surfaces (17).

Should isolated etch pits develop on an atomically flat surface, the path of the electron beam may be that of $ABCDE$ shown in Fig. 10(*b*). When the facet $S'S''$ makes an angle β greater than about 10° with the surface plane SS', the deviation of the beam CDE passing across the surface $S'S''$ is negligible. Under such conditions the angular displacement of the beam from the direction in the absence of refraction ($FBCDE$) is $(\theta-\phi)$. If the angle β has values between 0 and 10° the beam suffers refraction displacements varying between $2(\theta-\phi)$ and $(\theta-\phi)$.

A more markedly etched surface may be composed entirely of structures of the type Fig. 10(*c*). The electron beam will suffer no apparent change in direction on passing across the facets SS' or $S''S'''$ providing the angles β and β' are greater than about 10°. If the facets $S'S''$, parallel to the surface, are not developed, all refraction effects should

Can. J. Chem. Downloaded from www.nrcresearchpress.com by 176.9.209.113 on 09/04/12
For personal use only.

Can. J. Chem. Downloaded from www.nrcresearchpress.com by 176.9.209.113 on 09/04/12
For personal use only.

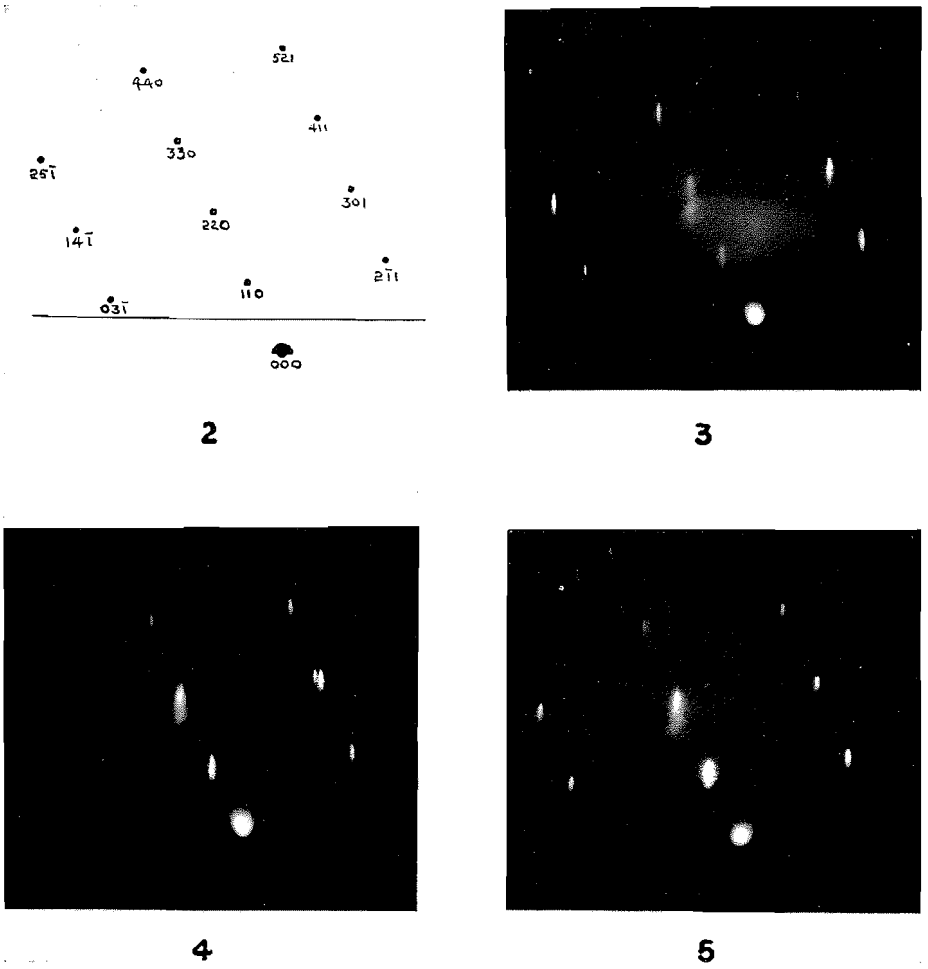

FIG. 2. Indexed diffraction pattern from iron surface almost parallel to (521) plane. Electron beam parallel to [113] zone axis.
FIG. 3. Electron diffraction pattern of freshly electropolished surface.
FIG. 4. As Fig. 3 plus 15-second etch in 0.05% nitric acid.
FIG. 5. As Fig. 4 plus 15-second etch in 0.05% nitric acid.

Can. J. Chem. Downloaded from www.nrcresearchpress.com by 176.9.209.113 on 09/04/12
For personal use only.

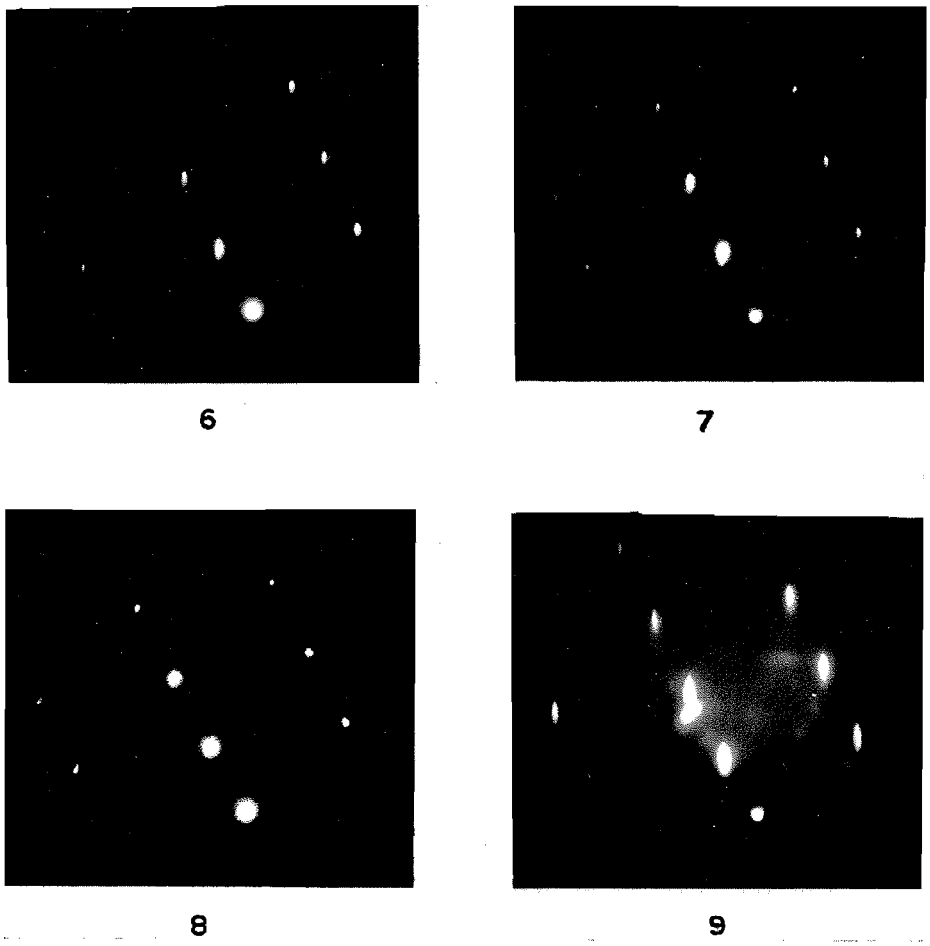

FIG. 6. As Fig. 5 plus 15-second etch in 0.05% nitric acid.
FIG. 7. As Fig. 6 plus 15-second etch in 0.05% nitric acid.
FIG. 8. As Fig. 7 plus 30-second etch (total 90-second etch).
FIG. 9. Diffraction pattern of electropolished specimen after exposure to dry air at room temperature for 17 hours.

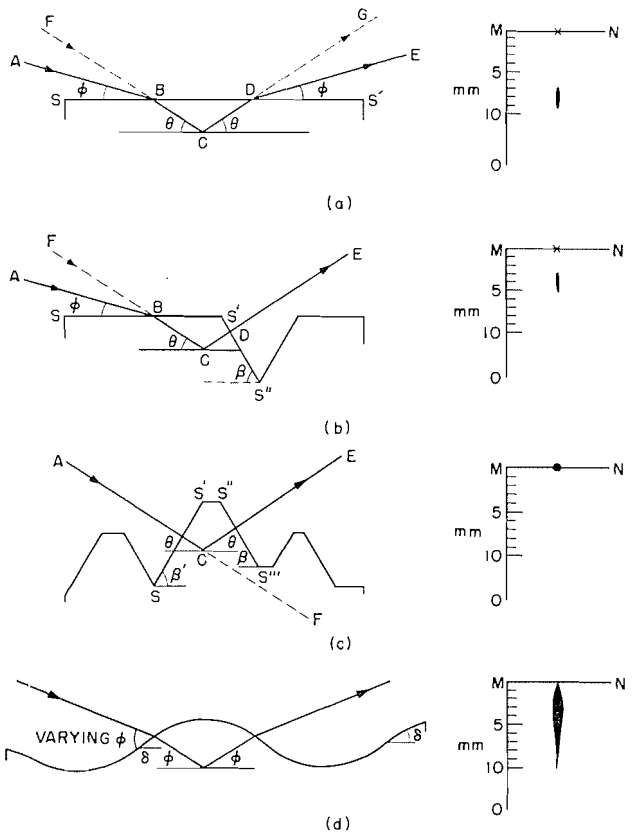

FIG. 10. Idealized models of specimen surfaces showing path of electron beam. Corresponding spot shape is illustrated. Reference line MN shows spot position in absence of refraction. Direction MO represents refraction displacement towards the shadow edge.
(*a*) Atomically flat surface; (*b*) very lightly etched flat surface; (*c*) heavily etched surface; (*d*) slightly rolling surface characteristic of electropolishing.

be absent. Small circular diffraction spots should appear in the positions calculated from the normal Bragg relationship ($n\lambda = 2d \sin \theta$). The beam suffers a deviation of 2θ from the initial direction ACF (Fig. 10(*c*)).

The current concept of an electropolished or "atomically smooth" surface is illustrated in Fig. 10(*d*). The rolling nature of this surface gives rise to a range of angles of incidence (ϕ), which when considered in conjunction with a mosaic structure in the crystal, results in elongated diffraction spots of the type illustrated. The displacement of the region of maximum intensity in the spot from the normal Bragg position has been shown to be a function of the mean angle of slope (δ) of the rolling surface, the inner potential of the crystal, and the electron-accelerating voltage (16).

This explanation of refraction elongation of spots from electropolished surfaces is found to be at fault when considered in detail. The concept of a smooth rolling structure on a surface parallel to a major crystallographic plane becomes questionable when the mean angle of slope (δ) is of the order of 0 to 10°. These problems will be discussed more fully in a note to be published elsewhere.

For the present, an "atomically smooth" surface (Fig. 10(*d*)) would account for the shape of the diffraction spots observed from the electropolished surface of an iron single

Can. J. Chem. Downloaded from www.nrcresearchpress.com by 176.9.209.113 on 09/04/12
For personal use only.

crystal (Figs. 3 and 4). With etching, pits developing in the metal enable effects of the type Fig. 10(*b*) to contribute more strongly to the spot intensity. The observed spot elongation due to refraction is thus reduced (Figs. 5, 6, 7). Further etching covers the surface with structures of the type Fig. 10(*c*). If a suitable etchant is chosen so that no facets parallel to the surface are developed, no evidence of spot elongation should be apparent (Fig. 8).

At present it is not possible to determine from the shape of the diffraction spots the relative areas of the specimen surface giving rise to the separate effects Figs. 10(*a*), (*b*), (*c*), and (*d*). The change in spot elongation observed during etching serves only as an indication that intermediate states exist between that of an electropolished (Fig. 10(*d*)) and the completely etched state (Fig. 10(*c*)). It is hoped that the correlation of electron micrographs and electron diffraction photographs from such surfaces will enable a more accurate assessment of the surface microstructure.

(*2*) *Overgrowth*

The overgrowth material giving rise to the diffuse spot below the (220) iron reflection in Fig. 3 is probably an oxide film formed during electropolishing. The identification of this material is being attempted using similar results obtained from iron surfaces parallel to other crystal planes. On exposure of an electropolished surface to air for 17 hours at 20° C, the overgrowth thickens, resulting in Fig. 9. The diffuse spots due to the overgrowth in this pattern are in good agreement with either of the cubic oxides Fe_3O_4 or γ-Fe_2O_3, confirming the results of Nelson (18) and Haase (19). The (111) plane of the oxide is parallel to the (110) of the metal, and the $[11\bar{2}]$ azimuth of the oxide is parallel to the $[\bar{1}13]$ azimuth in the metal. This corresponds to an orientation of the close-packed oxygen planes in the oxide on the closest-packed (110) planes in the b.c.c. iron. A more complete investigation of this epitaxial relationship is in progress. Figure 9 illustrates the suitability of the electropolished surface for the investigation of thin oxide films. Cathodic reduction of such an air-formed film of oxide on iron shows it to be of the order of 10 to 20 Å thick.

After etching of the electropolished surface, a diffuse spot is still visible below the (220) iron reflection (Figs. 4 to 8). This spot is due to an overgrowth material developed during rinsing and air exposure as the specimen was loaded into the diffraction apparatus and the instrument evacuated. The film should develop to the same thickness on each exposure after etching. The observed decrease in intensity of the spot due to this material in Figs. 4 to 8 resulted from the decreased ratio of film to substrate which was traversed by the electron beam on the etched surface.

(*3*) *Electropolishing*

Electropolishing is generally considered to take place by the anodic dissolution of metal through a thin film of conversion product. During the process both metal and film dissolve. The composition of the film probably depends on both the current density and potential and is probably different from the film formed on air exposure. At voltages and current densities below the optimum there appears to be a thick polishing film which is uneven in thickness or conductivity and leads to both uneven polishing and high scattering of the electron beam. At higher than the optimum voltage and current density the polishing film is too thin to prevent etching of the metal by the highly acid polishing solution. Due to different activities of the different crystal planes some very light etching was occasionally observed on some grains even under good polishing conditions. This etching takes place first on grains with a (110) plane parallel to the specimen surface.

Can. J. Chem. Downloaded from www.nrcresearchpress.com by 176.9.209.113 on 09/04/12
For personal use only.

The strong refraction effect on the smooth electropolished surface results in broad banding in the electron diffraction patterns of randomly oriented polycrystalline specimens. It would appear that the assessment of electropolished surfaces by the use of electron diffraction should be made using large-grained polycrystals or single crystals.

CONCLUSION

Iron can be electropolished in the acetic–perchloric bath to give an "atomically smooth" surface with a very small amount of overgrowth. The film formed during electropolishing can be removed by treatment in dilute nitric acid. This treatment also etches the metal, thus changing the character of the diffraction pattern. On exposure to air, the film present after electropolishing thickens to form a cubic iron oxide with preferred orientation. On the basis of the electron diffraction evidence, the electropolishing and etching procedure developed above should serve as a proper method of specimen preparation for corrosion and oxidation studies.

REFERENCES

1. PASHLEY, D. W. Advances in Phys. **5**, 173 (1956).
2. KRANERT, W., LEISE, K. H., and RAETHER, H. Z. Physik, **122**, 248 (1944).
3. FINCH, G. I. J. Chem. Soc. 1137 (1938).
4. RAETHER, H. J. phys. radium, **11**, 11 (1950).
5. LUCAS, L. N. D. Proc. Phys. Soc. (London), A, **64**, 943 (1951).
6. LADAGE, A. Z. Physik, **144**, 354 (1956).
7. BOSWELL, F. W. Proc. Am. Soc. Testing Materials, **56**, 426 (1956).
8. JACQUET, P. A. and ROCQUET, P. Compt. rend. **208**, 1012 (1939).
9. COHEN, M. J. Phys. Chem. **56**, 451 (1952).
10. CAULE, E. J. and COHEN, M. Can. J. Chem. **31**, 237 (1953).
11. EVANS, D. M., LAYTON, D. N., and WILMAN, H. Proc. Roy. Soc. (London), A, **205**, 205 (1951).
12. AGAWALA, R. P. and WILMAN, H. Proc. Roy. Soc. (London), A, **223**, 167 (1954).
13. AGAWALA, R. P. and WILMAN, H. J. Iron Steel Inst. (London), **179**, 124 (1955).
14. THOMSON, G. P. and COCHRANE, W. Theory and practice of electron diffraction. Macmillan & Co., Ltd., London. 1933.
15. PINSKER, Z. G. Electron diffraction. Butterworth Scientific Publications, London. 1953.
16. YOSHIDA, S. J. Phys. Soc. Japan, **11**, 129 (1956).
17. YAMAGUTI, T. Proc. Phys.-Math. Soc. Japan, **14**, 433 (1941).
18. NELSON, H. R. J. Chem. Phys. **5**, 252 (1937).
19. HAASE, O. Z. Naturforsch, **11a**, 46 (1956).

Can. J. Chem. Downloaded from www.nrcresearchpress.com by 176.9.209.113 on 09/04/12
For personal use only.

Can. J. Chem. Downloaded from www.nrcresearchpress.com by 176.9.209.113 on 09/04/12
For personal use only.

OXIDATION OF D-GALACTURONIC ACID WITH SOME DELIGNIFYING AND BLEACHING AGENTS[1]

R. H. ZIENIUS[2] AND C. B. PURVES

ABSTRACT

D-Galacturonic acid was oxidized with decreasing ease, and in the approximate order shown, by excess of the following agents: sodium chlorite near pH 2.8 and 75°; sodium hypochlorite at pH 10–11 and 25°; chlorine dioxide, pH 1.3 or 5 at 75°; chlorine near 0° and pH 5 (slight); and hydrogen peroxide at pH 10–11 and 25° (negligible). Some uronic acid was always recovered unchanged, even from conditions that would have oxidized glucose quantitatively to gluconic acid. The only other products were mucic acid, together with DL-tartaric acid and tartronic acid presumably derived therefrom. Chlorine dioxide, however, never produced tartronic acid. Methyl-α-D-galacturonoside methyl ester yielded some galacturonic acid when exposed to alkaline hypochlorite or peroxide, and this cleavage of the glycosidic group was tentatively attributed to the oxidants rather than to the alkalinity of the systems.

Anhydrous bromine degraded the silver salt of methyl-α-D-galacturonoside in poor yield to a syrup which was probably L-arabotrihydroxyglutaric dialdehyde.

INTRODUCTION

In connection with a study of the action on pectic acid of agents used for delignifying wood and for bleaching cellulose, it seemed desirable to conduct some preliminary experiments with D-galacturonic acid and its methyl-α-glycoside methyl ester. The presence of the carboxyl group in the sixth position of these substances would be expected to make the fifth position more readily oxidizable than the corresponding position in non-acidic carbohydrates. As Link and his collaborators pointed out (1), oxidation of uronic acids with periodic acid yielded a dialdehyde in which the fifth position lay between an aldehyde and the carboxyl group. Such enhancement of the effect produced by the carboxyl group alone probably explained why the fifth position was then oxidizable even by an agent as mild as periodic acid. This assumption received solid support from later work on the overoxidation of uronides (2, 3), and the oxidation of the methylene group in malonic acid (4) by periodate; also from the oxidation of acetylacetone by lead tetraacetate (5). D-Galacturonic acid was, of course, oxidized by many agents to mucic acid, and could also be degraded in high yield to L-araboglutaric acid even by oxygen in aqueous barium hydroxide (6).

In the present experiments, a solution of pure galacturonic acid in a 10-fold molar amount of aqueous sodium chlorite buffered near pH 2.8 was kept at 70–75° for 150 minutes. These conditions resembled those used for delignifying wood meals by Wise's method (7). After excess oxidant and all cations were removed by appropriate methods described below, the solution was concentrated and the mucic acid that separated was removed. The concentrate was then resolved into its components by passage through a column of anion-exchange resin followed by paper partition chromatography. Galacturonic acid, DL-tartaric acid, and tartronic acid were recovered in pure crystalline form, the identities of the last two being confirmed by preparing the crystalline di-*p*-nitrobenzyl ester, and the crystalline dimethyl ester, respectively. The recovery of unchanged galacturonic acid was unexpected, because the conditions of the oxidation would have oxidized the aldehyde group in glucose (8) or in veratraldehyde (9) swiftly and almost quantitatively to carboxylic acid.

[1]*Manuscript received July 13, 1959.*
Contribution from the Division of Industrial and Cellulose Chemistry, McGill University, and the Wood Chemistry Division, Pulp and Paper Research Institute of Canada, Montreal, Quebec. Abstracted from the Ph.D. thesis submitted by R.H.Z. to the University in April, 1959.
[2]*Present address: Canadian Industries Limited, McMasterville, Quebec.*

Can. J. Chem. Downloaded from www.nrcresearchpress.com by 176.9.209.113 on 09/04/12
For personal use only.

A similar oxidation employed a 10-fold molar amount of aqueous chlorine dioxide, buffered near pH 2.7 and kept at 70–75° for 150 minutes. Some unchanged galacturonic acid was recovered, as might have been expected from the resistance of glucose to oxidation with chlorine dioxide at 20° (8); also some mucic acid and DL-tartaric acid, but tartronic acid was absent. The pure, crystalline methyl ester of methyl-α-D-galacturonoside, when oxidized for 2 hours at 25° with a 3-fold molar amount of sodium hypochlorite at pH 11.5, yielded DL-tartaric acid and tartronic acid, but, in addition, acidic methyl-α-D-galacturonoside and galacturonic acid itself, all of which were crystallized and carefully identified. Mucic acid was absent. The appearance of galacturonic acid in this experiment was attributed to oxidation, since small amounts of glucose were isolated from methyl-β-D-glucopyranoside (10) and cellulose (11) oxidized with hypochlorite at pH 4–4.5. When the methyl ester methyl glycoside of galacturonic acid was kept at 25° for several hours in 1% sodium hydroxide (pH 12), free galacturonic acid formed only if traces of air were present. This observation contrasted sharply with the relatively great resistance of uronosides to acid hydrolysis (12) and with the claim that methyl-α-D-galacturonoside and its methyl ester were both non-reducing to Fehling's solution (13). Although the methyl ester of methylglucopyranuronoside was also non-reducing and required the proper amount of alkali when saponified, the 3,6 lactones of methyl-β-D-glucofuranoside and 1,2-di-*O*-isopropylidene glucofururonic acid both reduced Fehling's solution and slowly neutralized more than the theoretical amount of alkali (14). The instability toward alkali of methyl pectate was discussed in the review by Whistler and BeMiller (15). In the present case, the action of alkali alone on galacturonic acid, its methyl glycoside, and methyl glycoside methyl ester, could well be the subject of a separate research. After treatment with 1% sodium hydroxide, the product from the methyl glycoside methyl ester, for example, yielded paper chromatograms showing only the spots characteristic of the acidic methyl glycoside and of galacturonic acid, and there was no clear evidence of either saccharinic acids or Lobry de Bruyn inversion products derived from galacturonic acid. Chromatographic evidence of such inversion products would be expected if an aldohexose had been submitted to the same conditions.

Since the only tartaric acid isolated in the above three oxidations was the DL-isomer, whose purity and optical inactivity were always carefully checked, it followed that the galacturonic acid or its methyl glycoside had been cleaved at equal rates at the 2,3- and 4,5-positions. Such symmetrical cleavage suggested that one of the initial products of oxidation was mucic acid, whose symmetry made it inevitable that the 2,3- and 5,6-positions would be equally liable to further oxidation. Oxidative cleavage at the 3,4-position would give the tartronic acid found. Mucic acid, when oxidized with chlorine dioxide, did, in fact, yield paper chromatograms with the spot characteristic of DL-tartaric acid; oxidation with chlorite and with alkaline hypochlorite yielded traces of tartronic acid, as well as of DL-tartaric acid. Structures I, II, and III illustrate these suggestions. Parallel test oxidations with glucurone showed that the phenomena discussed above were probably valid for uronic acids in general, though, of course, the products from glucurone were not the same as those from galacturonic acid.

When butanol – formic acid – water was the solvent in paper chromatography, the R_F values for galacturonic acid, its methyl-α-glycoside, DL-tartaric acid, and tartronic acids were well spaced at 0.04, 0.11, 0.21, and 0.38–44, respectively, and these compounds were easily distinguished from each other. A series of small-scale oxidations of galacturonic acid yielded chromatograms with spots at one or more of the four positions but no chromatogram contained additional spots at other R_F values. The chromatograms

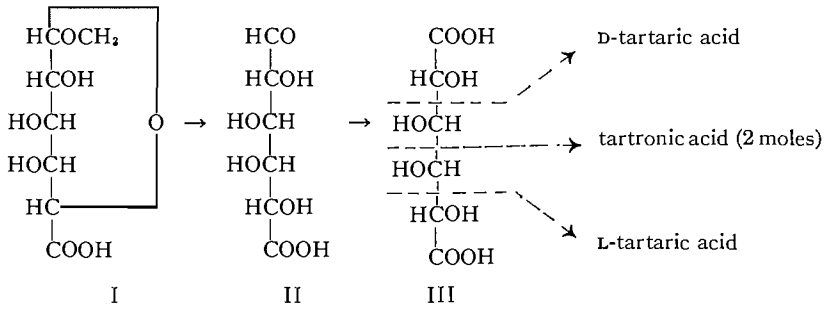

I II III

were also sprayed with *o*-aminodiphenyl to detect any carbonyl compounds formed, but the results were uniformly negative. Although all of the oxidants tried thus yielded one or more of the same acids, and no others, it should be emphasized that the yields were small, and that any non-reducing, non-acidic products would not have been detected. As before, mucic acid was isolated directly from the concentrated liquors.

The results (Table I) showed that the behavior of chlorine dioxide depended to some extent on the hydrogen ion concentration of the solution. The production of some mucic acid near pH 1.3 agreed with the slow conversion of aldoses to aldonic acids by this

TABLE I

Oxidation products from D-galacturonic acid and its methyl-α-glycoside methyl ester[a]

Aqueous oxidant	Unchanged acid	Mucic acid	Sugar acids[b]	
			R_F 0.21	R_F 0.38–0.44
Chlorine dioxide, 10 moles[c] at 75°				
Uronic acid, pH 1.3–1.4	+++	++	+	0
pH 2.6–2.9	+++	+	+	0
pH 4.5–4.8	+++	+++[d]	++	0
pH 9[e]	+++	0	+	0
Sodium chlorite, 10 moles at 75°				
Uronic acid, pH 2.3–2.9	+++	+++	+	+++
Chlorine, large excess near 0°				
Uronic acid, pH ~ 5	+++	+	+	0
Hypochlorite, 3 moles[c] at 25° and pH 10–11				
Uronic acid	++	+++	++	+++
Methyl glycoside ester[e]	++	0	++	+++
Hydrogen peroxide, 1.1 moles[c] at 25° and pH 9–12				
Uronic acid	+++	0	0	0
Methyl glycoside ester[e]	++	0	+	0
Sodium hydroxide, excess at 25° and pH 12 (1%)[f]				
Methyl glycoside ester[e]	++	0	0	0

[a]Oxidations lasted 90 or 150 minutes. A relatively large or intense spot on paper chromatogram denoted by +++; a fair amount by ++; a trace by +.

[b]DL-Tartaric acid, R_F 0.21; tartronic acid, R_F 0.38–0.44 with butanol – formic acid – water system.

[c]Per mole of uronic acid or uronide.

[d]Mucic acid yield 20%, and maximum yield of tartaric acid.

[e]Spot for unchanged methyl glycoside methyl ester ++ at R_F 0.11.

[f]For several hours; traces of air were probably present.

oxidant in strongly acidic conditions (8), but a maximum formation of mucic acid and DL-tartaric acid near pH 4.5 was not anticipated. The generalization (16) that chlorine

Can. J. Chem. Downloaded from www.nrcresearchpress.com by 176.9.209.113 on 09/04/12
For personal use only.

dioxide had no effect on sugars and polysaccharides thus did not apply strictly to galacturonic acid. Attempts to oxidize galacturonic acid at room temperature in a sodium borate buffer at pH 9, in 1% ammonium hydroxide (pH 10.5), or by continuously bubbling the gas through an ammonium hydroxide – sodium hydroxide solution kept near pH 12, yielded little or no mucic acid, and only traces of tartaric acid. As expected (8, 9), sodium chlorite readily oxidized the aldehyde group in galacturonic acid to give mucic acid as a major product, but the other major product was tartronic acid, no trace of which had been observed at any pH when the oxidant was chlorine dioxide. The result supported the opinion (8, 9) that sodium chlorite was an oxidant in its own right, and its effects could not be completely attributed to by-product chlorine dioxide. The possibility that the latter was exclusively responsible for the trace of DL-tartaric acid formed was not investigated.

Only traces of oxidation were observed when chlorine gas was bubbled through a solution of galacturonic acid kept near 0° and pH 5, conditions reminiscent of those used to delignify wood by one or other of the chlorination processes (17, 18). At pH 10–12 and 25°, however, hypochlorite produced relatively extensive oxidation to mucic and tartronic acids, with lesser amounts of DL-tartaric acid, and thus resembled acidified sodium chlorite in its action. The resemblance included the survival of some of the galacturonic acid in circumstances where glucose would have been rapidly and almost quantitatively oxidized to gluconic acid. Alkaline hydrogen peroxide appeared incapable of oxidizing galacturonic acid at 25°, although some of this acid was produced from the corresponding methyl-α-glycoside methyl ester. As in the case of alkaline hypochlorite, the loss of the glycosidic methyl group was tentatively attributed to the oxidant rather than to the alkalinity.

Kleinberg (19) reviewed the degradation of the anhydrous silver salts of many organic acids to the lower halides by elemental chlorine, bromine, or iodine,

$$RCOOAg + Br_2 \rightarrow RBr + CO_2 + AgBr,$$

and the reaction was extended to alginic acid, penta-*O*-acetyl gluconic acid, and an oxycellulose acetate by Rice and Johnson (20). A mixture of the anhydrous acid chloride and silver oxide could be substituted for the silver salts in these reactions (20). Since salts of simple uronic acids had apparently not been degraded in this way, a few preliminary experiments were carried out with galacturonic acid and its methyl glycoside. Little or no action occurred when dry calcium galacturonate was suspended in carbon tetrachloride containing an equimolar amount of bromine. The same reagent, however, caused the quick evolution of carbon dioxide from the silver salt of methyl-α-D-galacturonic acid. Extraction of the product with water gave a neutral, strongly reducing solution, free of silver and bromide ions, from which a clear syrup was isolated by paper chromatography. This syrup was free of methoxyl groups and yielded a crystalline phenylhydrazone melting at 128–129°. By analogy with the earlier work, the methyl galacturonide (I) would first be degraded to an acetobromo derivative (IV), which probably decomposed during isolation to yield the methoxyl-free dialdehyde (V). The yield of the crystalline di-phenylhydrazone, however, was only 8–10% of theory, the compound was not pure, and the work was discontinued. The product appeared to be of the same type as the xylotrihydroxyglutardialdehyde bis-phenylhydrazone derived from the oxidation of 1,2-*O*-isopropylidene-D-glucofuranose with lead tetraacetate (21) or sodium periodate (22, 23).

Can. J. Chem. Downloaded from www.nrcresearchpress.com by 176.9.209.113 on 09/04/12
For personal use only.

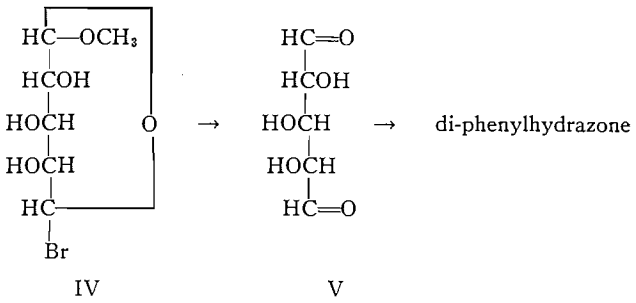

IV V

EXPERIMENTAL

All solutions and eluents were concentrated in a rotatory film evaporator under diminished pressure at not more than 50°. Melting points were corrected and analyses were quoted as the mean of concordant determinations.

Materials and Methods

The methyl ester of methyl-α-D-galacturonopyranoside monohydrate was prepared by boiling crystalline D-galacturonic acid, 25 g, in methanolic hydrogen chloride (13, 24), and after recrystallization from water had m.p. 142–144°, and specific rotation in water $[\alpha]_D^{20}$ +122° (*c*, 1.0%).

To prepare the silver salt, 1.1 g of the methyl ester was saponified by solution for 1 hour at room temperature in 50 ml of 0.1 *N* sodium hydroxide in a nitrogen atmosphere. Silver acetate, 0.72 g dissolved in 50 ml of hot water, was then added and a few minutes later the solution was filtered. Evaporation of the filtrate to small volume caused the white salt to separate. Yield, 0.7 g or 67%. Found: Ag, 33.5%. Calc.: Ag, 34.3%.

Di-(*p*-nitrobenzyl)-DL-tartrate, prepared from the crystalline disodium salt and *p*-nitrobenzyl bromide (25), after recrystallization from 63% ethanol melted correctly at 146–148°. The dimethyl ester of tartronic acid, also required for reference purposes, was prepared by boiling 0.1 g of the free acid under reflux for 2 hours in 3% methanolic hydrogen chloride. After removing halide ions as the silver salt and any residual cations by an ion-exchange resin, the liquid was concentrated and chilled. The crystalline dimethyl ester separated, and its melting point was correct at 43–45° (26).

Chlorine-free, 0.25–0.35 *M* solutions of chlorine dioxide were prepared from Schacherl's mixture of potassium chlorate, oxalic acid, and 33% sulphuric acid with the precautions noted elsewhere (27) and were standardized iodometrically. Chlorine dioxide was assumed to have five oxidizing equivalents in this standardization, whereas sodium chlorite had only four (27). Solutions of sodium hypochlorite were standardized either iodometrically or by the method employing arsenite.

Paper partition chromatography, employing Whatman No. 1 paper, and 10 lambda (10^{-2} ml) aliquots, was carried out by conventional methods. The solvent system was butanol – formic acid – water (500:115:385 vol.) (28), and the chromatograms after being dried *in vacuo* at 115° were sprayed with bromphenol blue in 90% ethanol (29). This spray gave yellow spots with sugar acids, and was stable indefinitely if stored in the dark at −10°. Residual traces of hydrochloric and chloric acids were retained at or near the starting line in these chromatograms. The best separations by column chromatography were obtained with a 50–100 mesh Dowex 1-4X anion-exchange resin which was converted from the chloride to the acetate form by washing in succession with 5% sodium hydroxide, water, *N* acetic acid, and water.

Can. J. Chem. Downloaded from www.nrcresearchpress.com by 176.9.209.113 on 09/04/12
For personal use only.

Oxidations of D-*Galacturonic Acid*

(*a*) *With Chlorine Dioxide*

Galacturonic acid, 18 g (93 mmole), was dissolved in a 10-fold molar amount of aqueous 0.3 *M* chlorine dioxide adjusted to pH 5 with acetic acid and kept at 70–75°. After 150 minutes the solution was cooled, and excess chlorine dioxide was removed by the passage of nitrogen gas. Concentration then caused the separation of crystalline mucic acid, decomp. 214–217°, and a paper chromatogram of the filtrate showed it to contain only unchanged galacturonic acid, R_F 0.04, a tartaric acid, R_F 0.21, and traces of inorganic acids.

A few grams of Dowex 1-4X anion-exchange resin (acetate form) was dispersed in the concentrate, and several hours later the resin with the absorbed acids was recovered and added to the top of a 102 cm × 5 cm column of the same resin. Elution of the column with water, and then with increasing concentrations of acetic acid, failed to remove any sugar acids until *N* acetic acid was used. Twelve 1-liter fractions then contained the galacturonic acid, which crystallized when the combined fractions were concentrated and chilled. After recrystallization, the galacturonic acid had the correct m.p., 158–159°, and the correct initial specific rotation of $[\alpha]_D^{20}$ +97° in 1% aqueous solution. The sample when oxidized with nitric acid gave mucic acid, decomp. 215–217°.

More concentrated acetic acid, *N* to 3 *N*, failed to remove sugar acids from the column, but elution with 0.5 *N* trifluoroacetic acid, 100 ml fractions being collected, removed both DL-tartaric acid and inorganic acids. These eluates were combined, concentrated to a very small volume, and spotted on sheets of Whatman No. 3MM chromatography paper, 50 mg being in each spot. The portions of paper containing the tartaric acid were extracted with water, and the product crystallized from the concentrate. After recrystallization, the m.p., 203–204°, the neutralization equivalent, 75, and the optical inactivity in water (*c*, 1%) were correct for DL-tartaric acid. A mixed melting point with an authentic sample was undepressed, and the m.p., 146–148°, of the crystalline di-(*p*-nitrobenzyl)-DL-tartrate was also satisfactory.

Several experiments with 0.35-g samples of galacturonic acid were carried out at room temperature and different pH values, and the results were assessed by paper chromatograms (Table I). A larger quantity of acetic acid was used to maintain pH 1.3. The buffer for pH 5 consisted of acetic acid and 3.2% aqueous sodium acetate, the sodium ions being afterwards removed by Amberlite IR-120 cation-exchange resin. In an experiment at pH 9, 0.35 g of galacturonic acid was dissolved in 70 ml of a potassium chloride – boric acid – sodium hydroxide buffer (30), but as soon as 20 ml of 0.27 *M* chlorine dioxide was added the pH decreased and more sodium hydroxide had to be added. Two further additions of the same amount of chlorine dioxide were made at intervals of 30 minutes, with additions of alkali to maintain pH 9, and after 2 hours the solution was shaken with silver carbonate. Insoluble silver salts were removed, and the filtrate was evaporated to dryness. The residue was taken up in 100 ml of acidified methanol and the solution was evaporated to dryness; several such cycles sufficed to remove all boric acid as the volatile methyl ester. An aqueous solution of the residue was then prepared for chromatography by passage through Amberlite IR-120 cation-exchange resin. An experiment that yielded only a trace of tartaric acid, R_F 0.21, consisted of adding a solution of 0.35 g of galacturonic acid in 100 ml of 1% ammonium hydroxide to 50 ml of 0.21 *M* chlorine dioxide (6-fold amount). After 2 hours at 70–75° the solution was colorless, but on acidification to pH 2–3 with acetic acid the characteristic odor and color of chlorine dioxide reappeared. A similar ammonia solution was kept at pH 12 by

Can. J. Chem. Downloaded from www.nrcresearchpress.com by 176.9.209.113 on 09/04/12
For personal use only.

the continuous addition of sodium hydroxide while chlorine dioxide was bubbled through it, but little or no oxidation of the galacturonic acid occurred.

(*b*) *With Sodium Chlorite*

A solution of galacturonic acid, 5.5 g, and 18.7 g of sodium chlorite (10-fold molar amount) in 1430 ml of 10% acetic acid (pH 2.7–2.9) was kept at 70–75° for 150 minutes. By-product chlorine dioxide then was expelled by the passage of nitrogen gas, and any remaining oxidizing agents were destroyed by the addition of a little cold, 48% hydriodic acid, the liberated iodine being promptly extracted with ether. After the removal of halides as the silver salts, the filtered solution was passed through a column of Amberlite IR-120 cation-exchange resin, and was concentrated. Mucic acid, decomp. 215–218°, separated, and after further concentration the filtrate was separated on a 91.5 cm × 5 cm column of Dowex 1-4X resin (acetate form) as described in the oxidation with chlorine dioxide. Galacturonic acid again crystallized from the *N* acetic acid eluates and after recrystallization had the correct melting point and specific rotation. Oxidation with nitric acid yielded mucic acid.

DL-Tartaric acid and tartronic acid occurred together in the 0.5 *N* trifluoroacetic acid eluates, and were separated by paper chromatography. After recrystallization, the DL-tartaric acid was optically inactive, melted correctly at 204–205°, had the correct neutralization equivalent, and yielded the crystalline di-(*p*-nitrobenzyl) derivative with the proper melting point. The tartronic acid solution was evaporated to dryness because no crystallization occurred on cooling of the concentrated liquor. A solution of the residue in water was evaporated to dryness several times to eliminate formic acid, and the tartronic acid then crystallized. After recrystallization from water, the product had the correct m.p., 141–143°, and neutralization equivalent, 61.0, and was optically inactive (water, *c*, 1%). Its identity was confirmed by conversion to dimethyl tartronate, m.p. 44–45°.

(*c*) *With Chlorine*

A solution of 0.35 g of galacturonic acid in 100 ml of water buffered to pH 5 with acetic acid – sodium acetate was kept near 0° while chlorine gas was bubbled through it for 10 minutes. Most of the gas was removed by the passage of nitrogen, and any residual oxidant was destroyed by the addition of a small amount of hydriodic acid, liberated iodine being extracted with ether. After neutralization with silver carbonate, the clarified liquor was passed through Amberlite IR-120 resin, and the cation-free effluent was concentrated. A small amount of mucic acid, decomp. 215–216°, separated, and after its removal the concentrate was chromatographed on paper.

(*d*) *With Sodium Hypochlorite*

Galacturonic acid, 0.35 g, was dissolved in 50 ml of water and the solution was adjusted to pH 11.7 with aqueous sodium hydroxide. After 8 ml of 0.75 *M* sodium hypochlorite (3-fold molar amount) had been added the mixture was kept at 25° for 2 hours, during which period the pH decreased to 11.3. The solution was acidified, treated with dilute hydriodic acid and silver carbonate, and freed of cations as described above. A large amount of mucic acid, decomp. 214–216°, was removed prior to chromatography.

(*e*) *With Hydrogen Peroxide*

A solution of 0.35 g of galacturonic acid in 100 ml of water, adjusted to pH 9.9 with aqueous sodium hydroxide, was mixed with 2 ml of 0.98 *M* hydrogen peroxide (1.1 molar amount), and kept at 25° for 90 minutes. After acidification with acetic acid, the excess oxidant was reduced by the addition of a little 48% hydriodic acid, 30 minutes

Can. J. Chem. Downloaded from www.nrcresearchpress.com by 176.9.209.113 on 09/04/12
For personal use only.

being required for this reaction to become complete. The iodine formed was extracted with ether. Neutralization, the removal of cations, and concentration yielded a solution containing unchanged galacturonic acid.

Methyl-α-D-galacturonoside Methyl Ester and Sodium Hypochlorite

Five grams of the crystalline methyl glycoside methyl ester monohydrate was oxidized at pH 11.7 and 25° with a 3-fold molar amount of aqueous sodium hypochlorite, and the products were recovered, as in the parallel oxidation of galacturonic acid. These products were: acidic methyl galacturonoside, m.p. 112–114°, $[\alpha]_D^{20}$ +130° in water (*c*, 1.0%); galacturonic acid, m.p. 158–159°, initial $[\alpha]_D^{20}$ +97° in water (*c*, 1.0%); optically inactive DL-tartaric acid (1% aqueous solution), neutralization equivalent, 75.8, and m.p. 203–204°; and optically inactive tartronic acid, m.p. 142–144°, and neutralization equivalent 61.0. All these constants were in good agreement with those of authentic samples.

Attempted Decarboxylations with Bromine

In a typical experiment, 1 g of the dry silver salt of methyl-α-D-galacturonoside, dispersed in 100 ml of anhydrous carbon tetrachloride, was treated with 0.3 ml, or the equimolar amount, of bromine (31). A rapid reaction occurred initially, with the evolution of some heat and carbon dioxide. After the mixture had been warmed for 10 minutes at the end of this reaction, the insoluble portion was washed with carbon tetrachloride and dried over silica gel. The yellow-white solid, 0.9 g, was extracted with three 75-ml volumes of water to remove insoluble silver salts. The combined extracts were free of silver and bromine ions, and gave a negative test for carboxylic acid groups, but a strongly positive test for aldehydic groups. No solid separated when the extracts were concentrated, but a small aliquot when chromatographed on paper yielded a single spot of R_F 0.84 (butanol – formic acid – water system, *o*-aminodiphenyl spray).

An orange precipitate immediately formed when the above concentrate was mixed with 5 ml of water containing 0.5 g of phenylhydrazine hydrochloride and 0.8 g of sodium acetate. After being dried, this precipitate weighed 0.1 g (10%), and melted at 129–130°. Found: OCH_3, 0.0; N, 23.7%. Calc. for the bis-phenylhydrazone of a trihydroxyglutardialdehyde, $C_{17}H_{20}N_4O_3$: OCH_3, 0.0; N, 17.1%.

When the molar ratio of bromine to the silver salt of the methyl galacturonoside was doubled, the yield of the crystalline phenylhydrazone was 8%. Found: OCH_3, 0.0; N, 20.5%.

ACKNOWLEDGMENTS

One of us (R.H.Z.) wishes to thank the National Research Council of Canada for assistance in the form of a bursary and two Summer Maintenance grants; also the Celanese Corporation of America for the fellowships awarded to him in 1957 and 1958.

REFERENCES

1. HUEBNER, C. F., LOHMAR, R., DIMLER, R. J., MOORE, S., and LINK, K. P. J. Biol. Chem. **159**, 503 (1945).
2. HALSALL, T. G., HIRST, E. L., and JONES, J. K. N. J. Chem. Soc. 1427 (1947).
3. EDINGTON, R. A., HIRST, E. L., and PERCIVAL, E. E. J. Chem. Soc. 2281 (1955).
4. SPRINSON, D. B. and CHARGAFF, E. J. Biol. Chem. **164**, 433 (1946).
5. HOCKETT, R. C., NICKERSON, M. H., and REEDER, W. H. J. Am. Chem. Soc. **66**, 472 (1944).
6. HARDEGGAR, E., KREIS, K., and SPITZ, D. Helv. Chim. Acta, **35**, 958 (1952).
7. WISE, L. E. Ind. Eng. Chem. Anal. Ed. **17**, 63 (1945).
8. JEANES, A. and ISBELL, H. S. J. Research Natl. Bur. Standards, **27**, 125 (1941).
9. LOGAN, C. D., HUSBAND, R. M., and PURVES, C. B. Can. J. Chem. **33**, 82 (1955).
10. HENDERSON, J. T. J. Am. Chem. Soc. **79**, 5304 (1957).
11. BARKER, S. A., BOURNE, E. J., and THEANDER, O. J. Chem. Soc. 4276 (1955).

Can. J. Chem. Downloaded from www.nrcresearchpress.com by 176.9.209.113 on 09/04/12
For personal use only.

12. WHISTLER, R. L. and RICHARDS, G. M. J. Am. Chem. Soc. **80**, 4888 (1958).
13. MORELL, S. and LINK, K. P. J. Biol. Chem. **100**, 385 (1933).
14. OWEN, L. N., PEAT, S., and (in part) JONES, W. J. G. J. Chem. Soc. 339 (1941).
15. WHISTLER, R. L. and BEMILLER, J. N. Advances in Carbohydrate Chem. **13**, 289 (1958).
16. SCHMIDT, E. and GRAUMANN, E. Ber. **54**, 1860 (1921).
17. RITTER, G. J. and KURTH, E. F. Ind. Eng. Chem. **25**, 1250 (1933).
18. SITCH, D. A. Pulp Paper Mag. Can. **50**, 234 (1949).
19. KLEINBERG, J. Chem. Revs. **40**, 381 (1947).
20. RICE, F. A. H. and JOHNSON, A. R. J. Am. Chem. Soc. **78**, 428 (1956); **79**, 5049 (1959).
21. IWADARE, K. Bull. Chem. Soc. Japan, **16**, 40 (1941). Chem. Abstr. **35**, 4740 (1941).
22. SOWDEN, J. C. J. Am. Chem. Soc. **74**, 4377 (1952).
23. MESTER, L. and MÓCZÁR, E. J. Chem. Soc. 3228 (1956).
24. JONES, J. K. N. and STACEY, M. J. Chem. Soc. 1340 (1947).
25. LYMAN, R. J. Am. Chem. Soc. **39**, 709 (1917).
26. PINNER, A. Ber. **18**, 2854 (1885).
27. HUSBAND, R. M., LOGAN, C. D., and PURVES, C. B. Can. J. Chem. **33**, 68 (1955).
28. EDINGTON, R. A. and PERCIVAL, E. E. J. Chem. Soc. 3554 (1955).
29. AYRES, A., DINGLE, J., PHIPPS, A., and REID, W. W. Nature, **170**, 834 (1952).
30. VOGEL, A. I. Quantitative inorganic analysis. 2nd ed. Longmans, Green & Co., Inc., New York. 1948.
31. LÜTTRINGHAUS, A. and SHADE, D. Ber. **74**, 1565 (1941).

Can. J. Chem. Downloaded from www.nrcresearchpress.com by 176.9.209.113 on 09/04/12
For personal use only.

Can. J. Chem. Downloaded from www.nrcresearchpress.com by 176.9.209.113 on 09/04/12
For personal use only.

THE EXCHANGE OF OXYGEN-18 BETWEEN CELLULOSE, ADSORBED WATER, AND WATER VAPOR[1]

A. R. G. LANG AND S. G. MASON

ABSTRACT

The adsorption on regenerated cellulose of water at vapor pressures of 0 to 40 μ Hg has been measured by an oxygen-18 dilution technique. The results showed that cellulose may be dried to less than 0.04% moisture by evacuation at 70° C. The adsorption isotherm was compared with that of Taylor for viscose rayon.

It was also shown that oxygen-18 does not exchange between cellulose and water.

INTRODUCTION

The experiments described in this note provided supplementary information for a study of the exchange of tritium between cellulose and water vapor described elsewhere (1). In order to correct the experimental data for the exchange occurring between the water vapor and the water adsorbed on the cellulose even after prolonged evacuation, it was necessary to know the amount of water adsorbed under the conditions of the experiments.

The published values for the amount of adsorbed water present on cellulose at very low vapor pressures (2–5) actually represent the incremental adsorption above a certain minimum defined by the method of drying; there still exists, however, some doubt as to whether cellulose can be completely freed from adsorbed water. In the usual method of drying by heating to 105–110° C, in an air oven, up to 0.5% by weight of water remains as a result of the small but nevertheless significant water vapor pressure (6, 7). On the other hand, it is generally considered that cellulose is completely dried by prolonged desiccation over phosphorus pentoxide at room temperature (6) or at elevated temperatures (8), by heating in a stream of dry gas (8), or by extended evacuation (2–5, 7). However, in all these measurements the sole criterion of dryness was that the mass of cellulose had reached a minimum value. Recently it was reported from the direct titration of cellulose by the Karl Fischer reagent that 1% adsorbed water remained on cellulose dried over phosphorus pentoxide (9).

In the present experiments, these uncertainties were eliminated by measuring the dilution of oxygen-18 when oxygen-18-enriched water was mixed with the adsorbed water *in situ*. The method requires, however, that the oxygen atoms of cellulose do not exchange with those of water, and it was therefore first necessary to determine whether or not such exchange was taking place.

Oxygen-18 generally does not exchange between alcohols and water (10). However, only one author (11) has studied the system cellulose/water and a critical study of his data showed that less than 6% of the cellulose oxygens reacted. Since this precision was inadequate for the present work, it was necessary to extend the measurements.

PROCEDURE

In the method used, known quantities of dried cellulose and O^{18}-enriched water were reacted together, the water recovered, and the dilution of the O^{18} measured mass spectrometrically. Dilution could be caused both by exchange with the oxygen atoms of the

[1]*Manuscript received July 6, 1959.*
Contribution from the Physical Chemistry Division, Pulp and Paper Research Institute of Canada, Montreal, Que., and the Department of Chemistry, McGill University, Montreal, Quebec.

cellulose molecules, and by mixture with adsorbed water. The quantities were chosen so that an adsorption of 1 mg water per g cellulose would cause a 10% change in the concentration of O^{18}.

Figure 1 shows the apparatus. It was made of brass and copper, except for the Pyrex glass jacket (F) of the trap and the tared recovery tube (H). The train could be broken at E so that the reaction vessel could be connected directly to the vacuum system, which

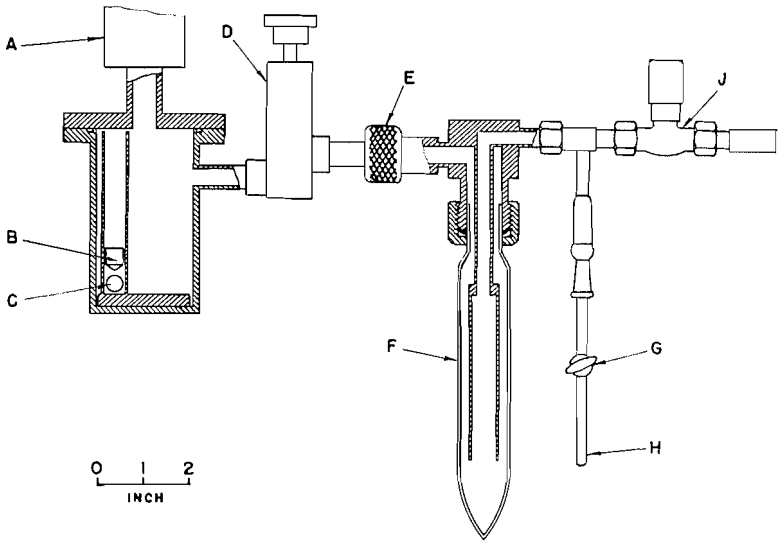

FIG. 1. Apparatus. A, Pirani gauge; B, plunger; C, ampoule; D, valve; E, vacuum coupling; F, trap; G, stopcock; H, tared glass tube; J, valve.

consisted of a mechanical pump, a two-stage oil diffusion pump, and a liquid-air trap.

Air-dried gel cellulose film was used, made from viscose and neither plasticized nor coated. This sample was identical with sample *c* used previously (1). For each experiment, strips 7.5 cm wide by 23 μ thick and weighing 2 g on a dry basis (oven-dried at 105° C) were folded backwards and forwards on themselves and placed in the reaction vessel together with a thin-walled Pyrex ampoule (C) containing 0.02 g of water having an O atom content of 9.4% O^{18}. The masses of cellulose and water (with the necessary correction for buoyancy of the evacuated ampoule) were determined within 1%.

The cellulose was dried to various degrees by evacuating the reaction vessel. In one case the reaction vessel was heated to about 70° C during the reaction; in all other cases the temperature was about 25° C. Details including times of evacuation are given in Table I. After the evacuation, the cellulose was isolated by closing valve D, and the gas pressure was measured at intervals for a total time of up to 3 hours with an Edwards Pirani gauge, Type MA-5 (A, in Fig. 1), which had been calibrated against a McLeod gauge. Since the empty reaction vessel leaked air (0.071 μ Hg per minute), the equilibrium water vapor pressure was obtained as follows: The pressure was plotted against time to yield curves illustrated in Fig. 2. When the slope of a curve reached the constant value of 0.071 μ Hg per minute, measurements were discontinued; the linear part of the graph was then extrapolated back to zero time and the intercept on the pressure axis taken as the equilibrium water vapor pressure.

To bring about the exchange the reaction vessel was shaken until the stainless steel plunger (B, Fig. 1) broke the ampoule of water (C). The reaction continued for 8 to 8.5

Can. J. Chem. Downloaded from www.nrcresearchpress.com by 176.9.209.113 on 09/04/12
For personal use only.

TABLE I

Adsorption of water on cellulose at low vapor pressures

Experiment	Sample	Evacuation: Time, hours	Evacuation: Temp., °C	P equilibrium H_2O, μ Hg	Oxygen-18 in recovered water, atom fraction	m/M*	Water adsorbed at P, mg/g
1	Blank	21	25	0	0.0941	—	0
2	Cellulose	59	70	< 0.1	0.0932	0.0089	0.10
3	Cellulose	47	23	4	0.0815	0.0104	1.61
4	Cellulose	40	24	6.5	0.0693	0.0099	3.52
5	Cellulose	35	25	16	0.0681	0.0104	3.95
6	Cellulose	23	27	41	0.0589	0.0108	6.46

*m/M = (mass of water in ampoule, g)/(mass of dry cellulose, g).

hours at 23 to 27° C, and then the water was collected by evacuating the reaction vessel through the trap (F) cooled with a Dewar flask of liquid air. Valves D and J were then closed and the Dewar of liquid air moved from the trap to the lower end of the tared tube (H) so that the water distilled into it. Stopcock G was then closed and the tared tube (H) removed from its matching ground-glass joint and weighed. Between 50 and 60% of the total water reacted with the cellulose was recovered. The isotope effect in this distillation is negligible: calculations assuming the extreme case of equilibrium distillation (1) and using the values of the vapor pressures of the H_2O^{18} and H_2O^{16} given by Huffman and Urey (12) show that the concentration of O^{18} in the distillate after 50% recovery is the same (within 0.6%) as before distillation.

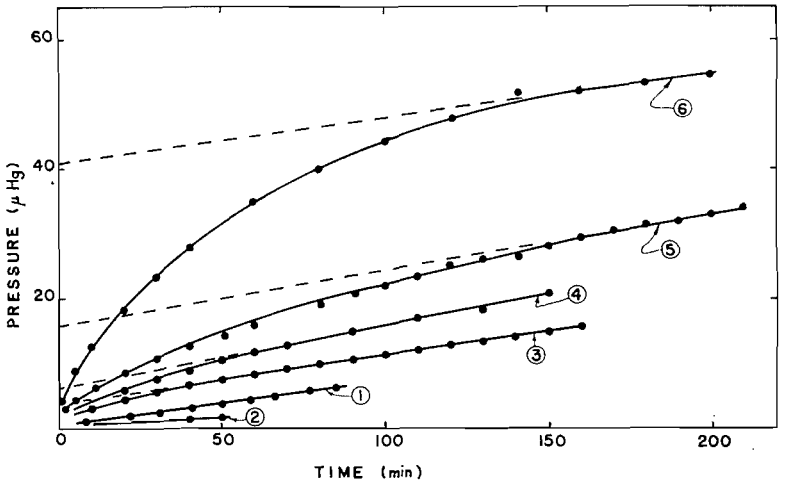

FIG. 2. Estimation of equilibrium pressure. Circled figures are experiment numbers.

The concentration of the O^{18} in the water in tube H was determined by the method of Dostrovsky and Klein (13). The water was exchanged with carbon dioxide, then the ratio of the 44/46 mass peaks of the carbon dioxide was measured four times in a mass spectrometer. The concentration of the O^{18} in the water was calculated from relationships given by Dostrovsky and Klein.

RESULTS AND DISCUSSION

The results are summarized in Table I.

When the sample was evacuated until the vapor pressure was practically zero (experi-

Can. J. Chem. Downloaded from www.nrcresearchpress.com by 176.9.209.113 on 09/04/12
For personal use only.

ment 2), almost no dilution of the O^{18} occurred. This experiment showed simultaneously that no exchange occurred between the oxygen atoms of the water and the cellulose (less than 0.08% of the cellulose oxygens), and that no water (less than 0.4 mg per g) remained adsorbed in the cellulose. The amount of adsorbed water on the cellulose for experiments 2 to 6 was therefore given from an O^{18} balance as:

$$A = \frac{m}{M}\{(N_i/N_f)-1\}$$

where A is the adsorbed water (milligrams per gram of cellulose), m the mass of water in the ampoule (milligrams), M the mass of cellulose on an oven-dry (105° C) basis (grams), and N_i and N_f the initial and final atom fractions of O^{18}.

The zero adsorption of water in experiment 2 removed any reasonable doubt that cellulose can be completely dried by evacuation with heat. Since this fact was assumed in the low-pressure adsorption studies of Taylor (2, 3, 4) and Neale and Springfellow (5) its establishment adds reliance to their experimental values.

Figure 3 shows the relationship between the amount of adsorbed water and the estimated vapor pressure. Except for the zero value the vapor pressures were probably less

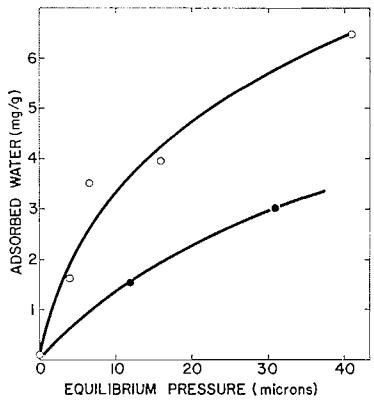

FIG. 3. Graph of adsorbed water on cellulose versus water vapor pressure. —○— Oxygen-18 dilution method (desorption branch). —●— Results of Taylor (2) for viscose rayon (reproducible adsorption branch).

than the true equilibrium values, because, although it takes several days to reach equilibrium (2), in the present experiments only 3 hours were allowed. The sorption values reported here are, therefore, upper limits for the desorption branch of the sorption cycle. This is supported by the comparison with the somewhat lower "reproducible adsorption" values for viscose rayon reported by Taylor (2), who also demonstrated that appreciable sorption hysterisis occurred at these low pressures.

ACKNOWLEDGMENT

The authors are indebted to Dr. H. I. Schiff, Chemistry Department, McGill University, for performing the mass spectrometric analyses.

REFERENCES

1. LANG, A. R. G. and MASON, S. G. To be published.
2. TAYLOR, J. B. J. Textile Inst. **43**, T489 (1952).
3. TAYLOR, J. B. J. Textile Inst. **45**, T642 (1954).
4. TAYLOR, J. B. J. Textile Inst. **47**, T147 (1956).

Can. J. Chem. Downloaded from www.nrcresearchpress.com by 176.9.209.113 on 09/04/12
For personal use only.

5. NEALE, S. M. and SPRINGFELLOW, W. A. Trans. Faraday Soc. **37**, 525 (1941).
6. DAVIDSON, G. F. and SHORTER, S. A. J. Textile Inst. **21**, T165 (1930).
7. NELSON, O. A. and HULETT, G. A. Ind. Eng. Chem. **12**, 40 (1920).
8. HERMANS, P. H. Contribution to the physics of cellulose fibers. Elsevier Pub. Co., Inc., Amsterdam. 1946.
9. BRICKMAN, W. J., DUNFORD, H. B., TORY, E. M., MORRISON, J. L., and BROWN, R. K. Can. J. Chem. **31**, 550 (1953).
10. TAUBE, H. Ann. Rev. Nuclear Sci. **6**, 277 (1956).
11. MAKOLKIN, I. A. J. Gen. Chem. (USSR), **12**, 365 (1942).
12. HUFFMAN, J. R. and UREY, H. C. Ind. Eng. Chem. **29**, 531 (1937).
13. DOSTROVSKY, I. and KLEIN, F. S. Anal. Chem. **24**, 414 (1952).

Can. J. Chem. Downloaded from www.nrcresearchpress.com by 176.9.209.113 on 09/04/12
For personal use only.

Can. J. Chem. Downloaded from www.nrcresearchpress.com by 176.9.209.113 on 09/04/12
For personal use only.

THE MERCURY-PHOTOSENSITIZED DECOMPOSITIONS OF PROPANE AND ETHANE[1]

R. A. BACK[2]

ABSTRACT

The mercury-photosensitized decompositions of propane and ethane have been studied at pressures of 300 and 600 mm, at 24° C, at very low conversions. Hydrogen was the only product identified and measured. The hydrogen yield fell rapidly at first, with increasing time of irradiation, and finally became constant. This behavior is attributed to the accumulation in the system of propylene or ethylene formed by the disproportionation of propyl or ethyl radicals, and the constant rate of hydrogen production finally achieved is thought to correspond to a steady-state concentration of the unsaturate. Previous values of the quantum yields of these decompositions were probably measured in this steady-state region, and must be corrected upwards.

Relative values have been estimated for the various rate constants involved in this mechanism. There is some evidence that energy-rich radicals, formed by the addition of hydrogen atoms to the unsaturates, tend to disproportionate rather than dimerize.

INTRODUCTION

In a previous study of the mercury-photosensitized decomposition of *n*-pentane at very low conversion, the hydrogen production decreased rapidly at first, then more slowly, and finally became constant after about 0.5% reaction (1). This was attributed to the accumulation in the system of pentene, formed by disproportionation of pentyl radicals, and the final constant rate of hydrogen production was thought to correspond to a low, steady-state concentration of pentene. The hydrogen yield was reduced, and pentene consumed, by the addition of hydrogen atoms to pentene. Similar behavior has been observed with the cyclo-alkanes (2), and more recently with *n*-butane (3). Previous studies of the mercury-photosensitized decomposition of propane and ethane did not show this effect, as hydrogen production was independent of time (4). However, rough calculations from the relative rates of the reactions concerned suggest that even the smallest conversions achieved in these experiments were probably much too large for the initial behavior to be observed. It was decided to study these reactions at very low conversions to see whether they behaved in the same way.

EXPERIMENTAL

The apparatus, a conventional static system, and the method were essentially similar to those described previously (1). Two reaction vessels, of 38- and 180-cc volume, were used in the course of the work, the larger volume permitting measurements to be made at lower conversion. After irradiation, gases non-condensable at −210° C were removed and analyzed, and the hydrocarbon, together with any condensable products, was returned to the reaction vessel for further irradiation. In this way, the hydrogen yield could be studied as a function of total irradiation time, using a single sample of hydrocarbon. Concentrations of hydrogen and unsaturates produced in the system were always low enough so that all quenching of the excited mercury atoms was by the hydrocarbon alone. Measurements were made with propane at 300- and 600-mm pressure, and with ethane at 305-mm pressure, all at 24° C. In some experiments, unsaturates (propylene or ethylene) were added.

[1]*Manuscript received July 17, 1959.*
Contribution from the Physical Chemistry Laboratory, McGill University, Montreal, Que.
[2]*Present address: Division of Pure Chemistry, National Research Council, Ottawa, Canada.*

Phillips Research-grade propane was used without further purification. A sample treated with $HgSO_4$–H_2SO_4 solution to remove unsaturates gave the same results as the untreated gas. Phillips Research-grade ethane was found to contain appreciable amounts of methane and ethylene. The former was removed by repeated trap-to-trap distillation and prolonged pumping at −210° C. The latter was removed by condensing the ethane onto charcoal previously treated with bromine.

RESULTS

Propane

The non-condensable gas was never less than 99.5% hydrogen, measured by diffusion through a Pd thimble at 300° C. Careful analysis with a low temperature still failed to detect any C_2 hydrocarbons, so that hydrogen was the only product detected and measured. Hydrogen yield is shown as a function of total time of irradiation in Figs. 1 and 2 for propane at 600- and 300-mm pressure respectively. The effect of adding propylene to the system is shown in Fig. 3.

Ethane

When care was taken to remove all the methane present initially, the non-condensable gas produced was never less than 99% hydrogen, and this was again the only product detected and measured. The hydrogen yield is shown in Fig. 4 as a function of total time of irradiation for ethane carefully purified to remove ethylene. For comparison, the hydrogen yield from Research-grade ethane, used without purification, is shown in the same figure.

Under conditions of high pressure, low light intensity, and low temperature, and consequent absence of hydrogen atom "cracking" reactions and other complicating processes, the simple mechanism suggested previously (1) seems to account adequately for the observed behavior of both compounds.

$$h\nu + Hg \longrightarrow Hg^* \quad [1]$$

$$Hg^* + RH \xrightarrow{\text{rate} = K} \dot{R} + H + Hg \quad [2]$$

$$H + RH \xrightarrow{k_3} H_2 + \dot{R} \quad [3]$$

$$\dot{R} + \dot{R} \xrightarrow{k_4} R_2 \quad [4]$$

$$\dot{R} + \dot{R} \xrightarrow{k_5} RH + R' \quad [5]$$

RH is an alkane, $\dot{R}$ is an alkyl radical, and R′ is an olefin. As the olefin accumulates in or is added to the system, the following additional reactions may become important.

$$H + R' \xrightarrow{k_6} \dot{R} \quad [6]$$

$$H + R' \xrightarrow{k_7} H_2 + \dot{R}' \quad [7]$$

$$\dot{R} + R' \xrightarrow{k_8} \dot{R}_2 \quad [8]$$

$$\dot{R} + \dot{R}' \xrightarrow{k_9} R'_2 \quad [9]$$

where $\dot{R}'$ is an unsaturated radical, $\dot{R}_2$ is a dimer radical, and $\dot{R}'_2$ is an unsaturated dimer. From the mechanism, it may be shown that

$$[1] \qquad dH_2/dt = K(k_3[RH]+k_7[R'])/(k_3[RH]+(k_6+k_7)[R']).$$

Thus dH_2/dt is equal to K initially, decreases as R′ accumulates, and becomes constant if R′ attains a steady-state concentration before depletion of RH becomes appreciable.

Can. J. Chem. Downloaded from www.nrcresearchpress.com by 176.9.209.113 on 09/04/12
For personal use only.

This behavior was shown by propane and ethane, Figs. 1, 2, and 4, and the reduction of the hydrogen yield in the steady state may be taken as a measure of the extent of reaction 6. Furthermore, if loss of R′ via reaction 8 is neglected, the reduction of the hydrogen yield is also a measure of the rate of disappearance of R′, and since it is a steady state, of the rate of formation of R′ by reaction 5. Thus we may obtain the relative rates of reactions 4 and 5 directly from Figs. 1, 2, and 4, as shown.

Interesting confirmation that the plateaux do represent steady-state concentrations of

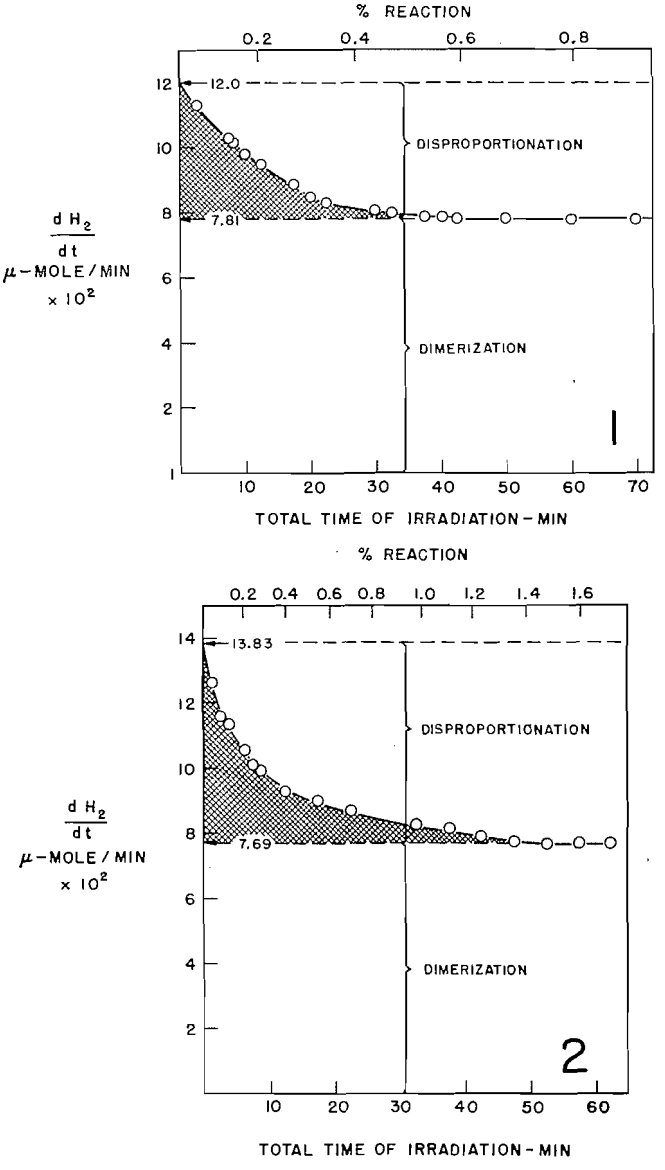

FIG. 1. Rate of production of hydrogen vs. total time of irradiation for the mercury-photosensitized decomposition of propane at 600-mm pressure.

FIG. 2. Rate of production of hydrogen vs. total time of irradiation for the mercury-photosensitized decomposition of propane at 300-mm pressure.

Can. J. Chem. Downloaded from www.nrcresearchpress.com by 176.9.209.113 on 09/04/12
For personal use only.

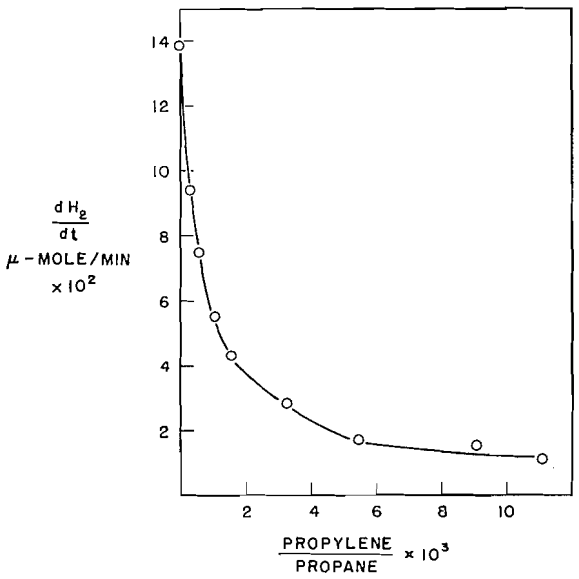

FIG. 3. The effect of added propylene on the rate of hydrogen production from the mercury-photosensitized decomposition of propane at 300-mm pressure.

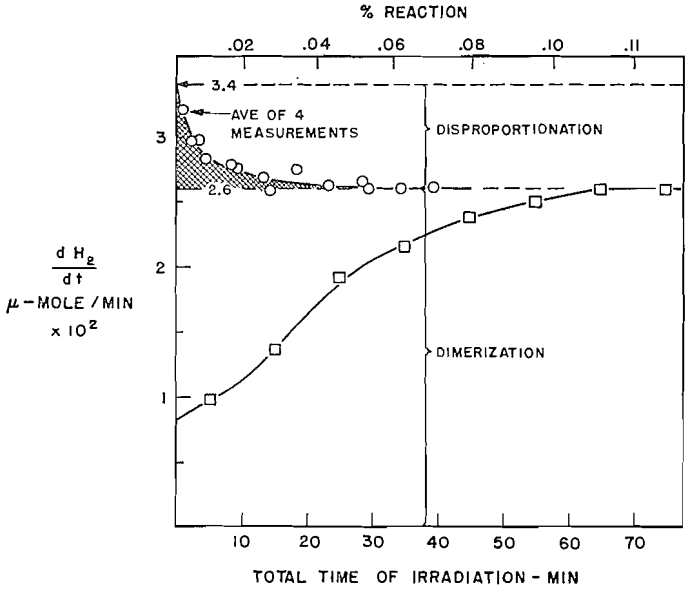

FIG. 4. Rate of production of hydrogen vs. total time of irradiation for the mercury-photosensitized decomposition of ethane at 305-mm pressure; ○ pure ethane, □ Research-grade ethane.

unsaturates is seen in the behavior of the impure Research-grade ethane (Fig. 4). Upon repeated irradiation, the ethylene in excess of the steady-state value was slowly used up, until finally the hydrogen yield rose to the same steady-state value as before. In another experiment, a sample of pure ethane was irradiated until the hydrogen yield had attained the plateau value. At this point, a small amount (0.02%) of ethylene was added, whereupon the hydrogen yield was reduced to 0.0042 micromoles/minute. Upon repeated

Can. J. Chem. Downloaded from www.nrcresearchpress.com by 176.9.209.113 on 09/04/12
For personal use only.

irradiation, the hydrogen yield slowly increased, following the same curve as the sample of impure ethane, and again attained the same limiting value. Thus the same steady state, which is a function only of the ratio k_4/k_5, was approached in three different ways.

Equation 1 may be rewritten as

$$[2] \qquad (K-d\mathrm{H}_2/dt)\,[\mathrm{RH}]/[\mathrm{R}'] = A(d\mathrm{H}_2/dt)-BK$$

where $A = (k_6+k_7)/k_3$ and $B = k_7/k_3$. Plots of this equation for the experiments with propane–propylene mixtures are shown in Figs. 5 and 6. Ratios of rate constants calculated from the slopes and intercepts of these plots are shown in Table I, together with values of k_5/k_4.

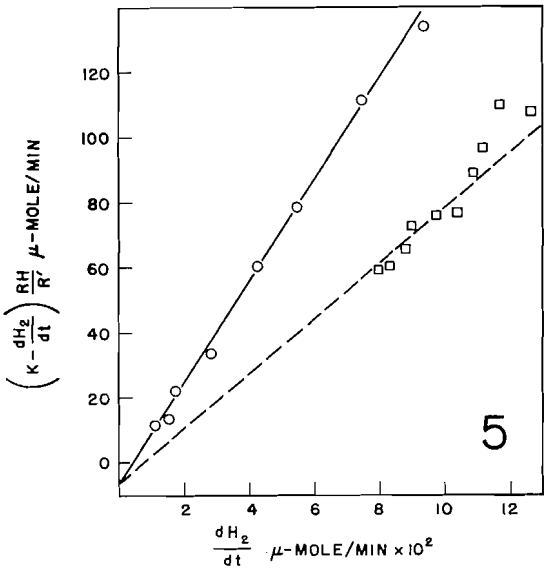

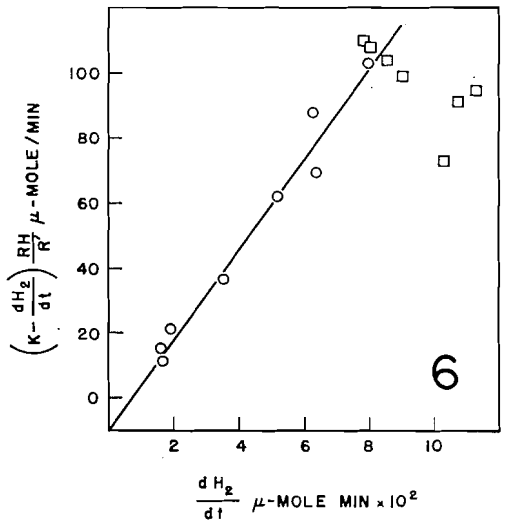

FIG. 5. A plot of equation 2 for propane at 300-mm pressure; □ pure propane, ○ added propylene.
FIG. 6. A plot of equation 2 for propane at 600-mm pressure; □ pure propane, ○ added propylene.

Can. J. Chem. Downloaded from www.nrcresearchpress.com by 176.9.209.113 on 09/04/12
For personal use only.

The same ratios of rate constants may be calculated in a different way from the experiments with pure propane and ethane. If one assumes a constant rate of formation of R′ by reaction 5, and a loss of R′ equal at any time to the net decrease in hydrogen production (thus neglecting reaction 8), it may be shown that the net rate of production of R′ is given by

$$[3] \qquad dR'/dt = d_2H/dt - (dH_2/dt)_S$$

where $(dH_2/dt)_S$ is the rate of production of hydrogen in the steady state. R′ may then be evaluated as a function of time by a graphical integration of this equation, represented by the shaded areas in Figs. 1, 2, and 4. Using values of R′ obtained in this way, the data were plotted according to equation 2 and are shown in Figs. 5 and 6, for propane, and Fig. 7 for ethane. A similar graphical integration of the data for the impure ethane,

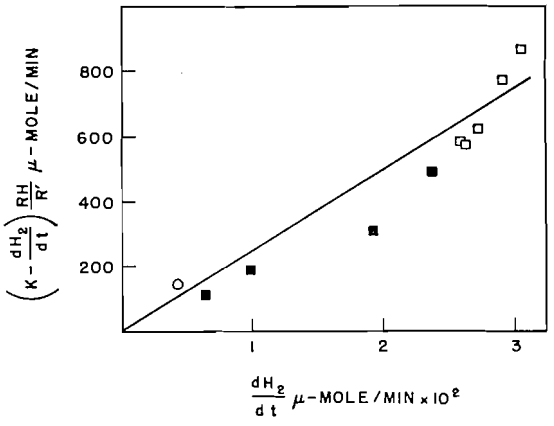

FIG. 7. A plot of equation 2 for ethane at 305-mm pressure; □ pure ethane, ■ Research-grade ethane, ○ added ethylene.

integrating backwards from the steady state, permitted calculation of ethylene concentrations in this system. These data are also plotted in Fig. 7, together with a single point obtained in the experiment, mentioned previously, when ethylene was added to ethane already irradiated until the steady state had been reached. From the pure ethane data, a rough value of $k_6/k_3 = 25{,}000$ was estimated from a straight line drawn through the origin (since k_7 is zero for ethylene). All ratios of rate constants are summarized in Table I.

DISCUSSION

The mercury-photosensitized decompositions of propane and ethane both show the same initial behavior that has been observed with *n*-pentane (1), *n*-butane (3), and some cyclo-alkanes (2). Because of the larger values of k_6/k_3, this was observed only at very low conversions (shown as upper abscissae in Figs. 1, 2, and 4). This was especially true for ethane, with which the steady state was attained after about 0.05% reaction, with an estimated steady-state concentration of ethylene of one part in 80,000. All previous studies of these reactions, in which hydrogen production was observed to be linear with time, were undoubtedly made in the steady-state region, and the measured quantum yields must be corrected upwards by the factor $(k_4+k_5)/k_4$, as indeed the authors anticipated. Bywater and Steacie reported a pressure-independent quantum yield of 0.50

Can. J. Chem. Downloaded from www.nrcresearchpress.com by 176.9.209.113 on 09/04/12
For personal use only.

Can. J. Chem. Downloaded from www.nrcresearchpress.com by 176.9.209.113 on 09/04/12
For personal use only.

for hydrogen production from propane at high pressures and room temperature (4), from which values of the initial quantum yield of 0.90 and 0.77 at 300 and 600 mm, respectively, may now be estimated. It may be noted that while the steady-state hydrogen yields at the two pressures are almost identical, confirming the pressure independence observed by Bywater and Steacie, the initial quantum yield appears to decrease with increasing pressure, suggesting, perhaps, the intermediate formation of an excited propane molecule of appreciable lifetime in the primary process. The quantum yields for the ethane decomposition reported by Darwent and Steacie (4), which tended towards unity at high pressure, should be revised upward in a similar way, although the correction here is smaller than for propane.

Values of k_5/k_4 for both ethyl and propyl radicals appear to be rather higher than those observed for thermally equilibrated radicals (5, 6, 7, 8). Some of this discrepancy may be attributed to inaccuracy in the extrapolation to zero time. However, it should be noted that in the steady-state region, where this ratio is estimated, a fraction $k_5/2(k_5+k_4)$ of the radicals in the system were formed via reaction 6, and would be vibrationally excited until stabilized by collisions. It has clearly been shown by several authors that such "hot" radicals tend to disproportionate rather than dimerize, and that these effects can persist to quite high pressures (9, 10, 11). The decrease in k_5/k_4 for propane in going from 300- to 600-mm pressure lends support to such an explanation. It might be noted, incidentally, that the "propyl" radicals in the present study are very probably isopropyl radicals (9).

Values of k_6/k_3 obtained from the experiments with propane–propylene mixtures (Table I) are in fair agreement with a value of about 3000 which may be estimated

TABLE I

Ratios of rate constants

Hydrocarbon	k_6/k_3	$k_7/(k_6+k_7)$	k_5/k_4
Propane, 300 mm	1515	0.032	0.08
Propane, 600 mm	1304	0.061	0.54
Ethane, 305 mm	25000	—	0.31

from separate measurements of the two rate constants by Schiff and Steacie (12), and Bradley, Melville, and Robb (13). The values of $k_7/(k_6+k_7)$, the fraction of hydrogen atoms reacting with propylene which abstract hydrogen (Table I), are rather lower than previous estimates of this ratio (14). The variation with pressure is probably not significant, considering the relatively long extrapolation which is involved.

The data from the experiments with pure propane at 300 mm, plotted in Fig. 5, using calculated values of the propylene concentration, lie considerably below the data from the experiments with added propylene, and, taking the same intercept, would lead to values of k_6/k_3 about half as large. A similar behavior was previously observed with *n*-pentane at 300 mm, which was tentatively attributed to the formation of 2-pentene in the disproportionation reaction (1). Such an explanation is impossible with propylene, and another cause must be sought. The values of the propylene concentration were calculated assuming, first, disappearance of propylene by reaction 6 only, and secondly, a constant rate of formation of propylene equal to that in the steady state. If propylene disappeared by other reactions, such as 8, or by direct photosensitized decomposition, the calculated values of propylene concentration would be too high, and k_6/k_3 would be low, as observed. It is doubtful, however, that reaction 8 would occur to such an extent,

Can. J. Chem. Downloaded from www.nrcresearchpress.com by 176.9.209.113 on 09/04/12
For personal use only.

and the very low concentrations of propylene eliminate the possibility of direct decomposition. It may be noted that the reaction sequence, 7+9, would merely substitute hexene for propylene, which would not have a large effect.

The second assumption, that the rate of production of propylene is constant, is more likely at fault. The high value of k_5/k_4 noted previously was attributed to preferential disproportionation of "hot" propyl radicals formed by reaction 6. Initially, however, all the propyl radicals were formed by reactions 2 and 3, and reaction 6 only becomes important as propylene accumulates in the system. Thus if "hot" propyl radicals were the cause of the high values of k_5/k_4 in the steady state, the rate of formation of propylene may have been much lower in the earlier stages of the reaction, and the graphical integration may have thus overestimated the concentration of propylene quite considerably. In support of this explanation is the improved agreement of the two sets of data at 600-mm pressure, where a lower value of k_5/k_4 was observed, and, presumably, "hot" radical reactions were less important. It seems that a similar explanation is probably valid for *n*-pentane. With ethane, at 305 mm, only one experiment was done with added ethylene, and it again lies somewhat above the data for pure ethane using calculated concentrations of ethylene. It should be noted, finally, that all these data for low concentrations of unsaturates lie in an inherently inaccurate region for the plot of equation 2, towards the right-hand side of Figs. 5, 6, and 7.

The value of k_6/k_3 of 25,000, calculated from the data obtained with pure ethane, may also be compared with values calculated from the literature. Berlie and LeRoy measured k_3 over a range of temperature, and from their data a collision yield of 4.5×10^{-8} at 24° C may be estimated (15). Bradley, Melville, and Robb estimated a collision yield of 9.3×10^{-5} for reaction 6 (13), which, assuming similar collision numbers, gives $k_6/k_3 = 2100$, an order of magnitude lower than found in the present study. Pursuing the discrepancy further, the collision yield of 4.5×10^{-8} for reaction 3, with ethane, is almost identical with the value 4.6×10^{-8} found by Schiff and Steacie for the same reaction with propane (12). From the results of Darwent and Roberts, however, a ratio k_3(propane)/k_3(ethane) of about 19, at 24° C, may be calculated (14). Taking a value of the ratio k_6(propylene)/k_6(ethylene) of 1.5 (13), from the present results a value of k_3(propane)/k_3(ethane) of about 25 may be estimated, in fair agreement with Darwent and Roberts, but much higher than the value of about 1 indicated from the combined results of Berlie and LeRoy, and Schiff and Steacie. One would expect the reaction of hydrogen atoms with the primary hydrogen atoms of ethane to be considerably slower than with the secondary hydrogen atoms of propane, and it would appear that the values of k_3 (ethane) found by Berlie and LeRoy may be too high, as has been suggested elsewhere (16), although perhaps the discrepancies are simply an indication of the rather unsatisfactory knowledge of accurate absolute values for the rates of hydrogen atom reactions.

It may be noted that all the relative rate constants measured in the present work are dependent upon the values chosen for K, the initial rate of hydrogen production. The sharply rising nature of the curves (Figs. 1, 2, and 4) makes this extrapolation to zero time inherently inaccurate, while the presence of even minute amounts of unsaturates initially present in the hydrocarbon could seriously reduce the observed value of K. The reasonable agreement between values of k_5/k_4 observed, and those measured by other methods suggests that the initial extrapolations were not grossly in error. The value of 0.9 for the initial quantum yield estimated for propane at 300 mm puts an upper limit on the possible value of K for that particular system. The reaction

$$H + R + M \rightarrow RH + M \qquad [10]$$

may be of some importance, especially with ethane (6), and probably accounts for the decrease in quantum yield with decreasing ethane pressure observed by Bywater and Steacie (4). The occurrence of this reaction would not seriously affect the kinetics and rate constants observed in the present study, since for a given pressure and light intensity, it may be regarded, to a first approximation, simply as a constant factor reducing the extent of reaction 2.

A careful measurement of initial quantum yields of the mercury-photosensitized decompositions of the simple alkanes would be of obvious value in determining the exact nature of the primary process, and it is perhaps worth while to note briefly the conditions essential for such measurements as indicated by the present study. These are: (1) very low conversions, preferably 10 or 100 times lower than in the present work, in order to improve the accuracy of the extrapolation to zero time; (2) rigorous purification of hydrocarbons to eliminate trace amounts of unsaturates; and (3) low light intensities, sufficiently low to make reaction 10 negligible.

The author wishes to thank Miss M. Cooper and Miss M. Bilevicius, summer research assistants in 1957 and 1958 respectively, who performed some of the experimental work. The author also gratefully acknowledges tenure of a National Research Council of Canada postdoctoral fellowship.

REFERENCES

1. BACK, R. A. Trans. Faraday Soc. **54**, 512 (1958).
2. BECK, P. W., KNIEBES, D. V., and GUNNING, H. E. J. Chem. Phys. **22**, 672 (1954).
3. CVETANOVIĆ, R. To be published. (Reported, in part, at the 1958 annual meeting of the Royal Society of Canada at Edmonton.)
4. BYWATER, S. and STEACIE, E. W. R. J. Chem. Phys. **19**, 319, 326 (1951).
5. BRINTON, R. K. and STEACIE, E. W. R. Can. J. Chem. **33**, 1840 (1955).
6. SMITH, M. J., BEATTY, P. M., PINDER, J. A., and LEROY, D. J. Can. J. Chem. **33**, 821 (1955).
7. DURHAM, R. W. and STEACIE, E. W. R. Can. J. Chem. **31**, 377 (1953).
8. BLACET, F. E. and CALVERT, J. G. J. Am. Chem. Soc. **73**, 661 (1951).
9. BRADLEY, J. N., MELVILLE, H. W., and ROBB, J. C. Proc. Roy. Soc. A, **236**, 318, 339 (1956).
10. HOEY, G. R. and LEROY, D. J. Can. J. Chem. **33**, 580 (1955).
11. TURNER, A. H. and CVETANOVIĆ, R. Can. J. Chem. **37**, 1075 (1959).
12. SCHIFF, H. I. and STEACIE, E. W. R. Can. J. Chem. **29**, 1 (1951).
13. BRADLEY, J. N., MELVILLE, H. W., and ROBB, J. C. Proc. Roy. Soc. A, **236**, 454 (1956).
14. DARWENT, B. de B. and ROBERTS, R. Discussions Faraday Soc. **14**, 55 (1953).
15. BERLIE, M. R. and LEROY, D. J. Discussions Faraday Soc. **14**, 50 (1953).
16. TROTMAN-DICKENSON, A. F. Gas kinetics. Butterworth Scientific Publications. London. 1955.

Can. J. Chem. Downloaded from www.nrcresearchpress.com by 176.9.209.113 on 09/04/12
For personal use only.

Can. J. Chem. Downloaded from www.nrcresearchpress.com by 176.9.209.113 on 09/04/12
For personal use only.

THE ABSOLUTE CONFIGURATION OF (+)-DES-(OXYMETHYLENE)-LYCOCTONINE HYDRIODIDE MONOHYDRATE AND (+)-DEMETHANOLACONINONE HYDRIODIDE TRIHYDRATE[1]

MARIA PRZYBYLSKA AND LÉO MARION

ABSTRACT

By X-ray analyses it has been possible to derive the absolute configuration of (+)-des-(oxymethylene)-lycoctonine and that of (+)-demethanolaconinone. These are shown in Figs. 2 and 3.

The detailed X-ray analyses of (+)-des-(oxymethylene)-lycoctonine hydriodide monohydrate (1) and (+)-demethanolaconinone hydriodide trihydrate (2) showed that these compounds have the same carbon–nitrogen ring structure (Fig. 1). The determinations of absolute configuration have since been carried out in order to establish whether the skeleton in Fig. 1 or its mirror image represents the ring structure of these compounds.

The principle on which it is possible to distinguish between optical isomers by means of X-rays in the case of anomalous dispersion was outlined by Bijvoet (3) and since then the absolute configuration of several compounds has been established (4, 5, 6).

The equi-inclination Weissenberg films were indexed taking into account the rotation of the crystal, the translation of the film, the position of the film, and the direction of the inclination of the camera (7). On the examination of Weissenberg films eight reflections corresponding to a right-handed set of axes were chosen for each compound and the intensities I_H and $I_{\bar{H}}$ were estimated by visual comparison with an intensity strip. In each case the shortened and lengthened diffraction spots were measured and then averaged.

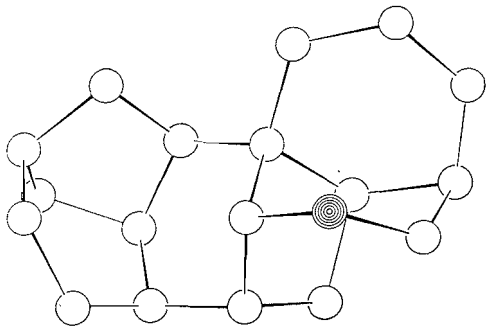

FIG. 1. The carbon–nitrogen skeleton of des-(oxymethylene)-lycoctonine and demethanolaconinone.

The intensities $I_H = KF_H.F_H^*$ and $I_{\bar{H}} = KF_{\bar{H}}.F_{\bar{H}}^*$ were calculated using the refined atomic co-ordinates obtained from the X-ray analyses. They corresponded to molecular models in right-handed sets of axes, the photographs of which were already published (1, 2). Their carbon–nitrogen skeleton is shown in Fig. 1. The contribution made by the hydrogen atoms was not taken into account, but it would certainly be small and considering large differences observed in intensities between I_H and $I_{\bar{H}}$, it could safely be neglected.

[1]*Manuscript received August 13, 1959.*
Contribution from the Division of Pure Chemistry, National Research Council, Ottawa, Canada.
Issued as N.R.C. No. 5360.

The values for the real and imaginary dispersion corrections were those given by Dauben and Templeton (8). For the scattering factor for the iodine atom and CuK_α radiation they were $\Delta f' = -1.1$ e.Å^{-2} and $\Delta f'' = 7.2$ e.Å^{-2}.

(+)-Des-(oxymethylene)-lycoctonine Hydriodide Monohydrate

(+)-Des-(oxymethylene)-lycoctonine hydriodide monohydrate, $C_{24}H_{39}O_6N.HI.H_2O$, crystallizes in the space group $P2_1$. The authenticated sample was kindly provided by Dr. O. E. Edwards, who found the optical rotation of the anhydrous compound to be: $[\alpha]_D^{28}$ +6±2° (*c*, 1.0 in absolute ethanol). The *b* axis was taken as unique, polar axis and therefore the reflections which showed the violation of Friedel's law were *hkl* and $h\bar{k}l$ ($I_{h\bar{k}l} = I_{\bar{h}\bar{k}\bar{l}}$). They were obtained by inclining the Weissenberg camera in opposite ways with respect to the X-ray beam. The films were exposed for identical periods of time and developed simultaneously. The crystal used was very small, roughly cylindrical in shape, about 0.06 mm in diameter, hence absorption corrections were not applied. The observed and calculated ratios of intensities are given in Table I.

TABLE I

(+)-Des-(oxymethylene)-lycoctonine hydriodide monohydrate

hkl	$I_{hkl}/I_{h\bar{k}\bar{l}}$, calculated	$I_{hkl}/I_{h\bar{k}\bar{l}}$, observed
$11\bar{2}$	1.7	2.2
213	0.4	0.5
510	1.2	1.2
$31\bar{4}$	1.5	1.6
$41\bar{4}$	0.6	0.6
610	0.8	0.7
$51\bar{4}$	2.0	2.4
$61\bar{4}$	1.3	1.3

The agreement is satisfactory and it can be concluded that the molecular model used for calculation represents the absolute configuration of this compound. The structural formula emphasizing the diterpenoid character of the (+)-isomer is therefore as shown in Fig. 2. It should be noted that if the mirror image of that molecule was used for calculation, the ratio $I_H/I_{\bar{H}}$ would be inverted.

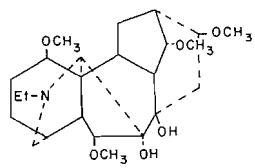

FIG. 2. (+)-Des-(oxymethylene)-lycoctonine.

(+)-Demethanolaconinone Hydriodide Trihydrate

The crystals of (+)-demethanolaconinone hydriodide trihydrate, $C_{24}H_{35}O_8N.HI.3H_2O$, were prepared and authenticated by Dr. H. Mayer, who found the rotation was $[\alpha]_D^{25}$ +59.2±1.5° (*c*, 1.04 in water) (9). The space group of this compound is $P2_12_12_1$. The three axes of the unit cell are polar and therefore $I_{\bar{h}kl} = I_{h\bar{k}l} = I_{hk\bar{l}} = I_{\bar{h}\bar{k}\bar{l}}$.

The crystal used was cylindrical in shape, about 0.12 mm in diameter, and the absorption corrections were not applied.

Can. J. Chem. Downloaded from www.nrcresearchpress.com by 176.9.209.113 on 09/04/12
For personal use only.

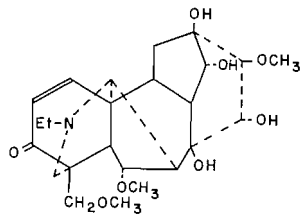

FIG. 3. (+)-Demethanolaconinone.

The results in Table II indicate that the (+)-isomer can be represented by the formula in Fig. 3 and its carbon–nitrogen skeleton by Fig. 1.

It is of interest to note that Dvornik and Edwards have concluded on molecular rotation grounds that the *Aconitum* alkaloid atisine (10) and the *Delphinium* alkaloid

TABLE II

(+)-Demethanolaconinone hydriodide trihydrate

hkl	$I_{hkl}/I_{\bar{h}kl}$, calculated	$I_{hkl}/I_{\bar{h}kl}$, observed
511	1.8	2.2
513	0.5	0.5
611	0.4	0.3
2, 10, 2	0.4	0.3
751	3.0	3.5
821	5.7	3.2
822	1.6	1.5
912	0.6	0.7

ajaconine (11) also bear mirror image relationship to the common diterpenes. The biosynthesis of the lycoctonine family of alkaloids undoubtedly proceeds via intermediates with the atisine-type skeleton (12, 13) and the above correspondence of absolute configuration is in agreement with this.

REFERENCES

1. PRZYBYLSKA, M. and MARION, L. Can. J. Chem. **34**, 185 (1956).
2. PRZYBYLSKA, M. and MARION, L. Can. J. Chem. **37**, 1116 (1959).
3. BIJVOET, J. M. Proc. Acad. Sci. Amsterdam, **52**, 313 (1949).
4. TROMMEL, J. and BIJVOET, J. M. Acta Cryst. **7**, 703 (1954).
5. PEEDERMAN, A. F. Acta Cryst. **9**, 824 (1956).
6. HANSON, A. W. and AHMED, F. R. Acta Cryst. **11**, 724 (1958).
7. PEEDERMAN, A. F. and BIJVOET, J. M. Acta Cryst. **9**, 1012 (1956).
8. DAUBEN, C. H. and TEMPLETON, D. H. Acta Cryst. **8**, 841 (1955).
9. MAYER, H. and MARION, L. Can. J. Chem. **37**, 856 (1959).
10. DVORNIK, D. and EDWARDS, O. E. Chem. & Ind. 623 (1958).
11. DVORNIK, D. and EDWARDS, O. E. Proc. Chem. Soc. 280 (1958).
12. COOKSON, R. C. and TREVETT, M. E. J. Chem. Soc. 3121 (1956).
13. VALENTA, Z. and WIESNER, K. Chem. & Ind. 354 (1956).

Can. J. Chem. Downloaded from www.nrcresearchpress.com by 176.9.209.113 on 09/04/12
For personal use only.

Can. J. Chem. Downloaded from www.nrcresearchpress.com by 176.9.209.113 on 09/04/12
For personal use only.

THERMAL DECOMPOSITION OF 1-HEXANETHIOL[1]

PAUL E. GAGNON, JEAN L. BOIVIN,[2] AND DONALD C. WATSON[3]

ABSTRACT

The uncatalyzed thermal decomposition of 1-hexanethiol was studied at temperature varying from 300 to 700° C and was observed to give 42% of olefinic hydrocarbons at 600° C. Dialkyl sulphides were also obtained at 550° C with a maximum yield of 13.3% at 650° C. The effect of sulphide catalyst was investigated and nickel sulphide was found to be the most effective: at low temperature (150–450° C) dihexylsulphide was produced and at higher temperature (450–600° C) olefinic hydrocarbons were obtained. Very little catalytic effect was observed with molybdenum and cadmium sulphides.

INTRODUCTION

The thermal decomposition of aliphatic mercaptans has been extensively studied by several investigators (1 to 12), but it appears from the various results obtained that additional studies of this pyrolysis should be made in the absence or presence of catalysts at temperature of 150 to 750° C using 1-hexanethiol.

EXPERIMENTAL

1-Hexanethiol was distilled and the fraction boiling at 153–154° C was used in the pyrolysis. Other materials had to be prepared for purpose of identification and analysis: dihexyl sulphide (13), dihexyl disulphide (14), and 1-hexene (15).

The apparatus used in the thermal decomposition of 1-hexanethiol was essentially the same as the one described in an earlier paper (12), together with the general procedure.

The liquid pyrolyzate was analyzed for mercaptan by the method of Kimball, Kramer, and Reid (16) and also by an amperometric method (17, 18) and for the olefinic material by an iodine method (19). Dialkyl sulphide was estimated by the bromide–bromate reagent (20), dialkyl disulphide by the Kolthoff method (21), and sulphur by a colorimetric method using sodium cyanide (22).

The gaseous pyrolyzate was analyzed by the Orsat apparatus (12).

For the uncatalyzed thermal decomposition, the pyrolysis tube was filled with Pyrex glass helices forming a column 40 cm high in the reaction zone; then 1-hexanethiol was dropped into the vaporizing flask at the rate of 0.5 g per minute. The liquid and gaseous pyrolyzates were analyzed and sampled for infrared measurements. Tables I and II show the composition of the liquid and gaseous products as a function of the temperature. Elemental sulphur could not be detected in the pyrolyzate residue until the pyrolysis temperature had risen to 500° C. At 550° C, the pyrolyzate contained 0.1% sulphur and only 0.3 at 650° C.

In the metal sulphide catalyzed decompositions, the pyrolysis tube was packed as follows: a 2-cm-thick plug of glass wool was placed in the pyrolysis tube at the lower end of the decomposition zone. A 3-cm layer of 8-mm glass helices was placed on top of the plug, followed by a 3-cm layer of the metal sulphide catalyst. The placing of alternate layers of glass helices and catalyst was continued until a column 40 cm high was built up

[1]*Manuscript received July 6, 1959.*
Contribution from the Department of Chemistry, Laval University, Quebec, Que., with financial assistance from the Defence Research Board and the National Research Council of Canada. This paper constitutes part of a thesis submitted to the Graduate School, Laval University, in partial fulfillment of the requirements for the degree of Doctor of Science.
[2]*Defence Research Board, Canadian Armament Research and Development Establishment, Valcartier, Que.*
[3]*St. Patrick's College, University of Ottawa, Ottawa, Ont.*

in the decomposition tube. This type of packing was used in preference to a solid column of metal sulphide catalyst in order to prevent channeling and hence loss of catalyst contact of the vaporized mercaptan. The results obtained are shown in Tables I and II for the composition of liquid and gaseous pyrolyzates. With the sulphide catalysts, elemental sulphur was not detected in pyrolyzate liquids at temperatures below 400° C. At a decomposition temperature of 550° C, the sulphur content was only 0.1% with NiS and 0.2 with MoS_3 and CdS.

TABLE I

Liquid products of 1-hexanethiol decomposition

Catalyst	Temp., °C	Liquid recovery, %	Percentage composition of liquid products			
			Mercaptan	Olefin	Sulphide	Disulphide
Nil	300	90.7	100.0	—	—	—
	350	90.6	100.0	—	—	—
	400	88.4	100.0	—	—	—
	450	87.3	94.5	0.7	0.0	0.2
	500	77.5	87.7	8.9	0.0	1.8
	550	61.0	57.8	27.4	0.1	2.5
	600	25.4	15.3	42.3	8.1	2.5
	650	11.9	0.0	27.0	13.5	2.7
	700	6.8	0.0	18.5	0.1	2.7
NiS	200	86.9	71.1	0.0	21.5	0.0
	250	85.8	20.9	0.0	35.2	0.0
	300	83.5	17.7	2.3	34.0	0.0
	350	72.2	29.2	10.4	25.4	0.0
	400	64.1	44.0	16.9	12.2	3.0
	450	58.9	57.0	23.0	0.0	9.5
	500	45.7	48.2	26.2	0.0	16.1
	550	32.8	21.0	17.7	0.0	14.0
	600	14.8	0.0	5.4	0.0	12.8
MoS_3	300	82.6	89.0	3.2	0.3	0.0
	350	78.4	66.2	6.2	9.3	1.3
	400	74.6	40.7	9.1	12.8	4.8
	450	70.6	30.7	19.1	15.4	6.9
	500	65.3	15.8	28.0	28.7	7.0
	550	40.7	13.2	24.4	32.6	9.0
	600	12.4	0.0	22.2	34.0	12.8
CdS	300	87.6	85.2	1.0	0.0	0.0
	350	82.6	68.2	4.8	2.3	0.0
	400	78.2	52.0	9.8	10.7	1.3
	450	66.7	40.8	18.7	17.3	2.4
	500	38.5	27.6	29.2	27.4	3.6
	550	29.6	14.0	22.6	26.6	13.0
	600	17.4	0.0	6.7	20.0	16.2

DISCUSSION

There is a general agreement that the thermal decomposition of an aliphatic mercaptan will result in the formation of a dialkyl sulphide and an unsaturated hydrocarbon. Several investigators (1, 2, 12) have pointed out that at a high decomposition temperature, the mercaptan undergoes loss of hydrogen sulphide, which results in the formation of an unsaturated hydrocarbon as the main product. At a lower decomposition temperature, there is only partial desulphurization, and a dialkyl sulphide is the major product formed. As a result of the present investigation, this generalization has been found to be true only under certain conditions.

In the thermal decomposition of 1-hexanethiol without catalyst, it was found that unsaturated hydrocarbons were produced at lower temperatures than the dialkyl

Can. J. Chem. Downloaded from www.nrcresearchpress.com by 176.9.209.113 on 09/04/12
For personal use only.

TABLE II

Gaseous products of 1-hexanethiol decomposition

Catalyst	Temp., ° C	Gas produced, % by weight	Percentage composition of gaseous products			
			Hydrogen sulphide	Olefin	Hydrogen	Residual
Nil	450	4.7	90.0	0.0	0.0	10.0
	500	14.5	79.8	7.0	0.4	12.8
	550	31.0	61.2	18.5	2.4	17.9
	600	66.6	44.0	27.1	2.7	26.2
	650	80.1	33.4	27.8	2.9	36.2
	700	85.2	30.1	26.1	2.2	41.4
NiS	350	13.5	81.2	0.4	0.4	18.0
	400	21.6	70.0	5.6	6.1	18.3
	450	26.8	56.8	9.2	10.2	23.8
	500	40.0	46.2	14.8	13.4	25.6
	550	52.9	30.6	26.4	11.8	31.2
	600	70.9	20.2	34.8	2.8	42.2
MoS_3	350	11.2	87.5	0.1	0.0	12.4
	400	15.2	83.3	3.9	1.3	11.8
	450	20.5	80.0	9.7	3.8	6.5
	500	45.1	71.2	15.8	6.8	6.2
	550	73.4	49.8	21.2	6.4	22.6
	600	82.6	14.4	26.1	7.3	52.2
CdS	400	11.8	78.6	1.3	1.6	18.5
	450	23.3	75.0	8.0	5.2	11.8
	500	51.5	50.8	15.2	6.3	27.7
	550	60.4	36.0	22.6	6.5	34.9
	600	72.6	25.2	28.1	6.8	39.9

sulphides. Olefinic hydrocarbons were first detected at 450° C, and reached a maximum concentration of 42.3% at a decomposition temperature of 600° C. On the other hand, dihexyl sulphide was not formed until 550° C, and the maximum content of 8.1% was obtained at a decomposition temperature of 600° C.

These observations were not found true of the subsequent catalytic studies. With nickel sulphide as catalyst, dialkyl sulphide formation began as low as 200° C and increased to give a maximum pyrolyzate concentration of over 35% at 250° C to 300° C, the temperature range at which olefinic hydrocarbon formation began. In the case of the molybdenum and cadmium sulphide catalysts, analysis of the liquid residues indicated that sulphide and unsaturated hydrocarbons were both formed at the same decomposition temperature range, i.e., between 300 and 350° C.

It then appears that in non-catalytic decompositions, unsaturated hydrocarbons are produced at a lower temperature than the dialkyl sulphides. A very active catalyst like nickel sulphide reverses this, causing sulphides to be produced at the lower temperature. Molybdenum and cadmium sulphides, on the same basis, are classed as possessing only moderate catalytic activity, in that sulphides and olefins are produced at the same temperature.

The effect of the catalyst on the decomposition of 1-hexanethiol is also indicated by the residual thiol content of the liquid samples. As noted from the analytical results, 1-hexanethiol undergoes marked decomposition without catalyst in a very narrow temperature range of 100° C, i.e., between 500 and 600° C. In the studies with nickel sulphide, decomposition took place in two stages. The first decomposition, which was accompanied by considerable sulphide formation, was determined as catalytic, extending from 150 to

Can. J. Chem. Downloaded from www.nrcresearchpress.com by 176.9.209.113 on 09/04/12
For personal use only.

450° C. The second stage was determined to be thermal, extending from 450 to 600° C. However, in molybdenum and cadmium sulphide decompositions, thiol decomposition is considered as a one-stage process, due mainly to a thermal effect. The decomposition range extended over a much wider temperature zone, from about 300 to 600° C.

Similar conclusions regarding the activities of the different catalysts were indicated from dialkyl disulphide formation. During the non-catalytic decompositions, very little disulphide was produced. The disulphide content did not rise above 3% of the total pyrolyzate, and therefore could not be considered as a major decomposition product. However, in nickel sulphide decomposition studies, disulphide was formed in moderate quantities in the 450 to 600° C temperature range. With the sulphides of molybdenum and cadmium, the disulphide content accounted for over 10% of the total only in the final 50° C decomposition range studied, i.e., from 550 to 600° C.

From the analytical results, it should be noted that there were a number of liquid and gaseous samples obtained during the pyrolysis of 1-hexanethiol, in which the known components, analyzed by chemical means, constituted less than 75% of the total sample weight. In most cases, these were obtained from high temperature decomposition studies, both with and without catalyst. Infrared analysis indicated the formation of many decomposition products containing less than six carbon atoms. These smaller fragments included the saturated hydrocarbon gases, methane, ethane, propane, and butane, as well as the olefinic hydrocarbons, ethylene, propylene, and butylene. A number of sulphur-containing compounds such as thiophene and carbon disulphide were also identified by infrared examination.

The formation of hydrogen sulphide could be considered as a function of carbon–sulphur cleavage whereas gaseous hydrocarbon formation would indicate carbon–carbon cleavage. The relative quantities of these two components in any given sample indicated the major point of cleavage at a particular decomposition temperature. In non-catalytic pyrolysis, hydrogen sulphide was produced at 450° C, and remained the main gaseous component until a temperature of 600° C had been reached. In the 600 to 700° C range, hydrocarbons formed the greater part of the effluent gas, indicating that the above 600° C cleavage of the carbon chain occurred more readily than that of the carbon–sulphur bond. From the results of gas analysis with the sulphide catalysts, the same generalization holds true, with the exception that lower temperatures were required. Hydrogen sulphide was produced at about 350° C and carbon–carbon cleavage did not become the predominant reaction until a decomposition temperature of 500° C had been reached.

One final difference between catalytic and non-catalytic decomposition was indicated by the hydrogen content of the effluent gas. In non-catalytic decomposition, less than 3% hydrogen was produced throughout the temperature range studied. Sulphide catalysts, however, gave an increased hydrogen content of the effluent gas. With nickel sulphide, 15% hydrogen was produced at 500° C; approximately half this quantity was obtained with molybdenum and cadmium sulphide catalysts.

REFERENCES

1. SABATIER, P. and MAILHE, A. Compt. rend. **150**, 1569 (1910).
2. KAHN, H. Bull. soc. chim. Roumanie, **5**, 70 (1923).
3. FARAGHER, W. F., MORRELL, J. C., and COMAY, S. Ind. Eng. Chem. **20**, 527 (1928).
4. HURD, C. D. The pyrolysis of carbon compounds. The Chemical Catalog Co., Inc., New York. 1929.
5. ELGIN, J. C. Ind. Eng. Chem. **22**, 1290 (1930).
6. ELGIN, J. C., WILDER, G. W., and TAYLOR, H. S. Ind. Eng. Chem. **22**, 1284 (1930).
7. MALISOFF, W. M. and MARKS, E. M. Ind. Eng. Chem. **23**, 114 (1931).
8. TITS-SKVORTSOVA, I. N., LEVINA, S. YA., LEONOVA, A. I., and KARASEVA, E. A. Zhur. Obshcheĭ Khim. **21**, 242 (1950).

Can. J. Chem. Downloaded from www.nrcresearchpress.com by 176.9.209.113 on 09/04/12
For personal use only.

9. TITS-SKVORTSOVA, I. N., LEONOVA, A. I., and LEVINA, S. YA. Doklady Akad. Nauk S.S.S.R. **84**, 741 (1952).
10. THOMPSON, C. J., MEYER, R. A., and BALL, J. S. J. Am. Chem. Soc. **74**, 3284 (1952).
11. THOMPSON, C. J., MEYER, R. A., and BALL, J. S. J. Am. Chem. Soc. **74**, 3287 (1952).
12. BOIVIN, J. L. and MACDONALD, R. Can. J. Chem. **33**, 1281 (1955).
13. FEHNEL, E. A. and CARMACK, M. J. Am. Chem. Soc. **71**, 92 (1949).
14. STUTZ, R. E. and SHRINER, R. L. J. Am. Chem. Soc. **55**, 1243 (1933).
15. SCHMITT, C. G. and BOORD, C. E. J. Am. Chem. Soc. **54**, 754 (1932).
16. KIMBALL, J. W., KRAMER, R. L., and REID, E. E. J. Am. Chem. Soc. **43**, 1199 (1921).
17. BIRCH, S. F. and NORRIS, W. S. G. P. J. Chem. Soc. **129**, 2545 (1929).
18. BORGSTROM, P. and REIK, E. E. Ind. Eng. Chem. Anal. Ed. **1**, 186 (1929).
19. MCILHINEY, P. C. J. Am. Chem. Soc. **21**, 1084 (1899).
20. SIGGIA, S. and EDSBERG, R. L. Anal. Chem. **20**, 938 (1948).
21. KOLTHOFF, I. M., MAY, D. R., MORGAN, P., LAITENEN, H. A., and O'BRIEN, A. S. Ind. Eng. Chem. Anal. Ed. **18**, 442 (1946).
22. BARTLETT, J. K. and SKOOG, D. A. Anal. Chem. **26**, 1008 (1954).

Can. J. Chem. Downloaded from www.nrcresearchpress.com by 176.9.209.113 on 09/04/12
For personal use only.

Can. J. Chem. Downloaded from www.nrcresearchpress.com by 176.9.209.113 on 09/04/12
For personal use only.

A SYNTHESIS OF HARMALINE[1]

IAN D. SPENSER

ABSTRACT

The synthesis of 1-methyl-3,4-dihydro-β-carboline (harmalan) and of two of its derivatives by dehydration of the corresponding 1-hydroxymethyl-1,2,3,4-tetrahydro-β-carbolines is described. Harmalan was also obtained by oxidative decarboxylation of 1-methyl-1,2,3,4-tetrahydro-β-carboline-1-carboxylic acid.

Harmalol (I), isolated from *Peganum harmala* L. (1), and the corresponding methyl ether harmaline (II), obtained from the same plant (1), as well as from *Banisteria caapi* Spruce (2), are the only 3,4-dihydro-β-carboline derivatives hitherto found to occur in nature. All other naturally occurring compounds containing the β-carboline ring system are either fully aromatic (IV) or contain a 1,2,3,4-tetrahydro-structure (VI) (3*a*). Amongst the structurally analogous isoquinoline alkaloids only two, psychotrine and O-methyl-psychotrine (3*b*) have so far been recognized as 3,4-dihydro-derivatives. The 3,4-dihydro-structure thus represents a rare oxidation state in these plant bases.

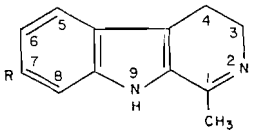

I R = OH
II R = OCH_3
III R = H

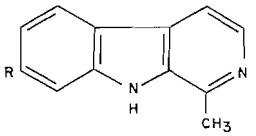

IV R = H
V R = OCH_3

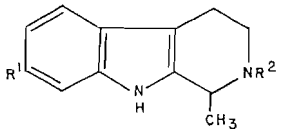

VI $R^1 = R^2 = H$
VII $R^1 = H$, $R^2 = CH_3$
VIII $R^1 = OCH_3$, $R^2 = H$

Although the biosynthesis of the β-carboline alkaloids has not so far been investigated, it has long been assumed (4) that the nucleus arises in the plant by a Mannich-type condensation of tryptamine or oxytryptamine with an aldehyde to yield a tetrahydro-β-carboline derivative. Such condensations have been carried out in vitro under mild conditions of temperature and pH (e.g. (5)), and a number of tetrahydro-β-carbolines have been found in plants (e.g. 1-methyl-1,2,3,4-tetrahydro-β-carboline (eleagnine) (VI) (6, 7, 8), 1,2-dimethyl-1,2,3,4-tetrahydro-β-carboline (leptocladine) (VII) (9), and 1-methyl-7-methoxy-1,2,3,4-tetrahydro-β-carboline (tetrahydroharmine) (VIII) (2, 8)).

Partial dehydrogenation of these tetrahydro-derivatives has been postulated (4, 7, 10) to account for the origin of the dihydro-derivatives harmaline (II) and harmalol (I), and further loss of hydrogen for that of the β-carbolines (e.g. 1-methyl-β-carboline (harman) (IV) (3*a*) and its 7-methoxy-derivative (harmine) (V) (3*a*)).

If this stepwise oxidation sequence were indeed to represent the biosynthetic origin of dihydro-β-carbolines and β-carbolines, the former might be expected to accompany the latter frequently in the plant. The comparative rarity of the dihydro-derivatives is thus puzzling and led us to consider other possible biogenetic routes.

Neither of the reported syntheses of harmaline (II) can be regarded as models for in vivo formation. The synthetic base was first obtained (11) by cyclization of 1-acetyl-2-

[1]*Manuscript received July 2, 1959.*
Contribution from the Department of Chemistry, McMaster University, Hamilton, Ontario.

aminoethyl-6-methoxyindole (IX), and later by Bischler–Napieralski ring closure of

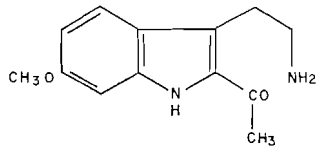

(IX)

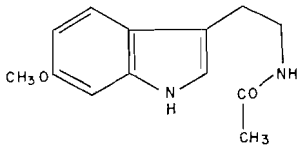

(X)

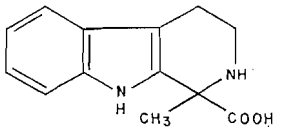

(XI)

N_β-acetyl-6-methoxytryptamine (X) (12). Much earlier Perkin and Robinson (4) had obtained the compound by oxidation of tetrahydroharmine (VIII) with permanganate in acetone. Under nonacidic conditions dihydro-β-carbolines thus appear to be stable to oxidizing agents. This stability has now been confirmed: 1-methyl-3,4-dihydro-β-carboline (III) (harmalan) was obtained in good yield both by oxidation of 1-methyl-1,2,3,4-tetrahydro-β-carboline (VI) (13) in acetone with permanganate, and also by oxidative decarboxylation of 1-methyl-1,2,3,4-tetrahydro-β-carboline-1-carboxylic acid (XI) (5) with silver oxide in aqueous solution. This latter synthesis of a dihydro-β-carboline was modelled on our studies of oxidative decarboxylation of amino acids (14).

Under acid conditions (nitric acid (15), chromic acid (16), acid permanganate (12, 17)) dihydro-β-carbolines are oxidized to β-carbolines. Oxidation of tetrahydro-β-carbolines under similar conditions does not take place as readily (12) and leads to β-carbolines in poor yield (18). β-Carbolines are obtained in good yield by acid dichromate oxidation of tetrahydro-β-carboline-3-carboxylic acids (XII), decarboxylation accompanying the reaction (19). The biogenetic origin of β-carbolines, without intermediate formation of dihydro-β-carbolines, has been proposed in analogy to this reaction sequence (20).

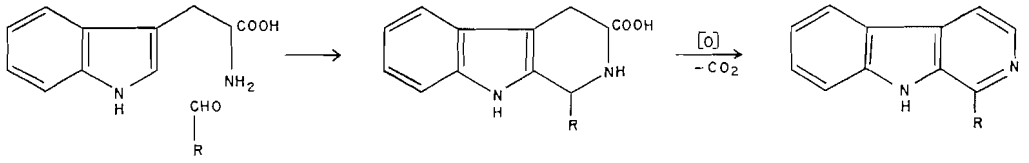

(XII) (IV)

In the present synthesis harmaline was obtained in two physiologically possible steps, the C=N double bond being introduced by dehydration, rather than oxidatively: 6-Methoxytryptamine (21)[2] was condensed with glycolaldehyde to give (±)-1-hydroxymethyl-7-methoxy-1,2,3,4-tetrahydro-β-carboline (XIV) in good yield. This step involves the usual Mannich reaction between a biogenetic amine and an aldehyde. The latter, glycolaldehyde, is known to arise enzymically *inter alia* by decarboxylation of hydroxypyruvic acid (22), a metabolic precursor of serine (23).

In a similar manner tryptamine gave (±)-1-hydroxymethyl-1,2,3,4-tetrahydro-β-carboline (XIII), and *dl*-tryptophan yielded the corresponding 3-carboxylic acid (XV) (24).

[2]*I am grateful to Dr. R. A. Abramovitch, University of Saskatchewan, for a specimen of this material.*

Can. J. Chem. Downloaded from www.nrcresearchpress.com by 176.9.209.113 on 09/04/12
For personal use only.

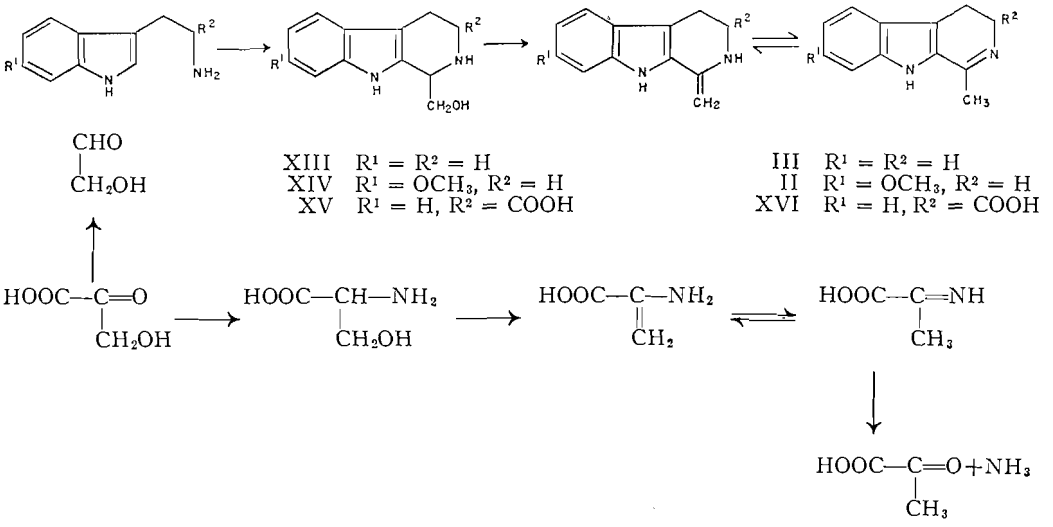

Dehydration of these tetrahydro-derivatives gave the corresponding 3,4-dihydro-β-carbolines. Harmaline (II) was obtained in 70% yield with 90% w/w phosphoric acid, harmalan (III) in 75% yield with phosphoric acid and in 25% yield with 50% w/v sulphuric acid. In each instance the product was indistinguishable from an authentic specimen.[3] 1-Methyl-3,4-dihydro-β-carboline-3-carboxylic acid (XVI) was obtained in moderate yield with 50% w/v sulphuric acid. The course of the dehydration reaction was followed in each case by observing the change in ultraviolet absorption (Figs. 1 and 2).

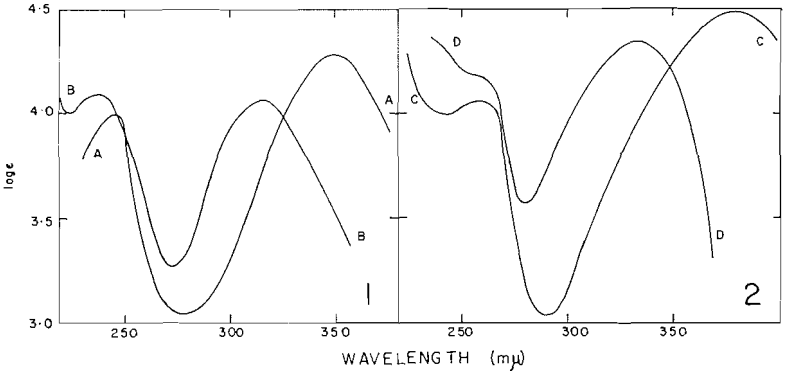

FIG. 1. 1-Methyl-3,4-dihydro-β-carboline (harmalan). Curve A, in 0.1 *N* HCl in aqueous ethanol; curve B, in 0.1 *N* NaOH in aqueous ethanol.
FIG. 2. 1-Methyl-7-methoxy-3,4-dihydro-β-carboline (harmaline). Curve C, in 0.1 *N* HCl in aqueous ethanol; curve D, in 0.1 *N* NaOH in aqueous ethanol.

The dihydro-β-carboline (XVI) derived from tryptophan had not hitherto been described. Another synthetic route was therefore sought to confirm its identity. Bischler–Napieralski ring closure of N_β-acetyltryptophan was not suitable since it has proved unsuccessful with classical dehydrating agents (24, 25) while with polyphosphoric acid

[3]*I am greatly indebted to Dr. T. M. Sharp, Wellcome Laboratories, London, England, for a sample of natural harmaline.*

Can. J. Chem. Downloaded from www.nrcresearchpress.com by 176.9.209.113 on 09/04/12
For personal use only.

it was accompanied by decarboxylation and aromatization (26) to yield 1-methyl-β-carboline (IV) instead of the desired product. However, cyclization of ethyl α-acetamido-α-carbethoxy-β-(3-indolyl)-propionate (XVII) (27) gave 1-methyl-3,3-dicarbethoxy-3,4-dihydro-β-carboline (XVIII) (28) and the latter was saponified and decarboxylated, to give a 65% yield of the desired compound (XVI), identical with a specimen obtained by dehydration.

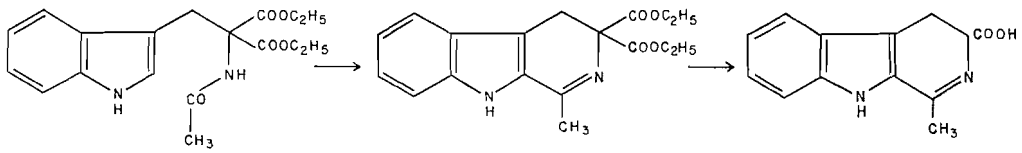

(XVII) (XVIII) (XVI)

A second, as yet unidentified material, differing in infrared and ultraviolet absorption from the main product was also isolated in this reaction.

The dehydration step in the present harmaline synthesis parallels the catabolic pathway of serine (29), enzymatic dehydration to α-aminoacrylic acid, and rearrangement to α-iminopropionic acid. Whereas this compound spontaneously hydrolyzes to pyruvic acid and ammonia, the imino-linkage in harmaline is stabilized by conjugation with the indole system. In vitro this dehydration of serine requires strong acid (30).

The synthesis of harmaline here described is put forward as a possible biogenetic route and an alternative to the oxidative pathway postulated by earlier authors (4, 7, 10). The recent confirmation (31) of the structure of calycotomine as 1-hydroxymethyl-6,7-dimethoxy-1,2,3,4-tetrahydroisoquinoline, analogous to the intermediate in the present synthesis, lends additional interest to this hypothesis.

EXPERIMENTAL

1-Methyl-3,4-dihydro-β-carboline (harmalan) (III)

(1) By Dehydration of 1-Hydroxymethyl-1,2,3,4-tetrahydro-β-carboline (XIII)

(±)-1-Hydroxymethyl-1,2,3,4-tetrahydro-β-carboline

Tryptamine hydrochloride (5.9 g, 0.03 moles) was dissolved in 250 ml warm water containing 15 ml 2 *N* HCl (1.095 g, 0.03 moles) and the solution was filtered. To the cold solution was added an aqueous solution of 1.90 g (0.032 moles) glycolaldehyde (32) and the mixture was kept on the steam bath (2 hours) until a sample no longer gave a precipitate with dinitrophenylhydrazine. The cooled solution was then treated with charcoal, filtered, extracted with ether to remove nonbasic impurities, concentrated, and treated with excess of 20% NaOH, when the product precipitated as an oil which crystallized on standing. It was taken up in ether, and the solution was dried with KOH and concentrated to yield an oil which crystallized on digestion with warm water to give the trihydrate of 1-hydroxymethyl-1,2,3,4-tetrahydro-β-carboline (6.25 g, 81%) melting at 138–139° after sintering below 100°. Recrystallization from aqueous ethanol did not raise the melting point. Distillation of a small sample at 2.10^{-2} mm and 140–150° gave an oil, crystallizing into a white solid, melting at 144–145°, which still retained water of crystallization. (Found: H_2O, 19.18. $C_{12}H_{14}ON_2,3H_2O$ requires H_2O, 21.10%. After drying at 120° found: C, 71.5; H, 6.8. $C_{12}H_{14}ON_2$ requires C, 71.5; H, 7.0%.)

Can. J. Chem. Downloaded from www.nrcresearchpress.com by 176.9.209.113 on 09/04/12
For personal use only.

The hydrochloride, recrystallized from ethanol, melted at 215–216° after darkening from 205°. (Found: C, 56.3; H, 6.8; N, 10.5. $C_{12}H_{15}ON_2Cl,H_2O$ requires C, 56.1; H, 6.7; N, 10.9%.)

Harmalan

(*i*) *90% w/w* H_3PO_4.—The above tetrahydro-β-carboline trihydrate (3.37 g, 0.013 moles) was wetted with 10 ml water, 100 ml 90% H_3PO_4 was added, and the suspension was kept on the steam bath until the absorption band at 280 mμ, characteristic of the indole chromophore of the starting material, had disappeared. The reaction was complete after 2 hours. The dark brown solution was diluted with water, extracted with ether, treated with charcoal, and made alkaline with 20% NaOH. The precipitate was collected, dried in air, and extracted in the Soxhlet extractor with 70–100° petroleum ether, from which harmalan crystallized in fluffy needles, melting at 178–179° in a total yield of 1.80 g (75%). For analysis a sample was sublimed at 1.10^{-3} mm and 90° C. (Found: C, 77.9; H, 6.4; N, 15.1. Calc. for $C_{12}H_{12}N_2$: C, 78.2; H, 6.6; N, 15.2%.) Infrared absorption (Nujol) (cm^{-1}): 1622 (m), 1605 (m), 1570 (m), 1550 (s). Ultraviolet absorption (Fig. 1) (λ_{max}, mμ (log ε)); in 0.1 *N* HCl: 245 (4.04); 350 (4.28); in 0.1 *N* NaOH: 240 (4.09), 315 (4.06).

(*ii*) *50% w/v* H_2SO_4.—The tetrahydro-β-carboline (0.11 g, 0.00043 moles) was treated with an ice-cold mixture of 2 ml 95% H_2SO_4 and 4 ml water. After 2 hours on the steam bath and standing overnight, the solution showed a strong dihydro-β-carboline peak at 350 mμ, but the indole peak at 280 mμ was still apparent. The latter had disappeared after a further 2 hours on the steam bath with an additional 1 ml of 95% H_2SO_4. The solution was diluted with water, treated with charcoal, and the product precipitated by addition of a little 20% NaOH, when harmalan, melting at 176–177°, was obtained in poor yield (25%). When the experiment was carried out at room temperature, even after 1 week unchanged starting material was recovered.

(*2*) *By Oxidation of 1-Methyl-tetrahydro-β-carboline* (VI)

1-Methyl-1,2,3,4-tetrahydro-β-carboline (13) (0.186 g, 0.001 moles) was dissolved in acetone. To the ice-cold solution was added 0.11 g (0.0007 moles) powdered $KMnO_4$. When reaction was complete, MnO_2 was filtered off, the solution evaporated, the residue taken up in ether, dried over NaOH, the solvent removed, and the residual solid extracted with boiling ligroin, from which harmalan (0.11 g, 65%), melting at 176–178°, crystallized.

(*3*) *By Oxidative Decarboxylation of 1-Methyl-1,2,3,4-tetrahydro-β-carboline-1-carboxylic Acid* (XI)

1-Methyl-1,2,3,4-tetrahydro-β-carboline-1-carboxylic Acid

Cooled aqueous solutions of tryptamine hydrochloride (0.98 g, 0.005 moles) and pyruvic acid (0.48 g, 0.0055 moles) were mixed and left at 37° overnight when the product had separated in 85% yield (0.96 g) as colorless crystals, melting with decarboxylation at 217–219°. Recrystallization from dilute aqueous ammonia did not raise the melting point, which is reported as 220° (5).

Harmalan

The above amino acid (0.115 g, 0.0005 moles) in 20 ml water was refluxed 24 hours with freshly precipitated Ag_2O (0.23 g, 0.001 moles). Metallic silver deposited, and the solution gave an ultraviolet absorption curve characteristic of a dihydro-β-carboline. The mixture was filtered hot. On cooling a solid precipitated, which on recrystallization from boiling petroleum ether gave 0.079 g (85%) of harmalan, melting at 178–180°.

Can. J. Chem. Downloaded from www.nrcresearchpress.com by 176.9.209.113 on 09/04/12
For personal use only.

The products obtained from each of the above experiments were compared with a sample of harmalan prepared from N_β-acetyltryptamine (12) and were found to have identical ultraviolet (Fig. 1) and infrared (Nujol) spectra, melting points, and mixed melting points.

1-Methyl-7-methoxy-3,4-dihydro-β-carboline (harmaline) (II)

6-Methoxytryptamine (21) (0.033 g, 0.00017 moles) was dissolved in 3.5 ml 0.1 *N* HCl (0.00035 moles) and heated on the steam bath with 0.011 g (0.00019 moles) glycolaldehyde, until a sample no longer gave a precipitate with dinitrophenylhydrazine (1½ hours). The solution was filtered, concentrated, washed into a continuous extractor, overlayered with ether, and made alkaline with 10 ml 0.5 *N* NaOH. Eighteen hours' extraction, drying over KOH and removal of solvent, gave 50 mg of a white crystalline solid, melting at 170–175°, after sintering at 85°, presumably a hydrate of 1-hydroxymethyl-7-methoxy-1,2,3,4-tetrahydro-β-carboline (XIV). (Ultraviolet absorption (λ_{max}, mμ (log ε)): 225 (4.37), 275 (3.53), 295 (3.65) in ethanol.) Without further purification, this base was treated with 2.5 ml 90% H_3PO_4 and kept on the steam bath for 2 hours, when the solution gave an ultraviolet curve identical with that of natural harmaline (footnote 2). The solution was diluted with water, placed in a continuous extractor, made alkaline with 20% NaOH, and the product was extracted into ether. The ether extract was dried, the solvent removed, and the product distilled at 10^{-3} mm and 120–140° to yield 27 mg (72%) harmaline, melting at 235–237°, identical with an authentic specimen in infrared and ultraviolet absorption (Fig. 2), R_f value (0.89) in 95% ethanol/.880 ammonia (99:1), melting point and mixed melting point. (Found: C, 72.6; H, 6.6; N, 13.1. Calc. for $C_{13}H_{14}ON_2$: C, 72.8; H, 6.6; N, 13.1%.) Infrared absorption in (Nujol) (cm^{-1}): 1620 (s), 1600 (m), 1570 (m), 1535 (s). Ultraviolet absorption (Fig. 2) (λ_{max}, mμ (log ε)): in 0.1 *N* HCl: 260 (4.07), 380 (4.49); in 0.1 *N* NaOH: 260 (4.18) (shoulder), 335 (4.34).

A portion was converted to the picrate, orange needles, melting at 228–229° after sintering at 215°, after recrystallization from aqueous ethanol, identical with the picrate derived from the authentic sample.

1-Methyl-3,4-dihydro-β-carboline-3-carboxylic acid (XVI)

(*1*) *By Dehydration of 1-Hydroxymethyl-1,2,3,4-tetrahydro-β-carboline-3-carboxylic Acid* (XV)

1-Hydroxymethyl-1,2,3,4-tetrahydro-β-carboline-3-carboxylic Acid

dl-Tryptophan (1.02 g, 0.005 moles) was dissolved in *N* HCl (5 ml, 0.005 moles), 0.33 g glycolaldehyde (0.0055 moles) was added, and the mixture was kept on the steam bath for 2 hours when a sample no longer gave a precipitate with dinitrophenylhydrazine. The dark solution was treated with charcoal, the pH of the filtrate was adjusted to pH 7, and a small amount of precipitate was removed by filtration. On concentration the product crystallized, and on recrystallization from boiling water was obtained in 51% yield (0.63 g) as long needles, decomposition 256–257° after darkening from 235°. No attempt was made to separate the diastereoisomers. A melting point of 234° was reported (24) for the product derived from *l*-tryptophan. (Found: C, 63.1; H, 5.7; N, 11.6. Calc. for $C_{13}H_{14}O_3N_2$: C, 63.4; H, 5.7; N, 11.4%.)

1-Methyl-3,4-dihydro-β-carboline-3-carboxylic Acid

The above amino acid (0.37 g, 0.0015 moles) was treated with an ice-cold solution of 2 ml 95% H_2SO_4 in 5 ml H_2O. After keeping this solution at room temperature for 48 hours no absorption at 355 mμ was observed. The solution was then kept on the steam bath for

Can. J. Chem. Downloaded from www.nrcresearchpress.com by 176.9.209.113 on 09/04/12
For personal use only.

2 hours, when absorption at 355 mμ appeared, but since the ultraviolet absorption band at 280 mμ was still strong, a further 1 ml 95% H_2SO_4 was added. After 2 hours the reaction was complete. The solution was diluted with water, absorbed on a Zeocarb cation exchange resin in the acid form, and eluted with ammonia. The eluate was concentrated and the residue taken up in aqueous ethanol, treated with charcoal and allowed to stand at 0°, giving 88 mg (26%) of yellow crystals, melting at 189–190° after darkening at 185°, of the dihydrate of 1-methyl-3,4-dihydro-β-carboline-3-carboxylic acid. (Found: H_2O, 14.0. $C_{13}H_{12}O_2N_2,2H_2O$ requires H_2O, 13.6%. After drying at 100° found: C, 68.2; H, 5.4; N, 12.0. $C_{13}H_{12}O_2N_2$ requires C, 68.4; H, 5.3; N, 12.3%.) Infrared absorption (Nujol) (cm^{-1}): 1655 (m), 1632 (m), 1615 (m), 1592 (s), 1570 (s), 1523 (m), 1445 (s). Ultraviolet absorption (λ_{max}, mμ (log ε)): in 0.1 *N* HCl: 245 (3.97), 355 (4.29); in 0.1 *N* NaOH: 235 (4.10), 315 (4.07).

(2) By Malonic Ester Synthesis

Ethyl α-Acetamido-α-carbethoxy-β-(3-indolyl)-propionate (XVII)

This was prepared by the pyridine method of Howe, Zambito, Snyder, and Tishler (27) which was found more satisfactory than their other methods. It was obtained as colorless crystals, melting at 142–144°.

1-Methyl-3,3-dicarbethoxy-3,4-dihydro-β-carboline (XVIII) (*cf.* (*28*))

Ethyl α-acetamido-α-carbethoxy-β-(3-indolyl)-propionate (1.04 g, 0.003 moles) was gently warmed with 5 ml $POCl_3$ for 45 minutes, when the band at 280 mμ in the ultraviolet spectrum of the original solution had been completely replaced by the band at 355 mμ. The reaction mixture had become dark brown. Excess $POCl_3$ was distilled off at room temperature at 10^{-3} mm, and the brown tarry residue triturated with excess NH_3. On standing overnight the tarry salt had been converted into the solid, crude base, which was filtered off and taken up in ether. The ether solution was washed with dilute NH_3 and H_2O, and the product then extracted into 0.02 *N* HCl. The acid solution was immediately treated with dilute ammonia, and the product re-extracted into ether and dried over Na_2SO_4. Removal of solvent gave a yellow solid which was dissolved in acetone. Addition of 70–100° petroleum ether and cooling gave the product as long yellow needles, melting at 154–156°, which was identical in infrared and ultraviolet absorption with the product described by Hardegger and Corrodi (28), melting at 147–149°[4] (yield 0.45 g, 44%). (Found: C, 65.6; H, 6.3; N, 8.7. Calc. for $C_{18}H_{20}O_4N_2$: C, 65. 8; H, 6.1; N, 8.5%.) Infrared absorption (cm^{-1}) 1725 (s), 1612 (w), 1595 (m), 1570 (w), 1540 (m), 1500 (w). Ultraviolet absorption (λ_{max}, mμ (log ε)): in 0.1 *N* HCl: 245 (4.11), 355 (4.40); in 0.1 *N* NaOH: 240 (4.18), 318 (4.22).

1-Methyl-3,4-dihydro-β-carboline-3-carboxylic Acid

1-Methyl-3,3-dicarbethoxy-3,4-dihydro-β-carboline (0.2 g, 0.00061 moles) was wetted with a little ethanol, suspended in 1.22 ml *N* NaOH (0.00122 moles), and warmed for 2 hours. A small quantity of tarry material was filtered off and the filtrate acidified by addition of 19 ml 0.982 *N* HCl (0.00183 moles) and decarboxylation accelerated by keeping the mixture on a steam bath for 30 minutes. A small amount of solid was filtered off. The solution was applied to a column of Dowex 50, was washed free of chloride ion, and the product eluted with *M* NH_3. Concentration gave a small amount of a substance, crystallizing as long needles and melting at 188–190°, which gave an infrared spectrum ((Nujol) (cm^{-1}): 1620 (m), 1545 (m), 1510 (w)) different from that of the expected product (*vide supra*) and an ultraviolet absorption which even after repeated recrystallization of

[4]*I thank Dr. E. Hardegger for a reference sample of this material.*

Can. J. Chem. Downloaded from www.nrcresearchpress.com by 176.9.209.113 on 09/04/12
For personal use only.

the substance showed, in addition to the dihydro-β-carboline bands at 245 mμ and 355 mμ in acid solution and 240 mμ and 318 mμ in alkaline solution, another band at 278 mμ in acid solution and at 256 mμ (shoulder) in alkaline solution.

Further concentration of the solution gave the desired product (0.09 g, 64%) as yellow crystals, melting at 186–188°, identical in infrared (Nujol) and ultraviolet absorption (*vide supra*), melting point, and mixed melting point with that obtained by dehydration.

ACKNOWLEDGMENTS

Financial assistance by the National Research Council of Canada and by the Ontario Research Foundation is gratefully acknowledged.

REFERENCES

1. GOEBEL, F. Ann. **38**, 363 (1841).
2. HOCHSTEIN, F. A. and PARADIES, A. M. J. Am. Chem. Soc. **79**, 5735 (1957).
3. (*a*) HENRY, T. A. The plant alkaloids. Churchill, London. 1949. MANSKE, R. H. F. and HOLMES, H. L. (*Editors*). The alkaloids. Academic Press Inc., New York. 1952. (*b*) BATTERSBY, A. R., DAVIDSON, G. C., and HARPER, B. J. T. J. Chem. Soc. 1744 (1959).
4. PERKIN, W. H. and ROBINSON, R. J. Chem. Soc. **115**, 933 (1919).
5. HAHN, G., BÄRWALD, L., SCHALES, O., and WERNER, H. Ann. **520**, 107 (1935).
6. MENSHIKOV, G. P., GUREVITCH, E. L., and SAMSONOVA, G. A. J. Gen. Chem. (U.S.S.R.) **20**, 1927 (1950).
7. BADGER, G. M. and BEECHAM, A. F. Nature, **168**, 517 (1951).
8. PARIS, R. R., PERCHERON, F., MAINIL, J., and GOUTAREL, R. Bull. soc. chim. France, 780 (1957).
9. YURASHEVSKI, N. K. J. Gen. Chem. (U.S.S.R.) **11**, 157 (1941).
10. GUGGENHEIM, M. Die Biogenen Amine. S. Karger, Basel. 1951. p. 587.
11. MANSKE, R. H. F., PERKIN, W. H., and ROBINSON, R. J. Chem. Soc. 1 (1927).
12. SPÄTH, E. and LEDERER, E. Ber. **63**, 120 (1930).
13. AKABORI, S. and SAITO, K. Ber. **63**, 2245 (1930).
14. SPENSER, I. D., CRAWHALL, J. C., and SMYTH, D. G. Chem. & Ind. 796 (1956).
15. FISCHER, O. Ber. **22**, 637 (1889).
16. HASENFRATZ, V. and SUTRA, R. Compt. rend. **182**, 703 (1926). MANSKE, R. H. F. Can. J. Research, **5**, 592 (1931. KONOVALOVA, R., PROSKURINA, N., and ORECHOV, A. Arch. Pharm. **273**, 156 (1935).
17. FISCHER, O. Ber. **30**, 2481 (1897).
18. ASHLEY, J. N. and ROBINSON, R. J. Chem. Soc. 1376 (1928).
19. KERMACK, W. O., PERKIN, W. H., and ROBINSON, R. J. Chem. Soc. **119**, 1602 (1921). JACOBS, W. A. and CRAIG, L. C. J. Biol. Chem. **113**, 759 (1936).
20. ROBINSON, R. Congress Lectures, 1st Intern. Biochem. Congr., Cambridge, 32 (1949).
21. ABRAMOVITCH, R. A. J. Chem. Soc. 4593 (1956).
22. DE LA HABA, G., LEDER, I. G., and RACKER, E. J. Biol. Chem. **214**, 409 (1955).
23. SALLACH, H. J. J. Biol. Chem. **223**, 1101 (1956). ICHIHARA, A. and GREENBERG, D. M. J. Biol. Chem. **224**, 331 (1957).
24. HARVEY, D. G., MILLER, E. J., and ROBSON, W. J. Chem. Soc. 153 (1941).
25. SNYDER, H. R., HANSCH, C. H., KATZ, L., PARMERTER, S. M., and SPAETH, E. C. J. Am. Chem. Soc. **70**, 219 (1948).
26. SNYDER, H. R. and WERBER, F. X. J. Am. Chem. Soc. **72**, 2962 (1950).
27. HOWE, E. E., ZAMBITO, A. J., SNYDER, H. R., and TISHLER, M. J. Am. Chem. Soc. **67**, 38 (1945).
28. HARDEGGER, E. and CORRODI, H. Helv. Chim. Acta, **39**, 984 (1956).
29. CHARGAFF, E. and SPRINSON, D. B. J. Biol. Chem. **151**, 273 (1943).
30. BERGMANN, M. and DELIS, D. Ann. **458**, 76 (1927).
31. BATTERSBY, A. R. and EDWARDS, T. P. J. Chem. Soc. 1909 (1959).
32. POWERS, H. H., TABAKOGLU, G., and SABLE, H. Z. Biochem. Preparations, **4**, 56 (1955).

Can. J. Chem. Downloaded from www.nrcresearchpress.com by 176.9.209.113 on 09/04/12
For personal use only.

Can. J. Chem. Downloaded from www.nrcresearchpress.com by 176.9.209.113 on 09/04/12
For personal use only.

PHYSICAL PROPERTIES OF ALKYL PYRROLES AND THEIR SALTS[1]

R. J. ABRAHAM,[2] E. BULLOCK,[2] AND S. S. MITRA[2]

ABSTRACT

The structures of the ions formed by several alkyl pyrroles in hydrochloric acid are deduced from proton resonance spectra. Basicity values for three alkyl pyrroles are determined from ultraviolet spectra of their salts in buffer solutions. An attempt is made to estimate the basicity of other pyrroles from the variation of the —OD stretching frequency of methanol-*d* in solution in the pyrroles. Variations of the free and bonded NH frequencies of alkyl pyrroles are shown to be a simple function of the positions and number of the substituents.

INTRODUCTION

The basic nature of substituted pyrroles has been emphasized recently (1, 2, 3, 4, 5) and suggestions made about the structures of the protonated forms (3, 4, 5, 6). Proton magnetic resonance seemed to present a good method for defining these structures, which are probably the activated forms of pyrroles in acid (3, 4, 6).

The proton magnetic resonance spectra of pyrrole and some substituted pyrroles have been given in a previous publication (12) and the frequencies completely assigned. The spectra of the methyl-substituted pyrroles given here can be interpreted on the same basis and need not be discussed in detail. However, the pyrrole hydrochlorides give much more complex spectra and these will be discussed here. The striking differences between the spectra of the hydrochlorides and of the parent compounds show immediately that the methyl pyrroles in acid solution do not form merely loose addition complexes, but true salts, and the structure of the cations can be found from the interpretation of the proton magnetic resonance spectra.

Basicity constants for two substituted pyrroles have been reported (5) and in addition to a redetermination of these values, two further pyrroles have been examined. Since the application of the ultraviolet method is very limited (by instability of the solutions) in the pyrrole series, a correlation with infrared measurements was desirable (7, 8). In view of a possible relationship between hydrogen-bonding and basicity, the NH frequencies of the pyrroles were examined.

Materials

Substituted pyrroles were synthesized by standard methods (9) or recent variations on these methods (10, 11). Pyrrole was a commercial sample (Fisher) repeatedly redistilled to give a fraction of 1° boiling range; other liquid compounds were distilled similarly. Tetramethyl pyrrole was crystallized from heptane.

The hydrochlorides were prepared as described earlier (5). 2,3,4,5-Tetramethyl pyrrole hydrochloride forms deliquescent white needles of low melting point and regenerates the parent base (melting point and mixed melting point) on treatment of the salt with sodium acetate. The salt slowly decomposed when stored *in vacuo*; the decomposition is not obvious from the condition of the solid but is observed by a slow decrease in the intensity of the ultraviolet absorption.

Infrared spectrum of II*b* ($R_2 = R_3 = R_4 = CH_3$, $R_5 = H$) (fluorolube mull): 2860, 2810, 2680, 2610 (broad), 1755, 1650, 1574, 1478, 1446, 1412, 1382 cm^{-1}.

[1]*Manuscript received June 30, 1959.*
Contribution from the Division of Pure Chemistry, National Research Council, Ottawa, Canada. Issued as N.R.C. No. 5369.
[2]*National Research Council Postdoctorate Fellow.*

Infrared spectrum of II*b* ($R_n = CH_3$) (nujol mull); 2680, 2490 (broad), 1780, 1655, 1580, 1415 cm^{-1}.

CH_3OD and DCl in D_2O were kindly provided by Dr. L. C. Leitch.

EXPERIMENTAL

The NMR spectrometer has been described previously (12). The spectra were measured at 60 Mc/s and the chemical shifts are given in c.p.s. from an internal dioxane reference, high field being positive. The internal reference was used in order to remove bulk susceptibility corrections. However, the position of the dioxane reference may change with the change in the acidity of the medium. This change would be expected to be only of the order of a few c.p.s. but must be taken into account in any correlation of the chemical shifts of the parent compound and the hydrochloride.

Most of the ultraviolet measurements were made on a Beckmann DU spectrometer, the remainder being determined on a Cary Model 11M instrument.

Buffer solutions, pH 2.2, 2.8, 3.4, and 4.0 were McIlvaine's citric acid – phosphate standards.

Solutions of the solid hydrochlorides containing 0.8–2.5 mg/25 ml were used.

A Perkin–Elmer model 12C infrared spectrometer equipped with LiF prism was used. Very dilute solutions in carbon tetrachloride were used for the determination of the free NH stretching mode of the pyrroles. The condition of infinite dilution was attained by increasing the dilution until the frequency was unaffected by further dilution. To determine the extent of association, a few drops of the liquids were pressed between rock salt plates and the spectrum of the thin film was taken.

In an attempt to measure the basicity of the different pyrroles, a solution of methanol-*d* was made in each pyrrole and the —OD stretching frequency was examined at 'infinite dilution' to ensure the absence of solute–solute interaction (8).

RESULTS

(*i*) *NMR Spectroscopy*

The chemical shifts for the parent compounds are shown in Table I. The spin coupling constants are observed only in two cases. In 3,4-dimethyl pyrrole $J_{12} = J_{15} = 2.3$ c.p.s.

TABLE I

The chemical shifts of methyl pyrroles

		Ring protons		Methyls	
Compound	N–H	α	β	α	β
2,4-Dimethyl pyrrole	−220	−166	−138	80	84
3,4-Dimethyl pyrrole		−161			95
2,3,4-Trimethyl pyrrole*	−221	−155		92	96, 100
2,3,5-Trimethyl pyrrole			−127	91, 94	96
2,3,4,5-Tetramethyl pyrrole*				94	104

*In carbon tetrachloride solution; all the others were pure liquids.

and in 2,3,5-trimethyl pyrrole $J_{14} = 2.1$ c.p.s. In the other ring proton peaks, this interaction is obscured by the additional interactions of the ring protons with the nitrogen nucleus and the methyl protons. The couplings of the methyls to the ring protons are known to be very small (~1 c.p.s.) and are not observed in these spectra. The chemical shift values serve as reference points for the shifts in the hydrochlorides and the coupling

Can. J. Chem. Downloaded from www.nrcresearchpress.com by 176.9.209.113 on 09/04/12
For personal use only.

constants are also useful in assigning the various lines. Note that the α-methyl groups and the α-ring protons always come to low field of the corresponding β-positions.

The most probable structures for the pyrrole hydrochlorides are shown in Fig. 1. The structure formed by a loose association of the pyrrole ring with a bare proton is not shown and need not be considered as it does not explain the observed spectra. The structures shown, therefore, are formed by the attachment of the proton to I, the nitrogen atom; II*a* and *b*, the α-carbon atoms; III*a* and *b*, the β-carbon atoms. The chemical evidence supports structures I or II (3, 4, 5); however, we include III for completeness.

2,3,4,5-Tetramethyl Pyrrole

This is the simplest case to consider. Here all the R groups in Fig. 1 are methyl groups and thus structures II*a* and *b* are equivalent as are also III*a* and *b*. Thus we need to

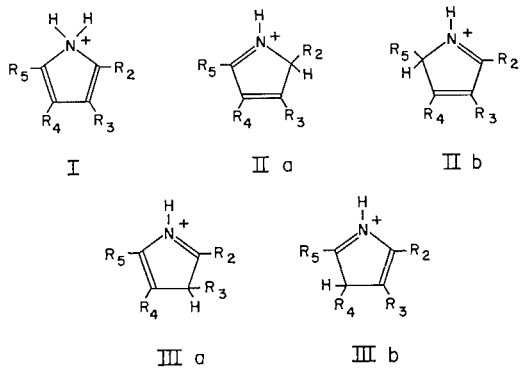

FIG. 1. Possible structures for pyrrole hydrochloride ion.

consider only three possible structures for the hydrochloride. Due to its symmetry the free base has only two methyl resonances, of the α- and β-methyl groups, at +94 and +104 c.p.s. respectively. If the hydrochloride had structure I this symmetry would be preserved and there would be only two peaks corresponding to the methyl groups, with possibly some fine structure.

The observed spectrum (Fig. 2*a*) is much too complex to be explained by this structure, which therefore is eliminated. In the observed spectrum, it is difficult to distinguish chemical shift separations from those due to spin interactions. In order to resolve this uncertainty the pyrrole was dissolved in DCl/D_2O. Any spin interaction with an exchangeable proton (i.e. all protons except those on the methyl groups) will now be reduced by a factor of six. The spectrum of the deuterated pyrrole salt (Fig. 2*b*) has the same methyl resonances, apart from a spurious peak due to some acetic acid impurity, but the original doublets at +71 and +138 are now broad single lines, proving conclusively the existence of four distinct methyl resonances, two of which are doublets due to spin–spin interaction.

Consider now structures II and III. Both structures would be expected to give rise to four different methyl peaks, one of which (the 2-methyl in II and the 3-methyl in III) will lie to high field, as it is attached to a saturated carbon atom, and give a doublet pattern of separation around 8 c.p.s. due to interaction with the nearest proton. This doublet is seen in the observed spectrum (at +134, +141 c.p.s.) and is strong support for one of these structures. The remaining peaks of the spectrum are less clearly assigned.

Can. J. Chem. Downloaded from www.nrcresearchpress.com by 176.9.209.113 on 09/04/12
For personal use only.

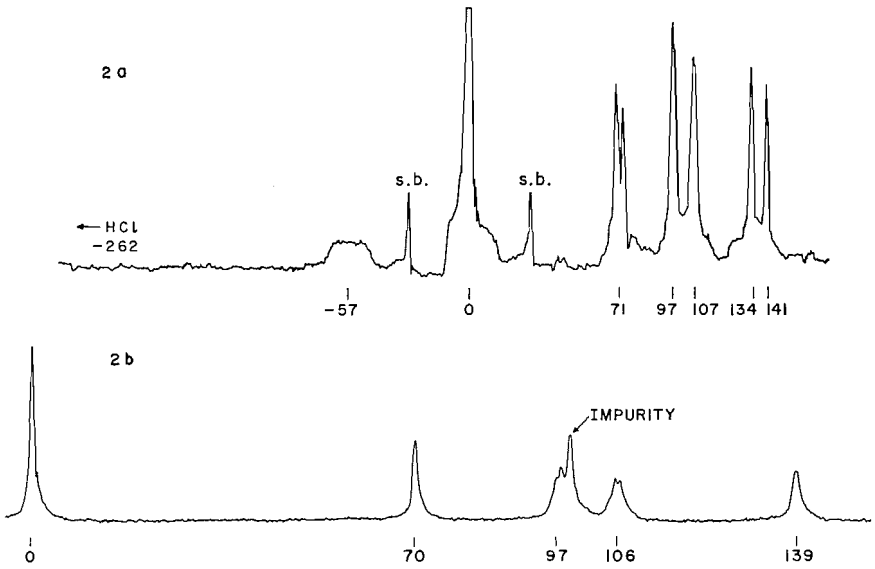

FIG. 2. The NMR spectrum of (*a*) 2,3,4,5-tetramethyl pyrrole in concentrated HCl, (*b*) 2,3,4,5-tetramethyl pyrrole in concentrated DCl.

In structure II either of the 3- or 5-methyl peaks could be the low field signal at +71 c.p.s., the 3-methyl as it is now in an α-position in the ring, and the 5-methyl as it is adjacent to a positively charged nitrogen atom, whilst in structure III it would be expected to be due to the 2-methyl peak. The remaining methyl peaks will be essentially unchanged. Thus from the chemical shift data both structures are possible. However, the doublet fine structure of this signal does provide a further clue. The spin coupling constants in these types of compound are not completely known, but for planar molecules, the methyl ring proton interactions are very small (less than 1 c.p.s. (12)). Thus the 3-c.p.s. splitting of this low field methyl peak is very likely the result of the interaction of the methyl protons with a ring proton which is not in the plane of the ring, i.e. proton 2 or 3, in structure II and III respectively.

However, in structure III, the 3-proton will couple equally with the methyl groups in positions 2 and 4, and thus two of the methyl peaks should be doublets. This is not observed and thus structure III may be discarded.

Thus the ion is very probably structure II. The assignment of the spectrum is then that the low field methyl peak (at +71 c.p.s.) is due to the 3-methyl group, and the remaining methyl peaks at 97 and 107 c.p.s. are assigned to methyls 5 and 4 respectively. The broad hump at −57 is the 2-proton. This has a complex fine structure which would not be expected to be resolved. The N–H proton signal is not observed and the interaction with the nitrogen quadrupole moment would be expected to broaden the peak to such an extent that it would not be observed. The spectrum of the hydrochloride is unchanged on dilution and is given on dissolving the pyrrole hydrochloride in dilute hydrochloric acid. Thus this salt is quite stable in acid solution, in agreement with the chemical evidence.

2,3,4-Trimethyl Pyrrole

The free base has three distinct methyl peaks at 92, 96, and 100 c.p.s. which can be reasonably assigned to the methyl groups in positions 2, 4, and 3 respectively, the 3-methyl being the most shielded. The spectrum of the hydrochloride in concentrated hydrochloric

Can. J. Chem. Downloaded from www.nrcresearchpress.com by 176.9.209.113 on 09/04/12
For personal use only.

acid is shown in Fig. 3. The striking feature of this spectrum is the triplet of 2.8-c.p.s. separation given by the low field methyl group.

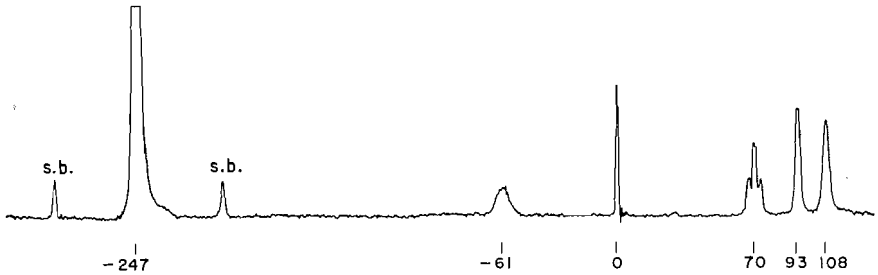

FIG. 3. The NMR spectrum of 2,3,4-trimethyl pyrrole in concentrated HCl.

Consider the possible structures for this ion (Fig. 1). In this case R_2, R_3, and R_4 are methyl groups whilst R_5 is a proton. Structures II*a*, III*a*, and III*b* can be eliminated immediately as they would all give the high field doublet observed in the tetramethyl pyrrole hydrochloride. The two remaining possibilities (structures I and II*b*) are very similar. Both structures may be expected to give a low field triplet methyl resonance (from the 2-methyl in I and the 4-methyl in II*b*), and the other methyl resonances will not differ appreciably from those in the free base; however, the structures can be differentiated by considering the chemical shifts of the ring protons. The resonances of ethylenic protons and protons attached to a positive nitrogen atom are known to lie at very low fields; on the scale used here, at around -150 c.p.s. (Table I) and -260 c.p.s (13) respectively. Thus there are no protons in structure I which would explain the broad peak at -61 c.p.s. However, this can be assigned very simply on structure II*b* as due to the CH_2 protons. The peak is in the correct region (compare the tetramethyl pyrrole hydrochloride in which the corresponding proton is found at -57 c.p.s.), and a further check is provided by the intensity of the peak. The three methyl peaks in Fig. 3 have intensities, in arbitrary units, of 216, 239, and 227 respectively giving an average of 227 ± 12. The intensity of the low field peak in the same units is equal to 157, which corresponds almost exactly to two-thirds of the intensity of the methyl, i.e. to two protons. The remaining peaks at $+93$ and $+108$ c.p.s. can be assigned to the 2- and 3-methyl groups respectively. Their fine structure can arise from coupling between themselves or with the nitrogen hydrogen, in any case it is expected to be small.

Thus the proton magnetic resonance spectrum strongly supports structure II*b* in which, as in the case of the tetramethyl pyrrole hydrochloride, the extra proton adds on to an α-carbon atom in the ring. The spectrum of this salt also does not change appreciably in different solutions, but in very concentrated solutions the individual line widths increase until eventually all the fine structure is obscured. This is probably due to intermolecular interactions rather than to any changes in the structure of the ion.

2,3,5-Trimethyl Pyrrole

The free base has again three distinct methyl peaks at 91, 94, and 96 c.p.s. which can be assigned to the 5-, 2-, and 3-methyl groups, the 3-methyl being the most shielded. The spectrum of the hydrochloride in concentrated hydrochloric acid (Fig. 4) is almost identical with that of the tetramethyl pyrrole hydrochloride with one methyl group missing. This is strong support for the proposed structure of the tetramethyl hydrochloride, as it is the 4-methyl peak in the tetramethyl case which should be missing here

Can. J. Chem. Downloaded from www.nrcresearchpress.com by 176.9.209.113 on 09/04/12
For personal use only.

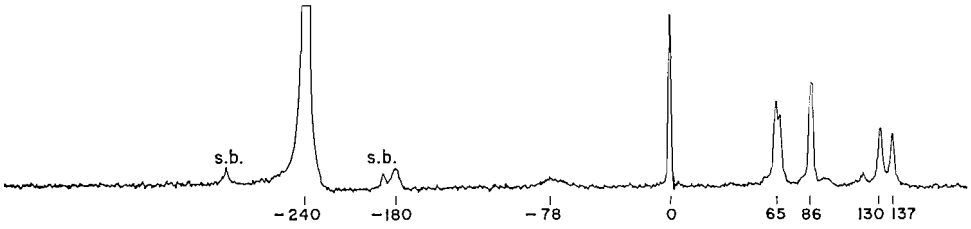

FIG. 4. The NMR spectrum of 2,3,5-trimethyl pyrrole in concentrated HCl.

(if the trimethyl hydrochloride has the same type of structure), and this is what is observed. Thus we may conclude that this structure has again the additional proton on the α-carbon atom. There are now two possible structures II*a* and II*b*, i.e. the additional proton is on either the 2- or 5-position. These can be differentiated. The doublet methyl peak at +65 c.p.s. cannot be explained on structure II*b*, assuming the values of the ring coupling constants mentioned earlier, but finds a reasonable assignment on structure II*a* as the 3-methyl group. The rest of the spectrum is assigned as follows. The 2- and 5-methyl resonances occur at +134 and +86 c.p.s. respectively, the 2-proton is at −78 c.p.s. and the 4-proton at −180 c.p.s.

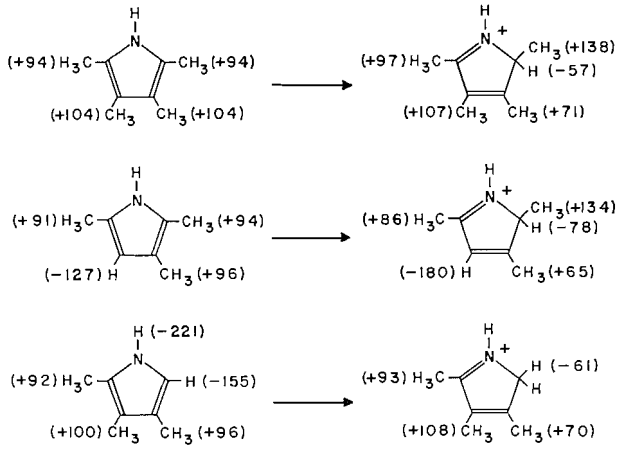

FIG. 5. The chemical shifts and assignments of the protons in the proton magnetic resonance spectra of 2,3,4- and 2,3,5-trimethyl and 2,3,4,5-tetramethyl pyrrole and their hydrochloride ions.

The structures of the remaining pyrrole hydrochlorides studied cannot be determined from their proton magnetic resonance spectra with the same certainty. However, before giving these results, the results for the tri- and tetra-methyl pyrroles are summarized in Fig. 5. Here the chemical shifts and assignments for the free bases and the hydrochlorides are given. The 2,3,4-trimethyl pyrrole formula has been written reversed in the figure so that the similarity with the other structures is more obvious. The figure shows that the differences in chemical shift on going from free bases to hydrochlorides are consistent in these compounds (allowing for the small chemical shift differences in concentration of the solutions and any shift in the internal standard), and these results can now be used to obtain some idea of the structures of the remaining pyrroles studied.

Can. J. Chem. Downloaded from www.nrcresearchpress.com by 176.9.209.113 on 09/04/12
For personal use only.

2,4-Dimethyl Pyrrole

The spectrum of the hydrochloride in concentrated hydrochloric acid is shown in Fig. 6 (note that the methyl groups are given on a different field scale from the rest of the

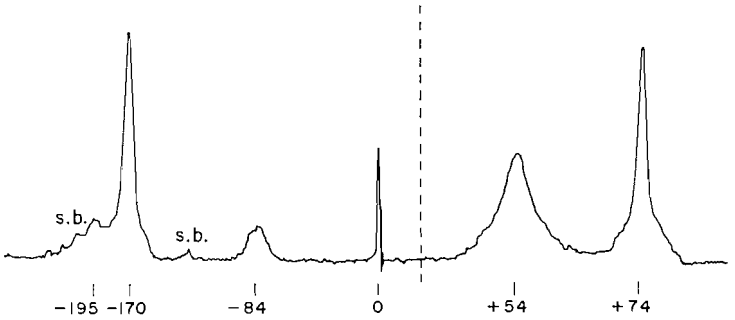

FIG. 6. The NMR spectrum of 2,4-dimethyl pyrrole in concentrated HCl.

spectrum, but that the vertical scale is the same throughout). By exactly similar reasoning to that used in the 2,3,4-trimethyl pyrrole case, it can be shown that the observed spectrum, and in particular the absence of a doublet methyl peak to high field, the breadth of the methyl peak at +54 c.p.s., and the broad peak of intensity two at −84 c.p.s., is explained only by structure II*b*, and is inconsistent with any of the other structures. The other dimethyl pyrroles give very different spectra in acid solution. Pyrrole itself is known to trimerize in acid solution (6), and the spectra of the acid solutions of 2,5- and 3,4-dimethyl pyrrole suggest that some reaction has occurred other than the formation of a positive ion. In particular, both compounds give many peaks in the methyl region, 3,4-dimethyl pyrrole gives four broad peaks at +82, 99, 109, and 125 c.p.s. and 2,5-dimethyl pyrrole three main peaks with a considerable amount of fine structure. This suggests that a reaction has occurred with the formation of compounds in which the environment of the methyl groups has changed radically. However, the spectra are difficult to interpret without further chemical evidence.

(*ii*) pK_a *Values*

The method reported previously (5) suffers from two disadvantages: (*a*) The difficulty of ensuring complete solution of the base in the very dilute hydrochloric acid used, and (*b*) the very limited pH range available, which prevents any check on the values obtained.

The solid salts of the tri- and tetra-substituted pyrroles were dissolved in phosphate–citric acid buffers at pH 2.8, 3.4, and 4.0. The results given in Table II are the average of at least nine determinations per compound (several concentrations). The 'error' quoted represents the spread of values obtained and is not a standard deviation. 2,4-Dimethyl pyrrole was checked by the former method at five different concentrations.

TABLE II
pK_a's of alkyl pyrroles

Pyrrole	λ_{max} (mμ)	pK_a
2,4-Dimethyl pyrrole	249	$1.9_8 \pm .14$
Cryptopyrrole	260	$3.5_4 \pm .14$
2,3,4-Trimethyl pyrrole	261	$3.9_4 \pm .07$
2,3,4,5-Tetramethyl pyrrole	265	$3.7_7 \pm .16$

Can. J. Chem. Downloaded from www.nrcresearchpress.com by 176.9.209.113 on 09/04/12
For personal use only.

It is clear from these values that the incorrect figure reported previously for cryptopyrrole (5) is due to the fact that at the pH used the degree of dissociation being measured was comparable with the error in the method.

(iii) OD *Stretching Frequency for Methanol-d Dissolved in the Pyrroles*

Having established reference pK_a values by the ultraviolet method, an attempt was made to determine at least the order of the pK_a's for other substituted compounds.

The —OD bonding method of Gordy (7) is known to give reasonable agreement within a series of closely related compounds (8). The results recorded in Table III include the

TABLE III

The OD stretching frequency for methanol-*d* at infinite dilution in pyrroles and CCl_4

Solvent	ν_{OD} str. (cm^{-1})	$\Delta\nu_{OD}$ (cm^{-1})
CCl_4	2689.5	—
Pyrrole	2522.5*	167
α-Methyl pyrrole	2516	173.5
2,3-Dimethyl pyrrole	2513.5	176
2,4-Dimethyl pyrrole	2516	173.5
2,5-Dimethyl pyrrole	2514.5	175
3,4-Dimethyl pyrrole	2513.5	176
2,3,4-Trimethyl pyrrole	2511.5	178
2,3,5-Trimethyl pyrrole	2514	175.5
Cryptopyrrole	2513	176.5

*Tamres *et al.* (8) give 2528 cm^{-1}.

decrease in ν_{OD} with respect to the value in CCl_4. The range of frequency from pyrrole to 2,3,4-trimethyl pyrrole is only 11 cm^{-1} and since the OD peaks often coincided with solvent peaks and were found by manual plotting, it is not likely that the accuracy obtained ($\sim \pm 1$ cm^{-1}) permits any conclusion to be drawn about the relative basicities; indeed, the $\Delta\nu_{OD}$ appears to be quite unrelated to the substitution of the pyrrole.

(iv) Free and Bonded —NH *Stretching Frequencies*

In view of the inconclusive results above, the extent of association in the substituted pyrroles was determined by measurement of the —NH stretching frequencies in two extreme cases. Table IV gives NH stretching frequencies for the pyrroles at infinite

TABLE IV

Compound	ν_{NH} str. (infinite dilution in CCl_4) Obs. (cm^{-1})	ν_{NH} str. (infinite dilution in CCl_4) Calc. (cm^{-1})	ν_{NH} str. (assoc.) pure liquid (cm^{-1})	$\Delta\nu$ Obs. (cm^{-1})	$\Delta\nu$ Calc. (cm^{-1})
Pyrrole (cf. 15)	3497	3497	3395	102	102
3,4-Dimethyl pyrrole	3501	3501	3393	108	110
2,3-Dimethyl pyrrole	3489	3489	3378	111	111
2,3,4-Trimethyl pyrrole	3490	3491	3375	115	115
2,4-Dimethyl pyrrole	3488	3489	3377	111	111
α-Methyl pyrrole	3486	3487	3379	107	107
Cryptopyrrole	3491	—	3380	111	—
2,5-Dimethyl pyrrole	3477	3477	3365	112	112
2,3,5-Trimethyl pyrrole	3479	3479	3364	115	116
Tetramethyl pyrrole	3480	3481	3360	120	120

dilution in carbon tetrachloride (free molecules) and in the pure liquid (fully associated molecules). The separation $\Delta\nu_{NH}$ between the free and bonded values is large enough,

Can. J. Chem. Downloaded from www.nrcresearchpress.com by 176.9.209.113 on 09/04/12
For personal use only.

according to the Sutherland (28) criterion of $\Delta\nu/\nu \geqslant 3\%$, to show the existence of hydrogen bonding. The values of $\Delta\nu_{NH}$, which are considered to be a measure of the strength of the hydrogen bond, are included in Table IV.

The NH stretching frequencies of the free molecules and the $\Delta\nu_{NH}$ values can be expressed as linear functions of the numbers of α- and β-substituents. The values are well reproduced by the following formulae

$$[1] \qquad \nu_{NH\ str} = 3497 - 10n_\alpha + 2n_\beta$$

$$[2] \qquad \Delta\nu_{NH} = 102 + 5n_\alpha + 4n_\beta$$

where n_α and n_β are the numbers of α- and β-substituents respectively.

$\Delta\nu_{NH}$ for 2,5-dimethyl pyrrole is considerably greater than that of pyrrole and the value for 2,3,4,5-tetramethyl pyrrole is the highest of all. Since the strength of the hydrogen bond must increase with $\Delta\nu_{NH}$ it seems that steric hindrance by α-methyl groups has no appreciable inhibitory effect on the strength of the hydrogen bond. This point is emphasized by the fact that the linearity relation (2) is obeyed almost exactly (within the limits of experimental accuracy).

Many suggestions have been made concerning the nature of the association in pyrrole (15–27) and the latest work (27) proposes a zigzag polymer form.

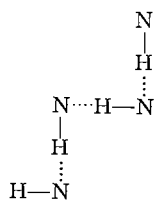

This proposal is also consistent with the results given here for the alkyl pyrroles.

DISCUSSION

The ions formed from all four pyrroles which remained as monomers in the aqueous acid are shown to be very probably ions in which the new proton is attached at an α-carbon in the ring.*

In a series of experiments using pyrroles which were activated by formation of a Grignard derivative, it has been shown (29) that alkylation by an alkyl halide always occurs at an α-position. In these cases the new alkyl group could be inserted at a substituted α-position about as easily as at an unsubstituted one when both were available on the same pyrrole. In the protonation reaction, the new proton always adds to the unsubstituted α-position when the choice exists.

The mull spectra of three hydrochlorides in the crystalline state are so similar in the region 3000–1400 cm^{-1} as to leave no doubt that the ring structures are identical. The assignments of infrared bands made earlier (5) are still valid, however, and it must be considered possible that the solid phase salts are different in orientation from the salts in solution. In this connection one chemical observation is pertinent. Thus, treatment of 2,3,4,5-tetramethyl pyrrole hydrochloride with water gives an immediate precipitate of the *free base* (melting point) which slowly redissolves in the acid solution. Although this does not prove the hypothesis, it indicates at least that a two-step process involving dissociation and reassociation occurs on dissolution of this salt.

**Professor G. W. Kenner has kindly informed us that he has also reached this conclusion by similar methods.*

Can. J. Chem. Downloaded from www.nrcresearchpress.com by 176.9.209.113 on 09/04/12
For personal use only.

This structural assignment gives strong support to the reaction mechanism proposed by Treibs and his co-workers (*inter alios*, 2, 3, 4) by confirming the initial postulate of salt formation.

It was expected that the mechanism of hydrogen bonding in the liquid pyrroles and between methanol-*d* and pyrrole molecules would be very similar, since energetically the processes are presumably almost equivalent. The methanol-*d* solution probably represents the insertion of CH_3OD units into the pyrrole chains, i.e.,

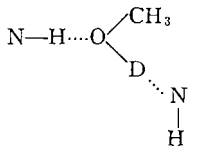

The small range of $\Delta\nu_{NH}$ (Table IV) and $\Delta\nu_{OD}$ (Table III) agrees with this hypothesis. Thus $\Delta\nu_{OD}$ should show the same regular variation with substitution as does $\Delta\nu_{NH}$ and it is probably the inaccuracy inherent in the former measurement which prevents this correlation.

It is found that for three pyrroles, the pK_a versus $\Delta\nu_{OD}$ plot is approximately linear and

$$\Delta\nu_{OD} = 2.3\ pK_a + 168. \qquad [3]$$

Interpolation of other $\Delta\nu_{OD}$ values into this equation gives values of pK_a which are apparently unrelated to the substitution and do not follow any logical additive principle such as is found for the methyl pyridines (14).

From the known structure of the pyrrole ions, it is reasonable to suggest that a mono-α-substituted pyrrole would form an ion more readily than would a di-α-substituted compound, since the latter involves displacement of a methyl group from the plane of the ring. Thus two distinct series of pK_a variations would be expected. This expectation is borne out by the measured pK_a values for 2,3,4- and 2,3,4,5-substituted compounds. The $\Delta\nu_{NH}$ measurement, which should also reflect basicity, does not show any steric effect of this type and hence does not relate to the basicity measured in solution.

The variations in absorption maximum of the salts with increasing methyl substitution are unusual. Thus (Table II) the addition of the 3-methyl to 2,4-dimethyl pyrrole changes the λ_{max} by 12 mμ whilst adding the fourth methyl produces a bathochromic shift of only 4 mμ (cf. 30). The large increment in pK_a accompanying the addition of the third methyl group is also unusual, and the relative positions of substituents, therefore, has a great influence on the salts and also on the ease of salt formation.

The results recorded here add another limit to the value of the hydrogen bonding method for determination of basicity, i.e., that it is necessary to be certain that the hydrogen bond formation is not a radically different process from the salt formation.

ACKNOWLEDGMENTS

The authors are indebted to Dr. S. F. MacDonald and Dr. H. J. Bernstein for their interest and helpful suggestions, and to Mr. R. Lauzon for the solid phase infrared spectra.

REFERENCES

1. STEDMAN, R. J. and MACDONALD, S. F. Can. J. Chem. **33**, 468 (1955).
2. TREIBS, A., HERRMANN, E., MEISSNER, E., and KUHN, A. Ann. **602**, 153 (1957).
3. TREIBS, A. and KOLM, H. G. Ann. **606**, 166 (1957).

Can. J. Chem. Downloaded from www.nrcresearchpress.com by 176.9.209.113 on 09/04/12
For personal use only.

4. TREIBS, A. and FRITZ, G. Ann. **611**, 162 (1957).
5. BULLOCK, E. Can. J. Chem. **36**, 1686 (1958).
6. SMITH, G. F. and POTTS, H. A. J. Chem. Soc. 4018 (1957).
7. GORDY, W. J. Chem. Phys. **7**, 93 (1939).
8. TAMRES, M., SEARLES, S., LEIGHLEY, E. M., and MOHRMAN, D. W. J. Am. Chem. Soc. **76**, 3985 (1954).
9. FISCHER, H. and ORTH, H. Die chemie des pyrrols. Vol. I, Akademische Verlags gesellschaft M.B.H., Leipzig. 1934.
10. TREIBS, A. and SCHMIDT, R. Ann. **577**, 105 (1952).
11. JOHNSON, A. W., MARKHAM, E., PRICE, R., and SHAW, K. B. J. Chem. Soc. 4254 (1958).
12. ABRAHAM, R. J. and BERNSTEIN, H. J. Can. J. Chem. **37**, 1056 (1959).
13. TAKEDA, M. and JARDETSKY, O. J. Chem. Phys. **26**, 1346 (1957).
14. IKEKAWA, N., SATO, Y., and MAEDA, T. Pharm. Bull. (Japan), **2**, 205 (1954).
15. FUSON, N., JOSIEN, M., POWELL, R. L., and UTTERBACK, E. J. Chem. Phys. **20**, 145 (1952).
16. ROBERTSON, J. M. J. Chem. Soc. 615 (1935); 1195 (1936).
17. LECOMTE, J. Bull soc. chim. France, **13**, 415 (1946).
18. JOSIEN, M. L. and FUSON, N. J. Chem. Phys. **22**, 1169 (1954).
19. JOSIEN, M. L. and FUSON, N. J. Chem. Phys. **22**, 1264 (1954).
20. MIRONE, P. Atti accad. nazl. Lincei, Rend. Classe sci. fis. mat. e nat. **11**, 365, (1951).
21. MIRONE, P. and VAMPIRI, M. Atti accad. nazl. Lincei, Rend. Classe sci. fis. mat. e nat. **12**, 405 (1952).
22. TUOMIKOSKI, P. J. Chem. Phys. **20**, 1054 (1952).
23. TUOMIKOSKI, P. J. Phys. Radium, **15**, 318 (1954).
24. TUOMIKOSKI, P. J. Chem. Phys. **22**, 2096 (1954).
25. TUOMIKOSKI, P. Mikrochem. Acta, 505 (1955).
26. TUOMIKOSKI, P. J. Phys. Radium, **16**, 347 (1955).
27. JOSIEN, M., PINEAU, P., PATY, M., and NELSON F. J. Chem. Phys. **24**, 1261 (1956).
28. SUTHERLAND, G. B. B. M. Trans. Faraday Soc. **38**, 889 (1940).
29. IKEKAWA, N., MARUYAMA, M., and SATO, Y. Pharm. Bull. (Japan), **2**, 209 (1954).
30. BOOTH H., JOHNSON, A. W., MARKHAM, E., and PRICE, R. J. Chem. Soc. 1587 (1959).

Can. J. Chem. Downloaded from www.nrcresearchpress.com by 176.9.209.113 on 09/04/12
For personal use only.

Can. J. Chem. Downloaded from www.nrcresearchpress.com by 176.9.209.113 on 09/04/12
For personal use only.

SYNTHESES IN THE TERPENE SERIES

VIII. SYNTHESIS OF THE *CIS*- AND *TRANS*-ISOMERS OF 7,7,10-TRIMETHYLDECAL-1-ONE. A CONVENIENT MODIFICATION OF THE BROWN HYDRATION REACTION[1, 2]

FRANZ SONDHEIMER AND SAUL WOLFE[3]

ABSTRACT

7,7,10-Trimethyl-$\Delta^{1(9)}$-octal-2-one (VII) was converted to the cycloethylenedithioketal (VIII), which on Raney nickel reduction yielded 7,7,10-trimethyl-$\Delta^{1(9)}$-octalin (IX). Oxidation with perbenzoic acid led to the corresponding oxide (X), which could be rearranged in low yield to an equilibrium mixture of 7,7,10-trimethyldecal-1-one consisting essentially of the *trans*-isomer (XI).

A convenient modification of the Brown hydration reaction is described, whereby the necessity of generating diborane or of using diglyme is avoided. 7,7,10-Trimethyl-$\Delta^{1(9)}$-octalin (IX) on Brown hydration using this modification stereospecifically furnished 7,7,10β-trimethyl-*cis*-decal-1β-ol (XII), which was oxidized to 7,7,10-trimethyl-*cis*-decal-1-one (XIII). Isomerization resulted in the above-described equilibrium mixture containing at least 90% of the *trans*-isomer (XI). Similarly, the previously described 10-methyl-$\Delta^{1(9)}$-octalin (XVI) yielded a mixture of the *cis*- and *trans*-isomers of 10-methyldecal-1-one (XIX). Syntheses of 2-methylene-7,7,10-trimethyl-$\Delta^{1(9)}$-octalin (XIV) and of 7,7,10-trimethyl-*cis*-decal-2,3-dione 3-dithiotrimethylene ketal (XXII) are also described.

In Part V of this series (1) stereospecific syntheses of the bicyclic ketones (I*a*) and (I*b*) were described, compounds which could become rings A and B of triterpenes of the β-amyrin (III) type. For the construction of rings D and E, ketones of type (II)

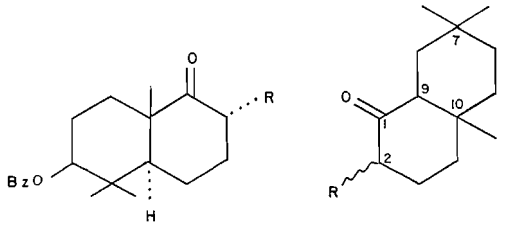

(Ia) R = H
(Ib) R = Me

(IIa) R = H
(IIb) R = Me

(III)

are required which are to be joined to the ketones (I) by a two-carbon unit, probably best introduced as acetylene. In this connection a study of the synthesis and stability of 10-methyldecal-1-one has already been carried out (2).

The substances of particular interest are the ketones (II*a*) and (II*b*) of the *cis*-configuration. Conformational considerations show that the derived acetylenic carbinols on dehydration should give vinyl-acetylenes with the double bond at the required $\Delta^{1(2)}$-position, whereas the corresponding *trans*-ketones would be expected to give vinyl-acetylenes with the double bond at the less desirable $\Delta^{1(9)}$-position. In this paper we

[1]*Manuscript received July 13, 1959.*
Contribution from the Daniel Sieff Research Institute, The Weizmann Institute of Science, Rehovoth, Israel.
[2]*Part VII: Sondheimer, F. and Elad, D. J. Am. Chem. Soc.* **81**, *4429 (1959).*
[3]*National Research Council of Canada Postdoctorate Overseas Fellow, 57–1958.*

describe a synthesis in good yield of the key intermediate 7,7,10-trimethyl-*cis*-decal-1-one (*cis*-II*a* = XIII) as well as its inversion to the corresponding *trans*-isomer (*trans*-II*a* = XI).

The starting material for our work was 7,7,10-trimethyl-$\Delta^{1(9)}$-octal-2-one (VII), obtained by Halsall and Thomas (3) by the route (IV) → (V) → (VI) → (VII). The conversion of 2,5,5-trimethylcyclohexane-1,3-dione (IV) to 2,5,5-trimethylcyclohexanone (VI) has been carried out by two methods (3), the preferred one involving conversion to the enol chloride (V) and subsequent reduction with lithium in ammonia–ethanol and reoxidation. The hydrogenation of the enol chloride (V) over palladium – calcium carbonate in the presence of pyridine (cf. (4)) was reported not to yield (VI). However, in our hands the corresponding reaction when carried out over palladium–charcoal in the absence of pyridine smoothly produced 2,5,5-trimethylcyclohexanone (VI) in 75% yield and this was found to be the best preparative method for obtaining the latter compound. It was found further that the condensation between the ketone (VI) and 4-diethylaminobutan-2-one methiodide could be effected conveniently by the potassium *tert*-butoxide-*tert*-butanol method (2, 5), whereby the octalone (VII) was obtained in 34% yield, corrected for unchanged (VI).

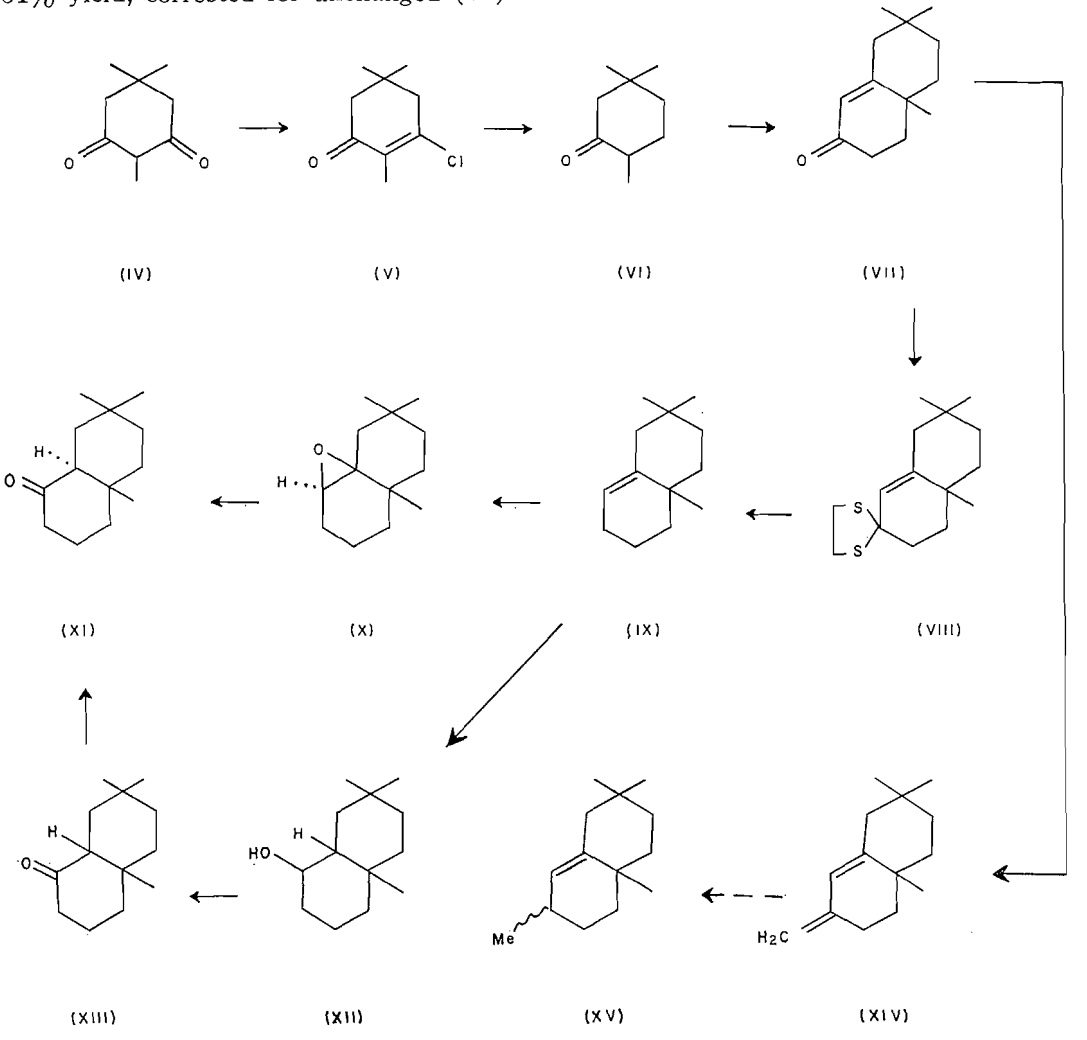

Can. J. Chem. Downloaded from www.nrcresearchpress.com by 176.9.209.113 on 09/04/12
For personal use only.

Can. J. Chem. Downloaded from www.nrcresearchpress.com by 176.9.209.113 on 09/04/12
For personal use only.

Our first experiments designed to convert the octalone (VII) to 7,7,10-trimethyl-*cis*-decal-1-one (XIII) were modelled after those which led to the successful transformation of 10-methyl-$\Delta^{1(9)}$-octal-2-one (VII without the 7,7-dimethyl group) to a mixture of the *cis*- and *trans*-isomers of 10-methyldecal-1-one (XIX) (2). Thus, treatment of (VII) with ethanedithiol in the presence of boron trifluoride etherate gave in 91% yield the cycloethylenedithioketal (VIII), m.p. 71°, which on reduction with Raney nickel produced over 80% of 7,7,10-trimethyl-$\Delta^{1(9)}$-octalin (IX). It has been shown that no shift of the double bond occurs in this type of transformation (6).

Oxidation of the octalin (IX) with perbenzoic acid gave a liquid oxide. A model of the olefin (IX) reveals the double bond to be considerably more hindered from the α- than from the β-side[4] and the oxide is therefore most probably largely, if not completely, the β-oxide (X). The rearrangement of this oxide with boron trifluoride etherate was investigated under a variety of conditions, but in all cases the yield of ketonic material was rather unsatisfactory. Under the optimum conditions (see Experimental) about a 10% yield of a liquid ketone was obtained after chromatography on alumina, Girard separation, conversion to the semicarbazone, and pyruvic acid regeneration. This ketone, the infrared spectrum of which is reproduced in Fig. 1, is an equilibrium mixture of 7,7,10-trimethyldecal-1-one containing at least 90% of the *trans*-isomer (XI) (see below). The material appeared to be reasonably homogeneous, as evidenced by the fact that it yielded directly the pure semicarbazone on being reconverted to this derivative. This is in contrast to the situation which was observed with 10-methyldecal-1-one (XIX) (2).

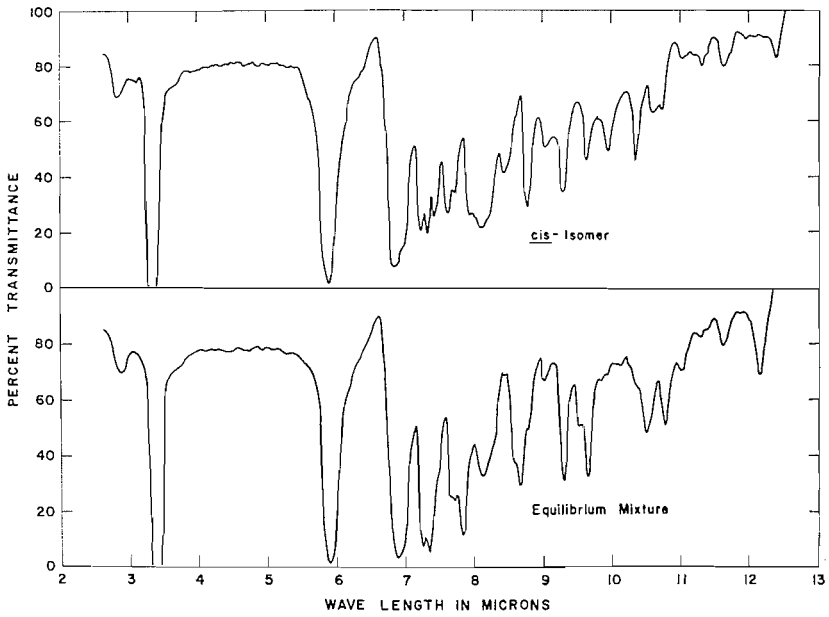

FIG. 1. Infrared spectra of 7,7,10-trimethyldecal-1-ones (in chloroform).

This route to 7,7,10-trimethyldecal-1-one suffers from two disadvantages. Firstly, the yield is poor. Secondly, it has been shown that the rearrangement of oxides to ketones

[4]*It may be noted that a model of 10-methyl-$\Delta^{1(9)}$-octalin* (XVI) *shows the double bond to be about equally hindered from both sides, and, in fact, hydrogenation proceeds about equally from the α- and the β-side (2). In 7,7,10-trimethyl-$\Delta^{1(9)}$-octalin* (IX), *the additional equatorial 7β-methyl group appears to make little difference, whereas the axial 7α-methyl group would be expected effectively to block attack from the α-side.*

proceeds by *cis*-shift of hydrogen (7). The β-oxide (X) will therefore produce the *trans*-decalone (XI) directly, even if care were taken to avoid equilibration of the product during its isolation. This fact, taken together with the apparent stability of the *trans*-ketone (XI), indicates that the more desirable *cis*-isomer (XIII) cannot be obtained by the present method. For these reasons another route to ketones of type (XI) and (XIII) was worked out, as described in the sequel.

An excellent method for the hydration of double bonds has recently been described by H. C. Brown and co-workers. This involves the conversion of the olefin dissolved in an ether to the corresponding trialkylborane by passing in diborane (generated from sodium borohydride and boron trifluoride etherate in diglyme) (8, 9), or alternatively allowing the olefin in diglyme solution to react *in situ* with sodium borohydride and aluminum chloride (10) or with sodium borohydride and boron trifluoride (11). The trialkylborane without purification is then oxidized with alkaline hydrogen peroxide to the borate ester, which under the reaction conditions is hydrolyzed to the corresponding alcohol. The hydration has been shown to proceed by over-all *cis*-addition of water from the less hindered side of the molecule,[5] the hydroxyl function being introduced at the less substituted position (anti-Markownikoff).

Application of the Brown hydration method to $\Delta^{1(9)}$-octalins of type (IX) seemed to offer a simple route to ketones of type (XI) and (XIII). However, since no diglyme (diethylene glycol dimethyl ether) was available to us and since the ether-soluble lithium aluminum hydride with boron trifluoride is known also to produce diborane (12), the following modification was made, as exemplified with cyclohexene (for a preliminary communication, see (13)). The latter olefin in ether solution was treated with boron trifluoride etherate and then gradually with an ethereal lithium aluminum hydride solution. The product on oxidation with alkaline hydrogen peroxide then gave cyclohexanol in over 80% yield. Similarly 1-octene was converted to 1-octanol in excellent yield. In this way the necessity of generating diborane separately or of using the high-boiling diglyme (b.p. 160–162° (740 mm)) *in situ* is avoided.

Application of this modification to 10-methyl-$\Delta^{1(9)}$-octalin (XVI) (2) gave 85% of an alcohol, which judging from our experience in the steroid series (13) and the known

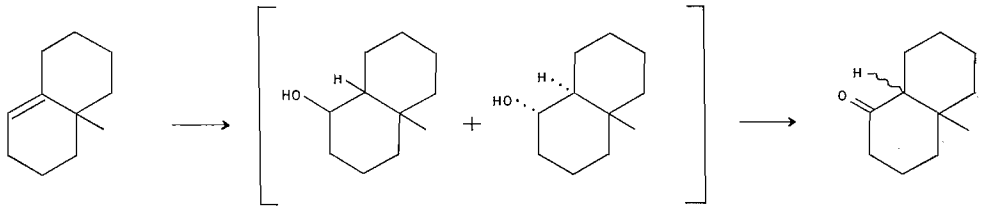

(XVI) (XVII) (XVIII) (XIX)

course of hydrogenation of (XVI) (2) is most probably a mixture of 10β-methyl-*cis*-decal-1β-ol (XVII) and 10β-methyl-*trans*-decal-1α-ol (XVIII). Oxidation of this material with chromium trioxide – pyridine then smoothly yielded 10-methyldecal-1-one (XIX),

[5]*The experiments of Brown, H. C. and Zweifel, G. (J. Am. Chem. Soc.* **81**, *247 (1959)) do not provide unequivocal proof that this mode of addition operates in all cases, since they involve flexible monocyclic systems and lead to alcohols in all of which the hydroxyl group is presumably equatorial. Rigid proof for over-all cis-addition from the less hindered side (involving cis-addition of diborane, followed by oxidation and hydrolysis with retention of configuration) was provided by the demonstration that Δ5-cholestene derivatives on Brown hydration yield the corresponding axial 6β-hydroxycoprostane as well as the equatorial 6α-hydroxycholestane derivatives (Wechter, W. J. Chem. & Ind. 294 (1959); Wolfe, S., Nussim, M., Mazur, Y., and Sondheimer, F., J. Org. Chem.* **24**, *1034 (1959)).*

Can. J. Chem. Downloaded from www.nrcresearchpress.com by 176.9.209.113 on 09/04/12
For personal use only.

probably as a mixture of the *cis*- and *trans*-isomers, which gave the same semicarbazone as obtained previously from the equilibrium mixture (2).

Finally our modification of the Brown hydration method was applied to 7,7,10-trimethyl-$\Delta^{1(9)}$-octalin (IX). A crystalline alcohol, m.p. 83°, was readily obtained in 80% yield, which must be 7,7,10β-trimethyl-*cis*-decal-1β-ol (XII) in view of the known steric course of the reaction (9, 13) and the fact that the α-side of (IX) is considerably more hindered than the β-side.[6] Oxidation of the alcohol (XII) with chromium trioxide – pyridine and direct crystallization of the product then gave 80% of 7,7,10-trimethyl-*cis*-decal-1-one (XIII), m.p. 43°. The infrared spectrum of this ketone, reproduced in Fig. 1, is considerably different from that of the 7,7,10-trimethyldecal-1-one obtained by the first method.

Adsorption of the crystalline *cis*-ketone (XIII) on alkaline alumina resulted in isomerization and yielded the equilibrated product, which was identified with the ketone obtained by the first method in view of the complete identity of the infrared spectra (Fig. 1) and of crystalline derivatives. Comparison of the infrared spectrum of the equilibrated product with that of the crystalline *cis*-ketone (XIII) shows that no more than about 10% of the latter can be present and consequently that it consists essentially of the *trans*-ketone (XI).

Of the two conformations A and B which can be written for the *cis*-ketone (XIII), the latter is undoubtedly the preferred one. It contains three methyl–hydrogen and three methylene – hydrogen 1,3-diaxial interactions, whereas the *trans*-ketone (XI) (conformation C) contains five methyl–hydrogen interactions. The observed greater stability of the latter isomer is therefore in keeping with expectation.

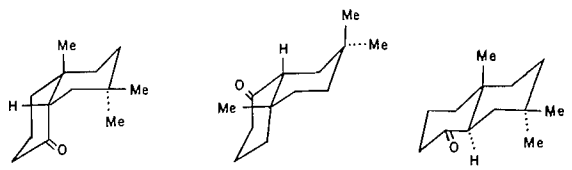

A B C

The methylation of the *cis*- and *trans*-isomers of 7,7,10-trimethyldecal-1-one (type II*a*) to the corresponding 2,7,7,10-tetramethyl-ketones (type II*b*) is now being studied. Some experiments designed to obtain the latter directly have also been carried out and are briefly reported in the sequel, although the desired objective was not reached.

Thus, 7,7,10-trimethyl-$\Delta^{1(9)}$-octal-2-one (VII) on being subjected to the Wittig reaction (14) with triphenylphosphinemethylene yielded 70% of 2-methylene-7,7,10-trimethyl-$\Delta^{1(9)}$-octalin (XIV). This diene proved to be rather unstable and it was not possible to effect its partial hydrogenation to the corresponding 2-methyl compound (XV), which we intended to hydrate by the Brown reaction.

Hydrogenation of 7,7,10-trimethyl-$\Delta^{1(9)}$-octal-2-one (VII) with palladium–charcoal in ethanol gave the known 7,7,10-trimethyl-*cis*-decal-2-one (XX), m.p. 68° (3). The 3-position of this compound was blocked through conversion to the 3-hydroxymethylene-ketone (XXI),[7] which with the toluene-*p*-thiosulphonate of propane-1,3-dithiol yielded

[6]*See footnote 4.*

[7]*The formulation of this compound as* (XXI) *follows from the fact that condensation of cis-decal-2-one with ethyl oxalate is known to occur at the 3-position (Stork, G. and Hill, R. K. J. Am. Chem. Soc.* **79**, *495 (1957)), and in the case of 7,7,10-trimethyl-cis-decal-2-one* (XX) *even normal alkylation and bromination takes place at this position (3).*

Can. J. Chem. Downloaded from www.nrcresearchpress.com by 176.9.209.113 on 09/04/12
For personal use only.

the dithioketal (XXII), m.p. 121° (method of Woodward *et al.* (15)). This thioketal appears to be a useful substance for further synthetic studies.

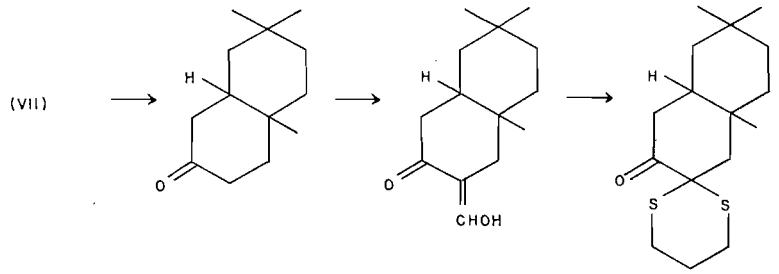

(XX) (XXI) (XXII)

EXPERIMENTAL

Melting points and boiling points are uncorrected. The alumina used for all chromatograms was prepared from Alcoa activated alumina, grade F-20 (Aluminum Co. of America, Pittsburgh, Pa.) through neutralization by means of ethyl acetate and reactivation for 4 hours at 200° (35 mm). Ultraviolet spectra were measured in 95% ethanol solution on a Unicam model S.P. 500 spectrophotometer and infrared spectra in chloroform solution on a Baird double-beam recording spectrophotometer. Analyses were carried out in our microanalytical department under the direction of Mr. Erich Meier.

2,5,5-Trimethyl-3-chlorocyclohex-2-en-1-one (V)

2,5,5-Trimethylcyclohexane-1,3-dione (IV) was prepared by the methylation of dimedone (3, 16, 17). The reaction of (IV) with phosphorus trichloride was best carried out on a 30–35 g scale under the conditions described by Halsall and Thomas (3). The yield could be improved by azeotropic distillation with dry chloroform of traces of moisture in the ketone (IV) before the addition of the phosphorus trichloride. By taking this precaution, there were obtained from a total of 165 g of IV a total of 125 g (68%) of 2,5,5-trimethyl-3-chlorocyclohex-2-en-1-one, b.p. 78–80° at 2 mm, n_D^{22} 1.4963; reported (3): b.p. 76–78° at 5 mm, n_D^{20} 1.4962.

2,5,5-Trimethylcyclohexanone (VI)

A solution of 15 g of 2,5,5-trimethyl-3-chlorocyclohex-2-en-1-one (V) in 165 ml of absolute methanol was shaken with 2 g of a 5% palladium–charcoal catalyst in hydrogen at 22° and 758 mm. The absorption of hydrogen had become very slow after 1 hour, by which time 2.09 molar equivalents of gas had been absorbed. The catalyst was removed and washed well with ethanol. Most of the solvent was removed by fractional distillation through a 12-inch Vigreux column. The residue was dissolved in ether and the solution was washed with water, dried, and evaporated. Distillation of the residue yielded 9.1 g (75%) of 2,5,5-trimethylcyclohexanone, b.p. 79–80° at 21 mm, n_D^{24} 1.4458; reported (3): b.p. 71–73° at 12 mm, n_D^{20} 1.4460. The semicarbazone showed m.p. 179–180°; reported (3): m.p. 173–177°.

7,7,10-Trimethyl-$\Delta^{1(9)}$-octal-2-one (VII)

A solution of potassium *tert*-butoxide in *tert*-butanol (1000 ml of 0.86 *N*) was added all at once to a boiling solution of 120 g (0.857 mole) of 2,5,5-trimethylcyclohexanone in

Can. J. Chem. Downloaded from www.nrcresearchpress.com by 176.9.209.113 on 09/04/12
For personal use only.

Can. J. Chem. Downloaded from www.nrcresearchpress.com by 176.9.209.113 on 09/04/12
For personal use only.

200 ml of dry *tert*-butanol under nitrogen. The mixture was boiled for 1 hour under nitrogen and the resulting clear orange solution was allowed to cool to room temperature during the next 2 hours. During this time a solution of 4-diethylaminobutan-2-one methiodide in *tert*-butanol was prepared by the addition of 236 g (1.64 moles) of 4-diethylaminobutan-2-one (18) in 200 ml of dry *tert*-butanol to 230 g (1.62 moles) of methyl iodide in 150 ml of *tert*-butanol, followed by stirring under nitrogen at 0° for 1 hour. The resulting non-viscous two-phase system was added gradually during 1 hour to the solution of the enol, with stirring, whereby the temperature rose to 60° and a reddish suspension resulted. The mixture was stirred in nitrogen at room temperature for 70 hours. It was then poured onto cracked ice containing 180 ml of concentrated hydrochloric acid, and the mixture was well extracted with ether. The organic layer, containing ether and *tert*-butanol, was evaporated, the residue was diluted with ether, and the solution was washed with water, dried, and evaporated. The dark residue was distilled through a small column under reduced pressure. The first fraction after redistillation gave 55 g (46%) of unreacted 2,5,5-trimethylcyclohexanone (b.p. 62–64° at 10 mm; semicarbazone, m.p. 177–179°, undepressed on admixture with an authentic sample). The next fraction (60.5 g) consisted of the crude ketone VII, b.p. 120–125° at 0.7 mm, λ_{max} 241 mμ (ε 9800). This fraction was converted to the semicarbazone in the usual way. The crude derivative after being filtered and dried weighed 46 g and showed m.p. 208–212°. The derivative could be purified by crystallization, but in practice it was found wasteful and unnecessary to do so. The total crude derivative was therefore boiled under reflux for 30 minutes with 52 g of fused sodium acetate and 40 g of freshly distilled pyruvic acid in 1 l. of glacial acetic acid containing 200 ml of water. Most of the solvent was removed by distillation at 30 mm and ether and water were added to the residue. The ether extract was washed with sodium bicarbonate solution and water, dried, and evaporated. Distillation of the residue yielded 30.2 g (34%, corrected for recovered starting material) of the ketone (VII), b.p. 122–124° at 3 mm, n_D^{22} 1.5068, λ_{max} 241 mμ (ε, 16,400); reported (3): b.p. 110–115° (bath) at 0.5 mm, n_D^{20} 1.5070, λ_{max} 243 mμ (ε, 17,000). The semicarbazone after crystallization from ethanol showed m.p. 226–227°. Anal. Calc. for $C_{14}H_{23}N_3O$: C, 67.43; H, 9.30. Found: C, 67.22; H, 9.35.

7,7,10-Trimethyl-$\Delta^{1(9)}$*-octal-2-one Cyclоethylenedithioketal* (VIII)

Boron trifluoride etherate (2 cc) was added to a mixture of 5 g of the unsaturated ketone VII and 4.25 cc of ethanedithiol, with ice-cooling, and the mixture was then allowed to stand at 0° for 30 minutes. The crystalline mass was diluted with 25 cc of dry methanol, cooled, and filtered. This procedure yielded 6.38 g (91%) of the dithioketal (VIII), m.p. 67–69°, which was used in the next step. Crystallization of a small sample from methanol led to the analytical specimen, m.p. 70.5–71°, no high-intensity absorption in the ultraviolet. Anal. Calc. for $C_{15}H_{24}S_2$: C, 67.10; H, 9.01. Found: C, 66.86; H, 8.84.

7,7,10-Trimethyl-$\Delta^{1(9)}$*-octalin* (IX)

The dithioketal (VIII) (6.3 g), W-2 Raney nickel (ca. 50 g), and absolute ethanol (450 cc) were boiled under reflux for 14 hours. The nickel was removed, washed with absolute ethanol, and the solvent was evaporated through a 12-inch Vigreux column. Pentane was added to the residue, the mixture was filtered, and the filtrate evaporated. Distillation of the residue at 120–130° (bath temperature) at 30 mm yielded 3.40 g (81%) of the olefin (IX), n_D^{22} 1.4951, infrared band at 6.00 and 12.44 μ (trisubstituted double bond). Anal. Calc. for $C_{13}H_{22}$: C, 87.56; H, 12.44. Found: C, 87.42; H, 12.20.

The olefin could also be purified by chromatography on alumina and elution with pentane.

1β,9β-Oxido-7,7,10-trimethyldecalin (X)

7,7,10-Trimethyl-$\Delta^{1(9)}$-octalin (IX) (2 g) (0.0112 mole) in benzene (40 ml) was added during 15 minutes to a solution of perbenzoic acid (0.0123 mole) in benzene (40 ml) cooled to 5°. The solution was then allowed to reach room temperature. Aliquots (0.1 cc each) were removed at intervals and titrated against standard sodium thiosulphate solution. After 15, 30, and 150 minutes the extent of reaction was 88, 95, and 104%, respectively. After the last titration, the solution was washed with 2 *N* potassium hydroxide solution and water and was then dried and evaporated. Evaporation of the solvent yielded 2.16 g (99%) of the crude oxide (X), which was used for the next step. A small sample was purified by chromatography on alumina, followed by elution with pentane and pentane–benzene (9:1) and finally distillation at 120° (bath temperature) at 23 mm. The purified oxide showed n_D^{18} 1.4868, no infrared band in the 6-μ region. Anal. Calc. for $C_{13}H_{22}O$: C, 80.35; H, 11.41. Found: C, 80.30; H, 11.53.

Rearrangement of 1β,9β-Oxido-7,7,10-trimethyldecalin (X) *to 7,7,10-Trimethyl-trans-decal-1-one* (XI)

Boron trifluoride etherate (1.78 g) in dry chloroform (25 ml) was added to a solution of the crude oxide (X) (2.0 g) in dry chloroform (25 ml) kept at 0° by ice-cooling. The solution, which rapidly turned orange, was maintained at 0° for 30 minutes and was then poured into 100 ml of a saturated sodium bicarbonate solution. Ether was added and the organic extract was washed with water, dried, and evaporated. The residue (2.02 g) was chromatographed on 80 g of alumina, a procedure which showed it to be a complex mixture. The only ketonic fraction (0.84 g; strong infrared band at 5.84 μ) was eluted with pentane–ether (3:1). This fraction did not yield a crystalline semicarbazone. It was therefore boiled under reflux for 1 hour with 2 g of Girard reagent P in 40 cc of absolute methanol containing 4 g of glacial acetic acid. The solution was cooled and added to 5.05 g of sodium bicarbonate dissolved in 250 ml of ice-cold water. The mixture was extracted with ether, and the aqueous layer was then acidified with dilute hydrochloric acid, allowed to stand for 30 minutes, and extracted well with ether. The latter extract was washed with water, dried, and evaporated. The resulting ketone (0.29 g; 14.5%) was converted in about 80% yield into the semicarbazone of the ketone XI, which after crystallization from ethanol showed m.p. 221–222°. Anal. Calc. for $C_{14}H_{25}N_3O$: C, 66.89; H, 10.03. Found: C, 66.81; H, 10.21.

The ketone was regenerated from the semicarbazone in over 80% yield with pyruvic acid as described above for the octalone (VII). It showed b.p. 84–86° at 0.1 mm, n_D^{22} 1.4905. The infrared spectrum is reproduced in Fig. 1. Anal. Calc. for $C_{13}H_{22}O$: C, 80.35; H, 11.41. Found: C, 80.51; H, 11.43.

Reconversion to the semicarbazone, followed by one crystallization from ethanol, yielded the pure derivative, m.p. 220–222°. The 2,4-dinitrophenylhydrazone after crystallization from ethanol formed orange needles, m.p. 197–198°. Anal. Calc. for $C_{19}H_{26}N_4O_4$: C, 60.94; H, 7.00. Found: C, 61.10; H, 6.92.

Conversion of Cyclohexene to Cyclohexanol with Lithium Aluminum Hydride and Boron Trifluoride

Boron trifluoride etherate (3.4 g; 0.024 mole) was added to a solution of cyclohexene (4 g; 0.049 mole) in 100 ml of dry ether. A solution of lithium aluminum hydride (0.7 g; 0.018 mole) in 70 ml of ether was then added dropwise during 20 minutes, under

Can. J. Chem. Downloaded from www.nrcresearchpress.com by 176.9.209.113 on 09/04/12
For personal use only.

nitrogen, with stirring and ice-cooling. The mixture was stirred at room temperature under nitrogen for a further 2 hours, when 20 ml of acetone were added carefully to destroy excess reagent. A saturated solution of sodium sulphate was added, followed by solid sodium sulphate. The mixture was filtered, the precipitate was washed with ether, and the clear filtrate was evaporated. The residue was dissolved in 30 ml of 90% ethanol containing 0.8 g of sodium hydroxide, and 10.2 ml of 20% aqueous hydrogen peroxide was then added during 5 minutes with stirring, whereby the mixture heated spontaneously to about 70°. The temperature was maintained at this point for 5 minutes longer by external heating and the flask was then cooled. Water and ether were added, the ether extract was washed with water, dried, and evaporated through a Vigreux column. Distillation of the residue yielded 4.0 g (82%) of cyclohexanol, m.p. 20–23°, b.p. 161–162°, n_D^{22} 1.4656, identified with an authentic sample through non-depression of the melting point on admixture and by the complete identity of the infrared spectra.

In exactly the same way, 1-octene was converted in 80% yield to *n*-octanol (b.p. 194–196°, n_D^{25} 1.4295) identified through the infrared spectrum with an authentic sample.

Conversion of 10-Methyl-$\Delta^{1(9)}$*-octalin* (XVI) *to cis- and trans-10-Methyldecal-1-one* (XIX) *by the Diborane Reaction*

A solution of 0.45 g (0.0032 mole) of boron trifluoride etherate in 5 ml of ether was added to 0.5 g (0.0033 mole) of 10-methyl-$\Delta^{1(9)}$-octalin (XVI) (2) in 15 ml of ether. A solution of 0.2 g (0.005 mole) of lithium aluminum hydride in 20 ml of ether was then added during 10 minutes under nitrogen with stirring and the mixture was stirred at room temperature for 3 hours more. The product, isolated as before, was dissolved in 15 ml of 90% ethanol containing 0.4 g of sodium hydroxide. The solution was heated to 70° and 1 ml of 20% aqueous hydrogen peroxide was added dropwise. Heating at 70° was continued for 5 minutes and the product was then isolated as above. The resulting material (0.52 g) was chromatographed on 25 g of alumina. Elution with pentane yielded 0.08 g (16%) of unchanged octalin (XVI), while elution with pentane–ether (3:1) gave 0.40 g (71%; 85% corrected for recovered starting material) of a liquid mixture of the carbinols (XVII) and (XVIII), showing a strong hydroxyl band in the infrared.

This material was dissolved in 12 ml of dry pyridine and added dropwise during 10 minutes to a mixture of 0.6 g of chromic acid and 12 ml of pyridine, with stirring and ice-cooling. The mixture was allowed to stand overnight and was then diluted with water and extracted repeatedly with ether. The organic extract was filtered through Celite and evaporated. Distillation of the product at 90–100° (bath temperature) at 3 mm yielded 0.33 g (83%) of a mixture of the *cis*- and *trans*-isomers of 10-methyldecal-1-one (XIX), the infrared spectrum of which was almost identical with that of the previously described equilibrium mixture (2). Conversion to the semicarbazone gave about an 80% yield of derivative, m.p. 198–204°, which after several crystallizations from ethanol rose to 209–210°. The melting point was undepressed on admixture with an authentic sample (m.p. 209–211°) (2).

7,7,10β-Trimethyl-cis-decal-1β-ol (XII) *from 7,7,10-Trimethyl-*$\Delta^{1(9)}$*-octalin* (IX)[8]

Boron trifluoride etherate (5 ml) was added to a solution of 2 g of the octalin (IX) in 40 ml of ether. A solution of 1.1 g of lithium aluminum hydride in 70 ml of ether was then added during 45 minutes, with stirring under nitrogen, and the mixture was stirred for another 2 hours at room temperature. The product, isolated as before, was dissolved in 30 ml of 90% ethanol containing 1.2 g of sodium hydroxide. Hydrogen peroxide (7 ml

[8]*This experiment was done in collaboration with Dr. E. Ghera.*

Can. J. Chem. Downloaded from www.nrcresearchpress.com by 176.9.209.113 on 09/04/12
For personal use only.

Can. J. Chem. Downloaded from www.nrcresearchpress.com by 176.9.209.113 on 09/04/12
For personal use only.

of a 20% solution) was added, and the mixture was allowed to stand at room temperature for 1 hour. Isolation with ether then gave 2.1 g of a product which was chromatographed on 80 g of alumina. Elution with pentane gave 0.12 g (6%) of unchanged octalin (IX), while elution with pentane–ether (4:1) gave 1.65 g (75%; 80% corrected for recovered starting material) of the crystalline alcohol (XII), m.p. 78–81°. Crystallization from pentane gave the analytical sample, m.p. 82–83°, strong hydroxyl band in the infrared. Anal. Calc. for $C_{13}H_{24}O$: C, 79.53; H, 12.32. Found: C, 79.87; H, 12.32.

7,7,10-Trimethyl-cis-decal-1-one (XIII) *from 7,7,10-Trimethyl-cis-decal-1β-ol* (XII)

A solution of 2.4 g of the carbinol (XII) in 20 ml of dry pyridine was added during 10 minutes to a mixture of 3 g of chromic acid and 40 ml of pyridine, with stirring and ice-cooling, and the mixture was then allowed to stand at room temperature for 24 hours. The product, isolated as described above, on crystallization from pentane yielded 1.54 g of the *cis*-ketone (XIII), m.p. 40–42°. Distillation of the mother liquors at 120–130° at 25 mm and subsequent crystallization from pentane gave another 0.36 g (total yield, 80%), m.p. 39–42°. Further crystallization from pentane gave large plates, m.p. 42–43°, with the infrared spectrum shown in Fig. 1. Anal. Calc. for $C_{13}H_{22}O$: C, 80.35; H, 11.41. Found: C, 80.36; H, 11.23.

Isomerization of 7,7,10-Trimethyl-cis-decal-1-one (XIII) *to the trans-Isomer* (XI)

The crystalline *cis*-ketone (XIII) (0.5 g) dissolved in 10 cc of pentane was absorbed on a column of 50 g of alkaline alumina (Grade F-20, Aluminum Co. of America, Pittsburgh, Pa.), prepared with pentane. The column was then allowed to stand for 12 hours. Elution with pentane and then with pentane–benzene (2:3) yielded 0.47 g (94%) of the liquid equilibrated product, consisting essentially of the *trans*-ketone (XI). The infrared spectrum was identical in every respect with that of the ketone obtained by the boron trifluoride isomerization method. The semicarbazone after crystallization from ethanol formed needles, m.p. 221–222°. The 2,4-dinitrophenylhydrazone formed orange needles from ethanol, m.p. 196–197°. Neither of these melting points were depressed on admixture with the corresponding derivatives of the ketone (XI) obtained from the oxide (X).

2-Methylene-7,7,10-trimethyl-$\Delta^{1(9)}$*-octalin* (XIV)

An ethereal solution of *n*-butyllithium (35 ml of 0.68 *N*; 0.024 mole) was added to a suspension of 10 g (0.028 mole) of methyltriphenylphosphonium bromide (prepared from methyl bromide and triphenylphosphine (14)) in 160 ml of dry ether, with swirling under nitrogen. The mixture was stirred in nitrogen for 1½ hours and a solution of 0.96 g (0.005 mole) of the octalone (VII) in 50 ml of ether was added. Stirring at room temperature was continued for 20 hours and 200 ml of dry tetrahydrofuran were then added at the same time as most of the ether was removed by distillation. The resulting mixture was boiled under reflux for 10 hours, cooled, and diluted with water. The product was extracted with ether and the ether layer was washed with dilute hydrochloric acid and water, dried, and evaporated. The orange oily residue was heated with 500 ml of dry pentane, the mixture was cooled, and the triphenylphosphine oxide which had precipitated was removed. Evaporation of the solvent and distillation of the residue gave 0.67 g (71%) of the diene (XIV), b.p. 130–140° (bath temperature), at 23 mm n_D^{24} 1.5100, infrared bands at 6.08 and 11.35 μ. Anal. Calc. for $C_{14}H_{22}$: C, 88.35; H, 11.65. Found: C, 88.60; H, 11.42.

The diene polymerized on attempted chromatographic purification on alkaline alumina and also on being allowed to stand for 1 week in light and air at room temperature.

7,7,10-Trimethyl-cis-decal-2,3-dione 3-Dithiotrimethylene Ketal (XXII)

7,7,10-Trimethyl-$\Delta^{1(9)}$-octal-2-one (1 g) in 200 ml of absolute ethanol was shaken in hydrogen over 0.6 g of a 10% palladium–charcoal catalyst at 755 mm and 25°. After 20 minutes, 1.01 molar equivalents of hydrogen had been absorbed and uptake stopped. The catalyst was removed, the filtrate was evaporated, and the resulting crystalline residue on sublimation at 60° (bath temperature) at 23 mm gave 7,7,10-trimethyl-*cis*-decal-2-one (XX) (0.74 g) as needles, m.p. 65–67°, infrared band at 5.83 μ; reported (3): m.p. 67.5–68°.

A solution containing 0.62 g of the *cis*-ketone (XX) and 0.75 ml of freshly distilled ethyl formate in 15 ml of dry benzene was stirred in nitrogen with 0.4 g of sodium hydride at room temperature for 65 hours. Excess hydride was then destroyed by the dropwise addition of methanol, and ether and cold 3% sodium hydroxide solution was added. The aqueous layer was separated, acidified with cold 5% hydrochloric acid, and again extracted with ether. The latter ether extract on being washed with water, dried, and evaporated yielded 1.13 g of the crude hydroxymethylene-ketone (XXI), admixed with formic acid, λ_{max} 282 mμ (ϵ, 5500). This material was dissolved in 25 ml of absolute ethanol, 1.67 g of propane-1,3-dithiol toluene-*p*-thiosulphonate was added, and then a solution of 2.4 g of freshly fused potassium acetate in 10 ml of ethanol. The resulting mixture was boiled under reflux for 5 hours and then evaporated nearly to dryness. Ether and water were added, the organic layer was washed with water, dried, and evaporated. The residue was chromatographed on 30 g of alumina. Elution with benzene yielded 0.42 g (44%) of the dithioketal (XXII) as a crystalline solid, m.p. 100–110°. Two crystallizations from methanol gave the analytical sample as long needles, m.p. 120–121°. Anal. Calc. for $C_{16}H_{26}OS_2$: C, 64.38; H, 8.78. Found: C, 64.08; H, 8.59.

ACKNOWLEDGMENTS

We are indebted to Professor Gilbert Stork, Columbia University, for valuable discussions. Thanks are also due to Dr. B. Altman for his skillful technical assistance.

REFERENCES

1. SONDHEIMER, F. and ELAD, D. J. Am. Chem. Soc. **80**, 1967 (1958).
2. SONDHEIMER, F. and ROSENTHAL, D. J. Am. Chem. Soc. **80**, 3995 (1958).
3. HALSALL, T. G. and THOMAS, D. B. J. Chem. Soc. 2431 (1956).
4. STEINER, U. and WILLHALM, B. Helv. Chim. Acta, **35**, 1752 (1952). FAVRE, H. and SCHINZ, H. Helv. Chim. Acta, **35**, 2388 (1952).
5. HUSSEY, A. S., LIAO, H. P., and BAKER, R. H. J. Am. Chem. Soc. **75**, 4727 (1953).
6. HAUPTMANN, H. J. Am. Chem. Soc. **69**, 562 (1947).
7. HENBEST, H. B. and WRIGLEY, T. I. J. Chem. Soc. 4596 (1957).
8. BROWN, H. C. and SUBBA RAO, B. C. J. Org. Chem. **22**, 1136, 1137 (1957).
9. BROWN, H. C. and ZWEIFEL, G. J. Am. Chem. Soc. **81**, 247 (1959).
10. BROWN, H. C. and SUBBA RAO, B. C. J. Am. Chem. Soc. **78**, 5694 (1956).
11. BROWN, H. C. and ZWEIFEL, G. Abstracts of Papers, 135th Meeting of the American Chemical Society, Boston, Mass., April, 1959. p. 39.
12. SHAPIRO, I., WEISS, H. G., SCHMICH, M., SKOLNIK, S., and SMITH, G. B. L. J. Am. Chem. Soc. **74**, 901 (1952).
13. WOLFE, S., NUSSIM, M., MAZUR, Y., and SONDHEIMER, F. J. Org. Chem. **24**, 1034 (1959).
14. SCHOLLKOPF, U. Angew. Chemie, **71**, 260 (1959).
15. WOODWARD, R. B., PATCHETT, A. A., BARTON, D. H. R., IVES, D. A. J., and KELLY, R. B. J. Chem. Soc. 1131 (1957).
16. DESAI, R. D. J. Chem. Soc. 1079 (1932).
17. MEEK, E. G., TURNBULL, J. H., and WILSON, W. J. Chem. Soc. 811 (1953).
18. WILDS, A. L. and SHUNK, C. H. J. Am. Chem. Soc. **65**, 469 (1943).

Can. J. Chem. Downloaded from www.nrcresearchpress.com by 176.9.209.113 on 09/04/12
For personal use only.

Can. J. Chem. Downloaded from www.nrcresearchpress.com by 176.9.209.113 on 09/04/12
For personal use only.

MYCOCHRYSONE

II. CARBON SKELETON, PRINCIPAL CHROMOPHORE, AND OXYGEN FUNCTIONS[1]

G. READ[2] AND L. C. VINING

ABSTRACT

A mono- and di-methyl ether and two diacetates of mycochrysone have been prepared. Elemental analyses of these derivatives and of the purified pigment itself are consistent with a revised $C_{20}H_{12}O_7$ formula for mycochrysone.

The formation of a leucohexaacetate suggests that the molecule contains two hydroxyl or potential hydroxyl oxygen functions in addition to the quinonoid and phenolic (or enolic) groups already shown to be present. The infrared spectra of mycochrysone and derivatives provide evidence that the remaining oxygen atom is ketonic. The principal chromophore of mycochrysone is related to 8-hydroxy-1,2-naphthoquinone. Hydrogenation experiments indicate that the pigment has a perylene carbon skeleton.

INTRODUCTION

In part I of this series (1) it was proposed that mycochrysone is a $C_{20}H_{14}O_7$ peri-hydroxylated orthoquinone containing a second, more acidic, hydroxyl, and since perylene was formed on zinc – zinc chloride fusion, it was concluded that the carbon skeleton was that of either perylene or 1,1′-dinaphthyl.

Several derivatives of the pigment have now been prepared and repeated analyses have given lower hydrogen values than expected for a parent compound of the above formula. Re-examination of the purity of the pigment preparations used in earlier work has now shown that a persistent minor contaminant, not removed by recrystallization from cold chloroform, is responsible for this inconsistency. Recrystallizing the pigment from cold aqueous acetone or by concentrating an ethereal solution at room temperature, or chromatographic purification on silicic acid, has given material analyzing for $C_{20}H_{12}O_7$, the molecular formula expected from the analysis of derivatives. The best solvent for purification was cold aqueous acetone. Low and variable carbon analyses had been obtained for the quinoxaline derivative crystallized from methanol (1) and preparations from ethyl acetate give similar results. The derivative is hygroscopic and it appears that complete dessiccation cannot be obtained.

Methylation of the pigment with silver oxide and methyl iodide at room temperature gave two crystalline compounds, separable by chromatography on silicic acid. The minor product was shown to be a monomethyl ether with properties indicating methylation of the more acidic hydroxyl. The second compound, a dimethyl ether, showed a pronounced hypsochromic shift of the quinonoid absorption band, and tests indicated that in this product the *peri*-hydroxyl group had also been methylated. The monomethyl ether could be readily converted to the dimethyl ether by refluxing with silver oxide in methyl iodide. The incomplete substitution in the cold is not surprising for methylation of *peri*-hydroxyl groups is frequently difficult (2). Both methyl ethers formed quinoxaline derivatives, providing additional evidence for the orthoquinonoid group in mycochrysone. Methylation of mycochrysone quinoxaline at room temperature gave a single

[1]*Manuscript received July 10, 1959.*
Contribution from the National Research Council of Canada, Prairie Regional Laboratory, Saskatoon, Saskatchewan.
Issued as N.R.C. No. 5368.
[2]*National Research Council of Canada Postdoctorate Fellow, 1957–59. Present address: The Dyson Perrins Laboratory, Oxford University, England.*

product shown to be identical with the quinoxaline of the monomethyl ether, a result consistent with the presence of a *peri*-hydroxyl group.

Acetylation by standard techniques failed to yield solid derivatives, and examination of the reactions by paper chromatography indicated that extensive decomposition of the pigment had taken place. The use of silver carbonate with acetic anhydride, however, gave two principal products (mycochrysone acetates I and II) which were separated on a silicic acid – Celite column and found to be isomeric diacetates. Re-examination of the products from acetylation with acetic anhydride and sodium acetate at room temperature by paper chromatography showed that, under these conditions, some mycochrysone acetate I was formed.

Paper chromatographic examination of the crude product from reductive acetylation showed a large number of components. The ultraviolet spectrum of the material indicated that a perylene chromophore was present in low concentration, and in view of the relatively mild reaction conditions this suggested a perylene skeleton in the starting material. The major product, separated by countercurrent distribution, was a hexa-acetate. The hydrogen values favored a $C_{32}H_{28}O_{13}$ formula, but in view of the slightly high carbon analyses and the difficulty experienced with the parent pigment, the compound may be the simple acetylated leucomycochrysone, $C_{32}H_{26}O_{13}$. If so the parent compound should contain four hydroxyl groups. The seventh oxygen atom is most probably present in a ketone group since the carbonyl stretching region of the infrared spectra of mycochrysone and all of the derivatives described above contain maxima at or near 1690 cm^{-1} (s). Should the $C_{32}H_{28}O_{13}$ formula be correct, it is possible that one or both of the hydroxyl groups not revealed by methylation may have been generated during reduction.

The ultraviolet absorption spectrum of the leucoacetate resembles that of naphthalene, and the principal chromophore of the pigment is therefore similar to that of diosquinone (I),* isolated from the shrub *Diospyros tricolor* Hiern (Ebenaceae) (3). A comparison between the absorption spectra of these two compounds is shown in Fig. 1. The authors

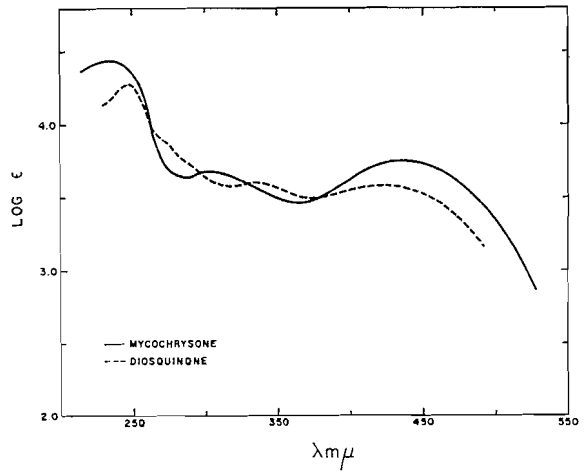

FIG. 1. Absorption spectra in ethanol of mycochrysone and diosquinone (redrawn from (4)).

have observed that the ultraviolet spectral properties of a sample of diosquinone changed over a period of several months. Some reservations should therefore be made in accepting

This structure has not yet been confirmed by synthesis.

Can. J. Chem. Downloaded from www.nrcresearchpress.com by 176.9.209.113 on 09/04/12
For personal use only.

the data obtained by Prista (4), and reproduced here, as an accurate spectrum of this sensitive pigment. Although the two spectra are alike, a closer similarity might have been expected if the naphthaquinone system were the only chromophore present in mycochrysone. In view of the unsaturation in the remainder of the molecule, the differences may be due to an extension of the conjugated system or to an independent chromophore.

The formation of perylene from the pigment by zinc – zinc chloride fusion (1) did not exclude the possibility that mycochrysone is a derivative of 1,1′-dinaphthyl. The identification of the carbon skeleton by a series of reactions less likely to result in cyclized artifacts was therefore sought. It could be expected that hydrogenation followed by dehydration would remove most of the oxygen atoms so that subsequent dehydrogenation of the product might proceed unambiguously to yield the parent hydrocarbon (5). When the pigment was hydrogenated in ethanol or dioxane over Raney nickel, a dark red tarry product was obtained and it was evident that decomposition had occurred. However, under similar conditions mycochrysone dimethyl ether reduced smoothly to a colorless oil which yielded a small amount of solid product on trituration with methanol. The solid proved to be tetradecahydroperylene, obtained in 12.5% yield and identified by comparison with an authentic sample. This unexpected result in itself provided convincing evidence for the perylene skeleton, while the production of considerable quantities of perylene from the residual oil on dehydration and dehydrogenation supported the finding. From the dimethyl ether, under somewhat milder conditions, there was obtained a complex mixture of products, some of which appeared to retain the quinol system. Dehydration and dehydrogenation again gave perylene but in lower yields. On no occasion could 1,1′-dinaphthyl be detected.

From a consideration of the results given above, II is suggested as the most probable partial structure for mycochrysone, although the hydroxylic character of two oxygen functions requires confirmation.

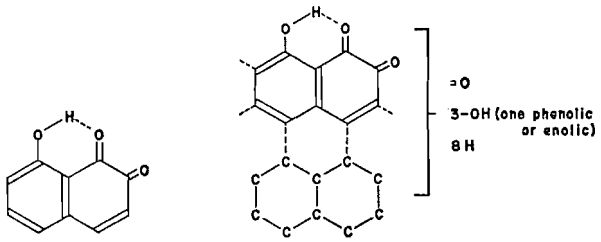

(I) (II)

EXPERIMENTAL

Unless otherwise indicated, the petroleum ether referred to in this section has a 60–80° C boiling range.

Whatman No. 1 filter paper disks (32 cm diameter), impregnated with formamide (adjusted with formic acid to pH 6.0), were used for paper chromatograms.

Melting and decomposition points were determined on a Leitz hot stage instrument. Figures given in cases of slow decomposition refer to the first appearance of decomposition. This temperature is largely dependent on the crystal size and is of little diagnostic value.

Can. J. Chem. Downloaded from www.nrcresearchpress.com by 176.9.209.113 on 09/04/12
For personal use only.

Can. J. Chem. Downloaded from www.nrcresearchpress.com by 176.9.209.113 on 09/04/12
For personal use only.

Mycochrysone

The following purifications gave satisfactory products.

(*a*) Crude mycochrysone, isolated by chloroform extraction (1), was dissolved in acetone and filtered free from a trace of dark impurity. Water was added to the filtrate until it became faintly cloudy and crystals began to form. The solution was refiltered and, on standing overnight at 4° C, gave the bulk of the compound as fine red needles. The crystallization was repeated to give a product slowly decomposing above 195° C. Found: C, 66.00, 66.04%; H, 3.47, 3.37%. $C_{20}H_{12}O_7$ requires: C, 65.94%; H, 3.32%. Ultraviolet absorption spectrum in ethanol showed λ_{max} 236, 303, 438 mμ; log ε 4.49, 3.75, and 3.80, respectively.

(*b*) A solution of crude mycochrysone dissolved in "analar" chloroform was filtered and concentrated. The product, which was slowly deposited as orange microcrystals, was redissolved in a large volume of ether. Filtration and concentration of the ethereal solution at room temperature gave mycochrysone as short orange-brown rods, decomposing slowly above 200° C. Found: C, 66.00, 66.27%; H, 3.45, 3.49%.

(*c*) Crude mycochrysone was adsorbed on a silicic acid column from benzene–chloroform (1:1) and the pigment slowly eluted with chloroform containing 2% ethanol. The product was dissolved in a small volume of acetone and rapidly precipitated with petroleum ether to give mycochrysone as a red amorphous powder decomposing slowly above 175° C. Found: C, 65.92, 65.60%; H, 3.71, 3.69%.

Mycochrysone Quinoxaline

The derivative was prepared as in (1); the crude product (100 mg) dissolved in chloroform was applied to a silicic acid column (2.2×6.0 cm). Elution with chloroform – 4% ethanol gave the quinoxaline which was crystallized twice from a small volume of ethyl acetate as prisms, slowly decomposing above 228° C.

A sample dried for 16 hours at 140° C and cooled to room temperature under high vacuum was observed to increase steadily in weight while being weighed for analysis. Found: C, 70.68%; H, 3.86%. $C_{26}H_{16}O_5N_2 . 1/3H_2O$ requires: C, 70.61%; H, 3.80%. A sample (590.08 mg), dried as above, gained 3.26 mg in weight on standing in an open sample tube for 24 hours. Ultraviolet absorption spectrum in ethanol – 4% dioxane showed λ_{max} 240, 266.5, 443, λ_{infl} 330 mμ; log ε 4.64, 4.70, 4.17, and 3.95, respectively.

Methylation (Typical Run)

Mycochrysone (0.25 g) was shaken for 12 hours at room temperature with silver oxide (0.25 g) and methyl iodide (30 ml) free from hydrogen iodide. The products were washed into chloroform (100 ml Analar), filtered from silver iodide and excess silver oxide, and the filtrate applied to a silicic acid column (4×15 cm). The chloroform eluate gave mycochrysone monomethyl ether (35 mg), deep red needles decomposing slowly above 170° C after three crystallizations from methanol. Found: C, 66.43, 66.74, 66.83%; H, 3.98, 3.86, 3.63%; CH_3O, 8.79, 9.28%. $C_{21}H_{14}O_7$ requires: C, 66.67%; H, 3.73%; CH_3O, 8.21%. Ultraviolet absorption in ethanol showed λ_{max} 235, 301, 443 mμ; log ε 4.50, 3.78, and 3.80, respectively. The monomethyl ether was readily soluble in acetone, dioxane, chloroform, ether, and benzene. In concentrated sulphuric acid, ferric chloride, and sodium hydroxide or sodium carbonate solutions it gave blue, brown, and purple colorations, respectively. It was not extracted from chloroform by sodium bicarbonate solution, and gave a purple solution but no precipitate with methanolic lead acetate.

Development of the column with chloroform containing 3% ethanol eluted mycochrysone dimethyl ether (135 mg), obtained as small, yellow needles, m.p. 251–252° C

(decomp.) after three crystallizations from acetone. Found: C, 67.31, 67.41, 67.47%; H, 4.03, 4.06, 4.16%; CH_3O, 15.08, 15.95%. $C_{22}H_{16}O_7$ requires: C, 67.34%; H, 4.11%; CH_3O, 15.82%. Ultraviolet absorption in ethanol containing 4% dioxane showed λ_{max} 234, 330, 419 mμ; log ε 4.58, 3.70, and 3.85, respectively. The dimethyl ether gave a blue solution with concentrated sulphuric acid, dissolved slowly with decomposition in sodium hydroxide, and gave a colorless solution with concentrated ammonia.

Mycochrysone monomethyl ether, mycochrysone dimethyl ether, and mycochrysone had R_f values of 0.42, 0.20, and 0.07, respectively, when chromatographed on paper by the circular technique using benzene–chloroform (3:1) as mobile phase.

Mycochrysone Monomethyl Ether Quinoxaline

The quinoxaline of mycochrysone monomethyl ether was prepared in ethanol, purified by elution from a silicic acid column with chloroform, and crystallized from methanol–chloroform (1:1) as needles, m.p. 276–277° C (decomp.). Found: C, 71.69, 71.95%; H, 4.09, 4.07%; N, 6.19%. $C_{27}H_{18}O_5N_2$ requires: C, 71.99%; H, 4.03%; N, 6.22%. Ultraviolet absorption in ethanol containing 4% dioxane showed λ_{max} 237.5, 266, 443, λ_{infl} 330 mμ; log ε 4.65, 4.71, 4.11, and 4.00, respectively. The quinoxaline was sparingly soluble in ether, ethyl acetate, benzene, methanol, and ethanol.

Methylation of mycochrysone quinoxaline as above gave a monomethyl ether as needles, m.p. 275–277° C (decomp.). Found: C, 71.75%; H, 4.27%. The ultraviolet and infrared spectra and R_f of this product were indistinguishable from those of the quinoxaline obtained from mycochrysone monomethyl ether.

Mycochrysone Dimethyl Ether Quinoxaline

The quinoxaline of mycochrysone dimethyl ether was prepared in glacial acetic acid and purified on a silicic acid column developed with chloroform. The compound was very soluble in common solvents with the exception of ether and petroleum ether and was precipitated from chloroform by petroleum ether as a bright yellow powder, m.p. 175° C. Found: C, 72.26%; H, 4.57%; N, 6.16%. $C_{28}H_{20}O_5N_2$ requires: C, 72.40%; H, 4.34%; N, 6.03%. Ultraviolet absorption in ethanol showed λ_{max} 232, 265.5, 423, λ_{infl} 324 mμ; log ε 4.68, 4.73, 4.17, and 4.02, respectively.

The quinoxalines of mycochrysone monomethyl ether, mycochrysone dimethyl ether, and mycochrysone had R_f values of 0.64, 0.34, and 0.08, respectively, when developed on circular paper chromatograms using petroleum ether – benzene (2:1).

Acetylation with Silver Carbonate and Acetic Anhydride

Silver carbonate (100 mg) was added to a refluxing solution of mycochrysone (0.5 g) in acetic anhydride (15 ml). After 0.25 hour the solution was cooled, filtered, and poured onto ice. When the acetic anhydride had decomposed, the product (440 mg) was separated by extraction into chloroform and evaporation to dryness under reduced pressure. It showed two main components, acetate I (R_f 0.37) and acetate II (R_f 0.61), when developed on paper chromatograms with petroleum ether – benzene (1:1). The product was dissolved in benzene and adsorbed on a column (38×2.3 cm) of silicic acid – Celite (1:1). Benzene–chloroform (2:1) eluted acetate II which, upon evaporation of the solvent, was left as a brown viscous gum, unstable in hot solvents. Since it could not be crystallized even after further chromatography, it was dissolved in chloroform (5 ml), passed through a fine sintered glass filter, and precipitated by the addition of petroleum ether as a yellow powder (65 mg), m.p. 127–129° C. Found: C, 64.45, 64.50%; H, 3.79, 3.83%; acetyl (Kuhn Roth), 18.52%. $C_{24}H_{16}O_9$ requires: C, 64.29%; H, 3.60%; $(OAc)_2$, 19.2%. Ultraviolet absorption in ethanol showed λ_{max} 244, 296.5, 442 mμ; log ε 4.37, 3.85, and 3.76, respectively.

Can. J. Chem. Downloaded from www.nrcresearchpress.com by 176.9.209.113 on 09/04/12
For personal use only.

Elution of the silicic acid – Celite column with benzene–chloroform (1:1) gave additional acetate II followed by acetate I. After rechromatography on silicic acid the latter product, which was also thermolabile and could not be obtained crystalline, was precipitated as above to give a yellow powder (205 mg), m.p. 142–144° C. Found: C, 64.42, 64.23%; H, 3.74, 3.79%; acetyl (Kuhn Roth), 19.54%. Ultraviolet absorption in ethanol showed λ_{max} 245, 292, 443 mμ; log ϵ 4.39, 3.79, and 3.75, respectively.

Reductive Acetylation

A solution of mycochrysone (0.4 g) in acetic anhydride (60 ml) was shaken with zinc dust (5 g) for 30 minutes, when it became pale yellow with a bright green fluorescence. Sodium acetate (5 g) was added, the mixture shaken for 30 minutes, and then heated for 40 minutes on a water bath. After cooling and filtration, the solution was poured onto ice and, on decomposition of the acetic anhydride, extracted with chloroform (4×50 ml) and the extract evaporated to dryness under reduced pressure. Paper chromatography using petroleum ether – benzene (2:1) showed eight fluorescent bands detected under ultraviolet light in addition to two principal non-fluorescent bands detected by alkali spray.

Countercurrent fractionation through 200 transfers in the solvent system, water – ethanol – benzene – petroleum ether (2:6:5:3), gave the main component (252 mg) in tubes 66 to 92, with peak concentration in tubes 77 and 78. The material in tubes 76 to 79 (83 mg) was considered pure and was precipitated with petroleum ether (100–120° C) as a colorless powder. It could not be crystallized but melted at 133–135° C. Found: C, 62.14, 62.12%; H, 4.68, 4.63%; acetyl, 43.3, 42.0%. $C_{32}H_{26}O_{13}$ requires: C, 62.14%; H, 4.24%; $(OAc)_6$, 41.7%. Ultraviolet absorption in ethanol showed λ_{max} 227, 292, λ_{infl} 326 mμ; log ϵ 4.95, 4.12, and 3.57, respectively.

Hydrogenation of Mycochrysone Dimethyl Ether

Mycochrysone dimethyl ether (1 g) was hydrogenated in ethanol (60 ml) with Raney nickel for 10 hours at 2000 lb/sq. in. and 200° C. Evaporation of the solvent yielded a colorless viscous oil which on trituration with methanol deposited a solid (85 mg). Crystallization from methanol and sublimation (110° C; 0.05 mm) raised the melting point from 155° to 170° C. Found: C, 89.99%; H, 9.96%. $C_{20}H_{26}$ requires: C, 90.16%; H, 9.84%. Ultraviolet absorption spectrum in heptane showed λ_{max} 274 mμ; log ϵ 3.07. The melting point of this product was undepressed on admixing with an authentic sample of tetradecahydroperylene obtained by hydrogenating perylene (100 mg) under the same conditions. Found: C, 90.35%; H, 9.89%. The ultraviolet and infrared absorption spectra of the two materials were indistinguishable. Literature gives m.p. 175–177° C (6) and λ_{max} 270 mμ; log ϵ 3.38 for the ultraviolet absorption in hexane (7).

The residual oil from the reaction was refluxed for 2 hours with a small amount of cymene over freshly fused and powdered potassium hydrogen sulphate at 180° C. On cooling, the products were freed from inorganic salt by extraction into benzene and chromatographed on an alumina column (45×2.3 cm). In addition to cymene, four fractions were collected: (*a*) 145 mg and (*b*) 86 mg in the benzene eluate, (*c*) 74 mg in the chloroform–ethanol (1:1), and (*d*) 80 mg in the ethanol eluates, respectively. Fractions (*a*) and (*b*) gave perylene (78 and 40 mg, respectively) on heating for 3 hours with selenium powder at 290° C, while (*c*) and (*d*) yielded small amounts of perylene together with unidentified oils under the same conditions. The perylene was isolated by column chromatography and identified by melting point and ultraviolet absorption (1).

Can. J. Chem. Downloaded from www.nrcresearchpress.com by 176.9.209.113 on 09/04/12
For personal use only.

ACKNOWLEDGMENTS

A sample of diosquinone was generously donated by Dr. R. H. Thomson, the University of Aberdeen. The authors also wish to express their appreciation to Dr. R. H. Haskins and to Mr. M. Mazurek, of this laboratory, for the production in large quantities of the fungus from which mycochrysone was isolated, and for the microanalyses, respectively.

REFERENCES

1. READ, G., SHU, P., VINING, L. C., and HASKINS, R. H. Can. J. Chem. **37**, 731 (1959).
2. GARDEN, J. F. and THOMSON, R. H. J. Chem. Soc. 2483 (1957).
3. PARIS, R. and PRISTA, L. V. N. Ann. pharm. franç. **12**, 375 (1954).
4. PRISTA, L. V. N. Anais fac. farm. Porto, **17**, 5 (1958).
5. READ, G. Ph.D. thesis, Nottingham, 1957.
6. ZINKE, A. and BENNDORF, O. Monatsh. Chem. **59**, 241 (1932).
7. CONRAD-BILLROTH, H. Z. physik. Chem. B, **15**, 1 (1931).

Can. J. Chem. Downloaded from www.nrcresearchpress.com by 176.9.209.113 on 09/04/12
For personal use only.

Can. J. Chem. Downloaded from www.nrcresearchpress.com by 176.9.209.113 on 09/04/12
For personal use only.

CONDUCTANCES OF DILUTE SOLUTIONS OF POTASSIUM IODATE IN WATER AND WATER–DIOXANE MIXTURES AT 25° C[1]

E. Bock

ABSTRACT

Conductances of dilute solutions of potassium iodate in water and water–dioxane solutions, extending over the dielectric constant range from $D = 78.54$ to $D = 29.71$, have been measured over the concentration range from zero up to $Ka < 0.2$ at 25.00° C. By applying the Fuoss–Onsager treatment to the data obtained, the association constants for the electrolyte in the various solvents, as well as $\mathring{a}$, the distance of closest approach of the ions, have been determined.

INTRODUCTION

In the literature are recorded several attempts at calculating association constants of a number of moderately strong electrolytes by means of conductance data. According to the latest refinement of the electrolytic conductance theory by Fuoss and Onsager (1) all these earlier attempts have yielded erroneous association constants, since in their derivation an incomplete equivalent conductance function was used. More specifically, the early association constants were forced to carry transcendental as well as linear terms of the conductance function, terms which have now become calculable. The Fuoss–Onsager conductance equation provides a means of determining all three parameters usually encountered in conductance work, viz. the limiting equivalent conductance Λ_0, the association constant K_A, and $\mathring{a}$ the distance of closest approach of the ions.

The assumption that salts of the oxyacids belong to the class of moderately strong electrolytes is of long standing. Thus T. Shedlovsky (2) in 1932 interpreted the anomalous course of the phoreograms of $AgNO_3$ and KNO_3 by assuming ion association. More recently Monk (3), Krieger and Kilpatrick (4), and especially Spiro (5) have addressed themselves to the problem of determining the extent of ion-association of potassium iodate in aqueous solution. However, since, as already pointed out above, in all these efforts the incomplete conductance function was used, it was thought worth while to reinvestigate the potassium iodate problem, and as it was apparent from the papers of the above workers as well as from results of experiments carried out in this laboratory (6) that the association constant of potassium iodate in aqueous solution is of the order of unity, it was necessary to obtain conductance data in solvents of varying dielectric constants. Moreover as rather reliable dielectric constants (7) as well as viscosity and density (8) data for water–dioxane mixtures were available in the literature, it was decided to study the conductance of potassium iodate in these media.

EXPERIMENTAL

The experimental technique employed has been recorded elsewhere (9), with the exception that instead of preparing dilute solutions by weight dilution these were prepared by direct addition of dry salt in platinum cups, to the solvent, contained in a Shedlovsky-type conductance cell. The salt, dried in a vacuum oven at 80° C for 36 hours, was weighed out on a Mettler M-5 Grammatic micro-balance having a 2-μg sensitivity.

The dioxane of spectro quality was further purified according to the scheme proposed

[1]*Manuscript received July 13, 1959.*
Contribution from the Department of Chemistry, University of Manitoba, Winnipeg, Manitoba.

by Hess and Frahm (10). After purification the dioxane had a melting point of 11.75° C and a refractive index of $n_D^{20} = 1.42246$. In each and every preparation of a water–dioxane mixture only dioxane freshly distilled from sodium was used. The water–dioxane mixtures were prepared by first passing a stream of nitrogen, which was purified by passage through alkaline pyrogallol, sulphuric acid, ascarite, and two tall water saturators (the latter situated in the same bath in which the conductance measurements were carried out), through conductance water, contained in the conductance cell, for several hours until a steady low conductance value was obtained, usually of the order of 2.5–3 $\times 10^{-7}$ mho. Then dioxane freshly distilled from sodium was added to the water by means of a container similar in design to that described by Martel and Kraus (11). The dielectric constants were interpolated from the work of Critchfield, Gibson, and Hall (7), and the viscosities and densities, the former corrected for the latest value of the viscosity of water (12), from the work of Geddes (8).

The conductances were measured on a Jones conductivity bridge, an oscilloscope serving as a detector. The cell constant was determined using the equation for conductances of dilute aqueous solutions of KCl, proposed by Fuoss *et al.* (13).

The temperature was read on a platinum resistance thermometer calibrated by the National Research Council of Canada.

RESULTS AND DISCUSSION

The experimental results are summarized in Table I. Figure 1 shows the plots of y vs. x,

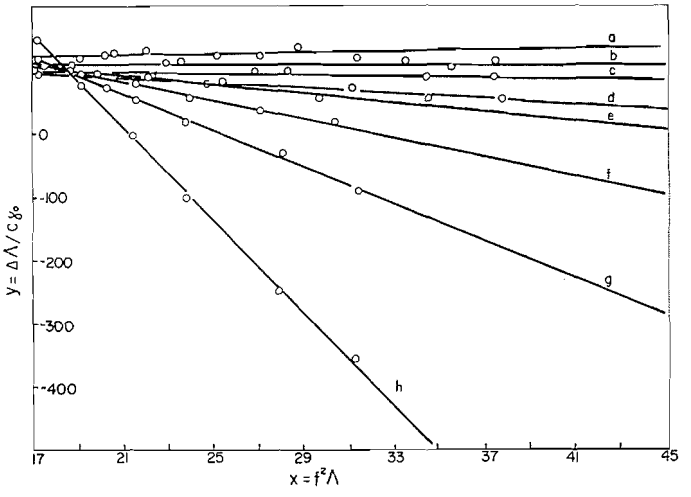

FIG. 1. Plots of y vs. x.
Graph: (*a*) 0% Dioxane. (*b*) 9.53% Dioxane. (*c*) 17.94% Dioxane. (*d*) 29.91% Dioxane. (*e*) 37.20% Dioxane. (*f*) 43.79% Dioxane. (*g*) 49.56% Dioxane. (*h*) 57.12% Dioxane.

where

$$y = \Delta\Lambda/C\gamma_0 \quad [1]$$

$$\Delta\Lambda = \Lambda + Sc^{\frac{1}{2}}\gamma_0^{\frac{1}{2}} - Ec\gamma_0 \log C\gamma_0 - \Lambda_0 \quad [2]$$

$$x = f^2\Lambda. \quad [3]$$

Can. J. Chem. Downloaded from www.nrcresearchpress.com by 176.9.209.113 on 09/04/12
For personal use only.

TABLE I

Equivalent conductances of potassium iodate at various concentrations in different water–dioxane mixtures at 25.00° C

Concentration in moles/l. $\times 10^4$	Equivalent conductance in mhos/equiv.	Concentration in moles/l. $\times 10^4$	Equivalent conductance in mhos/equiv.
0% Dioxane		29.91% Dioxane	
0.86082	113.62	1.74644	67.08_1
2.05973	113.17	5.17687	66.32_7
3.14043	112.90	10.4873	65.56_5
4.69655	112.55	28.9172	63.82_7
6.58631	112.21	40.4107	63.03_2
8.66525	111.87	54.2107	62.24_2
10.8189	111.59	71.0788	61.41_2
12.9277	111.33		
14.1154	111.19	9.53% Dioxane	
15.6428	111.02	3.87079	95.357
16.8869	111.88	6.40851	94.89_7
		9.34022	94.48_3
17.94% Dioxane		13.3625	94.00_9
4.13496	82.278	25.6002	92.84_7
8.17181	81.63_2	39.8083	91.88_4
22.8563	80.14_2	58.6903	90.84_5
41.7615	78.48_3		
81.9495	76.87_6	49.56% Dioxane	
		10.6227	46.16_9
14.3407	50.66_6	21.7473	44.58_1
23.9384	49.58_8	33.7206	43.32_6
37.0447	48.42_6	45.2947	42.34_4
52.4081	47.35_9	53.7218	41.72_7
68.0228	46.44_4	67.3286	40.85_8
83.5281	45.67_3	79.2354	40.18_4
37.20% Dioxane		57.12% Dioxane	
17.3233	56.73_0	8.05120	40.694
31.7963	55.48_6	14.0987	39.343
47.2423	54.42_8	26.3997	37.365
61.7318	53.60_6	36.9684	36.127
80.0696	52.71_6	50.7410	34.822
		67.0938	33.595

NOTE: These data were taken from a previous publication, see ref. 9.

In Figs. 2 to 6 are shown the graphs of Λ_J vs. $C\gamma_0$ where

$$\Lambda_J = \Lambda + Sc^{\frac{1}{2}}\gamma_0^{\frac{1}{2}} - Ec\,\gamma_0 \log C\,\gamma_0 + K_A\,C\,\gamma_0 f^2\,\Lambda \quad [4]$$

and γ_0 the degree of association is given by

$$\gamma_0 = \frac{\Lambda}{\Lambda_0 - (S(\Lambda c)^{\frac{1}{2}}/\Lambda_0^{\frac{1}{2}})}. \quad [5]$$

Figure 7 shows the plot of log K_A vs. $1/D$, where K_A is the association constant for the equilibrium

$$A^+ + B^- \rightleftarrows AB. \quad [6]$$

Lastly Table II summarizes the derived values of K_A, Λ_0, and $\mathring{a}$; also included are the values of $\mathring{a}$ and the corresponding dielectric constants, as well as the weight per cent composition of the solvent, and the Walden product.

As is apparent from Fig. 7, log K_A is a linear function of $1/D$, a behavior first predicted on theoretical grounds by Denison and Ramsay (14) and later verified experimentally by Kraus *et al.* (15). The linear character of the log K_A vs. $1/D$ plot of course means, as one would expect, that the chief forces involved in ion-pair formation are electrostatic in nature.

Can. J. Chem. Downloaded from www.nrcresearchpress.com by 176.9.209.113 on 09/04/12
For personal use only.

Can. J. Chem. Downloaded from www.nrcresearchpress.com by 176.9.209.113 on 09/04/12
For personal use only.

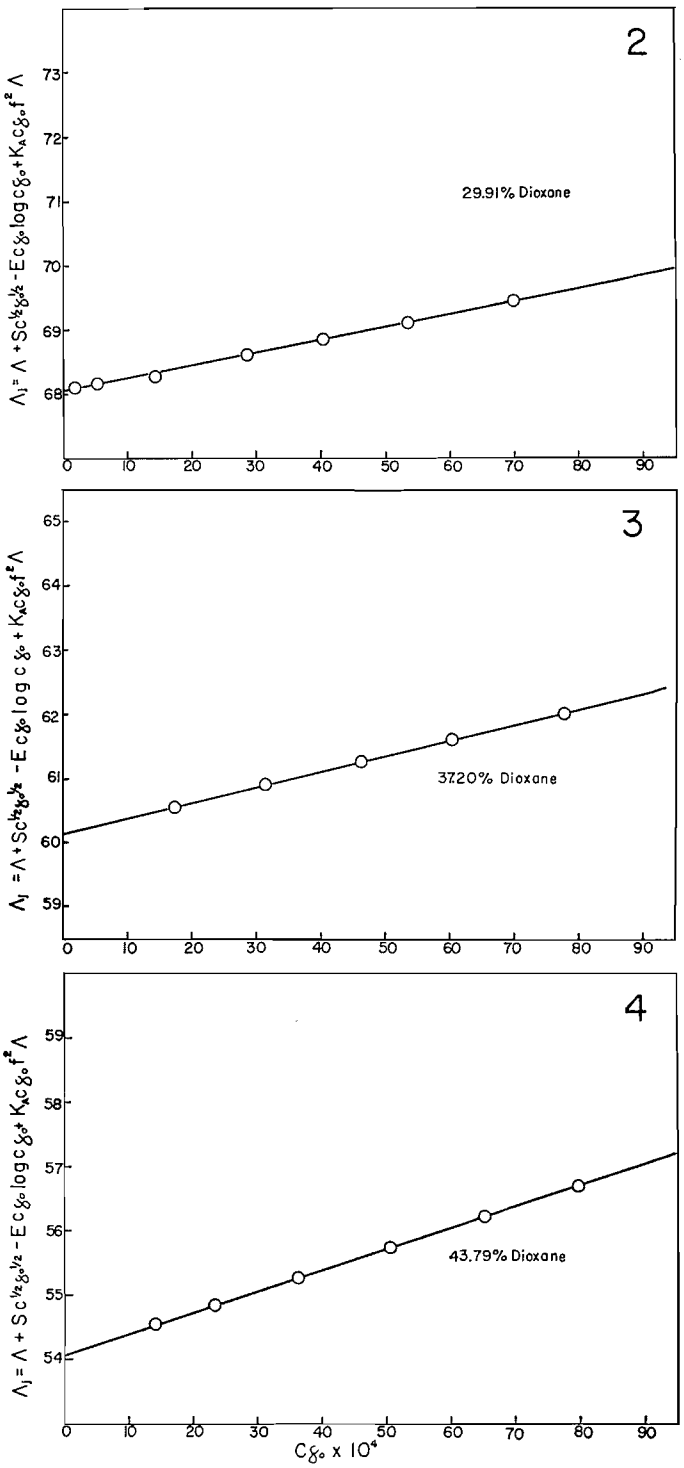

FIG. 2. Plot of Λ_j vs. $c \times 10^2$ (29.91% dioxane).

FIG. 3. Plot of Λ_j vs. $c \times 10^2$ (37.20% dioxane).

FIG. 4. Plot of Λ_j vs. $c \times 10^2$ (43.79% dioxane).

Can. J. Chem. Downloaded from www.nrcresearchpress.com by 176.9.209.113 on 09/04/12
For personal use only.

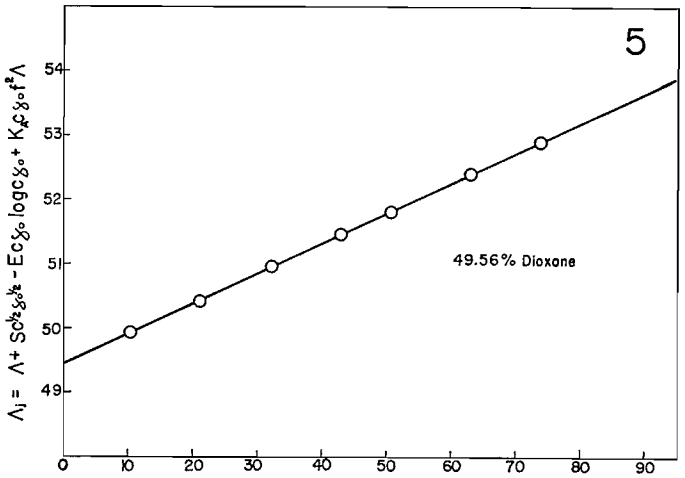

FIG. 5. Plot of Λ_j vs. $c \times 10^2$ (49.56% dioxane).

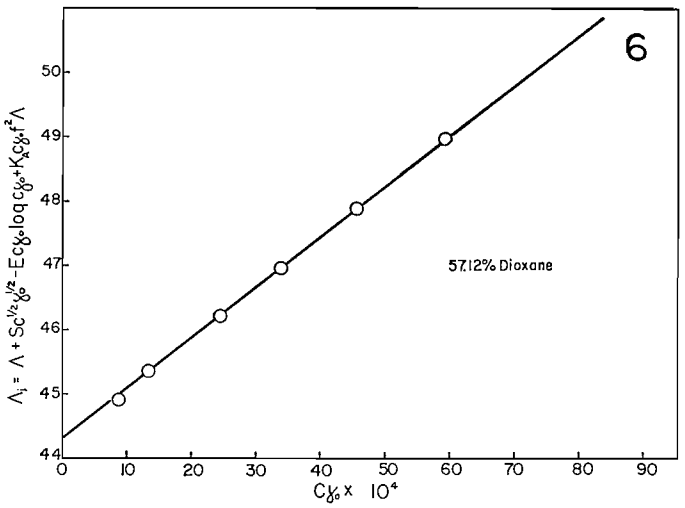

FIG. 6. Plot of Λ_j vs. $c \times 10^2$ (57.12% dioxane).

TABLE II

Summary of derived quantities

Wt. % dioxane	D	$J(\mathring{a})$	$\mathring{a}$	K_A	Λ_0	$\Lambda_0\eta_0 \times 10^2$
0	78.54	172	(3.2)	.41	114.43	102.27
9.53	70.71	178	(3.2)	.77	96.84	103.85
17.94	63.61	204	(3.2)	1.46	83.84	104.40
29.91	53.27	200	2.8	2.32	68.07	103.09
37.20	41.05	241	2.0	3.92	60.14_5	100.75
43.79	41.26	330	3.00	7.85	54.05_0	97.91
49.56	36.26	467	3.35	15.1	49.45_5	94.53
57.12	29.71	775	3.60	36.8	44.32_0	87.94

The graph of log K_A vs. $1/D$ was constructed from the values of K_A for the five lower dielectric constant media, viz. for mixtures containing 29.91% to 57.12% dioxane. The latter were derived according to the procedure recommended by Fuoss (16) from the slope of the y vs. x plot. Only mixtures containing more than 29.91% dioxane yielded a graph of y vs. x with a reasonable slope; for a mixture poorer in dioxane than 29.91 the

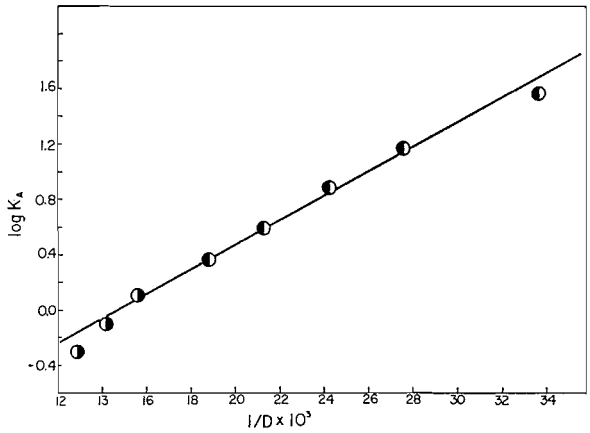

FIG. 7. log K_A vs. $1/D \times 10^3$. ◐ From Λ_j vs. $c\gamma_0$ plots. ◑ From y vs. plots assuming an $\mathring{a}$ of 3.2 Å.

slope of the y vs. x plots were so nearly horizontal that no reliable value of K_A could be obtained. In these latter cases the K_A's were obtained by an alternative procedure, viz. first obtaining the value of $y(0)$ through extrapolation of the y vs. x curve. Then, since at $x = \Lambda_0 y = y(0) = (J(\mathring{a}) - K_A\Lambda_0)$, K_A could be calculated by assuming a value for $\mathring{a}$ and calculating $J(\mathring{a})$. The selection of $\mathring{a}$ was in turn guided by the series of $\mathring{a}$ values derived from the slope of the Λ_j vs. $C\gamma_0$ curve for the five lower dielectric constant mixtures. The limiting equivalent conductances were also derived from these plots. When the logarithms of the association constants thus calculated are plotted vs. $1/D$ the points fall reasonably close to the straight line of log K_A vs. $1/D$ drawn through the log K_A points for the five lower dielectric constant solvents.

From a perusal of Table II it will be noticed that $\mathring{a}$, the distance of closest approach of the ions, is not constant for the various dielectric constant mixtures, but exhibits a slow increase with decreasing dielectric constant. A similar behavior was noticed by Fuoss and Kraus (17) for $NaBrO_3$ (although the increase for this salt was slight it was still noticeable), tetrabutyl ammonium iodide, tetrabutyl ammonium bromide, and tetraisoamyl ammonium nitrate. The change in $\mathring{a}$ in the latter three cases was attributed by the above authors to the disparity of the cationic and anionic sizes. In the case of Bu_4NI it was further suggested that additional induction forces on the periphery of the cation as well as possible specific interactions with the solvent molecules were also causing $\mathring{a}$ to increase in the low dielectric constant region.

Whether similar effects are causing an increase in $\mathring{a}$ in the present case is difficult to say. From an examination of the origin of the $\mathring{a}$ term it would seem that one would expect a change in the magnitude of $\mathring{a}$ with change in the composition of the solvent medium, since $\mathring{a}$ arises out of specifying a boundary condition which demands equality of electrical potential and intensity originating inside and outside a sphere of radius $\mathring{a}$, on the surface of this sphere. Thus $\mathring{a}$ measures, in a sense, the electrical influence of an ion, an influence which one would expect to change with a change in dielectric constant. The present investigation is of course too incomplete to permit a definite determination of the causes of the increase of $\mathring{a}$ with changing solvent composition, if only because of the fact that all calculations presented in this paper were carried out manually and no second and third approximations in γ_0 and Λ_0 were attempted. Moreover, $\Lambda\eta = \Lambda(1+Fc)$ was approximated to Λ by neglecting the Fc term for lack of viscosity data but this latter

Can. J. Chem. Downloaded from www.nrcresearchpress.com by 176.9.209.113 on 09/04/12
For personal use only.

approximation should not prove too serious in the present case since as suggested by Fuoss (16), for relatively small inorganic ions the Fc term is unimportant. From the slope of log K_A vs. $1/D$, $\mathring{a}$ results as 2.8 Å; a value which seems to be unrealistically small. But if as suggested by Fuoss and Kraus, the internal dipole of the iodate ion is taken into account then the steepness of the log K_A plot becomes more understandable. Since, if an internal dipole moment is present in one of the ions K_A should be written as

$$K_A = K_0 \exp (U_1 + U_2)/kT,$$

where $U_1 = e^2/aD$ is the electrostatic energy of ion-pair dipole in the absence of an internal dipole in one of the ions and $U_2 = \mu/d^2D$ is the additional energy term resulting from the interaction of the cation with μ the internal dipole of the anion. Here d is the distance from the center of the cation to the electrostatic center of the anion dipole.

There still remains, however, the difficulty of interpreting the equally small $\mathring{a}$ values derived from the y vs. x plots, and the gradual increase of $\mathring{a}$ with decrease in dielectric constant. Thus the average value of $\mathring{a}$ derived from y vs. x plots results as 3.2 Å which is some 0.3 Å smaller than the sum of the crystallographic radii of the potassium ion (1.33 Å), and the iodate ion (2.2 Å). This latter value was calculated on the assumption that iodate ion has the shape of a regular tetrahedron of edgelengths 3.35 Å (18).

CONCLUSION

In conclusion it may be said that the present paper certainly bears out the predictions of the Fuoss–Onsager conductance equation. There is some difficulty, however, in interpreting the rather small magnitude of $\mathring{a}$. If some sort of interpenetration of ionic shells takes place, a possibility which does not seem too inconceivable in the case of the iodate ion considering its tetrahedral or perhaps more correctly, pyramidal structure, then the small value of $\mathring{a}$ would find an explanation, but this of course is mere conjecture. Further studies of potassium iodate conductances especially in other than water–dioxane mixtures should prove interesting.

Concerning the change of the size of $\mathring{a}$ with change in dielectric constant of the mixture, attention should be drawn to the fact that the Walden product, almost constant in the region of higher dielectric constants, drops more or less sharply in lower dielectric constant mixtures. Now an increase in $\mathring{a}$ would of course result in a lowering of the ionic mobility which in turn would result in a decrease of the Walden product. This correlation seems to suggest that the increase of $\mathring{a}$ in the lower dielectric constant region is perhaps real and does not arise out of some inaccuracies in the experimental data, or the theoretical treatment thereof.

ACKNOWLEDGMENTS

The author wishes to thank Professor A. N. Campbell and Dr. E. M. Kartzmark for their interest and encouragement. Furthermore, the financial assistance of the National Research Council of Canada is gratefully acknowledged.

REFERENCES

1. Fuoss, R. M. and Onsager, L. J. Phys. Chem. **61**, 668 (1957).
2. Shedlovsky, T. J. Am. Chem. Soc. **54**, 1411 (1932).
3. Monk, C. B. J. Am. Chem. Soc. **70**, 3281 (1948).
4. Krieger, K. A. and Kilpatrick, M. J. Am. Chem. Soc. **64**, 7 (1942).
5. Spiro, M. J. Phys. Chem. **60**, 976, 1673 (1956).
6. Bock, E. and Campbell, A. N. Can. J. Chem. **37**, 889 (1959).
7. Critchfield, F. E., Gibson, J. A., Jr., and Hall, J. L. J. Am. Chem. Soc. **75**, 1991 (1953).

Can. J. Chem. Downloaded from www.nrcresearchpress.com by 176.9.209.113 on 09/04/12
For personal use only.

8. GEDDES, J. A. J. Am. Chem. Soc. **55**, 4832 (1933).
9. CAMPBELL, A. N. and BOCK, E. Can. J. Chem. **36**, 1277 (1958).
10. HESS, K. and FRAHM, H. Ber. B, **71**, 2627 (1938).
11. MARTEL, R. W. and KRAUS, C. A. Proc. Natl. Acad. Sci. **41**, 9 (1955).
12. SWINDELL, J. F., COX, J. R., JR., and GODFREY, T. B. J. Research Natl. Bur. Standards, **48**, 1 (1952).
13. LIND, J. E., JR., ZWOLENIK, J. J., and FUOSS, R. M. J. Am. Chem. Soc. **81**, 1557 (1959).
14. DENISON, J. T. and RAMSEY, J. B. J. Am. Chem. Soc. **77**, 2615 (1955).
15. MARTEL, R. W. and KRAUS, C. A. Proc. Natl. Acad. Sci. **41**, 9 (1955). MORIER, P. L. and KRAUS, C. A. Proc. Natl. Acad. Sci. **41**, 1033 (1955). KRAUS, C. A. and FUOSS, R. M. J. Am. Chem. Soc. **55**, 21 (1933).
16. FUOSS, R. M. J. Am. Chem. Soc. **81**, 2659 (1958).
17. FUOSS, R. M. and KRAUS, C. A. J. Am. Chem. Soc. **79**, 2304 (1957).
18. NARAY-SROBO, I. and NEUGEBOUER, J. J. Am. Chem. Soc. **69**, 1280 (1947).

Can. J. Chem. Downloaded from www.nrcresearchpress.com by 176.9.209.113 on 09/04/12
For personal use only.

Can. J. Chem. Downloaded from www.nrcresearchpress.com by 176.9.209.113 on 09/04/12
For personal use only.

SENSITIVE VIBRATIONAL FREQUENCIES

IV. MASS EFFECTS[1]

J. K. WILMSHURST[2]

ABSTRACT

The correlation of vibrational frequencies with atomic properties of substituent atoms in the molecular system is critically examined for reality in the light of possible mass effects. The general rule is formulated that only frequencies continuously characteristic of a grouping in the mass–frequency plot can be used in such correlations. Calculated mass–frequency plots are presented for the systems XC≡N, XC≡CX, XC≡CY, $X_2C{=}CX_2$, $X_2C{=}O$, $X_3P{=}O$, XCH_3, X_2CH_2, X_3CH.

A number of empirical relations between molecular vibrational frequencies and some property of a substituent atom or radical in the molecular system have recently been reported (1–18), the most common properties used being Hammett's σ-constant (1–7), electronegativity (10–17), and ionization potential (18). However, since all these properties decrease down any column of the periodic table, while any vibrational frequency (for example, ν_{CO} in the system $X_2C{=}O$) will decrease as a substituent (X) in the molecular system is altered down the periodic table, due only to the increasing mass, care must be taken when expressing these empirical relations to ensure that they are indeed real. Ideally, of course, force constants should be evaluated and used (15), but, unfortunately, this is often impracticable for most systems of interest. However, in the absence of force constant data, the characteristic frequency of a bond or group can be used in the empirical correlations provided that firstly its dependence upon the mass of the substituent it is intended to vary is checked. This can be done simply by choosing a potential energy function for the molecular system and plotting the vibrational frequencies as a function of the mass of the substituent which is to be varied. Any significant variation in the slope of the plot of the experimental frequencies from that calculated would then indicate some change in the potential energies of the systems and would hence justify some attempt at a correlation.

In the present investigation calculated plots of frequency versus mass are given for a number of common systems assuming a simple valence force field. These plots show the mass sensitivity of the molecular vibrations and illustrate the phenomenon of "vibrational coupling". Rules are derived to permit rapid qualitative estimates of the mass insensitiveness of vibrations and the types of vibrational coupling that may occur in the general case.

Secular Determinants

The secular determinants usually encountered in normal co-ordinate calculations are of the form (19):

$$[1] \qquad \begin{vmatrix} A_{11}-\lambda, & A_{12}, & \cdots\cdots & A_{1_n} \\ A_{12}, & A_{22}-\lambda, & \cdots\cdots & A_{2_n} \\ \vdots & \vdots & & \vdots \\ A_{1_n}, & A_{2_n}, & \cdots\cdots & A_{nn}-\lambda \end{vmatrix} = 0$$

[1]*Manuscript received August 5, 1959.*
Contribution from the Department of Chemistry, Auckland University College, Auckland, New Zealand. This work was performed in part at the University of Auckland with financial assistance from the New Zealand University Research Grants Committee.

[2]*Present address: Research Laboratories, National Carbon Company, Division of Union Carbide Corporation, P.O. Box 6116, Cleveland 1, Ohio.*

where the A_{ii} are functions of the force constant and masses of a diparticle system (2 atoms for stretching, two bonds for bending, etc.) and $\lambda = 4\pi^2c^2M\nu^2$ ($= 5.8894\times10^{-2}\nu^2$) (19). The A_{ij} are also functions of the masses and force constants, but are in general smaller than the corresponding A_{ii} or A_{jj}.

It is a general property (20) of such symmetrical determinants that the roots of the nth order determinant are separated by the roots of the diagonal $(n-1)$th order determinants which roots are again separated by those of the diagonal $(n-2)$th order determinants, and so on. In particular, for the second order determinant:

$$\begin{vmatrix} A_{11}-\lambda & A_{12} \\ A_{12} & A_{22}-\lambda \end{vmatrix} = 0$$

having roots λ_1, λ_2 ($\lambda_1 > \lambda_2$), then

$$\begin{aligned} &\lambda_1 > A_{11} > \lambda_2 \\ &\lambda_1 > A_{22} > \lambda_2. \end{aligned} \qquad [2]$$

Thus, in a symmetry species containing only two vibrational modes, the vibrational frequencies are separated by the frequencies of the two diatom modes. Further, if the frequency–mass plots of the two diatom modes cross (e.g., σ-frequencies in Fig. 1*a*), then the pair of frequencies of the system cannot cross, but instead change their vibrational character and in this cross-over region can no longer be defined as approaching a particular diatom mode, but rather are only characteristic of the system as a whole. This is commonly called "vibrational coupling".

If a third order secular equation has roots λ_1, λ_2, λ_3 ($\lambda_1 > \lambda_2 > \lambda_3$) then these are separated by the roots of the three diagonal second order determinants σ_1, σ_2 ($\sigma_1 > \sigma_2$); τ_1, τ_2 ($\tau_1 > \tau_2$); and ω_1, ω_2 ($\omega_1 > \omega_2$) which are in turn separated by the roots of the first order determinants, giving the following set of inequalities:

$$\begin{aligned} &\lambda_1 > \sigma_1, \tau_1, \omega_1 > \lambda_2 > \sigma_2, \tau_2, \omega_2 > \lambda_3 \\ &\sigma_1 > A_{11}, A_{22} > \sigma_2 \\ &\tau_1 > A_{22}, A_{33} > \tau_2 \\ &\omega_1 > A_{11}, A_{33} > \omega_2. \end{aligned} \qquad [3]$$

As with two vibrations in a symmetry species, so in this case with three vibrations it is seen that non-crossing rules apply in the mass–frequency plots. This can be easily extended to higher order determinants and inequality relations similar to eq. [2] and [3] obtained. These inequalities afford a very quick qualitative estimate to be made of the mass–frequency plot and the regions in which vibrational coupling will occur.

Using secular equations derived elsewhere (19, 21, 22, 23, 24) mass–frequency plots have been calculated[3] for a number of simple systems which appear most amenable to empirical correlations, and these are shown in Fig. 1 (XC≡N, XC≡CX, XC≡CY); Fig. 2 ($X_2C{=}CX_2$, $X_2C{=}O$, $X_3P{=}O$); and Fig. 3 (XCH_3, CH_2X_2, HCX_3).

DISCUSSION

A comparison of the data calculated here with the published empirical correlations shows that in every case the experimental "sensitive" frequency chosen for the empirical correlation varies by a much larger extent than if it were only dependent on mass. Thus,

[3]*Though more theoretical significance is attached to the plot of frequency versus* $1/\sqrt{M_X}$, *in order to obtain a better magnification of the curves the frequency was plotted against log* M_X *in the present work. In the symmetry species containing a bending mode the term* $1/r^2_{CX}$ *appears and in the calculation of the curves in Figs. 1 and 2a, this has been varied as* M_X *varies the standard curve for its variation being obtained by plotting* r_{CX} *for the bonds* C—H, C—F, C—Cl, C—Br, C—I *against the mass of* X.

Can. J. Chem. Downloaded from www.nrcresearchpress.com by 176.9.209.113 on 09/04/12
For personal use only.

Can. J. Chem. Downloaded from www.nrcresearchpress.com by 176.9.209.113 on 09/04/12
For personal use only.

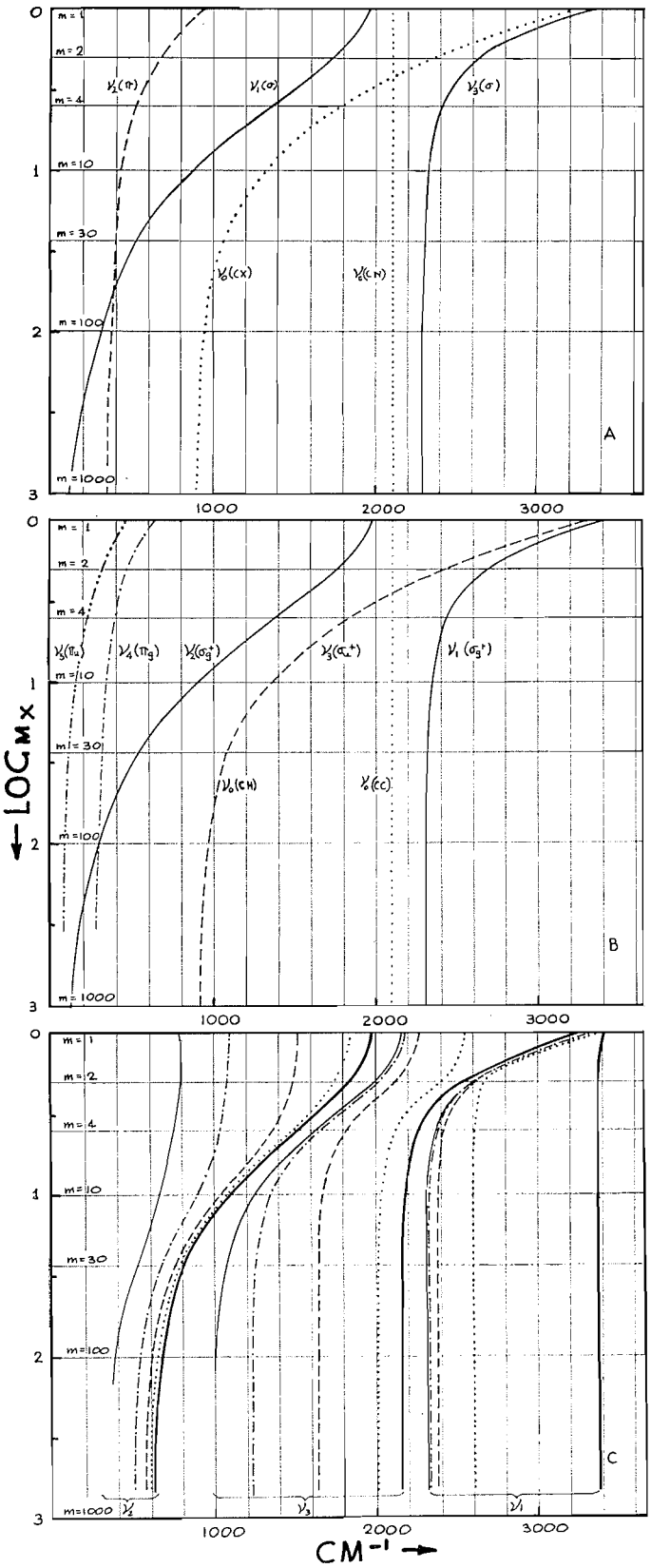

(*a*) XC≡N (k_{CN} = 17.0×10⁵, k_{CX} = 5.6×10⁵ dynes cm^{-1}; k_δ = 0.35×10^{-11} dynes cm radian^{-1}).

(*b*) XC≡CX (k_{CC} = 15.8×10⁵, k_{CX} = 5.9×10⁵ dynes cm^{-1}; k_δ = 0.13×10^{-11} dynes cm radian^{-1}).

(*c*) σ-Type frequencies for XC≡CY, (k_{CC} = 15.8×10⁵, k_{CX} = k_{CY} = 5.9×10⁵ dynes cm^{-1}) ——— M_Y = 1; . . . . M_Y = 2; – – – M_Y = 4; ·–·–·– M_Y = 10; ——— M_Y = 30.

FIG. 1. Calculated mass–frequency curves for:

Can. J. Chem. Downloaded from www.nrcresearchpress.com by 176.9.209.113 on 09/04/12
For personal use only.

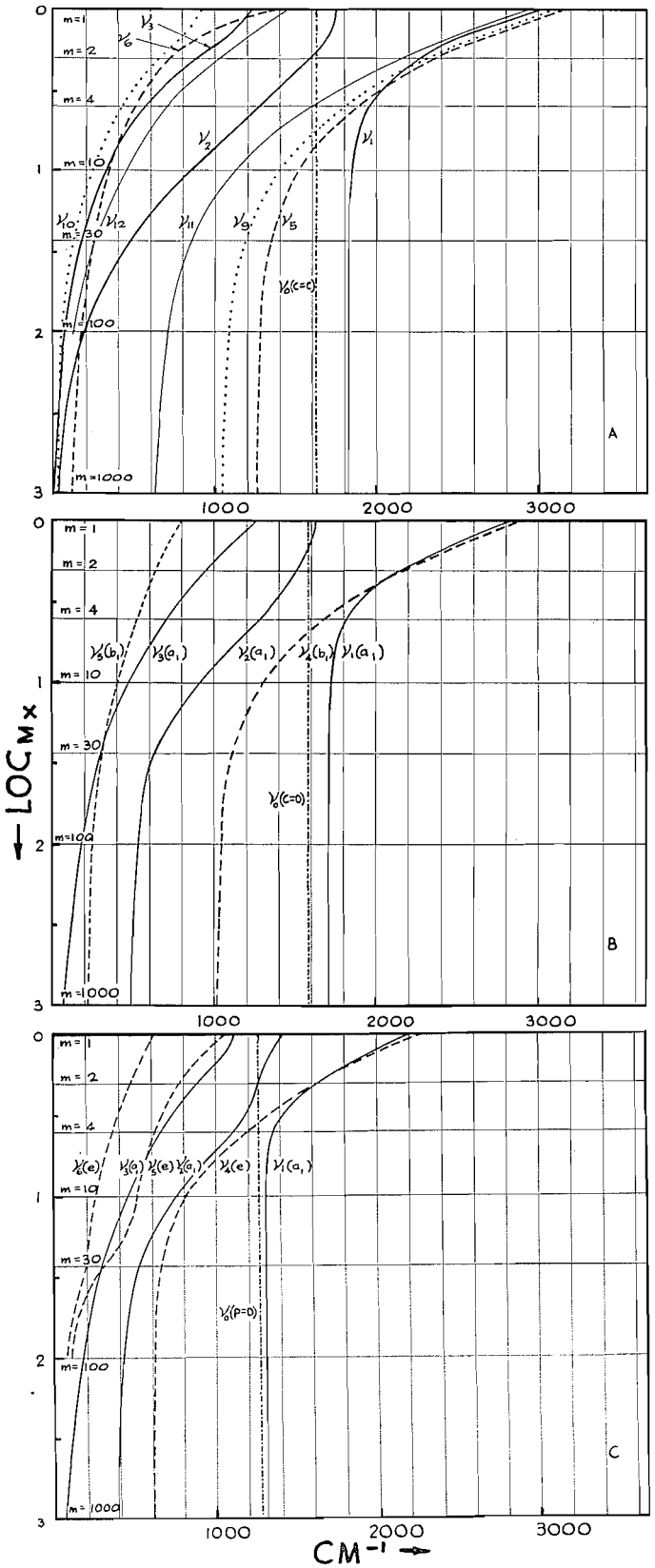

(*a*) $X_2C{=}CX_2$ ($k_{CC} = 9.5\times10^5$, $k_{C-X} = 5.15\times10^5$ dynes cm^{-1}; $\delta_{XCX} = 0.34\times10^{-11}$, $\delta_{XCC} = 0.57\times10^{-11}$ dynes cm radian^{-1}) ——— a_g; – – – b_{1g}; . . . . b_{2u}; ——— b_{3u}.

(*b*) $X_2C{=}O$ ($k_{C-O} = 10\times10^5$, $k_{C-X} = 4.45\times10^5$, $\delta_{XCX}/r^2_{CX} = 0.38\times10^5$, $\delta_{XCO}/r^2_{CX} = 0.25\times10^5$ dynes cm^{-1}).

(*c*) $X_3P{=}O$ ($k_{P=O} = 10\times10^5$, $k_{P-X} = 3\times10^5$, δ_{XPX}/r^2_{PX}, $\delta_{XPO}/r^2_{PX} = 0.36\times10^5$ dynes cm^{-1}).

FIG. 2. Calculated mass-frequency curves for:

Can. J. Chem. Downloaded from www.nrcresearchpress.com by 176.9.209.113 on 09/04/12
For personal use only.

in every case it appears the variation of the sensitive frequency with substituent is reflecting a change in potential energy of the system. However, although the variation of vibrational frequency in these systems can then be considered as expressing a variation of potential energy, one fundamental consideration must be remembered before starting any correlations. The region of vibrational coupling in the mass–frequency plot is a cross-over region in which the two interacting frequencies mix, losing their initial characters and emerging with the opposite characters (e.g. Fig. 1*a*, ν_3 is a C—X stretching vibration for $M_X = 1$ and a C≡N stretching vibration for $M_X > 10$, while ν_1 is a C≡N stretching vibration for $M_X = 1$ and a C—X stretching vibration for $M_X > 10$). If these frequencies are the only two in the symmetry species, or if no interaction with other frequencies in the symmetry species occurs, then they must lie on opposite sides of the corresponding diatom plots (Fig. 1*a*). In other systems where additional interactions occur, this is modified, but the following general rule still applies. *A frequency characteristic of a particular grouping can only be used in an empirical correlation in that region of the mass–frequency plot where it is continuously characteristic of the vibrational mode.* Thus, in the system XC≡N any correlation of $\nu_{C\equiv N}$ with some property of X cannot plot $\nu_{C\equiv N}$ for HCN on the same curve as $\nu_{C\equiv N}$ for systems with $M_X > 10$ (Fig. 1*a*).

This rule has been overlooked in some cases and plots of characteristic frequency versus some atomic property have been constructed using frequencies which are not continuously characteristic of the vibrational mode (10, 11, 12). The apparent agreement of these "improper" points must be considered in these cases as fairly fortuitous, e.g. in the series $X_2C{=}O$, $\nu_{C=O}$ for $H_2C{=}O$ or for $HXC{=}O$ should not be included on the plots of $\nu_{C=O}$ derived for $X_2C{=}O$ and $XYC{=}O$ where M_X, $M_Y > 10$. The agreement in this case fortuitously arises from the additional interaction of $\nu_{C=O}$ with δ_{HCH} shifting $\nu_{C=O}$ to higher frequencies.

In other systems such as the benzonitriles where $\nu_{C\equiv N}$ is correlated with Hammett's σ-constant of meta- and para-aromatic ring substituents (1, 7) the secular equation virtually factorizes due to the smallness of the interaction (off diagonal) terms between the nitrile group and the ring substituents. In this case the vibrational coupling between $\nu_{C\equiv N}$ and the frequencies of the ring substituent will be extremely small and while the non-crossing rule will still apply, both branches of the nitrile curve in the mass–frequency plot will approximate the same straight line for virtually all masses of the substituent and the correlation can be made for all masses of ring substituent. This state of affairs will occur in most cases where the group whose characteristic frequency is being considered is placed a number of atoms away (and is away in space also) from the group whose atomic property is to be correlated. However, since the effect of any group on the characteristic frequency of a vibrating unit decreases rapidly as the group is separated from the vibrating center by atoms in a chain or by space, this approximate factorization is only of interest in conjugated or aromatic systems. In other systems the group affecting the frequency of the vibrating center must be either closely bonded to the center or close in space to it to actually produce any effect on the frequency, and in both cases vibrational coupling will, in general, need to be considered. In the case of orthosubstituted benzonitriles, for instance, the nitrile frequency is not only affected by effects transmitted through the atomic chain, but also because the ortho substituent is close in space to the nitrile group it is affected by the field effect across space. Thus, the approximate factorization will not apply here, as a strong interaction or central force will exist between the nitrile group and the substituent and vibrational coupling will need to be considered in any empirical correlation.

Can. J. Chem. Downloaded from www.nrcresearchpress.com by 176.9.209.113 on 09/04/12
For personal use only.

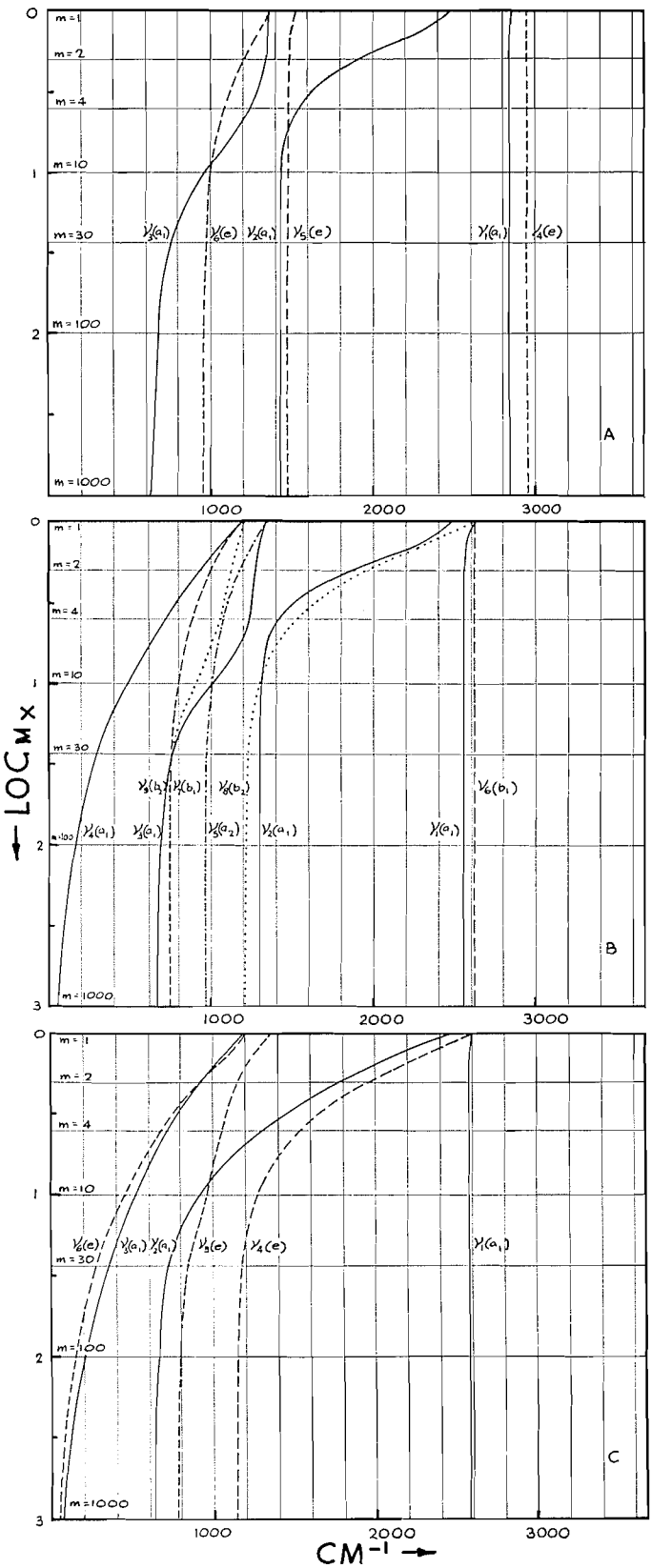

(*a*) CH_3X ($k_{C-X} = 3.6\times10^5$, $k_{CH} = 4.58\times10^5$, $\delta_{XCH}/r^2_{CH} = \delta_{HCH}/r^2_{CH} = 0.46\times10^5$ dynes cm^{-1}).

(*b*) CH_2X_2 ($k_{C-X} = 3.6\times10^5$, $k_{CH} = 3.6\times10^5$, $\delta_{HCH}/r^2_{CH} = \delta_{XCX}/r^2_{CX} = \delta_{HCX}/r^2_{CH} = 0.36\times10^5$ dynes cm^{-1}).

(*c*) HCX_3 ($k_{C-X} = 3.6\times10^5$, $k_{CH} = 3.6\times10^5$, $\delta_{HCX}/r^2_{CX} = \delta_{XCX}/r^2_{CX} = 0.36\times10^5$ dynes cm^{-1}).

FIG. 3. Calculated mass–frequency curves for:

In conclusion it should be pointed out that while any variation of a vibrational frequency with changing atomic substituents in a molecular system in excess of that predicted, assuming it were dependent only on mass alone, does reflect a real change in potential energy of the system, any correlation of this sensitive frequency with an atomic property cannot, in general, be verified regardless of how good the correlation appears. In fact, it may quite possibly be fortuitous. As an example, consider the series (13) of methyl derivatives, CH_3X, where the squares of the rocking and symmetrical deformation frequencies for X = F, Cl, Br, and I, were each found to be linearly dependent on the electronegativity of the halogen. It can be quickly seen on comparison (19) of the experimental data with Fig. 3*a* that these frequencies in these molecules are varying by a much greater extent than if they were dependent on mass changes alone and are, therefore, reflecting a real variation in potential energy. However, whether this real variation in potential energy is dependent on the electronegativity of X as suggested (13) is not established. Fitting other sensitive methyl frequencies to these empirical relations produced estimates of group electronegativities, but the meaning of such group electronegativities is open to the original question of the reality of the relation between potential energy and electronegativity. However, the fact that group electronegativities were later calculated (25) by a completely unrelated method and were found to be in good agreement with those predicted from the empirical frequency versus electronegativity relations does give more credulence to the reality of the empirical relations in this case, but it by no means proves them. Although similar uncertainty must be placed on all data obtained from such empirical relations, there is still considerable value in these relations.

As another example, a number of frequency–frequency plots have been obtained (9, 11, 26) and these are often of considerable use to the spectroscopist. However, in setting up these plots care must be taken to obey the non-crossing rule while in using them it must be remembered that an assumption is involved, namely, that the frequencies concerned each depend on the same atomic or molecular properties. This assumption cannot in general be proven and may or may not be valid, a point which should not be forgotten in using these types of relations.

REFERENCES

1. FLETT, M. ST. C. Trans. Faraday Soc. **44**, 767 (1948).
2. DAVISON, W. H. T. J. Chem. Soc. 2456 (1951).
3. FUSON, N., JOSIEN, M. L., and SHELTON, E. M. J. Am. Chem. Soc. **76**, 2526 (1954).
4. BELLAMY, L. J. J. Chem. Soc. 2818 (1955).
5. SCROCCO, M. and LIBERTI, A. Ricerca Sci. **24**, 1687 (1954).
6. INGRAHAM, L. L., CORSE, J., BAILEY, G. F., and STITT, F. J. Am. Chem. Soc. **74**, 2297 (1952).
7. THOMPSON, H. W. and STEEL, G. Trans. Faraday Soc. **52**, 1451 (1956).
8. GOULDEN, J. D. S. Spectrochim. Acta, **6**, 129 (1954).
9. BELLAMY, L. J. and WILLIAMS, R. L. J. Chem. Soc. 2753 (1956).
10. BELL, J. V., HEISLER, J., TANNENBAUM, H., and GOLDENSON, J. J. Am. Chem. Soc. **76**, 5185 (1954).
11. BELLAMY, L. J. J. Chem. Soc. 4221 (1955).
12. KAGARISE, R. E. J. Am. Chem. Soc. **77**, 1377 (1955).
13. WILMSHURST, J. K. J. Chem. Phys. **26**, 426 (1957).
14. WILMSHURST, J. K. Can. J. Chem. **35**, 937 (1957).
15. WILMSHURST, J. K. J. Chem. Phys. **28**, 733 (1958).
16. SHEPPARD, N. Trans. Faraday Soc. **51**, 1465 (1955).
17. DAASCH, L. W. Symposium on Molecular Structure and Spectroscopy, Ohio, 1957.
18. COOK, D. J. Am. Chem. Soc. **80**, 49 (1958).
19. HERZBERG, G. Infrared and Raman spectra of polyatomic molecules. D. Van Nostrand Co., Inc., New York, N.Y. 1945.
20. BARNARD, S. and CHILD, J. M. Higher algebra. MacMillan and Co., Ltd., London, 1949. p. 140.
21. LECHNER, F. Wien. Ber. **141**, 633 (1932).
22. WAGNER, J. Z. physik. Chem. B, **40**, 36 (1938).
23. WAGNER, J. Z. physik. Chem. B, **45**, 69 (1940).
24. WAGNER, J. Z. physik. Chem. B, **45**, 341 (1940).
25. WILMSHURST, J. K. J. Chem. Phys. **27**, 1129 (1957).
26. BELLAMY, L. J. and WILLIAMS, R. L. J. Chem. Soc. 863 (1957).

Can. J. Chem. Downloaded from www.nrcresearchpress.com by 176.9.209.113 on 09/04/12
For personal use only.

Can. J. Chem. Downloaded from www.nrcresearchpress.com by 176.9.209.113 on 09/04/12
For personal use only.

CATALYSIS OF THE *CIS-TRANS* ISOMERIZATION OF AZOBENZENE BY ACIDS AND CUPRIC SALTS[1]

STEFANIA CICCONE AND J. HALPERN

ABSTRACT

The catalytic effects of various acids and metal salts on the *cis–trans* isomerization of azobenzene in aqueous ethanol were examined kinetically. The effect of perchloric acid is apparently due to H^+ ions and is interpreted in terms of a catalytic mechanism involving the conjugate acid of azobenzene. The much greater catalytic effect found for hydrochloric acid is attributed to an additional path involving catalysis by the undissociated acid. Acetic acid was found to be inactive. Of the metal salts examined only those of Cu^{++} showed pronounced activity which was attributed to co-ordination with the azo group. Kinetic evidence was obtained for a catalytic path involving Cu^{++} and H^+ simultaneously.

INTRODUCTION

It has been reported (1, 2) that the *cis–trans* isomerization of azobenzene, which proceeds spontaneously in solution, is susceptible to catalysis by acids, certain metal salts, and a variety of other inorganic and organic substances. However, while the kinetics of the uncatalyzed isomerization have been examined extensively (1, 3), few quantitative measurements have been made on the catalyzed reactions whose mechanisms are thus for the most part unresolved. This paper describes a kinetic study of the catalysis of the isomerization of azobenzene in aqueous alcohol solution by acids and cupric salts and an attempt is made to elucidate the mechanisms of the catalytic effects in these systems.

EXPERIMENTAL

Cis-azobenzene was prepared by the method of Hartley (1) and recrystallized from petroleum ether to a constant melting point of 70°. Distilled water and ethanol, redistilled from KOH, were used as solvents. Cupric perchlorate (G. F. Smith Reagent) was recrystallized from perchloric acid. The acids and other reagents were of reagent grade.

The kinetics of the isomerization reaction were measured using the procedure described earlier (3). The absorption spectra of *cis*- and *trans*-azobenzene were determined in each of the media used and were found to be substantially unaffected by the added acids and metal salts. Solutions of azobenzene were prepared, and all experiments performed, in the dark to prevent photochemical isomerization.

RESULTS AND DISCUSSION

All the kinetic experiments were made at 60°. The solvent was generally aqueous alcohol in which both azobenzene and the catalysts were conveniently soluble. A few experiments were also made in benzene solution.

Typical rate plots for the uncatalyzed and catalyzed reactions are shown in Fig. 1. The kinetics were generally first order in *cis*-azobenzene yielding a pseudo first order rate constant, k, which contained contributions from both the uncatalyzed (k_0) and catalyzed

[1]*Manuscript received August 10, 1959.*
Contribution from the Department of Chemistry, University of British Columbia, Vancouver, B.C., Canada, with financial assistance from the National Research Council of Canada.

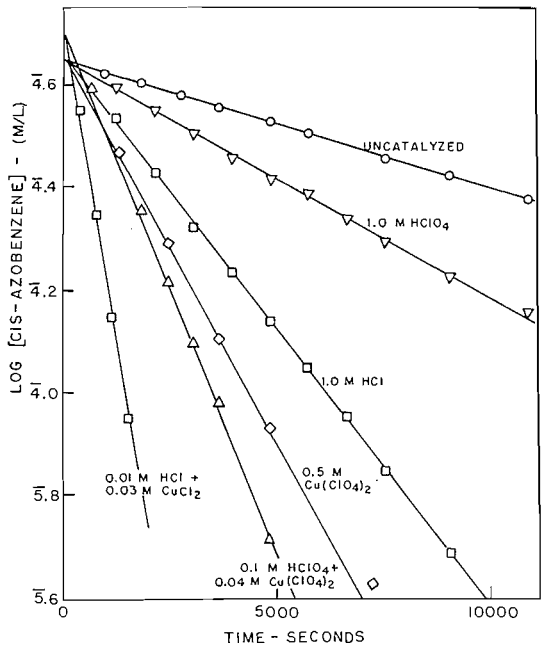

FIG. 1. First order kinetic plots for the uncatalyzed and catalyzed *cis–trans* isomerization of azobenzene in 50 mole% EtOH at 60°.

(k_{cat}) paths, i.e.

[1] $$-d\,[cis\text{-A}]/dt = k\,[cis\text{-A}]$$

where

[2] $$k = k_0 + k_{cat}\,,$$

k_0 was measured separately and k_{cat} determined by difference.

Deviations from first order kinetics were sometimes observed at high catalyst concentrations (particularly with perchloric acid), possibly due to side reactions of azobenzene with the catalyst. In such cases only the region of first order behavior was investigated and the range of results reported below reflects this limitation.

Table I summarizes some of the observed catalytic effects. Of the three acids examined in aqueous alcohol, namely $HClO_4$, HCl, and CH_3COOH (selected as typical strong, intermediate, and weak acids), the first two showed pronounced catalytic activity while the last was inactive. The unimportance of ionic strength effects is indicated by the observation that 0.5 *M* $NaClO_4$ or 0.2 *M* NaCl, either alone or in the presence of equivalent concentrations of the corresponding acid, were substantially without effect.

Since it seemed likely that the acid catalysis was associated with protonation of the azo group, salts of a number of metal ions (Cu^{++}, Co^{++}, Ag^{+}) with known tendency to coordinate with nitrogen were also examined for catalytic effects. Of these only the cupric salts showed pronounced activity, which was further enhanced in the presence of acids. These effects are discussed further below.

Perchloric Acid

The results for this acid, in solvents of various compositions, are summarized in Fig. 2. The range of catalyst concentrations in each case is that for which the kinetics remained first order in *cis*-azobenzene. In this region the catalytic effect conforms to the rate law,

[3] $$k_{cat} = k_{H^+}\,[HClO_4]$$

Can. J. Chem. Downloaded from www.nrcresearchpress.com by 176.9.209.113 on 09/04/12
For personal use only.

TABLE I

Some catalytic effects at 60°

Solvent	Catalyst	10^5k (sec^{-1})	10^5k_{cat} (sec^{-1})
50 mole% EtOH	None	5.8	0.0
50 mole% EtOH	0.1 *M* $HClO_4$	6.4	0.6
50 mole% EtOH	0.5 *M* $HClO_4$	8.6	2.8
50 mole% EtOH	1.0 *M* $HClO_4$	11.2	5.4
50 mole% EtOH	0.5 *M* $NaClO_4$	5.8	0.0
50 mole% EtOH	0.5 *M* $HClO_4$ + 0.5 *M* $NaClO_4$	8.6	2.8
50 mole% EtOH	0.2 *M* HCl	6.4	0.6
50 mole% EtOH	1.0 *M* HCl	24.2	18.4
50 mole% EtOH	0.2 *M* NaCl	5.5	−0.3
50 mole% EtOH	0.2 *M* HCl + 0.2 *M* NaCl	6.7	0.9
50 mole% EtOH	0.5 *M* HOAc	5.5	−0.3
50 mole% EtOH	0.5 *M* KI	5.8	0.0
50 mole% EtOH	0.5 *M* $Cu(ClO_4)_2$	35.0	29.2
50 mole% EtOH	0.04 *M* $Cu(ClO_4)_2$ + 0.1 *M* $HClO_4$	46.0	40.2
50 mole% EtOH	0.03 *M* $CuCl_2$ + 0.01 *M* HCl	101	95
50 mole% EtOH	0.2 *M* $Cu(OAc)_2$ + 0.5 *M* HOAc	15.3	9.5
50 mole% EtOH	0.5 *M* $Co(ClO_4)_2$ + 0.1 *M* $HClO_4$	6.4	0.6
50 mole% EtOH	0.5 *M* $AgClO_4$ + 0.1 *M* $HClO_4$	8.3	2.5
Benzene	None	12.7	0.0
Benzene	0.2 *M* heptanoic acid	11.2	−1.5
Benzene	0.2 *M* heptanoic acid + 0.2 *M* cupric heptanoate	14.3	1.6

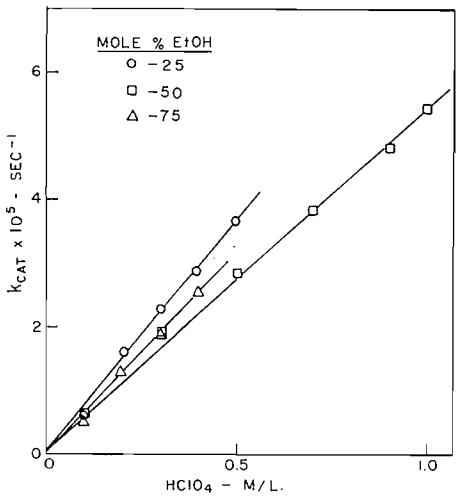

FIG. 2. Catalytic effect of perchloric acid at 60°.

where the values of $10^5k_{H^+}$ are 7.4, 5.1, and 6.5 l. $mole^{-1}$ sec^{-1} in 25, 50, and 75 mole per cent EtOH, respectively.

It seems likely that $HClO_4$ is completely dissociated in these solutions and hence that the observed catalytic effect is due to H^+ (i.e. H_3O^+ or $EtOH_2^+$) ions. A plausible mechanism, depicted below, assumes that the catalyzed isomerization proceeds through the conjugate acid of azobenzene (AH^+), formed in a rapid pre-equilibrium step, i.e.

$$cis\text{-A} + H^+ \rightleftharpoons cis\text{-AH}^+ \text{ (fast)} \quad [4]$$

$$cis\text{-AH}^+ \rightarrow trans\text{-AH}^+ \text{ (slow)} \quad [5]$$

$$trans\text{-AH}^+ \rightleftharpoons trans\text{-A} + H^+ \text{ (fast).} \quad [6]$$

Can. J. Chem. Downloaded from www.nrcresearchpress.com by 176.9.209.113 on 09/04/12
For personal use only.

The protonation equilibrium of azobenzene in acidic solutions is well known (4, 5) although, because of the rapid isomerization, it can be studied only for the *trans* isomer. Spectrophotometric measurements have yielded values of -2.5 (4) and -1.6 (5) for pK_a of AH^+ at 25°. The equilibrium concentration of AH^+ in our solutions is thus very small ($\sim$1% at 1 *M* H^+) and is not detected spectrophotometrically.

The structure of AH^+ has not been conclusively established. Klotz (4) has proposed structure (I) in which the proton is localized on one of the N atoms through a bond involving lone pair electrons. On the other hand Jaffé (5, 6), on the basis of convincing evidence, favors the non-classical structure (II) in which H is attached to both N atoms through

(I) (II)

delocalized bonds. Enhanced ease of isomerization is more readily explained in terms of the first model where some reduction in the degree of double bond character of the azo bond might be expected through polarization. It is less obvious why structure (II) should lead to enhanced isomerization particularly if, as suggested by Jaffé (5, 6), the *cis*-conformation of this structure is the more stable one.

An alternative description of the slow isomerization step, which we are inclined to favor, involves the attack of a solvent molecule (S) on AH^+ to give an intermediate (III) in which free rotation about the N—N bond is possible, i.e.

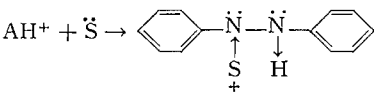

[7]

(III)

This mechanism is readily consistent with either structure (I) or (II) for AH^+.

Zucker and Hammett (7, 8) have suggested a criterion for distinguishing between a mechanism of the type represented by equations [4], [5], and [6] and one in which the rate-determining step [5] is replaced by step [7] involving attack on the conjugate acid by a solvent molecule. This is based on the expectation of a linear dependence of k_{cat} on h_0 (related to the Hammett acidity function H_0 (9, 10) by $H_0 = -\log h_0$) in the first case and on $[H^+]$ in the second. Unfortunately this criterion is not readily applicable here in view of the limited acidity range accessible to kinetic measurement and of the absence of h_0 data for mixed solvents. In aqueous solution the dependence of h_0 on $[H^+]$ does diverge appreciably from linearity even below 1 *M* $HClO_4$ and this divergence is not reflected in plots in Fig. 2. On the other hand the dependence of k_{cat} on solvent composition appears to follow h_0 which, at least for HCl, has been shown to pass through a minimum in the vicinity of equimolar concentrations of H_2O and EtOH (11). Because of their conflicting nature, and because of the questionable theoretical validity of the Zucker–Hammett hypothesis (8), these indications are considered as inconclusive. An alternative kinetic interpretation, namely that the protonation step [4] is rate determining, also leads to an expected h_0, rather than $[H^+]$, dependence but is considered unlikely in view of the low rates.

Can. J. Chem. Downloaded from www.nrcresearchpress.com by 176.9.209.113 on 09/04/12
For personal use only.

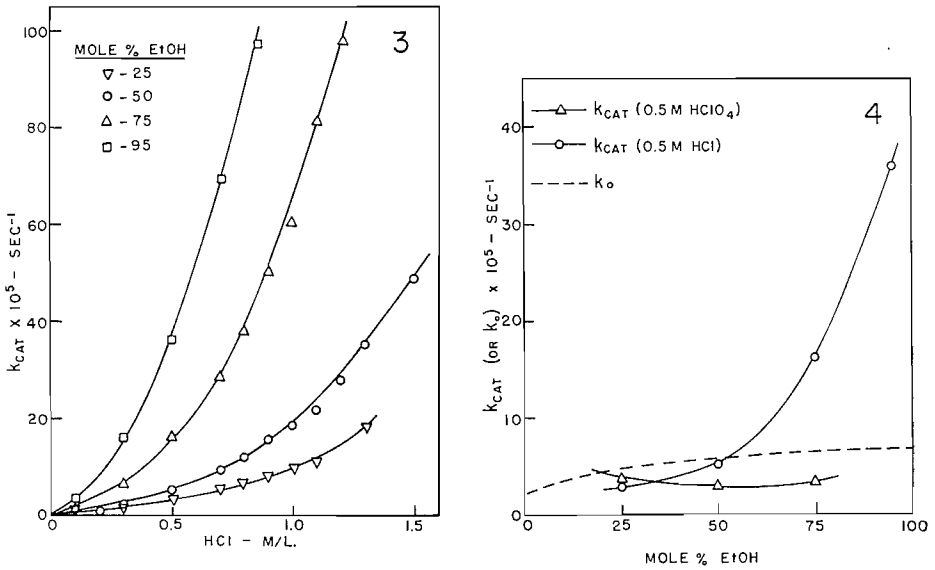

FIG. 3. Catalytic effect of hydrochloric acid at 60°.
FIG. 4. Solvent dependence of the catalytic effects of perchloric and hydrochloric acids at 60°. The broken line depicts the solvent dependence of the uncatalyzed rate (k_0).

Hydrochloric Acid

The results for this acid are depicted in Figs. 3 and 4. Attention is directed to the following features.

(1) Except at very low concentrations, the catalytic activity of HCl is greater than that of $HClO_4$.

(2) the kinetic dependence of k_{cat} on the total HCl concentration, $[HCl]_0$, is apparently greater than first order.

(3) The catalytic effect increases markedly with the EtOH content of the medium. At low EtOH content it approaches that of $HClO_4$.

This behavior can be interpreted in terms of a catalytic contribution due to undissociated HCl in addition to that due to H^+. The predicted rate law is then

$$[8] \qquad k_{cat} = k_{H^+}[H^+] + k_{HCl}[HCl]$$

$$[9] \qquad = k_{H^+}[H^+] + (k_{HCl}/K)[H^+][Cl^-],$$

where K is the dissociation constant of HCl. If the fraction of undissociated HCl is small, $[H^+] \sim [Cl^-] \sim [HCl]_0$, and equation [9] becomes

$$[10] \qquad k_{cat} = k_{H^+}[HCl]_0 + (k_{HCl}/K)[HCl]_0^2$$

or

$$[11] \qquad k_{cat}/[HCl]_0 = k_{H^+} + (k_{HCl}/K)[HCl]_0.$$

The linear plots of $k_{cat}/[HCl]_0$ vs. $[HCl]_0$ in Fig. 5 are, on the whole, in accord with this, although their intercepts yield values of k_{H^+} which are somewhat lower than those obtained with $HClO_4$ (like the latter, however, these pass through a minimum at 50 mole per cent EtOH). Again this may be due to the fact that the H^+-catalyzed reaction follows h_0 rather than $[H^+]$ and that in these media the former is appreciably lower for HCl than for $HClO_4$ even at low concentrations.

Can. J. Chem. Downloaded from www.nrcresearchpress.com by 176.9.209.113 on 09/04/12
For personal use only.

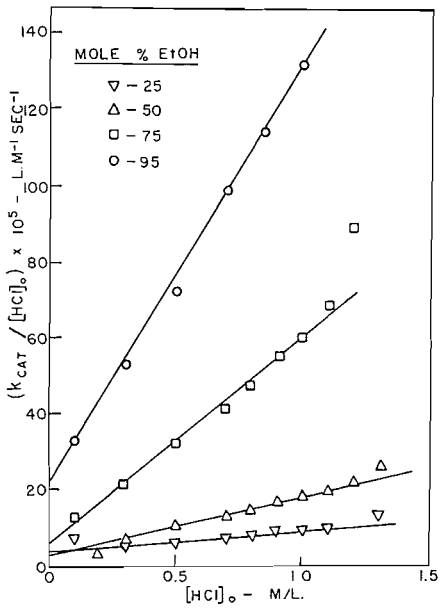

FIG. 5. Concentration-dependence of HCl catalysis plotted according to equation [11].

A plausible mechanism for the catalysis by undissociated HCl involves protonation, coupled with simultaneous co-ordination of Cl^-, to give an intermediate (IV), analogous to (III), in which the role of the solvent molecule is effectively assumed by Cl^-.

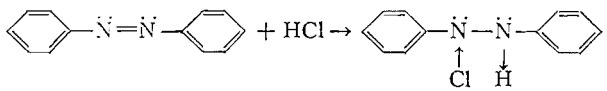

[12]

(IV)

A similar mechanism may account for the combined catalytic effect of H^+ and thiourea on the *cis–trans* isomerization of azobenzene, observed by Schulte-Frohlinde (2). This has the kinetic form, $k_{cat} = [H^+]$ [thiourea] and may involve a reaction analogous to equation [12] between azobenzene and the conjugate acid of thiourea.

It is also of interest that the above pattern of catalytic effects for $HClO_4$ and HCl resembles that found by Nozaki and Ogg (12) for the *cis–trans* isomerization of maleic acid. In the latter case also a mechanism involving simultaneous co-ordination of H^+ and Cl^- (although not at adjacent positions) was proposed to account for the higher activity of HCl. Analogous mechanisms have also been proposed (13, 14) for the catalysis by secondary amines of the *cis–trans* isomerization of diethyl and dimethyl maleate.

Cupric Salts

Figure 6 depicts the catalytic effect due to cupric perchlorate. The kinetic dependence of k_{cat} on the cupric perchlorate concentration is greater than first order (approximately 1.5) implying some contribution from a path involving more than one Cu^{++} ion. As for H^+, it seems plausible to interpret the catalytic effect of Cu^{++} in terms of a mechanism involving co-ordination of Cu^{++} with the azo nitrogen atoms to give intermediates analogous to (III). The significance of the higher order path is not clear but a plausible interpretation is in terms of a complex, azobenzene.$2Cu^{++}$, in which Cu^{++} ions are

Can. J. Chem. Downloaded from www.nrcresearchpress.com by 176.9.209.113 on 09/04/12
For personal use only.

co-ordinated to both N atoms of the azobenzene molecule. The existence of an analogous cuprous complex of azomethane (azomethane.$2Cu^+$) has been reported (15).

A similar complex, involving simultaneous co-ordination of H^+ and Cu^{++} with the two N atoms of azobenzene, may account for the unexpected and very marked enhancement of the catalytic activity of cupric perchlorate by perchloric acid shown in Fig. 7. Over a considerable range of concentrations the combined effect of the two catalysts is much greater than the sum of their separate effects and the predominant contribution to k_{cat} is of the kinetic form, k $[H^+]$ $[Cu^{++}]$, implying a catalytic path involving H^+ and Cu^{++} simultaneously.

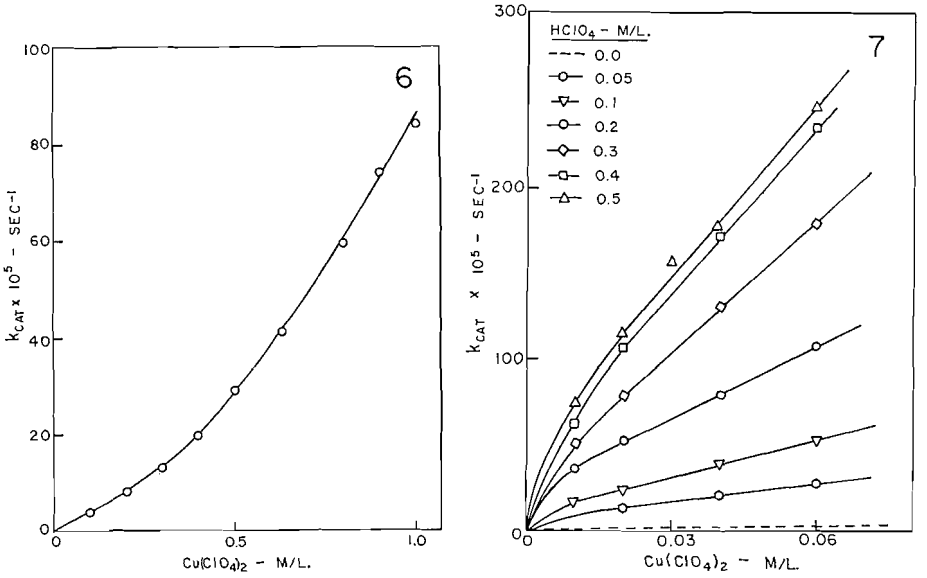

FIG. 6. Catalytic effect of cupric perchlorate in 50 mole% EtOH at 60°.
FIG. 7. Combined catalytic effects of cupric perchlorate and perchloric acid in 50 mole% EtOH at 60°.

Because of solubility limitations the effect of $CuCl_2$ in aqueous ethanol could be examined only in the presence of HCl. The results are shown in Fig. 8 and again reveal a

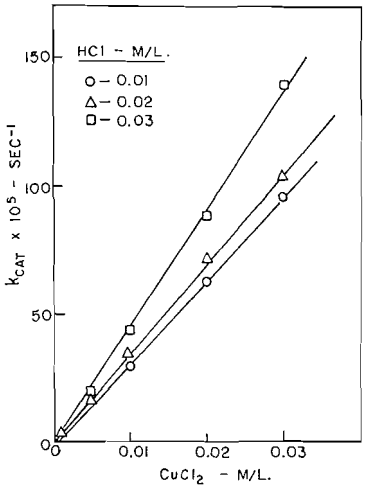

Catalytic effect of cupric chloride in 50 mole% EtOH at 60°.

Can. J. Chem. Downloaded from www.nrcresearchpress.com by 176.9.209.113 on 09/04/12
For personal use only.

tendency, although less marked than for cupric perchlorate, for the catalytic activity to be enhanced by the acid. At low HCl concentrations k_{cat} is first order in $CuCl_2$ and is much greater than for $Cu(ClO_4)_2$ at comparable $HClO_4$ concentrations.

Cupric acetate in aqueous ethanol and cupric heptanoate in benzene (in each case in the presence of the corresponding acid which by itself was without effect) were also found to catalyze the isomerization reaction (Table I), but their effects were not examined quantitatively.

Co-ordination of the catalyst to the azo nitrogen atoms appears to be a common feature of all the catalytic effects described and the low catalytic activities of Co^{++} and Ag^{+}, relative to Cu^{++} (Table I), may be related to their much smaller tendencies to form complexes with nitrogen ligands in general.

REFERENCES

1. HARTLEY, G. S. J. Chem. Soc. 633 (1938).
2. SCHULTE-FROHLINDE, D. Ann. Chem. Liebigs, **612**, 131, 138 (1958).
3. HALPERN, J., BRADY, G. W., and WINKLER, C. A. Can. J. Research, B, **28**, 140 (1950).
4. KLOTZ, I. M., FIESS, H. A., CHEN HO, J. Y., and MELLODY, M. J. Am. Chem. Soc. **76**, 5136 (1954).
5. JAFFÉ, H. H. and GARDNER, R. W. J. Am. Chem. Soc. **80**, 319 (1958).
6. JAFFÉ, H. H., YEH, SI-JUNG, and GARDNER, R. W. Mol. Spectroscopy, **2**, 120 (1958).
7. ZUCKER, L. and HAMMETT, L. P. J. Am. Chem. Soc. **61**, 2779, 2785, 2791 (1939).
8. LONG, F. A. and PAUL, M. A. Chem. Revs. **57**, 935 (1957).
9. HAMMETT, L. P. and DEYRUP, A. J. J. Am. Chem. Soc. **54**, 2721 (1932).
10. PAUL, M. A. and LONG, F. A. Chem. Revs. **57**, 935 (1957).
11. BRAUDE, E. A. and STERN, E. S. J. Chem. Soc. 1976 (1948).
12. NOZAKI, K. and OGG, R., JR. J. Am. Chem. Soc. **63**, 2583 (1941).
13. NOZAKI, K. J. Am. Chem. Soc. **63**, 2681 (1941).
14. DAVIES, M. and EVANS, F. P. Trans. Faraday Soc. **51**, 1506 (1955).
15. DUNITZ, J. D. Unpublished. (1957). *Quoted by* Orgel, L. E. *in* Metals and enzyme activity. Biochemical Society Symposium No. 15, Cambridge University Press. 1958. p. 8.

Can. J. Chem. Downloaded from www.nrcresearchpress.com by 176.9.209.113 on 09/04/12
For personal use only.

Can. J. Chem. Downloaded from www.nrcresearchpress.com by 176.9.209.113 on 09/04/12
For personal use only.

ENTROPY PRODUCTION IN A SPONTANEOUS, ADIABATIC (NON-ISOTHERMAL) CHEMICAL REACTION[1]

D. H. EVERETT[2]

ABSTRACT

When a chemical reaction occurs spontaneously and isothermally the loss of useful work is equal to the decrease in free energy of the system. If the same reaction, supposed for example to be exothermic, occurs adiabatically the temperature rises and the system can be used as a source of heat to operate a heat engine: as heat is withdrawn the temperature of the system falls and eventually returns to its initial value. Part of the free energy of the reaction has been recovered as useful work, part lost in the spontaneous irreversible step. Expressions are derived for the loss of useful work and the entropy production in the adiabatic irreversible step, and it is shown that the work lost is equal to $T_0\times$(entropy produced) where T_0 is the temperature *of the surroundings*. Some consequences of these ideas in relation to the definition of the efficiency of internal combustion engines are considered briefly.

When a chemical reaction proceeds spontaneously under isothermal conditions the irreversible production of entropy in a finite change ($\Delta_i S$) is related both to the "loss of useful work" and to the "decrease in free energy" (1). For a reaction which proceeds spontaneously at a temperature T,

$$T\Delta_i S = \Delta W(\text{rev.}) - \Delta W(\text{irrev.}) = -\Delta F, \qquad [1]$$

where ΔW(rev.) is the work which can be obtained if the process takes place reversibly and ΔW(irrev.) the work done by the system in an irreversible change between the same initial and final states. F is the Helmholtz free energy.

However, as pointed out by Prigogine and Defay (2), these equations cannot be applied immediately to a non-isothermal process, and a more general relationship involves the affinity of reaction (**A**). For an infinitesimal process:

$$Td_i S = \mathbf{A}d\xi, \qquad [2]$$

where

$$\mathbf{A} = -(\partial F/\partial \xi)_{T,V} \qquad [3]$$

and ξ is the extent of reaction.

In practice, we often have to deal with reactions which occur more or less adiabatically (e.g. in an internal combustion engine) so that it is instructive to see whether an equation of the form [1] can be derived for this case, and whether Prigogine and Defay's objection to this equation can be overcome.

Consider, for the sake of simplicity, an exothermic reaction

$$\mathrm{A} \rightarrow \mathrm{B}$$

whose equilibrium position lies far to the right. We start with 1 mole of A at a temperature T_0 (state α), and allow it to react spontaneously at constant volume in an adiabatic container, whose heat capacity is negligible compared with that of A or B. The final equilibrium state of the system (β) is one in which ξ_e moles of A have reacted to form

[1]*Manuscript received May 13, 1959.*
Contribution from the Division of Pure Chemistry, National Research Council, Ottawa, Canada.
Issued as N.R.C. No. 5372.
[2]*Visiting Scientist, National Research Council, Ottawa, Canada. Permanent address: Department of Physical and Inorganic Chemistry, The University, Bristol, England.*

B, while the temperature has risen from T_0 to T_1. Again, for simplicity, we suppose that the molar heat capacities of A and B are equal (c) and that the heat of reaction at constant volume ($u^0_{T,V}$) is independent of ξ; it will also be independent of T. The temperature rise is then given by

$$T_1-T_0 = (-u^0_{T,V}/c)\xi_e; \qquad [4]$$

or since we suppose $\xi_e \rightarrow 1$,

$$T_1-T_0 = -u^0_{T,V}/c. \qquad [5]$$

The entropy produced in this process may be obtained by integrating [2].

$$\Delta_1 S \text{ (chem. adiab.)} = \int_0^{\xi_e} \frac{\mathbf{A}}{T} d\xi \text{ (adiabatic conditions)} \qquad [6]$$

where

$$\mathbf{A} = \mathbf{A}^0 + RT \ln (1-\xi)/\xi,$$

and

$$\mathbf{A}^0 = -u^0_{T,V} + Ts^0_{T,V}.$$

Here $\mathbf{A}^0$ is the standard affinity of reaction and $s^0_{T,V}$ the standard entropy of reaction at constant volume, which is also independent of T. Remembering that $(-u^0_{T,V})d\xi = cdT$ under adiabatic conditions, it is readily shown that subject to the above assumptions

$$\Delta_1 S \text{ (chem. adiab.)} = \xi_e s^0_{T,V} + c \ln (T_1/T_0) - \mathbf{R}[\xi_e \ln \xi_e + (1-\xi_e) \ln (1-\xi_e)]. \qquad [7]$$

When $\xi_e \rightarrow 1$, this reduces to

$$\Delta_1 S \text{ (chem. adiab.)} = s^0_{T,V} + c \ln (T_1/T_0). \qquad [8]$$

The same equation is obtained from the consideration that, since the process is adiabatic, the only way in which the entropy of the system can change is by the internal production of entropy which must therefore be equal to the difference between the total entropy of final and initial states.

The system in state β can now be cooled to T_0 (state γ) in two ways. First consider reversible cooling using the system as the source of entropy working a reversible heat engine whose sink temperature is T_0: the source temperature is initially T_1 but falls eventually to T_0. It may then be shown (3) that the work obtainable in this way is given by

$$\Delta^\gamma_\beta W(\text{rev.}) = c(T_1-T_0)\left[1-\frac{T_0}{T_1-T_0}\ln\frac{T_1}{T_0}\right], \qquad [9]$$

which, from [4], reduces to

$$\Delta^\gamma_\beta W(\text{rev.}) = -u^0_{T,V} - cT_0 \ln (T_1/T_0). \qquad [10]$$

On the other hand, if $\beta \rightarrow \gamma$ is carried out irreversibly, i.e. by placing the system in thermal contact with the surroundings at T_0 so that thermal equilibrium is established by heat conduction, then it can be shown that the entropy produced in this process, $\Delta_1 S$ (heat cond.), is given by

$$\Delta_1 S(\text{heat cond.}) = \Delta^\gamma_\beta W(\text{rev.})/T_0, \qquad [11]$$

$$= -(u^0_{T,V}/T_0) - c \ln (T_1/T_0). \qquad [12]$$

Can. J. Chem. Downloaded from www.nrcresearchpress.com by 176.9.209.113 on 09/04/12
For personal use only.

We now compare this two-stage path between α and γ with the reversible isothermal path, e.g. using a van't Hoff equilibrium box, or a reversible electrochemical cell, in which the amount of work done by the system is

$$[13] \qquad \Delta_\alpha^\gamma W(\text{isothermal rev.}) = \int_0^{\xi_e} \mathbf{A} d\xi = \xi_e \mathbf{A}^0 - \mathbf{R}T[\xi_e \ln \xi_e + (1-\xi_e) \ln (1-\xi_e)].$$

Here ξ_e is the equilibrium extent of reaction at T_0 rather than T_1, but since we suppose $\xi_e \to 1$, we do not have to elaborate the argument to take account of this. Equation [13] thus reduces to

$$[14] \qquad \Delta_\alpha^\gamma W(\text{isothermal rev.}) = \mathbf{A}^0(T_0).$$

We may now identify the "loss of useful work" associated with the irreversible step $\alpha \to \beta$ with the difference between the work done by the system in the reversible, isothermal change $\alpha \to \gamma$, and that done when the process follows the path $\alpha \overset{\text{irrev.}}{\to} \beta \overset{\text{rev.}}{\to} \gamma$.

Thus:

[Loss of useful work in adiabatic, spontaneous chemical reaction]

$$= \Delta_\alpha^\gamma W(\text{isothermal rev.}) - \Delta_\beta^\gamma W(\text{rev.})$$

$$= \mathbf{A}^0(T_0) + u^0_{T,V} + cT_0 \ln (T_1/T_0)$$

$$[15] \qquad = T_0 s^0_{T,V} + cT_0 \ln (T_1/T_0)$$

which, from [8],

$$[16] \qquad = T_0 \Delta_t S \text{ (chem. adiab.)}.$$

Hence, the first number of equation [1] can be generalized to a non-isothermal process by identifying T not with the temperature of the system but with T_0, that of the surroundings. We note in passing that if both $\alpha \to \beta$ and $\beta \to \gamma$ are carried out irreversibly, then the entropy production (and the loss of useful work) is the same as when the process $\alpha \to \gamma$ is allowed to proceed spontaneously at constant temperature.

As an example of the above discussion we consider the irreversible freezing of supercooled water. This process, carried out isothermally, is a frequently quoted example in standard texts on chemical thermodynamics. When carried out adiabatically the freezing process is accompanied by a rise in temperature until the equilibrium freezing point is reached. To the approximation employed here, the fraction (ϕ) of the liquid which solidifies for a given degree of supercooling ($T_f - T$) is

$$[17] \qquad \phi = c(T_f - T)/\Delta_f h$$

where $\Delta_f h$ is the heat of fusion. It is then readily shown that the entropy production in this irreversible process is

$$[18] \qquad \Delta_i S = -\phi \Delta_f s + c \ln (T_f/T).$$

The entropy produced per mole of ice formed is thus

$$[19] \qquad \frac{\Delta_i S}{\phi} = -\Delta_f s + \frac{c}{\phi} \ln \frac{T_f}{T}$$

$$= -\Delta_f s + \frac{\Delta_f h}{T_f - T} \ln \frac{T_f}{T}$$

Can. J. Chem. Downloaded from www.nrcresearchpress.com by 176.9.209.113 on 09/04/12
For personal use only.

which tends to zero as $T \rightarrow T_t$. $\Delta_i S/\phi$ is shown as a function of the degree of supercooling in Fig. 1.

The present considerations are also relevant to the question of the efficiency of internal combustion (or more generally, chemical reaction) engines. Thus the processes $\alpha \overset{\text{irrev.}}{\rightarrow} \beta \overset{\text{rev.}}{\rightarrow} \gamma$ may be regarded as the basic steps in the operation of an "ideal internal combustion engine", and the work derivable from this series of changes is the maximum which can be obtained from any engine involving a spontaneous chemical reaction. The magnitude of this work depends not only on the heat of reaction, but also upon the

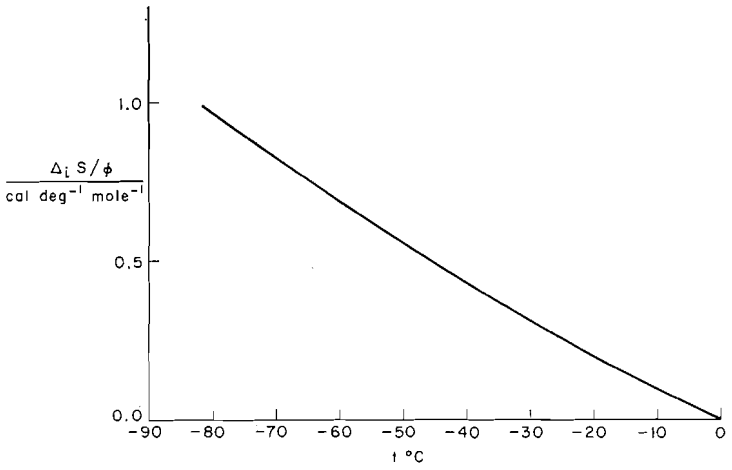

FIG. 1. Entropy production per mole of ice formed when water cooled to $t°$ C freezes spontaneously under adiabatic conditions.

heat capacities of the components: it therefore takes a much more specific account of the nature of the chemical reaction than do other treatments. In discussions of the Otto and Diesel cycles, for example, the only characteristic of the reaction which enters specifically is the heat of reaction. Conventionally, the efficiency of an internal combustion engine may be defined in relation to the heat of reaction

$$\theta_H = \frac{\Delta_\beta^\gamma W(\text{rev.})}{(-u^0_{T,V})} = 1-\frac{T_0}{T_1-T_0}\ln\frac{T_1}{T_0} \qquad [20]$$

$$= 1-\left(\frac{cT_0}{-u^0_{T,V}}\right)\ln\left[1+\left(\frac{-u^0_{T,V}}{cT_0}\right)\right].$$

A more fundamental definition of efficiency (θ_A) is the ratio of the work obtained to that which could be obtained in an isothermal, reversible process (e.g. in an ideal reversible fuel cell):

$$\theta_A = \frac{\Delta_\beta^\gamma W(\text{rev.})}{\mathbf{A}^0} = \frac{-u^0_{T,V}}{\mathbf{A}^0}\left\{1-\left(\frac{cT_0}{-u^0_{T,V}}\right)\ln\left[1+\left(\frac{-u^0_{T,V}}{cT_0}\right)\right]\right\} \qquad [21]$$

$$= \frac{-u^0_{T,V}}{\mathbf{A}^0}\theta_H.$$

The two efficiencies are equal when the standard entropy of reaction is zero. Alter-

Can. J. Chem. Downloaded from www.nrcresearchpress.com by 176.9.209.113 on 09/04/12
For personal use only.

native equations are

$$\theta_A = 1 - \frac{T_0 \Delta_1 S(\text{chem. adiab.})}{\mathbf{A}^0}; \quad [22]$$

$$\theta_A = 1 - \frac{T_0}{\mathbf{A}^0}\left[s^0_{T,V} + c \ln \frac{T_1}{T_0} \right]. \quad [23]$$

θ_A may be regarded, therefore, as the ratio of the maximum fuel cell efficiency to the maximum efficiency of converting chemical energy to work via an engine involving a spontaneous chemical reaction. To illustrate the way in which the nature of the chemical reaction determines the maximum efficiency, the following table gives the results of calculations (making the approximations mentioned above) of θ_H and θ_A for some typical reactions, when $T_0 = 300°$ K. We notice that in the highly exothermic combination of H atoms, which because of low heat capacities involved leads to a large temperature rise, only 1% of the available "chemical energy" is lost in the irreversible step.

TABLE

Reaction	$-u^0_{T,V}$ kcal	c_V cal deg^{-1}	θ_H	θ_A
$2H \rightarrow H_2$	103	5.5	0.934	0.990
$H_2 + \frac{1}{2}O_2 \rightarrow H_2O$	57.5	6.6	0.883	0.930
$CH_4 + 2O_2 \rightarrow CO_2 + 2H_2O$	191.8	17	0.914	0.915

In the above discussion, consideration has been limited to exothermic reactions. For an endothermic reaction similar arguments apply, except that $T_1 < T_0$, and in the step $\beta \rightarrow \gamma$ the system is used as the sink of the heat engine whose temperature rises steadily from T_1 to T_0. A chemical reaction for which $u^0_{T,V} = 0$ cannot form the basis of an internal combustion engine: in this case $\mathbf{A}^0 = T_0 \Delta_1 S$ (chem. adiab.) and $\theta_A = 0$.

In the present note, we have not elaborated the argument by taking account of incomplete reaction ($\xi_e \neq 1$) or of the variation of heat of reaction with temperature, although there would be no difficulty in doing so for the purposes of more precise calculations.

REFERENCES

1. SCHOTTKY, W., ULICH, H., and WAGNER, C. Thermodynamik. Springer–Verlag, Berlin. 1929.
2. PRIGOGINE, I. and DEFAY, R. Chemical thermodynamics. Longmans, Green & Co., Ltd., London. 1954. p. 43. DEFAY, R. and PRIGOGINE, I. Bull. classe sci. Acad. roy. Belg. (Ce. Sc.), **33** (5), 222 (1947).
3. EVERETT, D. H. Nature, **182**, 1084 (1958).

Can. J. Chem. Downloaded from www.nrcresearchpress.com by 176.9.209.113 on 09/04/12
For personal use only.

Can. J. Chem. Downloaded from www.nrcresearchpress.com by 176.9.209.113 on 09/04/12
For personal use only.

THE INFLUENCE OF TEMPERATURE ON THE KINETICS OF CHEMISORPTION OF HYDROGEN ON ZINC OXIDE[1]

MANFRED J. D. LOW

ABSTRACT

The kinetics of hydrogen adsorption by ZnO have been measured at constant pressures of 403 mm Hg over temperatures from 0° C to 257° C. Two distinct consecutive kinetic stages occur at all temperatures, each stage being precisely expressed by the Elovich equation. The rates and extents of adsorption increase in the temperature ranges 0–80° C and 110–200° C and decrease in the range 80–110° C. The change with temperature of the constants a and $1/\alpha$ of the Elovich equation parallels changes in the amount adsorbed with temperature.

INTRODUCTION

It has been found (1) that the kinetics of many chemisorption processes can be described by the Elovich equation,

$$(dq/dt) = a\, e^{-\alpha q},$$

where q is the amount of gas adsorbed at time t. The parameters a and α were found (1–5) to be affected by changes in initial gas pressure and in temperature. It was suggested (2, 3, 4) that the direction of change of the parameters with temperature might be bound up with a similar change of the isobar. Previous investigations were made mainly over temperature regions corresponding to increasing or to decreasing regions of the isobar, and it was consequently thought desirable to measure chemisorption kinetics in a temperature region in which an adsorption maximum or minimum existed. The system hydrogen – zinc oxide was chosen because two maxima and one minimum were known to exist (7, 8, 9) in the chemisorption region of about 0°–300° C.

EXPERIMENTAL DETAILS

The course of hydrogen adsorption was followed by measuring the disappearance of gas in a constant pressure system of the type described by Taylor and Strother (8). The electrolysis cell of that system was modified by addition of a water jacket in order to cool the electrolyte. The latter consisted of a concentrated solution of sodium acetate in glacial acetic acid and was electrolyzed by a current of 5–8 amps at 40–60 v a-c. Gold electrodes of $\sim$ 300 mm^2 area, about 3 cm apart, were used. Electrolytic tank hydrogen was purified by passage over palladized asbestos, Ascarite, Drierite, and glass wool at the temperature of liquid nitrogen. Helium, used for measurement of dead space in the usual fashion, was purified by passage over charcoal at the temperature of liquid nitrogen. During an adsorption experiment the catalyst was kept at the described temperature to within ± 0.1° C by the vapor of a boiling liquid. A Wheelco Amplitrol Model 152 was used to regulate temperatures to within about 5° C during degassing. Two sets of experiments were made. The first, set A, is incomplete because experiments became irreproducible, probably due to accidental exposure of the catalyst to air. Except where specifically noted, all reference is to the data of the second set, B.

The adsorbent was prepared by decomposing zinc oxalate *in vacuo* by heating at the following schedule: 20–100° C, 1 hour; 100–200°, 1 hour; 200–300°, 1.5 hours; at 400°,

[1]*Manuscript received July 24, 1959.*
Contribution from the Texaco Research Center, Beacon, N.Y.

4 hours; at 450°, 15 hours. Evolution of gas began at about 150°, and continued until 400° had been reached. After the 450° treatment the catalyst was cooled *in vacuo*. For set B, a 19.76-g sample of the preparation was placed in a tube which was then sealed to the adsorption system. This catalyst was degassed at 450° for 2 days, was then cooled to 300°, and exposed to hydrogen at $\frac{1}{2}$ atm for about 30 minutes. The catalyst was then degassed at 420° C for 20 hours. This "activation" procedure was repeated twice. Residual pressures $\leqslant 10^{-6}$ mm Hg were attained. Between runs the catalyst was degassed at 420° C overnight. The adsorbent had a nitrogen B.E.T. surface area of 16 m^2/g. Experiments were made at constant pressure of 403 mm Hg.

EXPERIMENTS, RESULTS, AND DISCUSSION

Kinetics of Chemisorption

At the lower temperatures the plots of q vs. t showed the characteristics of "normal" adsorption, namely a rapid adsorption at short times that quickly decelerated. Each of the q–t curves of runs at the higher temperatures, however, shows a distinct "dip", or change in rate, after some 20 to 80 minutes, shown in the plots of Fig. 1. Similar dips

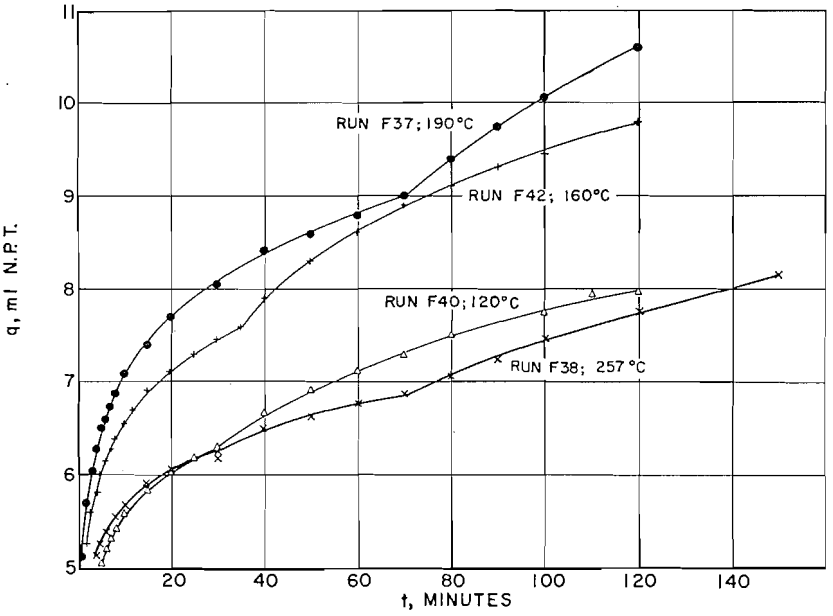

FIG. 1. Adsorption rate data: typical runs. The points of F42, F38, and F40 are displaced by 1, 4, and 5 minutes, respectively.

are noticeable in the q–t data of hydrogen adsorption on ZnO of Taylor and Sickman (6) and Taylor and Strother (8). These authors drew smooth curves through the data, ignoring the dip. Indeed, on cursory examination the dips might be ascribed to experimental scatter, especially in the plots of data at the lower temperatures. However, as shown by Fig. 2, plots of q vs. $\log_{10}t$ show the presence of two distinct kinetic stages. After some time the q–$\log_{10}t$ line changes in slope, and such discontinuities, or "breaks", are present in the data of all runs, and are also found in the q–$\log_{10}t$ plots of the data of other studies (6, 8). Each linear portion of a q–$\log_{10}t$ plot can be described by the Elovich equation (1).

Can. J. Chem. Downloaded from www.nrcresearchpress.com by 176.9.209.113 on 09/04/12
For personal use only.

Isobars

Plots of amounts adsorbed after a specific time, q_t, against temperature reveal the double-humped isobars first described by Taylor and Strother (8). Figure 3 shows curves

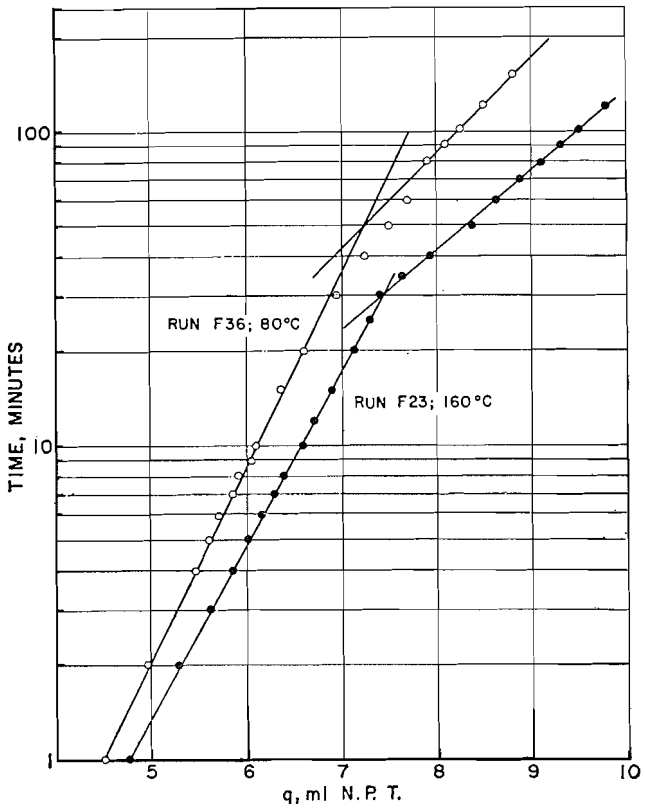

FIG. 2. Adsorption rate data: Elovich plots.

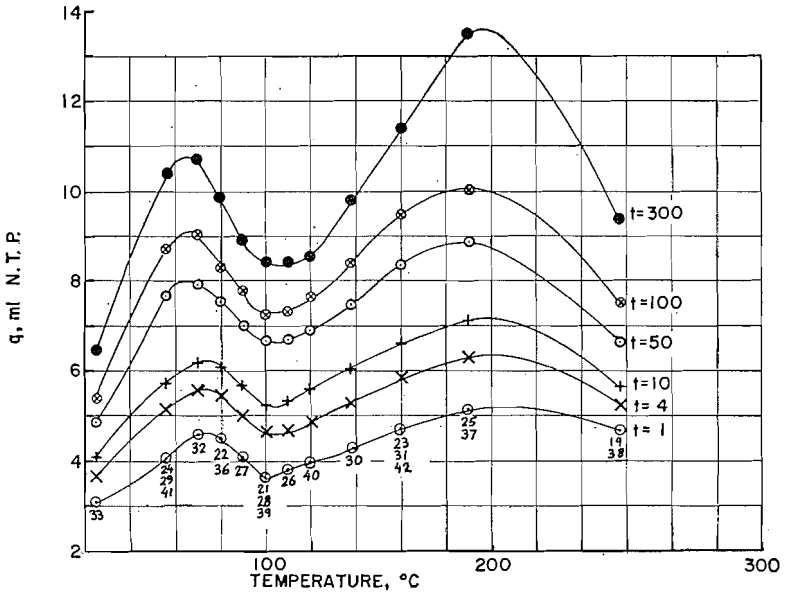

FIG. 3. H_2–ZnO isobars. The numbers next to points of the $t = 1$ curve are those of the experiments, which were numbered consecutively in order of their execution.

Can. J. Chem. Downloaded from www.nrcresearchpress.com by 176.9.209.113 on 09/04/12
For personal use only.

representing amounts adsorbed after 1, 4, 10, 50, 100, and 300 minutes at each temperature. Adsorption maxima appear at about 70° and 200°, and a minimum appears at about 105°. Inspection of Table I reveals small temperature differences in isobar positions. Cimino, Cipollini, and Molinari (9) were able to displace the position of their isobar by about 20° by sintering their adsorbent at 900°. The relatively small differences in isobar positions of pure ZnO suggests that the maxima are not very sensitive to catalyst preparation variables, although it has been shown (9) that the structure of the isobar is severely affected by doping the ZnO.

TABLE I
Temperatures of occurrence of the maxima and the minimum of the adsorption isobar of hydrogen on zinc oxide

Investigation*	Maximum, ° C	Minimum, ° C	Maximum, ° C
(*a*) Taylor and Strother (8)	80	97	218
(*b*) Wicke (7)	70	100	260
(*c*) Cimino *et al.* (9)	50	105	—
(*c, d*) Cimino *et al.* (9)	70	135	190
(*e*) Present experiments	70	105	200
(*f*) Present experiments	80	110	200

*(*a*) Measured after 1000 minutes; pressure: 1 atm.
(*b*) Measured after 600 minutes; pressure: 1 atm.
(*c*) Measured after 900 minutes; pressure: 1 atm.
(*d*) After sintering the catalyst at 900° C.
(*e*) Set B measured after 300 minutes.
(*f*) Set A measured after 500 minutes.

Effect of Temperature on Rate Constants

Values of the constants a and α were calculated (10) for each linear portion of an Elovich plot, and are given graphically as functions of temperature in Figs. 4, 5, and 6.

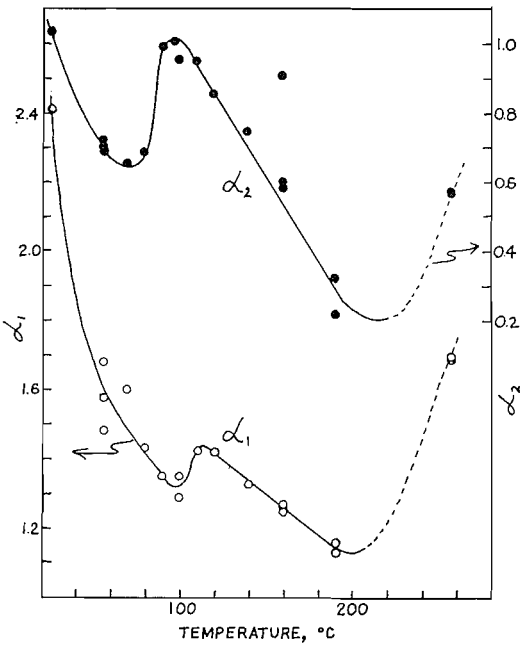

FIG. 4. The effect of temperature on α.

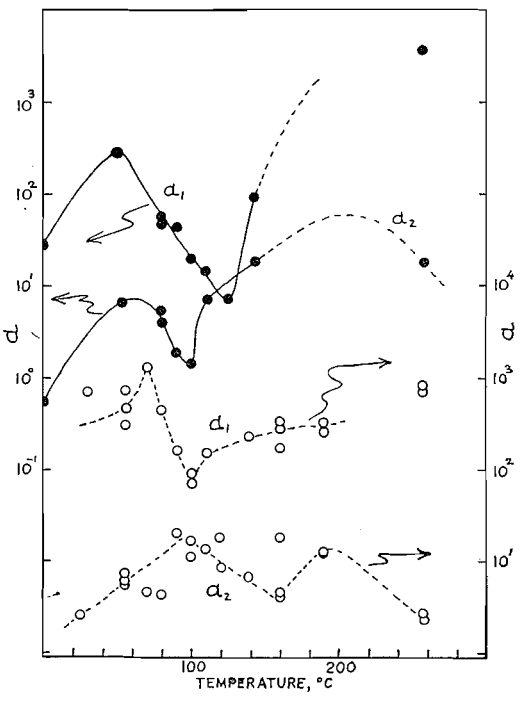

FIG. 5. The effect of temperature on a. ●, Data of set A. ○, Data of set B. The catalyst of set A consisted of 31.30 g ZnO ex oxalate.

Can. J. Chem. Downloaded from www.nrcresearchpress.com by 176.9.209.113 on 09/04/12
For personal use only.

The subscripts 1 and 2 refer to the constants for the first and second lines of Elovich plots, respectively. The structure shown by the α–T plots of Fig. 4 is similar but inverse of that of the isobar. The plots of Fig. 5 of the more sensitive (2, 3, 4) values of a against temperature similarly reflect the isobar structure, but show more scatter. In Fig. 5 the lower two curves formed by open circle refer to the data of set B, while the upper two curves refer to the incomplete set A, shown here to illustrate the trends in a–T relations. The ratio of the rate of the second kinetic process to that of the first process is α_1/α_2. Figure 6 shows the α_1/α_2–T relation: undulations similar to those of the isobar are apparent, so that the effect of temperature on the second kinetic process is greater than that on the first process. Figure 7 shows values of the co-ordinates q_b and t_b of the break

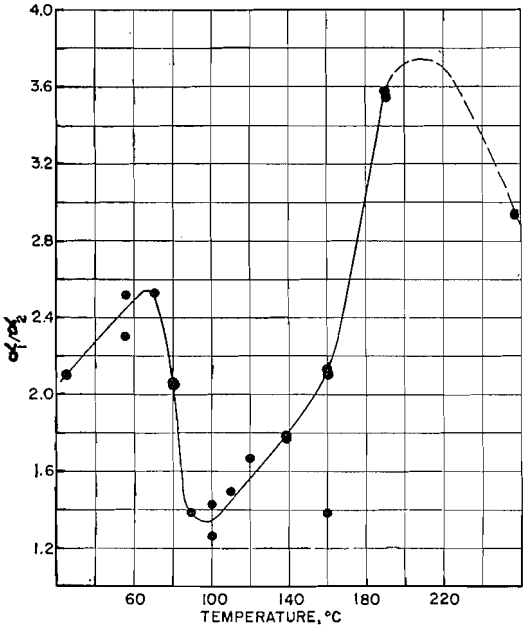

FIG. 6. The effect of temperature on (α_1/α_2).

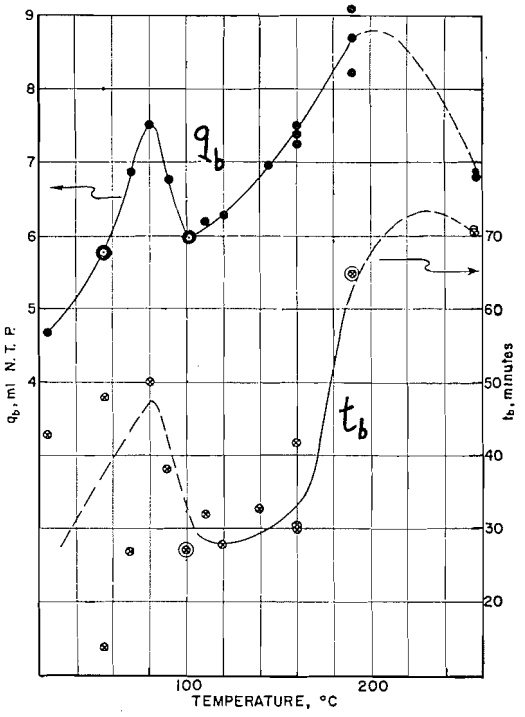

FIG. 7. The variation of the co-ordinates of the break with temperature.

of Elovich plots at various temperatures. The q_b–T plot shows structures similar to that of the isobar. The t_b–T plot shows some variations but, because of the exponential effect of scatter of a values on those of t_b, the trends are not well defined. In general, then, in the present system of H_2–ZnO, the rates of adsorption vary with temperature in a fashion similar to the variation of the extents of adsorption after long times.

It is obvious that the temperature dependencies of the rate parameters can be more complex than had been previously believed. Earlier studies (1–4) show simple relations

$$\alpha = A+B/T$$
$$\log a = C+D/T \qquad A, B, C, D = \text{constants}$$

to hold over ranges of temperatures covering about 200° C. Such studies, however, had been made in a temperature region of continuously increasing or decreasing adsorption. Such linear equations can be constructed for the present data. The constants α_1 and α_2

Can. J. Chem. Downloaded from www.nrcresearchpress.com by 176.9.209.113 on 09/04/12
For personal use only.

over the range 120–190° C, for example, vary inversely with temperature. In view of the undulations of the isobar, however, such equations are pointless in this case. Similarly pointless are calculations of activation energies of adsorption, particularly in the region 80–110° C, where negative activation energies are obtained. By analogy one may expect similar undulant variations of rate parameters with temperature to occur with the adsorption of hydrogen on iron synthetic ammonia catalyst (11), the only other system known to exhibit the double-humped isobar. Also, a consistent reversal of temperature coefficients in the vicinity of a normal adsorption isobar maximum seems plausible. However, because no adequate general explanation of these phenomena is apparent, the sign and magnitude of the temperature coefficients in both the ascending and the descending portions of the isobar cannot be predicted.

The Effect of Continuously Changing Temperature

Taylor and Liang (12) found that if the temperature of a sample of ZnO almost saturated with hydrogen was suddenly increased, a desorption followed by a readsorption of gas occurred. When the temperature was decreased, increased adsorption was found. It was thought of interest to perform several experiments in order to determine if similar results would be obtained when (*a*) the temperature was changed relatively slowly and in continuous fashion; (*b*) the adsorbent was in a state relatively far removed from complete coverage.

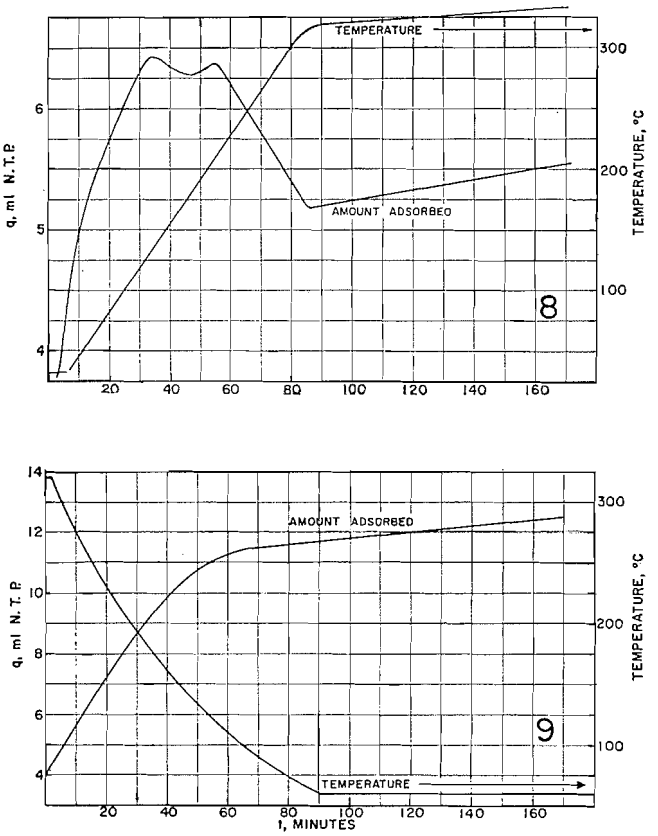

FIG. 8. The effect of continuously increasing temperature.
FIG. 9. The effect of continuously decreasing temperature.

Can. J. Chem. Downloaded from www.nrcresearchpress.com by 176.9.209.113 on 09/04/12
For personal use only.

Run F34 was started in normal fashion, with the catalyst degassed, at a temperature of 33° C. However, instead of keeping the temperature constant as in a normal run, the temperature was raised at a rate of about 4°/minute to about 314° C. Readings were made every minute except after 85 minutes. The numerous q data as well as the prevailing furnace temperature are shown in Fig. 8 as smoothed plots as functions of time. Adsorption ceases to increase at about 130°, and a continual decline in q is found after about 205° C. The significance of the small dip in the q–t curve at about 180° is not clear: the decline in q between 140° and 180° is only about 0.15 ml. Further, it may be expected that the temperature of the catalyst will not be uniform and will be at a slightly lower temperature than that of the furnace.

Run F35 was started at 323° C in normal fashion, but the temperature was allowed to fall to 69° C. In Fig. 9 the smoothed q–t plot of the numerous data shows continuous increase in adsorption with time. The rate of adsorption declines slowly and becomes roughly constant in the constant temperature region after 100 minutes. The results of the two experiments are thus comparable to those of the experiments of Taylor and Liang. Apparently quite drastic departures from the techniques of those authors will not bring about significantly different results.

REFERENCES

1. Taylor, H. A. and Thon, N. J. Am. Chem. Soc. **74**, 4169 (1952).
2. Leibowitz, L., Low, M. J. D., and Taylor, H. A. J. Phys. Chem. **62**, 471 (1958).
3. Low, M. J. D. and Taylor, H. A. Can. J. Chem. **37**, 544 (1959).
4. Low, M. J. D. and Taylor, H. A. Can. J. Chem. **37**, 915 (1959).
5. Low, M. J. D. and Taylor, H. A. J. Electrochem. Soc. **106**, 524 (1959).
6. Taylor, H. S. and Sickman, D. V. J. Am. Chem. Soc. **54**, 602 (1932).
7. Wicke, E. Z. Electrochem. **53**, 279 (1949).
8. Taylor, H. S. and Strother, C. O. J. Am. Chem. Soc. **56**, 586 (1934).
9. Cimino, A., Cipollini, E., and Molinari, E. Naturwissenschaften, **43**, 58 (1956).
10. Sarmousakis, J. N. and Low, M. J. D. J. Chem. Phys. **25**, 178 (1956).
11. Emmett, P. H. and Harkness, R. W. J. Am. Chem. Soc. **57**, 1631 (1935).
12. Taylor, H. S. and Liang, S. C. J. Am. Chem. Soc. **69**, 1306 (1947).

Can. J. Chem. Downloaded from www.nrcresearchpress.com by 176.9.209.113 on 09/04/12
For personal use only.

Can. J. Chem. Downloaded from www.nrcresearchpress.com by 176.9.209.113 on 09/04/12
For personal use only.

THE THIRD LAW ENTROPY AND STRUCTURE OF IRON PENTACARBONYL[1]

A. J. LEADBETTER[2] AND J. E. SPICE[3]

ABSTRACT

The heat capacity of solid and liquid iron pentacarbonyl has been measured from 20° to 290° K. The heat of fusion was also measured and found to be 3161±3 cal/mole. From an investigation of the change of temperature of the sample during melting the triple point of iron pentacarbonyl was estimated to be 253.15° K and the purity of the sample 99.9 mole%. An anomalous absorption of energy amounting to 4.8 cal/mole was observed at about 230° K; this is shown to be due to an unknown impurity in the sample. The vapor pressure of the liquid was measured in the vicinity of room temperature and from these results the heat of vaporization at 25° C was estimated to be 9.1±0.1 kcal/mole.

The entropy of iron pentacarbonyl as an ideal gas at 1 atm pressure and 25° C computed from the thermal measurements is 106.4±0.8 cal/mole deg. Comparison of this quantity with values calculated from spectroscopic data indicates that the iron pentacarbonyl molecule has the form of a trigonal bipyramid rather than that of a square pyramid.

INTRODUCTION

The iron pentacarbonyl molecule, one of the few of type AX_5, might on general grounds be either a trigonal bipyramid or a square pyramid. An electron diffraction study (1) indicated a trigonal bipyramid structure but this does not appear to be consistent with the reported dipole moment of 0.8 Debye (2). An attempt has been made to use nuclear resonance techniques to determine the structure but the results were inconclusive (3).

Many spectroscopic investigations have been reported but the photosensitivity of iron pentacarbonyl has made it difficult to obtain the Raman spectrum which is necessary for an unambiguous frequency assignment. However, the weight of spectroscopic evidence favors the bipyramidal structure (3, 4, 5, 6) although O'Dwyer (7) has recently claimed that his infrared results can best be interpreted on the basis of the square pyramid structure.

It has thus not been possible to establish conclusively the structure of the iron pentacarbonyl molecule from spectroscopic data alone. A comparison of the Third Law entropy with the statistical value calculated on the basis of the two possible structures and the corresponding frequency assignments might therefore help to decide between the two structures.

EXPERIMENTAL

The Material

We are grateful to the Mond Nickel Co. Ltd. for supplying the sample of iron pentacarbonyl. It was supplied in the form of the pure liquid, and an analysis of the freezing curve by the method of Taylor and Rossini (8) indicated the purity to be 99.9 mole%. The sample was therefore used without further purification; a subsequent study of the melting curve confirmed the above value for the purity.

The Calorimetric Method

The cryostat contained a miniature hydrogen liquefier of the type used by Jones[4]

[1]*Manuscript received July 16, 1959.*
Contribution from the Department of Inorganic and Physical Chemistry, The University of Liverpool, Liverpool, England.
[2]*Present address: Department of Physical and Inorganic Chemistry, The University of Bristol, Bristol 8, England.*
[3]*Present address: The Science School, Winchester College, Winchester, England.*
[4]*We are grateful to Professor G. O. Jones for his help while we were designing and constructing the liquefier.*

(9). The calorimetric measurements were made with a conventional vacuum adiabatic calorimeter by standard methods. All of the measurements were made with a White double potentiometer. Time of energy input was determined with a Venner mechanical stop clock, the solenoid switching mechanism of which was coupled directly to the switch controlling the heater current. The clock was calibrated by comparison with the B.B.C. time signals. The platinum resistance thermometer was calibrated on the International Temperature Scale above 90° K and on the thermodynamic scale below this temperature. The calorimetric apparatus and the establishment of the temperature scale below 90° K will be fully described elsewhere (10).

The copper calorimeter vessel, weighing 240 g, was filled with 0.5906 mole of sample in a dimly lit, dry atmosphere. It was sealed by pinching shut and sealing with solder a short length of thin-walled nickel tubing previously soldered into the neck of the vessel. The heat capacity of the calorimeter amounted to 17% of the total at 20° K and to 39% at 290° K. Temperature increments of between 4° and 8° were generally used except in the region of 230° K, where smaller increments were used in order to investigate the anomalous energy absorption.

The Vapor Pressure Measurements

The vapor pressure of the liquid was measured between 20° and 33° C using a mercury manometer of 17-mm-bore tubing. Pressures were measured using a comparator telescope and a glass scale, etched in 0.5-mm divisions, which was freely suspended between the arms of the manometer; the accuracy of pressure measurement is estimated to be ±0.05 mm. The temperature of the sample was maintained constant to ±0.02° for each pressure determination, by means of a water thermostat. The vapor space was always maintained at a slightly higher temperature than the liquid. Temperatures were measured to ±0.02° with a mercury-in-glass thermometer, the ice point reading of which had been found correct within these limits. In order to prevent photochemical decomposition light was excluded from these portions of the apparatus containing the iron pentacarbonyl; as a check against possible decomposition, measurements were made after both warming and cooling the sample.

RESULTS

The Heat Capacity

The experimental results are given in Table I (the ice point was taken as 273.16° K and the calorie as 4.1840 absolute joules). The maximum deviation of any point from a smoothed curve is 0.4% and the average deviation ±0.1%, except in the anomalous region where the measurements were somewhat less precise. The accuracy of the results is estimated to be ±0.5% for $20° K < T < 50° K$ and ±0.3% for $T > 50° K$. The heat capacity curve shows a quite regular behavior except for a very small peak at about 230° K, associated with the absorption of an "extra" energy of 4.8 cal/mole over a narrow temperature range. A preliminary investigation of the heat capacity of iron pentacarbonyl, made in this laboratory by McGowan (11), had indicated the presence of a much larger anomaly in the heat capacity curve. It was shown in the present work, by determination of the heat capacity after cooling through the anomalous region at different rates and to different temperatures, that the size of the anomaly was independent of the previous history of the sample. The data obtained on the apparent anomaly in the two investigations are compared in Table II. T_{max} is the temperature at which the heat capacity in the anomalous region reaches its maximum value. The amount of impurity in each specimen was estimated from the depression of the melting point.

Can. J. Chem. Downloaded from www.nrcresearchpress.com by 176.9.209.113 on 09/04/12
For personal use only.

TABLE I

The heat capacity of $Fe(CO)_5$

Temp. (° K)	C_p (cal/mole deg)	Temp. (° K)	C_p (cal/mole deg)
22.59	6.66	213.84	40.89
27.47	9.39	217.24	41.09
38.15	13.77	219.29	41.57
44.19	15.76	220.42	41.57
49.32	17.20	222.58	41.60
53.86	18.20	223.61	41.87
59.91	19.51	225.84	42.60
67.30	20.86	226.81	42.53
73.96	21.83	227.80	43.53
85.07	23.42	228.57	43.35
88.55	23.84	229.33	43.36
99.21	25.01	229.97	44.02
104.33	25.72	230.13	43.63
109.25	26.26	230.90	42.67
116.83	27.48	232.07	42.72
126.98	29.00	233.11	43.28
136.62	30.39	233.49	43.45
145.87	31.80	236.24	43.72
154.78	33.22	236.59	43.58
158.52	33.98	241.61	45.11
163.34	34.47	248.14	53.47
166.96	35.15	253.15	Fusion
169.65	35.34	258.58	55.86
175.20	36.27	269.33	56.10
183.20	37.18	275.35	56.57
191.05	38.11	281.35	56.82
198.74	39.06	287.33	56.89
206.32	39.93		

TABLE II

The apparent anomaly in $Fe(CO)_5$ at 230° K

T_{max} (° K)	ΔH (cal/mole)	Impurity (mole%)	
229.9±0.1	4.84±0.05	0.1	This work
229.7±0.3	124 ±1	3.4	McGowan

Within the limits of experimental uncertainty the size of the anomaly is directly related to the amount of impurity in the specimen, showing that the anomaly must be caused in some way by the impurity and is not an intrinsic property of pure iron pentacarbonyl. The most probable explanation of the anomaly is that it is due to the melting of an eutectic mixture present in a small amount. Unfortunately, the nature of the impurity is not known but the most likely impurities in iron pentacarbonyl are nickel carbonyl and $Fe_2(CO)_9$ formed in the photochemical decomposition of the pentacarbonyl. Since both samples were obtained from the same source it seems unlikely that they initially contained such differing amounts of impurity and this would suggest that $Fe_2(CO)_9$ is the most likely impurity. However, without additional experimental data further speculation would appear to be of little value. In addition, it should be noted that the entropy associated with the anomaly (0.02 cal/mole deg) is quite negligible in the determination of the standard entropy.

Can. J. Chem. Downloaded from www.nrcresearchpress.com by 176.9.209.113 on 09/04/12
For personal use only.

The Triple Point and Heat of Fusion

The equilibrium temperatures as a function of the fraction of the sample melted are shown in Table III. From these results the calculated triple point of iron pentacarbonyl is 253.15° K.

TABLE III

The melting point of $Fe(CO)_5$

% Melted	T° K
31	253.018
50	253.062
67	253.084
84	253.097
100	253.11

NOTE: Impurity: 0.1 mole%. Triple point: 253.15° K.

The heat of fusion was determined in the usual manner, the premelting energy being included in the heat of fusion. Two determinations gave respectively 3158.7 and 3162.6 cal/mole, or a mean value of 3161±3 cal/mole. The only previously published value for the heat of fusion is 3250±40 cal/mole reported by Mittasch (12).

The Vapor Pressure

The experimental results are given in Table IV. Pressures are expressed in terms of the height of a column of mercury under standard gravity at 0° C. The results may be represented within their experimental uncertainty by the formula

$$\log P \text{ (mm)} = 8.514 - (2105/T)$$

as is shown in Table IV.

TABLE IV

The vapor pressure of $Fe(CO)_5$

Temp. (° K)	P_{obs} (mm)	P_{calc} (mm)	Temp. (° K)	P_{obs} (mm)	P_{calc} (mm)
293.47	21.95	21.90	301.44	34.00	33.89
294.36	23.01	23.02	302.71	36.38	36.25
295.99	25.38	25.21	302.91	36.65	36.64
296.94	26.45	26.56	303.48	37.88	37.77
297.98	28.05	28.12	304.01	38.70	38.83
298.30	28.68	28.62	305.24	41.37	41.41
299.60	30.56	30.70	305.30	42.73	41.53
300.26	31.67	31.82	306.32	43.60	43.78

The above formula has been compared with vapor pressure data reported by Dewar and Jones (13) between −7° and 78° C, Eyber (14) between −15° and 20° C, and Trautz and Badstübner (15) between 46° and 104° C. The results of Dewar and Jones appear to be too high below about 40° C, while those of Eyber are in excellent agreement with the present work. The results of Trautz and Badstübner are higher by about 1% at 46° C and the deviation increases with temperature. This, however, may only represent the inadequacy of a two-constant expression for log P over any but a restricted temperature range.

The heat of vaporization at 25° C was calculated by means of the Clausius–Clapeyron equation, the Berthelot equation of state being used to correct for gas imperfection. The

Can. J. Chem. Downloaded from www.nrcresearchpress.com by 176.9.209.113 on 09/04/12
For personal use only.

values of the critical constants used were $T_c = 560°$ K and $P_c = 29.6$ atm (13). The heat of vaporization of iron pentacarbonyl was found to be $9.6_0 \pm 0.1$ kcal/mole.

DISCUSSION

The Third Law Entropy of $Fe(CO)_5$

The computation of the entropy of iron pentacarbonyl as an ideal gas at 1 atm pressure and 25° C is summarized in Table V. The extrapolation of the heat capacity from 22.59° to 0° K was carried out by means of a Debye function with 18 degrees of freedom and $\Theta = 155°$ K.

TABLE V

The Third Law entropy of $Fe(CO)_5$

	cal/mole deg	
ΔS (0° to 22.59° K) Debye extrapolation	2.7 ±0.2	
ΔS (22.59° to 253.15° K) solid	56.3 ±0.2	
$\Delta S_{253.15}$ (3161/253.15) fusion	12.49±0.02	
ΔS (253.15° to 298.16° K) liquid	9.26±0.03	
$\Delta S_{298.16}$ (960_0/298.16) vaporization	32.2 ±0.3	
Entropy of real gas at 28.4 mm and 298.16° K		$112.9_5 \pm 0.7_5$
$\Delta S_{\text{compression}}$ R ln (28.4/760)	−6.53±0.01	
Correction for gas imperfection	0.01	
Entropy of the ideal gas at 1 atm and 298.16° K		106.4±0.8

The Statistical Entropy of $Fe(CO)_5$

The standard entropy of iron pentacarbonyl has been calculated from spectroscopic data by standard methods, using the rigid rotator – harmonic oscillator approximation. The values of the fundamental constants were taken from the tables of Kaye and Laby (16).

The computation was carried out for both the trigonal bypiramid model (symmetry D_{3h}) and the square pyramid model (symmetry C_{4v}) and in both cases the following interatomic distances were used (1): Fe—C, 1.84 Å and C—O, 1.15 Å; the Fe—C—O groups were assumed linear. The D_{3h} model was precisely that proposed by Ewens and Lister (1) on the basis of their electron diffraction studies, while for the C_{4v} model the four equivalent CO groups were assumed coplanar with the Fe atom and the remaining CO group perpendicular to the plane. This is a reasonable assumption since the C—Fe—C angle would not be expected to differ greatly from 180° and numerical values of entropy are not sensitive to small changes in bond angles. In fact, the difference in the moments of inertia of the D_{3h} and C_{4v} models contributes less than 0.01 cal/mole deg to the difference in the rotational entropies of the two structures; almost the whole difference is due to the change of symmetry number from 6 to 4.

A serious deficiency in the frequency assignments of King and Lippincott (4, 5), Murata and Kawai (6), Edgell and Wilson (see ref. 5), and O'Dwyer (7) is the lack of experimental data on the low frequency C—Fe—C deformation modes, to which the thermodynamic properties at normal temperatures are most sensitive. Only one of these fundamentals was directly observed, the remainder being obtained from infrared combination bands or by comparison with similar molecules. Very recently, however, Cotton Danti, Waugh, and Fessenden (3) have reported the observation of these low frequency fundamentals. They conclude that these and other (unpublished) results at higher frequencies are more consistent with the D_{3h} than the C_{4v} model and have accordingly

Can. J. Chem. Downloaded from www.nrcresearchpress.com by 176.9.209.113 on 09/04/12
For personal use only.

assigned the observed fundamentals on this basis. The various assignments proposed for the C—Fe—C deformation modes on the basis of both molecular models are given in Table VI, where the numbering is taken from the original papers.

TABLE VI

C—Fe—C deformation frequencies

	D_{3h}					C_{4v}	
		Frequency (cm^{-1})					
	Symmetry	King and Lippincott	Murata and Kawai	Edgell and Wilson	Cotton *et al.*	Symmetry	Frequency (cm^{-1}), O'Dwyer
ν_9	A_2''	100	100	115	93	ν_6 A_1	79
ν_{14}	E'	110	110	92	72	ν_{11} B_1	185
ν_{15}	E'	100	63	102	104	ν_{13} B_2	146
ν_{18}	E''	110	95	110	112	ν_{19} E	103
						ν_{20} E	71

The vibrational entropy for the D_{3h} model has been calculated using each of the proposed frequency assignments, first as published and then corrected to include the observed low frequency fundamentals reported by Cotton *et al.* For the C_{4v} model O'Dwyer's assignment has first been used to calculate the vibrational entropy, but in order to provide a fair comparison of the two models it is necessary to correct his assignment to incorporate the new spectroscopic results for the low frequency fundamentals and calculate the entropy on this basis also. This may be done most reasonably by assigning the observed fundamentals to ν_6 (93 cm^{-1}), ν_{13} (112 cm^{-1}), ν_{19} (104 cm^{-1}), and ν_{20} (72 cm^{-1}) but it must be emphasized that such an assignment does not appear to be consistent with the spectroscopic results. The results of the entropy calculations are summarized in Table VII, the final column contains the entropies calculated using the frequency assignments corrected to incorporate the observed values for the low frequency fundamentals.

TABLE VII

The statistical entropy of $Fe(CO)_5$

	Moments of inertia (g cm^2 $\times 10^{40}$)		$S°_{trans+rot}$ (cal/mole deg)		$S°_{vib}$ (cal/mole deg)	$S°$ (cal/mole deg)	$S°_{corr}$ (cal/mole deg)
Model	I_A	$I_B = I_C$		Frequency assignment			
C_{4v}	1220	861	69.5_4	O'Dwyer	35.5_2	105.1	105.2
D_{3h}	915	1067	68.9_0	King and Lippincott*	35.4_7	104.4	106.0
				Murata and Kawai	34.5_2	103.4	102.6
				Edgell and Wilson	36.0_1	104.9	106.1
				Third Law entropy		106.4±0.8	

*The values of $S°$ and $-(F°-E_0°)/T$ quoted by King and Lippincott (4) are too high at all temperatures by 1.9 cal/mole deg.

The comparison of the Third Law entropy with the statistical value, calculated using the new results of Cotton *et al.* for the C—Fe—C deformation frequencies, provides strong support for the D_{3h} rather than the C_{4v} model for the iron pentacarbonyl molecule. In view of the evidence from electron diffraction and spectroscopic studies, which alone were not conclusive, and the new evidence presented here from thermodynamic studies, it can now be concluded with reasonable certainty that the structure of the iron pentacarbonyl molecule is a trigonal bipyramid.

Can. J. Chem. Downloaded from www.nrcresearchpress.com by 176.9.209.113 on 09/04/12
For personal use only.

The above comparison cannot help to resolve the details of the frequency assignment since the entropies calculated on the basis of the assignments of King and Lippincott and Edgell and Wilson are very close, while the frequency assignments differ considerably in detail. However, it can be concluded that the assignment proposed by Murata and Kawai based on the same experimental data as that of King and Lippincott, must be seriously in error.

ACKNOWLEDGMENT

One of us (A.J.L.) wishes to thank the University of Liverpool for the award of the Goodlass–Wall Research Studentship.

REFERENCES

1. EWENS, R. V. G. and LISTER, M. W. Trans. Faraday Soc. **35**, 681 (1939).
2. WEISS, E. Z. anorg. u. allgem. Chem. **287**, 223 (1956).
3. COTTON, F. A., DANTI, A., WAUGH, J. S., and FESSENDEN, R. W. J. Chem. Phys. **29**, 1427 (1958).
4. KING, F. T. and LIPPINCOTT, E. R. J. Am. Chem. Soc. **78**, 4192 (1956).
5. FATELEY, W. G. and LIPPINCOTT, E. R. Spectrochim. Acta, **10**, 8 (1957).
6. MURATA, H. and KAWAI, K. J. Chem. Phys. **28**, 516 (1958).
7. O'DWYER, M. F. J. Mol. Spectroscopy, **2**, 144 (1958).
8. TAYLOR, W. J. and ROSSINI, F. D. J. Research Natl. Bur. Standards, **32**, 197 (1944).
9. CHESTER, P. F. and JONES, G. O. Proc. Phys. Soc. **66**, 296 (1953).
10. LEADBETTER, A. J., SMITH, K. A., and SPICE, J. E. To be published.
11. MCGOWAN, C. R. Thesis, University of Liverpool, 1954.
12. MITTASCH, A. Angew. Chem. **41**, 827 (1928).
13. DEWAR, J. and JONES, H. O. Proc. Roy. Soc. A, **76**, 558 (1905).
14. EYBER, G. Z. physik. Chem. A, **144**, 1 (1929).
15. TRAUTZ, M. and BADSTÜBNER, W. Z. Elektrochem. **35**, 799 (1929).
16. KAYE, G. W. C. and LABY, T. H. Tables of physical and chemical constants. 11th ed. Longmans, Green & Co., Ltd., London. 1956.

Can. J. Chem. Downloaded from www.nrcresearchpress.com by 176.9.209.113 on 09/04/12
For personal use only.

Can. J. Chem. Downloaded from www.nrcresearchpress.com by 176.9.209.113 on 09/04/12
For personal use only.

CONFIGURATION OF GLYCOSIDIC LINKAGES IN OLIGOSACCHARIDES
VIII. SYNTHESIS OF α-D-MANNOPYRANOSYL- AND α-L-RHAMNOPYRANOSYL-DISACCHARIDES BY THE KÖNIGS–KNORR REACTION*

P. A. J. Gorin and A. S. Perlin

6-*O*-β-D-Mannopyranosyl-D-glucose was required for studies on oligosaccharide structure. A synthesis of the octa-*O*-acetyl derivative of this disaccharide via the Königs–Knorr reaction (1) has been reported by Talley, Reynolds, and Evans (2), who condensed 2,3,4,6-tetra-*O*-acetyl-α-D-mannopyranosyl bromide with 1,2,3,4-tetra-*O*-acetyl-β-D-glucose in the presence of silver oxide. The procedure of these earlier workers has now been repeated, and the disaccharide fraction produced was deacetylated and isolated by column chromatography on cellulose (3). The amorphous material, which contained a major and a minor component (chromatographic evidence), showed an unexpectedly strong dextrorotation ($[\alpha]_D$ +64°). Examined by the periodate oxidation procedure described in Part I of this series (4), it yielded a product ($[\alpha]_D$ +63°) which corresponded in optical rotation much more closely to that (I, free trialdehyde form) given by (1 → 6)-α-D-aldohexopyranosyl disaccharides (for example, No. 1, Table I), than by the β-D-anomers

TABLE I
Specific rotations of the products obtained by periodate oxidation of disaccharides and methyl glycosides

	Compound	$[\alpha]_D$	$[\alpha]_D$[a] oxidized	Ref.
1.	6-*O*-α-D-Glucopyranosyl-D-glucose	+120°	+85°	4
2.	6-*O*-α-D-Mannopyranosyl-D-glucose	+75°	+85°	[b]
3.	6-*O*-β-D-Glucopyranosyl-D-glucose	+8°	+109°	4
4.	6-*O*-α-D-Mannopyranosyl-D-mannose	+57°	+82°	[b]
5.	6-*O*-(6-Deoxy-α-L-mannopyranosyl)-D-glucose	−0.1°	−110°	[b]
6.	6-*O*-(6-Deoxy-α-D-galactopyranosyl)-D-glucose[c]	+125°	+100°	[b]
7.	6-*O*-(6-Deoxy-β-D-glucopyranosyl)-D-glucose[d]	−6°	−30°	[b]
8.	Methyl 6-deoxy-α-L-mannopyranoside	−63°	−143°	13
9.	Methyl 6-deoxy-β-L-galactopyranoside	+14°	+89°	13
10.	Methyl 6-deoxy-β-D-glucopyranoside	−55°	−88°	13

[a]Based on the assumption that the compound on oxidation yields the corresponding di- or tri-aldehyde in quantitative yield (4).

[b]Present work.

[c]Prepared in low yield as a chromatographically pure syrup from 6-*O*-α-D-galactopyranosyl-D-glucose, via a series of reactions utilized commonly for preparation of ω-deoxy sugars and derivatives (cf. (28)), i.e., tritylation, acetylation, detritylation, tosylation, iodination, reduction, deacetylation; intermediate products were not isolated.

[d]Obtained as the β-hepta-*O*-acetate (m.p. 175–176° C; $[\alpha]_D^{25}$ −2° (*c*, 1.4, chloroform). Calculated for $C_{26}H_{36}O_{17}$: C, 50.32%; H, 5.85%. Found: C, 50.35%; H, 5.93%) by condensation of 2,3,4-tri-*O*-acetyl(6-deoxy-α-D-glucopyranosyl)-bromide ((m.p. 152–155° C; $[\alpha]_D^{25}$ +268° (*c*, 1.3, chloroform). Calculated for $C_{12}H_{17}O_7Br$: C, 40.81%; H, 4.85%. Found: C, 40.98%; H, 4.95%)) with 1,2,3,4-tetra-*O*-acetyl β-D-glucose, according to the procedure of Talley, Reynolds, and Evans (2).

(for example, No. 3, Table I). A sample of the disaccharide octaacetate† prepared by Talley, Reynolds, and Evans was deacetylated and oxidized as described previously (4)

*Issued as N.R.C. No. 5354.

†*Obtained through the kindness of Professor M. L. Wolfrom.*

for isomaltose octaacetate. The rotatory power of the oxidation product (No. 2, Table I) showed that the disaccharide possesses the α-D-linkage, rather than the β-D-linkage assigned (2).

A (1 → 6)-mannobiose octaacetate (designated (1 → 6)-β-D-) was synthesized in the same manner by these earlier workers (2), and examination of this disaccharide* (No. 4, Table I) showed that it too must be assigned the α-D-linkage. This disaccharide has been obtained by acid reversion of D-mannose and partial hydrolysis of yeast mannan (5), its configuration having been confirmed earlier by the periodate oxidation method (4).

Two trisaccharides have been synthesized by Talley and Evans (6) through condensation of the α-acetobromo derivative of their 6-*O*-D-mannopyranosyl-D-glucose with 1,2,3,4-tetra-*O*-acetyl-D-glucose or -D-mannose. These trimers may now be redesignated, therefore, *O*-α-D-mannopyranosyl-(1 → 6)-β-D-glucopyranosyl-(1 → 6)-D-glucose, and *O*-α-D-mannopyranosyl-(1 → 6)-β-D-glucopyranosyl-(1 → 6)-D-mannose. The trisaccharides were thought (6) to be isomeric, or identical, with two oligosaccharides prepared (7) by acetolysis of the glucomannan from *Amorphophallus konjac*. Recently, however, it has been shown that the parent polysaccharide contains (1 → 4)-, but not (1 → 6)-, glycosidic linkages (8).

Reducing disaccharides which contain L-rhamnopyranose(6-deoxy-L-mannopyranose) as the non-reducing end unit have also been prepared by the Königs–Knorr reaction. Rutinose, the sugar moiety of the flavone glycoside, rutin, has been synthesized (9) from 2,3,4-tri-*O*-acetyl-α-L-rhamnopyranosyl bromide and 1,2,3,4-tetra-*O*-acetyl-β-D-glucose in the presence of mercuric acetate (the Zemplen modification (10)) and its linkage assigned a β-configuration. Similarly, the related disaccharide robinobiose, a component of the flavonoid robinin, has been synthesized and designated 6-*O*-β-L-rhamnopyranosyl-D-galactose (11). On periodate oxidation these disaccharides theoretically should yield a trialdehyde (II, α-L-anomer) which is closely related structurally to that (I) produced from (1 → 6)-linked aldohexose disaccharides, or to the dialdehyde produced from the corresponding methyl L-rhamnopyranoside (III, α-L-anomer). Examined by the oxidation procedure, rutinose† afforded a strongly levorotatory product (No. 5, Table I) which, by comparison with the products prepared from methyl 6-deoxy-α- and β-L-glycopyranosides (13) (Nos. 8 and 9, Table I), was to be expected for the α-L-isomer. Confirmation of this possibility was provided by the fact that 6-*O*-(6-deoxy-

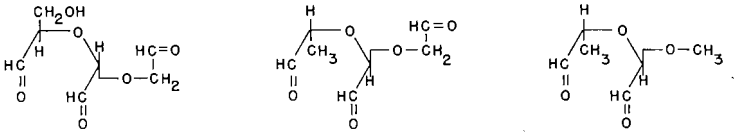

I II III

α-D-galactopyranosyl)-D-glucose (No. 6, Table I) on oxidation yielded a product having a specific rotation approximately equal and opposite to that produced from rutinose. In addition, the oxidation product derived from 6-*O*-(6-deoxy-β-D-glucopyranosyl)-D-glucose (No. 7, Table I) possessed a negative specific rotation of much smaller magnitude than that shown by the α-L- (or α-D-) isomers, which parallels the properties of the corresponding methyl β-D- and β-L-glycosides (Nos. 9 and 10, Table I). These findings

Obtained through the kindness of Professor M. L. Wolfrom.
†Prepared by enzymic hydrolysis of rutin (12).

Can. J. Chem. Downloaded from www.nrcresearchpress.com by 176.9.209.113 on 09/04/12
For personal use only.

show, therefore, that rutinose is an α-L- (rather than a β-L-) rhamnoside and, by analogy, that robinobiose most probably also is an α-L-rhamnoside.*

In most applications of the Königs–Knorr reaction it has been found that a Walden inversion accompanies replacement of the halide group, and the glycosidic linkage formed thus possesses a configuration opposite that of the parent glycosyl halide (16, 17, 18, 19, 20). Several reactions have been reported, however, in which the anomeric configuration of the product is the same as in the glycosyl halide used (for example, 21, 22, 23, 24, 25). Syntheses of the oligosaccharides considered above, using poly-*O*-acetyl-α-D-mannopyranosyl- or α-L-rhamnopyranosyl-bromide, clearly represent yet other examples in which configuration is retained. The latter two glycosyl halides may also undergo replacement with inversion, nonetheless, since on methanolysis the respective β-glycosides (together with orthoesters) have been obtained (24, 26, 27). These conflicting results are related possibly to the fact that different reaction conditions have been used in preparing the two classes of compounds. For methyl glycoside formation, the methanol served also as the reaction medium (24, 26, 27), whereas a less polar solvent (benzene or chloroform) was used in synthesis of the disaccharides (2, 9, 11). Isbell and Frush have shown (24) that use of a diluent (for example, benzene or ether) alters the course of the methanolysis of tetra-*O*-acetyl-α-D-mannopyranosyl bromide, promoting synthesis of the α-D-glycoside and a lower yield of the β-D-glycoside and orthoacetate. They suggested that the diluent interacts with an orthoester-type intermediate, formed with participation of the 2-*O*-acetyl group, permitting the reaction with methanol to proceed without a Walden inversion.† In the light of these observations, therefore, the formation of α-D-mannosyl- and α-L-rhamnosyl-disaccharides by the Königs–Knorr reaction is understandable.

The authors are grateful to Professor M. L. Wolfrom and Drs. G. L. Talbot and F. J. Simpson for the gift of samples, and to J. W. L. C. Christ and Sheila Lubin for technical assistance. Microanalyses were performed by M. Mazurek.

1. KÖNIGS, W. and KNORR, E. Ber. **34**, 957 (1901).
2. TALLEY, E. A., REYNOLDS, D. D., and EVANS, W. L. J. Am. Chem. Soc. **65**, 575 (1943).
3. HOUGH, L., JONES, J. K. N., and WADMAN, W. H. J. Chem. Soc. 2511 (1949).
4. CHARLSON, A. J. and PERLIN, A. S. Can. J. Chem. **34**, 1804 (1956).
5. JONES, J. K. N. and NICHOLSON, W. H. J. Chem. Soc. 27 (1958).
6. TALLEY, E. A. and EVANS, W. L. J. Am. Chem. Soc. **65**, 573 (1943).
7. NISHIDA, K. and HASHIMA, H. J. Dept. Agr. Kyushu Imp. Univ. **2**, 277 (1930); Chem. Abstr. **25**, 498 (1931).
8. SMITH, F. and SRIVASTAVA, H. C. J. Am. Chem. Soc. **81**, 1715 (1959).
9. ZEMPLEN, G. and GERECS, A. Ber. **67**, 2049 (1934); **68**, 1318 (1935).
10. ZEMPLEN, G. Ber. **62**, 990 (1929).
11. ZEMPLEN, G., GERECS, A., and FLESCH, H. Ber. **71**, 774 (1938).
12. TALBOT, G. L. and SIMPSON, F. J. 42nd Annual Conference, C.I.C., Halifax, May 26, 1959. p. 36.
13. MACLAY, W. D., HANN, R. M., and HUDSON, C. S. J. Am. Chem. Soc. **61**, 1660 (1939).
14. HUDSON, C. S. J. Am. Chem. Soc. **38**, 1566 (1916).
15. CHARLSON, A. J. Ph.D. Thesis, University of Capetown. 1954.
16. FRUSH, H. L. and ISBELL, H. S. J. Research Natl. Bur. Standards, **27**, 413 (1941).
17. PACSU, E. Advances in Carbohydrate Chem. **1**, 77 (1945).
18. EVANS, W. L., REYNOLDS, D. D., and TALLEY, E. A. Advances in Carbohydrate Chem. **6**, 27 (1951).
19. LEMIEUX, R. U. Advances in Carbohydrate Chem. **9**, 1 (1954).
20. HAYNES, L. J. and NEWTH, F. H. Advances in Carbohydrate Chem. **10**, 207 (1955).
21. LEVENE, P. A. and WOLFROM, M. L. J. Biol. Chem. **78**, 525 (1928).

**The specific rotation of rutinose, when correlated with Hudson's observations on the configuration of disaccharides (14), suggests that the compound possesses the α-L-linkage (15). Similarly, the specific rotations of the D-mannopyranosyl disaccharides considered above, are much more in accord with assignment of the α-D-linkage, rather than the β-D-linkage, to these bioses.*

†*Alternatively, retention of configuration has been ascribed (20) to formation initially of a cyclic orthoester ion (17, 19) which undergoes further solvolysis, so that two successive Walden inversions occur. However, this mechanism does not account for the solvent effects noted above.*

Can. J. Chem. Downloaded from www.nrcresearchpress.com by 176.9.209.113 on 09/04/12
For personal use only.

22. HELFERICH, B. and BREDERECK, H. Ann. **465**, 166 (1928).
23. ZEMPLEN, G. and GERECS, A. Ber. **63**, 2720 (1930).
24. ISBELL, H. S. and FRUSH, H. L. J. Research Natl. Bur. Standards, **43**, 161 (1949).
25. NESS, R. K., FLETCHER, H. G., JR., and HUDSON, C. S. J. Am. Chem. Soc. **72**, 2200 (1950).
26. FISCHER, E., BERGMANN, M., and RABE, A. Ber. **53**, 2362 (1920).
27. DALE, J. K. J. Am. Chem. Soc. **46**, 1046 (1924).
28. BREDERECK, H. Ber. **63**, 959 (1930).

RECEIVED JULY 22, 1959.
NATIONAL RESEARCH COUNCIL OF CANADA,
PRAIRIE REGIONAL LABORATORY,
SASKATOON, SASKATCHEWAN.

Can. J. Chem. Downloaded from www.nrcresearchpress.com by 176.9.209.113 on 09/04/12
For personal use only.

CATALYTIC ACTIVATION OF MOLECULAR HYDROGEN IN SOLUTION BY CHLORORHODATE(III) COMPLEXES

J. F. HARROD AND J. HALPERN

We have found that rhodium (III) chloride, in aqueous solutions containing hydrochloric acid, activates molecular hydrogen homogeneously. Its behavior is qualitatively very similar to that observed earlier (1) for palladium (II) chloride and the same procedure (i.e. determination of the rate of catalytic reduction of ferric chloride by measuring the volume of hydrogen taken up at constant pressure) was employed to study the kinetics. The results are summarized in Table I.

The kinetics of the catalyzed reduction of ferric chloride were found to be of the form

$$-d\,[H_2]/dt = k\,[H_2]\,[Rh(III)].$$

Typical hydrogen uptake rate plots are shown in Fig. 1. Simultaneous spectrophotometric measurements confirmed that the hydrogen taken up is consumed in the reduction of

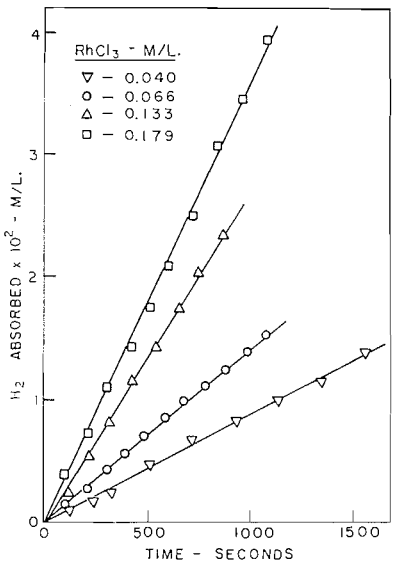

FIG. 1. Rhodium (III) chloride catalyzed reduction of ferric chloride at 80°, 450 mm Hg.

22. HELFERICH, B. and BREDERECK, H. Ann. **465**, 166 (1928).
23. ZEMPLEN, G. and GERECS, A. Ber. **63**, 2720 (1930).
24. ISBELL, H. S. and FRUSH, H. L. J. Research Natl. Bur. Standards, **43**, 161 (1949).
25. NESS, R. K., FLETCHER, H. G., JR., and HUDSON, C. S. J. Am. Chem. Soc. **72**, 2200 (1950).
26. FISCHER, E., BERGMANN, M., and RABE, A. Ber. **53**, 2362 (1920).
27. DALE, J. K. J. Am. Chem. Soc. **46**, 1046 (1924).
28. BREDERECK, H. Ber. **63**, 959 (1930).

RECEIVED JULY 22, 1959.
NATIONAL RESEARCH COUNCIL OF CANADA,
PRAIRIE REGIONAL LABORATORY,
SASKATOON, SASKATCHEWAN.

Can. J. Chem. Downloaded from www.nrcresearchpress.com by 176.9.209.113 on 09/04/12
For personal use only.

CATALYTIC ACTIVATION OF MOLECULAR HYDROGEN IN SOLUTION BY CHLORORHODATE(III) COMPLEXES

J. F. HARROD AND J. HALPERN

We have found that rhodium (III) chloride, in aqueous solutions containing hydrochloric acid, activates molecular hydrogen homogeneously. Its behavior is qualitatively very similar to that observed earlier (1) for palladium (II) chloride and the same procedure (i.e. determination of the rate of catalytic reduction of ferric chloride by measuring the volume of hydrogen taken up at constant pressure) was employed to study the kinetics. The results are summarized in Table I.

The kinetics of the catalyzed reduction of ferric chloride were found to be of the form

$$-d\,[H_2]/dt = k\,[H_2]\,[Rh(III)].$$

Typical hydrogen uptake rate plots are shown in Fig. 1. Simultaneous spectrophotometric measurements confirmed that the hydrogen taken up is consumed in the reduction of

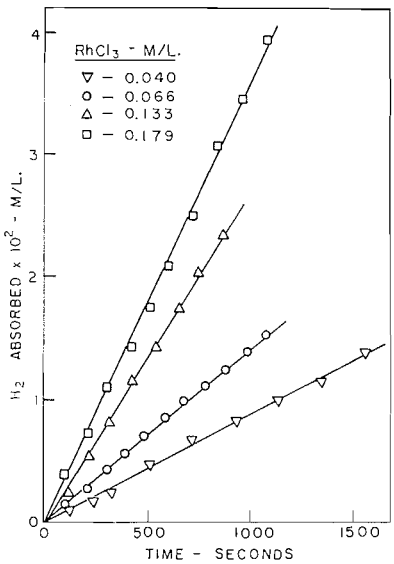

FIG. 1. Rhodium (III) chloride catalyzed reduction of ferric chloride at 80°, 450 mm Hg.

Fe(III) to Fe(II) and that the concentration of Rh(III) remains constant. The reaction under these conditions is clearly homogeneous (providing the HCl concentration exceeded 3 *M*, the reduction of Rh(III) to metallic Rh, a powerful heterogeneous catalyst, did not commence until the reduction of Fe(III) to Fe(II) was nearly complete), and since the concentrations of Rh(III) and of H_2 remain constant, the kinetics are of pseudo-zero order. Values of k are listed in Table I and are seen to be substantially independent of the concentrations of Fe(III), H_2, and Rh(III). The slight dependence on the HCl concentration and the effects of added electrolytes follow much the same pattern as found for Pd(II) and are attributable to variations in the solubility of hydrogen (1). Measurements of k over the temperature range 61.5° to 85.0° (Table I) yielded a good Arrhenius plot fitted by,

$$k = 2.3 \times 10^{15} \exp[-25{,}200/RT] \text{ l. mole}^{-1} \text{ sec}^{-1}$$

corresponding to an entropy of activation of +9 e.u.

TABLE I

Summary of kinetic data

Temp. (° C)	$[RhCl_3]$ (m/l.)	$[FeCl_3]$ (m/l.)	H_2 (mm)	$[H_2]\times10^4$ (m/l.)[a]	Medium	Rate$\times10^6$ (m l.$^{-1}$ sec^{-1})	k (l. m^{-1} sec^{-1})
80.0	0.040	0.17	450	3.6	3 *M* HCl	9.0	0.63
80.0	0.066	0.17	450	3.6	3 *M* HCl	13.6	0.57
80.0	0.133	0.17	450	3.6	3 *M* HCl	27.0	0.56
80.0	0.133	0.085	450	3.6	3 *M* HCl	26.0	0.54
80.0	0.179	0.17	450	3.6	3 *M* HCl	36.0	0.56
80.0	0.067	0.17	192	1.5	3 *M* HCl	6.0	0.59
61.5	0.179	0.17	625	4.8	3 *M* HCl	7.0	0.081
68.4	0.133	0.085	570	4.4	3 *M* HCl	11.4	0.195
74.6	0.133	0.085	510	3.9	3 *M* HCl	19.0	0.36
85.0	0.067	0.085	380	3.1	3 *M* HCl	21.0	1.01
80.0	0.067	0.15	450	3.6	5 *M* HCl	12.8	0.53
80.0	0.067	0.17	450	3.6	3 *M* HCl; 2 *M* NaCl	5.4	0.22
80.0	0.067	0.17	450	3.6	3 *M* HCl; 2 *M* LiCl	9.0	0.37
80.0	0.067	0.085	450	3.6	3 *M* HCl; 2 *M* $NaClO_4$	8.5	0.35
80.0	0.067	0.085	450	3.6	3 *M* HCl; 2 *M* $HClO_4$	17.0	0.70

[a]Based on solubility of hydrogen in 3 *M* HCl estimated as described earlier (1).

The insensitiveness of the rate to the HCl concentration in the region where $RhCl_6^{---}$ is the predominant species (2, 3) suggests that the major catalytic contribution is due to this species, although it is not possible to rule out some contributions also from lower chloro complexes (particularly $RhCl_5(H_2O)^{--}$ which is probably present in appreciable concentrations). It seems likely that the mechanism is of the same type as proposed earlier (1, 4) for kinetically analogous reactions of hydrogen involving other metal ions and complexes (including $PdCl_4^{--}$) as catalysts. This involves heterolytic splitting of hydrogen by the catalyst in the rate-determining step with formation of a catalyst–hydride complex (in this case $HRhCl_5^{---}$) which is reoxidized in subsequent rapid reactions with the substrate.

The abnormally high frequency factor of the present reaction is in contrast to the "normal" values ($\sim10^{11}$ l. mole^{-1} sec^{-1}) found for $PdCl_4^{--}$ (1) and for most of the other catalytic species previously examined (5), and its significance is not clear. It may reflect the higher charge of the present catalytic species and imply some spreading out of the charge (resulting in a decrease in the electrostriction of the surrounding solvent) in the activated complex, such as would result from separation of one of the Cl^- ligands. This

Can. J. Chem. Downloaded from www.nrcresearchpress.com by 176.9.209.113 on 09/04/12
For personal use only.

is consistent with earlier suggestions concerning the configuration of the activated complex in reactions of this type (4).

Grateful acknowledgment is made to the National Research Council of Canada and to the donors of the Petroleum Research Fund, administered by the American Chemical Society, for support of this research.

1. HALPERN, J., HARROD, J. F., and POTTER, P. E. Can. J. Chem. **37**, 1446 (1959).
2. COZZI, D. and PANTANI, F. J. Inorg. & Nuclear Chem. **8**, 385 (1958).
3. JORGENSEN, C. K. Acta Chem. Scand. **10**, 500 (1956).
4. HALPERN, J. J. Phys. Chem. **63**, 398 (1959).
5. HALPERN, J. Quart. Revs. (London), **10**, 463 (1956). Advances in Catalysis, (1959). In press.

RECEIVED AUGUST 10, 1959.
DEPARTMENT OF CHEMISTRY,
UNIVERSITY OF BRITISH COLUMBIA,
VANCOUVER, B.C., CANADA.

Can. J. Chem. Downloaded from www.nrcresearchpress.com by 176.9.209.113 on 09/04/12
For personal use only.

Can. J. Chem. Downloaded from www.nrcresearchpress.com by 176.9.209.113 on 09/04/12
For personal use only.

Canadian Journal of Chemistry

Issued by THE NATIONAL RESEARCH COUNCIL OF CANADA

VOLUME 37 DECEMBER 1959 NUMBER 12

PROFILES AND AREAS OF INTERFACES IN THE DU NOÜY RING METHOD[1]

F. VAN ZEGGEREN, C. DE COURVAL, AND E. D. GODDARD

ABSTRACT

Profiles and areas of interfaces subjected to interfacial tension measurements by the du Noüy ring method, were calculated with the aid of a digital computer. The computations were based on a solution of a set of two simultaneous, first order, ordinary differential equations. Area corrections amounted to from 5 to 17% of the total area calculated on the assumption of planar contact. These corrections permit more precise evaluation of the molecular area of monolayers spread at such interfaces. Two interfaces, viz. benzene–water and hexane–water, were taken as examples. Profiles of curves around the rings were also determined experimentally by means of an electrical contact micromanipulator method. Theoretically computed and measured profiles show very good agreement.

INTRODUCTION

Of the procedures available for investigating insoluble monolayers at the oil/water interface, that developed by Alexander and Teorell (1) is the most satisfactory. This utilizes the ring method for determination of the interfacial tension. For calculation of the area per molecule of the monolayer, it is necessary to allow for the fact that the interface is not completely planar; corrections must be made for the increase in interfacial area around the ring and also for that at the walls of the containing vessel. By using a vessel of large cross-sectional area, the correction for contours around the ring can be made relatively small, but even with a vessel of area 300 cm², Crisp (2) has estimated that the over-all correction to the planar area can be greater than 10%.

The shape of a surface between two fluids is given by the Laplace equation:

$$[1] \qquad (1/R_1)+(1/R_2) = P/\gamma$$

where R_1 and R_2 are the radii of curvature in vertical and horizontal directions, respectively, P is the hydrostatic pressure difference, and γ is the interfacial tension.

Thomas (3) has given a solution to this equation for flat-walled vessels; here R_2 is infinite and the equation becomes quite simple. Bashforth and Adams (4) have used an approximate Taylor expansion of the equation, but their publication is very old and almost inaccessible on this continent. Also, it only applies to drops. Freud and Freud (5) in their theory of the ring method, have used a Taylor expansion of the Laplace equation to calculate the total volume of liquid raised by the ring. However, their publication does not give many details about the manner in which profile calculations were performed. As far as we can determine, no treatment has been presented for the calculation of the area of interface raised by the ring, and it is the purpose of this paper to present a treatment which will allow both this calculation and also that of the area increase due to curvature of the interface at the walls of the containing vessel.

[1]*Manuscript received August 10, 1959.*
Contribution from Canadian Industries Limited, Central Research Laboratory, McMasterville, Quebec.

Can. J. Chem. Downloaded from www.nrcresearchpress.com by 176.9.209.113 on 09/04/12
For personal use only.

THEORETICAL DERIVATION OF EQUATIONS

The Laplace equation [1] can be written in the form:

$$[2] \qquad \frac{d \sin \phi}{dx} + \frac{\sin \phi}{x} = \frac{P}{\gamma}$$

where x is the horizontal distance from the center of cylindrical symmetry to any point on the surface, and ϕ is the angle that the tangent to the surface makes with the horizontal plane. Now $P = \pm g(d_2 - d_1)y$, where g is the constant of gravity (980.6 cm/sec^2), d_2 and d_1 are the densities of the two liquids under study, and y is the vertical distance from the planar contact region to the point on the surface. With $\sin \phi = u$ the equation becomes:

$$[3] \qquad \frac{du}{dx} + \frac{u}{x} = \pm\frac{g(d_2 - d_1)y}{\gamma}$$

or

$$\frac{du}{dx} + \frac{u}{x} = \pm By$$

where B is a constant for a certain interface of two fluids.

It is readily shown that the expression for the interfacial area, A, is given by

$$[4] \qquad A = 2\pi \int \frac{x dx}{\sqrt{1-u^2}}.$$

The boundary values of the integral depend on whether the area inside the ring, outside the ring, or at the wall is desired.

In equation [3] x, y, and u are interrelated variables. Hence, this equation cannot be solved unless one of the variables can be expressed explicitly as a function of the other two. The obvious choice for such an expression is:

$$[5] \qquad \frac{dy}{dx} = \pm \tan \phi = \frac{\pm u}{\sqrt{1-u^2}}.$$

The importance of this equation has only been assessed before by Lohnstein (6) who used a Taylor expansion of the expression for the calculation of profiles and volumes of drops.

The set of equations [3] and [5] can be combined into one second order differential equation with two variables.

Differentiating equation [3] with respect to x gives:

$$[6] \qquad \frac{d^2u}{dx^2} + \frac{1}{x}\frac{du}{dx} - \frac{u}{x^2} = \pm B\frac{dy}{dx}.$$

Combining [5] and [6] and rearranging terms yields:

$$[7] \qquad x^2\frac{d^2u}{dx^2} + x\frac{du}{dx} + u\left(-1 - \frac{Bx^2}{\sqrt{1-u^2}}\right) = 0.$$

This equation has the general appearance of a Bessel equation but for the awkward term $\sqrt{1-u^2}$. No solution for an equation of this type could be found in the literature, nor could we arrive at an analytical solution.

However, a numerical solution to the problem can be obtained. Bashforth and Adams

have used Taylor's theorem to calculate approximate solutions for equation [3]. We have attempted to use a more exact method to find u (and y) at distinct values of x.

Equations [3] and [5] are a set of two simultaneous first order ordinary differential equations.

For the inside of the ring the equations are:

$$\left.\begin{aligned} \frac{du}{dx} + \frac{u}{x} &= +By \\ \frac{dy}{dx} &= \frac{+u}{\sqrt{1-u^2}} \end{aligned}\right\} \quad [8]$$

outside the ring they are:

$$\left.\begin{aligned} \frac{du}{dx} + \frac{u}{x} &= -By \\ \frac{dy}{dx} &= \frac{-u}{\sqrt{1-u^2}} . \end{aligned}\right\} \quad [9]$$

At the walls of a circular vessel the set of equations [8] holds; if the vessel is flat-sided $u/x = 0$.

In each case the equations can be written:

$$\left.\begin{aligned} \frac{dy}{dx} &= f(u) \\ \frac{du}{dx} &= g(x, y, u). \end{aligned}\right\} \quad [10]$$

These equations may be solved by the Runge–Kutta method (see, e.g., ref. 7), and this method has been used in the present work.

Boundary values x_0, y_0, and u_0 for the starting point of the calculations were the values of the variables x, y, and u at the ring or wall, depending on the interfacial region being considered. In the former case x_0 is the radius of the ring; y_0 is the height to which the ring is pulled up in the interfacial tension measurements; and u_0 is the sine of the angle ϕ at the ring surface. The value of u_0 is not known in advance, but it is determined by the boundary conditions.

For the inside of the ring the calculation proceeds as follows: A value of u_0 between 0 and 1 is chosen, and the region between $x = x_0$ and $x = 0$ is divided into 10 equal intervals. Corresponding to each of these x values, values of y and u are computed. After 10 of these steps at the point where $x = 0$, i.e. the ring center, the value of u should be zero. If u does not become zero, the value chosen for u_0 is incorrect, and another value must be estimated. Usually it is not necessary to go through all 10 steps before the correctness of u_0 can be evaluated. After two or three steps u either increases again (it should decrease) or it decreases too fast. Suitable interpolation between extreme values of u_0 chosen leads to an accurate value in about six or seven estimates (accurate to four decimal places). The u value at the ring center is then usually less than ± 0.005.

Then, 11 correct values of u at 10 intervals of x are obtained and the integral in equation [4] can be evaluated numerically using a simple Simpson's one-third rule.

For the area outside the ring the calculation proceeds very similarly with the aid of equations [9], but now both y and u have to go to zero as x increases. If one of these variables becomes zero while the other remains positive, the chosen u_0 value was wrong, and another value has to be estimated. Six or seven successively closer estimates normally lead to an initial u_0 value correct to four decimal places.

Can. J. Chem. Downloaded from www.nrcresearchpress.com by 176.9.209.113 on 09/04/12
For personal use only.

For the area at the walls of a circular vessel, equations [8] are used, and the above described procedure is followed.

CALCULATIONS

Hand calculations of the equations as outlined in the preceding section would undoubtedly be a very laborious and time-consuming undertaking. The time required for the calculation of one curve for the inside of the ring, for instance, would take about six hours. However, the Runge–Kutta procedure can be handled extremely well on a digital computer. All calculations described below were performed on a Burroughs E-101 digital computer. Although this machine is relatively slow, it computed a curve inside the ring in approximately twenty-five minutes, which indicates a time saving factor of about fifteen.

The computations were carried out for a number of different parameters.

(*a*) *Various Liquids*

Benzene–water (B = 3.308) and hexane–water (B = 6.462) were studied.

(*b*) *Various Ring Sizes*

The platinum rings supplied for the du Noüy tensiometer usually have a circumference of 4 or 6 cm, corresponding to radii of 0.6366 and 0.954 cm, respectively. Alexander and Teorell (1) published results of tension measurements with a ring radius 1.501 cm. Our calculations were carried out for these three ring sizes.

(*c*) *Various Ring Heights*

The heights ($y_0 = h_2$) to which the rings are raised from the heavier liquid (water)

TABLE I

Area increase for various ring heights

	Benzene/water, B = 3.308					Hexane/water, B = 6.462				
	Inside ring			Outside ring		Inside ring			Outside ring	
h_2	u_0	y (min)	ΔA	u_0	ΔA	u_0	y (min)	ΔA	u_0	ΔA
					Ring radius 0.6366 cm					
0.3	—	—	—	—	—	0.4685	0.1654	0.0638	0.8445	0.3807
0.4	0.3613	0.2907	0.0398	0.8620	0.5288	0.6159	0.2160	0.1203	0.9648	0.7913
0.5	0.4500	0.3615	0.0641	0.9619	0.9293	0.7536	0.2614	0.2045	0.99014	1.3707
0.6	0.53755	0.4304	0.0958	0.98985	1.5321	0.8748	0.2997	0.3327	0.99514	1.8711
0.7	0.6234	0.4971	0.1408	0.99574	2.1814	0.9643	0.3273	0.5656	0.996756	2.2398
0.8	0.70665	0.5619	0.1903	0.99756	2.7708	—	—	—	—	—
					Ring radius 0.954 cm					
0.4	0.4647	0.2027	0.1372	0.8115	0.6759	0.7224	0.1173	0.3308	0.9520	0.9745
0.45	—	—	—	—	—	0.7962	0.1277	0.4367	0.9809	1.3745
0.5	0.5746	0.2513	0.2225	0.9238	1.1998	0.8623	0.1359	0.5695	0.9911	1.8381
0.55	—	—	—	—	—	0.9179	0.1445	0.7437	0.9949	2.2931
0.6	0.6797	0.2962	0.3367	0.9740	1.9607	0.95886	0.1492	0.9938	0.99662	2.7266
0.7	0.7780	0.3353	0.4893	0.98856	2.8180	—	—	—	—	—
0.8	0.8659	0.3713	0.6958	0.99332	3.5832	—	—	—	—	—
					Ring radius 1.501 cm					
0.3	—	—	—	0.6044	0.5279	0.6204	0.0339	0.3982	0.7709	0.7167
0.4	0.5537	0.0981	0.3939	0.7670	0.9470	0.7897	0.0343	0.7576	0.9231	1.4210
0.5	0.6772	0.1171	0.6396	0.8936	1.5554	0.9160	0.0375	1.3549	0.9791	2.6043
0.6	0.7887	0.1368	0.9702	0.9663	2.5498	0.97503	0.0426	2.3997	0.99101	3.8017
0.7	0.8832	0.1483	1.4317	0.9887	3.9202	0.98983	0.0454	3.5883	0.99444	4.7123
0.8	0.9512	0.1558	2.1493	—	—	—	—	—	—	—

NOTE: Heights in cm, areas in cm².

Can. J. Chem. Downloaded from www.nrcresearchpress.com by 176.9.209.113 on 09/04/12
For personal use only.

in the tension measurements are dependent upon the monolayer present at the interface. For future reference, we have compiled data for various heights (five for each set of the other parameters) from which the value for a particular measured height can be obtained by interpolation, provided the change in interfacial tension due to the presence of the monolayer is not too great. See (*ii*) under Discussion.

(*d*) *Various Elevations at the Wall*

For the same reasons as mentioned under (*c*) we proceeded with calculations at the wall, using five different heights of elevation of the interface at the vessel wall.

Typical results of profile calculations are shown in Fig. 2 for a curve outside the ring. (Tables and curves for other sets of parameters can be obtained from the authors upon request.)

The results of the area calculations are given in Tables I and II.

TABLE II

Area increase for various elevations at vessel wall

	$B = 3.308$			$B = 6.462$		
Height (cm)	u_0	Δ area (cm²)	% increase	u_0	Δ area (cm²)	% increase
0.3	0.5066	1.769	1.057	0.6890	2.618	1.564
0.4	0.6560	3.205	1.914	0.85767	5.009	2.992
0.5	0.7873	5.165	3.085	0.95715	9.205	5.498
0.6	0.8932	7.893	4.715	0.98626	15.207	9.083
0.7	0.96116	12.071	7.210	0.993004	20.465	12.224

NOTE: Vessel radius 7.30 cm.
$\Delta x = 0.146$ cm.

EXPERIMENTAL

For a particular oil/water interface there are three heights which require experimental determination for present purposes. These are the height of the interface at the wall of the vessel, h_1; and at the position of maximum pull on the ring, the height of the ring, h_2, and the lowest point of the interface drawn up inside the ring, h_3 (see Fig. 1). Heights h_1 and h_2 can be determined optically, but because of the complex

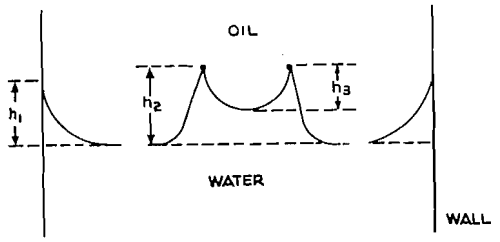

FIG. 1. Diagram showing the heights requiring experimental determination.

curvature around the ring, optical determination of h_3 appeared difficult if not impossible. After experimenting with photographic methods, the use of a cathetometer, and simple observation with a scale placed in contact with the outside wall of the vessel, it was concluded that determination of h_1 is best carried out by the simple scale method. This method can also be used fairly reliably for h_2, but in the present work the more convenient and accurate method developed for the determination of h_3 was used for

Can. J. Chem. Downloaded from www.nrcresearchpress.com by 176.9.209.113 on 09/04/12
For personal use only.

h_2 as well. This makes use of an electrical probe and depends on the fact that the electrical conductivity of distilled water is much greater than that of a hydrocarbon liquid. The device was as follows: a platinum electrode (1 cm × 1 cm) was placed in the water in the bottom of the vessel and connected through a 20-v dry cell to one terminal of

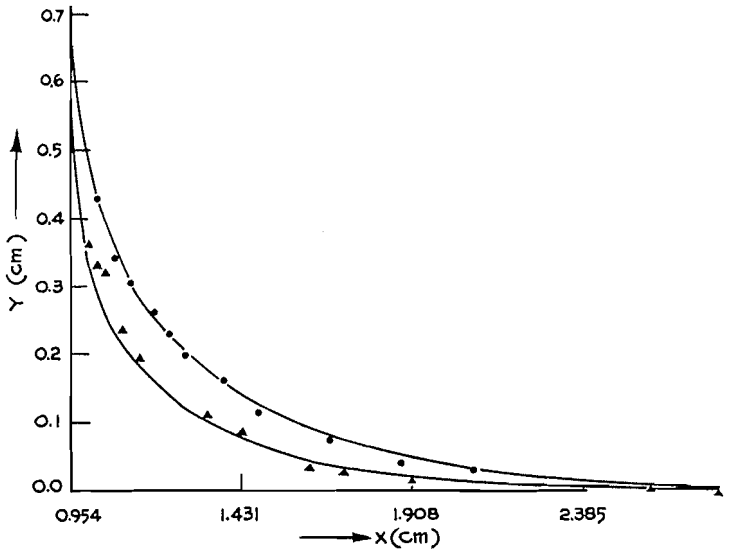

FIG. 2. Calculated and experimentally determined profiles of the interface outside the ring. The solid lines were computed. The dots are experimental points for a benzene/water interface, the triangles for a hexane/water interface.

an electrometer-type vacuum tube voltmeter (Keithley, VTVM, input impedance ca. 10^{14} Ω). A second electrode, the probe, in the form of a fine platinum wire, was connected to the other terminal of the voltmeter. The probe was attached to a micromanipulator which permitted movement in three perpendicular directions, each movement being equipped with a scale and vernier. The system was found to be very sensitive; when the probe was in the oil, no movement of the electrometer needle was detectable, but at the instant contact was made with the water interface, the instrument registered a reading of 20 v. This method was suitable not only for determining heights h_2 and h_3 but could be used for mapping the profile of the interface; this was done for the region just outside the ring, see Fig. 2.

TABLE III

	Heights (cm)		
Liquids	h_1	h_2	h_3
Benzene–water	0.68±0.04	0.72±0.02	0.40±0.02
Hexane–water	0.54±0.04	0.55±0.02	0.41±0.01

The water used in the determinations was distilled and then passed through a mixed bed ion exchange column; the organic solvents, benzene and *n*-hexane, were Fisher reagent and were distilled just before use; measured interfacial tensions against water agreed with published values. The dimensions of the Cenco platinum–iridium ring were: circumference of ring 5.998 cm, circumference of wire .1118 cm. The glass vessel used had a diameter of 14.60 cm.

The results of the determinations are given in Table III.

Can. J. Chem. Downloaded from www.nrcresearchpress.com by 176.9.209.113 on 09/04/12
For personal use only.

Can. J. Chem. Downloaded from www.nrcresearchpress.com by 176.9.209.113 on 09/04/12
For personal use only.

DISCUSSION

From Fig. 2 it can be seen that the theoretically computed and experimentally determined curves more or less coincide, so that it may be assumed that the calculated results represent the Laplace equation quite well and that any deviations will be due to experimental inaccuracies rather than to computational errors.

Computing errors that may have arisen are due to the following.

(*a*) *The Interval Size Taken*

For the region inside the ring the interval was chosen as one-tenth of the radius of the ring. In one case ($x_0 = 0.954$, $y_0 = 0.45$ cm, $B = 6.462$) the region was split up in 20 intervals, and it was found that the curve obtained was almost identical to the one obtained from the 10-interval calculation, and that the area increase was 0.4317 cm², as compared to 0.4367 cm² for the double interval size. For the region outside the ring, using the parameters, $x_0 = 0.954$, $y_0 = 0.5$, $B = 3.308$, an area increase of 1.199 cm² was calculated for the small interval computation, whereas for twice as large intervals it was 1.156 cm². Thus, the finer division only affected the corrections by 1 to 4%, i.e. about 0.04% of the total area of the interface in a vessel of radius 7.30 cm, which is quite negligible.

(*b*) *The Accuracy of the Iterated u_0 Value*

In some cases the u_0 value chosen leads to a y value of zero before u reaches zero, or vice versa, particularly at the wall of the vessel. This means that the initial u_0 value was in error by about 0.0001. The effect of such an error has been studied for one case at the wall ($x_0 = 7.30$ cm, $y_0 = 0.5$ cm, $B = 3.308$), and it was found that for $u_0 = 0.7872$ the area increase was 5.157 cm², whereas for $u_0 = 0.7874$ the area increase was 5.175 cm². For one case outside the ring ($x_0 = 0.954$, $y_0 = 0.45$, $B = 6.462$) the following results were found: for $u_0 = 0.9810$, $\Delta A = 1.3792$ cm²; for $u_0 = 0.9808$, $\Delta A = 1.3698$ cm². In both cases a difference of 0.0001 in u_0 amounted to a difference of about 0.004% of the total area.

(*c*) *The Value of B*

For a benzene–water interface the value of B was taken to be 3.308 and for a hexane–water interface 6.462 at a temperature of 18° C. These values were calculated from

$$B = \frac{g(d_2 - d_1)}{\gamma}$$

where $g = 980.6$ cm/sec², d_2 = density of water, d_1 = density of benzene or hexane, and γ is the interfacial tension; d_2 and d_1 and γ are dependent upon the temperature. For a 1° increase in temperature B(benzene) increases by about 0.6%, and B(hexane) by about 0.2%. The effect of small changes in B on the area increments has been investigated, and it was found that area increases augmented by 0.6–1.0% for benzene–water interfaces and by 0.2–0.6% for hexane–water interfaces, which indicates that the corrections expressed as a percentage of the total area amount to about 0.005–0.01% per degree for both interfaces. This may be quite a considerable correction for an operator working far outside the ordinary temperature range, but it is felt that for most purposes the correction is negligible.

Thus all possible corrections amount to a negligible change in the ΔA values given in the tables.

The corrections for oil–water interfaces can be obtained from the tables by means

of suitable interpolation for the heights h_1 and h_2 determined; e.g. for the heights observed by us with a 0.954-cm radius ring, and 167.5-cm² area dish:

Benzene–water	$h_1 = 0.68$ cm	$\rightarrow \Delta A = 11.24$	total correction 14.74 cm², i.e. 8.82%
	$h_2 = 0.72$, $h_3 = 0.40$	$\rightarrow \Delta A = 3.50$	
Hexane–water	$h_1 = 0.54$	$\rightarrow \Delta A = 11.61$	total correction 14.65 cm², i.e. 8.75%.
	$h_2 = 0.55$, $h_3 = 0.41$	$\rightarrow \Delta A = 3.04$	

These percentage increases come close to the 10% estimated by Crisp (2) for vessels of area 300 cm². It is likely that above 100 cm² the percentage increase will decrease only very slightly with increasing vessel size.

It is interesting to compare the computed values for $h_2 - h_3$ with the experimental ones. For benzene–water the values are 0.342 and 0.320, respectively, for hexane–water 0.144 and 0.140, respectively. In view of the experimental inaccuracies (see Table III) this is very satisfactory agreement.

A few points of general interest may be reported here.

(*i*) The size of the vessel can influence the elevation of the ring. For the particular vessel used by us, radius 7.30 cm, the interface at the wall curves downward to reach the planar part asymptotically. At a distance of 2.04 cm the elevation has become negligibly small. At a distance of 2.86 cm from the ring outward the elevation of the interface is negligibly small as well. As $2.04+2.86 < 7.30-0.954$, the two curves will not overlap. However, when the radius of the vessel becomes smaller than 5.85 cm, the curves will overlap, and the ring height will be affected. Thus it is advisable to use vessels of radius larger than 5.85 cm, with a ring of radius 0.954 cm.

(*ii*) If, as a result of the presence of an interfacial monolayer, the lowering of the interfacial tension becomes too great, it will no longer be permissible to use the data tabulated in this paper, as these were obtained using the capillary constant characteristic

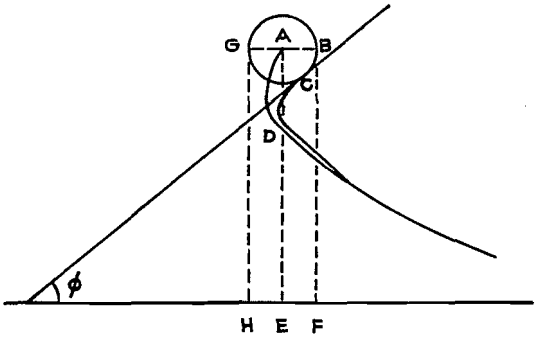

FIG. 3. Diagram illustrating the curving effect at the ring surface, for finite wire diameter (observed in experiments) and for zero wire diameter (indicated by Freud and Freud).

of the uncontaminated interface between the two liquids. For interfacial pressures up to about 5 dynes/cm, the tabulated area values would probably be acceptable for most purposes; however, in cases where the lowering of the interfacial tension is considerable, further computation using a program similar to that described in this paper, would be necessary. The measured value of the interfacial tension would be required for calculation of the constant B, see equation [3].

Can. J. Chem. Downloaded from www.nrcresearchpress.com by 176.9.209.113 on 09/04/12
For personal use only.

(*iii*) The peculiar effect found by Freud and Freud (5) that the interface at the ring can curve inwards beyond AE (see Fig. 3), cannot be explained from considerations of the Laplace equation alone. For such behavior the equation $dy = -udx/\sqrt{1-u^2}$ should yield a finite negative value for dy (AD) when dx becomes infinitely small. This can only be the case when u becomes 1 as dx goes to zero. But $u = \sin\phi$ and hence ϕ should become 90°. This in turn indicates that the tangent should be vertical, and this means that the curve cannot extend beyond AE. Also in no instance was an angle of 90° computed, i.e. u_0 was always smaller than 1.

The fact that there can be a region where the interface around the ring curves inwards beyond AE, i.e. where $\phi > 90°$, can only be explained on the basis of the finite wire diameter of the ring, a constant which has not been considered in the present treatment. Thus, if the curve starts at the point C, where the interface leaves the wire, and the contact angle is small or zero, it is apparent that the interface can curve inwards. Such curvature has in fact been observed in the present studies, but it was noted that the interface did not curve in beyond the vertical line GH.

(*iv*) The equations could have been solved with the center of symmetry as a starting point, but then the boundary value of u/x becomes doubtful. It may be assumed that the value is given by l'Hopital's rule:

$$\frac{u}{x} = \frac{B(h_2-h_3)}{2}$$

but since h_2-h_3 is even less accurate than h_2 alone, and since small errors in h_2-h_3 lead to wide spreads in the curves obtained, this method of approach was abandoned in favor of the one reported here.

ACKNOWLEDGMENT

The authors are indebted to Dr. D. C. West for helpful suggestions and comments.

REFERENCES

1. ALEXANDER, A. E. and TEORELL, T. Trans. Faraday Soc. **35**, 727 (1939).
2. CRISP, D. J. J. Colloid Sci. **1**, 49, 161 (1946).
3. THOMAS, A. G. Nature, **179**, 776 (1957).
4. BASHFORTH, F. and ADAMS, J. C. Attempt to test theories of capillary action. Cambridge University Press. 1883.
5. FREUD, B. B. and FREUD, H. Z. J. Am. Chem. Soc. **52**, 1772 (1930).
6. LOHNSTEIN, T. Ann. Physik, **20**, 237 (1906).
7. KUNZ, K. S. Numerical analysis. McGraw-Hill Book Co., Inc., New York. 1958. p. 188.

Can. J. Chem. Downloaded from www.nrcresearchpress.com by 176.9.209.113 on 09/04/12
For personal use only.

Can. J. Chem. Downloaded from www.nrcresearchpress.com by 176.9.209.113 on 09/04/12
For personal use only.

MECHANISM OF FORMATION OF ANTHOCYANIDINS FROM FLAVAN-3,4-DIOLS[1]

A. V. ROBERTSON[2]

ABSTRACT

Conversion by hydrochloric acid in 2-propanol of 5,7:3′,4′-tetramethoxyflavan-3,4-diol (I; R = OMe) into cyanidin chloride 5,7:3′,4′-tetramethyl ether is examined. The diol is wholly changed into the anthocyanidin. The over-all reaction mechanism must therefore be oxidative, since the alternative of disproportionation is excluded. Fading of this anthocyanidin in solution is studied. Attempts to synthesize flavan-3-one derivatives are briefly described.

Interest in the mechanism of conversion of flavan-3,4-diols (e.g. I; R = OH) into anthocyanidins (e.g. II; R = OH) arises from the possible biogenetic relation between natural leucoanthocyanins and anthocyanins and the need for satisfactory analytical procedures for leucoanthocyanins in plant materials. The usual qualitative test for leucoanthocyanins depends on the production of anthocyanidins by treatment with hot hydrochloric acid, and as late as 1953 the leuco-compounds had to be defined as colorless substances giving this reaction (1). Since then several leucoanthocyanins have been structurally identified as flavan-3,4-diol derivatives (2). An important feature of the chemistry of the leucoanthocyanins is that the anthocyanidins produced from them have lost the 4-hydroxyl and retained the 3-hydroxyl group, and Bauer, Birch, and Hillis suggested that the mechanism is an initial acid-catalyzed dehydration to a flavan-3-one (e.g. III) (3). The mechanism for the required direction of dehydration has been discussed by Birch for the corresponding tetrahydronaphthalenes (4). Flavan-3-ones, like flavan-3,4-diols, are in the same oxidation state as dihydroanthocyanidins so that the flavylium salt must be produced by oxidation. Over-all mechanistic possibilities are direct oxidation and disproportionation (3, 5). Production of anthocyanidins from leucoanthocyanins seems independent of the presence of oxygen in some cases, but not in others (6, 7). The reduced substance from disproportionation of a flavan-3-one would be at the catechin (e.g. IV; R = OH) level of oxidation. The detection of catechins among the products from the action of acid on cacao leucocyanidin (8) is no longer support for the disproportionation hypothesis (3, 5, 9), since Forsyth and Roberts (10) have shown that this leucoanthocyanin contains an epicatechin unit bound as a semiacetal

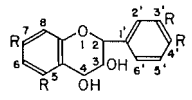

(I)

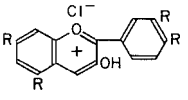

(II)

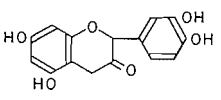

(III)

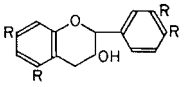

(IV)

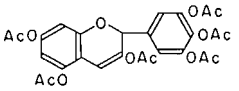

(V)

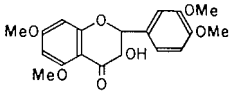

(VI)

[1]*Manuscript received July 21, 1959.*
Contribution from the Department of Organic Chemistry, University of Sydney, New South Wales.
[2]*Present address: N.I.A.M.D., National Institutes of Health, Bethesda 14, Md., U.S.A.*

Can. J. Chem. Downloaded from www.nrcresearchpress.com by 176.9.209.113 on 09/04/12
For personal use only.

to what is probably a flavan-2-ol-3-one. Roux and Bill (11) have recently obtained evidence for the initial dehydration step by demonstrating that increased yields of anthocyanidins result when treatment of several flavan-3,4-diols with acid is conducted under anhydrous conditions. The low yield of anthocyanidins from leuco-compounds is generally considered to be due to a competing reaction leading to condensed tannins. This is explicable if flavan-3-ones are intermediates for, by analogy with the naphthalene analogues (β-tetralones), they would be very unstable, polymerization occurring by aldol-type condensations of the ketone group with the phloroglucinol nucleus (3). Direct polymerization of flavan-3,4-diols can also be expected to occur by routes similar to the acid-catalyzed self-condensations of catechins, suggested mechanisms for which have been reviewed by Freudenberg and Weinges (12). Much higher yields of anthocyanidins have recently been obtained by Laumas and Seshadri (13), who first converted the flavan-3,4-diols into flav-3-en-3-ol acetates (e.g. V). In such flavan-3-one derivatives competing self-condensations are inhibited because of the lowered reactivity of the acetylated phenolic rings. Other products may also be produced by acid treatment of leucoanthocyanins, and some of these have been identified as flavonols and more highly condensed leucoanthocyanins (14, 15). The reaction is thus most complex, since different kinds and ratios of flavonoid substances can be formed depending on the precise experimental conditions and the particular leucoanthocyanin being studied.

This paper reports a study of the action of acid on the tetramethoxyflavan-3,4-diol (I; R = OMe) and of attempts to synthesize certain flavan-3-ones. Birch has briefly described some of these experiments (16).

The diol (I; R = OMe) was prepared by reduction of taxifolin tetramethyl ether (VI) with either lithium aluminum hydride or sodium borohydride. The crystalline product was considered to be a mixture of stereoisomers because of the melting range (175–190°; compare Swain (14)) of analytically pure material, and because spots of the compound on paper chromatograms were always somewhat streaked (chromatographic examination by Mr. W. E. Hillis). Ganguly and Seshadri have recently separated two isomers of m.p. 172° and 198° from this reduction (17). The proportions and ease of separation of the isomers may depend on the optical purity of the starting material as well as the exact experimental conditions. The present taxifolin tetramethyl ether had $[\alpha]_D$ −14° (2.5% in chloroform) and the recrystallized diol was optically inactive (polarimetric examination by Dr. J. W. Clark-Lewis).

The action of hydrochloric acid in 2-propanol on the diol gave cyanidin tetramethyl ether (II; R = OMe), which could be separated from the other product of the reaction, a neutral polymer, by normal partition methods. The flavylium salt was obtained as the crystalline dihydrate and its identity was proved by analysis and comparison of the ultraviolet and visible spectrum, color reactions, and paper chromatographic behavior with these properties for a synthetic specimen. The neutral by-product was reddish-purple and produced more flavylium salt on further acid treatment. The salt was separated and the neutral fraction was again heated with acid. After the third acid treatment no more anthocyanidin was formed, and the combined yield of cyanidin tetramethyl ether amounted to about 40% (percentage yields have been calculated throughout for this reaction by assuming a diol:anthocyanidin stoichiometry of 1:1). Neutral material remaining at this stage was quite intractable and attempts to prepare crystalline derivatives were unsuccessful.

The anthocyanidin is unstable under the conditions of its formation: the yield (12%) after 5 hours' refluxing with the reagent with free exposure to air was slightly lower

Can. J. Chem. Downloaded from www.nrcresearchpress.com by 176.9.209.113 on 09/04/12
For personal use only.

than that (15%) after 1 hour under the same conditions and, more significantly, the neutral fraction no longer produced a red color with acid. Production of the anthocyanidin is dependent on the presence of oxygen for only a trace (3%) was isolated after 1 hour in an atmosphere of nitrogen.

Failure to obtain more than 50% of the diol as anthocyanidin is therefore a result of decomposition of the product and not evidence for disproportionation. In any case, disproportionation would lead to one or more of the stereoisomeric catechin tetramethyl ethers (IV; R = OMe), but no evidence for their presence in the reaction products was obtained. (+)-Catechin tetramethyl ether is also unstable under the reaction conditions, but the rate of decomposition is sufficiently slow to allow isolation of the compound if it were present.

It is possible that considerably greater yields of anthocyanidin could be obtained by frequent interruption of the reaction, but such preparative experiments are tedious and lead to inaccuracies due to losses during extraction and isolation of products. Spectrophotometric examination appeared to offer a more convenient and accurate method of measuring the yield of anthocyanidin. In practice, complications arose through fading of the anthocyanidin but the results confirm the conclusion from the preparative experiments.

When the flavan-3,4-diol (I; R = OMe) was refluxed in the acid solvent in diffuse daylight, the anthocyanidin concentration at first rapidly increased but fell off as the rate of decomposition became greater than the rate of formation. The maximum intensity occurred at 30 minutes and corresponded to a 25% yield of anthocyanidin. The spectrum of the solution was recorded when the optical density at the visible absorption peak had become constant (Fig. 1, curve D). Under the same conditions pure tetramethylcyanidin gave a nearly identical spectrum (curve C). A trace of color remained in each solution after prolonged boiling. After similar treatment (+)-catechin tetramethyl ether had the spectrum shown in curve E. The spectrum of pure tetramethylcatechin closely resembles that of pure diol (I; R = OMe) (curve B). The high intensity absorption of curves C

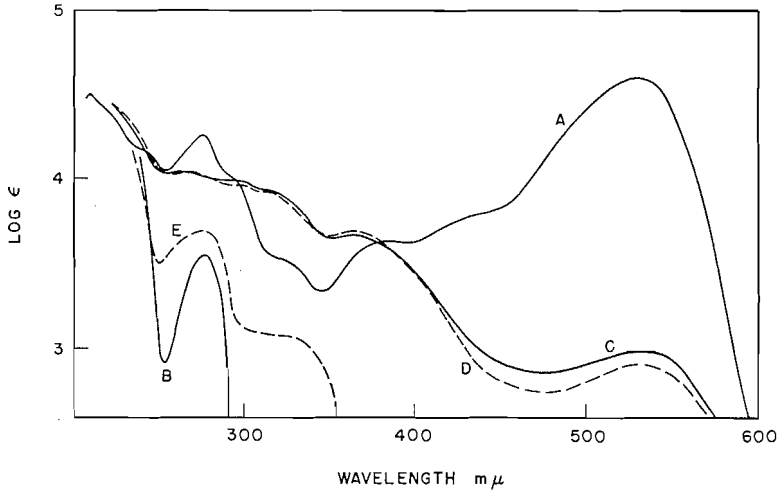

FIG. 1. (A) Tetramethylcyanidin chloride (II; R = OMe) in acidified 2-propanol. (B) Tetramethoxyflavan-3,4-diol (I; R = OMe) in ethanol. (C) (II; R = OMe) after 15 hours' refluxing in acidified 2-propanol. (D) (I; R = OMe) after 15 hours' refluxing in acidified 2-propanol. (E) Tetramethylcatechin (IV; R = OMe) after 15 hours' refluxing in acidified 2-propanol.

Can. J. Chem. Downloaded from www.nrcresearchpress.com by 176.9.209.113 on 09/04/12
For personal use only.

and D is unresolved and due to mixtures. Disproportionation of the diol into tetramethylcyanidin and tetramethylcatechin would lead to a mixture of decomposition products whose spectrum would be the sum derived from curves C and E at halved concentrations. The only reasonable conclusion from the fact that curves C and D are essentially superposable is that they represent the same mixture of decomposition products. In other words the diol must be wholly converted into anthocyanidin which then decomposes into unknown products. The possibility of any disproportionation of this flavan-3,4-diol under these conditions is clearly excluded. The conclusion from the earlier preparative scale experiments is supported: the final neutral material was largely a decomposition product of anthocyanidin already formed, and no weight should be attached to the failure to isolate more than 50% of anthocyanidin, since this value merely represents the quantity isolable when the reaction mixtures were worked up at the arbitrary times used.

The degree to which these conclusions may be extrapolated to the reactions of phenolic flavan-3,4-diol is difficult to assess. The tetramethyl ether used in the present work is deactivated towards competing side reactions such as self-condensations involving active methylene groups. Nevertheless, the yield of flavylium salt as determined spectrophotometrically may not measure the total conversion of leucoanthocyanins into anthocyanidins, and the need for blank fading experiments with the latter compounds is obvious.

It is generally known that solutions of anthocyanidins are unstable, and fade particularly under the influence of light. The phenomenon has not been studied extensively although Spaeth and Rosenblatt (18), Nordström (19), and Hillis (15) have investigated the matter in order to establish satisfactory analytical methods for anthocyanidins and leucoanthocyanins. Nordström found that solutions of cyanidin chloride (II; R = OH) in 0.1–2.0 *N* hydrochloric acid were stable in the dark at room temperature or 100°, but on 6 hours' exposure to diffuse light the intensity of color decreased by 10%, and by 95% in sunlight. Slightly less fading occurred under nitrogen. Hillis reports somewhat faster fading for 3,7,8:3′,4′-pentahydroxyflavylium chloride in acidified 2-propanol. The presence of other materials can greatly influence the rate of fading. For example, after reduction of quercetin penta-acetate in tetrahydrofuran with lithium aluminum hydride (3), a 50% yield of cyanidin chloride (compare King and White (20)) can be obtained by partition between hydrochloric acid, amyl alcohol, and light petroleum if the acidified reaction mixture is worked up immediately; when the aqueous acid fraction is left for 3 hours in diffuse light, the cyanidin chloride decomposes and leaves a light orange solution.

Cyanidin tetramethyl ether (II; R = OMe) in acidified 2-propanol was stable in the dark at room temperature. Nevertheless, at reflux temperature (80°) in darkness the color faded only slightly more slowly than at 80° in duffuse daylight. Fading was only slightly faster under oxygen and only slightly slower under nitrogen. In sunlight the anthocyanidin solution was decolorized very rapidly and the process was considerably slower under nitrogen. The rate of fading in sunlight at room temperature was faster than the rate at 80°. Cyanidin chloride and 3,7,8:3′,4′-pentahydroxyflavylium chloride behaved similarly in the above tests, but qualitative comparisons showed that the free phenols fade at a noticeably slower rate than tetramethylcyanidin chloride.

It was hoped to obtain further information about the conversion by acid of flavan-3,4-diols into anthocyanidins by examination of the properties of synthetic flavan-3-

ones. Such information has added interest in view of the recent work by Laumas and Sheshadri on flavan-3-one enol acetates (e.g. V) (13). There are few other reports of syntheses in this field. Karrer and Fatzer claimed to have prepared the flavan-3-one (VIII) by catalytic reduction of the anthocyanidin (VII) (21). Fonsenka hydrogenated

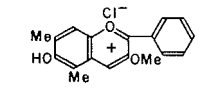

(VII)

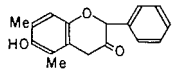

(VIII)

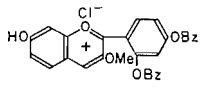

(IX)

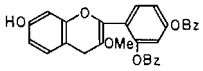

(X)

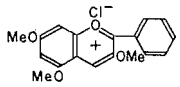

(XI)

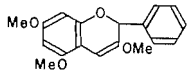

(XII)

the flavylium salt (IX) over platinum and obtained a crystalline compound to which he assigned the structure of the enol ether (X) on the basis of scanty evidence (22). Karrer and Seyhan reduced three 3-methoxyflavylium salts (e.g. XI) with lithium aluminum hydride and obtained crystalline dihydro products which were allotted structures of the corresponding flavan-3-one enol ethers (e.g. XII) (23). Elementary analysis and analogy with the reduction of quinolinium and isoquinolinium salts (24) were the only pieces of evidence used to support these formulations.

We have been unable to prepare crystalline flavan-3-ones or corresponding enol ethers. Reduction of flavylium salts (XI), (II; R = OH) and (II; R = OMe) with complex metal hydrides, hydrogen in the presence of catalysts, or combinations of these methods, gave oils or gums from which the flavylium salts were sometimes regenerated by the action of acids. Oxidative methods were also unsuccessful. The tetramethyl ethers (IV; R = OMe) of (+)-catechin and (−)-epicatechin resisted oxidation by the methods of Oppenauer and Sarett. Details of these unfruitful experiments are given below.

EXPERIMENTAL

Absorption spectra were measured with a Hilger Uvispek spectrophotometer. The term "acid reagent" is used to describe the solvent mixture 2-propanol:10 *N* hydrochloric acid (9:1).

5,7:3′,4′-Tetramethoxyflavan-3,4-diol (I; R = OMe)

Taxifolin tetramethyl ether (3.0 g) in tetrahydrofuran (100 ml) was added dropwise to a stirred slurry of lithium aluminum hydride (0.5 g) in tetrahydrofuran (50 ml) at 0°. Excess of reagent was decomposed with water after 1 hour and the mixture was poured into dilute hydrochloric acid at 0°. The mixture was immediately extracted with chloroform and after removal of solvent the slightly pink product (2.8 g) was recrystallized three times from ethanol to give the diol (I; R = OMe) as white feathery needles having m.p. 175–190° after drying *in vacuo* at 100°. (Found: C, 62.7; H, 6.3; OMe, 34.5%; *M* (Rast), 390. Calc. for $C_{19}H_{22}O_7$: C, 63.0; H, 6.1; 4OMe, 34.3%; *M*, 362.) The diol is moderately soluble in alcohol, but is very difficult to dissolve. For recrystallization it was convenient to add ethanol (50 ml) to a solution of the compound (1 g) in hot acetone (10 ml) and reduce the volume to 30 ml by boiling.

Can. J. Chem. Downloaded from www.nrcresearchpress.com by 176.9.209.113 on 09/04/12
For personal use only.

Can. J. Chem. Downloaded from www.nrcresearchpress.com by 176.9.209.113 on 09/04/12
For personal use only.

5,7:3′,4′-Tetramethylcyanidin Chloride (II; R = OMe)

Karrer and his co-workers (25) claimed to have prepared this compound by methylation of cyanidin, but Hayashi (26) obtained a compound having different properties by condensation of the appropriate phloroglucinaldehyde and acetophenone derivatives. Hayashi's work has been substantiated in this laboratory and, as his paper was available only in abstract, the synthesis is reported in full.

Phloroglucinaldehyde 2,4-dimethyl ether was prepared from phloroglucinol dimethyl ether (27), by the method of Gruber (28). ω-Acetoxyacetoveratrone (29) was prepared from acetoveratrone (30) via ω-bromoacetoveratrone (31). A solution of phloroglucinaldehyde 2,4-dimethyl ether (2.7 g) and ω-acetoxyacetoveratrone (3.6 g) in ethyl acetate (50 ml) and ethanol (10 ml) was saturated at 0° with hydrogen chloride and left in the refrigerator. Three days later the precipitate (2.5 g) was collected, recrystallization from ethanol:10 *N* hydrochloric acid (1:1) giving cyanidin tetramethyl ether dihydrate, after drying to constant weight *in vacuo* at room temperature, as red-brown microcrystals having a golden luster. (Found: C, 55.0, 55.0; H, 5.5, 5.6; Cl, 8.5; OMe, 25.1, 24.8; MeCO, 0. Calc. for $C_{19}H_{19}O_6Cl.2H_2O$: C, 55.0; H, 5.6; Cl, 8.6; 4OMe, 29.9%.) Light absorption in ethanol:10 *N* hydrochloric acid (9:1): λ_{max} 209 (log ε 4.50), 276 (4.25), 381 (3.63), and 532 mμ (4.59). Dilution with ether of the mother liquors from the reaction mixture gave further crude flavylium salt (2 g). Attempts to prepare the anhydrous anthocyanidin by drying the dihydrate *in vacuo* at elevated temperatures were unsuccessful owing to general decomposition. The pure dihydrate sintered at 140°, softened at 170°, but was not completely molten until 200° (decomp.), on a Kofler block. The structure of the compound was confirmed by reduction to tetramethylepicatechin.

(±)-*Epicatechin 5,7:3′,4′-Tetramethyl Ether*

Tetramethylcyanidin chloride dihydrate (0.41 g) in ethanol (30 ml) was hydrogenated at room temperature and pressure over platinum black (0.3 g). When reduction was complete (1 hour), the catalyst was removed and the filtrate was evaporated at reduced pressure. The residue, dissolved in ether, was washed with aqueous sodium hydroxide and water. Removal of the ether left a light yellow gum (0.35 g) which was chromatographed in benzene on alumina. Elution with benzene:ether (4:1) gave (±)-epicatechin 5,7:3′,4′-tetramethyl ether (0.118 g, 34%) which after recrystallization from aqueous methanol had m.p. 136–139°. (Found: C, 65.7; H, 6.4. Calc. for $C_{19}H_{22}O_6$: C, 65.9; H, 6.4%.) The infrared absorption spectra in Nujol of the (±)-compound and authentic (−)-epicatechin tetramethyl ether showed an exact correspondence.

Stability of 5,7:3′,4′-(+)-Catechin Tetramethyl Ether to Acid Reagent

Tetramethylcatechin (50 mg) was refluxed for 1 hour in acid reagent (25 ml). The colorless solution was evaporated to dryness under reduced pressure and the partly crystalline residue was chromatographed in benzene on alumina. Elution with benzene–ether (4:1) gave starting material (27.5 mg, 55% recovery).

Reactions of Flavan-3,4-diol (I; R = OMe) *with Acid Reagent*

A typical experiment is described. The flavandiol (200 mg) was dissolved in boiling 2-propanol (90 ml) in a flask shaded from direct light, and concentrated hydrochloric acid (10 ml) was added. An immediate red coloration was observed which became more intense as the solution was refluxed (1 hour). Most of the solvent was removed *in vacuo* and, after addition of amyl alcohol (10 ml) and light petroleum (100 ml; b.p. 60–80°), the flavylium salt was extracted into 2 *N* hydrochloric acid (4×25 ml). The antho-

cyanidin (35 mg, 15%) was purified by further partitioning in the usual way between amyl alcohol, light petroleum, and dilute hydrochloric acid, and was finally obtained as the dihydrate of tetramethylcyanidin (II, R = OMe) by crystallization and drying as for the synthetic sample above. (Found: C, 55.4; H, 5.6; Cl, 9.0.) The light absorption, color reactions, and paper chromatographic behavior were identical with those for the synthetic specimen; R_F 0.69 in 2 *N* hydrochloric acid:acetic acid (7:3) (lit., (14) 0.62), and 0.93 in water:acetic acid:10 *N* hydrochloric acid (10:30:3) (lit., (19) 0.82). The material that remained in the first light petroleum layer was a reddish-purple amorphous solid (160 mg) which yielded further flavylium salt on repetition of the above treatment. The neutral fraction (125 mg) which was separated still furnished tetramethylcyanidin, but after a third treatment as above the neutral fraction (93 mg) gave no red color on heating with the acid reagent. It was a brown gum which resisted crystallization and could not be purified by chromatography on alumina, or by acetylation. The total yield of crude flavylium salt was 88 mg. Other reactions with slight experimental modifications gave much the same results. In one experiment, the neutral fraction after the first hour's heating was chromatographed, but no crystalline compounds were obtained. When the initial heating was continued for 5 hours, 12% of anthocyanidin was isolated, but the dark neutral fraction no longer gave a red color on heating with the acid reagent. When a moderate stream of oxygen was passed through the reaction mixture the yield of anthocyanidin in 1 hour was 18%. Under purified nitrogen, the yield in 1 hour was 3% in either a sealed flask, or with a stream of gas through the solution; the solvents in each case were freed from oxygen by refluxing for 1 hour with passage of purified nitrogen before the diol was added.

Spectrophotometric and Fading Experiments

Beer's law was valid within ±2% for cyanidin tetramethyl ether over the range of optical densities 0.1–2.0 at the visible absorption peak. The reactions with tetramethyl cyanidin, the diol (I; R = OMe), and tetramethylcatechin were performed by refluxing 1- to 2-mg samples, accurately weighed, in 40 ml of acid reagent. The volumes were finally made up to 50 ml to eliminate solvent evaporation errors. Log ϵ values of decomposition products were calculated using molar concentrations of starting materials. The rate of fading of refluxing tetramethylcyanidin solution in diffuse daylight was: 40% in 1 hour; 60% in 2 hours; 70% in 3 hours; 90% in 6 hours; and 98% in 12 hours. The last trace of color remained even after the solution was heated a further 12 hours. In sunlight, the anthocyanidin solution in a pyrex tube was completely decolorized in 20 minutes at room temperature and 45 minutes at reflux temperature. When oxygen was passed through the cold solution in sunlight fading was complete in 6 minutes, but under nitrogen 80 minutes were required.

Reduction of Anthocyanidins

Karrer and Seyhan prepared the enol ether (XII) by treating a suspension of 3,5,7-trimethoxyflavylium chloride (XI) (27) in ether with lithium aluminum hydride (23). In our hands no reaction occurred under these conditions, presumably because of the complete insolubility of the anthocyanidin which was recovered by acid extraction and the usual partition methods after decomposing the excess of reagent. The anthocyanidin was soluble in tetrahydrofuran, but numerous reduction experiments with lithium aluminum hydride gave yellow or red oils which resisted crystallization and which darkened rapidly on exposure to air. Treatment of these oils with aqueous or alcoholic hydrochloric acid, or acetic acid gave the original flavylium salt having R_F 0.80 in 2 *N* hydrochloric acid:acetic

Can. J. Chem. Downloaded from www.nrcresearchpress.com by 176.9.209.113 on 09/04/12
For personal use only.

acid (7:3). Color developed after a few minutes in the cold and very rapidly on heating. These properties were not changed under nitrogen. 3,5,7-Trimethoxyflavylium ferrichloride was formed when the oils were treated with anhydrous ferric chloride in glacial acetic acid. The compound had m.p. 176–178° (lit., (27) 174°) after recrystallization from acetic acid. (Found: C, 43.8; H, 3.2. Calc. for $C_{18}H_{17}O_4Cl_4Fe$: C, 43.7; H, 3.4%.) The melting point was not depressed by admixture with an authentic specimen. Similar oils were obtained when the anthocyanidin in tetrahydrofuran was reduced with sodium borohydride in water. When the flavylium salt in ethanol was treated with sodium borohydride in water, 3,5,7-trimethoxyflavylium pseudo base ethyl ether was obtained as white prisms of m.p. 90–91° after recrystallization from aqueous alcohol. (Found: C, 69.4; H, 6.4. $C_{20}H_{22}O_5$ requires C, 70.2; H, 6.5%.) This compound regenerated the anthocyanidin (XI) immediately with cold acid.

At room temperature and pressure, solutions in ethanol of flavylium salts (XI), (II; R = OH) and (II; R = OMe), were decolorized by 1 mole of hydrogen over Adam's catalyst or platinum black, but only unstable red gums were isolated. An attempt to provide evidence for the fugitive existence of the flavan-3-ones from cyanidin and tetramethylcyanidin was made by adding sodium borohydride to solutions in ethanol which had absorbed 1 mole of hydrogen over platinum and then been neutralized. Only dark amorphous material was isolated even after acetylation or methylation, and no indication of the presence of catechin derivatives was obtained.

Attempted Oxidation of Catechins

(+)-Catechin 5,7:3′,4′-tetramethyl ether (1 g) was unchanged after being refluxed (40 hours) with aluminum isopropoxide (2 g) and cyclohexanone (5 ml) in toluene (50 ml). The tetramethyl ether (1 g) in pyridine (10 ml) was treated with chromic oxide (1 g) in pyridine (10 ml) according to the method of Sarett and his co-workers (32). The substance isolated (0.7 g) was starting material. (−)-Epicatechin 5,7:3′,4′-tetramethyl ether behaved similarly toward these reagents; no ketonic fraction was obtained when the material isolated was treated in each case with Girard P reagent.

ACKNOWLEDGMENTS

I am indebted to Professor A. J. Birch and Dr. E. Ritchie for advice; to Monsanto Chemicals (Australia) Ltd. for the award of a scholarship; and to Dr. E. F. Kurth, Dr. W. G. C. Forsyth, and Mr. W. E. Hillis for samples of natural taxifolin, epicatechin, and catechin respectively. Microanalyses were performed by Miss B. Stevenson and the C.S.I.R.O. Microanalytical Service.

REFERENCES

1. Bate-Smith, E. C. J. Exptl. Botany, **4**, 1 (1953).
2. Clark-Lewis, J. W. and Roux, D. G. J. Chem. Soc. 1402 (1959).
3. Bauer, L., Birch, A. J., and Hillis, W. E. Chem. & Ind. 433 (1954).
4. Birch, A. J. Ann. Repts. on Progr. Chem. **47**, 184 (1950).
5. King, F. E. and Bottomley, W. J. Chem. Soc. 1399 (1954).
6. Swain, T. and Bate-Smith, E. C. The chemistry of vegetable tannins. Society of Leather Trades' Chemists, Cambridge Symposium, 1956. p. 114.
7. Hillis, W. E. J. Soc. Leather Trades' Chemists, **38**, 91 (1954).
8. Forsyth, W. G. C. Nature, **172**, 726 (1953).
9. King, F. E. and Clark-Lewis, J. W. J. Chem. Soc. 3387 (1955).
10. Forsyth, W. G. C. and Roberts, J. B. Chem. & Ind. 755 (1958).
11. Roux, D. G. and Bill, M. C. Nature, **183**, 42 (1959).
12. Freudenberg, K. and Weinges, K. Fortschr. Chem. org. Naturstoffe, **16**, 1 (1958).
13. Laumas, K. R. and Seshadri, T. R. Proc. Indian Acad. Sci. A, **49**, 47 (1959).
14. Swain, T. Chem. & Ind. 1144 (1954).
15. Hillis, W. E. Australian J. Biol. Sci. **9**, 269 (1956).

Can. J. Chem. Downloaded from www.nrcresearchpress.com by 176.9.209.113 on 09/04/12
For personal use only.

16. BIRCH, A. J. Fortschr. Chem. org. Naturstoffe, **14**, 210 (1957).
17. GANGULY, A. K. and SESHADRI, T. R. Tetrahedron, **6**, 21 (1959).
18. SPAETH, E. C. and ROSENBLATT, D. H. Anal. Chem. **22**, 1321 (1950).
19. NORDSTRÖM, C. G. Acta Chem. Scand. **10**, 1491 (1956).
20. KING, H. C. G. and WHITE, T. J. Chem. Soc. 3901 (1957).
21. KARRER, P. and FATZER, W. Helv. Chim. Acta, **25**, 1129 (1942).
22. FONSENKA, E. L. J. Chem. Soc. 1683 (1947).
23. KARRER, P. and SEYHAN, M. Helv. Chim. Acta, **33**, 2209 (1950).
24. SCHMIDT, H. and KARRER, P. Helv. Chim. Acta, **32**, 960 (1949).
25. KARRER, P., WIDMER, R., HELFENSTEIN, A., HURLIMAN, W., NIEVERGELT, O., and MONSARRAT-THOMS, P. Helv. Chim. Acta, **10**, 729 (1927).
26. HAYASHI, K. Acta Phytochim. (Japan), **8**, 65 (1934); Chem. Abstr. **29**, 1251 (1935).
27. PRATT, D. D. and ROBINSON, R. J. Chem. Soc. 188 (1924).
28. GRUBER, W. Ber. **76**, 135 (1943).
29. KAUFMANN, A. and MULLER, H. Ber. **51**, 123 (1918).
30. KOEPFLI, J. B. and PERKIN, W. H. J. Chem. Soc. 2995 (1928).
31. MANNICH, C. and HAHN, F. L. Ber. **44**, 1549 (1911).
32. POOS, G. I., ARTH, G. E., BEYLER, R. E., and SARETT, L. H. J. Am. Chem. Soc. **75**, 422 (1953).

Can. J. Chem. Downloaded from www.nrcresearchpress.com by 176.9.209.113 on 09/04/12
For personal use only.

Can. J. Chem. Downloaded from www.nrcresearchpress.com by 176.9.209.113 on 09/04/12
For personal use only.

THE SYNTHESIS OF 5-*O*-METHYL-L-ARABINOSE[1]

G. G. S. DUTTON, Y. TANAKA, AND K. YATES

ABSTRACT

5-*O*-Methyl-L-arabinose is thought to occur in the hydrolysis products of methylated wheat bran hemicellulose. This sugar has now been synthesized from ethyl 2,3-di-*O*-acetyl-5-*O*-trityl-α-L-arabinoside by detritylation, methylation, and hydrolysis. The free sugar was obtained as a sirup and was characterized by periodate oxidation together with the preparation of a crystalline osazone and a crystalline lactone.

In 1955 Adams (1) reported the probable occurrence of 5-*O*-methyl-L-arabinose, together with another monomethylarabinose, in the hydrolysis products of methylated wheat bran hemicellulose. It was not possible to separate these compounds and no constants for 5-*O*-methyl-L-arabinose were available so that positive identification was not possible.

We have now synthesized this compound from L-arabinose diethylmercaptal in 16% over-all yield by the following series of reactions:

L-arabinose diethyl mercaptal (I) → ethyl α-L-arabofuranoside (II) → ethyl 2,3-di-*O*-acetyl-5-*O*-trityl-α-L-arabinoside (III) → ethyl 2,3-di-*O*-acetyl-α-L-arabinoside (IV) → ethyl 2,3-di-*O*-acetyl-5-*O*-methyl-α-L-arabinoside (V) → 5-*O*-methyl-L-arabinose (VI).

Tritylation and acetylation of (II), which was readily obtained from (I) by the action of ethanol, mercuric chloride, and mercuric oxide, afforded (III) in high yield as a sirup. Although detritylation of (III) with hydrogen bromide in acetic acid was not satisfactory and gave positively rotating sirups the use of 80% acetic acid gave (IV) in high yield. Two treatments with Purdie's reagents gave a sirup which showed no hydroxyl band in the infrared. Successive hydrolyses with alkali and acid gave a sirup which showed a strong *p*-anisidine positive spot with R_f 0.30 (butanone–water azeotrope) and several weak spots which were not further examined. By chromatography on a column of cellulose–hydrocellulose (2) the component of R_f 0.30 was obtained pure.

A sample of this compound was oxidized with sodium metaperiodate and rapidly consumed 3 moles of periodate yielding 3 moles of formic acid. These results can be expected only from the 5-*O*-methyl derivative. Confirmation of this structure was obtained from the infrared spectrum of the lactone obtained by bromine oxidation. It has been reported that γ-lactones of aldonic acids show their C=O band in the range of 5.59–5.68 μ while for δ-lactones this is in the range of 5.68–5.79 μ (3). The C=O band of our mono-*O*-methyl-L-arabonolactone was at 5.62 μ, in agreement with the assigned structure of 5-*O*-methyl-L-arabinose. This was further supported by the fact that the lactone showed no change in rotation in aqueous solution after 20 hours.

It may be noted that the 5-*O*-methyl ether has a much higher R_f value than the corresponding 2-*O*-methyl derivative and that this is consistent with sugars which can only exist in the furanose form. Although sugar acetates may undergo acetyl migration even in the presence of such a weak base as silver oxide (4, 5) there was no indication of such migration in the preparation described here. It is obvious that this preparation might be shortened

[1]*Manuscript received June 22, 1959.*
Contribution from the Department of Chemistry, University of British Columbia, Vancouver, British Columbia. Presented at the 136th American Chemical Society meeting in Atlantic City, New Jersey, September, 1959.

by starting from an equilibrium mixture of arabofuranosides but we preferred to use a pure anomeric form in the hope that any intermediates would be crystalline. This hope was not realized. The ethyl furanoside was preferred to the methyl because of the hygroscopic nature of the latter (6, 7).

The related 2- and 3-*O*-methyl-L-arabinoses have been known for some time and only the 4-isomer remains to be synthesized.

EXPERIMENTAL

Ethyl α,L-Arabofuranoside (6)

L-Arabinose diethylmercaptal (4.90 g) was shaken for 4 hours at room temperature in absolute ethanol (50 ml) with mercuric chloride (11 g), yellow mercuric oxide (4.7 g), and drierite (1.5 g). The inorganic salts were removed by filtration and the filtrate was concentrated *in vacuo* to sirup. The sirup was dissolved in chloroform (60 ml) to remove inorganic salts and evaporation of the solution gave a light yellow sirup (3.05 g, 90%) which crystallized slowly on standing after seeding. R_f values of the sirup were 0.042 (very weak), 0.386 (very weak), and 0.543 (strong) (butanone–water azeotrope). M.p. 66–69° C, $[\alpha]_D^{25}$ −114.1° (*c*, 0.918 in water). Lit. (6) m.p. 68–69° C, $[\alpha]_D^{20}$ −116.0° (*c*, 7.055 in water).

Ethyl 2,3-Di-O-acetyl-5-O-trityl-α,L-arabinoside (8)

Ethyl α,L-arabofuranoside (3.05 g, 0.0172 mole) was dissolved in dry pyridine (20 ml) and the solution was kept at room temperature for 24 hours after addition of trityl chloride (5.25 g, 0.0188 mole). During this period pyridine hydrochloride precipitated out of the solution. Acetic anhydride (20 ml) was added and the solution was kept at room temperature for a further 24 hours. The acetylated solution was poured into ice water and extracted with chloroform (20 ml × 5). The chloroform solution was washed with aqueous sodium bicarbonate solution, washed with water, dried over anhydrous sodium sulphate, and evaporated *in vacuo* to give a yellow sirup (8.30 g, 96%), $[\alpha]_D^{25}$ −82.9° (*c*, 0.362 in chloroform).

Ethyl 2,3-Di-O-acetyl-α,L-arabinoside (8)

To ethyl 2,3-di-*O*-acetyl-5-*O*-trityl-α,L-arabinoside (8.30 g) were added water (62 ml) and glacial acetic acid (250 ml) and the mixture was heated for 1 hour in boiling water. The solution was concentrated *in vacuo* to give a mixture of tritanol and yellow sirup. The mixture was dissolved in chloroform (10 ml) and adsorbed on an alumina column (3.5×20 cm) which was washed with benzene. Tritanol was eluted first with benzene (800 ml) and the detritylated compound was eluted with chloroform (1500 ml). Evaporation of the eluate gave a yellow sirup (3.59 g, 83%) $[\alpha]_D^{25}$ −58.8° (*c*, 0.218 in chloroform). Lit. (8) $[\alpha]_D^{20}$ −30° (*c*, 1.7 in chloroform). Infrared spectrum of the sirup showed complete lack of aromatic character.

Ethyl 2,3-Di-O-acetyl-5-O-methyl-α,L-arabinoside

Ethyl 2,3-di-*O*-acetyl-α,L-arabinoside (3.59 g) and drierite (5 g) were stirred under reflux in methyl iodide (50 ml) for 6 hours. Silver oxide (10 g) was added in 10 portions at about 30-minute intervals. Excess methyl iodide was removed by distillation and the residue was extracted five times with 50 ml each of chloroform. Evaporation of the solvent gave a yellow sirup (2.99 g).

The procedure was repeated again under the same conditions and the yellow sirup (2.48 g, 65.5%), $[\alpha]_D^{25}$ −49.0° (*c*, 0.306 in chloroform), showed no free hydroxyl band on the infrared spectrum.

Can. J. Chem. Downloaded from www.nrcresearchpress.com by 176.9.209.113 on 09/04/12
For personal use only.

Can. J. Chem. Downloaded from www.nrcresearchpress.com by 176.9.209.113 on 09/04/12
For personal use only.

Hydrolysis of Ethyl 2,3-Di-O-acetyl-5-O-methyl-α,L-arabinoside

Ethyl 2,3-di-*O*-acetyl-5-*O*-methyl-α,L-arabinoside (2.48 g) was heated in a mixture of 2 *N* sodium hydroxide (20 ml), water (20 ml), and methanol (40 ml) for 1 hour in boiling water, and then neutralized with IR-120 resin (Rohm and Haas). The neutral solution was concentrated *in vacuo* to a volume of 65 ml and 1 *N* hydrochloric acid (65 ml) was added. The mixture was heated in boiling water and the hydrolysis was followed polarimetrically. The initial rotation (−1.440° in 1-dm tube) changed after 4 hours to a constant value (−0.155° in 0.5-dm tube). The acidic solution was neutralized with Duolite A-4 resin (Chemical Process Co.) and then concentrated *in vacuo* to a sirup (1.10 g, 74%). Paper chromatography (butanone–water azeotrope) of the sirup showed a strong spot of R_f 0.30 and weak spots of R_f's 0.64, 0.53, 0.22, and 0.12.

Separation of 5-O-Methyl-L-arabinose by Chromatography

The hydrolysis product (1.1 g) was dissolved in methanol (2 ml) and was chromatographed on a cellulose–hydrocellulose column (3×40 cm) using butanone–water azeotrope as developing solvent (rate of flow, 10 ml/30 minutes). Each fraction (10 ml) was checked by paper chromatography. In tubes No. 13–23 a compound with R_f 0.30 was found with others having R_f 0.64 and R_f 0.53, but in tubes No. 24–40 only the compound with R_f 0.30 was observed. On evaporation of the fractions No. 24–40 a colorless sirup (387 mg) was obtained. Rechromatography of fractions No. 13–23 under the same conditions gave a further quantity of sirup (120 mg). Both were chromatographically pure (R_f 0.30) and the total yield of the sirup was 507 mg (46%). Anal. calc. for $C_6H_{12}O_5$: OMe, 18.9%. Found: OMe, 18.8, 19.0%. $[\alpha]_D^{25}$ −32.0° (*c*, 0.484 in water). The R_f value in butan-1-ol–ethanol–water–ammonia (40:11:19:1) was 0.48.

Periodate Oxidation of 5-O-Methyl-L-arabinose

All reactions were carried out in the dark and at 5° C.

(*i*) *Determination of periodate consumed.*—5-*O*-Methyl-L-arabinose (7.5 mg) was dissolved in water (10 ml), and 0.23 *M* sodium metaperiodate solution (1 ml) was added to the solution. A blank was run concurrently. Aliquot portions (1 ml) were withdrawn at intervals and the consumption of periodate was determined by means of the arsenite method (8). The results are shown in Table I.

(*ii*) *Estimation of formic acid produced.*—After reacting overnight, an aliquot was titrated with 0.01 *N* sodium hydroxide solution using methyl red as an indicator. The results are shown in Table I.

TABLE I

Periodate oxidation of the mono-*O*-methyl-L-arabinose

	Periodate consumption					Formic acid production
Time, hour	0	1	2	3	Overnight	Overnight
Moles	1.97	2.68	2.70	2.86	2.86	3.09

5-O-Methyl-L-arabinose Phenylosazone

5-*O*-Methyl-L-arabinose (111 mg) was dissolved in 20% acetic acid (5 ml), and sodium bisulphite (110 mg) and phenylhydrazine (1 ml) were added. The solution was kept for 1 hour at 80° C and then at room temperature overnight. The precipitated yellow crystals (50 mg) were filtered and recrystallized from aqueous acetone, m.p. 154.5°, $[\alpha]_D^{25}$ −16.6°

(*c*, 0.4 in methanol). Dilution of the filtrate with water gave a further 70 mg of the crystals which showed m.p. 154.5° after recrystallization from aqueous acetone. Total yield of the phenylosazone was 120 mg (52%). Anal. calc. for $C_{18}H_{22}O_3N_4$: C, 63.1; H, 6.5; N, 16.4; OMe, 9.1%. Found: C, 62.9; H, 6.4; N, 16.3, 16.6; OMe, 9.0, 9.2%. (C, H, and N by Drs. Weiler and Strauss, Oxford).

*5-O-Methyl-*L*-arabonolactone*

5-*O*-Methyl-L-arabinose (120 mg) was dissolved in water (2 ml) and kept at room temperature in the dark, after addition of bromine (10 drops). The oxidation was complete after 30 hours (paper chromatography) and water (10 ml) was added. Excess bromine was removed by aeration, and the solution was treated with silver carbonate and centrifuged. After hydrogen sulphide was passed through the solution and after centrifugation, the solution was concentrated *in vacuo* to dryness to give a solid (77 mg) which by recrystallization from acetone–petroleum ether gave colorless needles, m.p. 135° C, $[\alpha]_D^{25}$ −76.2° (*c*, 0.22 in water) (no change after 20 hours); $[\alpha]_D^{25}$ −43.7° (*c*, 0.27 in acetone); γ Nujol max. 5.62 μ. Anal. calc. for $C_6H_{10}O_5$: OMe, 19.2%. Found: OMe, 19.1, 19.3%.

ACKNOWLEDGMENTS

The financial support of the National Research Council is gratefully acknowledged. We wish to thank Dr. F. Smith for a gift of ethyl α-L-arabofuranoside.

REFERENCES

1. Adams, R. A. Can. J. Chem. **33**, 56 (1955).
2. Geerdes, J. D., Lewis, B. A., Montgomery, R., and Smith, F. Anal. Chem. **26**, 264 (1954).
3. Baker, S. A., Bourne, E. J., Pinkard, R. M., and Whiffen, D. H. Chem. & Ind. 658 (1958).
4. Whistler, R. L. and Kazeniac, S. J. J. Am. Chem. Soc. **76**, 5812 (1954).
5. Bouveng, H. O., Lindberg, B., and Theander, O. Acta Chem. Scand. **11**, 1788 (1957).
6. Green, J. W. and Pacsu, E. J. Am. Chem. Soc. **60**, 2056 (1938).
7. Augestad, I. and Berner, E. Acta Chem. Scand. **8**, 251 (1954).
8. Goldstein, I. J., Smith, F., and Srivastava, H. C. J. Am. Chem. Soc. **79**, 3858 (1957).
9. Jackson, E. L. Organic reactions. Vol. 2. John Wiley & Sons, Inc., New York. 1944. p. 341.

Can. J. Chem. Downloaded from www.nrcresearchpress.com by 176.9.209.113 on 09/04/12
For personal use only.

Can. J. Chem. Downloaded from www.nrcresearchpress.com by 176.9.209.113 on 09/04/12
For personal use only.

TRANSFERENCE NUMBERS AND CONDUCTANCES IN CONCENTRATED SOLUTIONS: SILVER NITRATE AND SILVER PERCHLORATE AT 25.00° C[1]

A. N. Campbell and K. P. Singh[2]

ABSTRACT

The transference numbers, equivalent conductances, densities, and viscosities of aqueous solutions of silver nitrate and of silver perchlorate have been determined from a concentration of 0.1 *M* up to 7.6 *M*, for silver nitrate, and up to 5.6 *M* for silver perchlorate. In both cases the cation transference number increases considerably with increasing concentration. Certain anomalies in the results for silver perchlorate raise the possibility of complex ion formation here. Similar anomalies appear in the behavior of equivalent conductance with respect to concentration.

The results of the conductance measurements have been compared with the values calculated from the equations of Wishaw and Stokes and of Falkenhagen and Leist.

Little experimental work has been done on transference numbers in concentrated solution. Elementary textbooks make such statements as, "They [transference numbers] vary somewhat with concentration, but the variation is in general not large. As a rule, the transference numbers that are large in dilute solution increase with rise in concentration, while those which are small decrease." (1). This statement seems to rest principally on the results of Longsworth, which extend only to a concentration of 0.2 *M* (2); a few results from other sources extend to 1.0 *M*. Apart from the present work, the only references to work in really concentrated solutions are those of Stokes and Levien (3), who determined the transference numbers of the ions of zinc perchlorate, by the E.M.F. method, between the concentration limits 0.1 *M* to 4 *M*; of Lee and Millen (4), who determined the data for nitric acid, between the concentrations 0.1 *M* to 1.8 *M*, by a form of the Hittorf method; and Fritz and Fuget (5), who measured the transference numbers of copper sulphate, by the moving boundary method, between 0.1 and 0.5 *M*.

EXPERIMENTAL

Two years of work with the moving boundary method, using both sheared and autogenic boundaries, and both rising and falling boundaries, convinced us that this method is not suitable for measurements in concentrated solution. The E.M.F. method rests on a not completely satisfactory theoretical basis and, in any case, for accurate results calls for a very high degree of precision in E.M.F. measurements. We were therefore forced to make use of the Hittorf method.

It is sometimes claimed that the Hittorf method cannot be used in concentrated solution because the relative change of concentration becomes inappreciable with respect to the high concentration of electrolyte. This statement, however, is the result of careless thinking. It would be true if the same cell were used both for dilute and concentrated solutions. In dilute solutions, it is true that anode and cathode compartments must be relatively large, and widely separated, in order to preserve the necessary constancy of concentration in the middle compartment. If, however, one considers the well-known equation used in determining transference numbers by the moving boundary method, viz.

$$t_+ = (V \times C \times F)/1000\,Q$$

[1]*Manuscript received July 24, 1959.*
Contribution from the Department of Chemistry, University of Manitoba, Winnipeg, Manitoba.
[2]*N.R.C. Postdoctorate Fellow, 1957–59.*

and solves this for V, the volume swept out by the moving boundary, i.e.

$$V = t_+ 1000\, Q/CF,$$

one sees that for a fixed Q the volume through which the boundary moves is inversely proportional to the concentration of the electrolyte. It is therefore only necessary to reduce the volumes of anode and cathode chambers as the concentration increases, in order to preserve constant the relative change in concentration. We therefore built Hittorf cells with smaller and smaller chambers. A limit is of course set to this by the necessity of having a chamber sufficiently large to hold the electrode. About 8 ml was the smallest volume of electrode chamber used by us.

Other modifications of the usual method were as follows: Since the coulometer has been virtually abandoned as an instrument for measuring quantity of electricity in the moving boundary method, we saw no reason for retaining what is in practice a rather clumsy instrument. When working with the moving boundary method we were accommodated, thanks to the kindness of Dr. G. Ballard and his associates of the National Research Council, with a constant current source which yielded constant current (maximum variation equal to $\pm 0.02\%$) within the limits 1.5 ma to 15 ma, the potential at the same time altering between 1 and 500 v. Time was measured by means of a railway watch, whose maximum variation was 15 seconds in a week. In short, our determination of the quantity $Q = Ct$ is practically without error. In some of our experiments, the experiment continued as long as 20 hours. In all cases, the central compartment was analyzed and absence of change there demonstrated.

As a means of analysis we used the specific conductance. The contents of the anode and cathode chambers were run into separate containers and weighed and the specific conductance determined. As a preliminary, curves of specific conductance versus concentration were determined, for silver nitrate and for silver perchlorate. Since it was now only necessary to determine, in addition to the above data, the density of the solutions, in order to obtain the equivalent conductance, this was done. It should be added that anode and cathode chambers were washed out and titrated with potassium thiocyanate to determine the silver salt adhering to the walls of the chamber.

While the measurements with silver nitrate were pushed with ease up to a concentration of 7.640 molar, great discrepancies at first appeared in our results for silver perchlorate. These discrepancies were traced to the presence in the silver perchlorate (supplied as pure) of free acid, presumably perchloric acid. It was found quite easy to free the silver perchlorate from adhering acid by recrystallization from benzene. Examination of the purified product with a series of indicators showed it to be neutral. (The pH meter gives wavering and uncertain results with silver perchlorate.) The results with the purified product were consistent and reproducible but we found a certain lack of agreement between the results from anode and cathode chambers, in the more concentrated solutions, an effect we did not observe with silver nitrate.

While the silver nitrate solutions were made up by direct weighing, it was not possible to do this with silver perchlorate because of its extremely hygroscopic nature. Accordingly, a very concentrated stock solution was made up and analyzed gravimetrically in quadruplicate, by precipitation of silver as silver chloride, a method known for its accuracy. From this stock solution other solutions were prepared by weight dilution.

EXPERIMENTAL RESULTS

The results of the transference number experiments are contained in Table I.

Can. J. Chem. Downloaded from www.nrcresearchpress.com by 176.9.209.113 on 09/04/12
For personal use only.

Can. J. Chem. Downloaded from www.nrcresearchpress.com by 176.9.209.113 on 09/04/12
For personal use only.

TABLE I

Transference numbers of silver nitrate and of silver perchlorate at different concentrations and at 25.00° C

Concn. in moles/liter	Transference number	
	From anode	From cathode
	Silver nitrate	
0.1000	0.469	0.470
0.4916	0.479	0.480
1.0515	0.484	0.485
1.6723	0.505	0.504
2.0163	0.508	0.509
2.7833	0.528	0.531
3.5913	0.544	0.548
4.3256	0.547	—
4.9518	0.550	0.557
4.9880	0.552	—
6.3476	0.564	—
6.5660	0.566	0.558
7.6388	0.576	—
	Silver perchlorate	
0.1074	0.475	0.486
0.2348	0.468	0.510
0.5847	0.464	—
0.9001	0.470	0.518
1.4230	0.476	0.510
2.4027	0.522	0.505
3.0731	0.550	0.475
4.1797	0.613	—

NOTE: The results of conductance measurements are contained in Table II.

TABLE II

Specific and equivalent conductances, densities, and viscosities (relative) of aqueous solutions of silver nitrate and of silver perchlorate at 25.00° C

Concn. in wt. %	Density	Concn. in moles/liter	$k \times 10^2$ mhos/cm	Λ_{exp} mhos/cm	Relative viscosity
		Silver nitrate			
1.680	1.0110	0.1000	1.091	109.1	1.009
7.835	1.0658	0.4916	4.409	89.69	1.033
15.618	1.1427	1.0515	8.069	76.74	1.078
23.120	1.2288	1.6723	11.36	67.91	1.132
26.702	1.2743	2.0163	12.85	63.74	1.168
34.265	1.3806	2.7833	15.84	56.90	1.260
40.978	1.4888	3.5913	18.37	51.15	1.382
46.237	1.5874	4.3256	20.20	46.69	1.464
50.333	1.6713	4.9518	21.55	43.43	1.632
50.557	1.6760	4.9880	21.61	43.32	1.638
58.080	1.8566	6.3476	23.70	37.34	1.942
59.162	1.8855	6.5660	23.95	36.47	1.990
64.030	2.0267	7.6388	24.84	32.52	2.264
68.380	2.1713	8.7400	25.23	28.87	2.740
		Silver perchlorate			
2.195	1.0144	0.1074	1.182	110.1	1.002
4.702	1.0353	0.2348	2.453	104.4	1.006
8.992	1.0733	0.4649	4.562	98.15	1.014
10.859	1.1164	0.5847	5.611	96.26	1.021
16.316	1.1439	0.9001	8.166	90.70	1.044
24.000	1.2294	1.4230	11.99	84.23	1.070
31.832	1.3284	2.0394	15.68	76.90	1.142
35.921	1.3861	2.4027	17.48	72.71	1.194
42.624	1.4947	3.0731	20.23	65.83	1.302
46.641	1.5662	3.5231	21.60	61.31	1.399
51.852	1.6713	4.1797	22.95	54.91	1.571
61.224	1.8962	5.6000	23.49	41.95	2.134

Can. J. Chem. Downloaded from www.nrcresearchpress.com by 176.9.209.113 on 09/04/12
For personal use only.

DISCUSSION

When transference numbers are plotted against concentration the transference number of silver ion in silver nitrate is seen to increase continuously from about 0.46 at zero concentration to about 0.56 at 7.5 molar, while the transference number of silver ion in silver perchlorate starts with a value of about 0.47 at zero concentration, passes through a minimum value of 0.46 at about 0.5 molar and then increases continuously and rather rapidly to a value of 0.61 at 4.0 molar. The increase in the transference number of silver ion in silver nitrate with increasing concentration is in agreement with the result of Laity and Duke (6), who found that in molten silver nitrate the cation carries three-quarters of the current. The behavior of silver perchlorate points to some abnormality in the structure of silver perchlorate solutions, possibly complex anion formation. This hypothesis would also account for our inability to obtain agreement in the results from anode and cathode for this salt.

The graph of equivalent conductance versus concentration (Fig. 1) is perfectly normal for silver nitrate, i.e. the curve flattens out towards a constant value as saturation is

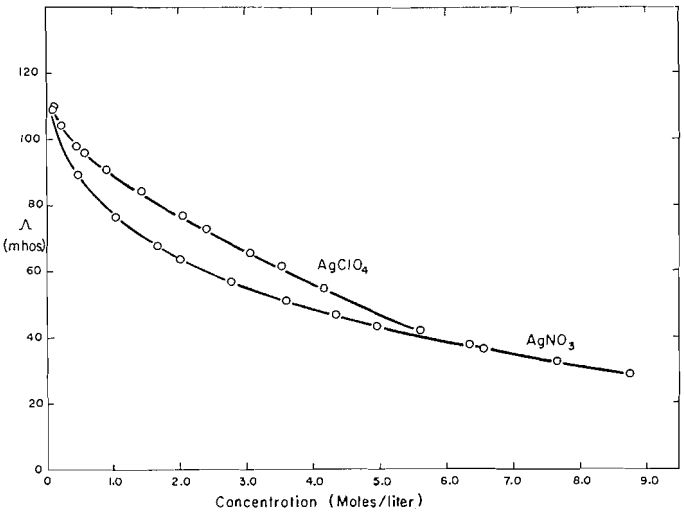

FIG. 1.

approached and the curve is convex towards the axis of concentration. The curve for silver perchlorate, on the other hand, is much less convex to the axis of concentration; indeed, the curve becomes actually concave if, instead of concentration, the square root of concentration is used as abscissa. This may be connected with our postulated complex ion formation.

As usual, in work proceeding from this laboratory the conductance results have been compared with the results calculated from the equations of Wishaw and Stokes and of Falkenhagen. The results are given in Table III. The agreement is good up to a concentration greater than 1 *M*. In order to obtain this correspondence, it has been necessary to assume an $\mathring{a}$ value of 4.5 (Stokes) and 3.7 (Falkenhagen) for silver perchlorate, as against 2.18 and 1.88 for silver nitrate, and this is in harmony with the belief that the radius of the perchlorate ion must be greater than that of the nitrate ion. The common device of introducing 1 solvent molecule between anion and cation in the ion-pair is obviously not applicable to silver nitrate, since $\mathring{a}$ is so small, but it might well be done

TABLE III

Calculated and observed equivalent conductances of silver nitrate and of silver perchlorate

Concn. moles/liter	Λ_{exp}	Λ_{calc} (Stokes)		Λ_{calc} (Falkenhagen)	
		Silver nitrate			
0.1000	109.1	109.6	($\mathring{a}$ = 2.18 Å)	109.3	($\mathring{a}$ = 1.88 Å)
0.4916	89.69	90.13		89.68	
1.0515	76.74	76.91		76.80	
1.6723	67.91	67.54		67.85	
2.0163	63.74	63.21		63.70	
2.7833	56.90	54.99		56.00	
3.5913	51.15	47.52		48.96	
4.3256	46.69	43.08		44.85	
4.9518	43.43	37.95		39.38	
4.9880	43.32	37.44		39.18	
6.3476	37.34	29.73		31.83	
6.5660	36.47	28.63		30.90	
7.6388	32.52	24.36		26.56	
8.7400	28.87	19.44		21.52	
		Silver perchlorate			
0.1074	110.1	109.4	($\mathring{a}$ = 4.5 Å)	109.5	($\mathring{a}$ = 3.7 Å)
0.2348	104.4	103.5		104.1	
0.4649	98.15	97.52		98.81	
0.5847	96.26	95.15		96.52	
0.9001	90.70	90.00		92.10	
1.4230	84.23	83.95		87.60	
2.0394	76.90	75.91		80.28	
2.4027	72.91	71.56		76.50	
3.0731	65.83	63.79		69.37	
3.5231	61.31	58.44		64.11	
4.1797	54.91	51.00		56.78	
5.6000	41.95	36.14		41.28	

with silver perchlorate. The fact that agreement between observed and calculated results is poorer for silver perchlorate is again in agreement with the assumption of the existence of complex anion in the more concentrated solutions of silver perchlorate.

Despite the contention that the Debye–Hückel–Onsager concepts cannot apply to concentrated solutions, and that therefore the above conductance equations can only be considered empirical equations, the fact that the $\mathring{a}$ values which it is necessary to assume for these equations are always in at least qualitative agreement with the sums of the crystallographic radii (with a certain allowance for ionic hydration) inclines us to believe that there is more than a measure of truth in these equations. Perhaps the full story will refer to effects not yet accounted for but the final treatment may be of the same form. At least, this is possible.

It is common practice to express the product of equivalent conductance and viscosity as a function of concentration. It is not very obvious why this is done, since there is no reason why the product should be constant; it never is and usually passes through a minimum. This is the behavior observed here, for both electrolytes.

REFERENCES

1. MARON, S. H. and PRUTTON, C. F. Principles of physical chemistry. 3rd ed. The Macmillan Co., New York. 1958. p. 443.
2. LONGSWORTH, L. G. J. Am. Chem. Soc. **54**, 2741 (1932); **57**, 1185 (1935).
3. STOKES, R. H. and LEVIEN, B. J. Am. Chem. Soc. **68**, 333 (1946).
4. LEE, W. H. and MILLEN, D. J. J. Chem. Soc. 2248 (1958).
5. FRITZ, J. J. and FUGET, C. R. J. Phys. Chem. **62**, 303 (1958).
6. LAITY, R. W. and DUKE, F. R. J. Electrochem. Soc. **105** (No. 2), 97 (1958).

Can. J. Chem. Downloaded from www.nrcresearchpress.com by 176.9.209.113 on 09/04/12
For personal use only.

Can. J. Chem. Downloaded from www.nrcresearchpress.com by 69.46.99.164 on 09/04/12
For personal use only.

1′,2;3,6;3′,6′-TRIANHYDROSUCROSE[1,2]

R. U. Lemieux and J. P. Barrette

ABSTRACT

The "trianhydrosucrose" obtained on treatment of amorphous "sucrose tritosylate" with sodium methoxide was found to be 1′,2;3,6;3′,6′-trianhydrosucrose.

The preparation of two "trianhydrosucroses" was reported (1) in a previous publication. The compound which was obtained on the alkaline alcoholysis of 1′,4,6′-tri-*O*-tosyl sucrose was shown (1) to be 3,6-anhydro-α-D-galactosyl 1,4;3,6-dianhydro-β-D-fructoside. The purpose of this communication is to present evidence that 1′,2;3,6;3′,6′-trianhydrosucrose (II) is formed on the alkaline alcoholysis of 6,1′,6′-tri-*O*-tosyl sucrose (I). Compound I is a component of the so-called tri-*O*-tosyl sucrose which is obtained on reaction of sucrose with 3 moles of tosyl chloride in pyridine (2, 3, 4).

The trianhydride (II), m.p. 163–164.5°, $[\alpha]_D$ +117°, R_f value = 0.42–0.48 (butanol–water), was extremely sensitive to acid hydrolysis (about 200 times more rapid in 0.01 *N* hydrochloric acid at 25° than sucrose (5), measured polarimetrically). The initial rapid hydrolysis led to a reducing (Fehling's solution) compound (III) (R_f = 0.32–0.38 (butanol–water)), which resisted crystallization. The chromatographically pure compound (III) very rapidly consumed 2 moles of periodate without formation of either formic acid or formaldehyde. Since the trianhydride (II) resisted periodate oxidation at pH 7 or higher, it was evident that the acid hydrolysis liberated two isolated α-glycol groups. Furthermore, the lack of formation of formic acid or formaldehyde showed the absence of —CHOH—CH_2—OH, —CHOH—CHO, or —CO—CH_2OH groups. Since acid hydrolysis of II produced readily only one compound (III), it was apparent that the anhydrization had produced an ether linkage between the glucose and fructose residues. It seemed likely that this linkage would be between the 2- and 1′-positions of sucrose, since Helferich and Werner (6) have shown that reaction of both the α- and β-anomers of 2-chloroethyl-D-glucopyranoside with alkali proceed with participation of the 2-oxygen atom to form 1,2-*O*-ethylene derivatives of D-glucopyranose.

The compound III was reduced with sodium borohydride to a non-reducing substance (IV) (R_f = 0.20–0.24 (butanol–water)) which, like III, very rapidly consumed 2 moles of periodate. Again no formaldehyde nor formic acid was liberated in the oxidation.

The acetolysis and subsequent deacetylation of substance IV gave a crystalline dihexitol ether (V), m.p. 110–114° (dimorphic), $[\alpha]_D$ −12.6 (in water), which on periodate oxidation produced 2 moles of formaldehyde, 5 moles of formic acid, and an aldehydic residue (VI) (7) which was reduced with sodium borohydride to 2-(β-hydroxyethoxy)-1,3-propanediol (VII). The identity of VII was proved from its synthesis through periodate oxidation and subsequent sodium borohydride reduction of polygallitol (VIII) (1,5-anhydro-D-glucitol). These results established the existence of the 1′,2 aliphatic-type ether linkage between the anhydrohexopyranose and the anhydroketohexofuranose residues of II.

[1]*Manuscript received August 7, 1959.*
Contribution from the Chemistry Department, University of Ottawa, Ottawa, Ontario.
[2]*To comprise a portion of a thesis to be submitted by J.P.B. in partial fulfillment of the requirements for the Ph.D. degree.*

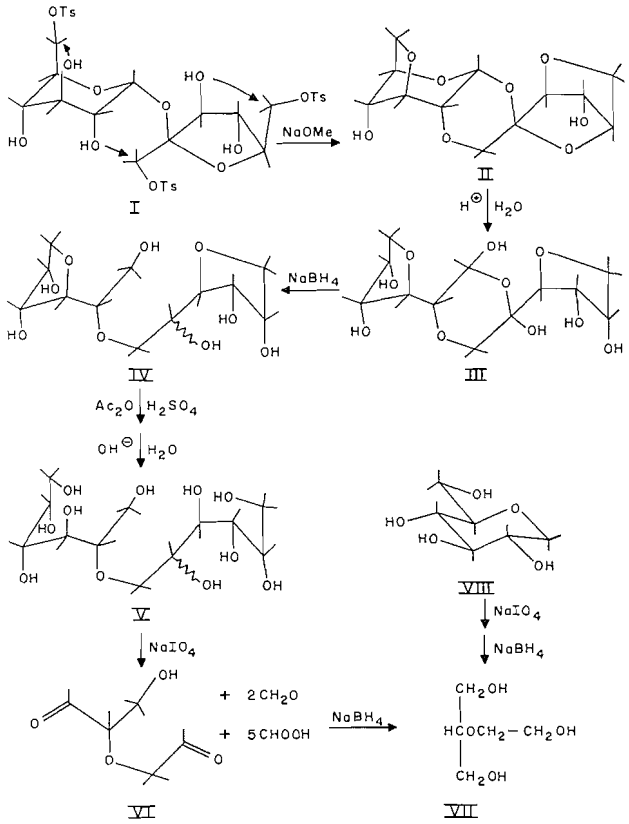

The infrared spectrum of II gave no indication of unsaturation and the absence of epoxide ring was indicated by the substance's resistance to prolonged treatment both with 25% alkali and hydrazine at 100°. The ditosylate of II, m.p. 164.5–166° (decomp.), was unaffected by either sodium iodide in acetone or hydrazine at 100°. It could then be concluded that neither of the two free hydroxyl groups in II were at the 6- or 6′-position (2).

The extremely rapid periodate consumption by compounds III and IV (90% uptake, 2 minutes in 0.025 *M* sodium metaperiodate at 0°) was clearly indicative of *cis*-α-glycols (8, 9) situated on five-membered rings. Consequently, these results require structures III and IV to possess free *cis*-glycol groups at the 4,5- and 4′,5′-positions. Compound III showed no absorption in the infrared characteristic of carbonyl groups. It seems probable that the carbonyls were masked through the formation of a hydrate as shown in the formula for III.

The results require that both the glucose and fructose residues of II possess 3,6-anhydro rings. In view of these rings, the fact that the configurations at the 5- and 5′-positions were in all likelihood not affected in the formation of II, and the fact that the 4- and 4′-hydroxyl groups are in *cis*-relationship to the 5- and 5′-oxygens, respectively, it can be concluded that configurations at the positions 3, 4, 5, 3′, 4′, and 5′ in II are the same as in sucrose. Although methyl 3,6-anhydro-α-D-glucopyranoside is known readily to undergo both α-to-β anomerization (10) and pyranoside-to-furanoside ring contraction (10) under acid conditions, there can be no doubt that such isomerizations would not

Can. J. Chem. Downloaded from www.nrcresearchpress.com by 69.46.99.164 on 09/04/12
For personal use only.

occur under the alkaline conditions used to prepare the trianhydride II. Therefore, only the configuration at the 2-position of the glucose residue was reasonably in need of verification. Information on this point of structure was provided by the nuclear magnetic resonance spectrum for the di-*O*-acetyl derivative of II. Our experience with the nuclear magnetic resonance spectra of sugar derivatives (11) enables us to assign the doublet of total intensity 1 at 76.9 and 79.5 c.p.s. (60 Mc/s) (the lowest field signal in the spectrum) to the anomeric hydrogen of the glucose residue. The spacing for the doublet was found to be 2.9 ± 0.1 c.p.s. both at 40 Mc/s and 60 Mc/s. This requires that the spacing represents a true spin–spin coupling constant. The magnitude of the coupling is that characteristic for two neighboring hydrogens in gauche or skewed relationship (11). In view of the 3,6-anhydro ring, the glucose residue must reside in that conformation which possesses the anomeric hydrogen in axial orientation. It follows, therefore, that the 2-hydrogen is in equatorial orientation since if it were in axial orientation, the coupling with the anomeric hydrogen would have been two to three times stronger (11) than that observed. It follows that the sucrose trianhydride (II) possesses the configuration of sucrose and must have formed from 6,1′,6′-tri-*O*-tosyl sucrose (I). All attempts to obtain 4-*O*-methyl-D-hexose by acetolysis of the methyl ether of the trianhydride (II) met with failure because of the high resistance of the 1′,2 ether linkage to acetolyzing reagents.

It is of interest to note that titration of the solution obtained on the periodate oxidation of III suggested that 1 mole of acid was liberated in the periodate oxidation. However, *no* formic acid could be detected in the mixture. The details of the effort to characterize the formic acid are reported since they provide a convenient method for the estimation of formic acid and formaldehyde produced in periodate oxidations. Our results render obvious the need for the application of such a technique in experiments designed to elucidate points of structure in carbohydrates through a measure of the formic acid produced in a periodate oxidation.

EXPERIMENTAL

All melting points are uncorrected. The rotations were measured at room temperature, 20–25°, using the D-line of sodium. Infrared spectra were obtained with a Perkin–Elmer single beam double pass instrument. Optical densities for colorimetric determinations were obtained from a Coleman Junior spectrophotometer. Microanalysis for carbon and hydrogen were carried out by Geller Laboratories, West Englewood, N.J. The n.m.r. spectra were measured with Varian Associates' high resolution spectrometers and the chemical shifts are from the signal for chloroform as an internal standard.

Acid Hydrolysis of II

1′,2;3,6;3′,6′-Trianhydrosucrose (II) (1), 53 mg, m.p. 163–164.5°, $[\alpha]_D$ +117° (*c*, 0.92 in chloroform), was dissolved in 5 ml of 0.01 *N* hydrochloric acid at 25°. The change in rotation of this solution was observed at intervals and the rotation became constant after 8 hours. The final specific rotation, based on the concentration of II at the start of the hydrolysis was +87.0 (*c*, 1.063 in 0.04 *N* HCl). Sucrose in 0.05 *N* hydrochloric acid at 25° requires about 1600 hours (6) for 99.99% inversion.

The solution was deionized by percolating through a small column of Dowex 1X8 anion exchange resin (quaternary ammonium type) and evaporated *in vacuo* to a syrup (54.6 mg). Paper chromatography (butanol–water) of this syrupy product showed only one major component, $R_f = 0.36$, when examined with aniline phthalate spray reagent (12). A faint streak appeared from the origin to $R_f = 0.45$. The material was chromatographed on a 25-g Celite column in the manner described by Lemieux, Bishop, and

Can. J. Chem. Downloaded from www.nrcresearchpress.com by 69.46.99.164 on 09/04/12
For personal use only.

Can. J. Chem. Downloaded from www.nrcresearchpress.com by 69.46.99.164 on 09/04/12
For personal use only.

Pelletier (13). The main band was obtained in 39.1 mg yield, $[\alpha]_D$ +87 (c = 0.69 in water), R_f value 0.36 (butanol–water), and reduced Fehling's solution. The chromatographically pure compound (III) resisted crystallization. Periodate oxidation of III in 0.025 N sodium metaperiodate at 0° consumed 1.73, 1.85, 1.88, 1.90, and 1.92 moles of the oxidant per mole, after 2, 10, 60, 120, and 720 minutes. Titration of the reaction mixture, after destroying the excess periodate with ethylene glycol, suggested the formation of 1 mole of carboxylic acid per mole of III oxidized. However, no formic acid or formaldehyde could be detected using the following procedures.

A weighed sample of the compound, ca. 0.05 mmole, is dissolved in 2 ml of 0.2 M sodium metaperiodate and left to oxidize for the required time. When the oxidation has progressed to the desired extent, the oxidation mixture is quantitatively transferred into the "microvacuum distillation" apparatus described by Grant (14), and the solution is frozen in an acetone – dry ice mixture. The apparatus is then evacuated to less than 1 mm. The arm of the apparatus which contains the frozen reaction mixture is then removed from the freezing mixture and the other arm is kept in the freezing mixture until all the volatile components have sublimed to the cold portion of the apparatus. The distillate, after thawing, is quantitatively transferred to a 25-ml volumetric flask and aliquots are titrated with standard 0.01 N sodium hydroxide to estimate the total amount of acid present in the distillate. The acid can be conveniently characterized by converting a suitable aliquot to sodium salt, 1–2 mg, and dissolving the salt in 4 ml of 10% aqueous potassium bromide, freeze-drying, and pressing the residue into a window in the usual manner (15). The formaldehyde content is conveniently determined using the chromotropic acid reagent (16).

Compound IV

The trianhydride (II), 100 mg, was hydrolyzed in 0.001 N hydrochloric acid to constant rotation in order to obtain crude compound III. The solution was neutralized with 0.05 N sodium hydroxide and then treated with a twofold excess of sodium borohydride at 0° for 36 hours. The excess sodium borohydride was destroyed with acetic acid and the resulting solution was evaporated *in vacuo* to dryness. The dry residue was acetylated using 5 ml acetic anhydride, and 5 ml pyridine. The acetylated product, 92.4 mg, was isolated in the usual manner and deacetylated in dry methanol, 10 ml, saturated at 0° with ammonia. Paper chromatography of the crude product (IV), 60 mg, indicated a main component with R_f value = 0.26 (butanol–water). There was a faint streak from the origin to R_f = 0.28. This syrupy product was chromatographed on a 25-g column of Celite in the usual manner (13). The resulting product (IV) did not reduce Fehling's solution and failed to crystallize. Periodate oxidation of IV in 0.025 N sodium metaperiodate at 0° consumed 1.8, 1.85, 1.91, 1.95, and 1.96 moles of the oxidant per mole after 2, 15, 30, 60, 120, and 720 minutes. No formic acid nor formaldehyde was produced in this oxidation.

Periodate oxidation of erythritan (8), (1,4-anhydroerythritol) in 0.025 N sodium metaperiodate at 0° consumed 0.95, 0.97, 0.99, 0.99, 0.99, and 0.99 mole of the oxidant per mole after 2, 5, 10, 30, 60, and 120 minutes. However, oxidation of threitan (8) (1,4-anhydrothreitol) in 0.025 N sodium metaperiodate at 0° consumed 0.135, 0.153, 0.168, 0.210, 0.434, 0.930, and 0.99 mole of the oxidant after 2, 5, 15, 70 minutes and 2.5, 11, and 22 hours.

Dihexitol Ether V

The crude acetyl derivative of IV, 96 mg (prepared as described above from a 100 mg of the trianhydride (II)), was treated with acetic anhydride, 1 ml, and concentrated

sulphuric acid, 0.08 ml, at 0° for 3 days. The resulting acetolysis products were isolated in the usual manner and deacetylated by percolating through a column of Dowex 1X8 anion exchange resin to yield 63.8 mg of syrupy polyol. This was chromatographed on a 25-g Celite column (butanol–water) (13). The main band, $R_f = 0.24$, gave 39.7 mg of crystalline dihexitol ether (V), m.p. 105–109°. After two recrystallizations from ethanol the melting point was 110–114° (dimorphic), $[\alpha]_D^{25} - 12.6°$ (c, 0.48 in water). The periodate oxidation of V produced 5 moles of formic acid and 2 moles of formaldehyde per mole, based on the assumption that the compound corresponds to structure V and using the above described lyophilization procedure. The elementary analyses were unsatisfactory, probably because of solvent of crystallization. The following experiment together with the periodate oxidation can leave no doubt as to the structure of V.

2-(β-Hydroxyethoxy)-1,3-propanediol (VII)

The dihexitol ether (V), 20.2 mg, was dissolved in 2 ml of 0.11 *M* sodium metaperiodate and left to oxidize to a final rotation of 0°. Excess sodium borohydride, 250 mg, was added to reduce the oxidation products (VI) and the solution was left for 18 hours before acidification with acetic acid to destroy the excess sodium borohydride. The resulting solution was evaporated *in vacuo* to a dry cake, which was acetylated with acetic anhydride in pyridine in the usual manner to yield 12.1 mg of syrupy acetate. This syrupy acetate was distilled at a bath temperature of 125–135° and 0.3 mm pressure to yield 8.2 mg of yellowish syrup. The infrared spectrum of this syrupy acetate was almost identical with that of 2-(β-hydroxyethoxy)-1,3-propanediol triacetate prepared by an identical treatment of polygallitol (VIII) (1,5-anhydrosorbitol). The syrupy triacetate was then deacetylated in absolute methanol, 3 ml, saturated with ammonia. The resulting syrupy triol was chromatographed on Celite in the usual manner (13). The main product, 2-(β-hydroxyethoxy)-1,3-propanediol (VII), had the same $R_f = 0.48$ (butanol–water) and identical infrared spectrum as the authentic specimen prepared in similar manner from polygallitol. Reacetylation of VII, produced a substance with a spectrum identical with that of the authentic triacetate prepared from polygallitol.

Stability of Trianhydrosucrose (II) *and its Ditosylate Derivative toward Nucleophilic Reagents*

Substance II remained unchanged when heated at 100° in 25% potassium hydroxide for 24 hours as well as in 85% hydrazine at 100° for 36 hours. Similarly the ditosylate of II, m.p. 164.5–166°, when heated to 100° with sodium iodide in acetone or with hydrazine in sealed tubes for 24 hours, remained unchanged.

4,4′-Di-O-methyl-1′,2;3,6;3′,6′-trianhydrosucrose

The trianhydride (II), 200 mg, was methylated using the procedure described in a previous communication (1), to yield 147 mg of di-*O*-methyl trianhydrosucrose, m.p. 179–181°, $[\alpha]_D^{24} +140°$ (c, 1.9 in chloroform). Anal: Calc. for $C_{14}H_{20}O_8$: methoxyl, 19.62%. Found: methoxyl, 19.78, 20.05%.

ACKNOWLEDGMENT

This work was conducted as part of Project No. 88 sponsored by the Sugar Research Foundation, New York, N.Y.

REFERENCES

1. LEMIEUX, R. U. and BARRETTE, J. P. J. Am. Chem. Soc. **80**, 2243 (1958).
2. RAYMOND, A. L. and SCHROEDER, E. F. U.S. Patent No. 2, 365, 776 (1944).
3. HOCKETT, R. C. and ZIEF, M. J. Am. Chem. Soc. **72**, 1839 (1950).

Can. J. Chem. Downloaded from www.nrcresearchpress.com by 69.46.99.164 on 09/04/12
For personal use only.

4. BRAGG, P. D. and JONES, J. K. N. Can. J. Chem. **37**, 575 (1959).
5. JACKSON, R. F. and GILLIS, C. K. Bur. Stand. Sci. Papers, No. 375, 125 (1920).
6. HELFERICH, B. and WERNER, J. Ber. B, **75**, 1446 (1942).
7. CARSON, J. F. and MACLAY, W. D. J. Am. Chem. Soc. **67**, 1808 (1945).
8. KLOSTERMAN, H. and SMITH, F. J. Am. Chem. Soc. **74**, 5336 (1952).
9. BULGRIN, V. C. J. Phys. Chem. **61**, 702 (1957).
10. HAWORTH, W. N., OWEN, L. N., and SMITH, F. J. Chem. Soc. 88 (1941).
11. LEMIEUX, R. U., KULLNIG, R. K., BERNSTEIN, H. J., and SCHNEIDER, W. G. J. Am. Chem. Soc. **80**, 6098 (1958).
12. PARTRIDGE, S. M. Nature, **164**, 443 (1949).
13. LEMIEUX, R. U., BISHOP, C. T., and PELLETIER, G. E. Can. J. Chem. **34**, 1365 (1956).
14. GRANT, W. M. Ind. Eng. Chem. Anal. Ed. **18**, 729 (1946).
15. LEMIEUX, R. U., EPP, A., and BAUER, H. F. Abstracts of papers. Fall meeting of the American Chemical Society, Sept. 12–16, 1955, Minneapolis, Minn.
16. BRICKER, C. E. and VAIL, W. A. Anal. Chem. **22**, 720 (1950).

Can. J. Chem. Downloaded from www.nrcresearchpress.com by 69.46.99.164 on 09/04/12
For personal use only.

Can. J. Chem. Downloaded from www.nrcresearchpress.com by 176.9.209.113 on 09/04/12
For personal use only.

VOLUCRISPORIN

ISOLATION, STRUCTURE, AND SYNTHESIS OF THE METHYL ETHER[1]

P. V. DIVEKAR,[2] G. READ,[3] L. C. VINING, AND R. H. HASKINS

ABSTRACT

A new pigment, volucrisporin, has been isolated from shaken cultures of the Hyphomycete *Volucrispora aurantiaca* Haskins, and characterized as 2,5-(*m*-hydroxyphenyl)-1,4-benzoquinone. The structure has been confirmed by synthesis of the dimethyl ether.

Volucrispora aurantiaca Haskins (1), a new genus and species of Hyphomycete, produces a red pigment which has been named "volucrisporin" (2). This represents approximately two per cent of the dry weight of mycelia from cultures grown in shaken flasks in a suitable liquid medium and could be readily obtained by hot extraction of the dried culture solids with acetone. Subsequent crystallization from pyridine afforded the pigment as red rhombic plates. Preliminary defatting with petroleum ether yielded a product which was shown to contain ergosterol in the non-saponifiable fraction.

Elemental analyses of the pigment together with analyses and molecular weight estimations on derivatives indicated a molecular formula $C_{18}H_{12}O_4$. Neither C-methyl nor O-methyl groups were present. A quinone group in the substance was considered likely since reduction with zinc and acetic acid gave a colorless unstable dihydro compound which could be readily reoxidized to the original pigment with chromic acid in acetic acid. Acetylation of volucrisporin gave a yellow diacetate and reductive acetylation of this derivative or of the original pigment yielded a colorless dihydrotetraacetate. With methyl iodide and silver oxide a yellow dimethyl ether was obtained. These results provided further evidence for the presence of a quinone group and indicated that both remaining oxygen atoms were present as hydroxyls.

Distillation of volucrisporin with zinc dust yielded *p*-terphenyl, thus establishing the carbon skeleton of the pigment. The ultraviolet absorption spectrum of the leucoacetate was similar to those of acetoxylated *p*-terphenyls (3, 4), and the position of the single absorption maximum at 258.5 mμ was consistent with a terphenyl quinone structure containing no further substituents in either the central quinone ring or in the ortho positions of the phenyl rings. From the lack of solubility of volucrisporin in sodium carbonate, failure to react with diazomethane, and negative tests for chelation with ferric chloride or lead acetate, it was evident that the quinone ring did not contain a vinylogous acid group.

Oxidation of volucrisporin with alkaline peroxide yielded *m*-hydroxybenzoic acid, which was shown by paper chromatography to be the only hydroxybenzoic acid formed. Structure (I, R = H) was therefore assigned to the pigment.

[1]*Manuscript received August 26, 1959.*
Contribution from the National Research Council of Canada, Prairie Regional Laboratory, Saskatoon, Saskatchewan.
Issued as N.R.C. No. 5397.
Presented in part before the Division of Organic Chemistry, 47th Annual Conference of the Chemical Institute of Canada, Halifax, N.S., May 26, 1959. A summary of the results has also appeared in Chem. & Ind. 731 (1959).
[2]*National Research Council of Canada Postdoctorate Fellow, 1957–59.*
[3]*National Research Council of Canada Postdoctorate Fellow, 1957–59. Present address: The Dyson Perrins Laboratory, Oxford University, Oxford, England.*

The infrared spectrum of the dimethyl ether in potassium bromide showed the carbonyl maximum at 1649 cm^{-1} (s) expected for a 2,5-disubstituted *p*-benzoquinone (5). In the pigment itself intermolecular hydrogen bonding was evident, since the carbonyl region showed a split peak at 1630 (s) and 1637 (s) cm^{-1} and the hydroxyl absorption occurred at 3280 cm^{-1} (s).

Unsuccessful attempts were made to synthesize the dimethyl ether of volucrisporin by a single-step arylation of *p*-benzoquinone with 2 moles of diazotized *m*-anisidine. Failure was attributed to the instability of the diazonium salt, particularly in the organic solvents which it was necessary to use to overcome the low solubility of the intermediate monosubstituted quinone. In aqueous solution (6) the diazonium salt of *m*-anisidine was sufficiently stable to give the 2-(*m*-methoxyphenyl)-1,4-benzoquinone in a yield of 37%, but attempts to introduce the second aryl ring into the quinone again met with difficulty. Paper chromatographic examination of the products from reactions carried out under a variety of conditions established that in aqueous acetone at low temperature, as recommended by Brassard and L'Écuyer (7), detectable amounts of a material with the desired R_f value were formed. Chromatography failed to separate this completely from other reaction products but a fraction was isolated which contained the compound contaminated only with a large amount of unreacted monoaryl derivative. The starting material was removed by sublimation leaving a product which, after purification, was indistinguishable from the dimethyl ether of volucrisporin (I, R = CH_3).

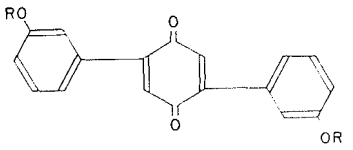

(I)

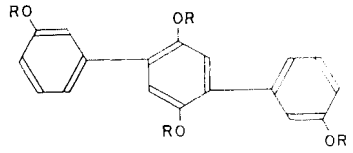

(II)

Volucrisporin is the first terphenyl quinone to be found in a hyphomycetous fungus, and differs from those isolated from Basidiomycetes and lichens (8) in the absence of hydroxyl groups on the quinone ring and in the unusual metasubstitution of the outer rings. It is accompanied in the mold by the leuco form (II, R = H) which was occasionally found to crystallize from the pyridine mother liquors after the separation of volucrisporin. The occurrence of atromentin in both oxidized and reduced forms has already been noted in *Paxillus atrotomentosus* (Batsch) Fr. (9), and the substituted quinols of aurantiacin (10) and leucomelone (11) occur with the corresponding quinones in *Hydnum aurantiacum* Batsch and *Polyporus leucomelas* Pers. ex Fr., respectively.

Derivatives of meta-hydroxybenzoic acid are rare in nature and, to the authors' knowledge, have been found only in the beaver castor (12), the urine of animals (13, 14), and recently in cultures of *Penicillium griseofulvum* Dierckx (15). Their appearance in urine was associated with the administration of 3,4-dihydroxyphenyl derivatives and was suggested to result from removal of the *p*-hydroxy group (16), a mechanism which may also be of significance in the biosynthesis of volucrisporin.

Can. J. Chem. Downloaded from www.nrcresearchpress.com by 176.9.209.113 on 09/04/12
For personal use only.

Solutions of volucrisporin in dilute aqueous sodium hydroxide are very unstable and when neutralized after only a few minutes yield a mixture of products. One of these has been isolated and appears to be 3-hydroxy-2,5-(*m*-hydroxyphenyl)-1,4-benzoquinone. This ease of hydroxylation emphasizes the need for caution when isolating quinones, particularly terphenylquinones, by treatment of the fungus or crude extracts with sodium hydroxide solution (9).

EXPERIMENTAL

Medium

The medium used for production runs consisted of distilled water 2000 ml, soil extract 200 ml, peptone 10 g, soluble starch 2 g, and glucose 100 g. The soil extract incorporated in the medium was prepared in the following manner. A beaker, two-thirds full of garden soil, was filled with tap water. The contents were stirred well and the mixture was autoclaved for an hour at 15 lb per square inch pressure. On cooling, the liquid was decanted, mixed with Celite, and filtered.

The medium was dispensed in 25-ml aliquots into 250-ml conical flasks which were then plugged and sterilized in the usual manner. While the medium is obviously not a precise one, its use resulted in yields exceeding those obtained from a number of others tested.

Inoculation

The initial inoculum was prepared by blending in sterile distilled water in Waring blendors several 3-week-old cultures of *Volucrispora aurantiaca* Haskins growing on Difco potato dextrose agar. Inoculum was added to the growth medium at the rate of 5% volume for volume, and the inoculated flasks were shaken for 6 days at 28° C on a rotary shaker operating at 220 r.p.m. describing a radius of motion of 1 inch. The organism also grew well in stirred aerated tank fermentors, but under the conditions tested, the growing mycelium collected in the foam at the surface of the liquid and yields of the pigment were considerably less than in shake flasks.

Subsequently the inoculum was prepared by blending 6-day-old shake flask cultures from production runs with an equal volume of sterile, distilled water. By always selecting flasks showing the greatest pigment production for use as inoculum, yields of pigment have been increased considerably.

Isolation of Volucrisporin

At the end of 6 days' incubation, the cultures were bulked and filtered. The orange-colored mycelium obtained by filtration was freeze-dried and pulverized in a Wiley mill.

In a typical isolation procedure, the pulverized mycelium (40 g obtained from 270 flasks), packed in a hot extractor, was defatted (16 hours) with petroleum ether (35–50° C), and then extracted (6 hours) with ether, which removed a small quantity of colored impurities. The bulk of the pigment was subsequently extracted from the mycelium with acetone (40 hours), the mycelium becoming practically colorless.

The acetone extracts (350 ml), on concentration *in vacuo* to about 50 ml and cooling, deposited an amorphous brick-red precipitate (2.1 g). This was crystallized twice from pyridine to give volucrisporin as rhombic plates (0.85 g) which did not melt below 300° C. Found: C, 74.3%; H, 4.1%; active H (Zerewitinoff), 0.57%; no N, methoxyl, or C-methyl. Calculated for $C_{18}H_{12}O_4$: C, 74.0%; H, 4.1%; two active H, 0.68%. Ultraviolet maxima in dioxane at 281.5 and 329 mμ, inflexions at 234 and 377 mμ; log ε 4.00, 3.90, 4.47, and 3.45, respectively. Infrared maxima (KBr disk) at 3280 (s), 1637 (s), 1630 (shoulder, s), 1590 (s), 882 (s), 790 (s), 727 (m), and 683 (s) cm^{-1}.

Can. J. Chem. Downloaded from www.nrcresearchpress.com by 176.9.209.113 on 09/04/12
For personal use only.

Volucrisporin is sparingly soluble or insoluble in most common organic solvents with the exception of pyridine or dioxane. It is insoluble in cold sodium carbonate solution but dissolves readily in dilute sodium hydroxide giving a purple color.

Isolation of Ergosterol

The petroleum ether extract of the mycelium was evaporated to dryness. A portion of the dried extract (1 g) was boiled for 3 hours with 100 ml of 10% methanolic potash, the reaction mixture concentrated, diluted with water, and extracted with two 50-ml portions of ether. The crystals obtained by evaporation of the ethereal extract were washed with petroleum ether and crystallized from ethanol to give colorless plates (20 mg), m.p. 160–162° C, undepressed on admixture with an authentic sample of ergosterol. The color reaction with the Liebermann–Burchard reagent and wavelengths of the ultraviolet absorption maxima were also identical with those of ergosterol.

Leucovolucrisporin

(*i*) When the mother liquors of the initial crystallization of volucrisporin were allowed to evaporate slowly, a crop of colorless needles was obtained. These were recrystallized from pyridine to give a product m.p. 253–255° C which was stable as a solid but slowly converted in solutions exposed to air to volucrisporin. Found: C, 73.2%; H, 5.0%. Calculated for $C_{18}H_{14}O_4$: C, 73.5%; H, 4.8%.

(*ii*) Volucrisporin (30 mg) was boiled for 20 minutes with 3 ml of glacial acetic acid and zinc dust when the pigment slowly dissolved giving a colorless solution. This was filtered and poured into ice water. The precipitate was collected and crystallized from pyridine as colorless needles (20 mg), m.p. 253–255° C, undepressed on admixture with a sample of leucovolucrisporin isolated from *V. aurantiaca*. Found: C, 73.2%; H, 4.8%.

The dihydro compound was reoxidized to volucrisporin by brief warming with CrO_3 in glacial acetic acid.

Volucrisporin Diacetate

A mixture of volucrisporin (50 mg) and acetic anhydride (3 ml) was boiled for 15 minutes, when a clear solution resulted. When the mixture was cooled, yellow crystals were obtained. They were filtered and recrystallized from glacial acetic acid as glistening yellow needles (45 mg), m.p. 223° C, insoluble in sodium hydroxide. Found: C, 70.3%; H, 4.5%; CH_3CO, 24.0%; mol. wt. (Rast), 312. Calculated for $C_{22}H_{16}O_6$: C, 70.2%; H, 4.3%; $2CH_3CO$, 22.8%; mol. wt., 376. Ultraviolet absorption in dioxane shows λ_{max} 236 and 330 mμ; log ϵ 4.51 and 3.99, respectively.

When the compound was hydrolyzed by boiling for 2 hours with methanol containing a drop of concentrated sulphuric acid, volucrisporin was obtained.

Dihydrovolucrisporin Tetraacetate

Volucrisporin (50 mg) was boiled for $\frac{1}{2}$ hour with acetic anhydride (3 ml) and zinc dust giving a colorless solution which was filtered and poured into ice water. The precipitate was collected and crystallized from methanol as colorless plates (40 mg), m.p. 161–162° C, showing bright green fluorescence under ultraviolet light. Found: C, 67.4%; H, 5.1%; CH_3CO, 35.9%; mol. wt. (Rast), 438. Calculated for $C_{26}H_{22}O_8$: C, 67.5%; H, 4.8%; $4CH_3CO$, 37.2%; mol. wt., 462. Ultraviolet absorption maximum in dioxane at 258.5 mμ; log ϵ 4.42.

Volucrisporin Dimethyl Ether

A mixture of volucrisporin (60 mg), methyl iodide (4 ml), and silver oxide (500 mg) was refluxed for 2 hours. The resulting orange solution was filtered and evaporated to

Can. J. Chem. Downloaded from www.nrcresearchpress.com by 176.9.209.113 on 09/04/12
For personal use only.

dryness. The crude product thus obtained was crystallized twice from glacial acetic acid as glistening orange cubes (40 mg), m.p. 172–174° C. The analytical sample was sublimed in high vacuum at 120° C. Found: C, 75.0%; H, 5.3%; OCH_3, 18.3%. Calculated for $C_{20}H_{16}O_4$: C, 75.0%; H, 5.0%; $2OCH_3$, 19.4%. Ultraviolet absorption in ether shows λ_{max} at 279 and 326, λ_{Infl} at 235 and 371 mμ; log ε 4.22, 4.16, 4.82, and 3.72, respectively. Infrared maxima (KBr disk) at 1649 (s), 1580 (s), 871 (s), 860 (s), 809 (s), 778 (s), 730 (m), and 688 (s) cm^{-1}.

Zinc Dust Distillation

Volucrisporin (100 mg) was mixed intimately with zinc dust (6 g) and the mixture divided into 10 parts. Each was distilled in an open test tube and the distillates collected and crystallized from glacial acetic acid as colorless plates (10 mg). This product was purified by repeated sublimation in high vacuum at 120° C to give *p*-terphenyl, m.p. 209° C, undepressed on admixture with an authentic sample. Found: C, 93.4%; H, 6.4%. Calculated for $C_{18}H_{14}$: C, 93.9%; H, 6.1%. Ultraviolet absorption spectrum in ether showed λ_{max} 277 mμ, log ε 4.44, and was identical with that of an authentic sample of *p*-terphenyl. The infrared spectrum of the product was also identical with that given by *p*-terphenyl.

Alkaline Peroxide Oxidation

Three per cent hydrogen peroxide (1.5 ml; 7.3 moles) was added to a solution of volucrisporin (50 mg) in 0.1 *N* NaOH (10 ml). After 14 hours at room temperature in the dark the solution was neutralized with 1 *N* HCl and excess hydrogen peroxide decomposed with a small amount of palladized charcoal. An aliquot was spotted onto paper (Whatman No. 1) together with samples of the monohydroxybenzoic acids and the chromatogram developed in *i*-propanol – concentrated NH_4OH – water (8:1:1) (17). After the paper was dried and sprayed with diazotized *p*-nitraniline (18), the principal spot from the reaction mixture was found to correspond in R_f value (0.45) and color to that of *m*-hydroxybenzoic acid. Of the minor spots present, none corresponded to *o*- or *p*-hydroxybenzoic acids.

The aqueous solution was evaporated to dryness and the product (9.2 mg) sublimed directly from the mixture at 110–120° C/0.05 mm. Resublimed material melted at 199–201° C. Found: C, 60.9%; H, 4.6%. Calculated for $C_7H_6O_3$: C, 60.9%; H, 4.4%. The compound was indistinguishable from a sample of *m*-hydroxybenzoic acid in ultraviolet and infrared spectra and the melting point, on admixture with an authentic sample, was undepressed.

Sodium Hydroxide Treatment

Volucrisporin (100 mg) was dissolved in normal sodium hydroxide (5 ml) and the dark purplish solution filtered, neutralized with normal hydrochloric acid (5 ml), and extracted with ether until the aqueous layer became colorless. The reddish brown ethereal solution was extracted three times with 5% $NaHCO_3$. The purple bicarbonate extract was acidified with hydrochloric acid and left overnight in the refrigerator. The precipitate was filtered, dried, and crystallized three times from aqueous methanol as small reddish brown plates, (42 mg), m.p. 294–296° C. Found: C, 69.8%; H, 3.5%. Calculated for $C_{18}H_{12}O_5$: C, 70.1%; H, 3.9%.

An alcoholic solution of the compound gave a light green color with alcoholic $FeCl_3$. Distillation with zinc dust yielded *p*-terphenyl. The leucoacetate, prepared by boiling with zinc and acetic anhydride, crystallized from aqueous methanol as colorless needles,

Can. J. Chem. Downloaded from www.nrcresearchpress.com by 176.9.209.113 on 09/04/12
For personal use only.

m.p. 78° C. Found: C, 65.0%; H, 4.9%. Calculated for $C_{28}H_{24}O_{10}$: C, 64.6%; H, 4.7%. Attempts to crystallize the bicarbonate-insoluble fraction which was obtained by evaporation of the ethereal layer failed.

2-(m-Methoxyphenyl)-1,4-benzoquinone

m-Anisidine (12.3 g), prepared by the method of Meldola and Stephens (19) and dissolved in concentrated hydrochloric acid (25 ml) and water (50 ml), was diazotized at 0° C by dropwise addition, under vigorous stirring, of a solution of sodium nitrite (7.0 g) in water (25 ml). This solution was then added at 10° C to a well-stirred suspension of *p*-benzoquinone (13 g) in water (1 liter) containing sodium acetate (18 g). After 1 hour the temperature was allowed to rise slowly to ambient, and after all evolution of nitrogen had ceased (approximately 4 hours), the residue was filtered off, washed well with water, and dried. (Yield of crude product, 17.4 g.) This was extracted in a Soxhlet with petroleum ether (b.p. 30–60° C) and, after cooling, the supernatant solution was decanted onto a short column (4 cm × 8 cm) of activated alumina. The partially crystalline residue was dissolved in benzene and applied to the same column. Elution of the yellow product was continued with fresh benzene until impurities giving a dark red zone reached the bottom of the column. The eluate was then evaporated to dryness and the residual solid crystallized from acetone as yellow needles, m.p. 115–115.5° C. Concentration of the mother liquor to half volume yielded a second crop of crystals of the same melting point. (Total yield, 9.3 g = 37%.) Found: C, 73.0%; H, 4.8%; OCH_3, 14.0%. Calculated for $C_{13}H_{10}O_3$: C, 72.9%; H, 4.7%; $1OCH_3$, 14.5%. Ultraviolet spectrum in ether shows λ_{max} 273 and 362, λ_{Infl} at 230 and 303 mμ; log ε 3.64, 3.27, 4.17, and 3.14, respectively. Infrared spectrum (KBr disk) shows maxima at 1650 (s), 1593 (s), 1575 (s), 873 (s), 837 (m), 769 (s), and 687 (s) cm^{-1}.

2,5-Bis-(m-methoxyphenyl)-1,4-benzoquinone

2-(*m*-Methoxyphenyl)-1,4-benzoquinone (2.72 g) in acetone (85 ml) cooled to −5° C was poured into a well-stirred solution of *m*-anisidine (1.75 g) in concentrated hydrochloric acid (3.5 ml) and water (7.5 ml) which had been diazotized as above with a solution of sodium nitrite (1 g) in water (4.5 ml). Stirring was continued and the reaction mixture kept at −8° C during the addition of sodium acetate (3.5 g) in 10 equal portions over a period of 20 minutes. Water (10 ml) was then added to avoid a separation into two phases and the mixture allowed to warm up very slowly to room temperature. After all evolution of nitrogen had ceased, the reaction mixture was diluted with water and extracted several times with benzene. The benzene solution was evaporated to dryness and applied in chloroform to a column (4.5 cm × 30 cm) of silicic acid (Mallinckrodt 2847). Development with chloroform eventually eluted a bright red zone which was shown, by circular paper chromatography using formamide impregnated Whatman No. 1 filter disks (32 cm diameter) and petroleum ether (b.p. 100–120° C) as mobile phase, to contain a mixture of the desired product (R_f 0.70) together with unreacted monosubstituted benzoquinone (R_f 0.45). This fraction was concentrated to dryness and the residue (1.29 g) sublimed for 12 hours at 80° C in high vacuum. The unsublimed residue (0.36 g) was washed with benzene and crystallized from glacial acetic acid and then chloroform – carbon tetrachloride (1:2) to give yellow needles (99 mg), m.p. 175–176° C. Mixed melting point with dimethylvolucrisporin 173–174.5° C. Found: C, 75.0%; H, 5.1%; OCH_3, 18.9%. The ultraviolet and infrared spectra were identical with those of the dimethyl ether prepared from the natural pigment.

Can. J. Chem. Downloaded from www.nrcresearchpress.com by 176.9.209.113 on 09/04/12
For personal use only.

ACKNOWLEDGMENTS

The authors wish to express their appreciation to Mr. A. Funk and Mr. L. R. Nesbitt for technical assistance, and to Miss I. M. Gaffney, Mr. M. Granat, and Mr. M. Mazurek for measurement of infrared spectra and microanalyses.

REFERENCES

1. HASKINS, R. H. Can. J. Microbiol. **4**, 273 (1958).
2. DIVEKAR, P. V., READ, G., and VINING, L. C. Chem. & Ind. 731 (1959).
3. GRIPENBERG, J. Acta. Chem. Scand. **12**, 1762 (1958).
4. ERDTMAN, H., GRANATH, M., and SCHULTZ, G. Acta Chem. Scand. **8**, 1442 (1954).
5. BARCHEWITZ, P., TATIBOÜET, F., and SOUCHAY, P. Compt. rend. **236**, 1652 (1953).
6. BRASSARD, P. and L'ÉCUYER, P. Can. J. Chem. **36**, 700 (1958).
7. BRASSARD, P. and L'ÉCUYER, P. Can. J. Chem. **36**, 709 (1958).
8. THOMSON, R. H. Naturally occurring quinones. Butterworth Scientific Publications, London. 1957 p. 26.
9. KÖGL, F. and POSTOWSKY, J. J. Ann. **440**, 19 (1924).
10. GRIPENBERG, J. Acta Chem. Scand. **12**, 1411 (1958).
11. AKAGI, M. J. Pharm. Soc. Japan, **62**, 129 (1942).
12. LEDERER, E. J. Chem. Soc. 2115 (1949).
13. ARMSTRONG, M. D. and SHAW, K. N. F. J. Biol. Chem. **225**, 269 (1957).
14. DEEDS, F., BOOTH, A. N., and JONES, F. T. J. Biol. Chem. **225**, 615 (1957).
15. SIMONART, P. and WIAUX, A. Bull. soc. chim. biol. **41**, 537 (1959).
16. BOOTH, A. N., EMERSON, O. H., JONES, F. T., and DEEDS, F. J. Biol. Chem. **229**, 51 (1957).
17. ARMSTRONG, M. D., SHAW, K. N. F., and WALL, P. E. J. Biol. Chem. **218**, 293 (1956).
18. BRAY, H. G., THORPE, W. V., and WHITE, K. Biochem. J. **46**, 271 (1950).
19. MELDOLA, R. and STEPHENS, F. G. C. J. Chem. Soc. 923 (1906).

Can. J. Chem. Downloaded from www.nrcresearchpress.com by 176.9.209.113 on 09/04/12
For personal use only.

Can. J. Chem. Downloaded from www.nrcresearchpress.com by 176.9.209.113 on 09/04/12
For personal use only.

LIGHT ABSORPTION STUDIES

PART XVI. THE ULTRAVIOLET ABSORPTION SPECTRA OF FLUOROBENZENES[1]

W. F. FORBES[2]

ABSTRACT

The ultraviolet absorption spectra of a series of fluorobenzenes are determined. It is found that as a first approximation a fluoro substituent does not appreciably affect the benzenoid absorption. The spectra are discussed on the assumption that the mesomeric effect of the fluorine atom is small.

INTRODUCTION

It has previously been noted in studies of the ultraviolet absorption spectra of a number of *p*-substituted halobenzenes that the implied order of the over-all electron release for the halogens is I (greatest release) > Br > Cl > F (1, 2, 3, 4, 5). This order is difficult to reconcile with the currently accepted order of the relevant mesomeric effects, which is F > Cl > Br > I (cf. refs. 1, 3 and see also Ingold, C. K. Structure and mechanism in organic chemistry. Cornell Univ. Press, Ithaca, New York. 1953. p. 75). One attempt to reconcile the conflicting orders has been made by Burawoy, Schubert, and co-workers (1, 2, 3), who do not use the concept of the mesomeric effect but instead interpret the spectra in terms of what is known as an inductomeric effect. The order of the inductomeric effect is I > Br > Cl > F and in this way the spectral results are not at variance with the conclusions deduced from reactivity measurements, which suggest the reverse order for the mesomeric interactions.

In our own studies, on the other hand, it was found helpful to correlate spectral changes in the main ultraviolet absorption band primarily with mesomeric and steric effects. Mesomeric effects were defined in general terms as associated with electron mobility acting along systems of conjugated bonds, and classical resonance structures were found to account satisfactorily for a large number of the spectral changes. For example, the spectral changes for a number of disubstituted benzene derivatives are consistently greatest in the *p*-isomers. Two difficulties became apparent in our approach. First, it was found necessary to postulate that frequently, for steric or other reasons, absorption spectra are determined by what have been termed locally excited states. For example, the main absorption band of phenol has been interpreted as being caused predominantly by locally excited states involving only the benzene ring, with the hydroxy group exerting merely a secondary effect (6). Secondly, it was found necessary to postulate that the mesomeric effect of the halogen atoms is in the order I > Br > Cl > F, that is, not in the order generally accepted. This implies that the activated complexes involved in the chemical reactions (cf., for example, ref. 7 and references cited there), which differ from the excited states involved in electronic absorption spectra, are also affected in a different manner by the halogen atoms. This hypothesis is evidently not entirely satisfactory but it is preferred since at least it provides a consistent explanation of a variety of different spectral effects. The purpose of the present paper is to show how the spectra of fluorobenzenes can be interpreted on the basis of our general hypotheses.

[1]*Manuscript received June 29, 1959.*
Contribution from the Memorial University of Newfoundland, St. John's, Newfoundland. Presented in part at the meetings of the Chemical Institute of Canada, Halifax, Nova Scotia, May, 1959.
[2]*Present address: Division of Protein Chemistry, C.S.I.R.O., Parkville, N. 2, Victoria, Australia.*

Can. J. Chem. Downloaded from www.nrcresearchpress.com by 176.9.209.113 on 09/04/12
For personal use only.

THE SPECTRUM OF FLUOROBENZENE

The spectra of fluorobenzene in different solvents are listed in Table I.

TABLE I

Absorption maxima of fluorobenzene in various solvents*

	B-Band†,§		*C*-Band†	
Solvent	λ_{max}(mμ)	ϵ_{max}	λ_{max}(mμ)	ϵ_{max}
Vapor phase	206	‡	247 253 259 265	‡
Cyclohexane	204	*ca.* 8000	248 254 259 266	450 850 1300 1150
Ether	207	*ca.* 3000	248 253 259 265	250 450 750 750
Ethanol	204	*ca.* 8000	248 254 259 266	600 1000 1300 1200
Water	202	*ca.* 3000	*248* 253 258 265	*150* 275 390 300

*Values in italics represent inflections in this and the subsequent table.
†For band nomenclature used, see previous parts of this series of papers.
‡Intensities not determined.
§See "Experimental" concerning the accuracy of maximal wavelengths below 210 mμ.

The similarity of the *C*-bands for fluorobenzene and benzene in inert media has previously been noted (8), and Fig. 1 now records both *B*- and *C*-bands as also the *B*- and *C*-bands of iodobenzene.

Table I shows that the *B*-band location of fluorobenzene is not appreciably affected by solvent changes. Figure 1 indicates that any effect which the fluorine atom has on the benzene spectrum is less than the effect of the other halogens since the latter all cause appreciable spectral changes particularly on the *B*-band as illustrated, for example, by the spectrum of iodobenzene. The small wavelength displacement caused by the fluorine atom on the benzene *B*-band (*ca.* 2 mμ) is ascribed to secondary interaction (cf. ref. 6), and this displacement is similar to the effect which the fluorine atom has on a number of other benzenoid spectra in the absence of appreciable mesomeric interaction (see next sections). Both *B*- and *C*-bands of fluorobenzene appear to be less intense in ether or aqueous solutions.

THE SPECTRA OF PARASUBSTITUTED FLUOROBENZENES

The spectra of substituted fluorobenzenes are listed in Table II.

Table II shows that the maximal locations of the *B*-bands of *p*-substituted fluorobenzenes are all similar to the locations of the *B*-bands of the corresponding non-fluoro-substituted analogues as a first approximation (cf. also ref. 5). However, closer inspection

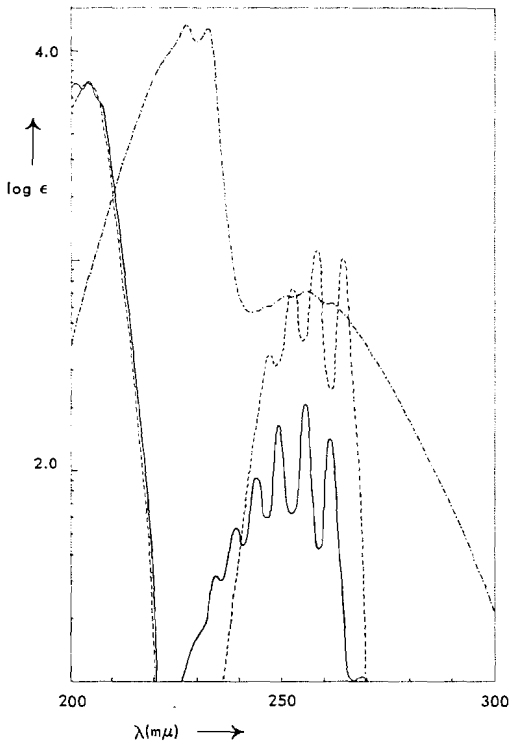

FIG. 1. The ultraviolet absorption spectra of benzene (——) in *n*-heptane solution, and of fluorobenzene (– – –) and of iodobenzene (—·—·) in cyclohexane solution.

allows a subdivision into two classes:

(i) If the *p*-substituent is electron-donating, a *hypsochromic* wavelength displacement is frequently observed in the *B*-band with respect to the non-fluorosubstituted parent compound. For example, in hexane solution Burawoy and Thompson (3) report the wavelength changes in the *B*-band for *p*-fluoroaniline, *p*-fluoroanisole, and *p*-iodofluorobenzene to be -3.5, -3.5, and -3.8 mμ compared with the *B*-bands of aniline, anisole, and iodobenzene respectively. To explain these wavelength displacements it may be assumed that resonance forms of type I contribute predominantly to the electronic excited state. These resonance forms represent locally excited states, in the example shown that of aniline, and the fluorine atom is assumed to exert only a secondary effect. Since the fluorine atom may be expected to withdraw electrons from the neighboring carbon atom, and since further this electron withdrawal will hinder the formation of a negative charge on the carbon atom, the secondary effect may be anticipated to raise the transition energy and in this way the observed slight hypsochromic wavelength displacement in the *B*-band can be rationalized.

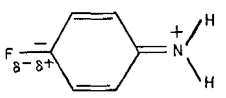

(I)

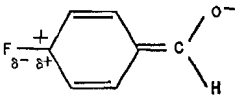

(II)

Can. J. Chem. Downloaded from www.nrcresearchpress.com by 176.9.209.113 on 09/04/12
For personal use only.

Can. J. Chem. Downloaded from www.nrcresearchpress.com by 176.9.209.113 on 09/04/12
For personal use only.

TABLE II

Absorption maxima of substituted fluorobenzenes in cyclohexane solution

	Para isomer				Meta isomer						Ortho isomer					
	B-Band		*C*-Band		*B*-Band		2nd *B*-band		*C*-Band		*B*-Band		2nd *B*-band		*C*-Band	
Substituent	$\lambda_{max}(m\mu)$	ϵ_{max}	$\lambda_{max}(m\mu)$	ϵ_{max}	$\lambda_{max}(m\mu)$	ϵ_{max}	$\lambda_{max}(m\mu)$	ϵ_{max}	$\lambda_{max}(m\mu)$	ϵ_{max}	$\lambda_{max}(m\mu)$	ϵ_{max}	$\lambda_{max}(m\mu)$	ϵ_{max}	$\lambda_{max}(m\mu)$	ϵ_{max}
-F	204	*ca.*7000	*ca.248*	*500*	203	*ca.*8000	—	—	254	700						
			ca.251	*725*					260	1000						
			253	1000					265	1000						
			258	1650												
			261	2100												
			264	2000												
			267	3000												
			273	2600												
-Cl	209	5500	*258*	*450*			211	8500					210	10,000		
	215	5500	263	780			215	8500	258	600			214	10,000	260	1000
	ca.218	*4500*	271	1100					265	1000					266	1400
			277	1150					272	1000					272	1500
-Br	215	7000	265	800			213	8000	260	700						
			271	1050			*ca.215*	7500	266	1000						
			278	900					273	800						
-I	226	10,500	*ca.251*	*1750*												
	ca.230	*8500*	255	1900												
			258	1950												
			ca.262	*1900*												
			266	1850												
			ca.271	*1600*												
			ca.280	*1000*												
$-CH_3$	206	7250	253	510			207	*ca.*7500*	257	600			206	8000*	257	700
			256	625					262	850					262	1000
			259	900					269	950					268	1000
			261	1000												
			264	1100												
			267	1700												
			273	1650												

Can. J. Chem. Downloaded from www.nrcresearchpress.com by 176.9.209.113 on 09/04/12
For personal use only.

TABLE II (*concluded*)

Absorption maxima of substituted fluorobenzenes in cyclohexane solution

	Para isomer				Meta isomer						Ortho isomer					
	B-Band		*C*-Band		*B*-Band		2nd *B*-band		*C*-Band		*B*-Band		2nd *B*-band		*C*-Band	
Substituent	λ_{max}(mμ)	ϵ_{max}	λ_{max}(mμ)	ϵ_{max}	λ_{max}(mμ)	ϵ_{max}	λ_{max}(mμ)	ϵ_{max}	λ_{max}(mμ)	ϵ_{max}	λ_{max}(mμ)	ϵ_{max}	λ_{max}(mμ)	ϵ_{max}	λ_{max}(mμ)	ϵ_{max}
-OH	212–213	4200	*270*	*1700*												
	ca.217	*3600*	272.5	2200			213.5	5200	*ca.266*	*1150*			214	5800	265	1250
			275.5	2500					269.5	1450					269	1600
			278.5	2750					275	1300					275	1400
			281.5	3100												
			ca.285	*2000*												
			288	2600												
-OCH_3	*ca.213*	*5000**	*ca.270*	*1650*			220	7500	*ca.266*	*1250*			219.5	7100	267.5	1450
	218–219	5400	272.5	2150					269.5	1550					271	1700
			275.5	2500					275.5	1450					276	1450
			278	2750												
			281.5	3200												
			287.5	2750												
-NH_2	230	7000	293	2200			234	10,000	*ca.280*	*1800*			230	11,000	281	2500
			296	2200					283	1900						
			ca.300	*2100*												
-$COCH_3$	240	12,000	266	550			235	10,500	280	1700			233	9500	279	1600
									290	1250						
-CHO	244	13,000					238	12,800	282–283	2100			240	13,300	284	2400
							246	11,600	290	1750			*ca.247*	*9700*	291	2000
									ca.293	*1700*					294	2000
-NO_2	256	9500	—	—	210	8000*	250	8500	284	1850			242	7250	278	1850†
-COOH‡	232	12,000	263	650			230	11,200	279	2000			227	11,000	278	1950
			269	400			*ca.235*	*10,300*	286	1700					*ca.283*	*1500*

**B*-Band assignment doubtful; cf. also "Experimental". †Reference 10 (in isooctane solution). ‡These bands are concentration dependent; values quoted are those at relatively small solute concentrations.

(ii) If, on the other hand, the non-fluoro substituent is electron-withdrawing, the reverse effect would be expected. That is, resonance forms of type II would be favored by the electron-withdrawing effect of the fluorine atom and this may cause a slight *bathochromic* wavelength displacement. Examples to support this suggestion are provided by the data of Burawoy and Thompson (3), who report bathochromic displacements in hexane of 3.1 and 5.6 mμ for the *B*-bands of the spectra of *p*-fluorobenzaldehyde and *p*-fluoronitrobenzene compared with the spectra of benzaldehyde and nitrobenzene respectively. It might be noted that the small wavelength displacement from benzene to fluorobenzene in inert media (see previous section) can similarly be explained.

In addition to the wavelength displacement of the *B*-band caused by the fluorine atom, the fluorine atom also generally appears to decrease the extinction coefficient (ϵ_{max}) of the *B*-band of the fluorosubstituted benzene derivative compared with the ϵ_{max} value of the *B*-band of the non-fluorosubstituted parent compound (see Table II and refs. 3 and 5). This effect may again be ascribed to the electron-withdrawing ability of the fluorine atom which may be assumed to decrease the proportion of available π-electrons in the benzene ring and in this way decrease the over-all absorption probability of the transition involving the benzene ring.

Significant spectral changes between the *p*-substituted fluorobenzene and the non-fluorosubstituted parent compound are also observed in the *C*-band; for example, the fine structure is frequently increased characteristically. This is shown by the data in Table II and is further illustrated by Fig. 2 which records the spectra of phenol and *p*-fluorophenol. Figure 2 shows that while the *B*-bands remain similar, the *C*-band fine structure in *p*-fluorophenol is appreciably increased.

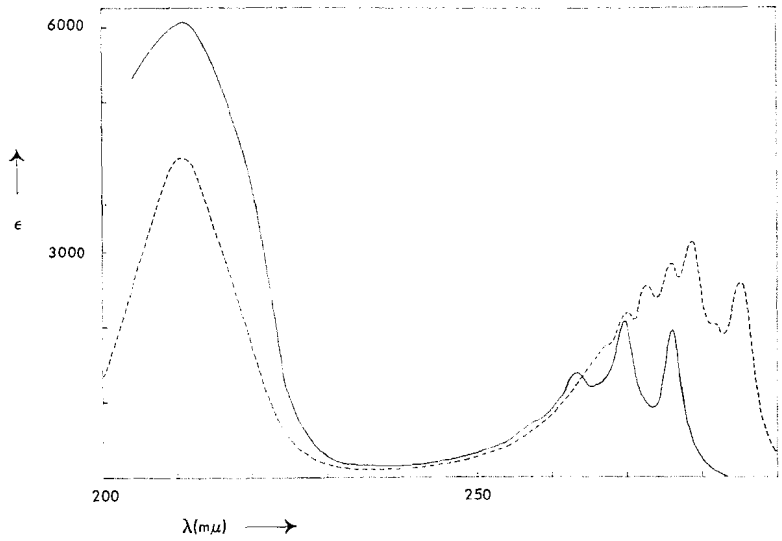

FIG. 2. The ultraviolet absorption spectra of phenol (——) and *p*-fluorophenol (– – –) in cyclohexane solution.

THE SPECTRA OF METASUBSTITUTED FLUOROBENZENES

The spectra of *m*-substituted fluorobenzenes, as other previously discussed spectra of *m*-disubstituted benzene derivatives, might be expected to show two *B*-bands corresponding to the two monosubstituted parent compounds. Unfortunately, the fluorobenzene *B*-band cannot usually be identified with any degree of confidence, because it occurs at a wavelength at which it is not readily identified.

Can. J. Chem. Downloaded from www.nrcresearchpress.com by 176.9.209.113 on 09/04/12
For personal use only.

The location of the maximal absorption of the second, non-fluorobenzene, *B*-band again does not appear to be appreciably affected by the fluorine atom as a first approximation. More careful examination of the data, however, indicates that the second *B*-band is frequently *hypsochromically* displaced if the non-fluoro substituent is *electron-withdrawing*. For example, *m*-fluorobenzaldehyde absorbs at shorter wavelength than benzaldehyde (9), and *m*-fluoronitrobenzene absorbs at shorter wavelength than nitrobenzene (10, 11). These slight hypsochromic displacements are in a different direction from the displacements observed in the corresponding *p*-isomers (see previous section), but this is not unexpected if resonance forms of type III are assumed to be predominantly

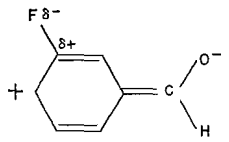

(III)

involved in the transitions leading to the observed absorption. This follows because the electron-withdrawing effect of the fluorine atom will now favor the formation of a positive charge on a *different* carbon atom (cf. the related resonance form II in the previous section), which in turn will tend to hinder the positive charge formation associated with resonance forms II and III.

Conversely, if the non-fluoro substituent is *electron-donating* a slight *bathochromic* wavelength displacement is usually observed for the *m*-substituted fluorobenzenes (see Table II, and previous parts of this series for the relevant *B*-bands of the non-fluoro-substituted parent compounds). It may also be noted that opposite wavelength displacements in the meta and para isomers are sometimes observed in the infrared spectra. For example, Krueger and Thompson (12) report that the amino group stretching vibrations of *p*-fluoroaniline occur at *lower* frequency than for aniline, but that those of *m*-fluoroaniline occur at *higher* frequency compared with the stretching vibrations of aniline.

The extinction coefficient (ϵ_{max}) of the second *B*-band is again generally decreased compared with the *B*-band of the corresponding non-fluorosubstituted parent compound (see Tables I and II).

Whereas, with the exception of the above-mentioned minor spectral changes, the *B*-band remains essentially unaltered, the *C*-bands of *m*-substituted fluorobenzenes are frequently profoundly altered on introducing a substituent (see Table II and cf. also ref. 13 for a discussion of the fluorobenzene band). For example, in *m*-fluorobenzaldehyde compared with benzaldehyde, the *C*-band is bathochromically displaced and the extinction coefficient is almost doubled (see Table II and ref. 9). The *C*-band in the *o*-isomers incidentally appears frequently to undergo similar spectral changes.

THE SPECTRA OF ORTHOSUBSTITUTED FLUOROBENZENES

In the absence of direct mesomeric interaction two *B*-bands are again possible (see previous section), but again the *B*-bands associated with fluorobenzene absorption can only be identified with difficulty. As a first approximation, the second *B*-band is only slightly altered because of the fluorine atom.

Closer inspection of the data shows that this second *B*-band, compared with the same *B*-band in the *m*-isomer, usually occurs at slightly shorter wavelength and with slightly

Can. J. Chem. Downloaded from www.nrcresearchpress.com by 176.9.209.113 on 09/04/12
For personal use only.

Can. J. Chem. Downloaded from www.nrcresearchpress.com by 176.9.209.113 on 09/04/12
For personal use only.

reduced absorption intensity. Since this effect appears to be more pronounced when the non-fluoro substituent is large and electronegative, it seems reasonable to ascribe this secondary spectral effect to electrostatic repulsions and/or steric interactions between the fluorine atom and the *o*-substituent. This is illustrated by the data in Table II for the relevant *B*-bands (see also refs. 14, 15, and 16 for the spectra and a full discussion of diphenyl, fluorosubstituted diphenyls and related compounds). The effect of the size of the substituent may be deduced from the aniline spectra where an *o*-fluoro substituent causes an increased extinction coefficient, whereas an *o*-fluoro substituent in the larger N,N-dimethylaniline is reported to cause a reduced extinction coefficient (ϵ_{max} 11,600) compared with the relevant extinction coefficient in N,N-dimethylaniline (ϵ_{max} 13,750) (cf. Klevens and Platt (17), who assume a certain degree of non-planarity for *o*-fluoro-N,N-dimethylaniline). Likewise the spectra of *o*-fluorobenzaldehyde and *o*-fluoroacetophenone, which may be assumed to possess similar conformations,* indicate that *o*-fluoroacetophenone is less planar because the characteristic hypsochromic wavelength displacement and ϵ decrease only occur in the *B*-band of the acetophenone.

The data also again show that the *B*-band spectral changes can be explained as a first approximation without taking into account the effects of intramolecular hydrogen bonding or of inductive effects involving the fluorine atom. For example, compounds like *o*-fluorophenol and *o*-fluorobenzoic acid, which are believed to form an intramolecular hydrogen bond (19, 20), possess spectra similar to those of the corresponding *m*-isomers (see Table II). This is illustrated in Fig. 3, which shows that the *B*-band of *o*-fluorobenzoic acid is not very different from the *B*-bands of either *m*-fluorobenzoic acid or even benzoic acid itself.

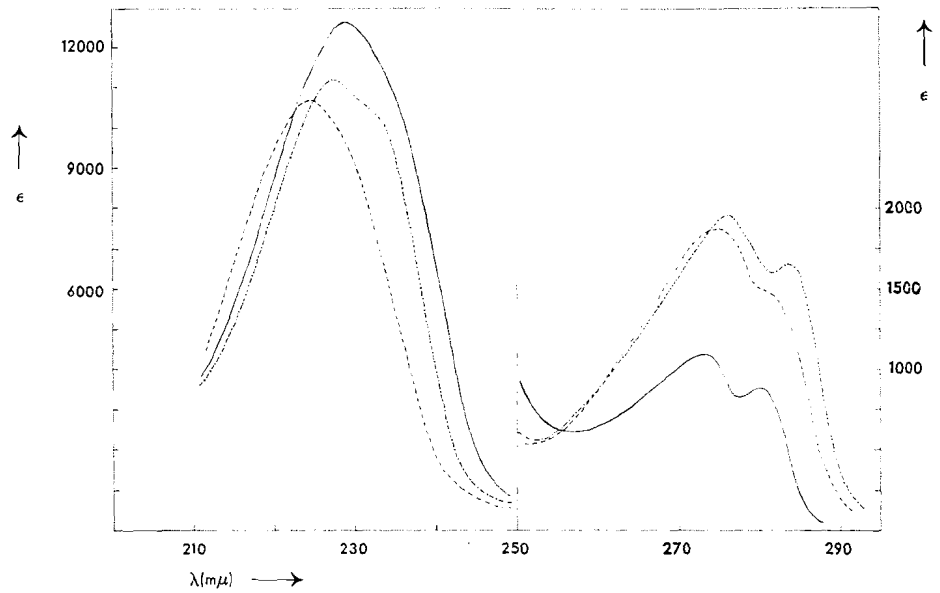

FIG. 3. The ultraviolet absorption spectra of benzoic acid (——), *o*-fluorobenzoic acid (– – –), and *m*-fluorobenzoic acid in cyclohexane solution.

**The infrared carbonyl band of o-fluorobenzaldehyde in carbon tetrachloride solution showed only one intense peak at 1701 cm^{-1}. By analogous reasoning as employed in the interpretation of the infrared carbonyl band of o-fluoroacetophenone at 1692 cm^{-1} (18), we assume that both compounds exist predominantly in one conformation with the C=O and C—F dipoles aligned in opposite directions. Since on the basis of steric considerations alone o-fluorobenzaldehyde might be expected to exist in two s-cis, s-trans conformations, this further suggests that the electrostatic repulsive forces associated with the fluorine atom are sufficiently important to tend to maintain the molecule predominantly in only one conformation.*

This then provides additional evidence that, as a first approximation, *B*-bands of the type discussed in this paper are determined predominantly by mesomeric and steric interactions (cf. refs. 4 and 21).

EXPERIMENTAL

The ultraviolet absorption spectra were determined by standard methods using a Unicam SP500 or a Beckman Model DU spectrophotometer. For each compound at least two independent sets of observations were made. Some of the spectra have previously been described in this series. The Unicam SP500 instrument was calibrated against a didymium filter and wavelength readings obtained on the Unicam and Beckman instruments were found to be within 1 mμ of each other. The values given in this paper should replace earlier wavelength values (6) which were determined on an uncalibrated SP500 spectrophotometer. Difficulty was encountered in obtaining maximal absorptions below 210 mμ since on both instruments the location of the maximal absorption frequently changed with concentration. The values quoted were determined in 1-mm cells for absorption maxima below 210 mμ but otherwise in 1-cm cells. Apart from the maximal wavelengths below 210 mμ, the accuracy of λ_{max} values is estimated to be ± 0.5 mμ, and the precision of ϵ_{max} values $\pm 5\%$ or better. Values were reproducible in most cases to $\pm 2\%$.

The infrared spectrum was determined on a Unicam SP100 instrument, using a NaCl prism and a diffraction grating.

The fluorobenzenes were either prepared by standard methods or were commercially available; they were purified by distillation or recrystallization until their boiling points and refractive indices or melting points showed them to be sufficiently pure. The solvents used were spectroanalyzed cyclohexane (Fisher) or other commercially available spectroanalyzed solvents.

ACKNOWLEDGMENTS

The author is greatly indebted to Miss Florence Jackman for very competent technical assistance in the determination of the spectral data. Thanks are also due to Mr. D. L. Coffen for determining the infrared spectrum and to Mr. J. C. Dearden, who prepared the diagrams and also obtained some of the spectral data.

The financial assistance of the National Research Council is again gratefully acknowledged.

REFERENCES

1. SCHUBERT, W. M., CRAVEN, J. M., and STEADLY, H. J. Am. Chem. Soc. **81**, 2695 (1959).
2. SCHUBERT, W. M., CRAVEN, J. M., STEADLY, H., and ROBINS, J. J. Org. Chem. **22**, 1285 (1957).
3. BURAWOY, A. and THOMPSON, A. R. J. Chem. Soc. 4314 (1956).
4. FORBES, W. F. and MUELLER, W. A. Can. J. Chem. **35**, 488 (1957).
5. FORBES, W. F. and RALPH, A. S. Can. J. Chem. **34**, 1447 (1956).
6. DEARDEN, J. C. and FORBES, W. F. Can. J. Chem. **37**, 1294 (1959).
7. BRAUDE, E. A. and STERN, E. S. J. Chem. Soc. 1096 (1947).
8. ROBIN, M. J. Chem. Educ. **33**, 526 (1956).
9. DEARDEN, J. C. and FORBES, W. F. Can. J. Chem. **36**, 1362 (1958).
10. GRUBER, W. Can. J. Chem. **31**, 1020 (1953).
11. FORBES, W. F. Can. J. Chem. **36**, 1350 (1958).
12. KRUEGER, P. J. and THOMPSON, H. W. Proc. Roy. Soc. A, **243**, 143 (1957).
13. KLEVENS, H. B. and ZIMRING, L. J. J. Chem. Phys. **49**, 377 (1952).
14. BEAVAN, G. H. and HALL, D. M. J. Chem. Soc. 4637 (1957).
15. BROWNSTEIN, S. J. Am. Chem. Soc. **80**, 2300 (1958).
16. BILBO, A. J. and WYMAN, G. M. J. Am. Chem. Soc. **75**, 5312 (1953).
17. KLEVENS, H. B. and PLATT, J. R. J. Am. Chem. Soc. **71**, 1714 (1949).
18. JONES, R. N., FORBES, W. F., and MUELLER, W. A. Can. J. Chem. **35**, 504 (1957).
19. BAKER, A. W. J. Am. Chem. Soc. **80**, 3598 (1958).
20. MARYOTT, A. A., HOBBS, M. E., and GROSS, P. M. J. Chem. Phys. **9**, 415 (1941).
21. RAO, C. N. R. and RAMACHANDRA, J. J. Sci. Ind. Research, B, **17**, 56 (1958).

Can. J. Chem. Downloaded from www.nrcresearchpress.com by 176.9.209.113 on 09/04/12
For personal use only.

Can. J. Chem. Downloaded from www.nrcresearchpress.com by 176.9.209.113 on 09/04/12
For personal use only.

THE NATURE OF THE SPECIFICITY OF ADSORPTION OF ALKYL ORANGE DYES ON SILICA GEL[1]

JOHN L. MORRISON,[2] M. WORSLEY,[3] D. R. SHAW,[4] AND G. W. HODGSON[5]

ABSTRACT

The properties of silica gels sensitized by methyl orange and its homologues were critically examined in order to decide between the alternative hypotheses of a lock and key mechanism and an association mechanism to explain the enhancement of adsorption. Evidence appears to favor an association mechanism in which the unextractable dye particles act as centers to attract their own kind more strongly than one of their homologues. Nitrogen area measurements show that less than 0.5% of the gel surface area is used in adsorbing dye molecules. The dye series from methyl to butyl orange have a very sharp increase in solubility from ethyl to propyl when dissolved in 5% aqueous acetic acid solution (pH = 2.3).

INTRODUCTION

The preparation of solid adsorbents specific to predetermined substances has both theoretical and practical interest (1). Dickey (2, 3) has reported the preparation of silica gels that specifically adsorb their sensitizing alkyl orange dyes. Haldeman and Emmett (4) attempted to correlate dye adsorption with nitrogen area measurements.

In his original communication (2), Dickey compared his adsorbents by making single adsorption measurements from solutions of the same *initial* concentration; this magnified any differences in adsorption. He interprets the phenomenon in terms of a "lock and key" or "footprint" mechanism.

There is, no doubt, a production of some specificity in adsorption, but our experiments show that an alternative explanation of the specificity may be found in the fact that a relatively appreciable amount of the sensitizing dye is permanently retained by the adsorbent.

EXPERIMENTAL

Preparation of Silica Gels

Following Dickey (2, 3), silica gels were prepared by the acetic acid and the oxalate methods. In each case, sodium silicate solution (J. T. Baker Chemical Co., Technical, 40°–42° Bé) with and without a sensitizing dye was acidified by an acid to produce a gel.

Two modifications were made in the procedure: one, the mixture of sodium silicate solution and dye was heated nearly to boiling before adding the acid. This was necessary to ensure more complete solution of the dyes. When the acid was added, there was a precipitation of much of the methyl orange, less of the ethyl orange, and the propyl and butyl orange solutions gave clear gels.

The other modification was to wash the gel thoroughly with distilled water after it had been dried, ground, and sieved. It was found that methanol extraction alone did not

[1]*Manuscript received July 20, 1959.*
Contribution from the Department of Chemistry, University of Alberta, Edmonton, Alberta. Part of this paper was taken from the thesis of M. Worsley, presented in partial fulfillment of the requirement for the degree of M.Sc., May, 1952. Presented at the 39th Annual Conference, Chemical Institute of Canada, Montreal, Que., May 28–30, 1956.
[2]*Present address: Connaught Medical Research Laboratories, Toronto, Ontario.*
[3]*Present address: Hooker Electrochemical Co., Niagara Falls, N.Y.*
[4]*Present address: Alberta Petroleum and Natural Gas Conservation Board, Edmonton, Alberta.*
[5]*Associate Research Officer, Research Council of Alberta, Edmonton, Alberta.*

remove all of the residual sodium acetate in the acetic acid method. As a result, in the absence of water washing, both the weight of the gel and the concentration of dye solutions used in the subsequent adsorption experiments were in doubt. The pH of these solutions shifted from 2.3 (5% acetic acid solution) to about 4 with an indeterminate effect on the concentration measurements by the spectrophotometer (Beckman model DU).

A similar washing procedure was used for the oxalate gels.

Adsorption Measurements with Dye Solutions

The alkyl orange dyes were prepared by the method of Slotta and Franke (5). The dyes were purified (6) and analyzed by a semimicro Nesslar method. Purity of 98–100% was obtained, and the extinction coefficients were similar to those reported by Klotz *et al.* (7).

Dye solutions for adsorption measurements were prepared in 5% acetic acid, pH 2.3. At this pH, the absorption maxima at about 510 μ for the four dyes were used for analysis. In some of the later experiments, corrections were made for small deviations from Beer's Law.

For the series A acetic acid gels, each adsorption measurement was made on a separate gel sample (1 g). As a result, there was a considerable sampling error which for this method could only be overcome by using larger samples.

For the series B acetic acid gels and the oxalate gels, the same gel sample was used with each dye (4). Thus, for example, 100 ml of 1×10^{-5} molar dye solution was added to 1 g silica gel, and equilibrated with occasional shaking at 25.0° C for 3 days. After centrifugation, 80 ml of supernatant was removed and analyzed, and 80 ml of the next higher concentration (2×10^{-5}) was added. A repetition of this procedure for 3 and 5×10^{-5} molar solutions completed the adsorption measurements. A much smoother adsorption isotherm curve was obtained by this serial procedure than by the batch method.

Acid-washing of the Gels

The effect of acid(HCl)-washing (3) was determined by dividing the gel samples into two parts, one part which was immersed in 1 *N* HCl for 1 day, then carefully washed with distilled water, and the other part washed with distilled water only.

Residual Dye Content

Following Haldeman and Emmett (4), the residual dye content of each gel was determined by dissolving a weighed sample in 1 *N* NaOH solution. The sample was neutralized, adjusted to pH 2.3 and analyzed spectrophotometrically.

Nitrogen Areas

Nitrogen adsorption isotherms were measured at −195° C on all samples of series B acetic acid gels and oxalate gels. The Brunauer–Emmett–Teller equation (8) was applied to determine the amount of nitrogen adsorbed in a monolayer. In contrast to Haldeman and Emmett (4), who heated their gels to 200° C for 1 hour, a temperature and time which "would be sufficient to destroy the specificity of the sample . . .", we evacuated the gels at room temperature for at least 16 hours to remove adsorbed gases. The measurements were made as soon as possible after the gels were prepared.

Dye Solubilities

The solubilities of the alkyl orange dyes in 5% acetic acid at 25° C were determined spectrophotometrically, and are given in Table I. In each case, excess solid dye was

Can. J. Chem. Downloaded from www.nrcresearchpress.com by 176.9.209.113 on 09/04/12
For personal use only.

added to the acetic acid solution at 75° C, then cooled to the bath temperature and kept in contact, with occasional shaking, for 3 days.

TABLE I

Dye solubilities in 5% aqueous acetic acid at 25° C

Dye	Concentration of saturated solution (moles/liter)
Methyl orange	8.17×10^{-5}
Ethyl orange	7.75×10^{-5}
Propyl orange	22.5×10^{-5}
Butyl orange	34.8×10^{-5}

RESULTS AND DISCUSSION

Adsorption Isotherms

The adsorption isotherms are reversible (4) as illustrated in Fig. 1 by the batch measurements for ethyl orange on an ethyl-orange-sensitized gel.

In general, the adsorption isotherms of the dyes on sensitized gels are concave to the concentration axis and then they increase approximately linearly. The isotherms of methyl and ethyl orange dyes on control gels are approximately linear from zero concentration (3). However, propyl and butyl orange dyes also show concavity on control gels.

The isotherms increase approximately linearly up to saturated solutions of adsorbate. This is illustrated by Figs. 1 and 2. In the latter case, an equilibrium concentration of 17×10^{-5} molar was achieved.

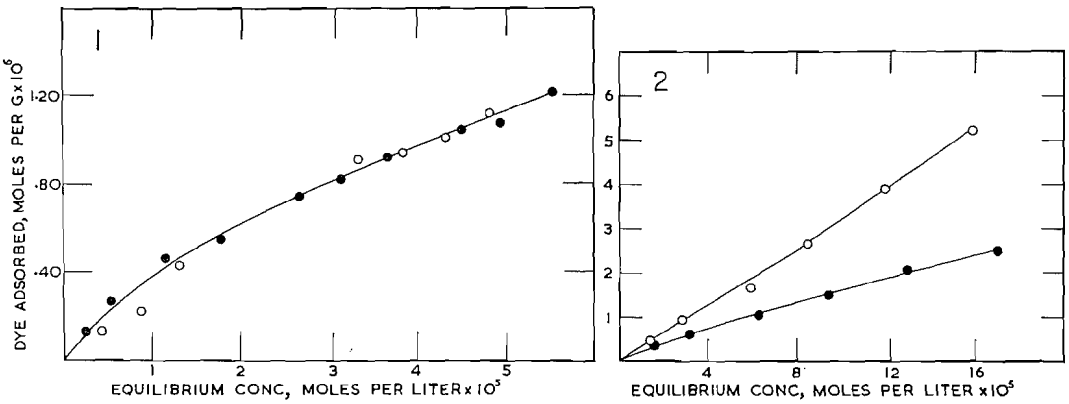

FIG. 1. The sorption isotherm of ethyl orange dye on an ethyl orange silica gel (series A, acetic acid, water-treated). ● Adsorption. ○ Desorption.

FIG. 2. Adsorption isotherms of propyl orange dye extended to relatively high concentrations. ○ A methyl orange, acetic acid, water-treated gel. ● A propyl orange, oxalate, HCl-treated gel.

Absolute Amounts Adsorbed

The absolute magnitudes of adsorption are given in Table II for 1.5×10^{-5} molar equilibrium concentration as interpolated on the isotherms.

It is not possible to determine the absolute magnitudes from Dickey's original paper (2), but more recently (3) he reported absolute measurements for methyl and ethyl dyes and gels. Our results are very similar to his for the dye-sensitized gels, and much higher for control gels. Thus, we conclude that our modification of heating the dye – sodium

Can. J. Chem. Downloaded from www.nrcresearchpress.com by 176.9.209.113 on 09/04/12
For personal use only.

Can. J. Chem. Downloaded from www.nrcresearchpress.com by 176.9.209.113 on 09/04/12
For personal use only.

TABLE II

Adsorption of dyes on silica gels at 1.5×10^{-5} molar concentration

Silica gel	Series A acetic (H_2O)				Series B acetic (H_2O)				Series B acetic (HCl)				Oxalate (H_2O)				Oxalate (HCl)			
	M.	E.	P.	B.	M.	E.	P.	B.	M.	E.	P.	B.	M.	E.	P.	B.	M.	E.	P.	B.
(A) Absolute dye adsorption, moles $\times10^6$ per g																				
Control	0.25	0.19	0.48	0.50	0.40	0.40	0.92	1.25	0.22	0.21	0.51	0.68	0.12	0.09	0.20	0.31	0.13	0.033	0.15	0.27
Methyl	0.40	0.25	0.44	0.42	0.35	0.37	0.77	0.90	0.34	0.31	0.57	0.72	0.33	0.16	0.09	0.35	0.34	0.16	0.13	0.25
Ethyl	0.50	0.51	0.62	0.92	0.32	0.35	0.62	0.77	0.36	0.42	0.75	0.64	0.29	0.22	0.45	0.33	0.32	0.32	0.32	0.29
Propyl	0.37	0.43	1.08	1.28	0.33	0.31	0.75	0.86	0.38	0.48	1.05	1.34	0.21	0.26	0.46	0.38	0.18	0.14	0.32	0.44
Butyl	0.34	0.35	0.78	0.72	0.34	0.31	0.73	0.90	0.33	0.34	0.98	1.30	0.29	0.24	0.59	0.80	0.19	0.22	0.45	0.65
(B) Relative adsorption power																				
Methyl	1.6	1.3	0.92	0.84	0.88	0.94	0.84	0.72	1.6	1.5	1.1	1.1	2.8	1.8	0.45	1.1	2.6	4.9	0.87	0.93
Ethyl	2.0	2.7	1.3	1.8	0.80	0.88	0.68	0.62	1.6	2.0	1.5	0.9	2.4	2.4	2.2	1.1	2.5	9.7	2.1	1.1
Propyl	1.5	2.3	2.3	2.6	0.83	0.78	0.82	0.69	1.7	2.3	2.1	2.0	1.8	2.9	2.3	1.2	1.4	4.2	2.1	1.6
Butyl	1.4	1.8	1.6	1.4	0.85	0.79	0.79	0.72	1.5	1.6	1.9	1.9	2.4	2.7	3.0	2.6	1.5	6.7	3.0	2.4

silicate solutions before adding the acid is not a significant one insofar as specific effects are concerned.

Relative Adsorption Power

The relative adsorption powers given in Table II are defined as the ratio of the adsorptions for the sensitized and control gels at 1.5×10^{-5} molar equilibrium concentration.* Dickey (3) used 0.5×10^{-5} molar and Haldeman and Emmett (4) used 1×10^{-5}. The value 1.5×10^{-5} was chosen here because it was in a region of greater accuracy, although it is recognized that it tends to give somewhat lower values for the relative adsorption power.

Specificity of Adsorption

In general, the sensitizing process enhances adsorption by $1\frac{1}{2}$ to 2 times compared with the control gels. Higher degrees of enhancement are more apparent than real. For example, a relative adsorption power of 9.7 for ethyl orange on ethyl orange oxalate (HCl) gel arises from an extremely low value for the adsorption on the control. The absolute value (0.32×10^{-6} mole per g) on this ethyl orange gel is lower than the absolute values on all of the other ethyl orange gels except the oxalate (H_2O) gel.

The specificity is so low that it can be masked by gel fluctuations. It was found that two controls when prepared under identical conditions from the same batch of sodium silicate may differ by as much as 25% and two sensitized gels also identically prepared may differ by as much as 50%.

Nitrogen Areas

Nitrogen area measurements were made to test the postulate by Dickey that the specificity of adsorption was due to footprints or imprints left in the gel structure by the dye molecules.

The nitrogen areas of a number of our gels are given in Table III. Haldeman and

TABLE III

Nitrogen surface areas, square meters per g

	Series B acetic acid gels		Oxalate gels	
Silica gel	(H_2O)	(HCl)	(H_2O)	(HCl)
Control	715	746	484	457
Methyl	(*a*) 574	(*a*) 702	695	471
	(*b*) 574	(*b*) 631	674	
Ethyl	574	662	674	461
Propyl	584	675	492	550
Butyl	588	649	554	588

NOTE: Basis: N_2 molecular adsorption area = 16.2 Å^2.

Emmett also measured the nitrogen areas of a number of Dickey's silica gels (4). They obtained the same area, 980 sq. m per g, for all the gels. Our gel areas are significantly lower, and are very similar to those obtained by Sing and Madeley (10). The latter workers used freshly prepared gels, but, like Haldeman and Emmett, they heated the

**Dickey in his original paper and Haldeman and Emmett in some of their measurements have used the same initial concentration. This misleadingly magnifies the specificity, and the more so, the lower the initial concentration. Dickey acknowledges this magnifying effect (ref. 3, p. 698), but he and Bernhard (9), and also Haldeman and Emmett, continue to accept the original announcement and perpetuate the misleading method. Dickey (Table I in ref. 4) confuses the problem even further by using a variety of initial concentrations for the different dye solutions.*

Can. J. Chem. Downloaded from www.nrcresearchpress.com by 176.9.209.113 on 09/04/12
For personal use only.

gels to 200° C for 1 to 2 hours. It would appear that the gel gradually disintegrates in time to produce a larger surface area.

It is questionable that nitrogen area measurements will reveal anything concerning the *specificity* of adsorption on sensitized silica gels. What they do show is that the fraction of gel surface used in the adsorption of the alkyl oranges is very small.

For example, the highest adsorption we observed, which was for propyl orange approaching saturation concentration, was 5.2×10^{-6} mole dye per g gel. Assuming like Haldeman and Emmett that the molecular adsorption area of each dye molecule is 100 Å^2, and that they adsorb in a monolayer, we find that in this case only 0.4% of the surface is covered by dye molecules.

Nitrogen area measurements on the same sample vary by as much as 1% and the variations observed here from one gel preparation to another, and even from water to acid washing on the same gel are as much as 40%. Obviously, it would be very difficult to distinguish by means of nitrogen areas between the presence of "footprints" in a sensitized gel and their absence in a control gel, and even more so, the difference of the "imprints" of two methylene groups in gels sensitized to two successive dye homologues.

Unextractable Dye

The residual dye content of two series of sensitized gels, both water- and acid-washed, are given in Table IV. Acid-washing does not alter the amount of residual dye.

TABLE IV

Unextractable dye contents, moles $\times10^8$ per g

	Series B acetic acid gels		Oxalate gels	
Silica gel	(H_2O)	(HCl)	(H_2O)	(HCl)
Methyl	3	8	8	7
Ethyl	15	10	24	26
Propyl	31	29	70	72
Butyl	23	21	67	75

In general, contrary to Dickey's statement "that more than one hundred times as much dye may be specifically adsorbed as is unextractably retained" (ref. 3, p. 705), we find that the amount of residual dye is an appreciable fraction of the amount of dye specifically adsorbed.

For example, in Fig. 3, the amount of propyl dye *specifically* adsorbed on a propyl

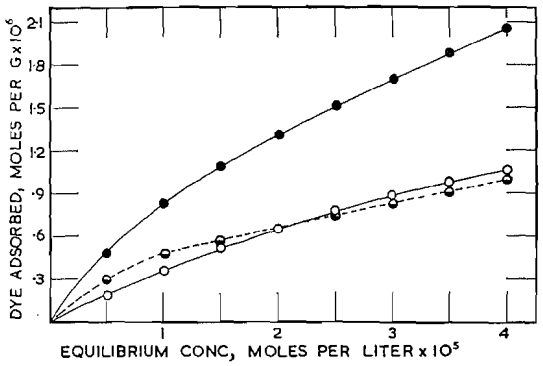

FIG. 3. Specifically adsorbed propyl orange dye. ● Propyl orange gel (series B, acetic acid, HCl-treated). ○ Control gel (same type). ◒ Difference between the two curves. All points are from smoothed curves.

Can. J. Chem. Downloaded from www.nrcresearchpress.com by 176.9.209.113 on 09/04/12
For personal use only.

gel is given as the difference between the amounts actually adsorbed on the propyl gel and on the control gel. The extrapolated value of the linear portion of the resultant isotherm at zero equilibrium concentration is 0.3×10^{-6} moles per g gel, which practically coincides with the amount of residual dye. Of course, this is an accidental coincidence but it serves to emphasize the fact that the amount of unextractable dye is not negligible.

Acid-washing of the Gel

Dickey claims that acid-washing (with HCl) is "found to preserve the specific adsorption property". Included in Table II are the acetic acid B series and the oxalate series of gels in each of which one part was water-washed and the other part HCl-washed and then water-washed.

Acid-washing does not have much effect on the adsorption of dyes on the oxalate gels. Similarly, the nitrogen areas of the oxalate gels show no general trend as a result of acid-washing (Table III).

The effect of acid-washing is more definite for the acetic acid gels. In general, dye adsorption is enhanced on the dye-sensitized gels and reduced on the control gels. Acid-washing noticeably enhances nitrogen adsorption on the dye-sensitized gels, but only slightly affects that on the control gel.

It is difficult to account for an *enhancement* of adsorption by acid-washing in terms of "footprints" left by the dye. A more plausible explanation could be given in terms of the effect of acid-washing on the unextractable dye. It was already noted that acid-washing does not extract any dye. Possibly this treatment exposes more dye to the external surface by corroding the gel; concomitantly, the control gel becomes somewhat less active by the same corroding action.

Although there is much more unextractable dye in the oxalate gels than in the acetic acid gels, it appears that this dye is either more deeply buried or in a less active form (the oxalate gels are prepared at a significantly higher pH value than the acetic acid gels). Thus, the oxalate gels have lower absolute dye adsorptions and they are almost totally insensitive to the action of acid-washing.

The Nature of the Dyes as Adsorbates

It was generally observed that the adsorption of the orange dyes on the control gels increased with increasing molecular weight; moreover, methyl and ethyl were grouped together followed by a gap after which propyl and butyl were grouped. This grouping is also largely maintained among the sensitized gels.

A similar grouping occurs for the amounts of unextractable dye retained by the sensitized gels (Table IV) and for the solubilities of the dyes in 5% aqueous acetic acid solutions (Table I).

It is very unusual to find that the more soluble adsorbates of a homologous series are the ones adsorbed in the larger amounts. For example, Hansen and Craig (11) found that the adsorptions of slightly soluble homologues were congruent functions of their *reduced* concentrations (equilibrium concentration divided by saturation concentration). They reported on the adsorption of the monobasic aliphatic acids on non-porous carbons.

When the same method was applied to one of our sets of isotherms on a single gel, the isotherms became more divergent (Fig. 4).

Hansen and Craig point out that congruency of the adsorption isotherms is to be expected if the adsorbent acts on the same functional group of the adsorbate. Apparently, in the present case, one must use an entirely different mechanism to account for the

Can. J. Chem. Downloaded from www.nrcresearchpress.com by 176.9.209.113 on 09/04/12
For personal use only.

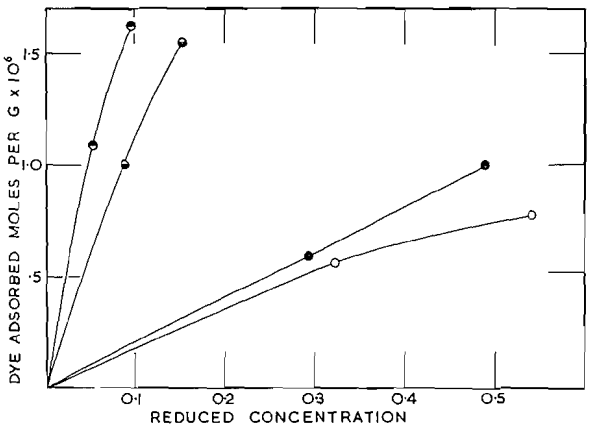

FIG. 4. Adsorption on a methyl orange gel plotted against reduced concentration (methyl orange gel, series B, acetic acid, water-treated); ● methyl, ○ ethyl, ◒ propyl, and ◓ butyl orange dyes.

adsorption of the methyl orange homologues on silica gel. Our results suggest that such a mechanism will be very dependent on properties of the adsorbate molecules.

The striking increase in solubility from ethyl to propyl orange recalls a rule of Blitz and Herzog (12) that the diffusibility of dyes with more than 45 to 50 atoms suddenly decreases in comparison with those of less than this number of atoms. We are suggesting that the sudden increase in solubility is due to a sudden increase in the degree of association of the propyl and butyl orange dye molecules in comparison with the methyl and ethyl orange molecules.

Such an increase could largely account for the greater adsorbability of these two dyes compared with their methyl and ethyl homologues. The adsorption of the larger aggregates of propyl and butyl oranges would thus partially mask any specificity.

Moreover, a general tendency for association would be one way of accounting for the unextractable dye playing a role as attraction centers in specific adsorption.

A similar explanation for specific adsorption is the suggestion of Singer (ref. 3, footnote, p. 702) that the unextractable dye molecules act as centers for a phenomenon akin to crystallization.

The Effect of Other Unextractable Substances

Dickey (3) rejects the suggestion that the unextractable dye plays a role in the enhancement of adsorption; his rejection is largely based on a single experiment, in which decolorizing of the unextractable dye by ozone did not alter the amount of adsorption. He suggests that the dye "has been destroyed" without altering the footprints.

However, this experiment does not ensure the *removal* of the decolorized molecules from the gel, and these may still act as centers for adsorption.

Bernhard (9) and Beckett and Anderson (13) have shown that the sensitization of the gel by similarly structured molecules gave similar adsorptive properties.

We prepared gels in the presence of sulphanilic acid and of *p,p'* diaminodiphenyl and compared their adsorptive properties to methyl and ethyl orange dyes by measuring complete isotherms. The adsorptions at 1.5×10^{-5} molar equilibrium concentration are given in Table V. It is quite apparent that both these substances, and particularly sulphanilic acid, enhance the adsorption as much as do the two orange dyes.

Can. J. Chem. Downloaded from www.nrcresearchpress.com by 176.9.209.113 on 09/04/12
For personal use only.

TABLE V

Adsorption on various gels at 1.5×10^{-5} molar equilibrium concentration

	Adsorbate dye	
Sensitized silica gel	Methyl orange	Ethyl orange
Control	0.25	0.19
Methyl orange	0.40	0.25
Ethyl orange	0.50	0.51
p,p' diaminodiphenyl	0.38	0.42
Sulphanilic acid	0.50	0.55

We have concluded from these experiments that unless the unextractable dye is completely removed, and not merely decolorized, one cannot unequivocally reject its role in enhancing adsorption. Unfortunately, it does not appear possible to remove the dye completely without destroying the gel. Moreover, the drastic treatments necessary to decolorize the unextractable dye bring into question the survival of "footprints".

CONCLUSION

According to Martin (1) the "finding of stationery phases of high specificity . . . " is "an extremely difficult field, as difficult as it is obviously rewarding". Therefore, much care should be taken particularly in the interpretation of any observations of specificity; for, a correct interpretation should be more fruitful than an incorrect one in developing new specific adsorbents.

In the present case, neither of the participants in the specific adsorption phenomena is a simple substance.

Silica gel is extremely complex; in its formation under the present conditions it undergoes about a 30-fold shrinkage. It is very difficult to envisage the survival of matching structures to the dye molecules in such a gel. However, some of the dye particles remain trapped within the gel structure during this shrinkage and become unextractable. Until the effect of such unextractable material has been unequivocally disproved, one must, we believe, follow the simpler hypothesis that the specificity arises from the retained dye.

The methyl orange homologues have been found to be complex substances. For example, Burkhard, Burgert, and Levitt (14) have shown in connection with dye–protein interactions that, at pH 6.8 and 7.3, methyl orange does not form micelles whereas butyl orange does so. We are reporting the unusual solubility behavior of the dye series, and it is interesting to note that Dickey in his second paper has only dealt with methyl and ethyl orange dyes (3).

If the specificity in the silica gels is due to unextractable substances, then the development of tailor-made adsorbents might follow a different path from that suggested by the "footprint" hypothesis.

ACKNOWLEDGMENTS

Financial assistance from the National Research Council is acknowledged. We also wish to thank the Research Council of Alberta for the use of some facilities.

Can. J. Chem. Downloaded from www.nrcresearchpress.com by 176.9.209.113 on 09/04/12
For personal use only.

REFERENCES

1. MARTIN, A. J. P. 1957 International Gas Chromatography Symposium, Michigan State University. *In* Proc. Instr. Soc. Am. 203 (1957).
2. DICKEY, F. H. Proc. Nat. Acad. Sci. U.S. **35**, 227 (1949).
3. DICKEY, F. H. J. Phys. Chem. **59**, 695 (1955).
4. HALDEMAN, R. G. and EMMETT, P. H. J. Phys. Chem. **59**, 1039 (1955).
5. SLOTTA, K. H. and FRANKE, W. Ber. B, **66**, 104 (1933).
6. WORSLEY, M. M.Sc. Thesis, University of Alberta, Edmonton, 1952.
7. KLOTZ, I. M., BURKHARD, R. K., and URQUHART, J. M. J. Am. Chem. Soc. 74, 202 (1952).
8. BRUNAUER, S., EMMETT, P. H., and TELLER, E. J. Am. Chem. Soc. **60**, 309 (1938).
9. BERNHARD, S. A. J. Am. Chem. Soc. **74**, 4946 (1952).
10. SING, K. S. W. and MADELEY, J. D. J. Appl. Chem. **3**, 549 (1953).
11. HANSEN, R. S. and CRAIG, R. P. J. Phys. Chem. **58**, 211 (1954).
12. BLITZ, W. and HERZOG, R. O. *Referred to in* Colloid and capillary chemistry. H. Freundlich. Methuen & Co., Ltd., London, 1926. p. 550.
13. BECKETT, A. H. and ANDERSON, P. Nature, **179**, 1074 (1957).
14. BURKHARD, R. K., BURGERT, B. E., and LEVITT, J. S. J. Am. Chem. Soc. **75**, 2977 (1953).

Can. J. Chem. Downloaded from www.nrcresearchpress.com by 176.9.209.113 on 09/04/12
For personal use only.

Can. J. Chem. Downloaded from www.nrcresearchpress.com by 176.9.209.113 on 09/04/12
For personal use only.

HYDROXYLYCOCTONINE[1]

O. E. Edwards, M. Los,[2] and Léo Marion

ABSTRACT

The structures of isolycoctonine and hydroxylycoctonine salts have been shown to be VII and X respectively. These structures and the δ-lactone character of the products of lead tetraacetate cleavage of hydroxylycoctonam are in harmony with structure XI for hydroxylycoctonine.

Most of the chemistry of the alkaloid lycoctonine (1, 2, 3) has been accounted for on the basis of structure I (R = CH_2OH).[3] However, one of the remaining sets of facts not readily reconciled with this structure centered around the base hydroxylycoctonine.

This product of silver oxide (5) or lead tetraacetate (1, 6) oxidation of lycoctonine contained one more oxygen than the parent alkaloid, and had many characteristics of a carbinolamine. The marked drop in pK_a in going from lycoctonine to hydroxylycoctonine (3.3 units) indicated that the extra oxygen was close to the nitrogen. The fact that the base could be oxidized to a lactam, which on acid hydrolysis gave ethylamine (1), proved the presence of the system:

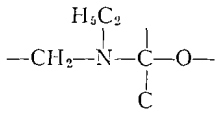

Suginome (7) treated hydroxylycoctonine with methanolic hydrogen chloride and obtained what appeared to be a carbinolamine ether. In addition, when hydroxylycoctonine was heated in mildly alkaline solution formaldehyde, acetaldehyde, lycoctonine, and des(oxymethylene)-lycoctonine were among the compounds formed (1). The aldehydes obviously arose from the carbinolamines II (R = CH_2OH) and III. Since only a trace of lactam was produced it was suggested (1) that II (R = CH_2OH) was reduced by the above aldehydes in a crossed Cannizzaro reaction to lycoctonine, while the carbinolamine II (R = H) formed by retroaldol fission was similarly reduced to des(oxymethylene)-lycoctonine (I, R = H).

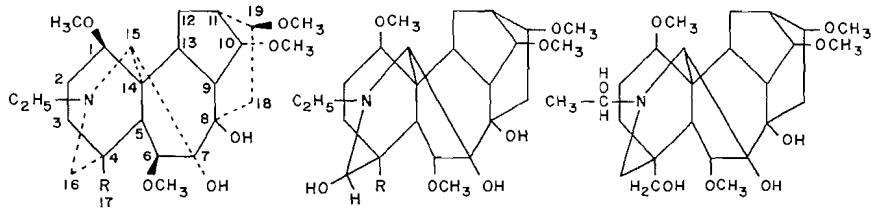

I II III

[1]*Manuscript received July 29, 1959.*
Contribution from the Division of Pure Chemistry, National Research Council, Ottawa, Canada.
Issued as N.R.C. No. 5402.
[2]*National Research Council Postdoctorate Fellow.*
[3]*The numbering system used herein has been decided upon recently (4). The absolute stereochemistry denoted by* I *has been demonstrated using X-ray crystallography (Przybylska, M. and Marion, L. Can. J. Chem.* **37**, *1843 (1959)).*

Finally, the presence of a vicinal diol in hydroxylycoctonam was demonstrated, suggesting that the original lycoctonine skeleton was intact. On this basis, structure IV was advanced for hydroxylycoctonine (1). This structure is consistent with the above facts provided it is possible for the immonium salt V to exist as a transient intermediate in the formation of IV. This assumption would also be required to account for the rearrangement of IV to the immonium ion VI which must be the precursor of II, and for the comparable formation of III. However, four pieces of evidence were not readily reconcilable with structure IV for hydroxylycoctonine.

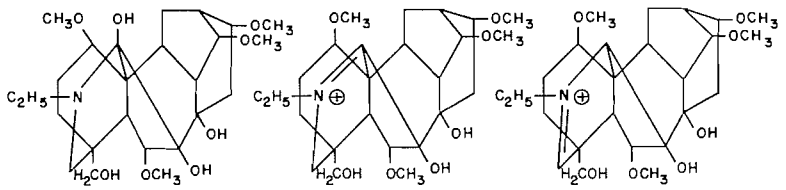

IV V VI

(*a*) The salts of hydroxylycoctonine were anhydronium salts (i.e. involved loss of a molecule of water), and these salts had unusual ultraviolet and infrared spectra (1, 6) (see below). The corresponding anhydronium salt structure V is extremely strained.

(*b*) A solution of hydroxylycoctonine in acetic acid over platinum rapidly absorbed 1 mole of hydrogen, giving an isomer of lycoctonine "isolycoctonine" (5), which proved to be a ketone. Lithium aluminum hydride reduced hydroxylycoctonine salts[4] to dihydroisolycoctonine[5] (carbonyl reduced to the secondary alcohol).

(*c*) Although structure IV contains a vicinal triol system, glycol cleavage reagents failed to cleave more than one vicinal diol in the molecule (1). The main products gave monoacetates whose infrared spectra contained no hydroxyl absorption bands.

(*d*) A marked change in saponification rate exists between methyl lycoctonamate and methyl hydroxylycoctonamate (1).

In an attempt to account for these observations we undertook the study of the structure of isolycoctonine. This base had a pK_a' of 6.7 (0.9 unit higher than hydroxylycoctonine), was inert to nitrous acid, and gave no amide with acetic anhydride. It thus appeared to be a simple tertiary amine. Its infrared spectrum demonstrated the presence of a carbonyl in a six-membered or larger ring.

Permanganate oxidation of isolycoctonine gave a neutral compound without loss of carbon. Since vigorous hydrolysis of this compound yielded no acetic acid or volatile amine it was a lactam (named isolycoctonam), and hence the nitrogen was flanked by two skeletal carbons as in lycoctonine itself.

The environment of the carbonyl was next proved by a series of experiments. The action of lead tetraacetate in wet acetic acid on isolycoctonam resulted in the consumption of 1 mole of reagent and the production of a keto acid. This spontaneously cyclized on handling giving a lactone, which in view of this ease of formation and its infrared absorption at 1737 cm^{-1} was undoubtedly a δ-lactone. The keto lactone lost the elements of methanol when heated with dilute mineral acid, giving rise to a compound containing the lactone ring and a lightly substituted α-β unsaturated ketone

[4]*Leonard and co-workers showed that immonium salts are reduced by this reagent to the tertiary amine (8).*
[5]*We cordially thank Dr. D. K. R. Stewart, who performed this experiment.*

Can. J. Chem. Downloaded from www.nrcresearchpress.com by 176.9.209.113 on 09/04/12
For personal use only.

(λ_{Infl} 225 mμ). 17-Desoxylycoctonine (I, R = CH_3) gave an exactly parallel series of reactions, except that no lactone formed. The lactone formation thus indicates a 1,5 relation between the primary hydroxyl and the carbonyl.

Zinc and refluxing acetic anhydride removed the tertiary hydroxyl α to the carbonyl in isolycoctonam. When the product was hydrolyzed and then treated with 5% sodium amalgam in ethanol one methoxyl was removed and the ketone carbonyl reduced. Since isolycoctonam is stable to base, this reaction proved that a methoxyl was α to the carbonyl.[6]

The above evidence defines the sequence

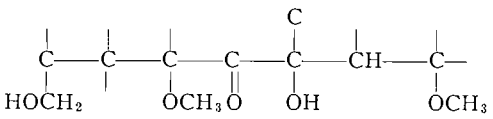

in isolycoctonine. This sequence is present in lycoctonine if the C(7)–C(15) bridge is ruptured. In view of the gentle conditions under which lycoctonine can be transformed into isolycoctonine, it seems unlikely that a deep-seated skeletal rearrangement takes place, hence VII is a very plausible structure for isolycoctonine. The α-β unsaturated keto-δ-lactone must then be VIII, and the product of the successive Zn–Ac_2O and $Na(Hg)_x$ treatment of isolycoctonam is IX.

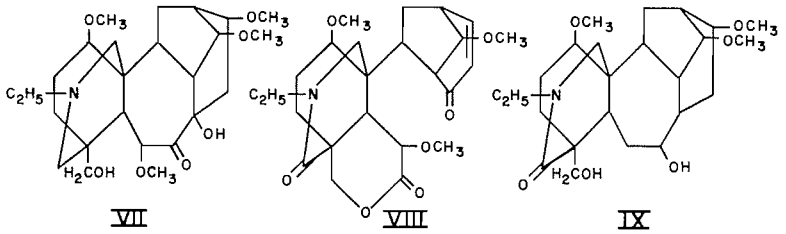

VII VIII IX

The infrared spectrum of salts of hydroxylycoctonine had two absorption bands at 1670 cm^{-1} and 1712 cm^{-1}. The former correspond to the $\rangle C{=}N^{\oplus}\langle$ stretching vibration (9, 10), but the latter was not easily accounted for. Solution of the salts in alcohol, or of the base in acetic acid, had a carbonyl absorption band in the ultraviolet at the abnormally long wavelength of 330 mμ. The very rapid catalytic reduction of hydroxylycoctonine in acid solution to VII, and the course of the lithium aluminum hydride reduction of hydroxylycoctonine salts, coupled with the above spectroscopic evidence, led to the conclusion that the salts must have structure X. Thus the IR band with ν_{max} 1712 cm^{-1} is the $\rangle C{=}O$ stretching absorption and the catalytic hydrogenation reduces the immonium bond.

While the above results prove the structure of isolycoctonine and hydroxylycoctonine salts, acceptance of structure IV for hydroxylycoctonine still demands the invoking of the highly strained immonium ion of V as a transient intermediate (see above), and no explanation of points (*c*) and (*d*) above is provided. While the preliminary communication of the above results (11) was in press, Professor G. Büchi suggested to us that

[6]*The reductive removal of a methoxyl α to a ketone carbonyl has been used previously in lycoctonine chemistry (2). In this case, and in the original work of Kondo, the carbonyl was not reduced. However, in the present work it was not found possible to avoid reduction to the secondary alcohol.*

Can. J. Chem. Downloaded from www.nrcresearchpress.com by 176.9.209.113 on 09/04/12
For personal use only.

an initial complex between the nitrogen of lycoctonine and $Pb(OAc)_4$ led directly to the "open" structure X(X = OAc) as shown. Hydroxylycoctonine would then be XI and the product of lead tetraacetate cleavage of hydroxylycoctonam would be XII. In

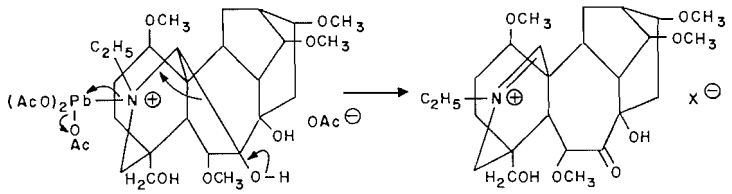

X

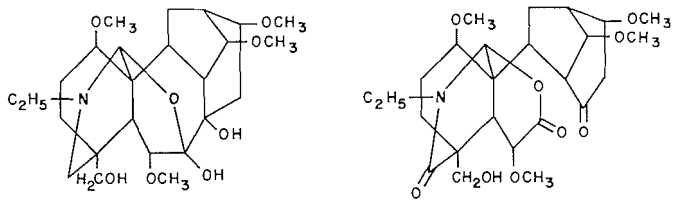

XI XII

a recent communication (12) Valenta has drawn the same conclusion about the structure of hydroxylycoctonine and its salts. These very convincing rationalizations were quickly established to be correct by alkaline hydrolysis of the compound XIII which we had called desmethanol *seco*hydroxylycoctonam diketone monoacetate.[7] A nearly quantitative yield of acid was obtained, which spontaneously cyclized to a new crystalline lactone, presumably XIV.

In view of the new structure for hydroxylycoctonine it appeared that the more strongly adsorbed compound lacking the primary hydroxyl (not acetylatable) produced in the

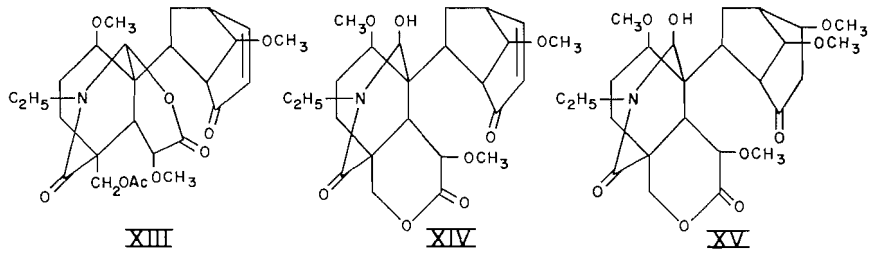

XIII XIV XV

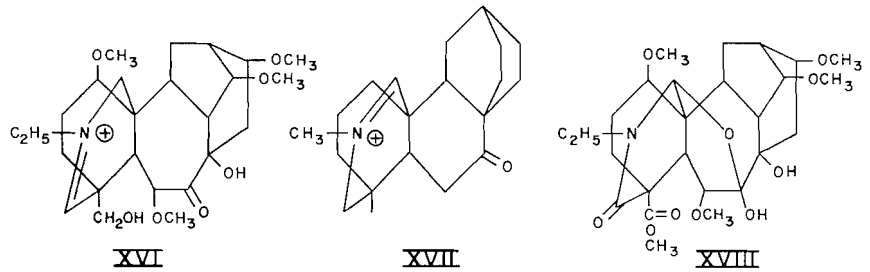

XVI XVII XVIII

[7]*By mistake this compound was called des(oxymethylene) hydroxysecolycoctonam diketone monoacetate in several places in reference 1.*

Can. J. Chem. Downloaded from www.nrcresearchpress.com by 176.9.209.113 on 09/04/12
For personal use only.

lead tetraacetate cleavage of hydroxylycoctonam (1) might have structure XV. The compound even after 8 hours' drying at 100° in high vacuum still gave carbon values 0.5% low for this possibility. However, the compound was shown to be a lactone by alkaline hydrolysis to an acid. Flash pyrolysis of the compound *in vacuo* gave a mixture from which XIV was obtained by crystallization. Thus structure XV is confirmed.

N-Bromosuccinimide (13) rapidly oxidized isolycoctonine. The product gave a hydrochloride which appeared to be a mixture of the salt of N-desethyl isolycoctonine (ν_{max} 2680, 2470, and 1602 cm^{-1}, ascribable to $\rangle\overset{\oplus}{N}H_2$) and of immonium salt XVI (ν_{max} 1673 cm^{-1}). Attempts to rearrange the immonium salt to the readily crystallizable hydroxylycoctonine salts by heating the mixture in dimethylformamide failed, although the corresponding transformation in the atisine series is facile (14). This gives some support to our contention that hydroxylycoctonine salts represent a high energy state (see below).

Considerable driving force for the formation of hydroxylycoctonine must come from the relief of non-bonded interaction between the ring A hydrogens and the ethyl group in going from lycoctonine to X. Examination of Courtauld's models, however, suggested that this was offset by an increase in other non-bonded interactions and in ring strain[8] in going from lycoctonine to X. The expected course of the lead tetraacetate oxidation by analogy to the attack of other oxidizing agents on the lycoctonine (5, 15), atisine (16, 17), and garrya (18) groups of alkaloids would lead to initial formation of the immonium ion VI. This ion is strain free, has no serious non-bonded interactions, and gives the same relief of crowding of the N-ethyl group as the formation of X. Hence it is not clear why the oxidation goes rapidly and nearly quantitatively to X. The possibility exists that VI is the primary product, which rearranges rapidly to X, but this still leaves the question unsettled as to why X is formed.

The low basicity of hydroxylycoctonine is more readily understood. The basic strength of carbinolamines (13, 19) and oxazolidines (9, 16, 19) derived from tertiary bases is 2 to 4 units greater than that of the parent saturated bases.[9] The higher values pertain when the salt formation relieves strain or reduces non-bonded interaction (19). In the case of hydroxylycoctonine, salt formation relieves the interaction of the ethyl group with ring A hydrogens, hence we might expect a pK_a' at least 3 units greater than that of the saturated analogue. However, the presence of the carbonyl should lower the basicity by approximately 1 unit,[10] leaving a net increase of 2 pK_a units. Using dihydroisolycoctonine XVI as the reference base (pK_a' 7.4) we would thus expect a pK_a' of hydroxylycoctonine of at least 9.4. (The pK_a' of base XVII (20) derived from ajaconine which has very similar N to CO distance and orientation is 11.7 in aqueous alcohol.) Thus a discrepancy of a minimum of 3 units exists between the actual pK_a' (5.8) and the estimated value. Since inductive effects must be negligible we attribute this difference to the ring strain and increased non-bonded interactions in the salt[11] relative to the hemiketal structure of hydroxylycoctonine (XI), thus destabilizing the salt.

[8]*The hydrogen on* C-*6 was very crowded and there was serious interaction between the* C-*15 and* C-*12 hydrogens. In addition, considerable distortion of bond angles was necessary to form the skeleton.*

[9]*This is only true if there is no violation of Bredt's rule or no introduction of new serious non-bonded interaction in forming the anhydronium salts.*

[10]*The difference in pK_a' between the azomethine ketone from which* XVII *is derived and the corresponding alcohol is 0.9 unit. In this case the carbon of the carbonyl is slightly closer to the nitrogen than in hydroxylycoctonine salts. The nitrogen lies close to the axis of the carbonyl and on the positive end of the dipole, conditions that should favor the maximum field effect. Isolycoctonine* (VII) *is weaker (pK_a' 6.7) than the corresponding alcohol dihydroisolycoctonine (pK_a' 7.4) by 0.7 unit.*

[11]*See footnote 8.*

Can. J. Chem. Downloaded from www.nrcresearchpress.com by 176.9.209.113 on 09/04/12
For personal use only.

Comparison of Courtauld models of lycoctonine and hydroxylycoctonine showed increased crowding of the C-6 hydrogen and methoxyl against the functions on C-17 in the latter. This gave a possible explanation of the fact that methyl hydroxylycoctonamate (XVIII) was hydrolyzed much more slowly than methyl lycoctonamate (point (*d*) above).

The mechanism of the oxidation of lycoctonine to hydroxylycoctonine by silver oxide remains obscure. The fact that silver ammonium ion did not oxidize the base suggested that here, too, a silver–amine complex is a necessary intermediate. However, the way in which two silver atoms participate to accept the pair of electrons is not clear.

The transformation of hydroxylycoctonine salts (X) to lycoctonine etc. suggests an alternative to aldol condensation (21, 22) for the formation of the C-7:C-15 bridge in the biosynthesis of lycoctonine from diterpenoid precursors.

EXPERIMENTAL

Isolycoctonine (VII)

Adams' catalyst (25 mg) in 3 ml of acetic acid was prereduced and 105 mg of hydroxylycoctonine added. One mole of hydrogen was absorbed in 4 minutes, after which the reduction was stopped. The catalyst was removed by filtration, the solvent evaporated, and the residue dissolved in methylene chloride. This was washed with dilute sodium carbonate solution, dried, and evaporated to give 90 mg of syrup. Crystallization from aqueous methanol gave plates identical in melting point, mixed melting point, and rotation with isolycoctonine previously described (5). ν_{max} (Nujol): 3470 and 3420 (OH), 1713 (ketone).

Dihydroisolycoctonine

Isolycoctonine (97 mg) in 5 ml of acetic acid was hydrogenated in the presence of 25 mg of Adams' catalyst. One mole of hydrogen was absorbed in 16 hours. The catalyst was removed by filtration and the filtrate concentrated under reduced pressure. The residue was dissolved in methylene chloride, washed with dilute sodium carbonate solution, dried, and evaporated. Four crystallizations from acetone gave 50 mg of colorless plates, m.p. 176–179° C. pK_a 7.35 in 50% aqueous methanol, $[\alpha]_D^{23}$ −21° (*c*, 1.07). Found: C, 63.98; H, 9.20; OCH_3, 26.14. Calc. for $C_{25}H_{43}O_7N$: C, 63.94; H, 9.23; $4OCH_3$, 26.42.

Dihydroisolycoctonine could be obtained more readily by the reduction of isolycoctonine with sodium borohydride in 50% aqueous methanol for ½ hour at room temperature.

Reduction of Hydroxylycoctonine Hydriodide by $LiAlH_4$[12]

Hydroxylycoctonine hydriodide (120 mg) was dissolved in hot purified dioxane. $LiAlH_4$ ether solution (15 cc) was added and the temperature raised until the ether evaporated. The solution was refluxed for ½ hour. Excess $LiAlH_4$ was destroyed using methanol and the solvent removed *in vacuo*. The residue was suspended in saturated Rochelle salt solution and extracted with methylene chloride yielding 89 mg of clear glass. This crystallized from aqueous methanol giving 50 mg, m.p. 164–171°. After two recrystallizations the product melted at 174–177° and had $[\alpha]_D$ −21° (*c*, 1.25). It did not depress the melting point of dihydroisolycoctonine, described above, and the infrared spectra of the two compounds were identical.

[12]*See footnote 5.*

Can. J. Chem. Downloaded from www.nrcresearchpress.com by 176.9.209.113 on 09/04/12
For personal use only.

Can. J. Chem. Downloaded from www.nrcresearchpress.com by 176.9.209.113 on 09/04/12
For personal use only.

Isolycoctonam

Isolycoctonine (3.23 g) was dissolved in 130 ml of acetone containing 1 ml of acetic acid and 1 ml of water. Powdered potassium permanganate (1.94 g) was then added portionwise over a period of 3 hours. The last portion persisted for ¾ hour. Sulphur dioxide was then passed into the solution to destroy excess permanganate, and the solution filtered and evaporated. The residue was dissolved in methylene chloride, washed first with dilute H_2SO_4, and then with dilute Na_2CO_3 solution. After drying (Na_2SO_4) the methylene chloride was removed to give 2.40 g of neutral product. Crystallization from acetone–hexane gave 2.02 g of white crystalline material m.p. 181–184°. Recrystallization from the same solvent raised the m.p. to 182–184°. Found: C, 62.21; H, 7.99. Calc. for $C_{25}H_{39}O_8N$: C, 62.35; H, 8.16%. $[\alpha]_D^{24}$ +45.2° (*c*, 0.93 in ethanol); ν_{max} (Nujol): 3410 (OH), 1702 (ketone), 1620 and 1640 (lactam). The dilute sulphuric acid solution when made alkaline and extracted with methylene chloride yielded 0.346 g of isolycoctonine (melting point and mixed melting point).

Isolycoctonam Acetate

When prepared using acetic anhydride – pyridine, this compound crystallized from acetone–hexane as blades, m.p. 180–181°. Found: C, 61.79; H, 7.77. Calc. for $C_{27}H_{41}O_9N$: C, 61.93; H, 7.89.

17-Desoxyhydroxylycoctonine

A solution of 310 mg of 17-desoxylycoctonine (I, R = CH_3) in 10 ml of acetic acid and 20 ml of a saturated solution of lead tetraacetate in acetic acid was allowed to stand at room temperature for ¾ hour. Excess tetraacetate was then destroyed with a saturated aqueous solution of sodium bisulphite and lead salts precipitated by the addition of a saturated aqueous solution of sodium sulphate. The precipitate was removed by centrifugation. The precipitate was thoroughly washed with acetic acid and the solutions combined and evaporated. The residue was then dissolved in methylene chloride and washed with dilute sodium carbonate solution and water. After the methylene chloride solution was dried, (Na_2SO_4) it was evaporated leaving a froth (313 mg). The base was not obtained in the crystalline form but its perchlorate crystallized readily from acetone – ethyl acetate as colorless prisms (283 mg) m.p. 199–209°. Three recrystallizations raised the melting point to 203–207° C. Found: C, 54.67; H, 7.2. Calc. for $C_{25}H_{40}O_{10}NCl$: C, 54.55; H, 7.23. Infrared spectrum (Nujol): 3410 (OH), 1715 (ketone), 1673 ($\rangle C{=}\overset{\oplus}{N}\langle$).

17-Desoxyisolycoctonine

17-Desoxyhydroxylycoctonine (220 mg) was reduced with hydrogen and prereduced PtO_2 (120 mg) in acetic acid (18 ml). One mole of hydrogen was absorbed in 20 minutes. After the solvent was removed the residue was dissolved in methylene chloride and washed with dilute sodium carbonate solution and water. Evaporation of the solution after drying (Na_2SO_4) gave a syrup (231 mg) which crystallized as colorless prisms from acetone–hexane, m.p. 155–161° C. Two further crystallizations gave a pure product (184 mg), m.p. 162–164° C. Found: C, 66.54; H, 8.97. Calc. for $C_{25}H_{41}O_6N$: C, 66.49; H, 9.15%. $[\alpha]_D^{27}$ +41.7° (*c*, 0.96). Infrared spectrum (Nujol): 3425 (OH), 1715 (ketone).

17-Desoxyisolycoctonam

17-Desoxyisolycoctonine (320 mg) was dissolved in pyridine (5 ml) and to this was added at 0° C the complex derived from chromic anhydride (321 mg) and pyridine (5 ml).

After standing at room temperature for 24 hours, sulphur dioxide was bubbled through the solution, the solution evaporated, and the residue dissolved in 3 *N* sulphuric acid. This was extracted with methylene chloride, the methylene chloride washed with dilute sodium carbonate solution, dried, and evaporated. The neutral material (254 mg) was chromatographed on alumina (3 g, activity II). Benzene (150 ml) and 5% $CHCl_3$–benzene eluted material (220 mg) which crystallized from acetone–hexane in colorless prisms, m.p. 145–148° C. Two recrystallizations raised the melting point to 147–149° C. Found: C, 64.55; H, 8.15. Calc. for $C_{25}H_{39}O_7N$: C, 64.49; H, 8.44. Infrared spectrum (Nujol): 3410 (OH), 1707 (ketone), 1649 (lactam).

Environment of the Nitrogen

(*a*) Isolycoctonine was recovered quantitatively after 1 hour in aqueous nitrous acid solution.

(*b*) Desoxyisolycoctonine was recovered in 84% yield after 4 hours' heating at 100° with 50% acetic anhydride – pyridine mixture.

(*c*) Desoxyisolycoctonam (75 mg) in 1 ml of methanol and 4 ml of 1 *N* sulphuric acid was heated for 24 hours at 100° C and 24 hours at 160° C in a sealed tube. The filtered solution was basified and distilled until approximately 1 ml remained. Picric acid (70 mg) was added to the distillate and the solution evaporated. Extraction of the dry residue with ether left no residue of ethylamine picrate.

The residue after the initial distillation was acidified with sulphuric acid and again distilled. The distillate was neutral showing the absence of acetic acid.

Lead Tetraacetate on Isolycoctonam Monoacetate

A solution of 12.6 mg of the acetate in 10 ml of a saturated solution of lead tetraacetate in glacial acetic acid to which had been added 0.5 ml of water was titrated at intervals. The mole ratio of lead tetraacetate consumed was 0.31 (28 hours), 0.68 (73 hours), 0.94 (96 hours).

Lead Tetraacetate Cleavage of Isolycoctonam

Isolycoctonam (200 mg) was dissolved in 40 ml of a saturated solution of lead tetraacetate in glacial acetic acid containing 2.4 ml of water. After 120 hours at room temperature, hydrogen sulphide was passed into the solution until the precipitation of lead sulphide was complete. The solution was filtered through Hyflo Supercel, the acetic acid removed, and the residue taken up in dilute sodium carbonate. After the carbonate solution was washed with chloroform, it was acidified with dilute H_2SO_4 and extracted with chloroform. Evaporation of the dried extract gave 195 mg of a white froth. This crystallized from benzene–hexane as white prisms m.p. 162–172°. ν_{max} ($CHCl_3$), 1737 (lactone), 1704 (ketone), 1670 (α-β unsaturated ketone), 1635 (lactam). Found: C, 63.91; H, 7.76. Calc. for $C_{25}H_{37}O_8N$: C, 62.61; H, 7.78. This indicates the product to be a mixture of the expected *seco*ketolactone and its desmethanol derivative VIII.

Desmethanol Keto Lactone (VIII)

Crude acidic material (500 mg) as obtained above was dissolved in 1 ml of ethanol, 20 ml of 6 *N* H_2SO_4 was added, and the solution heated at 90° C for $\frac{1}{2}$ hour. After extraction with $CHCl_3$, washing with water, and drying (Na_2SO_4), the extract yielded 477 mg of froth. Crystallization from acetone–hexane gave 376 mg of crystalline material. After three recrystallizations it had a melting point of 255–258°. Found: C, 64.87; H, 7.29; OCH_3, 20.64. Calc. for $C_{24}H_{33}O_7N$: C, 64.41; H 7.43; $3OCH_3$, 20.8. $[\alpha]_D^{24}$ −104°; ν_{max} ($CHCl_3$), 1738 (lactone), 1671 (α-β unsaturated ketone), 1635 (lactam); λ_{infl} 225 mμ (ϵ 8230), λ_{max} 305 mμ (ϵ 57).

Can. J. Chem. Downloaded from www.nrcresearchpress.com by 176.9.209.113 on 09/04/12
For personal use only.

Can. J. Chem. Downloaded from www.nrcresearchpress.com by 176.9.209.113 on 09/04/12
For personal use only.

Action of Lead Tetraacetate on 17-Desoxyisolycoctonam

17-Desoxyisolycoctonam (556 mg) was treated with lead tetraacetate in the same manner as described for isolycoctonam. Separation of the product into neutral and acidic fractions gave 320 mg of starting material and 120 mg of acidic material.

The acidic material (100 mg) was heated at 70° C for ½ hour with 6 *N* sulphuric acid (5 cc). Extraction of the cold solution with chloroform followed by washing with water, drying (Na_2SO_4), and evaporation of the chloroform yielded 38 mg froth which crystallized from acetone–hexane as colorless plates, m.p. 248–252°. Two further recrystallizations gave material of m.p. 251–253 (decomp.). Found: C, 63.99; H, 7.69. Calc. for $C_{24}H_{35}O_7N$: C, 64.12; H, 7.85. Infrared spectrum (Nujol): no OH, 1732 (—COOH), 1677 (α-β unsaturated ketone), 1597 (lactam), 692 (*cis*-disubstituted double bond).

8-Deoxyisolycoctonam

Isolycoctonam (302 mg) in a mixture of acetic acid and 10 ml of acetic anhydride was heated under reflux, and then zinc dust (15 g) was added portionwise over a period of 1½ hours. The cold solution was filtered and evaporated. Methanol was added and the solution evaporated. The residue was then dissolved in methylene chloride, washed with dilute sodium carbonate solution, dried (Na_2SO_4), and evaporated to give 327 mg of a colorless oil.

Hydrolysis of this material was accomplished by refluxing for 1 hour a solution of the above oil in 3% potassium hydroxide in 60% aqueous methanol. After most of the methanol was removed, water (15 ml) was added and the solution extracted with methylene chloride. Evaporation of the dried extract gave 273 mg of a colorless froth which was chromatographed on alumina (8.2 g activity III). Chloroform and chloroform–methanol eluted 192 mg of material which crystallized from ether. Recrystallization from ether–hexane gave colorless prisms, m.p. 110–125°. Found: C, 64.62; H, 8.44; OCH_3, 26.46. Calc. for $C_{25}H_{39}O_7N$: C, 64.49; H, 8.44; $4OCH_3$, 26.63. Infrared spectrum (Nujol): 3360 (OH), 1695 (ketone), 1645 (lactam).

Action of Sodium Amalgam on 8-Deoxyisolycoctonam

8-Deoxyisolycoctonam (50 mg) was dissolved in 5 ml absolute ethanol, and 5% sodium amalgam (600 mg) added. After the solution was shaken for 1½ hours it was filtered, evaporated to 1 ml, diluted with water, and extracted with methylene chloride. The dried extract yielded 38 mg of froth. This crystallized from ether as plates, m.p. 176–189°. Two recrystallizations from acetone–ether raised the melting point to 197–199°. $[\alpha]_D^{24}$ −29.1° (*c*, 0.79 in ethanol). Found: C, 66.08; H, 8.83; OCH_3, 21.63. Calc. for $C_{24}H_{39}O_6N$: C, 65.87; H, 8.98; $3OCH_3$, 21.27%. Infrared spectrum (Nujol): 3365 and 3480 (OH), 1605 (lactam).

Desmethanol secohydroxylycoctonam Ketolactone Isomer (XIV)

A solution of 37 mg of desmethanol *seco*hydroxylycoctonam "diketone" monoacetate (1) in a mixture of 5 ml of methanol and 5 ml of 2.5% aqueous potassium hydroxide was refluxed for 40 minutes. After the methanol was removed, the solution was extracted with chloroform. This extract, after drying, yielded 1 mg of material. The aqueous solution was acidified (H_2SO_4), extracted with chloroform, the extract washed with water, dried, and evaporated. The residue, 34 mg, crystallized from acetone–hexane and after two recrystallizations had m.p. 235–242° C. Its infrared spectrum (1745 (lactone), 1708 (ketone) (weak), 1675 (α-β unsaturated ketone), 1650 (lactam)) showed this to be predominantly an α-β unsaturated keto-δ-lactone. The compound was dried

for 7 hours at 140°, 1×10^{-3} mm. Found: C, 60.61; H, 7.66. Calc. for $C_{24}H_{33}O_8N.\frac{1}{2}H_2O$: C, 61.01; H, 7.25.

Strongly Adsorbed Lead Tetraacetate Cleavage Product

(*a*) A solution of 13 mg of the compound (dried for 10 hours at 100°, 1×10^{-3} mm; found: C, 60.07; H, 7.40; calc. for $C_{25}H_{37}O_9N$: C, 60.59; H, 7.53) in 2 ml of 2.5% potassium hydroxide solution was heated on the steam bath for 55 minutes. The yellow solution was extracted thoroughly with chloroform and the chloroform extracts backwashed with dilute alkali. The combined aqueous layers were acidified and extracted with chloroform giving 11 mg of acid which could not be induced to crystallize.

(*b*) Adsorption of the compound on a 25-fold ratio of acid-washed alumina, activity 3, failed to eliminate cleanly the elements of methanol.

(*c*) The compound was subjected to flash pyrolysis at 220°, 1×10^{-3} mm in 5-mg lots. The colorless glass which distilled out of the hot zone crystallized readily from acetone–ether giving a first crop, m.p. up to 220°. After two recrystallizations the compound melted at 235° with sintering at 225°, ν_{max} 3440, 1745, 1673, 1650 cm^{-1}. This did not depress the melting point of the 242° lactone (XIV) and the two gave identical X-ray powder patterns.

Action of N-*Bromosuccinimide on 17-Desoxyisolycoctonine*

A solution of 18 mg N-bromosuccinimide in 3 ml of dry ethanol-free chloroform was added to a solution of 37 mg of 17-desoxyisolycoctonine in 1 ml dry, ethanol-free chloroform. An immediate yellow color developed which slowly faded and was replaced by a slight pink coloration. After 5 minutes no N-bromosuccinimide remained (starch–iodide test), and the solution was diluted with chloroform, washed with dilute Na_2SO_3 solution, dried, and evaporated. The residual 42 mg of oil was converted to its perchlorate, which could not be induced to crystallize. The corresponding hydrochloride had ν_{max} 2680, 2470, 1602 cm^{-1} ($\rangle\overset{\oplus}{N}H_2$) and 1673 cm^{-1} ($\rangle C{=}\overset{\oplus}{N}\langle$).

The product obtained by refluxing a solution of the amorphous hydrochloride in dimethylformamide for more than 1 hour failed to crystallize or give a crystalline perchlorate. Isoatisine hydrochloride was 50% isomerized (by rotation) on refluxing for $\frac{1}{2}$ hour in this solvent.

Parallel experiments using osmium tetroxide as oxidizing agent were similarly unsuccessful.

ACKNOWLEDGMENTS

The authors are grateful to Professor G. Büchi for informing us of his conclusions regarding the structure of hydroxylycoctonine. We thank Mr. R. Lauzon for obtaining the infrared spectra, Mr. H. Seguin for the analyses, Mr. M. Lesage and Mr. Allan Knoll for technical assistance, and Dr. M. Przybylska for the comparison of X-ray powder patterns.

REFERENCES

1. Edwards, O. E., Marion, L., and Stewart, D. K. R. Can. J. Chem. **34**, 1315 (1956).
2. Edwards, O. E., Marion, L., and Palmer, K. H. Can. J. Chem. **36**, 1097 (1958).
3. Edwards, O. E., Marion, L., and Palmer, K. H. J. Org. Chem. **22**, 1372 (1957).
4. Mayer, H. and Marion, L. Can. J. Chem. **37**, 856 (1959).
5. Edwards, O. E. and Marion, L. Can. J. Chem. **30**, 627 (1952).
6. Cookson, R. C. and Trevett, M. E. Chem. & Ind. 276 (1956).
7. Suginome, H. and Ohno, K. J. Fac. Sci. Hokkaido Imp. Univ. Ser. III, **4**, 36 (1950).
8. Leonard, N. J., Hay, A. S., Fulmer, R. W., and Gash, V. W. J. Am. Chem. Soc. **77**, 439 (1955).

Can. J. Chem. Downloaded from www.nrcresearchpress.com by 176.9.209.113 on 09/04/12
For personal use only.

9. EDWARDS, O. E. and SINGH, T. Can. J. Chem. **32**, 465 (1954).
10. LEONARD, N. J. and GASH, V. W. J. Am. Chem. Soc. **76**, 2781 (1954).
11. EDWARDS, O. E., LOS, M., and MARION, L. Proc. Chem. Soc. 192 (1959).
12. VALENTA, Z. Chem. & Ind. 633 (1959).
13. EDWARDS, O. E., CLARKE, F. H., and DOUGLAS, B. Can. J. Chem. **32**, 235 (1954).
14. EDWARDS, O. E. and SINGH, T. Can. J. Chem. **33**, 448 (1955).
15. SPARATORE, F., GREENHALGH, R., and MARION, L. Tetrahedron, **4**, 157 (1958).
16. PELLETIER, S. W. and JACOBS, W. J. Am. Chem. Soc. **78**, 4139 (1956).
17. PELLETIER, S. W. and JACOBS, W. J. Am. Chem. Soc. **78**, 4144 (1956).
18. WIESNER, K., TAYLOR, W. I., FIGDOR, S. K., BARTLETT, M. F., ARMSTRONG, J. R., and EDWARDS, J. A. Ber. **86**, 800 (1953).
19. DVORNIK, D. and EDWARDS, O. E. Can. J. Chem. **35**, 860 (1957).
20. DVORNIK, D. and EDWARDS, O. E. Proc. Chem. Soc. 280 (1958).
21. COOKSON, R. C. and TREVETT, M. E. J. Chem. Soc. 3121 (1956).
22. VALENTA, Z. and WIESNER, K. Chem. & Ind. 354 (1956).

Can. J. Chem. Downloaded from www.nrcresearchpress.com by 176.9.209.113 on 09/04/12
For personal use only.

Can. J. Chem. Downloaded from www.nrcresearchpress.com by 176.9.209.113 on 09/04/12
For personal use only.

THE CARBONYL STRETCHING BANDS IN THE INFRARED SPECTRA OF UNSATURATED LACTONES[1]

R. N. JONES, C. L. ANGELL,[2] T. ITO,[2] AND R. J. D. SMITH[3]

ABSTRACT

Certain types of unsaturated lactones exhibit two bands in the region of the spectrum associated with the C=O stretching vibrational mode. This is observed both in the infrared and Raman spectra.

The infrared spectra of 23 simple saturated and unsaturated lactones have been examined in an attempt to determine the structural features with which this carbonyl band splitting is associated. It appears to be common to most unsaturated five- and six-membered ring lactones in which the double bond is conjugated with the carbonyl group, though one well-established exception has been observed. The relative intensities of the two bands are extremely sensitive to changes in the polarity of the solvent; they also vary reversibly with temperature but are independent of concentration.

The splitting of the C=O stretching band is attributed to an intramolecular vibrational effect similar to that which occurs in cyclopentanone and in certain Δ^2-cyclopentenone derivatives. Its possible dependence on Fermi resonance with the overtone of a lower lying fundamental vibration is discussed.

Similar effects occur in other types of carbonyl compounds, such as benzoyl chloride and cyclic five-membered ring anhydrides, and care is needed to distinguish carbonyl band splitting of this kind from that associated with equilibria between conformational isomers.

INTRODUCTION

In the course of a systematic survey of the infrared spectra of steroids, it was observed (1, 2) that compounds containing the unsaturated lactone rings of I and II show anomalous absorption in the region of the carbonyl stretching bands. The single absorption band

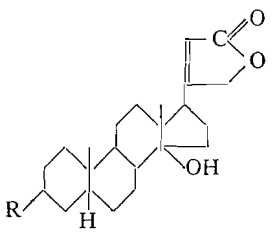

I

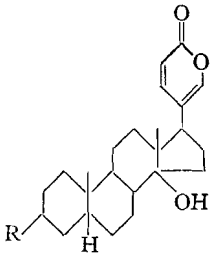

II

expected for the stretching vibration of the lactone carbonyl is replaced by two bands, the relative intensities of which are extremely sensitive to the solvent polarity.

The steroids in which the effect was first observed contained hydroxy and acetoxy groups in addition to the lactone ring; this complicated study of the lactone carbonyl absorption and suggested that the bands might involve inter- or intra-molecular hydrogen bonding, or some other interaction between the lactone and the functional groups of the ring system. The spectra of a series of simple model compounds have therefore been

[1]*Manuscript received June 29, 1959.*
Contribution from the Division of Pure Chemistry, National Research Council of Canada, Ottawa, Canada. Presented, in part, at the International Conference of the European Molecular Spectroscopy Group, Freiburg-im-Breisgau, Germany, July 1957.
Issued as N.R.C. No. 5363.
[2]*National Research Council Guest Worker.*
[3]*National Research Council Postdoctorate Fellow.*

investigated. These compounds show the same anomalies as the steroid lactones, and the effects of solvent, temperature, and small structural changes on the carbonyl stretching band system have been investigated.

EXPERIMENTAL

The compounds examined have the structures III–XXV; they include four saturated γ-lactones (III–VI), 13 unsaturated γ-lactones (VII–XIX), one saturated δ-lactone (XX), and five unsaturated δ-lactones (XXI–XXV). The majority of these compounds were synthesized specifically for this investigation, and the preparative details and structural characterization are noted briefly below.

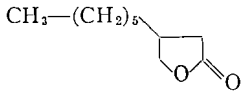

III

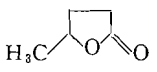

IV

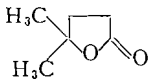

V

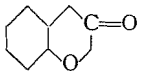

VI

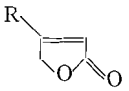

VII R = —H
VIII R = —$(CH_2)_3$—CH_3
IX R = —$(CH_2)_5$—CH_3

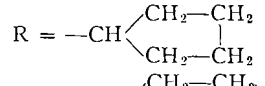

X R = —

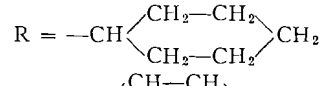

XI R = —

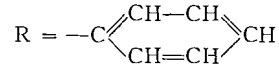

XII R = —

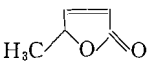

XIII

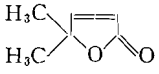

XIV

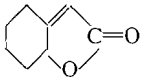

XV

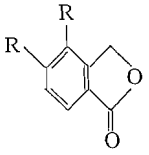

XVI R = —H
XVII R = —OCH_3

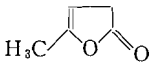

XVIII

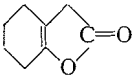

XIX

XX

XXI

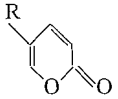

XXII R = —H
XXIII R = —CH_3

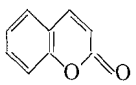

XXIV

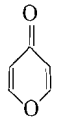

XXV

Can. J. Chem. Downloaded from www.nrcresearchpress.com by 176.9.209.113 on 09/04/12
For personal use only.

Can. J. Chem. Downloaded from www.nrcresearchpress.com by 176.9.209.113 on 09/04/12
For personal use only.

Synthesis and Characterization of Compounds

III. *β-n-Hexyl-butanolide.*—Prepared by hydrogenation of VIII with 5% Pd on charcoal in methanol at 1 atm H_2.

IV. *γ-Methyl-butanolide.*—Prepared from XIII by hydrogenation under the same conditions as III, b.p. 83° (10 mm).

V. *γ,γ-Dimethyl-butanolide.*—Prepared as III from XIV, b.p. 80° (10 mm).

VI. *trans-Cyclohexanol-2-acetic acid lactone.*—Prepared as described by Newman and VanderWerf (3), b.p. 142° (20 mm).

VII. *$\Delta^{\alpha\beta}$-Butenolide.*—Prepared as described by Smith and Jones (4), b.p. 86–87° (12 mm). Found: C, 57.03%; H, 4.94%. Calc.: C, 57.14%; H, 4.80%.

VIII. *β-n-Butyl-$\Delta^{\alpha\beta}$-butenolide.*—Prepared as described by Rubin, Paist, and Elderfield (5); the product was repeatedly distilled until free from bromine, b.p. 101–101.5° (1 mm) n_D^{20} 1.4715.

IX. *β-n-Hexyl-$\Delta^{\alpha\beta}$-butenolide.*—Prepared as VIII, b.p. 120–121° (2 mm). Found: C, 70.99%; H, 9.63%. Calc.: C, 71.40%; H, 9.59%.

X. *β-Cyclopentyl-$\Delta^{\alpha\beta}$-butenolide.*—Prepared as VIII, b.p. 120–121° (2 mm). Found: C, 70.18%; H, 8.00%. Calc.: C, 71.02%; H, 7.95%.

XI. *β-Cyclohexyl-$\Delta^{\alpha\beta}$-butenolide.*—Prepared as VIII, b.p. 143–144° (5 mm). Found: C, 72.36%; H, 8.61%. Calc.: C, 72.28%; H, 8.43%. Ultraviolet spectrum: λ_{max} 2215 Å log ϵ_{max} 3.33 (*n*-heptane solution).

XII. *β-Phenyl-$\Delta^{\alpha\beta}$-butenolide.*—Prepared as VIII. Recrystallized five times from 75% aqueous methanol, m.p. 94°. Ultraviolet spectrum: λ_{max} 2020 Å log ϵ_{max} 4.34; λ_{max} 2070 Å log ϵ_{max} 4.24; λ_{max} 2530 Å (broad) log ϵ_{max} 4.37 (*n*-heptane solution).

XIII. *β-Angelica lactone.*—Prepared by isomerization of the α-isomer with triethylamine (6). Some residual α-isomer was removed by hydrolysis and redistillation (7) but the product still contained 7–10% of the α-isomer as estimated from the infrared spectrum, b.p. 83° (10 mm).

XIV. *γ,γ-Dimethyl-$\Delta^{\alpha\beta}$-butenolide.*—Prepared as described by Haynes and Jones (8) and purified by chromatography on a neutralized alumina column from petroleum ether – benzene (2:1), b.p. 80° (10 mm).

XV. *(2-Hydroxy-1-cyclohexylidine)-acetic acid lactone.*—Prepared as described by Newman and VanderWerf (3), b.p. 130° (5 mm); m.p. 30°. Ultraviolet spectrum: λ_{max} 2215 Å log ϵ_{max} 3.26 (*n*-heptane solution).

XVI. *Phthalide.*—Commercial sample recrystallized twice from water, m.p. 72°.

XVII. *5,6-Dimethoxyphthalide.*—Sample provided by Dr. O. E. Edwards. Recrystallized twice from water, m.p. 156–157°.

XVIII. *α-Angelica lactone.*—Commercial sample purified by distillation, b.p. 52° (10 mm); m.p. 18°.

XIX. *2-Hydroxy-(Δ^1-cyclohexenyl)-acetic acid lactone.*—Prepared as described by Newman and VanderWerf (3), b.p. 110° (5 mm).

XX. *δ-Valerolactone.*—Prepared by hydrogenation of XXI under the same conditions as III, b.p. 107° (7 mm).

XXI. *5,6-Dihydro-α-pyrone.*—Prepared as described by Haynes and Jones (8), b.p. 105° (7 mm). Ultraviolet spectrum: λ_{max} 2195 Å log ϵ_{max} 2.87 (*n*-heptane solution).

XXII. *α-Pyrone.*—Prepared as described by von Pechmann (9), m.p. 5°.

XXIII. *5-Methyl-α-pyrone.*—Prepared as described by Fried and Elderfield (10), m.p. 17–19°.

XXIV. *Coumarin.*—Commercial sample purified by vacuum sublimation, m.p. 70°.

XXV. *γ-Pyrone.*—Sample supplied by Dr. O. E. Edwards, m.p. 32°.

Can. J. Chem. Downloaded from www.nrcresearchpress.com by 176.9.209.113 on 09/04/12
For personal use only.

Spectroscopic Measurements

Most of the infrared spectra were measured in carbon tetrachloride, carbon disulphide, or chloroform solution on a Perkin–Elmer 112 spectrometer. A calcium fluoride prism was used above 1300 cm^{-1} and a sodium chloride prism below. After correction for background and solvent absorption the spectra were plotted as apparent molecular extinction coefficient against wave number (11). Several of the spectra were also determined as thin liquid films on a Perkin–Elmer Model 21 spectrophotometer with sodium chloride prism. The estimated precision of the carbonyl band positions reported in Tables I and II is ± 2 cm^{-1}. Only portions of selected spectra are shown here, but the complete series of spectra will be published separately (12). A standard Perkin–Elmer heated cell was used to obtain the spectra of liquid films at elevated temperatures, and the spectrum of β-phenyl-$\Delta^{\alpha\beta}$-butenolide at liquid nitrogen temperature was measured on equipment kindly made available to us by Dr. H. J. Bernstein.

TABLE I

Positions and intensities of absorption bands between 1850 and 1550 cm^{-1} in the infrared spectra of lactones exhibiting "doublet carbonyl" absorption

Compound	Solvent	Band *A* ν_{max} (cm^{-1})	Band *A* $\epsilon^{(a)}_{max}$ (cm^{-1})	Band *B* ν_{max} (cm^{-1})	Band *B* $\epsilon^{(a)}_{max}$ (cm^{-1})	Intensity ratio*	Other bands†
VII $\Delta^{\alpha\beta}$-Butenolide	CCl_4	1784.5	1240	1742	98	12.6	
	$CHCl_3$	1777.5	790	1745	565	1.4	1618(18); 1601(31)
VIII β-*n*-Butyl-$\Delta^{\alpha\beta}$-butenolide	CCl_4	1785	1075	1752	430	2.5	1643(96)
	$CHCl_3$	1784	335	1748	900	0.37	1638(125)
IX β-*n*-Hexyl-$\Delta^{\alpha\beta}$-butenolide	CCl_4	1787	1000	1754	405	2.45	1642(116)
	$CHCl_3$	1785	330	1750	915	0.36	1639(122)
X β-Cyclopentyl-$\Delta^{\alpha\beta}$-butenolide	CCl_4	1785	1175	1756	495	2.4	1638(117)
	$CHCl_3$	1784	335	1750	920	0.36	1636(136)
XI β-Cyclohexyl-$\Delta^{\alpha\beta}$-butenolide	CCl_4	1785	695	1764	540	1.30	1648(50); 1636(53)
	$CHCl_3$	1782	225	1748	850	0.26	1647(56); 1633(66)
XII β-Phenyl-$\Delta^{\alpha\beta}$-butenolide	CCl_4	1786	1805	1758	975	1.85	1694(25); 1628(180)
	$CHCl_3$	1789	335	1751	1400	0.24	1712(75); 1626(275)
XIII β-Angelica lactone	CCl_4	1782	900	1765	470	1.92	1735(220)
	$CHCl_3$	1783	270	1759	940	0.29	1742(490); 1634(60); 1602(138)
XIV γ,γ-Dimethyl-$\Delta^{\alpha\beta}$-butenolide	CCl_4	1776	635	1764	650	0.96	
	$CHCl_3$	1774	295	1754	975	0.30	1604(27)
XV (2-Hydroxy-cyclohexylidine)-acetic acid lactone	CCl_4	1779	855	1764	605	1.41	1653(183)
	$CHCl_3$	1755	640	1740	830	0.77	1649(205)
XXII α-Pyrone	CCl_4	1752	1480	1716	115	12.8	1780(114); 1640(60); 1622(55)
	$CHCl_3$	1739	1080	1721	920	1.17	1785(46); 1640(45); 1625(100)
XXIII 5-Methyl-α-pyrone	CCl_4	1753	1505	1731	445	3.4	1657(65); 1647(50)‡
	$CHCl_3$	1750	440	1719	990	0.45	1648(135); 1640(45);‡ 1544(190)
XXIV Coumarin	CCl_4	1757	1100	1743	1290	0.85	
	$CHCl_3$	1757	275	1731	1000	0.275	
XXV γ-Pyrone	CCl_4	1678	1270	1657	320	3.7	1730(22); 1695(180); 1619(87)
	$CHCl_3$	1674	980	1661	1210	0.81	1740(18); 1698(63); 1632(180); 1613(216)

*$\epsilon^{(a)}_{max}$ Band *A*/$\epsilon^{(a)}_{max}$ Band *B*.
†Band positions are reported in cm^{-1} followed by intensities ($\epsilon^{(a)}_{max}$) in parentheses.
‡Inflection.

The Raman spectra were measured in 0.2-ml cells on a Cary Model 81 spectrophotometer using Hg 4358-Å excitation at a spectral slit width of 6 cm^{-1}. Ultraviolet spectra, determined for identification purposes only, were measured on a Cary Model 12C spectrophotometer in ethanol and *n*-heptane solution; these spectra were in good accord with those reported previously in the literature (8, 13). Most previous investigators

TABLE II

Positions and intensities of absorption bands between 1850 and 1550 cm^{-1} in the infrared spectra of lactones exhibiting "singlet carbonyl" absorption

	Compound	Solvent	Carbonyl band ν_{max} (cm^{-1})	Carbonyl band $\epsilon^{(a)}_{max}$ (cm^{-1})	Other bands*
III	β-*n*-Hexyl-butanolide	CS_2	1792	—	
		$CHCl_3$	1777	—	
IV	γ-Methyl-butanolide	CS_2	1790	—	
		$CHCl_3$	1775	—	
V	γ,γ-Dimethyl-butanolide	CS_2	1785	—	
		$CHCl_3$	1775	—	
VI	*trans*-Cyclohexanol-2-acetic acid lactone	CCl_4	1793	1050	1710(20)
		$CHCl_3$	1779	780	1716(40)
XVI	Phthalide	CCl_4	1778	—	
		$CHCl_3$	1761	—	
XVII	5,6-Dimethoxyphthalide	CCl_4	1772	—	
		$CHCl_3$	1752	—	
XVIII	α-Angelica lactone	CCl_4	1806	675	1722(27); 1686(60); 1678(45)
		$CHCl_3$	1796	435	1722(110); 1683(57)
XIX	2-Hydroxy-(Δ¹-cyclohexene-1-yl)-acetic acid lactone	CCl_4	1819†	470	1708(65)
		$CHCl_3$	1798†	450	1709(335)
XX	δ-Valerolactone	CS_2	1750	—	
		$CHCl_3$	1732	—	
XXI	5,6-Dihydro-α-pyrone	CCl_4	1743	1080	
		$CHCl_3$	1729	830	

*Band positions are reported in cm^{-1}, followed by intensities ($\epsilon^{(a)}_{max}$) in parentheses.
†Broad unsymmetrical band.

have measured the ultraviolet absorption spectra of $\Delta^{\alpha\beta}$-butenolides in ethanol solution, and under these conditions the maximum occurs near 2100 Å. The band is displaced bathochromically to 2200–2215 Å in *n*-heptane, where it is more easily observed and more precisely measured. A representative ultraviolet spectrum in *n*-heptane has been published elsewhere (4).

Molecular Weight Measurements

Molecular weights in solution were kindly determined for us by Dr. A. F. Sirianni of the Applied Chemistry Division of the National Research Council by measurement of the depression of the solvent vapor pressure, using the technique developed by Puddington (14).

RESULTS

The typical doublet carbonyl absorption of the conjugated unsaturated γ- and δ-lactones is illustrated by the infrared spectra of $\Delta^{\alpha\beta}$-butenolide (VII), β-cyclopentyl-$\Delta^{\alpha\beta}$-butenolide (X), and 5-methyl-α-pyrone (XXIII) in Figs. 1–3. It is characteristic of this absorption that the high frequency component (Band *A*) is more intense in carbon tetrachloride, and the relative intensities tend to reverse in chloroform solution. This is identical with the behavior of the lactone carbonyl bands of the steroids I and II. The positions and intensities of these bands for all lactones exhibiting the doublet absorption are given in Table I, while the carbonyl bands of lactones showing normal behavior are summarized in Table II.

Before discussing this absorption it will be convenient first to record some additional experiments that illustrate the effect of various environmental factors on these bands.

Can. J. Chem. Downloaded from www.nrcresearchpress.com by 176.9.209.113 on 09/04/12
For personal use only.

Can. J. Chem. Downloaded from www.nrcresearchpress.com by 176.9.209.113 on 09/04/12
For personal use only.

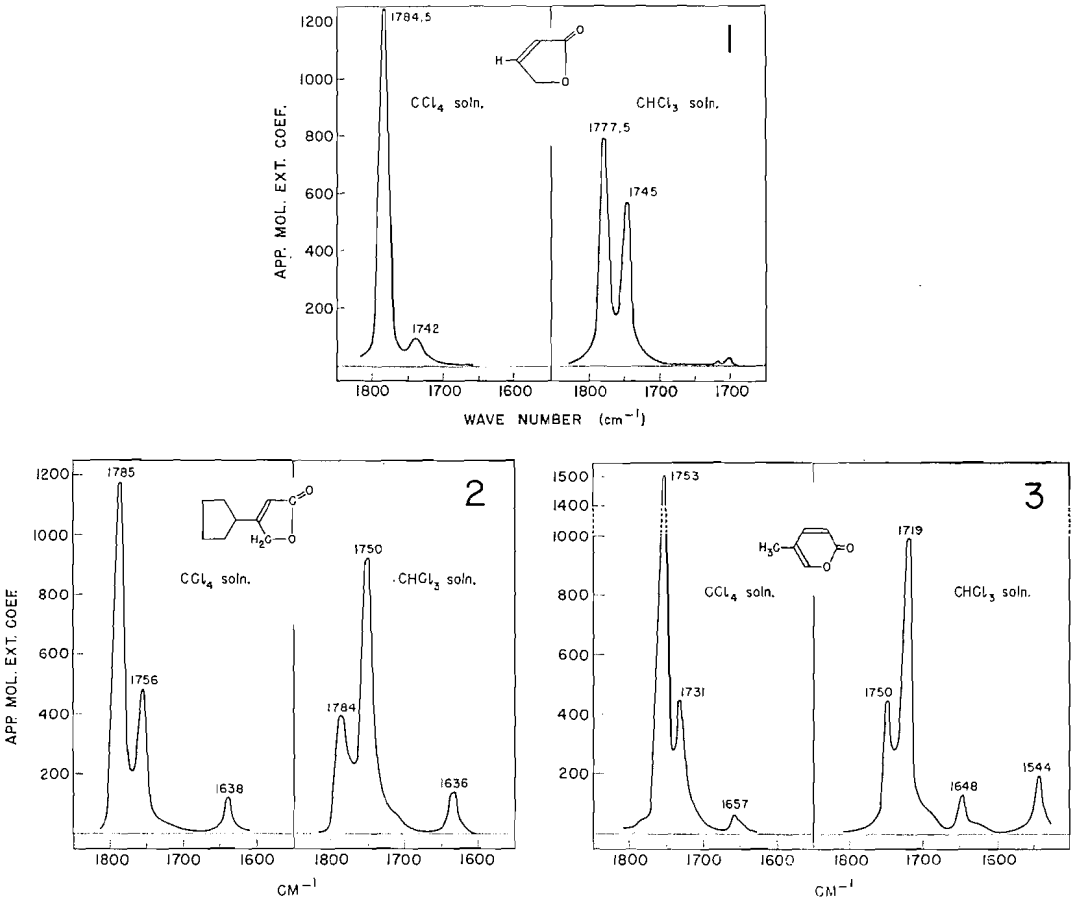

FIG. 1. Infrared spectrum of $\Delta^{\alpha\beta}$-butenolide in the region of the C=O stretching absorption.
FIG. 2. Infrared spectrum of β-cyclopentyl-$\Delta^{\alpha\beta}$-butenolide in the region of the C=O stretching absorption.
FIG. 3. Infrared spectrum of 5-methyl-γ-pyrone in the region of the C=O stretching absorption.

Most of these measurements were made with β-*n*-hexyl-$\Delta^{\alpha\beta}$-butenolide (IX), as this was the lactone in most plentiful supply. The phenyl derivative (XII) with melting point 94° was used for solid phase studies since most of the other lactones are liquids or low melting solids. We are satisfied, however, that these effects are general to all the lactones exhibiting the split carbonyl bands.

Solvent Effects

In carbon disulphide the spectrum of β-*n*-hexyl-$\Delta^{\alpha\beta}$-butenolide in the region of the carbonyl bands is similar to that in carbon tetrachloride, while the spectrum of the pure liquid is similar to that in chloroform. The spectrum in acetonitrile and methanol also resembles the spectrum of the chloroform solution, but the inversion of the band intensities is more accentuated (Table III). These band intensity changes are reversible when the same sample of lactone is examined successively in a series of different solvents.

In the last two columns of Table III are given the dipole moments and dielectric constants of the solvents. Although the relative intensity of the low frequency band (Band *B*) increases with the solvent polarity, the relationship is not a simple one. This, however,

TABLE III

Doublet carbonyl absorption of β-*n*-hexyl-$\Delta^{\alpha\beta}$-butenolide in various solvents

Solvent	Band *A* ν_{max} (cm^{-1})	Band *A* $\epsilon^{(a)}_{max}$ (cm^{-1})	Band *B* ν_{max} (cm^{-1})	Band *B* $\epsilon^{(a)}_{max}$ (cm^{-1})	Intensity ratio (Band *A*/ Band *B*)	Dielectric constant of solvent	Dipole moment of solvent (Debye)
CCl_4	1787	1000	1754	405	2.5	2.238 (20° C)	0.0
CS_2	1782	1120	1750	410	2.7	2.641 (20° C)	0.0
$CHCl_3$	1785	330	1750	900	0.37	4.806 (20° C)	1.20
CH_3OH	1783	185	1741	750	0.25	32.03 (25° C)	3.01
CH_3CN	1783	325	1750	1050	0.31	37.5 (20° C)	3.4/3.5*
CCl_4 sat. HCl	1786	980	1752	460	2.1	—	—
$CHCl_3$ sat. HCl	1785	310	1749	880	0.35	—	—
$CHCl_3$(20%)/CCl_4(80%)†	1785	695	1751	785	0.89	—	—
$CHCl_3$(50%)/CCl_4(50%)	1785	470	1752	865	0.54	—	—

*Benzene solution.
†Percentage by weight.

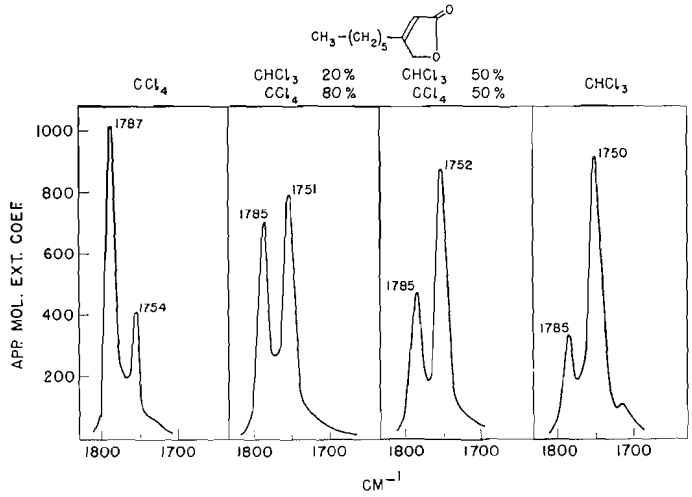

FIG. 4. Effect of solvent on the C=O stretching absorption of β-*n*-hexyl-$\Delta^{\alpha\beta}$-butenolide.

would hardly be expected in the light of recent studies of solvent effects (15). The sensitivity of the bands to the solvent polarity is illustrated by the curves for mixed carbon tetrachloride/chloroform solvents shown in Fig. 4. With increase in the chloroform concentration the relative intensities of the bands change progressively; the position of Band *A* remains unchanged while Band *B* shifts slightly from 1754 cm^{-1} to 1750 cm^{-1}. Saturation of either solvent with dry hydrogen chloride, which might catalyze a chemical bond shift, has no effect on the band positions or intensities.

Concentration Effects

The spectrum of β-*n*-hexyl-$\Delta^{\alpha\beta}$-butenolide in the region of the carbonyl stretching bands was measured both in carbon tetrachloride and in chloroform solution over a concentration range from 0.001 *M* to 0.03 *M*, and no significant change in the ratios of the band intensities was observed. When this is considered in conjunction with the similarity of the spectrum of the pure liquid to that of the dilute solutions in chloroform, it strongly suggests that we are not dealing with an association phenomenon; this is borne out also by the molecular weight measurements discussed below.

Can. J. Chem. Downloaded from www.nrcresearchpress.com by 176.9.209.113 on 09/04/12
For personal use only.

Temperature Effects

The effect of temperature increase on the spectra of liquid films of β-*n*-hexyl-$\Delta^{\alpha\beta}$-butenolide and 5-methyl-α-pyrone is shown in Figs. 5 and 6. In both cases there is a pronounced enhancement of the relative intensity of the high frequency component as the temperature rises. This effect is reversed on cooling. The decrease in the absolute intensity in the heated film in Fig. 5 is a secondary consequence of the decrease in the thickness of the capillary film layer.

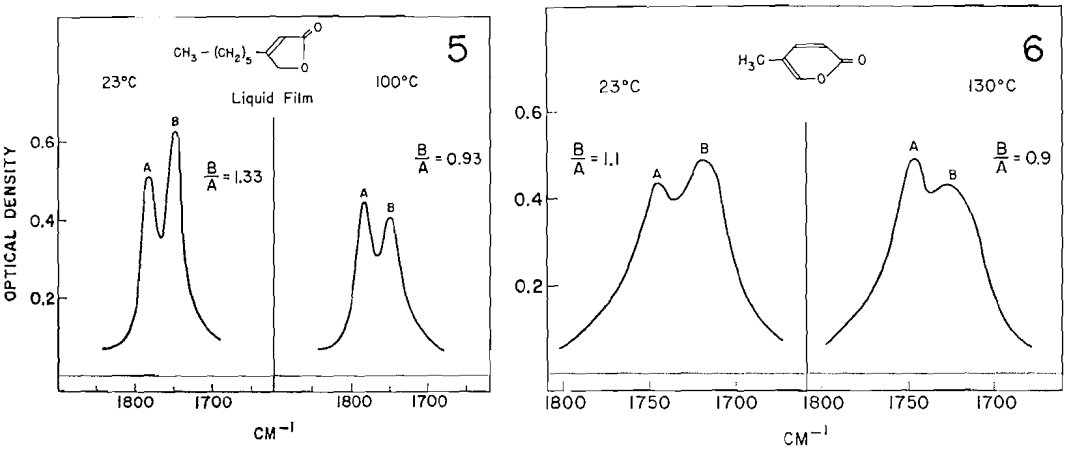

FIG. 5. Effect of temperature on the C=O stretching absorption of a liquid film of β-*n*-hexyl-$\Delta^{\alpha\beta}$-butenolide.

FIG. 6. Effect of temperature on the C=O stretching absorption of a liquid film of 5-methyl-γ-pyrone.

The spectrum of β-phenyl-$\Delta^{\alpha\beta}$-butenolide, measured as a crystalline film at room temperature and when cooled with liquid air, is shown in Fig. 7. Both spectra show the doublet carbonyl peaks. The minor bands and inflection may be due to incomplete compensation for water vapor absorption.

Raman Spectra

The Raman spectra of $\Delta^{\alpha\beta}$-butenolide and its β-*n*-butyl derivative have been determined for the pure liquids and for solutions in carbon tetrachloride and chloroform. The

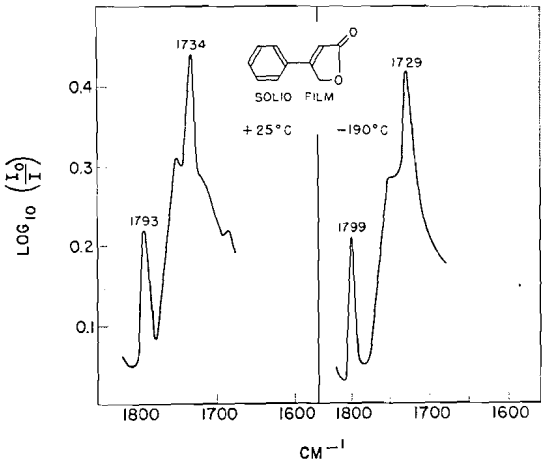

FIG. 7. Effect of temperature on the C=O stretching absorption of a solid crystalline film of β-phenyl-$\Delta^{\alpha\beta}$-butenolide.

Can. J. Chem. Downloaded from www.nrcresearchpress.com by 176.9.209.113 on 09/04/12
For personal use only.

Raman spectrum of β-phenyl-$\Delta^{\alpha\beta}$-butenolide was also measured in both solvents. These spectra show the same doublet carbonyl bands as do the infrared spectra with intensity variations in the same sense. The C=C stretching bands are relatively more intense than in the infrared spectrum, as is normally the case. A representative pair of Raman spectra is shown in Fig. 8.

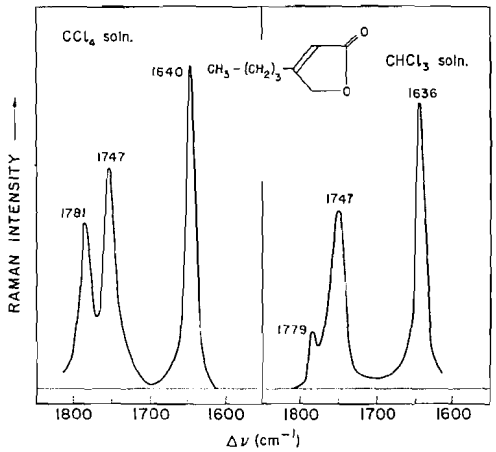

FIG. 8. Effect of solvent on the C=O stretching bands in the Raman spectrum of β-*n*-butyl-$\Delta^{\alpha\beta}$-butenolide.

TABLE IV

Molecular weights of $\Delta^{\alpha\beta}$-butenolides in solution

Solvent	Concn. (mg/100 mg of solution)	Temp. (° C)	Mol. wt.
(A) β-Phenyl-$\Delta^{\alpha\beta}$-butenolide (XII)*			
Benzene	1.360	38	169.5
	0.735	38	166.5
	0.64	38	172.2
	0.765	36	173.9
	0.735	36	175.8
	0.570	36	174.3
Ethanol	1.309	38	183.5
	1.00	38	184.6
	0.754	38	185.6
	0.756	36	167.3
	0.696	36	178.0
	0.542	36	178.5
(B) Digitoxigenin acetate (I)†			
Toluene	2.31	50	511
	1.6	50	485
	1.55	50	479
	2.15	70	470
	1.65	70	436
	1.5	70	423
	1.32	70	445
	1.13	70	447
Ethanol	3.02	50	454
	2.35	50	411
	1.67	50	422

*Mol. wt. of monomer (calc.) 160.
†Mol. wt. of monomer (calc.) 416.

Can. J. Chem. Downloaded from www.nrcresearchpress.com by 176.9.209.113 on 09/04/12
For personal use only.

Molecular Weights in Solution

Accurate molecular weight determinations on solutions of the lower melting and liquid lactones could not be obtained because of their finite vapor pressure. Measurements are reported in Table IV for β-phenyl-$\Delta^{\alpha\beta}$-butenolide (m.p. 74°) and for digitoxigenin acetate (I) (R = —OAc) (m.p. 217°). Although these data all indicate some degree of association in solution, there is no significant difference between the measurements in the more polar and less polar solvents that might reasonably be correlated with the spectral changes. The spectrum of β-phenyl-$\Delta^{\alpha\beta}$-butenolide in benzene shows the typical non-polar solvent pattern with strong reversal of the band intensity in ethanol. These molecular weight measurements therefore exclude any explanation of the carbonyl band splitting based on dimeric or polymeric association.

DISCUSSION

The infrared literature contains numerous examples of monocarbonyl compounds that exhibit two or more prominent bands between 1900 and 1650 cm^{-1}. In the absence of other acceptable explanations, both bands are usually assigned to vibrations involving the carbonyl group. In a number of cases these doublet carbonyl peaks have been attributed to equilibria between conformational isomers.

This interpretation is usually based on the demonstration that the relative intensities of the two peaks are temperature- and solvent-dependent, but are independent of the concentration. It must also be possible to write a pair of conformationally isomeric structures that are plausible on both thermodynamic and spectroscopic grounds. This requires that the energy difference between the two forms will be small enough to allow a significant concentration of the less stable form to exist in equilibrium at room temperature, while the energy barrier to interconversion must be small enough to permit rapid attainment of the equilibrium. It is also necessary that the inductive, mesomeric, and field effects on the carbonyl group must differ sufficiently in the two forms to induce a significant displacement of the two carbonyl frequencies.

The doublet carbonyl peaks of the lactones considered here do show the necessary solvent and temperature dependence and concentration independence, but for them it is not possible to write pairs of stable conformationally isomeric structures within the framework of current views of molecular structure. A similar situation occurs for cyclopentanone (16), which also exhibits a split carbonyl band, and for certain Δ^2-cyclopentenones that have been studied by Yates and his collaborators (17, 18). In both the latter cases it has been shown that the splitting of the carbonyl band must involve an intramolecular vibrational property of the molecule, since it disappears when certain of the hydrogen atoms are exchanged for deuterium. So far our attempts to introduce deuterium into the αβ-unsaturated-γ-lactone ring have been unsuccessful, but there can be little doubt that the nature of the carbonyl band splitting is similar to that in cyclopentanone and in the Δ^2-cyclopentenones.

Assuming that an intramolecular vibrational effect is involved, it must depend on some form of coupling between the carbonyl stretching mode and another vibration. This would seem to require an accidental degeneracy between the C=O stretching mode and an overtone or combination band, i.e. a Fermi resonance. We have come to accept this explanation for the lactone spectra with some reluctance, since, a priori, it seemed highly unlikely that such accidental degeneracy would occur through such a wide range of different types of structure. Thus it is necessary that the overtone or combination band must be entirely uninfluenced by the nature of the substituent on the

Can. J. Chem. Downloaded from www.nrcresearchpress.com by 176.9.209.113 on 09/04/12
For personal use only.

Can. J. Chem. Downloaded from www.nrcresearchpress.com by 176.9.209.113 on 09/04/12
For personal use only.

β-carbon atom. The lack of coupling between the vibrations in the ring and in the β-side chain of the $\Delta^{\alpha\beta}$-butenolides is demonstrated in the spectrum of the β-phenyl derivative. The carbonyl bands of this compound show practically no shift from those of compounds containing β-alkyl groups (cf. VIII and XII in Table I). Models demonstrate that in β-phenyl-$\Delta^{\alpha\beta}$-butenolide there is no steric hindrance to a structure in which the aromatic and lactone rings are coplanar, but nevertheless there must be negligible π-electron flow between the rings in the ground state of the molecule.

In terms of a Fermi resonance hypothesis, it is also surprising that the perturbation effects on the five- and six-membered ring lactones should be identical (cf. Figs. 2 and 3). In looking for common structural features among the compounds in Table I we do observe that all contain the partial structure XXVI, and this closely resembles XXVII which Yates and Williams have demonstrated to be necessary for carbonyl band splitting in Δ^2-cyclopentenones (18). On the other hand it must also be noted that the $\alpha\beta$-un-

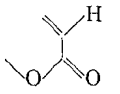

XXVI

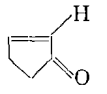

XXVII

saturated-δ-lactone XXI which does contain the partial structure XXVI shows the normal singlet carbonyl maximum. The possibility must be considered that an element of fortuitousness exists in the seemingly similar behavior of the γ- and δ-lactones, and this will arise again when numerical relationships with possible low-lying fundamental vibrations are considered. In γ,γ-dimethyl-$\Delta^{\alpha\beta}$-butenolide (XIV) the doublet is also rather poorly resolved.

In the infrared spectra of the saturated five-membered ring lactones (III–VI) the singlet carbonyl peak occurs at 1795–1785 cm^{-1} in carbon tetrachloride solution. In the absence of vibrational perturbation effects, this frequency would be expected to fall by about 20 cm^{-1} on introduction of the conjugated double bond to form the $\Delta^{\alpha\beta}$-butenolide ring. This would place the "normal" $\Delta^{\alpha\beta}$-butenolide carbonyl band in the range 1775–1765 cm^{-1}. However, the shortening of the $\alpha\beta$-bond will reduce the internal ring angles, and this will have a secondary effect, changing the hybridization to put more sp^2 character into the external bonds, and raising the carbonyl frequency slightly, perhaps to 1780–1770 cm^{-1}.

A survey of the complete spectra of the $\Delta^{\alpha\beta}$-butenolides (12) shows that there is usually a band (ν_2) in the region 900–875 cm^{-1}, the first overtone of which ($2\nu_2$) might couple with the carbonyl stretching mode to provide the postulated Fermi resonance split. These frequency relationships are summarized in Table V. In most of the compounds ν_2 is one of the strongest bands in this region of the spectrum. It might be identified with the out-of-plane deformation vibration of the hydrogen atom on the α-carbon atom, and this would be consistent with the presence of structure XXVI. In some of the compounds, however (notably XIII and XIV), the band is weak.

From Table V it will be seen that ν_2 is displaced upwards with change from carbon tetrachloride to chloroform solvent, while ν_1, the arithmetical mean of the two carbonyl frequencies, moves in the opposite direction. In the last column of Table V the difference $\nu_1 - 2\nu_2$ is given. In the absence of anharmonicity, the Fermi resonance coupling should depend inversely on the numerical value of this difference, irrespective of the sign. This might be changed if $2\nu_2$ is lowered below ν_1 by a strong anharmonicity term. $\Delta^{\alpha\beta}$-Butenolide itself is an exception, and for this compound stronger coupling would be expected

TABLE V

Relationships between positions of carbonyl bands and other bands that might enter into Fermi resonance

Compound	Solvent*	Mean carbonyl frequency $\nu_1 = \frac{1}{2}(\nu_A + \nu_B)$	ν_2	$2\nu_2$	$\nu_1 - 2\nu_2$
$\Delta^{\alpha\beta}$-Butenolide (VII)	CCl_4	1763 (cm^{-1})	869	1738	−25
	$CHCl_3$	1761	877	1754	− 7
β-*n*-Butyl-$\Delta^{\alpha\beta}$-butenolide (VIII)	CCl_4	1768	878	1756	+12
	$CHCl_3$	1766	891	1782	−16
β-*n*-Hexyl-$\Delta^{\alpha\beta}$-butenolide (IX)	CCl_4	1770	881	1762	+ 8
	$CHCl_3$	1767	894	1788	−21
β-Cyclopentyl-$\Delta^{\alpha\beta}$-butenolide (X)	CCl_4	1770	882	1764	+ 6
	$CHCl_3$	1767	893	1786	−19
β-Cyclohexyl-$\Delta^{\alpha\beta}$-butenolide (XI)	CCl_4	1774	878	1756	+18
	$CHCl_3$	1765	899	1798	−33
β-Phenyl-$\Delta^{\alpha\beta}$-butenolide (XII)	CCl_4	1772	886	1772	0
	$CHCl_3$	1770	895	1790	−20
β-Angelica lactone (XIII)	CCl_4	1773	878†	1756	+17
	$CHCl_3$	1771	887†	1774	− 3
γ,γ-Dimethyl-$\Delta^{\alpha\beta}$-butenolide (XIV)	CCl_4	1770	885†	1770	0
	$CHCl_3$	1764	890†	1780	−16
(2-Hydroxy-1-cyclohexylidine)-acetic acid lactone (XV)	CCl_4	1771	881	1762	+ 9
	$CHCl_3$	1747	894	1788	−41
α-Pyrone (XXII)	CCl_4	1734	833	1866	+68
	$CHCl_3$	1730	—	—	—
5-Methyl-α-pyrone (XXIII)	CCl_4	1742	822	1644	+98
	$CHCl_3$	1735	828	1656	+79
γ-Pyrone (XXV)	CCl_4	1667	846	1692	−25
	$CHCl_3$	1667	851	1702	−35

*Where the carbonyl frequency is measured in CCl_4 the value of ν_2 was taken from measurements in CS_2. For the measurements in $CHCl_3$ ν_2 was determined in the same solvent at a higher concentration in an 0.1-mm cell; these measurements were made through regions where the solvent is also absorbing, and the band positions may be displaced slightly on this account.

†These bands are weaker than those designated ν_2 in the spectra of the other compounds and their appearance suggests they are of a different origin (see reference 12).

in chloroform. The spectra in Figs. 1 and 2 give no indication of different behavior from the substituted $\Delta^{\alpha\beta}$-butenolides.

If we are indeed dealing with a Fermi resonance effect, the anharmonicity of the overtone vibration must be a major factor in connection with the sensitive solvent effects. The differential solvent displacements of the two unperturbed combining frequencies will influence the magnitude of the coupling, but in addition the resonance involves a perturbation function (designated w_{n1} by Herzberg (19)) which depends on the cubic and quartic terms of the potential energy. These terms may be considerably modified by the force fields in the solvent–solute complex, particularly in polar media. In regard to the effect of temperature on the resonance coupling, it will be noted from Figs. 4–6 that an increase in temperature alters the band intensities in the same sense as a decrease in solvent polarity. The temperature effect on the spectrum may therefore be an indirect consequence of the reduction of the polarity of the molecular environment at the higher temperature.

Additional difficulties appear when the δ-lactones are considered. Comparisons of the curves for β-cyclopentyl-$\Delta^{\alpha\beta}$-butenolide in Fig. 2 and 5-methyl-α-pyrone in Fig. 3 can leave little doubt that essentially the same phenomenon is involved in both cases. However, in the δ-lactone infrared spectra the bands that might reasonably be assigned to the out-of-plane C—H deformation of the α-hydrogen are displaced to 850–820 cm^{-1}. This would place the pure harmonic overtone at 1700–1640 cm^{-1}, and it would be necessary

Can. J. Chem. Downloaded from www.nrcresearchpress.com by 176.9.209.113 on 09/04/12
For personal use only.

to invoke a large negative anharmonicity to raise this sufficiently to allow Fermi resonance with the carbonyl frequency. In the infrared spectra of the unsaturated δ-lactones there are no suitable infrared active bands nearer to the required position. It is of course possible that combination bands rather than overtone bands may be involved, or bands inactive in the infrared, as probably occurs in cyclopentanone (16). As yet we have had no opportunity to look for such bands in the Raman spectra.

Similar Effects in Other Compounds

A survey of other compounds has shown that this type of carbonyl band splitting may be much more widespread than is generally recognized.

In open chain acid anhydrides, the appearance of two carbonyl stretching bands is well known and, although probably a vibrational resonance phenomenon, it is distinct from the effect we are considering here. In five-membered ring cyclic anhydrides, however, it was noted first by Cooke (20) that the carbonyl band of lower frequency can itself be resolved into a doublet if the spectrum is measured with good dispersion. We have studied this band in maleic anhydride, phthalic anhydride, and naphthalene-1,2-dicarboxylic anhydride, and observe that the two components of the low frequency carbonyl band of these compounds show an intensity reversal with solvent change identical with that of the unsaturated lactones. This is illustrated for maleic anhydride in Fig. 9. This is not observed with the open chain anhydrides, and the cyclic structure seems to be essential.

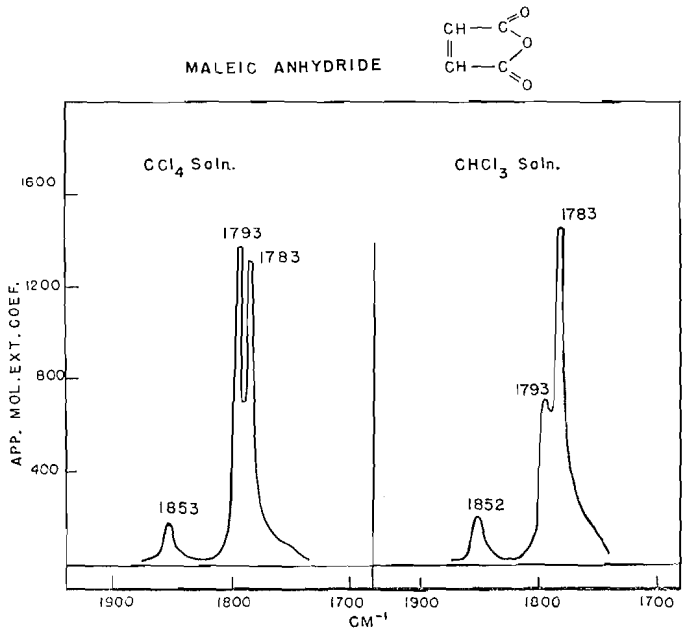

FIG. 9. Effect of solvent on the C=O stretching absorption of maleic anhydride.

The doubling of the carbonyl band in benzoyl chloride and some of its derivatives was first noted in the Raman spectrum by D. D. Thompson and J. F. Norris (21) in 1936, and subsequently by Flett in the infrared spectrum (22). We have confirmed Flett's observation, and it will be seen from Fig. 10 that with change of solvent from carbon tetrachloride to chloroform the low frequency "carbonyl" band of benzoyl chloride

Can. J. Chem. Downloaded from www.nrcresearchpress.com by 176.9.209.113 on 09/04/12
For personal use only.

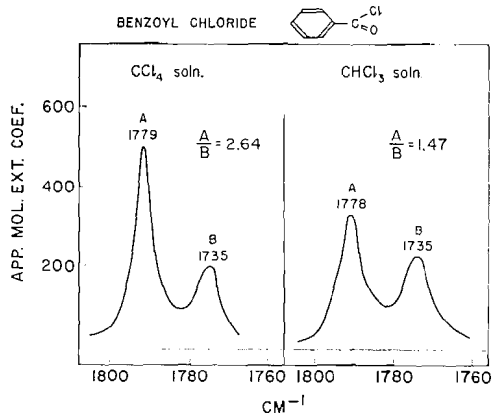

FIG. 10. Effect of solvent on the C=O stretching absorption of benzoyl chloride.

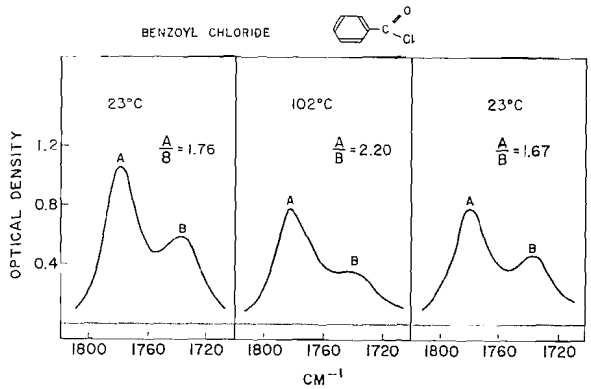

FIG. 11. Effect of temperature on the C=O stretching absorption of a liquid film of benzoyl chloride. The first spectrum at 23° C was determined before heating, and the second one after heating.

gains in intensity at the expense of the high frequency band. In both solvents the relative intensities of the "carbonyl" bands of benzoyl chloride have been shown to be independent of concentration over a 200-fold range. The two bands in the spectrum of the pure liquid show a reversible temperature effect, the high frequency band increasing relative to the low with rising temperature (Fig. 11). This also parallels the behavior of the unsaturated lactones. For benzoyl chloride one cannot write conformational equilibria involving *cis* $\rightleftharpoons$ *gauche* or *s-cis* $\rightleftharpoons$ *s-trans* forms, unless stable structures differing only in the angle between the chlorocarbonyl group and the benzene ring are considered; these are highly unlikely and here again we must resort to an interpretation based on an intramolecular vibrational phenomenon. It should be added that the possibility of the second carbonyl peak in the benzoyl chloride spectrum resulting from partial hydrolysis to benzoic acid has been disproved by the observation that on addition of small quantities of benzoic acid to liquid benzoyl chloride a third band appeared at 1695 cm^{-1}.*

We wish to thank Dr. K. Noack for making these measurements.

Can. J. Chem. Downloaded from www.nrcresearchpress.com by 176.9.209.113 on 09/04/12
For personal use only.

Can. J. Chem. Downloaded from www.nrcresearchpress.com by 176.9.209.113 on 09/04/12
For personal use only.

CONCLUSIONS

It will be apparent from the above discussion that we are not satisfied that the Fermi resonance hypothesis provides a full explanation of these effects, though there can be little doubt that some type of intramolecular vibrational effect is involved. It is to be hoped that experimental work of this kind will stimulate a more detailed theoretical study of vibrational resonance effects in complex molecules, with particular respect to the influence of solvent–solute interactions and other intermolecular force fields in the liquid phase.

The organic chemist, who is making increasing use of infrared spectra in the study of conformational isomerism and intermolecular association, must be on his guard for effects of the type discussed here. Even where it is possible to explain solvent- and temperature-dependent changes in spectra in terms of plausible conformational equilibria, such interpretations should not be accepted without further investigation. The demonstration that temperature- and concentration-dependent spectral changes can be observed in several widely separated regions of the spectrum will strongly substantiate an interpretation based on conformational isomerism. If, on the other hand, the spectral anomalies can be removed by selective deuteration, it must indicate that they have their origin in an intramolecular vibrational effect.

Finally, we must recognize that cases may arise where this type of vibrational resonance effect may be insufficient to induce a complete splitting of a band, but may broaden the band and modify its intensity and contour. This may explain the marked difference

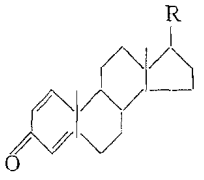

XXVIII

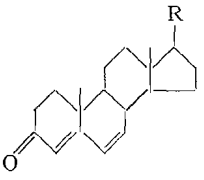

XXIX

in the contours of the carbonyl bands associated with the steroid structures XXVIII and XXIX which are illustrated in Fig. 99 of reference 29.

It has been shown recently (23, 24) that the various kinetic "σ-constants" of Hammett, Taft, and Roberts can be evaluated from measurements of the intensities, positions, and half-widths of infrared absorption bands associated with vibrations localized in the reactive functional group (23, 24). As work of this kind is extended, it will be particularly important to watch for small perturbation effects of vibrational resonance which would probably have little if any effects on the chemical reactivity of the group, and may cause discrepancies between σ-constants derived from spectrographic and kinetic measurements.

ACKNOWLEDGMENTS

We wish to thank Mr. R. Lauzon and Mrs. M. A. MacKenzie for technical assistance with the measurement of the spectra. We are also grateful to Dr. A. F. Sirianni and Dr. I. E. Puddington of the Applied Chemistry Division of the National Research Council for the molecular weight measurements, Dr. O. E. Edwards for samples of 5,6-dimethoxyphthalide and γ-pyrone, and Mr. H. Seguin for carbon and hydrogen analyses.

REFERENCES

1. DOBRINER, K., KATZENELLENBOGEN, E. R., and JONES, R. N. Infrared absorption spectra of steroids—an atlas. Interscience Publishers, Inc., New York—London. 1953. p. xii.
2. JONES, R. N. and GALLAGHER, B. S. J. Am. Chem. Soc. In press.
3. NEWMAN, M. S. and VANDERWERF, C. A. J. Am. Chem. Soc. **67**, 233 (1945).
4. SMITH, R. J. D. and JONES, R. N. Can. J. Chem. This issue.
5. RUBIN, M., PAIST, W. D., and ELDERFIELD, R. C. J. Org. Chem. **6**, 260 (1941).
6. THIELE, VON J., TISCHBEIN, R., and LOSSOW, E. Ann. **319**, 192 (1901).
7. WOLFF, L. Ann. **229**, 249 (1885).
8. HAYNES, L. J. and JONES, E. R. H. J. Chem. Soc. 954 (1946).
9. VON PECHMANN, H. Ann. **264**, 261 (1891).
10. FRIED, J. and ELDERFIELD, R. C. J. Org. Chem. **6**, 566 (1941).
11. JONES, R. N. Spectrochim. Acta, **9**, 235 (1957).
12. ANGELL, C. L., ITO, T., SMITH, R. J. D., and JONES, R. N. National Research Council of Canada Bulletin No. 7, (1959).
13. PAIST, W. D., BLOUT, E. R., UHLE, F. C., and ELDERFIELD, R. C. J. Org. Chem. **6**, 273 (1941).
14. PUDDINGTON, I. E. Can. J. Research, B, **27**, 151 (1949).
15. BELLAMY L. J. The infrared spectra of complex molecules. Methuen & Co., Ltd., London. 1954; 2nd ed. John Wiley & Sons, Inc., New York. 1958. pp. 380–382.
16. ANGELL, C. L., KRUEGER, P. J., LAUZON, R., LEITCH, L. C., NOACK, K., SMITH, R. J. D., and JONES, R. N. Spectrochim. Acta. In press.
17. YATES, P., YODA, N., BROWN, W., and MANN, B. J. Am. Chem. Soc. **80**, 202 (1958).
18. YATES, P. and WILLIAMS, L. L. J. Am. Chem. Soc. **80**, 5896 (1958).
19. HERZBERG, G. Infrared and Raman spectra of polyatomic molecules. D. Van Nostrand Company, Inc., New York. 1945. p. 215.
20. COOKE, R. G. Chem. & Ind. 142 (1955).
21. THOMPSON, D. D. and NORRIS, J. F. J. Am. Chem. Soc. **58**, 1953 (1936).
22. FLETT, M. ST. C. Trans. Faraday Soc. **44**, 767 (1948).
23. THOMPSON, H. W. Conference on molecular spectroscopy. *Edited by* E. Thornton and H. W. Thompson. Pergamon Press, Ltd., London. 1959. pp. 173–177.
24. KRUEGER, P. J. and THOMPSON, H. W. Proc. Roy. Soc. A, **250**, 22 (1959).

Can. J. Chem. Downloaded from www.nrcresearchpress.com by 176.9.209.113 on 09/04/12
For personal use only.

Can. J. Chem. Downloaded from www.nrcresearchpress.com by 176.9.209.113 on 09/04/12
For personal use only.

ALIPHATIC CHEMISTRY OF FLUORENE

PART I. DERIVATIVES OF 9-BENZOYLFLUORENE[1]

P. M. G. Bavin

ABSTRACT

Several C-alkylation products of 9-benzoylfluorene have been prepared. 9-Methyl-9-benzoylfluorene has been transformed into 9-methyl-10-phenylphenanthrene, 9-phenylphenanthrene-10-carboxylic acid, and 1,2:3,4-dibenzfluorenone.

Phenyl-9-allyl-9-fluorenylmethanol has been cyclized and rearranged in one step to 14-methyl-13,14-dihydrodibenz[a,c]phenanthrene.

Phenyl-9-methyl-9-fluorenylmethyl chloride readily decomposes to 9-methyl-10-phenylphenanthrene when heated alone or in formic acid, but reacts with silver or mercuric acetates to give unrearranged acetate.

This series of papers will be concerned with reactions of fluorene anions (I), particularly where R is an electron-demanding group, and with systems potentially capable of forming cations (II), the products being utilized in the synthesis of complex polycyclic systems.

We have shown that methyl fluorene-9-carboxylate anion (I, R = CO_2CH_3) reacts rapidly with a very wide range of alkyl halides (1, 2). Of particular interest was the formation in good yield of the 9-*t*-butyl derivative (1). Experiments with 9-benzoylfluorene anion (I, R = $CO \cdot C_6H_5$) are now reported.

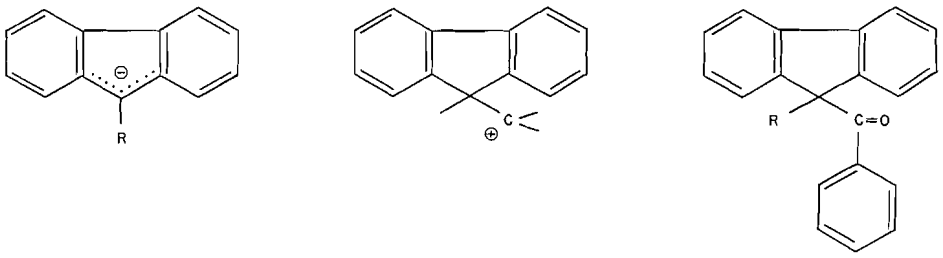

(I) (II) (III)

The keto form of 9-benzoylfluorene crystallizes from acetone as colorless needles which are insoluble in aqueous sodium hydroxide. The enol has been reported only as an oil which rapidly passes into the keto form. Solutions of either tautomer in alcoholic sodium alkoxide are deep orange, with the color attributed to the anion (I, R = $CO \cdot C_6H_5$) (3, 4), also referred to as the enolate ion.

Initial attempts to alkylate the anion (I, R = $CO \cdot C_6H_5$) with methyl or isopropyl iodides gave very low yields of the desired products, even when only 1 equivalent of methoxide ion was used to generate (I). The low yields were attributed to facile cleavage by strong base of the non-enolizable ketonic products, the cleavage being facilitated and its direction controlled by the formation of the mesomeric anion (I, R = alkyl), Fig. 1. These conclusions found support in the isolation of methyl benzoate and 9-methylfluorene among the products of attempted methylation.

[1]*Manuscript received August 24, 1959.*
Contribution from the Department of Chemistry, the University, Hull, East Yorkshire, England.

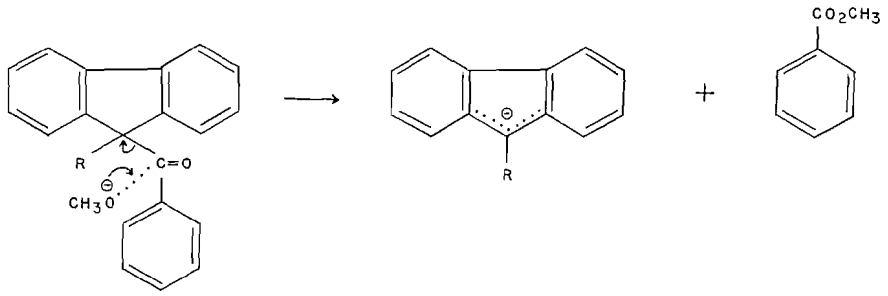

FIG. 1.

Weaker bases were next examined. Pyridine, piperidine, and triethylamine generated the anion (I) from 9-benzoylfluorene as shown by the color of methanolic solutions, but apparently formed quaternary salts too rapidly to permit C-alkylation. Suitable conditions were eventually found in the mixed solvent acetone–methanol containing a little water, with potassium carbonate as base. The 9-alkyl-9-benzoylfluorenes (III, R = alkyl) prepared in this way were methyl, ethyl, isopropyl, allyl, benzyl, and cyclohexyl, all in satisfactory yields. The reaction with *t*-butyl chloride followed a different course and will be discussed in a later paper.

The structures of the products were shown by their lack of color (the enol ethers would be yellow like other 9-fluorenylidene compounds, e.g. see (5)) and by the presence of carbonyl stretching absorption bands in their infrared spectra. In particular, the 9-methyl derivative formed an oxime in pyridine solution, was cleaved by strong base to 9-methylfluorene, and was reduced to an alcohol by lithium aluminum hydride.

Compounds of structure (IV) are potential phenanthrene intermediates through the cation (II). The transformations of 9-methyl-9-benzoylfluorene are summarized for clarity in Fig. 2. Reduction to the alcohol (IV, R = methyl; X = OH) followed by dehydration–rearrangement brought about by phosphorus pentoxide in boiling xylene gave 9-methyl-10-phenylphenanthrene, which was oxidized* by aqueous sodium dichromate at 250° to a mixture of 9-phenylphenanthrene-10-carboxylic acid (5–10%) and 1,2:3,4-dibenzfluorenone (70–80%). The acid cyclizes particularly readily, even in cold thionyl chloride. Although 1,2:3,4-dibenzfluorenone becomes readily available by this route, insufficient of the acid was obtained to allow synthesis of the phenol (V, R = OH), a potential carcinogen.

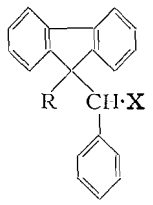

(IV)

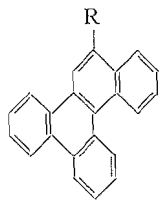

(V)

The chloride (IV, R = CH_3; X = Cl), prepared from the alcohol by the action of warm thionyl chloride, proved to be particularly interesting. It melted with slow decomposition in the range 90–100°, varying with the sample. The decomposition was rapid at 150° and gave 9-methyl-10-phenylphenanthrene in essentially quantitative yield. Related toluenesulphonates also melt with decomposition to phenanthrene derivatives

The author is indebted to Dr. D. Fishel of the State University of South Dakota for details of this oxidation procedure (6).

Can. J. Chem. Downloaded from www.nrcresearchpress.com by 176.9.209.113 on 09/04/12
For personal use only.

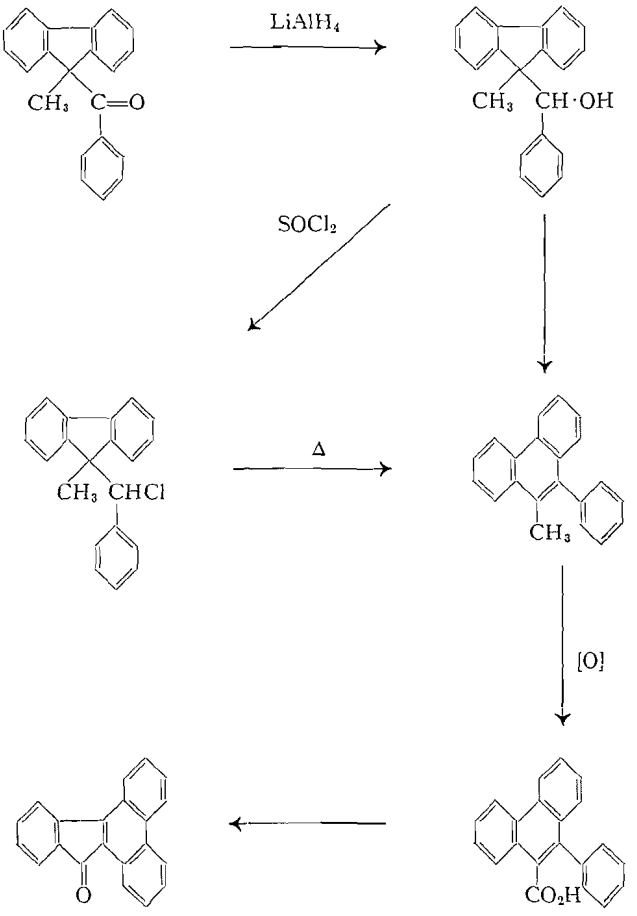

FIG. 2.

(1), but attempts to prepare the toluene- or methane-sulphonate of (IV, R = CH_3; X = OH) were not successful. The formate and acetate have been prepared. The chloride was recovered essentially unchanged after heating with methanol, acetic acid, pyridine, or quinoline and did not react with sodium iodide in acetone. Decomposition to 9-methyl-10-phenylphenanthrene in hot formic acid was complete in 2 hours. It reacted rapidly with silver or mercuric acetates in dry acetic acid to give the *unrearranged acetate* (IV, R = CH_3; X = $O\cdot CO\cdot CH_3$), the structure of which has been confirmed by esterification of the alcohol with acetic anhydride and by reduction of the acetate with lithium aluminum hydride back to the alcohol. Under similar conditions neopentyl chloride reacts with silver acetate to give the *rearranged* *t*-amyl acetate (7). The difference in behavior is tentatively attributed to stabilization of the cation (II) by the phenyl group. Experiments designed to test this postulate are under way.

When heated with phosphorus pentoxide and xylene, the allyl derivative (IV, R = $CH_2CH{=}CH_2$; X = OH) underwent dehydration–rearrangement and cyclization in one step to 14-methyl-13,14-dihydrodibenz[a,c]phenanthrene (VI, R = CH_3), isolated as the picrate in almost 90% yield. Like Bradsher and Rapoport (8) and despite rigorous purification procedures the hydrocarbon was not obtained crystalline. Dehydrogenation gave 14-methyldibenz[a,c]phenanthrene (V, R = CH_3) of m.p. 115–116°. Through the

Can. J. Chem. Downloaded from www.nrcresearchpress.com by 176.9.209.113 on 09/04/12
For personal use only.

kindness of Professor Bradsher it has been established beyond doubt that this is a metastable form, the stable form showing m.p. 150–151° (see Experimental for details). The ultraviolet spectrum showed good agreement with that of dibenz[a,c]phenanthrene having the bathochromic shift of approximately 3 mμ associated with the introduction of a methyl group.

The spiro-alcohol (VII) undergoes dehydration–rearrangement under the action of phosphorus pentoxide to give 13,14-dihydrodibenz[a,c]phenanthrene (VI, R = H) (2). Consequently the reaction of (IV, R = $CH_2CH{=}CH_2$; X = OH) may follow either of the sequences rearrangement–cyclization or cyclization–rearrangement. Cyclization must proceed through the cation $R\cdot CH_2\overset{+}{C}HCH_3$ and it is surprising that the mesomeric ion $R\cdot\overset{+}{C}HCH_2CH_3$ is not formed, leading to a derivative of 1,2:3,4-dibenzfluorene.

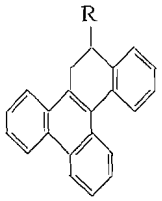

(VI)

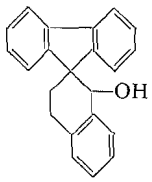

(VII)

Oxidation of (V, R = CH_3) with aqueous sodium dichromate at 250° gave the pale yellow very sparingly soluble acid, characterized as its methyl ester.

The transformations of (IV, R = $CH_2CH{=}CH_2$; X = OH) are summarized in Fig. 3. The corresponding chloride (IV, R = $CH_2CH{=}CH_2$; X = Cl) failed to yield decomposition products useful for the synthesis of (V, R = OH).

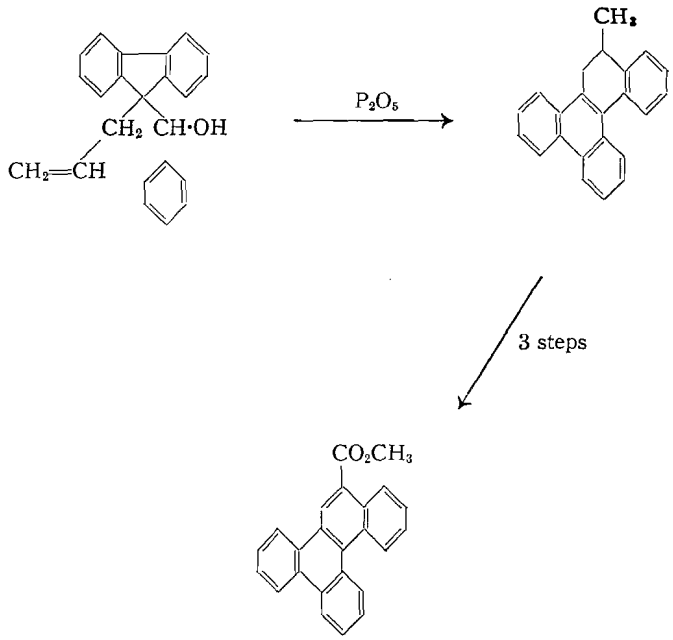

FIG. 3.

Can. J. Chem. Downloaded from www.nrcresearchpress.com by 176.9.209.113 on 09/04/12
For personal use only.

Can. J. Chem. Downloaded from www.nrcresearchpress.com by 176.9.209.113 on 09/04/12
For personal use only.

EXPERIMENTAL

9-Methyl-9-benzoylfluorene

To a boiling solution of 9-benzoylfluorene (20 g) (9) in acetone (200 ml) were added successively hot methanol (200 ml), a solution of potassium carbonate (15 g, anhydrous) in hot water (30 ml), and methyl iodide (25 g). The mixture was boiled gently under an efficient reflux condenser for 1 hour during which time the initial deep orange color faded to pale yellow. The mixture was diluted with water (800 ml) and a rapid stream of air passed through overnight. Next day the crystalline *ketone* was collected, washed, and crystallized from acetone–methanol, from which it separated as large colorless tablets (17 g, 81%), m.p. 99–101°, raised to 101–102° by two further crystallizations. Found: C, 89.48; H, 5.72%. Calculated for $C_{21}H_{16}O$: C, 88.70; H, 5.67%. Carbonyl stretching frequency: 1665 cm^{-1}.

The ketone was first obtained by alkylating 9-benzoylfluorene (2.7 g) in cold methanol containing sodium methoxide (from sodium, 0.23 g, 1 equivalent) with methyl iodide (3 g). The product crystallized from chloroform–hexane as colorless prisms (0.4 g), m.p. and mixed m.p. 99–101°. Methyl benzoate and 9-methylfluorene (see below) were obtained by distilling the mother liquors.

The *oxime*, prepared in pyridine, crystallized from chloroform–hexane as colorless needles, more rarely as prisms, m.p. 206–207°. Found: C, 84.66; H, 5.66%. Calculated for $C_{21}H_{17}NO$: C, 84.25; H, 5.73%.

After the ketone (2 g) was warmed for a few minutes with potassium hydroxide (2 g) in 95% alcohol (10 ml), isolation and distillation of the neutral product gave 9-methylfluorene as a rapidly crystallizing oil, which formed bipyramidal prisms from methanol, m.p. 45–47°. (Lit. m.p. 45–47° (10).)

Phenyl-9-methyl-9-fluorenylmethanol

Reduction of the ketone with ethereal lithium aluminum hydride gave an almost quantitative yield of the *alcohol*, which crystallized from hexane as colorless needles, m.p. 100–101°. Found: C, 87.60; H, 5.90%. Calculated for $C_{21}H_{18}O$: C, 88.08; H, 6.33%. Hydroxyl stretching frequency: 3350 cm^{-1}.

Phenyl-9-methyl-9-fluorenylmethyl Chloride

The alcohol was warmed for a few minutes with four times its weight of thionyl chloride. After excess reagent was destroyed with water, a solution of the product in hexane was passed through a column of activated alumina. The *chloride* crystallized from the eluant as massive colorless prisms (70–85%), melting point with decomposition in the range 91–99°, varying with the sample. Found, for two preparations: C, 83.03, 82.60; H, 5.70, 5.36%. Calculated for $C_{21}H_{17}Cl$: C, 82.74; H, 5.62%.

The chloride was recovered essentially unchanged after the solution was boiled with moist methanol, acetic acid, pyridine, or quinoline, or with a solution of sodium iodide in acetone. More fruitful experiments are recorded below.

9-Methyl-10-phenylphenanthrene

(*i*) The alcohol (10 g) and phosphorus pentoxide (10 g) were boiled under reflux for 3 hours with xylene (100 ml). The *hydrocarbon*, isolated in the usual way, crystallized from acetone–methanol as colorless blades (8.7 g), m.p. 98–99°, depressed to 84–90° by addition of the alcohol. Found: C, 93.73; H, 6.01%. Calculated for $C_{21}H_{16}$: C, 93.99; H, 6.01%.

The *1,3,5-trinitrobenzene complex* crystallized from methanol as bright yellow silky

needles, m.p. 126–128°. Found: C, 67.62; H, 4.15%. Calculated for $C_{27}H_{19}N_3O_6$: C, 67.35; H, 3.98%.

(*ii*) The chloride (1 g) was carefully pyrolyzed over a microburner until evolution of hydrogen chloride ceased. Crystallization of the residue from acetone–methanol gave blades (0.7 g), m.p. and mixed m.p. 97–99°.

(*iii*) The chloride (0.2 g) was boiled under reflux for 2 hours with 98% formic acid (100 ml). The product crystallized from hexane as blades (0.15 g), m.p. and mixed m.p. 96–98°.

Phenyl-9-methyl-9-fluorenylmethyl Acetate

(*i*) The chloride (1 g) was boiled for 5 minutes with silver or mercuric acetate (2 g) in anhydrous acetic acid (100 ml). The *acetate* slowly crystallized from hexane as colorless prisms, m.p. 80–81° after three crystallizations. Found: C, 84.06; H, 5.98%. Calculated for $C_{23}H_{20}O_2$: C, 84.12; H, 6.14%. No trace of the easily crystallized 9-methyl-10-phenylphenanthrene could be found.

(*ii*) The alcohol (0.2 g) was warmed for 12 hours with acetic anhydride (4 ml) containing 1 drop of concentrated sulphuric acid. The colorless prisms obtained by crystallization from hexane had m.p. and mixed m.p. 78–80°.

Reduction of the acetate with ethereal lithium aluminum hydride gave the original alcohol, identified by melting point and mixed melting point.

Phenyl-9-methyl-9-fluorenylmethyl Formate

Attempts to esterify the alcohol with *p*-toluenesulphonyl or methanesulphonyl chloride in pyridine under a range of conditions were unsuccessful. Boiling the crude products with 98% formic acid usually gave only unchanged alcohol but occasionally the *formate* was obtained, which slowly crystallized from cyclohexane as massive colorless prisms, m.p. 126–128°. Found: C, 84.24; H, 5.83%. Calculated for $C_{22}H_{18}O_2$: C, 84.05; H, 5.77%.

9-Phenylphenanthrene-10-carboxylic Acid and 1,2:3,4-Dibenzfluorenone

In a typical experiment, 9-methyl-10-phenylphenanthrene (13.4 g) was heated at 250–260° for 8 hours with technical sodium dichromate (25 g) and water (250 ml) in a 500-ml, rotating autoclave. After the container was cooled and opened, the contents were heated to boiling with the addition of 1250 ml water. Chromium sesquioxide was removed by filtration, acidification of the filtrate with dilute sulphuric acid precipitating the *phenanthroic acid* (5–10%). It formed colorless prisms from benzene–hexane, m.p. 192–193° after two crystallizations. Found: C, 84.65; H, 4.85%. Calculated for $C_{21}H_{14}O_2$: C, 84.54; H, 4.73%.

The acid dissolved in cold thionyl chloride to give an orange solution, dilution of which with water precipitated 1,2:3,4-dibenzfluorenone, orange needles from heptane, m.p. 185–187° (Lit. m.p. 185–186° (11).)

The chromium sesquioxide formed in the oxidation was contaminated with an orange gum, removed by percolation with methylene chloride. The extracted material formed orange rods from benzene–hexane (10.1 g), m.p. and mixed m.p. 184–186°.

The following ketones were prepared as described for the methyl analogue:

9-Ethyl-9-benzoylfluorene, white needles from hexane, m.p. 129–130°. Found: C, 88.34; H, 5.91%. Calculated for $C_{22}H_{18}O$: C, 88.56; H, 6.08%. Carbonyl stretching frequency: 1663 cm^{-1}.

9-Isopropyl-9-benzoylfluorene, small colorless prisms from acetone–methanol, m.p. 226–227°. Found: C, 88.17; H, 6.40%. Calculated for $C_{23}H_{20}O$: C, 88.42; H, 6.45%. Carbonyl stretching frequency: 1630 cm^{-1}.

Can. J. Chem. Downloaded from www.nrcresearchpress.com by 176.9.209.113 on 09/04/12
For personal use only.

9-Benzyl-9-benzoylfluorene, white prisms from acetone–methanol, m.p. 134–135°. Found: C, 89.81; H, 5.78%. Calculated for $C_{27}H_{20}O$: C, 89.97; H, 5.59%. Carbonyl stretching frequency: 1665 cm^{-1}.

9-Cyclohexyl-9-benzoylfluorene, colorless prisms from methanol, m.p. 121–122°. Found: C, 88.33; H, 6.78%. Calculated for $C_{26}H_{24}O$: C, 88.60; H, 6.86%. Carbonyl stretching frequency: 1675 cm^{-1}.

9-Allyl-9-benzoylfluorene, long colorless needles from acetone–methanol, m.p. 91–92°. Found: C, 89.11; H, 6.00%. Calculated for $C_{23}H_{18}O$: C, 89.00; H, 5.84%. Carbonyl stretching frequency: 1670 cm^{-1}.

Phenyl-9-allyl-9-fluorenylmethanol crystallized as irregular prisms from benzene–hexane, m.p. 132–134°. Found: C, 88.46; H, 6.33%. Calculated for $C_{23}H_{20}O$: C, 88.43; H, 6.45%.

Phenyl-9-allyl-9-fluorenylmethyl chloride formed lustrous plates from methanol, m.p. 81–82°. Found: C, 83.49; H, 5.78%. Calculated for $C_{23}H_{19}Cl$: C, 83.50; H, 5.79%. Decomposition of the chloride by pyrolysis or by boiling with formic acid gave only gums, from which nothing useful was obtained by oxidation.

14-Methyl-13,14-dihydrodibenz[a,c]phenanthrene

The allyl alcohol (20 g) and phosphorus pentoxide (30 g) were boiled under reflux for 1 hour with xylene (100 ml). The product was a pale yellow viscous oil which formed a *1,3,5-trinitrobenzene complex*, crystallizing as vermilion rods from methanol, m.p. 194–195°. Found: C, 68.48; H, 4.23%. Calculated for $C_{29}H_{21}N_3O_6$: C, 68.63; H, 4.17%. This complex was not decomposed by passing a hexane solution through a column of activated alumina.

The *picrate* crystallized from ethanol as maroon needles, m.p. 174–175°. (Lit. m.p. 170.5–171.0°, corr. (8).) Decomposition of the picrate by passing a benzene solution through a column of alumina and evaporation of the eluant gave a colorless oil which has defied prolonged attempts to induce crystallization (cf. (8)).

14-Methyldibenz[a,c]phenanthrene, (9-Methyl-1,2:3,4-dibenzphenanthrene)

Prepared in almost quantitative yield by dehydrogenating the preceding hydrocarbon at 280–300° over 10% palladium-on-charcoal, 14-methyldibenz[a,c]phenanthrene slowly crystallized from benzene–methanol as large colorless prisms, m.p. 115–116°, not raised by further crystallizations. Subsequently, recrystallization with seeding by Bradsher's preparation gave small prisms, m.p. 150–151°. (Lit. m.p. 150.5–151.5°, corr. (8).)

The ultraviolet spectrum showed excellent agreement with that of dibenz[a,c]phenanthrene (12, 13); with peaks at:

Dibenzphenanthrene	276.5	286	308	321	334	352	371 mμ
Methyl derivative	278	288	311	323	337	354*	373 mμ

The *picrate* crystallized from ethanol as bright red needles, m.p. 212–213°. (Lit. m.p. 207.5–208.5°, corr. (8).)

The *1,3,5-trinitrobenzene complex* formed slender orange needles from methanol, m.p. 234–235.5°. Found: C, 68.91; H, 3.81%. Calculated for $C_{29}H_{19}N_3O_6$: C, 68.91; H, 3.79%.

An impure sample of Professor Bradsher's original preparation was converted to the picrate (m.p. and mixed m.p. 212–213°) from which the hydrocarbon was regenerated on alumina. Crystallization from benzene–methanol gave small prisms, m.p. 149–150°, not depressed by either the low or high melting forms described above.

**Inflexion.*

Can. J. Chem. Downloaded from www.nrcresearchpress.com by 176.9.209.113 on 09/04/12
For personal use only.

Methyl Dibenz[a,c]phenanthrene-14-carboxylate

14-Methyldibenz[a,c]phenanthrene (5 g) was oxidized with sodium dichromate (20 g) as described for the methylphenylphenanthrene. The pale yellow acid (4.6 g) was very sparingly soluble but was esterified by boiling with methanol (1500 ml) for 4 hours while dry hydrogen chloride was bubbled in. A solution of the crude product in benzene–hexane (5:1) was passed through a short column of alumina to remove traces of tar. Crystallization of the eluted material from acetone–methanol gave pale orange elongated prisms, m.p. 155–156°. Found: C, 85.75; H, 5.04%. Calculated for $C_{24}H_{16}O_2$: C, 85.69; H, 4.80%.

ACKNOWLEDGMENTS

The author is grateful to Professor N. B. Chapman for his interest and encouragement and to the University, Kingston-upon-Hull, for the award of an I.C.I. Fellowship. He is indebted to Dr. G. W. Gray for taking the infrared spectra and to Dr. K. Clarke for criticizing the manuscript. Sincere thanks are offered to Professor C. K. Bradsher for his sample of 14-methyldibenz[a,c]phenanthrene.

REFERENCES

1. ANET, F. A. L. and BAVIN, P. M. G. Can. J. Chem. **34**, 991 (1956).
2. BAVIN, P. M. G. Unpublished data.
3. LEY, H. and MANECKE, W. Ber. **56**, 779 (1923).
4. MEYER, K. H. and GOTTLIEB-BILLROTH, H. Ber. **54**, 577 (1921).
5. MILLER, F. D. and WAGNER, E. C. J. Org. Chem. **16**, 279 (1951).
6. SHECHTER, H., FISHEL, D., and FRIEDMAN, L. Unpublished data.
7. WHITMORE, F. C. and FLEMING, G. H. J. Chem. Soc. 1269 (1934).
8. BRADSHER, C. K. and RAPOPORT, H. J. Am. Chem. Soc. **66**, 1281 (1944).
9. WISLICENUS, W. and FEHRLE, A. Ber. **48**, 1321 (1915).
10. GREENHOW, E. J., WHITE, E. N., and MCNEIL, D. J. Chem. Soc. 2848 (1951).
11. MARTIN, R. H. and VASSART, S. Bull. soc. chim. Belges, **61**, 234 (1952).
12. CLAR, E. Aromatische Kohlenwasserstoffe. 2nd ed. Springer-Verlag, Berlin. 1952.
13. BAVIN, P. M. G. Thesis, London. 1954.

Can. J. Chem. Downloaded from www.nrcresearchpress.com by 176.9.209.113 on 09/04/12
For personal use only.

Can. J. Chem. Downloaded from www.nrcresearchpress.com by 176.9.209.113 on 09/04/12
For personal use only.

STEROIDS AND RELATED PRODUCTS

XI. THE SYNTHESIS OF 3,9,12,20-TETRAOXYGENATED 9,12-*SECO*-STEROIDS. PART I[1, 2]

CH. R. ENGEL[3] AND W. W. HUCULAK[4]

ABSTRACT

The synthesis of 3α,20β-dihydroxy-9-oxo-9,12-*seco*-12-pregnanoic acid (XV) and some of its derivatives, from 3α,12α-diacetoxy-20-oxopregnane, is described. The fission of ring C was achieved by ozonolysis of a 9,11-unsaturated 12-ketone. In the course of this work evidence was found that the rearrangement of certain 11-hydroxy-12-ketones to 12β-hydroxy-11-ketones, under the influence of alkali, can occur in high yield, even at room temperature.

For synthetic experiments which will be described at a later date, we needed 3,20-dioxygenated pregnane derivatives in which ring C of the original steroid nucleus had been opened in such a manner as to give a 9,12-*seco*-9-keto-12-acid derivative of the following general formula I:

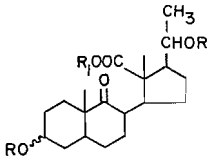

I, R = H, acyl; R_1 = H, alkyl

Wieland *et al.* (2, compare also 3) had already obtained a similar 9,12-*seco* derivative, but without oxygen functions in positions 3 and 20, in the course of their elucidations of the structure of bile acids. The German authors brominated 12-oxocholanic acid (partial formula II) and hydrolyzed the resulting bromoketone (III)[5] with methanolic potassium hydroxide at reflux temperature. Since it is known that, under these relatively vigorous conditions, 11-hydroxy-12-ketones of structure IV rearrange to 12β-hydroxy-11-ketones (7, 8), one has to assign to the hydrolysis product structure V, in contrast to Wieland's original formulation as IV. Oxidation led Wieland and his co-workers to the 11,12-diketo derivative VIII, which they enolized to VII; treatment with potassium permanganate or chromic acid resulted in the 9-oxo-9,12-*seco*-12-acid derivative of cholanic acid (partial formula VI).

We wished to investigate the possibility of using this method for preparative purposes and, in particular, of employing it for the synthesis of 3,20-dioxygenated 9,12-*seco*-steroids. Since we intended to prepare a product with alcohol functions in positions 3 and 20, it seemed important to isolate in our series the unrearranged ketol of type IV. We considered that this would allow us to acetylate positions 3 and 20 selectively,

[1]*Manuscript received August 25, 1959.*
Contribution from the Collip Medical Research Laboratory and the Department of Chemistry, the University of Western Ontario, London, Ontario. The subject of this communication was part of a paper presented at the 40th annual conference of the Chemical Institute of Canada, Vancouver, B.C., June 1957.
[2]*For paper X of this series see reference 1.*
[3]*Present address: Department of Chemistry, Laval University, Quebec, Canada. Correspondence should be addressed to this author.*
[4]*This paper is abbreviated from a portion of the M.Sc. thesis of W. W. Huculak, presented to the Faculty of Graduate Studies of the University of Western Ontario in April, 1959.*
[5]*In accordance with the now-accepted stereochemical course of brominations of 12-ketones (4, 5, 6), one has to assign the α-configuration to Wieland's main bromination product.*

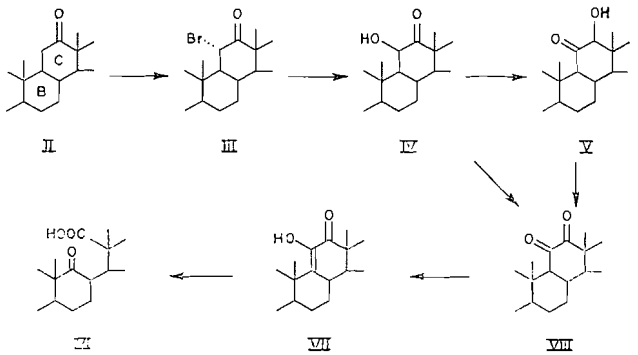

since it is known that an 11β-hydroxy group generally resists acetylation with acetic anhydride in pyridine under mild conditions, and to oxidize subsequently the 11-hydroxy group without affecting the protected alcohol functions in 3 and 20.

The readily available bile acid derivative, 3α,12α-diacetoxy-20-oxopregnane (IX*a*), served as starting material. Reaction with an excess of lithium aluminum hydride afforded predominantly 3α,12α,20β-trihydroxypregnane (X), further characterized by its triacetate X*a*. The configuration in position 20 of the main reduction product was assigned on the basis of molecular rotational analysis. Upon acetylation of X to the triacetate X*a* we observed an increment in the molecular rotation of +435°; since a computation of the data available in the literature indicates that the increment due to diacetylation in positions 3α and 12α lies between 230 and 360°, the contribution of acetylation in position 20 to the observed increment lies between +75 and +205°. Sarett (9) has shown that acetylation of a 20β-hydroxy function produces an increment of molecular rotation of the same order of magnitude, whereas acetylation of a 20α-hydroxy function is accompanied by a decrease of the molecular rotation.

Succinylation of the triol X afforded in good yield a dihemisuccinate (X*b*), readily methylated to the bis-methylsuccinate X*c*. The assignment of structures X*b* and X*c* to the disuccinates is legitimate because, under the succinylation conditions employed, a 12α-hydroxy group remains unchanged (compare for instance 10 and 11), as also confirmed by the monosuccinylation of 3α,12α-dihydroxy-20-oxopregnane (IX) to the 12α-hydroxy derivative IX*b*.

Oxidation of the bis-methylsuccinate X*c* with chromic acid in acetic acid gave in high yield the monoketone XI, which was brominated with 1 equivalent of bromine in acetic acid, at 55°. The amorphous reaction product, presumably containing predominantly the 11α-bromoketone XIV (compare 4, 5, 6), was hydrolyzed directly with aqueous ethanolic potassium hydroxide, at room temperature. The neutral reaction product was acetylated with acetic anhydride in pyridine at room temperature; instead of a mixture containing mainly the desired 3,20-diacetate XIII*d*, a product composed predominantly of a triacetate (M_D +235°) was obtained.

Gallagher (7, compare also article 8, by Wintersteiner *et al.*) proved that, under the influence of hot aqueous alcoholic potassium hydroxide, 11α- and 11β-hydroxy-12-ketones rearranged to 12β-hydroxy-11-ketones. We assumed that such a rearrangement must have occurred in our case at room temperature, as otherwise no appreciable amount of triacetate should have been obtained; it seemed indeed improbable that the 11β-hydroxy function would have been acetylated smoothly under the conditions employed. Furthermore, even if this had been the case, the reaction product should also have

Can. J. Chem. Downloaded from www.nrcresearchpress.com by 176.9.209.113 on 09/04/12
For personal use only.

contained some 3α,11α,20β-triacetoxy ketone XIII*b*, since it is known that bromination of a 12-keto group does not proceed stereospecifically and since the crude bromination product, containing some 11β-bromide, had been hydrolyzed with potassium hydroxide. We were, however, unable to isolate a second triacetate. The homogeneity of the triacetate obtained can be explained by a rearrangement of the originally formed ketols XIII*a* and XIII to ketol XII*a*, as it has been established (7) that both 11α- and 11β-hydroxy-12-ketones can be rearranged to the same 12β-hydroxy-11-ketone.

Recently, Schindler (12) reported a case in the etianic acid series where, under the influence of a 12-keto group, an 11β-hydroxy function was acetylated with acetic anhydride in pyridine at room temperature; this could weaken our argument in favor of

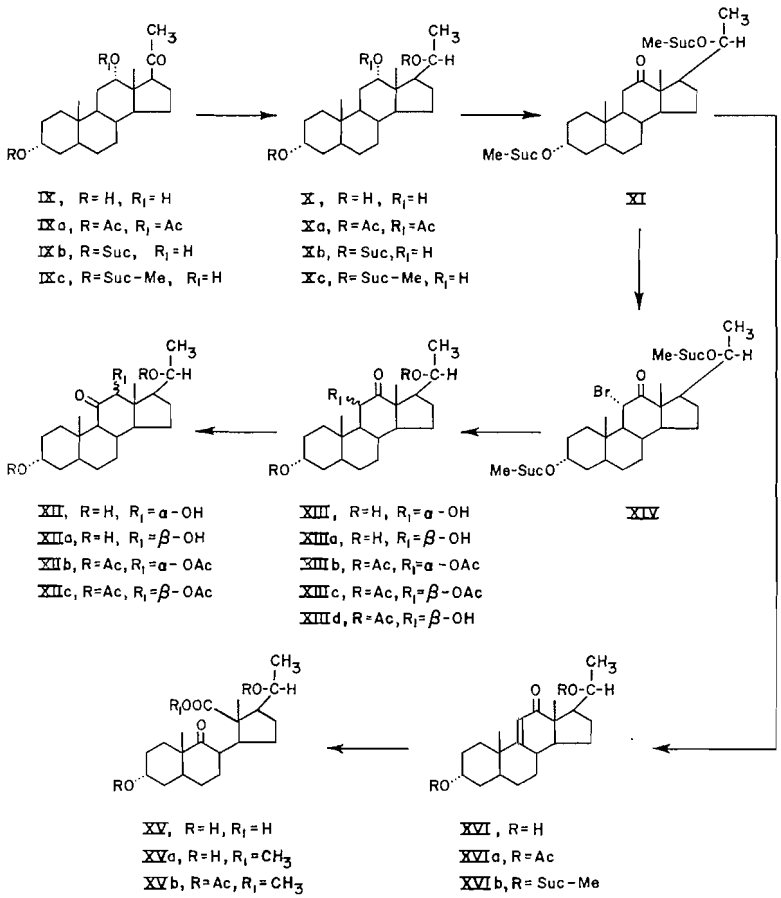

structure XII*c* for the triacetate. However, Baumgartner, Tamm, and Schindler (12, 13) also showed that the constitution and configuration of 11,12-ketol acetates can be determined with the help of ultraviolet and molecular rotational analyses. Thus Schindler (12) tabulated the molecular rotational differences between ring C-acetoxylated and ring C-unsubstituted 11- and 12-ketones of the cholanic acid series; he used these values for calculating the expected molecular rotations of 11,12-ketol acetates of the 3β-hydroxy-etianic acid series from the known rotations of the corresponding non-acetoxylated ketones. Schindler further demonstrated that a definite assignment of constitution and con-

Can. J. Chem. Downloaded from www.nrcresearchpress.com by 176.9.209.113 on 09/04/12
For personal use only.

figuration of ring C ketol acetates was, in general, not possible by molecular rotational analysis alone, but that conclusive deductions could be made by also determining the position of the weak ultraviolet maximum of the keto function.

According to the literature, the molecular rotations of methyl 3α-acetoxy-11-oxoetianate (12, 14) and of 3α,20β-diacetoxy-11-oxopregnane (9) are 385° and 340° respectively; if one assumes a similar relationship between the molecular rotations of methyl etianates and 20β-acetoxypregnanes in the 12-keto series, one can calculate, from the known molecular rotation of methyl 3α-acetoxy-12-oxoetianate (595°) (12, 15), the molecular rotation of 3α,20β-diacetoxy-12-oxopregnane to be approximately 550°. If one now adds to this value the decrement, respectively increment, for additional 11α- and 11β-acetoxy substituents (12, 13) and accordingly to the molecular rotation of 3α,20β-di-

TABLE I

Calculated molecular rotations and expected ultraviolet maxima of 11,12-ketol acetates

Substance		$[M]_D$ calc.	λ_{max} (theor.)
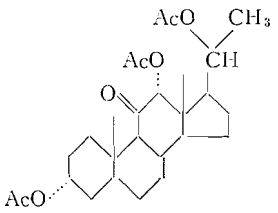	XII*b*	+660°	308 mμ
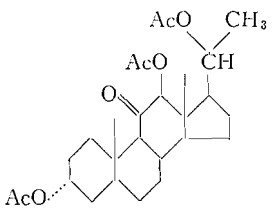	XII*c*	+315°	292–294 mμ
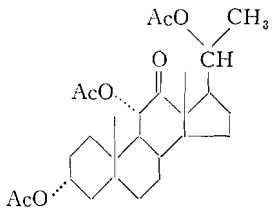	XIII*b*	+270°	285 mμ
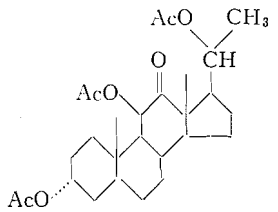	XIII*c*	+710°	298 mμ

Can. J. Chem. Downloaded from www.nrcresearchpress.com by 176.9.209.113 on 09/04/12
For personal use only.

Can. J. Chem. Downloaded from www.nrcresearchpress.com by 176.9.209.113 on 09/04/12
For personal use only.

acetoxy-11-oxopregnane (9) the increment and decrement of additional 12α- and 12β-acetoxy groups (12, 13), one obtains calculated approximate values for the molecular rotations of the four isomeric ketol acetates XII*b*, XII*c*, XIII*b*, and XIII*c* (cf. Table I).[6] It can be seen from Table I that the molecular rotation of our triacetylated hydrolysis product of the crude 11-bromo-12-ketone XIV can correspond only to structure XII*c* or XIII*b*. On the other hand, the position of the weak maximum of ketol acetates of type XII*c* should be at 292–294 mμ and that of ketol acetates of type XIII*b* at 285 mμ (compare Table I). Since the corresponding absorption maximum of our triacetylated hydrolysis product of the crude bromoketone XIV was at 293 mμ, our original assignment of structure of this product as 3α,12β,20β-triacetoxy-11-oxopregnane (XII*c*) is confirmed and we must assume that, even under the mild reaction conditions employed, the mixture of 11-hydroxy-12-ketones (containing presumably mostly the 11β-hydroxy-12-ketone XIII*a*) formed initially by hydrolysis of the 11-bromo-12-ketone was rearranged extensively to the 12β-hydroxy-11-ketone XII*a*.[7]

It thus appeared that the preparation in good yield of the intermediate 3α,20β-diacetoxy-11β-hydroxy-12-oxopregnane (XIII*d*) would present serious difficulties, and we therefore abandoned Wieland's pathway to 9,12-*seco*-steroids of type I.

We now decided to effect the cleavage of ring C to the desired 9,12-*seco* derivatives (compare I and XV) by ozonolysis of a 9,11-unsaturated 12-ketone (compare XVI), in analogy to the successful cleavage of ring A of Δ^4-3-keto steroids with ozone, yielding 3,5-*seco*-5-oxo-3-acid derivatives (compare 16–23). The 9,11-double bond was introduced in good yield by dehydrogenating the saturated 12-ketone XI with selenium dioxide, according to a modification by McKenzie *et al.* (24) of Schwenk and Stahl's method (25). Treatment of XVI*b* with approximately twenty equivalents of ozone at $-15°$ for 70 minutes in acetic acid – ethyl acetate, followed by reaction with hydrogen peroxide, was not successful, the majority of the starting material being recovered. When approximately a hundred equivalents of ozone were used at 0° there was obtained, after partial purification and complete hydrolysis of the reaction product, an acidic fraction in approximately 25% yield. However, it was not possible to obtain the acid in a crystalline state; neither could its methyl ester and acetylated methyl ester be crystallized.

We considered it more promising to employ the diacetate XVI*a*, instead of the bismethylsuccinate XVI*b*, for the reaction with ozone. Hydrolysis of XVI*b* with potassium hydroxide readily gave the diol XVI, which was easily acetylated to XVI*a*. Treatment with 22–27 equivalents of ozone at $-10°$, over a period of 5–7 hours, afforded in approximately 25% yield a crude acidic material (compare XV) which, upon methylation with diazomethane and reacetylation, gave, in an over-all yield of 2–4% from XVI*a* (10%, considering the recovery of starting material), crystalline methyl 3α,20β-diacetoxy-9-oxo-9,12-*seco*-pregnane-12-oate (XV*b*). Its structure was substantiated by combustion analysis and by its infrared spectrum, as well as by the infrared spectra of the intermediates XV and XV*a*, which all showed very clearly the absorption band of a 6-membered ring ketone.

[6]*Molecular rotations are calculated to the nearest 5° and are based on median values of specific rotations. Relatively large errors are introduced into the calculations because some of the rotations reported in the literature were not taken in chloroform.*

[7]*Baumgartner and Tamm (13) recently reported the presence of the rearranged ketol in the product of hydrolysis at room temperature of methyl 11α-bromo-3α-acetoxy-12-oxocholanate. In the 3β-hydroxy-etianic acid series Schindler (12) found that at room temperature the hydrolysis of an 11-bromo-12-ketone led predominantly to the unrearranged ketol (type* IV*) only when the reaction time did not exceed 20 minutes; otherwise the rearranged ketol (type* V*) constituted the major component of the mixture. These observations are in good accord with our above-discussed finding.*

Can. J. Chem. Downloaded from www.nrcresearchpress.com by 176.9.209.113 on 09/04/12
For personal use only.

EXPERIMENTAL[8, 9, 10]

3α,12α-Dihydroxy-20-oxopregnane-3α-methylsuccinate (IX*c*)

A quantity of 591 mg of 3α,12α-diacetoxy-20-oxopregnane (IX*a*) was refluxed for 2 hours with 25 cc of a 5.4% methanolic potassium hydroxide solution. The usual working up gave 486 mg of crude *3α,12α-dihydroxy-20-oxopregnane* (IX) (27), m.p. 150–156°, which upon recrystallization from ether–hexane afforded 380 mg (81%) of pure dihydroxy ketone IX, m.p. 168–169°. The analytical sample melted at 169–170°, $[\alpha]_D^{20}$ +158° (*c* 0.50 in $CHCl_3$). Anal. Calc. for $C_{21}H_{34}O_3$: C, 75.40; H, 10.25. Found: C, 75.31; H, 10.17.

A solution of 240 mg of IX, m.p. 168–169°, in 5 cc of pyridine, was heated with 560 mg of succinic anhydride to 90° for 2 hours, with the exclusion of moisture, and then allowed to stand overnight at room temperature. Ice was added and the mixture was poured after 30 minutes into 400 cc of water. The precipitate was extracted with ether and the organic extract was washed with iced hydrochloric acid and water and dried over sodium sulphate. Upon removal of the solvent, 305 mg of crude amorphous *3α,12α-dihydroxy-20-oxopregnane-3-hemisuccinate* (IX*b*) was obtained, which was dissolved in 10 cc of absolute ether and treated with 16.5 cc of a 0.6% ethereal diazomethane solution. The mixture was kept for 20 minutes at room temperature, the excess diazomethane was decomposed with acetic acid, and the solvent was removed *in vacuo*. The amorphous residue (320 mg) was chromatographed on 6.5 g of aluminum oxide. Petroleum ether – benzene, benzene, benzene–ether, ether, and ether – ethyl acetate (4:1) elutions gave 250 mg of crystalline *3α,12α-dihydroxy-20-oxopregnane-3α-methylsuccinate* (IX*c*), m.p. 118.5–122°. A sample was recrystallized three times from ether–hexane for analysis; m.p. 126–128°, $[\alpha]_D^{23}$ +139° (*c* 1.00 in $CHCl_3$). Anal. Calc. for $C_{26}H_{40}O_6$: C, 69.61; H, 8.99. Found: C, 69.53; H, 8.85.

3α,12α,20β-Trihydroxypregnane (X)[11]

To a slurry of 11 g of lithium aluminum hydride in 700 cc of absolute tetrahydrofuran was added over a period of 50 minutes, dropwise and with stirring, 10.02 g of 3α,12α-diacetoxy-20-oxopregnane (IX*a*) in 500 cc of absolute tetrahydrofuran. The mixture was refluxed for 1 hour with stirring and then allowed to stand overnight. There was added, at 0°, 25 cc of ethyl acetate and a small quantity of ice. After addition of 150 cc of 2 *N* sulphuric acid, the volume of the solution was reduced *in vacuo*, at 40°, to 600 cc and the mixture poured into 2 l. of water. The steroid was extracted with ether, and the organic solution was washed with dilute sulphuric acid, sodium bicarbonate solution, and water, and dried over sodium sulphate. During the removal of the solvent, crystals formed, which were repeatedly removed from the mother liquors. Thus there was obtained a batch of 3.86 g of crystals melting at 236–238° and another batch of 4.857 g of less pure material, m.p. 226–229°. The latter was recrystallized from acetone–hexane and afforded another 2.502 g of crystals, melting at 236–238° (total yield 78%). A sample was recrystallized for analysis; m.p. 236°, $[\alpha]_D^{24}$ +31° (*c* 1.06 in $CHCl_3$). Anal. Calc. for $C_{21}H_{36}O_3$: C, 74.95; H, 10.78. Found: C, 74.72; H, 10.49. In another run, 10 g of IX*a* gave various fractions (6.152 g, 76% yield) of X, melting between 230 and 236°. From the mother liquors, 470 mg of another substance, m.p. 97–98°/218–219°, representing probably the 20α-isomer, was isolated. This product was not further investigated.

[8]*The melting points were taken in evacuated capillaries and the temperatures were corrected.*

[9]*The microanalyses were performed by Mr. J. F. Alicino, Metuchen, N.J., to whom we express our appreciation.*

[10]*The aluminum oxide used for chromatography was treated as described under footnote 31 of reference 26. We thank Messrs. Merck and Co., Montreal, for their kindness in providing us with their activated aluminum oxide.*

[11]*This product was first prepared by Mr. George Montandon, in this laboratory.*

Can. J. Chem. Downloaded from www.nrcresearchpress.com by 176.9.209.113 on 09/04/12
For personal use only.

Acetylation (*Triacetate* X*a*)[12]

A solution of 300 mg of triol X in 10 cc of pyridine was refluxed with 5 cc of acetic anhydride for 1.5 hours. The usual working up gave an amorphous product crystallizing from ethanol. Recrystallization afforded 260 mg (63%) of pure *3α,12α,20β-triacetoxypregnane*, m.p. 193–195°, and 70 mg (17%) of less pure crystals, m.p. 177–187°. A sample was recrystallized three times for analysis; m.p. 199–200°, $[\alpha]_D^{23}$ +116.7° (*c* 0.556 in $CHCl_3$). Anal. Calc. for $C_{27}H_{42}O_6$: C, 70.10; H, 9.15. Found: C, 70.40; H, 9.06.

3α,12α,20β-Trihydroxypregnane-3α,20β-bis-methylsuccinate (X*c*)[13]

A solution of 3.636 g of dried triol X, m.p. 236–238°, in 31.6 cc of absolute pyridine was heated with 8.32 g of succinic anhydride for 2 hours at 90° and subsequently left overnight at room temperature. Ice was added, and after 45 minutes the mixture was poured into 1 l. of water. The precipitate was extracted with ether, and the ethereal solution was washed repeatedly with cold dilute sulphuric acid and with water and was dried over sodium sulphate. During the removal of the ether, 3.54 g of crude, crystalline *3α,12α,20β-trihydroxypregnane-3α,20β-bis-hemisuccinate* (X*b*), m.p. 175–176°, was separated. The greatest part of the mother liquors (2.38 g) crystallized upon trituration with acetone–hexane. Repeated recrystallizations of both batches from acetone–hexane afforded 4.225 g of pure bis-hemisuccinate X*b*, m.p. 182–184°, and 1.5 g of mother liquors. The latter were subjected anew to succinylation under the conditions described above, and 1.58 g of crude bis-hemisuccinate X*b* was obtained.

The two batches of bis-hemisuccinate X*b* were methylated in the usual fashion with diazomethane. Separate recrystallizations of the reaction products from ether–hexane afforded 5.144 g (84.5% from X) of pure *3α,12α,20β-trihydroxypregnane-3α,20β-bis-methylsuccinate* (X*c*), m.p. 95–98°. A sample was recrystallized three times from ether–hexane and pure hexane for analysis; m.p. 95–96°, $[\alpha]_D^{22}$ +71° (*c* 1.01 in $CHCl_3$). Anal. Calc. for $C_{31}H_{48}O_9$: C, 65.93; H, 8.57. Found: C, 66.02; H, 8.54.

When the crude bis-hemisuccinate X*b* was methylated without having been purified, comparable results were obtained but, in general, chromatography of the product was necessary and the over-all yield was slightly lower.

3α,20β-Dihydroxy-12-oxopregnane-3,20-bis-methylsuccinate (XI)[14]

To a solution of 7.262 g of 3α,12α,20β-trihydroxypregnane-3α,20β-bis-methylsuccinate (X*c*) in 250 cc of glacial acetic acid was added 1.419 g of chromic acid in 14 cc of 90% acetic acid at 17°. After 15 hours, 5 cc of methanol was added and the product stirred into 3.5 l. of water. Filtration afforded 6.507 g of colorless leaflets, m.p. 107–108.5°; extraction of the filtrate afforded 605 mg of crude product, which upon recrystallization from ether–hexane gave 395 mg of XI, m.p. 105.5–106.5° (total yield 95%). A sample was recrystallized three times from ether–hexane for analysis; m.p. 113–114°, $[\alpha]_D^{25}$ +107.5° (*c* 0.975 in $CHCl_3$). Anal. Calc. for $C_{31}H_{46}O_9$: C, 66.17; H, 8.24. Found: C, 66.14; H, 8.34.

Bromination of 3α,20β-Dihydroxy-12-oxopregnane-3,20-bis-methylsuccinate (*Bromide* XIV)

To a solution of 2.002 g of ketone XI, m.p. 110–111°, in 30 cc of acetic acid, were added 2 drops of a hydrogen bromide solution in acetic acid and subsequently, at 55–60°, 8.6 cc of a 0.75 *M* bromine solution in acetic acid. The solution was kept at the same temperature for 5.5 hours and then allowed to cool to room temperature. The product was decolorized with a few drops of sodium thiosulphate solution and poured into 600 cc

[12]*See footnote 11.*

[13]*With the co-operation of Mr. K. D. Burell, whose contribution towards this project represented part of his B.Sc. thesis, submitted to the Department of Chemistry of the University of Western Ontario in May, 1955.*

[14]*See footnote 13.*

of water. The precipitate was extracted with chloroform, and the organic layer was washed with water, iced sodium bicarbonate solution, a small quantity of cold 1% sodium hydroxide solution, and with water, and was dried over sodium sulphate. The solvent was removed *in vacuo* and 2.243 g of an amorphous residue, representing crude XIV, was obtained.

Debromination

To a solution of 278 mg of the above-described crude bromo ketone (compare XIV) in 6 cc of 90% acetic acid was added, in small amounts and with repeated shaking, at 80°, 583 mg of zinc dust. The mixture was heated for another 45 minutes to 90°, with repeated shaking. The zinc was removed by filtration, and the filtrate extracted with ether. The ethereal solution was washed with water, cold dilute hydrochloric acid, cold bicarbonate solution, and with water, and was dried over sodium sulphate. Removal of the solvent afforded 224 mg of crude ketone XI, giving no depression of melting point upon admixture of authentic material.

Hydrolysis of the Bromination Product

To a solution of 1.387 g of the above-described bromide (compare XIV) in 55.4 cc of ethanol was added a solution of 2.16 g of potassium hydroxide in 10 cc of water and 20 cc of ethanol. The mixture was allowed to stand at room temperature for 48 hours. The usual working up afforded 634 mg of neutral material and 95 mg of an acidic product.

Acetylation

The above-described neutral hydrolysis product of bromide XIV (634 mg) was dissolved in 4.5 cc of pyridine and treated with 3.5 cc of acetic anhydride at room temperature. After 18 hours, the mixture was worked up in the usual fashion and afforded 776 mg of a product which was chromatographed on 22 g of aluminum oxide. Petroleum ether – benzene elutions afforded, after recrystallization, 477 mg of *3α,12β,20β-triacetoxy-11-oxopregnane* (XII*c*), m.p. 172–174.5°, and 70 mg of crystals melting between 158 and 166° which gave no depression of melting point upon admixture with XII*c*. From the latter crystals another batch of 22 mg of pure XII*c*, m.p. 172–174.5°, was obtained by recrystallization.

A sample was recrystallized three times for analysis; colorless needles, m.p. 179–180.5°, $[\alpha]_D^{22}$ +49° ($CHCl_3$) λ_{max}^{EtOH} 293 mμ (log ε 1.2). Anal. Calc. for $C_{27}H_{40}O_7$: C, 68.04; H, 8.46. Found: C, 68.14; H, 8.42.

$\Delta^{9,11}$-3α,20β-Dihydroxy-12-oxopregnene-3α,20β-bis-methylsuccinate (XVI*b*)

To a solution of 2.583 g of 3α,20β-dihydroxy-12-oxopregnane-3α,20β-bis-methylsuccinate (XI), m.p. 105–106.5°, in 26 cc of an 0.0006 *N* hydrogen chloride solution in acetic acid was added 1.505 g of selenium dioxide. The mixture was refluxed for 20 hours, cooled, diluted with 2 l. of ether, and filtered over sodium sulphate. The filtrate was further diluted with ether and the solution was washed with water, iced dilute hydrochloric acid, cold sodium bicarbonate solution, and with water, and was dried over sodium sulphate. Removal of the solvent gave 2.498 g of a yellow oil which yielded, upon recrystallization from ether, 455 mg of $\Delta^{9,11}$-3α,20β-dihydroxy-12-oxopregnene-3α,20β-bis-methylsuccinate (XVI*b*), m.p. 94–95°. The amorphous mother liquors (1.966 g) were dissolved in 23.5 cc of a mixture composed of 80% chlorobenzene and 20% acetic acid. To this was added 9.6 g of chromic acid in 9.6 cc of water. The mixture was shaken for 2 hours at room temperature; then 4.8 g of chromic acid in 4.8 cc of water was added and the flask was shaken again for another 2 hours. The product was diluted with 2 l.

Can. J. Chem. Downloaded from www.nrcresearchpress.com by 176.9.209.113 on 09/04/12
For personal use only.

of ether and filtered over sodium sulphate. The filtrate was washed with water, iced sodium bicarbonate solution, and water, and was dried over sodium sulphate. Removal of the solvent afforded 1.941 g of crystalline XVI*b*, m.p. 90–93° (total yield of crystalline XVI*b*, 91%). The batch melting at 90–93° was chromatographed on 58 g of aluminum oxide. Recrystallization of the petroleum ether – benzene (1:4) and benzene fractions yielded 1.027 g of pure XVI*b* (m.p. 94.5–95.5°; total yield of highly purified XVI*b*: 58%). A sample was recrystallized twice from ether for analysis; m.p. 95.5–96.5°, $[\alpha]_D^{22}$ +155° (*c* 1.0 in $CHCl_3$) λ_{max}^{EtOH} 239 mμ (log ε 4.1). Anal. Calc. for $C_{31}H_{44}O_9$: C, 66.40; H, 7.91. Found: C, 66.30; H, 7.87.

$\Delta^{9,11}$-3α,20β-Dihydroxy-12-oxopregnene (XVI)

To a solution of 3.509 g of $\Delta^{9,11}$-3α,20β-dihydroxy-12-oxopregnene-3α,20β-bis-methylsuccinate (XVI*b*) in 70 cc of methanol was added 4.39 g of potassium carbonate in 50 cc of water. The mixture was refluxed for 17 hours, cooled to room temperature, and extracted with 2 l. of ether. The ethereal solution was washed with water and dried. The solvent was removed and 1.992 g (95.5% yield) of crystalline dihydroxy ketone XVI, m.p. 232–234.5°, was obtained. Recrystallization from ether afforded 1.487 g of fine needles, m.p. 238–240°. A sample was recrystallized twice for analysis; m.p. 242–243°, λ_{max}^{EtOH} 242 mμ (log ε 4.04). Anal. Calc. for $C_{21}H_{32}O_3$: C, 75.86; H, 9.70. Found: C, 75.65; H, 9.74.

Acetylation

The dihydroxy ketone XVI (2.253 g, m.p. 238–240°) was acetylated overnight at room temperature with 152 cc of acetic anhydride in 225 cc of pyridine. The usual working up afforded 2.8 g of crystalline *$\Delta^{9,11}$-3α,20β-diacetoxy-12-oxopregnene* (XVI*a*), m.p. 179–183°. Recrystallization and chromatography of the mother liquors yielded 1.976 g of broad needles, m.p. 180–200°. A sample was recrystallized twice for analysis; m.p. 200.5–201.5°, λ_{max}^{EtOH} 244 mμ (log ε 4.02). Anal. Calc. for $C_{25}H_{36}O_5$: C, 72.10; H, 8.71. Found: C, 72.01; H, 8.90.

Ozonolysis of $\Delta^{9,11}$-3α,20β-Dihydroxy-12-oxopregnene-3α,20β-bis-methylsuccinate (XVI*b*)

(*a*) At −15°, a stream of oxygen containing 8% of ozone was passed over a period of 70 minutes through a solution of 1.194 g of $\Delta^{9,11}$-3α,20β-dihydroxy-12-oxopregnene-3α,20β-bis-methylsuccinate (XVI*b*), m.p. 94.5–95.5°, in 15 cc of glacial acetic acid and 15 cc of ethyl acetate (40 equivalents of ozone). Subsequently, 4.5 cc of water and 0.45 cc of a 30% hydrogen peroxide solution were added and the mixture was allowed to stand for 19 hours at room temperature. The product was extracted with ether, the ethereal solution was washed repeatedly with water and subsequently extracted with 2 *N* sodium hydroxide solution. The remaining ethereal solution was washed to neutral and dried over sodium sulphate. Evaporation of the solvent gave 950 mg (80%) of starting material XVI*b*, m.p. 91–93°, not depressed upon admixture of an authentic sample. The sodium hydroxide extract was acidified and worked up in the usual way to give 98 mg of an amorphous product.

(*b*) A solution of 950 mg of XVI*b* in 13 cc of acetic acid and 13 cc of ethyl acetate was flushed for 5 hours, at 0°, with an oxygen stream (flow rate 180 cc per minute) containing 8.3% of ozone (100 equivalents). After treatment of the product with 4 cc of water and 0.5 cc of a 30% hydrogen peroxide solution for 18 hours, the product was worked up as described above, yielding 300 mg of neutral material and 412 mg of a crude acid fraction. A quantity of 348 mg of the latter was treated for 24 hours with

Can. J. Chem. Downloaded from www.nrcresearchpress.com by 176.9.209.113 on 09/04/12
For personal use only.

30 cc of a 5% aqueous sodium hydroxide solution. The usual working up afforded 20 mg of neutral material and 210 mg of an acidic product, the infrared spectrum of which was in agreement with structure XV but which resisted all attempts of crystallization.

The product was dissolved in 7 cc of absolute benzene and methylated in the usual fashion with an ethereal diazomethane solution. After 17 hours, the product was worked up and there was obtained 214 mg of a methyl ester (compare XV*a*), which could not be crystallized. A solution of this product in 5 cc of pyridine was treated overnight with 2.5 cc of acetic anhydride. The crude reaction product (234 mg) was chromatographed on 6.9 g of aluminum oxide but none of the fractions could be induced to crystallization.

Methyl 3α,20β-Diacetoxy-9-oxo-9,12-seco-pregnane-12-oate (XV*b*) *from* XVI*a*, *via the Intermediates* XV *and* XV*a*

At −10°, a current of oxygen (180 cc per minute) containing 8.3% of ozone was passed for 5 hours and 22 minutes through a solution of 3.611 g of $\Delta^{9,11}$-3α,20β-diacetoxy-12-oxopregnene (XVI*a*) in 50 cc of glacial acetic acid and 50 cc of absolute ethyl acetate (22 equivalents of ozone). Water (15 cc) and a 30% hydrogen peroxide solution (1.8 cc) were added and the mixture was allowed to stand at room temperature overnight. The usual working up afforded 2.431 g of an amorphous neutral material and 1.041 g of a crude amorphous acidic fraction which resisted crystallization. This product was dissolved in 35 cc of absolute benzene and treated with 20 cc of a 2.5% ethereal diazomethane solution at 0° for 15 hours. The usual working up gave 1.061 g of an amorphous product which was dissolved in 8 cc of pyridine and acetylated in the usual fashion with 5 cc of acetic anhydride. There was obtained 1.07 g of an amorphous product which was chromatographed on 31 g of aluminum oxide. Benzene and benzene–ether (4:1) gave 51 mg (1.3% yield from XVI*a*) of methyl 3α,20β-diacetoxy-9-oxo-9,12-*seco*-pregnane-12-oate (XV*b*), m.p. 125–128.5°. Recrystallization for analysis afforded very fine needles, m.p. 126–127°, $[\alpha]_D^{22}$ +30° (*c* 0.891 in $CHCl_3$), weak ultraviolet absorption maximum at 282 mμ, ν_{max}^{KBr} 1242 cm^{-1} (acetate absorption), 1701 cm^{-1} (9-ketone), 1722 cm^{-1} (12-methyl ester). Anal. Calc. for $C_{25}H_{38}O_7$: C, 66.64; H, 8.50. Found: C, 66.60; H, 8.27.

The major portion (2.39 g) of the neutral reaction product from the ozonolysis was dissolved in 64 cc of a 1:1 mixture of acetic acid and ethyl acetate, and ozonized at −10° over a period of 7 hours and 52 minutes with an oxygen stream (160 cc per minute) containing 7.9% of ozone (27 equivalents). The product was worked up as described above, and there was obtained 93 mg of XV*b*, m.p. 124–126° (3.7% yield), identical with the above-described XV*b*.

ACKNOWLEDGMENTS

We wish to acknowledge with sincere thanks the valuable co-operation of Mr. G. Montandon and Mr. K. D. Burell; the expert technical assistance of Mrs. J. Capitaine and Mr. R. Heckadon; and the highly appreciated help of Mr. R. W. White, Science Service Laboratory, London, Ontario, with the infrared analyses. We are greatly indebted to the Federal–Provincial Departments of National Health and Welfare, Ottawa and Toronto; to Ayerst, McKenna and Harrison Limited, Montreal; and to the Canadian Life Insurance Officers Association, for financial support; and to CIBA Limited, Basle, for kindly providing us with starting materials. Dean J. B. Collip's active interest and Dr. J. Gunton's kindness in making the facilities of his department available were highly appreciated.

Can. J. Chem. Downloaded from www.nrcresearchpress.com by 176.9.209.113 on 09/04/12
For personal use only.

REFERENCES

1. ENGEL, CH. R. and JAHNKE, H. Can. J. Biochem. and Physiol. **35**, 1047 (1957).
2. WIELAND, H. and POSTERNAK, TH. Z. physiol. Chem. **197**, 17 (1931).
3. WIELAND, H. and DANE, E. Z. physiol. Chem. **216**, 91 (1933).
4. SEEBECK, E. and REICHSTEIN, T. Helv. Chim. Acta, **26**, 536 (1943).
5. GALLAGHER, T. F. and LONG, W. P. J. Biol. Chem. **162**, 495 (1946).
6. GALLAGHER, T. F. and LONG, W. P. J. Biol. Chem. **162**, 521 (1946).
7. GALLAGHER, T. F. J. Biol. Chem. **162**, 539 (1946).
8. WINTERSTEINER, O., MOORE, M., and REINHARDT, K. J. Biol. Chem. **162**, 707 (1946).
9. SARETT, L. H. J. Am. Chem. Soc. **71**, 1175 (1949).
10. SCHWENK, E., RIEGEL, B., MOFFETT, R. B., and STAHL, E. J. Am. Chem. Soc. **65**, 549 (1943).
11. SORKIN, M. and REICHSTEIN, T. Helv. Chim. Acta, **31**, 1890 (1948).
12. SCHINDLER, O. Helv. Chim. Acta, **39**, 1698 (1956).
13. BAUMGARTNER, G. and TAMM, CH. Helv. Chim. Acta, **38**, 441 (1955).
14. LARDON, A. and REICHSTEIN, T. Helv. Chim. Acta, **26**, 705 (1943).
15. WENNER, V. and REICHSTEIN, T. Helv. Chim. Acta, **27**, 965 (1944).
16. DORÉE, C. and GARDNER, J. A. J. Chem. Soc. **93**, 1328 (1908).
17. BOLT, C. C. Rec. trav. chim. **57**, 905 (1938).
18. REICHSTEIN, T. and FUCHS, H. G. Helv. Chim. Acta, **23**, 676 (1940).
19. TURNER, R. B. J. Am. Chem. Soc. **72**, 579 (1950).
20. HEARD, R. D. H. and ZIEGLER, P. J. Am. Chem. Soc. **72**, 4328 (1950).
21. GUT, M. Helv. Chim. Acta, **36**, 906 (1953).
22. FUJUMOTO, L. P. and PRAGER, J. J. Am. Chem. Soc. **75**, 3259 (1953).
23. THOMPSON, L. M., YATES, C. H., and ODELL, A. D. J. Am. Chem. Soc. **76**, 1194 (1954).
24. MCKENZIE, B. F., MATTOX, V. R., ENGEL, L. L., and KENDALL, E. C. J. Biol. Chem. **173**, 271 (1948).
25. SCHWENK, E. and STAHL, E. Arch. Biochem. **14**, 125 (1947).
26. ENGEL, CH. R. and JUST, G. J. Am. Chem. Soc. **76**, 4909 (1954).
27. HOEHN, W. M. and MASON, H. L. J. Am. Chem. Soc. **60**, 1493 (1938).

Can. J. Chem. Downloaded from www.nrcresearchpress.com by 176.9.209.113 on 09/04/12
For personal use only.

Can. J. Chem. Downloaded from www.nrcresearchpress.com by 69.46.99.164 on 09/04/12
For personal use only.

SOME CARBOXYLIC ACIDS PRESENT IN ROYAL JELLY[1]

WILLIAM H. BROWN[2] AND ROBERT J. FREURE[3]

ABSTRACT

Only one carboxylic acid, 10-hydroxy-2-decenoic acid, has previously been isolated from royal jelly. Small amounts of two additional acids, sebacic and 2-decendioic acid, have now been found in the ether-soluble portion of this special bee foodstuff. Evidence is presented in favor of the *trans*-configuration for naturally occurring 10-hydroxy-2-decenoic acid. Chromic acid oxidation of the hydroxy acid yields 2-decendioic acid.

The chemical nature of the components of royal jelly has received considerable attention over the past 20 years. Townsend and Lucas (1) reported the isolation of a carboxylic acid, $C_{10}H_{18}O_3$, from the mixture of acids obtained from royal jelly by extraction with ether. Abbott and French (2) and Abbott (3) confirmed this finding and attempted by oxidative means to establish a structure for the acid. However, their efforts were unsuccessful. More recently Butenandt and Rembold (4) have characterized the compound as 10-hydroxy-2-decenoic acid (I).

This year Barker, Foster, and Lamb (5) have independently confirmed the structure proposed by Butenandt and Rembold for I and have speculated on the olefinic configuration.

In view of the increasing interest in royal jelly from a therapeutic standpoint and the findings recently reported by Townsend, Morgan, and Hazlett (6) on the activity of I against experimental leukaemia and ascitic tumors we are reporting the results of our investigation into the chemical nature of additional carboxylic acids which we have discovered in royal jelly.

Besides 10-hydroxy-2-decenoic acid (I) we have isolated, by chromatographic means, sebacic acid (II) and 2-decendioic acid (III) from the mixture of acids obtained from lyophilized royal jelly by ether extraction.

$$HO—CH_2—(CH_2)_6—CH=CH—COOH \qquad I$$
$$HOOC—(CH_2)_6—CH_2—CH_2—COOH \qquad II$$
$$HOOC—(CH_2)_6—CH=CH—COOH \qquad III$$

Barker *et al.* (5) have reported that I comprises approximately 70% of the mixture of ether-soluble acids and approximately 15% of royal jelly. We find that I is present to a greater extent in the mixture of ether-soluble acids, 90%, whereas it is present only in the amount of 3% in whole royal jelly (7% of lyophilized royal jelly). A variety of melting points have been reported for this compound: 46–58° (1); 61–62° (3); 54–56° (4); 52° (5). When I is separated chromatographically from the other ether-soluble acids with which it is associated in royal jelly and subsequently crystallized from water, the pure material has m.p. 62.0–62.5°.

Only Barker *et al.* (5) have considered the olefinic configurations of I but were unable to make a firm assignment. We have found that I, when irradiated in acetone solution, is converted slowly to another isomer (IV). This latter compound, m.p. 43–46°, slowly reverts to I when allowed to stand at room temperature even in the solid state. In the case of IV, absorption is strong in the region 300–340 mμ while I is relatively transparent

[1]*Manuscript received June 29, 1959.*
Contribution from the Department of Chemistry, Ontario Agricultural College, Guelph, Ontario.
[2]*Associate Professor of Chemistry, Ontario Agricultural College, Guelph, Ontario.*
[3]*Graduate student, Department of Chemistry, Ontario Agricultural College, Guelph, Ontario.*

over the same range. Both I and IV show strong end absorption (220–290 mμ) in the ultraviolet. Infrared absorption spectra of I and IV were run on mineral oil mulls and are summarized in Table I.

TABLE I

Infrared spectra of 10-hydroxy-2-decenoic acid

Peaks, cm^{-1}	
Naturally occurring (I)	Irradiated with sunlight (IV)
3390	3390
1710	1710
1658	1658
976	976
—	830

The medium peak observed at 830 cm^{-1} in the spectrum of IV is not present in that of I. Allan, Meakins, and Whiting (7) have determined the infrared absorption spectra of a number of α,β-unsaturated carboxylic acids and have established that a peak in the region 830 cm^{-1} indicates an olefinic C—H out-of-plane bending for *cis*-α,β-unsaturated acids. The presence of a peak at 976 cm^{-1} in the spectra of both I and IV indicates that IV is contaminated with I (incomplete conversion). A peak in this latter region has been well established as being characteristic of *trans*-substituted ethylenic structures (8). Based on these observations we postulate that naturally occurring 10-hydroxy-2-decenoic acid exists in the *trans*-form.

The presence of sebacic acid (II) in royal jelly is interesting since its occurrence in other natural foodstuffs is limited to the fat portion of milk from buffalo and cow (9). It has been reported by Stählin and Blievernicht (10) that the free sebacic acid content of rape and turnip seed rises as it becomes moldy.

The third acid, 2-decendioic acid (III), found in royal jelly, has previously been reported only twice. It was synthesized by English (11), who was investigating homologues of traumatic acid ($HOOC-(CH_2)_8-CH=CH-COOH$). The latter compound is a factor involved in plant growth phenomena.

Cram and Tishler (12) isolated III from the acetone-soluble fraction of clinical penicillin. Chromic acid oxidation of 10-hydroxy-2-decenoic acid (I) readily yields III. This reaction was originally reported by Abbott (3), but no structures were known at that time.

It is significant that the three acids in royal jelly are all closely related, 10-carbon compounds. The concentration of each acid is given in Table II.

TABLE II

Acid	Conc. (p.p.m.) (basis lyophilized royal jelly)
I	70,000
II	200
III	300

The chemotherapeutic value of II and III is being investigated by our co-workers, Townsend, Morgan, and Hazlett (6) and will be reported elsewhere.

Can. J. Chem. Downloaded from www.nrcresearchpress.com by 69.46.99.164 on 09/04/12
For personal use only.

EXPERIMENTAL

(All melting points have been corrected against reliable standards.)

Isolation of Carboxylic Acids (A) from Royal Jelly

Lyophilized royal jelly was placed in a Pyrex 3885 Soxhlet extractor in 2-inch layers alternated with glass wool and was extracted with ether for 26 hours. The resulting straw-colored extract, approximately 2 l. in volume, was concentrated to 200 ml and processed as shown in the following flowsheet.

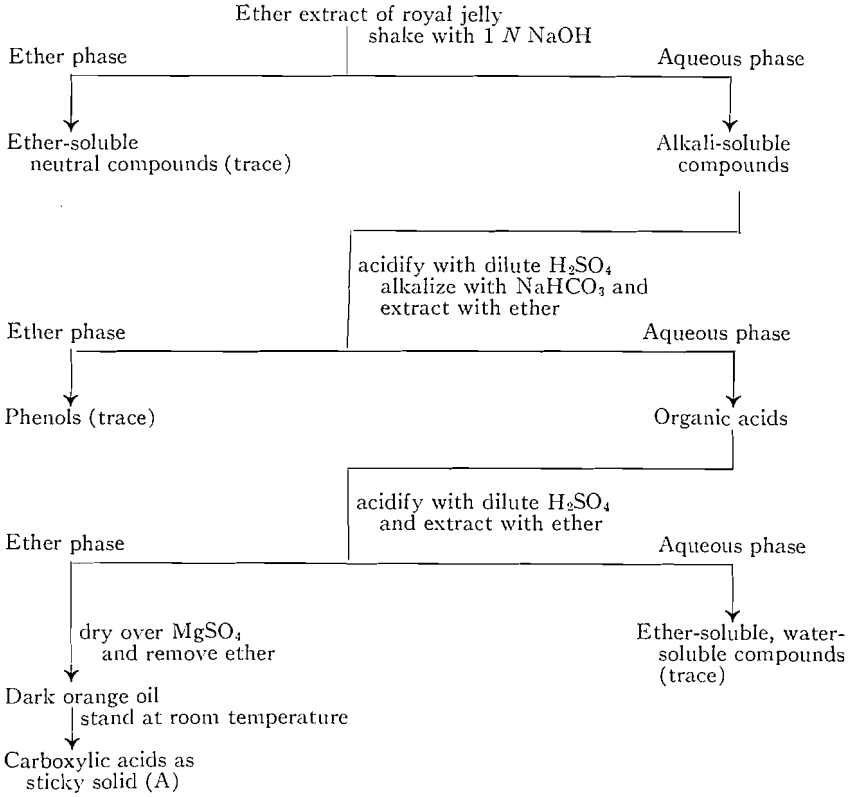

The final ether extract was dried over anhydrous magnesium sulphate, filtered, and the ether removed in a current of air. The residue, (A), a dark orange oil, crystallized after standing overnight at 25°.

A number of samples of lyophilized royal jelly extracted with ether and the ether extract processed as already described showed an average of 7% ether-soluble organic acids. This represents 3% of whole royal jelly which averages 65% moisture and 35% solids.

Isolation and Identification of Sebacic Acid (II) *as the p-Bromophenacyl Ester*

The crystalline mixture of acids, (A), (7.7 g), was taken up in hot hexane–ether and refrigerated to 5°. While the solution was cooling, seeds of 10-hydroxy-2-decenoic acid were introduced. The resulting white crystalline solid, 3.8 g, was removed by filtration, m.p. 43–46°. A further crystallization of the solid gave 2.8 g (36% by wt.) of impure 10-hydroxy-2-decenoic acid, m.p. 55–59°. The mother liquor from the first crystallization

Can. J. Chem. Downloaded from www.nrcresearchpress.com by 69.46.99.164 on 09/04/12
For personal use only.

was concentrated and cooled, yielding 1.7 g of white crystalline solid, m.p. 39–63°. A second crystallization of the latter solid using the same mixed solvent gave 1.2 g of white crystals, m.p. 45–72°. Crystallization from benzene–hexane raised the m.p. to 51–78°.

When 0.37 g of the material, m.p. 51–78°, was treated with *p*-bromophenacyl bromide by the usual procedure, a white solid was formed in the hot reaction mixture and was removed by filtration before cooling. It weighed 0.050 g, m.p. 146–150°. Crystallization from absolute ethanol and acetone raised the m.p. to 150–151°.

A mixture melting point of the latter compound with authentic *p*-bromophenacyl ester of sebacic acid was not depressed.

Isolation and Identification of Sebacic Acid (II) *and 2-Decendioic Acid* (III) *from A by Chromatography*

Isolation of III was achieved by chromatographic separation of A on Whatman seed test paper (1/16 inch) using a 7:3 ratio by volume of propanol and concentrated aqueous ammonia as the developing solvent. Isherwood and Hanes (13) have described the use of this solvent system.

A concentration of 700 mg of A per 9×22.5-inch sheet gave adequate separation of II and III from I. Acid I comprises approximately 90% of A. The various regions containing the acids were located on the paper by cutting out a quarter-inch strip from the center of the sheet and spraying it with a 0.1% solution of thymol blue adjusted to pH 10. No significant separation of II from III was achieved at this concentration.

The region containing acids II and III was cut out and the acids extracted from the paper with propanol in a Soxhlet apparatus. The extract was evaporated to dryness, the residue taken up in 5% aqueous sodium hydroxide solution, acidified with dilute sulphuric acid, and extracted with ether. From 2.7 g of A, 91 mg of the mixture of II and III was obtained. Fractional crystallization from chloroform removed most of II. The resulting crude III was fractionated on Whatman 3 MM chromatography paper using the same solvent system as previously described to remove the residual II.

Compound III was extracted from the paper, m.p. 161–168°. After crystallization from chloroform 25 mg of pure III was obtained, m.p. 172–173°.

The infrared spectrum, mull in mineral oil, of III shows maximum absorptions at 1,710 cm^{-1} (carboxylic acid), 1,655 cm^{-1} (unsaturation), and 1,198 cm^{-1} (carboxylic acid). Anal. calc. for $C_{10}H_{16}O_4$: C, 60.0; H, 8.00. Found: C, 59.9; H, 7.92.

The identity of III was confirmed by mixture melting point with 2-decendioic acid, m.p. 172–173°, prepared by chromic acid oxidation of 10-hydroxy-2-decenoic acid.

Sebacic acid (II) was also isolated by the same procedure and identified as the *p*-bromophenacyl ester.

Using Whatman No. 1 chromatography paper and the same developing solvent as before, R_f values are I, 0.79; II, 0.43; and III, 0.38 at 25°.

Oxidation of 10-Hydroxy-2-decenoic Acid (I) *to 2-Decendioic Acid* (III)

A mixture of 0.93 g (0.0050 mole) of 10-hydroxy-2-decenoic acid and 1.0 g (0.0034 mole) of potassium dichromate, dissolved in a solution of 0.9 ml of C.P. concentrated sulphuric acid in 15 ml of water, was heated in a 50-ml round-bottomed flask on a steam bath for 3 hours. After the reaction mixture was allowed to stand at room temperature for 10 hours a solid product was removed by filtration. It weighed 0.43 g, m.p. 145–160°. The crude material was crystallized from hot water including treatment with activated charcoal. In this manner 0.20 g (20%) of small white rosettes, m.p. 171–172° was obtained.

Can. J. Chem. Downloaded from www.nrcresearchpress.com by 69.46.99.164 on 09/04/12
For personal use only.

Effect of Ultraviolet Irradiation on Naturally Occurring 10-Hydroxy-2-decenoic Acid (I)

When 10-hydroxy-2-decenoic acid (I), m.p. 62°, isolated from A, was irradiated with sunlight in a thin-walled Pyrex bulb in acetone solution for a total of 20 hours, the melting point of I dropped to 43–46°, suggesting a conversion of the acid from *trans*- to *cis*-configuration. After the solution had been standing for a three-week period the melting point of the irradiated material (IV) rose to 44–54° indicating slow reversion to the more stable *trans*-isomer.

p-Bromophenacyl Ester of 10-Hydroxy-2-decenoic Acid (I)

The *p*-bromophenacyl ester of I has been prepared by Abbott (3) but no melting point has been reported. The ester is readily obtained by treating the sodium salt of I with *p*-bromophenacyl bromide in hot dilute ethanol solution. It has m.p. 89–90°.

ACKNOWLEDGMENTS

We are indebted to Prof. G. F. Townsend and Dr. R. W. Shuel, Department of Apiculture, Ontario Agricultural College, Guelph, for generous supplies of whole and lyophilized royal jelly and 10-hydroxy-2-decenoic acid. Naugatuck Chemicals, Elmira, determinated the infrared spectra. W. C. Hardesty Co. of Canada, Limited, supplied generous samples of pure sebacic acid and esters of sebacic acid.

REFERENCES

1. Townsend, G. F. and Lucas, C. C. Biochem. J. **34**, 1155 (1940).
2. Abbott, O. D. and French, R. B. Ann. Rept. Florida Agr. Expt. Station, 69 (1945).
3. Abbott, O. D. Royal jelly unpublished data. Florida Agr. Expt. Station, Gainsville, (1954).
4. Butenandt, A. and Rembold, H. Z. physiol. Chem. **308**, 284 (1957).
5. Barker, S. A., Foster, A. B., and Lamb, D. C. Nature, **183**, No. 4, 996 (1959).
6. Townsend, G. F., Morgan, J. F., and Hazlett, B. Nature, **183**, No. 5, 1270 (1959).
7. Allan, J. L. H., Meakins, G. D., and Whiting, M. C. J. Chem. Soc. 1874 (1955).
8. Sinclair, R. G., McKay, A. F., Myers, G. S., and Jones, R. N. J. Am. Chem. Soc. **74**, 2578 (1952).
9. Phatak, S. S. and Patwardhan, V. N. Nature, **172**, 456 (1953).
10. Stählin, A. and Blievernicht, L. Forschungsdienst, **16**, 220 (1943).
11. English, J., Jr. J. Am. Chem. Soc. **63**, 941 (1941).
12. Cram, J. and Tishler, M. J. Am. Chem. Soc. **70**, 4238 (1948).
13. Isherwood, F. A. and Hanes, C. S. Biochem. J. **55**, 824 (1953).

Can. J. Chem. Downloaded from www.nrcresearchpress.com by 69.46.99.164 on 09/04/12
For personal use only.

Can. J. Chem. Downloaded from www.nrcresearchpress.com by 69.46.99.164 on 09/04/12
For personal use only.

THE REACTION OF SUCROSE WITH GLYCOL-CLEAVING OXIDANTS[1]

A. K. MITRA[2] AND A. S. PERLIN

ABSTRACT

Lead tetraacetate in acetic acid is reduced at an unusually rapid rate by sucrose, due to a vigorous preferential cleavage of the 3,4-glycol group in the D-fructofuranosyl moiety. By contrast, periodate attacks the D-glucopyranosyl unit more readily. These marked variations are exhibited also in the same solvent and, therefore, appear to be related to the characteristics of the oxidants themselves. The mechanism of the action of lead tetraacetate is discussed with reference to the stereochemistry of the D-fructofuranose unit. Selective oxidation provides a chemical method for controlled degradation of the sucrose molecule and affords products in which either the D-fructose or the D-glucose residue is modified.

An earlier paper (1) described the chemical degradation of raffinose and stachyose to give sucrose, the method being dependent on selective oxidation by glycol-cleaving agents of the α-D-galactopyranosyl residues present. However, lead tetraacetate promoted a more vigorous oxidation of the sucrose moiety in these oligosaccharides than did periodate. This observation has led to a comparison of the action of these two closely related reagents on sucrose itself.

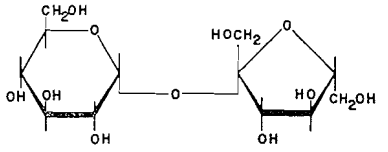

I

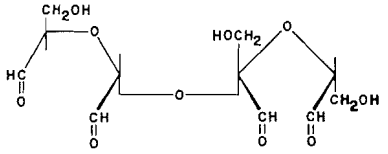

II

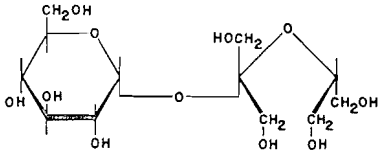

III

In the presence of excess periodate or lead tetraacetate, sucrose (I) undergoes normal glycol-cleavage and forms the expected tetraaldehyde (II) in high yield (2, 3). With a limited proportion of oxidant, however, differences become apparent in the *sequence* of attack by the two reagents. Lead tetraacetate in acetic acid is reduced at a relatively rapid rate by the sugar (Table I) due to a vigorous preferential splitting of the 3,4-glycol group in the D-fructofuranosyl unit. This specificity is suggested from a comparison of the

[1]*Manuscript received August 19, 1959.*
Contribution from the National Research Council of Canada, Prairie Regional Laboratory, Saskatoon, Saskatchewan. Presented at the 134th Meeting of the American Chemical Society, Chicago, September, 1958. Release requested June 19, 1959.
Issued as N.R.C. No. 5408.
[2]*National Research Council of Canada Postdoctorate Fellow, 1956–58.*

TABLE I

Rate of oxidation of sucrose and related sugars

Reagent	Time (minutes)	Moles oxidant consumed/mole		
		Sucrose	MF[a]	MG[b]
Lead tetraacetate	30	0.54	0.34	—
	60	0.88	0.65	0.08
	120	1.10	0.88	0.11
Sodium periodate	30	0.36	0.05	0.23
	90	0.71	0.13	0.46
	150	1.04	0.21	0.61

[a]Methyl β-D-fructofuranoside (chromatographically pure syrup); the compound was over-oxidized by prolonged treatment, possibly due to partial hydrolysis.
[b]Methyl α-D-glucopyranoside.

rates of oxidation of methyl-β-D-fructofuranoside and methyl α-D-glucopyranoside ((4) see also Table I), and is demonstrated by the fact that reaction with only 1 mole of lead tetraacetate per mole (theoretical uptake, 3 moles/mole) causes oxidation of 90% of the fructose units (Table II). The dialdehyde formed as the major product in the latter reaction was reduced catalytically or with sodium borohydride (5), and the polyol (III) produced was isolated as a crystalline octaacetate. Confirmation of the structure of III was obtained from the fact that it was not attacked by invertase, that methanolysis yielded methyl α-D-glucopyranoside, and hydrolysis followed by bromine oxidation gave 1,3-dihydroxy-2-propanone but not D-fructose. The D-glucose unit of III is intact, but the partially degraded D-fructose unit no longer possesses an asymmetric center. Accordingly, the molecular rotation of the compound ($[M]_D$ of the octaacetate is +45,000) is in close agreement with that expected for the α-D-glucopyranosyl residue in sucrose (6, 7, 8, 9).*

In contrast to the foregoing results, sodium periodate attacks the D-fructose unit even less readily than the D-glucose unit, the latter utilizing as much as 77% of 1 mole of oxidant added per mole (Table II). A relatively high resistance of the β-D-fructofuranosyl

TABLE II

Oxidation of sucrose by 1 mole of glycol-cleaving reagent

Reagent	Solvent	% Fructose oxidized
Lead tetraacetate	50% acetic	90
	98% acetic	70
Sodium periodate	50% acetic	30
	50% ethanol	23
	50% ethanol*	44
	Water	39

*Two moles of periodate used.

structure to periodate cleavage is illustrated also in the comparatively slow oxidation rate for the corresponding methyl glycoside (Table I).† This marked difference from the action of lead tetraacetate did not appear to be related to solvent, as shown by the variation obtained when each oxidant was used in 50% acetic acid (Table II). On treat-

**For example, 2,3,4,6-tetra-O-acetyl methyl α-D-glucopyranoside has $[M]_D$ +47,300; the β-D-glucoside tetraacetate has $[M]_D$ −6600.*

†*Methyl α-L-arabofuranoside, another furanoside containing a trans-glycol group, is also attacked by periodate more slowly than methyl glycopyranosides (10).*

Can. J. Chem. Downloaded from www.nrcresearchpress.com by 69.46.99.164 on 09/04/12
For personal use only.

ment with 1 or 2 moles of periodate in 50% ethanol, followed by reduction, sucrose afforded a mixture of several compounds. Some of the products contained intact D-fructose residues, but were present in low proportion and were difficult to isolate from the mixture. The low yield of D-fructose-containing products shows that both glycol groups of the D-glucose unit consume a substantial proportion of the periodate added, and also that they are, on the average, only slightly more reactive than the single glycol group of the D-fructose unit.

From the stereochemical viewpoint, the *trans*-1,2-glycol group of the D-fructofuranose unit should be less-favorably oriented than those of the D-glucopyranosyl ring for forming a cyclic complex with glycol-cleaving oxidants (11, 12, 13), since the *trans*-glycol group on a 6-membered ring (projected angle of 60°) should approach coplanarity more closely than that on a 5-membered ring (projected angle of 120°) (13). The periodate data is consistent with these considerations.

Lead tetraacetate appears to exhibit anomalous behavior in its preferential attack on the D-fructofuranosyl residue. However, earlier studies of the reaction of lead tetraacetate with cyclic 1,2-diols (14, 15, 16) have shown a similar inconsistency. *trans*-1,2-Cyclopentanediol, for example, consumes lead tetraacetate at about 60 times the rate for *trans*-1,2-cyclohexanediol (14). These and other comparative rate data have been cited (16) as evidence that glycol-cleavage by lead tetraacetate need not involve an intermediate cyclic lead complex. By contrast, the marked resistance to oxidation shown by rigidly fixed *trans*-glycol groups on a 5-membered ring, as in bicyclic systems (16, 17), has been ascribed to an orientation unsuitable for complexing.

If a cyclic intermediate is involved, its formation should be favored by such distortion of the ring which would force the adjacent hydroxyl groups toward the eclipsed state, rendering the glycol structure more nearly coplanar (13). X-ray crystallography has shown (6) that in the D-fructosyl residue of sucrose sodium bromide dihydrate, the ring oxygen atom and carbons-2, -3, and -5 lie essentially in one plane and the ring is puckered at carbon-4 so that the C3—O and C4—O bonds are forced towards coplanarity. In addition, the angles which the 3- and 4-hydroxyl groups make with the adjacent ring bonds are unusually high, tending further to bring the glycol group into the mean plane of the residue. Most probably this conformation is imposed by forces within the crystal lattice and may not represent the D-fructofuranosyl unit in solution. Nevertheless, it is clear that under suitable conditions the furanose ring *can be* distorted so as to afford a glycol group having a projected angle much smaller than 120°, which might occur in the lead-complex transition state. Hence, the "anomalous" lead tetraacetate oxidation behavior of *trans*-1,2-diols on 5-membered rings need not be regarded as inconsistent with a cyclic intermediate pathway. Differences between lead tetraacetate and periodate exhibited in their attack on sucrose, therefore, may be due to factors such as variations in steric requirements of the two reagents, or to the relative ease with which the intermediate complexes decompose to products (18), and not to fundamental differences in reaction mechanism.

EXPERIMENTAL

Paper chromatography was carried out using Whatman No. 1 paper, and benzene–butanol–pyridine–water (19) as solvent. Urea oxalate (20) was used to detect fructose-containing oligosaccharides on chromatograms, and ammoniacal silver nitrate (21) as a general spray.

Can. J. Chem. Downloaded from www.nrcresearchpress.com by 69.46.99.164 on 09/04/12
For personal use only.

Measurement of Oxidation Rates

(*a*) *Lead Tetraacetate*

The sugar (10–15 mg) in water (0.2 ml) was taken up in acetic acid (10 ml). A solution of lead tetraacetate (0.2 g) in acetic acid (10 ml) was added, and at chosen intervals aliquots of the reaction mixture were withdrawn and the oxidant content determined iodometrically (11). Results are given in Table I.

(*b*) *Periodate*

The sugar (10–15 mg) in water (5 ml) was taken up in ethanol (10 ml), and a solution of sodium periodate (60 mg) in water (5 ml) added. At chosen intervals aliquots of the reaction mixture were added to phosphate buffer (pH 7.0) (22) and the iodine released titrated. Results are given in Table I.

Partial Oxidation of Sucrose with Lead Tetraacetate and Catalytic Reduction of the Dialdehyde

Sucrose (10 g, 29.2 mmoles) was dissolved in water (500 ml), the solution was diluted with acetic acid (500 ml), and lead tetraacetate (12.4 g, 28.0 mmoles) added with stirring at room temperature. Oxidant was found to be consumed within 0.5 hour (negative starch – potassium iodide test), and excess Amberlite IR-120 was then added to remove divalent lead. The filtered solution was concentrated *in vacuo* at 45°, and most of the residual acetic acid and water removed by codistillation several times with ethanol and toluene, the product being obtained as a white crust (9.5 g). On a paper chromatogram the product streaked heavily, and a small proportion of unoxidized sucrose was detected.

The oxidation product (8.0 g), absolute ethanol (125 ml), and Raney nickel (2.5 g, wet weight) were heated together at 120° in the presence of hydrogen (1800 p.s.i.) for 12 hours. After removal of the catalyst and evaporation of the solvent, the syrup obtained was found to contain a major component (R_{sucrose} 2.5) which gave a negative ketohexose test (urea oxalate spray), together with a small proportion of sucrose. The syrup (6.5 g) in acetic anhydride (75 ml) was heated with anhydrous sodium acetate (6.0 g) on a steam bath for 2 hours. Slow addition of the cooled acetylation mixture to a vigorously stirred ice slurry afforded a solid product which, after 8 hours of continued stirring, was filtered off, washed well with water, and dried. Weight, 9.0 g. The product crystallized rapidly from ethanol as large plates (weight, 7.1 g); when powdered and heated slowly (1°/3–4 minutes) the crystals had m.p. 56–60°, unchanged by two further crystallizations from ethanol $[\alpha]_D^{25}$ +67.2 (*c*, 2.6, chloroform). Calculated for $C_{28}H_{40}O_{19}$: acetyl, 50.40%. Found: acetyl (sapon.), 50.27%. The melting point was virtually unchanged also by two recrystallizations from ether, m.p. 56–59°. Calculated for $C_{28}H_{40}O_{19}$: C, 49.40%; H, 5.92%; acetyl, 50.40%. Found: C, 49.19%; H, 5.97%; acetyl (sapon.), 50.55%.

On deacetylation with sodium methoxide the syrupy polyol was found to be chromatographically pure, and was not attacked by an active preparation of invertase.

Reduction of the Dialdehyde with Sodium Borohydride

Partially oxidized sucrose (above) (6.0 g) in water (50 ml) was added to a cold solution of sodium borohydride (3.5 g in 50 ml ice water) over a period of 45 minutes. After 18 hours acetic acid was added slowly to pH of about 7 and the solution was concentrated *in vacuo* at 45° to dryness.* Borate was removed as volatile methyl borate by repeated (5 times) addition and evaporation of methanol. Acetic anhydride (75 ml) and anhydrous sodium acetate (5.0 g) were added to the dry residue, the mixture was heated on the

**Use of Amberlite IR-120 to remove sodium ions at this stage, as in the usual procedure, resulted in extensive hydrolysis of the reduction product.*

Can. J. Chem. Downloaded from www.nrcresearchpress.com by 69.46.99.164 on 09/04/12
For personal use only.

steam bath for 2 hours, and the acetate was isolated as described above and recrystallized from ethanol (weight, 4.5 g). Recrystallized twice from ether the acetate had m.p. 56–60°, $[\alpha]_D^{25}$ +65.0 (*c*, 2.7, chloroform); the X-ray diffraction pattern was indistinguishable from that of the octaacetate prepared via catalytic reduction. Calculated for $C_{28}H_{40}O_{19}$: C, 49.40%; H, 5.92%; acetyl, 50.40%. Found: C, 49.25%; H, 6.02%; acetyl (sapon.), 50.49%.

Degradation of III

The octaacetate of III (1.5 g) in dry methanol (15 ml) was treated with sodium methoxide (3 ml, 0.5 *N*) in the cold for 30 hours. An aliquot (8 ml) of the solution was acidified with 2% methanolic hydrogen chloride (10 ml) and heated under reflux for 12 hours. Ethereal diazomethane was then added to neutrality, and additional ether to cause turbidity. A crystalline product (0.11 g) obtained by cooling was recrystallized from ethanol, m.p. 164–165°, undepressed by admixture with methyl α-D-glucopyranoside; the X-ray diffraction pattern was indistinguishable from that of the D-glucoside. Calculated for $C_7H_{14}O_6$: C, 43.29%; H, 7.27%. Found: C, 43.50%; H, 7.40%. Paper chromatographic examination of the mother liquor (silver nitrate spray) indicated the presence of glyceritol, methyl glucoside, and a third component (faint streak slightly slower than glyceritol), which was presumed to be 1,3-dihydroxy-2-propanone dimethylketal.

A second aliquot (5 ml) of the deacetylation mixture was concentrated to give a syrup (0.20 g), 0.1 *N* sulphuric acid (10 ml) was added, the solution heated on the steam bath for 5 hours, and neutralized with Dowex-1 (bicarbonate form). The hydrolyzate appeared (paper chromatogram) to contain glucose, 1,3-dihydroxy-2-propanone, and glyceritol. Calcium benzoate (23) (1.0 g) was added, followed by bromine (0.5 ml) and, after 6 hours at room temperature with occasional shaking, excess bromine was removed *in vacuo*. The solution was filtered, treated with a mixture of Amberlite IR-120 and Dowex-1 (bicarbonate form), and concentrated to a volume of 5 ml. Phenylhydrazine (0.8 ml) and acetic acid (0.8 ml) were added and the solution was heated on the steam bath for 0.5 hour. After cooling, a yellow precipitate which formed was collected, dried, and recrystallized three times from benzene, m.p. 131–133°; the X-ray diffraction pattern was indistinguishable from that of triose (1,3-dihydroxy-2-propanone) phenylosazone. Calculated for $C_{15}H_{16}ON_4$: C, 67.14%; H, 6.01%. Found: C, 67.20%; H, 5.96%.

Partial Oxidation of Sucrose with Periodate and Reduction of the Product

Sucrose (3.4 g) in 50% ethanol (100 ml) was treated at 0° in the dark for 30 hours with sodium periodate (2.1 g in 43 ml of 50% ethanol). A precipitate which formed was filtered off, a slight excess of hot strontium hydroxide solution was added slowly with efficient stirring, the reaction mixture filtered, and the filtrate treated with a mixture of Amberlite-IR-120 and Dowex-1 (bicarbonate form). The final filtrate and washings were concentrated *in vacuo* at 40°. Weight, 3.0 g.

The partially oxidized sucrose (0.6 g) was reduced with sodium borohydride, followed by acetylation, as described above for lead-tetraacetate-oxidized sucrose. The syrupy acetate (1.0 g), on deacetylation with sodium methoxide, was found (paper chromatogram) to consist of one major and two minor components in addition to a large proportion of unoxidized sucrose. The major product ($R_{sucrose}$ 3.0) was detected on the chromatogram with silver nitrate but not with urea oxalate or *p*-anisidine hydrochloride, and hence appeared to be the polyol derived via oxidation of sucrose by 3 moles periodate per mole. One of the minor components ($R_{sucrose}$ 1.7) contained unoxidized fructose as shown by its color reaction with urea oxalate; the third product ($R_{sucrose}$ 2.4) corresponded on the

Can. J. Chem. Downloaded from www.nrcresearchpress.com by 69.46.99.164 on 09/04/12
For personal use only.

chromatogram to compound III, giving a yellow-brown color with *p*-anisidine hydrochloride and a negative ketohexose test with urea oxalate.

When sucrose was oxidized with 2 moles of sodium periodate, reduced, acetylated, and deacetylated (as above) the proportion of sucrose unoxidized was lower, and of the compound ($R_{sucrose}$ 3.0), increased slightly. The compounds having $R_{sucrose}$ 1.7 and 2.4 were now present in relatively higher proportion and a second fructose-containing product ($R_{sucrose}$ 2.0) was detected also. This mixture was not resolved satisfactorily by chromatography on a cellulose column (24) using butanol, containing varying percentages of water, as eluent.

ACKNOWLEDGMENTS

Dr. D. J. Bell very kindly provided a sample of methyl β-D-fructofuranoside. The authors express thanks to J. W. L. C. Christ for technical assistance, to M. Mazurek for microanalyses, and to Miss I. Gaffney, for preparing X-ray diffraction diagrams.

REFERENCES

1. MITRA, A. K. and PERLIN, A. S. Can. J. Chem. **36**, 1079 (1957).
2. FLEURY, P. F. and COURTOIS, J. E. Compt. rend. **214**, 366 (1942).
3. HOCKETT, R. C. and ZIEF, M. J. Am. Chem. Soc. **72**, 2130 (1950).
4. HOCKETT, R. C. and MCCLENAHAN, W. S. J. Am. Chem. Soc. **61**, 1667 (1939).
5. WOLFROM, M. L. and WOOD, H. B. J. Am. Chem. Soc. **73**, 2933 (1951).
6. BEEVERS, C. A. and COCHRAN, W. Proc. Roy. Soc. (London), A, **190**, 257 (1947).
7. LEVI, I. and PURVES, C. B. Advances in carbohydrate chemistry. Vol. 4. *Edited by* W. W. Pigman and M. L. Wolfrom. Academic Press, Inc., New York. 1949. p. 27.
8. LEMIEUX, R. U. and HUBER, G. J. Am. Chem. Soc. **75**, 4118 (1953).
9. WOLFROM, M. L. and SHAFIZADEH, F. J. Org. Chem. **21**, 88 (1956).
10. JACKSON, E. L. and HUDSON, C. S. J. Am. Chem. Soc. **59**, 994 (1937).
11. CRIEGEE, R., KRAFT, L., and RANK, B. Ann. **507**, 159 (1933).
12. HEIDT, L. J., GLADDING, E. K., and PURVES, C. B. Tappi, **121**, 81 (1945).
13. REEVES, R. E. Advances in carbohydrate chemistry. Vol. 6. *Edited by* W. W. Pigman and M. L. Wolfrom. Academic Press, Inc., New York. 1951. p. 115.
14. CRIEGEE, R., BÜCHNER, E., and WALTHER, W. Ber. **73**, 571 (1940).
15. CRIEGEE, R., HÖGER, E., HUBER, G., KRUCK, P., MARKTSCHEFFEL, F., and SCHELLENBERGER, H. Ann. **599**, 81 (1956).
16. LEVESLEY, P., WATERS, W. A., and WRIGHT, A. N. J. Chem. Soc. 840 (1956).
17. DIMLER, R. J. Advances in carbohydrate chemistry. Vol. 7. *Edited by* W. W. Pigman and M. L. Wolfrom. Academic Press, Inc., New York. 1952. p. 49.
18. BUIST, G. J., BUNTON, C. A., and MILES, J. H. J. Chem. Soc. 743 (1959).
19. DE WHALLEY, H. C. S., ALBON, N., and GROSS, D. Analyst, **76**, 293 (1951).
20. HIRST, E. L., MCGILVRAY, D. I., and PERCIVAL, E. G. V. J. Chem. Soc. 1297 (1950).
21. PARTRIDGE, S. M. Nature, **158**, 270 (1946).
22. NEUMÜLLER, G. and VASSEUR, E. Arkiv Kemi, **5**, 235 (1953).
23. HUDSON, C. S. and ISBELL, H. S. Bur. Standards J. Research, **3**, 57 (1929).
24. HOUGH, L., JONES, J. K. N., and WADMAN, W. H. J. Chem. Soc. 254 (1949).

Can. J. Chem. Downloaded from www.nrcresearchpress.com by 69.46.99.164 on 09/04/12
For personal use only.

Can. J. Chem. Downloaded from www.nrcresearchpress.com by 69.46.99.164 on 09/04/12
For personal use only.

PYRROLE CHEMISTRY

II. 2-PYRROLECARBONITRILE, 1-METHYL-2-PYRROLECARBONITRILE, AND THEIR NITRATION PRODUCTS[1]

HUGH J. ANDERSON

ABSTRACT

The 2-nitriles of pyrrole and 1-methylpyrrole have been prepared by the dehydration of the corresponding aldoximes. These compounds have been nitrated and the ratios of 4- and 5-nitro isomers have been determined. The 2-cyano group appears to be less strongly "meta"-directing (i.e. toward the 4-position) during nitration in the pyrrole series than in the benzene ring.

In a previous paper some investigations were reported concerning directive effects in the pyrrole ring system. These researches have now been extended by the nitration of pyrrole and 1-methylpyrrole possessing a cyano group in the 2-position. The strongly meta-directing effect of this group tending to place an incoming substitutent in the 4-position is thus competing with the normally α-directing hetero atom which would place it in the 5-position. Although many substituted cyanides of pyrrole are known, neither 2-pyrrolecarbonitrile nor 1-methyl-2-pyrrolecarbonitrile are reported in the literature.

These two compounds (I and II) have now been prepared through the dehydration of the oximes of their readily available aldehydes. Fischer and Orth (2) have reported that heating 2-pyrrolecarboxaldoxime with a mixture of acetic anhydride and sodium acetate produced only 5-acetyl-2-pyrrolecarbonitrile, but acetic anhydride alone gave us a good yield of the desired product. Both this nitrile and the 1-methyl homologue could be hydrolyzed by potassium hydroxide in ethylene glycol at 130–140° to moderate yields of the known acids. Attempted acid hydrolysis leads to extensive decomposition. Several authors (3) have reported that substituted nitriles of pyrrole resist hydrolysis, however, these were mostly alkyl-substituted 3-pyrrolecarbonitriles.

It was hoped that a one-step preparation of these nitriles might be developed by an adaption of the procedure of Lettré, Jungmann, and Salfeld (4), who used N-phenyl-N-methylcyanamide and phenyllithium to prepare benzonitrile. We hoped that it might be possible to substitute the readily available N,N-dimethylcyanamide for their reagent, which is difficult to prepare. However, a trial using a 2-thienyllithium produced no neutral fraction, and another with 2-pyrrylmagnesium bromide also failed to give any of the desired nitrile. Presumably the amidines were formed instead.

As pointed out previously (1, 5) the proportions of 4- and 5-nitro derivatives formed through the reaction of acetyl nitrate and pyrroles possessing a meta-directing substituent in the 2-position are similar to those formed from the corresponding thiophenes although the α-directing effect of the N-atom is somewhat less than that of the sulphur. When a methyl group replaces the N-hydrogen there is a large increase in the proportion of the 4-nitro derivative.

Two fairly recent papers have reported the nitration of 2-thiophenecarbonitrile but their results are totally different. Reynaud and Delaby (6) isolated 80% 4-nitro and

[1]*Manuscript received August 17, 1959.*
Contribution from the Chemistry Department, Memorial University of Newfoundland, St. John's, Newfoundland.

20% 5-nitro, identifying their products by conversion to known substances. On the other hand Tirouflet (7) established the ratio of 42% 4- to 58% 5-nitro by means of a polarographic reduction, having first standardized against the pure compounds.

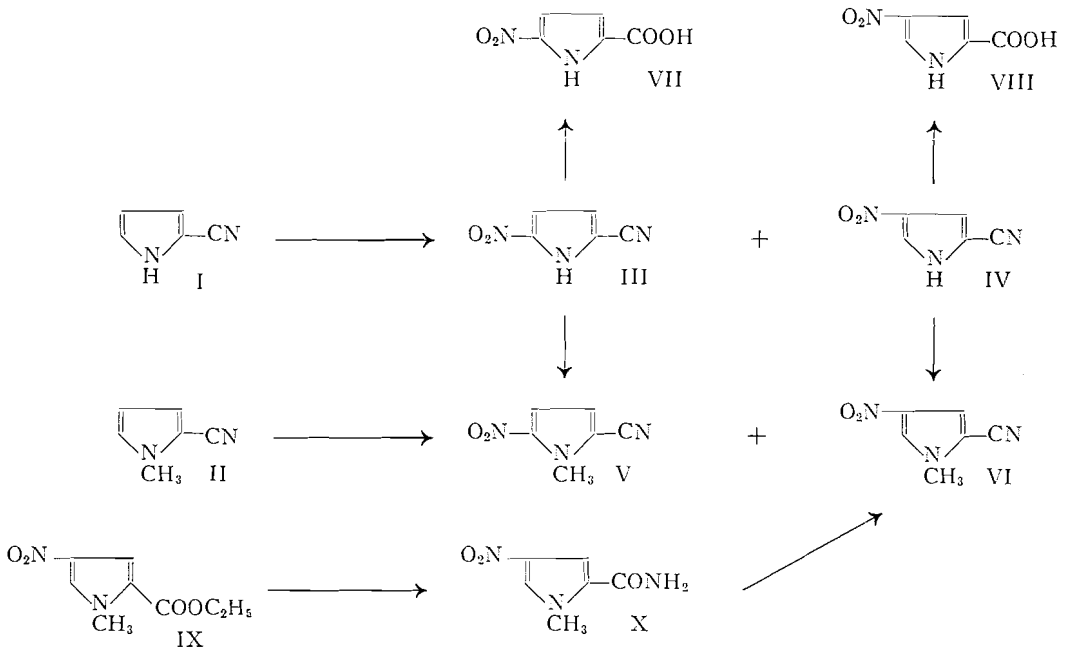

The nitration of 2-pyrrolecarbonitrile with "acetyl nitrate" (fuming nitric acid/acetic anhydride) at 0–10° proceeded normally and chromatography was attempted on alumina.

This method had proved satisfactory in previous separations of nitrated pyrrole derivatives and has the advantage of removing the dark tarry by-products as well. However, from the column we isolated only a single product, 4-nitro-2-pyrrolecarbonitrile (IV), using the usual benzene and benzene/ethyl acetate eluants. When we progressed to ethyl acetate and later to 1:1 ethanol/ethyl acetate a bright yellow solid was obtained. This substance was recrystallized from benzene/ethyl acetate and melted at 292°. It proved to be the sodium salt of 5-nitro-2-pyrrolecarbonitrile. The sodium salt was very soluble and quite stable in water. The desired product (III) could be obtained by ether extraction from the acidified aqueous solution.

The very weakly acidic nature of pyrrole is strengthened by the presence of an electron-withdrawing group in the 2-position which decreases the electron density at the nitrogen and facilitates the loss of the proton from the nitrogen. This situation is similar to the behavior of the corresponding *p*-substituted phenol. The same type of group in the 3-position of pyrrole has considerably less effect and thus α-nitro-substituted pyrroles are more acidic than β-nitro ones. Rinkes (5) made use of this observation in separating isomers from the nitration of 2-acetylpyrrole and other compounds. In these mixtures the 4-nitro could be extracted by ether from a basic aqueous solution while the 5-nitro isomer remained behind. The dinitropyrroles were found to be much more acidic, and separation was achieved by extracting 2,4-dinitropyrrole from an aqueous sodium

Can. J. Chem. Downloaded from www.nrcresearchpress.com by 69.46.99.164 on 09/04/12
For personal use only.

acetate solution leaving 2,5-dinitropyrrole behind. Thus it is not surprising that 5-nitro-2-pyrrolecarbonitrile with two strongly electron-withdrawing groups in α-positions should be quite acidic. Nevertheless, the isolation of such a stable sodium salt is somewhat unusual in the pyrrole series where most preparations have made use of sodium or sodium alkoxide under anhydrous conditions (8, 9).

When the nitrated 1-methylpyrrole was chromatographed it was found that even a long column did not provide a clear separation of the isomers, so eventually a simplified fractional crystallization from petroleum pentanes was used successfully.

The melting points of our 4- and 5-nitro-2-pyrrolecarbonitriles (III and IV) coincide with those recently reported by Tirouflet and Fournari (10), who prepared them by dehydration of the corresponding nitroaldoximes. Hydrolysis in concentrated hydrochloric acid was successful and mixed melting points with authentic specimens of the known nitroacids (VII and VIII) were undepressed.

The 1-methyl analogs (V and VI) would not hydrolyze in acid solution and base destroyed them as it does most nitrated pyrroles. Consequently, we N-methylated the nitro-2-pyrrolecarbonitriles (III and IV) and confirmed the identity of (V and VI) by mixed melting points. In addition it was possible to nitrate ethyl 1-methyl-2-pyrrolecarboxylate although only the 4-nitro isomer (IX) could be isolated. This ester (IX) was then ammonolyzed to the amide (X) and dehydrated with phosphorus oxychloride and pyridine to 4-nitro-1-methyl-2-pyrrolecarbonitrile (VI) which was identical with one of our isomers.

From the nitration of 2-pyrrolecarbonitrile we found that the 4-nitro isomer constituted about 40% of the mononitro fraction. Thus the —CN group seems to have somewhat less meta-directing ability in the pyrrole ring nitration than has the carbomethoxy and considerably less than acetyl or nitro groups. This is quite different from the benzene series where the meta-directing ability of the cyano group lies between nitro and acetyl in nitrations (12). However, it is similar to the proportion found in the thiophene series by Tirouflet, although not by Reynaud and Delaby.

As expected, the proportion of 4-nitro isomer was much higher for 1-methyl-2-carbonitrile—about 70% of the mononitro product. This also falls below the percentage of 4-isomer formed during nitration by the analogous 2-acetyl compound.

EXPERIMENTAL

2-Pyrrolealdoxime

A solution of hydroxylamine hydrochloride (7.5 g, 0.11 *M*) and sodium acetate trihydrate (15 g, 0.11 *M*) in 30 ml water was shaken vigorously with 2-pyrrolealdehyde (9.0 g, 0.095 *M*) for 5 minutes, then refrigerated overnight. The crude product weighed 9.2 g (84%). After recrystallization from benzene its melting point was 164–164.5°. Literature 165–166° (13).

1-Methyl-2-pyrrolealdoxime

This compound was prepared from the corresponding aldehyde by the same procedure. After recrystallization from water its melting point was 148.5–149.5°. Calc. for $C_6H_8N_2O$: C, 58.05; H, 6.49; N, 22.57; O, 12.89. Found: C, 58.10; H, 6.45; N, 22.38%.

2-Pyrrolecarbonitrile (I)

2-Pyrrolealdoxime (9.2 g, 0.084 *M*) in acetic anhydride (30 ml) was warmed slowly and then refluxed gently for 20 minutes. The cooled reaction product was poured into 200 ml cold water, extracted three times with 20-ml portions of ether, and dried over

Can. J. Chem. Downloaded from www.nrcresearchpress.com by 69.46.99.164 on 09/04/12
For personal use only.

sodium sulphate. After removal of the ether the residue was vacuum-distilled and the fraction, b.p. 89–90° at 1.5 mm, was collected. Yield 4.7 g (61%). Calc. for $C_5H_4N_2$: C, 65.20; H, 4.38; N, 30.42. Found: C, 65.09; H, 4.36; N, 30.25%.

The nitrile (0.5 g) was heated at 165–180° with potassium hydroxide (5 g) in ethylene glycol (10 ml) for 1 hour. The crude acid (0.28 g) obtained from this hydrolysis melted at 203–204° (decomp.) after several recrystallizations from water. The mixed melting point with an authentic specimen of 2-pyrrolecarboxylic acid was undepressed.

1-Methyl-2-pyrrolecarbonitrile (II)

1-Methyl-2-pyrrolealdoxime (10 g, 0.079 *M*) was dehydrated with acetic anhydride in the manner described above. The product weighed 5.2 g (61%) and had b.p. 86–88° at 11 mm. Calc. for $C_6H_6N_2$: C, 67.90; H, 5.70; N, 26.40. Found: C, 67.88; H, 5.72; N, 26.35%.

The nitrile (0.5 g) was hydrolyzed as before at 130–140° for 1 hour. The crude product weighed 0.55 g and on recrystallization from aqueous ethanol had m.p. 135–136°. The mixed melting point with authentic 1-methyl-2-pyrrolecarboxylic acid was undepressed.

Nitration of 2-Pyrrolecarbonitrile

The nitrile (1.2 g, 0.011 *M*) was dissolved in acetic anhydride (7 ml) and chilled to 0°. To this was added a mixture of fuming nitric acid (d = 1.5, 1.5 g, 0.023 *M*) and acetic anhydride (2.0 ml) while the temperature was kept below 10°. The dark solution was poured into 25 ml ice water with vigorous stirring and extracted with three 15-ml portions of ether and dried. After removal of all solvents under reduced pressure the crude red solid weighed 1.55 g.

Chromatography was commenced on alumina (150 g) using benzene and later 1:1 benzene/ethyl acetate as eluants. From these fractions a total of 0.5 g of pale yellow solid was obtained. Pure ethyl acetate gave no further solid, however, 1:3 ethanol/ethyl acetate and later 1:1 ethanol/ethyl acetate produced about 0.8 g of a bright yellow solid with a very high melting point (292° from benzene/ethyl acetate).

The first solid, 4-nitro-2-pyrrolecarbonitrile (IV), was recrystallized from water, m.p. 150.5–151°. (Tirouflet reported 152°.) Calc. for $C_5H_3N_3O_2$: C, 43.80; H, 2.21; N, 30.65; O, 23.34. Found: C, 43.84; H, 2.20; N, 30.40%. A small amount of this nitrile was refluxed with concentrated hydrochloric acid for 30 minutes. From the hydrolysis was obtained an acid which, after several recrystallizations from water, was a pale cream solid m.p. 210–212° (slight decomp.). Rinkes found 216° for 4-nitro-2-pyrrolecarboxylic acid.

The second solid from the chromatography was dissolved in a small amount of water, cooled, and acidified with concentrated hydrochloric acid. The colorless solid obtained was filtered, dried, and recrystallized from water. Its melting point was 172.5–173°. (Tirouflet found 174° for 5-nitro-2-pyrrolecarbonitrile (III) and a greenish-yellow color.) Calc. for $C_5H_3N_3O_2$: C, 43.80; H, 2.21; N, 30.65; O, 23.34. Found: C, 43.65; H, 2.28; N, 30.41%. A small amount of this nitrile was hydrolyzed in concentrated hydrochloric acid. The pale cream-colored product after recrystallizing from water melted at 159–161°. Rinkes gives m.p. 161° for 5-nitro-2-pyrrolecarboxylic acid.

Nitration of 1-Methyl-2-pyrrolecarbonitrile

The nitrile (1.3 g, 0.021 *M*) was nitrated and worked up in the manner described above, and the crude product (1.50 g) chromatographed on alumina (150 g). Elution with benzene/petroleum pentanes produced no real separation nor did rechromatography of the first six fractions. Consequently all fractions were extracted repeatedly with small amounts of hot petroleum pentanes. From these extracts 0.36 g of solid was obtained,

Can. J. Chem. Downloaded from www.nrcresearchpress.com by 69.46.99.164 on 09/04/12
For personal use only.

m.p. 86–86.5° after several recrystallizations from water. This was compound V. Calc. for $C_6H_5N_3O_2$: C, 47.68; H, 3.34; N, 27.81; O, 21.17. Found: C, 47.51; H, 3.19; N, 27.60%. Compound V failed to undergo hydrolysis in concentrated hydrochloric acid and was destroyed by hot base.

The less soluble fraction was recrystallized from benzene/petroleum hexanes and weighed 0.86 g. After a final recrystallization from water it had m.p. 157.5–158°. This was compound VI. Calc. for $C_6H_5N_3O_2$: C, 47.68; H, 3.34; N, 27.81; O, 21.17. Found: C, 47.55; H, 3.27; N, 27.68%. Compound VI also failed to undergo hydrolysis to the corresponding acid.

Preparation of Compounds V *and* VI *by* N-*Methylation*

To a solution of 4-nitro-2-pyrrolecarbonitrile (50 mg) in toluene (10 ml) was added a solution of sodium metal (100 mg) in ethanol (1 ml). The mixture was refluxed gently for 3 minutes, methyl sulphate (0.3 g) added, and refluxed 5 minutes longer. The cooled mixture was extracted twice with 5-ml portions of 1 *N* sodium hydroxide solution. The organic layer was dried over sodium sulphate and nearly all solvent removed in vacuum. At this point an excess of petroleum pentanes was added and the precipitate filtered. After recrystallization from water the 4-nitro-1-methyl-2-pyrrolecarbonitrile (25 mg) melted at 156–158° and mixed melting point with compound VI was 156–158°.

In a similar manner 5-nitro-2-pyrrolecarbonitrile was converted to the 1-methyl analog m.p. 83–84° (from water). Mixed melting point with compound V 83–84°.

Nitration of Ethyl 1-Methyl-2-pyrrolecarboxylate

Ethyl 1-methyl-2-pyrrolecarboxylate (1.53 g, 0.01 *M*) in acetic anhydride (8 ml) was treated with a mixture of fuming nitric acid (1.1 g, 0.018 *M*) and acetic anhydride (2.0 ml) keeping the temperature below −5°. After hydrolysis in cold water the product was extracted with ether, dried over sodium sulphate, and all solvent removed under vacuum. The crude red solid (1.33 g) was chromatographed on alumina (150 g) using benzene/petroleum pentanes as eluant. From the chromatogram 0.35 g of unreacted ester was recovered and 0.52 g of a product (IX) which on recrystallization from aqueous alcohol had m.p. 112.5–113°. The reported melting point of ethyl 4-nitro-1-methyl-2-pyrrolecarboxylate is 113–114° (11). In addition the chromatogram produced a small amount of acidic material presumably resulting from the hydrolysis of the ester. It was not identified. None of the isomeric 5-nitro ester was found.

Ammonolysis of the Ester IX

A solution of the 4-nitro ester (0.4 g) was dissolved in methanol (10 ml) and cooled during saturation with ammonia gas. The flask was stoppered tightly and allowed to stand for a week at room temperature. A bright yellow solid which had separated was completely precipitated by the addition of 5 ml water. After several recrystallizations the pale yellow 4-nitro-1-methyl-2-pyrrolecarboxamide (X) (0.32 g) had m.p. 224–225°. Calc. for $C_6H_7N_3O_3$: C, 42.61; H, 4.18; N, 24.85; O, 28.37. Found: C, 42.43; H, 4.15; N, 24.50%.

Dehydration of the Amide (X)

The amide (0.3 g) was dissolved in freshly dried pyridine (3 ml). To this was added phosphorus oxychloride (0.4 g) resulting in vigorous reaction. After this had subsided the mixture was cooled, diluted with 10 ml water, chilled again, and filtered. The crude solid (0.18 g) was recrystallized from water, m.p. 155–157°. A mixed melting point with product VI from the nitration of 1-methyl-2-pyrrolecarbonitrile was undepressed confirming the latter as 4-nitro-1-methyl-2-pyrrolecarbonitrile.

Can. J. Chem. Downloaded from www.nrcresearchpress.com by 69.46.99.164 on 09/04/12
For personal use only.

REFERENCES

1. ANDERSON, H. J. Can. J. Chem. **35**, 21 (1957).
2. FISCHER, H. and ORTH, H. Ann. **502**, 237 (1933).
3. CURRY, T. H. Ph.D. Thesis. The Ohio State University. 1953. Mic 58-694, pp. 12–13.
4. LETTRÉ, H., JUNGMAN, P., and SALFELD, J.-C. Chem. Ber. **85**, 397 (1952).
5. RINKES, I. J. Rec. trav. chim. **53**, 1167 (1934).
6. REYNAUD, P. and DELABY, R. Bull. soc. chim. France, 1614 (1955).
7. TIROUFLET, J. Bull. soc. chim. France, 1066 (1958).
8. TREIBS, A. and KOLM, H. G. Ann. **606**, 166 (1957).
9. CORWIN, A. H. and QUATTLEBAUM, W. M., JR. J. Am. Chem. Soc. **58**, 1081 (1936).
10. TIROUFLET, J. and FOURNARI, P. Compt. rend. **248**, 1182 (1959).
11. WEISS, M. J., WEBB, J. S., and SMITH, J. M., JR. J. Am. Chem. Soc. **79**, 1266 (1957).
12. FERGUSON, L. N. Electron structures of organic molecules. Prentice-Hall, Inc., New York. 1952. p. 302. Table 10.3.
13. SILVERSTEIN, R. M., RYSKIEWICZ, E. E., and CHAIKEN, S. W. J. Am. Chem. Soc. **76**, 4485 (1954).

Can. J. Chem. Downloaded from www.nrcresearchpress.com by 69.46.99.164 on 09/04/12
For personal use only.

Can. J. Chem. Downloaded from www.nrcresearchpress.com by 176.9.209.113 on 09/04/12
For personal use only.

THE DECAY OF ACTIVE NITROGEN AT HIGH TEMPERATURES[1]

R. A. BACK,[2] W. DUTTON, AND C. A. WINKLER

ABSTRACT

Previous studies of the decay of active nitrogen have been extended to higher temperatures. A more detailed treatment of the results suggests that surface recombination of nitrogen atoms may be either first or zero order. Rate constants for both the surface and the homogeneous recombination of nitrogen atoms are reported. The latter shows a slight positive temperature coefficient.

In a previous paper from this laboratory (1), a method was described for measuring the rate of decay of active nitrogen. Measurements were made at 55° C and 400° C, and rate constants for the recombination of nitrogen atoms on the surface and in the gas phase were reported. In the present paper, similar measurements at higher temperatures are described, together with a slightly revised treatment of the previous data.

EXPERIMENTAL

The apparatus and method were similar to those used previously, with a few minor changes. Active nitrogen was produced in a condensed discharge in a fast-flow system under conditions of complete initial dissociation of the nitrogen. It was passed through a "decay tube" of fixed dimensions into a reaction vessel, where the atom concentration was measured chemically using the reaction with ethylene at 400° C. By studying the decay over a range of pressures, it was possible to separate homogeneous and heterogeneous decay processes. A Vycor discharge tube and decay tube permitted measurements up to 1000° C. Much improved estimation and control of the temperature of the decay tube was possible with a concentric thermocouple well, combined with a sectionally wound furnace. The decay tube was larger (455 cc) than in the previous experiments, in anticipation of a shorter contact time at higher temperatures.

It was hoped originally to compare decay rates at various temperatures under the same surface conditions. However, the instability of most poisons above 400° C caused serious difficulty; Na_2HPO_4, which behaved very reproducibly at 55 and 400° C, deteriorated badly at 700° C, and Na_3PO_4 was no better. Although $AlPO_4$ was slightly more stable at 700° C, and consistent data could be obtained from experiments done in a single day, it was completely ineffective as a poison at 1000° C. The most stable poison at 700° C, was $Mg_3(PO_4)_2$ and this was the only substance that was at all effective at 1000° C, at which temperature, however, it deteriorated rapidly.

When a good poison, stable at 400° C, was heated for some time to 700° C or 1000° C, it was practically ineffective when used again at 400° C. Thus, an irreversible physical change in the poison at high temperature was involved, rather than simply a reversible increase in γ, the recombination efficiency.

THEORY

The theory of nitrogen atom decay in a similar apparatus has been treated previously

[1]*Manuscript received August 21, 1959.*
Contribution from the Physical Chemistry Laboratory, McGill University. This research was supported in part by the Defence Research Board of Canada, Grant No. 9530-21, Project D-44-95-30-21, and in part by Imperial Oil Ltd., Sarnia, Ontario.
[2]*Postdoctoral Fellow. Present address: Division of Pure Chemistry, National Research Council, Ottawa.*

Can. J. Chem. Downloaded from www.nrcresearchpress.com by 176.9.209.113 on 09/04/12
For personal use only.

(1), and will be used here with one or two modifications. Kelly and Winkler considered two possible modes of surface decay, first order and second order in nitrogen atoms. Homogeneous decay was assumed to be second order in nitrogen atoms, and termolecular. Two extreme cases were considered, the first of which assumed nitrogen atoms and nitrogen molecules to be equally effective as third bodies, while the second assumed nitrogen atoms to be completely ineffective. For simplicity, only the former case will be considered in the present work, and the two differential equations for first and second order surface decay are, respectively,

$$[1] \qquad -dN/dt = k_1\mathrm{N} + k_2\mathrm{N}^2p,$$

$$[2] \qquad -dN/dt = k_3\mathrm{N}^2 + k_2\mathrm{N}^2p.$$

A third possible mode of surface decay, not considered previously, is zero order in nitrogen atoms, and for this

$$[3] \qquad -dN/dt = k_4 + k_2\mathrm{N}^2p.$$

Upon integration of these equations over a time of decay, t, assuming initial complete dissociation of the nitrogen, and expressing N atom concentration as partial pressure,

$$[4] \qquad p/p_\mathrm{N} = e^{k_1t} + p^2(e^{k_1t}-1)k_2/k_1$$

$$[5] \qquad 1/p_\mathrm{N} - 1/p = (k_3 + k_2p)t$$

$$[6] \qquad (p-p_\mathrm{N})/t = (k_4 + p_\mathrm{N}p^2k_2)\ (\tan\theta)/\theta$$

where p = total pressure, p_N = partial pressure of nitrogen atoms, and $\theta = t(k_4k_2p)^{\frac{1}{2}}$.

In the previous study, t was taken to be approximately constant, independent of pressure, whereupon it is easily shown that

$$\lim_{p\to 0} \quad p_\mathrm{N}/p = 1, \text{ for equation [5]}$$
$$= e^{-k_1t}, \text{ for equation [4]}$$
$$= 0, \text{ for equation [6]}.$$

Since p_N clearly did not approach p as the pressure was reduced, second order surface decay was ruled out. Since a zero order surface decay had not been considered, it was concluded that the surface decay was first order, and k_1 and k_2 were evaluated from suitable plots of equation [4].

The assumption of constant decay time, while it simplified the treatment considerably, may perhaps introduce appreciable errors under some conditions. The decay time varied considerably with pressure, and increased rather sharply at very low pressures. This could affect both the determination of the order of the surface decay, by affecting the limiting value of p_N/p, and the numerical values of the rate constants. In the present paper, therefore, the variation of t with pressure is taken into account. Decay time was measured, and each of equations [4], [5], and [6] in turn was plotted in a suitable way to determine the order of surface decay and values of the decay constants. If surface decay were first order, a plot of $(p/p_\mathrm{N}) - e^{k_1t}$ versus $(e^{k_1t}-1)p^2$ should be linear, and pass through the origin, with slope k_2/k_1. The value of k_1 could be determined by successive approximations to give the best extrapolation to the origin. If surface decay were second order, a plot of $(1/p_\mathrm{N} - 1/p)/t$ versus p should be linear, with intercept k_3 and slope k_2. If surface decay were zero order, a plot of $(p-p_\mathrm{N})/t$ against $p_\mathrm{N}p^2$ should

be approximately linear. The factor $(\tan\theta)/\theta$, and thence values of k_4 and k_2, could be evaluated by a method of successive approximations.

RESULTS

Consistent data were obtained with Na_2HPO_4 and $Mg_3(PO_4)_2$ poisons at 400° C, and with $AlPO_4$ and $Mg_3(PO_4)_2$ at 700° C, and these were treated in the manner described above. No poisons were sufficiently stable at 1000° C to permit calculation of rate constants. The previous data of Kelly and Winkler, using Na_2HPO_4 poison at 55° C and 400° C, were also treated in the same way, taking into account the variation of t and the possibility of zero order surface decay.

In every case, the plot of equation [5] yielded a curve with negative slope at low pressures, while at higher pressures the slope became positive, which clearly indicates that the surface decay was not second order.

Plots of equation [4], representing first order surface decay, always had positive slopes, and showed considerable curvature. Such curvature may be attributed, as before, to the deviation, with increasing pressure, from required conditions such as complete initial dissociation, negligible radial concentration gradients, and others (1). Rate constants were thus determined from the slopes and intercepts of low pressure asymptotes of these curves.

Plots of equation [6], corresponding to zero order surface decay, also showed positive slopes and some curvature, and rate constants were again estimated from low pressure asymptotes. Some of this curvature is due to the variation of $(\tan\theta)/\theta$ with pressure. These plots were neither more nor less linear than those of equation [4], and it appears impossible to distinguish between first and zero order surface decay by the present method, although the data are clearly incompatible with a second order process.

TABLE I

Rate constants for homogeneous atom combination

Temp., ° C	Surface poison	Source of data	Values of k_2 (molecules^{-2}. cc^2. sec^{-1}) $\times 10^{33}$		
			1st order surface decay, neglecting change in t	1st order surface decay, allowing for change in t	Zero order surface decay
55	Na_2HPO_4	Ref. 1	1.32	2.98	8.21
400	Na_2HPO_4	Ref. 1	8.6	16.7	40.3
	Na_2HPO_4	This work	7.0	11.7	22.8
	$Mg_3(PO_4)_2$	This work	12.1	27.2	33.0
700	$Mg_3(PO_4)_2$	This work	14.4	112	145
	$AlPO_4$	This work	9.3	119	147

In Table I are shown values for k_2, the termolecular rate constants for the homogeneous recombination of nitrogen atoms, assuming either first or zero order surface decay. Two sets of values are reported for the first order surface decay, one calculated by the simpler method of Kelly and Winkler, the other corrected for the variation of decay time with pressure. It should be noted that nitrogen atoms and molecules are assumed to be equally effective as third bodies in this treatment. If nitrogen atoms were completely ineffective, values of k_2 would be approximately doubled.

In Table II are shown values of the surface recombination efficiency, γ, defined in

Can. J. Chem. Downloaded from www.nrcresearchpress.com by 176.9.209.113 on 09/04/12
For personal use only.

the usual way (1), for first order surface decay, again for the two methods of calculation.

TABLE II

Values of γ, the recombination efficiency, for first order surface decay

Temp., ° C	Surface poison	Source of data	$\gamma \times 10^4$ Neglecting change in t	$\gamma \times 10^4$ Allowing for change in t
55	Na_2HPO_4	Ref. 1	2.65	2.32
400	Na_2HPO_4	Ref. 1	2.86	2.49
	Na_2HPO_4	This work	1.94	1.70
	$Mg_3(PO_4)_2$	This work	1.70	1.23
700	$Mg_3(PO_4)_2$	This work	3.50	2.10
	$AlPO_4$	This work	4.40	3.10

In Table III are shown values of the rate constant for zero order surface decay, expressed as a rate per unit area, molecules $\cdot$ sec^{-1} $\cdot$ cm^{-2}.

TABLE III

Rate constants for zero order surface decay

Temp., ° C	Surface poison	Source of data	Rate (molecules $\cdot$ sec^{-1} $\cdot$ cm^{-2}) $\times 10^{-16}$
55	Na_2HPO_4	Ref. 1	5.9
400	Na_2HPO_4	Ref. 1	7.0
	Na_2HPO_4	This work	2.3
	$Mg_3(PO_4)_2$	This work	2.9
700	$Mg_3(PO_4)_2$	This work	1.9
	$AlPO_4$	This work	2.4

DISCUSSION

The general effect of neglecting the variation of decay time with pressure (Tables I and II) was to lower the values of k_2 and raise the values of γ. The largest error was introduced in the value of k_2, where it amounted to a factor of 10 at 700° C and a factor of about two at the lower temperatures. The effect on the values of γ was much less pronounced, the largest error being a factor of about 1.5 at 700° C.

The values of k_2 are affected considerably by the order assumed for the surface decay. Zero order surface decay requires a larger value of k_2 than does first order surface decay, the difference being more pronounced at lower temperatures. With both orders, k_2 appeared to increase markedly with increasing temperature. An Arrhenius plot was not linear, and was only slightly improved by plotting log $(k_2/t^{\frac{1}{2}})$ to allow for the increase in the termolecular collision rate with temperature. "Activation energies" of between 0.5 and 2 kcal may be estimated from these plots, although undoubtedly the variation of k_2 with temperature is too complex to be described by a simple exponential temperature dependence. If the termolecular recombination proceeds through the $^5\Sigma$ state of N_2 (2, 3), the radiationless transition to the $^3\pi$ state might depend in a critical way on the vibrational energy of the former state, and hence on the temperature. It is perhaps interesting that other termolecular atom combination processes, which proceed simply through the ground state of the diatomic molecule, show the expected small negative temperature coefficient (4, 5, 6).

Values of k_2 in Table I may be compared with values of 200×10^{-33} (7), 33×10^{-33} (8),

Can. J. Chem. Downloaded from www.nrcresearchpress.com by 176.9.209.113 on 09/04/12
For personal use only.

17×10^{-33} (9), and 15×10^{-33} (10) (molecules^{-2}.cc^2.sec^{-1}), measured by a variety of methods, all at about room temperature. In some of these methods, surface recombination was perhaps not adequately taken into account, and high values were obtained. Atom concentrations were measured in the first two cases by a calorimetric probe technique, of somewhat doubtful efficiency, while the latter two used the nitric oxide flame titration, which yields atom concentrations about 1.5 times those measured by the ethylene reaction (11). Herron *et al.* reported no temperature dependence of k_2 between 25° and 180° C (10).

The surface decay constants showed surprisingly little temperature dependence. A first order surface recombination of atoms is usually interpreted as a reaction between gas-phase atoms and adsorbed atoms on a fully covered surface (12). A zero order surface combination implies a bimolecular surface reaction between adsorbed atoms, again on a fully covered surface. It may be noted that with either mechanism, a sparsely covered surface leads to a second order process, which clearly does not fit the experimental results. Both mechanisms thus require a fully covered surface, over a considerable range of temperature and atom concentration, which implies a very strong adsorption, probably chemisorption, of the nitrogen atoms. The small temperature dependence of the decay constants is in accord with this view.

The observed values of γ are quite compatible with the suggested first order mechanism, and are of the same order of magnitude as those measured for similar recombinations of oxygen and hydrogen atoms (13, 14, 15). The zero order mechanism, on the other hand, perhaps presents some difficulties. In bimolecular surface reactions on a sparsely covered surface, the adsorption of one atom onto a site adjacent to another one is usually thought to be the rate-controlling step. Obviously, in a zero order process, with a fully covered surface, this is no longer true, and the rate must be controlled by the rate of interaction of atoms already adsorbed on adjacent sites. The values of γ, the fraction of collisions with the surface leading to combination, at least permit a rate of combination much slower than the rate of adsorption, if the adsorption process were highly efficient. A bimolecular surface reaction on a fully covered surface would require a high surface concentration of atoms, as the strongly chemisorbed atoms would have little mobility. Superficially, the zero order process seems rather less likely, mechanistically, than the first order one, but it must be emphasized that the present data clearly do not enable distinction between the two.

Finally, the limited accuracy of the present method should be pointed out. Because of inherent approximations and errors, an accuracy of perhaps $\pm50\%$ should be assigned to the numerical values of the decay constants. It might be noted that the variation of k_2 with temperature seems well beyond these limits.

REFERENCES

1. KELLY, R. and WINKLER, C. A. Can. J. Chem. **37**, 62 (1959).
2. BERKOWITZ, J., CHUPKA, W. A., and KISTIAKOWSKI, G. B. J. Chem. Phys. **25**, 457 (1956).
3. KISTIAKOWSKI, G. B. and WARNECK, P. J. Chem. Phys. **27**, 1417 (1957).
4. RUSSELL, K. E. and SIMONS, J. Proc. Roy. Soc. A, **217**, 271 (1953).
5. STRONG, R. L., CHIEN, J. C. W., GRAF, P. E., and WILLARD, J. E. J. Chem. Phys. **26**, 1287 (1957).
6. BRITTON, D., DAVIDSON, N., and SCHOTT, G. Discussions Faraday Soc. **17**, 58 (1954).
7. SAXE, M. H. and LICHTIN, N. N. Abstracts of Am. Chem. Soc. Spring meeting, April, 1959.
8. WENTINK, T. W., SULLIVAN, J. O., and WRAY, K. L. J. Chem. Phys. **29**, 231 (1958).
9. HARTECK, P., REEVES, R. R., and MANNELLA, G. J. Chem. Phys. **29**, 608 (1958).
10. HERRON, J. T., FRANKLIN, J. L., BRADT, P., and DIBELER, V. H. J. Chem. Phys. **29**, 230 (1958).
11. VERBECKE, G. and WINKLER, C. A. In press.
12. LAIDLER, K. J. Chemical kinetics. 1st ed. McGraw-Hill Book Co., Inc., New York. 1950.
13. SMITH, W. V. J. Chem. Phys. **11**, 110 (1943).
14. LAIDLER, K. J. J. Phys. Chem. **53**, 712 (1949).
15. LINNETT, J. W. and MARSDEN, D. G. H. Proc. Roy. Soc. A, **234**, 504 (1956).

Can. J. Chem. Downloaded from www.nrcresearchpress.com by 176.9.209.113 on 09/04/12
For personal use only.

Can. J. Chem. Downloaded from www.nrcresearchpress.com by 176.9.209.113 on 09/04/12
For personal use only.

TERNARY COMPOUNDS IN THE SYSTEM NH_3–H_2O_2–H_2O[1]

PAUL A. GIGUÈRE AND DAVID CHIN

ABSTRACT

A thermal analysis of the three-component system ammonia – hydrogen peroxide – water was carried out by adding anhydrous ammonia to the hydrate $H_2O_2 \cdot 2H_2O$. A first compound was found, with formula $NH_3 \cdot 3H_2O_2.6H_2O$, melting at −28.9° C; another compound melting around 15° appears to be a hydrate of ammonium peroxide, $(NH_4)_2O_2 \cdot 2H_2O$. The eutectics are at −54.5°, 0.7% NH_3, and −33.4°, 12.5% NH_3. Careful redeterminations have confirmed that the melting point of the hydrate $H_2O_2 \cdot 2H_2O$ is −52°, not −50° as was sometimes claimed. The latent heat of fusion of that compound is estimated to be 3.9 kcal and the degree of dissociation on melting, about one-third.

Following various investigations, the phase equilibria are now fairly well established for the three binary systems NH_3–H_2O (1, 2), H_2O_2–H_2O (3), and NH_3–H_2O_2 (4, 5). For reference the three phase diagrams are illustrated in Fig. 1. No work has been reported yet on the corresponding three-component system, although formation of ternary

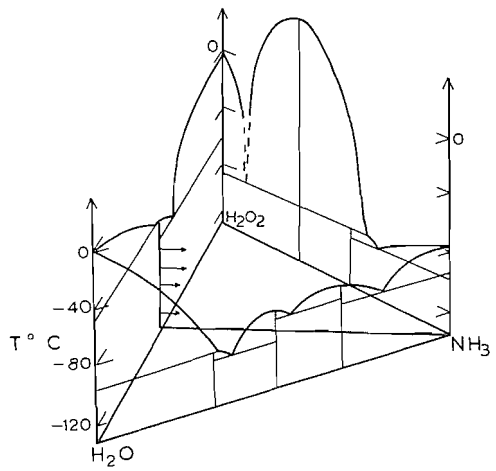

FIG. 1. Phase equilibria in the three binary systems formed between ammonia, hydrogen peroxide, and water. The present investigation was carried out along the plane marked by the arrows.

compounds was to be expected. Some evidence in that connection was detected in a recent spectroscopic study of crystalline ammonium hydroperoxide (6). Using the same thermal analysis apparatus as previously (7) the melting-point curve along the plane NH_3–$H_2O_2 \cdot 2H_2O$ was determined up to 20% ammonia.* Beyond that concentration the method used was impracticable due to the high partial pressure of ammonia over the solutions.

EXPERIMENTAL

The compound $H_2O_2 \cdot 2H_2O$ was selected as the starting point in preference to the

[1]*Manuscript received August 10, 1959.*
Contribution from the Department of Chemistry, Laval University, Québec, Que., with financial assistance from the National Research Council.
**Throughout this paper the compositions are given in weight%.*

Can. J. Chem. Downloaded from www.nrcresearchpress.com by 176.9.209.113 on 09/04/12
For personal use only.

hydrates of ammonia which melt at much lower temperatures; as for ammonium hydroperoxide, m.p. 25° (4), preliminary tests indicated that it decomposes badly when small amounts of water are added. On the contrary, a stable stock solution of hydrogen peroxide 48.6% in water is easily prepared. Anhydrous ammonia gas from a commercial cylinder was first dried over pellets of caustic potash and bubbled slowly through the solution of hydrogen peroxide in the freezing tube. The latter was cooled in ice to prevent decomposition of the peroxide by the heat of solution. A precision bore flow-rator was used to meter the ammonia gas, and the final composition of the solution was determined by titration of an aliquot with 0.1 *N* HCl using methyl orange as indicator; there was no noticeable interference from the hydrogen peroxide. Because of the strong tendency of the solutions to supercool, seeding was required in most cases.

DISCUSSION OF RESULTS

Some 20 melting-point determinations are listed in Table I and shown on the phase diagram in Fig. 2. The first compound encountered at 7.5% NH_3 separated out as a fine white powder that settled at the bottom of the freezing tube. Existence of a definite

TABLE I

Freezing points in the system NH_3–$H_2O_2 \cdot 2H_2O$

% NH_3	$T°$ C	% NH_3	$T°$ C
0.0	−52.2	7.5	−28.9
0.30	−53.1	8.93	−29.1
0.58	−54.0	10.4	−30.2
0.70	−54.3	11.3	−31.5
1.08	−51.8	12.5	−32.5
1.56	−48.5	13.7	−24.4
1.80	−47.4	14.6	−17.1
2.28	−45.6	17.0	− 9.7
3.1	−41.3	18.2	− 6.7
6.2	−29.9	19.8	− 4.0

compound with formula $NH_3 \cdot 3(H_2O_2 \cdot 2H_2O)$ was in a way unexpected since the corresponding binary compounds have not been found, either in the ammonia–water or in the ammonia – hydrogen peroxide systems. However, the latter two-component system has not been investigated thoroughly in the low ammonia concentration range. Maass and Hatcher (4) reported no measurement from 4.3 to 18% NH_3, and in the more recent work of Mironov (5) a single determination was carried out at 9.7% NH_3 which pointed to a much lower eutectic temperature, −93°, than at first thought, −47° (4). The difficulty here comes from the extreme viscosity and the turbidity of these solutions at low temperatures so that they cannot be made to crystallize cleanly. A couple of attempts yielded melting points of −17.6° and −4.2° respectively for solutions of 4.5% and 13.9% NH_3 in anhydrous hydrogen peroxide, in fair agreement with the data of Maass and Hatcher. Although that portion of the phase diagram remains unsettled it seems very doubtful, from the trend of the liquidus, if a compound $NH_3 \cdot 3H_2O_2$ exists.

The other ternary compound appeared when solutions containing over 15% NH_3 were cooled. In the melting-point apparatus it separated out as white granular crystals much denser than the liquid; when grown slowly from the appropriate solutions at around −10° it resembled a lump of sugar and was indefinitely stable at 0°. Several melting-point measurements gave only an approximate value. At 12° the crystals looked damp

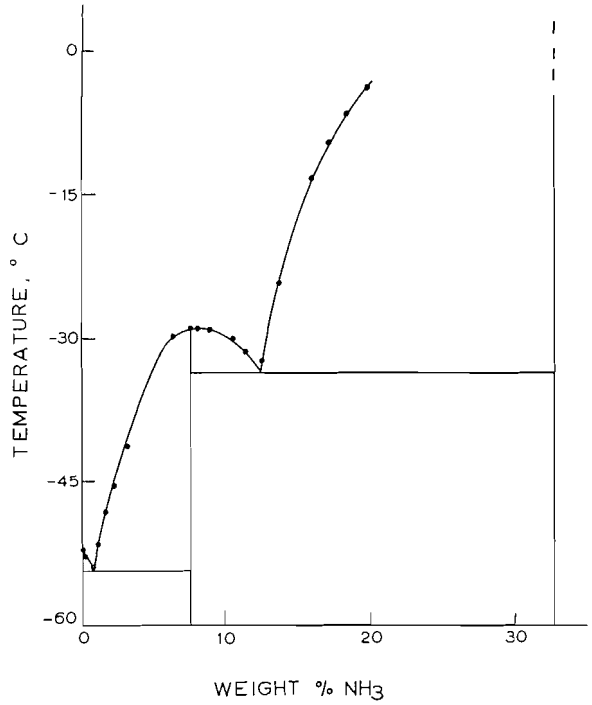

FIG. 2. Melting point curve for the system NH_3–$H_2O_2 \cdot 2H_2O$.

and seemed to wet the glass capillary; at that stage there was some gas evolution. Liquefaction was complete by 15°. The premelting was no doubt caused by some trapped mother liquor as shown by the chemical analysis: 31.5% NH_3 against the theoretical 32.7% for the ratio $2NH_3/H_2O_2 \cdot 2H_2O$.

The nature of the two ternary compounds is of some interest in relation to the various binary compounds of the three systems under consideration. The solid hydrates of ammonia have been proved by spectroscopy (8) and other physical methods (9, 10) to exist as molecular crystals; likewise the dihydrate of hydrogen peroxide is of the molecular type in the solid state (11). On the other hand, the 1:1 ammonia – hydrogen peroxide compound, although molecular in the molten state (12), is actually ionic when solid, NH_4O_2H (6, 13) due, probably, to the mild acid–base character of the two components. As for the meritectic 2:1 ammonia – hydrogen peroxide compound (Fig. 1) discovered recently by Mironov (5) it must have a molecular structure considering its low melting point, −93°, and narrow range of existence. Now, these two criteria point to the same conclusion as far as the first ternary compound $NH_3 \cdot 3H_2O_2 \cdot 6H_2O$ is concerned. For the other ternary compound, however, the apparently sharp melting curve and good thermal stability denote rather some degree of ionic character as would be expected in the hydrate of ammonium peroxide, $(NH_4)_2O_2 \cdot 2H_2O$. An attempt was made to establish that structure by infrared spectroscopy in the 3μ region, but due to difficulties in preparing a suitable sample of the solid, together with strong absorption from the water of crystallization, only vague indications could be found of the characteristic bands of the NH_4^+ ion. It is not clear why the presence of water of crystallization should favor an ionic structure while the anhydrous ammonium peroxide does not exist.

Can. J. Chem. Downloaded from www.nrcresearchpress.com by 176.9.209.113 on 09/04/12
For personal use only.

This time again a very careful redetermination of the melting point of the hydrate $H_2O_2 \cdot 2H_2O$ has confirmed the value $-52°$ found previously in this laboratory by two different methods (7, 14). The higher value $-50.2°$ reported at first (3), and again recently, by Mironov (15, 16) must be discarded for reasons already set forth (7). In addition, further results from the same author on the ammonia–water system (17) show the same systematic discrepancy of 2° with all other published data (2). Lastly, the heat of fusion of the hydrate $H_2O_2 \cdot 2H_2O$ was estimated to be 3.9 kcal from the average of a few calculations based either on its melting curve, after correction for the presence of the solute (H_2O_2) in the solid phase, or on the lowering of its melting point by methanol. Two determinations with the latter gave a $\Delta T_f = 1.42°$ for a 0.838 molal solution and 2.73° for a 1.58 molal solution of CH_3OH in $H_2O_2 \cdot 2H_2O$. By means of the van Laar equation (18) the degree of dissociation of the hydrate on melting is found to be about one-third.

RÉSUMÉ

L'analyse thermique du système NH_3–$H_2O_2 \cdot 2H_2O$ a prouvé l'existence de deux composés ternaires; l'un, $NH_3 \cdot 3H_2O_2 \cdot 6H_2O$ fond à $-28.8°$ C, l'autre, probablement un hydrate du peroxyde d'ammonium, $(NH_4)_2O_2 \cdot 2H_2O$, fond aux environs de 15°. Deux points eutectiques se trouvent à 0.7% de NH_3 et $-54.5°$, et à 12.5% de NH_3 et $-33.4°$. On a de nouveau vérifié que le point de fusion de l'hydrate $H_2O_2 \cdot 2H_2O$ est bien $-52°$ et non pas $-50°$. La chaleur de fusion de ce composé est d'environ 3.9 kcal et il se dissocie dans la proportion d'un tiers en fondant.

ACKNOWLEDGMENT

The preliminary measurements in this investigation were carried out by Mr. Robert Drouin.

REFERENCES

1. POSTMA, S. Rec. trav. chim. **39**, 516 (1920).
2. ROLLET, A. P. and VUILLARD, G. Compt. rend. **243**, 383 (1956).
3. SCHUMB, W. S., SATTERFIELD, C. N., and WENTWORTH, R. L. Hydrogen peroxide. Reinhold Publishing Corp., New York. 1955.
4. MAASS, O. and HATCHER, W. H. J. Am. Chem. Soc. **44**, 2472 (1922).
5. MIRONOV, K. E. Zhur. Neorg. Khim. **4**, 153 (1959).
6. KNOP, O. and GIGUÈRE, P. A. Can. J. Chem. **37**, 1794 (1959).
7. GIGUÈRE, P. A. and SECCO, E. A. Can. J. Chem. **32**, 553 (1954).
8. WALDRON, R. L. and HORNIG, D. J. J. Am. Chem. Soc. **75**, 6079 (1953).
9. SIEMONS, W. J. and TEMPLETON, D. H. Acta Cryst. **7**, 194 (1954).
10. GUTOWSKY, H. S. and FUJIWARA, S. J. Chem. Phys. **22**, 1782 (1954).
11. GIGUÈRE, P. A. and HARVEY, K. B. J. Mol. Spectroscopy, **3**, 36 (1959).
12. SIMON, A. and MARCHAND, M. Z. anorg. Chem. **262**, 191 (1950).
13. SIMON, A. and KRIEGSMAN, H. Naturwiss. **42**, 14 (1955).
14. FOLEY, W. T. and GIGUÈRE, P. A. Can. J. Chem. **29**, 123 (1951).
15. MIRONOV, K. E. and BERGMAN, A. G. Doklady Akad. Nauk S.S.S.R. **81**, 1081 (1951).
16. MIRONOV, K. E. Izvest. Sektora Fiz.-Khim. Anal., Inst. Obshcheĭ Neorg. Khim., Akad. Nauk S.S.S.R. **26**, 215 (1955).
17. MIRONOV, K. E. Zhur. Obshcheĭ Khim. **25**, 1081 (1955).
18. GLASSTONE, S. Text-book of physical chemistry. D. van Nostrand Company, Inc., New York. 1940. p. 748.

Can. J. Chem. Downloaded from www.nrcresearchpress.com by 176.9.209.113 on 09/04/12
For personal use only.

Can. J. Chem. Downloaded from www.nrcresearchpress.com by 176.9.209.113 on 09/04/12
For personal use only.

L'ARYLATION DES QUINONES PAR LES SELS DE DIAZONIUM

VI. SUR L'IDENTIFICATION DE L'ISOMÈRE OBTENU PAR L'ARYLATION DE LA TOLUQUINONE[1]

K. HOEGERLE[2] ET P. L'ÉCUYER

RÉSUMÉ

Les trois phényltoluquinones isomères ont été synthétisées à partir de diverses nitroluidines. Ces amines ont donné successivement, par condensation avec le benzène, des méthylnitrobiphényles, par réduction, des méthyl-aminobiphényles et finalement, par oxydation, la 2-méthyl-3-phényl-1,4-benzoquinone, la 2-méthyl-5-phényl-1,4-benzoquinone et la 2-méthyl-6-phényl-1,4-benzoquinone. La 2-méthyl-5-phényl-1,4-benzoquinone ainsi préparée et la phényltoluquinone obtenue par la réaction de la toluquinone avec le chlorure de benzène-diazonium sont identiques.

Une série de réactions analogues à partir de la 4-chloro-2-nitraniline a donné naissance successivement au 4-chloro-2-nitrobiphényle, au 4-chloro-2-aminobiphényle et à la 2-chloro-5-phényle-1,4-benzoquinone. Cette phénylchloroquinone est identique à l'isomère principal isolé de la réaction entre la chloroquinone et le chlorure de benzène-diazonium.

Dans un travail précédent (1) nous avons décrit la réaction de la toluquinone (I, X = CH_3) avec des sels de diazonium aromatiques en milieu tampon aqueux, réaction qui donne des monoaryltoluquinones (II, X = CH_3). Il était déjà connu que, suivant des conditions semblables, des monoaryl-1,4-benzoquinones (I, X = Ar) donnent naissance à des 2,5-bisaryl-1,4-benzoquinones (II, X = Ar) (2, 3, 4, 5) et que la chloroquinone (I, X = Cl) produit des monoarylchloroquinones (II, X = Cl) isomères (6).

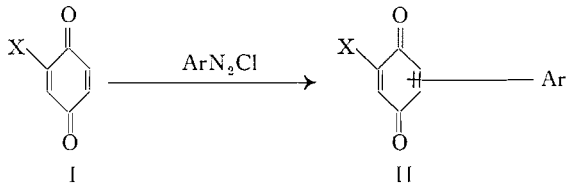

I II

X = CH_3, Cl ou Ar Ar: groupe aryle ou phényle

Toutefois, ces résultats ne permettaient pas de déduire d'une façon certaine lequel des trois isomères possibles, la 3-aryl-2-méthyl-1,4-benzoquinone (III), la 5-aryl-2-méthyl-1,4-benzoquinone (IV) ou la 6-aryl-2-méthyl-1,4-benzoquinone (V), est isolé du produit de la réaction de la toluquinone avec les sels de diazonium. Dans le but d'établir la constitution de cet isomère, nous avons synthétisé les trois phényltoluquinones XXI, XXII et XXIII par une suite de réactions non équivoques. Quant aux autres aryltoluquinones qui se forment au cours de l'arylation de la toluquinone avec les sels de diazonium préparés à partir de diverses anilines substituées, il est fort probable qu'elles ont la même structure que la phényltoluquinone (II, X = CH_3, Ar = ϕ) obtenue par la phénylation de la toluquinone (1).

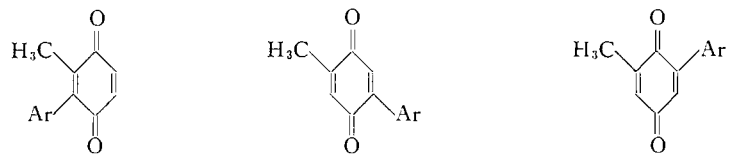

III IV V

[1]*Manuscrit reçu le 10 août, 1959.*
Contribution du Département de Chimie, Faculté des Sciences, Université Laval, Québec, Qué.
[2]*Bénéficiaire d'une bourse postdoctorale du Conseil National de Recherches du Canada.*

Can. J. Chem. Downloaded from www.nrcresearchpress.com by 176.9.209.113 on 09/04/12
For personal use only.

En suivant la modification d'Ellis *et al.* (7), apportée à la réaction de Gomberg (8), nous avons fait agir le benzène sur le chlorure de diazonium provenant de la 3-méthyl-5-nitraniline (VI), de la 4-méthyl-3-nitraniline (VII), de la 4-méthyl-2-nitraniline (VIII), de la 2-méthyl-3-nitraniline (IX) et de la 6-méthyl-2-nitraniline (X). Ainsi nous avons obtenu respectivement le 3-méthyl-5-nitrobiphényle (XI), le 4-méthyl-3-nitrobiphényle (XII), le 4-méthyl-2-nitrobiphényle (XIII) et le 2-méthyl-3-nitrobiphényle (XIV).

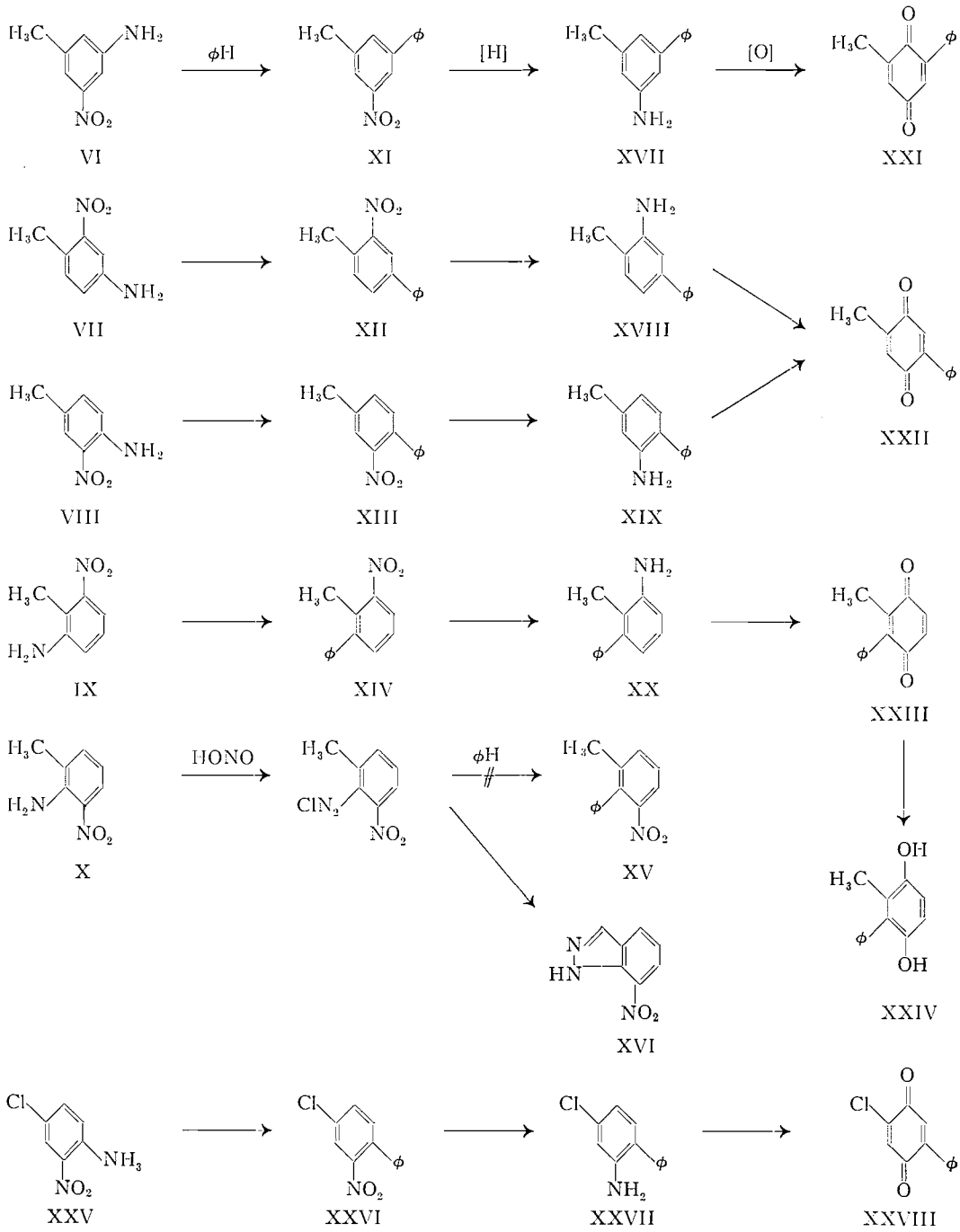

Toutefois, exécutée avec la 6-méthyl-2-nitraniline (X), la réaction a conduit à la formation du 7-nitroindazole (XVI), (9, 10) au lieu du 6-méthyl-2-nitrobiphényle (XV).

La réduction catalytique des méthylnitrobiphényles dans l'éthanol en présence de palladium a donné avec de bons rendements le 3-méthyl-5-aminobiphényle (XVII), le 4-méthyl-3-aminobiphényle (XVIII), le 4-méthyl-2-aminobiphényle (XIX) et le 2-méthyl-3-aminobiphényle (XX) correspondants.

L'oxydation de ces méthyl-aminobiphényles par le peroxyde de plomb dans l'acide sulfurique 50% selon la méthode de Willstätter et Dorogi (11) a permis d'obtenir les trois phényltoluquinones isomères désirées, soient la 2-méthyl-6-phényl-1,4-benzoquinone (XXI), la 2-méthyl-5-phényl-1,4-benzoquinone (XXII) et la 2-méthyl-3-phényl-1,4-benzoquinone (XXIII).

La 2-méthyl-5-phényl-1,4-benzoquinone (XXII) ainsi obtenue et la phényltoluquinone isolée du produit de la réaction de la toluquinone avec le chlorure de benzène-diazonium se révélèrent identiques par leur point de fusion, le point de fusion mixte et leur spectre infrarouge (Fig. 1).

C'est aussi fort probablement l'isomère correspondant, c'est-à-dire la 2-méthyl-5-aryl-1,4-benzoquinone (IV), que l'on isole comme produit principal à la suite de la réaction entre la toluquinone et le chlorure de diazonium obtenu d'une aniline substituée (1).

Nous avons observé que la 2-méthyl-3-phényl-1,4-benzoquinone (XXIII) est instable. Lorsque la quinone est exposée à la lumière solaire, soit à l'état solide, soit en solution dans l'eau, l'acétone ou l'éther, elle se transforme assez rapidement en l'hydroquinone (XXIV) incolore correspondante, comme le démontre l'analyse. Fieser *et al.* (12) mentionnent une observation analogue faite au cours de la purification de la 2,3-diméthyl-1,4-benzoquinone. D'après ces auteurs, cette substance, lorsqu'elle est exposée au soleil, se décomposerait en un polymère incolore; mais il nous semble probable qu'elle se transforme plutôt en 2,3-diméthyl-hydroquinone.

Au cours de l'arylation de la toluquinone (1) nous avons constaté à plusieurs reprises l'apparition d'un film blanc à la surface d'échantillons d'aryltoluquinones conservés à la lumière du jour. Ces aryltoluquinones avaient été purifiées au préalable, mais n'avaient pas encore un point de fusion constant. Ceci nous fait supposer la présence de l'isomère 2-méthyl-3-aryle dans le produit de la réaction.

Une série de réactions analogue à celle qui a servi à la synthèse des phényltoluquinones a été exécutée à partir de la 4-chloro-2-nitraniline (XXV). Elle a donné successivement, par condensation avec le benzène, le 4-chloro-2-nitrobiphényle (XXVI), par réduction avec le fer activé (13), le 4-chloro-2-aminobiphényle (XXVII) et, finalement, par oxydation avec du peroxyde de plomb, la 2-chloro-5-phényl-1,4-benzoquinone (XXVIII). Le point de fusion de cette phénylchloroquinone et celui de produit principal obtenu de la réaction entre la chloroquinone et le chlorure de benzène-diazonium que l'on croyait être la 2-chloro-6-phényl-1,4-benzoquinone (6) est le même. Le point de fusion mixte et les spectres infrarouges (Fig. 2) confirment l'identité des deux composés.

La préparation de la 2-méthyl-3-nitraniline (IX) à partir du 1,3,5-trinitrotoluène selon la méthode décrite dans la littérature (14) n'a donné que de mauvais résultats. En particulier, il a été impossible de réaliser le rendement mentionné pour la réduction du trinitrotoluène en 4-méthyl-3,5-dinitraniline. Pour cette raison nous donnons dans la partie expérimentale une description améliorée de sa synthèse par les intermédiaires 4-méthyl-3,5-dinitraniline et 2,6-dinitrotoluène.

Can. J. Chem. Downloaded from www.nrcresearchpress.com by 176.9.209.113 on 09/04/12
For personal use only.

Can. J. Chem. Downloaded from www.nrcresearchpress.com by 176.9.209.113 on 09/04/12
For personal use only.

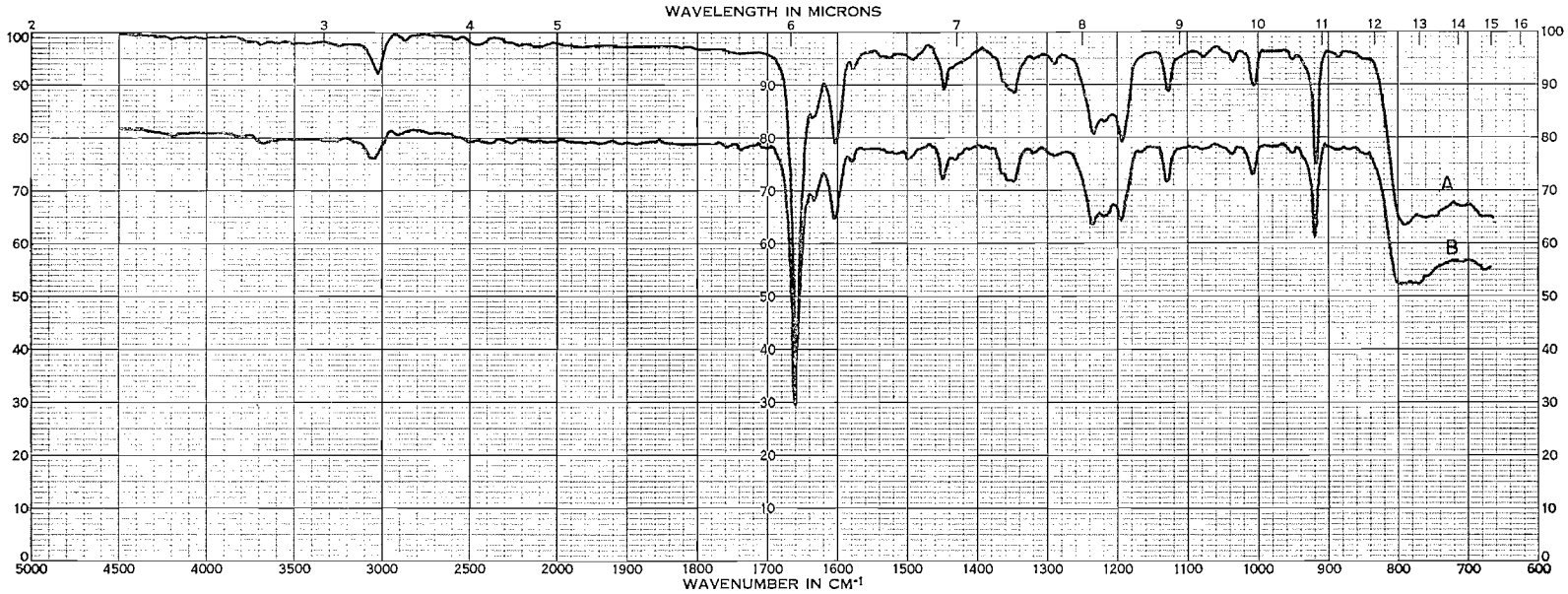

FIG. 1. Spectres infrarouges. (A) 2-Méthyl-5-phényl-1,4-benzoquinone obtenue par phénylation de la toluquinone par le chlorure de benzène-diazonium. (B) 2-Méthyl-5-phényl-1,4-benzoquinone obtenue par l'oxydation du 4-méthyl-2-amino- ou du 4-méthyl-3-amino-biphényle.

Can. J. Chem. Downloaded from www.nrcresearchpress.com by 176.9.209.113 on 09/04/12
For personal use only.

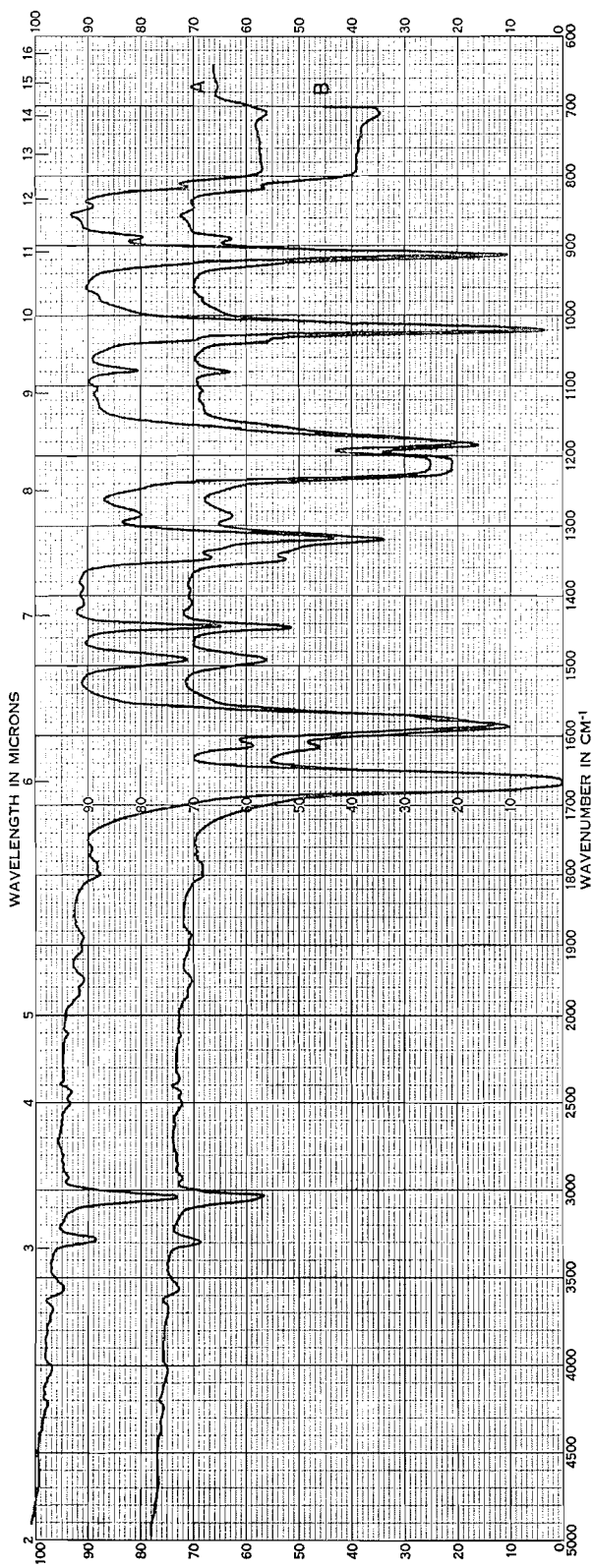

FIG. 2. Spectres infrarouges. (A) 2-Chloro-5-phényl-1,4-benzoquinone obtenue par phénylation de la chloroquinone par le chlorure de benzène-diazonium. (B) 2-Chloro-5-phényl-1,4-benzoquinone obtenue par l'oxydation du 4-chloro-2-aminobiphényle.

Can. J. Chem. Downloaded from www.nrcresearchpress.com by 176.9.209.113 on 09/04/12
For personal use only.

PARTIE EXPÉRIMENTALE[3]

3,5-Dinitro-4-méthylaniline

La réduction du 2,4,6-trinitrotoluène (410 g) est exécutée selon la description donnée par Lowe (15) jusqu'à l'essoration du produit brut. Celui-ci est alors agité vigoureusement avec 2000 ml d'acide chlorhydrique 10% à environ 75° et la solution est filtrée à chaud. On extrait le solide deux autres fois de la même façon et les filtrats réunis sont ensuite versés dans environ six fois leur quantité d'eau froide. L'amine brute se sépare alors sous la forme d'un solide jaune de p.f. 135–165°. Celui-ci est dissous à chaud dans de l'éthanol et la solution bouillie avec du noir animal, filtrée et diluée avec un cinquième de son volume d'eau. La 4-méthyl-3,5-dinitraniline (rendement, 76 g; 78.6% de la théorie) cristallise en aiguilles rouges de p.f. 169–171° (p.f. lit. 171–172° (14)).

2,6-Dinitrotoluène

À de la 4-méthyl-3,5-dinitraniline (59.1 g) triturée avec 450 ml d'acide chlorhydrique concentré, on ajoute 130 ml d'eau et 120 g de glace et on diazote à 0° avec 21.6 g de nitrite de sodium solide (½ heure). Dans la solution bien agitée mécaniquement et refroidie à 0° (bain réfrigérant) on laisse dégoutter une solution froide (400 ml) d'acide hypophosreux à 30%. Après l'addition de 150 ml de cette solution un fort dégagement d'azote commence à se produire. Une fois l'addition de l'acide hypophosreux terminée on continue d'agiter pendant 20 heures à la température ambiante. Le précipité rouge-brunâtre formé est alors essoré, séché, dissous dans du benzène et chromatographié sur 300 g d'alumine. Par élution avec le même solvant (500 ml), on recueille 41 g (75% de la théorie) de 2,6-dinitrotoluène de p.f. 66° (lit. 65–66° (14)).

2-Méthyl-3-nitraniline (IX)

Tout en faisant barboter un courant d'acide sulfhydrique gazeux dans une solution de 2,6-dinitrotoluène (59.72 g) dans de l'éthanol (200 ml) bouillie à reflux, on introduit lentement une solution de sulfure d'ammonium (50 ml d'ammoniaque concentrée fraîchement saturée d'acide sulfhydrique). On continue de faire barboter l'acide sulfhydrique pendant 1½ heure, à la température d'ébullition, on filtre ensuite le soufre précipité, le lave deux fois à l'alcool et évapore le filtrat à siccité. Le résidu est extrait deux fois à chaud avec 300 ml d'acide chlorhydrique dilué (1:1). Les extraits réunis sont traités à l'ammoniaque concentrée jusqu'à l'apparition d'un précipité brun. On filtre la solution et la neutralise à l'ammoniaque (pH = 7). On obtient 42.7 g (86% de la théorie) de 2-méthyl-3-nitraniline de p.f. 86–88° (lit. 90–91° (14)).

2-Méthyl-3-nitrobiphényle (XIV)

On triture de la 2-méthyl-3-nitraniline (42.7 g) avec 150 ml d'acide chlorhydrique concentré, on ajoute à cette pâte 80 g de glace et, tout en agitant vigoureusement et en maintenant le mélange à environ 3–4° (bain réfrigérant), on diazote avec 20.5 g de nitrite de sodium solide. À la solution diazoïque filtrée on ajoute 800 ml de benzène et une solution de 200 g d'acétate de sodium trihydraté dans 700 ml d'eau et on continue d'agiter pendant 2 heures à 5° et durant 20 heures à la température ambiante. Ensuite, on chauffe à 70° l'émulsion formée, décante la couche benzénique, extrait la phase aqueuse au benzène chaud et réunit les extraits benzéniques. Ceux-ci sont lavés successivement à la soude 2 *N*, à l'eau, à l'acide chlorhydrique 2 *N* et finalement à l'eau. On évapore le benzène et distille l'huile rouge résiduelle (12.3 g). On recueille ainsi, 4.0 g (12% de la théorie) d'une huile jaune de p.é. 116–118°/0.0001 mm. Le 2-méthyl-3-nitrobiphényle cristallise dans le méthanol en lamelles jaunes de p.f. 72.5–73°. Calculé pour $C_{13}H_{11}O_2N$: C, 73.22%; H, 5.20%; N, 6.57%. Trouvé: C, 73.26%; H, 5.33%; N, 6.57%.

[3]*Les points de fusion (p.f.) ont été pris en tubes capillaires et ne sont, ainsi que les points d'ébullition (p.é.), pas corrigés. Les microanalyses ont été effectuées par M. W. Manser, Zürich, Suisse.*

4-Méthyl-2-nitrobiphényle (XIII)

À 38.04 g de 4-méthyl-2-nitraniline (16) triturée avec 80 ml d'acide chlorhydrique concentré, on ajoute 45 g de glace et diazote à 0–5° avec une solution de 18 g de nitrite de sodium dans 50 ml d'eau. On filtre la solution diazoïque, ajoute 550 ml de benzène et 80 g d'acétate de sodium trihydraté dissous dans 200 ml d'eau et agite pendant 3 heures à 5–10° et 45 heures à la température ambiante. On brise l'émulsion formée en la filtrant dans un entonnoir en verre poreux. La phase benzénique est séparée et lavée successivement à la soude 2 *N*, à l'eau, à l'acide chlorhydrique 2 *N* et à l'eau. En évaporant le solvant et en distillant le résidu on obtient 23.47 g (43.5% de la théorie) d'une huile jaune de p.é. 126–128°/0.0003 mm. (Ritchie (17) donne le p.é. 207–209°/28 mm.)

4-Méthyl-3-nitrobiphényle (XII)

De la 4-méthyl-3-nitraniline (34.25 g) est diazotée et condensée avec le benzène comme il est décrit précédemment pour le 2-méthyl-3-nitrobiphényle. Par distillation du produit brut on obtient 10.3 g (21.5% de la théorie) d'une huile de p.é. 132–134°/0.0003 mm. Le 4-méthyl-3-nitrobiphényle forme dans l'éthanol des cristaux jaunâtres de p.f. 63.5–64.5°. Calculé pour $C_{13}H_{11}O_2N$: C, 73.22%; H, 5.20%; N, 6.57%. Trouvé: C, 73.17%; H, 5.30%; N, 6.66%. Cette substance a déjà été préparée par Wessely *et al.* (18) qui donnent le p.f. 61–62°, mais ni analyse, ni rendement.

3-Méthyl-5-nitrobiphényle (XI)

De la 4-méthyl-2,6-dinitraniline (19) est désaminée dans un mélange alcool – acide sulfurique (1:1) avec du nitrite de sodium solide. Le 3,5-dinitrotoluène est isolé et partiellement réduit selon la méthode utilisée précédemment pour la 2-méthyl-3-nitraniline. On diazote la 5-méthyl-3-nitraniline (23 g) ainsi obtenue et condense son sel de diazonium avec le benzène (500 ml) en présence de 100 g d'acétate de sodium cristallisé. Après 24 heures d'agitation la réaction est terminée. On isole le produit comme il est décrit précédemment dans le cas du 4-méthyl-2-nitrobiphényle et recueille 17 g (54% de la théorie) d'une huile jaune pâle de p.é. 140–143°/0.002 mm. Dans le méthanol le 3-méthyl-5-nitrobiphényle donne des cristaux jaunes pâles de p.f. 85.5–86°. Calculé pour $C_{13}H_{11}O_2N$: C, 73.22%; H, 5.20%; N, 6.57%. Trouvé: C, 73.22%; H, 5.19%; N, 6.62%.

4-Chloro-2-nitrobiphényle (XXVI)

De la 4-chloro-2-nitraniline (52 g) est diazotée selon Fierz-David (20, p. 236). On filtre la solution diazoïque et lui ajoute 750 ml de benzène. Dans ce mélange bien agité et refroidi à 5°, on introduit assez rapidement 100 g d'acétate de sodium trihydraté et agite 2 heures à cette température et 12 heures à la température ambiante. Le produit de la réaction est isolé comme précédemment et distillé. On recueille, à 135–137°/0.0002 mm, 32.78 g (44% de la théorie) de 4-chloro-2-nitrobiphényle, qui cristallise dans le méthanol sous forme de prismes de p.f. 52–53°. Calculé pour $C_{12}H_8O_2NCl$: C, 61.68%; H, 3.45%; N, 6.00%. Trouvé: C, 61.71%; H, 3.65%; N, 6.19%.

7-Nitroindazole (XVI)

De la 2-méthyl-6-nitraniline (21) (56.8 g) est diazotée et condensée avec le benzène tel que décrit précédemment dans le cas du 4-méthyl-2-nitrobiphényle. Après 45 heures d'agitation à la température ambiante, on porte le mélange à 70–80° pour briser l'émulsion et dissoudre le précipité formé. La couche benzénique est décantée et la phase aqueuse extraite une autre fois au benzène chaud. Les extraits réunis sont lavés à la soude et à l'acide, et ensuite concentrés à 200 ml. De cette solution on obtient 14.7 g d'une substance qui, recristallisée dans le benzène et dans le méthanol (noir animal), donne 13 g de

Can. J. Chem. Downloaded from www.nrcresearchpress.com by 176.9.209.113 on 09/04/12
For personal use only.

cristaux jaunes pâles de p.f. 185–187°. L'analyse démontre qu'il ne s'agit pas du 2-méthyl-6-nitrobiphényle attendu, mais du 7-nitroindazole (p.f. lit. 186.5–187.5° (10)). Calculé pour: $C_7H_5O_2N_3$: C, 51.54%; H, 3.09%; N, 25.76%. Trouvé: C, 51.57%; H, 2.84%; N, 25.51%.

4-Méthyl-2-aminobiphényle (XIX)

Du 4-méthyl-2-nitrobiphényle (26.10 g), dissous dans 50 ml d'éthanol, est réduit catalytiquement en présence de 1 g de chlorure de palladium. La réduction terminée, on essore le catalyseur et évapore le solvant sous pression réduite. Le résidu est repris par de l'éther et traité à l'acide chlorhydrique gazeux. Le p.f. du chlorhydrate ainsi obtenu (25.5 g) est 196–198°, et celui du picrate cristallisé dans l'éthanol est 159–161° (lit. 161° (17)).

Le dérivé acétylé, préparé à partir de 200 mg de la base et de 1 ml d'anhydride acétique et cristallisé dans le méthanol, fond à 145.5–146.5°. Calculé pour $C_{15}H_{15}ON$: C, 79.97%; H, 6.71%; N, 6.22%. Trouvé: C, 79.96%; H, 6.77%; N, 6.24%.

4-Méthyl-3-aminobiphényle (XVIII)

Du 4-méthyl-3-nitrobiphényle (10.30 g) est réduit et l'amine formée isolée comme il est décrit précédemment. On obtient 10.6 g (100% de la théorie) de chlorhydrate de 4-méthyl-3-aminobiphényle. En chauffant ce sel, la base se sublime en belles lamelles incolores de p.f. 59–60° (lit. 54–55° (18)).

3-Méthyl-5-aminobiphényle (XVII)

Du 3-méthyl-5-nitrobiphényle (16.8 g) est réduit en présence de palladium et la base formée est isolée à l'état de sulfate (14 g) dans de l'éther anhydre. Le sulfate fond à 196–200°, le chlorhydrate à 220–223° et la base, après cristallisation dans l'éther de pétrole, à 79–82° (lit. 80–82° (22)). Calculé pour $C_{13}H_{13}N$: C, 85.20%; H, 7.15%; N, 5.64%. Trouvé C, 85.14%; H, 7.17%; N, 7.69%.

4-Chloro-2-aminobiphényle (XXVII)

De la poudre de fer (passée au tamis de 40 mailles) (150 g) est activée (13) et ajoutée à une solution de 15 g de 4-chloro-2-nitrobiphényle dans 500 ml de benzène. Le mélange est agité mécaniquement et bouilli à reflux. Au cours de 7 heures on ajoute en petites portions 60 ml d'eau et continue de chauffer et d'agiter pendant 12 heures. La solution est ensuite filtrée et évaporée à siccité. L'huile résiduelle (11.73 g) (90% de la théorie) distille à 105–106°/0.0002 mm. Calculé pour $C_{12}H_{10}NCl$: C, 70.73%; H, 4.95%; N, 6.88%; Cl, 17.41%. Trouvé: C, 70.52%; H, 5.06%; N, 7.00%; Cl, 17.54%.

2-Méthyl-3-phényl-1,4-benzoquinone (XXIII)

Du 2-méthyl-3-nitrobiphényle (3.25 g) est dissous dans 50 ml d'éthanol et réduit catalytiquement à la pression atmosphérique en présence de 300 mg d'oxyde de platine. L'hydrogénation terminée, le catalyseur est éliminé par filtration et la solution de l'amine évaporée à sec. On reprend le résidue à l'éther et ajoute quelques millilitres d'un mélange d'acide sulfurique concentré et d'éthanol (1:1). Le sulfate ainsi obtenu est oxydé sans aucune purification. On l'agite pendant 40 heures à 0° avec 12 g de peroxyde de plomb dans 200 ml d'acide sulfurique à 50%. On dilue ensuite le mélange réactionnel avec deux fois sa quantité d'eau et on le filtre. Le résidu et le filtrat sont épuisés à l'éther et les extraits réunis séchés sur du sulfate de sodium anhydre et évaporés. On recueille ainsi 600 mg de quinone qui, cristallisée plusieurs fois dans de l'acétone aqueux (1:1) et ensuite dans de l'éther de pétrole, fond à 79–81°. Calculé pour $C_{13}H_{10}O_2$: C, 78.77%; H, 5.09%; O, 16.14%. Trouvé: C, 78.57%; H, 5.05%; O, 16.42%.

Can. J. Chem. Downloaded from www.nrcresearchpress.com by 176.9.209.113 on 09/04/12
For personal use only.

2-Méthyl-3-phénylhydroquinone (XXIV)

Une solution aqueuse de la 2-méthyl-3-phényl-1,4-benzoquinone (XXIII) est exposée à la lumière solaire. En quelques jours la solution se décolore et l'hydroquinone correspondante cristallise en longues aiguilles incolores de p.f. 133–134°. Calculé pour $C_{13}H_{12}O_2$: C, 77.98%; H, 6.04%. Trouvé: C, 77.91%; H, 6.04%.

2-Méthyl-5-phényl-1,4-benzoquinone (XXII)

(*A*) Du 4-méthyl-2-aminobiphényle (5.83 g) est agité pendant 55 heures à 0–5° avec 32 g de peroxyde de plomb dans 150 ml d'acide sulfurique à 50%. On extrait la phase solide et liquide séparément au benzène, réunit les extrait et les lave une fois à l'eau. Une fois le solvant évaporé, on distille le résidu à la vapeur d'eau et épuise le distillat à l'éther. La solution éthérée fournit 1.5 g de quinone qui, après plusieurs cristallisations dans du méthanol (noir animal), a le p.f. 111–112°. Calculé pour $C_{13}H_{10}O_2$: C, 78.77%; H, 5.09%. Trouvé: C, 78.78%; H, 5.03%. Le p.f. mixte de cette substance avec le produit de p.f. 109–111° obtenu par phénylation de la toluquinone (1) est 109–112°.

(*B*) Comme précédemment, on oxyde le 4-méthyl-3-aminobiphényle (5.61 g) pendant 24 heures avec 31 g de peroxyde de plomb dans 150 ml d'acide sulfurique à 50%. Le rendement de la quinone brute est 5.27 g (86% de la théorie). La substance, cristallisée quelques fois dans un mélange acétone–eau (1:1) (noir animal) et ensuite dans du méthanol, fond à 108–111°. Les p.f. mixtes de cette substance avec le produit obtenu par phénylation de la toluquinone (1) et par la méthode (*A*), ne sont pas abaissés. Les spectres infrarouges (solution à 10% dans le chloroforme) sont également identiques.

2-Méthyl-6-phényl-1,4-benzoquinone (XXI)

Du sulfate de 3-méthyl-5-aminobiphényle (8 g) est oxydé par 32 g de peroxyde de plomb dans 300 ml d'acide sulfurique à 50% et le produit de la réaction est isolé comme il est décrit précédemment. Le produit pur (0.5 g) cristallise dans le méthanol en aiguilles jaune-orange de p.f. 57–58°. Calculé pour $C_{13}H_{10}O_2$: C, 78.77%; H, 5.09%. Trouvé: C, 78.75%; H, 5.05%.

2-Chloro-5-phényl-1,4-benzoquinone (XXVIII)

L'oxydation du sulfate de 4-chloro-2-aminobiphényle (10 g) par 40 g de peroxyde de plomb dans 300 ml d'acide sulfurique à 50% selon le procédé habituel donne 7.1 g de quinone brute. Un échantillon de ce produit, distillé à la vapeur d'eau et cristallisé dans un mélange acétone–méthanol, donne la 2-chloro-5-phényl-1,4-benzoquinone pure de p.f. 130–131.5°. Calculé pour $C_{12}H_7O_2Cl$: C, 65.92%; H, 3.23%; Cl, 16.22%. Trouvé: C, 65.66%; H, 3.19%; Cl, 16.18%. Le p.f. mixte de cette substance et du produit principal isolé de la réaction entre la chloro-1,4-benzoquinone et le chlorure de benzène-diazonium (6) n'est pas abaissé, et les spectres infrarouges des deux (solution à 10% dans le chloroforme) sont de plus identiques.

REMERCIEMENTS

Nous remercions le Conseil National de Recherches du Canada pour une bourse d'études postdoctorales qu'il a accordée à l'un de nous (K. H.).

BIBLIOGRAPHIE

1. Brassard, P. et L'Écuyer, P. Can. J. Chem. **37**, 1505 (1959).
2. Günther, F. Brevet allemand, 508,395 (1924); Frdl. **17**, 557 (1930).
3. Kvalnes, D. E. J. Am. Chem. Soc. **56**, 2478 (1934).
4. Schimmelschmidt, K. Ann. **566**, 184 (1950).
5. Brassard, P. et L'Écuyer, P. Can. J. Chem. **36**, 709 (1958).

Can. J. Chem. Downloaded from www.nrcresearchpress.com by 176.9.209.113 on 09/04/12
For personal use only.

6. BRASSARD, P. et L'ÉCUYER, P. Can. J. Chem. **36**, 814 (1958).
7. ELLIS, J., HAWORTH, J. W. et HEY, D. H. J. Chem. Soc. 1284 (1940).
8. GOMBERG, M. et BACHMANN, E. W. J. Am. Chem. Soc. **46**, 2339 (1924); GOMBERG, M. et PERNERT, J. C. J. Am. Chem. Soc. **48**, 1372 (1926).
9. NOELTING, E. Ber. **37**, 2558, 2575 (1904).
10. AUWERS, K. et SCHWEGLER, K. Ber. **52**, 1225 (1920).
11. WILLSTÄTTER, R. et DOROGI, S. Ber. **42**, 2147 (1909).
12. FIESER, L. F. et ARDAO, M. I. J. Am. Chem. Soc. **78**, 774 (1956).
13. HAZLET, S. E. et DORNFELD, C. A. J. Am. Chem. Soc. **66**, 1781 (1944).
14. FOSTER, R. J., ROSICKY, F. G. et NIEMANN, C. J. Am. Chem. Soc. **72**, 3959 (1950).
15. LOWE, E. W. Brevet U.S. 2,699,584; Chem. Abstr. **49**, 3246 (1955).
16. NOYES, W. A. Am. Chem. J. **10**, 472 (1888).
17. RITCHIE, E. J. Proc. Roy. Soc. New South Wales, **78**, 168 (1945); Chem. Abstr. **40**, 8805 (1945).
18. WESSELY, F., HOLZER, C. et VILCOCK, H. Monatsh. Chem. **83**, 1253 (1952).
19. BEILSTEIN, F. et KUHLBERG, A. Ann. **158**, 335 (1871).
20. FIERZ-DAVID, H. E. et BLANGEY, L. Grundlagende Operationen der Farbenchemie, Springer-Verlag, Wien. 1946.
21. ORG. SYNTHESES, **35**, 3 (1955).
22. BERINGER, F. M. et UGELOW, J. J. Am. Chem. Soc. **75**, 2635 (1953).

Can. J. Chem. Downloaded from www.nrcresearchpress.com by 176.9.209.113 on 09/04/12
For personal use only.

Can. J. Chem. Downloaded from www.nrcresearchpress.com by 176.9.209.113 on 09/04/12
For personal use only.

ON THE COUPLING BETWEEN H^1 AND F^{19} NUCLEI IN *p*-FLUOROTOLUENE. II[1]

T. SCHAEFER[2] AND W. G. SCHNEIDER

ABSTRACT

By making use of specific solvent interaction effects it has been found possible to vary the relative chemical shift between ortho and meta protons in *p*-fluorotoluene continuously from about 0.2 p.p.m. to zero. The values of the HF coupling constants were found to be $J_{ortho}^{HF} = 8.7$ c/s and $J_{meta}^{HF} = 5.8$ c/s. As the internal chemical shift goes to zero the ring proton spectrum collapses to two lines with a separation of 7.3 c/s. This splitting is interpreted as equal to $\frac{1}{2}(J_o^{HF} + J_m^{HF})$. Corresponding changes observed in the CH_3 proton spectrum are consistent with this interpretation.

INTRODUCTION

The proton and fluorine high resolution nuclear magnetic resonance spectra of liquid *p*-fluorotoluene at 29.92 Mc/s (for H^1) have recently been interpreted on the basis of a negligible internal chemical shift in the ring proton spectrum and with $J_m^{HF} = J_o^{HF} = 7.4$ c/s (a better value is 7.3 c/s)* (1). The latter condition was sufficient to explain the distribution and intensities of the lines. In addition, there was a coupling of about 0.9 c/s between the methyl protons and the fluorine.

It is known that normally $J_m^{HF} < J_o^{HF}$. In *p*-fluoroaniline, for instance, $J_m^{HF} = 5.1$ c/s and $J_o^{HF} = 8.6$ c/s (2). If one considers a three-spin $\frac{1}{2}$ system such that two of the spins see a field H_2 but are unequally coupled to the third at field H_1 one notes that, under certain circumstances, the *splitting* of the lines is equal to an *average* of the two coupling constants (this does not mean that the coupling between the nuclei is averaged). An approximate example is the ring proton spectrum of 2,5-dichloronitrobenzene (3). The question arises whether the spacing of 7.3 c/s between the two lines of the ring proton spectrum of *p*-fluorotoluene might not also be an average of J_m^{HF} and J_o^{HF}.

If one could change the internal chemical shift in the ring continuously in some way from zero to a relatively large value, some information on this matter should be obtainable. This was found possible by making use of specific solvent effects (4). Dilution of *p*-fluorotoluene in acetone shows a large increase in the relative shift between the protons ortho and meta to the fluorine atom, while dilution in benzene shows a progressive decrease of the shift to zero. It is the purpose of this work to show (*a*) that the values of the proton–fluorine coupling constants are $J_m^{HF} = 5.8$ c/s and $J_o^{HF} = 8.7$ c/s, and (*b*) that in the limit of zero internal chemical shift the line separation of the ring proton spectrum is equal to $\frac{1}{2}(J_m^{HF} + J_o^{HF}) = 7.3$ c/s. Inherent in the analysis is the assumption that solvent effects, while changing the relative chemical shifts, do not perceptibly alter the spin-coupling constants. This assumption is consistent with experimental observations to date.

[1]*Manuscript received August 4, 1959.*
Contribution from Division of Pure Chemistry, National Research Council, Ottawa, Canada.
Issued as N.R.C. No. 5409.
[2]*Research associate, summer 1959. Present address: Chemistry Department, University of Manitoba, Winnipeg, Manitoba.*
J_m^{HF} and J_o^{HF} refer to the proton–fluorine coupling constant when the proton is respectively meta and ortho relative to the fluorine atom.

Can. J. Chem. Downloaded from www.nrcresearchpress.com by 176.9.209.113 on 09/04/12
For personal use only.

EXPERIMENTAL

The methyl and ring proton spectra of *p*-fluorotoluene in the pure liquid and at various dilutions in acetone and benzene were measured at 60 Mc/s on a Varian High Resolution NMR spectrometer. The line separations were measured by the side-band technique. The concentrations by volume were approximate since the solvent was used only to change the ring proton shift.

RESULTS

The ring proton and methyl proton spectra of *p*-fluorotoluene at the various concentrations in acetone and benzene are shown in Figs. 1 and 2. The caption 1:35 benzene, for instance, denotes a solution consisting of 1 volume of *p*-fluorotoluene dissolved in 35 volumes of benzene. The relevant line separations are given in c/s. The main field H_0 increases from left to right.

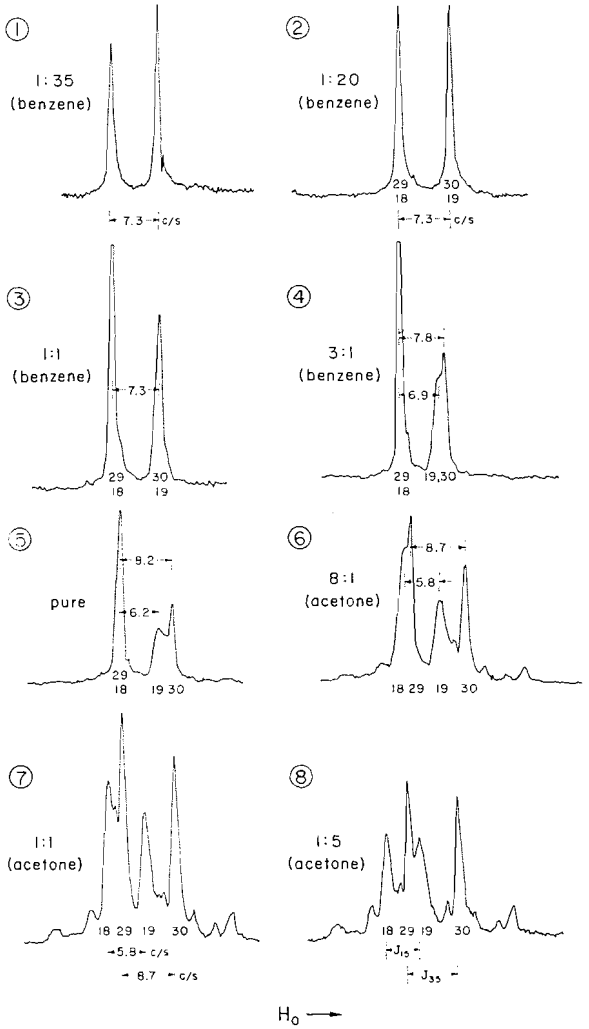

FIG. 1. Ring proton resonance spectra (at 60 Mc/s) of *p*-fluorotoluene and of *p*-fluorotoluene at various concentrations in benzene and acetone. At a concentration of 1:20 in benzene the relative chemical shift of ortho and meta protons is zero.

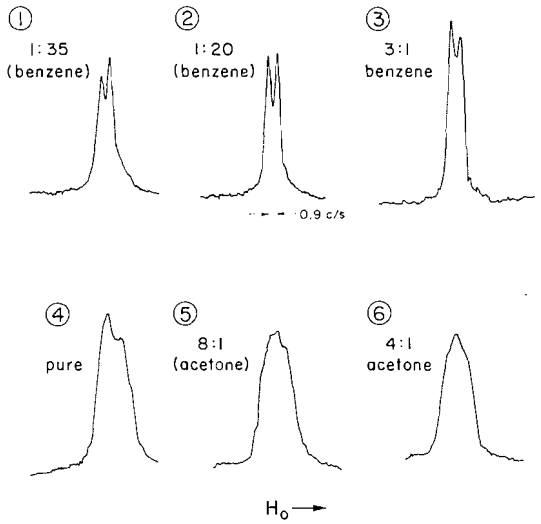

FIG. 2. Proton resonance spectra (at 60 Mc/s) of the methyl group of *p*-fluorotoluene at various concentrations in benzene and acetone.

DISCUSSION

(*a*) *Analytics*

As in reference 1, the following labelling and notation is employed.

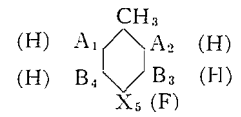

I

for $\sigma_B > \sigma_A$
$J_{15} = J_m^{HF}$, $J_{35} = J_o^{HF}$
$J_{13} = J_p^{HH}$, $J_{23} = J_o^{HH}$

The ring proton spectrum at, say, 1:1 of acetone (Fig. 1.7) is the A_2B_2 part of an A_2B_2X spectrum (5). This case with the screening constants $\sigma_A > \sigma_B$ has been fully discussed for *p*-fluoroaniline (2). The case $\sigma_A = \sigma_B$ (i.e. $A_2A_2'X$) has been discussed for pure *p*-fluorotoluene measured at 29.92 Mc/s (1). In acetone solutions we have the case $\sigma_B > \sigma_A$: the protons ortho to fluorine are most shielded. We can limit our discussion to the four most intense lines in the proton spectrum, since their separations depend on $(\sigma_B - \sigma_A)$ and on J_m^{HF} and J_o^{HF}. (The other lines go to zero intensity when $\sigma_B = \sigma_A$, as discussed in reference 1.)

From Table VI in reference 1 these four transitions correspond to lines 18, 19, 29, and 30. The energies of these transitions contain corrective terms, A and B, whose values depend on the sign of $\sigma_B - \sigma_A$, which was taken as negative to correspond with the *p*-fluoroaniline case. When $\sigma_B - \sigma_A > 0$, as for *p*-fluorotoluene in acetone, the definitions of A and B as positive quantities change to

$$\begin{aligned} A\cos 2\theta &= \tfrac{1}{2}\nu_0(\sigma_B-\sigma_A)-\tfrac{1}{4}(J_{35}-J_{15}) \\ A\sin 2\theta &= \tfrac{1}{2}(J_{23}+J_{13}) \\ B\cos 2\phi &= \tfrac{1}{2}\nu_0(\sigma_B-\sigma_A)+\tfrac{1}{4}(J_{35}-J_{15}) \\ B\sin 2\phi &= \tfrac{1}{2}(J_{23}+J_{13}). \end{aligned} \qquad [1]$$

Hence the signs of A and B in transitions 18, 19, 29, and 30 must be changed. The

Can. J. Chem. Downloaded from www.nrcresearchpress.com by 176.9.209.113 on 09/04/12
For personal use only.

intensity of transition 18, for instance, changes from a value of $2(1-\sin 2\theta)$ to $2(1+\sin 2\theta)$. The energies of the transitions then become

18. $\frac{1}{2}\nu_0(2-\sigma_B-\sigma_A)+\frac{1}{4}(-2J_{13}-2J_{23}+J_{15}+J_{35})+A$
19. $\frac{1}{2}\nu_0(2-\sigma_B-\sigma_A)+\frac{1}{4}(-2J_{13}-2J_{23}-J_{15}-J_{35})+B$
29. $\frac{1}{2}\nu_0(2-\sigma_B-\sigma_A)+\frac{1}{4}(2J_{13}+2J_{23}+J_{15}+J_{35})-A$
30. $\frac{1}{2}\nu_0(2-\sigma_B-\sigma_A)+\frac{1}{4}(2J_{13}+2J_{23}-J_{15}-J_{35})-B.$

These four lines coalesce to two when $\sigma_B \rightarrow \sigma_A$ as shown below in II.

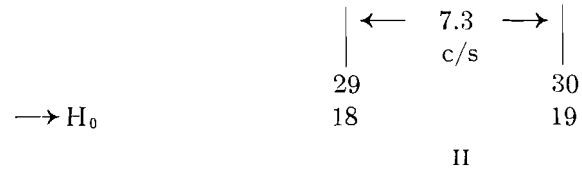

II

(b) The Ring Proton Spectrum

Consider the series of spectra in Fig. 1, beginning with the solution containing 1:20 of benzene. This spectrum corresponds to the case $\sigma_B-\sigma_A = 0$, as discussed in reference 1. There it was shown that this spectrum is consistent with $J_m^{HF} = J_o^{HF} = 7.3$ c/s and $A = B = \frac{1}{2}(J_{23}+J_{13})$, with the four transitions as in II. However, we now know that when $\nu_0(\sigma_B-\sigma_A)$ is about 0.2 p.p.m. (Fig. 1.8), $J_o^{HF} = J_{35} = 8.7$ c/s and $J_m^{HF} = J_{15} = 5.8$ c/s. It is apparent from the definitions of A and B that these values of J_{15} and J_{35} will also reproduce the ring proton spectrum. Substituting these values into [1] for $\sigma_B-\sigma_A = 0$ we see that $\sin 2\theta$ and $\sin 2\phi$ are very nearly 1 and A and B are very nearly $\frac{1}{2}(J_{23}+J_{13})$. The deviations will be undetectable experimentally. Since $\frac{1}{2}(J_{23}+J_{13})$ is large compared to $\frac{1}{4}(J_{35}-J_{15})$, the analysis yields virtually the same results whether we consider $J_{15} = J_{35}$ or $J_{15} \neq J_{35}$. Physically it is clearly more reasonable to assume J_{15} and J_{35} independent of $\sigma_B-\sigma_A$.*

From the definitions [1] and the transitions 18 to 30 it is also clear that the analysis will yield J_{35} and J_{15} individually (and not only their sum) when $\sigma_B-\sigma_A$ becomes large enough relative to $\frac{1}{2}(J_{23}+J_{13})$. This is illustrated by the series of spectra in Fig. 1. Figure 1.6 corresponds roughly to the smallest value of $\sigma_B-\sigma_A$ at which values of J_{15}, J_{35}, and J_{23} can be extracted. The shift is approximately 8 c/s and shows that we must have $\frac{1}{2}\nu_0(\sigma_B-\sigma_A)+\frac{1}{4}(J_{35}-J_{15}) \approx \frac{1}{2}(J_{23}+J_{13})$ since $J_{23} \approx 8.5$ c/s and $J_{13} \approx 0$.†

It can be seen that in Fig. 1 the lines from the protons ortho to the CH_3 group, i.e., those at low field, are broader than those ortho to the fluorine atom because of a weak coupling to the CH_3 protons. The coupling $J_m^{CH_3,H}$ is not noticeable. When $\sigma_B-\sigma_A \rightarrow 0$, however, we again have the situation that the spectrum will only yield $\frac{1}{2}(J_o^{CH_3,H}+J_m^{CH_3,H})$. Since $J_m^{CH_3,H} \approx 0$ and $J_o^{CH_3,H}$ is about 0.25 c/s at most, the lines of the ring proton spectrum are quite narrow when $\sigma_B-\sigma_A = 0$ (Fig. 1.2).

J_{15} and J_{35} need not always be independent of $\sigma_B-\sigma_A$. An example is formamide (6) where, at sufficiently high temperatures, rotation about the C—N bond results in zero relative shift for the N—H protons while, at the same time, the two coupling constants to the aldehyde proton are "mechanically" averaged from widely different values. These two coupling constants correspond to J_{15} and J_{35} in the present case.

†*We can predict, therefore, that in order to obtain individual coupling constants in similar situations even when $\sigma_B-\sigma_A$ approaches zero, we must have the two protons only weakly coupled. A substituted fluorobenzene with two protons arranged para to one another and meta and ortho to the fluorine atom would be expected to behave in the required way. Such molecules are being investigated.*

Can. J. Chem. Downloaded from www.nrcresearchpress.com by 176.9.209.113 on 09/04/12
For personal use only.

(*c*) *The Methyl Spectrum*

The third illustration afforded by *p*-fluorotoluene of an apparent but unreal averaging of coupling constants occurs in the methyl spectrum (Fig. 2). The CH_3 spectrum at 1:20 dilution in benzene is a doublet with a splitting of 0.9 c/s due to coupling to the F^{19} nucleus. This gives $J_p^{F,CH_3} = 0.9$ c/s. The lines are narrow for the reason given in the preceding paragraph.

As $\sigma_B - \sigma_A$ becomes positive the doublet becomes asymmetrical and both lines broaden (e.g. in the pure liquid at 60 Mc/s). Finally the doublet is washed out in the 8:1 acetone solution because of coupling to the ortho protons of the ring. This behavior agrees with that of the ring proton spectrum.

At high dilutions in benzene (1:35) there is a reversal in sign of the chemical shift, i.e. $\sigma_B - \sigma_A < 0$. The protons ortho to the fluorine atom are becoming less shielded than the meta protons.

CONCLUSIONS

$J_m^{HF} = 5.8$ c/s and $J_o^{HF} = 8.7$ c/s in *p*-fluorotoluene. These values are independent of chemical shift in the ring, although at zero chemical shift the line separations yield only the sum of J_m^{HF} and J_o^{HF}. The latter still have the individual values given above. The same behavior is shown by the line splittings due to $J_o^{CH_3,H}$ and $J_m^{CH_3,H}$ when the ring proton chemical shift changes. We conclude that a coupling constant can affect a spectrum significantly even though *it is non-detectable*, viz. $J_m^{CH_3,H}$.

The problem of solvent effects on internal chemical shifts of substituted benzenes has also been investigated and will be discussed in a forthcoming publication.

ACKNOWLEDGMENTS

We wish to thank Dr. R. Abraham and Dr. H. J. Bernstein for stimulating discussion in connection with this work.

REFERENCES

1. SCHAEFER, T. Can. J. Chem. **37**, 882 (1959).
2. RICHARDS, R. E. and SCHAEFER, T. Proc. Roy. Soc. A, **246**, 429 (1958).
3. RICHARDS, R. E. and SCHAEFER, T. Molecular Phys. **1**, 331 (1958).
4. SCHAEFER, T. and SCHNEIDER, W. G. To be published.
5. BERNSTEIN, H. J., POPLE, J. A., and SCHNEIDER, W. G. Can. J. Chem. **35**, 65 (1957).
6. SCHNEIDER, W. G. and SUNNERS, B. To be published.

Can. J. Chem. Downloaded from www.nrcresearchpress.com by 176.9.209.113 on 09/04/12
For personal use only.

Can. J. Chem. Downloaded from www.nrcresearchpress.com by 176.9.209.113 on 09/04/12
For personal use only.

NOTES

SOLUBILIZATION IN AQUEOUS BUTYRIC ACID SOLUTIONS*

D. MOULE† AND G. C. BENSON

INTRODUCTION

Bury and co-workers (1–3) have interpreted the concentration dependence of a number of the physical properties of aqueous butyric acid solutions as indicating micelle formation. Recent ultrasonic absorption measurements (4) have provided further evidence for the occurrence of some type of aggregation in this system.

The presence of a significant number of fairly large aggregates should have a marked effect on the capacity of aqueous butyric acid solutions to dissolve certain types of water-insoluble organic molecules. The convenience of a colorimetric method of analysis led to the choice of the dye *p*-dimethylaminoazobenzene (DMAB) for the present solubilization study. The solubility of this material in water is less than 1 mg/liter (5).

EXPERIMENTAL

The DMAB (Eastman Organic Chemicals) was purified by recrystallization from ethanol. Purification of the butyric acid has been described previously (4).

Aqueous solutions of the acid were prepared with concentrations in the range 0–7 molar. An excess of dye crystals was added to measured amounts of these solutions contained in long-necked glass vials. After the necks were sealed, the vials were mounted in a horizontal agitator and equilibrated in a thermostat for 4 or 5 days. At the end of this time the solid remaining was allowed to settle and a sample of the liquid was withdrawn through a sintered glass filter into a pipette heated to thermostat temperature. After dilution with a known amount of acidified ethanol the concentration of the solution was determined absorptiometrically using an Evelyn photoelectric colorimeter (6). For most of the concentration range studied duplicate determinations of the concentration agreed to better than 5%. Kolthoff and Stricks (5) have noted that the spectrum of DMAB in ethanol is altered by the presence of water. Errors due to this effect were negligible in the present work.

RESULTS AND DISCUSSION

The solubility of DMAB in butyric acid solutions at four temperatures (0°, 25°, 40°, and 60° C) is shown in Fig. 1. At low acid concentrations the dye is only slightly soluble but the amount solubilized increases noticeably at concentrations above 2 *M*. The solubility at 0° C reaches a maximum of 3.8 g/liter around 5.9 *M* (18 mole % acid) and then decreases. The curve at 25° C also shows a tendency to level off in the same region but this is followed by a further increase. At 40° and 60° C the solubilization rises to successively higher values as the butyric acid concentration is increased.

Kolthoff and Stricks (5) have investigated the solubilization of DMAB by a number of soaps and other detergents. These authors defined the solubilizing power at any detergent concentration as the slope of the solubilization curve at that concentration. They found that it was possible to identify the critical micelle concentration (CMC)

*Issued as N.R.C. No. 5436.
†*Present address: Department of Chemistry, McMaster University, Hamilton, Ontario, Canada.*

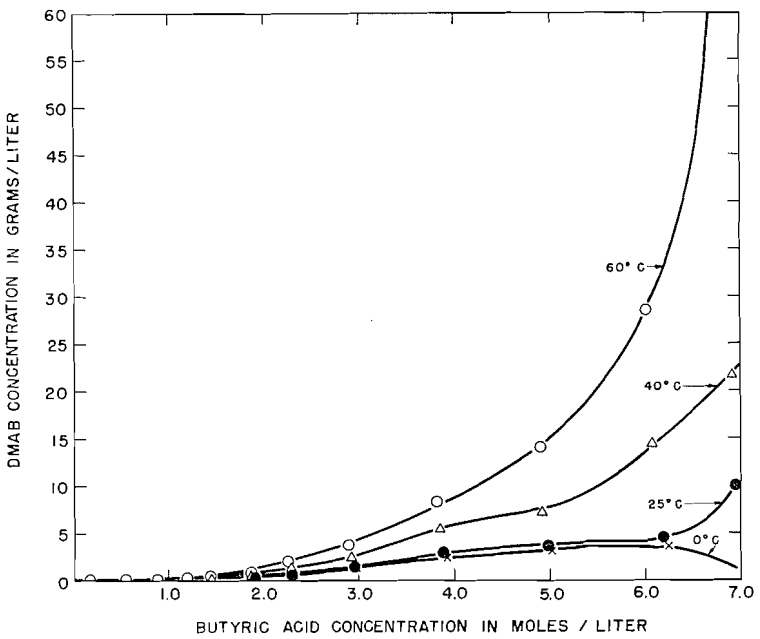

FIG. 1. The solubilization of DMAB in aqueous butyric acid solutions.

with the concentration where there was a rather sharp change in the solubilizing power of the detergent. Values of the CMC for butyric acid solutions obtained in this way are given in Table I along with the solubilizing power in the concentration range just

TABLE I

Data on the solubilization of DMAB in butyric acid solutions

Temp. (° C)	CMC		Solubilizing power (2–3.5 *M*)	
	Molarity	Mole %	(g dye/mole acid)	(molecules acid/molecule dye)
0	1.8_2	3.7_6	1.0_8	2100
25	1.7_5	3.5_9	1.1_5	2000
40	1.5_8	3.2_0	1.9_1	1200
60	1.6_2	3.2_9	3.0_6	740

above the CMC. The values of the CMC agree quite well with other estimates, i.e. 15 wt.% (3.5 mole %) from freezing point data (1), 12–15 wt.% (2.7–3.5 mole %) from density measurements (2), and 13 wt.% (3.0 mole %) from specific heat measurements (3). The solubilizing power of butyric acid for DMAB is of comparable magnitude to values for this dye in a variety of detergents (5).

Figure 2 illustrates the similarity between the concentration dependence of the solubilization of DMAB (curve A) and that for the absorption of ultrasound of frequency 3 mc/sec (curve C, data taken from ref. 4) in butyric acid solutions at 0° C. White, Moule, and Benson (4) in discussing the ultrasonic results noted that the concentration corresponding to the absorption peak (13 mole %) is the same as that of the upper con-

Can. J. Chem. Downloaded from www.nrcresearchpress.com by 176.9.209.113 on 09/04/12
For personal use only.

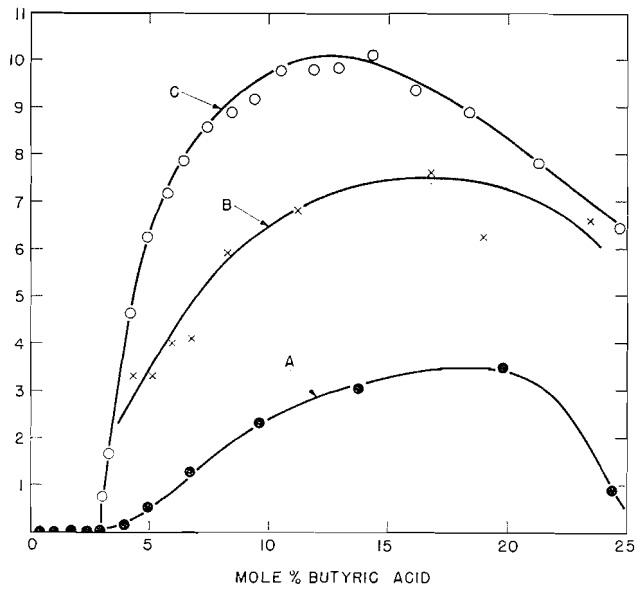

FIG. 2. Comparison of solubilization results with ultrasonic absorption and mean micellar aggregation number. Curve A: solubilization of DMAB at 0° C stated as g dye/liter of solution. Curve B: mean micellar aggregation number $\times 10^{-1}$ (data taken from ref. 8). Curve C: ultrasonic absorption at frequency of 3 mc/sec and 0° C stated in db/cm (data taken from ref. 4).

solute point (7) for the butyric acid – water system and suggested that clusters of acid molecules persist in these solutions at temperatures considerably above the critical region. Curve B in Fig. 2 is taken from the work of Davies and Griffiths (8). These authors applied Kreuzer's analysis (9) to the freezing point data for butyric acid solutions and obtained an estimate of the average micellar aggregation number. At 0° C this changed from 33 at 5 mole % to about 76 at 17 mole % and then decreased slightly as the concentration was increased still further.

White, Moule, and Benson (4) found that with increasing temperature the ultrasonic absorption peak at 13 mole % decreased and that a second maximum developed at about 50 mole %. The disappearance of the maximum in the solubilization curve at higher temperatures roughly parallels the ultrasonic behavior but the solubilization does not show any tendency to decrease as the temperature is raised. This is not surprising since the solubilization process must involve several factors. A change of temperature will not only alter the micellar characteristics of the solution but also the interaction between a solubilizate molecule and a micelle. The present investigation did not extend to high enough acid concentrations to make any comparison between solubilization and ultrasonic behavior in the region of the second absorption maximum.

Finally it should be noted that the solubilizing powers given in Table I must not be taken to indicate a minimum micellar size of 2000 acid molecules required to solubilize 1 dye molecule at 25° C. The error of this interpretation has been pointed out by McBain and Hutchinson (10). From a purely geometric point of view an aggregate of 70 or 80 molecules as estimated by Davies and Griffiths (8) should be able to solubilize at least 1 dye molecule. The larger mole ratios (acid/dye) observed experimentally suggest that there is a fairly broad distribution of aggregate sizes.

Can. J. Chem. Downloaded from www.nrcresearchpress.com by 176.9.209.113 on 09/04/12
For personal use only.

1. JONES, E. R. and BURY, C. R. Phil. Mag. **4**, 841 (1927).
2. GRINDLEY, J. and BURY, C. R. J. Chem. Soc. 679 (1929).
3. BURY, C. R. and DAVIES, D. G. J. Chem. Soc. 2413 (1932).
4. WHITE, P., MOULE, D., and BENSON, G. C. Trans. Faraday Soc. **54**, 1638 (1958).
5. KOLTHOFF, I. M. and STRICKS, W. J. Phys. & Colloid Chem. **52**, 915 (1948).
6. EVELYN, K. A. J. Biol. Chem. **115**, 63 (1936).
7. FAUCON, A. Ann. chim. et phys. **19**, 70 (1910).
8. DAVIES, M. and GRIFFITHS, D. M. L. Z. physik. Chem. (Frankfurt), (N.S.), **6**, 143 (1956).
9. KREUZER, J. Z. physik. Chem. (Leipzig), B, **53**, 213 (1943).
10. MCBAIN, M. E. L. and HUTCHINSON, E. Solubilization. Academic Press Inc., New York. 1955. pp. 78, 94.

RECEIVED JUNE 17, 1959.
DIVISION OF PURE CHEMISTRY,
NATIONAL RESEARCH COUNCIL,
OTTAWA, CANADA.

Can. J. Chem. Downloaded from www.nrcresearchpress.com by 176.9.209.113 on 09/04/12
For personal use only.

VAPOR PRESSURES OF AQUEOUS POTASSIUM OCTANOATE SOLUTIONS[1]

D. MOULE,[2] P. WHITE,[3] AND G. C. BENSON

Recent calorimetric studies in these laboratories (1–3) have yielded thermodynamic data for aqueous potassium octanoate solutions. The present osmotic investigation was undertaken in order to provide independent and supplementary thermodynamic information about this system.

EXPERIMENTAL

Vapor pressure depressions of a series of potassium octanoate solutions were measured with a pair of thermistors in an apparatus similar to that described by several previous workers (4–6). The present form of this consisted of an all-glass cell into which was inserted a long glass tube with a pair of Veco (32A1, 2000 ohm) thermistors projecting from a rubber stopper at the lower end. The upper chamber of the cell was connected by a long neck to a Dewar vessel which served as the solvent well. The response time of the thermistors was reduced by carefully grinding and etching away the main part of the glass coating. The thermistors were placed in the adjacent arms of a Wheatstone bridge to which 0.2 v was applied from a lead storage battery and rheostat. A Leeds and Northrup d-c. amplifier coupled to a Speedomax recorder provided a continuous record of the changes in bridge balance. With this arrangement a resistance change of 0.1 ohm which corresponded to about 1×10^{-3}° C could be detected easily.

The vapor pressure apparatus and all the solutions were kept in an oil thermostat controlled to ±0.01° C. During a measurement, the thermistor tips were washed with water, wiped dry, a drop of solution placed on one thermistor and a drop of water on the other. Measurements were attempted over the range 10° C to 50° C; however, the results much above or below room temperature were not reproducible, and the investigation had to be restricted to the interval 20° to 30° C. For measurements in this range steady resistance values were generally obtained within 30 minutes after the drops were placed on the thermistors.

The apparatus was calibrated with NaCl. Values of the practical osmotic coefficient ϕ for aqueous solutions of this material were taken from the data compiled by Harned and

[1]*Issued as N.R.C. No. 5407.*
[2]*Present address: Department of Chemistry, McMaster University, Hamilton, Ontario, Canada.*
[3]*National Research Council of Canada Postdoctorate Fellow 1956–58; present address: International Business Machines Corporation, Research Laboratories, Poughkeepsie, N. Y., U.S.A.*

1. JONES, E. R. and BURY, C. R. Phil. Mag. **4**, 841 (1927).
2. GRINDLEY, J. and BURY, C. R. J. Chem. Soc. 679 (1929).
3. BURY, C. R. and DAVIES, D. G. J. Chem. Soc. 2413 (1932).
4. WHITE, P., MOULE, D., and BENSON, G. C. Trans. Faraday Soc. **54**, 1638 (1958).
5. KOLTHOFF, I. M. and STRICKS, W. J. Phys. & Colloid Chem. **52**, 915 (1948).
6. EVELYN, K. A. J. Biol. Chem. **115**, 63 (1936).
7. FAUCON, A. Ann. chim. et phys. **19**, 70 (1910).
8. DAVIES, M. and GRIFFITHS, D. M. L. Z. physik. Chem. (Frankfurt), (N.S.), **6**, 143 (1956).
9. KREUZER, J. Z. physik. Chem. (Leipzig), B, **53**, 213 (1943).
10. MCBAIN, M. E. L. and HUTCHINSON, E. Solubilization. Academic Press Inc., New York. 1955. pp. 78, 94.

RECEIVED JUNE 17, 1959.
DIVISION OF PURE CHEMISTRY,
NATIONAL RESEARCH COUNCIL,
OTTAWA, CANADA.

Can. J. Chem. Downloaded from www.nrcresearchpress.com by 69.46.99.164 on 09/04/12
For personal use only.

VAPOR PRESSURES OF AQUEOUS POTASSIUM OCTANOATE SOLUTIONS[1]

D. MOULE,[2] P. WHITE,[3] AND G. C. BENSON

Recent calorimetric studies in these laboratories (1–3) have yielded thermodynamic data for aqueous potassium octanoate solutions. The present osmotic investigation was undertaken in order to provide independent and supplementary thermodynamic information about this system.

EXPERIMENTAL

Vapor pressure depressions of a series of potassium octanoate solutions were measured with a pair of thermistors in an apparatus similar to that described by several previous workers (4–6). The present form of this consisted of an all-glass cell into which was inserted a long glass tube with a pair of Veco (32A1, 2000 ohm) thermistors projecting from a rubber stopper at the lower end. The upper chamber of the cell was connected by a long neck to a Dewar vessel which served as the solvent well. The response time of the thermistors was reduced by carefully grinding and etching away the main part of the glass coating. The thermistors were placed in the adjacent arms of a Wheatstone bridge to which 0.2 v was applied from a lead storage battery and rheostat. A Leeds and Northrup d-c. amplifier coupled to a Speedomax recorder provided a continuous record of the changes in bridge balance. With this arrangement a resistance change of 0.1 ohm which corresponded to about 1×10^{-3}° C could be detected easily.

The vapor pressure apparatus and all the solutions were kept in an oil thermostat controlled to ±0.01° C. During a measurement, the thermistor tips were washed with water, wiped dry, a drop of solution placed on one thermistor and a drop of water on the other. Measurements were attempted over the range 10° C to 50° C; however, the results much above or below room temperature were not reproducible, and the investigation had to be restricted to the interval 20° to 30° C. For measurements in this range steady resistance values were generally obtained within 30 minutes after the drops were placed on the thermistors.

The apparatus was calibrated with NaCl. Values of the practical osmotic coefficient ϕ for aqueous solutions of this material were taken from the data compiled by Harned and

[1]*Issued as N.R.C. No. 5407.*
[2]*Present address: Department of Chemistry, McMaster University, Hamilton, Ontario, Canada.*
[3]*National Research Council of Canada Postdoctorate Fellow 1956–58; present address: International Business Machines Corporation, Research Laboratories, Poughkeepsie, N. Y., U.S.A.*

Owen (7). Plots of observed resistance change against ϕm were good straight lines over the concentration range 0 to 0.5 molal at both 20 and 30° C.

The preparation of the potassium octanoate has been described previously (1, 2). Vapor pressure lowerings were determined for solutions with concentrations 0 to 0.7 molal. All solutions contained an excess of potassium hydroxide (0.042 molal) to suppress hydrolysis, and the osmotic coefficients measured were corrected for the presence of this alkali.

RESULTS AND DISCUSSION

The osmotic results at 20° and 30° C are shown in Fig. 1 as a plot of ϕm against m. The results at 30° have been displaced vertically 0.1 unit for clarity. Osmotic data for NaCl are shown as dashed lines. Within the experimental error the data for potassium octanoate

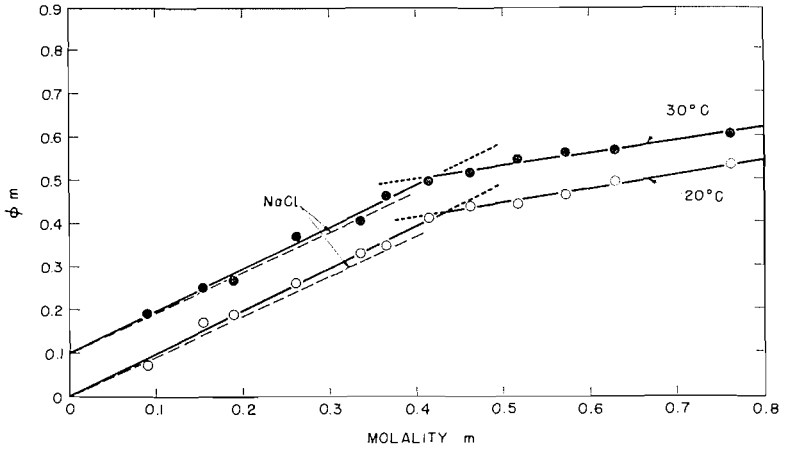

FIG. 1. Osmotic data for aqueous potassium octanoate solutions at 20° and 30° C. The results at 30° C have been increased 0.1 unit.

at each temperature can be fitted by two straight lines as shown. Similar behavior has been observed for a number of detergent systems by Fineman and McBain (8) and by Huff, McBain, and Brady (9), who identified the intersection of the lines with the critical micelle concentration CMC.

The lines in Fig. 1 were fitted with equations of the form

[1] $$\phi m = cm$$

below CMC and

[2] $$\phi m = a + bm$$

above the CMC. The values of the constants a, b, and c are listed in Table I along with

TABLE I

Values of the constants a, b, and c in eqs. [1] and [2]

T° C	a (molality)	b	c	CMC (molality)
20	0.282	0.325	0.973	0.43
30	0.275	0.306	0.961	0.42

Can. J. Chem. Downloaded from www.nrcresearchpress.com by 69.46.99.164 on 09/04/12
For personal use only.

values of the CMC calculated from them. It should be noted that the representation of the data below the CMC by eq. [1] with c different from unity is an approximation which cannot hold strictly at low concentration. The values of the CMC given in Table I are somewhat higher than results at 25° C obtained from measurements of refractive index 0.39 (10), heat of dilution 0.38[4] (1), and conductivity 0.35 (3) but lower than the value 0.47 from density determinations (11).

Mean molal activity coefficients $\gamma_{\pm}$ were calculated from the osmotic data at 20° C and at 30° C. The relative partial molal enthalpy of the solute at 25° C was then estimated from the temperature variation of $\gamma_{\pm}$. The results are shown in curve A of Fig. 2, where the difference in partial molal enthalpy $\bar{H}_2-\bar{H}_2^*$ is plotted against molality. The asterisk is used to indicate a reference concentration $m^* = 0.1$. In view of the rather limited accuracy of the original osmotic results the enthalpy data derived in this way are only of a semiquantitative nature. Values of $\bar{H}_2-\bar{H}_2^*$ taken from calorimetric measurements (1) are also shown in Fig. 2 (curve B). Both curves show an increase in enthalpy when micellization occurs. Curve A gives a value of 0.8 kcal mole^{-1} for the enthalpy of micellization ΔH_M which is smaller by a factor of 2 than the value (1.7 kcal mole^{-1}) estimated previously (1) from the calorimetric data. The abrupt step in curve A is due to the discontinuous change in slope at the CMC for the straight line approximations adopted in Fig. 1.

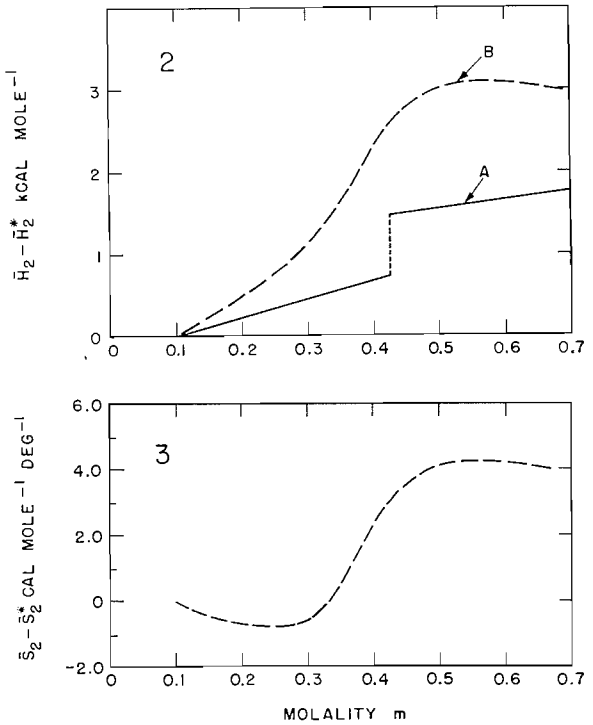

FIG. 2. Plot of the partial molal enthalpy difference $\bar{H}_2-\bar{H}_2^*$ against molality for potassium octanoate solutions at 25° C. Reference concentration is $m^* = 0.1$. Curve A estimated from osmotic data. Curve B calorimetric results from ref. 1.

FIG. 3. Plot of partial molal entropy difference $\bar{S}_2-\bar{S}_2^*$ against molality for potassium octanoate solutions at 25° C. Reference concentration is $m^* = 0.1$.

[4]*This result refers to the point of inflection of a plot of partial molal enthalpy against molality.*

Can. J. Chem. Downloaded from www.nrcresearchpress.com by 69.46.99.164 on 09/04/12
For personal use only.

Assuming the activity coefficients $\gamma_{\pm}$ at 25° C to be the average of results at 20° C and 30° C, changes in partial molal entropy were calculated from the expression

$$[3] \qquad \bar{S}_2 - \bar{S}_2^* = (\bar{H}_2 - \bar{H}_2^*)/T - 3.972 \ln (\gamma_{\pm} m/\gamma_{\pm}^* m^*).$$

The calorimetric results (1) were used for the enthalpy difference rather than the estimates of this quantity from osmotic data. The resulting curve is plotted in Fig. 3. The increase in entropy on micellization is about 5.5 cal mole^{-1} deg^{-1} and is of course equal to $\Delta H_M/T$. Goddard, Hoeve, and Benson (1) have drawn attention to the importance of changes in solvent structure in the process of micelle formation. The observed increase in entropy is explicable on this basis.

1. Goddard, E. D., Hoeve, C. A. J., and Benson, G. C. J. Phys. Chem. **61**, 593 (1957).
2. White, P. and Benson, G. C. J. Colloid Sci. **13**, 584 (1958).
3. White, P. and Benson, G. C. Trans. Faraday Soc. **55**, 1025 (1959).
4. Brady, A. P., Huff, H., and McBain, J. W. J. Phys. & Colloid Chem. **55**, 304 (1951).
5. Davies, M. and Thomas, D. K. J. Phys. Chem. **60**, 767 (1956).
6. Kitahara, A. Bull. Chem. Soc. Japan, **31**, 288 (1958).
7. Harned, H. S. and Owen, B. B. The physical chemistry of electrolytic solutions. 3rd ed. Reinhold Publishing Corp., New York. 1958.
8. Fineman, M. N. and McBain, J. W. J. Phys. & Colloid Chem. **52**, 881 (1948).
9. Huff, H., McBain, J. W., and Brady, A. P. J. Phys. & Colloid Chem. **55**, 311 (1951).
10. Klevens, H. B. J. Phys. & Colloid Chem. **52**, 130 (1948).
11. Davies, D. G. and Bury, C. R. J. Chem. Soc. 2263 (1930).

Received September 1, 1959.
Division of Pure Chemistry,
National Research Council,
Ottawa, Canada.

THE SYNTHESIS OF A LIGNIN MODEL SUBSTANCE: 3-HYDROXY-1-(4-HYDROXY-3,5-DIMETHOXYPHENYL)-2-PROPANONE

E. W. Gorecki and J. M. Pepper

A study of the ethanolysis (1) of 3-hydroxy-1-(4-hydroxy-3-methoxyphenyl)-2-propanone (I (R)) (β-oxyconiferyl alcohol) has provided considerable evidence for the presence in the lignin complex of the side chain —CH_2—CO—CH_2OH or its enolic form. Gardner has shown (1) that the four Hibbert monomers (II–V) are produced by the ethanolysis of I.

(R = 4-hydroxy-3-methoxyphenyl, R′ = 4-hydroxy-3,5-dimethoxyphenyl)

They have been shown previously to be released by the ethanolysis of spruce wood and various isolated lignins (2). Hibbert has proposed a series of interconversions (3) relating the production of II–V from I. Such a scheme would account for the proved absence of primary alcoholic groups in these isolated propylphenyl lignin monomers as contrasted with the presence of such groups in lignin derivatives obtained by other degradation procedures such as hydrogenation (2) and as evidenced from general analytical data. It

Can. J. Chem. Downloaded from www.nrcresearchpress.com by 69.46.99.164 on 09/04/12
For personal use only.

Assuming the activity coefficients $\gamma_{\pm}$ at 25° C to be the average of results at 20° C and 30° C, changes in partial molal entropy were calculated from the expression

$$[3] \qquad \bar{S}_2 - \bar{S}_2^* = (\bar{H}_2 - \bar{H}_2^*)/T - 3.972 \ln (\gamma_{\pm} m / \gamma_{\pm}^* m^*).$$

The calorimetric results (1) were used for the enthalpy difference rather than the estimates of this quantity from osmotic data. The resulting curve is plotted in Fig. 3. The increase in entropy on micellization is about 5.5 cal mole^{-1} deg^{-1} and is of course equal to $\Delta H_M/T$. Goddard, Hoeve, and Benson (1) have drawn attention to the importance of changes in solvent structure in the process of micelle formation. The observed increase in entropy is explicable on this basis.

1. Goddard, E. D., Hoeve, C. A. J., and Benson, G. C. J. Phys. Chem. **61**, 593 (1957).
2. White, P. and Benson, G. C. J. Colloid Sci. **13**, 584 (1958).
3. White, P. and Benson, G. C. Trans. Faraday Soc. **55**, 1025 (1959).
4. Brady, A. P., Huff, H., and McBain, J. W. J. Phys. & Colloid Chem. **55**, 304 (1951).
5. Davies, M. and Thomas, D. K. J. Phys. Chem. **60**, 767 (1956).
6. Kitahara, A. Bull. Chem. Soc. Japan, **31**, 288 (1958).
7. Harned, H. S. and Owen, B. B. The physical chemistry of electrolytic solutions. 3rd ed. Reinhold Publishing Corp., New York. 1958.
8. Fineman, M. N. and McBain, J. W. J. Phys. & Colloid Chem. **52**, 881 (1948).
9. Huff, H., McBain, J. W., and Brady, A. P. J. Phys. & Colloid Chem. **55**, 311 (1951).
10. Klevens, H. B. J. Phys. & Colloid Chem. **52**, 130 (1948).
11. Davies, D. G. and Bury, C. R. J. Chem. Soc. 2263 (1930).

Received September 1, 1959.
Division of Pure Chemistry,
National Research Council,
Ottawa, Canada.

THE SYNTHESIS OF A LIGNIN MODEL SUBSTANCE: 3-HYDROXY-1-(4-HYDROXY-3,5-DIMETHOXYPHENYL)-2-PROPANONE

E. W. Gorecki and J. M. Pepper

A study of the ethanolysis (1) of 3-hydroxy-1-(4-hydroxy-3-methoxyphenyl)-2-propanone (I (R)) (β-oxyconiferyl alcohol) has provided considerable evidence for the presence in the lignin complex of the side chain —CH_2—CO—CH_2OH or its enolic form. Gardner has shown (1) that the four Hibbert monomers (II–V) are produced by the ethanolysis of I.

(R = 4-hydroxy-3-methoxyphenyl, R′ = 4-hydroxy-3,5-dimethoxyphenyl)

They have been shown previously to be released by the ethanolysis of spruce wood and various isolated lignins (2). Hibbert has proposed a series of interconversions (3) relating the production of II–V from I. Such a scheme would account for the proved absence of primary alcoholic groups in these isolated propylphenyl lignin monomers as contrasted with the presence of such groups in lignin derivatives obtained by other degradation procedures such as hydrogenation (2) and as evidenced from general analytical data. It

Can. J. Chem. Downloaded from www.nrcresearchpress.com by 176.9.209.113 on 09/04/12
For personal use only.

Can. J. Chem. Downloaded from www.nrcresearchpress.com by 176.9.209.113 on 09/04/12
For personal use only.

also explains the fact that carbon–methyl groups are present in these ethanolysis products and in other isolated lignins (4, 5) but not in protolignin itself (4).

From maple wood, by ethanolysis, the corresponding syringyl (R′ = 4-hydroxy-3,5-dimethoxyphenyl) analogues were isolated in addition to, and in greater yield than, the guaiacyl members, II–V (2). Although it is logical to assume that these monomers would be produced by the ethanolysis of the previously unreported 3-hydroxy-1-(4-hydroxy-3,5-dimethoxyphenyl)-2-propanone (VI), this assumption has yet to be proved. Of greater interest would be the comparison in yield of the rearrangement products obtained through ethanolysis of the two analogues. In the degradation of hardwood lignins, syringyl derivatives are obtained in greater abundance than are the corresponding guaiacyl members. A comparative study of the yield of the products obtained by the various established techniques of ethanolysis, oxidation, and hydrogenation as applied to I (R and R′) would assist in estimating the ratio of guaiacyl to syringyl nuclei in angiosperm protolignin.

This note records the synthesis of 3-hydroxy-1-(4-hydroxy-3,5-dimethoxyphenyl)-2-propanone. The method is similar to that used to prepare the analogous β-oxyconiferyl alcohol (6). Homosyringic acid, prepared by three different routes, was acetylated, then converted via the acid chloride, through the diazomethyl ketone, to the O-acetyl derivative of I (R′) which on hydrolysis gave I (R′). Several of the intermediate compounds are reported here for the first time. The yields of the syringyl derivatives are consistently lower than those of the corresponding guaiacyl compounds.

EXPERIMENTAL

All melting points are uncorrected. Infrared spectra were measured with a Perkin–Elmer Model 21 spectrophotometer using sodium chloride optics.

Syntheses of Homosyringic Acid

Via Willgerodt Reaction (Kindler Modification)

Homosyringic acid was obtained starting from acetosyringone (7) by the adoption of the method used by Schwenk and Papa (8) to synthesize *p*-hydroxyphenylacetic. The product, obtained in only 6.7% yield, was recrystallized from water (Norite) to give fluffy white crystals, m.p. 130–131°; reported m.p. 132.5–134.5° (9). Previously a similar synthesis in these laboratories of homovanillic acid from acetovanillone had been achieved in a 43% yield. Arlt *et al.* (9) also reported the synthesis of homovanillic acid by this method.

Via Syringal Rhodanine

Syringal rhodanine.—To a mixture of syringaldehyde (41.0 g), rhodanine (29.9 g), and freshly fused sodium acetate (51.3 g) was added glacial acetic acid (365 ml) and the mixture refluxed for 40 minutes. The hot reaction mixture was decanted into vigorously stirred water (1030 ml), and after the mixture had been stirred for 3 hours, the product was collected, washed well with water, and dried under vacuum. The yield of crude syringal rhodanine was 59.4 g (89%), m.p. 242–246° (decomp.). Three recrystallizations from *n*-butanol (Norite) gave orange microcrystals, m.p. 258–258.5° (decomp.). Calc. for $C_{12}H_{11}NO_4S_2$: C, 48.5; H, 3.72; OCH_3, 20.9%. Found: C, 48.5; H, 3.74; OCH_3, 21.0%.

α-Thioketo-β-(4-hydroxy-3,5-dimethoxyphenyl)-pyruvic acid.—To syringal rhodanine (3.0 g) was added 15% sodium hydroxide (19 ml) and the mixture refluxed for 45 minutes. The red solution was cooled to 0° and acidified rapidly using 10% hydrochloric acid. The yield of the crude precipitated thioketo acid was 2.4 g (92.7%), m.p. 123–125°.

Several reprecipitations of the product from saturated sodium bicarbonate solution yielded dense, orange-yellow crystals, m.p. 130–131°. Calc. for $C_{11}H_{12}O_5S$: C, 51.5; OCH_3, 24.2%. Found: C, 51.1; OCH_3, 24.1%.

α-Oximo-β-(4-hydroxy-3,5-dimethoxyphenyl)-pyruvic acid.—Hydroxylamine hydrochloride (4.1 g) was dissolved in water (4.3 ml) and neutralized with a solution of sodium (1.75 g) in ethanol (45 ml). After filtration, the base was added to α-thioketo-β-(4-hydroxy-3,5-dimethoxyphenyl)-pyruvic acid (5.67 g) and the mixture refluxed on a steam bath for 60 minutes. Cooling to 0° gave fluffy white crystals, which were filtered, washed with ethanol, and dried. From the mother liquor was obtained a further 0.6 g, the combined yield being 4.2 g (75%), m.p. 219–220° (decomp.). Calc. for $C_{11}H_{13}NO_6$: OCH_3, 24.3%. Found: OCH_3, 24.2%.

Acetylhomosyringonitrile.—α-Oximino-β-(4-hydroxy-3,5-dimethoxyphenyl)-pyruvic acid (8.7 g) was treated with acetic anhydride (32.8 ml), the mixture warmed gently until solution of the oximino acid and the evolution of carbon dioxide were complete and then refluxed for 2 hours. Removal of the excess acetic anhydride yielded the crude nitrile, m.p. 84–89°. Several recrystallizations from petroleum ether (80–100°) (Norite) gave white crystals, m.p. 96–96.5°. Calc. for $C_{12}H_{13}NO_4$: OCH_3, 26.4%. Found: OCH_3, 25.8%.

Homosyringic acid.—Potassium hydroxide (7.84 g) was dissolved in a mixture of water (46.8 ml) and ethanol (52.1 ml) and this solution added to acetylhomosyringonitrile (6.0 g). After it was refluxed for 13 hours the solution was concentrated, under reduced pressure, to remove the ethanol. After it had cooled, the reaction mixture was acidified with dilute hydrochloric acid (40 ml) and the precipitated acid collected at 0° and dried. The yield of crude acid was 4.4 g (81.5%), m.p. 100–104°. Four recrystallizations from water (Norite) gave white needles, m.p. 126–128°.

Via Azlactone Synthesis

Homosyringic acid was also prepared from syringaldehyde by means of the intermediate azlactone (9). Recrystallizations of this product from water (Norite) gave white crystals, m.p. 130.5–132°.

Syntheses of 3-Hydroxy-1-(4-hydroxy-3,5-dimethoxyphenyl)-2-propanone

Acetylhomosyringic Acid

Homosyringic acid (1.17 g) was dissolved in 37% sodium hydroxide (2 ml) containing crushed ice (ca. 3 g). After the addition of acetic anhydride (0.75 ml) the cooled solution was shaken for 2–3 minutes. Acidification with 6 *N* hydrochloric acid (5.3 ml) produced an oil which crystallized slowly. The yield of crude acetylhomosyringic acid was 0.92 g (65.6%), m.p. 117–119.5°. Recrystallization from water (Norite) gave white flakes, m.p. 120–121°. Calc. for $C_{12}H_{14}O_6$: C, 56.7; H, 5.55; OCH_3, 24.4%. Found: C, 55.9; H, 5.68; OCH_3, 24.3%.

Acetylhomosyringoyl Chloride

To a solution of acetylhomosyringic acid (1.5 g) in dry benzene (3.0 ml) was added freshly purified thionyl chloride (1.35 ml). The resulting solution was refluxed, under nitrogen, for 1.5 hours. The excess thionyl chloride was removed by the successive addition and distillation of 5×2.0 ml of benzene. Removal of the excess benzene left the crude acyl chloride as a red, viscous oil weighing 1.63 g.

Acetylhomosyringoyl Diazomethane

The above acetylhomosyringoyl chloride (1.63 g) was dissolved in dry benzene (4.3 ml) and the solution added dropwise to a vigorously stirred solution of diazomethane, at 0°, prepared by dissolving the diazomethane from 5.1 g of N-nitrosomethylurea in 60 ml of

Can. J. Chem. Downloaded from www.nrcresearchpress.com by 176.9.209.113 on 09/04/12
For personal use only.

diethyl ether. The solution was allowed to warm slowly to room temperature and react overnight. Removal of the solvents under reduced pressure (nitrogen) left a viscous, red oil weighing 1.7 g.

3-Hydroxy-1-(4-hydroxy-3,5-dimethoxyphenyl)-2-propanone

Acetylhomosyringoyl diazomethane (1.7 g) was dissolved in chloroform (2.15 ml) and this solution added dropwise, with vigorous mechanical stirring, to water (45 ml) in a three-necked flask fitted with a stirrer and a condenser. The mixture was heated on a steam bath at 93° for 4 hours. Dilute hydrochloric acid (0.76 ml) was added to bring the solution to pH 1 and the heating and stirring continued for 1 hour. Decolorizing carbon (0.75 g) was added and the heating continued for a further 1 hour. The hot solution was filtered, the yellow filtrate cooled to 5°, and exhaustively extracted with 6×25-ml portions of ethyl acetate. These combined extracts were dried over anhydrous magnesium sulphate and the solvent removed under reduced pressure at room temperature to leave a viscous, pale red oil. Considerable difficulty was experienced in effecting crystallization, but after thorough drying by the addition and evaporation of three successive portions of dry benzene followed by cooling in a dry ice – acetone bath, with scratching, the oil crystallized (0.46 g). Five recrystallizations from dry benzene gave cream-colored crystals, m.p. 106.5–107.5°. Calc. for $C_{11}H_{14}O_5$: C, 58.4; H, 6.23%. Found: C, 58.8; H, 6.46%. Infrared spectrum: 3455 cm^{-1} (broad) and 3295 cm^{-1} (broad) (hydroxyls); 1700 cm^{-1} (carbonyl); 1611 cm^{-1} and 1515 cm^{-1} (aromatic ring).

The authors are grateful to the Saskatchewan Research Council for continued financial assistance and to the Ontario Paper Company Limited for their donation of acetovanillone.

1. GARDNER, J. A. F. Can. J. Chem. **32**, 532 (1954).
2. BRAUNS, F. The chemistry of lignin. Academic Press Inc., New York. 1952.
3. HIBBERT, H. Ann. Rev. Biochem. **11**, 183 (1942).
4. MCGREGOR, W. S., EVANS, T. H., and HIBBERT, H. J. Am. Chem. Soc. **66**, 41 (1944).
5. PEPPER, J. M., BAYLIS, P. E. T., and ADLER, E. Can. J. Chem. **37**, 1241 (1959).
6. FISHER, H. E. and HIBBERT, H. J. Am. Chem. Soc. **69**, 1208 (1947).
7. CRAWFORD, L. W., EATON, E. O., and PEPPER, J. M. Can. J. Chem. **34**, 1562 (1956).
8. SCHWENK, E. and PAPA, D. J. Org. Chem. **11**, 798 (1946).
9. ARLT, H. G., JR., GROSS, S. K., and SCHUERCH, C. Tappi, **41**, 64 (1958).

RECEIVED AUGUST 4, 1959.
DEPARTMENT OF CHEMISTRY,
UNIVERSITY OF SASKATCHEWAN,
SASKATOON, SASKATCHEWAN.

THE PREPARATION OF $\Delta^{\alpha\beta}$-BUTENOLIDE[1]

R. J. D. SMITH[2] AND R. N. JONES

The syntheses of β-substituted derivatives of $\Delta^{\alpha\beta}$-butenolide (I) have been described by Rubin, Paist, and Elderfield (1). These investigators prepared the β-*n*-butyl,

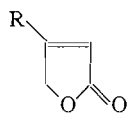

I

[1]*Issued as N.R.C. No. 5371.*
[2]*National Research Council Postdoctorate Fellow.*

Can. J. Chem. Downloaded from www.nrcresearchpress.com by 176.9.209.113 on 09/04/12
For personal use only.

diethyl ether. The solution was allowed to warm slowly to room temperature and react overnight. Removal of the solvents under reduced pressure (nitrogen) left a viscous, red oil weighing 1.7 g.

3-Hydroxy-1-(4-hydroxy-3,5-dimethoxyphenyl)-2-propanone

Acetylhomosyringoyl diazomethane (1.7 g) was dissolved in chloroform (2.15 ml) and this solution added dropwise, with vigorous mechanical stirring, to water (45 ml) in a three-necked flask fitted with a stirrer and a condenser. The mixture was heated on a steam bath at 93° for 4 hours. Dilute hydrochloric acid (0.76 ml) was added to bring the solution to pH 1 and the heating and stirring continued for 1 hour. Decolorizing carbon (0.75 g) was added and the heating continued for a further 1 hour. The hot solution was filtered, the yellow filtrate cooled to 5°, and exhaustively extracted with 6×25-ml portions of ethyl acetate. These combined extracts were dried over anhydrous magnesium sulphate and the solvent removed under reduced pressure at room temperature to leave a viscous, pale red oil. Considerable difficulty was experienced in effecting crystallization, but after thorough drying by the addition and evaporation of three successive portions of dry benzene followed by cooling in a dry ice – acetone bath, with scratching, the oil crystallized (0.46 g). Five recrystallizations from dry benzene gave cream-colored crystals, m.p. 106.5–107.5°. Calc. for $C_{11}H_{14}O_5$: C, 58.4; H, 6.23%. Found: C, 58.8; H, 6.46%. Infrared spectrum: 3455 cm^{-1} (broad) and 3295 cm^{-1} (broad) (hydroxyls); 1700 cm^{-1} (carbonyl); 1611 cm^{-1} and 1515 cm^{-1} (aromatic ring).

The authors are grateful to the Saskatchewan Research Council for continued financial assistance and to the Ontario Paper Company Limited for their donation of acetovanillone.

1. GARDNER, J. A. F. Can. J. Chem. **32**, 532 (1954).
2. BRAUNS, F. The chemistry of lignin. Academic Press Inc., New York. 1952.
3. HIBBERT, H. Ann. Rev. Biochem. **11**, 183 (1942).
4. MCGREGOR, W. S., EVANS, T. H., and HIBBERT, H. J. Am. Chem. Soc. **66**, 41 (1944).
5. PEPPER, J. M., BAYLIS, P. E. T., and ADLER, E. Can. J. Chem. **37**, 1241 (1959).
6. FISHER, H. E. and HIBBERT, H. J. Am. Chem. Soc. **69**, 1208 (1947).
7. CRAWFORD, L. W., EATON, E. O., and PEPPER, J. M. Can. J. Chem. **34**, 1562 (1956).
8. SCHWENK, E. and PAPA, D. J. Org. Chem. **11**, 798 (1946).
9. ARLT, H. G., JR., GROSS, S. K., and SCHUERCH, C. Tappi, **41**, 64 (1958).

RECEIVED AUGUST 4, 1959.
DEPARTMENT OF CHEMISTRY,
UNIVERSITY OF SASKATCHEWAN,
SASKATOON, SASKATCHEWAN.

THE PREPARATION OF $\Delta^{\alpha\beta}$-BUTENOLIDE[1]

R. J. D. SMITH[2] AND R. N. JONES

The syntheses of β-substituted derivatives of $\Delta^{\alpha\beta}$-butenolide (I) have been described by Rubin, Paist, and Elderfield (1). These investigators prepared the β-*n*-butyl,

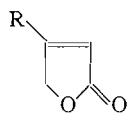

I

[1]*Issued as N.R.C. No. 5371.*
[2]*National Research Council Postdoctorate Fellow.*

Can. J. Chem. Downloaded from www.nrcresearchpress.com by 69.46.99.164 on 09/04/12
For personal use only.

β-*n*-phenyl, β-cyclopentyl, and β-cyclohexyl derivatives. These syntheses have subsequently been repeated in our laboratory and in addition the β-*n*-hexyl compound was prepared by the same method. We were not successful in obtaining the β-methyl compound; only tarry products were obtained from which no lactone could be isolated. Syntheses of the same type have been carried out in the steroid series by Ruzicka, Reichstein, and Fürst (2).

~~Unsubstituted $\Delta^{\alpha\beta}$-butenolide (I, R = H) has not previously been synthesized~~, and the object of this note is to describe its preparation by the procedure I–VII. Starting

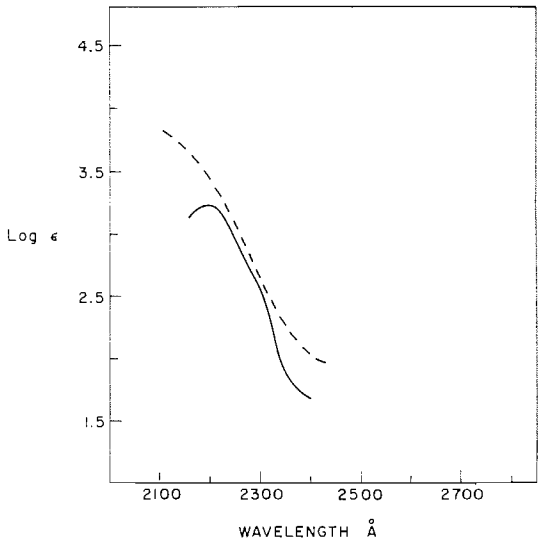

FIG. 1. Ultraviolet absorption spectrum of $\Delta^{\alpha\beta}$-butenolide.
-------- Ethanol solution.
——— *n*-Heptane solution.

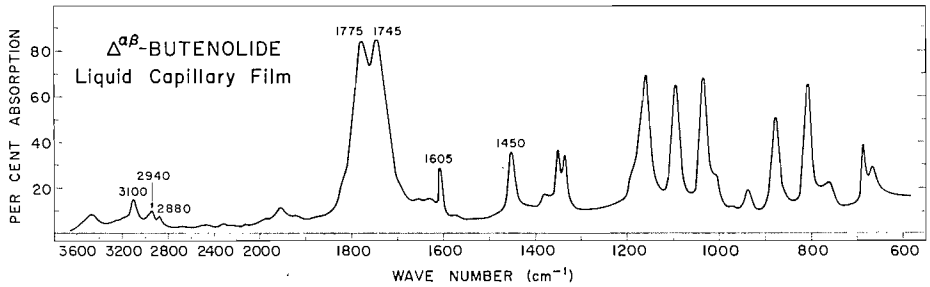

FIG. 2. Infrared absorption spectrum of $\Delta^{\alpha\beta}$-butenolide. (3100 cm^{-1} ethylenic C—H stretch; 2940, 2880 cm^{-1} methylene C—H stretch; 1775, 1745 cm^{-1} split C=O stretching band; 1605 cm^{-1} C=C stretch; 1450 cm^{-1} methylene C—H scissor vibration.)

from ethyl bromide and propargyl alcohol, the lactone was obtained as a colorless liquid in 37% over-all yield based on the alcohol. The product had b.p. 86–87° (12 mm), $n_D^{20} = 1.4670$, and ultraviolet spectrum λ_{max} 2200 Å log ϵ_{max} 3.22 in *n*-heptane solution (Fig. 1). The infrared spectrum shown in Fig. 2 exhibits the solvent-sensitive splitting

Can. J. Chem. Downloaded from www.nrcresearchpress.com by 69.46.99.164 on 09/04/12
For personal use only.

of the C=O stretching band characteristic of the $\Delta^{\alpha\beta}$-butenolide ring system (3); the principal group vibration frequencies are noted in the legend to Fig. 2.

$C_2H_5MgBr + HC{\equiv}C{-}CH_2OH$

$\downarrow$

$BrMgC{\equiv}C{-}CH_2OMgBr$ (I)

$\downarrow CO_2$

$BrMgO.CO.C{\equiv}C{-}CH_2OMgBr$ (II)

$\downarrow H_2O$

$HOOC{-}C{\equiv}C{-}CH_2OH$ (III)

$\downarrow H_2/Pd.BaSO_4$

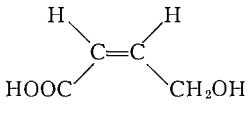

(IV)

$\downarrow \Delta$

I (R = H)

EXPERIMENTAL

Ethylmagnesium bromide was prepared from magnesium (24 g) and ethyl bromide (110 g) in anhydrous ether (250 ml). The ether was removed by distillation with simultaneous addition of benzene (200 ml). The product was cooled with ice, and propargyl alcohol (28 g) added slowly with vigorous stirring. The mixture was next heated for 2 hours on a steam bath with continuous stirring, during which time a pasty solid was deposited. This product was transferred to a 1-liter stainless steel bomb and sealed with solid carbon dioxide (250 g) for 24 hours. The pressure was released slowly, the product scraped from the bomb, and decomposed with 15% sulphuric acid (400 ml) at 0° C. This solution was next saturated with sodium chloride and extracted continuously with ether for 24 hours, after which the ether layer was separated and reextracted with aqueous sodium hydrogen carbonate solution. The aqueous phase after acidification with dilute hydrochloric acid was extracted continuously with ether for 24 hours. The ethereal solution of the acid was next dried with anhydrous magnesium sulphate and the ether removed *in vacuo* to yield 4-hydroxy-2-butynoic acid (III) (22 g) as a crystalline product.

Compound III (10 g) was dissolved in methanol (50 ml), 5% $Pd/BaSO_4$ (1 g) added, and hydrogenated at room temperature and pressure until the theoretical amount of hydrogen for semihydrogenation had been absorbed (2.4 liters). The methanol was removed *in vacuo* and the residue distilled to yield $\Delta^{\alpha\beta}$-butenolide (I, R = H) (5.8 g) as a colorless liquid, b.p. 86–87° (12 mm) n_D^{20} 1.4670. Found: C, 57.03%; H, 4.94%. Calc.: C, 57.14%; H, 4.80%.

We wish to thank Mr. H. Seguin for the carbon and hydrogen analyses.

1. Rubin, M., Paist, W. D., and Elderfield, R. C. J. Org. Chem. **6**, 260 (1941).
2. Ruzicka, L., Reichstein, T., and Fürst, A. Helv. Chim. Acta, **24**, 76 (1941).
3. Jones, R. N., Angell, C. L., Ito, T., and Smith, R. J. D. Can. J. Chem. **37**, 2007 (1959).

Received June 29, 1959.
Division of Pure Chemistry,
National Research Council of Canada,
Ottawa, Canada.

Can. J. Chem. Downloaded from www.nrcresearchpress.com by 69.46.99.164 on 09/04/12
For personal use only.

THE PROTON MAGNETIC RESONANCE SPECTRUM OF THIOPHENE*

R. J. ABRAHAM† AND H. J. BERNSTEIN

In this note, the complete analysis of the proton magnetic resonance spectrum of thiophene in solution is presented as a typical example of the analysis of an A_2B_2 spectrum.

The spectrum of liquid thiophene is too complex to analyze with certainty even at 60 Mc/s. However, in acetone solution the chemical shift difference between the A and B protons increases, and the spectrum shown (Fig. 1) of a 1:1 solution of thiophene in acetone at 60 Mc/s can be analyzed quite easily following the standard A_2B_2 analysis (1).

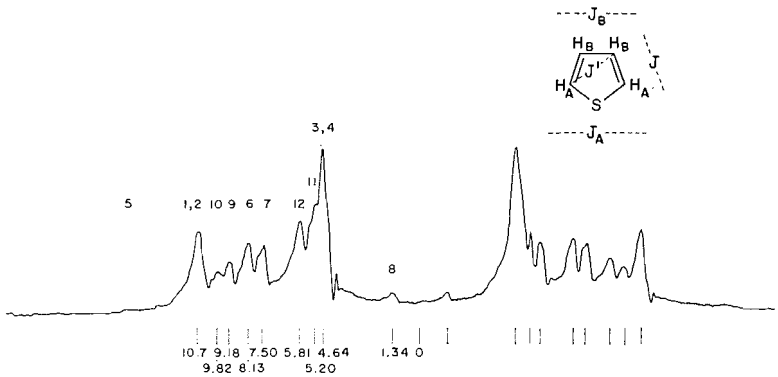

FIG. 1. The proton resonance spectrum of thiophene in a 1:1 mixture of thiophene in acetone at 60 Mc/s.

The nomenclature which will be used is shown in Fig. 1. It is convenient to define the following constants: $K = J_A+J_B$, $L = J-J'$, $M = J_A-J_B$, $N = J+J'$, and $\delta = \sigma_B - \sigma_A$.

By analogy with other five-membered heterocyclic compounds such as furan and pyrrole (2) the spectrum would be expected to be of the type for which $J_B > J_A$ and $J > J'$. This is of use in assigning the lines in the spectrum. A further check on the assignments shown (Fig. 1) is given by comparing the values of the coupling constants obtained with the results of Gronowitz and Hoffman (3) for the coupling constants in substituted thiophenes (viz.: $J_B = 3.8\pm0.3$ c.p.s., $J_A = 2.7\pm0.4$ c.p.s., $J = 5.4\pm0.6$ c.p.s., and $J' = 1.6\pm0.3$ c.p.s.).

From the assignment shown and following the analysis given in reference 1,

$$N-E_1-E_3 = 6.06$$
$$\{(\eta H_0\delta)^2+N^2)\}^{\frac{1}{2}} = E_1+E_3 = 15.34.$$

Hence

$$\eta H_0\delta = 14.1$$

also

$$[1] \qquad (M^2+L^2)^{\frac{1}{2}} = \left\{ \begin{matrix} E_9-E_{11} = 3.98 \\ E_{10}-E_{12} = 4.01 \end{matrix} \right\} = 4.00$$

Issued as N.R.C. No. 5406.

†*National Research Council Postdoctorate Fellow, 1957–59.*

Can. J. Chem. Downloaded from www.nrcresearchpress.com by 176.9.209.113 on 09/04/12
For personal use only.

and

$$[2] \qquad \{(\eta H_0\delta+M)^2+L^2\}^{\frac{1}{2}} = E_9+E_{11} = 14.38$$

$$[3] \qquad \{(\eta H_0\delta-M)^2+L^2\}^{\frac{1}{2}} = E_{10}+E_{12} = 15.63.$$

The best fit of equations [1], [2], and [3] gives

$$M = -0.67 \text{ and } L = 3.93.$$

The remaining constant K cannot be found explicitly from the spectrum. From the results of Gronowitz, we will take $K = 6.0$ c.p.s. The energies and intensities for the spectrum can now be calculated directly. These are shown with the observed values, in Table I. The agreement between calculated and observed energies is excellent, but

TABLE I

Observed and calculated energies and intensities for thiophene

	Energy relative to center of band (c.p.s.)		Relative intensity	
Transition	Calc.	Obs.	Calc.	Obs.*
1	10.70	10.70	.61	1.38
2	10.60	10.70	1.99	
3	4.64	4.64	1.40	2.74
4	4.33	4.64	1.54	
5	14.02		0.23	
6	8.07	8.13	1.56	1.18
7	7.27	7.50	1.72	1.19
8	1.32	1.34	0.31	0.33
9	8.99	9.18	.28	0.87
10	9.61	9.82	.45	0.73
11	5.01	5.20	.72	1.59
12	5.63	5.81	.55	1.35

*Normalized to the same total as the calculated values.

there is only fair agreement between the calculated and observed intensities. This is due to two factors. The values for the observed intensities shown in Table I are very approximate. The values shown are the individual peak heights as those are better defined than the integrated intensities for such an unresolved spectrum. However, these obviously only give approximate values for the intensities in such a spectrum. Also a different relaxation time may be associated with each peak in the spectrum. Thus, even when the individual lines are well resolved the observed intensities need not necessarily be the true intensities as relaxation phenomena may affect these values.

The values of the coupling constants obtained from this analysis are, in c.p.s., $J_A = 2.7$; $J_B = 3.3$; $J = 5.0$; $J' = 1.1$. As in the furan ring (2), these values are in close agreement with those obtained for the substituted compounds.

The A_2B_2 analysis provides a means of obtaining approximately the chemical shift difference between the A and B protons of thiophene in an unresolved thiophene spectrum. For example, the spectrum of thiophene in cyclohexane solution at 40 Mc/s has been given by Gronowitz and Hoffman (3). Here the chemical shift difference between the A and B protons is so small that the two parts of the spectrum start to overlap. However, transitions 3 and 4 can still be assigned to the strong central line and transitions 1 and 2 to the weak outermost line. This gives

$$N = E_1-E_3 = 5.5 \text{ c.p.s.}$$

Can. J. Chem. Downloaded from www.nrcresearchpress.com by 176.9.209.113 on 09/04/12
For personal use only.

and

$$\{(\eta H_0\delta)^2+N^2\}^{\frac{1}{2}} = E_1+E_3 = 7.4 \text{ c.p.s.}$$
$$\text{i.e. } \eta H_0\delta = 5.0 \text{ c.p.s.}$$

The value of N obtained is in good agreement with the value found above (6.0 c.p.s.), thus confirming the assignment. The above analysis, however, only gives the numerical value of $\eta H_0\delta$ and does not say which of the protons in the thiophene ring give the low field signal. By analogy with the results for furan and pyrrole (2), it may be assumed that the A protons are to low field. This conclusion is supported by the results of Gronowitz and Hoffman, who find that the A proton signal in 3,4-dibromothiophene is to low field of the B proton signal in the analogous compound, 2,5-dibromothiophene. However, the difference between the A and B proton chemical shifts is much less in thiophene (5.0 c.p.s.) than in these dibromo compounds (19 c.p.s.). Gronowitz and Hoffman have taken the ring proton signals in these compounds as the reference chemical shifts in determining the influence of substituents on the ring proton chemical shifts. Thus, the values obtained need to be altered slightly, but this does not affect their general conclusions.

1. Pople, J. A., Schneider, W. G., and Bernstein, H. J. Can. J. Chem. **35**, 1060 (1957).
2. Abraham, R. J. and Bernstein, H. J. Can. J. Chem. **37**, 1056 (1959).
3. Gronowitz, S. and Hoffman, R. A. Arkiv Kemi, **13**, 279 (1958).

Received August 4, 1959.
Division of Pure Chemistry,
National Research Council,
Ottawa, Canada.

Can. J. Chem. Downloaded from www.nrcresearchpress.com by 176.9.209.113 on 09/04/12
For personal use only.

OOSPOREIN FROM AN ACREMONIUM SP.*

P. V. Divekar,† R. H. Haskins, and L. C. Vining

Stationary liquid cultures of a fungus isolated in this laboratory as an air contaminant excreted into the medium a purple pigment which could be extracted with ether and purified by crystallization from aqueous methanol. Analyses and molecular weight estimations on the pigment and derivatives best fitted a molecular formula $C_{14}H_{10}O_8$. A tetraacetate and tetramethyl ether were prepared, and reductive acetylation gave a colorless dihydrooctaacetate with an ultraviolet absorption spectrum similar to that of dibenzoquinone leucoacetate (1). These properties suggested that the pigment might be oosporein, a substance of known chemical structure produced by *Oospora colorans* van Beyma (2) and by *Chaetomium aureum* Chivers (3). Direct comparisons with authentic samples confirmed the identification. Infrared, ultraviolet, and visible absorption maxima of oosporein and of the derivatives mentioned above are reported.

The fungus (PRL 1699) belongs to the family Moniliaceae. As far as can be determined from available literature, it is a member of the genus *Acremonium* and a complete study of its morphology and development will appear as part of a comparative study of the various species of *Acremonium*, a number of which are known to produce purple pig-

*Issued as N.R.C. No. 5405.
†*National Research Council of Canada Postdoctorate Fellow, 1957–59.*

and

$$\{(\eta H_0\delta)^2+N^2\}^{\frac{1}{2}} = E_1+E_3 = 7.4 \text{ c.p.s.}$$
$$\text{i.e. } \eta H_0\delta = 5.0 \text{ c.p.s.}$$

The value of N obtained is in good agreement with the value found above (6.0 c.p.s.), thus confirming the assignment. The above analysis, however, only gives the numerical value of $\eta H_0\delta$ and does not say which of the protons in the thiophene ring give the low field signal. By analogy with the results for furan and pyrrole (2), it may be assumed that the A protons are to low field. This conclusion is supported by the results of Gronowitz and Hoffman, who find that the A proton signal in 3,4-dibromothiophene is to low field of the B proton signal in the analogous compound, 2,5-dibromothiophene. However, the difference between the A and B proton chemical shifts is much less in thiophene (5.0 c.p.s.) than in these dibromo compounds (19 c.p.s.). Gronowitz and Hoffman have taken the ring proton signals in these compounds as the reference chemical shifts in determining the influence of substituents on the ring proton chemical shifts. Thus, the values obtained need to be altered slightly, but this does not affect their general conclusions.

1. Pople, J. A., Schneider, W. G., and Bernstein, H. J. Can. J. Chem. **35**, 1060 (1957).
2. Abraham, R. J. and Bernstein, H. J. Can. J. Chem. **37**, 1056 (1959).
3. Gronowitz, S. and Hoffman, R. A. Arkiv Kemi, **13**, 279 (1958).

Received August 4, 1959.
Division of Pure Chemistry,
National Research Council,
Ottawa, Canada.

Can. J. Chem. Downloaded from www.nrcresearchpress.com by 176.9.209.113 on 09/04/12
For personal use only.

OOSPOREIN FROM AN ACREMONIUM SP.*

P. V. Divekar,† R. H. Haskins, and L. C. Vining

Stationary liquid cultures of a fungus isolated in this laboratory as an air contaminant excreted into the medium a purple pigment which could be extracted with ether and purified by crystallization from aqueous methanol. Analyses and molecular weight estimations on the pigment and derivatives best fitted a molecular formula $C_{14}H_{10}O_8$. A tetraacetate and tetramethyl ether were prepared, and reductive acetylation gave a colorless dihydrooctaacetate with an ultraviolet absorption spectrum similar to that of dibenzoquinone leucoacetate (1). These properties suggested that the pigment might be oosporein, a substance of known chemical structure produced by *Oospora colorans* van Beyma (2) and by *Chaetomium aureum* Chivers (3). Direct comparisons with authentic samples confirmed the identification. Infrared, ultraviolet, and visible absorption maxima of oosporein and of the derivatives mentioned above are reported.

The fungus (PRL 1699) belongs to the family Moniliaceae. As far as can be determined from available literature, it is a member of the genus *Acremonium* and a complete study of its morphology and development will appear as part of a comparative study of the various species of *Acremonium*, a number of which are known to produce purple pig-

*Issued as N.R.C. No. 5405.
†*National Research Council of Canada Postdoctorate Fellow, 1957–59.*

ments diffusible in the agar medium on which they are growing (4). Although oosporein has recently been reisolated from *Chaetomium* and other species (5), to the authors' knowledge, its production by an *Acremonium* has not previously been described.

EXPERIMENTAL

Production and Isolation

A batch of twenty 1-liter conical flasks, each containing 350 ml of Czapek-Dox solution (glucose, 50 g; $NaNO_3$, 2 g; KH_2PO_4, 1 g; KCl, 0.5 g; $MgSO_4.7H_2O$, 0.5 g; $FeSO_4.7H_2O$, 0.01 g; and distilled water, 1 liter), were sterilized and inoculated with *Acremonium* sp. (PRL 1699). After incubation in the dark at 24° C for 15 days the wine-red culture fluid (6.4 liters) was filtered, acidified with concentrated hydrochloric acid, and extracted twice with 2-liter portions of ether. The ethereal extract was evaporated to dryness and the reddish-brown amorphous powder (3 g) crystallized three times from aqueous methanol as bronze plates (1.8 g), m.p. 290–295° C, undepressed on admixture with authentic samples of oosporein. Found: C, 55.0%; H, 3.2%; C—CH_3, 9.8%. Calculated for $C_{14}H_{10}O_8$: C, 54.9%; H, 3.3%; 2C—CH_3, 9.8%. Absorption maxima in ethanol 216 and 287 mμ, inflexions at 372 and 415 mμ, log ε 3.51, 4.67, 2.94, and 2.79, respectively. In aqueous solution the inflexion at 415 mμ is displaced bathochromically and appears as a maximum at 500 mμ (log ε, 3.05). Other maxima appear at 244 and 291 mμ, with an inflexion at 374 mμ; log ε 4.09, 4.47, and 3.35, respectively. The pigment has principal infrared maxima (KBr disk) at 3310 (s), 1648 (s), 1625 (s), 1387 (s), 1329 (s), 1297 (s), 1242 (s), 1070 (s), 929 (m), 764 (m), 740 (w), 708 (w) cm^{-1}. No differences were detected between the spectral properties of the pigment and those of authentic samples of oosporein.

Acetate

The pigment (50 mg) boiled for 10 minutes with acetic anhydride (3 ml) gave a pale red solution which, when poured into ice water, deposited yellow crystals (55 mg). These were recrystallized from methanol as bright yellow needles (45 mg), m.p. 190° C, undepressed by an authentic sample of oosporein tetraacetate. Found: C, 55.7%; H, 3.9%; CH_3CO, 36.0%. The molecular weight determined by isothermal distillation in acetone (6) was 463, and by the Rast method in camphor, 428. Calculated for $C_{22}H_{18}O_{12}$: C, 55.7%; H, 3.8%; $4CH_3CO$, 36.3%; mol. wt., 474. Ultraviolet absorption maximum in ethanol at 262 mμ, inflexion at 330 mμ; log ε 4.41 and 3.05, respectively. Infrared absorption maxima (KBr disk) at 1791 (shoulder, s), 1778 (s), 1675 (s), 1640 (w), 1620 (m) cm^{-1}. These spectral properties were indistinguishable from those of authentic samples of oosporein tetraacetate.

Leucoacetate

The pigment (50 mg) was boiled with acetic anhydride (3 ml) and zinc dust for 1 hour. The colorless solution was filtered and poured into ice water giving an amorphous white precipitate (80 mg) which was crystallized twice from methanol to yield small colorless cubes (55 mg), m.p. 243° C. Found: C, 55.7%; H, 4.8%; CH_3CO, 54.6%. Calculated for $C_{30}H_{30}O_{16}$: C, 55.7%; H, 4.7%; $8CH_3CO$, 53.3%. Ultraviolet absorption maximum in ethanol at 270 mμ, inflexion at 234 mμ; log ε 3.42 and 4.17, respectively.

Methyl Ether

Ethereal diazomethane (from 0.5 g of nitrosomethyl urea) was added to the pigment (50 mg) suspended in 2 ml of methanol. After half an hour at room temperature the solution was evaporated to dryness and the product in benzene (50 ml) passed through

Can. J. Chem. Downloaded from www.nrcresearchpress.com by 176.9.209.113 on 09/04/12
For personal use only.

a short column of neutral alumina. The eluate was evaporated to dryness and crystallized three times from aqueous methanol to give orange needles (20 mg), m.p. 123° C. Found: C, 60.0%; H, 5.3%; OCH_3, 31.5%. Calculated for $C_{18}H_{18}O_8$: C, 59.7%; H, 5.0%; $4OCH_3$, 34.2%. Ultraviolet absorption maxima in ethanol at 285.5 and 394 mμ; log ε 4.40 and 2.98, respectively. Infrared absorption maxima (KBr disk) at 1654 (s), 1614 (w), 1588 (s).

The authors are indebted to Mr. A. Funk for the isolation of PRL 1699 and also wish to thank Dr. W. B. Whalley, University of Liverpool, and Prof. F. Kögl, Organisch-chemisch Laboratorium der Rijksuniversiteit, Utrecht, for generously supplying samples of oosporein and its acetate. Analyses were done by Mr. M. Mazurek and infrared spectra by Miss I. M. Gaffney of this laboratory.

1. Erdtman, H., Granath, M., and Schultz, G. Acta Chem. Scand. **8**, 1442 (1954).
2. Kögl, F. and Van Wessen, G. C. Rec. trav. chim. **63**, 5 (1944).
3. Lloyd, G., Robertson, A., Sankey, G. B., and Whalley, W. B. J. Chem. Soc. 2163 (1955).
4. Petch, T. Brit. Mycol. Soc. Trans. **16**, 209 (1932).
5. Thomson, R. H. University of Aberdeen. Personal communication.
6. Childs, C. E. Anal. Chem. **26**, 1963 (1954).

Received August 21, 1959.
Prairie Regional Laboratory,
National Research Council,
Saskatoon, Saskatchewan.

SYNTHESIS OF POLYMETHYLENEBISISOTHIOCYANATES*

G. D. Thorn and B. Huston

Alkyl isothiocyanates are most conveniently prepared by reacting aqueous alkyldithiocarbamic acid salts with ethyl chloroformate to give carbethoxydithiocarbamates, which undergo fission to the isothiocyanate, carbon oxysulphide, and ethanol (1, 2):

$$RNHCS_2Na + ClCO_2C_2H_5 \rightarrow RNHCS_2CO_2C_2H_5 \rightarrow RNCS + COS + C_2H_5OH.$$

The decomposition reaction can be effected by heating the isolated ester *in vacuo* (3) or with aqueous alkali (4, 5). The decomposition of carbethoxybutyldithiocarbamate was found also to proceed very quickly in chloroform solution containing anhydrous triethylamine (4).

Ethylenebisisothiocyanate has been prepared by the thermal decomposition of the carbethoxy compound (6, 7). In order to obtain yields approaching those reported in the literature it was our experience that the carbethoxy derivative must be purified through several crystallizations before attempting the batchwise thermal cleavage. In this note, two procedures are reported upon for preparation of ethylene- and other polymethylene-bisisothiocyanates which obviate the necessity of purifying the carbethoxy compound.

In method A, the isolated but crude oily carbethoxydithiocarbamate is put through a falling-film molecular still *in vacuo* with the heating surface kept at a temperature a few degrees above the boiling point of the bisisothiocyanate, or at 100–105°, whichever is the higher. Decomposition of the carbethoxy compound and distillation of the resultant

*Contribution No. 164, Pesticide Research Institute.

Can. J. Chem. Downloaded from www.nrcresearchpress.com by 176.9.209.113 on 09/04/12
For personal use only.

a short column of neutral alumina. The eluate was evaporated to dryness and crystallized three times from aqueous methanol to give orange needles (20 mg), m.p. 123° C. Found: C, 60.0%; H, 5.3%; OCH_3, 31.5%. Calculated for $C_{18}H_{18}O_8$: C, 59.7%; H, 5.0%; $4OCH_3$, 34.2%. Ultraviolet absorption maxima in ethanol at 285.5 and 394 mμ; log ε 4.40 and 2.98, respectively. Infrared absorption maxima (KBr disk) at 1654 (s), 1614 (w), 1588 (s).

The authors are indebted to Mr. A. Funk for the isolation of PRL 1699 and also wish to thank Dr. W. B. Whalley, University of Liverpool, and Prof. F. Kögl, Organisch-chemisch Laboratorium der Rijksuniversiteit, Utrecht, for generously supplying samples of oosporein and its acetate. Analyses were done by Mr. M. Mazurek and infrared spectra by Miss I. M. Gaffney of this laboratory.

1. Erdtman, H., Granath, M., and Schultz, G. Acta Chem. Scand. **8**, 1442 (1954).
2. Kögl, F. and Van Wessen, G. C. Rec. trav. chim. **63**, 5 (1944).
3. Lloyd, G., Robertson, A., Sankey, G. B., and Whalley, W. B. J. Chem. Soc. 2163 (1955).
4. Petch, T. Brit. Mycol. Soc. Trans. **16**, 209 (1932).
5. Thomson, R. H. University of Aberdeen. Personal communication.
6. Childs, C. E. Anal. Chem. **26**, 1963 (1954).

Received August 21, 1959.
Prairie Regional Laboratory,
National Research Council,
Saskatoon, Saskatchewan.

SYNTHESIS OF POLYMETHYLENEBISISOTHIOCYANATES*

G. D. Thorn and B. Huston

Alkyl isothiocyanates are most conveniently prepared by reacting aqueous alkyldithiocarbamic acid salts with ethyl chloroformate to give carbethoxydithiocarbamates, which undergo fission to the isothiocyanate, carbon oxysulphide, and ethanol (1, 2):

$$RNHCS_2Na + ClCO_2C_2H_5 \rightarrow RNHCS_2CO_2C_2H_5 \rightarrow RNCS + COS + C_2H_5OH.$$

The decomposition reaction can be effected by heating the isolated ester *in vacuo* (3) or with aqueous alkali (4, 5). The decomposition of carbethoxybutyldithiocarbamate was found also to proceed very quickly in chloroform solution containing anhydrous triethylamine (4).

Ethylenebisisothiocyanate has been prepared by the thermal decomposition of the carbethoxy compound (6, 7). In order to obtain yields approaching those reported in the literature it was our experience that the carbethoxy derivative must be purified through several crystallizations before attempting the batchwise thermal cleavage. In this note, two procedures are reported upon for preparation of ethylene- and other polymethylene-bisisothiocyanates which obviate the necessity of purifying the carbethoxy compound.

In method A, the isolated but crude oily carbethoxydithiocarbamate is put through a falling-film molecular still *in vacuo* with the heating surface kept at a temperature a few degrees above the boiling point of the bisisothiocyanate, or at 100–105°, whichever is the higher. Decomposition of the carbethoxy compound and distillation of the resultant

*Contribution No. 164, Pesticide Research Institute.

Can. J. Chem. Downloaded from www.nrcresearchpress.com by 176.9.209.113 on 09/04/12
For personal use only.

isothiocyanate are immediate. Thus, reaction of the formed isothiocyanate with impurities or by self-condensation at elevated temperatures as obtained in the "batch" method is avoided.

In method B, the crude carbethoxy compound is added to cold 20% aqueous potassium hydroxide. After several minutes, the mixture is extracted with benzene and the organic layer dried with anhydrous sodium sulphate. The residue obtained by removal of the solvent (as in a rotary evaporator) is then subjected to distillation at reduced pressure.

The procedure followed for the preparation of the carbethoxydithiocarbamates is typically that of several examples in the literature. Briefly, the diamine (1.0 mole), carbon disulphide (2.2 mole), and sodium hydroxide (2.0 mole) are reacted together at 35–45° for 3 hours in sufficient water to end up with an approximately 20% solution of the disodium polymethylenebisdithiocarbamate. The solution is then chilled and treated dropwise, with adequate stirring, with 2.0 mole of ethyl chloroformate. After a further reaction period of an hour, the carbethoxy derivative is isolated either by filtration or extraction with benzene.

TABLE I

Aliphatic bisisothiocyanates, SCN—X—NCS

X	B.p./mm	n_D	Log ϵ_{max}	Method	% Yield	Anal. (N%) Calc.	Found
Ethylene	71.5–72/0.3	1.6265/22.8°*	3.30†	A	77	19.45	19.25
Propylene	77–9/0.1	1.5750/23°	3.33	A	23	17.75	17.73
Tetramethylene	102–4/0.1	1.5930/23°	3.32	B	50	16.30	16.05
Pentamethylene	124–30/0.3	1.5680/23.5°	—	A	18	15.05	14.8
Hexamethylene	119–22/0.1	1.5630/26°	3.28	B	41	14.00	13.9

*Yakubovitch and Klimova (6) give b.p. 144° at 10 mm and n_D^{20} 1.6271.

†The isothiocyanates possess a single absorption peak in the ultraviolet region, at 247 mμ. Solvent, ethyl ether.

Table I gives the aliphatic bisisothiocyanates prepared by these methods. It might be noted that, except in the preparation of ethylenebisisothiocyanate, some diethyl polymethylenebisurethane was always obtained, requiring fractional distillation of the isothiocyanate. The urethane arises from incomplete reaction of the diamine with carbon disulphide, and can be avoided either by extending the reaction time for the dithiocarbamate or by purification of the carbethoxy derivative.

The authors wish to thank R. W. White for checking the purity of the isothiocyanates by infrared analysis, and Dorle Bongart for the microanalyses.

1. Andreasch, R. Monatsh. **27**, 1211 (1906).
2. Kaluza, L. Monatsh. **33**, 363 (1912).
3. Slotta, K. H. and Dressler, H. Ber. B, **63**, 888 (1930).
4. Hodgkins, J. E. and Ettlinger, M. G. J. Org. Chem. **21**, 404 (1956).
5. Ettlinger, M. G. and Hodgkins, J. E. J. Am. Chem. Soc. **77**, 1831 (1955).
6. Yakubovitch, A. Ya. and Klimova, V. A. J. Gen. Chem. U.S.S.R. **9**, 1777 (1939).
7. Klopping, H. Chemical constitution and antifungal action of organic sulphur compounds. Thesis. Utrecht, (1951).

Received September 11, 1959.
Pesticide Research Institute,
Canada Department of Agriculture,
London, Ontario.

Can. J. Chem. Downloaded from www.nrcresearchpress.com by 176.9.209.113 on 09/04/12
For personal use only.

THE EFFECT OF HEAT TREATMENT ON THE ACTIVITY OF A SILVER CATALYST*

E. ECHIGOYA,† C. H. AMBERG, AND G. L. OSBERG

Can. J. Chem. Downloaded from www.nrcresearchpress.com by 69.46.99.164 on 09/04/12
For personal use only.

In carrying out the oxidation of ethylene on silver catalysts it is customary to stabilize the catalyst in the reacting gas mixture over periods up to several days. Among the few workers that have reported studies of catalytic activity during pretreatment, Orzechowski and MacCormack (1) have given a detailed account of the attendant slow changes. In an earlier paper Murray (2) examined the first few hours of reaction and found an increase in selectivity.‡

In the present study it has been attempted to demonstrate the similarity of activity changes during the first few hours of reaction with changes induced by short periods of preliminary heat treatment. It is important to note that the similar reaction patterns found both by Murray and in this laboratory differ from the common case in which all activity is diminished through destruction of the surface with heating.

The reported experiments were made along with a more detailed examination of ethylene oxidation in fluidized bed reactors (3).

EXPERIMENTAL

The method of catalyst preparation from Ag–Ca alloys has been discussed previously (4). The present batch contained 0.17% Ca and had been derived from a powdered alloy containing 8.05% Ca.

The reactor was a fluidized bed consisting of a mixture of 5 cc (12.2 g) of the 100- to 200-mesh catalyst powder and 20 cc (31.8 g) of 100- to 200-mesh "Scotchlite" glass beads contained in a 1-in. diameter, pyrex column. The glass beads served to inhibit agglomeration of the catalyst granules (5). An air flow of 3.4 l./minute was maintained throughout both the pretreatment and reaction periods, and an air-to-ethylene ratio of 40:1 with maximum fluctuations of ±4% was used for the reaction. All reactions were carried out at 250±2° C and the products analyzed by gas chromatography (6). Pretreatment temperatures and periods are indicated in Fig. 2. Fresh portions of catalyst from the same batch were used for each pretreatment.

A sample of 48- to 100-mesh catalyst (0.21% Ca) was used to follow changes in B.E.T. surface area with prolonged outgassing at 250° C. A conventional volumetric apparatus was employed for the purpose and argon at −195° C was used as the adsorbate.

RESULTS AND DISCUSSION

Figure 1 shows the initial selectivity and total conversion values at 250° C for the different portions of catalyst plotted against the temperature of pretreatment. Since the two curves qualitatively resembled those found for the reaction at, say, 250° C over a period of several hours, it was tempting to assume that the short heat treatments had produced very similar surfaces, but had done so far more rapidly.

That this is so, at least in terms of catalytic activity, was demonstrated by following the selectivity and conversion changes with time of reaction at 250° C for each pretreated batch. Figure 2 shows these changes superimposed on the two curves drawn for

*Issued as N.R.C. No. 5414.
†National Research Council Postdoctorate Fellow 1957–59.
‡Ethylene oxide as per cent of converted ethylene.

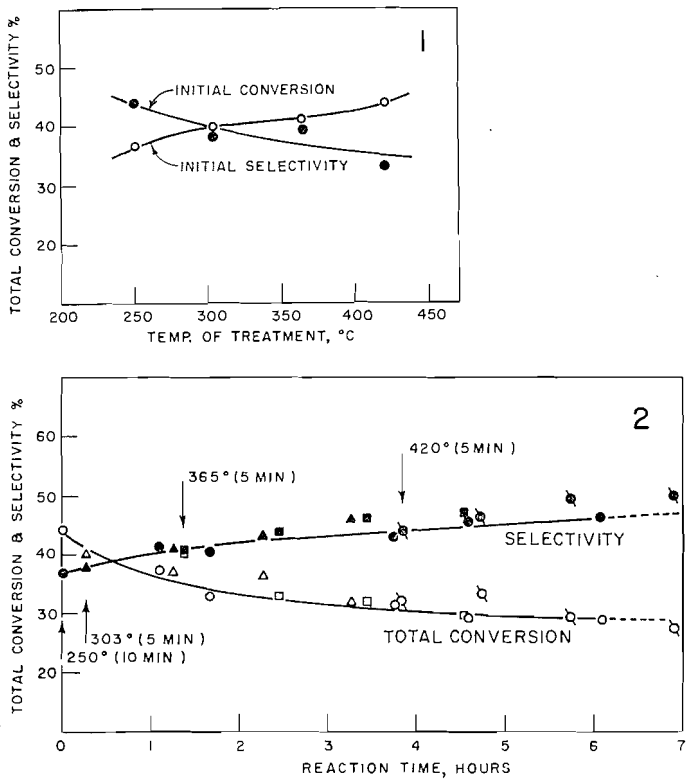

FIG. 1. Silver-catalyzed oxidation of ethylene at 250° C. Initial total conversion (filled-in circles) and initial selectivity (open circles) for catalysts pretreated at different temperatures.

FIG. 2. Silver-catalyzed oxidation of ethylene at 250° C. Changes in total conversion (open points) and selectivity (filled-in points) for catalysts pretreated at different temperatures. Periods of pretreatment given in parentheses. Zero reaction time indicated by arrows. Circles: Pretreatment at 250° for 10 minutes. Triangles: Pretreatment at 303° for 5 minutes. Squares: Pretreatment at 365° for 5 minutes. Dashed circles: Pretreatment at 420° for 5 minutes.

the original catalyst that had never been heated beyond 250° C (solid lines, fitted to circles only). The time axes were shifted so that the initial selectivities would fall on the original selectivity curve (arrows). The grouping of the remaining selectivity and total conversion values near the respective 250° C curves indicates that the catalytic "histories" match that of the original catalyst. This, in turn, supports our original assumption, namely, that the heat treatments merely served to speed up surface changes also occurring during the course of the reaction at 250° C.

Although the data do not warrant a unique mechanistic interpretation of these surface changes, a few additional observations will be found to narrow down the range of possible causes.

(1) The small particle size required for fluidization ensured that leaching of the calcium had taken place throughout the bulk of the granule. Coupled with the fact that catalysts in the 0.1–0.2% range of calcium content show little variation in activity with change in calcium content (7), this means that diffusion of calcium from particle interior to active surface during the course of the reaction can be discounted as a possible explanation for the observed changes.

Can. J. Chem. Downloaded from www.nrcresearchpress.com by 69.46.99.164 on 09/04/12
For personal use only.

(2) The observed changes are almost entirely attributable to a decrease in CO_2 production with time, ethylene oxide remaining virtually constant. Any model that is ultimately adopted must incorporate a capacity for undergoing surface modifications resulting in selective changes of this type. For instance, if one were to adopt Twigg's model (8) of two-point contact of C_2H_4 molecules on a silver oxide surface to produce CO_2, this might mean that the number of two-point configurations in the surface has decreased with surface rearrangement, leaving unchanged the available single centers for ethylene oxide production.

It is interesting to note that the rate of CO_2 production decreased linearly as the logarithm of reaction time. This function is formally the same as the Elovich equation, applicable in many cases to the increase with time of the amount of gas chemisorbed on a solid surface. Whether this is significant in terms of selective poisoning in our case cannot, of course, be decided on the basis of the available information.

(3) When the temperatures and times of preliminary heat treatment (both shown in Fig. 2) were combined with their equivalent times at 250° (marked by arrows in Fig. 2) in three Arrhenius-type plots, the maximum spread in slopes was found to be only 10%. Although we do not wish to attach any significance to the absolute value obtained from two-point plots (17 kcal/mole), its relative lack of variation suggests that an essentially uniform change has taken place on the catalyst surface during heat treatment and reaction. This change may well have been complex in nature, involving such processes as recrystallization, diffusion, and chemisorption.

(4) A sample of catalyst was outgassed for 100 hours at 250° C. During the first half of this period its B.E.T. surface area decreased from 0.54 m^2/g by about 6% and during the second half by a further 1%. These data indicate maintenance of a stable skeletal structure of the silver catalyst at 250° C. It must be kept in mind that B.E.T. measurements may not be too sensitive to changes in the fine-structure of the surface. In the present case they serve merely to confirm that gross surface destruction did not take place at 250°. Smeltzer *et al.* (9) found that their catalyst No. I retained about 80% of its original sorption capacity for oxygen after heating at 300° C for over 100 days, thus exhibiting properties similar to those shown by the catalyst in the present work, if one makes allowances for somewhat different conditions. Though chemisorbed oxygen takes part in the oxidation of ethylene, even this set of adsorption experiments was not strictly applicable to the oxidation reaction. The latter takes place on a surface at least partially covered with oxygen and in an environment of other gases. Nevertheless, sorption experiments on out-gassed surfaces are useful, provided their limited applicability to systems under reaction conditions is clearly recognized.

1. Orzechowski, A. and MacCormack, K. E. Can. J. Chem. **32**, 388 (1954).
2. Murray, K. E. Australian J. Sci. Research, A, **3**, 433 (1950).
3. Echigoya, E. and Osberg, G. L. To be published.
4. Cambron, A. and McKim, F. L. W. U.S. Patent No. 2,562,857 (1951); Can. Patent No. 475,366 (1951).
5. Echigoya, E. and Osberg, G. L. To be published.
6. Amberg, C. H., Echigoya, E., and Kulawic, D. Can. J. Chem. **37**, 708 (1959).
7. Cvetanović, R. J. and Chenier, J. H. B. Unpublished results.
8. Twigg, G. H. Trans. Faraday Soc. **42**, 284 (1946).
9. Smeltzer, W. W., Tollefson, E. L., and Cambron, A. Can. J. Chem. **34**, 1046 (1956).

Received July 17, 1959.
Division of Applied Chemistry,
National Research Council of Canada,
Ottawa, Canada.

Can. J. Chem. Downloaded from www.nrcresearchpress.com by 69.46.99.164 on 09/04/12
For personal use only.